

Until the supplement has been able to undergo proper copyediting, typesetting, and author proofing, readers should be aware that the specific preprint information below may contain errors and has not been finalized by authors.

Regular and Young Investigator Award Abstracts

Ethics Approval Stained samples were commercially available.

<http://dx.doi.org/10.1136/jitc-2022-SITC2022.0001>

Biomarkers, Immune Monitoring and Novel Technologies

1 CAPTURING THE SPATIAL LANDSCAPE OF TUMOR AND IMMUNE CELL LINEAGES IN THE MICROENVIRONMENT OF HUMAN CANCER TISSUES

¹Reggie Prioli*, ¹Lisa Arvidson*, ¹Sam Jensen, ²Michael Smith*, ²Katie White, ²Richard Heil-Chapdelaine, ²Melinda Angus-Hill. ¹*Cell Signaling Technology, Danvers, MA, USA*; ²*Leica Microsystems Inc, Bellevue, WA, USA*

Background Immune system response to cancer therapies can indicate whether a patient will have positive outcomes following therapy. Understanding how the tumor microenvironment (TME) evolves during tumorigenesis and therapeutic response is crucial to developing personalized treatments with the goal of improving cancer therapy. With robust and comprehensive multiplexed imaging technologies, immune biomarkers can be used to interrogate myeloid and lymphoid cell lineages and structures, and when combined with specific oncology biomarkers, can capture the immune response within the TME in a variety of neoplasms. The availability of cell type specific biomarkers, combined with the ability to interrogate using multiplexed tissue imaging, provides unprecedented and novel insights into immune cell populations and spatial cell interactions with many cell types in the TME.

Cell DIVETM Multiplex Imaging Solution allows probing and imaging of dozens of biomarkers on a whole single tissue section with an iterative staining and dye inactivation workflow. At its core, Cell DIVE is a precise and adaptable open multiplexing solution that enables flexibility in antibody selection of biomarker panels used in a multiplexed imaging study. Cell Signaling Technology (CST) has a broad portfolio of IHC-validated antibodies to detect key proteins in the TME, enabling immune cell detection and phenotyping in tissue. CST offers off the shelf (OTS), ready-to-ship antibody conjugates that have been verified to work on Cell DIVE and offers custom conjugation of IHC-validated antibodies to fluorophores and other detection reagents. CST employs a rigorous approach to IHC validation, followed by verification on the Cell DIVE platform to ensure successful detection of proteins. Here, we demonstrate multiplexed Cell DIVE imaging using a novel panel of dozens of CST biomarkers across multiple tissue types.

Methods Sections were stained using conjugated antibodies (Cell Signaling Technology) to various biomarkers in 4 channels plus DAPI and imaged using Cell DIVE. Multiple rounds of staining and imaging were accomplished using the Cell DIVE workflow (Leica Microsystems).

Results Development of the multiplexed panel required minimal optimization, enabled the identification of complex cell types and revealed their cell-to-cell interactions within the tumor microenvironment.

Conclusions Multiplexed whole slide imaging allows deep analysis of immune cell lineages and provided new insights into immune and tumor cell-to-cell interactions within the tumor microenvironment.

2

CHARACTERIZATION OF THE TUMOR MICROENVIRONMENT IN PANCREATIC DUCTAL ADENOCARCINOMA USING MULTIPLEXED IMAGING

Michael J Smith*, Katie O White, Richard A Heil-Chapdelaine, Melinda L Angus-Hill. *Leica Microsystems Inc, Bellevue, WA, USA*

Background The pancreas is surrounded by highly vascularized organs such as the duodenum and the common bile duct. Pancreatic cancer often invades and metastasizes to these organs, and to more distant organs such as the liver, peritonium, lung, brain, kidney and bone. Conventional chemotherapy plus radiation, or in advanced disease chemotherapy plus targeted drug therapy can lengthen patient survival. However, even in patients that only have local disease, the 5-year survival rate is only around 40%, demonstrating that there is need for improved conventional and immune therapies for all pancreatic cancer patients. Tumor cells can evade treatments and continue to grow. Additionally, stromal cells in the tumor microenvironment are a critical support niche for continued tumor growth. Understanding all cells in the tumor microenvironment is essential for understanding tumor metastasis and improving cancer therapies, especially immunotherapies. In this study, dozens of biomarkers have been used to probe tumor heterogeneity in pancreatic ductal adenocarcinoma (PDAC) tissue. With Cell DIVETM multiplexed imaging, dozens of biomarkers can characterize cell heterogeneity, cellular activity and cell-to-cell spatial context within the TME.

Methods Sections were stained using conjugated antibodies (from multiple vendors) to various biomarkers in 4 channels plus DAPI and imaged using Cell DIVE. Multiple rounds of staining and imaging were accomplished using the Cell DIVE workflow (Leica Microsystems).

Results We examined the tumor, stromal compartment and immune cell contributions to the tumor microenvironment (TME). The panel enabled the examination of tumor associated stromal components and tumor infiltrating lymphocytes (TIL), angiogenesis, metastasis, invasion, inflammation, hypoxia, metabolism, and the immune response. We found that these heterogenous activities are often intertwined. For example, subregions within the tumor adapt to hypoxic conditions and can gain dominance by uncontrolled cell growth. Additionally, these hypoxic regions are devoid of immune cells.

Conclusions Taken together, multiplexed whole slide imaging enables spatially resolved tissue analysis of cellular activities in the TME, including new insights into cell-to-cell interactions and immune cell profile.

Ethics Approval Human samples were commercially available.

<http://dx.doi.org/10.1136/jitc-2022-SITC2022.0002>

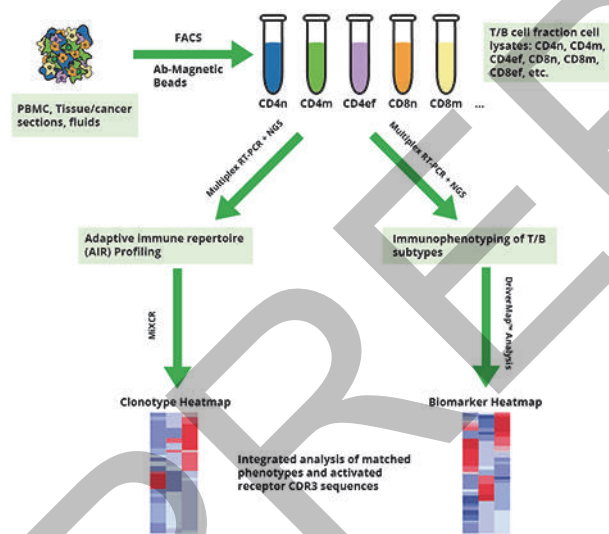
3 ADAPTIVE IMMUNE RECEPTOR REPERTOIRE PROFILING FOR BIOMARKER DISCOVERY

Alex Chenchik*, Mikhail Makhanov, Dongfang Hu, Tianbing Liu, Lester Kobzik. *Cellecta, Inc., Mountain View, CA, USA*

Background Adaptive Immune Receptor (AIR) Repertoire profiling and characterization of antigen-activated immune cells is essential for the discovery of novel prognostic and predictive biomarkers and for studying immune response mechanisms in cancer, auto-immune and other diseases.

Methods To facilitate these studies, we developed a novel technology for combined, unbiased profiling of all human TCR and BCR variable regions; and phenotypic characterization of immune cells in bulk, sorted fraction and single immune cells (figure 1). This method involves multiplex RT-PCR amplification and sequencing of CDR3 regions of TCR and BCR genes along with immunophenotyping with a set 500 highly expressed T- and B-cell subtyping and activation marker genes. Bioinformatic analysis of next-generation sequencing (NGS) data allows comprehensive AIR repertoire profiling, identification of antigen-activated TCR and BCR clonotypes, and detailed phenotypic characterization of T and B cells induced by adaptive immune responses.

Results Preliminary phenotypic AIR profiling studies in metastatic tumor samples and Humira®-treated rheumatoid arthritis cases indicate that AIR immunophenotyping technology has unparalleled throughput and sensitivity for the discovery of immunity biomarkers.



Abstract 3 Figure 1 Integrated AIR repertoire profiling & immunophenotyping

Fig. 1 The workflow illustrates integrated adaptive immune receptor (AIR) repertoire profiling and immunophenotyping directly in sorted cells without RNA purification using multiplex RT-PCR. High-resolution immunophenotyping (matching) of top TCR/BCR clonotypes is based on the expression of 300 key cell typing and activation T and B markers. Candidates were selected from a set of 3000 candidate genes described in >100 public databases, commercial assays, and peer-reviewed publications

<http://dx.doi.org/10.1136/jitc-2022-SITC2022.0003>

Abstracts

4 POTENTIATION OF THE IMMUNE CHECKPOINT BLOCKADE RESPONSE BY TUMOR ACIDOSIS AND HYPOXIA MODULATION IS PREDICTABLE USING MOLECULAR IMAGING

Renee Chin*, Xiaofei Liang, Tianzhe Li, Jorge de la Cerda, F William Schuler, Mark Pagel. University of Texas MD Anderson Cancer Center, Houston, TX, USA

Background While immune checkpoint blockade (ICB) treatments such as programmed death-1 (α PD-1) and cytotoxic T lymphocyte antigen-4 blockade (α CTLA-4) shifted the paradigm of cancer treatment, this ICB combination produces objective response rates of only 35.9% for patients with non-small cell lung cancer,¹ and 58% for melanoma patients.² Tumors are able to suppress the anti-tumor T cells that drive ICB through the reduction extracellular tumor pH,³⁻⁵ and by promoting hypoxia in the tumor microenvironment,⁶ both of which are functions inherent to tumor cells due to the Warburg effect. We thus hypothesize that the magnitude of tumor acidosis and hypoxia modulation influences ICB response.

Methods To interrogate modulation of acidity in combination with ICB, we screened a panel of six inhibitors that interfere with tumor cell mechanisms that reduce pH, termed pH sensitizers, using Seahorse, cell viability assay, and T cell suppression assay. We probed the effect of our pH sensitizer candidate in combination with α PD-1 and α CTLA-4 blockade for changes in immunogenicity, tumor control, and correlation between acidity and tumor response or immune cell infiltrate. Tumor pH is measured using a modified Chemical Exchange Saturation Transfer Magnetic Resonance Imaging technique, or acidoCEST MRI, which tracks tumor pH non-invasively. To interrogate the modulation of hypoxia, we measured the correlation between oxygen saturation and immune cell infiltrate and the tumor growth kinetics of myo-inositol trispyrophosphate (ITPP) in combination with α PD-1 and α CTLA-4 blockade. Oxygen saturation is monitored non-invasively using Multispectral Optoacoustic Tomography, or MSOT.

Results Out of the pH sensitizers, we found that esomeprazole significantly reduced proton efflux rate without inducing cytotoxicity or T cell suppression. Furthermore, esomeprazole significantly reduced tumor burden when given one day prior to starting α PD-1 and α CTLA-4 treatment (figure 1), an effect mediated by decreasing the frequencies of tumoral Ly6C+ myeloid cells. We also observed that post-esomeprazole pH correlated with tumor mass (figure 2) and the frequencies of TCF-1+ effector CD4 and CD8 T cells in the tumors following α PD-1 and α CTLA-4 treatment. Lastly, we found that ITPP is able to significantly delay tumor growth, and that tumor immunogenicity increases in correlation with oxygen saturation induced by ITPP.

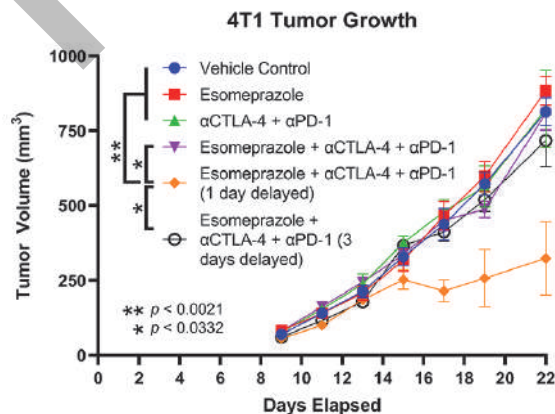
Conclusions AcidoCEST MRI can predict tumor control in the combination treatment of esomeprazole followed by α PD-1 and α CTLA-4 one day afterwards, with TCF-1+ effector CD4 and CD8 T cells being possible biomarkers for treatment success as well. MSOT may also indicate α PD-1 and α CTLA-4 tumor control by determining changes in tumor oxygenation by ITPP.

Acknowledgements We would like to thank the Small Animal Imaging Facility at the MD Anderson Cancer Center for their support conducting imaging studies.

REFERENCES

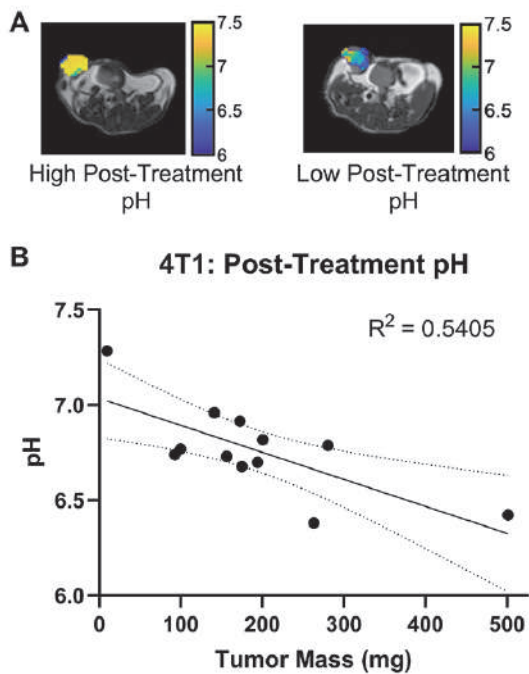
1. Hellmann MD, Paz-Ares L, Bernabe Caro R, Zurawski B, Kim SW, Carcereny Costa E, Park K, Alexandru A, Lupinacci L, de la Mora Jimenez E, Sakai H, Albert I, Vergnenegre A, Peters S, Syrigos K, Barlesi F, Reck M, Borghaei H, Brahmer JR, O'Byrne KJ, Geese WJ, Bhagavatheswaran P, Rabinدران SK, Kasinathan RS, Nathan FE, Ramalingam SS. Nivolumab plus Ipilimumab in Advanced Non-Small-Cell Lung Cancer. *N Engl J Med*. 2019;**381**:2020–31.
2. Hodi FS, Chiarion-Sileni V, Gonzalez R, Grob JJ, Rutkowski P, Cowey CL, Lao CD, Schadendorf D, Waggstaff J, Dummer R, Ferrucci PF, Smylie M, Hill A, Hogg D, Marquez-Rodas I, Jiang J, Rizzo J, Larkin J, Wolchok JD. Nivolumab plus ipilimumab or nivolumab alone versus ipilimumab alone in advanced melanoma (Check-Mate 067): 4-year outcomes of a multicentre, randomised, phase 3 trial. *Lancet Oncol*. 2018;**19**:1480–92.
3. Gerweck LE, Seetharaman K. Cellular pH gradient in tumor versus normal tissue: potential exploitation for the treatment of cancer. *Cancer Res*. 1996;**56**:1194–8.
4. Huntington KE, Louie A, Zhou L, Seyhan AA, Maxwell AW, El-Deiry WS. Colorectal cancer extracellular acidosis decreases immune cell killing and is partially ameliorated by pH-modulating agents that modify tumor cell cytokine profiles. *Am J Cancer Res*. 2022;**12**:138–51.
5. Pilon-Thomas S, Kodumudi KN, El-Kenawi AE, Russell S, Weber AM, Luddy K, Damaghi M, Wojtkowiak JW, Mulé JJ, Ibrahim-Hashim A, Gillies RJ. Neutralization of Tumor Acidity Improves Antitumor Responses to Immunotherapy. *Cancer Res*. 2016;**76**:1381–90.
6. Jayaprakash P, Vignali PDA, Delgoffe GM, Curran MA. Hypoxia Reduction Sensitizes Refractory Cancers to Immunotherapy. *Annu Rev Med*. 2022;**73**:251–65.

Ethics Approval The study was approved by the Institutional Animal Care & Use Committee, protocol numbers 00001998-RN00 and 00001779-RN01.



Abstract 4 Figure 1 Esomeprazole and delayed ICB reduces tumor growth

Balb/c mice orthotopically implanted with 4T1 tumor cells were treated with the respective treatments listed above and the resulting tumor growth kinetics are shown, $n = 4 - 5$



Abstract 4 Figure 2 Post-esomeprazole pH predicts treatment efficacy

A) AcidoCEST MRI images depicting tumor pH distribution after esomeprazole treatment in a responsive (left) and unresponsive (right) 4T1 tumor. B) Average pH from acidoCEST MRI after esomeprazole treatment compared to tumor mass after three treatments of ICB in 4T1-bearing mice, $n = 12$

<http://dx.doi.org/10.1136/jitc-2022-SITC2022.0004>

5 DEVELOPMENT OF A VACCINE TO INTERCEPT ORAL CANCER

¹Traci Hilton*, ²Andrew Gunderson, ¹Mark Schmidt, ¹Christopher Paustian, ¹Sam Bookhardt, ¹Glenna McDonnell, ³Tarsem Moudgil, ¹Hong-Ming Hu, ³Bryan Bell, ⁴Bernard Fox. ¹UbiVac, Portland, OR, USA; ²UbiVac, Portland, OR, USA, The Ohio State University Comprehensive Cancer Center, Columbus, Ohio, USA; ³Providence Cancer Institute, Portland, OR, USA; ⁴UbiVac, Portland, OR, USA, Providence Can Institute, Earle A. Chiles Research Institute, Portland, OR, USA

Background Oral cavity cancer is diagnosed in more than 300,000 people each year worldwide and approximately half of these will die within five years despite standard treatment. These cancers are often preceded by the appearance of a pre-malignant dysplastic lesion, which offers a unique opportunity to identify patients at high risk of developing cancer and offer them a vaccine that may prevent development of this non-viral malignancy. Lesions can be removed but because of a 'field effect' their entire oral mucosa is at risk – thus the vaccine. Recent studies have identified genes that are differentially expressed during progression from normal tissue to oral cancer providing a roadmap to developing a preventative vaccine [PMID: 27027432]

Methods We have manufactured and performed initial characterization of a DC-targeted microvesicle vaccine, DPV-007, made specifically to intercept the progression of oral dysplasia to oral cancer. DPV-007 is manufactured using platform vaccine technology that is in the clinic. This technology captures short-lived and non-canonical proteins that make up the dominant epitopes presented by HLA and packages them in microvesicles containing DAMPs and molecular chaperones. Characterization of DPV-007 included molecular, proteogenomic, biochemical and functional assessments. Preclinical studies were performed evaluating prevention of tumor development in the 4NQO-induced tumor model.

Results The DPV-007 microvesicle vaccine contains more than 200 proteins for genes that are upregulated in oral dysplasia and oral cancer. Preliminary data suggests that the vaccine may contain as many as 30 somatic variants identified as somatic mutations in the COSMIC Database. Additionally, the vaccine contains at least 11 NCI prioritized cancer antigens and has agonist activity for TLR 2, 3, and 9. In the 4NQO preclinical model, vaccination including relevant antigens and agonist activity, provided significant ($p < 0.02$) protection from lesion onset and tumor outgrowth.

Conclusions The identification of genes associated with the progression of pre-cancerous lesions to cancer provides targets for active immunotherapy of this disease. In preclinical models we have shown that this vaccine strategy is effective in both protection and therapy studies [PMID: 21810919; PMID: 27874054; PMID: 31747946]. A clinical trial of a similar vaccine, DPV-001, administered as a single agent as adjuvant therapy for NSCLC, documented induction of immunity to a large number of cancer antigens contained in the vaccine and did not identify serious adverse events. Based on data summarized above, we propose to vaccinate patients with dysplastic lesions and investigate whether vaccination reduces lesion recurrence.

Acknowledgements Research support was provided by Janssen Research and Development, Johnson & Johnson.

Ethics Approval The Institutional Animal Care & Use Committee of the Earle A. Chiles Research Institute approved the above noted studies. Protocol 55.

<http://dx.doi.org/10.1136/jitc-2022-SITC2022.0005>

6 USE OF REAL-WORLD (RW) DATA TO ASSESS THE ABILITY OF CIRCULATING CELL-FREE TUMOR DNA (CTDNA) MOLECULAR RESPONSE TO ASSESS THERAPEUTIC OUTCOMES IN PATIENTS WITH NON-SMALL CELL LUNG CANCER (NSCLC)

Caroline Weipert*, Leylah Drusbosky, Leslie Bucheit, Kyle Chang, Shaun Forbes, Sean Gordon. *Guardant Health, Redwood City, CA, USA*

Background Data suggests that changes in ctDNA quantity correlate with response to therapy in patients with advanced solid malignancies. However, there is little consistency on how to calculate and interpret such changes. Here, we apply a clinically-validated molecular response algorithm to a RW cohort of patients with NSCLC to further evaluate its ability to assess treatment outcomes.

Methods We queried the Guardant INFORM database, which comprises aggregated commercial payer health claims and de-identified records from over 173,000 individuals with comprehensive ctDNA testing via Guardant360 (G360) from September 2018-March 2022. Patients with NSCLC treated with either EGFR tyrosine kinase inhibitors (TKI) or immune checkpoint inhibitors (ICI) (monotherapy or in combination) who received a ctDNA test within 15 weeks prior to treatment initiation and a second test 3–15 weeks after treatment initiation were retrospectively evaluated using the G360 Response algorithm. Cox proportional hazards (CPH) were used for RW time to next treatment (TTNT) and time to treatment discontinuation (TTD) analyses. A >50% decrease in mean variant allele fraction ratio from pre-treatment to on-treatment was used to define the molecular response categorical variable. Gender, age, line of therapy (LOT) and comorbidities were included as covariates. Median TTNT and TTD were calculated by Kaplan Meier.

Results 282 patients with NSCLC were identified: 38% of patients received ICI, 26% received an EGFR-TKI, and 36% received other therapies. Of patients receiving either EGFR-TKI or ICI, 34% were classified as molecular responders, 47% were non-responders, and 19% were not evaluable by the algorithm due to no/low ctDNA at one or both time-points. Molecular responders had significantly longer TTNT on EGFR TKIs and ICI compared to non-responders receiving the same therapy. TTD was significantly longer for molecular responders compared to non-responders in the EGFR-TKI cohort (table 1).

Conclusions Patients with NSCLC classified as molecular responders via the G360 Response algorithm had prolonged TTD and TTNT on both EGFR-TKI and ICI compared to non-responders. This data supports the use of ctDNA molecular response, as calculated by this algorithm, in assessing patient response to therapy; exploration of the utility of this algorithm in adaptive clinical trial design to evaluate the impact of early treatment interventions on patient outcome is ongoing.

Ethics Approval This research was approved by the Quorum Institutional Review Board (IRB) for the generation of de-identified datasets for research purposes.

Abstract 6 Table 1

Treatment Cohort	Clinical Outcome	Median TTNT/TTD, 95% CI (months)	CPH HR, 95% CI	CPH HR, p-value
EGFR-TKI	TTNT	responder (n=30) = 9.8 [5.9-23.6]	0.26 [0.11-0.60]	< 0.005
		non-responder (n=33) = 4.7 [2.7-6.3]		
EGFR-TKI	TTD	responder (n=30) = 6.6 [4-11.8]	0.33 [0.16-0.66]	< 0.005
		non-responder (n=33) = 3.4 [2.6-4.8]		
ICI	TTNT	responder (n=31) = not reached [6.4-inf]	0.43 [0.18-0.99]	0.049
		non-responder (n=52) = 4.7 [3.1-8.4]		
ICI	TTD	responder (n=31) = 5.5 [4.0-6.8]	0.54 [0.28-1.06]	0.073
		non-responder (n=52) = 2.8 [2.1-4.9]		

Abbreviations
CI = confidence interval, CPH = Cox proportional hazards model, ctDNA = circulating cell-free tumor DNA, EGFR-TKI = Epidermal growth factor receptor-tyrosine kinase inhibitors, G360 = Guardant360, HR = hazard ratio, ICI = immune checkpoint inhibitor, inf = infinity, NSCLC = non-small cell lung cancer, TTD = time to discontinuation, TTNT = time to next treatment

TTNT and TTD for molecular responders versus non-responders in NSCLC patients treated with either EGFR-TKI or ICI.

<http://dx.doi.org/10.1136/jitc-2022-SITC2022.0006>

7

ANTI-PD1 TREATMENT RESPONSE PREDICTION AND MONITORING IN NON-SMALL CELL LUNG CANCER PATIENTS USING PLASMA CELL-FREE DNA HYDROXYMETHYLATION

Gulfem Guler*, Yuhong Ning, David Haan, Michael Kesling, Ceyda Coruh, Giuliana Mognol, Tierney Phillips, Kyle Hazen, Wayne Volkmuth, Samuel Levy. *Bluestar Genomics, San Mateo, CA, USA*

Background Treatment with immune checkpoint inhibitors (ICIs) targeting programmed death-1 (PD-1) can yield remarkable anti-tumor responses in lung cancer patients, however, not all patients respond to ICIs. Biomarkers currently used in clinical practice are insufficient in determining patient populations who may benefit from anti-PD-1 treatment. Non-invasive liquid biopsy approaches for therapy response prediction present key advantages over methods that rely on tumor biopsy, especially in cancer types such as lung cancer, where the location of the tumor may impact both patient compliance and the health risks involved with the procedure. Liquid biopsies offer a simple and convenient alternative and can also help overcome challenges hampering tumor biopsy dependent biomarker discovery and development such as tumor heterogeneity and difficulty in longitudinal sampling over the course of treatment.

Methods 151 whole blood samples were collected from 31 non-small cell lung cancer (NSCLC) patients, prior to therapy start and while on anti-PD1 therapy, namely pembrolizumab or nivolumab (up to 5 timepoints). cfDNA was extracted from plasma, followed by fragment enrichment using 5-hydroxymethyl-cytosine (5hmC)-based epigenomic platform technology. As part of this analysis, both 5hmC and low pass whole genome libraries were generated and sequenced.

Results Here, we investigated the utility of 5-hydroxymethyl-cytosine (5hmC) signatures obtained from plasma-derived cell free DNA (cfDNA) for non-invasive prediction and monitoring of anti-PD-1 treatment response. Comparison of pre-treatment 5hmC profiles from responders to non-responders revealed differential hydroxymethylation, many of which localized to genes in pathways important for immune response. While anti-PD1 treatment induced changes in hydroxymethylomes of both responding and non-responding patients, these changes were distinct. Upon anti-PD1 treatment, 5hmC further accumulated over genes involved in immune activation such as IFN γ and IFN α response, inflammatory response and TNF α signaling, in responding patients but strikingly not in non-responders. On the other hand, non-responder plasma cfDNA had 5hmC increase over genes involved in epithelial to mesenchymal transition, which is associated with metastasis and drug resistance. These pathway-based changes in responders and non-responders are consistent with previous data from tumor tissue analysis. Furthermore, anti-PD1 treatment induced differential 5hmC changes in responders relative to non-responders starting from the first cycle of treatment, suggesting that 5hmC can help monitor treatment response.

Conclusions Our results demonstrate that 5hmC profiling can capture tumor-associated immune response signals in plasma without the need for tissue biopsy. Altogether, these findings show that 5hmC profiling of plasma-derived cfDNA enables non-invasive monitoring of immunotherapy response and can provide putative patient selection biomarkers from blood.

<http://dx.doi.org/10.1136/jitc-2022-SITC2022.0007>

8 **UNIVERSAL LCMS-BASED ASSAY PLATFORM, REFMAB-Q NSMOL, FOR MONITORING MONOCLONAL ANTIBODY THERAPEUTICS USING ONE REFERENCE ANTIBODY**

¹Noriko Iwamoto, ²Yoshinobu Koguchi, ¹Kotoko Yokoyama, ³Akinobu Hamada, ⁴Atsushi Yonezawa, ²Brian Piening, ²Eric Tran, ²Bernard Fox, ²William Redmond, ¹Takashi Shimada*. ¹Shimadzu Corporation, Kyoto, Japan; ²Providence Cancer Institute, Portland, OR, USA; ³National Cancer Center Research Institute, Tokyo, Japan; ⁴Kyoto University Hospital, Kyoto, Japan

Background The US FDA has approved more than 100 antibody therapeutics (mAbs) and nearly 900 of them are currently being investigated in clinical trials. Accurate quantitation of antibody is critical for pharmacokinetics studies during the development of mAbs. In clinical settings, mAb monitoring has been applied to the dose adjustment for autoimmune disease. We recently showed that trough levels of mAbs can be a biomarker for cancer immunotherapy.¹ Thus, the deployment of a rapid and universal platform for mAb monitoring may help streamlining processes ranging from drug development to clinical practice for a wide spectrum of diseases. However, mAb monitoring often depends on the development of an individual ligand binding assay, which is impractical to scale.² Previously, we developed a method for mAbs quantitation that uses Fab-selective proteolysis of mAb followed by detection of signature peptides by LC-MS called nSMOL (nano-surface and molecular-orientation limited proteolysis) technology.³ So far, we have established the validated LC-MS conditions for over 35 mAbs.

Methods We confirmed that count per second (CPS) ratio between different signature peptides were constant thanks to negligible matrix effect in nSMOL assay. Therefore, we hypothesized that we could select optimal reference antibody and use that as a universal reference antibody for highly multiplexed mAb quantitation. To select a universal reference mAb (refmAb-Q), we picked 18 mAbs and compared quantitative reproducibility of each mAb from singleplex and 18-plex nSMOL assay with a concentration from LLOQ to HQC.

Results We found that the CPS ratio to trastuzumab was unique to each mAb and consistent when we arbitrarily picked trastuzumab. We identified optimal reference mAb candidates based on the several physicochemical properties of signature peptides. The refmAb-Q nSMOL assay showed perfect concordance with the conventional nSMOL with an authentic reference in clinical sample from ipilimumab-treated patients (NCT00495066), pembrolizumab-treated patients (NCT02575404), and patients with the combination immunotherapy of ipilimumab and nivolumab.

Conclusions This innovative refmAb-Q nSMOL platform may provide a practical solution for quantitating an ever-increasing number of mAbs from developmental to clinical use settings. We envision that wide adaptation of refmAb-Q nSMOL is possible for PK and TDM assays for mAbs in the treatment of cancer and autoimmune diseases. Furthermore, refmAb-Q nSMOL can be applied to the quantitation and structural analysis of individual autoantibodies and neutralizing antibodies.

REFERENCES

1. Koguchi Y, Iwamoto N, Shimada T, Chang SC, Cha J, Curti BD, Urba WJ, Piening BD, Redmond WL. Trough levels of ipilimumab in serum as a potential biomarker of clinical outcomes for patients with advanced melanoma after treatment with ipilimumab. *J Immunother Cancer*. 2021 Oct;**9**(10):e002663.
2. Curti BD, Koguchi Y, Leidner RS, Rolig AS, Sturgill ER, Sun Z, Wu Y, Rajamannickam V, Bernard B, Hilgart-Martiszus I, Fountain CB, Morris G, Iwamoto N, Shimada T, Chang S, Traber PG, Zomer E, Horton JR, Shlevin H, Redmond WL. Enhancing clinical and immunological effects of anti-PD-1 with belapectin, a galectin-3 inhibitor. *J Immunother Cancer*. 2021 Apr;**9**(4):e002371.

3. Iwamoto N, Shimada T. Structure-Indicated LC-MS/MS Bioanalysis of Therapeutic Antibodies. *Methods Mol Biol*. 2022;**2313**:187–205.

<http://dx.doi.org/10.1136/jitc-2022-SITC2022.0008>

9 **A PAN-CANCER MULTI-OMIC IMMUNE SINGLE-CELL ATLAS FOR CANCER IMMUNOTHERAPY: FOCUS ON CD4 + T CELLS**

¹Roberta Zappasodi, ²Lydia Mok student*, ¹Andrea Orlando, ²Julian Lehrer, ²Joshua Stuart, ³Nils-Petter Rudqvist, ⁴Benjamin Vincent, ⁵Anne Monette, ⁶Yasin Senbabaoglu, ⁷Kellie Smith, ⁸Paul Thomas, ⁹Nicholas Tschernia, ¹⁰Vesteinn Thorsson, ²Vanessa Jonsson. ¹Weill Cornell Medical College, New York, NY, USA; ²University of California, Santa Cruz, CA, USA; ³MD Anderson, Houston, TX, USA; ⁴University of North Carolina at Chapel Hill, Chapel Hill, NC, USA; ⁵Jewish General Hospital, Montreal, Canada; ⁶Genentech, South San Francisco, CA, USA; ⁷Bloomberg-Kimmel Institute for Cancer Immunotherapy, Baltimore, MD, USA; ⁸St. Jude Children's Research Hospital, Memphis, TN, USA; ⁹Center for Immunology, National Cancer Institute, Bethesda, MD, USA; ¹⁰Institute for Systems Biology, Seattle, WA, USA

Background Despite the success of immunotherapy, clinical responses remain difficult to predict, likely due to diverging tumor immune cell composition and function. Advances in single-cell analysis have revealed heterogeneous immune cell activity within and across individuals with cancer. While CD8 + tumor-infiltrating lymphocytes (TILs) have been extensively studied,¹⁻⁴ a pan-cancer consensus annotation of CD4+ TIL in immunotherapy is lacking. Robust identification of CD4+ T-cells from admixed single-cell transcriptomes is challenging due to low CD4 transcript expression and CD4+CD8+ T cells. Poor harmonization of CD4+ T-cell annotations across datasets compromises reproducibility and generalization. Here, we present the Cancer Immunotherapy T-cell Atlas (CITA), a harmonized, metadata-rich, pan-cancer, single-cell omics resource, spanning over 1.3M T cells, aimed at discovering CD4+ T-cell related features impacting immunotherapy response.

Methods Publicly available single-cell RNA sequencing (scRNA-seq) data were used to generate the CD4+ T-cell consensus re-annotation and the CITA. Raw count data and metadata were obtained from the Gene Expression Omnibus (GEO) or manuscript supplementary data. Individual datasets were processed using standardized bioinformatics workflow for quality control, integration, normalization, and batch correction.

Results We collected scRNAseq data and clinical metadata from 23 published datasets from 320 donors, across 30 different cancers, 20 immunotherapies, and from diverse tissue types and sequencing platforms^{3,5-25} (figure 1). Existing immune cell annotations were harmonized by mapping to our reference cell identity labels, and T cells were subsetted for the CITA. To enable consensus-driven annotation, we resolved precise CD4+ T-cell transcriptional profiles from publicly available, FACS-sorted CD4+ T-cell scRNAseq datasets from liver, lung, and colorectal cancers.^{21,22,26} We found CD4+ T cells homogeneously distributed in 12 main clusters across cancer types (figure 2). Foxp3+ regulatory T cells (Tregs) segregated into circulating/naive, tissue-resident, and effector Tregs, consistent with prior studies.²⁷ Moreover, we resolved naive, central, effector, tissue-resident, activated, and highly proliferating CD4+Foxp3- T cells, as well as Tbet+ Th1, and T follicular helper (Tfh) cells, co-expressing cytotoxic or canonical Tfh genes respectively (figure 2).

Conclusions The CITA provides the foundation for pan-cancer, harmonized, metadata-rich compendium of single-cell omics T-cell data from treatment-naive and immunotherapy-treated patients. Our CD4+ T-cell consensus re-annotation in conjunction with existing and new machine-learning-based classification methods automates annotation of new and existing CD4+T-cell datasets. CITA will be a publicly available software

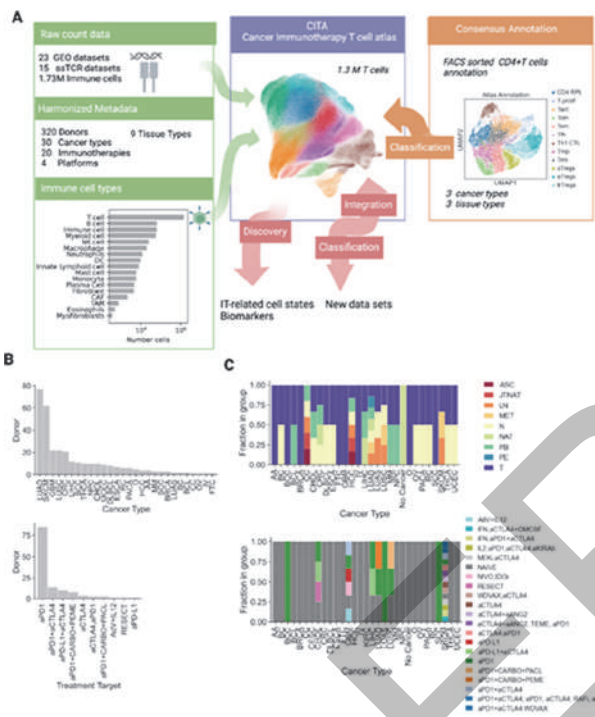
and data resource at <http://cita.cells.ucsc.edu> and will include new datasets as they are released.

Acknowledgements We thank SITC Sparkathon for supporting this work. L.M. is supported by the Regents fellowship for the Program in Biomedical Sciences & Engineering, Biomolecular Engineering & Bioinformatics Ph.D. at the University of California, Santa Cruz. R.Z. is supported by the Parker Institute for Cancer Immunotherapy Bridge Fellows Award. R.Z. acknowledges funding from the NCI SPORE (P50-CA192937) and the Leukemia & Lymphoma Society and receives grant support from Bristol Myers Squibb and AstraZeneca.

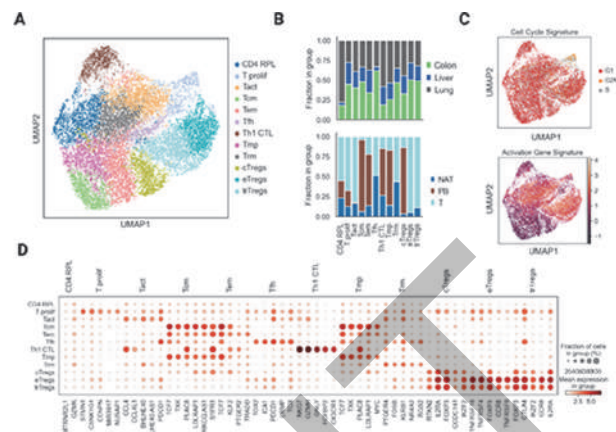
REFERENCES

- Giles JR, Manne S, Freilich E, Oldridge DA, Baxter AE, George S, et al. Human epigenetic and transcriptional T cell differentiation atlas for identifying functional T cell-specific enhancers. *Immunity*. 2022;**55**: 557–574.e7.
- Developmental Relationships of Four Exhausted CD8+ T Cell Subsets Reveals Underlying Transcriptional and Epigenetic Landscape Control Mechanisms. *Immunity*. 2020;**52**: 825–841.e8.
- Zheng L, Qin S, Si W, Wang A, Xing B, Gao R, et al. Pan-cancer single-cell landscape of tumor-infiltrating T cells. *Science*. 2021;**374**: abe6474.
- Leun AM van der, van der Leun AM, Thommen DS, Schumacher TN. CD8 T cell states in human cancer: insights from single-cell analysis. *Nature Reviews Cancer*. 2020. pp. 218–232. doi:10.1038/s41568-019-0235-4.
- Jerby-Arnon L, Shah P, Cuoco MS, Rodman C, Su M-J, Melms JC, et al. A Cancer Cell Program Promotes T Cell Exclusion and Resistance to Checkpoint Blockade. *Cell*. 2018. pp. 984–997.e24. doi:10.1016/j.cell.2018.09.006.
- Zhang L, Yu X, Zheng L, Zhang Y, Li Y, Fang Q, et al. Lineage tracking reveals dynamic relationships of T cells in colorectal cancer. *Nature*. 2018;**564**: 268–272.
- Azizi E, Carr AJ, Plitas G, Cornish AE, Konopacki C, Prabhakaran S, et al. Single-Cell Map of Diverse Immune Phenotypes in the Breast Tumor Microenvironment. *Cell*. 2018;**174**: 1293–1308.e36.
- Borchertding N, Vishwakarma A, Voigt AP, Bellizzi A, Kaplan J, Nepple K, et al. Mapping the immune environment in clear cell renal carcinoma by single-cell genomics. *Commun Biol*. 2021;**4**: 122.
- Li H, van der Leun AM, Yofe I, Lubling Y, Gelbard-Solodkin D, van Akkooi ACJ, et al. Dysfunctional CD8 T Cells Form a Proliferative, Dynamically Regulated Compartment within Human Melanoma. *Cell*. 2020. p. 747. doi:10.1016/j.cell.2020.04.017.
- Yost KE, Satpathy AT, Wells DK, Qi Y, Wang C, Gageyama R, et al. Clonal replacement of tumor-specific T cells following PD-1 blockade. *Nat Med*. 2019;**25**: 1251–1259.
- Ma L, Hernandez MO, Zhao Y, Mehta M, Tran B, Kelly M, et al. Tumor Cell Biodiversity Drives Microenvironmental Reprogramming in Liver Cancer. *Cancer Cell*. 2019;**36**: 418–430.e6.
- Zilionis R, Engblom C, Pfirschke C, Savova V, Zemmour D, Saatioglu HD, et al. Single-Cell Transcriptomics of Human and Mouse Lung Cancers Reveals Conserved Myeloid Populations across Individuals and Species. *Immunity*. 2019;**50**: 1317–1334.e10.
- Vieira Braga FA, Kar G, Berg M, Carpaij OA, Polanski K, Simon LM, et al. A cellular census of human lungs identifies novel cell states in health and in asthma. *Nat Med*. 2019;**25**: 1153–1163.
- Wu TD, Madireddi S, de Almeida PE, Banchereau R, Chen Y-JJ, Chitre AS, et al. Peripheral T cell expansion predicts tumour infiltration and clinical response. *Nature*. 2020;**579**: 274–278.
- Mahuron KM, Moreau JM, Glasgow JE, Boda DP, Pauli ML, Gourand V, et al. Layilin augments integrin activation to promote antitumor immunity. *J Exp Med*. 2020;**217**. doi:10.1084/jem.20192080
- Mathewson ND, Ashenberg O, Tirosh I, Gritsch S, Perez EM, Marx S, et al. Inhibitory CD161 receptor identified in glioma-infiltrating T cells by single-cell analysis. *Cell*. 2021;**184**: 1281–1298.e26.
- Wu SZ, Al-Eryani G, Roden DL, Junankar S, Harvey K, Andersson A, et al. A single-cell and spatially resolved atlas of human breast cancers. *Nat Genet*. 2021;**53**: 1334–1347.
- Liu B, Hu X, Feng K, Gao R, Xue Z, Zhang S, et al. Temporal single-cell tracing reveals clonal revival and expansion of precursor exhausted T cells during anti-PD-1 therapy in lung cancer. *Nat Cancer*. 2022;**3**: 108–121.
- Steen CB, Luca BA, Esfahani MS, Azizi A, Sworder BJ, Nabet BY, et al. The landscape of tumor cell states and ecosystems in diffuse large B cell lymphoma. *Cancer Cell*. 2021;**39**: 1422–1437.e10.
- Schad SE, Chow A, Mangarin L, Pan H, Zhang J, Ceglia N, et al. Tumor-induced double positive T cells display distinct lineage commitment mechanisms and functions. *J Exp Med*. 2022;**219**. doi:10.1084/jem.20212169.
- Zheng C, Zheng L, Yoo J-K, Guo H, Zhang Y, Guo X, et al. Landscape of Infiltrating T Cells in Liver Cancer Revealed by Single-Cell Sequencing. *Cell*. 2017;**169**: 1342–1356.e16.

22. Guo X, Zhang Y, Zheng L, Zheng C, Song J, Zhang Q, *et al.* Global characterization of T cells in non-small-cell lung cancer by single-cell sequencing. *Nat Med.* 2018;**24**: 978–985.
23. Tirosch I, Venteicher AS, Hebert C, Escalante LE, Patel AP, Yizhak K, *et al.* Single-cell RNA-seq supports a developmental hierarchy in human oligodendrogloma. *Nature.* 2016;**539**: 309–313.
24. Caushi JX, Zhang J, Ji Z, Vaghiasa A, Zhang B, Hsiue EH-C, *et al.* Transcriptional programs of neoantigen-specific TIL in anti-PD-1-treated lung cancers. *Nature.* 2021;**596**: 126–132.
25. Oliveira G, Stromhaug K, Cieri N, Iorgulescu JB, Klaeger S, Wolff JO, *et al.* Landscape of helper and regulatory antitumor CD4 T cells in melanoma. *Nature.* 2022;**605**: 532–538.
26. Zhang Y, Zheng L, Zhang L, Hu X, Ren X, Zhang Z. Deep single-cell RNA sequencing data of individual T cells from treatment-naïve colorectal cancer patients. *Sci Data.* 2019;**6**: 131.
27. Single-Cell Transcriptomics of Regulatory T Cells Reveals Trajectories of Tissue Adaptation. *Immunity.* 2019;**50**: 493–504.e7.



Abstract 9 Figure 1 Composition of the CITA
 A. Pipeline for the Cancer Immunotherapy T-cell Atlas (CITA) integration including the use of consensus annotated CD4+ T-cell states based on FACS-sorted CD4 single-cell datasets. UMAP of 1.3M T cells from 23 single cell datasets from individuals with cancer, for 30 different cancer types and 9 tissue types (center). B,C. CITA harmonized metadata overview, with sampled tissue type per cancer type and treatment type by cancer type. LUAD: lung adenocarcinoma; SKCM, skin cancer melanoma; GBM, glioblastoma; LUSC, lung squamous cell carcinoma; CC/CRC, colorectal carcinoma; LIHC, liver hepatocellular carcinoma; BC/BCC, basal cell carcinoma; THCA, thyroid carcinoma; NPC, nasopharyngeal cancer; CHOL, cholangiocarcinoma; UCEC, uterine corpus endometrial carcinoma; DLBCL, diffuse large B cell lymphoma; ESCA, esophageal cancer; RC, renal cancer; PACA, pancreatic adenocarcinoma; O, oligodendrogloma; HCC, hepatocellular carcinoma; AA, anaplastic astrocytoma; MM, multiple myeloma; SCC, squamous cell carcinoma; BRCA, breast cancer; LUAS, lung adeno/squamous carcinoma; BC, basal cell carcinoma; BCL, B cell lymphoma; OV, ovarian serous cystadenocarcinoma; IV, glioma stage 4; FTC, fallopian tube carcinoma; ASC, ascite; JTNAT, joint tumor normal tissue; LN, lymph node; MET, metastasis; N, normal; NAT, normal adjacent tissue; PB, peripheral blood; PE, pleural effusion; T, tumor; CARBO, carboplatin; PEME, Pemetrexed; PAcl, paclitaxel; Adv, adenovirus; RESECT, resection



Abstract 9 Figure 2 Pan-cancer CD4+ T-cell consensus annotation
 A. UMAP of consensus annotation of CD4+ sorted cells from peripheral blood (PB), tumor (T) and normal adjacent tissue (NAT) from individuals with lung, colorectal or liver cancer.^{21,22,26} CD4 RPL: high ribosomal protein, T prolif: proliferating, Tmp: memory precursors; Tcm: central memory, Tact: activated, Tem: effector memory, Tfh: follicular helper, Th1 CTL: T helper 1 cytolytic lymphocytes, Trm: tissue resident memory, cTregs: circulating regulatory T cells, eTregs: effector regulatory T cells, trTregs: tissue resident regulatory T cells. B. Barplot of cancer type and tissue type fractions for each cell annotation. C. UMAP of gene signature scores for cell cycle and a curated T-cell activation/terminal differentiation gene signature (n=26 genes) consisting of terminal differentiation transcription factors (e.g. ID2, RUNX3, PRDM1, TOX), cytolytic markers (e.g. GZMA, GZMB, GZMH, PRF1), co-stimulatory receptors (e.g. ICOS, TNFRSF18, TNFRSF4), and chemokines/chemokine receptors (e.g. CXCR3, CX3CR1, CXCL13) for dataset described in (A). D. Dotplot of the five most significant differentially expressed genes for each cell annotation contrasted against each other cell annotation

<http://dx.doi.org/10.1136/jitc-2022-SITC2022.0009>

10 **AUTOMATED DETECTION OF RNA, DNA, AND PROTEIN TARGETS IN TISSUES ON THE ONCORE PROX**

Julio Masabanda*, Jason Ramos. *Biocare Medical, Pacheco, CA, USA*

Background A detailed assessment of the biological status of tissues can be achieved by performing as many multiple target detections as possible on the same tissue slide of protein, DNA, and RNA. However, the tests methods, can be labor intensive. When applying commercial kits, such as RNAscope from ACD for mRNA detection, the basic manual protocol takes about 8 hours. Here we show the utility of the ONCORE ProX – an open, fully automated slide staining platform – for developing detection protocols of mRNA using different RNAscope kits. Additionally, we developed protocols for the combined detection of Protein/mRNA and Protein/DNA/mRNA on the same slide.

Methods

FFPE tissues used Tonsil, breast MTA. Antibodies used: mouse IG kappa, rabbit ERBB2. FISH probe used: ERBB2/Copy Control 17 red/green in ZipFISH fast hybridization buffer. mRNA probes from ACD: IGK, ERBB2, CD3, CD20. RNA detection and visualization was performed following the main RNAscope protocols¹ for manual applications adapted for performance on the ONCORE ProX. The basic RNAscope protocol for DAB detection was adapted for the combined detection of Protein/mRNA, and for detection of Protein/DNA/mRNA.

Results The RNAscope procedure¹ involves steps present also in IHC and FISH protocols, thus we used this protocol as backbone for the development of protocols for the combined detection of protein and DNA targets. The basic RNAscope protocol for detection of a single mRNA type (e.g., ERBB2) takes 7–8 hours on the ONCORE ProX. We have additionally developed protocols for the sequential detection of protein and mRNA targets (IGK) and this takes about 9 hours. Furthermore, we detected on the same slide protein (ERBB2), DNA (ERBB2/copy control17 FISH probe) and mRNA (ERBB2). This complex procedure takes about 11 hours, and it is possible thanks to ZipFISH buffer for FISH. Additionally, we have performed the RNAscope chromogenic detection of IGK mRNA in DAB and Red, as well as Chromogenic and Immunofluorescent Multiplex detection of CD3 and CD20 mRNAs.

Conclusions In addition to the established function for fully automated IHC, we have demonstrated the suitability of the ONCORE ProX for performing successfully and with relative ease, complex technologies such as RNAscope and furthermore the combined detection on the same slide of multiple targets such as protein (IF), DNA (ZipFISH) and RNA probes (RNAscope).

These features of the ONCORE ProX show its versatility and make it suitable for performing complex protocols to satisfy the needs of a rapidly developing field of molecular histology.

REFERENCE

1. <https://acdbio.com/manual-assays-rnascope>

<http://dx.doi.org/10.1136/jitc-2022-SITC2022.0010>

11

TERTIARY LYMPHOID STRUCTURES IN MELANOMAS HARBOR INCREASED PROPORTIONS OF STEM-LIKE EFFECTOR T-CELLS COMPARED TO TUMOR-INFILTRATING LYMPHOCYTES

Ileana Mauldin*, Priya Kaytal, Nicole Edmonds, Craig Slingluff. *University of Virginia, Charlottesville, VA, USA*

Background Tertiary lymphoid structures (TLS) in melanoma are associated with improved survival and response to checkpoint blockade therapy (CBT). However, whether and how TLS contribute to this response is unknown. If TLS contribute to the responses, they may be expected to contain higher proportions of T-cells with therapeutic potential, than tumor infiltrating lymphocytes outside of TLS. TCF1/TCF7 has been identified as a marker for a stem cell-like T-cell that mediates the proliferative response post-CBT in tumor infiltrating cells. We hypothesized that TLS would contain higher fractions of stem-like TCF7⁺ and TCF7⁺TOX⁺ T-cells poised to respond post-CBT. To address this hypothesis, we evaluated TLS and tumor sites of both desmoplastic and non-desmoplastic melanomas, for markers of stem like T-cells (TCF7, TOX).

Methods Primary desmoplastic melanomas (PDM) and non-desmoplastic metastatic melanomas (NDMM) were evaluated for TLS presence (yes/no) and immune markers, by 7-color multiplex Immunofluorescence histology. Specimens were stained with the following two panels: TLS panel: CD20, CD3, CD8, PNA^d, DC-Lamp, Ki67, and DAPI; T cell activity panel: CD3, CD8, CD20, Granzyme-b, TOX, TCF7, and DAPI. Lymphoid aggregates were identified as TLS if possessing organized T-cell and B-cell regions in addition to high endothelial venule-like vasculature (PNA^{d+}). Cells were enumerated from TLS and tumor regions of TLS⁺ tumor specimens from PDM, and NDMM, with Halo software (Indica Labs). CD3⁺CD8⁺ (CD8⁺) cells and CD3⁺CD8⁻ (CD4⁺) cells were evaluated for activation markers, and the proportions of cells expressing activation markers was calculated. Statistical comparisons were done with unpaired Wilcoxon tests in RStudio.

Results TLS were identified in 25 out of 39 evaluated (64%) PDM, and 37 of 111 (33%) NDMM. Comparing TLS to tumor outside the TLS, we found that PDM TLS contain significantly elevated proportions of CD8⁺TCF7⁺ cells and CD4⁺TCF7⁺ cells compared to tumor (table 1). NDMM TLS also contain elevated proportions of CD8⁺TCF7⁺ cells and CD4⁺TCF7⁺ cells relative to tumor (table 1). In addition, TLS in PDM and NDMM contain elevated proportions of CD8⁺TOX⁺TCF7⁺ cells and CD4⁺TOX⁺TCF7⁺ cells relative to their respective tumor (table 1).

Conclusions The elevated proportion of TCF7⁺ T-cells, and TCF7⁺TOX⁺ T-cells in TLS from PDM and NDMM relative to their tumor suggests that stem-like T-cells are enriched in TLS, and that T-cell regeneration may be occurring there. Additionally, TLS may be helping in the maintenance or generation of TCF7⁺ T-cells in the tumor microenvironment.

Abstract 11 Table 1 Proportion of T- or B-cells expressing markers of activation or exhaustion within TLS and tumor (median)

Table 1. Proportion of T- or B-cells expressing markers of activation or exhaustion within TLS and tumor (median)

	PDM Tumor	PDM TLS	P value	NDMM Tumor	NDMM TLS	P value
CD3+CD8+TCF7+	33%	53%	0.007	6%	31%	0.001
CD3+CD8-TCF7+	29%	61%	<0.001	10%	49%	<0.001
CD3+CD8+TOX+	41%	39%	1.000	46%	37%	0.020
CD3+CD8-TOX+	37%	48%	0.146	25%	30%	0.9129
CD3+CD8+TOX+TCF7+	12%	22%	0.006	1%	7%	0.013
CD3+CD8-TOX+TCF7+	12%	27%	<0.001	3%	16%	<0.001
CD3+CD8+GRANB+	8%	6%	0.302	13%	3%	<0.001
CD3+CD8-GRANB+	3%	3%	0.615	6%	1%	<0.001
TOX+CD20+	39%	44%	0.193	30%	25%	0.355

*p values are from unpaired Wilcoxon tests comparing cell proportions in TLS to their respective tumor. Abbreviations: Granzyme-b (GRANB), TLS (tertiary lymphoid structure)

<http://dx.doi.org/10.1136/jitc-2022-SITC2022.0011>

12 **EVALUATING THE CONTRIBUTION OF EXTRACELLULAR MATRIX INVASION FOR KILLING OF TUMOR CELLS BY NATURAL KILLER CELLS**

Jyothi Mony*, Yama Abassi, Brandon Lamarche. *Agilent Technologies, San Diego, CA, USA*

Background Extracellular matrix (ECM) is a generic term for the diverse types of acellular structural component in tissues that play an important role in homeostasis. The ECM in solid tumors is greatly altered and can contribute to the modulation of immune cell function in the tumor microenvironment. Lymphocytes such as the cytotoxic natural killer and CD8+ T cells that are harnessed in immunotherapy can be regulated by the ECM. We hypothesized that matrigel layer presents a challenge for the NK cells and increasing the distance for invasion would delay the kinetics of tumor cell killing. Furthermore, invasion and killing of tumor targets would depend on their ability to remodel the matrix with matrix-metalloproteinases.

Methods Briefly, increasing volumes (50–110 μL /well) of matrigel (6mg/mL) representing increasing distance for invasion was layered over MCF7-red target tumor cells expressing nuclear-localized mKate2 (red fluorescent protein). NK92 cells were seeded over the solidified matrigel layer at E:T of 3:1. Agilent eLive Green (1 μL /mL) was added to the wells. NK cell invasion and function was evaluated using impedance-based measurements of immune cell killing and live cell imaging data collected on xCELLigence RTCA eSight.

Results Impedance increases with time as MCF7 target cells adhere and proliferate. The addition of NK92 cells results in a drop in impedance due to killing of the target cells. Total time taken for impedance levels to fall to levels at the time of NK92 addition increased progressively from 46h for 50 μL /well to 72 h for 110 μL /well. The eLive green stained NK cells and dead cells, but not healthy MCF7 targets. Consistent with impedance data, the loss of red fluorescence from target cells and increase in green fluorescence was progressively delayed with increasing volume of matrigel. A similar delay in kinetics was achieved with the broad spectrum MMP inhibitor GM6001 (2 μM and 10 μM), suggesting that MMPs played a role in the NK function. Interestingly, the NK-92 cells induce significant morphological changes in MCF7-red target cells prior to invading all the way through the Matrigel, suggesting an early distal effect.

Conclusions The results suggest a role for effector functions of NK cells potentially involving cytokines, that is independent from invasion and/or ability to degrade the matrix, for the killing of susceptible target cells. The assay also demonstrates the potential for adapting the RTCA eSight platform to study various ECM interactions with immune cells.

<http://dx.doi.org/10.1136/jitc-2022-SITC2022.0012>

13 REAL-WORLD TISSUE-BASED CIRCULATING TUMOR DNA (CTDNA) MINIMAL RESIDUAL DISEASE (MRD) ASSAY PREDICTS OUTCOME IN LUNG CANCER PATIENTS WHO HAD CURATIVE TREATMENTS

¹Youjin Oh, ¹Liam Il-Young Chung*, ²Soowon Lee, ³Timothy Hong, ⁴Leesul Kim, ¹Sung Mi Yoon, ¹Joo Hee Park, ¹Trie Ami Djunadi, ¹Young Kwang Chae. ¹Feinberg School of Medicine, Northwestern University, Chicago, IL, USA; ²Baylor University, WACO, TX, USA; ³Northwestern University, Evanston, IL, USA; ⁴Ascension Saint Francis Hospital Evanston, Evanston, IL, USA

Background As highly sensitive liquid biopsy assays have been developed, minimal residual disease (MRD) has emerged as a novel tool to predict the prognosis of cancer patients.¹ Monitoring MRD during post-curative-intent treatment can help detect relapse of disease many months earlier compared to radiological imaging evaluation.^{1,2,5} Recurrence remains a challenge among early-stage non-small cell lung cancer (NSCLC) patients who are treated with curative intent.³ Some patients with seemingly successful treatment of early-stage cancer can have occult micrometastases or MRD that persists after the initial therapy which can be a potential source of subsequent metastatic relapse at distant sites.⁴ This study compares longitudinal changes in tissue-based ctDNA levels of thirty NSCLC patients.

Methods Thirty patients included in this study were treated with concurrent chemoradiotherapy or surgery and/or neoadjuvant or adjuvant chemotherapy for stage I-IV lung cancer. The patients underwent a multiplex polymerase chain reaction (mPCR) assay for detection of ctDNA in plasma, where 16 individual-specific mutation signatures were identified by upfront tissue sampling. These were matched to normal whole-exome sequencing to identify progression or relapse of disease (SignateraTM, Natera, Austin, Texas). Patients who were MRD-positive at any time point after curative treatment were defined as ‘MRD positive (MP)’. Among patients who were monitored for two or more times, patients whose MRD was persistently detected in blood were classified as ‘MRD persistently positive (MPP)’.

Results ctDNA was evaluated one time in fifteen patients (42.9%) and two or more times in twenty patients (57.1%). MRD was detectable among nine patients (25.7%) after curative treatment at a median of 4 months (range 0–41 months). Among nine MP patients, six experienced progressions. In twenty-nine patients with NSCLC who did not relapse after surgery, the assay confirmed MRD negativity at 71 of 73-time points. Three patients were MPP, ctDNA was continuously detectable in three out of twenty patients, and all of them showed progression, including one patient who died (figure 1). MRD positive patients had marginally worse overall survival (OS) and progression-free survival (PFS) ($p=0.092$ and $p=0.04$, respectively). However, persistent MRD positivity showed a stronger correlation with poor OS and PFS ($p=0.037$ and $p < 0.001$, respectively) (figure 2).

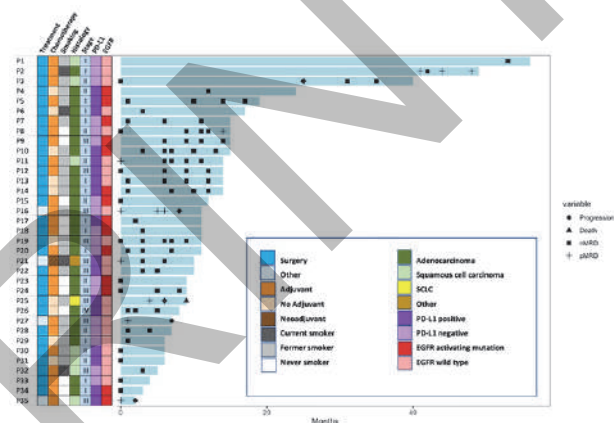
Conclusions This is the first report of real-world data on tissue-based ctDNA MRD assay among NSCLC patients treated curatively. The results indicate that post-curative-intent treatment ctDNA MRD monitoring can be predictive of clinical prognosis including OS or PFS.

REFERENCES

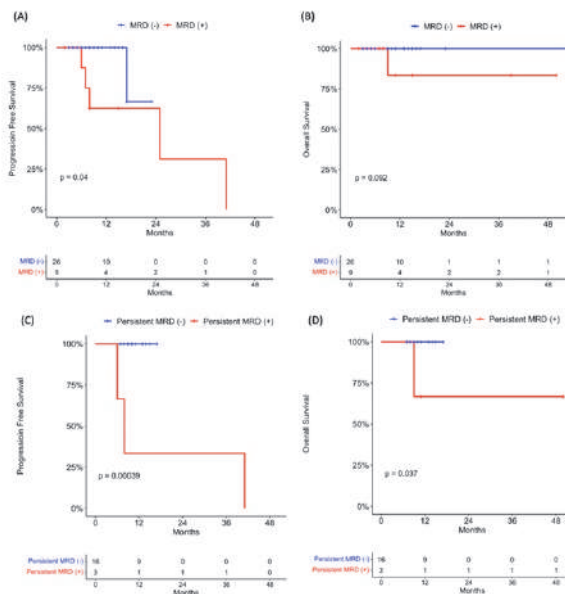
1. Zviran A, Schulman RC, Shah M, Hill STK, Deochand S, Khamnei CC, *et al.* Genome-wide cell-free DNA mutational integration enables ultra-sensitive cancer monitoring. *Nat Med.* 2020 Jul;**26**(7):1114–24.

2. Phallen J, Sausen M, Adleff V, Leal A, Hruban C, White J, *et al.* Direct detection of early-stage cancers using circulating tumor DNA. *Sci Transl Med.* 2017 Aug 16;**9**(403):ean2415.
 3. Chaudhuri AA, Chabon JJ, Lovejoy AF, Newman AM, Stehr H, Azad TD, *et al.* Early Detection of Molecular Residual Disease in Localized Lung Cancer by Circulating Tumor DNA Profiling. *Cancer Discov.* 2017 Dec;**7**(12):1394–403.
 4. Abbosh C, Frankell A, Garnett A, Harrison T, Weichert M, Licon A, *et al.* Abstract CT023: Phylogenetic tracking and minimal residual disease detection using ctDNA in early-stage NSCLC: A lung TRACERx study. *Cancer Res.* 2020 Aug 15;**80**(16_Supplement):CT023.
 5. Rolfo C, Mack PC, Scagliotti GV, Baas P, Barlesi F, Bivona TG, *et al.* Liquid Biopsy for Advanced Non-Small Cell Lung Cancer (NSCLC): A Statement Paper from the IASLC. *J Thorac Oncol.* 2018 Sep 1;**13**(9):1248–68.

Ethics Approval The study was approved by Northwestern University’s Institutional Review Board, study number STU00207117.



Abstract 13 Figure 1 Patient Characteristics and MRD monitoring



Abstract 13 Figure 2 Overall survival and progression-free survival between MRD positive and MRD negative patients, and MRD persistently positive and non-MRD persistently positive patients

<http://dx.doi.org/10.1136/jitc-2022-SITC2022.0013>

Abstracts

14 **EXPLORING REAL-WORLD CONCORDANCE OF TUMOR MUTATION BURDEN (TMB) FROM BLOOD AND TISSUE IN PATIENTS WITH SOLID TUMORS**

¹Youjin Oh, ¹Jewel Park, ¹Liam Il-Young Chung*, ²Soowon Lee, ³Timothy Hong, ¹Young Kwang Chae. ¹Feinberg School of Medicine, Northwestern University, Chicago, IL, USA; ²Baylor University, Waco, TX, USA; ³Northwestern University, Evanston, IL, USA

Background Tumor mutational burden (TMB) is an approved biomarker for immunotherapy in metastatic cancer patients.¹ While initially measured from tissue (tTMB), TMB derived from circulating tumor DNA (ctDNA) – also known as blood TMB (bTMB) – is increasingly being used in the clinic. Currently, real-world concordance between tTMB and bTMB is not well understood.^{2,3}

Methods From October 2020 to July 2022, cancer patients who had both tTMB and bTMB results were selected. Commercial next generation sequencing (NGS) testing for both tissue and blood, i.e. by Tempus xT (Tempus; Chicago, IL) and Guardant360 (Guardant Health; Redwood City, CA) were utilized. Patients were classified according to clinical variables and tumor burden, and correlation analyses or tests of independence were performed. To explore the significance of concordant and discordant bTMB:tTMB ratio, patients were divided into tertiles based on their bTMB:tTMB ratio as ‘low’, ‘mid’, and ‘high’. ‘Low’ and ‘high’ subgroups were considered to be discordant while ‘mid’ was considered to be concordant.

Results From a total of 95 patients included in the study, 69 patients (72.6%) had lung carcinoma and 26 (27.4%) had other cancers, including but not limited to thyroid, brain, and cervical cancer. Median bTMB was 9.6 mut/MB and median tTMB was 4.0 mut/Mb. The distributions of bTMB and tTMB differed significantly (Wilcoxon signed-rank $V=268.5$, $n=95$, $p<0.001$). bTMB was moderately correlated with tTMB (Spearman $\rho=0.49$, $p < 0.001$) (figure 1). Twelve patients had tTMB > 10 mut/Mb while 45 patients had bTMB > 10 mut/Mb. When patients were divided according to cancer type, moderate correlation between bTMB and tTMB remained statistically significant for both lung adenocarcinoma, lung squamous cell carcinoma, and other lung cancer types. The regression lines for lung cancer subtypes displayed marked differences in slope. Dividing patients by site of tissue biopsy revealed that the degree of correlation was pronounced for tissue samples from primary and metastatic sites, not from the lymph nodes. Correlation appeared equivalent between smoker and never smokers. However, dividing patients by concordant and discordant bTMB:tTMB ratio did not reveal any significant differences in clinical variables or tumor burden (table 1).

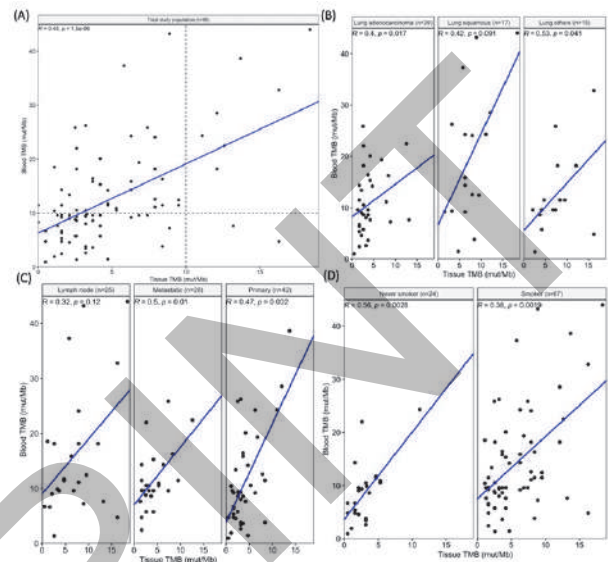
Conclusions Cancer type and site of tissue biopsy may influence concordance between tTMB and bTMB. Future studies with more patients may help define the optimal bTMB threshold for receiving immunotherapy, which may be different from the tTMB threshold.

REFERENCES

1. Goodman AM, Kato S, Bazhenova L, et al: Tumor mutational burden as an independent predictor of response to immunotherapy in diverse cancers. *Mol Cancer Ther* 16:2598–2608, 2017.
2. Davis AA, Chae YK, Agte S, et al: Comparison of tumor mutational burden (TMB) across tumor tissue and circulating tumor DNA (ctDNA). [Internet]. *J Clin Oncol* 35:e23028–e23028, 2017 Available from: https://doi.org/10.1200/JCO.2017.35.15_suppl.e23028.
3. Chae YK, Davis AA, Agte S, et al: Clinical Implications of Circulating Tumor DNA Tumor Mutational Burden (ctDNA TMB) in Non-Small Cell Lung Cancer [Internet].

Oncologist 24:820–828, 2019 Available from: <https://pubmed.ncbi.nlm.nih.gov/30867242>.

Ethics Approval The study was approved by Northwestern University’s Institutional Review Board, study number STU00207117.



Abstract 14 Figure 1 Correlation between tumor mutational burden from blood and tissue

Spearman correlations were examined in A) the total study population, B) patients divided by cancer type, C) patients divided by site of tissue biopsy, and D) patients divided by smoking history. Dotted lines in figure 1A represent the >10 mut/MB cutoff for TMB. TMB, tumor mutational burden

Abstract 14 Table 1 Distribution of patient characteristics and tumor burden according to bTMB:tTMB ratio divided into tertiles

	Low (0.0-2.0)	Mid (2.0-3.8)	High(3.8-16.8)	P-value
<i>Patient characteristics</i>				
Gender				0.842
Female	15	15	17	
Male	16	16	14	
Cancer type				0.432
Lung adenocarcinoma	13	11	15	
Lung SCC	5	7	5	
Other lung cancers	8	5	2	
Other cancers	5	8	9	
Site of tissue biopsy				0.964
Primary tumor	13	14	14	
Metastatic tumor	9	8	10	
Lymph node	9	9	7	
Sampling interval				0.594
<30 days	15	17	19	
≥30 days	16	14	12	
Smoking				0.499
Never smoker	7	11	8	
Former/current smoker	24	20	23	

<http://dx.doi.org/10.1136/jitc-2022-SITC2022.0014>

15 **INTEGRATION OF MULTIPLE IMMUNE-ASSOCIATED BIOMARKERS FACILITATES CLASSIFICATION OF SOLID TUMORS BY PRIMARY IMMUNE ESCAPE MODE AND PREDICTION OF PATIENT OUTCOMES**

RJ Seager*, Maria-Fernanda Senosain, Erik Van Roey, Shuang Gao, Mary Nesline, Jeffrey Conroy, Sarabjot Pabla. *OmnSeq, Inc., Buffalo, NY, USA*

Background Many individual biomarkers describe the idiosyncrasies of each tumor and its interactions with the tumor microenvironment (TME). However, tumors often evade immunotherapy through multiple immune escape mechanisms. Here, we present a method of integrating immune and neoplastic biomarkers that classify tumor and immune activity in the TME.

Methods Standard-of-care comprehensive genomic and immune profiling was performed on 5450 FFPE tumors representing 39 histologic types, assessing expression levels of 395 immune genes and >500 tumor-associated genes. From this data, three previously published gene expression signatures were calculated: cell proliferation (CP), tumor immunogenic signature (TIGS), and cancer testis antigen burden (CTAB). PD-L1 status of each tumor was assessed by IHC, and tumor mutational burden (TMB) was calculated. Principle component analysis (PCA) and unsupervised clustering revealed four distinct biological groups. Subsequently, a nearest neighbor method was used to classify an immune checkpoint inhibitor (ICI) treated 242-patient validation cohort (Lung cancer, melanoma and renal cell carcinoma) into these groups, the association between these groups and ICI treatment response was determined by overrepresentation analysis, and overall survival was assessed using Kaplan-Meier and CoxPH analyses.

Results PCA and clustering generated four groups: 1) Tumor-dominant, exhibiting high CTAB, TMB, and CP, and low PD-L1 and TIGS; 2) Proliferative, exhibiting high CP and low TIGS, PD-L1, CTAB, and TMB; 3) Inflamed, exhibiting high TIGS and low CP, PD-L1, CTAB, and TMB; and 4) Checkpoint, exhibiting high PD-L1, TIGS, and TMB, and low CTAB. Classifying the validation cohort into these groups, significant association with ICI response was found, with the checkpoint group overrepresented by the highest proportion of disease control [$p=0.0313$]. Kaplan-Meier survival analysis suggested a significant relationship between these groups and overall survival [$p=0.035$], with the proliferative and checkpoint groups demonstrating increased survival over tumor-dominant and inflamed groups. CoxPH analysis showed the checkpoint group to have a significantly decreased hazard ratio [HR=0.28; $p=0.024$] for ICI treatment. In all Kaplan-Meier and CoxPH analyses, this approach outperformed any of its constituent biomarkers as a survival predictor.

Conclusions Our study demonstrated that an integrated approach combining comprehensive tumor profiling and emerging biomarkers better predicts ICI response and survival in multiple histologies. Divergent outcomes between the resulting groups are likely the result of distinct tumor-immune interaction modalities. As we further validate this methodology, we hope to produce a treatment decision and clinical trial selection tool leveraging tumor-immune interactions in solid tumors to outperform single marker testing.

<http://dx.doi.org/10.1136/jitc-2022-SITC2022.0015>

MULTI-DIMENSIONAL ANALYSIS OF CD19-CAR T CELLS AT SINGLE CELL RESOLUTION ON THE BERKELEY LIGHTS PLATFORM ENABLE UNIQUE INSIGHTS INTO RELATIONSHIPS BETWEEN CYTOTOXICITY KINETICS AND CYTOKINE SECRETION

Joseph Valdez*, Guido Stadler, Milton Quintanilla, Pei-Yu Lin, Aribet De Jesus, Deric Griffin, Sapna Tandon, Yiyang Xu. *Berkeley Lights, Emeryville, CA, USA*

Background CD-19 CARs have tremendous efficacy in the clinic and complete clinical responses persisting for >10 years. However, outcome of clinical response cannot be predicted. Traditional analytical methods are complex, labor/cost intensive, with high sample requirements, thus generating deep characterization datasets to define critical quality attributes is an unmet need. In addition, linking parameters at single-cell resolution has not been possible. We show here the ability to rapidly measure and link analytes at single-cell resolution for thousands of cells in parallel.

Methods T cells from a healthy donor were activated with CD3/CD28 beads and transduced with lentivirus encoding CD-19 CAR. Single control or CD-19 CAR T cells were loaded on OptoSelect® chips and placed in co-culture with Raji CD19+ or Raji CD19-KO single cells and a bead conjugated to anti-IFN- γ antibody. Co-cultures were under perfusion media culture containing Caspase-3 detection reagent over 22-hour timelapse with 30-minute imaging intervals. Time to detection of Caspase-3 signal and mean fluorescent intensity of anti-IFN- γ -PE was recorded.

Results Hundreds to thousands of single cell co-cultures of the populations described above were obtained. Detectable IFN- γ signal was observed in 45% of the co-culture events in the CAR-T+CD-19 Raji group while all others were below 1%. Cytotoxicity was observed in 25% of the co-culture events in the CAR-T+CD-19 Raji group, 10% of the co-culture events in the CAR-T+CD-19-KO Raji group and $\leq 1\%$ in the other groups. Rapid cytotoxicity (≤ 7 hours) was enriched in the CAR-T+CD-19 Raji group >6 fold compared to the CD-19-KO control. Slow cytotoxicity (>7 hours) showed no significant difference between the CD-19+ and KO groups. Co-cultures double positive for IFN- γ and cytotoxicity comprised 13% of the CAR-T + CD-19 Raji population and not present in any others. Significant clustering of rapid killers with low IFN- γ secretion was observed.

Conclusions We demonstrate the ability to characterize T cells in co-culture with antigen-presenting cells (APCs) at single-cell resolution. Classic functions of antigen-dependent interactions between CAR-T cells and APCs such as IFN- γ secretion and cytotoxicity are enriched when both CAR and antigen are present but largely absent in mismatches as expected. Evaluation of cytotoxicity kinetics and semi-quantitative measurements of cytokines enable identification of potential multi-modal mechanisms of action and insights into potency of cell products. This deep characterization dataset can be generated in two days with limited numbers of cells which will enable definition of critical quality attributes to drive next-generation cell therapies.

<http://dx.doi.org/10.1136/jitc-2022-SITC2022.0016>

17

ISOLATION AND EXPANSION OF CIRCULATING TUMOR-REACTIVE LYMPHOCYTES FOR ADOPTIVE CELL THERAPY

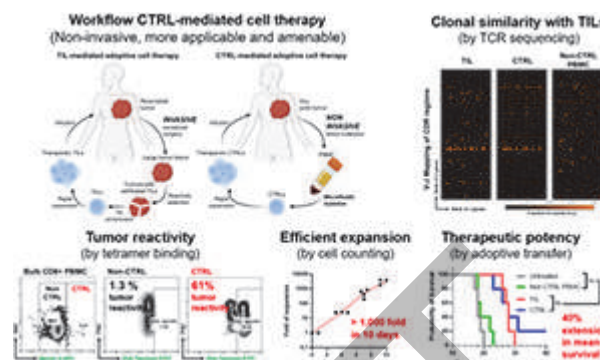
Shana Kelley, Zongjie Wang*. Northwestern University, Evanston, IL, USA

Background The autologous transplantation of tumor-infiltrating lymphocytes (TILs) expanded from resected tumors has become a promising therapeutic modality in the clinic. The clinical outcome is extremely encouraging so far – long-term complete responses have been observed in subsets of melanoma patients. Despite positive results in the clinic, the use of tumor-infiltrating lymphocytes (TILs) to treat solid tumors is limited by the use of fresh, large, viable tumor fractions from invasive resectable surgery, which is not often feasible in patients with unresectable tumors or recurrent metastases. Recent studies on peripheral T cell dynamics have revealed a string result – a subset of peripheral lymphocytes shares clonotypes with TILs and their expansion is highly correlated with response to treatment. However, these circulating tumor-reactive lymphocytes (CTRLs) are extremely rare in peripheral T cell populations (as low as 0.002%), and their molecular signature and therapeutic potency are yet to be examined.

Methods Conventional cell sorting is infeasible to enrich CTRLs with high purity as they due to their rarity. We developed a novel approach, named microfluidic immunomagnetic cell sorting (MICS), that efficiently isolates CTRLs from blood circulation for molecular assay, rapid expansion and cellular therapy (figure 1).

Results With the high recovery and purity of MICS, we identified that the expression of CD8⁺MarkerA⁺ almost exclusively defines the CTRL population in circulation. This population has a tissue-resident-like (T_{rm}-like) phenotype and can re-enter blood circulation from primary tumors and accumulate in secondary tumors. We successfully expanded the isolated CTRLs through a feeder-based rapid expansion protocol (REP) and found CTRLs have strong therapeutic potency in multiple adoptive cell transfer models in mice. The cocktail of CTRLs and immune checkpoint blockade successfully achieved an 80% complete response (CR) rate in the mouse colon cancer model. In addition, we also confirmed that the human CD8⁺ MarkerA⁺ lymphocytes in blood circulation have higher tumor reactivity, by comparing the level of interferon-gamma (IFN- γ) secretion and clonal similarity.

Conclusions In this work, we adapted our MICS technology for the isolation of CTRLs, a rare tumor-targeting cell population in blood circulation, and deconvolute their molecular signature comprehensively. In addition, we developed the protocols to expand rare CTRLs to a therapeutic scale for the first time. The successful expansion and administration of CTRLs promise to transfer adoptive cell therapy by eliminating invasive surgery and potentially providing a more amenable therapeutic modality that is broadly applicable to all patients.



Abstract 17 Figure 1 Circulating tumor-reactive lymphocytes Figure 1. Circulating tumor-reactive lymphocytes from blood circulation as a mean for cellular therapy. CTRLs cover major TIL clonotypes, are highly tumor-reactive and expandable, and deliver potent anti-tumor efficacy in vivo. Compared to conventional TIL-mediated therapy, CTRL-mediated are non-invasive, more amenable and broadly applicable to all cancer stages

<http://dx.doi.org/10.1136/jitc-2022-SITC2022.0017>

18 IDENTIFICATION AND CHARACTERIZATION OF CIRCULAR RNAs AS NOVEL PUTATIVE BIOMARKERS TO PREDICT THE SURVIVAL BENEFIT AMONG METASTATIC MELANOMA PATIENTS TREATED WITH ANTI-PD-1 MONOTHERAPY

¹Jian-Guo Zhou*, ²Udo Gaipl, ³Hu Ma, ⁴Haitao Wang. ¹The Second Affiliated Hospital of Zunyi Medical University, Zunyi, China; ²Universitätsklinikum Erlangen, Erlangen, Germany; ³The Second Affiliated Hospital of Zunyi, Zunyi, China; ⁴National Institutes of Health, Bethesda, MD, United States

Background Melanoma is the most aggressive skin malignancy with high morbidity. Anti-programmed cell death protein 1 (PD-1) monotherapy has been applied in metastatic melanoma, however, most patients do not respond to anti-PD-1 and the availability of the present approved biomarkers is limited.

Methods Here we combined the transcriptomic and clinical data in 163 advanced melanoma patients receiving anti-PD-1 from phs000452 (122 patients) as the training and internal validation cohort, and PRJEB23709 (41 patients) as the external validation cohort, respectively.

Results 74,243 circular RNAs (circRNA) were identified with NCLscan and CIRCexplorer2, 70 circRNAs significantly associated with progression-free survival and overall survival as novel putative candidates to predict the survival benefit of immunotherapy. The prognostic circRNAs signature (HSA_CIRCpedia_1497, HSA_CIRCpedia_12559, HSA_CIRCpedia_43640, HSA_CIRCpedia_43070, and HSA_CIRCpedia_21660) was determined with LASSO regression. This signature was a prognostic factor of overall survival and progression-free survival among advanced melanoma patients, and the concordance indexes also confirms its credibility and accuracy. Enrichment analysis showed that immune response and currently known pathways were enriched.

Conclusions We constructed and validated a novel prognostic circRNAs signature to serve as a predictor for advanced melanoma patients treated with anti-PD-1 immunotherapy.

<http://dx.doi.org/10.1136/jitc-2022-SITC2022.0018>

19

PERIPHERAL LYMPHOCYTES AND LACTATE DEHYDROGENASE CORRELATE WITH IMPROVED RESPONSE AND SURVIVAL IN HEAD AND NECK CANCER TREATED WITH IMMUNE CHECKPOINT INHIBITORS

¹Cassie Pan*, ²Qian 'Vicky' Wu, ²Jenna Voutsinas, ¹Jeffrey Houlton, ¹Brittany Barber, ¹Zain Rizvi, ¹Emily Marchiano, ¹Neal Futran, ¹George Laramore, ¹Jay Liao, ¹Upendra Parvathaneni, ³Renato Martins, ¹Jonathan Fromm, ¹Cristina Rodriguez. ¹University of Washington, Seattle, WA, USA; ²Fred Hutchinson Cancer Research Center, Seattle, WA, USA; ³Virginia Commonwealth University, Richmond, VA, USA

Background Little is known regarding peripheral blood biomarkers (PBBMs) for oncologic outcomes in recurrent/metastatic head and neck squamous cell carcinoma (R/M HNSCC) treated with immune checkpoint inhibitors (ICIs). We explored associations of PBBMs with outcomes and toxicities in R/M HNSCC treated with ICIs.

Methods In this single-institution retrospective cohort study, records of 186 adult patients with R/M HNSCC treated with ICIs between 08/2012–03/2021 were reviewed. Pretreatment PBBMs investigated included lactate dehydrogenase (LDH), platelets, neutrophils, lymphocytes, monocytes, eosinophils, neutrophil-to-lymphocyte ratio (NLR), and prognostic nutritional index (PNI). Percent (%) and absolute (abs) values for each cell type were examined. Cox regression was performed to explore associations with time-to-event outcomes, including overall survival (OS) and progression-free survival (PFS). Logistic regression was performed for binary outcomes, including objective response (ORR) by RECIST 1.1 and grade ≥ 3 toxicities ($G \geq 3AE$) by CTCAEv5 within 100 days of treatment initiation. Multivariable models for each outcome were created using elastic net variable selection method.

Results Median age was 64 (range 24–90), 145 (78%) were male, 149 (82%) had ECOG ≤ 1 , 81 (44%) were never-smokers, and 60 (33%) had p16-positive tumors. Single-agent pembrolizumab or nivolumab was used in 140 (75%) patients. Combined positive score (CPS) was available in 33 patients, with median CPS 31 (range 0–100). Univariate analyses adjusted for ECOG, p16, and smoking revealed that baseline higher LDH ($p=0.025$), neutrophils (%: $p=0.002$, abs: $p=0.001$), monocytes (abs: $p=0.043$), and NLR ($p<0.001$), and lower lymphocytes (%: $p<0.001$, abs: $p=0.005$), eosinophils (%: $p=0.046$), and PNI ($p=0.005$) correlated with worse OS. Elevated platelets ($p=0.010$), neutrophils (%: $p=0.010$, abs: $p<0.001$), and NLR ($p<0.001$), and decreased lymphocytes (%: $p<0.001$) and PNI ($p=0.007$) correlated with worse PFS. No peripheral blood parameter reached significance for $G \geq 3AE$ s or ORR, although% lymphocytes, absolute neutrophils, and LDH were borderline significant for ORR ($p=0.066$, $p=0.055$, $p=0.069$, respectively). Refitted multivariable models adjusted for ECOG, p16, and smoking confirmed that lower% lymphocytes and higher LDH and absolute neutrophils correlated with worse OS and PFS. Lower% lymphocytes and higher LDH also correlated with worse ORR.

Conclusions In the largest cohort to date of R/M HNSCCs treated with ICIs, our variable selection method showed that baseline lower% lymphocytes and higher LDH and absolute neutrophils correlated with worse OS and PFS, and lower% lymphocytes and higher LDH correlated with worse ORR. PBBMs are promising prognostic tools for immunotherapy in HNSCC and warrant further investigation in a large, prospective study along with validation with CPS biomarker.

<http://dx.doi.org/10.1136/jitc-2022-SITC2022.0019>

DEVELOPMENT OF VISTA-CENTRIC TUMOR IMMUNOPHENOTYPING AS A NOVEL APPROACH FOR IDENTIFICATION OF POTENTIAL BIOMARKERS FOR ANTI-VISTA THERAPY

¹Andrey Ugolkov*, ¹Hok, ¹Reinhard von Roemeling, ²Alexander Martin, ¹Robert Martell. ¹Curis, Lexington, MA, USA; ²Tufts Medical Center, Boston, MA, USA

Background V-domain immunoglobulin suppressor of T cell activation (VISTA) is a negative checkpoint regulator of immune cells. VISTA has been recognized as a potential mediator of resistance to anti-PD-1 and anti-CTLA-4 immunotherapies in cancer patients. Targeting the VISTA signaling pathway has been suggested as a promising approach for overcoming resistance to current immune checkpoint therapies. Herein, we report the design, development, and analytical algorithm for comprehensive VISTA-centric tumor immunophenotyping to explore potential tumor biomarkers for novel anti-VISTA therapeutic antibody CI-8993, currently under clinical development in Phase 1 trial.

Methods Formalin-fixed paraffin embedded (FFPE) tumor tissue sections from 10 cases of non-small cell lung carcinoma (NSCLC) were purchased from NovoVita Histopath Laboratory. Serial tumor tissue sections were double-immunostained with VISTA combined with CD8 (cytotoxic T cell marker), CD4 (T helper cell marker), CD11b (myeloid cell marker), CD68 (monocyte/macrophage marker), CD56 (NK cell marker), CD19 (B cell marker) or Programmed Death-Ligand 1 (PD-L1).

Results Immunohistochemical analysis revealed the presence of CD8+ cells (9/10 cases), CD4+ cells (3/10 cases), CD11b+ cells (10/10 cases), CD68+ cells (10/10 cases), CD56+ cells (4/10 cases) and CD19+ cells (8/10 cases) in lung tumors. Using double IHC staining, we found that VISTA was expressed in CD8+ cells (5/9 tumors), CD11b+ cells (5/10 tumors) and CD19+ cells (5/8 tumors), whereas VISTA was hardly detectable in CD4+, CD68+ or CD56+ cells. Expression of PD-L1 was detected in cancer cells in 6/10 tumors, whereas VISTA-pos cancer cells were revealed in 1/10 tumors. We developed an algorithm for evaluation of VISTA-centric tumor immunophenotyping and demonstrated that every tumor has a unique cell-type-specific pattern of VISTA expression which could serve as a potential biomarker.

Conclusions Our results demonstrate that comprehensive VISTA-centric immunophenotyping enables spatially resolved and cell-type-specific characterization of VISTA expression in solid tumors and can serve as applicable bioanalytical approach for identification of potential biomarkers to guide anti-VISTA therapeutic treatment decisions.

<http://dx.doi.org/10.1136/jitc-2022-SITC2022.0020>

21 **IL-6 AS PROGNOSTIC FACTOR IN ADJUVANT OR METASTATIC SKIN CANCER PATIENTS TREATED WITH IMMUNOTHERAPY – A REAL LIFE STUDY**

Domenico Mallardo*, Maria Antonietta Isgrò, Vito Vanella, Marilena Tuffanelli, Lucia Festino, Maria Grazia Vitale, Grazia D'angelo, Francesca Sparano, Mario Mallardo, Eleonora Cioli, Benedetta Alfano, Claudia Trojaniello, Alfredo Budillon, Ester Simeone, Corrado Caracò, Ernesta Cavalcanti, Paolo Ascierto. *Istituto Nazionale Tumori IRCCS Pascale, Napoli, Italy*

Background The immune checkpoint inhibitors revolutioned cancer therapeutic landscape and substantially improved the survival of patients with advanced malignancies, especially in skin cancer patients.¹⁻⁵ Several predictive biomarkers are under evaluation, in order to identify patients who can derive benefit from ICI while also limiting exposure and toxicity. IL-6 is a pleiotropic cytokine involved not only in immune responses but it is also a major player in chronic inflammatory diseases.⁶⁻⁷ Additionally, elevated levels of IL-6 are observed in a large number of patients (pts) with solid tumours.⁸ The purpose of this study is to retrospectively investigate the relationships between IL-6 serum concentration and outcome in skin cancer patients treated with immunotherapy.

Methods From June 2020 to October 2021 at INT IRCCS Pascale, Naples, we analyzed interleukin -6 from 265 consecutive serum samples in different skin cancer pts before and during immunotherapy treatment. We included pts with cutaneous squamous cell carcinoma (SCC) treated with cemiplimab (n=32), melanoma in adjuvant setting (n=61), metastatic melanoma treated with: anti-PD1 (n=103), combo ipi+nivo (n=36) and ipilimumab alone (n=32). All patients signed informed consent. Patients baseline characteristics are listed in table 1. IL6 ere measured by Electrochemiluminescence immunoassays (ECLIA) from Roche Cobas. ROC curves were used to determine the best cut off. Survival rates were analyzed using the Kaplan-Meier method and differences among curves were assessed by the log-rank test. Hazard Ratios (HR) and their 95% confidence intervals (CI) were estimated using a Cox regression model.

Results Among 265 pts, lower serum concentration of interleukin-6 was associated with a better PFS (15.07 months (95% CI 9,76 to 18,86) versus 8.01 months (95% CI 2,80 to 4,03), HR = 0.34 (CI 0,23–0,50, p<0.0001), OS (19.83 months (95% CI 18.57 to 21.03) versus 14.53 months (95% CI 12.38 to 16.68), HR = 0.41 (CI 0,26–0,64, p=0.0001) and ORR (95% CI 6.86 to 13.30, p<0.001). Similarly, IL6 (p <0.01) and ORR (p <0.01) are significantly associated with OS and PFS in the multivariate analysis. We also confirmed the association between IL6 with PFS and OS in adjuvant setting. Moreover, pts with an IL-6 ratio (on treatment/baseline) ≤1 have a better PFS and OS.

Conclusions In this retrospective study, we found that lower IL-6 level are associated with better OS, PFS and ORR. In addition, minimum variation of IL-6 during immunotherapy are strongly associated to outcome. Further investigations are needed to get additional information.

Acknowledgements We thank the Italian Ministry of Health (IT-MOH) through support of ‘Ricerca Corrente’

REFERENCES

1. James Larkin, Vanna Chiarion-Sileni, Rene Gonzalez, Jean Jacques Grob, C. Lance Cowey et al. Combined Nivolumab and Ipilimumab or Monotherapy in Untreated Melanoma. *N Engl J Med.* 2015 Jul 2;**373**(1):23–34.
2. Robert C, Long GV, Brady B, Dutriaux C, Maio M et al. Nivolumab in previously untreated melanoma without BRAF mutation. *N Engl J Med.* 2015 Jan 22;**372**(4):320–30.

3. Weber JS, D'Angelo SP, Minor D, Hodi FS, Gutzmer R. Nivolumab versus chemotherapy in patients with advanced melanoma who progressed after anti-CTLA-4 treatment (CheckMate 037): a randomised, controlled, open-label, phase 3 trial. *Lancet Oncol.* 2015 Apr;**16**(4):375–84.
4. Weber J, Mandala M, Del Vecchio M, Gogas HJ, Arance AM, Cowey CL, Dalle S, Schenker M, Chiarion-Sileni V, Marquez-Rodas I, Grob JJ, Butler MO et al. CheckMate 238 Collaborators. Adjuvant Nivolumab versus Ipilimumab in Resected Stage III or IV Melanoma. *N Engl J Med.* 2017 Nov 9;**377**(19):1824–1835.
5. Larkin J, Chiarion-Sileni V, Gonzalez R, Grob JJ, Cowey CL, et al. Combined Nivolumab and Ipilimumab or Monotherapy in Untreated Melanoma. *N Engl J Med.* 2015 Jul 2;**373**(1):23–34.
6. Hirano T. Interleukin 6 and its receptor: ten years later. *Int Rev Immunol.* 1998;**16**(3–4):249–84.
7. Hunter CA, Jones SA. IL-6 as a keystone cytokine in health and disease. *Nat Immunol.* 2015 May;**16**(5):448–57.
8. Kumari N, Dwarakanath BS, Das A, Bhatt AN. Role of interleukin-6 in cancer progression and therapeutic resistance. *Tumour Biol.* 2016 Sep;**37**(9):11553–11572.

Ethics Approval This study was approved by the Ethics Committee of Istituto Nazionale Tumori – IRCCS – Fondazione ‘G. Pascale’, Naples, Italy, protocol number 17/17 oss.

Abstract 21 Table 1 Patients clinical parameters

Parameter	N = 265
Patient characteristics	
Median age	62 (range 23-96)
Gender: female:male, n (%)	96/169 (36/64)
BRAF Status	
Wild type	104 (39)
Mutation, n (%)	77 (29)
NA, n (%)	84 (32)
Line of treatment in mts pts	N=207
1st line treatment, anti-PD1	77 (38)
pretreated, anti-PD1	26 (13)
1st line treatment, anti-CTLA4	2 (1)
pretreated, anti-CTLA4	30 (15)
1st line treatment, ipi+nivo	22 (11)
pretreated, ipi+nivo	14 (7)
1st line treatment, Cemiplimab	25 (12)
pretreated, Cemiplimab	7 (3)
Response rate at 1st assessment in mts	
Complete response, n (%)	5 (2)
Partial response, n (%)	45 (21)
Stable disease, n (%)	36 (17)
Progression disease, n (%)	119 (60)
ORR, n (%)	48 (25)
DCR, n (%)	69 (34)
Patient characteristics adjuvant focus	N = 61
Median age	57 (range 44-81)
Gender: female:male, n (%)	25/36 (41/59)
BRAF Status	
Wild type, n (%)	30 (50)
Mutation, n (%)	24 (39)
NA, n (%)	7 (11)
Response rate	
Progression disease, n (%)	19 (31)
Median PFS	8.16 Months

<http://dx.doi.org/10.1136/jitc-2022-SITC2022.0021>

ACTIVITY OF THE TUMOR-INTRINSIC NLRP3 INFLAMMASOME PATHWAY PREDICTS FOR RESPONSE TO CHECKPOINT INHIBITOR IMMUNOTHERAPY IN MELANOMA PATIENTS

Tarek Haykal*, Nagendra Yarla, Nicholas DeVito, Georgia Beasley, April Salama, Brent Hanks, Balamayooran Theivanthiran. *Duke University, Durham, NC, USA*

Background We have previously determined that activation of a novel tumor-intrinsic NOD-, LRR- and pyrin domain-containing protein-3 (NLRP3) inflammasome-heat shock protein-70 (HSP70) signaling axis in response to PD-1 blockade triggers the recruitment of granulocytic myeloid-derived suppressor cells (PMN-MDSCs) into the tumor microenvironment, suppresses anti-tumor immunity and, in select settings, promotes tumor hyperprogression. We, therefore, sought to determine whether the activity of the tumor-intrinsic NLRP3-HSP70 pathway may correlate with anti-PD-1 response by interrogating clinical specimens derived from advanced melanoma patients undergoing anti-PD-1 monotherapy.

Methods Three independent approaches were utilized to measure the activity of the tumor-intrinsic NLRP3-HSP70 signaling pathway in 60 advanced melanoma patients undergoing either pembrolizumab or nivolumab monotherapy: 1. baseline week 0 plasma HSP70 levels were measured by ELISA, 2. germline PCR-based genotyping was performed to detect the single-nucleotide polymorphism (SNP), rs12239046, previously associated with enhanced *NLRP3* expression, 3. PCR-based proximity ligation assay (PLA) analysis targeting the NLRP3-ASC proteins in baseline formalin-fixed paraffin-embedded tumor tissue specimens. Detection of the rs12239046 SNP was correlated with progression-free survival (PFS) while plasma HSP70 and NLRP3-ASC PLA levels were correlated with objective response (OR) based on RECIST1.1 assessment of week-12 CT imaging as well as PFS and overall survival (OS).

Results Our studies demonstrate that elevated baseline plasma HSP70 levels ($P = 0.0008$) and elevated baseline tissue NLRP3-ASC PLA levels ($P = 0.0014$) independently correlate with resistance to anti-PD-1 immunotherapy (ICI) based on week-12 OR in melanoma patients. Importantly, melanoma patients developing disease hyperprogression ($n=5$) in response to ICI exhibited elevations in baseline plasma HSP70 levels ($P = <0.0001$) and baseline tissue NLRP3-ASC PLA levels ($P = <0.0001$) relative to patients with week-12 disease progression ($n=10$). Above median baseline tissue NLRP3-ASC PLA levels were determined to correlate with both inferior PFS (HR 0.12, $P = 0.0008$) and OS (HR 0.16, $P = 0.0456$) in advanced melanoma patients undergoing ICI. Germline PCR detection of the rs12239046-C SNP was found to be associated with elevated plasma HSP70 levels and trended toward a correlation with inferior PFS (HR 0.50, $P = 0.07$).

Conclusions Baseline markers of the tumor-intrinsic NLRP3-HSP70 signaling pathway correlate with resistance and disease hyperprogression in melanoma patients undergoing anti-PD-1 immunotherapy. These data strongly support the important role of the tumor-intrinsic NLRP3 inflammasome in regulating responses to anti-PD-1 therapy and verify its relevance as a pharmacologic target to enhance immunotherapy efficacy. Expanded studies are warranted to confirm these findings in a larger patient cohort.

<http://dx.doi.org/10.1136/jitc-2022-SITC2022.0022>

23

CLUES FROM THE MATRIX – PERIPHERAL COLLAGEN FRAGMENTS ORIGINATING FROM ACTIVITY OF LYMPHOID CELLS, MYELOID CELLS, AND FIBROBLASTS MAY HAVE BIOMARKER POTENTIAL FOR CANCER IMMUNOTHERAPY

Jeppe Thorlacius-Ussing, Nicholas Willumsen*, Neel Nissen, Christina Jensen, Morten Karsdal. *Nordic Bioscience, Herlev, Denmark*

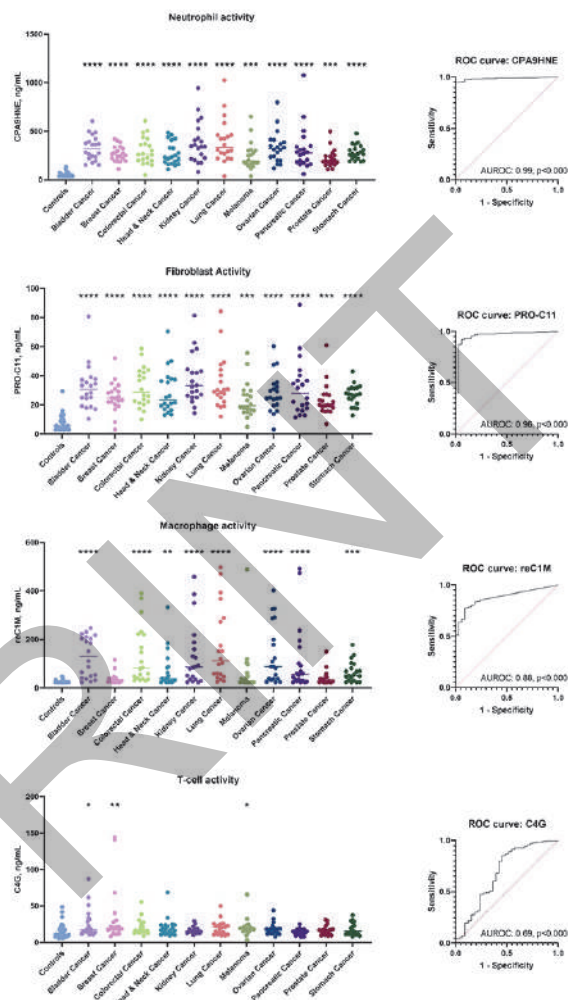
Background Solid tumors have a high tissue turnover due to increased recruitment and activity of cells related to the fibro-inflammatory axis. The high tissue turnover generates small extracellular matrix (ECM) fragments, primarily from collagens, that are released into circulation. By mapping and quantifying collagen fragments with neo-epitopes that are generated by proteases from specific cell types, it is possible to develop peripheral biomarkers that reflect the activity of lymphoid cells, myeloid cells, and fibroblasts in the tumor microenvironment. Here we investigated the distribution of such biomarkers across 11 different cancer indications.

Methods ECM or collagen fragments related to activity of T-cells (C4G: Collagen-4 degraded by Granzyme B), Neutrophils (CPA9-HNE: Calprotectin degraded by neutrophil elastase), Macrophages (reC1M: Collagen-1 degraded by MMPs) and Cancer Associated Fibroblasts (PRO-C11: pro-peptide from Collagen-11) were measured by ELISA/ECLIA in pre-treatment serum from patients with various solid tumor types (n=220) including stage 1–4 bladder-, breast- colorectal-, head and neck-, kidney-, lung-, ovarian-, pancreatic, stomach-, prostate-cancer, and melanoma and compared to age-matched healthy controls (n=33) by ANOVA and AUROC.

Results As shown in figure 1, biomarkers of neutrophil and fibroblast activity were significantly increased in all solid tumor types ($p < 0.001-0.0001$) and with an overall AUROC of 0.99 ($p < 0.0001$) and 0.96 ($p < 0.0001$), respectively. The macrophage activity marker was significantly elevated in most types of cancer and with an AUROC of 0.88 ($p < 0.0001$). The T-cell activity marker was only slightly elevated in a few indications ($p < 0.05-0.01$) and with an AUROC of 0.69 ($p = 0.0006$). All biomarker levels were independent of age and disease stage (not shown).

Conclusions ECM fragments in serum that are derived from proteolytic activity of myeloid cells and fibroblasts, and to lesser extent lymphoid cells, are altered in serum from patients with cancer. If validated, such tools may increase the understanding of response and resistance mechanism associated to the fibro-inflammatory axis and serve as predictive and pharmacodynamic biomarkers in clinical trials investigating cancer immunotherapy.

Ethics Approval Sample collection was approved by an Institutional Review Board or Independent Ethical Committee and patients gave their informed consent: Russian Oncological Research Centre n.a. Blokhin RAMS (PG-ONC 2003/1) and Western Institutional Review Board, Inc. (WIRB® Protocol #20161665).



Abstract 23 Figure 1 Biomarker levels and AUROC for patients with various types ECM or collagen fragments related to activity of T-cells (C4G), Neutrophils (CPA9-HNE), Macrophages (reC1M) and Cancer Associated Fibroblasts (PRO-C11) in pre-treatment serum from patients with various solid tumor types and healthy controls. * $p < 0.05$

<http://dx.doi.org/10.1136/jitc-2022-SITC2022.0023>

24 PROTEOMIC ANALYSIS OF BREAST CANCER BASED ON IMMUNE SUBTYPES

Yeonjin Jeon*, Hee Jin Lee. *Asan Medical Center, Songpa-gu, Korea, Republic of*

Background Immunotherapy was recently conducted on breast cancer to defeat the limitations of survival gain of other treatment modalities like surgery, chemotherapy and targeted therapy. With immunotherapy, a tumour can be classified into immune inflamed, immune excluded and immune desert based on the distribution of immune cells. We assessed the clinicopathological features, each subtype's prognostic value, and differentially expressed proteins between the immune subtypes.

Methods A total of 56 cases of breast cancer with neoadjuvant chemotherapy, including all intrinsic subtypes, between 2014 and 2018 were retrieved from Asan Medical Center. The immune subtype was established based on the tumour-infiltrating lymphocytes' level and Klintrup criteria. Correlation between clinicopathological factors and immune subtypes and each subtype's prognostic value were investigated. Mass spectrometry was used to identify differentially expressed proteins in formalin-fixed paraffin-embedded biopsy tissues.

Results Thirty-one cases (55%) were immune inflamed, 21 cases (38%) were immune excluded, and 2 cases (4%) were immune desert. Only age demonstrated a statistical difference between immune inflamed and excluded/desert, among clinicopathological factors. The old age (age \geq 50) ratio was higher in immune inflamed than in immune excluded/desert ($p=.039$). In the Kaplan-Meier survival analysis, there was no difference in the overall survival rate and relapse-free survival (RFS) rates between immune subtypes. Welch's t-test revealed two differentially expressed proteins between immune inflamed and immune excluded/desert. *CORO1A* and *SERPINA1* were up-regulated in immune inflamed (adjusted $p=.008$) and immune excluded/desert (adjusted $p=.008$), respectively. *TNN* was up-regulated in pCR than non-pCR among immune inflamed subtypes (adjusted $p=.036$).

Conclusions Through proteomic analysis using formalin fixed paraffin embedded breast cancer samples, *CORO1A* showed up-regulation in immune inflamed and *SERPINA1* showed up-regulation in immune excluded/desert. *TNN* was up-regulated in pCR than non-pCR in immune inflamed and probably related to favorable prognosis. Further studies in large representative cohorts needs to be performed to validate these findings.

Ethics Approval Informed consent was obtained from all patients. This study was approved by the Institutional Review Board of Asan Medical Center (2019-1480).

<http://dx.doi.org/10.1136/jitc-2022-SITC2022.0024>

25 POTENTIAL PREDICTIVE BIOMARKERS FOR BXCL701 IN ACUTE MYELOID LEUKEMIA (AML)

Veena Agarwal*, Shubhendu Trivedi, Dimple Bhatia, Zeenia Jagga, Moses Donkor, Vincent O'Neill. *BiXcel Therapeutics, New Haven, CT, USA*

Background BXCL701 (talabostat), an oral innate immune activator is currently in a Phase 2 trial in combination with PD-1 checkpoint inhibitor in metastatic castration-resistant prostate cancer patients. In solid tumors, preclinical data suggest that BXCL701 inhibition of dipeptidyl peptidases (DPPs) enhances antitumor immune responses via two mechanisms: (1) DPP4 inhibition increases tumor content of CXCL9/10, which recruits CXCR3⁺ NK and T cells, and (2) DPP8/9 inhibition activates the inflammasome resulting in immune cell pyroptosis followed by Th1 proinflammatory cytokine release, and dendritic cells (DCs) activation which further enhances the CXCL9/10-CXCR3 axis¹. Recent studies show that BXCL701 exhibits single agent cytotoxicity against human AML cells through a similar pyroptotic mechanism². Here, we report the identification of potential predictive biomarkers by using BXCL701-responsive and -nonresponsive human leukemic cell lines.

Methods The cytotoxic activity of BXCL701 was evaluated in a panel of 170 hematological and non-hematological cell lines and confirmed that mostly but not all the leukemic cells were responsive to BXCL701. Four responding cell lines (KG1, MV4-11, THP1 and EOL-1, IC₅₀ = 100 – 700 nM) and 2 non-responding cell lines (K562 and Kasumi1, IC₅₀ >60 μM) were selected based on the cytotoxicity data and their gene expression profiles were compared to identify predictive biomarkers for BXCL701. Nanostring analysis was performed followed by qRT-PCR using cDNA from the cell lines.

Results The analysis identified 20 genes as potential predictive biomarkers. These, include 5 genes (DPP9, DPP8, caspase 1, CARD8 and PYCARD) involved in the inflammasome – pyroptosis pathway that is activated by BXCL701 and correlate with the BXCL701 cytotoxic activity. Most of the genes have 2-to-1,000-fold higher expression in at least 3 responding cell lines in comparison to non-responding cell lines. On the other hand, EPCAM gene has 7,000-fold higher expression in non-responding cell lines vs responding cell lines. Further, copy number was evaluated for BXCL701 target genes (DPP8, DPP9, DPP4 and FAP) by RT-PCR in 11 responding leukemic cell lines and 6 non-responding cell lines. The DPP9 copy number variation (CNV) was found to be directly correlated with BXCL701 cytotoxicity in BXCL701-responding human leukemic cell lines with correlation coefficient (R²) of 0.813.

Conclusions A gene panel consisting of genes involved in BXCL701 mechanism of action has been identified as a potential predictive biomarker for BXCL701 in leukemia, which can help in selecting patients susceptible to respond to BXCL701 treatment.

REFERENCES

1. Fitzgerald AA, Wang S, Agarwal V, et al. DPP inhibition alters the CXCR3 axis and enhances NK and CD8+ T cell infiltration to improve anti-PD1 efficacy in murine models of pancreatic ductal adenocarcinoma. *J Immunother. Can* 2021, **9** (11): e002837
2. Johnson DC, Taabazuin CY, Okondo MAC, et al. DPP8/DPP9 inhibitor-induced pyroptosis for treatment of acute myeloid leukemia. *Nat Med.* 2018; **24**:1151–1156.

<http://dx.doi.org/10.1136/jitc-2022-SITC2022.0025>

26

TUMOR INFILTRATING CD8/CD103/TIM-3 EXPRESSING LYMPHOCYTES IN EPITHELIAL OVARIAN CANCER CO-EXPRESS CXCL13 AND ASSOCIATE WITH IMPROVED SURVIVAL

Vrouyr Bilemjian*, Edwin Bremer. *University of Groningen, Berlin, Germany*

Background Reactivation of tumor infiltrating T lymphocytes (TILs) with immune checkpoint inhibitors or co-stimulators has proven to be an effective anti-cancer strategy for a broad range of malignancies. However, epithelial ovarian cancer (EOC) remains largely refractory to current T cell-targeting immunotherapeutics. Therefore, identification of novel immune checkpoint targets and biomarkers with prognostic value for EOC is warranted. TIL populations in many cancers often express checkpoint receptor TIM-3. However, TIM-3 expression in TILs and the biological consequences thereof are subject of debate, as associations with both poor and favorable prognosis have been reported across multiple malignancies. Here, we identified a small population of CD8/CD103/TIM3 triple-positive T cells in EOC tissue using immunofluorescence microscopy. Upon analysis of an EOC Tissue Micro Array, tumor infiltration of this immune cell subset associated with improved patient survival.

Methods Methods used in my research are the following:

- Analysis of Single Cell mRNA Sequencing Data
- Multicolor immunofluorescent staining
- Perform Flow Cytometry analysis after isolating Tumor Infiltrated Lymphocytes (TILs) from Fresh Tumor Tissues.

Results Combining multicolor immunofluorescent staining's with single cell RNA-sequencing analysis, we here identified a TIM-3/CXCL13-positive tissue-resident memory (CD8/CD103-positive) T cell (T_{rm}) population in EOC. Analysis of a cohort of ~175 patients with high-grade serous EOC revealed TIM-3-positive T_{rm} were significantly associated with improved patient survival. As CXCL13-positive CD8-positive T cells have been strongly linked to patient response to anti-PD1 immune checkpoint blockade, combinatorial TIM-3 and PD-1 blockade therapy may be of interest for the (re)activation of anti-cancer immunity in EOC.

Conclusions We identified a small set of CD8/CD103/TIM-3-expressing tumor infiltrated T cells in EOC patients associated with improved EOC patient survival. Therefore, CD8/CD103/TIM-3 triple-positive TILs may be a prognostic marker for EOC and represents a target population of interest for reactivation by immunotherapeutics. Further, differential gene expression (DEG) analysis revealed upregulated expression of co-stimulatory, cytotoxic, and exhaustive genes, and notably that of CXCL13 within the terminally exhausted CD8-positive T cell fraction. Due to the co-expression pattern of TIM-3 and CXCL13, TIM-3 might also serve as a surrogate marker for prognostically favorable CXCL13-positive CD8-positive TILs.

<http://dx.doi.org/10.1136/jitc-2022-SITC2022.0026>

27 **TUMOR AGNOSTIC CD8 IMMUNE-PHENOTYPE RELATED GENE SIGNATURE DEFINES CLINICAL OUTCOME ACROSS EARLY AND LATE PHASE CLINICAL TRIALS**

Andreas Roller*, Iakov Davydov, Martha Serrano-Serrano, Astrid Heller, Nicolas Staedler, Claudia Ferreira, Gabriele Dietmann, Irina Klamann, Konstanty Korski, Petra Schwalie, Michael Cannarile. *Roche, Basel, Switzerland*

Background A key question in cancer immunotherapy is the general immune status of the patient's tumor-microenvironment prior to therapy. The patient's underlying tumor immune-contexture may therefore a) guide the therapeutic intervention and b) help to identify potential resistance mechanisms to immune-therapies. The most commonly used classification of the patients' immune status is based on the CD8 tumor infiltrating lymphocytes status referring to either 'cold' or 'hot' tumors.

Methods In this study, we systematically analyzed the CD8 immune-phenotype in 628 patients from 11 Phase 1 clinical trials using immunohistochemistry (IHC) and matched gene expression profiling by RNA-seq. The CD8 immune-phenotype was classified by pathologist assessment into cold (CD8 deserts) and hot (CD8 excluded and inflamed) tumors using CD8+/Ki67+ IHC staining in epithelial and stromal areas of the tumor.

Results In total, we observed 193 inflamed, 144 excluded, and 291 desert CD8 immune-phenotype from 49 different indications. The main source of tumor biopsy tissues was liver metastasis (N=174), lymph node (N=51) and lung tumor tissue (N=69). Further, we developed a RNA-seq based classification as a surrogate to the IHC based CD8 immune-phenotype classification. Using regularized logistic regression (ElasticNet), we identified a 92 gene signature that accurately predicts the CD8 immune-phenotype in primary and metastatic samples (AUC inflamed = 0.846; AUC Excluded = 0.712; AUC Desert = 0.855). Using our new gene signature, we demonstrate prolonged overall survival (ORR) of patients with CD8 inflamed tumors across The Cancer Genome Atlas (TCGA; Hazard-Ratio 0.89; 95%CI [0.80–0.98]) as well as a better ORR to Checkpoint inhibitors (CPI) in the randomized Phase III OAK study in Non-Small-Cell lung cancer patients (Hazard-Ratio 0,75; 95%CI [0.58–0.97]).

Conclusions In summary, we identified a novel prognostic and predictive gene signature accurately predicting the IHC based CD8 immune-phenotype in primary and metastatic tumor samples. Survival analysis indicated that the predicted CD8 inflamed phenotype results in prolonged survival in independent patient cohorts. Our analysis provides important insights and a new precision immune phenotyping tool to characterize the impact of the tissue origin with regards to the tumor microenvironment. The new signature enables multiplex analyses and may be used for retrospective, reverse translation approaches as well as for prospective patient enrichment to identify resistance mechanisms to cancer immunotherapy.

Ethics Approval All patients provided written informed consent. The trials were approved by each center's ethics committee or institutional review board and were performed in compliance with the Declaration of Helsinki and International Conference on Harmonisation Guidelines for Good Clinical Practice.

<http://dx.doi.org/10.1136/jitc-2022-SITC2022.0027>

IDENTIFICATION AND FUNCTIONAL VALIDATION OF NEOANTIGENS-SPECIFIC T-CELL RECEPTORS IN LYNCH SYNDROME

Fahriye Duzagac*, Krishna Sinha, Ana Bolivar, Nan Deng, Laura Reyes Uribe, Alexandre Reuben, Eduardo Vilar-Sanchez. MD Anderson Cancer Center, Houston, TX, USA

Background Lynch syndrome (LS) is the most common cause of hereditary colorectal cancer (CRC), with >1 million estimated carriers in the US.¹ Normal cells in LS patients become MMR-deficient (MMRd) after acquiring a somatic 'second hit' in the same MMR gene, thus generating thousands of small insertion/deletion (indels) mutations. Indels occurring in coding microsatellite regions give rise to immunogenic frameshift peptides (FSPs) that become mutated neoantigens (neoAg).² LS elicits a distinct immune response directed against FSP neoantigens stimulating the adaptive immune cells through recognition by T cell receptors (TCR) of cytotoxic CD8⁺ T cells.³⁻⁴ Despite the recent advances in silico prediction algorithms for identifying candidate neoAg peptides, large-scale validation of these peptides is still challenging due to low frequency of Neoag-specific T cells and limited availability of patient samples.⁵ Our objective was to characterize neoAg-specific T cells response in LS carriers and to validate the functionality of recurrent and shared mutated neoantigens-specific T cells and their TCRs.

Methods We have identified and validated recurrent and shared MHC-I restricted mutated neoAgs in a cohort of LS patients diagnosed with pre-cancer and colorectal cancers using an enzyme-linked immunospot (ELISPOT) assay. NeoAgs validated for eliciting in vitro immunogenicity were used to prime autologous naïve T cells from healthy donors. NeoAg-specific T cells were detected and isolated using Flex-T™ HLA-A*02:01 UVX biotinylated monomers derived peptide-MHC (pMHC) multimers staining. Cytotoxicity and infiltration of isolated NeoAg-specific T cells were measured using innovative NeoAg-specific T cell-mediated co-culture assays in a physiologically relevant microfluidic setup. NeoAgs that showed high cytotoxic activity were used for downstream single-cell TCR sequencing (10x Genomics).

Results We used healthy donor T cell repertoires to eliminate the hurdle in identifying immunogenic and reactive NeoAg. We have validated a set of novel recurrent NeoAg such as RNF43 that showed in vitro immunogenicity with a threshold >30 SFU in ELISPOT assay. Then, we identified and isolated Neoag-specific T cells that recognize endogenously processed and presented epitopes using peptide-MHC (pMHC) multimer staining. Our results showed 5 to 8% CD8⁺ NeoAg specific T cells enrichment. Robustly enriched and isolated T cells showed cytotoxicity against LS patient-derived organoids that expressed determined NeoAgs. We profiled TCR sequences of validated NeoAg with single-cell TCR sequencing that will serve to perform immune monitoring and early cancer detection.

Conclusions This data suggest that identified neoepitopes and corresponding TCRs provide robust candidate biomarkers to track immunogenicity after vaccination and TCR-based immune monitoring for LS carriers

REFERENCES

1. Lynch HT, Snyder CL, Shaw TG, Heinen CD, and Hitchins MP. Milestones of Lynch syndrome: 1895–2015. *Nat Rev Cancer*. 2015;**15**(3):181–94.
2. Bonadona V, Bonaiti B, Olschwang S, Grandjouan S, Huiart L, Longy M, et al. Cancer risks associated with germline mutations in MLH1, MSH2, and MSH6 genes in Lynch syndrome. *JAMA*. 2011;**305**(22):2304–10.

3. Yarchoan M, Johnson BA, 3rd, Lutz ER, Laheru DA, and Jaffee EM. Targeting neoantigens to augment antitumour immunity. *Nat Rev Cancer*. 2017;**17**(9):569.
4. Gebert J, Gelincik O, Oezcan-Wahlbrink M, Marshall JD, Hernandez-Sanchez A, Urban K, Long M, Cortes E, Tosti E, Katzenmaier EM, Song Y, Elsaadi A, Deng N, Vilar E, Fuchs V, Nelius N, Yuan YP, Ahadova A, Sei S, Shoemaker RH, Umar A, Wei L, Liu S, Bork P, Edelmann W, von Knebel Doeberitz M, Lipkin SM, Kloor M. Recurrent Frameshift Neoantigen Vaccine Elicits Protective Immunity With Reduced Tumor Burden and Improved Overall Survival in a Lynch Syndrome Mouse Model. *Gastroenterology*. 2021 Oct;**161**(4):1288–1302.e13.
5. Karpanen T, Olweus J. The Potential of Donor T-Cell Repertoires in Neoantigen-Targeted Cancer Immunotherapy. *Front Immunol*. 2017 Dec 11;**8**:1718.

Ethics Approval NeoAgs were identified using paired whole-exome sequencing (WES) and mRNAseq in 10 LS CRC (stage I-III) and 33 precancers (7 advanced adenomas and 26 adenomas). A total of 43 patient samples were recruited during their routine screening colonoscopy to an IRB-approved biospecimen protocol (MDACC IRB# PA12–0327).

<http://dx.doi.org/10.1136/jitc-2022-SITC2022.0028>

29 **LUNG-MAP COMPOSITE SIGNATURE FOR IMMUNE CHECKPOINT INHIBITOR (ICI) EFFICACY IN ADVANCED SQUAMOUS CELL LUNG CANCER (SCC)**

¹David Gandara*, ²Xing Hua, ³Khaled Tolba, ³David Fabrizio, ³Lee Albacker, ³Ryan Brennick, ³Meagan Montesion, ³Geoff Oxnard, ⁴Stacey Adam, ⁵Fred Hirsch, ⁶Karen Kelly, ⁷Roy Herbst, ⁸Michael LeBlanc, ⁸Mary Redman, ⁸Michael Wu, ⁹David Kozono. ¹University of California Davis Cancer Center, Sacramento, CA, USA; ²Fred Hutchinson Org, Seattle, WA, USA; ³Foundation Medicine, Cambridge, MA, USA; ⁴Foundation for the NIH, North Bethesda, MD, USA; ⁵Mount Sinai Health System, New York, NY, USA; ⁶International Association for the Study, Denver, CO, USA; ⁷Yale School of Medicine, New Haven, CT, USA; ⁸Fred Hutchinson Cancer Center, Seattle, WA, USA; ⁹Brigham and Women's Hospital Harvard Med, Boston, MA, USA

Background Predictive biomarkers for ICI regimens in NSCLC, namely PD-L1 and tumor mutational burden (TMB), remain suboptimal, leaving oncologists with limited decision-making tools. We sought to develop a more comprehensive solution, integrating genomic alterations detected by comprehensive genomic profiling (CGP), to enrich for association with progression-free survival (PFS) and overall survival (OS).

Methods Lung Master Protocol (Lung-MAP) is an NCI-sponsored public-private partnership evaluating new therapies for previously-treated advanced stage NSCLC. In this analysis, 320 SCC patients from sub-studies S1400A (n=68; durvalumab) and S1400I (n=252; nivolumab ± ipilimumab) had tissue CGP data by Foundation Medicine. 204 patients from S1400A (n=43; SP263) and S1400I (n=161; 28–8 pharmDX) had PD-L1 IHC. We evaluated TMB (0–9, 10–20, >20 mut/Mb), PD-L1 IHC, HLA loss of heterozygosity (LOH) of ≥ 1 gene (evaluable for n=206), mutations in KEAP1/NFE2L2, DNA damage response genes, ARID1A, and loss of CDKN2A as potential ICI biomarkers. Wilcoxon and Fisher's exact tests assessed association between continuous TMB/PDL1 IHC (<1%, 1–49%, ≥50%) and each binary biomarker, and between pairs of binary markers. Cox proportional hazards model evaluated the association between each biomarker and OS/PFS, adjusting for age, sex, smoking status, and stage. Based on significance (at the nominal 0.1 level without correction for multiplicity) from univariate analysis, multiple combination signatures were analyzed using a predetermined scoring system. Biomarkers in the most significant combination signature was further examined by adjusting for TMB and PD-L1, to demonstrate if they provided additional value.

Results Despite associations between TMB and ARID1A mutations (P = 0.009), PD-L1 and KEAP1/NFE2L2 mutations (P = 0.007) and ARID1A mutations and KEAP1/NFE2L2 mutations (OR = 2.89; 95% CI, 1.43 – 5.91, P = 0.0016), the magnitude of correlation was modest, thus representing complementary predictors. Higher TMB (>20 vs. 10–20 vs. 0–9) was the most significant positive predictor of OS (HR=0.79; 95% CI, 0.65–0.95, p=0.01). A composite combinatorial signature (ICIsig) inclusive of TMB, PD-L1, HLA LOH, ARID1A, and KEAP1/NFE2L2 mutations was associated with better OS (HR=0.76; 95% CI, 0.63–0.92, p=0.005) and PFS (HR=0.84; 95% CI, 0.70–0.99, p=0.048). Landmark 3-year OS rates were 29% vs. 6% in ICIsig high vs. low. ICIsig high represented 39% of the evaluable population.

Conclusions We show that a composite ICIsig extending beyond TMB and PD-L1 captures NSCLC patients benefiting from ICI therapy more effectively than single biomarkers. ICIsig could inform treatment selection in today's rapidly expanding therapeutic landscape. Validation from a large randomized Phase III trial is ongoing.

Acknowledgements We would like to acknowledge funding from: NIH/NCI grants U10CA180888, U10CA180819, U10CA180820, U10CA180821, U10CA180868; and by Astra-Zeneca and Bristol-Myers Squibb Company, through the Foundation for the National Institutes of Health, in partnership with Friends of Cancer Research.

<http://dx.doi.org/10.1136/jitc-2022-SITC2022.0029>

30

SINGLE CELL MULTIOMIC PROFILING OF THE ANTIGEN-SPECIFIC IMMUNE RESPONSE USING ANTIGEN SPECIFIC DCODE DEXTRAMER® (RIO) REAGENTS AND BD® ABSEQ REAGENTS ON THE BD RHAPSODY™ SINGLE-CELL ANALYSIS SYSTEM

Kivin Jacobsen*, Dilek Inekci, Liselotte Brix. *Immudex aps, Virum, Denmark*

Background Understanding the specific T- and B- cellular immunity during an induced cellular immune response is important for development of anti-tumor immunity in personalized immunotherapy. Advanced single-cell genomics technologies have enabled researchers to do single cells immune profiling, by assessing cell surface proteins, the transcriptome and TCR and/or BCR gene clonotypes. However, understanding antigen-specific recognition at the immune synapse is key to understand the specific immune response in cancer. The dCODE MHC Dextramer® technology combine single-cell genomic profiling with antigen-recognition allowing deep analysis of antigen-specific T-, and B-cells at the single cell level pairing TCR recognition adding to unveil the antigen specific immune response, in cancer and infectious diseases.

Methods We have combined two powerful technologies, Immudex® dCODE Dextramer® (RiO) Reagents and the BD Rhapsody™ Single-Cell Analysis System, to detect and characterize low-frequency antigen-specific T- and B cells, including the full sequences of the V(D)J gene segments of the antigen-specific T- and B cell receptors, as well as profile transcriptome and cell phenotyping by surface protein expression. We used a panel of dCODE Dextramer® (RiO) reagents directed against 10 virus-specific antigens + 6 negative control reagents, spanning MHCI and MHCII, to profile two HPBMC samples, together with 15 BD® AbSeq immune related antibodies, and over 350 immune related genes.

Results We identified 10 different virus-specific T-cell responses over the two samples and revealed major clonotypes of all responses in the two samples, alongside with phenotypic activation profile using the BD® AbSeq reagents and immune target gene expression of the antigen-specific T cells identified by the dCODE® (RiO) Dextramer reagents. Data on antigen-specific B-cell responses is pending.

Conclusions Here we show an assay with the ability to analyze antigen-specific immune cells, by applying combined antigen-specific detection, with surface phenotyping, and gene expression, resulting in a deep phenotypic characterization of the immune cells in the donor. The ability to do high-resolution B and T cell profiling has broader implications and utility in immuno-oncology, infectious diseases, and autoimmunity.

For Research Use Only. Not for use in therapeutic or diagnostic procedures

-Immudex®, Dextramer®, dCODE®, Klickmer™ and U Load™ are trademarks owned by Immudex ApS

<http://dx.doi.org/10.1136/jitc-2022-SITC2022.0030>

31 CELLULAR COMPOSITION OF MALIGNANT PLEURAL EFFUSIONS SHOW A SIMILAR LANDSCAPE TO THAT OF THEIR PRIMARY TUMOR SITES: A PILOT STUDY

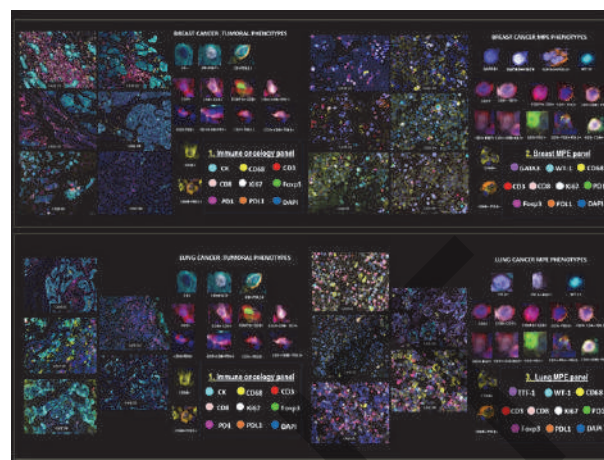
Caddie Laberiano- Fernández, Qiong Gan, Auriole Tamegnon, Sinchita Roy Chowdhuri, Edwin Parra*. MD Anderson Cancer Center, Houston, TX, USA

Background Malignant pleural effusion (MPE) is a frequent complication of advanced malignancy with significant associated morbidity and mortality. Metastases from lung cancer are the most common cause of MPE, followed by breast cancer. This pilot study aims to characterize the immune landscape of stage IV primary tumors (PT) and their MPE counterparts, to compare the cellular and immune landscape of these tumors.

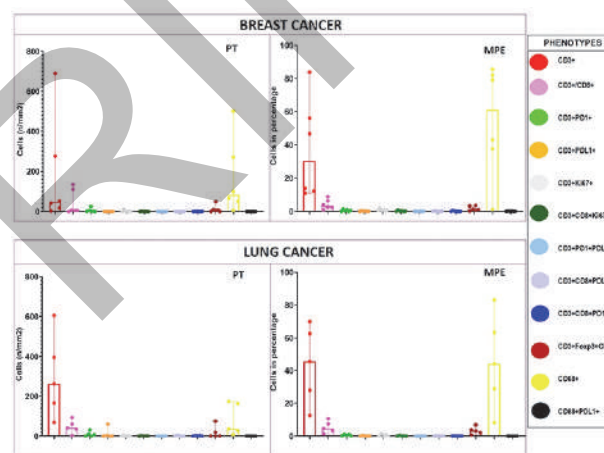
Methods We studied the immune contecture of six breast carcinoma and five lung adenocarcinoma PT samples and their respective MPEs using three immune-oncology multiplex immunofluorescence panels (figure 1). The slides were scanned using Vectra Polaris and analyzed by InForm image analysis software. We characterized the cellular composition to compare PT and MPE samples (figure 1). In addition, we use the densities of cell phenotypes from PTs and the percentages from MPE to correlate with clinicopathologic characteristics (table 1).

Results Overall, the immune cell phenotypes were similar between PT and their respective MPE samples, as shown in figure 2. The predominant cell densities for CD3+ T-cells (45.5%) and CD3+CD8+ cytotoxic T-cells (4.7%) were observed in lung MPEs, while in the PTs the same phenotypes showed a median, 262 cells/mm² and 42 cells/mm², respectively. CD68+ macrophages were found mainly in breast MPE (61%) and in their PTs (median 82.5 cells/mm²). However, two breast carcinoma cases showed suppressive components related to regulatory T-cells CD3+Foxp3+CD8^{neg} expression in their MPEs but not in their PTs; whereas in one case T cell antigen-experienced CD3+PD1+ was present in the breast PT but not in the corresponding MPE. One lung MPE showed T cell antigen-experienced CD3+PD1+ while this expression was absent in the PT. In contrast, one lung MPE case had no expression of CD3+PD-L1+, CD3+CD8+PD-L1+ or T regulatory CD3+Foxp3+CD8^{neg} cells, but these cells were present in their respective lung PTs. No correlation was observed with clinicopathologic characteristics.

Conclusions While our results showed some differences in cellular compositions between MPE and their corresponding PT, the overall cellular compositions showed a similar landscape. Therefore, our results suggest that MPE may be used as a surrogate for PT to explore new target options or predict treatment responses. A more extensive study with a larger dataset would be necessary to confirm our results.



Abstract 31 Figure 1— MPE and PT cases and Immuno-oncology panels



Abstract 31 Figure 2 Results : MPEs vs PTs in breast and lung cancer

Abstract 31 Table 1 Clinical information of lung and breast cancer patients

CLINICAL INFORMATION		
	Breast cancer patients, n=6 (%)	Lung cancer patients n=5 (%)
Sex		
Female	6 (100)	4 (80)
Male	0 (0)	1 (20)
Age (median)	68	75
Localization		
Right	4 (67)	2 (40)
Left	2 (33)	3 (60)
Smoker		
Yes	0 (0)	2 (40)
No	0 (0)	2 (40)
N/A	6 (100)	1 (20)
Histopathology		
Invasive ductal carcinoma	5 (83)	N/A
Invasive lobular carcinoma	1 (17)	N/A
Adenocarcinoma	N/A	5 (100)
Stage at diagnosis		
I	0 (0)	1 (20)
II	1 (17)	0 (0)
III	1 (17)	0 (0)
IV	4 (67)	2 (40)
N/A	0 (0)	2 (40)
Treatment		
Chemotherapy	3 (33)	1 (20)
Chemotherapy + surgery	4 (67)	0 (0)
Chemotherapy + radiotherapy	0 (0)	2 (40)
N/A	0 (0)	2 (40)
Survival after MPE collection (median) in months	4.5	16.5
IHC/molecular test in primary tumor		
ER: (+), PR: (-), HER2: (-)	1 (17)	N/A
ER: (+), PR: (+), HER2: (-)	3 (50)	N/A
ER: (+), PR: (+), HER2: (+)	1 (17)	N/A
ER: (-), PR: (-), HER2: (-)	1 (17)	N/A
EGFR positive	N/A	1 (20)
EGFR negative	N/A	1 (20)
N/A	0	3 (60)
Period between biopsy and MPE (median) in months	37	57
Overall survival in months (median)	53.5	55.5

<http://dx.doi.org/10.1136/jitc-2022-SITC2022.0031>

Abstracts

32

REAL-WORLD PREVALENCE OF DEFICIENT MISMATCH REPAIR ACROSS 5 SOLID TUMOR TYPES IN CHINA

¹Xiaohua Shi*, ²Xiang-Hong Yang, ³Jing-Ping Yun, ⁴Xiang-Shan Fan, ⁵Ying-Yong Hou, ²Zhe Wang, ³Peng Li, ⁴Jie-Yu Chen, ⁵Juan Yu, ¹Longyun Chen, ⁶Yan Wang, ⁷Rubentiran Ramar, ⁷Michael Wong, ¹Zhiyong Liang. ¹*Peking Union Medical College Hospital, Chinese Academy of Medical Sciences, and Peking Union Medical College, Beijing, China, Beijing, China*; ²*Shengjing Hospital of China Medical University, Shenyang, China, Shenyang, China*; ³*Sun Yat-sen University Cancer Center, Guangzhou, China, Guangzhou, China*; ⁴*The Affiliated Drum Tower Hospital of Nanjing University Medical University, Nanjing, China, Nanjing, China*; ⁵*Zhongshan Hospital, Fudan University, Shanghai, China, Shanghai, China*; ⁶*MSD China, Shanghai, China, Shanghai, China*; ⁷*MSD International GmbH, Singapore, Singapore*

Background The anti-PD-1 monoclonal antibody pembrolizumab has a tumor-agnostic approval by the US FDA for previously treated advanced tumors characterized as microsatellite instability-high (MSI-H)/deficient mismatch repair (dMMR). Although several studies have reported on the global prevalence of MSI-H/dMMR, data on the prevalence of dMMR across advanced solid tumor types in Chinese patients are limited. Here, we report real-world data on dMMR across 5 tumor types in Chinese patients.

Methods Adult patients with treatment-naïve or previously treated advanced (stage III/IV) biliary tract, cervical, endometrial, gastric, or ovarian cancer from 5 study centers in China were included in this analysis. MMR testing was performed on archival formalin-fixed, paraffin-embedded tissue samples using the Ventana MMR RxDx panel. The primary objective of this study was to determine the prevalence of dMMR. Secondary objectives were to assess clinicopathologic characteristics and treatment patterns.

Results Of 748 patients who had tissue samples evaluable for MMR status, 314 (42.0%) had gastrointestinal (GI) tumors and 434 (58.0%) had gynecologic (GYN) tumors. The prevalence of dMMR was 9.4% (70/748) overall, 4.1% (13/314) in GI tumors (4.3% [8/186] biliary tract, 3.9% [5/128] gastric) and 13.1% (57/434) in GYN tumors (2.7% [6/221] cervical, 29.9% [49/164] endometrial, 4.1% [2/49] ovarian). In the dMMR population (n = 70), most patients were aged 18–65 years (88.6%), had stage III disease at diagnosis (78.6%), and had undergone surgery (91.4%). At the protein level, the frequency of a co-occurring loss of MLH1 and PMS2 in patients with dMMR tumors was 68.6% (table 1), which is consistent with global reports in colorectal cancer. Evaluation of the treatment history of dMMR versus the proficient mismatch repair populations showed that a higher proportion of patients with dMMR tumors received radiation (40.0% vs 23.0%), chemotherapy (70.0% vs 48.5%), and/or treatment with immune checkpoint inhibitors (11.4% vs 4.6%) at some point since their initial diagnosis.

Conclusions Prevalence of dMMR and co-occurring loss of MLH1 and PMS2 at the protein level across the 5 different tumor types in Chinese patients are consistent with reports in the literature.

Acknowledgements Medical writing and/or editorial assistance was provided by Obinna T. Ezeokoli, PhD, and Holly C. Cappelli, PhD, CMPP of ApotheCom (Yardley, PA, USA). This assistance was funded by Merck Sharp & Dohme LLC, a subsidiary of Merck & Co., Inc., Rahway, NJ, USA.

Consent Written informed consent was provided by all patients before use/analysis of tumor specimen.

Abstract 32 Table 1 Frequency of MLH1/PMS2/MSH2/MSH6 deficiency in patients with dMMR tumors

n (%)	MLH1 and PMS2	PMS2	MSH2 and MSH6	MSH6
Overall dMMR population (N = 70)	48 (69)	5 (7)	13 (19)	4 (6)
Biliary tract (n = 8)	5 (63)	0 (0)	3 (38)	0 (0)
Gastric (n = 5)	4 (80)	1 (20)	0 (0)	0 (0)
Cervical (n = 6)	4 (67)	1 (17)	1 (17)	0 (0)
Endometrial (n = 49)	35 (71)	2 (4)	9 (18)	3 (6)
Ovarian (n = 2)	0 (0)	1 (50)	0 (0)	1 (50)

<http://dx.doi.org/10.1136/jitc-2022-SITC2022.0032>

33 **ROLE OF PLASMA T-CELL-DERIVED CIRCULATING DNA LEVEL IN ANTI-PD(L)1 IMMUNOTHERAPY IN ADVANCED STAGE NON-SMALL CELL LUNG CANCER**

Nuthchaya Mejun, Nophol Leelayuwatanakul, Pongsakorn Ouwongprayoon, Chanida Vinayanuwattikun, Nattiya Hirankarn. *Chulalongkorn University, Bangkok, Thailand*

Background We previously published prognostic impact of T-cell-derived circulating DNA (T-cirDNA) and its correlation with intra-tumoral CD8 tumor-infiltrating lymphocyte (TIL) in advanced stage non-small cell lung cancer (NSCLC). Currently, PD-L1 staining is solely the standard biomarker of anti-PD-(L) 1 immunotherapy treatment response. However, not perfect correlation in individual patient.

Methods We prospectively explored plasma T-cirDNA and cirDNA (total circulating DNA), using real-time PCR with Taqman assay-specific rearranged TCR-beta CDR3 region in 47 advanced NSCLC patients treated with anti-PD-(L)1 immunotherapy. We defined patients into undetectable, low ($\leq 1\%$ ratio) and high ($> 1\%$ ratio) T-cirDNA/cirDNA based on previous study. Demographic characteristics such as sex, age, ECOG performance status, smoking, histology, PD-L1 staining, treatment regimen were integrated with T-cirDNA/cirDNA into the cox-regression analysis model.

Results Out of 47 patients, 60% of participants had detectable plasma T-cirDNA/cirDNA with a median of 0.03 [range 0–4.7] ngml^{-1} (table 1). Undetectable group was significantly correlated with the longest overall survival (OS) with a median of 25.5 [range 8–73.7] months (p-value 0.05) (figure 1). Multivariate analysis of progression-free survival (PFS) revealed 0–1 ECOG performance status and undetectable T-cirDNA correlated with favorable outcome, hazard ratio (HR) of 0.05 [95% CI 0.007–0.4, p-value 0.005] and 0.1 [95% CI 0.01–0.7, p-value 0.02] respectively. High amount of circulating DNA which represented high tumor burden and mono-anti-PD-(L)1 immunotherapy were correlated with unfavorable disease control with the HR of 6.6 [95% CI 1.1–37.9, p-value 0.03] and 6.3 [95% CI 1.3–29.1, p-value 0.01] respectively. For detectable T-cirDNA group, high level correlated with better disease control than low level (HR 0.1 [95% CI 0.02–0.8, p-value 0.03]) (table 2). We did observe paradoxical effect in predictive implication in undetectable and high level of T-cirDNA/cirDNA%ratio.

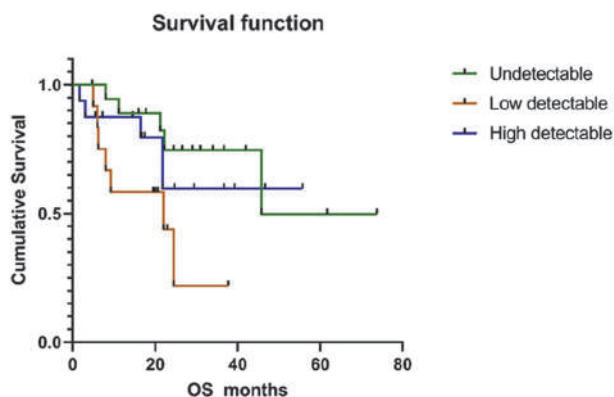
Conclusions Incorporate with demographic characteristic, T-cell-derived circulating DNA could be adopted for predictive implication of anti-PD(L)1 immunotherapy usage.

Acknowledgements This research was supported by the National Research Council of Thailand (Grant number 347/2564) to CV and NH. Biospecimen collection was supported by Biobank, Faculty of Medicine, Chulalongkorn University, Bangkok, Thailand.

Ethics Approval All methods were carried out in accordance with the declarations of Helsinki. The Institutional Review Board (IRB), Faculty of Medicine, Chulalongkorn University approved the study protocol (IRB 385/63).

Abstract 33 Table 1 Demographic characteristics of detectable plasma circulating DNA from 47 advanced NSCLC patients categorized by %ratio of T-cirDNA/cirDNA into undetectable, low ($\leq 1\%$ ratio) and high ($> 1\%$ ratio)

Demographic characteristic	Undetectable	Low detectable	High detectable	p value
	T-cirDNA/cirDNA (%) (n=18)	T-cirDNA/cirDNA (%) (n=13)	T-cirDNA/cirDNA (%) (n=16)	
Sex				0.909
Male	13(72.22)	10(76.92)	13(81.25)	
Female	5(27.78)	3(23.08)	3(18.75)	
Age at diagnosis				0.489
<60 years	3(16.67)	1(7.69)	4(25.00)	
≥60 years	15(83.33)	12(93.31)	12(75.00)	
ECOG performance status				0.720
0-1	15(83.33)	12(93.31)	15(93.75)	
>2	3(16.67)	1(7.69)	1(6.25)	
Smoking status				0.337
Never	6(33.33)	4(30.77)	2(12.50)	
Former/Current smoker	12(66.67)	9(69.23)	14(87.50)	
Histology				0.398
Adenocarcinoma	16(88.89)	12(93.31)	12(75.00)	
Non-adenocarcinoma	2(11.11)	1(7.69)	4(25.00)	
Driver alteration (EGFR/ALK)				1.000
Present	1(5.56)	0(0.00)	0(0.00)	
Absent	17(94.44)	13(100.00)	16(100.00)	
PD-L1 staining				0.464
Positive	3(16.67)	6(46.15)	5(31.25)	
Negative	7(38.89)	2(15.39)	4(25.00)	
Missing data	8(44.44)	5(38.46)	7(43.75)	
No. of lines of treatment				0.179
<2 lines	2(11.11)	5(38.46)	5(31.25)	
≥2 lines	16(88.89)	8(61.54)	11(68.75)	
Total amount of cirDNA				0.030*
High(>4.5 ngml^{-1})	1(6.11)	13(100.00)	13(81.25)	
Low($\leq 4.5 \text{ngml}^{-1}$)	7(38.89)	0(0.00)	3(18.75)	
Total amount of cirDNA				0.000*
RPP30, median (range)	6.71	27.18	14.54	
(0-18.08)		(8.25-52.37)	(0.00-120.57)	
TCRβ, median (range)	0.00	0.08	0.47	
(0.00-0.00)		(0.00-0.32)	(0.01-41.37)	
Therapy				0.423
Single I/O	14(77.78)	7(53.85)	11(68.75)	
Combined I/O	4(22.22)	6(46.15)	5(31.25)	
Response to I/O				0.944
Complete/ Partial response	5(27.78)	2(15.38)	4(25.00)	
Stable disease	5(27.78)	4(30.77)	4(25.00)	
Progression disease	8(44.44)	7(53.85)	8(50.00)	
PFS months, median (range)	3.75(0.50-28.25)	3.00(0.75-8.25)	3.63(0.75-19.25)	0.727
OS months, median (range)	25.50(8.00-73.75)	19.50(4.75-37.75)	19.63(1.75-55.75)	0.050*



Abstract 33 Figure 1 A cumulative survival curve comparison of % ratio of T-cirDNA/cirDNA; undetectable, low and high by using overall survival (Kaplan–Meier method and Log rank test, p-value 0.071)

Abstracts

Abstract 33 Table 2 Univariate and multivariate analysis of prognostic factors by progression-free survival including demographic characteristics, treatment and ratio of T-cirDNA/cirDNA using cox proportion hazards regression analysis

Variables	Univariate, HR [95% CI]	p value	Multivariate, HR [95% CI]	p value
Sex (male vs. female)	0.730 [0.363-1.471]	0.379	1.266 [1.390-11.537]	0.835
Age (< 60 vs. ≥ 60)	1.954 [0.877-4.355]	0.101	2.246 [0.557-9.054]	0.255
ECOG (0-1 vs. > 2)	0.375 [0.142-0.989]	0.047*	0.052 [0.007-0.403]	0.005*
Smoking status (never smoker vs. former/current smoker)	1.457 [0.735-2.889]	0.281	0.447 [0.052-3.813]	0.461
Histology (adenocarcinoma vs non-adenocarcinoma)	0.941 [0.364-2.431]	0.900	0.109 [0.011-1.103]	0.061
PD-L1 (negative vs. positive)	0.821 [0.357-1.888]	0.642	0.410 [0.067-2.508]	0.335
Lines of treatment (< 2 vs. ≥ 2)	0.539 [0.247-1.174]	0.120	0.185 [0.028-1.241]	0.082
T-cirDNA/cirDNA %ratio				
Low (≤ 1%)	-	0.358	-	0.048*
Undetectable	0.675 [0.313-1.457]	0.317	0.102 [0.015-0.718]	0.022*
High (> 1%)	0.522 [0.241-1.261]	0.159	0.133 [0.021-0.849]	0.033*
circDNA (> 4.5 ng/ml ¹ vs. ≤ 4.5 ng/ml ¹)	1.094 [0.513-2.332]	0.816	6.623 [1.155-37.977]	0.034*
Treatment (single I/O vs. combined I/O)	2.083 [1.033-4.202]	0.040*	6.359 [1.387-29.149]	0.017*

<http://dx.doi.org/10.1136/jitc-2022-SITC2022.0033>

34

NEUTROPHIL-TO-EOSINOPHIL RATIO AS A BIOMARKER FOR CLINICAL OUTCOMES IN ADVANCED STAGE MELANOMA PATIENTS TREATED WITH ANTI-PD-1 THERAPY

Vincent Pozorski*, Yeonhee Park, Dahlia Tesfamichael, Yusuf Mohamoud, Vincent Ma. University of Wisconsin, Madison, WI, USA

Background An association between lower neutrophil-to-eosinophil ratios (NER) and improved clinical outcomes in patients with metastatic renal cell carcinoma treated with combination ipilimumab/nivolumab (I/N) was recently reported.¹ While neutrophil-to-lymphocyte ratios (NLR) and eosinophil counts have been associated with improved survival in melanoma patients treated with immunotherapy^{2, 3}, no studies have investigated NER as a predictor of outcomes in advanced melanoma patients receiving anti-PD-1 therapy.

Methods We conducted a single-center, retrospective review of unresectable stage III and IV melanoma patients treated with anti-PD-1 monotherapy (nivolumab or pembrolizumab) or I/N between 2011 and 2022. Overall survival (OS) and progression-free survival (PFS) were measured from the first dose of treatment to date of death and clinical or radiographic progression, respectively. Treatment-related adverse events (trAEs) of grade ≥3 were also assessed. Baseline NLR and NER were measured relative to anti-PD-1 treatment start date. Change in NLR and NER from baseline were measured at 3-months follow up. Patients were divided into groups by median NLR and NER at baseline (<mNER vs ≥mNER) and analyzed for OS and PFS using univariate and multivariate analyses with Cox proportional hazard (CPH) models. Logistic regression models were used to evaluate risk differences for trAEs. The multivariate analyses accounted for the following covariates: Age, gender, anti-PD-1 therapy type, primary melanoma type, pre-treatment LDH, BRAF status, presence of brain or liver metastasis, and prior adjuvant or non-anti-PD-1 treatment for advanced-stage melanoma.

Results 190 patients were identified. Lower NER at baseline, relative to the mNER of 30.7, was associated with improved OS [HR: 0.330, 95% CI: 0.175–0.623, p=0.0006] but not PFS (table 1). Both PFS and OS differed between groups relative to the mNER and an explicit NER cut-off of 35 on univariate analysis (figure 1). Neither PFS nor OS differed between groups based on baseline NLR. A trend towards decreased grade ≥3 trAEs was associated with lower NER at baseline [OR: 0.411, 95% CI: 0.157–1.022, p=0.061]. Baseline NLR was not associated with trAEs. Change in the NLR and NER at three months relative to baseline was not associated with clinical outcomes.

Conclusions Lower pre-treatment NER is associated with improved OS in patients with advanced-stage melanoma treated with anti-PD-1 based regimens. Survival outcomes may differ with an explicit NER cut-off of 35. Higher baseline NER may be associated with high-grade trAEs. Further validation is warranted to evaluate NER as a predictive marker for clinical outcomes in melanoma patients treated with immune checkpoint inhibitors.

REFERENCES

1. Tucker MD, Brown LC, Chen YW. *et al.* Association of baseline neutrophil-to-eosinophil ratio with response to nivolumab plus ipilimumab in patients with metastatic renal cell carcinoma. *Biomark Res.* 2021 Nov 3;**9**(1):80.
2. Ferrucci PF, Gandini S, Cocorocchio E, *et al.* Baseline relative eosinophil count as a predictive biomarker for ipilimumab treatment in advanced melanoma. *Oncotarget.* 2017 Aug 1;**8**(45):79809–79815.

3. Cohen JT, Miner TJ, Vezeridis MP. Is the neutrophil-to-lymphocyte ratio a useful prognostic indicator in melanoma patients? *Melanoma Manag.* 2020 Aug 25;**7**(3):MMT47.

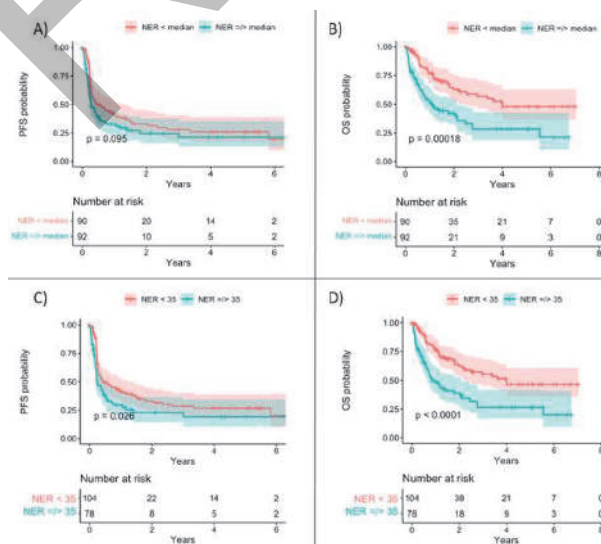
Ethics Approval The study was approved by the University of Wisconsin institutional ethical guidelines and patients' consents were waived following Institutional Review Board protocol review (UW21110).

Abstract 34 Table 1 Multivariate Cox proportional hazard regression models for progression-free survival (PFS) and overall survival (OS), and odds ratios for multivariate logistic regression models for grade ≥3 treatment toxicity

Variables	Progression Free Survival		Overall Survival		Grade ≥3 Treatment Toxicity	
	HR (95% CI)	p-value	HR (95% CI)	p-value	OR (95% CI)	p-value
Anti-PD-1 Treatment Type (I/N vs Anti-PD-1 Monotherapy)	0.573 (0.367-0.884)	0.014*	0.705 (0.416-1.194)	0.193	5.880 (2.616-14.548)	3.87e10**
Prior Non-Anti-PD-1 Treatment for Advanced Melanoma (yes vs no)	1.678 (1.026-2.720)	0.036*	2.008 (1.181-3.409)	0.010*	1.977 (0.704-5.531)	0.191
Prior Adjuvant Treatment (yes vs no)	1.561 (0.946-2.578)	0.062	1.227 (0.661-2.277)	0.516	0.763 (0.370-1.919)	0.549
Age (45 vs ≥65)	0.947 (0.629-1.422)	0.796	1.120 (0.681-1.870)	0.639	1.246 (0.637-2.879)	0.584
Gender (male vs female)	0.983 (0.653-1.481)	0.939	0.951 (0.589-1.544)	0.839	0.832 (0.371-1.865)	0.653
BRAF status (mutant vs WT)	1.101 (0.736-1.647)	0.639	0.959 (0.616-1.606)	0.985	0.796 (0.344-1.781)	0.585
Primary melanoma type (Cutaneous vs Mucosal or Unknown)	0.830 (0.517-1.333)	0.441	0.519 (0.294-0.916)	0.024*	1.165 (0.479-2.961)	0.741
Pre-treatment LDH level† (≥ULN vs normal)	1.560 (1.034-2.363)	0.034*	2.300 (1.428-3.708)	0.0006*	0.800 (0.348-1.800)	0.593
Brain metastases (yes vs no)	0.941 (0.679-1.529)	0.805	1.031 (0.587-1.812)	0.914	1.053 (0.411-2.603)	0.913
Liver metastases (yes vs no)	1.305 (0.843-2.021)	0.232	1.818 (1.105-2.986)	0.019*	0.671 (0.264-1.616)	0.386
Pre-treatment NLR (median NLR vs ≥median NLR)	0.620 (0.599-1.429)	0.712	0.683 (0.407-1.149)	0.148	1.642 (0.725-3.774)	0.237
NLRs at 3 months (median NLR vs ≥median NLR)	0.707 (0.457-1.094)	0.12	0.589 (0.313-1.034)	0.064	0.635 (0.253-1.672)	0.327
Pre-treatment NER (median NER vs ≥median NER)	0.727 (0.447-1.185)	0.201	0.330 (0.175-0.623)	0.0006*	0.411 (0.157-1.022)	0.061
NERs at 3 months (median NER vs ≥median NER)	0.767 (0.507-1.283)	0.327	0.624 (0.321-1.242)	0.789	0.529 (0.197-2.204)	0.873

*Normal means of significance of p<0.05.

Abbreviations: CI, confidence interval; HR, hazard ratio; I/N, ipilimumab/nivolumab; LDH, lactate dehydrogenase; NER, neutrophil-to-eosinophil ratio; NLR, neutrophil-to-lymphocyte ratio; OR, odds ratio; OS, overall survival; PFS, progression-free survival; ULN, upper limit of normal; WT, wildtype.



Abstract 34 Figure 1 Kaplan-Meier curves comparing progression-free survival (PFS) and overall survival (OS) between patients based on baseline neutrophil-to-eosinophil ratios (NER). A) PFS difference between patients with lower baseline median NER

<http://dx.doi.org/10.1136/jitc-2022-SITC2022.0034>

Abstracts

35

EARLY PHARMACODYNAMIC CHANGES MEASURED BY RNA SEQUENCING IN PERIPHERAL BLOOD FROM PATIENTS IN A PHASE 1 STUDY WITH MITAZALIMAB, A POTENT CD40 AGONISTIC IGG1 MONOCLONAL ANTIBODY

¹Malin Lindstedt*, ²Peter Ellmark, ¹Aastha Sobti, ²Karin Enell Smith, ²Yago Pico de Coaña, ²Sumeet Ambarkhane. ¹Lund University, Lund, Sweden; ²Alligator Bioscience, Lund, Sweden

Background Mitazalimab is a human FcγR crosslinking-dependent human IgG1 CD40 agonistic antibody developed for cancer immunotherapy.^{1–3} Mitazalimab has demonstrated a manageable safety profile when administered once every 2 weeks both with or without corticosteroid pre-treatment.³ Treatment with mitazalimab induces transient increases in levels of selected chemokines and activation of peripheral B cells.³ An ongoing phase 2 study (OPTIMIZE-1) is currently evaluating the efficacy of mitazalimab in patients with metastatic pancreatic cancer (NCT04888312).

Methods Cell-free RNA from whole blood was collected from subjects both pre- and post-treatment in a dose escalation study of mitazalimab in patients with solid tumors (NCT02829099). The whole transcriptome sequencing was conducted according to Illumina TruSeq Stranded protocol. Samples obtained pretreatment and one day after treatment from cohorts receiving 75, 200, 600 and 900 μg/kg mitazalimab without corticosteroid pretreatment (pre/post treatment; 75 μg: n=3/3, 200 μg: n=5/5, 600 μg: n=10/11 and 900 μg: n=13/14) and 600 μg/kg mitazalimab with corticosteroid pre-treatment were analyzed (pre/post treatment; n=10/5). The normalized data was analyzed utilizing the edgeR limma workflow on R software. Differentially expressed genes were analyzed according to dose level and corticosteroid (yes vs no) administration. Cell phenotyping was conducted according to CIBERSORTX and Xcell cell signatures. Gene expression results were further correlated with peripheral blood concentrations of 15 cytokines 24 hours after treatment.

Results Significant mitazalimab treatment-induced transcriptional activity was identified using pre-selected gene signatures related to event associated to CD40 biology at the 600 and 900 μg/kg dose levels without corticoid pre-treatment. In contrast, the number of significantly expressed genes in the lower dose groups were limited. Gene signatures related to activation of B cell- and myeloid/dendritic activation were upregulated post treatment, confirming the CD40 agonistic activity of mitazalimab. Additionally, corticosteroid pre-treatment significantly reduced the magnitude of the mitazalimab treatment induced changes in gene expression in circulating immune cells in patients. This was confirmed at the protein level for circulating cytokines.

Conclusions The analysis of RNAseq data obtained from whole blood clearly demonstrated that mitazalimab induce strong CD40-mediated responses, such as activation of myeloid cells and B cells in patients. Furthermore, corticosteroid pretreatment reduced the immune stimulatory activity of mitazalimab. The presented gene expression data confirms the biological activity of mitazalimab, further strengthening the proof of mechanism.

REFERENCES

1. Mangsbo SM, Broos S, Fletcher E, *et al.* The human agonistic CD40 antibody ADC-1013 eradicates bladder tumors and generates T-cell-dependent tumor immunity. *Clin Cancer Res* 2015;**21**:1115–1126.
2. Irenaeus SMM, Nielsen D, Ellmark P, *et al.* First-in-human study with intratumoral administration of a CD40 agonistic antibody, ADC-1013, in advanced solid malignancies. *Int J Cancer* 2019.

3. Calvo E, Moreno V, Perets R, *et al.* A phase I study to assess safety, pharmacokinetics (PK), and pharmacodynamics (PD) of JNJ-64457107, a CD40 agonistic monoclonal antibody, in patients (pts) with advanced solid tumors. *Journal of Clinical Oncology* 2019;**37**:2527–2527.

Ethics Approval The study protocol and amendments were reviewed and approved by an Independent Ethics Committee. The study was conducted in accordance with the ethical principles that have their origin in the Declaration of Helsinki and that are consistent with Good Clinical Practices and applicable regulatory requirements. Subjects or their legally acceptable representatives provided their written consent to participate in the study after having been informed about the nature and purpose of the study, participation/termination conditions, and risks and benefits of treatment. ClinicalTrials ID: NCT02829099

<http://dx.doi.org/10.1136/jitc-2022-SITC2022.0035>

36

ANALYSIS OF T-CELL RECEPTOR SEQUENCES IDENTIFIES SIGNATURES ASSOCIATED WITH NEOANTIGEN EXPOSURE IN PERIPHERAL BLOOD OF LYNCH SYNDROME PATIENTS

Ana Bolivar*, Eduardo Vilar-Sanchez, Krishna Sinha, Laura Reyes Uribe, Nan Deng, Fahriye Duzagac, Alexandre Reuben. MD Anderson Cancer Center, Houston, TX, USA

Background Lynch Syndrome (LS) is the most common inherited colorectal cancer (CRC) syndrome. It constitutes the perfect model to understand DNA mismatch repair deficient (dMMR) carcinogenesis, which underlies 15% of early-stage CRC.¹ LS patients develop dMMR tumors with high loads of shared neoantigens, which are recognized by the immune system.² Elucidating the role and molecular landscape of public T-cell receptors (TCRs), provides potential as a diagnostic strategy for exposure to viruses and other immune-related phenotypes^{3–5}. This study aims to characterize the TCR beta chain (TCRB) landscape of LS patients and to identify the presence of cancer-specific TCRB clones in the peripheral blood of LS carriers.

Methods A total of 122 PBMCs and 29 colorectal tissue samples have been collected from patients enrolled during their routine screening colonoscopy to an ongoing IRB-approved biospecimen protocol (MDACC IRB# PA12–0327). All TCRB repertoires were sequenced using the Immunoseq TCRB assay (Adaptive Biotechnologies). Bioinformatics analyses were performed using the immunarch R package^{6,7} and the immuneML software⁸ by comparing the TCRB repertoires among LS cancer survivors, LS healthy carriers (with no cancer history), and controls with no cancer and no family history of LS. To validate some of the identified TCRBs, a viral peptide and a cancer neoantigen predicted to be recognized by these public TCRBs were used to isolate peripheral T-cells from healthy human donors using pMHC-tetramer assays and single-cell TCR sequencing.

Results Our data show that LS cancer survivors have less diverse TCRB repertoires compared to LS healthy carriers due to the presence of hyper-expanded TCRBs in the group of survivors. Our results also show that a set of highly expanded cancer-specific public TCRBs is detectable in the peripheral blood of LS cancer survivors after annotation to the McPAS-TCR database⁹. We observe an overlap of TCRBs between the tissue (precancers and cancers) and PBMCs in patients for which both types of samples were collected at the same time-point. Finally, with our pMHC-tetramer assays, we are capable of isolating TCRBs that were initially identified with bulk-TCR sequencing.

Conclusions Overall, our data suggest that the T-cell response of LS patients against developing cancers is not entirely restricted to their tumor microenvironment, with expanded cancer-specific public TCRBs being detectable in the peripheral blood of LS cancer survivors. This is the first step toward identifying a TCR signature that serves as a biomarker of early cancer detection in LS patients.

REFERENCES

1. Lynch HT, Snyder CL, Shaw TG, Heinen CD, Hitchins MP. Milestones of Lynch syndrome: 1895–2015. *Nat Rev Cancer [Internet]*. 2015 Feb 12;**15**:181. Available from: <https://doi.org/10.1038/nrc3878>
2. Ballhausen A, Przybilla MJ, Jendrusch M, Haupt S, Pfaffendorf E, Seidler F, et al. The shared frameshift mutation landscape of microsatellite-unstable cancers suggests immunoediting during tumor evolution. *Nat Commun [Internet]*. 2020;**11**(1):4740. Available from: <https://doi.org/10.1038/s41467-020-18514-5>
3. Woodsworth DJ, Castellarin M, Holt RA. Sequence analysis of T-cell repertoires in health and disease. *Genome Med*. 2013;**5**(10).

4. Emerson RO, DeWitt WS, Vignali M, Gravley J, Hu JK, Osborne EJ, et al. Immuno-sequencing identifies signatures of cytomegalovirus exposure history and HLA-mediated effects on the T cell repertoire. *Nat Genet [Internet]*. 2017;**49**(5):659–65. Available from: <http://dx.doi.org/10.1038/ng.3822>
5. Cui JH, Lin KR, Yuan SH, Jin Y Bin, Chen XP, Su XK, et al. TCR repertoire as a novel indicator for immune monitoring and prognosis assessment of patients with cervical cancer. *Front Immunol*. 2018;**9**(NOV):1–11.
6. Nazarov V, immunarch.bot, Rumynskiy E. immunarch: An R Package for Painless Analysis of Large-Scale Immune Repertoire Data. *Zenodo [Internet]*. 2019 Jan 20 [cited 2020 Mar 30]; Available from: https://doi.org/10.5281/zenodo.3613560#.XoJ_oycykjl.mendeley
7. Nazarov VI, Pogorelyy M V., Komech EA, Zvyagin I V., Bolotin DA, Shugay M, et al. tcR: An R package for T cell receptor repertoire advanced data analysis. *BMC Bioinformatics [Internet]*. 2015;**16**(1):1–5. Available from: ???
8. Pavlovic M, Scheffer L, Motwani K, Kanduri C, Kompova R, Vazov N, et al. The immuneML ecosystem for machine learning analysis of adaptive immune receptor repertoires. *Nat Mach Intell*. 2021;
9. Tickotsky N, Sagiv T, Prilusky J, Shifrut E, Friedman N. McPAS-TCR: a manually curated catalogue of pathology-associated T cell receptor sequences. *Bioinformatics [Internet]*. 2017 May 8;**33**(18):2924–9. Available from: <https://doi.org/10.1093/bioinformatics/btx286>

Ethics Approval All patients included in this study provided written informed consent at The University of Texas MD Anderson Cancer Center (MDACC). All samples were obtained from study participants through an Institutional Review Board (IRB) approved protocol at MDACC (Protocol PA12–0327).

<http://dx.doi.org/10.1136/jitc-2022-SITC2022.0036>

37 **SIGNAL AMPLIFICATION STRATEGIES FOR IN SITU DETECTION OF LOW-EXPRESSED MARKERS IN MULTIPLEX IMMUNOFLUORESCENCE**

Pino Bordignon*, Paula Juričić, Alexandre Kehren, Victor de Gautard, Saska Brajkovic, Diego Dupouy. *Lunaphore Technologies, Tolochenaz, Switzerland*

Background The characterization of the tumor microenvironment is essential for a deep understanding of tumor biology and the identification of personalized targeted therapies. By means of new spatial proteomic approaches, a detailed mapping of the different immune cells has been made possible¹. Among them, multiplex immunofluorescence has emerged as a key technology, maximizing the amount of extractable information from a cancer tissue section². While lineage markers can usually be easily detected via canonical indirect immunofluorescence, functional markers often show much lower levels of expression and would benefit from a signal amplification strategy³. Combining the possibility to amplify low-expressed markers with a system capable of performing multiplex staining could provide significantly improved tumor immunoprofiling with detailed information on immune cell activation and exhaustion.

Here, we aim to implement amplification technologies on the COMET™ system, capable of performing automated multiplex immunofluorescence, to improve the detection of low-expressed markers.

Methods The COMET™ platform is a microfluidic-based system that enables fully automated sequential immunofluorescent (seqIF™) assays based on iterative series of fast tissue staining, imaging, and antibody elution cycles on the same tissue section. Two amplification technologies were automated: Fluorescent Signal Amplification via Cyclic Staining of Target Molecules (FRACTAL)⁴, and enzymatic Tyramide-based Signal Amplification (TSA)⁵, also testing different commercially available TSA kits. The effects of amplification on low-expressed markers were evaluated with respect to standard assays on multiple human FFPE tissues. Normalized Mean Intensity and Signal to Background ratio have been used as parameters for the evaluation.

Results The two amplification technologies, FRACTAL and TSA, were successfully automated and optimized on COMET™. The signal intensity of multiple challenging markers, including FoxP3, PD1, PD-L1, and IDO-1 – though being detectable by standard seqIF™ – was significantly amplified by the two techniques. Overall, FRACTAL appeared to be the most suitable technology as shown by the better performance in terms of signal amplification (by NMI or SBR quantification) over the TSA amplification tested on COMET™. Importantly, optimization of the elution step resulted in efficient removal of all antibody layers employed in the FRACTAL method from the stained tissues, therefore allowing its use in sequential staining cycles on the same section.

Conclusions The implementation of amplification technologies in the COMET™ workflow for hyper-plex panel development will allow the detection of difficult-to-target biomarkers, such as functional markers with low-expression levels. This strategy can provide a significant improvement in immune cell profiling of tumor samples.

REFERENCES

1. Lundberg E, Borner GH. Spatial proteomics: a powerful discovery tool for cell biology. *Nat Rev Mol Cell Biol.* 2019; **20**(5):285–302.
2. Francisco-Cruz A, Parra ER, Tetzlaff MT, Wistuba II. Multiplex Immunofluorescence Assays. *Methods Mol Biol.* 2020; **2055**:467–495.

3. Stack EC, Wang C, Roman KA, Hoyt CC. Multiplexed immunohistochemistry, imaging, and quantitation: a review, with an assessment of Tyramide signal amplification, multispectral imaging and multiplex analysis. *Methods.* 2014; **70** (1):46–58.
4. Cho Y, Seo J, Sim Y, Chung J, Park CE, Park CG, Kim D, Chang JB. FRACTAL: Signal amplification of immunofluorescence via cyclic staining of target molecules. *Nanoscale.* 2020; **12**(46):23506–23513.
5. Wang G, Achim CL, Hamilton RL, Wiley CA, Soontornniyomkij V. Tyramide signal amplification method in multiple-label immunofluorescence confocal microscopy. *Methods.* 1999; **18**(4):459–64.

<http://dx.doi.org/10.1136/jitc-2022-SITC2022.0037>

38 FULLY AUTOMATED SPATIAL MULTI-OMICS ANALYSIS TO MAP THE TUMOR MICROENVIRONMENT WITH SINGLE-CELL RESOLUTION

Pino Bordignon*, Alice Comberlato, Saska Brajkovic, Diego Dupouy. Lunaphore Technologies, Tolochenaz, Switzerland

Background The tumor and its microenvironment are distinguished by highly heterogeneous cell types in dynamic evolution¹. In the past decades, the adoption of single-cell RNA sequencing technologies improved our understanding of intra- and inter-patient variations, refining cancer diagnosis and targeted therapy, while still lacking spatial context information². The spatial analysis of single-cell gene expression provides previously missing information on cell interactions, crucial for innovative treatment opportunities. However, the large-scale implementation of these assays is hampered by the lack of automated and user-friendly workflow solutions³.

Here, we aim at automating an *in situ* transcriptomic assay and integrating it with a proteomic workflow on the COMET™ platform for easy and comprehensive mapping of the tumor microenvironment.

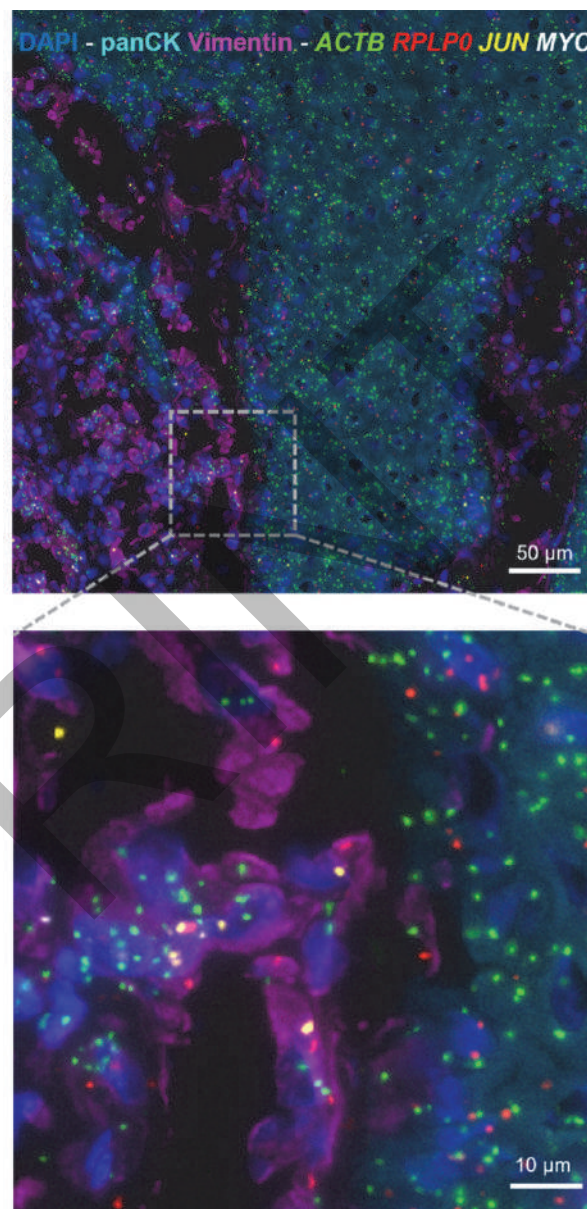
Methods COMET™ is a microfluidic-based instrument capable of automated sequential immunofluorescence (seqIF™) assays. The *in situ* RNA detection was based on DNA padlock probe hybridization and ligation, followed by rolling circle amplification and gene detection with fluorophore-tagged probes. A panel of probes targeting various immune-oncology genes was designed and the gene expression was evaluated in combination with a high-plex seqIF™ analysis.

Results The protocol for *in situ* RNA detection was automated and optimized on COMET™, resulting in specific detection of multiple transcripts (cell-type specific markers, transcription factors, secreted cytokines) on various tumor samples, with a signal quality that allows downstream computational analysis of gene expression signals. The transcriptomic assay was then integrated with a seqIF™ workflow for the co-detection of several target proteins for tumor microenvironment characterization on the same tissue section (figure 1). Double RNA and protein analysis allowed to examine the expression of biomarkers for which no good antibody clones are available, validation of new antibodies by detecting RNA and protein colocalization, in addition to the identification of the cellular source of secreted molecules. Compared to the manual protocol, the combined automated workflow resulted in a drastic time reduction being based on iterative fast cycles of detection and imaging of two transcripts or proteins each, lasting approximately 30 and 40 minutes, respectively.

Conclusions We showed here that *in situ* spatial transcriptomics assays can be fully automated and combined with spatial proteomics on the COMET™ platform for a multi-omics approach with advantages in terms of time and complexity reduction with respect to manual protocols. This combinatorial automated detection of RNAs and proteins of pivotal biomarkers provides a powerful new tool for a simpler and better mapping of the tissue spatial context.

REFERENCES

1. Janiszewska M. The microcosmos of intratumor heterogeneity: the space-time of cancer evolution. *Oncogene*. 2020 Mar;**39**(10):2031–2039.
2. Rao A, Barkley D, França GS, Yanai I. Exploring tissue architecture using spatial transcriptomics. *Nature*. 2021 Aug;**596**(7871):211–220.
3. Asp M, Bergenstråhle J, Lundberg J. Spatially Resolved Transcriptomes-Next Generation Tools for Tissue Exploration. *Bioessays*. 2020 Oct;**42**(10):e1900221.



Abstract 38 Figure 1 Automated and simultaneous *in situ* detection of RNA and protein (ACTB, RPLP0, JUN, MYC) and protein (panCK and Vimentin) targets are co-detected on a human melanoma frozen section with a fully automated workflow on the COMET™ platform. Background autofluorescence was subtracted and brightness adjusted for visualization purposes

<http://dx.doi.org/10.1136/jitc-2022-SITC2022.0038>

39 INTERROGATING ELITE RESPONDER HUMORAL RESPONSES TO IDENTIFY NOVEL TARGETS AND THERAPEUTIC ANTIBODIES FOR THE TREATMENT OF CANCER

Ramya Chandrasekaran*, Darbie Whitman, Ray Fox, Tom Graddis, Kamal Puri. *OncResponse, Seattle, WA, USA*

Background The development of checkpoint inhibitors (CPIs) has transformed the treatment landscape for certain cancers. However, the response rates are modest for most cancers and some cancers are not amenable to CPIs and represent a significant unmet medical need.^{1,2} CPIs promote anti-tumor adaptive responses by lifting the brakes off immune activation, which is known to break tolerance to self-antigens and induce autoantibody formation.^{3–5} A subset of these autoantibodies may mediate anti-tumor responses and enhance CPI efficacy. B cells and tertiary lymphoid structures have been shown to contribute to CPI efficacy.^{6–8} We have evaluated serum autoantibody profiles of cancer patients who responded well to CPI therapy and interrogated their memory B cell repertoires to identify novel targets, epitopes, biomarkers, and immunomodulatory anti-cancer antibodies.

Methods Solid tumor patients who remain on CPI therapy for at least 6 months with stable disease, or at least 3 months with a partial or complete response were designated as Elite Responders for this study. Serum samples from healthy donors and matched serum and peripheral blood mononuclear cells from Elite Responders were collected. For novel targets, epitopes, and biomarker discovery, serum samples were tested on proteome microarrays containing >21,000 unique full length human proteins. Serum samples were also probed for binding, by flow cytometry, to a panel of myeloid cells. Elite Responders with seroreactivity specific to suppressive myeloid cells were selected for B cell activations and antibody discovery using the OncoResponse platform. Myeloid-targeting antibodies were subsequently cloned, expressed and evaluated for anti-tumor activity in functional assays.

Results Autoantibody profiling using the microarrays corroborated some targets known to have immunomodulatory activities in the TME across several cancer types, e.g., LILRB2, VSIG1, CD47, Siglec, and identified additional immune-oncology targets of interest. Some autoantigens exhibited broad serological responses across several solid tumor types, while others were specific to a cancer type. The functional importance of the Elite Responder's humoral response was demonstrated by the discovery of a myeloid-targeting antibody, OR2805, which specifically binds immunosuppressive M2 macrophages and converts them into an immunostimulatory phenotype. In M2 macrophage/T cell coculture assays, OR2805 rescues T cell activation and proliferation and amplifies anti-PD-1 activity. A phase 1–2 dose escalation-expansion study of OR2805 alone or in combination in subjects with advanced solid tumors is ongoing (NCT05094804).

Conclusions Interrogation of humoral responses in cancer Elite Responders is an attractive strategy for discovery of novel targets and therapeutic antibodies for the treatment of cancer.

REFERENCES

1. Das S, Johnson DB. Immune-related adverse events and anti-tumor efficacy of immune checkpoint inhibitors. *J Immunother Cancer*. 2019 Nov 15;**7**(1):306.
2. Johnson DB, Nebhan CA, Moslehi JJ, Balko JM. Immune-checkpoint inhibitors: long-term implications of toxicity. *Nat Rev Clin Oncol*. 2022 Apr;**19**(4):254–267.
3. Schoenfeld J, Jinushi M, Nakazaki Y, Wiener D, Park J, Soiffer R, Neuberger D, Mihm M, Hodi FS, Dranoff G. Active immunotherapy induces antibody responses that target tumor angiogenesis. *Cancer Res*. 2010 Dec 15;**70**(24):10150–60.

4. Kwek SS, Dao V, Roy R, Hou Y, Alajajian D, Simko JP, Small EJ, Fong L. Diversity of antigen-specific responses induced in vivo with CTLA-4 blockade in prostate cancer patients. *J Immunol*. 2012 Oct 1;**189**(7):3759–66.
5. Wu X, Giobbie-Hurder A, Connolly EM, Li J, Liao X, Severgnini M, Zhou J, Rodig S, Hodi FS. Anti-CTLA-4 based therapy elicits humoral immunity to galectin-3 in patients with metastatic melanoma. *Oncoimmunology*. 2018 Mar 13;**7**(7):e1440930.
6. Helmink BA, Reddy SM, Gao J, Zhang S *et al*. B cells and tertiary lymphoid structures promote immunotherapy response. *Nature*. 2020 Jan;**577**(7791):549–555.
7. Petitprez F, de Reyniès A, Keung EZ *et al*. B cells are associated with survival and immunotherapy response in sarcoma. *Nature*. 2020 Jan;**577**(7791):556–560.
8. Cabrita R, Lauss M, Sanna A *et al*. Tertiary lymphoid structures improve immunotherapy and survival in melanoma. *Nature*. 2020 Jan;**577**(7791):561–565.

<http://dx.doi.org/10.1136/jitc-2022-SITC2022.0039>

40 NGS-BASED IMMUNOLOGY PANEL: APPLICATIONS IN PRECLINICAL IMMUNO-ONCOLOGY RESEARCH

¹Jia Xue*, ¹Xiaobo Chen, ¹Xiaoyu An, ¹Jingjing Wang, ²Henry Li, ¹Sheng Guo. ¹*Crown Bioscience Inc., Suzhou, China*; ²*Hanx Biopharmaceuticals, Inc., Wuhan, China*

Background Cancer immunogenomics encompassing tumor cells and tumor microenvironment (TME) is critical for unravelling the complexity of tumor immunity, understanding the mechanism of action (MOA) for immunotherapies, and revealing potential predictive/pharmacodynamic biomarkers. We previously described a new and comprehensive 1080 mouse immuno-oncology (I/O) gene RNA-Seq panel (mouse I/O RNA-Seq panel) that has an improved dynamic range for rare IO transcripts and is more cost effective over conventional microarray assays (e.g., NanoString nCounter Mouse Pan-Cancer IO 360™ Panel) when analyzing bulk tumor samples. In this study, we set out to explore its applications in preclinical IO studies evaluating immune checkpoint inhibitor (ICI) response.

Methods A panel of 14 mouse syngeneic tumors was profiled using the mouse I/O RNA-Seq panel to benchmark the baseline expression of IO transcripts and compared to the tumor-infiltrate leukocyte (TIL) analysis of the same tumors by flow cytometry. The pharmacodynamic profiles of selected syngeneic models upon ICI and CD4+ cell depletion treatment was also examined to reveal potential MOAs.

Results The panel of syngeneic models had a differential profile of response to ICI, TIL infiltration and IO gene expression. The mouse I/O RNA-Seq panel gene expression highly correlated with that from whole transcriptome sequencing (RNA-Seq) across the panel of syngeneic models, but mouse I/O RNA-Seq panel showed generally > 12x higher sensitivity for comparable sequencing data sizes. Using a collection of comprehensive gene signatures for TIL lineage identification, the mouse I/O RNA-Seq panel revealed rich TIL components in syngeneic mouse tumors that were confirmed by flow cytometry demonstrating the value and depth of coverage in studying TME at the gene expression level without the need for a wide array of antibodies and complex gating operations in flow cytometry and also the potential scalability of mouse I/O RNA-Seq assay. The mouse I/O RNA-Seq panel was then used for pharmacodynamic profiling upon anti-PD-1 antibody and CD4+ cell depletion treatment, and revealed different IO related pathway activity changes, with higher accuracy than the NanoString 360™ Panel.

Conclusions With NGS-based technology becoming ubiquitous, our mouse I/O RNA-Seq panel can be a powerful, fast and cost-effective solution in the preclinical IO research, improving our understanding of the tumor and immune cell interactions in unprecedented detail and in response to immunotherapeutics.

<http://dx.doi.org/10.1136/jitc-2022-SITC2022.0040>

41 **EXTERNAL REPRODUCIBILITY OF PD-L1 IHC 22C3 PHARMDX FOR CERVICAL CANCER AT CPS \geq 1 AND CPS \geq 10**

¹Greg Cherryholmes*, ¹Alexander Posch, ¹Siena Tabuena-Frolli, ¹Jesse Vasquez, ¹Tiffany Evans, ¹Chris La Placa, ¹Kristopher Kersch, ¹Angeliki Apostolaki, ²Jonathan Juco, ¹Karina Kulangara. ¹Agilent Technologies, Inc., Carpinteria, CA, USA; ²Merck and Co., Inc., Kenilworth, NJ, USA

Background Despite advancements in cervical cancer care, women with persistent, recurrent, or metastatic cervical cancer face difficult prognoses with limited treatment options. Recent results from clinical trials KEYNOTE-158 (NCT02628067) and KEYNOTE-826 (NCT03635567) have demonstrated clinically meaningful results in patients with recurrent or metastatic cervical cancer whose tumors express PD-L1 with a Combined Positive Score (CPS) \geq 1. Here we give evidence of the reproducibility of PD-L1 expression determination in cervical cancer utilizing PD-L1 IHC 22C3 pharmDx at the CPS \geq 1 and CPS \geq 10 cutoffs.

Methods External reproducibility studies tested the inter-site, intra-site, inter-observer, and intra-observer assay reproducibility for cervical cancer at CPS \geq 1 and CPS \geq 10. To test inter- and intra-site reproducibility, five replicate sets of a blinded and randomized cervical cancer specimen set were tested at each of the three external sites. For inter- and intra-observer reproducibility, three external sites evaluated one pre-stained set of cervical cancer specimens. Percent agreement was calculated using Negative Percent Agreement (NPA), Positive Percent Agreement (PPA), and Overall Percent Agreement (OA). Pre-specified acceptance criteria (AC) for all components of the analyses were \geq 85.0% for the lower bound value of a 95% two-tailed percentile bootstrap confidence interval (CI) of each percent agreement point.

Results At the CPS \geq 1 cutoff: (i) inter- and intra-site NPA/PPA/OA met AC with point estimates (PE) \geq 97.5% and CI lower bounds \geq 94.7%, and (ii) inter- and intra-observer NPA/PPA/OA met AC with PE \geq 98.1% and CI lower bounds \geq 94.9%. At the CPS \geq 10 cutoff: (i) inter- and intra-site NPA/PPA/OA met AC, with PE \geq 92.8% and CI lower bounds \geq 86.7%, and (ii) inter- and intra-observer NPA/PPA/OA met AC, with PE \geq 98.4% and CI lower bounds \geq 95.9%.

Conclusions This study demonstrates high external lab reproducibility of PD-L1 IHC 22C3 pharmDx with respect to expression determination in cervical cancer at CPS \geq 1 and CPS \geq 10 cutoffs.

Ethics Approval The external reproducibility study was approved by WCG IRB, study numbers 1284639, 1284652, and 1284653.

<http://dx.doi.org/10.1136/jitc-2022-SITC2022.0041>

42

MODULATION OF FIBROSIS AND ANGIOGENESIS IN POST-ISCHAEMIC EXTRACELLULAR MATRIX

¹Paolo Contessotto*, ²Doriana Orbanic, ³Mark Da Costa, ⁴Chunsheng Jin, ³Peter Owens, ⁴Niclas Karlsson, ²José Carlos Rodríguez-Cabello, ³Peter Dockery, ³Michelle Kilcoyne, ³Abhay Pandit. ¹University of Padova, Padova, Italy; ²University of Valladolid, Valladolid, Spain; ³NUI, Galway, Galway, Ireland; ⁴University of Gothenburg, Gothenburg, Sweden

Background Modulation of post-ischaemic remodelling is a significant clinical need.¹ Ischaemia results in the loss of millions of living cells as a result of the hypoxic condition.¹ However, our tissue is programmed to compensate for this loss by activating a remodelling program which leads to the formation of a fibrotic scar.¹ Inspired by the natural extracellular matrix, we have developed an injectable elastin-based hydrogel which showed marked functional and biological improvements in the ischaemic hearts by using a large animal model.²

Methods Focal infarcts were induced in male sheep by multiple suture ligations of side branches of the left anterior descending coronary artery. Functional data of ejection fraction and fractional shortening were obtained using transthoracic echocardiography prior to the induction of infarcts, prior to intervention, and at three weeks after intervention. Samples were analysed by bulk RNA-seq, LC-ESI-MS/MS proteomics and N-glycomics. Histology included Masson's Trichrome, anti-CD31 and lectin histochemistry.

Results ELRs-treated sheep showed less fibrosis and more angiogenesis compared to the untreated ones, as validated by expression, proteomic, glycomic, and histological analyses [3]. Remarkably, the effects of the hydrogel injection were already significant 21 days post-treatment, thus in the acute phase of the disease. Since our ELRs-hydrogel also contained matrix metalloproteinase-responsive motifs (MMP-2 and -9), this study showed that the combination of ELRs sequences together with MMP-2 and -9 responsive motifs in the cross-linked hydrogel network enabled the recruitment of endothelial cells to promote an angiogenic effect (figure 1). The enhancement of a stable angiogenic response resulted in a protective effect towards the cardiomyocytes located in the border zone of the infarct that play a crucial role in the functional recovery of the infarcted heart. Here, an unbiased approach based on RNA-sequencing and proteomic analyses enabled us to identify GATA4 as the most relevant regulator of the improved response in the hydrogel-treated sample. We have validated our molecular analysis by evaluating the preserved mitochondrial integrity in the GATA4+ cardiomyocytes in the border zone of the hydrogel-treated animals.

Conclusions In this up-to-date scenario, our ELRs-hydrogel has a distinct advantage for its translational potential due to its marked benefit despite the absence of any stem cell or growth factor. Our study highlighted the elastin-derived molecular signalling advantages, thus acting as a timely reminder not to underestimate the potential of ECM proteins which were only partially studied when compared with paracrine effect-dependent cellular systems.

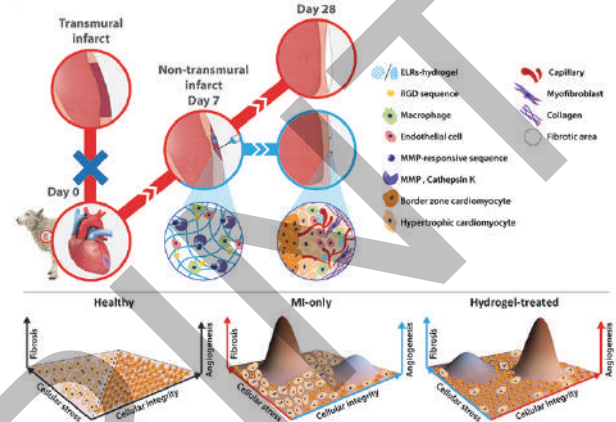
Acknowledgements Seventh Framework Programme Grant Agreement no.: 317304; Centre for Microscopy & Imaging funded by NUI Galway and PRTL, Cycles 4 and 5, National Development Plan 2007–2013; Science Foundation Ireland (SFI) and European Regional Development Fund under Grant Number 13/RC/2073.

REFERENCES

1. Contessotto P, Pandit A, Therapies to prevent post-infarction remodelling: From repair to regeneration. *Biomaterials* 2021;**275**:120906

2. Contessotto P *et al.* Elastin-like recombinamers-based hydrogel modulates post-ischaemic remodeling in a non-transmural myocardial infarction in sheep. *Sci. Transl. Med.* 2021;**13**:581

Ethics Approval All experiments in this study were performed following the regulations established by the European Union directive on the protection of animals for scientific research (2010/63/EU). All animal procedures and treatments were approved by the ethics committee at the Lithuanian University of Health Sciences.



Abstract 42 Figure 1 Modulation of fibrosis and angiogenesis Schematics of the ELRs-hydrogel intervention in focal infarcts. Lower plots show the entity of the effects of the treatment on fibrosis, angiogenesis and cellular stress/integrity compared with the MI-only pathological condition

<http://dx.doi.org/10.1136/jitc-2022-SITC2022.0042>

43 **TUMOR MUTATIONAL BURDEN CORRECTED FOR HUMAN LEUKOCYTE ANTIGEN SOMATIC DEFECTS PREDICTS RESPONSE TO CHECKPOINT BLOCKADE IN ADVANCED NON-SMALL CELL LUNG CANCER**

Yinjie Gao*, Ramit Bharanikumar, Aly Khan, Michelle Stein. *Tempus Labs, Los Angeles, CA, USA*

Background Tumor mutational burden (TMB) has been proposed as a biomarker for predicting response to immune checkpoint blockade (ICB) therapies in patients with non-small cell lung cancer (NSCLC). However, a subset of patients with high TMB tumors do not have a long-term response to ICB. Several studies have hypothesized that somatic events in the antigen processing machinery may contribute to ICB resistance. In this study, we determined that TMB adjusted for the number of neoantigens lost due to human leukocyte antigen (HLA) somatic defects better predicted response to ICB.

Methods Using the real-world Tempus Database, we selected a cohort of 378 de-identified NSCLC patient records with DNA data and recorded outcomes following ICB. Loss of heterozygosity in HLA-I genes (HLA-LOH) were identified in this cohort. TMB was adjusted to match the proportion of neoantigens estimated to escape HLA presentation due to loss of specific HLA alleles. Cox proportional hazards models were fitted to determine the relationship between HLA-adjusted TMB and time to progression (TTP), with hazard ratios (HRs) and confidence intervals (CIs) reported. In addition, immune inflammation signatures were calculated for 249 patients for whom paired RNA data were available.

Results HLA-LOH was observed in 27% of late-stage NSCLC tumors. Notably, the presence of HLA-LOH was significantly associated with shorter TTP in TMB-high (>10mut/Mb) tumors versus TMB-high, HLA-stable tumors (HR [CI]=2.99 [1.39–6.40]). This association was not observed in tumors with low levels of TMB (HR [CI]=0.75 [0.46–1.20]). In addition, HLA-adjusted TMB improved the estimated risk ratio in comparison to unadjusted TMB. Binarization of HLA-adjusted TMB further stratified TMB-low and TMB-high groups (TMB-low HR[CI]=1.67[1.09–2.56]; HLA-adjusted TMB-low HR[CI]=2.08[1.19–3.08]). Immune-inflamed environment was also associated with longer TTP in the HLA-adjusted TMB-low group (HR[CI]=0.58 [0.36–0.92]), indicating that HLA-adjusted TMB can be used in conjunction with immune phenotypes to predict outcomes to ICB.

Conclusions In this study, we observed that high TMB, HLA-stable patients had a longer TTP in NSCLC. Furthermore, we discovered that HLA-adjusted TMB outperformed unadjusted TMB in predicting ICB response, and that an inflamed immune phenotype was associated with longer TTP within HLA-adjusted TMB subgroups. Our findings suggest that HLA-adjusted TMB can be used alone as a DNA-based biomarker or in combination with immune signatures to better predict ICB response in NSCLC patients.

<http://dx.doi.org/10.1136/jitc-2022-SITC2022.0043>

44

IMMUNE SIGNATURES OF SEVERE IMMUNE-RELATED ADVERSE EVENTS DETECTED BY MASS CYTOMETRY IMMUNE PROFILING IN BLOOD IN PATIENTS WITH ADVANCED MELANOMA TREATED WITH IMMUNOTHERAPY

<http://dx.doi.org/10.1136/jitc-2022-SITC2022.0044>

¹Connor Healy*, ^{2,3}Magdalena Kovacovics*, ¹Natalia Sigal, ¹Li-Chun Cheng, ¹Shane Evans, ³John Marsiglio, ²Berit Gibson, ²Yoko DeRose, ³Annaleah Larson, ¹Carlos Medina, ¹Jolien Sweere, ¹Ramji Srinivasan, ⁴Matthew Spitzer, ²John Hyngstrom, ²Siwen Hu-Lieskovan. ¹Teiko Bio, Salt Lake City, UT, USA; ²Huntsman Cancer Institute, Salt Lake City, UT, USA; ³University of Utah, Salt Lake City, UT, USA; ⁴University of California San Francisco, Chan Zuckerberg Biohub, Parker Institute for Cancer Immunotherapy, San Francisco, CA, USA

Background Immune-related adverse events (irAE) are major barriers of clinical management and further development of cancer immunotherapy. In this study, we used mass cytometry to characterize the immune system before and during presentation of severe (grade 3+ that required clinical intervention) irAE to identify cell signatures correlated with irAE development.

Methods We performed analysis on banked peripheral blood mononuclear cells (PBMCs) from 29 patients with melanoma undergoing checkpoint inhibitor (CPI) therapy, of which 18 developed severe irAEs (3 gastrointestinal, 5 endocrine, 4 cutaneous, 9 hepatobiliary, 4 musculoskeletal, 1 pulmonary irAEs and 1 acquired lipodystrophy) while 11 did not. Samples were taken at initiation of CPI (pre-treatment), before onset of irAE (pre-irAE) and at presentation of irAE (irAE max). The median number of CPI cycles per patient was 5 for patients with severe irAEs and 11 for patients without severe irAEs. We used a 44-marker mass cytometry panel designed to capture cell subsets and activation states across the innate and adaptive immune system, with both supervised analysis of manually gated immune cell subpopulations and unsupervised analysis by Clustering LARge Applications (CLARA) clustering.

Results At the peak of irAE presentation, patients with severe irAE demonstrated significantly more CD38+ (marker of immune activation) CD4+ central memory T cells (TCM), CD39+ (marker of tumor antigen-specificity) and HLA-DR+ (marker of activation) CD8 TCM cells, and CCR7+ (marker of migration) CD4+ T cells compared to patients with no or non-severe irAEs. Conversely, patients with severe irAEs had significantly fewer CD16+ NK cells and CD161+ (marker of inhibition) CD4+ T cells. Interestingly, patients with severe irAEs already had fewer CD16+ NK cells and CD161+ CD4+ T cells pre-treatment, and more CCR7+ CD4+ T cells pre-irAE. Presentation of severe irAEs was also correlated with significantly lower levels of TIGIT+ regulatory T (Treg) cells pre-treatment, and more CD4+ T naïve cells at all three timepoints.

Conclusions Development of severe irAE in melanoma could be the result of reduced inhibitory immune capacity pre-treatment, marked by fewer regulatory TIGIT+ Treg cells and CD161+ CD4+ T cells, leading to dysregulated increase in migratory CCR7+ CD4+ T, activated CD38+ and tumor-reactive CD39+ TCM cells, and activated CD16+ NK cells. This study demonstrates that high-dimensional immune profiling can detect novel blood-based immune signatures associated with presentation of severe irAEs.

Ethics Approval The study was approved by Huntsman Cancer Institute's Ethics board, approval number IRB_00010924. Participants gave informed consent before taking part in the study.

45 PREVALENT BINDING MOTIF IN C57BL6 MICE CURED OF B78 MELANOMA VIA IMMUNOTHERAPY

¹Anna Hoefges*, ¹Nicholas Mathers, ¹Sean McIlwain, ²Richard Pinapati, ²Bradley Garcia, ²Jigar Patel, ¹Amy Erbe, ¹Irene Ong, ¹Paul Sondel. ¹University of Wisconsin Madison, Madison, WI, USA; ²Nimble Therapeutics, Inc, Madison, WI, USA

Background Using a high-density peptide array, we assessed potential protein-targets for antibodies detected in mice cured of melanoma through a combined immunotherapy regimen. Our goal was to determine the linear peptide sequences recognized by anti-tumor antibodies produced in mice cured of melanoma following immunotherapy.

Methods Mice bearing B78 melanoma tumors were treated with a combination immunotherapy (local radiation therapy + intratumoral anti-GD2 mAb linked to IL2) capable of inducing an 'in situ vaccine' effect (ISV), enabling mice to be cured of their tumors with long-term immune memory.¹ Naïve (prior to tumor injection) and immune (post-rechallenge/after cure) sera were collected from these mice. Using flow cytometry, immune sera showed strong antibody-binding against B16 (parental cell line of B78) and B78. These sera were then used on a Nimble Therapeutics' whole-proteome peptide-array to determine specific antibody-binding sites, and data were analyzed using a dynamic programming method that scans adjacent peptides to determine whether a peptide is bound by antibodies. Epitopes were selected if peptides were bound using immune sera but not bound, or significantly less, with the sera from naïve mice.

Results We identified many binding epitopes only present in immune mice. Among the epitopes found, we noticed a repeating motif consisting of 4 amino acids that made up over 60% of epitopes that are present in at least 50% of mice in our most restrictive binding category. However, the 4 amino acid long motif is not the only reason for binding as some peptides including this motif do not show binding. The amino acid (aa) sequence before and the 2aa sequences following the motif seem to be important for binding. Using an unrelated cohort of mice we were able to show binding of some additional immune mouse samples to selected peptides containing the identified motif

Conclusions We think that this motif might be an important piece in anti-tumor immunity to B78 melanoma. We are further investigating what causes binding vs no binding to the motif, and if the antibodies against it originated at one specific site vs multiple sites. The presence of antibodies against this motif might be a useful biomarker to predict response to our ISV regimen and might have the potential to be used for other immunotherapy treatments.

REFERENCE

1. Morris ZS, Guy EI, Gressett MM, Werner LR, Carmichael LL, Yang RK, Armstrong EA, Huang S, Navid F, Gillies SD, Korman A, Hank JA, Rakhmilevich AL, Harari PM, Sondel PM. In Situ Tumor Vaccination by Combining Local Radiation and Tumor-Specific Antibody or Immunocytokine Treatments. *Cancer Res* (2016) **76** (13): 3929–3941.

<http://dx.doi.org/10.1136/jitc-2022-SITC2022.0045>

46

GENETIC ANALYSIS OF TUMOR CELLS DERIVED FROM THE STRESS OF IMMUNE RESPONSE FOR UNDERSTANDING OF IMMUNOTHERAPY

¹Tomoyuki Ishiguro*, ¹Daisuke Takayanagi, ¹Toshiaki Tsurui, ¹Risako Suzuki, ¹Nana Iriguchi, ¹Yuya Hirasawa, ¹Ryotaro Ohkuma, ¹Hirotsugu Ariizumi, ¹Yutaro Kubota, ¹Kazuyuki Hamada, ¹Atsushi Horiike, ¹Satoshi Wada, ¹Kiyoshi Yoshimura, ²Kazuyoshi Takeda, ¹Takuya Tsunoda. ¹Showa University, Tokyo, Japan; ²Juntendo University, Tokyo, Japan

Background Cancer immunotherapy with immune checkpoint inhibitors (ICIs), unlike conventional anticancer agents and molecular targeted drugs, shows Kaplan-Meier curves characteristic of long-term survival in patients with advanced stage IV cancer, which is so-called the ‘kangaroo tail phenomenon’. However, the response rate of ICI is limited at only 20–30%, and improvement of therapeutic efficacy needs to be developed. We believed that a thorough elucidation of the mechanism of the kangaroo tail phenomenon would be one of the most important aspects to improve the therapeutic efficacy of ICIs.

Methods Using a mouse model of breast cancer 4T1 cells subcutaneously transplanted into wild type (natural immunological response) and immunocompromised mice with CTL transferred (tumor specific immunological response) (RAG-/- + ACT), we isolated tumor cells that had shrunk once and then re-expanded in two systems and performed whole exon RNA sequencing using tumor cells immediately after transplantation as controls. We analyzed the genetic changes induced by anti-tumor immune stress that tumors undergo from natural immune response.

Results In all samples, Tumor Mutational Burden and MSI scores increased compared to the control which is under no immunological stress, and many new genetic mutations were observed. In addition, the immunogenicity was maintained, with high affinity between neoantigens and MHC, which was inferred from the mutation information with amino acid changes. This suggests that the kangaroo tail phenomenon is caused by the repeated recognition and cytotoxic activity of neoantigens by CTLs with 10^{18} repertoire T cell receptors.

On the other hand, the genetic mutations common to each sample appeared the genes related to immune response, and mutations were also found in genes related to repair mechanisms such as DNA repair. For elective splicing, intron retention was found to have more genes related to DNA repair, while exon skipping had more genes related to DNA repair and the cell cycle. Copy number analysis also showed loss of heterozygosity in chromosome 17, which is located at MHC. These results were suggested that immune evasion by immunological pressure may be derived from the mutations such as abnormal immune response and loss of antigen-presenting ability.

Conclusions This study provides the first molecular biological insights into the mechanisms by which ICI produces long-term survivors. Furthermore, this study also provides clues to further improve the response rate of ICI through the understanding of the mechanism of action of ICIs in effective cases, at the same time understanding the immune evasive mechanism that occurs in ineffective cases.

<http://dx.doi.org/10.1136/jitc-2022-SITC2022.0046>

47

MULTISPECTRAL IMAGING TO DETECT IMMUNE PHENOTYPES ASSOCIATED WITH THE TUMOR MICROENVIRONMENT IN A MULTI-TISSUE STUDY: A FULL AUTOMATED 7-COLOR MIF IMMUNO-ONCOLOGY WORKFLOW

¹Navi Mehra*, ¹Bhavika Patel, ¹Stephanie Allen, ¹Noah Ramirez, ²Najiba Mammadova, ²Agnes Haggerty. ¹Lanterne Dx, Boulder, CO, USA; ²Akoya Biosciences, Menlo Park, CA, USA

Background Immunotherapy and precision medicine are rapidly developing approaches to cancer therapy. Biomarkers that detect the tumor and tumor microenvironment allow for the development of strategies that accelerate the advancement of treatments to enhance a patient's immune system. Akoya's MOTiF™ PD-1/PD-L1 Panel is a validated, multiplex immunoassay enabling detection of the 6 most clinically relevant immuno-oncology and spatial biomarkers: PD-1, PD-L1, FoxP3, CD8, CD68, and PanCK.

Methods The MOTiF™ PD-1/PD-L1 Panel was used to analyze the tumor microenvironment and specifically assess immune phenotypes of different types of cancers: non-small cell lung cancer (NSCLC), colon adenocarcinoma, head and neck squamous cell carcinoma (HNSCC), and breast cancer.

Results We demonstrate the utility of Akoya's MOTiF™ PD-1/PD-L1 panel kit in studying the cellular diversity of various cancers while retaining spatial context. Stained slides were analyzed using the InForm® and PhenoptrReports image analysis platforms to identify and better understand spatial relationships between a variety of simple and complex cell phenotypes. The MOTiF™ PD-1/PD-L1 panel kit provides reproducibility across different tissue types.

Conclusions These data provide insight into the innate and adaptive immune environment for targeted design of new immunotherapies and have implications for improving the treatment paradigm across many tumor types.

<http://dx.doi.org/10.1136/jitc-2022-SITC2022.0047>

48

WHOLE-SLIDE MULTISPECTRAL IMAGING REVEALS THE IMMUNE SUBTYPES OF MELANOMA ASSOCIATED WITH THE TUMOR MICROENVIRONMENT: AN AUTOMATED 7-COLOR MIF ASSAY

¹Navi Mehra*, ¹Bhavika Patel, ¹Stephanie Allen, ¹Noah Ramirez, ²Najiba Mammadova, ²Agnes Haggerty. ¹Lanterne Dx, Boulder, CO, USA; ²Akoya Biosciences, Menlo Park, CA, USA

Background Immunotherapy and precision medicine are rapidly developing approaches to cancer therapy. Biomarkers that detect the tumor and tumor microenvironment allow for the development of strategies that accelerate the advancement of treatments to enhance a patient's immune system. Akoya's MOTiF™ PD-1/PD-L1 Auto Melanoma Kit is a validated, multiplex immunoassay enabling detection of the 6 most clinically relevant immuno-oncology and spatial biomarkers: FoxP3, PD-L1, Sox10/S100, PD-1, CD8 and CD68.

Methods In this study, the MOTiF™ PD-1/PD-L1 panel was used to analyze the tumor microenvironment and specifically assess immune phenotypes within melanoma samples from 3 patients. This study demonstrates a fully optimized and end-to-end workflow solution for biomarker discovery in melanoma.

Results We demonstrate the utility of Akoya's MOTiF™ PD-1/PD-L1 Melanoma panel kit in studying the cellular diversity while retaining spatial context. Stained slides were analyzed using the InForm® and PhenoptR Reports image analysis platforms to identify phenotypes and better understand spatial relationships between cell phenotypes. The MOTiF™ PD-1/PD-L1 panel kit provides reproducibility across different patient samples.

Conclusions This data provides insight into the innate and adaptive immune landscape for targeted design of new immunotherapies as well as improved efficacy and reduced toxicity in the treatment of melanoma.

<http://dx.doi.org/10.1136/jitc-2022-SITC2022.0048>

49 **IMMUNO-ONCOLOGY IMAGING MASS CYTOMETRY
STUDY OF THE STRUCTURAL AND CELLULAR
COMPOSITION OF THE TUMOR MICROENVIRONMENT IN
HUMAN CANCERS**

Thomas Pfister*, Christina Loh, Sam Lim, Qanber Raza, Shaida Ouladan, Nick Zabinyakov.
Standard BioTools, Toronto, Canada

Background Multiplex imaging is becoming an increasingly valuable tool to study the tumor microenvironment (TME) in immuno-oncology. Imaging Mass Cytometry™ (IMC™) provides a means for visualization and analysis of the complex spatial biology of the TME. IMC permits detailed assessment of cell phenotype and function using 40-plus markers simultaneously at subcellular resolution on a single slide without spectral overlap or background autofluorescence. The ability to analyze multiple markers can facilitate accurate prediction of disease progression and clinical outcome measures from precious tissue samples and microarrays. Here, we demonstrate how our reagents support these applications.

Methods Antibodies targeting T cells, natural killer cells, myeloid cells, immune checkpoint markers, epithelial-to-mesenchymal transition (EMT) and extracellular matrix (ECM) proteins were used to study the immune microenvironment in multiple cancer histologies. Antibodies were selected from the Maxpar® and Maxpar OnDemand™ catalog. Data acquisition was performed using a Hyperion™ Imaging System (Standard BioTools™). To facilitate cell segmentation, an IMC Cell Segmentation Kit (Standard BioTools) was applied to enhance nucleus and cell membrane boundaries. Single-cell analysis was completed using custom MATLAB® script for pixel classification, CellProfiler™ for cell segmentation and histoCAT™ for phenograph clustering.

Results IMC analysis of human cancer tumor microarrays (TMAs) stained with panels of Maxpar and Maxpar OnDemand antibodies is presented here. We identified major cell populations and phenotypes via clustering (PhenoGraph). Immune cell phenotype and ECM staining data are overlaid on IMC images and complemented with t-SNE embeddings and signal intensity heat map. Additionally, we classified the activation state of immune cell populations, EMT progression and molecular composition of the TME ECM.

Conclusions Highly multiplexed IMC has enabled us to compare the TME across cancer histologies. Spatial analysis of the tumor architecture revealed details of tumor immune cell interaction at single-cell resolution. This work demonstrates the capability of IMC for quantitative and spatial identification of multiple immune parameters and detailed analysis of the TME from a single slide from cancer patients.

<http://dx.doi.org/10.1136/jitc-2022-SITC2022.0049>

50

MERKEL CELL POLYOMAVIRUS-SPECIFIC CD8 T CELLS IN BLOOD, BUT NOT IN TUMORS, CORRELATE WITH IMMUNOTHERAPY RESPONSE IN MERKEL CELL CARCINOMA

¹Thomas Pulliam*, ¹Saumya Jani, ¹Lichen Jing, ²Jiajia Zhang, ¹Rima Kulikuskas, ¹Candice Church, ³Charlie Garnett-Benson, ⁴Kelly Paulson, ²Kellie Smith, ²Andrew Pardoll, ¹David Koelle, ²Suzanne Topalian, ¹Paul Nghiem. ¹University of Washington, Seattle, WA, USA; ²Johns Hopkins University, Baltimore, MD, USA; ³Bristol Myers Squibb, Princeton, NJ, USA; ⁴Swedish Health Services, Edmonds, WA, USA

Background PD-1 pathway blockade has revolutionized oncology, though most patients do not derive durable benefit. Accurate prediction of response is not currently possible. Cancer-specific CD8 T cells can mediate tumor regression, however, identifying these cells is difficult because many tumor antigens are patient-specific. Merkel cell carcinoma (MCC), driven by Merkel cell polyomavirus (MCPyV) oncoproteins in ~80% of cases, is an attractive cancer for studying tumor-specific T cells due to shared, viral antigens and a low tumor mutational burden. Using samples from a recent trial of neoadjuvant nivolumab in MCC (NCT02488759), we studied anti-PD-1 resistance by interrogating MCPyV-specific CD8 T cells before and during therapy.

Methods MCPyV-specific CD8 T cells were identified using an expanded panel of 16 MCPyV-specific HLA class I multimers. PBMC from 21 patients with suitable multimers (among 35 patients assessed) collected before, 2 and 4 weeks after initiating anti-PD-1 were stained with MCPyV-multimers in 26-plex flow cytometry. Intratumoral MCPyV-specific T cell frequency was calculated using a combination of 1) HLA-I multimers and paired T cell receptor (TCR)-seq of phytohemagglutinin-expanded tumor infiltrating lymphocytes to identify virus-specific TCRs and 2) beta-TCRseq of formalin-fixed tumors to determine T cell clone frequency. To study phenotypic differences between cancer-specific CD8 T cells found in tumors versus blood, single cell RNAseq and paired TCRseq were performed on a separate cohort of 7 MCC patients.

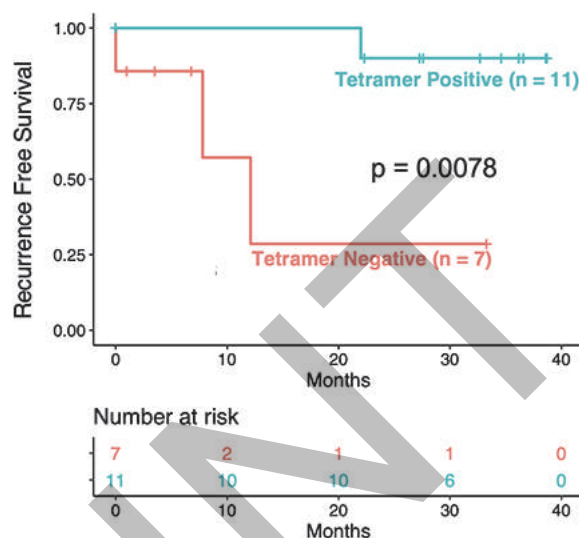
Results Patients without detectable circulating MCPyV-specific CD8 T cells before treatment had shorter recurrence-free survival (RFS; figure 1; median RFS=12 months; n=7) than patients with detectable MCPyV-specific cells (median RFS not reached; n=11; p=0.0078). In contrast, response was not associated with intratumoral, MCPyV-specific CD8 T cells (13% [mean] of intratumoral T cells in patients with pathological complete response versus 23% in those without response; p=NS). T cells were considered 'dysfunctional/exhausted' if they fell within single cell RNAseq clusters characterized by TOX, PD-1, and LAG-3 transcripts. MCPyV-specific T cells were significantly more likely to be dysfunctional/exhausted if they were intratumoral (>90% dysfunctional) versus in blood (0–50%; p=0.002).

Conclusions MCC-specific CD8 T cells in blood were less dysfunctional than their intratumoral counterparts. The frequency of pre-existing MCC-specific CD8 T cells in blood strongly correlated with anti-PD-1 response, while their frequency within tumors was unrelated to response. These results suggest that approaches to increase the number of circulating, less exhausted, cancer-specific T cells may benefit patients with anti-PD-(L)1-refractory MCC, and the frequency of these cells may be a predictive marker of anti-PD-(L)1 response.

Trial Registration NCT02488759

Ethics Approval This study was approved by the Fred Hutchinson Cancer Center's Institutional Review Board, approval

number 6585. All patients represented here participated with written informed consent.



Abstract 50 Figure 1 T cell frequency and response
Frequency of Merkel cell polyomavirus-specific CD8 T cells in blood predicts response to neoadjuvant PD-1 pathway blockade. Kaplan Meier curve showing survival of patients who had MCPyV-specific CD8 T cells in blood above (tetramer positive; blue) or below (tetramer negative; red) the limit of detection (0.01% of CD8 T cells; p=0.0078 via log-rank test)

<http://dx.doi.org/10.1136/jitc-2022-SITC2022.0050>

51

A COMBINATION OF ANTIGEN PRESENTATION AND T-CELL RECOGNITION FEATURES IMPROVES NEOANTIGEN IMMUNOGENICITY PREDICTIONS

Neeraja Ravi*, Rachel Pyke, Steven Dea, Prateek Tandon, Richard Chen, Sean Boyle. *Personalis, San Francisco, CA, USA*

Background The assessment of tumor neoantigen burden has been shown to outperform tumor mutational burden in predicting patient response to checkpoint inhibitor immunotherapy by better capturing the biological mechanism underlying response.¹ However, immune recognition of neoantigens by T-cells requires more than antigen presentation, which has been the focus of tumor neoantigen burden assessment to date. Here, we extend the existing SHERPA[®] MHC-presentation framework.² To include a model for the prediction of neoantigen immunogenicity.

Methods For feature engineering, training and validation, we utilized two datasets containing peptides experimentally validated for immunogenicity. The first dataset, curated by Schmidt et al.,³ aggregates experiments from 17 different sources, identifying 1282 immunogenic peptides across 67 MHC alleles. While the diversity of this dataset enables generalizability, a lack of associated sequencing data limits the features that can be investigated. The second dataset, curated by the TESLA consortium, contains 37 immunogenic peptides across 13 MHC alleles and patient-specific exome and transcriptome sequencing data, broadening the potential feature landscape.⁴ Using both datasets, we developed and validated features associated with antigen availability, processing, presentation and recognition. To inform the assessment of antigen availability, we measured gene expression level and variant allele fraction. We built a cleavage probability predictor from immunopeptidomics data for antigen processing, while SHERPA MHC binding probability was used to quantify antigen presentation. Finally, we included measures to predict T-cell recognition based on antigen hydrophobicity, agreotopicity, dissimilarity to self antigens and similarity to known foreign antigens. We utilized a two-tiered machine learning model that selectively learns the weights of features from the dataset that is most informative and least biased.

Results The Schmidt et al. dataset was used in the first tier of the model to develop an immunogenicity score using peptide-derived features. The first tier score distinguished immunogenic peptides with an area under the precision recall curve (AUPRC) of 0.74, far greater than SHERPA or NetMHCpan-4.1 alone (0.48 and 0.39 respectively). The second tier of the model was trained on the TESLA dataset and used the first tier score as a feature along with other patient-specific features. Cross validation yielded a 37% fold increase in AUPRC over the method developed by the TESLA consortium.

Conclusions By combining antigen presentation and T-cell recognition features in a two-tiered model, we can better predict immunogenic neoantigens and make progress towards using neoantigens as biomarkers to assess checkpoint inhibitor efficacy.

REFERENCES

1. Abbott, C.W. *et al.* Prediction of Immunotherapy Response in Melanoma through Combined Modeling of Neoantigen Burden and Immune-Related Resistance Mechanisms. *Clin Cancer Res.* 2021; **27**(15):4265–4276.
2. Pyke, R.M. *et al.* Precision Neoantigen Discovery Using Large-scale Immunopeptidomics and Composite Modeling of MHC Peptide Presentation. *Mol Cell Proteomics.* 2021;**20**:100111.

3. Schmidt, J. *et al.* Prediction of neo-epitope immunogenicity reveals TCR recognition determinants and provides insight into immunoeediting. *Cell Rep Med.* 2021;**2**(2):100194.
4. Wells, D. *et al.* Key Parameters of Tumor Epitope Immunogenicity Revealed Through a Consortium Approach Improves Neoantigen Prediction. *Cell.* 2020 Oct 29;**183**(3):818–834.e13.

<http://dx.doi.org/10.1136/jitc-2022-SITC2022.0051>

52 DIGITAL PATHOLOGY TRAINING EFFECTIVENESS FOR THE EVALUATION OF PD-L1 EXPRESSION IN MULTIPLE TUMOR INDICATIONS

Jennifer Robinson*, Edward Manna, Charlotte Roach, Ryan Marczak, Arkendra De, Joshua Littrell, Micki Adams. *Agilent Technologies, Inc., Oxnard, CA, USA*

Background In-person pathologist trainings during the COVID-19 pandemic became impossible, necessitating a shift to remote-digital whole slide image (WSI) training. High concordance between WSI and glass slide scores from the same specimens stained with PD-L1 IHC 22C3 pharmDx (SK006) across multiple tumor indications supported the validity of digital training.¹ However, in-person microscope (glass-slide) training versus remote-digital (WSI) training effectiveness must be assessed. Collated testing data on specimens (SK006 stained) spanning multiple indications scored by external pathologists during Agilent led training and testing (T&T) sessions via glass slides were compared to sessions utilizing WSIs.

Methods Stained slides (30 unique specimens per tumor indication) were scanned on an Aperio AT2 scanner to generate WSIs for digital T&T. Remote T&T sessions used WebEx and PathcoreScholar's online platform to discuss scoring guidelines and WSI training cases. Subsequently, external pathologists evaluated WSIs in PathcoreScholar for PD-L1 expression using either Tumor Proportion Score (TPS) or Combined Positive Score (CPS) scoring algorithms and interpreted these scores at predefined cutoffs (figure 1). In both glass and WSI scoring test modalities, passing is defined as inter and intra-observer overall agreement (OA) ≥85%. Training effectiveness pass rates from glass slide data (2018–2020) and WSI data (2021–2022) spanning multiple indications and scoring algorithms were calculated and then compared using the Fisher-Freeman-Halton test, with a significance threshold of 0.05. Only data from initial pathologist tests were included in the pass rate calculation; data from re-tests executed after initial test failure were excluded.

Results The differences between pass rates for microscope (glass slide) and digital (WSI) testing were not statistically significant (p-value > 0.05) (tables 1 and 2). Testing pass rates for indications scored with TPS or CPS using microscope glass slide vs digital WSI T&T was not statistically significant (p-value > 0.05) (table 3).

Conclusions No statistically significant differences in pathologist training effectiveness for PD-L1 were observed between remote and in-person trainings across multiple tumor indications, scoring algorithms, and cutoffs. These results demonstrate the effectiveness and equivalency of remote-digital pathologist trainings for evaluation of PD-L1 expression as detected by PD-L1 IHC 22C3 pharmDx in multiple tumor indications when compared to in-person-microscope glass slide T&T. Use of digital training and scoring proficiency testing can provide pathologists around the world with access to high-quality, interactive training from leading experts in PD-L1 expression evaluation.

Acknowledgements We would like to thank our colleagues at Agilent Technologies, Inc. and all the pathologists who completed Agilent scoring certification training and testing for their valuable contributions to this study.

Tissue samples were provided by the Cooperative Human Tissue Network which is funded by the National Cancer Institute. Other investigators may have received specimens from the same subjects.

Tissue samples supplied by BioIVT (Hicksville, NY, USA).

The data and biospecimens used in this project were provided by Centre Hospitalier Universitaire (CHU) de Nice (Nice, France), US Biolab (Gaithersburg, MD, USA), Contract Research Ltd (Charlestown, Nevis), Centre Hospitalier Universitaire (CHU) de Nice (Nice, France), IOM Ricera (Viagrande, Italy), National BioService LLC (Saint Petersburg, Russia), SageBio LLC (Sharon, MA, USA, Tumorothèque Régionale de Franche-Comté (Besançon, France), Centre Antoine Lacassagne (CAL; Nice, France, GLAS (Winston-Salem, NC, USA), Maine Medical, Hospices Civils de Lyon (Lyon, France), Sofia Bio LLC (New York, NY, USA), SELARL DIAG (Nice, France), and Clin-Path Diagnostics (Tempe, AZ, USA) with appropriate ethics approval and through Azenta Life Sciences.

Biological materials were provided by the Ontario Tumour Bank, which is supported by the Ontario Institute for Cancer Research (Toronto, Ontario, Canada) through funding provided by the Government of Ontario.

Abstract 52 Table 1 Pass rates of microscope (glass slide) vs digital (WSI) testing

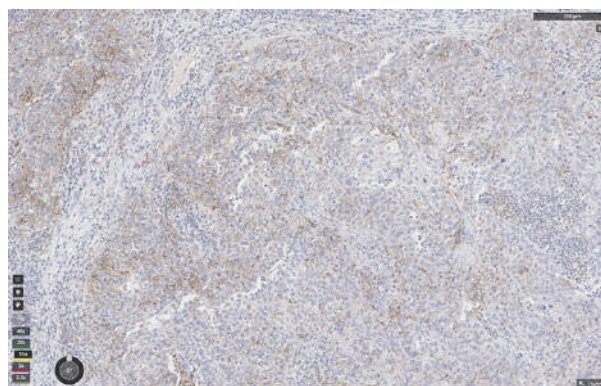
Training and Testing Modality	Pass Rate (Participants: Passing/Total)
Glass (in-person)	100*(97/102) = 95.1%
Digital (remote)	100*(110/111) = 99.1%

Abstract 52 Table 2 Glass and digital pass rates by indication

Indication	Scoring Algorithm	2018-2020 Glass Pass Rate (Participants: Passing/Total)	2021-2022 Digital Pass Rate (Participants: Passing/Total)
Colorectal carcinoma (CRC)	CPS	No data	100*(20/20) = 100%
Cervical cancer	CPS	100*(6/6) = 100%	100*(3/4) = 75%
Biliary tract adenocarcinoma (BTAC)	CPS	100*(7/8) = 88%	100*(16/16) = 100%
Urothelial carcinoma (UC)	CPS	100*(3/3) = 100%	100*(2/2) = 100%
Non-small cell lung cancer (NSCLC)	TPS	100*(6/6) = 100%	100*(22/22) = 100%
Esophageal cancer	CPS	100*(6/6) = 100%	100*(21/21) = 100%
Head and neck squamous cell carcinoma (HNSCC)	TPS	100*(16/19) = 84%	100*(16/16) = 100%
Pan-breast carcinoma (including triple-negative breast cancer, TNBC)	CPS	100*(44/44) = 100%	100*(10/10) = 100%
NSCLC cytology	TPS	100*(8/8) = 100%	No data
Small cell lung cancer (SCLC)	CPS	100*(4/4) = 100%	No data
Gastric adenocarcinoma	CPS	100*(7/8) = 88%	No data

Abstract 52 Table 3 Pass rates of microscope (glass slide) vs digital (WSI) testing for indications scored with CPS or TPS

Scoring Algorithm	Microscope (Glass) Pass Rate (Participants: Passing/Total)	Digital (WSI) Pass Rate (Participants: Passing/Total)
CPS	(80/85)*100 = 94.4%	(88/89)*100 = 98.8%
TPS	(17/17)*100 = 100%	(22/22)*100 = 100%



Abstract 52 Figure 1 Digital (WSI) of a triple-negative breast cancer (TNBC) specimen stained with PD-L1 IHC 22C3 pharmDx primary antibody and scored on PathcoreScholar online platform with

Abstracts

corresponding H&E and negative control reagent (NCR) WSIs for use as aids in the interpretation of PD-L1 staining

REFERENCE

1. Adams M, Moquin D, Littrell J, et al 36 Digital Whole Slide Image (WSI) scoring is equivalent to microscope glass slide scoring for evaluation of programmed death-ligand 1 (PD-L1) expression across multiple tumor indications. *Journal for Immunotherapy of Cancer* 2021;**9**: doi: 10.1136/jitc-2021-SITC2021.036.

<http://dx.doi.org/10.1136/jitc-2022-SITC2022.0052>

PREPRINT

53

EVALUATION OF TUMOR ANTIGEN-SPECIFIC ANTIBODY RESPONSES IN PATIENTS WITH METASTATIC TRIPLE NEGATIVE BREAST CANCER TREATED WITH CYCLOPHOSPHAMIDE AND PEMBROLIZUMAB

Eric Routh*, Benjamin Vincent, Jonathan Serody, Mark Woodcock. *UNC-Chapel Hill, Chapel Hill, NC, USA*

Background Although T cells have been a central focus of cancer immunotherapy studies, there is a growing appreciation for the role of B cells in anti-tumor immunity. We recently reported that increased B cell gene signature expression and B cell receptor diversity in pretreatment samples were associated with clinical response to immune checkpoint blockade (ICB) in triple negative breast cancer (TNBC).¹ In murine models of TNBC, ICB response has been found to be dependent upon B cell responses.² Beyond TNBC, intratumoral presence of tertiary lymphoid structures (TLS; enriched with B cells, T cells and dendritic cells (DCs)) have been associated with ICB response in various cancer types.^{3–7} Deeper understanding of B cell responses in the context of ICB is needed.

Methods We evaluated tumor antigen-specific antibody responses in patients with metastatic triple negative breast cancer treated with pembrolizumab following low dose cyclophosphamide therapy using custom peptide arrays (figure 1).

Results We found that a minority of predicted linear epitopes were associated with antibody signal, and antibody signal was associated with both mutated epitopes and self epitopes. No associations were observed between antibody signal and subcellular localization or RNA expression of parent proteins (figure 2). Patient-specific patterns of antibody signal boostability (e. g., antibody signal increase on-therapy) were observed and were independent of clinical response (figure 3). Intriguingly, measures of cumulative antibody signal intensity relative to immunotherapy treatment showed that the one complete responder in the trial had the greatest increase in total antibody signal (figure 3), which supports a putative association between ICB-dependent antibody boosting and clinical response. The antibody boost in the complete responder was largely driven by increased levels of IgG specific to a sequence of N-terminal residues in native Epidermal Growth Factor Receptor Pathway Substrate 8 (EPS8) protein (figure 4), a known oncogene in several cancer types including breast cancer. Structural protein prediction analysis showed that the antibody-targeted region of EPS8 was in a region of the protein with mixed linear/helical structure, and that this region was solvent-exposed and not predicted to bind to interacting macromolecules (figure 4).

Conclusions High-throughput peptide arrays can be used to map tumor antigen-specific antibody responses. This study highlights the potential importance of humoral immune responses recognizing neoantigen epitopes and unmutated self protein epitopes in anti-tumor immunity. Future studies will be needed to better elucidate the role of tumor antigen-specific antibodies in tumor growth inhibition and immunotherapy response.

Acknowledgements

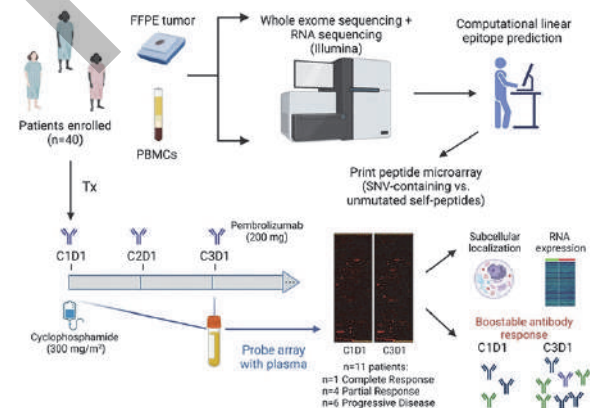
Funding Merck Sharp & Dohme, a subsidiary of Merck & Co, Kenilworth, NJ, USA (MSD) provided financial support for the clinical trial under which samples from this study were acquired. This work was also supported by Susan G. Komen for the Cure (BV), V Foundation for Cancer Research (BV), and UNC University Cancer Research Fund (MW, JS, BV).

The authors thank Ken Fowler and Karen McKinnon with the Immune Monitoring and Genomics Facility (IMGF) at UNC-Chapel Hill for their assistance with this study. We also thank the patients in this study and their families, without whom this study would not have been possible.

REFERENCES

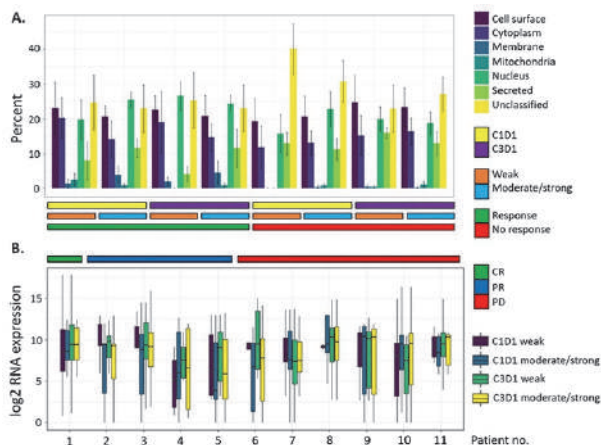
- Anders CK, Woodcock MG, Van Swearingen AED, Moore DT, Sambade MJ, Laurie S, *et al.* Evaluating the efficacy of a priming dose of cyclophosphamide prior to pembrolizumab to treat metastatic triple negative breast cancer. *Journal for immunotherapy of cancer.* 2022;**10**(2).
- Hollern DP, Xu N, Thennavan A, Glodowski C, Garcia-Recio S, Mott KR, *et al.* B Cells and T Follicular Helper Cells Mediate Response to Checkpoint Inhibitors in High Mutation Burden Mouse Models of Breast Cancer. *Cell.* 2019;**179**(5):1191–206.e21.
- Cabrera R, Lauss M, Sanna A, Donia M, Skaarup Larsen M, Mitra S, *et al.* Tertiary lymphoid structures improve immunotherapy and survival in melanoma. *Nature.* 2020;**577**(7791):561–5.
- Helmink BA, Reddy SM, Gao J, Zhang S, Basar R, Thakur R, *et al.* B cells and tertiary lymphoid structures promote immunotherapy response. *Nature.* 2020;**577**(7791):549–55.
- Vanhersecke L, Brunet M, Guégan JP, Rey C, Bouguin A, Cousin S, *et al.* Mature tertiary lymphoid structures predict immune checkpoint inhibitor efficacy in solid tumors independently of PD-L1 expression. *Nat Cancer.* 2021;**2**(8):794–802.
- Petitprez F, de Reyniès A, Keung EZ, Chen TW, Sun CM, Calderaro J, *et al.* B cells are associated with survival and immunotherapy response in sarcoma. *Nature.* 2020;**577**(7791):556–60.
- Meylan M, Petitprez F, Becht E, Bouguin A, Pupier G, Calvez A, *et al.* Tertiary lymphoid structures generate and propagate anti-tumor antibody-producing plasma cells in renal cell cancer. *Immunity.* 2022;**55**(3):527–41.e5.

Ethics Approval This study was approved by UNC IRB #16-1025.

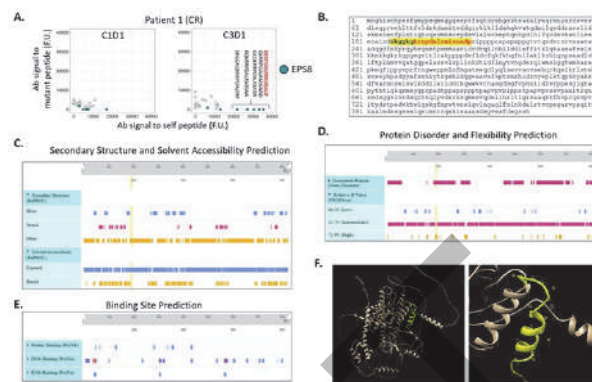


Abstract 53 Figure 1 Experimental approach to examine neoantigen-specific antibody responses. Patients with metastatic triple negative breast cancer underwent a clinical trial to examine the efficacy of regulatory T cell depletion with cyclophosphamide plus PD-1 inhibition with pembrolizumab. Eleven patients from this cohort were selected based on clinical response for analysis of tumor antigen-specific antibody responses via multiplex ELISA (peptide arrays). Downstream analyses included examination of protein subcellular localization and RNA expression, as well as antibody boostability relative to immunotherapy treatment. Antibody responses were seen at baseline, and in some patients, increased after therapy

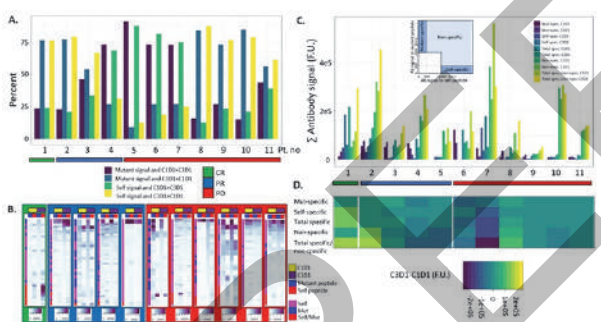
Abstracts



Abstract 53 Figure 2 Subcellular protein localization and RNA expression do not associate with antibody signal or response group. (A) Subcellular localization of parent proteins of self/mutant peptide pairs subset based on associated antibody signal level (weak vs. moderate/strong), and further categorized by treatment time point and response. Peptide pairs were considered to have moderate/strong signal if either peptide of the pair (self or mutant) had >2,000 F.U. signal intensity. Peptide pairs were considered to have weak signal if both peptides of the pair (self and mutant) had signal intensity >500 F.U. and <2000 F.U. Error bars represent standard error (n=5 for responders; n=6 for non-responders). (B) Distribution of RNA expression of parent proteins categorized according to antibody signal level, treatment time point and response



Abstract 53 Figure 4 Complete responder displayed ICB-dependent boostability of both mutant and self-peptides, with particularly strong boost of IgG specific to native EPS8 peptides. (A) Relative antibody signal to self- versus mutant peptides at C1D1 and C3D1. Annotation shows ICB-dependent boost of antibody signal to self-EPS8 peptides. Peptides with greatest boost corresponding to S187-P107 residues are shown. (B) Primary protein structure of EPS8, with S187-P107 highlighted. The primary structure for EPS8 protein was input into PredictProtein (<https://predictprotein.org>) to query secondary structure and solvent accessibility (C), protein disorder and flexibility (D), and macromolecular binding site predictions (E). (F) Tertiary structure of EPS8 as predicted by AlphaFold Protein Structure Database (<https://alphafold.com>), with S187-P107 highlighted in yellow. 3D structure was visualized and annotated using Chimera v1.16 software (<https://www.cgl.ucsf.edu/chimera/>)



Abstract 53 Figure 3 Boostability of antibody response relative to ICB treatment. (A) Percentage of mutant or self-peptides that had associated antibody signal (>500 F.U. at either C1D1 or C3D1) and greater signal relative to the other time point. (B) Heatmap depiction of antibody signal relative to treatment time point. Signal was ranked according to intensity of signal to C3D1 mutant peptide. A peptide pair was included if there was any signal >2,000 F.U. for either self or mutant peptide at either C1D1 or C3D1 time point. Colored sidebar denotes whether antibody signal was associated with mutant peptide, self peptide or both. (C) Absolute antibody signal (summed) categorized by signal specificity, treatment time point and response. Inlay depicts signal thresholds that were used to denote specificity classes. (D) ICB-associated boostability difference in antibody signal, which is derived by subtracting C1D1 antibody signal from C3D1 signal for respective specificity classes

<http://dx.doi.org/10.1136/jitc-2022-SITC2022.0053>

54 **PROGNOSTIC VALUE OF T CELL IMMUNOSCORE ESTIMATED FROM TRANSCRIPTOMIC DATA IN PATIENTS WITH ADVANCED MALIGNANCIES TREATED WITH IMMUNE CHECKPOINT INHIBITORS**

¹Ahmad Tarhini*, ²Payman Ghasemi Saghand, ¹Aik Choon Tan, ²James Chen, ³Aakrosh Ratan, ⁴Martin McCarter, ⁵John Carpton, ⁶Howard Colman, ⁷Alexandra Ikeguchi, ⁸Igor Puzanov, ⁹Susanne Arnold, ¹⁰Michelle Churchman, ¹Patrick Hwu, ¹Jose Conejo-Garcia, ¹⁰William (Bill) Dalton, ¹¹George Weiner, ¹Issam El Naqa. ¹H. Lee Moffitt Cancer Center and Research Institute, Tampa, FL, USA; ²The Ohio State University, Columbus, OH, USA; ³University of Virginia, Charlottesville, VA, USA; ⁴University of Colorado Cancer Center, Aurora, CO, USA; ⁵USC Norris Comprehensive Cancer Center, Los Angeles, CA, USA; ⁶Huntsman Cancer Institute, Salt Lake City, UT, USA; ⁷Stephenson Cancer Center, Oklahoma City, OK, USA; ⁸Roswell Park Comprehensive Cancer Center, Buffalo, NY, USA; ⁹Markey Cancer Center, Lexington, KY, USA; ¹⁰M2Gen, ORIEN, Tampa, FL, USA; ¹¹University of Iowa Holden Cancer Center, Iowa City, IA, USA

Background Evidence supports the association between tumor-infiltrating lymphocytes with disease prognosis and response to immunotherapy. Here, we evaluated the prognostic value of an immunoscore reflecting CD3+ and CD8+ T cell density in patients with advanced malignancies treated with immune checkpoint inhibitors (ICIs).

Methods We utilized real-world clinical and transcriptomic data collected under the Total Cancer Care Protocol (NCT03977402) and Avatar® project within the Oncology Research Information Exchange Network (ORIEN) of 18 cancer centers to which all included subjects provided a written informed consent at their participating institutions. The immunoscore for each patient was calculated based on the estimated densities of tumor CD3+ and CD8+ T cells (Galon, 2020) utilizing CIBERSORTx and the LM22 gene signature matrix. Overall survival (OS) predictions were assessed using Harrell's concordance index (C-index). Kaplan-Meier (KM) curves and the log-rank test were used to assess the immunoscore ability to stratify risk groups.

Results Patients (n=522) with 4 cancer types including melanoma (n=125), renal cell carcinoma (n=149), non-small cell lung cancer (n=128) and head and neck cancer (n=120) treated with 6 immune checkpoint inhibitor (ICI) regimens were included in this analysis. ICI regimens were nivolumab (n=219), pembrolizumab (n=202), ipilimumab+nivolumab (n=69), ipilimumab (n=30), avelumab (n=1) and cemiplimab (n=1). Table 1 summarizes the overall C-index and associated 95% CIs and log-rank p values for the entire cohort resulting from estimated immunoscore categorizations. KM analyses of the entire cohort are displayed in figure 1. We compared the performance of the immunoscore as a prognostic biomarker in the 4 cancer types, with significant results seen only in the melanoma and head and neck cancer cohorts (table 2, figure 2).

Conclusions The CD3+, CD8+ T Cell immunoscore estimated from transcriptomic data represents a prognostic biomarker for estimating overall survival in patients with metastatic melanoma and head and neck cancer treated with ICIs in a real-world setting and can be used as a reference in prognostic biomarker development. Integration with other biomarker candidates that may guide the choice of ICI regimen (anti-PD1 monotherapy versus combinations) is underway.

Acknowledgements We are grateful to the participating patients and their family members as well as all research staff supporting the conduct of the Total Cancer Care protocol.

Trial Registration NCT03977402

Ethics Approval We utilized real-world clinical and transcriptomic data collected under the Total Cancer Care Protocol

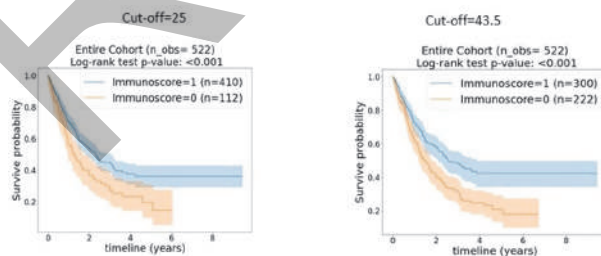
(NCT03977402) and Avatar® project within the Oncology Research Information Exchange Network (ORIEN) of 18 cancer centers to which all included subjects provided an IRB-approved written informed consent at their participating institutions.

Abstract 54 Table 1 Overall C-index and associated 95% CIs and log-rank

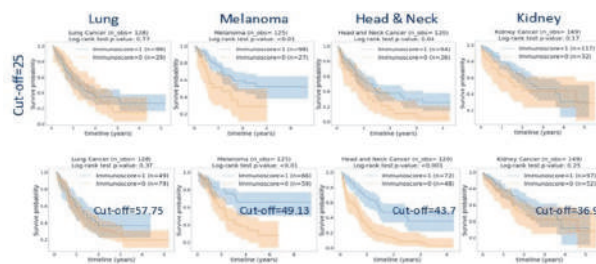
	Avg. C-index	95% CI	Log-rank test p-value
Cut-off = 25	0.5402	(0.5345 , 0.5459)	<0.001
Cut-off = 43.5	0.5528	(0.5466 , 0.5591)	<0.001

Abstract 54 Table 2 Overall C-index and associated 95% CIs and log-rank

	Cut-off	Avg. C-index	95% CI	Log-rank test p-value
Lung	57.75	0.5083	(0.4973 , 0.5194)	0.37
Melanoma	49.13	0.5857	(0.5721 , 0.5993)	0.002
Head & Neck	43.7	0.6264	(0.6154 , 0.6375)	<0.001
Kidney	36.9	0.5209	(0.5487 , 0.5762)	0.17



Abstract 54 Figure 1 Kaplan-Meier analysis for the entire cohort



Abstract 54 Figure 2 Cancer-specific Kaplan Meier plots

<http://dx.doi.org/10.1136/jitc-2022-SITC2022.0054>

IDENTIFICATION OF THE O-GLYCAN EPIOTOPE TARGETED BY AN ANTI-HUMAN CARCINOMA MONOCLONAL ANTIBODY (MAB) NEO-201

¹Massimo Fantini*, ¹Anjum Zaki, ¹Sharon Mavroukakis, ²Christina Annunziata, ¹Philip Arlen, ¹Kwong Tsang, ¹Kwong Tsang. ¹*Precision Biologics, Inc., Bethesda, MD, USA;* ²*National Cancer Institute, Bethesda, MD, USA*

Background NEO-201 is a humanized IgG1 mAb reactive against multiple human carcinomas, but not normal epithelial tissues. NEO-201 can mediate antitumor activity through multiple mechanisms such as antibody-dependent cellular cytotoxicity, complement dependent cytotoxicity, and blockade of the CEACAM5/CEACAM1 immune checkpoint inhibitory pathway. In addition to solid tumors, flow cytometry analysis has demonstrated that NEO-201 binds to 98.9% of CD15⁺ granulocytes, human regulatory T cells as well as various human hematological neoplastic cell lines. However, NEO-201 does not bind to other immune subsets and to the majority of CD4⁺ T cells. Furthermore, we have demonstrated that NEO-201 binds to mammalian expressed rhCEACAM6 but not bacterial expressed rhCEACAM6. These findings suggest that NEO-201 binds to glycans linked to specific proteins. Glycosylation is an important post-translation modification of protein and is affected by oncogenesis. Aberrant O-glycans may serve as potential targets to improve the monitoring and treatment of cancers. Based on this information, this study was designed to focus on the identification of the O-glycan binding epitope of NEO-201.

Methods An O-glycan array consisting of 94 O-glycans was used to identify the O-glycans targeted by NEO-201. O-glycan profiles were elucidated from human pancreatic cancer cell line (CFPAC-1), human hematological neoplastic cell lines (HL60, U937, K562) and human neutrophils. Different truncated C-terminus of CEACAM6 and CEACAM5 gene constructs were designed and the truncated CEACAM6 and CEACAM5 proteins were expressed in mammalian expression system to identify the NEO-201 binding region in CEACAM6 and CEACAM5.

Results The O-glycan array analysis shows that NEO-201 interacts with O-glycans 01, 02 (Tn antigens), 06 (Core 1), 023 (Core 2), 026 (Core 3) and 039 (Core 4). The Core-1 binding interaction was the strongest of any observed. The O-glycan profiling studies demonstrated that CFPAC-1 and human neutrophils express mostly the Core 1 profile. HL-60 expresses mainly the extended Core 1 profile, U937 expresses mainly the extended Core 1 and Core 2 profiles and K562 expresses only the Core 2 profile. Flow cytometry analysis demonstrated that NEO-201 binds to CFPAC-1, human neutrophils, HL60 and U937 cells but not to K562. We also proved that in both CEACAM5 and CEACAM6 NEO-201 binds to regions containing threonine. GalNAc residue can be added onto threonine to form O-glycans.

Conclusions This study demonstrated that NEO-201 binds strongly to Core 1 and/or extended Core 1 O-glycans and confirms our finding that NEO-201 binds only mammalian expressed rhCEACAM6 express O-glycans.

<http://dx.doi.org/10.1136/jitc-2022-SITC2022.0055>

56

HIGH PRETREATMENT DHEA LEVEL IS ASSOCIATED WITH SHORTER OVERALL SURVIVAL IN NEWLY DIAGNOSED METASTATIC NON-SMALL CELL LUNG CANCER PATIENTS RECEIVING IMMUNE CHECKPOINT INHIBITORS

Yumeng Zhang*, Lancia Darville, Stephanie Hogue, Julie Hallanger Johnson, Youngchul Kim, Jhanelle Gray, Lary Robinson. *Moffitt Cancer Center, Tampa, FL, USA*

Background Sex is an important factor in determining response to immune checkpoint inhibitors (ICI) in cancer patients.¹ Sex hormones can modulate the immune response in preclinical studies.² Our study aimed to determine if the pretreatment sex hormone level can predict outcomes in metastatic non-small cell lung cancer (mNSCLC) patients undergoing ICI therapies.

Methods This study included 61 patients with newly diagnosed mNSCLC who received ICI as part of the upfront therapy. Pretreatment plasma and fecal samples were collected before the first ICI infusion, and we measured sex hormone levels using ultra-high-performance liquid chromatography high-resolution mass spectrometry. Sex hormone levels were compared between the clinical benefit and no clinical benefit group. Patients were then divided into high DHEA and low DHEA groups based on the sex-specific median of the cohort. Overall survival (OS) and progression-free survival (PFS) were compared between high DHEA and low DHEA using Kaplan Meier's methods. A similar analysis was based on the 5-androstenediol level. We used the univariate and multivariate Cox proportional hazards (PH) model to measure hazard ratios (HRs) for PFS and OS.

Results Pretreatment plasma samples were collected from 61 patients, and 31 patients were female (table 1). Among them, 30 plasma samples had measurable DHEA levels, and 46 patients had measurable 5-androstenediol levels (table 2). Patients in the clinical benefit group had significantly higher plasma DHEA levels and 5-androstenediol levels than those in the no clinical benefit group (figure 1)

The high DHEA group had fewer patients with clinical benefits from ICI therapy (27% vs. 87% in the high DHEA and low DHEA groups, respectively) (figure 2). Patients with high DHEA also had shorter OS (mOS: 11.4mo vs. not reached for high DHEA and low DHEA group respectively, p=0.0001) and shorter PFS (mPFS: 4.1mo vs. 2.2mo for the high DHEA and low DHEA groups, respectively, p<0.0001). High 5-androstenediol also had fewer patients with clinical benefit (46% vs 72% for the high 5-androstenediol and low 5-androstenediol groups, respectively).

Univariate Cox PH analysis confirmed our observation. High DHEA level was associated with poor OS (HR=8.29, 95% CI:2.31–29.79) and PFS (HR=10.23, 95% CI:3.4–30.74). High 5-androstenediol level was associated with shorter PFS (HR=2.26, 95% CI: 1.07–4.75) (table 3).

Conclusions Pretreatment DHEA level and 5-androstenediol level were significantly lower in patients with clinical benefit from ICI. Our study supports the use of pretreatment DHEA as a promising predictive biomarker in patients with metastatic NSCLC receiving ICI therapies.

REFERENCES

1. Klein, S. L. and K. L. Flanagan (2016). Sex differences in immune responses. *Nat Rev Immunol* **16**(10): 626–638.
2. Ben-Batalla, I., M. E. Vargas-Delgado, G. von Amsberg, M. Janning and S. Loges (2020). Influence of Androgens on Immunity to Self and Foreign: Effects on Immunity and Cancer. *Front Immunol* **11**: 1184.

Ethics Approval This study was approved by Advarra IRB (MCC 18611, PRO00017235).

Abstract 56 Table 1 Patient Demographics and Clinical Characteristics of 61 enrolled patients based on clinic benefit

	clinical benefit N=28	no clinical benefit N=33	P value
age at diagnosis median, range	68(49,84)	67 (52.8, 82.1)	0.89
Male Sex, %	15 (45.5)	15 (53.6)	0.527
Race			0.074
White	31 (94)	23 (82)	
Black	1 (3)	3 (11)	
BMI (median, 95% CI) at the time of treatment	26.1 [18.7, 36.9]	23.8 [16.9, 46.9]	0.36
Smoking Status			0.803
Current	9 (32.1)	8 (24.2)	
former	15 (53.6)	21 (63.6)	
never	4 (14.3)	4 (12.1)	
ECOG performance status			0.353
0	5 (15.2)	2 (7.1)	
1	28 (84.8)	25 (89.3)	
Histology:			0.529
non-squamous, %	28 (85)	24 (86)	
Squamous, %	5 (15)	4 (14)	
CNS involvement	4 (14.3)	2 (6.3)	0.282
Laboratory Evaluation			
Absolute Neutrophil Count, e3/DL, median, 95% CI	5.1 [2.3, 11.7]	5.1 [3.2, 10.5]	0.34
Absolute Lymphocyte Count, e3/DL, median, 95% CI	1.2 [0.3, 2.8]	1.05 [0.3, 2.7]	0.61
Absolute Eosinophil Count, e3/DL, median, 95% CI	0.17 [0.0, 0.92]	0.15 [0.01, 0.84]	0.32
Absolute Platelet Count, e6/DL, median, 95% CI	282 [109.1, 526.2]	251 [114.4, 469.4]	0.99
Neutrophil to Lymphocyte ratio (median, 95% CI)	4.2 [1.8, 14.8]	4.9 [1.6, 13.7]	0.85
Platelet to Lymphocyte ratio (median, 95% CI)	245.6 [62.2, 1104.2]	229.9 [105.7, 796.2]	0.81
Co-morbidities			
COPO	12 (36)	16 (57)	0.11
HLI	22 (66.7)	17 (60.7)	0.63
OSA	6 (18.2)	5 (17.9)	0.97
M/Heart Failure	3 (9.1)	6 (21.4)	0.18
DM	4 (12.1)	10 (36)	0.038
Prior therapy including neoadjuvant and adjuvant			
Prior chemotherapy	24 (42.9)	20 (61)	0.406
Prior Radiation Therapy	10 (36)	9 (27)	0.478
PD-L1 positive (>1%)	20/27 (74)	14/24 (58)	0.84
if positive, PD-L1 = 50 %, median, 95% CI	9 (32)	10 (30)	0.88
Other mutation			
ALK fusion	1/19	1/20	0.93
EGFR	5/24	2/31	0.16
KRAS	6/19	7/31	0.07
NRAS	0/14	0/15	0.72
TP53	6/11	6/15	0.95

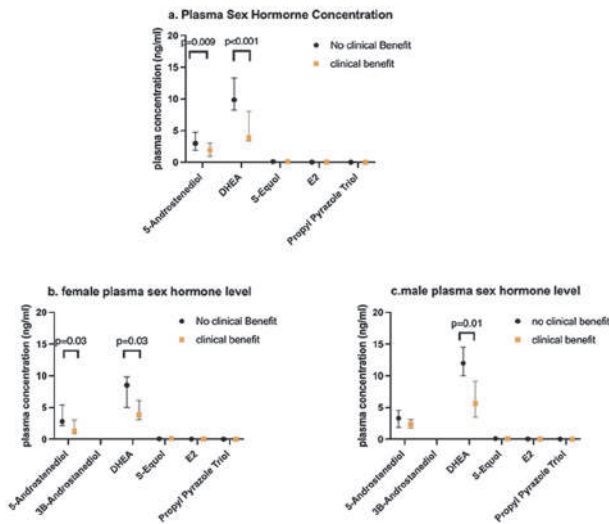
Abstract 56 Table 2 Plasma sex hormone level and stool phytoestrogen level of patients based on clinical benefit

	clinical benefit N=28	No clinical benefit N=33	P value
Plasma			
DHEA level (ng/ml), median, 95% CI	3.7 (2.1-8.3)	9.6 (3.8-16.6)	<0.001
5-androstenediol level (ng/ml), median, 95% CI	2.7 (0.66-5.0)	2.3 (0.87-5.5)	0.01
S-equal level (ng/ml), median, 95% CI	0.11 (0.006-0.32)	0.11 (0.027-0.7)	0.73
Propyl Pyrazole Triol level (ng/ml), median, 95% CI	0.015 (0.0016-0.056)	0.0080 (0.0017-0.079)	0.95
E2 level (ng/ml), median, 95% CI	0.043 (0.013, 0.079)	0.03 (0.009-0.12)	0.43
Stool phytoestrogen level normalized to Daidzein			
Quercetin level, median, 95% CI	0.89 (0.096-129)	0.86 (0.007-15.0)	0.43
Naringenin level, median, 95% CI	1.18 (0.1-48)	0.91 (0.03-29)	0.36
Genestein, median, 95% CI	2.1 (0.07-21)	1.46 (0.07-20)	0.68
S-equal, median, 95% CI	7.81 (0.70-703)	7.38 (0.1-747)	0.58

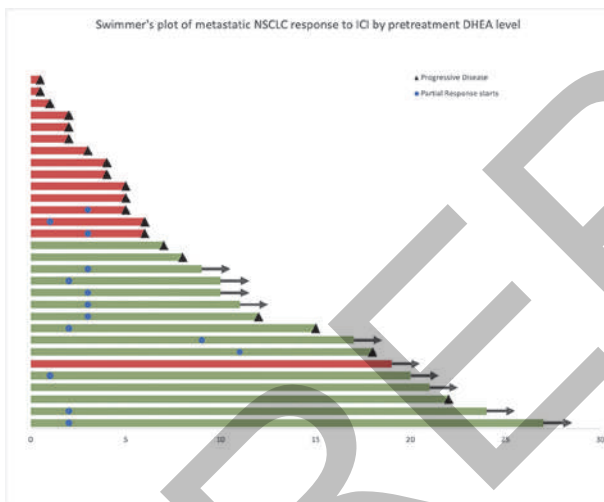
Abstract 56 Table 3 Univariate and multivariate analysis of clinical factors affecting progress-free survival and overall survival in metastatic non-small cell lung cancer undergoing first line immune checkpoint inhibitor therapy

Clinical Factors	Progression Free Survival			no of events/ cases
	no of events/ no of cases	Univariable HR (95% CI)	Multivariable HR (95% CI)	
age	45/61	1.01 (0.98-1.05)	1.11 (1.01,1.23)	34/61
sex				
male	21/30	1	1	17/30
female	24/31	0.85 (0.47,1.53)	1.12 (0.32,3.89)	17/31
p for trend		0.58	0.86	
BMI	45/61	1.00 (0.95,1.06)	1.09 (0.97, 1.22)	34/61
Smoking Status				
current	13/17	1	1	12/17
former	27/36	0.92 (0.47,1.79)	0.25 (0.037, 1.72)	18/36
never	0/625	0.84 (0.30,2.36)	0.20 (0.018, 2.12)	4/8
p for trend		0.94	0.29	
Medical Comorbidities				
DM present	10/14	1.74 (0.85,3.59)	1.14 (0.23,5.68)	10/14
DM absent	35/47	1	1	24/47
p for trend		0.13	0.87	
MIR	45/61	1.01 (0.93,1.09)	1.15 (0.88,1.50)	34/61
PLR	45/61	1.00 (0.99, 1.00)	1.00(0.99, 1.01)	34/61
Systemic therapy within 1 year of immunotherapy initiation				
yes	23/29	1.12 (0.62, 2.02)	1.39 (0.41, 4.7)	21/29
no	22/32	1	1	13/32
p for trend		0.77	0.59	

Abstracts



Abstract 56 Figure 1 Plasma sex hormone concentration in clinical benefit and no clinical benefit group. a) all patients b) female only c) male only. The dots/square represents the median and the error bar represented the interquartile changes. The clinical benefit group had significantly lower DHEA and 5-androstenediol plasma concentration



Abstract 56 Figure 2 Swimmer's plot. Patients are color-labeled based on their DHEA level. Patients are arranged based on their duration on therapy. X-axis represented their duration on therapy in months. Red bar represented individual with high DHEA. Green bar represented individual with low DHEA

<http://dx.doi.org/10.1136/jitc-2022-SITC2022.0056>

57

CD8+FOXP3+ CELLS REPRESENT EARLY, EFFECTOR T-CELLS AND PREDICT OUTCOMES IN PATIENTS WITH RESECTABLE NON-SMALL CELL LUNG CARCINOMA (NSCLC) RECEIVING NEOADJUVANT ANTI-PD-1-BASED THERAPY

¹Emily Cohen, ²Daphne Wang, ²Elizabeth Engle, ²Benjamin Green, ²Justina Caushi, ²Jijia Zhang, ²Joel Sunshine, ¹Sonali Uttam, ¹Michael Fotheringham, ³Alexa Fiorante, ¹Nicole Espinosa, ³Bhakti Pandey, ¹Teodora Popa, ²Aleksandra Ogurtsova, ²Sigfredo Soto-Diaz, ²Jose Loyola, ²Jeffrey Roskes, ²Margaret Eminizer, ²Dmitry Medvedev, ⁴Jamie Chaft, ²Julie Brahmer, ²Joshua Reuss, ²Patrick Forde, ²Alexander Szalay, ²Andrew Pardoll, ²Kellie Smith, ²Janis Taube, ¹Tricia Cottrell*. ¹Queen's University, Kingston, Canada; ²Johns Hopkins University, Baltimore, MD, USA; ³University of Toronto, Toronto, Canada; ⁴Memorial Sloan-Kettering Cancer Center, New York City, USA

Background PD-1/PD-L1 pathway blockade has improved survival in patients with advanced NSCLC. Neoadjuvant (pre-operative) anti-PD-1 plus chemotherapy was also recently approved for patients with resectable stage II/III NSCLC. However, among patients receiving neoadjuvant anti-PD-1-based therapy, only 33–45% achieved a major pathologic response (MPR, $\leq 10\%$ of residual viable tumor), highlighting the need for biomarkers predicting response.^{1,3} Based upon recent results in advanced melanoma showing that CD8 +FoxP3+ cells were strongly associated with therapeutic response,⁴ we hypothesized that these cells would also be predictive of response in resectable NSCLC. Additionally, we performed single-cell RNA sequencing (scRNAseq) to define the phenotype of CD8+FoxP3+ cells, given reports suggesting an immunosuppressive role.

Methods Pre-treatment formalin-fixed paraffin-embedded tumor specimens from the first-in-human clinical trial of neoadjuvant anti-PD-1 (nivolumab) +/- anti-CTLA-4 (ipilimumab) in NSCLC (NCT02259621)^{1,3} were stained with a 6-marker multiplex immunofluorescence mIF panel (PD-1, PD-L1, CD8, CD163, FoxP3, and cytokeratin). Eight specimens were from patients demonstrating MPRs and 17 were from patients with non-MPRs. The densities of immune cell populations within the tumor microenvironment (TME) were analyzed using the AstroPath platform and the area under the receiver operating characteristic curve (AUC) for each possible cell phenotype was calculated for predicting MPR.⁴ The association for cell phenotypes with event-free survival (EFS) and overall survival (OS) was determined using the log-rank test. scRNAseq analyses were performed on freshly collected CD3+ TIL from 15 of the same NSCLC patients. T-cells were clustered by UMAP and were queried for co-expression of CD8 and FoxP3.

Results The density of CD8+FoxP3+ T-cells was significantly elevated in patients achieving MPR (AUC=0.78, $p=0.014$, $N=25$). This association was strongest in the PD-1(+) (AUC=0.83, $p=0.004$) and PD-L1(-) (AUC=0.81, $p=0.007$) subsets. The AUCs for CD8+FoxP3+ cells were stronger than any other cell phenotype labeled by this 6-plex mIF assay. Patients whose TMEs contained CD8+FoxP3+ cells ($n=18$) when compared to those lacking this phenotype ($n=7$) had improved EFS and OS (41 vs. 8 months, $p=0.041$; and 26 vs. 8 months, $p=0.074$, respectively). scRNAseq studies of the CD8+FoxP3+ T-cell subset revealed a transcriptome compatible with a highly-activated, cytotoxic phenotype (*CCL5*, *CD8A*, *GZMB*, *NKG7*, *CTSW*, *CD8B*, *LINC02446*, *GZMK* all highly expressed).

Conclusions CD8+FoxP3+ T-cells in the NSCLC TME do not represent immunosuppressive cells, as has been previously reported, but instead represent highly-potent early, effector T-cells. When detected by mIF in pre-treatment NSCLC tumor

specimens, these cells associate with major pathologic response and improved survival outcomes following neoadjuvant anti-PD-1.

REFERENCES

1. Forde, P. M., Chaft, J. E., Smith, K. N., Anagnostou, V., Cottrell, T. R., Hellmann, M. D., Zahurak, M., Yang, S. C., Jones, D. R., Broderick, S., Battafarano, R. J., Velez, M. J., Rekhman, N., Olah, Z., Naidoo, J., Marrone, K. A., Verde, F., Guo, H., Zhang, J., Caushi, J. X., ... Pardoll, D. M. Neoadjuvant PD-1 Blockade in Resectable Lung Cancer. *N Engl J Med*. 2018; **378**, 1976–1986.
2. Forde, P. M., Spicer, J., Lu, S., Provencio, M., Mitsudomi, T., Awad, M. M., Felip, E., Broderick, S. R., Brahmer, J. R., Swanson, S. J., Kerr, K., Wang, C., Ciuleanu, T.-E., Saylor, G. B., Tanaka, F., Ito, H., Chen, K.-N., Liberman, M., Vokes, E. E., ... Girard, N. Neoadjuvant Nivolumab plus Chemotherapy in Resectable Lung Cancer. *N Engl J Med*. 2022; **386**, 1973–1985.
3. Reuss, J. E., Anagnostou, V., Cottrell, T. R., Smith, K. N., Verde, F., Zahurak, M., Lanis, M., Murray, J. C., Chan, H. Y., McCarthy, C., Wang, D., White, J. R., Yang, S., Battafarano, R., Broderick, S., Bush, E., Brock, M., Ha, J., Jones, D., Merghoub, T., ... Forde, P. M. (2020). Neoadjuvant nivolumab plus ipilimumab in resectable non-small cell lung cancer. *J Immunother Cancer*. 2020; **8**, e001282.
4. Berry, S., Giraldo, N. A., Green, B. F., Cottrell, T. R., Stein, J. E., Engle, E. L., Xu, H., Ogurtsova, A., Roberts, C., Wang, D., Nguyen, P., Zhu, Q., Soto-Diaz, S., Loyola, J., Sander, I. B., Wong, P. F., Jessel, S., Doyle, J., Signer, D., ... Taube, J. M. Analysis of multispectral imaging with the AstroPath platform informs efficacy of PD1 blockade. *Science*. 2021; **372**, eaba2609.

Ethics Approval This study was conducted in accordance with the Declaration of Helsinki and was performed following Johns Hopkins University IRB approval (#NA_00085595). This protocol allows for the retrieval of tissue from archives from patients who signed an informed written consent or with waiver of consent.

<http://dx.doi.org/10.1136/jitc-2022-SITC2022.0057>

58 EXAMINING ELEVATED TMB AND CLINICAL BENEFIT OF 1L IMMUNE CHECKPOINT INHIBITOR IN ADVANCED NSCLC

¹David Carbone*, ²Jacob Sands, ³Gerald Li, ³Alexa Schrock, ³Ryon Graf, ³Liangliang Zhang, ³Karthikeyan Murugesan, ³Jeffrey Ross, ³Khaled Tolba, ³Geoffrey Oxnard, ³Richard Huang, ⁴David Spigel. ¹The Ohio State University, Columbus, OH, USA; ²Dana-Farber Cancer Institute, Boston, MA, USA; ³Foundation Medicine, Cambridge, MA, USA; ⁴Sarah Cannon Research Institute, Nashville, TN, USA

Background For patients with advanced non-small cell lung carcinoma (NSCLC), immune check point inhibitor (ICPI) and chemotherapy (chemo)-ICPI represent 2 distinct first-line standard-of-care regimens without clear and established biomarkers to inform the optimal choice for individual patients. Here, we examined the complementary roles of tumor mutational burden (TMB) and PD-L1 immunohistochemistry (IHC) to inform first-line therapy using a large real-world (rw) data set.

Methods The study included patients with NSCLC from the Flatiron Health (FH)-Foundation Medicine (FMI) de-identified clinico-genomic database (CGDB). All patients underwent genomic testing using FMI's tissue comprehensive genomic profiling (CGP) assay and PD-L1 IHC assay scored for tumor cell staining (TS).

Results Of 2,165 patients included in the analysis, 150 exhibited durable benefit from first line ICPI regimens (these patients were enriched for PD-L1 TS ≥ 50 , non-squamous histology, and TMB ≥ 20 mutations/Megabase [muts/Mb]). Comparing low TMB (< 10 muts/Mb), high TMB (10–19 muts/Mb), and very high TMB (≥ 20 muts/Mb) receiving ICPI alone, we observed a stepwise increase in median rwPFS (real world-progression free survival) (6.5, 7.5, 17.2 months) and rwOS (real world-overall survival) (10.1, 11.8, 26.9 months) as TMB increased. In the low PD-L1 (TS $< 50\%$) cohort, TMB < 10 muts/Mb (HR:0.70 [0.54–0.92]) and 10–19 muts/Mb (HR:0.48 [0.32–0.72]) showed a more favorable rwPFS on chemoICPI when compared to ICPI alone while no significant additional increases in rwPFS is observed when adding chemo onto ICPI in the TMB ≥ 20 muts/Mb (HR:1.18 [0.56–2.48]) cohort.

Conclusions This study provides evidence that higher TMB cut-offs, such as 20 muts/Mb, can identify patients with prolonged benefit. TMB ≥ 20 muts/Mb may identify patients in whom an ICPI without chemo could be considered, even in the setting of lower PD-L1 levels. Prospective validation of these findings could increase access to chemo-sparing regimens for the first-line treatment of advanced NSCLC.

Ethics Approval Institutional Review Board approval of the study protocol was obtained prior to study conduct and included a waiver of informed consent.

<http://dx.doi.org/10.1136/jitc-2022-SITC2022.0058>

59 **DETERMAIO (IO SCORE) IS ASSOCIATED WITH EFFICACY OF ICI MONOTHERAPY IN ADVANCED NSCLC PATIENTS: A RETROSPECTIVE BC CANCER STUDY**

¹David Saltman*, ²Nicole Croteau, ¹Heather Lockyer, ³Rob Seitz, ³Frank McMahon, ³Jeremy Spille, ³Andrea Dickey, ³Jordan Jennings, ³Matthew Varga, ³Kimberly McGregor, ³Tyler Nielsen, ³David Hout, ³Brock Schweitzer, ³Douglas Ross, ⁴David Gandara. ¹BC Cancer, Victoria, Canada; ²The University of British Columbia, Vancouver, Canada; ³Oncocyte Corporation, Nashville, TN, USA; ⁴University of California, Davis, Sacramento, CA, USA

Background Immune checkpoint inhibitors (ICI), either as monotherapy or in combination with platinum-based chemotherapy, is standard of care in aNSCLC. However, most patients do not respond to ICI therapy, even when PD-L1 \geq 50% (PD-L1 high). At BC Cancer, only those patients with PD-L1 high are eligible for first line (1L) ICI monotherapy, offering an opportunity to study potential new biomarkers in a relatively unbiased cohort of patients treated by ICI without chemotherapy. DetermaIO (IO score) is a 27-gene RT-qPCR immuno-oncology assay that classifies the tumor immune microenvironment (TIME) as IO+ or IO- and has been previously shown to associate with clinical benefit to ICI therapy in multiple tumor types.

Methods All available FFPE blocks were assembled for ECOG \leq 2 patients treated with at least one cycle of ICI monotherapy in the 1L (required to be PD-L1 \geq 50%) or later line (2L+). DetermaIO was performed using a CAP/CLIA validated RT-qPCR assay for cases where sufficient tissue was available. IO score classification was analyzed for association with PFS and OS in patients treated in the 1L.

Results Considering the entire cohort of 147 patients, DetermaIO was significantly associated with OS (HR=0.68, 95%CI 0.47–0.89, $p=0.042$) and PFS (HR=0.62, 95%CI 0.43–0.88, $p=0.0069$). When examining the cohort by line of therapy, 78 (53%) were treated in 1L with ICI monotherapy and were all PD-L1 high. DetermaIO in this subgroup was significantly associated with PFS (HR=0.55, 95%CI 0.32–0.94, $p=0.028$) and demonstrated meaningful clinical benefit when measuring OS (HR=0.60, 95%CI 0.34–1.06, $p=0.078$). The objective response rate in the 1L subgroup was 53% for IO+ (2CR, 28PR out of 56 patients) and 23% for IO- (5PR out of 22 patients). The net reclassification rate of IO- amongst the PD-L1 high 1L group was 54.5% (12/22, $p<0.01$) for response.

Conclusions Retrospective analysis of outcomes of aNSCLC patients treated 1L with ICI monotherapy found that DetermaIO was significantly associated with PFS and trended towards significance for OS. First-line PD-L1 high patients who were IO- had significantly worse outcomes for PFS than PD-L1 high IO+ patients potentially informing the selection of combination therapy in PD-L1 high patients. These data confirm and expand previous studies of DetermaIO in advanced NSCLC and suggest IO score classification may offer significant incremental information for helping to make complex treatment decisions in aNSCLC.

Ethics Approval This study was approved by the Research Ethics Board (REB) of University of British Columbia (H20–02635). Individual consent for this retrospective analysis and the use of tumor samples for the IO score assay was required for live patients. Consent was waived by the REB for deceased patients.

<http://dx.doi.org/10.1136/jitc-2022-SITC2022.0059>

60 **ENABLEMENT OF SINGLE-CELL SPATIAL INSIGHT ADDRESSING T-CELL AND CAF INVOLVEMENT IN PANCREATIC INVASIVE DUCTAL ADENOCARCINOMA USING AI-BASED DEEP LEARNING IMAGE ANALYSIS**

¹Andrew Quong*, ¹Smriti Kala, ¹Nina Lane, ¹Michelle Macpherson, ²Gourab Chatterjee, ²Devan Fleury, ²Kirsteen Maclean, ³Dan Winkowski, ³Fabian Schneider, ³Jeppe Thagaard, ³James Mansfield. ¹Standard BioTools, South San Francisco, CA, USA; ²Ultivue, Cambridge, MA, USA; ³Visiopharm, Roanoke, VA, USA

Background As the fourth most common cause of death in developed countries, pancreatic cancer remains a deadly disease due to difficulties hindering its early diagnosis, giving way to metastasis of the tumor, resulting in poor prognosis. Pancreatic invasive ductal adenocarcinoma (PDAC) is the most common of pancreatic neoplasms and treatment options are few, with poor overall survival. While it is clear that immunotherapy has revolutionized the treatment of solid tumors by leading to cures where none existed a decade ago, optimally selecting patients as candidates for immunotherapy-chemotherapy combinations remains a critical challenge.

The complexities of the tumor microenvironment (TME) have been implicated in the failure of treatments options. The TME of PDAC is especially rich with multiple interactions between pancreatic epithelial/cancer cells, stromal cells, immune cells, and the extracellular matrix (ECM). PDACs are characterized by a complex ECM of desmoplastic reaction consisting of an extensive and dense fibrotic stroma that surrounds and infiltrates clusters of malignant epithelial cells, together with the loss of basement membrane integrity and an abnormal vasculature. As critical players in the development of PDACs, cancer-associated fibroblasts (CAFs) are the predominant cell type within the tumor stroma; they exhibit considerable heterogeneity that can have both tumor-promoting and tumor-repressing functions. Given that these effects are potentially affected by the tumor-stromal crosstalk and the spatial context of other cell types, a deeper understanding with respect to the different cell types present and their relationship to each other will help uncover the much-needed therapeutic approaches for this disease.

Methods Herein, we demonstrate a spatial phenotyping workflow combining complementary methods that can unravel the complexity of the PDAC TME, in particular the important spatial relationships of different T cells subsets and CAFs. We highlight the utility, robustness, and ability to derive meaningful biological and actionable insights in PDAC samples using the InSituPlex[®] (ISP), Imaging Mass Cytometry[®] (IMC) spatial technologies coupled to Oncotopix Discovery[®] A.I.-based multiplex image analysis.

Results This workflow utilizes a 4-plex whole-slide ISP assay with image analysis to define regions of interest for a comprehensive 40-plex IMC imaging and analysis. Both assays were analyzed using a workflow that includes tissue region and cellular segmentations followed by cellular phenotyping and spatial analyses.

Conclusions Our novel tissue imaging workflow affords the comprehensive and multiparametric *in situ* exploration of the TME at the single cell level, but importantly alludes to a better understanding of PDAC tumor immunology and potential optimization of immunotherapy protocols for this disease.

<http://dx.doi.org/10.1136/jitc-2022-SITC2022.0060>

61

COMBINATION OF NOVEL BIOMARKERS OF COLLAGEN FIBER AND IMMUNE ARCHITECTURE ARE ASSOCIATED WITH CLINICALLY RELEVANT OUTCOMES IN GYNECOLOGICAL CANCERS TREATED WITH IMMUNOTHERAPY

¹Arpit Aggarwal*, ²Sepideh Azarianpour-Esfahani, ³Haojia Li, ²Pingfu Fu, ²Mojgan Mokhtari, ²Stefanie Avril, ³Haider Mahdi, ⁴Anant Madabhushi. ¹Georgia Tech and Emory University, Atlanta, GA, USA; ²Case Western Reserve University, Cleveland, OH, USA; ³University of Pittsburgh, Pittsburgh, PA, USA; ⁴Emory University, Atlanta, GA, USA

Background Qualitative studies suggest collagen fiber organization (CFO) is associated with gynecological cancer (GC) prognosis.^{1, 2} Previous studies have shown the prognostic role of quantitative characterization of architecture of tumor-infiltrating-lymphocytes and their interplay with cancer cells in GC prognosis, known as ArcTIL.³ However, combination of CFO and immune architecture in GC prognosis is not yet studied. In this work, we use computational and machine learning tools to develop quantitative biomarkers combining collagen fiber orientation disorder (CFOD) and ArcTIL features from H&E slides and evaluate its association with progression-free-survival (PFS) in women undergoing surgical resection followed by immunotherapy.

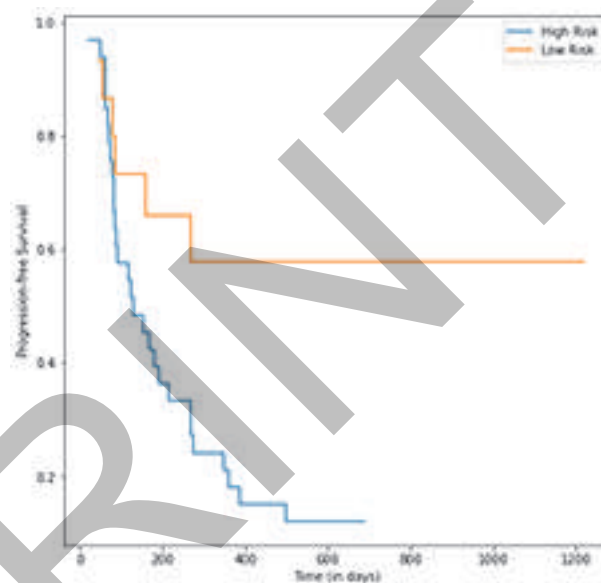
Methods Whole-Slide-Images (WSIs) of H&E slides from surgically-resected ovarian cancer treated with adjuvant chemotherapy were obtained from TCGA used for training (St, n=95) and surgically-resected GC treated with adjuvant immunotherapy were obtained from Cleveland Clinic Foundation used for validation (Sv, n=48). ArcTIL features were derived from cell cluster graphs of nuclei within epithelial nests, surrounding stroma, and invasive tumor front compartments of WSI. The ArcTIL model previously developed by our group,³ was used for this study and prognostic subset having 7 features was selected. For calculating CFOD, WSI was partitioned into array of tumor neighborhoods and then entropy of fiber orientations in stromal regions was quantified within each neighborhood using derivative-of-Gaussian model. The first-order-statistics of CFOD feature maps were extracted for 9 different neighborhood sizes, yielding 27 features. Using these features, three Cox Regression models (CRM+LASSO) were trained that assigned risk of recurrence to each patient in St. The CRM+LASSO model trained using CFOD features selected 9 features, model trained using ArcTIL features selected 4 features and model trained using CFOD+ArcTIL features selected 6 features (4 ArcTIL and 2 CFOD features) for predicting risk scores in St and Sv. For each model, the mean risk score obtained in St was used to stratify patients as low, high-risk in Sv.

Results In Sv (figure 1, table 1), univariate analysis yielded Hazard-Ratio= 2.74, p-value= 0.03 for high-risk CFOD+ArcTIL. Multivariable analysis controlling for prognostic clinical variables, FIGO Stage (I, II, III, IV) and Tumor Grade (1, 2, 3), showed CFOD+ArcTIL (Hazard-Ratio= 2.84, p-value= 0.02) was independently associated with PFS.

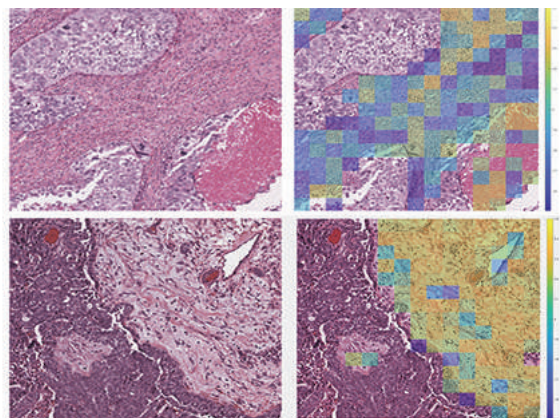
Conclusions Our results found that CFO is more ordered in high-risk patients (figure 2) and evenly distributed, smaller clusters in ArcTIL-defined low-risk patients. Independent multi-site validation should allow for deployment of CFOD+ArcTIL as a prognostic decision support tool for management of GC patients treated with immunotherapy.

REFERENCES

1. Alkmin S, Brodziski R, Simon H. Role of Collagen Fiber Morphology on Ovarian Cancer Cell Migration Using Image-Based Models of the Extracellular Matrix. *Cancers (Basel)*. 2020;**12**(6):1390
2. Ricciardelli C, Rodgers R.J. Extracellular matrix of ovarian tumors. *Semin. Reprod. Med.* 2006;**24**:270–282
3. Azarianpour S, Corredor G, Bera K. Computational image features of immune architecture is associated with clinical benefit and survival in gynecological cancers across treatment modalities. *Journal for ImmunoTherapy of Cancer*. 2022;**10**: e003833



Abstract 61 Figure 1 Kaplan Meier Curve of CFOD+ArcTIL model, validated on 48 patients of Cleveland Clinic Foundation cohort treated with immunotherapy (p-value= 0.03, Hazard-Ratio= 2.74, 95% Confidence Interval= 1.13–6.6)



Abstract 61 Figure 2 Example 3000x3000 tile of High-risk patient (top) and Low-risk patient (bottom) predicted by the CFOD+ArcTIL model. We observe CFO to be more ordered for high-risk patients as compared to low-risk patients (as seen in the right sub-figures which is the heatmap representing the disorder in CFO)

Abstracts

Abstract 61 Table 1 Performance of CFOD, ArcTIL and CFOD +ArcTIL models, validated on 48 patients of Cleveland Clinic Foundation cohort treated with immunotherapy (Sv)

Features	C-Index	p-value	Hazard Ratio (95% Confidence Interval)
CFOD	0.54	0.38	1.35 (0.69-2.6)
ArcTIL	0.59	0.13	1.79 (0.84-3.8)
CFOD + ArcTIL	0.6	0.03	2.74 (1.13-6.6)

<http://dx.doi.org/10.1136/jitc-2022-SITC2022.0061>

62

RESISTANCE TO FRAMESHIFT NEOANTIGEN-SPECIFIC T CELL SURVEILLANCE IN MICROSATELLITE UNSTABLE CANCERS

Matthew Brown*, Leandra Velazquez, Mona Saleh, Alexandros Polydorides, Aimee Lucas, Cansu Cimen Bozkus, Robert Samstein, Nina Bhardwaj. *Icahn School of Medicine at Mount Sinai, New York, NY, USA*

Background Patients with Lynch syndrome (LS), characterized by germline inactivation of one allele of the mismatch repair (MMR) genes, have an increased risk (up to 80%) of developing cancers with high microsatellite instability (MSI-H).¹ MSI-H tumors account for 15–30% of all colon, endometrial, and gastric cancers.² Due to unrepaired frameshift (fs) mutations, these cancers possess a high tumor mutational burden which has enabled microsatellite instability to emerge as a biomarker of immune checkpoint blockade (ICB) response. However, there is still a significant population of MSI-H patients unresponsive to ICB treatment.^{3,4} Therefore, novel strategies to prevent LS-associated tumor development and predict ICB resistance are urgently needed. T cell surveillance in LS is evidenced by (i) elevated fs-loads in MMR-deficient (MMRd) nonneoplastic tissue⁵ and (ii) a correlation between increased T cell infiltration into normal mucosa of LS patients and delayed onset of colorectal cancer.⁶ We previously characterized unique immunogenic fs-peptides shared in MSI-H cancers⁷ and identified T cell receptors (TCRs) specific to MSI-H-associated fs-peptides. Utilizing TCR sequencing, we demonstrated that fs-specific T cells were present in the primary tumor, draining lymph nodes, and metastases of an LS patient. However, tumor growth in the presence of these fs-specific T cell clones suggests suboptimal T cell surveillance.

Methods Our hypothesis is that MMRd precancerous and malignant lesions expressing fs-neoantigens escape immune surveillance due to suppression of T cell infiltration and activity. We investigated whether this is the result of immunosuppressive activity from innate immune cell populations and/or T cell dysfunction. Using normal, precancerous, and tumor tissue collected from our cohort of LS and sporadic MSI-H cancer patients we are leveraging whole-exome sequencing, spatial transcriptomics, and multiplexed immunohistochemistry.

Results This has allowed us to begin to define the spatiotemporal landscape of fs-neoantigen expression, innate immune cell localization, and T cell dysfunction in the course of MSI-H tumor development to explain how MMRd lesions escape T cell surveillance. Additionally, our analysis of MSI-H tumors from The Cancer Genome Atlas (TCGA) with high fs-neoantigen loads but low cytotoxic T lymphocyte (CTL) signatures (assessing granzyme and perforin expression) have revealed lower immune-stimulatory macrophage and higher activated mast cell-related gene signatures. We have also observed high frequencies of exhausted (PD-1+TIM-3+) tumor infiltrating lymphocytes in advanced MSI-H tumors assessed by flow cytometry.

Conclusions This work supports the development of fs-neoantigen-based vaccination/immunomodulation strategies to prevent LS-associated tumor development and identifies potential ICB resistance biomarkers for advanced MSI-H tumors.

REFERENCES

1. Roudko V, Cimen Bozkus C, Greenbaum B, Lucas A, Samstein R, Bhardwaj N, Lynch Syndrome and MSI-H Cancers: From Mechanisms to 'Off-The-Shelf' Cancer Vaccines. *Frontiers in Immunology*. 2021;**12**:3946.
2. Bonneville R, Krook MA, Kautto EA, Miya J, Wing MR, Chen HZ, et al., Landscape of Microsatellite Instability Across 39 Cancer Types. *JCO Precis Oncol*. 2017.

3. Bellone S, Roque DM, Siegel ER, Buza N, Hui P, Bonazzoli E, et al., A phase 2 evaluation of pembrolizumab for recurrent Lynch-like versus sporadic endometrial cancers with microsatellite instability. *Cancer*. 2021.
4. Le DT, Uram JN, Wang H, Bartlett BR, Kemberling H, Eyring AD, et al. PD-1 Blockade in Tumors with Mismatch-Repair Deficiency. *N Engl J Med*. 2015;**372**:2509–20.
5. Lee BCH, Robinson PS, Coorens THH, Yan HHN, Olafsson S, Lee-Six H, et al., Mutational landscape of normal epithelial cells in Lynch Syndrome patients. *Nat Commun*. 2022;**13**:2710.
6. Bohaumilitzky L, Kluck K, Hüneburg R, Gallon R, Nattermann J, Kirchner M, et al., The Different Immune Profiles of Normal Colonic Mucosa in Cancer-Free Lynch Syndrome Carriers and Lynch Syndrome Colorectal Cancer Patients. *Gastroenterology*. 2022;**162**:907–19.
7. Roudko V, Bozkus CC, Orfanelli T, McClain CB, Carr C, O'Donnell T, et al., Shared Immunogenic Poly-Epitope Frameshift Mutations in Microsatellite Unstable Tumors. *Cell*. 2020;**183**:1634–49.

Ethics Approval The study was approved by the Icahn School of Medicine at Mount Sinai Institutional Review Board, approval numbers: STUDY-21–01317 and STUDY-19–00936-CR001. Informed consent was given by all participants in this research study.

<http://dx.doi.org/10.1136/jitc-2022-SITC2022.0062>

EPISCAN: A SYNTHETIC BIOLOGY PLATFORM FOR TARGETED IMMUNOPEPTIDOMICS

¹Peter Bruno*, ²Richard Timms, ³Nouran Abdelfattah, ⁴Yumei Leng, ⁴Felipe Lelis, ⁴Duane Wesemann, ⁵Xu Yu, ¹Stephen Elledge. ¹Department of Genetics, Harvard Medical School and Division of Genetics, Brigham and Women's Hospital, Boston, MA, USA, and Howard Hughes Medical Institute, Chevy Chase, MD, USA; ²University of Cambridge, Cambridge, UK; ³Harvard Medical School, Boston, MA, USA; ⁴Brigham and Women's Hospital, Boston, MA, USA; ⁵Ragon Institute of MGH, MIT and Harvard, Boston, MA, USA

Background Identification of CD8⁺ T-cell epitopes is critical for the development of immunotherapeutics. Existing methods for empirical determination of peptide binding are time-intensive, expensive and highly specialized. Mass spectrometry, the predominant high-throughput approach for MHC-I ligand discovery, is unable to easily interrogate defined subsets of proteins. Thus, we sought a high-throughput, accessible method for the identification of MHC-I ligands derived from user chosen, synthetically encoded sources of peptides. Here we present EpiScan, a programmable genetic strategy to identify MHC-I ligands amongst predetermined starting pools comprising >100,000 peptides.

Methods To accomplish this, we used CRISPR-Cas9 to create 'EpiScan cells' that lack both endogenous MHC-I and short peptides in ER. Then, separate lentiviral introduction of an MHC-I allele and a single exogenous short peptide into the ER restores cell surface MHC-I levels according to the affinity of the peptide to the chosen MHC-I allele. We exploited the programmability of EpiScan to screen 12 different MHC-I alleles with large peptide libraries including the entire SARS-CoV-2 proteome.

Results These screens uncovered an unappreciated role for cysteine that increases the number of predicted ligands by 12–21%, revealed affinity hierarchies by analysis of biased-anchor peptide libraries, and identified conserved, high-affinity, T-cell reactive SARS-CoV-2 epitopes. Using these data, we generated and iteratively refined peptide binding predictions to create EpiScan Predictor, or ESP. ESP performed comparably to other state-of-the-art MHC-I peptide binding prediction algorithms while not suffering from underrepresentation of cysteine-containing peptides. Overall, the new specificities identified by EpiScan and ESP increase the number of peptides predicted to bind MHCs by over 15% on average. This significantly expands the potential human epitope landscape, facilitating epitope discovery efforts and the design of immunotherapeutics.

Conclusions Our work significantly expands the potential human epitope landscape, facilitating epitope discovery efforts and the design of immunotherapeutics.

Ethics Approval Peripheral blood was provided by collaborators from Ragon Institute of MGH that were PCR-confirmed COVID-19 cases. All study participants provided verbal and/or written informed consent. Participation in these studies was voluntary and the study protocols have been approved by the Partners Institutional Review Board.

<http://dx.doi.org/10.1136/jitc-2022-SITC2022.0063>

64

SPATIAL WHOLE TRANSCRIPTOME PROFILING OF THE TUMOR MICROENVIRONMENT IN ARCHIVED AND FRESHLY-MOUNTED FFPE TISSUES

Jun Chiang*, Augusto Tentori, Hardeep Singh, Anuj Patel, Han Lu, Alex Hermes. *xgenomics, Pleasanton, CA, USA*

Background The tumor microenvironment (TME) is composed of highly heterogeneous cell types that dynamically interact with each other. The constant interaction between a tumor and its microenvironment plays a critical role in how the cancer develops, progresses, and responds to therapies. Traditional tissue-based studies of the TME can be limited to a small number of target analytes, which can limit biological insights. In this work, we used the Visium CytAssist instrument and Visium Spatial Solutions from 10x Genomics which enable whole transcriptome gene expression and immunofluorescence-based protein expression profiling from archival and freshly preserved FFPE cancer tissues. Our data provided a more comprehensive understanding of cellular behavior in and around tumors yielding new insights into disease progression and therapeutic response.

Methods Tumor FFPE tissues (breast, liver, lung, and ovarian cancer) were spatially profiled using the Visium CytAssist instrument and Visium Spatial Solutions. Tissues were mounted on glass slides, H&E or IF stained, and imaged to select the target region for whole transcriptome analysis. Following decrosslinking and probe hybridization, the samples were prepared for probe transfer to spatially barcoded Visium slides with 6.5 x 6.5 or 11 x 11 (mm x mm) capture areas. The captured probes were used in a downstream genomics workflow to generate sequencing-ready libraries.

Results We applied this method to measure gene expression within the TME of archived human lung and ovarian cancer FFPE samples. Normalized gene expression levels superimposed on the H&E images demonstrated similar clustering patterns delineating the tumor and stromal region. In the lung cancer sample, canonical gene makers, *TP63* and *KRT5*, confirmed the general phenotype of non-small cell carcinoma. In addition, other keratin and mucin genes revealed intra-tumor heterogeneity. In the same lung cancer sample, immune response genes were expressed in the stromal region, adjacent to the tumor bed, identifying the presence of immune cell subsets such as activated T, B, and regulatory dendritic cells. Freshly prepared breast and liver cancer samples were screened with fluorescently labeled antibodies in addition to transcriptomic profiling. In particular, PCNA and Vimentin showed the precision and accuracy of probe transfer using the Visium for FFPE spatial solution.

Conclusions The data highlights that Visium CytAssist can retrieve transcriptome information from archived and freshly prepared FFPE sections in a spatial context. Visium CytAssist provides a more comprehensive understanding of clinical tissue samples and provides novel insights into architectural and cellular heterogeneity across multiple diseases.

<http://dx.doi.org/10.1136/jitc-2022-SITC2022.0064>

SURFACE NANOTOPOGRAPHY AND CELL SHAPE MODULATE TUMOR CELL SUSCEPTIBILITY TO NK CELL CYTOTOXICITY

¹Jeehun Park*, ¹Junsang Doh, ²Yongbum Cho. ¹Seoul National University, Seoul, Korea, Republic of, ²Pohang University of Science and Engineer, Pohang, Kosovo, Republic of

Background Natural killer (NK) cells are innate cytotoxic lymphocytes exerting cytotoxicity against virally infected cells and tumor cells.¹ NK cell cytotoxicity is primarily determined by biochemical signals received by ligands expressed on target cell surfaces. In addition to the biochemical signals, NK cell cytotoxicity could be regulated by biophysical environments of tumor cells such as nanoscale surface topography typically existing on extracellular matrixes (ECMs) or cell morphology determined by ECM or cell density. Matrixes.^{2, 3} Engineered surfaces, including soft substrates with various rigidities, nanostructured surfaces, and micropatterned surfaces, may serve as alternative tools to further dissecting the roles of biophysical cues in tumor microenvironment in NK cell cytotoxicity.

Methods To test this possibility, we used engineered surfaces that allowed control of cell shape and surface nanotopography to investigate how NK cell cytotoxicity is regulated by tumor cell shape and surface nanotopography.^{4, 5} Tumor cells were plated on flat vs. nanogrooved surfaces, or micropatterned into circular vs. elliptical geometries, and the effects of surface topography and tumor cell morphology on NK cell cytotoxicity were investigated. Cell morphology and cytotoxicity of NK cells were analyzed by live fluorescence imaging. For the filamentous actin intensity measurement, patterned cells were fixed and permeabilized and stained with fluorescence labeled phalloidin.

Results NK cells exhibited significantly higher cytotoxicity against tumor cells on nanogrooved surfaces than those on flat surfaces. However, it was not clear whether nanotopography underlying tumor cells itself was a major factor for enhanced NK cell cytotoxicity or not, as cells cultured on nanogrooved surfaces typically exhibit elongated morphologies. To directly test whether elongated morphology of tumor cells is sufficient for enhanced NK cell cytotoxicity, we manipulated tumor cell shape to circular and elliptical. NK cell exhibited significantly higher cytotoxicity against tumor cells on tumor cells in elliptical patterns than tumor cells in circular patterns. Both nanogrooved surfaces and elongated morphology of tumor cells induced stress fiber formation, which in turn increase cytoskeletal tension. Thus, we checked correlation between stress fiber formation and cytotoxicity, and found positive correlation between them.

Conclusions These results indicate that tumor cells in elliptical micropatterns or on nanogrooved surfaces are more susceptible for NK cell-mediated cytotoxicity due to increased cellular tension by stress fiber formation. These results suggest that biophysical microenvironments surround tumor cells influence NK cell cytotoxicity against tumor cells by cytoskeletal tension regulation.

REFERENCES

1. Miller J, Lanier L, Natural Killer Cells in Cancer Immunotherapy, *Annu. Rev. Cancer Biol.* 2019; **3**:77–103.
2. Anderson N, Simon M, The tumor microenvironment, *Curr. Biol.* 2020;**30**:R921–R925.
3. Winkler J, Abisoye-Ogunniyan A, Metcalf K, Werb Z, Concepts of extracellular matrix remodelling in tumour progression and metastasis, *Nat. Comm.* 2020; **11**:5120.

4. Kweon SH, Song K, Park HJ, Choi J-C, Doh J, Dynamic Micropatterning of Cells on Nanostructured Surfaces Using a Cell-friendly Photoresist, *ACS Appl. Mater. Interfaces.* 2016; **8**:4266–4274.
5. Kim M, Choi J-C, Jung H-R, Katz J, Kim M-G, Doh J, Addressable micropatterning of multiple proteins and cells by microscope projection photolithography based on a protein friendly photoresist, *Langmuir.* 2010; **2**:12112–12118.

<http://dx.doi.org/10.1136/jitc-2022-SITC2022.0066>

67 **GERMLINE MUTATIONS IN DNA DAMAGE RESPONSE AND REPAIR GENES ARE ASSOCIATED WITH INCREASED CLINICAL BENEFIT FROM IMMUNE CHECKPOINT INHIBITORS**

Michael Dennis*, Sophia Bylsma, Lisa Madlensky, Sandip Patel. *University of California San Diego, La Jolla, CA, USA*

Background Impaired DNA damage response (DDR) can impact the efficacy of immune checkpoint inhibitors (ICIs). Defects in the DDR pathway can also lead to heightened immune activation. The purpose of this study was to determine if pathogenic germline mutations in DDR pathways would increase the efficacy or toxicity of ICIs.

Methods We performed a single-institution retrospective analysis of all patients for whom germline DNA testing was available and who were treated with ICIs between January 1st, 2014 and September 1st, 2022. Patients without measurable disease were excluded. The best response to therapy and the incidence of immune-related adverse events (irAEs) were compared between patients that had pathogenic germline mutations in DDR genes (DDR+) and those who did not (DDR-). Clinical benefit (CB) was defined as stable disease, partial response, or complete response as determined by the treating physician. irAEs were graded according to the Common Terminology Criteria for Adverse Events v5.0.

Results We identified 152 patients that met the inclusion criteria. Forty-two patients were DDR+, of which 25 had mutations in homologous recombination genes (HRD), and 11 had mutations in mismatch repair genes (dMMR). DDR+ patients were more likely to derive CB than DDR- patients in univariate and multivariate analysis (table 1) (81% vs 53%, unadjusted odds ratio [OR] = 3.81; 95% CI, 1.59 to 9.11; adjusted OR 3.58; 95% CI, 1.29 to 9.93). Adjustments were made for the line of therapy, tumor mutational burden, and history of tyrosine kinase inhibitor (all associated with CB in univariate analysis, $p \leq 0.05$). Similar results were observed in HRD patients (76% HRD vs 53% DDR-, adjusted OR = 3.16; 95% CI, 1.00 to 9.94). dMMR patients were more likely to receive CB from ICIs in the univariate analysis (91% dMMR vs 53% DDR-, OR = 8.96; 95% CI, 1.10 to 72.89), but this did not reach statistical significance in multivariate analysis (OR = 4.99; 95% CI, 0.49 to 51.17). When dMMR patients were removed from the DDR+ group (DDR+MMR-), there remained a significant difference in CB from ICIs (77% DDR+MMR- vs 53% DDR-, adjusted OR 3.35, 95% CI 1.13 to 9.95). There were no significant differences in the rate of irAEs for DDR+ patients regardless of the subgroup.

Conclusions Patients with germline pathogenic DDR mutations are more likely to derive CB from ICIs without added immune toxicity. The fact that MMR intact germline DDR mutations are associated with significant CB is a novel finding.

Abstract 67 Table 1 Association of germline pathogenic mutations and clinical benefit

			Unadjusted		Adjusted*	
	No CB	CB ^b	OR (95% CI)	p-value	OR (95% CI)	p-value
DDR- (n=91)	43 (47)	48 (53)	-	-	-	-
DDR+ (n=42)	8 (19)	34 (81)	3.81 (1.59-9.11)	<0.01	3.58 (1.29-9.93)	0.01
HRD (n=25)	6 (24)	19 (76)	2.84 (1.04-7.76)	0.04	3.16 (1.00-9.94)	0.049
dMMR (n=11)	1 (9)	10 (91)	8.96 (1.10-72.89)	0.04	4.99 (0.49-51.17)	0.18
DDR+MMR- (n=31)	7 (23)	24 (77)	3.07 (1.20-7.84)	0.02	3.35 (1.13-9.95)	0.03

*adjusted for metastatic disease, line of therapy, TMB status, and history of tyrosine kinase inhibitor
^bClinical benefit data was not available for 19 patients
 CB, clinical benefit; OR, odds ratio; CI, confidence interval; DDR, DNA damage response; HRD, homologous recombination deficient; dMMR, mismatch repair deficient; (*) indicates the presence of a pathogenic mutation

<http://dx.doi.org/10.1136/jitc-2022-SITC2022.0067>

69 A HIGH CONTENT SCREENING PLATFORM FOR TESTING IMMUNOTHERAPIES IN PATIENT-DERIVED ORGANOIDS

Gera Goverse*, Saskia de Man, Tomas Veenendaal, Nataliia Beztsinna, Daniel Okkes, Ashgard Weterings, Kuan Yan, Leo Price. *Crown Bioscience, Leiden, Netherlands*

Background Patient-derived organoids (PDOs) are advanced 3D cell culture models, which have high predictive value of patient drug responses in the clinic. In this study a high throughput screening platform is presented, which allows testing of cancer immunotherapies in co-cultures of human organoids with immune cells. Incorporating diverse cellular players from the immune system and stromal compartment, such as cancer associated fibroblasts (CAFs), allows the reconstitution of complex cellular interactions that occur in the tumor micro-environment (TME). Our proprietary, automated high content imaging (HCI)-based analysis provides visualization and quantification of immune cell-mediated effects in this complex physiological relevant 3D screening platform. Functional readouts such as migration of immune cells towards organoids, infiltration into the organoids and their killing are obtained, allowing for a better understanding of the immunomodulatory profile of immuno-oncology drugs.

Methods PDOs, obtained from HUB Organoid Technology, generated from different cancer indications among colon and ovarian were cultured in protein hydrogel. Partially HLA-matched immune cells isolated from different healthy PBMC donors were labelled and added (naïve or activated) to the 3D culture after incorporation of different suppressive populations, including pre-labelled CAFs and myeloid cells. High content microscopy combined with morphometric image analysis software was used to quantify the capacity of immune cells to infiltrate and subsequently kill the organoids.

Results Differences in the sensitivity and kinetics of organoid models from the same indication and from different indications towards the killing by immune cells was profiled. Pre-activation or reactivation of immune cells within the 3D co-cultures increased the sensitivity towards killing of the organoids, while incorporation of suppressive cellular players within the TME could reduce immune cell mediated killing effects. Moreover, testing of different immune cell donors, although showing slight donor-to-donor variability, indicated an overall consistency of organoid sensitivity towards immune cell-mediated killing effects. Additionally, quantitative readouts strictly dependent on a 3D environment such as immune cell migration and infiltration could be measured and analyzed upon treatment with different immune modulators such as T cell engagers.

Conclusions HCI of complex *in vitro* 3D co-cultured organoids enables rapid, reproducible, physiologically relevant and spatial readouts for testing various cancer immunotherapies within different cancer indications. Visualization and quantification of these complex cellular interactions within the TME via our high content screening platform is a powerful tool for immunotherapeutic drug development in patient-relevant models to select the most promising candidates, better understand their mechanism of action, and ultimately stratify patient cohorts for clinical success.

<http://dx.doi.org/10.1136/jitc-2022-SITC2022.0069>

70

WHOLE GENOME CRISPR-CAS9 SCREENS IN A CANCER CELL LINE PANEL CO-CULTURED WITH ANTIGEN-SPECIFIC CYTOTOXIC CD8 T CELLS ARE A POWERFUL ENGINE FOR IMMUNO-ONCOLOGY DRUG TARGET DISCOVERY

Serge Gueroussov*, Chengyin Min, Alan Huang, Samuel Meier, Jessica Finkler, Lei Ji, Ashley Choi, Tenzing Khendru, Disha Subramanya, Shangtao Liu, Binzhang Shen, Teng Teng, Xuewen Pan, Yi Yu. *Tango Therapeutics, Cambridge, MA, USA*

Background Cytotoxic T lymphocytes (CTLs) are a key driver of the anti-tumor immune response. Understanding the molecular mechanisms mediating this process can reveal therapeutic targets whose pharmacological inhibition can increase responses to immunotherapy. In recent years, forward genetic screens with CRISPR-Cas9 have been successfully applied to study the interaction between tumor cells and CTLs *in vitro*. Here, we extend this approach to a broad panel of human cancer cell lines and define methods for prioritization and validation of immuno-oncology therapeutic targets.

Methods A panel of seven HLA-A*02 cancer cell lines were prioritized to span multiple cancer lineages. Tumor cells were infected with a whole-genome CRISPR-Cas9 library and co-cultured with primary human CD8+ T cells expressing the NYESO1 HLA-A*02-restricted T cell receptor. Next-generation sequencing and statistical analysis were used to define the top genes that affected tumor cell killing by CTLs. We validated the top hits from the screen *in vitro* and developed an adoptive cell transfer model to validate the sensitizing effects *in vivo*.

Results Comparison of screen hits uncovered both known and novel pathways that sensitize tumor cell lines to CTL killing, including surface checkpoint molecules, epigenetic regulators, genes that control cytokine response, autophagy, post-transcriptional regulation, and cell surface glycosylation. We prioritized genes for validation based on effect size, druggability, and TCGA correlation between target expression and an immune-deficient tumor microenvironment. We showcase our approach using the known immune regulator, PTPN2. PTPN2 knockout in tumor cells sensitized them to CTL-mediated killing in co-culture assay *in vitro* and adoptive cell transfer model *in vivo*.

Conclusions Our cancer cell and T cell co-culture CRISPR screening platform revealed multiple known as well as novel genes to comprehensively characterize the mechanisms regulating tumor cell killing by CTLs, providing a rich resource of therapeutic targets to advance into drug discovery.

<http://dx.doi.org/10.1136/jitc-2022-SITC2022.0070>

Abstracts

71

HIGH SCORING PRECISION DEMONSTRATED IN MULTIPLE TUMOR INDICATIONS STAINED WITH PD-L1 IHC 22C3 PHARMDX USED IN CONJUNCTION WITH COMBINED POSITIVE SCORE

Julia Hand*, Francisco Ponce, Stephanie Hund, Lindsay Peltz, Micki Adams, Deanna Moquin, Megan Kalpakoff, Siena Tabuena-Frolli, Jay Milo, Angeliki Apostolaki, Karina Kulangara. *Agilent Technologies, Carpinteria, CA, USA*

Background PD-L1 22C3 IHC pharmDx (SK006) is a qualitative immunohistochemical (IHC) assay using anti-PD-L1, Clone 22C3 to detect PD-L1 in formalin-fixed, paraffin-embedded (FFPE) tumor tissues using the Autostainer Link 48. PD-L1 expression is determined by Combined Positive Score (CPS), which is the number of PD-L1 staining cells (tumor cells, lymphocytes, macrophages) divided by the total number of viable tumor cells, multiplied by 100.¹ SK006 has been analytically validated using CPS across multiple tumor indications and diagnostic cutoffs and is used as an aid in identifying patients for treatment with KEYTRUDA®. A previous publication presents the analytical performance of the following indications: gastric or gastroesophageal junction (GC/GEJ) adenocarcinoma (CPS ≥ 1), cervical cancer (CPS ≥ 1), head and neck squamous cell carcinoma (HNSCC) (CPS ≥ 1), esophageal cancer (EC/ESCC) (CPS ≥ 10), and triple-negative breast cancer (TNBC) (CPS ≥ 10).² This study evaluated the analytical performance of the SK006 assay for an additional five individual tumor indications (ovarian carcinoma (OC), prostate cancer (PC), colorectal carcinoma (CRC), renal cell carcinoma (RCC), biliary tract adeno cancer (BTAC)) and a group of 11 rare tumor indications in a basket trial (BT).³ Two CPS cutoffs were evaluated: CPS ≥ 1 (OC, PC, CRC, RCC, BTAC and BT [3]) and CPS ≥ 10 (OC, CRC and BTAC).

Methods Combined precision measured inter-instrument, -operator, -day and -lot variation. Intra-run measured repeatability and Inter/Intra-Observer measured scoring reproducibility. Negative percent agreement (NPA), positive percent agreement (PPA), and overall agreement (OA) with two-sided 95% bootstrap confidence intervals (CIs) were used for data analysis, based on the PD-L1 binary status at the evaluated cutoffs. Each tumor indication and cutoff pair was analyzed individually for Combined Precision, and Intra-Run and Inter/Intra Observer reproducibility. Meta-analysis was also performed on pooled data from all indications per study and cutoff.

Results Analyses for each indication/cutoff pair showed NPA, PPA, OA point estimates (PE) of ≥89.6% and CI lower bounds (CILB) of ≥81.8%. Meta-analyses for all indications and cutoffs showed NPA, PPA, OA PE of ≥92.5% and CILB of ≥89.3%. Table 1 summarizes the PD-L1 binary status results for all indications and the pooled meta-analysis.

Conclusions PD-L1 IHC 22C3 pharmDx used in conjunction with CPS provides high precision for evaluating PD-L1 expression across multiple tumor indications and cutoffs under standard, day-to-day laboratory testing conditions.

Abstract 71 Table 1 PD-L1 binary status results for all indications and results of meta-analysis pooled data

Table 1: PD-L1 binary status results for all indications and results of meta-analysis pooled data.

Cutoff	Study	Indication	NPA ¹	PPA ¹	OA ¹
1	Combined Precision	Basket Trial	97.4% (93.5%, 100%)	97.4% (93.5%, 100%)	97.4% (94.8%, 99.3%)
		BTAC	98.0% (94.1%, 100%)	100% (92.1%, 100%)	98.9% (96.8%, 100%)
		CRC	98.3% (94.8%, 100%)	96.4% (91.2%, 100%)	97.4% (94.0%, 100%)
		OC	98.2% (94.7%, 100%)	100% (93.6%, 100%)	99.1% (97.3%, 100%)
		PC	96.0% (90.1%, 100%)	90.9% (81.8%, 100%)	94.0% (89.2%, 98.8%)
		RCC	95.4% (90.9%, 100%)	97.6% (92.8%, 100%)	96.2% (92.5%, 99.0%)
	Intra-Run	Basket Trial	100% (92.8%, 100%)	98.5% (95.7%, 100%)	99.1% (97.5%, 100%)
		BTAC	100% (95.4%, 100%)	100% (95.4%, 100%)	100% (97.6%, 100%)
		CRC	100% (96.0%, 100%)	100% (96.3%, 100%)	100% (98.0%, 100%)
		OC	100% (96.1%, 100%)	100% (96.1%, 100%)	100% (98.0%, 100%)
		PC	97.3% (93.3%, 100%)	96.9% (92.3%, 100%)	97.1% (94.2%, 99.3%)
		RCC	98.8% (96.4%, 100%)	100% (96.3%, 100%)	99.4% (98.3%, 100%)
	Inter-Observer	Basket Trial	99.6% (98.8%, 100%)	95.6% (91.9%, 98.4%)	97.6% (95.8%, 99.2%)
		BTAC	99.5% (98.5%, 100%)	98.6% (96.6%, 100%)	99.0% (97.4%, 100%)
		CRC	95.4% (90.9%, 99.3%)	99.6% (98.9%, 100%)	97.5% (95.3%, 99.4%)
		OC	100% (98.5%, 100%)	97.1% (93.2%, 100%)	98.5% (96.5%, 100%)
		PC	95.0% (90.9%, 98.3%)	93.9% (90.2%, 97.3%)	94.4% (91.6%, 96.8%)
		RCC	96.0% (91.7%, 99.6%)	94.6% (90.9%, 97.9%)	95.3% (92.5%, 97.7%)
	Intra-Observer	Basket Trial	98.8% (97.5%, 100%)	98.3% (96.7%, 99.5%)	98.6% (97.6%, 99.4%)
		BTAC	99.5% (98.5%, 100%)	100% (98.2%, 100%)	99.7% (99.3%, 100%)
		CRC	97.8% (95.6%, 99.3%)	98.9% (97.7%, 100%)	98.4% (97.0%, 99.6%)
		OC	100% (98.6%, 100%)	99.2% (98.1%, 100%)	99.6% (99.0%, 100%)
		PC	97.1% (94.0%, 99.2%)	95.6% (93.0%, 97.9%)	96.2% (94.4%, 97.9%)
		RCC	97.8% (96.2%, 99.2%)	97.2% (94.9%, 99.0%)	97.5% (96.0%, 98.8%)
10	Combined Precision	BTAC	100% (92.9%, 100%)	100% (92.1%, 100%)	100% (96.1%, 100%)
		CRC	100% (94.8%, 100%)	100% (92.5%, 100%)	100% (96.6%, 100%)
		OC	95.8% (92.0%, 100%)	94.1% (88.2%, 100%)	95.6% (92.1%, 99.1%)
	Intra-Run	BTAC	97.1% (91.4%, 100%)	100% (95.9%, 100%)	98.7% (96.2%, 100%)
		CRC	99.1% (97.3%, 100%)	100% (95.6%, 100%)	99.4% (98.4%, 100%)
		OC	100% (96.4%, 100%)	97.6% (92.9%, 100%)	98.9% (96.8%, 100%)
	Inter-Observer	BTAC	96.1% (92.3%, 99.0%)	96.8% (93.3%, 99.5%)	96.5% (93.9%, 98.6%)
		CRC	91.3% (85.4%, 95.5%)	89.5% (84.0%, 94.4%)	90.4% (86.4%, 94.0%)
		OC	91.2% (85.9%, 95.9%)	93.7% (88.8%, 97.5%)	92.1% (88.4%, 95.1%)
	Intra-Observer	BTAC	98.5% (96.0%, 100%)	96.5% (93.9%, 98.7%)	97.4% (95.6%, 99.0%)
		CRC	94.8% (92.0%, 97.4%)	95.0% (92.3%, 97.4%)	94.9% (92.8%, 96.8%)
		OC	97.1% (95.0%, 98.8%)	94.2% (91.0%, 97.2%)	95.9% (93.9%, 97.7%)
1 (Meta-analysis)	Combined Precision	BTAC, CRC, OC, PC, RCC	97.2% (95.5%, 98.6%)	97.4% (95.5%, 99.0%)	97.3% (96.1%, 98.3%)
10 (Meta-analysis)	Intra-Run	Basket Trial	99.3% (98.5%, 100%)	99.4% (98.6%, 100%)	99.3% (98.8%, 99.7%)
		BTAC, CRC, OC, PC, RCC			
		BTAC, CRC, OC, PC, RCC	97.5% (96.1%, 98.7%)	96.5% (95.1%, 97.7%)	97.0% (96.0%, 97.8%)
10 (Meta-analysis)	Inter-Observer	Basket Trial	98.5% (97.8%, 99.1%)	98.1% (97.4%, 98.8%)	98.3% (97.7%, 98.8%)
		BTAC, CRC, OC, PC, RCC			
		BTAC, CRC, OC	98.5% (97.2%, 100%)	97.5% (95.1%, 100%)	98.4% (96.9%, 99.6%)
10 (Meta-analysis)	Intra-Run	BTAC, CRC, OC	98.9% (97.2%, 100%)	99.2% (97.6%, 100%)	99.0% (97.8%, 100%)
		BTAC, CRC, OC	92.4% (89.3%, 95.3%)	93.0% (90.1%, 95.6%)	92.7% (90.6%, 94.6%)
		BTAC, CRC, OC	96.6% (95.2%, 97.9%)	95.2% (93.5%, 96.8%)	96.0% (94.8%, 97.1%)

1. Percent agreement [lower-bound, upper-bound]

REFERENCES

- [1] CPS = #PD-L1 staining cells (tumor cells, lymphocytes, macrophages) x 100 / Total # viable tumor cells
- [2] Ponce F, Hund S, Peltz L, et al 60 Use of Combined Positive Score (CPS) with the companion diagnostic PD-L1 IHC 22C3 pharmDx provides precise evaluation of PD-L1 expression across multiple tumor indications and cutoffs. *Journal for ImmunoTherapy of Cancer* 2021;9: 10.1136/jitc-2021-SITC2021.060
- [3] Basket trial consists of 11 rare tumor indications: anal canal squamous cell carcinoma, biliary adenocarcinoma, cervical squamous cell carcinoma, endometrial carcinoma, mesothelioma, neuroendocrine carcinoma, salivary gland squamous cell carcinoma, Salivary gland adenocarcinoma, small cell lung carcinoma, thyroid adenocarcinoma, vulvar squamous cell carcinoma.

<http://dx.doi.org/10.1136/jitc-2022-SITC2022.0071>

72 **INTRAVITAL MULTIPHOTON AUTOFLUORESCENCE IMAGING IS SENSITIVE TO CHANGES IN CD8 T CELL AND TUMOR CELL METABOLISM DURING IMMUNOTHERAPY IN A MURINE MELANOMA MODEL**

^{1,2}Alexa Heaton*, ²Anna Hoefges, ¹Peter Rehani, ²Nathaniel Burkard, ²Arika Feils, ²Dan Spiegelman, ²Noah Tsarovsky, ²Alina Hampton, ²Amy Erbe, ²Alexander Rakhmievich, ²Paul Sondel, ¹Melissa Skala. ¹Morgridge Institute for Research and University of Wisconsin, Madison, WI, USA; ²University of Wisconsin, Madison, WI, USA

Background Intravital multiphoton autofluorescence microscopy provides *in vivo*, label free, single cell imaging of metabolic changes. These metabolic changes are quantified via the metabolic coenzymes NAD(P)H and FAD which are autofluorescent molecules endogenous to all cells. Metabolic reprogramming of tumor and immune cells is closely associated with cancer progression and cell phenotype.¹⁻³ We aim to study metabolic changes during administration of an effective, triple-combination immunotherapy within murine melanoma tumors.⁴ This therapy includes external beam radiation, intratumoral hu14.18-IL2 immunocytokine (anti-GD2 mAb fused to IL2), and intraperitoneal anti-CTLA-4 leading to *in situ* vaccination and cure of GD2 + murine tumors.⁵ Previous work has shown that a T cell response is critical to the efficacy of this therapy⁴⁻⁵, so we created an mCherry-labeled T cell mouse model to study this response. Here, intravital multiphoton metabolic imaging was used to image concurrent tumor and CD8+ T cell metabolic trends during administration of immunotherapy.

Methods We implanted syngeneic B78 (GD2+) melanoma cells into the flanks of mCherry-labeled CD8+ T cell reporter mice (C57Bl/6 background) to induce tumors. Under anesthesia, skin flap surgery was performed and tumors were imaged at several time points during therapy. Multiphoton imaging was performed to collect NAD(P)H, FAD, mCherry, and collagen signal through a 40X objective (figure 1A). Fluorescence lifetime data was collected using time correlated single photon counting electronics. Tissues were harvested and analyzed via flow cytometry and multiplex immunofluorescence to corroborate intravital imaging findings and characterize the immune infiltrate.

Results Here we demonstrate that our intravital imaging is sensitive to metabolic changes in both B78 melanoma and CD8 T cells from immunotherapy treated tumors versus control tumors. These metabolic differences include changes in protein binding and redox balance (figure 1B) within treated tumors. We also show remodeling of collagen (figure 1C), a major component of the extracellular matrix, during immunotherapy that may be explained by an observed decrease in macrophages. Flow cytometry and multiplex immunofluorescence illustrate changes in the immune infiltrate composition, activation, and cytotoxicity during therapy (figure 1D).

Conclusions These results show that intravital metabolic imaging enables single cell quantification of metabolic changes in tumor and immune cells during therapy. Combined with other traditional assays, we can elucidate key immune cell populations and the crucial timepoints during therapy where changes are occurring. With continued efforts, this imaging platform may be leveraged to develop new combinations of immunotherapies.

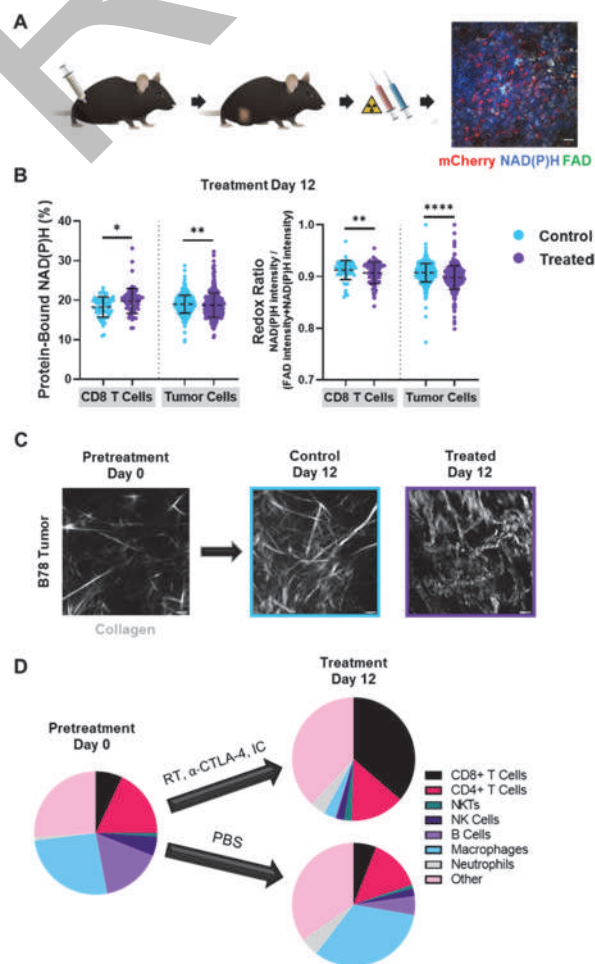
Acknowledgements This work is supported by the Morgridge Institute for Research (Interdisciplinary Fellowship awarded to A.R.H.) and the NIH (R01 CA205101 and R35 CA197078). The authors thank the University of Wisconsin Carbone Cancer Center (UWCCC) Support Grant P30 CA014520, the UWCCC Translational Research Initiatives in Pathology

laboratory – supported by the UW Department of Pathology and Laboratory Medicine and the Office of The Director NIH (S10OD023526), the UWCCC Flow Cytometry Laboratory, and the Genome Editing and Animal Models Laboratory for core services.

REFERENCES

1. Renner K, Singer K, Koehl GE, Geissler EK, Peter K, Siska PJ, Kreutz M. Metabolic Hallmarks of Tumor and Immune Cells in the Tumor Microenvironment. *Front. Immunol.* 2017, **8** (MAR), 1–11.
2. Mockler MB, Conroy MJ, Lysaght J. Targeting T Cell Immunometabolism for Cancer Immunotherapy; Understanding the Impact of the Tumor Microenvironment. *Front. Oncol.* 2014, **4** (May), 1–11.
3. Ghesquière B, Wong BW, Kuchnio A, Carmeliet P. Metabolism of Stromal and Immune Cells in Health and Disease. *Nature* 2014, **511** (7508), 167–176.
4. Morris ZS, Guy EI, Francis DM, Gressett MM, Werner LR, Carmichael LL, Yang RK, Armstrong EA, Huang S, Navid F, Gillies SD, Korman AJ, Hank JA, Rakhmievich AL, Harari PM, Sondel PM. In Situ Tumor Vaccination by Combining Local Radiation and Tumor-Specific Antibody or Immunocytokine Treatments. *Cancer Res.* 2016, **76** (13), 3929–3941.
5. Morris ZS, Guy EI, Werner LR, Carlson PM, Heinze CM, Kler JS, Busche SM, Jaquish AA, Sriramaneni RN, Carmichael LL, Loibner H, Gillies SD, Korman AJ, Erbe AK, Hank JA, Rakhmievich AL, Harari PM, Sondel PM. Tumor-Specific Inhibition of In Situ Vaccination by Distant Untreated Tumor Sites. *Cancer Immunol. Res.* 2018, **6** (7), 825–834.

Ethics Approval All animal work was approved by the University of Wisconsin Institutional Animal Care and Use Committees.



Abstract 72 Figure 1 *In vivo* multiphoton imaging and flow cytometry of tumor and CD8 T cell populations during immunotherapy. A) Experimental workflow showing B78 flank tumor implantation and growth, administration of triple therapy, and representative *in vivo*

Abstracts

fluorescence intensity image of B78 melanoma tumor growing in a mCherry reporter mouse. Image shows mCherry-expressing CD8 T cells (red) infiltrating tumor tissue as well as autofluorescent metabolic coenzymes NAD(P)H (blue) and FAD (green) expressed by the tumor and T cells. Scale bar 25 μm . B) *In vivo* single cell B78 tumor fluorescence lifetime data shows increased NAD(P)H protein binding in treated CD8 T cells with decreased protein binding in treated tumor cells (left panel). Corresponding *in vivo* optical redox ratio fluorescence intensity data shows redox balance within the tumor microenvironment (right panel). Both CD8 T cells and tumor cells from treated tumors exhibited a decreased optical redox ratio, compared to control tumors, indicating they are more oxidized ($n = 2$ mice, B78 tumor cells = 1039, CD8 T cells = 132, mean \pm SD, Mann-Whitney U Test). C) *In vivo* second harmonic generation images of B78 tumors show collagen morphology and alignment without labels. Collagen fibers from control tumors show little change from Day 0 pretreatment to Day 12 of PBS treatment while collagen fibers from treated tumors show remodeling of collagen towards a healthier tissue phenotype by Day 12 of immunotherapy treatment (healthy tissue collagen is typically very tortuous while tumor tissue collagen is typically very aligned). D) Flow cytometry data of B78 tumors shows differences in immune infiltrate populations in immunotherapy treated mice at Day 12 versus PBS control mice at Day 12 ($n = 4$ mice per condition, average%CD45+ cells). Immunotherapy treated mice show an increase in CD8 T cells and NKTs while macrophage numbers decrease.

<http://dx.doi.org/10.1136/jitc-2022-SITC2022.0072>

73

DELTA-RADIOMICS PREDICTS RESPONSE AND OVERALL SURVIVAL IN ADVANCED NON-SMALL CELL LUNG CANCER PATIENTS TREATED WITH DURVALUMAB

¹Mohammadhadi Khorrami, ¹Vidya Sankar Viswanathan*, ²Amit Gupta, ³Qin Li, ³Ashok Gupta, ³Ikbel Achour, ³Brian Fitzgerald, ⁴Vamsidhar Velcheti, ¹Anant Madabhushi. ¹Emory University, Atlanta, GA, USA; ²University Hospitals Cleveland, Cleveland, OH, USA; ³AstraZeneca, Cambridge, MA, USA; ⁴New York University, Pepper Pike, OH, USA

Background Immune checkpoint inhibitors (ICI) are the standard of care for advanced non-small cell lung cancer (NSCLC). However, the response rates to these immuno-oncology agents remain modest (~45% in the frontline setting and ~20% in the second line setting). The ability to determine early response during treatment is important to allow early adjustment of treatment regimens. Currently, there is a lack of objective methods for early evaluation of clinical benefits from ICI treatments. In this study, we evaluated the performance of a CT-based delta-radiomics model for predicting early response in advanced NSCLC patients enrolled in CP1108 durvalumab nonrandomized phase 1/2 trial (NCT01693562) as an independent validation set.¹ Change of feature statistics between baseline and post-treatment scans was defined as the delta radiomic features.

Methods Baseline and first post-treatment chest CT scans from 225 NSCLC patients were acquired from 3 sites. A maximum of 2 lung lesions were annotated on both scans as per RECIST v1.1 and patients with objective response were defined as 'responders', and those with progressive disease or stable disease were defined as 'non-responders'. Patients lacking follow-up scans or measurable lung lesions were excluded. A previously trained classifier on D1=111 patients from two institutions (Cleveland Clinic Foundation and University of Pennsylvania Health System)² was validated on D2=114 cases from CP1108 durvalumab study¹ to assess the probability of treatment response using ROC curve as AUC. 454 intratumoral and 7426 peritumoral texture features were extracted from the scans and relative radiomic differences were computed to yield a set of 'delta-radiomic' features. A Cox regression model that was previously trained was used to evaluate the overall survival on CP1108 durvalumab study and relative HR with 95% confidence intervals (CI) was reported. A blinded validation was performed by AstraZeneca.

Results A combination of peritumoral and intratumoral delta radiomic features yielded an AUC of 0.77 ± 0.07 in D1 and a corresponding AUC of 0.7 in D2, respectively. Univariate Cox regression analysis indicated that delta-radiomic signature was significantly associated with OS in D1 set [HR: 1.95; 95% CI, 1.5–2.5; $P < 0.001$; C-index=0.70) and D2 set [HR: 1.34; 95% CI, 1.05–1.7; $P = 0.018$; C-index=0.55).

Conclusions We validated that a delta-radiomics based prediction model enables the identification of advanced NSCLC patients who respond to durvalumab treatment. Our study demonstrates the potential of radiomics and delta-radiomics as non-invasive imaging biomarkers to assess response and overall survival to immune checkpoint inhibitors including durvalumab.

REFERENCES

1. Antonia SJ, Balmanoukian A, Brahmer J, Ou SI, Hellmann MD, Kim SW, Ahn MJ, Kim DW, Gutierrez M, Liu SV, Schöffski P, Jäger D, Jamal R, Jerusalem G, Lutzky J, Nemunaitis J, Calabrò L, Weiss J, Gadgeel S, Bhosle J, Ascierto PA, Rebalatto MC, Narwal R, Liang M, Xiao F, Antal J, Abdullah S, Angra N, Gupta AK, Khleif SN, Segal NH. Clinical Activity, Tolerability, and Long-Term Follow-Up of Durvalumab in Patients With Advanced NSCLC. *J Thorac Oncol*. 2019 Oct; **14**(10):1794–1806. doi: 10.1016/j.jtho.2019.06.010. Epub 2019 Jun 20. PMID: 31228626.

2. Khorrami M, Prasanna P, Gupta A, Patil P, Velu PD, Thawani R, Corredor G, Allou M, Bera K, Fu P, Feldman M, Velcheti V, Madabhushi A. Changes in CT Radiomic Features Associated with Lymphocyte Distribution Predict Overall Survival and Response to Immunotherapy in Non-Small Cell Lung Cancer. *Cancer Immunol Res*. 2020 Jan; **8**(1):108–119. doi: 10.1158/2326-6066.CIR-19-0476. Epub 2019 Nov 12. PMID: 31719058; PMCID: PMC7718609.

Ethics Approval The study included de-identified data from human participants. An exempt determination was made by Case Western Reserve University under the Exempt category '(4) Secondary research on data or specimens (no consent required)'.

<http://dx.doi.org/10.1136/jitc-2022-SITC2022.0073>

74 DEEPTCRMATCH: AN EFFECTIVE WAY OF COMPUTING T CELLS ANTIGEN SPECIFICITY

¹Seungtae Park*, ²Sungsik Kim, ³Hee Joon Jeon, ³Na Ri Yoon, ²Bo Ryeong Lee, ²Sungmin Kim, ²Woong-Yang Park, ⁴Hyung Ju Hwang. ¹Pohang University of Science and Technology, Pohang, Korea, Republic of; ²Geninus Inc., Seoul, Korea, Republic of; ³AMSquare Inc., Pohang, Korea, Republic of; ⁴Pohang University of Science and Technology and AMSquare Inc., Pohang, Korea, Republic of

Background To determine the specificity of T cells based on their receptor sequence is a demanding task due to cross-reactivity, complicated patterns and limited size of public dataset. An effective computational model, which finds CDR3 patterns of shared antigen specificity in the existing dataset, can predict specificity of T cells accurately. In this work, we developed a deep learning methodology that computes the similarity among T cells in terms of antigen specificity using *k*-mer features.

Methods Our model consists of two parts. First, it encodes every overlapping *k*-mers of CDR3 into numerical vectors. We parallelize such *k*-mer encodings into several allowable ways, so that the independent semantics of each *k*-mers are effectively learned. Second, among the encoded *k*-mer features, we select only meaningful *k*-mers using a self-attention structure. By doing this, we remove unwanted correlations among overlapping *k*-mers.

We train our model with preprocessed public datasets: IEDB, VDJdb and McPAS. We optimize the overall process to find an optimal contrastive predictive coding, which is an unsupervised objective function. After optimization, we define a kernel function of *k*-mer features to define similarity between two CDR3s.

Results We designed an one-of-many unsupervised task: for a given arbitrary CDR3 sequence, whether our model can correctly select CDR3 with a similar specificity among *N* randomly sampled candidates. With *N*=10, our model achieves accuracy 0.3 for an independent dataset. We also test supervised task: whether our model can induce probable cognate antigens for a given CDR3. Our model achieves precision 0.7.

Conclusions Our deep learning model can extract *k*-mer information that only represents antigen specificity. This information is an invaluable numerical vector for computing similarity of antigen specificity. By doing this, our model can solve the one-of-many problem and predict the antigen specificity. In the future, our model will improve its performance as a size of training dataset grows.

<http://dx.doi.org/10.1136/jitc-2022-SITC2022.0074>

75 **METHODS TO IMPROVE CO-EXPRESSION EFFICACY OF GENES MODULATING PROMOTER AND LINKER**

Suji Kim, ¹Grad Student*, ¹Jong Moo Hong, ²Kwanghee Kim, ³Hee Jin Lee, ²Hee Jin Lee, ³Gyungyub Gong. ¹University of Ulsan College of Medicine, Seoul, Korea, Republic of; ²NeogenTC cop., Seoul, Korea, Republic of; ³Asan Medical Center, Seoul, Korea, Republic of

Background Adoptive T cell therapy is an important modality of cancer immunotherapy. Engineering of various genes associated with improved T cell function, such as viability, sustainability, migration potential, and target specificity is important. Therefore, we need to identify effective methods for multi-gene transfer to T cells. The selection of appropriate promoters or linkers in the production of virus vectors is critical for efficacy of multigene expression.

Methods In order to optimize vectors that can increase the expression efficiency of multigenes, we intended to compare the expression amount of each gene with different promoters and linkers. The expression of each gene was compared when 1G4 TCR (alpha and beta chains are linked by furin-SGSG-P2A) and CCR10 were linked using IRES, T2A, or furin-SGSG-T2A. Three cloning vectors were produced using one EF1a, one EFS, or two EFS to express 1G4 and CCR10 genes simultaneously with T2A. Transfection was performed on Lenti-x 293T and transduction was performed in Jurkat cells to measure the difference in expression of the 1G4 with mouse TCR constant antibody and CCR10 protein by flow cytometry. Finally, 1G4 and CCR10 dual expressing cells were sorted and cultured to see the persistence of expression on the day of culture, day 6, and day 12.

Results Since CCR10 was not expressed with the vector using IRES, T2A was selected. In addition, differences in protein expression between T2A and furin-SGSG-T2A were not observed. Using two EFS promotors, 1G4 and CCR10 were expressed at 4.3% and 33.4%, respectively, so they were not studied further. When using one EFS promotor, 1G4 was expressed at 97.6%, but CCR10 (downstream of T2A) was expressed significantly lower at 26.1% on the transduction day. When using the EF1a, the expression of 1G4 was decreased to 74.2%, but CCR10 expression was increased to 37.4%. After sorting of dual expressing cells, the expression of 1G4 and CCR10 with the EFS decreased from 100% and 86.1% (day 0) to 89.5% and 2.66%, respectively (day 12). However, with the EF1a, the expression of 1G4 was almost the same from 99.2% (day 0) to 99.7% (day 12), and CCR10 expression decreased slightly from 94.6% (day 0) to 73.5% (day 12).

Conclusions T2A showed better gene expression efficiency for downstream gene than IRES. EF1a was better than EFS and it was associated durable transduction efficacy. Comparison of linkers and promoters are necessary to improve multigene transfer to T cells for adoptive T cell therapy.

<http://dx.doi.org/10.1136/jitc-2022-SITC2022.0075>

Abstracts

76

DISCOVERY OF BLOOD PHARMACODYNAMIC BIOMARKERS FOR ATR INHIBITORS

¹Ya Kong, ¹Lulu Jiang, ²Bin Jiang*, ¹Hui Yuwen, ³Jay Mei, ³Bo Shan, ³Bing Hou. ¹Shanghai Antengene Corporation Limited, Shanghai, China; ²Antengene Biotech LLC, Doylestown, PA, USA; ³Antengene Corporation Co., Ltd, Shaoxing, China

Background The ataxia telangiectasia and rad3-related kinase (ATR) is a critical mediator of DNA damage response (DDR), which induce cell cycle arrest and facilitate DNA repair via downstream targets. Targeting ATR has become an attractive therapeutic strategy in cancer treatment and ATR inhibitors are currently being tested as anti-cancer agents in clinical trials, where pharmacodynamic (PD) biomarkers are crucial to help guide dose and scheduling and support mechanism of action studies. Tumor is the obvious tissue in which to measure PD effect but collecting tumor biopsies is often challenging for the patients.¹ Phosphorylation of Chk1 or γ H2AX has been reported to be PD markers of ATR inhibitors. However, these markers are difficult to measure directly using blood samples. ATG-018 is an oral, potent and selective small-molecule inhibitor of ATR. In this study, to identify clinically easy-to-use blood PD biomarkers of ATR inhibitor, we screened the gene expression changes *in vitro* using peripheral blood mononuclear cells (PBMCs) treated by different concentrations of ATG-018 and validated the marker in *in vivo* mouse models.

Methods We first assessed gene expression changes induced by ATG-018 on human PBMCs *in vitro*. Human PBMCs from three different donors were treated with different concentrations of ATG-018 (10, 100, 300, 1000 ng/ml), and NanoString technology was used for high-throughput gene expression profiling at transcriptional level. To further validate the identified potential biomarkers, wild type mice were treated with ATG-018 and Meso Scale Discovery was used to detect the protein expression of potential PD markers in plasma.

Results In *in vitro* test, a series of genes were found to change in a dose-dependent manner in response to ATG-018 in PBMCs (figure 1A). ATG-018 significantly inhibited the expression of chemokine genes, especially CCL2, CCL3/L1 and CCL4. Under the condition of 1000 ng/mL ATG-018 treatment, the log₂ fold change of these three genes was more than -1.5 compared with the control group (figure 1B). In *in vivo* assay, the inhibition of CCL2, CCL3 and CCL4 protein expression could still be observed in plasma from Balb/c mice orally treated with ATG-018. Expression of CCL4 was significantly downregulated after administration of ATG-018 compared with the control group.

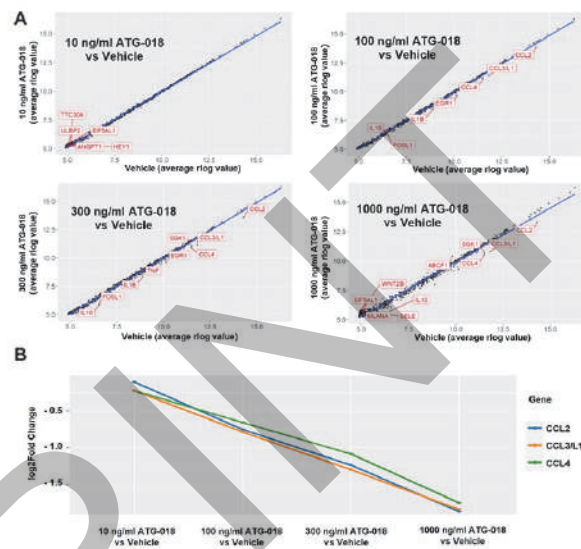
Conclusions In this study, we found the expression of chemokines, especially CCL2, CCL3/L1, and CCL4 are potential novel PD biomarkers of ATG-018, which could be detected in unmanipulated blood samples, and may guide dose and scheduling and support mechanism of action studies of both ATG-018 and other ATR inhibitors in clinic.

REFERENCE

1. Chen T, Middleton FK, Falcon S, Reaper PM, Pollard JR, Curtin NJ. Development of pharmacodynamic biomarkers for ATR inhibitors. *Mol Oncol*. 2015 Feb;9(2):463–72.

Ethics Approval The protocol and any amendment(s) or procedures involving the care and use of animals in this study were reviewed and approved by the Institutional Animal Care and Use Committee (IACUC) of CrownBio to execution with an

AUP number or IACUC approval number for each animal study. During the study, the care and use of animals were conducted in accordance with the regulations of the Association for Assessment and Accreditation of Laboratory Animal Care (AAALAC). All studies were conducted following an approved IACUC protocol. AUP NO.:2104–09–2108.



Abstract 76 Figure 1 ATG-018 regulates the gene expression of hPBMC *in vitro*
A. Top up- and down- regulated genes (defined as $p_{\text{adjust}} < 0.05$ and the absolute value of fold change > 1.5) in hPBMCs in response to ATG-018, detected by Nanostring. B. Fold change of CCL gene expression (ATG-018 vs. Vehicle). Data from A

<http://dx.doi.org/10.1136/jitc-2022-SITC2022.0076>

77

AN NGS ASSAY TO IDENTIFY HLA LOSS OF HETEROZYGOSITY FOR FUTURE CEA AND MSLN LOGIC-GATED CAR-T SOLID TUMOR PROTOCOLS DESIGNED FOR REDUCED ON-TARGET, OFF-TUMOR TOXICITY

¹Scott Kopetz*, ¹Maria Pia Morelli, ²Julian Molina, ³Diane Simeone, ⁴J Randolph Hecht, ⁵Kedar Kirtane, ⁶Mitesh Borad, ³Theodore Welling, ⁴Edward Garon, ⁷Armen Mardiros, ⁷Xueyin Wang, ⁷Eric Ng, ⁸Tyler Daneke, ⁸Shannon Gallagher, ⁸Ariane Lozac'hmeur, ⁸Karl Beutner, ⁷John Welch, ⁹David Maloney, ⁷William Go, ¹⁰Sandip Patel. ¹The University of Texas MD Anderson Cancer Center, Houston, TX, USA; ²Mayo Clinic, Rochester, MN, USA; ³New York University Langone Health, New York, NY, USA; ⁴University of California at Los Angeles, Los Angeles, CA, USA; ⁵H. Lee Moffitt Cancer Center, Tampa, FL, USA; ⁶Mayo Clinic Cancer Center, Scottsdale, AZ, USA; ⁷A2 Biotherapeutics, Inc., Agoura Hills, CA, USA; ⁸Tempus, Chicago, IL, USA; ⁹Fred Hutchinson Cancer Research Center, Seattle, WA, USA; ¹⁰University of California San Diego, La Jolla, CA, USA

Background Chimeric antigen receptor (CAR) T-cell therapy has shown clinical efficacy in hematologic cancers, but success is limited in solid tumors due to a lack of tumor-specific targets that distinguish cancer from normal cells and an immunosuppressive tumor microenvironment.¹ Integrating synthetic biology and comprehensive molecular profiling of tumors may provide active and tolerable approaches to CAR T-cell therapy in patients with solid tumors.

Human leukocyte antigen (HLA) loss of heterozygosity (LOH) in tumors offers a definitive tumor vs normal discriminator target for CAR T-cell therapy.² The Tmod platform^{3,4} is a modular logic-gated CAR T system comprising different versions including a carcinoembryonic antigen (CEA)- or mesothelin (MSLN)-targeting CAR activator and a separate blocker receptor targeting HLA-A*02 or other HLA alleles to protect normal cells. Compared with existing immunohistochemistry (IHC) tests, Tempus xT-Onco is a standard-of-care next-generation sequencing (NGS) assay⁵ that detects somatic alterations including HLA LOH and generates whole transcriptome RNA data (eg, CEA or MSLN expression) and a tumor immune infiltration profile, which can effectively identify patients appropriate for Tmod CAR T-cell therapy.

Methods HLA LOH in solid tumors was assessed with paired germline and somatic DNA sequencing. Common driver mutations, microsatellite instability status, and tumor mutational burden were examined in HLA-A LOH or HLA-A intact cohorts. Tumor expression of CEA and MSLN was evaluated via RNA sequencing and compared with immunohistochemistry (IHC) results.

Results A total of 21,053 tumor samples in the Tempus database were compared with their matched-normal samples. HLA-A LOH was detected in 16% of 10,867 advanced solid tumors (table 1) and similar LOH frequencies were observed among common HLA-A alleles. Clinical factors and molecular biomarkers were similar between HLA-A LOH and HLA-A intact cohorts. High CEA expression was seen in IHC-positive patients.

Conclusions The frequency of HLA-A LOH in solid tumors in the Tempus database is similar to that reported in the Cancer Genome Atlas.⁶ Tempus xT-Onco reliably detects HLA LOH and quantifies CEA and MSLN expression. Based on these data, patients with solid tumors are now being prospectively screened for HLA LOH using xT-Onco in an ongoing tissue banking study (BASECAMP-1, NCT04981119), preparing for future interventional protocols.

REFERENCES

1. Martinez M, Moon EK. CAR T cells for solid tumors: new strategies for finding, infiltrating, and surviving in the tumor microenvironment. Review. *Front Immunol.* 2019;**10**:128.

2. Hwang MS, Mog BJ, Douglass J, et al. Targeting loss of heterozygosity for cancer-specific immunotherapy. *Proc Natl Acad Sci U S A.* 2021;**118**(12): e2022410118
3. Hamburger A, DiAndreth B, Cui J, et al. Engineered T cells directed at tumors with defined allelic loss. *Mol Immunol.* 2020;**128**:298–310.
4. DiAndreth B, Hamburger AE, Xu H, Kamb A. The Tmod cellular logic gate as a solution for tumor-selective immunotherapy. *Clin Immunol.* 2022;**241**:109030.
5. Beaubier N, Tell R, Lau D, et al. Clinical validation of the tempus xT next-generation targeted oncology sequencing assay. *Oncotarget.* 2019;**10**(24):2384–2396.
6. The Cancer Genome Atlas (TCGA) Research Network [Internet]. <https://www.cancer.gov/tcga>. Accessed June 2022.

Abstract 77 Table 1 Solid tumor samples (n) and HLA-A LOH frequency (%)

Table 1. Solid tumor samples (n) and HLA-A LOH frequency (%)

	Tempus advanced disease real-world n (%)	TCGA Primary tumors n (%)
Average	10,867 (16)	10,844 (13)
Non-small cell lung cancer	1,915 (23)	501 (25)
Head and neck cancer	208 (26)	522 (16)
Breast cancer	1,447 (12)	1,080 (14)
Ovarian cancer	569 (16)	579 (17)
Colorectal cancer	1,854 (16)	615 (10)
Pancreatic cancer	675 (20)	184 (33)
Gastroesophageal cancer	506 (21)	625 (16)
Mesothelioma	7 (14)	87 (11)

HLA-A, human leukocyte antigen A; LOH, loss of heterozygosity; TCGA, the Cancer Genome Atlas.

<http://dx.doi.org/10.1136/jitc-2022-SITC2022.0077>

MAPPING THE TISSUE COMPOSITION WITH HYPERPLEX IMMUNOFLUORESCENCE ON DELICATE SAMPLES

Joanna Kowal*, Diego Dupouy, Jonathan Mignot, Benjamin Pelz. *Lunaphore Technologies, Tolochenaz, Switzerland*

composition and tissue organization: a primer for multiplexed antibody-based imaging. *Nat Methods*. 2022; **19**: 284–295.

<http://dx.doi.org/10.1136/jitc-2022-SITC2022.0078>

Background In health and disease, cells are interacting with their microenvironment, which shapes their homeostasis and response to any stimuli.¹ Deciphering the tissue architecture emerged as a crucial step to better understand tissue biology and harness it in a future therapeutic intervention.²

Recently, advancements were made to interrogate the tissue spatial composition with the development of immunofluorescence-based hyperplex assays,^{3,4} allowing the investigation of dozens of biomarkers on a single tissue slide. There is a growing interest to apply hyperplex assay on fresh frozen sections (FS), yet harsh procedures used in manual protocols are detrimental to tissue morphology and limit the use of this application.⁵ Furthermore, manual protocols are laborious and time-consuming, allowing to process a limited number of samples.

Here, we describe the capability to perform automated hyperplex assays for up to 32 biomarkers on fragile FS tissues as a cogent case combining staining quality with tissue preservation.

Methods COMET™ platform allows performing sequential immunofluorescence (seqIF™) assays based on an iterative series of fast tissue staining, imaging, and antibody elution cycles. Fresh frozen tissue sections of human and murine origins were fixed and permeabilized prior to loading on the device for automated staining protocols. Multiplex assay was performed for up to 32 biomarkers on a single tissue slide. To assess the tissue morphology preservation, standard hematoxylin and eosin (H&E) staining was performed on FS freshly processed or post-staining protocol.

Results In this study, a sequential immunofluorescence protocol was automated and optimized on COMET™ for both human and mouse frozen tissue sections. Murine spleen, brain and lung tissues were stained with multiplex panels of up to 6 proteins and showed an accurate detection of both common immune and organ-specific biomarkers. For a deep characterization of human lung cancer, 32 biomarkers were simultaneously detected on a single FS with optimal staining and a total procedure time of 23 hours. An H&E staining performed on the slide retrieved from the platform after the multiplex protocol showed excellent preservation of the tissue architecture in comparison with an unprocessed FS slide.

Conclusions This work proves the feasibility of performing automated hyper-plex assays on a variety of delicate frozen samples with high-quality results. With this new toolbox, we aim to support and hasten discovery studies across multiple research fields overcoming current limitations in tissue spatial biology.

REFERENCES

1. Quail DF, Joyce JA. Microenvironmental regulation of tumor progression and metastasis. *Nat Med*. 2013; **19**(11):1423–37.
2. Allam M, Cai S, Coskun AF. Multiplex bioimaging of single-cell spatial profiles for precision cancer diagnostics and therapeutics. *npj Precis. Onc*. 2020; **4**(11).
3. Mund A, Brunner AD, Mann Unbiased spatial proteomics with single-cell resolution in tissues. *Molecular Cell* 2022; **82**:2335–2349.
4. Palla G, Fischer DS, Regev A, Theis FB. Spatial component of molecular tissue biology. *Nat Biotech*. 2022; **40**: 308–318.
5. Hickey JK, Neumann EK, Radtke AJ, Camarillo JM, Beuschel RT, Albanese A, McDonough E, Hatler J, Wiblin AE, Fisher J, Croteau J, Small EC, Sood A, Caprioli RM, Angelo RM, Nolan GP, Chung K, Hewitt SM, Germain RN, Spraggins JM, Lundberg E, Snyder MP, Kelleher NL, Saka SK. Spatial mapping of protein

79

HIGH-DIMENSIONAL SPATIAL PHENOTYPING OF CUTANEOUS SQUAMOUS CELL CARCINOMA FROM IMMUNE-COMPETENT AND IMMUNOCOMPROMISED PATIENTS

¹Arutha Kulasinghe, ²Niyati Jhaveri*, ²Dmytro Klymyshyn, ²Bassem Ben Cheikh, ³Rahul Ladwa, ³Howard Liu, ³Caroline Cooper, ¹Gabrielle Belz, ³Sandro Porceddu, ²Oliver Braubach. ¹The University of Queensland, Brisbane, Australia; ²Akoya Biosciences, Menlo Park, CA, USA; ³Princess Alexandra Hospital, Brisbane, Australia

Background Cutaneous squamous cell carcinoma (cSCC) is the second most common non-melanoma skin cancer and represents a major global health burden. Approximately 50% of cSCC patients develop primary resistance and 20% will develop secondary resistance to immune checkpoint inhibitors (ICI). There are few biomarkers that reflect the tumor dynamics predictive of response to ICI therapy and we thus need to better understand the cSCC tumor microenvironment (TME).

Methods Our retrospective study profiled tissues from 50 patients at the Princess Alexandra Hospital (Brisbane, AU). Study groups included patients with de novo local cSCC (n=10) and regional nodal metastasis (n=10) who have remained disease free for >2 years. Additional groups included patients with locoregional recurrent disease (n=10), recurrent and/or metastatic disease (n=10) treated with immunotherapy, and immunocompromised de novo or recurrent disease (n=10). In this exploratory study, we designed a high-dimensional >40-plex antibody panel identifying cell lineages, activation states, and checkpoints, as well as markers for cell metabolism, vasculature, and tissue structure. Whole-slide spatial phenotyping was conducted on the PhenoCycler[®]-Fusion spatial biology system and spatial features, including spatial phenotypic composition, cell-to-cell localization, and cellular neighborhoods were analyzed and compared against clinicopathological findings and response to ICI therapy

Results We have profiled the TME of cSCC via ultrahigh-plex, single-cell spatial analyses of whole tissues. Our data have revealed unique cell phenotype compositions within the TME of different patient cohorts. Additionally, spatial phenotyping analysis revealed distinct cellular neighborhoods within the tissue cohorts. Taken together, this high-dimensional imaging approach of the cSCC TME has revealed new tissue insights

Conclusions There is a need to understand the immune contexture of the cSCC immune microenvironment. Here we identify distinct cellular phenotypic compositions and cellular neighbourhoods in tissues from immune-competent and immunocompromised cSCC. We thereby confirm biological differences in tissue composition and cellular interactions between these tissues and provide putative new biomarkers for cSCC patient stratification.

Ethics Approval This study has Metro South Human Research Ethics Committee (HREC) Approval (LNR/2020/QMS/66612) and The University of Queensland ethics ratification.

<http://dx.doi.org/10.1136/jitc-2022-SITC2022.0079>

Abstracts

80

TUMOR-SPECIFIC ALTERNATIVE SPLICING GENERATES IMMUNOGENIC SPATIALLY-CONSERVED HLA-BINDING NEOANTIGENS DETECTED THROUGH INTEGRATIVE TRANSCRIPTOMIC AND PROTEOMIC ANALYSES

Darwin Kwok*, Takahide Nejo, Chibo Hong, Aidan Du, Maggie Colton, James Woo, Joseph Costello, Hideho Okada. *University of California San Francisco, San Francisco, CA, USA*

Background While immunotherapy is profoundly efficacious in certain cancers, its success is limited in cancers with lower mutational burdens, such as gliomas.¹ Therefore, investigating neoantigens beyond those from somatic mutations can expand the repertoire of immunotherapy targets. Recent studies detected alternative-splicing (AS) events in various cancer types that could potentially translate into tumor-specific proteins.^{2, 3} Our study investigates AS within glioma to identify novel MHC-I-presented neoantigens through an integrative transcriptomic and proteomic computational pipeline, complemented by an extensive spatiotemporal analysis of the AS candidates.

Methods Bulk RNA-seq of high tumor purity TCGA-GBM/LGG (n=429) were analyzed through a novel systematic pipeline, and tumor-specific splicing junctions (neojunctions) were identified *in silico* by cross-referencing with bulk RNA-seq of GTEx normal tissue (n=9,166). Two HLA-binding prediction algorithms were subsequently incorporated to predict peptide sequences with a high likelihood for HLA presentation. Investigation of the tumor-wide clonality and temporal stability of the candidates was performed on extensive RNA-seq data from our spatially mapped intratumoral samples and longitudinally collected tumor tissue RNA-seq. Proteomic validation was conducted through mass-spec analysis of the Clinical Proteomic Tumor Analysis Consortium (CPTAC)-GBM repository (n=99).

Results Our analysis of TCGA-GBM/LGG bulk RNA-seq identified 249 putative neojunctions that translate into 222 cancer-specific peptide sequences encoding 21,489 tumor-specific numbers (8–11 amino acids in length, figure 1). Both prediction algorithms concurrently identified 271 n-mers likely to bind and be presented by HLA*A0101, HLA*A0201, HLA*A0301, HLA*A1101, or HLA*A2402. We confirmed the expression of 17 out of 74 HLA*A0201-binding candidates in RNA-seq of two HLA*A0201+ patient-derived glioma cell lines with a subset of candidates found tumor-wide (figure 2). Analysis of CPTAC-GBM mass-spec data detected 42 tumor-specific peptides generated specifically from 23 GBM-specific splicing events (figure 3). 4 candidates were selected for downstream immunogenicity analysis and were selected based on high *in silico* HLA-presentation scores and detection in RNA sequencing and mass spectrometry. *In vitro* sensitization of healthy donor-derived CD8+ T-cells was performed with the 4 candidates along with an influenza positive control condition and a no peptide negative control condition. 1 of the 4 neoantigen candidates, mutant-RPL22, was shown to elicit a CD8+ T-cell-specific immune response based on IFN γ ELISA assay analysis (figure 4).

Conclusions Tumor-specific neojunctions identified in our unique integrative pipeline present novel candidate immunotherapy targets for gliomas and offer a new avenue in neoantigen discovery across cancer types.

REFERENCES

- Alexandrov LB, Nik-Zainal S, Wedge DC, Aparicio SA, Behjati S, Biankin AV, Bignell GR, Bolli N, Borg A, Borresen-Dale AL, Boyault S, Burkhardt B, Butler AP, Caldas C, Davies HR, Desmedt C, Eils R, Eyfjörd JE, Foekens JA, Greaves M,

Hosoda F, Hutter B, Ilicic T, Imbeaud S, Imielinski M, Jäger N, Jones DT, Jones D, Knappskog S, Kool M, Lakhani SR, López-Otin C, Martin S, Munshi NC, Nakamura H, Northcott PA, Pajic M, Papaemmanuil E, Paradiso A, Pearson JV, Puente XS, Raine K, Ramakrishna M, Richardson AL, Richter J, Rosenstiel P, Schlesner M, Schumacher TN, Span PN, Teague JW, Totoki Y, Tutt AN, Valdés-Mas R, van Buuren MM, van 't Veer L, Vincent-Salomon A, Waddell N, Yates LR; Australian Pancreatic Cancer Genome Initiative; ICGC Breast Cancer Consortium; ICGC MMLL-Seq Consortium; ICGC PedBrain, Zucman-Rossi J, Futreal PA, McDermott U, Lichter P, Meyerson M, Grimmond SM, Siebert R, Campo E, Shibata T, Pfister SM, Campbell PJ, Stratton MR. Signatures of mutational processes in human cancer. *Nature*. 2013 Aug 22;**500**(7463):415–21. doi: 10.1038/nature12477. Epub 2013 Aug 14. Erratum in: *Nature*. 2013 Oct 10;502(7470):258. Imielinski M, Marcin [corrected to Imielinski, Marcin]. PMID: 23945592; PMCID: PMC3776390.

- Kahles A, Lehmann KV, Toussaint NC, Hüser M, Stark SG, Sachsenberg T, Stegle O, Kohlbacher O, Sander C; Cancer Genome Atlas Research Network, Ratsch G. Comprehensive Analysis of Alternative Splicing Across Tumors from 8,705 Patients. *Cancer Cell*. 2018 Aug 13;**34**(2):211–224.e6. doi: 10.1016/j.ccell.2018.07.001. Epub 2018 Aug 2. PMID: 30078747.
- Bigot J, Lalanne AI, Lucibello F, Gueguen P, Houy A, Dayot S, Ganier O, Gilet J, Tosello J, Nemati F, Pierron G, Waterfall JJ, Barnhill R, Gardrat S, Piperno-Neumann S, Popova T, Masson V, Loew D, Mariani P, Cassoux N, Amigorena S, Rodrigues M, Alsafadi S, Stern MH, Lantz O. Splicing Patterns in SF3B1-Mutated Uveal Melanoma Generate Shared Immunogenic Tumor-Specific Neoepitopes. *Cancer Discov*. 2021 Aug;**11**(8):1938–1951. doi: 10.1158/2159-8290.CD-20-0555. Epub 2021 Apr 2. Erratum in: *Cancer Discov*. 2022 Mar 1;**12**(3):872. PMID: 33811047.

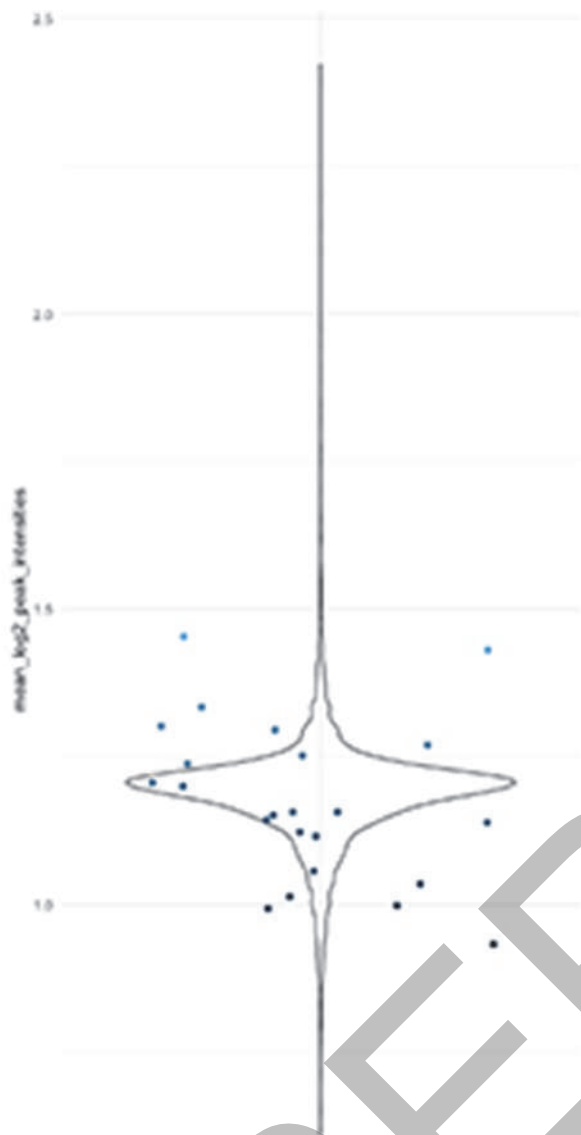


Abstract 80 Figure 1 Identification of top HLA-presented neoantigens. Neoantigen sequences were predicted from glioma-specific neojunctions identified from our novel *in silico* pipeline. 398 top-candidates were selected based on high HLA-presentation scores identified in two independent HLA-prediction algorithms.



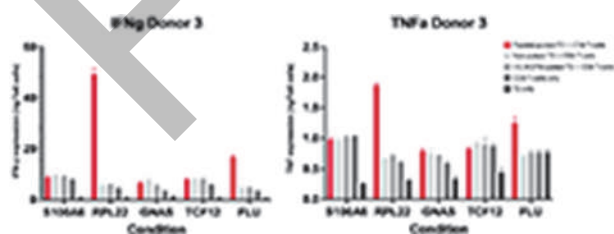
Abstract 80 Figure 2 RNA-level validation of neojunctions. RNA-expression of neojunctions was validated by analyzing RNA-sequencing data from two patient-derived HLA-A*0201 glioma cell lines. 74 of the 398 top candidates were shown to bind strongly to HLA-A*0201. Neojunctions expressing 14 of the candidates were detected in either cell lines.

<http://dx.doi.org/10.1136/jitc-2022-SITC2022.0080>



Abstract 80 Figure 3 Peptide-level validation of NJ-derived neoantigens

Protein-level expression of the neojunctions was detected by analyzing mass-spectrometry data from CPTAC. Mass spectrometry data of GBM patients (n=99) detected 42 peptides that are uniquely derived from 23 unique neojunctions



Abstract 80 Figure 4 NJ-derived neoantigens elicit CD8+ T-cell response

Four neojunction-derived neoantigen candidates demonstrated high HLA-presentation scores and were detected on both an RNA- and peptide-level. Neoantigen sensitization was performed on donor derived PBMCs, and neojunction-derived mutant-RPL22 elicited a CD8+ T-cell-specific immune response

T CELL STIMULATION ASSAY AND IMMUNOASSAYS COMPARISON FOR SOLUBLE CYTOKINES PROFILING IN DRUG DISCOVERY

Celine Lefranc, Nicole Meritet, Karine Berthelot, Odile Flamand, Jeremy Baudhuin, Jack Pollard, Luc Canard, Angelique Biancotto*. *Sanofi, Paris, France*

Background T cell stimulation assays are commonly used in invitro pharmacological assays to understand immunomodulatory functions of drugs in development.¹⁻³ Assays read outs are common activation markers measured by flow cytometry and cytokines secretion detected in culture supernatants. In addition to monitoring activation markers, cytokines and their expression are critical for biomarker discovery and essential in understanding immune biology in addition to being commonly used as a read out in T cell stimulation.

Methods In this work, we report CD25 CD69 expression after stimulation at 24,48,72h and IL-4, IL-2, TNFa, IFNg production from 33 healthy donors. We used a subset of samples to compare 4 technologies used in drug discovery; Meso Scale Discovery [MSD], Cytometric Bead Array [CBA] and Sartorius Q Beads Plexscreen. Through experimental data analysis, several assay features were compared, including sensitivity, dynamic range, and robustness.

Results Out of all parameters monitored, we identified that measurement of IL-2 at 48h was the best read out using these assay features to quantify T cell stimulation level. Our studies revealed normal range of cytokines production after CD3 CD28 stimulation of isolated T cells. Comparing cytokines measurement technologies, we showed that MSD has the best sensitivity in the low detection limit and the broadest dynamic range, while CBA and Luminex also demonstrate superior performance in the sensitivity and dynamic range. Additional aspects of these technologies, including assay principles, formats, throughputs, robustness, costs, and multiplexing capabilities, were also reviewed, and compared. MSD was the most sensitive technology for IL-4, while CBA was the most suitable one for cytokine high-throughput screening with multiplexing capability.

Conclusions This report aims to help readers understand analyte variance in healthy donors at baseline and upon stimulation, to select the proper cytokines secretion method for their specific applications.

REFERENCES

1. Boyman, O., *et al.*, Selective stimulation of T cell subsets with antibody-cytokine immune complexes. *Science*, 2006. **311**(5769): p. 1924–7.
2. Raulf, M., T Cell: Primary Culture from Peripheral Blood. *Methods Mol Biol*, 2019. **2020**: p. 17–31.
3. Zappasodi, R., *et al.*, In vitro assays for effector T cell functions and activity of immunomodulatory antibodies. *Methods Enzymol*, 2020. **631**: p. 43–59.

<http://dx.doi.org/10.1136/jitc-2022-SITC2022.0081>

82

DIFFERENTIAL EXPRESSION AND FUNCTION OF TOLL-LIKE RECEPTOR 3 WITHIN TUMOR IMMUNE MICROENVIRONMENT OF CLEAR CELL RENAL CELL CARCINOMA

Mingjia Li*, Patrick Stevens, Maciej Pietrzak, Jinesh Gheeya, Amir Mortazavi, Ming Yin, Steven Clinton, Daniel Spakowicz, Anil Parwani, Zihai Li, Yuanquan Yang. *Ohio State University, Columbus, OH, USA*

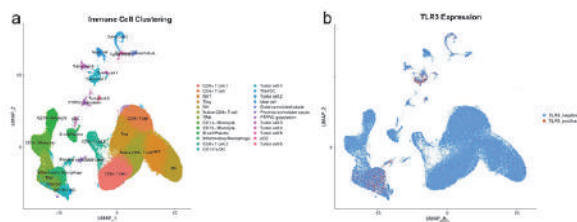
Background High intratumoral toll-like receptor 3 (TLR3) expression is associated with improved survival in patients with clear cell renal cell carcinoma (ccRCC). However, the function of TLR3 in the tumor immune microenvironment is poorly understood. Here, we assessed the expression of TLR3 in tumor-infiltrating immune cell subsets, and the differential gene expressions comparing TLR3+ VS TLR3- cells within each subset.

Methods Single-cell RNA-Seq dataset was obtained from the publication by Braun et al (PMI 33711273). Seurat version 4.0.4 was used for analysis. Uniform Manifold appreciation (UMAP) and projection reduction were performed with principal component analysis independent from previous work. Clusters were identified at a resolution of 0.8 with the Louvain algorithm using 1:20 dimensions in function. Clusters were labeled based on a combination of previous cell barcode annotation and our input. Differential gene expression was performed on normalized gene expression using FindMarkers function (only.pos = FALSE, min.pct = 0.15, logfc.threshold= 0.15) from each cluster/condition tested against all other cells. Genes were significantly elevated when Log2 fold change ≥ 0.20 with corrected p-value ≤ 0.05 . Cells were segregated based on TLR3 expression if a cell has at least 1 expression unit of TLR3. Quiagen IPA was used to perform pathway analysis. IPA Z-scores of ≥ 2 and ≤ -2 were used to determine the significance of activation and inhibition, respectfully.

Results A total of 164,722 cells from 13 patients with early (n=8) and advanced stage (n=5) ccRCC were included. TLR3 expression was enriched in myeloid compartment (figure 1). The top three TLR3 expressing immune cell types were: inflammatory macrophages (IM) with 636 out of 3309 cells (19.2%), CD141+ dendritic cells (DC) with 541 out of 3010 cells (18.0%), and tumor-associated macrophages (TAM) with 1209 out of 9749 cells (12.4%) (table 1). In IPA analysis, TLR3 positivity was associated with increased function of cell adhesion in DC141+DC (Z-score=2.0), response of antigen presentation in TAM (z score=2.2), and cell migration of IM (Z-score=2.2). Whereas TLR3 negativity was associated with inhibited cell movement of DC (Z-score= -2.1). The top differentially expressed genes between TLR3+ vs TLR3- cells of each subset was shown in figure 2-4.

Conclusions TLR3 expression is enriched in macrophages and dendritic cells within ccRCC tumor microenvironment. TLR3 signaling may promote cell adhesion, migration, and antigen presentation function of these cells.

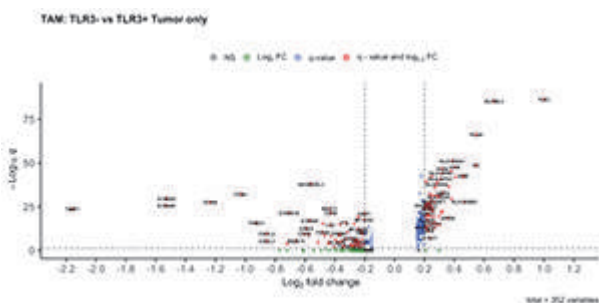
Ethics Approval This research was exempt from IRB review per institutional policy. This study utilized previously published and publicly available data. Data contained in this study is not individually identifiable or potentially identifiable.



Abstract 82 Figure 1 a). UMAP of the cell clustering. b). TLR3 expression (in red) is enriched in myeloid compartment and a subset of tumor cells

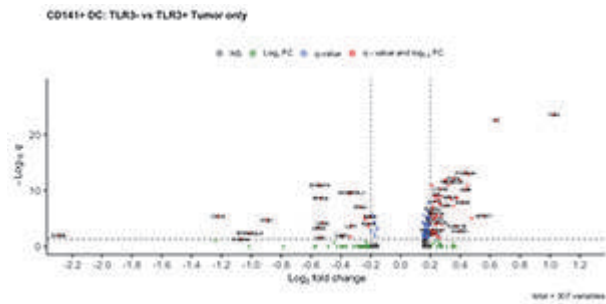
Abstract 82 Table 1 TLR3 expression (negative or positive) in the immune cell subtypes. Abbreviation: dendritic cell (DC), tumor-associated macrophages (TAM), protein tyrosine phosphatase – receptor type C (PTPRC or CD45), natural killer cells (NK), natural killer T cell (NKT), regulatory T cell (Treg), plasmacytoid dendritic cell (pDC)

	TLR-	TLR3+	Percent +
Tumor	4486	1373	23.4%
Inflammatory Macrophages	2673	636	19.2%
CD141+ DC	2469	541	18.0%
TAM	8540	1209	12.4%
PTPRC	785	38	4.6%
TAM/DC	1922	67	3.4%
distal convoluted tubule	1037	19	1.8%
CD8 T cell.2	3160	53	1.6%
NK	15075	202	1.3%
Mast Cell	1414	17	1.2%
NKT	19328	185	0.9%
CD8 T cell.1	28473	242	0.8%
Native CD8 T cell	14659	112	0.8%
Treg	16587	78	0.5%
CD4 T cell	20773	69	0.3%
pDC	380	1	0.3%
CD14+ Monocyte	7874	17	0.2%
Proximal convoluted tubule	1015	2	0.2%
B-cell/Plasma	3817	6	0.2%
CD16 Monocyte	5380	8	0.1%

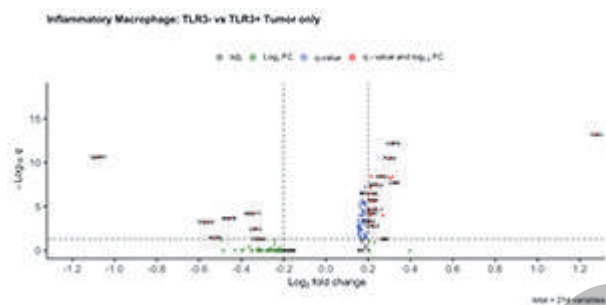


Abstract 82 Figure 2 Volcano plot showing the differential gene expression of TLR3+ vs TLR3- tumor associated macrophages (TAM). Y-axis showing corrected p-value expressed in $-\text{Log}_{10}q$, and X-axis showing the difference in gene expression measured Log_2 fold change. All significant change in gene expression were colored in red

Abstracts



Abstract 82 Figure 3 Volcano plot showing the differential gene expression of TLR3+ vs TLR3- CD141+ dendritic cells (DC). Y-axis showing corrected p-value expressed in $-\text{Log}_{10}q$, and X-axis showing the difference in gene expression measured Log_2 fold change. All significant change in gene expression were colored in red



Abstract 82 Figure 4 Volcano plot showing the differential gene expression of TLR3+ vs TLR3- inflammatory macrophages. Y-axis showing corrected p-value expressed in $-\text{Log}_{10}q$, and X-axis showing the difference in gene expression measured Log_2 fold change. All significant change in gene expression were colored in red

<http://dx.doi.org/10.1136/jitc-2022-SITC2022.0082>

83

IMMUNOTHERAPY ELUTING INTRATUMORAL NANOSEED ACHIEVES LOCAL AND SYSTEMIC TUMOR CONTROL OF PANCREATIC CANCER

Hsuan-Chen Liu, Daniel Davila Gonzalez, Robin Vander Pol, Dixita Viswanath, Shani Saunders, Corrine Ying Xuan Chua*, Alessandro Grattoni. *Houston Methodist Research Institute, Houston, TX, USA*

Background Intratumoral immunotherapy is a clinically investigated approach based on the premise that local priming of the antitumor immune response can yield durable systemic immunity and avoid toxicities associated with systemic administration. However, direct intratumoral injection rapidly disseminates from the tumor, resulting in diminished efficacy and undesirable systemic exposure.¹ Variations in intratumoral injection methods as well as lesion type and location could further affect local bioavailability and consequently, clinical outcome.² Moreover, clinical protocols typically require repeated administration, which could be challenging for hard to reach tumors. To address these challenges, we present an immunotherapy eluting intratumoral ‘nanoseed’ for in situ treatment.^{3–5} Sustained intratumoral immunotherapy release occurs autonomously through diffusion across a nanofluidic membrane mounted on the nanoseed without requiring pumps, ports or manipulation after implantation. We posit that nanoseed-mediated sustained intratumoral release of agonist CD40 antibody could promote local and systemic antitumor responses for effective tumor control.

Methods We investigated our approach using the syngeneic KPC pancreatic cancer murine model. When tumor volumes approximated ~140 mm³, nanoseed containing agonist CD40 antibody was intratumorally implanted in a one-time minimally invasive trocar procedure for sustained in situ delivery (8 ug/day), in comparison to systemic administration (100 ug every other day for a total of 4 doses) and vehicle controls. Treatment response and adverse effects were evaluated using tumor volume, flow cytometry and imaging mass cytometry assessment of immune activity, serum ELISA, liver histology and Kaplan Meier survival analysis.

Results Sustained release of agonist CD40 antibody directly into the tumor microenvironment through the nanoseed resulted in significant tumor burden reduction and prolonged survival of KPC mice without toxicities. With nanoseed-CD40 treatment, local tumor immune microenvironment modulation was observed with increased intratumoral CD8⁺ effector T cells and M1 macrophages, as well as decreased M2 macrophages and Foxp3⁺ Treg. Moreover, local treatment with nanoseed-CD40 yielded systemic reduction of M2 macrophages. As opposed to systemically treated mice, which showed inflammatory liver histology and elevated serum IL-6, IFN- γ , TNF α , and M-CSF levels indicative of cytokine storm, nanoseed-CD40 cohort were comparable to vehicle controls. Further, in a bilateral KPC model, nanoseed-CD40 treatment significantly inhibited growth of the contralateral untreated tumor, suggestive of a systemic antitumor response.

Conclusions Overall, our results support further development of the nanoseed as a clinically viable approach for intratumoral immunotherapy delivery in a safe and effective manner to locally modulate tumor immune microenvironment for systemic antitumor effects.

REFERENCES

1. Sheth RA, Murthy R, Hong DS, *et al.* Assessment of Image-Guided Intratumoral Delivery of Immunotherapeutics in Patients With Cancer. *JAMA Network Open* 2020;**3**(7):e207911-e207911.

2. Muñoz NM, Williams M, Dixon K, *et al.* Influence of injection technique, drug formulation and tumor microenvironment on intratumoral immunotherapy delivery and efficacy. *Journal for ImmunoTherapy of Cancer*. 2021;**9**(2):e001800.
3. Chua CYX, Jain P, Susnjar A, *et al.* Nanofluidic drug-eluting seed for sustained intratumoral immunotherapy in triple negative breast cancer. *Journal of Controlled Release*. 2018;**285**:23–34.
4. Liu HC, Viswanath DI, Pesaresi F, *et al.* Potentiating Antitumor Efficacy Through Radiation and Sustained Intratumoral Delivery of Anti-CD40 and Anti-PDL1. *Int J Radiat Oncol Biol Phys*. 2021;**110**(2):492–506.
5. Chua CYX, Ho JS, Demaria S, Ferrari M, Grattoni A. Emerging technologies for local cancer treatment. *Advanced Therapeutics*. 2020.

<http://dx.doi.org/10.1136/jitc-2022-SITC2022.0083>

Abstracts

84

SYSTEMIC LEVELS OF THE SOLUBLE CO-INHIBITORY AND CO-STIMULATORY IMMUNE CHECKPOINT MOLECULES IN BASAL CELL CARCINOMA

¹Nonkululeko Z Malinga, ¹Bernardo Rapoport*, ¹Siwela Shalette, ¹Helen Steel, ¹Luyanda Kwofie, ¹Pieter Meyer, ¹Ronald Anderson, ¹Mahlatse Kgokolo, ²Teresa Smit. ¹University of Pretoria, Pretoria, South Africa; ²The Medical Oncology Centre of Rosebank, Johannesburg, South Africa

Background Although co-inhibitory immune checkpoint proteins are primarily involved in promoting inhibitory cell-cell interactions in adaptive immunity, especially tumor immunity, the soluble cell-free variants of these molecules are also detectable in the circulation of cancer patients where they retain immunosuppressive activity. Nevertheless, little is known about the systemic levels of these soluble co-inhibitory immune checkpoints in patients with various subtypes of basal cell carcinoma (BCC), which is the most invasive and treatment-resistant type of this most commonly occurring malignancy.

Methods We have measured the systemic concentrations of five prominent co-inhibitory immune checkpoints, namely CTLA-4, LAG-3, PD-1/PD-L1, and TIM-3, as well as those of C-reactive protein (CRP) and vitamin D (VD), in a cohort of patients (n = 40) with BCC, relative to those of a group of control participants (n = 20), using the combination of multiplex bead array, laser nephelometry, and ELISA technologies, respectively. Additionally, in the subsequent study, we measured co-stimulatory checkpoints (CD27, CD28, CD40, ICOS, GITR, GITRL, CD8.6, and CD80), co-inhibitory checkpoints (PD-1, PD-L1, CTLA-4, TIM-3, LAG-3, BTLA-4) and dual checkpoints (TRL-2 and HVEM).

Results The median systemic concentrations of CRP and VD were comparable between the two groups; however, those of all five immune checkpoints were significantly elevated ($P=0.0184 - P < 0.00001$), with those of CTLA-4 and PD-1 being highly correlated ($r = 0.87; P < 0.00001$) (table 1). The levels of CD27, CD28, CD40, and other immune checkpoint levels will be presented at the time of the meeting as this study is ongoing.

Conclusions This novel finding identifies the existence of systemic dysregulation in BCC and underscores the therapeutic promise of immune checkpoint targeted therapy, as well as the potential of these immune checkpoint molecules to serve as prognostic/predictive biomarkers in BCC.

Ethics Approval Ethics approval was granted by The Research Ethics Committee, Faculty of Health Sciences, University of Pretoria (Ethics Committee Approval Numbers 326/2016, 251/2019 and 510/2020).

Abstract 84 Table 1 Comparing the median levels of systemic soluble immune checkpoints in basal cell carcinoma patients with those of healthy controls

Table 1: Comparing the median levels of systemic soluble immune checkpoints in basal cell carcinoma patients with those of healthy controls.

ICM	BCC (n=40)	Controls (n=20)		p value
		Median (pg/ml)	Median (pg/ml)	
Co-stimulatory	CD27	3360,865 (2363.64 - 4970.73)	1410.54 (1259.16 - 2172.74)	0,0002
	CD28	170,47,05 (8487,16 - 30677,1)	11314.17 (7239,45 - 14933,96)	0,2523
	CD40	1508,8 (668,17 - 1778,77)	1222,253 (769,43 - 1349,26)	0,4148
	ICOS	15359,79 (7591,11 - 20398,75)	12902,86 (7980,59 - 15316,63)	0,3428
	GITR	1217,4 (664,31 - 1795,54)	898,205 (228,01 - 1222,24)	0,0538
	GITRL	2527,32 (1470,48 - 3599,4)	2107,325 (1784,1 - 2724,34)	0,3799
	CD8.6	2215,865 (793,93 - 3092,67)	1638,05 (781,54 - 2144,3)	0,2427
	CD80	1480,26 (863,6 - 2161,26)	1212,29 (781,71 - 1590,1)	0,3428
	PD-1	16978,21 (5714,48 - 14351,17)	2524,89 (1832,95 - 3038,34)	0,0000
	PD-L1	1740,25 (773,982 - 1930,649)	228,67 (139,01 - 274,86)	0,0000
Co-inhibitory	PD-L2	14125,27 (18102,68 - 16375,87)	12008,07 (10670,4 - 14023,9)	0,0011
	CTLA-4	744,82 (422,08 - 1129,16)	126,49 (56,24 - 241,25)	0,0000
	TIM-3	7519,74 (6019,869 - 8157,925)	12008,07 (10670,4 - 14023,9)	0,0000
	LAG-3	388288,90 (243248,3 - 640480,6)	11108,96 (6995,67 - 15093,31)	0,0000
	BTLA-4	12284,97 (8758,07 - 16181,59)	26439,74 (17274,89 - 32427,56)	0,0061
Dual	TLR-2	17896,28 (10473,49 - 24211,18)	15731,88 (12262,72 - 19913,19)	0,6437
	HVEM	2052,45 (1894,5 - 2317,55)	1290,11 (1263,46 - 1488,04)	0,0000
Other	Arginase	25,52 (25,52 - 25,8505)	25,52 (25,52 - 72,15)	0,2897
	RANTES	131,46 (97,26 - 174,9144)	90,83 (70,78 - 148,74)	0,2097
	TGF-β1	7,54 (4,549417 - 10,79543)	5,83 (4,18 - 8,83)	0,1469
	FAP	115,67 (94,02 - 130,19)	109,04 (70,83 - 127,33)	0,2425

<http://dx.doi.org/10.1136/jitc-2022-SITC2022.0084>

85

MAPPING THE TUMOR MICROENVIRONMENT WITH SEQUENTIAL IMMUNOFLUORESCENCE, AN AUTOMATED IMAGE ANALYSIS PIPELINE, AND SPATIAL METRICS

¹Joanna Kowal*, ¹Diego Dupouy, ¹Pedro Machado Almeida, ²James Mansfield, ¹Benjamin Pelz, ²Fabian Schneider, ²David Mason. ¹Lunaphore Technologies, Tolothenaz, Switzerland; ²Visiopharm A/S, Horsholm, Denmark

Background Spatial biology enables the interrogation of tissue composition at a single cell level with preservation of spatial context, which opens new avenues for tumor microenvironment (TME) studies.¹ Biomarkers' composition of the tissue can be interrogated with hyperplexed immunofluorescence, wherein an imaging detection is performed for each marker on the same slide. The COMET™ platform performs sequential immunofluorescence (seqIF™) and enables full automation of such workflow, where: up to 40 biomarkers can be detected with full automation from staining to data acquisition. The resulting hyperplex images are rich sources of data about the specimens. To extract information from such a dataset, Oncotopix® Discovery (Visiopharm) has a dedicated pipeline for image analysis that delivers single cell phenotypic information and biodistribution, providing access to the spatial composition of the TME.

Methods An FFPE Lung Tissue Microarray underwent sequential cycles of staining and imaging with COMET™ platform seqIF™ assay. Iterative cycles of staining, imaging and antibody elution allowed the detection of 20 antigens spanning across epithelial tumor and immune markers (panCK, E-Cad, aSMA, CD31, CD3, CD4, CD8, FoxP3, CD20, HLA-DR, Ki67, Vimentin, CD16, CD68, CD11b, CD163, CD14, CD11c, PD-1, PD-L1). The resulting image contains 23 channels: nuclear detection with DAPI, 2 channels of tissue autofluorescence (AF), and 20 marker channels. All layers were aligned and stitched into a single ome.tiff automatically by the COMET™ control software. Subsequent AF subtraction was performed in the Viewer by Lunaphore. The AF-subtracted image was analyzed using Oncotopix Discovery. The analysis pipeline consisted of a deep-learning (DL)-based tissue segmentation (tumor, stroma, necrosis, etc.), a pre-trained DL DAPI nuclear segmentation step, cellular phenotyping, and spatial metrics among the various cell types.

Results We interrogated tumor composition with the use of COMET™ platform and Oncotopix Discovery Software from Visiopharm. Specific cellular phenotypes of interest are proliferating tumor cells, proliferating T cells, immunosuppressive macrophages and antigen-presenting cells and their interactions with a focus on the PD-(L)1 pathway.

Conclusions The combination of hyperplex staining and advanced image analysis and in situ cellular phenotyping allows the identification of tissue composition. It is a crucial step for understanding and harnessing tissue biology. Being able to analyze the spatial distribution of specifically phenotyped cells in the TME enables to identify reliable biomarkers as predictive factors of response to therapies.

REFERENCE

1. Mund A, Brunner AD, Mann Unbiased spatial proteomics with single-cell resolution in tissues. *Molecular Cell* 2022; **82**:2335–2349.

<http://dx.doi.org/10.1136/jitc-2022-SITC2022.0085>

86

HPV16 E1 AND E2 ELICIT A ROBUST CYTOTOXIC IMMUNE RESPONSE IN VIRALLY DRIVEN OROPHARYNGEAL SQUAMOUS CELL CARCINOMA

¹Christine McInnis*, ¹Shilpa Bhatia, ¹Brinda Vijaykumar, ¹Qiaomu Tian, ¹Yanbo Sun, ¹Del Leistriz-Edwards, ²Charles Quinn, ²Sean Donnelly, ²Ravindra Uppaluri, ²Ann Marie Egloff, ¹Daniel Pregibon, ¹Lakshmi Srinivasan, ¹Anthony Coyle, ²Glenn Hanna. ¹Repertoire Immune Medicines, Cambridge, MA, USA; ²Dana Farber Cancer Institute, Boston, MA, USA

Background Human papillomavirus (HPV) infection is a risk factor for oropharyngeal squamous cell carcinoma (OPSCC). HPV+ OPSCC is characterized by distinct biology, a heterogeneous immune landscape, and accounts for approximately 14,400 new diagnoses per year in the U.S. For patients with locoregional recurrence or distant metastasis, systemic treatment options beyond immune checkpoint inhibitors are limited. Though a decline in HPV+ HNSCC is expected due to HPV vaccination campaigns, incidence is currently increasing, prompting a wave of therapeutic development. While most therapeutic efforts have been focused on eliciting a cellular response to HPV early antigens E6 and E7, we sought to identify additional highly prevalent, immunogenic targets in both early stage as well as in relapsed/refractory HPV+ HNSCC.

Methods Treatment-naïve HPV+ OPSCC patients (n=19) were prospectively enrolled under an institutional review board (IRB)-approved tissue collection protocol (DF/HCC#09-472) for collection of surgical specimens. Tumor tissue from a biopsy or definitive oncologic transoral robotic-assisted resection specimen was collected prospectively for analysis. Multiplexed, barcoded peptide-MHC-I tetramer libraries containing epitopes derived from the HPV16 genome were used to probe dissociated tumors followed by single cell RNA sequencing using the 10x Genomics platform. SingleR and published gene marker sets were used to phenotype and perform broad lineage assignment.

Results We found broad T-cell reactivity to several HPV proteins across multiple HLA alleles and epitopes. E1 and E2-reactive T-cells were cytotoxic and highly expanded, whereas E5, E6 and E7-reactive T-cells were rare and displayed exhausted or naïve phenotypes. Cytotoxic E2 T-cell responses were associated with loss of E2 expression in at least one tumor suggesting functional capacity of these T-cells. We also identified evidence of pseudo-public TCR sequences, as TCR alpha, beta or paired CDR3 sequences associated with E2 reactivity were shared across multiple patients with common HLAs. TCR specificity was confirmed for several TCR-epitope interactions using recombinant TCRs and cognate peptide.

Conclusions We employed high-throughput, single-cell immune synapse profiling to characterize the cellular response to HPV + HNSCC across common HLA haplotypes and identified new candidates for immunotherapeutic intervention. We found that HPV16 proteins E1 and E2 induce robust, effective cytotoxic responses in HPV16-driven OPSCC. These findings indicate HPV16 E1 and E2-directed immunotherapy may be effective among patients with OPSCC expressing these antigens.

Ethics Approval Patients were consented and enrolled under an institutional review board (IRB)-approved tissue collection protocol (DF/HCC#09-472).

<http://dx.doi.org/10.1136/jitc-2022-SITC2022.0086>

87 **DEEP PHENOTYPING AND SPATIAL IMMUNE
CONTEXTURE THROUGH A COMBINED MULTIPLEX
IMMUNOFLUORESCENCE APPROACH**

Harry Nunns, Arezoo Hanifi, Erinn Parnell, Nam Tran, Sara Pollan, Qingyan Au*.
NeGenomics Laboratories Inc., Aliso Viejo, CA, USA

Background Tertiary lymphoid structures (TLS) have been observed in a variety of solid tumors and growing evidence has shown that TLS can be promising prognostic indicators of positive outcomes for patients with solid tumors including colorectal cancer (CRC).¹ Large-scale retrospective analysis shows patients with mature TLS in particular respond to PD-1/PD-L1 antibody treatment with improved objective response, progression-free and overall survival.² Since not all patients respond to immune checkpoint blockade (ICB) therapy, identifying patients with TLS can be clinically relevant as it enables selection of patients likely to respond. In this study, we demonstrate a tissue-based phenotyping workflow combining two complementary multiplex immunofluorescence (mIF) platforms to enable identification of TLS, characterization of TLS maturation stage and spatial phenotyping of tumor infiltrating lymphocytes (TIL) on whole slide scan.

Methods In this study, 40 CRC patients were first stained with an in-house developed PhenoImager™ mIF panel detecting CD20, CD21, CD23, CD3 and Cytokeratin. Whole slide scan was acquired using PhenoImager HT, followed by biomarker classification and TLS identification using custom analytics algorithm generated with Indica HALO® platform.

An adjacent section of tumor sample was then stained and analyzed with a 17-plex MultiOmyx™ mIF panel. Using the MultiOmyx assay in combination with proprietary deep-learning-based image analysis (NeoLYTX), we further characterized the TLS maturation stage and interrogated the correlation of the TLS presence with subtypes of TIL expression in the CRC samples.

Results PhenoImager 5-plex TLS panel combined with Halo custom analysis successfully identified TLS in the tumor microenvironment (TME) of CRC samples and led to the strategic selection of regions of interest (ROI) for further characterization by high-plex assay. The TLS detection was found to be concordant between both mIF platforms in the CRC samples. MultiOmyx 17-plex analysis was able to provide a detailed picture of TLS and enabled further classification of TLS into different maturation stages based on biomarker expression and spatial organization of immune cells in the CRC samples.

Conclusions Combination of PhenoImager and MultiOmyx IF provides a complementary and powerful solution to study cellular composition within the TME. PhenoImager assay characterizes the immunophenotypes and visualizes the spatial distribution of TIL at single-cell resolution on whole slides. High dimensional analysis by MultiOmyx can provide greater understanding of the immune contexture within the TME and deeper insights into the correlations between biomarkers. This combined approach may have broad application and provides novel insights into the complex TME.

REFERENCES

1. *Oncoimmunology*. 2020; **9**(1): 1724763.
2. *Nat Cancer*. **2**, 794–802 (2021).

<http://dx.doi.org/10.1136/jitc-2022-SITC2022.0087>

88 **GENETIC ASSOCIATION BETWEEN VITILIGO GENETIC SUSCEPTIBILITY AND RESPONSE TO IMMUNE-CHECKPOINT INHIBITOR THERAPY IN ADVANCED MELANOMA PATIENTS**

¹Wouter Ouwerkerk*, ¹Saskia Chielie, ¹Marcel Bekken, ²Remco van Doorn, ³Christian Blank, ³John Haanen, ⁴Karijn de Joode, ⁴Ron Mathijssen, ⁴Astrid van der Veldt, ²Ellen Kapiteijn, ⁵Karijn Suijkerbuijk, ⁶Kalijn Bol, ⁷Geke Hospers, ⁸Tomas Kirchoff, ¹Rosalie Luiten. ¹Amsterdam UMC, Amsterdam, Netherlands; ²LUMC, Leiden, Netherlands; ³NKI, Amsterdam, Netherlands; ⁴Erasmus MC, Rotterdam, Netherlands; ⁵University Medical Centre Utrecht, Utrecht, Netherlands; ⁶Radboudumc, Nijmegen, Netherlands; ⁷UMCG, Groningen, Netherlands; ⁸Perlmutter Cancer Center, New York, NY, USA

Background Only ~50% of advanced melanoma patients show objective responses to immune checkpoint inhibitor (ICI) therapy. Currently, there are still no reliable predictive biomarkers explaining ICI response heterogeneity. Vitiligo development during ICI therapy is associated with a better prognosis in melanoma patients. Genetic susceptibility to vitiligo has been well-characterized using multiple large GWAS studies, and includes genes that are also associated to other autoimmune diseases.

Objective To test if the germline genetic association to vitiligo is able to predict response to ICI in patients with advanced melanoma.

Methods Data from >1,000 patients from 6 melanoma centers in the Netherlands participating in the international IO-GEM melanoma consortium were analyzed in this study. DNA was extracted from blood or saliva and genotyped by Illumina GSA MD v3.0. Clinical data was obtained from the Dutch Melanoma Treatment Registry. We developed a polygenetic vitiligo-susceptibility score using a pre-defined set of 54 vitiligo-associated single nucleotide polymorphisms (SNPs) predicting overall survival.

Results We found a significant protective relation of the unweighted vitiligo-susceptibility score to all-cause mortality. Weighted for the association to vitiligo, the vitiligo-susceptibility score outperformed the unweighted score in predicting all-cause mortality.

Conclusions These results suggest that genetic susceptibility to vitiligo may be associated with more favorable survival outcome in melanoma patients upon ICI treatment. The risk scores will be validated in the remaining part of IO-GEM.

<http://dx.doi.org/10.1136/jitc-2022-SITC2022.0088>

89 **MULTIPLEXED ION BEAM IMAGING (MIBI) UNCOVERS ADAPTIVE IMMUNE RESPONSES ASSOCIATED WITH CLINICAL OUTCOMES IN ORAL CAVITY SQUAMOUS CELL CARCINOMA TREATED WITH NEOADJUVANT PD-1 INHIBITOR**

¹Raghav Padmanabhan, ²Hannah Knochelmann*, ¹Monirath Hav, ¹Mate Nagy, ¹Peng Si, ¹Sweta Bajaj, ³Gregory Lesinski, ⁴David Neskey, ³Chrystal Paulos. ¹Ionpath, Inc., Menlo Park, CA, USA; ²Emory University, Charleston, SC, USA; ³Emory University School of Medicine, Atlanta, GA, USA; ⁴Sarah Cannon Research Institute, Charleston, SC, USA

Background Oral cavity squamous cell carcinoma (OCSCC) is a subset of head and neck cancer with high recurrence rates. Recent evidence suggests that effective anti-tumor immunity can be induced by neoadjuvant immunotherapy in subsets of head and neck cancer patients, though immune mechanisms of response remain unclear. CD26, a novel costimulatory molecule, marks T cells with potent antitumor activity; therefore, we hypothesized that tumor infiltration by CD26+ T cells and other immune subsets may be related to treatment responsiveness. Here, using Multiplexed Ion Beam Imaging (MIBI), we report a first-in-class analysis of CD26 expression in relation to the immune and spatial architecture of the OCSCC micro-environment in patients treated with neoadjuvant nivolumab.

Methods Surgical pathology specimens from 8 OCSCC patients treated with pre-surgical nivolumab were stained with a panel of 31 metal-labeled antibodies. Tissues were imaged using MIBITM, and single cell segmentation was performed using a machine learning based tool that enabled downstream enumeration of 35 cell populations and quantitative analyses of both the costimulatory protein CD26 and immune checkpoint proteins as well as their spatial distribution. Cell population, protein expression, and spatial architectural differences were compared between patients with progressive disease and those with partial response.

Results A higher density of proliferating tumor cells was found in tumors from patients with progressive disease ($p=0.01$). Conversely, tumors from patients with partial response contained higher densities of cytotoxic T cells ($p=0.004$), particularly the activated and CD26+ cytotoxic T cell subsets. Evaluation of checkpoint expression across all populations showed that CD26 was predominantly expressed on T cells although a few of the myeloid subsets also expressed high CD26, particularly in patients with partial response. Finally, spatial analysis revealed pronounced interaction between tumor cells and cytotoxic T cells, notably of the activated cytotoxic T cell phenotype, in the samples from patients with partial response.

Conclusions MIBITM offers high-parameter tissue imaging, with a sensitivity and resolution suited to understanding the differences in the tumor immune landscape between patients with varied responsiveness to immunotherapies. In this study, OCSCC tumors from patients with partial response to neoadjuvant PD-1 inhibition showed evidence of adaptive immune responses with significant increases in infiltration of activated cytotoxic T cells and CD26+ cytotoxic T cells as well as greater interaction between activated cytotoxic T cells and tumor cells.

<http://dx.doi.org/10.1136/jitc-2022-SITC2022.0089>

Abstracts

90

CIRCULATING ALTRUISTIC STEM CELLS AS A MARKER OF IMMUNOSUPPRESSION IN ORAL CANCER

¹Lekhika Pathak*, ¹Seema Bhuyan, ²Bidisha Pal, ¹Partha Saikia, ¹Sukanya Gayan, ¹Shirsajit Mitra, ¹Tutumoni Baishya, ²Ramana Chilakamarti, ¹Bikul Das. ¹KaviKrishna Laboratory, Guwahati, India; ²Thoreau Laboratory for Global Health, Boston, MA, USA

Background Head & neck cancer is the 4th cancer, and most of them are diagnosed late, and treated with cisplatin monotherapy. In these subsets of patients, immunotherapy has been tried, but without major success.¹ We speculate that circulating altruistic stem cells may serve as biomarker for immunotherapy. Previously, we showed that oral cancer CSCs reprogram MSCs to altruistic phenotype,^{2, 3} an embryonic stem cell like phenotype having niche defending ability.⁵ Here, we propose to test the immunosuppressive ability of ASCs, and their detection in the circulation of head & neck cancer subjects undergoing platinum based chemotherapy.

Methods We obtained ASCs by culturing CD271+ BM-MSCs with the conditioned media of EPCAM+/ABCG2+ CSCs of SCC-25 cancer cell line or primary tumors as previously described.² The immunosuppression test: immunosuppressive secretory factors, mixed lymphocyte reaction (MLR) assay, and a Boyden chamber based co-culture assay with NK cells.⁴ Next, we obtained circulating CD271+/CD45- cells of stage IV head and neck cancer subjects (n=20) (5). Kaplan-Meier survival analysis and log-rank test to find association between the presence of circulatory ASCs and overall survival (OS).

Results CSCs including primary tumor obtained CSCs reprogram CD271+ MSCs to ASC phenotype; these cells secrete high level of Nitric oxide, IDO, TGF-beta, IL-10 and PGE-2. ASCs exhibited marked immunosuppression in the MLR test. In Boyden chamber assay, ASCs markedly decreased the number of NKG2D+ NK cells, and CD8+ T cells by 4-5 fold (p<0.02; n=3), whereas increased the CD4+/FoxP3/CD25- T-reg cells by 3-fold (p<0.05, n= 4). Moreover, ASCs, upon co-culture, increases the clonogenic capacity of non-CSCs (EPCAM+/ABCG2-/ALDH-) cells by 5-fold (p<0.02; n=4), while significantly decreasing the secretion of NKG2DL of these cancer cells. Next, we isolated circulating CD271+/CD45- cells from the 12/20 subjects with oral cancer and confirmed their ASC phenotype (figure 1A-E). These cells were in vitro cultured (figure 1D), and the conditioned media obtained showed marked immunosuppressive activities including significant reduction of NKG2D+ NK cells in the in vitro Boyden chamber assay. Importantly, these 12 out of 20 patients showed poor treatment response to platinum therapy. The OS at 6 months was 24.6% for circulating ASC-positive patients and 47.4% for circulating ASC-negative patients (log-rank test, p<0.001).

Conclusions The circulatory ASCs could be a promising biomarkers for immunotherapy.

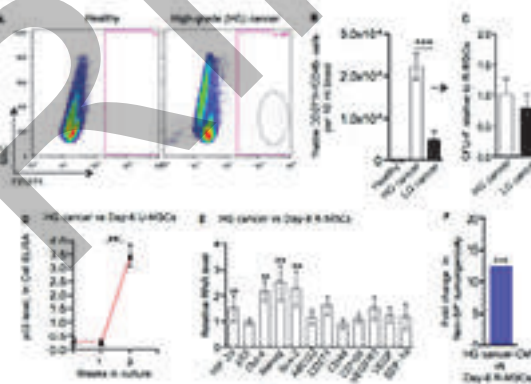
Acknowledgements We thank the staffs of KaviKrishna Telemedicine Care, Sualkuchi, Assam, India for their support in patient selection for the study, obtaining consent, sample collection and patient follow up. For funding, we thank KaviKrishna foundation, Sualkuchi, Assam, India, Department of Biotechnology, Govt of India and KaviKrishna USA Foundation.

REFERENCES

1. Bhuyan S, Pal B, Pathak L, Saikia PJ, Mitra S, Gayan S, Mokhtari RB, Li H, Ramana CV, Baishya D, Das B*. Targeting tumor stemness switch phenotype by activating pathogen induced stem cell niche defense. *bioRxiv* 2022.03.25.485829; doi: <https://doi.org/10.1101/2022.03.25.485829>

2. Talukdar J *et al.* Migratory cancer side population cells induces stem cell altruism in bone marrow mesenchymal stem cells to resist therapy, and enhance tumorigenic potential of non-tumorigenic cells. [abstract]. in *Cancer Res*, L.P.P.A. New Orleans, Editor. 2016 Apr 16–20; : In: *Proceedings of the 107th Annual Meeting of the American Association for Cancer Research*; . p. 920. <https://doi.org/10.1158/1538-7445.AM2016-920>
3. Pal B, Sandhya S, Talukdar S, Pathak L, Li H, Das B. Developing micro-fluidic chip to understand altruistic stem cell reprogramming. (https://cancerres.aacrjournals.org/content/79/13_Supplement/5154).
4. Bhuyan S, Pal B, Li H, Bhuyan R, Pathak L, Gayan S, Baishya D, Das B. Mesenchymal stem cell altruism mediates a novel HMGB1/NKG2D immune response in oral cancer (<https://doi.org/10.1158/1538-7445.AM2020-5539>).
5. Pathak L, Gayan S, Pal B, Talukdar J, Bhuyan S, Sandhya S, Yeger H, Baishya D, Das B*. Coronavirus Activates an Altruistic Stem Cell-Mediated Defense Mechanism that Reactivates Dormant Tuberculosis: Implications in Coronavirus Disease 2019 Pandemic. *Am J Pathol*. 2021 Jul; **191**(7):1255–1268. doi: 10.1016/j.ajpath.2021.03.011. Epub 2021 Apr 19. PMID: 33887214. (<https://pubmed.ncbi.nlm.nih.gov/33887214/>).

Ethics Approval The clinical study was approved by ‘Institutional Ethics Committee’ of KaviKrishna Laboratory, Guwahati, India and KaviKrishna Telemedicine Care, Sualkuchi, Assam, India. The stem cell study was conducted following the guidelines of NAC-SCRT and was approved by Institutional Committee for Stem Cell Research (ICSCR), KaviKrishna



Abstract 90 Figure 1 Subjects with advanced oral squamous cell cancer e

A. Representative flow cytometry profile depicting the presence of CD271+ cells in a population of EpCam-/CD45- cells sorted from peripheral blood mononuclear cells (PB-MNCs) of subjects with Oral cancer (supplementary table 4). The PB-MNCs were subjected to immunomagnetic sorting for EpCam-/CD45- cells. The sorted population was then mixed with CD271-/CD45+ cells recovered from the same subject for 1-day in serum free medium, fixed in 4% formaldehyde, and subjected to CD271 staining. The mixing with CD271-/CD45+ cell was done to minimize cell loss during flow cytometry procedure. B. The quantitative data of viable circulating CD271+/CD45- cells was estimated by trypan blue exclusion assay. Healthy subjects did not exhibit circulating CD271+/CD45- cells. C. Relative CFU-F was estimated in the isolated circulating CD271+/CD45- cells to confirm the mesenchymal phenotype. High Grade Oral Cancer (HG cancer) CFUs: $4.2 \pm 1.5/10^3$ cells (n=4). D. Relative protein level of p53 as measured by In-cell ELISA of CD271+/CD45- cells cultured in vitro in serum free medium. E. Gene expression profiles of circulating CD271+/CD45- cells. Note that circulating CD271+ cells exhibited enhanced expression of HIF-2 α , Nanog, Sox-2 and Oct-4. The CD271+/CD45- cells were cultured in the serum free StemSpan medium for one week to obtain mRNA. The values were compared with Day-8 CM treated MSCs. F. CM of circulating CD271+/CD45- cells obtained from HG- cancer exhibited higher capacity to enhance the tumorigenicity of non-SP cells compared to CM of R-MSCs (Day-8, reprogrammed by SCC-25 ABCG2+CSC-CM).

<http://dx.doi.org/10.1136/jitc-2022-SITC2022.0090>

91

CIRCULATING LIPID PROFILE AS A PROGNOSTIC FACTOR IN PATIENTS WITH ADVANCED SOLID TUMORS TREATED WITH IMMUNE CHECKPOINT INHIBITORS

¹Federica Pecci*, ¹Luca Cantini, ¹Valeria Cognigni, ²Fabiana Perrone, ¹Veronica Agostinelli, ²Giulia Mazzaschi, ²Elda Favari, ²Michele Maffezzoli, ³Alessio Cortellini, ¹Francesca Rossi, ¹Rebecca Chiarotti, ¹Francesco Venanzi, ¹Giulia Mentrasti, ⁴Giuseppe Lo Russo, ⁴Giulia Galli, ⁴Claudia Proto, ⁴Monica Ganzinelli, ¹Francesca Tronconi, ¹Francesca Morgese, ⁵Carla Campolucci, ⁵Marco Moretti, ¹Arianna Vignini, ⁶Melissa Bersanelli, ²Sebastiano Buti, ¹Rossana Berardi. ¹Università Politecnica delle Marche, Ancona, MA, USA; ²University of Parma, Parma, Italy; ³Imperial College London, London, UK; ⁴IRCCS Istituto Nazionale dei Tumori, Milano, Italy; ⁵A.O.U. Ospedali Riuniti, Ancona, Italy; ⁶University Hospital of Parma, Parma, Italy

Background Components of lipid profile seem to impact differently on phenotype and activity of immune cells in cancer.^{1,2} Their prognostic role in solid cancer patients treated with immune checkpoint inhibitors (ICIs) is still matter of debate.

Methods We retrospectively collected baseline clinicopathological characteristics including circulating lipid profile [total cholesterol (TC), triglycerides (TGs), low-density lipoproteins (LDL), high-density lipoproteins (HDL)] of consecutive solid cancer patients treated with ICIs and we investigated their impact on clinical outcomes. Cut-off values showing alteration of plasma lipid profile were ≥ 200 mg/dl for TC, ≥ 170 mg/dl for TGs, ≥ 130 mg/dl for LDL, < 40 mg/dl for HDL in males, < 45 mg/dl for HDL in females.

Results Among 432 patients enrolled, 67% (N=289) were men, 61% (N=266) were diagnosed with advanced non-small cell lung cancer and 86.6% (N=374) of patients were treated with ICIs as monotherapy. Patients' circulating lipid assessments were described in tables (tables 1–3). At a median follow-up of 46 months, patients with $TC \geq 200$ mg/dl showed an improved, although not significant, progression free survival (PFS) (6.61 versus 4.67 months, $p=0.4$) and longer overall survival (OS) (19.4 versus 10.8 months, $p=0.02$) compared to those with $TC < 200$ mg/dl. Conversely, patients with $TGs \geq 170$ mg/dl showed a shorter PFS (2.8 versus 5.07 months, $p=0.006$) and OS (5.92 versus 12.99 months, $p < 0.001$) compared to those with $TGs < 170$ mg/dl. Then, we combined TC and TGs in a LIPID-score that identified three subgroups: good risk (GR) ($TC \geq 200$ mg/dl and $TGs < 170$ mg/dl), intermediate risk (IR) ($TC < 200$ mg/dl and $TGs < 170$ mg/dl or $TC \geq 200$ mg/dl and $TGs \geq 170$ mg/dl) and poor risk (PR) ($TC < 200$ mg/dl and $TGs \geq 170$ mg/dl). The median PFS of GR, IR and PR groups was 7.76, 4.18 and 2.40 months, respectively ($p < 0.001$). Moreover, median OS of GR, IR and PR was 20.36, 11.18 and 4.14 months, respectively ($p < 0.001$) (figure 1). At multivariate analyses, after adjusting for baseline performance status, histology, treatment line, sex, statin use, number of metastatic sites and body mass index, the impact of LIPID score remained significant for both PFS and OS (table 4). Looking at TC components, HDL and LDL, a significant association was detected only for HDL and OS, with patients characterized by higher HDL levels showing longer OS (15.3 vs 10.1 months, $p=0.02$).

Conclusions LIPID score seems to strongly define subgroups of patients treated with ICIs with different prognosis. Further mechanistic insights are needed to clarify the prognostic and predictive role of lipid profile components in patients treated with ICIs.

REFERENCES

- Howie D, Ten Bokum A, Necula AS, Cobbold SP, Waldmann H. The Role of Lipid Metabolism in T Lymphocyte Differentiation and Survival. *Front Immunol.* 2018;**8**:1949. Published 2018 Jan 12. doi:10.3389/fimmu.2017.01949
- Bonacina F, Coe D, Wang G, et al. Myeloid apolipoprotein E controls dendritic cell antigen presentation and T cell activation. *Nat Commun.* 2018;**9**(1):3083. Published 2018 Aug 6. doi:10.1038/s41467-018-05322-1

Ethics Approval Ethical approval to conduct this study was obtained by the respective local ethical committees on human experimentation of each participating center, after previous approval by the coordinating center ('Comitato Etico Regionale delle Marche – C.E.R.M.', Reference Number 792). All study related procedures and data collection were conducted in accordance with the Declaration of Helsinki and in accordance with Good Clinical Practice.

Consent Not applicable

Abstract 91 Tables 1,2,3 Patients circulating lipid assessment

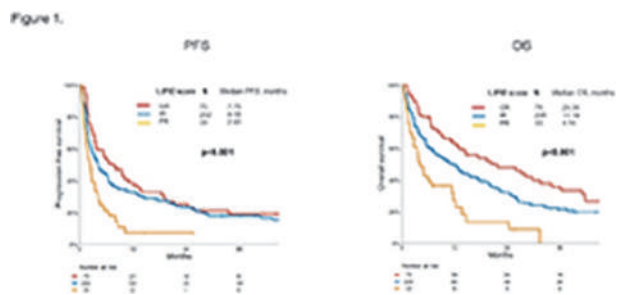
BMI, body mass index; TC, total cholesterol; TGs, triglycerides; LDL, low-density lipoproteins; HDL, high-density lipoproteins, NA, not available

Abstract 91 Table 4 Multivariate analysis for PFS and OS

Test variables	PFS			OS		
	HR	95% CI	p	HR	95% CI	p
Histology						
NSCLC/Other*	0.58	0.44-0.80	<0.001	0.58	0.42-0.79	<0.001
Sex						
Female (ref: Male)	1.11	0.87-1.42	0.516	1.45	1.17-1.80	0.001
Treatment line						
1st/2nd (ref: 3rd)	1.32	1.05-1.60	0.022	1.30	1.10-1.51	0.001
ECOG PS						
0-1 (ref: 2)	2.41	1.42-3.99	<0.001	2.41	1.67-3.49	<0.001
Metastatic sites						
0-1 (ref: 2)	1.58	1.07-2.32	0.021	1.80	1.17-2.75	0.007
BMI						
<25 (ref: 25-)	0.40	0.25-0.74	0.001	0.76	0.58-1.04	0.001
Statin use						
Yes (ref: No)	1.02	0.76-1.36	0.918	0.80	0.65-1.01	0.045
LIPID score						
GR (ref)						
IR	1.21	0.86-1.68	0.279	1.55	1.05-2.27	0.028
PR	2.01	1.26-3.20	0.004	2.81	1.71-4.54	<0.001

PFS, progression free survival; OS, overall survival; HR, hazard ratio; CI, confidence interval; NSCLC, non-small cell lung cancer; ECOG PS; Eastern Cooperative Oncology Group Performance Status; BMI, body mass index; GR, good risk; IR, intermediate risk; PR, poor risk. All variables referred to baseline characteristics of patients. *Others: melanoma, renal cell carcinoma, urothelial carcinoma, head and neck cancer. Statistically significant ($P < 0.05$).

Abstracts



Abstract 91 Figure 1 PFS and OS according to LIPID score
GR, good risk; IR, intermediate risk; PR, poor risk

<http://dx.doi.org/10.1136/jitc-2022-SITC2022.0091>

PREPRINT

NOVEL RNA-SEQ PLATFORM ENABLES REPURPOSING OF APPROVED DRUGS IN RARE CANCERS, IMPROVING OUTCOMES

Gitte Pedersen*. *Genomic Expression Inc, Beverly, MA, USA*

Background Rare cancers are those that affect fewer than 40,000 people per year in the U.S. As a group, they make up just over 25% of all cancers and are responsible for 25% of all cancer deaths each year. There are few effective drug treatment options for rare cancers, whereas over 300 drugs have been approved by the FDA for treating non-rare cancers. Repurposing already approved cancer drugs to treat rare cancers is much faster and cost-effective than developing new drugs, but success depends on matching these drugs to rare cancers with the corresponding drug targets.

RNA sequencing has the potential to identify many clinically actionable molecular changes, whereas DNA sequencing is limited to some targeted drugs and typically misses the identification of aberrantly expressed checkpoint inhibitors, tumor antigens, and fusion events.

To enable RNA-sequencing in clinical samples, we had to overcome two issues: 1) tissue samples are typically embedded in FFPE, which results in highly fragmented RNA, making sequencing of samples difficult; 2) how best to interpret aberrant gene expression events and translate these results into clinical action.

Methods We address this issue through the implementation of our CLIA-validated *quantitative* OneRNA[®]-sequencing platform for treatment navigation. The OneRNA platform is an end-to-end integration of 1) CLIA-validated quantitative mRNA sequencing chemistry optimized for FFPE tumor specimens and low input liquid biopsy samples, such as blood, saliva, or urine, and 2) a validated bioinformatics pipeline, normalization methods, and an interpretative database that matches aberrant gene expression events to already approved drugs. Actionable genes are defined as genes that code proteins or nucleic acids that (1) are direct targets of drugs, (2) are ligands for the drug targets, or (3) are treatment selection biomarkers listed on the FDA label.

Results This study demonstrates the potential clinical utility of OneRNA[®] in detecting aberrant gene expression events and connecting them through a drug target and biomarker database to already approved drugs. Examples of improved outcomes in rare cancers are presented. The potential impact includes truly individualized treatment options in rare cancers. OneRNA[®] typically identifies 5 or more already approved drugs in all patients, whereas DNA sequencing only identifies 1 drug in 80% of the patients.

Conclusions The OneRNA[®] Platform can be used to expand treatment options for patients with rare cancers and with refractory cancers by matching tumors to existing drug targets, and by identifying high penetrance gene expression variants that may serve as targets for future drugs.

<http://dx.doi.org/10.1136/jitc-2022-SITC2022.0092>

Abstracts

93

PCR ASSAY TO IDENTIFY WOODCHUCK HEPATITIS VIRUS POSTTRANSCRIPTIONAL REGULATORY ELEMENT IN CAR-T AND TCR-T CELLS FOR FRESH AND FORMALIN-FIXED SAMPLES

¹Shalini Pullarkat*, ¹Jocelyn Wright, ¹David Woolston, ¹Erik Kimble, ¹Bo Lee, ¹Alexandre Hirayama, ¹Aude Chapuis, ¹Denise Buenostro, ¹Graeme Black, ¹Marie Bleakley, ¹Brandon Seaton, ²Jennifer Specht, ¹Cameron Turtle, ¹Cecilia Yeung, ¹Fred Hutchinson Cancer Center, Seattle, WA, USA; ²University of Washington, Seattle, WA, USA

Background Chimeric antigen receptor T-cell (CART) and engineered T-cell receptor cytotoxic T cell (TCRT) therapy are adoptive cellular therapies developed by modifying T-cells to target surface antigens of cancer cells in CART, and both cell surface and intracellular antigens in the case of TCRT.¹ Producing CART and TCRT cells involves transduction with viral vectors that usually contain the Woodchuck Hepatitis Virus Posttranscriptional Regulatory Element (WPRE) to enhance transcription.² As adoptive cellular therapies become more widely used in cancer care, adverse events (AE) and safety monitoring questions have been raised requiring methods to quantify the amount of CART and TCRTs in patient tissues. We developed a PCR assay to target WPRE for use on archival formalin-fixed, paraffin embedded (FFPE) tissues with the goal of providing valuable information regarding CART/TCRT localization and AEs as most engineered cell products used at our institution are transduced with a viral vector containing WPRE.

Methods DNA from 4 pre-infusion CART (JCAR14 and Kymriah anti-CD19 CARTs) and TCRT (HA-1 TCRT, and MAGEA1 TCRT) products along with unmodified peripheral blood mononuclear cells (PBMC) were extracted.^{3,4,5} WPRE primers were designed to generate short amplicon of 159 base pairs for use on FFPE tissues. Using Phusion High-Fidelity PCR Kit (ThermoFisher Scientific) per manufacture protocol, we verified the assay with fresh DNA as well as FFPE samples. FFPE DNA was extracted from curls cut from paraffin blocks containing cell pellet admixtures of CART or TCRT products and human PBMCs resuspended in Histogel and embedded to mimic cells in fixed tissues.

Results Our PCR protocol detects CART/TCRT constructs in fresh and FFPE samples for JCAR14 CART, Novartis (Kymriah) CART, HA-1 TCRT, MAGEA1 TCRT products. Through limit-of-detection experiments, we detected fresh CART DNA in dilution up to 0.1% (figure 1a) in JCAR14 products. Using fresh TCR-T samples, we detected TCR DNA up to 0.1% (figure 1b) in HA-1 TCRT products. For FFPE-derived DNA, we detected WPRE sequences (figure 1c, d) in four samples with an input amount of 25ng CART/TCRT DNA and various CART/TCRT admixtures confirmed by WPRE-ISH on RNA-scope (table 1).

Conclusions Detecting CART/TCRT using a WPRE PCR assay optimized for use on FFPE is a novel yet simple technique suitable for clinical application in understanding AEs and tumor localization of the adoptive cellular therapy. In detecting CART and TCRT in FFPE, we are now able to study trafficking of these immune effector cells when AE occurs or when post-treatment biopsies are available.

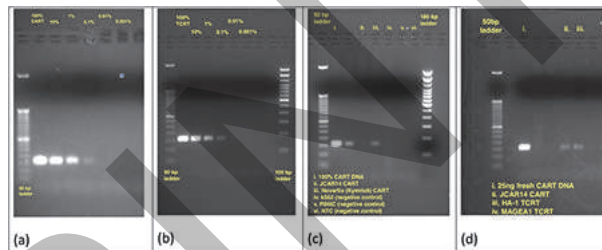
REFERENCES

1. Barrett DM, Grupp SA, June CH. Chimeric antigen receptor- and TCR-modified T cells enter Main Street and wall street. *The Journal of Immunology*. 2015;**195**(3):755–61.
2. Wright JH, Huang L-Y, Weaver S, Archila LD, McAfee MS, Hirayama AV, et al. Detection of engineered T cells in FFPE tissue by multiplex in situ hybridization

and Immunohistochemistry. *Journal of Immunological Methods*. 2021;**492**:112955.

3. Hirayama AV, Gauthier J, Hay KA, Sheih A, Cherian S, Chen X, et al. Efficacy and toxicity of JCAR014 in combination with durvalumab for the treatment of patients with relapsed/refractory aggressive B-cell Non-Hodgkin Lymphoma. *Blood*. 2018;**132**(Supplement 1):1680.
4. Schuster SJ, Tam CS, Borchmann P, Worel N, McGuirk JP, Holte H, et al. Long-term clinical outcomes of Tisagenlecleucel in patients with relapsed or refractory aggressive B-cell lymphomas (Juliet): A Multicentre, open-label, single-ARM, phase 2 study. *The Lancet Oncology*. 2021;**22**(10):1403–15.
5. Biernacki MA, Brault M, Bleakley M. T-cell receptor-based immunotherapy for hematologic malignancies. *The Cancer Journal*. 2019;**25**(3):179–90.

Ethics Approval This study was approved by the University of Washington ethics review board. This study does not involve the use of animal or human subjects.



Abstract 93 Figure 1 (a) Limit of detection dilution series on fresh CART (JCAR14 product). Detection occurred to 0.1% CART, (b) Limit of detection dilution series on fresh TCR (HA-1). Detection occurred to 0.1% TCRT, (c) WPRE assay on FFPE tissues. Tested on 100% CART (+ control), JCAR14, and Novartis (Kymriah) CART products, (d) WPRE assay on FFPE tissues. Tested on 100% CART (+ control), Muc1*, Novartis (Kymriah), JCAR14, CD20 CART, and MAGEA1 TCRT

Abstract 93 Table 1 CART/TCRT products extracted from FFPE, with configuration of block as well as percentage of curl DNA made up of CART/TCRT DNA

Product	Target	FFPE block configuration	Approximate % CART/TCRT in curl
JCAR14	CD19	0%, 66.6% CAR-T	33
Kymriah	CD19	0%, 67% CAR-T	33
HA-1 TCRT	HA1	0%, 20%, 100% TCR-T	40
MAGEA1 TCRT	MAGEA1	0%, 18%, 45% TCR-T	21

<http://dx.doi.org/10.1136/jitc-2022-SITC2022.0093>

94

CYTOF AND SERUM PROTEOMICS SHOW DISTINCT DIFFERENCES IN IMMUNE RESPONSES BETWEEN MYCOSIS FUNGOIDES AND SEZARY SYNDROME TO MONO- AND COMBINATION ANTI-PD-1 IMMUNOTHERAPY

¹Nirasha Ramchurren*, ¹Rachael Parks, ¹Laura Islas, ¹Steven Fling, ²Michael Khodadoust, ¹Evan Newell, ¹David Glass. ¹Fred Hutch Cancer Center, Seattle, WA, USA; ²Stanford University, Palo Alto, CA, USA

Background Cutaneous T cell Lymphoma (CTCL) is a rare malignancy of CD4+ T cells that has few treatment options. Mycosis Fungoides (MF) and Sezary Syndrome (SS) are the most common subtypes of CTCL, with MF confined to the skin and SS a leukemic variant. The PD-1 checkpoint inhibitor, Pembrolizumab, used as a single agent or in combination with Interferon Gamma (IFN γ) to treat CTCL in two Cancer Immunotherapy Trials Network (CITN) studies produced positive clinical outcomes of ~38% in each trial. Additional therapeutic approaches are needed to treat patients refractory to therapy, and informative biomarkers are essential to predict patient response. Here we describe findings from multi-omic studies conducted in the two CITN trials that were designed to elucidate such biomarkers.

Methods A mass cytometry (CyTOF) antibody panel targeting phenotypic, metabolic, and functional proteins expressed by reactive and neoplastic human T cells was developed. This panel was used to interrogate PBMC at several longitudinal timepoints. The serum proteome was also evaluated at these time-points using the Olink platform.

Results CyTOF revealed that the neoplastic T cells, while having patient-specific phenotypic profiles, tended to overexpress checkpoint and exhaustion molecules as compared to reactive T cells. IFN γ therapy induced robust activation of innate immune cells, while anti-PD-1 preferentially activated CD8+ T cells. Neither therapy had significant effect on the activation state of neoplastic T cells. PD-1 expression dropped dramatically across most T cell subsets, including neoplastic T cells, following anti-PD-1 therapy. Serum proteomic evaluation revealed that high levels of the chemokines CXCL9, CXCL10 and CXCL11 at baseline were associated with negative and positive clinical outcomes in MF and SS subjects respectively following anti-PD-1 therapy as a single agent. Though not statistically significant, treatment with exogenous IFN γ may have reversed this trend.

Conclusions We describe features of the immune response as seen in MF and SS subjects following anti-PD-1 monotherapy and in combination with IFN γ and emphasize that these subtypes behave as two distinct diseases in response to therapy. It is therefore important to analyze biomarkers in SS separately from MF as combining the diseases may cloud putative signatures.

Ethics Approval These studies were approved Fred Hutch IRB; CITN-10 (anti-PD-1 monotherapy) approval number 8268 and CITN-13 (anti-PD-1 plus IFN γ combination therapy) approval number 8588.

<http://dx.doi.org/10.1136/jitc-2022-SITC2022.0094>

CHARACTERIZATION OF HUMAN BREAST CANCER TISSUE WITH THE XENIUM IN SITU PLATFORM REVEALS A NOVEL MARKER FOR INVASIVENESS

Robert Henley*, Nicole Rapicavoli, Amanda Janesick, Robert Shelansky, Albert Kim, Janine Hensel, Francesca Meschi, Navid Farahani, Vijay Kumar, Xiaoyan Qian, Sarah Taylor.
x Genomics, Pleasanton, CA, USA

Background Breast cancer became the most diagnosed cancer globally for the first time in 2020. Of these breast cancers, approximately 20% are ductal carcinoma in situ (DCIS). Within the mammary gland ducts, myoepithelial cells and their surrounding basement membrane form a layer separating the breast epithelium from the surrounding stroma.¹ Using Xenium, an in situ analysis platform capable of detecting gene expression patterns of hundreds of RNA targets with subcellular spatial resolution, we investigated the myoepithelial layer of human DCIS breast cancer tissue and observed gene expression alterations that may serve as markers of a transition to tumor invasiveness.

Methods Ten micron thick FFPE tissue sections were prepared from breast tissue blocks containing DCIS and invasive tumor areas. Tissue sections were screened using a Xenium In Situ gene panel of 205 markers and subsequently stained with H&E and imaged at 20X magnification using a light microscope. RNA expression was analyzed with Xenium Explorer software.

Results We analyzed FFPE sections of human DCIS tissues with invasive and non-invasive tumor regions with both H&E staining and with Xenium In Situ for spatial RNA expression profiles. Our data-driven and curated Xenium In Situ gene panel design allowed for the annotation of multiple cell types, including lymphocytes and macrophages, with specific immune subpopulations surrounding the cancerous lesions. In DCIS non-invasive tumor areas, we observed high KRT14 expression and intact myoepithelial tissue. Conversely, in invasive tumor areas, we observed low KRT14 expression and a disrupted myoepithelial layer. The same areas of low KRT14 expression were also positive for progesterone receptor (PGR).

Conclusions Progesterone receptor has previously been identified as playing a role in driving luminal B cell proliferation and invasion.² In our study, Xenium In Situ analysis reveals that PGR is associated with regions where the myoepithelial layer appears to have broken down and may represent a novel marker for the transition between DCIS and invasive cancer in human breast tissue.

REFERENCES

1. Pandey, P. R., Saidou, J. and Watabe, K. Role of myoepithelial cells in breast tumor progression, *Frontiers in Bioscience*, 2010, Jan 1; **15**:226–236.
2. McFall, T., Patki, M., Rosati R., and Ratnam, M., Role of the short isoform of the progesterone receptor in breast cancer cell invasiveness at estrogen and progesterone levels in the pre- and post-menopausal ranges, 2015, Oct 20: **6** (32):33146–64.

<http://dx.doi.org/10.1136/jitc-2022-SITC2022.0095>

96

METASTATIC BREAST CANCER IS ASSOCIATED WITH INCREASED LEVELS OF SOLUBLE INHIBITORY IMMUNE CHECKPOINT PROTEINS AND DECREASED LEVELS OF SOLUBLE STIMULATORY IMMUNE CHECKPOINT PROTEINS

¹Bernardo Rapoport*, ¹Helen Steel, ²Carol Benn, ³Liezi Heyman, ³Teresa Smit, ¹Ronald Anderson. ¹University of Pretoria, Pretoria, South Africa; ²Netcare Breast Care Centre, Johannesburg, South Africa; ³The Medical Oncology Centre of Rosebank, Johannesburg, South Africa

Background Checkpoint proteins regulate the immune system. Breast cancer (BC) cells exploit the up-regulation or down-regulation of these proteins to evade anti-tumor immune responses. Soluble forms of immune checkpoint molecules (ICM) can be measured in human plasma; however, their biological and clinical significance remain essentially unknown. The present analysis aimed to measure plasma ICMs in metastatic BC patients (pts) and compare them to healthy controls. **Methods** Soluble forms of ICM and RANTES, arginase and TGF- β 1 were measured using Multiplex[®] bead array and ELISA technologies, respectively. Plasma samples from 20 metastatic breast cancer (MBC) pts and 45 healthy controls were analyzed for each protein. Data was prospectively obtained. Measured levels were compared between MBC pts and healthy controls using a non-parametric test (Mann-Whitney), p-values below 0.05 were considered statistically significant.

Results The median age of the cohort was 53 years (range 34–79 years). The main metastatic sites included liver (10 pts), bone (8 pts), and lung (6pts), with brain-, nodal-, rectum- and skin metastasis presenting in one patient each. The performance status was as follows; PS=0 (11 patients), PS=1 (7 patients,) and PS=2 (2 patients). The median neutrophil-lymphocyte ratio (NLR) was 3.18 (range 0.35 – 10.97). The soluble co-stimulatory molecules, GITR (p<0.0011), GITRL (p< 0.0000), CD27 (p< 0.0039), CD28 (p<0.0069), CD40 (p< 0.0022), CD86 (p< 0.0000) and ICOS (p< 0.0157), as well as the co-inhibitory molecules, PD-L1 (p< 0.0002), CTLA-4 (p< 0.0002) and BTLA (p<0.0145) levels were significantly lower in MBC pts compared to healthy controls. Inhibitory molecules TIM-3 (p< 0.0001) and LAG-3 (p<0.0000) were significantly higher than those of healthy controls. Other biomarkers with raised serum concentrations included TLR (p<0.0039). Serum CD80 (p<0.0992), PD-1 (p<0.2325), HVEM (p<0.062,6) and RANTES (p<0.4861) levels were not significantly different between the MBC pts and the healthy controls (table 1).

Conclusions We identified lower levels of CD27, CD28, CD40, ICOS, GITR, GITRL, CD86, PD-L1, CTLA-4, BTLA, arginase, and TGF- β 1, and higher levels of TIM-3 and LAG-3 immune checkpoint molecules in MBC pts compared to healthy controls. These results indicate that a down-regulation of soluble ICM pathways and an up-regulation of some inhibitory ICM pathways are associated with MBC patients. To our knowledge, this is the first study to describe soluble immune checkpoint molecules in MBC pts.

Ethics Approval Ethics approval was granted by The Research Ethics Committee, Faculty of Health Sciences, University of Pretoria (Ethics Committee Approval Numbers 517/2017).

Abstract 96 Table 1 Comparing the median levels of systemic soluble immune checkpoints in metastatic breast cancer patients with those of healthy controls

Table 1: Comparing the median levels of systemic soluble immune checkpoints in metastatic breast cancer patients with those of healthy controls.

	ICM	Metastatic Breast Cancer (n=20)		Controls (n=45)		p-value
		Median pg/ml (95%CI)	Median pg/ml (95%CI)	Median pg/ml (95%CI)	Median pg/ml (95%CI)	
Co-stimulatory	CD27	DOWN	2364.87 (1214.96 - 4249.63)	4577.35 (3391.13 - 5784.85)		0.0039
	CD28	DOWN	21106.20 (13421.92 - 36668.75)	46136.18 (27210.29 - 67544.1)		0.0069
	CD40	DOWN	1285.74 (836.51 - 1924.37)	1977.08 (1404.82 - 2569.56)		0.0022
	ICOS	DOWN	16001.67 (8033.1 - 25988.1)	28206.65 (15897.52 - 31725.99)		0.0157
	GITR	DOWN	1621.68 (266.85 - 2390.84)	3797.68 (1993.96 - 5396.86)		0.0011
	GITRL	DOWN	3207.48 (1092.21 - 4795.97)	7151.12 (1092.21 - 4795.97)		0.0000
	CD86	DOWN	2930.8 (762.93 - 5579.81)	14297.09 (9391.46 - 20525.14)		0.0000
	CD80	DOWN	1933.18 (459.93 - 3030.69)	2320.77 (1395.51 - 3042.87)		0.0992
	Co-inhibitory	PD-1	DOWN	13350.79 (3695.61 - 20379.82)	14917.48 (7874.92 - 21795.02)	
PD-L1		DOWN	1016.5 (546.89 - 2807.31)	3342.02 (2628.64 - 4750.96)		0.0002
CTLA-4		DOWN	910.96 (220.6 - 1742.46)	2618.23 (1578.44 - 3110.47)		0.0002
TIM-3		UP	7438.2 (6430.35 - 9885.27)	5046.87 (4732.72 - 5958.87)		0.0001
LAG-3		UP	460708.67 (245454.27 - 873316.46)	150416.02 (94508.53 - 187997.23)		0.0000
BTLA		DOWN	12380.49 (2788.14 - 17513.4)	18147.26 (11461.86 - 25180.69)		0.0145
Dual	TLR-2	DOWN	19061.48 (10368.32 - 33291.28)	30477.2 (20928.44 - 50302.64)		0.0039
	HVEM	DOWN	2115.98 (1744.07 - 2332.1)	2290.19 (2079.46 - 2618.44)		0.0626
Other	Arginase	DOWN	25.52 (25.52 - 25.52)	78.64 (38.03 - 195.47)		0.0033
	RANTES	UP	51.95 (39.31 - 62.88)	48.72 (36.3 - 66.96)		0.4861
	TGF- β 1	DOWN	5443.42 (16184.42 - 36390.72)	23785.83 (36113.79 - 11090.75)		0.0000

<http://dx.doi.org/10.1136/jitc-2022-SITC2022.0096>

Abstracts

97

EFFECT OF ADMINISTRATION OF NEOADJUVANT CHEMOTHERAPY TO NEWLY DIAGNOSED EARLY BREAST CANCER PATIENTS ON THE DEPRESSED PLASMA LEVELS OF SOLUBLE CO-STIMULATORY AND CO-INHIBITORY IMMUNE CHECKPOINT MOLECULES

¹Bernardo Rapoport*, ¹Helen Steel, ²Carol Benn, ³Simon Nayler, ⁴Teresa Smit, ⁴Liezl Heyman, ¹Annette Theron, ¹Nomsa Hlatshwayo, ¹Luyanda Kwofie, ¹Pieter Meyer, ¹Ronald Anderson. ¹University of Pretoria, Pretoria, South Africa; ²Netcare Breast Care Centre, Johannesburg, South Africa; ³Dr's Gritzman and Thatcher Inc, Johannesburg, South Africa; ⁴The Medical Oncology Centre of Rosebank, Johannesburg, South Africa

Background Neoadjuvant chemotherapy (NAC) may alter the immune landscape of patients with early breast cancer (BC), potentially setting the scene for more effective implementation of checkpoint-targeted immunotherapy, albeit by largely unexplored mechanisms.

Methods This study investigated which alterations in the plasma concentrations of 16 soluble co-stimulatory and co-inhibitory, immune checkpoints were measured in a cohort of newly diagnosed, early BC patients (n=72) pre-treatment, post-NAC, and post-surgery using a Multiplex[®] bead array platform.

Results Relative to a group of healthy control subjects (n=45), the median pre-treatment levels (table 1) of 5 co-stimulatory (CD27, CD40, GITRL, ICOS, GITR) and 3 co-inhibitory (TIM-3, CTLA-4, PD-L1) soluble checkpoints were significantly lower in the BC patients vs. controls ($p < 0.021 - p < 0.0001$; and $p < 0.008 - p < 0.00001$, respectively). Following NAC (table 2), the plasma levels of 6 soluble co-stimulatory checkpoints (CD28, CD40, ICOS, CD27, CD80, GITR), all involved in activation of CD8⁺ cytotoxic T cells, were significantly increased relative to pre-treatment levels ($p < 0.04 - p < 0.00001$), being comparable with control values and remaining at these levels post-surgery (table 3). Of the soluble co-inhibitory checkpoints, 3 (LAG-3, PD-L1, TIM-3) increased significantly post-NAC, while PD-1 was unchanged and BTLA and CTLA-4 were significantly decreased ($p < 0.03$ and $p < 0.00001$, respectively). A pathological complete response was documented in 65% of patients (mostly TNBC).

Conclusions Normalization of soluble co-stimulatory immune checkpoints is seemingly indicative of reversal of systemic immune dysregulation following administration of NAC in early BC, independent of response to treatment, while recovery of immune homeostasis may explain the increased levels of several negative checkpoint proteins, albeit with the exceptions of CTLA-4 and PD-1.

Ethics Approval Ethics approval was granted by The Research Ethics Committee, Faculty of Health Sciences, University of Pretoria (Ethics Committee Approval Numbers 517/2017).

Abstract 97 Table 1 Difference in median plasma concentrations of soluble systemic immune checkpoint molecules in newly diagnosed breast cancer patients and healthy controls.

Table 1.

ICM	Breast Cancer newly diagnosed (n=72)	Controls (n=45)	p value		
	Median pg/ml (95%CI)	Median pg/ml (95%CI)			
Co-stimulatory	CD27	3342,45 (2808,61 - 4107,68)	4577,35 (3391,13 - 5784,85)	0,0243	
	CD28	32914,45 (29326,9 - 42636,04)	46135,18 (27210,29 - 67544,1)	0,1248	
	CD40	1523,32 (1298,16 - 1777,45)	1977,68 (1404,82 - 2669,56)	0,0210	
	ICOS	15123,78 (12471,47 - 19942,11)	26506,66 (16897,52 - 31725,99)	0,0087	
	GITR	1497,40 (1053,33 - 1969,52)	3797,68 (1993,96 - 6396,86)	0,0001	
	GITRL	5886,13 (4959,23 - 6681,22)	7151,12 (5528,36 - 9878,41)	0,0199	
	CD86	11585,17 (9938,61 - 14646,29)	14297,09 (9391,46 - 20525,14)	0,1734	
	CD80	1678,33 (1422,82 - 2039,65)	2329,77 (1395,01 - 3042,87)	0,0735	
	Co-inhibitory	PD-1	12305,41 (10260,08 - 15798,61)	14917,48 (7874,92 - 21795,02)	0,5158
		PD-L1	1647,14 (1269,54 - 2228,88)	3342,62 (2628,64 - 4750,96)	0,0001
CTLA-4		1566,38 (1314,46 - 1890,81)	2618,23 (1578,44 - 3110,47)	0,0079	
TIM-3		3897,66 (3169,51 - 4330,5)	5046,87 (4732,72 - 5958,87)	0,0005	
LAG-3		131275,90 (106666,3 - 156881,5)	150416,00 (94508,53 - 187997,2)	0,5888	
BTLA		13021,75 (10277,82 - 18548,68)	18147,26 (11461,86 - 25180,69)	0,2349	
Dual		TLR-2	26831,35 (21172,1 - 32396,97)	30477,20 (20928,44 - 50302,64)	0,1806
	HVEM	1865,22 (1671,15 - 2038,38)	2290,19 (2079,46 - 2618,44)	0,0004	

Abstract 97 Table 2 Difference in median plasma concentrations of soluble systemic immune checkpoint molecules in pre-treatment and post-treatment breast cancer patients

Table 2.

ICM	Breast Cancer newly diagnosed (n=72)	Post-NAC (n=72)	p value		
	Median pg/ml (95%CI)	Median pg/ml (95%CI)			
Co-stimulatory	CD27	3342,45 (2808,61 - 4107,68)	5351,47 (4678,25 - 5894,37)	0,0001	
	CD28	32914,45 (29326,9 - 42636,04)	44277,76 (38319,44 - 51220,42)	0,0416	
	CD40	1523,32 (1298,16 - 1777,45)	2030,72 (1792,5 - 2199,04)	0,0003	
	ICOS	15123,78 (12471,47 - 19942,11)	26586,28 (20912,88 - 31335,04)	0,0002	
	GITR	1497,40 (1053,33 - 1969,52)	4035,98 (3198,29 - 5204,35)	0,0001	
	GITRL	5886,13 (4959,23 - 6681,22)	5339,99 (4728,24 - 6121)	0,8044	
	CD86	11585,17 (9938,61 - 14646,29)	9922,61 (7890,54 - 11990,77)	0,2789	
	CD80	1678,33 (1422,82 - 2039,65)	3048,74 (2522,82 - 3520,25)	0,0001	
	Co-inhibitory	PD-1	12305,41 (10260,08 - 15798,61)	13350,55 (10537,37 - 15491,33)	0,7859
		PD-L1	1647,14 (1269,54 - 2228,88)	4794,97 (4162,41 - 5731,71)	0,0001
CTLA-4		1566,38 (1314,46 - 1890,81)	598,20 (472,91 - 768,78)	0,0001	
TIM-3		3897,66 (3169,51 - 4330,5)	9975,90 (8793,62 - 10515,7)	0,0001	
LAG-3		131275,90 (106666,3 - 156881,5)	464880,70 (309218,5 - 580137,6)	0,0001	
BTLA		13021,75 (10277,82 - 18548,68)	9987,98 (8255,35 - 12554,33)	0,0367	
Dual		TLR-2	26831,35 (21172,1 - 32396,97)	33837,86 (28228,61 - 39571,02)	0,0258
	HVEM	1865,22 (1671,15 - 2038,38)	4047,29 (3610,92 - 4445,29)	0,0001	

Abstract 97 Table 3 Difference in median plasma concentrations of soluble systemic immune checkpoint molecules in post-treatment- and post-surgery breast cancer patients

Table 3.

ICM	Post-NAC (n=72)	Post-Surgery (n=72)	p value	
	Median pg/ml (95%CI)	Median pg/ml (95%CI)		
Co-stimulatory	CD27	5351,47 (4678,25 - 5894,37)	5427,68 (4411,67 - 6317,06)	0,8105
	CD28	44277,76 (38319,44 - 51220,42)	50058,18 (34830,52 - 64706,44)	0,5705
	CD40	2030,72 (1792,5 - 2199,04)	2054,12 (1820,74 - 2383,79)	0,6203
	ICOS	26586,28 (20912,88 - 31335,04)	29746,46 (24270,58 - 33438,89)	0,3751
	GITR	4035,98 (3198,29 - 5204,35)	4434,89 (3354,37 - 6046,58)	0,9777
	GITRL	5339,99 (4728,24 - 6121)	5927,89 (4860,76 - 7008,59)	0,5226
	CD86	9922,61 (7890,94 - 11990,77)	12439,80 (9586,36 - 14837,24)	0,2276
	CD80	3048,74 (2522,82 - 3520,25)	3611,23 (2754,67 - 4138,41)	0,6459
	Co-inhibitory	PD-1	13350,55 (10537,37 - 15491,33)	15076,64 (12077,71 - 19383,37)
PD-L1		4794,97 (4182,41 - 5731,71)	5215,05 (4239,88 - 5969,17)	0,8667
CTLA-4		598,20 (472,91 - 768,78)	687,76 (550,45 - 828,91)	0,8292
TIM-3		9975,90 (8793,62 - 10515,7)	9615,77 (8440,15 - 10984,92)	1,0000
LAG-3		464880,70 (309218,5 - 590137,6)	500133,40 (466624,6 - 500748,6)	0,5992
BTLA		9987,98 (8255,35 - 12554,33)	12777,20 (9507,29 - 15003,63)	0,3217
Dual		TLR-2	33837,86 (28228,61 - 39571,02)	37042,86 (29069,2 - 45880,29)
	HVEM	4047,29 (3610,92 - 4445,29)	3950,36 (3611,92 - 4381,72)	0,6259

<http://dx.doi.org/10.1136/jitc-2022-SITC2022.0097>

98 **IMAGING MASS CYTOMETRY IDENTIFIES IMMUNO-ONCOLOGY-BASED PATHOPHYSIOLOGICAL FEATURES OF THE MOUSE TUMOR TISSUE MICROENVIRONMENT**

Thomas Pfister*, Christina Loh, Michael Cohen, Sam Lim, Qanber Raza. *Standard BioTools, Toronto, Canada*

Background Mouse tumor models are widely utilized as the preferred model organism for cancer studies and pre-clinical drug development. An obstacle in predicting therapeutic drug efficacy is the ability to quantitatively evaluate the multi-parametric post-treatment response in the tumor microenvironment (TME). Particularly, identification of immunological and oncological processes that dictate tumor growth, metastasis and immune response are essential for selecting promising drug candidates for further clinical evaluation. Imaging Mass Cytometry™ (IMC™) enables analysis of 40-plus distinct tissue and cellular markers simultaneously on tumor samples, providing a thorough assessment of the spatial landscape of the TME on a single slide without spectral overlap or background autofluorescence. Here, we showcase application of the Mouse Immuno-Oncology (IO) IMC Panel Kit for identification of pathophysiological features of the mouse TME.

Methods We compiled the Maxpar® OnDemand™ Mouse Immuno-Oncology IMC Panel Kit to quantitatively assess IO-related processes and applied it to a tissue microarray containing multiple mouse tumors. Antibodies in panel kits were selected from the Maxpar and Maxpar OnDemand catalog. Data acquisition was performed using a Hyperion™ Imaging System (Standard BioTools™). To facilitate cell segmentation, the IMC Cell Segmentation Kit (Standard BioTools) was applied to enhance nuclear and cell membrane demarcation. Single-cell analysis was completed using a custom MATLAB® script for pixel classification, CellProfiler™ for cell segmentation and histoCAT™ for PhenoGraph clustering.

Results The Maxpar OnDemand Mouse Immuno-Oncology IMC Panel Kit successfully identified pathophysiological processes such as immune cell infiltration and activation, signaling pathway activation, biomarkers of epithelial to mesenchymal transition, metabolic activity, growth and the tissue architecture of the TME. Single-cell analysis of non-small-cell lung carcinoma and B cell lymphoma separated distinct cellular clusters representing tumor, immune, stromal and vascular cells. Based on expression of activation markers in the panel kits, cellular processes associated with signaling, growth and metastasis were identified in tumor cells. In addition, cytotoxic and inflammatory activation in lymphoid and myeloid immune cell subtypes was detected.

Conclusions Application of IMC based multiparametric analysis successfully identified the spatial landscape of the TME at single-cell resolution. Quantitative analysis of tumor composition revealed critical insights regarding prognostic parameters such as metastatic and growth potential of tumors, and identification and activation of immune cell infiltrates. Overall, this work demonstrates the power of IMC technology and provides evidence of its successful application in mouse tumor models.

<http://dx.doi.org/10.1136/jitc-2022-SITC2022.0098>

99

**SPATIAL INSIGHTS INTO TUMOR IMMUNE EVASION
ILLUMINATED WITH THE COSMX™ SPATIAL
MOLECULAR IMAGER PLATFORM**

Jason Reeves*, Patrick Danaher, Shanshan He, Sean Kim, Michael Patrick, Julian Preciado, Justin Jenkins, Rachel Liu, Sarah Murphy, Christine Kang, Byron Hartman, Vik Devgan, Youngmi Kim, Michael Rhodes, Joseph Beechem. *NanString Technologies, Seattle, WA, USA*

Background Patient response to immunotherapy has been revolutionary but remains limited due to the inability to convert excluded or cold tumors into ones which would be permissive to therapeutic intervention. To treat patients that evade immune therapy, comprehensive understanding of their tumor microenvironment (TME) is needed. To date, most profiling efforts have lacked the ability to capture high-plex 'omics data while retaining the spatial architecture of the TME. We developed the CosMx™ Spatial Molecular Imager for analyzing formalin-fixed paraffin-embedded (FFPE) or fresh-frozen (FF) tissue and capturing the expression of over 1000 RNA targets simultaneously with subcellular resolution from a single histopathology slide.

Methods We profiled a cohort of 10 patient samples with CosMx using the Human Universal Cell Characterization Panel across a range of solid tumors. This cohort represents a diverse array of patients which include both infiltrated and excluded tumors. We included technical replicates for 5 of the samples to better understand reproducibility of the assay. We were able to characterize over 1.8 million cells, and detected on average over 80% of the panel per patient and assigning more than 95% of the transcripts profiled to unique cells across these samples.

Results We were able to robustly identify more than 20 cell types by integrating our data with previous single-cell sequencing projects from the human cell atlas. We demonstrate robust delineation of critical immune cell populations from across lymphoid and myeloid lineages, as well as stromal cell populations, including cell types frequently missed using dissociated cell sequencing, such as vascular endothelium associated with immune cell migration into the tumor bed. We leveraged 450 + genes from our panel dedicated to cell lineage, cell-cell interaction, and ligand-receptor signaling to identify unique interactions happening at different scales between the tumor and the TME. These include evidence of direct inhibition of T-cell function through the PDL1 axis between tumor, and tumor intrinsic and extrinsic interactions that mediate tissue architecture and T-cell exclusion.

Conclusions The CosMx platform for profiling tissue allows for robust resolution of critical immunogenic signaling cascades and cellular interactions that are necessary to truly understand the tumor architecture. By maintaining the tissue structure, we can directly measure cellular interactions and capture cells commonly missed during dissociative studies. With this new platform, we are better poised than ever to truly understand the molecular mechanisms which drive tumor response to intervention.

FOR RESEARCH USE ONLY Not for use in diagnostic procedures.

<http://dx.doi.org/10.1136/jitc-2022-SITC2022.0099>

¹Guilhem Richard*, ²Gary Steinberg, ¹Nicole Ruggiero, ¹William Martin, ¹Anne de Groot. ¹EpiVax Therapeutics, Inc., Providence, RI, USA; ²NYU Langone Health, NYC, NY, USA

Background As tumor genomes are shaped by their interaction with the immune system, a phenomenon known as immunoeediting, it is critical to understand how immunotherapies impact this process. Checkpoint inhibitors directly influence T cells responding to neoantigens, as such, these therapies drastically affect the genomes of surviving tumor clones. Similar to the concept of immune camouflage, where genomes of pathogens evolve in a way to avoid immune detection, we hypothesized that tumor clones surviving checkpoint inhibition therapy harbor mutations more prone to immune avoidance.

Methods We analyzed a published cohort of Nivolumab-treated melanoma patients (n=41) for which tumor samples were collected from the same site prior ('Pre' samples) and during ('On' samples) Nivolumab therapy.¹ The immunogenic and tolerance potential of mutations from the Pre and On samples were evaluated with the Ancer neoantigen screening platform,² which includes the EpiMatrix algorithm to identify HLA class I and HLA class II neopeptides and the JanusMatrix algorithm to evaluate neopeptides for homology with the self genome. Prior work with JanusMatrix showed that neoantigens highly homologous to self might be inhibitory.³

Results Tumor samples collected during Nivolumab therapy demonstrated increased homology (self-like) scores from their matched pre-therapy samples (paired t test, p=0.0475). While this increase in homology with self was significant across the cohort, the effect was more pronounced in patients exhibiting complete (CR) or partial responses (PR), compared to patients with stable (SD) or progressive disease (PD). An ANOVA analysis confirmed that increase in homology after Nivolumab therapy was significantly greater in CR/PR patients, as opposed to SD or PD patients (p=0.0005). This observation was supported by Receiver Operating Characteristic (ROC) analysis discriminating CR/PR patients from SD/PD patients based on differences in homology with self between Pre and On treatment samples (AUC=0.7484, p=0.0313). A comparative ROC analysis employing baseline patient tumor mutation burden (TMB) yielded non-conclusive results (AUC= 0.5054, p=0.9613).

Conclusions Our Ancer analysis highlights that Nivolumab therapy affects the tolerance profile of tumors in a manner that is consistent with the concepts of immunoeediting and immune camouflage. Interestingly, tumors in patients with favorable outcomes demonstrated the greatest increase in self-like neopeptides. This observation suggests that collecting tumor biopsies shortly after the initiation of checkpoint inhibitor therapy and evaluating their tolerance profile may be employed as a prognostic biomarker. Furthermore, this approach highlights in silico tools may distinguish effector from tolerance inducing neopeptides, a critical feature for designing novel neoantigen-based precision immunotherapies.

REFERENCES

1. Riaz N, Havel JJ, Makarov V, et al., Tumor and Microenvironment Evolution during Immunotherapy with Nivolumab. *Cell*. 2017 Nov 2;**171**(4):934–949.
2. Richard G, Princiotta MF, Bridon D, et al., Neoantigen-based personalized cancer vaccines: the emergence of precision cancer immunotherapy. *Expert Rev Vaccines*. 2022 Feb;**21**(2):173–184.
3. De Groot AS, Rosenberg AS, Miah SMS, et al., Identification of a potent regulatory T cell epitope in factor V that modulates CD4+ and CD8+ memory T cell responses. *Clin Immunol*. 2021 Mar;**224**:108661.

101 **DETERMAIO (IO SCORE) IS ASSOCIATED WITH EFFICACY OF ICI MONOTHERAPY IN ADVANCED NSCLC PATIENTS WITH ECOG 2**

¹David Saltman*, ²Rob Seitz, ²Tyler Nielsen, ²Matthew Varga, ³Nicole Croteau, ¹Heather Lockyer, ²David Hout, ²Brock Schweitzer, ²Douglas Ross, ⁴Amit Jain, ⁴Gregory Vidal, ⁵David Gandara. ¹BC Cancer, Victoria, Canada; ²Oncocyte Corporation, Nashville, TN, USA; ³University of British Columbia, Vancouver, Canada; ⁴West Cancer Center, Memphis, USA; ⁵University of California, Davis, Sacramento, CA, USA

Background Immune checkpoint inhibitor (ICI) therapy is an attractive option for aNSCLC patients with poor performance status (ECOG 2) but several studies have failed to demonstrate benefit. DetermaIO (IO score) is a 27-gene RT-qPCR immuno-oncology tumor immune microenvironment (TIME) RNA expression classifier that has been previously shown to be associated with clinical response to ICI therapy in multiple tumor types. This study was performed to explore the possibility that the IO score (IO+/IO-) could identify responders in patients with ECOG 2 whose overall poor outcome might otherwise obscure detecting a significant clinical benefit.

Methods Available FFPE specimens with ECOG 2 from two studies of advanced NSCLC patients treated with ICI monotherapy were analyzed independently. The first, composed of 46 patients from BC Cancer (BCCA), was split into two cohorts due to the differences in treatment and PD-L1 status: Cohort 1 was composed of patients with PD-L1 \geq 50% who received 1st line ICI monotherapy (n=26). Cohort 2 was composed of mostly PD-L1 negative or 1–49% patients who received ICI monotherapy in the 2nd+ line (n=20). Cohort 3 was comprised of thirteen patients of mixed PD-L1 phenotype and mixed line of therapy from an independent center, West Cancer Center (WCC). In total, 59 patients treated with ICI monotherapy from the three cohorts were analyzed separately for association with PFS using Cox proportional hazards.

Results Overall, 35 of 59 patients were IO+ (cohort 1 = 18/26, cohort 2 = 10/20 cohort 3 = 7/13). Median PFS improved for IO+ versus IO- in each of the three cohorts (cohort 1 IO- = 67, IO+ = 357; cohort 2 IO- = 100, IO+ = 189; cohort 3 IO- = 127, IO+ = 404). The Cox proportional hazard for cohort 1 was 0.27 (95%CI 0.10 to 0.72, p=0.0095), cohort 2 was 0.51 (95%CI 0.20 to 1.32, p=0.17), and cohort 3 was 0.14 (95%CI 0.027 to 0.76, p=0.023).

Conclusions DetermaIO has identified significant benefit for PFS from two cohorts of ECOG 2 patients and trended towards significance in a 3rd cohort treated in the 2nd+ line. While each cohort alone is modestly powered, the consistent results in three independent cohorts, separated for analysis to control for other confounding prognostic variables, suggests that DetermaIO is worthy of further study as a biomarker to better identify ECOG 2 patients likely to benefit from ICI therapy.

Ethics Approval This study was approved by the Research Ethics Board (REB) of University of British Columbia (H20-02635). Individual consent for this retrospective analysis and the use of tumor samples for the IO score assay was required for live patients. Consent was waived by the REB for deceased patients.

<http://dx.doi.org/10.1136/jitc-2022-SITC2022.0101>

EXPLORING THE SPATIAL HETEROGENEITY OF IMMUNE CELLS IN NASOPHARYNGEAL TUMOURS

Aastha Sobti*, Christina Sakellariou, Johan Nilsson, David Askmyr, Lennart Greiff, Malin Lindstedt. *Lund university, Lund, Sweden*

Background Nasopharyngeal cancer (NPC) is a squamous cell carcinoma of the upper pharynx, strongly associated with Epstein-Barr virus (EBV), and with varying incidences in the world. We have previously investigated the presence and distribution of CD8⁺ T cells in NPC and found that an 'inflamed profile', with CD8⁺ T cells in and around cancer cell areas, was associated with better disease-free survival (*cf.* non-inflamed 'desert' tumours). In this study, we explore immune-related biomarkers in a spatial context to assess distribution of cell types and quantify selected biomarkers within the NPC.

Methods Using the GeoMx Digital Spatial Profiler (DSP), 49 target proteins were digitally quantified on an NPC tissue microarray consisting of 30 unique biopsies. DSP combines spatial and molecular profiling technologies and enable assessment of different features of intratumoral structures in a cell type-specific manner while simultaneously performing protein expression analysis on selected regions-of-interest (ROIs). A total of 96 ROIs were obtained based on morphological staining using CD45, CD8, and PanCK antibodies, and a quantitative analysis was performed between ROIs within the tumour area and outside/stroma.

Results To evaluate unbiased grouping of segments, principal component analysis and k-means clustering were conducted. Protein targets CD56, CD20, CD68, PD-1, FOXP3, and Ki-67 were the most differentially expressed in the CD45⁺ segments within the tumour area, suggesting a presence of B cells, NK cells, macrophages, and regulatory T cells in the tumour area. In contrast, B7-H3, fibronectin, CD163, CD4, VISTA, LAG3, and TIM3 were higher in the CD45⁺ segments outside the tumour barrier, indicating a presence of suppressive populations of myeloid cells and T cells. Additionally, the expression of B7-H3 correlated best with a presence of CD14, fibronectin, and CD163. Interestingly, the presence of PD-1 was limited to within tumour-rich regions, in contrast to other 'immune regulatory' proteins like LAG3, VISTA, and TIM3, which were found on the tumour border and in the stroma. The detected proteins were validated with multiplexed staining.

Conclusions This study considers the spatial heterogeneity of the NPC immune microenvironment and demonstrates a variable expression of immune checkpoint markers in NPC. The identified immune profiles and highlighted biomarkers may be of relevance as a prognostic tool and for therapeutic targeting.

Ethics Approval The collection of biobank samples from Lund University was approved by ethics committee Dnr 2014/117.

Consent In accordance with the ethics approval, informed consent was not required, but the study was advertised in print media with the option to opt-out

<http://dx.doi.org/10.1136/jitc-2022-SITC2022.0102>

103

**SPATIAL PROTEIN ANALYSIS OF THE TUMOR
MICROENVIRONMENT AND BIOMARKERS IN
HODGKIN'S LYMPHOMA**

¹Alexander Xu*, ²Tomohiro Aoki, ²Aixiang Jiang, ¹Alicia Gamboa, ¹Anthony Colombo, ²Christian Stiedl, ¹Akil Merchant. ¹Cedars Sinai Medical Center, Los Angeles, CA, USA; ²BC Cancer, Vancouver, Canada

Background The tumor microenvironment (TME) is the milieu of cells and molecules surrounding the tumor. Single cell methods have been used to identify subpopulations of cells that have pro- or anti-tumor properties, and modulating these is critical to immunotherapy. However, there is limited information on the spatial organization of these subpopulations, which determines how they signal and their therapeutic potential. **Single cell spatial computational analysis is needed to describe the interactions of the TME and their effect on patient outcomes.** Hodgkin's Lymphoma presents a unique TME due to the sparse distribution of Hodgkin's Reed-Sternberg tumor cells. Though it is difficult to disentangle signaling in Hodgkin's tumor cells from the immune TME, Hodgkin's is receptive to checkpoint inhibitors among lymphomas and insights gleaned from the Hodgkin's TME could inform immunotherapies across lymphomas.

Methods Here we apply Imaging Mass Cytometry (IMC), a technology to perform ~40-plex protein analysis with 1 micron resolution in tissue, to study a cohort of 260 matched samples at diagnosis and after relapse from 90 patients with relapsed/refractory Hodgkin's Lymphoma. We developed a computational pipeline to perform cell phenotyping, spatial analysis, and biostatistics, to describe tumor architecture and propose putative biomarkers of Hodgkin's clinical response and relapse. A novel feature of the pipeline is to quantify proteins and spatial analysis on the same numerical scale for each cell, to generate hybrid biomarkers.

Results We analyzed over 7 million cells for their phenotype and spatial organization. We use IMC to describe spatial features of the tumor that correlate to clinical outcomes. We identify proteins such as CXCR5 that correlate to survival in spatial contexts, and we describe spatial reorganization from diagnosis to the relapsed tumor as it relates to survival and relevant clinical factors such as MHC expression and EBV infection. A significant conceptual advance was to use spatial metrics to perform 'digital biopsies', a selection of tumor regions comparable across patients. We validated multiple existing biomarkers in the literature using our data set and proposed novel biomarkers using IMC data.

Conclusions Spatial analysis of the HL microenvironment revealed composite features of the TME that predict clinical outcomes. These features cannot be described using single cell tools or low-plexed imaging, and represent a truer picture of HL biology. The pipeline developed here can be applied to other spatial protein data for biomarker discovery and analysis.

<http://dx.doi.org/10.1136/jitc-2022-SITC2022.0103>

104

COMPREHENSIVE SINGLE-CELL IMMUNE PROFILING OF LYMPHOID AND PERIPHERAL TISSUES OF AGED MICE USING HIGH-PARAMETER FLOW CYTOMETRY BY CYTOF TECHNOLOGY

Wenxi Xu, Stephen Li, Alexandre Bouzekri, Thomas Pfister*, Christina Loh. *Standard BioTools Inc., Markham, Canada*

Background High-parameter flow cytometry is a major tool used in human and mouse studies to discover novel immunological mechanisms of infectious diseases, cancer and immunosenescence. Fluorescence-based cytometry can be especially challenging in mouse model studies due to the large amount of cell samples needed for single-stained controls. CyTOF[®] technology has transformed high-parameter flow cytometry by enabling 50-plus-marker analysis per tube of sample, with easy panel design and no need for single-stained or autofluorescence controls. Flow cytometry by CyTOF thus provides an efficient and unbiased approach to discovering novel cell populations and unique functional states of immune cells with minimal cell number requirements. Here we present how Standard BioTools[™] commercially available mouse antibody products can be incorporated into a high-parameter panel, enabling comprehensive single-cell immune profiling of both lymphoid and peripheral tissues of individual aged mice.

Methods Antibodies from the Maxpar[®] and Maxpar OnDemand[™] catalogs were used to create a panel identifying lymphocytes, myeloid cells, functional markers and immune checkpoint markers (for example, PD-1 and PD-L1). Lymphoid and peripheral tissues (for example, lung and spleen) from young adult and aged mice were harvested and processed for cell staining with a 42-parameter cytometry panel. Sample acquisition was performed using the Helios[™] mass cytometer. High-dimensional single-cell data analysis was carried out with Maxpar Pathsetter[™] and R package PhenoGraph and UMAP.

Results In young adult and aged mice, we identified more than 10 major immune cell populations, including lymphocytes and myeloid cells in multiple lymphoid and peripheral tissues, by unsupervised high-dimensional data clustering. We further defined and quantified more than 30 immune cell clusters with distinct phenotypes (for example, naive, effector, effector memory and central memory T cells). The frequency, activation and checkpoint marker status of these cell clusters were analyzed and compared between young adult and aged mice to identify the age-related changes in the immune system of multiple organs.

Conclusions This work demonstrates that by using CyTOF technology together with Maxpar and Maxpar OnDemand mouse antibodies, comprehensive single-cell phenotyping of the immune system in multiple distinct tissues of individual aged mice is easily accomplished. Moreover, the high-parameter panel can be further customized for deep functional characterization of specific lymphocytes and myeloid cell subsets. Thus, by utilizing the well-curated collection of Maxpar and Maxpar OnDemand mouse antibodies, flow cytometry by CyTOF can significantly facilitate the mechanistical studies of mouse models and expand our understanding of age-related human diseases, infection and cancer.

<http://dx.doi.org/10.1136/jitc-2022-SITC2022.0104>

105

PREVALENCE OF CLAUDIN18.2 AND PD-L1 EXPRESSION IN CHINESE GASTRIC/GASTROESOPHAGEAL JUNCTION ADENOCARCINOMA

Linlin Mao*, Wei Yi, Xu-Alan Lin, Ying Gu, Zhenzhong Xia, Chuan Qi, Michael Shi, Steven Yu, Xueming Qian. *Suzhou Transcenta Therapeutics Co., Limited, Suzhou, China*

Ethics Approval This study obtained ethics approval by Shanghai AKM Laboratory Ethics Committee (number: AKMLL202207001).

<http://dx.doi.org/10.1136/jitc-2022-SITC2022.0105>

Background Claudin18.2 (CLDN18.2), a tight junction protein highly specific to gastric mucosa, is a promising target for gastric cancer (GC) treatment.¹ Immunotherapy targeting PD-1 combined with chemotherapy has been approved as the first line treatment of GC.² Understanding the expression profiles of CLDN18.2 and PD-L1 could offer guidance for the development of combination therapies that maximize the benefits of both agents. This study investigated the prevalence of CLDN18.2 expression in gastric/gastroesophageal junction (GC/GEJ) adenocarcinoma and its correlation with PD-L1 expression in Chinese patients.

Methods Expression of CLDN18.2 in formalin-fixed, paraffin-embedded (FFPE) GC/GEJ tissue samples was detected by immunohistochemistry (IHC) using an in-house anti-CLDN18.2 antibody (Clone14G11) on the Leica Bond III IHC stainer. Both the staining intensity (0, 1+, 2+, 3+) and the percentage of positive tumor cells were evaluated. CLDN18.2 positivity was defined as expression of CLDN18.2 in $\geq 10\%$ tumor cells with intensity $\geq 1+$. Samples with moderate-to-strong CLDN18.2 membrane staining (intensity $\geq 2+$) in $\geq 40\%$ tumor cells were also analyzed. PD-L1 expression was assessed based on combined positive score (CPS) using Agilent's PD-L1 IHC 28–8 pharmDx.

Results A total of 300 GC/GEJ resected tissue samples were assessed, 89 (30%) were histologically classified as intestinal, 158 (52%) diffuse, 33 (11%) mixed, and 20 (7%) others. 295 (98%, 286 GC, 9 GEJ) samples were from primary site, 5 (2%) samples were from metastatic site (ovary, lymph node, omentum or left adnexa). CLDN18.2 staining was positive in 216 (72%), and negative in 84 (28%) of the tissue samples. 136 (45%) samples showed moderate-to-strong CLDN18.2 membrane staining in $\geq 40\%$ tumor cells. CLDN18.2 positivity prevalence was 75% ($n = 119/158$) in diffuse and 61% ($n=54/89$) in intestinal subtypes. Moderate-to-strong CLDN18.2 membrane staining in $\geq 40\%$ tumor cells was observed in 48% ($n=76/158$) diffuse subtypes, and in 39% ($n=35/89$) intestinal subtypes. For PD-L1 expression, 51 (17%) had PD-L1 CPS ≥ 5 . 19% ($n=41/216$) of the CLDN18.2 positive samples also showed PD-L1 CPS ≥ 5 . In the CLDN18.2 subgroup with moderate-to-strong CLDN18.2 membrane staining in $\geq 40\%$ tumor cells, 21% ($n=28/136$) had PD-L1 CPS ≥ 5 . It appears that the distribution of CLDN18.2 expression is independent of PD-L1 status.

Conclusions High prevalence of CLDN18.2 expression in Chinese patients with GC/GEJ adenocarcinoma was observed. About 80% CLDN18.2 positive tumors had PD-L1 CPS < 5 . These results support the value of CLDN18.2-targeted therapy in gastric cancer, especially for those patients who may not benefit from anti-PD-1/PD-L1 immuno-checkpoint therapy.

REFERENCES

1. Zhang JW, Dong RL, Shen L. Evaluation and reflection on claudin 18.2 targeting therapy in advanced gastric cancer. *Chin J Cancer Res.* 2020;**32**:263–270.
2. Janjigian YY, Shitara K, Moehler M, et al. Firstline nivolumab plus chemotherapy versus chemotherapy alone for advanced gastric, gastroesophageal junction, and oesophageal adenocarcinoma (CheckMate 649): a randomised, openlabel, phase 3 trial. *Lancet.* 2021;**398**:27–40.

106

DEVELOPMENT OF RO ASSAY FOR ANTI-PD-1 MAB AND ANTI-PD-1×CD47 BSAB UTILIZING HPD-1/HCD47 DUAL HUMANIZED MICE, AT PRECLINICAL SETTING TO FACILITATE CLINICAL VALIDATION

¹Xiaoyu An*, ¹Mingfa Zang, ²Ke Hang, ³Xianfei He, ³Ruilin Sun, ³Jian Fei, ²Henry Li, ¹Haijuan Yu. ¹Crown Bioscience Inc, san diego, CA, USA; ²Hanx Biopharmaceuticals, Wuhan, China; ³Shanghai Model Organisms Center, Inc, Shanghai, China

Background One of the most relevant pharmacokinetic (PK) parameters for antibody-based therapy in the clinics is receptor occupancy (RO). Each specific therapeutics usually requires a tailored RO assay, an PD-1 RO assay for anti-PD-1 antibody treatment. For bispecific antibody (BsAb) treatment, the needed RO assays can include each receptor RO and total RO combining the two different receptors. Due to the complexity and challenges in developing such assays using clinical samples, it would be prudent to develop a model system to test RO assay methods *in vivo* at the preclinical stage prior to clinical validation, since it may simulate dosing process in human and also provide opportunity to correlate RO to tumor model efficacy if tumor pharmacology is also conducted simultaneously. Surface expressing CD47 and PD-1 receptors are recognized two most important checkpoints for both innate and adaptive immunity suppressing tumor immunity, and have been explored for immunotherapies, in the cases of investigational drugs, HX008 (PD-1 mAb) and HX009 (CD47×PD1 BsAb).¹⁻⁴ In order to facilitate development of RO assay for the clinics, we explored preclinical modelling RO assays using hPD-1/hCD47 dual humanized mouse model for testing these two species-restricted investigational drugs.

Methods The brief procedures are as followed: 1) Non-tumor bearing hPD1×hCD47 dual humanized mice were single administrated via *i.p.* injection with test antibodies at different dose levels; 2) PBMCs were collected and prepared from the animals at different timepoints (pre-dosing, 2 hours post dosing and 7 days post dosing; 3) one half of the PBMC samples were added into the vials containing over-saturating amount of test antibody, and the other half were added into the vials containing PBS, followed by mixing; 4) add defined amount of fluorescence-labeled test antibody, followed by washing and flow cytometry analysis, and the %RO being determined. The test antibodies could be anti-human PD-1 antibody, anti-human CD47 antibody or anti-human PD-1×CD47 BsAb for measuring the respective RO values.

Results Preliminary results demonstrated that HX008 RO assays showed anticipated dose dependent RO values at both timepoints, suggesting this assay development is highly doable and predictive using the preclinical humanized models. Further detailed to be analyzed, including HX009 RO values for PD-1 receptor only, CD47 receptor only and total for combining both receptors.

Conclusions Supposing further data from HX-009 RO modelling proven valid, RO assay using humanized mice could become a standard method of choice for RO assay development at the preclinical stage, enabling simpler/efficient clinical development.

REFERENCES

1. Feng, M., Jiang, W., Kim, B. Y. S., Zhang, C. C., Fu, Y. X., and Weissman, I. L. (2019). Phagocytosis checkpoints as new targets for cancer immunotherapy. *Nat Rev Cancer* 19, 568–586.
2. Liu, B., Guo, H., Xu, J., Qin, T., Guo, Q., Gu, N., Zhang, D., Qian, W., Dai, J., Hou, S., et al. (2018). Elimination of tumor by CD47/PD-L1 dual-targeting fusion protein that engages innate and adaptive immune responses. *MAbs* 10, 315–324.

3. Liu, X., Pu, Y., Cron, K., Deng, L., Kline, J., Frazier, W. A., Xu, H., Peng, H., Fu, Y. X., and Xu, M. M. (2015). CD47 blockade triggers T cell-mediated destruction of immunogenic tumors. *Nat Med* 21, 1209–1215.
4. Roohullah, A., et al., (2021). First-in-human phase I dose escalation study of HX009, a novel recombinant humanized anti-CD47/PD-1 bispecific antibody, in patients with advanced malignancies. ASCO 2021 Annual Meeting.

<http://dx.doi.org/10.1136/jitc-2022-SITC2022.0106>

107

TUMOR SPECIFIC MHC-I EXPRESSION DETERMINES THE LOCAL IMMUNE MICROENVIRONMENT IN BREAST CANCER

Xiaopeng Sun*, Brandie Taylor, Paula Gonzalez Ericsson, Violeta Sanchez, Justin Balko. Vanderbilt University Medical Center, Nashville, TN, USA

Background Tumors employ various immune escape mechanisms, including downregulation of major histocompatibility complex I (MHC-I) expression, to avoid T cell-mediated anti-tumor immunity. Although complete MHC-I loss is possible, most tumors express MHC-I in a heterogeneous manner, with a mix of MHC-I high, mid, and low expressing tumor cells. However, the intratumor MHC-I heterogeneity and its impact on the immune microenvironment still require further study. The goal of this study is to investigate MHC-I expressional heterogeneity in breast cancer and characterize the immune landscape, with a focus on CD8 T cells, which target MHC-I expressing tumor cells, and NK cells, which target MHC-I negative/low tumor cells, in a spatial manner within the tumor microenvironment.

Methods We performed quantitative immunofluorescence for MHC-I, CD8, CD56 (NK cell marker), and pan-cytokeratin on breast cancer tumors (n=314) from diverse subtypes to obtain single-cell resolution MHC-I expression and spatial information of tumor and immune cells. Ripley's K function was used to analyze the spatial distribution of MHC-I high, mid, and low expressing tumor cells. We also performed density-based clustering to arrange neighboring tumor cells into clusters and subsequently examine the local immune cell infiltration.

Results All clinical breast cancer subtypes showed high variability in MHC-I expression, with triple-negative breast cancer (TNBC) having the highest MHC-I expression and the largest percentage of tumors with multimodal MHC-I expression (consisting of MHC-I high, mid, and low expressing tumor cells). Both MHC-I high and low expressing tumor cells, especially those in TNBC, tend to cluster and create tumoral MHC-I hot and cold spots. Meanwhile, the MHC-I high-expressing stromal cells and CD8 T cells clustered with tumoral MHC-I hot spots, while MHC-I cold spots exhibited the lowest lymphocyte infiltration and clustered with MHC-I low-expressing stromal cells. Interestingly, heterogeneous MHC-I tumor clusters (those with mixed high and low expressing cells) had the highest levels of infiltrating NK cells.

Conclusions Our work reveals the heterogeneity of MHC-I expression among different breast cancer subtypes. TNBC, the immune checkpoint inhibitor (ICI)-sensitive subtype, is characterized by the highest MHC-I expression and well-defined MHC-I hot and cold spots. Additionally, the local immune landscape around MHC-I hot, cold, and heterogeneous clusters are significantly different. Increased NK cell infiltration in areas where tumor cells heterogeneously express MHC-I was also consistent with our preclinical heterogeneous MHC-I mammary tumor model. Those results suggested that immunotherapy-resistant, MHC-I heterogeneous tumors may be sensitized by combining an NK cell activation drug, such as anti-NKG2A, with already-available ICIs.

Ethics Approval Samples involved in this study are under IRB030747 and INEN 10-018

<http://dx.doi.org/10.1136/jitc-2022-SITC2022.0107>

Abstracts

108

PREDICTION OF CANCER IMMUNOTHERAPY RESPONSE USING ULTRASOUND IMAGING OF TUMOR STIFFNESS AND PERFUSION

¹Chrysovalantis Voutouri*, ¹Triantafyllos Stylianopoulos, ¹Fotios Mpekris, ¹Myrofora Panagi, ¹Christina Michael, ²John Martin. ¹University of Cyprus, Aglantzia, Nicosia, Cyprus; ²Materia Therapeutics, Las Vegas, Nevada, Las Vegas, NV, USA

Background Solid tumors are highly heterogeneous tissues that might differ considerably between different types or even among tumors of the same type. As a result, while in some patients (responders) a particular treatment may be very effective, in other patients (non-responders) the same treatment may not be beneficial and in many cases. Emerging technologies have been used towards the development of new biomarkers mainly through analyzing the human genome or biological markers, such as the expression of PD-L1/PD-1, but so far most of them have failed to translate into clinical tools¹ and only a limited number has managed to be approved for cancer prediction.^{2, 3} Here, we hypothesize that aspects of the tumor microenvironment, and particularly the tumor stiffness and perfusion can be used as biomarkers predictive of response to immune checkpoint inhibition in desmoplastic (i. e., rich in extracellular fibers) murine tumor models.

To modulate tumor stiffness and improve perfusion, strategies based on the use of drugs that inhibit CAF-stimulating signaling factors to normalize the levels of intratumor extracellular matrix have been developed. These therapeutics are known as mechanotherapeutics, because they normalize mechanical abnormalities in the TME, i.e., stiffness and blood flow.^{4, 5} Towards the development of this novel therapeutic class, several generic drugs with decades of safe use in other diseases have been repurposed to act as cancer mechanotherapeutics, including the anti-hypertensives losartan and bosentan, the corticosteroid dexamethasone, the antihistamine ranitidine and the antifibrotic pirfenidone.^{6–11}

Methods In this study, we employed clinically-applied ultrasound shear wave elastography (SWE) and contrast-enhanced ultrasound (CEUS) to demonstrate in four orthotopic murine tumor models of breast cancer (4T1 and E0771), sarcoma (MCA205) and melanoma (B16F10) that specific measures of stiffness and perfusion can predict the efficacy of immune checkpoint inhibition.

Results Interestingly, we further show that these correlations between tumor stiffness/perfusion and therapeutic efficacy are valid even when data from all tumor models are considered together (figure 1). SWE and CEUS are non-invasive imaging modalities that are employed for diagnostic purposes in the clinical practice in oncology, cardiology and other diseases.^{12–15}

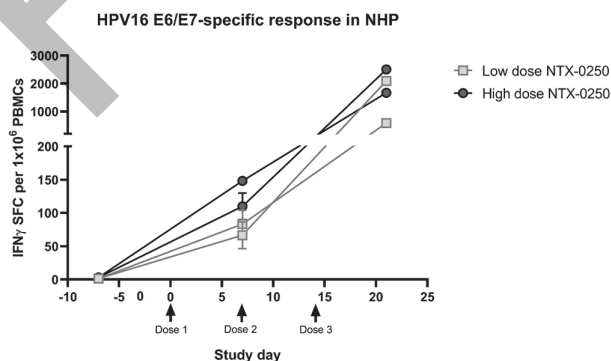
Conclusions Furthermore, SWE has been investigated in patients with breast cancer as a marker of response to chemotherapy.¹⁶ Therefore, the results of our study are highly transferable to the clinic.

Acknowledgements This project received funding from the European Research Council (ERC) under the European Union's Horizon 2020 research and innovation programme (grant agreement nos. 863955 and 101069207 to T.S.).

REFERENCES

1. Feldman R & Kim ES (2017) Prognostic and predictive biomarkers post curative intent therapy. *Annals of Translational Medicine* **5**(18):374.
2. Borrebaeck CAK (2017) Precision diagnostics: Moving towards protein biomarker signatures of clinical utility in cancer. *Nature Reviews Cancer* **17**(3):199–204.
3. Prelaj A, et al. (2019) Predictive biomarkers of response for immune checkpoint inhibitors in non-small-cell lung cancer. *Eur J Cancer* **106**:144–159.

4. Sheridan C (2019) Pancreatic cancer provides testbed for first mechanotherapeutics. *Nat Biotechnol* **37**(8):829–831.
5. Jain RK, Martin JD, & Stylianopoulos T (2014) The role of mechanical forces in tumor growth and therapy. *Annu Rev Biomed Eng* **16**:321–346.
6. Chauhan VP, et al. (2013) Angiotensin inhibition enhances drug delivery and potentiates chemotherapy by decompressing tumor blood vessels. *Nature Communications* **4**(2516):10.1038/ncomms.3516.
7. Martin JD, et al. (2019) Dexamethasone Increases Cisplatin-Loaded Nanocarrier Delivery and Efficacy in Metastatic Breast Cancer by Normalizing the Tumor Microenvironment. *ACS Nano* **13**(6):6396–6408.
8. Mpekris F, et al. (2021) Normalizing the Microenvironment Overcomes Vessel Compression and Resistance to Nano-immunotherapy in Breast Cancer Lung Metastasis. *Adv Sci (Weinh)* **8**(3):2001917.
9. Panagi M, et al. (2020) TGF- β inhibition combined with cytotoxic nanomedicine normalizes triple negative breast cancer microenvironment towards anti-tumor immunity. *Theranostics* **10**(4):1910–1922.
10. Voutouri C, et al. (2021) Endothelin Inhibition Potentiates Cancer Immunotherapy Revealing Mechanical Biomarkers Predictive of Response. *Advanced Therapeutics* 2000289.
11. Polydorou C, Mpekris F, Papageorgis P, Voutouri C, & Stylianopoulos T (2017) Pirfenidone normalizes the tumor microenvironment to improve chemotherapy. *Oncotarget* **8**(15):24506–24517.
12. Averkiou MA, Bruce MF, Powers JE, Sheeran PS, & Burns PN (2020) Imaging Methods for Ultrasound Contrast Agents. *Ultrasound Med Biol* **46**(3):498–517.
13. Malone CD, et al. (2020) Contrast-enhanced US for the Interventional Radiologist: Current and Emerging Applications. *Radiographics* **40**(2):562–588.
14. Carlsen J, et al. (2015) Ultrasound Elastography in Breast Cancer Diagnosis. *Ultraschall Med* **36**(6):550–562; quiz 563–555.
15. Gandhi J, Zaidi S, Shah J, Joshi G, & Khan SA (2018) The Evolving Role of Shear Wave Elastography in the Diagnosis and Treatment of Prostate Cancer. *Ultrasound Q* **34**(4):245–249.
16. Evans A, et al. (2013) Can shear-wave elastography predict response to neoadjuvant chemotherapy in women with invasive breast cancer? *Br J Cancer* **109**(11):2798–2802.



Abstract 108 Figure 1 Tumor stiffness strongly correlates to perfusion markers independently of heterogeneities among tumor types. Plots of the stiffness (in terms of elastic modulus) of 4T1, E0771, MCA205 and B16F10 tumors as a function of the values of the perfusion measures of mean transit time and rise time demonstrate the strong linear correlation even when data from all tumor types are considered together. The Pearson's r value and the R^2 value of the best linear fit to the experimental data is shown to quantify the strength of the correlations. A Pearson's r value >0.8 denotes a very strong correlation

<http://dx.doi.org/10.1136/jitc-2022-SITC2022.0108>

109

QUANTITATIVE SPATIAL ASSESSMENT OF THE TUMOR-IMMUNE MICROENVIRONMENT IN THE METASTATIC MELANOMA LYMPH NODE

¹Rachel Maus*, ¹Raymond Moore, ¹Alexey Leontovich, ¹Zachary Fogarty, ¹Ruifeng Guo, ¹Chathu Dona, ¹Burak Tekin, ¹Jill Schimke, ¹Betty Dicke, ²Benjamin Chen, ¹Svetomir Markovic. ¹Mayo Clinic, Rochester, MN, USA; ²Bristol-Myers Squibb, Cambridge, MA, USA

Background Lymph nodes often serve as the first site of metastasis in solid tumors despite being specialized peripheral immune organs. Evaluating tumor-immune interactions within distinct architectural regions of the lymph node has the potential to inform the clinical heterogeneity observed in metastatic cancer response to immunotherapy. Here, we applied multiplexed immunofluorescence (MxIF) to melanoma lymph node (LN) tissue specimens to quantify tumor-immune interactions contributing to recurrence risk in patients receiving anti-PD1 immunotherapy.

Methods Whole, excisional lymph node biopsies were obtained from 33 treatment-naïve patients with metastatic melanoma who underwent subsequent anti-PD1 therapy. A single 5µm formalin-fixed paraffin embedded LN tissue section was used to assess a panel of 45 analytes by cyclic MxIF. Fields of view (~1mm²) were selected from pathologist-annotated regions of the tumor core (n=447), tumor-immune interface (n=298) and adjacent lymphoid tissue (n=339). Pixel-based single cell segmentation and a supervised classifier approach was applied to resolve 10 distinct tumor, stromal and immune cell phenotypes and functional states (e.g. PD1, PDL1, LAG3) in 5.5 million cells.

Results Stratification based on responsiveness to anti-PD1 therapy resulted in 15 patients experiencing melanoma recurrence by 12 month follow-up. Single cell quantification of the tumor cell fraction was reflective of the pathologist-annotated histology (tumor: 69.7 ± 21.7%, interface: 20.9 ± 13.0%, lymphoid: 0.7 ± 2.5%). Similarly, the distribution of T cell subsets (cytotoxic T, T helper, Tregs) followed conventional histology patterns (tumor 5.3 ± 7.0%, interface: 32.0 ± 16.2%, lymphoid: 51.6 ± 20.9%). Within tumor regions, B and T cell counts displayed a high concordance with pathologist TIL scores as calculated by ANOVA (p-value=0.012). Functional expression of PD1 on T cells was observed in all histologies (tumor: 15.1%, interface: 8.9%, lymphoid: 2.8%). Notably, the percentage of PD1+ T cells was significantly higher in the interface histology of patients that did not experience recurrence (11.5% vs 5.8%) and lymphoid tissue (4.5% vs 1.4%) and lower in the tumor core (14.3% vs 17.7%) suggesting distinctive spatial localization patterns for PD1+ T cells correlate with clinical outcomes (p<0.001). Ongoing analyses will evaluate the diverse cellular interactions across these histologies to determine unique spatial signatures that correlate with recurrence.

Conclusions Spatial distribution of PD1+ T cells is regionally enriched at the tumor-immune interface among patients that did not experience recurrence following anti-PD1 therapy. The metastatic lymph node represents an ideal tissue landscape to apply cyclic MxIF and study tumor-immune cellular interactions that inform recurrence risk following immunotherapy.

Acknowledgements The authors would like to thank the physicians of the Mayo Clinic Melanoma Oncology division who treated the patients included in this study. We also wish to extend our gratitude to the patients and their families for entrusting us with their tissue and for their unwavering commitment to scientific advances in metastatic melanoma.

Ethics Approval The study was approved by Mayo Clinic's Institutional Review Board, approval number 20-002866.

<http://dx.doi.org/10.1136/jitc-2022-SITC2022.0109>

110

CHARACTERIZATION OF HPV-SPECIFIC T-CELLS IN BLOOD AND TISSUE IN UGANDAN WOMEN LIVING WITH HIV WITH CERVICAL LOW GRADE SQUAMOUS INTRAEPITHELIAL LESIONS

¹Amy Codd*, ¹Scott Adams, ¹Cecilia Yeung, ¹Lauri Aicher, ²Corey Casper, ³Lisa Frenkel, ⁴Thomas Uldrick, ¹Evan Newell. ¹Fred Hutch Cancer Center, Seattle, WA, USA; ²Infectious Disease Research Institute, Seattle, WA, USA; ³Seattle Children's Research Institute, Seattle, WA, USA; ⁴Regeneron, Bethesda, MD, USA

Background Cervical cancer (CC) is the most common cancer in women living with HIV (WLWH) and the leading cause of cancer mortality in women in Uganda.^{1,2} CC occurs in a fraction of unresolved high-risk human papilloma virus (hrHPV) infections. HIV is a risk factor for hrHPV infection, however, infection and early stage, low grade squamous epithelial lesions (LSIL), can be resolved by a competent immune response. Nevertheless, WLWH with immune function restored by antiretroviral therapy (ART) remain at higher risk for persistent hrHPV infection, LSIL and progression to high grade squamous epithelial lesions (HSIL).³ Therefore, we hypothesize that the immune response differs between WLWH, on ART, who progress from LSIL to HSIL/ICC, compared to WLWH, on ART, who experience LSIL regression.

Methods Recently, a cohort (n=304) of Ugandan WLWH and HIV seronegative counterparts was established to categorize hrHPV status and examine associations with the immune response.⁴ When stratified by degree of dysplasia, hrHPV infection was more prevalent in WLWH with LSIL (cervical intraepithelial neoplasia (CIN) 0/1), compared to seronegative women, than the same comparison in HSIL (CIN2/3).⁴ Due to the scale of this study, immune parameters analyzed were limited to CD4 and CD8 counts and ratio. This prompted us to design a pilot study, subsampling the cohort, for in-depth interrogation of the immune response in LSIL. The study involves analysis of formalin fixed paraffin embedded (FFPE) cervical tissue and peripheral blood mononuclear cells (PBMC) from WLWH, on ART, diagnosed with LSIL associated with hrHPV infection with progression (n=4) or regression (n=4) or WLWH with no dysplasia diagnosis (n=4).

Results We developed a mass cytometry panel incorporating markers of T cell dysregulation and mucosal homing and leveraged combinatorial tetramer technology to analyze PBMC-derived T cell responses to antigens from various hrHPV types. Further functional analysis is being performed using cytokine intracellular staining (ICS) flow cytometry. FFPE-derived DNA and RNA are subject to TCR sequencing and immunology gene focused-Nanostring analysis, respectively, to complement peripheral immune response data. Owing to complexities of sample procurement, data analysis is ongoing.

Conclusions LSIL represents a reversible stage in the development of CC, with recent data³ suggesting this may be associated with poorer resolution of hrHPV infection in WLWH, compared to seronegative women. In this pilot study, we expect to identify features of immune dysregulation underlying increased risk of malignant progression from LSIL, which could propel larger scale high dimensional analysis of the cohort.

REFERENCES

1. C. de Martel, M. Plummer, J. Vignat, and S. Franceschi, Worldwide burden of cancer attributable to HPV by site, country and HPV type, *Int. J. Cancer*, **vol. 141**, no. 4, pp. 664–670, Aug. 2017, doi: 10.1002/ijc.30716.
2. F. Bray, J. Ferlay, I. Soerjomataram, R. L. Siegel, L. A. Torre, and A. Jemal, Global cancer statistics 2018: GLOBOCAN estimates of incidence and mortality

worldwide for 36 cancers in 185 countries, *CA. Cancer J. Clin.*, **vol. 68**, no. 6, pp. 394–424, 2018, doi: 10.3322/caac.21492.

3. S. Blitz *et al.*, Evaluation of HIV and highly active antiretroviral therapy on the natural history of human papillomavirus infection and cervical cytopathologic findings in HIV-positive and high-risk HIV-negative women, *J. Infect. Dis.*, **vol. 208**, no. 3, pp. 454–462, Aug. 2013, doi: 10.1093/infdis/jit181.
4. C. Nakisige *et al.*, Multiple High-Risk HPV Types Contribute to Cervical Dysplasia in Ugandan Women Living With HIV on Antiretroviral Therapy, *J. Acquir. Immune Defic. Syndr.* 1999, **vol. 90**, no. 3, pp. 333–342, Jul. 2022, doi: 10.1097/QAI.0000000000002941.

Ethics Approval This study including the informed consent process and consent forms in English and Luganda was approved by the Fred Hutchinson Cancer Research Center Institutional Review Office, the UCI Research Ethics Committee and the Uganda National Council for Science and Technology. All participants gave informed consent.

Consent De-identified patient information from this cohort was obtained through approval by the institutional review board at the Fred Hutchinson Cancer Center (IR File#: 10496)

<http://dx.doi.org/10.1136/jitc-2022-SITC2022.0110>

111

INTEGRATING MULTIDIMENSIONAL MASS CYTOMETRY AND MULTIPLEX IMMUNOHISTOCHEMISTRY TO INFER SPATIAL RELATIONSHIPS BETWEEN HUMAN GLIOBLASTOMA INFILTRATING IMMUNE CELLS THAT CORRELATE WITH PATIENT OUTCOME

Todd Bartkowiak*, Asa Brockman, Sierra Lima, Madeline Hayes, Caroline Roe, Justine Sinnaeve, Akshikumar Mistry, Nalin Leelatian, Bret Mobley, Lola Chambless, Reid Thompson, Kyle Weaver, Rebecca Ihrie, Jonathan Irish. *Vanderbilt University Medical Center, Nashville, TN, USA*

Background Glioblastomas (GBM) account for ~60% of adult primary brain tumors. With few advances in therapeutics, median overall survival remains 15-months post-diagnosis. Immunotherapies may provide therapeutic benefit; however, no predictive immune features have informed therapeutic stratification. Radiographic tumor contact with the lateral ventricle (C-GBM) correlates with 7-months worse prognosis compared to patients with ventricle non-contacting GBM (NC-GBM), yet the influence of ventricle contact on anti-tumor immunity is unknown. This study characterized the GBM immune micro-environment and identified targetable mechanisms of immunosuppression correlating with worse outcomes in C-GBM patients.

Methods Primary glioblastoma tissue was provided with written informed consent in accordance with the Declaration of Helsinki and with approval of the Vanderbilt Institutional Review Board (IRB #131870). Seventeen patients presented with primary, IDH-wildtype C-GBM and 15 with NC-GBM. Machine learning integrated 1) mass cytometry immunophenotyping, 2) metabolic phenotypes, 3) immune cytokine response patterns and induced intracellular signaling networks, and 4) matched multiplex immunohistochemistry on FFPE embedded tissue to identify phenotypic, functional, and spatial biomarkers correlating with patient outcome.

Results C-GBM tumors were enriched in STAT3-driven CD32+CD44+HLA-DR+ monocyte-derived macrophages (MDM) compared to NC-GBM ($19 \pm 8\%$ vs. $6 \pm 2\%$; $p < 0.001$) and depleted in lymphocytes including subsets of T, B and NK cells ($2.9 \pm 1\%$ vs. $7.6 \pm 2\%$; $p < 0.001$) and tissue-resident microglia ($1.8 \pm 0.3\%$ vs. $7 \pm 3\%$; $p < 0.001$). Moreover, 45% of exhausted T cells in C-GBM co-expressed the checkpoint receptors PD-1 and TIGIT despite exhibiting metabolic activity consistent with retained functional capacity. As an orthogonal approach, we used multiplex IHC to identify the spatial distribution of immune cells throughout the GBM tumor tissue. K-means clustering identified 10 immunological niches in GBM tumors. Macrophage-tumor niches were most common in C-GBM (17.93% of niches), followed by T cell-microglia-tumor niches (17.72%). Within NC-GBM niches, T cell-T cell interactions were more prevalent in NC-GBM tumors (log odds ratio = 0.90) and correlated with improved survival outcome.

Conclusions These findings suggest that factors within the periventricular space negatively influence the immune micro-environment within GBM tumors. Clinically targetable immune biomarkers (e.g. PD-1) were identified in C-GBM. Notably, this work highlights the potential impact of radiologic assessment of lateral ventricle contact as a guide for clinical trial design for immunotherapies in neuro-oncology based on tumor proximity to the lateral ventricle wall.

Ethics Approval Primary glioblastoma tissue was provided with written informed consent in accordance with the Declaration of Helsinki and with approval of the Vanderbilt Institutional Review Board (IRB #131870).

Consent No sensitive or identifiable information is included in this study.

<http://dx.doi.org/10.1136/jitc-2022-SITC2022.0111>

Abstracts

112

CIRCULATING AND MOLECULAR MARKERS OF INFLAMMATION: IMPACT ON TREATMENT RESPONSE AND SURVIVAL AMONG OLDER PATIENTS WITH CANCER TREATED WITH IMMUNE CHECKPOINT INHIBITORS

¹Khalil Choucair*, ²Caroline Nebhan, ³Alessio Cortellini, ⁴Stijn Hentzen, ⁵Yinghong Wang, ⁶April Salama, ⁷Andrew Elliott, ⁷Matthew Oberley, ⁷Phillip Walker, ⁵Raza Bokhari, ⁸Raffaele Giusti, ⁹Marco Filetti, ¹⁰Paolo Ascierto, ¹¹Vito Vannella, ¹²Domenico Galetta, ¹²Annamaria Catino, ¹²Pamela Pizzutilo, ¹³Carlo Genova, ¹⁴Melissa Bersanelli, ¹⁴Sebastiano Buti, ¹⁵Azhaar Saeed, ¹⁶Wafik El-Deiry, ¹⁷Himisha Beltran, ⁷Chadi Nabhan, ²Douglas Johnson, ¹⁸Claudia Fulgenzi, ¹⁸David Pinato, ⁴Maluki Radford, ¹⁹Stephen Liu, ¹⁹Chul Kim, ²⁰Rafah Naqash, ²¹Anwaar Saeed. ¹Karmanos Cancer Institute/Wayne State University, Detroit, MI, USA; ²Vanderbilt-Ingram Cancer Center, Nashville, TN, USA; ³Hammersmith Hospital, Imperial College London; Fondazione Policlinico Campus Bio-Medico, London, UK; ⁴Kansas University Medical Center, Kansas City, KS, USA; ⁵UT MD Anderson Cancer Center, Houston, TX, USA; ⁶Duke Cancer Institute, Durham, NC, USA; ⁷Caris Life Sciences, Phoenix, AZ, USA; ⁸Azienda Ospedaliero Universitaria Sant'Andrea, Rome, Italy; ⁹Fondazione Policlinico Universitario Agostino Gemelli, IRCC, Rome, Italy; ¹⁰Istituto Nazionale Tumori-Fondazione Pascale, Milan, Italy; ¹¹Istituto Nazionale Tumori IRCCS Fondazione Pascale, Napoli, Italy; ¹²IRCCS Istituto Tumori Giovanni Paolo II, Bari, Italy; ¹³UOC Clinica di Oncologia Medica, IRCCS Ospedale Policlinico San Martino, Genova, Italy; ¹⁴University Hospital of Parma, Parma, Italy; ¹⁵University of Minnesota, Minneapolis, MN, USA; ¹⁶Cancer Center at Brown University, Providence, RI, USA; ¹⁷Dana Farber Cancer Institute, Boston, MA, USA; ¹⁸Hammersmith Hospital Campus, Imperial College London, London, UK; ¹⁹Georgetown University, Washington, DC, USA; ²⁰University of Oklahoma/ Stephenson Cancer Center, Oklahoma, OK, USA; ²¹Kansas University Cancer Center, Fairway, KS, USA

Background Age-associated pro-inflammatory states may result in decreased response to immune checkpoint inhibitors (ICI) in older patients (pts) with cancer. We explored the association of circulating inflammatory markers with response to ICIs, and investigate potential differences in transcriptional and TME signatures of pts ≥80-years (yr) of age and younger.

Methods We built a multicenter, international database of pts with different tumors treated with ICIs monotherapy between 2011 and 2021 from 11 academic centers in the US and Europe. Retrospective analysis of 885 pts compared objective response rates (ORR; iRECIST), median progression-free survival (mPFS) and overall survival (mOS) between pts ≥80-yr and <80-yr, and stratified them across serum pre-treatment levels of neutrophil-to-lymphocyte ratio (NLR), platelet-to-lymphocyte ratio (PLR), monocyte-to-lymphocyte ratio (MLR) and systemic immune-inflammation index (SII=PxN/L). Optimal cut-off values for high (H) vs. low (L) levels were determined using receiver operating characteristic curves.

DNA (592-gene panel/whole exome) and RNA (whole transcriptome) next-generation sequencing, immunohistochemistry (IHC) and TME analysis (MCP-counter) were performed on 24,123 independent samples of non-small cell lung cancer (NSCLC), melanoma (MEL) and renal cell carcinoma (RCC) submitted to a CLIA-certified laboratory (Caris Life Sciences, Phoenix, AZ). Results were compared between pts ≥80-yr and <80-yr.

Results Table 1 summarizes pts baseline characteristics. Pts <80-yr had better ORR ($P<0.01$), but comparable mOS and mPFS to ≥80-yr (table 2). In pts ≥80-yr, NLR-L and SII-L were associated with higher ORR ($P<0.01$ and $P<0.05$; figure 1). All pts with NLR-L, PLR-L and SII-L, had longer mOS ($P<0.01$; figure 2). All PLR-L and SII-L pts had significantly longer mPFS ($P<0.01$; figure 3).

Compared to pts <80-yr, NSCLC ≥80-yr had increased abundance of fibroblasts, dendritic cells and macrophages ($P<0.01$) in their TME and lower TMB-H ($P<0.001$). MEL

≥80-yr pts had fewer TME infiltrating T-lymphocytes ($P=0.02$), a1.24-fold increased expression of IL-6. RCC ≥80-yr pts had 0.56-fold decreased expression of GZMB, and lower PD-L1 (IHC-SP142, ≥2+|5%) expression ($P<0.05$; figure 4). Additional correlative biomarkers will be reported in the poster.

Conclusions Lower levels of circulating inflammatory markers associated with significantly longer survival and better response rates to ICIs. SII-L and NLR-L specifically are potential biomarkers of response to ICI in pts ≥80-yr. This is the first study to evaluate the role of serum markers of inflammation as potential biomarkers of response to ICI in older pts with cancer, along with molecular correlate. Circulating inflammatory markers, and associated gene expression and TME composition suggest potential unique, cancer-specific biomarkers of response to ICIs in this population.

Ethics Approval The study was approved by the institutional review board at each participating institution. Written informed consent was waived, given the retrospective nature of the study and the de-identified status of collected data.

Abstract 112 Table 1 Baseline characteristics of patients

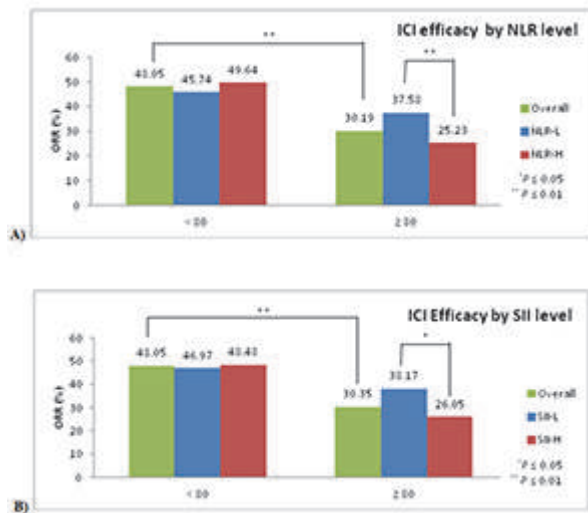
	Overall	<80 years	≥ 80 years	P-value
Number of patients (N)	885	417	468	-
Age (years) at ICI start, median (range)	80.0 (16.0-94.6)	65.0 (16.0-79.9)	82.8 (80.0-94.6)	<0.001
Sex (n=697; %)				0.012
M	446/697 (64.0)	141/244 (57.8)	305/453 (67.3)	
F	251/697 (36.0)	103/244 (42.2)	148/453 (32.7)	
ECOG (n=743; %)				<0.001
0-1	638/743 (85.87)	275/296 (92.9)	363/447 (81.2)	
2	90/743 (12.11)	20/296 (6.76)	70/447 (15.67)	
>2	15/743 (2.02)	1/296 (0.34)	14/447 (3.16)	
Tumor types, N (%)				<0.001
Melanoma	323 (36.5)	118 (28.3)	205 (43.80)	
NSCLC	502 (56.72)	282 (67.62)	220 (47)	
SCLC	17 (1.92)	15 (3.60)	2 (0.43)	
RCC	10 (1.13)	1 (0.24)	9 (1.92)	
Bladder/GU	22 (2.49)	1 (0.24)	21 (4.49)	
Tongue/Larynx/glottis	3 (0.34)	-	3 (0.64)	
Gastric/esophageal	3 (0.34)	-	3 (0.64)	
HCC	3 (0.34)	-	3 (0.64)	
Sarcoma	2 (0.22)	-	2 (0.44)	
Stage (n=882; %)				0.123
I	17 (1.93)	7/414 (1.69)	10/468 (2.14)	
II	33 (3.74)	11/414 (2.90)	21/468 (4.49)	
IIIa	81 (9.18)	47/414 (11.35)	34/468 (7.26)	
IIIb/c	90 (10.2)	46/414 (11.11)	44/468 (9.4)	
IV	661 (74.95)	302/414 (72.95)	359/468 (76.71)	
Prior lines of therapy (n=749; %)				0.028
0	425/749 (56.74)	176/296 (59.46)	249/453 (54.97)	
1	261/749 (34.85)	106/296 (35.81)	155/453 (34.22)	
2	39/749 (5.21)	9/296 (3.04)	30/453 (6.62)	
≥3	24/749 (3.20)	5/296 (1.69)	19/453 (4.19)	
ICI (n=696; %)				<0.001
Pembrolizumab	327/696 (46.99)	100/244 (40.98)	227/452 (50.22)	
Ipilimumab	21/696 (3.02)	4/244 (1.64)	17/452 (3.76)	
Nivolumab	239/696 (34.34)	79/244 (32.38)	160/452 (35.40)	
Atezolizumab	34/696 (4.88)	15/244 (6.15)	19/452 (4.20)	
Avelumab	1/696 (0.14)	1/244 (0.41)	0	
Durvalumab	43/696 (6.18)	36/244 (14.75)	7/452 (1.55)	
Cemiplimab	3/696 (0.43)	0	3/452 (0.67)	
ICI combination	28/696 (4.02)	9/244 (3.69)	19/452 (4.20)	
Time (months) on ICI, median (range)				<0.001
(n=697)	7.50 (1.0-82.0)	11.0 (1.0-82)	4.55 (1.0-61.4)	

ICI: Immune checkpoint inhibitor; M: male; F: female; ECOG: Eastern Cooperative Oncology Group; NSCLC: non-small cell lung carcinoma; SCLC: small-cell lung carcinoma; RCC: renal cell carcinoma; GU: genitourinary; HCC: hepatocellular carcinoma.

Abstract 112 Table 2 Treatment response and survival

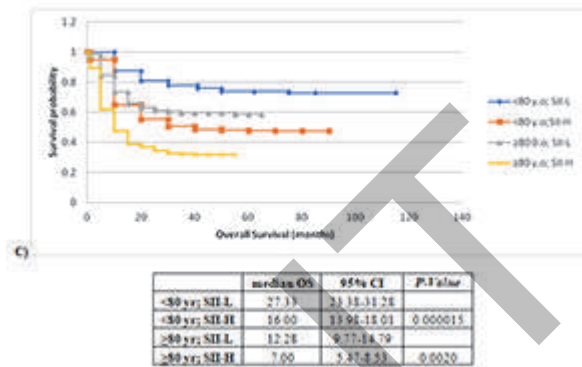
	Overall (n=885)	<80 years (n=417)	≥ 80 years (n=468)	P-value
mOS (months; [95% CI])	12.88 [11.74-14.02]	14.30 [12.62-15.98]	12.80 [11.23-14.37]	
mPFS (months; [95% CI])	8.60 [7.52-9.68]	9.33 [7.73-10.93]	8.33 [6.84-9.82]	
DCR, (n=638, (%))	69.6 (444/638)	94.09 (223/227)	55.11 (221/401)	<0.001
CR	53 (8.31)	14 (5.91)	39 (9.73)	
PR	176 (27.59)	100 (42.19)	76 (18.95)	
SD	215 (33.7)	109 (45.99)	106 (26.43)	
ORR, (n=638, (%))	229 (35.89)	114/237 (48.1)	115/401 (28.68)	<0.001

mOS: median overall survival; mPFS: median progression-free survival; DCR: disease control rate; CR: complete response; PR: partial response; SD: stable disease; ORR: Objective response rate; CI: confidence interval

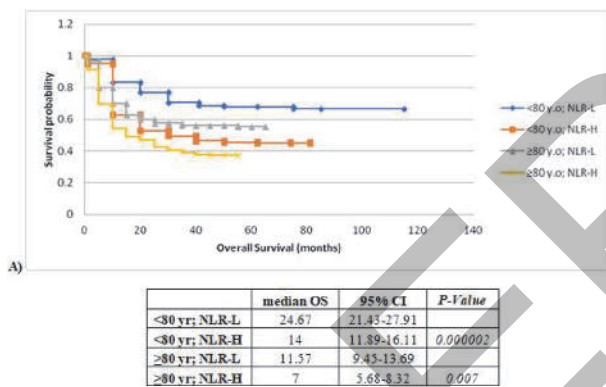


Abstract 112 Figure 1 Objective response rates (ORR) Objective response rates (ORR) in patients < 80 vs. ≥ 80 years, stratified by pre-treatment levels of inflammatory markers: ICI: immune checkpoint inhibitor; NLR: neutrophil-to-lymphocyte ratio; H: high; L: low

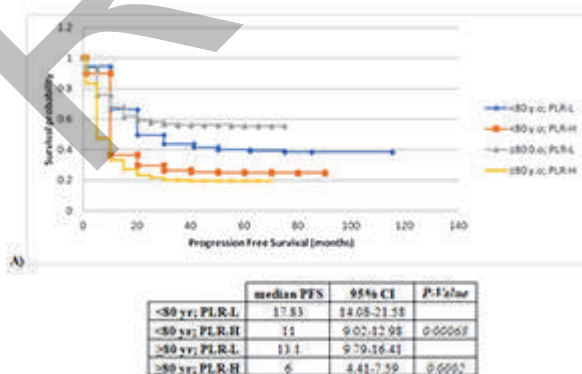
< 80 and ≥ 80 years, stratified according to pre-treatment MLR levels: ICI: immune checkpoint inhibitor; MLR: monocyte-to-lymphocyte ratio; H: high; L: low; 95%CI: 95% confidence interval



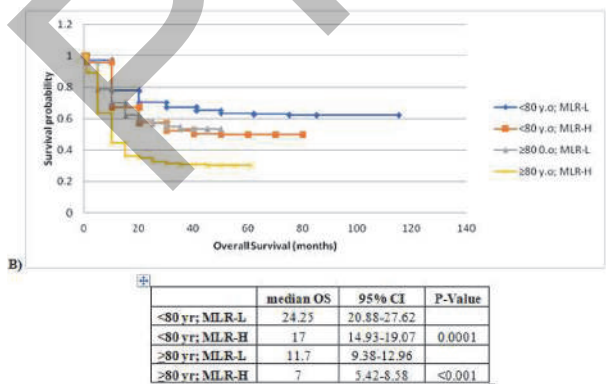
Abstract 112 Figure 2C Kaplan-Meier plot of overall survival by SII level Kaplan-Meier plot of overall survival (OS) from ICI initiation, for patients < 80 and ≥ 80 years, stratified according to pre-treatment SII levels: ICI: immune checkpoint inhibitor; SII: Systemic immune-inflammatory index; H: high; L: low; 95%CI: 95% confidence interval



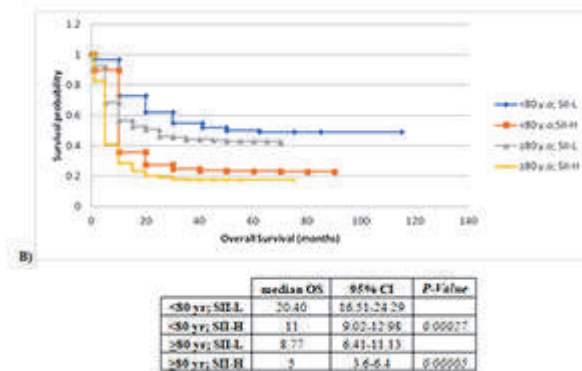
Abstract 112 Figure 2A Kaplan-Meier plot of overall survival by NLR level Kaplan-Meier plot of overall survival (OS) from ICI initiation, for patients < 80 and ≥ 80 years, stratified according to pre-treatment NLR levels: ICI: immune checkpoint inhibitor; NLR: neutrophil-to-lymphocyte ratio; H: high; L: low; 95%CI: 95% confidence interval



Abstract 112 Figure 3A Kaplan-Meier plot of PFS by PLR level Kaplan-Meier plot of progression-free survival (PFS) from ICI initiation, for patients < 80 and ≥ 80 years, stratified according to pre-treatment PLR levels: ICI: immune checkpoint inhibitor; PLR: platelets-to-lymphocyte ratio; H: high; L: low; 95%CI: 95% confidence interval



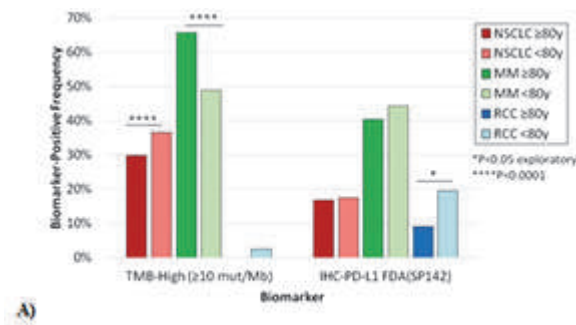
Abstract 112 Figure 2B Kaplan-Meier plot of overall survival by MLR level Kaplan-Meier plot of overall survival (OS) from ICI initiation, for patients



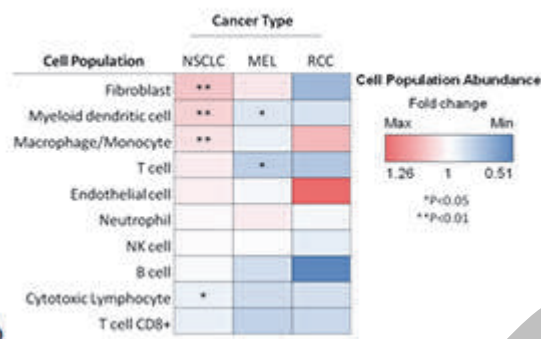
Abstract 112 Figure 3B Kaplan-Meier plot of PFS by SII level Kaplan-Meier plot of progression-free survival (PFS) from ICI initiation, for patients < 80 and ≥ 80 years, stratified according to pre-treatment

Abstracts

SII levels: ICI: immune checkpoint inhibitor; SII: systemic immune-inflammation index; H: high; L: low; 95%CI: 95% confidence interval



A)



B)

Abstract 112 Figure 4 ICI-related biomarkers (A) and (B)TME composition

ICI-related biomarkers (A) and composition of the TME (B) in patients ≥ 80 and < 80 years: Fold-changes represent the median value of patients ≥ 80 years compared to those < 80 years. ICI: immune checkpoint inhibitor; TME: tumor microenvironment; TMB-H: high tumor mutation burden; NSCLC: non-small cell lung cancer; MEL: melanoma; PD-L1: programmed-death ligand-1; RCC: renal cell carcinoma

<http://dx.doi.org/10.1136/jitc-2022-SITC2022.0112>

113

UNCOVERING THE DARK IMMUNOPEPTIDOME OF HEAD AND NECK SQUAMOUS CELL CARCINOMA (HNSCC): RELEVANCE FOR UNIVERSAL CANCER VACCINES, IMMUNOLOGICAL MONITORING AND TIL THERAPY

¹Noriko Iwamoto*, ¹Takashi Shimada, ²Tarsem Moudgil, ²Ryan Meng, ²Tanisha Christie, ²Alexa Dowell, ²Rom Leidner, ²Bryan Bell, ²William Redmond, ²Eric Tran, ³Hong-Ming Hu, ³Traci Hilton, ²Brian Piening, ²Yoshinobu Koguchi, ³Bernard Fox. ¹Shimadzu Corporation, Kyoto, Japan; ²Providence Cancer Institute, Portland, OR, USA; ³UbiVac/Providence Cancer Institute, Portland, OR, USA

Background Discoveries of the last two years have initiated a renaissance in our understanding of the targets T cells recognize on cancer cells. Identification of HLA-presented non-canonical or cryptic peptides that are non-mutated and have high interpatient sharing in AML [PMID: 33740418], coupled with their absence from the thymus, led them to be designated as alternative neoantigens with potential for being universal cancer vaccines [PMID: 33852826]. These cryptic genes, in some cases, appear to play a role in promoting malignancy, further strengthening the rationale for their identification and use as targets for immunotherapy. Our group seeks to identify the Dark Immunopeptidome of HNSCC. Over the last several months we have swithed from exome-capture RNA-Seq, which fails to detect non-canonical gene sequences, to ribo-Seq, which can capture these cryptic transcripts.

Methods HNSCC cells were lysed and recovered lysates were treated with detergent in the presence of protease inhibitor. HLA peptides were collected from HLA complexes purified by anti-HLA-I antibody (w6/32). Recovered HLA peptides were analyzed by the microLC-QTOF MS (LCMS-9030, Shimadzu Corporation). Ribo-Seq was performed on HNSCC and full cryptic protein databases were generated using a modified version of the pipeline described in Scull et al. [PMID: 34509645]. Libraries were aligned to the GRCh38 reference genome using STAR [PMID: 23104886] in two-pass mode and both a reference guided assembly and a de-novo assembly were generated using Cufflinks [PMID:22383036]. Variant calling was performed using GATK Best Practices Workflow 'RNASeq short variant discovery (SNPs + Indels)' utilizing Mutect2 [PMID:23396013] for variant calling and subsequent filtering. The reference guided assembly, de-novo assembly, and the variant calling output were turned into transcriptome assemblies utilizing gffread [PMID: 32489650], and underwent three frame translation using triple_translate (Scull et al.). The resulting three-frame translated fasta files were merged and had any duplicates or redundancies removed using squish (Scull et al.) for database generation to be used in PEAKS [PMID: 14558135].

Results We have completed ribo-Seq on 2 HNSCC cells lines and are preparing to interrogate the microLC-QTOF MS-generated spectra for HLA-presented peptides of the HNSCC cell lines.

Conclusions While data are still being generated and evaluated using different assessment tools, our group considers this proteogenomic approach to assess the Dark Immunopeptidome for HNSCC holds substantial promise for uncovering targets of anti-cancer immunity. In addition to applications for immunological monitoring, this has potential therapeutic application for cancer vaccines or as vaccine boosters for patients receiving TIL.

Acknowledgements Funding Support from Shimadzu Corporation, The Harder Family, Robert and Elsie Franz, Wes and Nancy Lematta, Lynn and Jack Loacker, The Chiles Foundation, The Providence Portland Medical Foundation, the Oral

and Maxillofacial Surgery Foundation, and The Murdock Trust.

Ethics Approval The study was approved by the institutional review board of the Providence Portland Medical Center (06-108).

<http://dx.doi.org/10.1136/jitc-2022-SITC2022.0113>

114

CHARACTERIZATION OF SUPPRESSIVE MYELOID CELLS IN SOLID TUMORS TO REFINE DISEASE SELECTION IN A PHASE 1 STUDY OF THE MULTI-SIGLEC INHIBITOR AL009

Julie Huang*, Sam Nalle, Helen Lam, Arnon Rosenthal, Daniel Maslyar. *Alector, South San Francisco, CA, USA*

Background Inhibitory sialic acid-binding immunoglobulin-type lectins (Siglecs) are a subset of the Siglec family of cell surface receptors expressed predominantly on myeloid cells that potentiate immune suppression. Tumors increase the expression of sialic acid glycans and co-opt the immunosuppressive effects of Siglecs, driving tumor resident immune cells toward a cancer permissive phenotype. Disrupting Siglec-sialic acid signaling could confer a therapeutic benefit in cancer, particularly those cancers with high levels of myeloid derived suppressor cells (MDSCs). To accomplish this, we designed AL009, an engineered Siglec Fc fusion molecule that acts as a sialic acid trap and a multi-Siglec inhibitor, repolarizing suppressive myeloid cells and activating an anti-cancer response. The safety, tolerability, and efficacy of AL009 in patients with solid tumors will be evaluated in an upcoming Phase 1 study. Here we present data that help to refine disease selection for the Phase 1 study and efforts in testing potential predictive biomarkers for clinical use.

Methods Tissue microarrays from patients with various solid tumors were analyzed by immunohistochemistry (IHC). Markers detected included CD163, CD68, and a representative Siglec for multi-Siglec expression. IHC scoring methodology was prespecified focusing on proportion of cells expressing each of the above markers. Scoring was on a 4-point scale and based upon the number of cells stained with the marker of interest in reasonable proximity to the tumor (tissue without tumor was not scored).

Results Tumor profiling by IHC identified squamous cell lung cancer, colorectal cancer, ovarian cancer, kidney cancer as indications rich in MDSCs marked by high levels of CD163, CD68, and Siglec expression. These cancer indications may be particularly responsive to AL009. The use of PD-L1 expression data from The Cancer Genome Atlas for these various cancer indications provides further guidance on potential effective combination therapies coupled with AL009.

Conclusions We employed an IHC panel that marks CD163, CD68, and Siglecs to identify cancer indications rich in MDSCs. As AL009's mechanism of action is to disrupt the Siglec-sialic acid signaling of MDSCs, we believe that patients with these particular cancers will be most likely to respond to AL009 treatment. This IHC panel will be utilized to retrospectively explore Siglecs, CD163, and CD68 as predictive biomarkers in an upcoming Phase 1 study.

Ethics Approval The human tissue microarrays were procured from a commercial vendor that collect human samples with the following ethical considerations: informed donor consent, IRB/EC approval, fully anonymized, and compliant with current US (HIPAA) International and EU regulations.

<http://dx.doi.org/10.1136/jitc-2022-SITC2022.0114>

SPATIAL DISSECTION OF T CELL CLONOTYPE IDENTITY, TRANSCRIPTIONAL PROFILES, AND CELL-CELL INTERACTIONS IN THE TUMOR MICROENVIRONMENT AND TERTIARY LYMPHOID STRUCTURES

¹Bryan Iorgulescu*, ²Sophia Liu, ³Shuqiang Li, ³Mehdi Borji, ²Irving Barrera-Lopez, ²Vignesh Shanmugam, ³Haoliang Lyu, ²Julia Morriss, ²Zoe Garcia, ²Evan Murray, ³David Reardon, ³Charles Yoon, ⁴David Braun, ³Ken Livak, ³Catherine Wu, ²Fei Chen. ¹MD Anderson Cancer Center, Houston, TX, USA; ²Broad Institute, Cambridge, USA; ³Dana-Farber Cancer Institute, Boston, MA, USA; ⁴Yale, Boston, MA, USA

Background Determining the spatial interactions of T cell clonotypes in tumor microenvironments and tertiary lymphoid structures (TLSs) is essential to understanding adaptive anti-tumoral immune responses, but existing spatial sequencing methods remain unable to profile the TCR repertoire at high resolution.

Methods We previously described the development of Slide-TCR-seq, which integrates Slide-seqV2 (spatially-resolved RNA capture by a DNA-barcoded bead array with 10 μ m resolution) with rhTCRseq (highly sensitive targeted capture of TCR sequences)^{2,3,4} to facilitate amplification of the TCR transcript from CDR3 to the 3' end. This approach enables the simultaneous measurement of cellular transcriptomes, T cell clonotypes, and spatial location at 10 μ m resolution. We examined melanoma and renal cell carcinoma (RCC) tumors with Slide-TCR-seq to understand the spatial relationships between T cell clonotypes, tumor cells, and immune cells in the tumor microenvironment and TLSs.

Results We applied Slide-TCR-seq to melanoma and RCC metastases because of the well-characterized roles played by T cell phenotype and TCR repertoire in their immune microenvironments.^{5,6} By histology and Slide-TCR-seq, we identified TLSs in both melanoma and RCC metastases. We observed that T cells located within the tumor regions were more clonally expanded than those in the TLSs. Furthermore, T cells in TLSs tended to be CD4+ T cells, while those infiltrating into tumor tended to be CD8+ T cells with an exhausted phenotype ($p < 0.05$ by FDR-corrected t-test)—together suggesting unique immunological roles of TLSs in tumors.

In the melanoma metastasis, one T cell clone (CDR3 sequence CASRASNEQFF) was preferentially enriched in one of the two tumor lobes that were examined ($p = 1 \times 10^{-102}$). Compared to other clonotypes, GZMB ($p = 1 \times 10^{-8}$; associated with cytotoxic T cell function) and STAT3 ($p = 7 \times 10^{-7}$; associated with activated T cells' survival) were prominently upregulated in CASRASNEQFF.

CASRASNEQFF T cells additionally exhibited unique cell non-autonomous mechanisms: monocytes neighboring CASRASNEQFF T cells displayed elevated CXCL10 chemokine expression ($p = 5 \times 10^{-21}$), which can recruit tumor-reactive effector T cells.⁷ Notably, monocytic expression of CXCL10 was higher in the same lobe that was enriched with CASRASNEQFF T cells, implicating a preferential interaction between the two. Melanoma cells neighboring the CASRASNEQFF T cells also displayed differential gene expression, including downregulated MGST1 expression ($p = 3 \times 10^{-15}$).

Conclusions Slide-TCR-seq enables spatially-resolved transcriptomics and TCR clonotyping. Our findings suggest that TLS T cells' phenotype and TCR repertoire are distinct from tumor-infiltrating T cells, and that the transcriptional profiles of T cells, monocytes, and tumor cells may depend on their spatial relationships to one another in the tumor microenvironment.

REFERENCES

1. Liu S, Iorgulescu B, Li S, et al. 76 Spatial mapping of T cell receptors and transcriptomes in renal cell carcinoma following immune checkpoint inhibitor therapy. *Journal for Immunotherapy of Cancer* 2021;9:doi: 10.1136/jitc-2021-SITC2021.076
2. Stickels, R. R. et al. Highly sensitive spatial transcriptomics at near-cellular resolution with Slide-seqV2. *Nat. Biotechnol.* (2020) doi:10.1038/s41587-020-0739-1.
3. Rodrigues SG, Stickels RR, Goeva A, Martin CA, Murray E, Vanderburg CR, Welch J, Chen LM, Chen F, Macosko EZ. Slide-seq: A scalable technology for measuring genome-wide expression at high spatial resolution. *Science*. 2019 Mar 29;363(6434):1463–1467. doi: 10.1126/science.aaw1219. Epub 2019 Mar 28. PMID: 30923225; PMCID: PMC6927209.
4. Li, S. et al. RNase H-dependent PCR-enabled T-cell receptor sequencing for highly specific and efficient targeted sequencing of T-cell receptor mRNA for single-cell and repertoire analysis. *Nat. Protoc.* **14**, 2571–2594 (2019).
5. Braun, D. A. et al. Progressive immune dysfunction with advancing disease stage in renal cell carcinoma. *Cancer Cell* (2021) doi:10.1016/j.ccell.2021.02.013.
6. Oliveira, G. et al. Phenotype, specificity and avidity of antitumour CD8+ T cells in melanoma. *Nature* (2021) doi:10.1038/s41586-021-03704-y.
7. Spranger, S., Dai, D., Horton, B. & Gajewski, T. F. Tumor-Residing Batf3 Dendritic Cells Are Required for Effector T Cell Trafficking and Adoptive T Cell Therapy. *Cancer Cell* **31**, 711–723.e4 (2017).

Ethics Approval This study was approved by MGB/DFCI/Broad institution's Ethics Board; approval number 2019P000017.

<http://dx.doi.org/10.1136/jitc-2022-SITC2022.0115>

116

DEEP HIGH-PLEX SPATIAL PHENOTYPING OF GLIOBLASTOMA MULTIFORME PROVIDES NEW INSIGHTS INTO THE IMMUNE LANDSCAPE AND TUMOR HETEROGENEITY

¹Dmytro Klymyshyn*, ¹Niyati Jhaveri, ¹Yasmin Kassim, ¹Bassem Ben Cheikh, ¹Oliver Braubach, ²Keith Black, ²Tao Sun. ¹Akoya Biosciences, Menlo Park, CA, USA; ²Cedars-Sinai Medical Center, Los Angeles, CA, USA

Background Highly multiplexed spatial biology technologies have become key to unveiling unique cellular phenotypes and cellular neighborhoods in healthy and diseased tissues. Glioblastoma (GBM), the most prevalent and aggressive brain tumor in adults, is characterized by high intra- and inter-tumoral heterogeneity. Along with the highly infiltrative nature of these tumors, the immunosuppressive microenvironment leads to poor clinical outcomes with median survival of less than 15 months with current standard-of-care treatments. While immunotherapies have been approved for the treatment of various types of cancer, clinical trials in GBM treatment yielded little to no success.

Methods Using the Phenocycler[®]-Fusion, an integrated spatial biology system, we performed deep analysis of over 50+ proteins to interrogate the immune, vascular, and tumor landscapes in primary and recurrent GBMs. Antibody panels included markers for cell lineage, immune checkpoints, tissue structure, and cellular activation states which, when analyzed, provided comprehensive information of the tumor microenvironments' phenotypic constituents as well as their spatial relationship.

Results Most of the tumor tissues exhibited high levels of glial marker GFAP, indicative of their cell-of-origin. In some tumors, GFAP expression overlapped with Vimentin and CD44, two characteristic markers for the mesenchymal subtype of GBM associated with poor prognosis. GBM tumors also showed varying degrees of proliferation and angiogenesis as evidenced by Ki67 and CD31 staining, respectively. MMP9 expression was very common in most tumors and MMP9 positive cells were found to be associated with the vasculature. Infiltrating T cells also varied significantly from almost non-detectable to a large presence in certain tumors. Both residential microglia and infiltrating monocytes/macrophages could be found across most of the tumors. Intriguingly, some GBM samples showed high expression of β -catenin and exhibited a remarkable infiltration of myeloid-derived suppressor cells (MDSCs; CD14^{high}/HLA-DR^{low}), a large amount of glioma-associated macrophages (CD163⁺) and a high percentage of FoxP3⁺ Tregs.

Conclusions Deep spatial phenotyping of GBM tumors revealed a high degree of cellular heterogeneity in both intra and inter-tumoral fashion. This unbiased, whole-slide approach of analyzing multiple proteins simultaneously within complex GBM tissue structures will greatly enhance our understanding of the immune-suppressive tumor microenvironment in GBM. Further investigation of the immune landscape before and after immunotherapy treatment will help us understand the mechanism of therapy resistance and guide new drug development.

Ethics Approval This study was performed in accordance with Cedars-Sinai IRB protocol No STUDY00001892

<http://dx.doi.org/10.1136/jitc-2022-SITC2022.0116>

117

HIGH-PLEX SPATIAL PROTEOMIC PROFILING OF IMMUNOTHERAPY RESPONSE GROUPS IN HEAD AND NECK CANCER IDENTIFIES TISSUE SIGNATURES ASSOCIATED WITH THERAPY RESPONSE

¹Arutha Kulasinghe*, ¹Habib Sadeghirad, ²Ning Liu, ¹James Monkman, ²Chin Wee Tan, ³Caroline Cooper, ⁴Sarah Church, ²Fabian Schneider, ⁵Jeppe Thaaagard, ³James Mansfield, ³Kenneth O'byrne, ²Melissa Davis, ⁶Brett Hughes. ¹The University of Queensland, Brisbane, Australia; ²WEHI, Melbourne, Australia; ³The Princess Alexandra Hospital, Brisbane, Australia; ⁴Nanostring Technologies, Seattle, WA, USA; ⁵Visiopharm, Horsholm, Denmark; ⁶The Royal Brisbane and Women's Hospital, Brisbane, Australia

Background Immunotherapies have improved the treatment landscape for recurrent and metastatic head and neck cancers (HNC). Immune checkpoint inhibitors (ICI) have led to durable benefit in approximately 20% of HNSCC patients. Therefore, predictive biomarkers are needed to identify those likely to respond or develop resistance to ICI therapy.

Methods Our retrospective study profiled pre-treatment formalin-fixed paraffin-embedded (FFPE) tissues from metastatic HNC patients treated with immunotherapy at the Royal Brisbane and Women's Hospital. Here, we used image analytics tool (Oncotopix Discovery[®]) to demarcate gross structures from H&E images (tumour, stroma, tertiary lymphoid structures, muscle, fat and vasculature) and per-region cell counts, which informed our high-plex profiling of the tumour microenvironment using the Nanostring GeoMx Digital Spatial Profiler. Tumour and stromal compartments were measured for 80-proteins simultaneously spanning immune cell typing, immuno-oncology drug targets, immune activation, pan-tumour, cell death, and PI3K/AKT panels. Each GeoMx ROI (H&E and 4-plex IF (DNA, PanCK, CD8 and CD3)) was analysed for percent tissue type (tumour, stroma, etc), per-subregion cell counts, simple cellular phenotypes, and spatial metrics between cell types. The protein findings were measured against response to ICI therapy (RECIST criteria) and overall survival parameters to identify tissue signatures associated with patient outcomes. High-plex validation of markers was performed using orthogonal multiplex tools.

Results Our data revealed robust structural segmentation strategies to annotate tissues using H&E, which may sit upstream of high-plex spatial proteomic assays to identify regions of interest for selection and profiling. The study identified VISTA, CD66b, CD44 which were upregulated, and PD-L1, PD-L2, IDO-1 were downregulated in the progressive disease (PD) vs partial response (PR) comparison, respectively. Within the tumour microenvironment compartment, BAD, BIM and Phospho-PRAS40 were upregulated in the PD group, whereas Cleaved Caspase 9, HLA-DR and CD68 was upregulated in the PR group. A multi-marker signature composed of Pan-CK, PD-1, PD-L2 and cleaved caspase 9, co-localised in the tumour compartment was associated with a worse overall survival.

Conclusions There is an increasing need to comprehensively profile tumour tissues from HNC using high-plex automated imaging and tissue profiling methodologies. Our study demonstrates a new combined workflow enabling the development of tissue-based signatures predictive of response/resistance to ICI therapy.

Ethics Approval This study has Human Research Ethics Approval (LNR/2020/QRBW/66744) from the Royal Brisbane and Women's Hospital Human Research Ethics Committee (RBWH HREC) and the University of Queensland

<http://dx.doi.org/10.1136/jitc-2022-SITC2022.0117>

118

DELINEATION OF SPATIAL TISSUE SIGNATURES OF IMMUNOTHERAPY RESPONSE GROUPS IN NON-SMALL CELL LUNG CANCER (NSCLC)

¹Arutha Kulasinghe*, ¹James Monkman, ²Honesty Kim, ²Aaron Mayer, ¹Ahmed Mehdi, ³Marie Cumberbatch, ³Milan Bhagat, ⁴Fabian Schneider, ⁴Jeppe Thaaagard, ⁴James Mansfield, ⁵Rahul Ladwa, ⁶Scott Mueller, ⁷Mark Adams, ⁵Kenneth O'byme. ¹The University of Queensland, Brisbane, Australia; ²Enable Medicine, California, CA, USA; ³Tristar Technologies, London, DC, UK; ⁴Visiopharm, Horsholm, Denmark; ⁵The Princess Alexandra Hospital, Brisbane, Australia; ⁶University of Melbourne, Melbourne, Australia; ⁷Queensland University of Technology, Brisbane, Australia

Background Lung cancers remain the leading cause of cancer related mortality and have a poor 5-year survival. Immunotherapies have led to durable benefit in a cohort of non-small cell lung cancer (NSCLC) patients. Identifying those patient likely to achieve benefit remains a clinical unmet need. Whilst predictive biomarkers such as PD-L1 and tumour mutation burden (TMB) have shown utility, the underlying tumour-immune biology is unlikely represented. The composition and activation status of the cellular milieu contained within the tumour microenvironment (TME) is becoming increasingly recognised as a driving factor dictating response to immunotherapies.

Methods In this study, we employed multiplex IHC (mIHC), and digital spatial profiling (DSP) to capture the targeted immune proteome and transcriptome of tumour and TME compartments from ICI-treated (n=41) and standard of care (n=47) NSCLC patient cohorts. Oncotopix[®] Discovery was also used to analyse the highplex imagery. The analysis pipeline consisted of tissue segmentation (tumor, stroma, necrosis, etc), nuclear detection using a deep-learning algorithm for DAPI, a threshold-based cellular phenotyping step, and spatial analyses.

Results Patients sensitive to ICI therapy expressed higher levels of IL2 receptor alpha (CD25, p=0.028) within the tumour compartments, which corresponded with increased *IL2* mRNA (p=0.001) within their stroma. *IL2* mRNA levels within the stroma positively correlated with the expression of pro-apoptotic markers cleaved caspase 9 (p=2e-5) and BAD (p=5.5e-4) and negatively with levels of memory T cells (CD45RO) (p=7e-4). Immuno-inhibitory markers CTLA-4 (p=0.021) and IDO-1 (p=0.023) were suppressed in ICI-responsive patients. Tumour CD44 (p=0.02) was depleted in the response group and corresponded inversely with higher stromal expression of one of its ligands, *SPP1*(osteopontin, p=0.008). Cox survival analysis indicated tumour CD44 expression was associated with poorer prognosis (HR=1.61, p=0.01), consistent with its depletion in ICI sensitive patients. The SOC cohort paralleled similar roles for immune checkpoints and pro-apoptotic markers, with LAG3 (HR=3.81, p=0.04) indicating poorer outcome, and BIM (HR=0.16, p=0.014) with improved outcome.

Conclusions Through multi-modal approaches, we have dissected the characteristics of NSCLC treatment groups and provide evidence for the role of several markers including *IL2*, CD25, CD44 and *SPP1* in the efficacy of current generations of ICI therapy. The signatures are being validated in prospective larger cohort studies.

Consent This study has Queensland University of Technology (QUT) Human Research Ethics Committee Approval (UHREC #2000000494).

<http://dx.doi.org/10.1136/jitc-2022-SITC2022.0118>

119

SENSITIVE PREDICTION OF IMMUNOTHERAPY RESPONSE BY INTEGRATING IMMUNE INFILTRATION AND NEOANTIGEN PRESENTATION SCORE IN LATE-STAGE MELANOMA

¹Bailiang Li*, ¹Charles Abbott, ¹Lee McDaniel, ¹Rachel Pyke, ¹Fabio Navarro, ¹Hima Anbunathan, ²Michael Synder, ³Sekwon Jang, ¹Sean Boyle, ¹Richard Chen. ¹Personalis, Inc, Menlo Park, CA, USA; ²Stanford University, Palo Alto, CA, USA; ³Inova Schar Cancer Institute, Fairfax, VA, USA

Background Single-modality biomarkers such as tumor mutational burden (TMB) often fail to reliably predict response to immune checkpoint blockade (ICB), likely due to incomplete characterization of the complex tumor-immune interactions that influence treatment efficacy. We previously developed the composite biomarker, neoantigen presentation score (NEOPSTM), which integrates neoantigen processing and presentation potency and showed it outperformed TMB and other single-modality biomarkers in predicting ICB response in melanoma.^{1,2} Here, we combined NEOPS with the assessment of tumor immune infiltration, and demonstrated more accurate patient stratification for ICB response.

Methods We assessed the interaction effect of 17 immune and stromal cell types on NEOPS, as measured with the ImmunID NeXT Platform[®], using logistic regression in a retrospective cohort of 45 stage III/IV melanoma patients who received anti-PD1 therapy. Next, we evaluated the impact of the resulting immune-selected phenotype on the accuracy of NEOPS, built integrated models, and validated them in a cohort of 109 anti-PD1 treated late-stage melanoma.

Results The predictive value of NEOPS was increased in patients with higher levels of naïve CD4/CD8 T cell, exhausted CD8 T cell, and CD8 T cell gene expression signatures. Correlated cell signatures were further engineered into features reflecting naïve T lymphocytes (naïve CD4/8 T) and total CD8 (exhausted and CD8 T) T cell infiltrations. Both features were shown to independently boost the accuracy of NEOPS in the validation cohort (naïve: $p_{\text{interaction}} < 0.05$; CD8: $p_{\text{interaction}} = 0.11$). In immune-selected patients displaying both high naïve and CD8 features, NEOPS achieved an improved accuracy of 77.2% (vs 69.7% baseline performance, $p < 0.05$) and an AUC of 0.74 (vs 0.66, $p < 0.1$) in the validation cohort (table 1). In anti-CTLA4 treatment naïve patients, NEOPS prediction in the immune-selected group was also enhanced with an accuracy of 81.8% (vs 70.6%, $p < 0.05$) and an AUC of 0.89 (vs 0.68, $p < 0.01$) in the validation cohort (table 1). Integrating NEOPS with naïve and CD8 features into a single composite biomarker results in an AUC of 0.82 (cross validation: 0.78 vs 0.71).

Conclusions Identifying immune-selected patients based on cellular composition of the tumor microenvironment significantly increased the accuracy of our neoantigen-based biomarker of ICB response, NEOPS. These data highlight the potential utility of integrating tumor microenvironment data with neoantigen information into an extended composite biomarker to provide more accurate prediction of immunotherapy response.

REFERENCES

- Abbott CW, Boyle SM, Pyke RM, McDaniel LD, Levy E, Navarro FCP, et al. Prediction of immunotherapy response in melanoma through combined modeling of neoantigen burden and immune-related resistance mechanisms. *Clinical Cancer Research. American Association for Cancer Research Inc.*; 2021;**27**:4265–76.
- Pyke RM, Mellacheruvu D, Dea S, Abbott CW, Zhang S v., Phillips NA, et al. Precision neoantigen discovery using large-scale immunopeptidomes and composite modeling of MHC peptide presentation. *Molecular and Cellular Proteomics. American Society for Biochemistry and Molecular Biology Inc.*; 2021;20.

Abstract 119 Table 1 NEOPS performances in different immune groups

		Discovery		Validation	
		Full	Immune-selected	Full	Immune-selected
All	n	45	26	109	57
	Accuracy	76%	89%	70%	77%
	AUC	0.79	0.95	0.66	0.74
anti-CTLA4 naïve	n	38	22	66	33
	Accuracy	76%	91%	71%	82%
	AUC	0.85	0.94	0.68	0.89
	C-index (PFS)	0.68	0.74	0.58	0.62
	C-index (PFS)	0.69	0.73	0.59	0.61

<http://dx.doi.org/10.1136/jitc-2022-SITC2022.0119>

120

DECODING IMMUNOTHERAPY RESPONSES WITH HIGH-DIMENSIONAL AND HIGH-THROUGHPUT SPATIAL PHENOTYPING OF NON-SMALL CELL LUNG CANCER (NSCLC)

¹Ning Ma*, ¹Aditya Pratapa, ²James Monkman, ³Ken O'Byrne, ¹Oliver Braubach, ²Arutha Kulasinghe. ¹*Akoya Biosciences, Menlo Park, CA, USA*; ²*University of Queensland, Brisbane, Australia*; ³*Princess Alexandra Hospital, Brisbane, Australia*

Background Lung cancers are the leading cause of cancer-related deaths globally and have a 5-year survival of ~20%. Whilst immunotherapies have led to durable and prolonged survival, only a subset of patients remain responsive. Additional biomarkers are needed to better predict which patients will respond or develop resistance against immune checkpoint inhibitor (ICI) therapies. Spatial phenotyping of the tumor microenvironment (TME) is now recognized as a key factor in understanding immunological composition and status that are predictive of ICI therapy benefits.

Methods Here, we profiled biopsies from a cohort of non-small cell lung cancer (NSCLC) patients treated with single-agent Nivolumab. We developed high-dimensional immune profiling (57 antibody panel) and conducted whole-tissue PhenoCycler®-Fusion spatial phenotyping. Spatial features, including cellular composition and cellular neighborhoods were analyzed and compared against clinicopathological findings and response to immunotherapy.

We then expanded our spatial analysis to a larger NSCLC cohort using customizable PhenoCode™ Signature Panels (PSP) for high-throughput immunoprofiling (CD3/CD8/CD20/CD68/PanCK + CD4 add-in) and immunocontexture (CD8/CD68/PD-L1/FoxP3/PanCK + PD-1 add-in) imaging. The PSP panel content combines the barcode-based antibody chemistry from the PhenoCycler® platform with the signal amplification of Opal chemistry from the PhenoImager® platform. The PSP panel was profiled across 20 biopsies to investigate correlations between spatial phenotypic signatures, clinicopathological findings, and response to ICI therapy.

Results Our PhenoCycler®-Fusion data revealed more than 10 unique phenotypes within the TMEs of ICI therapy response groups. High-dimensional spatial analyses furthermore revealed intratumoral and intertumoral heterogeneity and cell-specific metabolic signatures. Concurrently, multispectral spatial analysis of PSP panel data uncovered putative spatial signatures within NSCLC cohorts, indicating the enrichment and significance of certain phenotypic frequencies and cellular interactions associated with therapy response.

Conclusions There is an increasing need for the development of predictive biomarkers of response to ICI therapy. We demonstrate the complementary use of high-dimensional, deep spatial phenotyping analysis with high-throughput multiplex imaging for identifying new spatial signatures with the immune landscape of NSCLC. These methods are amenable to revealing novel cell types and spatial signatures that can be associated with ICI outcomes and therefore serve as clinical biomarkers.

Ethics Approval This study has Metro South Human Research Ethics Committee (HREC) Approval (LNR/2019/QMS/51117) and University of Queensland ethics ratification.

<http://dx.doi.org/10.1136/jitc-2022-SITC2022.0120>

121

TETRASPANIN MOLECULE CD9 AS A NOVEL MARKER OF TUMOR-REACTIVE T CELLS

<http://dx.doi.org/10.1136/jitc-2022-SITC2022.0121>

¹Yoshihiro Miyahara*, ¹Makiko Yamane, ¹Tae Hayashi, ¹Yuji Toiyama, ²Kazushi Hiranuka, ³Hirofumi Kishi, ¹Hiroshi Shiku. ¹Mie Univ. Graduate School of Medicine, Tsu, Japan; ²BrightPath Biotherapeutics Co., Ltd., Kawasaki, Japan; ³University of Toyama, Toyama, Japan

Background Overcoming 'heterogeneity of tumor antigen' by infusion of a variety of T cells that recognize multiple tumor antigens would be beneficial for patients with solid tumor. To this end, two major approaches aiming to comprehensively obtain tumor-reactive T cells (or TCRs) from TIL/PBMC have been examined so far. One approach is to use cell surface molecules such as exhaustion marker PD-1, and the other is to utilize single cell analysis for selecting tumor-reactive T cells with characteristic RNA expression profiles. Although significant progress has been made, it is still required to deepen the understanding of anti-tumor immunity for development of an effective immunotherapy.

Methods We applied the following strategies to dissect human colorectal TIL. (1) Obtain TCRs from single cell sorted CD8⁺ TIL ex vivo by using cell surface molecules, (2) Analyze tumor reactivity by using autologous tumor organoids, (3) Determine the specificity to neoantigens, and (4) Identify molecules preferentially expressed by neoantigen-specific T cells.

Results We obtained neoantigen-specific 5 TCRs from 4 cases among of 8 tumor-reactive TCRs from 6 cases. Notably, tumor-specific CD8⁺ TILs were most enriched in the PD-1⁺ and 4-1BB⁺ (DP) population in all cases, and further analysis revealed that the frequency of DP cells in CD8⁺ TIL tend to correlate with patient survival. Interestingly, scRNA-seq and TCR-seq analysis of TIL in which about 5% of whole CD8⁺ TILs are neoantigen-specific uncovered that CD9, a member of tetraspanin, was significantly expressed in these T cells. Indeed, addition of CD9 to DP sorting further enriched tumor-specific T cells. To our best knowledge, tetraspanin molecule has not been reported as a marker of tumor-reactive T cells. Therefore, these data prompted us to examine CD9 expression on neoantigen-specific CD8⁺ T cells in mice. Indeed, not only CD9 but also CD81, another member of tetraspanin, is preferentially expressed on these T cells in a mouse model we previously reported.¹ Furthermore, we successfully identified tumor-reactive TCRs from splenic CD8⁺CD9⁺CD81⁺ T cells in two independent tumor bearing mice models (CMS7 and CT26), in which one TCR recognized AH-1 epitope in the case of CT26 tumor bearing mice. **Conclusions** We report that tetraspanin molecules would be novel markers of tumor-reactive T cells. Our data strongly indicate that tetraspanin molecules play unexpected roles in the interaction of T cells with tumor, although further analysis is required. Finally, we hope that these findings would be useful for development of an effective personalized cancer immunotherapy in near future.

REFERENCE

1. Fujii K, Miyahara Y, Identification of an immunogenic neo-epitope encoded by mouse sarcoma using CXCR3 ligand mRNAs as sensors. *Oncoimmunology*. 2017 Mar 20;**6**(5):e1306617.

Ethics Approval Written informed consents were obtained from patients and healthy volunteers according to the guidelines of the Declaration of Helsinki. The experimental protocol (ID:3037) was approved by the Institutional Review Board at the Mie University School of Medicine.

THE NEXT GENERATION OF IMMUNOTHERAPY RESPONSE SIGNATURES REVEALED BY BIOPHYSICAL SIMULATIONS

Gregory Norris, John Pfeiffer, Joseph Peterson, Nicole Liadis, Matthew Biancalana, Dorys Lopez-Ramos, Anuja Antony, Daniel Cook*. *SiBiSys, Inc., Chicago, IL, USA*

Background Although immunotherapy has become standard-of-care for many cancers, the number of benefiting patients remains relatively small. Current biomarkers of response (e.g., PD-L1) have proven only modestly useful for distinguishing IO-responders vs. non-responders.¹ Here, we present a proof-of-concept approach for the rapid, non-invasive assessment of immunotherapy response prediction using biomarker imaging signatures.

Methods We used publicly available datasets (ISPY1 and ISPY2 non-IO-treated patients)^{2,3} to calculate the expression levels of gene signatures across breast cancer subtypes. We analyzed these imaging datasets using TumorScope, a biophysical simulation engine, to identify biomarkers (features) present within IO-responsive tumors. We then correlated this response to biological processes and hallmark cancer gene signatures. TumorScope uses patient standard-of-care data, including high spatiotemporal resolution medical images (e.g., DCE-MRIs) to predict a patient's probability of achieving a pathological complete response (pCR).⁴ Next, we calculated the spatial distribution of these features across tumors. To specifically identify the IO-response signatures, we calculated the feature thresholds associated with pCR in response to IO using the ISPY2 IO-treated patient dataset (linear regression of the training set, n=63). This spatial biomarker-based approach, SimbIOScope, showed comparable predictive power as the traditional biopsy-based transcriptomic approach. We further validated this approach in an independent cohort from a single center (n=12), and applied our method to a large IO-naïve population (n=292) to assess the model's predictive capability.

Results Spatially-resolved biomarkers of immune evasion in triple negative breast cancer (TNBC) and HR+/HER2- tumors identified individuals with resistance to IO therapy, and had similar predictive power to transcriptomic analysis. We found that baseline (prior to therapy) high levels of immune evasion signatures in IO non-responders are associated with hypoxia ($r=0.45$, $p<1\times 10^{-6}$) and autophagy in TNBC patients, and with low angiogenesis ($r=-0.40$, $p=0.006$) in HR+/HER2-patients. When tested on an independent patient cohort (n=12), SimbIOScope correctly predicted pCR in over 91% of cases. In a larger reference cohort (n=292), SimbIOScope predictions of pCR were consistent with the empirical increase observed in clinical trials. Our analysis predicted a 14% increase in pCR for TNBC tumors over baseline with the addition of the checkpoint inhibitor pembrolizumab, as compared to the 13.6% pCR increase observed in clinical trials (Keynote 522).⁵

Conclusions SimbIOScope imaging biomarkers and analyses efficiently identify the cohort of patients likely to respond to immunotherapy. Its imaging analytic capabilities position SimbIOScope as a critical tool when planning cancer treatment options, and expands IO-response prediction beyond traditional biomarkers.

REFERENCES

1. A Marra GVGC. Recent advances in triple negative breast cancer: the immunotherapy era. *BMC Med.* 2019;**17**(1):1–9. doi:10.1186/s12916-019-1326-5
2. Esserman LJ, Berry DA, DeMichele A, et al. Pathologic Complete Response Predicts Recurrence-Free Survival More Effectively by Cancer Subset: Results From the

I-SPY 1 TRIAL—CALGB 150007/150012, ACRIN 6657. *J Clin Oncol.* 2012;**30**(26):3242. doi:10.1200/JCO.2011.39.2779

3. Wang H, Yee D. I-SPY 2: a Neoadjuvant Adaptive Clinical Trial Designed to Improve Outcomes in High-Risk Breast Cancer. *Curr Breast Cancer Rep.* 2019;**11**(4):303. doi:10.1007/s12609-019-00334-2
4. Spring LM, Fell G, Arfe A, et al. Pathologic Complete Response after Neoadjuvant Chemotherapy and Impact on Breast Cancer Recurrence and Survival: A Comprehensive Meta-analysis. *Clin Cancer Res.* 2020;**26**(12):2838–2848. doi:10.1158/1078-0432.CCR-19-3492
5. Schmid P, Cortes J, Pusztai L, et al. Pembrolizumab for Early Triple-Negative Breast Cancer. <https://doi.org/10.1056/NEJMoa1910549>. 2020;**382**(9):810–821. doi:10.1056/NEJMoa1910549

<http://dx.doi.org/10.1136/jitc-2022-SITC2022.0122>

123

LANDSCAPE ANALYSIS OF THE NEOEPITOPE-SPECIFIC T CELL RESPONSES IN PATIENTS WITH AND WITHOUT CLINICAL BENEFIT FROM IMMUNE CHECKPOINT BLOCKADE THERAPY

¹Cristina Puig Saus*, ²Barbara Sennino, ²Songming Peng, ²Zheng Pan, ²Benjamin Yuen, ²Bhamini Purandare, ²Kyle Jacoby, ²Olivier Dalmás, ²Duo An, ²Boi Quach, ²Clifford Wang, ³Huiming Xia, ¹Sameeha Jilani, ²Diana Nguyen, ²Kevin Shao, ²Claire McHugh, ²John Greer, ²Phillip Peabody, ²Saparya Nayak, ²Jonaathan Hoover, ²Sara Said, ²Susan Foy, ²Andrew Conroy, ²Michael Yi, ²Christine Shieh, ²William Lu, ²Katharine Heeringa, ²Yan Ma, ²Shahab Chizari, ²Melissa Pilling, ²Marc Ting, ²Ramya Tunuguntla, ²Salemiz Sandoval, ²Robert Moot, ²Theresa Hunter, ³Sidi Zhao, ¹Justin Saco, ¹Ivan Perez-García, ¹Agustin Vega-Crespo, ¹Ignacio Baselga, ¹Gabriel Abril-Rodríguez, ¹Grace Cherry, ¹Deborah Wong, ³Jasreet Hundal, ¹Bartosz Chmielowski, ¹Daniel Speiser, ²Michael Bethune, ²Xiaoyan Bao, ⁴Alena Gros, ³Obi Griffith, ³Malachi Griffith, ³James Heath, ²Alex Franzusoff, ²Stefanie Mandl, ¹Antoni Ribas. ¹University of California, Los Angeles, Los Angeles, CA, USA; ²PACT Pharma, South San Francisco, CA, USA; ³Washington University School of Medicine, St. Louis, USA; ⁴VHIO, Barcelona, Spain; ⁵Institute for Systems Biology, Pasadena, CA, USA

Background The primary target of T-cell responses to cancer cells are peptides derived from non-synonymous mutations presented by HLA. However, the large diversity of HLA alleles and restricted availability of clinical samples has limited the study of the antigenic determinants recognized by T cells (termed neoepitopes) at the scale needed for a landscape analysis of antitumor immune responses in patients.

Methods We applied a newly developed technology to perform a longitudinal landscape analysis of the neoepitope-specific T cells in peripheral blood and tumor from 11 patients with metastatic melanoma, 7 with response (R) or 4 with no response (NR) to immune checkpoint blockade (ICB) immunotherapy. Briefly, based on the computational prediction of patient-specific putative neoepitopes, hundreds of capture reagents were made consisting of the patient HLA class I subtypes loaded with the corresponding predicted neoepitope; neoepitope-specific T cells were then isolated, and the TCR alpha and beta sequenced. The tumor reactivity of the isolated neoepitope-specific TCRs (neoTCR) was assessed upon co-culture of autologous melanoma cell lines from each patient with primary human T cells expressing the neoTCRs generated using a CRISPR-based non-viral precision genome engineering to replace the endogenous TCRs.

Results The tumor mutation burden ranged between 2562 and 54 and 297 to 31 for patients with R and NR, respectively. We screened an average of 157 (range 243 to 17) predicted neoepitope-HLA per patient across their 6 HLA molecules, and isolated neoTCRs in all 11 patients. The number of mutations targeted ranged between 13 and 1. We assessed tumor reactivity in samples from 3 R and 3 NR; 39 of the 64 neoTCRs demonstrated specific recognition and cytotoxicity to patient-matched melanoma cell lines. Multiple T cells with different neoTCRs (T cell clonotypes) recognized a limited number of mutations in 7 patients with R (average of 31 different neoTCR clonotypes per patient). These T cell specificities were recurrently detected at different time points in blood and tumors. Samples from 4 patients with NR also demonstrated neoepitope-specific T cell responses in blood and tumor to a similarly restricted number of mutations but lacked TCR polyclonality (average 3 neoTCR clonotypes per patient) and were not recurrently detected in sequential samples.

Conclusions Effective ICB therapy is associated with polyclonal neoepitope-specific T cell responses in the tumor and blood that recognize a limited number of immunodominant mutations and are recurrently recognized over time.

Ethics Approval Patients with metastatic melanoma were selected as they signed an informed consent to collect PBMC and tumour biopsies while receiving therapy with anti-PD-1 therapy alone or in combination with other drugs. Biopsies and blood samples were collected under the University of California, Los Angeles (UCLA) Institutional Review Board approvals 11-003254.

<http://dx.doi.org/10.1136/jitc-2022-SITC2022.0123>

Abstracts

124

IDENTIFICATION OF TUMOR ANTIGENS FROM MULTIPLE GENOMICS SOURCES USING LENS (LANDSCAPE OF EFFECTIVE NEOANTIGENS SOFTWARE)

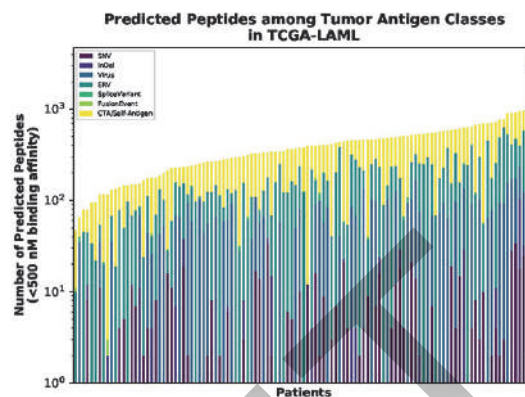
¹Benjamin Vincent, ¹Steven Vensko*, ¹Kelly Olsen, ¹Dante Bortone, ²Christof Smith, ³Shengjie Chai, ¹Alexander Rubinsteyn. ¹University of North Carolina School of M, Chapel Hill, NC, USA; ²Brigham and Women's Hospital, Boston, MA, USA; ³Uber, Inc., San Francisco, CA, USA

Background Elimination of cancer cells by T cells is a critical mechanism of antitumor immunity and cancer immunotherapy response. T cells recognize cancer cells via engagement of T cell receptors with peptide epitopes presented by major histocompatibility complex (MHC) molecules on the cancer cell surface. Discovery of the full landscape of tumor antigens in any given individual will be important for understanding response to immunotherapy and optimizing strategies for antigen-specific immunotherapy development. Although T cell epitopes can be derived from antigen proteins coded for by multiple genomic sources, bioinformatics tools used to identify tumor-specific epitopes using DNA and RNA sequencing data have largely focused on epitopes derived from somatic variants.

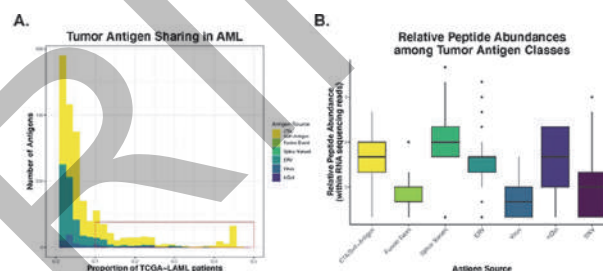
Methods We report here an open-source workflow utilizing the Nextflow DSL2 workflow manager, Landscape of Effective Neoantigen Software (LENS), which predicts tumor-specific and tumor-associated antigens from single nucleotide variants (SNVs), insertions and deletions (InDels), gene fusions, splice variants, cancer testis antigens (CTAs), overexpressed self-antigens, viruses, and human endogenous retroviruses (hERVs). The main advantage of LENS is that it extends the breadth of genomic sources of tumor antigens that may be discovered using genomics data. Other advantages include modularity, extensibility, ease of use, incorporation of phasing and germline variant information in epitope identification, and harmonization of relative expression level and immunogenicity prediction across multiple genomic sources (table 1). LENS is open-source and freely available for academic use (<https://gitlab.com/bgv-lens>).

Results To demonstrate the utility of LENS, we present an analysis of the predicted antigen landscape in 115 acute myeloid leukemia (AML) samples. AML was chosen due its low somatic mutation rate and dearth of classical (SNV-derived) neoantigens. Predicted tumor antigens were distributed unevenly across genomic sources (figure 1). The highest degree of antigen sharing was found in those derived from aberrantly expressed endogenous retroviral genes, which were also highly-expressed in the RNA-seq data (figure 2). A small number of gene fusion-derived antigens were also highly expressed with high predicted binding affinity (figure 3).

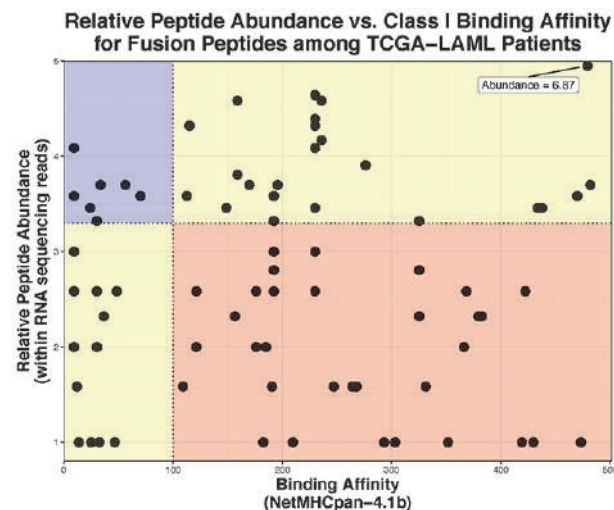
Conclusions We expect that LENS will be a valuable platform and resource for analysis of polypeptopic T cell responses across the full immunodominance hierarchy, antigen selection for therapeutic neoantigen vaccination, and T cell epitope discovery, especially in cancers with few somatic mutations and increased importance of tumor-specific epitopes from genomic sources beyond single nucleotide variants. In AML specifically, our results support further development of hERV and gene fusion-based tools for immune monitoring and therapeutics going forward.



Abstract 124 Figure 1 TCGA AML tumor antigen distribution by patient sample. Tumor antigen distributions across 115 TCGA-LAML samples are shown. Predicted neoantigen number ranges between 40 to 2,433 peptides with a median of 319 peptides per patient



Abstract 124 Figure 2 Antigen sharing in AML. (A) The number of AML antigens predicted to be presented in multiple TCGA AML samples are shown along with their genomic sources. Antigens identified in more than 10% of samples are enclosed by the red box. (B) RNA expression of predicted AML antigens by genomic source



Abstract 124 Figure 3 Fusion peptide read support vs. HLA Class I binding affinity across patients. Several predicted fusion-derived peptides show both relatively high binding affinity and high relative peptide abundance (blue). Others show either high expression and low affinity or low expression and high affinity (light red), or both low expression and low affinity (red)

Abstract 124 Table 1 Comparison between LENS and other Neoantigen workflows LENS generally offers similar or improved functionality compared to other popular neoantigen workflows. Specifically, LENS supports more tumor antigen sources, includes a harmonized estimate of antigen expression, does not require end-user pre-processing of input data, and is a both modular and extensible workflow. It is worth noting that all the included workflows are open-source and may subjectively be classified as modular and extensible as a result. We classify LENS as modular and extensible as these were desired features that drove design and development rather than consequences of code availability. The 'Hybrid' classification for nextNEOpI's containerization metric is due to some components, like pVACTools and NeoFuse, having self-contained containers while other tools (e.g. variant callers) are all contained within a single container.

Workflow	Input	HTS data support	Protein data support	Workflow language	Containerized	Automated Pipeline Execution (CI/CD)	Modular (components)	Open source	Publicly available (GitHub)	Hybrid	Containerized	Modular	Open source	Publicly available (GitHub)	Hybrid	Containerized	Modular	Open source	Publicly available (GitHub)
LENS	HTS (raw or aligned), RNA-seq (raw or aligned), Protein (raw or aligned)	✓	✓	Nextflow/Snakemake	✓	✓	✓	✓	✓	✓	✓	✓	✓	✓	✓	✓	✓	✓	✓
NeoAntigen	HTS (raw or aligned), RNA-seq (raw or aligned), Protein (raw or aligned)	✓	✓	Nextflow/Snakemake	✓	✓	✓	✓	✓	✓	✓	✓	✓	✓	✓	✓	✓	✓	✓
NeoProphet	HTS (raw or aligned), RNA-seq (raw or aligned), Protein (raw or aligned)	✓	✓	Nextflow/Snakemake	✓	✓	✓	✓	✓	✓	✓	✓	✓	✓	✓	✓	✓	✓	✓
NeoPepTools	HTS (raw or aligned), RNA-seq (raw or aligned), Protein (raw or aligned)	✓	✓	Nextflow/Snakemake	✓	✓	✓	✓	✓	✓	✓	✓	✓	✓	✓	✓	✓	✓	✓

<http://dx.doi.org/10.1136/jitc-2022-SITC2022.0124>

125

CHARACTERIZATION AND LABEL-FREE ISOLATION OF PHENOTYPICALLY DEFINED HUMAN IMMUNE CELLS USING GHOST CYTOMETRY, A NOVEL AI POWERED FLOW CYTOMETRY TECHNOLOGY

¹Keisuke Wagatsuma, ¹Hiroko Nomaru, ¹Kazuki Teranishi, ²Satoru Akai, ¹Yuri An, ²Kaoru Komoriya, ¹Yoko Kawamura, ²Asako Tsubouchi, ¹Andy Wu*, ¹Sadao Ota. ¹ThinkCyte Inc, Tokyo, Japan; ²ThinkCyte Inc., San Carlos, CA, USA

Background Background: Identification and isolation of specific human immune cell populations with technologies that are minimally disruptive to native biological states are a critical requirement in modern cellular immunotherapy approaches. For both early-stage cell therapy research and the development of autologous and allogenic cellular therapeutics, technologies that can isolate specific immune cell subsets while preserving their native biological and functional properties are needed to improve the quality and efficacy of cell therapy drug products.

Methods

Methods Here we applied Ghost Cytometry, a novel method of analyzing and sorting cells using high dimensional image information, to isolate human immune cell subsets with minimal external perturbation. Ghost Cytometry leverages a combination of proprietary optics and artificial intelligence to capture digital-optical profiles (Ghost Motion Imaging (GMI) signals) from individual immune cells. The approach generates a novel, multi-dimensional data set for individual cells, which can be leveraged to enable label-free sorting of defined phenotypic cell populations for downstream R&D

Results

Results We characterized human T-cells and generated 'ground truth' functional profiles for 1) glycolysis level (by depletion of a glucose analog), 2) exhaustion state (by PD-1 and LAG3 expression), 3) activation or resting profiles (by CD25 expression) and 4) viability (by propidium iodide exclusion and Annexin V expression) based on their unique GMI signals. From this, we developed a set of machine-learning derived classifiers for identification of unlabeled T-cell subsets. The classifiers showed area under the curve (AUC) performance ranges between 0.923 and 0.995, demonstrating high classification accuracy.

Conclusions

Conclusions Here we report on a novel method to characterize and isolate human immune cell subsets with enhanced therapeutic potential. This approach enables isolation of target T-cell subsets with defined phenotypic profiles in an unperturbed state, without the requirement of using external fluorescent markers. The results described here have practical applications for investigators and drug developers in cell therapy research and development.

<http://dx.doi.org/10.1136/jitc-2022-SITC2022.0125>

126

PROGNOSTIC GENE SIGNATURE REFLECTING CD8+ T CELL ENRICHMENT IN EARLY-STAGE TRIPLE-NEGATIVE BREAST CANCER

<http://dx.doi.org/10.1136/jitc-2022-SITC2022.0126>

¹Chang Kim*, ¹Yun Suk Yu, ¹Jin Young Park, ²Kyong Hwa Park. ¹CbsBioscience, Daejeon, Korea, Republic of; ²Korea university anam hospital, Seoul, Korea, Republic of

Background Triple-negative breast cancer (TNBC) is the most challenging subtype of breast cancer, and its prognosis is poor compared to the other subtypes.¹ Immune cells have critical role in tumor rejection and prognosis of patient with TNBC.² In early TNBC, CD8+ T cells infiltration is positively associated with response to neo-adjuvant chemotherapy and prognosis of patients.³ Recently, combination of immune checkpoint inhibitor, pembrolizumab, with standard chemotherapy has been approved for the neo-adjuvant setting.⁴ However, there are no valid prognostic biomarkers that reflect the CD8+ T cell enriched tumor in patients with early TNBC. To establish an elaborate therapeutic strategy for TNBC, identification of biomarkers that reflecting feature of CD8+ T cell enriched TNBC is needed.

Methods 76 patients with TNBC were enrolled for gene expression profiles and GSE 169246 data were collected for single cell RNA (scRNA) profiles. Median Follow-up period of enrolled patients was 51.5 months (range: 4.6–230.8). Of the enrolled patients, 13 patients had recurrence or metastasis. Using the HiSeq 4000 sequencer, RNA sequencing was conducted to analyze the gene expression profiles of tumor samples from TNBC patients. Single cell RNA analysis was performed using Seurat package (v.4.0.5). Differentially expressed genes (DEGs) were defined as satisfying both conditions that satisfying in Cox regression analysis and Wilcoxon analysis in gene expression profiles, and that satisfying in logistic regression analysis in CD8+ t cell profiles of scRNA analysis. Gene signature was analyzed by combination of above DEGs. Gene signature was marked on t-SNE of scRNA profiles. Statistical analyses were conducted using R language (v.3.4.3).

Results We identified gene signature reflecting CD8+ T cell enriched feature that stratified patients with TNBC by risk score. Gene-set signatures related to CD8+ T cells were identified as following; GADD45B_H2AFX_PTPRA_RILPL2_RORA_ZC3H13_ZHX2 (sensitivity = 92.31%; specificity = 93.65%; accuracy = 93.42%). In Kaplan Meier (KM) analysis, patients with tumors with high-risk gene signatures (n=16, median iDFS = 42.7) showed significantly shorter iDFS than those with low-risk gene signatures (n=60, median iDFS not reached). CD8+ t cells related gene signature was marked on CD8+ T cell near the CD4+ T cell in t-SNE.

Conclusions the gene-set signatures reflecting CD8+ T cells enrichment showed high performance to predict prognosis of TNBC. Further analysis of gene signatures related to macrophages will be additionally presented at the conference.

REFERENCES

1. Yin L, Duan J, Bian X, et al. Triple-negative breast cancer molecular subtyping and treatment progress. *Breast Cancer Res.* 2020;**22**:61.
2. Oshi M, Asaoka M, Tokumaru Y, et al. CD8 T Cell Score as a Prognostic Biomarker for Triple Negative Breast Cancer. *Int. J. Mol. Sci.* 2020;**21**:6968.
3. Hueatas-Caro C, Ramirez M, Gonzalez-Torres H, et al. Immune Lymphocyte Infiltrate and its Prognostic Value in Triple-Negative Breast Cancer. *Front. Oncol.* 2022;**12**:910976.
4. Tarantino P, Corti C, Schmid P, et al. Immunotherapy for early triple negative breast cancer: research agenda for the next decade. *npj Breast Cancer.* 2022;**8**:23.

SPATIAL-SPECIFIC GENE SIGNATURES OUTPERFORM BULK-MRNA SIGNATURES TO DEFINE RESISTANCE TO IMMUNOTHERAPY IN MELANOMA PATIENTS

Thazin Aung*, Jonathan Warrell, Sandra Martinez-Morilla, Niki Gavrielatou, Ioannis Vathiotis, Nay Chan, Harriet Kluger, David Rimm. *Yale University, New Haven, CT, USA*

Background Gene signatures have been shown to predict the response/resistance to immunotherapies but with only modest accuracy.^{1–3} However, gene signatures are devoid of spatial information, and the inability to distinguish tumor genes from TME genes is likely to decrease the prediction accuracy. Here we collect spatially defined genes and determine if the addition of spatial information can improve prediction.

Methods The Digital Spatial Profiling (DSP) of GeoMX Whole Transcriptome Atlas (WTA), a new technology for transcriptome-wide spatial profiling of tissues, is used to generate a transcriptomic map of 55-immunotherapy-treated melanoma samples. DSP-WTA approach enables *in situ* hybridization against 18,190 genes in several areas of interest (i.e., CD68+ macrophages, CD45+ lymphocytes and S100+ tumor cells) at high throughput using a sequencing readout. We developed a computational pipeline to discover cell-type (compartment) specific signature models. To estimate the classification accuracy, the models were built using a split sample approach with 100 different Lasso logistic regression binomial models. Response Evaluation Criteria in Solid Tumors (RECIST) 1.1 was used to identify objective response. We then developed a compartment signature matrix to deconvolve bulk-RNA-seq into compartmentalized-RNA expression using CIBERSORTx (*in silico* tissue dissection)⁴ to simulate compartment-derived gene expression data. We then compare the CIBERSORT results to actual spatially collected gene signatures.

Results We achieved AUC (area under the curve) > 0.9 for all compartment-specific signatures. The AUCs for each signature are 0.94 (CD45), 0.97 (CD68), 0.93 (S100B), 0.98 (pseudostroma) and 0.92 (pseudo-bulk). Cross-testing in different compartments (i.e., CD45 signature in CD68, S100B, pseudo-bulk and pseudo-stroma compartments, etc.) showed poor performance indicating the signatures are compartment-specific. Then these signatures were validated in an independent immunotherapy-treated melanoma cohort (N=90)⁵ by deconvolving bulk-RNA-seq into compartmentalized gene expression. Our 8-gene pseudo-bulk signature validated with AUC:0.74 (CI:0.64–0.84), our 8-gene CD68 signature with AUC:0.83 (CI:0.75–0.91), and our S100B 8-gene signature with AUC:0.66 (CI:0.54–0.77), respectively. To evaluate the deconvolution platform with real compartment RNA-seq data, our pseudo-bulk data were deconvolved into pseudo-compartments using CIBERSORTx cell-type decomposition and tested with compartment-specific signatures. We noted poor performances with AUC:0.59 (CD45), AUC:0.56 (CD68) and AUC:0.65 (S100B), respectively.

Conclusions Compartmentalized CD45-, CD68- and S100B-signatures show strikingly high AUC compared to bulk mRNA signatures. These high spatially de novo signatures far outperform the signatures that can be achieved by computational deconvolution. We believe that the spatially informed signatures differentially evaluates the tumor vs the TME and may be much more accurate in the prediction of response/resistance to immunotherapy.

Acknowledgements This study was funded by Yale Melanoma SPORE and sponsor research agreement from NextCure, Navigate and Cepheid.

REFERENCES

1. Ayers M, Luceford J, Nebozhyn M, Murphy E, Loboda A, Kaufman DR, et al. IFN- γ -related mRNA profile predicts clinical response to PD-1 blockade. *The Journal of clinical investigation* 2017;**127**(8):2930–40.
2. Newell F, da Silva IP, Johansson PA, Menzies AM, Wilmott JS, Addala V, et al. Multiomic profiling of checkpoint inhibitor-treated melanoma: Identifying predictors of response and resistance, and markers of biological discordance. *Cancer cell*. 2022;**40**(1):88–102. e7.
3. Garg M, Couturier D-L, Nsengimana J, Fonseca NA, Wongchenko M, Yan Y, et al. Tumour gene expression signature in primary melanoma predicts long-term outcomes. *Nature communications*. 2021;**12**(1):1–14.
4. Newman AM, Steen CB, Liu CL, Gentles AJ, Chaudhuri AA, Scherer F, et al. Determining cell type abundance and expression from bulk tissues with digital cytometry. *Nature biotechnology*. 2019;**37**(7):773–82.
5. Gide TN, Quek C, Menzies AM, Tasker AT, Shang P, Holst J, et al. Distinct immune cell populations define response to anti-PD-1 monotherapy and anti-PD-1/anti-CTLA-4 combined therapy. *Cancer cell*. 2019;**35**(2):238–55. e6.

Ethics Approval This study was approved by Yale Human Investigation IRB protocol ID 9505008219.

Consent Written informed consent was obtained from the patients for publication of this abstract and any accompanying images. A copy of the written consent is available for review by the Editor of this journal.

<http://dx.doi.org/10.1136/jitc-2022-SITC2022.0127>

128

MULTIOMIC SPATIAL INTERROGATION OF TUMOR-INFILTRATED IMMUNE CELLS USING THE RNASCOPE™ CO-DETECTION ASSAY WITH VIVID DYES

¹Anushka Dikshit*, ²Sayantani Basak, ¹Emerald Doolittle. ¹*Advanced Cell Diagnostics, a Bio-Techne, Newark, CA, USA;* ²*Bio-Techne, Newark, CA, USA*

Background Interrogating complex tumor microenvironment requires a multi-omics approach that can provide high level of sensitivity and specificity. Identifying immune cell subsets within the tumor can be vital for predicting response and determining therapeutic efficacy. Detecting target immune cell markers using immunohistochemistry/Immunofluorescence (IHC/IF) and visualizing cytokine expression with *in situ* hybridization (ISH) can provide comprehensive information about the activation states of immune cells. Here, we demonstrate a newly developed integrated ISH and IHC/IF workflow compatible with manual and automated platforms that can substantially improve RNA-protein co-detection.

Methods We demonstrate the use of our RNA-Protein Co-detection assay in combination with the automated and manual RNAscope Multiplex Fluorescent v2 assay and the RNAscope Chromogenic Duplex assay. The RNAscope Multiplex Fluorescent v2 assay was also combined with the new TSA Vivid dyes for detection of cytokines and immune cells. The co-detection assays enabled detection of T cell markers, macrophage markers and checkpoint markers in the tumor microenvironment by using a tumor microarray.

Results We identified CD4+ helper T cells and CD8+ cytotoxic T lymphocytes using CD3, CD8 and CD4 antibodies. Additionally, we determine the activation states of CD8+ T cells by visualizing *IFNG*, *GZMB* and *IL-2* RNA expression. We were also able to identify macrophages detected by CD68 protein expression, *CD163* and *ITGAM* RNA expression. We could also delineate tumor-stroma border in the samples by using the Pan-CK probe which distinctly marks the tumor cells and visualize the expression of immunoregulatory receptors PD-L1 and *CTLA4* in the tumor cells. The new TSA Vivid dyes demonstrated much brighter signals when compared to than other TSA-based dyes enabling robust detection of immune cell and low-abundance cytokine markers.

Conclusions The RNA-protein co-detection assay is enabled for multi-omic detection of target biomarkers with both chromogenic and fluorescent RNAscope assays. The new TSA vivid dyes improve the robustness of target detection using the RNAscope Multiplex V2 assay with co-detection by effectively boosting signal intensity. Overall, the new RNAscope RNA-protein co-detection workflow and reagents allow optimized simultaneous visualization of RNA and protein targets by enhancing the compatibility of antibodies with RNAscope.

<http://dx.doi.org/10.1136/jitc-2022-SITC2022.0128>

129

PLATFORM TO CONDITIONALLY INDUCE LUNG TUMORS IN GENETICALLY ENGINEERED MOUSE MODELS USING CRE MRNA CONTAINING NANOPARTICLES

Vidit Bhandarkar*, Elen Torres-Mejia, Namita Nabar, Tamara Dacoba, Paula Hammond, Stefani Spranger. *Massachusetts Institute of Technology, Cambridge, MA, USA*

Background Pre-clinical models are crucial for better understanding and treating human diseases such as cancer. Autochthonous models of lung cancer are excellent tools to study tumor progression and evolution. However, current approaches rely on intra-tracheal, viral delivery of Cre recombinase to initiate tumorigenesis by activating oncogenes and deleting tumor suppressor genes.¹ Two caveats of this technique are the lack of cell-type specificity of viral vectors and the resulting immunogenicity of these vectors. We have demonstrated that lentiviral delivery of Cre recombinase (Cre-LV) to the lungs of mice results in infection of dendritic cells (DCs) and macrophages and innate immune activation. To study the immune response to naturally progressing lung cancer while controlling for the confounding immunogenicity of viral vectors, we have developed a virus-free platform to induce lung tumors in genetically engineered mice.

Methods We encapsulated Cre mRNA in polymeric nanoparticles (NPs) made from a Poly(Beta-Amino Ester) (PBAE). The resulting cationic NPs were layered with anionic poly-aspartic acid (PLD) to preferentially target epithelial cells and reduce immunogenicity by decreasing interactions with immune cells.² To optimize particle size and mRNA packaging for efficient *in-vivo* delivery, we screened different mRNA:PBAE ratios. Top candidates were then tested *in-vitro* on the Green-Go reporter cell line, which becomes GFP⁺ upon Cre expression, to determine the transfection efficiency of these NPs.³ To induce lung tumors, we intra-tracheally injected the optimized PLD-layered Cre mRNA-NPs (PLD Cre-NPs) into *Kras*^{LSL-G12D}; *p53*^{fl}; *TdTomato*^{fl} (*KP*^{TdTomato}) reporter mice.¹ We compared tumor initiating capacity of these NPs to Cre-LV and analyzed tumor progression, innate immune activation and cell-type specific infection.

Results PLD Cre-NPs efficiently formed tumors in *KP*^{TdTomato} mice, with comparable histology to Cre-LV induced tumors. However, unlike Cre-LV induced tumors, PLD Cre-NP administration resulted in fewer lesions at late timepoints, which better recapitulates human disease. Further, PLD Cre-NPs primarily infect epithelial cells and minimally infect myeloid cells such as DCs and macrophages. Finally, compared to Cre-LV infection, PLD Cre-NP administration reduces innate immune activation.

Conclusions Current approaches to induce lung tumors in autochthonous mouse models rely on viral delivery of Cre which elicits an immune response. PLD Cre-NPs are efficient at forming lung tumors without activating and infecting innate immune cells, enabling a more controlled characterization of the immune landscape in lung cancer. This technology can also be extended to other conditional mouse models of cancer where delivery of the NPs can be localized to the tissue of origin.

REFERENCES

1. DuPage, M., Dooley, A. L. & Jacks, T. Conditional mouse lung cancer models using adenoviral or lentiviral delivery of Cre recombinase. *Nat Protoc* **4**, 1064–1072 (2009).
2. Dacoba, T. G., Olivera, A., Torres, D., Crecente-Campo, J. & Alonso, M. J. Modulating the immune system through nanotechnology. *Seminars in Immunology* **34**, 78–102 (2017).

3. Sánchez-Rivera, F. J. *et al.* Rapid modeling of cooperating genetic events in cancer through somatic genome editing. *Nature* **516**, 428–431 (2014).

Ethics Approval All mouse experiments were approved by MIT's Committee on Animal Care (CAC) – DHHS Animal Welfare Assurance # D16–00078

<http://dx.doi.org/10.1136/jitc-2022-SITC2022.0129>

130

PRECISE SPATIAL MULTIPLEXING FOR IMMUNE CELL PROFILING OF THE TUMOR MICROENVIRONMENT WITH CHIPCYTOMETRY

Thomas Campbell*, Nancy Stanslowski, Jennifer Brooks. *Canopy Biosciences – A Bruker Company, Saint Louis, MO, USA*

Background Understanding the spatial distribution of key immune cell populations is critical in advancing our understanding of cancer to inform the development of novel therapeutics. Historically, the spatial analysis of the tumor microenvironment has been limited to relatively low-plex immunohistochemical (IHC) or immunofluorescent (IF) assays, which were inadequate for deep immune cell profiling of the tumor microenvironment.

Methods Here we present the analysis of human breast carcinoma samples with a 60-plex protein assay using a novel precise spatial multiplexing technology called ChipCytometry™, which combines iterative immuno-fluorescent staining with high dynamic range imaging to facilitate quantitative phenotyping with single-cell resolution. In addition to traditional pathology review of the high-plex dataset, standard FCS files are generated from multichannel OME-TIFF images, enabling identification and quantification of cellular phenotypes via flow cytometry-like hierarchical gating.

Results The results show precise expression levels for each of the 60 markers in the assay in each individual cell in the sample, maintaining spatial information about each cell. Dozens of immune cell subtypes were identified and quantified based on protein expression profiles. Spatial analysis of the samples reveals quantifiable heterogeneity of immune cell infiltration within the tumor samples, demonstrating the utility of the ChipCytometry platform for in-depth immune profiling in clinical samples.

Conclusions The ChipCytometry platform enables simultaneous detection of multiple protein markers on a single tissue section for deep immune cell profiling in the tumor microenvironment. Combined with the single-cell spatial information, such data sets provide an opportunity for the discovery of new complex multiplexed biomarker signatures to inform therapeutic development.

<http://dx.doi.org/10.1136/jitc-2022-SITC2022.0130>

131 **QUANTITATIVE SPATIAL PROFILING OF THE TUMOR MICROENVIRONMENT IN NSCLC TISSUE MICROARRAY CORES USING A 6-PLEX MULTIPLEX IMAGING TECHNOLOGY AND AI-POWERED PHENOTYPING ANALYSIS**

Nicole Couper*, Bethany Remeniuk, Karen McClymont, Bei Hopkins, Natalie Monteiro, Lorcan Sherry, Darren Locke. ¹OracleBio, Glasgow, UK; Akoya Biosciences, Marlborough, MA, USA

Background Non-small cell lung cancer (NSCLC) patients can have impaired immune responses within the tumor microenvironment (TME), leading to a progression of tumor growth and poorer prognosis. Accurate cell phenotyping combined with spatial profiling of the immune contexture and checkpoint expression, can provide a deeper understanding of complex cellular interactions underpinning the tumor-immune response. The aim of this study was to utilize spatial multiplexed imaging technology and associated data analysis methods to identify populations of immune cells, their functional status, as well as their interactions with the tumor in a set of NSCLC tissue cores from patients treated with first line standard-of-care chemotherapy, and second line immuno-oncology treatment.

Methods Formalin-fixed paraffin-embedded (FFPE) NSCLC tissue microarrays (TMA), comprised of n=41 cores containing a range of carcinomas and pathological Tumor-Node-Metastasis (pTNM) stages, were stained on a Leica Bond RX™ using the Akoya PhenoCode™ Signature Immuno-contexture Human Protein Panel, which includes markers for CD8, CD68, PD-1, PD-L1, FoxP3, and PanCK as a tumor indicator. Stained TMAs were scanned at 20x magnification on a PhenoImager HT multispectral imaging system. Image analysis was performed using Visiopharm software deep learning algorithms for multiplexed images to segment specific tissue regions of interest (ROI) and to perform accurate detection and classification of different cell phenotypes. Cell object data files per core were exported for spatial and heterogeneity analysis using proprietary python scripts.

Results Immune cell counts, phenotypes and spatial interactions were identified within the tumor and stroma ROI per core. Data included total and negative cell phenotype counts, cell density in tumor and stroma, as well as cell distance and clustering spatial interactions in each of the 41 cores in the TMA set. Specific immune cell subsets of interest quantified included CD8+/PD-1+, CD8+/FoxP3+/PD-1+ and CD68+/PD-L1+, FoxP3+, and FoxP3+/PD-1+. Tumor cells of interest included PanCK+ and PanCK+/PD-L1 +.

Conclusions The combination of high quality, spatial multiplex imaging data provided by the PhenoCode Panel, coupled with deep learning quantitative image analysis techniques, enables detailed characterization of the complex cellular interactions, at both the functional and spatial level, within the TME of IO-treated NSCLC tissue. This study further highlights the importance of a robust technical workflow to deliver optimal staining, imaging, cell detection and phenotyping in generating high quality data to facilitate spatial profiling and interpretation in pathologically complex tissue samples.

Ethics Approval Commercially sourced TMA from Tr-Star Technology Group

<http://dx.doi.org/10.1136/jitc-2022-SITC2022.0131>

132

RACIAL DIFFERENCES IN TMB MEASURES BETWEEN PAIRED TUMOR/NORMAL AND TUMOR-ONLY SEQUENCING ACROSS ENDOMETRIAL, BLADDER, AND NON-SMALL CELL LUNG CANCERS

¹Francisco De La Vega, ¹Yannick Pouliot, ²Chad Reichard, ¹Rotem Ben-Shachar, ¹Brooke Rhead, ¹Kenneth Carson, ¹Matheww Cooney, ¹Kristiyana Kaneva, ³Afshin Dowlati, ¹Justin Guinney*. ¹Tempus Labs, Inc., Chicago, IL, USA; ²Urology of Indiana, Indianapolis, IN, USA; ³Case Western Reserve University, Cleveland, OH, USA

Background Tumor mutational burden (TMB), defined as the number of somatic mutations per megabase of a tumor, is routinely used as a predictive biomarker for immunotherapy response in metastatic cancer patients. Sequencing of paired tumor and normal specimens allows for correction of TMB estimates with patient-specific germline variants. For tumor only assays, TMB estimates are corrected using germline variant annotations derived from population-scale germline variant surveys. These surveys often underrepresent minorities and individuals of non-European descent, leading to potential inaccuracies in TMB estimates in these populations.

Methods Our cohort includes patients who underwent tumor genomic profiling with the Tempus xT Next Generation Sequencing (NGS) assay and diagnosed with non-small cell lung (NSCLC, n=4,583) endometrial (n=3,084), or urothelial (n=2,806) cancer. We used 654 ancestry informative markers selected to overlap the target regions of the 648-gene Tempus xT NGS assay to infer global continental ancestry proportions and imputed race/ethnicity categories using ancestry admixture thresholds. TMB differences in paired sequencing (PS) and tumor-only sequencing (TOS) were evaluated for each imputed race/ethnicity category and cancer type. Statistical comparisons of TMB distributions were assessed using the Kruskal-Wallis test.

Results Among the entire cohort, 6,126 patients had PS performed, and 4,347 had TOS performed. The imputed ethnicities were 4% Asian (A), 10% Black (B), 5% Hispanic/Latino (H) and 81% White (W). In NSCLC, median TMB for A, B, H, and W patients was 1.9, 4.2, 3.2, and 3.8 for PS and 4.9, 7.6, 4.9, and 5.4 for TOS. Among endometrial cancers, median TMB for A, B, H, and W patients was 2.1, 2.7, 2.6, and 3.5 for PS and 5.0, 5.4, 5.4, and 5.4 for TOS. Median TMB for A, B, H, and W patients was 3.1, 3.5, 3.5, and 4.2 for PS and 7.3, 6.1, 6.9, and 5.6 for TOS in urothelial cancers. Differences across PS and TOS were significant in each cancer type ($p < 0.0001$). When all cancer types were combined, the mean inflation of TMB median values was 1.7 for White whereas non-White patients was 3.4 ($p < 0001$).

Conclusions Paired tumor sequencing reduces estimated TMB compared to tumor-only sequencing across all racial groups, more significantly for non-White patients.

<http://dx.doi.org/10.1136/jitc-2022-SITC2022.0132>

133

SPATIALLY DEFINED GENE SIGNATURES UNCOVER THE ASSOCIATION OF EXTRACELLULAR MATRIX GENES WITH IMMUNOTHERAPY RESISTANCE IN HEAD AND NECK SQUAMOUS CELL CARCINOMA

¹Niki Gavrielatou*, ²Jonathan Warrell, ¹Thazin Aung, ¹Ioannis Vathiotis, ³Panagiota Economopoulou, ⁴Barbara Burtness, ³Amanda Psyrris, ¹David Rimm. ¹Yale School of Medicine, New Haven, CT, USA; ²Yale University, New Haven, CT, USA; ³Attikon University Hospital, NKUA, Athens, Greece; ⁴Yale School of Medicine, Yale Cancer Center, New Haven, CT, USA

Background Immune-checkpoint inhibition (ICI) only benefits a subgroup of patients with head and neck squamous cell carcinoma (HNSCC). Several molecular and cellular components of the tumor microenvironment (TME) have been hypothesized to drive either response or resistance. Here, spatially defined whole transcriptome data were analysed in search of associations of compartment-specific gene-signatures with HNSCC immunotherapy outcomes

Methods Pre-treatment biopsy samples from 50 immunotherapy-treated recurrent or metastatic HNSCC patients as well as 12 matched post-treatment biopsies obtained after 4 weeks of treatment, constructed in tissue microarray format (YTMA496), were included in the study. The GeoMx Human Whole Transcriptome Atlas (NanoString Technologies) assay was performed on samples to allow RNA quantification of 18,677 protein encoding genes, using in situ hybridization, in three molecularly defined tissue compartments; tumor (CK), leukocyte (CD45), macrophage (CD68). Differentially expressed genes (DEGs) ($P < 0.05$) between pre- and post-treatment biopsies in each of the tissue compartments were identified. Next, these DEGs were used as a 'biological' filter for the initial 18,677 gene set and analysed using LASSO logistic regression models with the aim to obtain pre-treatment gene expression signatures for best overall response (RECIST 1.1.). The performance of each compartment signature was evaluated using the receiver operating characteristic (ROC) curve and AUCs were calculated for Best Overall Response (BOR) to ICI. Genes comprising the highest performing signature were investigated for correlations with immune cell genes extracted from the 'Single Cell RNA-Seq HNSCC' (CIBERSORTx) gene matrix.

Results A six-gene signature (*DDX4*, *COL17A1*, *HBA1*, *MMP1*, *GPNMB*, *TTN*) in the CD45 compartment presented the highest AUC (0.83), followed by signatures in the CK and CD68 compartments (AUC: 0.72 and 0.68, respectively). Cross-testing of the CD45 signature in the other two compartments, as well as in a third, artificially generated 'pseudo-bulk' compartment (all compartments combined), showed poor performance, indicating spatial specificity. Interestingly, the CD45 signature included three extracellular-matrix protein-encoding genes (*MMP1*, *COL17A1*, *TTN*), all associated with resistance (negative coefficients in the BOR model) to ICI. Fibroblast and dendritic cell populations, characterized using the CIBERSORTx gene matrix, were the immune phenotypes most closely associated with the CD45 signature.

Conclusions Our results indicate that CD45 molecular tissue compartment gene expression demonstrates increased association with ICI resistance in HNSCC. Extracellular matrix genes rather than immune-cell related genes dominated the CD45 compartment signature, highlighting the importance of non-immune stromal components within the TME and the importance of the use of spatial information in the understanding of ICI resistance.

Acknowledgements This study was funded by Yale Head and Neck SPORE.

Ethics Approval This study was approved by Yale Human Investigation IRB protocol ID 9505008219.

<http://dx.doi.org/10.1136/jitc-2022-SITC2022.0133>

134

B AND MYELOID CELL POPULATIONS DOMINATE IN THE METASTASIS COMPARED TO PRIMARY TUMORS OF PATIENTS WITH PANCREATIC CANCER

¹Emily Greene*, ¹Deon Doxie, ¹Maria Diab, ²Bassel El-Rayes, ¹Shishir Maithel, ¹Juan Sarmiento, ¹Olatunji Alese, ¹Jayden Kim, ³Cameron Herting, ¹Kavita Dhodapkar, ¹Madhav Dhodapkar, ¹Haydn Kissick, ¹Chrystal Paulos, ¹Gregory Lesinski. ¹Emory University, Atlanta, GA, USA; ²University of Alabama at Birmingham, Birmingham, AL, USA; ³Eli Lilly, Decatur, GA, USA

Background Pancreatic ductal adenocarcinoma (PDAC) is a lethal malignancy with 5-year survival rate of only 11% for patients. To date, nominal data on the immune profile within metastatic PDAC of patients exists. Since most patients present with late-stage disease, defining the immunological landscape of metastatic disease could inform next-generation immunotherapy for PDAC patients.

Methods Using a 37-marker mass cytometry panel, freshly digested tumor tissue from surgically resected primary (n=6) and untreated liver punch biopsy metastatic (n=10) PDAC samples were evaluated for various immune features at the single cell level. Stained samples were fixed, run on a Helios™ mass cytometer and analyzed via FlowJo and Cytobank software.

Results Fewer CD45⁺ cells were present in metastatic compared to primary PDAC tumors. CD19⁺ B Cells (3.65% ± 5.19 of live cells) dominated among other immune populations in metastases. Yet these B cells appeared less activated in metastatic PDAC, signified by fewer B cells expressing HLA-DR⁺ (57.67% ± 26.49 of CD19⁺) versus the primary cohort (84.95% ± 21.19 of CD19⁺). Primary samples had significantly more myeloid, NK and T cells (p=0.017, p<0.01 and p=0.015, respectively) versus metastases. Moreover, primary tumors had significantly higher CD38⁺CD4⁺ and CD38⁺CD8⁺ T cells (consistent with an exhausted phenotype), while ICOS and TIGIT were elevated on T reg from primary vs. metastatic tumors. A survey of checkpoints revealed that LAG-3, TIGIT, and PD-1 were the most prevalent markers across both CD4⁺ and CD8⁺ T cells. Further analysis revealed proliferative (Ki67⁺) CD11b⁺ cells at both tumor sites. Metastatic sites had prevalent PMN-MDSC-like myeloid cells, but few M-MDSC-like myeloid cells. In-depth analysis of T cell populations revealed more CD4⁺Tbet⁺ Th1-like cells in primary (37.83% ± 34.13 of CD4⁺) as compared to metastatic samples (12.34% ± 31.43 of CD4⁺). Antigen-exposed CD45RO⁺PD-1⁺ T cells (CD4⁺: 60% ± 33.28; CD8⁺: 44.17% ± 23.38) and TCF-1⁺PD-1⁺CD8⁺T cells (37.88% ± 33.27 of CD8⁺) were also predominant in primary samples.

Conclusions These data indicate for the first time that metastatic PDAC is dominated by B and myeloid cells. While T cells were more evident in primary tumors, these cells harbored phenotypic properties of exhaustion. This work lays the foundation for a detailed spatial investigation into primary and metastatic PDAC tumors and could identify actionable targets to improve immunotherapy for PDAC patients.

<http://dx.doi.org/10.1136/jitc-2022-SITC2022.0134>

135 IDENTIFICATION OF SUPER-EXHAUSTED T CELLS: A NOVEL POPULATION PREDICTIVE OF RESPONSE TO IMMUNOTHERAPY

¹Alban Bessede, ²Florent Peyraud*, ¹Jean Philippe Guegan, ¹Christophe Rey, ³Sylvestre Le Moulec, ⁴Fabrice Barlesi, ²Sophie Cousin, ²Guilhem Roubaud, ²Mathilde Cabart, ²Maxime Brunet, ⁵Ezogelin Gruyters, ⁵Ariel Savina, ⁶Berengère Dadone-Montaudon, ⁴Aurélien Marabelle, ⁴Jean Charles Soria, ⁴Yohann Loriot, ⁴Jean-Yves Scoazec, ²François Le Loarer, ²Antoine Italiano. ¹Explicyte, Bordeaux, France; ²Institut Bergonié, Bordeaux, France; ³Clinique Marzet, Pau, France; ⁴Institut Gustave Roussy, Villejuif, France; ⁵Astrazeneca, Rahway, NJ, USA; ⁶CHU Nice, Nice, France

Background Given that most of cancer patients treated with anti-PD1/PD-L1 immune checkpoint blockers (ICB) do not derive benefit, there is a crucial need to identify reliable predictive biomarker of responses. Besides PD-1, several key immune checkpoints, such as CTLA4, LAG3, TIM3 and TIGIT, are associated with a T cell exhausted phenotype and play a crucial role in leading to cancer immune evasion. The impact of simultaneous expression by T cells of distinct inhibitory receptors on outcome of patients treated with ICB is still unknown.

Methods We analyzed the tissue samples, collected before ICB initiation, from patients with solid tumors and included in an institutional molecular profiling program (NCT02534649). We used multiplexed-immunohistofluorescence with the following panel CD3/PD1/TIM3/LAG3/TIGIT/CTLA4, and performed immune cell characterization using multispectral images analysis. We then investigated the correlation between coexpression of T cell-associated exhaustion markers, clinical response rate, progression-free survival (PFS) and overall survival (OS) by Cox proportional hazards models.

Results Four hundred thirty five patients were included in the analysis (NSCLC: n=207, 47.6%; sarcoma: n=42, 9.7%; urothelial: n=30, 6.9%; others: n=156, 35.9%). Digital pathology analysis allowed us to identify a population of 'super-exhausted' T cells characterized by the co-expression of PD1, LAG3, TIGIT and TIM3 which was enriched in 125 cases (28.7%), and was significantly associated with better PFS (HR 1.60, CI95 1.26–2.04, p<0.001) and OS (HR 1.42, CI95 1.07–1.89, p=0.016) in the whole cohort. Patients with super-exhausted high tumors had higher objective response rate (38.4%) compared to super-exhausted low tumors (19.7%, p<0.001). The presence of super-exhausted T cells was significantly higher in responders (10%) versus non responders (4%, p<0.001). Correlation with better outcome was observed whatever the subgroup considered (NSCLC vs other tumors, CD8 T cells density and presence of tertiary lymphoid structure [TLS]). In multivariate analysis (n=372, 85.5%), increased tumor infiltration by super-exhausted T cells (>1%) was significantly associated with better PFS (HR 0.61, CI95 0.46–0.81, p<0.001) and OS (HR 0.68, CI95 0.48–0.97, p=0.033).

Conclusions The presence of super-exhausted T cells may represent a new predictive biomarker of response to ICB and pave the way for the development of effective ICB combinations. Data from an independent validation cohort will be presented at the meeting.

<http://dx.doi.org/10.1136/jitc-2022-SITC2022.0135>

136

A PLASMA PROTEOMIC BASED PREDICTIVE BIOMARKER FOR RESPONSE TO IMMUNOTHERAPY IN NSCLC

<http://dx.doi.org/10.1136/jitc-2022-SITC2022.0136>

¹Michal Harel*, ¹Coren Lahav, ²Ido Wolf, ³Ella Tepper, ⁴Maya Gottfried, ⁵Raya Leibowitz, ⁶Mahmoud Abu-Amna, ⁷Abed Agbarya, ⁸Rivka Katzenelson, ⁹Michal Lotem, ¹⁰Mor Moskovitz, ¹¹Alona Zer, ¹²Ina Koch, ¹²Niels Reinmuth, ¹³Adam Dicker, ¹⁴David Gandara, ¹⁵Petros Christopoulos, ¹⁶David Carbone. ¹*Oncohost LTD, Binyamina, Israel*; ²*Tel Aviv Sourasky Medical Center, Tel Aviv Yafo, Israel*; ³*Assuta Ramat HaHayal Hospital, Tel Aviv Yafo, Israel*; ⁴*Meir Medical Center, Kfar Saba, Israel*; ⁵*Shamir Medical Center, Zerifin, Israel*; ⁶*Emek Medical Center, Afula, Israel*; ⁷*Bnai-Zion Medical Center, Haifa, Israel*; ⁸*Kaplan Medical Center, Rehovot, Israel*; ⁹*Hadassah Medical Center, Jerusalem, Israel*; ¹⁰*Rabin Medical center, Petah Tikva, Israel*; ¹¹*Rambam Health Care Campus, Haifa, Israel*; ¹²*Asklepios Klinik Gauting GmbH, Munich-Gauting, Germany*; ¹³*Thomas Jefferson University, Philadelphia, PA, USA*; ¹⁴*UC Davis Comprehensive Cancer Center, Sacramento, CA, USA*; ¹⁵*Thoraxklinik Heidelberg gGmbH, Heidelberg, Germany*; ¹⁶*The Ohio State University, Columbus, OH, USA*

Background To date, predicting response to immune checkpoint blockade (ICB) therapy in non-small cell lung cancer (NSCLC) patients is based on tumor PD-L1 levels. However, available assays are only moderately predictive, and most require a tumor biopsy. Here, we describe a novel machine learning-based biomarker model that analyzes proteomic profiles in blood plasma to predict ICB response in NSCLC patients.

Methods We collected plasma samples and clinical data from 339 ICB-treated NSCLC patients via a multi-center clinical study (PROPHETIC; NCT04056247; approved by local IRB committees from each site), 60% of them received combination of ICB-chemotherapy and the rest received ICB alone. Patients displaying disease progression were classified as non-responders and the rest as responders. Proteomic profiling was performed by the SOMAscan assay. A machine-learning-based model for clinical response prediction was developed based on protein expression level in patient's plasma. Using a proprietary algorithm, we identified Response Associated Proteins (RAPs), that serve as potential indicators of clinical response depending on their plasma level in the individual patient. The output of the model provides a patient-specific response probability for 3, 6, and 12 months after starting treatment.

Results The RAP-based model displayed strong predictive power over the first year of ICB-based therapy, as indicated by area under the curve (AUC) of the receiver operating characteristics (ROC) plot of 0.71, 0.77 and 0.78 for 3-, 6- and 12-months following treatment initiation, respectively, and a high goodness of fit between predicted response probability and observed response rate ($R^2 = 0.97$). Patients with low and high response probability predictions displayed a significant difference in overall survival and progression-free survival. The RAP-based model outperformed a PD-L1-based model (AUC of 0.5, 0.6 and 0.55 for 3-, 6- and 12- months, respectively). Notably, in a subgroup of patients with PD-L1-high tumors (>50% PD-L1) receiving monotherapy, patients with high response probability predictions survived significantly longer than patients with low response probability predictions (p-value 0.0002, 0.0036 and 0.0115 for 3-, 6- and 12-months, respectively) who had similar overall survival as patients with PD-L1-low tumors (<50% PD-L1).

Conclusions Altogether, we have developed a novel predictive model for ICB response in NSCLC patients based on proteomic profiling of blood plasma. The model offers two main clinical utilities. First, it provides response predictions for three time points over the first year of treatment. Second, it identifies a subgroup of high PD-L1 patients who may benefit more from combination therapy.

137 **FC γ RIIA-SPECIFIC DARPINS AS A NOVEL TOOL TOWARD SPECIFIC GENE DELIVERY INTO HIV RESERVOIR CELLS**

¹Arezoo Jamali*, ¹Vanessa Riechert, ¹Samuel Theuerkauf, ¹Sascha Hein, ²Philipp Adams, ²Elena Herrercarrillo, ²Ben Berkhout, ¹Klaus Cichutek, ¹Jessica Hartmann, ¹Christian Buchholz. ¹Paul Ehrlich Institut, Langen (Hessen), Germany; ²University of Amsterdam, Amsterdam, Netherlands

Background Fc γ RIIa (CD32a) has recently been identified as a cellular marker for the latent HIV-1 reservoir.¹ Its relevance as a marker has been challenged, due to technical problems complicated by T-B cell conjugates, and trogocytosis, as well as the lack of reliable antibodies, to distinguish the a and b isoforms. Thus, there remains a need for specific Fc γ RIIa-binders for diagnostic and therapeutic strategies, including targeted gene delivery. Receptor-targeted viral vectors can mediate highly selective gene delivery into target-receptor positive cells not only ex vivo but also in vivo.

Methods Libraries of designed ankyrin repeat proteins (DAR-Pins) were screened for binding to human Fc γ RIIa using ribosomal display. Binders unable to discriminate between isoforms were eliminated by counter selection against Fc γ RIIb. Specific binders were identified on cell lines artificially expressing Fc γ RIIa or Fc γ RIIb and by surface plasmon resonance. The binding epitopes were localized through chimeric Fc γ RIIa a/b proteins expressed on SupT1 cells. The most promising DAR-Pins were inserted into the glycoprotein of Nipah virus to generate Fc γ RIIa receptor-targeted viral vector. Targeting Fc γ RIIa receptor on pure or mixed expressing cell lines as well as primary human PBMC was monitored.

Results The identified DARPins discriminated between Fc γ RIIa and Fc γ RII b in protein and cellular binding assays with no detectable off-target activities. Their affinities for human Fc γ RIIa were in the low nanomolar range. In flow cytometry, the DARPins detected Fc γ RIIa + cells even when they made up less than 1% of the cell population. The difference between Fc γ RIIa and Fc γ RIIb is due to a single amino acid moiety. DARPins detected Fc γ RIIa⁺ cells could discriminate this even when they made up less than 1% of the cell population in flow cytometry. Lentiviral vectors, displaying the DAR-Pin mediated highly selective gene delivery into Fc γ RIIa + cells in the presence of a large surplus of Fc γ RIIb+ cells. On primary cells, between 0.03% – 1.26% (PBMC) and 0.14% – 3.46% of CD4⁺ T cells were transduced. Such frequencies are well within expectation for Fc γ RIIa⁺ cells among T lymphocytes.

Conclusions In summary, well-characterized high-affinity selected Fc γ RIIa- DARPins have become available offering the potential to become unique tools for the detection of and drug delivery into the latent cellular HIV-1 reservoir. Their application for cell detection supports the presence of Fc γ RIIa-positive T cells.

REFERENCE

1. Descours B, Petitjean G, López-Zaragoza JL, Bruel T, Raffel R, Psomas C, Reyes J, Lacabaratz C, Levy Y, Schwartz O, Lelievre JD, Benkirane M. CD32a is a marker of a CD4 T-cell HIV reservoir harboring replication-competent proviruses. *Nature* 2017 Mar 23; **543** (7646):564–567

<http://dx.doi.org/10.1136/jitc-2022-SITC2022.0137>

138

PLASMA YKL-40 IS ASSOCIATED WITH PROGNOSIS IN PATIENTS WITH METASTATIC PANCREATIC CANCER RECEIVING IMMUNE CHECKPOINT INHIBITORS IN COMBINATION WITH RADIOTHERAPY

¹Astrid Johansen*, ²Sif Novitski, ²Jessica Hjaltelin, ³Susann Theile, ³Mogens Boisen, ²Søren Brunak, ¹Daniel Madsen, ³Dorte Nielsen, ³Inna Chen. ¹Center for Cancer Immune Therapy, Herlev, Denmark; ²NNF Center for Protein Research, Copenhagen, Denmark; ³Department of Oncology, Herlev, Denmark

Background YKL-40, also known as chitinase-3 like-1 protein (CHI3L1), is a secreted glycoprotein produced by various cell types including stromal, immune, and cancer cells. It contributes to cancer progression through tumor-promoting inflammation. YKL-40 has been shown to inhibit the cytotoxic function of T and NK lymphocytes, and in vivo studies have demonstrated synergistic anti-cancer effects of blocking YKL-40 in combination with immune checkpoint inhibitors (ICIs). Biomarkers for the prediction of the response to ICIs are highly needed. We investigated the association between plasma YKL-40 levels clinical benefit and survival in patients with metastatic pancreatic cancer (mPC) receiving ICIs combined with stereotactic body radiotherapy (SBRT).

Methods Blood samples were collected from 84 patients with mPC who participated in the randomized phase II CheckPAC study, in which patients received nivolumab with or without ipilimumab combined with a single fraction of SBRT (15 Gy). Blood samples were collected at baseline, after 2 weeks, and then every 8 weeks until disease progression. Plasma YKL-40 was measured using a commercial ELISA kit.

Results Median plasma YKL-40 was higher after 8 weeks of treatment in patients with progressive disease than in patients with clinical benefit, defined as stable disease, partial or complete response ($p < 0.05$). Elevated baseline plasma YKL-40 was an independent predictor of shorter overall survival (OS) (HR 2.06, 95% confidence interval 1.15–3.7). A $\geq 40\%$ decrease in plasma YKL-40 was associated with longer OS ($p = 0.0025$) compared to stable ($< 40\%$ decrease to $\leq 40\%$ increase) and $> 40\%$ increasing plasma YKL-40. There was no correlation between plasma YKL-40 and the tumor burden marker CA19–9 at baseline or during treatment.

Conclusions This study contributes new knowledge regarding plasma YKL-40 as a predictor of clinical benefit from ICIs combined with radiotherapy. These exploratory results warrant further investigation of YKL-40 as a biomarker for patients treated with immunotherapies.

Ethics Approval The CheckPAC study was approved by the Danish Ethics Committee (VEK, j.nr. H-16031247) and the Danish Data Protection Agency (j.nr. 2012–58–0004; HGH-2016–112; I-Suite j.nr. 05088).

Consent Signed informed consent was obtained from each participant.

<http://dx.doi.org/10.1136/jitc-2022-SITC2022.0138>

139

IDENTIFICATION OF DISTINCT TISSUE PHENOTYPES IN LUNG AND COLORECTAL CANCERS BY IMAGING MASS CYTOMETRY IS CONSISTENT ACROSS SERIAL SECTIONS

¹Smriti Kala*, ²Rasmus Lyngby, ²Rasmus Sorensen, ¹Andrew Quong, ¹Sam Lim, ¹Clinton Hupple, ¹Nina Lane, ²Jeppe Thagaard, ²Johan Dore-Hansen, ²James Mansfield, ²Fabian Schneider, ¹Michelle Macpherson. ¹Standard BioTools, San Francisco, CA, USA; ²Visiopharm, Hørsholm, Denmark

Background The growth in cancer immunotherapy agents requires an understanding of the immune contexture of the tumor microenvironment (TME). Imaging Mass Cytometry™ (IMC™) is a powerful tool for the study of complex cellular interactions in the TME and in the discovery of biomarkers that can predict disease outcome or response to therapy. The Hyperion Imaging System (Standard BioTools) utilizes CyTOF® technology to simultaneously assess 40+ protein markers at subcellular resolution without spectral overlap or background autofluorescence, thus providing unprecedented insight into the organization and function of the TME. However, despite the advances in staining and imaging methods, developments in analysis software had not kept pace, as a complete, user-defined workflow in a single software package for the analysis of highplex imaging data was lacking.

Methods This study demonstrates a tissue phenotyping workflow in highly autofluorescent lung and colorectal cancer tissues using highplex IMC, which offers the advantage of zero autofluorescence, and hence more reliable results. The data analysis pipeline uses Oncotopix® Discovery (Visiopharm) software for easy, accurate and quantifiable phenotyping. Serial sections of both tissue types were stained with a 40-marker panel comprised of structural, tumor, stroma, and immune cell markers, including immunoregulatory proteins that are targets of immunotherapy. The IMC cell segmentation kit was included in the panel for improved nucleus and plasma membrane demarcation. The analysis pipeline consisted of tissue segmentation (tumor, stroma, necrosis, etc), nuclear detection using a deep-learning algorithm pre-trained on IMC DNA channels, a threshold-based cellular phenotyping step, and spatial analyses.

Results In this work, we have shown that analysis of IMC images from lung and colorectal cancer tissues can uncover tissue phenotypic signatures of the TME through the determination of immune cell types found in the vicinity of cancerous cells and their numbers. Moreover, cell counts and tissue phenotypes were highly consistent across the serial sections, demonstrating the power of IMC in generating robust data.

Conclusions Overall, this work demonstrates that even for highly autofluorescent tissues, IMC can generate high-quality data, consistent across serial sections, which can be easily and accurately analyzed using a single software package, thus empowering IMC users to be confident in biological interpretation of high-dimensional proteomic data. This study showcases the capability of IMC technology combined with Oncotopix Discovery analysis in classification of cellular components within the TME, which is important for development of systematic digital profiling of the spatial TME.

<http://dx.doi.org/10.1136/jitc-2022-SITC2022.0139>

140

ASSESSMENT OF DIFFERENCES IN TUMOR MUTATIONAL BURDEN IDENTIFIED ON LIQUID BIOPSY IN 16,870 PATIENTS NEWLY DIAGNOSED WITH METASTATIC CANCER

¹Eugene Kwon, ¹Daniel Childs, ¹Bradley Stish, ¹Stephen Boorjian, ¹Matthew Tollefson, ¹Cameron Britton, ¹Ahmed Mahmoud, ²Angela Thompson, ²Reagan Barnett, ²Leylah Drusbosky, ²Leslie Bucheit*. ¹Mayo Clinic, Rochester, MN, USA; ²Guardant Health, Redwood City, CA, USA

Background Tumor mutational burden (TMB) has emerged as a biomarker of response to immune checkpoint inhibition (ICI), with pembrolizumab approved for patients with a TMB of >10 mut/Mb regardless of solid tumor type. Predictive TMB cutoffs have not been optimized to account for differences in results based on genetic platform, manner of collection (tissue versus blood-based), or tumor type, though some data suggest disease-specific cut-offs may better identify patients who are likely to benefit from ICI. While described in tissue-based assays, blood-based TMB (bTMB) values and histology-specific differences are not well characterized for those newly diagnosed metastatic solid tumors. Here, we present results of bTMB assessment in nearly 17,000 newly diagnosed patients.

Methods Genomic results were queried for patients with newly diagnosed metastatic non-small cell lung cancer (NSCLC), colorectal, breast, prostate, gastric, melanoma or bladder cancer (as designated by ordering clinicians on requisition forms), who had Guardant360 (Guardant Health) testing between October 1, 2020, and June 1, 2022. Three factors were assessed across cancer types: 1) rate of evaluable bTMB, 2) median bTMB at diagnosis, and 3) percentage of patients whose initial bTMB value was above disease-specific cut-offs generated from prior Guardant cohorts¹ (≥ 80 th percentile bTMB values in mut/Mb – NSCLC: 20.2, CRC: 20.1, breast: 15.3, prostate: 13.4, gastric: 13.8, melanoma: 23.8, bladder: 20.2).

Results 16,870 patients were included, most diagnosed with NSCLC (table 1). Newly diagnosed patients with prostate cancer had the lowest rate of evaluable bTMB (<75%); all other cancer types were near or above 80% evaluable. Newly diagnosed patients with bladder cancer and melanoma had the highest median bTMB, while the lowest values were observed for breast and prostate cancers. Less than 20% of newly diagnosed patients with prostate or colorectal cancers had bTMB values above the cancer-type specific cut-off; all other cancer types had >20% of patients with bTMB values above cut-offs.

Conclusions bTMB is evaluable in most patients with newly diagnosed metastatic disease, supporting the feasibility of using circulating tumor DNA to determine TMB. Approximately 20% had a bTMB value above the cancer-specific cut-offs, suggesting potential responsiveness to ICI. Notably, prostate cancer was low across all factors assessed which may reflect its ‘cold’ biology; assessment of bTMB over time, rather than only at diagnosis, may better inform bTMB utility for patients with certain cancers. Further studies are needed to explore the utility of serial TMB assessment and correlate bTMB values with clinical treatment and outcomes.

REFERENCE

1. Drusbosky L, et al. *Journal of Clinical Oncology* 39, no. 15_suppl. 2021; 3040–3040. DOI: 10.1200/JCO.2021.39.15_suppl.3040

Abstract 140 Table 1 bTMB values in patients newly diagnosed with metast

Cancer type	bTMB evaluable	Median bTMB (mut/Mb)	Number of patients who had bTMB greater than cancer type cut-off
NSCLC	8509/10,333 (82%)	12.44	1825 (21%)
Colorectal	1978/2281 (87%)	9.57	95 (13%)
Breast	1621/1984 (82%)	7.89	298 (21%)
Prostate	856/1155 (74%)	7.99	149 (17%)
Gastric	433/525 (82%)	8.61	95 (22%)
Melanoma	274/347 (79%)	14.94	99 (26%)
Bladder	208/245 (85%)	19.36	61 (29%)

<http://dx.doi.org/10.1136/jitc-2022-SITC2022.0140>

141 **INDOLEAMINE 2,3 DIOXYGENASE EXPRESSION PREDICTS RESPONSE TO IMMUNE CHECKPOINT BLOCKERS IN ADVANCED NON-SMALL CELL LUNG CANCER**

¹Alban Bessedé*, ²Sylvestre Le Moulec, ¹Jean Philippe Guegan, ³Isabelle Soubeyran, ³Florent Peyraud, ¹Christophe Rey, ³Antoine Italiano. ¹Explicyte, Bordeaux, France; ²Clinique Marzet, Pau, France; ³Institut Bergonié, Bordeaux, France

Background In the era of immuno-oncology, it's now crucial to identify primary resistance mechanisms to Immune Checkpoint Blockers (ICB) in order to i) delineate novel pathways that can be targeted to improve current rate of response and to ii) identify predictive biomarkers to select patients who might benefit from ICB. The Indoleamine 2,3 dioxygenase (Ido) – a tryptophan degrading enzyme – has been well described to exert immunosuppressive functions and is considered as a therapeutic target to improve ICB benefit. However, despite important drug development efforts, little is known about Ido expression and its association with clinical response to ICB.

Methods We analyzed through a digital pathology approach the tumor samples obtained at immunotherapy onset from 55 patients (pts) with stage III/IV NSCLC enrolled in an institutional molecular profiling program (BIP: NCT02534649, sponsor: Institut Bergonié, Bordeaux, France). A multiplexed immunohistofluorescence panel consisting of the following markers PDL1, IDO1, CD8 and PanCK was developed, validated, and applied on each available tissue sample. Images were captured through slide digitization (PhenoImager HT, Akoya Biosciences) and analyzed for correlation with clinical outcome (Progression Free Survival and Overall Survival).

Results High PDL1 expression was correlated with a better PFS (19.60 months vs 4 months, $p=0,018$) and OS (not reached vs 21.2 months, $p=0,017$) than PDL1^{Low} pts. This study confirmed that pts with a higher abundance of CD8 within the stroma were more responsive to ICB than pts with a lower CD8 infiltration level. Strikingly, high levels of IDO1 expression within the tumor region – as defined through PanCK staining – was associated with a better PFS (not reached vs 4.40 months, $p=0,039$). Additional image analysis is currently ongoing for the evaluation of the association between the spatial distribution of PDL1+, IDO1+ and CD8+ cells and clinical outcome.

Conclusions Our results indicate that high IDO1 expression in the tumor compartment is associated with improved outcome in patients with advanced NSCLC. Inhibiting IDO may not be a relevant approach to improve ICB efficacy in NSCLC.

<http://dx.doi.org/10.1136/jitc-2022-SITC2022.0141>

142

DEMONSTRATING THE ROLE OF SPATIAL CONTEXTURE IN DETERMINING RESPONSE TO IMMUNE CHECK POINT INHIBITORS USING A TUMOR HISTOCULTURE PLATFORM

¹Satish Sankaran*, ¹Oliyarasi M, ¹Rajashekar M, ¹Ritu Malhotra, ¹Kowshik Jaganathan, ¹Gowri Shankar K, ¹Vasanth K, ²Manjula BV, ³MS Ganesh, ³Amritha Prabha, ⁴Prakash BV, ⁵C Jaya Prakash, ¹Arjun Chakraborty, ¹Syamkumar V, ¹Biswajit Das, ¹Aditi Satish, ¹Nandini Basak. ¹Farcast Biosciences, Bangalore, India; ²Bangalore Baptist Hospital, Bangalore, India; ³Vydehi Multi Speciality Hospital, Bangalore, India; ⁴Sri Lakshmi Multi Speciality Hospital, Bangalore, India; ⁵DBR and SK Super Speciality Hospital, Bangalore, India

Background Baseline signatures have so far failed to accurately predict response to immune checkpoint inhibitors. A model that mimics the clinical response of tumor immune microenvironment (TiME) upon treatment in culture, would dramatically improve the chances of identifying true responders. Tumor histocultures capture the complex interactions between various tumor microenvironment components effectively. They retain the immune cell repertoire along with spatial context, both of which are adequately represented in Farcast™ TiME histoculture platform.

Methods Farcast™ head and neck squamous cell carcinoma histoculture platform was used to evaluate response to treatment with anti-PD1 (Nivolumab) alone or in combination with anti-CTLA4 (Ipilimumab) in culture. Multiple assays including spatial analysis was performed post-treatment.

Results Interferon gamma (IFN γ) cytokine release, that classically defines T- cell response, was used to stratify samples for response to treatment with Nivolumab (n=45). Histopathological evaluation revealed that 4 of 45 (9%) samples showed an increase in tumor infiltrating immune cells by 1.5 folds, with a concomitant increase in IFN γ secretion (Log₂FC \pm SD, 1.67 \pm 0.8), and CD8+GranzymeB+ cells estimated by flow cytometry. Three out of these 4 samples showed an increase in tumoricidal response. To capture the complex spatial interplay between TiME components and the intra-cellular signals that determine response, a 72-protein marker GeoMx DSP (nanoString) panel was used on two samples (one recurrent and a primary) treated with Nivolumab. panCK was used for tumor segmentation. An increased expression of FoxP3 (Treg marker), IDO and phosphorylated tumor markers was observed in the recurrent sample within the tumor nest, suggestive of immune suppressive microenvironment post treatment. Interestingly, the primary sample exhibited increase in checkpoint and T-cell costimulatory molecules within the tumor nest along with a significant decrease in FoxP3 and tumor marker EGFR, suggestive of enhanced T- cell mediated tumor cytotoxicity. To map the relative spatial distribution of CD8+ and FoxP3+ cell populations, multiplex IHC assay was performed, and data analyzed using QuPath. Decrease in distance between CD8+ cells from tumor nest with a concomitant increase in distance between FoxP3+ and CD8+ cells were observed in a high IFN γ and GranzymeB secreting sample.

Conclusions In summary, our data suggests that though IFN γ secretion was observed in multiple samples post treatment, spatial contexture influenced T-cell response mediated tumor cytotoxicity. Farcast TiME thus provides a unique platform that can combine spatial dynamics of immune cells overlaid with bulk data, providing important insights into understanding underlying mechanisms that counter T-cell response to immune check point inhibitors.

Acknowledgements Technical support from nanoString for performing the GeoMx DSP experiment and analysis is acknowledged.

Ethics Approval All patient samples used in this study was obtained with prior approvals from individual institutional review boards of participating hospitals.

<http://dx.doi.org/10.1136/jitc-2022-SITC2022.0142>

143

A COMPREHENSIVE WORKFLOW FOR HIGHPLEX IMAGING, TISSUE SEGMENTATION, AND MULTIPLEX CELLULAR PHENOTYPING FOR TUMOR MICROENVIRONMENT ANALYSIS

Fabian Schneider*, Rasmus Lyngby, Rasmus Sorensen, Andrew Quong, Smriti Kala, Sam Lim, Clinton Hupple, Nina Lane, Michelle Macpherson, Jeppe Thagaard, Johan Dore-Hansen, James Mansfield. ¹Visiopharm, Horsholm, Denmark; ²Standard BioTools, South San Francisco, CA, USA

Background The growth in cancer immunotherapy agents requires an understanding of the immune contexture of the tumor microenvironment (TME). One way to understand immune contexture is to use multiplex staining, imaging, and analysis to obtain multi-marker phenotypes of specific cells and analyze their biodistribution in the TME. Imaging Mass Cytometry™ (IMC) is the method of choice for single-step staining and highplex imaging of FFPE tissues. FFPE tissue is autofluorescent, which limits the utility of immunofluorescence methods, particularly when done without amplification. Lung and colorectal tissue (and bone, skin, etc) are highly autofluorescence, and therefore are a good target for IMC imaging, which has no autofluorescence issues. However, developments in analysis software with a single-package workflow for highplex imagery have not kept pace. We present here a comprehensive workflow in the Oncotopix® Discovery platform designed specifically for highplex IMC image analysis, covering tissue segmentation, cell segmentation based on IMC DNA images, cellular phenotyping, and spatial analyses.

Methods Lung and colorectal tissue sections with a 40-marker panel comprised of structural, tumor, stroma, immune cell markers, and immunoregulatory proteins that are targets of immunotherapy, were imaged (Hyperion, Standard BioTools). Highplex image analysis was performed as a multi-step workflow in a single software package that includes: conversion of IMC images to pyramidal format; easy visualization methods for displaying different marker subsets; a paint-to-train algorithm for tissue segmentation (into tumor, stroma, necrosis, etc); deep-learning-based nuclear segmentation pre-trained specifically on IMC DNA channels; cellular phenotyping based on thresholds set based on visual assessment of positivity; spatial biodistribution metrics for cell populations; and a flexible set of outputs for further downstream analysis.

Results This study demonstrates that a simple workflow can be used to analyze highplex images of different tissue types with no programming knowledge and few changes between tissue types. Visualization templates for the marker subsets and the pre-trained IMC nuclear segmentation are reusable. A new tissue segmentation algorithm for each tissue type is required, as are new thresholds for biomarker positivity. Spatial biodistribution metrics and heatmaps were generated for each tissue type with a minimum of work required.

Conclusions IMC highplex imaging of lung and colorectal tumor samples is a simple and effective means of obtaining highplex images without interfering autofluorescence. Having a comprehensive workflow for the analysis of this complex data makes obtaining useful results from highplex images more accessible to biologists and immunologists by circumventing the requirement for expert programming for each specific application.

<http://dx.doi.org/10.1136/jitc-2022-SITC2022.0143>

144

CD3 HUMANIZED MOUSE MODELS AS VALIDATED TOOLS TO ASSESS IMMUNE-RELATED ADVERSE EVENTS OF T CELL ENGAGERS

Perrine Martin-Jeantet, Gaele Martin, Angela Pappalardo, Florence Renart-depontieu, Patricia Isnard-Petit, Yacine Cherifi, Fabiane Sónego, Kader Thiam*.

genOway, Lyon, France

Background T cell engagers show high efficacy in B cells malignancies. Immune-related adverse events (IrAE), including cytokine release syndrome (CRS), is reported in patients due to on-target off-site effects of T cell engagers (TCE). Translational and predictive assays to assess IrAE of TCE are key to avoid pitfalls in clinical trials. Knock-in humanized mouse models enable the assessment of human-target antibodies in a fully immunocompetent mouse. Indeed, immune responses in CD3 humanized model have been extensively evaluated, and humanization of CD3 has not impaired immune cell distribution. Furthermore, immunization studies showed that T-B cell cooperation is functional in these mice. CD3-TCR complex is also functional, as anti-human CD3 antibodies induce T cell activation. Different classes of TCE showed tumor cell killing *ex vivo*, as well as tumor growth inhibition *in vivo*. Here we report the use of CD3 humanized models to assess CRS *ex vivo* and *in vivo*.

Methods Two CD3 humanized mice developed by knock-in were used for *ex vivo* and *in vivo* investigation of cytokine production. While one of the models is restricted to one clone of anti-human CD3, the other has been shown to bind several clones of anti-human CD3. *Ex vivo*, T-cell dependent cellular cytotoxicity assay was performed using different TCE concentrations on splenocytes from CD3 humanized mice. *In vivo*, CD3 humanized mice were treated with anti-human CD3 and cytokine release in blood, clinical monitoring, body weight and temperature were assessed.

Results Cytokine release in cytotoxicity assay showed that splenocytes from CD3 humanized mice produced IFN- γ , TNF- α , IL-6, IL-1 β , IL-10 and IL-12p70 in a TCE concentration-dependent manner. *In vivo*, cytokine production was also observed in blood of CD3 humanized mice treated with anti-human CD3. Kinetic of secretion was dependent on the detected cytokine (IFN- γ , IFN- α , IL-6, IL-10) and chemokine (CXCL9, CXCL10, CCL3, CCL2, CCL4). An anti-CD3 dose-effect on cytokine levels of secretion was demonstrated. In parallel, body temperature drop at early timepoints and increase in late timepoints were observed upon treatment with anti-CD3.

Conclusions Cytokine release and some clinical signs of CRS are reproduced in the two CD3 humanized models described here, validating their value to assess IrAE of TCE. Although the fully functional immune system is one of the main advantages of this model, assessment of mouse biology is a drawback. As a complementary approach, BRGSF-HIS mice, an immunodeficient mouse model reconstituted with human CD34⁺ cells, showed to reproduce both clinical signs and cytokine production of human TCE-induced CRS.

<http://dx.doi.org/10.1136/jitc-2022-SITC2022.0144>

NADUNOLIMAB INHIBITS IL-1 α / β -INDUCED CXCR1/2 LIGAND EXPRESSION AND REDUCES SERUM LEVELS OF CXCL1 AND CXCL5 IN NSCLC AND PDAC PATIENTS

Camilla Millrud*, Elin Gyllenbäck, Petter Skoog, Annika Sanfridson, David Liberg. *Cantargia AB, Lund, Sweden*

Background Interleukin-1 receptor accessory protein (IL1RAP) is expressed on tumor cells and stromal cells in most solid tumors, including PDAC and NSCLC. IL1RAP is a co-receptor of the IL-1 receptor (IL1R1), and its dimerization with IL1R1 is required for IL-1 signaling. IL-1 is expressed in the tumor microenvironment and contribute to chemoresistance and an immune-suppressive tumor microenvironment. The chemokine receptors CXCR1 and CXCR2 and their ligands are crucial for the migration of immune-suppressive cells into the tumor and thereby influences tumor progression and metastasis. CXCR1/2 ligands can be expressed by cells in the tumor microenvironment and are downstream of IL-1 signaling. Nadunolimab is a fully humanized ADCC-enhanced monoclonal IgG1 antibody targeting IL1RAP and disrupting both IL-1 α and IL-1 β signaling. Currently, nadunolimab is evaluated in phase II for PDAC and NSCLC (NCT03267316) in combination with gemcitabine + Nab-paclitaxel or gemcitabine + cisplatin, respectively.

Methods Whole blood and PBMC from healthy donors as well as cancer-associated fibroblasts (CAFs) were stimulated with IL-1 α or IL-1 β with or without nadunolimab followed by assessment of CXCR1/2 ligands. Serum samples collected before start of treatment and after 2 weeks of treatment from 11 NSCLC patients treated with nadunolimab in combination with gemcitabine + cisplatin, and 16 PDAC patients treated with nadunolimab and gemcitabine + Nab-paclitaxel, were analyzed for the presence of CXCL1, CXCL5 and CXCL8.

Results The inhibitory effect of nadunolimab on IL-1 α and IL-1 β induced CXCR1/2 ligands was evaluated in different cell systems. IL-1 α and IL-1 β induced the secretion of the CXCR1/2 ligands CXCL1, CXCL2, CXCL5, CXCL6 and CXCL8 in CAFs. This increase was normalized with the addition of nadunolimab. In a similar fashion, nadunolimab significantly blocked the IL-1 α and IL-1 β induced levels of CXCL1, CXCL5 and CXCL8 from PBMC and whole blood. Therefore, CXCL1, CXCL5 and CXCL8 were evaluated as potential biomarkers in serum from patients treated with nadunolimab. Similar to the in vitro results, serum levels of CXCL1 and CXCL5 were significantly decreased in patient on treatment with nadunolimab and chemotherapy. However, levels of CXCL8 were not affected after 2 weeks of treatment.

Conclusions Nadunolimab was demonstrated to decrease the levels of CXCR1/2 ligands across different cell systems, and a reduction in CXCL1 and CXCL5 was detected in both NSCLC and PDAC patients during treatment with nadunolimab. This is in line with an effect of nadunolimab on the tumor microenvironment and indicates the potential of CXCL1 and CXCL5 as serum biomarkers for treatment with nadunolimab.

Trial Registration NCT03267316

Ethics Approval The study was approved by the Ethics committees of the concerned countries and an informed consent was obtained from all individuals included in this study. Clinical trial number NCT03267316.

<http://dx.doi.org/10.1136/jitc-2022-SITC2022.0145>

146

TRANSCRIPTOME AUGMENTATION PROVIDES ACCURATE AND SENSITIVE QUANTIFICATION OF GENES ASSOCIATED WITH THE TUMOR MICROENVIRONMENT

Fabio Navarro*, Pamela Milani, Koichi Hashikawa, Shruti Bhide, Upasana Dutta, Dave Delano, Charles Abbott, Robin Li, Zeid Rusan, John West, John Lyle, Sean Boyle, Richard Chen. *Personalis, Inc, Menlo Park, CA, USA*

Background Tumors harbor a complex and dynamic ecosystem of malignant, immune, and stromal cells. While malignant cells dictate much of the tumor biology, there is evidence that the tumor microenvironment (TME) also plays a significant role in disease progression and response to therapy. The role of the immune cells is particularly relevant in immunotherapy, and multiple transcriptome-based biomarkers have shown utility in predicting the efficacy of immune checkpoint blockade. However, little is known about the benefits of enhancing the depth and uniformity of transcriptome sequencing coverage for quantifying the TME cell type composition.

Methods We have developed the ImmunoID NeXT Platform®, which combines high-quality exome and transcriptome sequencing with advanced informatics designed for immunoncology to comprehensively characterize the tumor and TME from a single FFPE tumor sample. Proprietary augmentation technology was applied to bolster sequencing depth in regions of low coverage across approximately 20,000 genes, enhancing transcriptome coverage uniformity. We processed and sequenced 32 PBMC samples, in-vitro cell mixtures (CD8, CD4, Tregs, B-cells), and over 100 purified cell types to assess the biases and performance of gene expression quantification using the augmented transcriptome. Immune cell composition was validated using flow cytometry. Using purified cell types, we applied differential expression analysis to identify genes preferentially expressed in target cell types. Finally, we confirmed the augmented transcriptome identifies well-established cell-type marker genes and novel cell-type enrichment genes fit for deconvolution.

Results We observed that the ImmunoID NeXT Platform benefits read coverage and uniformity for the majority of genes as compared to both PBMC (PolyA+) and tumor samples (rRNA-depletion). We identified genes preferentially expressed in immune, stromal and granulocyte cell types, showing high overlap with previous literature, and we describe over 1,000 new potential markers fit to assess cell type enrichment in reference samples. To demonstrate that coverage augmentation did not introduce biases disrupting the collinearity between cell fractions and gene expression, we profiled in-vitro cell mixtures. We found that marker genes for Tregs, CD4, CD8, and B-cells are linearly correlated with the fraction of cells mixed and verified by flow cytometry. For instance, well-established CD8 markers show a strong correlation between cell fraction and expression (CD8A corr=0.947 p-value=2.55e-12).

Conclusions We show that ImmunoID NeXT® accurately captures and augments the transcriptome of PBMC and FFPE samples. Applying augmented transcriptome coverage to the assessment of the TME benefited the identification of marker genes for cell type enrichment analysis without introducing bias.

<http://dx.doi.org/10.1136/jitc-2022-SITC2022.0146>

COMPREHENSIVE *IN SITU* IMMUNE PHENOTYPING WITH THE COSMX™ HIGH PLEX PROTEIN ASSAY

¹Tien Phan-Everson*, ¹Jianji Chen, ¹Zachary Lewis, ¹Gary Geiss, ¹Yan Liang, ¹Emily Brown, ¹Liuliu Pan, ¹Stefan Phelan, ¹Charlie Glaser, ¹Mithra Korukonda, ¹Carl Brown, ¹Dwayne Dunaway, ¹Joseph Phan, ¹Alyssa Rosenbloom, ¹Brian Filanoski, ¹Rhonda Meredith, ¹Kan Chantranuvatana, ¹Brian Birditt, ¹Giang Ong, ¹Hye Son Yi, ¹Erin Piazza, ¹Jason Reeves, ²Subham Basu, ¹Christine Kang, ¹Vik Devgan, ¹Edward Zhao, ¹Michael Rhodes, ¹Joseph Beechem. ¹*NanoString, Seattle, WA, USA*; ²*Abcam, Cambridge, UK*

Background The spatial interactions between the immune system and tumor cells greatly influence antitumoral immunity, patient prognosis, and therapeutic efficacy. However, few methods exist to query large numbers of immune biomarkers at subcellular spatial resolution. Launched earlier this year, the CosMx™ Spatial Molecular Imager (SMI) platform captures high-plex single cell and subcellular detection of proteins from FFPE tissues. To detect these key drivers of cancer progression and immune cell activation states and functions, we designed and validated a high-plex protein panel for the CosMx SMI platform. This panel contains 4 markers for cell segmentation and pre-experimental imaging and 64 barcoded antibodies emphasizing immuno-oncology focused targets.

Methods The CosMx protein assay uses antibodies conjugated with oligonucleotides, which are detected using universal, multi-analyte CosMx readout reagents. The fully automated CosMx instrument carries a widefield water immersion objective with 1.1 NA. The CosMx Human Immuno-oncology panel was optimized to comprehensively phenotype lymphoid and stromal lineages within the tumor microenvironment. The CosMx protein assay reagents were validated on multi-organ FFPE tissue microarrays covering prevalent solid tumor types and matched controls, and 52 human FFPE cell lines, including overexpression lines for key targets such as GITR, CD278, PD-L1, and PD-1.

Results We achieved 86% sensitivity and 90% specificity across well-characterized human cell lines compared to GeoMx spatial profiling, and further benchmarked to multiple orthogonal datasets (e.g., the Human Protein Atlas, low-plex IHC). Within the tissue sample profiled, we captured immune cell localization across and within the tumor, key signaling markers related to lymphoid and myeloid activation such as checkpoint engagement, and myeloid cell polarization and antigen cross-presentation markers. We made the data from the study profiling cancer tissue freely available online. This includes the protein images, AI-based cell segmentation, and the per-cell protein abundance profiles.

Conclusions CosMx SMI is a high-plex spatial multiomics platform that enables detection of more than 64 proteins at subcellular resolution in real-world FFPE tissues. Our 64-plex human immuno-oncology protein panel enables in-depth study of the tumor microenvironment, including markers covering cell typing and lineage, immune activation, and checkpoints. This new platform will enable researchers to collect high-plex protein immunophenotyping data and understand immune molecular mechanisms with full spatial context.

FOR RESEARCH USE ONLY.

Not for use in diagnostic procedures.

<http://dx.doi.org/10.1136/jitc-2022-SITC2022.0147>

148 **TAP2 DEFICIENCY MEDIATES ADAPTIVE IMMUNE EVASION AND IMMUNOTHERAPY RESISTANCE IN HUMAN NON-SMALL CELL LUNG CANCER**

¹Kishu Ranjan*, ¹Imad ud Deen, ¹Miguel López de Rodas, ¹Nicole Gianino, ²Soldano Ferrone, ³Kurt Schalper. ¹Yale University School of Medicine, New Haven, CT, USA; ²Massachusetts General Hospital, Boston, MA, USA

Background The recognition of cancer-cells by T-cells and the therapeutic efficacy of PD-1 axis blockers for cancer treatment are dependent on a fully functional HLA class-I antigen processing machinery (APM). The APM has been found to be defective in many types of human malignancies; however, there is limited information in non-small cell lung cancer (NSCLC). Here we studied cancer-cell APM defects in NSCLC focusing on transporter associated with antigen processing proteins TAP1 and TAP2.

Methods We utilized quantitative and spatially resolved multiplex quantitative immunofluorescence (mQIF) to simultaneously analyze the markers DAPI, cytokeratin (CK), CD8, TAP1 and TAP2 in >1,100 primary NSCLCs from 6 independent cohorts represented in tissue microarrays. Three cohorts (Cohorts #1–3) included 881 tumors from patients treated with standard of care non-immunotherapy and two cohorts included 139 cases treated with PD-1 axis blockers (Cohorts #4–5). One additional cohort included 130 primary lung adenocarcinomas clinically tested for oncogenic mutations in *EGFR* and *KRAS* (Cohort #6). The association between cancer-cell selective TAP1 and TAP2 protein downregulation, clinicopathologic variables and outcomes were studied. To investigate the functional consequences of TAP1 and/or TAP2 deficiency in lung cancer cells, we analyzed the surface peptide-HLA complex levels, functional phenotype/transcriptomic profile, and sensitivity to tumor-antigen specific T-cell killing of cultured tumor cells with targeted TAP1 and/or TAP2 silencing using siRNA or CRISPR-Cas9 based targeted gene deletion.

Results mQIF analysis revealed cancer-cell selective downregulation of TAP1 and TAP2 proteins in ~5% and ~45% of immunotherapy naïve primary NSCLCs, respectively. Cases with TAP2 downregulation showed lower CD8+ T-cell infiltration and shorter survival after PD-1 axis blockers. This effect was not seen in tumors with cancer-cell selective TAP1 downregulation or in cases treated without immunotherapy. Targeted silencing or genetic deletion of *TAP2*, but not *TAP1* in human HER2⁺/HLA⁺ A549 lung cancer cells reduced the baseline and cytokine induced surface levels of the peptide-HLA complexes formed by the HER2_{369–377} nonamer and HLA-A2 recognized using flow cytometry. In addition, *TAP2* silencing was associated with a marked reduction in tumor cell killing after co-culture with human HLA-A2-positive CD8 + T-cells expressing the T-cell receptor recognizing the HER2_{369–377} peptide. Targeted immune transcriptomic analysis of *TAP2* deficient A549 cells revealed prominent alterations in IFN γ sensitivity and cytokine/chemokine expression.

Conclusions Cancer-cell selective TAP2 downregulation is common in NSCLC and mediates immune evasion and immunotherapy resistance *via* reduced antigen presentation and defective IFN γ responses. TAP2 deficiency in NSCLC has prominent biomarker and therapeutic potential.

Ethics Approval This study was carried out in accordance with the principles of the Declaration of Helsinki and all tissue and clinical information were used in a de-identified fashion after approval from the Yale Internal Review Board (Yale Human

Investigation Committee) protocols #9505008219 and #1608018220 or local institutional protocols, which approved the patient consent forms or waiver of consent.

<http://dx.doi.org/10.1136/jitc-2022-SITC2022.0148>

COMPLEMENTARY PHENOCODE SIGNATURE PANELS COMPREHENSIVELY MAP CELL INTERACTIONS AND IDENTIFY SPATIAL PHENOTYPIC SIGNATURES IN THE TUMOR MICROENVIRONMENT

analysis. *JAMA Oncol.* 2019; 5(8):1195–1204. <https://jamanetwork.com/journals/jamaoncology/fullarticle/2738418>

<http://dx.doi.org/10.1136/jitc-2022-SITC2022.0149>

Bethany Remeniuk*, Bei Hopkins, Natalie Monteiro, Darren Locke. *Akoya Biosciences, Marlborough, MA, USA*

Background Spatial biology using multiplexed imaging provides advantages over other biomarker modalities by enabling deeper interrogation of cellular- and protein-level co-expression, localization, and arrangements within the tumor microenvironment (TME). An emerging new biomarker class in the TME are Spatial Phenotypic Signatures (SPS), defined by the measurement of the interactions between, and cell densities of, tumor and immune cells. Akoya's PhenoCode™ Signature Panels have been designed to enable comprehensive mapping of the TME and to help identify SPS. Three PhenoCode Signature Panels were used to investigate SPS for immune checkpoint inhibitor (ICI) therapy in non-small cell lung cancer (NSCLC) patients where ICI have shown durable benefit.

Methods PhenoCode Signature Panels provide off-the-shelf multiplexed imaging customization (6-plex Panel via 5-plex core plus 1 open channel configuration) with minimal user development requirements. PhenoCode uses barcode-based antibody chemistry from Akoya's PhenoCycler® platform integrated with the signal amplification capabilities of Opal chemistry from Akoya's PhenoImager® platform. A tissue microarray (TMA) comprising 41 formalin-fixed paraffin-embedded (FFPE) pre-treatment samples from second-line PD-L1/PD-1 ICI-treated NSCLC cohorts (Durvalumab, Nivolumab, or Pembrolizumab, 16 responders and 25 non-responders) was screened with three PhenoCode Signature Panels. The PhenoCode Signature Panels were: Immuno-contexture Human Protein Panel (CD8/CD68/PDL1/FoxP3/CK core + CD20 or PD1 in the open channel) and Immune Profile Human Protein Panel (CD3/CD8/CD20/CD68/CK core + CD4 in the open channel). FFPE TMAs were stained on a Leica Bond RX™. Slides were imaged on a Phenoimager HT multispectral imaging system and analysis algorithms were developed using inForm®, with cell counts, densities, and spatial parameters calculated using PhenoptrReports.

Results Meta-analysis¹ on anti-PD-1/PD-L1 therapy data pooled from 50+ studies (10+ tumor types and 8,000+ patients) examined the predictive value of single-marker immunohistochemistry (PDL1), tumor mutation burden (TMB), gene expression profiling (GEP) and multiplexed imaging; findings revealed that spatial approaches performed significantly better compared to the other assay types. Multispectral spatial analysis of FFPE TMA samples using PhenoCode Signature Panels uncovered putative SPS within ICI-sensitive NSCLC, indicating enrichment and significance of cell frequencies and cell interactions in responder/non-responder cohorts.

Conclusions A new frontier of biomarker discovery based on spatial biology presents a path toward the use of multiplexed imaging in the clinic, as multiplexing technologies and workflows become more practical, high-throughput, and analytically robust. The ability to deploy Signature Panels supported by PhenoCode chemistry to investigate the immune landscape of the TME will accelerate the finding of SPS that may reliably predict response for ICI therapy.

REFERENCE

1. Lu S, Stein JE, Rimm DL, *et al.* Comparison of Biomarker Modalities for Predicting Response to PD-1/PD-L1 Checkpoint Blockade: A Systematic Review and Meta-

150

**CIRCULATORY PLASMA PROTEOMIC BIOMARKERS
PREDICT RESPONSE TO IMMUNOTHERAPY IN
MELANOMA PATIENTS AND REVEAL BIOLOGICAL
INSIGHTS INTO THE TUMOR MICROENVIRONMENT**

¹Arnav Mehta*, ²Marijana Rucevic, ²Emmett Sprecher, ³Nir Hacohen, ⁴Genevieve Boland, ³Milan Parikh, ¹Jiajia Chen, ⁴Dennie Frederick, ⁴Elliot Woods, ³Lynn Bi, ³David Lieb, ²Lina Hultin-Rosenberg, ²Jamey Guess, ³Ryan Park, ³Alexis Schneider, ⁴William Michaud, ⁴Benchun Miao, ⁴Gyulnara Kasumova, ⁴Michelle Kim, ⁴Xue Bai, ⁴Russell Jenkins, ⁴Samuel Klempner, ⁴Anna Gonye, ⁵Keren Yizhak, ³Moshe Sade-Feldman, ¹David Liu, ⁴Ryan Sullivan, ⁴Keith Flaherty. ¹Dana-Farber Cancer Institute, Boston, MA, USA; ²Olink Proteomics, Boston, USA; ³Broad Institute of MIT and Harvard, Boston, USA; ⁴Massachusetts General Hospital, Boston, MA, USA; ⁵Technion Israel Institute of Technology, Haifa, Israel

Background The majority of patients treated with immunotherapy do not have durable treatment responses. Therefore, there is an urgent need to identify early non-invasive biomarkers for treatment response.

Methods In this study, we performed plasma proteomic analysis of >700 proteins at three timepoints on 174 metastatic melanoma patients treated with immune checkpoint blockade (ICB). We then expanded our analyses to >3000 proteins performed on a larger cohort of 250 patients for deeper exploration of baseline and early on-treatment predictive biomarkers for response to ICB treatment. As a result, we built a predictor of immunotherapy response that outperforms several tissue-based approaches.

Results From the differentially expressed proteins between ICB responders (R) and non-responders (NR), we identified a co-regulated module of proteins associated with treatment resistance comprising IL-6, IL-8, MIA, LIF and GDF-15 enriched in certain NR patients. By analyzing single-cell RNA-sequencing data of tumor biopsies from 32 patients and bulk RNA-sequencing data from 70 patients, we determined the relative contribution of cells in the tumor to proteins in circulation, and associated plasma protein levels with tumor immune microenvironment (TME) phenotypes. The major TME subsets driving the expression of the non-response module proteins were tumor and myeloid cells. Amongst myeloid cells, a subset of tumor-associated macrophages (TAMs) with a suppressive phenotype were identified as potential key drivers of non-response, having the highest expression of all the proteins in the co-regulated NR module.

Conclusions In summary, an integrated longitudinal analyses of circulatory plasma proteins, combined with TME transcriptomics, provides deeper insight into the biology of immunotherapy resistance, and demonstrates prognostic significance and utility of plasma proteomics in biomarker discovery for cancer immunotherapy.

<http://dx.doi.org/10.1136/jitc-2022-SITC2022.0150>

151 USING ADDITIONAL MORPHOLOGY MARKERS IN NANOSTRING® GEOMX® WHOLE TRANSCRIPTOME ATLAS ASSAY TO ASSESS NSCLC TUMOR SUBTYPE

Jessica Runyon*, Christian Nievera, Vijay Baichwal. *Canopy Biosciences, St. Louis, MO, USA*

Background Recent publications have discussed techniques to identify tumor subtypes and a potential correlation with tumor immunity and immunotherapy success. Several techniques have been used for tumor subtype identification including RNA Seq, NanoString® nCounter®, and newer multi-omics approaches. NanoString's GeoMx® DSP platform provides spatial context about cells and their interactions within a tumor while also producing high-plex gene expression data. Expansion of existing morphology markers used with GeoMx DSP enables more precise segmentation of tumors based on key characteristics and provides a better understanding of the tumor's interaction with surrounding tissue. The subsequent transcriptomic profile from the Whole Transcriptome Atlas (WTA) panel may help identify characteristics that impact immunotherapies and the development of treatment screening tests. Lung cancer is still the leading cause of cancer death in the United States.¹ As classified by the WHO/International Association for the Study of Lung Cancer (IASLC),² there are three main subtypes of malignant NSCLS including squamous cell carcinoma (25% of lung cancers) and adenocarcinoma (40% of lung cancers).

Methods To evaluate the capability of this technology to selectively enrich specific cell types, we stained sections of non-small-cell lung cancer tumor (NSCLS) subtypes. Since molecular subtyping of NSCLC tumors is critical for targeted therapy and IHC biomarkers play a key role in the diagnosis and subclassification of lung cancer, we investigated if a histological approach combined with molecular profiling could assess both subtypes while identifying unique markers to each tumor subtype. NSCLC tissue was stained with P40 and TTF-1 antibodies to differentiate between squamous cell carcinoma and adenocarcinoma subtypes.^{3, 4} For all experiments, transcriptional profiles were assessed with the WTA panel for GeoMx DSP, covering over 18,000 genes and enabling oncology pathway analysis to profile the tumor, tumor microenvironment, and immune response. Analysis of this data set was performed using the GeoMx DSP Analysis Suite software.

Results The transcriptional profiles of these samples were then compared, and significant differences were revealed between these two tumor cell types.

Conclusions The findings support the notion that custom morphology markers enable better tumor stratification providing more meaningful gene expression analysis data. This gene expression data can then be integrated with gene signatures which are being developed for key targets of IO treatments to predict the utility of various immunotherapies for individual patient tumors. Studies with additional tumor types and markers are ongoing to further explore the utility of this technology for analyzing gene expression in different tumor types.

REFERENCES

1. Siegel RL, Miller KD, Jemal A. Cancer statistics, 2019. *CA Cancer J Clin.* 2019 Jan; **69**(1):7–34. doi: 10.3322/caac.21551. Epub 2019 Jan 8. PMID: 30620402.
2. Travis WD, Brambilla E, Nicholson AG, Yatabe Y, Austin JHM, Beasley MB, Chiriac LR, Dacic S, Duhig E, Flieder DB, Geisinger K, Hirsch FR, Ishikawa Y, Kerr KM, Noguchi M, Pelosi G, Powell CA, Tsao MS, Wistuba I; WHO Panel. The 2015 World Health Organization Classification of Lung Tumors: Impact of Genetic, Clinical and Radiologic Advances Since the 2004 Classification. *J Thorac Oncol.* 2015 Sep; **10**(9):1243–1260. doi: 10.1097/JTO.0000000000000630. PMID: 26291008.

3. Affandi KA, Tizen NMS, Mustangin M, Zin RRMRM. p40 Immunohistochemistry Is an Excellent Marker in Primary Lung Squamous Cell Carcinoma. *J Pathol Transl Med.* 2018 Sep; **52**(5):283–289. doi: 10.4132/jptm.2018.08.14. Epub 2018 Aug 31. PMID: 30235512; PMCID: PMC6166010.
4. Ordóñez NG. Value of thyroid transcription factor-1 immunostaining in tumor diagnosis: a review and update. *Appl Immunohistochem Mol Morphol.* 2012 Oct; **20**(5):429–44. doi: 10.1097/PAI.0b013e31825439bc. PMID: 22531688.

<http://dx.doi.org/10.1136/jitc-2022-SITC2022.0151>

THE IMMUNE EXPRESSION LANDSCAPE OF SOLID TUMORS WITH TERTIARY LYMPHOID STRUCTURES

Maria-Fernanda Senosain*, RJ Seager, Erik Van Roey, Shuang Gao, Mary Nesline, Jeffrey Conroy, Sarabjot Pabla. *Labcorp/Omniseq, Nashville, TN, USA*

Background Tertiary lymphoid structures (TLS) are lymphoid organs that develop in non-lymphoid structures in chronically inflamed areas such as tumors. These organized aggregates of T and B cells have the potential to be used as prognostic and predictive cancer factors and could even be targeted for activation and differentiation to increase the antitumor immune response. One current challenge is to identify TLS biomarkers that can discriminate between tumors with strong immune infiltration and those with true TLS structures. In this study, we identified genes and pathways that could potentially be used to categorize tumors as TLS-positive.

Methods Targeted RNA-seq of 398 immune genes was performed on 167 FFPE tumors representing 5 histologies, composed of melanoma (51.5%), lung cancer (29.9%), kidney cancer (16.2%), bladder cancer (1.8%), and head and neck cancer (0.6%). These tumors had different degrees of T-cell immune infiltration patterns as determined by H&E and CD8 IHC review: TLSs (14.4%), strongly infiltrating (7.2%), infiltrating apparent (29.9%), infiltrating not apparent (22.2%), and not infiltrating (26.3%). We then identified differentially expressed genes comparing TLS-positive tumors with TLS-negative tumors (including infiltration patterns), and TLS-positive tumors with strongly infiltrated tumors, followed by pathway analysis with the REACTOME database.

Results When comparing TLS-positive with TLS-negative tumors, TLS-positive tumors were significantly enriched in pathways associated with the adaptive immune system and T cell receptor signaling, whereas TLS-negative tumors were enriched in cytokine and interferon signaling. Crucially, when comparing TLS-positive tumors with strongly infiltrated tumors, we observed that TLS-positive tumors were significantly enriched in pathways associated with cell cycle, mitosis, and proliferation signaling hinting at active antigen recognition and anti-tumor response.

Conclusions Our results suggest that tumors with TLS have an upregulation of pathways associated with cell cycle and proliferation, and downregulation of interferon and cytokine signaling pathways compared to strongly immune infiltrated tumors without TLS. Genes associated with these pathways could be potential biomarkers for use in identifying TLS-positive tumors. Future directions are to continue the refinement of these signatures using larger datasets, and explore their value in predicting clinical outcomes in patients treated with immune checkpoint therapy.

<http://dx.doi.org/10.1136/jitc-2022-SITC2022.0152>

CLINICAL IMPLICATION OF EXHAUSTIVE T-CELL ENVIRONMENT IN UVEAL MELANOMA PATIENTS

¹Mithalesh Singh*, ²Seema Kashyap, ²Nikhil Kumar, ²Jayanti Jha, ²Neiwete Lomi, ²Lata Singh. ¹University of California, Irvine, CA, USA; ²All India Institute of Medical Sciences, New Delhi, India

Background Despite recent advancements in the clinical use of immunotherapies, the role of exhausted T cells in the immunobiology of uveal melanoma is still unclear. Exhausted T lymphocytes in the tumor microenvironment exhibit activation of inhibitory receptors, decreased effector cytokine production, and cytolytic activity, resulting in failure of cancer cell elimination. Therefore, the goal of this study was to examine the predictive value of LAG3, CTLA-4, and T-cell markers (CD4, CD8, CD3, and FOXP3) expression in UM patients.

Methods Prospective analysis of 54 UM tumor and blood specimens were taken for this study. Immunohistochemical analysis of exhausted T-cell targets (LAG3 and CTLA-4), and T-cell markers (CD3, CD4, CD8, and FOXP3) were performed on formalin-fixed paraffin-embedded specimens, and expression of exhausted T-cell targets were validated by western blotting. Transcriptional analysis was investigated by qRT-PCR on all the cases for *LAG3* and *CTLA-4* genes. We also checked the expression of CTLA-4, CCR8, and LAG3 at serum levels by sandwich-ELISA assay. Statistical analysis was performed to correlate tumor targets with clinicopathological parameters and patient outcomes.

Results CD3, CD4, CD8, and FOXP3 expression was found in 41%, 35%, 50%, and 39% of the patients, respectively. TIL-positive UM appears to have more CD8-positive cells than other TIL markers. Furthermore, patients lacking nBAP1 who had these TILs exhibited aggressive behavior, which may be associated to shorter metastasis-free survival (MFS). LAG3 and CTLA-4 expression was found in both tumor cells and the lymphocytic environment of UM tissues. Higher LAG3 expression was found to be statistically significant with the presence of epithelioid cells ($p=0.033$), a high mitotic count ($p=0.006$), CD34 positive ($p=0.001$), and nBAP1 loss ($p=0.007$), respectively. While CTLA-4 expression was associated with ciliary body invasion ($p=0.013$) and CD34 positivity ($p=0.031$). Similarly, to protein expression, increased mRNA expression of *LAG3* and *CTLA-4* gene was found in high-risk UM. sLAG3 was considerably higher in metastatic UM (MUM) than in primary UM (PUM) ($p<0.001$). sCCR8 levels were significantly lower in MUM ($p<0.05$) than in PUM. Our data suggest that MFS rates were 60% and 57% in patients having LAG3 immunoexpression and BAP1 loss, respectively. MFS rates were 80% and 56%, respectively, for those who had mRNA expression of *LAG3* and *CTLA-4* with nBAP1 loss.

Conclusions Our findings suggest LAG3 as a promising biomarker to specifically identify functionally exhausted T cells and has a prognostic significance in UM.

Ethics Approval This study was approved by Institute's Ethical Committee, AIIMS (Ref. No. IEC-424/RP-6/2016)

Consent Written consent was obtained from all the patient's guardian

<http://dx.doi.org/10.1136/jitc-2022-SITC2022.0153>

154

GENERATION OF HUMANIZED MOUSE MODELS FOR THE PRECLINICAL EVALUATION OF NOVEL IMMUNE CHECKPOINT INHIBITORS, IMMUNE CELL ENGAGERS AND CELL THERAPIES

Maria Stecklum, Annika Wulf-Goldenberg, Bernadette Brzezicha, Christian Rupp*, Wolfgang Walther, Jens Hoffmann. *Experimental Pharmacology and Oncology Berlin-Buch GmbH, Berlin-Buch, Germany*

Background The preclinical evaluation of many novel immune therapies requires the use mouse models with a functional human immune system. In previous studies we have demonstrated that either peripheral blood mononuclear cells (PBMCs) or subpopulations of PBMCs such as T- and NK-cells or hematopoietic stem cells (HSC) can be used to establish a humanized immune system in immunodeficient mice system with functional T-, B-, and NK cells as well as monocytes and dendritic cells. By transplanting either cell-line or patient-derived tumor xenografts into humanized mice, we successfully generated a fully human tumor-immune-cell model for several tumor entities. Finally, we validated the functionality of these models using either immune-checkpoint inhibitors, cell therapies, or immune cell engagers.

Methods HSC-humanized mice were generated by i.v. injection of CD34+ stem cells into immunodeficient NOG mice. PBMCs or enriched T- or NK-cell populations from a curated set of blood donors were used to humanize mice by either single or multiple i.v. injections. CDX and PDX models from different entities (i.e. lymphoma, neuroblastoma, and breast cancer) were transplanted into these humanized mice which were used to evaluate novel immune therapy options. The presence of immune cells and their activation status was analyzed by flow cytometry in blood and tumor samples

Results Injected HSCs successfully engrafted and established a functional human immune system with proliferating and differentiating immune cell populations. Fourteen weeks after injection, up to 20% of the human immune cells in the blood were functional T-cells. Several CDX and PDX models successfully engrafted in these humanized mice without significant differences regarding tumor growth compared to non-humanized mice. Checkpoint inhibitor treatment led to tumor growth delay in selected models and flow cytometry analysis of tumor samples revealed a high number of tumor infiltrating T-cells. A comparison of checkpoint inhibitor activity in a pancreatic cancer PDX model using four different humanized mouse models in parallel (HSC, PBMC, T-or NK cell humanized) revealed most convincing results in terms of tumor growth inhibition for the HSC humanized model.

Conclusions We have established fully human tumor-immune-cell models for different tumor entities in combination with different donor derived immune cell subsets as effector cells and have demonstrated successful long term engraftment of HSCs. All models have been used for the evaluation of either novel checkpoint inhibitors, cell therapies or immune cell engagers and will allow preclinical and translational studies for the identification of novel therapy options, drug combinations and biomarkers.

<http://dx.doi.org/10.1136/jitc-2022-SITC2022.0154>

MHC CLASS I ANTIGEN PRESENTATION IS ASSOCIATED WITH AN INFLAMED SCLC TUMOR MICROENVIRONMENT CHARACTERIZED BY A HIGHER DENSITY OF CYTOTOXIC T-CELLS IN CLOSER PROXIMITY TO TUMOR CELLS

Markus Schick*, Miljenka Vuko*, Mingchao Xie, Monica Azqueta Gavaldon, Felix Segerer, Andreas Spitzmüller, Harald Hessel, Marco Testori, Johannes Zimmermann, Michael Surace, Mari Heininen-Brown, Jaime Rodriguez Canales, Shashank Saran, Helen Angell, Guenter Schmidt, Hadassah Sade, J Carl Barrett, Giulia Fabbri. *AstrZeneca, Munich, Germany*

Background Small cell lung cancer (SCLC) is generally known to exclude immune cells and durable responses to immunotherapies are rare. Only very few biomarkers to inform immuno-oncology (IO) treatments are established in clinical practice thus far. Recently, four major SCLC subtypes (SCLC-A, SCLC-N, SCLC-P and SCLC-I) were described. Whereas the first three are characterized by activation of specific transcription factors, the SCLC-I (inflamed) subtype is characterized by an inflamed gene signature, high expression of MHC class I (MHC-I) antigen presentation and shows the greatest benefit from addition of immunotherapy to chemotherapy treatment [1,2]. Importantly, MHC-I is epigenetically silenced in the vast majority of SCLC and the presence of MHC-I could serve as a biomarker for the identification of SCLC-I cases. [2]. Here, we aimed to assess the biology of MHC-I high SCLC cases to investigate its role as a biomarker to inform cancer immunotherapies.

Methods We combined the power of artificial intelligence (AI)-driven computational pathology with multiplex immunofluorescence (mIF) to gain critical insight into the tumor microenvironment (TME) of SCLC. 125 SCLC formalin-fixed, paraffin-embedded tissue samples were stained with a mIF panel consisting of six markers: PanCK, CD8, CD68, PD-1, PD-L1, and Ki67. We assessed the phenotype and spatial location of each cell in the pathologist-annotated tumor center and within the AI-segmented stroma and tumor epithelium. Pathologists classified immunohistochemically stained MHC-I slides from the same tissue blocks as MHC-I high, medium, or low according to their H-scores (low: ≤ 30 ; medium: 31–139; high: ≥ 140). TME characteristics between those groups were compared.

Results In all measured regions, we found higher densities of CD8+ and particularly PD-1/CD8 double positive T-cells in the MHC-I high group. Moreover, we observed the highest proportion of PD-1 positivity among cytotoxic T-cells in the tumor epithelium of MHC-I high samples, which also showed a high density of PD-L1+ tumor cells. Average distance of PD-1+ T-cells to their nearest tumor cell was lowest in the MHC-I high group. In the same group, an average of 19.3% of tumor cells in the epithelium had at least one PD-1+ T-cell within a 50 μm radius, while in the MHC-I low group this average was only 8.9%.

Conclusions We utilized cutting-edge computational pathology to establish MHC-I as orchestrator of the composition and spatial arrangement of an inflamed SCLC TME. Beyond that, our findings corroborate the role of MHC-I as a potential biomarker for inflamed SCLC cases, which benefit most from cancer immunotherapies.

REFERENCES

1. Gay CM, Stewart CA, Park EM, Diao L, Groves SM, Heeke S, Nabet BY, Fujimoto J, Solis LM, Lu W, Xi Y, Cardnell RJ, Wang Q, Fabbri G, Cargill KR, Vokes NI, Ramkumar K, Zhang B, Della Corte CM, Robson P, Swisher SG, Roth JA, Glisson BS, Shames DS, Wistuba II, Wang J, Quaranta V, Minna J, Heymach JV, Byers LA. Patterns of transcription factor programs and immune pathway activation define

four major subtypes of SCLC with distinct therapeutic vulnerabilities. *Cancer Cell*. 2021 Mar 8;39(3):346–360.e7. doi: 10.1016/j.ccell.2020.12.014. Epub 2021 Jan 21. PMID: 33482121; PMCID: PMC8143037.

2. Mahadevan NR, Knelson EH, Wolff JO, Vajdi A, Saigi M, Campisi M, Hong D, Thai TC, Piel B, Han S, Reinhold BB, Duke-Cohan JS, Poitras MJ, Taus LJ, Lizotte PH, Portell A, Quadros V, Santucci AD, Murayama T, Cañadas I, Kitajima S, Akitsu A, Fridrikh M, Watanabe H, Reardon B, Gokhale PC, Pawletz CP, Awad MM, Van Allen EM, Lako A, Wang XT, Chen B, Hong F, Sholl LM, Tolstourov MY, Pfaff K, Jänne PA, Gjini E, Edwards R, Rodig S, Reinherz EL, Oser MG, Barbie DA. Intrinsic Immunogenicity of Small Cell Lung Carcinoma Revealed by Its Cellular Plasticity. *Cancer Discov*. 2021 Aug;11(8):1952–1969. doi: 10.1158/2159-8290.CD-20-0913. Epub 2021 Mar 11. PMID: 33707236; PMCID: PMC8338750.

Ethics Approval All samples from which data in this report were generated, were obtained from an internal repository. All protocols, amendments, and participant informed consent documents were approved by the appropriate institutional review boards.

<http://dx.doi.org/10.1136/jitc-2022-SITC2022.0155>

156 ESTABLISHMENT OF AN IMMUNE CELL PHENOTYPING MULTIPLEXED IMMUNOFLUORESCENCE ASSAY AND DIGITAL IMAGE ANALYSIS WORKFLOW TO INVESTIGATE THE TUMOR MICROENVIRONMENT IN SOLID TUMORS

Dirk Zielinski, Suso Platero*. *Discovery Life Sciences, Kassel, Germany*

Background The advent of immune-oncology had a significant impact on the stratification of cancer patients, in the past few years. Immune phenotyping of the tumor microenvironment is becoming a tool for the identification of novel predictive biomarkers for cancer immunotherapy. One promising approach is the usage of multiplexed immunofluorescence (mIF) assays for the semi-quantitative assessment of spatial distribution patterns.

Methods Akoya's Opal fluorophores were optimized for the Ventana Discovery ULTRA for use with human control tissues as well as several cancer tumors. The panel consisted of CD4 (clone SP35), CD8 (clone C8/144B), CD68 (clone PG-M1), FoxP3 (clone SP97), PD-L1 (clone SP263) and pan-Cytokeratin (clones AE1/AE3). Each marker was independently validated using single plex bright field immunohistochemistry and adequate stripping efficiency, of the previous applied primary and secondary antibody complex, was confirmed.

Automated image analysis was performed using a workflow of several custom Visiopharm applications, after optimization of segmentation in regions of interest, like tumor invasive margins, or surrounding microenvironment.

Results 6-plex mIF, followed by automated image analysis, was performed in controls and cancer tissue. The ability to multiplex allows for the detection of new immunophenotypes in the tumor and surrounding microenvironment. Such phenotypes, together with the validation of the markers and the image analysis workflow will be presented.

Conclusions Individual mIF immune marker panels and automated image analysis identify a broad number of different immune phenotypes, including rare double- or triple-positive cell subtypes, yielding new insights into the complexity of the tumor microenvironment. Such results could in the future improve cancer patient stratification in immunotherapy.

<http://dx.doi.org/10.1136/jitc-2022-SITC2022.0156>

157

INTERROGATION OF THE TUMOR IMMUNE MICROENVIRONMENT AND *EX VIVO* PROFILING OF PD-1 BLOCKADE USING THE 3D-EXPLORE *EX VIVO* PLATFORM OF FRESH PATIENT TUMOR TISSUE

Brittney Ruedlinger*, Jasmin D'Andrea, Jared Ehrhart, Soner Altioik. *Nilogen Oncosystems, Tampa, FL, USA*

Background The patient derived 3D-EXplore *ex vivo* platform that incorporates features of the tumor microenvironment provides the multifaceted approach required to model the dynamic response to immune checkpoint blockade. For many patients resistance to PD-1/PD-L1 blockade remains a challenge and new approaches are needed to guide treatment. Here, we demonstrate feasibility of the 3D-EXplore platform utilizing fresh patient tumoroids to interrogate the impact of PD-1 blockade on the tumor immune microenvironment in Non-Small Cell Lung Cancer (NSCLC).

Methods Tumoroids measuring 150 μm in size were generated using a proprietary mechanical process without any enzymatic digestion or propagation from fresh NSCLC samples (n=70). This study was approved by Vanderbilt University Ethics Board; approval number 031078 and Ohio State University Ethics Board: 2014J0130. 3D-EXplore *ex vivo* studies were performed with anti-PD-1 monoclonal antibodies nivolumab or pembrolizumab and multiparameter flow cytometry analysis was carried out to assess the treatment-mediated changes in the tumor resident T lymphocytes, Tregs, NK/NKT and myeloid cell populations. Furthermore, we performed multiplex cytokine release assays with supernatants collected from the *ex vivo* treated tumoroid cultures.

Results Multiplex flow cytometric analysis demonstrated the heterogeneity of the tumor immune cell populations including myelomonocytic and leukocyte lineages in different patient tumor samples. 3D *ex vivo* samples treated with nivolumab and pembrolizumab demonstrated PD1 occupation on CD3 T-cells, while approximately 20% of tumors showed increased CD8 T-cell activation upon *ex vivo* treatment that correlated with proinflammatory cytokine release in the conditioned media. The *ex vivo* response to PD1 inhibitors was correlated with changes in the expression of other immune checkpoint proteins, such as CTLA4, immune scoring, tumor mutation burden, tumor pathologic stage, and PD-L1 expression assessed by E1L3N IHC in FFPE tumor sections.

Conclusions Our data demonstrated that 3D-EXplore is as a clinically relevant platform for examining the efficacy of immunotherapeutic interventions. As shown here, PD-1 blockade had tumor and donor specific treatment efficacies with respect to overcoming the suppressive tumor environments. Furthermore, the 3D-EXplore platform provides keen insight into the intact tumor microenvironments, facilitating the development and efficacy of immunotherapeutic agents in cancer.

Ethics Approval All tissues in the study were collected under patient consent approval by Vanderbilt University Ethics Board; approval number 031078 and Ohio State University Ethics Board: 2014J0130

<http://dx.doi.org/10.1136/jitc-2022-SITC2022.0157>

158

A NOVEL, HIGHLY ACCURATE LIQUID BIOPSY-BASED GLYCOPROTEOMIC PREDICTOR OF CHECKPOINT INHIBITOR TREATMENT BENEFIT IN ADVANCED NON-SMALL CELL LUNG CANCER

Klaus Lindpaintner*, Apoorva Srinivasan, Alan Mitchell, Apurva Dixit, Gege Xu, Xin Cong, Daniel Serie. *InteVenn Bioscience, South San Francisco, CA, USA*

Background Protein glycosylation is the most abundant and complex form of post-translational protein modification. Glycosylation profoundly affects protein structure, conformation, and function. The elucidation of the potential role of differential protein glycosylation as biomarkers has been limited by the technical complexity of generating and interpreting this information. We have recently established a novel, powerful platform that combines liquid chromatography-mass spectrometry with a proprietary artificial-intelligence-based data processing engine that allows, for the first time, highly scalable interrogation of the glycoproteome. Here we report the performance of this platform to predict likely benefit from immune-checkpoint inhibitor (ICI) therapy in advanced non-small cell lung cancer (NSCLC).

Methods Our platform was utilized to assess 532 glycopeptide (GP) and peptide signatures representing 75 serum proteins in pretreatment blood samples from a cohort of 125 individuals (54 females, 71 males, age range 60 to 75 years). Inclusion criteria were as follows: a diagnosis of unresectable stage 3 or 4 NSCLC, treatment with pembrolizumab monotherapy (27 patients), or treatment with combination pembrolizumab-chemotherapy (98 patients). Overall survival (OS) data were available for all patients. Samples and de-identified clinical data were obtained from Tempus Labs (Chicago, IL).

Results A multivariable-model-based classifier for OS was created utilizing 70% of the cohort as a training set and seven glycopeptide and non-glycosylated peptide biomarker features selected from a generalized additive model. The classifier yielded a hazard ratio (HR) for prediction of likely ICI benefit of 3.96 at $p < 0.0001$. Additionally, the classifier was validated using a test set comprised of the withheld 30% of patients, yielding a HR of 3.86 at $p < 0.01$ which separated patients likely benefiting from ICI therapy from those likely not benefiting from ICI therapy (median OS of 23.2 vs. 5.9 months, respectively, based on classifier score above/below cutoff).

Conclusions The glycoproteomic classifier described here predicts with high sensitivity which patients are likely to benefit from ICI therapy. In addition to potentially reducing the use of ICIs in a safe manner in patients who would be unnecessarily subjected to possible adverse drug reactions, our classifier simultaneously has the potential of reducing the burden of health care expenditures. Our results indicate that glycoproteomics holds a strong promise as a predictor for ICI treatment benefit which appears to significantly outperform other currently pursued biomarker approaches.

Ethics Approval The study was conducted under IRB approval obtained by Tempus Labs, with all patients involved providing informed consent for the use of their blood samples for biomarker research.

<http://dx.doi.org/10.1136/jitc-2022-SITC2022.0158>

Abstracts

159

XERNA TUMOR MICROENVIRONMENT SUBTYPES AS A BIOMARKER IN LUNG CANCER PATIENTS

¹Mark Landers*, ¹Patrick Eimerman, ¹Steve Mastrian, ¹Tracey White, ¹Janine LoBello, ¹Gargi Basu, ¹Szabolcs Szelinger, ¹Jessica Aldrich, ¹Matthew Halbert, ¹Jess Hoag, ¹David Hall, ²Farjana Fattah, ³Daniel Pointing, ³Luka Ausec, ³Anze Gregorc, ⁴Seema Iyer, ⁴Mark Uhlik, ⁴Laura Benjamin, ¹Rick Baehner. ¹Exact Sciences, Madison, WI, USA; ²Simmons Comprehensive Cancer Center, UT Southwestern, Dallas, TX, USA; ³Genialis Inc., New York, NY, USA; ⁴OncXerna Therapeutics, Waltham, MA, USA

Background Despite immune checkpoint inhibitor (ICI) monotherapy approvals in NSCLC, SOC predominately utilizes combinations of ICI with non-targeted chemotherapy or precision therapies targeting oncogenic drivers. Biomarkers guiding these clinical decisions rely on tumor genotyping to identify actionable mutations, tumor mutational burden (TMB) and on immunohistochemistry for PD-L1 expression. Currently, neither PD-L1 nor TMB perform adequately for ICI patient selection.¹ Emerging evidence indicates a more complete profile of the tumor microenvironment (TME) may improve selection of patients likely to respond to ICI.² The Xerna machine learning-based RNA sequencing biomarker assay classifies tumors into four TME subtypes; Immune Active (IA), Immune Suppressed (IS), Immune Desert (ID) and Angiogenic (A). This classification identifies tumors likely to benefit from ICI (IA and IS) or anti-angiogenic agents (ID and A).³ We examined the distribution of actionable oncogenic driver mutations across Xerna TME subtypes to investigate the potential use for therapy selection.

Methods Biomarker prevalence, and Xerna TME subtype classification, were determined for 104 metastatic lung cancer cases previously analyzed using the Oncomap™ ExTra test, tumor-normal whole-exome and whole-transcriptome sequencing. DNA variants and high TMB (≥10 mut/Mb) were identified from DNA sequencing, and RNA expression levels were used to assign tumors to Xerna subtypes. Biomarker and associations were compared using Fisher’s Exact Test. The study was approved by WCG IRB Ethics Board, approval number 20181863.

Results In total, 53% of cases had high (IA+IS) vs. low (ID+A) Xerna immune subtypes and 60% harbored targetable oncogenic driver mutations (table 1). Actionable EGFR and KRAS mutations were detected in 31% and 20% of cases respectively, while high TMB was detected in 27% of cases. High TMB was significantly higher in IA (62%) vs. IS (14%) or A (13%) categories (p<0.05). Although no significant associations between Xerna subtype and oncogenic drivers were observed, EGFR mutations were least frequent in IA tumors (15%) while 33% of the IS subtype contained KRAS mutations (10% G12C).

Conclusions The Xerna TME panel identified a high prevalence of patients who may benefit from ICI (IA+IS) and harbored actionable oncogenic drivers. Within this group, the prevalence of targetable oncogenic drivers within the IS phenotype, such as KRAS G12C, may represent the potential for novel ICI combination therapies.⁴ These findings further highlight the importance of adding TME analysis to comprehensive biomarker testing in NSCLC

REFERENCES

1. Steuer CE, Ramalingam SS. Advances in Immunotherapy and Implications for Current Practice in Non-Small-Cell Lung Cancer. *JCO Oncol Pract.* 2021 Nov;**17**(11):662–668. doi: 10.1200/OP.21.00305. Epub 2021 Jun 25. Erratum in: *JCO Oncol Pract.* 2022 Mar;**18**(3):244.

2. Horvath L, Thienpont B, Zhao L, Wolf D, Pircher A. Overcoming immunotherapy resistance in non-small cell lung cancer (NSCLC) – novel approaches and future outlook. *Mol Cancer.* 2020 Sep 11;**19**(1):141.
 3. Iyer, S., Ausec, L., Pointing, D., Zganec, M., Cvitkovic, R., Stajdohar, M., ... & Uhlik, M. T. (2022). Xerna? TME Panel: A pan-cancer RNA-based investigational assay designed to predict patient responses to angiogenic and immune targeted therapies. *Cancer Research*, **82**(12_Supplement), 1232–1232.
 4. Mugarza E, van Maldegem F, Boumelha J, Moore C, Rana S, Llorian Sopena M, East P, Ambler R, Anastasiou P, Romero-Clavijo P, Valand K, Cole M, Molina-Arcas M, Downward J. Therapeutic KRASG12C?inhibition drives effective interferon-mediated antitumor immunity in immunogenic lung cancers. *Sci Adv.* 2022 Jul 22;**8**(29)

Ethics Approval The study was approved by WCG IRB Ethics Board, approval number 20181863.

Abstract 159 Table 1 Actionable genomic biomarkers across Xerna TME subtypes

Table 1: Actionable genomic biomarkers across Xerna TME categories

Biomarker*	Xerna category					
	A (n=15)	IA (n=13)	ID (n=34)	IS (n=42)	Immune score high IA+IS (n=55)	Immune score low ID+A (n=49)
TMB high	7 (13.3%)	8 (61.5%)	12 (35.3%)	6 (14.3%)	14 (25.5%)	14 (28.6%)
EGFR	7 (46.7%)	2 (15.4%)	7 (20.6%)	16 (38.1%)	18 (32.7%)	14 (28.6%)
KRAS	2 (13.3%)	1 (7.7%)	4 (11.8%)	14 (33.3%)	15 (27.3%)	6 (12.2%)
BRAF	0 (0.0%)	0 (0.0%)	2 (5.9%)	1 (2.4%)	1 (1.8%)	2 (4.1%)
MET	1 (6.7%)	0 (0.0%)	0 (0.0%)	1 (2.4%)	1 (1.8%)	1 (2.0%)
RET	0 (0.0%)	1 (7.7%)	0 (0.0%)	1 (2.4%)	2 (3.6%)	0 (0.0%)
FGFR1/2/3	0 (0.0%)	1 (7.7%)	0 (0.0%)	1 (2.4%)	2 (3.6%)	0 (0.0%)

*Biomarkers not observed ALK, DDR2, ERBB2, NTRK1, PIK3CA, PTEN, ROS
 Xerna TME subtypes: A=Angiogenic, IA=Immune Active, ID=Immune Desert, IS=Immune Suppressed

<http://dx.doi.org/10.1136/jitc-2022-SITC2022.0159>

160

NOVEL, HIGH-PLEX, AND FLEXIBLE BIOMARKER PANELS FOR RAPID DEVELOPMENT OF SPATIAL SIGNATURES TO IMPROVE STRATIFICATION OF RESPONSE TO COMBINATION THERAPIES

Rachel Schaefer*, Jacob Circelli, Oscar Perez, Linying Liu, Michael McLane, Yi Zheng. *Akoya Biosciences, Marlborough, MA, USA*

Background Pre-clinical and clinical studies into new checkpoints as therapeutic targets have raised the possibility that combining immune checkpoint inhibitors or other immunotherapies may be an effective strategy in improving both the response and survival rates. The development of clinically useful biomarkers to select responders for combination therapies will be critical for the advancement of such treatments. Profiling the tumor microenvironment (TME) by assessing spatial relationships and protein co-expression within specific cellular subsets could lead to improved patient stratification of response to these combination therapies. To provide researchers with an end-to-end, automated workflow for the functional evaluation of tumors in the context of patient immunity, we have developed a new single-cell multiplexed staining method.

Methods PhenoCode Signature panels utilize barcode-based antibody labeling chemistry, allowing primary antibodies to be applied as a cocktail in a single incubation step followed by amplified detection using Opal fluorescent dye technology. These panels feature a flexible design component allowing for the easy integration of a novel checkpoint or immune cell marker into a 5-plex panel, resulting in the detection of up to six biomarkers simultaneously on a single tissue section. Human formalin-fixed, paraffin-embedded (FFPE) lung cancer tissues were stained using the PhenoCode Signature panels and DAB. Staining was performed on the Leica BOND RX™ automated stainer. Multispectral imaging was performed on the PhenoImager® platform, and image analysis was performed with a phenotyping algorithm in inForm® software. Intensity analysis was performed in R using Phenoptr and PhenoptrReports.

Results Three PhenoCode Signature 6-plex panels were developed and applied to lung cancer samples to help characterize distinct immune landscapes. We demonstrate a fully automated, yet robust and flexible workflow for assessing spatial relationships and profiling the tumor microenvironment. The staining of each marker within the panels qualitatively matches chromogenic DAB staining. High assay reproducibility was demonstrated by both qualitative and quantitative analysis of staining quality. Single markers were substituted from each panel to show the flexibility of the panel design.

Conclusions In this study, we demonstrate the utility of three 6-plex PhenoCode Signature panels for easy and reproducible profiling of the TME. The flexible design component of the panels allows for the substitution of a single biomarker enabling the rapid assessment of additional cell phenotypes. The flexible configuration combined with shortened assay development time are designed to enable researchers to rapidly develop more predictive spatial phenotypic signatures, aiding in the development of more targeted combination immunotherapies

<http://dx.doi.org/10.1136/jitc-2022-SITC2022.0160>

161

SINGLE-CELL SPATIAL IN SITU TRANSCRIPTOMICS UNRAVELS VULVAR HSIL COMPOSITION ASSOCIATED WITH COMPLETE RESPONSE TO THERAPEUTIC VACCINATION

¹Ziena Abdulrahman*, ²Mariette IE van Poelgeest, ²Marij JP Welters, ¹Sjoerd H van der Burg. ¹Leiden University Medical Center, Oncode, Leiden, Netherlands; ²Leiden University Medical Center, Leiden, Netherlands

Background Vulvar High-grade Squamous Intraepithelial Lesion (vHSIL) is predominantly induced by high-risk Human Papilloma Virus type 16 (HPV16). In two independent trials, therapeutic vaccination against the HPV16 E6 and E7 oncoproteins resulted in objective partial and complete responses in half of the HPV16+ vHSIL patients at 12 months follow-up. Here, the pre-vaccination vHSIL tumor microenvironment in relation to the vaccine-induced clinical response was in-depth investigated.

Methods A unique novel high-plex spatial molecular imaging technique, CosMx (Nanostring), was applied, which for the first time allows the visualization of 1000 RNA transcripts at a subcellular resolution in situ on FFPE pre-immunotherapy tissue, using cyclic fluorescent in situ hybridization. This allowed both the discovery of new cell types in the tumor microenvironment of vHSIL, as well as the investigation of their spatial interactions. We studied a cohort of 20 pre-immunotherapy vHSIL samples, 6 complete responders, 7 partial responders and 7 non-responders. Data was analyzed with the R Giotto package for spatial transcriptomics, applying unsupervised clustering for cell identification and machine learning to unravel spatial patterns in the tissue.

Results The tumor microenvironment of complete responders is characterized by the presence of distinct pro-inflammatory dendritic cells, macrophages and T cells, whereas these cells are scarce in non-responders. Moreover, also the spatial composition of these patient groups differed significantly, the tumor microenvironment of complete responders harbors direct spatial interactions between pro-inflammatory innate and adaptive immune cells indicating an adequate ongoing anti-tumor immune response, which is lacking in non-responders.

Conclusions Single-cell in situ transcriptomics identified the key importance of multiple pro-inflammatory immune cell types for response of vHSIL to therapeutic vaccination, as well as the importance of the spatial organisation of these immune cells in order to be able to execute their pro-inflammatory function. This indicates that a well coordinated immune response on multiple levels, i.e. having sufficient numbers of both pro-inflammatory myeloid and lymphoid cells, as well as their spatial architecture, is pivotal for successful response to immunotherapy.

Ethics Approval Ethics approval was provided by the Leiden University Medical Center. Patients were included in this study after providing written informed consent. This study was conducted in accordance with the Declaration of Helsinki and in accordance with Dutch law.

<http://dx.doi.org/10.1136/jitc-2022-SITC2022.0161>

162

DETECTING T-CELL REINVIGORATION AND PERSISTENCE USING PATIENT DERIVED EX VIVO THREE-DIMENSIONAL SPHEROID MODELS

Katy Lassahn*, Ashley Elrod, Tessa DesRochers, Kathryn Appleton. *Kiyatec, Greenville, SC, USA*

Background Immune checkpoint blockade is shifting the paradigm for cancer treatment. However, this class of therapeutics is limited by insufficient or dysfunctional antitumor T-cells with impaired memory formation. Adoptive cell therapy is a treatment option for patients with exhausted resident T-cells, yet the effective use of this immunotherapy for the treatment of solid tumors is still in early stages. A durable patient response is possible when T-cell products successfully persist following recursive tumor cell exposure and resist differentiation and exhaustion.¹ Due to the variability of personalized cellular immunotherapies, verification of T-cell function would facilitate selection of the most desirable product for clinical use. Herein, we report a tissue agnostic ex vivo three-dimensional model which recapitulates the tumor microenvironment for the assessment of T-cell performance.

Methods Spheroids were generated using primary patient-derived tumor cells or patient-derived xenografts and cultured with immune cells, expanded tumor-infiltrating lymphocytes or CAR-Ts. Reinvigoration was determined via increased T-cell activation and proliferation as detected by flow cytometry. Low effector to target ratios were utilized to mimic a high tumor burden. T-cell persistence was tested following multiple rounds of tumor cell challenge in a repetitive antigen exposure assay. Granzyme B levels, degranulation and annexin V were evaluated to measure antitumor efficacy. T-cell susceptibility to differentiate was determined by detecting memory markers CD62L and CCR7. Finally, T-cell products that were prone to exhaustion were identified by monitoring expression of checkpoint proteins.

Results Patient samples capable of reinvigoration responded to PD-1 blockade as determined by increases in T-cell proliferation, 4-1BB, and degranulation. Decreased expression of the memory markers CD62L and CCR7 was observed on CD45RO+/CD8+ T-cells when challenged with high tumor burden, but not with low tumor burden exposure. Responding T-cells persisted with higher absolute numbers compared to low tumor burden models. Using our repetitive antigen challenge platform, we detected no significant change in T-cell function with a single rechallenge of tumor cell exposure. Upon multiple challenges, varying degrees of T-cell degranulation, granzyme B levels, and T-cell viability were observed compared to lesser challenged T-cells demonstrating inherent differences in donor T-cell persistence.

Conclusions This complex three-dimensional platform has the ability to 1) test patient-specific T-cell reinvigoration and 2) closely monitor and assess candidate cell therapy products during development. This platform can provide a cost-effective method to expedite new cell therapy products through pre-clinical pipelines.

REFERENCES

1. Wagner J, Wickman E, DeRenzo C, Gottschalk S. CAR T Cell Therapy for Solid Tumors: Bright Future or Dark Reality? *Mol Ther*. 2020;**28**(11):2320–39.

Ethics Approval Written informed consent was obtained from patients in accordance with the Institutional Review Board (IRB) approved biology protocols by Prisma Health, formally known as Greenville Health System, Cancer Institute (IRB-

Committee C). Where applicable, additional tissue for this study was procured from commercial vendors who maintain strict ethical compliance, including fully de-identified materials and stringent IRB and Ethics Committee compliance.

<http://dx.doi.org/10.1136/jitc-2022-SITC2022.0162>

IMMUNE-BASED BIOMARKER ACCURATELY PREDICTS RESPONSE TO IMIQUIMOD IMMUNOTHERAPY IN CERVICAL HIGH-GRADE SQUAMOUS INTRAEPITHELIAL LESIONS

<http://dx.doi.org/10.1136/jitc-2022-SITC2022.0163>

¹Ziena Abdulrahman*, ²Natasja Hendriks, ²Arnold J Kruse, ³Antonios Somarakis, ⁴Anna JM van de Sande, ⁴Heleen van Beekhuizen, ³Jurgen MJ Piek, ³Noel FCC de Miranda, ²Loes FS Kooreman, ²Brigitte FM Slangen, ¹Sjoerd H van der Burg, ²Peggy J de Vos van Steenwijk, ⁵Edith MG van Esch. ¹Leiden University Medical Center, Oncode, Leiden, Netherlands; ²Maastricht University Medical Center, Maastricht, Netherlands; ³Leiden University Medical Center, Leiden, Netherlands; ⁴Erasmus University Medical Center, Rotterdam, Netherlands; ⁵Catharina Hospital, Eindhoven, Netherlands

Background The complete response rate of cervical high-grade squamous intraepithelial lesion (cHSIL) patients to imiquimod immunotherapy is 60%. Consequently, many patients are exposed to unnecessary adverse effects of imiquimod. On the other hand, conventional surgical large loop excision therapy is associated with increased risk of premature births in subsequent pregnancies. An in-depth analysis of the cHSIL immune microenvironment was performed in order to identify and develop a predictive biomarker for response to imiquimod, to maximize therapy efficacy and avoid adverse effects in patients unlikely to respond.

Methods Biopsies of 35 cHSIL patients, before and 10 weeks on imiquimod treatment, were comprehensively analyzed by two multispectral seven-color immunofluorescence panels for T cell and myeloid cell composition in relation to treatment response. Based on these results a simplified immunohistochemical detection protocol was developed. Samples were scanned with the Vectra multispectral imaging system, and cells were automatically identified using machine learning.

Results The immune microenvironment of complete responders (CR) prior to imiquimod is characterized by a strong and coordinated infiltration by T helper cells (activated PD1⁺/type 1 Tbet⁺), M1-like macrophages (CD68⁺CD163⁻) and dendritic cells (CD11c⁺). The lesions of non-responders (NR) displayed a high infiltration of CD3⁺FOXP3⁺ regulatory T cells. At 10 weeks on imiquimod treatment, a strong influx of intraepithelial and stromal CD4⁺ T cells was observed in CR but not NR patients. A steep decrease in macrophages occurred both in CR and NR patients, leveling the pre-existing differences in myeloid cell composition between the two groups. Based on the pre-existing immune composition differences, the sum of intraepithelial CD4⁺ T cell, macrophage and dendritic cell counts was used to develop a quantitative simplified one color immunohistochemical biomarker, the CHSIL Immune Biomarker for Imiquimod (CIBI), which can be automatically and unbiasedly quantified and has an excellent predictive capacity (ROC AUC 0.95, p<0.0001).

Conclusions The capacity of cHSIL patients to respond to imiquimod is associated with a pre-existing coordinated local immune process, fostering an imiquimod-mediated increase in local T cell infiltration. The CIBI immunohistochemical biomarker has strong potential to select cHSIL patients with a high likelihood to experience a complete response to imiquimod immunotherapy.

Ethics Approval Ethics approval was provided by all the participating hospitals: Maastricht University Medical Center, Erasmus University Medical Center Rotterdam and Catharina Hospital Eindhoven. Patients were included in this study after providing written informed consent. This study was conducted in accordance with the Declaration of Helsinki and in accordance with Dutch law.

164

EVALUATION OF LIQUID BIOPSY-BASED PLASMA COPY NUMBER BURDEN, DNA METHYLATION AND PERSONALIZED MINIMAL RESIDUAL DISEASE APPROACH FOR MONITORING MOLECULAR RESPONSE TO DIFFERENT DRUG REGIMENS IN METASTATIC COLORECTAL CANCER PATIENT

¹Zheng Feng*, ²Neil Smith, ³Giancarlo Bonora, ²Juergen Scheuenpflug, ³Pan Du. ¹EMD Serono, A business of Merck KGaA, Darmstadt, Germany, Billerica, MA, USA; ²Merck Healthcare KGaA, Darmstadt, Germany, Darmstadt, Germany; ³Predicine, Inc, Hayward, CA, USA

Background Liquid biopsy (LBx) based low pass whole genome sequencing (LP-WGS) derived blood copy number burden (bCNB) with defined clinical cut-offs provides a genome-wide overview for monitoring molecular response. LBx DNA methylation analysis promises sensitivity for monitoring treatment response and possibly provides tissue of origin (TOO) insights. The potential clinical utility of the multi-faceted approaches to monitor molecular response using bCNB and DNA methylation in the metastatic colorectal cancer (mCRC) palliative treatment setting were investigated.

Methods Seventy longitudinal (baseline, on-treatment, and end of treatment (EOT)) plasma samples were collected from 14 mCRC patients treated with chemotherapy (CTx) alone or in combination with one or more targeted agents and PD-L1 blockade (figure 1). bCNB and DNA methylation were analyzed at all timepoints, respectively. bCNB is calculated based on the genome-wide copy number abnormalities, normalized by the LP-WGS profiles from healthy donors. Furthermore, a clinical applicable cut-off can be defined for molecular response monitoring. DNA methylation provides whole-genome methylation profiles using input amounts as low as 1 ng. Personalized MRD which uses patient-specific mutation and fixed panels, was utilized to generate MRD data for the 11 baselines, time points and EOT samples.

Results Using bCNB, eight patients treated with CTx in combination with different therapies such as targeted agents and PD-L1 blockade showed a consistent reduction in tumor burden compared to baseline, with post-treatment bCNB values below the cut-off of 5.2 (log₂) derived from healthy donors (figure 2). DNA Methylation determined TOO, exemplified by the preliminary data detected the enrichment of SMAD4-associated hypermethylated DNA fragments in a patient with metastasis. A cut-off of 9.5 (log₂) was defined based on abnormally methylated fragments, which correlated with bCNB ($R^2=0.83$; figure 2). Additionally, indication specific tiered cut-offs for molecular responses can be defined. Tumor fraction estimates using Personalized MRD showed a correspondence with both bCNB (patient-wise correlation, Pearson $r=0.87$) and abnormal DNA Methylation cut-offs (patient-wise correlation, Pearson $r = 0.82$) for patients with matching data points, respectively.

Conclusions bCNB is a feasible approach for assessing molecular response with cut-off determination, and its low cfDNA input requirement enables clinical utilities. Preliminary data supported that DNA methylation assay detected TOO and demonstrated potential clinically applicable cut-off definitions. bCNB, DNA methylation and Personalized MRD demonstrated concordance and provided a comprehensive suite of solutions for molecular response and MRD monitoring. Collectively, the holistic LBx approaches with clinical applicable cut-off definition would possibly facilitate the selection of patient-centric tailored treatments.

Ethics Approval The study protocol was in accordance with the tenets of the Declaration of Helsinki. Commercial samples used in this study were procured from Indivumed GmbH following protocols approved by the local Institutional Review Board (IRB) committee. Informed consent forms were obtained from all the human subjects in this study.

Consent Written informed consent was obtained from the patient for publication of the abstract and any accompanying images. A copy of the written consent is available for review by the Editor of this journal.

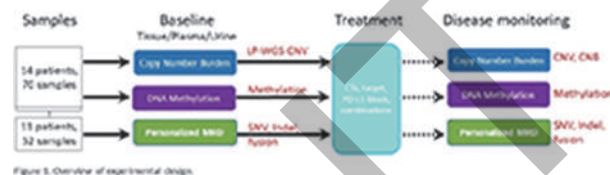


Figure 1. Overview of experimental design.

Abstract 164 Figure 1 Overview of experimental design

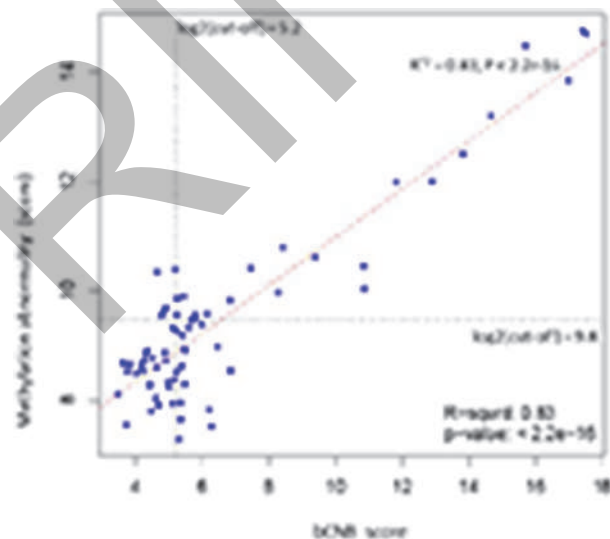


Figure 2. Methylation abnormality scores by plotted against bCNB score show their strong concordance. Vertical and horizontal dashed lines indicate defined cut-off values of each assay.

Abstract 164 Figure 2 Methylation abnormality scores by plotted against bCNB score show their strong concordance. Vertical and horizontal dashed lines indicate defined cut-off values of each assay

<http://dx.doi.org/10.1136/jitc-2022-SITC2022.0164>

165 PAHR: THE PAN-CANCER AHR SIGNATURE PIPELINE

¹Peter Schulz-Knappe, ¹Christiane Opitz*, ²Saskia Trump, ¹Ahmed Sadik. ¹DKFZ, Heidelberg, Germany; ²Charite, Berlin, Germany

<http://dx.doi.org/10.1136/jitc-2022-SITC2022.0165>

Background The ligand-activated transcription factor, AHR (aryl hydrocarbon receptor) is an important regulator of different biological process including angiogenesis, hematopoiesis, drug and lipid metabolism, cell motility, and immune modulation. AHR activating ligands are found in the environment (e. g., dioxin), but are also generated endogenously, for example by tryptophan catabolizing enzymes (e.g., IDO1, TDO2, IL4I1).^{1,2,3} AHR activation can lead to immunosuppression, thus limiting response to therapy. AHR activity is increased in cancer and efforts are ongoing to decipher the AHR-mediated immune modulation in the crosstalk between cancer and the tumor microenvironment.

Methods By combining analysis of gene expression data from over 10,000 tumors in 32 different cancers and natural language processing we developed a pan-cancer AHR transcriptional gene signature (PAHR) that allows detecting the status of AHR activation in a cell and ligand independent manner. We built a plug & play pipeline using PAHR, which employs multiple machine learning methods for AHR target biomarker discovery.

Results Using PAHR, we profiled transcriptomics and amino acid metabolic profiles of 32 different cancers that associate with the production of AHR activating ligands. Furthermore, we used PAHR to characterize AHR specific cancer subtypes showing various AHR-mediated immunosuppressive functions.

In most cancers, the AHR cancer subtypes reflected worse overall survival outcome with increasing AHR activity. Functional characterization of bladder cancer AHR subtypes showed that AHR mediates different transcriptional programs leading to similar survival outcomes using different immunosuppressive modules. Some cancer subtypes showed better survival outcome associated with high AHR activity, indicating that AHR can play both tumor promoting and suppressive roles.

Conclusions PAHR integrative analysis detects different patterns of AHR activities across cancers with significant induction of immunosuppression in cancers leading to the development of distinct patient strata on a pan-cancer level.

We conclude that assessment of AHR-activity by way of PAHR presents as a new stratification strategy in immune oncology. PAHR will improve patient selection in clinical trials, and therapy selection of todays and future cancer immunotherapies to improve response to treatment for the individual patient.

REFERENCES

1. Sadik A, Somarrivas Patterson LF, Öztürk S, Mohapatra SR, ...Trump S, Seiffert M, Opitz CA. IL4I1 Is a Metabolic Immune Checkpoint that Activates the AHR and Promotes Tumor Progression. *Cell*. 2020 Aug 17;50092–8674(20)30946–6.
2. Opitz CA, Litztenburger UM, ..., Wick W, Platten M. An endogenous tumour-promoting ligand of the human aryl hydrocarbon receptor. *Nature*. 2011 Oct 5;478(7368):197–203.
3. Panitz V, Končarević S, Sadik , ...Platten M, Wick W, Opitz CA. Tryptophan metabolism is inversely regulated in the tumor and blood of patients with glioblastoma. *Theranostics*. 2021 Sep 3;11(19):9217–9233.

Ethics Approval Metastatic melanoma samples were obtained from the section of dermatooncology in the National Center for Tumor Diseases (NCT), Heidelberg, Germany, under the ethics board approval S-207/2005. Participants gave informed consent before taking part in the study.

167

COMPREHENSIVE PROFILING OF CANCER-ASSOCIATED FIBROBLASTS IN CD8+ T CELL-EXCLUSIVE NON-SMALL CELL LUNG CANCER TUMOR MICROENVIRONMENTS USING THE NANOSTRING GEOMX® DIGITAL SPATIAL PROFILER

Christina Cho*, Gavitt Woodard, Francesc Lopez-Giraldez, Ti Badri, Matthew Vesely, Lieping Chen. *Yale School of Medicine, New Haven, CT, USA*

Background Cancer-associated fibroblasts (CAFs) are a major component of the non-small cell lung cancer (NSCLC) tumor microenvironment (TME).¹⁻⁴ Recent studies indicate that CAFs play a role in generating a CD8+ T cell (CTL)-exclusive TME.⁵⁻⁹ Given that immune-checkpoint inhibitors (ICIs) rely on CTLs, an abundance of CAFs in the TME may result in reduced ICI efficacy. Although CAFs are considered potential targets for therapy, attempts to deplete CAFs have largely failed.¹⁰ This is due to the fact that CAFs are a heterogeneous population of cells and depletion of the wrong subpopulation could worsen disease.¹ Thus, to enhance ICI efficacy and improve patient outcome, we must identify and target CAF subtypes that promote CTL exclusion. Single-cell RNA sequencing (scRNAseq) has improved our understanding of CAF heterogeneity¹¹⁻¹³; yet this technology cannot provide a comprehensive profile of CAF subtypes within the TME. For scRNAseq, tumor tissues are digested, causing cell death, and the resultant transcriptomic profile is incomplete. To generate a holistic profile of CAF subtypes within NSCLC, and identify the subpopulation that promotes CTL exclusion, we have utilized the GeoMX® Digital Spatial Profiler (DSP)¹⁴⁻¹⁷, a state-of-the-art platform that allows for spatially resolved, high-plexed molecular profiling of intact tumor tissues.

Methods We performed digital spatial profiling on a tissue microarray (TMA) slide containing fifty-five cores of human lung tumors. We performed in-situ hybridization (ISH) on the slide with the GeoMx Whole Transcriptome Atlas (WTA), a mixture of photocleavable oligo-linked RNA probes that covers 18,000+ protein-coding human genes. Next, we stained the slide with fluorescent antibodies against Vimentin (VIM, a CAF marker), CD8, and SYTO (nuclear dye). Each core was a region of interest (ROI), and UV-light was masked to focus on CD8+ and VIM+ areas within each ROI to generate distinct areas of illumination (AOI) that were read out separately. NSG data was analyzed with DESeq2 to identify genes that were differentially expressed in CAFs living in CTL-exclusive tumors.

Results We identified 441 genes that were differentially expressed in CAFs residing in CTL-exclusive tumors compared to CAFs in CTL-inclusive tumors. Ingenuity Pathway Analysis (IPA) of those genes revealed several pathways which were inactivated in CTL-exclusive CAFs, including Leukocyte Extravasation Signaling and Ephrin Receptor Signaling, both of which could contribute to reduced CTL migration and infiltration.

Conclusions The GeoMX DSP can be used to identify CAF subpopulations that contribute to the formation of immune-exclusive TMEs and reveal novel molecular targets for immunotherapy.

REFERENCES

1. Sahai E, Atsaturov I, Cukierman E, et al (2020) A framework for advancing our understanding of cancer-associated fibroblasts. *Nat Rev Cancer* **20**:174–186.
2. Kilvaer TK, Khanekhenari MR, Hellevik T, Al-Saad S, Paulsen E-E, Bremnes RM, Busund L-T, Donnem T, Martinez IZ (2015) Cancer Associated Fibroblasts in Stage I-III NSCLC: Prognostic Impact and Their Correlations with Tumor Molecular Markers. *PLoS One* **10**:e0134965.

3. Schulze AB, Schmidt LH, Heikötter B, et al (2020) Prognostic impact of CD34 and SMA in cancer-associated fibroblasts in stage I-III NSCLC. *Thorac Cancer* **11**:120–129.
4. Li L, Lu G, Liu Y, Gong L, Zheng X, Zheng H, Gu W, Yang L (2021) Low Infiltration of CD8+ PD-L1+ T Cells and M2 Macrophages Predicts Improved Clinical Outcomes After Immune Checkpoint Inhibitor Therapy in Non-Small Cell Lung Carcinoma. *Front Oncol* **11**:1513.
5. Puré E, Lo A (2016) Can targeting stroma pave the way to enhanced antitumor immunity and immunotherapy of solid tumors? *Cancer Immunol Res* **4**:269–278.
6. Kilvaer TK, Rakae M, Hellevik T, Østman A, Strell C, Bremnes RM, Busund LT, Dønnem T, Martinez-Zubiaurre I (2018) Tissue analyses reveal a potential immune-adjutant function of FAP-1 positive fibroblasts in non-small cell lung cancer. *PLoS One* **13**:e0192157.
7. Barret RL, Pure E (2020) Cancer-associated fibroblasts and their influence on tumor immunity and immunotherapy. *Elife* **9**:1–20.
8. Monteran L, Erez N (2019) The dark side of fibroblasts: Cancer-associated fibroblasts as mediators of immunosuppression in the tumor microenvironment. *Front Immunol*. <https://doi.org/10.3389/fimmu.2019.01835>.
9. De Jaeghere EA, Denys HG, De Wever O (2019) Fibroblasts Fuel Immune Escape in the Tumor Microenvironment. *Trends in Cancer* **5**:704–723.
10. Shah K, Mallik SB, Gupta P, Iyer A (2022) Targeting Tumour-Associated Fibroblasts in Cancers. *Front Oncol* **12**:908156.
11. Lambrechts D, Wauters E, Boeckx B, et al (2018) Phenotype molding of stromal cells in the lung tumor microenvironment. *Nat Med* **24**:1277–1289.
12. D'Ó A H-S, G B, et al (2017) Distinct populations of inflammatory fibroblasts and myofibroblasts in pancreatic cancer. *J Exp Med* **214**:579–596.
13. Elyada E, Bolisetty M, Laise P, et al (2019) Cross-species single-cell analysis of pancreatic ductal adenocarcinoma reveals antigen-presenting cancer-associated fibroblasts. *Cancer Discov* **9**:1102–1123.
14. Zollinger DR, Lingle SE, Sorg K, Beechem JM, Merritt CR (2020) GeoMx™ RNA Assay: High Multiplex, Digital, Spatial Analysis of RNA in FFPE Tissue. In: *Methods Mol. Biol.*, Springer US, pp 331–345.
15. Wang N, Li X, Wang R, Ding Z (2021) Spatial transcriptomics and proteomics technologies for deconvoluting the tumor microenvironment. *Biotechnol J*. <https://doi.org/10.1002/biot.202100041>.
16. Bergholtz H, Carter JM, Cesano A, et al (2021) Best Practices for Spatial Profiling for Breast Cancer Research with the GeoMx® Digital Spatial Profiler. *Cancers (Basel)*. <https://doi.org/10.3390/CANCERS13174456>.
17. Monkman J, Taheri T, Warkiani ME, O'leary C, Ladwa R, Richard D, O'Byrne K, Kulasingha A (2020) High-Plex and High-Throughput Digital Spatial Profiling of Non-Small-Cell Lung Cancer (NSCLC). *Cancers (Basel)* **12**:1–14

<http://dx.doi.org/10.1136/jitc-2022-SITC2022.0167>

EXPLORING FEATURES AND PARAMETERS FOR NEIGHBORHOOD ANALYSIS IN HUMAN CANCER MULTIPLEXED IMMUNOFLUORESCENCE DATA

¹Ian Dryg*, ¹Madison Turner, ¹Ann-Elizabeth Le, ¹Anne Carlisle, ¹Kathleen Pfaff, ¹Jason Weirather, ¹F Stephen Hodi, ²Scott Rodig. ¹Dana-Farber Cancer Institute, Boston, MA, USA; ²Brigham and Women's Hospital, Boston, MA, USA

Background The tumor microenvironment (TME) contains an elaborate mixture of varied cell phenotypes, whose spatial organization plays an important but incompletely understood role in disease outcome and response to therapy. Neighborhood Analysis is a promising new spatial analysis method used to extract broad features from a spatial dataset and summarize recurring regions that may be important in the TME [Schürch et al 2020, Griffin et al 2021, Patel et al 2019, Oyler-Yaniv et al 2018].¹⁻⁴ However, it remains unclear which neighborhood sizes provide the best insights. Schürch et al 2020 used 19 nearest neighbors plus self, which is a small spatial neighborhood. Our group has previously used a circular area with radius of 75 microns, which is a larger spatial neighborhood. Primarily, we aim to explore how neighborhood size can affect neighborhood analysis results and interpretations. Secondly, we propose to explore other new features in neighborhood analysis.

Methods The Human Tumor Atlas Network's (HTAN) efforts to establish a cancer atlas 3-dimensionally and over disease progression presents the opportunity to mine spatial datasets across cancer types and explore parameters used in neighborhood analysis. As part of the HTAN consortium, DFCI focused on three diseases to investigate with paired sequencing and spatial analyses: metastatic breast, melanoma, and colorectal cancers. Patient FFPE samples were stained and imaged using Akoya Biosciences Phenoptics mIF platform. Two panels were used: a macrophage-oriented panel including CD3, CD68, Tumor marker (SOX10 or Cytokeratin), PDL1, CD163, and Ki67; and a T cell-focused panel including CD8, PDL1, PD1, FOXP3, and Tumor marker. mIF images were thresholded and phenotyped using inForm software from Akoya Biosciences. Pythologist python package [https://github.com/dfci/pythologist] was used to ingest inForm outputs and to perform neighborhood analysis.

Results A pilot comparison of $r=45$ microns (r_{45}) and $r=75$ microns (r_{75}) revealed that r_{45} neighborhoods contained approximately 1/3 the number of cells of r_{75} neighborhoods and were more susceptible to one cell of a certain phenotype influencing that entire neighborhood cluster.

Conclusions Primarily, we postulate that smaller neighborhoods may lead to more granular results, perhaps describing small locales better, but leading to less interpretable overall conclusions than larger neighborhoods. Secondly, we hypothesize that new features measured from neighborhoods may be used to identify boundaries in different tissue regions such as the tumor/margin/stroma borders. By exploring parameters and features for neighborhood analysis, we aim to improve interpretability of these analyses, to provide new features to use, and to strengthen rationale for picking certain neighborhood sizes in future spatial studies.

Acknowledgements This work is supported through the Human Tumor Atlas Network, grant U2CCA233195.

REFERENCES

1. Schürch, Christian M., et al. Coordinated Cellular Neighborhoods Orchestrate Antitumoral Immunity at the Colorectal Cancer Invasive Front. *Cell*, vol. **182**, no. 5, 3 Sept. 2020, https://doi.org/10.1016/j.cell.2020.07.005.

2. Griffin, Gabriel K., et al. Spatial Signatures Identify Immune Escape via PD-1 as a Defining Feature of T-Cell/Histiocyte-Rich Large B-Cell Lymphoma. *Blood*, vol. **137**, no. 10, 2021, pp. 1353–1364., https://doi.org/10.1182/blood.2020006464.
3. Patel, Sanjay S., et al. The Microenvironmental Niche in Classic Hodgkin Lymphoma Is Enriched for CTLA-4-Positive T-Cells That Are PD-1-Negative. *Blood*, 2019, https://doi.org/10.1182/blood.2019002206.
4. Oyler-Yaniv, Alon and Krichevsky, Oleg. Imaging Cytokine Concentration Fields Using PlaneView Imaging Devices. *Bio Protoc.* 2018 Apr 5; **8**(7): e2788. doi: 10.21769/BioProtoc.2788

Pythologist python package https://github.com/dfci/pythologist

Ethics Approval The HTAN study is approved by the DFCI Institutional Review Board as protocol 18-452.

<http://dx.doi.org/10.1136/jitc-2022-SITC2022.0168>

169

IMMUNOTHERAPEUTIC POTENTIAL OF THE HUMANIZED ANTI-MUC16 ANTIBODY AR9.6 AGAINST PDAC

¹Christabelle Rajesh*, ¹Satish Sagar, ²Cory Brooks, ¹Michael Hollingsworth, ¹Prakash Radhakrishnan. ¹University of Nebraska Medical Center, Omaha, NE, USA; ²California State University Fresno, Fresno, CA, USA

Background Pancreatic ductal adenocarcinoma (PDAC) is a lethal disease with poor overall survival, owing partly to its late-stage presentation and resistance to standard of care.¹ Mucins are largely glycosylated proteins that have been found to be aberrantly expressed in multiple adenocarcinomas, including PDAC.² Mucin-16 (MUC16/CA125) is one such heavily glycosylated member that is overexpressed in >65% of PDACs and has been shown to correlate to poor prognosis.³ This study investigates the tumor mitigating mechanisms and thereby, therapeutic potential of the humanized anti-MUC16 monoclonal antibody (huAR9.6) in models of PDAC. **Methods** The enzyme-linked immunosorbent assay (ELISA) was performed using recombinantly produced MUC16 epitopes to assess the binding affinity of huAR9.6, as described previously.⁴ The wound healing assay using isogenic PDAC cell lines treated with huAR9.6, isotype control huIgG and vehicle was performed to assess the effect on cell migration. To determine the *in vivo* therapeutic potency, PDAC cells were orthotopically implanted into the pancreas of athymic nude mice which were then randomized to huAR9.6, isotype control huIgG, and vehicle treatment groups. Furthermore, *in vitro* functional assays to assess the antibody-dependent cellular cytotoxicity (ADCC) and complement-dependent cytotoxicity (CDC) capacity of huAR9.6 were performed using PDAC cell lines.

Results huAR9.6 showed a strong binding affinity to the tandem repeat region of the SEA domain 5 of MUC16. Treatment of PDAC cells with huAR9.6 reduced their migratory potential, indicating its anti-tumorigenic role. Mice treated with huAR9.6 showed a significant decrease in tumor weight and volume as compared to the huIgG and vehicle treated groups. The proliferative marker Ki67 was also significantly lowered in the pancreatic tumors of huAR9.6 treated mice, as compared to controls. Further, *in vitro* ADCC assays using freshly isolated human peripheral blood mononuclear cells (PBMCs) as effector cells showed an increase in cell death of PDAC cells treated with huAR9.6, as compared to cells treated with huIgG control. CDC assays using human serum also showed increased cytotoxicity of PDAC cells in the presence of the huAR9.6 antibody as compared to controls.

Conclusions The results strongly suggest that huAR9.6 binds to MUC16 and limits PDAC growth via cytotoxicity mechanisms including ADCC and CDC. This validates the therapeutic potential of huAR9.6 in models of PDAC and adds value to the previously established diagnostic ability of this antibody [5]. These studies are conducted with the overarching goal of facilitating the translation of huAR9.6 to treat PDAC in the clinic.

REFERENCES

1. A. N. Hosein, S. K. Dougan, A. J. Aguirre, and A. Maitra, Translational advances in pancreatic ductal adenocarcinoma therapy, *Nature Cancer* 2022; 3:3, no. 3, pp. 272–286, Mar. 2022, doi: 10.1038/s43018-022-00349-2.
2. M. A. Hollingsworth and B. J. Swanson, Mucins in cancer: protection and control of the cell surface, *Nature Reviews Cancer* 2004; 4:1, vol. 4, no. 1, pp. 45–60, 2004, doi: 10.1038/nrc1251.
3. D. Thomas *et al.* Isoforms of MUC16 activate oncogenic signaling through EGF receptors to enhance the progression of pancreatic cancer, *Molecular Therapy*, vol. 29, no. 4, pp. 1557–1571, Apr. 2021, doi: 10.1016/j.ymt.2020.12.029/ATTACHMENT/632DD631-FCE4-4079-AC9E-940B42278BB0/MMC1.PDF.

4. B. White, M. Patterson, S. Karnwal, and C. L. Brooks, 'Crystal structure of a human MUC16 SEA domain reveals insight into the nature of the CA125 tumor marker,' *Proteins: Structure, Function, and Bioinformatics*, vol. 90, no. 5, pp. 1210–1218, May 2022, doi: 10.1002/prot.26303.
5. S. K. Sharma *et al.*, ImmunoPET of Ovarian and Pancreatic Cancer with AR9.6, a Novel MUC16-Targeted Therapeutic Antibody, *Clinical Cancer Research*, vol. 28, no. 5, pp. 948–959, Mar. 2022, doi: 10.1158/1078-0432.CCR-21-1798/3019395/CCR-21-1798.PDF.

<http://dx.doi.org/10.1136/jitc-2022-SITC2022.0169>

Abstracts

171

TUMOR MICROENVIRONMENT IMMUNE CELL LANDSCAPE VARIES AMONG MOLECULAR SUBTYPES IN GASTRIC CANCER

Sanyog Dwivedi*. UNAM, Mexico City, Mexico

Background Immune interactions in the tumor microenvironment (TME) are a major factor in deciding the fate of immunotherapy. Heterogeneity and molecular subtypes, especially in solid tumors like gastric cancer (GC), involve substantial modification in TME. Hence understanding the immune cell populations infiltrating the TME of different molecular subtypes will help to develop more effective and targeted therapies

Methods CBioPortal^{1,2} was used to extract and analyze The Cancer Genome Atlas (TCGA) Stomach Adenocarcinoma Pan-Cancer Atlas Data (STAD). Immune Metagene signatures from previous publications³ were used to analyze the immune infiltration landscape in different GC molecular subtypes- chromosomal instability (CIN)(n=223), microsatellite instable (MSI) (n=73), genomically stable (GS)(n=50), Epstein-Barr virus (EBV) associated (n=30). GraphPad Prism9 and MS Excel were used to analyze the data and generate the figures.

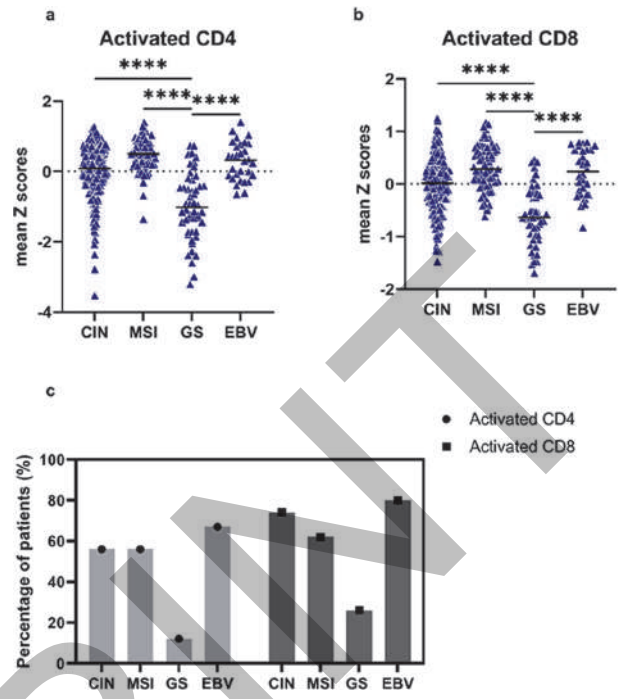
Results We analyzed the infiltration landscape of Natural Killer (NK) cells, T cells (CD4⁺, CD8⁺, Th1, Th2, Th17), immune suppressive Myeloid-derived suppressor cells (MDSC), and Regulatory T cells (Tregs) in GC molecular subtypes. The results showed that CD8⁺ cytotoxic T cells and CD4⁺ helper T cells were highly downregulated in the GS subtype in comparison to other molecular subtypes (figure 1). Cytokine secreting T helper cell subsets, Th1, Th2, and Th17 demonstrate a dissimilar infiltration pattern among subtypes (figure 2). Th1 cells were highly expressed in the EBV subtype as compared to Th1 infiltration in the other subtypes (figure 3). GS and EBV both depict higher infiltration of Th2 cells and lower infiltration of Th17 cells in comparison to CIN and MSI subtypes (figure 2). GS subtype along with EBV has a superior infiltration of immune suppressive MDSC and Tregs (figure 3). Both cytotoxic NK^{56dim} and cytokine secreting immune modulating NK^{56bright} cells were the lowest infiltrating the GS molecular subtype (figure 4). Intriguingly, NK^{56bright} infiltration markers don't differ significantly between subtypes. It was worth observing that in general, there is more infiltration of NK^{56dim} over NK^{56bright} cells in GC patients (figure 4).

Conclusions TME of the GS molecular subtype of GC contains less cytotoxic cells (NK56^{Dim} and CD8⁺ T) and higher infiltration of immune suppressive cells (Tregs and MDSCs).

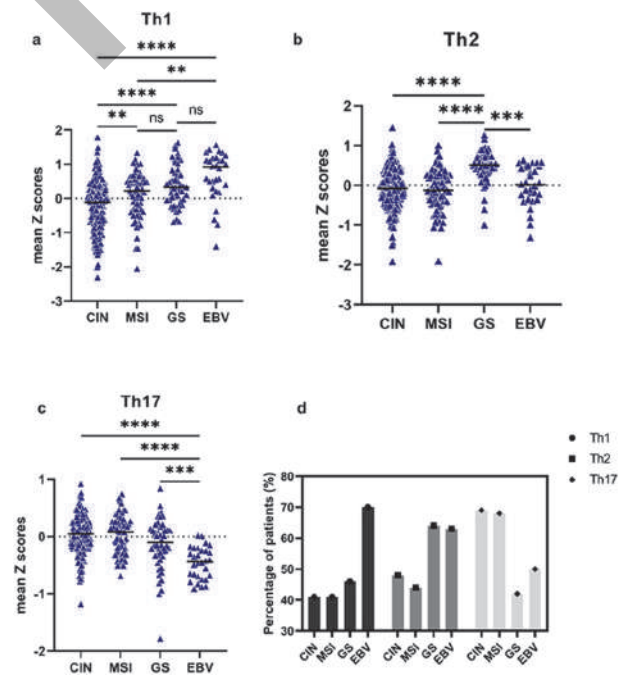
Acknowledgements This research was supported by UNAM DGAPA grant to Dr. Sanyog Dwivedi (Feb 2022- Jan 2023).

REFERENCES

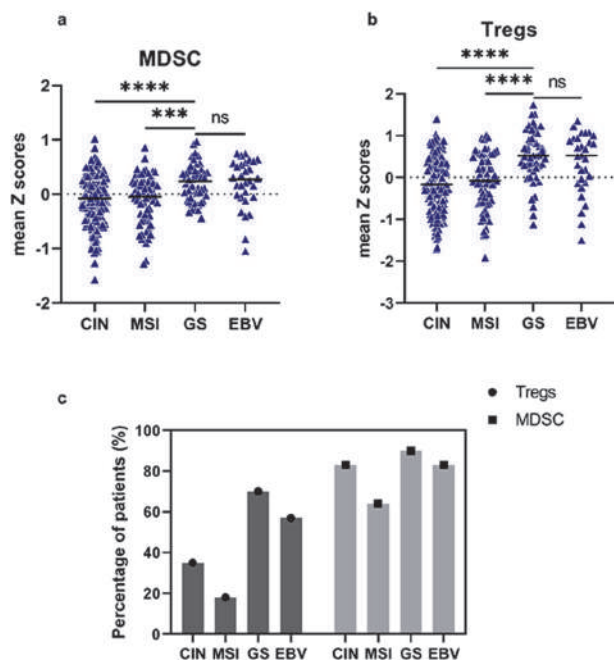
1. Cerami, Ethan, Jianjiong Gao, Ugur Dogrusoz, Benjamin E. Gross, Selcuk Onur Sumer, Bülent Arman Aksoy, Anders Jacobsen, *et al.* The CBio Cancer Genomics Portal: An Open Platform for Exploring Multidimensional Cancer Genomics Data. *Cancer Discovery* **2**, no. 5 (May 2012): 401-4. <https://doi.org/10.1158/2159-8290.CD-12-0095>.
2. Chae, Young Kwang, Wooyoung M. Choi, William H. Bae, Jonathan Anker, Andrew A. Davis, Sarita Agte, Wade T. Iams, Marcelo Cruz, Maria Matsangou, and Francis J. Giles. Overexpression of Adhesion Molecules and Barrier Molecules Is Associated with Differential Infiltration of Immune Cells in Non-Small Cell Lung Cancer. *Scientific Reports* **8**, no. 1 (2018): 1023. <https://doi.org/10.1038/s41598-018-19454-3>.
3. Gao, Jianjiong, Bülent Arman Aksoy, Ugur Dogrusoz, Gideon Dresdner, Benjamin Gross, S. Onur Sumer, Yichao Sun, *et al.* Integrative Analysis of Complex Cancer Genomics and Clinical Profiles Using the CBioPortal. *Science Signaling* **6**, no. 269 (April 2, 2013): pl1. <https://doi.org/10.1126/scisignal.2004088>.



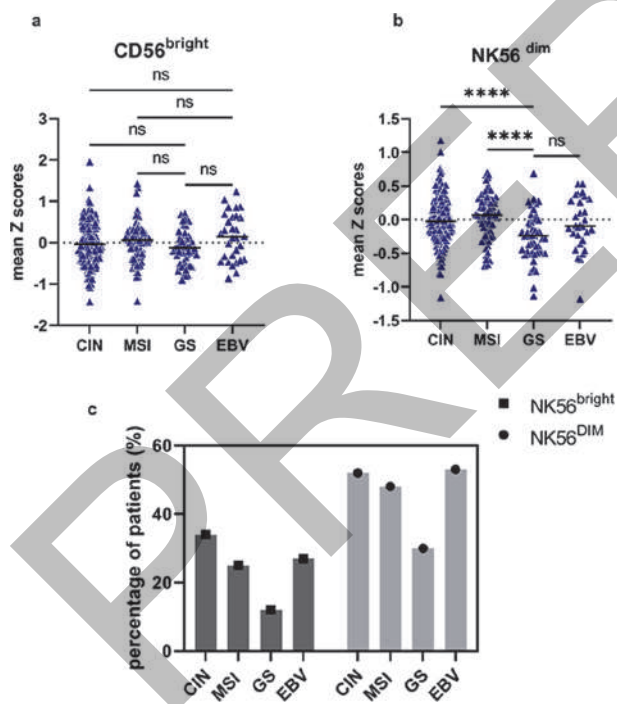
Abstract 171 Figure 1 Immune cell infiltration landscape of T cells (CD4⁺, CD8⁺) cells by GC molecular subtypes. Statistical significance was confirmed using one-way ANOVA, P-Value, **** <0.0001



Abstract 171 Figure 2 Immune cell infiltration landscape of Th1, Th2, and Th17 cells by GC molecular subtypes. Statistical significance was confirmed using one-way ANOVA, P-Value, **-0.0045, ***-0.0002, **** <0.0001



Abstract 171 Figure 3 Immune cell infiltration landscape of MDSC and Tregs by GC molecular subtypes. Statistical significance was confirmed using one-way ANOVA, P-Value, **-0.0045, ***-0.0002, **** <0.0001



Abstract 171 Figure 4 Immune cell infiltration landscape of NK56^{bright} and NK56^{dim} cells by GC molecular subtypes. Statistical significance was confirmed using one-way ANOVA, P-Value, **** <0.0001

<http://dx.doi.org/10.1136/jitc-2022-SITC2022.0171>

Abstracts

172

BODY MASS INDEX (BMI) AND SERUM ALBUMIN LEVEL AS A PREDICTOR OF SURVIVAL OUTCOMES IN ADVANCED-STAGE MELANOMA PATIENTS TREATED WITH ANTI-PD1 THERAPY

Yusuf Mohamoud*, Yeonhee Park, Dahlia Tesfamichael, Vincent Pozorski, Vincent Ma. University of Wisconsin, Madison, WI, USA

Background Body mass index (BMI) and serum albumin are common measurements used to evaluate nutritional status. Recent studies have shown conflicting results correlating nutritional status with immune checkpoint inhibitor (ICI) therapy outcomes.^{1,2} In this study, we investigate if baseline and change in BMI and serum albumin levels correlate with survival outcomes in advanced stage melanoma patients treated with anti-PD-1 therapy.

Methods We conducted a single-center, retrospective review of unresectable stage III and IV melanoma patients treated with anti-PD-1 monotherapy (nivolumab or pembrolizumab) or ipilimumab/nivolumab (I/N) between 2011 and 2022. Overall survival (OS) and progression-free survival (PFS) were measured from the first dose of treatment to date of death and clinical or radiographic progression, respectively. The effect of baseline BMI, serum albumin levels, and their respective percentage change at 3 months from treatment initiation on PFS and OS was assessed on a continuum level. Multivariate analyses were performed using Cox proportional hazard models, accounting for the following covariates: Age, gender, anti-PD-1 therapy type, primary melanoma type, pre-treatment LDH, BRAF status, presence of brain or liver metastasis, and prior adjuvant or non-anti-PD-1 treatment for advanced-stage melanoma.

Results 202 patients were identified. Mean BMI was 30.1 and mean albumin level was 3.63 g/dL. Higher baseline BMI (HR 0.9825, 95% CI: 0.9657–0.9996, p=0.0445) and lower baseline albumin level (HR 2.4498, 95% CI: 1.2606–4.7619, p=0.0082) was associated with worse PFS [table 1]. Change in BMI and albumin level at 3 months was not associated with PFS outcomes. Lower baseline albumin level was associated with worse OS outcomes [HR 2.4814, 95% CI: 1.1161–5.5157 p=0.0258]. Higher change in albumin level at 3 months was also associated with worse OS [HR 0.9389, 95% CI: 0.9109–0.9677, p=0.00004]. Our univariate analysis showed lower baseline albumin level and decreasing albumin change from the baseline mean at 3 months was associated with worse PFS and OS [figure 1].

Conclusions Nutritional status may have a predictive role on survival in advanced melanoma patients treated with anti-PD-1 therapy. Baseline albumin and decreasing albumin levels at 3 months is associated with worse survival. Unlike previous studies, we found that higher baseline BMI may lead to worse PFS outcomes in immunotherapy treated patients. Interventional studies are warranted to see if nutritional status optimization prior to and during anti-PD-1 therapy can affect clinical outcomes.

REFERENCES

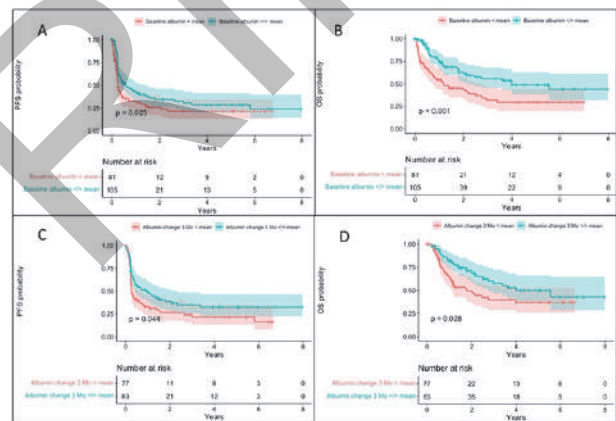
1. Kondo T, Nomura M, Otsuka A, et al. (2019). Predicting marker for early progression in unresectable melanoma treated with nivolumab. *Int J Clin Oncol*. 2019 Mar;24(3):323–327.
2. McQuade JL, Daniel CR, Hess KR, et al. Association of body-mass index and outcomes in patients with metastatic melanoma treated with targeted therapy, immunotherapy, or chemotherapy: a retrospective, multicohort analysis. *Lancet Oncol*. 2018 Mar;19(3):310–322.

Ethics Approval The study was approved by the University of Wisconsin institutional ethical guidelines and patients' consents were waived following Institutional Review Board protocol review (UW21110).

Abstract 172 Table 1

Variables	Progression Free Survival		Overall Survival	
	HR (95% CI)	p-value	HR (95% CI)	p-value
Anti-PD-1 Treatment Type (I/N vs Anti-PD-1 Monotherapy)	0.6031 (0.3142, 1.1580)	0.1287	0.705 (0.416–1.194)	0.0002*
Prior Non-Anti-PD-1 Treatment for Advanced Melanoma (yes vs no)	2.1245 (1.1989–3.7649)	0.0098	2.006 (1.181–3.405)	0.0744
Prior Adjuvant Treatment (yes vs no)	1.8687 (1.0764–3.3140)	0.0267*	1.3445 (0.6913–2.6149)	0.3831
Age (<65 vs ≥65)	0.8766 (0.5503–1.3964)	0.8794	1.0933 (0.6140–1.9489)	0.7618
Gender (male vs female)	0.9284 (0.5896–1.4657)	0.7403	1.2059 (0.6620–2.1968)	0.5406
BRAF status (mutant vs WT)	1.0336 (0.6655–1.6299)	0.8868	0.5731 (0.3203–1.0254)	0.0608
Primary melanoma type (Cutaneous vs Mucosal or Unknown)	0.8050 (0.4775–1.3669)	0.4195	0.7097 (0.3608–1.3958)	0.3204
Pre-treatment LDH level (>ULN vs normal)	1.5201 (0.9678–2.3876)	0.0691	2.6213 (1.4604–4.7050)	0.0012*
Brain metastases (yes vs no)	0.9747 (0.5474–1.7357)	0.9307	1.2712 (0.6361–2.5402)	0.4969
Liver metastases (yes vs no)	1.3610 (0.8354–2.2174)	0.2158	1.3743 (0.7534–2.5067)	0.2999
Baseline BMI (lower vs higher)	0.9825 (0.9657–0.9996)	0.0445*	0.9517 (0.9154–1.0103)	0.1209
Baseline albumin level (lower vs higher)	2.4498 (1.2606–4.7619)	0.0082*	2.4814 (1.1161–5.5157)	0.0258*
Percent change in BMI at 3 months from baseline (lower vs higher)	1.0205 (0.9697–1.0739)	0.4363	0.9896 (0.9277–1.0537)	0.7518
Percent change in albumin level at 3 months from baseline (lower vs higher)	0.9814 (0.9579–1.0054)	0.1274	0.9389 (0.9109–0.9677)	4.31x10 ⁻⁴ *

Multivariate Cox proportional hazard regression models for progression-free survival and overall survival. *Indicates statistical significance of p<0.05. ‡Normal limits of LDH <240 U/L. Abbreviations: CI, confidence interval; HR, hazard ratio; I/N, ipilimumab/nivolumab; LDH, lactate dehydrogenase; BMI, body mass index; OS, overall survival; PFS, progression-free survival; ULN, upper limit of normal; WT, wildtype.



Abstract 172 Figure 1 Kaplan-Meier curves of progression-free survival (PFS) and overall survival (OS) comparing patients based on baseline albumin levels and percent albumin change at 3 months. Mean albumin level was 3.63 g/dL. A) PFS difference between patients with baseline albumin below the mean and those with baseline albumin above the mean. B) OS difference between patients with baseline albumin below the mean and those with baseline albumin above the mean. C) PFS difference between patients with percent albumin change 3 months below the mean and those with percent albumin change 3 months above the mean. D) OS difference between patients with percent albumin change 3 months below the mean and those with percent albumin change 3 months above the mean

<http://dx.doi.org/10.1136/jitc-2022-SITC2022.0172>

173

SENSITIVITY AND CONCORDANCE OF *CD274* EXPRESSION BY RNA SEQUENCING (RNA-SEQ) IN COMPARISON WITH THREE PD-L1 IMMUNOHISTOCHEMISTRY METHODS IN HEAD AND NECK SQUAMOUS CELL CARCINOMA (HNSCC)

<http://dx.doi.org/10.1136/jitc-2022-SITC2022.0173>

¹Mary Nesline*, ¹Sarabjot Pabla, ¹Jeffrey Conroy, ¹Paul DePietro, ¹Shengle Zhang, ¹Roger Klein, ²Achyut Bhagelu, ²Rebecca Previs, ²Prasanth Reddy, ²Shakti Ramkissoon, ²Eric Severson. ¹OmniSeq, Inc., Buffalo, NY, USA; ²Labcorp, Durham, NC, USA

Background PD-L1 expression by immunohistochemistry (IHC) is associated with HNSCC immunotherapy response.¹ The performance of different PD-L1 IHC clones has shown variability and poor concordance for immune vs. tumor cell scoring in HNSCC. Crucially, this leads to poor reproducibility in the combined positive score (CPS) method by the PD-L1 IHC 22C3 companion diagnostic.² We explored the clinical sensitivity and concordance of *CD274* (PD-L1) expression by RNA-sequencing compared to three PD-L1 IHC methods.

Methods A retrospective cohort of HNSCC patients (n=258) with FFPE tissue was tested by comprehensive immune profiling³(2017–2022), including *CD274* by RNA-seq (normalized percentile rank 0–100). IHC was performed with either the 28–8 or 22C3 PD-L1 clones. 28–8 was scored with% tumor cells stained (TC, n=34), while 22C3 was scored with either tumor proportion score (TPS, n=61) or combined positive score (CPS, n=163). For 22C3, CPS \geq 1 is low positive, and \geq 20 is high positive. For 28–8 TC and 22C3 TPS, \geq 1 is low positive, and \geq 50 is high positive. ROC models for each IHC method were constructed for 5 sets of patients with different pairwise interpretation groups and used to determine RNA-seq cutoffs based on individual PD-L1 IHC scoring methods and accuracy at those cutoffs. Concordance between standard IHC scoring methods and *CD274* by RNA-seq was also assessed.

Results PD-L1 IHC results varied depending on the clone and scoring method used. Not surprisingly, CPS had the fewest negative cases (2.7%) and most high cases (47.2%). Tumor cell scoring by TPS (29.5% negative, 24.6% high) and TC (17.6% negative, 26.5% high) was similar for high vs. not high. For all three IHC approaches, PD-L1 RNA-seq classified IHC high v negative, high v low, and high v not high status with at least fair range of AUC (0.758–0.981), sensitivity (0.636–1.00), and specificity (0.785–1.00). RNA-seq could not discern between IHC low v negative status for any method. Pairwise comparisons showed significant concordance between median RNA-seq percentile ranks for IHC high v low and high v negative status for all IHC methods. By RNA-seq, the frequency of PD-L1 high cases for each scoring method increased from 47% to 55% (CPS), 24.6% to 42.6% (TPS) and 26.5% to 47.1% (TC) based on modeled RNA-seq cutoffs.

Conclusions RNA-seq accurately discerns PD-L1 high vs. not high HNSCC tumors based on IHC scoring methods and may more reliably identify patients for frontline immunotherapy.

REFERENCES

1. NCCN, 'NCCN Clinical Practice Guidelines in Oncology (NCCN Guidelines[®]) Head and Neck Cancers, Version 2.2022,' National Comprehensive Cancer Network, Fort Washington, Pennsylvania, Version 2.2022, Mar.
2. J. Ribbat-Idel *et al.*, Performance of Different Diagnostic PD-L1 Clones in Head and Neck Squamous Cell Carcinoma, *Front. Med.*, vol. **8**, no. April, pp. 1–8, 2021.
3. J. M. Conroy *et al.* Analytical Validation of a Next-Generation Sequencing Assay to Monitor Immune Responses in Solid Tumors, *J. Mol. Diagnostics*, vol. **20**, no. 1, pp. 95–109, Jan. 2018.

174

SINGLE CELL FFPE AND SPATIAL TRANSCRIPTOMIC PROFILING OF AN INVASIVE DUCTAL CARCINOMA ENHANCES CELLULAR AND SPATIAL INSIGHTS

Ryan Stott*, Jawad Abousoud, Stephen Williams, Shamoni Maheshwari, Valeria Giangarra, Sarah Taylor, Andrew Kohlway, 10x Genomics, Pleasanton, CA, USA

Background Invasive ductal carcinoma (IDC) is the most common type of breast cancer, accounting for 80% of all breast cancer diagnoses. Formalin-fixed paraffin-embedded (FFPE) samples are a valuable resource for diagnosing breast cancers. FFPE samples are often available with patient metadata and clinical outcomes, thus providing a critical sample resource for disease studies. Here we demonstrate the potential of single-cell transcriptomics on dissociated FFPE tissues. We also assessed the same FFPE breast IDC tissue block using the Chromium Single Cell Fixed RNA Profiling and Visium Spatial Gene Expression assays for more accurate estimation of cell-type proportions for each Visium spot.

Methods FFPE scrolls (2 x 25- μ m) of human breast IDC were dissociated into a single cell suspension using a combination of enzymatic digestion and mechanical dissociation. Cells were then processed using the Chromium Fixed RNA Profiling workflow. A section from the same FFPE IDC block was processed using the Visium Spatial Gene Expression Solution for FFPE.

Results Clustering analysis of the single cell FFPE data identified 17 distinct cell populations, including luminal epithelial progenitors, mature luminal epithelia, basal cells, fibroblasts, pericytes, and immune cells. Applying the Prediction Analysis of Microarray 50 (PAM50) subtype predictor to these clusters, we identified one cluster showing a strong correlation with a basal-like cancer subtype whereas all other clusters correlated with a normal signature. To compare single cell and spatial data, we utilized Robust Cell Type Decomposition to estimate cell-type proportions for each Visium gene expression spot. Distinct regions were observed for mature and progenitor luminal cells. Interestingly, the mature luminal cells mapped specifically to the region annotated by a pathologist as invasive carcinoma while T and B cells colocalized outside of the carcinogenic region, which may have implications on the patient's prognosis.

Conclusions Our studies show that transcriptome-wide gene expression at a single-cell resolution on FFPE-preserved tissue adds a whole new axis of information to clinical studies, providing new opportunities for the analysis of large biobanked cohorts and longitudinal samples of clinical relevance. Additionally, assessing the same FFPE tissue blocks by combining Chromium Single Cell Fixed RNA Profiling with Visium Spatial Gene Expression assays enables a comprehensive dataset with more precise cell type profiling in the spatial context.

<http://dx.doi.org/10.1136/jitc-2022-SITC2022.0174>

Cell Therapies

175 CAR-T ENGAGER PROTEINS OPTIMIZE ANTI-CD19 CAR-T CELL THERAPIES FOR LYMPHOMA

Paul Rennert*, Lihe Su, Lan Wu, Roy Lobb, Christine Ambrose. *Aleta Biotherapeutics, Natick, MA, USA*

Background B cell lymphoma therapy has been transformed by CD19-targeting cellular therapeutics that induce high clinical response rates and impressive remissions in relapsed and refractory patients. However, approximately half of all patients who respond to CD19-directed cell therapy relapse, the majority within six months. One characteristic of relapse is loss or reduction of CD19 expression on malignant B cells. We designed a novel biologic, a CAR T Engager, that binds CD20 and displays the CD19 extracellular domain. This approach increases the apparent CD19 antigen density on CD19-positive/CD20-positive lymphoma cells, and prevents antigen-loss induced relapse, as CD19 bound to CD20 remains present on the cell surface. We demonstrate that this novel therapeutic prevents and reverses lymphoma relapse *in vitro* and prevents CD19-negative lymphoma growth and relapse *in vivo*.

Methods The CTE biologic has three functional domains: a modified CD19 ECD, an anti-CD20 binding domain and an anti-albumin binding domain. The protein, termed a CAR-19-CD20 T cell Engager (CTE-19.20), binds to CD20 and displays the CD19 ECD and increases CD19 antigen density on target lymphoma cells regardless of their level of CD19 expression.

Results CTE-19.20 proteins potently triggered CD19-negative lymphoma cell death in the presence of CAR-19 T cells *in vitro* and prevented antigen-loss relapse in an *in vitro* model of lymphoma escape from CAR-19 therapy. Using *in vivo* modeling we show that CTE-19.20 protein given alongside CAR-19 T cells prevented CD19-negative lymphoma expansion, eliminated disease, and significantly impacted survival. CTE-19.20 was readily expressed and secreted by transfected mammalian cells, was efficiently purified and demonstrated favorable biophysical properties.

Conclusions Patient relapse from CAR-19 therapy occurs rapidly, often within the first months following therapy. The kinetics of relapse offer the potential to intervene using CTE-19.20 protein, using several different clinical designs. In the first instance we are developing this molecule with the goal of treating patients who have already received a CAR-19 therapy, by evaluating their clinical response through the first few months post CAR infusion. Diverse biomarkers can be used to track response and risk of relapse. PET imaging and ctDNA analyses have emerged as sensitive means of tracking lymphoma and leukemia regression. This is an optimal and straightforward approach to productive and sustained activation of CAR-19 T cells, using a potent CD19-anti-CD20 bridging protein with an extended half-life.

<http://dx.doi.org/10.1136/jitc-2022-SITC2022.0175>

176

IMMUNE ACTIVATION BY ANTIGEN-SPECIFIC T CELLS ELICITED IN PATIENTS RECEIVING STANDARD THERAPY FOR PEDIATRIC SOLID TUMORS

Jillian Smith*, Amy Hont, Catherine Bollard. *Children's National Hospital, Washington, DC, USA*

Background Immunotherapy in the form of immune checkpoint inhibitors and chimeric antigen receptor (CAR) T-cells has revolutionized the treatment of select malignancies.¹⁻² However, beyond CD19+ cancers, clinical responses to CAR-T have been modest in pediatric cancers, likely due to lower mutational burden. Antigen spreading, an expanded anti-tumor immune response through exposure to neoantigens, has been observed in patients following treatment with immunotherapy agents or chemotherapy for malignancies with typically higher mutational burdens.³⁻⁶ However, this has not been observed in pediatric patients with solid tumors after standard treatment. We demonstrated the safety of autologous tumor-associated antigen-specific T lymphocytes (TAA-T) specific for WT1, PRAME, and Survivin in Phase I studies.⁷ We also identified antigen spreading post-infusion with increased T cells specific for non-targeted antigens MAGE-A3, MAGE-A4, SSX-2, and SOX-2, all expressed on solid tumors.⁸⁻¹² We hypothesized that antigen spreading would be greater in patients who received TAA-T than in those who received standard chemotherapy or radiation therapy.

Methods Fourteen patients with pediatric solid tumors who received standard-of-care therapy were enrolled on the standard chemotherapy arm and compared to fourteen relapsed/refractory patients who received TAA-T infusion. Peripheral blood samples were taken prior to therapy, during therapy, and off therapy if available, and these were evaluated for the presence of T cells specific to MAGE-A3, MAGE-A4, SSX-2, and SOX-2 as measured by IFN- γ ELISPOT.

Results Our results demonstrate the presence of antigen spreading in newly diagnosed patients who receive standard therapy as evidenced by T cells specific for MAGE-A3 (mean: 28.2, range: 0–137 IFN- γ SFC/1e5 cells (SFC)), MAGE-A4 (mean: 31.8, range: 0–270 SFC), SSX-2 (mean: 22.8, range: 0–100 SFC) and SOX-2 (mean: 7.2, range: 0–46 SFC). Similar levels of antigen spreading were also identified in relapsed/refractory patients post TAA-T infusion detecting T cells specific for MAGE-A3 (mean: 30.7, range: 0–249 SFC), MAGE-A4 (mean: 27.6, range: 0–230 SFC), SSX-2 (mean: 33.9, range: 0–200 SFC) and SOX-2 (mean: 39.5, range: 0–270 SFC).

Conclusions These results demonstrate immune activation as evidenced by antigen spreading in newly diagnosed pediatric patients with solid tumors receiving standard-of-care chemotherapy and radiation therapy, the majority of which remain in remission following treatment. Similar levels of antigen spreading were also observed in responding patients who received TAA-T for relapsed/refractory disease. This data provides further support for the role of immunotherapy in the treatment of pediatric solid tumors and the strong anti-tumor response these therapies can potentiate.

REFERENCES

1. Lee DW, Kochenderfer JN, Stetler-Stevenson M, et al. T cells expressing CD19 chimeric antigen receptors for acute lymphoblastic leukaemia in children and young adults: a phase 1 dose-escalation trial. *The Lancet*. 2015; **385**(9967): 517–528.
2. Davis KL, Fox E, Merchant MS, et al. Nivolumab in children and young adults with relapsed or refractory solid tumours or lymphoma (ADVL1412): a multicentre, open-label, single-arm, phase 1–2 trial. *The Lancet Oncology*. 2020; **21**(4): 474–476.

3. Li AM, Hucks GE, Dinofia AM, et al. Checkpoint Inhibitors Augment CD19-Directed Chimeric Antigen Receptor (CAR) T Cell Therapy in Relapsed B-Cell Acute Lymphoblastic Leukemia. *Blood*. 2018; **132**:556
4. Jackaman C, Majewski D, Fox SA, et al. Chemotherapy broadens the range of tumor antigens seen by cytotoxic CD8+ T cells in vivo. *Cancer Immunol Immunother*. 2012; **61**(12):2343–2356.
5. Gulley JL, Madan RA, Pachynski R, et al. Role of Antigen Spread and Distinctive Characteristics of Immunotherapy in Cancer Treatment. *J Natl Cancer Inst*. 2017; **109**(4):1–9.
6. Brossart, P. The Role of Antigen Spreading in the Efficacy of Immunotherapies. *Clin Cancer Res*. 2020; **26**(17):4442–4447.
7. Hont AB, Cruz CR, Ulrey R, et al. Immunotherapy of Relapsed and Refractory Solid Tumors With Ex Vivo Expanded Multiantigen-Associated Specific Cytotoxic T Lymphocytes: A Phase I Study. *J Clin Oncol*. 2019; **37**(26):2349–2359.
8. Dalerba P, Frascella E, Macino B, et al. MAGE, BAGE and GAGE Gene Expression in Human Rhabdomyosarcomas. *Int J Cancer*. 2001; **93**(1):85–90.
9. Jacobs JFM, Brasseur F, Hulsbergen-van de Kaa CA, et al. Cancer-germline gene expression in pediatric solid tumors using quantitative real-time PCR. *Int J Cancer*. 2006; **120**(1):67–74.
10. Naka N, Araki N, Nakanishi H, et al. Expression of SSX Genes in Human Osteosarcomas. *Int J Cancer*. 2002; **98**(4):640–642.
11. Zayed H, Petersen I. Stem cell transcription factor SOX2 in synovial sarcoma and other soft tissue tumors. *Pathology – Research and Practice*. 2018; **214**(7):1000–1007.
12. Weon JL & Potts PR. The MAGE Family of Proteins and Cancer. *Current Opinions in Cell Biology*. 2015; **37**: 1–8.

<http://dx.doi.org/10.1136/jitc-2022-SITC2022.0176>

177

PRECLINICAL CHARACTERIZATION OF CYT-100 IPSC DERIVED NK CELLS ALONE AND IN COMBINATION WITH CYT-303 NK CELL ENGAGER FOR HEPATOCELLULAR CARCINOMA (HCC)

Liang Lin*, Andrea Chambers, Marshall Chao Ma, Hao-Ming Chang, David Zou, Preeti Ashok, Elizabetta Burchi, Armin Rath, Stanley Frankel, Jean Kadouche, Daniel Tepper, Nejmi Dilmac, Antonio Arulanandam, Wei Li. *Cytovia Therapeutics, Natick, MA, USA*

Background CYT-100 is a first-generation iPSC derived NK cell product in development for use in combination with NK cell engager antibody (NKE) CYT-303 targeted against NKp46 activation receptor on NK cells and Glypican-3 (GPC3) expressed in the tumor for treatment of hepatocellular carcinoma (HCC). The combination of CYT-100 and CYT-303 is expected to activate endogenous NK cells and provide additional functional NK cells in the HCC microenvironment. Here we describe preclinical characterization of CYT-100 alone or in combination with CYT-303. In addition, we compared CYT-100 expansion capacity potential to PBNKs (peripheral blood natural killer cells).

Methods CYT-100 immunophenotyping was conducted by flow cytometry using a panel of NK cell directed antibodies. Intracellular signaling following stimulation of CYT-100 with rIL-2 or rIL-15 was assessed using a phospho STAT-5 antibody by flow cytometry and cell growth monitored by counting cells using the flow cytometer or a cell counting kit (CCK8). Hep3B tumor spheroids were formed in special U-bottom adhesive plates and tumor spheroid killing assays were conducted using the Incucyte™ Live Cell Analysis System. Serial killing assays were conducted by repeatedly adding the same CYT-100 cells to fresh tumor cells following each round of tumor killing. The chromosome telomere length was assessed by a q-PCR assay.

Results CYT-100 immunophenotyping results showed > 95% expression of CD56/CD45, high expression of all activating receptors, except CD16, and some chemokine receptors including CXCR3, and minimal expression of most inhibiting receptors. Stimulation with rIL-2 or rIL-15 resulted in tyrosine phosphorylation of STAT-5 and increased cell growth over a period of 6 days, comparable to PBNKs, demonstrating the capacity of these cells to expand in the presence of cytokines. CYT-100 showed increased time-dependent killing of Hep3B tumor spheroids that peaked 2–3 days following of initiation of killing. This killing was enhanced in the presence of CYT-303 in a dose dependent manner. Furthermore, CYT-100 showed serial killing of Hep3B tumors and this was enhanced in combination with CYT-303. Chromosome telomere length analysis of CYT-100 showed greater telomere length compared to that of PBNKs, suggesting greater expansion capacity potential of these cells.

Conclusions The allogeneic iPSC derived NK cell product CYT-100 demonstrates cytotoxicity against hepatocellular carcinoma Hep3B cells, sensitivity to cytokine activation and expansion potential. The cytotoxicity of this iNK product is further enhanced by combination with the NK cell engager antibody CYT-303. These data support further development of the combination of iNK cells and NKEs as therapeutics for HCC.

<http://dx.doi.org/10.1136/jitc-2022-SITC2022.0177>

TARGETING ER-MITOCHONDRIAL DYNAMICS TO IMPROVE RESPONSES TO IMMUNE CHECKPOINT BLOCKADE

Katherine Cook, Elizabeth Stirling, Jessica Mackert, Mitra Kooshki, Adam Wilson, Wei Zhang, Pierre Triozzi, David Soto-Pantoja*. *Wake Forest School of Medicine, Winston-Salem, NC, USA*

Background One of the top challenges in cancer immunotherapy is ‘understanding the molecular and cellular drivers of primary vs. secondary immune escape to immune checkpoint blockade therapies.’ Although durable responses indicating immunologic memory are reported, most patients do not respond with tumor regression. In addition, recurrences are observed after initial response, suggesting the emergence of acquired resistance. Therefore, novel therapeutics are needed to enhance ICB treatment to halt melanoma progression and increase patient survival rates. Oxidative stress and hypoxia in the tumor microenvironment resulting in endoplasmic reticulum (ER) stress signaling associated with cancer therapy resistance. PKR-like endoplasmic reticulum kinase actions in the tumor microenvironment can occur by activation of the Unfolded Response (UPR). However, PERK also has functions that are not linked to canonical activation of UPR signaling. PERK is involved in the maintenance of ER with mitochondria-associated membranes (MAMs). This is important in glucose sensing and could impair metabolic reprogramming during T cell activation if disrupted.

Methods To determine ER-stress markers of patient response, we analyzed Peripheral Blood Mononuclear Cells by single-cell RNA sequencing (scRNAseq), 3D electron, and confocal microscopy to determine mitochondria/ER interactions. Antigen-mediated CD8+ T cell toxicity assay was performed using Pmel-1 transgenic mice. LC-MS Metabolomics and Seahorse mitochondrial respiration assays were used to determine CD8+ cellular energetics treated with anti-PD-1 in the presence or absence of PERK blockade. An in vivo murine tumor model (B16) was developed to determine whether PERK blockade sensitizes tumors to anti-PD1 therapy.

Results UMAP clustering of our scRNAseq data indicates a ~3-fold increase in PERK expression after the first treatment cycle in patients who did not respond to anti-PD-1 therapy (n=12, *p<0.05). This was confirmed by plasma ELISA assay in a different cohort of patients (N=50, *p<0.001). Furthermore, the expression of PERK in non-responder patients was associated with increased expression of TOX1 in the T-cell population, and induction of ER stress caused a transcriptional increase in TOX1 in T cells suggesting that ER stress may be associated with T cell dysfunction. Induction of ER stress limited antigen-mediated CD8+ T cell killing; however, blockade of PERK enhanced the cytolytic capacity of CD8+ T cells over 4-fold, clearing tumor cells even under ER stress-induced circumstances (n=4, *p<0.01). Examination of ER-mitochondria interactions by confocal and 3D electron microscopy suggested increased co-localization of these two organelles in lymphocytes of responder patients to anti-PD1 therapy. Blockade of PERK in combination with anti-PD1 treatment resulted in a 64% reduction in tumor volume compared to control and an over 40% reduction compared to anti-PD1 monotherapy (n=7, *p<0.002). This suggests that blockade of PERK enhances α PD-1 efficacy. PCA from metabolomics of tumor-infiltrating T cells suggested a differential metabolic signature that separates the PD1 treated group from control, PERK blockade, and combination-treated animals. Furthermore,

blockade of PERK increased glycolytic flux and mitochondrial respiration of CD8+ T cells. Thus, blockade of PERK supports metabolic reprogramming to support T cell effector function under ER stress conditions.

Conclusions Our data show that PERK expression may serve as a potential clinical marker of ICB response. Our preliminary evidence indicates that Targeting PERK improved the efficacy of anti-PD1 therapy by modulating metabolic signaling of CD8+ T cells. Thus, targeting PERK in the tumor microenvironment may inhibit pro-oncogenic and immunosuppressive signaling from enhancing ICB responsiveness.

<http://dx.doi.org/10.1136/jitc-2022-SITC2022.0178>

179

T-CELLS DERIVED FROM MALIGNANT PLEURAL EFFUSIONS (MPE) ARE READILY EXPANDABLE, POLYFUNCTIONAL AND CYTOTOXIC TO AUTOLOGOUS TUMOR

<http://dx.doi.org/10.1136/jitc-2022-SITC2022.0179>

¹Vera Donnenberg*, ¹Albert Donnenberg, ¹James Luketich, ¹Shannon Puhalla, ¹Yasa Mutlu, ²David Bartlett. ¹University of Pittsburgh, Pittsburgh, PA, USA; ²Ahn Research Institute, Pittsburgh, PA, USA

Background We have shown that malignant pleural effusions (MPE) are characterized by a distinct and complex pleural secretome¹⁻³ dominated by IL-6, sIL-6R α , CCL2, CXCL10, TGF β , CCL22, IL-8. These cytokines favor tumor epithelial to mesenchymal transition, invasion and suppression of anti-tumor response among the abundant infiltrating T cells. The goal of this study was to determine whether brief ex vivo activation could induce potent effector activity.

Methods Pleural T cells were isolated from freshly drained pleural effusions from 6 breast cancer patients. Autologous pleural tumor was expanded in vitro using the Mammary Epithelial Growth Medium (Lonza). Pleural T cells were stimulated using antiCD3CD28 Dynal beads and low dose IL-2 (60 Cetus U/ml) for 2,4,7, 14 or 21 days. Expanded tumor targets (p0 and p1) were plated at 10,000 cells/96well cultured overnight before the addition of pleural effector T cells at effector to target ratios of 0.1, 3, 6, 12.5, 25 and 50. Cytotoxicity was assessed using a colorimetric assay for lactate dehydrogenase (LDH) release (PromegaCyttox-96). Pleural T cells phenotype and activation/exhaustion markers. Cytokine secretion was measured by flow cytometry and (Luminex).

Results Ex vivo expanded pleural T cells were effector-memory phenotype (CD45RA-CD27-) and were highly cytotoxic against autologous tumor (89-100% Specific Lysis). Even a 2-day ex vivo activation generated highly cytotoxic T cells. The effectors were mostly CD4+ cells (62-90%). Majority of CD8+ T cells were central memory (CD45RA-/CD27-) or effector memory (CD45RA+/CD27-); a majority co-expressed intracellular granzyme B and perforin, 20-60% expressed PD-1. Most CD4+ co-expressed granzyme B and perforin, suggesting cytotoxic CD4+ T cells and were PD-1+. The in vitro cytotoxicity of expanded pleural T cells was highly reproducible among patients of significantly varied age (37 - 94) as well as patients with different molecular subtypes (triple negative, ER+PR+Her2-, ER+PR-Her2+, ER+PR+Her2+, ER+AR+PR-Her2-). Supernatants from cytotoxicity cultures evidenced secretion of G-CSF, IL-6, CXCL10, IFN γ , MCP-3, MIP1 α and beta, IL-13, IL-2 and TNF α in a dose dependent fashion. Polyfunctional T cells (single cells secreting IL-2, TNF α , IFN γ , but not IL-10) were detectable among ex vivo expanded T cells.

Conclusions Pleural T cells are not exhausted and can be stimulated to become potent anti-tumor effectors that may be useful for adoptive cellular therapy.

REFERENCES

1. Donnenberg, A. D., Luketich, J. D., Dhupar, R., and Donnenberg, V. S. (2019) Treatment of malignant pleural effusions: the case for localized immunotherapy. *Journal for ImmunoTherapy of Cancer* **7**, 110
2. Donnenberg, A. D. V. S. (2019) The secretome of malignant pleural effusions: Clues to targets of therapy. *Leukemia Research* **85**, S11-S12
3. Donnenberg, A. D., Luketich, J. D., and Donnenberg, V. S. (2019) Secretome of pleural effusions associated with non-small cell lung cancer (NSCLC) and malignant mesothelioma: therapeutic implications. *Oncotarget* **10**, 6456-6465

Ethics Approval Some samples were anonymized by an honest broker while some participants gave consent.

180

THE IN-VITRO MEASURE OF T CELL AVIDITY BETWEEN TUMOR-EFFECTOR PAIRS, NOT AFFINITY, PREDICTS OPTIMAL ANTI-TUMOR RESPONSE IN VIVO

Justin Moser*, Yotam Bar-Ephraim, Jens Eberlein, Keith Bailey, Song-My Hoang, Andrea Candelli, Will Singleterry. *LUMICKS, Waltham, MA, USA*

Background With the increasing complexity of cell therapy construct design, novel methodologies to accelerate screening and improve evaluation of lead candidates for clinical benefit are needed. Several methods are currently employed including receptor-ligand affinity measurements. However, affinity between T cell receptors (TCRs) and peptide-MHC complexes (pMHC) has shown to be a poor predictor of T cell functional capacity.

Methods We have developed the z-Movi Cell Avidity Analyzer to directly measure the overall binding strength, or cellular avidity, of effector to their target. Unlike affinity, cellular avidity is driven by the overall strength of dynamic surface interactions between effector cells and their targets; this novel biomarker integrates receptor density, the sum of individual affinities, and engagement of the multitude of co-receptors within the immunological synapse to characterize the interaction in a more biologically relevant context.

Results We will discuss how increased specific cellular avidity, i.e., TCRs with the strongest antigen binding and the lowest background binding, correlated with improved effector function in vitro and in vivo. Another application of measuring cell avidity explored the effect of changes to the glycosylation pattern on the cell surface of BMDC on T cell activation. Here, altered glycosylation patterns on BMDC increased avidity towards T cells leading to enhanced T cell function upon Ag recognition. These results demonstrated the benefits of understanding cell avidity to predict and select potent T cell candidates or bispecific antibodies.

Conclusions These results demonstrated the benefits of understanding cell avidity to predict and select potent T cell candidates or bispecific antibodies.

<http://dx.doi.org/10.1136/jitc-2022-SITC2022.0180>

181 HIGH THROUGHPUT SCREENING STRATEGIES IN THE DEVELOPMENT OF LOGIC GATED CELL THERAPIES

Rona Harari-Steinfeld*, Laura Lim, Angela Boroughs, Sofia Kyriazopoulou Panagiotopoulou, Cate Sue, Jamie Thomas, Jon Chen, Aaron Cooper, Ryan Fong, Mary Chua, Ed Yashin, Christine Shieh, Sophie Xu, Nicholas Haining. *Arsenal Biosciences, South San Francisco, CA, USA*

Background Generating potent clinical responses against solid tumors remains a challenge for CAR T cell therapy. This lack of efficacy is likely due in part to reduced on-tumor activity in the tumor microenvironment and the lack of appropriate target antigens that are expressed on tumor cells but not on critical healthy tissues. We addressed the second of these challenges by engineering T cells to target tumors only upon recognition of two antigens through AND Boolean logic.

Methods In our efforts to develop logic gated cell therapies we generated hundreds of binders for the priming receptor (PrimeR) and the CAR receptor. Here we demonstrate two strategies used for functional screening of PrimeR binders to identify binders with desired sensitivity and fidelity in driving the specific on-target expression of a fixed CAR.

In an arrayed strategy, we engineered T cells from 4 donors in multiwell plates using CRISPR-mediated, non-viral, site-specific integration of circuits bearing ~1000 PrimeR binders and receptor architectures with a fixed MSLN CAR. In addition, we employed a pooled screening strategy in which we engineered 2 donors of T-cells with a pool containing a subset of >300 unique PrimeR binders with a fixed MSLN CAR, using a similar engineering protocol.

Engineered T cells from both strategies were co-cultured with target cell lines to evaluate targeting fidelity and on-target functionality. In the arrayed setting, functional readouts (activation markers, cytokine secretion) were measured and reported directly. In the pooled setting, sorting based on functional markers was performed at end-point and sequencing was used to determine the enrichment of specific binders. Circuit fidelity was assessed by the lack of CAR expression and/or T-cell activation in response to target cell lines expressing the cytolytic antigen alone, or neither target antigens. On-target functionality was assessed by quantifying secretion of key cytokines in response to dual antigen stimulation.

Results We combined these metrics to filter out PrimeRs that allowed for CAR expression in the absence of logic gate activation, and to rank the remaining binders by their ability to drive CAR expression in the presence of both antigens. To account for multiple criteria when ranking binders, we used desirability functions, scaling each measurement to a (0–1) range, and using geometric means to combine desirabilities across different criteria.

Conclusions As each strategy comes with a different set of limitations and advantages, both serve as important tools for the effective selection of binders and receptors in the development of novel cell therapies.

<http://dx.doi.org/10.1136/jitc-2022-SITC2022.0181>

182

DISCOVERY OF TSC-203-A02: A PRAME-SPECIFIC TCR-T CELL THERAPY CANDIDATE FOR THE TREATMENT OF SOLID TUMORS

Mollie Jurewicz, Elizabeth Hall, Alexandra Luther, Kimberly Cirelli, Vivin Karthik, Kenneth Jahan, Tary Traore, Maytal Bowman, Victor Ospina, Sonal Jangalwe, Shubhangi Kamalia, Sadie Lee, Daniel Pollacksmith, Sida Liao, Amy Virbasius, Kristen Murray, Jillian Oliveira, Lisa Nip, Christina Lam, Livio Dukaj, Danielle Ramsdell, Jin He, Joel Sher, Ribhu Nayar, Qikai Xu, Yifan Wang, Antoine Boudot, Cagan Gurer, Gavin MacBeath*. *TScan Therapeutics, Waltham, MA, USA*

Background The cancer/testis antigen PRAME exemplifies an ideal TCR-T cell therapy target due to its high expression in multiple malignancies and its absence in normal tissues. Initially identified in metastatic cutaneous melanoma,¹ PRAME is highly expressed in various additional solid tumors including lung, head & neck, and ovarian cancers. PRAME plays a pivotal role in multiple cellular processes and has been demonstrated to exhibit protumorigenic function primarily through inhibition of retinoic acid receptor signaling.² Targeting of PRAME in solid tumors, particularly when performed as part of a TCR-T multiplexing strategy, represents a promising therapeutic approach in the treatment of many cancer indications.

Methods We discovered TCRs specific for 5 different A*02:01-restricted PRAME-derived epitopes using TScan's proprietary ReceptorScan platform. Using an activation-based screening technology termed ActivScan, we identified the most functional TCRs from a library of 1300 PRAME-specific TCRs to select for TCRs with greatest avidity and expression. These highly active TCRs were examined for their cytotoxic function using a panel of PRAME-expressing A*02:01-positive cell lines. Lead TCRs were assessed for potential off-target reactivity using our proprietary SafetyScan platform, in which off-target recognition of antigens derived from all proteins that comprise the human proteome is evaluated. Safety was further confirmed by examining alloreactivity to high-frequency class I HLAs and by testing TCR reactivity to a panel of normal primary human cells. Lastly, we tested TCR-T cells for their ability to control tumor growth *in vivo* using PRAME-expressing xenograft mouse models.

Results We screened 871 million naïve CD8⁺ T cells from 16 unique healthy donors in ReceptorScan to identify 5706 TCRs specific for 5 PRAME epitopes. PRAME₄₂₅₋₄₃₄-specific TCRs demonstrated superior recognition of a PRAME-expressing cell line compared to all other PRAME epitopes tested. Following selection of high-expressing and high avidity PRAME₄₂₅₋₄₃₄-specific TCRs in ActivScan, TCRs were evaluated for their cytotoxic function, and two TCRs compared favorably to a clinical-stage benchmark TCR with respect to cytotoxicity, cytokine release, and T cell proliferation. Safety assessment demonstrated that few off-target peptides were recognized by lead TCRs, minimal alloreactivity was observed to 110 allotypes tested, and no reactivity to normal primary human cells was found. PRAME₄₂₅₋₄₃₄-specific TCR-T cells were also able to control tumor growth *in vivo* following infusion into immunodeficient mice implanted with PRAME-expressing xenografts.

Conclusions Based on its demonstrated activity *in vitro* and *in vivo*, this autologous TCR-T cell therapy candidate, TSC-203-A02, has been advanced to IND-enabling studies.

REFERENCES

1. Ikeda H, Lethé B, Lehmann F, van Baren N, Baurain JF, de Smet C, *et al.* Characterization of an antigen that is recognized on a melanoma showing partial HLA loss by CTL expressing an NK inhibitory receptor. *Immunity*. 1997;**6**(2):199–208.

2. Epping MT, Wang L, Edel MJ, Carlee L, Hernandez M, Bernards R. The human tumor antigen PRAME is a dominant repressor of retinoic acid receptor signaling. *Cell*. 2005;**122**(6):835–47.

<http://dx.doi.org/10.1136/jitc-2022-SITC2022.0182>

183

CANCER-MUTATION-SPECIFIC T CELLS: NOVEL IMMUNOTHERAPY APPROACH FOR LOW MUTATIONAL BURDEN PATIENTS

Alfred Slanetz*, Walter Barry, Benjamin Schwarz, Farzonai Muzaffar, Ryan Campbell, Abenezer Abera. *Geneius Biotechnology, Inc., Natick, MA, USA*

Background Immune checkpoint inhibitors, such as anti-PD1 antibodies, have revolutionized cancer immunotherapy. Their success demonstrates that a patient's own T cells recognize and treat cancer. However, anti-PD1 therapy is most effective in the treatment of cancers with high mutational burden, ~5% of all malignancies. Therefore, an alternative strategy is necessary to target cancer with lower mutational burden. Importantly, the efficacy of PD-1 blockade is associated with the recruitment of new T cells from the blood rather than the activation of pre-existing tumor infiltrating lymphocytes (Yost K.E., *et al.* Nat. Med. 2019).

Methods Our approach is to prime and expand T cells from the blood to cancer-specific mutations *ex vivo*.

Results We can generate T cell populations reactive to as few as 8 and as many as 40 cancer-specific mutant proteins in a single production run. *In vitro*, these T cells have mutation-specific cytotoxicity and do not kill the normal cells. These T cells express homing receptors that allow them to infiltrate the tumor and express high levels of TNF α and IFN γ , both of which are associated with effective tumor cytotoxicity and pro-inflammatory modification of the tumor microenvironment. The predominant immunophenotype of these cells is consistent with central and effector memory, CD4 $^{+}$ and CD8 $^{+}$ T cells, with almost no regulatory or exhausted T cells.

Conclusions We believe these T cells can be used as a cellular therapy in conjunction with, or as an alternative to, immune checkpoint inhibitors to treat lower mutational burden cancers that comprise most patients' tumors.

<http://dx.doi.org/10.1136/jitc-2022-SITC2022.0183>

184

DISCOVERY, CLONING AND FUNCTIONAL VALIDATION OF A NEOANTIGEN SPECIFIC PATIENT DERIVED TCR ON THE BERKELEY LIGHTS PLATFORM, WITH IMPLICATIONS IN PERSONALIZED CANCER IMMUNOTHERAPY

¹Joseph Valdez*, ¹Guido Stadler, ¹Pei-Yu (Kate) Lin, ¹Milton Quintanilla, ¹Tyler Helmann, ²Xiuli Zhang, ^{2S}Peter Goedegebuure, ²Malachi Griffith, ²William Gillanders, ³William Hoos, ¹Yiyang Xu. ¹Berkeley Lights, Emeryville, CA, USA; ²Washington University in St. Louis, St. Louis, USA; ³Jaime Leandro Foundation, Scotts Valley, CA, USA

Background Pancreatic ductal adenocarcinoma (PDAC) has the poorest prognosis of all human cancers and requires new therapeutic options. Several immune-based treatments including personalized neoantigen vaccines and adoptive T cell transfer are currently being investigated. Recently, complete clinical response was reported in a patient with HER2+ metastatic PDAC treated with a neoantigen vaccine in combination with radiation and dual checkpoint (<https://doi.org/10.1101/2021.12.16.21267326>). Here we describe a sensitive method for post-vaccination functional characterization of neoantigen-specific T cells from minimal quantity of patient peripheral blood at the single cell level using a microfluidic device on the Beacon[®] optofluidic system from Berkeley Lights.

Methods Peripheral blood was obtained from a patient with metastatic PDAC in complete response following neoantigen DNA vaccine therapy. T cells were pre-enriched by stimulating with a cocktail of peptides corresponding to 7 neoantigens. Subsequently, single T cells were investigated over 2 days using a microfluidic device featuring nanoliter-scale NanoPen[®] chambers in co-culture with autologous dendritic cells or partially HLA-matched allogeneic antigen presenting cells (APCs) pulsed with the neoantigen peptides. Antigen-responsive T cells were isolated based on expression of CD137, a known T cell activation-associated marker, cytokine secretion and cytotoxicity profile. TCRs of selected T cells were recovered, synthesized, cloned into a lentiviral expression vector, expressed in primary T cells from an unrelated donor, and validated using peptide pulsed APCs.

Results A quantitative dataset including CD137 expression, IFN- γ secretion and real time cytotoxicity was generated for single T cells from the peripheral blood of a cancer patient in co-culture with single APCs. Candidates were ranked based on strength of phenotype, isolated and TCR sequences were generated. The top TCR candidate, restricted to HLA-A*02:01, post-engineering was effective in recapitulating the same potency criteria (99% cytotoxicity, 74% CD137+ as compared to <1% for controls and >15,000 fold enrichment of IFN γ /TNF α /IL-2 as compared to controls) against a lymphoma derived cell line presenting a single peptide from the cancer vaccine. Importantly, this TCR was not active against the other neoantigen peptides or a well characterized oncogenic peptide MART-1 demonstrating specificity.

Conclusions We demonstrate the ability to characterize T cells in co-culture with APCs at single cell resolution. A TCR which exhibited strong functional behavior during screening was also effective and specific to a single neoantigen peptide post engineering. This workflow may enable personalized TCR to be realized by reducing the timeframe and finding better candidates to be used independently or in combination with cancer vaccines and other interventions.

<http://dx.doi.org/10.1136/jitc-2022-SITC2022.0184>

185 **TUNING THE CELL-CELL DISTANCE VIA THE NON-SIGNALING EXTRACELLULAR SPACER DOMAIN OF CHIMERIC ANTIGEN RECEPTORS IS CRITICAL FOR OPTIMAL ACTIVITY**

¹Jason Yokoyama*, ¹Lisa Song, ²Quinn Walker, ²Bijan Boldajipour, ¹Howell Moffett, ¹Brian Weitzner, ¹Scott Boyken, ¹Marc Lajoie. ¹Outpace Bio, Seattle, WA, USA; ²Lyell Immunopharma, San Francisco, CA, USA

Background Chimeric antigen receptors (CARs) are synthetic receptors that target engineered immune cell effector functions against target cells expressing specific antigens. CAR activity can be significantly improved by optimization of multiple parameters, including geometry of the immunologic synapse, biophysical properties of the extracellular domains, and signaling properties of the intracellular domains. Native T cell activation is driven by adhesion molecules and T cell Receptors (TCRs) binding to peptides displayed on the Major Histocompatibility Complex (MHC) of target cells, with a well-defined cell-cell distance of 14–15 nm in synaptic contact areas. However, the optimal synaptic distance, and the importance of cell-cell synaptic distance for CAR activity has not been systematically determined. Here we investigate the role of spacer length on the recognition of clinically relevant tumor antigens using a panel of 4 previously-published spacers and 41 novel spacers derived from human extracellular proteins and ranging in length from 3.6–30.6 nm.

Methods We tested all of these spacers with five known CAR targeting domains that bind epitopes at varying distances from the cell membrane on the target cells, including three ROR1 CARs (R11, R12, 2A2), one CD19 CAR (FMC63) and one HER2 CAR (herceptin). Additionally, we developed a model system in which a single linear epitope could be systematically presented at different distances from the target cell membrane using our spacer sequences. In this model, an anti-HA scFv (clone 2E2) was used as the CAR binding domain and an HA peptide (YPYDVPDYA) was used as a model epitope. We tested all possible CAR constructs *in vitro* by evaluating cytokine production and target cell killing kinetics (primary and serial restimulation). Additionally, we tested whether our *in vitro* observations are predictive of *in vivo* performance by choosing five spacers that cover a wide range of performance for two CARs with different predicted optimal spacer lengths in the *in vitro* study (R12, FMC63) and tested them in mouse xenograft models.

Results We demonstrate that both *in vitro* and *in vivo* CAR activity is dependent on spacer length, with optimal activity observed at a synaptic distance of about 20 nm, substantially longer than the 14–15 nm TCR:MHC complex. Furthermore, the optimal range of synaptic distances is far narrower than previously appreciated.

Conclusions We identified spacers that led to improved activity over the current state-of-the-art CAR sequences, suggesting that our biophysically-optimized spacers can be used to rapidly create optimal CAR constructs for arbitrary binder-epitope pairs.

Ethics Approval All animal procedures and housing were conducted in accordance with the Lyell/Explora umbrella IACUC protocol ID EB17–010–117.

<http://dx.doi.org/10.1136/jitc-2022-SITC2022.0185>

186

TUMOR REACTIVE, CYTOKINE INDUCED, ENGINEERED HUMAN NATURAL KILLER CELLS DEMONSTRATE SERIAL CYTOTOXICITY AGAINST LIQUID AND SOLID TUMOR CELL TARGETS

¹Ting Lu*, ¹Christian Bustillos, ¹Zhiyao Li, ¹Jianying Zhang, ²Lei Zhang, ²Li Chen, ¹Jianhua Yu, ¹Michael Caligiuri. ¹City of Hope National Medical Center, Los Angeles, CA, USA; ²CytolImmune Therapeutics, Inc., Monrovia, CA, USA

Background Expression of PD-L1 on human natural killer (NK) cells identifies a subset that are selectively reactive to tumors. PD-L1(+) NK cells have increased CD107a expression, cytotoxicity, and interferon-gamma secretion vs. the PD-L1(-) fraction. PD-L1(+) NK cells are manufactured for patient administration using cytokine stimulation under GMP conditions and in vivo survival sustained by engineering these tumor-reactive, cytokine-induced killer (TRACK) NK cells to express soluble (s)IL-15. Cryopreserved, off-the-shelf allogeneic TRACK NK cells expressing sIL-15 are being assessed in a phase 1 trial in patients with relapsed/refractory non-small cell lung cancer (NSCLC; NCT05334329). Here, we assess phenotype and function of human TRACK NK cells and demonstrate serial natural cytotoxicity and antibody-dependent cellular cytotoxicity (ADCC) lymphoma and NSCLC targets.

Methods TRACK NK cells were manufactured from umbilical cord blood NK cells by activation and expansion of NK cells over a feeder cell line, engineering to secrete sIL-15, followed by cytokine activation before cryopreservation. Serial TRACK NK cell cytotoxicity was measured as killer frequency, defined as the average number of tumor target cells killed per single TRACK NK cell over 8–40 hours.¹

Results Fresh TRACK NK cells expressed >90% CD16 immediately prior to cryopreservation; following thaw, resting NK cell CD16 expression was >60% at T₀ but rose significantly to >75% following culture at 37C for 6h and >82% at 24h (p<0.05), mimicking upregulations as would likely occur in vivo. Similar statistically significant upregulation of NKp44 and NKp46 (p<0.05) was observed on TRACK NK cells, whereas very high expression of NKp30, NKG2D, and DNAM-1 remained stable. CD57 and PD-1 expression remained low (~1–5%). TRACK NK cells performed robust ADCC against both CD20(+) at various E:T in the presence of anti-CD20 and anti-EGFR, respectively, significantly better than NK killing of either target. Substantial TRACK NK cell cyto-reduction of NSCLC was also demonstrated in vivo. In addition, antibody independent serial cytotoxicity and antibody-dependent serial cytotoxicity by TRACK NK cells was demonstrated against both lymphoma and NSCLC lines.

Conclusions Under various conditions, each TRACK NK cell was able to kill a multitude of lymphoma cells via ADCC in the presence of anti-CD20 mAb or a multitude of NSCLC in the absence or presence of antibody. These data support the use of the TRACK-NK cells in the clinic using both their natural cytotoxicity and their ADCC mechanism of action against both liquid and solid tumors.

REFERENCE

1. Navarrete-Galvin et al. *J Transl Med* **20**, 151; 2022.

<http://dx.doi.org/10.1136/jitc-2022-SITC2022.0186>

187 **A LIVE TUMOR FRAGMENT PLATFORM SUITABLE FOR ASSESSING RESPONSE TO T-CELL THERAPIES**

Christopher Zahm*, Laura Hrycniak, Ellen Wargowski, Dinesh Joshi, Team Adstamongkonkul, Greg Ochs, Gabriella Stueber, Debra Bloom, Ryan Fischer, Christina Scribano, Christin Johnson, Anura Shrestha, Nathan Marhefke, Aariah Law, Jonathan Oliner. *Elephas Bio, Madison, WI, USA*

Background T-cell therapies have shown efficacy in numerous clinical settings. However, predictive biomarkers of response are lacking, and determining which T-cell therapy each cancer patient will respond to has been hindered by the absence of model systems that maintain the specific immunosuppressive features of each patient's tumor microenvironment (TME). The Elephas live tumor fragment (LTF) platform is designed to enable prediction of clinical response to many types of immunotherapies, including cellular therapies and checkpoint blockade. The experiments described here examine T-cell activation, cytokine production, and tumor-cell killing following co-culture of LTFs with T-cell therapies.

Methods Transgenic T-cells: LTFs were generated from two tumors that differ only by the presence or absence of a recombinantly expressed protein selectively recognized by targeted transgenic T cells. Transgenic and wildtype (WT) T-cells were isolated and co-cultured at 1:1, 5:1, and 10:1 T-cell:target-cell ratios using LTFs from both tumor types and assessed for T-cell activation and tumor cell viability using flow cytometry and cytokine/chemokine secretion profiling.

TILs: Tumors were collected and processed for TIL expansion, which was conducted in the presence of IL-2 for 10 days. Following expansion, CD8 T-cells were isolated and co-cultured for 48h at a 1:1 ratio with LTFs from the same tumor. Tumor killing and T-cell activation were measured by flow cytometry.

All animal studies were carried out in accordance with animal welfare guidelines and approved by the IACUC at Excelsior Labs.

Results Transgenic T-cells: Flow cytometry revealed an increase in activation markers (CD25, CD69, ICOS, PD1, and CD137) on the surface of transgenic CD8 T-cells incubated with target-positive tumors, but not target-negative tumors, while WT T-cells displayed no increases when incubated with either tumor type. Secretome profiling demonstrated similar changes, with an increase in cytokine and chemokine secretion (IFN γ , CXCL1, CCL4, and CXCL5) as the ratio of transgenic CD8 T-cells to target-cells increased, using target-positive, but not target-negative, LTFs. Decreases in tumor cell viability were also detected at higher T-cell:Target-cell ratios and were again only observed with target-positive LTFs.

TILs: CD8 T-cells isolated from TILs, but not WT T-cells, that were co-cultured with LTFs demonstrated increased activation and resulted in a decrease in tumor cell number following 48h of culture.

Conclusions We have verified target-specific transgenic T-cell activation, as well as reduced tumor viability in expanded TILs following co-culture with LTFs. These data lay the groundwork for future studies using the Elephas LTF platform to predict individual clinical responses to various T-cell therapies.

Ethics Approval All animal studies were carried out in accordance with animal welfare guidelines and approved by the IACUC at Excelsior Labs.

<http://dx.doi.org/10.1136/jitc-2022-SITC2022.0187>

188 **ARGININE PRE-CONDITIONING ENHANCES T-CELL POTENCY AND METABOLIC FITNESS**

Rashmi Pillai*, Xiaoyu Zhang, Brandon Lamarche, Yama Abassi. *Agilent, San Diego, CA, USA*

Background Enhanced T-cell performance is imperative for the success of adoptive T-cell-based therapies. Here we assessed the killing efficiency of MART-1 specific TCR T-cells after Arg, Gln, and Leu pre-conditioning using the Agilent xCELLigence RTCA eSight (eSight). The eSight system can simultaneously capture live-cell images and measure cellular impedance, which determines the changes in cell number, morphology, and attachment. In parallel, the status of metabolism of the pre-conditioned T-cell was determined by Seahorse XF assays.

Methods Briefly, CD3⁺ T-cells (Hemacare, Seattle, WA) were transduced with retrovirus SAMEN-DMF5 with a CD34 marker gene, against MART-1. The T-cells were pre-conditioned in a range of concentrations varying between 0–6mM with Arg, Glu and Leu for 7 days, followed by a killing assay using MART-1 expressing melanoma cell line as target cells (624.38) engineered to express a red-fluorescent nuclear protein, and Seahorse XF Cell MitoStress and T-cell metabolic profiling assays. The comparison was made with the controls, including transduced T-cells grown in RPMI but with no amino acids during pre-conditioning (TCR_RPMI), and non-transduced T-cells (Non_TCR).

Results Our data show Arg supplementation enhanced T-cell killing of target cells while Leu and Gln suppressed T-cell mediated killing. Specific cytolysis (5:1, E:T ratio) at 60h for TCR_RPMI and 6 mM Arg pre-conditioned T cells (TCR_ARG) were 35% and 76%, respectively. We further determined the impact of the duration of pre-conditioning. 2 and 4 days of pre-conditioning with 6 mM Arg were done along with the 7-day method. The percentages of cytolysis of TCR_ARG (6 mM) at 60 hr were 29, 68, and 81 on days 2, 4, and 7, respectively, indicating that improved killing potency of the T-cells started as early as 4 days with Arg. The Seahorse XF assays were performed to determine metabolic fitness and persistence. Arg (6mM) supplementation increased the spare respiratory capacity 1.7 and 2.6 times compared to TCR_RPMI control on days 4 and 7 respectively.

Conclusions In summary, Arg at 6mM concentration was effective with the highest percentage of cytolysis and a higher spare respiratory capacity and Gln and Leu conditioning suppressed T-cell killing. Consistently, Arg fuels the TCA cycle and thus, shifts metabolism towards mitochondrial respiration.

<http://dx.doi.org/10.1136/jitc-2022-SITC2022.0188>

189

CRISPR-MEDIATED METABOLIC REPROGRAMING OF ADOPTIVELY TRANSFERRED T CELLS TO POTENTIATE ANTITUMOR RESPONSE

Soraya Zorro Manrique*, Yunfei Wang, Ana Dominguez, Debra Armendariz, Patrick Hwu. Moffitt Cancer Center, Tampa, FL, USA

Background The signaling of key metabolic pathways in T cells within the tumor microenvironment (TME), strongly impacts their antitumor response. Cancer cells compete with T cells for essential nutrients such as glucose and amino acids; in addition, cancer cells produce T-cell inhibitory metabolites such as lactate and adenosine. Therefore, metabolic reprogramming of T cells to confer adaptability to the TME is a promising therapeutic strategy for advanced cancers.

Methods To identify detrimental metabolic genes for T-cell tumor infiltration, we performed an *in vivo* shRNA screen with a pooled metabolome library (~300 genes) in Pmel CD8 T cells adoptively transferred into B16 tumor-bearing mice. We identified genes whose disruption in T cells resulted in increased infiltration in B16 melanoma.

Results We found that disruption of the PDHB gene enhances T-cell tumor infiltration. Pdhb encodes for the E1 Subunit Beta of the Pyruvate Dehydrogenase (PDHB), an enzyme linking glycolysis and the tricarboxylic acid cycle. We validated this result using CRISPR/Cas9 RNP transfection (>90% knockout efficacy) to knockout (KO) Pdhb in Pmel CD8 T cells. Our *in vivo* studies showed that PDHB KO improves T-cell infiltration and tumor rejection, vs non-targeting control T cells. PDHB KO cells produced higher IFN γ levels and displayed improved tumoricidal capacity. The functional metabolomic analyses (seahorse assays) indicated that PDHB KO cells have an impaired mitochondrial function (reduced respiratory and FAO capacities) while having an increased glycolytic activity. The transcriptome and pathway analyses indicated that PDHB disruption, strongly induced lipid biosynthesis. Analyzing the most upregulated metabolites in the PDHB KO cells revealed that inosine, a product of adenosine metabolism, reported to serve as an alternative carbon source for T cells, was within the top 5 upregulated metabolites. The integrated transcriptome, metabolomics and pathway analyses indicated that PDHB KO cells display a metabolic reprogramming with upregulation of unsaturated fatty acid biosynthesis, glycolysis/gluconeogenesis, pyruvate metabolism, chemokine signaling and purine metabolism. Remarkably, the transcriptome analysis suggests that the PDHB KO T cells have an expression pattern of Tscm/Tcm cells which might be associated with their capacity to survive within tumors.

Conclusions In tumors characterized by glucose deprivation, the inosine upregulation by PDHB KO T cells might support T-cell function. Overall, our data suggests that PDHB disruption in T cells could contribute improving adoptive cell therapy. Thus, our study indicates that CRISPR-mediated metabolic reprogramming of T cells could be a powerful approach for generating T cells able to overcome tumor-driven metabolic restrictions.

Ethics Approval Animal protocol was approved by the University of South Florida, IACUC IS00008501.

<http://dx.doi.org/10.1136/jitc-2022-SITC2022.0189>

NOVEL CELLULAR IMMUNOTHERAPY WITH ANTI-MESOTHELIN CAR-KILLER LYMPHOCYTES AGAINST ADVANCED CHOLANGIOCARCINOMA

^{1,2}Annamaria Massa*, ³Valeria Leuci, ²Federica Galvagno, ²Chiara Donini, ²Francesca Vita, ²Ramona Rotolo, ²Alessia Proment, ⁴Letizia Vitali, ³Elisabetta Fenocchio, ²Elisa Vigna, ³Giuliana Cavalloni, ⁵Massimo Aglietta, ²Dario Sangiolo. ¹University of Turin, Orbassano (Torino), Italy; ²University of Turin, Turin, Italy; ³Candiolo Cancer Institute, FPO-IRCCS, Candiolo, Italy; ⁴University of Turin, Candiolo, Italy; ⁵Università di Turin, Turin, Italy

Background Cholangiocarcinoma (CCA) is a biliary epithelial tumor with poor prognosis, for which there are not effective therapeutic options in advanced stages.¹ Innovative therapeutic strategies are highly needed. Cellular immunotherapy holds great promise for the treatment of solid tumors.² Among various cellular immunotherapy approaches, our group contributed to the development and testing of Cytokine Induced Killer lymphocytes (CIK) endowed with intrinsic MHC-unrestricted tumor killing activity.³ Recently, it was reported that CIK may be engineered with Chimeric Antigen Receptors (CARs) generating immune effectors with double antitumor potentiality,^{4,5} strategically important to counteract the frequent heterogeneity of tumor antigen expression. To this end, in the context of CCA mesothelin (MSLN) is emerging as a promising CAR target.^{6,7}

Here, we hypothesized to generate a novel and effective cell therapy strategy against CCA redirecting patient-derived CIK, with a CAR against MSLN acting as relevant CCA target.

Methods

MSLN-CAR CIK were generated from patients' PBMC and were transduced with a lentiviral vector encoding for the second generation anti-MSLN CAR including the co-stimulatory domain 4-1BB. CAR expression and extended phenotype of mature CAR-CIK were assessed by flow cytometry. The expression of MSLN, were assessed in CCA cell lines and CCA surgical specimens. In parallel, target molecules recognized by CIK (MICA/B, ULBPs) were evaluated.

Tumor killing in 2D models was evaluated at different effector:target ratio by flow-cytometry and bioluminescence-based assays. In order to increase the complexity of CCA models 3D tumor spheroids were generated from different CCA cells bearing a reporter gene (RFP) and co-incubated with effector cells at ratio 2:1. Fluorescence images were acquired at different times using fluorescence microscopy.

Results We successfully generated MSLN-CAR.CIK from peripheral blood of tumor patients (n=5) (figure 1A). CAR.CIK immunophenotype was comparable to unmodified controls (NTD.CIK): (42±5)% CAR+, (49±8)% CD3+CD56+, (77±6)% CD3+CD8+ and (83±7)% NKG2D+. We found high (>90%) membrane expression of MSLN in 6/7 CCA cell lines that were all effectively killed by MSLN-CAR.CIK in 2D assays. The observed tumor lysis was significantly enhanced (n=12) compared to NTD.CIK: 80% vs 30% (E/T 2.5:1), 70% vs 20% (E/T 1:2, p< 0.0001) (figure 1B). The intense activity, along with tumor infiltration, by MSLN-CAR.CIK was observed also against CCA 3D spheroids.

Conclusions We report that MSLN-CAR.CIK effectively targets CCA cells in both 2D assays as well as in 3D models. Our findings provide translational bases to support clinical cellular immunotherapy studies with MSLN-CAR.CIK in the challenging field of advanced CCA.

REFERENCES

1. Brindley PJ, Bachini M, Ilyas SI, Khan SA, Loukas A, Sirica AE, Teh BT, Wongkham S, Gores GJ. Cholangiocarcinoma. *Nat Rev Dis Primers*. 2021 Sep 9;7(1):65.
2. Menon S, Shin S, Dy G. Advances in Cancer Immunotherapy in Solid Tumors. *Cancers (Basel)*. 2016 Nov 24;8(12):106.
3. Giraudo L, Gammaitoni L, Cangemi M, Rotolo R, Aglietta M, Sangiolo D. Cytokine-induced killer cells as immunotherapy for solid tumors: current evidence and perspectives. *Immunotherapy*. 2015;7(9):999–1010.
4. Leuci V, Donini C, Grignani G, Rotolo R, Mesiano G, Fiorino E, Gammaitoni L, D'Ambrosio L, Merlini A, Landoni E, Medico E, Capellero S, Giraudo L, Cattaneo G, Iaia I, Pignochino Y, Basiricò M, Vigna E, Pisacane A, Fagioli F, Ferrone S, Aglietta M, Dotti G, Sangiolo D. CSPG4-Specific CAR.CIK Lymphocytes as a Novel Therapy for the Treatment of Multiple Soft-Tissue Sarcoma Histotypes. *Clin Cancer Res*. 2020 Dec 1;26(23):6321–6334.
5. Leuci V, Casucci GM, Grignani G, Rotolo R, Rossotti U, Vigna E, Gammaitoni L, Mesiano G, Fiorino E, Donini C, Pisacane A, Ambrosio LD, Pignochino Y, Aglietta M, Bondanza A, Sangiolo D. CD44v6 as innovative sarcoma target for CAR-redirectioned CIK cells. *Oncoimmunology*. 2018 Feb 15;7(5):e1423167.
6. Mandrekar P, Cardinale V. Periostin and mesothelin: Potential predictors of malignant progression in intrahepatic cholangiocarcinoma. *Hepatol Commun*. 2018 Apr 25;2(5):481–483.
7. Yu L, Feng M, Kim H, Phung Y, Kleiner DE, Gores GJ, Qian M, Wang XW, Ho M. Mesothelin as a potential therapeutic target in human cholangiocarcinoma. *J Cancer*. 2010 Oct 1;1:141–9.

Ethics Approval We received approval for collection of patient samples and the associated informed consent document from the Institutional Review Board (IRB) per Declaration of Helsinki guidelines (Prot. Number 225/2015).

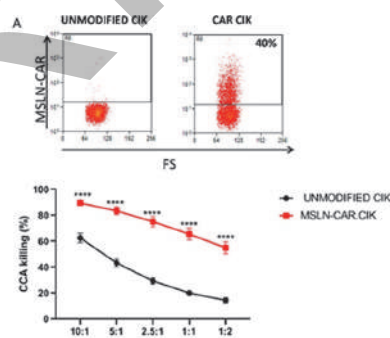


Figure 1. Generation and anti-CCA activity of CAR.MSLN CIK. A) Representative flow-cytometry showing that patient-derived MSLN-CAR.CIK. B) In vitro MSLN-CAR.CIK intensely killed CCA cells even at very low effector/target ratio (p<0.0001 as compared with controls).

Abstract 190 Figure 1 Generation and anti-CCA activity of CAR.MSLN CIK. A) Representative flow-cytometry showing that patient-derived MSLN-CAR.CIK. B) In vitro MSLN-CAR.CIK intensely killed CCA cells even at very low effector/target ratio (p<0.0001 as compared with controls)

<http://dx.doi.org/10.1136/jitc-2022-SITC2022.0190>

191

TARGETING MYELOID-DERIVED SUPPRESSOR CELLS (MDSCS) IN BLADDER CANCER TO ENHANCE EFFICACY OF ADOPTIVE CELL THERAPY (ACT)

<http://dx.doi.org/10.1136/jitc-2022-SITC2022.0191>

Sarah Bazargan Candidate*, Brittany Bunch, Jamie Blauvelt, Annick Landin, Johannes Ali, Dominique Abrahams, Amy Hall, Matthew Beatty, Michael Poch, Shari Pilon-Thomas. *Moffitt Cancer Center, Tampa, FL, USA*

Background MDSCs are a significant barrier to adoptive cell therapy (ACT) due to their suppressive effects on T-cells. We predict that there is an enrichment of MDSCs within bladder tumors and depletion of MDSCs may augment anti-tumor responses after intravesical ACT with tumor reactive T-cells.

Methods For murine studies, orthotopic MB49-OVA bladder tumors were collected, stained for MDSCs, and analyzed by flow cytometry. Urine samples from bladder cancer patients were also collected and stained for MDSCs. From mice, purified MDSCs and OT-I T-cells were cocultured and from bladder cancer patients, purified urine MDSCs and CD3-stimulated peripheral blood T-cells were cocultured to assess suppression of T-cell proliferation or IFN-gamma secretion. Mice bearing MB49-OVA tumors were treated with intravesical instillation of gemcitabine and/or OT-I T-cells and tumor growth was monitored via ultrasound.

Results In mice bearing MB49-OVA tumors, the levels of polymorphonuclear (PMN)-MDSCs averaged between 11.1–23.5% of live cells and monocytic (M)-MDSCs averaged 7.6% of live cells, demonstrating that nearly 20–30% of live cells within murine bladder tumors are MDSCs. In the urine of bladder cancer patients, PMN-MDSCs predominantly make up the live cell population, averaging 71.7%, demonstrating an enrichment for MDSCs within the microenvironment of human bladder cancer. In murine coculture assays, MDSCs reduced the proliferation of OT-I T-cells and in human cocultures, MDSCs reduced T-cell IFN-gamma production to a fourth of control levels. Therefore, MDSCs from bladder tumors suppress anti-tumor T-cells by inhibiting proliferation and reactivity. In mice bearing large MB49-OVA tumors (>50mm³), pretreatment with gemcitabine improved anti-tumor response in combination with intravesical ACT with OT-I T cells in comparison to treatment with gemcitabine only ($p=0.0387$), OT-I only ($p=0.0148$), and untreated ($p=.0039$). In smaller MB49-OVA tumors (<50mm³), gemcitabine pretreatment provided little added benefit to ACT in comparison to treatment with gemcitabine only ($p>0.05$) and OT-I only ($p>0.05$). All p-values generated by performing Mann-Whitney tests on tumor volumes at final time points.

Conclusions MDSCs make up a significant proportion of the immune population within bladder tumors and exert suppressive effects on T-cells. Our studies support the selective targeting of MDSCs via gemcitabine to improve the anti-tumor effects of ACT. While we show that a single instillation of gemcitabine and ACT improves anti-tumor responses, we predict that this effect will be further enhanced with multiple instillations of T-cells.

Acknowledgements This study was supported by funds from the NIH/NCI R01CA259387. This work was supported in part by the Tissue Core Facility at the Moffitt Cancer Center, and in part by the Cancer Center Support Grant P30 CA076292 from the National Cancer Institute.

Ethics Approval This study was approved by the Advarra IRB; approval number IRB# 00000971 and the University of South Florida IACUC, approval number R IS00007685.

CHARACTERIZATION OF ANTIBODIES AGAINST BTN2A1 FOR V δ 2⁺ γ δ T CELL-BASED TUMOR IMMUNOTHERAPY

¹Kok Fei Chan*, ¹Simone Ostrouska, ²Ranjeeta Prasad, ²Daria Kurtov, ²Andrew Hammet, ³Marc Rigau, ³Adam Aldrich, ¹Andreas Behren. ¹Olivia Newton-John Cancer Research Institute, and School of Cancer Medicine, La Trobe University, Heidelberg, Victoria, Australia, Melbourne, Australia; ²CSL Limited at the Bio21 Molecular Science and Biotechnology Institute, The University of Melbourne, Parkville, Victoria 3010, Australia, Melbourne, Australia; ³Department of Microbiology and Immunology at the Peter Doherty Institute for Infection and Immunity, The University of Melbourne, Parkville, Victoria 3010, Australia, Melbourne, Australia

Background Human γ δ T cells are ideal candidates for tumor immunotherapy because of their natural tropism for tumor microenvironment, elicit rapid innate-like immune responses upon tumor recognition and the ability to orchestrate other tumor-infiltrating immune cells for tumor cell killing.¹ Our group has recently defined aspects of the mechanism of T-cell receptor (TCR) dependent activation of V γ 9V δ 2⁺ T cells by tumors following the presentation of phosphoantigens via the B7 immunoglobulin family-like butyrophilin 2A1 (BTN2A1) and BTN3A1.² Dysregulation of the mevalonate pathway in tumors can cause activation of V γ 9V δ 2⁺ T cells via phosphoantigen accumulation and induces γ δ T cell chemotaxis toward tumor cells.^{3, 4} Most clinical studies so far have used aminobisphosphonates (to promote accumulation of phosphoantigens in cells) or synthetic phosphoantigen analogues such as bromohydrin pyrophosphate (BrHPP) and 2-methyl-3-butenyl-1-pyrophosphate (2M3B1PP) to activate V γ 9V δ 2⁺ T cells in cancer patients.^{5–8} More recently, agonist antibodies against BTN3A (e.g., clone 20.1, ICT-01 and CTX-2026) have been identified and used as a phosphoantigen-independent approach to activate V γ 9V δ 2⁺ T cells for targeted cell killing.¹

Methods We are currently characterizing a number of anti-BTN2A1 antibodies that can potentially be used to modulate the activity of V γ 9V δ 2⁺ T cells in *in vitro* assays.

Results We have also established a pre-clinical humanized tumor model using NOD scid gamma (NSG) mice and showed delayed tumor growth in mice that received 4 rounds of human V δ 2⁺ γ δ T cell adoptive cell transfer in combination with clone 20.1 agonist antibody, which will allow further characterization of our anti-BTN2A1 antibodies.

Conclusions Taken together, our study has demonstrated the potential to target BTN2A1 and BTN3A1 for V γ 9V δ 2⁺ T cell-based cancer immunotherapy development.

REFERENCES

1. Chan KF, Da Gama Duarte J, Ostrouska S, Behren A. Gamma-delta T cells in the tumor microenvironment—interactions with other immune cells. *Frontiers in Immunology*. 2022;**13**:3598.
2. Rigau M, Ostrouska S, Fulford TS, Johnson DN, Woods K, Ruan Z, et al. Butyrophilin 2A1 is essential for phosphoantigen reactivity by γ δ T cells. *Science*. 2020;**367**(6478):eaay5516.
3. Benzaid I, Mönkkönen H, Stresing V, Bonnelye E, Green J, Mönkkönen J, et al. High phosphoantigen levels in bisphosphonate-treated human breast tumors promote V γ 9V δ 2 T-cell chemotaxis and cytotoxicity *in vivo*. *Cancer research*. 2011;**71**(13):4562–72.
4. Ashihara E, Munaka T, Kimura S, Nakagawa S, Nakagawa Y, Kanai M, et al. Isopentenyl pyrophosphate secreted from Zoledronate-stimulated myeloma cells, activates the chemotaxis of γ δ T cells. *Biochemical and biophysical research communications*. 2015;**463**(4):650–5.
5. Abe Y, Muto M, Nieda M, Nakagawa Y, Nicol A, Kaneko T, et al. Clinical and immunological evaluation of zoledronate-activated V γ 9 γ δ T-cell-based immunotherapy for patients with multiple myeloma. *Experimental Hematology*. 2009;**37**(8):956–68.
6. Meraviglia S, Eberl M, Vermijlen D, Todaro M, Buccheri S, Cicero G, et al. *In vivo* manipulation of V γ 9V δ 2 T cells with zoledronate and low-dose interleukin-2 for

immunotherapy of advanced breast cancer patients. *Clinical & Experimental Immunology*. 2010;**161**(2):290–7.

7. Sebestyen Z, Prinz I, Déchanet-Merville J, Silva-Santos B, Kuball J. Translating gammadelta (γ δ) T cells and their receptors into cancer cell therapies. *Nature Reviews Drug Discovery*. 2020;**19**(3):169–84.
8. Yazdanifar M, Barbarito G, Bertaina A, Airolidi I. γ δ T cells: the ideal tool for cancer immunotherapy. *Cells*. 2020;**9**(5):1305.

Ethics Approval ‘This study was approved by Australian Red Cross for the isolation of human V δ 2+ γ δ T cells from healthy donors’ peripheral blood mononuclear cells, agreement number: 21–07VIC-09.’

‘This study was approved by Austin Health Animal Ethics Committee for adoptive cell transfer of human V δ 2+ γ δ T cells into NSG mice, AEC Reference number: A2020/05661.’

<http://dx.doi.org/10.1136/jitc-2022-SITC2022.0192>

193

CAR-T MANUFACTURED FROM FROZEN PBMC YIELD EFFICIENT FUNCTION WITH DELAYED *IN VITRO* EXPANSION

¹Julieta Abraham-Miranda*, ¹Meghan Menges, ¹Reginald Atkins, ²Mike Mattie, ²Justyna Kanska, ¹Joel Turner, ¹Melanie Hidalgo-Vargas, ¹Frederick Locke. ¹Moffitt Cancer Center, Tampa, FL, USA; ²Kite Pharma, Santa Monica, CA, USA

Background Chimeric antigen receptor (CAR)-T cells are engineered T cells that can identify and eliminate cells expressing a target antigen. Cryopreservation of CAR-T cells preceding infusion is a widely used practice since it allows flexible scheduling time of patient infusions.¹ Using frozen PBMCs from patients prior to standard therapies could impact the fitness and function of the final CAR-T product² but provides flexibility in scheduling both leukapheresis and manufacture.³ The impact of cryopreserved PBMCs on the quality of the final CAR-T product is incompletely characterized and needs to be further studied.

Methods We performed a prospective study using PBMCs from 20 healthy donors (HDs) to examine if manufacture of CAR-T cells using frozen (2X) vs. fresh (1X) PBMCs affects the quality and functionality of the product. The CAR-T manufacturing process is detailed in figure 1. We analyzed second generation CD19-targeted human CAR-T cells with CD28 (h1928z) co-stimulation for transduction efficiency, product expansion, immune-phenotype, activation induced cell death (AICD) and metabolic fitness (MF). We compared functionality by measuring markers of activation (4-1BB, CD107a and pAKT measured by flow cytometry, and cytokine release measured by ELLA) and their cytotoxic capacity (measured by xCELLigence Real-Time Cell Analysis) against hCD19 target-expressing cells.

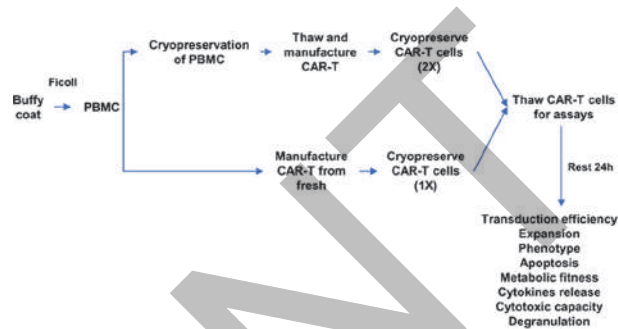
Results We found that freezing PBMCs delayed expansion during manufacture, with a doubling time 1.25-fold higher in 2X h1928z compared to 1X h1928z CAR-T cells (figure 2B). Transduction efficiency (figure 2A), CD4/CD8 ratio (figure 2C), CAR-T cell phenotype (figure 2D-E), AICD (figure 2F) and MF (figure 2G) were not affected by freezing PBMCs prior to CAR-T manufacture. Moreover, freezing PBMCs did not affect expression of 4-1BB (figure 2H), CD107a (figure 2I) or pAKT (figure 2J) after CAR engagement. IFN- γ and TNF- α production was reduced in 2X h1928z CAR-T cells after hCD19 mediated activation (figure 2K) without compromising their cytotoxic capacity (figure 2L-M).

Conclusions Freezing PBMCs prior to CAR-T production slows cell expansion during manufacture and decreases IFN- γ and TNF- α production, without disturbing CAR-T cell immune-phenotype, activation, or *in vitro* anti-tumor function. As CAR-T immunotherapy continues to expand, the necessity to store PBMCs to improve manufacturing logistics as well as to allow collection from patients at an early clinical stage will grow. This study supports the concept that cryopreservation of PBMCs is a valid solution to these issues without compromising the quality of the final product.

Acknowledgements Dr. Locke is supported by the Leukemia and Lymphoma Society as a Clinical Scholar. This study was supported by research funding from Kite Pharma to F.L. Locke. The authors thank the team at Kite Pharma for helpful and critical scientific discussions. We would like to thank the Flow Cytometry Core at Moffitt Cancer Center.

REFERENCES

1. Roddie, C., O'Reilly, M., Dias Alves Pinto, J., Vispute, K., & Lowdell, M. (2019). Manufacturing chimeric antigen receptor T cells: issues and challenges. *Cytotherapy*, 327–340.
2. Palen, K., Zurko, J., Johnson, B. D., Hari, P., & Shah, N. N. (2021). Manufacturing chimeric antigen receptor T cells from cryopreserved peripheral blood cells: time for a collect-and-freeze model? *Cytotherapy*, 985–990.
3. Tyagarajan, S., Schmitt, D., Acker, C., & Rutjens, E. (2019). Autologous cryopreserved leukapheresis cellular material for chimeric antigen receptor-T cell manufacture. *Cytotherapy*, 1198–1205.

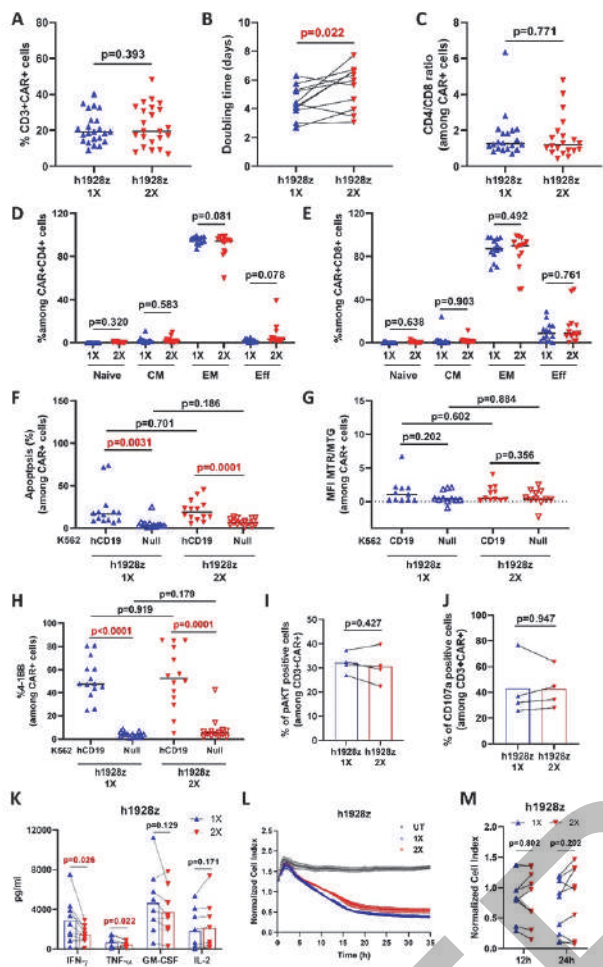


Abstract 193 Figure 1 CAR-T cell manufacture schematic representation

PBMCs were collected from healthy donor buffy coats after ficoll process. Cells were either used fresh to prepare CAR-T cells (1X) or cryopreserved to prepare CAR-T cells from frozen PBMCs (2X). After CAR-T cells expansion, they were cryopreserved, and then thawed 24h prior experimental analysis.

Abstracts

<http://dx.doi.org/10.1136/jitc-2022-SITC2022.0193>



Abstract 193 Figure 2 Comparison between CAR-T cells manufactured from fresh (1X) or cryopreserved (2X) PBMC. A. CAR expression was determined by flow cytometry using anti-FMC63 mAb. *# B. Doubling time was calculated as day 7/day 1 ratio. * C. CD4/CD8 ratio on live CD3+CAR+ cells determined by flow cytometry. *# D-E. CD4+ (D) and CD8+ (E) CAR-T cells immune-phenotype determined by flow cytometry. *# Naive (CCR7+CD45RO-), CM: central memory (CCR7+CD45RO+), EM: effector memory (CCR7-CD45RO+), Eff: terminally differentiated effector (CCR7-CD45RO-). F-H. CAR-T cells were stimulated with irradiated hCD19 target cells for 72h. Cells were then collected, and activation induced cell death (F), metabolic fitness (G) and 4-1BB expression (H) were analyzed by flow cytometry. *# I. Percentages of phosphorylated AKT cells within CD3+CAR+ cells. CAR-T cells were stimulated with OCI-LY3 target cells for 20 minutes and analyzed by phospho flow cytometry. * J. Percentages of CD107a cells within CD3+CAR+ cells. Degranulation was measured by CD107a staining upon incubation of h1928z CAR-T cells with OCI-LY3 target cells for 4h. * K. CAR-T cells were stimulated with hCD19-expressing 3T3 target cells for 24 h before supernatant was collected and analyzed by ELISA immunoassay to quantify IFN- γ , TNF- α , GM-CSF and IL-2. * L-M. The xCELLigence real-time cell analysis system monitored real-time cytotoxicity of CAR-T cells co-cultured with irradiated hCD19-expressing 3T3 target cells at 1:1 E:T ratio. (L) Representative RTCA comparing killing activity of untransduced (UT), 1X and 2X CAR-T cells. (M) Comparison of the killing activity of 1X and 2X CAR-T cells at 12h and 24h. *
*A paired t test was used. Each symbol represents an individual healthy donor, and the p values are indicated in each graph. #The middle line denoted the median.

194

PRE-CLINICAL DEVELOPMENT OF CT-1119, A MESOTHELIN TARGETING CHIMERIC ANTIGEN RECEPTOR MACROPHAGE (CAR-M), FOR SOLID TUMOR IMMUNOTHERAPY

Nicholas Anderson*, Michael Klichinsky, Kerri Ciccaglione, Stefano Pierini, Brinda Shah, Alison Worth, Rashid Gabbasov, Brett Menchel, Daniel Blumenthal, Sabrina DeLong, Sascha Abramson, Thomas Condamine. *Carisma Therapeutics, Philadelphia, PA, USA*

Background Despite significant success in treating hematological malignancies, adoptive cell therapies have yielded limited efficacy in solid tumors.¹ Macrophages are myeloid cells of the innate immune system and are naturally recruited to solid tumors,² where they have the potential to phagocytose tumor cells, activate the tumor microenvironment (TME), and prime a broad anti-tumor adaptive immune response via T cell recruitment and activation. We have previously developed chimeric antigen receptor macrophages (CAR-M) targeting HER2 and showed efficacy in a variety of pre-clinical models,³ with a Phase I clinical trial ongoing. Mesothelin is overexpressed in a variety of solid tumors, including mesothelioma, lung, pancreatic, and ovarian cancers.⁴ Here, we present preclinical data summarizing the development of CT-1119, a mesothelin targeted CAR-M for solid tumors.

Methods Using the chimeric adenoviral vector Ad5f35, we engineered primary human macrophages to express a CAR comprising a human scFv targeted against human mesothelin. To assess the activity of CT-1119, *in vitro* cell based assays and *in vivo* murine xenograft models were utilized. Donor-matched untransduced (UTD) macrophages served as controls.

Results Primary human CAR-M engineered with an Ad5f35 vector demonstrated high CAR expression, high viability, upregulated M1 (anti-tumor) macrophage markers, and downregulated M2 (pro-tumor) macrophage markers. CT-1119 demonstrated increased resistance to repolarization by M2 (pro-tumor) polarizing cytokines as compared to donor matched UTD macrophages. CT-1119 specifically bound mesothelin and binding was not impacted by mesothelin shedding. CT-1119 specifically phagocytosed multiple mesothelin expressing tumor cell lines in a CAR-dependent and antigen-dependent manner. CT-1119 demonstrated robust *in vitro* killing of the relevant tumor cell lines A549 and MES-OV expressing mesothelin. CAR engagement also induced the release of pro-inflammatory cytokines such as TNF α following stimulation with mesothelin in both cell-free and cell-based contexts in a dose-dependent manner. *In vivo*, CT-1119 significantly reduced tumor burden in a murine xenograft model of lung cancer. Similarly, human monocytes targeting mesothelin were successfully generated using the same Ad5f35 vector and demonstrated specific activity against mesothelin positive tumor cells.

Conclusions The presented results demonstrate that CT-1119, an autologous human anti-mesothelin CAR-M, can cause phagocytosis, tumor cell killing, and pro-inflammatory cytokine release in response to stimulation with mesothelin. These results show that CAR-M is a feasible approach for the treatment of mesothelin expressing solid tumors via the potential for induction of a systemic anti-tumor response.

REFERENCES

1. Hou A, Chen L, Chen Y, Navigating CAR-T cells through the solid-tumour micro-environment, *Nat Rev Drug Discov.* 2021; **20**:531–550.
2. Biswas S, Allavena P, Mantovani A, Tumor associated macrophages: functional diversity, clinical significance, and open questions, *Semin Immunopathol.* 2013; **35**:585–600.
3. Klichinsky M, et al, Human chimeric antigen receptor macrophages for cancer immunotherapy, *Nat Biotechnol.* 2020: 1–7.

4. Lv J, Li P, Mesothelin as a biomarker for targeted therapy, *Biomarker Res.* 2019; **7**: 1–18.

Ethics Approval All studies involving animals were approved by the IACUC of the Wistar Institute (protocol 201364).

<http://dx.doi.org/10.1136/jitc-2022-SITC2022.0194>

CHARACTERIZATION OF WU-NK-101, A FEEDER CELL-FREE EXPANDED ALLOGENEIC MEMORY NK CELL PRODUCT WITH POTENT ANTI-TUMOR ACTIVITY

<http://dx.doi.org/10.1136/jitc-2022-SITC2022.0195>

¹Laura Arthur*, ¹Mary Mathyer, ¹Celeste Dufour, ¹Bryan Cruz, ²Melissa Berrien-Elliott, ²Mark Foster, ¹Nitin Mahajan, ¹Alun Carter, ¹Matthew Cooper, ¹Ryan Sullivan. ¹Wugen Inc., Saint Louis, MO, USA; ²Washington University in St. Louis, St. Louis, MO, USA

Background Cytokine-induced memory NK cells, like WU-NK-101, offer several advantages over conventional NK cells.^{1, 2} These advantages include enhanced functional persistence, efficacy, and metabolic fitness that improve their survival and activity in liquid and solid tumor microenvironments.^{3, 4} Additionally, unlike conventional NK (cNK) cells derived from iPSC, cord blood, or adult peripheral blood, WU-NK-101 does not require engineering to enable anti-tumor activity.

The Moneta™ Platform is a feeder cell-free system of fusion protein complexes to generate, expand, phenotypically maintain, and cryopreserve memory NK cells for an ‘off-the-shelf’ allogeneic drug product. Here we define the molecular characteristics of WU-NK-101, through RNA and protein phenotyping, and elucidate pathways involved in memory NK cell expansion and activity.

Methods WU-NK-101 was generated from previously frozen NK cells derived from healthy donor whole blood using the Moneta™ platform. We evaluated pre- and post-expansion phenotype by flow cytometry, CyTOF, and RNA-Seq. We further assessed post-thaw functionality by cytokine secretion and cancer cell cytotoxicity in the absence or presence of monoclonal antibodies.

Results CyTOF analysis revealed that WU-NK-101 have an expression profile distinct from cNK. Compared to cNK, WU-NK-101 have elevated expression of Memory NK markers (CD25, CD69, NKG2A), cytotoxic molecules (GzmB, TRAIL), activating receptors (NKp30, NKp44, NKG2D), and nutrient transporters (CD71, CD98), providing mechanistic rationale for their enhanced anti-tumor activity and metabolic flexibility. Flow cytometry and RNAseq analysis confirm this phenotype. When stimulated by cancer cells, WU-NK-101 have enhanced secretion of IFN- γ , MIP-1 α , and TNF α ; and also demonstrate improved cytotoxicity compared to cNK. WU-NK-101 is able to utilize monoclonal antibodies to effectively drive antibody-dependent cellular cytotoxicity against solid tumor cancer cell lines.

Conclusions The Moneta™ platform expands memory NK cells while maintaining their cytokine-induced memory phenotype, as identified by RNA-Seq, flow cytometry, and CyTOF. As a result, WU-NK-101 demonstrates improved anti-tumor activity compared to cNK cells, even within the adverse tumor microenvironment. These data support the clinical development of WU-NK-101, an allogeneic Memory NK cell therapy in both liquid and in solid tumors, as a monotherapy and in combination with monoclonal antibodies, solid tumor engagers, or other anti-tumor modalities.

REFERENCES

1. Romee R, et al. Cytokine-induced memory-like natural killer cells exhibit enhanced responses against myeloid leukemia. *Science translational medicine* 8.357 (2016): 357ra123–357ra123.
2. Berrien-Elliott, M, et al. Multidimensional Analyses of Donor Memory-Like NK Cells Reveal New Associations with Response after Adoptive Immunotherapy for Leukemia *Cancer discovery* 10.12 (2020): 1854–1871.
3. Terren I, et al. Metabolic changes of Interleukin-12/15/18-stimulated human NK cells. *Sci Rep* 2021
4. Rutella S, et al. WU-NK-101: An Enhanced NK Cell Therapy Optimized for Function in the Tumor Microenvironment (TME). *ESMO Congress* (2022).

196

EXPANSION OF TUMOR-INFILTRATING LYMPHOCYTES FROM COLORECTAL CANCER LIVER METASTASIS; CHARACTERISTICS AND POTENTIAL HISTOLOGIC MARKER OF SUCCESSFUL CELL EXPANSION

¹Jina Baek*, ²Hyun Lee, ¹Gyungyub Gong, ²Chae-Lyul Lim, ¹Hee Jin Lee. ¹University of Ulsan College of Medicine, Seoul, Korea, Republic of; ²NeogenTC Corp, Gyeonggi-do, hanam-si, Korea, Republic of

Background Colorectal cancer is the 3rd most common cancer worldwide. In recent years, adoptive cell therapy (ACT) of tumor-infiltrating lymphocytes (TILs) has been successful in treatment of metastatic melanoma. We cultured TILs from colorectal cancer liver metastasis. We evaluated the numbers and subsets of expanded TILs and their relationship with the original tumors' histologic findings.

Methods Fifteen samples of colorectal cancer liver metastasis were collected at a single institute. Cancer tissues were cut into 1 to 2-mm fragments and underwent initial expansion of TILs for 2 weeks. The number of the TILs per fragment was counted and checked for successful expansion at cutoff of 0.8×10^5 cells per fragment. Their characteristics were evaluated by flow cytometry. Remnant cancer tissues were made into hematoxylin and eosin-stained slides. The slides were reviewed for histologic findings including the level of stromal TILs and inflammatory cell infiltrate at the invasive margin, using the Klintrup-Makinen (KM) assessment. KM score was assessed in a 4-point scale, from 0 (no increase) to 3 (florid infiltrate at invasive edge with cancer cell destructions).

Results The median number of expanded TILs per fragment after initial expansion was 1.1×10^5 cells (range: $0.16 - 8.75 \times 10^5$). With cutoff value of 0.8×10^5 cells per fragment, successful culture rate was 66.7% (10 of 15 cases). The mean proportion of CD4+ and CD8+ T cells were 69.4% and 32.5%, respectively. The mean proportion of effector memory, effector, central memory, and naïve T cells were 73.1%, 7.8%, 1.4%, and 0.8%, respectively. Number of expanded TILs per fragment and the level of stromal TILs showed no statistical correlation (Kruskal-Wallis test, $p=0.258$). However, number of expanded TILs per fragment and KM score showed significant association ($p=0.006$). Histologically, intratumoral percentage of tumor cells, stroma, necrosis, and mucin showed no statistical correlation to expanded TILs per fragment ($p=0.36$, $p=0.286$, $p=0.563$, and $p=0.27$, respectively), and tumor size also did not show statistical correlation to expanded TILs per fragment (simple regression, $p=0.122$). We also reviewed patients' MSI status and history of chemotherapy after metastasis, and neither showed statistical correlation (Mann-Whitney U test, $p=0.782$ and $p=0.661$, respectively).

Conclusions Expansion of TILs from colorectal cancer liver metastasis was successfully performed, and assessment of inflammatory cell infiltrate at the invasive margin may be helpful in estimating the number of obtainable TILs before the initial expansion. Together, these data could be used for further studies to establish the effective ACT in colorectal cancer patients.

<http://dx.doi.org/10.1136/jitc-2022-SITC2022.0196>

197

PRELIMINARY SAFETY AND EFFICACY OF AUTOLOGOUS ANTI-MSLN T CELL ENGAGER-LOADED T CELLS (CAB-T) IN PATIENTS WITH MESOTHELIN-EXPRESSING ADVANCED SOLID TUMORS

¹Xuanwen Bao, ¹Lulu Liu, ²Jialin Gu, ²Mei Li, ¹Zhou Tong, ¹Hangyu Zhang, ²Yalin Li, ²Xinjiang Gong, ²Peng Wang, ³Andy Tsun, ⁴Guoqiang Hu, ⁴Chuan-Chu Chou*, ²Zhiyuan Li, ¹Weijia Fang. ¹The First Affiliated Hospital, Hangzhou, China; ²CABT-Bio, Haikou, China; ³Biotheus Inc, Zhuhai, China; ⁴Biotheus Inc., Shanghai, China

Ethics Approval Clinical Research Ethics Committee of the First Affiliated Hospital, College of Medicine, Zhejiang University.

<http://dx.doi.org/10.1136/jitc-2022-SITC2022.0197>

Background Mesothelin (MSLN) is highly expressed in various solid tumor types with low levels of expression in some normal healthy tissues. Our CAB-T platform is a novel, proprietary T cell based anti-CD3 bispecific T cell engager (TCE) delivery system. Our preclinical studies indicated its superior anti-tumor efficacy over traditional 2nd-generation CAR-T formats. Here, we report the preliminary safety and efficacy of MSLN-targeting CAB-T (MSLN-CAB-T) in patients with MSLN-expressing advanced solid tumors during an investigator-initiated trial (IIT).

Methods This is an open-label, single-center study with an accelerated dose titration followed by a 3+3 design. Patients were enrolled with MSLN+ advanced or metastatic solid tumors (detected by IHC; 2+/3+ \geq 30% in viable tumor cells). MSLN-CAB-T cells were manufactured using autologous PBMC that were freshly isolated from leukapheresis. Following lymphodepletion, MSLN-CAB-T cells were administered intravenously followed by safety and efficacy observations, and the detection of MSLN-CAB-T expansion and cytokine/TCE levels in patient sera. Primary objectives included safety and tolerability to determine the maximum tolerated dose (MTD). Secondary objectives included overall safety, preliminary efficacy, and PK.

Results From Apr, 2021 to Nov, 2021, seven patients had enrolled (4, ovarian cancer; 1, colon cancer; 2, duodenal carcinoma). 4/7 received \geq 4 prior lines of therapy, 2/7 received anti-PD1 treatment. Dose levels included 3×10^5 cells/kg (n=1); 1×10^6 cells/kg (n=1); 3×10^6 cells/kg (n=3); 5×10^6 cells/kg (n=1), and 1×10^7 cells/kg (n=1). There were no dose-limiting toxicities (DLT) or treatment-related deaths. Treatment-related adverse events (TRAEs) of \geq Grade 3 were reported in two patients (1×10^6 cells/kg and 1×10^7 cells/kg). Grade 1 cytokine release syndrome (CRS) was reported in all of the patients $\geq 3 \times 10^6$ cells/kg and only one patient dosed at 1×10^7 cells/kg developed Grade 3 CRS (quickly recovered after treatment with corticosteroid and tocilizumab). Post-infusion, MSLN-CAB-T expansion peaked in peripheral blood within 5–19 days. In five evaluable patients (4, ovarian cancer; 1, colon cancer), the best overall response was stable disease (n=1); two ovarian cancer patients dosed at 3×10^6 cells/kg showed tumor shrinkage with one patient whose tumor reduced in size of $\sim 26.89\%$ at the first assessment. Dose-dependent PK and TCE levels correlated with MSLN positivity and tumor burden.

Conclusions MSLN-CAB-T showed good preliminary safety in subjects with MSLN+ solid tumors, and MTD has not yet been reached. This provides the rationale to expand the study, especially for patients with tumors expressing higher levels of MSLN ($\geq 60\%$ in viable tumor cells) as a monotherapy or in combination with other agents.

Acknowledgements We would like to thank the trial patients and their families for their contribution to this clinical study. This trial was funded by Hainan Kaibo Biotechnology Co., Ltd. and Biotheus Inc.

Trial Registration ChiCTR. org.cn: ChiCTR2100043956

198

INNATE-ENHANCED CHIMERIC ADAPTORS (CAD): A NEWLY-DESCRIBED APPROACH FOR AUGMENTING POTENCY OF $\gamma\delta$ T CELL IMMUNOTHERAPY

Marissa Herman*, Taylor Barca, Xue (Cher) Yang, Maryam Tabrizizad, Morgan Smith-Boeck, Louise Kiru, Jonathan Wong, Ramandeep Kaur, Smitha Gundurao, Gauri Lamture, Aruna Azameera, Kevin Nishimoto, Arun Bhat, Blake Aftab. *Adicet Bio, Inc., Menlo Park, CA, United States*

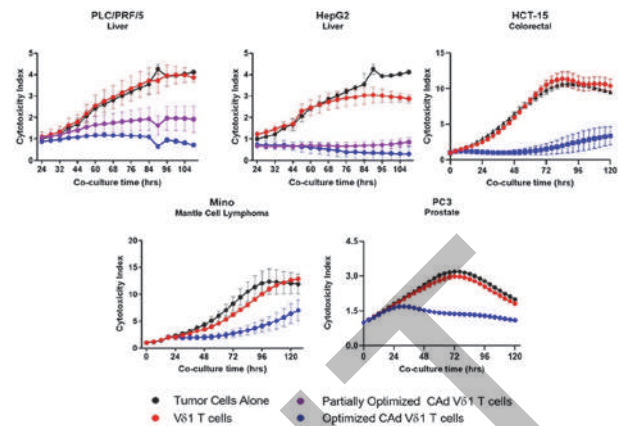
Background $\gamma\delta$ T cells are a clinically active cytotoxic effector subtype with intrinsic tumoricidal activity and are correlated to improved survival in solid and hematologic malignancies. $\gamma\delta$ T cells target tumors through innate and adaptive mechanisms. Notably, the innate receptor NKG2D is highly expressed on $\gamma\delta$ T cells and recognizes a family of target proteins commonly upregulated on tumors. NKG2D specifically associates with intracellular DAP10, a binding partner necessary for signal transduction and activation. Here we describe a novel form of cell engineering incorporating an enhanced intracellular DAP10 chimeric adaptor (CA δ) protein, comprising DAP10 domain modifications and inclusion of 4-1BB and modified CD3 ζ co-stimulation, designed to amplify potency for tumor targeting via endogenous NKG2D receptors.

Methods V δ 1 T cells were expanded from donor PBMCs and transduced with enhanced DAP10 CA δ s. CA δ expression and association with NKG2D were confirmed by western blot and blocking studies. *In vitro* characterization included co-culture assays, flow cytometric phenotyping, and cytokine production by multiplexed immunoassay. Anti-tumor potency of CA δ V δ 1 T cells was evaluated in a panel of human tumor xenograft models. Xenograft and murine tissues were analyzed for V δ 1 homing and proliferation by flow cytometry.

Results CA δ -enhanced V δ 1 T cells showed robust expansion and transduction, routinely reaching >80% V δ 1 purity prior to depletion steps, while maintaining a primarily naïve-like phenotype. CA δ -enhanced V δ 1 T cells displayed robust *in vitro* proliferation, cytokine production, and cytotoxic activity across a broad array of solid and heme tumor lines with significantly increased potency compared to unmodified V δ 1 T cells (figure 1). *In vivo*, CA δ -enhanced V δ 1 T cells primarily accumulated and specifically proliferated in tumors, with a single dose demonstrating control of tumor burden (figure 2).

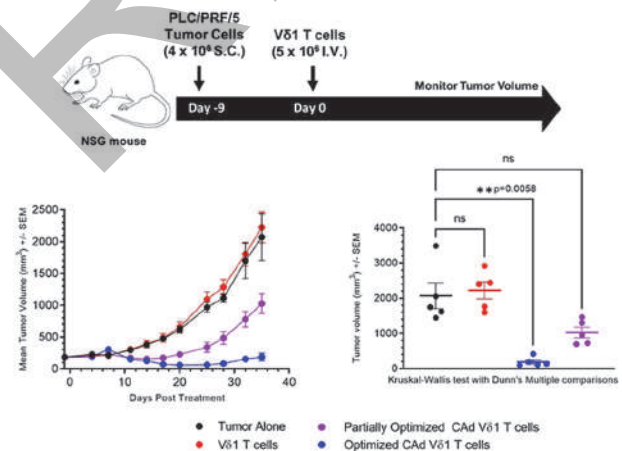
Conclusions Innate-enhanced V δ 1 T cells engineered with a newly-described DAP10-based chimeric adaptor technology represents a potent and potentially broadly-applicable ‘off-the-shelf’ cell therapy with marked increase in cytolytic activity via endogenously expressed innate cytotoxicity receptors. These data support continued development and further investigation in the clinic across a range of hematologic and solid tumor indications.

Ethics Approval All mouse experiments were performed in accordance with the Guide for the Care and Use of Laboratory Animals and followed all institutional and national guidelines with appropriate protocol review and approval.



Abstract 198 Figure 1 *in vitro* cytotoxicity with innate-enhanced V δ 1 T cells

An array of tumor cell lines across multiple indications were cocultured with unmodified V δ 1 T cells or innate-enhanced DAP10 CA δ V δ 1 T cells and tumor cell growth was tracked using Incucyte. The cell line and tumor origin are indicated in the title of each graph. The difference between partially optimized CA δ V δ 1 and optimized CA δ V δ 1 groups is incorporation of additional DAP10 modifications into the CA δ construct design



Abstract 198 Figure 2 *in vivo* efficacy in hepatocellular carcinoma model

Top panel schematic provides details of study design and bottom panel reports tumor volumes throughout study (left) and statistical comparisons of treatment groups relative to tumor alone control at study termination (right). The difference between partially optimized CA δ V δ 1 and optimized CA δ V δ 1 groups is incorporation of additional DAP10 modifications into the CA δ construct design

<http://dx.doi.org/10.1136/jitc-2022-SITC2022.0198>

3D *EX VIVO* PATIENT TISSUE PLATFORM FOR IMMUNO-ONCOLOGY DRUG TESTING

¹Sander Basten*, ¹Natalia Beztinna, ²Fanny Grillet, ¹Kuan Yan, ¹Niels Meesters, ²Donny van der Meer, ¹Emma Spanjaard, ²Willemijn Vader, ¹Leo Price. ¹CrownBioscience, Leiden, Netherlands; ²vitroscaan B.V., Leiden, Netherlands

Background Many immuno-oncology drugs fail in clinical trials, which is partly due to the lack of *in vitro* and *in vivo* models that sufficiently recapitulate the tumor microenvironment (TME). To bridge this gap in translational model systems, a 3D *ex vivo* patient tissue platform was developed which uses 3D *ex vivo* tumor cultures, where tumor endogenous cells of the TME are preserved. These TME components can affect tumor drug responses with potentially novel targets for drug development, making them a crucial component to be presented upon drug efficacy evaluations.

Methods Patient tumor tissues, both solid resection and liquid biopsies from metastatic disease, were processed within 24 hours of surgery or fluid drainage. Following minimal processing small tumor clusters and single cells remain, that were manipulated in liquid handling robotics. The material was embedded in a protein-rich hydrogel and exposed to panels of drug treatments in a 384-well format for 5–7 days until samples were fixed. Tissue responses were quantified using a Crown Bioscience proprietary high content image (HCI)-based analysis platform. In addition, histology and FACS were used to characterize primary samples at baseline. Cytokine measurements were performed on the tumor supernatants.

Results Freshly isolated tumor cells from various cancer patients were exposed to tissue relevant treatments, such as standard of care, targeted therapies, and immunomodulatory drugs. Endpoint analysis of fixed and stained material allowed for phenotypic measurement of responses such as tumor cell volume reduction, indicating cell killing, and more in-depth effects including growth arrest, and immune cell proliferation. Differential responses of tumor tissues to various classes of drugs targeting the tumor and/or the TME were demonstrated. In addition, validation of the various TME components for different cancers was confirmed. Using FACS, the presence of tumor cells accompanied by immune-profiling of the TME, including presence of tumor infiltrating lymphocytes, macrophages, and other immune cells was observed. Similarly, biomarker staining using IHC indicated the presence of tumor cells, fibroblasts, and various immune cell types. Cytokine measurement at experimental endpoint aligns with the measured responses of tumor reduction upon certain drug treatments.

Conclusions The 3D *ex vivo* patient tissue platform offers a rapid, reliable and patient-relevant approach to test preclinical drug candidates (e.g., antibodies, antibody-drug conjugates and small molecules) for different solid tumour types. It has the potential to significantly improve the preclinical evaluation of drugs and support the decision-making process during progression of drug candidates to the clinic.

Ethics Approval National Bioethics Committee in Romania, approval number 9S/4 from 25.11.2019

<http://dx.doi.org/10.1136/jitc-2022-SITC2022.0199>

200

A UNIQUE CRISPR-BASED NUCLEASE WITH A NON-NGG PAM EFFICIENTLY TARGETS MULTIPLE EXCLUSIVE GENOMIC SITES FOR IMMUNO-ONCOLOGY BASED THERAPY

<http://dx.doi.org/10.1136/jitc-2022-SITC2022.0200>

Rachel Diamant*, Lior Lior Izhar, Ira Gotliv, Yonit Ben David, Sigal Cohen, Maya Noff, Nir Shahar, Rafi Emmanuel, Bar Ben Baruch. *Emendo Biotherapeutics, Rehovot, Israel*

Background Chimeric antigen receptor (CAR)-T cell therapy is a recent clinically successful approach to tackling cancer, in which T cells are genetically modified to allow specific recognition and efficient killing of cancer cells via tumor associated antigens.¹ Current CAR-based treatments require costly and time-consuming autologous cell transfer. Patients' own cells are frequently of low quality and difficult to obtain, further supporting the advantage of an allogeneic transplantation. To prevent graft versus host reactions and avoid host-mediated rejection of healthy donor-derived allogeneic cells, these cells must be adjusted by eliminating the expression of endogenous recognition components, such as T cell receptor alpha constant (TRAC or TCR) and CD3, and of HLA class I molecules such as β -2 microglobulin (B2M).^{2,3} In this study, we tested the feasibility of gene editing in allogeneic cells using our novel high-fidelity CRISPR-associated nuclease OMNIA4. OMNIA4 is a highly active nuclease with a unique non-NGG PAM recognition domain. The unique PAM allows gene-editing in exclusive genomic sequences that are not accessible by commonly used nucleases. Our strategy involves disrupting endogenous T cell recognition elements as well as checkpoint receptors and exhaustion genes that restrict anti-tumor T cell response.

Methods RNA guides (gRNAs) were designed for several of such genes of interest and their editing via OMNIA4 nuclease was evaluated by NGS in HeLa cells. Ribonucleoproteins (RNPs), including OMNIA4 and gRNAs designed to target distinctive sites in either TRAC, CD3e or B2M genes, were applied to primary T cells. The resulting editing outcome was evaluated by measuring T cell receptor (TCR), CD3e or B2M surface expression by flow cytometry. In addition, an unbiased analysis was performed to identify 'off-targets' edited by the nuclease.

Results Our gRNA screening yielded at least one (and up to five) active gRNA for each gene of interest, with editing level >70%. Flow cytometric analysis showed that editing in primary T cells resulted in about 94% TCR negative cells, about 85% CD3e negative cells and about 95% B2M negative cells. An unbiased assay revealed no off-targets for neither of the guides.

Conclusions These findings demonstrate efficient, accurate and safe impairment of a self-presenting element and endogenous T cell recognition components. Our approach offers gene editing at unique targets as a tool to generate universal allogeneic T cells that could be employed in the development of 'off-the-shelf' 'ready-to-use' CAR-T therapeutic agents for large-scale clinical applications.

REFERENCES

1. Labanieh, L., Majzner, R.G., and Mackall, C.L. (2018). Programming CAR-T cells to kill cancer. *Nat. Biomed. Eng.* **2**, 377–391.
2. Liu, X., Zhang, Y., Cheng, C., Cheng, A.W., Zhang, X., Li, N., Xia, C., Wei, X., Liu, X., and Wang, H. (2017). CRISPR-Cas9-mediated multiplex gene editing in CAR-T cells. *Cell Res.* **27**, 154–157.
3. Depil, S., Duchateau, P., Grupp, S.A., Mufti, G., and Poirot, L. (2020). 'Off-the-shelf' allogeneic CAR T cells: development and challenges. *Nat. Rev. Drug Discov.* **19**, 185–199

201 DEVELOPMENT OF GUCY2C-TAC T CELLS FOR THE TREATMENT OF COLORECTAL CANCER

Tania Benatar*, Ling Wang, Thanyashanthi Nitya-Nootan, Heather MacGregor, Suzanna Prosser, Philbert IP, Prabha Lal, Stacey Xu, Laura Shaver, Sadhak Sengupta, Christopher Helsen, Andreas Bader. *Triumvira Immunologics, Inc., Hamilton, ON, Canada*

Background The T cell antigen coupler (TAC) is a novel, proprietary chimeric receptor that facilitates the re-direction of T cells to tumor cells and activates T cells by co-opting the endogenous T cell receptor complex with the goal to elicit safe and durable anti-tumor responses. TAC01-HER2, a first-in-class TAC T product targeting HER2 (ERBB2), has entered a phase I/II clinical trial in patients with HER2-positive solid tumors. Here, we present the development of a new TAC T product targeting guanylyl cyclase 2C (GUCY2C) to treat colorectal cancer. GUCY2C belongs to a family of membrane-bound mucosal guanylate cyclase receptors and is selectively expressed on the apical brush border of intestinal epithelia, a site inaccessible to T cells. In cancer, however, GUCY2C is frequently overexpressed in primary and metastatic colorectal carcinomas and, thus, a preferred antigen for the specific targeting of tumor cells via TAC T cells.

Methods GUCY2C-TAC receptor functionality was characterized using a variety of *in vitro* and *in vivo* assays. *In vitro* assays were based on flow cytometric analysis of TAC surface staining, CD69 upregulation and T cell proliferation. Cytotoxicity was assessed via real-time microscopy co-culture assays. *In vivo* studies examined the anti-tumor effect of TAC-engineered T-cells against established GUCY2C-expressing tumor xenografts.

Results The GUCY2C-TAC receptor showed strong surface expression and specific activation when co-cultured with a variety of cancer cells expressing GUCY2C *in vitro*. Upregulation of the activation-induced CD69 marker was comparable with levels induced by activated control TAC T cells. Proliferation of GUCY2C-TAC T cells was induced by co-culture with naturally expressing GUCY2C target cell lines as well as GUCY2C-engineered cell lines. *In vitro* cytotoxicity assay demonstrated a strong anti-GUCY2C response and killing of GUCY2C-expressing target cell lines. No increases in T cell activation, proliferation and no cytotoxicity were observed in non-transduced T cells and GUCY2C-TAC T cells co-cultured with GUCY2C-negative target cells, indicating that the T cell response is specific to the GUCY2C antigen. Intravenous administration of GUCY2C-TAC T cells in mice carrying GUCY2C -positive tumor xenografts led to a sustained anti-tumor response.

Conclusions The *in vitro* and *in vivo* data confirm strong and specific activity of GUCY2C-targeted TAC T cells against GUCY2C-expressing tumor models and highlight the versatility of the TAC platform for therapeutic applications in solid tumors.

Ethics Approval AUP number 20–10–37, approved by McMaster University's Animal Research Ethics Board.

<http://dx.doi.org/10.1136/jitc-2022-SITC2022.0201>

202

SINGLE STEP KNOCK-IN OF NEXT GENERATION INDUCIBLE IL-12 ARMORED CAR T CONSTRUCTS

Alexander Benton*, Anze Smole, Mathilde Poussin, Monika Eiva, Daniel Powell. *University of Pennsylvania, Philadelphia, PA, USA*

Background While CAR-T cell cancer immunotherapy has been successful in treating hematological malignancies, there have been significant difficulties in adapting these therapies for the treatment of solid tumors. Several factors are responsible for this challenge including increased tumor burden, immunosuppression in the tumor microenvironment, and heterogeneity of tumor associated antigens. Various approaches have been developed to address these challenges, including endowment of CAR T cells with expression of accessory molecules that enhance their function, such as IL-12, to make “armored CARs”. These approaches currently rely on constitutive IL-12 expression, or in case of inducible systems, use of multiple viral vectors, resulting in unregulated delivery or product heterogeneity respectively. Either of these methods can add significant risk of poor activity or toxicity.

Methods To resolve these issues, we developed genetic systems that combine antigen-induced production of an accessory molecule via a synthetic nuclear factor of activated T cells (NFAT) promoter, along with constitutive CAR expression, in a single lentiviral vector referred to as Uni-Vect. We demonstrate the therapeutic application of Uni-Vect *in vivo* by transient activation-dependent expression of IL-12 in an ovarian cancer model. In a previous clinical trial tumor infiltrating-lymphocytes engineered with NFAT inducible IL-12 expression were tested and clinical activity was observed.¹ However, severe toxicity accompanied by high serum levels of IL-12 and IFN- γ limited further development. We address this challenge by eliminating endogenous TCR-driven activation, which may lead to triggering of undesired NFAT-inducible IL-12 expression. Further, we utilize a genome-editing approach with homology-directed repair as a means of gene integration, to achieve single-step generation of TCR disrupted-inducible IL-12 armored CAR T cells.

Results We compare the Uni-Vect platform to standard methods for arming CAR-T cells and demonstrate enhanced control over accessory molecule expression *in vitro*. Further, we demonstrate the functionality of our lentiviral and knock-in products in our *in vitro* and *in vivo* models of ovarian cancer. We found that knock-in inducible IL-12 CAR T cells were able to eliminate tumors in all mice while avoiding lethal toxicity due to dysregulated T cell activation.

Conclusions We demonstrate the feasibility of non-viral knock-in of large Uni-Vect constructs that share the benefits of inducible arming and gene disruption. The modular Uni-Vect platform will set a foundation for potent next generation CAR T cellular products. Our added safety layers and an optimized manufacturing process will support clinical translation for patients with ovarian cancer and beyond.

Acknowledgements Special thanks to The UPenn Human Immunology and Stem Cell and Xenograft Cores for their services and materials provided

REFERENCE

1. Zhang, L., *et al.* Tumor-infiltrating lymphocytes genetically engineered with an inducible gene encoding interleukin-12 for the immunotherapy of metastatic melanoma. 2015; *Clin. Cancer Res.* **21**, 2278–2288.

<http://dx.doi.org/10.1136/jitc-2022-SITC2022.0202>

Abstracts

203

PRECLINICAL DISCOVERY AND CHARACTERIZATION OF ALLOGENEIC ANTI-PSMA $\gamma\delta$ CAR T THERAPY FOR PROSTATE CANCER

Nitya Ramadoss*, Aruna Azameera, Alexander Teague, Jonathan Wong, Atrish Bagchi, Tonya Capillo, Morgan Smith-Boeck, Michael Salum, Erika Meaddough, Elizabeth Speltz, Matthew Hoopes, Katherine Wang, Ramandeep Kaur, Smitha Gundurao, Marissa Herrman, Yvan Chanthery, Blake Aftab, Kevin Nishimoto, Arun Bhat. *Adicet Bio, Inc., Redwood City, CA, USA*

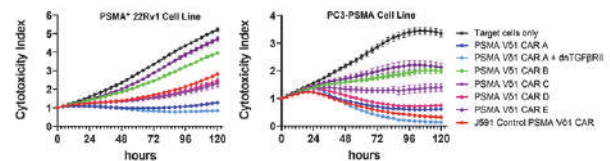
Background Prostate-specific membrane antigen (PSMA) is a transmembrane glycosylated homodimer overexpressed in >80% of prostate cancers. PSMA expression is increased in advanced stages of the disease, making it an attractive therapeutic target. Clinically, autologous anti-PSMA $\alpha\beta$ CAR T cells have shown initial efficacy with significant CRS-like dose-limiting toxicities. Compared to $\alpha\beta$ T cells and other innate cells, $\gamma\delta$ T cells are associated with multifunctional innate and adaptive targeting and differentiated biodistribution into tumor-associated tissues. Additionally, $\gamma\delta$ CAR T cells have demonstrated enhanced tumoricidal activity and tailored activation-induced cytokine profiles that may decrease toxicities associated with CRS. We characterized $\gamma\delta$ T cells modified from a set of novel scFv-based CARs targeting PSMA for prostate cancer.

Methods We used phage panning to identify a library of anti-PSMA scFv sequences, which were reformatted into CARs in VH-VL and VL-VH orientations and screened in Jurkat-Lucia™ NFAT cells to assess CAR expression and activation in the context of target cell-based stimulation. We transduced a set of functional CARs into V δ 1 T cells, a primarily tissue-resident subset, activated and expanded from healthy donor PBMCs. We performed *in vitro* cell-based cytotoxicity assays and phenotypic assessments of CAR V δ 1 T cells using flow cytometry. Potency was also assessed in NSG mice bearing subcutaneous PSMA-expressing xenografts.

Results Anti-PSMA scFvs ranged in apparent affinities from the low nanomolar to the sub-micromolar range. CAR-expressing Jurkat cells showed target-specific NFAT activation and low tonicity. CAR-engineered V δ 1 T cells demonstrated robust expansion, *in vitro* cytotoxicity and antigen-specific proliferation against PSMA⁺ cell lines in a manner comparable to, or greater than, J591 scFv-based V δ 1 CAR. *In vitro* potency correlated with the release of multiple effector cytokines. Notably, IL-6 and IL-10 production by anti-PSMA V δ 1 CAR T cells was negligible, while TNF α production was low, further supporting the potential of the $\gamma\delta$ CAR T platform to demonstrate a favorable cytokine-associated safety profile. Anti-PSMA V δ 1 CAR T cells were also found to be predominantly naïve, with low levels of exhaustion marker expression. Additionally, *in vitro* (figure 1) and *in vivo* (figure 2) potency of anti-PSMA V δ 1 CAR T cells was investigated upon co-expression of dominant negative TGF β R2 (dnTGF β R2). In xenograft models, anti-PSMA V δ 1 CAR T cells demonstrated potent anti-tumor efficacy.

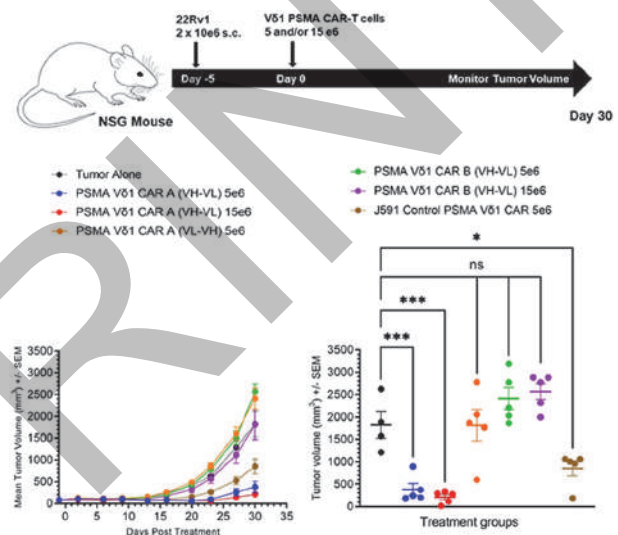
Conclusions We have engineered, screened and demonstrated preclinical efficacy for “off-the-shelf” PSMA-targeting $\gamma\delta$ CAR T cells. Resulting $\gamma\delta$ CAR T constructs identified here are candidates for further preclinical and clinical development in the context of armoring technologies.

Ethics Approval All mouse experiments were performed in accordance with the Guide for the Care and Use of Laboratory Animals and followed all institutional and national guidelines with appropriate protocol review and approval.



Abstract 203 Figure 1 In vitro cytotoxicity of PSMA-targeting V δ 1 CAR-T cells

Demonstration of *in vitro* potency at 1:1 E:T ratio of PSMA-targeting V δ 1 CAR-T cells (including CAR A co-expressing dnTGF β R2) when co-cultured with PSMA-expressing target cell lines, 22Rv1 (left) and TGF β -secreting PC3 cells engineered to express PSMA (right)



Abstract 203 Figure 2 *in vivo* potency of V δ 1 CAR-T cells in 22Rv1 PCa model

Demonstration of *in vivo* potency in a 22Rv1 PCa xenograft model (low, heterogenous PSMA expression) with PSMA-targeting V δ 1 CAR-T cells. Schematic outlines the study design (top panel). Graphs detail tumor volumes determined for the entire study duration (bottom, left panel) as well as statistical comparison of treatment groups relative to the untreated tumor alone control at study termination (bottom, right panel).

<http://dx.doi.org/10.1136/jitc-2022-SITC2022.0203>

204

COMBINING FT536, A PAN-TUMOR TARGETING CAR NK CELL THERAPY, WITH CD16 ENGAGERS PROVIDES A COORDINATED TARGETING STRATEGY TO OVERCOME TUMOR HETEROGENEITY

¹John Goulding*, ¹Bryan Hancock, ¹Robert Blum, ¹Wen-I Yeh, ¹Chia-Wei Chang, ¹Mochtar Pribadi, ¹Yijia Pan, ¹Hui-Yi Chu, ¹Shohreh Sikaroodi, ¹Thomas Dailey, ¹Miguel Meza, ²Lucas Ferrari de Andrade, ¹Peter Szabo, ¹Sarah Cooley, ¹Jeffrey Chou, ³John Powderly, ¹Yu-Waye Chu, ¹Tom Lee, ¹Ryan Bjordahl, ⁴Kai Wucherpfennig, ¹Bob Valamehr. ¹Fate Therapeutics, San Diego, CA, USA; ²Icahn School of Medicine at Mount Sinai, New York, NY, USA; ³Caroline BioOncology Institute, Huntersville, NC, USA; ⁴Dana Farber Cancer Institute, Boston, MA, USA

Background The hurdles of tumor antigen heterogeneity, a paucity of tumor-specific antigens, and pervasive immune evasion remain as significant challenges to the successful development of solid tumor immunotherapies. Despite clinical success against hematological malignancies, broader clinical application and efficacy of autologous chimeric antigen receptor (CAR)-T cell therapy remains limited. To remedy these intrinsic challenges, CAR-T cell therapy, immune checkpoint inhibition, and bi-specific engagers are being utilized in combination to extend their therapeutic application to solid tumors.

Methods We have previously presented FT536, a multiplex-engineered clonal master induced pluripotent stem cell (iPSC)-derived NK cell product candidate that incorporates a novel CAR targeting the pan-tumor associated MICA and MICB (MICA/B) stress proteins (3MICA/B CAR). FT536 has been shown to overcome multiple tumor immune evasion mechanisms, to elicit significant and broad CAR-mediated anti-tumor cytotoxic effector function, and to provide multi-antigen targeting capability through expression of a high-affinity, non-cleavable CD16 (hnCD16) Fc receptor.

Results In addition to innate cytotoxicity and MICA/B-specific activity against multiple solid tumor targets, we here demonstrate that the combination of FT536 with multiple Fc receptor engagers results in potent ADCC as well as CAR activity. ADCC was established using monoclonal antibodies (mAbs) targeting EGFR and HER2, a bi-specific c-met/EGFR mAb (amivantamab), and bi-specific NK cell engagers. Combining FT536 with conventional mAbs, bi-specific mAbs such as amivantamab, and/or bispecific NK cell engagers provides additional non-clinical evidence that multi-antigen-specific tumor targeting affords potent cytotoxicity responses in preclinical models that recapitulate patient tumor heterogeneity and antigen expression variation. We hypothesize that multi-antigen targeting of solid tumors could provide a novel approach to minimize antigen selection and immune escape.

Conclusions To assess the clinical translation potency of multi-antigen targeting and combinatorial therapeutic application of FT536 in humans, a phase I first-in-human, dose-escalation clinical study of FT536 as monotherapy and in combination with tumor-targeting mAb therapy, including amivantamab, for the treatment of multiple solid tumor indications was designed and is currently enrolling (NCT05395052).

<http://dx.doi.org/10.1136/jitc-2022-SITC2022.0204>

Abstracts

205

SPECIFIC AMPK AGONISM DURING CART *IN VITRO* EXPANSION ENHANCES OXIDATIVE METABOLISM AND IMPROVES *IN VIVO* LEUKEMIA CLEARANCE

Erica Braverman*, Harrison Brown, Manda Ramsey, Craig Byersdorfer. University of Pittsburgh, Pittsburgh, PA, USA

Background While chimeric antigen receptor (CAR)T therapy has seen great success in pediatric leukemia, relapses continue to occur in up to 1/3 of patients.¹ CART persistence *in vivo* correlates with ongoing remission, and promoting oxidative metabolism and mitochondrial health during *in vitro* expansion creates more functional and persistent CARTs *in vivo*.² AMP-activated protein kinase (AMPK) is a cellular energy sensor with prominent roles in mitochondrial health and biogenesis.³ We hypothesized that promoting AMPK activity during CART expansion would enhance mitochondrial metabolism, leading to improved anti-leukemia clearance *in vivo*.

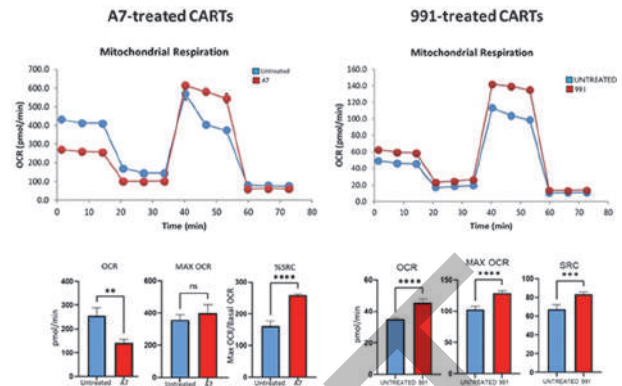
Methods Healthy human T cells underwent lentiviral transduction with a CD19-targeting CAR containing the CD28 costimulatory domain. Transduced CARTs were expanded in complete media supplemented with IL2 and either AMPK agonist Compound 991 (991), AMPK agonist A769662 (A7), or DMSO (control). After expansion, cells were assessed for metabolic function *in vitro* using the Seahorse Metabolic Analyzer. *In vitro* cytotoxicity against NALM6 targets expressing zGreen was measured by monitoring mean fluorescence intensity using the Incucyte. For *in vivo* studies, NSG mice were injected on Day -7 with luciferase+ NALM6 leukemia cells followed by CARTs +/- agonist on Day 0, with luminescence followed weekly by IVIS imaging.

Results 991 treatment enhanced CART oxidative metabolism over DMSO-treated controls, while A7 treatment significantly reduced initial oxygen consumption, leading to 991 treatment being chosen for further study (figure 1). Despite this potential metabolic advantage, 991-treated CARTs showed reduced *in vitro* cytotoxicity against NALM6 targets compared to DMSO-treated controls, which interestingly mimicked the cytotoxicity advantage of CD28-costimulated CARTs compared to 41BB-costimulated CARTs (figure 2). Given 41BB-CARTs show enhanced persistence over CD28-CARTs *in vivo* (2), we pursued further *in vivo* studies with our agonist-treated CARTs. Indeed, despite the slower killing *in vitro*, 991-treated CARTs outperformed the DMSO-treated control CARTs *in vivo*, with significantly reduced luminescence by IVIS imaging and improved overall survival (figure 3).

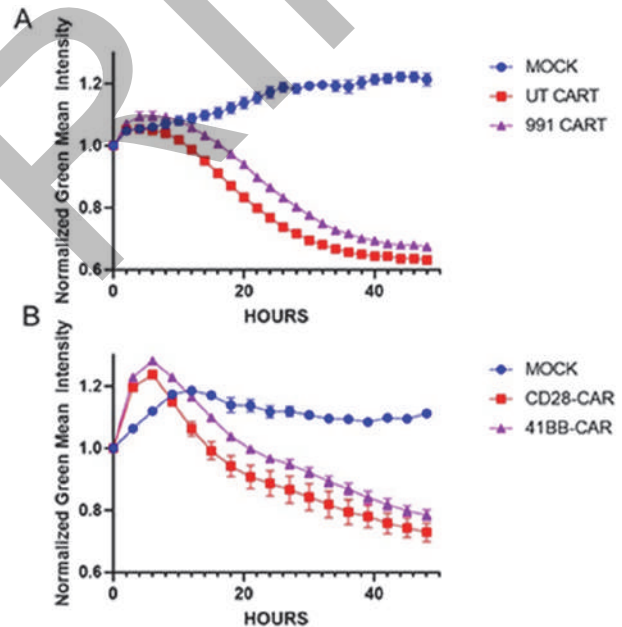
Conclusions AMPK agonism during *in vitro* expansion of CARTs with 991, but not A7, creates metabolically desirable CARTs for immunotherapy. This was demonstrated by increased oxidative metabolism after expansion *in vitro* and improved leukemia clearance *in vivo*. However, anti-leukemia activity appeared decreased with *in vitro* assessments. These studies identify AMPK as an attractive target in immunotherapy, with attention paid to how this pathway is activated, and also suggest the potentially limited utility in using *in vitro* cytotoxicity as a predictor of *in vivo* function in leukemia.

REFERENCES

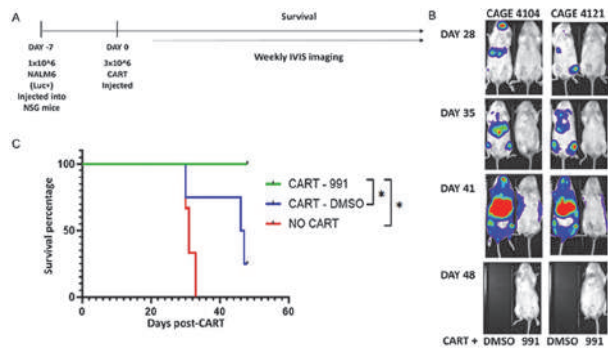
- Maude SL, Frey N, Shaw PA, Aplenc R, Barrett DM, Bunin NJ, et al. Chimeric antigen receptor T cells for sustained remissions in leukemia. *N Engl J Med*. 2014; **371**(16):1507–1517.
- Kawalekar OU, O'Connor RS, Fraietta JA, Guo L, McGettigan SE, Posey AD, et al. Distinct signaling of coreceptors regulates specific metabolism pathways and impacts memory development in CAR T cells. *Immunity*. 2016; **44**(2):380–390.
- Herzig S, Shaw RJ. AMPK: guardian of metabolism and mitochondrial homeostasis. *Nat Rev Mol Cell Biol*. 2018; **19**(2):121–135.



Abstract 205 Figure 1 991 treatment, but not A7 treatment, enhances CART cell oxidative metabolism. Human CART cells were generated from healthy human donor T cells through lentiviral transduction, and then expanded in either DMSO (untreated), A769662 (A7), or Compound 991 (991). CARTs then underwent restimulation overnight before assessment utilizing the mitostress kit for the Seahorse Metabolic Analyzer. ** p<0.01, *** p<0.001, **** p<0.0001



Abstract 205 Figure 2 AMPK-agonist treated CARTs show decreased cytotoxicity vs untreated CARTs *in vitro*, which is mimicked by the cytotoxicity of 41BB vs CD28 CARTs. (A) CD28-costimulated CARTs were generated and expanded with or without 991. After expansion, cells were placed in the Incucyte against zGreen+NALM6 targets, with green fluorescence followed to measure cell killing over 48 hours. (B) The experiment was repeated using CD28-costimulated and 41BB-costimulated CARTs. In both experiments, mock transduced human T cells were plated against NALM6 targets as a control.



Abstract 205 Figure 3 991-treated CART cells outperform standard CARTs in vivo. Luciferase+ NALM6 cells were injected into NSG mice on Day -7, followed by injection with either 991-treated CARTs or DMSO-treated control CARTs on Day 0 (A). Tumor burden was followed weekly with IVIS imaging (B), and overall survival was determined (C). N= 3-4 mice per group. * p < 0.05.

<http://dx.doi.org/10.1136/jitc-2022-SITC2022.0205>

Abstracts

206

NOVEL INTERMEDIATE-AVIDITY GLYPICAN-3 SPECIFIC CARTS RESIST EXHAUSTION AND MEDIATE DURABLE ANTITUMOR EFFECTS AGAINST HUMAN HEPATOCELLULAR CARCINOMA

¹Leidy Caraballo-Galva, ¹Xiaotao Jiang, ¹Mohamed Hussein, ²Huajun Zhang, ¹Rui Mao, ¹Pierce Brody, ¹Yibing Peng, ³Alwu He, ¹Mercy Kehinde-Ige, ¹Ramses Sadek, ²Xiangguo Qiu, ¹Huidong Shi, ¹Yukai He*. ¹Augusta University, Augusta, GA, USA; ²University of Manitoba, Winnipeg, Canada; ³Georgetown University, Washington DC, USA

Background Despite intensive effort, current chimeric antigen receptor modified T cells (CARTs) do not work well for solid tumors. In blood cancers, CARTs easily access to target cells and can “take a break” after each killing of individual tumor cells. In contrast, solid tumor mass limits CART infiltration and create a persistent and multi-dimensional engagement between CART and tumor cells. After CARTs manage infiltrate into tumor mass, they are surrounded by tumor cells, and their movement is further restrained by tumor stroma matrix, which force them under constant stimulation and drive them into exhaustion and death. Conventionally, most CARTs are built from high-affinity monoclonal antibodies (mAb). While such high-avidity CARTs may detect and kill tumor cells of low antigen, they are more prone to exhaustion and death in solid tumors. The aims of this study is to develop proper intermediate-affinity mAbs and intermediate-avidity CARTs for hepatocellular carcinoma (HCC), the 3rd leading cause of cancer death and to test the hypothesis that intermediate-avidity CARTs can resist exhaustion and apoptosis and maintain functions in solid tumors, generating more durable antitumor effects.

Methods We developed 3 new human glypican-3 (hGPC3)-specific mAbs from immunized mice. The mAbs only stained HCC tumors, but not the adjacent normal liver tissues. One of them, 8F8, bound an epitope close to that of GC33, the frequently used high-affinity mAb, but with ~17 fold lower affinity. We then built and compared the intermediate-avidity 8F8 CARTs to high-avidity GC33 CARTs for their *in vitro* function and antitumor effects (1).

Results *In vitro*, 8F8 CARTs killed both hGPC3^{high} and hGPC3^{low} HCC cells to the same extent as GC33 CARTs, but produced lower cytokines. However, the expansion of 8F8 CARTs was 3-5 folds more than GC33 CARTs after engaging with target cells. 8F8 CARTs were less exhausted and less apoptotic than high-avidity GC33 CARTs. The expansion advantage of 8F8 CARTs was maintained under hypoxia culture condition. Importantly, the 8F8 CARTs also expanded and persisted to a greater extent than GC33 CARTs *in vivo*, resulting in durable responses against HCC xenografts. Compared to GC33 CARTs, there were 5 folds more 8F8-BBz CARTs in the tumor mass for a longer period of time (figure 1). Remarkably, the tumor infiltrating 8F8 CARTs were much less exhausted and apoptotic, and more functional than GC33 CARTs.

Conclusions The novel intermediate-avidity 8F8-BBz CART resists exhaustion and apoptosis inside solid tumors, demonstrating a greater and durable therapeutic potential than high-avidity CARTs.

REFERENCE

1. Caraballo Galva, L.D., et al. (2022) Novel low-avidity glypican-3 specific CARTs resist exhaustion and mediate durable antitumor effects against HCC. *Hepatology* 76(2), 330-44

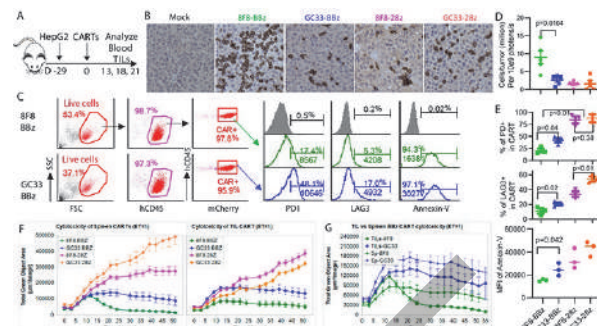


Fig. 1. More functional 8F8-BBz CARTs are in tumors. (A) Experimental scheme. (B) IHC staining of human CD8 in tumor. (C) Gating strategy of analyzing TIL CART exhaustion and apoptosis. (D) CART number was calculated by dividing the total CARTs in the single cell suspension of each tumor by tumor BLL. (E) A summary of the %s of PD1+, LAG3+, and MFI of Annexin-V on CARTs. (F) 8F8 CARTs have stronger cytotoxicity than GC33 CARTs, and BBz CARTs have better function than 2Bz CARTs. (G) BBz CARTs in the spleen had better function than BBz CARTs in the tumor.

Abstract 206 Figure 1 More functional 8F8-BBz CARTs are in tumors.
More functional 8F8-BBz CARTs are in tumors.

<http://dx.doi.org/10.1136/jitc-2022-SITC2022.0206>

207

CLAUDIN18.2-TARGETING CAB-T CELLS HAVE SUPERIOR SAFETY OVER TRADITIONAL CAR-T, WHILE MAINTAINING POTENT *IN VIVO* ANTI-TUMOR EFFICACY

¹Jitian Chai, ¹Weifeng Huang, ¹Shaogang Peng, ¹Zhenqing Zhang, ²Yao Yan, ²Chuan-Chu Chou*, ²Andy Tsun, ¹Zhiyuan Li. ¹Biotheus (Suzhou) Co., Ltd., Suzhou, China; ²Biotheus Inc., Zhuhai, China

Background We have developed a proprietary T cell-based anti-CD3 T cell engager delivery platform (named CAB-T), which includes two elements: a chimeric CD3e/signaling component and a CD3-based bispecific T cell engager (TCE). We have previously shown the efficacy *vs.* safety advantages of the CAB-T system over a traditional second-generation CAR-T format by targeting claudin18.2 (CLDN18.2) (poster no. 206, SITC2021). However, a comprehensive comparison between CAB-T *vs.* CAR-T had not been investigated. Here, in multiple independent *in vivo* tumor mouse models, we aimed to assess the safety and efficacy of our CAB-T platform using CLDN18.2-CAB-T cells.

Methods A sequence encoding for an anti-human CLDN18.2 scFv was engineered into CAB-T (CLDN18.2-CAB-T) and CAR-T (CLDN18.2-CAR-T) expression systems and generated via lentiviral transduction of T cells followed by cell expansion. Cytokine release and TCE levels were determined by ELISA and a cytometric bead array, while T cell killing was tested by the detection of LDH release. *In vivo* studies using CLDN18.2+ tumor cells were tested in humanized mouse models (NCG or NOG mice). T cell infiltration into tumors or normal gastric tissue were detected by immunohistochemistry with an anti-FLAG antibody.

Results Both CLDN18.2-targeting CAB-T and CAR-T cells displayed excellent dose-dependent *in vivo* anti-tumor efficacy towards CLDN18.2-positive tumor cells. However, CLDN18.2-CAB-T cells had a superior safety profile over its CAR-T equivalent. More specifically, mid (1×10^6 cells) to high (5×10^6 cells) single doses of CLDN18.2-CAR-T cells were lethal to mice, whereas all the dose levels of CAB-T cells were safe. CLDN18.2-CAB-T cells released less inflammatory cytokines than CLDN18.2-CAR-T, including IL-6, TNF α and IL-2, in *in vitro* co-culture assays with NUGC4 tumor cell targets. Mice treated with CLDN18.2-CAB-T also showed higher levels of serum GM-CSF and IFN γ compared to those treated with CLDN18.2-CAR-T. Meanwhile, CLDN18.2-CAR-T induced severe immune cell infiltration in normal gastric tissue, whereas CLDN18.2-CAB-T did not. This suggests that CAB-T may provide a wider therapeutic dosing window than traditional CAR-T platforms.

Conclusions We show that CLDN18.2-CAB-T has superior safety traits over CLDN18.2-CAR-T while maintaining high levels of *in vivo* anti-tumor efficacy, suggesting that CAB-T cells may offer better safety for patients in the clinic. CLDN18.2-CAB-T is currently undergoing an investigator-initiated trial to test its safety and efficacy for subjects with CLDN18.2+ solid tumors.

Ethics Approval All mice were maintained under specified pathogen-free conditions, and all studies were approved by the Animal Care and Use Committee of HUST-Suzhou Institute for Brainmatics.

<http://dx.doi.org/10.1136/jitc-2022-SITC2022.0207>

208

T-SIGN VECTOR-MEDIATED ANTIGEN “SPRAY PAINTING” AND TUMOR MICROENVIRONMENT (TME) REPROGRAMMING TO ENABLE CAR-T CELL TARGETING OF SOLID TUMORS

<http://dx.doi.org/10.1136/jitc-2022-SITC2022.0208>

Maria Stella Sasso, Rachel Bergin, Manuela Zonca, Eva Vainiute, Tae Hyun Jang, Zahra Oubihl, Meg Snowden, Alice Muntzer, Carla Cerqueira, Rochelle Lear, Katy West, Brian Champion*. *PsOxus Therapeutics Ltd, Abingdon, UK*

Background Multiple barriers in the tumor microenvironment (TME) have hampered development of CAR-T cell therapies for solid tumors. These challenges include an immunosuppressive TME, poor trafficking of CAR-T cells to the tumor and shortage of highly expressed tumor-specific antigens. We recently demonstrated that Tumor-Specific Immuno-Gene (T-SIGn) viral vectors encoding immunostimulatory cytokines, costimulators and chemokines can reprogram the TME towards a pro-inflammatory phenotype resulting in a markedly increased therapeutic efficacy of CAR-T cells in a A549 human tumor xenograft and lung metastasis model.¹ Here we further explored the potential of the T-SIGn platform in combination with CAR-T cell therapy by developing and characterizing a T-SIGn viral vector that simultaneously expresses immunostimulatory cytokines/chemokines and a secreted bispecific protein incorporating a CAR-T cell target antigen. This secreted ligand binds to (“spray paints”) tumor cells to enable recognition by CAR-T cells.

Methods We used a T-SIGn virus (NG-1125) expressing a secreted anti-HER2-CD19 fusion protein (saH2-19), as a model “spray paint” antigen, encoded together with IFN α and CXCL9 as example cytokine/chemokines. *In vitro*, human tumor cell lines were used to assess the ability of T-SIGn viruses to induce tumor-specific expression and activity of saH2-19 as CAR-T cell target antigen. We quantified T-SIGn vector-encoded CD19 expression on tumor cell surfaces using flow cytometry and CAR-T mediated killing via xCELLigence.

In vivo, expression of CD19 fusion protein and transferred CD19 CAR-T cells in tumors were assessed by flow cytometry analysis and immunohistochemistry of A549 tumor xenografts.

Results Using *in vitro* human cell culture models, the NG-1125 vector led to efficient expression of saH2-19 on tumor cell surfaces, both on vector-infected and non-infected or non-permissive cells. This enabled effective antigen-specific tumor cytotoxicity by CD19-specific CAR-T cells. Using an *in vivo* human A549 lung tumor xenograft model adoptively transferred with human CD19-specific CAR-T cells, NG-1125 induced tumor-specific CD19 expression on both vector infected and non-infected cells (demonstrating antigen “spray painting”) together with accumulation of activated T cells. This accumulation of T cells was not seen with a vector only expressing the saH2-19 transgene.

Conclusions Together, our data provide a proof of concept that T-SIGn vectors can be designed to deliver TME-modifying immunomodulators together with “spray paint” antigens that effectively enable tumor cell recognition and destruction by CAR-T cells specific for target antigens not endogenously expressed by tumors. Further studies are exploring the full potential of this “spray painting” approach to enable CAR-T cell therapy for of solid tumors.

REFERENCE

1. Sonzogni O, Zak DE, Sasso MS, Lear R, Muntzer A, Zonca M, West K, Champion BR, Rottman JB. T-SIGn tumor reengineering therapy and CAR T cells synergize in combination therapy to clear human lung tumor xenografts and lung metastases in NSG mice. *Oncoimmunology* 2022; **11**. <https://doi.org/10.1080/2162402X.2022.2029070>

209 ANTI-ALPP CAR-T CELL IMMUNOTHERAPY FOR OVARIAN AND ENDOMETRIAL CANCER

¹Si Li*, ²Qi-Jing Li, ¹Nicole Palmer, ¹Johnny Guan, ³Zhenbo Su, ¹Peter Alexander, ¹Rui Chen, ¹Lixia Zhao. ¹TCRCure Biopharma Corp., Los Angeles, CA, USA; ²A*STAR, Proteos, Singapore; ³Guangdong TCRCure Biopharma Technology C, Guangzhou, China

Background Ovarian and endometrial cancers are commonly occurring cancers in women with very limited treatment options for relapse and metastasis. While immune checkpoint inhibitors have generated unprecedented responses in certain other cancer types, results from early attempts in ovarian and endometrial cancers have been suboptimal. To develop a CAR-T therapy against these cancers, multi-omics data mining identified ALPP (alkaline phosphatase, placental), a cell surface protein with expression restricted to female reproductive tissues, as a potential target.

Methods To validate its tumor-specific expression, immunohistochemical arrays were performed to assess cell surface display of ALPP in normal and cancerous tissues. An anti-ALPP CAR (TC-A101) was developed and validated for its targeting specificity against multiple ALP homologs, as well as its killing efficacy in vitro. The pre-clinical efficacy of TC-A101 was validated in an animal model of ovarian cancer peritoneal metastasis. The CAR structure was further optimized through alternative hinge and transmembrane domains for lower tonic signaling and better stability of CAR expression.

Results Preclinical models demonstrate that TC-A101 T cells specifically recognize and kill ALPP-expressing tumor targets, and their administration significantly reduces tumor burdens and extends the survival of mice bearing metastatic SiHa tumors and ascites. CAR structure optimization, particularly incorporating a CD28 hinge domain (TC-A103), further potentiates CAR-T cells with stabilized CAR surface expression, lowered tonic signaling, and augmented antitumor efficacy.

Conclusions The preclinical findings reported here indicate that ALPP could be a good target and anti-ALPP CAR-T cell immunotherapy is potentially safe and efficacious against female reproductive cancers expressing ALPP.

Ethics Approval All in vivo experiments in this study were conducted according to guidelines under a protocol approved by Mispro Biotech Services Institutional Animal Care and Use Committee.

<http://dx.doi.org/10.1136/jitc-2022-SITC2022.0209>

210

GENERATION OF HYPOIMMUNOGENIC ALLOGENEIC CAR T CELLS BY INACTIVATION OF TRANSCRIPTIONAL REGULATORS OF HLA CLASS I AND II GENES

Hsinyuan Cheng*, Michael Yi, Michael Bethune, Eric Gschweng, Melinda Au, Duy Nguyen, Kristen Zhang, Tanu Shenoy, Barbra Sasu, Thomas Van Blarcom, Cesar Sommer. *Allogene Therapeutics, South San Francisco, CA, USA*

Background Autologous CAR T cell therapies have revolutionized the treatment landscape in hematological malignancies. Using the patient's own T cells for manufacturing, however, poses limitations on the widespread use of these therapies. Off-the-shelf allogeneic CAR T cells could potentially address these issues by using healthy donor T cells as starting material, consistency of product, immediate availability, and cost and convenience of scalable manufacturing. However, expansion and persistence of infused allogeneic CAR T cells may be limited by immune rejection. Immune "cloaking" strategies centered on deletion of β 2-microglobulin can avoid rejection by CD8 T cells but may elicit strong NK cell rejection. Moreover, HLA Class II expression can be induced upon T cell activation to increase the risk of CD4 T cell rejection. Here, we propose an alternative approach to immune evasion by selectively targeting NLRC5 and RFX5, transcriptional regulators controlling expression of HLA molecules.

Methods CRISPR/Cas9 technology was used to knockout NLRC5, RFX5, B2M, CIITA, and/or TRAC. Survival of hypoimmunogenic cells was assessed in mixed lymphocyte reaction (MLR) assays with allogeneic T cells, NK cells, or PBMCs. For in vivo evaluation, mice were engrafted with human T cells and Raji tumor cells followed by administration of hypoimmunogenic CD19 CAR T cells, and CAR T cell persistence and tumor growth were monitored over time.

Results Deletion of NLRC5 and RFX5 resulted in substantial and stable downmodulation, but not complete ablation, of HLA Class I expression. RFX5 KO cells also exhibited downregulation of HLA Class II expression. NLRC5 KO and RFX5 KO T cells showed enhanced survival against allogeneic T cells but elicited only minor NK cell reactivity. When co-cultured with HLA-mismatched PBMCs, NLRC5 KO and RFX5 KO cells effectively mitigated rejection, whereas uncloned control and B2M KO cells were eliminated by allogeneic T and NK cells, respectively. These findings were replicated in T cells expressing a CD19 CAR. Inactivation of NLRC5 or RFX5 did not impact CAR T cell phenotype or cytotoxic activity. In vivo, hypoimmunogenic CAR T cells demonstrated superior persistence and antitumor efficacy compared to uncloned control CAR T cells in the presence of allogeneic T cells.

Conclusions Hypoimmunogenic CAR T cells can be successfully generated by targeted deletion of NLRC5 or RFX5, which reduces T cell rejection without triggering substantial NK cell rejection and does not affect CAR T cell function. The improved persistence of hypoimmunogenic allogeneic CAR T cells may increase the therapeutic efficacy of off-the-shelf products.

<http://dx.doi.org/10.1136/jitc-2022-SITC2022.0210>

211 CHEMICAL PRIMING OF NATURAL KILLER CELLS FOR CANCER IMMUNOTHERAPY

Seung Hee Choi*, Eun-Su Ko, Joo Dong Park, Kyung-Soon Park. *CHA University, Seongnam, Republic of Korea*

Background Due to their powerful immune surveillance activity and ability to kill and clear cancer cells, natural killer (NK) cells are an emerging anticancer immunotherapeutic agent.^{1,2} Therefore, there is much interest in developing efficient technologies that further enhance the therapeutic antitumor efficacy of NK cells. One of these technologies is a priming strategy that pre-activates NK cells using a cytokine cocktail or cancer cell lysates.^{3,4}

Methods Chem_NK refers to ex vivo NK92MI or primary NK cells that have been chemically primed by 25KDa branched polyethylenimine (25KbPEI). The priming activity of 25KbPEI was evaluated by receptor expression, perforin accumulation, chemotaxis and the antitumor efficacy of Chem_NK. The priming mechanism was studied regarding 25KbPEI mediated calcium influx and subsequent activation of multiple signaling pathways.

Results Chem_NK showed increased perforin accumulation, interferon- γ expression and activating/adhesion/chemokine related receptor expression. In line with these phenotypes, Chem_NK had potent in vivo antitumor efficacy toward ovarian cancers and triple negative breast cancers. The major mechanism for 25KbPEI to prime NK cells was identified as a calcium influx via the Ca²⁺-permeable nonselective cation channel transient receptor potential melastatin 2 (TRPM2). We confirmed that 25KbPEI mediated calcium-influx is associated with activation of ERK and mTOR signaling, which is directly linked to the translational initiation of immune response-related proteins of NK cells (figure 1).

Conclusions NK cells can be chemically primed with 25KbPEI to become 'ready to fight' state. Because PEI is a biocompatible and FDA-approved chemical for biomedical use, our results suggest a cost-effective and simple method of producing therapeutic NK cells.

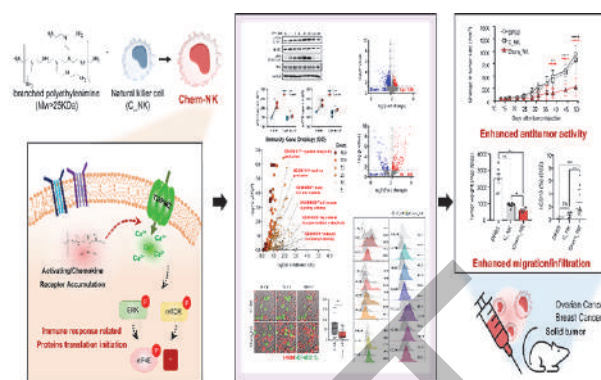
Acknowledgements This work was supported by Samsung Research Funding & Incubation Center of Samsung Electronics under Project Number SRFC_MA2102_06.

REFERENCES

1. Lanier, L.L. Up on the tightrope: natural killer cell activation and inhibition. *Nat Immunol* **9**, 495-502 (2008).
2. Lusty, E. *et al.* IL-18/IL-15/IL-12 synergy induces elevated and prolonged IFN-gamma production by ex vivo expanded NK cells which is not due to enhanced STAT4 activation. *Mol Immunol* **88**, 138-147 (2017).
3. Ni, J. *et al.* Sustained effector function of IL-12/15/18-preactivated natural killer cells against established tumors. *J Exp Med* **209**, 2351-2365 (2012)
4. North J. *et al.* Tumor-priming human natural killer cells lyse NK-resistant tumor targets: evidence of a two-stage process in resting NK cell activation. *J Immunol* **178**, 85-94 (2007)

Ethics Approval All animal experiments were approved by the Institutional Animal Care and Use Committee of the laboratory animal research center at CHA University. Primary NK cells were isolated from peripheral blood mononuclear cells obtained from healthy donors. This research was reviewed and approved by the institutional review board of CHA University.

Consent All healthy blood donors provided informed consent.



Abstract 211 Figure 1

<http://dx.doi.org/10.1136/jitc-2022-SITC2022.0211>

212

ADOPTIVELY TRANSFERRED TH17 CELLS COOPERATE WITH HOST B CELLS TO MEDIATE ROBUST IMMUNITY TO TUMORS

¹Anna Cole*, ²Hannah Knochelmann, ³Amalia Rivera-Reyes, ⁴Aubrey Smith, ¹Megan Wyatt, ²Guillermo Rangel Rivera, ¹Jeremy Boss, ¹Gregory Lesinski, ¹Chrystal Paulos. ¹Emory University, Atlanta, GA, USA; ²Medical University of South Carolina, Charleston, SC, USA; ³University of Colorado, Aurora, CO, USA; ⁴Orange Grove Bio, Cincinnati, OH, USA

Background Adoptive T cell transfer therapy mediates potent immunity in some patients with aggressive malignancies, but many individuals do not respond, or may relapse. One reason for therapy failure is due to lack of T cell persistence. To overcome this problem, we aimed to generate a cell product that will lead to long term antitumor immunity in aggressive models. Accordingly, our team reported that a subset of CD4⁺ T cells termed Th17 cells, persist long term and can eradicate solid tumors when infused into mice. However, how Th17 cells mediate tumor immunity is unclear.

Methods To model Th17 cell adoptive T cell transfer therapy, we use a transgenic mouse model in which CD4⁺ cells express a T cell receptor (TCR) that recognizes tyrosinase-related protein 1 (TRP-1) expressed on melanoma, and polarized naïve CD4⁺ T cell to Th17 cells. These cells are infused into mice bearing B16F10 melanoma tumors that received non-myeloablative lymphodepleting total body irradiation. Tumor growth is measured over time or tumors, spleen, and lymph nodes are analyzed 12 days post cell transfer.

Results To understand how Th17 cells elicit robust antitumor activity, we performed an unbiased analysis of RNA transcripts on tumor-draining lymph nodes of mice treated with Th17 cells. Surprisingly, we found that mice infused with anti-tumor Th17 cells have increased transcripts associated with B cells, and factors that trigger B cell maturation, antibody-secretion, and enhanced antigen presentation. Furthermore, host B cells, but not CD8⁺ T cells, were surprisingly critical in sustaining long-term immunity, as their depletion significantly impaired survival. B cells enhance Th17 cell persistence and promote their differentiation into IFN-g producers and away from regulatory IL-10 production. Th17 cells induce B cell activation and maturation in an IL-21-dependent manner, causing the production of class switched antibodies which can alone partially protect against tumor challenge. Finally, we found that IL-21, ICOS, and IFN-g are required for this antitumor response as inhibition of any of these three abrogates durable tumor immunity.

Conclusions Altogether, this suggests a cooperative relationship between transferred Th17 cells and host B cells in mediating long term tumor immunity. Our novel findings highlight Th17 cell therapy as a way to harness both T and B cell responses against cancer. Ongoing experiments will further determine the mechanism of how B cells collaborate with Th17 cells to mediate superior antitumor activity.

Acknowledgements We would like to acknowledge Emory University, The Winship Cancer Institute, and the Pediatrics/Winship Flow Cytometry Core.

Ethics Approval All animal procedures were approved by the Institutional Animal Care and Use Committee of Emory University, protocol number 201900225.

<http://dx.doi.org/10.1136/jitc-2022-SITC2022.0212>

213

DESIGN, CHARACTERIZATION AND PRECLINICAL VALIDATION OF A COMBINATORIAL CAR-BASED IMMUNOTHERAPY AGAINST COLORECTAL CANCER WITH HER2 AMPLIFICATION

¹Marco Cortese*, ²Erica Torchiario, ²Simonetta Leto, ²Consalvo Petti, Alice D'Andrea, ²Master Degree, ²Federica Invrea, ¹Sabrina Arena, ¹Enzo Medico. ¹University of Turin, Turin, Italy; ²Candiolo Cancer Center, Turin, Italy

Italian Ministry of Health approved protocol (Authorization n°225/2021-PR).

<http://dx.doi.org/10.1136/jitc-2022-SITC2022.0213>

Background Adoptive immunotherapy based on chimeric antigen receptor (CAR)-T cells has led to successful treatment of different hematological malignancies. However, it remains extremely challenging for solid tumors, mostly because of “on-target off-tumour” toxicity, as observed in the case of anti-HER2 CAR-T treatment of HER2-amplified colorectal cancer (HER2_{amp} CRC).¹ To enable adoptive immunotherapy against HER2_{amp} CRC, we therefore considered a combinatorial strategy based on the synNotch-based artificial regulatory network. A synthetic Notch receptor including anti-HER2 scFv as extracellular domain and the GAL4-VP64 artificial transcription factor as intracellular domain was employed.² Engagement of the anti-HER2 domain by target cells drives GAL4-VP64 cleavage and translocation to the nucleus, leading to the expression of a CAR under a GAL4-responsive promoter. In this way, only cells co-expressing both HER2 and the CAR target are killed. As a CRC-specific CAR target we selected CEA, product of the CEACAM5 gene. CEA expression is restricted to the digestive tract and is increased in cancer.

Methods For the generation of HER2-synNotch CEA-CAR effectors, we chose the natural killer cell line NK-92 and transduced it with two lentiviral vectors, encoding respectively the HER2 synNotch and the second-generation anti-CEA CAR with CD28 costimulatory domain. Transduced cells were repeatedly sorted in the ON and OFF state to select those with the best CAR induction after synNotch engagement; cloning of sorted cells led to identification of an optimally responsive clone (clone 5F).

Results *In vitro*, the 5F clone showed no basal CEA-CAR expression and massive induction in the presence of HER2_{amp} cancer cells. It also displayed selective cytotoxicity against HER2_{amp}/CEA_{pos} CRC cells, with minimal killing activity against HER2_{amp}/CEA_{neg} breast cancer cells, or against CRC cells expressing CEA but without HER2 amplification. *In vitro* 3D models highlighted better recruitment and infiltration by clone 5F respect to NK-92 WT cells, only of HER2_{amp} organoids. *In vivo*, the clone 5F significantly impaired tumor growth in two different HER2_{amp} CRC models.

Conclusions The observed selective efficacy both *in vitro* and *in vivo* of the HER2-synNotch/CEA-CAR approach opens a perspective for possible clinical applications for HER2_{amp} CRC displaying primary or secondary resistance to HER2/EGFR blockade.

REFERENCES

1. Morgan RA, Yang JC, Kitano M, Dudley ME, Laurencot CM, Rosenberg SA. Case Report of a Serious Adverse Event Following the Administration of T Cells Transduced With a Chimeric Antigen Receptor Recognizing ErbB2. *Mol. Ther.* 2010; **18**:843-851.
2. Roybal KT, Williams JZ, Morsut L, Rupp LJ, Kolinko I, Choe JH, Walker WJ, McNally KA, Lim WA. Engineering T Cells with Customized Therapeutic Response Programs Using Synthetic Notch Receptors. *Cell.* 2016; **167**:419-432.

Ethics Approval All the experiments were performed in compliance with institutional guidelines under the Ethical committee of Candiolo Cancer Institute consensus and under the

**INVESTIGATING THE CONSEQUENCES OF TIM-3
EXPRESSION ON MTOR ACTIVATION AND NK CELL
CYTOTOXICITY AGAINST GLIOBLASTOMA**

Tram Dao*, Sandro Matosevic. *Purdue University, West Lafayette, IN, USA*

Background Natural killer (NK) cells hold potential as one of the next generation adoptive cell therapy candidates due to their allogeneity, capability to lyse target without prior sensitization, and low risk of host-versus-graft disease. Thus, being able to utilize NK cell receptors to drive their cytotoxicity remains crucial. Additionally, for treatments of solid tumors, NK cells need to retain their viability against the suppressive tumor microenvironment. One method to modulate NK cell immunometabolism is to leverage the surface receptor TIM-3, which lies at the intersection of NK cytotoxic functions and metabolism – the mTOR-associated pathways.

Methods NK cells were isolated from healthy adult peripheral blood, and expanded in K562-based feeder media. Flow cytometry was used to phenotype TIM-3 expression and phosphorylation of mTOR, Akt, and ribosomal protein S6 (rpS6). CCK-8 assay was used to assess mTOR inhibition against patient-derived glioblastoma cells (GBM43). NK co-operative activities with mTOR inhibitors against GBM43 were evaluated through target lysis, degranulation, and cytokine secretion. TIM-3 *knock-out* (TIM-3 KO) NK cells were generated by electroporating CRISPR/Cas9 ribonucleoprotein complexes.

Results We first explored the link between TIM-3 expression on NK cells and mTOR proteins, including mTOR itself, rpS6, and Akt, which were linked to TIM-3 regulation in T cells. Previously, we had reported that TIM-3 downregulation was associated with lower IFN- γ production. As changes in phosphorylation of rpS6 was linked to lower IFN- γ mRNA levels, we hypothesized that TIM-3 expression leads to increased rpS6 phosphorylation, thus encouraging higher IFN- γ production. Here, we report changes in phosphorylation levels of Akt and rpS6 as consequences of TIM-3 KO, and how these changes can affect NK cell cytotoxicity against GBM43. We also cross-examine these findings using specific pharmacological inhibitors of mTOR, including rapamycin, JR-AB2-011, and torin-1, against mTORC1, mTORC2, and both complexes, respectively, to demonstrate that TIM-3 expression could provide some functional protection against activities these inhibitors through retention of NK cell activity. Lastly, to show that these inhibitions would not compromise NK cell functions, we show GBM43 lysis by NK cells with mTOR inhibitor adjuvants.

Conclusions We have found that TIM-3 expression can exert some control over the mTOR pathway on *ex vivo* NK cells, and this affects NK cells' cytokine production capacity. Since the tumor microenvironment is highly immunosuppressive, the protection against mTOR inhibition by TIM-3 allowed tumor-infiltrating NK cells to remain metabolically and functionally viable, and affords an opportunity to leverage mTOR inhibitors as adjuvants with NK cell therapy against GBM.

Ethics Approval IRB #1804020540

<http://dx.doi.org/10.1136/jitc-2022-SITC2022.0214>

215 **TARGETING OVARIAN CARCINOMA WITH GDT002, A FIRST-IN-CLASS $\gamma\delta$ TCR-BASED T CELL THERAPY**

Esther Drent, Sabine Middendorp*, Andrea Bisso, Sjoerd Baardman, Dagmar Verweij, Estefania Salcedo, Chris Coomans, Steven Braem, Sander van de Weg, Menno Meijer, Natalie Proost, Marieke van de Ven, Haakan Norell, Marleen van Loenen, Nia Emami, Sara Melief, Stefania Gobessi, Mark Throsby. ¹Gadeta, Utrecht, Netherlands; The Netherlands Cancer Institute, Amsterdam, Netherlands

Background Broad application of cell therapies like CAR-T have been hampered by a lack of tumor-specific targets. Gadeta leverages the natural HLA-independent tumor recognition capabilities of $\gamma\delta$ TCRs combined with the proliferative capacity and robust tumor killing of $\alpha\beta$ T cells to develop tumor-specific cell therapies.¹ The most abundant peripheral $\gamma\delta$ T cells express V γ 9V δ 2 TCRs, which sense the presence of phosphoantigens (pAgs) upregulated in malignant cells due to a dysregulated mevalonate pathway.²⁻⁴ The V γ 9V δ 2 TCR expressed by GDT002 was selected for its broad and strong tumor reactivity.⁵ In addition, GDT002 demonstrated effective control of tumor growth in an aggressive systemic xenograft MM mouse model.

Currently GDT002 is being evaluated in a multicenter first-in-human phase 1/2 study for the treatment of multiple myeloma (NCT04688853). This ongoing FIH trial has completed the first dose cohort of 7E7 GDT002 cells without any safety concerns. To broaden the applicability of GDT002, we conducted preclinical studies to identify potential solid tumor indications.

Methods The specificity and anti-tumor activity of GDT002 was evaluated in various cell lines from solid cancer types and primary cells from healthy tissues. Tumor reactivity was tested in 2D co-cultures in the presence or absence of pamidronate, a clinically approved aminobisphosphonate that boosts pAgs levels. Target killing was determined by an xCELLigence-based cytotoxicity assay and T cell activity by cytokine release. Furthermore, GDT002 tumor reactivity and infiltration capacity was assessed in more complex 3D co-culture systems, such as a broad panel of patient-derived tumor organoids and ovarian carcinoma tumoroids, which were subjected to high-content imaging.

Results Significant GDT002 reactivity was observed against 10/15 adherent tumor targets in the presence of pamidronate. In contrast, no GDT002 reactivity was observed against primary cells from healthy tissue. In 3D organoid co-culture assays, GDT002 displayed significant reactivity towards most organoids, with an exceptionally high (90%) response rate towards ovarian cancer organoids. In addition, high-content quantitative imaging showed efficient aminobisphosphonate- and CD277-dependent cytotoxic activity of GDT002 in tumoroids with evidence of infiltration and expansion of GDT002 in the 3D cellular matrix.

Conclusions We demonstrate that GDT002 has potent anti-tumor activity across a broad spectrum of solid tumors. Based on the unmet clinical need and preclinical studies, recurrent ovarian cancer was selected as the first solid tumor indication to evaluate the efficacy of GDT002.

REFERENCES

1. Marcu-Malina V, *et al.* Redirecting $\alpha\beta$ T cells against cancer cells by transfer of a broadly tumor-reactive $\gamma\delta$ T-cell receptor. *Blood*. 2011; **118**:50-59.
2. Gu S, *et al.* Phosphoantigen-induced conformational change of butyrophilin 3A1 (BTN3A1) and its implication on V γ 9V δ 2 T cell activation. *PNAS*. 2017; **114**:E7311-7320.

3. Karunakaran MM, *et al.* Butyrophilin-2A1 Directly Binds Germline-Encoded Regions of the V γ 9V δ 2 TCR and Is Essential for Phosphoantigen Sensing. *Immunity*. 2020; **52**:487-498.
4. Rigau M, *et al.* Butyrophilin 2A1 is essential for phosphoantigen reactivity by $\gamma\delta$ T cells. *Science*. 2020; **367**:eaay5516.
5. Grunder C *et al.* gamma9 and d2CDR3 domains regulate functional avidity of T cells harboring gamma9d2TCRs. *Blood*. 2012; **120**:5153-62

Ethics Approval This study was approved by the Ethics Board of the Mouse Clinic for Cancer and Aging (MCCA), The Netherlands Cancer Institute, Amsterdam, The Netherlands; approval number AVD3010020165407 -165001, study EGP 1.1.9705, 1.5.9012 and 1.5.9421

<http://dx.doi.org/10.1136/jitc-2022-SITC2022.0215>

216

DUAL TARGETING OF CAR-NK CELLS TO PD-L1 AND ERBB2 FACILITATES SPECIFIC ELIMINATION OF CANCER CELLS OF SOLID TUMOR ORIGIN AND OVERCOMES IMMUNE ESCAPE BY ANTIGEN LOSS

¹Jiri Eitler*, ¹Kristin Freudenberg, ¹Paola Ortiz Montero, ¹Wiebke Rackwitz, ²Winfried Wels, ¹Torsten Tonn. ¹Carl Gustav Carus, Dresden, Germany; ²Goethe University, Frankfurt, Germany

Background Retargeting of natural killer (NK) cells with chimeric antigen receptors (CARs) can be a powerful approach to overcome NK-cell resistance of tumor cells. However, targeting a single tumor-associated antigen may be insufficient for some tumors to trigger effective NK-cell activation or result in the selection of antigen-loss variants and tumor immune escape.

Methods To overcome this hurdle, here we generated CAR-NK cells carrying two CARs that target the tumor-associated antigens PD-L1 and ErbB2 (HER2), respectively (figure 1A). NK-92 cells were transduced with lentiviral CAR constructs, and their cytotoxicity against cancer cell lines of different solid tumor origins was compared to that of parental NK-92 and corresponding single-target CAR variants.

Results Dual targeting significantly increased *in vitro* cytotoxicity against PD-L1 and ErbB2 double-positive tumor cell lines including breast, ovarian, pancreatic and gastric cancer cells when compared to single-target CAR variants (Figure 1B,C). These results were also confirmed with 3D spheroid tumor models. Off-target cytotoxicity was not observed. On a molecular level, this enhanced cell killing may be explained by synergistic activation of PLC γ and MAPK pathways. Incubation of cancer cells with IFN- γ further improved killing efficacy due to upregulation of PD-L1 expression. Furthermore, blocking experiments revealed that dual PD-L1/ErbB2-CAR NK-92 cells can overcome immune escape based on loss or inaccessibility of a single target antigen.

Conclusions Altogether, we showed that dual targeting of PD-L1 and ErbB2 improves efficacy of CAR-NK cells against otherwise difficult to treat tumors, and counteracts potential resistance and immune escape mechanisms of cancer cells.

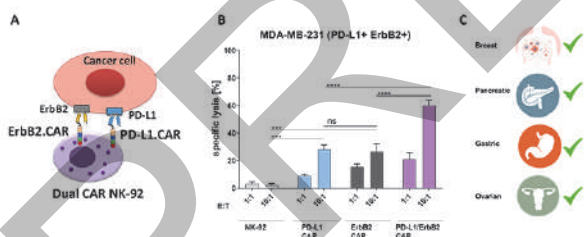


Figure 1: A) schematic representation of Dual CAR NK-92 targeting ErbB2 and PD-L1 molecules on human cancer cell. B) Functional killing assay against human breast carcinoma cell line MDA-MB-231. C) Specific cytotoxicity of PD-L1/ErbB2.CAR NK-92 was confirmed against cancer cell lines of different origin.

Abstract 216 Figure 1

<http://dx.doi.org/10.1136/jitc-2022-SITC2022.0216>

217

MULTI-ARMORED ALLOGENEIC MUC-1 CAR T-CELLS EFFICIENTLY CONTROL TRIPLE NEGATIVE BREAST CANCER TUMOR GROWTH

<http://dx.doi.org/10.1136/jitc-2022-SITC2022.0217>

Piril Erler*, Tomasz Kurcon, Jordan Skinner, Chantel Dixon, Steven Grudman, Ben Mumford, Shipra Das, Alexander Boyne, Alexandre Juillerat, Roman Galetto, Julien Valton, Hana Cho, Laurent Poirot, Beatriz Aranda-Orgilles. *Collectis, New York, NY, USA*

Background CAR T-cell therapy success in solid tumors has been limited due to their complex biology. In solid tumors, lack of tumor-specific antigens, tumor heterogeneity, and immuno-inhibitory nature of tumor microenvironment (TME) demand an optimal therapeutic window where CAR T-cells can be highly efficient while ensuring safety. To address these challenges, we engineered CAR T-cells that i) use the tumor-specific MUC-1 antigen as a discriminatory target and ii) have enhanced therapeutic properties provided by multiple attributes. We focused on TNBC due to poor prognosis and over-expression of MUC1 (~67%) [1]. Here, we describe a universal CAR T-cell therapy for TNBC that can overcome both the host immune rejection and key inhibitory signals from the TME.

Methods We first screened several tumor-specific scFVs for MUC-1 CARs, assessing their binding and safety profiles. Then, we generated allogenic CAR T-cells by leveraging our TALEN® technology. TCR-alpha and B2M were knocked-out to prevent host-versus-graft disease, and to evade host T-cell attack. HLA-E was knocked-in at the B2M-KO site to provide resistance to host NK cell rejection. To increase activity and to overcome inhibitory signals from the TME, we introduced a PD-1 knock-out, a tumor-specific IL-12 release, and TGFBR2 knock-out. We tested these CAR T-cells *in vitro* using target specificity and cytotoxic assays, and *in vivo* by assessing tumor growth, survival, and tumor infiltration.

Results Three scFVs we prioritized showed efficient dose-dependent killing of breast cancer cells *in vitro*. Next, we used subcutaneous and orthotopic models to test CAR T-cells armored with IL-12 inducible release *in vivo*. Efficient tumor control and increased CAR-T cell infiltration extended mice survival, and notably antitumor response followed a dose-dependent pattern. Importantly, we introduced multiple edits in CAR-T cells with a high degree of efficacy, and precision using TALEN®. Functionally validating these edits, we demonstrated that TGFBR2-KO circumvents the inhibitory effects of TGFβ1, and IL-12 release follows a CAR T-cell activation pattern restricting it to the tumor site for increased safety.

Conclusions Overall, our data demonstrate that we can efficiently generate allogenic CAR T-cells and equip them through complex engineering to overcome key challenges of solid tumors. We show that MUC-1 CAR T-cells control tumor growth, while infiltrating tumors more efficiently when enhanced with attributes catered towards the TME of TNBC tumors. Altogether, these pre-clinical data suggest that enhanced MUC-1 CAR T-cells could address some of the current challenges in development of CAR-Ts for TNBC patients with unmet medical needs.

REFERENCE

1. Siroy, A., Abdul-Karim, F. W., Miedler, J., Fong, N., Fu, P., Gilmore, H., & Baar, J. MUC1 is expressed at high frequency in early-stage basal-like triple-negative breast cancer. *Human Pathology* 2013; **44**:54.

Ethics Approval All animals in this study were treated humanely and in agreement with IACUC guidelines. IACUC Protocol #:2019-05-10-CEL-02

Inaki Etxeberria*, Lauren Banks, Smita Chandran, Arianna Correa, Bryan Novak, Jessica Fleischman, Alexander Drilon, Jedd Wolchok, Taha Merghoub, Christopher Klebanoff. *Memorial Sloan Kettering Cancer Center (MSKCC), New York, NY, USA*

Background The NRAS driver oncogene is frequently mutated in diverse cancer types of high unmet medical need, including colorectal cancer, thyroid cancer, and ~25% of cutaneous melanomas. Most colorectal and thyroid cancers fail to respond to immune checkpoint inhibitors. Further, unlike other genomic variants of melanoma, those that harbor mutant NRAS respond poorly to current immunotherapies. Public neoantigens (NeoAgs) represent an elite class of clonally conserved, cancer-specific epitopes derived from recurrently mutated driver genes. Because public NeoAgs are restricted by prevalent HLA alleles they are shared among cancer patients and can be therapeutically targeted using off-the-shelf reagents. Here, we report on the immunogenic landscape and T cell responses to public NeoAgs resulting from recurrent NRAS (Q61) hotspot mutations in cancer patients.

Methods We combined a mass spectrometry screen, dextramer-based T cell detection, single-cells RNA sequencing, and functional immune validation assays to determine the immunogenicity of NRAS(Q61) epitopes. As part of these efforts, we assembled and performed comprehensive immune monitoring of peripheral blood and tumor samples from $n=26$ HLA-A*01⁺ patients with an NRAS(61) mutated cancer.

Results We discovered that neopeptides derived from the three most common NRAS(Q61) hotspot substitutions (R, K, and L) are naturally processed and presented in the context of HLA-A*01, an allele expressed by ~25% of North Americans. Immune monitoring demonstrated that NRAS public NeoAg-specific T cell responses occur in ~50% of patients, including subjects with melanoma and non-melanoma cancers. Responses occurred at comparable frequencies whether the mutated NRAS residue was basic or aliphatic. Using single-cell sequencing, we retrieved and functionally validated a panel of $n=18$ TCRs from patient samples that confer specific recognition to cancer cells that express an NRAS Q61 public neopeptide. All of the patient-derived TCRs are high-affinity and function in a CD8 co-receptor-independent manner. Moreover, a subset TCR candidates demonstrate "cross-protection" towards multiple NRAS Q61 mutated variants, allowing a single receptor to provide therapeutic coverage for >90% of NRAS mutations. Mechanistically, we demonstrate that NRAS public NeoAg TCR cross-protection is tuned by expression of the CD8 $\alpha\beta$ co-receptor and requires recruitment of LCK.

Conclusions Collectively, our results demonstrate that multiple NRAS(Q61) hotspot mutations give rise to immunogenic public NeoAgs that can be studied across patients and therapeutically targeted using a TCR-based approach. These findings establish the foundation for an innovative new class of precision immune-genomic treatments for mutant NRAS cancers.

Ethics Approval All patients provided written informed consent for tumor and white blood cell sequencing and review of patient medical records for demographic, pathological and treatment information under a Memorial Sloan Kettering Cancer Center (MSKCC) institutional review board-approved biospecimen umbrella protocol (protocol 12-245; ClinicalTrials.gov ID: NCT01775072).

219 THE FUNCTIONAL ACTIVITY OF GAVO-CEL TRUC-T CELLS IS NOT IMPAIRED BY SOLUBLE MESOTHELIN

Michael Lofgren*, Robert Tighe, Robert Hofmeister, Jian Ding, Nate Bagge, Alec Andrews, Michelle Fleury, Courtney Anderson. *TCR2 Therapeutics, Cambridge, MA, USA*

Background Gavo-cel is an autologous and HLA-independent T-Cell Receptor Fusion Construct (TRuCTM) T cell therapy that targets mesothelin-expressing tumors and is under Phase 2 evaluation for treatment-resistant MPM, NSCLC, cholangiocarcinoma, and ovarian cancer tumors (NCT03907852). Mesothelin (MSLN) is a 71 kDa GPI-anchored membrane protein that undergoes proteolytic membrane shedding to generate soluble mesothelin-related peptides (sMRPs) whose levels are correlated with tumor burden in MPM. sMRPs contain the juxtamembrane epitope of that is recognized by the MH1 binder domain of the gavo-cel TRuC and whose levels are correlated with tumor burden in MPM. Because shed MSLN has been implicated as a potential obstacle to successful anti-MSLN therapies, including cell therapies, we assessed the impact of soluble MSLN (sMSLN) on the function of gavo-cel and or allogeneic anti-MSLN TRuC, MH1gd.

Methods In this study, we generated primary human TRuC-T cells modeling MSLN-targeting clinical agent gavo-cel or that express MH1gd TRuC, and then measured the impact of soluble MSLN on the *in vitro* activation, cytotoxicity, and cytokine response of gavo-cel or MH1gd during acute and chronic challenge with antigen-expressing tumor cells. We also evaluated whether sMRP in human serum impacts the *in vitro* cytotoxicity and cytokine response of gavo-cel in response to MSLN-expressing tumor cell lines.

Results High, supraphysiological levels of the full-length shed domain of MSLN, sMSLN, does not impair, block, or disrupt the effector function of gavo-cel or MH1gd TRuC-T cells with respect to *in vitro* cytotoxicity or cytokine production. Furthermore, gavo-cel demonstrates potent efficacy *in vivo* in a tumor model characterized by circulating sMSLN.

Conclusions Our data indicate that both gavo-cel and allogeneic MSLN-targeting TRuC-T cells are not susceptible to functional suppression by sMRPs, even at supraphysiological levels that far exceed those found in cancer patients.

<http://dx.doi.org/10.1136/jitc-2022-SITC2022.0219>

LUCIFERASE REPORTER CANCER CELL LINES FACILITATE CAR-T DEVELOPMENT

John Foulke*, Luping Chen, Brian Della Fera, Hyeoun Chang, Kevin Tyo, Zhizhan Gu, Fang Tian. ATCC (American Type Culture Collection), Gaithersburg, MD, USA

Background Chimeric antigen receptor (CAR)-T cells have displayed remarkable efficacy in treating malignant cancers, particularly liquid tumors. CAR-T cells have proven to be a new type of “living” therapeutic by harnessing the patient’s immune system to recognize specific tumor associated antigens and redirect the engineered T cells to more specifically targeted tumor cells. Considerable research efforts have been invested into developing new CAR structures to increase the scope of targeted cancer types and raise their anti-tumor efficacy. Evaluating the biofunction of CAR-T cells in vitro typically involves a series of labor-intensive co-culture experiments and immunoassays, where reproducibility remains a challenge during the validation of new CAR-T cells due to donor-to-donor variations and other possible factors. In this study, we present a panel of luciferase reporter tumor cell lines that can be utilized to examine the function of CAR-T cells. The panel of selected human tumor cell lines naturally express high levels of clinically relevant CAR-T target antigens on cell surface, such as CD19, CD20 and HER2.

Methods The panel of selected human tumor cell lines naturally express high levels of clinically relevant CAR-T target antigens on cell surface, such as CD19, CD20 and HER2. Antibiotic selection and single cell sorting were performed to isolate stable clones with high luciferase expression via the introduction of a Lenti-LUC2 luciferase reporter into the parental cell lines. The target antigen and luciferase were verified to have expression stability by comparing the low passage and the high passage reporter cells. In addition, these reporter cell lines were characterized and authenticated using cell morphology, growth kinetics, and STR profile. To verify the performance of the target luciferase reporter cell lines, we used the cancer and T cell co-culture experiments. Commercially available CAR-T cells targeting CD19, CD20, and HER2 were employed in this study, with which empty vector-transduced T cells from the same donor were paired as controls. The cytotoxicity of the CAR-T cells against target tumor cells was measured using a luciferase assay, a commercially available potency assay, and a bright field and fluorescence live cell imaging assay.

Results Our results demonstrate that the luciferase reporter system is a simple, robust, and highly sensitive means to measure biological processes in cancer and T cell ex vivo co-cultures.

Conclusions In summary, CAR-T target antigen luciferase reporter cell lines from ATCC provide the well-characterized tools with high reproducibility for studying CAR-T biofunction and validating new CAR-T agents for cancer immunotherapy.

<http://dx.doi.org/10.1136/jitc-2022-SITC2022.0220>

221

SENTI-401, AN ALLOGENEIC LOGIC-GATED AND MULTI-ARMED CAR-NK CELL THERAPY FOR THE TREATMENT OF CEA-EXPRESSING SOLID TUMORS WITH ENHANCED SELECTIVITY AND EFFICACY

Alba Gonzalez Junca*, Nicholas Frankel, Maelig Morvan, Assen Roguev, Michelle Hung, Russell Gordley, Miguel Palermo, Tyler Santomaso, Pearley Chinta, Aldo Sotelo, Marcus Gainer, Derrick Lee, Tony Hua, Andrew Banicki, Mengxi Tian, Niran Almudhar, Atahualpa Contreras, Chen-Ting Lee, Timothy Lu. *Senti Biosciences, South San Francisco, CA, USA*

Background Chimeric Antigen Receptor (CAR)-based cell-therapies have demonstrated clinical benefit in select blood cancers. Unfortunately, their success has yet to be translated to solid tumors. Poor antigen specificity and immune-suppressive mechanisms in the tumor microenvironment (TME) pose key challenges for cell-therapies in the treatment of solid tumors.

Methods SENTI-401, a CAR-NK cell-therapy with NOT Logic Gating and Multi-Arming gene circuits, is designed to overcome the above challenges. SENTI-401 targets CEACAM5 (CEA), a tumor-associated antigen (TAA) highly expressed in solid tumors, including colorectal, pancreatic and lung cancers. SENTI-401 also incorporates NOT Gate technology to overcome on-target off-tumor toxicity from CEA expression by healthy epithelial cells, which has been previously reported when targeting CEA in the clinic.¹ Senti is evaluating the effects of multi-arming CAR-NK cells with immunostimulatory payloads to potentially overcome the immunosuppressive TME.

Senti's novel NOT-Gate technology incorporates an activating (aCAR) targeting a TAA, paired with an inhibitory (iCAR) that recognizes a safety antigen (SA) uniquely expressed on the surface of healthy cells. The NOT-Gate significantly reduces CAR-mediated killing of target cells in a SA-dependent manner, thus mitigating on-target, off-tumor toxicity and allowing targeting of tumor antigens that are broadly expressed by healthy cells.

Results Using our Tumor-Associated Antigen and Safety Antigen Discovery Platform, we discovered and validated VSIG2, a protein on the surface of CEA-expressing healthy epithelial cells and not on tumor cells.

NK cells expressing CEA-targeting aCARs and VSIG2-targeting iCARs receptor pairs had significantly reduced CAR-mediated killing of target cells expressing both CEA and the SA VSIG2, *in vitro* and *in vivo*.

To enhance persistence and activity of CAR-NK cells, we developed, calibrated release (cr) technology, which can be coupled to cytokines such as IL-15, resulting in a desired ratio of secreted and surface-bound cytokine to provide autocrine and paracrine functions. The combination of crIL-15 and IL-21 resulted in increased survival and activation of anti-CEA CAR-NK cells, and leading to significantly increased target-cell killing in serial-killing assays. *In vivo*, anti-CEA CAR-NK cells expressing the both cytokines had superior activity and longer persistence compared to anti-CEA CAR-NK cells. Similarly, we optimized gene-circuits to confer resistance to the immunosuppressive effects of TGF β ; anti-CEA CAR-NK cells armed with TGF β -blocking constructs sustained target-cell killing in the continuous presence of TGF β .

Conclusions SENTI-401 incorporates NOT-Gating and Multi-Arming gene-circuits into CAR-NK cells in order to improve the therapeutic window and efficacy of CEA-targeting cell-therapies for the treatment of solid tumors.

REFERENCE

1. Parkhurst MR, Yang JC, Langan RC, *et al* T cells targeting carcinoembryonic antigen can mediate regression of metastatic colorectal cancer but induce severe transient colitis. *Mol Ther.* 2011 Mar;**19**(3):620-6 [doi: 10.1038/mt.2010.272.]

<http://dx.doi.org/10.1136/jitc-2022-SITC2022.0221>

**DEVELOPING AN ADOPTIVE CELL TRANSFER
IMMUNOTHERAPY FOR PEDIATRIC HIGH-GRADE
GLIOMAS**

Stephen Frederico*, Chaim Sneiderman, Ian Pollack, Gary Kohanbash. *University of Pittsburgh, Pittsburgh, PA, USA*

Background Pediatric high-grade gliomas (HGGs) are one of the deadliest brain tumors that arise in children, with an average five-year survival for this disease being less than 20%.¹ HGGs expresses glioma-associated antigens (GAAs) which can be targeted by the immune system. These include IL-13Ra2, Survivin, and EphA2 [2]. Previously, our research group conducted a clinical trial where HLA-A2 positive pediatric patients were vaccinated with these GAA epitopes when newly diagnosed with HGG [2]. Our group observed many patients enrolled in the study showed positive anti-GAA immune responses to IL-13Ra2, EphA2, and Survivin. The findings from this trial highlighted that the sparsity of T-cells within the tumor microenvironment may pose a major challenge to improving immuno-therapeutic outcomes.

Methods In this study we engaged in identifying TCR sequences targeted to IL-13Ra2, Survivin, or EphA2. To accomplish this, a single cell-suspension of CD8 T-cells tetramer stained for Survivin, IL13Ra2, or EphA2 were obtained using FACS from PBMCS taken from individual patients who underwent vaccination. Single-cell RNA-sequencing (ScRNA-Seq) was performed on these samples to determine the phenotype of the T-cells. We also assessed T-Cell expansion and obtained the nucleotide sequence for the CDR3 region. Following acquisition of the nucleotide sequence, we developed retroviral TCR-vectors and viral particles to enable transduction of T cells. We confirmed the presence of TCRs on the T-cell surface via tetramer staining and flow cytometric analysis. We then performed *in vitro* killing assays by co-culturing transduced T-cells with U87 cells and assessed for LDH within our samples.

Results ScRNA-seq allowed us to identify a cluster of T-cells consisting of PRF1+ (Perforin) & GZMB+ (Granzyme b), as well as a cluster of PDCD1+ (PD-1) & TIGIT+ cells. Our tetramer staining confirmed the presence of our TCRs on the T-cell surface. *In vitro* killing assays demonstrated T-cell cytotoxicity as T-cells with U87 cells in 10:1, 4:1 and 1:1 ratios had a percentage cytotoxicity of 30.95%, 22.59% and 9.37% respectively. When pairing T-cells with U87 cells while blocking HLA-A2, there was a marginal decrease in cytotoxicity.

Conclusions TCRs targeted to IL-13Ra2, Survivin, or EphA2 were positively identified on the surface of transduced T-cells and demonstrated a cytotoxic response during *in vitro* killing assays. We now intend to grow these cells into large numbers and adoptively transfer them into tumor-bearing mice in hopes this will provide a survival benefit.

Acknowledgements This research was supported by the American Brain Tumor Association Jack & Fay Netchin Medical Student Summer Fellowship in memory of Jeffrey Ragan Frost.

REFERENCES

1. Huang TY, Piunti A, Qi J, Morgan M, Bartom E, Shilatifard A, Saratsis AM. Effects of H3.3G34V mutation on genomic H3K36 and H3K27 methylation patterns in isogenic pediatric glioma cells. *Acta Neuropathol Commun.* 2020 Dec 7;8(1):219. doi: 10.1186/s40478-020-01092-4. PMID: 33287886; PMCID: PMC7722426.
2. Pollack IF, Jakacki RI, Butterfield LH, Hamilton RL, Panigrahy A, Potter DM, Connelly AK, Dibridge SA, Whiteside TL, Okada H. Antigen-specific immune responses and clinical outcome after vaccination with glioma-associated antigen peptides and polyinosinic-polycytidylic acid stabilized by lysine and carboxymethylcellulose in children with newly diagnosed malignant brainstem and nonbrainstem gliomas.

J Clin Oncol. 2014 Jul 1;32(19):2050-8. doi: 10.1200/JCO.2013.54.0526. Epub 2014 Jun 2. PMID: 24888813; PMCID: PMC4067943.

Ethics Approval All experiments were carried out in conformity with the principles set out in the World Medical Association's Declaration of Helsinki as well as the Department of Health and Human Services Belmont Report. The University of Pittsburgh Institutional Review Board approved sample use (PRO08030085). Informed written consent was provided by all patients prior to inclusion in the study.

<http://dx.doi.org/10.1136/jitc-2022-SITC2022.0222>

223

ANTI-TNMUC1 CAR-T CELLS THAT ARE CONDITIONALLY ARMED WITH IL12 ELIMINATE ADENOCARCINOMAS IN PRECLINICAL MODELS

Albert Gacerez, Eytan Herzig, Tiger Ren, Nicole Grant, Jay Danao, Daniel Roche, Daeun Nam, Krista McNally, Ben Wang, Melissa Fardy, Gus Zeiner*. *Chimera Bioengineering, South San Francisco, CA, USA*

Background Chimeric antigen receptor T (CAR-T) cell therapeutics have been successful at driving remissions in several B cell malignancies, but their efficacy against most tumor types remains limited. An emerging strategy to increase CAR-T efficacy against solid tumors is to arm CAR-T cells with additional transgenes encoding immunomodulatory payloads such as IL-12, that weaken the tumor and its supportive microenvironment, and enhance the anti-tumor effector functions of T cells. However, several clinical trials investigating the use of armed T cell therapeutics have demonstrated that immunomodulatory payload arming necessitates stringent payload expression control to prevent systemic payload exposures, which can limit therapeutic efficacy and persistence, and simultaneously drive toxicity and severe adverse events.

Methods Here we report the repurposing of a native T cell gene regulatory node, that operates post-transcriptionally to prevent effector cytokine expression in quiescent T cells, as a cellular engineering platform that conditionally affects transgenic payload expression exclusively in activated CAR-T cells. We have applied this cellular engineering platform to develop aTnMuc1 CAR-T cells armed conditionally with IL-12. TnMuc1 is a hypoglycosylated variant of MUC1, an antigen expressed by many Adenocarcinomas but not by healthy cells.

Results Our anti-TnMuc1 CAR-T cells armed conditionally with IL-12 dramatically outperformed cognate unarmed aTnMuc1 CAR-T cells *in vitro* and *in vivo*. anti-TnMuc1 CAR-Ts armed conditionally with IL-12 exhibit very low levels basal IL-12 expression in quiescent states, and efficiently cleared tumors at low CAR-T doses in multiple preclinical Adenocarcinoma models; cognate unarmed anti-TnMuc1 CAR-T cells were unable to clear these tumors at any dose level. Additionally, tumor-bearing mice dosed with anti-TnMuc1 CAR-T cells armed conditionally with IL-12 demonstrated no weight loss and had low serum IL-12 levels.

Conclusions These data demonstrate the utility of applying a native T cell gene regulatory mechanism to produce highly efficacious, conditionally armed CAR-T cells. Based on the results of our preclinical data, we are advancing anti-TnMuc1 CAR-T cells armed conditionally with IL-12 for clinical trials to confirm these results in humans.

<http://dx.doi.org/10.1136/jitc-2022-SITC2022.0223>

GENERATION OF CELL THERAPIES FOR DIVERSE APPLICATIONS USING MICROFLUIDIC CELL SQUEEZE® MANUFACTURING TECHNOLOGY

Jonathan Gilbert*, Maisam Dadgar, Scott Loughhead, Ipsita Roymoulik, Devin Bridgen, Howard Bernstein, Armon Sharei. *SQZ Biotechnologies, Watertown, MA, USA*

Background Cellular therapies require precise and versatile biological engineering at scale to generate effective and accessible products. However, current cell delivery approaches are often limited in the types of biology and range of cells they can engineer and have significant scale-up challenges. Microfluidic deformation using the Cell Squeeze® technology effectively delivers a variety of payloads to diverse cell types at scale while preserving cell health and function.

Methods We tested preclinically the performance of the Cell Squeeze technology in many cell types including T cells, PBMCs, HSCs, iPSCs, red blood cells, and TILs. We evaluated the efficiency of delivery of many materials including mRNA, gene editing factors, transcription factors, and membrane-bound cytokines. We further investigated the integration of our scaled cGMP process into an integrated manufacturing system for the rapid and cost-effective production of cell therapy drug products (point-of-care system).

Results We showed highly efficient mRNA delivery (>80%) to T cells, iPSCs, PBMCs, HSCs, and TILs while also maintaining cell function. Cell Squeeze technology also demonstrated efficient gene editing in multiple cell types. The technology further demonstrated engineering ~10B cells/minute and has been used in 3 clinical trials generating distinct investigational products. Furthermore, our point-of-care system demonstrated a fully closed automated unit for manufacturing cell therapies that integrates cell isolation, cell washing, cell delivery and bag filling. This portable system used a single-use sterile disposable tubing set and has the potential to be operated outside of a clean room. Our point-of-care system also reduced our operator hours by 90% and process time by ~50% to < 6 hours.

Conclusions Cell Squeeze technology has shown differentiated capabilities in applications such as therapeutic vaccines, immune tolerance, effector cell engineering, and directed differentiation of iPSCs. These results support a continued expansion of clinical impact of the Cell Squeeze technology leveraging the flexibility of the delivery platform. Our automated, point-of-care system incorporating the Cell Squeeze® technology could potentially further streamline manufacturing time and costs to achieve greater cell therapy accessibility and therapeutic impact potential.

<http://dx.doi.org/10.1136/jitc-2022-SITC2022.0224>

225

KILLER CELL IMMUNOGLOBULIN-LIKE RECEPTOR 2DL2 (KIR2DL2) IMMUNE CHECKPOINT AS A MODULATOR OF T-CELL EFFECTOR FUNCTION

Miguel Gomez Fontela*, Sebastian Snedal, Daniel Abate-Daga. *H. Lee Moffitt Cancer Center, Tampa, FL, USA*

Background Killer immunoglobulin-like receptors (KIRs) are a family of regulatory cell surface molecules expressed on natural killer (NK) cells and in subsets of memory T cells.^{1,2} Interaction of KIR2DL2 with its HLA-C1 ligands leads to inhibition of NK cell activation and decoupling of T cell effector function by inhibiting actin cytoskeleton rearrangement and modifying T cell transcriptional profile.³⁻⁵ Here we assess the effect of KIR2DL2 on CAR-T cell effector function both *in vitro* and *in vivo* and propose KIR2DL2 as an immune checkpoint. We have developed a strategy for genomic ablation of KIR2DL2 during T cell manufacturing as a method for enhancement of adoptive cell immunotherapy (ACT).

Methods We generated prostate stem cell antigen (PSCA)-CAR-T cells, alone or in combination with KIR2DL2, using a bicistronic retroviral vector. We tested KIR2DL2 *in vitro* inhibitory role in presence or absence of HLA-C1 using real time cytotoxicity assays at different effector:target ratios (2.5:1, 1:1, 0.5:1, 0.25:1). We evaluated IFN- γ production by ELISA. To assess the inhibitory role of KIR2DL2 *in vitro* we used a mouse model bearing HLA-C1⁺ or HLA-C1⁻ subcutaneous xenografts of human pancreatic adenocarcinoma (HPAC) cells, treated with 5 \times 10⁶ KIR2DL2⁺ or KIR2DL2⁻ CAR-T cells. We used GFP-transduced T cells as a negative control. CRISPR/Cas9 genome editing was used for KIR2DL2 ablation in CAR-T cells.

Results *In vitro*, KIR2DL2 impaired CAR-T cell responses in an HLA-C1-dependent manner. KIR2DL2⁺ PSCA-CAR-T cells were significantly less cytotoxic in presence of HLA-C1 and secreted less IFN- γ than their KIR2DL2⁻ counterparts. *In vivo*, KIR2DL2⁺ PSCA-CAR-T cells injected in NSG mice harboring PSCA⁺/HLA-C1⁺ pancreatic tumors were not able to eliminate tumors in the presence of HLA-C1. In contrast, KIR2DL2⁺ CAR-T cells transferred to mice harboring PSCA⁺/HLA-C1⁻ tumor cells performed as well as their KIR2DL2⁻ counterparts. We designed guide RNAs targeting KIR2DL2 and developed a strategy for KIR2DL2 abrogation during adoptively transferred CAR-T cell manufacturing.

Conclusions We evaluated for the first time the biological and molecular function of KIR2DL2 within adoptively transferred T cells. Engagement of KIR2DL2 with its HLA-C1 ligand(s) impaired CAR-T cell effector function both *in vitro* and *in vivo*, as CAR⁺/KIR2DL2⁺ cells were less cytotoxic and secreted less IFN- γ than their CAR⁺/KIR2DL2⁻ counterparts. KIR2DL2 abrogation in CAR-T cells may enhance ACT by limiting its inhibitory signaling. Current efforts are focused on evaluating the impact of KIR2DL2 ablation on the therapeutic effect of CAR- and TCR-T cells.

Acknowledgements This work has been supported in part by the Flow Cytometry and Comparative Medicine Core Facilities at Moffitt Cancer, a National Cancer Institute (NCI) designated Comprehensive Cancer Center (P30 CA076292); and by a donation by the Steinman Family Foundation.

REFERENCES

1. van der Veken, L.T., *et al.*, Functional analysis of killer Ig-like receptor-expressing cytomegalovirus-specific CD8⁺ T cells. *J Immunol*, 2009; **182**(1): p. 92-101.
2. Bjorkstrom, N.K., *et al.*, CD8 T cells express randomly selected KIRs with distinct specificities compared with NK cells. *Blood*, 2012; **120**(17): p. 3455-65.

3. Burshtyn, D.N., *et al.*, Recruitment of tyrosine phosphatase HCP by the killer cell inhibitor receptor. *Immunity*, 1996; **4**(1): p. 77-85.
4. Olcese, L., *et al.*, Human and mouse killer-cell inhibitory receptors recruit PTP1C and PTP1D protein tyrosine phosphatases. *J Immunol*, 1996; **156**(12): p. 4531-4.
5. Stebbins, C.C., *et al.*, Vav1 dephosphorylation by the tyrosine phosphatase SHP-1 as a mechanism for inhibition of cellular cytotoxicity. *Mol Cell Biol*, 2003; **23**(17): p. 6291-9.

Ethics Approval This study was approved by the Institutional Animal Care and Use Committee (IACUC); approval number R ISO00010727.

<http://dx.doi.org/10.1136/jitc-2022-SITC2022.0225>

227

HUNTR™: A HYPERPLEX PLATFORM FOR THE DISCOVERY OF NEOANTIGEN-REACTIVE T-CELL RECEPTORS

Guowei Gu*, Julissa Simmons, Kristen Rimaila, Gaby Garland, Ugochi Ibekwe, Donghyun Joo, An Lu, Amanda Montoya, Pretty Mathew, Hao Zhao, Beatriz Santillan, Matthew Collinson-Pautz, Drew Deniger. *Alaunos Therapeutics, Houston, TX, USA*

Background Solid tumors harbor mutations that can give rise to neoantigens recognized by T-cell receptors (TCRs) expressed on tumor infiltrating lymphocytes (TILs). We have developed a library of TCR-T cells targeting hotspot mutations based on the non-viral *Sleeping Beauty* transposon/transposase system, which is presently being evaluated in a first-in-human phase 1/2 study in patients with non-small cell lung, colorectal, endometrial, pancreatic, ovarian, and bile duct cancers. Current methods of TCR discovery require large volume blood draws or immortalization of primary cells with live viruses to make antigen presenting cells (APCs), limiting the ability to efficiently discover new TCRs and is only applicable to some patients. We developed hunTR™ (human neoantigen T-cell Receptor), a rapid, hyperplex platform for the discovery of neoantigen-reactive TCRs from limited starting material.

Methods TILs sorted from dissociated tumor specimens were processed to obtain TCR sequences and gene expression profiles on a single cell basis. These data were fed into a novel bioinformatics pipeline that identifies TCRs with predicted neoantigen reactivity. TCRs were reconstructed in *Sleeping Beauty* transposon plasmids and expressed in TCR cells, an engineered cell line capable of detecting TCR reactivity to both class I and class II HLA-restricted neoepitopes. Somatic single nucleotide variants, short insertions/deletions, and germline class I and II HLA alleles were called for each patient. neoAPCs were engineered to express relevant patient-derived neoantigens and HLA molecules. TCR cells were cocultured with a matrix of neoAPCs, and conditions yielding a neoantigen reactivity were identified.

Results A total of 3.1×10^5 TCR+HLA+neoantigen combinations were evaluated in seven patients with a mean plexity of 4.4×10^4 per patient. All specimens screened (colorectal n=3, endometrial n=2, breast n=2) yielded at least one neoantigen-reactive TCR. The 57 neoantigen-reactive TCRs (19% of 304 total TCRs screened) identified targeted 20 mutations, including one shared *KRAS* and 19 personal mutations. Of these, 81% were restricted by HLA class II while 19% were restricted by class I. A median reactive hit rate of 14% was achieved per patient (range 5-31%) with an average of three unique neoantigen specificities (range 1-6).

Conclusions In conclusion, hunTR is a hyperplex screening platform that identifies neoantigen-reactive TCRs. hunTR allows for the expansion of our hotspot mutation-targeted TCR library, increasing the addressable population of solid tumor patients (with matching hotspot mutation and HLA allele) eligible for TCR-T cell treatment. In addition, hunTR is applicable for personalized TCR-T therapy such that most solid tumor patients could be eligible for mutation-targeted cell therapy.

Ethics Approval Human-derived specimens were obtained through a commercial source that adheres to all applicable regulations and guidelines of the relevant countries including the US.

<http://dx.doi.org/10.1136/jitc-2022-SITC2022.0227>

228

MULTI-ARMING AND REGULATOR DIAL GENE CIRCUITS TACKLE KEY CHALLENGES IN SOLID TUMORS

Marcela Guzman Ayala*, Michelle Hung, Deepika Kaveri, Rebecca Cottman, Elizabeth Leitner, Priscilla Wong, Ronni Ponek, Enping Hong, Manan Shah, Andrew Banicki, Lawrence Naitmazi, Kelly Lee, Wesley Gorman, Russell Gordley, Philip Lee, Timothy Lu. *Senti Biosciences, South San Francisco, CA, USA*

Background Chimeric antigen receptor (CAR) cell therapy for solid tumors is hampered by the immunosuppressive tumor microenvironment (TME), which can inhibit the function of endogenous and therapeutic immune cells, as well as a paucity of targets. The use of potent immunomodulators to transform the TME, such as interleukin (IL)-12, is limited by the need for regulation to avoid systemic toxicities.

Methods To address these challenges, Senti Bio is developing CAR-NK therapies that include Multi-Arming with calibrated release (cr)IL-15 and a Regulator Dial gene circuit to control the expression of crIL-12. Senti's proprietary calibrated release technology enables cytokines to be expressed in both membrane-bound and secreted forms, providing multi-factorial activity via autocrine and paracrine stimulation to increase CAR-NK cell function and activation of endogenous immune cells in the TME. In addition, we have designed a Regulator Dial gene circuit that expresses crIL-12 under the control of grazoprevir (GRZ), an FDA-approved small molecule drug.

Results We have tested our Multi-Arming and Regulator Dial gene circuits in combination with a CAR targeting GPC3, a hepatocellular carcinoma (HCC)-relevant target. We observed crIL-15 to promote NK cell persistence and proliferation in an autocrine fashion, while also activating other immune cells in a paracrine manner. In addition, crIL-15 was observed to enhance GPC3 CAR-NK tumor killing in a serial killing assay compared to wild-type secreted IL-15 and showed enhanced antitumor function and increased survival over control groups *in vivo*.

GPC3 CAR-NK cells containing the Regulator Dial gene circuit expressed low crIL-12 levels in the absence of GRZ (<100 pg/1e6 cells/48h), while induction with GRZ led to a 1000-fold increase of crIL-12 expression under the same conditions. The ON and OFF kinetics of crIL-12 induction were determined *in vitro*. 4 hours of GRZ-treatment was sufficient to induce >600-fold increase in crIL-12 concentrations. By day 3 post-GRZ removal, crIL-12 reverted to basal levels. Lastly, the role of crIL-12 in reversing immunosuppression was validated in a co-culture assay. Specifically, GRZ-induced crIL12 restored CAR-NK cells that were suppressed in the presence of M2 macrophages.

Conclusions We have engineered off-the-shelf CAR-NK cell therapies that target GPC3 and express crIL-15. To increase the therapeutic window of the potent immune effector IL-12 in the TME, we have designed a Regulator Dial gene circuit to controllably produce crIL-12. These gene circuits have complementary mechanisms of action to enhance CAR-NK anti-tumor function and potentially overcome the immunosuppressive TME in solid tumors such as HCC.

<http://dx.doi.org/10.1136/jitc-2022-SITC2022.0228>

229

A2B530, AN AUTOLOGOUS CEA-DIRECTED TMOD T-CELL THERAPY WITH AN INHIBITORY RECEPTOR GATED BY HLA-A*02 TO TARGET COLORECTAL, PANCREATIC, AND LUNG CANCER

¹J Randolph Hecht, ²Mark Sandberg, ²Xueyin Wang, ²Aaron Martin, ²Daniel Nampe, ²Grant Gabrelow, ²Chuck Li, ²Michele Mcelvain, ²Wen-Hua Lee, ²Sanam Shafaatalab, ²Sara Martire, ²Fernando Fisher, ²Yuta Ando, ²Edwin Liu, ²David Ju, ²Jing-Ping Hsin, ²Alexandre Zampieri, ³Diane Simeone, ⁴Scott Kopetz, ⁴Maria Pia Morelli, ⁵Mitesh Borad, ³Theodore Welling, ⁶Sandip Patel, ¹Edward Garon, ⁷Kedar Kirtane, ⁷Frederick Locke, ²John Welch, ²Eric Ng, ²William Go, ²Armen Mardiros*, ⁸David Maloney, ²Lu-Min Wong, ²Alexander Kamb, ²Han Xu, ⁹Julian Molina. ¹University of California at Los Angeles, Los Angeles, CA, USA; ²A2 Biotherapeutics, Inc., Agoura Hills, CA, USA; ³New York University Langone Health, New York, NY, USA; ⁴The University of Texas MD Anderson Cancer Center, Houston, TX, USA; ⁵Mayo Clinic Cancer Center, Scottsdale, AZ, USA; ⁶University of California San Diego, La Jolla, CA, USA; ⁷H. Lee Moffit Cancer Center, Tampa, FL, USA; ⁸Fred Hutchinson Cancer Research Center, Seattle, WA, USA; ⁹Mayo Clinic, Rochester, MN, USA

Background Nearly all colorectal and most pancreatic and lung cancers express carcinoembryonic antigen (CEA). However, due to its expression in normal gut epithelial cells, CEA-targeted therapies have resulted in on-target, off-tumor toxicity. To overcome this, we have developed Tmod™, a logic-gated T-cell therapy platform. Tmod constructs are composed of an activating CAR or T-cell receptor that targets a tumor antigen and an inhibitory receptor recognizing an antigen expressed on normal healthy tissues, but not on tumor cells due to loss of heterozygosity (LOH).^{1,2} A2B530 is a CEA-directed Tmod construct utilizing an LIR-1-based inhibitory receptor (blocker) targeting human leukocyte antigen A*02 (HLA-A*02).

Methods To generate CEA Tmod, T cells from HLA-A*02(+) donors were transduced with a single lentivirus to express i) the CAR, ii) the blocker, and iii) an shRNA targeting β2M. Cytotoxicity was measured by culturing CEA(+) target cell line pairs (A*02[-] and A*02[+]), expressing either GFP or RFP, with engineered T cells and quantifying live target cells over time. *In vivo* activity was examined using NSG mice subcutaneously implanted with “normal” (CEA[+]A*02[+]) and tumor cells (CEA[+]A*02[-]), in the right and left flanks. Mice were treated intravenously with CEA Tmod cells or control T cells.

Results Control CEA CAR T cells killed CEA(+) target cell lines *in vitro* irrespective of HLA-A*02 expression. In contrast, CEA Tmod cells selectively killed tumor cells (CEA[+]A*02[-]) while sparing “normal” cells (CEA[+]A*02[+]). In mixed target cell cultures, CEA Tmod cells killed only the A*02(-) target cells, whereas the CEA CAR T cells killed both the A*02(-) and A*02(+) cell lines. Further, CEA Tmod cells exhibited bidirectional control between the activated and blocked states. While mice treated with control CEA CAR T cells experienced a reduction in volume and bioluminescence of both normal and tumor grafts, CEA Tmod cells specifically cleared A*02(-) tumors in mice (table 1). Finally, although expansion of Tmod cells in peripheral blood trended lower than CAR and TCR controls, anti-tumor activity was comparable in these groups.

Conclusions A2B530 is an autologous CEA Tmod cell product that exploits common LOH at the HLA locus in cancer cells, enabling these engineered T cells to discriminate between normal and tumor cells. BASECAMP-1 (NCT04981119), an observational study identifying patients with somatic HLA LOH, is recruiting. Eligible patients with metastatic colorectal, pancreatic, or non-small cell lung cancer will be apheresed for a future A2B530 EVEREST-1 interventional study.

REFERENCES

1. Hamburger A, DiAndreth B, Cui J, *et al.* Engineered T cells directed at tumors with defined allelic loss. *Mol Immunol.* 2020;**128**:298-310.
2. DiAndreth B, Hamburger AE, Xu H, Kamb A. The Tmod cellular logic gate as a solution for tumor-selective immunotherapy. *Clin Immunol.* 2022;**241**:109030.

Abstract 229 Table 1

Table 1: Mean graft bioluminescence percentage change in mice from Day 24 (day of T cell infusion) to Day 50

	Normal graft CEA(+)A*02(+)	Tumor graft CEA(+)A*02(-)
Untransduced	98	143
CEA TCR	-99	162
CEA CAR	-94	-100
CEA Tmod	221	-92

CAR, chimeric antigen receptor; CEA, carcinoembryonic antigen; TCR, T cell receptor.

<http://dx.doi.org/10.1136/jitc-2022-SITC2022.0229>

230 TCR-LIKE CHIMERIC-ANTIGEN-RECEPTOR TO RECOGNIZE NEOEPITOPES DERIVED FROM DRIVER MUTATIONS

David Hou, Yafei Hou*. *Immunosynth, LLC, San Carlos, CA, USA*

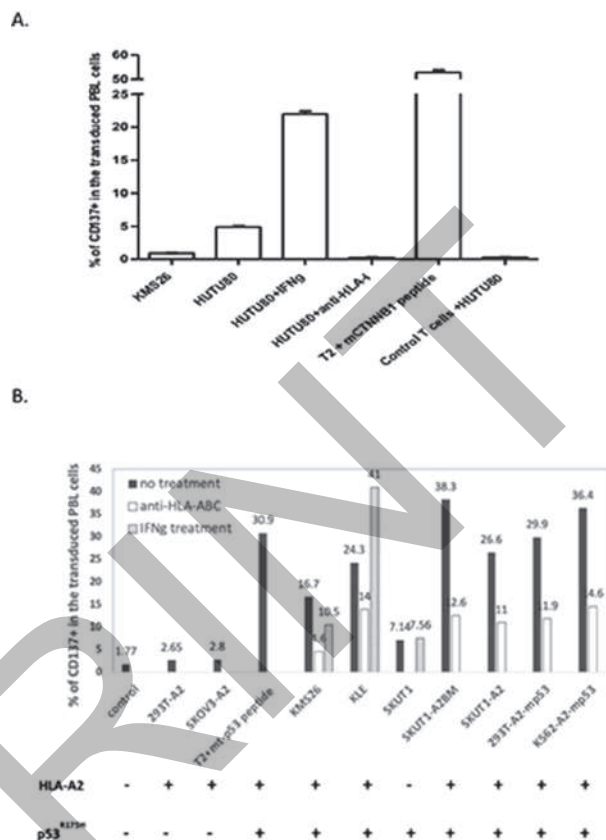
Background T cell receptor (TCR)-based cell therapy to treat solid tumors by targeting tumor neoantigens is gaining momentum. While there is an urgent need for discovering novel TCRs, one challenge is that the exogenous TCR may compete with the endogenous TCR for CD3 signaling components and form mixed dimers with potential toxicities. Additionally, the activity of T cells highly depends on signaling machinery only present in T cells, which restricts the scope of eligible therapeutic cells. We developed a TCR-like chimeric-antigen-receptor to both overcome the mispairing of TCR α/β chains and to expand the scope of TCR-based cell therapy to other immune cells.

Methods To identify novel TCRs, a monoclonal TCR discovery platform was developed. A high avidity TCR of a neoepitope-specific CD8+ T cell clone (CTL) that was generated from donor PBMCs was isolated and sequenced. A chimeric-antigen-receptor comprising an antigen binding domain (which is a portion of the identified TCR), a CD28 segment containing the hinge/transmembrane domain, and a cytoplasmic signaling domain containing a Dap10 and a Dap12 intracellular domains. To augment the avidity of the antigen receptor, a chimeric co-receptor was constructed by combining HLA-I binding domains of CD8 α with the hinge/transmembrane/cytoplasmic domains of CD4. T cell line (J.RT3-T3.5) and NK cell line (KYGH-1) were transduced by a lentivirus encoding the chimeric-antigen-receptor and co-receptor to assess their expression and function.

Results Two novel TCRs specific for CTNNB1^{S37F} peptide (YLDSGIHFGA) and for p53^{R175H} peptide (HMTEVVRHC) respectively were identified; both are high-avidity and can recognize the endogenous neoepitope presented by HLA-A2 in tumor cells (figure 1A and B). A chimeric-antigen-receptor specific for CTNNB1^{S37F} neoepitope/HLA-A2 was expressed on the surface of 293T cells independent of endogenous CD3 (figure 2A). However, its avidity to recognize CTNNB1^{S37F} neoepitope was approximately 5 folds lower than that of the native TCR (figure 3A). Co-expression of the co-receptor could significantly enhance the avidity of the chimeric-antigen-receptor and make it capable of recognizing endogenously presented neoepitope in tumor cells (figure 3B). In addition, NK cells re-directed with the chimeric-antigen-receptor could also recognize the neoepitope peptide in the context of HLA-A2 (figure 2B and 4).

Conclusions We validated a TCR-like chimeric-antigen-receptor that can be expressed on cells independent of endogenous CD3 and can recognize neoepitope/HLA-A2. We also designed and tested a co-receptor that can enhance the avidity of the chimeric-antigen-receptor. To further leverage the avidity of the chimeric-antigen-receptor, testing of new configurations of the chimeric-antigen-receptor and co-receptor is underway.

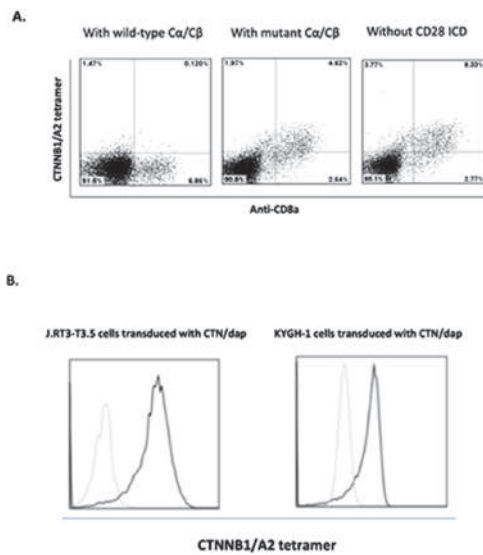
Figure 1.



Abstract 230 Figure 1 TCRs specific for a neoepitope peptide presented by HAL-A2 PBLs re-directed to express a specific TCR can be activated by the endogenous neoepitope peptide/HLA-A2+ in tumor cells. Fig. 1A shows T cells transduced with a TCR specific for a CTNNB1S37F neoepitope peptide in the context of HLA-A2 can be activated to express CD137 against HLA-A2+ tumor cell line (HuTu80 cells pre-treated with IFN γ) with the CTNNB1S37F mutation. Fig. 1B shows T cells transduced with a TCR specific for a p53R175 neoepitope peptide in the context of HLA-A2 can be activated to express CD137 against HLA-A2+ tumor cell lines with the p53R175 peptide mutation.

Abstracts

Figure 2

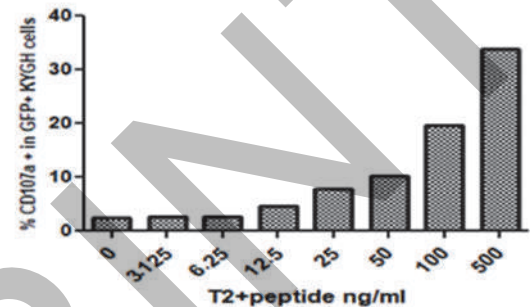


Abstract 230 Figure 2 Expression of a TCR-like chimeric-antigen-receptor.

TCR-like chimeric-antigen-receptor can be expressed on cell surface independent of endogenous CD3 components. Fig. 2A shows that a chimeric-antigen-receptor specific for the CTNNB1S37F neopeptide peptide in the context of HLA-A2 can be expressed on 293T cells. The additional disulfide bond formed between Ca and Cβs of the TCR is essential for the stable expression of the chimeric-antigen-receptor while the intracellular domains of CD28 have no effect. Fig. 2B shows that both T cells (J.RT3.5) and NK cells (KYGH-1) can be re-directed to express exogenous TCR-like chimeric-antigen-receptor to bind the epitope peptide/HLA-I

TCR-like chimeric-antigen-receptor on T cells can functionally recognize the neopeptide peptide presented by HLA-I. Fig. 3A shows that a chimeric-antigen-receptor specific for the CTNNB1S37F neopeptide peptide in the context of HLA-A2 (JRT-CTN/dap) can be activated by the neopeptide peptide and its avidity can be enhanced by a co-receptor which is a CD8a/CD4 fusion receptor (CD8/4). Fig. 3B shows that with the help of the co-receptor, the avidity of the chimeric-antigen-receptor is comparable to the native TCR and capable of recognize the neopeptide peptide presented by HAL-A endogenously in tumor cells

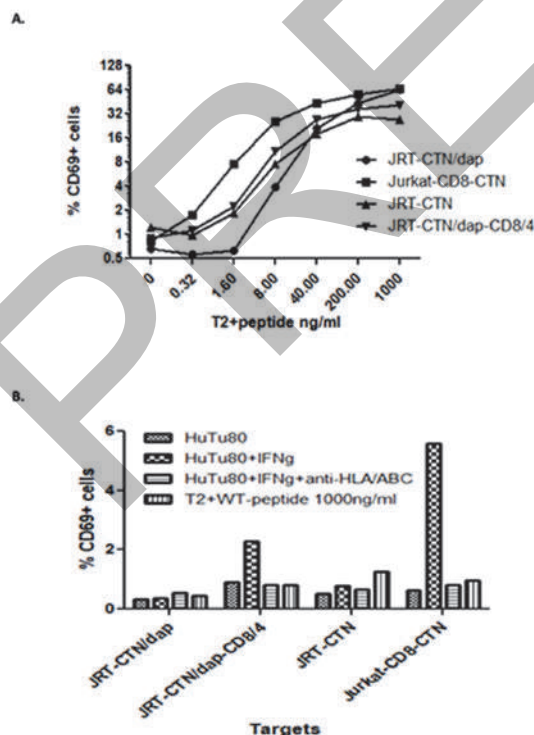
Figure 4



Abstract 230 Figure 4 Function of a TCR-like chimeric-antigen-receptor on NK cells

TCR-like chimeric-antigen-receptor on NK cells can functionally recognize the neopeptide peptide presented by HLA-I. NK cells (KYGH-1) that re-directed to express a chimeric-antigen-receptor specific for the CTNNB1S37F neopeptide peptide in the context of HLA-A2 (JRT-CTN/dap) can be activated by the neopeptide peptide presented by HLA-A2 on the target T2 cells

Figure 3



Abstract 230 Figure 3 Function of a TCR-like chimeric-antigen-receptor on T cells

<http://dx.doi.org/10.1136/jitc-2022-SITC2022.0230>

231

DYSFUNCTIONAL IMMUNE SYNAPSES RESTRAIN ANTI-DIPG ACTIVITY OF CAR T CELLS

Jorge Ibanez*, Haley Houke, Michaela Meehl, Jennifer Ocasio, Nikhil Hebbar, Paulina Velasquez, Suzanne Baker, Giedre Krenciute. *St. Jude Children's Research Hospital, Memphis, TN, USA*

Background Diffuse intrinsic pontine gliomas (DIPGs) are highly lethal pediatric brain tumors. Thus, there is an urgent need for novel therapeutics. While chimeric antigen receptor (CAR) T-cell therapy has the potential to meet this need, early phase clinical studies with CAR T cells has shown limited anti-tumor activity for brain tumors. T cells require three signals for optimal activity, being (1) T cell activation, (2) costimulation, and (3) cytokines. While numerous investigators have focused on improving signals 2 and 3, the goal of this study was to investigate the role of immune synapse (IS) formation, which is critical for proper T cell activation, in the context of DIPG-targeted CAR T cell therapy.

Methods We generated GRP78-CAR T cells by expressing a 2nd generation CAR with a CD28.z signaling domain, which recognize an endoplasmic reticulum chaperone protein that is broadly expressed on the cell surface of DIPGs. We compared the effector function of GRP78-CAR T cells against U87 glioma and the patient-derived DIPG007 cell line, which are both positive for GRP78. Then we evaluated *in vitro* CAR T cell effector functions by MTS-based assays (cytotoxicity), repeated stimulation assays (persistence), and Milliplex (cytokine secretion). To gain mechanistic insight into tumor and CAR T cell interaction, we analyzed IS formation by live cell imaging confocal microscopy.

Results Our *in vivo* studies demonstrated that GRP78-CAR T cells eradicate orthotopic U87 brain tumors but have no anti-tumor activity against DIPG007, despite that GRP78-CAR T cells efficiently killed U87 and DIPG007 cells *in vitro*. However, the total cytokine production was significantly lower post DIPG007 activation (28 fold) when compared to U87 activation with IFN γ , GM-CSF, TNF α , IL-2 and IL-13 being the most significantly suppressed in DIPG setting. In concordance, CAR T cells were only able to expand and retain their cytolytic activity in the presence of U87 cells. When we look at the CART:DIPG007 IS resulted in a significantly lower calcium flux in comparison to CART:U87 synapses. Likewise, the recruitment of lysosomes to CART:DIPG007 IS was significantly diminished. Importantly, we observe the same dysfunctional IS formation regardless of CAR T cell specificity and targeted antigen expression level indicating that the suppressive effect is DIPG-tumor mediated.

Conclusions Our study demonstrates that DIPG tumors suppress CAR T cell effector function by damping T cell activation through dysfunctional immune synapse formation. We are now testing other CARs and genetic engineering approaches directed at improving IS formation to overcome the suppressive effects of DIPGs.

<http://dx.doi.org/10.1136/jitc-2022-SITC2022.0231>

232

**INCREASED POTENCY AND FUNCTIONAL PERSISTENCE
IN VITRO OF A NEXT-GENERATION NY-ESO-1-SPECIFIC
TCR THERAPY INCORPORATING GEN-R™ GENETIC
REPROGRAMMING TECHNOLOGY**

¹Helle Jensen*, ¹Rachel Fukuda, ¹Megan Murt, ¹Xiao Wang, ¹Lora Zhao, ¹Sheila Lou, ¹Purnima Sundar, ¹Christopher Navas, ¹Andrew Jimena, ¹Amanda Sims, ¹Travis Beckett, ¹Shobha Potluri, ¹Rowena Martinez, ¹David Chian, ¹Candace Sims, ¹Quinn Walker, ¹Abira Bandyopadhyay, ¹Breanna Pamintuan, ¹Bijan Boldajipour, ¹Chang-Chih Wu, ¹Martin Wohlfahrt, ¹Young Ryu, ¹Viola C Lam, ¹Rachel C Lynn, ¹Hajime Hiraragi, ²Johannes Breuning, ²Ashley Hamilton, ²Fotini Kouri, ²Jack Euesden, ²Sara Brett, ¹Blythe Sather. ¹Lyell Immunopharma, Inc, South San Francisco, CA, USA; ²GSK, Stevenage, UK

Background Letetresgene autoleucel (lete-cel; GSK3377794) is a first-generation (1st gen) NY-ESO-1-specific T-cell receptor (TCR) therapy with demonstrated clinical activity in solid tumors.¹⁻² Next-generation T-cell therapies are in development with the goal of further improving response rates and durability. Gen-R is an *ex vivo* genetic reprogramming technology in which T cells are engineered to overexpress c-Jun, a member of the activator protein 1 (AP-1) family of transcription factors. Dysregulation of AP-1 family members is implicated in chimeric antigen receptor (CAR) T-cell exhaustion, and previous studies demonstrate that overexpressing c-Jun can delay functional exhaustion, thereby improving anti-tumor efficacy and CAR T-cell persistence in pre-clinical solid tumor models.³ LYL331 (GSK4349560) is a next-generation NY-ESO-1-specific TCR therapy that incorporates Gen-R technology. Here we show pre-clinical data for LYL331 evaluating the impact of c-Jun overexpression on primary and long-term durable T-cell functions *in vitro*.

Methods Donor T cells were transduced with a lentiviral vector encoding EF1 α _NY-ESO-1 (1st gen NY-ESO-1 TCR control) or EF1 α _c-JunWT_NY-ESO-1 (LYL331) and characterized for primary functional activities (cytotoxicity, cytokine secretion, and proliferation) and NY-ESO-1 antigen sensitivity. In addition, we used an *in vitro* serial re-stimulation assay as a model for measuring features of T-cell exhaustion and evaluating long-term durable functions.

Results LYL331 displayed stable and high expression of c-Jun and showed multiple enhancements to primary T-cell functions *in vitro* compared to the control, including superior cytotoxic activity, as well as increased cytokine secretion (IFN γ and IL-2), proliferative capacity, and sensitivity towards the NY-ESO-1 peptide. Enhanced proliferation was observed in both CD4+ and CD8+ T cell populations, indicating that overexpressing c-Jun can improve T-cell functions in CD4+ T cells transduced with an HLA class I restricted NY-ESO-1 TCR. In addition, while the control displayed characteristics of exhaustion (i.e., loss of cytotoxic activity and cytokine secretion and increased expression of multiple exhaustion markers) in the serial re-stimulation assay, LYL331 maintained the ability to kill and secrete cytokines and displayed reduced expression of exhaustion markers TIGIT, PD-1, and CD39.

Conclusions In addition to supporting the hypothesis that genetic reprogramming with Gen-R technology can delay the onset of exhaustion and improve the long-term durable functions of LYL331, these data show that c-Jun overexpression can provide immediate benefits to the NY-ESO-1-specific TCR therapy during primary stimulation *in vitro*. Based on these promising pre-clinical data, LYL331 may have the potential to improve clinical responses in patients with solid tumor malignancies.

REFERENCES

1. D'Angelo SP, Melchiori L, Merchant MS, Bernstein D, Glod J, Kaplan R, Grupp S, Tap WD, Chagin K, Binder GK, Basu S, Lowther DE, Wang R, Bath N, Tipping A, Betts G, Ramachandran I, Navenot J-M, Zhang H, Wells DK, Winkle EV, Kari G, Trivedi T, Holdich T, Pandite L, Amado R, Mackall CL, Antitumor Activity Associated with Prolonged Persistence of Adoptively Transferred NY-ESO-1 c259 T Cells in Synovial Sarcoma. *Cancer Discov.* 2018;**8**(8): 944–57.
2. Stadtmauer EA, Fajt TH, Lowther DE, Badros AZ, Chagin K, Dengel K, Iyengar M, Melchiori L, Navenot J-M, Norry E, Trivedi T, Wang R, Binder GK, Amado R, Rapoport AP, Long-term safety and activity of NY-ESO-1 SPEAR T cells after autologous stem cell transplant for myeloma. *Blood Advances.* 2019;**3**(13): 2022–34.
3. Lynn RC, Weber EW, Sotillo E, Gennert D, Xu P, Good Z, Anbunathan H, Lattin J, Jones R, Tieu V, Nagaraja S, Granja J, de Bourcy CFA, Majzner R, Satpathy AT, Quake SR, Monje M, Chang HY, Mackall CL, c-Jun overexpression in CAR T cells induces exhaustion resistance. *Nature.* 2019;**576**: 293–300.

Ethics Approval Experiments presented in this abstract relied on human donor material that was obtained from commercial vendors. These vendors use their own IRB-approved protocol and consent process.

<http://dx.doi.org/10.1136/jitc-2022-SITC2022.0232>

233

A REAL-WORLD CASE OF SECOND CHIMERIC ANTIGEN RECEPTOR T-CELL THERAPY

Jacinth Joseph, Dennis Marjoncu, Kori Holman, Sara Leidy*. *Methodist University Hospital, Memphis, TN, USA*

Background CD19-directed Chimeric Antigen Receptor T-Cell (CAR-T) therapy has emerged as a promising and novel treatment for relapsed and refractory (r/r) B-cell malignancies. Efforts are directed towards increasing persistence of CAR-T cells, which is known to lead to durable responses. Repeat CAR-T infusions have been explored in clinical trials.¹⁻¹⁴ Here, we report a second CD19-directed CAR-T treatment in a patient with diffuse large B-cell lymphoma (DLBCL).

Methods A 60-year old man diagnosed with r/r DLBCL received a CAR-T infusion with tisagenlecleucel having a cell viability of 75%, not meeting FDA specifications of $\geq 80\%$. After relapse, the same patient received a second CAR-T with axicabtagene ciloleucel (axi-cel). For both infusions, the patient received appropriate lymphodepletion. Throughout and following both infusions, the patient was monitored for cytokine release syndrome (CRS) or immune effector associated neurotoxicity syndrome (ICANS). mEASIX scores (figure 1) were calculated to evaluate association with developing CRS/ICANS and disease response. Appropriate imaging and additional follow-up of response was completed.

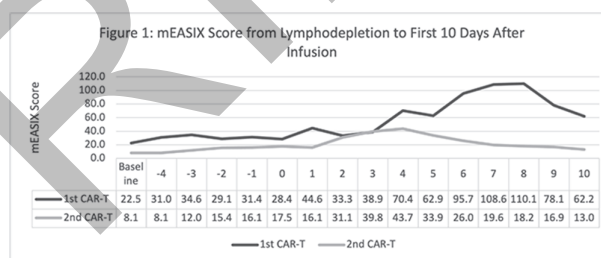
Results Following the patient's first CAR-T, he had no CRS or ICANS. He was discharged on day +9, then presented on day +84 with cough and dyspnea. Imaging showed an increase in lung lesion and pleural effusion. Biopsy of the lesion confirmed active lymphoma. Due to progression following CAR-T, he received two cycles of polatuzumab vedotin and rituximab for salvage. He then received his second CAR-T cell with axi-cel. On day +4, he developed grade 1 CRS, consisting of fever. CRS symptoms resolved on day +5 and he was discharged on day +12 without complications. Positron Emission Tomography (PET) scans on day +30, 3 and 6-months showed complete metabolic response (CMR), with persistently avid lesion at the L1 spine. This was biopsied showing no active lymphoma. Nine-month PET and 12-month CT showed no new findings to suggest active lymphoma and the patient remains in remission.

Conclusions Here, we present a case of a patient with r/r DLBCL who received two infusions of CAR-T cells. A second CAR-T treatment with a different product was used to treat relapse after first CAR-T in order to harness potential benefit from inherent differences between the 2 available commercial products, achieve adequate CAR-T cell dose, and avoid the higher-risk associated with the alternative treatment of allogeneic hematopoietic stem cell transplantation. As of 1-year post-second CAR-T the patient remains in a remission. This report reflects the benefit of a second infusion of CAR-T therapy in certain cases.

REFERENCES

1. June CH and Sadelain, M. Chimeric Antigen Receptor Therapy. *N Engl J Med* 2018; **379**:64-73. Doi: 10.1056/NEJMra1706169
2. Oluwole OO, Bishop MR, Gisselbrecht, C, et al. A phase 3 randomized trial of axicabtagene ciloleucel versus standard-of-care therapy in patients with relapsed/refractory diffuse large B cell lymphoma. *Journal of Clinical Oncology* **36**, no. 15_suppl. Doi: 10.1200/JCO.2018; 36.15_suppl.TPS7585.
3. Neelapu SS, Locke FL, Bartlett NL, et al. Axicabtagene Ciloleucel CAR T-Cell Therapy in Refractory Large B-Cell Lymphoma. *N Engl J Med* 2017; **377**:2531-2544. Doi: 10.1056/NEJMoa1707447
4. Schuster SJ, Bishop MR, Tam CS, et al. Tisagenlecleucel in Adult Relapsed or Refractory Diffuse Large B-Cell Lymphoma. *N Engl J Med* 2019; **380**:45-56. Doi: 10.1056/NEJMoa1804980

5. Abramson JS, Palomba ML, Gordon LI, et al. Lisocabtagene maraleucel for patients with relapsed or refractory large B-cell lymphomas. *Lancet*. 2020; Sep 19; **396**(10254):839-852. Doi: 10.1016/S0140-6736(20)31366-0.
6. Joseph Melenhorst J, Chen GM, Wang M, et al. Decade-long leukaemia remissions with persistence of CD4+ CAR T cells. *Nature*. 2022; Feb; **602**(7897):503-509. Doi: 10.1038/s41586-021-04390-6.
7. Zhao S, Wang C, Lu P, et al. Switch receptor T3/28 improves long-term persistence and antitumor efficacy of CAR-T cells. *J Immunother Cancer*. 2021; Nov; **9**(12):e003176. Doi: 10.1136/jitc-2021-003176.
8. Casucci M and Ciceri F. A second CD19 CAR T-cell infusion: yes or no? *Blood* (2021); **137** (3): 284-286. Doi: 10.1182/blood.2020009206
9. Gauthier J, Bezerra ED, Hirayama AV, et al. Factors associated with outcomes after a second CD19-targeted CAR T-cell infusion for refractory B-cell malignancies. *Blood* (2021); **137** (3): 323-335. Doi: 10.1182/blood.2020006770
10. Xu X, Sun Q, Liang X, et al. Mechanisms of relapse after CD19 CAR T-cell therapy for acute lymphoblastic leukemia and its prevention and treatment strategies. *Front Immunol*. 2019; **10**:2664.
11. Yu H, Sotillo E, Harrington C, et al. Repeated loss of target surface antigen after immunotherapy in primary mediastinal B cell lymphoma. *Am J Hematol*. 2017; **92** (1):E11-E13.
12. Pennisi M, Sanchez-Escamilla M, Flynn JR, et al. Modified EASIX predicts severe cytokine release syndrome and neurotoxicity after chimeric antigen receptor T cells. *Blood Adv*. 2021; **5**(17):3397-3406.
13. Sarkar RR, Gloude NJ, Schiff D, et al. Cost-effectiveness of chimeric antigen receptor T-cell therapy in pediatric relapsed/refractory B-cell acute lymphoblastic leukemia. *J Natl Cancer Inst*. 2019; **111**(7):719-726.
14. Baumgardner JR, Brauer MS, Zhang J, et al. CAR-T therapy and historical trends in effectiveness and cost-effectiveness of oncology treatments. *J Comp Eff Res*. 2020; **9**(5):327-340.



Abstract 233 Figure 1

<http://dx.doi.org/10.1136/jitc-2022-SITC2022.0233>

234

BEAD-BOUND ANTIBODY-ACTIVATION OF T CELLS PROVIDES SUB-OPTIMAL METABOLIC PROGRAMMING AND TUMOUR CONTROL COMPARED TO DENDRITIC CELL-ACTIVATED T CELLS

Meghan Kates*, Gavin Yuen, Michael St Paul, Alisha Elford, Pamela Ohashi, Sam Saibil. University Health Network, Toronto, ON, Canada

Background Adoptive cell therapies (ACT), including chimeric antigen receptor (CAR) or T cell receptor (TCR) transgenic T cells, have demonstrated impressive efficacy for the treatment of cancer. Unfortunately, ACT still does not result in durable responses for many patients.¹ Much investigation has centered around defining the characteristics of T cells that drive the clinical efficacy of ACT. Metabolic programming, and particularly oxidative metabolism, has emerged as a hallmark of T cells associated with superior performance in ACT due to important associations with *in vivo* persistence and metabolic resiliency in nutrient limiting environments.^{2–7} However, further investigation is required to define the optimal *ex vivo* activation conditions to impart optimal metabolic programming on the T cells used for ACT. We therefore interrogated the difference in metabolic programming resulting from activation with antibody-coated beads versus peptide-pulsed dendritic cells (DCs).

Methods CD8+ T cells were isolated from P14 TCR transgenic mice (recognizing H2-D^b gp33 peptide from lymphocytic choriomeningitis virus). T cells were activated with either bone-marrow derived DCs pulsed with gp33 peptide (1:10 DC:T cells) or with bead-bound anti-CD3/anti-CD28 antibodies (1:1 beads:T cells). Oxidative and glycolytic metabolism were measured by Seahorse Extracellular Flux analyzer. These data were used to calculate ATP production rate. *In vivo*, we examined the performance of these differentially activated P14 T cells to control the growth of subcutaneously implanted B16-gp33 melanoma tumours.

Results DC-activated T cells showed increased oxidative and glycolytic metabolism compared to bead-bound antibody-activated T cells. This resulted in an enhanced rate of ATP production in the DC-activated T cells. These metabolic data were associated with efficacy in the B16-gp33 model of ACT. Mice treated with DC-activated T cells had significantly diminished tumour growth and improved survival when compared to the bead-bound antibody-activation treatment condition. The latter treatment provided little advantage over the control (no treatment) group.

Conclusions Bead-bound antibody activation of T cells at a ratio of 1:1 (beads:T cells) provides sub-optimal metabolic priming which is associated with decreased performance in ACT, particularly when compared to DC-activated T cells. Further investigation into the metabolic programming of T cells by different activation conditions may reveal metabolic or signaling modules that can be modified in these conditions to improve therapy. This is relevant to the efficacy of CAR T cell therapy which often uses bead-activation of T cells for clinical protocols.

REFERENCES

1. C. H. June, R. S. O'Connor, O. U. Kawalekar, S. Ghassemi, and M. C. Milone, "CAR T cell immunotherapy for human cancer," *Science*, vol. **359**, no. 6382, pp. 1361–1365, Mar. 2018; doi: 10.1126/science.aar6711.
2. S. D. Saibil *et al.*, "Activation of Peroxisome Proliferator-Activated Receptors α and δ Synergizes with Inflammatory Signals to Enhance Adoptive Cell Therapy," *Cancer Res*, vol. **79**, no. 3, pp. 445–451, Feb. 2019; doi: 10.1158/0008-5472.CAN-17-3053.

3. M. St Paul *et al.*, "Coenzyme A fuels T cell anti-tumor immunity," *Cell Metab*, vol. **33**, no. 12, pp. 2415–2427.e6, Dec. 2021; doi: 10.1016/j.cmet.2021.11.010.
4. G. J. W. van der Windt *et al.*, "Mitochondrial Respiratory Capacity Is a Critical Regulator of CD8+ T Cell Memory Development," *Immunity*, vol. **36**, no. 1, pp. 68–78, Jan. 2012; doi: 10.1016/j.immuni.2011.12.007.
5. Y. Zhang *et al.*, "Enhancing CD8+ T Cell Fatty Acid Catabolism within a Metabolically Challenging Tumor Microenvironment Increases the Efficacy of Melanoma Immunotherapy," *Cancer Cell*, vol. **32**, no. 3, pp. 377–391.e9, Sep. 2017; doi: 10.1016/j.ccell.2017.08.004.
6. Y. Sun *et al.*, "Zbtb20 Restrains CD8 T Cell Immunometabolism and Restricts Memory Differentiation and Antitumor Immunity," *The Journal of Immunology*, vol. **205**, no. 10, pp. 2649–2666, Nov. 2020; doi: 10.4049/jimmunol.2000459.
7. M. D. Buck *et al.*, "Mitochondrial Dynamics Controls T Cell Fate through Metabolic Programming," *Cell*, vol. **166**, no. 1, pp. 63–76, Jun. 2016; doi: 10.1016/j.cell.2016.05.035.

Ethics Approval This study was approved by The University Health Network Animal Care Committee; approval number 929.

<http://dx.doi.org/10.1136/jitc-2022-SITC2022.0234>

235

CRISPR-MEDIATED INSERTION OF IL-12 INTO THE *PDCD1* LOCUS IMPROVES THE ANTITUMOR ACTIVITY OF TCR-T CELLS AGAINST SOLID TUMORS

Segi Kim*, Choi Park, Sunhwa Lee, Hyeongryeol Choi, Chan Hyuk Kim. *Korea Advanced Institute of Science and Technology, Daejeon, Republic of Korea*

Background Interleukin-12 (IL-12) is a powerful immunostimulatory cytokine that has been expressed ectopically in genetically engineered T cells to enhance their antitumor activity. However, the constitutive production of IL-12 by engineered T cells caused severe adverse effects in patients. Thus, to fully harness the immunostimulatory potential of IL-12 while avoiding systemic toxicity, we inserted *IL-12* gene into the *PDCD1* locus in T cell receptor (TCR)-engineered T cells using the CRISPR/Cas9-based genome editing tool, which allows for IL-12 secretion to be induced strictly in a T cell activation-dependent manner.

Methods As a model TCR, we used a monoclonal TCR that is specific to the NY-ESO-1 (SLLMWITQV) peptide. The PD1-edited NY-ESO-1-specific TCR-T cells were generated by sequential lentiviral transduction and Cas9 RNP/AAV6-based knock-in into human primary T cells. The resulting TCR-T cells were co-cultured with an A375 cell line expressing NY-ESO-1 antigen to evaluate cytokine production, cytotoxicity, and proliferation *in vitro*. *In vivo* antitumor activity of the TCR-T cells was investigated in A375 xenograft models using NSG mice.

Results The *PDCD1* locus was successfully edited in NY-ESO-1 TCR-T cells by replacing the endogenous PD-1 gene with a single-chain IL-12 transgene, without affecting the viability or expansion of the engineered T cells. Upon recognition of the target cells, the IL-12 transgene was expressed successfully, resulting in the strong phosphorylation of STAT-4 in the TCR-T cells. As compared to control TCR-T cells, these Δ PD-1-IL-12 NY-ESO-1 T cells displayed enhanced *in vitro* effector function, including increased secretion of IFN γ , TNF, and IL-10 as well as faster tumor cell lysis. In addition, Δ PD-1-IL-12 NY-ESO-1 T cells expanded more robustly after repeated challenges with PD-L1 overexpressing target cells. In xenograft models, Δ PD-1-IL12 NY-ESO-1 T cells potently eliminated established tumors and demonstrated increased tumor infiltration compared to control TCR-T cells.

Conclusions Using the CRISPR/Cas9 system, we demonstrated that the upregulation of PD-1, an immune-suppressive event in T cells, could be reprogrammed to secrete immunostimulatory IL-12 in TCR-T cells. In both *in vitro* assays and *in vivo* mouse xenograft studies, these PD-1-edited TCR-T cells demonstrated enhanced cytotoxic activity. Our approach may offer a novel engineering option for adoptive T cell therapy against solid tumors.

<http://dx.doi.org/10.1136/jitc-2022-SITC2022.0235>

236

EXPANSION OF TUMOR-INFILTRATING LYMPHOCYTES FROM HEAD AND NECK SQUAMOUS CELL CARCINOMA TO ASSESS THE SUCCESSFUL EXPANSION FACTORS FOR DEVELOPING ADOPTIVE CELL THERAPY

¹Mofazzal Hossain*, ¹Jong Hyeok Kim, ²Hyun Lee, ²Chae-Lyul Lim, ³Gyungyub Gong, ³Hee Jin Lee. ¹University of Ulsan College of Medicine, Seoul, Republic of Korea; ²NeogenTC corp, Gyeonggi-do, hanam-si, Republic of Korea; ³Asan Medical Center, Seoul, Republic of Korea

Background Adoptive transfer of *in vitro* expanded tumor-infiltrating lymphocytes (TILs) has been effective in regressing several types of malignant tumors, which was first applied to metastatic melanoma more than three decades ago. Promising results of such adoptive cell therapies have intrigued us to evaluate their feasibility in unexplored cancer types that are difficult to treat with existing treatment options. Hence, we evaluated the possibility of TIL expansion from head and neck squamous cell carcinoma (HNSCC), the factors affecting their successful expansion, and the immune phenotypes of expanded TILs.

Methods We tried to expand TILs from 51 specimens (36 patients) of surgically resected HNSCC of three different anatomical location groups, including primary tumors and their metastasized lymph nodes (LNs). Cancer tissues were cut into small pieces (1-2 mm each) and underwent initial expansion for 2 weeks with gentamycin (400-1600 µg/ml). The cutoff value of successful expansion was 0.8×10^5 TILs per fragment. Factors affecting the successful expansion or contamination were determined mainly by focusing on the location of the samples. The characteristics of expanded cells were evaluated by flow cytometry.

Results TILs were successfully expanded from 35% of the samples (18 of 51). Mean number of TILs per fragment in successful cases of LNs was $6.1 \pm 4.6 \times 10^5$ (n=9), whereas the value was $4.3 \pm 3.8 \times 10^5$ (n=9) in primary tumors. Among three location groups of the primary tumors, the success rate was higher in samples of oropharynx & larynx than those of oral cavity (44%, 33%, and 19%, respectively). Mean percentage of CD4+ T cells was 60% in compared to 30% for CD8+ T cells. Mean proportion of T_{EM}, T_{EFF}, T_{CM}, and T_{NAIVE} were 88.5%, 4.7%, 4.8%, and 1.8% in CD4+ T cells, while 80.0%, 13.4%, 3.6%, and 2.9%, respectively in CD8+ T cells. However, 27% of the total samples were contaminated, and the rate was higher in tumor samples than in LN samples, 36%, and 11%, respectively.

Conclusions We could expand TILs from a third of primary tumors and LN samples of HNSCC. LN samples generated slightly more TILs per fragment than primary tumors while getting less contaminated. To use primary HNSCCs as a source of TIL therapy, a setting of clinically applicable antibiotic treatment during the manufacturing process is necessary. Varied success rates were observed according to the location of the cancer tissues, but those remain to be checked statistically with a large number of samples.

<http://dx.doi.org/10.1136/jitc-2022-SITC2022.0236>

237

NEOANTIGEN-SPECIFIC EXPANSION OF TUMOR-INFILTRATING LYMPHOCYTES ENABLES EFFECTIVE TREATMENT OF P53-MUTANT CANCER IN MICE

Peter Kim*, Noam Levin, Nolan Vale, Steven Rosenberg. *NCI, Bethesda, MD, USA*

Background Adoptive cell therapy (ACT) targeting neoantigens can achieve durable clinical responses in patients with advanced solid cancer.¹⁻³ However, many T cells among the tumor infiltrating lymphocytes (TIL) are not specific for tumor antigens.⁴⁻⁶ Additionally, *ex vivo* expansion of TILs often results in further reduction and differentiation of TILs specific for neoantigens.⁷ The low frequencies and/or differentiated phenotype of TILs can contribute to ineffective ACT.

Methods We developed a protocol to selectively expand neoantigen-specific TILs by *in vitro* stimulation of target neoantigens, termed NeoExpand. As a proof-of-concept we performed NeoExpand on p53 neoantigen-specific TILs. TILs were incubated with antigen presenting cells either electroporated with tandem minigene RNAs encoding multiple p53 neoantigens in 25mers or pulsed with mutant peptides (25mers or minimal epitopes) and cultured in media containing 300-1000 IU interleukin (IL) 2 and 30 ng/mL IL-21 for 14 days.

Results We retrospectively determined the frequencies of neoantigen-reactive TILs in 10 patient infusion products by *CDR3B* deep sequencing. 62% (41/61) of neoantigen-reactive clones were <1% in the infusion products. TILs from patient 4196 initially containing ~2% of TILs recognizing p53^{R175H}, one of the “hotspot” p53 mutations, were subjected to NeoExpand and the rapid expansion protocol (REP) with feeder cells, OKT3 and IL-2. Following REP, 0.4% of 4196 T cells were reactive with p53^{R175H}, indicating that REP decreased the frequency of the p53^{R175H}-reactive clones. In contrast, the 4196 TILs following NeoExpand contained 8% TILs reactive with p53^{R175H}, which was a 4-fold increase in the p53^{R175H}-reactive cells relative to the starting population and 20-fold higher than that of REP. While conventional TIL screening identified 3 T-cell receptors (TCRs),⁸⁻¹⁰ NeoExpand enabled identification of 7 TCRs including the 3 TCRs identified by conventional screening. *In vivo*, 4196 TIL expanded through REP was ineffective in treating established TYK-nu human ovarian cancer cells that naturally expressed p53^{R175H},⁷ while the 4196 NeoExpand TILs effectively regressed the tumor in NSG mice. Single cell transcriptome analysis demonstrated that NeoExpand led to expansion of central memory/stem-like populations among the mutant p53-reactive clones in the 4196 TILs, while REP led to the depletion of the central memory/stem-like population. In total, we identified 18 TCRs recognizing various p53 neoantigens, including 7 uniquely identified by NeoExpand from 6 patient samples.

Conclusions In conclusion, these data indicate that TILs specific for neoantigens can be preferentially expanded by NeoExpand, enabling effective TCR isolation and treatment of p53-mutant cancer in mice.

Trial Registration Patient samples and healthy donor peripheral lymphocytes were obtained through the tissue procurement protocol NCT00068003.

REFERENCES

1. Tran, E., *et al.*, T-Cell Transfer Therapy Targeting Mutant KRAS in Cancer. *N Engl J Med*, 2016; **375**(23): p. 2255-2262.
2. Tran, E., *et al.*, Cancer immunotherapy based on mutation-specific CD4+ T cells in a patient with epithelial cancer. *Science*, 2014; **344**(6184): p. 641-5.

3. Zacharakis, N., *et al.*, Immune recognition of somatic mutations leading to complete durable regression in metastatic breast cancer. *Nat Med*, 2018; **24**(6): p. 724-730.
4. Scheper, W., *et al.*, Low and variable tumor reactivity of the intratumoral TCR repertoire in human cancers. *Nat Med*, 2019; **25**(1): p. 89-94.
5. Lowery, F.J., *et al.*, Molecular signatures of antitumor neoantigen-reactive T cells from metastatic human cancers. *Science*, 2022; **375**(6583): p. 877-884.
6. Simoni, Y., *et al.*, Bystander CD8(+) T cells are abundant and phenotypically distinct in human tumour infiltrates. *Nature*, 2018; **557**(7706): p. 575-579.
7. Kim, S.P.V., N.R.; Zacharakis, N.; Krishna, S.; Yu, Z.; Gasmil, B.; Gartner, J.J.; Sindiri, S.; Malekzadeh, P.; Deniger, D.C.; Lowery, F.J.; Parkhurst, M.R.; Ngo, L.T.; Ray, S.; Yong, L.; Hill, V.; Florentin, M.; Masi, R.V.; Paria, B.C.; Levin N.; Bera, A.; Hedges, E.; Choi, A.; Chatani, P.D.; Parikh, A.Y.; Levi, S.; Seitter, S.; Lu, Y.; Zheng, Z.; Prickett, T. D.; Jia, L.; Hernandez, J.M.; Hoang, C.D.; Robbins, P.F.; Goff, S.L.; Sherry, R.M.; Yang, J.C.; Rosenberg, S.A., Adoptive cell therapy of autologous tumor infiltrating lymphocytes and T cell receptor-engineered T cells targeting common p53 neoantigens in human solid cancers. *Cancer Immunology Research*, 2022; Accepted.
8. Parkhurst, M.R., *et al.*, Unique Neoantigens Arise from Somatic Mutations in Patients with Gastrointestinal Cancers. *Cancer Discov*, 2019; **9**(8): p. 1022-1035.
9. Zacharakis, N., *et al.*, Breast Cancers Are Immunogenic: Immunologic Analyses and a Phase II Pilot Clinical Trial Using Mutation-Reactive Autologous Lymphocytes. *J Clin Oncol*, 2022; p. JCO2102170.
10. Lo, W., *et al.*, Immunologic Recognition of a Shared p53 Mutated Neoantigen in a Patient with Metastatic Colorectal Cancer. *Cancer Immunol Res*, 2019; **7**(4): p. 534-543.

Ethics Approval Written, informed consent was obtained from all study participants, and all studies were conducted in accordance with The Declaration of Helsinki, The Belmont Report, and the U.S. Common Rule. This study was approved by the Investigational Review Board at the NCI in accordance with an assurance filed with and approved by the U.S. Department of Health and Human Services and was registered at <https://clinicaltrials.gov> under NCT00068003. Animal experiments were approved by the Institutional Animal Care and Use Committees of the NCI and performed in accordance with the NIH guidelines.

<http://dx.doi.org/10.1136/jitc-2022-SITC2022.0237>

238

EXOGENOUS GOT2 IN CAR-T CELLS IMPROVES METABOLIC FUNCTION AND PRESERVES EARLY MEMORY T CELL SUBSETS

John Hinds*, Sujatha Muralidharan, Ann Ranger, Jennifer Coccia, Thomas Giordano, Emily Kuiper, Pratirodh Koirala. *SOTIO Biotech Inc., Cambridge, MA, USA*

Background To overcome the challenges of a hostile solid tumor microenvironment, we have engineered CAR-T cells to co-express mitochondrial enzyme glutamic-oxaloacetic-transaminase 2 (GOT2). GOT2 is hypothesized to improve CAR-T cell fitness by maintaining cellular redox balance under oxidative stress and fueling the tricarboxylic acid (TCA) cycle via glutaminolysis. *In vivo* preclinical studies have shown improved anti-tumor activity of glypican-3 (GPC3)-targeting CAR-T cells co-expressing GOT2 (BOXR1030) compared to Control GPC3 CAR-T cells. In this study, we have characterized the cellular phenotype and mitochondrial function of BOXR1030 T cells compared to Control CAR-T cells to better understand the contribution of GOT2 to improved CAR-T function.

Methods Phenotype and function of BOXR1030 and Control CAR-T cells (n=3 donors) were assessed at the end of standard CAR-T cell manufacturing process, after repetitive stimulation with anti-idiotype antibody (up to 5 stimulations over 15 days) and co-culturing with GPC3-expressing Hep3B cells (2D) or Hep3B spheroids (3D) in standard or low glucose culture conditions. T cell differentiation status was assessed by flow cytometry using CD45RA, CD45RO, CCR7, CD27, CD28 and CD95. Mitochondrial health was measured by analyzing mitochondrial mass, membrane potential and reactive oxygen species (ROS) generation. Cytotoxic function in terms of tumor cell killing and Granzyme B secretion in culture supernatant were measured by Incucyte and MSD respectively.

Results At the end of manufacturing, BOXR1030 T cells have a higher frequency of T stem cell memory (CD45RA+CCR7+CD27+CD95+) and T central memory (CD45RO+CCR7+CD27+) in CD8+ populations relative to Control CAR-T cells. BOXR1030 T cells also have a lower frequency of terminally differentiated CD27-CD28- T cells. Following *in vitro* stimulation or Hep3B co-culture in standard and low glucose culture conditions, BOXR1030 T cells showed preservation of early memory populations, reduced CD27-CD28- senescent cells and improved cytotoxic function relative to Control CAR-T cells. Since changes in mitochondrial function are associated with T cell differentiation and senescence, we explored mitochondrial health of BOXR1030 T cells *in vitro*. In low glucose culture conditions, BOXR1030 T cells showed reduced ROS levels and reduced loss of mitochondrial membrane potential compared to Control CAR-T cells.

Conclusions BOXR1030 CD8+ T cells contain a higher frequency of early memory cells with fewer terminally differentiated senescent cells and show improved mitochondrial health compared to Control CAR-T cells. These data suggest potentially increased fitness of BOXR1030 T cells enabling enhanced *in vivo* T cell persistence and antitumor activity. BOXR1030 is currently in Phase 1 trials to assess safety and preliminary efficacy (NCT05120271).

<http://dx.doi.org/10.1136/jitc-2022-SITC2022.0238>

239

ENGINEERING OF POTENCY-ENHANCED TCR-EDITED T CELLS FOR SHARED NEOANTIGEN-TARGETED CANCER IMMUNOTHERAPY

Lianne Kok*, Sander Eshuis, Paula Kroon, Vanessa Tubb, Xiangjun Kong, Carsten Linnemann, Gavin Bendle, Jeroen van Heijst. *Neogene Therapeutics, Amsterdam, Netherlands*

Background Human cancers can express both private and shared mutation-associated neoantigens, the latter being derived from recurrent cancer driver gene mutations, with the R175H mutation in the human *TP53* tumor-suppressor gene being the most frequently shared between patients across cancer types. This makes the generation and subsequent adoptive transfer of TCR-engineered T cells reactive to an HLA-A*02:01-restricted TP53^{R175H} epitope a highly attractive cancer immunotherapy approach. However, the combined immunosuppressive tumor-microenvironment and the low levels of neoantigen presentation by solid cancers compromise the activation and reactivity of TCR-engineered T cells, posing a major hurdle for these cells to eradicate tumor lesions. A substantial body of work has highlighted that inactivation of negative regulators of TCR signaling can augment T cell functionality and anti-tumor reactivity.

Methods Aiming to develop a highly potent anti-cancer T cell product, we applied CRISPR genome engineering to specifically introduce a TP53^{R175H}-specific TCR into the TRAC locus of primary human T cells, while simultaneously inactivating negative regulators of TCR signaling. After validating successful introduction of the TP53^{R175H} TCR and inactivation of endogenous TCR chains and the TCR inhibiting genes of interest, the ability of edited T cells to proliferate, produce cytokines and control tumor growth were assessed in vitro.

Results We found that inactivation of TCR signaling inhibitory genes significantly enhanced the ability of TCR-edited T cells to proliferate and produce the cytokines IFN- γ , TNF and IL-2, both in response to anti-CD3/anti-CD28 stimulation and HLA-A*02:01⁺ tumor cell lines that express the TP53^{R175H} mutation. Notably, T cells that had lost expression of negative regulators of TCR signaling were also superior in serial killing of TP53^{R175H}-positive tumor cells in vitro, while these T cells did not inhibit tumor cells that overexpressed a TP53 R175 WT epitope.

Conclusions Taken together, our findings show that inactivation of negative regulators of the TCR signaling pathway can enhance the reactivity of TCR-edited T cells against shared neoantigen-expressing tumor cells, thereby providing a promising new approach to increase the efficacy of TCR therapy directed against solid human cancers.

Ethics Approval Samples were obtained through a supply agreement with Sanquin Bloedvoorziening Amsterdam. These samples were collected only from voluntary, non-remunerated, adult donors who provided written informed consent as part of routine donor selection and blood collection procedures, that were approved by the Ethics Advisory Council of Sanquin Blood Supply Foundation.

<http://dx.doi.org/10.1136/jitc-2022-SITC2022.0239>

240

HUMANIZED CD30 CHIMERIC ANTIGEN RECEPTOR T CELLS WITH A NOVEL 4-1BB DERIVED SPACER HAVE IMPROVED ACTIVITY AND SAFETY AGAINST CD30-POSITIVE LYMPHOMAS

Lindsay Kua*, Chee Hoe Ng, Jin Wei Tan, Richard Ong, Cheah Chen Seh, Fiona Wong, Don Sim, Ivan David Horak, Lionel Low, Kar Wai Tan. *Tessa Therapeutics, Singapore, Singapore*

Background Autologous T cells expressing chimeric antigen receptors (CARs) against CD30 have demonstrated high clinical efficacy in the treatment of relapsed or refractory CD30-positive classical Hodgkin lymphoma (cHL) [1]. In the allogeneic setting, we have treated nine CD30-positive lymphoma patients in an ongoing Phase 1 study (NCT04288726) with Epstein-Barr virus specific T cells (EBVST) expressing a CD30-specific CAR derived from the murine HRS-3 antibody. These allogeneic CD30.CAR EBVSTs show promising signs of efficacy with a favorable safety profile and no evidence of graft versus host disease (GVHD). However, low levels of infused CD30.CAR EBVSTs were detected in the peripheral blood of most patients seven days post infusion, suggesting that durable persistence of these cells remains a challenge. In this study, we seek to improve the persistence of the CD30.CAR EBVSTs with the humanization of the murine HRS-3 scFv to minimize immunogenicity, and the replacement of the current IgG1 spacer with a novel 4-1BB derived spacer to eliminate any off-target interactions.

Methods CD30.CARs with humanized scFvs and novel spacers were designed and evaluated on their *in vitro* cytolytic potency and cytokine secretion profile. Top candidates were further tested for *in vivo* efficacy and safety in CD30-high tumor models.

Results CD30.CARs with humanized scFvs preserved specificity and efficacy, and exhibited improved stability as compared to the parent HRS-3 CAR. We found that HRS-3 binds to the cysteine-rich domain 5 of the CD30 molecule, which enabled informed design of novel spacer candidates. In combination with the murine HRS-3 scFv, the novel spacer derived from the 4-1BB receptor decreased basal cytokine secretion compared to the current IgG1 spacer, while retaining cytolytic activity *in vitro*. Humanized CD30.CARs combined with the 4-1BB-derived spacer did not exhibit any nonspecific interactions with CD16+ immune cells, while displaying superior efficacy *in vitro*, better persistence *in vivo* in various humanized mouse models, and more importantly an improved safety profile in a leukemia model with high tumor burden.

Conclusions Our re-engineered CD30.CAR construct, consisting of a humanized CD30.CAR and a 4-1BB-derived spacer, is likely to improve allogeneic CD30.CAR EBVST performance.

REFERENCE

1. Ramos CA, Grover NS, Beaven AW, Lulla PD, Wu MF, Ivanova A, Wang T, Shea TC, Rooney CM, Dittus C, Park SI, Gee AP, Eldridge PW, McKay KL, Mehta B, Cheng CJ, Buchanan FB, Grilley BJ, Morrison K, Brenner MK, Serody JS, Dotti G, Heslop HE, Savoldo B. Anti-CD30 CAR-T Cell Therapy in Relapsed and Refractory Hodgkin Lymphoma. *J Clin Oncol*. 2020; Nov 10;**38**(32):3794-3804. PubMed PMID: 32701411.

Ethics Approval This study was approved by the Agency for Science, Technology and Research (A*STAR) Institutional Animal Care and Use Committee (IACUC) under project approval number 211593.

<http://dx.doi.org/10.1136/jitc-2022-SITC2022.0240>

241 DEVELOPMENT OF A PERSONALIZED NEOANTIGEN-SPECIFIC TCR DISCOVERY PLATFORM

¹Robbert Spaapen*, ¹Thomas Kuilman, ¹Bo Schrikkema, ¹Jules Gadiot, ¹Raquel Gomez, ¹Julia Walker, ¹Laura Bies, ¹Oscar Krijgsman, ¹Yvonne Claassen, ¹Milena Viyacheva, ¹Demi Houg, ¹Manuel Soarnil, ¹Huiwen Ding, ¹Bas Stringer, ¹Gavin Bendle, ¹Carsten Linnemann, ²Ton Schumacher. ¹*Neogene Therapeutics, Amsterdam, Netherlands*; ²*Netherlands Cancer Institute, Amsterdam, Netherlands*

Background Tumor-infiltrating lymphocyte (TIL) therapy can mediate tumor regression in a range of solid cancers, most notably in melanoma. However, its wider application and efficacy has been limited by the low frequency and exhausted phenotype of tumor-specific T cells in the final product. Here, we developed a personalized, neoantigen-specific TCR discovery platform that will enable engineering of multiple TCRs into autologous peripheral blood T cells. This allows for the generation of a fitter T cell product with a high frequency of tumor-reactive TCRs of defined specificity.

Methods Our platform first identifies tumor-specific mutations and TIL-derived TCR repertoires from non-viable tumor specimens using next-generation sequencing (NGS), which are subsequently recreated using synthetic biology technology. The synthesized TCR libraries are expressed in reporter T cells, whereas neoantigen libraries are engineered in autologous APCs. Following coculture of these cells, activated and non-activated T cells are separated, followed by neoantigen-specific TCR identification using NGS-based analysis.

Results We validated the high sensitivity and specificity of this platform by successfully identifying multiple TCRs and their cognate neoantigens from high tumor mutational burden (TMB) cancers including melanoma. Notably, we show that the platform is agnostic to the type of mutation and HLA class restriction. Importantly, neoantigen-specific TCRs can also be isolated from a panel of low TMB microsatellite-stable colorectal cancers, underscoring the pan-cancer potential of this approach.

Conclusions We commenced applying this approach in a clinical study in which patients will be treated with functional autologous T cells engineered with neoantigen-specific TCRs of defined specificity and composition.

<http://dx.doi.org/10.1136/jitc-2022-SITC2022.0241>

DEVELOPMENT OF POOLED SCREENING PLATFORM FOR DISCOVERING THE NEXT GENERATION CHIMERIC ANTIGEN RECEPTORS

Taeyoon Kyung*, Nicole Wong, Andreas Rolfs, Lucas Hartsough, Joshua Mace, Jai Raman, Adam Scheidegger, Adam Meyer, Siqi Zhao, Lauren Baugh, Keith Robison, Narendra Maheshri, Shawdee Eshghi. *Ginkgo Bioworks, Cambridge, MA, USA*

Background Signaling cascades triggered by intracellular domains (ICDs) of Chimeric Antigen Receptor (CAR) in immune cells drive cell behaviors that correspond to different therapeutic outcomes. While canonical CAR-T ICD combinations 4-1BB-CD3z (BBz) and CD28-CD3z (28z) have achieved clinical success in a limited number of hematologic indications, CAR-based cell therapies have not yet been successful in more challenging indications. Systematic discovery of novel ICD combinations that drive more favorable T cell phenotypes has been onerous due to technical constraints in high-throughput screening and scaling.

Methods Here, we developed a versatile platform that allows parallel comparison of 10,000 different 2nd generation CAR ICD combinations in primary CD8+ T cells. We utilized combinatorial genetics en masse (CombiGEM) to assemble multiple DNA-barcoded lentiviral libraries of CAR ICDs distinguished by the affinity of extracellular binder and the length of hinge/spacer. We screened CAR ICD libraries for T cell persistence and fitness in a serial tumor rechallenge assay in a pooled manner.

Results Precisely tracking enriched barcodes over the course of 20 days allowed us to identify novel CAR clones with superior T cell proliferation and survival relative to conventional BBz and 28z CARs. Hits were validated in downstream arrayed studies with additional functional characterization including cytotoxicity, cytokine secretion, and T cell memory and exhaustion phenotypes in the serial tumor rechallenge assay.

Conclusions We believe our approach is readily applicable to diverse immune cell types, including T cell subsets, NK cells and macrophages, as well as different CAR domains including binders, structural components, and armoring components in addition to ICDs. Rapid and systematic generation and comparison of synthetic molecules at scale in pooled libraries via our platform will further elucidate design principles to guide next generation cell therapies engineering strategies.

<http://dx.doi.org/10.1136/jitc-2022-SITC2022.0242>

243

NR4A3 GENE EDITING AND C-JUN OVEREXPRESSION SYNERGIZE TO LIMIT EXHAUSTION AND ENHANCE FUNCTIONAL ACTIVITY OF ROR1 CAR T CELLS *IN VITRO* AND *IN VIVO*

Viola Lam*, Jessica Barragan, Christina Cheung, Jia Lu, David Chian, Rowena Martinez, Candace Sims, Purnima Sundar, Hajime Hiramagi, Shobha Potluri, Rachel Lynn. *Lyell Immunopharma, Inc., South San Francisco, CA, USA*

Background Next-generation strategies to improve T-cell functional activity, persistence, and durability are needed for effective cellular immunotherapy against solid tumors. Overexpression of the activator protein 1 (AP-1) family transcription factor c-Jun reduces chimeric antigen receptor (CAR) T-cell exhaustion thereby improving functional activity in multiple preclinical models.¹ Nuclear receptor subfamily 4A (NR4A) transcription factors may contribute to exhaustion and limit T-cell function by restraining expression of AP-1 regulated genes.^{2,3} Thus, we hypothesize that NR4A knockout (KO) and c-Jun overexpression may synergize to further limit exhaustion and enhance CAR T-cell function.

Methods Healthy donor T cells were transduced with a ROR1 CAR lentiviral vector with (+) or without (-) c-Jun overexpression. NR4A family genes (NR4A1, NR4A2, or NR4A3) were disrupted using CRISPR/Cas9 ribonucleoprotein delivery via electroporation (EP). CAR T-cell cytotoxicity and cytokine production were evaluated *in vitro* after primary and repeated antigen-stimulation assays designed to promote exhaustion. Cell phenotypes (flow cytometry) and transcriptional profiling (bulk and single-cell RNA-Seq) were also assessed. Finally, CAR T cells were evaluated *in vivo* using a ROR1-expressing H1975 lung cancer xenograft model in mice.

Results NR4A3 KO ROR1 CAR T cells consistently demonstrated superior cytotoxic activity and prolonged cytokine production upon repeated antigen stimulation compared to NR4A1 KO, NR4A2 KO, and EP control ROR1 CAR T cells. NR4A3 KO showed significant synergy in ROR1 CAR T cells overexpressing c-Jun (figure 1).

NR4A3 KO + c-Jun ROR1 CAR T cells were phenotypically and functionally indistinguishable at primary antigen stimulation. However, this combination resulted in the highest levels of cytokine production (IFN- γ , IL-2, and TNF- α), increased CAR T-cell persistence, and reduced surface expression of inhibitory receptors after repetitive antigen stimulation, suggesting a mechanism of resistance to exhaustion-induced dysfunction. Transcriptomic analysis indicated that NR4A3 KO + c-Jun increased effector and interferon response-associated T-cell subsets, yet reduced terminal exhaustion compared to control + c-Jun ROR1 CAR T cells following antigen restimulation.

NR4A3 KO + c-Jun ROR1 CAR T cells showed the most robust anti-tumor efficacy *in vivo* with activity at a 7-fold reduced CAR T-cell dose and demonstrated more than 20-fold greater CAR T-cell expansion in blood compared to control + c-Jun ROR1 CAR T cells (figure 2).

Conclusions These data suggest that reducing NR4A3 expression in combination with c-Jun overexpression has the potential to further limit exhaustion and provide durable ROR1 CAR T-cell functional activity compared to either strategy alone, which may improve cellular immunotherapy against ROR1-expressing solid tumors.

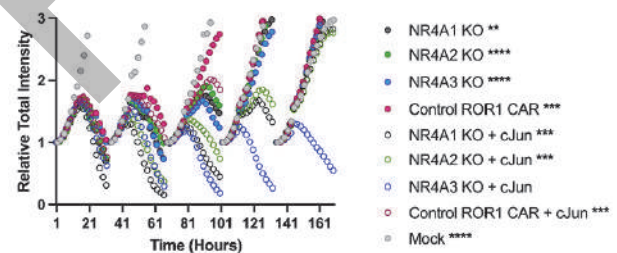
Acknowledgements We thank members of Lyell Immunopharma's In Vivo Pharmacology team (Abira Bandyopadhyay, Shawn Anderson, Jacob Corpuz, and Quinn Walker), NGS/

Flow team (Amir Figueroa, Elizabeth Hernandez, Andrew Jimena, Amanda Sims, Emily Fu-Sum, Yi-Dong Lin, Sheila Lou, Stefan Siebert, Ken Xiong, and Lora Zhao), Research team (Rachel Fukuda, Helle Jensen, Megan Murt, Spencer Park, Blythe Sather, Courtney Simianer, Sydney Spadinger, and Nicole Zhang), and Vector Sciences team (David Anderson, Martin Wohlfahrt, and Chang-Chi Wu) for their experimental contributions.

REFERENCES

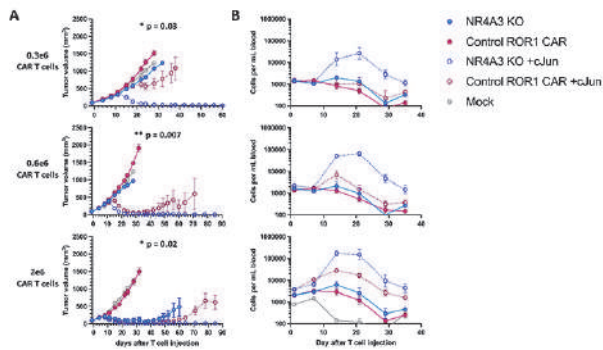
- Lynn RC, Weber EW, Sotillo E, Gennert D, Xu P, Good Z, Anbunathan H, Lattin J, Jones R, Tieu V, Nagaraja S, Granja J, de Bourcy CFA, Majzner R, Satpathy AT, Quake SR, Monje M, Chang HY, and Mackall CL. c-Jun overexpressing CAR-T cells are exhaustion-resistant and mediate enhanced antitumor activity. *Nature*. 2019;**576**:293–300.
- Chen J, Lopez-Moyado IF, Seo H, Lió, CJ, Hempleman LJ, Sekiya T, Yoshimura A, Scott-Browne JP, Rao A. NR4A transcription factors limit CAR T cell function in solid tumors. *Nature*. 2019;**567**:530-534.
- Liu X, Wang Y, Lu H, Li J, Yan X, Xiao M, Hao J, Alekseev A, Khong H, Chen T, Huang R, Wu J, Zhao Q, Wu Q, Xu S, Wang X, Jin W, Yu S, Wang Y, Wei L, Wang A, Zhong B, Ni L, Liu X, Nurieva R, Ye L, Tian Q, Bian X, Dong C. Genome-wide analysis identifies NR4A1 as a key mediator of T cell dysfunction. *Nature*. 2019;**567**:525-529.

Ethics Approval Experiments presented in this abstract relied on human donor material that was obtained from commercial vendors. These vendors use their own IRB-approved protocol and consent process. *In vivo* experiments presented in this abstract were approved by Lyell Immunopharma's IACUC (EB17-010-117).



Abstract 243 Figure 1 Successive lysis of ROR1-expressing H1975-NuLight Red (NLR) target cells by NR4A1 KO, NR4A2 KO, NR4A3 KO, or control unedited ROR1 CAR T-cells with (+) or without (-) c-Jun overexpression, and mock untransduced T cells in one representative donor of four donors tested. Lysis of H1975-NLR target cells was quantified by measuring total NLR intensity. NLR intensity was normalized relative to the starting intensity after replating for each round of stimulation. NR4A3 KO + c-Jun showed significant synergy at the last timepoint of the fifth stimulation compared to other T-cells tested. Asterisks represent p-value significance of each condition compared to NR4A3 KO + c-Jun (unpaired t-test, ** p < 0.005, *** p < 0.001, **** p < 0.0001).

Abstracts



Abstract 243 Figure 2 Anti-tumor efficacy at three CAR T-cell doses (A) and CAR T-cell expansion (B) of NR4A3 KO or control edited ROR1 CAR T cells with (+) or without (-) c-Jun overexpression, and mock untransduced T cells in one representative experiment (n=3 healthy donors) tested in an in vivo H1975 xenograft model. NR4A3 KO + c-Jun CAR T cells significantly impaired tumor growth at all three CAR T cell doses tested compared to control + c-Jun (* p < 0.05, ** p < 0.005, Tukey one-way ANOVA). At the 0.6x10⁶ CAR T-cell dose, NR4A3 KO + c-Jun CAR T cells demonstrated a significantly higher day 21-fold expansion compared to control + c-Jun (mean of 40.1 vs 1.7, ****p < 0.0001, unpaired t-test, n=10 mice per group). Day 21-fold expansion was normalized relative to day 1.

<http://dx.doi.org/10.1136/jitc-2022-SITC2022.0243>

244

AFNT-111, A SAFE AND EFFECTIVE TCR-ENGINEERED T CELL THERAPY TARGETING THE ONCOGENIC DRIVER KRAS G12V MUTATION

Boards, approval number EB17-010-303 and PROTO000050898, respectively.

<http://dx.doi.org/10.1136/jitc-2022-SITC2022.0244>

¹Hubert Lam*, ¹Xingyue He, ¹Cheryl Black, ¹Michele Hoffmann, ¹Joshua Francis, ¹James Parsons, ¹Christian Roy, ¹Jinsheng Liang, ¹Hongjing Qu, ¹Martin Campbell, ¹Tomasz Sewastianik, ²Jessica Webb, ²Aude Chapuis, ²Thomas Schmitt, ²Phillip Greenberg, ¹Damien Hallet, ¹Markus Vallaster, ¹Piotr Pierog, ¹Gary Shapiro, ¹Loic Vincent. ¹Affini-T Therapeutics, Watertown, MA, USA; ²Fred Hutchinson Cancer Research Center, Seattle, WA, USA

Background Mutations in the RAS family of genes are responsible for approximately 30% of all human cancers. Mutated RAS proteins are truncal oncogenic driver antigens essential for cancer development and progression making them optimal targets for cancer therapies by limiting tumor escape. The AFNT-111 cell therapy consists of autologous CD8⁺ and CD4⁺ T cells expressing a TCR specific for the highly prevalent KRAS_{G12V} mutation presented by HLA-A*11:01, one of the most common HLA alleles worldwide. AFNT-111 is also engineered to express the CD8 α / β coreceptor, enabling a coordinated CD4⁺/CD8⁺ tumor response that aims to promote increased T cell activity and persistence while minimizing T cell exhaustion.

Methods Lentiviral vector was used to transduce primary human CD4⁺ and CD8⁺ T cells with the KRAS_{G12V}-specific TCR and CD8 α / β coreceptor. Engineered T cells were assessed against KRAS_{G12V} peptide and a panel of KRAS_{G12V}-expressing tumor cell lines for *in vitro* activation, proliferation, and cytotoxicity. *In vitro* safety studies were performed to evaluate self-peptide cross-reactivity and alloreactivity and *in vivo* efficacy studies were conducted using human KRAS_{G12V} xenografts in NSG mice.

Results AFNT-111 demonstrated potent functional avidity for KRAS_{G12V} peptide with no reactivity to wildtype KRAS. Several naturally expressing KRAS_{G12V} human tumor cell lines, derived from lung, colorectal, and pancreatic cancer, triggered significant AFNT-111 T cell activation and proliferation, and potent cytotoxicity towards tumor cells. *In vitro* killing by AFNT-111 was consistently observed even after repeated tumor cell challenge. Robust *in vivo* anti-tumor efficacy was also observed in two established mouse xenograft tumor models. XScan studies using amino acid substitutions of the reference KRAS_{G12V} peptide revealed a restrictive TCR recognition motif limiting risk of promiscuous off-target activation. Further, potentially cross-reactive self-peptides in the human proteome matching this motif were tested and no cross-reactivities with significant avidity were identified. A large lymphoblastoid cell line library covering >95% of the most common HLA alleles was assessed with no alloreactive responses detected. For clinical studies, a robust manufacturing process has been developed in which CD4⁺/CD8⁺ T cell ratios are controlled, and the final AFNT-111 drug product preserves stem-like properties.

Conclusions AFNT-111 preclinical data demonstrate a highly potent and specific TCR-engineered T cell product that is cytotoxic to KRAS_{G12V}-expressing tumor cells both *in vitro* and *in vivo*. Cross-reactivity and alloreactivity assessments established a strong safety profile of AFNT-111, supporting clinical translation. First-in-human clinical studies will focus on advanced or metastatic pancreatic, colorectal, and lung cancer indications.

Ethics Approval These studies were approved by Affini-T Therapeutics and Fred Hutchinson Cancer Research Center Ethics

245

CORD BLOOD CD34⁺ STEM CELLS ARE EFFICIENTLY TRANSDUCED WITH ANTI-CD19-CAR AND EXPANDED AND DIFFERENTIATED INTO VIVENK™ NATURAL KILLER CELLS WHICH DISPLAY SELECTIVE CYTOTOXICITY AGAINST B-CELL LEUKEMIA

Monica Raimo*, Nina Lamers-Kok, Didem Özkazanc, Daniëlle Steenmans, Greis Shahini, Amanda van Vliet, Denise Panella, Arianna Micciché, Youri van Waardenburg, Anna-Maria Georgoudaki, Jan Spanholtz, Adil Duru. *Glycostem Therapeutics, Oss, Netherlands*

Background Chimeric antigen receptor (CAR)-engineered Natural Killer (NK) cells are a highly promising option for adoptive cancer immunotherapy. Glycostem Therapeutics has developed a closed, automated, and feeder-free system for ex vivo expansion and differentiation of umbilical cord blood-derived CD34⁺ stem cells into highly functional NK cells, currently evaluated in a Phase I/II clinical study (ClinicalTrials.gov ID: NCT04632316). The introduction of a genetic engineering step during early culture stages makes the system suitable for CAR-NK products, for the generation of billions of off-the-shelf viveNK™ cells for antigen-directed tumor targeting.

Methods To enhance the ability of NK therapies to kill resistant B-cell leukemia cells, we generated anti-CD19-CAR viveNK™ cells via lentiviral transduction with multiple second- and third-generation CARs carrying different hinge, transmembrane and intracellular domains. CAR cassettes were cloned into Glycostem's own clinically suitable lentiviral transfer plasmid; promoter analysis identified MNDU3 as the optimal transgene driver.

Results Engineered cells showed high expansion potential and fast differentiation into functional NK cells expressing specific surface markers. CAR surface expression increased up to 83% (n=8 donors) with higher Multiplicity of Infection (MOI) in a range of 1-20, but was sustained even at low (<5) MOI. CAR transgene genome integration (Vector Copy Number) and transcriptional efficiency was evaluated via quantitative Polymerase Chain Reaction (PCR). Exposure of CD19-viveNK™ cells to antigen-expressing B-cell leukemia cell lines resulted in increased degranulation and very potent antigen-specific cytotoxicity. Additionally, inherent innate NK cell phenotype and responses and the mechanism of action driving CD19-CAR viveNK™ cytotoxicity were investigated via flow cytometry-based analysis and single-cell RNA-sequencing (scRNA-Seq) of CAR-transduced vs non-transduced donors.

Conclusions Our data show how off-the-shelf, highly functional, and antigen-directed CAR-NK cells can be generated ex vivo, offering an option to target cancers which are often resistant or difficult to treat with standard immunotherapy.

<http://dx.doi.org/10.1136/jitc-2022-SITC2022.0245>

246 ALLOGENEIC "OFF-THE-SHELF" $\gamma\delta$ T CELLS MODIFIED WITH CD27-CONTAINING CAR FOR TARGETING CD70⁺ CANCERS

Gauri Lamture, Alexander Teague, Morgan Smith-Boeck, Michael Salum, Ramandeep Kaur, Smitha Gundurao, Pannaga Parthasarathy, Yvan Chanthery, Marissa Herrman, Blake Aftab, Arun Bhat, Kevin Nishimoto*. *Adicet Bio, Inc., Redwood City, CA, USA*

Background CD70, a member of the TNF receptor ligand family, represents a compelling target for the development of CAR T cell therapies due to its high expression in multiple solid and hematologic malignancies. Although CAR T cells have shown remarkable clinical benefit in hematologic malignancies, efficacy in solid tumors has highlighted key challenges. Among the emerging strategies to improve clinical responses is the use of alternative cytotoxic effector cells with multifunctional tumoricidal activity. $\gamma\delta$ T cells combine innate and adaptive immunity to recognize and kill malignant cells. In addition, the infiltration of $\gamma\delta$ T cells into various cancer types, including those expressing CD70, significantly correlates with survival. Strategies for targeting CD70 have explored scFvs or engineering its natural receptor (CD27) as the antigen-recognition moiety of a CAR. Recent studies demonstrate improved preclinical antitumor activity using the CD27 ligand compared to scFv-based CAR, suggesting functional advantages associated with a CD27-based CAR approach.¹ Here we report on the functional characterization and manufacturability of $\gamma\delta$ T cells expressing CD27-based CAR for targeting a set of CD70⁺ cancers.

Methods Healthy donor PBMCs were used to activate, expand, and engineer cytotoxic V δ 1 T cells to express CD27-containing CAR. In vitro phenotype and antitumor functionality of V δ 1 CAR T cells were determined using flow cytometry and cell-based cytotoxicity assays against a panel of cell lines having a broad range of CD70 expression. Human tumor xenograft models in immunodeficient mice were used to evaluate in vivo efficacy after a single dose of CD27-containing CAR V δ 1 T cells.

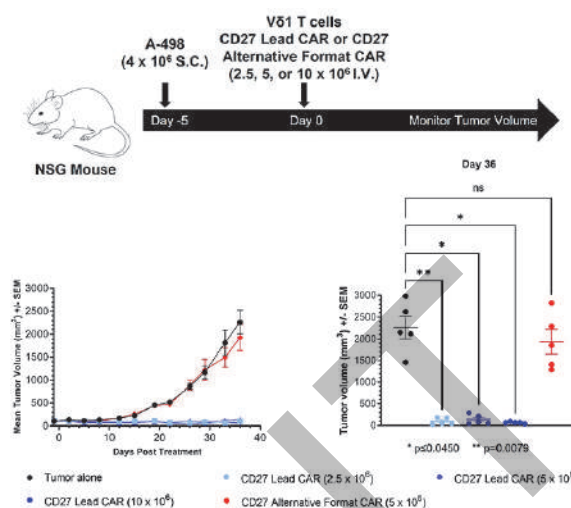
Results V δ 1 T cells modified to express CD27-containing CAR were successfully generated and expanded, indicating product expansion was not hindered by putative risks for CD70-mediated fratricide. The resulting V δ 1 CAR T cells expressed a predominant naïve-like memory phenotype and were associated with potent in vitro cytotoxicity, production of proinflammatory cytokines, and proliferation against CD70⁺ tumor cell lines. To assess the potential impacts of soluble CD27 (sCD27) on cytotoxicity, exogenously added sCD27 resulted in no change in anti-tumor activity. Lastly, highly potent tumor growth inhibition was observed against tumor xenografts in immunodeficient mice (figure 1).

Conclusions In summary, these preclinical data support further development and clinical evaluation of an allogeneic $\gamma\delta$ CAR T cell therapy utilizing the CD27 natural receptor CAR format for targeting CD70⁺ cancers.

REFERENCE

1. Sauer T, Parikh K, Sharma S, Omer B, Sedloev D, Chen Q, Angenendt L, Schliekmann C, Schmitt M, Müller-Tidow C, Gottschalk S, Rooney CM. CD70-specific CAR T cells have potent activity against acute myeloid leukemia without HSC toxicity. *Blood*. 2021; Jul 29;138(4):318-330.

Ethics Approval All mouse experiments were performed in accordance with the Guide for the Care and Use of Laboratory Animals and followed all institutional and national guidelines with appropriate protocol review and approval.



Abstract 246 Figure 1 Efficacy of CD27-containing CAR V δ 1 T cells in an RCC Model
The top panel illustrates the study design, and the bottom panels report the average tumor volumes for the duration of the study (left) and statistical comparison between treatment groups and the tumor alone control group at the end of the study (right).

<http://dx.doi.org/10.1136/jitc-2022-SITC2022.0246>

Abstracts

247

PRECLINICAL DISCOVERY AND EVALUATION OF ALLOGENEIC "OFF-THE-SHELF" $\gamma\delta$ CAR T CELLS TARGETING B7-H6⁺ TUMORS

Gauri Lamture, Alexander Teague, Jonathan Wong, Morgan Smith-Boeck, Michael Salum, Erika Meaddough, Pannaga Parthasarathy, Atrish Bagchi, Matthew Hoopes, Elizabeth Speltz, Ramandeep Kaur, Smitha Gundurao, Nitya Ramadoss, Marissa Herrman, Blake Aftab, Arun Bhat, Kevin Nishimoto*. *Adicet Bio, Inc., Redwood City, CA, USA*

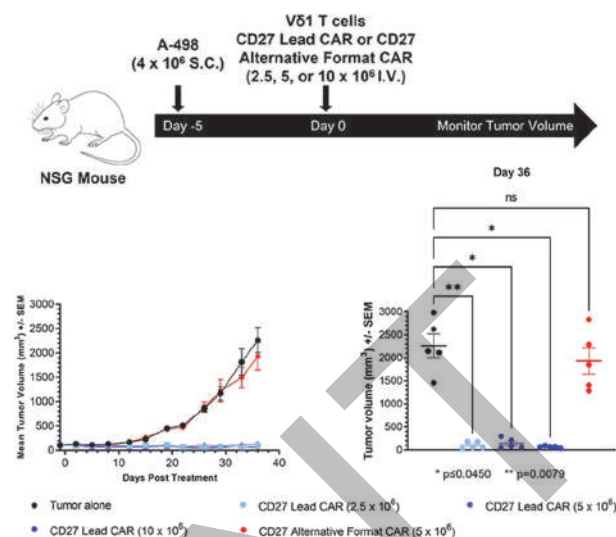
Background B7-Homolog 6 (B7-H6) is a B7 family member and the natural ligand for NK cell-activation receptor, NKp30. B7-H6 is expressed on multiple tumor types but has limited expression in normal tissues. Given this tumor specificity, B7-H6 represents an attractive target for CAR T therapy. CAR T cell therapy is associated with high clinical response rates in hematologic malignancies, but opportunities for improved efficacy in solid tumors remain. $\gamma\delta$ T cells, whose solid tumor infiltration has demonstrated a significant correlation with survival, combine innate and adaptive mechanisms to recognize and kill tumors. In addition, $\gamma\delta$ T cells engineered with CARs have shown enhanced tumoricidal activity and compelling clinical efficacy. Here, we evaluated the antitumor activity of $\gamma\delta$ T cells modified with a set of novel scFv-based CARs targeting B7-H6, potentially applicable against multiple cancer indications for which natural tissue tropism of $\gamma\delta$ T cells may offer advantages.

Methods Phage-display libraries were used to identify scFvs against B7-H6 epitopes. To confirm activation upon target engagement, scFvs formatted into CARs were evaluated in a Jurkat-Lucia™ NFAT reporter cell line. PBMCs from healthy donors were used to activate, expand, and engineer V δ 1 T cells to express libraries of CAR constructs representing permuted scFv arrangements. V δ 1 CAR T cells were assessed for phenotype and in vitro activity using flow cytometry and cell-based assays. Tumor xenograft models were further used to evaluate and assess CAR candidates for in vivo efficacy.

Results Phage-display derived scFvs showed a diverse range of affinities against multiple B7-H6 epitopes. Increased NFAT activity post-activation and minimal tonic signaling was observed in the majority of CAR-modified Jurkat-Lucia™ cells. V δ 1 CAR T cells manufactured from healthy PBMC donors demonstrated a predominant naïve-like phenotype with low levels of exhaustion-associated markers. Upon in vitro stimulation with B7-H6⁺ cell lines, leading V δ 1 CAR T cells inhibited tumor cell growth, demonstrated antigen associated proliferation, and released proinflammatory cytokines. Robust tumor growth inhibition was also observed for a subset of active constructs against tumor xenografts in immunodeficient mice (figure 1).

Conclusions In summary, we present the preclinical discovery, optimization, and generation of allogeneic $\gamma\delta$ CAR T cells targeting B7-H6 with potential applications across a broad set of cancer indications. Based on these data, continued preclinical development of a clinical lead candidate is ongoing for future evaluation in the clinic.

Ethics Approval All mouse experiments were performed in accordance with the Guide for the Care and Use of Laboratory Animals and followed all institutional and national guidelines with appropriate protocol review and approval.



Abstract 247 Figure 1 Efficacy of B7-H6 V δ 1 CAR T Candidates in HCT-15

The study design is described in the top panel and the bottom panels report tumor volumes throughout the study (left) and statistical comparisons of treatment groups to the tumor alone control group at study termination (right).

<http://dx.doi.org/10.1136/jitc-2022-SITC2022.0247>

248 **INTRATHECAL DELIVERY OF DENDRITIC CELL VACCINE ERADICATES TUMOR GROWTH AND PROTECTS AGAINST LEPTOMENINGEAL DISEASE RE-INOCULATION IN IMMUNOCOMPETENT HER2+ AND TRIPLE NEGATIVE BREAST CANCER LMD XENOGRAFT MODELS**

Vincent Law, Krithika Kodumudi, Colin Snyder, Brian Czerniecki, Peter Forsyth*, H. Lee Moffitt Cancer Center and Research Institute, Tampa, FL, USA

Background Leptomeningeal disease (LMD) occurs in approx. 5% of patients with breast cancer (BC) with median survival of 2-4 months. Here we investigated intrathecal (IT) delivery of HER2/HER3-dendritic cell vaccine (DCV) in BC-LMD murine model.

Methods HER2+ and triple negative breast cancer (TNBC) murine BC cells were injected into CSF of BALB/c mice to render LMD. We developed an murine Ommaya device that mimics the Ommaya reservoir in patients for the IT administration of DCV into CSF.

Results HER2-/HER3-DCV was able to rescue disease mice (71% in HER2+ breast cancer-LMD and 28% in triple negative breast cancer-LMD) with complete tumor regression. Surviving mice also exhibited adaptive immunity against tumor rechallenge.

Conclusions Our preclinical data supported a clinical trial (submitted) of the IT delivery of DCV in breast cancer patients with LMD.

Ethics Approval For animal use, Institutional Animal Care and Use Committee (IACUC) approval was obtained from the University of South Florida (IS00010398) as well as been reviewed by the Department of Defense Animal Care and Use Review Office.

<http://dx.doi.org/10.1136/jitc-2022-SITC2022.0248>

249 HETEROGENEITY AND CHANGES OF T-CELL SUBSET PROPORTION DURING THE EXPANSION OF TUMOR-INFILTRATING LYMPHOCYTES IN NON-SMALL CELL LUNG CANCER

¹Hyun Lee*, ²Gyungyub Gong, ¹Chae-Lyul Lim, ²Hee Jin Lee. ¹NeogenTC Corp, Gyeonggi-do, hanam-si, Republic of Korea; ²Asan Medical Center, Seoul, Republic of Korea

Background Adoptive cell therapy (ACT) using tumor-infiltrating lymphocytes (TILs) has emerged as an additional treatment option for non-small cell lung cancer (NSCLC). However, the absence of predictive factors for therapeutic efficacy and successful expansion and lack of knowledge of changes in TILs characteristics during expansion are hurdles to the clinical introduction of TIL therapy. Herein, we report the characteristics of TILs and their changes during manufacturing.

Methods 103 cases of NSCLC operational specimens were prospectively collected at the single institute. In the initial expansion (IE) step, lung cancer tissues were cut into 1 to 2-mm diameter fragments and expanded within 2 hours of surgery. In the rapid expansion (REP) step, post-IE TILs were cultured with allogeneic peripheral blood mononuclear cells, interleukin-2, and human anti-CD3 antibody. The memory subsets and PD-1 expression status of TILs were estimated via flow cytometry (CD3, CD4, CD8, CD45, CD45RA, CCR7, and PD-1). IFN- γ ELISA assay with TILs (4.0×10^5) and autologous cancer cells (1.0×10^5) was evaluated. We investigated clinicopathologic characteristics including the level of stromal TIL (sTIL) and tertiary lymphoid structures (TLS) in hematoxylin and eosin stained slides.

Results The median IE cells per fragment were 2.5×10^5 (range $0.02 \sim 30.8 \times 10^5$), and the success rate of IE is 81.6% (84 of 103 cases, cut-off value of 0.8×10^5). The sTIL and IE cells per fragment showed positive correlation (Pearson's $r=0.215$, $p=0.029$). Increased TLS grades were associated with IE cells per fragment (Jonchheere-Terpstra test, $p=0.008$). Effector memory type was a major subset in both IE ($n=39$; CD8+, mean 72.4%; CD4+, mean 86.1%) and REP ($n=29$; CD8+, mean 85.6%; CD4+, mean 91.6%). Mean PD-1+ cells were 30.4% in IE ($n=25$) and 12.6% in REP ($n=20$). 75% (12 of 16) of the REP TIL cases showed a more than 2-fold increase of IFN- γ secretion against autologous cancer cells. Cases with less than 2-fold increased IFN- γ secretion showed higher PD-1+ cell proportion ($n=2$, 47.3%) in REP than cases with above 2-fold increase ($n=6$, 2.0%). Cases with higher IFN- γ fold change showed a decrease of PD-1+ cell proportion during IE to REP ($n=3$).

Conclusions We successfully manufactured expanded TILs from NSCLC specimens for TIL therapy. The TLS and sTIL may be potential markers for the prediction of successful TIL expansion in NSCLC. Effector memory cells were the main subset of therapeutic TIL products. PD-1 expression was decreased during REP and it was associated with higher IFN- γ secretion against autologous cancer cells.

<http://dx.doi.org/10.1136/jitc-2022-SITC2022.0249>

250

CHIMERIC ANTIGEN RECEPTORS CONTAINING CD30-DERIVED COSTIMULATORY DOMAIN ELICIT AUGMENTED T CELL EFFECTOR FUNCTIONS AND ANTI-TUMOR EFFICACY

Hyun-Il Cho, Chung-Hyo Kang*, Sang-Eun Lee, In-Sil Song, Jung-Min Ha, Hyun-Jung Sohn, Tai-Gyu Kim. *VGeCell Inc., Seoul, Republic of Korea*

Background Adoptive cell therapy utilizing chimeric antigen receptor (CAR)-engineered T cells has demonstrated a feasible, attractive “off-the-shelf” approach against numerous types of cancers. Successful tumor eradication depends primarily on providing optimized costimulatory signals capable of achieving robust CAR-T cell proliferation, persistence, and antitumor reactivity. Here, we assessed the capability of a novel CD30-derived costimulatory domain, a known TNFR superfamily member involved in anti-apoptosis as well as cell activation and proliferation, to generate effective CAR-T cells.

Methods We designed CD19-redirecting second-generation CARs incorporating the intracellular signaling domain of CD30 and evaluated the immune-phenotype, cytokine secretion, and real-time cytolytic activity of CAR-transduced T cells against CD19-expressing cells in comparison with other CARs containing CD28 or 4-1BB costimulatory domains. Subsequently, their therapeutic efficacy was assessed with a pre-clinical Nalm-6-bearing xenogeneic model. We also engineered third-generation CARs combining CD30 and either CD28 or 4-1BB and conducted multiple repeat in vitro experiments evaluating their proliferation and cytolytic functionality against CD19-expressing tumors. Further, we tested the efficacy of third-generation CAR signaling after alteration with glypican-3 or mesothelin-targeting single chain fragment variable (scFv) domains.

Results T cells activated by a CD30- ζ signaling-CAR displayed enhanced effector functions with similar levels of proliferation, cytolytic efficacies, and cytokine secretion in vitro against CD19-expressing cancer cells as those of other CARs with CD28 or 4-1BB costimulatory domain, which are currently in clinical use. Administration of CD30-containing CAR-T cells into tumor-bearing mice resulted in improved human T cell persistence and tumor regression in a xenogeneic allograft model, which was similar to those achieved with CD28- or 4-1BB-signaling CAR-T cells. Furthermore, third-generation CARs including CD30 with either CD28 or 4-1BB costimulatory domain retained potent antitumor efficacies independent of their position. More significantly, CAR-T cells containing CD30-signaling revealed effective cytolytic activities against several solid cancer cell lines based on its scFv fragments.

Conclusions Our results demonstrate that the CD30-derived costimulatory domain could be an alternative for developing CAR-engineered therapeutics which may be applicable for various design of CAR constructs, with an emphasis on effectiveness against solid tumors.

<http://dx.doi.org/10.1136/jitc-2022-SITC2022.0250>

251 APPLICATION OF ANTIBODY-CELL CONJUGATION TECHNOLOGY IN A NOVEL OFF-THE-SHELF CD20-TARGETING GAMMA DELTA T CELL THERAPY ACE1831

Hao-Kang Li, Tai-Sheng Wu, Yi-Chiu Kuo, Ching-Wen Hsiao, Hsiu-Ping Yang, Chia-Yun Lee, Pei-Ju Leng, Zih-Fei Cheng, Sen-Han Yang, Yang-Liang Lin, Shih-Chia Hsiao, Sai-Wen Tang*. *Acepodia Biotech Inc., Alameda, CA, USA*

Background Chimeric antigen receptor T cells (CAR-T) therapy has been applied in the treatment of B cell lymphoma; however, CAR-T manufacturing requires virus or non-virus based genetic modification which causes high manufacturing cost and potential safety concerns. The novel antibody cell conjugation (ACC) technology has the advantage to direct innate immune cells, such as $\gamma\delta$ T and NK cells, to find and erase cancer cells by linking cancer-targeting antibodies on cell surface proteins without genetic modification. In this study, ACC technology was applied to generate a novel off-the-shelf CD20-targeting $\gamma\delta$ T cell therapy ACE1831, and the potential mechanism of ACC-mediated cytotoxicity was elucidated.

Methods PBMC-derived $\gamma\delta$ T cells were expanded from healthy donors. DNA linker-1 and linker-2 were conjugated to $\gamma\delta$ T cells and Rituximab, respectively. Linker-1 conjugated Rituximab was attached to linker-2 conjugated $\gamma\delta$ T cells by DNA hybridization to generate off-the-shelf CD20-targeting $\gamma\delta$ T cell product, ACE1831. *In vitro* and *in vivo* potency of ACE1831 against CD20-expressing cancer cells was evaluated in B cell lymphoma models. Mass spectrometry analysis was performed to identify Rituximab-linked surface proteins of $\gamma\delta$ T cells. Jurkat T cells expressing a luciferase reporter driven by an NFAT-response element were used to examine the mechanism of ACC-mediated T cell activation.

Results ACE1831 exhibited CD20-specific binding activity and viability after recovery from cryopreservation. *In vitro* cytotoxicity analysis demonstrated the superior potency of ACE1831 against B cell lymphoma including Raji, Rituximab-resistant Raji and Daudi cells, while no significant off-target toxicity against CD20-negative cells or PBMCs was observed. The enhanced secretion of IFN γ and TNF α has been detected when ACE1831 encountered Raji cells, whereas IL-6 remained undetectable. Furthermore, ACE1831 showed excellent *in vivo* potency in B cell lymphoma xenograft model, and ACE1831-treated mice remained cancer-free to the end of the study. By mass spectrometry analysis, Rituximab-linked proteins were identified, and the protein functions were mainly related to cell activation and immune synapse. Additionally, NFAT signaling was significantly activated when Rituximab-linked Jurkat cells encountered CD20-expressing cancer cells. Blocking TCR $\gamma\delta$ activation partially inhibited ACE1831-mediated cytotoxicity, indicating both TCR $\gamma\delta$ and external ACC-linked Rituximab involved in ACE1831 potency against B cell lymphoma.

Conclusions This study provides the evidence for the efficacy and safety of ACE1831 to support the clinical application against CD20-expressing tumors and elucidates the potential mechanism of ACC-mediated activation and cytotoxicity. ACE1831 will be evaluated in clinical trials for relapsed/refractory B cell lymphomas.

Ethics Approval SCID-Beige mice were purchased and housed under the regulation of the Institutional Animal Care and Use Committee (IACUC) of the contract research organizations.

<http://dx.doi.org/10.1136/jitc-2022-SITC2022.0251>

252

ENGINEERING POTENT CAR T-CELL THERAPIES BY CONTROLLING T-CELL ACTIVATION SIGNALING PARAMETERS USING THE STIM-R™ TECHNOLOGY, A PROGRAMMABLE SYNTHETIC CELL-SIGNALING PLATFORM

Aileen Li*, Jessica Briones, Jia Lu, Candace Sims, Quinn Walker, Rowena Martinez, Stefan Siebert, Lora Zhao, Emily Fu-Sum, Sheila Lou, Andrew Jimena, Elizabeth Pedrosa, Purnima Sundar, Hajime Hiraragi, Shobha Potluri, Bijan Boldajipour, Omar Ali, Alexander Cheung. *Lyell Immunopharma, South San Francisco, CA, USA*

Background CART-cell therapy has shown clinical success in treating hematologic cancers. However, more effective CAR T-cell therapies are needed for the treatment of solid tumors. T-cell activation is a formative event that directs cell fate and function in mature T cells. In the context of cellular product derivation, these decisions critically impact the phenotypic and functional quality of the T-cell drug product. We hypothesized that optimization of signaling parameters during T-cell activation can generate more potent CAR T cells.

Methods To control signaling during T-cell activation, we employed our platform, the Stim-R technology, a synthetic cell mimic that mediates precise signal molecule presentation (figure 1). We designed and fabricated Stim-R technology formulations to present T-cell activating signals engaging CD3 and CD28 at different densities and stoichiometries. Utilizing these formulation variants, we generated arrays of diverse ROR1-targeted CAR T-cell products which we profiled phenotypically and functionally. Based on these metrics, we compared Stim-R-generated CAR T cells to CAR T cells generated using a conventional bead-based activator to identify lead formulations showing superior *in vitro* function. We interrogated the mechanisms underlying this improved function by performing transcriptomic analysis of Stim-R CAR T cells following multiple rounds of tumor cell stimulation *in vitro* and validated the Stim-R CAR T cells *in vivo* in an H1975 lung tumor xenograft model in mice.

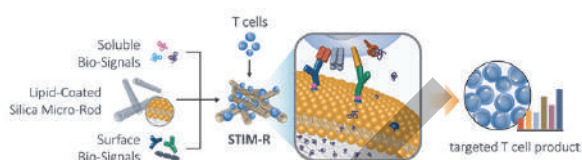
Results *In vitro*, Stim-R CAR T cells exhibited increased polyfunctionality in response to ROR1⁺ target-cell stimulation. Stim-R CAR T cells also demonstrated enhanced expansion and cytotoxicity in response to repeated ROR1⁺ target-cell stimulation. Transcriptomic analysis revealed that Stim-R CAR T cells retained a unique subset of stem-like cells with effector-associated gene signatures and also displayed down-regulation of exhaustion-associated gene sets compared to conventional CAR T cells, following repeat antigen stimulation. *In vivo*, Stim-R-generated CAR T cells exhibited 10-40x greater peak T-cell numbers in the blood, prolonged persistence, and improved tumor control over two months.

Conclusions Potent CAR T-cell therapies may be engineered by optimizing signaling events during T-cell activation to direct the phenotypic and functional qualities of the resultant cell product. Stim-R technology formulations mediating optimized signal presentation enabled the production of ROR1-targeted CAR T cells with improved polyfunctionality, persistence, and anti-tumor activity that retained a stem-like subpopulation with effector-associated gene signatures and showed reduced exhaustion, following repeated antigen stimulation. Such enhanced T-cell products may result in improved therapeutic benefit against solid tumors.

Acknowledgements We acknowledge Brianna Parish, Carson Harms, and Melissa DeFrancesco for their help with Stim-R technology process development. We also acknowledge Blythe Sather, Suman Vodnala, Gary Lee, Stan Riddell, Stephen Hill,

and Nick Restifo for their scientific input and strategic guidance.

Ethics Approval Animal studies were conducted in Explora BioLabs vivariums and are approved by Explora's IACUC under Core protocol amendment EB17-010.



Abstract 252 Figure 1 The Stim-R technology is a programmable cell-signaling platform. The technology comprises biodegradable lipid-coated silica micro-rods that can combinatorially present signals in precise densities and stoichiometries. Soluble signals are released in a controlled manner while surface-anchored signals are presented on a synthetic lipid membrane, mimicking physiologic presentation. By using the Stim-R technology to control cell-signaling parameters during T-cell activation, T-cell products with targeted phenotypic and functional profiles may be engineered.

<http://dx.doi.org/10.1136/jitc-2022-SITC2022.0252>

253

FULLY HUMAN CD123 CAR T CELLS IRRADICATE AML IN PRE-CLINICAL MODELS AND EXHIBIT A FAVORABLE SAFETY PROFILE

Genqing Liang*, Peirong Hu, Ngoc Tran, Hasan Mahmud, Pradyot Dash, Dina Schneider. *Lentigen Technology Inc, a Miltenyi Biotec Company, Gaithersburg, MD, USA*

Background CD123, the interleukin-3 receptor alpha chain (IL-3Ra), is widely overexpressed in hematologic malignancies including acute myeloid leukemia (AML), at both the level of leukemic stem cells (LSCs) and leukemic blasts. This makes CD123 an attractive therapeutic target. Monoclonal antibodies directed against CD123, and CD123 chimeric antigen receptor (CAR)-modified T cells are explored for new immunotherapies for the treatment of AML. Here, we developed a second generation anti-CD123 CAR comprising a fully human CD123 targeting scFv domain, a 4-1BB (CD137) co-stimulatory domain, and CD3 ζ activation domain, and investigated its potency against AML.

Methods Primary human T cells from healthy donors were enriched and transduced with lentiviral vector encoding the CD123 CAR, and CAR expression was detected by flow cytometry. CAR123 T cells or untransduced UTD control T cells co-cultured with the CD123⁺ MOLM-14 and KG1a AML cells, or the CD123⁺293T cells for 18h, were evaluated by luciferase assay, and cytokine production was measured by ELISA. Supernatants were collected from co-cultures of CAR T cells with CD123⁺ MOLM-14 target cells, and the concentration of cytokines IL-2, IFN- γ , and TNF- α was determined. CAR123 T cell functionality *in vivo* was evaluated in a MOLM-14 acute myeloid leukemia NSG xenograft model exhibiting CD123⁺ phenotype. In addition, myelotoxicity was investigated in colony-forming unit assays.

Results Lentiviral transduction resulted in robust expression of CD123 CAR in the transduced T cells. The CD123 CAR T cells showed potent *in vitro* killing of CD123⁺ AML cell lines MOLM-14 and KG1a, but no killing of the CD123⁺293T cells, indicating CD123-dependent efficacy. The TNF- α was modestly elevated in culture supernatants from CD123 CAR T cells co-incubated with target cells, however there was no significant induction of IL-2 or IFN- γ , suggesting low risk of cytokine release syndrome. Colony-forming unit assays utilizing peripheral blood CD34⁺ hematopoietic stem cells from healthy donors treated with CAR123 T cells overnight, yielded similar numbers of BFU-E erythroid and CFU-GM myeloid colonies to an untransduced T cell control, indicating an absence of CAR123-associated myelotoxicity. Moreover, CAR123 T cells showed efficient tumor clearance, expansion and persistence *in vivo*, and no apparent toxicity.

Conclusions In summary, the fully human CAR123 T cells are highly potent against AML *in vitro* and *in vivo*, manifest the desired safety attributes, and are a promising modality for AML therapy.

<http://dx.doi.org/10.1136/jitc-2022-SITC2022.0253>

254

THE CBL-B INHIBITOR, NX-0255, ENHANCES HUMAN DRUG ENHANCED TUMOR INFILTRATING LYMPHOCYTE (DETIL) EXPANSION AND T CELL FUNCTION IN FULL-SCALE RUNS

Xiaoyan Liang*, Xianzhu Wu, Jeevitha Jeevan, Samuel Butler, Pranav Murthy, Arthur Sands, Michael Lotze. *Nurix Therapeutics, San Francisco, CA, USA*

Background Ex-vivo expanded autologous tumor-infiltrating lymphocyte (TIL) therapy is one type of adoptive cellular therapy (ACT) which has demonstrated encouraging clinical responses in patients with melanoma or those with epithelial tumors. Effective methods to obtain sufficient TIL of suitable quality and diversity from tumor samples remains a challenge. The E3 ubiquitin ligase, Casitas B lineage lymphoma B (CBL-B) is expressed in T cells where it regulates signaling through the T Cell Receptor (TCR), limiting T cell activation and differentiation. Our previous studies (Whelan S., SITC; 2021) demonstrated that addition of NX-0255, our highly potent CBL-B inhibitor, during ex-vivo TIL expansion resulted in a favorable TIL phenotype and higher cell yields.

Methods Here we evaluated the comparative effects of the addition of the CBL-B inhibitor NX-0255 on expansion and phenotype of drug-enhanced TIL (DeTIL), in multiple full-scale processes. Six full-scale studies were conducted. All six runs were performed in parallel in TIL expanded either solely in the presence of 3,000-6000 IU/ml rHu IL-2 (TIL arm), or in the presence of rHu IL-2 and 1 μ M NX-0255 (DeTIL-0255 arm). DeTIL-0255 and TIL harvested on day 22 were assessed for total cell number, viability, phenotype, and function.

Results Compared with the TIL arm, the addition of NX-0255 increased the total viable cell count on Day 22 in five out of six full-scale experiments. Significant increases in the total number of CD8⁺ T cells as well as those with a central memory phenotype were observed in all six runs. A significant increase in the proportion of CD4⁺ central memory DeTIL-0255 was also demonstrated. No significant differences in effector memory populations were observed. DeTIL-0255 have a significantly ($p < 0.05$) higher stem-like population of CD39⁻CD69⁻ 'double negative' CD8⁺ cells as compared to TIL upon TCR and CD28 co-stimulation. CD8⁺ T cells in DeTIL-0255 displayed higher intracellular expression of granzyme B as well as co-expression of granzyme B and the cell surface CD107 α when compared to TIL. Furthermore, significant increases in intracellular IFN- γ expression were observed in activated DeTIL-0255 when compared to TIL using flow cytometric assessment.

Conclusions DeTIL-0255 demonstrates a superior phenotype and greater yield when compared with conventional TIL and is suitable for testing in clinical trials. We have initiated a clinical trial with DeTIL-0255 in patients with gynecologic malignancies. NCT05107739

<http://dx.doi.org/10.1136/jitc-2022-SITC2022.0254>

255

EXPRESS™: AN ACCELERATED PROCESS FOR THE MANUFACTURE OF KSQ-001, A CRISPR/CAS9-EDITED ETIL™ PRODUCT

Sharon Lin, Leila Williams, Mitali Ghose, Hugh Gannon, Conor Calnan, Angelina Pizzo, Pei-Lun Kao, Mallory Brady, Katri Sofjan, Anne Dodson, Sol Shenker, Michael Schlabach, Fiona Sharp, Frank Stegmeier, Micah Benson*, Karrie Wong. *KSQ Therapeutics, Cambridge, MA, USA*

Background Adoptive cell therapy with ex vivo expanded tumor infiltrating lymphocytes (TIL) offers a potentially curative treatment for cancer. To improve the clinical durability of TIL, we have developed KSQ-001, a CRISPR/Cas9 engineered TIL (eTIL) product with inactivation of *SOCS1* gene. *SOCS1* is a negative regulator of cytokine signaling in T cells that we previously identified as a top target restraining T cell in vivo anti-tumor function and long-term persistence in genome-wide in vivo CRISPR screens. The clinical manufacture of TIL has historically required a complex multi-step baseline process involving a pre-Rapid Expansion Protocol (pre-REP) followed by a Rapid Expansion Protocol (REP) with feeder cells. To simplify and shorten the manufacture of KSQ-001, we developed a next-generation ExPRESS manufacturing process involving fewer steps and eliminating the use of feeder cells. We demonstrated that ExPRESS can robustly manufacture KSQ-001 with high functional potency at clinical scale from tumor starting material in 21 days or less across multiple solid tumor types.

Methods Vially-cryopreserved-tumor-fragments (VCTF) from different solid tumor indications were used as starting materials for eTIL manufacture. T cells in the tumor fragments are activated to propagate for 7-11 days, after which TIL were electroporated with ribonucleoprotein (RNP) complexes containing the *SOCS1*-targeting guide RNA (gRNA). Following electroporation, TIL were further expanded for an additional 7-11 days prior to cryopreservation. The editing level, phenotypic characteristics, and functionality of KSQ-001 was assessed by NGS, flow cytometry, and in vitro functional assays.

Results KSQ-001 was successfully manufactured from 10/11 VCTF starting materials from melanoma and NSCLC samples to clinically relevant doses, demonstrating robust viability at the time of cryopreservation and following thaw. KSQ-001 manufactured using ExPRESS showed >90% editing of the *SOCS1* gene as well as complete knockdown of *SOCS1* protein in all donors tested. Importantly, KSQ-001 manufactured using ExPRESS exhibited heightened anti-tumor function when compared to un-engineered TIL, including increased production of IFN γ and anti-tumor potency in an in vitro TIL/tumor co-culture system. KSQ-001 also retained high diversity of the TCR repertoire and specificity for autologous tumor. Lastly, adoptively transferred eTIL showed enhanced persistence and anti-tumor efficacy in immunodeficient mouse tumor models.

Conclusions We describe a shortened and streamlined process for the manufacture of CRISPR/Cas9-edited eTIL. KSQ-001 can be manufactured at clinically relevant doses in 21 days or less and displays enhanced functional potency. These data support evaluating KSQ-001 manufactured by the ExPRESS process in the treatment of patients with metastatic treatment-refractory solid tumors.

<http://dx.doi.org/10.1136/jitc-2022-SITC2022.0255>

256 **IN VIVO EXPANSION OF ENDOGENOUS ANTIGEN-SPECIFIC CD8+ T CELLS USING ARTIFICIAL T-CELL STIMULATING MICROPARTICLES**

Natalie Livingston*, John Hickey, Hajin Sim, Hai-Quan Mao, Jonathan Schneck. *Johns Hopkins University, Baltimore, MD, USA*

Background T cell-based immunotherapies such as chimeric antigen receptor T cell therapy (CAR T), have seen some clinical success; however, these therapies are still currently limited to a select few cancer types and have price tags that further limit accessibility for patients. Here, we create a novel biomaterials-based platform for the *in vivo* activation of naïve, antigen-specific T cells, removing the need for expensive and lengthy *ex vivo* expansion steps.

Methods Thiol-modified HA is cross-linked with PEDGA in the presence of thiol-modified signals 1 (here, KbOVA) and 2 (anti CD28).¹ The cross-linked gel is passed through a mesh to form microparticles (MPs) (figure 1A). MPs are mixed with naïve B6 CD8+ T cells and injected subcutaneously into mice. Eight days after injection, target cells expressing OVA antigen are injected i.v. On day 9, mice are sacrificed and analyzed for enrichment of antigen-specific cells and killing of target cells. MPs were also tested therapeutic tumor model, in which MC-38 OVA tumor cells were injected on day 0 and naïve OT I CD8s plus MPs were injected on day 6.

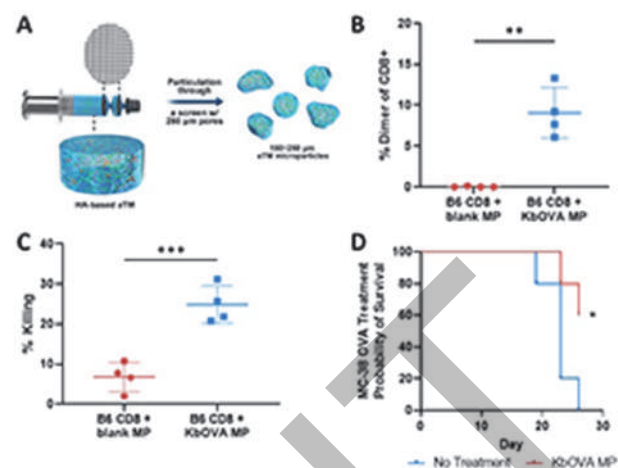
Results Nine days after co-injecting naïve B6 CD8+ T cells with KbOVA MPs, we can detect a significant enrichment of OVA-specific T cells via flow cytometry (figure 1B). Cells expanded *in vivo* showed significant and robust killing of target splenocytes (figure 1C). In the MC-38 OVA cancer treatment model, injection of naïve OT I CD8+ T cells with OVA MPs increased survival compared with naïve OT I CD8+ cells injected with blank MPs (figure 1D).

Conclusions We have developed an injectable, LN-mimicking MP platform that incorporates T-cell activation signals and critical ECM cues of the LN. These MPs are capable of expanding antigen-specific T cells from a fully endogenous B6 repertoire, and these cells are able to robustly kill target splenocytes as well as reduce tumor growth and extend survival in a therapeutic cancer model. Developing a system for the *in vivo* activation of antigen-specific T cells reduces both cost of T cell-based therapies as well as the time to treatment for patients.

Acknowledgements NKL is supported by the NSF GRFP and NIH F31 Fellowships.

REFERENCE

1. Hickey JW, Dong Y, Chung JW, Salathe SF, Pruitt HC, Li X, Chang C, Fraser AK, Bessell CA, Ewald AJ, Gerecht S, Mao H, Schneck JP. Engineering an Artificial T-Cell Stimulating Matrix for Immunotherapy. *Adv Mater.* 2019; Apr 10;1807359.



Abstract 256 Figure 1 (A) Schematic of the preparation of T cell-stimulating MPs. (B) Enrichment of OVA-specific T cells within the biomaterial site 9 days after injection. (C) In vivo killing of OVA-pulsed splenocytes after 9 days of in vivo expansion of OVA-specific T cells. (D) Survival plot after mice are injected with MC-38 OVA tumor cells on day 0 and naïve OT I CD8s plus MPs on day 6.

<http://dx.doi.org/10.1136/jitc-2022-SITC2022.0256>

257

AN OFF-THE-SHELF PERSONALIZED CELLULAR APPROACH TO IMMUNOTHERAPY FOR THE TREATMENT OF ADVANCED SOLID TUMORS

Miguel Lopez-Lago*, William Williams, Giuseppe del Priore, Sagarika Pachhal, Vikas Bhardwaj, Xiaoyi Zheng, Mingjin Chang, Charles Wiseman. *BriCell Therapeutics Corp., Philadelphia, PA, USA*

Background BriCell is developing off-the-shelf personalized cellular immunotherapies based on our most advanced lead candidate—SV-BR-1-GM, which is in Phase I/IIa clinical trial in patients with metastatic or locally recurrent breast cancer. SV-BR-1-GM is a breast cancer cell line with features of an antigen presenting cell (APC) which has been stably transfected with the CSF2 gene encoding GM-CSF (SV-BR1-GM). We have recently reported favorable clinical outcomes in patient populations that match SV-BR-1-GM at one or more HLA alleles. This clinical observation, together with the fact that SV-BR-1-GM cells can directly activate CD4+ T-cells in an antigen-specific HLA-restricted manner, as demonstrated by an in vitro antigen presentation assay,¹ lead us to hypothesize that SV-BR-1-GM can function as an APC. We propose a therapeutic approach in which a patient will be treated with a cell line expressing HLA class I and II molecules matched to their genotype. Also, to further enhance direct antigen presentation to T-cells, the parent SV-BR-1 cells were genetically modified to express co-stimulatory molecules and additional immune-modulatory cytokines.

Methods Using CRISPR/Cas9 technology we have inactivated several endogenous *HLA-A* and *HLA-DRB* alleles present in five cancer cell lines (SV-BR-1, PC-3, LNCaP, SK-MEL-24, and NCI-H2228). Cells with inactivated *HLA-A/DRB* genes were transduced with lentiviral based vectors expressing selected cytokines and costimulatory molecules (GM-CSF, INF α , CD80, CD86, IL-12, IL-7, HLA-DRA, and 4-1BBL). Next, unique combinations of *HLA-A* and *HLA-DRB3/4/5* alleles were transduced into the cells using lentiviral based vectors to generate a collection of cell lines that will match over 99% of the patient population for at least one HLA allele. Expression and functionality of the stimulatory molecules and transgenic HLA alleles was established using flow cytometry and cell-based assays.

Results Four cell lines (for each tumor type) that secreted GM-CSF, INF α , IL12, IL7 and expressed CD80, CD86, 4-1BBL, and different combinations of both Class I and Class II HLA alleles were selected. Using cell-based assays – including mixed lymphocyte reaction assays –, we demonstrated that the generated cells stimulate naïve T-cells.

Conclusions We have successfully generated “off the shelf” personalized cell-based therapeutic cancer vaccines that induce potent T-cell responses. These modified cancer cell lines will be used in clinical studies designed to first evaluate the safety of intradermal inoculation with the irradiated cells and later combined with other agents to augment the immune response.

REFERENCE

1. Lacher MD *et al*, *Front Immunol*. 2018; May 15;9:776

<http://dx.doi.org/10.1136/jitc-2022-SITC2022.0257>

258

INDUCTION OF TUMOR CELL AUTOSIS BY MYXOMA VIRUS-INFECTED CAR-T AND TCR-T CELLS TO OVERCOME PRIMARY AND ACQUIRED RESISTANCE IN SOLID TUMORS

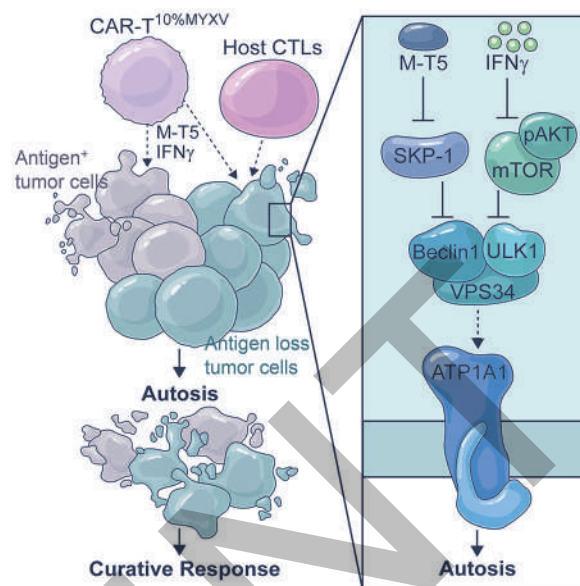
¹Yong Lu, ²Ningbo Zheng*. ¹Houston Methodist Research Institute/Weill Cornell Medicine, Houston, TX, USA; ²Wake Forest School of Medicine, Winston-Salem, NC, USA

Background Cytotoxicity of tumor-specific T cells requires tumor cell-to-T cell contact-dependent induction of classic tumor cell apoptosis and pyroptosis. However, such canonical mechanisms may not trigger sufficient primary responses of solid tumors to adoptive cell therapy (ACT) and prevent tumor antigen escape-mediated acquired resistance.

Methods One of the candidate oncolytic viruses is myxoma virus (MYXV), a DNA virus, which has a highly restricted host range and is only pathogenic to European rabbits (Stanford et al., 2007). In this study, we investigated the potential to exploit CAR-T and TCR-T cells as myxoma virus (MYXV)-delivery carrier cells by pre-infecting the T cells with MYXV *ex vivo* by a spin-infection protocol (CAR-T^{MYXV} and TCR-T^{MYXV}).

Results Here, we demonstrate that myxoma virus (MYXV)-infected tumor-specific T (T^{MYXV}) cells, expressing chimeric-antigen-receptor (CAR) or T-cell-receptor (TCR), which systemically deliver MYXV into solid tumors to overcome primary resistance. In addition to T cell-induced apoptosis and pyroptosis, tumor eradication by CAR/TCR-T^{MYXV} cells is also attributed to tumor cell autosis induction, a special cell death unleashed by this unexpected novel T-cell-cytotoxic machinery. Mechanistically, T cell-derived IFN- γ /AKT signaling synergizes with MYXV-induced M-T5/SKP-1/VPS34 signaling to trigger robust tumor cell autosis. Moreover, CAR/TCR-T^{MYXV}-elicited autosis also functions as a potent bystander killing to restrain antigen escape.

Conclusions Collectively, our results highlight a pivotal role of CAR-T^{10%MYXV} cells in improving the efficacy of ACT by: (1) delivering MYXV into tumor beds; (2) recognizing and inducing classic tumor cell apoptosis and pyroptosis to antigen-positive tumor cells accompanied by IFN γ secretion; (3) inducing autosis in antigen-positive and antigen-negative cancer cells; and (4) potentially eliminating ALV cells by autosis and adaptive antitumor immunity. Thus far, our data suggest the existence of a tumor cell autosis-triggering strategy dependent on both MYXV and antigen-programmed CAR-T cells, which strategically incorporates MYXV and tumor-specific T cells to overcome therapeutic resistance in solid tumors (figure 1).



Abstract 258 Figure 1 Graphical Abstract

- CAR-T^{MYXV} cells systemically deliver MYXV into cognate antigen-expressing tumors
- T cell-derived IFN γ synergizes with MYXV-derived M-T5 to trigger tumor cell autosis
- Autosis is a potent bystander killing to eradicate antigen-negative tumor cells
- CAR/TCR-T^{10%MYXV} induces autosis and adaptive immunity to restrain antigen escape

<http://dx.doi.org/10.1136/jitc-2022-SITC2022.0258>

259

IPSC-DERIVED NK CELLS ENGINEERED WITH A NOVEL TGF β SIGNAL REDIRECTOR RECEPTOR EXHIBIT ENHANCED PERFORMANCE AGAINST SOLID TUMORS

Eigen Peralta*, Dan Lu, Hui-Yi Chu, Justin Rahman, Diana Galvan, Amit Mehta, Eric Sung, Jeffrey Chen, Masanao Tsuda, Elena Demeester, Earl Avramis, Alec Witt, Tom Lee, Bob Valamehr. *Fate Therapeutics Inc., San Diego, CA, USA*

Background Transforming growth factor beta (TGF β) is an immuno-suppressive cytokine commonly present in the tumor microenvironment (TME) that creates considerable challenges for the treatment of solid tumors. Here we describe a unique strategy where induced pluripotent stem cell (iPSC)-derived NK (iNK) and T (iT) cells engineered to express a chimeric TGF β signal redirector receptor (TGF β -SRR) block the TGF β -mediated repressive signaling and redirect the signal to potentiate effector cell function and improve cell fitness.

Methods To identify iNK cell-specific pathways for TGF β signal redirection, candidate cytokines were tested for their ability to mitigate suppression of iNK cell anti-tumor activity in the presence of recombinant TGF β . Next, we developed TGF β -SRR constructs where selected cytokine endodomains were fused to TGFBR2 ectodomain. TGF β -SRR constructs were then engineered into iPSCs and differentiated into iNK cells. Phospho-flow for pSMAD2/3 was used to test for blockade of TGF β signaling in recombinant TGF β -treated cells. Antibody-dependent cellular cytotoxicity (ADCC) from TGF β -SRR iNK cells was tested in co-cultures with SKOV-3, PC3, and MDA-MB-231 targets, then measured using xCELLigence readout. Innate killing mechanism was tested via serial restimulation assay with Raji targets and measured by flow cytometry. Co-cultures were performed in the presence of recombinant TGF β .

Results Engineered iPSCs expressing candidate TGF β -SRR constructs were successfully differentiated into iNK cells (>95% CD56+), uniformly expressing TGF β -SRR transgene (TGF β -SRR; >95% positive). Analysis for pSMAD2/3 in recombinant TGF β -treated cells showed 95% reduction of SMAD2/3 phosphorylation in top performing TGF β -SRR motif, indicating successful blockade of TGF β signaling. Evaluation of ADCC toward multiple solid tumor lines and using various monoclonal antibodies (Herceptin, Cetuximab, and Avelumab) showed superiority of TGF β -SRR iNK cells (>80% cytotoxicity) over parental iNK cell control (<40% cytotoxicity) in the presence of recombinant TGF β . Innate killing mechanism was tested in the serial restimulation assay, where TGF β -SRR iNK cells expanded 3.5-fold over parental iNK cells after the first round of co-culture. Notably, the TGF β -SRR iNK cells exhibited enhanced functional persistence, completely controlling tumor growth through three rounds of co-culture despite the addition of suppressive quantities of recombinant TGF β , unlike parental iNK cells which failed to control tumor growth after the first round.

Conclusions Collectively, the data illustrate that a customized TGF β -SRR construct can redirect TGF β -mediated suppression and potentiate effector cell function to enhance the anti-tumor activity of iNK cells. This novel synthetic receptor represents an innovative strategy to enable adoptively-transferred cell therapy to overcome the immunosuppressive TME for the successful treatment of bulky tumors.

<http://dx.doi.org/10.1136/jitc-2022-SITC2022.0259>

260

INVESTIGATING CANCER CELL AUTONOMOUS CAR T CELL THERAPY RESISTANCE IN DLBCL *IN VITRO*

Fabiana Lueoend*, Youngchul Song, Beverly Nguyen, Xiaoyan Li, Andreas Raue, Jennifer Brogdon, Glenn Dranoff, Matthew Niederst, Louise Treanor. *Novartis Institutes for Biomedical Research, Cambridge, MA, USA*

Background CD19 CAR T cell therapy has greatly improved the outcome of r/r DLBCL patients, but durable responses are achieved in only 40% of cases. Relapses can be due to declining T cell fitness and/or cancer cells becoming inherently refractory. However, besides antigen loss, cancer cell autonomous resistance mechanisms are poorly understood.

Methods We generated DLBCL cell lines that are refractory to CD19 targeting CAR T cells by longterm co-culture *in vitro*. We assessed response to alternative CAR T cells targeting other antigens and performed RNAseq of resistant cancer cell lines to identify yet unknown resistance mechanisms.

Results Our *in vitro* longterm co-cultures recapitulate common resistance mechanisms observed in the clinics including CD19 loss. Interestingly, we do observe CD19 positive resistance and multiple of our CD19 CAR T cell resistant cell lines had become less sensitive also to alternative CAR T cells. Moreover, our RNAseq data indicate that the majority of transcriptional changes are associated with a common resistant phenotype rather than a specific resistance mechanism (e.g., antigen loss).

Conclusions Our results suggest that besides CD19 loss, DLBCL cells evolve mechanisms to overcome T cell killing which may render them cross-resistant to CAR T cells targeting other antigens. Analysis of our RNAseq data will allow us to characterize these mechanisms.

<http://dx.doi.org/10.1136/jitc-2022-SITC2022.0260>

261 EVIDENCE FOR DURABLE ANTI-TUMOR RESPONSES BY TAC-T CELLS IN PRECLINICAL MODELS OF SOLID TUMORS

¹Heather MacGregor*, ²Duane Moogk, ¹Stacey Xu, ²Joanne Hammill, ¹Philbert Ip, ¹Ling Wang, ¹Swati Shetty, ¹Kyle MacDonald, ¹Laura Shaver, ¹Sailaja Pirati, ¹Prabha Lal, ¹Christopher Helsen, ^{1,2}Jonathan Bramson, ¹Sadhak Sengupta, ¹Andreas Bader. ¹Triumvira Immunologics Inc., Hamilton, ON, Canada; ²McMaster University, Hamilton, ON, Canada

Background T cell antigen coupler (TAC) is a chimeric receptor that redirects T cells (TAC-T) towards surface-expressed tumor antigens to create safe and durable anti-cancer immune responses. The TAC activates T cells by co-opting the endogenous T cell receptor machinery via a CD3 ϵ -specific binding motif and a cytoplasmic co-receptor tail. TAC01-HER2, a first-in-class TAC-T product targeting HER2 (ERBB2), has entered a phase I/II clinical trial. Here, we have characterized the fate of TAC-T cells during anti-tumor responses *in vitro* and *in vivo*.

Methods *In vitro*, HER2-specific TAC-T products were challenged with HER2-expressing and HER2-negative tumors. Kinetics of proliferation, degranulation, activation, differentiation, and memory generation was assessed by flow cytometry. TAC-T products were subjected to multiple rounds of tumor cell exposure *in vitro* to test the durability of the T-cell-mediated immune response. Bioinformatic clustering analysis of flow cytometry data was performed to identify T cell populations and track them over time.

T cell expansion in blood, tumor, bone marrow, and spleen were evaluated *in vivo* after primary xenograft tumor treatment and secondary tumor rechallenge. Tumor- and spleen-infiltrating or circulating T cells were phenotyped by flow cytometry after treatment with TAC-T cells.

Results Co-culture studies revealed that TAC-T products become rapidly activated and degranulate upon contact with HER2-expressing, but not HER2-negative, cell lines. Activation coincided with rapid downregulation of the TAC receptor. A large proportion of the T cells expressed activation markers, and a majority of these also expressed degranulation markers, indicating ongoing cytotoxicity. *In vitro* and *in vivo* studies demonstrated a CD8-biased response characterized by a considerable expansion in the activated CD8 population enriched at the tumor site. Later, activation and differentiation markers returned to baseline concurrently with the re-emergence of surface TAC expression, initiating T cell proliferation. Importantly, central memory T cells were expanded, and stem-like cells were maintained, suggesting strong self-renewal potential. *In vitro* serial cytotoxicity assays showed that TAC-T products could repeatedly kill tumor cells up to several rounds. In tumor rechallenge experiments, a single dose of TAC-T cells expanded to clear solid tumor xenografts and protected mice from a second tumor challenge 30 days post initial tumor clearance, indicating long-lasting T cell persistence.

Conclusions The TAC-T product mounts an effective anti-tumor response in multiple preclinical models, comprising activated TAC-T cells that do not become terminally exhausted but are dominated by an activated CD8 response and supported by the expansion of a memory population, indicating robust self-renewal capacity.

Ethics Approval Animal studies were approved by McMaster University's Animal Research Ethics Board under AUP 20-10-37.

<http://dx.doi.org/10.1136/jitc-2022-SITC2022.0261>

262

MULTIPLE TARGETING OF SOLID TUMORS WITH iPSC-DERIVED GAMMA DELTA CAR T CELLS IN COMBINATION WITH THERAPEUTIC ANTIBODIES

Hillary Millar Quinn*, Justin Bianchini, Liam Campion, Katherine Santostefano, Toshinobu Nishimura, Sydney Bucher, Buddha Gurung, Shelby Keating, Rebecca Genovese, Steven DeLuca, Bruno Bonanno, David Walker, Marilda Beqiri, Chris Dower, Kaitlin Idank, Tomas Aramburu, Michael Naso, Luis Borges, Mark Wallet. *Century Therapeutics, Philadelphia, PA, USA*

Background CAR-T cell therapies have proven safe and efficacious for hematologic malignancies, but there remains a significant unmet need for effective cell therapy options for solid tumors. CAR-engineered induced pluripotent stem cell (iPSC)-derived effector cells allow for the treatment of cancer as an off-the-shelf allogeneic cell therapy. Gamma delta ($\gamma\delta$) T cells exhibit the cytolytic features of conventional alpha beta ($\alpha\beta$) CD8⁺ T cells with additional capabilities for innate recognition of tumors. For example, expression of CD16 on $\gamma\delta$ T cells can mediate antibody-dependent cellular cytotoxicity (ADCC) against tumors. Here we describe development of an iPSC-derived CAR $\gamma\delta$ T cell platform which can target solid tumors through both CAR-mediated recognition and ADCC when combined with a therapeutic antibody.

Methods Primary $\gamma\delta$ T cells were enriched and expanded in culture to enable reprogramming to iPSCs by delivery of pluripotency genes. These T cell derived iPSCs (TiPSCs) were used to produce $\gamma\delta$ T cells using a proprietary differentiation process. The TiPSC line was engineered with a CAR targeting EGFR and a membrane bound form of IL-15 to enhance T cell persistence. Tumor spheroids were generated from EGFR⁺Her-2⁺ SKOV-3 ovarian tumor cells. Cytolysis of spheroids was evaluated using CAR-T cells alone or in combination with anti-HER2 antibody (trastuzumab).

Results Batches of CAR-T cells were generated using a proprietary differentiation process yielding >90% pure CAR⁺ $\gamma\delta$ T cells. The TiPSCs contained the rearranged $\gamma\delta$ TCR gene and upon differentiation to T cells, uniformly expressed a V γ 9V δ 2 TCR and expressed high levels of CD16. CAR $\gamma\delta$ T cells were effective in killing SKOV-3 spheroids. When cultured with SKOV-3 spheroids in an ADCC assay, CAR $\gamma\delta$ T cells exhibited enhanced cytotoxicity in the presence of trastuzumab but not isotype control antibody. Activity of the $\gamma\delta$ T cells was not reliant on additional exogenous cytokine due to the engineered form of membrane-associated IL-15.

Conclusions We have demonstrated that iPSC-derived $\gamma\delta$ T cells mediate anti-tumor activity in human solid tumor models through multiple pathways. The combination of two modes of tumor recognition (CAR and CD16/antibody) enabled more potent killing of solid tumor spheroids. The ability to manufacture large batches of iPSC derived CAR $\gamma\delta$ T cells will enable a true off-the-shelf allogeneic cell therapy for solid tumors.

<http://dx.doi.org/10.1136/jitc-2022-SITC2022.0262>

Abstracts

263

A2B694, AN AUTOLOGOUS LOGIC-GATED CELL THERAPY TARGETING MESOTHELIN

¹Julian Molina, ²Talar Tokatlian*, ²Jason Wang, ²Shruti Sharma, ²Diane Manry, ²Martin Naradikian, ²Grace Asuelime, ²Breanna DiAndreth, ²Aaron Winters, ²Tisha San Miguel, ²Armen Mardiros, ³Sandip Patel, ⁴Edward Garon, ⁵Diane Simeone, ⁶Scott Kopetz, ⁶Maria Pia Morelli, ⁵Theodore Welling, ⁷Mitesh Borad, ⁸Kedar Kirtane, ²Eric Ng, ²John Welch, ⁹David Maloney, ²William Go, ¹⁰Alexander Kamb, ²Agi Hamburger, ⁴J Randolph Hecht. ¹Mayo Clinic, Rochester, MN, USA; ²A2 Biotherapeutics, Inc., Agoura Hills, CA, USA; ³University of California San Diego, La Jolla, CA, USA; ⁴University of California at Los Angeles, Los Angeles, CA, USA; ⁵New York University Langone Health, New York, NY, USA; ⁶University of Texas MD Anderson Cancer, Houston, TX, USA; ⁷Mayo Clinic Cancer Center, Scottsdale, AZ, USA; ⁸H. Lee Moffitt Cancer Center, Tampa, FL, USA; ⁹Fred Hutchinson Cancer Research Center, Seattle, WA, USA; ¹⁰A2 Biotherapeutics, Inc., Westlake Village, CA, USA

Background Mesothelin (MSLN) is expressed on a variety of solid tumors, including mesothelioma and ovarian, uterine, gastric, pancreatic, and lung cancers.¹ However, efforts to target MSLN using cellular therapies have been hampered by severe on-target, off-tumor toxicities associated with damage to normal tissues expressing MSLN.² To avoid these toxicities, we have developed a logic-gated engineered cell therapy, Tmod™, which is composed of two chimeric antigen receptors (CARs): an activator that targets a tumor-associated antigen and an inhibitory receptor (blocker) gated by an antigen expressed on normal tissue but lost in tumor cells due to loss of heterozygosity (LOH). A2B694 is an MSLN-specific Tmod construct combining a third-generation MSLN CAR with an LIR-1-based inhibitory receptor specific for human leukocyte antigen A*02 (HLA-A*02).

Methods Lentivirus encoding i) the CAR, ii) the blocker, and iii) an shRNA targeting $\beta 2M$ was used to transduce T cells from HLA-A*02 donors and generate MSLN Tmod cells. In vitro cytotoxicity measurements were performed using fluorescence-based imaging and luciferase readouts. In vivo assessments were performed in NSG mice subcutaneously implanted with “normal” cells (MSLN[+]A*02[+]), or tumor cells (MSLN[+]A*02[-]), in the left and right flanks, respectively. Following engraftment, mice were randomized and treated intravenously with MSLN Tmod cells or controls. Grafts were measured via caliper.

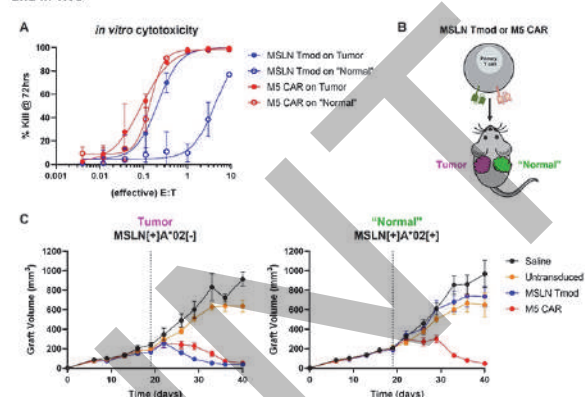
Results MSLN Tmod cells preferentially killed tumor cells (MSLN[+]A*02[-]) over “normal” cells (MSLN[+]A*02[+]) in vitro, unlike clinically active comparator M5 CAR T cells, which indiscriminately killed both target cell types (figure 1A). Soluble MSLN, tested across a 0-2 $\mu\text{g}/\text{mL}$ range, did not impact MSLN Tmod function. Additionally, in mixed cell cultures where T cells and tumor and “normal” cells were simultaneously cultured (1:1:1 ratio), MSLN Tmod cells selectively killed tumor targets while sparing “normal” cells. Further, MSLN Tmod cells cycled between activated and blocked states in vitro when repeatedly challenged with tumor or “normal” target cells. Finally, while MSLN CAR T cells killed both “normal” and tumor grafts in vivo, MSLN Tmod cells selectively killed tumor grafts while sparing “normal” grafts (figure 1B, C).

Conclusions A2B694 is an autologous MSLN Tmod cell product that leverages LOH at the HLA locus in cancer cells, providing a mechanism to discriminate between normal and tumor cells. BASECAMP-1 (NCT04981119), an observational study that will identify patients with somatic HLA LOH, is currently recruiting. Eligible patients with metastatic colorectal, pancreatic, or non-small cell lung cancer will be apheresed for a future A2B694 interventional study (EVEREST-2).

REFERENCES

- Hassan R *et al.* Mesothelin immunotherapy for cancer: Ready for prime time? *J Clin Oncol.* 2016;**34**(34):4171-4179.
- Tanyi JL *et al.* Phase I study of autologous T cells bearing fully-humanized chimeric antigen receptors targeting mesothelin in mesothelin-expressing cancers. Presented at: Cellicon Valley '21: The Future of Cell and Gene Therapies; May 6-7, 2021; virtual symposium.

Figure 1. MSLN Tmod demonstrates selective killing of tumor vs “normal” cells in vitro and in vivo



(A) MSLN Tmod and M5 CAR killing of MSLN[+]A*02(-)luciferase(+) tumor and MSLN[+]A*02(+)luciferase(+) “normal” MS751 target cells at various E:T. Cytotoxicity was measured 72 hours after co-culture via luminescence. Data shown are for a representative donor. (B) Schematic diagram of the dual-flank tumor and “normal” MS751 xenograft model. (C) Graft sizes assessed via caliper. Left: MSLN Tmod cells kill tumor cells equivalently to M5 CAR cells. Right: M5 CAR cells kill while MSLN Tmod cells spare “normal” cells. Data shown are mean \pm SEM (n=10 animals per group).

CAR, chimeric antigen receptor; E:T, effector-to-target ratio; MSLN, mesothelin; SEM, standard error of the mean.

Abstract 263 Figure 1

<http://dx.doi.org/10.1136/jitc-2022-SITC2022.0263>

264

ALLOGENEIC NATURAL KILLER CELLS ENGINEERED TO EXPRESS HER2-DIRECTED CAR, INTERLEUKIN-15 AND TGF β DOMINANT NEGATIVE RECEPTOR EFFECTIVELY CONTROL HER2+ TUMORS

<http://dx.doi.org/10.1136/jitc-2022-SITC2022.0264>

Finola Moore*, Andres Alvarez, Alexia Barandiaran, Luke Barron, Eugene Choi, Krista Daniel, Charlotte Franco, Bashar Hamza, Jennifer Johnson, Annie Khamhoung, Marilyn Marques, Henry Moreno, Angela Nunez, Dominic Picarella Jared Sewell, Alex Storer, Meghan Walsh, Finola Moore, Vipin Suri. *Catamaran Bio, Boston, MA, USA*

Background The remarkable clinical responses of chimeric antigen receptor (CAR)-engineered immune cell therapies in hematological malignancies have not been replicated in solid tumors. Engineered, off-the-shelf, allogeneic natural killer (NK) cells are particularly attractive as a chassis for effective cell therapies for solid tumors given their clinical safety, efficacy, and ability to reduce tumor escape through inherent multimodal recognition of tumor cells.

We describe here preclinical efficacy and pharmacodynamics of CAT-179, a novel CAR-NK cell therapy, in multiple models of HER2-amplified ovarian and gastric cancer. CAT-179 cells are engineered to express three transgenes: a HER2-directed CAR to effectively target tumor cells, a transforming growth factor β (TGF β) dominant negative receptor (DNR) for resistance to TGF β -mediated immune suppression in the tumor microenvironment, and interleukin-15 (IL15) to enhance NK cell persistence and activity for durable response.

Methods PBMC-derived NK cells were engineered with a tricistronic construct expressing HER2-directed CAR, TGF β DNR, and IL15 under the control of a MND promoter using TcBuster™ transposase. CAT-179 activity was assessed in vitro by quantifying cytotoxicity and cytokine production upon coculture with HER2-expressing cell lines. TGF β DNR activity was assayed by quantifying TGF β -induced SMAD phosphorylation and DNAM1 receptor expression. In vivo persistence and anti-tumor efficacy was evaluated in NSG mice. Anti-tumor efficacy was tested against luciferase-engineered SKOV-3 ovarian cancer cells (SKOV-3-luc) and N87 gastric carcinoma xenografts.

Results CAT-179 demonstrates both CAR-dependent and innate NK receptor-dependent tumor cell killing in vitro, reducing the likelihood of tumor escape through antigen loss. CAT-179 demonstrated high CAR-dependent cytotoxicity as well as TNF α and IFN γ production when co-incubated with multiple HER2-expressing cell lines. Engineered NK cells demonstrated 75% reduction (relative to control NK cells) in TGF β -induced SMAD2 phosphorylation, prevented TGF β -induced downregulation of NK cell activating receptors, and restored NK cell cytotoxic activity. Furthermore, TGF β DNR protected bystander cells from TGF β -induced phenotypic changes. After a single IV dose, CAT-179 cells persisted for more than two months and retained cytotoxic activity. CAT-179 effectively reduced SKOV-3-luc tumor burden in NSG mice (95% AUC, $p < 0.0001$ for survival).

Conclusions CAT-179 is a promising demonstration of the Catamaran CAR-NK platform, as a novel off-the-shelf cell therapy to overcome the challenges associated with solid tumors.

Acknowledgements We would like to acknowledge the contribution of Tucker Ezell, Taeyoon Kyung, and Celeste Richardson to this work.

Ethics Approval We confirm that legal and ethical requirements have been met with regards to the humane treatment of mice described in this work, according to regulations within IACUC.

265

EMPOWERING iPSC-DERIVED iNK CELLS WITH MULTIPLE GENE EDITS TO IMPROVE PERSISTENCE AND ANTI-TUMOR EFFICACY

Buddha Gurung*, Annalise Jethon, Maisha Harris, Shelby Keating, Spencer Moros, Rebecca Genovese, Steven DeLuca, Arden Edgerton, Nicholas Alexander, Chiamin Bullaughey, Barry Morse, Liam Campion, Mark Mendonca, Kaitlin Idank, Hillary J, Millar Quinn, Diana Chin, Jill Carton, Michael Naso, Mark Wallet, Luis Borges. *Century Therapeutics, Chalfont, PA, United States*

Background A unique attribute of iPSCs is the ability to perform sequential gene edits thus enabling development of highly engineered cell therapies. Here, we describe our next generation platform for iPSC-derived NK cells (iNK cells) that include genetic enhancements for improved allo-evasion, cell fitness, tumor targeting, in vivo imaging, and safety. By adopting a common progenitor strategy, an engineered iPSC master cell bank will be used as the starting point for future therapies across diverse indications.

Methods Clinical grade iPSC lines were engineered using Mad7 CRISPR endonuclease. $\beta 2$ microglobulin was disrupted and a bicistronic transgene encoding both HLA-E and HLA-G was inserted. The gene encoding CIITA was disrupted and a bicistronic transgene encoding HSV-TK and PSMA ectodomain was inserted. A transgene encoding IL-15/IL-15Ra was delivered into the NKG2A locus, and a bicistronic transgene encoding CD16 and NKG2D was delivered into the CD70 locus.

Results iNK cells exhibited uniform expression of each transgene. Functional studies demonstrated that HLA-E/G enabled evasion of allogenic NK cells; IL-15/IL-15RA enhanced persistence of iNK cells both in vitro and in vivo; PSMA expression on the cell surface was confirmed through binding of a PSMA-specific fluorescent tracer; HSV-TK enabled the elimination of iNK cells in culture in the presence of ganciclovir; NKG2D enhanced elimination of tumor lines expressing the stress ligands MICA/MICB; and high-affinity CD16 enabled ADCC-mediated killing of CD20-expressing target cells in the presence of rituximab. HLA-A/B/C, HLA-DR/DP/DQ, NKG2A, and CD70 were absent from iNK cells.

Conclusions A clonal iPSC line was derived with eleven total genetic modifications to improve allogeneic cell therapy for cancer. Future iNK cell therapies will be derived from the common progenitor by addition of a CAR(s) for indication-specific tumor targeting.

<http://dx.doi.org/10.1136/jitc-2022-SITC2022.0265>

266

STING ACTIVATION IMPROVES T CELL ENGAGING IMMUNOTHERAPY OF ACUTE MYELOID LEUKEMIA

¹Daniel Nixdorf*, ²Andreas Linder, ²Niklas Kuhl, ¹TengTeng Xu, ³Roman Kischel, ¹Veit Bücklein, ²Thomas Carell, ²Veit Hornung, ¹Marion Subklewe med. ¹University Hospital LMU, Munich, Germany; ²LMU, Munich, Germany; ³AMGEN Research Munich GmbH, Munich, Germany

Background The treatment landscape for Acute myeloid leukemia (AML) patients has changed dramatically in recent years, however the majority of patients will eventually relapse. Allogeneic stem cell transplantation has proven the power of T-cells in eradicating residual leukemic cells, but alternative strategies based on T-cell recruiting bispecifics have failed to replicate these responses. Resistance is mediated by the immunosuppressive tumor-microenvironment and secretion of immune dampening metabolites by AML cells. We hypothesized that combining the CD33 BiTE construct AMG 330 with a cGAS-STING agonist has the potential to reverse immunosuppressive mechanisms and augment anti-leukemic activity.

Methods *In vitro* co-culture assays of human T-cells and AML cell lines were performed to study the effect of AMG 330 in combination with the STING-agonist cGAMP. Cytotoxicity, degranulation, and cytokine secretion were assessed by flow-cytometry. Transcriptomic analysis and systematic CRISPRCas9 knockout-studies were conducted.

Results We observed markedly increased target cell lysis upon simultaneous addition of cGAMP and AMG 330. Notably the cGAMP-dependent enhancement of AML cell lysis increased over time and was most pronounced at low effector-to-target ratio. Moreover, cGAMP improved AMG 330 mediated killing of primary AML cells. We noted increased T-cell degranulation, as well as increased T-cell intrinsic levels of Granzyme B and IFN γ in the presence of cGAMP. In addition, we observed a strong increase in inflammatory cytokine (IFN γ , TNF α , IL-4) secretion.

RNA-sequencing of AMG 330 and cGAMP stimulated target (HL-60) and effector cells revealed type-I-IFN signatures in both cell types, while HL-60 cells also displayed a signature of IFN γ signaling. We observed a distinct activated T-cell phenotype with markedly increased TNF α , IFN γ and GZMB expression induced by the co-treatment.

Knockout-studies revealed that the enhanced phenotype was fully dependent on target cell intrinsic STING/IRF3 signaling and functional IFN γ /TNF α signaling. Increased T-cell mediated IFN γ production upon combinatory treatment was also dependent on functional target cell STING and IFN γ /TNF α signaling, implying a crosstalk between effector and target cells. Most notably, the effector cytokines IFN γ and TNF α in turn boosted the expression of ISGs, as well as the secretion of type-I-interferons (IFN α , IFN β) by HL-60 cells in the presence of cGAMP.

Conclusions We propose a novel mechanism by which AMG 330-activated T-cells prime and sensitize AML target cells in a forward feedback loop towards STING activation, leading to increased type-I-IFN production. This leads to pronounced expression of effector cytokines and an overall cytotoxic T-cell phenotype, contributing to the beneficial effect of cGAMP in enhancing BiTE construct-mediated lysis.

Ethics Approval Peripheral blood or bone marrow samples were collected from healthy donors and patients with acute myeloid leukemia at initial diagnosis, relapse, or complete remission after written informed consent was received in accordance with the Declaration of Helsinki and approval was

granted by the Institutional Review Board of the Ludwig-Maximilian-Universität (Munich, Germany, reference number: 216-08).

<http://dx.doi.org/10.1136/jitc-2022-SITC2022.0266>

MRNAS ENCODING IL-12 AND A DECOY-RESISTANT VARIANT OF IL-18 SYNERGIZE TO ENGINEER T CELLS FOR EFFICACIOUS INTRATUMORAL ADOPTIVE IMMUNOTHERAPY

¹Irene Olivera*, ¹Elixabet Bolanos, ¹Jose González-Gomariz, ¹Sandra Hervas-Stubbs, ²Karina V Mariño, ¹Carlos Luri-Rey, ¹Iñaki Etxeberria, ¹Assunta Cirella, ¹Josune Egea, ¹Javier Glez-Vaz, ¹Saray Garasa, ¹Maite Alvarez, ¹Iñaki Eguren-Santamaria, ³Sonia Guedan, ¹Miguel F Sanmamed, ¹Pedro Berraondo, ²Gabriel Rabinovich, ¹Alvaro Teixeira, ¹Ignacio Melero. ¹Center for Applied Medical Research (CIMA), Pamplona, Spain; ²IBYME, Buenos Aires, Argentina; ³IDIBAPS, Barcelona, Spain

Background Interleukin-12 (IL-12) is a potent immunotherapeutic cytokine in mouse models which application as a systemic agent in the clinical setting is hampered by IFN γ -dependent toxicity.¹ Engineering T cells with IL-12 is highly efficacious in mouse models² but has resulted in serious adverse events in clinical settings.³ On the other hand, IL-18 is a myeloid-derived cytokine that elicits IFN- γ expression on T and NK lymphocytes.⁴

IL-12 and IL-18 are known to synergize in terms of eliciting massive IFN γ production.⁵ For cancer immunotherapy, IL-18 has the caveat of being down-regulated in its function by a decoy receptor termed IL-18BP,⁶ which is reportedly abundant in tumor tissues.^{7,8} Recently, a mutant sequence of mouse IL-18 termed DRIL18 which preserves its bioactivity but lacks binding to IL-18BP has been reported to exert T-cell-dependent antitumor activity upon systemic delivery.⁷

We previously reported that transient engineering of tumor-specific CD8 T cells with IL-12 mRNA enhanced their systemic therapeutic efficacy when delivered intratumorally.⁹ In this study, we sought to improve the therapeutic strategy of intratumoral delivery of T cells transiently engineered to express IL-12 with IL-18 mRNA electroporation.

Methods We mixed CD8⁺ T cells (TCR transgenic, TILs and CAR-T) engineered with mRNAs to transiently express either single-chain IL-12 (scIL-12) or an IL-18 decoy-resistant variant (DRIL18) that is not functionally hampered by IL-18BP. CD8⁺ T cells were injected repeatedly into mouse tumors for antitumor efficacy experiments. RNA-seq was performed to assess the functional changes induced after mRNA electroporation. Additionally, T-cell metabolic modifications and glycosylation profile functional changes were analyzed using Seahorse and cell adhesion assays.

Results Pmel-1 TCR-transgenic T cells electroporated with scIL-12 or DRIL18 mRNAs exerted powerful therapeutic effects in local and distant melanoma lesions. These effects were associated with T-cell metabolic fitness, enhanced miR-155 control of immunosuppressive target genes, enhanced expression of various cytokines and unique changes in the glycosylation profile of surface proteins, enabling enhanced adhesiveness to E-selectin. Efficacy of this intratumoral immunotherapeutic strategy was recapitulated using other clinically relevant adoptive T cell therapies as tumor-infiltrating lymphocytes (TILs) and CAR T cells upon IL-12 and DRIL18 mRNA electroporation.

Conclusions We report on a substantial improvement of adoptive T-cell therapies strategy based on mRNA transient gene-transfer and repeated intratumoral delivery. The synergistic immunobiology of IL-12 and IL-18, best represented in the form of DRIL18, holds promise for efficacious outcomes in the treatment of metastatic cancer patients.

Acknowledgements This project has been supported by MINECO SAF2017-83267-C2-1-R and PID2020-112892RB-I00 (AEI/FEDER, UE), by Instituto de Salud Carlos III (PI19/

01128), by the I-ON network supported by Bristol Myers Squibb to I.M. and cofinanced by Fondos FEDER "A way to make Europe". This project has received funding from the European Union's Horizon 2020 research and innovation program (grant agreement n° 945393- T2EVOLVE) and (Marie-Sklodowska-Curie grant agreement n° 765394), Fundación de la Asociación Española Contra el Cáncer (AECC) GCB15152947MELE, Fundación La Caixa and Fundación BBVA, Gobierno de Navarra Salud, Gobierno de Navarra Proyecto LINTERNA Ref: 0011-1411-2020-000075, Mark Foundation, Fundación BBVA and Fundación Olga Torres

REFERENCES

1. Del Vecchio M, Bajetta E, Canova S, Lotze MT, Wesa A, Parmiani G, et al. Interleukin-12: Biological Properties and Clinical Application. *Clinical Cancer Research. American Association for Cancer Research*; 2007;**13**:4677–85.
2. Kerker SP, Goldszmid RS, Muranski P, Chinnasamy D, Yu Z, Reger RN, et al. IL-12 triggers a programmatic change in dysfunctional myeloid-derived cells within mouse tumors. *Journal of Clinical Investigation. American Society for Clinical Investigation*; 2011;**121**:4746–57.
3. Zhang L, Morgan RA, Beane JD, Zheng Z, Dudley ME, Kassim SH, et al. Tumor-Infiltrating Lymphocytes Genetically Engineered with an Inducible Gene Encoding Interleukin-12 for the Immunotherapy of Metastatic Melanoma. *Clinical Cancer Research. American Association for Cancer Research Inc.*; 2015;**21**:2278–88.
4. Novick D, Kim S, Kaplanski G, Dinarello CA. Interleukin-18, more than a Th1 cytokine. *Seminars in Immunology. Academic Press*; 2013;**25**:439–48.
5. Chaix J, Tessmer MS, Hoebe K, Fuséri N, Ryffel B, Dalod M, et al. Cutting Edge: Priming of NK Cells by IL-18. *The Journal of Immunology. American Association of Immunologists*; 2008;**181**:1627–31.
6. Detry S, Andries J, Bloch Y, Gabay C, Clancy DM, Savvides SN. Structural basis of human IL-18 sequestration by the decoy receptor IL-18 binding protein in inflammation and tumor immunity. *Journal of Biological Chemistry. Elsevier*; 2022;**298**:101908.
7. Zhou T, Damsky W, Weizman O-E, McGeary MK, Hartmann KP, Rosen CE, et al. IL-18BP is a secreted immune checkpoint and barrier to IL-18 immunotherapy. *Nature. Nature Publishing Group*; 2020;**583**:609–14.
8. Carbotti G, Barisione G, Orengo AM, Brizzolara A, Airolidi I, Bagnoli M, et al. The IL-18 Antagonist IL-18-Binding Protein Is Produced in the Human Ovarian Cancer Microenvironment. *Clinical Cancer Research. American Association for Cancer Research*; 2013;**19**:4611–20.
9. Etxeberria I, Bolaños E, Quetglas JI, Gros A, Villanueva A, Palomero J, et al. Intratumor Adoptive Transfer of IL-12 mRNA Transiently Engineered Antitumor CD8⁺ T Cells. *Cancer Cell. Cell Press*; 2019;**36**:613-629.e7.

<http://dx.doi.org/10.1136/jitc-2022-SITC2022.0267>

268

HARNESSING CD39 FOR THE TREATMENT OF COLORECTAL CANCER AND LIVER METASTASES BY ENGINEERED T CELLS

Alessia Potenza*, Chiara Bonini, Chiara Balestrieri, Luca Albarello, Federica Pedica, Martina Spiga, Francesco Manfredi, Beatrice Cianciotti, Claudia De Lalla, Lorena Stasi, Elena Tassi, Silvia Bonfiglio, Giulia Scotti, Miriam Redegalli, Donatella Biancolini, Danilo Abbati, Fabio Simeoni, Dejan Lazarevic, Ugo Elmore, Guido Fiorentini, Giulia Di Lullo, Giulia Casorati, Paolo Dellabona, Claudio Doglioni, Giovanni Tonon, Riccardo Rosati, Luca Aldrighetti, Eliana Ruggiero. *IRCCS San Raffaele Scientific Institute, Milan, Italy*

Background Colorectal cancer (CRC) is the 2nd cause of cancer-related death. Despite standard therapies, more than 50% of patients experience relapse, eventually with metastatic disease. Colorectal tumours are densely infiltrated by immune cells that have a role in surveillance and modulation of tumour progression, correlating with an improved overall survival. However, exhaustion mechanisms acting within the tumour microenvironment impede their functional capacity against tumour cells.

Methods We paired high-dimensional flow cytometry, RNA sequencing, immunohistochemistry and immunofluorescence to describe the T cell functional landscape in tumour and peritumoral tissues from primary colorectal cancers and liver metastases. By CRISPR/Cas9 genome engineering techniques, we redirected the specificity of T cells towards a tumor-specific antigen while disrupting inhibitory molecules, to counteract the immune-suppressive tumor microenvironment.

Results Analysis of the healthy, peritumoral and neoplastic tissues of treatment-naïve primary CRCs and of the peritumoral and tumoral tissues of CRC patients undergoing surgery for liver metastases revealed extensive transcriptional and spatial remodeling across tumors, being metabolic pathways among the major drivers of this variance. Regarding the immune infiltrate, we found that T cells are mainly localized at the front edge and that tumour-infiltrating T cells co-express multiple inhibitory receptors. Unsupervised analysis of flow cytometry data performed by an advanced pipeline of data handling by dimensionality reduction and clustering algorithms allowed the definition of a peculiar inhibitory receptors signature in TILs enriched both in primary CRCs and liver metastases. Among the highly co-expressed inhibitory receptors, CD39 was found to represent the major driver of exhaustion in both primary and metastatic colorectal tumours. CD39 is a diphosphohydrolase converting ATP into AMP that is emerging as exhaustion marker for tumor-specific T cells, thus highlighting its relevance as molecular target for T cells engineering. By CRISPR/Cas9 genome editing tools, we simultaneously redirected T cell specificity by disrupting the alpha and beta genes of the endogenous T cell receptor with >90% efficiency, and disrupted CD39 with 100% efficiency, generating triple-knockout engineered lymphocytes. By lentiviral transduction, we redirected the specificity of our engineered T cell product employing a novel T-cell receptor targeting the HER-2 antigen. Gene-edited, HER2-redirected T cells were challenged against HER2+ patient-derived organoids (PDOs) *in vitro* and *in vivo*: CD39-disrupted, HER2-redirected T cells displayed a functional advantage in recognizing and killing CRC PDOs and enhancing mice survival, compared to CD39-competent, HER2-redirected T cells.

Conclusions The CD39 axis is relevant for further exploitation in adoptive T-cell therapy to treat primary and metastatic colorectal cancer.

Ethics Approval The present study was approved by IRCCS San Raffaele Ethical Committee, protocols ACTxCRC and NCT04622423.

<http://dx.doi.org/10.1136/jitc-2022-SITC2022.0268>

MITOCHONDRIAL APOPTOSIS MEDIATES CAR T CELL CYTOTOXICITY

¹Alexandra Pourzia, ¹Michael Olson*, ²Stefanie Bailey, ¹Aditi Aryal, ¹Jeremy Ryan, ²Marcela Maus, ¹Anthony Letai MD. ¹Dana-Farber Cancer Institute, Boston, MA, USA; ²Massachusetts General Hospital, Charlestown, MA, USA

Background CAR T cell therapy has greatly improved outcomes in relapsed hematologic malignancies, yet some patients do not respond to treatment. Dysregulation of apoptotic signaling pathways has been implicated in reduced sensitivity to chemotherapeutics in many hematologic malignancies, however, whether these pathways are also perturbed as a mechanism of resistance to CAR T cell therapy remains unclear. Here, we investigated the importance of mitochondrial apoptosis in CAR T cell anti-tumor cytotoxicity.

Methods Given that knockout of the pro-apoptotic proteins Bak and Bax is sufficient to significantly dampen mitochondrial apoptosis, we generated HeLa, HCT-116, JeKo-1 and NALM6 cells lacking Bak and Bax and cultured them with CAR T cells in order to determine the relevance of mitochondrial apoptosis to CAR T cell cytotoxicity. Cytotoxicity was measured by Annexin V/Hoechst staining, impedance assays and colony formation assays.

Results HeLa cells expressing CD19 and lacking Bak and Bax (HeLa-19-DKO) exhibited significantly enhanced resistance to killing by CD19 CAR T cells when compared to cells expressing endogenous levels of Bak and Bax. Given the protection from CAR T cell cytotoxicity conferred by loss of the pro-apoptotic proteins Bak and Bax, we next conversely sought to determine if overexpression of the anti-apoptotic proteins Bcl-2 and Bcl-XL would similarly confer protection. Consistent with our findings using DKO cells, HeLa-19 cells overexpressing Bcl-2 and Bcl-XL were more resistant to killing by CD19 CAR T cells, demonstrating that mitochondrial apoptosis is relevant to CAR T cell cytotoxicity.

We next sought to validate the importance of mitochondrial apoptosis in CAR T cell cytotoxicity by targeting an endogenously expressed CAR T cell target, namely EGFR. Coculture of EGFR CAR T cells with wild type and DKO HeLa and HCT-116 cells revealed significant resistance to CAR T cells by DKO target cells. Given the protective effect of dampening mitochondrial apoptosis in two solid cancer models, we finally sought to determine whether CAR T cells similarly utilize mitochondrial apoptosis to induce cell death in liquid cancers. In contrast with our solid cancer models, knockout of Bak and Bax in the liquid cell lines JeKo-1 and NALM6 did not result in enhanced resistance to CD19 CAR T cell cytotoxicity.

Conclusions Taken together, these data demonstrate that mitochondrial apoptosis plays a role in how CAR T cells kill solid but not liquid tumors, suggesting that cancer type may be an important factor in considering combinatorial treatments using CAR T cells and pro-apoptotic drugs.

<http://dx.doi.org/10.1136/jitc-2022-SITC2022.0269>

270

DEVELOPING PLACENTAL CD34⁺-DERIVED NATURAL KILLER CELLS WITH HIGH AFFINITY AND CLEAVAGE RESISTANT CD16 (CYNK-101) IN COMBINATION WITH AVELUMAB FOR ENHANCED THERAPY AGAINST PD-L1⁺ SOLID TUMORS

Irene Raitman*, Gavin Foley, Eric He, Hemlata Rana, Niranjan Ghimire, Xuan Guo, Robert Harii, Lin Kang. *Celularity Inc., Florham Park, NJ, USA*

Background Natural killer (NK) cells play a key role in antibody dependent cellular cytotoxicity (ADCC) via their CD16 Fc receptor. NK cell therapies can be targeted to tumors via tumor specific antibodies. Celularity Inc. is developing human placental CD34⁺-derived, cryopreserved, off-the-shelf, allogenic NK cells (CYNK-101) with a high IgG binding affinity and proteinase cleavage resistant CD16 variant (CD16VP) for cancer treatment. We hypothesize that expression of CD16VP on CYNK-101 augments its anti-tumor ADCC activity.

Methods Here, we evaluated anti-tumor activity of CYNK-101 in combination with Avelumab, an anti-PD-L1 antibody, against PD-L1⁺ lung, breast, and bladder cancer cell lines. Furthermore, the PI3-kinase inhibitor Wortmannin was used to investigate the molecular mechanism underlying CYNK-101-mediated cytotoxicity.

Results *In vitro* ADCC activity of CYNK-101 against PD-L1⁺ targets was assessed in combination with Avelumab. At 4h, at an effector to target (E:T) ratio of 5:1, CYNK-101 displayed increased cytotoxicity against the lung cancer cell line NCI-H1975, 56.7 ± 19.3% with Avelumab vs. 37.3 ± 6.4% with IgG control (n=6 donors, p<0.05). For the breast cancer cell line MDA-MB-231, cytotoxicity with Avelumab at the 5:1 ratio was 64.4 ± 17.1% vs. 51.1 ± 15.7% with IgG control (n=6 donors, p<0.005). For the bladder cancer cell lines, the cytotoxicity with Avelumab compared to IgG control was 78.3 ± 16.9% vs. 10.4 ± 20.2% for 5637 (p<0.005), 57.8 ± 22.8% vs. 37.2 ± 19.4% for T-24 (p<0.005), and 38.1 ± 20.0% vs. 28.7 ± 14.3% for RT-112 (p<0.05), respectively (n=6 donors). CYNK-101 in the presence of Avelumab also secreted significantly higher levels of GM-CSF and IFN-gamma when co-cultured for 24h with NCI-H1975 and MDA-MB-231 compared to that of the IgG control (n=6 donors, p<0.05). The enhanced cytotoxicity of CYNK-101 was PI3-kinase pathway-dependent as Wortmannin (0.1 μM) significantly decreased the 24h cytotoxicity for NCI-H1975 with Avelumab from 92.4 ± 13.1% to 66.3 ± 16.7% at the E:T ratio of 5:1, such a decrease was also observed at E:T ratios from 2.5:1 to 0.6:1 (n=3 donors, p<0.05).

Conclusions Our results demonstrate that CYNK-101 has enhanced Avelumab-mediated ADCC activity against PD-L1⁺ tumor cell lines, such as lung, breast, and bladder cancers. Further development of the combinational therapy for PD-L1⁺ solid tumor indications is warranted.

<http://dx.doi.org/10.1136/jitc-2022-SITC2022.0270>

271 **B CELL PRIMED CD8 T CELLS GENERATE SIMILAR PHENOTYPE, FUNCTION AND ANTI-TUMOR RESPONSES TO DC PRIMED CD8 T CELLS**

Ichwaku Rastogi*, Douglas McNeel. *University of Wisconsin-Madison, Madison, WI, USA*

Background Exogenous peptide-loaded antigen presenting cells (APCs) have been under investigation as a therapeutic approach for the treatment of cancer patients. However, in general APC vaccines have demonstrated limited efficacy in clinical trials. To date, only one APC based vaccine, Sipuleucel-T, has been approved by FDA for the treatment of cancer, in this case castrate-resistant metastatic prostate cancer. Dendritic cells (DCs), best known for their cross priming ability, have been the ultimate choice for APC based vaccine research. However, B cells, which also serve as professional APC and can function similarly to activate CD4 and CD8 T cells, remain largely understudied. We compared the phenotype and function of activated T cells that resulted from epitope-specific priming through either B cells or DCs.

Methods We isolated B cells and DCs from C57Bl/6 mice, which were either treated or not with LPS for maturation. These cells were then either loaded or not with SIINFEKL peptide (dominant ovalbumin epitope) for priming CD8 T cells isolated from OT-1 mice (transgenic for TCR specific for SIINFEKL). Resulting T cells were analyzed for their phenotype, function, and anti-tumor efficacy via flow cytometry, ELISA, and E.G7-OVA murine tumor model respectively.

Results We report that priming through peptide-pulsed immature B cells or immature DCs similarly activated antigen-specific CD8 T cells. However, priming through mature DCs resulted in generation of a stronger CD8 T cell activation profile when compared to priming through mature B cells. Similarly, we report that CD8 T cell priming through B cells or DCs resulted in comparable expression of exhaustion and checkpoint related markers on activated CD8 T cells, and similar expression of pro-inflammatory and cytotoxicity related cell surface proteins and intracellular cytokines. Lastly, we report that CD8 T cells primed through immature B cells, immature DCs or mature DCs, all generated a similar anti-tumor response upon adoptive transfer to tumor-bearing mice.

Conclusions Collectively, our data indicated that both B cells and DCs are equally capable of activating CD8 T cells and generating an anti-tumor response. Given that B cells are relatively easier to culture and expand when compared to DCs, our study warrants further investigation into the APC function of B cells and their potential use as APC-based vaccines.

Ethics Approval All experiments involving animals were performed under IACUC approved protocol no. M005690.

<http://dx.doi.org/10.1136/jitc-2022-SITC2022.0271>

272

PRE-CLINICAL EVALUATION AND FIRST-IN-DOG CLINICAL TRIALS OF INTRAVENOUS INFUSION OF PBMC-EXPANDED ADOPTIVE NK CELL THERAPY IN DOGS WITH CANCER

<http://dx.doi.org/10.1136/jitc-2022-SITC2022.0272>

Aryana Razmara*, Lauren Farley, Rayna Harris, Sean Judge, Marshall Lammers, Cordelia Dunai, William Murphy, Robert Rebhun, Michael Kent, Robert Canter. *UC Davis, Davis, CA, USA*

Background Natural killer (NK) cells are cytotoxic immune cells capable of recognizing heterogeneous cancer targets without prior sensitization, making them promising prospects for use in cellular immunotherapy. Previously, CD5 depletion of peripheral blood mononuclear cells (PBMCs) has been used in dogs to isolate and expand a CD5^{dim}-expressing NK subset prior to co-culture with an irradiated feeder line, but this can limit the yield of the final NK product. This study aimed to assess NK activation, expansion, and preliminary clinical activity in first-in-dog clinical trials using unmanipulated PBMCs without CD5 depletion to generate our NK cell product.

Methods Starting populations of CD5-depleted cells and PBMCs from 12 matched healthy beagle donors were co-cultured with irradiated K562-C9-mIL21 cells and 100IU/mL rhIL-2 for 14 days. Phenotype, cytotoxicity, and cytokine secretion were measured, and samples were sequenced using the 3'-Tag-RNA-Seq protocol for gene profiling. In addition, two first-in-dog feasibility clinical trials were performed in dogs with melanoma (MEL, N=5) and osteosarcoma (OSA, N=9) using autologous and allogeneic NK cells, respectively, expanded from unmanipulated PBMCs.

Results Calculated cell counts, overall fold change, and viability in NK expansions displayed higher means at day 14 using PBMCs versus CD5-depleted cells, reaching a peak mean of 677×10^6 cells from 5×10^6 starting cells (P=NS). Flow analysis showed similar upregulation of Nkp46 and Granzyme B expression in both groups, reaching >90%. Killing assays against M5 (MEL) and OSCA78 (OSA) canine tumor targets demonstrated comparable percent killing >50% among both subsets of day 14 NK cells (P=NS). Median production of canonical NK cytokines, IFN- γ and GM-CSF, at day 14 was over 5-fold greater in PBMC-expanded (IFN- γ =316.7pg/mL, GM-CSF=267.0pg/mL) compared to CD5-depleted NK cells (IFN- γ =59.6pg/mL, GM-CSF=48.7pg/mL) (P=NS). Sequencing data showed principal component sample variance based on time points and upregulation of NK pathways related to activation, crosstalk, and glycolytic function in both groups. PBMC-expanded NK cells for first-in-dog clinical trials showed sufficient expansion for multiple NK cell transfers at 7.5×10^6 cells/kg with no serious adverse events. We also observed preliminary data for efficacy, particularly in the allogeneic setting where peripheral blood gene expression significantly changed post-transfer and one dog survived 445 days post-treatment.

Conclusions Overall, the use of unmanipulated PBMCs appears safe and potentially effective for canine NK immunotherapy, with equivalent or superior results to CD5 depletion in NK expansion, activation, and cytotoxicity. Our pre-clinical and clinical data support further evaluation of this technique as a novel platform for optimizing NK immunotherapy in dogs.

Ethics Approval Clinical trials involving dog patients were IACUC and Clinical Trials Review Board-approved (Protocols #21620 and #22157). Dog owners gave informed consent before taking part.

273

GDA-501: ENGINEERED NAM-NK CELLS WITH HER2-CAR EXPRESSION DEMONSTRATE INCREASED CYTOTOXICITY AGAINST HER2-EXPRESSING SOLID TUMORS

Julia Rifman*. *Gamida Cell, Jerusalem, Israel*

Background Natural killer (NK) cells have generated considerable interest as potential adoptive cell immunotherapy. *Ex vivo* expansion of allogeneic NK cells using our proprietary nicotinamide (NAM) platform enhances NK cell functionality by preventing cell exhaustion, enhancing cytotoxic activity, generating a protective effect against oxidative stress, and exhibiting improved homing to lymphoid tissues. These attributes provide opportunities to enhance the therapeutic potential of NK cells in the clinic.

The success of immunotherapy in solid tumors has been limited due to several barriers, including immunosuppressive tumor microenvironment, inefficient trafficking, and heterogeneity of tumor antigens. A number of therapeutic approaches to overcome these limitations have emerged.

Gene modification strategies of NK cells may further enhance their functionality and provide a promising next-generation immunotherapeutic tool. The use of chimeric antigen receptors (CARs) can target specific antigens on tumors. Human epidermal growth factor receptor 2 (HER2)-CAR may be used to target HER2⁺ solid tumors, such as breast, gastric, and ovarian carcinomas.

Methods HER2-CAR-NK cells were developed based on a single-chain variable fragment (scFv) of the widely used humanized monoclonal antibody trastuzumab. To construct our HER2-CAR-NK cells, we used the same binding domain present in trastuzumab, and designed different constructs in a modular way, optimized by modifying the hinge, transmembrane, and cytoplasmic domains with NK cell-related activating molecules to specifically enrich the cytotoxicity of NK cells.

Results Our engineered HER2-CAR NAM-NK cells (GDA-501) displayed significantly enhanced *in vitro* cytotoxicity when cocultured with HER2⁺ target cells such as ovarian adenocarcinoma cell line SKOV3. Elevated levels of the degranulation marker CD107a and proinflammatory cytokines including interferon (IFN)- γ and tumor necrosis factor (TNF)- α were observed, signifying increased potency of GDA-501 compared with control cells. Furthermore, increased cytotoxicity and potency persisted for up to 5 days post electroporation.

The specificity of the cytotoxic effect was evaluated. No significant elevation of HER2-CAR NK cell activation was detected when cultured with HER2⁻ tumor cell lines or normal lymphocytes.

Conclusions GDA-501 is a genetically modified NAM-NK targeting HER2. By optimizing downstream signaling, we were able to directly enhance NK cell activity. *In vitro* data demonstrated potent cytotoxicity against HER2-expressing cells. These results suggest that GDA-501 represents a unique allogeneic cell therapy potentially targeting HER2⁺ solid tumors.

Ethics Approval For the present study NK cells were collected from peripheral blood leukapheresis of individual donors. Ethics approval has been obtained from the local ethics committee (EC) at each of the sites (Hadassah Medical Center [0483-16-HMO], Rambam Medical Center [0641-18-RBM], Ichilov Sourasky Medical Center Tel-Aviv [0025-17-TLV]) prior to any study related activities.

The working procedures of the EC at the sites for conduct of clinical studies are in due compliance with local regulations (Israeli Ministry of Health) and provisions of Harmonized

International Guidelines for Good Clinical Practice. Sites follow EC conditions & requirements in terms of submissions, notifications, and approval renewals. Participants gave informed consent (approved by the EC) before taking part in the study. Informed consent has been approved by the ECs. The Israeli template of informed consent is in used and it includes study specific information (e.g. study goal, design, method, duration, risks, etc.).

<http://dx.doi.org/10.1136/jitc-2022-SITC2022.0273>

274

LCK KNOCKOUT CAR-T CELLS AS A NOVEL ALLOGENEIC PLATFORM

Previtha Dawn Sakthi Vale*, Ling Wu, Vivian Jia Yi Tan, Benson Chua, Liangzhe Wu, Jia Chi Tan, Clara Kai Ting Koh, June Ong, Nicholas Gascoigne. *National University of Singapore, Singapore, Singapore*

Background Chimeric antigen receptor (CAR) T therapy has shown remarkable success in treating liquid tumours but current approved therapies rely on autologous T cells which are expensive, difficult to manufacture and not readily available for patients whose disease progress rapidly. The production of safe and effective allogeneic CAR-T cells is needed to increase accessibility of CAR-T therapy and broaden its application. The main approach to generate allogeneic CAR-T therapy is by disrupting T cell receptor (TCR) expression to minimize Graft-versus-Host Disease (GVHD) mediated through the TCR of donor cells against the recipient's major histocompatibility complex (MHC). However, the TCR disruption approach has shown limited persistence *in vivo* [1] and in clinical trials [2] unlike the long term durability of autologous CAR-T cells. Here, we propose a novel platform for allogeneic CAR-T therapy that retains the TCR but inhibits TCR signalling by knocking out the Lymphocyte-specific protein tyrosine kinase (LCK) – a well-established kinase for proximal TCR activation. This builds on the discovery that our second generation CD28-CAR can be activated independently of LCK unlike the endogenous TCR.

Methods We utilise the CRISPR-Cas9 system to knockout LCK and TCR in both mouse and human primary T cells. We show how this difference in CAR and TCR signalling can be exploited to generate LCK knockout CAR-T cells that showed similar or enhanced *in vitro* and *in vivo* efficacy against tumour cells compared to conventional CAR-T cells of both human and mouse T cell origin.

Results LCK knockout T cells have reduced proliferation and intracellular cytokine staining against allogeneic PBMCs compared to T cells, suggesting comparable suppression of TCR-mediated alloreactivity to TCR knockout T cells. In the immunodeficient mouse model where human T cells cause xenogeneic GVHD, LCK knockout T cells showed reduced xenogeneic GVHD comparable to TCR knockout T cells. Murine LCK knockout T cells showed the same suppression of TCR signalling as TCR knockout T cells *in vitro*. In murine major mismatched allogeneic models, murine LCK knockout T cells showed a reduction in GVHD symptoms compared to wild-type T cells. Compared to TCR knockout T cells, the LCK knockout T cells showed superior persistence and higher engraftment in allogeneic recipient mice.

Conclusions Our study suggests LCK knockout CAR-T cells inhibits TCR-mediated alloreactivity and retains the TCR for improved persistence while maintaining CAR activation potential which results in a superior allogeneic CAR-T therapy compared to TCR knockout CAR-T cells.

REFERENCES

1. Stenger, D, Stief, T A, Kaeuferle, T, Willier, S, Rataj, F, Schober, K, Vick, B, Lotfi, R, Wagner, B, Grünwald, T G P, Kobold, S, Busch, D H, Jeremias, I, Blaeschke, F, & Feuchtinger, T. Endogenous TCR promotes *in vivo* persistence of CD19-CAR-T cells compared to a CRISPR/Cas9-mediated TCR knockout CAR. *Blood*. 2020;**136**(12):1407-1418.
2. Wang, Z, Li, N, Feng, K, Chen, M, Zhang, Y, Liu, Y, Yang, Q, Nie, J, Tang, N, Zhang, X, Cheng, C, Shen, L, He, J, Ye, X, Cao, W, Wang, H, & Han, W. Phase I study of CAR-T cells with PD-1 and TCR disruption in mesothelin-positive solid tumors. *Cell Mol Immunol*. 2021;**18**(9):2188-2198.

Ethics Approval Animal Protocols were approved by NUS IACUC (R20-1303). Use of human primary T cells was approved by Institutional Review Board (IRB) (H-19-026).

<http://dx.doi.org/10.1136/jitc-2022-SITC2022.0274>

275 **MANUFACTURE OF ALLOGENEIC, HLA-MATCHED, TCR-EDITED T-CELL THERAPY REACTIVE AGAINST MINOR HISTOCOMPATIBILITY ANTIGEN 1 TO TREAT ACUTE MYELOID LEUKEMIA IN COMBINATION WITH CD34 HSCT WITH THE POTENTIAL FOR HIGH POTENCY AND DURABILITY**

¹Robert Keefe*, ¹Tim Mayall, ¹Egidio Cofano, ¹Marlyn Anguelov, ²Constantinos Panousis, ¹Paola Sette. ¹BlueSphere Bio, Walkersville, MD, USA; ²BlueSphere Bio, Pittsburgh, PA, USA

Background BlueSphere Bio (BSB) has developed a proprietary high-throughput T cell receptor (TCR) capture and screening platform to enable T-cell therapy for the treatment of cancer. Our TCX-101 program develops allogeneic TCR T-cells to enhance the beneficial alloreactive T cell response observed with allogeneic hematopoietic stem cell transplantation (alloSCT). The therapeutic goal is to promote a graft-versus-leukemia effect, whilst reducing the risk of graft versus host disease. The first product in the platform, BSB-1001, targets the hematopoietically-restricted minor HA-1 (HA-1 TCR). HA-1 is restricted by a common human HLA type A*02:01 and covers approximately 50% of the that population. BSB-1001 is currently in development for clinical testing in Acute Myeloid Leukemia (AML).

Methods BSB-1001 is generated by activation of healthy donor PBMCs from a mobilized apheresis, using anti-CD3 OKT3. Following the activation, CD8 T-cells are isolated, and the endogenous TCR knocked out with CRISPR edits, using formulated Cas9/guide RNA, RiboNuclear Particles (RNP). Cells are then transduced with the anti-miHA-1 TCR lentivector (Yposkesi). Cells are cultured and expanded and cryopreserved on harvest day using CryoStor10 in a controlled rate freezer. The product is co-administered with CD34 cells isolated from the same donor apheresis.

Results BSB-1001 was developed and generated at BSB. PBMCs derived from fresh APH are activated using OKT3, with T-cells over 90% by CD69 upregulation. CD8+ T-cells were isolated, and endogenous TCR knockout using RNP, and then transduced with anti-HA1 TCR lenti viral vector. Integrated vector copy number in these cells is under 5 copies/cell. After culture, day 12 harvest, and cryopreservation, cells are thawed and tested in QC. Phenotype of these cells demonstrates a generally stem-cell like phenotype (Tcm, Tem, Tscm), with Tscm cells predominating. BSB-1001 cells showed efficient killing of HA-1+ LCL222 cells, but not HA-1 -/- LCL224 cells. Log-scale plots shows strong IC50 points on the killing curve as low as 0.1:1 Effector:Target ratios. Continued culture of the cells after killing is measured, by the addition more LCL cells, shows that the cytolytic potency of the cells is maintained for at least an additional 20 days (32 days from initial activation).

Conclusions Taken together, the results indicate that BSB-1001 is an active, highly potent drug product candidate, with a potential to be effective in treating HA-1+ HLA-A*02:01 AML patients in the setting of alloSCT. The phenotype and high cytolytic bioactivity indicate that the clinical response has a potential to be very potent and durable.

<http://dx.doi.org/10.1136/jitc-2022-SITC2022.0275>

276

ENGINEERING OF SYNTHETIC CHEMOKINE RECEPTORS INTO iPSC-DERIVED CAR-T CELLS TO INCREASE HOMING AND ENHANCE TRAFFICKING INTO SOLID TUMORS

¹Soheila Shirinbak*, ¹Joy Grant, ²Angela Gentile, ¹Bishwas Shrestha, ¹Philip Chu, ¹Amit Mehta, ¹Yijia Pan, ¹Bjoern Gaertner, ¹Mochtar Pribadi, ¹Joyee Yao, ¹Matthew Denholtz, ¹Alec Witty, ¹Layton Smith, ¹Tom Lee, ¹Eigen Peralta, ¹Martin Hosking, ¹Bob Valamehr. ¹Fate Therapeutics Inc. (FHQ1), San Diego, CA, USA; ²Fate Therapeutics, Inc. (FTP1), San Diego, CA, USA

Background Despite the success of chimeric antigen receptor (CAR)-T cells in treating hematological malignancies, the efficacious treatment of solid tumors has been hampered by lack of CAR-T cell persistence, tumor-associated antigen heterogeneity, and the immuno-suppressive tumor microenvironment (TME). In addition, trafficking of CAR-T cells to solid tumors, potentially due to a chemokine-chemokine receptor mismatch between the tumor and the CAR-T cells, has proven ineffective. Early and sustained detection of T cells within a solid tumor has been associated with better outcomes across several clinical trials, suggesting that strategies focused on enabling CAR-T cell homing and trafficking can generate significant therapeutic benefit.

Methods IL8/CXCL8, a ligand for the chemokine receptor CXCR2, has been detected in many cancer types including ovarian, breast, prostate and renal and is often associated with poor prognosis and overall survival. We have previously shown high baseline expression and inducible upregulation of IL8 following chemo- or radiotherapy conditioning in multiple tumor lines. We therefore engineered CXCR2 into induced pluripotent stem cell (iPSC)-derived CAR-T (CAR iT) cells to express a synthetic CXCR2 transgene.

Results CXCR2-engineered iPSCs were differentiated to manufacture alpha-beta CAR iT cells expressing uniform and high levels of the chemokine receptor (>90% CXCR2 expression). Importantly, CXCR2 expression did not affect CAR-dependent effector function. CXCR2 engineered CAR iT cells demonstrated specific and functional *in vitro* chemotactic migration to recombinant IL8 and tumor preconditioned media (up to 3 fold increase compared to control CAR iT cells). In preclinical *in vivo* assessment with either (i) an aggressive ovarian xenograft model that produces high levels of CXCL8, or (ii) a triple negative breast cancer xenograft model that expresses CXCL8 following cyclophosphamide/fludarabine preconditioning, CXCR2-engineered CAR iT cells demonstrated enhanced infiltration (SKOV3 model; 6.01e6 cells/gr tumor vs 0.94e6 cells/gr tumor with CXCR2+ CAR iT cells vs control CAR iT cells, respectively) and increased retention specifically within the solid tumor microenvironment, resulting in improved tumor control (SKOV3 model; 81.3% TGI vs 60.9% TGI with CXCR2+ CAR iT cells vs control CAR iT cells, respectively).

Conclusions Preclinical data demonstrate that the engineering of synthetic chemokine receptors to further direct off-the-shelf CAR iT cells to the tumor site is an exciting strategy to improve anti-tumor activity, including as part of a multiplexed-engineering strategy for overcoming challenges in treating solid tumors.

<http://dx.doi.org/10.1136/jitc-2022-SITC2022.0276>

277

DEVELOPMENT OF A ROBUST MANUFACTURING PROCESS FOR AB-1015, AN INTEGRATED CIRCUIT T CELL (ICT) PRODUCT, USING TARGETED, CRISPR INTEGRATION OF TRANSGENES BY ELECTROPORATION (CITE) EDITING

Alice Chang*, Sophia Phillips, Max Lee, Elizabeth Huang, Navneet Anand, Hayden Ko, Stella Tran, Lindsay Rios, Rory Dai, Anton Nguyen, Anu Vasudevan, Rona Harari Steinfeld, Dina Polyak, Jessica Fuhrman, Hongruo Yun, Jun Feng, Haixia Wang, Ben Tran, Jenessa Smith, Tim Sirichoche. *ArsenaBio, South San Francisco, CA, USA*

Background AB-1015 is an autologous, integrated circuit T cell (ICT) product for the treatment of platinum-resistant ovarian cancer. AB-1015 includes a transgene cassette with two functional modules: an "AND" logic gate designed to limit off-tumor toxicity through dual tumor antigen recognition, and a dual shRNA-miR designed to resist TME suppression and to improve ICT cell function. ICT cells are generated via CRISPR integration of transgenes by electroporation (CITE), a non-viral and site-specific integration approach that provides enhanced safety, increased cargo capacity, and reduced cost. A scalable, semi-closed, and semi-automated manufacturing process was developed to support GMP manufacture of AB-1015 for Ph1 clinical evaluation.

Methods Clinical-scale, end-to-end runs were performed in healthy donors using ArsenalBio's manufacturing process for AB-1015. On Day 0, CD4 and CD8 positive cells were isolated from fresh apheresis from healthy donors. Cells were activated using CD3/CD28 stimulation, electroporated with Cas9 protein, sgRNA targeting a safe harbor site (GS94), and plasmid DNA encoding the transgene. Cells were expanded until harvest and formulated into drug product. Frozen cell drug product was thawed and characterized using flow cytometry, in vitro functional assays, and in vivo tumor efficacy models.

Results Processing of healthy donor apheresis from more than 20 donors using the AB-1015 manufacturing process resulted in average knock-in efficiencies of approximately 25% and total therapeutic yields exceeding 2.5e9 transgene positive cells. In addition to robust IFN- γ production and tumor cell killing in dual antigen-specific co-culture, AB-1015 ICT cells retained favorable memory phenotype (CCR7+) at harvest. Furthermore, AB-1015 ICT cells demonstrated potent anti-tumor responses in a xenograft in vivo model.

Conclusions A robust, 10-day manufacturing process was successfully developed for AB-1015 that enables high knock-in efficiencies of a large (> 6 kb) transgene using a site-specific, non-viral integration approach. Billions of ICT cells can be generated from a single healthy donor in a semi-closed, semi-automated fashion and these ICT cells display potent anti-tumor activity in vitro and in vivo with high specificity. AB-1015 will be evaluated in clinical trials for treatment of platinum-resistant ovarian cancer.

<http://dx.doi.org/10.1136/jitc-2022-SITC2022.0277>

278

PHARMACOLOGICALLY-CONTROLLED EXPRESSION OF MEMBRANE-BOUND IL-12 RESULTS IN T-CELL THERAPY WITH ENHANCED POTENCY IN PRECLINICAL SOLID TUMOR MODELS

Sean Smith*, Benjamin Primack, Theresa Ross, Patricia Timpug, Dexue Sun, Dan Jun Li, Scott Lajoie, Violet Young, Meghan Langley, Jeremy Tchaicha, Dhruv Sethi, Jan ter Meulen, Michelle Ols. *Obsidian Therapeutics, Cambridge, MA, USA*

Background Solid tumors remain a challenging frontier for adoptive cellular therapies (ACT). Armoring T-cells with cytokines, such as interleukin 12 (IL-12), to remodel the tumor microenvironment (TME) has demonstrated preclinical efficacy against solid tumors. However, the clinical utility of IL-12 is limited by systemic toxicities, requiring tight control of expression. Herein, we show that T-cells armored with a small molecule-controlled membrane bound IL-12 (mbIL-12) drives regulation of pharmacodynamic markers and solid tumor efficacy in xenograft and syngeneic solid tumor models.

Methods We regulated mbIL-12 expression using Obsidian's cytoDRIVE® technology. In this system, a drug responsive domain (DRD) is fused to a protein of interest. In the "off-state" the fusion protein is rapidly degraded by the proteasome. Adding a small molecule ligand stabilizes the complex, enabling expression (the "on-state"). Here, we use a DRD derived from carbonic anhydrase 2 and the FDA-approved inhibitor acetazolamide (ACZ) as a stabilizing ligand. Unlike most other regulation systems, cytoDRIVE® is both fully human, reducing immunogenicity, and induced pharmacologically, allowing on-demand control. Adding oligomerization domains increases the local density of DRDs to form modulation-hubs that further increase the regulation of mbIL-12.

Cytokine levels were determined using flow cytometry and Meso Scale Discovery assays. Human mbIL-12 modulation hubs and CD19-CARs were transduced in peripheral blood T-cells and evaluated *in vivo* against subcutaneous Raji xenografts that form solid tumors in NSG mice after inoculation in Matrigel. Mouse constructs were evaluated in CD8 gp100 (PMEL) TCR transgenic cells against subcutaneous B16-F10 melanoma in C57BL6 mice.

Results In the xenograft setting, ACZ dosing resulted in 35-fold regulation of IL-12 in the plasma and showed remarkable ACZ-dependent anti-tumor efficacy against large, solid Raji tumors at a 10x lower cell dose than unarmored CAR-Ts. In the immunocompetent PMEL/B16 model, IL-12 modulation-hub PMEL cells slowed tumor growth over unarmored PMEL cells and showed improved tolerability over secreted IL-12. Animals receiving IL-12 modulation-hub cells showed ACZ-dependent regulation of IL-12 and IFN γ in the plasma with levels 100-fold and 20-fold less, respectively, than with constitutive secreted IL-12 cells. This regulation led to functional impacts at the cellular level, including an increase in circulating antigen presenting cells.

Conclusions The cytoDRIVE® platform enables enhanced regulation of IL-12 armored T-cells in multiple preclinical solid tumor models, potentiating an improved therapeutic window for IL12 in ACT.

Ethics Approval All animals studies were IACUC approved.

<http://dx.doi.org/10.1136/jitc-2022-SITC2022.0278>

279

PRECLINICAL *IN VIVO* MODEL DEVELOPMENT: HIGHLIGHTING SUCCESS AND DISCUSSING XENOGRAFT ADVANCEMENTS, A STEP CLOSER TO PREDICTING PATIENT OUTCOMES

Thomas Dailey*, Angela Gentile, Lexe Linderhof, Layton Smith, Bob Valamehr. *Fate Therapeutics Inc., San Diego, CA, USA*

Background Immunotherapy, in particular chimeric-antigen receptor (CAR) T-cells, has been shown as an effective strategy for the treatment of cancer. However, the full therapeutic potential of these innovative therapies has not yet been fulfilled. This is particularly true of complex solid tumors. In comparison with hematologic tumors, solid tumors are more complex with unique three-dimensional structures, an immunosuppressive microenvironment and cellular heterogeneity that extends to the expression of tumor-associated antigens.¹ Therefore, robust preclinical models with a high degree of fidelity towards the clinical presentation of the tumor are required for the accurate evaluation and translation of next-generation immunotherapies, including advancement of *in vivo* xenograft mouse models that more closely recapitulate disease as it is observed in the clinical setting.

Methods We have developed an orthotopic, mammary fat pad #4 (MFP#4) xenograft model utilizing an engineered tumor cell line based on the MDA-MB-231 triple negative breast cancer (TNBC) to assess epithelial cancer progression. Using this anatomically implanted human tumor model, we evaluated tumor growth kinetics, body weight, metastases and control of tumor with bioluminescence imaging.

Results The established MFP#4 xenograft model yields consistent, uniform tumor growth that produces disease progression and secondary metastases *in vivo*. Importantly, the model produced secondary tumors in both the lung and liver, recapitulating human disease in distal sites where 31.4% and 26% of patients show metastases. Moreover, we observed metastases in the axillary lymph node, a hallmark sign for diagnosing and staging breast cancer in patients. In the initial proof of concept study, administration of induced pluripotent stem cell-derived CAR T (CAR iT) cells, which had been successful in demonstrating tumor growth inhibition in various other disseminated and subcutaneous *in vivo* tumor models, significantly reduced the size of the primary tumor burden and the secondary tumor nodes.

Conclusions This work demonstrates that our engineered TNBC cell line in the MFP#4 xenograft model recapitulates much of the human disease phenotype. Importantly, the model demonstrated metastatic disease consistent with clinical presentation. Furthermore, administration of CAR iT-cells resulted in a decrease in overall tumor burden, validating the use of the orthotopic tumor xenograft as a preclinical model of TNBC with a high degree of clinical translatability.

REFERENCE

1. Chen, M *et al.*. Comparison of patterns and prognosis among distant metastatic breast cancer patients by age groups: a SEER population-based analysis. *Sci Rep* 2017; Aug 23;7(1):9254.

Ethics Approval All animal studies were conducted under the approval of the IACUC at Fate Therapeutics.

<http://dx.doi.org/10.1136/jitc-2022-SITC2022.0279>

280

**RAPID AND SIMPLIFIED PROCESS FOR
MANUFACTURING MULTI-TUMOR-ASSOCIATED
ANTIGEN SPECIFIC T CELLS**

Anastasiya Smith*, Tara Shahim, Jeanette Crisostomo, Eric Smith, Jennifer Pickering, Anna Wilga-Savitski, Tsvetelina Hoang, Juan Vera. *Marker Therapeutics, Inc., Houston, TX, USA*

Background Marker Therapeutics, Inc. has developed MT-401, a multi-tumor-associated antigen (multiTAA)-specific allogeneic T cell product capable of recognizing multiple targets expressed on the tumor simultaneously, minimizing tumor escape. Currently, MT-401 is being used for treatment of AML patients following allogeneic stem-cell transplant in both the adjuvant and active disease settings. Although MT-401 has shown promising clinical results, the manufacturing process is time prohibitive for cancer patients with rapid disease progression. Here we demonstrate how additional process improvements streamlined the manufacturing process and resulted in products with superior T cell phenotype and potency, both of which have the potential to enhance clinical responses.

The original manufacturing process for multiTAA-specific T cell products is derived from Baylor College of Medicine studies and begins with the purification of PBMCs from leukapheresis material. Subsequently, dendritic cells (DCs) are matured and pulsed with a pool of exogenous peptides spanning the entire primary sequence of target antigens (Ags). The mature DCs expressing the antigens are co-cultured with T cells in a Gas Permeable Rapid Expansion Device (G-Rex[®]) to stimulate and expand antigen-specific T cells. For MT-401, the following four antigens are used: PRAME, NY-ESO-1, Survivin and WT1. This 36-day manufacturing process results in products containing an average of 83% CD3+ T cells with a predominantly effector memory T cell phenotype, and an average specificity for 4 tumor Ags of 179 spot-forming units (SFU) per 2e5 cells.

Methods We have now simplified the manufacture of multi-TAA-specific T cells and eliminated the need to generate DCs in vitro prior to T cell stimulation.

Results The improved 9-day manufacturing process produces superior T cell products with an average%CD3+ purity of 96%, T cell phenotype showing a uniform distribution of naïve, central memory and effector memory T cells, increased Ag specificity (5-fold), Ag diversity and killing potential.

Conclusions These process improvements significantly reduced the number of interventions needed during manufacturing, thereby decreasing both the possibility of manufacturing failures and product manufacturing time, which translates to faster patient treatment. This sophisticated and rapid manufacturing approach has shown to be reproducible regardless of the tumor antigen combination, enabling the extension of this technology to other clinical indications.

<http://dx.doi.org/10.1136/jitc-2022-SITC2022.0280>

281

THE TWO SIDES OF THE COIN: PRO-INFLAMMATORY STIMULI LEAD TO UPREGULATION OF CD70 IN AML, BUT ALSO REDUCE NK-CELL-BASED IMMUNOTHERAPY EFFICACY

¹Monika Sponheimer*, ¹Gerulf Hänel, ¹Lisa Rohrbacher, ¹Nora Philipp, ¹Daniel Nixdorf, ¹Anetta Marcinek, ¹Christian Wichmann, ¹Andreas Humpe Med, ²Shyra Gardai, ²Daniel Diolaiti, ¹Veit Leonhardt Bücklein, ¹Marion Subklewe. ¹University Hospital LMU Munich, Munich, Germany; ²Seagen, Bothell, WA, USA

Background Novel immune cell-based treatment options are evolving for patients with acute myeloid leukemia (AML). The identification of a suitable target antigen with a restricted expression profile is still a major challenge and a prerequisite for success. CD70, which is transiently expressed in activated T-, B-, and NK cells, has been reported to be aberrantly expressed on AML and leukemic stem cells.¹⁻³ While the mechanism driving its expression in AML is not defined, its restricted profile in normal tissues makes it an ideal target for immunotherapeutic strategies.

Methods We evaluated CD70 expression by flow cytometry on primary AML cells from initial diagnosis (ID, n = 123) and relapse (RL, n = 14). NK cell-mediated antibody-dependent cellular cytotoxicity (ADCC) assays utilizing a sugar-engineered anti CD70 antibody with a nonfucosylated Fc backbone (SEA-CD70) were performed against AML cell lines with varying CD70 expression levels and primary AML cells (n=6). Modulation of CD70 and CD33 expression and susceptibility to ADCC were analyzed in a pro-inflammatory environment achieved by either supplementation of tumor necrosis factor alpha (TNF-alpha) and interferon gamma (IFN-gamma) or by the addition of conditioned media (CM) from a CD33xCD3 bispecific-based model system for T-cell activation.⁴

Results The percentage of CD45^{dim}SSC^{lo} AML cells expressing CD70 ranged between 0.2 – 89.6% (mean = 15.2%) at ID and 0.3 – 90.3 (mean = 25.4%) at time of RL. SEA-CD70-mediated ADCC against AML cell lines was dependent on antigen expression level and antibody concentration (n= 4, CD70^{bright}93.1%, CD70^{dim}47.6%). Specific lysis of primary AML cells ranged from 9.5 to 33.2% (mean = 20.1%). Interestingly, pre-conditioning with TNF-alpha/IFN-gamma or CM from CD33xCD3-activated T cells resulted in a significant increase of CD70, but not CD33 expression on AML cell lines (fold change in MFI ratio: 2.7, n=5). However, CM or TNF-alpha/IFN-gamma treatment also reduces NK cell ADCC activity in a target-independent manner resulting in a reduction of CD70-mediated cell lysis from 74.8% to 36.5% (n=4), and CD33-mediated cell lysis from 81.8% to 30.5% (n=4).

Conclusions Our findings validate CD70 as a target antigen in the setting of AML and show that pro-inflammatory stimuli lead to an upregulation of CD70 expression on AML cells. However, these pro-inflammatory stimuli inhibit NK-mediated ADCC activity. This data warrant future studies to understand how modulation of the TME may be utilized as a strategy to enhance target expression without negatively impacting effector cell functions.

REFERENCES

1. Sauer, T., K. Parikh, S. Sharma, B. Omer, D. Sedloev, Q. Chen, L. Angenendt, C. Schliemann, M. Schmitt, C. Muller-Tidow, S. Gottschalk and C. M. Rooney (2021). "CD70-specific CAR T cells have potent activity against acute myeloid leukemia without HSC toxicity." *Blood* **138**(4): 318-330.
2. Riether, C., C. M. Schurch, E. D. Bührer, M. Hinterbrandner, A. L. Huguenin, S. Hoepner, I. Zlobec, T. Pabst, R. Radpour and A. F. Ochsenbein (2017); "CD70/

CD27 signaling promotes blast stemness and is a viable therapeutic target in acute myeloid leukemia." *J Exp Med* **214**(2): 359-380.

3. Perna, F., S. H. Berman, R. K. Soni, J. Mansilla-Soto, J. Eyquem, M. Hamieh, R. C. Hendrickson, C. W. Brennan and M. Sadelain (2017); "Integrating Proteomics and Transcriptomics for Systematic Combinatorial Chimeric Antigen Receptor Therapy of AML." *Cancer Cell* **32**(4): 506-519 e505
4. Herrmann, M., C. Krupka, K. Deiser, B. Brauchle, A. Marcinek, A. Ogrinc Wagner, F. Rataj, R. Mocikat, K. H. Metzeler, K. Spiekermann, S. Kobold, N. C. Fenn, K. P. Hopfner and M. Subklewe (2018); "Bifunctional PD-1 x alphaCD3 x alphaCD33 fusion protein reverses adaptive immune escape in acute myeloid leukemia." *Blood* **132**(23): 2484-2494.

Ethics Approval Peripheral blood or bone marrow samples were collected from healthy donors and patients with acute myeloid leukemia at initial diagnosis, relapse, or complete remission after written informed consent was received in accordance with the Declaration of Helsinki and approval was granted by the Institutional Review Board of the Ludwig-Maximilian-Universität (Munich, Germany, reference number: 216-08).

<http://dx.doi.org/10.1136/jitc-2022-SITC2022.0281>

282

ANTI-FOLATE RECEPTOR ALPHA (FR α) COSTIMULATORY ANTIGEN RECEPTOR (COSTAR) IMPROVES T-CELL FUNCTION ACROSS PHYSIOLOGICALLY RELEVANT RANGES OF FR α EXPRESSION AND T-CELL RECEPTOR (TCR) AFFINITIES

Martina Sykороva*, Michelle Mojadidi, Leyuan Bao, Eric Gschwend, Milena Kalaitidou, Gray Kueberuwa, Xingliang Zhou, Rubén Alvarez-Rodríguez, John Bridgeman. *Instil Bio, Inc., Dallas, TX, USA*

Background ITIL-306 is a genetically engineered autologous TIL cell therapy that amplifies TCR-specific antigen recognition (Signal 1) with an FR α -specific CoStimulatory Antigen Receptor (CoStAR; Signal 2).¹ T-cell activation through the endogenous TCR is dependent on the concentration of cognate peptide-MHC antigen. This study examined T-cell activation across a range of physiologically relevant FR α expression levels and characterized whether functional T-cell avidity (response to cognate antigen concentration) was impacted with CoStAR engagement.

Methods In vitro cocultures were used to determine T-cell response to variations in strength of Signal 1 and Signal 2. To evaluate the role of FR α on amplification of T-cell responses, stable cell lines expressing membrane-anchored OKT3 and different FR α levels were established. Healthy donor (HD) T cells transduced with anti-FR α CoStAR or non-transduced (control) were used as effector cells. Cytolytic activity and cytokine levels (IL-2, IFN- γ , TNF- α) were assessed.

To assess the effect of CoStAR on TCR functional avidity, HD T cells were non-transduced or transduced with a defined TCR recognizing HLA-A*02/MART-1 antigen, anti-FR α CoStAR, or both. Parental T2 or FR α -transduced T2 cells were used as targets. Target cells were pulsed with titrated concentrations of 4 different MART-1-altered peptide ligands of varying antigenicity. Cytokine secretion after coculture was measured, and antigen half-maximal effective concentration (EC₅₀) was calculated.

Results CoStAR amplified T-cell responses at all FR α expression levels. IL-2 secretion was significantly higher at any FR α expression level versus no FR α ($P < .0001$). CoStAR-transduced and non-transduced T cells were not activated in coculture with cells expressing any level of FR α alone. Kinetic activation studies demonstrated that engaging CoStAR (Signal 2) followed by TCR activation (Signal 1) at a later time resulted in amplified T-cell activity.

Cytokine secretion was increased from MART-1-TCR +CoStAR T cells versus MART-1-TCR T cells when cocultured with T2-FR α cells pulsed with titrated concentrations of all cognate peptides evaluated. EC₅₀ was not impacted by CoStAR for cognate peptides with EC₅₀ between 10⁻¹⁰ to 10⁻⁷ M.

Conclusions CoStAR augmented T-cell function across a range of physiologically relevant FR α expression levels and TCR/cognate peptide affinities. TCR/cognate antigen affinity (EC₅₀) was unchanged by CoStAR, suggesting that CoStAR TIL will have identical specificity as unmodified TIL. Further, CoStAR improved T-cell function at low FR α expression levels, supporting the evaluation of ITIL-306 activity across multiple tumors, including those with low FR α expression. These results are being explored in a first-in-human clinical study with ITIL-306 (NCT05397093).

Acknowledgements The authors would like to thank Akshata Udyavar, MS, PhD; Sujita Sukumaran, PhD; Clare Yarka, MS; Stella Ouyang, MS; Owen Moon, PhD, BSc Hons; and

Michael King, PhD, for help with experimental execution and abstract writing. Medical writing support was provided by Nexus Global Group Science, with funding from Instil Bio, Inc.

REFERENCE

1. Sukumaran S, Kalaitidou M, Mojadidi M, *et al.* Costimulatory antigen receptor (CoStAR): a novel platform that enhances the activity of tumor infiltrating lymphocytes (TILs). *J Immunother Cancer*. 2021;9(Suppl 2):198.

<http://dx.doi.org/10.1136/jitc-2022-SITC2022.0282>

283

GENOME-WIDE CRISPR SCREENS OF CYTOTOXIC T CELLS IDENTIFY A NOVEL REGULATOR THAT ENHANCES T CELL EFFECTOR FUNCTION

Vivian Jia Yi Tan*, Ling Wu, Clara Kai Ting Koh, Yen Leong Chua, Liangzhe Wu, June Xu Hui Ong, Nicholas Gascoigne. *NUS, Singapore, Singapore*

Background Despite the immense therapeutic potential of cytotoxic T lymphocytes (CTLs) in anti-tumor immune response, it remains under-exploited given the limited knowledge we have on genes that regulate its function. Current immunotherapies modulating CTL functions are promising anti-tumor treatment options, but they are severely underutilized due to the lack of druggable targets and potential side effects associated with the treatments. Moreover, the development of new immunotherapies is highly driven by our improved understanding of genetic programs that influences T cell function. Therefore, identifying new immunotherapeutic gene targets is crucial to open new avenues for immunotherapies.

Methods In this study, we first performed an *in vitro* CRISPR-based genome-wide screen for negative regulators of CD8 T cell effector function by sorting for transduced cells with an increased expression of CD107a and tumor necrosis factor (TNF) after gene editing. Using next-generation sequencing, enriched genes in the respective populations were identified and ranked using the available PinAPL-Py platform.¹ To validate and characterize hundreds of the top ranked hits from genome-wide screen at greater details, we created a custom sgRNA mini-pool with newly designed sgRNA sequences for the screened hits. We repeated the screens with the mini-pool against various cancer cell lines as antigen presenting cells to validate the gene targets as well as *in vivo* mice tumour models to examine its effect on tumour infiltration.

Results Our screens robustly identified a gene target which encodes for an actin-binding domain and signal-mediator scaffolding protein that is important in regulating CTL's cytotoxic function. Preliminary data suggests that knocking out the gene target in mouse CD8 T cells showed increased degranulation and production of effector cytokines. Gene-KO T cells also exhibited greater killing efficacy against mouse B16 melanoma cells at various effector to target ratios compared to the control group transduced with non-targeting sgRNA. Further mechanistic studies and validation in mouse tumor models are currently in progress to support the findings.

Conclusions Overall, our data demonstrate that genetic screens for immunotherapeutic gene target discovery is essential to identify new regulators of CTLs. We also showed that our identified gene target plays an important role in modulating the effector function of CTLs and suggests that manipulation of the gene would improve cancer immunotherapy.

REFERENCE

1. Spahn PN, Bath T, Weiss RJ, Kim J, Esko JD, Lewis NE, Harismendy O. PinAPL-Py: A comprehensive web-application for the analysis of CRISPR/Cas9 screens. *Sci Rep.* 2017; Nov 20;7(1):15854. doi: 10.1038/s41598-017-16193-9. PMID: 29158538; PMCID: PMC5696473.

<http://dx.doi.org/10.1136/jitc-2022-SITC2022.0283>

284

EPSTEIN BARR VIRUS SPECIFIC T CELLS (EBVSTs) EXPRESSING B7-H3 TARGETING CHIMERIC ANTIGEN RECEPTORS (CAR) EXHIBIT GOOD PRE-CLINICAL ACTIVITY AND SAFETY AGAINST B7-H3 POSITIVE SOLID TUMORS

Kar Wai Tan*, Lionel Low, Xin Yu Koh, Lindsay Kua, Jin Wei Tan, Siok Ping Yeo, Joanna Kristyn Lim, May Delos Santos, Fiona Wong, Chek Meng Poh, Ivan David Horak, Angeline Goh. *Tessa Therapeutics, Singapore, Singapore*

Background The B7 homolog 3 protein (B7-H3, CD276) is an immune checkpoint member of the B7 and CD28 families that is minimally expressed in healthy tissues. In contrast, B7-H3 is found to be widely over-expressed in multiple types of human cancers, making it an excellent target for CAR T cell therapy.¹ Allogeneic EBVSTs have demonstrated good safety and efficacy in clinical trials and hold the promise to enable broad application of CAR-based T cell therapy in the allogeneic setting.

Methods With the goal of creating off-the shelf allogeneic CAR T cell therapy for solid tumors, we developed Epstein-Barr Virus Specific T cells (EBVSTs) expressing a nanobody-based CAR (B7-H3 CAR EBVSTs) to target B7-H3 positive solid tumors.

Results Our optimised cell manufacturing protocol produced good cell expansion with more than 80% of EBVSTs expressing B7-H3 targeting CAR. B7-H3 CAR EBVSTs demonstrated excellent killing of several B7-H3 expressing colorectal, gastric, non-small cell lung and triple negative breast cancer cell lines while cytotoxicity of B7-H3 knockout counterparts of these cell lines were attenuated. In addition, EBVSTs expressing a truncated B7-H3 CAR that did not contain any intracellular signalling domains was devoid of activity against these cell lines. B7-H3 CAR EBVSTs retained good specificity and reactivity to EBV antigens, evident by abundant production of Tumor Necrosis Factor α and/or Interferon- γ in response to EBV but not to irrelevant HIV pepmixes stimulation.

To assess *in vivo* anti-tumor efficacy, immunodeficient mice were randomized to receive no treatment or treatment with un-transduced or B7-H3 CAR EBVSTs following xenografting of colorectal (HT-29 and SW480) or gastric cancer cell lines (NCI-N87) or triple negative breast cancer (MDA-MB-468) cells. Treatment with B7-H3 CAR EBVSTs induced significant tumor regression in all models compared to the unabated growth in mice that received un-transduced EBVSTs. Further evaluation revealed significantly greater numbers of B7-H3 CAR EBVSTs in blood, liver, lung, spleen and tumors of mice compared to un-transduced EBVST. Body weight of mice from all treatment groups was stable in the days post treatment in all studies, indicating the absence of major tolerability issues.

Conclusions Altogether, our data provides first proof that we are able to generate B7-H3 CAR EBVSTs with good *in vitro* and *in vivo* activity against B7-H3 expressing solid tumors. Given the excellent activity and tolerable safety profile observed, we believe that B7-H3 CAR EBVSTs is a promising candidate for allogeneic CAR T cell therapy against solid tumors.

REFERENCE

1. Seaman S, Zhu Z, Saha S, Zhang X, Yang MY, Hilton MB *et al.* Eradication of Tumors through Simultaneous Ablation of CD276/B7-H3-Positive Tumor Cells and Tumor Vasculature. *Cancer Cell.* 2017; Apr 10;**31**(4):501-515

Ethics Approval This study was approved by Agency for Science, Technology and Research (A*STAR) Institutional Animal Care and Use Committee (IACUC) approval number: 211593.

<http://dx.doi.org/10.1136/jitc-2022-SITC2022.0284>

285

MULTIOMIC ANALYSIS OF TIL SUGGESTS THAT CD4+ POLARIZATION REPRESSES TIL EXPANSION AND CD8+ ACTIVATION AND IS ASSOCIATED WITH PROGRESSION OF DISEASE

¹Brian Thompson*, ²David Woods, ¹Ann Strange, ¹Carol Amato, ¹Jonathan Hester-McCullough, ³Jeffrey Weber, ⁴Amod Sarnaik. ¹CU Anschutz, Aurora, CO, USA; ²University of Colorado School of Medicine, Aurora, CO, USA; ³NYU Langone, New York, NY, USA; ⁴H. Lee Moffitt Cancer Center and Research Institute, Tampa, FL, USA

Background Tumor Infiltrating Lymphocyte (TIL) Adoptive Cell Transfer (ACT) is effective in treating malignant melanoma and other solid tumors. The success of TIL ACT relies on the adequate expansion of TIL, with previous studies showing a positive association between number of TIL infused and patient response. To identify characteristics important for TIL expansion, we performed a multiomic analysis of patients' TIL product.

Methods Expanded TIL products from metastatic melanoma patients enrolled in clinical trials at Moffitt Cancer Center were collected before infusion. CD4+ and CD8+ were isolated and analyzed by RNA-seq (n=13) and pan-acetyl histone 3 ChIP-seq (n=20). The number of TIL, percentage of CD4/CD8 infused, progression free survival (PFS), and overall survival (OS) were recorded. To more evenly divide both RNA-Seq and ChIP-seq samples between groups, patients were categorized into "TIL high" vs "TIL low" based on division at the geometric mean of the number of TIL infused (geometric mean= 4.6e10, range= 9.05e+09 – 1.13e+11). Log2 fold changes of ± 0.5 and q-values of <0.1 were considered significant.

Results Individuals in the "TIL high" group had longer (PFS) (median=92 vs 4, $p < 0.0001$) and OS (OS median=92 vs 10 months, $p < 0.0001$) than those in the "TIL low" group, and the percentage of CD4+ infused was negatively correlated with the number of TIL infused ($R^2 = -0.72$, $p = 7.7e-05$). RNA-seq revealed 30 differentially expressed genes (DEGs) in CD4+ between groups. The upregulated genes in the "TIL low" group included *TNFRSF4*, *PTGDR2*, *IL5*, and *CCL4*, which are associated with Th2 and T_{reg} phenotypes. Pathway analysis of the RNA-seq data further suggested increased Th2 and Th17 polarization in the "TIL low" group. ChIP-seq showed 18 differentially acetylated genes (DAGs) between "TIL high" and "TIL low" CD4+, including increased acetylation at known inducers of T_{regs} *CD200R1*, *IL12RB2*. RNA-seq revealed 3 DEGs between CD8+ in the "TIL high" and "TIL low" groups. ChIP-seq revealed 18 DAGs between "TIL high" and "TIL low" CD8+, with increased acetylation at genes known to be upregulated during CD8+ activation (e.g., *SLC4A10*, *TIGIT* and *P2RY1*).

Conclusions Our results and those of other groups have shown that increased number of TIL infused are associated with positive patient outcomes. Our results further indicate that CD4+ Th2, Th17 and T_{reg} phenotypes in the TIL product are associated with decreased numbers of TIL achieved during expansion. Consequently, we hypothesize that approaches to directing T-cell polarization during TIL expansion may increase patient response rates.

Ethics Approval IRB exempt

<http://dx.doi.org/10.1136/jitc-2022-SITC2022.0285>

286

SYSTEMIC DISTRIBUTION OF GAMMA-DELTA PSCA-CAR T CELLS IN COMBINATION WITH ZOLEDRONATE IN A MODEL OF BONE METASTATIC PROSTATE CANCER

Leticia Tordesillas* Junior Cianne, Jeremy Frieling, Xiomar Bustos, Conor Lynch, Daniel Abate-Daga. *H. Lee Moffitt Cancer Center and Research Institute, Tampa, FL, USA*

Background Metastatic castrate resistant prostate cancer (mCRPC) frequently manifests in the bone, leading to increased morbidity and mortality. We have previously demonstrated that gd Chimeric Antigen Receptor (CAR) T cells targeting prostate stem cell antigen (PSCA) led to significant regression of established prostate cancer cells in the bone. Regression was further increased by combination with the bisphosphonate zoledronate (ZOL), usually administered to mCRPC patients to skeletal related events. To further optimize the use of gd CAR T cells for mCRPC, we aimed to determine the kinetics of gd CAR T cell accumulation and activation in a mouse model of bone metastatic prostate cancer, either as single treatment or in combination with ZOL.

Methods Male NSG mice were intratibial injected with C4-2B prostate cancer cells expressing PSCA and luciferase with the contralateral tibia receiving PBS. ZOL (25 ug/kg) was injected every other day subcutaneously in half of the mice and was discontinued one day prior to administering T cells. When tumors were established, mice received gd PSCA-CAR T cells, gd untransduced (UT) T cells or were left untreated. Bone marrow from tumor-bearing or naïve tibias, femur, spleen and blood were recovered at multiple time points, and the number of gd T cells and their activation status were analyzed by flow cytometry.

Results gd CAR T cells showed an accumulation in the bone marrow recovered from tumor-bearing tibias, with 3 times more gd T cells detected compared to mice treated with gd UT cells ($p=0.0002$). The number of gd T cells peaked at 5 days post infusion and could still be detected after 21 days. Increased gd CAR T cell accumulation was not observed in tumor naïve bone marrows, spleen or blood, suggesting a preferential localization of gd CAR T cells at tumor sites. Moreover, gd CAR T cells presented increased expression of CD25, PD1 and CD56 in comparison with gd UT after only 5 days ($p<0.001$) suggesting their enhance activation. Treatment with ZOL did not significantly affect the number of gd T cells accumulated in bone.

Conclusions gd PSCA-CAR T cells quickly accumulate and become activated at tumor sites with limited distribution outside the bone. ZOL does not appear to impact gd PSCA-CAR T distribution kinetics. Taken together, our data further support the suitability for treatment of bone metastasis.

Ethics Approval The study was approved by University of South Florida IACUC, approval number R7429.

<http://dx.doi.org/10.1136/jitc-2022-SITC2022.0286>

287

NOVEL, BOOSTED, FULLY HUMAN ROR1-TARGETING CAR T CELLS EFFECTIVELY ELIMINATE HEMATOLOGIC AND SOLID TUMORS, AND RESIST TUMOR MICROENVIRONMENT

Tri Tran*, Bal Krishna Chand Thakuri, Saule Nurmukhambetova, Brittany Steimle, Ngoc Tran, Darong Wu, Peirong Hu, Pradyot Dash, Dina Schneider. *Lentigen, Gaithersburg, MD, USA*

Background Receptor tyrosine kinase-like Orphan Receptor 1 (ROR1) is widely expressed in various hematologic and solid tumors. A clinical trial employing ROR1-CAR T-cells with scFv-R12 binder showed poor tumor infiltration and dysfunctionality of CAR T-cells in NSCLC & TNBC patients,¹ suggesting that further CAR-binder/construct optimization may be required to improve CAR T-cell persistence and control of T-cell inhibitory factors in the tumor microenvironment.

Methods We designed new ROR1-CAR constructs, either non-boosted (CAR-1), or boosted with TGFβRII Dominant Negative fragment (TGFβRIIDN), or membrane-bound IL-7 (mbIL7), to overcome the TGFβ1 inhibitory effect in the tumor microenvironment, and to enhance T-cell persistence, respectively. We also designed ROR1-CAR with R12 binder¹ (CAR-2) as control. The ROR1-CARs were transduced into human primary T-cells using lentiviral vectors. *In vitro* cytotoxicity was assessed by co-culture with hematologic mantle cell lymphoma (MCL, Jeko-1), or solid ovarian (OVCAR-3), pancreatic (CAPAN-2) or lung (NCI-H226) tumor cell lines; TNF-α, IFN-γ and IL-2 cytokine release was assessed by ELISA. To simulate tumor microenvironment, CAR T-cells were challenged with TGFβ1 or cultured without exogenous IL-2. *In vivo* xenograft studies were performed in NSG mice bearing Jeko-1 or OVCAR-3 xenografts; tumor progression was monitored, and CAR T cells expansion in mouse peripheral blood was analyzed by flow cytometry.

Results CAR-1-transduced T-cells showed enhanced activation and cytotoxicity against Jeko-1 MCL as compared to CAR-2 *in vitro*, and eliminated tumors in the Jeko-1 model *in vivo*. CAR-1 also mediated potent killing and enhanced cytokine release as compared to CAR-2 upon incubation with OVCAR-3, CAPAN-2, and NCI-H226 solid tumor cell lines *in vitro*. Surprisingly, in *in vivo* ovarian OVCAR-3 xenograft model, CAR-2 failed to reject tumors, whereas CAR-1 mediated remissions; analysis of CAR T-cells in peripheral blood revealed rapid expansion of CAR⁺T-cell population and enrichment for the central memory phenotype in CAR-1 as compared to CAR-2. In addition, we successfully boosted CAR-1 with TGFβRIIDN, which attenuated the inhibitory effect of TGFβ1 on CAR T-cell cytotoxic activity *in vitro*. We also equipped CAR-1 with mbIL7, which enhanced cytotoxic activity and mediated extended functionality of the CAR T-cells without exogenous IL-2 for up to 18 days.

Conclusions The novel fully human ROR1-CAR1 T-cells effectively eliminated both hematologic and solid tumors *in vivo*, and were superior to ROR1-CAR-2 T cells. Furthermore, the boosting elements TGFβRIIDN and mbIL7 are promising tools to overcome the inhibitory effects of tumor microenvironment and sustain CAR T-cell persistence.

REFERENCE

1. Srivastava S *et al.*, Immunogenic Chemotherapy Enhances Recruitment of CAR-T Cells to Lung Tumors and Improves Antitumor Efficacy when Combined with Checkpoint Blockade. *Cancer Cell*, 2021, **39**, 193–208.

<http://dx.doi.org/10.1136/jitc-2022-SITC2022.0287>

288

TARGETING COLD TUMORS USING iPSC-DERIVED CAR T CELLS DIRECTED TO THE IMMUNE CHECKPOINT MOLECULE AND TUMOR-ASSOCIATED ANTIGEN B7-H3

^{1,3}Jon Tuncel*, ¹Bahram Valamehr, ¹Xu Yuan, ¹Francisco Martinez, ¹Nicholas Brookhouser, ¹Philip Chu, ¹Duygu Ozmadenci, ²Zachary Davis, ¹Robert Blum, ¹Bryan Hancock, ¹Bjoern Gaertner, ²Nicholas Zorko, ¹Shohreh Sikaroodi, ¹Miguel Meza, ¹Thomas Dailey, ²Martin Felices, ²Frank Cichocki, ¹Lauren Fong, ¹Tom Lee, ¹Raedun Clarke, ¹John Goulding, ¹Ryan Bjordahl, ²Jeffrey Miller. ¹Fate Therapeutics, Inc. (FHQ1), San Diego, CA, USA; ²University of Minnesota, Minneapolis, USA; ³Fate Therapeutics, Inc. (FTP1), San Diego, CA, USA

Background B7 homolog 3 protein (B7-H3) is a cell-surface protein that is broadly expressed on tumors as well as tumor-associated stromal cells, where it provides inhibitory signals to T and NK cells. Inhibition of B7-H3 using antibody-based modalities has shown promising, albeit incomplete, suppression of tumor progression in clinical studies. Induced pluripotent stem cell (iPSC)-derived chimeric antigen receptor T (CAR-T) cells targeting B7-H3 antigen may offer a unique approach for the treatment of immunologically cold tumors, as treatment may provide an influx of CAR-T cells to tumors that are largely devoid of endogenous infiltrating lymphocytes.

Methods Here we used a unique iPSC engineering strategy to deliver a single tricistronic expression cassette encoding a highly tuned CAR construct consisting of a single-domain camelid antibody against B7-H3 fused to a (CD28-CD3z-1XX) signaling domain, an interleukin (IL)-7 receptor fusion protein, and a high affinity non-cleavable version of the CD16 Fc receptor (hnCD16) into the T-cell receptor α constant (TRAC) locus. These engineered iPSC-derived CAR-T cells demonstrate high potency and fitness and can, unlike naturally occurring T cells, mediate antibody-dependent cell-mediated cytotoxicity (ADCC) to enable combination with monoclonal antibody therapy for treatment of heterogeneous tumors.

Results In preclinical studies, these multi-functional B7-H3 single-domain/1XX iPSC-derived CAR-T cells demonstrated improved tumor control compared to MGA271-scFv/1XX CAR-T cells. Additional preclinical studies confirmed antigen specificity and broad application in targeting various tumor lines. Furthermore, coactivation of hnCD16 markedly improved cytotoxicity against a variety of target cells both in vitro and in vivo, illustrating the potency of coordinated expression of these two pathways in CAR-T cells. Further preclinical studies are ongoing and will be discussed.

Conclusions Taken together, these results provide a tantalizing outlook for the effectiveness of multiplexed-engineered, iPSC-derived CAR-T cells targeting B7-H3, including in combination with therapeutic antibodies, for off-the-shelf treatment of solid tumors.

Ethics Approval All animal experiments were reviewed and approved by Fate Therapeutics Animal Care Committee (IACUC) under the protocol 2019-11-01 O'Rourke.

<http://dx.doi.org/10.1136/jitc-2022-SITC2022.0288>

CLINICAL EXPANSION AND PERSISTENCE OF CAR T-CELLS: AN ESSENTIAL BIOMARKER IN NEED OF STANDARDIZATION

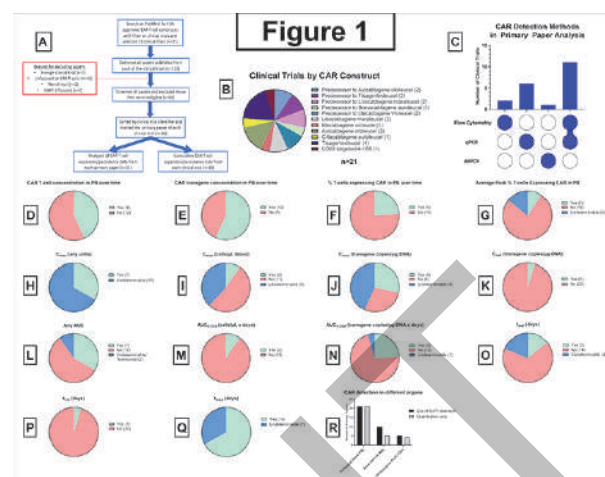
¹David Turicek*, ¹Victoria Giordani, ¹Naomi Taylor, ²Nirali Shah. ¹National Cancer Institute, Bethesda, MD, USA; ²National Institutes of Health, Bethesda, MD, USA

Background *In vivo* CAR T-cell expansion and persistence are associated with response, toxicity, and long-term efficacy. As such, the tools used to detect CAR T-cells are fundamental for optimizing this therapeutic approach. Nevertheless, despite the critical value of this essential biomarker, there is significant variability in CAR T-cell detection methods and the frequency and intervals of testing. Furthermore, heterogeneity in the reporting of quantitative data adds layers of complexity that limit inter-trial and inter-construct comparisons.

Methods We sought to assess the heterogeneity of CAR T-cell expansion and persistence data in a scoping review using the PRISMA-ScR checklist. Based on 21 clinical trials from the United States featuring a Food and Drug Administration-approved CAR T-cell construct or one of its predecessors, 112 papers were screened and 60 were selected for analysis based on the inclusion of CAR T-cell expansion and persistence data (figure 1A). Paper identifiers, CAR construct and antigen targeted, detection technique(s), detection frequency, expansion data and persistence data were all captured in the analysis.

Results Across a wide array of CAR T-cell constructs (figure 1B) and based on the first/primary publication, flow cytometry and quantitative polymerase chain reaction (qPCR) were identified as the two primary techniques for detecting CAR T-cells (figure 1C). Despite apparent uniformity in detection techniques, the specific methods used were highly variable. Further, detection timepoints and the number of evaluated timepoints ranged broadly. Additionally, quantitative data for the parameters assessed were often not reported (figure 1D-R). To evaluate whether subsequent papers from a trial resolve this issue, we analyzed all remaining papers reporting on a clinical trial, recording all expansion and persistence data. Flow cytometry and qPCR remained the most common CAR T-cell detection techniques; however, additional methods included droplet digital PCR, NanoString, and single-cell RNA sequencing. Inconsistencies, however, with detection timepoints and frequency remained, and a significant amount of quantitative data was still not readily available (data not shown).

Conclusions Our findings highlight the critical need to establish a universal standard for reporting on CAR T-cell detection in patients on early phase studies. The current reporting of non-interconvertible metrics and limited provision of quantitative data make cross-trial and cross-CAR T-cell construct comparisons extremely challenging. While unique attributes of CAR T-cells may limit how they can be detected across various constructs, establishing a standardized approach for collecting and reporting data is urgently needed and would represent a substantial advancement in the ability to evaluate cross-trial outcomes.



Abstract 289 Figure 1 1A. Manuscript selection
 1B. CAR T-cell constructs analyzed
 1C. CAR T-cell detection methodologies
 1D-1R. Results for primary analysis evaluating reporting on and methods used for CAR T-cell detection

<http://dx.doi.org/10.1136/jitc-2022-SITC2022.0289>

290

A NOVEL iPSC-DERIVED CAR-INVARIANT NATURAL KILLER T (iNKT) CELL THERAPY PLATFORM FOR HEMATOLOGIC MALIGNANCIES AND SOLID TUMORS

Akane Urakami, Tomokuni Shigeura, Makoto Kondo, Mari Isomi, Yuko Kokubu, Ken-ichi Suzuki*, Haruhiko Koseki. *BrightPath Biotherapeutics Co., Ltd., Kawasaki-Ku, Kawasaki-Shi, Japan;* ²*Riken, Yokohama, Japan*

Background Following a success of autologous chimeric antigen receptor (CAR)-T cells in hematologic malignancies, allogeneic CAR-transduced cells have been developed with various immune cells including induced pluripotent stem cell (iPSC)-derived NK cells and T cells. We have developed a novel platform of first-in-class iPSC-derived CAR-invariant natural killer T (iNKT) cells. iNKT cells are a rare subset of innate lymphocytes that bridge innate and adaptive immune response. iNKT cells can recognize and kill tumor cells, and further enhance antitumor activities of host endogenous immune cells by; cross-talking with dendritic cells; cross-priming tumor-specific CD8⁺T cells; transactivating NK cells; and reprogramming pro-tumor myeloid cells. These intrinsic functions of iNKT cells possibly lead to high persistence and durability of allogeneic CAR-T cell therapy especially for solid tumors in the immunosuppressive tumor microenvironment. Usage of iPSC derived from iNKT cells is an ideal strategy to realize clinical scale production of functional iNKT cells from such a rare cell population. A Phase 1 study of the iPSC-derived non-transduced iNKT cells is currently ongoing in patients with head and neck squamous cell carcinoma. To demonstrate that CAR-transduced iPSC-derived iNKT cells provide a novel platform for effective cancer immunotherapy, the killing activities of CD19-CAR or HER2-CAR-transduced iPSC-derived iNKT cells were investigated in this first set of study.

sMethods iNKT-derived iPSCs were engineered to express CD19-CAR or HER2-CAR by targeting the adeno-associated virus integration site-1 locus using genome editing method. CAR-iNKT cells were obtained by differentiation from CAR-introduced iPSCs under feeder cells free culture condition. The expressions of CAR and iNKT cell surface markers were examined by flow cytometry analysis. *In vitro* cytotoxicity of CAR-iNKT cells against cancer cell lines was examined by xCELLigence[®] real-time cell analyzer.

Results CD19-CAR or HER2-CAR molecules were continuously expressed on engineered CAR-iPSCs. Both CAR-iPSCs were successfully differentiated into iNKT cells in feeder cell-free culture system without losing CAR expression. CAR-iNKT cells showed similar phenotypic properties to iPSC-derived non-transduced iNKT cells. Cytotoxic assay revealed that CAR-iNKT cells possessed enhanced antigen-specific killing activities against target molecule expressing cancer cell lines, such as CD19 positive NALM6 (B cell leukemia) or HER2 positive U-2 OS (Osteosarcoma), compared with iPSC-derived non-transduced iNKT cells.

Conclusions This study showed the first successful delivery of a CAR construct into iPSC cells that differentiate precisely into iNKT cells with enhanced cytotoxicity. iPSC-derived CAR-iNKT cells is demonstrated to become a novel allogeneic cell therapy platform.

Acknowledgements We would like thank Dr. Takahiro Aoki at RIKEN for helpful discussions.

<http://dx.doi.org/10.1136/jitc-2022-SITC2022.0290>

CAR T CELLS AS A SURGICAL ADJUVANT FOR UNRESECTABLE ADENOCARCINOMA

Ugur Uslu*, Tong Da, Charles-Antoine Assenmacher, John Scholler, Regina Young, Julia Tchou, Carl June. *University of Pennsylvania, Philadelphia, PA, USA*

Background Unresectable tumor or incomplete surgical excision of solid tumors are risk factors for primary treatment failure. For those patients, treatment options to clear residual tumor cells following incomplete surgical excision which could be administered promptly and safely in an intraoperative setting would be beneficial. Approaches that could simultaneously clear positive margins without raising safety concerns and interfering with wound healing would be ideal. Here we have tested the hypothesis that the local, intraoperative use of chimeric antigen receptor (CAR) T cell therapy might be an effective surgical adjuvant, based on their emergence as an effective systemic immunotherapy for several hematological malignancies.

Methods We have optimized the use of tissue adhesives as a CAR T cell carrier, which could be applied intraoperatively on the wound surface without the need for intratumoral injection and have evaluated fibrin glue, a biologic tissue adhesive which was found to be an effective sealant and topical hemostatic agent. We then tested the feasibility of this approach in partial resection xenograft models of pancreatic adenocarcinoma and triple negative breast cancer using mesothelin-specific CAR T cells. In addition, we developed a novel in vivo toxicity model to evaluate safety of this approach and effects on wound healing in immunocompetent C57BL/6 mice.

Results We found that the local delivery of CAR T cells in a fibrin-glue based carrier (fibrin gel) applied within the resection cavity was effective in clearing residual cancer cells following incomplete surgical excision of subcutaneous tumors. This resulted in significantly longer overall survival when compared to mice treated with surgery and direct intracavitary CAR T cell injection without fibrin gel. Importantly, on-target off-tumor toxicity was diminished compared to mice treated with systemically administered CAR T cells. In addition, wound healing complications were not seen in any of the immunocompromised or immunocompetent mice.

Conclusions In summary, CAR T cells can be effectively and safely used as a surgical adjuvant in adenocarcinomas that cannot be completely excised. Based on these promising observations, a clinical trial in patients with locally advanced breast cancer is planned.

<http://dx.doi.org/10.1136/jitc-2022-SITC2022.0291>

292

DISCOVERY AND DEVELOPMENT OF T CELL RECEPTORS FOR ADOPTIVE T CELL THERAPY AGAINST SOLID TUMORS

Juliana Velez Lujan*, Hannah Fields, Kan Xing Wu, Natalie Epstein, Florence Chioh, Nicholas Tan, Daniel Carbajo, Neeraja Kulkarni, Lorenz Gerber, Yovita Purwanti, Alessandra Nardin, Michael Fehlings, Katja Fink, Dan Macleod. *Immunoscape, San Diego, CA, USA*

Background T cell receptors (TCRs) have the potential to recognize epitopes derived from both intracellular and cell surface antigens. This facilitates targeting a wide range of tumor antigen classes including overexpressed, differentiation and cancer-testis antigens as well as antigens derived from driver mutations, frameshift mutations, splice variants and human endogenous retroviral elements (HERV). Despite this array of potentially targetable shared antigens, TCR-based anti-tumor therapies have to date only focused on a very limited number of target epitopes. The discovery of clinically relevant TCRs has been challenging due to the limitations in novel tumor antigen discovery and low throughput TCR screening approaches in addition to the inherently low frequency of tumor-reactive T cells in tumor samples and in peripheral blood.

Methods We employ our sensitive and high-throughput Deep Immunomics platform using a mass-cytometry-based multiplexed tetramer staining approach to screen and characterize CD8+ T cells in peripheral blood mononuclear cells (PBMC) for reactivity against >500 potential T cell targets per sample. Downstream single cell sequencing of identified tumor antigen-specific T cells enables a combined analysis of T cell phenotype, transcriptome, TCR specificity and TCR sequence. TCRs identified using this approach are transduced for expression in engineered Jurkat reporter cells and primary T cells and evaluated for activation and effector function, respectively.

Results We have utilized this approach to discover novel TCRs targeting a diverse list of potential tumor epitopes. We identified a TCR recognizing an HLA-A*02-restricted epitope derived from an HERV that is reported to be expressed across many cancer types. In Jurkat reporter cells, this TCR is activated specifically in the presence of the same epitope initially used to identify this TCR, but also through a related epitope variant from the same HERV subfamily. Furthermore, we have identified multiple TCRs that recognize an epitope resulting from alternative splicing of the target antigen in multiple cancers with mutations in a specific splicing factor. Primary T cells expressing these transgenic tumor specific TCR candidates demonstrated killing activity when exposed to target cells presenting the specific cognate peptide.

Conclusions Our Deep Immunomics platform allows us to identify, characterize, and confirm the activity of TCR candidates against novel and therapeutically relevant shared cancer antigens. These findings validate our discovery workflow leading to a portfolio of potential clinical candidates that are currently under preclinical development.

<http://dx.doi.org/10.1136/jitc-2022-SITC2022.0292>

Abstracts

293

THE EFFECTS OF NEGATIVE ISOLATION AND AGGREGATE STRAINERS ON EXPANDED GAMMA/DELTA T CELLS AND THEIR CANCER CELL CYTOTOXICITY

¹Georg von Massow*, ¹Kent Gustafsson, ¹Jack Firth, ²Steve Oh, ³Alan Lam. ¹UCL, London, UK; ²BTI A-Star, Singapore, Singapore; ³A-Star, Singapore, Singapore

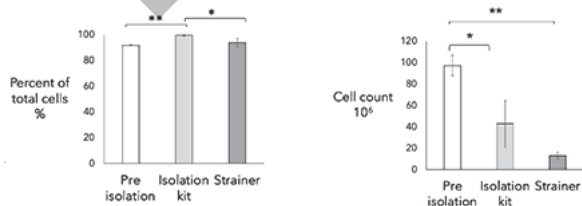
Background One of the most effective ways to purify gd T cells after their expansion, is through negative selection isolation kits. However, even though the target gd T cells are not stained themselves, they appear to suffer stress during the process. An alternative method is to use aggregate strainers which filter cell aggregates through a membrane. This is based on the concept that expanding activated gd T cells, aggregate together. In the context of gd T cells ability to kill cancer cells, the potential stress caused by these methods could affect their functionality.

To shed light on this topic we here analysed the viability, purity, and the functionality of 14 days expanded gd T cells with 24h killing assays on HER2 positive SKBR3 breast cancer cells.

Methods Gd T cells were expanded for 14 days with Zoledronate added on day 0 and IL-2 added every 3 days. Negative isolation was performed using EasySep™ Human Gamma/Delta T Cell Isolation Kit from StemCell Technologies. StemCell Technologies 37mm Reversible Strainers were used for the aggregate isolation. An MTS assay with 1:1 target to effector, with 24h incubation was performed to analyse the killing capacity.

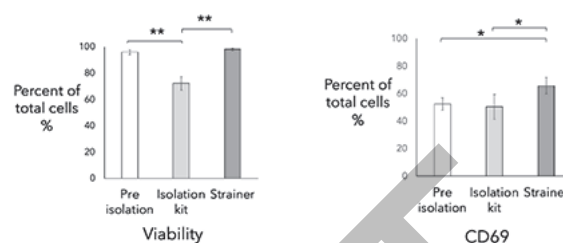
Results The negative isolation showed the highest reliability in generating a near 100% purity of gd T cells (figure 1). The aggregate strainer increased the purity significantly with donors with low gd T cells yield before isolation from 40% to 70%, but could not purify donors with high purity before isolation over 92%. While not statistically significant, the CD69 expression was elevated on the aggregate strainer isolated gd T cells compared to the negative selection isolated gd T cells (figure 2). The viability was significantly reduced after negative selection isolation but was not affected by the aggregate strainer isolation. The killing capacity of gd T cells was significantly reduced for 2 donors after isolation via the negative selection isolation, compared to the gd T cells isolated via aggregate strainers (figure 3). The absolute number of cells isolated was significantly reduced in the aggregate strainer isolation.

Conclusions This indicates that negative selection isolation, while generating a high purity, has a negative impact on the functionality of gd T cells. Aggregate strainers on the other hand can purify gd T cells not to the same purity as negative selection isolation, however retain a high viability in the cell population and show higher killing capacity against SKBR3 cancer cells.



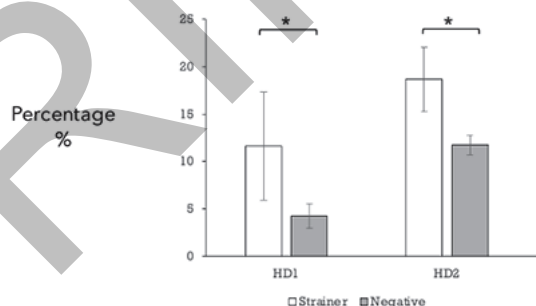
Abstract 293 Figure 1 Purity and absolute cell count
The left graph shows the percent of gd T cells before and after isolation with negative isolation kit and aggregate strainers. The right shows the

absolute cell count before and after isolation with the methods mentioned above.



Abstract 293 Figure 2 The Viability and CD69 expression of gd T cells

The left graph shows the viability before isolation as well as after negative isolation and aggregate strainer isolation in percentage. The right graph shows the expression of CD69 on the same three conditions as the left graph. (* p<0.05; ** p<0.005; n=3)



Abstract 293 Figure 3 Percentage of killing of SKBR3 cells by gd T cells

The killing of SKBR3 cancer cells after 24h with a target to effector ratio of 1:1 is shown for two donors. The killing was analysed via MTS assay.

<http://dx.doi.org/10.1136/jitc-2022-SITC2022.0293>

294

PRECLINICAL STUDIES OF TAC01-CLDN18.2, AN AUTOLOGOUS CLAUDIN 18.2-DIRECTED TAC T CELL THERAPY, IN THE TREATMENT OF GASTRIC CANCER

Ling Wang*, Stacey Xu, Tania Benatar, Suzanna Prosser, Laura Shaver, Ritu Randhawa, Philbert Ip, Prabha Lal, Thanyashanthi Nitya-Nootan, Heather MacGregor, Sadhak Sengupta, Christopher Helsen, Andreas Bader. *Triumvira Immunologics Inc, Hamilton, ON, Canada*

Background The T cell antigen coupler (TAC) is a novel, proprietary chimeric receptor that facilitates the re-direction of T cells to tumor cells and activates T cells by co-opting the endogenous T cell receptor complex with the goal to elicit safe and durable anti-tumor responses. TAC01-HER2, a first-in-class TAC T product targeting HER2 (ERBB2), has entered a phase I/II clinical trial in patients with HER2-positive solid tumors. The subject of this presentation is a new TAC T product, TAC01-CLDN18.2 targeting Claudin 18.2 (CLDN18.2) to treat gastric cancer. CLDN18.2 belongs to a family of Claudin tight junction proteins and is naturally restricted to epithelia of normal stomach. In gastric cancer cells, CLDN18.2 expression can go awry, is no longer confined to tight junctions and, thus, targetable by CLDN18.2-TAC T cells.

Methods CLDN18.2-TAC T cells were evaluated using a variety of *in vitro* and *in vivo* assays. *In vitro* assays were based on flow cytometric analysis of T cell proliferation and surface activation marker expression. Cytotoxicity was assessed via a real-time microscopy-based co-culture assay. *In vivo* studies examined the anti-tumor effect of CLDN18.2-TAC T cells against established solid CLDN18.2-expressing tumors.

Results CLDN18.2-TAC T cells showed a specific anti-CLDN18.2 response as no cytotoxicity, increase in proliferation or activation was observed when they were co-cultured with CLDN18.2-negative target cells. While CLDN18.2-TAC T cells showed cross-reactivity *in vitro* towards target cells expressing murine CLDN18.2, mice showed no signs of toxicity, suggesting that CLDN18.2-TAC T cells do not induce off-tumor effects.

The *in vitro* repeat killing assay demonstrated strong and persistent anti-tumor activity of CLDN18.2-TAC T cells against CLDN18.2 expressing target cells. Lastly, treatment with CLDN18.2-TAC T cells in MHC DKO mice bearing CLDN18.2-positive tumors led to complete and sustained tumor clearance, even after a secondary tumor re-challenge, indicating long-term persistence of TAC cells up to 56 days after initial dosing.

Conclusions The *in vitro* and *in vivo* data confirm strong and specific activity of CLDN18.2-targeted TAC T cells against CLDN18.2-expressing solid tumor models and highlight the versatility of the TAC platform for therapeutic applications in solid tumors.

Ethics Approval The animal study was approved by McMaster University's Animal Research Ethics Board (AUP 20-10-37).

<http://dx.doi.org/10.1136/jitc-2022-SITC2022.0294>

AFFINITY FINE-TUNING ANTI-CAIX CAR-T CELLS MITIGATE ON-TARGET OFF-TUMOR SIDE EFFECTS

¹Yufei Wang*, ¹Alicia Buck, ²Michael Lynch, ¹Gabriella Kastrunes, ³Jae-Won Cho, ¹Marion Grimaud, ⁴David Braun, ¹Cecile Razimbaud, ¹Matthew Chang, ¹Atef Fayed, ¹Audrey Apollon, ¹Ze-Hua Li, ¹Luann Zerefa, ¹Brandon Piel, ¹Elena Ivanova, ¹Dennis Bonal, ¹Kristen Jones, ¹Quang-De Nguyen, ³Zhu Zhu, ³Kevin Wei, ¹Rebecca Jennings, ¹Miriam Ficial, ¹Maura Aliezh Sticco-Ivins, ³Sabina Signoretti, ¹Catherine Wu, ¹Toni Choueiri, ³Jon Wee, ¹Cloud Paweletz, ³Martin Hemberg, ²Aedin Culhane, ¹David Barbie, ¹Gordon Freeman, ¹Wayne Marasco. ¹Dana-Farber Cancer Institute, Boston, MA, USA; ²University of Limerick, Limerick, Ireland; ³Brigham and Women's Hospital, Boston, MA, USA; ⁴Yale University, New Haven, CT, USA

Background Chimeric Antigen Receptor (CAR) T cell therapy is a new type of “living drug” that has proven to be a powerful immunotherapy for hematologic malignancies. To date, there are six CAR-T products approved by FDA, four CD19 targeted CAR-T cells, and two targeting B-cell maturation antigen (BCMA).¹⁻⁸ However, this success has not yet been transferred to solid tumors. A major hurdle is the on-target off-tumor toxicities due to the shared expression of target antigen on healthy tissues.

Methods Here, we assessed the *in vitro* cytotoxicity of carbonic anhydrase IX (CAIX) targeted CAR-T cells generated from a series of single chain fragment variables (scFvs) that have various affinities against CAIX. In addition, we studied the avidity of CAR-T cells using a cell avidity analyzer. We established a tetracycline (Tet)-On inducible CAIX expressing system that provides different CAIX levels on the cell surface covering the range from the density on CAIX-high skrc-59 cells to the one on CAIX-low MMNK-1 cholangiocytes. To assess the therapeutic effect of CAR-T on patient samples, we generated patient derived organotypic spheroids (PDOTS) *ex vivo* cultures and tested CAR-T cell migration and cytokine release using these miniature tumors.

Results We identified a low affinity, high avidity anti-CAIX CAR G9, which only kills CAIX high tumor cells but not CAIX-low normal tissues *in vitro*. G9 demonstrates a CAIX density dependent response on Tet-On inducible CAIX expressing cell lines. G9 CAR has a wider therapeutic window compared to G250 that caused serious adverse events in the first anti-CAIX CAR-T clinical trial.⁹⁻¹¹ G9 exhibits superior efficacy *ex vivo* on ccRCC PDOTS 3D cultures which recapitulates ccRCC patient tumor microenvironment (TME), as well as mitigating toxicity on cholangiectasis spheroids.

Conclusions In summary, affinity fine-tuned CAR-T cell therapy holds the promise to achieve cures of ccRCC by killing ccRCC tumor cells and mitigating on-target off-tumor toxicity on normal tissues.

REFERENCES

1. Maude, S. L., Laetsch, T. W., Buechner, J., Rives, S., Boyer, M., Bittencourt, H. *et al.* Tisagenlecleucel in Children and Young Adults with B-Cell Lymphoblastic Leukemia. *N Engl J Med.* 2018; Feb 1; **378**: 439-448, doi:10.1056/NEJMoa1709866.
2. Schuster, S. J., Bishop, M. R., Tam, C. S., Waller, E. K., Borchmann, P., McGuirk, J. P. *et al.* Tisagenlecleucel in Adult Relapsed or Refractory Diffuse Large B-Cell Lymphoma. *N Engl J Med.* 2019; Jan 3; **380**: 45-56, doi:10.1056/NEJMoa1804980
3. Wang, M., Munoz, J., Goy, A., Locke, F. L., Jacobson, C. A., Hill, B. T. *et al.* KTE-X19 CAR T-Cell Therapy in Relapsed or Refractory Mantle-Cell Lymphoma. *N Engl J Med.* 2020; Apr 2; **382**: 1331-1342, doi:10.1056/NEJMoa1914347.
4. Abramson, J. S., Palomba, M. L., Gordon, L. I., Lunning, M. A., Wang, M., Aramson, J. *et al.* Lisocabtagene maraleucel for patients with relapsed or refractory large B-cell lymphomas (TRANSCEND NHL 001): a multicentre seamless design study. *Lancet.* 2020; Sep 19; **396**: 839-852, doi:10.1016/s0140-6736(20)31366-0
5. Neelapu, S. S., Locke, F. L., Bartlett, N. L., Lekakis, L. J., Miklos, D. B., Jacobson, C. A. *et al.* Axicabtagene Ciloleucel CAR T-Cell Therapy in Refractory Large B-Cell

- Lymphoma. *N Engl J Med.* 2017; Dec 28; **377**: 2531-2544, doi:10.1056/NEJMoa1707447.
6. Locke, F. L., Ghobadi, A., Jacobson, C. A., Miklos, D. B., Lekakis, L. J., Oluwole, O. O. *et al.* Long-term safety and activity of axicabtagene ciloleucel in refractory large B-cell lymphoma (ZUMA-1): a single-arm, multicentre, phase 1-2 trial. *Lancet Oncol.* 2019; Jan; **20**: 31-42, doi:10.1016/s1470-2045(18)30864-7.
7. FDA Approves First Cell-Based Gene Therapy for Adult Patients With Multiple Myeloma. 2021; Mar 27. Available at: <https://www.fda.gov/news-events/press-announcements/fda-approves-first-cell-based-gene-therapy-adult-patients-multiple-myeloma>.
8. Berdeja, J. G., Madduri, D., Usmani, S. Z., Jakubowiak, A., Agha, M., Cohen, A. D. *et al.* Ciltacabtagene autoleucel, a B-cell maturation antigen-directed chimeric antigen receptor T-cell therapy in patients with relapsed or refractory multiple myeloma (CARITUDE-1): a phase 1b/2 open-label study. *Lancet.* 2021; Jul 24; **398**: 314-324, doi:10.1016/s0140-6736(21)00933-8
9. Lamers, C. H., Klaver, Y., Gratama, J. W., Sleijfer, S. & Debets, R. Treatment of metastatic renal cell carcinoma (mRCC) with CAIX CAR-engineered T-cells-a completed study overview. *Biochem Soc Trans.* 2016; Jun 15; **44**: 951-959, doi:10.1042/bst20160037
10. Lamers, C. H., Sleijfer, S., Vulto, A. G., Kruit, W. H., Kliffen, M., Debets, R. *et al.* Treatment of metastatic renal cell carcinoma with autologous T-lymphocytes genetically retargeted against carbonic anhydrase IX: first clinical experience. *J Clin Oncol.* 2006; May 1; **24**: e20-22, doi:10.1200/jco.2006.05.9964
11. Lamers, C. H., Willemsen, R., van Elzakker, P., van Steenberghe-Langeveld, S., Broerjtes, M., Oosterwijk-Wakka, J. *et al.* Immune responses to transgene and retroviral vector in patients treated with ex vivo-engineered T cells. *Blood.* 2011; Jan 6; **117**: 72-82, doi:10.1182/blood-2010-07-294520

Ethics Approval The study obtained DFCI Office for Human Research Studies (OHRS) approval (IRB protocol #19-194).

<http://dx.doi.org/10.1136/jitc-2022-SITC2022.0295>

296

TARGETING B-CELL MALIGNANCIES WITH ANTI-ROR1 CAR T-CELL THERAPY

Jinsheng Weng*, Ow Hofasa Agbedia, Jingjing Cao, Xiaoyun Cheng, Shao Qing Kuang, Fuliang Chu, Sridevi Patchv, Yongfu Tang, Divyam Bansal, Jingwei Liu, Neeraj Saini, Sattva Neelapu. *The University of Texas MD Anderson Cancer Center, Houston, TX, USA*

Background Anti-CD19 chimeric antigen receptor (CAR) T cell therapy has been shown to induce high complete response rates in the majority of B-cell lymphoma patients. However, over 50% of patients relapse within one year. A major cause of failure appears to be due to loss of CD19 expression on the tumor cell surface. This indicates that novel therapeutic strategies are still needed in clinic. Receptor tyrosine kinase like orphan receptor 1 (ROR1) is an oncofetal receptor for Wnt5 α that is expressed in multiple embryonic tissues but absent in virtually all adult tissues. However, ROR1 is expressed at high levels in chronic lymphocytic leukemia (CLL), mantle cell lymphoma (MCL), diffuse Large B-Cell Lymphoma (DLBCL), and several solid tumors. The high expression level of ROR1 in tumor cells is associated with adverse clinical prognosis. In addition, a small percentage of cancer cells with characteristics of undifferentiated leukemia cells or cancer stem cells were found to overexpress ROR1.

Methods Using hybridoma technology, we generated an anti-ROR1 monoclonal antibody that specifically recognized ROR1 protein. The antibody bound to ROR1-expressing MCL cell lines but not to normal donor T cells, B cells, or monocytes, indicating the specificity of the antibody. Lentiviral transduction of a CAR molecule derived from the anti-ROR1 antibody into primary human T cells redirected their specificity against B-cell lymphoma cell lines.

Results We found the anti-ROR1 CAR T cells specifically lysed B-cell lymphoma tumor cells at high efficiency but not normal B cells. At an effector: target ratio of 1:1, the anti-ROR1 CAR T cells lysed over 95% of B-cell lymphoma tumor cells during 3-days of coculture. To determine the optimal CAR construct, we evaluated various hinge, transmembrane, and costimulatory domains in the CAR molecule. We found that incorporation of the CD28 hinge and transmembrane domain in the CAR construct dramatically enhanced the *in vitro* lysis efficiency of anti-ROR1 CAR-T cells.

Conclusions In conclusion, we developed a novel and potent anti-ROR1 CAR T-cell therapy product that may be used for treatment of various B-cell malignancies and ROR1-expressing solid tumors.

Acknowledgements This work was supported by MD Anderson Internal Research grant 2020 (J. Weng).

<http://dx.doi.org/10.1136/jitc-2022-SITC2022.0296>

MANUFACTURE OF KSQ-001, A CRISPR/CAS9-ENGINEERED TIL (ETIL) THERAPY, FOR THE TREATMENT OF HEAD AND NECK SQUAMOUS CELL CARCINOMA

¹Karrie Wong*, ¹Leila Williams, ¹Nick Constant, ¹Mitali Ghose, ¹Sharon Lin, ¹Frank Thompson, ¹Conor Calnan, ¹Fiona Sharp, ²Sean Donnelly, ²Charles Quinn, ²Glenn Hanna, ¹Frank Stegmeier, ¹Micah Benson. ¹KSQ Therapeutics, Cambridge, MA, USA; ²Dana-Farber Cancer Institute, Boston, USA

Background Head and neck squamous cell carcinoma (HNSCC) is characterized by frequent immune infiltration and an immunosuppressive tumor microenvironment. In recent years, adoptive cell therapy with ex vivo expanded tumor infiltrating lymphocytes (TIL) has shown clinical efficacy among HNSCC patients (pts), although the durability of responses to TIL therapy remains limited. To address this issue, we developed KSQ-001, a novel engineered TIL (eTIL) product with CRISPR/Cas9 mediated inactivation of *SOCS1* gene. This gene was identified as a top target for enhancing T cell anti-tumor potency and persistence in vivo from our genome-wide CRISPRomics screens.

Methods Viably cryopreserved primary tumors and/or metastatic lymph nodes (mLN) from HNSCC pts were processed into small fragments and cultured in the presence of IL-2 through the pre-Rapid Expansion Protocol (pre-REP). TILs were then electroporated with ribonucleoprotein (RNP) complex containing the *SOCS1*-targeting guide RNA (gRNA). Following electroporation, engineered TIL (KSQ-001), and an unengineered control TIL were expanded under the REP. Both KSQ-001 and control TIL were harvested on day 27 and cryopreserved. *SOCS1* editing in KSQ-001 was assessed by Next Generation Sequencing (NGS). The phenotypic characteristics and functionality of thawed KSQ-001 drug product from HNSCC tumors were assessed by flow cytometry, TCR sequencing, *in vitro* functional assays, and in *in vivo* models.

Results KSQ-001 was successfully manufactured from 7/8 (88%) of HNSCC tumors with an average of 2000-fold post-electroporation expansion at the REP phase and an average of 95.2% editing at the *SOCS1* locus as assessed by NGS. KSQ-001 from all donors showed levels of TCR diversity similar to those of the matched unedited TIL, and displayed hypersensitivity to IL-12 with elevated pSTAT4 levels upon stimulation. In comparison to donor-matched TIL, KSQ-001 showed greater cytotoxicity and enhanced IFN γ production against 3D tumor spheroids *in vitro*. Further, after infusion into immunocompromised mice, KSQ-001 was detected in circulation at a significantly higher level than control TIL at 7-days post infusion, suggesting hyperresponsiveness to IL-2 and greater persistence *in vivo*.

Conclusions We demonstrated feasibility and robust manufacture of KSQ-001, a *SOCS1*-edited eTIL product, from HNSCC tumors at clinical scale. KSQ-001 from HNSCC tumors consistently displayed enhanced functional potency while retaining a highly diverse TCR repertoire. These data provide a compelling rationale for evaluating KSQ-001 as a therapeutic strategy for patients with HNSCC.

<http://dx.doi.org/10.1136/jitc-2022-SITC2022.0297>

298

**ONCOMETABOLITES IN THE TUMOR
MICROENVIRONMENT DRIVE ALTERED NATURAL KILLER
CELL FUNCTIONAL CAPACITY**

Xinyu Wu*, Sandro Matosevic, Xinyu Wu. *Purdue University, West Lafayette, IN, USA*

Background Natural killer (NK) cells are part of innate immunity with high cytolytic activity against tumor cells, along with the ability to secrete cytokines and chemokines. However, solid tumors have been largely resistant to treatment, owing to unfavorable interactions between immune cells and tumors driven by an immunosuppressive tumor microenvironment (TME). Among tumor-driving metabolites, we have found that adenosine (ADO), has the ability to alter the phenotypic profile of NK cells in solid tumors and enhance their cytotoxicity via inhibiting LAG-3 expression. At the same time, targeting these in the TME of solid tumors with CAR-engineered NK cells enables tumor control and the identification of drivers of resistance to CAR-NK cell killing.

Methods NK cells from lung cancer patients were isolated from blood samples. To study the effect and role of oncometabolites, we treated NK cells with various concentrations of ADO for 24 hours before either removing or leaving them in the medium. NK cell phenotyping, including LAG-3 expression, was measured using flow cytometry. Subsequently, we generated dual-specific CAR-NK cells and identified drivers of resistance to CAR-NK-mediated killing via a genome-based CRISPR screen involving patient-derived GBM.

Using the same conditions as above, NK cells from both groups were then co-cultured with wild type and CD73 knockout (KO) lung carcinoma cell line A549 (A549 WT and A549 CD73KO).

Results Our results showed that NK cell phenotype is altered in response to ADO, including increasing cytotoxicity and aberrant expression of LAG-3, which was downregulated upon ADO treatment, and could be partially recovered upon removal of ADO from the culture medium.

Finally, genome-based CRISPR screening of dual-specific CAR-NK cells co-targeting CD73 identified metabolic drivers of GBM response to NK attack and could represent new targets for adoptive cell therapy with NK cells.

Conclusions Our data showed that metabolites affect NK cell killing capacity. Interestingly, we found that ADO heterogeneously modulates the killing ability of NK cells, suggesting that context- and receptor-specific activation – such as the continued presence of cytokines and metabolites – drives NK cell responses to metabolic factors in the TME. We corroborated these findings with the phenotypic characterization of NK cells isolated from tumors of lung cancer patients and revealed a dysfunctional state linked with an inability of NK cells to support proliferative or cytolytic functions. This dysfunction could be repaired by targeting new transcriptional drivers of GBM resistance to NK cell attack.

<http://dx.doi.org/10.1136/jitc-2022-SITC2022.0298>

3D *IN VITRO* TUMOR MICROENVIRONMENT MODELS FOR SCREENING CAR-T CELL THERAPY EFFICACY

¹Bin Xue, ²Sophie Vermond, ²Ulrike Herbrand, ²David Harris, ²Gemma Moiset, ¹Kolin Hribar*, ²Julia Schuler. ¹Cypre Inc., San Francisco, CA, USA; ²Charles River Laboratories International Inc., Leiden, Netherlands

Background T cells that are genetically modified to express chimeric antigen receptors (CARs) show promising results for treating hematological tumors, however CAR-T cell therapy have thus far demonstrated limited anti-tumor activity in solid tumors.¹ The immunosuppressive tumor microenvironment (TME)² and T cell dysfunction, driven by chronic antigen exposure in solid tumor, likely contribute to the CAR-T resistance. In order to advance the CAR-T therapy into patients with solid tumors, we need models which accurately represent the TME to evaluate CAR-T efficacy at the discovery, preclinical and translational stages of R&D.

Methods Using a proprietary 3D hydrogel patterning technology,³ a 3D in vitro tumor model was generated in 96-well plates utilizing breast cancer cells and human dermal fibroblasts to reflect the tumor and stromal compartments, respectively, of the tumor microenvironment. Specifically, the commercially available HER2-positive breast cancer cell line, JIMT-1, and the triple-negative patient-derived xenograft (PDX) cell line MAXFTN 401, were utilized in these 3D TME models and subsequently interrogated with HER2-specific CAR-T cells as well as untransduced T cells. 5,000, 10,000, or 25,000 T cells were added to each well of the 3D in vitro models and apoptosis via Caspase 3/7 staining was analyzed at day 4 endpoint using high content imaging.

Results T cell-mediated killing in the respective models was highly dependent on their HER2 status – HER2-positive JIMT-1 demonstrated a dose dependent effect in apoptosis (Caspase 3/7 marker) and up to 42% of JIMT-1 cells underwent apoptosis in response to HER2-specific CAR-T cells, while less than 5% of HER2-negative MAXFTN 401 showed a response to any therapeutic dose of the CAR-T cells. Moreover, inclusion of fibroblasts in the 3D TME model enhanced the CAR-T mediated tumor killing in JIMT-1 model. Finally, the untransduced T cells demonstrated negligible effects (<2% in the JIMT-1 model), highlighting the specificity of the HER2-targeting CAR-T cells.

Conclusions A novel 3D in vitro tumor model platform has been described for assaying CAR-T efficacy. In this case, the platform demonstrated the highly specific nature of the CAR-T cells in targeting HER2-positive tumors cells in a translationally relevant 3D in vitro TME model.

REFERENCES

1. Rodriguez-Garcia, A, Palazon, A, Noguera-Ortega, E, Powell, DJ, & Guedan, S, CAR-T Cells Hit the Tumor Microenvironment: Strategies to Overcome Tumor Escape. *Front Immunol.* 2020; **11**:1109.
2. Pitt, JM, Marabelle, A, Eggermont, A, Soria, JC, Kroemer, G, Zitvogel, L, Targeting the tumor microenvironment: Removing obstruction to anticancer immune responses and immunotherapy. *Annal Oncol.* 2016; **27**:1482-1492.
3. Hribar, KC, Wheeler, CJ, Bazarov, A, Varshneya, K, Yamada, R, Buckley, P, Patil, CG, A simple three-dimensional hydrogel platform enables ex vivo cell culture of patient and PDX tumors for assaying their response to clinically relevant therapies. *Mol Cancer Ther.* 2019; **18**:718-725.

<http://dx.doi.org/10.1136/jitc-2022-SITC2022.0299>

300

TRI-MODAL CAR⁺TCR⁺HNCD16⁺ IPSC-DERIVED T CELLS CO-TARGETING SURFACE AND INTRACELLULAR/NEOANTIGENS DEMONSTRATE ADDITIVE EFFECT ON OVERCOMING TUMOR HETEROGENEITY AND CANCER ESCAPE

Bi-Huei Yang*, Soheila Shirinbak, Wen-I Yeh, Alma Gutierrez, Mochtar Pribadi, Bjoern Gaertner, Hui-Yi Chu, David Gonzalez, Angela Liao, Tom Lee, Eigen Peralta, Ryan Bjordahl, Martin Hosking, Chia-Wei Chang, Bob Valamehr. *Fate Therapeutics Inc., San Diego, CA, USA*

Background Antigen escape and tumor heterogeneity remain significant hurdles to the development of curative treatments in many cancers. To address tumor heterogeneity, the introduction of pairs of chimeric antigen receptors (CARs) in donor T cells has been demonstrated, however, this adds complexity to a manufacturing process already challenged by cellular product consistency. To tackle tumor heterogeneity while maintaining product purity, we applied our induced pluripotent stem cell (iPSC)-derived T cell (iT) platform to design an off-the-shelf cell therapy capable of targeting multiple tumor antigens through complementary activation pathways, including targeting of both cell-surface antigens as well as intracellular/neoantigens.

Methods A CAR construct targeting BCMA or MICA/B, a T-cell receptor (TCR) $\alpha\beta$ targeting NYESO1 (1G4) or tumor-associated metabolite presented by MR1 (MC.7.G5), and a high-affinity non-cleavable (hnCD16) to promote antibody-dependent cellular cytotoxicity (ADCC) were engineered into iPSCs for use as a renewable starting source in deriving uniformly-engineered T cells. Resulting multiplexed-engineered CAR⁺TCR⁺hnCD16⁺ (tri-modal) iPSCs were differentiated into T cells and the function of each individual edit was evaluated by preclinical models designed to represent tumor heterogeneity. In addition to *in vitro* mix-culture assays, a mixed cell disseminated *in vivo* model was used to mimic cancer heterogeneity and to evaluate the *in vivo* potency of tri-modal iT cells at mitigating tumor heterogeneity and antigen escape.

Results Assessment of individual edits in tri-modal iT cells demonstrated independent functionality by exhibiting increased antigen-mediated IFN γ and TNF α production, and degranulation compared to the control group ($p < 0.0001$). Using 9-day daily restimulation assay, each edit produced significant tumor reduction compared to tumor only control ($p < 0.0001$). By stimulating tri-modal iT cells with multiple antigens simultaneously using various solid tumor lines (A549, Caski and MDA-MB-231), we found that co-activation by two or three targeting edits significantly enhanced tumor killing ($p < 0.0001$). Furthermore, when challenged with *in vivo* heterogenous tumor models, we found that the co-activation of all three targeting moieties in tri-modal iT cells achieved nearly complete tumor clearance ($p < 0.0001$). *Ex vivo* bone marrow analysis further confirmed antigen-specific target elimination, reinforcing the specificity and potency of the tri-modal iT cells.

Conclusions Our data highlight the potency and broad applicability of tri-modal iT cell expressing CAR, TCR, and hnCD16. This consistent and scalable approach to multiplex-engineered T-cell therapy is an ideal strategy to mitigate antigen escape and combat difficult to treat heterogeneous solid tumors.

<http://dx.doi.org/10.1136/jitc-2022-SITC2022.0300>

301

SINGLE-CELL RNA STUDY OF TRANSCRIPTIONAL ACTIVITIES ASSOCIATED WITH ANAKINRA PROPHYLAXIS AND AXICABTAGENE CILOLEUCEL IN PATIENTS WITH RELAPSED OR REFRACTORY LARGE B-CELL LYMPHOMA

^{1,2,3}Ning Yao*, ⁴Matthew Frigault, ⁴Marc Wehrli, ⁴Kathleen Gallagher, ⁴Charlotte Graham, ⁵Caron Jacobson, ⁶Rhine Shen, ⁶Simone Filosto, ⁶Justin Budka, ⁶Sao-Mai Nyugen-Mau, ⁶Jenny Nater, ⁶Mike Mattie, ^{3,4,7}Gad Getz, ³Nicholas Haradhvala, ^{3,4,7}Marcela Maus. ¹Harvard T.H. Chan School of Public Health, New York, NY, USA; ²Tri-Institutional PhD Training Program, New York, NY, USA; ³The Broad Institute, New York, NY, USA; ⁴Massachusetts General Hospital Cancer Center, Boston, MA, USA; ⁵Dana Farber Cancer Institute, Boston, MA, USA; ⁶Kite, a Gilead Company, Santa Monica, CA, USA; ⁷Harvard Medical School, Boston, MA, USA

Background Chimeric antigen receptor T-cell (CAR-T) therapy has shown unprecedented treatment outcomes for B-cell malignancies. The wider utilization of CAR-T, however, is limited by CAR-T-induced adverse events including cytokine release syndrome (CRS). Tocilizumab, a monoclonal antibody blocking Interleukin (IL)-6 receptor, is the only approved treatment for CRS. Recent animal studies suggest that anakinra, a recombinant form of IL-1 receptor antagonist, could have potential benefit in managing toxicity, with or without tocilizumab. We have opened a clinical trial (NCT04150913) testing the use of prophylactic anakinra in patients with relapsed or refractory large B-cell lymphoma eligible to receive axicabtagene ciloleucel (axi-cel) as per the registration study ZUMA-1. Here, we used single-cell RNA sequencing (scRNA-seq) on clinical samples of the first ten subjects on the study¹ to probe the molecular pathways altered by anakinra and to discover potential mediators of breakthrough cases of CRS.

Methods We conducted scRNA-seq on the peripheral blood mononuclear cells (PBMCs) of 10 patients 7 days post infusion (D7) and the infusion products (IP). We compared data from the trial subjects to 4 control samples from the same institution along with our previously generated scRNA-seq IPs and D7 PBMCs from 19 subjects that were treated with axicel without prophylaxis for toxicity.² We utilized pseudo-bulk differential expression analysis of major immune cell types to reveal transcriptional signals associated with CRS and anakinra treatment.

Results Our study revealed that IL-4 and IL-10 anti-inflammatory pathways in IPs of both anakinra and non-anakinra cohorts were negatively associated with breakthrough CRS. We further observed that the same pathways were enriched at D7 in anakinra-treated CAR+ CD4+ T cells populations. Anakinra prophylaxis had little effect on the overall CAR+ T-cell compositions from IPs to D7, but was associated with an increased proportion of CAR+ regulatory T cells (Tregs). Expression of interferon gamma (IFN γ) pathways, cytokine levels of IFN γ and IFN γ -induced protein 10 (CXCL10) in CD14+ monocytes were significantly enriched in patients with breakthrough CRS treated with tocilizumab in the anakinra cohort. Differential cell-cell interaction analysis further showed the association of IFN γ ligand receptor activities with breakthrough toxicity uniquely among anakinra- and tocilizumab-treated patients.

Conclusions We identified key molecular pathways and immune cell populations that were possibly modulated by anakinra, including the upregulation of IL-10 signaling pathway in CAR+ CD4+ T cells and increased abundance of Tregs. IFN γ enrichment in patients with breakthrough CRS further suggests that this pathway is also targetable and not inhibited by anakinra alone.

Acknowledgements The clinical trial is funded by Kite Pharma and the correlative studies are funded by R01CA252940. **Trial Registration** NCT04150913 (A Phase 2 Trial of Anakinra for the Prevention of CAR-T Cell Mediated Neurotoxicity)

REFERENCES

1. Frigault, M. J. *et al.* A Phase II Trial of Anakinra for the Prevention of CAR-T Cell Mediated Neurotoxicity. *Blood*. 2021;**138**:2814.
2. Haradhvala, N. J. *et al.* Distinct cellular dynamics associated with response to CAR-T therapy for refractory B-cell lymphoma. *Nature Medicine*. 2022; in press. <http://medrxiv.org/lookup/doi/10.1101/2022.04.04.22273422>. doi:10.1101/2022.04.04.22273422.

Ethics Approval The clinical study complies with IRB-approved protocol (19-348) at the Dana-Farber/Harvard Cancer Center.

<http://dx.doi.org/10.1136/jitc-2022-SITC2022.0301>

302 ALLOGENIC ADOPTIVE NK CELLS AND IRRADIATION
JOIN FORCE TO CONTROL TRIPLE NEGATIVE BREAST
CANCER STEM CELLS

Meesun Yoon*. Chonnam National University Medical School, Hwasun-gun, Korea, Republic of Korea

Background Previously, our group has shown the long-term synergistic effects of allogeneic expanded natural Killer (NK) cells and Irradiation in a human triple-negative breast cancer (TNBC) model. Primary tumor irradiation enhanced the migration and infiltration of adoptive NK cells into tumor microenvironment (TME), hence increasing the NK cell's ability to lyse tumor cells. Although RT alone successfully controlled primary tumor, however, the primary tumor bioluminescence intensity was significantly reduced only in the RT+NK group compared to the RT alone. To clarify this phenomenon, we investigated cancer stem cells (CSC) population correlated with radioresistance and metastatic propensity.

Methods We analyzed CSC phenotype in human TNBC after irradiation in a time- and dose-dependent manner by using multiparameter flow cytometry. Ex vivo expansion of NK cells from human peripheral blood mononuclear cells was performed by co-culture with conventional K562 cells. NK cell cytotoxicity against CSCs were evaluated under irradiated TME. Mammosphere was generated to investigate the efficacy of combination therapy against CSC. Allogenic NK cells were i.v injected twice after local tumor irradiation in human TNBC xenograft model. Single cells suspension of tumors was prepared on day 14 after treatment and analyzed with flow cytometry

Results We identified ALDH+CD44+CD24- CSC phenotype showing increased absolute number of MDA-MB-231 CSCs population after fractionated RT compared to single-dose RT. Interestingly, NK cells effectively killed CD44+CD24- CSC population in response to an increased effector to target ratio. Combined NK cells with RT significantly decreased CD44+CD24- population of tumors both single-dose and fractionated RT ($p=0.0104$ and $p=0.0188$). We observed a significantly increase NK cells' lysis ability against TNBC mammosphere both single-dose RT ($p=0.0011$) and fractionated RT ($p=0.0145$) compared to non-irradiated group. However, there was no synergistic effect of NK cells and irradiation against parental TNBC cells. Moreover, allogenic NK cells prefer to lyse mammosphere but not parental cells when co-cultured sphere and parental cells together. NK cells combined with single-dose irradiation more effectively killed TNBC mammosphere than fractionated irradiation ($p=0.0212$).

Conclusions Allogenic NK cells effectively killed breast-stem like cells. Combination therapy enhances NK cells antitumor response against breast cancer stem-like cells, suggesting that elimination of stem like cells by NK cells is closely correlated to long-term primary tumor control under irradiated TME. For RT dose scheme when combined with NK therapy, single-dose irradiation improved antitumor response against breast cancer stem-like cells.

<http://dx.doi.org/10.1136/jitc-2022-SITC2022.0302>

Abstracts

303

TARGETING EWING SARCOMA WITH ANTI-IL1RAP CHIMERIC ANTIGEN RECEPTOR MODIFIED NATURAL KILLER CELLS

¹Wen Luo*, ²Poul Sorensen, ¹Mitchell Cairo, ¹Hai Hoang, ¹Yaya Chu, ¹Janet Ayello, ³Wei Li, ²Michael Lizardo, ²Renata Ribeiro, ²Melanie Rouleau, ³Dimitar Dimitrov, ⁴Dean Lee, ²Hai-Feng Zhang. ¹New York Medical College, Valhalla, NY, USA; ²BC Cancer Research Centre, Horsholm, Denmark; ³University of Pittsburgh, Pittsburgh, PA, USA; ⁴Nationwide Children's Hospital, Columbus, OH, USA

Background Metastatic and recurrent/refractory Ewing sarcoma (ES) has a dismal prognosis,¹ largely secondary to therapy resistance within the tumor microenvironment.² ES have heightened natural killer (NK) cell sensitivity,³ and increased abundance of activated NK cells in ES patient tumors are correlated with extended survival.⁴ Solid tumors are resistant to NK in large part due to the small number of active NK cells and lack of specific tumor targeting of NK cells.² Our group has developed a genetically engineered feeder cell to expand peripheral blood mononuclear cells (PBMCs) into NK cells,⁵ and demonstrated that expanded NK cells engineered to express chimeric antigen receptor (CAR) against various targets including CD20, GD2, ROR1 and MCAM had significantly enhanced cytotoxicity against lymphoma and sarcomas^{6,7} compared to mock NK. IL-1 receptor accessory protein (IL1RAP) is highly expressed on ES cells and minimally expressed in normal tissues as we previously reported.⁸

Methods Here we developed an anti-IL1RAP CAR NK cell and investigated its efficacy in promoting NK cell cytotoxicity against ES. PBMCs were expanded into NK cells using K562-mbIL21-41BBL artificial antigen presenting cells. The IL1RAP antibody VH domain DNA was codon optimized and synthesized to create the anti-IL1RAP CAR. CAR NK cells were generated by non-viral electroporation of CAR mRNA into expanded NK cells. CAR expression was analyzed by flow cytometry using biotinylated IL1RAP protein. Anti-IL1RAP CAR NK cytotoxicity was evaluated in vitro by luciferase based cytotoxicity assay. CRISPR-Cas9 mediated IL1RAP knockout (KO) in ES cells was utilized to evaluate the specificity of CAR NK targeting.

Results Electroporation resulted in CAR expression in 70% of expanded NK cells and the CAR expression lasted for at least 6 days (figure 1). We found a significantly increased cytotoxicity of anti-IL1RAP CAR NK cells compared to mock NK cells against ES A673 and SKNMC cells at various effector to target ratios after co-culturing for 4 hours (**p<0.01 and *p<0.05) (figure 2). In the IL1RAP KO A673 cells, we did not observe the significant increase in cytotoxicity with IL1RAP CAR NK compared to mock NK as we did in the wildtype (WT) A673 cells (figure 3), demonstrating the enhanced cytotoxic activity of CAR NK cells is due to specific targeting of IL1RAP.

Conclusions These findings demonstrate enhanced efficacy of anti-IL1RAP CAR NK cells compared to mock NK cells against ES and support a preclinical evaluation of anti-IL1RAP CAR NK in limiting ES xenograft tumor growth and/or metastasis and prolonging animal survival in vivo.

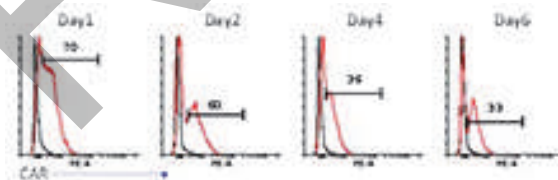
Acknowledgements This study is funded by NCI Cancer Moonshot U54 grant (CA232561-01A1).

REFERENCES

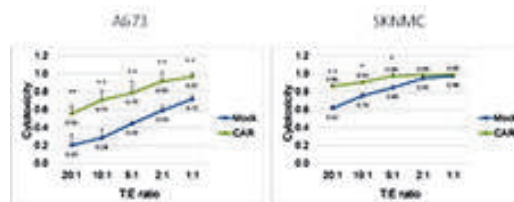
1. Ladenstein R, Potechger U, Le Deley MC, Whelan J, Paulussen M, Oberlin O, van den Berg H, Dirksen U, Hjorth L, Michon J, Lewis I, Craft A, Jurgens H: Primary disseminated multifocal Ewing sarcoma: results of the Euro-EWING 99 trial. *J Clin Oncol.* 2010; **28**:3284-3291. <http://www.ncbi.nlm.nih.gov/pubmed/20547982>

- Nayyar G, Chu Y, Cairo MS: Overcoming Resistance to Natural Killer Cell Based Immunotherapies for Solid Tumors. *Front Oncol.* 2019; **9**:51. <https://www.ncbi.nlm.nih.gov/pubmed/30805309>
- Cho D, Shook DR, Shimasaki N, Chang YH, Fujisaki H, Campana D: Cytotoxicity of activated natural killer cells against pediatric solid tumors. *Clin Cancer Res.* 2010; **16**:3901-3909. 3168562, <http://www.ncbi.nlm.nih.gov/pubmed/20542985>
- Stahl D, Gentles AJ, Thiele R, Gutgemann I: Prognostic profiling of the immune cell microenvironment in Ewing's Sarcoma Family of Tumors. *Oncoimmunology.* 2019; **8**:e1674113. 6844324, <http://www.ncbi.nlm.nih.gov/pubmed/31741777>
- Chu Y, Flower A, Cairo MS: Modification of expanded NK cells with chimeric antigen receptor mRNA for adoptive cellular therapy, in Somanchi S (ed): *Methods in Molecular Biology. Natural Killer Cells: Methods and Protocols.* New York, Humana Press, Springer, 2016, pp 215-230
- Chu Y, Hochberg J, Yahr A, Ayello J, van de Ven C, Barth M, Czuczman M, Cairo MS: Targeting CD20+ Aggressive B-cell Non-Hodgkin Lymphoma by Anti-CD20 CAR mRNA-Modified Expanded Natural Killer Cells In Vitro and in NSG Mice. *Cancer Immunol Res.* 2015; **3**:333-344. <http://www.ncbi.nlm.nih.gov/pubmed/25492700>
- Gardenswartz A, Luo W, Rosenblum JM, Ayello J, and Cairo MS. Targeting Ewing sarcoma and osteosarcoma with anti-MCAM chimeric antigen receptor modified NK cells. *Cancer Research* 2020;80.
- Zhang HF, Hughes CS, Li W, He JZ, Surdez D, El-Naggar AM, Cheng H, Prudova A, Delaidelli A, Negri GL, Li X, Orum-Madsen MS, Lizardo MM, Oo HZ, Colborne S, Shyp T, Scopim-Ribeiro R, Hammond CA, Dhez AC, Langman S, Lim JKM, Kung SHY, Li A, Steino A, Daugaard M, Parker SJ, Gelfink RIK, Orentas RJ, Xu LY, Morin GB, Delattre O, Dimitrov DS, Sorensen PH. Proteomic Screens for Suppressors of Anoikis Identify IL1RAP as a Promising Surface Target in Ewing Sarcoma. *Cancer Discov.* 2021;**11**(11):2884-2903.

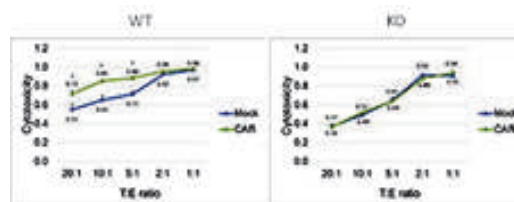
Ethics Approval This study was approved by the New York Medical College Institutional Animal Care and Use Committee (protocol number 13911).



Abstract 303 Figure 1 Anti-IL1RAP CAR expression on ex vivo expanded NK cells on day 1 to 6 post electroporation



Abstract 303 Figure 2 In vitro cytotoxicity of anti-IL1RAP CAR NK and mock NK cells against ES A673 and SKNMC cells. **p<0.01, *p<0.05.



Abstract 303 Figure 3 In vitro cytotoxicity of anti-IL1RAP CAR NK and mock NK cells against A673 IL1RAP WT and KO cells. *p<0.05.

<http://dx.doi.org/10.1136/jitc-2022-SITC2022.0303>

304

OFF-THE-SHELF IPSC-DERIVED CAR-T CELLS CONTAINING SEVEN FUNCTIONAL EDITS OVERCOME ANTIGEN HETEROGENEITY, IMPROVE TRAFFICKING, AND WITHSTAND IMMUNOSUPPRESSION ASSOCIATED WITH FAILED TUMOR TREATMENT

Martin Hosking*, Soheila Shirinbak, Bishwas Shrestha, Joy Grant, Kyla Omilusik, Hannah Keegan, Demetrio Cardenas, Angela Gentile, Shilpi Chandra, Lorraine Loter, Lexe Linderhof, Nicholas Brookhouser, Stephanie Kennedy, Francisco Martinez, Loraine Campanati, Chris Ecker, Xu Yuan, Karina Palomares, Yi-Shin Lai, Lauren Fong, Yijia Pan, Shohreh Sikaroodi, Mark Jelcic, Philip Chu, Amit Mehta, Layton Smith, Eigen Peralta, Tom Lee, Ramzey Abujarour, Raedun Clarke, Bob Valamehr. *Fate Therapeutics, Inc, San Diego, CA, USA*

Background Although chimeric antigen receptor (CAR) T-cell therapy has shown remarkable efficacy in liquid tumors, its wider application to solid tumors has been hampered by tumor-associated antigen (TAA) heterogeneity, inefficient CAR-T cell trafficking to the tumor, and immunosuppression inherent to the tumor microenvironment. Moreover, the often-dysfunctional and heterogenous yield of highly-edited (*e.g.* >2 transgenes) CAR-T cells necessary to address these obstacles has limited their efficacy and wider clinical investigation.

Methods T-cell derived induced pluripotent stem cells (TiPSCs) were engineered to express a CAR targeting a novel TAA domain and an interleukin-7 receptor fusion protein (IL7RF) under the regulation of the T-cell receptor alpha chain constant locus. Additionally, these TiPSCs were engineered to express TGF β -signal redirection receptor (TGF β -SRR), high-affinity non-cleavable CD16A (hnCD16), and CXCR2 within the CD38 locus enabling TGF β resistance, secondary TAA targeting via antibody-dependent cell cytotoxicity (ADCC), and solid tumor specific trafficking, respectively. Engineered TiPSCs were differentiated into alpha-beta T (iT) cells, uniformly expressing all engineered transgenes and completely lacking both CD38 and T-cell receptor expression, avoiding the potential risk of graft-versus-host disease in an allogeneic setting.

Results Functional evaluation of these multiplexed-engineered CAR iT cells demonstrated broad, potent, and specific CAR based efficacy across multiple solid tumor indications. Importantly, hnCD16 activation with multiple therapeutic antibodies further augmented anti-tumor efficacy across target cell lines with heterogenous CAR antigen expression, underscoring the broad efficacy, applicability, and multi-antigen targeting capability of these CAR iT cells. Additionally, engineered CAR iT cells maintained high levels of anti-tumor efficacy over multiple rounds of tumor challenge, even in the presence of high and suppressive levels of TGF β (Round 3 challenge with TGF β : 90% cytolysis with TGF β -SRR expressing CAR iT cells vs. 10% cytolysis with control CAR iT cells), demonstrating potent resistance to TGF β -mediated effector suppression. CXCR2 expression enabled specific and potent migration to the CXCR2 ligand IL-8 (2-fold specific migration, 10ng/ml) that has been associated with, along with other CXCR2 ligands, poor outcomes in diverse tumor indications. Furthermore, we demonstrate robust anti-tumor efficacy in an aggressive ovarian cancer xenograft model which, when coupled with the activation of hnCD16 via therapeutic antibody, reached complete tumor clearance.

Conclusions Together these results demonstrate that a multiplexed-engineered CAR-iT cell product tailored for solid tumors can promote trafficking, overcome tumor microenvironment resistance, and elicit enhanced anti-tumor activity.

Ethics Approval These studies were approved by Fate Therapeutics Institutional Animal Care and Use Committee and

were carried out in accordance with the National Institutes of Health's Guide for the Care and Use of Laboratory Animals.

<http://dx.doi.org/10.1136/jitc-2022-SITC2022.0304>

305 **COMBINATION IMMUNOTHERAPY USING A NOVEL CHIMERIC ONCOLYTIC VIRUS TO REDIRECT CD19 BISPECIFIC T CELL ENGAGERS TO TARGET SOLID TUMORS**

¹Anthony Park*, ¹Saul Priceman, ²Leslie Chong, ¹Yuman Fong, ¹Isabel Monroy, ¹Colin Cook, ²Monil Shah. ¹City of Hope, Duarte, CA, USA; ²Imugene, Sydney, Australia

Background Bispecific T cell engager (BiTE) monoclonal antibodies have emerged as a promising immunotherapy strategy for the treatment of hematological malignancies. Blinatumomab, an FDA approved BiTE carrying CD19 and CD3 epitopes has shown durable clinical responses for the treatment of B-cell acute lymphoblastic leukemia (B-ALL) and non-Hodgkins lymphomas. Despite a wide array of research in hematological malignancies, BiTE therapies for the treatment of solid tumors have remained a significant challenge in demonstrating comparable efficacy. Solid tumors often lack amenable and targetable tumor antigens, and in many solid tumors the tumor microenvironment (TME) is largely known to be immunologically “cold” and a barrier to immunotherapy responses. Oncolytic viruses have recently gained traction in the field for the treatment of solid tumors because of their ability to target tumor-intrinsic properties and reshape the immunosuppressive TME. We have previously described the use of a chimeric oncolytic vaccinia virus (CF33) for the treatment of a variety of tumor cell types, including triple-negative breast cancer, lung cancer, and liver cancer. Building on this, we generated an OV that expresses a non-signaling, truncated CD19 antigen (CF33-CD19t or onCARlytics, in collaboration with Imugene Limited), onto the surface of infected tumor cells prior to virus mediated tumor lysis, which redirected CD19-targeting chimeric antigen receptor (CAR) T cell activity against solid tumors (Park *et al.* STM 2020). Using this combination, we have created a universal system that is agnostic to solid tumor type and can be provided with a targetable and well-characterized antigen. We now show that blinatumomab can be redirected to solid tumors with CF33-CD19t, enabling an off-the-shelf combinatorial immunotherapy strategy.

Methods For preclinical testing, we utilized *in vitro* co-culture assays using human healthy donor-derived T cells and human triple-negative breast cancer cells treated with CF33-CD19t and blinatumomab. We evaluated tumor cell killing and T cell activation using flow cytometry and cytokine assays. Humanized NSG mice were used to evaluate anti-tumor activity of the combination *in vivo*.

Results Tumors infected with CF33-CD19t along with blinatumomab show specific tumor cell killing *in vitro* and robust anti-tumor efficacy using *in vivo* human triple-negative breast cancer xenograft models.

Conclusions Using this approach, we show that a clinically-approved CD19-directed BiTE can be combined with oncolytic viruses to activate and redirect endogenous anti-tumor immunity against solid tumors.

<http://dx.doi.org/10.1136/jitc-2022-SITC2022.0305>

306

EVALUATION OF AB-101, AN ALLOGENEIC CORD BLOOD-DERIVED NATURAL KILLER (NK) CELL THERAPY, AS AN ADCC ENHANCER IN HEMATOLOGIC AND SOLID TUMORS

¹Paul Rogers, ²Bitna Yang, ²Hyojin Kim, ²Yusun Kim, ²Sunglim Cho, ¹Bret Morin, ¹Amanda Conerty, ³Lavakumar Karyampudi, ¹Lisa Guerretaz, ¹Peter Flynn, ²Bokyung Min, ¹Heather Raymon*. ¹Artiva Biotherapeutics, San Diego, CA, USA; ²GC Cell, Seoul, Republic of Korea; ³Moffitt Cancer Center, Tampa, FL, USA

Background AB-101 is a non-engineered, allogeneic, off-the-shelf, cryopreserved cord blood-derived natural killer (NK)-cell therapy in development as a cancer therapeutic. A highly scaled manufacturing process enables production of 1000s of doses from a single donor cord blood unit (CBU). AB-101 has been optimized for combination with monoclonal antibodies (mAbs) to enhance antibody-dependent cellular cytotoxicity (ADCC) and anti-tumor responses through selection of key attributes in the CBU. These include a KIR-B haplotype and natural high-affinity variant of CD16 (158V/V polymorphism), which are associated with improved anti-tumor activity and ADCC enhancement. Administration of AB-101 to patients in combination with mAbs has the potential to enhance the ADCC response thereby increasing anti-tumor activity. Here we present preclinical data to support development of AB-101 in combination with mAbs as an ADCC enhancer in hematologic malignancies and solid tumor indications.

Methods AB-101 was expanded utilizing a proprietary engineered feeder-cell line. In vitro characterization of AB-101 included evaluation of the purity and expression of cell surface markers by flow cytometry. In vitro ADCC assays were performed at various effector to target ratios against hematologic (Raji, ARH-77) and solid tumor (MDA-MB-468) cell lines in the presence of approved therapeutic antibodies. In addition, AB-101 efficacy was assessed in vivo in established hematologic (Raji) and ovarian (SKOV-3) xenograft models.

Results AB-101 was $\geq 95\%$ CD3-CD56+ with $\geq 80\%$ CD56+CD16+ and high expression of NK activating receptors such as NKG2D, NKp30, NKp44 and DNAM-1 was observed. Cytotoxicity assays were used to demonstrate the ADCC mechanism of activity in combination with approved therapeutic antibodies. In the Raji cell line, when AB-101 was combined with rituximab, $\sim 90\%$ of target cell lysis was observed vs $\sim 79\%$ with AB-101 alone. Similar cell killing activity was observed against ARH-77 and MDA-MB-468 cell lines in combination with obinutuzumab and cetuximab, respectively. In addition, in vivo efficacy of AB-101 and AB-101 in combination with rituximab demonstrated enhanced median survival in the Raji xenograft model and AB-101 in combination with trastuzumab led to enhanced survival in the SKOV-3 xenograft model.

Conclusions Data presented suggests that AB-101 is a pure and readily expandable NK cell product that has the potential to be effective in combination with mAbs to treat both hematologic and solid tumors without the need for engineering. AB-101 is currently in a Ph1 clinical trial to evaluate the safety and anti-tumor activity alone and in combination with rituximab in patients with relapsed or refractory NHL (ClinicalTrials.gov: NCT04673617).

Ethics Approval All animal work was conducted under reviewed IACUC protocol and with approval of an IACUC committee at each center where the studies took place.

<http://dx.doi.org/10.1136/jitc-2022-SITC2022.0306>

307

IL12 GENETICALLY ENGINEERED MYELOID CELLS EFFECTIVELY TARGET THE MYELOID-ENRICHED TUMOR AND METASTATIC MICROENVIRONMENT IN AN IMMUNE-COMPETENT MURINE MODEL OF OSTEOSARCOMA

Kristin Wessel*, Miranda Clements, Wei Ju, Sabina Kaczanowska, Rosandra Kaplan. National Institutes of Health, Bethesda, MD, USA

conducted in specific pathogen-free conditions at the NIH animal facility.

<http://dx.doi.org/10.1136/jitc-2022-SITC2022.0307>

Background Osteosarcoma is the most common bone tumor in children and adolescents. Outcomes for patients presenting with metastatic and recurrent disease are poor and have not improved over the past forty years; therefore, novel therapies are urgently needed. Immunotherapy has shown promise for some solid malignancies, however, durable responses are often rare and several challenges, including an immune-suppressive microenvironment, limit efficacy. We hypothesized that Genetically Engineered Myeloid cells (GEMys) could be used as a platform to locally deliver the anti-tumor cytokine IL12 to primary tumor and metastatic sites. We aimed to profile the tumor and pre-metastatic immune microenvironments in a syngeneic murine model of osteosarcoma and to evaluate the effect of IL12-GEMys on tumor microenvironment dynamics and survival.

Methods We utilized a syngeneic orthotopic OS model (F40210 gifted by Dr. Yustein, Baylor College of Medicine) derived from a spontaneous tumor arising in Col2.3-Cre/p53^{fl/+} mice. C57BL/6 mice were inoculated with tumor cells via orthotopic intratibial injection. Immune populations in the primary tumor and pre-metastatic lung were profiled at various timepoints during tumor progression utilizing flow cytometry, immunofluorescence and RNAseq. We engineered myeloid cells with a lentiviral vector to express IL-12, a potent anti-tumor cytokine, and administered IL12-GEMys intravenously to mice inoculated with osteosarcoma tumors.

Results Our characterization of the tumor and pre-metastatic microenvironment revealed a dense vascular and stromal matrix with steady enrichment of myeloid cells during cancer progression. Analysis of the immune microenvironment revealed an abundance of tumor-associated macrophages that develop an increasingly immune-suppressive phenotype during tumor progression. CD8⁺ T cells in the tumor were relatively rare and showed increased expression of activation markers PD-1 and CD44 during tumor progression. The presence of F42010 orthotopic tumors was associated with pre-metastatic niche formation in lungs of tumor-bearing mice, as evidenced by increased macrophage infiltration and upregulation of a myeloid-mediated immune suppressive gene signature. In the pre-metastatic lung, IL12-GEMy treatment increased T and NK cell activation and increased myeloid MHCII expression. IL12-GEMy administration resulted in enhanced T and NK cell infiltration into the primary tumor microenvironment. Finally, IL12-GEMy monotherapy reduced tumor growth and prolonged survival compared to vector control GEMy cell therapy.

Conclusions These data provide insight into immune population dynamics and pre-metastatic niche formation in immune-competent murine model of osteosarcoma and show that IL12-GEMys represent a promising strategy to reverse or limit the immune-suppressive microenvironment in osteosarcoma.

Acknowledgements We would like to acknowledge the Children's Cancer Foundation for supporting this work.

Ethics Approval All animal studies were approved by the NCI Animal Care and Use Committee (Protocol PB-054) and were

308 **HARNESSING TUMOR LOCALIZED IL-12 TO ENHANCE STEAP1 CAR T CELL THERAPY FOR PROSTATE CANCER**

¹Vipul Bhatia*, ²Nikhil Kamat, ¹Tiffany Pariva, ¹Li-Ting Wu, ¹Annabelle Tsao, ³Koichi Sasaki, ¹Lauren Wiest, ¹Ailin Zhang, ¹Dmytro Rudoy, ²Lawrence True, ¹Radhika Patel, ²Martine Roudier, ¹Roman Gulati, ¹Michael Haffner, ¹Peter Nelson, ⁴Saul Priceman, ³Jun Ishihara, ¹John Lee. ¹Fred Hutchinson Cancer Center, Seattle, WA, USA; ²University of Washington, Seattle, WA, USA; ³Imperial College London, London, UK; ⁴City of Hope, Duarte, CA, USA

Background Surfaceome profiling of prostate cancer identified six transmembrane epithelial antigen of the prostate 1 (STEAP1) as a compelling prostate cancer-associated antigen. Adoptive transfer of chimeric antigen receptor (CAR) T cells has shown limited success in solid tumors, like prostate cancer due to the immunosuppressive tumor microenvironment (TME). Combining CAR T cell therapy with strategies that augment host immune responses and remodel immunologically “cold” TMEs may represent a promising treatment strategy for metastatic castration-resistant prostate cancer (mCRPC).

Methods We evaluated differences in the patterns of STEAP1 and prostate-specific membrane antigen (PSMA) expression using lethal mCRPC tissue microarrays. Second-generation STEAP1 CAR T cell therapy was developed and tested for its antitumor potency in various human prostate cancer disseminated mice models. We also generated a humanized STEAP1 knock-in (hSTEAP1-KI) mouse model and tested the potency and safety of murine STEAP1 CAR T cells. Systemic administration of a collagen binding domain-IL-12 (CBD-IL-12) fusion cytokine in combination with STEAP1 CAR T cells was assessed as a strategy to potentiate anti-tumor responses.

Results STEAP1 was found to be broadly expressed in ~87% of lethal mCRPC tissues compared to PSMA in 60%. CAR T cells targeting STEAP1 showed anti-tumor efficacy in various disseminated models tested with complete responses in the C4-2B model and substantial tumor growth inhibition in the 22Rv1 model with evidence of antigen loss in residual tumors. Mouse-in-mouse studies in hSTEAP1-KI mice bearing RM9-hSTEAP1 tumors treated with murine STEAP1 CAR T cell therapy showed preliminary safety without gross toxicity or architectural disruption and increased T cell infiltration at sites of systemic hSTEAP1 expression. Transient anti-tumor responses and a modest survival benefit were observed with progressive tumors demonstrating loss of STEAP1 expression. Concomitant treatment with STEAP1 CAR T cells and CBD-IL-12 showed enhanced anti-tumor effects by engaging host immune cells and increased epitope spreading.

Conclusions We generated STEAP1 CAR T cell therapy with promising potency in preclinical prostate cancer models and preliminary evidence of safety. We highlight antigen heterogeneity and escape as a major mechanism of resistance to effective STEAP1 CAR T cell therapy in prostate cancer. A strategy of combining CBD-IL-12 together with STEAP1 CAR T cell therapy enhances anti-tumor responses by remodeling the TME and engaging host immunity.

Ethics Approval All mouse studies were performed in accordance with protocols approved by the Fred Hutchinson Cancer Center Institutional Animal Care and Use Committee and regulations of Comparative Medicine.

<http://dx.doi.org/10.1136/jitc-2022-SITC2022.0308>

309

DETERMINING THE HISTOCOMPATIBILITY BARRIERS BETWEEN UNIVERSAL CAR T (UCART) CELLS AND NK CELLS

Kimberly Apodaca*, Chong Xu, Kelsey Stanton, Beatriz Carreno, Gerald Linette. *University of Pennsylvania, Philadelphia, PA, USA*

Background Chimeric antigen receptor (CAR) T cell adoptive therapies have proven efficacy in the treatment of hematological malignancies. However, there are challenges to the current CAR T cell manufacturing process, one being manufacturing failure due to dysfunctional, patient-derived T cells.¹ A proposed solution to overcoming this limitation is the development of universal CAR T (UCART) cells engineered from healthy, normal donor-derived T cells. Histocompatibility barriers must be addressed when creating the UCART cell. Ablation of the alpha/beta T cell receptor surface expression will prevent graft-versus-host disease while host-versus-graft responses will be mitigated by ablating the surface expression of the major histocompatibility complex (MHC) class I and II molecules.^{2,3} These triple knockout (TKO) T cells could serve as universal recipients for development of the UCART cell. Importantly, a consequence of MHC class I ablation is NK cell activation due to the “missing-self” response.⁴ HLA-E, a non-classical MHC class I molecule, is known to interact with the NK cell inhibitory receptor NKG2A and we propose its overexpression on UCART cells will mitigate NK cell activation.

Methods Because the HLA-E/NKG2A interaction is dependent upon the peptide presented by HLA-E, 10 HLA-E single-chain trimer (SCT) constructs expressing various peptide sequences were created to determine which HLA-E/peptide complex would result in significant NK cell inhibition.⁵ K562 cells transduced to express these HLA-E/peptide complexes were used as a model for UCART cells in preliminary experiments.

Results An HLA-E SCT presenting an HLA-C leader peptide (HLA-E/C) resulted in significant inhibition of NK cells as determined by flow cytometry-based NK cell degranulation (CD107a) assays. Decreased lysis of K562 HLA-E/C -expressing target cells in ⁵¹Cr release assays further validated the inhibitory effect of HLA-E/C complexes on NK cell activation. Finally, HLA-E/C complex expression on TKO T cells lead to protection against NK lytic activity.

Conclusions Altogether these data demonstrate the effectiveness of selected HLA-E/peptide complexes to inhibit NK cell activation due to the “missing-self” response. Modifications such as the one described here may prevent UCART cell clearance due to host recognition (NK cell activation) and may ultimately lead to a more potent, safe, and long-term persistent UCART cell therapy.

REFERENCES

1. Thommen DS, Schumacher TN. T cell dysfunction in cancer. *Cancer Cell*. 2018; **33**:547–562.
2. Abdelhakim H, Abdel-Azim H, Saad A. Role of $\alpha\beta$ T cell depletion in prevention of graft versus host disease. *Biomedicines*. 2017; **5**:35.
3. Wang D, Quan Y, Yan Q, Morales J. E, Wetsel RA. Targeted disruption of the $\beta 2$ -microglobulin gene minimizes the immunogenicity of human embryonic stem cells. *Stem Cells Transl Med*. 2015; **4**:1234–1245.
4. Ljunggren HG, Kärre K. In search of the ‘missing self’: MHC molecules and NK cell recognition. *Immunol Today*. 1990; **11**:237–244.
5. Borrego F, Ulbrecht M, Weiss EH, Coligan JE, Brooks AG. Recognition of human histocompatibility leukocyte antigen (HLA)-E complexed with HLA class I signal sequence-derived peptides by CD94/NKG2 confers protection from natural killer cell-mediated lysis. *J Exp Med* 1998; **187**:813–818.

<http://dx.doi.org/10.1136/jitc-2022-SITC2022.0309>

310

ENGINEERING OPTIMAL CAR T CELLS TO OVERCOME PANCREATIC TUMORS WITH SECRETED ANTAGONISTIC PEPTIDES

Heather Lin*, Ruby Freeman, Alysa Evans, Tenzin Passang Fnu, Tongrui Liu, Elyse Christensen, Raymond Fei, Tanisha Sinha, Sruthi Ravindranathan, Lily Yang, Edmund Waller, Sarwish Rafiq. *Emory University, Atlanta, GA, USA*

Background Chimeric antigen receptor (CAR) T cell therapies have shown remarkable clinical efficacy in hematological cancers, but still face significant obstacles in the treatment of solid tumors such as pancreatic ductal adenocarcinoma (PDAC). Two hurdles in developing effective CAR T therapies for PDAC are the identification of ideal tumor-associated antigens (TAA) to target and overcoming a complex tumor micro-environment (TME). We hypothesize that the optimal CAR T cell to treat PDAC both recognizes an ideal TAA and is protected from immune suppression from the TME. Here, we propose the ectodomain of Muc16 (Muc16CD) as a viable TAA expressed in PDAC tumors (figure 1) and antagonizing vasoactive intestinal peptide (VIP), an immunosuppressive neuropeptide,^{1,2} to overcome the PDAC TME.

Methods CAR T cells were generated to specifically target Muc16CD and express a novel, potent VIP receptor (VIPR) antagonist (antVIPR) peptide.³ CAR T cells were assayed *in vitro* and *in vivo* against human VIP-expressing PDAC cell lines (Panc1) and PDX cell lines.

Results We first assayed patient-derived xenograft (PDX) PDAC cell lines for Muc16CD and VIP expression to establish the clinical relevance of these targets (figure 1). Interestingly, despite modest Muc16CD expression on PDX lines, anti-Muc16CD CAR T cells had cytotoxic function *in vitro* (figure 1) and reduced tumor burden in mice engrafted with orthotopic PDX PDAC tumors. Next, we investigated whether VIP is immunosuppressive for CAR T cell function. VIP limits the proliferative capacity of CAR T cells, which can be reversed by treatment with VIPR antagonist peptides. We therefore engineered novel antVIPR-secreting CAR T cells that provide continuous and localized delivery of antVIPR peptides within the TME. AntVIPR expression by CAR T cells impacts their phenotype as these cells have improved cell viability and express less VIP and VIPRs at baseline. Functionally, antVIPR CAR T cells have a proliferative advantage after antigen-stimulation and enhanced activation compared to parental CAR T cells. Finally, treatment with antVIPR CAR T cells reduces tumor burden and improve overall survival in mice bearing human VIP-expressing PDAC tumors (figure 2).

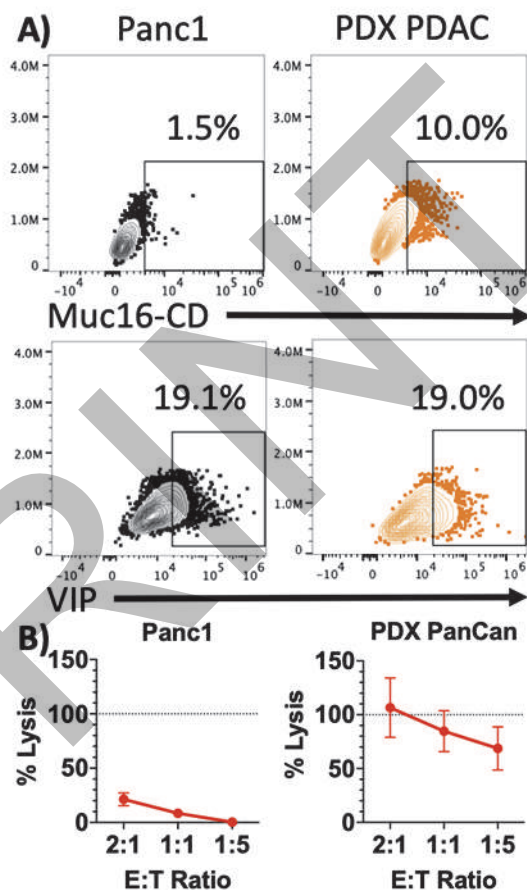
Conclusions Collectively, this data demonstrates that the combination of targeting Muc16CD and VIP with a novel CAR T cell can improve anti-tumor efficacy against PDAC. Ongoing experiments are determining the mechanisms by which locally secreted VIPR antagonists can modulate the PDAC TME using an orthotopic syngeneic PDAC mouse model with the long-term goal of translating antVIPR-secreting CAR T cells for the treatment of PDAC.

Acknowledgements The authors thank healthy volunteers and patients for blood samples. The authors also thank the shared resources at Emory University, namely the Emory Pediatrics/Winship Flow Cytometry Core (ECFCC) that provided services or instruments at subsidized cost to conduct some of the reported experiments.

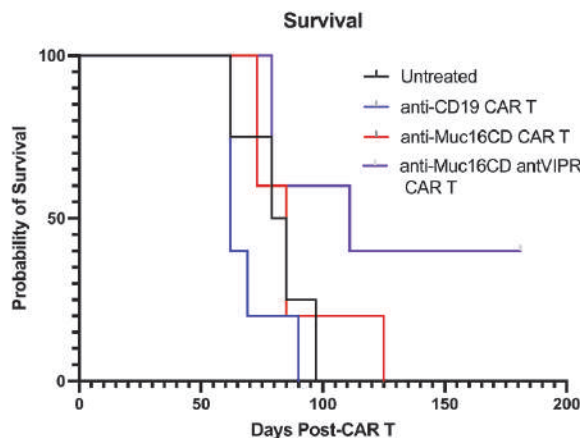
REFERENCES

- Delgado M, Ganea D. Vasoactive intestinal peptide: a neuropeptide with pleiotropic immune functions. *Amino Acids*. 2013; **45**: 25-39.

- Ravindranathan S, et al. 819 Targeting vasoactive intestinal peptide receptor signaling: a novel approach to enhance anti-tumor response in pancreatic ductal adenocarcinoma. *J Immunother Cancer*. 2020; **8**: A489.
- Fnu TP, Li J, Ravindranathan S, Waller EK. Inhibition of vasoactive intestinal peptide signaling with more potent inhibitors augments T-cell activation and prolongs survival in leukemic mice. *Blood*. 2021; **138**: 1868.



Abstract 310 Figure 1 (A) Unmodified Panc1 cells do not express Muc16CD but do express VIP. PDX PDAC cells express Muc16CD and VIP by flow cytometry. (B) Anti-Muc16CD CAR T cells are capable of cytotoxic function against PDX PDAC cells *in vitro*.



Abstract 310 Figure 2 Kaplan-Meier survival plot of SCID/Beige mice engrafted with VIP-expressing Panc1-Muc16CD+ tumor cells and treated 7 days later with CAR T. Anti-Muc16CD antVIPR-secreting CAR T cells

Abstracts

(purple) show improved survival compared to parental anti-Muc16CD CAR T cells (red).

<http://dx.doi.org/10.1136/jitc-2022-SITC2022.0310>

PREPRINT

311 PD-1 BLOCKADE PROTEIN COUPLED IN 4TH GENERATION ARMORED CAR-T CELLS ENHANCES CYTOTOXICITY EFFECT WITH *IN VITRO* RE-CHALLENGE SYSTEM

Zhifeng Zhao*, Jinyan Ma, Tiantian Wang, Ka Fung Noi, Jie Xu, Qingyang Gu. *WXi ApTec, Nantong, China*

Background Chimeric antigen receptor (CAR)-T cells are genetically engineered T cells expressing a receptor on their surface to recognize tumor-associated antigens (TAA). CAR-T cell therapy has been coined as a 'living drug' and have demonstrated remarkable success with hematological malignancies. However, limited headway has been made with solid tumors due to various challenges, including recognition of tumor-specific antigens, trafficking and penetration, and survival within an immunosuppressive tumor microenvironment (TME). Some overexpression of immunosuppressive cytokines/proteins, such as TGF- β and PD-L1, downregulates cytotoxic CD8+ T cells and reduces the efficacy of CAR-T cell therapy. Immune checkpoint inhibitors (ICIs), such as anti-PD-1/PD-L1 and anti-CTLA-4 antibodies have gathered immense attention due to their efficacy across multiple solid malignancies. Therefore, a combination of CAR-T and ICIs could be a viable strategy to overcome the unfavorable TME. Here, we have established a 4th generation, armored CAR-T coupled with a PD-1 blockade protein to enhance the anti-exhaustion effect of CAR-T cells.

Methods CAR-T cells were generated from primary human T cells which were isolated from human PBMC using a pan T cell isolation kit. Lentiviral particles containing the MSLN CAR gene with/without PD-1 transgene were generated in 293T cells. T cells were stimulated by CD3/CD28 beads for 2 days, followed by the addition of CAR lentiviral particles for an additional 24 hours, then further proliferated for 6 days. Cells were collected for surface marker analysis after the second stimulation or co-cultured with luciferase-transduced HCT-116 cells for re-challenge cytotoxicity assay.

Results • 4th generation CAR-T cells have reduced surface PD-1 available for binding, compared to 3rd generation CAR-T cells and untransduced T cells.

• CAR-negative 4th generation T cells also have reduced available PD-1 binding sites.

• 4th generation CAR-T cell retains >70% cytotoxicity effect, while 3rd and 2nd generation CAR-T cells have markedly reduced cytotoxicity effect after two re-challenges with HCT-116-luc cells.

Conclusions PD-1 immune checkpoint blockade enhances and prolongs CAR-T cells cytotoxic effect in an *in vitro* re-challenge assay. This research indicates the possibility of adding an immune checkpoint inhibitor transgene to the existing CAR gene to enhance CAR-T cytotoxicity.

<http://dx.doi.org/10.1136/jitc-2022-SITC2022.0311>

312

IDENTIFICATION OF NOVEL NSC LUNG CANCER DARK ANTIGENS™ WITH EXPRESSION IN MULTIPLE TUMOR TYPES, AS PROMISING TARGETS FOR IMMUNOTHERAPIES

¹Rachel Abbott*, ¹Okba Alassadi, ¹Matthew Davies, ¹Magdalena Von Essen, ¹Verónica Freire-Benítez, ¹Vicki Jefferson, ¹Samit Kundu, ¹Prathiba Kurupati, ²Ralf Leonhardt, ²Samuel Lukowski, ¹Fabio Marino, ¹Giulia Masi, ¹Rayner Queiroz, ¹Hayden Selvadurai, ¹Joana Senra, ¹Emily Tye, ¹Joseph Dukes. ¹Enara Bio Ltd, Oxford, UK; ²Boehringer Ingelheim RCV, Vienna, Austria

Background Recent advances in immunotherapy have led to the development of multiple therapeutic modalities that harness T cells to recognize and eliminate cancer cells, bringing benefit to cancer patients with unmet need. However, targeted immunotherapies have utilized traditional tumor-associated antigens, which lack cancer specificity and broad expression across patient populations.

We utilized Enara Bio's EDAPT™ (Enara Dark Antigen Platform Technology) platform to probe the genomic dark matter (genomic regions previously thought to be non-coding) and discover novel, cancer-specific antigens with validated presentation on Class I HLA of primary tumors.

Methods We created a *de novo* pan-cancer transcriptome assembly with RNA-seq reads from The Cancer Genome Atlas (TCGA) non-small cell (NSC) lung cancer projects. Transcript sequences were subject to differential expression analysis selecting those with enriched expression in tumors compared to a comprehensive panel of healthy tissues.

To discover *bona fide* Dark Antigens™ encoded by tumor-specific transcripts, we translated all possible open reading frames (ORFs) and interrogated these against mass spectrometry-based immunopeptidomics data, from primary NSC lung cancer samples, to identify peptides solely mapping to putative ORF sequences. Subsequent filtering was performed to extract those antigens with robust immunopeptidomic support, transcript expression prevalence, and cancer specificity.

Confirmation of tumor-specific expression of antigen-encoding transcripts was carried out using RNA *in situ* hybridization (ISH) and RT-qPCR. The immunogenicity of detected epitopes was assessed by characterization of antigen-specific T cell responses from healthy donors.

Results Our *de novo* assemblies identified >1,000 transcripts encoding >15,000 ORFs. Interrogation of these ORFs against MS immunopeptidomic datasets mapped HLA-bound peptides to hundreds of ORFs, demonstrating presentation of these novel antigens in multiple patient tumor samples. Many candidate antigens displayed promising expression across additional tumor types, supporting potential for broader clinical utility.

RNA ISH revealed tumor-specificity and intra-tumoral homogeneity at the transcript level, with little to no transcript expression identified across healthy tissues. Assessment of immunogenicity in healthy subject peripheral blood cells revealed reactive T cells, indicating a lack of central-tolerance deletion of T cells specific for these antigen-derived peptides.

Conclusions We identified a suite of candidate Dark Antigens™ that are expressed in a cancer-specific manner with evidence of processing and HLA presentation on the surface of tumor cells. T cells with specificity for these antigens can be detected in healthy subjects, and thus these antigens show promise as candidates for the development of targeted immunotherapies such as cancer vaccines, TCR-T cell and bi-specific T cell engager therapies.

Acknowledgements The results presented here are based in part upon data generated by The Cancer Genome Atlas

(TCGA) Research Network (<http://cancergenome.nih.gov/>); and the Genotype-Tissue Expression (GTEx) Project (supported by the Common Fund of the Office of the Director of the National Institutes of Health, and by NCI, NHGRI, NHLBI, NIDA, NIMH, and NINDS). Primary patient material utilized in this study was provided by the Royal Papworth Hospital Research Tissue Bank. Written consent was obtained for all samples.

Ethics Approval All work involving the use of human tissue was approved by the NHS Health Research Authority North-west Haydock Research Ethics Committee (reference number 19/NW/0216).

<http://dx.doi.org/10.1136/jitc-2022-SITC2022.0312>

313 EDIT-202, A MULTIPLEXED ASCAS12A EDITED IPSC DIFFERENTIATED iNK, DISPLAYS A MATURE PHENOTYPE, HIGH KIR EXPRESSION, AND ADCC TOWARDS MULTIPLE SOLID TUMOR LINES

Alex Allen*, Kaitlyn Izzo, Mrunali Jagdale, Scott Mordecai, Jared Getgano, Laura Blaha, Abhijit Dandapat, Mark Shearman, Kai-Hsin Chang. *Editas Medicine, Cambridge, MA, USA*

Background Chimeric antigen receptor (CAR)-T cells have demonstrated that cell therapy can achieve durable remissions in hematologic malignancies. CAR-T cell therapies have limited efficacy in solid tumors, however, and are often associated with severe toxicity, highlighting the need for safer, more efficacious cell therapies. Natural killer (NK) cells with high-affinity CD16 represent an attractive alternative therapy option to CAR-T cells due to their natural cytotoxic ability and low toxicity.

Methods Using our proprietary engineered AsCas12a, we generated a multiplexed edited iPSC clone(s) that includes four edits: high affinity, cleavable, CD16 KI (knock-in), membrane-bound IL-15 (mbIL-15) KI, TGFBR2 KO, and a CISH KO. The two gene knock-ins were enabled with our proprietary SeLECTION by Essential Exon Knock-in (SLEEK™) technology which enables high levels of KI, while expressing the cargo transgene consistently over time. Subsequently, we differentiated the iPSC clone(s) into iNK cells, termed EDIT-202, using a feeder-free differentiation process. We have previously demonstrated that this unique combination of edits in EDIT-202 results in an enhanced ability to overcome TGF- β -mediated immunosuppression, persist long-term without exogenous cytokine support, and control ovarian tumors in vitro and in vivo via natural and antibody-dependent cellular cytotoxicity.

Results The phenotype of EDIT-202 and its effector function against multiple solid tumor cell lines were further characterized. EDIT-202 expressed high levels of CD16 and KIR, which are commonly used markers for maturation. In addition, EDIT-202 expressed high levels of perforin, granzyme b, and T-bet, a critical transcription factor that helps control maturation in NK cells. Higher expression of KIR correlated to potent NK cell killing with an R^2 of 0.78 in a 3D tumor spheroid killing assay. Tumor cells from head and neck squamous cell carcinoma (HNSCC), gastric cancer, and non-small cell lung cancer (NSCLC) were screened against cryopreserved EDIT-202 cells. When combined with cetuximab (anti-EGFR antibody) against HNSCC and NSCLC, or with trastuzumab (anti-HER-2 antibody) against gastric cancer cells, EDIT-202 showed an approximately 10-fold increase in IFN- γ secretion compared with an EDIT-202 alone control. Moreover, there were significant increases in ADCC at multiple effectors to target ratios (E:T) when EDIT-202 cells were screened against the aforementioned solid tumor types.

Conclusions In conclusion, iPSC derived NK cells (iNK) have the unique advantage of being an off-the-shelf, and fully characterizable cell therapy amenable to multiplexed gene editing to enhance anti-tumor activity. EDIT-202 demonstrates a mature phenotype which translates to a highly potent and persistent iNK cell for potential treatment of multiple solid tumor types.

<http://dx.doi.org/10.1136/jitc-2022-SITC2022.0313>

314 CELL THERAPY DEVELOPMENT IN ONCOLOGY REQUIRES A COLLABORATION BETWEEN SPONSORS AND CELL THERAPY EXPERIENCED CRO

Jaikrishna Balkissoon*. PPD, Piedmont, CA, USA

Background From 2017 to 2022 the oncology community has seen a significant increase in the number of cell therapy clinical trials in both hematologic malignancies and solid tumors. With breakthrough designations, priority reviews and orphan drug status, cell therapy regulatory approvals in hematologic malignancies have also significantly increased during this time based on acceptable safety/tolerability and positive clinical efficacy data from single-arm studies with relatively small sample sizes. As a global CRO, PPD has gained a wealth of experience in the management of these complex cell therapy trials in hematologic malignancies and solid tumors. Project teams managing these complex trials are supported by our Immunology Cell and Gene Therapy Center of Excellence which provides a platform for sharing of knowledge and best practices as well as comprehensive cell therapy training. Through these cross-functional monthly meetings we review safety/tolerability between the different genetically modified cell therapies as well as those that are not genetically modified. We can also identify gaps in the management of cell therapy trials that could impact study timelines and create enrollment challenges. We demonstrate our comprehensive analysis of factors that could impact enrollment into our cell therapy trials and describe proposed solutions.

Methods We reviewed cell therapy approvals in relapsed/refractory DLBCL from 2017 to 2022 and the changing treatment options that could impact enrollment into current and future clinical trials using the IPSOS prescribing database. The Citeline-Trialtrove study database was then used to assess the number of studies competing for the same patient population.

Results From this evaluation we identified multiple factors that could impact enrollment requiring mitigation strategies to be implemented to prevent delays to study timelines (figure 8,9).

Conclusions By using a combination of experiential metrics and publicly available data, it is possible to identify remediable factors which could negatively impact enrollment. Rapid implementation of targeted measures can improve enrollment and keep study timelines on track (figure 9).

<http://dx.doi.org/10.1136/jitc-2022-SITC2022.0314>

315

CHARACTERIZATION OF CT-0508, AN ANTI-HER2 CHIMERIC ANTIGEN RECEPTOR MACROPHAGE (CAR-M), MANUFACTURED FROM PATIENTS ENROLLED IN THE PHASE 1, FIRST IN HUMAN, CLINICAL TRIAL OF CT-0508

Michael Ball*, Madison Kremp, Rehman Qureshi, Poonam Sonawane, Maggie Schmierer, Josh VanDuzer, Michael Lynch, Adam Pfendt, Melissa Christiano, Ken Locke, Ramona Swaby, Daniel Cushing, Michael Klichinsky, Thomas Condamine. *Carisma Therapeutics, Philadelphia, PA, USA*

Background Adoptive T cell therapies have led to remarkable advances among patients with hematologic malignancies but have had less success in those with solid tumors. Macrophages are actively recruited and abundantly present in the solid tumor microenvironment (sTME). Tumor associated macrophages are predominantly immunosuppressive and support tumor growth (M2), while a subset of proinflammatory macrophages enhance anti-tumor immunogenicity (M1). M1 macrophage function can be augmented by CAR expression to selectively recognize and phagocytose antigen overexpressing cancer cells. Moreover, CAR macrophages can reprogram the sTME and present neoantigens to T cells, leading to epitope spreading and anti-tumor immune memory. Human Epidermal Growth Factor Receptor 2 (HER2) overexpression promotes tumorigenesis in many solid tumors. CT-0508 is a cell product comprised of autologous monocyte-derived proinflammatory macrophages expressing an anti-HER2 CAR and is being investigated in a currently ongoing first in human clinical trial (NCT04660929).

Methods Using the chimeric adenoviral vector Ad5f35, we manufactured CT-0508 product from apheresis material collected from patients enrolled in group 1 of the CT-0508 phase 1 clinical trial. To assess the activity of pre-infusion CT-0508 products, *in vitro* cell based assays were utilized including killing, phagocytosis, cytokine secretion, and transcriptomics analysis. Donor-matched untransduced (UTD) macrophages served as controls. Additionally, healthy donor derived products were used in some experiments.

Results CT-0508 was successfully manufactured with high viability, purity and CAR expression for patients enrolled in group 1. CT-0508 products demonstrated enhanced killing and phagocytosis of HER2-expressing tumor cells over autologous UTD macrophages. CITE-Seq analysis of CT-0508 confirmed an M1 macrophage transcriptional signature compared with pre-manufacturing monocyte and apheresis populations. Using healthy donor derived CT-0508 products, cell product activation was demonstrated by ex vivo CAR engagement and led to an increase in secreted immunostimulatory cytokines and chemokines, consistent with pro-inflammatory macrophage activation including TNF, IL-6, MIP-1 α , and MIP-1 β . Secreted factor analysis also showed HER2 responsive changes in extracellular matrix remodeling factors and growth factors. Additionally, transcriptomic and proteomic analysis revealed that CAR engagement further enhanced CAR-M M1 polarization. CAR engagement mediated effects are also being investigated in patient derived products.

Conclusions Together, these results demonstrate that functional CT-0508 CAR-M were successfully manufactured with an M1 phenotype and that CAR-antigen interaction drives cell product activation and amplifies the M1 polarization status of CT-0508 CAR-M.

<http://dx.doi.org/10.1136/jitc-2022-SITC2022.0315>

316 **NEXT GENERATION CAR-T INCORPORATING AN INHIBITORY CAR (iCAR) FOR INCREASED SAFETY IN SOLID TUMORS**

David Bassan*, Michael Weist, Leehee Weinberger, Jason Yi, Gregor Adams, Tanya Kim, Caitlin Schnair, Kristina Vucci, Sarit Tabak, Neta Chaim, Nir Bujanover, Yael Lopesco, Limor Levy-Kanfo, Orit Foord, Jim Johnston, Frank Calzone, Rick Kendell, Adi Sharbi-Yunger. *ImPACT-Bio, Rehovot, Israel*

Background Chimeric antigen receptor (CAR)-T cell therapy has shown incredible clinical success for hematopoietic malignancies, but for solid tumors is limited by “on-target off-tumor” toxicity to vital organs due to lack of target specificity. We have developed dual CAR-T cells consisting of a canonical activating CAR (aCAR), intended to elicit efficacy in solid tumors, and an inhibitory CAR (iCAR) designed to effectively suppress aCAR activation in normal tissues. The iCAR and aCAR bind distinct cell-surface antigens that are widely co-expressed in normal tissues. The iCAR is allele specific, and targets an antigen that is commonly lost in cancer due to chromosomal loss-of heterozygosity (LOH). Therefore, whereas healthy cells express the iCAR antigen and are protected, tumors have irreversibly lost iCAR antigen expression via LOH and are killed.

Methods In this study we developed dual CARs with an aCAR targeting Her2 and iCAR targeting HLA-A2. We screened bicistronic dual CARs in human PBMCs following lentiviral transduction against target cell lines that express normal levels of both antigens paired with targets following CRISPR KO of the HLA-A2 to mimic LOH. *In-vitro* assays included Luciferase-based killing assays, live-imaging killing assays, and cytokine secretion. *In-vivo* studies were performed in NSG-mice inoculated with either the HLA-A2+ or HLA-A2 KO targets.

Results We optimized the iCAR scFv, hinge, signaling domain, and bicistronic linker to generate dual CARs with high potency and tumor-specificity. These dual CARs were highly active against HLA-A2 KO targets (“tumor”) and inhibited against HLA-A2+ targets (“normal tissue”).

Conclusions These results show that the iCAR enables the tremendous therapeutic potential of CAR-T therapy to transition to solid tumors while maintaining safety and tumor specificity.

<http://dx.doi.org/10.1136/jitc-2022-SITC2022.0316>

317

**ALK CHIMERIC ANTIGEN RECEPTOR T CELLS
COOPERATE WITH ALK INHIBITORS TO TARGET
NEUROBLASTOMA CELLS WITH LOW TARGET DENSITY**

<http://dx.doi.org/10.1136/jitc-2022-SITC2022.0317>

¹Elisa Bergaggio*, ¹Wei-Tien Tai, ¹Andrea Aroldi, ²Elisa Landoni, ¹Manuel Nuesch, ¹Ines Mota, ³Jasna Metovic, ⁴Leyuan Ma, ⁵Diego Alvarado, ³Chiara Ambrogio, ³Claudia Voena, ¹Rafael Blasco, ⁶Tongqing Li, ⁶Daryl Klein, ⁴Darrell Irvine, ³Mauro Papotti, ²Barbara Savoldo, ²Gianpietro Dotti, ¹Roberto Chiarle. ¹Boston Children's Hospital and Harvard Medical School, Cambridge, MA, USA; ²University of North Carolina Chapel Hill, Chapel Hill, NC, USA; ³University of Torino, Torino, Italy; ⁴Koch Institute and Massachusetts Institute of Technology, Cambridge, MA, USA; ⁵Celldex Therapeutics, New Haven, CT, USA; ⁶Yale University School of Medicine, New Haven, USA

Background Neuroblastoma is the most common extracranial solid tumor of childhood¹ and accounts for 12-15% of cancer-related deaths in children.² The survival of patients with refractory or relapsed neuroblastoma remains dismal.³ In neuroblastoma, chimeric antigen receptor (CAR) T cells against GD2 have shown encouraging clinical results, but relapses are associated with loss of antigen expression. The selection of the best target is critical for the therapeutic success of CAR-T cells in hematologic malignancies and solid tumors. The Anaplastic Lymphoma Kinase (ALK) receptor is expressed by most neuroblastoma while virtually absent in the majority of normal tissues. It is an oncogenic driver in neuroblastoma and ALK inhibitors show promising clinical activity. All these features render ALK a great candidate for CAR-T therapy.

Methods We generated seven ALK.CAR constructs using the single-chain variable fragment derived from different anti-ALK monoclonal antibodies that recognize the ALK extracellular domain into a CAR construct that included the CD28 costimulatory endodomain. Their ability to target and kill was tested in vitro and in vivo against neuroblastoma cells expressing different intensities of ALK. The activity of ALK.CAR-T cells was compared to GD2.CAR-T cells.

Results

ALK CAR-T cells showed potent activity without on-target or off-target toxicity against neuroblastoma with high ALK expression. Combination with ALK inhibitors specifically potentiated the activity of ALK.CAR-T cells, but not GD2.CAR-T cell, against neuroblastoma with low ALK expression in cell lines and in a patient-derived xenograft (PDX), where the combination of ALK inhibitors with ALK.CAR-Ts significantly reduced tumor growth and extended mice survival. Mechanistically, ALK inhibitors impaired tumor growth and upregulated the expression of ALK, thereby improving the targeting of neuroblastoma tumors by ALK.CAR-T cells.

Conclusions These data indicate that ALK.

CAR-T cells are effective and safe as monotherapy against neuroblastoma with high ALK expression. Furthermore, treatment with ALK inhibitors increases the efficacy of ALK.CAR-T cells by enhancing ALK targeting.

REFERENCES

1. Maris JM. Recent advances in neuroblastoma. *The New England Journal of Medicine* 2010; **362**:2202-2011.
2. Park JR, Eggert A, Caron H. Neuroblastoma: biology, prognosis, and treatment. *Pediatr Clin North Am* 2008;**55**:97-120.
3. Inwin MS, Park JR. Neuroblastoma: paradigm for precision medicine. *Pediatr Clin North Am* 2015;**62**:225-256.

Ethics Approval All mouse experiments were performed under protocols approved by the Institutional Animal Care and Use Committee (IACUC) of Boston Children's Hospital (Protocol 00001530).

Linara Gabitova*, Brett Menchel, Silvia Beghi, Larissa Ishikawa, Rehman Qureshi, Andrew Best, Sabrina DeLong, Sascha Abramson, Thomas Condamine, Daniel Blumenthal, Michael Klichinsky. *Carisma Therapeutics, Philadelphia, PA, USA*

Background Engineered cell therapies have demonstrated significant clinical activity against hematologic malignancies, but responses against solid tumors remain rare. Our previously developed human chimeric antigen receptor macrophage (CAR-M) platform has shown potent anti-tumor activity in pre-clinical solid tumor models,¹ and an anti-HER2 CAR-M product (CT-0508) is currently being evaluated in a Phase I trial. Use of myeloid cells for immunotherapy has the potential to overcome the main challenges presented by solid tumors – tumor infiltration, immunosuppression within the tumor microenvironment (TME), lymphocyte exclusion, and target antigen heterogeneity. Currently, CAR-M are generated in a week-long *ex-vivo* process in which peripheral blood monocytes are differentiated into macrophages prior to genetic manipulation. Here, we demonstrate the feasibility, phenotype, pharmacokinetics, durable CAR expression, cellular fate, specificity, and anti-tumor activity of human CD14+ CAR monocytes.

Methods Using the chimeric adenoviral vector Ad5f35, we engineered primary human CD14+ monocytes to durably express an anti-HER2 CAR (CAR-mono). Using a partially automated approach, we established a process that allowed for same day manufacturing (from Leukopak to cryopreserved CAR-mono cell product).

Results CAR-mono showed high CAR expression and viability (>90%), and efficiently differentiated into CAR-expressing macrophages. The production process was designed to precondition CAR-mono to differentiate into M1-like CAR macrophages with strong pro-inflammatory effector functions. CAR-mono derived CAR-M (cmdCAR-M) demonstrated potent anti-tumor activity regardless of exposure to GM-CSF or M-CSF, and were protected against M2 switching by immunosuppressive factors. Treating CAR-mono with GM-CSF and IL-4 resulted in their differentiation to monocyte-derived CAR-DCs with an activated phenotype, indicating that these cells retained their myeloid differentiation potential. *In vivo*, intravenous administrated CAR-mono demonstrated the ability to traffic to tumors and showed remarkable long-term CAR expression and persistence (>180 days) in both NSG and NSG-S mouse models, demonstrating lasting persistence and CAR expression irrespective of human cytokine support. CAR-mono differentiated into strong pro-inflammatory CAR-M even when injected directly into well-established tumors. Finally, CAR-mono induced anti-tumor activity in various HER2+ solid tumor xenograft models.

Conclusions The CAR-mono platform allows for a rapid, same-day manufacturing process while maintaining the key characteristics of CAR-M therapy. Ad5f35 engineered human CAR monocytes are primed toward M1 macrophage differentiation, demonstrate durable CAR expression and persistence, and produce a cell population highly similar to our established CT-0508 product. These data provide strong pre-clinical support to advance the CAR-mono platform into clinical testing.

REFERENCE

1. Klichinsky M, et al. Human chimeric antigen receptor macrophages for cancer immunotherapy. *Nature Biotechnology*. 2020; **38**: 947-953.

319 IMMUNOMETABOLIC MODULATION OF ENGINEERED IPSC-NK CELLS FOR IMMUNOTHERAPY OF SOLID TUMORS

¹Shambhavi Borde*, ¹Sandro Matosevic, ²Kyle Lupo. ¹Purdue University, West Lafayette, IN, USA; ²Memorial Sloan Kettering Cancer Center, New York, NY, USA

Background Natural killer (NK) cells have efficient intrinsic recognition capabilities towards abnormal cells. This fact makes them particularly attractive as safe effector cells for cancer immunotherapy. Despite being innately tumor-killing cells, sourcing them from human donors is a tedious and highly donor-specific process.¹ As an alternative, induced pluripotent stem cells (iPSCs) represent a universal source of NK cells. iPSC-NK cells can be prepared with homogenous quality and can be easily genetically modified to modulate their specificity and activity.² Despite their demonstrated potential, differentiation processes to generate NK cells from iPSCs require improvements in terms of NK cell yield. Our group has reported that chemically defined and serum- and feeder-free differentiation generates NK cells that are predominantly CD56+/CD16+/CD3- and which express NK activation markers NKG2D, NKp30, NKp44, NKp46, and DNAM-1. We also recently engineered these cells to express multi-specific CAR constructs and showed that they mediate strong anti-tumor activity and lead to improved survival in mouse xenografts of glioblastoma.³

Methods However, we also found that modulating the differentiation and genetic engineering processes can yield further improvements in terms of NK cell quality, yield, and activity. Here, we report our recent work on evaluating iPSC-NK protocol advancements to improve reproducibility and yield, as well as the generation of more efficient immunometabolically-reprogrammed CAR-iPSC-NK cells. These involve the addition of Interleukin-15 in the second stage of differentiation, where differentiating embryoid bodies transitions to the generation of NK cells. We are also modulating the activity of multi-specific CAR-iPSC-NK cells with small molecule inhibitors of metabolic activity, by targeting mitochondrial dysfunction.

Results The involvement of interleukin-15 and inhibition/silencing of metabolic activity with small molecule inhibitors generated metabolically resilient and functionally robust CAR-NK cells. In addition, these cells showed robust cell-mediated effector functions including cytotoxicity, degranulation, and IFN- γ production against patient-derived cancer cells.

Conclusions These advancements lead to improved NK cell quality and activity and represent a significant step toward off-the-shelf immunotherapies for solid tumors.

REFERENCES

1. Liu S, Galat V, Galat Y, Lee YKA, Wainwright D, Wu J. NK cell-based cancer immunotherapy: From basic biology to clinical development. *J Hematol Oncol.* 2021; **14**: 7.
2. Karagianni, P, Kim S-I. iPSC-derived natural killer cells for cancer immunotherapy. *Mol Cells.* 2021; **44**: 541–548.
3. Lupo KB, Moon J-I, Chambers AM, Matosevic S. Differentiation of natural killer cells from induced pluripotent stem cells under defined, serum- and feeder-free conditions. *Cytotherapy.* 2021; **23**: 939–952.

<http://dx.doi.org/10.1136/jitc-2022-SITC2022.0319>

320

RAPID IDENTIFICATION OF A TCR LIBRARY TARGETING THE HPV E6/E7 ONCOPROTEINS TO ENABLE MULTI-TCR T-CELL THERAPIES FOR PATIENTS WITH HPV16+ EPITHELIAL CANCERS

<http://dx.doi.org/10.1136/jitc-2022-SITC2022.0320>

Magnolia Bostick*, John Greer, Andrew Conroy, Mark Ting, Allison Xu, Kevin Shao, Claire McHugh, Rakesh Sudhakar, Connie Kong, Taylor Dowdell, Yvonne DaCosta, Shannon Sorn, Justin Win, Noha Elabed, Cheryl Kwan, Craig Fett, Evelyn Vilchez, Nimisha Gandhi, George Yam, Benjamin Yuen, Zheng Pan, Theresa Stueve, Papia Chakraborty, William Lu, Cliff Wang, Eric Stawiski, Stefanie Mandl, Eric Kunkel. *PACT Pharma, Inc., South San Francisco, CA, USA*

Background In the United States, the HPV16 strain is responsible for nearly 60% of newly diagnosed HPV-driven cancers. HPV16 drives oncogenesis through persistent expression of the E6 and E7 oncoproteins.¹ The viral antigens E6 and E7 are absent from healthy tissues, making them attractive targets for TCR T-cell therapy. Both oncoproteins are validated targets for TCR T-cell therapies based on clinical trials with objective clinical responses in 50% (6 of 12) of patients for an E7-directed TCR, however, durability of response and coverage of the patient population were limited.^{2,3} Both issues can be addressed by a larger TCR library that allows treatment of patients of all ethnicities with a multi-TCR product. Here we describe a suite of TCR discovery and validation platforms for the rapid generation of an off-the-shelf TCR library targeting the HPV16 E6 and E7 oncoproteins presented by the 16 most prevalent HLA alleles across all ethnicities in the US. This library of TCRs provides social equity for patients with HPV16-driven cancer, since it will enable more than 80% of the US population to receive a multi-TCR T-cell therapy product with the potential to mitigate tumor escape mechanisms, such as HLA mutation or loss of heterozygosity, for durable anti-tumor responses.

Methods E6- and E7-specific TCRs were identified using the rapid and highly sensitive imPACT Isolation Technology[®] (capable of capturing T cells at a frequency of 1 in 300,000 CD8+ T cells) and barcoded libraries of peptide-HLA proteins predicted to derive from the HPV16 E6 or E7 oncoproteins. Every identified TCR undergoes functional validation as well as safety and specificity testing using primary human T cells non-virally edited to express the TCR of interest.

Results We have identified potent TCRs specific for HPV16 E6 or E7 from both HPV+ cancer patients and healthy donors (+/- HPV infection). In one example, circulating T cells from an HPV+ cancer patient yielded three novel TCRs against related E6 peptides restricted by A*11:01 that exhibit clinically relevant T-cell functionality. Interestingly, in this patient, the A*11:01 allele in the tumor had a deleterious mutation allowing the tumor to escape killing by these TCRs further validating their biological relevance. However, as part of an off-the-shelf HPV library for use in a multi-TCR T-cell therapy product, these TCRs have the potential to be highly effective in patients with intact A*11:01 expression.

REFERENCES

1. Moody CA, Laimins LA. Human papillomavirus oncoproteins: pathways to transformation. *Nat Rev Cancer*. 2010; **10**: 550-560.
2. Nagarsheth NB, Norberg SM, Sinkoe AL, Adhikary S, Meyer TJ, Lack JB, Warner AC, Schweitzer C, Doran SL, Lorrapati S, Stevanovic, S, Trimble, CL, Kanakry, JA, Bagheri MH, Ferraro E, Astrow SH, Bot A, Faquin WC, Stroneck D, Gkitsas N, Highfill S, Hinrichs CS. TCR-engineered T cells targeting E7 for patients with metastatic HPV-associated epithelial cancers. *Nat Med*. 2021; **27**: 419-425.
3. Doran SL, Stevanovic S, Adhikary S, Gartner JJ, Jia L, Kwong MLM, Faquin WC, Hewitt SM, Sherry RM, Yang JC, Rosenberg SA, Hinrichs CS. T-Cell Receptor Gene Therapy for Human Papillomavirus-Associated Epithelial Cancers: A First-in-Human, Phase I/II Study. *J Clin Oncol*. 2019; **37**(30): 2759-2768.

321 SINGLE MRNA CONSTRUCTS ENCODING MULTIPLE LINKED ANTIGENS ALLOW FOR A MULTIANTIGEN-SPECIFIC CD8⁺ T CELL RESPONSE DRIVEN BY SQZ[®] EAPCS

Ashley Brate*, Michael Maloney, Carolyne Smith, Katarina Blagovic, Andrea Silva, Amber Martin, Jodie Wong, Scott Loughhead. *SQZ Biotechnologies, Watertown, MA, USA*

Background During cancer progression, genomic mutations develop that can generate immunogenic neoepitopes, which are potential targets for immunotherapies. In contrast to microbial and other exogenous antigens where most of the protein is immunogenic, neoepitopes are immunogenic in a narrow region of the protein due to self-tolerance for the flanking regions. Previously, we demonstrated that SQZ[®] eAPCs, produced from human peripheral blood mononuclear cells (PBMCs) with mRNA encoding for full-length viral antigens (98-561 aa in length), can elicit robust CD8⁺ T cell responses. To understand whether the smaller immunogenic regions of multiple neoepitopes (~25 aa) could be linked together in a single mRNA construct, we delivered various mRNA constructs encoding 5-10 model antigen fragments (*e. g.*, HPV16 E6, HPV16 E7, mutant KRAS, and Influenza M1) linked together into PBMCs to generate SQZ[®] eAPCs.

Methods Model antigen fragments with known CD8⁺ T cell epitopes were linked together to form a single mRNA. Cell Squeeze[®] technology was used to deliver the linked antigen mRNAs directly into the cytosol of all major cell subsets of PBMCs. Western blots were used to confirm the delivery and translation of the linked antigen mRNA constructs. The MHC-I presentation of epitopes on the SQZ[®] eAPCs was assessed *in vitro* by culturing SQZ[®] eAPCs with antigen-specific responder T cells or TCR-transduced Jurkat-Lucia NFAT reporter cells overnight before measuring the activation response of these T cells via luciferase or IFN γ ELISA.

Results We demonstrate simultaneous antigen presentation on MHC-I by SQZ[®] eAPCs with a single mRNA encoding for 5 or 10 linked antigen fragments. Multiple antigen-specific responder cells are activated after co-culture with PBMCs squeezed with linked antigen mRNA, as measured by an increase in the secretion of luciferase or IFN γ .

Conclusions SQZ[®] eAPCs with mRNA encoding for up to 10 linked antigen fragments allows for simultaneous antigen presentation and robust CD8⁺ T cell responses. These findings further enhance the versatility of the Cell Squeeze[®] technology to potentially target multiple tumor-associated neoantigens (*e. g.*, mutated KRAS) in a single mRNA construct.

<http://dx.doi.org/10.1136/jitc-2022-SITC2022.0321>

322

MiNK-413: A NEXT GENERATION ARMORED ALLOGENIC BCMA CAR iNKT PRODUCT

Eleni Chantzoura*, Efrat Altman Sharoni, Reed Masakayan, Martyna Popis, Darrian Moskowitz, Paul Ibbett, Sapana Kadel, Moira Pinzan Rossi, Deborah Wright, Burcu Yigit, Olivier Le Tonqueze, Xavier Michelet, Marc Van Dijk. *MiNK Therapeutics, Cambridge, MA, UK*

Background We are developing MiNK-413; a novel allogeneic CAR-iNKT product targeting BCMA and secreting soluble IL-15 for treatment of relapsed/refractory Multiple Myeloma (rrMM). Chimeric Antigen Receptor (CAR)-T cell therapy has revolutionized treatment of rrMM with two autologous products already approved by the FDA. However, current treatments come with significant toxicity, cost, and logistical challenge and many patients relapse, with 60% of relapsed patients still expressing BCMA. To address these, we propose the use of invariant Natural Killer T (iNKT) cells as a platform for BCMA-targeted allogeneic cell therapy for rrMM. iNKT cells have potent immunostimulatory activity and intrinsic CD1d- and NK receptor ligand targeted cytotoxicity, and do not cause Graft *versus* Host Disease due to their invariant T cell receptor. In our native iNKT cell (AgenT-797) clinical trials for COVID, solid tumors and Multiple Myeloma we observe excellent tolerability to up to 1 billion cell dosing with minimal treatment-related adverse events, absence of signs of CRS or peripheral neuropathy, and early signs of biological activity. AgenT-797 is administered without prior lymphodepletion, which is an approach we intend to pursue with MiNK-413.

Methods Our proprietary CARDIS™ platform consists of highly diverse ($>10^{10}$) scFv library screening followed by library-based direct functional selection in CAR format using mammalian display. Candidates can be further optimized using affinity tuning to ensure optimal and highly selective on-target/on-tumor activity. We developed a manufacturing approach to engineer and specifically expand CAR and soluble IL-15-expressing allogeneic iNKT cells. Lead candidates are assessed *in vitro* and *in vivo* for cytotoxicity, cytokine secretion, exhaustion, tumor homing and persistence.

Results Discovery using our CARDIS™ platform generated a fully human, potent, and specific anti-BCMA CAR which forms the basis for MiNK-413. Xenograft *in vivo* studies demonstrate effective bone marrow homing, and potent cytotoxic activity, with soluble IL-15 prolonging persistence. *In vitro* data show potent immunomodulatory activity and lack of exhaustion against BCMA+ human hematologic tumor cell lines *in vitro* and *in vivo*.

Conclusions Combination of our proprietary CARDIS™ and iNKT platforms enabled rapid discovery and development of MiNK-413, a next generation armored allogeneic BCMA-targeting CAR therapies. MiNK-413 is eligible to target a broader rrMM patient population due to intrinsic iNKT cell properties such as effective bone-marrow homing, high BCMA specific activity augmented by natural CD1d and NK receptor-ligand mediated activity. We believe MiNK-413 will provide additional benefits to rrMM patients beyond currently available treatments.

<http://dx.doi.org/10.1136/jitc-2022-SITC2022.0322>

323

TALEN[®]-BASED GENE EDITED IPSC-DERIVED NK (iNK) CELLS DEMONSTRATE ENHANCED ANTITUMOR ACTIVITY

¹An-Ping Chen*, ¹Peng Gao, ¹Preeti Ashok, ¹Marshall Chao Ma, ¹David Zou, ¹Andrea Chambers, ¹Liang Lin, ¹Hao-Ming Chang, ¹Antonio Arulanandam, ²Justin Eyquem, ¹Elisabetta Burchi, ¹Armin Rath, ¹Stanley Frankel, ³Alex Boyne, ³Alexandre Juillerat, ⁴Philippe Duchateau, ¹Daniel Teper, ¹Nejmi Dilmac, ¹Wei Li. ¹Cytovia Therapeutics, Natick, MA, USA; ²University of California San Francisco, San Francisco, CA, USA; ³Collectis Inc., New York, NY, USA; ⁴Collectis Inc., Paris, France

Background Natural killer (NK) cell therapies have shown a great promise for solid and liquid tumors in initial clinical trials. NK cells are innate immune cells with distinct potential safety and efficacy advantages compared to adoptive T-cell therapies. However, there are limitations with the persistence and immunosuppression of these cells in the tumor microenvironment. Furthermore, multiple sources of NK cells have been used in clinical trials and there are challenges with manufacturing homogeneous and high doses of these cells. Induced Pluripotent Stem Cell (iPSC)-derived NK cells offer an opportunity to generate unlimited and homogenous NK cells for allogeneic off-the-shelf therapies. We combined Cytovia's iNK cell platform with Collectis TALEN[®] gene editing technology to improve potency and the manufacturing process. Clonally edited iPSC lines were generated by knocking in IL-15 and knocking out TGFβR2 to improve the persistence and antitumor activity, respectively. Edited iPSCs were differentiated into iNK cells with high efficiency using Cytovia's proprietary platform.

Methods iPSCs were edited at the B2M locus with TALEN[®] pairs along with a template to knock in IL-15 by electroporation. Another TALEN[®] pair was sequentially used to knock out TGFβR2. Edited single cell iPSCs were printed, expanded, and screened for clone selection. Selected clones were sequence verified by NGS and samples were submitted for off-target assessment by GUIDE-seq. Expression of IL-15 and TGFβR2 was measured by ELISA and western blot, respectively. iPSCs were differentiated into iNK cells and analyzed by surface staining and flow cytometry. Cytotoxicity assay was performed against K562 tumor cells.

Results Several single and double gene edited iPSC lines were generated with high efficiency to produce NK cells: iPSC-IL-15 (+/+), iPSC-TGFβR2 (-/-) and iPSC-IL-15 (+/+)-TGFβR2 (-/-). These TALEN[®]-edited iPSCs kept their pluripotency, exhibited normal morphology and karyotype with no detected off-target effect. Edited iPSCs were differentiated into NK cells with high efficiency (CD56⁺/CD45⁺ >95%) and enhanced cytotoxicity against K562 tumor cells compared to unedited iNK cells. Moreover, TGFβR2 protein was not detected, while the expression of secreted IL-15 was observed in the edited iNK cells confirming the phenotype of these cells.

Conclusions Cytovia's iPSC-NK platform combined with TALEN[®] gene editing robustly and reliably generated single cell edited iPSC clones, which were expanded and differentiated into functionally improved iNK cells. The data indicated iNK cells edited with an IL-15 knock in and TGFβR2 knock out resulted in enhanced antitumor activity. The editing and manufacturing process will enable clinical evaluation of these product candidates.

<http://dx.doi.org/10.1136/jitc-2022-SITC2022.0323>

Abstracts

324

SENSITIZING POORLY DIFFERENTIATED THYROID CANCERS TO TSHR-CART CELL THERAPY WITH MEK INHIBITORS

John Copland, Kendall Schick, Justyna Gleba, Truc Huynh, James Miller, Erin Miller, Aylin Alasonyiallar Demirel, Erin Tapper, Reona Sakemura, Elizabeth Siegler, Michelle Cox, Carl Stewart, Ismail Can, Ekene Ogbodo, Claudia Manriquez Roman*, Bezerra Evandro, Cui Gaofeng, Mer Georges, Olivier Gloria, Yushi Qui, Robert Smallridge, Abba Zubair, Han Tun, Saad Kenderian. *Mayo Clinic, Jacksonville, FL, USA*

Background Thyroid cancer incidence is rising,¹ and most thyroid cancer deaths are attributed to a subset of de-differentiated, treatment-refractory, metastatic tumors. Thyroid stimulating hormone receptor (TSHR),^{2,3} making TSHR a compelling target for advanced thyroid cancer diagnostics and therapeutics. We therefore developed a novel TSHR-targeted chimeric antigen receptor (CAR) T cell therapy to treat these aggressive thyroid cancers.

Methods TSHR-CAR constructs were synthesized using a single chain variable fragment derived from thyroid auto-antibody clone KI-70 and cloned into a lentiviral CAR construct containing 4-1BB and CD3 ζ . We then generated TSHR-CART by transducing T cells derived from normal donors. TSHR-CART demonstrated potent antigen-specific in vitro and in vivo antitumor activity. NOD-SCID- γ -/- (NSG) mice were inoculated subcutaneously with a TSHR-overexpressing thyroid cancer cell line, THJ529, and were randomized by tumor volume to treatment with TSHR-CART cells or control untransduced T cells (UTD). Treatment with TSHR-CART cells resulted in dose-dependent antitumor activity and prolonged survival (figure 1).

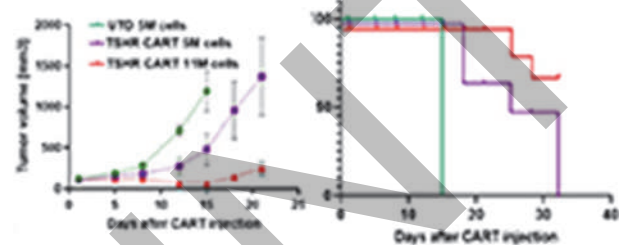
Results Anaplastic thyroid cancers (ATC) are reported to downregulate TSHR. Our TSHR immunohistochemistry results corroborated these findings and displayed attenuated or no TSHR protein expression, precluding successful TSHR-CART treatment (figure 2). We therefore sought to sensitize these tumors with mitogen-activated protein kinase (MEK) inhibitors, which have been shown to upregulate TSHR expression in patients with metastatic thyroid cancer.^{4,5} We verified that TSHR expression was upregulated in patient-derived xenograft (PDX) ATC models after one week of daily administration of the MEK inhibitors trametinib and R05126766 (figure 3). After confirming that MEK inhibition does not dampen TSHR-CART effector functions (not shown), we tested combination therapy of TSHR-CART with MEK and BRAF inhibition in vivo. NSG mice were engrafted with ATC BRAF-mutant PDX tumors and were randomized by tumor volume to daily oral treatment with placebo or trametinib (MEK inhibitor) plus dabrafenib (BRAF inhibitor). One week later, mice received either UTD or TSHR-CART. Because MEK/BRAF inhibitors alone inhibit tumor growth, treatment groups receiving placebo were implanted one week later than groups receiving MEK/BRAF inhibitors to achieve similar tumor volumes at the time of TSHR-CART treatment. Mice conditioned with trametinib plus dabrafenib and subsequently treated with TSHR-CART showed superior antitumor activity (figure 4).

Conclusions Collectively, our findings indicate that MEK/BRAF inhibition of de-differentiated thyroid cancers upregulated TSHR expression and enhanced TSHR-CART antitumor activity. This work represents a viable strategy to improve outcomes of patients with aggressive, metastatic thyroid cancers.

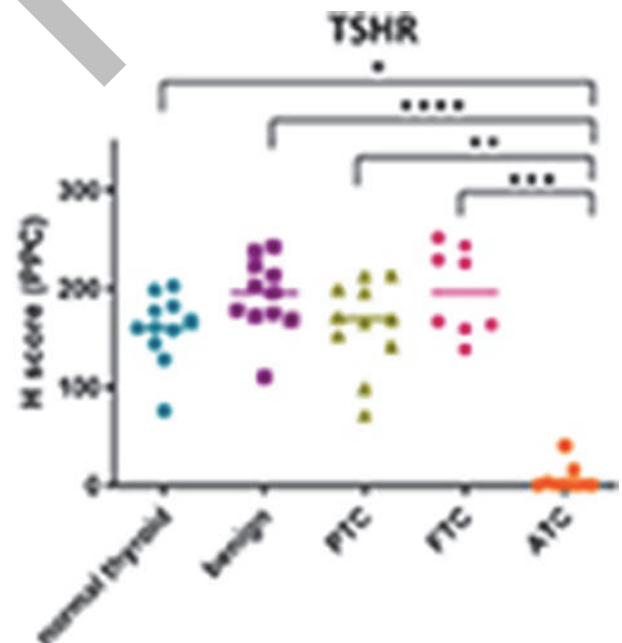
REFERENCES

1. Kim J, Gosnell JE, Roman SA. Geographic influences in the global rise of thyroid cancer. *Nat Rev Endocrinol*, 2020; **16**: 17-29.

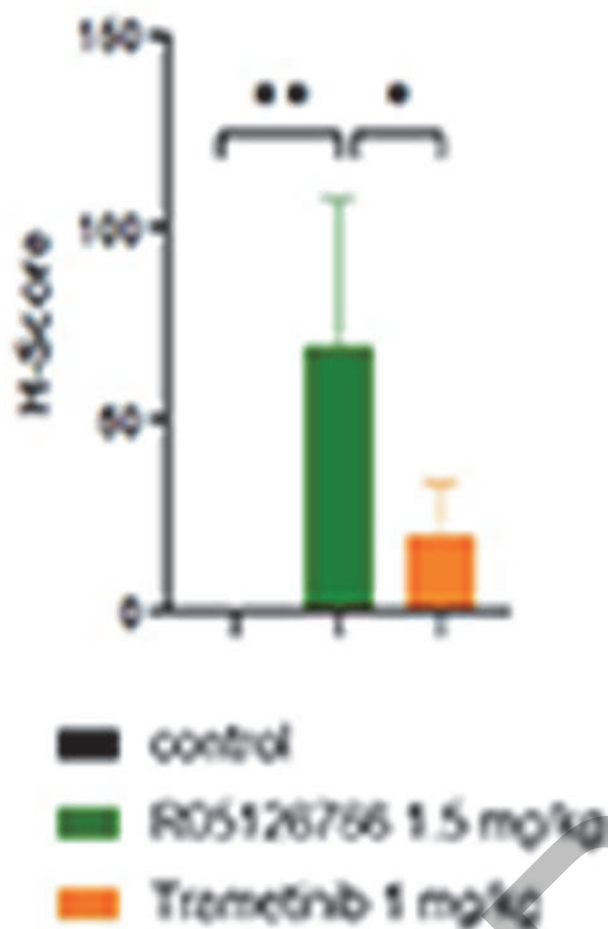
2. Li H, Zhou X, Wang G, Hua D, *et al*, CAR-T cells targeting thyroid-stimulating hormone receptor (TSHR) demonstrate safety and potent preclinical activity against differentiated thyroid cancer. *J Clin Endocrinol Metab*. 2022; **107**: 1110-1126.
3. Rowe CW, Paul JW, Gedye C, Tolosa JM, Bendinelli C, McGrath S, Smith R. Targeting the TSH receptor in thyroid cancer. *Endocr Relat Cancer*, 2017; **24**: R191-R202.
4. ElMokh O, Taelman V, Radojewski P, Roelli MA, Stoss A, Dumont RA, Dettmer MS, Phillips WA, Walter MA, Charles R-P. MEK inhibition induces therapeutic iodine uptake in a murine model of anaplastic thyroid cancer. *J Nucl Med*. 2019; **60**: 917-923.
5. Liu D, Hu S, Hou P, Jiang D, Condouris S, Xing M. Suppression of BRAF/MEK/ MAP kinase pathway restores expression of iodide-metabolizing genes in thyroid cells expressing the V600E BRAF mutant. *Clin Cancer Res*, 2007. **13**(4): 1341-1349.



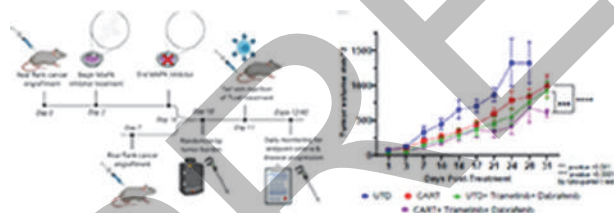
Abstract 324 Figure 1 TSHR-CART cells demonstrate potent antitumor activity in thyroid cancer TSHR< sup >+</sup >xenograft models. TSHR-CART cells exhibit dose-dependent antitumor activity (left panel) and prolonged survival (right panel) compared to untransduced (UTD) T cells in mice bearing subcutaneous TSHR+ THJ529 cells (n = 5 mice/group).



Abstract 324 Figure 2 TSHR expression is lost in advanced thyroid cancers. H-score quantitation of TSHR expression is shown. H-scores provided are based on 0 – 3 IHC scoring and percent of total areas each score (0x%0 + 1x%1 + 2x%2 + 3x%3 = H Score; 0 – 300 range with statistical analysis. * p = 0.0261, ** p = 0.0083, *** p = 0.0004, **** p < 0.0001, Kruskal-Wallis test.



Abstract 324 Figure 3 MEK inhibitors upregulate TSHR expression in ATC. H-score quantitation of TSHR expression (n=5 mice/group; * p<0.05, ** p<0.01).



Abstract 324 Figure 4 Sequential treatment of MEK/BRAF inhibition followed by TSHR-CART cell therapy demonstrates enhanced antitumor activity. Schema of treatment strategy (left panel). On day 0 or 7, NSG mice were engrafted with 5 mm³ ATC PDX. The day 0-innoculated mice, upon achieving tumor volume of ~100 mm³, were treated daily for 7 days with trametinib (1.5 mg/kg) plus dabrafenib (12.5 mg/kg) orally through ad libitum treated diet gel access to upregulate TSHR. On day 11, mice received 10 x 10⁶ cells of either UTD or CART intravenously. Tumor volume of mice treated with UTD or TSHR-CART +/- trametinib + dabrafenib (right panel).

<http://dx.doi.org/10.1136/jitc-2022-SITC2022.0324>

325 **TALEN-EDITED SMART CAR T-CELLS LEVERAGE SOLID TUMOR MICROENVIRONMENT FOR SPECIFIC AND EFFECTIVE IMMUNOTHERAPY**

¹Shipra Das*, ¹Sonal Dharani, ²Julien Valton, ²Philippe Duchateau, ²Laurent Poirot.
¹Collectis Inc, New York, NY, USA; ²Collectis, Paris, France

Background Adoptive cell therapy based on chimeric antigen receptor-engineered T (CAR-T) cells has proven to be life-saving for many cancer patients. However, its therapeutic efficacy has so far been restricted to only a few malignancies, with solid tumors proving to be especially recalcitrant to efficient therapy. Poor intra-tumor infiltration by T cells and T cell dysfunction due to an immunosuppressive microenvironment are key barriers against CAR-T cell success against solid tumors. Furthermore, low level expression of CAR-directed tumor-associated antigens (TAA) in normal tissues can result in “on-target off-tumor” cytotoxicity, raising potential safety concerns.

Methods Using our TALEN[®]-based gene editing platform, we present here innovative T cell engineering strategies that can combat some of the challenges posed by CAR-T cell development for solid tumors. These allogeneic ‘Smart CAR-T’ cells are designed to integrate locus-specific synthetic genes that can either respond to or take advantage of the unique cues localized to the solid tumor microenvironment (TME).

Results Inducible expression of a tumor-antigen directed CAR by a constitutive CAR specific to TME cues greatly enhanced anti-tumor activity, while limiting ‘on target, off-tumor’ cytotoxicity. Additionally, CAR induced gene expression could boost anti-tumor CAR-T only within the TME. Thus, our gene editing strategies could increase CAR-T cell persistence and anti-tumor activity while staying restricted to the tumor milieu.

Conclusions Our proof-of-concept study demonstrates the feasibility of developing CAR-T cell engineering strategies that can improve solid tumor targeting while mitigating potential safety risks, paving the way for clinical development.

Ethics Approval All procedures involving animals were performed in accordance with regulations and established guidelines and were reviewed and approved by the Collectis Institutional Animal Care and Use Committee (IACUC), as well as by the Animal Ethical Committee at Mispro-Biotech (New York, NY)

http://dx.doi.org/10.1136/jitc-2022-SITC2022_0325

326

OFF-THE-SHELF IPSC-DERIVED CAR-T CELLS TARGETING KLK2 DEMONSTRATE PROLONGED TUMOR CONTROL AND SURVIVAL IN XENOGRAFT MODELS OF PROSTATE CANCER

¹Charles Drake*, ²Alex Garcia, ²Chia-Wei Chang, ²Bi-Huei Yang, ²Samad Ibitokou, ²Cameron Pride, ²Spas Markov, ²Angela Liao, ²Mochtar Pribadi, ²Yijia Pan, ²Thomas Dailey, ²Tom Lee, ¹Szeman (Ruby) Chan, ¹Michael Ports, ²Jode Goodridge, ²Ryan Bjordahl, ¹Joseph Erhardt, ²Bahram Valamehr. ¹Janssen, USA, Spring House, PA, USA; ²Fate Therapeutics, Inc., San Diego, CA, USA

Background Human kallikrein-related peptidase 2 (KLK2) is an antigen with prostate-restricted expression which is maintained during prostate cancer progression – making it an attractive therapeutic target for chimeric antigen receptor (CAR) T cells. While CAR-T cell therapies have shown remarkable success in hematologic malignancies, application to solid tumors has been broadly unsuccessful. Cost of treatment, manufacturing consistency, and scalability remain significant hurdles to broader patient access. To overcome these challenges, we are developing a KLK2 targeted off-the-shelf CAR-T cell product using our induced pluripotent stem cell (iPSC)-derived immunotherapy platform.

Methods A clonal master iPSC line was derived by knock-in of a CAR construct targeting KLK2 into the T-cell receptor alpha constant chain (TRAC) locus in a bi-allelic manner. Specificity of the engineering strategy and testing for random donor vector integration and transgene copy number were confirmed by PCR and DNA sequencing. A clonal master iPSC line containing the TRAC-edits was differentiated into T cells (CAR-KLK2 iT cells) and subsequently expanded using a stage-specific protocol.

Results iPSC-derived CAR-KLK2 iT cells expressed a cell-surface profile consistent with a pure population of T lymphocytes; no TCR $\alpha\beta$ cell-surface expression was detected, cells showed homogenous expression of CD45/CD7 (>99%), and uniform CAR expression driven by TRAC (>99%). Notably, the complete loss of T-cell receptor expression by genetic knock-out eliminates the potential of graft-versus-host disease in an allogeneic setting. Preclinical *in vitro* analyses of these CAR-KLK2 iT cells demonstrated potent and specific cytotoxicity against multiple prostate cancer cell lines, including VCap cells which naturally express KLK2, PC3 cells engineered to express KLK2, and DU-145 cells engineered to express KLK2. *In vivo*, a multi-dose regimen of CAR-KLK2 iT cells controlled established (>100 mm³) VCap and PC3-KLK2 subcutaneous xenograft models with greater than 90% tumor growth inhibition and associated increased survival. Follow-up dose titration studies demonstrated that a single dose of CAR-KLK2 iT cells was sufficient to mediate approximately 70% tumor growth inhibition.

Conclusions These early preclinical *in vitro* and *in vivo* data suggest that CAR-KLK2 iT cells may have the potential to selectively eliminate prostate cancer cells. Since the behavior of engineered iT cells and additional edits in this novel platform are both currently not predictable, significant additional work is ongoing to generate an appropriate clinical candidate

<http://dx.doi.org/10.1136/jitc-2022-SITC2022.0326>

Abstracts

327

CLONAL EXPANSION OF CD22 CAR T-CELLS FOLLOWING LENTIVIRAL VECTOR INTEGRATION IN THE PWWP3A GENE

¹Alka Dwivedi*, ²Ling Su, ¹Justin Mirazee, ¹Mehdi Benzaoui, ¹Christopher Chien, ¹Nirali Shah, ²Xiaolin Wu, ¹Naomi Taylor. ¹National Cancer Institute, Rockville, MD, USA; ²Frederick National Laboratory for Cancer Research, Frederick, MD, USA

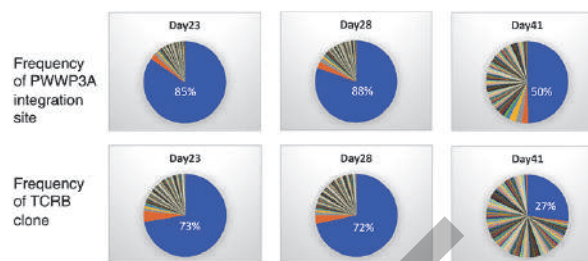
Background A 17-year-old female with multiply relapsed B-cell ALL following CD19 CAR T-cells and blinatumomab was treated with CD22 CAR T-cells (NCT02315612) for marrow and extramedullary disease (EMD). Following development of grade 2 cytokine release syndrome (on day +10) and resolution, she experienced a rapidly rising lymphocyte count at day 21 that was further evaluated.

Methods Following parental permission and minor assent, the patient was treated on a National Cancer Institute IRB approved protocol for a phase 1 trial of CD22 CAR T-cells. To evaluate for clonal expansion, TCR sequencing and integration site analysis were performed by ImmunoSEQ hsTCRB sequencing and a ddPCR assay, respectively. Evaluation of the mutant CAR and the novel endogenous protein generated by integration of the lentiviral vector was performed following their introduction into a lentiviral vector. Functional assays included cytotoxicity analyses, expansion analyses, and high throughput cytokine analyses.

Results The patient experienced full resolution of her clonal expansion and achieved a minimal residual disease negative CR in the bone marrow, with partial response at sites of EMD. TCR sequencing and integration site analyses revealed a single dominant T cell clone with lentivector integration in the PWWP domain-containing DNA repair factor 3A (PWWP3A) gene on chromosome 19 (figure 1) resulting in a fusion transcript, generated by a read-through from the EF-1a-driven CAR transcript. Additionally, a single glycine to serine mutation at position 51 (G51S) of the single chain variable fragment of CD22 CAR was detected. T cells engineered to express the mutant G51S CD22 CAR efficiently killed leukemic cells overexpressing CD22 but exhibited lower cytotoxicity against CD22+ leukemic cells. Furthermore, a high throughput dynamic evaluation of cytokine secretion revealed a significantly reduced secretion of IFN-g, IL-2, IL-10, IL-4, IL-8 and TNF-a of G51S CD22 CAR T-cells in response to CD22 antigen. Notably though, T cells engineered to express the G51S CD22 CAR exhibited an augmented cytokine-driven proliferation as compared to WT CD22 CAR T-cells.

Conclusions This is the second report of clonal expansion in the context of the CD22-CAR trial. Interestingly, in both this case and the previous one (PMID: 31387880), clonal expansion occurred in the setting of extramedullary disease and spontaneously resolved. In this patient, clonal expansion occurred secondary to a G51S CAR mutation and generation of a PWWP3A fusion transcript. The relative impact of these two events in promoting clonal T cell expansion in this CD22 CAR T-cell treated patient will be discussed.

Ethics Approval All human samples were obtained with informed consent and following institutional guidelines under protocols approved by the National Cancer Institute institutional review board and the National Institutes of Health Recombinant DNA Advisory Committee. The subject was also enrolled on an institutional review board-approved genomics protocol, which allowed for additional testing of blood samples. This trial was registered at clinicaltrials.gov as NCT02315612.



Abstract 327 Figure 1 Frequency of T cells wherein the CAR is integrated in the PWWP3A gene and frequency of the TCRB clone post CD22 CAR T-cell infusion.

<http://dx.doi.org/10.1136/jitc-2022-SITC2022.0327>

328

PROMOTING NK SURVIVAL AND FUNCTION WITHIN THE TUMOR MICROENVIRONMENT

Matthew Dysthe*, Ishwar Navin, Corrine Baumgartner, Stephanie Fetzko, Cliona Rooney, Robin Parihar. *Baylor College of Medicine, Houston, TX, USA*

Background The efficacy of CAR-NK cellular therapies in solid tumors is limited by insufficient survival and expansion within the suppressive tumor microenvironment (TME). To augment CAR-NK survival and anti-tumor function, CAR-NK cells are typically administered with exogenous cytokines or other signal modifiers that converge on signal transducer and activator of transcription-5 (STAT5) activation, an essential signaling node for NK survival and function.¹ However, systemic administration of these cytokines or signal modifiers is associated with toxicity,² unintended bolstering of TME components,³ and CAR-NK rejection.⁴ Thus, novel strategies to enhance CAR-NK function within the TME are needed. To promote CAR-NK survival and function in the TME while bypassing the need for exogenous signal dependency, we genetically modified GD2-specific CAR-NK cells to express a constitutively active IL-7 receptor complex, termed C7R (C7R.GD2-NK), that intrinsically confers persistent STAT5 activity within NK cells.

Methods To mimic challenges of the TME, we created an *in vitro* TME model by preconditioning CD14⁺ monocytes with CHLA255 neuroblastoma cells for 72 hours, converting them to an inhibitory M2-TAM phenotype expressing suppressive cytokines and ligands. 4 days after the addition of the C7R.GD2-NK cells to this immunosuppressive milieu, we assessed NK survival, expansion, cytokine secretion, and anti-tumor function.

Results Resting C7R.GD2-NK cells exhibited 3.4-fold (\pm 0.7; n=4 donors, $p < 0.005$) higher phosphorylated STAT5 (pSTAT5) compared to resting GD2-NK cells. C7R.GD2-NK cells alone in long-term culture expanded for 14 days without exogenous cytokine support but not indefinitely. In short-term co-cultures with GD2⁺ CHLA255 cells, C7R.GD2-NK demonstrated similar IFN γ levels as GD2-NK stimulated with exogenous IL-2 or IL-15 (mean% GD2-NK IFN γ ⁺ of 26.1, 21.2, and 22.4, respectively). In the *in vitro* TME model, C7R.GD2-NK cells expanded less than IL-15- or IL-2-stimulated GD2-NK cells (mean fold expansions of 2.8-, 4.5-, and 4.3-fold, respectively) but demonstrated similar anti-tumor activity. Furthermore, cell culture supernatants from C7R.GD2-NK treated conditions exhibited similar levels of NK effector cytokines IFN γ , TNF- α , and GM-CSF to exogenous cytokine-stimulated GD2-NK cells. Ongoing experiments in an *in vivo* TME xenograft model will assess the benefit of C7R in CAR-NK activity.

Conclusions C7R drives STAT5 activity in GD2 CAR-NK cells within TME conditions without the need for exogenous cytokines. The NK-intrinsic STAT5 signal is sufficient to promote NK survival, expansion, and function within the TME, potentially without the side effects of exogenous cytokines or cytokine modulators. Thus, C7R may be a viable alternative therapeutic strategy to augment CAR-NK efficacy in solid tumors.

REFERENCES

1. Gotthardt D, Sexl V. STATs in NK cells: The good, the bad, and the ugly. *Front Immunol.* 2017; **7**:694
2. Dutcher JP, Schwartzentruber DJ, Kaufman HL, Agarwala SS, Tarhini AA, Lowder JN, Atkins MB. High dose interleukin-2 (Aldesleukin) – expert consensus on best management practices-2014. *J Immunother Cancer.* 2014; **2**:26

3. Nelson B. IL-2, Regulatory T Cells, and Tolerance. *J Immunol.* 2004; **172**:3983-3988
4. Berrien-Elliott M, *et al.* Systemic IL-15 promotes allogeneic cell rejection in patients treated with natural killer cell adoptive therapy. *Blood.* 2022; **139**:1177-1183

<http://dx.doi.org/10.1136/jitc-2022-SITC2022.0328>

329

**SUPERKINE IL-2 AND IL-33 ARMORED CAR T CELLS
RESHAPE THE TUMOR MICROENVIRONMENT TO
UNIVERSALLY REDUCE SOLID TUMORS**

Shannon Ferry, Rachel Brog, Courtney Shiebout, Cameron Messier, W Cook, Charles Sentman, H Frost, Yina Huang*. *Dartmouth College, Lebanon, NH, USA*

Background CAR T cell efficacy against solid tumors is challenged by key obstacles present within the tumor microenvironment (TME). These include tumor-intrinsic expression of inhibitory ligands that induce T cell exhaustion, the heterogeneous expression of tumor antigens that contribute to immune evasion, the absence of essential nutrients required for T cell survival, and the presence of tumor associated immunosuppressive cells.

Methods To increase CAR T cell resistance to immunosuppression and broaden tumor recognition, we armored CAR T cells with a combination of the IL-2 superkine (Super2) and the alarmin IL-33. Super2+33 armored CAR T cells were transferred to mice with established primary or metastatic B16F10 melanoma or intradermal MC38 colon cell carcinoma without preconditioning regimens. Tumor growth, overall survival, and changes to tumor infiltrating leukocytes were assessed.

Results We show that a single dose of CAR T cells armored with Super2 and IL-33 promoted the control of solid tumors in immune competent mice without lymphodepletion or preconditioning regimens. Super2 and IL-33 synergized to expand adoptively transferred CAR T cells and shifted leukocyte proportions in the TME by recruiting and activating a broad repertoire of endogenous innate and adaptive immune cells. Tumors treated with Super2 and IL33 CAR T cells had significantly increased infiltration of endogenous CD8 T cells, including an effector subset with low expression levels of PD-1 and TIM-3. Super2 and IL33 synergy also resulted in reduced proportion of regulatory T cells and a phenotypic switch from M2-like to M1-like macrophages that expressed increased MHC class II. However, depletion of endogenous CD8 T cells or NK cells did not disrupt tumor control, suggesting that broad immune activation compensates for loss of individual subsets. Additionally, IFN γ , perforin, and CAR expression by transferred T cells were dispensable for the observed therapeutic effect of Super2 and IL33 expressing T cells, underscoring the contribution of endogenous immune cells in mediating tumor control.

Conclusions Super2 and IL-33 CAR T cells promoted antitumor immunity in multiple solid tumor models and was impervious to antigen loss, highlighting its potential as a universal CAR T cell platform for treatment of solid tumors. CAR T cells harnessing Super2 and IL33 synergy represent a novel strategy for improving the efficacy of CAR T cells in solid tumors by promoting the activation of endogenous immune cells.

<http://dx.doi.org/10.1136/jitc-2022-SITC2022.0329>

330 **REDIRECTING GLUCOSE USAGE DURING IN VITRO EXPANSION IMPROVES THE IN VIVO PERSISTENCE AND FUNCTION OF ADOPTIVE T CELL THERAPIES FOR CANCER**

¹Andrew Frisch*, ²Yiyang Wang, ¹Yupeng Wang, ³Konstantinos Lontos, ¹Greg Delgoffe.
¹University of Pittsburgh, Pittsburgh, PA, USA; ²Tsinghua University, Beijing, China; ³The University of Texas MD Anderson Cancer Center, Houston, TX, USA

Background While adoptive T cell therapies have shown impressive results in cancer therapy, persistence of cells remains a key feature of therapeutic efficacy. In all forms of cellular therapies, large numbers of cells are transferred to the patient, yet comparatively few can be detected within the body. We hypothesize this lack of survival and persistence is in part due to the hypermetabolic conditions, especially hyperglycemia, used to generate large numbers of T cells in vitro. Within this study, we aim to preserve a more in vivo-like metabolic state during T cell expansion so that upon transfer they may more easily re-enter the immune system and persist as a living drug.

Methods T cells were activated in culture with cognate peptide or *in vivo* with cognate antigen. The pyruvate dehydrogenase kinase (PDHK1) inhibitor dichloroacetate (DCA) was used to redirect glucose flux in vitro. Mouse tumor experiments were performed with gp100-specific pmel-1 TCR-Tg T cells transferred into B16-F10 -bearing mice. Mouse co-transfer experiments were performed with pmel-1 T cells on a congenically mismatched background. Human CAR-T experiments were performed using anti-hCD19 CAR-T cells transferred into immunodeficient mice bearing hCD19-A549 lung cancer cells.

Results Identical T cells stimulated in vitro or in vivo do not differ in effector function but differ heavily in their glycolytic metabolism. As direct inhibition of glycolysis severely hinders T cell expansion, the PDHK1 inhibitor DCA redirects glucose away from lactate production into mitochondrial metabolism, maintaining a robust expansion rate. Expansion under DCA improves cytokine production and promotes features of stemness. However, the most striking effect of expansion under DCA is evident after cells are transferred: improved immediate and long term survival of the transferred T cell product. These immediate changes in survival result in striking therapeutic efficacy, including increased tumor clearance, immunologic memory, and long-term cellular persistence in both mouse and human tumor models.

Conclusions We demonstrate that by redirecting glucose into mitochondria using DCA, T cells experience vastly reduced metabolic stress during expansion. This relatively simple energetic shift in vitro drastically improves the immediate survival and engraftment of T cells after infusion, resulting in enhanced anti-tumor efficacy and long-term memory. Our study not only suggests the current manufacturing process for cell therapies, utilizing hypermetabolic media, may hinder their ultimate therapeutic success, but provides potential solutions to bring the promise of cellular therapies to additional patients.

<http://dx.doi.org/10.1136/jitc-2022-SITC2022.0330>

331 **A NOVEL SMALL MOLECULE INHIBITOR OF CBL-B SHOWS POTENT ANTITUMOR ACTIVITY IN COMBINATION WITH PMEL-1 ADOPTIVE CELL TRANSFER IN AN AGGRESSIVE MOUSE MELANOMA MODEL**

Marilena Gallotta*, Jose Gomez Romo, Serena Ranucci, Austin Tenn-McClellan, Frederick Cohen, Gwenn Hansen, Arthur Sands, Ryan Rountree, Cristiana Guiducci. *Nurix Therapeutics, San Francisco, CA, USA*

Background Adoptive cell transfer (ACT) involving engineered T cells (CAR-T) or autologous tumor-specific lymphocytes (TIL) induces effective antitumor response in advanced cancer patients. However, tumors frequently relapse after an initial response due to suboptimal T-cell activation and expansion within the tumor microenvironment. Moreover, current ACT treatment paradigms require application of high dose bolus infusions of IL-2 which are associated with acute toxicities restricting the use of ACT in the clinic. The E3 ubiquitin ligase Casitas B-lineage lymphoma B (CBL-B) is highly expressed in T cells, where it functions as an intracellular checkpoint that constrains T-cell activation following T cell receptor (TCR) engagement, therefore limiting T cell-mediated antitumor responses.

Methods We have developed two highly potent small molecule inhibitors of CBL-B to increase T-cell antitumor function both *in vitro* (NX-0255) and *in vivo* (NX-1607).

Results We previously reported that addition of NX-0255 during *in vitro* treatment of tumor-specific T cells increases the frequency and absolute numbers of less exhausted CD8+ memory T cells, profoundly improving their functionality and ability to control tumor growth following ACT in tumor-bearing mice. Here, we hypothesized that CBL-B inhibition could reduce the requirement for IL-2 bolus and utilized the Pmel-1 ACT/B16 melanoma tumor model to compare the antitumor effect of post infusion *in vivo* treatments with NX-1607 to high dose IL-2. C57BL/6 mice were implanted with B16-OVA and received Pmel-1 CD8+ T cells activated *in vitro* using anti-CD3 stimulation and NX-0255 combined with IL-2, followed by systemic treatment with either IL-2 (IP, 150000 IU for three days, BID) or oral NX-1607 (30 mg/kg, QD). We found that ACT supported by *in vivo* treatment with NX-1607 increased the antitumor activity of Pmel-1 cells when compared to ACT alone. Importantly, the increased antitumor activity of NX-1607-supported ACT was comparable to IL-2. Spectral cytometry analysis performed at 7 and 14 days after ACT showed that following NX-1607, a larger fraction of circulating Pmel-1 cells had a central-memory phenotype and expressed high levels of Granzyme B. Interestingly, both *in vivo* treatments induced increased 4-1BB/CD137 expression that significantly correlates with antitumor response.

Conclusions These findings demonstrated that oral dosing of NX-1607 in combination with ACT can support the functionality of transferred cells providing a robust antitumor response in the aggressive B16-OVA model. Treatment with NX-1607 induces a more favorable T cell phenotype compared to IL-2 treatment and is well tolerated. The observed antitumor effects of NX-1607 support its potential use in combination with cell-based therapeutics.

<http://dx.doi.org/10.1136/jitc-2022-SITC2022.0331>

332

CRISPR/CAS9-BASED INTEGRATION OF A LARGE AND MODULAR CASSETTE INTO A SAFE HARBOR SITE TO IMPROVE CAR T CELL THERAPY EFFICACY AND SAFETY

Brendan Galvin*, Grace Zheng, Robby Moot, Michelle Nguyen, Michelle Tan, Rene Sit, Lionel Berthoin, David DeTomaso, Sofia Kyriazopoulou Panagiotopoulou, Shan Sabri, Jun Feng, Manching Ku, Anzhi Yao, Andrea Liu, Jennifer McDevitt, Matt Drever, Stephen Santoro, Aaron Cooper, Susie Jun, W Nicholas Haining, Tarjei Mikkelsen. *Arsenal Biosciences, South San Francisco, CA, USA*

Background Chimeric antigen receptor (CAR) T cell therapy has emerged as an important new tool in the treatment of cancers. However, the complexity of the enhancements used is limited by the amount of genetic information that can be integrated into the genome. Our approach utilizes Integrated Circuit T (ICT) cells, which are engineered to include a large DNA cassette that includes: receptor strategies to target multiple tumor antigens; transcriptional modifications that alter cell state; engineered cytokines and chemokines and variations in the CAR binding and signaling domains.

Our first ICT clinical program, AB-1015, is an autologous cell product for the treatment of ovarian cancer. The AB-1015 transgene cassette consists of a logic gate directed against ALPG/P and MSLN and an shRNA-miR module targeting FAS and PTPN2 that enhance potency and confer resistance to the tumor microenvironment. This transgene is delivered into primary T cells via non-viral, site-specific editing into a safe-harbor locus via CRISPR integration of transgenes by electroporation (CITE). CITE has many advantages over viral and other non-viral random integration methods, including more predictable transgene expression and function, reduced risk of unsafe insertional mutagenesis, and efficient integration of large cassettes.

Methods To identify candidate genomic loci for CITE-directed gene insertion we used epigenetic analysis, transcriptional profiling, and high-throughput gene-editing of primary T cells. Loci were further characterized using T cell functional assays. Knock-in efficiency and transgene expression stability in primary human T cells were evaluated for all loci. Lead candidate loci were tested for compatibility with complex T cell programs embodied by our integrated circuits, containing a priming receptor (PrimeR, ALPG/P) that triggers the expression of a CAR (MSLN) in response to a priming antigen. The top insertion site, GS94, was further characterized using in silico and empirical approaches.

Results GS94 was identified as an optimal locus for CITE-directed gene insertion based upon: 1) stable and high PrimeR expression; 2) high and inducible CAR expression; and 3) a superior T cell cytotoxic and cytokine secretion profile. We were unable to identify any off-target events generated by CITE at GS94, including off-target editing, knock-in and translocations, using a suite of molecular assays including iGUIDE, rhAMPseq, deep whole genome sequencing, and anchored-PCR.

Conclusions CITE editing at GS94 is specific and generates highly functional ICT cells. This novel approach to engineering tumor-specific T cells enables the generation of exceptional clinical candidates that both target new cancer types and improve efficacy.

<http://dx.doi.org/10.1136/jitc-2022-SITC2022.0332>

Abstracts

333 NOVEL PHYTOCHEMICALS-BASED CELL CULTURE MEDIUM MITIGATES NATURAL KILLER (NK) CELLULAR EXHAUSTION AND ENHANCES MATURE SUBPOPULATIONS, LEADING TO HIGHER ANTICANCER CYTOTOXIC ACTIVITY

Marc Gillig*, Rafet Amoor, Nicholas Ingala, Borom Chean, Rachit Ohri. *Enable Life Sciences LLC, Farmington, CT, USA*

Background The biological significance of the mitigation of NK cell dysfunction (exhaustion and/or anergy and/or senescence) is increased potential for solid tumor infiltration by NK cells, as well as decreased dysfunction of NK cells in the tumor microenvironment.^{1,2} Enable-NK, a novel phytochemicals-based culture medium that increases the cytotoxic activity of NK cells, has been previously demonstrated to mitigate cellular exhaustion in the NK cell line KHYG-1, as illustrated by the consistent downregulation of several exhaustion biomarkers (e.g. Tim-3, TIGIT, NKG2A). We evaluated the mitigation of exhaustion in human primary NK cells by culturing them in Enable-NK.

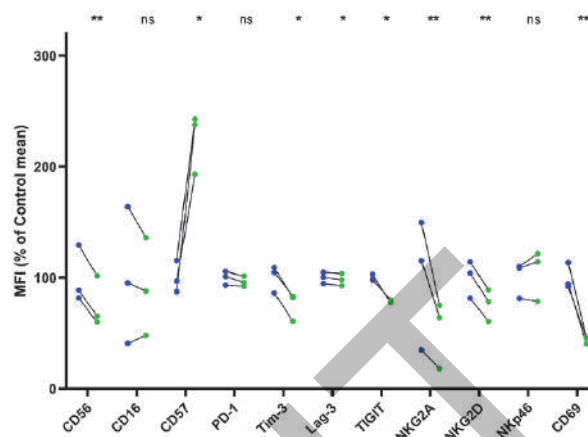
Methods Peripheral Blood Mononuclear Cells (PBMCs) were isolated from fresh buffy coats using density gradient centrifugation, and NK cells were enriched to ~90% purity using magnetic separation. Media conditions used were Enable-NK (DMEM/F12 supplemented with proprietary ingredients) or control (DMEM/F12). Cocultures were set up with K562-GFP target cells, undisturbed for several days using a 24-well G-Rex plate. Propidium iodide (PI) staining was used for cytotoxicity determination, and a panel of 12 antibodies for cellular exhaustion and subpopulation determination using surface biomarkers.

Results Several endpoints illustrate mitigation of cellular exhaustion when NK cells are cultured in Enable-NK media. Cell surface exhaustion markers (e.g. Tim-3, TIGIT, NKG2A) are consistently lower, and cytotoxicity-activating receptors (e.g. Nkp46) trend higher with the use of Enable-NK media (figure 1). The CD56dimCD16+CD57+ subpopulation is doubled in Enable-NK monocultures compared to control monocultures (figure 2), and also greatly expanded in cocultures. Finally, increased cytotoxic performance of Enable-NK-cultured NK cells, predicted based on the phenotypic differences and enrichment of the highly cytotoxic subpopulation, was confirmed by assessing the death of target cells in the cocultures by staining with propidium iodide (figure 3). Cytotoxic activity was initially equivalent to the control on Day 1, but it was boosted by over 40% in the Enable-NK group by Day 4 while remaining at the same level in the control group. Greatly enhanced cytotoxic activity was maintained through Day 7.

Conclusions The phenotypic and functional data indicate that cellular exhaustion in NK cells is significantly mitigated by culturing NK cells in the phytochemicals-based Enable-NK medium. By inducing downregulation of several inhibitory cell surface molecules, simultaneously inducing upregulation of cytotoxicity-activating receptors, and expanding cytotoxic subpopulations such as CD56dimCD16+CD57+, Enable-NK-cultured NK cells are better equipped to kill cancer cells.

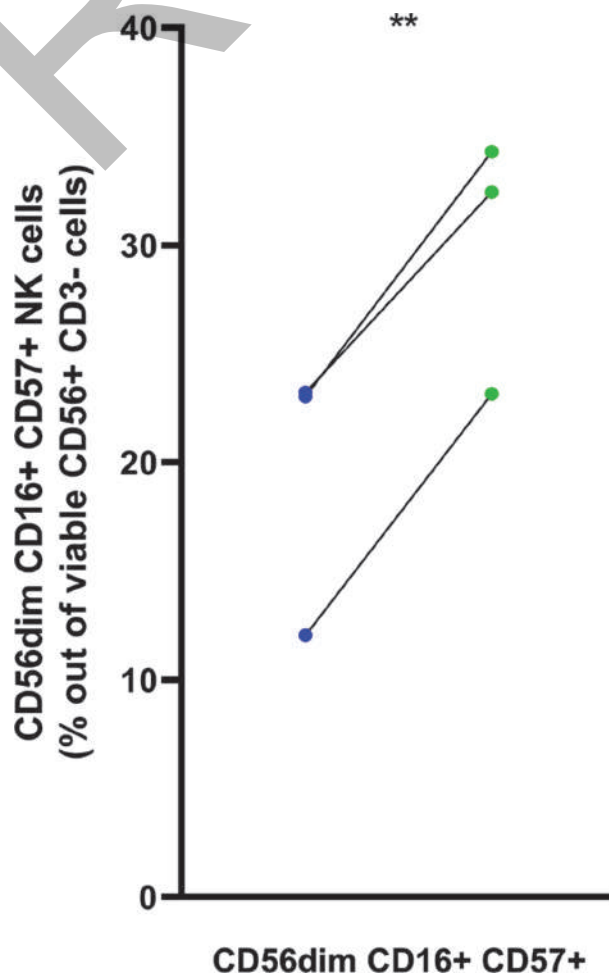
REFERENCES

1. Judge SJ, Murphy WJ, Canter RJ. Characterizing the dysfunctional NK cell: assessing the clinical relevance of exhaustion, anergy, and senescence. *Front Cell Infect Microbiol.* 2020;**10**:49.
2. Wang J, Matosevic S. Functional and metabolic targeting of natural killer cells to solid tumors. *Cell Oncol.* 2020;**43**(4):577-600.



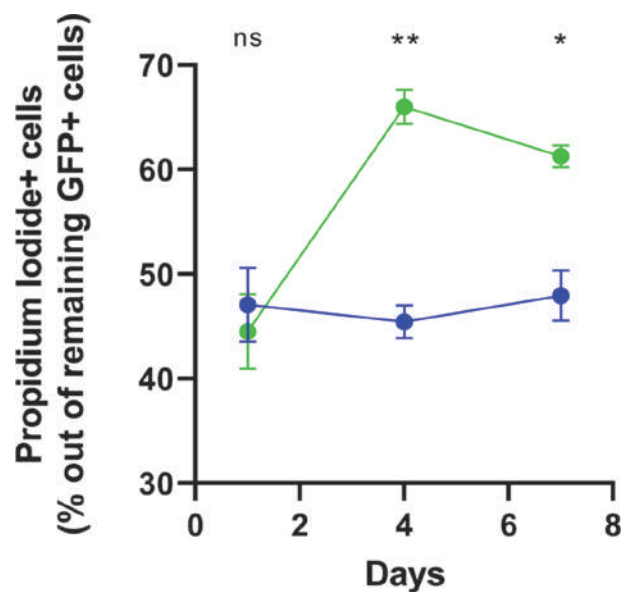
Abstract 333 Figure 1 Differences in surface marker expression in Enable-NK

The Mean Fluorescence Intensity comparison between surface marker levels on primary human NK cells, on day 3 of culture in control medium (blue) or Enable-NK (green). The represented data is for 3 healthy adult donors of primary NK cells, paired donor-wise between the two media conditions. The notation used for statistical significance is as follows (ratio paired t-test): ns is not significant, * $p < 0.05$, ** $p < 0.01$



Abstract 333 Figure 2 Enrichment of a mature cytotoxic subpopulation of NK cells
Comparison of the CD56dimCD16+CD57+ subpopulation between the control culture (blue) and Enable-NK culture (green) at day 3, as a

percentage of all NK cells (CD3-CD56+), with data paired donor-wise.
The notation used for statistical significance (paired t-test) is as follows:
**p<0.01



Abstract 333 Figure 3 Higher cytotoxic activity over time in Enable-NK coculture

Percentage of target cells which are dead, as a function of time, over the course of coculture of primary human NK effector cells with K562-GFP target cells. Cocultures were set up at an Effector:Target ratio of 1:1 on Day 0. Bars indicate Standard Error of Mean. Notation used for statistical significance (paired t-test): ns is not significant, *p<0.05, **p<0.01

<http://dx.doi.org/10.1136/jitc-2022-SITC2022.0333>

334

FUNCTIONAL VALIDATION OF SINGLE DOMAIN ANTIBODY-DERIVED CD33 SPECIFIC CAR-T CELLS FOR THE TREATMENT OF ACUTE MYELOID LEUKEMIA

<http://dx.doi.org/10.1136/jitc-2022-SITC2022.0334>

Brikena Gjenci*, Salar Khan, Julian Scherer, Tirtha Chakraborty. *Vor Biopharma, Cambridge, MA, USA*

Background Acute myeloid leukemia (AML) is an aggressive bone marrow malignancy with relapse rates >50% in treatment-responsive patients.¹ One promising new class of AML treatment is chimeric antigen receptor (CAR) T cell therapy, which has demonstrated success for certain leukemias, lymphomas, and myelomas. Conventional CAR-T cells are generated using single-chain variable fragments (scFv) derived from two domains (V_L and V_H) of monoclonal murine antibodies, potentially leading to misfolding and anti-CAR immunogenicity. In contrast, camelid-derived single domain antibodies (sdAbs) have high thermal stability and refolding capacity due to their reduced size. Single domain antibodies can access novel epitopes and exhibit reduced immunogenic potential,² suggesting their suitability as binders in CARs. Focusing on CARs targeting the AML-relevant antigen CD33, we here validate novel sdAb-derived CARs (sdCD33CAR) in a semi-automated multi-step process including cell-cell avidity and compare them to traditional scFv-derived CARs.

Methods A phage-display library containing $\sim 10^{11}$ vicuña sdAbs was panned against soluble and cell-associated CD33 to identify distinct sdAb binders by ELISA and FACS. Ten binders were selected, expressed as soluble human Fc tagged molecules, and screened for affinity by Octet. Five binders were used for sdCARs with 4-1BB costimulatory domains. Lentiviral vector (LVV) was generated with a liquid handler to express CARs in an IL-2 Reporter System (CAR-IRS cells). CAR-IRS cells enable functional CAR validation by activation-dependent induction of a fluorescent reporter. CAR-IRS activation was assessed by flow cytometry or continuous IncuCyte live cell imaging. CAR-IRS cells were also tested for cell-cell avidity against CD33-expressing target cells using the Z-Movi platform.

Results Octet analysis of sdAbs indicated affinity values (K_D range 2-13 nM) and binding kinetics favorable for CAR development. In the CAR-IRS assay, sdCD33CARs exhibited higher surface expression (up to 3-fold) and normalized activity (up to 70-fold) compared to scFv-based CD33CARs. Fluorescent reporter results were supported by CD69 staining (up to 15-fold increase). CAR-IRS flow cytometry was validated by IncuCyte imaging. Z-Movi analysis showed comparable avidity between the sdAb and scFv CARs, suggesting that sdCD33CARs represent a promising therapeutic approach.

Conclusions We have undertaken extensive *in vitro* validation of sdCD33CARs in an objective CAR-IRS background. Automated liquid handling allows for high-throughput LVV transduction to generate CAR-IRS cells, which enables reliable, fast, and economical comparisons across CAR constructs. We have identified one sdCD33CAR construct, which outperforms the traditional scFv-derived CD33CARs in our initial *in vitro* screens. These results provide promising *in vivo* screening candidates for future CAR-T cell therapies against AML.

REFERENCES

1. Thol F, Ganser A. Treatment of Relapsed Acute Myeloid Leukemia. *Curr Treat Options Oncol.* 2020; **21**:66.
2. Asaadi Y, Jouneghani FF, Janani S, Rahbarizadeh F. A comprehensive comparison between camelid nanobodies and single chain variable fragments. *Biomark Res.* 2021;**9**:87.

335

ANALYSES OF SEVERE IMMUNE-MEDIATED TOXICITY IN PATIENTS WITH ADVANCED MCRPC TREATED WITH A PSMA-TARGETED ARMORED CAR T-CELLS

¹Whitney Gladney*, ¹Adina Vultur, ²Michael Schweizer, ³Joseph Fraietta, ³Andrew Rech, ³Carl June, ¹Matthew O'Rourke, ¹Amy Roberts, ¹Hinel Patel, ¹Jamie Rosen, ¹Pam Hufner, ¹Yanping Luo, ¹David Barrett, ¹Thomas Fountaine, ¹Karen Chagin. ¹*Tmunity Therapeutics, Philadelphia, PA, USA*; ²*University of Washington, Seattle, WA, USA*; ³*University of Pennsylvania, Philadelphia, PA, USA*

Background We previously reported preliminary safety and efficacy results from a multi-center Phase 1 trial of CART-PSMA-TGF β RDN T-cells (TmPSMA-01; NCT04227275) in patients (pts) with metastatic castration resistant prostate cancer (mCRPC). Nine pts were dosed with TmPSMA-01 across three doses ranging from 1×10^7 - 3×10^8 CAR+ cells. Evidence of clinical activity was observed, however, two pts developed severe immune-mediated toxicity and experienced Grade (Gr) 5 events. These pts had no known clinically relevant risk-factors and demonstrated disparate pre- and post-infusion clinical courses. Translational research efforts to evaluate the mechanisms of immune-mediated toxicity to TmPSMA-01 were undertaken. Results are summarized herein.

Methods Pt samples collected per clinical protocol were subjected to correlative analysis platforms. Longitudinal serum and peripheral blood specimens were evaluated for soluble factors by immunoassays and TmPSMA-01 kinetics by molecular techniques, respectively. Biomarker comparisons between patients with Gr5 events and those without were made. As available, pt tissues (tumor and autopsy samples) were evaluated for TmPSMA-01 infiltration by RNA-ISH. Additionally, an *in vitro* model of immune toxicity was applied to evaluate TmPSMA-01 product potency and new CAR candidates.

Results Serum cytokines from all pts showed patterns consistent with an immune-effector response but pts with Gr5 events demonstrated an elevated inflammatory signature with higher levels of IL2, IL6, GM-CSF and IL-18, among others. Peripheral expansion of TmPSMA-01 was observed and kinetics correlated with cytokine response. Autopsy evaluation from one pt with a Gr5 event showed TmPSMA-01 lymph node tumor infiltration but no presence in the sampled brain, despite clinical presentation of immune effector cell associated neurotoxicity. Finally, *in vitro* modeling of immune-toxicity demonstrated higher cytokine levels in TmPSMA-01 cell products from Gr5 pts. Using the same assay, substituting CD2 for 41BB showed a reduction in cytokine levels without impacting efficacy.

Conclusions Correlative studies from pts who demonstrated severe immune-mediated toxicity following TmPSMA-01 revealed trends toward patient-intrinsic hyperinflammation. Biomarker findings suggest a contribution of IL-18 to TmPSMA-01-associated cytokine response which can be further explored for toxicity management. Moreover, we found no evidence of on-target, off-tumor involvement in the examined tissues. While a clear mechanism explaining the excessive immune-mediated response in 2 pts following TmPSMA-01 is not fully elucidated, our preclinical data demonstrate potential risk mitigation by replacing the 41BB co-stimulatory domain with CD2. Knowledge gained from these studies supported the development of a next-generation PSMA-targeting CAR, TmPSMA-02, to improve safety while maintaining anti-tumor activity and will be explored in a multi-center, Ph1/2 trial for pts with mCRPC.

Ethics Approval Patients were enrolled on a WCG Institutional Review Board (IRB) approved protocol, IRB#20191909, titled

“A Phase 1 Open-Label, Multi-Center Study of PSMA Targeted Genetically Modified Chimeric Antigen Receptor T Cells in Patients with Metastatic Castration Resistant Prostate Cancer.” This clinical study was designed and implemented, and the results of the trial reported in accordance with the International Conference on Harmonization (ICH) Harmonized Tripartite Guidelines for Good Clinical Practice with applicable local regulations and international guidances, including the 21 CFR and all ethical principles written in the Declaration of Helsinki. The clinical study protocol and the informed consent form (ICF) were both reviewed and approved by the properly chartered IRBs and Independent Ethics Committee before the study commenced. Patients enrolled in the study underwent the appropriate Screening procedures only after providing the appropriate written consent using the approved ICF for this study.

<http://dx.doi.org/10.1136/jitc-2022-SITC2022.0335>

Abstracts

336

A NOVEL METHOD FOR EFFICIENT CGMP PRODUCTION OF NATURAL KILLER CELLS FROM CLONAL MASTER INDUCED PLURIPOTENT STEM CELLS FOR NEXT GENERATION, OFF-THE-SHELF CANCER IMMUNOTHERAPY

¹Davide Bernareggi*, ¹Caryn Gonsalves, ¹Max Schabla, ¹Alejandra Gárate-Carrillo, ¹Mohammad El-Kalay, ²Dan Kaufman, ¹Robert Hollingsworth, ¹Huang Zhu. ¹Shoreline Bioscience, San Diego, CA, USA; ²University of California-San Diego, La Jolla, CA, USA

Background Natural killer (NK) cells are innate immune cells that play a key role in tumor immune surveillance. Recent advances allow for the derivation of immune cells, including NK cells, from human induced pluripotent stem cells that can be utilized for cancer immunotherapy. High doses of NK cells and multiple doses are both safe and likely necessary for clinical efficacy. Manufacturing large number of NK cells from a clonal master iPSC line provides a promising strategy to enable next generation, off-the-shelf, cancer immunotherapies.

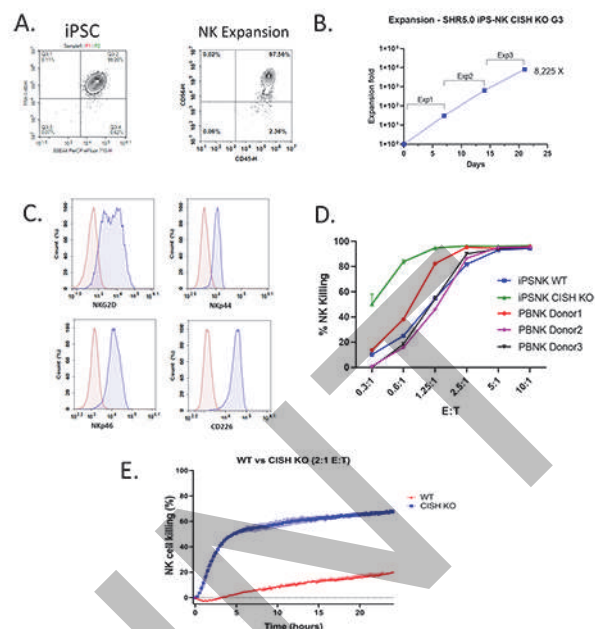
Methods We have developed a novel process to produce high purity, clinical scale NK cells efficiently and consistently. Briefly, hematopoietic progenitor cells are derived using an improved spin embryoid body (EB) method using defined cytokines including bone morphogenic protein-4 (BMP-4), stem cell factor (SCF), vascular endothelial growth factor (VEGF), fms-like tyrosine kinase 3 (FLT-3) etc. The hematopoietic progenitor cells are subsequently differentiated into mature NK cells using a second set of defined cytokines such as IL-3, IL-7, IL-15, SCF etc.

Results Using this novel method, fully functioning NK cells could be expanded more than 8,000-fold to enable us to produce 1×10^{12} NK cells starting from 1×10^6 undifferentiated iPSCs. This cell production scale can supply >200 clinical doses from one cGMP manufacturing campaign. NK cells produced using this method are CD56-positive and display the typical phenotype of NK cell activating receptors including NKG2D, NKp44, NKp46, DNAM-1. Importantly, these NK cells demonstrate better anti-tumor activities and produce higher levels of IFN γ and TNF α compared to peripheral blood-derived NK cells isolated from healthy donors. Moreover, this protocol has been adapted and optimized for clinical scale manufacturing of NK cells from a genetically engineered iPSC cell line bearing a knock-out of *CISH*, a key intracellular checkpoint of NK cell activation.¹ *CISH* KO NK cells produced using this optimized method show significantly better anti-tumor activities against multiple liquid and solid tumor cell lines (figure 1), including K562, Raji (B cell lymphoma), Daudi (B cell lymphoma), SUP-B15 (B cell lymphoma), MOLT-4 (T cell lymphoma), SKOV-3 (ovarian cancer), OVCAR-4 (ovarian cancer), HCC-827 (lung cancer), ZR-75 (breast cancer), and BT-474 (breast cancer), in standard cytotoxicity assays compared with unmodified NK cells.

Conclusions Overall, this novel cell production strategy paves the way for clinical trials using higher doses of iPSC-derived NK cells with increased potency, thus enabling next-generation CAR-NK cell-based immunotherapies.

REFERENCE

1. Zhu H, Blum R, Bernareggi D, Ask E, Wu Z, Hoel H, Meng Z, Wu C, Guan K, Malmberg KJ, Kaufman D. Metabolic reprogramming via deletion of CISH in human iPSC-derived NK cells promotes in vivo persistence and enhances anti-tumor activity. *Cell Stem Cell*. 2020; **27**: 224-237.



Abstract 336 Figure 1 CISH-KO iPSCs can be used to generate highly functional iNK

(A) Flow cytometric analysis of CISH KO iPSCs and iNK cells following differentiation and expansion. (B) Graph showing cumulative in vitro fold expansion of CISH-KO iNK cells over three expansion periods of 7d each. (C) Flow cytometric analysis of expression of indicated surface markers by CISH-KO iNK cells. (D) Comparison of cytotoxicity of WT iNK, CISH-KO iNK, and PBNK cells co-cultured with K562 cells using a flow cytometry killing assay. Error bars represent mean \pm SEM from three independent experiments. (E) xCELLigence killing assay comparing cytotoxicity of WT vs CISH-KO iNK cells co-cultured with BT474 target cells.

<http://dx.doi.org/10.1136/jitc-2022-SITC2022.0336>

337

DEVELOPMENT OF POTENT iPSC-DERIVED MACROPHAGES (iMACS) FOR OFF-THE-SHELF CANCER IMMUNOTHERAPY – A NEW CELL TYPE IN THE EVOCELLS PLATFORM

¹Kathrin Haake, ²Michela Mirenda, ²Julien Bousquet, ¹Philine Scheinpflug, ²Michael Esquerré, ¹Audrey Holtzinger, ¹Stefanie Pfaender, ²Michael Paillasse, ¹Daniel Sommermeyer, ²Oriane Bombarde, ³Loïc Ysebaert, ³Fabien Despas, ¹Matthias Austen, ¹Andreas Scheel, ¹Markus Dangl, ¹Monika Braun, ¹Nadja Wagner*. ¹Evotec International GmbH, Göttingen, Germany; ²Evotec France SAS, Toulouse, France; ³Oncopole (IUCT-O), Toulouse, France

Background Cellular immunotherapy has transformed the oncology landscape and provided promising treatment options for patients suffering from hematological malignancies in the form of chimeric antigen receptor (CAR)-T therapies, which involve the adoptive transfer of autologous patient-derived ab T cells equipped with a CAR for enhanced tumor cell targeting. However, the manufacturing complexity and logistical hurdles associated with such autologous products have shifted the focus to the development of allogenic therapies including off-the-shelf immune cells derived from induced pluripotent stem cells (iPSCs). Whilst CAR-Ts have been effective in treating a range of different blood cancers, they have demonstrated limited efficacy to date in solid tumors, which represent approximately 90% of all adult human cancers. Recently, CAR-directed autologous macrophages have emerged as a new potential treatment for solid tumors, as they carry many inherent characteristics beneficial for the penetration into and reprogramming of an immunosuppressive tumor microenvironment (TME). We aim to generate genetically modified iPSC-derived macrophages (iMACs) as an innovative, off-the-shelf cell source for cancer immunotherapy.

Methods Using a validated GMP iPSC line as starting material, we have established a proprietary feeder- and cell sorting-free 3D differentiation protocol that enables robust and large-scale production of iMACs. To ensure reproducible high quality and safety of our cells, we perform stringent monitoring of all process stages using flow cytometry, transcriptome analysis (scRNAseq), as well as an array of analytical methods to ensure genetic integrity of the cells. iMACs were polarized towards an M1-like phenotype and compared to blood-derived counterparts in functional assays, including antibody-dependent cellular phagocytosis (ADCP) and cytokine release.

Results Our iMACs exhibited the typical cell morphology and marker expression of fully differentiated macrophages at a homogeneous level. Transcriptome analysis confirmed the complete switch of iPSCs to cells with a macrophage-specific gene profile. The iMACs responded to M1 polarization by inducing expression of classic pro-inflammatory macrophage markers, showed a cytokine profile comparable to blood-derived macrophages and exhibited high phagocytic activity. In combination with clinically well-validated monoclonal antibodies, iMACs could be directed to target tumor cell lines as well as primary patient samples *in vitro*.

Conclusions Using our proprietary EVOcells iMAC differentiation process we were able to generate highly pure iMACs that can be polarized to M1-like macrophages with a pro-inflammatory phenotype and a high phagocytic capacity against cancer cell lines and primary tumor samples, indicating their great potential as a cell source for cancer immunotherapies.

<http://dx.doi.org/10.1136/jitc-2022-SITC2022.0337>

338 ANALYSIS OF CHEMOKINE EXPRESSION PROFILE OF NORMAL AND TUMOR TISSUE FOR EFFECTIVE ADOPTIVE CELL THERAPY

¹Do Yeon Han*, ^{1,2}Jung Han Seo, ²Cho Rong Hong, ²Hyeon Jin Lee, ¹Gyung Yub Gong, ^{1,2}Hee Jin Lee. ¹University of Ulsan College of Medicine, Seoul, Republic of Korea; ²NeogenTC Corp, Seoul, Republic of Korea

Background Adoptive cell therapy (ACT) is transfer of ex vivo expanded immune cells to treat cancers. In solid tumors, ACT is less effective because injected immune cells need to infiltrate to the tissue. To improve the ACT, engineering of chemokine receptors on immune cells has been developed. Since tumors secrete different chemokines, it is important to analyze frequently secreted chemokines and modulate their corresponding receptors. We analyzed and compared the chemokine expression in the normal and tumor tissues and proposed useful chemokine receptors for ACT.

Methods RNA sequencing data for tumor and normal tissues were obtained from the TCGA (n=9,807, pan-cancer) and GTEx (n=7,862, normal tissues from whole body). To identify chemokines expressed more in tumor tissues than normal tissues, we compared chemokine expression between TCGA and GTEx data. To identify chemokine receptors which are already expressed in activated T cells, we analyzed gene expression of expanded tumor-infiltrating lymphocytes (TILs) from 14 breast cancer patients.

Results Twenty-nine chemokines were expressed more than twice in tumors than normal tissues in pan-cancer analysis. Total 16 chemokine receptors are matched with these 29 chemokines. We checked expression of corresponding chemokines of 16 chemokine receptors. According to average expression in the normal and tumor tissues, 9 chemokine receptors that covered more than 80% of pan-cancer cases were considered to be useful for engineering of ACT. In RNA sequencing data of the TILs, 3 out of 9 chemokine receptors were highly expressed. About 98.1% of pan-cancer cases showed high expression of chemokines corresponding to these 6 chemokine receptors.

Conclusions Six chemokine receptors (CCR3, CCR4, CCR8, CXCR5, CXCR6, and XCR1) could be useful to modulate for ACT by enhancing cell trafficking.

Ethics Approval This study was approved by the Institutional Review Board of Asan Medical Center, approval number IRB#2015-0438.

<http://dx.doi.org/10.1136/jitc-2022-SITC2022.0338>

339

QUANTITATIVE ASSESSMENT OF CAR-T CELL THERAPY TARGETS USING COMPUTATIONAL PATHOLOGY

Nathalie Harder*, Markus Schick, Pallavi Sontakke, Alma Andoni, Karma DaCosta, Ruppen Nalbandian, Philipp Wortmann, Ansh Kapil, Gordon Moody, Maria Letizia Giardino Torchia, Martin Philip Lloyd, Nicholas Durham, Eric Tu. *AstrZeneca, Munich, Germany*

Background CAR-T cell-based therapies have improved the treatment of some advanced lymphomas and leukemias. While loss of CAR-T target expression is an established resistance mechanism, a large fraction of target-negative patients responded well to CAR-T cell therapy in early phase clinical trials revealing the urgent need for precise quantification of cell therapy targets as biomarkers. Typically, biomarkers are assessed by standard pathologist scoring of immunohistochemically stained tissue. However, this process is subjective, semi-quantitative and does not assess expression heterogeneity.

Methods To tackle this challenge, we used an automatic image analysis approach for Quantitative Continuous Scoring (QCS) of GPC3 and TGF- β expression in Hepatocellular carcinoma (HCC) patient-derived xenograft (PDX) samples. Our approach is based on supervised Deep Learning (DL) to precisely quantify GPC3 membrane expression and TGF- β membrane and cytoplasmic expression in tumor epithelium on digitized IHC whole slide images (WSI).¹ QCS consists of two supervised DL models which (1) identify epithelium versus non-epithelium regions and (2) segment tumor cells into cell nucleus, cytoplasm, and membrane compartments (figure 1). Based on this segmentation, GPC3 and TGF- β expression is computed as the mean optical density (OD) as a measure of brown staining intensity for each subcellular compartment. All WSIs used in this study have been scored by pathologists for validation.

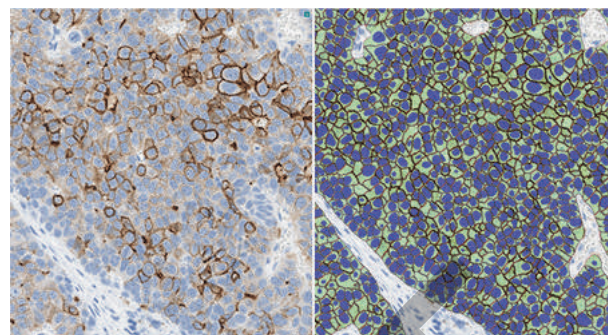
Results We validated our approach on a set of 23 WSIs by correlating the automatically computed mean GPC3 expression on membranes with pathologist's H-scores (Pearson correlation 0.93, 95% CI [0.85, 0.97]), as well as the computed TGF- β percentage positive cells (based on mean OD on membrane and cytoplasm, OD threshold=25) with the pathologist scoring of TGF- β percentage positive cells (Pearson correlation 0.95, 95% CI [0.89, 0.98]). Our automatic scoring provides continuous measurements of expression levels which allows us to reproduce the pathologist scoring, and provides additional resolution and enables analysis of expression heterogeneity.

Conclusions We adjusted QCS to precisely quantify GPC3 and TGF- β expression in HCC PDX samples and validated our approach based on pathologist's scoring and our automatic GPC3 scoring enables detailed and precise studies of CAR-T cell targets.

REFERENCE

1. Sade H, Kapil A, Wortmann P, Spitzmueller A, Triltsh N, Meinecke L, Haneder S, Shumilov A, Lesniak J, Bertani V, Tan TH, Hidalgo-Sastre A, Christ S, Storti A, Alleze R, Medrikova D, Chan J, Lanzmich S, Schick M, Schmidt G, Barrett JC. Quantitative assessment of IHC using computational pathology allows superior patient selection for biomarker-informed patients. *Cancer Res.* 2022;**82**: 468.

Ethics Approval All study protocols, amendments, and documents were approved by the appropriate institutional review boards.



Abstract 339 Figure 1 Example of segmentation result for GPC3 stained HCC sample
Left: raw image, right: overlay of automatic segmentation into cellular compartments nucleus (blue), cytoplasm (green), and membrane (red) after detection of epithelial regions.

<http://dx.doi.org/10.1136/jitc-2022-SITC2022.0339>

Abstracts

340

THE EPI-RTM TECHNOLOGY PRODUCES A POLYCLONAL TIL PRODUCT (LYL845) WITH DIVERSE TUMOR-REACTIVE CLONES THAT HAVE STEM-LIKE QUALITIES AND ANTI-TUMOR FUNCTION

Benjamin Harris*, Yogin Patel, Ngoc-Han Ha, Lora Zhao, Sheila Lou, Stefan Siebert, Emily Fu-Sum, Rigel Kishton, Purnima Sundar, Suman Kumar Vodnala, Shobha Potluri. *Lyell Immunopharma, South San Francisco, CA, USA*

Background Adoptive cell therapy using tumor-infiltrating lymphocytes (TIL) is a promising method for cancer treatment. Unlike other cell therapies that engineer the tumor-targeting receptor into the T cells, TIL therapy preserves and expands tumor-reactive T-cell clones from surgically resected tumors. TIL products that are highly enriched with tumor-reactive T-cell clones have been shown to mediate responses to treatment.¹⁻³ Additionally, stem-like qualities of T cells have been associated with improved outcomes in patients treated with cellular therapies, including TIL.⁴ Therefore, a polyclonal TIL product containing diverse, potent tumor-targeting clones with stem-like qualities is vital for improving clinical outcomes in TIL therapy. LYL845 is an autologous TIL product produced with our proprietary Epi-R[®] epigenetic reprogramming protocol, which was developed to preserve polyclonality and tumor-reactive clones with enhanced stem-like qualities and anti-tumor function.

Methods LYL845 was generated using Epi-R technology and compared with TIL product generated by a standard protocol (as control). To identify tumor-reactive clones, we primarily rely on surrogate measures of clonal frequency and clonal phenotype,⁵⁻⁷ but also used tumor co-culture assays to directly measure tumor-reactivity. Using bulk TCR sequencing and CITE-seq + scTCR-seq, LYL845 was assessed for retainment of tumor-reactive clones.

Results We observed that both the research and large-scale TIL products expanded from multiple tumor types (melanoma, lung, colon) using Epi-R technology were highly polyclonal. Furthermore, putative tumor-reactive clones identified from initial tumor samples were preserved in LYL845, both at research (n=13) and large-scale (n=3). Using tumor co-culture assays, we confirmed that our approach for identifying putative-tumor reactive clones is a good surrogate for true tumor reactivity. The cells from putative tumor-reactive clones (and true tumor-reactive clones defined from co-culture assays) in LYL845 demonstrate more stem-like and effector function and less exhaustion than the putative tumor-reactive clones in the control products. In tumor co-culture assays, LYL845 demonstrates potent antitumor function, including dose-dependent cytolytic activities and cytokine secretion (figure 1).

Conclusions Pre-clinical data show that LYL845 is an expanded TIL product that preserves tumor-reactive clones with stem-like qualities. Based on these promising preclinical data, we plan to evaluate LYL845 for safety, tolerability, and anti-tumor activity in an upcoming first-in-human Phase 1 clinical trial.

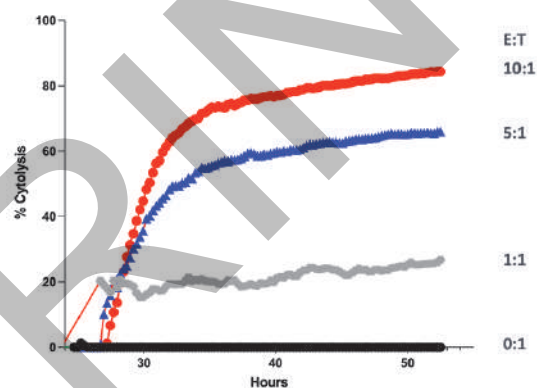
Acknowledgements We thank members of Lyell Immunopharma's flow cytometry core (Andrew Jimena, Elizabeth Pedrosa, Ken Xiong), process development team (Meritxell Galindo Casas, Carson Harms, Melissa DeFrancesco) and Queenie Vong for their experimental contributions.

REFERENCES

1. van den Berg JH, Heemskerk B, van Rooij N, *et al.* Tumor infiltrating lymphocytes (TIL) therapy in metastatic melanoma: boosting of neoantigen-specific T cell reactivity and long-term follow-up. *J Immunother Cancer.* 2020;**8**:e000848.

2. Tran E, Turcotte S, Gros A, *et al.* Cancer immunotherapy based on mutation-specific CD4+ T cells in a patient with epithelial cancer. *Clin Cancer Res.* 2014;**344**:641-645.
3. Zacharakis N, Chinnasamy H, Black M, *et al.* Immune recognition of somatic mutations leading to complete durable regression in metastatic breast cancer. *Nat Med.* 2018;**24**:724-730.
4. Krishna S, Lowery FJ, Copeland AR. Stem-like CD8 T cells mediate response of adoptive cell immunotherapy against human cancer. *Science.* 2020;**370**:1328-1334.
5. Oliviera G, Stromhaug K, Klaeger S, *et al.* Phenotype, specificity and avidity of antitumor CD8+ T cells in melanoma. *Nature.* 2021;**596**:119-125.
6. Pasetto A, Gros A, Robbins PF, *et al.* Tumor- and neoantigen-reactive T-cell receptors can be identified based on their frequency in fresh tumor. *Cancer Immunol Res.* 2016;**4**:734-743.
7. Lowery FJ, Krishna S, Yossef R, *et al.* Molecular signatures of antitumor neoantigen-reactive T cells from metastatic human cancers. *Science.* 2022;**875**:977-884.

Ethics Approval Research was performed with tissues obtained from patients through a procurement protocol approved by WCG IRB, tracking number 20210857



Abstract 340 Figure 1 Tumor recognition by the LYL845 product depicted as percent cytolysis with an autologous tumor cell line (metastatic melanoma). Tumor cell killing was observed in all E:T ratios compared to control- tumor only (0:1) in a dose-dependent manner.

<http://dx.doi.org/10.1136/jitc-2022-SITC2022.0340>

341

NOVEL IMMUNE RECONSTITUTION MODEL HIGHLIGHTS THE IMPORTANCE OF STEALTH STRATEGIES THAT POTENTIATE EFFECTOR CELL FUNCTION AND PROMOTE FUNCTIONAL PERSISTENCE OF NEXT-GENERATION ADOPTIVE CELL THERAPIES

¹Ken Hayama*, ¹Alan Williams*, ¹Yijia Pan, ¹Brian Groff, ¹Rina Mbofung, ¹Lauren Fong, ¹Nicholas Brookhouser, ¹Ramzey Abujarour, ¹Tom Lee, ¹Peter Szabo, ¹Lilly Wong, ²Maksim Mamonkin, ³Karl-Johan Malmberg, ¹Ryan Bjordahl, ¹Jode Goodridge, ¹Bob Valamehr. ¹Fate Therapeutics, San Diego, CA, USA; ²Baylor College of Medicine, Houston, TX, USA; ³University of Oslo, Oslo, Norway

Background Cyclophosphamide and Fludarabine (Cy/Flu)-based lymphodepletion conditioning (LDC) regimens are recognized as critical steps toward creating greater access to homeostatic cytokines and immune system modulation favorable for adoptively transferred, cell-based cancer therapy. However, protracted LDC has been associated with poor immune reconstitution and increased susceptibility to opportunistic infections. Therefore, the next-generation of cancer cell therapies should prioritize reducing the requirement for LDC regimens. Using a novel immune reconstitution *in vitro* assay, we provide promising evidence for unique stealth strategies designed to potentiate effector cell function without the need for Cy/Flu-based LDC; including, (1) engineering an alloimmune defense receptor (ADR)¹ which targets 4-1BB expressed on alloreactive immune cells and provides a CD3 ζ signaling boost to potentiate ADR-edited iPSC-derived NK (iNK) and T (iT) cells; (2) knockout of two costimulatory ligands to prevent immunological synapse formation; and (3) a combinatorial therapeutic strategy including CD38-null iNK and iT cells with the addition of anti-CD38 monoclonal antibody (mAb) to deplete alloreactive effector cells.

Methods By adjusting the dosage and temporal administration of Cy/Flu *in vitro*, we established a novel lymphodepletion model with a range of phosphoramidate mustard (the active metabolite of cyclophosphamide) and fludarabine-treated PBMCs to mimic the kinetics alloreactive immune depletion and reconstitution post-Cy/Flu LDC. Using high-resolution and mixed lineage- and source-detection flow cytometry panels, different sources and compartments of input cells were analyzed for persistence and activity.

Results Using our reconstitution model, preliminary data show that ADR potentiates iNK cells and extends functional persistence by selective targeting of 4-1BB-positive control or Cy/Flu-treated alloreactive immune cells. Double knockout of costimulatory ligands or supplementing PBMC and iNK cell co-cultures with anti-CD38 mAb protected costimulatory ligands-null and CD38-null iNK cells, respectively, and extended functional persistence by stagnating proliferation of alloreactive immune cells. Furthermore, we highlight translational data depicting the addition of anti-CD38 mAb to an LDC regimen further delays immune reconstitution in patients and may provide a prolonged window for therapeutic efficacy.

Conclusions Collectively, the data demonstrate that unique stealth strategies that potentiate effector cell function and promote functional persistence have the potential to eliminate the need for Cy/Flu mediated LDC. Notably, arming iNK cells with ADR extends functional persistence in the presence of an intact endogenous immune compartment. As exhibited by the immune reconstitution model, we show the first evidence of promising stealth strategies for allogeneic cell therapies that reduce or overcome the requirement of LDC while maintaining robust cytotoxic tumor responses.

REFERENCE

1. Mo F, et al. Engineering off-the-shelf therapeutic T cells resist host immune rejection. *Nat Biotechnol.* 2021;**39**:56-63.

<http://dx.doi.org/10.1136/jitc-2022-SITC2022.0341>

342

KRAS G12V T CELL RECEPTOR-ENGINEERED T CELLS EXPRESSING THE DURABILITY FAS-41BB SWITCH RECEPTOR EXHIBIT A POTENT, PERSISTENT, COORDINATED CD4/CD8 ANTI-TUMOR RESPONSE *IN VITRO* AND *IN VIVO*

¹Xingyue He, ¹Michelle Hoffmann, ¹Jinsheng Liang, ¹Hongjing Qu, ¹Allison Drain, ¹Hubert Lam, ²Shannon Oda, ³Thomas Schmitt, ³Aude Chapuis, ³Philip Greenberg, ¹Gary Shapiro*, ¹Loic Vincent. ¹Affini-T Therapeutics, Watertown, MA, USA; ²Seattle Children's Medical Research Institute, Seattle, WA, USA; ³Fred Hutchinson Cancer Research Center, Seattle, WA, USA

Background Adoptive cell therapy with genetically modified T cells has shown promising efficacy in solid tumors but has been limited by immunosuppressive mechanisms that interfere with sustained activity including FAS ligand-induced apoptosis of tumor-infiltrating, FAS receptor-positive lymphocytes.¹ As previously reported, T Cell Receptor (TCR)-engineered T cells expressing a FAS-41BB switch receptor, consisting of FAS extracellular and 41BB intracellular domains, demonstrated improved anti-tumor efficacy.² KRAS is a frequently mutated oncogene in cancers³ and recent clinical evidence suggests that it is immunogenic and targetable via TCR-engineered T cells.⁴ Targeting a mutated oncogenic driver such as KRAS G12V offers many advantages, including tumor dependence driving homogenous expression and decreasing risk of therapeutic escape. We are now reporting an optimized construct that achieves high functional co-expression of the KRAS TCR, CD8ab, and FAS-41BB switch receptor in a single viral vector. **Methods** Human T cells isolated from healthy volunteers were lentivirally transduced with constructs encoding the KRAS TCR, CD8ab chains, and FAS-41BB. Preclinical studies included peptide titrations with the index peptide and ones in which one residue was individually substituted to all possible amino acids (XScan), co-cultures with tumors or B-LCL, and *in vivo* subcutaneous xenografts.

Results Co-expression of CD8ab with the KRAS G12V-specific TCR allowed for efficient stimulation of CD4⁺ T cells, and further engineering with the FAS-41BB switch receptor increased sensitivity to low peptide concentrations. In tumor co-culture assays, the inclusion of FAS-41BB allowed for tumor control, even after re-challenge with fresh addition of tumor cells. In a repetitive T cell transfer/tumor exposure assay, continued proliferation and tumor control required both expression of FAS-41BB and inclusion of engineered CD4 and CD8 T cells, suggesting that CD8ab exogenous expression in CD4 T cells allowed for a coordinated T cell response able to resist exhaustion. Intravenous administration of engineered T cells prevented tumor outgrowth *in vivo*. Using the XScan assay, no off-target liabilities were identified upon co-incubation of A11-KRAS G12V/CD8ab/FAS-41BB switch receptor engineered T cells with all possible peptides in the human proteome matching the recognition motif, demonstrating the specificity of our TCR. No alloreactivity to the most prevalent HLA alleles was detected in B-LCL co-cultures.

Conclusions Preclinical development of the KRAS G12V-specific TCR with co-expression of CD8ab and the durability FAS-41BB switch receptor supports the clinical development of this first-in-class product for solid tumor patients with high unmet medical needs.

REFERENCES

1. Yamamoto TN, Lee P-H, Vodnala SK, Gurusamy D, Kishton RJ, Yu Z, Eidizadeh A, Eil R, Fioravanti J, Gattinoni L, Kochenderfer JN, Fry TJ, Aksoy BA, Hammerbacher J, Cruz AC, Siegel RM, Restifo NP, Klebanoff CA. T cells genetically engineered to

overcome death signaling enhance adoptive cancer immunotherapy. *J Clin Invest.* 2019;**129**:1551-1565.

2. Oda SK, Anderson KG, Ravikumar P, Bonson P, Garcia NM, Jenkins CM, Zhuang S, Daman AW, Chiu EY, Bates BM, Greenberg, PD. A Fas-4-1BB fusion protein converts a death to a pro-survival signal and enhances T cell therapy. *J Exp Med.* 2020;**217**:e20191166.
3. Prior IA, Hood FE, Hartley JL. The frequency of Ras mutations in cancer. *Cancer Res.* 2020; **80**: 2969–2974.
4. Leidner R, Sanjuan Silva N, Huang H, Sprott D, Zheng C, Shih Y-P, Leung A, Payne R, Sutcliffe K, Cramer J, Rosenberg SA, Fox BA, Urba WJ, Tran E. Neoantigen T-cell receptor gene therapy in pancreatic cancer. *N Engl J Med.* 2022;**386**, 2112–2119.

Ethics Approval These studies were approved by Affini-T Therapeutics and Fred Hutchinson Cancer Research Center Ethics Boards, approval number EB17-010-303 and PROTO000050898, respectively.

<http://dx.doi.org/10.1136/jitc-2022-SITC2022.0342>

343

IDENTIFICATION OF TUMOR-REACTIVE T CELLS TARGETING MELANOMA DARK ANTIGENS™ VALIDATES THIS NOVEL CLASS OF TARGETS FOR DEVELOPMENT OF IMMUNOTHERAPIES

¹Rachel Abbott*, ²Tom Hofland, ³Thomas Hulen, ⁴Elizabeth (Els) Verdegaal, ⁵Michael Crowther, ¹Joseph Dukes, ³Shawez Khan, ⁴Pita de Kok, ¹Giulia Masi, ³Özcan Met, ³Aimilia Schina, ¹Hayden Selvadurai, ⁴Marten Visser, ¹Katarzyna Ward, ¹Rachel Abbott, ⁴Sjoerd van der Burg, ²George Kassiotis, ³Inge Svane. ¹Enara Bio Ltd, Oxford, UK; ²The Francis Crick Institute, London, UK; ³Center for Cancer Immune Therapy, Herlev, Denmark; ⁴Leiden University Medical Centre, Leiden, Netherlands; ⁵National Center for Cancer Immune Therapy, Herlev, Denmark

Background Better solid tumor targets are needed to help realise the potential for TCR-directed immunotherapy. Dark Antigens™, encoded by regions of the genome previously thought to be non-coding, are promising targets for immunotherapy due to their cancer-specific expression and broad patient coverage.

Using our EDAPT™ (Enara Dark Antigen Platform Technology) platform, we have previously identified a number of melanoma-specific antigens, demonstrated their presentation on Class I HLA molecules of primary tumors using mass spectrometry-based immunopeptidomics data, validated their cancer-specificity and demonstrated homogenous tumor expression using RNA-Scope.¹⁻²

We sought to demonstrate that antigen-reactive T cells can be found in both the periphery of healthy donors and melanoma patient tumor material, and to further characterize these T cell responses.

Methods Tumor-infiltrating lymphocytes (TILs) expanded from twenty-one melanoma patients were screened by IFN γ ELISpot for reactivity against peptides from four different melanoma-specific antigens.

Healthy donor PBMCs were assessed for the presence of antigen-specific T cells using peptide-HLA tetramers, either directly *ex vivo* or following a period of peptide-specific stimulation and expansion.

T cell receptors (TCR) sequences were obtained from antigen-reactive isolated T cells using either iRepertoire or 10x Genomics, and are being screened for function against patient-derived tumor lines with endogenous expression of the cognate antigen.

Results We have shown that TILs expanded from two melanoma patients are reactive to a common epitope within EVA003, a melanoma-specific antigen. The autologous tumor lines derived from both patients were shown to be EVA003-positive.

Furthermore, we have identified T cells specific for two melanoma-specific antigens, EVA001 and EVA003, from PBMCs of several healthy donors.

TCRs have been sequenced, for further functional characterization, from T cells reactive to HLA-A3 and HLA-B7-restricted peptides from EVA003 and to an HLA-A2-restricted peptide from EVA001.

Conclusions We have identified T cells that are reactive against epitopes derived from melanoma-specific antigens in both patient TILs and peripheral blood of healthy subjects, supporting their relevance as cancer-specific antigens. TCRs isolated from these T cells are currently being assessed for reactivity against antigen-positive patient-derived melanoma tumor lines. This work highlights the promise of Dark Antigens™ as a novel class of targets for the development of targeted immunotherapies such as cancer vaccines, TCR-T cell and bi-specific T cell engager therapies, and our EDAPT™ platform is now

being employed to identify Dark Antigen™ targets in a range of other tumor types.

REFERENCES

1. Attig J, Young GR, Hosie L, Perkins D, Encheva-Yokoya V, Stoye JP, Srijders AP, Ternette N, Kassiotis G. LTR retroelement expansion of the human cancer transcriptome and immunopeptidome revealed by de novo transcript assembly. *Genome Research*. 2019; **29**:1578-1590.
2. Jupp R, Kassiotis G, Ternette N, Young G, Howie D, Marino F, Davies M, Selvadurai H, Sanchez A, Dodd J, Lozza L, Soileux E, Mason P, Pojasek K. Discovery of immunogenic ERV-derived antigens as targets for melanoma immunotherapy. *J Immunother Cancer*. 2019; **7**: P680.

Ethics Approval All work involving the use of human tissue was approved by the NHS Health Research Authority North-west Haydock Research Ethics Committee (reference number 19/NW/0216), London Bridge Research Ethics Committee (reference number 20/PR/0400), and the Medical Ethics Committee of the Leiden University Medical Center (reference number P04.085).

<http://dx.doi.org/10.1136/jitc-2022-SITC2022.0343>

344 **COMPARATIVE ASSESSMENT OF PRODUCT QUALITY ATTRIBUTES ASSOCIATED WITH PRODUCTION OF CHIMERIC ANTIGEN RECEPTOR T CELLS EXPRESSING SCFV CD-19 AND SCFV IL-13RA2 BY TWO MANUFACTURING PLATFORMS**

Sujin Hwang*, Heba Degheidy, Mondona McCann, Steven Bauer, Raj Puri, Bharat Joshi.
Food and Drug Administration, Silver Spring, MD, USA

Background The recent advances in adoptive immunotherapy of cancer have led to the FDA approval of chimeric antigen receptor modified T (CAR-T) cells targeting CD19 antigen on advanced hematological malignancies, which has resulted in dramatic responses in large numbers of patients. Because of several challenges and complexities in manufacturing for characterizing CAR-T cell products, it is important to optimize their manufacturing and critical quality attributes (CQAs). Herein, we performed a comparative assessment of scFv-CD-19-CAR-T and IL-13Ra2-CAR-T cells and manufactured using conventional and G-REX platforms.

Methods We manufactured lentiviral vectors (LVV) by employing common molecular biology techniques using HEK 293T as a producer cell line, transfected with scFVIL-13Ra2 or CD19 transgene plasmids along with three helper plasmids. The LVVs were used for transducing PBMCs from normal human blood donors after their activation and were expanded in T cell growth medium supplemented with cytokines including IL-2 or IL-2 + IL-15, IL-7 + IL-15 for specified durations. A battery of activation and exhaustion phenotype markers was studied at the end of expansion along with their potency to lyse the target cells and secrete Interferon-gamma in a co-culture assay.

Results Our results showed that the T cell activation was efficient by commercially available reagents such as anti-CD3/CD28 coated magnetic beads or nanoparticles and transduction either by retroinfection or Vectofusin. The CAR-T cell yields were at least two logs higher in the G-REX platform. Analysis of phenotype markers for T cells (CD3, CD4, CD8), T cell activation (CD25, CD45, CD69)/exhaustion markers (PD-1, LAG-3, TIM-3) and Central memory T cells, {CD45RA low, CD62L (CCR7 high)} revealed better health and yield of CAR-T cell products manufactured in G-REX platform.

Conclusions We conclude that G-REX platform was superior to conventional methods for manufacturing both types of CAR-T cells. The data also suggest that better activation and transduction by specific reagents and expansion in combination with selected cytokines are key issues associated in manufacturing healthy and potent CAR-T cell products.

Acknowledgements We thank Pamela Leland, former lab member in the Center for Biologics Evaluation and Research, FDA, Silver Spring, for her performance of the experiment.

<http://dx.doi.org/10.1136/jitc-2022-SITC2022.0344>

345 **CRS ASSESSMENT POST FAST-TRACK – CAR T CELLS APPLICATION IN NSG-SGM3 MOUSE MODEL**

Arezoo Jamali*, Naphang Ho, Angela Braun, Elham Adabi, Frederic Thalheimer, Christian Buchholz. *Paul Ehrlich Institut, Langen (Hessen), Germany*

Background CRS (Cytokine Release Syndrome) is considered as a recurrent side effect of CAR (Chimeric Antigen Receptor) T cell therapy. An experimental animal model for better investigating different aspects of CRS is still in demand. Besides CAR T cells' astonishing achievements, numerous efforts are determined on manufacturing hindrance, notably shortening production procedures. Here, we introduce a novel CRS mouse model employing the NSG-SGM3 strain to address adverse effects of FT- CAR T cells (Fast-Track CAR T).

Methods CD19-specific FT- CAR T cells were produced from 48 hours activated human PBMC plus 24h incubation with lentiviral vectors (LV). Cytotoxic activity of FT- CAR T cells was determined against Nalm-6 cells +/- same donor-derived monocyte supplementation allowed *in vitro* CRS assessment. Next, to launch a CRS mouse model, FT-CAR T cells were administered into NSG-SGM3 mice engrafted with Nalm-6 cells. Mice received 1×10^7 FT-CAR or activated T cells intravenously. Health condition assessment and body index calculation were regularly monitored using weight, and body temperature measurements. Human cytokines in plasma were determined by the LEGENDplex kit.

Results Flow cytometric analysis revealed that the majority of FT-CAR T cells were positive for the VSV-glycoprotein. Upon reactivation and further cultivation, 65% of all T cells converted into CAR-positive T cells by day 6. The FT-CAR T cells indicated significant cytotoxic activity against tumor cells compared to T cell control, without any contraction in presence of monocytes. The co-culture supernatant displayed significantly elevated amounts of pro-inflammatory cytokines, including IL-6, INF- γ , TNF- α , and IL-10. Next, we appointed the NSG-SGM3 mice to refine FT-CAR T cell competence in CRS induction. While all control mice were in good condition, detrimental side effects came up rapidly within 24h for all FT-CAR T-treated mice. Tremendous temperature change over 2°C and more than 10% weight loss led to termination of this group. Highly elevated cytokine levels were observed, notably enhanced for IFN- γ , TNF- α , IL-2, IL-10 (all $P < 0.0001$), and IL-6 ($P < 0.0121$).

Conclusions Our study introduces an appropriate CRS mouse model to substantiate the acute side effects of FT-CAR T cells. The key feature of this model is innate myeloid cells releasing cytokines upon interaction with CAR T cells. Our results suggest that FT-CAR T cells carry residual LV components and can induce at least as severe CRS as conventional CAR T cells.

<http://dx.doi.org/10.1136/jitc-2022-SITC2022.0345>

346

ENHANCED ANTI-TUMOR ACTIVITY OF HBSAG SPECIFIC TCR-T (SCG101) IN HEPATITIS B VIRUS (HBV) RELATED HEPATOCELLULAR CARCINOMA (HCC) BY PREVENTING T CELL EXHAUSTION THROUGH PD-1/PD-L1 AXIS BLOCKADE

¹Pin Xie, ¹Yanzhou Huang, ¹Lu Yang, ¹Karin Wisskirchen, ²Ulrike Protzer, ¹Ke Zhang, ¹Tao Jin*. ¹SCG Cell Therapy, Shanghai, China; ²Technical University of Munich, Munich, Germany

Background Checkpoint inhibitors as standard of care for hepatocellular carcinoma have limited tumor response, highlighting the importance of the tumor-reactive T cell abundance for effective treatment and the potential synergy with adoptive T cell therapy. SCG101 is a first-in-class, autologous TCR-T encoding a high-avidity TCR directed towards HLA-A*02-restricted HBsAg, with preliminary clinical benefits demonstrated in HBV related HCC patients. Given the profound immune-suppressive microenvironment of HCC, combining TCR-T cell therapy with PD-1/PD-L1 inhibition may have a synergistic effect by TCR-T cells potentially infiltrating immunogenically cold tumors, and checkpoint inhibitors reversing TCR-T cell exhaustion. Herein, we report results from preclinical combination therapy of SCG101 and checkpoint inhibition.

Methods SCG101 CD4⁺/CD8⁺ T cells were isolated via magnetic bead enrichment. T cell functionality was performed using Real Time Cellular Analysis (RTCA) and Cytometric Bead Array (CBA). Expression of PD-1 was analyzed on SCG101 cells after co-culturing with HBsAg⁺ HepG2 cells. For in vitro tumor rechallenge assay, the cytokine secretion and target cell lysis were performed to evaluate the functional impact of combining SCG101 cells and PD-1/PD-L1 inhibitors. In vivo, anti-tumor activities were evaluated in HBsAg⁺ PD-L1⁺ HepG2 cell xenograft mice by i.v. infusing pre-exhausted PD-1⁺ SCG101 with and without PD-1 (Pembrolizumab) or PD-L1 (Atezolizumab) inhibitors.

Results Both CD8⁺ and CD4⁺ SCG101 T cells exert profound anti-tumor activities via target cell lysis and cytokine secretion, while CD8⁺ SCG101 T cells confer stronger effects. The expression level of PD-1 was significantly and specifically elevated in TCR transduced SCG101 cells co-cultured with either HBsAg⁺ HepG2 cells or HBsAg⁺ PDL1⁺ HepG2 cells, comparing to the HepG2 cell control. The elevation was observed preferably in SCG101 CD8⁺ T cells. In tumor rechallenge assay, serial antigen stimulation led to dramatic decrease of the cytokine secretion and cytotoxic activity due to PD-1 induced T cell exhaustion, which could be restored by Pembrolizumab (anti-PD-1) or Atezolizumab (anti-PD-L1). This finding was confirmed in HBsAg⁺ PD-L1⁺ HepG2 CDX model, where a more prolonged antitumor effect was achieved when pre-exhausted SCG101 were co-administered with anti-PD1 or anti-PD-L1 inhibitors.

Conclusions Continuous antigen exposure under tumor microenvironment results in activation-induced cell death of T cells with hallmark features of exhaustion including reduced proliferation capacity and cytotoxicity, and severe defects in cytokine production. The benefit of PD-1/PD-L1 axis blockade on adoptively transferred T cells was demonstrated in vitro and in vivo xenograft models. Combination studies with PD-1/PD-L1 inhibitors is planned to augment SCG101 functionality and persistence in HBV related HCC patients.

Ethics Approval Here to clarify that the animal study is outsourced to WuXi AppTec (Nantong) Co., Ltd., which was

fully accredited by the Association for Assessment and Accreditation of Laboratory Animal Care International (AAALAC). Procedures used in this study were approved by the Institutional Animal Care and Use Committee (IACUC) at WuXi AppTec (Nantong) Co., Ltd. IACUC serial number: ON01-QD009-2020.

<http://dx.doi.org/10.1136/jitc-2022-SITC2022.0346>

347 DEVELOPMENT OF OPTIMIZED CAR T CELLS FOR THERAPY OF GLIOBLASTOMA

¹Jonathan Khan*, ¹Winson Cai, ¹Yanhong Yang, ¹Lauren Dong, ¹Kelsey Hopland, ¹Kenny Kwok-Hei Yu, ¹Ruby Freeman, ²Terence Purdon, ¹Viviane Tabar, ¹Taha Merghoub, ¹Jedd Wolchok, ²Renier Brentjens. ¹Memorial Sloan Kettering Cancer Center, Floral Park, NY, USA; ²Roswell Park Comprehensive Cancer Center, Buffalo, NY, USA

Background Glioblastoma (GBM) is the most lethal form of primary brain tumor in adults, with a 95% five-year mortality rate. Current therapy consists of surgical resection, chemotherapy, and radiotherapy. However, there remains an urgent need for novel therapies as recent trials have failed to improve overall survival.¹ A new approach to target GBM is the administration of Chimeric Antigen Receptor (CAR) T cells to treat relapsed/refractory disease.² To date, multiple clinical trials employing CAR T cells targeting disparate antigens in the context of GBM have been completed; and analysis of data accrued from these trials identified antigen loss and the upregulation of T cell inhibitory pathways to be major limitations of CAR T cell antitumor efficacy.^{3,4} Accordingly, we have identified B7-H3 as a potential target antigen for CAR T cell therapy of GBM, and the Programmed Death-1/Programmed Death Ligand-1 (PD-1/PD-L1) axis as an inhibitory pathway suitable for combinatorial immunotherapy with CAR T cell therapy of GBM.

Methods B7-H3 expression on U251, U87, and 4 primary GBM cells lines was evaluated by flow cytometry, while patient tumor samples were analyzed by immunofluorescence. B7-H3 targeting CAR T cells were engineered by transducing primary human T cells with a retroviral vector encoding either a CD28-based CAR, or a CD28-based CAR containing a PD-1 blocking scFv. *In vitro* luciferase-based killing assays, and Luminex-based quantification of cytokine release were used to characterize CAR function. NSG mice were engrafted with U251 GBM cell line and treated with a single peripheral infusion of CAR T cells. Tumors were harvested at various time points following CAR T cell treatment and characterized for T cell infiltrate, T cell phenotype, and expression of checkpoint pathways.

Results We demonstrate that B7-H3 is a suitable antigen for CAR T cell therapy of GBM, and that B7-H3-targeting CAR T cells are able to safely, and efficiently control disease progression in a disease-relevant xenograft model. We also show that GBM tumor cells upregulate PD-L1 in direct response to CAR T cell activity, and that CAR T cells upregulate PD-1 following activation through the CAR. We subsequently demonstrate that concomitant PD-1 blockade augments the antitumor capabilities of B7-H3-targeting CAR T cells through increased T cell engraftment and improved effector function to confer durable, long-term remissions in a disease-relevant preclinical model.

Conclusions These data demonstrate the concomitant PD-1 blockade is safe and efficient method for improving the antitumor capabilities of B7-H3 targeting CAR T cells in the context of GBM.

REFERENCES

1. Ostrom QT, Cioffi G, Waite K, Kruchko C, Barnholtz-Sloan, JS. CBTRUS statistical report: Primary brain and other central nervous system tumors diagnosed in the United States in 2014–2018. *Neuro Oncol.* 2021; **23**: iii1–iii105.
2. Bagley SJ, Desai AS, Linette GP, June CH, O'Rourke, DM. CAR T-cell therapy for glioblastoma: recent clinical advances and future challenges. *Neuro Oncol.* 2018; **20**: 1429–1438.
3. Brown CE, Badie B, Barish ME, Weng L, Ostberg JR, Chang W-C, Naranjo A, Starr R, Wagner J, Wright C, Zhai Y, Bading JR, Ressler JA, Porgnow J, D'Apuzzo

M, Forman SJ, Jensen MC. Bioactivity and safety of IL13R 2-redirected chimeric antigen receptor CD8+ T cells in patients with recurrent glioblastoma. *Clin Cancer Res.* 2015; **21**: 4062–4072.

4. O'Rourke DM, Nasrallah MP, Desai A, Melenhorst JJ, Mansfield K, Morrissette JJD, Martinez-Lage M, Brem S, Maloney E, Shen A, Isaacs R, Mohan S, Plesa G, Lacey SF, Navenot J-M, Zheng Z, Levine BL, Okada H, June CH, Brogdon JL, Maus MV. A single dose of peripherally infused EGFRvIII-directed CAR T cells mediates antigen loss and induces adaptive resistance in patients with recurrent glioblastoma. *Sci Transl Med.* 2017; **9**: eaaa0984.

Ethics Approval The human biospecimen analyses were approved by Memorial Sloan Kettering Cancer Center IRB #09-156.

<http://dx.doi.org/10.1136/jitc-2022-SITC2022.0347>

348

DEFINING T CELL RECOGNITION OF A HIGHLY CONSERVED FUSION NEOANTIGEN IN FIBROLAMELLAR CARCINOMA

¹Allison Kirk*, ¹Jeremy Crawford, ¹Ching-Heng Chou, ¹Phuong Nguyen, ¹Walid Awad, ¹E Kaitlynn Allen, ²Xiaoyu Zhang, ³Anthony Zamora, ¹Christopher DeRenzo, ⁴Scott Strome, ¹Paul Thomas. ¹St. Jude Children's Research Hospital, Memphis, TN, USA; ²University of Maryland School of Medicine, Baltimore, MD, USA; ³Medical College of Wisconsin, Milwaukee, WI, USA; ⁴University of Tennessee Health Science Center, Memphis, TN, USA

Background Fibrolamellar carcinoma (FLC) is a rare and fatal liver malignancy that primarily affects otherwise-healthy adolescents and young adults. No curative therapies are currently available, so novel treatments are needed to improve patient outcomes. In 2014, Honeyman et al.¹ identified the key genetic event in FLC tumorigenesis: a recurrent deletion in chromosome 19 that fuses *DNAJB1* to *PRKACA*. The resulting fusion protein, now known to be the essential driver mutation in FLC, is present in all cases and has an identical amino acid sequence in more than 90% of patients. We believe this highly conserved fusion protein is a potentially-ideal neoantigen target for T cell-based immunotherapy, and therefore sought to define fusion-specific T cell responses in FLC patients.

Methods To identify functional T cell responses to the *DNAJB1-PRKACA* fusion, tumor infiltrating lymphocytes (TILs) from an FLC patient tumor were expanded *ex vivo*, then stimulated with fusion peptides predicted to be presented by the patient's class I HLA alleles. We then used single cell gene expression profiling and T cell receptor (TCR) sequencing of patient TILs, and antigen-specific expansion² and peptide-HLA tetramer staining of patient peripheral blood T cells, to identify two fusion-specific TCRs. Both TCRs were reconstructed and expressed in cells, and their specificity and functionality were validated *in vitro* using peptide-HLA tetramer staining, intracellular cytokine staining, and killing assays. Finally, using a xenograft model in immunodeficient mice, we tested the ability of these TCRs to control the growth of fusion-expressing tumors *in vivo*.

Results We observed a small but robust T cell response to fusion peptide EIFDRYGEEV among patient TILs, and subsequently identified two TCRs in the patient that recognize this fusion peptide presented on HLA-A*68:02. These TCRs specifically bind their cognate tetramer and mediate both cytokine production and killing of fusion-expressing target cells *in vitro*, while sparing wild-type-expressing controls. Treating mice bearing fusion-expressing tumors with TCR-engineered T cells resulted in transient tumor clearance and significantly extended survival compared to mice treated with vehicle or mock-transduced T cells.

Conclusions We have identified, to our knowledge, the first reported endogenous T cell response to the *DNAJB1-PRKACA* fusion in an FLC patient. Further, we have defined two fusion-specific T cell receptors that hold promise for development in novel cell-based immunotherapies for FLC.

REFERENCES

1. Honeyman JN, Simon EP, Robine N, Chiaroni-Clarke R, Darcy DG, Lim II, Gleason CE, Murphy JM, Rosenberg BR, Teegan L, Takacs CN, Botero S, Belote R, Germer S, Emde AK, Vacic V, Bhanot U, LaQuaglia MP, Simon SM. Detection of a recurrent *DNAJB1-PRKACA* chimeric transcript in fibrolamellar hepatocellular carcinoma. *Science*. 2014; **343**:1010-1014.
2. Cimen Bozkus C, Blazquez AB, Enokida T, Bhardwaj N. A T-cell-based immunogenicity protocol for evaluating human antigen-specific responses. *STAR Protoc*. 2021; **2**:100758.

Ethics Approval Use of human samples in this study was approved by St. Jude Children's Research Hospital's Institutional Review Board (IRB); IRB number Pro00008980. All patients consented to the use of materials for research study. All animal studies were approved by and performed according to the guidelines of St. Jude Children's Research Hospital's Institutional Animal Care and Use Committee (IACUC); IACUC protocol number 640.

<http://dx.doi.org/10.1136/jitc-2022-SITC2022.0348>

349

HIGHLY POTENT TUMOR-TARGETING OPTIMALLY PRIMED NATURAL KILLER CELLS PRODUCED UNDER A FEEDER-CELL FREE CONDITION IN A 50L-SCALE BIOREACTOR WITH CYTOKINE-FUSION PROTEINS ELICITS ROBUST ANTI-TUMOR RESPONSE IN PRECLINICAL STUDY

¹Dongwoo Ko, ¹Jae Chan Park*, ¹Min-Kyong Hyon, ¹Young Hyun Park, ¹Gil-Jung Kim, ¹Jong Beom Ku, ¹Iseul Eom, ¹Su Bin Lee, ¹Jeong Mi Yun, ¹Dan Bee Park, ¹Do Yeon Kim, ¹HyeHyeon Jang, ¹Sora Lim, ¹Do Soo Jang, ¹Sung Yoo Cho, ¹Chun Pyo Hong, ²Myung Ho Jang. ¹GI Cell, Seongnam-si, Republic of Korea; ²GI Innovation, Seoul, Republic of Korea

Background The use of allogeneic natural killer (NK) cell as an adoptive immunotherapeutic is a promising strategy for a large pool of cancer patients, ensuring greater time- and cost-efficiency than autologous NK or T cell-based immunotherapies. However, large-scale production of clinical-grade NK cells is challenging with often use of genetically modified feeder cells, and the impairment of cytotoxic function in vivo due to exhaustion or senescence is a significant concern.

Methods We produced highly potent NK cells called Tumor-targeting Optimally Primed NK cell (T.O.P. NK), which are CD3-CD56+ cells directly derived from human PBMCs. These cells are expanded in a 50L bioreactor without feeder cells or genetic modification.

Results The T.O.P. NK demonstrates an increased expression of chemokine receptors, CCR5 and CXCR4, and NK activation markers, such as NKG2D, NKp46, and DNAM-1; the NK inhibitory and exhaustion markers such as CD57, PD-1, and TIM-3 maintained low expression levels after the harvest. The elevated expression of CCR5 and CXCR4 on T.O.P. NK elucidates its active migration in response to CCL5/RANTES and CXCL12/SDF-1 ligands, respectively, with high sensitivity. Furthermore, T.O.P. NK showed robust cytotoxicity in vitro and in vivo against various solid cancer cell lines even after recovery from cryopreservation. We observed strong anti-tumor activity of T.O.P. NK in short-term and long-term in vitro killing assays against solid cancer cell lines, including colorectal, breast, and head and neck cancers. Moreover, T.O.P. NK elicited strong anti-tumor effects in immunodeficient NOG mouse grafted with various human cancer cell lines.

Conclusions Collectively, we report T.O.P. NK, which are generated at clinical grade, with high productivity and purity while maintaining active phenotype and anti-tumor cytotoxicity. These findings suggest that the feeder-free expansion platform of T.O.P. NK proficiently generates allogeneic adoptive NK cells for the treatment of solid cancers.

Ethics Approval The study was approved by Ewha Womans University Medical Center's Ethics Board, approval number SEUMC 2021-04-026

<http://dx.doi.org/10.1136/jitc-2022-SITC2022.0349>

Abstracts

350

HARNESSING ARGININE METABOLISM TO OVERCOME HYPERTHERMIA-INDUCED METABOLIC DYSFUNCTION OF CAR T-CELLS

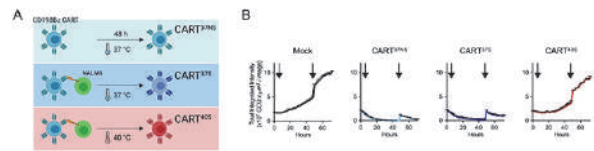
¹Taisuke Kondo*, ¹Justyn DuSold, ¹Sooraj Achar, ¹Serifat Adebola, ²Pedro Gonzalez-Menendes, ²Julie Perrault, ¹Bonnie Yates, ³Hannah Song, ¹Stephen Fox, ¹Xia Xu, ¹King Chan, ¹Abdalla Abdelmaksoud, ¹Christopher Chien, ¹Marie Pouzolles, ¹Haiying Qin, ³Steven Highfill, ¹Thorkell Andreasson, ¹Nirali Shah, ²Valérie Dardalhon, ¹Grégoire Altan-Bonnet, ¹Naomi Taylor. ¹National Cancer Institute, Bethesda, MD, USA; ²Université de Montpellier, Montpellier, France; ³National Institutes of Health Clinical Center, Bethesda, MD, USA

Background Chimeric antigen receptor (CAR) T-cells have shown remarkable success in the treatment of hematological malignancies, but many patients still relapse. One common adverse on-target effect of CAR T-cells is cytokine release syndrome (CRS), due to the triggering of a systemic inflammatory response. Importantly though, the impact of CRS, and especially the fever that is a hallmark of this syndrome, on CAR T-cell function is not known.

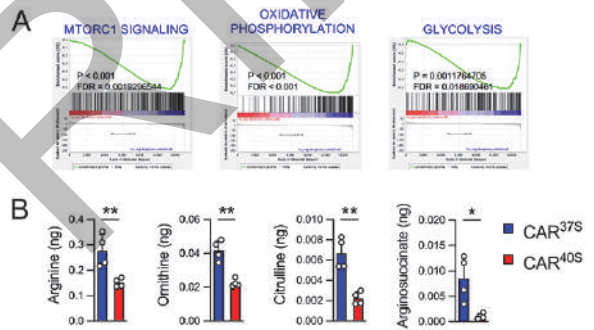
Methods T cells were generated to express an anti-CD19 (FMC63) CAR construct harboring the 4-1BB costimulatory domain. CD19CAR T-cells were exposed to hyperthermia (40°C) and their cytotoxic activity against CD19⁺ NALM6 leukemic cells was evaluated in both *ex-vivo* (Incucyte) and *in-vivo* (NSG mouse) models. Hyperthermia-induced changes in CAR T-cells were evaluated by cytokine secretion profiles, CyTOF, RNASeq, and metabolomic analyses. Arginine supplementation was performed as described.

Results Exposure of CD19CAR T-cells to hyperthermia significantly decreased their subsequent cytotoxicity against CD19⁺ leukemic cells at 37°C, both *ex-vivo* and *in-vivo* (figure 1). This was associated with reduced secretion of IL-2, IFNγ, and IL-8 by CD19CAR T-cells and high dimensional analyses revealed the induction of a terminally differentiated CD25^{Hi}CD39^{Hi}CD44^{Hi}TIM3^{Hi} CAR T cell. Mechanistically, gene profiling assays highlighted a negative enrichment of mTORC1, glycolysis, and oxidative phosphorylation gene sets in CAR T-cells subjected to hyperthermia (figure 2A), and these data were confirmed by functional metabolic assays. Furthermore, the metabolome of hyperthermia-exposed CAR T-cells unveiled significant reductions in arginine and urea cycle metabolites (figure 2B). Notably, pharmacological supplementation of arginine markedly enhanced the *ex-vivo* and *in-vivo* cytotoxicity of hyperthermia-exposed CAR T-cells. Moreover, in the absence of hyperthermia, short-term arginine supplementation to CAR T-cells during the expansion process enhanced metabolic fitness, promoting the potential of these CAR T-cells to respond to repetitive *ex-vivo* NALM6 stimulations (E/T=0.1) and enhancing *in-vivo* anti-leukemic activity under stress conditions (figure 3).

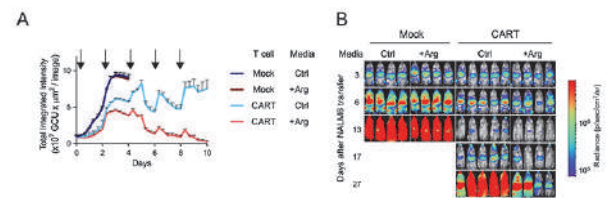
Conclusions Exposure of CAR T-cells to hyperthermia results in a metabolic reprogramming associated with attenuated cytotoxic function and the induction of a terminally differentiated state. We identify arginine metabolism as a critical pathway in CAR T-cells rendered dysfunctional by exposure to hyperthermia. On the basis of these data, we assessed the impact of short-term arginine supplementation on long-term CAR T-cell function, and our data highlight a significantly augmented CAR T persistence and cytotoxicity in stress conditions. Pharmacological arginine support will inform future iterations of CAR T-cell interventions.



Abstract 350 Figure 1 Hyperthermia-exposed CAR T-cells exhibit attenuated anti-leukemic cytotoxicity (A) Schema of the experimental strategy used to expose CAR T-cells to hyperthermia. Human peripheral T cells were transduced with a CD19-41BB-CAR lentiviral construct and the resulting CAR T-cells were stimulated (S) by co-culture with CD19⁺ NALM6 leukemic cells (GFP +Luc+) at an effector/target ratio of 1 in physiological (37°C, CART37S) or hyperthermic (40°C, CART40S) conditions. Non-stimulated (NS) CAR T-cells (CART37NS) were maintained at 37°C as a control. (B) The cytotoxic potential of pre-stimulated CART37S and CART40S was evaluated by Incucyte technology at a 1:1 effector/target ratio at 37 °C and non-transduced (Mock) T cells and non-stimulated CAR (CART37NS) were used as positive and negative controls, respectively. NALM6 cells were added at the indicated time points (arrows) and cytotoxicity is presented as a function of GFP intensity over time (n=73 technical replicates).



Abstract 350 Figure 2 Hyperthermia-exposed CAR T-cells exhibit a dysregulated metabolic state. (A) Hyperthermia-exposed CAR T-cells were stimulated with CD19⁺ NALM6 cells as shown in Fig. 1A and transcriptional changes were evaluated by RNASeq. Gene Set Enrichment Analysis (GSEA) plots of significantly altered metabolic pathways in CART40S relative to CART37S are presented (n = 3 biological replicates). (B) The metabolomes of CAR T-cells pre-exposed to 37°C (CART37S, blue) and 40°C (CART40S, red) were evaluated by mass spectrometry following a 48h stimulation by NALM6 cells at 37°C as shown in Fig. 1A. The abundance of urea cycle metabolites in CART37S and CART40S are presented (n = 4 biological replicates, statistical difference assessed by a two-tailed unpaired Student's t-test).



Abstract 350 Figure 3 Short-term arginine supplementation enhances CAR T-cell function under stress conditions. (A) Human peripheral T cells were transduced with CD19-41BB-CAR lentivirus and expanded from days 4-8 in either control media (blue) or in arginine-supplemented media (10mM, red). CD19CAR T-cells were then harvested and *ex-vivo* cytotoxicity against NALM6 was evaluated

in stress conditions, at a 1:10 effector/target (E: T) ratio in control media. Cytotoxicity was evaluated as a function of GFP intensity and NALM6 cells were added every 48h as indicated (arrows). Non-transduced (Mock) T cells, expanded in control (dark blue) or arginine-supplemented (dark red) conditions, were used as controls. (B) To evaluate in-vivo cytotoxicity of CD19CAR T-cells under stress conditions, suboptimal numbers of CAR T-cells (0.5×10^6), prepared as in panel A, were injected into NALM6 (GFP+Luc+)-bearing NSG mice at day 3 following engraftment. Tumor growth was monitored by bioluminescent imaging (BLI) using the Xenogen IVIS Lumina at the indicated time points and data were quantified by radiance (photons/cm²/sr).

<http://dx.doi.org/10.1136/jitc-2022-SITC2022.0350>

PREPRINT

351 **VITAMIN C TREATMENT PREVENTS CAR T CELL EXHAUSTION, MAINTAINS STEM CELL PHENOTYPE AND ENHANCES ANTITUMOR FUNCTION**

Leonce Kouakanou*, Hanmin Wang, Grace Sun, Tristan Chan, Jennifer Shepphird, Darya Alizadeh, Christine Brown, Leo Wang. *City of Hope, Duarte, CA, USA*

Background Chimeric antigen receptor (CAR) T cells have emerged as an effective therapy for B cell malignancies. However, major limitations to efficacy are lack of T cell persistence and T cell exhaustion, which result from epigenetic repression. Previous reports demonstrated that epigenetic remodeling can prevent T cell exhaustion and enhance CAR T antitumor activity.^{1,2,3} Vitamin C (VC) was previously described to modulate immune cell function through epigenetic modification.^{4,5}

Methods Here we sought to determine the effect of VC on CD19-CAR T cell functional differentiation. CD3+ T cells were activated and transduced with lentiviral supernatant in the presence of IL-2, low IL-15, and VC. The effect of VC on T cell differentiation was determined using flow cytometry, and on proliferation by direct cell count. To analyze functional differences between control (without VC) and VC-manufactured CD19-CAR T cells (VC-CD19-CAR T), we used a repeat challenge assay in which CAR T cells were cocultured with tumor cells, with fresh tumor cells reintroduced each week for four weeks in total. CAR T cell expansion, differentiation, and exhaustion were determined using flow cytometry and cell count. Cytotoxicity was assessed by measuring lactate dehydrogenase release. Whole-genome bisulfite sequencing was performed to analyze cell-intrinsic changes in CAR T cell DNA methylation as a result of VC treatment. Xenograft tumor mouse models were used to evaluate the long-term *in vivo* function of VC-CD19-CAR T cells.

Results Our data showed that addition of VC during CD19-CAR T cell production enforces a stem cell memory-like phenotype, characterized by increased expression of CD45RA⁺CD62L⁺ and CD27⁺CD62L⁺. VC-CD19-CAR T cells expanded more during manufacturing than controls, and their higher rate of expansion was preserved during the extended *in vitro* challenge. Interestingly, VC-CD19-CAR T cells were better at killing target cells in the first exposure to target cells, and retained their killing ability after subsequent stimulations while control CAR T cells did not. The improved function was mirrored by phenotypic analysis showing that stimulated VC-CD19-CAR T cells retained a stem cell memory-like phenotype with a lower expression of exhaustion markers after the last stimulation compared to control. *In vivo*, VC-CD19-CAR T cells efficiently delayed tumor growth resulting in superior overall survival compared with control.

Conclusions Our studies demonstrate that the addition of VC to CD19-CAR T production increased their expansion and prevented their exhaustion, resulting in enhanced antitumor function. Studies are ongoing to determine whether this occurs via epigenetic reprogramming.

REFERENCES

1. Pauken KE, Sammons MA, Odorizzi PM, Manne S, Godec J, Khan O, *et al.* Epigenetic stability of exhausted T cells limits durability of reinvigoration by PD-1 blockade. *Science*. 2016; **354**: 1160-1165.
2. Weber EW, Parker KR, Sotillo E, Lynn RC, Anbunathan H, Lattin J, *et al.* Transient rest restores functionality in exhausted CAR-T cells through epigenetic remodeling. *Science*. 2021; **372**: eaba1786.
3. Prinzing B, Zebley CC, Petersen CT, Fan Y, Anido AA, Yi Z, *et al.* Deleting DNMT3A in CAR T cells prevents exhaustion and enhances antitumor activity. *Sci Transl Med*. 2021; **13**: eabh0272.

4. Kouakanou L, Xu Y, Peters C, He J, Wu Y, Yin Z, *et al.* Vitamin C promotes the proliferation and effector functions of human gammadelta T cells. *Cell Mol Immunol*. 2020; **17**: 462-473.
5. Xu Y, Xiang Z, Alnaggar M, Kouakanou L, Li J, He J, *et al.* Allogeneic Vgamma9Vdelta2 T-cell immunotherapy exhibits promising clinical safety and prolongs the survival of patients with late-stage lung or liver cancer. *Cell Mol Immunol*. 2021; **18**: 427-439.

Ethics Approval Human samples were obtained from healthy donors under protocols approved by the City of Hope IRB (number 16025)

All mouse experiments were performed using protocols approved by the City of Hope IACUC (number 16081)

<http://dx.doi.org/10.1136/jitc-2022-SITC2022.0351>

352

STASH SELECT, A SIMPLE AND ROBUST METHOD OF PURIFYING CELLS ENGINEERED WITH MULTIPLE VECTORS USING A SINGLE SELECTION MARKER

Louai Labanieh*, Kaithlen Zen Pacheco, Robbie Majzner, Chris Fisher, Elena Sotillo, Peng Xu, Jennifer Cochran, Crystal Mackall. *Stanford University, Stanford, CA, USA*

Background CAR-T cell therapies have demonstrated remarkable clinical benefit in liquid tumors, but significant obstacles such as antigen loss, tumor heterogeneity, T cell exhaustion, and poor persistence limit the frequency and durability of complete responses. To overcome these challenges and expand this class of therapeutics to solid tumors, T cells will need to be multi-specific, resistant to exhaustion, and maintain their fitness in the tumor microenvironment. Engineering NextGen therapies with these enhanced capabilities will require the introduction of additional genetic modules that often do not fit within the payload capacity of a single vector, necessitating the use of multiple vectors. However, engineering cells with multiple vectors results in a heterogeneous cell product that requires purification for each vector, which is not currently possible in the clinical setting. Here, we present STASH Select, a simple method for enriching cells containing multiple genetic modifications using a single selection marker.

Methods Human CAR-T cells were generated from healthy donors and characterized by flow cytometry, ELISA, tumor killing assays, bulk RNAseq, and MACS.

Results The core principle of STASH-Select is the conditional cellular localization of a selectable marker. We integrate a protease cleavage site and an ER-Tag onto the C-terminus of the EGFRt selection marker, which “STASHes” it inside the cell. Co-expression of the cognate TEV protease results in cleavage of the ER Tag, which releases the EGFRt from the ER and allows it to translocate to the cell surface. Encoding the STASHed EGFRt on one vector and the protease on a second vector creates an AND gate system, where only cells transduced with both vectors express high levels of surface EGFRt that can be used as a selection handle for isolating double+ cells. We screened 22 ER retention domains and identified four novel, compact (<45aa) human ER tags that yield high performance STASH-Select systems. We tested the two-vector STASH-select in primary human T cells and were able to enrich an initial double+ population of 12.3% to 96.3% purity via EGFRt MACS. We expanded this approach to a three-vector STASH-Select using Split TEV protease. Configuring the STASHed EGFRt and the two TEV fragments onto three separate vectors produces a 3-vector AND gate which allowed for purification of three clinically relevant cargos with a single-step MACS selection, enriching an initial population of cells from 16.7% to >90% triple+.

Conclusions STASH-Select is a novel selection platform designed to propel NextGen smart therapies containing multiple enhancing modules into the clinic.

<http://dx.doi.org/10.1136/jitc-2022-SITC2022.0352>

ARTIFICIAL IMMUNE MODULATION ADOPTIVE CELL THERAPIES FOR VIRALLY DRIVEN MALIGNANCIES

David Langan*, Keshanti Tidwell, Alison Farrell, Selome Mitiku, Catrina Johnson, Pratima Kunwar, Ruipeng Wang, Sojung Kim, Mathias Oelke. *Neximmune, Gaithersburg, MD, USA*

Background NexImmune is developing novel, antigen-specific immunotherapies to meet serious unmet clinical needs. Here we report on the development of adoptive cell therapies (ACT) for virally driven malignancies. The proprietary Artificial Immune Modulation (AIM™) platform mimics natural T cell biology to target, activate and expand antigen-specific CD8⁺ T cells. EBV, HPV, and HTLV are estimated to contribute to 6-7% of global cancer cases. The targeted antigens are implicated in multiple malignancies including B cell lymphomas (EBV), adult T cell leukemia/lymphoma (HTLV1) as well as multiple HPV related malignancies such as oropharyngeal, cervical, and anal cancers.

Methods Using the paramagnetic AIM nanoparticle as an artificial antigen presenting cell (aAPC), in two-weeks T cells were enriched and expanded from HLA-A*02:01 donor apheresis material against immunodominant antigens of EBV, HTLV, and HPV. The memory phenotype of these cells was determined by CD45RA, CD62L, and CD95 expression. Antigen specific killing was observed on HLA-A2⁺ cell lines and polyfunctional activity characterized by an intracellular cytokine staining assay.

Results Greater than 90% of the total resulting CD8⁺ T cells display a phenotype of effector, central, or long-lived stem-like memory. From 8 independent healthy donor clinical scale manufacturing runs of NEXI-003, a pentavalent specific AIM ACT against the E6 and E7 antigens of both HPV-16 and HPV-18, as well as the tumor-associated antigen Survivin, 0.28E9 to 3.79E9 cells were generated. These cells showed dual HPV-16⁺ and HPV-18⁺ cancer antigen specificity and cytotoxic activity against HLA-A2⁺ cell lines, without significant cytotoxic activity against autologous PBMCs. With respect to EBV, using HLA-A2⁺ cell lines we further show antigen specific killing directed at LMP2, BRLF1, BMLF1, EBNA3, and LMP1 from a single healthy donor AIM ACT selected on 6 EBV antigens. In addition, these expanded memory T cells demonstrate a high degree of polyfunctional activity upon stimulation.

Conclusions NEXI-003 is an immunotherapy for HPV cancers in HLA*A02:01 patients that recently received IND clearance and it is anticipated to begin clinical trials in 2022. In addition to B cell lymphomas, B cells that are present in the plaques of multiple sclerosis patients have been found to express EBV antigens. Therefore, by directing a multivalent EBV T cell response there is the potential to treat other EBV-associated diseases using one AIM ACT product. Results reported here, will support the expansion of the AIM platform modalities for use in the treatment of virally driven malignancies, as well as potential virally associated autoimmune and infection diseases.

<http://dx.doi.org/10.1136/jitc-2022-SITC2022.0353>

354

PULLING THE LEVER ON ALL FRONTS: ICT01, A G9D2 T CELL-ACTIVATING MONOCLONAL ANTIBODY, IN COMBINATION WITH VENETOCLAX AND 5-AZACYTIDINE AS A NOVEL COMBINATION THERAPY FOR AML

¹Elisabeth Wieduwild*, ²Anne-Charlotte Le Floch, ¹Céline Garulli, ¹Sarah Bourass, ²Caroline Imbert, ¹Paul Frohna, ³Norbert Vey, ²Daniel Olive, ¹Aude de Gassart, ¹Loui Madakamutil. ¹Imcheck Therapeutics SAS, Marseille, FL, France; ²Inserm, Marseille, France; ³Institut Paoli-Calmettes, Marseille, France

Background Combination of Venetoclax, a BCL-2 inhibitor, and 5-Azacytidine, a hypomethylating agent, is the standard of care for patients with newly diagnosed acute myeloid leukemia (AML) who are not candidates for intensive chemotherapy.¹ In addition to their anti-leukemic activity, 5-Azacytidine was shown to improve cancer cell recognition by immune effector cells through induction of stress ligand expression,^{2,3} and Venetoclax was described to enhance T-cell and NK-cell-mediated cytotoxicity against AML blasts [3,4]. Among attractive mediators of anti-tumor immunity, g9d2 T-cells are emerging as effector cells that harbor strong cytolytic and pro-inflammatory activities and are associated with good prognosis in cancer patients.^{5,6} ICT01 is a first-in-class anti-BTN3A mAb activating g9d2 T-cells and is being evaluated in a Phase 1/2a clinical study in solid tumors and hematologic malignancies (NCT04243499).^{7,8}

Here, we explore the potential of combining ICT01 with Venetoclax and 5-Azacytidine to increase the anti-leukemic activity of g9d2 T-cells.

Methods Flow cytometry was used to assess the effects of Venetoclax and 5-Azacytidine on ICT01-mediated g9d2 T-cell activation after *in vitro* culture of healthy donor (HD) or patient derived PBMCs. AML cell lines' and primary AML blasts' sensitivity to ICT01-activated g9d2 T-cell killing was monitored after 4 or 24 hours of target:effector co-culture. Targets and/or effectors were pre-treated with Venetoclax, 5-Azacytidine or the combination. Expression of specific stress ligands upon treatment with Venetoclax, 5-Azacytidine or the combination was analyzed by flow cytometry.

Results First, we show that activation of g9d2 T-cells by ICT01 is unaltered in HD-PBMCs treated *in vitro* with Venetoclax or 5-Azacytidine, in naïve AML patients' PBMCs or in PBMCs from AML patients under respective treatment. In addition, ICT01-mediated activation of g9d2 T-cells improved resistance to Venetoclax-induced cell death, which is otherwise pronounced in resting g9d2 T-cells. Next, we identified several stress ligands to be upregulated on AML cell lines and primary AML blasts upon treatment with Venetoclax, 5-Azacytidine or the combination. Consequently, pre-treatment of AML (cell lines and primary) with Venetoclax, 5-Azacytidine or the combination improved g9d2 T-cell killing capacities, which confirms previous findings on NK- and T-cells and adds further mechanistic insights. Finally, activation of g9d2 T-cells with ICT01 in combination with Venetoclax and 5-Azacytidine treatment further increased apoptosis of AML cells.

Conclusions These results demonstrate the ability of Venetoclax and 5-Azacytidine to potentiate ICT01-mediated killing of AML cells by $\gamma\delta$ T-cells and support clinical evaluation of this combination as a novel therapeutic approach for AML patients.

REFERENCES

1. DiNardo CD, Jonas BA, Pullarkat V, Thirman MJ, Garcia JS, Wei AH, Konopleva M, Döhner H, Letai A, Fenaux P, Koller E, Havelange V, Leber B, Esteve J, Wang J, Pejsa V, Hájek R, Porkka K, Illés Á, Lavie D, Lemoli RM, Yamamoto K, Yoon

- SS, Jang JH, Yeh SP, Turgut M, Hong WJ, Zhou Y, Potluri J, Pratz KW. Azacitidine and Venetoclax in Previously Untreated Acute Myeloid Leukemia. *N Engl J Med*. 2020; **383**:617-629.
2. Gang AO, Frøsig TM, Brimnes MK, Lyngaa R, Treppendahl MB, Grønbaek K, Dufva IH, Straten PT, Hadrup SR. 5-Azacytidine treatment sensitizes tumor cells to T-cell mediated cytotoxicity and modulates NK cells in patients with myeloid malignancies. *Blood Cancer J*. 2014;**4**:e197.
3. Lee JB, Khan DH, Hurren R, Xu M, Na Y, Kang H, Mirali S, Wang X, Gronda M, Jitkova Y, MacLean N, Arruda A, Alaniz Z, Konopleva MY, Andreeff M, Minden MD, Zhang L, Schimmer AD. Venetoclax enhances T cell-mediated antileukemic activity by increasing ROS production. *Blood*. 2021; **138**:234-245.
4. Wu HY, Li KX, Pan WY, Guo MQ, Qiu DZ, He YJ, Li YH, Huang YX. Venetoclax enhances NK cell killing sensitivity of AML cells through the NKG2D/NKG2DL activation pathway. *Int Immunopharmacol*. 2022; **104**:108497.
5. Gentles AJ, Newman AM, Liu CL, Bratman SV, Feng W, Kim D, Nair VS, Xu Y, Khuong A, Hoang CD, Diehn M, West RB, Plevritis SK, Alizadeh AA. The prognostic landscape of genes and infiltrating immune cells across human cancers. *Nat Med*. 2015; **21**:938-945.
6. Tosolini M, Pont F, Poupot M, Vergez F, Nicolau-Travers ML, Vermijlen D, Sarry JE, Dieli F, Fournié JJ. Assessment of tumor-infiltrating TCRV γ 9V δ 2 $\gamma\delta$ lymphocyte abundance by deconvolution of human cancers microarrays. *Oncotarget*. 2017; **6**:e1284723.
7. De Gassart A, Le KS, Brune P, Agaugué S, Sims J, Goubard A, Castellano R, Joaland N, Scotet E, Collette Y, Valentin E, Ghigo C, Pasero C, Colazet M, Guillén J, Cano CE, Marabelle A, De Bonno J, Hoet R, Truneh A, Olive D, Frohna P. Development of ICT01, a first-in-class, anti-BTN3A antibody for activating V γ 9V δ 2 T cell-mediated antitumor immune response. *Sci Transl Med*. 2021; **13**:eabj0835.
8. Wermke M, Marabelle A, Jungels C, Bono JD, Vey N, Vicier C, et al. 503 Clinical activity of ICT01, an anti-BTN3A-targeted, $\gamma\delta$ -activating mAb, alone and in combination with pembrolizumab in patients with advanced/refractory solid tumors: EVICTION trial. *J Immunother Cancer*. 2021; **9**: A503

<http://dx.doi.org/10.1136/jitc-2022-SITC2022.0354>

355

TCR $\gamma\delta$ + TIL FROM PATIENTS WITH PANCREATIC CANCER RECOGNIZE AUTOLOGOUS TUMOR CELLS RESTRICTED BY CD1D

¹Joana Lérias*, ¹Patrícia António, ¹Jéssica Kamiki, ¹Rodrigo Eduardo, ¹Sara Cascais, ¹Bernardo Marinheiro, ¹Eric De Sousa, ¹Carolina Gorgulho, ¹Andreia Maia, ¹Mireia Castillo-Martin, ¹Markus Buechler, ¹Carlos Carvalho, ¹Antonio Beltran, ²Sam Jeong, ²Ridong Chen, ¹Markus Maeurer. ¹Champalimaud Center for the Unknown, Lisbon, Portugal; ²Human Cell Inc, Naperville, IL, USA

Background Pancreatic cancer is the 7th leading cause of cancer-related deaths worldwide. Treatment options are still limited; immunotherapeutic approaches using tumor infiltrating lymphocytes (TIL) represent a viable option for PDAC patients. TILs from PDAC lesions will include $\alpha\beta$ + and $\gamma\delta$ + T-cells, that recognize tumor cells restricted by non-classical MHC I molecules.^{1,2} $\gamma\delta$ + TILs are generally associated with a more favorable prognosis³ and present promising candidates for adoptive cellular therapy as cellular products, or by cloning the molecular blueprint of cancer-specific TCRs that could be transferred into recipient immune cells. The study focused on the expansion of TIL containing TCR $\gamma\delta$ +, molecular analysis of TCR $\gamma\delta$ + cells, and testing anti-tumor directed TIL specificity defined by IFN-gamma production upon NRLP3 pathway stimulation.

Methods Freshly harvested tumor tissue was used to propagate TIL using cytokines in combination with an NRLP3 pathway activator for 2-3 weeks. $\gamma\delta$ + T-cell expansion and T-cell activation/exhaustion were tested by flow cytometry and autologous tumor recognition assays were performed using blocking mAbs and IFN-gamma as the biological readout; molecular recognition analysis was performed using synthetic peptides derived from tumor exome sequencing. TCR deep sequencing was performed in sorted TCR $\gamma\delta$ + TIL. Tumor infiltration by TCR $\gamma\delta$ + was gauged by immunohistochemistry and spatial transcriptomics.

Results NRLP3 stimulation results in increased TCR $\gamma\delta$ + cells which – after sorting (>90% purity) – recognized autologous and allogeneic pancreatic cancer cells in a CD1d-restricted fashion defined by IFN-gamma production. TCR sequencing revealed a focused TCR repertoire with unusual Vgamma3 and Vgamma8 usage. NRLP3 stimulation increased the frequency of $\alpha\beta$ + T-cells against autologous tumor cells and mutant target epitopes defined by IFN-gamma production, abrogated with an NRLP3 inhibitor. Spatial transcriptomics revealed co-localization of CD1d and perforin+granzymeA +granzymeB $\gamma\delta$ + T-cells; TCR-sequencing of PDAC tissue and corresponding TIL exhibited an oligoclonal TCR repertoire. NRLP3 stimulation increased mRNA and protein expression of CXCL9 and CXCL10, which facilitates tissue invasion and favored CD1d restricted recognition of damaged mitochondria by $\gamma\delta$ + T-cells.

Conclusions NRLP3 pathway stimulation increased tumor-reactive and mutant epitope specific TILs, increased expression of chemokines facilitating tissue invasion and expansion of $\gamma\delta$ + TIL engaged in surveillance of damaged mitochondria. This allows a clinically relevant expansion of TIL for patients with PDAC that recognized tumor associated antigens restricted by classical and non-classical MHC molecules. CD1d restricted and tumor-reactive $\gamma\delta$ TCRs can be used as blueprints for anti-cancer directed receptors that could be transferred into recipient cells for active cellular immunotherapy for patients with PDAC.

REFERENCES

1. Zhao Y, Niu C, Cui J. Gamma-delta ($\gamma\delta$) T cells: friend or foe in cancer development? *J Transl Med.* 2018; **16**(1):3
2. Maeurer MJ, Martin D, Walter W, Liu K, Zitvogel L, Halusczyk K, Rabinowich H, Duquesnoy R, Storkus W, Lotze MT. Human intestinal Vdelta1+ lymphocytes recognize tumor cells of epithelial origin. *J Exp Med.* 1996; **183**(4):1681-1696
3. Lo Presti E, Pizzolato G, Corsale AM, Caccamo N, Sireci G, Dieli F, Meraviglia S. $\gamma\delta$ T cells and Tumor Microenvironment: From Immunosurveillance to Tumor Evacuation. *Front Immunol.* 2018; **9**:1395

Ethics Approval This study was approved by the Champalimaud Foundation's Ethics Committee. Research complied with the corresponding ethical principles and the applicable international, EU and national directive laws (EU Directive 2004/23/EC).

Consent Written informed consent was obtained from the patient for publication of this abstract and any accompanying images. A copy of the written consent is available for review by the Editor of this journal.

<http://dx.doi.org/10.1136/jitc-2022-SITC2022.0355>

356

GENERATION OF GD2-CAR NEUTROPHILS FROM HPSCS FOR TARGETED CANCER IMMUNOTHERAPY OF SOLID TUMORS

¹Asiri Majumder*, ¹Ho Sun Jung, ²Jue Zhang, ¹Kran Suknuntha, ²James Thomson, ¹Igor Slukvin. ¹University of Wisconsin, Madison, WI, USA; ²Morgridge Institute for Research, Madison, WI, USA

Background Chimeric antigen receptor (CAR) T cell and NK cell therapies already been successful in the eradication of lymphoid malignancies. However, many challenges remain in the applying CAR therapies for solid tumors, and responses with CAR-T cells have been limited to isolated exceptional cases. Thus, opportunities exist for new immunotherapies for specific targeting of solid tumors using CAR-weaponized neutrophils which are capable of cytotoxicity and migration into solid tumors. Human pluripotent stem cells (hPSCs) are a logical alternative for large-scale production of CAR neutrophils due to their renewability and uniform quality. In this study we explored a feasibility of generation GD2-CAR neutrophils from hPSCs with superior cytotoxic activities against GD2-expressing tumors *in vitro* and *in vivo*.

Methods We used CRISPR-Cas9 gene editing method to integrate a third generation GD2-CAR (anti-GD2-14g2A-CD28-OX40-CD3z) into AAVS1 locus of IISH2i-BM9 hiPSCs. GD2-CAR-hiPSCs differentiated into neutrophils in defined serum- and feeder-free conditions using ETV2 modified mRNA. The *in vitro* antitumor activity of CAR-M was evaluated by co-culture with GD2-expressing CHLA-20 neuroblastoma and WM266-4 melanoma and GD2-negative SKOV3 ovarian carcinoma and SK-BR3 breast carcinoma. To assess *in vivo* potential of GD2 CAR neutrophils, NSG mice were inoculated intraperitoneally (IP) with 3×10^5 Luc2-eGFP⁺ WM266-4 melanoma cells and engraftment was assessed by IVIS bioluminescent imaging. On day 4 post WM266-4 injection, mice were either treated with 10^7 WT or GD2-CAR neutrophils via IP injection every 7 days.

Results GD2-CAR hiPSCs differentiated into CAR-neutrophils with the same efficiency as unmodified hiPSCs. CAR-neutrophils demonstrated typical neutrophil morphology and phenotype, including expression CD15, lactoferrin and MPO. Neutrophils generated from GD2-CAR hiPSCs, as compared to unmodified neutrophils, demonstrated superior cytotoxicity *in vitro* against GD2⁺ WM266-4 melanoma and CHLA20 neuroblastoma, while minimal differences were observed in cytotoxicity against GD2-negative SKOV3 ovarian and SK-BR3 breast cancer cells between unmodified and CAR-neutrophils. Upon assessment of anti-tumor activities of GD2-CAR neutrophils in mice engrafted with WM266-4 melanoma over 30 days (figure 1), CAR neutrophil-treated mice showed significantly reduced tumor burden (figure 2) and prolonged survival (figure 3) compared to untreated mice or mice treated with unmodified iPSC-derived neutrophils.

Conclusions Our studies demonstrate that hiPSCs can be used to efficiently generate CAR-neutrophils with potent activity against solid tumors. Thus, hiPSCs provide a novel approach for generation CAR-neutrophil off-the-shelf product for targeted immunotherapy of solid tumors.

Acknowledgements This work is supported by funds from National Institute of Health, United States (R01HL142665, and P51 OD011106).

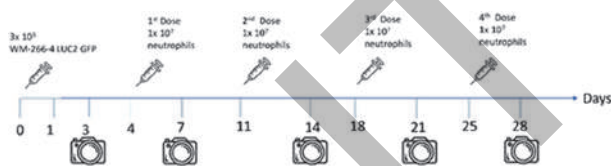
REFERENCES

- Hu K, Yu J, Suknuntha K, Tian S, Montgomery K, Choi KD, Stewart R, Thomson JA, Slukvin II. Efficient generation of transgene-free induced pluripotent stem cells

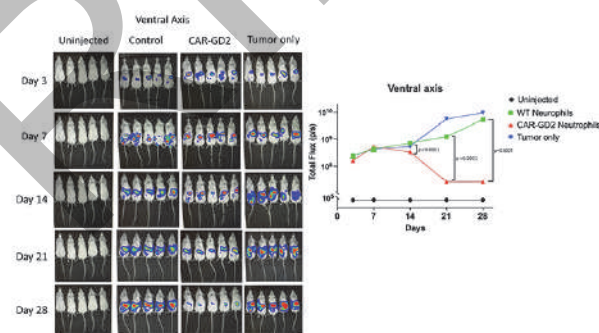
from normal and neoplastic bone marrow and cord blood mononuclear cells. *Blood*. 2011;**117**:e109–e119.

- Suknuntha K, Tao L, Brok-Volchanskaya V, D'Souza SS, Kumar A, Slukvin I. Optimization of synthetic mRNA for highly efficient translation and its application in the generation of endothelial and hematopoietic cells from human and primate pluripotent stem cells. *Stem Cell Rev*. 2018; **14**: 525–534.
- Brok-Volchanskaya V, Bennin DA, Suknuntha K, Klemm L, Huttenlocher A, Slukvin I. Effective and Rapid Generation of Functional Neutrophils from Induced Pluripotent Stem Cells Using ETV2-Modified mRNA. *Stem Cell Reports*. 2019; **13**:1099–1110.

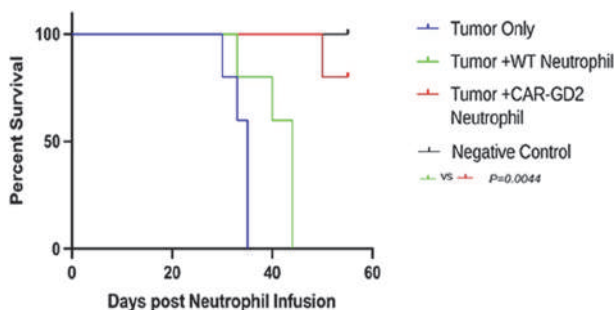
Ethics Approval The animal experiments were performed under approval from UW-Madison, Institutional Review Board.



Abstract 356 Figure 1 Schematic of the *in vivo* cytotoxicity assay. NSG mice inoculated IP with Luc2-GFP WM266-4 melanoma cells. On day 4 after melanoma injection, mice were left untreated, or treated with unmodified or CAR-N injected intraperitoneally every 7 days.



Abstract 356 Figure 2 *In vivo* evaluation of CAR-N cytotoxicity. Tumor burden was determined by bioluminescent imaging using IVIS imager showing total flux of the ventral axis.



Abstract 356 Figure 3 Kaplan-Meier curve for survival. Kaplan-Meier curve representing the percent survival of the experimental groups.

<http://dx.doi.org/10.1136/jitc-2022-SITC2022.0356>

357

PHOSPHORYLATION OF CD28-Y218 MODULATES IL-2 SECRETION AND ANTITUMOR EFFECT OF CAR-T CELLS, IN A PRECLINICAL MODEL OF PANCREATIC CANCER

Elena Martínez Planes*, Miguel Fontela, Cecilia Ramello, Daniel Abate-Daga. *H. Lee Moffitt Cancer Center, Tampa, FL, USA*

Background CD28-derived co-stimulation modules are frequently used as part of the signaling domain of chimeric antigen receptors (CAR). These modules contain well characterized tyrosine-containing moieties (YMN and PYAP) that become phosphorylated upon CAR activation, resulting in IL-2 secretion and T cell expansion.^{1,2} Previous work by our group has shown that an additional tyrosine residue, located in the C-terminus of CD28 (Y218), was also phosphorylated upon CAR activation.³ In this work we sought to evaluate the functional relevance and molecular mechanism of CD28-Y218 phosphorylation in CAR-T cells.

Methods We first analyzed the kinetics of Y218 phosphorylation. To that end, prostate stem cell antigen (PSCA) specific CAR-T cells were stimulated through co-culture with HPAC pancreatic cancer cells for 0, 1, 10, 30 and 60 minutes. Phosphorylation of Y218 was analyzed by Western blotting using a phospho-specific antibody. To determine the functional relevance of this phosphorylation event, we generated mutant CARs where the tyrosine residue was replaced with a non-phosphorylatable amino acid (Y218F) and evaluated its effects *in vivo* and *in vitro*. CAR-T cell cytotoxicity was monitored using the xCELLigence Real Time Cytotoxicity Assay (RTCA). A CD19-specific CAR was used as an alternative model, where NALM6 cells expressing firefly luciferase served as target cells. Luciferase activity was used as surrogate for target cell viability. In both models, we monitored cytokine production following overnight co-culture with target cells using the ELLA system (Biotechne, CA, USA). To evaluate *in vivo* antitumor effect of PSCA-specific CAR-T cells, NSG mice were injected (s.c.) with 1 HPAC cells and infused 14 days later with 5 CAR-T cells (i.v.). Tumor growth was monitored for 35 days.

Results We observed an antigen-dependent phosphorylation of Y218 which reached maximum levels approximately 10 min post-stimulation. Mutation of the CD28-Y218 residue did not affect CAR expression, cytotoxicity *in vitro*, or INF γ production. However, this mutation was associated with reduced IL-2 and TNF α secretion. *In vivo*, this mutation completely abrogated the therapeutic effect of these cells in the pancreatic cancer model.

Conclusions These results show that CD28-Y218 plays a role in CAR-T cell function, with direct impact on IL-2 secretion and antitumor efficacy. Future experiments will determine the specific signaling events that are triggered by Y218 phosphorylation.

Acknowledgements This work has been supported in part by the Flow Cytometry Core Facility at Moffitt Cancer Center, an NCI designated Comprehensive Cancer Center (P30-CA076292).

REFERENCES

1. Esensten JH, Helou YA, Chopra G, Weiss A, Bluestone JA. CD28 costimulation: From mechanism to therapy. *Immunity*. 2016; **44**:973-988.
2. Dong R, Libby KA, Blaeschke F, Fuchs W, Marson A, Vale RD, Su X. Rewired signaling network in T cells expressing the chimeric antigen receptor (CAR). *EMBO J*. 2020; **39**:e104730.
3. Ramello MC, Benzaid I, Kuenzi BM, Lienlaf-Moreno M, Kandell WM, Santiago DN, Pabón-Saldaña M, Darville L, Fang B, Rix U, Yoder S, Berglund A, Koomen

JM, Haura EB, Abate-Daga D. An immunoproteomic approach to characterize the CAR interactome and signalosome. *Sci Signal*. 2019; **12**:eaap9777.

Ethics Approval This study was approved by the Institutional Animal Care and Use Committee (IACUC); approval number R ISO00010727.

<http://dx.doi.org/10.1136/jitc-2022-SITC2022.0357>

358

DEVELOPMENT OF AN ALLOGENIC FAP CAR INKT PRODUCT TO TARGET TUMOR STROMA AND MODULATE THE TUMOR MICROENVIRONMENT

¹Xavier Michelet*, ¹Martyna Popis, ¹Shannon Boi, ¹Magda Niedzielska, ¹Reed Masakayan, ¹Efrat Altman Sharoni, ¹Paul Ibbett, ¹Deborah Wright, ²Barbara Barbara Kalinowska, ²Justin Keith, ²Bishnu Joshi, ¹Moira Pinzan Rossi, ¹Rachel Smith, ¹Burcu Yigit, ¹Olivier Le Tonqueze, ¹Eleni Chantzoura, ³Marc Van Dijk. ¹MiNK Therapeutics, Lexington, MA, USA; ²Agenus, Lexington, MA, USA; ³MiNK Therapeutics, Cambridge, UK

Background The emergence of antibodies targeting checkpoint modulators such as PD-1 and CTLA-4 has revolutionized solid tumor treatment and highlighted the importance of effectively engaging the immune system to drive durable responses. However, well over 50% of solid tumor patients do not respond adequately to checkpoint modulators; due to generally ascribed active immune suppression in the tumor microenvironment (TME). To overcome suppression and increase tumor control, we developed a highly selective and precisely tuned Chimeric Antigen Receptor (CAR), which targets Fibroblast Activating Protein (FAP) expressed on both tumor cells and immune-suppressive Cancer Associated Fibroblasts (CAFs). This novel allogeneic CAR-iNKT cell (invariant natural killer T cell) product is IL-15 secreting, in addition to being FAP binding, and is intended for treatment of solid tumors. iNKT cells were selected as hosts due to their natural resistance to exhaustion, tissue homing properties, selective cytotoxicity towards M2 macrophages and stimulation of dendritic cell maturation properties which are essential for effective solid tumor directed therapies. In addition, iNKT cells have intrinsic CD1d- and NK receptor ligand targeted cytotoxicity, while not causing Graft *versus* Host Disease due to the presence of invariant T cell receptors.

Methods Our proprietary CARDIS™ platform combines screening of highly diverse (>10¹⁰) fully human scFv libraries with library-based direct functional selection in CAR format using mammalian display. Candidates can be further optimized using affinity tuning to ensure optimal and highly selective on-target/on-tumor activity and full mouse cross-reactivity. We developed a scalable manufacturing approach to engineer and specifically expand CAR and soluble IL-15-expressing allogeneic iNKT cells.

Results Using our CARDIS™ platform, we generated a panel of fully human, potent, and highly selective anti-human FAP CARs with equivalent cross-reactivity towards mouse FAP. In xenograft mouse models our FAP-CAR-IL-15 iNKT cells effectively control FAP-expressing tumors, as well as FAP negative tumors with immune-suppressive stroma mediated by FAP+ CAFs, while soluble IL-15 prolongs persistence in immunocompromised mice. In addition, we show that FAP-CAR-IL-15 iNKT cells mediate the infiltration of tumor-specific T-cells and enhance their anti-tumor activity.

Conclusions We have used our CARDIS™ and iNKT platforms to develop a CAR-iNKT therapy effectively and selectively targeting FAP positive tumor cells and suppressive CAF subsets in the TME. We believe that combining the activity of our FAP-CAR with the potent natural activity of iNKT cells will enable a level of tumor control and immune engagement to solid tumor patients beyond currently available treatments.

<http://dx.doi.org/10.1136/jitc-2022-SITC2022.0358>

359

HYALURONIC ACID NANOGEL BASED CANCER VACCINE, IN COMBINATION WITH ADOPTIVE T CELL THERAPY TOTALLY SUPPRESSES ICI RESISTANT-TUMORS

¹Hiroshi Shiku*, ¹Fumiyasu Momose, ²Takashi Nakai, ²Kohei Yabuuchi, ²Toru Katsumata, ²Tsuyoshi Shimoboji. ¹Mie University Graduate School of Medicine, Tsu, Japan; ²Asahi Kasei Corporation, Fuji, Japan

Background In this study, we questioned efficacy of combination therapy of newly developed cancer vaccines for tumors refractory to immune checkpoint inhibitors (ICIs) and adoptive therapy of TCR-T cells. We have developed a nano-sized hydrogel particles (nanogels) to create novel nanomaterials for biomedical applications. In particular, HANG; Hyaluronic Acid partially hydrophobized by a chemical modification with cholesterol groups forms physically cross-linked NanoGel particles with a diameter of 30~100 nm via self-assembly in water. HANG efficiently forms a stable complex with antigenic polypeptides (HANG-V) through hydrophobic interactions. Two murine tumor models, B16F10 melanoma and CMS5a sarcoma, both of which are known to be refractory to ICI therapy and adoptive T cell therapy of TCR engineered T cells were studied.

Methods The peptides, gp100 or CMS5a neoantigens, in DMSO were added to the HANG aqueous solution and the mixture was incubated for 24 h at room temperature. After 0.22 µm filtration, the antigen peptide concentration was quantified by reverse phase chromatography analysis.

Results HANG-V cancer vaccine (HANG and gp100 long peptides) with TLR agonist were subcutaneously injected to B16F10-bearing C57BL/6 mice on days 7, 11, 15 and subsequently administered with CD8⁺ T cells obtained from Pmel-1 transgenic mice. B16F10 tumors more than 100 mm² became complete regression. This effect persisted for a long period without recurrence, by changing hair color of mice into white. Control non-vaccinated mice were all dead by day 25. The gp100-specific CTLs with effector phenotype and IFN-γ secretion, were observed with high frequency in LNs, spleen, PBMCs and TILs. Two months after last treatment of HANG-V, Ag-specific adoptive T cells were detected in circulating blood, which show effector memory/central memory phenotype. Furthermore, booster vaccination induces explosive expansion of these memory T cells. In similar experimental settings, BALB/c CMS5a tumor were treated with the HANG-V (HANG and mERK2 long peptides) plus TLR agonist with adoptive transfer of T cells from TCR transgenic DUC18, for CMS5a-specific mERK2 neoantigen, resulted in total suppression of tumor growth.

Conclusions HANG cancer vaccine (HANG-V) strongly enhances efficacy of adoptive TCR engineered T cell therapy against ICI refractory tumors leading to total tumor suppression. In addition, HANG-V induces potent and sustainable antigen-specific CTL systemically and intratumorally. Our studies may propose crucial insights for clinical application of HANG-V with adoptive T cell therapy for ICI-resistant and metastatic tumors with poor prognosis.

<http://dx.doi.org/10.1136/jitc-2022-SITC2022.0359>

360 **NOVEL IMMUNOTHERAPY FOR PROSTATE CANCER
COMBINING CAR T CELLS AND MYELOID CELL STAT3
INHIBITION**

John Murad*, Saul Priceman. *City of Hope, Duarte, CA, USA*

Background Poor prognosis for patients with metastatic castration resistant prostate cancer (mCRPC) has inspired efforts to develop effective treatments for advanced disease. Our lab has developed a chimeric antigen receptor (CAR)-engineered T cell targeting prostate stem cell antigen (PSCA), which is overexpressed in a majority of primary and metastatic prostate cancers. We believe PSCA-CAR T cells will provide a safe and effective strategy for improving clinical outcomes for mCRPC patients. While encouraged by clinical activity in our phase 1 trial (NCT03873805), the immunosuppressive tumor microenvironment (TME) will limit therapeutic potential. Central to tumor/immune cell interactions is the transcription factor, signal transduction and activation of transcription-3 (STAT3), recognized for its critical role in regulating multiple tumor-associated myeloid cell-related genes known to suppress anti-tumor immunity, including type-I IFNs, IL-10, IL-12, TGF β , and PD-L1. Thus, we hypothesized that TME modulation with a TLR9-guided STAT3 anti-sense oligonucleotide CpG-STAT3ASO (CSI3) would provide myeloid cell-selective STAT3 inhibition, which combined with PSCA-CAR T cells will improve responses in mCRPC.

Methods Using a PSCA knock-in (hPSCA-KI) immunocompetent mouse model of prostate cancer (*Murad et.al., 2021 Mol Ther*), we describe cyclophosphamide (Cy) preconditioning as crucial for unleashing the therapeutic potential of PSCA-CAR T cells, yet still achieving approximately 50% curative responses. Here, we interrogated synergy of Cy and PSCA-CAR T cells combined with targeted STAT3 inhibition with CSI3. Following dosing optimization, tumor reduction and survival kinetics in subcutaneous or intratibial prostate tumors were assessed. Modulation to tumor and systemic immune landscapes using CSI3 treatment was assessed via flow cytometry, Nanostring digital spatial profiling, and immunohistochemistry.

Results In an intratibial bone metastatic prostate cancer model, Cy and CAR T cell treatment was effective in curing 50% of mice. Impressively, we demonstrated 88% curative response rate when combined with CSI3 treatment. The benefit in survival via CSI3 necessitated Cy preconditioning, as only 25% of mice were cured when treated with the CAR T cell/CSI3 combination alone. Lastly, no cures were seen in single treated mice. Analysis is on-going to determine changes in the immune landscape when treated with Cy, PSCA-CAR T cells, and CSI3 combinations.

Conclusions Alone, PSCA-CAR T cell or CSI3 targeted approaches are insufficient in producing a robust immune response without dose limiting toxicities. Our data suggests that myeloid cell-selective STAT3 inhibition in combination with our PSCA-CAR T cells may synergize to improve overall responses and boost endogenous anti-tumor immunity. In sum, this approach presents an exciting avenue for clinical development in mCRPC.

<http://dx.doi.org/10.1136/jitc-2022-SITC2022.0360>

361 UNIVERSAL EXPANSION OF CBL-B-INHIBITED TUMOR INFILTRATING LYMPHOCYTES, DETIL-0255, FROM WOMEN WITH OVARIAN CANCER: PROCESS VALIDATION

¹Pranav Murthy*, ¹Nell Namitha Narasappa, ¹Xiaoyan Liang, ¹Xianzhu Wu, ¹Irene Luu, ¹Jeevitha Jeevan, ¹Sagar Sharma, ¹Alison Ross, ¹Caleb Lampenfeld, ¹Sam Zahn, ¹Thomas Musial, ¹Jennifer Bone, ²John Nakayama, ²David Bartlett, ³Jocelyn Chapman, ¹Greta Garrido, ¹Nicholas Shinnars, ¹Arthur Sands, ¹Michael Blackton, ¹Ena Wang, ¹Michael Lotze. ¹Nurix Therapeutics, San Francisco, CA, USA; ²Allegheny Health Network, Pittsburgh, PA, USA; ³UCSF Medical Center, San Francisco, CA, USA

Background Despite objective responses to immune checkpoint blockade in patients with ovarian cancer (OC), therapies providing durable clinical benefit are lacking.¹ An increased density of OC tumor infiltrating lymphocytes (TIL), specifically memory T cells with enhanced CD28 signaling, are associated with improved survival² and immunotherapy response.³ Adoptive cell therapy (ACT) utilizing *ex vivo* expanded TIL has demonstrated durable complete responses in several epithelial malignancies, but has shown limited clinical benefit in OC.^{4,5} This is due in part to extended manufacturing times and use of TIL products with a differentiated and exhausted phenotype.^{4,5} Casitas B lineage lymphoma-B (CBL-B) is an E3 ubiquitin ligase that limits T cell activation in the absence of CD28 co-stimulation following T cell receptor engagement. *Ex vivo* inhibition of CBL-B with the small molecule inhibitor NX-0255 increases the expansion of stem-like TIL with enhanced *in vivo* tumor cytotoxicity and persistence compared to conventional TIL expanded in IL-2 alone.^{6,7} Here we present our pre-clinical and early manufacturing experience of drug enhanced TIL therapy (DeTIL-0255) in OC.

Methods Tumor tissue from N=21 consenting patients undergoing resection for OC across multiple US clinical sites was fragmented and cultured with IL-2 and NX-0255 under research (N=20) or clinical scale (N=1) manufacturing conditions. Following 22 days of culture, DeTIL-0255 cell products were characterized by multiparameter spectral flow cytometry.

Results Even with as low as five input 2x2 mm³ tumor fragments, DeTIL-0255 was reproducibly expanded from primary and metastatic OC lesions with an average fold increase of 184±179 (mean ± SD) following the rapid expansion protocol and Day 22 total viable cell count of 8.0x10⁸±5.3x10⁸ cells (research scale) and 2.5x10¹⁰ cells (clinical scale). OC DeTIL-0255 was comprised of T (81.4±10.1%) and NKT (10.5±10.4%) cells with < 4% monocytes, NK, or B cells. OC DeTIL-0255 showed a balanced mixture of CD4 (53.4±28.9%) and CD8 (38.8±27.8%) T cells with heightened expression of the co-stimulatory marker CD226 (CD4: 87.4±12.6%; CD8: 86.0±16.4%), previously shown to predict immunotherapy response [8]. In contrast to prior OC TIL products, OC DeTIL-0255 were primarily effector memory (CD4: 59.7±30.6%; CD8: 55.6±29.8%) and central memory cells (CD4: 21.0±23.7%; CD8: 12.4±16.9%) displaying limited T cell exhaustion (CD4: PD-1 26.2±22.8%, LAG-3 15.1±13.5%, CD57 4.4±4.3%; CD8: PD-1 17.7±19.6%, LAG-3 45.4±28.4%, CD57 2.9±2.5%).

Conclusions OC DeTIL-0255 demonstrate a favorable phenotype amenable for ACT. A Phase 1 clinical study of DeTIL-0255 in women with recurrent/platinum resistant OC is ongoing (NCT05107739).

REFERENCES

1. Zamarin D, Burger RA, Sill MW, Powell DJ Jr, Lankes HA, Feldman MD, Zivanovic O, Gunderson C, Ko E, Mathews C, Sharma S, Hagemann AR, Khleif S,

Aghajanian C. Randomized phase II trial of nivolumab versus nivolumab and ipilimumab for recurrent or persistent ovarian cancer: An NRG oncology study. *J Clin Oncol*. 2020; **38**:1814-1823.

2. Anadon CM, Yu X, Hånggi K, Biswas S, Chaurio RA, Martin X, Payne KK, Mandal G, Innamarato P, Harro CM, Mine JA, Sprenger KB, Cortina C, Powers JJ, Costich TL, Perez BA, Gatenbee CD, Prabhakaran S, Marchion D, Heemskerck MHH, Curiel TJ, Anderson AR, Wenham RM, Rodriguez PC, Conejo-Garcia JR. Ovarian cancer immunogenicity is governed by a narrow subset of progenitor tissue-resident memory T cells. *Cancer Cell*. 2022;**40**:545-557.

3. Duraiswamy J, Turrini R, Minasyan A, Barras D, Crespo I, Grimm AJ, Casado J, Genolet R, Benedetti F, Wicky A, Ioannidou K, Castro W, Neal C, Moriot A, Renaud-Tissot S, Anstett V, Fahr N, Tanyi JL, Eiva MA, Jacobson CA, Montone KT, Westergaard MCW, Svane IM, Kandalaf LE, Delorenzi M, Sorger PK, Färkkilä A, Michielin O, Zoete V, Carmona SJ, Foukas PG, Powell DJ Jr, Rusakiewicz S, Doucey MA, Dangaj Laniti D, Coukos G. Myeloid antigen-presenting cell niches sustain antitumor T cells and license PD-1 blockade via CD28 costimulation. *Cancer Cell*. 2021;**39**: 1623-1642.

4. Kverneland AH, Pedersen M, Westergaard MCW, Nielsen M, Borch TH, Olsen LR, Aasbjerg G, Santegoets SJ, van der Burg SH, Milne K, Nelson BH, Met Ö, Donia M, Svane IM. Adoptive cell therapy in combination with checkpoint inhibitors in ovarian cancer. *Oncotarget*. 2020; **11**:2092-2105.

5. Pedersen M, Westergaard MCW, Milne K, Nielsen M, Borch TH, Poulsen LG, Hendel HW, Kennedy M, Briggs G, Ledoux S, Nøttrup TJ, Andersen P, Hasselager T, Met Ö, Nelson BH, Donia M, Svane IM. Adoptive cell therapy with tumor-infiltrating lymphocytes in patients with metastatic ovarian cancer: a pilot study. *Oncimmunology*. 2018; **7**:e1502905.

6. Whelan S, Gosling J, Mani M, Cohen F, Tenn-McClellan A, Powers J, Hansen G, Lotze M, Sands A. NX-0255, a small molecule CBL-B inhibitor, expands and enhances tumor infiltrating lymphocytes (TIL) for use in adoptive cancer immunotherapy. *J Immunother Cancer*. 2021; **9**: 98.

7. Gallotta M, Romo JG, Borodovsky A, Tenn-McClellan A, Stokes J, Gosling J, Hansen GM, Sands A, Rountree R, Guiducci C. Ex-vivo inhibition of CBL-B with a novel small molecule inhibitor, NX-0255, enhances persistence and anti-tumor activity of adoptively transferred CD8+ T cells in mouse tumor models. *Cancer Res*. 2022; **82**:573.

8. Banta KL, Xu X, Chitre AS, Au-Yeung A, Takahashi C, O’Gorman WE, Wu TD, Mittman S, Cubas R, Comps-Agrar L, Fulzele A, Bennett EJ, Grogan JL, Hui E, Chiang EY, Mellman I. Mechanistic convergence of the TIGIT and PD-1 inhibitory pathways necessitates co-blockade to optimize anti-tumor CD8+ T cell responses. *Immunity*. 2022;**55**:512-526.

Ethics Approval All studies were performed in full accordance with the guidelines for good clinical practice and the Declaration of Helsinki and approved by the cited institutional protocol review committee and IRB.

Consent Written informed consent was obtained from the patient for use of patient specimens for research and subsequent publication.

<http://dx.doi.org/10.1136/jitc-2022-SITC2022.0361>

362

DEFINING T CELL EXHAUSTION AND MEMORY CORRELATES OF GD2 CAR T CELL EXPANSION IN PEDIATRIC PATIENTS WITH SOLID TUMOR MALIGNANCIES

¹Tara Murty*, ¹Sneha Ramakrishna, ²Sabina Kaczanowska, ²Cristina Contreras, ¹Caroline Duault, ¹Priyanka Balasubrahmanyam, ¹Warren Reynolds, ¹Reema Baskar, ³Aashna Jhaveri, ³Yang Liu, ³Jennifer Altreuter, ³Franziska Michor, ¹Mina Pichavant, ¹Bitu Sahaf, ¹Sean Bendall, ¹Holden Maecker, ⁴Melinda Merchant, ¹Crystal Mackall, ²Rosandra Kaplan. ¹Stanford University School of Medicine, Stanford, CA, USA; ²National Cancer Institute, Bethesda, MD, USA; ³Dana-Farber Cancer Institute, Boston, MA, USA; ⁴Black Diamond Therapeutics, Cambridge, MA, USA

Background Chimeric antigen receptor T cells (CAR-Ts) hold promising therapeutic potential for solid tumors but have yet to produce consistent durable responses in patients. A major limitation to response in solid tumors remains the lack of CAR-T expansion, persistence, and anti-tumor cytotoxicity. Identifying molecular markers that correlate with CAR-T activity could elucidate key biological pathways and T cell populations central to the success of CAR-Ts in patients.

Methods A phase I trial (NCT02107963) was conducted to determine the feasibility of producing and safety of administering escalating doses of a third generation GD2 CAR-T (GD2-CAR.OX40.28.z.ICD9) in children and young adults with GD2+ solid tumors, including neuroblastoma and osteosarcoma. To understand biological differences correlating with CAR-T cell activity in patients, patient apheresis, CAR-T product, and post-treatment peripheral blood samples were analyzed for immune phenotype by mass cytometry (CyTOF), transcriptomic profile by RNA-sequencing (RNA-seq), and epigenetic landscape with Assay for Transposase-Accessible Chromatin using sequencing (ATAC-seq).

Results Across 4 dose levels, 15 patients (8-28 years old) were enrolled, of which 13 patients were infused. At Day 28 following GD2 CAR-T infusion, 23.1% (3/13) of evaluable patients had progressive disease and 76.9% (10/13) had stable disease (SD), but all patients eventually progressed. Despite limited GD2-CAR-T persistence, half of the patients had expansion similar to that seen in clinically active CD19 and CD22 CAR-Ts. Since a major barrier to CAR-T efficacy is inadequate CAR-T expansion, we comprehensively evaluated patient immune profiles to identify determinants of CAR-T expansion. Good CAR-T expansion was found to be associated with increased abundance of naïve CD8+ T cells in apheresis by CyTOF. Similarly, RNAseq demonstrated enrichment of naïve memory T cell pathways in the apheresis samples of good expanders. ATACseq identified epigenetic differences in apheresis that may predict good CAR-T expansion in patients. CAR-T products across all patients, regardless of CAR-T expansion, expressed activation/exhaustion markers by CyTOF. RNAseq of CAR-T products revealed an enhanced exhaustion signature in poor compared to good expanders. At post-treatment timepoints, poor expanders demonstrated increased expression of T cell exhaustion markers.

Conclusions Comprehensive analyses of patients' apheresis, product, and post-treatment timepoints enable characterization of the T cell immune compartment before CAR-T treatment, after CAR-T manufacturing, and after CAR-T infusion. We identified phenotypic, transcriptomic, and epigenetic T cell signatures correlating with CAR-T expansion. These data suggest key mechanisms of underlying T cell biology that may contribute to CAR-T activity in pediatric solid tumors.

Acknowledgements We are grateful to the study participants and their families, referring medical care teams, the faculty

and staff of the NCI CCR Pediatric Oncology Branch, NCI CCR Center for Cellular Engineering, and the data managers involved with this work. Clinical trial supported in part by: Intramural Research Program, National Cancer Institute, NIH Clinical Center, National Institutes of Health. Scientific and financial support for the CIMAC-CIDC Network are provided through the National Cancer Institute (NCI) Cooperative Agreements: U24CA224331 (to the Dana-Farber Cancer Institute CIMAC), U24CA224309 (to the Stanford University CIMAC), and U24CA224316 (to the CIDC at Dana-Farber Cancer Institute). Scientific and financial support for the Partnership for Accelerating Cancer Therapies (PACT) public-private partnership (PPP).

Trial Registration NCT02107963

Ethics Approval The phase I study protocol conformed to the Declaration of Helsinki, Good Clinical Practice guidelines, and was approved by the NCI Institutional Review Board (14-C-0059) and the FDA. All patients or their legal guardians signed a document of informed consent indicating their understanding of the investigational nature and risks of this study.

<http://dx.doi.org/10.1136/jitc-2022-SITC2022.0362>

Abstracts

363

LOCALIZED INTERLEUKIN-2 CYTOKINE FACTORIES ERADICATE MESOTHELIOMA TUMORS VIA ACTIVATION OF ADAPTIVE AND INNATE IMMUNE CELLS

¹Samira Aghlara-Fotovat*, ¹Amanda Nash, ¹Bertha Castillo, ¹Andrea Hernandez, ²Aarthi Pugazenthi, ²Hyun-Sung Lee, ²Hee-Jin Jang, ¹Annie Nguyen, ¹Alexander Lu, ²Bryan Burt, ²Ravi Ghanta, ¹Omid Veisheh. ¹Rice University, Houston, TX, USA; ²Baylor College of Medicine, Houston, TX, USA

Background High-dose interleukin-2 (IL-2) immunotherapy has previously demonstrated effective tumor lysis via activation of effector immune cells;¹ however, clinical utility is limited due to pharmacokinetic challenges and life-threatening toxicities experienced by patients.² To overcome these challenges, we developed a safe and clinically translatable localized IL-2 delivery system to boost the potency of therapy while minimizing systemic cytokine exposure.³

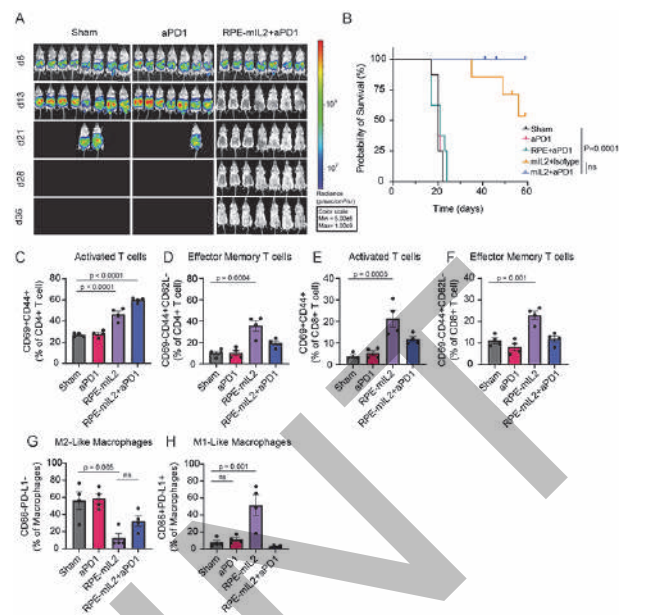
Methods We evaluated the therapeutic efficacy of hydrogel encapsulated, cell-based IL-2 cytokine factories in a mouse model of malignant mesothelioma. An effective and well tolerated dose was determined by tracking tumor burden in response to increasing doses of our cytokine factories. Therapeutic efficacy of the optimal dose was subsequently evaluated in combination with anti-PD1 checkpoint inhibitor. Changes in immune populations across groups were analyzed using time-of-flight mass cytometry (CyTOF). Finally, safety and translatability of the platform were evaluated following pleural implant in rats, using complete blood counts and serum chemistry analysis.

Results IL-2 cytokine factories enabled 150x higher IL-2 concentrations in the local compartment with limited leakage into systemic circulation. Additionally, AB1 tumor burden was reduced by 80% after one week of monotherapy treatment, and 7/7 animals exhibited tumor eradication when IL-2 cytokine factories were combined with aPD1 therapy (figure 1A). Resultantly, IL-2+aPD1 combination therapy led to significant improvements in tumor-free survival compared to controls (figure 1B). Further, CyTOF analysis showed an increase in CD69+CD44+ and CD69-CD44+CD62L- T cells (figure 1C-F), reduction of CD86-PD-L1- M2-like macrophages, and a corresponding increase in CD86+PD-L1+ M1-like macrophages (figure 1G and H) and MHC II+ dendritic cells after treatment. Finally, healthy blood chemistry ranges in rodents demonstrated the safety of cytokine factory treatment and reinforced its potential for clinical use.

Conclusions IL-2 cytokine factories led to eradication of aggressive mouse malignant mesothelioma tumors, protection from tumor recurrence, and increased the therapeutic efficacy of anti-PD1 checkpoint therapy. The results of this study provide support for clinical evaluation of our IL-2-based delivery system.

REFERENCES

- Berraondo P, Sanmamed MF, Ochoa MC, Etxeberria I, Aznar MA, Pérez-Gracia JL, Rodríguez-Ruiz ME, Ponz-Sarvisé M, Castañón E, Melero I. Cytokines in clinical cancer immunotherapy. *Br J Cancer*. 2019; **120**:6-15.
- Sivakumar PV, Garcia R, Waggle KS, Anderson-Haley M, Nelson A, Hughes SD. Comparison of vascular leak syndrome in mice treated with IL21 or IL2. *Comp Med*. 2013; **63**:13-21.
- Nash AM, Jarvis MI, Aghlara-Fotovat S, Mukherjee S, Hernandez A, Hecht AD, Rios PD, Ghani S, Joshi I, Isa D, Cui Y, Nouraein S, Lee JZ, Xu C, Zhang DY, Sheth RA, Peng W, Oberholzer J, Igoshin OA, Jazaeri AA, Veisheh O. Clinically translatable cytokine delivery platform for eradication of intraperitoneal tumors. *Sci Adv*. 2022; **8**:eabm1032.



Abstract 363 Figure 1 IL-2 Cytokine factories eradicate MM tumors. (A) Luminescent images tracking tumor burden over time. (B) Survival curves plotted as percent survival over time beginning after tumor injection (n=7-8). C-F) Comparison of activated, and effector memory CD4+ and CD8+ T cells across treatment groups. G & H) Comparison of M1-like and M2-like macrophages across treatment groups.

<http://dx.doi.org/10.1136/jitc-2022-SITC2022.0363>

364

ANTIGEN ABUNDANCE AND TCR AVIDITY IMPACT T CELL-MEDIATED TUMOR RECOGNITION IN NOVEL B16F10 ACT MODEL

¹Jenna Newman*, ¹John Finnigan, ²Andrew Ishizuka, ²Geoffrey Lynn, ³Alexander Rubinsteyn, ¹Timothy O'Donnell, ⁴Jeffrey Hammerbacher, ¹Nina Bhardwaj. ¹Icahn School of Medicine at Mount Sinai, New York, NY, USA; ²Avidea Technologies, Washington, USA; ³University of North Carolina at Chapel Hill, Chapel Hill, NC, USA; ⁴Medical University of South Carolina, Charleston, SC, USA

Background Adoptive cell transfer (ACT) of neoantigen-reactive CD8⁺ T cells has had some success in the clinic; however, mouse models recapitulating neoantigen-reactive CD8⁺ T cell ACT have been limited, especially in poorly immunogenic models such as the murine melanoma model B16F10. Further, direct comparison of neoantigen-reactive CD8⁺ T cell ACT versus ACT utilizing T cells reactive against overexpressed-self or heteroclitic tumor-associated antigen (TAA) peptides has been lacking. To address these gaps, we developed a model system to study neoantigen- and TAA-reactive CD8⁺ T cell ACT in parallel.

Methods Whole exome sequencing and RNA sequencing were employed to predict neoantigens present in B16F10. C57BL/6 mice were then administered charge-modified TLR7/8 conjugate vaccines targeting neoantigenic peptides predicted to elicit T cell responses. Vaccination against neoepitopes and previously characterized TAA epitopes elicited neoantigen- or TAA-reactive CD8⁺ T cells and modest tumor growth control; T cell receptors were isolated from neoantigen- and TAA-reactive CD8⁺ T cell clones. To develop an ACT model, we conducted CRISPR/Cas9-mediated knockdown of endogenous TCR and subsequent transduction (g-retrovirus encoding neoantigen- or TAA-reactive TCRs) in murine CD8⁺ T cells. T cells were expanded *in vitro* for use in downstream *in vitro* and *in vivo* applications.

Results Peptide stimulation *in vitro* of neoantigen- and TAA-reactive T cells revealed wide ranges of 1) specificity (vs. cross-reactivity to wild type peptide), and 2) avidity for cognate peptide. Neoantigen- and TAA-reactive T cells were able to recognize B16F10 cells *in vitro*, with the most robust recognition (readout: % T cells IFN γ ⁺) when target antigen is highly expressed by tumor cells. Ability of neoantigen- or TAA-reactive T cells to kill B16F10 *in vitro* was strongly dependent upon both tumor antigen expression and T cells' TCR avidity. Similarly, reduction of tumor growth *in vivo* required both high tumor antigen expression and transfer of high avidity neoantigen- or TAA-reactive CD8⁺ T cells.

Conclusions To conclude, we have created a novel model of neoantigen- and TAA-reactive ACT in immunotherapy-refractory B16F10 melanoma. Our data suggest that antigen abundance and TCR avidity are parameters that influence ACT efficacy; future research will be conducted to dissect the individual and summative contributions of these parameters and translate this knowledge towards improving ACT design in the clinic.

<http://dx.doi.org/10.1136/jitc-2022-SITC2022.0364>

365

COMPARISON OF VIRAL VECTOR TRANSDUCTION METHODS FOR TUMOR-INFILTRATING LYMPHOCYTES

¹Seung Eon Oh*, ²Won Seon Bang, ²Hee Jae Lee, ³Hee Jin Lee, ²Chae Lyul Lim. ¹University of Ulsan College of Medicine, Geoje-si, Republic of Korea; ²Neogen TC, Hanam, Republic of Korea; ³Asan Medical Center, Seoul, Republic of Korea

Background Tumor-infiltrating lymphocytes (TIL) therapy has been developed and its efficacy has been proven mainly for malignant melanoma. TILs are composed of various T cell clones with T cell receptors (TCRs) that can target tumor antigens. However, TILs are highly differentiated and exhausted. To improve the efficacy of TIL therapy, engineering various genes that are associated with immune activation and persistence is necessary. We tried to find methods to increase the gene transfer efficiency using lentiviral vectors.

Methods TILs were cultured in 2 steps; initial expansion and rapid expansion (REP). For initial expansion, tumor tissue from colorectal cancer patients was minced into fragments (1-2 mm) and cultured in a 24-well plate with IL-2 for 2 weeks. Gene transfer was conducted with initially expanded TILs with a lentiviral vector with Zsgreen. IL-2 and CD3/28 beads were used and compared for stimulation. Transduction efficiency was compared between protamine and retronectin during viral transduction. We compared three conditions with protamine according to the timing of viral transduction during REP (before, in the middle of, and after). We analyzed the fluorescence expression level of Zsgreen using a flow cytometer.

Results On post-transduction day 6, transduction efficiency for IL-2 stimulation was 4.3%, while CD3/28 beads achieved 13%. The doses of CD3/28 beads were compared and set as 1:1. Transduction efficiency was higher for protamine (17%) than retronectin (1.4%). For the timing of viral transduction, transduction in the middle of REP (17%) and before REP (16.8%) showed higher transduction efficiency than transduction after REP (5.6%).

Conclusions We showed different lentiviral transduction efficiency for TILs according to culture methods. Further studies with larger sample size and optimization of the culture protocol are necessary for better application of TIL therapy.

<http://dx.doi.org/10.1136/jitc-2022-SITC2022.0365>

366

SYNTHETIC RECEPTOR ENABLED DIFFERENTIATION (SHRED), A NOVEL PLATFORM FOR MANUFACTURING OF iPSC-DERIVED CYTOTOXIC INNATE LYMPHOCYTES FOR "OFF-THE-SHELF" CANCER IMMUNOTHERAPIES

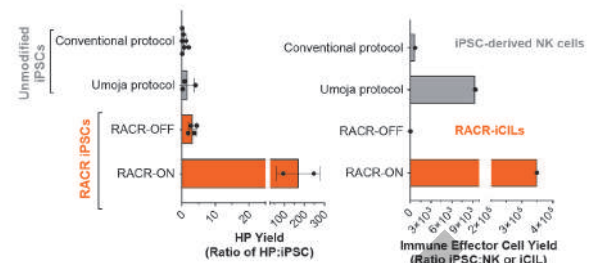
Sam O'Hara*, David Vereide, Teisha Rowland, Ashley Yingst, Dillon Jarrell, Ryan Koning, Cassidy Arnold, Susana Hernandez, Way Wu, Kristen Mittelsteadt, Chris Nicolai, Wai-Hang Leung, Shon Green, Laurie Beitz, Byoung Ryu, Christopher Garbe, Ryan Crisman, Andrew Scharenberg, Ryan Larson. *Umoja BiPharma, Boulder, CO, USA*

Background Induced pluripotent stem cells (iPSCs) are a renewable, modifiable, and scalable starting material for manufacturing cell-based therapies. However, current approaches for differentiating iPSCs into therapeutic immune effector cells, such as natural killer (NK) cells, require complex growth factors and feeder cells to achieve sufficient yields. Here, we present Synthetic Receptor Enabled Differentiation (ShRED), a directed differentiation and expansion process controlled by the Rapamycin-Activated Cytokine Receptor (RACRTM). RACR is activated via the addition of its synthetic ligand rapamycin, which induces a JAK/STAT signal that drives differentiation and expansion of cells into hematopoietic progenitors (HPs) and then into immune effector cells, termed RACR-induced Cytotoxic Innate Lymphocytes (RACR-iCILs). Furthermore, because rapamycin is a safe, effective, and approved therapeutic for immune suppression, we believe RACR can also be engaged *in vivo* through rapamycin dosing to increase the persistence of RACR-iCILs, while simultaneously protecting these cells from allogeneic rejection.

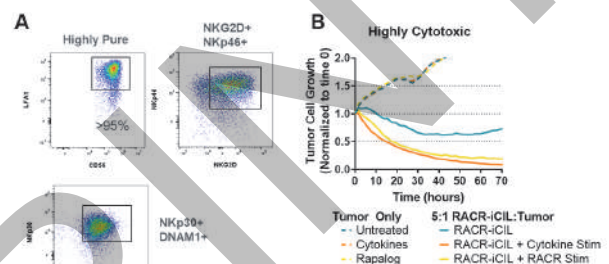
Methods RACR was introduced into iPSCs through CRISPR/Cas9 editing, enabling consistent expression of RACR throughout differentiation and expansion. Next, RACR was activated at the start of the manufacturing process, and the resulting differentiated cells were phenotyped by flow cytometry and assessed functionally in cytotoxicity assays.

Results Activating RACR in our engineered iPSCs resulted in enhanced HP differentiation, consistently producing a 300x yield of HPs (CD43+/CD45+/CD34+ cells) from iPSCs, two orders of magnitude greater than conventional protocols (figure 1). Continued engagement of RACR during differentiation resulted in >300,000x yield of RACR-iCILs (CD45+/CD56+/LFA1+ cells) from iPSCs in a completely feeder-free process (figure 1). These cells were highly pure and expressed receptors associated with NK cytotoxicity (figure 2A). Functionally, RACR-iCILs demonstrated potent cytotoxicity against solid tumors, and activation of RACR enhanced the cells' ability to clear tumor cells in a manner similar to potency-enhancing cytokines (figure 2B). Lastly, in a preclinical tumor xenograft model, RACR-NK cells demonstrated robust rapamycin-mediated expansion and clearance of breast adenocarcinoma tumors, highlighting RACR's ability to replace cytokine support and potentially increase cell persistence *in vivo*.

Conclusions These data demonstrate the potential of RACR to solve both the manufacturing and *in vivo* persistence challenges of iPSC-derived cell therapies. ShRED improves the manufacturing of iPSC-derived cells, producing unprecedented yields of immune effector cells (RACR-iCILs) and eliminating the need for complex cytokines and feeder expansions. *In vivo*, RACR activation increases the proliferation of RACR-expressing NK cells, potentially enhancing the persistence of cell immunotherapies and eliminating the need for cytokine dosing and lymphodepletion.



Abstract 366 Figure 1 Synthetic Receptor Enabled Differentiation (ShRED) enhances HP and effector cell generation to unprecedented yields.



Abstract 366 Figure 2 ShRED-generated RACR-iCILs are pure and cytotoxic against breast adenocarcinoma cells.

<http://dx.doi.org/10.1136/jitc-2022-SITC2022.0366>

367

CRISPR/CAS9 GENE-EDITED, ALLOGENEIC ANTI-CD83 CAR-T CELLS DEMONSTRATE POTENT ACTIVITY IN GVHD AND AML TUMOR MODELS

Ismael Oumzil*, Valerie Guerrero, Pooja Smruthi Keerthipati, Jaqlyn Colangelo, Brendan Lawler, Victoria Singson, Aditya Khedkar, Shweta Singh, Jonathan Terrett, Daniel Hostetter. *CRISPR Therapeutics, San Francisco, CA, USA*

Background CD83 is expressed on blood cancer cells, including acute myeloid leukemia (AML) blasts, and on allo-activated immune cells that are implicated in graft-versus-host disease (GvHD).¹ Targeting CD83 thus has the potential to improve outcomes in AML, as well as to reduce the risk of GvHD, which is a significant cause of mortality and morbidity in patients who undergo allogeneic hematopoietic cell transplant. The potential benefit of targeting CD83 is supported by literature showing that depletion of CD83+ cells in preclinical models of GvHD and AML is an effective therapeutic strategy.^{1,2}

Methods We assessed the effectiveness of CRISPR/Cas9 gene-edited, allogeneic anti-CD83 CAR-T cells against animal models of GvHD and AML, and whether additional gene edits could enhance CAR-T potency in these settings. Anti-CD83 CAR-T cells were made with *TRAC* disruption to reduce the risk of GvHD, *B2M* disruption to reduce allogeneic host rejection, and insertion of an anti-CD83 CAR construct into the *TRAC* locus. To assess whether CD83 expression on activated T cells causes CAR-mediated fratricide, the *CD83* gene was disrupted. To increase potency further, two additional gene disruptions were introduced: *ZC3H12A* (which encodes Regnase-1) and *TGFBR2* (which encodes TGFBR1).

Results We found that CD83 knockout (KO) improved the *in vitro* expansion of anti-CD83 CAR-T cells and enhanced *in vivo* activity. In a THP-1 tumor model, treatment with CD83 KO anti-CD83 CAR-T cells improved median survival when compared with wild-type cells (not reached vs. 59 days). In a xenogeneic GvHD model, CD83 KO cells were more effective at delaying GvHD at a dose of 1e6 CAR+ cells (median survival 71.5 vs. 51 days) and prevented GvHD entirely at a dose of 3e6 CAR+ cells. Activity could also be enhanced by combining CD83 KO cells with belatacept, a CTLA4-Fc fusion protein that blocks co-stimulation of T cells.

Anti-CD83 CAR-T cells with KO of Regnase-1, TGFBR1, and CD83 (R/T/83 KO cells) maintained robust expansion *in vitro*, demonstrated increased target cell killing *in vitro*, and showed enhanced *in vivo* activity. In a THP-1 tumor model, durable complete responses were observed in all animals (5/5) treated with R/T/83 KO cells and in 60% of animals (3/5) treated with CD83 KO cells. In a xenogeneic GvHD model, a single dose of 1e6 CAR+ R/T/83 KO cells prevented GvHD while CD83 KO cells delayed GvHD onset.

Conclusions Collectively, these data support the clinical evaluation of gene-edited, potency-enhanced, allogeneic anti-CD83 CAR-T cells in relapsed/refractory AML patients.

REFERENCES

1. Shrestha B, Walton K, Reff J, Sagatys EM, Tu N, Boucher J, Li G, Ghafoor T, Felices M, Miller JS, Pidala J, Blazar BR, Anasetti C, Betts BC, Davila ML. Human CD83-targeted chimeric antigen receptor T cells prevent and treat graft-versus-host disease. *J Clin Invest*. 2020; **130**:4652-4662.
2. Wilson J, Cullup H, Lourie R, Sheng Y, Palkova A, Radford KJ, Dickinson AM, Rice AM, Hart DN, Munster DJ. Antibody to the dendritic cell surface activation antigen CD83 prevents acute graft-versus-host disease. *J Exp Med*. 2009; **206**:387-398.

<http://dx.doi.org/10.1136/jitc-2022-SITC2022.0367>

368

CF33-CD19T ONCOLYTIC VIRUS (ONCARLYTICS) TARGETS HEPATOCELLULAR CARCINOMA (HCC) AND IN COMBINATION WITH ARTEMIS® CD19 T CELLS RESULTS IN SIGNIFICANT TUMOR KILLING

¹Isabel Monroy*, ¹Anthony Park, ¹Colin Cook, ²Guangyan Xiong, ²Vivien Chan, ²Cheng Liu, ¹Saul Priceman, ³Monil Shah, ³Nimali Withana, ³Leslie Chong, ¹Yuman Fong. ¹City of Hope, Duarte, CA, USA; ²Eureka Therapeutics, Emeryville, CA, USA; ³Imugene, Sydney, Australia

Background Hepatocellular carcinoma (HCC) is the second leading cause of cancer-related deaths in the world with a 5-year survival rate at less than 12%. Currently, curative treatments include ablation, surgical resection, and liver transplantation. For majority of patients with advanced-stage disease, treatment with agents such as sorafenib, lenvatinib, and atezolizumab/bevacizumab and other investigational agents yield modest success rates and justify the need for further development of new therapies. T cell therapy against HCC targeting antigens such as alpha-fetoprotein (AFP) and glypican-3 (GPC-3) have shown some efficacy in clinical trials with conventional challenges against solid tumors including antigen heterogeneity, the immunosuppressive tumor microenvironment, and off-tumor on-target activity. Therefore, novel therapies are desperately needed to improve clinical outcomes for patients with HCC.

Methods We have developed a novel chimeric vaccinia-based oncolytic virus, called onCARlytics (CF33-CD19t, Imugene Limited in collaboration with City of Hope), that delivers a non-signaling, truncated CD19t (CD19t) antigen to tumors that allows for targeting of solid tumors by CD19 T cells. Once the CD19 is expressed on solid tumor cells, to enable cell killing, we have combined onCARlytics with CD19 ARTEMIS® T cell, a CD19-targeting adoptive engineered T cell powered by the ARTEMIS® antibody-T-cell receptor (AbTCR) platform (Eureka Therapeutics, Inc). The ARTEMIS® AbTCR distinguishes itself from CAR by recruiting the endogenous CD3 complex and utilizing the same activation and regulatory signaling pathways employed by natural TCRs, which enables both potent killing activity against CD19+ tumor cells and a superior safety profile.

Results When administrated after onCARlytics, CD19 ARTEMIS® T cells were able to induce potent cytolytic activity against HCC tumor cells and demonstrated robust *in vivo* anti-tumor efficacy against human HCC tumor xenografts.

Conclusions In summary, ARTEMIS® CD19 T cells combined with onCARlytics is a potentially effective immunotherapy strategy for the treatment of patients with HCC and can be applied to other solid tumors.

<http://dx.doi.org/10.1136/jitc-2022-SITC2022.0368>

369

**ENHANCERS OF INNATE AND ADAPTIVE IMMUNITY
COMBINE WITH MEMBRANE BOUND IL15 TO INCREASE
THE EFFICACY OF TUMOR INFILTRATING LYMPHOCYTE
(TIL) THERAPY FOR TUMORS WITH
IMMUNOSUPPRESSIVE MICROENVIRONMENTS**

<http://dx.doi.org/10.1136/jitc-2022-SITC2022.0369>

Carmela Passaro*, Balazs Kosco, Sean Smith, Violet Young, Theresa Ross, Benjamin Primack, Natasha Ly, Patricia Timpug, Shabnam Davoodi, Rachel Burga, Gauri Kulkarni, Scott Lajoie, Meghan Langley, Nirzari Shah, Dexue Sun, Dan Jun Li, Raina Duan, Arman Aksoy, Mithun Khattar, Jeremy Tchaicha, Dhruv Sethi, Jan ter Meulen, Michelle Ols. *Obsidian Therapeutics, Cambridge, MA, USA*

Background The clinical impact of tumor infiltrating lymphocytes (TIL) cell products is currently limited by suboptimal persistence and potency, as well as the need for high-dose adjuvant IL-2 treatment, which is associated with severe toxicities. Thus, we engineered an IL-2-independent TIL product, based on regulated expression of interleukin 15 (cytoTIL15TM cells), which has shown anti-tumor efficacy and persistence in human melanoma PDX models. Since the immuno-suppressive tumor microenvironment (TME) hinders cell therapies, we hypothesized that combining pleotropic cytokines of the interferon (IFN), IL-1, or TNF families with IL-15 would further enhance antitumor activity and that our cytoDRiVE[®] platform would allow pharmacologic control of these potent immune mediators. We tested constitutive and regulated combinations of a representative member of these cytokines with IL-15 in human TIL for *in vitro* polyfunctionality and *in vivo* antigen-independent persistence. We also engineered mouse pmel-TCR cells with cytokine combinations for evaluation in the syngeneic B16 melanoma model.

Methods Human TIL were expanded and engineered with lentiviral vectors to express IL-15 with IFN-alpha, IL-18 (IL-1 family member) or undisclosed TNFSF-X (TNF superfamily member). Expanded TIL were immunophenotyped and assessed for polyfunctionality by flow cytometry after CD3/CD28 stimulation. Engineered TIL were transferred into NSG mice to assess antigen-independent TIL persistence in the absence of exogenous IL-2. Cytokines modified with our carbonic anhydrase 2 (CA2)-based cytoDRiVE[®] drug responsive domain (DRD) were evaluated for control of protein levels with the CA2 ligand, acetazolamide (ACZ). Cytokine expression was evaluated in flow cytometry and Meso Scale Discovery assays. To assess anti-tumor and TME remodeling capabilities, we used a syngeneic model with transduced pmel-TCR cells adoptively transferred into mice bearing B16 melanomas.

Results Engineered TIL expressing both IL-15 and either IFN-alpha, IL-18 or TNFSF-X showed similar fold expansion, immunophenotype and polyfunctionality *in vitro* as TIL expressing only IL-15. Combination cytokine-expressing TIL showed similar *in vivo* antigen-independent persistence in the absence of IL-2 as TIL engineered with only IL-15. As compared to control pmel cells, sub-optimal cell doses of pmel T cells expressing both IL-15 and either IFN-alpha or, IL-18, showed improved efficacy and TME remodeling, while combining IL-15 with TNFSF-X resulted in significant tumor growth arrest of B16 melanoma tumors without escape.

Conclusions While IL-15 drives expansion and persistence of cytoTIL15TM cells without IL-2, adding pleotropic and highly immune-stimulatory members of the IFN, IL-1 or TNF families may provide enhanced efficacy for patients with solid tumors marked by an immunosuppressive TME.

Ethics Approval All animal studies were IACUC approved

370

THE EPI-R™ TECHNOLOGY PRODUCES A POLYCLONAL TIL PRODUCT (LYL845) WITH A GREATER EXPANSION SUCCESS RATE ACROSS HOT AND COLD TUMORS, IMPROVED PRODUCT PHENOTYPE, AND MAINTENANCE OF TCR DIVERSITY

Yogin Patel*, Benjamin Harris, Melissa Bedard, Joanna Kritikou, Meritxell Galindo Casas, Carson Harms, Melissa DeFrancesco, Purnima Sundar, Nicholas Restifo, Gary Lee, Shobha Potluri, Suman Kumar Vodnala. *Lyell Immunopharma, South San Francisco, CA, USA*

Background Adoptive cell therapy (ACT) with tumor-infiltrating lymphocytes (TIL) can mediate durable responses in advanced solid tumors.¹⁻³ Effectiveness is driven by tumor-antigen recognition and maintenance of the diversity of T-cell receptors (TCR) found in the source tumor. As with all ACT, T-cell quality also impacts treatment efficacy, with more stem-like qualities associated with improved outcomes.⁴⁻⁵ Current rapid-expansion protocols reduce TIL stemness and TCR diversity through progressive differentiation during *ex vivo* expansion. Therefore, strategies that enrich for stemness and preserve polyclonality, while maintaining a high production success rate, are needed. LYL845 is an autologous TIL product produced with our proprietary Epi-R™ epigenetic reprogramming protocol, which was developed to preserve polyclonality and tumor-reactive clones and enhance stem-like qualities and anti-tumor function of manufactured TIL products.

Methods TIL products were produced from 3 different tumor types (melanoma, lung and colorectal cancer) treated with/without checkpoint inhibitors [CPI] using the Epi-R technology and standard protocol. Characteristics of the resulting products (LYL845 and control, respectively) were compared using a matrix of assays and methods, including flow cytometry, bulk RNA sequencing (RNA-seq), and TCR beta sequencing.

Results Epi-R technology resulted in 100% success rate of TIL expansion across all three tumor types, versus 70% with the control process. LYL845 was enriched for CD8+ T cells without compromising polyclonality compared to control TIL. LYL845 was also enriched for stem-like CD4+ and CD8+ T cells with reduced terminal differentiation and exhaustion, as demonstrated by flow data and transcriptomic profiling. In addition, LYL845 exhibited better metabolic fitness as evidenced by low glycolysis and hypoxia gene signatures. Metabolic fitness and enrichment of stemness indicate that LYL845 has attributes that correlated with positive clinical outcome in previous ACT trials. Furthermore, polyclonality was preserved in LYL845 as measured by Simpson clonality index using bulk TCR sequencing data. Finally, LYL845 maintained these favorable characteristics regardless of prior patient CPI use. These key product attributes were further translated to LYL845 large-scale products.

Conclusions Results from research- and large-scale productions demonstrate that the Epi-R technology enables successful TIL expansion from both immunologically hot and cold tumors, while maintaining a greater proportion of stem-like T cells that demonstrate better metabolic fitness with preserved polyclonality (i.e., maintenance of tumor-reactive TCR diversity) across all 3 tumor types investigated. These findings support the clinical development of LYL845 in an upcoming first-in-human Phase 1 clinical trial.

Acknowledgements We thank members of Lyell Immunopharma's next-gen sequencing core (Lora Zhao, Sheila Lou, Stefan Siebert and Emily Fu-Sum) and flow cytometry core (Andrew

Jimena, Elizabeth Pedrosa, Ken Xiong) for their experimental contributions

REFERENCES

1. Creelan BC, Wang C, Teer JK, *et al.* Tumor-infiltrating lymphocyte treatment for anti-PD-1-resistant metastatic lung cancer: a phase 1 trial. *Nat Med.* 2021;**27**:1410-1418.
2. Seitter SJ, Sherry RM, Yang JC, *et al.* Impact of prior treatment on the efficacy of adoptive transfer of tumor-infiltrating lymphocytes in patients with metastatic melanoma. *Clin Cancer Res.* 2021;**27**:5289-5298.
3. van den Berg JH, Heemskerk B, van Rooij N, *et al.* Tumor infiltrating lymphocytes (TIL) therapy in metastatic melanoma: boosting of neoantigen-specific T cell reactivity and long-term follow-up. *J Immunother Cancer.* 2020;**8**:e000848.
4. Krishna S, Lowery FJ, Copeland AR, *et al.* Stem-like CD8 T cells mediate response of adoptive cell immunotherapy against human cancer. *Science.* 2020;**370**:1328-1334.
5. Rosenberg SA, Yang JC, Sherry RM, *et al.* Durable complete responses in heavily pretreated patients with metastatic melanoma using T-cell transfer immunotherapy. *Clin Cancer Res.* 2011;**17**:4550-4557.

Ethics Approval Research was performed with tissues obtained from patients through a procurement protocol approved by WCG IRB, tracking number 20210857

<http://dx.doi.org/10.1136/jitc-2022-SITC2022.0370>

371

CHIMERIC ANTIGEN RECEPTOR MACROPHAGES (CAR-M) SENSITIZE SOLID TUMORS TO ANTI-PD1 IMMUNOTHERAPY

¹Stefano Pierini*, ¹Rashid Gabbasov, ¹Cecilia Nunes, ¹Alison Worth, ¹Yumi Ohtani, ¹Michael Ball, ¹Rehman Qureshi, ²Olga Shestova, ²Saar Gill, ³Serody Jonathan, ¹Sascha Abramson, ¹Thomas Condamine, ¹Michael Klichinsky. ¹*Carisma Therapeutics, Philadelphia, PA, USA*; ²*University of Pennsylvania, Philadelphia, PA, USA*; ³*UNC Lineberger Comprehensive Cancer Center, Chapel Hill, NC, USA*

Background Despite the remarkable efficacy achieved by CAR-T therapy in hematologic malignancies, application in solid tumors has been challenging. Given that CAR-M are M1-polarized macrophages with the potential to remodel the tumor microenvironment (TME) and act as professional antigen presenting cells, we developed an immunocompetent animal model to evaluate the interaction of CAR-M with the TME and the adaptive immune system. A Phase 1 FIH study evaluating the safety and feasibility of CT-0508 (a first in class CAR-M comprised of autologous human monocyte derived macrophages expressing an anti-HER2 CAR) is ongoing.¹

Methods Murine bone marrow-derived macrophages were engineered to express an anti-HER2 CAR using the chimeric adenoviral vector Ad5f35. To evaluate the safety and efficacy of CAR-M therapy, immunocompetent mice were engrafted with HER2+ tumors and treated with syngeneic CAR-M monotherapy or in combination with a PD1 blocking antibody. Tumors were collected at various time points and dynamic changes in the TME were assessed using flow cytometry, immunohistochemistry, multiplexed immunofluorescence, gene expression analysis and TCR sequencing.

Results CAR-M, but not control macrophages, phagocytosed and killed HER2-overexpressing tumor cell lines. CAR-M induced MHC-I expression on tumor cells and enhanced the cytotoxicity of CD8⁺T cells. In vivo, CAR-M led to significant tumor regression and improved overall survival in multiple syngeneic models. Analysis of the TME showed that CAR-M led to increased infiltration of intratumoral CD4⁺ and CD8⁺ T, NK, and dendritic cells as well as enhanced epitope spreading. Transcriptomic analysis of post-treatment biopsies collected from patients enrolled in the CT-0508 CAR-M Phase 1 clinical trial demonstrated remodeling of the TME, increased T cell infiltration, T cell activation/proliferation, and increased T cell clonality in the TME. In some patients, increased T cell exhaustion and increased expression of checkpoint receptors was detected post-treatment. Given these results, we evaluated the combination of CAR-M with anti-PD1 in tumors resistant to anti-PD1 monotherapy and found that the combination further reprogrammed the TME, significantly enhanced tumor control, and improved overall survival compared to monotherapy with either agent. Mice that achieved complete responses after CAR-M therapy were protected against antigen-negative relapse, indicating long-term anti-tumor immunity. Finally, the combination of CAR-M with anti-PD1 was well tolerated across numerous safety assessments.

Conclusions These results demonstrate that CAR-M reprogram the TME, induce epitope spreading, and orchestrate a systemic immune response against solid tumors. Moreover, our findings provide pre-clinical and clinical rationale for the combination of CAR-M with immune checkpoint inhibitors for the treatment of solid tumors.

REFERENCE

1. Reiss KA, Yuan Y, Ueno NT, Johnson ML, Gill S, Dees EC, Chao J, Angelos M, Shestova O, Serody JS, Priceman S, Barton D, Swaby RF, Ronczka A, Condamine

T, Cushing D, Qureshi R, Kemp M, Klichinsky M, Abdou Y. A phase 1, first-in-human (FIH) study of the anti-HER2 CAR macrophage CT-0508 in subjects with HER2 overexpressing solid tumors. *J Clin Oncol.* 2022; **40**:2533.

Ethics Approval All animal studies were approved by the IACUC (# 201364) and University Laboratory Animal Resources at the Winstar institute. Mice were treated in accordance with the Winstar institute guidelines.

<http://dx.doi.org/10.1136/jitc-2022-SITC2022.0371>

372

AGENT-797, A NATIVE ALLOGENEIC "OFF-THE-SHELF" INVARIANT NATURAL KILLER T (iNKT) CELL THERAPY PRODUCT IMPROVES EFFECTOR FUNCTIONS WITHIN THE TUMOR MICROENVIRONMENT

¹Sapana Pokharel*, ²John Chamberland, ²Yu Qin, ¹Darrian Moskowitz, ¹Reed Masakayan, ¹Xavier Michelet, ²Dhan Chand, ¹Burcu Yigit, ¹Marc Van Dijk. ¹*MiNK Therapeutics, Lexington, MA, USA*; ²*Agenus Inc, Lexington, MA, USA*

Background T cell exhaustion is a common phenomenon that occurs in the tumor microenvironment (TME) due to prolonged exposure of T cells to tumor antigen. This is in part governed by the suppressive microenvironment created by myeloid cells. Immune checkpoint inhibitors have shown promising outcomes in clinical trials treating patients with solid cancer. However, not all patients with cancer respond to checkpoint therapy, demonstrating an unmet need to optimize the current approaches including cell therapies and combination strategies. We show here that agenT-797 can reinvigorate exhausted T-cells and differentially target myeloid cells

Methods We developed a multi-platform to evaluate interaction of agenT-797 with exhausted antigen-specific T cells and myeloid cells. Briefly, we transduced pan T cells with an NY-ESO-1 specific TCR and co-cultured them for multiple rounds with melanoma cell line, A375 that endogenously expresses HLA-A*02:01 and NY-ESO-1 antigen. Killing capacity, cytokine profile and phenotype of T cells were analyzed at each round of antigen exposure. We observed progressively reduced activity with each successive round. To assess whether addition of agenT-797 rescues functional impairment of partially exhausted T cells, we performed co-culture experiments of agenT-797 (or conditioned media) with T cells and A375 cells and monitored tumor cell killing and activation of T cells. In addition, we generated M1 and M2 macrophages and DCs and co-cultured them with agenT-797 to monitor activation and killing.

Results NY-ESO-1 specific T cells with progressive degree of exhaustion show reduced proliferation and IFN γ production along with increased TIGIT expression. Upon addition of agenT-797 into co-culture (or conditioned media), we observed increased IFN-g production and activation of CD8 T cells followed by restored cytotoxic capacity of partially exhausted T cells. agenT-797 was observed to selectively kill M2 macrophages over M1 macrophages, while increasing DC activation.

Conclusions iNKT cells are known to modulate the tumor microenvironment they are part of. Immune-infiltrated tumors contain T cells in different exhaustion states as well as suppressive myeloid cells. We addressed whether iNKT cells can reinvigorate such exhausted T cells and target suppressive macrophages. Our data demonstrates that agenT-797 can improve the function of partially exhausted T cells, selectively kill M2 macrophages, and enhance DC activation in addition to exhibiting their intrinsic natural anti-tumor activity. This highlights the potential of iNKT cells as a cell therapy platform and sheds more light on the mechanisms by which they can act.

<http://dx.doi.org/10.1136/jitc-2022-SITC2022.0372>

373

COMBINATION VACCINE, ADOPTIVE NK CELL TRANSFER AND CHECKPOINT BLOCKADE REDUCE MURINE NEUROBLASTOMA PROGRESSION AFTER BONE MARROW TRANSPLANT

¹Aicha Quamine*, ¹Nicholas Mohrdieck, ¹Chloe King, ¹Anastasia Griggs, ¹Paul Bates, ¹Sean Rinella, ¹Katharine Tippins, ²Tyce Kearl, ²Byce Johnson, ¹Christian Capitini. ¹University of Wisconsin Madison, Madison, WI, USA; ²Medical College of Wisconsin, Milwaukee, USA

Background Despite use of intense multimodal therapy for treatment of high-risk neuroblastoma, poor survival outcomes persist. While autologous stem cell transplant (SCT) is standard of care for high risk patients, allogeneic SCT has been explored to produce a graft-versus-tumor (GVT) effect but has been hampered by tumor relapse and graft-versus-host disease (GVHD). We propose enhancing GVT by combining adoptive Natural Killer (NK) cells, anti-PD1 checkpoint blockade, and a neuroblastoma vaccine engineered to express CD54, CD80, CD86, and CD137L (AgN2a-4P) to stimulate donor T and NK cells.

Methods NK cells or T cells were isolated from C57BL/6 (B6) mice and expanded *in vitro* with IL-15/IL-15R α alone (NK), IL-2 (T cells) with/without AgN2a-4P for 7 days. All groups were analyzed by flow cytometry. For *in vivo* studies, on day +0, recipient mice received lethal radiation and either syngeneic (B6 to B6) or allogeneic (B6 to B6AJF1) SCT. Mice were inoculated with 9464D or NXS2 neuroblastomas to model relapse, and then treated with anti-PD1 antibody. Select groups received irradiated AgN2a-4P and/or donor-derived NK cells on days 14, 21, and 28. B6 Rag1^{-/-} mice were used as bone marrow donors to analyze the role of donor B and T cells, while select B6 recipients were injected with anti-NK1.1 every 4 days to analyze the role of NK cells. All groups were analyzed for tumor growth, GVHD and overall survival. Tumors were also analyzed for relative gene expression by bulk RNA-Seq.

Results T cells exposed to AgN2a-4P showed a significant increase in CD69, PD-1 and TIM-3 after 7 days, while NK cells exposed to AgN2a-4P expressed high levels of NKG2D and Nkp46 *in vitro*. After autologous and allogeneic SCT, combination NK cells, anti-PD1 and AgN2a-4P led to a significant decrease in tumor growth and increase in survival. Multiple NK infusions were superior to a single infusion. Usage of Rag1^{-/-} donors abrogated the benefits of combination immunotherapy on tumor growth, whereas depleting NK cells abrogated the benefits of AgN2a-4P alone more than AgN2a-4P and anti-PD1.

Conclusions AgN2a-4P vaccine activates both T and NK cells *in vitro*. Combination NK cell therapy with anti-PD1 and AgN2a-4P vaccination significantly decreases neuroblastoma tumor growth *in vivo*. T and NK cells are required for therapeutic benefit, and modulation of myeloid gene expression is observed within the TME. These studies provide the first evidence that adoptive NK cell therapy, checkpoint blockade and tumor vaccines show safety and efficacy in combination after SCT.

Acknowledgements This work was supported by grants from the NCI/NIH R01 CA215461, American Cancer Society Research Scholar grant RSG-18-104-01-LIB, St. Baldrick's – Stand up to Cancer Pediatric Dream Team Translational Research Grant SU2CAACR-DT-27-17, Hyundai Hope on Wheels and the MACC Fund (C.M.C). We would like to thank the UWCCC core facilities, who are supported in part through NCI/NIH P30 CA014520. Stand Up to Cancer is a

division of the Entertainment Industry Foundation. Research Grants are administered by the American Association for Cancer Research, the Scientific Partner of SU2C.

Ethics Approval The animal study M005915 was reviewed and approved by University of Wisconsin-Madison IACUC.

<http://dx.doi.org/10.1136/jitc-2022-SITC2022.0373>

374

DISCOVERY OF A PUBLIC HPV16-E6 DIRECTED T CELL RESPONSE THAT IS ASSOCIATED WITH OVERALL AND PROGRESSION FREE SURVIVAL

¹Klaudia A Szymonowicz, ¹Bo Jiang, ²Laurene Cheung, ¹Weihong Xiao, ¹Alexa J Halliday, ¹Emily Bontekoe, ¹Keiko Akagi, ¹Gregory Lizee, ²Kellie Smith, ¹Maura Gillison, ¹Nils-Petter Rudqvist*. ¹The University of Texas MD Anderson Cancer Center, Houston, TX, USA; ²Johns Hopkins School of Medicine, Baltimore, MD, USA

Background Human papillomavirus (HPV) infection causes at least 650,000 anogenital and oropharyngeal cancers (OPC) worldwide annually. Despite the viral immunological target, immune checkpoint inhibitors produce responses only in a minority of patients, and cancer therapies that directly target HPV-antigens represent an attractive alternative therapeutic approach. With this work, we introduce a high-throughput and epitope-agnostic pipeline for HPV16-reactive T cell discovery and validation.

Methods Using the FEST assay [1], T cell responses against HPV16 were assessed in 3 patients with HPV16-positive OPC that participated in an open-label phase I clinical trial studying the safety and immunogenicity of vaccination with a DNA-based HPV16-E7 vaccine. T cell receptor (TCR) motifs were constructed using GLIPH2 [2]. Enrichment of motifs in tumors and HLA alleles among patients was determined using Wilcoxon signed-rank test and Fisher Exact test, respectively. Association between TCR motifs and survival was assessed using a log-rank test. Single cell sequencing (sc-seq) was performed using the 10x platform. Expression of TCRs in effector cells was achieved using electroporation. All studies were approved by MD Anderson IRB (PA17-0149, PA19-0470, and 2019-1059).

Results Sixteen HPV16-reactive TCRs were identified in 3 patients with HPV16-positive OPC, and responses were found against most HPV16 proteins. Five clones were associated with commonly shared TCR motifs identified in our combined patient cohort. A TCR motif against HPV16-E6 (E6-TCR-motif) was found enriched in tumors ($p=0.007$; figure 1) of patients who expressed a common HLA allele ($p=0.0019$; figure 2). Strikingly, no patients that naturally harbor the E6-TCR-motif died ($p=0.04$) nor progressed ($p=0.023$; figure 3). Recognition of a region within E6 by a T cell belonging to the E6-TCR-motif was validated via transgenic TCR expression in Jurkat cells co-cultured with HLA-matched peptide-pulsed target cells, and eventually the minimal epitope was determined. Impressively, an interaction between TCR and epitope was still detectable at 10^{-15} M peptide concentration, a factor 1000 lower compared to our positive control TCR [3] against HPV16-E6 (figure 4).

Conclusions We have identified a common HPV16-E6 specific TCR motif shared among patients with HPV16-positive OPC cancer that is associated with survival. We are currently working to translate this finding to the clinic as an adoptive cellular therapy. Given the success of this approach, we are working to map the antigenic/TCR landscape in patients with HPV16-positive tumors, with the goal of developing a suite of TCR-based therapies restricted to common HLA alleles and to construct a therapeutic vaccine against persistent HPV16 infection.

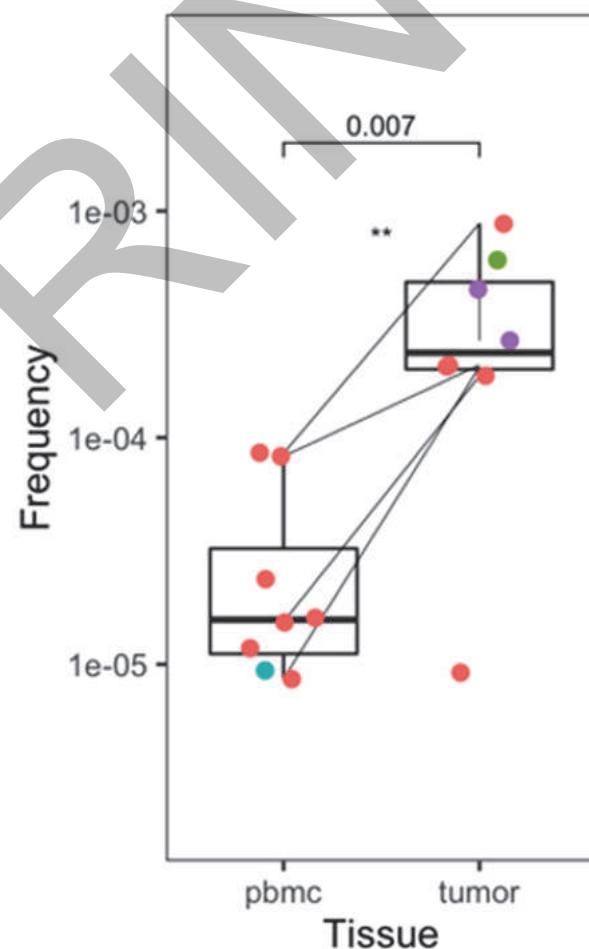
Acknowledgements This research was supported by The University MD Anderson HPV-Related Cancers Moon Shot, the MD Anderson Oropharynx Cancer Program, and Intramural Startup funds. FEST assays were performed by the FEST and TCR Immunogenomics core at Johns Hopkins University. We

would also like to thank Drs. Alexandre Reuben and Mingying Zhang for sharing reagents.

REFERENCES

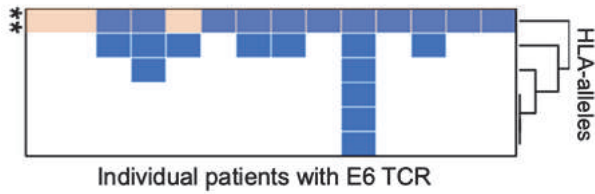
1. Danilova L, Anagnostou V, Caushi JX, Sidhom JW, Guo H, Chan HY, Suri P, Tam A, Zhang J, Asmar ME, Marrone KA, Naidoo J, Brahmer JR, Forde PM, Baras AS, Cope L, Velculescu VE, Pardoll DM, Housseau F, Smith KN. The mutation-associated neoantigen functional expansion of specific T cells (MANAFEST) assay: A sensitive platform for monitoring antitumor immunity. *Cancer Immunol Res.* 2018;**6**:888-899.
2. Huang H, Wang C, Rubelt F, Scriba TJ, Davis MM. Analyzing the Mycobacterium tuberculosis immune response by T-cell receptor clustering with GLIPH2 and genome-wide antigen screening. *Nat Biotechnol.* 2020; **38**:1194-1202.
3. Draper LM, Kwong ML, Gros A, Stevanović S, Tran E, Kerkar S, Raffeld M, Rosenberg SA, Hinrichs CS. Targeting of HPV-16+ epithelial cancer cells by TCR gene engineered T cells directed against E6. *Clin Cancer Res.* 2015; **21**:4431-4439.

Ethics Approval All studies were approved by MD Anderson IRB (PA17-0149, PA19-0470, and 2019-1059).

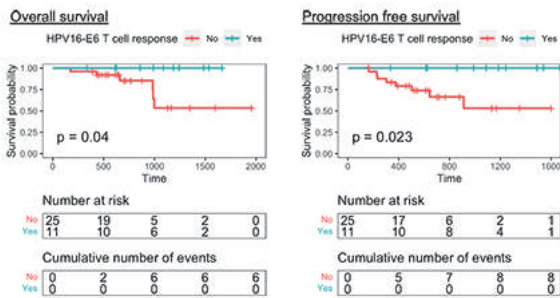


Abstract 374 Figure 1 HPV16-E6 TCR motif is enriched in tumors of patients with HPV16-positive oropharyngeal cancer. Frequency of T cell clones that belong to the HPV16-E6 TCR motif constructed using the GLIPH2 algorithm is shown. Statistical significance was determined using a Wilcoxon signed-rank test. Color represents data source (not shown). Line indicates paired tumor and blood data.

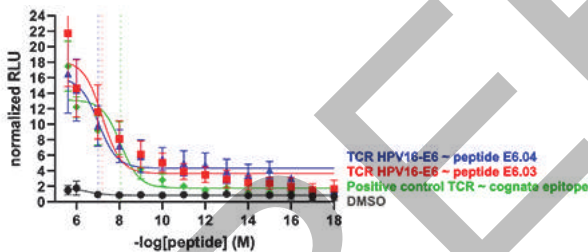
Abstracts



Abstract 374 Figure 2 Specific HLA-allele is enriched among patients that harbor HPV16-E6 TCR motif. Rows represent a specific HLA allele, columns represent individual patients. Enriched HLA allele is highlighted in orange (top row). Statistical significance was calculated using Fisher Exact test; ** indicate p-value < 0.01.



Abstract 374 Figure 3 Harboring the HPV16-E6 TCR motif is associated with survival. Natural presence of T cells from the HPV16-E6 TCR motif in tumors and/or blood was associated with overall (left) and progression free (right) survival in HPV16-positive oropharyngeal cancer patients that express the shared HLA allele.



Abstract 374 Figure 4 HPV16-E6 TCR motif T cells recognize their cognate epitope with high sensitivity. A full-length paired TCR belonging to the E6-TCR motif was expressed in Jurkat T cells without endogenous TCR expression and that has been genetically modified to produce luciferase upon TCR engagement. Peptide-pulsed and HLA-matched CD3 PBMC was used as target cells. DMSO (negative control) is shown in black and a positive control TCR that recognize the HPV16-E629-38 epitope [3] is shown in green. Blue and red represent the HPV16-E6 TCR we have discovered when pulsed with two different 15 amino acid long peptides that share a region of 11 amino acids; the minimal epitope reside in the overlapping region.

<http://dx.doi.org/10.1136/jitc-2022-SITC2022.0374>

375 **IN VIVO GENERATION OF UNIVERSAL CAR T CELLS THAT MEDIATE DURABLE ANTI-TUMOR IMMUNITY THROUGH COMBINATORIAL TARGETING WITH BISPECIFIC SMALL MOLECULE ADAPTERS**

Kristen Mittelsteadt*, Isabel Leung, Kelsey Lynch, Haiyan Chu, Chang-Chih Wu, Seungjin Shin, Ryan Larson, Andrew Scharenberg, Byoung Ryu, Laurie Beitz. *Umoja Biopharma, Seattle, WA, USA*

Background Chimeric antigen receptor (CAR) T cell therapies have demonstrated limited efficacy against solid tumors, in part due to challenges overcoming solid tumor heterogeneity and CAR T cell exhaustion associated with the immunosuppressive tumor microenvironment (TME). Our integrated platform aims to overcome these roadblocks by engineering T cells in vivo to express a universal TagCAR which binds to a common tag on bispecific adaptor TumorTags, bridging TagCAR T cells to TumorTag-bound tumor- and TME-associated antigens, including folate receptor (FR) which is upregulated on many tumor types as well as immunosuppressive tumor-associated macrophages. Additionally, our TagCAR T cells are engineered to express a rapamycin-activated cytokine receptor (RACR) which selectively provides survival signals to TagCAR T cells in the presence of rapamycin. Here, we identify a universal TagCAR that demonstrates potent in vitro and in vivo anti-tumor polyfunctionality against FR⁺ target cells with a folate receptor-targeting TumorTag (UB-TT170).

Methods PBMCs from healthy donors were transduced in vitro with surface-engineered lentiviral vectors with TagCAR/RACR payloads. Resultant TagCAR T cell anti-tumor activity and persistence was assessed using a co-culture approach with FR-expressing tumor cells and titrated doses of UB-TT170. To assess in vivo anti-tumor activity, lentiviral particles containing TagCAR/RACR payloads were administered to PBMC-humanized NSG mice with established FR⁺ xenograft solid tumors to generate TagCAR T cells in vivo. Mice were treated with UB-TT170 and efficacy was determined by assessing tumor regression and UB-TT170-mediated TagCAR T cell expansion.

Results TagCAR T cells containing a CD8 α hinge/transmembrane domain and 41bb ζ endodomain were superior to other construct candidates in eliminating FR⁺ target cells in the presence of UB-TT170 in vitro. These TagCAR T cells demonstrated UB-TT170-mediated expansion and proinflammatory cytokine production in the presence of FR⁺ target cells, and repeated elimination of target cells and enhanced persistence properties with serial antigen-exposure. Cells transduced with this vector exhibited RACR-mediated expansion and improved function in the presence of rapamycin. Administration of TagCAR/RACR payload-containing lentiviral particles to PBMC-humanized NSG mice resulted in generation of TagCAR T cells in vivo, which expanded and mediated clearance of FR⁺ solid tumors with UB-TT170.

Conclusions We have identified a universal TagCAR that displays robust anti-tumor activity and persistence qualities against FR⁺ target cells in vitro and in vivo with UB-TT170. These data support development of this platform as a new cellular therapy approach against solid tumors, using combinatorial targeting of tumor- and TME-associated antigens with an in vivo-generated universal TagCAR and multiple TumorTags.

<http://dx.doi.org/10.1136/jitc-2022-SITC2022.0375>

376 **MACROPHAGES ENGINEERED TO EXPRESS SYNTHETIC CYTOKINE SWITCH RECEPTORS ACT AS LIVING MICROENVIRONMENT CONVERTERS**

Chris Sloas*, Yuhao Huangfu, Thomas Condamine, Michael Klichinsky, Yumi Ohtani. *Carisma Therapeutics, Philadelphia, PA, USA*

Background Cytokines in tissue microenvironments regulate the balance between pro- and anti-inflammatory signaling. Dysregulated cytokine expression causes deleterious immunosuppression or inflammation, underpinning the pathophysiology of numerous diseases. As examples, anti-inflammatory cytokines in solid tumors suppress immune activation and safeguard the tumor, whereas pro-inflammatory cytokines in rheumatoid arthritis drive chronic inflammation. Rebalancing inflammation/immunosuppression by targeting aberrant cytokine signaling offers a generalizable approach to treating many diseases, but systemic cytokine blockade carries risks such as increased risk of infection. Cellular immunotherapies may offer a localized platform that could activate in response to cytokines then proportionately remodel the microenvironment's inflammatory state as needed. Macrophages are tissue-infiltrating homeostatic regulators responsible for initiating and resolving inflammation. Engineered macrophages have demonstrated a promising ability to target tumor cells utilizing chimeric antigen receptors. Here, we leveraged the ability of macrophages to regulate inflammation by generating macrophages that express synthetic cytokine switch receptors. We termed this platform "Engineered Microenvironment Converters" (EM-C) and evaluated its modular ability to convert immunosuppressive M2 signals into pro-inflammatory M1 responses for solid tumor microenvironment conversion, or *vice versa* for inflammatory disease.

Methods EM-C were generated by expressing switch receptors (SR) in primary human macrophages. To convert IL10, a prevalent immunosuppressive cytokine in the TME, into a pro-inflammatory signal, an IL10 SR was designed and delivered to macrophages using VPX-Lentiviral particles. The *in vitro* response of IL10 EM-Cs to IL10 was monitored using phenotypic characterization of surface molecules, measurement of cytokine production, and biochemical analysis of downstream signaling. To assess the ability of EM-Cs to alter the inflammatory status of their environment, *in vitro* co-culture assays were established with M2-polarized bystander cells, and the phenotype of bystanders and EM-Cs was assessed individually. Similarly, EM-Cs targeting TGF β or IFN γ were characterized.

Results IL10 EM-Cs converted IL10 into a pro-inflammatory signal. Unlike wildtype macrophages, IL10 EM-Cs treated with IL10 upregulated M1 markers and cytokines in a dose-dependent manner. Furthermore, IL10 EM-Cs repolarized bystander M2 macrophages towards a pro-inflammatory phenotype following co-culture. Additionally, TGF β EM-Cs were generated and converted TGF β to a pro-inflammatory signal. IFN γ EM-Cs were generated and converted IFN γ , a canonical M1 cytokine, into an M2 signal.

Conclusions We present for the first time a novel immunotherapy platform that harnesses macrophages as "living converters" to locally regulate inflammation for oncology and inflammatory applications. By demonstrating EM-Cs in the M2-to-M1 and M1-to-M2 direction, this platform offers modularity in controlling the inflammatory status of tissue microenvironments without systemic cytokine antagonism.

<http://dx.doi.org/10.1136/jitc-2022-SITC2022.0376>

377

ADOPTIVE CELL THERAPY WITH CYTOKINE-INDUCED KILLER CELLS RETARGETED WITH IMMUNOTOOLS AGAINST HER-2 POSITIVE BREAST CANCER

¹Roberta Sommaggio*, ²Elisa Cappuzzello, ²Annavera Ventura, ²Sara Perpinello, ¹Anna Dalla Pietà, ²Emilia Vigolo, ²Giulia D'accordio, ¹Pierangela Palmerini, ¹Antonio Rosato. ¹University of Padova, Padova, Italy; ²Veneto Institute of Oncology IOV-IRCCS, Padova, Italy

Background Cytokine-Induced Killer (CIK) cells are a heterogeneous population of CD3⁺CD56⁺ effector cells easy to expand from PBMCs in clinically relevant numbers, which are endowed with T and NK cells phenotypic and functional properties.¹ They show an MHC-unrestricted cytotoxicity and exert Antibody-Dependent Cell-mediated Cytotoxicity (ADCC) when combined with monoclonal antibodies (mAbs).² In the present study, CIK cells were combined either with Trastuzumab (TRS) or with the engineered TRS V90Lec13, which bears two amino acid substitutions (S239D/I332E) and lacks Fc fucosylation or with a bispecific antibody (bsAb) directed against HER-2 and CD3 (HER2xCD3).

Methods CIK cells were obtained from PBMCs by the addition of IFN γ , OKT3 and IL-2. The effector cell cytotoxicity and the dose-dependent activity of HER2xCD3 and TRS V90Lec13 were evaluated with a 4-hours Calcein-AM assay and with a 72-hours real-time cell analysis against HER-2-expressing breast cancer cell lines. The concentration of cytokines produced upon the co-culture of CIK cells with target cells was assessed with a multiplex assay. The biodistribution of the bsAb was evaluated in NSG mice upon the chemical conjugation of HER2xCD3 with a fluorophore.

Results The combination of CIK cells with HER2xCD3 or TRS V90Lec13 resulted in a significant improvement of the antigen-specific cytotoxic activity against breast cancer cell lines when compared to the combination of CIK cells with clinical mAb TRS. In particular, the real time analysis showed that even at a very low effector/target (E/T) ratio, such as 0.1:1 E/T ratio, CIK cells combined with HER2xCD3 showed a remarkable cytotoxicity, completely restraining target cells growth. Interestingly, TRS-resistant tumor cell lines showed to be sensitive to HER2xCD3-redirectioned CIK cell lytic activity. Moreover, bsAb resulted to be effective also at very low concentrations, and the cytokines released from CIK cells matched with a proinflammatory profile, with no significant concentration of cytokines correlated with Cytokines Release Syndrome (CRS), such as IL-6 and IL-5. The analysis of the *in vivo* biodistribution showed that the bsAb arrives efficiently at the tumor site where accumulates and reaches the maximum concentration 8 hours after i.v. injection.

Conclusions Taken together, these results highlight the potentiality of using recombinant immunotools to improve the antigen-specific cytotoxic activity of CIK cells against HER-2 positive tumor cells.

REFERENCES

1. Cappuzzello E, Sommaggio R, Zanovello P, Rosato A. Cytokines for the induction of antitumor effectors: The paradigm of Cytokine-Induced Killer (CIK) cells. *Cytokine Growth Factor Rev.* 2017; **36**:99-105.
2. Dalla Pietà A, Cappuzzello E, Palmerini P, Ventura A, Visentin A, Astori G, Chieragato K, Mozzo V, Perbellini O, Tisi MC, Trentin L, Visco C, Ruggeri M, Sommaggio R, Rosato A. Innovative therapeutic strategy for B-cell malignancies that combines obinutuzumab and cytokine-induced killer cells. *J Immunother Cancer.* 2021;**9**:e002475.

Ethics Approval Patient samples were obtained after written informed consent from Padua Hospital, Italy (Ethical Committee act n. 3529/AO/14). All the procedures involving animals

and their care were in conformity with institutional guidelines that comply with national and international laws and policies (D.L. 26/2014 and subsequent implementing circulars), and the experimental protocol (Authorization n. 118/2019-PR) was approved by the Italian Ministry of Health.

<http://dx.doi.org/10.1136/jitc-2022-SITC2022.0377>

378

CHIMERIC ENGULFMENT RECEPTOR (CER) T CELLS WITH A TLR2 DOMAIN SYNERGIZE WITH AN EGFR INHIBITOR TO TARGET NSCLC CELLS IN VITRO AND DEMONSTRATE APC-LIKE FUNCTION

Sunil Thomas*, Harini Kethar, Linh Nguyen, Brandon Cieniewicz, Alex Arballo, Priya Baichoo, Damoun Torabi, Ankit Bhatta, Daniel Corey. *Cero Therapeutics, South San Francisco, CA, USA*

Background A barrier to successful adoptive cell therapy for solid tumors is target antigen heterogeneity and antigen escape. Activated T cells, including CAR T cells, have limited innate antigen capture/presentation capabilities.¹ We engineered a novel TIM-4 CER that bears a toll/interleukin-1 (TIR) signaling domain from TLR2 designed to induce both direct cell-mediated cytotoxicity and initiate secondary immune responses, leading to improved solid tumor clearance and durability of response. CER-T cells offer potential pairing with multiple small molecule drugs to enhance the TIM-4 target ligand. We tested for antigen-presenting cell (APC)-like function, characterized transcriptional signatures, and quantified cytotoxic responses against EGFR-mutant NSCLC cells in combination with the epidermal growth factor inhibitor (EGFRi) osimertinib.

Methods CER-1236 contains a TIM-4 extracellular signaling domain fused with a TLR2-TIR domain, CD28 and CD3zeta. Using PS-coated beads labeled with a pH-sensitive dye (pHrodo), we quantified CER-1236 phagocytic uptake by FACs and fluorescent microscopy. Cytotoxic and proliferative responses against osimertinib-treated H1975 NSCLC cells was tested in vitro. We quantified APC activity by evaluating autologous HPV E7 TCR T cell activation and proliferation following CER-1236 co-culture with HLA-matched HPV-16 E7+ SCC152 tumor cells. To characterize transcriptional states, we performed bulk RNA-sequencing at rest and following activation. TLR2 inhibition was used to examine signaling pathway induction.

Results In combination with subtherapeutic osimertinib doses, CER-1236 eliminated 97% of targets by 72h at low effector:target ratios. EGFR inhibition drove target-dependent proliferation, production of TH1 cytokines (IFN-gamma, TNFalpha) and granzyme-B. Upon co-culture with PS-coated beads, 60% of CER-1236 T cells demonstrated increased bead uptake compared to untransduced or CER T cells expressing a TIM-4 PS-binding mutant ($p < 0.0001$), APC assays demonstrated higher activation of E7-TCR T cells by CER-1236 than untransduced T cells, indicating occurrence of antigen uptake and presentation. Both cytokine production and antigen presentation were inhibited by a TLR2 inhibitor. Finally, transcriptional profiling identified a distinct signature related to APC-like function upon CER-1236 stimulation with enrichment of NF-kB, MAP kinase, TNFalpha and chemokine signaling.

Conclusions Novel TIM-4-containing CER T cells that include a TLR2 signaling domain synergize with osimertinib to eliminate EGFR-mutant NSCLC cells in vitro. Notably, CER T cells capture and present tumor cell antigen, and demonstrate APC-like transcriptional signatures. Antigen presentation, alongside inducible, target-specific cytotoxic function in single T cells, represent a potential advantage to initiate host immune responses against novel antigens for solid tumors.

Acknowledgements The authors would like to acknowledge Edson Oliveira, Phani Kukutla and the CERo team for helpful suggestions.

REFERENCE

1. Lanzavecchia A, Roosnek E, Gregory T, Berman P, Abrignani S. T cells can present antigens such as HIV gp120 targeted to their own surface molecules. *Nature*. 1988; 334:530–532.

<http://dx.doi.org/10.1136/jitc-2022-SITC2022.0378>

379 ENGINEERING OF GAMMA/DELTA T CELLS DERIVED FROM CORD BLOOD FOR CHIMERIC ANTIGEN RECEPTOR-T CELL THERAPIES

¹Chelsia Qiuxia Wang*, ²Alice Cheung, ¹Andy Hee-Meng Tan. ¹*Bioprocessing Technology Institute (BTI), Singapore, Singapore;* ²*Singapore General Hospital (SGH), Singapore, Singapore*

Background Adoptive cellular immunotherapy as a new paradigm to treat tumors is exemplified by the FDA approval of six different chimeric antigen receptor (CAR)-T cell therapies targeting hematological malignancies in recent years. Conventional alpha/beta (ab) T cells applied in these therapies have proven efficacy but with hitherto disappointing outcomes when applied to solid tumors, largely due to poor survival and reduced efficacy of CAR-T cells in the immunosuppressive solid tumor microenvironment (TME). Moreover, these therapies are confined exclusively to autologous use since, upon infusion, they elicit devastating graft-versus-host disease (GvHD) in human leukocyte antigen (HLA)-mismatched patients. One way to overcome these challenges is to use allogeneic immune cell types, in particular gamma/delta (gd) T cells, which occupy the interface between innate and adaptive immune cells and recognize a wide variety of ligands expressed on transformed cells. Importantly, specific gd T cell subsets such as Vd1 T cells, have a natural propensity to home to solid tissues.

Methods We propose to harness these characteristics of gd T cells by generating CAR-T cells using cord blood (CB)- compared with peripheral blood (PB)-derived gd T cells. We expanded CB- and PB-gd T cells using a feeder cell-based protocol and transduced them with a HER2-targeting CAR bearing CD28 co-stimulatory endodomain and CD3z activation domain (4D5-28z CAR) via two-step retrovirus-based delivery. Both *in vitro* and *in vivo* cytotoxicity of 4D5-28z CB- and PB-gdT cells against selected solid tumor cell lines were assessed using bioluminescence-based methods.

Results We found that CB-gd cells were less amenable to CAR transduction, resulting in substantially lower frequencies of CAR-positive CB-gd T cells compared with PB-gd counterparts. Efforts are underway to optimize transduction to enhance CAR expression in CB-gd T cells. Despite fewer CAR-positive CB-gd T cells, we consistently observed that these cells exhibited increased *in vitro* cytotoxicity against SK-OV-3 ovarian tumor cells compared with non-CAR counterparts. However, our preliminary results demonstrated that both CAR- and non-CAR CB-gdT cells lacked persistence *in vivo*, alluding to the need for further genetic modifications of gd CAR-T cells to secrete cytokines which can help them overcome the immunosuppressive effects of TME and improve their *in vivo* functionality.

Conclusions Taken together, our findings highlight the potential of CB-gd T cells in allogeneic CAR immunotherapy by increasing the efficiency of their genetic engineering and *in vivo* anti-tumor efficacy.

Acknowledgements We thank staff of the Biological Resource Centre (BRC) for care and maintenance of mice and members of the laboratory for insightful discussions.

Ethics Approval Experiments with mice were approved by the Institutional Animal Care and Use Committee (IACUC) at BRC, A*STAR.

<http://dx.doi.org/10.1136/jitc-2022-SITC2022.0379>

Abstracts

380

DEVELOPMENT AND CHARACTERIZATION OF A CAR T CELL POTENCY ASSAY WITH 3D CANCER SPHEROID MODELS

Omari Weems, Denise Sullivan, Austin Passaro*, Stacie Chvatal, Daniel Millard. *Axion Biosystems, Atlanta, GA, USA*

Background The tumor microenvironment poses a significant challenge to immune therapies, like CAR T cells, for solid tumor indications. Development of in vitro 3D models may provide a more accurate assessment of CAR T potency. Here, we developed a real-time, label-free potency assay for evaluation of CAR T cell-mediated cytotoxicity of 3D cancer spheroids.

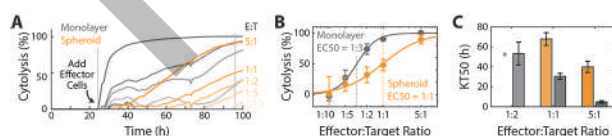
Methods In this study, the Maestro Z impedance system was used to develop a real-time, label-free potency assay for immune-cell mediated killing of 3D cancer spheroids. Cancer spheroids were produced with SKOV3 cells in ultra-low attachment U-bottom microplates for four days and then transferred to the CytoView-Z plate. The attachment and growth of SKOV3 spheroids was monitored using the resistance measurement of the Maestro Z. After 24 hours, the SKOV3 spheroid and monolayer groups were treated with HER2-specific CAR T cells at matched effector-to-target cell ratios and cytotoxicity was computed for the following 72 hours of real-time measurement.

Results The spheroid potency assay was used to compare CAR T cell-mediated cytotoxicity of SKOV3 spheroids and monolayer cultures with HER2-specific CAR T cells. The steady increase in resistance for the untreated group indicated continued spheroid growth after transfer to the CytoView-Z 96-well plate. CAR T effector cells were added at five E:T ratios at 24 hours post-plating of the target cells. The monolayer groups (gray) had higher rates of cytotoxicity than their respective spheroid groups (orange) for the same E:T ratios (figure 1A). Cytotoxicity was compared at 72 hours post-addition of the CAR T effector cells (figure 1B) and potency was quantified via a dose response regression. The EC₅₀ E:T ratio of the HER2-specific CAR T cells was 1:3 for the monolayer target cells and 1:1 for the spheroid target cells. These results suggest a decreased potency of HER2-specific CAR T cells against a 3D tumor model in vitro. CAR T potency was also evaluated via the KT₅₀, a measure of the kinetics of immune cell-mediated killing (figure 1C). There was a dose dependence of CAR T killing within the monolayer and spheroid groups, with monolayer groups having shorter KT₅₀s than the matched spheroid groups.

Conclusions These results suggest that 3D cancer spheroid had a higher resistance to CAR T killing than monolayer cultures, which may reflect an improved representation of the tumor microenvironment for an in vitro potency assay.

both groups and differences in duration to achieve 50% cytotoxicity between groups. *indicated 1:2 spheroid group did not reach a KT₅₀.

<http://dx.doi.org/10.1136/jitc-2022-SITC2022.0380>



Abstract 380 Figure 1 CAR T cells exhibit reduced cytotoxicity against spheroids

(A) Cytotoxicity over time of 10k SKOV3 spheroids and monolayers treated with 4-1BB (HER2 targeting) CAR T cells at effector-target ratios of 1:10, 1:5, 1:2, 1:1, and 5:1. (B) Cytotoxicity between spheroids and monolayer in respect to their effector-target ratios. EC₅₀ measured the 4-1BB CAR T ratio required to achieve 50% cytotoxicity. (C) KT₅₀ between spheroids and monolayer groups, displaying both dose dependence for

381 **LARGE-SCALE EXPANSION AND ENGINEERING OF HUMAN NK CELLS SOURCED FROM PERIPHERAL BLOOD VERSUS UMBILICAL CORD BLOOD**

Michael Whang*, Ming-Hong Xie, Kate Jamboretz, Chang Kim, Sombeet Sahu, Hadia Lemar, Nafees Rahman, Ivan Chan, Erik Whiteley, Ralph Brandenberger, Sasha Lazetic, James Trager. *Nkarta Therapeutics, South San Francisco, CA, USA*

Background Healthy adult peripheral blood natural killer (PBNK) cells are mature cytotoxic innate lymphocytes possessing an inherent capacity for tumor cell killing, making them attractive candidates for adoptive cell therapy. These NK cells are also amenable to chimeric antigen receptor (CAR) genomic engineering for enhanced functions. Moreover, NK cells possess an inherent capacity for off-the-shelf therapy since they are not known to cause graft-versus-host disease, unlike T cells. Approved CAR cell therapies are custom-made from each patient's own T cells, a process that can limit patient eligibility and contribute to product variability. In this study, we compare PBNK cells to umbilical cord blood NK (CBNK) cells to evaluate both as candidate starting materials for clinical and commercial supply of CAR NK cells.

Methods PBNK and CBNK cells were expanded using either a 14-day protocol and a single stimulation with Nkarta's NKSTIM cell line plus IL-2, or with 5 stimulations over 70 days.¹ IL-12 and IL-18 were added at the beginning and end of the 70-day expansion to drive memory-like NK cell differentiation. We transduced NK cells to express CD19-targeted CAR and membrane-bound IL-15 following the first NKSTIM pulse. We measured cytotoxicity against 3 tumor cell lines by IncuCyte, and phenotyped cells for NK markers including differentiation markers CD57 and NKG2C, and NKG2A and KIR.

Results Purified NK cells from 1 PBNK donor and 4 CBNK donors were successfully expanded and engineered to express high levels of CAR. The 70-day final product (FP) CBNK cells were CD57^{KIR^{lo/-}} and NKG2A⁺, consistent with an immature phenotype, whereas the FP PBNK cells were educated, at more than 80% NKG2A⁺ KIR⁺. CBNK cells expanded to approximately 11-million-fold, whereas PBNK cells surpassed 250-billion-fold expansion, without appearing to have reached a terminal expansion limit. At the end of the study, Nkarta's standard 14-day process (SP) cells [1], and FP PBNK cells were as potent or trended towards greater potency than CBNK cells against 3 different tumor targets in a 72-hour IncuCyte assay. Furthermore, FP PBNK cells were as or more potent than SP PBNK cells, depending on the tumor target.

Conclusions We demonstrate healthy donor-derived PBNK cells can expand over 250 billion-fold while maintaining potency. These results show robust expansion capability of educated, potent NK cells and provide a rationale for the development of off-the-shelf CAR NK cell therapies using NK cells from donors selected to provide optimal product characteristics.

REFERENCE

1. Whang M, Xie M, Jamboretz K, Lamar H, Guo C, Rahman N, Chan I, Whiteley E, Brandenberger R, Lazetic S, Trager J. 151 Potentiating the large-scale expansion and engineering of peripheral blood-derived CAR NK Cells for off-the-shelf application. *J Immunother Cancer*. 2021; **9**: 151.

<http://dx.doi.org/10.1136/jitc-2022-SITC2022.0381>

382

A NOVEL PERIPHERAL BLOOD MONONUCLEAR CELL HUMANIZED MOUSE MODEL FOR PRECLINICAL EFFICACY AND TOXICITY EVALUATION OF CHIMERIC ANTIGEN RECEPTOR T-CELL IMMUNOTHERAPY

¹Jiwon Yang*, ¹Won Lee, ²Heather Gustafson, ²Blair Amrstrong, ²Katelym Burleigh, ¹Mingshan Cheng, ¹James Keck. ¹The Jackson Laboratory, Sacramento, CA, United States; ²Seattle Children's Research Institute, Seattle, WA, United States

Background Chimeric antigen receptor T (CAR T)-cell therapy has emerged as a revolutionary treatment for certain hematological malignancies. While several CAR T therapies showed an efficacious response in selected patients, wider adoption of the therapy is challenged due to toxicity which can be life-threatening, and high relapse potentials (~50%). Clinically we are unable to predict CAR T-cell therapy-associated toxicities and efficacy and thus, need to be addressed and modeled at the individual level. Here, we developed a novel peripheral blood mononuclear cell (PBMC)-humanized mouse model to assess the efficacy and toxicity of CAR T-cell therapy simultaneously. This model reflects individual donor variations recapitulating observed clinical levels of toxicity and efficacy.

Methods NSG™ variants, including NSG™-MHC I/II-double knock-out mice that show delayed graft-versus-host disease, were humanized using human PBMCs. PBMC-humanized mice were treated with autologous CAR T-cells targeting CD19, and efficacy, toxicity, and CAR T-cell expansion were assessed. To evaluate these parameters in the presence of tumors, humanized mice were injected with luciferase-tagged human B-cell lymphoma Raji tumor cells.

Results Autologous CD19 CAR T-cell treatment in highly humanized mice showed significant mortality compared to the PBS treatment. When the humanization level was optimized by adjusting the number of PBMCs, the humanized mice showed great efficacy by reducing the target cells in the blood and spleen, and significant human cytokine release, including IFN- γ , IL-10, IL-6, IL-3, and RANTES. This model measures differential toxicity, human cytokine release, and CAR T-cell expansion in different PBMC donors, suggesting that the model can address the individual difference. In the presence of tumor, CAR T-cell treatment induced significantly higher human cytokines (IL-10: ~12,000 pg/mL, IL-6: ~850 pg/mL), as well as greater CAR T-cell expansion, compared to the mice without the tumor.

Conclusions In summary, we have developed a novel humanized mouse model to test the preclinical efficacy and toxicity of CAR T-cell immunotherapy. The assay is rapid that can be completed in 12-16 days. The model captures donor variability and CAR T dose-response, in both efficacy and toxicity, such as cytokine release and body weight loss. Our novel humanized mouse model can potentially be used to predict an outcome in the clinic at the individual level.

Ethics Approval The Jackson Laboratory Institutional Animal Care and Use Committee and institutional review board approved all protocols used.

<http://dx.doi.org/10.1136/jitc-2022-SITC2022.0382>

383 **TARGETING IGE-PRODUCING BLOOD CANCERS USING EMPD-SPECIFIC CHIMERIC ANTIGEN RECEPTOR T CELLS**

¹Shenyu Zhang*, ²Zhengyu Ma, ²Brittany Fay. ¹University of Delaware, Wilmington, DE, USA; ²Nemours Children's Hospital, Wilmington, DE, USA

Background Neoplasm of IgE-producing B lineage cells gives rise to IgE myeloma, chronic B cell leukemia and Hodgkin's lymphoma. Although several chimeric antigen receptor (CAR) T-cell therapies have been approved for treating B cell malignancies by targeting the B cell lineage marker CD19 or B cell maturation antigen (BCMA), these approaches indiscriminately eliminate both cancerous B cells and most normal B cells. This leads to general B cell and plasma aplasia and compromised humoral immune responses.

Methods To specifically target IgE-producing cancer cells, we developed a CAR that targets the extracellular membrane-proximal domain (EMPD) of membrane IgE (mIgE) expressed on the surfaces of IgE-producing cells. EMPD is a 52-residue peptide that exists only on mIgE but not on secreted IgE. Specifically, we generated a human EMPD-specific hybridoma 2E3E10, cloned the heavy and light chain variable regions, and constructed an EMPD-specific second-generation CAR with intracellular 4-1BB and CD3 ζ signaling domains. To determine the activity of the CAR, we used a human myeloma cell line U-266 expressing low levels of mIgE as target. In addition, to minimize alloreactive CD8⁺ T-cell-mediated background killings, we eliminated HLA class I expression on U266 cells by knocking out (KO) beta-2-microglobulin (β 2m) using CRISPR/Cas9. We also modified the U-266 cells to express firefly luciferase, enabling a bioluminescence-based killing assay.

Results Through lentiviral transduction, the EMPD-specific CAR was successfully expressed on more than 50% of primary human CD8⁺ and CD4⁺ T cells stimulated with anti-CD3/CD28 beads. The expression persisted for more than three weeks in cultures. Coculturing engineered U-266-b2mKO-luci target cells with primary human T cells that expressed the EMPD-specific CAR led to significant T cell cytokine production and target cell killing.

Conclusions The EMPD-specific CAR is capable of mediating primary human T cell activation and cytotoxicity through recognition of the mIgE on IgE-expressing cancer cells. The results demonstrate the proof-of-concept for using EMPD-specific CAR T cells to treat IgE-producing B cell malignancies. Although the CAR T cell eliminates both IgE-producing cancerous and normal B cells, since the vast majority of B cells produce IgG, this approach should not cause general B cell aplasia.

Acknowledgements The work is supported by NIH grants R21AI149243 and R03TR004206 and the Nemours Foundation.

<http://dx.doi.org/10.1136/jitc-2022-SITC2022.0383>

Abstracts

384

SYSTEMATIC, ANTIGEN-AGNOSTIC DISCOVERY OF TUMOR-REACTIVE TCRs POWERED BY REPERTOIRE-SCALE TCR GENE SYNTHESIS AND THE USE OF BANKED ALLOGENEIC CANCER CELL LINES

¹Xi Chen, ¹Yue Zhao, ¹Ely Porter*, ¹Danielle Cook, ¹Jiekun Xuan, ²Xiao-Wu Huang, ³Bin Li, ⁴Jingwei Zhang, ⁵Lili Ren, ⁵Teng Wei, ⁵Ning Li. ¹RootPath, Inc., Watertown, MA, USA; ²Zhongshan Hospital, Fudan University, Shanghai, China; ³Shanghai Jiao Tong University, Shanghai, China; ⁴Fudan University, Shanghai, China; ⁵Shenzhen People's Hospital, Shenzhen, China

Background Both neoantigen-reactive and wildtype tumor-associated antigen- (TAA) reactive TCRs contribute to anti-tumor immunity. While neoantigens can be identified by deep sequencing, the spectrum of TAA is harder to define. Although some TAAs are well studied, the majority of TAAs are likely undiscovered. Therefore it is difficult to survey the landscape of TAA-reactive TCRs for a given patient. Antigen-agnostic approaches have been reported,^{1,2} where patient-derived TCR genes are synthesized and used to make TCR-transgenic T cells, which are co-cultured with autologous tumor cells to observe cytokine secretion. However, these approaches are limited by the number of TCRs tested and the availability of autologous tumor cells.

Methods We have developed a new approach to solve both problems. First, we developed an ultrahigh-throughput TCR gene synthesis technology called PathFinder DNA AssemblyTM (figure 1, figure 2a), which bring the cost of TCR gene synthesis to <\$1 per TCR (100-fold lower than existing technologies). Second, we use banked cancer cell lines, which express a large swath of known and undiscovered TAAs. This method is justified in part by the similar gene expression profiles between many tumor tissues and many cell lines.^{4,5} We developed a simple method to inactivate the endogenous HLA genes of the cell lines and replace them with the HLA genes from the patient, a process we call 'HLA-personalization' (figure 2b, figure 2c).

Results For example, we have synthesized 1,575 TCRs from a liver cancer patient and screened them against HLA-personalized liver cancer cell lines HepG2, Huh6 and Huh7. We have discovered several tumor-reactive TCRs including one that reacts strongly to HepG2, restricted by HLA-C*03:04 (figure 3a). We further confirmed that this TCR can sense and kill HLA-C*03:04-expressing HepG2 cells and autologous tumor cells, but not PBMC of a C*03:04+ donor (figure 3b). We have similarly synthesized 1,053 TCRs from a cervical cancer patient and identified 4 TCRs reactive to HLA-personalized cervical cancer cell lines SiHA or C33A (figure 4). Two of these TCRs were confirmed to be reactive to HPV E7, restricted by HLA-B*38:15. Using this approach, we have synthesized ~50,000 TCRs from 9 patients and identified >70 tumor-reactive TCRs, restricted by a wide array of HLAs, from every patient tested.

Conclusions To our knowledge, this work represents the largest scale of TCR functional screening. The TCRs discovered may be used both as fully personalized TCR-T therapy, and as a repository of TAA-reactive TCRs for conventional TCR-T development after their deorphanization.^{6, 7}

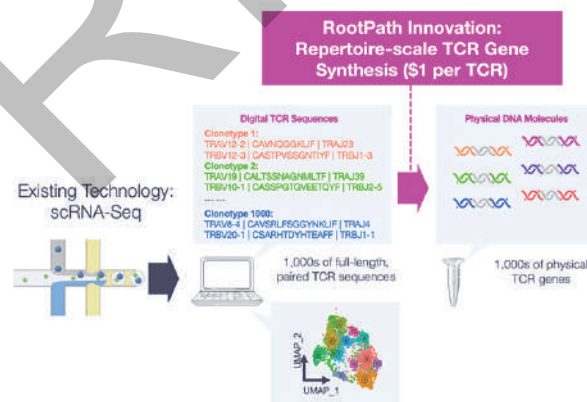
REFERENCES

1. Schepers W, Kelderman S, Fanchi LF, Linnemann C, Bendle G, de Rooij MAJ, Hirt C, Mezzadra R, Slagter M, Dijkstra K, Kluijn RJC, Snaebjornsson P, Milne K, Nelson BH, Zijlmans H, Kenter G, Voest EE, Haanen JBAG, Schumacher TN. Low and variable tumor reactivity of the intratumoral TCR repertoire in human cancers. *Nat Med*. 2019; **25**:89-94.

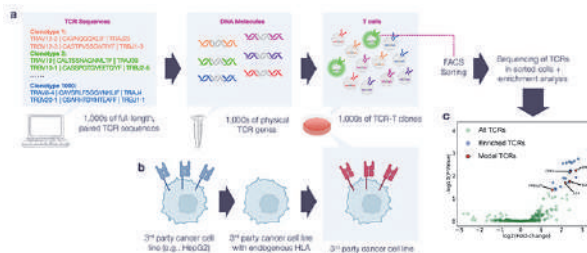
- Oliveira G, Stromhaug K, Klaeger S, Kula T, Frederick DT, Le PM, Forman J, Huang T, Li S, Zhang W, Xu Q, Cieri N, Clauser KR, Shukla SA, Neuberger D, Justesen S, MacBeath G, Carr SA, Fritsch EF, Hacohen N, Sade-Feldman M, Livak KJ, Boland GM, Ott PA, Keskin DB, Wu CJ. Phenotype, specificity and avidity of anti-tumour CD8+ T cells in melanoma. *Nature*. 2021; **596**:119-125.
- Chen X, Porter E. Compositions and methods for t-cell receptor gene assembly, WO2020206238A2
- Yu K, Chen B, Aran D, Charalel J, Yau C, Wolf DM, van't Veer LJ, Butte AJ, Goldstein T, Sirota M. Comprehensive transcriptomic analysis of cell lines as models of primary tumors across 22 tumor types. *Nat Commun*. 2019; **10**:3574
- Warren A, Chen Y, Jones A, Shibue T, Hahn WC, Boehm JS, Vazquez F, Tsherniak A, McFarland JM. Global computational alignment of tumor and cell line transcriptional profiles. *Nat Commun*. 2021; **12**:22
- Joglekar AV, Leonard MT, Jeppson JD, Swift M, Li G, Wong S, Peng S, Zaretsky JM, Heath JR, Ribas A, Bethune MT, Baltimore D. T cell antigen discovery via signaling and antigen-presenting bifunctional receptors. *Nat Methods*. 2019; **16**:191-198.
- Kula T, Dezfulian MH, Wang CI, Abdelfattah NS, Hartman ZC, Wucherpfennig KW, Lyerly HK, Elledge SJ. T-Scan: A Genome-wide method for the systematic discovery of T cell epitopes. *Cell*. 2019; **178**:1016-1028.

Ethics Approval The study obtained ethics approval by ethics committees at Shenzhen People's Hospital and Zhongshan Hospital.

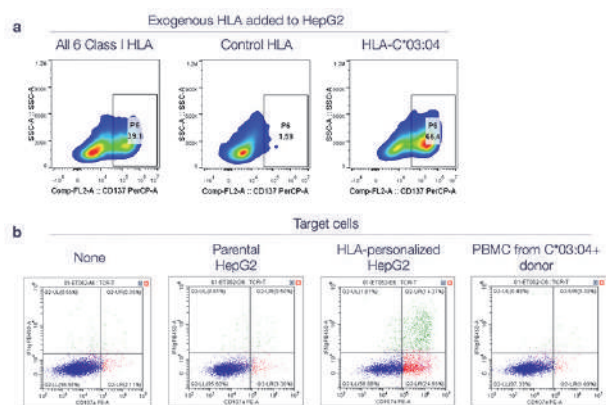
Consent Written informed consent was obtained from the patient for publication of this abstract and any accompanying images. A copy of the written consent is available for review by the Editor of this journal.



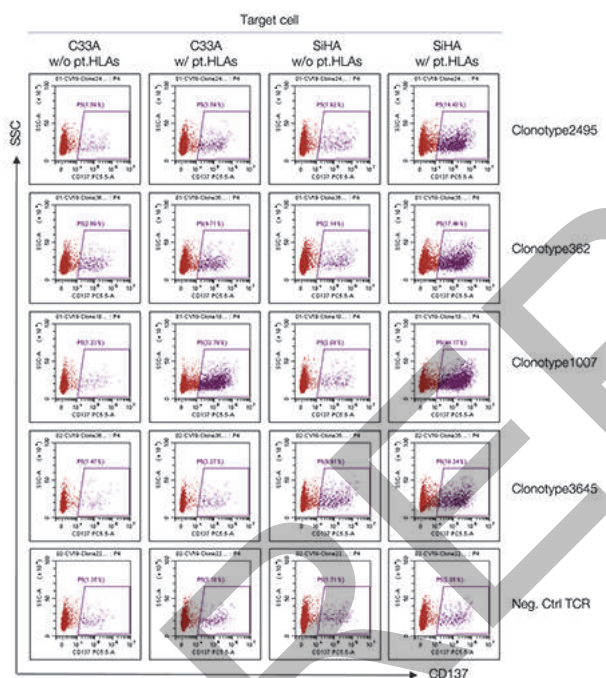
Abstract 384 Figure 1 Thousands of TCR genes can be synthesized simultaneously at a cost of <\$1 per TCR using our proprietary PathFinder DNA Assembly technology.



Abstract 384 Figure 2 Tumor-reactive TCRs can be identified by (a) producing thousands of TCR-T clones, (b) HLA-personalize a banked cell line through knocking out its endogenous HLA and expressing the patient-derived HLA sets, and (c) co-culturing the two, FACS-sort activated T cells, and identify TCRs enriched in the sorted cells.



Abstract 384 Figure 3 The tumor-reactive TCR we identified from the liver cancer patient is (a) restricted by HLA-C*03:04, and (b) capable of mediating effector function such as degranulation and IFN γ secretion up contacting HLA-personalized cell line, but not HLA-matched donor PBMC, suggesting tumor-specificity.



Abstract 384 Figure 4 4 TCRs identified from the TILs of a cervical cancer patient that can recognize cervical cancer cell line SiHA or C33A.

<http://dx.doi.org/10.1136/jitc-2022-SITC2022.0384>

Abstracts

385

ENGINEERING A TGF- β SWITCH RECEPTOR ENHANCES CAR-T CELL FUNCTION IN A SUPPRESSIVE TGF- β -ENRICHED TUMOR MICROENVIRONMENT

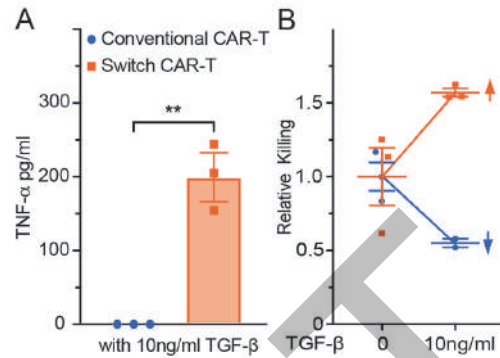
Joe Jiang Zhu*, Criselle DSouza, Vicky Qin, Niko Thio, Michael Kershaw, Joe Trapani, Phillip Darcy, Paul Neeson. Peter MacCallum Cancer Centre, Melbourne, Australia, Melbourne, Australia

Background Chimeric antigen receptor T (CAR-T) cells have performed poorly in patients with advanced solid cancers. A critical hurdle for CAR-T cell efficacy is the immunosuppressive tumor microenvironment (TME). CAR-T cell function is profoundly inhibited by transforming growth factor-beta (TGF- β) enriched in the TME. Current strategies to address this issue focus on the abrogation of TGF- β signaling. However, these strategies can have toxic side effects due to an imbalance in T cell homeostasis induced by complete blockade of TGF- β signaling.

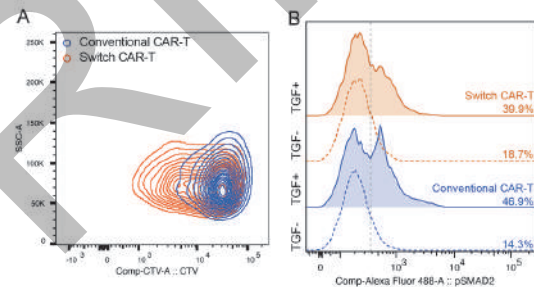
Methods We engineered a novel chimeric switch receptor comprising a TGF- β receptor domain and a T cell costimulatory domain to initiate T cell costimulation upon TGF- β binding. To maintain T cell homeostasis balance, we optimized the intracellular sequence of the switch receptor to reduce its effect on endogenous TGF- β signaling and decrease the potential side effects. The switch receptor was co-expressed in LeY-specific CAR-T cells (switch CAR-T). The *in vitro* function of switch CAR-T cells were investigated in the presence of TGF- β . We also performed RNAseq to explore genes involved in the switch receptor activation. Finally, we demonstrated the anti-tumor efficacy of switch CAR-T cells *in vivo*.

Results In the presence of TGF- β , switch CAR-T cells showed significantly enhanced cytotoxicity and higher levels of TNF secretion compared with conventional CAR-T cells (figure 1). In the presence of both CAR stimulation and TGF- β , but not TGF- β alone, switch CAR-T cells also had significantly higher proliferation and increased mitochondrial biogenesis, indicating an antigen-specific response. Furthermore, both switch and conventional CAR-T cells had equivalent levels of SMAD2 phosphorylation in response to TGF- β , indicating that switch CAR-T cells retained endogenous TGF- β signaling (figure 2). RNAseq analysis showed that switch CAR-T cells have a unique gene expression profile in response to CAR stimulation and TGF- β . Finally, tumor-bearing mice treated with switch CAR-T cells showed significantly better tumor control compared with conventional CAR-T cells (figure 3). This finding was associated with decreased TGF- β and increased IFN- γ levels within the tumor.

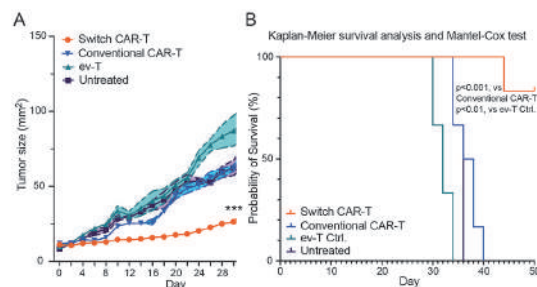
Conclusions The novel switch receptor activated CAR-T cells in response to immunosuppressive TGF- β leading to improved CAR-T cell function. This effect also required CAR-T cell activation through CAR-stimulation, suggesting a tumor-specific response. Furthermore, these switch CAR-T cells provided improved *in vivo* anti-tumor control. By fine-tuning the intracellular sequence of the switch receptor, we also successfully retained the endogenous TGF- β signaling. Switch CAR-T cells can preserve this important homeostatic mechanism and will be safe to use in the clinic.



Abstract 385 Figure 1 Switch CAR-T cells exhibited superior cytotoxicity and cytokine production. (A) Cytokine production of TNF- α after 16 hours of co-culture with LeY+ DU-145 cells and switch CAR-T cells or conventional CAR-T cells with or without TGF- β , measured by AlphaLISA assay (mean \pm SEM of triplicate cultures). (B) Relative lysis of LeY+ DU-145 after 16 hours co-culture, measured by 51Cr release assay (mean \pm SEM of triplicate cultures).



Abstract 385 Figure 2 The switch receptor enhanced the proliferation of switch CAR-T cells in the presence of TGF- β and maintained endogenous TGF- β signaling. (A) Contour plots showing proliferation of switch CAR-T cells and conventional CAR-T cells labelled with cell trace violet when cultured in the presence of TGF- β . (B) Histogram overlay of phosphorylated SMAD2 gated on CAR+ cells when cultured with TGF- β .



Abstract 385 Figure 3 Switch CAR-T cells showed significantly enhanced tumor control *in vivo*. (A) NSG mice were inoculated subcutaneously with DU-145 cells and treated with CAR-T cells when tumors were established. The growth kinetics was plotted (n=6). *** p<0.001. (B) Survival analysis was assessed, and the significance of Kaplan-Meier survival analysis was determined by log-rank Mantel-Cox test.

<http://dx.doi.org/10.1136/jitc-2022-SITC2022.0385>

386

EFFICIENT EX-VIVO EXPANSION OF ADAPTIVE NKG2C+/CD57+ NK CELLS FROM CMV-POSITIVE DONORS USING DENDRITIC CELLS DERIVED FROM THE ACUTE MYELOID CELL LINE DCONE

Haoxiao Zuo, Remco Bos, Alex Karlsson-Parra, Satwinder Kaur Singh*. *Mendus AB, Leiden, Netherlands*

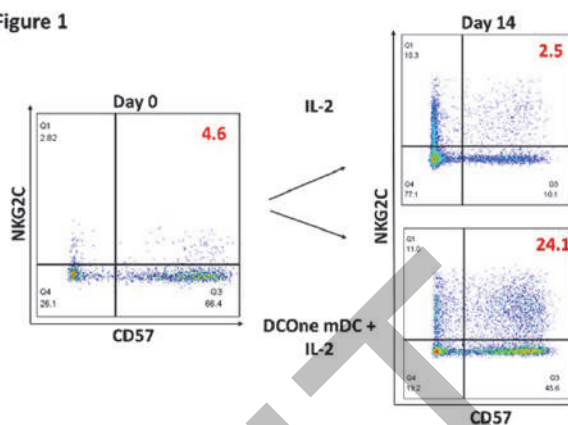
Background Human cytomegalovirus (CMV) infection profoundly affects NK cell compartment, as documented by the presence of a long-lived adaptive NK cell subset co-expressing NKG2C and CD57. Several features render adaptive NK cells a potentially attractive contributor to the efficacy of mAb-based therapeutic strategies and predict a lower sensitivity to immunosuppressive signals in the tumor microenvironment. Moreover, a recent work showed that CAR-transduced adaptive NK cells exhibit superior effector functions when compared to other NK subsets. The requirements for adaptive NK cell expansion ex vivo have however not been fully characterized. Ex-vivo expansion of NKG2C+ memory NK cells can be achieved by coculturing NK cells from CMV-positive subjects with CMV-infected fibroblasts + IL-2, HLA-E-transfected cell lines + IL-15, or IgG-opsonized tumor cells + IL-2. However, the reported fold-expansion after 14-21 days in culture in vitro is generally below 30-fold.

Methods PBMCs isolated from buffy coat of CMV-positive healthy donors. NK cells were co-cultured with or without DCOne-derived mature DCs (DCOne mDCs) in the presence of cytokines for 2 weeks. After 1 week, cells were restimulated by the addition of DCOne-derived mature DCs and cytokines. NK cell proliferation, viability and phenotype were monitored on day 7 and 14.

Results DCOne-derived mature DCs (high expression of HLA-DR, CD40/80/86 and CD83) were found to highly express CD58 and CD155, two ligands known to participate in adaptive NK cell activation and expansion. When these tumor cell/dendritic cell “hybrids” were co-cultured for 2 weeks with isolated NK cell from CMV-positive healthy donors, a selective (figure 1) and strong (>200-fold) median expansion (figure 2) of adaptive NKG2C+/CD57+ NK cells was found when cocultures were performed in medium supplemented with IL-2 or IL-15. Characterization of the functional profile, including ADCC, cytokine production and long-time survival, after target cell interaction by these expanded NKG2C+/CD57+ NK cells is ongoing.

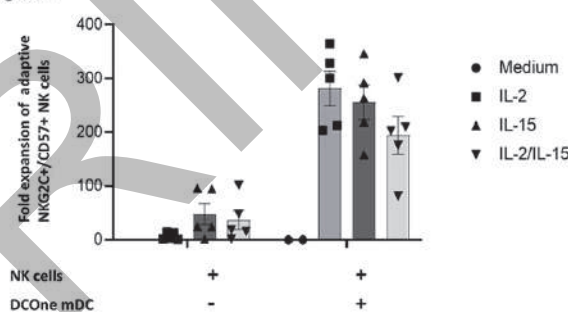
Conclusions The presented data indicate that DCOne-derived mature DCs are endowed with the capability to promote strong and selective ex vivo expansion of adaptive NKG2C+/CD57+ NK cells from healthy CMV+ donors. Such expanded NK cells could potentially be used for adoptive immunotherapy, including combinations with tumor-targeting antibodies, in different hematological and solid tumor indications.

Figure 1



Abstract 386 Figure 1 DCOne mDC lead to increased frequencies of adaptive NK cells

Figure 2



Abstract 386 Figure 2 DCOne-derived mature DCs boost expansion of adaptive NK cell

<http://dx.doi.org/10.1136/jitc-2022-SITC2022.0386>

387

EXPANSION AND IDENTIFICATION OF NEOANTIGEN REACTIVE TUMOR INFILTRATING LYMPHOCYTES (TIL) FROM METASTATIC COLORECTAL CANCER (CRC)

¹Matthew Beatty*, ¹MacLean Hall, ¹Holly Branthoover, ¹Mary Rau, ²Jake Nikota, ²James Bender, ²Jake Ceccarelli, ²Timothy Langer, ¹Jamie Teer, ¹Jason Fleming, ¹Shari Pilon-Thomas. ¹Moffitt Cancer Center, Tampa, FL, USA; ²Turnstone Biologics, Hamilton, Canada

Background Previously we have shown that neoantigen specific TIL can be enriched from cryopreserved TIL product from melanoma patients. TCGA data for colorectal cancer (CRC) show a median variant count of 111 but with a subset of patients having much higher mutation frequency. Additionally, patients with higher tumor mutation burden (TMB) have been shown to have improved response to immune checkpoint therapy compared to patients with low TMB. Thus, CRC samples with higher mutational frequency may be an ideal candidate for enrichment of neoantigen specific TIL. The purpose of this study is to expand, identify, and enrich neoantigen reactive TIL from CRC patients.

Methods Patient-derived CRC tissue and PBMC were collected at Moffitt Cancer Center under an Ethic's Board approved study (Advarra Pro00043972). TIL was expanded from digested tumor tissue. Whole exome sequencing and RNA sequencing were performed on DNA and RNA extracted from tumor tissue and autologous PBMC. Sequencing and expression data were utilized to identify protein-modifying mutations. Peptides were predicted for their ability to be presented on MHC molecules, prioritized, and synthesized. Neoantigen peptides were loaded onto patient-derived B-cells and co-cultured with autologous TIL. These TIL were then sorted by FACS by upregulation of 4-1BB and OX40 and expanded through the rapid expansion protocol (REP). Enriched TIL were screened for neoantigen reactivity and analyzed by flow cytometry for 4-1BB/OX40 upregulation and cytokine release and degranulation via the ELLA platform.

Results TIL expansion was successfully achieved in 9 of 10 liver metastasis (90%) while only 4 of 10 (40%) samples from the peritoneal cavity expanded TIL. Of the CRC samples that expanded TIL, one patient showed a high mutation frequency with 1710 mutations identified. Restimulation of enriched neoantigen-specific TIL resulted in upregulation of 4-1BB/OX40 from the positive sorted TIL but minimal upregulation from the negative control sorted TIL. This coincided with increased granzyme B, IFN γ , and TNF α in response when compared to their non-reactive TIL counterpart. Of the 196 peptides screened, one peptide corresponding to a known mutation in HDHD3 stimulated 4-1BB/OX40 enriched TIL.

Conclusions TIL from metastatic colorectal cancer patient samples were successfully expanded from multiple disease sites. TIL from these samples can be screened for neoantigens and enriched for neoantigen-reactive TIL. These enriched TIL maintained increased reactivity against these predicted peptides upon restimulation when compared non-reactive TIL. These data support further investigation into the use of neoantigen-enriched TIL products to enhance efficacy of ACT.

Ethics Approval The study was approved by Moffitt Cancer Center's Institutional Review Board, approval number 00043972. Patients gave informed consent before taking part in this protocol.

<http://dx.doi.org/10.1136/jitc-2022-SITC2022.0387>

388

TARGETED OVARIAN CANCER IMMUNOTHERAPY THROUGH ENGINEERING OF FOLLICLE STIMULATING HORMONE RECEPTOR (FSHR) ANTIBODY TO ENGAGE T CELLS

Devivasha Bordoloi*, Pratik Bhojnagarwala, Alfredo Perales-Puchalt, Abhijeet Kulkarni, Xizhou Zhu, Kevin Liaw, Ryan O'Connell, Daniel Park, Daniel Kulp, Rugang Zhang, David Weiner. *The Wistar Institute, Philadelphia, PA, USA*

Background Ovarian cancer is the deadliest gynecologic malignancy, resulting in the highest mortality among cancers of the female reproductive system. The most prevalent subtype of epithelial ovarian cancer (EOC) is high-grade serous cancer which results in 70–80% of cases.¹ OC is a high need area for novel therapeutic interventions; with a focus on identification of targets for immune therapy approaches expressed in the tumor microenvironment being of particular relevance. Follicle stimulating hormone receptor (FSHR) is one such important target with expression in 50-70% of serous OC cells.² To date just handful of studies have targeted FSHR. Here we describe development of biologics targeting FSHR and study their impact against multiple ovarian tumors.

Methods We developed monoclonal antibody clones which target FSHR and focused our studies on a potent FSHR cell binding clone for detailed characterization, including binding and evaluation of its effect on antibody dependent cellular cytotoxicity (ADCC). We expanded this work to develop bispecific T cell engager (TCE) targeting FSHR and evaluated for its specificity, functionality, and efficacy in OC models.

Results We observed that the anti-FSHR clone D2AP11 bound specifically to FSHR positive cells and tissues. D2AP11 IgG2a antibody could induce ADCC in OC cells (IC50: 28.5 µg/ml). We sought to improve on its potential through design of D2AP11-TCE. Besides exhibiting strong bidirectional binding, this TCE induced potent in vitro killing of multiple human OC cells; CaOV3, OVISe, Kuramochi, OVCAR3-FSHR, OVCAR4 and PEO-4 which exhibit resistance to different drugs targeting HDAC, microtubule stabilizer, DNA alkylating agents, mTORC, AKT, PARP etc. (table 1)^{3,4} and tumor lines harboring mutations in BRCA1&2. IC50 values of D2AP11-TCE killing were obtained at 24.7 and 15.9 ng/ml in OVISe-FSHR and OVCAR3 cells respectively, indicating 1000-fold higher efficacy than IgG2a FSHR biologic (figures 1 and 2). In the NSG in vivo tumor challenge studies, this TCE significantly attenuated tumor burden of a model K562-FSHR, and relevant OVISe-FSHR and OVCAR3-FSHR challenged mice. Median survival of D2AP11-TCE treated mice was increased by 10 days compared to control group.

Conclusions These studies extend published data that FSHR appears to be an important target for further study in the context of OC immunotherapy. We present new tools for studying FSHR in OC and report development of a potent TCE with pM activity to impact OC growth in multiple pre-clinical models. Additional studies of these new tools for different ovarian as well as other cancers expressing FSHR are of high interest.

REFERENCES

- Barnes BM, Nelson L, Tighe A, Burghel GJ, Lin IH, Desai S, *et al.* Distinct transcriptional programs stratify ovarian cancer cell lines into the five major histological subtypes. *Genome Med.* 2021;**13**:140.
- Perales-Puchalt A, Svoronos N, Rutkowski MR, Allegranza MJ, Tesone AJ, Payne KK, Wickramasinghe J, Nguyen JM, O'Brien SW, Gumireddy K, Huang Q, Cadungog MG, Connolly DC, Tchou J, Curiel TJ, Conejo-Garcia JR. Follicle-stimulating hormone receptor is expressed by most ovarian cancer subtypes and is a safe and effective immunotherapeutic target. *Clin Cancer Res.* 2017;**23**:441-453.

- CellModelPassports. Cell Model Passports: A Hub for Preclinical Cancer Models. <https://cellmodelpassports.sanger.ac.uk>. Accessed April 20, 2022.
- Sakai W, Swisher EM, Jacquemont C, Chandramohan KV, Couch FJ, Langdon SP, Wurz K, Higgins J, Villegas E, Taniguchi T. Functional restoration of BRCA2 protein by secondary BRCA2 mutations in BRCA2-mutated ovarian carcinoma. *Cancer Res.* 2009;**69**:6381-6386.

Abstract 388 Table 1 Different ovarian tumor lines used in the study and their drug resistance

Name	Resistant drugs	Resistant Drug targets	References
OVISe	FEN1_3940, Tanespimycin	FEN1, HSP90	[3]
CaOV3	Dacinostat	HDAC	[3]
Kuramochi	Dactolisib, Wee1 inhibitor, Buparlisib, UMI-77, Docetaxel, AZD5363, Gallibiscoquinazole, Mitoxantrone, Irinotecan, Emtinostat, Oxaliplatin	PI3K-class 1, mTORC1, mTORC2, WEEL1, CHEK1, PI3Kalpha, PI3Kdelta, PI3Kbeta, PI3Kgamma, MCL1, Microtubule stabilizer, CDK2, TOP1, HDAC1, HDAC3, DNA alkylating agent	[3]
OVCAR3	Sepantronium bromide, Foretinib, Belinostat, CAI10603, CUDC-101, JW-7-24-1, Omipalisib, QL-XII-47, THZ-2-102-1, AT-7519, UNC0638, QL-X-138, LDN-193189, KIN001-244, OSI-027, WZ3105, WZ3105	BIRC5, MET, KDR, TIE2, VEGFR3/FLT4, RON, PDGFR, FGFR1, EGFR, HDAC1/10, ERBB2, LCK, PI3K-class 1, mTORC1, mTORC2, BTK, BMX, CDK7, CDK1, CDK2, CDK4, CDK6, CDK9, G9a and GLP methyltransferases, BTK, BMP, PDK1, mTORC1, mTORC2, SRC, ROCK2, NTRK2, FLT3, IRAK1, SRC, ROCK2, NTRK2, FLT3, IRAK1	[3]
OVCAR4	Picitilisib, Eg5_9814, Taselisib, Mirin, AZD2014, AZ960, Famiposide, CDK9_5576, AZD5363, CDK9_5038	PI3K-class 1, KSP11, PI3K-beta sparing, MRE11, mTORC1, mTORC2, JAK2, JAK3, CDK9, AKT1, AKT2, AKT3, ROCK2, GSK3	[3]
PEO-4	Cisplatin, PARP inhibitor	DNA alkylating agent, PARP	[3], [4]

Figure 1

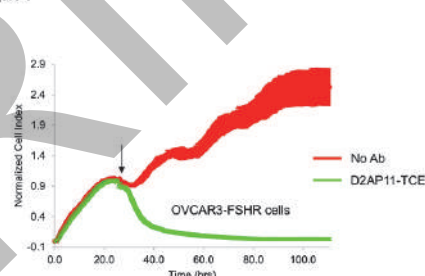


Figure 1: D2AP11-TCE mediated killing of OVCAR3-FSHR cells in the presence of human T cells. The real time cell killing was analyzed by xCelligence assay. Effector (E): target (T) = 10: 1. Arrow indicates the time at which effector cells and TCE were added. Red line indicates No antibody (only Effector + Target cells) whereas green line indicates treatment with D2AP11-TCE (Effector+Target+D2AP11-TCE).

Abstract 388 Figure 1 D2AP11-TCE mediated killing of OVCAR3-FSHR cells in the presence of human T cells.

Figure 2

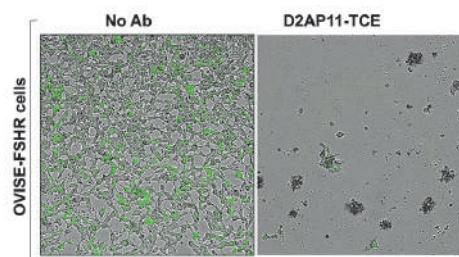


Figure 2: Representative images showing the cytotoxic effect of D2AP11-TCE on OVISe-FSHR cells (GFP+), 3 days post treatment. T cells were added to the target cells, Effector (E): target (T) = 10: 1. No viable cells are observed in D2AP11-TCE treated group. No Ab refers to Only effector + target cells.

Abstract 388 Figure 2 Representative images showing the cytotoxic effect of D2AP11-TCE on OVISe-FSHR cells

<http://dx.doi.org/10.1136/jitc-2022-SITC2022.0388>

389

MULTIPLEXED TCR-T CELL THERAPY TARGETING MAGEA1 AND PRAME ENHANCES THE ACTIVITY OF ADOPTIVE T CELL THERAPY IN PRE-CLINICAL MODELS

Cagan Gurer, Gavin MacBeath, Mollie Jurewicz, Nancy Nabils, Antoine Boudot, Jenny Tadros, Tary Traore, Maytal Bowman, Elizabeth Hall, Yifan Wang, Cagan Gurer*, Qikai Xu, Victor Ospina. *TScan Therapeutics, Waltham, MA, USA*

Background Adoptive cell transfer with genetically engineered T cells holds great promise for treating solid tumors. To date, clinical investigations of TCR-engineered T cell therapies (TCR-T) have targeted one antigen at a time and have produced response rates ranging from 30-50%. Unfortunately, complete responses have been rare, and responses are often short-lived. One possible reason why patients rapidly relapse is that their tumors exhibit substantial heterogeneity of antigen expression: not every cancer cell within a tumor expresses the target of a mono TCR therapy and, even when they do, the target is expressed at variable levels among the individual tumor cells. This suggests that TCR-T targeting one antigen could allow the cells lacking the treated antigen to escape and drive relapse.

Methods To address antigen heterogeneity, we are developing multiplexed TCR-T cell therapy in which a patient is treated with multiple TCR-T cell products, chosen from a collection of pre-vetted TCRs matched to the patient's tumor antigens and HLA type. As proof-of-concept, we selected two different cancer/testis antigens targeted by two different TCRs. One of these antigens, MAGEA1, was identified as the target of expanded tumor infiltrating T-cells from a head & neck cancer patient using TScan's screening technology.¹ The other one, PRAME, is highly expressed in a variety of cancers. Using our ReceptorScan platform, we developed two high affinity TCRs that recognize HLA-A*02:01-restricted epitopes from MAGEA1 and PRAME, and assessed the benefits of combining these two TCR-T cell products using a variety of pre-clinical models.

Results Individually, both TCRs show strong cytotoxic activity *in vitro* when co-cultured with HLA-matched cancer cell lines expressing endogenous MAGEA1 and PRAME. Additionally, in xenograft mouse models, each TCR was able to control the growth of tumors expressing their cognate antigens. To test whether the two TCRs exhibit additive or synergistic activity, we developed two different tumor models. In one model, we used a cancer cell line that expresses both MAGEA1 and PRAME. In the other model, a mixture of two different cell lines expressing either MAGEA1 or PRAME were grown as xenograft tumors in mice. Notably, when treated with multiplexed MAGEA1/PRAME TCR-T, the mice achieved longer lasting tumor control compared to TCR-T targeting a single antigen.

Conclusions These findings support the hypothesis that multiplexed TCR-T mimics the natural oligoclonal T-cell response to cancer and has the potential to overcome antigen heterogeneity, which may contribute to the observed lack of durability in monotherapy TCR-T clinical trials.

REFERENCE

1. Luoma AM, Suo S, Wang Y, Gunasti L, Porter CBM, Nabils N, Tadros J, Ferretti AP, Liao S, Gurer C, Chen YH, Criscitiello S, Ricker CA, Dionne D, Rozenblatt-Rosen O, Uppaluri R, Haddad RI, Ashenberg O, Regev A, Van Allen EM, MacBeath G, Schoenfeld JD, Wucherpfennig KW. Tissue-resident memory and circulating T cells are early responders to pre-surgical cancer immunotherapy. *Cell*. 2022;**185**:2918-2935.

<http://dx.doi.org/10.1136/jitc-2022-SITC2022.0389>

390

DIGITAL SPATIAL PROFILING AND ANTIGEN-DEPENDENT PHENOTYPIC ANALYSIS OF IL15-ENGINEERED TUMOR-INFILTRATING LYMPHOCYTES (CYTOTIL15[®] THERAPY) IN AN ALLOGENEIC MELANOMA PDX MODEL

<http://dx.doi.org/10.1136/jitc-2022-SITC2022.0390>

Rachel Burga*, Zheng Ao, Arman Aksoy, Scott Lajoie, Kyle Pedro, Jack Tremblay, Gauri Kulkarni, Alonso Villasmil Ocando, Benjamin Primack, Meghan Langley, Theresa Ross, Jeremy Tchaicha, Michelle Ols, Jan ter Meulen, Mithun Khattar. *Obsidian Therapeutics, Cambridge, MA, USA*

Background CytoTIL15[®] therapy is an IL2-independent, engineered TIL product which allows pharmacological control of membrane-bound IL15 (mbIL15). We have previously shown that cytoTIL15[®] TILs demonstrate enhanced persistence and anti-tumor efficacy in a human allogeneic melanoma PDX model. Here we use digital spatial profiling and single cell sequencing to characterize the RNA expression profile and phenotypic markers of tumor infiltrating immune cells as well as tumor cells in this model and compare the results to unengineered, IL2-dependent TIL.

Methods cytoTIL15[®] therapy contains TILs engineered with mbIL15 under the control of a carbonic-anhydrase-2 drug responsive domain, regulated by the ligand acetazolamide (ACZ). cytoTIL15[®] cells were generated from human melanomas through a proprietary rapid expansion process. Expanded TILs were phenotyped and assayed for *in vitro* polyfunctionality, cytotoxicity, and frequency of tumor-associated antigen-specific TCR. *In vivo* phenotype and anti-tumor functionality was examined through adoptive transfer of TILs into NSG mice bearing subcutaneous, HLA-matched, patient-derived-xenograft (PDX) tumors expressing melanoma-associated antigen MART-1, in IACUC approved animal studies. Tumors, spleen, bone marrow, and blood were harvested 14-21 days following adoptive cell transfer and assessed by flow cytometry, GeoMx digital spatial profiling, and single cell sequencing for characterization of TIL and the tumor microenvironment (TME).

Results cytoTIL15[®] cells demonstrated enrichment and reactivity for melanoma antigen-specific TCRs, while maintaining TCR β diversity. Fifteen days post-ACT, tumors from animals treated with cytoTIL15[®] cells exhibited significantly ($p=0.0175$) higher frequency (3.4-fold) of TILs, in which MART-1 tetramer positive cells demonstrated increased T-cell factor 1 (TCF-1) and CD69 expression, and secreted significantly greater amounts of IFN γ and TNF α cytokines into the TME, compared to unengineered TILs with IL2. In addition, cytoTIL15[®] TILs had a distinct differential gene expression profile, demonstrating an increase in effector genes such as IL2RB, GZMB, GNLY and CCL5 and reduction in exhaustion-related genes such as EOMES. cytoTIL15[®] cells accumulating in the bone marrow exhibited a lower frequency of CD39+ terminally differentiated CD8+ T cells, while maintaining higher levels of memory phenotype makers.

Conclusions In this allogeneic melanoma PDX model, cytoTIL15[®] cells showed a distinct profile of RNA expression and phenotypic markers, consistent with their increased persistence and anti-tumor efficacy. Interestingly, the subpopulation of cytoTIL15[®] cells reactive to tumor-associated antigen MART-1 displayed increased expression of TCF-1, which in melanoma patients has been associated with responses to immune checkpoint blockade, in addition to progression-free and overall survival.

Ethics Approval All animal studies were IACUC approved.

391 DEVELOPMENT OF A GMP-COMPATIBLE, VIRUS-FREE CRISPR CAR T CELL MANUFACTURING PROCESS

Dan Cappabianca*, Madison Bugel, Sarah Caroline Gomes de Lima, Ross Schwartz, Krishanu Saha, Christian Capitini. *University of Wisconsin-Madison, Madison, WI, USA*

Background Chimeric antigen receptor (CAR) T-cells are engineered immune cells that can be taken from a patient and redirected to fight cancer. Recently, we developed a virus-free process to create anti-GD2 CAR T cells using CRISPR-Cas9 ribonucleoproteins that endows cells with a stem cell memory-like and less exhausted phenotype that improves their ability to induce regression of GD2 positive solid tumors.

Methods To improve this workflow, we systematically modified the media conditions, electroporation timing, and small molecule treatment to improve the cell yield and memory-like characteristics of CAR T cells.

Results We find that optimal non-viral knock-in is dependent on activation time, and two key small molecule inhibitors.

Conclusions Key reagents have been made GMP-compatible, and therefore this process could be readily implemented in existing cell manufacturing facilities.

Ethics Approval The study was approved by the IRB at University of Wisconsin-Madison, approval number 2018-0103

<http://dx.doi.org/10.1136/jitc-2022-SITC2022.0391>

392

ENGINEERING CD70-DIRECTED CAR-NK CELLS FOR THE TREATMENT OF HEMATOLOGICAL AND SOLID MALIGNANCIES

¹Jae Woong Chang*, ¹Joshua Kreuger, ¹Joseph Skeate, ¹Erin Stelljes, ¹Walker Lahr, ¹Nicholas Slipek, ¹Emily Pomeroy, ²Meghan Walsh, ²Jennifer Johnson, ²Charlotte Franco, ²Simarjot Pabla, ²Jared Sewell, ²Eugene Choi, ²Vipin Suri, ¹Beau Webber, ¹Branden Moriarty. ¹University of Minnesota, Minneapolis, MN, USA; ²Catamaran Bio, Boston, MA, USA

Background While effective, CAR-T therapies are limited by a lack of scalability for patient-derived starting material. Alternatively, allogeneic CAR-NK cell therapies have the potential to overcome these limitations by providing an off-the-shelf product capable of delivering clinical benefits without the safety and manufacturing challenges associated with CAR-Ts. CAR-NK cell therapies are attractive in treating AML as the inherent graft-versus-leukemia activity of NK cells can be effectively augmented by a CAR directed to an AML-expressed antigen. CD70 is an attractive target for CAR therapy in AML since it is highly expressed on leukemic stem cells and blasts and is not detectable on normal bone marrow hematopoietic stem cells.¹ Additionally, aberrant CD70 expression is associated with several solid tumors and hematological malignancies, including AML and renal cell carcinoma (RCC) while expression in normal tissue is restricted to immune cells including T, B, DC, and NK cells.²

Methods Here we demonstrate that CD70 is not expressed in resting peripheral blood NK cells but is strongly upregulated in response to NK cell activation by engineered feeder cells. As such, integration of a CD70-targeting CAR into activated NK cells leads to substantial reduction of NK cell expansion due to fratricide. Knockout (KO) of CD70 by CRISPR/Cas9 editing does not inhibit NK cell expansion nor impair cytotoxicity against various types of tumor cells, therefore a successful engineering strategy where CAR integration and self-expression of the CAR ligand is knocked out via CRISPR/Cas9 would allow for successful propagation of such a CAR-NK therapy. Using the non-viral *TC Buster* transposon system, we were able to deliver transposons containing a CD70 CAR or CD70 CAR/IL15 expression cassette while simultaneously knocking out CD70 by CRISPR/Cas9 in primary human peripheral blood NK cells.

Results This single-step process resulted in >75% CD70 CAR integration/expression and >80% knockout of endogenous CD70. The resulting CD70 knockout CAR-NK cells were resistant to fratricide and expanded comparably to mock-engineered NK cells following feeder cell activation. The IL15 expression cassette enabled enhanced persistence of CAR-NK cells *in vitro* and *in vivo* without exogenous cytokine support. In functional assays, CD70 knockout CAR-NK cells mediated cytotoxicity against multiple CD70-positive tumor cell lines including AML and RCC both *in vitro* and *in vivo*.

Conclusions Overall, the results demonstrate the potential for targeting CD70 with CAR-NK cell therapy for the treatment of AML, RCC, and other CD70-positive malignancies while overcoming fratricide issues by engineering with a non-viral transposon delivery system in combination with CRISPR/Cas9 editing.

REFERENCES

1. Perna et al. 2017, *Cancer Cell*. **32**:506-519.
2. McEarchern et al. 2008, *Clin Cancer Res*. **14**(23):7763-7772.

<http://dx.doi.org/10.1136/jitc-2022-SITC2022.0392>

393

ATAK RECEPTORS, A NEW CLASS OF CHIMERIC ANTIGEN RECEPTOR THAT HARNESS INNATE IMMUNITY IN MYELOID CELLS TO TARGET CANCER

Neha Diwanji, Edward Cochran, Michael Gorgievski, Thomas Prod'homme, Yuxiao Wang*, Bruce McCreedy, Daniel Getts. *Myeloid Therapeutics, Cambridge, MA, USA*

Background For the majority of patients with advanced solid tumors, sustained clinical benefit with immunotherapy has yet to be achieved. Myeloid cells, including monocytes and macrophages are the primary orchestrators of immune responses and are found to accumulate in tumors, in some cases contributing up to 75% of the tumor mass. Myeloid cells express a wide range of innate immune sensors such as Toll-like receptors, RIG-I and cGAS-STING as well as co-stimulatory molecules like CD40. The activation of these innate immune pathways in myeloid cells can be associated with anti-tumor immune response. Notwithstanding the ability of the myeloid cells to infiltrate tumors and elicit broad immune responses, technologies capable of harnessing these cells to target cancer remains elusive.

Methods Here we designed and engineered a new class of chimeric antigen receptors that couple tumor recognition with multiple innate immune signal domains, referred to as Activate, Target, Attack & Kill (ATAKTM) receptors. By combining cancer recognition domains with intracellular signaling domains from innate immune receptors such as Fcγ, TLR and cytokine receptors, we show that myeloid cells can be controlled and programmed to recognize cancer and elicit a broad and tunable immune response. Critically, in mice with established, highly immunosuppressive B16 melanoma tumors, delivery of monocytes engineered to express ATAK receptors results in anti-tumor activity. Our data show the versatility of building ATAK receptors by harnessing innate immune pathways and support their clinical development in cell therapies.

<http://dx.doi.org/10.1136/jitc-2022-SITC2022.0393>

394 USING CO-STIMULATORY CARs IN NATURAL KILLER CELLS TO SAFELY TARGET SOFT-TISSUE SARCOMAS AND THEIR INHIBITORY MICROENVIRONMENTS

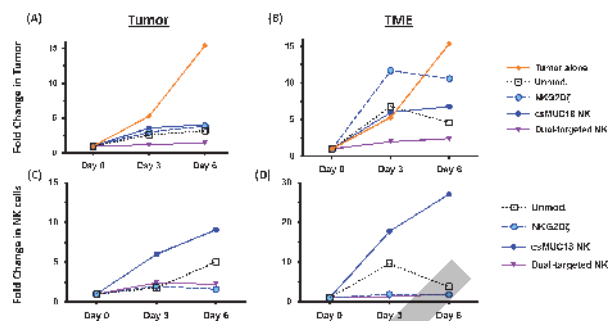
Stephanie Fetzko*, Ishwar Navin, Matthew Dysthe, Tim Sauer, Cliona Rooney, Robin Parihar. Baylor College of Medicine, Houston, TX, USA

Background Outcomes for patients with refractory or relapsed soft-tissue (ST) sarcomas are poor. Immunotherapy with chimeric antigen receptor (CAR)-expressing lymphocytes has shown promise in pre-clinical models. However, efficacy has been limited by the suppressive tumor microenvironment (TME). Furthermore, because sarcoma associated antigens are also expressed on normal tissues, maximizing tumor killing while minimizing off-tumor toxicity has been challenging with traditional CAR approaches. The current study aimed to (1) design a natural killer (NK) cell immunotherapy that utilizes a “co-stimulation only” CAR to safely target the sarcoma antigen, MUC18; (2) define the optimal endodomain for the co-stimulatory (cs) MUC18 CAR that enhances NK cell proliferation without adding cytotoxicity; and (3) combine an optimal MUC18-csCAR with a cytotoxic CAR, NKG2D.ζ, that simultaneously eliminates sarcoma cells and inhibitory cells of the TME such as myeloid-derived suppressor cells (MDSCs) and M2 macrophages (M2s). By using this novel combinatorial antigen-recognition approach, we hypothesized that dual-targeted NK cells (co-expressing MUC18-csCAR and NKG2D.ζ) would be activated only within the TME co-expressing MUC18 and TME-associated ligands, but not in MUC18+ normal tissues, resulting in enhanced anti-tumor efficacy against MUC18+ ST sarcomas without toxicity.

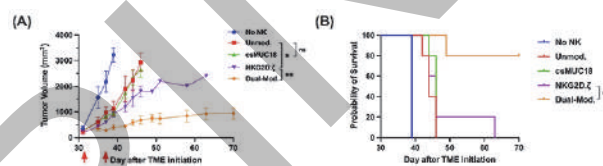
Methods We generated MUC18-cytotoxic and csCARs with 4-1BB, OX40, 2B4, and DNAM-1 endodomains and confirmed specificity and functionality using MUC18 overexpressing and knockout targets and a long-term TME co-culture comprised of alveolar rhabdomyosarcoma, Rh4, and inhibitory macrophages (M2s). Safety of MUC18-csCARs was tested against the MUC18+ liver sinusoidal endothelial cell (LSEC) line. Anti-tumor activity of dual-targeted NK cells compared to unmodified and singly-modified NK cells was assessed *in vivo* using a novel TME xenograft model with Rh4 and MDSCs.

Results MUC18 cytotoxic CAR-NK cells killed MUC+ high targets, while exhibiting low killing against an Rh4-MUC18 KO cell line, confirming CAR specificity and function. MUC18-OX40csCAR NK cells expanded without additional killing in the TME compared to NK cells with other co-stimulatory endodomains. MUC18-OX40csCAR NK cells did not exhibit killing of LSECs. Dual-targeted NK cells demonstrated enhanced tumor control in TME co-cultures (2.4-fold change in tumor vs. 4.6 by unmodified NK, 10.6 by NKG2D.ζ, and 6.8 by cs.MUC18) compared to either singly-modified NK population (figure 1). Dual-targeted NK cells demonstrated superior tumor control in the *in vivo* TME xenograft model compared to controls (p=0.007 versus NKG2D.ζ) and prolonged survival (p= <0.0001) (figure 2).

Conclusions Dual-targeted NK cells demonstrate enhanced anti-tumor activity without toxicity against normal tissue. Use of co-stimulation-only CARs in NK cells may allow exploitation of previously non-targetable sarcoma antigens.



Abstract 394 Figure 1 The dual-targeted CAR NK cells were compared to unmodified NK cells, NKG2D.ζ CAR NK cells, and csMUC18 CAR NK cells in a TME co-culture system. A) Rh4 fold expansion in the tumor alone conditions and B) in the TME conditions was determined for each time point. C) Fold change in NK cells in the tumor alone conditions. D) Fold change in NK cells in the TME conditions.



Abstract 394 Figure 2 (A) Mice (n=5 per treatment group) received two NK cells doses at 31 and 38 days post tumor inoculation and three times per week IL-2 and IL-15 to promote NK cell survival. (B) Survival probability of each treatment cohort.

<http://dx.doi.org/10.1136/jitc-2022-SITC2022.0394>

Abstracts

395

ENGINEERING NON-ACTIVATED CAR T CELLS WITH ENHANCED POTENCY AGAINST ADVANCED CANCERS

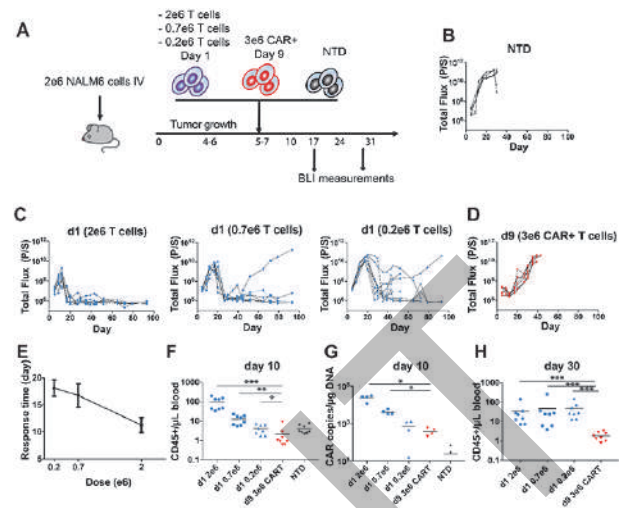
Saba Ghassemi*, Joseph Durgin, Frederic Bushman, Saar Gill, Roddy O'Connor, Michael Milone. *University of Pennsylvania, Philadelphia, PA, USA*

Background Chimeric antigen receptor (CAR) T cells can generate durable clinical responses in B-cell hematologic malignancies. The effectiveness of this approach led to several FDA-approved CAR T cell therapies against cancer. Despite their therapeutic promise in blood-based malignancies, CAR-T cells do not effectively kill solid tumors. Several factors contribute to success including tumor entry, CAR engagement, T cell expansion, and persistence. In several solid tumor models, CAR T cells can enter solid tumors and undergo antigen-specific stimulation. "Failure" coincides with a diminished ability to proliferative and persist.

Methods CAR T cell manufacturing is an iterative process with several important steps. Initially, T cells are activated through their T cell receptor, followed by lentiviral transduction and expansion ex vivo for several weeks. Unfortunately, activating and expanding CAR T cells in this manner drives differentiation with a corresponding loss of anti-tumor activity. Here we provide evidence that functional CAR T cells can be generated within 24 hours without any need for T cell activation or ex vivo expansion. We show that the efficiency of viral transduction in this process is substantially influenced by the formulation of the medium and the surface area-to-volume ratio of the culture vessel.

Results Remarkably, these cells exhibited higher anti-leukemic in vivo activity per cell than standard CAR T cells (activated and expanded for 9 days prior to adoptive transfer) in pre-clinical models of human leukemias (figure 1). Our preliminary findings position the non-activated system as a superior alternative against solid tumors where terminally differentiated T cells are so often ineffective. Our findings imply that quiescent T cells retain key attributes that influence engraftment and survival following adoptive transfer.

Conclusions In summary, the ability to generate genetically-modified T cells with superior therapeutic potential in a shorter time period has important implications for CAR-T manufacturing and therapy. Our results indicate that extended ex vivo culture is unnecessarily costly and redundant. Leveraging the unique ability of lentiviral vectors to enter and integrate into the genome of non-dividing cells, effective CAR-T cell products with durable engraftment in vivo can be generated in as little as one day. Minimizing ex vivo manipulation also conserves limited resources such as human serum and manufacturing space as expansion occurs entirely in vivo. Finally, more rapid product generation will lead to a shorter period of time between apheresis collection and re-infusion of CAR T cells. This will be of particular benefit to those patients with rapidly progressive disease.



Abstract 395 Figure 1 Non-activated CAR T cells induce durable remission (A) Schematic of the xenograft model and CART19 cell treatment in NSG mice. (B-D) serial quantification of disease burden by bioluminescence imaging. (B) Total bioluminescence flux in mice treated with non-transduced (NTD) control non-activated T cells. (C) Total bioluminescence flux in mice treated with a single high (2x10⁶), medium (0.7x10⁶) or low (0.2x10⁶) dose of non-activated T cells. (D) Total bioluminescence flux in mice treated with 3x10⁶ CAR+ T cells stimulated with anti-CD3/CD28 microbeads and expanded over 9 days. There are 8 mice in each group. (E) Time to initial anti-leukemic response (i.e. first reduction in bioluminescence) after infusion of non-activated CART19 in relationship to T cell dose. (F) Absolute peripheral blood CD45+ T cell counts in blood collected from mice at day 10 following T cell transfer. (G) Vector copy number in peripheral blood collected at day 10 measured by qPCR and normalized to DNA concentration. (H) Absolute peripheral blood CD45+ T cell counts in blood collected from mice on day 30 following T cell transfer. *P < 0.05, **P < 0.01 and ***P < 0.001. The mean of each group is indicated by the solid black line. Groups were compared using the two-tailed, unpaired Mann-Whitney test.

<http://dx.doi.org/10.1136/jitc-2022-SITC2022.0395>

396

INVESTIGATING THE ROLE OF THE ENDOGENOUS CD28 CO-STIMULATORY RECEPTOR IN ACHIEVING OPTIMAL CAR-T CELL THERAPEUTIC EFFICACY

¹Mackenzie Honikel*, ²Kelvin Lee, ¹Scott Olejniczak. ¹Roswell Park Comprehensive Cancer Center, Buffalo, NY, USA; ²Indiana University School of Medicine, Indianapolis, IN, USA

Background Multiple myeloma (MM) remains an incurable hematological malignancy by conventional chemotherapeutic approaches. Chimeric antigen receptor T (CAR-T) cells targeting B cell maturation antigen (BCMA) on MM have shown remarkable efficacy in relapsed/refractory patients, leading to the recent FDA approval of two CAR-T cell products. Despite initially promising responses, many MM patients fail to achieve durable remissions leading to relapse in the months following treatment, highlighting the need to better understand mechanisms of CAR-T cell failure.

CD28, the prototypical T cell co-stimulatory molecule, is commonly expressed on MM and was previously shown to protect MM from chemotherapy-induced cell death, implicating its role in promoting therapy resistance. However, the role of the endogenous CD28 receptor on CAR-T cells is largely unexplored.

Methods To specifically target CD28 on the surface of adoptively transferred CAR-T cells we employed a novel, inducible CD28^{-/-} genetically engineered mouse model as the T cell source.

Results We demonstrate that genetic deletion of the endogenous CD28 receptor does not impair CAR-T cell activation in response to stimulation by BCMA-expressing target cells, nor the subsequent cytotoxic response as assessed by intracellular cytokine production in two second-generation CAR-T cell models. However, the complete absence of a CD28 co-stimulatory signal has unveiled a previously uncharacterized role for the endogenous receptor in mediating an anti-tumor response *in vivo*. Specifically, CD28^{-/-} BCMA-targeted 4-1BB ζ CAR-T cells display a pronounced defect in their ability to control tumor growth in multiple disease models, while the function of CD28^{-/-} 28 ζ CAR-T cells is unaffected. Preliminary results suggest that CD28 deletion enhances persistence of the CAR-T cell population which may lend a more durable response to adoptive cellular therapies.

Conclusions These findings suggest that targeting the endogenous CD28 receptor with an FDA approved biologic CTLA4-Ig (Abatacept) may represent a viable clinical strategy to increase the efficacy of a potent 28 ζ CAR-T cell design through two independent mechanisms: 1) Blockade of CD28 on MM abrogates a critical survival signal in the bone marrow microenvironment which may enhance their sensitivity to CAR-T cell mediated killing 2) Blockade of CD28 on CAR-T cells dampens the CAR-T cell activation signal which may promote differentiation into longer-lived memory T cell subsets for enhanced therapeutic durability as compared to effector T cells.

This work has contributed to the unveiling of a novel CD28 axis in CAR-T cell biology and provides insight into identifying optimal levels of co-stimulation while offering a therapeutic strategy to improve adoptive cellular immunotherapeutics.

<http://dx.doi.org/10.1136/jitc-2022-SITC2022.0396>

397

DEEP MYELOID CELL PROFILING PROVIDES NEW INSIGHTS INTO MODULATORS OF CAR T CELL EXPANSION IN PATIENTS WITH SOLID TUMOR MALIGNANCIES

¹Sabina Kaczanowska*, ²Sneha Ramakrishna, ²Tara Murty, ¹Cristina Contreras, ³Ahmad Alimadadi, ³Norma Gutierrez, ⁴Aashna Jhaveri, ⁴Yang Liu, ⁴Jennifer Altreuter, ⁴Franziska Michor, ²Caroline Duault, ²Priyanka Balasubrahmanyam, ²Warren Reynolds, ²Reema Baskar, ²Mina Pichavant, ²Bitu Sahaf, ²Sean Bendall, ²Holden Maecker, ¹Melinda Merchant, ²Crystal Mackall, ³Catherine Hedrick, ¹Rosandra Kaplan. ¹National Cancer Institute, Bethesda, MD, USA; ²Stanford University School of Medicine, Palo Alto, CA, USA; ³La Jolla Institute for Immunology, La Jolla, CA, USA; ⁴Dana-Farber Cancer Institute, Boston, MA, USA

Background Chimeric antigen receptor (CAR) T cells have shown remarkable results in hematological malignancies but limited efficacy in the setting of solid tumors. GD2 is a tumor antigen expressed on neuroblastoma and osteosarcoma, and previous studies of T cells expressing 1st generation GD2-CAR were shown to be safe and mediated modest antitumor activity in patients with refractory neuroblastoma. Myeloid cells orchestrate immune responses with the ability to either activate or limit T cell responses. In the setting of solid tumors, myeloid-mediated immune suppression is known to play an important role in dampening antitumor activity. We hypothesized that myeloid cells impact CAR T cell expansion in patients with solid tumors.

Methods A phase I trial (NCT02107963) was performed to determine the feasibility and safety of administering 3rd generation GD2-CAR (GD2-CAR.OX40.28.z.ICD9) T cells in children and young adults with GD2⁺ neuroblastoma and osteosarcoma. Peripheral blood patient samples were analyzed retrospectively by qPCR for CAR expansion, multiplex ELISA for cytokine levels, mass cytometry (CyTOF) for phenotype analysis, ATAC-seq for epigenetic determination, and RNA-seq for transcriptomic evaluation.

Results 15 patients were enrolled on four dose levels, of which 13 patients were infused. While 76.9% of patients had stable disease by day 28, eventually all patients had disease progression. GD2-CAR T cells expanded in all patients receiving treatment, half of whom had expansion similar to that seen in clinically active CD19 and CD22 CAR T cells, but with limited persistence. To gain insight into the immune compartment in patients with good versus poor CAR T cell expansion, we evaluated immune profiles in patient pre-treatment apheresis and post-treatment peripheral blood samples. The main findings of this study indicate that a higher proportion of monocytes in pre-treatment apheresis was associated with poor CAR T cell expansion and CXCR3 expression on monocytes in pre-treatment apheresis was the most robust marker of good CAR T cell expansion in this cohort. Longitudinal analysis demonstrated that CXCR3⁺ monocytes were low following treatment in both good and poor CAR T cell expanders, demonstrating a transition in myeloid populations in response to GD2-CAR T cell treatment.

Conclusions Together, these data suggest that GD2-CAR T cell administration is associated with changes in the myeloid cell compartment in solid tumor patients. This study provides evidence of novel myeloid-based pre-treatment biomarkers of CAR T cell expansion and rationale for the combination of CAR T cells with myeloid-modulating therapies as a strategy to improve outcomes for patients with solid tumors.

Acknowledgements We are grateful to the study participants and their families, referring medical care teams, the faculty and staff of the NCI CCR Pediatric Oncology Branch, NCI

CCR Center for Cellular Engineering, and the data managers involved with this work. Clinical trial supported in part by: Intramural Research Program, National Cancer Institute, NIH Clinical Center, National Institutes of Health. Scientific and financial support for the CIMAC-CIDC Network are provided through the National Cancer Institute (NCI) Cooperative Agreements: U24CA224331 (to the Dana-Farber Cancer Institute CIMAC), U24CA224309 (to the Stanford University CIMAC), and U24CA224316 (to the CIDC at Dana-Farber Cancer Institute). Scientific and financial support for the Partnership for Accelerating Cancer Therapies (PACT) public-private partnership (PPP).

Trial Registration NCT02107963

Ethics Approval The phase I study protocol conformed to the Declaration of Helsinki, Good Clinical Practice guidelines, and was approved by the NCI Institutional Review Board (14-C-0059) and the FDA. All patients or their legal guardians signed a document of informed consent indicating their understanding of the investigational nature and risks of this study.

<http://dx.doi.org/10.1136/jitc-2022-SITC2022.0397>

398 **EXPANSION OF THERAPEUTIC NK CELL LINE UNDER HYPOXIC AND HYPERBARIC CULTURE CONDITIONS ENHANCES ANTI-TUMOR POTENCY**

James Lim, Ann Lu*, Yunmin Li, Yelena Bronevetsky. *Xcellbio, San Francisco, CA, USA*

Background Harnessing NK cells is proving to be an attractive strategy for cancer immunotherapy, either by activating endogenous NK cells or through adoptive cell transfer. NK cells can also be sourced from immortalized cell lines like NK-92 that are currently being evaluated in the clinic. However, the immunosuppressive solid tumor microenvironment (TME) can inhibit NK-92 function thereby limiting its cytolytic properties against tumor cells. To overcome the immunosuppressive effects of the TME, we applied a culturing strategy in which NK-92 cells were serially passaged and expanded under hypoxic and hyperbaric conditions. We then tested the potency of NK cells expanded under TME conditions.

Methods To investigate the short- and long-term effects of TME conditions on NK cell function, we cultured NK-92 cells under several environmental conditions and performed cytotoxic, transcriptional and protein expression analysis. NK-92 cells were either cultured in a conventional CO₂ incubator at 21% O₂ and 0 PSI, or in an AVATAR cell control system which can be precisely tuned to different O₂ and pressure levels that mimic TME conditions. We first assessed the effects of culture conditions on the ability of NK-92 cells to kill tumor cells in both normoxic and TME conditions. To this end we used the AVATAR AI instrument, which employs the environmental control of the AVATAR incubator paired with a specialized plate that enables real-time, label free cell killing analysis via electrical impedance.

Results In normoxic conditions, NK-92 cells that had been exposed to TME conditions for 24 hours exhibited reduced killing, as compared to controls, with slower kinetics of killing and lower total cytolysis. Interestingly, cells that had been adapted to TME conditions for more than 3 months exhibited increased cytotoxic activity, with faster killing kinetics and higher total cytolysis. When cell killing experiments were repeated under TME conditions, the differences between NK-92 culture conditions were even more stark. NK cells grown under standard conditions showed a reduction in total cytolysis, as compared to their killing activity under normoxic conditions. In contrast, TME-conditioned NK cells exhibited robust tumor cytolysis in both normoxic and TME conditions.

Conclusions This initial study supports the hypothesis that NK-92 cells can both react and adapt to different microenvironments. TME-adaptation strategies during cell expansion can enhance potency and efficacy of cell therapies designed to work in a solid tumor microenvironment.

<http://dx.doi.org/10.1136/jitc-2022-SITC2022.0398>

399

DEVELOPING A NEW TARGETED THERAPY FOR PEDIATRIC RHABDOMYOSARCOMA: α V β 3 AND HER2 AS PROMISING TARGETS FOR BISPECIFIC CAR T-CELL THERAPY

Amanda Lulu*, Joseph Caruso, Dustin Cobb, Daniel Lee. *University of Virginia, Charlottesville, VA, USA*

Background Even though rhabdomyosarcoma (RMS) is the most prevalent sarcoma in children, therapy relies on decades-old, multi-agent chemotherapy, radiation and surgery, which are ineffective in the salvage or metastatic disease setting, with only 30% of patients surviving three years[1]. Therefore, more effective treatments are desperately needed.

Chimeric antigen receptor T-cell (CAR-T) therapy has been highly successful for relapsed/refractory hematologic malignancies, but antigen downregulation by tumors have not uncommonly led to immunotherapy escape across several platforms [2–5]. We hypothesize that simultaneously targeting two RMS antigens with a bispecific CAR-T will provide a new treatment modality while reducing the likelihood of antigen escape. We previously established the efficacy of α v β 3 (CD133) and HER2 CAR-Ts against diffuse intrinsic pontine glioma/glioblastoma[6] and medulloblastoma[7], respectively. HER2 is known to be expressed on RMS[8], and one child with RMS experienced a temporary remission with HER2-CAR-T[9]. Therefore, targeting α v β 3 and HER2 using a bispecific CAR-T approach may be effective for RMS.

Methods Six alveolar and embryonal RMS cell lines were evaluated by flow cytometry for α v β 3 and HER2 expression. The *in vitro* kinetics of α v β 3 and HER2-CAR-T killing of RMS were assessed at varying effector-to-target ratios in an xCelligence analyzer, with CD19-CAR and non-transduced T-cells as controls. Antigen-specificity was evaluated by pre-incubating targets with α v β 3/HER2 blocking or control antibodies or by targeting *ITGB3* or *ERBB2* CRISPR knock out tumor cells. CAR-Ts were then evaluated for changes in activation marker expression by flow cytometry.

Results (1) α v β 3 and/or HER2 are expressed on 6/6 RMS cell lines. Five express both antigens (figure 1A). (2) Separately, α v β 3 and HER2-CAR-Ts rapidly and robustly kill antigen^{pos} RMS in an antigen- and dose-dependent manner. Furthermore, α v β 3 and HER2-CAR-Ts are sensitive, achieving 70% cytolysis at 300 and 1100 targets/cell, respectively (figure 1B) suggesting a lower likelihood of disease escape by antigen down-regulation. (3) Cytolysis is antigen-specific (figure 2). (4) Co-culture of both CARs with RMS drives increased expression of the activation markers CD107a, CD137, CD25, CD69 and PD-1, demonstrating antigen-driven induction of a strong effector response (figure 3).

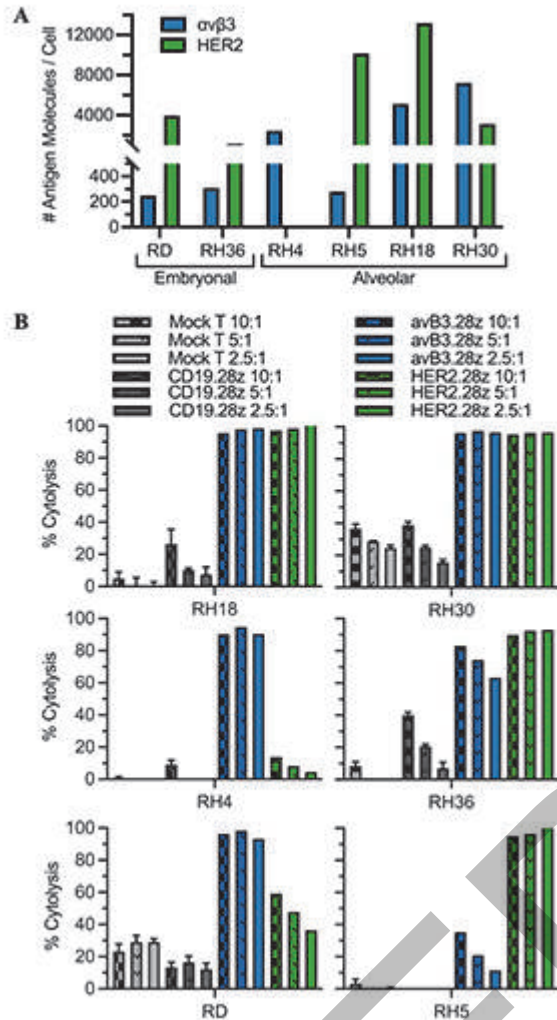
Conclusions Our data demonstrate that α v β 3 and HER2 are viable RMS targets for a bispecific CAR-T approach. α v β 3 and HER2 CAR-Ts independently control RMS well. They exhibited robust and low-level antigen-specific killing and effector cell activation *in vitro*, supporting further investigation into their control of RMS *in vivo*. α v β 3/HER2 bispecific CAR-Ts are being developed, which we expect to perform as well as or better than each CAR independently.

Acknowledgements This work was supported by a V Foundation Scholar Award (DWL), the Childhood Brain Tumor Foundation (DWL), and UVA Strategic Investment Funds (DWL). The authors thank Javed Khan for providing the rhabdomyosarcoma cell lines.

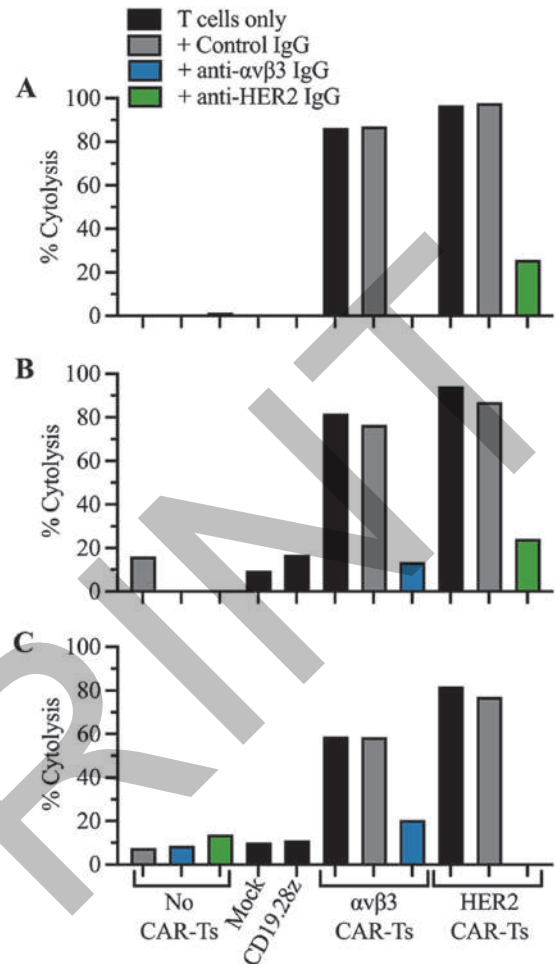
REFERENCES

1. Oberlin O, Rey A, Lyden E, Bisogno G, Stevens MCG, Meyer WH, *et al*. Prognostic Factors in Metastatic Rhabdomyosarcomas: Results of a Pooled Analysis From United States and European Cooperative Groups. *J Clin Oncol*. 2008;26:2384–9.
2. Brown CE, Alizadeh D, Starr R, Weng L, Wagner JR, Naranjo A, *et al*. Regression of Glioblastoma after Chimeric Antigen Receptor T-Cell Therapy. *N Engl J Med*. 2016;375:2561–9.
3. O'Rourke DM, Nasrallah MP, Desai A, Melenhorst JJ, Mansfield K, Morrissette JJD, *et al*. A single dose of peripherally infused EGFRvIII-directed CAR T cells mediates antigen loss and induces adaptive resistance in patients with recurrent glioblastoma. *Sci Transl Med*. 2017;9:eaaa0984.
4. Maude SL, Laetsch TW, Buechner J, Rives S, Boyer M, Bittencourt H, *et al*. Tisagenlecleucel in Children and Young Adults with B-Cell Lymphoblastic Leukemia. *N Engl J Med*. 2018;378:439–48.
5. Dourthe M-E, Rabian F, Yakouben K, Chevillon F, Cabannes-Hamy A, Méchinaud F, *et al*. Determinants of CD19-positive vs CD19-negative relapse after tisagenlecleucel for B-cell acute lymphoblastic leukemia. *Leukemia*. Nature Publishing Group; 2021;35:3383–93.
6. Cobb DA, de Rossi J, Liu L, An E, Lee DW. Targeting of the α v β 3 integrin complex by CAR-T cells leads to rapid regression of diffuse intrinsic pontine glioma and glioblastoma. *J Immunother Cancer*. 2022;10:e003816.
7. Nellan A, Rota C, Majzner R, Lester-McCully CM, Griesinger AM, Mulcahy Levy JM, *et al*. Durable regression of Medulloblastoma after regional and intravenous delivery of anti-HER2 chimeric antigen receptor T cells. *J Immunother Cancer*. 2018;6:30.
8. Ganti R, Skapek SX, Zhang J, Fuller CE, Wu J, Billups CA, *et al*. Expression and genomic status of EGFR and ErbB-2 in alveolar and embryonal rhabdomyosarcoma. *Mod Pathol Off J U S Can Acad Pathol Inc*. 2006;19:1213–20.
9. Hegde M, Joseph SK, Pashankar F, DeRenzo C, Sanber K, Navai S, *et al*. Tumor response and endogenous immune reactivity after administration of HER2 CAR T cells in a child with metastatic rhabdomyosarcoma. *Nat Commun*. 2020;11:3549.

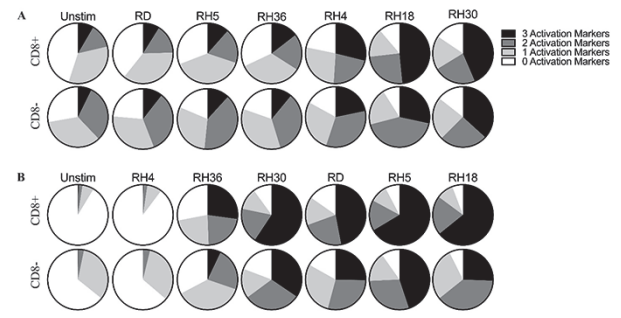
Ethics Approval The study was approved by the University of Virginia's Institutional Review Board, approval number 18842.



Abstract 399 Figure 1 avB3.28z and HER2.28z CAR-Ts robustly kill antigen+ rhabdomyosarcoma targets even at low effector-to-target ratios. A) RMS cells were analyzed for expression of avB3 and HER2 by flow cytometry. Antigen levels were quantified using BD QuantiBrite Beads. B) CAR-T cell cytotoxicity was measured via impedance assay in an xCelligence real time cell analyzer against RMS targets. Non-specific CD19 CAR-Ts (negative control) and mock (non-transduced) T-cells were used as controls.



Abstract 399 Figure 2 avB3.28z and HER2.28z CAR-T killing of RMS cells is antigen-specific. A) RH18, B) RH30 and C) RH36 tumor cells were pre-incubated with avB3- or HER2- blocking antibodies or with control IgG antibodies. CAR-Ts were evaluated for tumor cell killing after 12 hours co-culture at 2.5:1 effector:target ratio.



Abstract 399 Figure 3 Higher percentage of CAR-Ts express multiple activation markers with increased antigen expression on tumor cells. Cells were-cocultured for 24 hours at 2.5:1 effector:target ratio and then evaluated by flow cytometry for expression of CD25, CD137 and CD107a. Percentages of CD8+ and CD8- A) avB3.28z and B) HER2.28z CAR-Ts that were positive for 0-3 of the activation markers.

<http://dx.doi.org/10.1136/jitc-2022-SITC2022.0399>

Abstracts

400

PDGFR α -SPECIFIC CAR T CELL THERAPY OF PEDIATRIC HIGH-GRADE GLIOMA

Kathryn Eckholdt, Sara Mazrimas*, Paul Hauser, Wafik Zaky, Amer Najjar. MD Anderson Cancer Center, Houston, TX, USA

Background Platelet-derived growth factor receptor alpha (PDGFR α) is a tyrosine kinase receptor that plays a pivotal role in tumorigenesis and is associated with tumor proliferation and progression. Pediatric gliomas are known to express high levels of PDGFR α , designating the receptor a viable target for chimeric antigen receptor (CAR) T cell therapy.

Methods Lentiviral vectors encoding PDGFR α -specific CAR-coding sequences were constructed by fusion of a single chain Fv (scFv) to a human CD8a stalk and transmembrane domain linked to either a CD28 or CD137 intracellular signaling domain fused with a terminal CD3 ζ domain. PDGFR α -specific CAR T cells were expanded with IL-2 and artificial antigen presenting K562 cells (aAPC) expressing truncated PDGFR α . The cytotoxic function of PDGFR α -CAR T cells was assessed using *in vitro* killing assays. The therapeutic efficacy was evaluated in a mouse KNS42 glioma model. KNS42 cells expressing firefly luciferase and green fluorescent protein (ffLuc-GFP) were engrafted into the right parietal lobe of NSG mice using screw-guided injections. Intratumoral treatment with PDGFR α -CAR T cells was carried out one week later, and tumor growth was monitored weekly over the course of nine weeks by bioluminescence imaging.

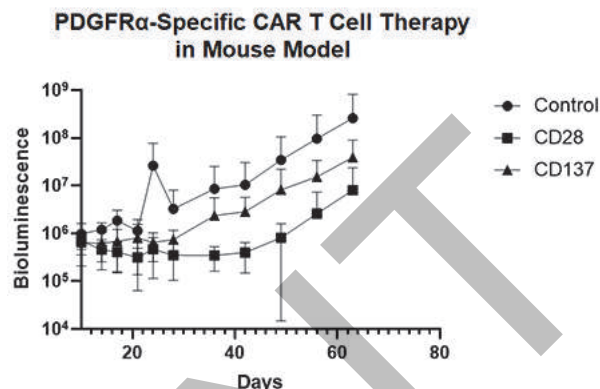
Results All CAR T cells demonstrated over 75% CAR expression two weeks following transduction and expansion. *In vitro* cytotoxicity assays demonstrated PDGFR α -specific lysis of KNS42 and PDGFR α -U87 glioma cells. PDGFR α -CAR T cells expressing the CD28 signaling domain exhibited a higher level of cytotoxicity against target KNS42 cells. Both PDGFR α -CD28 and -CD137 CAR T cell products resulted in decreased tumor progression when compared to the control mice injected with saline (figure 1). However, PDGFR α -CD28-CAR T cells exhibited a higher level of antitumor activity than PDGFR α -CD137 CAR T cells (97% vs 85% inhibition), consistent with the *in vitro* cytotoxicity observations (figure 1).

Conclusions In this study, we evaluated and compared the efficacy of PDGFR α -CAR T cells expressing the CD28 or CD137 costimulatory domains in controlling the growth of pediatric glioma cells. We have demonstrated that PDGFR α -CD28 CAR T cells exhibited more immediate anti-tumor response resulting in a more significant long-term reduction of tumor progression. Repeated administration of PDGFR α -CD28 CAR T cells may be warranted in future studies to further improve outcomes and preserve long-term responses. Our preclinical studies demonstrate the therapeutic potential for PDGFR α -CAR T cell in the treatment of pediatric high-grade glioma and set the stage for future clinical translation.

Acknowledgements We wish to acknowledge the staff of Small Animal Imaging Facility (SAIF) at MD Anderson Cancer Center for assistance in conducting all imaging-related aspects of our studies. We also wish to acknowledge the Department Veterinary Medicine and Surgery for facilitating all procedures related to our animal studies.

Ethics Approval All animal studies were conducted at MD Anderson with approval and in accordance with Institutional Animal Care and Use Committee (IACUC) guidelines. Mice were housed in pathogen-free conditions and were monitored daily for welfare and any signs of discomfort or pain. All efforts were made to minimize animal suffering, and moribund

mice were humanely euthanized according to IACUC guidelines. The ID number of approval for the animal study is 00001237-RN02.



Abstract 400 Figure 1 PDGFR α -Specific CAR T Cell Therapy in Mouse Model

Time-dependent quantification of KNS42 tumor burden following intratumoral injection of CAR T cells. NSG mice were implanted with 2x10⁵ KNS42 ffLuc-GFP cells in the right parietal lobe using skull screw-guided injections. One week later, intratumoral injections of PDGFR α -CD28 or PDGFR α -CD137 CAR T cells (2x10⁶ cells/5 μ L saline) were performed via the guide screws. Control mice received a 5 μ L injection of saline. Tumor growth was monitored weekly by bioluminescence imaging for 63 days.

<http://dx.doi.org/10.1136/jitc-2022-SITC2022.0400>

401

HINGE LENGTH: A NOVEL METHOD OF PREDICTING CYTOTOXICITY OF CAR CONSTRUCTS AGAINST ANTIGEN-LOW LEUKEMIA

¹Justin Mirazee*, ¹Dongya Jia, ²Xiang Chen, ¹Sooraj Achar, ¹Chris Chien, ¹Marie Pouzolles, ¹Kniya DeDe, ¹Philippe Youkharibache, ²Kylie Walters, ¹Grégoire Altan-Bonnet, ¹Naomi Taylor. ¹National Cancer Institute, Bethesda, MD, USA; ²Frederick National Laboratory for Cancer Research, Frederick, MD, USA

Background Genetic engineering of T-cells to target tumors through the expression of synthetic chimeric antigen receptors, or CARs, has led to a breakthrough in the treatment of relapsed/refractory B-cell leukemia. However, despite impressive initial clinical performance, 30-50% of patients eventually relapse, with the emergence of tumor cells expressing the targeted antigen at a level that is insufficient to induce CAR T responsiveness. We and others have shown that the hinge domain of CARs is critical in altering cytotoxic responsiveness of the CAR.^{1,2} Thus, we evaluated whether optimal hinge length could be evaluated for a given scFv *in-silico*, given the epitope location, thereby accelerating optimal CAR design.

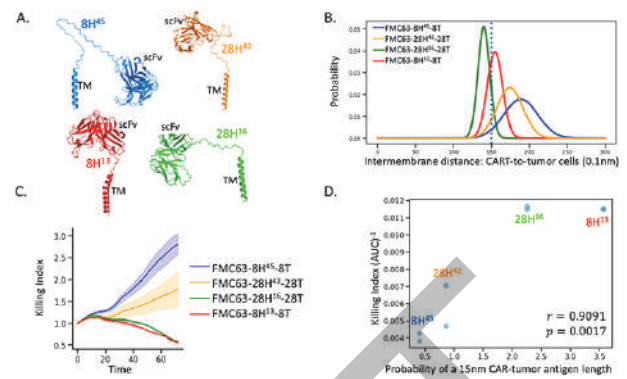
Methods Golden gate assembly was utilized to generate anti-CD19 (FMC63) and anti-CD22 (M971) CAR constructs. The lengths of the CD28 and CD8-alpha hinge domains were varied while intracellular 4-1BB and TCR-zeta signaling sequences remained constant. CAR structures were modeled with AlphaFold and intermembrane lengths modeled using Xplor-NIH. CAR function was evaluated by ex vivo cytotoxicity assays (Incucyte) against NALM6 cells engineered to express calibrated numbers of CD19 and CD22 molecules.

Results Through truncations and extensions of the CD28 and CD8-alpha hinge domains, we show that optimal hinge lengths for targeting CD19 and CD22 through their respective FMC63 and M971 scFvs are distinct and depend on the epitope location. Specifically, short and long hinges enhance cytotoxicity against membrane-distal epitope and membrane-proximal epitopes, respectively. Using Xplor-NIH and AlphaFold (figure 1A-1B), we were able to model hinge dynamics. As signaling of the TCR by MHC-presented peptide antigen (pMHC) is tightly regulated by the dimensions of the TCR-pMHC interaction, with an optimal intermembrane distance of 15nm,³ we assessed whether this distance would confer enhanced function to CAR T-cells following ligand encounter. Importantly, CAR constructs providing a predicted intermembrane CAR-ligand distance of 15nm exhibited enhanced cytotoxicity against antigen-low leukemic cells (figure 1C-1D).

Conclusions CAR responsiveness against a specific epitope can be modeled as a function of intermembrane distance, allowing a rapid optimization of CAR constructs by adjusting hinge length. The modeling presented here, based on epitope location and target protein dynamics, can be utilized to rapidly design CARs with optimized cytotoxic potential against a wide range of novel targets.

REFERENCES

1. Majzner, R. G., Rietberg, S. P., Sotillo, E., Dong, R., Vachharajani, V. T., Labanieh, L., Myklebust, J. H., Kadapakkam, M., Weber, E. W., Tousley, A. M., Richards, R. M., Heitzeneder, S., Nguyen, S. M., Wiebking, V., Theruvath, J., Lynn, R. C., Xu, P., Dunn, A. R., Vale, R. D., & Mackall, C. L. Tuning the Antigen Density Requirement for CAR T-cell Activity. *Cancer Discov.* 2020; 10: 702–723.
2. Chen, X., Mirazee, J. M., Skorupka, K. A., Matsuo, H., Youkharibache, P., Taylor, N., & Walters, K. J. The CD8 α hinge is intrinsically disordered with a dynamic exchange that includes proline cis-trans isomerization. *J. Magn. Reson.* 2022; 340: 107234.
3. Choudhuri, K., Wiseman, D., Brown, M. H., Gould, K., & van der Merwe, P. A. T-cell receptor triggering is critically dependent on the dimensions of its peptide-MHC ligand. *Nature.* 2005; 436: 578–582.



Abstract 401 Figure 1 Modeling of intermembrane CART-tumor cell distances promotes the generation of CAR constructs with increased cytotoxic potential. A: Alphafold-generated models of anti-CD19 (FMC63) CAR constructs reveal apparent differences in hinge length. CD8 α hinge = 8H; CD28 hinge = 28H; TM=transmembrane domain. Superscripts refer to the number of amino acids within the hinge. B: A distance of 15nm has been shown to optimize signaling secondary to TCR-MHC interaction³. Distributions of the end-to-end distances of hinges of variable lengths were combined with the distribution of the CD19 target epitope to predict the probability that the combined distribution is 15nm, as evaluated by Xplor-NIH. C: Anti-CD19 CAR constructs with altered hinge lengths exhibit significant differences in ex vivo killing, as evaluated against a CD19low leukemia cell line. Killing index was evaluated in an Incucyte assay and is presented as a function of time (E:T ratio = 1:2). D: Killing indices of anti-CD19 CAR constructs correlate significantly with the modeling prediction of a 15nm optimum CAR-antigen intermembrane length. Data are from two replicates and the identity of the hinges are indicated.

<http://dx.doi.org/10.1136/jitc-2022-SITC2022.0401>

402 T CELL KILLING IS FACILITATED BY MULTIPLE CYTOTOXIC PATHWAYS

Melisa Montalvo*, Irfan Bandey, Ali Rezvan, Kwan-Ling Wu, Arash Saeedi, Yongshuai Li, Rohan Kulkarni, Xingyue An, Navin Varadarajan. *University of Houston, Houston, TX, USA*

Background Chimeric antigen receptor (CAR) T cell therapies show remarkable progress in treating liquid tumors, with a complete remission rate of over 57%.¹ Translating the success of CAR T cells to solid tumors will need an understanding of the key mechanisms responsible for the cytotoxicity of CAR T cells. The primary factors contributing to tumor resistance against CAR T therapies are widely contested², therefore, we seek to explore the impact of different CAR T cell killing mechanisms of tumors.

Methods We examine CAR T cell killing of a leukemic cell line, NALM6, and an ovarian cancer cell line, SkOV3-CD19, in the presence of Granzyme B inhibitors and a Fas ligand inhibitor. We develop a fluorescent membrane reporter that translocates to the nucleus upon specific proteolytic cleaving by Granzyme A and B.

Results

- Overexpressing native Granzyme B inhibitor, Protease Inhibitor-9 (PI-9), in NALM6 and SkOV3-CD19 does not affect killing frequencies in CAR(19-41BB ζ and 19-28 ζ) T cell cytotoxicity assays.
- Treating 19-41BB ζ with a small molecule inhibitor of Granzyme B does not impact killing frequencies in cytotoxicity assays against NALM6 and SkOV3-CD19.
- Overexpressing PI-9 in NALM6 and SkOV3-CD19 does not affect 19-41BB ζ CAR T killing frequencies or killing kinetics in single cell time-lapse assays.
- Inhibition of Fas ligand on 19-41BB ζ CAR T cells does not impact killing frequencies against NALM6 and SkOV3-CD19.

Conclusions Our findings suggest that suppressing Granzyme B activity with small molecules or native proteins does not impair killing frequencies of 19-41BB ζ CAR T cells en masse or at the single cell level. We hypothesize that Granzyme A facilitates CAR T killing in the absence of Granzyme B, implying redundancy in granzyme expression. This study provides a comprehensive understanding of the main mechanisms associated with CAR T cell-mediated killing.

REFERENCES

1. Xu X, Huang S, Xiao X, Sun Q, Liang X, Chen S, Zhao Z, Huo Z, Tu S and Li Y. Challenges and clinical strategies of CAR T-cell therapy for acute lymphoblastic leukemia: overview and developments. *Front Immunol.* 2021; **11**:569117.
2. Shah NN, Fry TJ. Mechanisms of resistance to CAR T cell therapy. *Nat Rev Clin Oncol.* 2019;**16**(6):372–385.

<http://dx.doi.org/10.1136/jitc-2022-SITC2022.0402>

403 **RAPID AND MULTIPLEXED IDENTIFICATION OF NOVEL TCRS FOR TCR-T CELL THERAPY**

Tamson Moore*, Bindu Hegde, John Leonard, Nathan Katz, Akshay Sharathchandra, Bryan Xie, Joanna Dreux, May Khadilkar, Marvin Gee, Leah Sibener. *T Biosciences, South San Francisco, CA, USA*

Background T cell receptor (TCR)-based therapeutics have displayed clinical proof-of-concept, however challenges remain to robustly identify both novel targets and therapeutically active TCRs against endogenous targets.

Methods Here, we have developed a multi-plexed platform to efficiently identify novel TCRs towards non-mutated, tumor specific targets. We have developed a functional expansion protocol, combined with single cell sequencing, that enables the discovery of diverse TCRs in both function and sequence to multiple targets simultaneously.

Results These novel TCRs are highly sensitive, with sub-nanomolar EC50s. Furthermore, these novel TCRs display in vitro killing of target-bearing cells. To interrogate the specificity of these TCRs, we utilized 3T-TRACE, a highly diverse pHLA-target library platform to identify potential cross-reactive peptides that could identify potential liabilities pre-clinically. We find that although sequence distinct TCRs display the same on-target reactivity, they vary considerably in their cross-reactivity.

Conclusions Altogether, we have developed a robust platform to identify and select therapeutically active TCRs for TCR-T based therapy.

<http://dx.doi.org/10.1136/jitc-2022-SITC2022.0403>

404 ENRICHMENT OF NEOANTIGEN REACTIVE TIL IN A CRC PATIENT SAMPLE BY FACS: THE TIDAL-01 PROCESS

Jake Nikota*, Larissa Pikor, Anna Fritzsche, Zachary Jilesen, Sara Fallahi, Barbara Sennino, David Stojdl. *Turnstone Biologics, Hamilton, Canada*

Background Tumor infiltrating lymphocyte (TIL) therapy has proved to be most effective in melanoma. Additionally, enhancing tumor reactivity by selective expansion of individual TIL subpopulations, screened for neoantigen reactivity, has demonstrated some success in breast cancer.¹ However, while other solid tumors such as colorectal cancer (CRC) have been shown to contain neoantigen reactive TIL,² the ability to selectively enrich these cells has been challenging. Here we demonstrate that the TIDAL-01 process, which utilizes tumor-specific mutation containing peptides to select neoantigen reactive TIL by fluorescence-activated single cell sorting (FACS), can lead to a neoantigen targeted Selected TIL product in CRC.

Methods TIL were expanded from a cryopreserved dissociated CRC tumor sample and antigen presenting cells (APCs) were generated from patient-matched blood. Mutations were identified by sequencing and 13-40 amino acid peptides containing the mutation were generated. TIL were selected by FACS from a coculture of TIL and peptide pulsed APCs based on the activation markers CD134 and CD137. Selected TIL were cultured with a rapid expansion protocol (REP) and the expanded TIL were phenotyped and co-cultured with neoantigen pulsed APCs to confirm reactivity. The unselected TIL was expanded by REP as a bulk control for comparison.

Results A clear positive population of activated TIL (3.93%) were selected from the co-culture and expanded >1000 fold. The final TIL product was 93.6% CD4 cells and 4.60% CD8 cells and >90% of CD4 and CD8 cells expressed markers of an effector memory phenotype. Single cell sequencing of the T cell receptor repertoire revealed 12 clonotypes that were enriched in sorted TIL vs bulk TIL. In response to co-culture, 31.2% of CD8 cells and 25.6% of CD4 cells in the selected TIL product were positive for IFN- γ by intracellular cytokine staining. IFN- γ and TNF- α were 53 and 360-fold higher in the co-culture supernatants of selected TIL compared to bulk TIL, respectively. As a measure of killing potential, 20.9% of CD8 cells degranulated in co-culture based on CD107 expression and granzyme B secretion was increased 16.5-fold over bulk TIL. Deconvolution of the peptide pool identified one CD4 and one CD8 antigen driving the neoantigen reactivity.

Conclusions These data provide non-clinical proof of concept that neoantigen enriched TIL can be selected by FACS and expanded into a TIL product that contains a marked increase in neoantigen reactive TIL compared to bulk expanded TIL from a CRC tumor.

REFERENCES

1. Zacharakis N, Huq L M, Seitter SJ, Kim SP, Gartner JJ, Sindiri S, Hill VK, Li YF, Paria BC, Ray S, et al. Breast cancers are immunogenic: immunologic analyses and a phase ii pilot clinical trial using mutation-reactive autologous lymphocytes. *J Clin Oncol.* 2022;**40**(16):1741–1754
2. Parkhurst MR, Robbins PF, Tran E, Prickett TD, Gartner JJ, Jia L, Ivey G, Li YF, El-Gamil M, Lalani A, et al. Unique neoantigens arise from somatic mutations in patients with gastrointestinal cancers. *Cancer Discov.* 2019;**9**:1022–1035.

Ethics Approval All human material was obtained from a commercial source, Discovery Life Sciences, which ensures IRB and ethics committee compliance.

<http://dx.doi.org/10.1136/jitc-2022-SITC2022.0404>

405

**A NON-CANONICAL ROLE FOR CCL2 IN T CELL
MIGRATION: IMPROVING DUAL-INTERFERON-TREATED
AUTOLOGOUS MONOCYTES AS A THERAPY FOR
OVARIAN CANCER**

Franklin Ning*, Thomas Meyer, Brittney Harrington, Christina Annunziata. *National Cancer Institute, Bethesda, MD, USA*

Background Ovarian cancer is the fifth leading cause of cancer-related death in women in the US and the most lethal gynecologic malignancy. Although many patients respond initially to platinum-based chemotherapy, over 70% of patients diagnosed with advanced stage ovarian cancer relapse within 24 months and have limited second-line treatment options. Our group pioneered an approach manipulating innate immunity where autologous monocytes, interferon-gamma, and interferon-alpha2b (AMIGA) were given intraperitoneally to women with recurrent, ovarian cancer in order to directly kill tumor cells and mitigate the immunosuppressive tumor microenvironment.

Methods 18 patients were enrolled in the Phase 1 clinical trial (NCT02948426). Peripheral blood mononuclear cells (PBMCs) were collected from patients pre- and post-treatment cycles. Malignant ascites was collected when present. PBMCs were used for bulk and single-cell RNA-sequencing. Downstream analysis was completed on the NIH's Integrated Data Analysis Platform. LegendPlex Essential Immune Response kit (Biolegend #740930) was used to quantify ascites' cytokines. For migration assays, conditioned media from 2D and 3D ovarian cancer cell cultures treated with AMIGA was used to assess T cell migration. Migration was assayed 24 hours after T cells were exposed to conditioned media by flow cytometry or spinning disk confocal microscopy.

Results Of the 18 enrolled patients, two had partial responses and four had stable disease. Of these, both responders and two of the four patients with stable disease maintained clinical benefit for five or more months, and were thus labelled as long-term responders (LTRs). Through bulk-cell RNA-sequencing, the PBMCs of these LTRs showed increased levels of T cell activation and migration genes compared to the 14 non-responders (NRs). In light of this, we assessed patient malignant ascites for relevant chemokines and found CCL2, a known monocyte, and less so T cell, trafficking molecule, had increased in response to treatment. We then validated *in vitro* that CCL2 is significantly increased in the supernatants of AMIGA-treated ovarian cancer cells, but that this increase correlated with increased T cell, and not monocyte, migration. Furthermore, by manipulating the CCL2-CCR2 signaling axis *in vitro*, we were able to significantly alter T cell migration.

Conclusions Overall, our findings suggest AMIGA aids T cell migration towards ovarian cancer by increasing the production of CCL2. By further understanding how AMIGA contributes to T cell migration and function in the ovarian cancer tumor microenvironment, we seek to combine innate- and adaptive-based immunotherapies to improve the treatment options and, ultimately, survival of women with ovarian cancer.

<http://dx.doi.org/10.1136/jitc-2022-SITC2022.0405>

406

AN UNBIASED SURVEY OF TUMOR REACTIVITY AND TRANSCRIPTIONAL LANDSCAPE OF 1,000 CLONES OF PD-1^{hi} T-CELLS FROM PERIPHERAL BLOOD DURING ICB TREATMENT REVEALS BREATH AND DYNAMICS OF ANTI-TUMOR IMMUNITY

<http://dx.doi.org/10.1136/jitc-2022-SITC2022.0406>

¹Danielle Cook*, ²Immaculada Creus, ²Andrea Garcia-Garijo, ²Pierre Levy, ¹Seon Kinrot, ²Rodrigo Toledo, ²Elena Garralda, ¹Ely Porter, ¹Xi Chen, ²Alena Gros. ¹RootPath, Watertown, MA, United States; ²Vall d'Hebron Institute of Oncology, Barcelona, Spain

Background Immune checkpoint blockade (ICB) treatment often results in drastic changes in the TCR repertoire and T-cell phenotypes in the tumor and periphery. While scRNA-Seq allows the sequencing of thousands of T-cells, the high cost of TCR synthesis (>\$100 per TCR) makes it cost-prohibitive to identify which clones are tumor-reactive, particularly in peripheral blood where tumor-reactive cells are rarer. This severely hinders our mechanistic understanding of these treatments and the possibility to develop non-invasive personalized T-cell-based therapies. To solve this problem, we developed a novel technology, named PathFinder DNA Assembly™, that allows parallel synthesis and cloning of thousands of TCRs simultaneously for a cost of **under \$1 per TCR**. This enables the high-throughput experimental screening of up to 1000 TCRs for tumor reactivity. We have applied this technology to survey peripheral bulk or PD-1^{hi} T-cells from a melanoma patient before and after ICB treatment, since previous studies have demonstrated that PD-1 may be a biomarker for tumor-reactive T-cells from both tumor-infiltrating and peripheral T-cells.^{1 2}

Methods We obtained PBMCs of a melanoma patient at multiple time points before and after the ICB treatment. Next, we obtained scRNA-Seq data for both bulk CD3⁺ sorted and PD-1^{hi} sorted T-cells. We then synthesized, cloned, and expressed 1,000 TCR sequences in peripheral T-cells from unrelated donors while ensuring each T-cell only expresses a single TCR, creating polyclonal TCR-T-cells, which were then screened for tumor reactivity by co-culturing with autologous tumor or melanoma cell lines expressing the patient-matched HLAs. After co-culture, activated TCR-T-cells were sorted based on an activation marker, sequenced to identify the enriched TCRs, and then validated individually.

Results Both pre- and post-treatment PMBCs harbor T-cell clones that are also found in the tumor, with many emerging after ICB treatment. More than 30 TCRs were identified to be tumor-reactive, many of which emerged during the ICB treatment. Interestingly, 12 out of the 14 tumor-reactive TCRs obtained from screening on 3rdparty cancer cell lines also appeared to be reactive to the autologous tumor.

Conclusions These results not only reveal previously hidden details of ICB treatment but also exemplify the approach to affordably identify tumor-reactive TCRs for each patient without any tumor tissue resection. These TCRs can be used to produce highly potent, autologous, polyclonal TCR-T products that have the potential to be the next generation of adoptive cell therapy.

REFERENCES

1. Gros A, Robbins PF, Yao X, Li YF, Turcotte S, Tran E, Wunderlich JR, Mixon A, Farid S, Dudley ME, Hanada K, Almeida JR, Darko S, Douek DC, Yang JC, Rosenberg SA. PD-1 identifies the patient-specific CD8⁺ tumor-reactive repertoire infiltrating human tumors. *J Clin Invest*. 2014 May; **124**(5):2246–59.
2. Gros A, Parkhurst MR, Tran E, Pasetto A, Robbins PF, Ilyas S, Prickett TD, Gartner JJ, Crystal JS, Roberts IM, Trebska-McGowan K, Wunderlich JR, Yang JC, Rosenberg SA. Prospective identification of neoantigen-specific lymphocytes in the peripheral blood of melanoma patients. *Nat Med*. 2016 Apr; **22**(4):433–8.

407

MITOCHONDRIAL TRANSCRIPTION IS REQUIRED FOR THE ENHANCED ANTI-TUMOR ACTIVITY OF ADOPTIVELY TRANSFERRED STEM-LIKE MEMORY T CELLS

¹Guillermo Rangel Rivera*, ²Connor Dwyer, ¹Hannah Knochelmann, ³Aubrey Smith, ⁴Anna Cole, ⁴Megan Wyatt, ⁴Chrystal Paulos, ⁵Jessica Thaxton, ¹Shikhar Mehrotra, ⁴Haydn Kissick, ⁶Mark Rubinstein, ⁴Gregory Lesinski. ¹Medical University of South Carolina, Atlanta, GA, United States; ²Werewolf Therapeutics Inc., Watertown, MA, United States; ³Orange Grove Bio, Decatur, GA, United States; ⁴Emory University, Atlanta, GA, United States; ⁵University of North Carolina, Chapel Hill, NC, United States; ⁶The Ohio State University, Columbus, OH, United States

Background Durable responses have been observed with adoptive T cell therapy in chemotherapy and immunotherapy refractory patients. However, current T cell products do not always lead to therapeutic responses. T cell intrinsic factors that lead to failure in immunotherapy have been attributed to T cell exhaustion and poor mitochondrial quality. T cell mediated immunity can be impaired by overt PI3K δ signaling through altering transcriptional rewiring and metabolism. Recently, chronic PI3K signaling is associated with loss of mitochondrial transcription and mitochondrial DNA. We hypothesized that PI3K δ inhibition would generate stem-like memory T cells (T_{scm}) that provide protection against melanoma by sustaining stemness and enhancing mitochondrial fitness.

Methods To test this, we primed melanoma specific CD8⁺ pmel-1 T cells in the presence of increasing concentrations of Idelalisib, a PI3K δ specific inhibitor, and infused them into B16F10 tumor bearing, following non-myeloablative total body irradiation. We modeled both high and low immunogenic tumors using two different tumors lines of B16F10 melanoma (expressing low affinity mouse gp100) and a modified B16F10 line (expressing high affinity human gp100 antigen). *In vitro* we tested T cell stemness by flow cytometry and RNA sequencing. We assessed mitochondrial qualities such as mass, membrane potential, reactive oxygen species, and respiratory capacity. Mitochondrial transcription was measured via mitochondrial mRNA relative quantification and protein levels of electron transport proteins. We further tested the effect of ablating mitochondrial transcription by CRISPR knockout using guides against a known regulator of mitochondrial transcription.

Results We found that PI3K δ inhibited T cells provide potent antitumor activity in both poor and highly immunogenic tumor models of melanoma. The adoptively transferred T cells transcriptionally resemble intratumoral T_{scm} cells. Transcriptionally they showed elevated *Tcf7*, and *Lef1*, and suppressed *Havcr2*, and *Prdm1*. Metrics of improved mitochondrial quality were elevated in a dose dependent manner. Mitochondrially encoded electron transport chain gene expression was selectively enhanced at the RNA and protein level. Ablation of mitochondrial transcription vastly impaired the antitumor activity of stem-like memory T cells generated with PI3K δ inhibition.

Conclusions These findings indicate that blocking PI3K δ in T cells mediates lasting tumor immunity of adoptively transferred T cells by preserving stemness features and improving mitochondrial fitness. We discovered that enhanced mitochondrial transcription is required for T_{scm} anti-tumor immunity. These findings suggest that modulating mitochondrial transcription is a potential target to bolster the activity of tumor specific T cells.

Acknowledgements We would like to thank all the researchers and clinicians leading the way in translating immunological

principles into effective therapies, as well as the patients whose support is integral for the furthering of medicine.

Ethics Approval All animal procedures performed at the Medical University of South Carolina or Emory University were approved by each university's Institutional Animal Care & Use Committee, protocol number 0488 or 201900225, respectively

<http://dx.doi.org/10.1136/jitc-2022-SITC2022.0407>

408 **NEUTRALIZING OXIDATIVE DAMAGE AT TELOMERES PREVENTS T CELL DYSFUNCTION AND IMPROVES ADOPTIVE CELL THERAPY**

¹Dayana Rivadeneira*, ¹Sanjana Thosar, ²Konstantinos Lontos, ¹Jessica Jana, ³Marcel Bruchez, ¹Patricia Opreko, ¹Greg Delgoffe. ¹University of Pittsburgh, Pittsburgh, PA, United States; ²University of Pittsburgh Medical Center, Pittsburgh, PA United States; ³Carnegie Mellon University, Pittsburgh, PA, United States

Background The functional state of tumor infiltrating lymphocytes (TIL) is a critical determinant of antitumor immunity and response to immunotherapy. One of the key factors responsible for T cell dysfunction are metabolic barriers such as nutrient competition, low oxygen tension, and damaging byproducts in the tumor microenvironment. One of these metabolic barriers is the accumulation of oxidative stress, a critical contributor of T cell dysfunction observed during aging as well as in the tumor microenvironment. We and others have shown that accumulation of reactive oxygen species (ROS) accumulation drives T cell exhaustion. ROS can affect many cellular functions, but notably can induce DNA damage. We asked whether TIL accumulate DNA damage at telomeres as a consequence of terminal differentiation, and used a chemo-optogenetic approach to specifically induce telomeric DNA damage to explore its role in T cell biology, especially within the context of cancer.

Methods In this study we perform telomeric and centromeric FISH assays to analyze TIL for DNA damage accumulation. We used a chemo-optogenetic FAPS-TAPS to generate singlet oxygen and consequent 8-oxo-guanine lesions specifically at telomeres.¹ We tethered GPX1 to TRF1 to generate a telomere-guided antioxidant protein.

Results Telo-FISH analysis demonstrated an accumulation of telomeric DNA damage, but not telomere shortening, in exhausted TIL from B16 mouse tumors, coordinate with presence of 53BP1 and gammaH2AX. Our data show that specific induction of mitochondrial and telomeric ROS cause the accumulation of DNA damage at telomeres, and consequent development of telomere fragility. These cells ultimately become dysfunctional showing a diminished capability for cytokine production. Importantly, targeting the ROS scavenger GPX1 directly to telomeres reduced telomere fragility and improved the function of therapeutic T cells in the B16 melanoma model.

Conclusions Our data suggest that dysfunctional T cells in cancer are not classically senescent, bearing short telomeres, but rather harbor damaged telomeres due to exposure to oxidative stress. Telomeric damage is sufficient to drive a dysfunctional state in newly activated T cells. Protecting telomeres through expression of a telomere-targeted antioxidant protein may preserve T cell function in the tumor microenvironment and drive superior responses to immunotherapy.

REFERENCE

1. Fouquerel E, Barnes RP, Uttam S, Watkins SC, Bruchez MP, Opreko PL. Targeted and persistent 8-oxoguanine base damage at telomeres promotes telomere loss and crisis. *Mol Cell*. 2019 Jul 11;75(1):117–130.e6. doi: 10.1016/j.molcel.2019.04.024. Epub 2019 May 14. PMID: 31101499; PMCID: PMC6625854.

<http://dx.doi.org/10.1136/jitc-2022-SITC2022.0408>

409

MANUFACTURING OF A CLINICAL SCALE CD8 TIL PRODUCT, AGX148, WITH AND WITHOUT GENE SILENCING OF PD-1 USING SELF-DELIVERING RNAi INTASYL™ PH-762

¹Colin Thalhofer*, ²Simon Fricker, ¹Ryan Montler, ¹Elaine Ballinger, ¹Nick Morris, ¹Jake Moses, ²Dingxue Yan, ³Tarsem Moudgil, ³Bernard Fox, ³Nelson Sanjuan, ³Eric Tran, ²James Cardia, ¹Andrew Weinberg. ¹AgonOx Inc., Portland, OR, United States; ²Phio Pharmaceuticals, Marlborough, MA, United States; ³Providence Cancer Institute, Portland, OR, United States

Background Adoptive Cell Therapy (ACT) with Tumor Infiltrating Lymphocytes (TIL) can induce durable clinical responses in a percentage of patients with melanoma, however, the efficacy of standard TIL therapy (Bulk TILs) can be limited. We hypothesize that the therapeutic efficacy of TIL therapy is dependent on the abundance of tumor-reactive T cells in the ACT product, as well as the functionality of the T cells in the product. Our approach enriches for tumor-reactive TIL by sorting CD8+ T cells from patient tumors that co-express CD103 and CD39 prior to expansion of the ACT product,¹ termed AGX148. To mitigate PD-1-induced immune suppression in the Tumor Microenvironment (TME) and further enhance the therapeutic potential of AGX148 we have utilized Phio Pharmaceuticals' self-delivering RNAi INTASYL™ PH-762 to knock down PD-1 during the expansion.

Methods Surgically resected human tumor samples were provided through a collaboration with the Earle A. Chiles Research Institute's clinical research program at the Providence Cancer Institute. We have adapted our research expansion method into an optimized clinical manufacturing process. In collaboration with the Providence Cancer Institute's Cell Processing Facility and Phio Pharmaceuticals, we have completed three full scale IND-enabling manufacturing runs of our ACT product AGX148 w/wo PH-762 INTASYL™.

Results Our data demonstrate that the AGX148 ACT product can be successfully manufactured at a clinical scale and that AGX148 treated with PH-762 during the expansion process is effective at reducing the steady-state level of PD-1 protein. We also tested AGX148 ACT product for autologous tumor recognition and killing in co-culture assays in vitro and in vivo. AGX148 and AGX148 combined with PH-762 were able to recognize and kill autologous tumor lines in vitro and PH-762-treated cells had increased 4-1BB expression in TIL/tumor cocultures. PH-762 induced knockdown of PD-1 was observed in circulating T cells after ACT in a xenograft model with autologous tumor.

Conclusions We have generated a potent tumor-specific ACT TIL product (AGX148) at clinical scale through the isolation and selective expansion of tumor-reactive T cells. Knocking down PD-1 with PH-762 INTASYL™ has the potential to further enhance the function of the AGX148 product and this ACT product will soon be tested in cancer patients.

REFERENCE

1. Duhon T, Duhon R, Montler R, et al. Co-expression of CD39 and CD103 identifies tumor-reactive CD8 T cells in human solid tumors. *Nat Commun* 2018;**9**:2724.

Ethics Approval Human sample collection for this study was approved by the institutional review board, Providence St. Joseph Health IRB (FWA00029175), Study ID: PDX06-108. All patients provided informed consent for participation in this study. Experimental animal studies were performed according to the National Institutes of Health Guide for the Care and Use of Laboratory Animals and in accordance with

the EACRI Institutional Animal Care and Use Committee (Animal Welfare Assurance No. A3913-01) protocol# 51.

Summary: Name of IRB: Providence St. Joseph Health IRB (FWA00029175)

Study ID: PDX06-108

Most Recent IRB Submission ID: CR2022000115 (Continuing Review)

Date of most recent approval: 03/08/2022

The Institutional Animal Care and Use Committee (IACUC) of Providence Portland Medical Center

Study Protocol #51

Date of most recent approval: 03/28/2022

<http://dx.doi.org/10.1136/jitc-2022-SITC2022.0409>

410 **PRIMING OF SYNNOTCH CAR T CELLS VIA CNS-SPECIFIC ANTIGEN ALLOWS SPATIAL AND TEMPORAL REGULATION OF CAR EXPRESSION, EFFECTIVE HOMING AND PERSISTENCE OF T CELLS IN THE CNS, RESULTING IN THE COMPLETE ERADICATION OF AGGRESSIVE GLIOBLASTOMA**

Payal Watchmaker*, Milos Simic, David Diebold, Psalm Pineo-Cavanaugh, Jason Duecker, Wei Yu, Wendell Lim, Hideho Okada. *UCSF, San Francisco, CA, United States*

Background The CAR T cell therapies have failed to produce long-term remission in glioma patients. One of the key challenges in the development of an effective CAR-T therapy is the absence of target antigens that are tumor-specific and have homogenous expression. To safely target glioblastoma-associated antigens (GAAs) in the tumor without attacking normal tissue expressing the same GAAs outside of the brain, we adopted a novel synthetic Notch (synNotch) receptor system and established a “prime and kill” sequential two-receptor CAR circuit. We used glioblastoma- (GBM) specific neoantigen EGFRvIII as a priming signal for synNotch receptor and have reported robust antitumor response in the mice bearing intracerebral PDX tumor with heterogenous EGFRvIII expression. However, less than 20% of adult GBM cases express EGFRvIII. Furthermore, EGFRvIII expression can diminish over time even after its detection in the primary GBM, and the EGFRvIII-synNotch primed CAR T cells may deplete EGFRvIII-expressing GBM cells via their cytotoxic effects, thereby losing the priming signal. To overcome these inherent challenges of the EGFRvIII-priming strategy, we used CNS (Central Nervous System) tissue-specific antigens as the priming signal to drive localized expression of the CAR against EphA2 and IL-13R α 2 and bypassed the need for tumor-specific antigen.

Methods We have found BCAN (also known as Brevican) as the most promising priming antigen based on the specific and robust priming among several CNS-specific cell surface proteins that we evaluated. We created a synNotch-CAR circuit in which BCAN primes the T cells to induce expression of a CAR that recognizes IL-13R α 2 and EphA2.

Results When mice bearing intracerebral GBM6 PDX received a single intravenous (IV) infusion of T cells engineered with the α -BCAN synNotch α -EphA2/IL-13R α 2 CAR (B-SYNC) circuit, all mice (10/10) demonstrated complete regression of the tumor. Furthermore, these B-SYNC T cells were significantly more efficacious than constitutively expressed EphA2/IL-13R α 2 CAR T cells. The enhanced in vivo efficacy and superior persistence of B-SYNC T cells were associated with its tissue-resident and memory stem-cell-like phenotype.

Conclusions Taken together, the B-SYNC approach represents a robustly efficacious and conceptually novel T cell therapy with the CNS tissue-specific CAR activation. This also enhances the translational significance of synNotch-CAR T cells by widely extending the eligibility to EGFRvIII-negative glioma patients. We are currently developing a phase I study to evaluate the safety as well as the homing and priming status (i.e. expression of CAR) of the IV-infused B-SYNC T cells in patients with GBM.

<http://dx.doi.org/10.1136/jitc-2022-SITC2022.0410>

411 THE MULTI-OMICS ANALYSES OF "OFF-THE-SHELF" CD19-CAR-T CELLS IDENTIFIES THE SUBPOPULATION COMPLEXITY AND THE DEEP CHARACTERIZATION OF THE ANTI-TUMOR PROPERTIES

¹Asma Al Sulaiti, ¹Mohammed El-Anbari, ¹Shana Jacob, ¹Toufiq Mohamed, ¹Saroja Kotegar Balayya, ¹Suruchi Mohan, ¹Damilola Olagunju, ¹Chiara Cugno, ¹Sara Deola, ¹Jean-Charles Grivel, ¹Damien Chaussabel, ²Chiara Bonini, ²Monica Casucci, ¹Cristina Maccalli*. ¹Sidra Medicine, Doha, Qatar; ²San Raffaele Hospital, Milano, Italy

Background The goal of this study is to generate and optimize the manufacturing of "off-the-shelf" CD19-CAR-T cells utilizing umbilical cord blood (UCB) as starting material.

Methods T cells were isolated from UBCs (N=15) through negative magnetic selection and upon activation *in vitro* using CD3 and CD28 mAbs. The T lymphocytes were then transduced with lentiviral vectors encoding for CD19-CD28z-or CD19-4-1BBz-CARs. CD19-CAR-T cells were also generated from the peripheral blood lymphocytes (PBL; N=5) as reference. The multiparametric phenotype analysis was performed assessing the expression of markers associated with T cell differentiation and activation by CAR-T cells. Functional assays, through either Elispot, FluoroSpot or Luminex platforms, were carried out to assess cytokine, chemokine and cytotoxic profiles of the T cells. A machine learning technique called L0-regularized logistic regression,^{1,2} implemented in the R package L0Learn, was used to select the optimal values of the tuning parameters. The metabolomic and transcriptomic profiles of CD19-CAR-T cells was determined upon the antigen-specific or not engagement of the CARs.

Results The enrichment of both CD4⁺ and CD8⁺ CD19-CAR-T cells with stem memory-like or early stage of differentiation (CD45RA⁺) phenotype and co-expressing either ICOS or BTLA was observed in UCB- vs. PBL-derived CD19-CAR-T cells (p<0.0002-<0.05). Moreover, differential phenotype of CAR-T cells was associated with the variable costimulatory signals comprised in the structure of the CARs (CD28z or 4-1BBz). The differential antigen-specific anti-tumor activity of these CAR-T cells was identified, with diversities depending on the type and source of engineered T cells. Distinct metabolomic profiles, including pathways related to amino acid, tryptophan and nucleotide sugar metabolism and protein biosynthesis were detected in relation to the antigen-specific or unrelated stimulation and the manufacturing procedures. Integration of multi-omics results, including the transcriptomic profile allowed to identify the complexities of CD19-CAR-T cells phenotypes and functions.

Conclusions The characterization of phenotype and functional properties of CAR-T cells through multi-omics platforms allowed to prove the suitability of UCB to generate "off-the-shelf" CAR-T cells and to identify sub-populations endowed with superior anti-tumor activity.

REFERENCES

1. Hussein Hazim and Rahul Mazumder. Fast best subset selection: Coordinate descent and local combinatorial optimization algorithms. *Operations Research*, 2020;**68**(5):1517–1537.
2. Antoine Dedieu, Hussein Hazim, and Rahul Mazumder. Learning sparse classifiers: Continuous and mixed integer optimization perspectives. *Journal of Machine Learning Research*, 2021.

Ethics Approval The study obtained ethics approval from Sidra Medicine review board; approval #1500788. Participants to the study gave informed consent before taking part.

<http://dx.doi.org/10.1136/jitc-2022-SITC2022.0411>

412 **SYNTHETIC PD-1 CO-STIMULATORY MOLECULE PRESERVES A CYTOLYTIC CAR T CELL IMMUNE SYNAPSE WHILE REDUCING TONIC SIGNALING**

Rebecca Brock*, Jessica Morris, Ahmed Gad, Daniel Landi, Shoba Navai, Zeid Nawas, Sujith Joseph, Nabil Ahmed, Alexandre Carisey, Meenakshi Hegde. *Baylor College of Medicine, Houston, TX, United States*

Background It is well established that solid tumors upregulate checkpoint inhibitor ligands to suppress anti-tumoral immunity. This in turn can have a negative impact on the functionality of cell therapeutics such as chimeric antigen receptor (CAR) T cells by promoting exhaustion and cell death. In tumors such as glioblastoma (GBM), pro-inflammatory cytokines produced by T cells further contribute to this feedback loop, resulting in increased expression of PD-L1 and PD-L2. We have developed CAR T cells to modulate PD-1/PD-L1 (or PD-L2) signaling through engagement with a synthetic PD-1 molecule. Here, we hypothesize that the first generation CAR T cells with synthetic PD-1 co-stimulatory molecule form a functional immune synapse with tumor cells while maintaining a more physiological signaling state.

Methods HER2-specific CAR T cells expressing a synthetic PD-1 co-stimulatory molecule were generated from primary human T cells using a bicistronic vector and retroviral gene delivery. Appropriate control T cells were manufactured in parallel from the same donors under similar conditions. CAR T cell and HER2+ LN229-GBM cell conjugates (doublets) were studied using imaging flow cytometry for CAR immune synapse (CARIS) formation and composition. Phosphorylation of CD3 ζ was assessed at rest and over time after exposure to tumor cells by western blotting. Supernatant from T cell and HER2+ GBM co-cultures were analyzed using a multiplex assay to evaluate patterns of cytokine release.

Results Imaging of the CARIS revealed that PD-1 is recruited within 60 minutes of CAR T cell and tumor cell engagement. Synthetic PD-1 receptor was recruited to the CARIS within 60 minutes with tumor cells exhibiting constitutive/inducible PD-L1 or PD-L2 expression. Further, first generation CAR T cells with a PD-1 co-stimulatory molecule demonstrated enrichment of actin, indicative of “mature” immune synapse formation, comparable to a second-generation CAR. At baseline, PD-1 co-stimulatory molecule expressing CAR T cells with split signaling exhibit lower phosphoCD3 ζ compared to second generation control CAR T cells. Consistent with our imaging findings, CAR T cells with split signaling demonstrated robust CD3 ζ phosphorylation similar to that of second generation CAR T cells by 60 minutes. Upon additional assessment, we found that CAR T cells with split signaling showed a pattern of pro-inflammatory cytokine secretion distinct from second generation CAR T cells.

Conclusions Co-stimulation through synthetic PD-1 molecule confers a favorable functional profile to CAR T cells and may enhance their safety, longevity and antitumor function after adoptive transfer.

Ethics Approval This study was approved by Baylor College of Medicine's Ethics Board; approval number H-15280.

<http://dx.doi.org/10.1136/jitc-2022-SITC2022.0412>

413 **GENETIC DELETION OF TIGIT ENHANCES CAR-NK CELL FUNCTION IN THE SOLID TUMOR MICROENVIRONMENT**

Ishwar Navin*, Matthew Dysthe, Corrine Baumgartner, Robin Parihar. *Baylor College of Medicine, Houston, TX, United States*

Background Natural killer cells (NKs) expressing chimeric antigen receptors (CAR-NKs) were successful in hematological malignancies.¹ However, solid tumors resist CAR-NKs via a tumor microenvironment (TME) that includes myeloid derived suppressor cells (MDSCs) and M2 macrophages (M2s).² We demonstrated that ex vivo manufacture of therapeutic CAR-NKs significantly upregulated T cell immunoreceptor with Ig and ITIM domains (TIGIT), an inhibitory NK receptor. Analysis of pediatric neuroblastoma and sarcoma patient tumors confirmed high expression of TIGIT ligands on tumor cells and intra-tumoral MDSCs and M2s. *Our main objective* was to determine influence of TIGIT on CAR-NK function in the TME. Current TIGIT-targeting approaches using antibodies are handicapped by poor bioavailability and transient binding in the TME. *We hypothesized* that genetic deletion of TIGIT on CAR-NKs will lead to a more profound and durable anti-tumor response within the TME.³

Methods TIGIT knockout (KO) CAR-NKs expressing a GD2.4-1BB.zeta CAR were generated by concurrent CRISPR/Cas9 and retroviral transduction of expanded primary human NK cells. Degranulation (CD107a) and IFN- γ by TIGIT^{KO}. GD2.CAR-NK were assessed in short-term TME co-cultures containing LAN-1 neuroblastoma and human MDSCs. A novel long-term TME co-culture wherein human monocytes and CHLA255 neuroblastoma pre-established a suppressive TME for 72 hours prior to addition of TIGIT^{KO} GD2.CAR-NK was used to assess tumor growth and CAR-NK proliferation over 96 hours using Incucyte. We assessed phosphorylated mTOR (pMTOR) in CAR-NKs by intracellular flow cytometry.

Results CRISPR/Cas9 and retroviral transduction generated stable TIGIT^{KO}.CAR-NKs (>90% TIGIT deletion; 60% GD2.CAR expression). TIGIT^{KO} enhanced GD2.CAR-NK cytokine secretion but not degranulation in short-term TME co-cultures. In long-term tumor co-cultures, TIGIT^{KO}.GD2.CAR-NKs eliminated more tumor vs control NKs (<10% viable tumor vs 35% viable tumor, $p < 0.01$; $n = 4$ donors). In TME co-cultures, TIGIT^{KO}.GD2.CAR-NK rapidly proliferated and controlled tumor compared to TIGIT^{wt}.CAR-NKs (37% viable tumor vs 57% viable tumor, $p < 0.05$; $n = 4$ donors). TIGIT^{KO} did not increase CAR-NK degranulation or Fas ligand expression, nor did it alter CAR-NK surface expression of DNAM-1, NKG2D, NKG2A, TIM-3, PD-1 or LAG-3. While TIGIT^{wt}.CAR-NKs massively downregulated pMTOR within the TME, TIGIT^{KO}.CAR-NKs maintained pMTOR expression. Ongoing studies using a novel in vivo TME xenograft model of neuroblastoma will determine benefit of TIGIT^{KO} vs. TIGIT antibody therapy on CAR-NK activity.

Conclusions We defined a role for TIGIT in inhibition of CAR-NK function and suggest TIGIT deletion as a novel NK therapeutic platform to evade immune suppression in the TME. This highlights the potential of gene-edited CAR-NKs to improve clinical outcomes in patients with solid tumors.

REFERENCES

1. Liu E, Marin D, Banerjee P, Macapinlac HA, Thompson P, Basar R, Nassif Kerbaui L, Overman B, Thall P, Kaplan M, Nandivada V, Kaur I, Nunez Cortes A, Cao K, Daher M, Hosing C, Cohen EN, Kebriaei P, Mehta R, Neelapu S, Nieto Y, Wang M, Wierda W, Keating M, Champlin R, Shpall EJ, Rezvani K. Use of CAR-Transduced Natural Killer Cells in CD19-Positive Lymphoid Tumors. *N Engl J Med*. 2020;**382**: 545–553.

2. Beavis PA, Slaney CY, Kershaw MH, Gyorki D, Neeson PJ, Darcy PK. Reprogramming the tumor microenvironment to enhance adoptive cellular therapy. *Semin Immunol*. 2016;**28**: 64–72.
3. Chames P, Van Regenmortel M, Weiss E, Baty D. Therapeutic antibodies: successes, limitations and hopes for the future. *Br J Pharmacol*. 2009. **157**: 220–233.

<http://dx.doi.org/10.1136/jitc-2022-SITC2022.0413>

Abstracts

414 TARGET EPHRIN A3 ON CANCER CELLS AND TUMOR MICROENVIRONMENT IN BRAIN CANCER

Ekene Ogbodo*, Reona Sakamura, Michael Ruff, Claudia Roman, Truc Huynh Huynh, James Girsch, Olivia Sirpilla, Kun Yun, Carli Stewart, Ismail Can Can, Mohamad Adada, Lionel Fonkoua, Mehrdad Hefazi, Elizabeth Siegler, Saad Kenderian . *Mayo Clinic, Rochester, MN, United States*

Background Glioblastoma multiforme (GBM) is the most lethal form of brain cancer with a median survival of < 2 years despite treatment advances. Evidence indicates that GBM has been shown to reprogram immune responses to promote its progression. A predominant component of the immunosuppressive tumor microenvironment (TME) is glioblastoma-associated macrophages (GAM). GAM represents up to 50% of the bulk cell population in the GBM microenvironment and is crucial in tumor progression and persistence. We and others have shown the expression of the Ephrin A3 (EphA3) receptor in both tumor and GAM. We hypothesize that dual targeting of both the cancer cell and the immunosuppressive TME with EphA3-specific chimeric antigen receptor T (EphA3-CART) cells would enhance antitumor.

Methods We first investigated the expression of the EphA3 receptor on GBM patient-derived xenografts using immunohistochemistry (IHC) and Western blot. We then polarize primary monocyte or THP-1 monocytic cell line into M2-like macrophages and investigated the expression of the EphA3 receptor on both flow cytometry and then studied the effect of EphA3-CART against EphA3⁺ SNB-19 GBM cell line using the polarized macrophage. We also assessed the antitumor activity of the EphA3-CART in vivo. NSG mice were subcutaneously injected with 1 x 10⁶ Luc+ SNB-19 GBM cell line and monitored for tumor growth using bioluminescence imaging (BLI) and/or tumor size using vernier calipers. At BLI of >1 x10⁸ p/s and/or tumor volume of 200-300 mm³, mice were randomized and treated with 5 x 10⁶ EphA3-CAR T cells. And were further monitored by both BLI and/or tumor size using vernier calipers.

Results Our immunohistochemical analysis data revealed EphA3 expression on 26.623% of the PDX representing the area of the human cancer tissue and was confirmed using the western blot analysis of the selected GBM PDX lines in our biobank (figure 1). EphA3-CART cells exhibited potent antitumor activity against EphA3⁺ GBM cell line SNB-19 (figure 2). M2 polarized macrophage marker expressing a high level of CD206 as well as EphA3 compared to M1 polarized macrophages. EphA3-CART cells were effective in eliminating M2 macrophages (figure 3) and ameliorated M2-induced CART cell inhibition. Finally, EphA3-CART cells exhibited superior tumor control in GBM xenografts compared to the control un-transduced T cells (UTD), (figure 4).

Conclusions In summary, we have developed EphA3-CART cells that target both the tumor cells and GAM within GBM TME which holds promise in improving CART antitumor activity within the immunosuppressive solid tumor milieu.

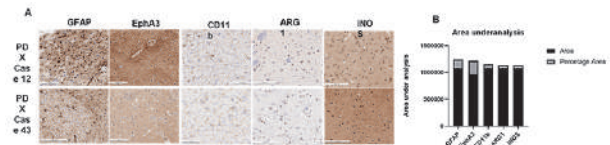


Figure 1. Results of immunohistochemical analysis of patient derived xenograft (PDX) passaged in the nude mice. Photomicrograph (A) and the result of statistical analyses (B) are shown. Immunohistochemical analyses demonstrate high expression levels of GFAP, EphA3, CD11b, ARG1 and iNOS. The EphA3 expression was shown to occupy most area. Original magnification, x20; scale bar, 100 µm.

Abstract 414 Figure 1 Results of Immunohistochemical analysis of patient derived xenograft (PDX) passaged in the nude mice. Photomicrograph (A) and the result of statistical analyses (B) are shown. Immunohistochemical analyses demonstrate high expression levels of GFAP, EphA3, CD11b, ARG1 and iNOS. The EphA3 expression was shown to occupy most area. Original magnification, x20; scale bar, 100 µm

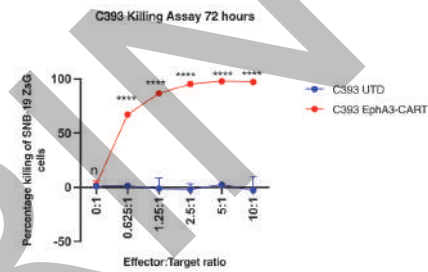


Figure 2. Cytotoxicity assay; SNB-19 ZsG was cocultured with increasing ratios of either EphA3-CART cells or the un-transduced (UTD) T cell control for 72 hours. 2-way ANOVA, ****P<0.0001.

Abstract 414 Figure 2 Cytotoxicity assay; SNB-19 ZsG was cocultures with increasing ratios of either EphA3-CART cells or the un-transduced (UTD) T cell control for 72 hours. 2-way ANOVA, ****P<0.0001

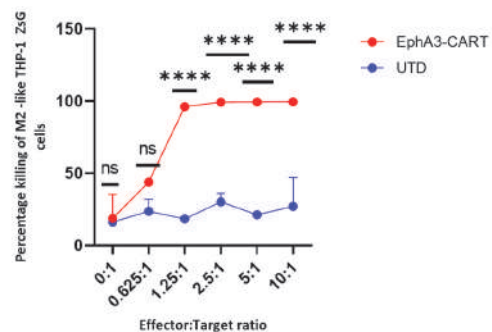


Figure 3. Cytotoxicity assay: M2-polarized THP-1 monocytic cells was cocultured with increasing ratios of either EphA3-CART cells or the un-transduced (UTD) T cell control 72 hours. 2-way ANOVA. ****P<0.0001.

Abstract 414 Figure 3 Cytotoxicity assay: M2-polarised THP-1 monocytic cells was cocultured with increasing ratios of either EphA3-CART cells or the un-transduced (UTD) T cell control 72 hours. 2-way ANOVA. ****P<0.0001

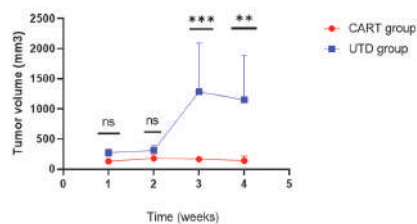


Figure 4. SNB-19 GBM cell line (1×10^6) was engrafted subcutaneously to into NSG mice. and When tumor burden reached 1×10^8 photon/second, mice were randomized to treatment of 5×10^6 cells EphA3-CART UTD. Tumors were monitored with bioluminescence imaging and vernier callipers. 2-way ANOVA. ** $P < 0.05$

Abstract 414 Figure 4 SNB-19 GBM cell line (1×10^6) was engrafted subcutaneously to into NSG mice and when tumor burden reached 1×10^8 photon/second, mice were randomized to treatment of 5×10^6 cells EphA3-CART UTD. Tumors were monitored with bioluminescence imaging and vernier callipers. 2-way ANOVA. ** $P < 0.05$

<http://dx.doi.org/10.1136/jitc-2022-SITC2022.0414>

Abstracts

415 PD-1 IMMUNE CHECKPOINT BLOCKADE ENHANCES ERADICATION OF DISSEMINATED OVARIAN CANCER

Rita Serda*. *University of New Mexico, Albuquerque, NM, United States*

Background Clinical trials for ovarian cancer using immune checkpoint inhibitors (ICI) as monotherapy have failed to show an improvement in survival, however, improved response rates and survival have been achieved with combination therapy. A novel cancer vaccine platform based on silicified cancer cells that are masked on the surface with microbial-associated molecules has been shown in preclinical trials to reduce tumor burden in mice with disseminated ovarian cancer.¹ Here we evaluate the therapeutic efficacy of combination ICI and vaccination.

Methods Female FVB mice were administered intraperitoneal (IP) injections of BR5-Akt-Luc cells. Mice were given two weekly IP vaccinations, with and without anti-mPD-1 antibody, beginning 8 days post tumor challenge. Bioluminescent imaging was performed using the IVIS Spectrum.

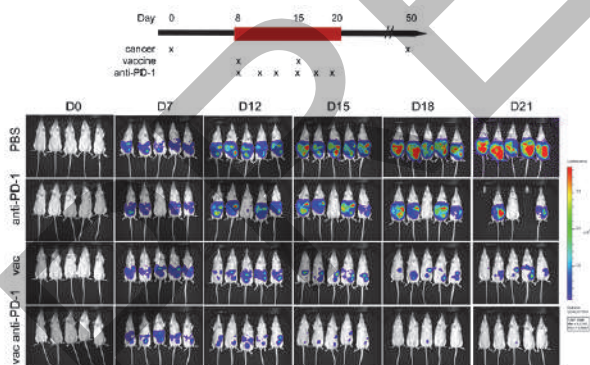
Results Bioluminescent imaging (figure 1) and animal weights indicated excessive tumor burden in untreated mice with animals sacrificed around 25 days post tumor challenge. ICI monotherapy provided no therapeutic benefit, however when combined with vaccination, tumor was undetectable in 80% of the mice 10 days post vaccination, with all mice surviving to Day 49. Tumor did not engraft in surviving mice when rechallenged on Day 50.

Conclusions A silicified cancer vaccine delivery system when combined with ICI is able to reduce tumor burden and enhance survival in mice with established ovarian cancer.

Acknowledgements This research is funded by the Oxnard Foundation

REFERENCE

1. Guo J, De May H, Franco S, Nouredine A, Tang L, Brinker CJ, Kusewitt DF, Adams SA, Serda RE. Cancer vaccines from cryogenically silicified tumour cells functionalized with pathogen-associated molecular patterns. *Nat Biomed Eng*, 2022; **6**(1):19–31.



Abstract 415 Figure 1 Immune checkpoint blockade promotes vaccine-induced eradication of disseminated ovarian cancer. (A) Study timeline. (B) Bioluminescent imaging of luciferase positive ovarian cancer in mice following therapeutic vaccination and immune checkpoint blockade

<http://dx.doi.org/10.1136/jitc-2022-SITC2022.0415>

417

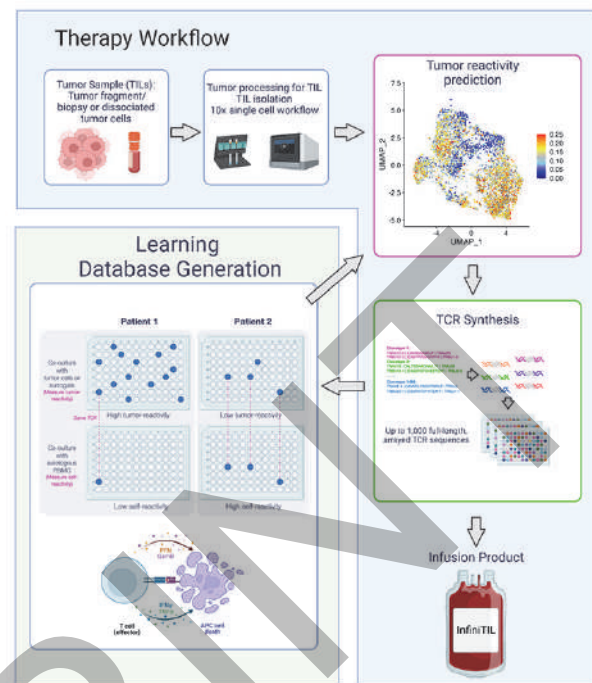
RAPID DISCOVERY OF PERSONALIZED TCRs THROUGH A SINGLE-CELL TRANSCRIPTOMIC SIGNATURE THAT PREDICTS TUMOR REACTIVITY

¹Ely Porter*, ¹Yue Zhao, ¹Danielle Cook, ¹Seon Kinrot, ¹Shuang Mao, ¹Yanzhen Ye, ¹Jiayu Ou, ²Dandan Hu, ¹Xi Chen. ¹RootPath, Inc., Watertown, MA, United States; ²State Key Laboratory of Oncology in South China, Guangzhou, China

Background Personalized T cell therapies are currently limited by complex manufacturing, unreliable potency, long timelines, and the associated high cost. An ideal personalized workflow would simplify this process by leveraging affordable sequencing and commoditized cell manufacturing, while still resulting in a potent therapeutic without time-consuming and costly experimental validation. The T cell population that mediates response, the cells containing tumor-reactive TCRs, is undefined by traditional phenotypic characterization. To better understand this cryptic population critical for therapy, we devised a workflow that involves scRNA-Seq of thousands of cells, synthesizing 1000s of TCRs per patient, and screening them for reactivity (figure 1). We then applied this workflow across a broad spectrum of cancer types. The synthesis of 100,000s of TCRs to enable this survey is cost-prohibitive using traditional vendors. To solve this problem, we developed a novel technology, named PathFinder DNA Assembly™, that allows parallel synthesis of thousands of TCRs simultaneously for a cost of **under \$1 per TCR**. The tumor-reactivity of these TCRs can then be experimentally tested, and their reactivity profile mapped back to high-complexity scRNA-Seq data to better define the population responsible for mediating therapeutic responses.

Methods To date, we've queried 26 patients across 10 different cancer types, synthesized between 350-2,800 TCRs per patient, and identified reactive TCRs against autologous tumor and allogeneic HLA matched cell lines. This database allows us to correlate the reactivity profile of a TCR with the transcriptomic profile of the original, unexpanded tumor infiltrating lymphocytes (TIL). In doing so, we've identified a transcriptomic profile (TR1.0) that enriches for tumor reactivity and is corroborated when we interrogating public scRNA-Seq datasets

Results To demonstrate the utility of our TR1.0 signature, we performed scRNA-Seq on a liver cancer sample, selected TCRs based on TR1.0, synthesized 192 TCRs from more than 4,500 cells encompassing high-scoring CD8 and CD4 populations, as well as TCRs predicted by other published metrics. Reactivity of the synthetic TCRs was established by ELISPOT assays against autologous tumor in a 384-well microplate and the highly reactive TCRs highlighted on the UMAP. The TR1.0 score correctly identifies the small population of T cells containing the reactive TCRs where other published metrics fail to predict the reactive population. This data, in combination with ongoing work, demonstrates the feasibility of a personalized therapy with simplified manufacturing and clinically viable timelines while maintaining a high potency of the product.



Abstract 417 Figure 1 RootPath InfiniTIL Workflow

Overview of the InfiniTIL workflow. Tumor samples are collected from as small amount of material as a biopsy, T cells selected, and single-cell sequenced. TCRs from T cells that score highly by TR1.0 metric are then selected for production. Additionally, each patients TCRs are screened in a companion assay to establish each TCR's reactivity profile. This establishes a database of reactivity information and it's correlation with transcriptomic and cell surface marker expression, that can then be leveraged to improve TR1.0 scoring and enable new therapies.

<http://dx.doi.org/10.1136/jitc-2022-SITC2022.0417>

Checkpoint Blockade Therapy

418 6-GINGEROL SUPPRESSES ANGIOGENESIS AND PROMOTES T-CELL CYTOTOXICITY IN MICE MODEL OF COLORECTAL CANCER

¹Babajide Ajayi*, ²Anuoluwapo Adeshina. ¹Ajayi Crowther University Oyo, Oyo, Nigeria; ²All Saint School of Medicine Dominica, Roseau, Dominica

Background Colorectal cancer (CRC) is the second most common adult cancer in women and the third most common in men, and it is the fourth leading cause of cancer death worldwide. Angiogenesis is a critical step in CRC progression and metastasis. Immune checkpoint proteins (ICP) such as programmed cell death 1 (PD1), PD1 ligand 1 (PD-L1) and cytotoxic T lymphocyte antigen 4 (CTLA4) act as inhibitory immunoreceptors that prevent cytotoxic T-cells from killing tumor cells. Studies have reported the contribution of angiogenesis and ICP to anti-tumor immunity. Indeed, targeting angiogenesis and use of ICP blockage have revolutionized colorectal cancer treatment and improved patients' survival. However, the use of immune checkpoint inhibitors has been shown to induce immune-related adverse reactions such as colitis. 6-gingerol (6G), the most pharmacologically active compound discovered in *Zingiber officinale* (ginger), We have reported the anti-tumor effects of 6-gingerol. However, there is a lack of information on the effect of 6G on angiogenic drivers and T-cell cytotoxicity in a mouse model of CRC. Herein, we investigated the effects of 6G angiogenesis and cytotoxic T-cell signaling in mice model of CRC.

Methods Male BALB/c mice were divided into three groups of 20 mice each. Group 1 mice served as controls Group 2 (CRC model) mice received a single dose of azoxymethane (AOM) 10mg/kg and, after one week, they received three cycles of dextran sulfate sodium (DSS) 4% in drinking water. Group 3 mice received 6G 10mg/kg/day by oral gavage in combination with AOM and three cycles of 4% DSS (W/V) in drinking water. The colons of the mice were observed daily for tumor development, and the experiment was terminated after confirmation of colorectal adenocarcinoma.

Results Tumor burden was observed to be decreased in CRC mice treated with 6G. Also, 6G decreases the expression of collagen (type I and I), vascular endothelial growth factor (VEGF), VEGF receptor, epidermal growth factor (EGF), and EGF receptor in mice with CRC when compared with control. Furthermore, mice administered 6G+AOM/DSS had increased expression of CD4 and CD8+ T-cells and decreased expression of tumor necrosis factor (TNF- α), cyclooxygenase-2 (COX-2), PD1, PD-L1, and CTLA4 when compared to mice with CRC. Using computational oncology, we observed a high binding affinity of 6G with VEGF, VEGFR, EGF, EGFR, PD1, PD-L1, and CTLA4.

Conclusions The result obtained from this study showed that 6-gingerol suppresses angiogenic drivers and promotes T-cell cytotoxicity in colorectal cancer.

Ethics Approval The work was approved by Ajayi Crowther Faculty of Natural Science Research Ethic Committee

<http://dx.doi.org/10.1136/jitc-2022-SITC2022.0418>

419

COMBINED ANTI-VEGF, ANTI-CTLA4 AND ANTI-PDL1 TREATMENT INDUCES STRONG IMMUNE RESPONSES IN PATIENTS WITH CHOLANGIOCARCINOMA: RESULTS FROM A CLINICAL TRIAL/IN DEPTH CORRELATIVE STUDIES AND MOUSE STUDIES

<http://dx.doi.org/10.1136/jitc-2022-SITC2022.0419>

¹Reda Benmebarek*, ²Tim Greten, ¹Cecilia Monge, ¹Benjamin Ruf, ¹Yuta Myojin, ²Cihan Oguz, ²Justin Lack, ¹William Telford, ¹Changqing Xie, ¹Tim Greten. ¹NCI, Bethesda, MD, United States; ²National Institutes of Health, Bethesda, MD, United States

Background The addition of durvalumab (anti-PD-L1) to chemotherapy with gemcitabine and cisplatin has become standard of care for patients with cholangiocarcinoma. Both anti-CTLA4/anti-PD-L1 and anti-VEGF/anti-PDL1 are FDA approved immune checkpoint inhibitor regimens. Here we tested the combination of anti-CTLA4 + anti-VEGF + anti-PD-L1 in patients with cholangiocarcinoma (CCA).

Methods In this open-label phase II study patients with histologically confirmed HCC and CCA were treated with 300 mg tremelimumab, 7.5 mg/kg bevacizumab and 1150 mg durvalumab on day 1 followed by 7.5 mg/kg bevacizumab and 1150 mg durvalumab every 3 weeks. Primary objective was the 6-month progression-free survival (PFS). Secondary endpoints include safety and correlative studies including single cell RNA-sequence analysis of PBMC, spectral flow cytometry analysis using a 22-color pan-immunological panel and a 25-color T cell-specific panel and multiplex serum cytokine analysis as well as bulk mRNA analysis from paired tumor biopsies. Immune and tumor responses were tested in mice with subcutaneously injected SB1 cholangiocarcinoma cells after treatment with anti-VEGF/anti-CTLA4 and anti-PD-L1.

Results A total of 7 patients (6 CCA and 1 HCC) were enrolled into this study before the study was halted for unexpected high rates of immune related AEs. 4/7 patients developed grade 3 AEs including 2 patients with myositis, 1 patient with colitis, 1 patient with hepatitis, 2 patients with thyroiditis and 1 patient who developed a myocarditis, myositis, myasthenia gravis and immune thrombocytopenia. Here we present the unexpected clinical responses in CCA with 2/6 CCA patients demonstrating long-lasting partial responses (10.3 and 3.5 months) and a median OS of 13.6 months despite early treatment discontinuation. Analysis of immune correlates are ongoing. Preliminary spectral flow cytometry results demonstrated a significantly higher frequency of regulatory T cells (Tregs), proliferating CD4⁺ and CD8⁺ T cells, as well as non-classical monocytes following anti-VEGF/anti-CTLA4/anti-PD-L1 treatment. Within the CD8 T cell compartment, a CD39⁺Ki67⁺PD-1^{hi} fraction expanded in the anti-VEGF/anti-CTLA4/anti-PD-L1 treated cohort. 10x single cell sequencing analysis confirmed the findings of the flow cytometric analysis and revealed expanded TCR clonotypes in the treated cohort. In murine studies anti-VEGF, anti-CTLA-4 and anti-PD-L1 combination resulted in marked tumor control in tumor-bearing mice mimicking results we obtained in patients with CCA.

Conclusions Here, we show that combined anti-VEGF, anti-CTLA4 and anti-PD-L1 induces exceptional immunological and therapeutic responses in patients with cholangiocarcinoma. The study is continuing to enroll with a modified dosing schedule. Murine studies will help better to further elucidate the immunological mechanism.

Trial Registration NCT03937830

Ethics Approval This study has been approved by the NIH review board (#NCI-19-C-0094)

420

**DOXYCYCLINE REGULATABLE β -CATENIN
DEMONSTRATES INDUCIBLE IMMUNE EVASION IN A
MELANOMA GEM MODEL**

¹Alexandra Cabanov*, ¹Thomas Gajewski, ²Stefani Spranger, ²Elen Torres-Mejia. ¹University of Chicago, Chicago, IL, United States; ²Koch Institute, Cambridge, MA, United States

Background Lack of response to checkpoint blockade immunotherapy has been linked to a deficiency of immune cell infiltration within the tumor microenvironment (TME). One demonstrated mechanism sufficient for the non-T cell inflamed TME is tumor cell-intrinsic activation of the β -catenin signaling pathway. Using genetically engineered mouse models (GEMMs), tumors constitutively expressing active β -catenin lack a robust endogenous T cell infiltrate and fail to respond to immunotherapies. In support of these mouse studies, human melanoma metastases with increased active β -catenin signaling exhibit decreased numbers of tumor infiltrating Batf3-driven cDC1 and CD3⁺ T cells. However, whether temporal activation and inactivation of β -catenin within the same developing tumor would alter immune cell infiltration is not known.

Methods A model was created in which tamoxifen-regulated Cre-recombinase mediates BRAF^{V600E} oncogene activation and PTEN tumor suppressor gene deletion as well as expression of a doxycycline regulatable reverse transactivator. Upon administration of doxycycline via the drinking water to these animals, a non-degradable form of nuclear β -catenin becomes expressed. Immunofluorescence assays were performed assessing the β -catenin expression status in the tumor cells as well as immune cell infiltration within the TME. Additionally, immunotherapy efficacy experiments were performed.

Results We observed that administration of doxycycline to these animals drove expression of an active form of nuclear β -catenin. Activation of nuclear β -catenin resulted in a 2-fold decrease in the overall CD3⁺ T cells infiltration into the TME. Moreover, this decrease in immune infiltration also resulted in loss of anti-PD-L1 + anti-CTLA-4 therapy efficacy. We next performed studies assessing the kinetics with which β -catenin levels diminish upon doxycycline removal. Switching animals to regular drinking water resulted in complete reduction of nuclear β -catenin levels seven days after doxycycline removal. Interestingly, once nuclear β -catenin levels diminished, we observed re-infiltration of the TME however, these tumors remained unresponsive to anti-PD-L1 + anti-CTLA-4 therapy.

Conclusions We describe a novel mouse model in which we induce autochthonous melanoma tumors in mice along with inducible expression of a non-degradable, nuclear β -catenin modulated by doxycycline in the drinking water. While removing doxycycline resulted in re-infiltration of CD3⁺ T cells within the TME, it did not result in restored anti-PD-L1 + anti-CTLA-4 efficacy. Single cell RNAseq and spatial transcriptomics are being performed to determine if an additional immune regulatory event becomes established when β -catenin is on from the birth of the tumor that needs to be overcome.

Acknowledgements This work was supported by the Wissler Fellowship from the University of Chicago (SS) K99/R00 (NCI; SS), and R35CA210098 (TG).

<http://dx.doi.org/10.1136/jitc-2022-SITC2022.0420>

422

KZR-540 IS A NOVEL ORAL SMALL MOLECULE INHIBITOR OF SEC61 COTRANSLATIONAL TRANSLOCATION THAT POTENTLY AND SELECTIVELY BLOCKS PD-1 EXPRESSION

Cristina Delgado-Martin*, Neel Anand, Janet Anderl, Chengguo Dong, Andrea Fan, Ying Fang, Christopher Kirk, Tony Muchamuel, Yu Qian, Jinhai Wang, Jennifer Whang, Patricia Zuno-Mitchell. *Kezar Life Sciences, South San Francisco, CA, United States*

Background Blocking the PD-1/PD-L1 pathway with antibodies has been effective in treating multiple types of cancers. However, orally administered small molecules can allow for better tumor penetrance and more convenient dosing than antibody-based therapies. Most secreted and transmembrane proteins utilize unique signal sequences (ss) to enable translocation through the Sec61 complex into the endoplasmic reticulum. Targeting Sec61 with small molecule inhibitors such as KZR-261, currently in a clinical trial for solid tumors (NCT05047536), has anti-tumor effects through inhibiting the expression of multiple therapeutic targets, including PD-1, in preclinical models. Here we describe KZR-540, an oral small molecule Sec61 inhibitor that potently and selectively blocks PD-1 expression.

Methods Inhibition of Sec61 clients was assayed in HEK-293 cells overexpressing the ss of interest fused to a luciferase reporter. Human T cells pre-treated *in vitro* with test compounds and stimulated were monitored for expression of PD-1 and other markers by flow cytometry and mass spectrometry (MS)-based proteomic profiling. Cytokine production was measured from allogeneic mixed lymphocyte reaction (MLR). T cell-mediated killing was assessed in co-culture assays with A375 cells. Pharmacokinetics (PK) was assessed using liquid chromatography-tandem MS. *In vivo* evaluation of PD-1 expression was conducted in humanized PBMC NSGTM and B-hPD-1 mice dosed orally with KZR-540 and treated with anti-CD3 antibody. Human PD-1 expression on T cells was assessed by flow cytometry of splenocytes.

Results We have discovered a series of Sec61 inhibitors that potently and selectively block ssPD-1 expression. In human T cells treated with these compounds *in vitro* prior to activation, surface expression of PD-1 was inhibited while other T cell activation markers were unaffected. KZR-540 demonstrated good liver microsome stability and a robust oral PK profile and was selected for further studies. The selectivity of KZR-540 was also demonstrated by global Sec61 client proteomic profiling of treated T cells. Treatment with KZR-540 increased IL-2 and IFN γ production in MLR and enhanced killing of A375 melanoma cells by human T cells. Furthermore, oral dosing of KZR-540 potently suppressed anti-CD3-induced PD-1 expression in both humanized NSG mice and human-PD-1 knock-in mice.

Conclusions KZR-540 is a small molecule inhibitor of Sec61 that can potently and selectively block PD-1 expression and increase T cell activity *in vitro*, as well as inhibit surface PD-1 expression when dosed orally *in vivo*. Future studies will examine whether there is an enhanced anti-tumor response in a tumor model.

Ethics Approval Animal studies were approved by the Institutional Animal Use and Care Committee.

<http://dx.doi.org/10.1136/jitc-2022-SITC2022.0422>

423

TREATMENT OF RELAPSED AND REFRACTORY LYMPHOMAS WITH NIVOLUMAB IN A LIMITED RECOURSE COUNTRY

¹Lusine Harutyunyan*, ¹Anahit Ter-Grigoryan, ¹Hayk Grigoryan, ¹Marina Kazaryan, ¹Miranush Saaryan, ¹Nerses Ghahramanyan, ²Artem Oganessian, ¹Levon Evoyan, ¹Marina Melik-Andreasyan, ¹Anahit Aynajyan, ¹Karapet Hakobyan, ¹Astghik Voskanyan, ¹Karen Meliksetyan, ¹Yervand Hakobyan. ¹Armenian Hematology Association, Yerevan, Armenia; ²Hematology Center aft. Prof. R. Yeolyan, Yerevan, Armenia; National Institute of Health, Yerevan, Armenia

Background Programmed cell death proteins and their ligands have been under research in recent years, as their inhibitors provide promising results in relapsed and refractory lymphoma treatment.¹ However, in Armenia, number of patients receiving Nivolumab is small and does not represent a real indication number, since it is problematic to provide it. The main aim of this monocenter retrospective study is to evaluate the outcome with Nivolumab among Armenian lymphoma cases.

Methods Data was taken from the Hematology Center after prof. R. Yeolyan ambulatory cards. Study duration: 2013-2021. Patient number: 10. Eight patients were diagnosed with Hodgkin's lymphoma (HL), one patient with Primary mediastinal B large cell lymphoma (PMBCL), another one with ALK-positive T-large cell anaplastic lymphoma (ALK+ ALCL). In all patients, the primary diagnosis was established in advanced stages.

Results Nivolumab performed after 2nd relapse in 5 patients, of which 4 were with HL and one with ALK+ ALCL. First-line therapy was started with BEACOPP scheme in all HL patients, after which BV, ABVD, VGPP, DHAP, CVPP, ViG-EPP3 were also the regimens of choice over Nivolumab. The PMBCL patient was treated with R-CHOEP, R-DHAP before Nivolumab + Venetoclax. At initial diagnosis he had skin necrosis of about 15 cm, which worsened after radiation, but partial skin recovery was observed after Nivolumab + Venetoclax regimen, skin biopsy showed no tumour activity. The patient with ALK+ ALCL was treated with R-CHOP, BV-CHP, BV before Nivolumab. 3 patients received Nivolumab after initial therapy failure, 1 of them with PMBCL and 2 with HL. One patient did not attend after Nivolumab+ BV courses, but no mortality status. One HL patient was diagnosed with HIV and is currently in partial remission (PR) after BEACOPP + Nivolumab + auto-HSCT. CR after Nivolumab was achieved in 3 patients, 2 of them with HL and 1 with PMBCL. PR was achieved in one HL patient. Progression after Nivolumab was observed in 5 patients, of which 4 had HL and one had ALK+ ALCL. Auto-HSCT was performed in 3 patients, 2 of them with HL and 1 with PMBCL, and CR was achieved in PMBCL.

Conclusions Overall, CR was achieved in 30% of lymphoma patients, among whom patients received Nivolumab at doses of 100, 160 and 200 mg. Some patients received reduced doses of Nivolumab 40 mg and did not respond to a treatment. Based on a limited number of patients, additional studies are needed for a definitive conclusion.

REFERENCE

1. Xie W, Medeiros LJ, Li S, Yin CC, Khoury JD, Xu J. PD-1/PD-L1 pathway and its blockade in patients with classic Hodgkin lymphoma and Non-Hodgkin large-cell lymphomas. *Current Hematologic Malignancy Reports*. 2020;**15**(4):372–81.

<http://dx.doi.org/10.1136/jitc-2022-SITC2022.0423>

424

AN ALLOSTERIC, ORALLY ADMINISTERED CBL-B INHIBITOR REMODELS THE TUMOR MICROENVIRONMENT AND ENHANCES IMMUNE-MEDIATED TUMOR GROWTH INHIBITION

Yilin Qi*, Jun Kuai, Yingzhi Bi, Huadong Sun, Samira Jaeger, David Greco, Ken Carson, Timothy Reilly, Geraldine Harriman, Fang Wang. *Hotspot Therapeutics, Boston, MA, United States*

Background Casitas B-lineage lymphoma proto-oncogene b (CBL-B), an E3 ubiquitin-protein ligase, is a critical regulator of immunity. Genetic ablation or inactivation of CBL-B bypasses the requirement of a co-stimulatory signal for T cell activation in an antigen-dependent manner. CBL-B knockout mice spontaneously reject tumor growth, and the effect is largely dependent on CD8+T cells. Therefore, CBL-B represents a novel target for cancer immunotherapy. Previously, Hotspot has disclosed a series of allosteric CBL-B inhibitors which exhibited potent *in vitro* and *in vivo* properties.

Methods Our CBL-B inhibitor (CBL-Bi) was evaluated in a set of syngeneic mouse tumor models. In addition to the measurement of tumor growth, tumor gene expression immune signatures were characterized by Nanostring analysis. Immunohistochemistry and flow-based immunophenotyping were used in profiling the tumor microenvironment.

Results CBL-Bi, as a single agent, demonstrated a spectrum of anti-tumor responses. It not only showed anti-tumor activity in immunologically hot tumor models, such as H22 and CT26, but also in immunologically cold tumor models, such as B16-F10. Responding tumors showed enhancement of antigen presentation, T cell cytotoxicity, and interferon and TNF pathway activation. Furthermore, an *in vivo* study using the CT26 model demonstrated that the anti-tumor effect was mediated by the immune system, as there was no tumor growth inhibition observed in immune deficient NCG mice. We further investigated the combinational effect of CBL-Bi with anti-PD1 in the CT26 syngeneic mouse tumor model. Additive or synergistic anti-tumor activity was observed. Tumor microenvironment profiling demonstrated significant enhancement of T cell tumor infiltration, and a shift of tumor associated macrophages to a pro-inflammatory status was observed in the combination group.

Conclusions Taken together, the pre-clinical *in vivo* data presented here demonstrate that inhibition of CBL-B induces immune mediated tumor growth inhibition; the anti-tumor effect is further enhanced when combined with anti-PD1. Thus, CBL-B inhibition has the potential to overcome the low-antigen and high immune suppressive tumor environment.

<http://dx.doi.org/10.1136/jitc-2022-SITC2022.0424>

425

KVA12.1: AN ANTI-VISTA MONOCLONAL ANTIBODY WITH STRONG SINGLE AGENT ANTI-TUMOR ACTIVITY AND NO EVIDENCE OF CYTOKINE MEDIATED TOXICITY

Thierry Guillaumeux*, Kurt Lustig, Emily Frazier, Neda Kabi, Chen Katz, David Peckham, Mei Xu, Shawn Iadonato. *Kineta Inc., Seattle, WA, United States*

Background V-domain Immunoglobulin Suppressor of T cell Activation (VISTA), an immune checkpoint regulator, is highly expressed in myeloid cells in the tumor microenvironment (TME). It has been shown in vitro and in vivo that VISTA inhibits T cell activation and prevent T cell recruitment into tumors. In patients, high VISTA expression is associated with poor prognosis and is also a potential mediator of resistance to current checkpoint therapies. VISTA is a very attractive new target for cancer immunotherapy.

Methods Kineta has developed a clinical candidate anti-VISTA monoclonal antibody, KVA12.1, which demonstrates in human VISTA KI mice strong anti-tumor activities as a single agent and in combination with other check-point inhibitors in multiple syngenic tumor models. KVA12.1 is an IgG1 antibody targeting a unique epitope on VISTA that has been engineered to extend its half-life and reduce its immunoreactivity. These modifications introduced in the IgG1 backbone of the antibody could prevent possible adverse events related to a Cytokine Release Syndrome (CRS) when injected into cancer patients.

Results We show here that the engineered IgG1 of KVA12.1 increases binding of the antibody to neonatal Fc-Receptor compared to the wild type IgG1 and reduces the binding to different FcRg receptors in particular FcγRIIIa involved in a strong immunoreactivity. We have also shown in previous work that KVA12.1 binds with the same potency and specificity to human and Non-human primate (NHP) VISTA. We have therefore conducted Non-GLP and GLP toxicological studies and demonstrated that KVA12.1 is very well tolerated in NHP, even after multiple high dose injections over a one-month period. No mortality or overt clinical signs have been observed, as well as no treatment-related findings for clinical pathology endpoints and no change of CRS cytokine levels, in particular IL6 and TNFα. The absence of CRS markers has also been confirmed in whole blood obtained from multiple human healthy donors. Besides, we have confirmed in these same NHP studies the extended PK of our antibody. KVA12.1 will be tested in a clinical trial in cancer patients with advanced solid tumors that have failed previous therapies with current standard of care. To guide our inclusion criteria, VISTA expression has been evaluated by immunohistochemistry on a large panel of human cancer tissue samples.

Conclusions The clinical trial will start by the end of 2022 and will evaluate the safety and tolerability of KVA12.1 injected alone or in combination with pembrolizumab, as well as the Recommended Phase 2 dose (RP2D) or maximum tolerated dose (MTD) as a primary objective. Pharmacokinetics, immunogenicity and tumor responses will also be evaluated in this trial.

<http://dx.doi.org/10.1136/jitc-2022-SITC2022.0425>

426

ES005, A HIGH AFFINITY ANTI-LAG3 MONOCLONAL ANTIBODY, INHIBITS THE INTERACTIONS BETWEEN LAG3 AND MULTIPLE LIGANDS AND ENHANCES ANTI-TUMOR ACTIVITY OF T CELLS IN PRECLINICAL MODELS

Xiaofeng Niu*, Chunlian Wang, Jinfeng Zhao, Yefeng Lu, Yingchao Liu, Rui Gao, Zhihao Wu, Yangsheng Qiu, Zheng Song, Hongtao Lu. *Elpiscience Biopharma, Shanghai, China*

Background Lymphocyte-activated gene 3 (LAG3) is a cell surface inhibitory receptor expressed by both activated and exhausted CD4⁺/CD8⁺ T cells, as well as regulatory T cells (Tregs). It plays an important role in regulating immune homeostasis with multiple biological activities related to T cell functions and is considered a next-generation immune checkpoint after programmed cell death protein 1 (PD-1) and cytotoxic T-cell lymphocyte antigen-4 (CTLA-4). The first identified LAG3 functional ligand is major histocompatibility complex class II (MHC-II). Recently other LAG3 ligands, like fibrinogen like 1 (FGL1), liver and lymph node sinusoidal endothelial cell C-type lectin (LSEctin), and galectin-3, were also found to be responsible for the inhibitory function of LAG3, suggesting that blocking these interactions simultaneously may bring greater clinical benefit in cancer treatment. We have developed a high affinity LAG3 blocking antibody ES005 that inhibits the interactions between LAG3 and multiple ligands and it enhances anti-tumor activity of T cells in preclinical models.

Methods LAG3 binding activity and affinity were evaluated by FACS and surface plasmon resonance system (Biacore). Blocking activity was determined by competition assay. *In vitro* functional activity was determined by NFAT reporter assay and antigen specific T cell activation assay. *In vivo* efficacy was evaluated in a syngeneic mouse breast tumor model with human LAG3 knock-in mice. Epitope analysis was performed by ELISA and hydrogen deuterium exchange mass spectrometry (HDX-MS). Lead clone was humanized via CDR grafting and back mutation screening. Non-human primates (NHPs) models were used to assess the safety and pharmacokinetics of the humanized candidate.

Results ES005 specifically recognizes human LAG3 with high affinity. It binds to a unique epitope on LAG3 that is distinct from known competitor molecules. ES005 potently blocks LAG3 binding to multiple ligands (MHC-II, LSEctin, FGL1). ES005 can reverse LAG3-driven inhibition of NFAT reporter gene expression and T cell activation in a dose-dependent manner. In a syngeneic mouse breast tumor model, ES005 significantly inhibited tumor growth *in vivo*. ES005 has excellent pharmacokinetics and safety profile in NHPs.

Conclusions In summary, anti-LAG3 mAb ES005 is a multiple-ligand blocker and demonstrated potent single-agent activity in *in vivo* mouse tumor models, indicating great potential to be used as next-generation immune checkpoint inhibitor in cancer treatment. We are currently advancing the development of ES005 into clinical candidate.

<http://dx.doi.org/10.1136/jitc-2022-SITC2022.0426>

427

APPROVAL TIMINGS AND REVIEW SPEED OF IMMUNE CHECKPOINT INHIBITORS (ICIS) IN CANCER THERAPY BETWEEN THE FOOD AND DRUG ADMINISTRATION (FDA) AND THE EUROPEAN MEDICINES AGENCY (EMA) FROM 2010-2022

cancer therapy approvals. *Journal of Clinical Oncology*. 2021;39(15_suppl):1575-1575. doi:10.1200/JCO.2021.39.15_suppl.1575

<http://dx.doi.org/10.1136/jitc-2022-SITC2022.0427>

¹Numair Rizwan, ²Ali Raza Khaki*, ³Aakash Desai, ⁴Jeremy Warner, ⁵Jonathan Krell, ⁵Mark Lythgoe. ¹Independent, Boston, MA, United States; ²Stanford, Stanford, CA, United States; ³Mayo Clinic, Rochester, MN, United States; ⁴Brown University, Providence, RI, United States; ⁵Imperial College London, London, UK

Background ICIs targeting cytotoxic T-lymphocyte-associated protein 4 (CTLA-4), programmed cell death protein 1 (PD-1) or its ligand (PD-L1) have transformed outcomes in many cancer types. Prompt regulatory approval is essential to ensure timely access for patients. We have previously shown that over the past decade most new oncology therapies are approved earlier and faster by the FDA compared to the EMA.^{1 2} However, less is known about the regulatory evaluation of ICIs, and if any significant review timing differences exist between initial and subsequent indication approval. In this study, we analyzed regulatory review and approval speed for ICIs at the FDA and EMA following the first ICI approval in 2011.

Methods We performed a cross-sectional analysis of regulatory databases for the FDA and EMA to identify approved ICIs, licensed indications and regulatory review time. ICIs with more than one indication by either the FDA or EMA were included. From each regulatory database we calculated number of approved indications, classified indications by tumor type and calculated the review speed (defined as time from application submission to approval) for each approval. We then compared the regulatory approval timings for initial and supplementary indications (pooled).

Results We identified 8 ICIs, including 7 anti-PD1/PDL1 and 1 anti-CTLA-4 monoclonal antibodies, approved for cancer indications by both the FDA and EMA. There were 93 approved subsequent indications for ICIs, across 14 tumor types with 3 agnostic indications by the FDA with 84 for anti-PD-1/PD-L1, 6 for anti-CTLA4/PD-1 combination therapy and 3 for anti-CTLA-4 monotherapy. This compared to 64 approved indications across 14 tumor types with 1 agnostic indication for the EMA, including 55 anti-PD1/PDL1, 6 for anti-CTLA4/PD-1 combination therapy and 3 for anti-CTLA-4 monotherapy. The median review time for initial ICI approval at the FDA and EMA was 195 days (IQR:172-228 days) and 440 days (IQR: 376-489 days), respectively. For supplementary ICI indication approval, the pooled review time was shorter for each regulator with 180 days (6% shorter) for FDA and 279 days (37% shorter) for the EMA.

Conclusions Eight ICIs have been approved, for similar cancer types, for use in the US and Europe, however, the US has ICIs approved for more indications and agnostic-use labels. ICIs are reviewed more quickly, for both initial and supplementary indications, by the FDA compared to the EMA. Compared to initial approval review, the regulatory review of supplementary indications was relatively unchanged by the FDA but faster by the EMA.

REFERENCES

1. Lythgoe MP, Desai A, Gyawali B, et al. Cancer therapy approval timings, review speed, and publication of pivotal registration trials in the US and Europe, 2010-2019. *JAMA Netw Open*. 2022;5(6):e2216183. doi:10.1001/jamanetworkopen.2022.16183
2. Lythgoe M, Krell J, Warner JL, Desai A, Khaki AR. Time intervals between U.S. Food and Drug Administration (FDA) and European Medicines Agency (EMA) new

428

DIFFUSING ALPHA-EMITTERS RADIATION THERAPY PROMOTES A PRO-IMMUNOGENIC TUMOR MICROENVIRONMENT AND SYNERGIZES WITH PD-1 BLOCKADE

¹Sara Roumani*, ¹Yossi Nishri, ¹Amit Shai, ¹Margalit Efrati, ²Itzhak Kelson, ²Yona Keisari, ¹Vered Domankevich, ¹Robert Den. ¹Alpha Tau Medical Ltd., Jerusalem, Israel; ²Tel Aviv University, Jerusalem, Israel

Background Diffusing alpha emitters radiation therapy (DaRT) utilizes Ra-224 loaded seeds that continuously release alpha-emitting atoms inside the tumor.¹ The treatment effectively ablates many types of human and mice xenografts² and shows 100% response rates in patients with recurrent and locally advanced squamous cell carcinoma (SCC) of the skin and head and neck.³ DaRT was previously shown to trigger specific- and systemic- antitumor immune responses in mice, that synergize with immunomodulation and immune stimulation.⁴⁻⁶ Nevertheless, the gene expression profile induced by DaRT treatment and its local and systemic immune response in combination with immune checkpoint inhibition by programmed cell death protein 1 (PD-1) blockade were not yet investigated.

Methods Balb/c mice bearing intracutaneous SCC murine tumors (SQ2 cells) were treated with an inert seed, a Ra-224 loaded DaRT seed, aPD-1 or DaRT+aPD-1. Anti-PD-1 or an isotype control was administered intraperitoneally at the dose of 10 mg/kg. Flow Cytometry Analysis (FACS) of dendritic cells, myeloid-derived suppressor cells (MDSCs) and lymphocytes was performed in tumors and spleens 16 days after DaRT/ inert seed insertion. Furthermore, tumors were subjected to IHC analysis for the detection of tumor infiltrating lymphocytes (TILs). In addition, similar FACS analysis and transcriptional profiling of immune-related target genes in tumor tissues were characterized using the Nanostring technology seven days post-DaRT seed insertion. Combination of DaRT with aPD-1 was also tested for retardation of tumor growth.

Results DaRT in combination with aPD-1 delayed tumor development, induced T lymphocytes infiltration and granzyme B secretion, and reduced systemic MDSCs more efficiently than each of the monotherapies. Gene expression and gene set enrichment analysis of mRNA levels 7 days after DaRT insertion indicated that DaRT upregulated apoptosis, p53 signalling, interferon signalling and myeloid related transcription, while downregulating DNA repair, cell proliferation and notch related transcription. Immunophenotyping analysis at this time-point showed that DaRT induced dendritic cell activation and affected the distribution of myeloid-derived suppressor cells populations.

Conclusions DaRT exerts a synergistic effect with aPD-1 in inhibiting tumor growth in a murine model of SCC and promotes a pro-immunogenic state both locally and systemically. DaRT potentiates not only a higher T-effector cells infiltration but also their cytotoxic potential under checkpoint molecule blockade. Therefore, the current study provides a rationale for a potential combination treatment in SCC patients.

REFERENCES

1. Arazi L, Cooks T, Schmidt M, Keisari Y, Kelson I. Treatment of solid tumors by interstitial release of recoiling short-lived alpha emitters. *Phys Med Biol*. 2007 Aug 21;**52**(16):5025–42.
2. Cooks T, Arazi L, Schmidt M, Marshak G, Kelson I, Keisari Y. Growth retardation and destruction of experimental squamous cell carcinoma by interstitial radioactive wires releasing diffusing alpha-emitting atoms. *Int J Cancer*. 2008 Apr 1;**122**(7):1657–64.

3. Popovtzer, A., Rosenfeld E, Mizrahi A, Bellia S R, Ben-Hur R, Feliciani G, Sarnelli A, Arazi L, Deutsch L, Kelson I, Keisari Y. Initial Safety and Tumor Control Results from a "First-in-Human" Multicenter Prospective Trial Evaluating a Novel Alpha-Emitting Radionuclide for the Treatment of Locally Advanced Recurrent Squamous Cell Carcinomas of the Skin and Head and Neck. *Int J Radiat Oncol Biol Phys*. 2020 Mar 1;**106**(3):571–578.
4. Confino, H, Hochman I, Efrati M, Schmidt M, Umansky V, Kelson I, Keisari Y. Tumor ablation by intratumoral Ra-224-loaded wires induces anti-tumor immunity against experimental metastatic tumors. *Cancer Immunol Immunother*. 2015;**64**(2):191–9.
5. Domankevich V, Cohen A, Efrati M, Schmidt M, Rammensee HG, Nair S, Tewari A, Kelson I, Keisari Y. Combining alpha radiation-based brachytherapy with immunomodulators promotes complete tumor regression in mice via tumor-specific long-term immune response. *Cancer Immunol Immunother*. 2019; **68**(12):1949–1958.
6. Domankevich V, Efrati M, Schmidt M, Glikson E, Mansour F, Shai A, Cohen A, Zilberstein Y, Flaisher E, Galalae R, Kelson I, Keisari Y. RIG-1-like receptor activation synergizes with intratumoral alpha radiation to induce pancreatic tumor rejection, triple-negative breast metastases clearance, and antitumor immune memory in mice. *Front Oncol*. 2020;**10**:990.

<http://dx.doi.org/10.1136/jitc-2022-SITC2022.0428>

429

HUMAN TUMOR RESPONSE TO A STANDARD MONOTHERAPY CHECKPOINT INHIBITOR IN A HUMANIZED HSC-NCG MOUSE MODEL ENGRAFTING ADULT HEALTHY DONOR-MOBILIZED HUMAN CD34⁺ HEMATOPOIETIC STEM CELLS

Jenny Rowe*, Christoph Eberle, Ann Fiore, Robert Mihalek, Brianna Schoen, Stephen Festin. Charles River Laboratories, Inc., Wilmington, MA, United States

Background Checkpoint inhibitors, including those of the PD-1/PD-L1 pathway, are immunotherapies used for the standard of care for cancer patients. New treatments or immunotherapies are compared to those that are currently approved for use. Continual focus is placed on cancers ranked amongst the most common worldwide, including breast, lung and colon cancer. In this study we assessed the ability of NCG mice to support engraftment of adult mobilized hCD34⁺ stem cells as a model for determining tumor growth modulation using anti-hPD-1 monotherapy driven cellular responses over time.

Methods We evaluated the anti-tumor effects of an anti-human PD-1 checkpoint inhibitor in three human tumors (A549 lung, Colo-205 colon and MDA-MB-436 breast cancer) in NCGs humanized with adult healthy donor-mobilized hCD34⁺ stem cells. Humanized mice were implanted subcutaneously with cancer cells, and tumor bearing mice (TBM) were randomized into treatment groups when the average tumor size reached comparable volumes for each tumor type. Vehicle control mice were treated with isotype control IgG antibody, whereas TBM were dosed with anti-hPD-1 antibody. Clinical observations, body weights and tumor growth kinetics were recorded throughout the study. At time of euthanasia whole blood, spleen and tumor tissues were collected and processed for immune profiling by multi-color flow cytometry.

Results In the mobilized hCD34⁺ humanized mice anti-hPD-1 monotherapy modulated tumor growth in lung, colon and breast cancer tumors compared to the IgG isotype control treated. We observed that growth kinetics varied between tumor types. At study termination common human lymphocytes were distributed in peripheral blood, spleen and tumors of surviving mice. After PMA/Ionomycin stimulation in vitro polyfunctional ex vivo T-cell responses were detected within tumor-infiltrating lymphocytes. NCG mice injected with adult healthy donor-mobilized hCD34⁺ stem cells sustained engraftment out to 34 weeks post-injection. The anticipated human immune cell types were detected in bone marrow, spleen and lung at ~18-19 weeks.

Conclusions Adult healthy donor-mobilized hCD34⁺ humanized mice can be successfully engrafted with human tumors and be used as a model for studying pharmacological interventions targeting immune cell responses. Levels of humanization were sustained throughout the course of the study. The ability to monitor tumor growth kinetics and observe a response to an anti-hPD-1 checkpoint inhibitor across multiple tumor types indicates that this model is useful when assessing immunotherapies. Future considerations of this model would expand upon monotherapies to evaluate additional treatment methods such as bispecific antibodies or cell-directed therapies.

Ethics Approval Animal studies were executed in compliance with local Charles River IACUC guidelines, IACUC number IO33.

<http://dx.doi.org/10.1136/jitc-2022-SITC2022.0429>

430

REAL-WORLD OUTCOMES OF PATIENTS WITH RESECTED STAGE IIIA MELANOMA TREATED WITH ADJUVANT NIVOLUMAB IN A US COMMUNITY SETTING

¹Wolfram Samlowski, ²Phillip Chan, ³Anna Pavlick*, ⁴Justin Moser, ²Nicholas Robert, ⁵Tayla Poreta, ⁵Andriy Moshyk, ⁵Leon Sakkal, ⁵Jennell Palaia, ²Nicole Niehoff, ²Jonathan Rajkumar, ⁶Asim Amin. ¹*Comprehensive Cancer Centers of Nevada, Las Vegas, NV, United States*; ²*Ontada, Irving, TX, United States*; ³*Weill Cornell Medical Center, New York, NY, United States*; ⁴*HonorHealth Research and Innovation Inst, Scottsdale, AZ, United States*; ⁵*Bristol Myers Squibb, Lawrenceville, NJ, United States*; ⁶*Atrium Health, Charlotte, NC, United States*

Background Nivolumab is approved in the US and EU for the adjuvant treatment of resected stage III-IV melanoma. Limited data is available regarding outcomes of patients with resected stage IIIA melanoma treated with adjuvant nivolumab. This observational study is an update to the prior study evaluating treatment patterns, outcomes, safety, and healthcare resource utilization in a US community oncology setting in resected stage IIIa patients who received adjuvant nivolumab.

Methods A follow-up to the previous study analysis was conducted by including an additional 15 months of follow-up data and newly matriculated patients. Data were sourced from The US Oncology Network chart review data examining patients with resected stage IIIA melanoma, treated with adjuvant nivolumab between 01-Jan-2018 and 31-Dec-2020, and followed until 30-June-2021. Patients were followed up to 42 months after their sentinel lymph node biopsy. Baseline demographic and clinical characteristics, treatment-related adverse events (TRAEs) and healthcare resource utilization were analyzed descriptively. Overall survival (OS), time to treatment discontinuation (TTD), and recurrence-free survival (RFS) were analyzed using the Kaplan-Meier method.

Results 40 stage IIIA melanoma patients treated with adjuvant nivolumab were included. The median age was 55 years (range 19,90+), 52.5% were male, and 77.5% were Caucasian. Among patients with a documented Eastern Cooperative Oncology Group (ECOG) performance status half had an ECOG score of 0 or 1. Median follow-up time was 27.7 months (range 2.8-39.0). Overall survival was not reached as no deaths occurred during the study period. The median TTD and RFS were also not reached. TRAEs were reported in 23 patients. Among all 40 patients, the most frequent TRAEs were rash (12.5%), hypothyroidism (12.5%), fatigue (10.0%), diarrhea (10.0%), and nausea (10.0%); the treatment-related hospitalization rate was 2.5%.

Conclusions This real-world analysis of patients with stage IIIA melanoma treated with adjuvant nivolumab demonstrated that the vast majority of patients were recurrence free and all patients were alive at the end of the study period, suggesting a favorable prognosis and low rates of healthcare resource utilization. Additional follow-up and investigations with other real-world data sources are warranted to substantiate the clinically relevant outcomes reported in this study of patients with resected stage IIIA melanoma.

Ethics Approval The study was approved by US Oncology, Inc. Institutional Review Board, approval number 20-020E-2020-0224-01.

<http://dx.doi.org/10.1136/jitc-2022-SITC2022.0430>

431 ESTIMATING SCENARIOS FOR SURVIVAL TIME IN PATIENTS WITH METASTATIC MELANOMA RECEIVING IMMUNOTHERAPY OR TARGETED THERAPY

¹Megan Smith-Uffen*, ²John Park, ²Andrew Parsonson, ³Anuradha Vasista. ¹McMaster University, Hamilton, Canada; ²Nepean Blue Mountains LHD, Penrith, Australia; ³NSW Health, Penrith, Australia

Background It is important for advanced cancer patients to understand their prognosis. This allows patients to plan appropriately for end-of-life. Unfortunately, many patients do not understand their life expectancy, often overestimating their likely survival time. Estimating survival in metastatic melanoma is particularly difficult, as immunotherapy and targeted therapies extend survival time and revolutionize care. We have previously shown that three survival scenarios (worst-case, typical, best-case), calculated using simple multiples of median overall survival ([OS], 0.25x, 0.5-2x, 3x, respectively), is a useful framework to estimate and communicate survival time to advanced cancer patients.

Methods This study aimed to determine whether three survival scenarios accurately estimate prognosis for metastatic melanoma patients receiving immunotherapy or targeted therapy. We searched Medline, EMBASE, and Cochrane Central Register of Controlled Trials for phase II/III randomized controlled trials (treatment arms $n \geq 90$) of patients with unresectable stage IIIC/IV cutaneous melanoma receiving immunotherapy or targeted therapy from January 2001 to February 2022. We extracted OS data from Kaplan Meier curves and compared it to our multiples of median OS.

Results 26 trials (12,345 patients) were included. Our estimates of worst-case scenarios ranged from 3.29 (interquartile range [IQR] 2.82-3.76) to 6.82 (IQR 4.48-18.93) months; most-likely lower-typical from 6.57 (IQR 5.64-7.52) to 13.64 (IQR 8.96-18.93) and upper-typical from 26.28 (IQR 22.58-30.07) to 54.55 (IQR 35.83-75.73) months; and best-case from 39.43 (IQR 33.87-45.11) to 81.83 (IQR 53.74-113.60) months, among patients receiving first-line targeted and immunotherapy, respectively. Our multiples of the median OS accurately estimated survival from anywhere between 16.7% to 100% of estimates.

Our scenarios tended to be more accurate for those receiving targeted (most between 70% to 100% accuracy) than immunotherapy (some as low as 16.7%); and second- (all between 50% to 100%) than first-line (some as low as 16.7%) treatment. We were unable to estimate scenarios for patients receiving first-line combination immunotherapy, as none of the treatment arms in this group met median OS. When we were inaccurate, we tended to overestimate survival.

Conclusions This study was limited by small sample sizes and immature data. The accuracy of our scenarios was more variable than previous work done by our team. Future research should include mature data and novel interventions when determining frameworks to communicate survival in metastatic melanoma.

<http://dx.doi.org/10.1136/jitc-2022-SITC2022.0431>

432 **EVALUATION OF NOVEL ANTI-TIGIT ANTIBODY M6223 AS A SINGLE AGENT AND IN COMBINATION WITH AVELUMAB ON HUMAN NATURAL KILLER (NK) CELL CYTOTOXICITY**

Anton Titov*, Nancy Sun, Christie Kelton, Mirek Jurzak, Hong Ma, Chunxiao Xu. *EMD Serono, Billerica, MA, United States*

Background M6223 is a fully human antagonistic anti-TIGIT immunoglobulin (Ig) G1 antibody with fragment crystallizable (Fc)-mediated effector function. Preclinical studies demonstrated that M6223 could induce an anti-tumor immune response through several mechanisms, including direct blockade of the TIGIT pathway, stimulation of CD226 dimerization/activation, and depletion of TIGIT+ immune subsets by Fc-mediated effector function. Avelumab is a human IgG1 anti-PD-L1 antibody with a wild-type Fc region that has been shown to induce antitumor activity *in vitro* via both adaptive effector cells (T cells) and innate immune effector cells (antibody-dependent cell-mediated cytotoxicity [ADCC] via NK cells). It is approved for urothelial carcinoma (UC), renal cell carcinoma, and Merkel cell carcinoma. We report an evaluation of the effects of M6223 as a single agent and in combination with avelumab on human NK cell cytotoxicity.

Methods NK cell anti-tumor cytotoxicity was measured against the cancer line MDA-MB-231 with beta-2 microglobulin (B2M) knockout using fluorescent live cell imaging. NK cells were treated with M6223 or its Fc effector null version PPB1791. Avelumab was also tested alone or at a single dose combination with M6223 to evaluate additive potential of these antibodies. A variety of CD155 (poliovirus receptor [PVR]) knockout and partial knockouts were generated to assess the dependence of anti-tumor cytotoxicity on expression of this ligand.

Results M6223 induced significant NK cell anti-tumor cytotoxicity in 4 different NK donors at doses above 0.3 mcg/mL (t-test: $p < 0.05$) with an EC50 value of approximately 100 ng/mL. There was limited *in vitro* NK fratricide. An Fc-mutant version of M6223 had reduced anti-tumor cytotoxicity (at 0.3 mcg/mL: $p = 0.28$). M6223 in combination with avelumab was more effective than either antibody alone, indicating that CD16-mediated ADCC is likely additive with TIGIT blockade. Anti-tumor cytotoxicity was retained with PVR (CD155) expression on target MDA-MB-231 cells at a wild-type level of 30–50% and was almost completely eliminated in CD155^{-/-} cells. CD112 alone did not facilitate significant M6223-induced anti-tumor cytotoxicity, consistent with a weaker role of DNAX accessory molecule 1 (DNAM-1)-mediated recognition of this receptor.

Conclusions This study confirmed that NK cell cytotoxicity plays an important role in the anti-tumor activity of M6223 and demonstrated the additive effect of avelumab and M6223 in enhancing NK cell activation, especially in CD155+ human leukocyte antigen (HLA) class I-deficient target tumors. Currently, M6223 plus avelumab is being studied as first-line maintenance therapy for advanced UC in the phase 2 JAVELIN Bladder Medley umbrella trial (NCT05327530).

<http://dx.doi.org/10.1136/jitc-2022-SITC2022.0432>

Abstracts

433

PREVALENCE OF PD-L1 EXPRESSION AMONG PATIENTS WITH RECURRENT AND METASTATIC HEAD AND NECK SQUAMOUS CELL CARCINOMA IN TAIWAN

¹Chia-Jui Yen, ²Ming-Yu Lien, ³Rebecca Cheng, ³Yu-Wen Su*, ³Han-Nan Lin, ⁴Michael Thomas Wong, ⁴Song Ling Poon, ⁵Chih-Yen Chien, ⁶Ruey-Long Hong. ¹National Cheng Kung University Hospital, Tainan City, Taiwan; ²China Medical University Hospital, Taichung, Taiwan; ³MSD (I.A.) LLC, Taipei, Taiwan; ⁴MSD International GmbH, Singapore, Singapore; ⁵Kaohsiung Chang Gung Memorial Hospital, taipei, Taiwan; ⁶National Taiwan University Hospital, Taipei, Taiwan

Background Tumor programmed death-receptor/ligand-1 (PD-1/PD-L1) expression negatively correlates with cancer prognosis and overall survival,¹⁻⁶ and has been shown to predict clinical responses to immunotherapy for head and neck cancers.⁷ In Taiwan, head and neck cancers continue to show a high prevalence associated with betel quid chewing, a practice endemic to the island. This study aims to evaluate the prevalence of PD-L1 expression in recurrent and metastatic head and neck squamous cell carcinoma (R/M HNSCC) patients in Taiwan.

Methods For this multi-centered prospective study, we recruited R/M HNSCC patients who are aged 20 years or older, have an Eastern Cooperative Oncology Group (ECOG) performance status of 0 or 1, are ineligible for re-irradiation or curative surgery, and had a biopsy obtained before treatment. PD-L1 expression measured by combined positive score (CPS) and tumor proportion score (TPS) was determined by the PD-L1 IHC 22C3 pharmDx™ kit. The primary endpoint was to estimate the prevalence of PD-L1 expression, characterized by CPS ≥ 1. Exploratory analyses were conducted to evaluate PD-L1 positivity by CPS ≥ 20 and TPS ≥ 50%, and to explore the association of prior first- or second-line systemic treatment and PD-L1 expression.

Results Between December 2019 and February 2021, 280 patients from 4 centers were enrolled, including 264 (94.3%) males with median age of 58.0 years. Notably, 211 (75.4%) had a history of betel nut chewing. The primary sites were oral cavity in 192 cases (68.5%), followed by oropharynx 43 (15.4%), hypopharynx 26 (9.3%), and larynx 20 (7.1%). Among patients with oropharyngeal cancer, 13 (30.2%) were p16 positive. Prior to enrollment, 171 (61.1%) patients had received first-line systemic treatment and 68 (24.3%) second-line. The prevalence of PD-L1 (CPS ≥ 1) was 94.3% (264/280) in the total cohort, 93.8% (198/211) in the betel nut exposed subgroup, and 96.6% (56/58) in the non-betel nut exposed subgroup. Furthermore, 46.1% (129/280) of all patients were CPS ≥ 20, and 17.1% (48/280) were TPS ≥ 50%. A total of 159 (93.0%) and 64 (94.1%) patients were CPS ≥ 1 among those that received first-line and second-line systemic treatment, respectively.

Conclusions PD-L1 expression was observed in a vast majority (94.3%) of R/M HNSCC patients. There is no difference in PD-L1 prevalence between those with betel nut exposure history and betel nut non-exposed patients. PD-L1 prevalence also does not differ in those that had received prior first-line or second-line therapy, compared to the overall study population.

Acknowledgements This study was funded by MSD. Cerner Enviza received funding for the conduct of the study and development of the abstract.

REFERENCES

1. Nakanishi J, Wada Y, Matsumoto K, Azuma M, Kikuchi K, Ueda S. Overexpression of B7- H1 (PD-L1) significantly associates with tumor grade and postoperative prognosis in human urothelial cancers. *Cancer Immunol Immunother* 2007;**56** (8):1173–82.

2. Nomi T, Sho M, Akahori T, Hamada K, Kubo A, Kanehiro H, et al. Clinical significance and therapeutic potential of the programmed death-1 ligand/programmed death-1 pathway in human pancreatic cancer. *Clin Cancer Res* 2007;**13**(7):2151–7.
3. Zeng Z, Shi F, Zhou L, Zhang MN, Chen Y, Chang XJ, et al. Upregulation of circulating PD- L1/PD-1 is associated with poor post-cryoablation prognosis in patients with HBV-related hepatocellular carcinoma. *PLoS One* 2011;**6**(9):e23621.
4. Hino R, Kabashima K, Kato Y, Yagi H, Nakamura M, Honjo T, et al. Tumor cell expression of programmed cell death-1 ligand 1 is a prognostic factor for malignant melanoma. *Cancer* 2010;**116**(7):1757–66.
5. Hamanishi J, Mandai M, Iwasaki M, Okazaki T, Tanaka Y, Yamaguchi K, et al. Programmed cell death 1 ligand 1 and tumor-infiltrating CD8+ T lymphocytes are prognostic factors of human ovarian cancer. *Proc Natl Acad Sci USA* 2007;**104** (9):3360–5.
6. Wu C, Zhu Y, Jiang J, et al. Immunohistochemical localization of programmed death-1 ligand-1 (PD-L1) in gastric carcinoma and its clinical significance. *Acta histochemica* 2006;**108**:19–24.
7. Burtress B, Harrington KJ, Greil R, et al. Pembrolizumab alone or with chemotherapy versus cetuximab with chemotherapy for recurrent or metastatic squamous cell carcinoma of the head and neck (KEYNOTE-048): a randomised, open-label, phase 3 study. *Lancet*. 2019;**394**(10212):1915–1928.

Ethics Approval The study received ethics approval from National Taiwan University Hospital (IRB number: 201909007RSA), China Medical University Hospital (IRB number: CMUH108-REC2-150), National Cheng Kung University Hospital (IRB number: B-ER-108-252), and Chang Gung Memorial Hospital Kaohsiung Branch (IRB number: 201901757B0C501).

<http://dx.doi.org/10.1136/jitc-2022-SITC2022.0433>

434

TARGETING THE EXPRESSION OF NEUROPILIN-1 BY LOCKED NUCLEIC ACID MODIFIED ANTISENSE OLIGONUCLEOTIDES RESULTS IN POTENT ANTI-TUMOR ACTIVITY IN VIVO

¹Richard Klar*, ²Clara Seger, ²Nicole Kirchhammer, ¹André Maaske, ¹Julia Festag, ²Laura Fernandez Rodriguez, ²Mélanie Buchi, ¹Monika Schell, ¹Stefanie Raith, ¹Sven Michel, ²Alfred Zippelius, ¹Frank Jaschinski. ¹Secarna Pharmaceuticals GmbH & Co. KG, Planegg / Martinsried, Germany; ²University Hospital Basel, Basel, Switzerland

Background Despite the remarkable success of immune modulating cancer therapies, the majority of patients does not benefit from the currently available therapies. Therefore, there is a high need for the identification of novel therapies targeting cancer-induced immunosuppression.

The membrane-bound protein neuropilin-1 (NRP1) is a molecule with diverse functions and interaction partners that has been shown to contribute to tumor cell migration and survival as well as neoangiogenesis. Furthermore, NRP1 contributes to the suppressive capacity of immune cells like e.g. tumor associated macrophages and regulatory T cells. As the different functions of NRP1 are mediated by multiple domains of NRP1, there is a conceptual advantage to downregulate the expression of the whole protein over the functional or steric blockade of individual domains e.g. by monoclonal antibodies.

Methods We used our in-house Oligofyer™ bioinformatics system to design human and mouse Nrp1-specific antisense oligonucleotides (ASOs). The ASOs were modified in the flanks with locked nucleic acids to increase stability and affinity to the target RNA. RNA knockdown efficacy in vitro was investigated in different cells without the use of a transfection reagent. We furthermore investigated the anti-tumor activity of selected mouse Nrp1-specific ASOs in different syngeneic mouse tumor models after systemic administration of unformulated ASOs. In vivo target knockdown in different cell types was investigated by flow cytometry.

Results Treatment of different cell types with LNA-modified ASOs in vitro led to downregulation of NRP1 mRNA as well as protein expression by >85%. Systemic treatment of immune-competent tumor bearing mice with mouse Nrp1-specific ASOs without the use of a delivery reagent strongly delayed tumor growth or completely eradicated tumors. Furthermore, long-term anti-tumor immunity has been observed in immune-competent responder mice after re-challenge with tumor cells. The anti-tumor effects were almost completely absent in immune-compromised NSG mice.

Conclusions Our encouraging results indicate that downregulation of NRP1 with LNA-modified ASOs has the potential to become a promising treatment option for patients in the future. Currently, further studies are performed to investigate therapeutic activity in additional tumor models, combination therapies as well as to fully elucidate the mechanisms that underlie the observed anti-tumor efficacy of ASO-mediated NRP1 downregulation.

<http://dx.doi.org/10.1136/jitc-2022-SITC2022.0434>

435 **INTRATUMORAL PLASMA CELLS PREDICT OUTCOMES TO PD-L1 BLOCKADE IN NON-SMALL CELL LUNG CANCER**

Namrata Patil*, Barzin Nabet, Sören Müller, Hartmut Koeppen, Wei Zou, Jennifer Giltane, Jason Cheng, Chikara Takahashi, Avantika Chitre, Linda Rangell, Sangeeta Jayakar, William O’Gorman, Marcus Ballinger, Romain Banchereau, David Shames. *Genentech Inc., South San Francisco, CA, United States*

Background Inhibitors of the programmed cell death-1 (PD-1/PD-L1) signaling axis are approved to treat non-small cell lung cancer (NSCLC) patients, based on their significant overall survival (OS) benefit. However, the mechanisms behind this efficacy are not completely understood and there remains a significant unmet need for patients who do not respond to these therapies.

Methods To better understand the mechanisms behind the survival benefit associated with atezolizumab, we performed transcriptomic analysis of 891 NSCLC tumors from patients treated with either the PD-L1 inhibitor atezolizumab or chemotherapy from two large randomized clinical trials.

Results We found a significant B cell association with extended OS with PD-L1 blockade, independent of CD8+ T cell signals. We then derived gene signatures corresponding to the dominant B cell subsets present in NSCLC from single-cell RNA-seq data. Importantly, increased plasma cell signatures were predictive of OS in patients treated with atezolizumab, but not chemotherapy. B cells were also associated with the presence of tertiary lymphoid structures (TLS) and organized lymphoid aggregates.

Conclusions Our results suggest an important contribution of B and plasma cells to PD-L1 blockade efficacy in NSCLC. The association of plasma cells and TLS with improved outcomes suggests that novel therapeutics targeting these mechanisms that can be combined with PD-(L)1 blockade to improve their overall efficacy.

Acknowledgements This study was performed using tissue samples from the open-label, randomized Phase 2 POPLAR (NCT01903993) and Phase 3 OAK trials (NCT02008227).

Trial Registration NCT01903993, NCT02008227

Ethics Approval Both the POPLAR and OAK studies were performed in full accordance with the guidelines for Good Clinical Practice and the Declaration of Helsinki, and all patients gave written informed consent. Protocol approval was obtained from independent ethics committees for each participating site for both studies and an independent data monitoring committee reviewed the safety data.

Consent Both the POPLAR and OAK studies were performed in full accordance with the guidelines for Good Clinical Practice and the Declaration of Helsinki, and all patients gave written informed consent.

<http://dx.doi.org/10.1136/jitc-2022-SITC2022.0435>

437

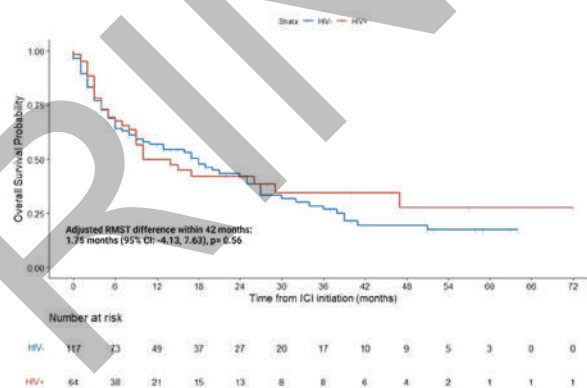
SAFETY AND EFFICACY OF IMMUNE CHECKPOINT INHIBITORS (ICI) IN PATIENTS LIVING WITH HIV (PLWH) AND METASTATIC NON-SMALL CELL LUNG CANCER (NSCLC): A MATCHED COHORT STUDY FROM THE INTERNATIONAL CATCH-IT CONSORTIUM

¹Talal El Zarif*, ²Amin Nassar, ³Elio Adib, ⁴Bailey Fitzgerald, ¹Jiaming Huang, ⁴Tarek Mouhieddine, ⁵Taylor Nonato, ⁵Rana McKay, ⁶Mingjia Li, ⁶Arjun Mittra, ⁶Dwight Owen, ⁷Michael Lorentsen, ⁷Christopher Dittus, ²Nazli Dizman, ²Brinda Emu, ⁸Adewunmi Falohun, ⁸Noha Abdel-Wahab, ⁹Anand Bankapur, ⁹Alexandra Reed, ⁹Ryan Dobbs, ¹⁰Chul Kim, ¹⁰Aakriti Arora, ¹¹Neil Shah, ¹²Edward El-Am, ¹²Elie Kozaily, ¹³Wassim Abdallah, ¹²Ahmad Al-Hader, ¹⁴Batool Abu Ghazal, ¹⁴Anwaar Saeed, ¹⁵Claire Drolen, ¹⁵Melissa Lechner, ¹⁶Javier Espinar, ¹⁷Caroline Nebhan, ¹⁷Douglas Johnson, ¹⁸Tarek Haykal, ¹⁸Michael Morse, ¹⁹Alessio Cortellini, ¹⁹David Pinato, ¹⁹Alessia Dalla Pria, ¹⁹Mark Bower, ²⁰Evan Hall, ²¹Veli Bakalov, ²¹Nathan Bahary, ²²Aarthi Rajkumar, ²²Ankit Mangla, ²³Vishal Shah, ²³Parminder Singh, ²⁴Frank Aboubakar Nana, ²⁵Nerea Lopetegui Lia, ²⁵Danai Dima, ²⁵Pauline Funchain, ²⁶Rabia Saleem, ²⁷Rachel Woodford, ²⁷Georgina Long AO, ²⁷Alexander Menzies, ²⁸Carlo Genova, ²⁸Giulia Barletta, ²⁹Sonam Puri, ²⁹Vaia Florou, ³⁰Dame Idossa, ³¹Paola Queirolo, ¹Giuseppe Lamberti, ³²Alfredo Addeo, ³³Melissa Bersanelli, ¹Dory Freeman, ¹Wanling Xie, ³⁴Ramy Ramaswami, ³⁵Thomas Marron, ¹Toni Choueiri, ³⁴Kathryn Lurain, ³Lindsey Baden, ¹Guru Sonpavde, ³⁶Abdul Rafah Naqash. ¹Dana-Farber Cancer Institute, Boston, MA, United States; ²Yale University School of Medicine, New Haven, CT, United States; ³Brigham and Women's Hospital, Boston, MA, United States; ⁴Tisch Cancer Institute, Mount Sinai, New York, NY, United States; ⁵University of California San Diego, La Jolla, CA, United States; ⁶The Ohio State University, Columbus, OH, United States; ⁷University of North Carolina-Chapel Hill, Chapel Hill, NC, United States; ⁸MD Anderson Cancer Center, Houston, TX, United States; ⁹Cook County Hospital, Chicago, IL, United States; ¹⁰Georgetown University, Washington, DC, DC, United States; ¹¹Memorial Sloan Kettering Cancer Center, New York, NY, United States; ¹²Indiana University, Indianapolis, IN, United States; ¹³Emory University, Atlanta, GA, United States; ¹⁴Kansas University Cancer Center, Kansas City, KS, United States; ¹⁵University of California Los Angeles, Los Angeles, CA, United States; ¹⁶Doce de Octubre University Hospital, Madrid, Spain; ¹⁷Vanderbilt University Medical Center, Nashville, TN, United States; ¹⁸Duke University Medical Center, Durham, NC, United States; ¹⁹Imperial College London, London, UK; ²⁰University of Washington, Seattle, WA, United States; ²¹Allegheny Health Network, Pittsburgh, PA, United States; ²²University Hospitals, Cleveland, OH, United States; ²³Mayo Clinic, Tucson, AZ, United States; ²⁴Université Catholique de Louvain (UCL), Brussels, Belgium; ²⁵Cleveland Clinic Foundation, Cleveland, OH, United States; ²⁶Oklahoma University Stephenson Cancer, Oklahoma, OK, United States; ²⁷Melanoma Institute of Australia, Sydney, Australia; ²⁸IRCCS Ospedale Policlinico San Martino, Genova, Italy; ²⁹Huntsman Cancer Institute, Salt Lake City, UT, United States; ³⁰University of California San Francisco, San Francisco, CA, United States; ³¹IEO European Institute of Oncology Milan, Milan, Italy; ³²Geneva University Hospitals, Geneva, Switzerland; ³³University Hospital of Parma, Parma, Italy; ³⁴Center for Cancer Research, Bethesda, MD, United States; ³⁵Cahn School of Medicine at Mount Sinai, New York, NY, United States; ³⁶Oklahoma University, Oklahoma City, OK, United States

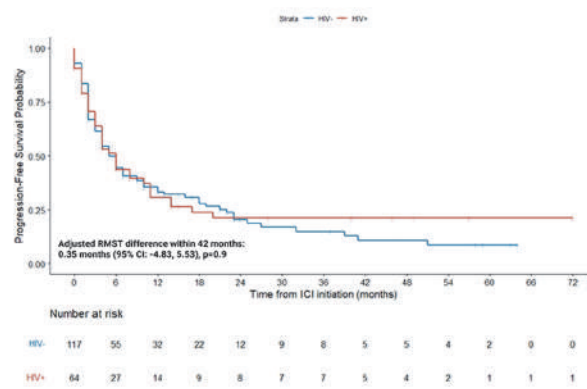
Background Due to limited inclusion of PLWH in most ICI clinical trials, there is a paucity of data evaluating their safety and efficacy in this unique population, especially among PLWH and metastatic NSCLC.

Methods In this retrospective, international multi-center study, we identified 64 HIV positive (HIV+) patients and 117 matched HIV negative (HIV-) controls with metastatic NSCLC treated with ICI between January 2015 and October 2021 at 16 institutions in the U.S. and Europe. At each institution, we matched 1 HIV+ patient to 2 or 1 HIV- controls (1:2 or 1:1 ratio) by age, sex, class of ICI, use of concurrent chemotherapy, and number of prior lines of systemic therapy. We estimated overall survival (OS) and progression-free survival (PFS) by the Kaplan-Meier method. When the proportional hazards assumption was violated, we used restricted mean survival time (RMST) to compare survival outcomes. We fitted a linear regression model with RMST as outcome and HIV infection as predictor, adjusting for race, ECOG performance status, histology, smoking status and PD-L1 expression. We compared categorical variables using chi-square tests.

Results In our cohort, median age was 60 years, 77% were males, 61% received ICI as 1st line therapy, 89% received anti-PD-1 based therapy, and 46% received concurrent chemotherapy. Blacks/African Americans were more represented among HIV+ vs. HIV- patients (42% vs 23%, p <0.01). At baseline, HIV+ patients had a median CD4 count = 386 cells/uL (range: 6 – 1,721), 19/31 had undetectable HIV viral load (VL) while 12/31 had a median detectable VL= 60 copies/mL (range: 10 – 223,408). Grade ≥3 immune-related adverse events occurred in 11% HIV+ vs. 9% HIV- patients. Overall response rate was similar between both groups (28% HIV+ vs. 37% HIV-, p=0.25). Comparing HIV+ vs. HIV- pts, the adjusted RMST difference within 42 months was 1.75 months (95% CI: -4.13, 7.63, p=0.56) for OS, and 0.35 months (95% CI: -4.83, 5.53, p=0.90) for PFS (figures 1 and 2). In addition, the 24-month OS rates were 41.7% for HIV+ vs. 42.9% for HIV- patients while the 24-month PFS rates were 18.1% HIV+ vs 18.7% HIV- patients.



Abstract 437 Figure 1 Kaplan-Meier curves for Overall Survival stratified by HIV status



Abstract 437 Figure 2 Kaplan-Meier curves for Progression-Free Survival stratified by HIV status

Conclusions In this matched cohort study, PLWH and metastatic NSCLC had similar toxicity profiles and clinical outcomes to HIV- counterparts receiving ICI supporting their use in PLWH and their inclusion in clinical trials. Larger

Abstracts

prospective studies are needed to inform a broader usage of ICI among PLWH presenting with other cancer types, low CD4 counts (i.e., <200 cells/uL) and high VL.

Ethics Approval Our study was exempt from institutional review board (IRB) review at DFCI (Protocol #21-342) and was approved by local IRBs at participating sites per institutional policy, according to the principles of the Declaration of Helsinki.

<http://dx.doi.org/10.1136/jitc-2022-SITC2022.0437>

PREPRINT

438 INTERROGATION OF IMMUNE TOXICITY IN PATIENTS WITH THYMIC EPITHELIAL TUMORS (TETS)

Meredith McAdams*, Shannon Swift, Madison Ballman, Abigail Wong-Rolle, Renee Donahue, Claudia Palena, Jeffrey Schlom, James Gullely, Arun Rajan, Chen Zhao. *National Cancer Institute, Bethesda, MD, United States*

Background Immune checkpoint inhibitors (ICIs) are well tolerated and clinically active against a wide variety of cancers. However, the risk of immune toxicity in patients with thymic epithelial tumors (TETs), especially thymomas, remains unacceptably high due to underlying defects in immune tolerance.¹⁻³ Mechanisms of immune toxicity remain poorly understood and the mainstay of treatment is immunosuppression with systemic corticosteroids, which can potentially impact the anti-tumor activity of ICIs.

Methods To understand mechanisms of organ-specific immune toxicity, we evaluated blood and tissue samples from patients with TETs enrolled in an ongoing NIH IRB-approved clinical trial (NCT03076554; NCI protocol number: 17C0066) of avelumab, an anti-PD-L1 antibody who developed multi-organ immune-related adverse events (irAEs) following treatment. Participants received avelumab 10 mg/kg IV every two weeks until disease progression or development of intolerable AEs. Toxicity was assessed with CTCAE 5.0. Immune profiling was conducted using one or more of the following methods: evaluation of biopsies with routine hematoxylin and eosin staining and immunohistochemistry (IHC), peripheral blood immune cell subset analysis by flow cytometry, RNAscope for IL-6, IL-8 and TGF-β1 mRNA expression, and spatial transcriptomics using the nanoString Digital Spatial Profiler platform to investigate T-cells' transcriptional profiles at tumor and irAE sites.

Results Between April 2017 and February 2022, 32 participants were enrolled (median age: 55 years; 16 female; 16 thymoma;). Five (16%) participants developed multiple irAEs during treatment. Objective anti-tumor responses were observed in 2 (40%) of 5 participants. table 1 includes clinical characteristics and results of immune analyses. Histopathology and IHC were notable for a T-cell infiltrate and paucity of B cells across irAE sites. IL-6 and TGF-β1 mRNA expression was variable in cases of upper gastrointestinal inflammation. Spatial transcriptomic analysis of 1811 genes in tumor and irAE samples (bone marrow) from subject 3 revealed distinct T-cell activation profiles in the bone marrow compared with tumor infiltrating T cells (figure 1).

Conclusions Organ-specific heterogeneity in mechanisms of ICI-related immune-mediated toxicity in individuals with TETs needs further evaluation. If confirmed, these findings highlight the need to tailor immunosuppressive treatments to specific irAEs and develop strategies for primary or secondary prophylaxis to decrease the risks associated with immunotherapy while maintaining clinical benefit in this population.

Acknowledgements This research was supported in part by the Intramural Research Program of the National Cancer Institute (Center for Cancer Research) and through a Cooperative Research and Development Agreement between the National Cancer Institute and EMD Serono (CrossRef Funder ID: 10.13039/100004755), as part of an alliance between the healthcare business of Merck KGaA, Darmstadt, Germany and Pfizer.

REFERENCES

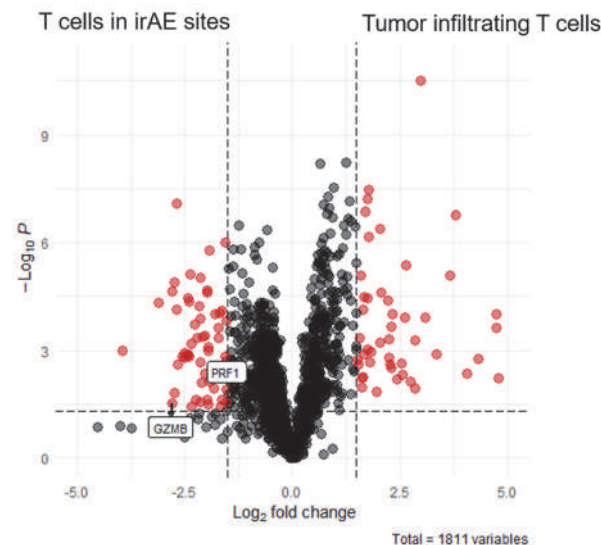
1. Ballman M, Zhao C, McAdams MJ, Rajan A. Immunotherapy for Management of Thymic Epithelial Tumors: A Double-Edged Sword. *Cancers*. 2022 Apr 20;14

(9):2060. doi: 10.3390/cancers14092060. PMID: 35565190; PMCID: PMC9105984.
 2. Rajan A, Heery CR, Thomas A, Mammen AL, Perry S, O'Sullivan Coyne G, Guha U, Berman A, Szabo E, Madan RA, Ballester LY, Pittaluga S, Donahue RN, Tsai YT, Lepone LM, Chin K, Ginty F, Sood A, Hewitt SM, Schlom J, Hassan R, Gullely JL. Efficacy and tolerability of anti-programmed death-ligand 1 (PD-L1) antibody (Avelumab) treatment in advanced thymoma. *J Immunother Cancer*. 2019 Oct 21;7(1):269. doi: 10.1186/s40425-019-0723-9. PMID: 31639039; PMCID: PMC6805423.
 3. Cho J, Kim HS, Ku BM, Choi YL, Cristescu R, Han J, Sun JM, Lee SH, Ahn JS, Park K, Ahn MJ. Pembrolizumab for Patients With Refractory or Relapsed Thymic Epithelial Tumor: An Open-Label Phase II Trial. *J Clin Oncol*. 2019 Aug 20;37(24):2162–2170. doi: 10.1200/JCO.2017.77.3184. Epub 2018 Jun 15. PMID 29906252.

Ethics Approval Samples used in this study were derived from an ongoing NIH IRB-approved clinical trial [NCT03076554; NCI protocol number: 17C0066]. Participants gave informed consent for participation in the clinical trial.

Abstract 438 Table 1 Clinical Characteristics and Results of Immune Analyses

Subject	WHO Type	Stage	Organ site	Area (cm ²)	Histopathology and IHC results	Additional Immune Analyses	Treatment	Outcomes	Other IHCs	Anti-tumor response	Adverse events
1	M1T	III	Lung/pleura	20	Extensive chronic inflammation	IL-6 mRNA analysis	Checkpoints	Partial response	TRAC	None	IR
2	M1T	III	Intestine	6	Small intestine, mucosal lymphocytic infiltration	High expression of CD45, CD3, CD8	Checkpoints	Partial response	CD3, CD8, CD45	None	IR
3	M1T	III	Intestine	10	Small intestine, mucosal lymphocytic infiltration	High expression of CD45, CD3, CD8	Checkpoints	Partial response	CD3, CD8, CD45	None	IR
4	M1T	III	Intestine	10	Small intestine, mucosal lymphocytic infiltration	High expression of CD45, CD3, CD8	Checkpoints	Partial response	CD3, CD8, CD45	None	IR
5	M1T	III	Intestine	10	Small intestine, mucosal lymphocytic infiltration	High expression of CD45, CD3, CD8	Checkpoints	Partial response	CD3, CD8, CD45	None	IR



Abstract 438 Figure 1 Volcano plot of T-cell genes enriched in primary tumor site versus organs affected by immune toxicity

<http://dx.doi.org/10.1136/jitc-2022-SITC2022.0438>

Abstracts

439

HEALTHCARE RESOURCE UTILIZATION IN PATIENTS WITH PRE-EXISTING AUTOIMMUNE DISEASES WHO RECEIVED IMMUNE CHECKPOINT INHIBITORS IN THE MARKETSCAN DATABASE

¹Jennell Palaia, ²Anna Pavlick*, ¹Radhika Pisupati, ¹Benjamin Fu, ¹Keith Wittstock, ¹Ying Zhang. ¹Bristol Myers Squibb, Lawrence Township, NJ, United States; ²Weill Cornell Medical Center, New York, NY, United States

Background Autoimmune diseases (ADs) affect more than 24 million people in the United States. As patients with ADs are excluded from clinical trials of immune checkpoint inhibitors (ICI), management of AD after ICI initiation is not well understood. Our study explored healthcare resource utilization (HCRU) before and after initiation of an ICI in cancer patients with pre-existing ADs.

Methods This retrospective, observational study included adult patients who were treated with ICIs and had ≥ 1 inpatient or ≥ 2 outpatient claims for melanoma (Mel), renal cell carcinoma, lung cancer (LC), head and neck cancer, hepatocellular carcinoma, or bladder cancer, between January 1, 2015 and March 31, 2020 in the MarketScan Commercial, Medicare Supplemental and Medicaid claims databases. Patients also had administrative claims for ADs (rheumatoid arthritis (RA), psoriasis/psoriatic arthritis (P/PA), multiple sclerosis (MS), Crohn's disease (CD)/ulcerative colitis (UC)/inflammatory bowel disease (IBD) and Others) within 12 months prior to the index date (first ICI treatment date). HCRU included outpatient visits, hospitalizations, and ER visits. Total HCRU and AD-related HCRU were calculated per patient per month (PPPM) for all patients. Generalized linear models (GLM) were used to calculate differences in HCRU pre- and post- ICI initiation over the entire follow-up period. Analyses were also conducted using the first 6 months of the pre- and post-index period.

Results Of the 525 eligible patients, mean age was 61 years, 58.9% were female; over half (50.7%) had a Charlson Comorbidity Index of 2+, 29.1% had Mel, and 55.6% had LC. The most common AD types were IBD/CD/UC (24.9%) and RA (19.0%). Mean total visits over the total follow-up period were 3.5 and 5.8 PPPM in the pre- and post-periods, respectively. Mean AD-related visits over the total follow-up period were 0.4 and 0.5 PPPM in the pre- and post-periods, respectively. Breakdown of outpatient visits, hospitalizations, and ER visits in the pre-and post-periods are described in (table 1). GLM showed that total HCRU increased in the post-period over total follow-up, but AD-related HCRU were not significantly different between pre-and post-periods, over the entire follow-up period.

Conclusions This real-world analysis is one of the largest claims-based analysis describing a patient population treated with ICI therapy with pre-existing ADs. Using HCRU as a proxy for management of the AD post ICI initiation, this study showed that care related to AD was similar in the prior and post periods.

Abstract 439 Table 1 Outpatient visits, hospitalizations, and ER visits in the pre-and post-periods

	Visit type	Mean (SD) Prior Period	Mean (SD) Post Period
All visits, PPPM	Outpatient	3.5 (3.5)	5.8 (4.6)
	Hospitalization	0.1 (0.1)	0.1 (0.2)
	ER	0.1 (0.2)	0.2 (0.3)
AD-related visits, PPPM	Outpatient	0.4 (1.3)	0.5 (1.7)
	Hospitalization	0.01 (0.01)	0.01 (0.01)
	ER	0.01 (0.01)	0.01 (0.01)

<http://dx.doi.org/10.1136/jitc-2022-SITC2022.0439>

440 **OUTCOMES IN PATIENTS WITH PRE-EXISTING AUTOIMMUNE DISEASES WHO RECEIVED IMMUNE CHECKPOINT INHIBITORS: A REAL-WORLD STUDY**

¹Anna Pavlick*, ²Jennell Palaia, ²Radhika Pisupati, ²Benjamin Fu, ²Keith Wittstock, ²Ying Zhang. ¹Weill Cornell Medical Center, New York, NY, United States; ²Bristol Myers Squibb, Lawrence Township, NJ, United States

Background Autoimmune diseases (ADs) affect more than 24 million people in the United States. Although patients with AD are usually excluded from ICI clinical trials, real world evidence suggests ICIs are used in this population. In this analysis, we describe the clinical outcomes of patients on ICI therapy with pre-existing ADs.

Methods This retrospective, observational study used the nationwide Flatiron Health electronic health record (EHR)-derived de-identified database to describe characteristics and outcomes in patients with pre-existing ADs (rheumatoid arthritis (RA), psoriasis/psoriatic arthritis (P/PA), multiple sclerosis (MS), Crohn's disease/ulcerative colitis/inflammatory bowel disease (CD/UC/IBD) and Others) who were treated with ICIs for advanced melanoma (aMel), metastatic renal cell carcinoma (mRCC), advanced non-small cell lung cancer (aNSCLC), hepatocellular carcinoma (HCC), or advanced bladder cancer (aBC). Overall survival (OS), Progression free survival (PFS), and Time to treatment discontinuation (TTD) were evaluated from the index date (first ICI treatment date). Baseline and clinical characteristics were analyzed using descriptive statistics, and time to event analysis for OS, PFS, and TTD were analyzed using Kaplan Meier methods. All analyses were conducted for the overall cohort and by subgroups including cancer type, AD type, line of therapy and ICI treatment group (monotherapy or combination). The ICI combination group included ICI + Chemo, ICI + targeted therapy, and ICI+ICI.

Results This study included 453 pts diagnosed with aMel, mRCC, aNSCLC, HCC, or aBC and treated with ICI from Jan 2015 to Oct 2021, with a pre-existing AD within 12 months of index date. Median age was 69.4 years; 55.4% were female and 76.8% were white. In the overall cohort, median OS was 11.1 months (95% CI: 9.0-14.0); median PFS was 4.2 months (95% CI: 3.5-4.8), and median TTD was 2.6 months (95% CI: 2.1-3.0). There were 301 patients who received ICI in the first line (1L) and 152 in the second line or later (2L+). OS and AD type by tumor type (1L and 2L+ combined) are described in (table 1).

Conclusions This real-world analysis is one of the largest studies describing clinical outcomes in patients with pre-existing ADs receiving ICI therapy. Further research is warranted to evaluate adverse event profiles and reasons for ICI discontinuation in this patient population.

Abstract 440 Table 1

	aMel (N=62)	mRCC (N=46)	aNSCLC (N=302)	HCC (N=21)	aBC (N=23)
Median OS, months (95% CI)	31.5 (15.8-NR)	18.9 (8.9-NR)	10.0 (7.8-12.8)	7.0 (1.7-17.3)	4.0 (2.1-17.5)
Median Follow-up Time from Index Date / Median Potential Follow-up time (months)	12.9 / 39.6	8.9 / 22.8	7.7 / 34.0	2.8 / 17.9	3.2 / 44.7
AD Type (%)					
RA	19.4	10.9	17.5	9.5	13.0
P/PA	17.7	39.4	16.6	23.8	13.0
MS	4.8	0	5.0	9.5	4.3
CD/UC/IBD	33.9	21.7	32.1	33.3	34.8
Other	32.3	37.6	32.5	23.8	34.8

Potential Follow-up time is defined as (data cut-off date - index date) +1

<http://dx.doi.org/10.1136/jitc-2022-SITC2022.0440>

441

CHECKPOINT INHIBITOR-ASSOCIATED INFLAMMATORY ARTHRITIS IS COMPRISED OF MULTIPLE CLINICAL ENDOTYPES CHARACTERIZED BY DISTINCT TRANSCRIPTIONAL PROGRAMS

Gary Reynolds*, Mazen Nasrallah, Neal Smith, Molly Thomas, Leyre Zubiri, Alice Tirard, John McGuire, Kasidet Manakongtreecheep, Jessica Tantivit, Steven Blum, Daniel Zlotoff, Elaina PuiYee Chan, Dejan Juric, Ryan Sullivan, Genevieve Boland, Andrew Luster, Sara Schoenfeld, Minna Kohler, Kerry Reynolds, Chloe Villani. *Massachusetts General Hospital, Boston, MA, United States*

Background Immune checkpoint inhibitor (ICI) therapy has revolutionized cancer treatment but is associated with a range of immune toxicities.¹ ICI-associated inflammatory arthritis (ICI-IA) is a complication that affects around 5% of patients on ICI therapy. Clinical manifestations mimic those of rheumatoid arthritis or seronegative spondyloarthropathies and often require treatment with glucocorticoids or other immunosuppressive medications. In severe cases, irArthritis results in interruption or discontinuation of ICI therapy and is a significant cause of morbidity. Understanding why ICI-IA develops and rationalizing our approach to its treatment could improve outcomes for this expanding patient cohort.

Methods Comprehensive clinical and demographic data were collected for patients with malignancy, treated with ICI, and subsequently diagnosed with inflammatory arthritis (n=41). Peripheral blood and synovial fluid were collected and profiled when possible. Presentations of ICI-IA included monoarthritis (n=5 total, n=4 profiled), oligoarthritis (n=10 total, n=5 profiled) and polyarthritis (n=26 total, n=7 profiled). Six additional patients with inflammatory arthritis after ICI that were not checkpoint-related were profiled. Samples were analyzed by paired single cell RNA sequencing, surface proteome of 204 protein targets, and T cell receptor (TCR) sequencing.

Results We captured data from 741,883 cells in total following quality-control (559,251 synovial fluid, 264,997 blood) and identified diverse cell populations in synovial fluid, including rare mast cells, AXL+SIGLEC6+ dendritic cells and cycling lymphocytes. Patients presenting with monoarthritis were ANA negative (0/6) with higher abundance of DC1 and DC2 (Dirichlet regression, $p=1.1 \times 10^{-3}$ and $p=8.1 \times 10^{-5}$), with DC1 having the highest per cell expression of *TNF* across all samples. Patients presenting with polyarthritis were significantly more likely to be antinuclear antibody positive (15/26, Fisher's test, $p=0.04$) with expansions of a macrophage population enriched for interferon response genes (*IFI44L*, *ISG15*) and peripheral helper CD4+T cells (*CXCL13*, *PDCD1*) previously described as expanded in seropositive rheumatoid arthritis.² TCR repertoire analysis demonstrated clonal expansion of specific CD8 T cell subsets, including shared clones across patients. Gene set enrichment analysis highlighted upregulation of distinct inflammatory pathways with existing biologic drugs in mono- and oligoarthritis presentations versus polyarthritis.

Conclusions These data demonstrate that ICI-IA is heterogeneous both in terms of clinical presentation and at the cellular and transcriptional level. It is likely that patients will benefit from better targeting of treatments that can simultaneously control arthritis and preserve anti-tumor efficacy and our data support new strategies for developing personalized medicine approaches for this patient population.

REFERENCES

1. Reynolds KL, et al. Immune-related adverse events associated with immune checkpoint inhibitors: a call to action for collecting and sharing clinical trial and real-world data. *J Immunother Cancer* 2021;**9**.

2. Rao DA, et al. Pathologically expanded peripheral T helper cell subset drives B cells in rheumatoid arthritis. *Nature* 2017;**542**:110–114.

Ethics Approval Patients involved in this study were consented to Dana-Farber Cancer Institute/Harvard Cancer Center collection protocols #11-181 and #13-416.

<http://dx.doi.org/10.1136/jitc-2022-SITC2022.0441>

442

PRE-TREATMENT INTERSTITIAL ABNORMALITIES IS A RISK FACTOR FOR IMMUNE CHECKPOINT INHIBITOR PNEUMONITIS IN PATIENTS WITH LUNG CANCER

¹Alexander Wong*, ²Maria Riley, ³Songzhu Zhao, ²Jessica Zimmer, ²Matthew Viveiros, ¹Jing Gennie Wang, ¹Vince Esguerra, ³Mingjia Li, ³Gabrielle Lopez, ³Gregory Otterson, ³Kari Kendra, ³Carolyn Presley, ³Lai Wei, ³Dwight Owen, ¹Kevin Ho. ¹The Ohio State University WMC, Columbus, OH, United States; ²The Ohio State University COM, Columbus, OH, United States; ³The Ohio State University James, Columbus, OH, United States

Background Immune checkpoint inhibitors (ICIs) are a first line and adjuvant treatment in advanced stage lung cancer. One of the main complications of ICI treatment is pneumonitis with an overall incidence of 2-5%; however, patient specific risk factors for developing ICI-pneumonitis (ICI-p) haven't been well elucidated. ^{1,2} We evaluated potential pre-treatment risk factors for ICI-p including pre-treatment interstitial abnormalities on computed tomography of the chest (CT chest).

Methods We conducted a retrospective cohort study of consecutive patients with lung cancer who received at least one dose of ICI between 2015-2020 at The Ohio State University. Potential risk factors for ICI-p were recorded and summarized between those with and without pneumonitis. Among patients who developed pneumonitis, these factors were compared between Grade <3 and Grade ≥3 severities as well as among patients with different cancer stage (3 vs 4). Multivariable survival analysis was used to examine the association of potential risk factors with pneumonitis. Pneumonitis cases were documented by the treating oncologist and retrospectively evaluated by an oncologist and pulmonologist.

Results 473 patients with lung cancer were included, 401 with Non-Small Cell Lung Cancer and 72 with Small Cell Lung Cancer. 38 developed ICI-p and 435 did not. Of the potential risk factors, the following were significantly associated with ICI-p: pre-existing interstitial abnormalities (30.8% vs 4.2%, p < 0.001), prior concurrent chemoradiation (17.7% vs 4.2%, p < 0.001), stage of cancer (19.8% for stage III vs 4.4% for stage IV, p < 0.001), and type of immunotherapy (12.5% for PD1 vs 3.6% for chemo-IO, p < 0.001) (table 1). Pre-existing interstitial abnormalities remained strongly correlated with development of pneumonitis on multivariable analysis including prior chemoradiation, pre-treatment interstitial abnormalities, and type of immunotherapy, (hazard ratio 8.54 [4.45-16.42], p<0.001) (table 2). Interstitial abnormalities also remained significant in subgroup analysis of both stage 3 and 4 lung cancer (p<0.001). Patients with grade 3/4 pneumonitis had decreased overall survival compared to those with grade 1/2 pneumonitis (p = 0.0342) (figure 1).

Conclusions Pre-existing interstitial abnormalities on CT chest is strongly associated with development of ICI-p in patients with lung cancer. It remains an independent risk factor after accounting for common treatment-related risk factors such as prior chemoradiation and chest radiation. Pre-treatment interstitial abnormalities could be utilized as a risk stratification tool to identify patients at highest risk for developing ICI-p, a devastating complication associated with higher mortality in more severe cases.

Acknowledgements This study was supported by the National Institutes of Health (P30CA016058 and K12 CA133250). Research support provided by the REDCap project and The Ohio State University Center for Clinical and Translational Science grant support (National Center for Advancing Translational Sciences, Grant UL1TR002733)

REFERENCES

1. Nishino M, Giobbie-Hurder A, Hatabu H, Ramaiya NH, Hodi FS. Incidence of Programmed Cell Death 1 Inhibitor-Related Pneumonitis in Patients With Advanced Cancer A Systematic Review and Meta-analysis. *JAMA Oncology*.2(12):1607–1616.
2. Wu J, Hong D, Zhang X, Lu X, Miao J. PD-1 inhibitors increase the incidence and risk of pneumonitis in cancer patients in a dose-independent manner: a meta-analysis. *Scientific Reports*.7(1).

Ethics Approval Human data was utilized in this project; CIRB approval was obtained and all participants provided informed consent prior to taking part in the study (Study number 2021C0069).

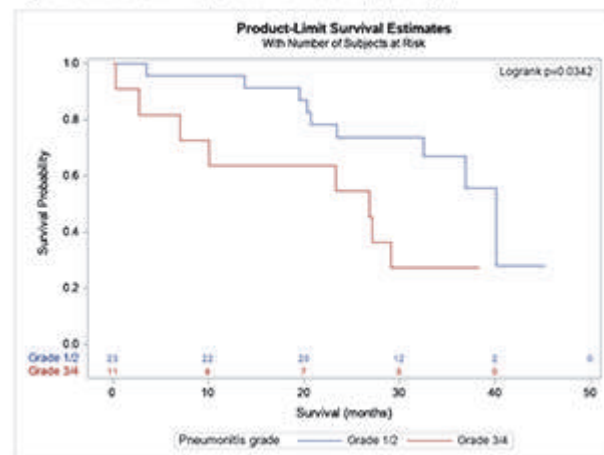
Abstract 442 Table 1 Pre-treatment risk factors for pneumonitis

Development of Pneumonitis	Yes	No	% of Total	p value
Pre-existing Interstitial Abnormalities	21	47	30.8%	<0.001
No Pre-existing Interstitial Abnormalities	16	562	4.2%	
Prior Chemoradiation	24	117	17.6%	<0.001
No Prior Chemoradiation	14	323	4.2%	
Type of Therapy: PD1	30	210	12.5%	<0.001
Type of Therapy: Chemo-IO	8	212	3.6%	
Stage 3 Lung Cancer	23	98	19.8%	<0.001
Stage 4 Lung Cancer	13	285	4.6%	

Abstract 442 Table 2 Multivariate analysis of risk factors

Parameter	Hazard Ratio	95% Hazard Ratio Confidence Limits	p-value
Pre-existing Interstitial Abnormalities	8.548	4.450 - 16.420	<.0001
Prior Chemoradiation	3.189	1.526 - 6.663	0.0020
Type of Therapy: Chemo-IO	0.482	0.206 - 1.131	0.0935

Figure 1: Overall Survival by Pneumonitis Grade (1/2 vs 3/4)



Abstract 442 Figure 1 Overall survival by pneumonitis grade

<http://dx.doi.org/10.1136/jitc-2022-SITC2022.0442>

444

TNG260, A COREST-SELECTIVE DEACETYLASE INHIBITOR, REVERSES ANTI-PD1 RESISTANCE DRIVEN BY LOSS OF STK11

Leanne Ahronian*, Xinyuan Wu, Minjie Zhang, Chengyin Min, Alice Tsai, Jacques Ermolieff, Patrick McCarren, Margaret Wyman, Ye Wang, Alborz Bejnood, Kenjie Amemiya, Brian McMillan, Nikitha Das, Brian Doyon, Andre Mignault, Colin Liang, Vassil Elitzin, Yi Yu, Samuel Meier, Ashley Choi, John Maxwell, Alan Huang. *Tango Therapeutics, Cambridge, MA, United States*

Background Histone deacetylase 1 (HDAC1) was identified from a novel *in vivo* CRISPR screening platform as a target gene whose inhibition reverses α -PD1 resistance driven by loss of STK11. Histone deacetylases are a well-studied class of oncology drug targets, but existing non-isoform-selective HDAC inhibitors have few approved clinical applications due to toxicities that limit sufficient exposure in solid tumors. Our data suggest that HDAC3, an essential gene, is a primary driver of bone marrow toxicity caused by HDAC inhibitors that target multiple isoforms.

Methods We discovered and developed TNG260, a small molecule which inhibits HDAC1 with 10-fold selectivity over HDAC3 in cells, and 500-fold selectivity for the CoREST complex over the other HDAC1-containing complexes, NuRD and Sin3. Due to its CoREST-selective deacetylase inhibition, we have termed TNG260 a CoreDAC inhibitor.

Results Treatment of an α -PD1 resistant STK11-mutant MC38 syngeneic tumor model with TNG260 re-sensitizes this model to treatment with α -PD1. The combination of TNG260 and α -PD1 led to durable complete tumor regressions in the majority of treated animals. All mice with complete responses remained tumor-free until tumor rechallenge (21 days) and rejected engraftment of tumor cells. Unlike previously developed HDAC inhibitors designed for tumor cell cytotoxicity, TNG260 has no anti-tumor efficacy in immunocompromised mice, indicating the tumor cell killing with TNG260 is immune-mediated and not due to direct cell killing. Immune profiling of tumors following treatment with TNG260 and α -PD1 showed a decoupling of T_{effector} and $T_{\text{regulatory}}$ cell recruitment caused by α -PD1 monotherapy, leading to a more active immune microenvironment. TNG260 also decreased intratumoral infiltration of neutrophils, an immune suppressive cell type associated with STK11-mutant NSCLC. Toxicity profiling of TNG260 shows it has less viability impact on erythroid and myeloid cells *in vitro* than other HDAC inhibitors, and *in vivo* toxicity studies showed bone marrow suppression only at TNG260 doses that are no longer selective for HDAC1/2.

Conclusions TNG260 is a potent, highly selective small molecule CoreDAC inhibitor with good drug-like properties. It reverses the immune evasion phenotype caused by loss of STK11 and induces tumor regressions in an STK11-mutant model in combination with α -PD1. The TNG260 clinical development plan will be among the first to combine the power of genetic patient selection and immunotherapy, evaluating patients with STK11 mutant cancers in a trial combining TNG260 and a checkpoint inhibitor.

<http://dx.doi.org/10.1136/jitc-2022-SITC2022.0444>

445

TREATMENT PATTERNS AND IMMUNOTHERAPY RECHALLENGE IN ADVANCED OR METASTATIC UPPER GASTROINTESTINAL CANCER IN A US REAL-WORLD SETTING

¹Jaffer Ajani*, ²Marley Boyd, ²Jenifer Wogen, ³Ilia Ferrusi, ⁴Peyman Nakhaei, ³Lakshmi Menon-Singh, ⁵Ailis Fagan. ¹The University of Texas MD Anderson Cancer Center, Houston, TX, United States; ²Genesis Research, Hoboken, NJ, United States; ³Novartis Pharmaceuticals Corporation, East Hanover, NJ, United States; ⁴Novartis Pharmaceuticals Canada Inc, Dorval, Canada; ⁵Novartis Ireland Limited, Dublin, Ireland

Background US regulatory approvals of immunotherapy (IO) for upper gastrointestinal (GI) cancers have notably increased treatment (tx) options. It is unknown which txs are often used in real-world practice. IO rechallenge shows potential efficacy in some cancers, although data are limited for upper GI cancers. We assessed tx patterns and use of IO rechallenge in patients (pts) with upper GI cancers in the US.

Methods This retrospective study evaluated pts aged ≥18 years with locally advanced or metastatic esophageal cancer (EC), gastric cancer (GC), or gastroesophageal junction cancer (GEJC) diagnosed on or after January 1, 2011. This study used the electronic health record-derived, de-identified Flatiron Health database (data cutoff: May 31, 2021). Eligible pts received ≥1 line of tx for advanced/metastatic disease and had tx data (or record of death) within 90 days of diagnosis. IO rechallenge was defined as IO given in any line after a prior IO-based regimen.

Results In total, 7672 pts with EC (46%), GC (30%), and GEJC (24%) were included (93% in community practices). Median follow-up after first-line (1L) tx start date was 8.8 mo. Median age was 69 years. Most pts had an Eastern Cooperative Oncology Group performance status of ≤1 (59%) and metastases (58%). The most common 1L chemotherapy was carboplatin + paclitaxel (2133/7672 [28%]) and IO was pembrolizumab alone (73/7672 [1%]). The most common 1L chemotherapy + IO regimen was fluorouracil + leucovorin + oxaliplatin + nivolumab (28/7672 [0.4%]). At the time of analysis, 3399 of 7672 pts (44%) had any second-line (2L) tx. The most common 2L chemotherapy was FOLFOX (458/3399 [13%]) and IO was pembrolizumab alone (286/3399 [8%]). A higher proportion of pts received IO in the post-IO approval period (2019; table 1). Overall, 1028 of 7672 (13%) had IO during any point on tx, most frequently first received in 2L (436/1028 [42%]); 75 of 1028 (7%) had IO rechallenge. The descriptive median time to rechallenge was 0.7 (IQR, 0.5-3.5) mo. Most pts (63/75 [84%]) had IO rechallenge in the immediate subsequent line of tx, with 2L to third line (3L) the most common setting (29/75 [39%]). Data from additional ongoing analyses will be presented.

Conclusions Analysis of tx patterns for upper GI cancers showed that few pts received 1L IO in the community setting. However, IO use and IO rechallenge are evolving in clinical practice. Further follow-up is warranted, including assessment of rechallenge effect on pt outcomes.

Abstract 445 Table 1

n/N (%)	Chemotherapy	IO Combination	IO Alone
1L tx, pre-IO approval*	6008/6076 (99)	24/6076 (<1)	44/6076 (1)
1L tx, post-IO approval*	1489/1596 (93)	57/1596 (4)	50/1596 (3)
Duration of 1L tx, median (IQR), mo	1.7 (1.0-4.2)	2.1 (0.6-4.1)	2.3 (0.7-6.2)
2L tx, pre-IO approval*	2571/2840 (91)	37/2840 (1)	232/2840 (8)
2L tx, post-IO approval*	378/559 (68)	65/559 (12)	116/559 (21)
Duration of 2L tx, median (IQR), mo	2.1 (1.0-4.4)	2.1 (0.9-3.9)	2.1 (0.7-5.0)
3L tx, pre-IO approval*	1097/1346 (82)	52/1346 (4)	197/1346 (15)
3L tx, post-IO approval*	101/167 (60)	11/167 (7)	55/167 (33)
Duration of 3L tx, median (IQR), mo	1.7 (0.7-3.8)	2.8 (1.4-5.6)	1.4 (0.03-3.4)

* 1L tx started before or after July 31, 2019 (date of first IO approval for EC).

<http://dx.doi.org/10.1136/jitc-2022-SITC2022.0445>

HR⁺BREAST CANCER: DEFINING INNATE AND ACQUIRED RESISTANCE TO IMMUNE CHECKPOINT INHIBITORS

¹Aitziber Buqué Martínez*, ¹Norma Bloy, ²Michal Hensler, ¹Giulia Petroni, ¹Ai Sato, ¹Takahiro Yamazaki, ¹Bhavneet Bhinder, ²Jitka Fucikova, ¹Olivier Elemento, ¹Silvia Formenti, ¹Lorenzo Galluzzi. ¹Weill Cornell Medicine, New York, NY, United States; ²Sotio Biotech, Prague, Czech Republic

Background Hormone receptor (HR)⁺breast cancer (BC) is responsible for the majority of BCs and -related deaths in the US.¹ Standard treatment for local disease involves surgery, followed by adjuvant endocrine therapy (ET) ± radiation therapy (RT) and/or chemotherapy (CT), depending on risk for relapse. However, many women receive CT and experience its severe side effect to benefit only a few. Immune checkpoint inhibitors (ICIs) have successfully been implemented in the management of other solid tumors like melanoma.² Conversely, the clinical experience with single-agent ICIs has been disappointing in patients with HR⁺ BC³, at least in part reflecting a limited immune infiltration at baseline and calling for the development of combinatorial regimens unlocking ICI efficacy in this patient population. In this setting, progress has also been hampered by the lack of a preclinical model that would faithfully recapitulated key immunobiological features of human HR⁺ BC. We have recently demonstrated that endogenous mammary carcinomas driven in immunocompetent mice by medroxyprogesterone acetate (M) plus 7,12-dimethylbenz[a]anthracene (D) represent a superior preclinical model to study HR⁺BC resistance to ICI and identify strategies to overcome it.⁴

Methods We established M/D-driven mammary carcinomas in immunocompetent, female C57BL/6 mice and randomized them to: (1) no treatment; (2) PD1 clockers (on d0/d3/d6 or d3/d6/d9); (3) RT (3x10 Gy on d0/d1/d2); (4) recombinant FLT3L (from d0-d9 or d3-d12), or all the 2- and 3-agent combinations thereof. Besides monitoring local and systemic tumor control, we collected tumors for RNAseq, and spleens for immunoprofiling by flow cytometry.

Results RT controls primary ICI-resistant M/D-driven carcinomas and extends the overall survival (OS) of the hosts, with marginal benefits from the addition of a PD-1 blocker. Recombinant FLT3L improves local tumor control by RT, but fails to ameliorate OS, mainly due to compromised control of distant, unirradiated lesions. RT followed by PD-1 blockage plus recombinant FLT3L is superior to all other approaches at primary tumor control and exhibits a trend for improved OS over RT alone, reflecting partial control of distant lesions.

Conclusions RT is highly effective in ICI-resistant HR⁺ BC tumors. Combination of RT with different immunotherapeutics alters the pattern of local vs systemic disease progression. This may define immunological signatures potentially linked to resistance/sensitivity and identify novel target to break through the resistance of HR⁺ BC to immunotherapy.

REFERENCES

1. Siegel RL, KD Miller, and A Jemal. Cancer statistics, 2020. *CA Cancer J Clin*, 2020. **70**(1): 7–30.
2. Girault I, et al. A PD-1/PD-L1 Proximity Assay as a Theranostic Marker for PD-1 Blockade in Patients with Metastatic Melanoma. *Clin Cancer Res*, 2022;**28**(3): 518–525.
3. Ascierto PA, et al. Perspectives in immunotherapy: meeting report from the immunotherapy bridge (December 2nd-3rd, 2020, Italy). *J Transl Med*, 2021;**19**(1): 238.
4. Buque A, et al. Immunoprophylactic and immunotherapeutic control of hormone receptor-positive breast cancer. *Nat Commun*, 2020. **11**(1): 3819.

Ethics Approval This study was approved by Weill Cornell Medical College Institutional Animal Care and Use Committee; Protocol Number 2018-0053

<http://dx.doi.org/10.1136/jitc-2022-SITC2022.0446>

447 **DUAL TARGETING OF PD-1 AND CTLA-4 SYNERGIZES WITH FOCAL RADIATION TO DURABLY INCREASE SURVIVAL AGAINST GLIOBLASTOMA**

¹Mara De Martino*, ¹Camille Daviaud, ²Claire Vanpouille-Box. ¹Weill Cornell Medicine, New York, NY, United States; ²Weill Cornell Medicine, Sandra and Edward Meyer Cancer Center, New York, NY, United States

Background The immunogenic role of ionizing radiation raised the use of radiation therapy (RT) as an immune adjuvant in multiple cancers. However, clinical trials testing RT and immune checkpoint blockers (ICB) combination failed to improve the survival of glioblastoma (GBM) patients. We have previously shown that cancer-cell intrinsic type I interferon (IFN-I) is a prerequisite for synergy between RT and ICB in murine breast cancer; a phenomenon that is RT-dose dependent.¹ Therefore, we hypothesized that failure of RT-ICB combinations in GBM is due to the use of a suboptimal RT regimen (i.e. 2Gyx30). Here, we compared various RT doses and schedules to determine the best immunogenic RT schedule for combination with ICB in murine models of GBM.

Methods First, GL261 and CT2A murine GBM cell lines were used to determine the release of IFN-I related cytokines and the accumulation of double stranded DNA (dsDNA) in the cytoplasm 24h after single (0-20Gy) or fractionated (8Gyx3 or 6Gyx5) RT regimens. Next, GBM intracranial tumors were established in syngeneic animals and treated with focal RT (10Gyx1, 8Gyx3 or 6Gyx5). In some settings, mice received anti-PD-1 and/or anti-CTLA-4. Mice were followed for survival or euthanized for flow cytometry analysis. Tumor-free animals were rechallenged with a fresh tumor inoculum.

Results *In vitro*, fractionation RT schedules enhanced the content of cytoplasmic dsDNA in GBM cells as compared to single RT doses, with 6Gyx5 resulting in the highest accumulation of dsDNA. Consistently, GBM cells irradiated with 6Gyx5 significantly improved the release of IFN-I cytokines as compared to any other RT schedules. *In vivo*, 6Gyx5 and 8Gyx3 RT regimens were superior in controlling GL261 or CT2A growth as compared to 10Gyx1. The addition of anti-PD-1 or anti-CTLA-4 to the immunogenic RT regimen of 6Gyx5 did not improve CT2A-bearing mice survival compared to RT alone. However, targeting both PD-1 and CTLA-4 with RT significantly improved survival with 100% of the animals being tumor-free. Tumor rechallenge confirmed the development of protective anti-tumor responses in anti-PD-1+anti-CTLA-4+RT treated animals. Tumor-infiltrating immune cells analysis revealed an increase of T cells in tumors treated with anti-PD-1+anti-CTLA-4+RT, thus reinforcing the role of T cells in this response.

Conclusions While 6Gyx5 RT combined with either anti-PD-1 or anti-CTLA-4 did not further improve mice survival, dual blockade of PD-1 and CTLA-4 successfully synergized with RT to durably increase survival against GBM. Overall, this study underscores the need to combine immunogenic RT with several ICB to elicit protective anti-tumor immunity against GBM.

REFERENCE

1. Vanpouille-Box C, Alard A, Aryankalayil MJ, et al. DNA exonuclease Trex1 regulates radiotherapy-induced tumour immunogenicity. *Nat Commun.* 2017;**8**:15618.

Ethics Approval All animal experiments were approved by the Institutional Animal Care and Use Committee (IACUC).

<http://dx.doi.org/10.1136/jitc-2022-SITC2022.0447>

DRIVER MUTATION ANALYSIS AS A SELECTIVE MARKER FOR IMMUNOTHERAPY IN PATIENTS WITH PHEOCHROMOCYTOMA AND PARANGLIOMA

¹Katerina Hadrava Vanova*, ¹Ondrej Uher, ¹Leah Meuter, ¹Suman Ghosal, ²Jiri Neuzil, ¹Karel Pacak. ¹NIH, Bethesda, MD, United States; ²Griffith University, Southport, Australia

Consent All patients provided written informed consent approved by the National Institutes of Health ethics committee.

<http://dx.doi.org/10.1136/jitc-2022-SITC2022.0448>

Background Metastatic pheochromocytomas and paragangliomas (PPGLs) are rare neuroendocrine tumors associated with poor prognosis and limited therapeutic options. Recent advances in oncology-related immunotherapy, specifically targeting of the programmed death 1 (PD-1)/ligand 1 (PD-L1) pathways, have uncovered new treatment potential for a variety of tumors. The expression of PD-L1 and PD-L2 was recently found to be present in 18% and 16% of PPGL, respectively, but only PD-L2 expression correlated with malignancy, hypoxia markers, and shorter survival.¹ However, PD-L1 was suggested to be a malignant proliferation biomarker for PPGLs in another study.² Given the promising outcomes of a clinical study in 9 cases of PPGL using pembrolizumab, a humanized IgG4κ monoclonal antibody that targets the PD-1/PD-L1 pathway,³ we examined the PD-Ls expression in our representative PPGL cohort to explore if PD-Ls expression can predict malignancy and/or be a predictive marker for PD-Ls targeted therapy in PPGL.

Methods The Cancer Genome Atlas (TCGA) provided 173 patient samples to allow for observation of gene expression across four PPGL driver mutation groups (Cluster I: SDHB, VHL; Cluster II: NF1, RET) and NAM samples. Tumor RNA from the 48-patient cohort (sporadic; Cluster I: SDHB, VHL, EPAS1; Cluster II: RET, NF1) was evaluated to validate the results.

Results Expression of PD-L1, but not PD-L2, was elevated in our PPGL cohort, which aligns with TCGA analysis. Expression of PD-L1 was decreased in Cluster I PPGLs but not in Cluster II, suggesting that sporadic and Cluster II PPGLs could benefit from PD-1/PD-L1 targeted therapy more than Cluster I PPGL tumors. Within Cluster I, expression of PD-L1 was significantly lower in SDHB- and VHL-mutated tumors compared to sporadic tumors. Expression of PD-L2 did not differ between PPGL clusters. Metastatic PPGLs had significantly elevated Ki-67 levels, however PD-Ls expression was not affected by malignancy status.

Conclusions We conclude that PD-Ls expression in our cohort of PPGL tumors was not linked to malignancy, however, driver mutation analysis could be a selective marker for PD-Ls-targeted therapy.

REFERENCES

1. Pinato DJ, Black JR, Trousil S, Dina RE, Trivedi P, Mauri FA, Sharma R. Programmed cell death ligands expression in pheochromocytomas and paragangliomas: Relationship with the hypoxic response, immune evasion and malignant behavior. *Oncoimmunology*. 2017;6(11):e1358332
2. Guo D, Zhao X, Wang A, Xie Q, Xu X, Sun J. PD-L1 expression and association with malignant behavior in pheochromocytomas/paragangliomas. *Hum. Pathol*. 2019; 86:155–162.
3. Naing A, Gainor JF, Gelderblom H, Forde PM, Butler MO, Lin CC, Sharma S, Ochoa de Olza M, Varga A, Taylor M, Schellens JHM, Wu H, Sun H, Silva AP, Faris J, Mataraza J, Cameron S, Bauer TM. A first-in-human phase 1 dose escalation study of spartalizumab (PDR001), an anti-PD-1 antibody, in patients with advanced solid tumors. *J Immunother Cancer*. 2020; 8(1):e000530.

Ethics Approval The study protocol was approved by the Eunice Kennedy Shriver National Institute of Child Health and Human Development Institutional Review Board (NIH Protocol 00-CH-0093).

449

CYCLIC DISRUPTION OF THE MITOGEN-ACTIVATED PROTEIN KINASE (MAPK) PATHWAY BY THE DUAL MEK INHIBITOR, IMM-6-415, ENHANCES PD1 AND CTLA4 CHECKPOINT BLOCKADE IN RAS MUTANT TUMORS

Brett Hall*, Anna Travesa, Amy Yamamura, Amy Axel, Sarah Kolitz, Jason Funt, Kevin Fowler, Matthew Nord, Praveen Nair, Scott Barrett, Benjamin Zeskind, Peter King. *Immuneering, San Diego, CA, United States*

Assessment and Accreditation of Laboratory Animal Care (AAALAC).

<http://dx.doi.org/10.1136/jitc-2022-SITC2022.0449>

Background KRAS is the most frequently altered RAS gene (~85%) and is often mutated in pancreatic ductal adenocarcinoma (PDAC; 95%), non-small cell lung cancer (NSCLC; 40%) and colorectal cancer (CRC; 45%). KRAS-G12C inhibitors (sotorasib/adagrasib) have demonstrated single-agent activity in all three tumor types. However, acquired resistance and limited biomarker positive patients (e.g., only 1-3% of PDAC and CRC) limit broader access and overall response to G12C inhibitors, prompting evaluation of combination partners including immune therapies. In contrast to G12C-mutant focused KRAS inhibitors, MEK inhibitors may broaden the potential for immune therapy in RAS-mutant tumors but have largely proven ineffective in this setting.

Methods IMM-6-415 is a novel, third-generation dual MEK inhibitor that reduces both pMEK and pERK in RAS-mutant tumor models at sub-100 nM potencies. IMM-6-415 drug-like properties have been evaluated across a series of preclinical *in vitro* and *in vivo* models focusing on activity in those with mutant RAS. Cell-based 2D and 3D biochemical and pharmacologic assays were performed across multiple models, and several *in vivo* studies have been completed, including: (1.) A549 (KRAS-G12S NSCLC) xenograft model, (2.) Colon-26 (KRAS-G12D CRC) syngeneic model, (3.) CT-26 (KRAS-G12D) syngeneic model. The CT-26 *in vivo* study evaluated both single-agent IMM-6-415 and combinations with PD1 or CTLA4 checkpoint inhibitors.

Results IMM-6-415 reduced pERK and pMEK across all RAS mutant models tested. Humanized 3D tumor models revealed a promising sensitivity profile for IMM-6-415 in RAS-mutant CRC and PDAC. The maximum tolerated dose (MTD) of IMM-6-415 was 175 to 180 mg/kg BID PO from the Colon-26 (96.4% TGI) and A549 (93.9% TGI) studies, yet the optimal MEKio combination dose/schedule was 120 mg/kg BID PO in the CT-26 study. At 28 days treatment, 33% (4/12) mice remained on study in either the (10 mg/kg BIW IP) anti-PD1 or anti-CTLA4 alone treated groups, whereas 58% (7/12) mice remained in the IMM-6-415 treatment arm at 120 mg/kg BID PO. However, 92% (11/12) and 83% (10/12) mice remained in the IMM-6-415 plus anti-PD1 or anti-CTLA4 combination at the same doses, respectively.

Conclusions We demonstrate that IMM-6-415 displays single-agent activity in multiple RAS-mutant models, has a 0.3h half-life, is well tolerated in mice, and when combined at sub-MTD levels with either PD1 or CTLA4 checkpoint inhibitors, significantly improved responses in the CT-26 model (p-value < 0.05). Our data suggest that moderated, cyclic inhibition of the MAPK pathway in RAS mutant tumors is active and may enhance therapeutic activity of immune checkpoint inhibitors.

Ethics Approval The protocol and any amendment(s) or procedures involving the care and use of animals in this study were reviewed and approved by the Institutional Animal Care and Use Committee (IACUC) of CrownBio prior to execution. During the study, the care and use of animals was conducted in accordance with the regulations of the Association for

450

INCREASED ACTIVITY OF THE ATX/LPA AXIS DIMINISHES CD8+ T CELL CYTOTOXICITY VIA LPAR5 SIGNALING, DRIVING IMMUNE CHECKPOINT BLOCKADE RESISTANCE IN NON-SMALL CELL LUNG CANCER

¹Jessica Konen*, ²B Leticia Rodriguez, ²Haoyi Wu, ²Jared Fradette, ²Lixia Diao, ²Jing Wang, ²Don Gibbons. ¹Emory University, Atlanta, GA, United States; ²MD Anderson Cancer Center, Houston, TX, United States

Background Targeting immunosuppressive checkpoints has proven to be an efficacious treatment strategy for non-small cell lung cancer (NSCLC), in which response rates are as high as 35% in patients harboring Kras/p53 (KP) mutations.¹ However, most patients demonstrate no or only partial response to immune checkpoint blockade (ICB), underscoring the need to better understand the suppressive mechanisms in the tumor-immune microenvironment. Murine models of KP mutant lung cancer demonstrate upfront sensitivity to PD-1 checkpoint blockade but rapidly acquire resistance², providing useful tools to discover tumor-intrinsic mechanisms of resistance.

Methods We generated new KP syngeneic and autochthonous lung tumor models with intrinsic resistance to anti-PD-1 treatment via *in vivo* passaging in the face of ICB treatment. Additionally, we analyzed transcriptome data from anti-PD-L1 treated KP tumors, identified differentially expressed genes between response and resistance timepoints, and queried these in the newly generated anti-PD-1 resistant tumor models. We utilized flow cytometry to characterize the tumor-infiltrating immune microenvironment with manipulation of candidate gene expression.

Results Our data identified a stable upregulation of the phosphodiesterase enzyme, autotaxin (ATX), and the metabolite that it generates, lysophosphatidic acid (LPA), in ICB resistant tumors. Analyses of lung adenocarcinoma patient datasets revealed a significant positive correlation between ATX and immune signatures, including a previously published dataset encompassing immune checkpoints and suppressive molecules³, suggesting that ATX is upregulated in the face of normal anti-tumor immunity. Mechanistic studies utilizing isogenic pairs of tumors demonstrated that ATX expression inversely correlated with CD8+ T cell proliferation and cytotoxic functionality, with ATX-overexpression in anti-PD-1 sensitive tumors promoting intrinsic resistance. We next sought to define LPA receptor (LPA) expression on T cells. Flow cytometry on tumor-infiltrating CD8+ T cells demonstrated significantly altered expression of LPA within anti-PD-1 resistant versus sensitive tumors, with upregulation of LPA5 and downregulation of LPA2. Additionally, analysis of previously published RNA-sequencing of CD8+ T cells from NSCLC patients⁴ revealed that lower LPA2 versus LPA5 correlated with worse response to ICB. Importantly, targeting ATX or LPA5 with PD-1 blockade caused significant tumor regressions in clinically relevant models of KP mutant lung cancer via invigoration of anti-tumor CD8+ T cells.

Conclusions Our data indicate that increased ATX/LPA activity occurs downstream of immune activation, which in turn stimulates LPA5 signaling on CD8+ T cells to diminish cytolytic functions. These results provide evidence that this axis acts as an immunosuppressive checkpoint, providing rationale that co-targeting it with ICB should improve anti-tumor immune response.

REFERENCES

1. Skoulidis F, Goldberg ME, Greenawalt DM, *et al.* STK11/LKB1 Mutations and PD-1 Inhibitor Resistance in KRAS-Mutant Lung Adenocarcinoma. *Cancer Discovery* 2018;CD-18-0099.
2. Chen L, Diao L, Yang Y, *et al.* CD38-mediated immunosuppression as a mechanism of tumor cell escape from PD-1/PD-L1 blockade. *Cancer Discovery* 2018.
3. Lou Y, Diao L, Cuentas ER, *et al.* Epithelial-mesenchymal transition is associated with a distinct tumor microenvironment including elevation of inflammatory signals and multiple immune checkpoints in lung adenocarcinoma. *Clinical Cancer Research : an Official Journal of the American Association For Cancer Research* 2016;22:3630-42.
4. Trefny MP, Rothschild SI, Uhlenbrock F, *et al.* A Variant of a Killer Cell Immunoglobulin-like Receptor Is Associated with Resistance to PD-1 Blockade in Lung Cancer. *Clinical Cancer Research* 2019;25:3026-34.

Ethics Approval All animal studies were completed under the approval of the University of Texas MD Anderson Cancer Center Institutional Animal Care and Use Committee (protocol# 1271).

<http://dx.doi.org/10.1136/jitc-2022-SITC2022.0450>

451

SERUM ALBUMIN PREDICTS OUTCOME IN PATIENTS WITH EXTENSIVE STAGE SMALL-CELL LUNG CANCER (ES-SCLC) RECEIVING FIRST-LINE COMBINATION OF PD-(L)1 INHIBITORS AND PLATINUM-ETOPOSIDE CHEMOTHERAPY

Giuseppe Lamberti*, Biagio Ricciuti, Victor Vaz, Joao Victor Alessi, Federica Pecci, Alessandro Di Federico, Mark Awad. Dana-Farber Cancer Institute, Boston, MA, United States

Background The combination of platinum-etoposide chemotherapy with PD-L1 inhibitors (chemoimmunotherapy) has become the new standard for first-line treatment of patients with extensive stage small-cell lung cancer (ES-SCLC). Nevertheless, factors associated with outcomes in this setting are lacking. We sought to identify clinicopathological and genomic factors associated with outcome to first-line chemoimmunotherapy in patients with ES-SCLC.

Methods Among patients at the Dana-Farber Cancer Institute with ES-SCLC who received a combination of platinum (carboplatin or cisplatin), etoposide, and a PD-(L)1 inhibitor (atezolizumab, durvalumab, or pembrolizumab), baseline clinicopathological and genomic features were correlated with objective response rate (ORR), progression-free survival (PFS), and overall survival (OS). For serum biomarkers (hemoglobin, sodium, albumin, lactate dehydrogenase [LDH]), and derived neutrophil-to-lymphocyte ratio [dNLR]) a blood draw performed within 10 days from treatment start was considered. Patients who were on corticosteroids at the time of blood draw were not assessed for dNLR.

Results Among 89 patients included in the study, 53% were female, median age was 66 years, 17% had an Eastern Cooperative Oncology Group performance status (ECOG PS) of 0, and 28% had baseline brain metastases (table 1). The most common treatment regimen was carboplatin-etoposide-atezolizumab in 82 patients (92%). Overall, ORR was 81% (N=71/88), median PFS was 5.0 months (95%CI: 4.7-5.6), and median OS 10.8 months (95%CI: 9.6-16.1), at a median follow-up time of 25.3 months (95%CI: 14.2-NA). Patients with an ECOG PS of 0 when compared to those with an ECOG PS of ≥1 had higher ORR (100% vs 77.0%, P=0.036), longer median PFS (6.2 vs 4.8 months; HR: 1.99 [95%CI: 1.07-3.70], P=0.029) and median OS (20.0 vs 10.3 months; HR: 3.36 [95%CI: 1.21-9.30], P=0.020) (figure 1). Patients with serum albumin levels ≥3.5g/dL (N=74 [84%]), compared to those with low albumin levels (<3.5g/dL, N=13 [16%]), had higher ORR (85% vs 54%, P=0.018), longer median PFS (5.5 vs 3.7 months; HR: 2.91 [95%CI: 1.53-5.53], P=0.001) and median OS (12.3 vs 5.9 months; HR: 4.32 [95%CI: 2.1-8.71], P<0.001). Neither dNLR (available in N=75 [84%]) nor tumor mutation burden (available in N=20 [22%]) were associated with outcome. After adjusting for confounding factors, a low albumin, but not ECOG PS, retained its association with ORR (adjusted odds ratio: 0.27 [95%CI: 0.07-0.96], P=0.025), PFS (adjusted HR: 2.58 [95%CI: 1.35-4.95], P=0.004), and OS (adjusted HR: 3.66 [95%CI: 1.80-7.44], P<0.001).

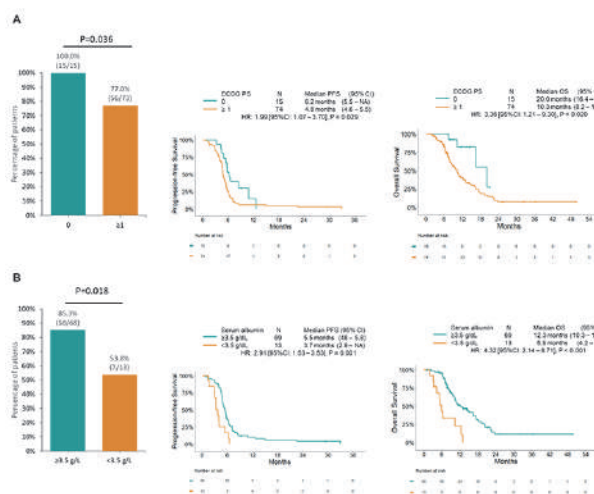
Conclusions Albumin levels might help predicting outcomes to first-line chemoimmunotherapy in patients with ES-SCLC. This can have implication in stratification of patients enrolled in prospective clinical trials.

Ethics Approval Patients at the Dana-Farber Cancer Institute who consented to institutional review board-approved protocols DF/HCC 02-180, 11-104, 13-364, and/or 17-000 which

allowed for conducting translational research and tumor next-generation sequencing, respectively, were included.

Abstract 451 Table 1 Patient characteristics

	Overall (N= 89)
Sex	
Female	47 (52.8%)
Male	42 (47.2%)
Age	
Median [Min, Max]	66 [42 - 84]
Smoking status	
Ever	83 (93.3%)
Never	6 (6.7%)
Packyears	
Median [Min, Max]	43.7 [10 - 180]
Stage at diagnosis	
Extensive	84 (94.4%)
Limited	5 (5.6%)
ECOG PS	
0	15 (16.9%)
≥1	74 (83.9%)
Metastases sites at dx	
Brain	25 (28.1%)
Liver	43 (48.3%)
Bone	45 (50.6%)
Treatment for ES-SCLC	
Carboplatin + Etoposide + Atezolizumab	82 (92.1%)
Carboplatin + Etoposide + Durvalumab	2 (2.3%)
Carboplatin + Etoposide + Pembrolizumab	3 (3.4%)
Cisplatin + Etoposide + Durvalumab	3 (2.3%)
dNLR	
Median [Min, Max]	4.3 [1.5, 16.4]
Serum prognostic markers	
Hb <12.0 g/dL	21 (25.3%)
Na+ <135 mEq/L	20 (24.4%)
Albumin <3.5 g/dL	13 (15.9%)
LDH >250 U/L	11 (57.9%)
IHC positivity	
TTF-1	62 (81.6%)
Synaptophysin	54 (81.8%)
Chromogranin A	46 (71.9%)
CD56/NCAM	23 (92.0%)



Abstract 451 Figure 1 Objective response rate (ORR) and Kaplan-Meier estimates of progression-free survival (PFS) and overall survival (OS) by (A) ECOG PS (0 vs ≥1) and (B) serum albumin level (low <3.5 g/dL vs normal = 3.5 g/dL).

<http://dx.doi.org/10.1136/jitc-2022-SITC2022.0451>

452

EFFICACY AND SAFETY OF CAMRELIZUMAB COMBINATION THERAPY IN PATIENTS WITH RECURRENT OR METASTATIC CERVICAL AND ENDOMETRIAL CARCINOMA: A RETROSPECTIVE STUDY

Shuhuai Niu, Zhaohui Fang, Xi Chen, Siyang Liu, Ge Jin, Yunfeng Guo, Qianying Zhang, Hong Liu*. *The Fourth Hospital of Hebei Medical University, Shijiazhuang, China*

Background Recurrent or metastatic cervical and endometrial carcinoma is largely an incurable disease due to lack of effective therapies. New treatment strategies are needed to provide long-term anti-tumor responses. Blocking the interaction between PD-1 and its ligands is a promising treatment strategy, and has previously shown encouraging antitumor activity in cervical and endometrial carcinoma. Camrelizumab is a humanised anti-programmed death-1 (anti PD-1) antibody. Therefore, this study aimed to assess the efficacy and safety of camrelizumab combination therapy in patients with recurrent or metastatic cervical and endometrial carcinoma.

Methods Patients (pts) with recurrent or metastatic cervical and endometrial carcinoma were enrolled. Eligible patients were aged 30–70 years with an Eastern Cooperative Oncology Group performance status of 0-2. Pts received camrelizumab (200mg iv d1 q2w) with concurrent chemoradiotherapy (CRT)/radiation/chemotherapy. Paclitaxel and carboplatin are delivered with 175mg/m² and AUC=5, respectively, d1, q3w for 6-8 cycles. Pts received radiation with external-beam radiotherapy 45~50.4Gy/25~28f, lymph node 60Gy/25~30f 5 times/week, brachytherapy 28~30Gy/4-5f. The primary endpoint was objective response (ORR). The secondary endpoints included disease control rate (DCR), median progression-free survival (mPFS) and safety.

Results 37 pts were enrolled from Sept. 2019 to Apr. 2022. 36 patients were evaluated for efficacy, the ORR and DCR was 53% (19/36) and 83% (30/36), respectively. In addition, 18 pts received camrelizumab combination CRT with the ORR of 76% (13/17) and DCR of 100% (17/17), and 8 pts received camrelizumab combination radiotherapy with the ORR of 12.5% (1/8) and DCR of 50% (4/8), and 11 pts received camrelizumab combination chemotherapy with the ORR of 45% (5/11) and DCR of 82% (9/11). 7 of 37 pts were still receiving the treatment, the mPFS was 12.5 months. Treatment-related adverse events occurred in 57% (21/37) of patients, and the most common adverse events were RCCEP (35%), Thyroid injury (14%) and diarrhea (14%). Treatment-related grade 3 adverse events occurred in 3% (1/37) of pts.

Conclusions Our Results indicates that Camrelizumab with chemoradiotherapy exhibits efficacy rather than combination with radiation/chemotherapy for recurrent or metastatic cervical and endometrial carcinoma. Further studies are planned to explore this new treatment option in a larger study population.

<http://dx.doi.org/10.1136/jitc-2022-SITC2022.0452>

453

PHARMACOLOGIC TUMOR PDL1 DEPLETION AS A TRANSLATIONAL APPROACH TO INHIBIT TUMOR-INTRINSIC PDL1 SIGNALS AND CREATE NOVEL TREATMENT VULNERABILITIES

¹Clare Murray*, ¹Haiyan Bai, ¹Anand Kornepati, ¹Carlos Ontiveros, ¹Yilun Deng, ¹Alvaro Padron, ¹Eva Galvan, ¹Myrna Garcia, ²Tyler Curiel. ¹UT Health San Antonio, Lebanon, NH, United States; ²Dartmouth College, Lebanon, NH, United States

Background Canonical tumor surface PDL1 signals to PD1 on immune cells to evade antitumor immunity are well-defined.¹ However, tumor-intrinsic PDL1 mediates additional pathologic signals.²⁻⁵ Our lab recently showed that tumor PDL1 promotes homologous recombination DNA damage repair and ATM/Chk2 DNA damage sensing. Genetic tumor PDL1 depletion rendered tumors sensitive to Chk1 and PARP inhibitors.^{6, 7} However, anti-PDL1 antibodies were unable to replicate treatment sensitivity,⁶ and genetic PDL1 depletion is not yet clinically feasible. We hypothesized that pharmacologic tumor PDL1 depletion could replicate genetic PDL1 depletion to sensitize tumors to therapy as a translational application of tumor PDL1 depletion.

Methods We conducted a high-throughput drug screen enriched for FDA-approved molecules in RFP-PDL1 B16 cells to identify PDL1 depleting drugs (PDDs).⁸ B16 cells were treated with 2.5 or 10 mM of screen drug for 48 hours, and RFP intensity was measured by fluorescence. We use various biochemical, cell biology, and genetic techniques to interrogate *in vitro* PDD mechanisms and *in vivo* studies of treatment and immune outcomes using human and transplantable murine cell lines of distinct cancers.

Results We identified the FDA-approved, structurally similar cephalosporin antibiotics cefepime and ceftazidime and the alkylating agent chlorambucil as PDDs with distinct signaling and treatment consequences. Cefepime and ceftazidime potently depleted PDL1 in several tumor lines and phenocopied genetic PDL1 depletion by inducing DNA damage and significantly depleting Chk2 protein. Cefepime and ceftazidime PDL1-dependently generated synthetic lethality to small molecule Chk1 inhibitors *in vitro*, and cefepime generated Chk1 inhibitor efficacy *in vivo*. Other beta-lactams failed to deplete PDL1, suggesting the beta-lactam ring is dispensable for PDL1 depletion. Cefepime and ceftazidime replicated additional genetic PDL1 depletion outcomes, including STING and autophagy induction and tumor stemness reduction *in vitro*. Cefepime induced an immune Th1 signature *in vivo* in tumor-bearing mice, consistent with STING induction and suggesting PDDs could improve immunotherapy efficacy. Strikingly, the PDD chlorambucil potently depleted ovarian cancer PDL1 and induced anti-PDL1 efficacy in PDL1-replete, anti-PDL1-resistant tumors through an NK-dependent mechanism. These data suggest tumor immunogenicity consequences of chlorambucil-mediated tumor PDL1 depletion.

Conclusions PDDs induce novel cancer treatment vulnerabilities with high clinical translational potential. We identify several FDA-approved drugs that deplete tumor PDL1, disrupt its pathogenic tumor-intrinsic signals, and induce small molecule synthetic lethality and anti-PDL1 efficacy improvement. We identified other PDDs offering opportunities as translational targets, which we are now progressing to phase I clinical trials.

Acknowledgements This research was funded by the National Center for Advancing Translational Sciences, National Institutes of Health, through Grant TL1 TR002647 (C.M.) and

the NIH T32GM113896 (STX MSTP) Award (C.M.). The Clayton Foundation (no grant number) and the NCI (CA204965, CA054515) supported T.C.

Flow cytometry data were generated at the UT Health San Antonio Flow Cytometry Shared Resource Facility, supported by the National Center for Advancing Translational Sciences, National Institutes of Health through Grant UL1 TR002645.

REFERENCES

1. Dong H, Strome SE, Salomao DR, Tamura H, Hirano F, Fljés DB, Roche PC, Lu J, Zhu G, Tamada K *et al.* Tumor-associated B7-H1 promotes T-cell apoptosis: a potential mechanism of immune evasion. *Nat Med.* 2002; **8**(8):793–800.
2. Clark CA, Gupta HB, Sareddy G, Pandeswara S, Lao S, Yuan B, Drerup JM, Padron A, Conejo-Garcia J, Murthy K *et al.* Tumor-Intrinsic PD-L1 signals regulate cell growth, pathogenesis, and autophagy in ovarian cancer and melanoma. *Cancer Res.* 2016; **76**(23):6964–6974.
3. Gupta HB, Clark CA, Yuan B, Sareddy G, Pandeswara S, Padron AS, Hurez V, Conejo-Garcia J, Vadlamudi R, Li R *et al.* Tumor cell-intrinsic PD-L1 promotes tumor-initiating cell generation and functions in melanoma and ovarian cancer. *Signal Transduct Target Ther.* 2016; **1**.
4. Zhang D, Reyes RM, Ostá E, Kari S, Gupta HB, Padron AS, Kornepati AVR, Kancharla A, Sun X, Deng Y *et al.* Bladder cancer cell-intrinsic PD-L1 signals promote mTOR and autophagy activation that can be inhibited to improve cytotoxic chemotherapy. *Cancer Med.* 2021; **10**(6):2137–2152.
5. Kornepati AVR, Vadlamudi RK, Curiel TJ. Programmed death ligand 1 signals in cancer cells. *Nat Rev Cancer.* 2022; **22**(3):174–189.
6. Kornepati AVR, Boyd JT, Murray CE, Saifetyarova J, de la Pena Avalos B, Rogers CM, Bai H, Padron AS, Liao Y, Ontiveros C *et al.* Tumor-intrinsic PD-L1 promotes DNA repair in distinct cancers and suppresses PARP inhibitor-induced synthetic lethality. *Cancer Res.* 2022; **82**(11): 2156–2170.
7. Anand Kornepati, Clare Murray, Barbara Avalos, Cody Rogers, Kavya Ramkumar, Harshita Gupta, Yilun Deng, Zexuan Liu, Alvaro Padron, Ratna Vadlamudi, Eloise Dray, Weixing Zhao, Patrick Sung, Lauren Byers, Tyler Curiel. Depleting non-canonical, cell-intrinsic PD-L1 signals induces synthetic lethality to small molecule DNA damage response inhibitors in an immune independent and dependent manner. *J Immunother.* 2021; **9**(2):A944.
8. Murray C, Galvan E, Ontiveros C, Deng Y, Bai H, Padron AS, Hinchee-Rodriguez K, Garcia MG, Kornepati A, Conejo-Garcia J *et al.* Pharmacologic Tumor PDL1 Depletion with Cefepime or Ceftazidime Promotes DNA Damage and Sensitivity to DNA-Damaging Agents. *Int J Mol Sci.* 2022; **23**(9).

Ethics Approval All animal studies were approved by the UT Health San Antonio Institutional Animal Care and Use Committee (Number 09128).

<http://dx.doi.org/10.1136/jitc-2022-SITC2022.0453>

Abstracts

454

REAL-WORLD TREATMENT PATTERNS AMONG PATIENTS WITH LOCALLY ADVANCED HEAD AND NECK SQUAMOUS CELL CARCINOMA (LA HNSCC) IN A COMMUNITY ONCOLOGY SETTING

¹Eric Nadler, ²Christopher Black*, ²Karthik Ramakrishnan, ³Wan-Yu Tseng, ³Chuck Wentworth, ³John Murphy, ³Nicole Fulcher, ²Liya Wang, ²Melannie Alexander, ⁴Gregory Patton. ¹Texas Oncology, Dallas, TX, United States; ²Merck & Co., Inc., Rahway, NJ, United States; ³Ontada, Irving, TX, United States; ⁴McKesson Life Sciences, The Woodlands, TX, United States

Background For patients with unresectable, locally advanced head and neck squamous cell carcinoma (LA HNSCC), concurrent chemotherapy with radiation therapy (CRT) is preferred. CRT that includes platinum-based chemotherapy is the standard of care. Cetuximab is the alternative for patients who cannot receive platinum-based treatment. This study describes demographics and treatment patterns of patients with LA HNSCC receiving CRT in a community oncology setting.

Methods This retrospective observational study examined patients with newly diagnosed de novo LA HNSCC who received CRT in The US Oncology Network within the period 2015–2017 and were followed up through 2021. All adult patients with LA HNSCC who initiated CRT with ≥2 visits were included. Index date was defined as the date of initiation of CRT at initial LA HNSCC diagnosis. Patients were stratified based on index treatments received. Demographic and clinical characteristics and time to next treatment (TTNT) were summarized.

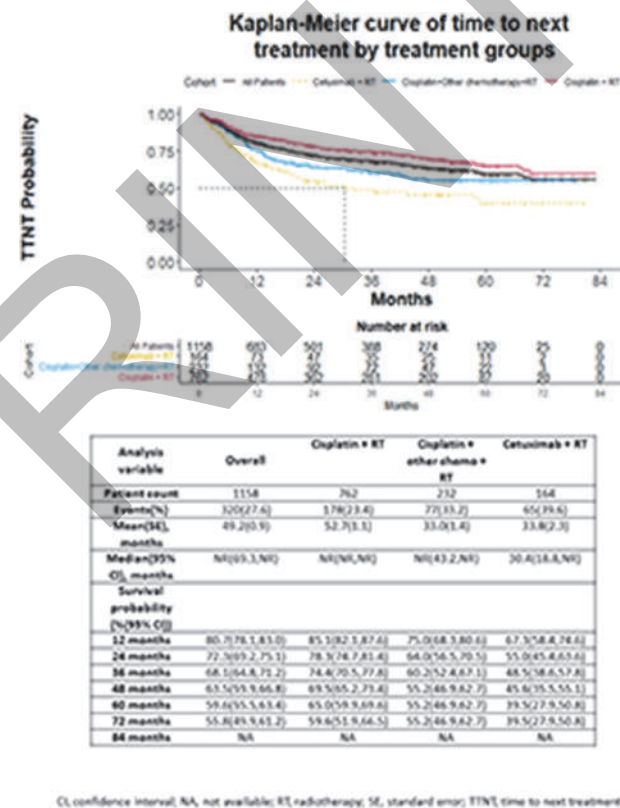
Results Table 1 summarizes demographic and clinical characteristics among the 1185 patients with LA HNSCC that met eligibility criteria, overall and by treatment groups. Overall, the median age was 61.8 (range 22.8–92.5) years, and the majority were male (n=952, 82.2%), Caucasian (n=947, 91.2%), had ECOG 0-1 at index (n=878, 89.4%), and had used or were using tobacco (n=783, 67.6%). Patients who received a cetuximab-containing regimen + radiotherapy (RT) (n=164, 14.2%) were slightly older and had a numerically higher Eastern Cooperative Oncology Group performance status (ECOG PS) score compared with cisplatin + RT (n=762, 65.8%) and cisplatin + other chemotherapy + RT (n=232, 20.0%). Distribution of patients by primary tumor site was consistent across the treatment groups, except that cetuximab + RT had a higher ratio of patients with laryngeal (n=32, 19.5%) to lip/oral cavity (n=10, 6.1%) compared to the other two treatment groups. The median TTNT was only reached by the cetuximab-containing regimen group, at 30.4 months. Overall, 80.7%, 68.1%, and 59.6% had initiated a subsequent treatment after index by 1, 3, and 5 years (figure 1).

Conclusions Patients who received a cetuximab-containing regimen + RT were slightly older and had numerically higher ECOG PS scores compared to the other treatment groups. This study provides real-world insights on patient profiles, treatment patterns, and TTNT among overall and by different CRT treatment groups for patients with LA HNSCC in the community oncology setting.

Ethics Approval All data were handled in compliance with the Health Insurance Portability and Accountability Act and the Health Information Technology for Economic and Clinical Health Act. The study protocol was granted an exemption and waiver of informed consent by the US Oncology Institutional Review Board on the basis of the use of deidentified patient data.

Abstract 454 Table 1 Patient demographic and clinical characteristics

Characteristic	Overall (n=1185)	Cisplatin + RT (n=762)	Cisplatin + Other chemotherapy + RT (n=232)	Cetuximab + RT (n=164)
Age (years)	61.8 (22.8-92.5)	61.8 (22.8-92.5)	61.8 (22.8-92.5)	61.8 (22.8-92.5)
Male (%)	82.2	82.2	82.2	82.2
Caucasian (%)	91.2	91.2	91.2	91.2
ECOG 0-1 (%)	89.4	89.4	89.4	89.4
Used or were using tobacco (%)	67.6	67.6	67.6	67.6
Primary tumor site (%)				
Lip/oral cavity	19.5	19.5	19.5	19.5
Larynx	19.5	19.5	19.5	19.5
Hypopharynx	19.5	19.5	19.5	19.5
Oropharynx	19.5	19.5	19.5	19.5
Nasopharynx	19.5	19.5	19.5	19.5
Unknown	19.5	19.5	19.5	19.5
ECOG PS score (%)				
0	19.5	19.5	19.5	19.5
1	19.5	19.5	19.5	19.5
2	19.5	19.5	19.5	19.5
3	19.5	19.5	19.5	19.5
4	19.5	19.5	19.5	19.5
5	19.5	19.5	19.5	19.5



Abstract 454 Figure 1 Time to next treatment by treatment group

<http://dx.doi.org/10.1136/jitc-2022-SITC2022.0454>

455 **FOSTROX (MIV-818) IN COMBINATION WITH ANTI-PD-1 SHOWS INCREASED EFFICACY IN NONCLINICAL TUMOR MODELS IN VIVO**

Fredrik Oberg*, Sujata Bhoi, Malene Jensen, Tom Morris, Karin Tunblad, Hans Wallberg. Medivir AB, Huddinge, Sweden

Background Fostroxacitabine bralpamide (fostrox) is an orally administered liver-targeted troxacitabine-based nucleotide pro-drug currently undergoing phase 1/2a clinical trial in advanced hepatocellular carcinoma (HCC), in combination with pembrolizumab or lenvatinib (NCT03781934). In phase 1 monotherapy fostrox has demonstrated proof-of-concept in advanced HCC, intrahepatic cholangiocarcinoma and liver metastasis from gastrointestinal solid tumors. Since liver-selective fostrox-induced DNA-damage and tumor cell killing has the potential to enhance the efficacy of checkpoint blockade we investigated the combination of fostrox with anti-PD1 in nonclinical tumor models in vivo.

Methods Combination of fostrox with anti-PD1 treatment was evaluated in the subcutaneous syngeneic mouse H22 model for HCC¹. Pharmacodynamic response to fostrox, induction of DNA-damage (phospho-ser139-H2AX), was assessed by immunohistochemistry (IHC). Changes in tumor microenvironment was assessed by targeted RNA-sequencing of a panel of 1080 genes representing different immune cell types. Anti-tumor efficacy of fostrox in combination with pembrolizumab was further investigated in the chicken chorioallantoic membrane (CAM) model using H460 human lung carcinoma cells. Tumor infiltrating T-cells (TILs) were assessed by immunohistochemistry (IHC).

Results Both fostrox (twice daily for 5 days, p.o.) and anti-PD1 (twice weekly for 3 weeks, i.p.) showed dose-dependent tumor growth inhibition in the H22 model. The combined treatment with fostrox and aPD1 showed a significantly improved anti-tumor efficacy in the H22 model. Analysis of immune-related gene expression indicated increased TILs and included upregulation of genes involved in cancer antigen presentation. Addition of fostrox to pembrolizumab treatment in the H460 CAM model showed enhancement of efficacy (reduction in tumor weight). Fostrox induced increased tumor infiltration of T-cells, and this was further increased with the combination of fostrox and pembrolizumab.

Conclusions The combination of fostrox with anti-PD1 showed enhanced efficacy in nonclinical tumor models, and changes in the tumor microenvironment consistent with increased immune-mediated anti-tumor activity. The results indicate a potential for combining anti-PD1 with fostrox in the treatment of HCC.

Ethics Approval The study was approved by the Institutional Animal Care and Use Committee (IACUC) of CrownBio UK, and conducted in accordance with the regulations of the Association for Assessment and Accreditation of Laboratory Animal Care (AAALAC)

<http://dx.doi.org/10.1136/jitc-2022-SITC2022.0455>

456

PATTERNS AND OUTCOMES OF PALLIATIVE RADIATION THERAPY WITH IMMUNOTHERAPY IN RECURRENT OR METASTATIC HEAD AND NECK SQUAMOUS CELL CARCINOMA

Logan Roof*, Anirudh Yalamanchali, David Buchberger, Shauna Campbell, Shlomo Koyfman, Neil Woody, Natalie Silver, Jessica Geiger, Emrullah Yilmaz. *Cleveland Clinic, Cleveland, OH, United States*

Background Immune checkpoint inhibitors (ICI) have been shown to improve outcomes in patients with recurrent or metastatic (R/M) head and neck squamous cell carcinoma (HNSCC). Radiation therapy (RT) is commonly incorporated into treatment of R/M HNSCC for symptom management and disease control. RT is a potential immunostimulatory treatment modality that may enhance the antitumor activity of ICI; however, ideal sequencing of RT and ICI in the palliative treatment setting is not defined. The objective of this study was to describe the patterns and outcomes of RT following ICI in R/M HNSCC.

Methods All adults (≥ 18 years) with HNSCC who received palliative ICI for R/M disease from 2015-2021 were identified from the institutional electronic medical record via ICD codes under an IRB approved protocol. Patients who received ICI for non-HNSCC, had synchronous primary tumors, or had history of hematologic malignancy or immunodeficiency were excluded. Patients without documentation of clinical outcomes after palliative RT were excluded. Retrospective data were collected and underwent descriptive analysis.

Results We identified 148 patients who received palliative ICI for R/M HNSCC. Of these patients, 55 received palliative RT with documentation of outcomes. Twenty-two of these patients underwent palliative RT while on ICI. Twelve of these 22 patients had re-irradiation of their neck, 5 had palliative RT to the lung, 4 to bone, 2 to brain, 1 to the retroperitoneum, and two to other sites. There were 15 grade 3 events. There was 1 patient (5%) with complete response (CR), 9 patients (41%) with partial response (PR), 5 (23%) with stable disease (SD), and 7 (32%) with progressive disease (PD) in the radiation site. Sixteen of the 33 patients who underwent palliative RT separately from IO had re-irradiation of their neck, 7 had palliative RT to the mediastinum, 5 to the lung, 2 to brain, 3 to liver, and 4 to other sites. There were 11 grade 3 events. There were 2 patients with CR (6%), 11 with PR (33%), 6 with SD (18%), and 14 with PD (42%) in the radiation site.

Conclusions These data suggest that concurrent ICI and palliative RT for R/M HNSCC is tolerated with a high disease control rate. Although there was a small number of patients who underwent concurrent ICI and RT, the disease control rate in this group was 68%, which is promising. Further study on the optimal type and sequence of palliative RT in this patient population is warranted.

REFERENCE

1. Clump D, Zandberg D, Skinner H, Ohr J, Fenton M, Normolle D, Beitler J, Bauman J, and Ferris R. A Randomized Phase II study evaluating concurrent or sequential fixed-dose immune therapy in combination with cisplatin and intensity-modulated radiotherapy in intermediate-or high-risk, previously untreated, locally advanced head and neck cancer. *JCO* 2022;**40**:16_suppl, 6007–6007.

<http://dx.doi.org/10.1136/jitc-2022-SITC2022.0456>

457

EFFICACY OF PEMBROLIZUMAB AS CROSS-LINE TREATMENT IN ADVANCED NON-SMALL CELL LUNG CANCER: A MULTI-CENTER NON-INTERVENTIONAL STUDY FROM CHINA

¹Xexin Ruan*, ¹Jing Zheng, ¹Jiaying Zhou, ²Yuping Li, ³Xiaodong Lv, ⁴Xiaoyu Wu, ⁵Liren Ding, ¹Jianya Zhou. ¹The First Affiliated Hospital, Zhejiang University School of Medicine, Hangzhou, China, Hangzhou, China; ²PCCM The first affiliated hospital of Wenzhou Medical College, Wenzhou, China, Wenzhou, China; ³The First Hospital of Jiaxing (The Affiliated Hospital of Jiaxing University), Jiaxing, China, Jiaxing, China; ⁴Zhe Jiang Jin Hua Guang Fu Tumor Hospital, Jinghua, China, Jinghua, China; ⁵The Second Affiliated Hospital, Zhejiang University School of Medicine, Hangzhou, China, Hangzhou, China

Background Pembrolizumab is a preferred drug in most major guidelines (e.g., NCCN, ESMO, Chinese consensus) for 1Line advanced non-small cell lung cancer (aNSCLC) patients (pts). However, whether Pembrolizumab treatment as cross-line is effective for aNSCLC has yet to be established.

Therefore, this study was conducted to describe the treatment patterns and determine the effectiveness of Pembrolizumab treatment as cross-line for aNSCLC in real-world setting in China.

Methods Data of the study was from a multi-center, non-interventional, ambispective cohort study (NCT04153097). aNSCLC pts who treated with Pembrolizumab and provide written informed consent will be included. The main objective of this study is to evaluate pembrolizumab efficacy and safety in the clinical practice and explore the prognosis-relevant factors.

Efficacy end points were Median Overall survival (mOS, defined as the length of time from the administration of the first-dose until death from any cause). Objective Response Rate (ORR, defined as the percentage of patients with complete response [iCR] and partial response [iPR] according to irRECIST), and Median Time to Treatment failure (mTTF, defined as the time from the start of first-dose to discontinuation for any reason, including disease progression, treatment toxicity, patient preference, or death.)

Results From May 2020 to May 2021, 224 NSCLC pts (including a 60 pts retrospective cohort from Mar 2018 to Jan 2020) were enrolled in this observational Study. 117 aNSCLC pts were treated with pembrolizumab in the 1line. 80 pts failed first-line therapy. 30 out of 80 treated with Pembrolizumab as cross-line therapy with different chemotherapy regimens and (or) angiogenesis inhibitor.

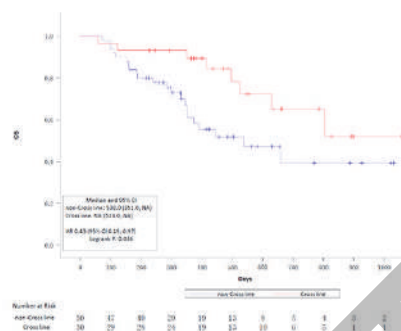
For the 30 pts of cross-line therapy, the 1line ORR was 50% (15/30), 1line mTTF 148 Day (95% CI: 121 to 216), 2line ORR 20% (6/30), 2line mTTF 120 Day (95% CI: 86 to 358).

For the other 50 non-cross-line pts, the 1line ORR was 60% (30/50), 1line mTTF 118 Day (95% CI: 75 to 158).

Compared with the 50 non-cross-line (mOS 538 Day [95%: 351 to NA]) pts, 30 cross-line (mOS NA [524 to NA]) pts showed a significant improvement (Logrank $p=0.036$) in survival benefits, HR (95% CI) 0.43 (0.19 to 0.97) (figure 1).

Conclusions In conclusion, the present study suggested that Pembrolizumab as cross-line treatment may serve as an option for aNSCLC patients to prolonged the OS. The efficacy should be confirmed in further investigations.

Acknowledgements Thanks MSD China Holding Co., Ltd. for scientific support.



Abstract 457 Figure 1 OS of Pembrolizumab cross line vs non-cross line in aNSCLC

<http://dx.doi.org/10.1136/jitc-2022-SITC2022.0457>

458

CHARACTERIZATION OF HZ-G206: A POTENT AND ORAL SMALL MOLECULE PD-L1 INHIBITOR

Yizhe Wu*, Xingguo Liu, Xinxin Jin, Jinglai Huang, Xinglu Zhou. *Hangzhou HealZen, Hangzhou, China*

Background Blocking of PD-1/PD-L1 protein-protein interaction has been proven as an effective therapeutic strategy in multiple types of cancer. More than ten PD-1 or PD-L1 antibody drugs have been approved worldwide. Contrasting to antibody drug, small molecule PD-L1 inhibitor has shown potential advantages, including increased tissue penetration, less immune-related adverse effect and better clinical compliance. In recent years, several small molecule PD-L1 inhibitors entered clinical stage study. Herein, we described our state-of-the-art work in discovery and identification of HZ-G206, which is a oral small molecule PD-L1 inhibitor and exhibited the potential of best-in-class.

Methods In vitro PD-1/PD-L1 inhibition potency was determined using ALPHAlisa assay. Surface PD-L1 internalization and degradation was carried out in hPD-L1-MC38 cell line and human PBMC through flow-cytometry. Immune-activation effect after PD-1/PD-L1 inhibition was evaluated in NFAT-reporter assay and cytokine production assay. The in-vivo anti-tumor efficacy was assessed in C57BL/c mice which were engrafted with hPD-L1-MC38 cell line and the tumor-bearing mice were administrated with different dosage of HZ-G206 followed by monitoring of tumor volume.

Results HZ-G206 binds and strongly blocks PD-1/PD-L1 interaction in in-vitro ALPHAlisa assay with the IC₅₀ value of 0.35nM. Binding of HZ-G206 in cell surface PD-L1 results in dimerization and destabilization of PD-L1 and followed by internalization and degradation in endosome, which is a distinct pharmacology effect comparing with traditional PD-L1 mAb drugs. HZ-G206 shows stronger PD-L1 internalization and degradation potency than clinical stage compounds INCB86550 and INCB99318 in hPD-L1-MC38 cell line and IFN-g stimulated human PBMC with IC₉₀ values of 18.1nM and 105.6nM respectively. HZ-G206 also exhibits enhanced T-cell activation effect after stimulation with CD3/CD28 in presence of PD-L1 overexpressed cells. In in-vivo anti-tumor evaluation, oral administration of HZ-G206 BID can significantly suppress the growth of tumor in a dose dependent manner, the TGI of middle dose group is comparable to Atezolizumab. In the end of experiment, the tumor tissue was also collected. The PD-L1 level in tumor cell and T cell infiltration were analyzed by flow-cytometry. For the mice treated with HZ-G206, the MFI of PD-L1 is significantly decreased. The ratio of CD3+T cells in tumor tissue is enhanced which is in accordance with Atezolizumab group.

Conclusions HZ-G206 is a novel small molecule PD-L1 inhibitor with good drug-like prosperities. The compound is identified with potent in-vitro activity which translates to anti-tumor efficacy in pre-clinical animal study. In conclusion, HZ-G206 is an excellent drug candidate for further clinical development.

Acknowledgements Prof. Xiaowu Dong(Institute of Drug Discovery and Design, College of Pharmaceutical Sciences, Zhejiang University, Hangzhou 310058, P. R. China)

Ethics Approval All animal studies were performed in strict accordance with the institutional guidelines as defined by the Institutional Animal Care and Use Committee (IACUC), approved by the Animal Care and Use Committee, Zhejiang University Laboratory Animal Center (Hangzhou, China),

approval ID: 19885. All participants gave informed consent before taking part.

<http://dx.doi.org/10.1136/jitc-2022-SITC2022.0458>

459

GENE THERAPY WITH P19ARF AND INTERFERON-BETA SENSITIZES CELLS TO PD-1 CHECKPOINT BLOCKADE AND ENHANCES ANTITUMOR IMMUNE RESPONSES IN RESISTANT MOUSE MODELS

¹Ana Domingues*, ²Nayara Tassarollo, ³Bryan Strauss. ¹Universidade de São Paulo, São Paulo, Brazil; ²Instituto Nacional de Câncer, Rio de Janeiro, Brazil; ³Instituto do Câncer do Estado de São Paulo, São Paulo, Brazil

Background Innate and acquired resistance are major concerns that limit the patient's response to immune checkpoint therapy.¹ Immune-boosting gene therapies have been shown to improve response in models of checkpoint blockade resistance.^{2, 3} Our group has previously shown that a combined gene therapy with p19Arf and interferon-beta promotes immunogenic cell death in melanoma models.⁴ However, even responsive mice often relapse, which we hypothesize to be partially due to PD-L1 superexpression. Thus, by combining our approach with anti-PD-1/PD-L1 monoclonal antibodies, we aim to overcome limitations of the gene therapy and increase sensibility to checkpoint blockade in resistant models.

Methods B16F10 cells were treated *in vitro* with non-replicating adenoviral vectors and were analyzed by flow cytometry. Tumor-bearing mice were treated *in situ* with the gene therapy and PD-L1 expression was analyzed by flow cytometry, RT-qPCR, and immunohistochemistry. Furthermore, tumor-bearing mice received intraperitoneal injections of the monoclonal antibodies and follow-up continued until reaching 1cm³. Blood serum was then collected for cytokine analysis and tumors were excised for immunophenotyping. Alternatively, B16OVA tumor-bearing animals were euthanatized on treatment day 12 and the splenocytes were pulsed with ovalbumin to assess specific tumor antigen presentation via MHC-I by antigen presenting cells by flow cytometry. Lastly, five different melanoma human cell lines were treated with the vectors and PD-L1 surface expression was analyzed by flow cytometry.

Results The analysis showed upregulation of PD-L1 both *in vitro* and *in vivo*, which led us to combine the gene therapy with PD-(L)1 inhibitors. In the *in vivo* model of B16F10, which is a known resistance model for PD-1 blockade, there was an increase of 10% and 20% responders when associating the gene therapy with anti-PD-L1 and anti-PD-1, respectively, in comparison to the gene therapy alone. Tumor immunophenotyping and cytokine profiling showed increased innate immune cell infiltrates in the conditions treated with the vectors and a high increase in NK cells and IFN gamma sera levels in the combination with both gene therapy and anti-PD-1. The gene therapy also increased tumor antigen presentation via MHC-I by antigen presenting cells, compared to mock group. Nevertheless, the gene therapy increased PD-L1 surface expression in all melanoma human cell lines analyzed.

Conclusions These data show that our immunogenic gene therapy approach increases sensibility to PD-1 and PD-L1 blockade in resistant mouse melanoma models and generates tumor antigen-specific immune responses, with further improved effector immune activity when combining it with checkpoint blockade.

Acknowledgements This work has been supported by the São Paulo Research Foundation (FAPESP).

REFERENCES

1. Barreto L, Caminero F, Cash L, Makris C, Lamichhane P, Deshmukh RR. Resistance to Checkpoint Inhibition in Cancer Immunotherapy. *Transl Oncol*. 2020; **13**(3): 100738.
2. Wenthe J, Naseri S, Hellström AC, Moreno R, Ullenhag G, Alemany R, Lövgren T, Eriksson E, Loskog A. Immune priming using DC- and T cell-targeting gene

therapy sensitizes both treated and distant B16 tumors to checkpoint inhibition. *Mol Ther Oncolytics*. 2022; **24**:429–442.

3. Chada S, Wiederhold D, Menander KB, et al. Tumor suppressor immune gene therapy to reverse immunotherapy resistance. *Cancer Gene Ther*. 2022; **29**:825–834.
4. Hunger A, Medrano R, Zanatta D, et al. Reestablishment of p53/Arf and interferon-β pathways mediated by a novel adenoviral vector potentiates antiviral response and immunogenic cell death. *Cell Death Discov*. 2017; **3**:17017.

Ethics Approval All procedures and conditions have been approved by the Ethics Committee for Animal Use (CEUA, FMUSP) under the protocol number 1300/2019 and by the National Technical Committee on Biosafety (CTNBio) under the process number 01250.034644/2019-31.

<http://dx.doi.org/10.1136/jitc-2022-SITC2022.0459>

460

**DISCOVERY OF POTENT CBL-B INHIBITORS
DEMONSTRATING ENHANCED IMMUNE CELL ACTIVITY
AND TUMOR GROWTH INHIBITION IN MURINE
SYNGENEIC MODELS**

Silvana Leit, David Ciccone*. *Nimbus Therapeutics, Cambridge, MA, United States*

Background Casitas B-lineage lymphoma b (Cbl-b), a RING finger E3 ligase and a member of a highly conserved family of Cbl proteins, catalyzes the ubiquitination of substrate proteins to regulate multiple signaling events in a variety of cell types, including immune cells. In T cells, Cbl-b negatively regulates adaptive immune system signaling by establishing the threshold for the activation of antigen receptors. Additionally, Cbl-b regulates the function of other immune cell types, including NK cells, dendritic cells (DC) and monocytes. Cbl-b deficient T cells no longer require a costimulatory signal to be fully activated. Cbl-b KO mice spontaneously reject tumors via an enhanced immune response. Taken together, these findings point to Cbl-b inhibitors as having the potential to be highly efficacious immuno-oncology agents.

Methods A structure-based drug design approach was used to identify potent inhibitors of Cbl-b. Biochemical and biophysical assays, in vitro cellular assays, as well as primary human and mouse immune cell assays were used to profile inhibitor compounds. *In vivo* activity of Cbl-b inhibitors was evaluated using an anti-CD3 mouse model and a CT-26 syngeneic mouse model.

Results Cbl-b inhibitors potently bind to Cbl-b, preventing Cbl-b phosphorylation and binding to E2. In cells, compound treatment results in enhanced transcriptional activity and robust cytokine secretion from primary human and mouse T cells. *In vivo*, an increase in cytokines and T cell activation markers was observed after a single dose of compound. Repeated dosing of compound showed dose-dependent anti-tumor activity in the colorectal CT-26 syngeneic model.

Conclusions Potent Cbl-b inhibitors demonstrate strong T cell activation and anti-tumor activity in a syngeneic tumor model. These data support Cbl-b inhibitors as a promising therapeutic opportunity for cancer treatment.

<http://dx.doi.org/10.1136/jitc-2022-SITC2022.0460>

461

GENERATION OF AZD7789, A NOVEL PD-1 AND TIM-3 TARGETING BISPECIFIC ANTIBODY, WHICH BINDS TO A DIFFERENTIATED EPIOTOPE OF TIM-3

¹Eleanor Clancy-Thompson*, ¹Trinity Perry, ¹Stacy Pryts, ²Ashvin Jaiswal, ¹Vaheh Oganessian, ¹Nydia van Dyk, ¹Chunning Yang, ¹Andrew Garcia, ¹Wenhan Yu, ¹James Moynihan, ¹Caroline Miller, ¹Kathy Mulgrew, ¹Mark Cobbold, ¹Yariv Mazor, ¹Scott Hammond, ¹Kristen Pollizzi. ¹AstraZeneca, Gaithersburg, MD, United States; ²Takeda, Cambridge, MA, United States

Background PD-1 and TIM-3 are expressed on tumor infiltrating lymphocytes (TIL) across multiple indications where dual receptor expression is associated with diminished functionality.^{1,2} Studies have demonstrated that TIM-3 acts as a compensatory inhibitory mechanism post PD-1 blockade to reduce anti-tumor T-cell responses.³ We developed a novel anti-TIM-3 antibody, O13, which engages the TIM-3 IgV domain without blocking phosphatidylserine (PS) binding, eliciting differential functionality. O13 was incorporated into AZD7789, a monovalent bispecific antibody that binds PD-1 and TIM-3. Herein we show preclinical work to support clinical investigation.

Methods Co-crystals of anti-TIM-3 antibodies and recombinant human TIM-3 IgV were generated by standard methods. TIM-3+ Jurkat T-cells were stimulated and treated with anti-TIM-3 antibodies and assessed for IL-2 production. PD-1+ TIM-3+ virally-reactive human T-cells were co-cultured with tumor cell lines expressing viral peptides in the presence of AZD7789 and controls to assess cytokine production and cytotoxicity of T-cells *in vitro*, and in immunodeficient mice for tumor growth inhibition and survival data *in vivo*. *In vitro*, monocyte-derived dendritic cells (Mo-DC) were assessed for the ability of AZD7789 to modulate efferocytosis and cross-presentation.

Results Crystallography revealed that O13 binds an epitope of human TIM-3 outside of the PS-binding cleft. This binding site confers unique biology. While O13 elicited enhanced IL-2 production from TIM-3+ Jurkat T-cells, a PS-blocking anti-TIM-3 antibody diminished IL-2 secretion. Recognition of PS was critical for this response as mutation of the PS-binding site in TIM-3, or use of T-cells that cannot expose extracellular PS, did not elicit an antibody-mediated effect. O13 and AZD7789 enhanced efferocytosis via TIM-3 recognition of PS on dying tumor cells, and increased cross-presentation of tumor antigen to T-cells. AZD7789 also increased anti-tumor T-cell responses compared to anti-PD-1 and a PD-1/TIM-3 bispecific antibody that blocks PS-binding to TIM-3. Additionally, subsequent AZD7789 treatment prolonged *in vivo* growth inhibition in tumors that progressed on anti-PD-1 monotherapy, and AZD7789 enhanced IFN-g secretion of *ex vivo* stimulated TIL derived from anti-PD-1 treated mice.

Conclusions AZD7789 enhanced primary human T-cell and Mo-DC anti-tumor responses over treatment with anti-PD-1 or a PD-1/TIM-3 bispecific antibody that blocks PS-binding to TIM-3. Our preclinical data shows AZD7789 modulates multiple immune functions, which may translate to clinical activity in both checkpoint inhibitor naïve and resistant tumors. AZD7789 is being tested in IO pretreated patients with NSCLC (NCT04931654) and cHL (NCT05216835).

Trial Registration NCT04931654; NCT05216835

REFERENCES

1. Thommen D, *et al.* A transcriptionally and functionally distinct PD-1+ CD8+ T cell pool with predictive potential in non-small-cell lung cancer treated with PD-1 blockade. *Nat Med.* 2018; **24**:994–1004.

2. Fourcade J, *et al.* Upregulation of TIM-3 and PD-1 expression is associated with tumor antigen-specific CD8+ T cell dysfunction in melanoma patients. *J Exp Med.* 2010; **207**: 2175–2186.
3. Koyama S, *et al.* Adaptive resistance to therapeutic PD-1 blockade is associated with upregulation of alternative immune checkpoints. *Nat Comm.* 2016; **7**:10501.

Ethics Approval All animal studies were conducted in accordance with IACUC protocol: AUP-21-15

<http://dx.doi.org/10.1136/jitc-2022-SITC2022.0461>

462

PD-L1/PD-L2 DUAL-SPECIFIC CYTOTOXIC ANTIBODIES AUGMENT SURVIVAL AND MEDIATE TUMOR REGRESSION ACROSS IMMUNE "HOT" AND "COLD" MURINE CANCERS

Coline Couillaud*, Anupallavi Srinivasamani, Shweta Hedge, Qinying Liu, Guillaume Trusz, Ashvin Jaiswal, Dongxing Zha, Michael Curran. *MD Anderson Cancer Center, Houston, TX, United States*

Background Inhibition of T cell activation and effector function via engagement of the co-inhibitory receptor PD-1 is a critical mechanism enabling tumors to evade host immunity. The two ligands for PD-1, PD-L1 and PD-L2, are expressed by a variety of immunosuppressive stromal cells, particularly the myeloid stroma and tumor endothelium, and by tumors themselves. In addition to PD-1, PD-L1 engages B7-1 in an additional co-inhibitory interaction. Blocking only PD-1 or only PD-L1 thus does not relieve all inhibitory components of this pathway. We hypothesized that dual-specific antibodies blocking both PD-L1 and PD-L2 could more fully restore tumor-specific T cell activation and potentiate anti-cancer immunotherapy. Furthermore, we speculated that enhancing the cytotoxic effector function of these antibodies might further enhance their efficacy through direct depletion of tumor cells and supportive stroma.

Methods We investigated the capacity of monoclonal antibodies capable of bivalent binding to both PD-L1 and PD-L2 to restore the function of PD-1-suppressed T cells *in vitro*. To assess the *in vivo* therapeutic efficiency of bispecific PD-Ligand antibodies with ADCC capacities, mouse IgG2a and effector enhanced human IgG1 versions were generated. Antitumor ADCC activity was assessed *in vitro* using a bioluminescent reporter assay, and therapeutic efficiency measured *in vivo* in syngeneic or human xenograft cancer models.

Results The dual-specific antibodies we generated restore the function of PD-1-suppressed T cells *in vitro* with equivalent efficiency to the FDA approved PD-1 antibody pembrolizumab. Moreover, our modified human dual-specific antibodies drive significantly higher FcγRIIa and FcγRIIIa activation and induction of NK cell ADCC versus FDA-approved PD-L1 antibodies *in vitro*. In syngeneic models of PD-L1/PD-L2 double positive colon carcinoma and melanoma, ADCC-capable PD-Ligand dual-specific antibodies demonstrate superiority to PD-1 blocking antibodies to limit tumor growth and increase survival. Furthermore, treatment with our dual-specific antibodies increases T cell proliferation and cytotoxicity and reduces density of immunosuppressive myeloid stroma *in vivo*. Our antibodies also suppress the growth of U2940 lymphoma in immunodeficient mice more efficiently than Rituximab.

Conclusions ADCC-capable PD-Ligand dual-specific antibodies display higher therapeutic potential than existing anti-PD-1 antibodies and represent a new class of PD-1 pathway therapeutics with significant potential to extend the efficacy of checkpoint immunotherapy to “cold” tumor patients.

<http://dx.doi.org/10.1136/jitc-2022-SITC2022.0462>

463

INVESTIGATING THE T CELL-INTRINSIC REGULATORY ROLE OF VISTA IN ANTI-TUMOR IMMUNITY

Cassandra Gilmour*, Yikun Wang, Sachin Patnaik, Sarah Stone, Li Wang. *Cleveland Clinic, Cleveland, OH, United States*

Background Cancer immunotherapies, specifically checkpoint blockade therapies, are extremely successful at treating subpopulations of specific cancers long term. The goal is to disrupt the negative regulation of T cells and restore cytotoxic abilities allowing killing of the cancer cells and formation of memory T cells. One major limitation to checkpoint blockade is that it has limited response rate, one theory as to why this is the case, is that there are multiple non-redundant pathways of T cell suppression. In response to the heterogeneous and suppressive tumor microenvironment (TME), T cells may enter a dysfunctional state which results in the concurrent expression of many checkpoint proteins, altered metabolic state, and lack of cytotoxic abilities.^{1, 2} One of the many checkpoint proteins which is expressed on these dysfunctional T cells and negatively regulates the T cell is V-domain Immunoglobulin Suppressor of T-cell Activation (VISTA). VISTA's expression on naïve CD4 T cells controls quiescence and peripheral tolerance, but VISTA's role on cytotoxic lymphocytes (CTL) populations in the TME is largely unknown.³

Methods Our studies explore VISTA's role on cytotoxic T cells in the TME in an antigen dependent and polyclonal manner using complementary in vivo models

Results Our results suggest that VISTA KO T cells proliferate more, persist longer, and maintain a more robust metabolic program which likely contributes to the observed reduced tumor burden and overall survival of the mouse. Additionally, our results indicate that genetic deletion of VISTA on T cells provide an advantage of protective immunity against a re-challenge of antigen compared to wildtype or naïvely challenged mice.

Conclusions These studies provide context to the mechanism by which VISTA contributes to the dysfunctional state of CTLs and reaffirms the value in studying VISTA on CTLs and developing VISTA blocking immunotherapies to broaden the scope in which checkpoint blockade immunotherapies are successful.

Acknowledgements Thank you to current and former members of the Wang lab whom I've inundated with questions and they so graciously answered: Hieu Ta, Dia Roy, Keman Zhang, and Jun Dong

REFERENCES

1. Blank CU, et al. Defining 'T cell exhaustion'. *Nature Reviews Immunology*, 2019. **19**(11): 665–674.
2. Yu Y-R, et al. Disturbed mitochondrial dynamics in CD8+ TILs reinforce T cell exhaustion. *Nature Immunology*, 2020. **21**(12): 1540–1551.
3. ElTanboly MA, et al., VISTA is a checkpoint regulator for naïve T cell quiescence and peripheral tolerance. *Science*, 2020. **367**(6475): eaay0524.

Ethics Approval All human data and animal work was collected analyzed and presented in accordance with Cleveland Clinic's IRB and ethics committee standards.

<http://dx.doi.org/10.1136/jitc-2022-SITC2022.0463>

464 ANTI-CTLA-4 THERAPY DEPLETES TREGS AND EXPANDS ICOS⁺ T-CELLS IN NEUROBLASTOMA TUMORS WITH INDUCED DNA MISMATCH REPAIR DEFICIENCY

Megan Hong*, Rene Figueredo, Saman Maleki. *Western University, London, Canada*

Background Cytotoxic T lymphocyte-associated protein 4 (CTLA-4) highly expressed on regulatory T-cells (Tregs) inhibit the activation of pro-inflammatory T-cells responsible for eliminating cancer cells. Anti-CTLA-4 can enhance T-cell activation by increasing CD28 co-stimulatory signaling through CTLA-4 blockade or depletion of Tregs by Fc-dependent effector mechanisms. Strategies to improve its therapeutic efficacy are needed as patient response rates to anti-CTLA-4 are low. Response to anti-CTLA-4 has been positively correlated with tumor mutation burden (TMB). Defects in the DNA mismatch repair (MMR) pathway can increase TMB and the production of neoantigens that promote anti-tumor immune responses. Here we investigate the underlying mechanism(s) to which induced MMR deficiency in an immunologically-cold and low TMB tumor model can enhance the therapeutic effect of anti-CTLA-4. We hypothesize that induced MMR deficiency in tumors enhances anti-CTLA-4-mediated Treg depletion and increases the infiltration and activation of effector T-cells.

Methods MMR deficiency was induced in a syngeneic murine neuro-2a neuroblastoma cell line by knocking-out *MLH1* expression using CRISPR-Cas9. Wildtype MMR-proficient (pMMR) or induced MMR-deficient (idMMR) neuro-2a cells were inoculated into immunocompetent A/J mice and treated with anti-CTLA-4. Tumors were immunophenotyped by flow cytometry and mixed-lymphocyte reaction assays were used to examine the effects of MMR deficiency and anti-CTLA-4 on T-cell activation and proliferation.

Results Induced MMR deficiency in neuroblastoma tumors enhances the anti-tumor immune response induced by anti-CTLA-4. MMR deficiency in neuroblastoma tumors promoted anti-CTLA-4-mediated Treg depletion and increased intratumoral CD3⁺ T-cells. idMMR neuroblastoma tumors had an increase of ICOS⁺ T-cells compared to pMMR tumors. In addition, ICOS⁺ T-cells were increased further with anti-CTLA-4 treatment.

Conclusions Our data show that inducing MMR deficiency in low TMB and immune-cold neuroblastoma tumors can enhance the anti-tumor effect of anti-CTLA-4 by increasing T-cell activation and depletion of Tregs. By understanding the underlying mechanism(s) of anti-CTLA-4 in idMMR tumors, it may justify targeting the MMR pathway to improve the response to immune checkpoint inhibitors in patients with immunologically-cold and/or low TMB tumors that are refractory to immunotherapy. Future studies will assess how inducing MMR deficiency alters the tumor microenvironment to enable anti-CTLA-4-mediated Treg depletion and the significance of ICOS⁺ T-cells in the efficacy of anti-CTLA-4 therapy in this setting.

<http://dx.doi.org/10.1136/jitc-2022-SITC2022.0464>

465

SYNERGISTIC APPROACH TO OVERCOME THE SOLID TUMOR MICROENVIRONMENT OF MESOTHELIOMA WITH NATURAL KILLER CELL-FOCUSED IMMUNOTHERAPY

Philippa (Pippa) Kennedy*, Quinlan Kile, Blake Jacobson, Brianna Ettestad, Sarah Miller, Jeffrey Miller, Manish Patel, Martin Felices. *University of Minnesota, Minneapolis, MN, United States*

Background Mesothelioma is a rare, but aggressive cancer that occurs in cells that surround internal organs. Immune checkpoint inhibitors (ICI) have been approved for the treatment of mesothelioma (nivolumab, ipilimumab and pembrolizumab), but currently approved strategies do not make use of natural killer (NK) cell mediated antibody-dependent cellular cytotoxicity (ADCC) of mesothelioma cells. We hypothesized that combining IL-15 treatment with an anti-PDL1 ICI that drives ADCC will enhance NK cell control of mesothelioma and lead to more robust immune control of the disease.

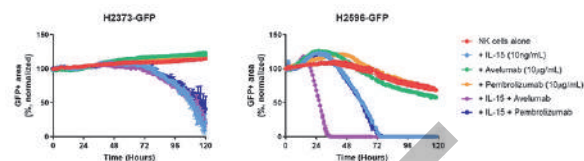
Methods In vitro assays challenged NK cells with three pleural mesothelioma lines, H2373, H2461 and H2596 and four peritoneal mesothelioma lines, ROB, YOU, HAY and ORT. Flow cytometry was used to assess degranulation and cytokine production by NK cells co-cultured with mesothelioma cells in short-term assays (5 hours). The tumor cells were treated overnight with IFN γ to mimic the inflammatory tumor microenvironment. Natural cytotoxicity was compared with ICI that do not drive ADCC (pembrolizumab), ICI that drive ADCC (avelumab) and IL-15, alone or in combination. Live cell imaging was used to track mesothelioma survival in three dimensional spheroids over 5 days when treated with NK cells and these drugs.

Results Mesothelioma lines showed a range of sensitivity to NK cell natural cytotoxicity, with H2373 cells being very resistant and H2596 being more sensitive. More resistant cells tended to have more HLA class I at the cell surface, which can inhibit NK cell function. IFN γ treatment increased the abundance of PDL1 and HLA class I on mesothelioma lines. Lines that lacked PDL1 and were resistant to avelumab treatment (ROB and YOU), were rendered sensitive by increased surface PDL1 following IFN γ treatment. However, lines that were already sensitive to avelumab treatment showed reduced NK cell responses with IFN γ (H2373 and ORT). In spheroid assays, H2596 and H2461, but not H2373, showed synergy between avelumab and IL-15 (figure 1).

Conclusions This study demonstrates a novel synergistic approach to treatment of mesothelioma, but variation in mesothelioma sensitivity to the combination of IL-15 and avelumab suggests other factors beyond PDL1 abundance are contributing to NK cell responses. Greater abundance of HLA class I decreased NK cell responses in our system, but would be beneficial for endogenous T cell responses. Optimizing for both the adaptive and innate arms of the immune response has the potential to limit tumor escape and enhance mesothelioma immunotherapy.

Acknowledgements Raffit Hassan (NIH) kindly provided the peritoneal mesothelioma lines. Daniel Vallera (University of Minnesota) kindly provided pleural mesothelioma lines. This project was supported in large part by the Meso Foundation and also by the Department of Defense (CA200922) and National Institutes of Health (R35 CA197292, P01 CA111412).

Ethics Approval This study was deemed not to constitute human research as determined by the University of Minnesota Institutional Review Board.



Abstract 465 Figure 1 NK cells with anti-PDL1 and IL-15 decrease the survival time of H2596 spheroids. Live imaging tracks the survival of three-dimensional spheroids made from GFP+ mesothelioma cells over 5 days. The relative two-dimension area observed in widefield microscopy images is plotted against time for one donor, representative of at least five donors.

<http://dx.doi.org/10.1136/jitc-2022-SITC2022.0465>

466

COMBINATION THERAPY WITH ANTI-VSIG4 AND ANTI-PD-L1 SUPPRESS GROWTH OF TUMOR VIA CONDITIONING OF TUMOR MICROENVIRONMENT

Byoung S Kwon, Hye Jeong Kim, Joong Won Lee*. *Eutilex Co.,Ltd., Seoul, Korea, Republic of*

Background V-set and immunoglobulin domain-containing 4 (VSIG4) is a B7 family-related protein which includes PDL1, VISTA and CTLA4 ligand. The known functions of VSIG4 are a receptor for complement to inhibit complement activity and negative regulation of proliferating T cell. Although VSIG4 is highly expressed in tissue-resident macrophage and tumor-associated macrophage (TAM), the mechanism of the signal transduction in tumor microenvironment (TME) is not fully elucidated.

Methods

Conversion assay CD14⁺ monocytes from PBMC were differentiated to M0 macrophages by rhM-CSF, and subsequently to M2 macrophages with rhIL-4/rhIL-13. The conversion of M2 macrophages to M1 was carried out by incubating the macrophages with LPS/rhIFN-gamma or EU103.

In vivo model Generation

PBMC-humanized mouse model shows a relative enrichment of human T cells but generally not enough numbers of human monocyte/macrophage. Therefore, a strategy of adding M2 macrophages was used in the tumor site. Human PBMC were injected i.v. into the NSG mice to humanize. To establish a lung cancer orthotopic model, A549-luci lung cancer cells were injected i.v. with differentiated M2 macrophages into the naïve NSG mice, followed by PBMC infusion. The degree of humanization was determined by measuring the ratio of human CD45⁺ cells in the mouse PBMC. Tumor size was measured using IVIS twice a week.

Results Here we investigate the pivotal roles of anti-VSIG4 therapeutic antibody, EU103 in TAM. EU103 engagement altered a broad range of type II macrophage (M2) transcriptome which was related to immune-tolerance and increased the proliferation of cytotoxic CD8⁺ T cells. EU103 induced phosphorylation of JNK and p38MAPK and in consequence, decreased the expression of M2 marker CD14, CSF-1R and CD163 while type I macrophage (M1) marker CD86 and CD40 were increased. In the PBMC-based humanized mouse, human orthotopic lung cancer model, stimulation of VSIG4 suppressed tumor growth and promoted infiltration of IFN-gamma-producing CD8⁺ T cells into tumor tissue. Furthermore, treatment of EU103 showed synergistic anti-cancer activity with an anti-PD-L1 therapy.

Conclusions Our finding suggests that EU103 directly act on TAM and induce repolarization of TAM to tumor suppressive M1 macrophages, leading to a CD8⁺ T cell proliferation and tumor suppression. Since the main cause of Immune Checkpoint Inhibitor (ICI) resistance is an immune-suppressive TME, EU103 could be an option for ICI-resistant patients, and synergistic anti-tumor effect could be expected with a combination with ICIs. Overall, targeting the VSIG4 would be an advantageous approach in cancer therapeutics.

<http://dx.doi.org/10.1136/jitc-2022-SITC2022.0466>

467 **YH38560, A NOVEL BISPECIFIC FUSION PROTEIN TARGETING 5T4 AND CD47 IN A TUMOR-SELECTIVE MANNER FOR THE TREATMENT OF SOLID CANCERS**

Narae Lee*, Eunjeong Jeong, Jung-Hoon Pyun, Minji Choi, Young Bong Park, Yoon ha Hwang, Eunjung Lee, Junhwan Kim, Se-Woong Oh. *Yuhan Corporation, Yongin-si, Korea, Republic of*

Background 5T4 (also known as trophoblast glycoprotein; TPBG) is highly expressed across a wide range of solid cancer indications, including NSCLC (non-small cell lung cancer), head and neck, colorectal, gastric, renal, pancreatic, bladder, breast, ovarian and cervical cancers, with limited expression in normal tissues, making it an attractive target as a tumor-specific antigen. CD47 (Cluster of Differentiation 47), a ubiquitously expressed innate immune checkpoint receptor, is also overexpressed in most solid and hematological cancers. CD47 interacts with signal-regulatory protein alpha (SIRP α) on myeloid cells, and this leads to the inhibition of tumor cell phagocytosis and anti-tumor immune responses. However, the development of novel treatment agents targeting CD47 is hampered by its ubiquitous expression, which often leads to rapid drug elimination and hemotoxicity including anemia or thrombocytopenia. Herein, YH38560 is a bispecific fusion protein targeting 5T4 and CD47 designed to overcome the on-target hematological toxicities and limited efficacies of monospecific CD47 blockers.

Methods *In vitro* binding potencies of YH3860 to human cancer cell lines and RBC (red blood cells) were analyzed by flow cytometry. The tumor selectivity of YH38560 was determined in co-culture system with human cancer cells and RBC *in vitro*. The Fc γ R-mediated activities of YH38560 were quantified with ADCC (antibody-dependent cellular cytotoxicity) and ADCP (antibody-dependent cellular phagocytosis) reporter bioassays. The tumor cell killing activities of YH38560 were measured in the co-culture system with NK (natural killer) cells or macrophages. *In vivo* anti-tumor effects of YH38560 were evaluated in human 5T4/CD47 expressing MC38 tumor model using hSIRP α knock-in (KI) mice as monotherapy and in combination with anti-PD-1 or PD-L1 antibody (Ab).

Results YH38560 exhibited stronger binding potency to human cancer cells than RBC and this is consistent with the preferential binding of YH38560 to cancer cells when co-cultured with RBC. YH38560 facilitated potent phagocytosis against tumor cells via CD47/SIRP α blockade and Fc γ RIIa-dependent ADCP. YH38560 demonstrated superior NK-mediated cytotoxicity to tumor cells through Fc γ RIIIa-dependent ADCC. Correspondingly, YH38560 alone showed significant tumor growth inhibition superior to monospecific CD47 blockers and it exerted synergistic and durable anti-tumor effects when combined with either anti-PD-1 or PD-L1 Ab in MC38 syngeneic mouse model.

Conclusions These findings suggest that YH38560 holds promising potential to improve patient outcomes over CD47-targeted therapies currently under development.

<http://dx.doi.org/10.1136/jitc-2022-SITC2022.0467>

468 APPLICATION OF ORGANOID-BASED DISCOVERY PLATFORM FOR INNOVATIVE SCREENING, EVALUATION, AND IDENTIFICATION (ODISEI) IN IMMUNOTHERAPY

Bo Eun Lee, Sarang Kim, Yuri Shin, Hee-Ra Lee, Suyoung Jo, Dong Wook Han*, Jongman Yoo. *ORGANOIDSCIENCES LTD., Seongnam, Korea, Republic of*

Background Immuno-oncologic therapies are known to activate patients' endogenous immune system, resulting in the enhanced tumor-killing effects in cancer patients. These therapeutic strategies have been gradually preferred as a prior regimen to cure cancer patients due to relatively fewer side effects and prolonged efficacy. Although many new immunotherapeutic drugs have been developed, almost all new drugs failed in clinical trials, strongly necessitating the development of *in vitro* screening platform for pre-evaluating the efficacy of the immunotherapeutic drug candidates.

Methods Moreover, for the precise efficacy prediction of immunotherapy, *in vitro* platform in which the interaction between patient-specific Major Histocompatibility Complex (MHC) and T-cell receptor (TCR) could be mirrored is essentially required. MHC, an antigen molecular in the tumor cells, binds to the TCR of the T-cells, and T-cells can exhibit their tumor-killing effects via MHC and TCR matching. However, tumor cells can evade T-cell-mediated tumor killing effects through the interaction between immune checkpoint (ICP) in tumor cells and their receptors in T-cells.

Results Here we describe a robust and novel efficacy evaluation platform, namely "ODISEI" in which patient-specific immune system could be recapitulated using tumor organoids and PBMC from same donors. The improved performance of our ODISEI platform as an efficacy evaluation platform of immunotherapy drugs was carefully examined using PD-1/PD-L1 blocker antibodies. Moreover, we also developed a series of ODISEI platforms in which the specific interactions between tumor organoids and each immune sub-populations (T-cells, macrophages, regulatory T-cells, dendritic cells) were replicated. Indeed, we were able to validate our ODISEI platforms using multiple drug candidates by assessing their tumor-killing effects through the specific interaction of tumor and reactive immune cell types.

Conclusions In conclusion, we have successfully established novel and robust ODISEI platforms which could serve as a useful efficacy screening platform for the immunotherapeutic drug candidates.

<http://dx.doi.org/10.1136/jitc-2022-SITC2022.0468>

469

PRECLINICAL STUDIES SUPPORT CLINICAL DEVELOPMENT OF AZD2936, A MONOVALENT BISPECIFIC HUMANIZED ANTIBODY TARGETING PD-1 AND TIGIT

¹Karin Lee, ¹Deepali Malhotra, ¹Stacy Pryts, ¹Eleanor Clancy-Thompson, ¹Bilal Omar, ¹Brian Naiman, ¹Michael Overstreet, ¹Devon Taylor, ¹Chunning Yang, ¹Kathy Mulgrew, ¹Zhan Xiao, ²Yue Wang, ¹Gordon Moody, ¹Mark Cobbold, ¹Yariv Mazor, ¹Scott Hammond, ¹Kristen Pollizzi*. ¹AstraZeneca, Gaithersburg, MD, United States; ²Innovent Biologics, Rockville, MD, United States

Background Although checkpoint inhibition has improved the treatment of metastatic non-small cell lung cancer (NSCLC), up to 65% of patients progress after initial response to PD-1/PD-L1 targeting strategies, suggesting additional immune therapies are required to further improve patient outcome.¹ TIGIT is a receptor of the Ig superfamily, which plays a role of limiting T cell and NK cell activity. TIGIT expression has high correlation with PD-1 and both are expressed on dysfunctional tumor-infiltrating lymphocytes.² Here we introduce AZD2936, a monovalent, bispecific, humanized IgG1 antibody that specifically binds to human TIGIT and PD-1 with high affinity and enhances T cell activity within preclinical models. AZD2936 is currently being evaluated in a Phase I/II study in participants with advanced or metastatic NSCLC, NCT04995523.

Methods Primary human immune cells and cells engineered to express either PD-1 and TIGIT or their ligands were co-cultured and incubated with AZD2936 to investigate its impact on T cell activation, cytokine production and cytotoxicity. Immune-compromised NSG mice bearing human tumors and administered human T cells were used to investigate the effect of AZD2936 on tumor growth and survival.

Results AZD2936 individually and concurrently bound TIGIT and PD-1 with high affinity and blocked interaction with their primary ligands, CD155 and PD-L1, respectively. The bispecific antibody triggered antigen-specific T cell-mediated lysis of tumor cell lines and enhanced IFN- γ release as compared to anti-PD-1 treatment. Co-culture of antigen specific T cells in a tumor spheroid model showed an increase in tumor cell killing with the addition of AZD2936. The activity of AZD2936 was also investigated in two xenograft mouse models of human cancer. In these models, administration of AZD2936 to animals significantly inhibited tumor growth compared to controls and a combination of parental antibodies.

Conclusions AZD2936 represents a novel immunotherapy engineered to target PD-1 and TIGIT with the potential to enhance anti-tumor immunity. These preclinical results support the ongoing clinical development of AZD2936 in patients with cancer.

Trial Registration NCT04995523

REFERENCES

1. Schoenfeld AJ, Hellmann MD. Acquired resistance to immune checkpoint inhibitors. *Cancer Cell*. 2020; **37**:443–455.
2. Johnston RJ, Comps-Agrar L, Hackney J, Yu X, Huseni M, Yang Y, Park S, Javinal V, Chiu H, Irving B, Eaton DL, Grogan J. The immunoreceptor TIGIT regulates antitumor and antiviral CD8(+) T cell effector function. 2014; **26**: 923–937.

Ethics Approval All animal studies were carried out in accordance to IACUC protocol 21-15

<http://dx.doi.org/10.1136/jitc-2022-SITC2022.0469>

470

BOTENSILIMAB, AN FC-ENHANCED CTLA-4 ANTIBODY, ENHANCES INNATE AND ADAPTIVE IMMUNE ACTIVATION TO PROMOTE SUPERIOR ANTI-TUMOR IMMUNITY IN COLD AND I-O REFRACTORY TUMORS

¹Chloe Delepine, ¹Daniel Levey*, ¹Shanmugarajan Krishnan, ²Kwang-Soo Kim, ²Adam Sonabend, ¹Margaret Wilkens, ¹Antoine Tanne, ¹Pilar Garcia-Brocano, ¹Claire Galand, ³Haiyong Han, ¹Christopher MacDermaid, ¹Jacky Chow, ¹Sylvia Vincent, ¹Shalu Karkwal, ⁴Yan Sun, ⁴Racehl Smith, ⁴Xavier Michelet, ¹Kah Teong, ¹Katherine Rosenthal, ¹David Savitsky, ¹Cailin Joyce, ¹Steven O'Day, ¹Joseph Grossman, ¹Jaymin Patel, ¹Dhan Chand, ¹Daniel Levey*. ¹Agenus Inc., Lexington, MA, United States; ²Northwestern University, Chicago, IL, United States; ³The Translational Genomics Research Institute, Phoenix, AZ, United States; ⁴Mink Therapeutics, Lexington, MA, United States

Background Botensilimab is a novel fragment crystallizable (Fc)-enhanced anti-cytotoxic T-lymphocyte antigen 4 (CTLA-4) antibody designed to promote superior immune activation and tumor killing relative to first-generation IgG1 CTLA-4 antibodies. In patients with advanced solid tumors, botensilimab ± balstilimab (anti-PD-1), demonstrated durable clinical responses across nine different immunotherapy-resistant or poorly immunogenic tumor types. The deep and broad activity observed with botensilimab is attributed to its enhanced binding to Fc gamma receptor IIIA (FcγRIIIA). This binding strengthens the immune synapse between CTLA-4-expressing T cells and FcγRIIIA-expressing antigen-presenting cells (APC) or natural killer (NK) cells, resulting in superior T cell priming, memory formation, intratumoral regulatory T cell (Treg) depletion, and APC functionality. We show that this diversity of immune functions, distinct from that of first-generation anti-CTLA-4, correlates with more effective control of 'cold' tumors alone or in combination with other therapies.

Methods Human *ex vivo* peripheral blood mononuclear cells (PBMCs) assays were used to assess effects of botensilimab on T cell responses, APC activation and Treg depletion. Pre- and post-treatment tumor biopsies and PBMCs from botensilimab-treated patients from a Phase 1 dose-escalation trial were analyzed by next-generation sequencing (NGS), flow cytometry or immunohistochemistry to assess neoantigen burden, immune gene signatures, T cell clonality and CD8:Treg ratios in the tumor. The efficacy of a mouse surrogate (ms) of botensilimab, alone or combined with other agents, was assessed in poorly immunogenic and anti-PD-1 refractory mouse tumor models.

Results In human *ex vivo* cell-based assays, botensilimab enhanced T cell responses as measured by IL-2 secretion, increased the frequency of activated FcγRIIIA+ CD11c+ myeloid cells as determined by CD40, HLA-DR and CD86 expression, and promoted Treg depletion superior to a first-generation IgG1 anti-CTLA-4 antibody. Tumor-bearing mice (CT26 colon carcinoma, MC38 colon carcinoma, and CT2A orthotopic glioblastoma) treated with botensilimab^{ms} showed superior tumor shrinkage and survival compared to mice treated with first-generation anti-CTLA-4. When combined with chemotherapy, radiotherapy, vaccines, adoptive cell therapy, tumor-targeted ultrasound or iNKT-activation, botensilimab^{ms} was therapeutically effective across several tumor models including GL261 glioblastoma, KPC pancreatic cancer and B16 melanoma. In both preclinical and clinical studies, botensilimab enhanced peripheral T cell clonality and expansion of T cell clonotypes and increased intratumoral CD8/Treg ratio. Concordant with preclinical observations, response to botensilimab in patients with advanced solid cancers was independent of FcγR polymorphism or neoantigen burden.

Conclusions Botensilimab demonstrates unprecedented activity in 'cold' and immunotherapy-resistant tumors consistent with its novel mechanism of action.

<http://dx.doi.org/10.1136/jitc-2022-SITC2022.0470>

471

TRANSIENT INHIBITION OF CYCLIN-DEPENDENT KINASE 4/6 WITH TRILACICLIB ENHANCES INHIBITORY RECEPTOR IMMUNOTHERAPY TO IMPROVE ANTITUMOR EFFICACY

¹Kun-Hui Lu*, ¹Catherine Dietrich, ²Sarah Ahn, ²Subing Cao, ²John Yi, ¹Shom Goel. ¹Peter MacCallum Cancer Centre, Melbourne, VIC, Australia; ²G1 Therapeutics, Inc., Research Triangle Park, NC, United States

Background Trilaciclib, an intravenously administered transient cyclin-dependent kinase (CDK)4/6 inhibitor, is indicated to decrease the incidence of chemotherapy-induced myelosuppression in adult patients with extensive-stage small cell lung cancer. In an open-label phase 2 trial in patients with metastatic triple-negative breast cancer, adding trilaciclib prior to gemcitabine plus carboplatin improved overall survival, potentially through protection and direct activation of immune function.¹

² Based on its broad effects on the cancer-immunity cycle, including enhanced antigen presentation and effector CD8 T-cell function, and sensitivity of Tregs to transient CDK4/6 inhibition, we hypothesized that trilaciclib may enhance the antitumor efficacy of inhibitory receptor immunotherapy (IRI).

Methods Syngeneic murine models of breast cancer (MMTV-PyMT) and colorectal cancer (CT26) were utilized to evaluate the synergy between trilaciclib and IRI. Trilaciclib 100 mg/kg was administered weekly, and α -PD-1 (5 mg/kg; clone RMP1-14), α -CD73 (5 mg/kg; clone TY/23), α -TIGIT (5 mg/kg; clone TY/23), α -TIM3 (5 mg/kg; clone RMT3-23), and α -LAG3 (10 mg/kg; clone C9B7W) administered biweekly. Treatment was administered intraperitoneally and continued until animals reached humane or study endpoint. Tumor volume and weight were measured 2–3 times a week.

Results In both MMTV-PyMT and CT26 models, adding trilaciclib to IRI delayed tumor growth and improved survival compared with treatment with IRI alone. In the CT26 model, the combination of trilaciclib plus α -PD-1 delayed tumor growth ($P=0.004$) and improved survival ($P=0.02$) versus α -PD-1 monotherapy. Additional benefit was observed when trilaciclib was added to α -TIGIT therapy compared with α -TIGIT alone, with delayed tumor growth ($P=0.007$) and improved survival ($P=0.002$; $P=0.04$) in the MMTV-PyMT and CT26 models, respectively. Trilaciclib plus α -LAG3 delayed tumor growth ($P=0.03$) compared with α -LAG3 alone in the CT26 model. When evaluating the combination of trilaciclib with multiple IRIs, an increase in survival was observed when trilaciclib was added to α -PD-1 plus α -CD73, α -TIGIT, or α -TIM3. Survival was significantly increased with trilaciclib plus α -PD-1 and α -LAG3 ($P=0.006$). Compared with α -TIGIT alone, trilaciclib plus α -PD-1 demonstrated efficacy irrespective of tumor model or starting day of treatment.

Conclusions Adding trilaciclib to IRI combinations heightened antitumor benefits. The combination of trilaciclib plus α -PD-1 was consistently effective, irrespective of when treatment was initiated, or the tumor model used. The data suggest that trilaciclib provides complementary immune modulatory benefits that support the mechanism of IRI and provide a rationale for combining trilaciclib with IRI to enhance clinical efficacy, including in populations resistant to checkpoint blockade or who have received prior IRI treatment.

REFERENCES

1. Tan AR, Wright GS, Thummala AR, *et al.* Trilaciclib plus chemotherapy versus chemotherapy alone in patients with metastatic triple-negative breast cancer: a multicentre, randomised, open-label, phase 2 trial. *Lancet Oncol.* 2019;**20**:1587–1601.

2. Tan AR, Wright GS, Thummala AR, *et al.* Trilaciclib prior to chemotherapy in patients with metastatic triple-negative breast cancer: final efficacy and subgroup analysis from a randomized phase II study. *Clin Cancer Res.* 2022;**28**:629–636.

Ethics Approval This study was performed in compliance with federal laws and institutional guidelines as approved by the Animal Ethics Experimentation Committee of the Peter MacCallum Cancer Centre.

<http://dx.doi.org/10.1136/jitc-2022-SITC2022.0471>

472

KNOCKDOWN OF VISTA PROTEIN USING ANTISENSE OLIGONUCLEOTIDES PROMOTES SUPERIOR ANTI-TUMOR IMMUNITY COMPARED TO ANTIBODY BLOCKADE

<http://dx.doi.org/10.1136/jitc-2022-SITC2022.0472>

¹Brittany Morrow*, ¹Michael Curran, ¹Priyamvada Jayaprakash, ²Alexey Revenko, ³Patrick Younan. ¹UT MD Anderson Cancer Center, Houston, TX, United States; ²Ionis Pharmaceuticals, Carlsbad, CA, United States; ³Seagen, Bothell, WA, United States

Background VISTA is an immunosuppressive checkpoint that can be expressed by a diverse array of immune cells, including CD4+ and CD8+ T cells, natural killer cells, macrophages, dendritic cells (DCs) and neutrophils.¹ VISTA expression is specifically upregulated on tumor infiltrating myeloid cells such as DCs, tumor associated macrophages (TAMs) and myeloid derived suppressor cells (MDSCs).¹ Previous studies showed that antibody blockade of VISTA could reduce tumor growth in multiple melanoma models and enhance T cell responses within the tumor microenvironment (TME).² Antibody blockade of VISTA, however, may be sub-optimal therapeutic solution as VISTA has been shown to co-localize with a recycling endosomal protein that contributes to its rapid turnover on and off the cell surface. Also, VISTA blockade in non-myeloid tissues has the potential to cause dose-limiting toxicities.¹

Methods We used a series of VISTA anti-sense oligonucleotides (ASO) to downregulate VISTA protein expression. Generation 2.5 Ionis ASO have minimal off-target inflammatory activity and are efficiently taken up by myeloid cells when delivered unformulated. We implanted C57Bl/6J mice with 1.5×10^5 B16-Ova melanoma cells subcutaneously on the flank and treated with anti-mouse VISTA antibody 13F3 for five injections or daily VISTA ASO over three weeks. Flow cytometry was performed to determine VISTA expression levels on TAMs, DC, and MDSCs. Tumor growth and survival were followed until tumor volume endpoints were reached.

Results Flow cytometric analysis confirmed ASO-mediated VISTA knockdown across the tumor myeloid compartment. Our results indicate that VISTA ASO regressed pre-implanted B16-OVA tumors and cured 40% of mice compared to minimal benefit with the 13F3 antibody. Overall, we observed a decrease in tumor growth and improved survival with VISTA ASO treatment compared to 13F3. VISTA ASO was well-tolerated at efficacious doses.

Conclusions Together, these data suggest VISTA expression in tumor myeloid stroma can be effectively downregulated using anti-sense oligonucleotides. Therapeutic approaches that reduce VISTA protein (e.g. VISTA ASOs) may provide superior efficacy and reduced off-target toxicity due to lack of ASO accessibility compared with monoclonal antibody-based approaches.

REFERENCES

1. ElTanbouly MA, Croteau W, Noelle RJ, Lines JL. VISTA: a novel immunotherapy target for normalizing innate and adaptive immunity. *Semin Immunol*. 2019 Apr;**42**:101308. doi: 10.1016/j.smim.2019.101308. PMID: 31604531; PMCID: PMC7233310.
2. Le Mercier I, Chen W, Lines JL, Day M, Li J, Sergent P, Noelle RJ, Wang L. VISTA Regulates the Development of Protective Antitumor Immunity. *Cancer Res*. 2014 Apr 1;**74**(7):1933–44. doi: 10.1158/0008-5472.CAN-13-1506. PMID: 24691994; PMCID: PMC4116689.

Ethics Approval All animal studies were approved by the MD Anderson Cancer Center Institutional Animal Care and Use Committee (Houston, Texas, USA) under protocol 00001378-RN00/1.

473 PD-1 BLOCKADE ADMINISTERED BEFORE OR AT THE TIME OF T CELL ACTIVATION ENHANCES ANTI-TUMOR IMMUNITY

Jena Moseman*, Douglas McNeel. *University of Wisconsin-Madison, Madison, WI, United States*

Background Immune checkpoint inhibitors as monotherapies have been a successful treatment strategy for some cancer types, but have not been as effective at treating immunologically “cold” tumors. This is likely due to low tumor mutational burden, a highly immunosuppressive microenvironment, and low numbers of infiltrating CD8+ T cells. Our group has implemented DNA vaccines as a means to generate antigen-specific CD8+ T cells. We and others have shown that PD-1 blockade in combination with T cell activating agents (vaccines) are more effective when these agents are administered simultaneously. However, optimal scheduling of vaccination in combination with checkpoint blockade and mechanisms thereof have not been thoroughly explored. Therefore, we sought to address whether administering PD-1 blockade prior to, simultaneously, or after immunization would affect anti-tumor immunity.

Methods C57Bl/6 mice were inoculated with E.G7-OVA. PDL1^{hi} tumors. Mice received naïve OT-1 splenocytes (with TCRs specific for SIINFEKL peptide) by adoptive transfer and were then immunized with SIINFEKL peptide. PD-1 blockade was administered to mice either at the same time as peptide immunization, two days prior, or two days later. In a separate model, isolated OT-1 CD8+ T cells were co-cultured with dendritic cells and activated in the presence of SIINFEKL peptide and PD-1 blockade. These resulting pre-activated T cells were then assessed for phenotype and IFN γ secretion *in vitro* and were adoptively transferred to tumor-bearing mice and assessed for tumor growth kinetics and tumor infiltrating lymphocyte (TIL) analysis.

Results Mice receiving pre- or simultaneous- treatment of PD-1 blockade had prolonged survival and delayed tumor growth in comparison to the control and late PD-1 blockade treatment groups. OT-1 CD8+ T cells activated *in vitro* in the presence of PD-1 blockade exhibited greater IFN γ secretion, and mice receiving transferred OT-1 CD8+ T cells pre-activated in the presence of PD-1 blockade exhibited greater anti-tumor responses than control mice or mice receiving late administration of PD-1 blockade. Mice receiving transferred T cells pre-activated in the presence of PD-1 blockade had an increased percentage of CD8+ TILs exhibiting an effector-memory and short-lived effector phenotype.

Conclusions These results indicate PD-1 blockade may be best employed when administered before or at the same time as T cell activating agents such as vaccines, and that blockade affects the phenotype and function of T cells at the time of vaccine activation.

<http://dx.doi.org/10.1136/jitc-2022-SITC2022.0473>

474

**FIRST-IN-CLASS ANTI-PVR MAB NTX1088 RESTORES
EXPRESSION OF DNAM1 AND AUGMENTS ANTITUMOR
IMMUNITY**

¹Akram Obeidat, ¹Anas Atieh, ¹Alon Vitenshtein, ¹Guy Cinamon, ¹Keren Paz, ²Tihana Roviš, ²Paola Brilc, ²Lea Hirs, ³Ofer Mandelboim, ²Stipan Jonjic, ¹Pini Tsukerman*. ¹*Nectin Therapeutics, Jerusalem, Israel*; ²*MEDRI, Rijeka, Croatia*; ³*HUJI, Jerusalem, Israel*

Background Poliovirus receptor (PVR, CD155) is a novel oncology target, differentially overexpressed in a wide range of solid tumors, which recently emerged as a main resistance mechanism to approved immune checkpoint inhibitors (ICIs). It is a key regulator of immune activation, that modifies function through multiple mechanisms, through interaction with the immune receptors DNAM1 (CD226), TIGIT and CD96. Increased PVR expression levels on tumor cells have been associated with resistance to anti-PD1 and PDL1 therapy in patients, while loss of PVR led to reduced tumor growth. Targeting PVR offers an attractive therapeutic approach for patients with advanced cancers, who are not responding to other ICIs.

NTX1088 is a first-in-class, humanized, anti-PVR mAb, currently investigated in a Phase I. By binding PVR with high affinity, NTX1088 has a multi-faceted immune-stimulating role. It blocks the interaction between PVR and its receptors, leading to the restoration of DNAM1 expression and its immune activation function, while simultaneously neutralizing TIGIT and CD96 inhibitory signals in immune cells. DNAM1 downmodulation by PVR was recently identified as a key effector of immune surveillance, and its distinctive restoration by NTX1088 was never seen before by other therapies.

Methods In vitro mechanistic studies demonstrated that NTX1088, as a monotherapy, significantly increased immune cell activation, and was superior to TIGIT, CD112R, and PD1 antibody blockade, leading to superior immune-mediated tumor cell killing, IFN γ release, and CD137 induction. Importantly, only NTX1088 was able to restore DNAM1 to the surface of immune cells in all settings. Synergy was observed when NTX1088 was combined with PD1 blockers or with the anti-CD112R mAb, NTX2R13, in line with the restoration of DNAM1 expression.

Results Numerous humanized murine xenograft models were investigated. NTX1088 as a monotherapy exhibited robust tumor growth inhibition of the PDAC cell line, HPAFII, co-grafted with human PBMC in NOD/SCID mice. The effect was significantly improved when NTX1088 was combined with a PD1 inhibitor. Furthermore, tumor growth inhibition by NTX1088 was observed in humanized A549 xenograft in which TIGIT and PD1 blockers failed to impact tumor growth. Tumor-infiltrating lymphocytes, harvested from NTX1088-treated mice, demonstrated a significantly higher prevalence of CD137+, DNAM1+, CD8+ T cells compared to all other interventions.

Conclusions These promising preclinical findings, together with a clean safety profile in cynomolgus monkeys, paved the way to a Ph1 clinical study in which NTX1088 is tested as a monotherapy and in combination with pembrolizumab, in patients with locally advanced and metastatic solid tumors (NCT05378425).

<http://dx.doi.org/10.1136/jitc-2022-SITC2022.0474>

475 **ANTI-TIGIT ANTIBODY TIRAGOLUMAB LEVERAGES MYELOID CELLS AND REGULATORY T CELLS TO IMPROVE PD-L1 CHECKPOINT BLOCKADE**

¹Namrata Patil*, ¹Raymond Meng, ¹Robert Johnston, ¹Patrick Chang, ¹Shyam Srivats, ¹Yoonha Choi, ¹Xiangnan Guan, ¹Barzin Nabet, ¹Lisa McGinnis, ¹Eugene Chiang, ¹Thinh Pham, ¹Alexis Dunkle, ¹Bill O’Gorman, ¹Ira Mellman, ¹Ruozhen Hu, ¹John Silva, ¹Joy Han, ¹Amelia Au-Yeung, ¹Chikara Takahashi, ¹Nandini Molden, ¹Pallavi Daggumati, ¹Wendy Connolly, ²Melissa Johnson, ³Delvys Rodriguez Abreu, ⁴Byoung Chul Cho, ⁵Antoine Italiano, ⁶Ignacio Gil Bazo, ⁷Enriqueta Felip, ¹Sanjeev Mariathasan, ¹Carlos Bais, ¹David Shames. ¹Genentech Inc., South San Francisco, CA, United States; ²Sarah Cannon Research Institute, Nashville, TN, United States; ³Hospital Universitario Insular, Las Palmas, Spain; ⁴Yonsei University College of Medicine, Seoul, Korea, Republic of; ⁵Institut Bergonie CLCC Bordeaux, Bordeaux, France; ⁶Clinica Universidad de Navarra, Pamplona, Spain; ⁷Vall d’Hebron Institute of Oncology, Barcelona, Spain

Background TIGIT is a co-inhibitory receptor and immune checkpoint associated with T cell and natural killer (NK) cell dysfunction in cancer. Tiragolumab is an anti-TIGIT antibody with an active, IgG1/kappa Fc. In a randomized double-blind phase 2 clinical trial in non-small cell lung cancer (NSCLC), tiragolumab + atezolizumab (anti-PD-L1) combination treatment demonstrated significant improvement relative to atezolizumab alone. However, the mechanisms underlying efficacy of this combination are not well understood.

Results Here, we show that tiragolumab functions as both a conventional checkpoint inhibitor and, via Fc gamma receptor (FcγR) engagement, as a modulator of immunosuppressive myeloid cells and T regulatory (Treg) cells. High levels of these cell subsets, which often mediate resistance to immunotherapy, were associated with treatment benefit in the tiragolumab + atezolizumab arm but not atezolizumab arm. Patients receiving the combination treatment exhibited transient on-treatment increases in serum proteins suggestive of myeloid cell activation, and decreases in circulating Treg cells. In pre-clinical experiments, treatment with Fc-active anti-TIGIT led to effector T cell and NK cell activation, Treg reduction, and proinflammatory modulation of myeloid cells and neutrophils.

Conclusions These findings reveal distinct mechanisms by which tiragolumab unleashes antitumor immune responses, and inform further clinical development of anti-TIGIT therapies.

Trial Registration NCT03563716

Ethics Approval Protocol approval was obtained from independent ethics committees for each participating site for both studies and an independent data monitoring committee reviewed the safety data.

<http://dx.doi.org/10.1136/jitc-2022-SITC2022.0475>

476 LAIR-1 INHIBITION ENHANCES ANTI-PD-1 EFFICACY

¹Yoshiko Takeuchi*, ¹Corazon Arthur, ¹Heather Kohlmeier, ¹James White, ²Betty Lee, ²Bin Fan, ²Jiawei Huang, ²James Sissons, ²Jonathan Sitrin, ²Lee Rivera, ¹Robert Schreiber. ¹Washington University School of Medicine, Saint Louis, MO, United States; ²NGM Biopharmaceuticals Inc., South San Francisco, CA, United States

Background Leukocyte-associated immunoglobulin-like receptor 1 (LAIR-1) is an immune inhibitory collagen-binding receptor that is aberrantly expressed in tumors. Recent work by others has led to conflicting views of immunoinhibitory versus immunoenhancing roles for LAIR-1 in solid tumors. Here, using well-defined syngeneic mouse tumor models, we assess the antitumor efficacy of LAIR-1 inhibition/depletion either alone or in combination with anti-PD-1.

Methods To evaluate the effect of LAIR-1 inhibition on *in vivo* tumor growth and control, we used either *Lair1*^{-/-} mice or a LAIR-1 blocking monoclonal antibody (mAb). We used two antigenically distinct MCA-induced C57Bl/6 strain sarcoma lines (1956 and 7347), a 129S6 strain sarcoma line (F244) and a PD-1 sensitive clone of C57Bl/6 MC38 (MC38-5s). To assess the effects of LAIR-1 deficiency on tumor immunity, we injected either 1956, 7347, or MC38-5s cells into either syngeneic *Lair1*^{-/-} or WT mice, and 10 days later, when tumor-bearing WT mice became insensitive to anti-PD-1 therapy, initiated either anti-PD-1 or Ctrl mAb therapy. To evaluate the efficacy of LAIR-1 blocking mAb as monotherapy or in combination with anti-PD-1, we treated 1956 or 7347 bearing WT C57Bl/6 mice and F244 bearing WT 129S6 mice continuously with either anti-LAIR-1 or Ctrl mAb. Ten-days after tumor inoculation, mice were additionally treated with either anti-PD-1 or Ctrl mAb.

Results Whereas 89% of anti-PD-1 treated *Lair1*^{-/-} mice rejected 1956 sarcomas, only 22% of Ctrl mAb treated *Lair1*^{-/-} mice and 6% of anti-PD-1 treated WT mice rejected their tumors. PD-1 blockade of *Lair1*^{-/-} mice bearing 7347 sarcomas or MC38-5s tumors induced similar rejection responses. In WT mice, the anti-LAIR-1 and anti-PD-1 combination induced better anti-tumor efficacy than anti-LAIR-1 or anti-PD-1 monotherapy. Flow cytometry analysis revealed that tumor-specific T cells were significantly increased in anti-PD-1 treated *Lair1*^{-/-} mice compared to anti-PD-1 treated WT mice. Depletion of CD4⁺ and/or CD8⁺ T cells in *Lair1*^{-/-} mice inhibited anti-PD-1 mediated tumor rejection. High dimensional profiling via CyTOF analyses of the myeloid cell compartment from 1956 tumors in *Lair1*^{-/-} mice treated with either anti-PD-1 or Ctrl mAb revealed a selective increase over similarly treated WT mice in a macrophage cluster expressing CD206 and folate receptor-b, suggesting that development of this macrophage cluster was LAIR-1 dependent.

Conclusions This study shows that inhibition of LAIR-1 in tumor bearing mice sensitizes advanced tumors to anti-PD-1 treatment.

<http://dx.doi.org/10.1136/jitc-2022-SITC2022.0476>

477

HBM1047, A NOVEL FULLY HUMAN ANTI-CD200R1 ANTAGONIST ANTIBODY WITH POTENT ANTI-TUMOR EFFICACY IN PRECLINICAL MODEL

Yuhua Wang, Qiumei Du, Hongjie Pan, Geetika Bajpai, Tao Liu, Jason Noon, Yao Lu, Jinqiu He, Yan Li, Qingfang Chen, Yongqiang Wang, Xingxing Jia, Fei Chen, Youhong Wang, Yiping Rong, Yun He, Joe Zhao, Musheng Bao*. *Harbour BioMed, Shanghai, China*

Background Immune checkpoint inhibitors have revolutionized cancer immunotherapy, however, only a small subset of patients respond to the treatment. There is still a high unmet medical need, especially for those who are resistant to immune checkpoint inhibitors. Developing new therapeutic targets are urgently needed. CD200-CD200R1 signaling pathway has been shown to inhibit the functions of T cells and myeloid cells, and represents a promising therapeutic target for cancer treatment. In a PD1-resistant mouse tumor model, CD200R1 expression is highly upregulated in tumor infiltrating T cells from PD1-resistant group.¹ Thus, blocking CD200-mediated CD200R1 inhibitory signaling pathway offers promising therapeutic potential for PD1-resistant patients. Moreover, CD200 is highly expressed in many human cancers such as non-small cell lung cancer, pancreatic cancer and brain cancer, which are potential indications for anti-CD200R1 antagonist antibody.²⁻⁴

Methods Utilizing the unique Harbour Mice[®] antibody discovery platform, we generated fully human anti-CD200R1 antibodies that efficiently blocked CD200-CD200R1 interaction. After further characterization and functional screening, we identified a novel fully human anti-CD200R1 antagonistic antibody – HBM1047.

Results HBM1047 demonstrated high binding affinity to both human and cyno CD200R1. It efficiently blocked CD200-CD200R1 interaction and inhibited CD200-induced CD200R1 reporter activity. In human primary cell assays, HBM1047 enhanced T cell activation when combined with anti-PD1 antibody. Furthermore, HBM1047 selectively bound to CD8+ T cells and myeloid cells in human tumor infiltrating lymphocytes from a variety of cancer types. More importantly, when used as monotherapy in preclinical models, HBM1047 showed potent anti-tumor efficacy in both CD200+ and CD200-humanized CDX models. In addition, HBM1047 had a favorable PK profile in mice and exhibited good developability properties.

Conclusions In conclusion, HBM1047 represents a novel fully human anti-CD200R1 antagonistic antibody with promising therapeutic potential for the treatment of cancer.

REFERENCES

1. Markowitz GJ, Havel LS, Crowley MJ, *et al.* Immune reprogramming via PD-1 inhibition enhances early-stage lung cancer survival. *JCI Insight.* 2018;**3**(13):1–21.
2. Vathiotis IA, Macneil T, Zugazagoitia J, *et al.* Quantitative assessment of cd200 and cd200r expression in lung cancer. *Cancers (Basel).* 2021;**13**(5):1–15.
3. Choueiry F, Torok M, Shakya R, *et al.* CD200 promotes immunosuppression in the pancreatic tumor microenvironment. *J Immunother Cancer.* 2020;**8**(1):1–12.
4. Xin C, Zhu J, Gu S, *et al.* CD200 is overexpressed in neuroblastoma and regulates tumor immune microenvironment. *Cancer Immunol Immunother.* 2020;**69**(11):2333–2343.

Ethics Approval This study obtained ethics approval and all participants gave informed consent before taking part. IRB NO: 3764. IRB protocol: MTG-015

<http://dx.doi.org/10.1136/jitc-2022-SITC2022.0477>

Abstracts

478 REAL-WORLD OUTCOMES IN PATIENTS WITH PENILE SQUAMOUS CELL CARCINOMA (PSCC) RECEIVING IMMUNE CHECKPOINT INHIBITORS (ICI)

Tony Zhuang*, Subir Goyal, Jacqueline Brown, Bradley Carthon, Omer Kucuk, Greta McClintock, Lauren Yantorni, Mehmet Bilen, Viraj Master, Bassel Nazha. Emory University School of Medicine, Atlanta, GA, United States

Background Penile squamous cell carcinoma (pSCC) is a rare and aggressive neoplasm with poor outcomes in advanced settings and limited treatment options beyond TIP chemotherapy (paclitaxel/ifosfamide/cisplatin). We evaluated real-world outcomes in patients treated with immune checkpoint inhibitors (ICI) for pSCC.

Methods We performed a retrospective review of patients with pSCC who received ICI from 2012-2022 at the Winship Cancer Institute at Emory University. Clinical benefit was defined as complete response, partial response, or stable disease based on RECIST 1.1 criteria. Overall survival(OS) and progression-free survival(PFS) were assessed by Kaplan-Meier method and univariate Cox regression(UVA).

Results Of 21 patients, 71.4% were white, 28.6% were black. Median age at diagnosis was 55 years (37-82). The majority (65%) had ECOG performance status ≥ 2 . Most common histological subtype was keratinizing (42.9%). Eight of 9 (89%) patients were HPV+. Median tumor size was 6.75cm (0.30-19.5). At diagnosis, 4.8%/33.3%/61.9% were stage 2/3/4 respectively. Eight patients had initial distal metastases. At ICI initiation, the median level of C-reactive protein was 43.1 $\mu\text{g}/\text{mL}$ (0-201.9), lactate dehydrogenase: 140.5 units/L (99-414), and neutrophil-to-lymphocyte ratio (NLR): 6.87 (2.49-45.46). Seven of 11 patients (63.6%) were PD-L1+. Median follow-up was 8.16 months(mo) and median time to ICI treatment from diagnosis was 15.6mo. Median OS and PFS for overall cohort were 8.2mo and 1.9mo respectively. Median OS was 8.4mo in white patients and not reached(NR) in black patients (1.3, NA). Median PFS was 2mo in white patients and NR in black patients (0, NA). On UVA, no differences were seen in outcomes with respect to race (figures 1,2) and PD-L1 status (figures 3,4). Three patients (14.3%) had clinical benefit and 76.2% progressed post-ICI. Only 14.3% were alive at last contact. Nearly all patients previously received chemotherapy. ICI was 1st line(1L) in 1 patient(4.8%), 2L in 13(61.9%), 3L in 6(28.6%), 4L in 1(4.8). Monotherapy with nivolumab or pembrolizumab was the most common regimen, others included combination ICI, cemiplimab, or clinical trial. Two patients received a second ICI regimen. Sites of progression included local invasion (66.7%), lymphadenopathy (57.1%), retroperitoneum (47.6%), lung (42.9%), and bone (42.9%). Three patients (14.3%) developed grade 3/4 ICI-related adverse events. Higher NLR and larger resection size were associated with shorter OS (table 1).

Conclusions Our real-world analysis confirms poor response rates of pSCC to ICI in an unselected approach and the critical need for biomarkers. NLR may be a potential biomarker to assess ICI response in pSCC. More prospective and multi-center studies are needed for confirmation.

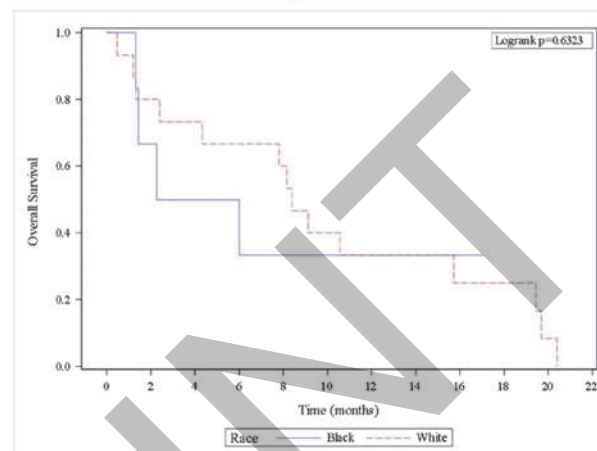
Acknowledgements Dr. Bassel Nazha and Dr. Viraj A. Master contributed equally to this work as senior authors.

Research reported in this publication was supported in part by the Biostatistics Shared Resource of Winship Cancer Institute of Emory University and NIH/NCI under award number P30CA138292. The content is solely the responsibility of the

authors and does not necessarily represent the official views of the National Institutes of Health.

Ethics Approval This study was approved by Emory's institution's Ethics Board; approval number 5355-21.

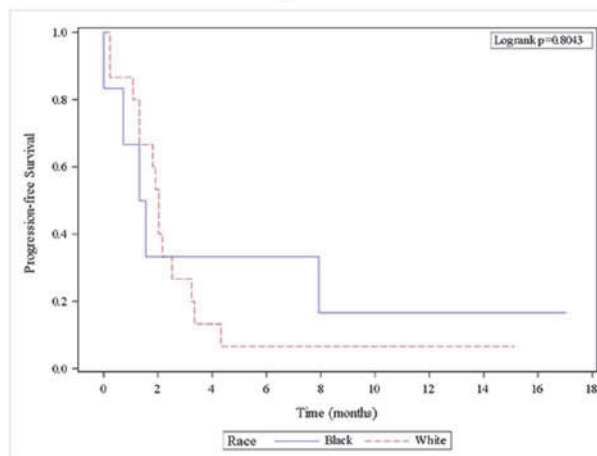
Figure 1



Race	No. of Subject	Event	Censored	Median Survival (95% CI)
Black	6	4 (67%)	2 (33%)	4.1 (1.3, NA)
White	15	14 (93%)	1 (7%)	8.4 (1.3, 15.7)

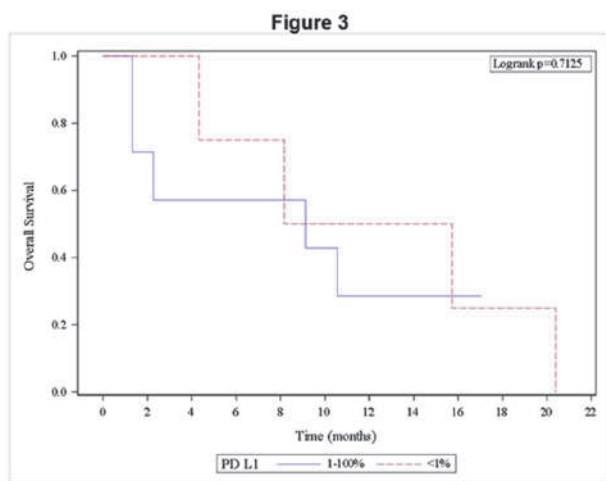
Abstract 478 Figure 1 Kaplan-Meier curve of OS stratified by race. No significant difference in OS was observed between white and black patients ($p=0.6323$).

Figure 2



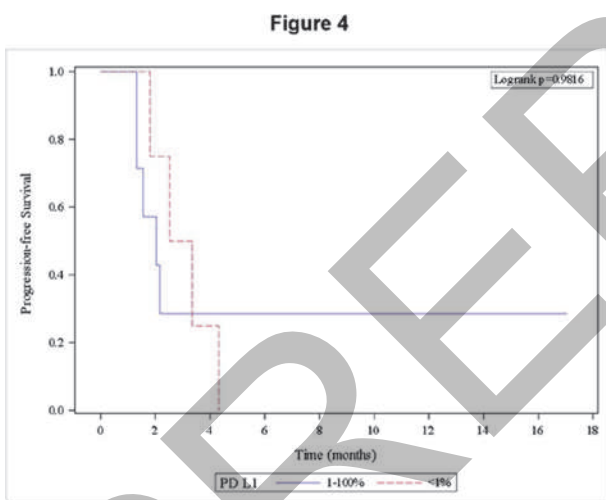
Race	No. of Subject	Event	Censored	Median Survival (95% CI)
Black	6	5 (83%)	1 (17%)	1.4 (0, NA)
White	15	14 (93%)	1 (7%)	2 (1.1, 2.5)

Abstract 478 Figure 2 Kaplan-Meier curve of PFS stratified by race. No significant difference in PFS was observed between white and black patients ($p=0.8043$).



PD L1	No. of Subject	Event	Censored	Median Survival (95% CI)
1-100%	7	5 (71%)	2 (29%)	9.1 (1.3, NA)
<1%	4	4 (100%)	0 (0%)	11.9 (4.3, 20.4)

Abstract 478 Figure 3 Kaplan-Meier curve of OS stratified by PD-L1. No significant difference in OS was observed between PD-L1+ and PD-L1 (-) patients ($p=0.7125$)



PD L1	No. of Subject	Event	Censored	Median Survival (95% CI)
1-100%	7	5 (71%)	2 (29%)	2 (1.3, NA)
<1%	4	4 (100%)	0 (0%)	2.9 (1.8, 4.3)

Abstract 478 Figure 4 Kaplan-Meier curve of PFS stratified by PD-L1. No significant difference in PFS was observed between PD-L1+ and PD-L1 (-) patients ($p=0.9816$).

Abstract 478 Table 1 Tabulated OS and PFS by NLR and resection size at ICI initiation. Higher NLR and higher resection sizes were associated with decreased overall survival.

Table 1. Tabulated OS and PFS by NLR and resection size at ICI initiation.

Covariates	PFS UVA		OS UVA	
	HR	p-value ^a	HR	p-value
NLR ^b	1.08 (95% CI: 1.03-1.15)	0.006	1.10 (95% CI: 1.04-1.19)	0.008
Resection size (cm) ^b	1.06 (95%CI: 0.93-1.17)	0.366	1.15 (95% CI: 1.00-1.30)	0.042

^aStatistical significance at alpha <0.05.

^bNLR and resection size were treated as continuous variables.

<http://dx.doi.org/10.1136/jitc-2022-SITC2022.0478>

479

EXPRESSION OF LEUCINE-RICH REPEATS AND IMMUNOGLOBULIN-LIKE DOMAINS PROTEIN 1 (LRIG1) ON CD4+/CD8+ T CELLS MAY ASSOCIATE WITH PATHOLOGICAL CHARACTERISTICS OF DIFFERENT TYPES OF CANCER

<http://dx.doi.org/10.1136/jitc-2022-SITC2022.0479>

Dia Roy*, Hieu Ta, Cassandra Gilmour, Timothy Chan, Keman Zhang, Li Wang, Sarah Stone. *Lerner Research Institute, Cleveland, OH, United States*

Background The tumor microenvironment (TME) gets infiltrated with numerous components of adaptive and innate immune system. However, the immune surveillance imparted by these components are often suppressed by numerous mechanisms in the TME in a context dependent manner. The tumor cells can mediate the signaling suppression of the immune cells which is reflected by the reduction in the activity of stimulatory immune-receptors and the concomitant activation of the inhibitory immune-receptors. In case of T cells, for instance, tumor cells facilitate the inhibition of the TCR-mediated activation signaling. Alongside, the tumor cells can also facilitate the up tuning of numerous inhibitory checkpoint receptors (ICRs). Several ICRs like CTLA-4, PD-1, and LAG3 have been studied in context of cancer immunotherapy in past decades. However, a great many drawbacks have begun to come to light with the gradual increase in accumulation of clinical data-the most obvious gridlock being its low response rate in most cancers thereby urging the need for the discovery of novel immune checkpoint molecules.

Methods Multi panel flow cytometry and Western blot analysis was done to check LRIG1 expression.¹ Bioinformatics analysis was done on the RNA seq data from the study by *Feldman et al.*²

Results The current study manifested the expression of Leucine-rich repeats and immunoglobulin-like domains protein 1 (LRIG1) on both CD4+ and CD8+T cells. Expression of LRIG1 can be detected in the tumor infiltrating lymphocytes (TILs) and also on the in-vitro activated T cells from both human and murine cancer models. Within the CD4 compartment, expression of this molecule on the immunosuppressive regulatory T cell was highly upregulated.

Further, the single cell RNA seq data from melanoma patients reanalyzed from the study obtained by *Feldman et al.* revealed the exclusive expression of LRIG1 among other exhausted markers such as TIM3, LAG3 and TIGIT.²

Conclusions LRIG1 has been identified as a potent immune suppressor molecule in numerous tissue but its role remains widely unexplored in context of the immune cells.

Detection of LRIG1 in different subsets of CD4⁺ and CD8⁺ might lead to interesting findings about its role in context of mounting anti-tumor immune response.

Acknowledgements The Wang lab is funded by American Cancer Society RSG-18-045-01-LIB, NIH/NCI (7 R01CA223804, 5 R01CA164225, 1 R21CA258618-01), Department of Defense (W81XWH-21-LCRP-IITRA and W81XWH-21-MRP-MCAA).

REFERENCES

1. Y Wang, EJ Poulin, RJ Coffey. LRIG1 is a triple threat: ERBB negative regulator, intestinal stem cell marker and tumour suppressor. 2013 May 14;**108**(9):1765–70.
2. Moshe Sade-Feldman *et al.* Defining T Cell States Associated with Response to Checkpoint Immunotherapy in Melanoma. *Cell* 2018 Nov 1;**175**(4):998–1013. e20.

Ethics Approval The human samples were obtained from Cleveland clinic after ethical approval.

480

IMPACT OF INFECTIONS IN PATIENTS WITH ADVANCED OR METASTATIC NON-SMALL CELL LUNG CANCER (NSCLC) RECEIVING PEMBROLIZUMAB-BASED THERAPIES

¹Ethan Burns*, ²Jiaqiong Xu, ¹Ryan Kieser, ³Ibrahim Muhsen, ³Shivan Shah, ¹Godsfavour Umore, ³Charisma Mylavarapu, ³Yuqi Zhang, ³Aubrey Crenshaw, ¹Kai Sun, ¹Abdullah Esmail, ¹Carlo Guerrero, ¹Zimu Gong, ³Kelly Gee, ¹Kirk Heyne, ¹Monisha Singh, ¹Jun Zhang, ¹Eric Bernicker, ¹Maen Abdelrahim. ¹Houston Methodist Neal Cancer Center, Houston, TX, United States; ²Houston Methodist Research Institute, Houston, TX, United States; ³Houston Methodist Hospital, Houston, TX, United States

Background Immune checkpoint inhibitor (ICI) therapy has improved outcomes in patients with NSCLC, particularly with the programmed death-1 inhibitor pembrolizumab. However, this therapy is not benign and while immune related toxicities are well-described, infections, a common cause of morbidity and mortality amongst patients with solid organ malignancies, are seldom studied. Herein, we investigate the incidence, risk factors, and impact of infections in patients receiving pembrolizumab regimens for NSCLC.

Methods Patients receiving pembrolizumab regimens for advanced/metastatic NSCLC from January 2017 through August 2021 across a seven-hospital network were retrospectively identified and dichotomized into infection and non-infection cohorts. Covariates included age, gender, race, comorbidities, ECOG, chronic infections, line of therapy, monotherapy/combination therapy, anti-infectives at ICI initiation, and growth factor use. Outcomes included all-cause emergency department (ED), inpatient, or intensive care unit (ICU) visits, median number of treatment cycles, overall survival (OS), and progression free survival (PFS). Univariable and multivariable analysis with reported odds ratio (OR) and 95% confidence intervals (CI) evaluated risk of developing infection, and OS/PFS was assessed via Kaplan-Meier methodology. P-value <0.05 was considered statistically significant.

Results Among 243 patients, 111 (45.7%) had ≥ 1 reported infection, with median time to first infection of 1.9 (0-48.8) months. Demographics were similar between cohorts. Compared to non-infected, infected patients had more ED [37 (33.3%) vs 26 (19.7%), $p=0.016$], hospital [87 (78.4%) vs 53 (40.1%), $p<0.001$], and ICU [31 (27.9%) vs 5 (3.8%), $p<0.001$] visits. During course of infection, there were treatment delays and discontinuation in 56 (50.4%) and 28 (25.2%) patients. Median treatment cycles received by infected and non-infected was 5 (2-13) and 8 (4-12) ($p=0.057$), respectively. Median OS and PFS in infected and non-infected patients was 11 (95% CI 6.4-16.7) and 21 (95% CI: 14.7-24.2) ($p=0.023$), and 13.03 (95% CI 10.03-19.73) and 9.7 (95% CI: 7.13-12.83) ($p=0.54$) months, respectively. Anti-infective therapy (OR 3.32, [95% CI: 1.26-8.76], $p=0.015$) and ECOG of 2 (OR 5.79, [95% CI 1.72-19.47], $p=0.005$) at ICI initiation had higher associations with infection; no other covariates were significant. At last evaluation, 74 (66.7%) infected and 70 (53.0%) non-infected died ($p=0.031$). Of these, infection caused death in 11 (14.9%) and 4 (5.7%) patients ($p=0.041$), respectively.

Conclusions Infections are common in NSCLC patients receiving pembrolizumab regimens and associated with greater morbidity, treatment interruptions, and poorer survival. Risks factors included poorer baseline ECOG status and anti-infective therapies at ICI initiation. Prospective studies assessing infectious process prevention and anti-infective stewardship programs may be valuable to augment ICI benefit.

Ethics Approval This retrospective study was an institutional review board approved study (Approval ID: PRO00028635). Informed consent was not obtained due to the retrospective nature of this study.

<http://dx.doi.org/10.1136/jitc-2022-SITC2022.0480>

481 AN AFFINITY-OPTIMIZED CD47XPD-L1 BISPECIFIC ANTIBODY FOR DUAL IMMUNE CHECKPOINT BLOCKADE

¹Xavier Chaudet, ¹Sebastien Calloud, ¹Margaux Legrand, ¹Laura Cons, ¹Laurence Chatel, ¹Adeline Lesnier, ¹Nicolas Bosson, ¹Pauline Lloveras, ¹Pauline Malinge, ¹Ulla Ravn, ¹Valery Moine, ¹Bruno Daubeuf, ¹Yves Poitevin, ¹Giovanni Magistrelli, ¹Susana Salgado-Pires, ²Dmitry Shchelokov, ²Oleg Demin, ¹Limin Shang, ¹Krzysztof Masternak, ¹Walter Ferlin*. ¹Light Chain Bioscience-Novimmune SA, Geneva, Switzerland; ²InsysBio UK Ltd, Edinburgh, UK

Background To enhance efficacy of anti-PD-1/PD-L1 antibodies, many combinations with various therapeutic agents are being investigated. Blocking the CD47/SIRP α checkpoint with monoclonal antibodies (mAbs) or decoy receptors is emerging as an effective approach to mobilize myeloid cells and support T-cell mediated antitumor responses. The benefit of combining CD47/SIRP α and PD-1/PD-L1 blockade to improve tumor control has been demonstrated in preclinical models and is being explored in patients. However, CD47 mAbs are hindered by ubiquitous CD47 expression leading to pharmacokinetic (PK) and safety issues.

Methods NI-2901, an IgG4 CD47xPD-L1 bsAb of optimized affinity, was generated using the κ L body platform.¹ *In vitro* assays were used to characterize its binding profile and checkpoint inhibition as well as its capacity to enhance T-cell activation and macrophage-mediated phagocytosis of tumor cells. PD-L1-independent CD47 antitumor activity was assessed *in vivo* in a PD-L1-negative xenograft model and compared to the humanized IgG4 anti-CD47 antibody, magrolimab. PK and tolerability of NI-2901 were evaluated in non-human primates (NHP), allowing for comprehensive modeling and simulations in humans.

Results Consistent with its intermediate CD47 affinity, NI-2901 shows low binding to red blood cells as compared to anti-CD47 mAbs and induces CD47/SIRP α blockade on PD-L1-negative cells, that is significantly enhanced once PD-L1 is expressed. As a result, the bsAb is able to enhance the phagocytosis of PD-L1-negative and -positive tumor cell lines induced by mAbs targeting tumor-associated antigens (e.g. CD20, HER2 and CD19) and demonstrates *in vivo* anti-tumor activity in the Raji B-cell lymphoma xenograft model. Given its high affinity for PD-L1, NI-2901 triggers effective blockade of the PD-1/PD-L1 interaction on cells, inducing T-cell activation *in vitro* similar to the anti-PD-L1 antibodies, atezolizumab and avelumab. After 4-weekly 30mg/kg injections in NHP, NI-2901 was well-tolerated showing no signs of hemotoxicity, while magrolimab induced a significant drop in RBC after a single 10mg/kg injection. Translational PK modelling and simulations from NHP to human suggest a more favorable dosing regimen is possible as compared to benchmark CD47-targeted approaches.

Conclusions As a dual immune checkpoint inhibitor, NI-2901 triggers effective T-cell activation, enhances phagocytosis of tumor cells and is expected to have improved efficacy over PD-1/PD-L1 blockade alone. The bsAb is well-tolerated in NHP at predicted therapeutic doses without inducing RBC or platelet depletion.

REFERENCE

1. Fischer N, *et al.* Exploiting light chains for the scalable generation and platform purification of native human bispecific IgG. *Nat. Commun.* 2015 May;6(1):6113.

Ethics Approval Studies in mouse models were performed at the sponsor's animal facility in accordance with the Swiss Federal Veterinary Office guidelines and approved by the animal

research committee of the Geneva canton, Switzerland (ID numbers: GE43 and GE/131/19)

Studies in non-human primates were outsourced and performed by Accelerera S.r.l., Italy and approved by the local Animal Welfare Body before approval by the Italian Ministry of Health (ID number: 215/2021-PR)

<http://dx.doi.org/10.1136/jitc-2022-SITC2022.0481>

482

ATG-031, A FIRST-IN-CLASS ANTI-CD24 ANTIBODY, SHOWED POTENT PRECLINICAL ANTI-TUMOR EFFICACY BY BLOCKING "DON'T-EAT-ME" SIGNAL

¹Peng Chen, ¹Min Deng, ¹Yun Liu, ¹Jiamei Luo, ¹Rong Guo, ²Jay Mei, ²Bo Shan, ²Bing Hou*. ¹Shanghai Antengene Corporation Limited, Shanghai, China; ²Antengene Corporation Co., Ltd, Shaoxing, China

Background By overexpressing anti-phagocytic surface proteins, often known as "don't eat me" signals, cancer cells can evade macrophage-mediated elimination. Therapeutic antibodies targeting "don't eat me" protein, such as CD47, demonstrates promising anti-tumor efficacy in preclinical models and in clinic. However, the clinical development of anti-CD47 mAbs that retain substantial FcR activating capacity (e.g. human IgG1) has been hampered by the on-target-off-tumor toxicity, such as erythrocyte depletion.¹ CD24, a GPI-anchored, highly glycosylated surface protein interacting with Siglec-10 on innate immune cells, was reported to be a novel "don't eat me" protein. CD24 is over-expressed in multiple tumor types. Knock-out of CD24 or blockade of CD24/Siglec-10 interaction enhances macrophage-mediated phagocytosis of tumor cells.² In this study, we developed a first-in-class, humanized anti-CD24 antibody, ATG-031. The *in vitro* and *in vivo* anti-tumor activity of ATG-031 was evaluated in preclinical models.

Methods The affinity of ATG-031 was measured using Surface Plasmon Resonance (SPR). Cell-based binding to HEK293, HEK293-CD24, human red blood cell (hRBC) and a panel of tumor cells was evaluated by flow cytometry. The ability of ATG-031 in enhancing macrophage-mediated phagocytosis of tumor cells was evaluated using human monocyte-derived M2 macrophage. *in vivo* efficacy of ATG-031 was tested in mouse bearing MC38 murine syngeneic colorectal cancer cells stably-expressing human CD24 (MC38-hCD24). Expression profile of CD24 in human tumor and normal tissues were analyzed using TCGA/GTEX database or using an in-house developed companion diagnostic antibody on tissue microarray (TMA) by IHC staining.

Results CD24 is overexpressed in multiple types of solid tumors and hematological malignancies. ATG-031 specifically binds to human CD24 with a single-digit nM affinity. ATG-031 potently binds to CD24-positive tumor cells, while showed no binding with parental HEK293 cells or hRBC. ATG-031 blocks the interaction between CD24 and Siglec-10 and induced potent macrophage-dependent tumor cell phagocytosis (figure 1A, B). Upon phagocytosis, M2 macrophages start to release M1-like cytokines suggesting a repolarization from M2 to M1. ATG-031 significantly inhibited *in vivo* tumor growth in MC38-hCD24 mouse model. A dose of 3mg/kg ATG-031 administered biweekly induced tumor regression (figure 1C).

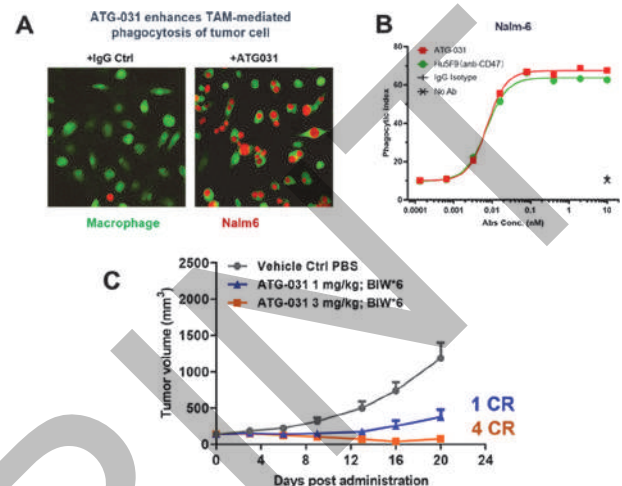
Conclusions Blocking CD24 by ATG-031 enhances macrophage-mediated phagocytosis of cancer cells, and polarized M2 macrophage towards anti-tumor M1 subtype (figure 2). It demonstrates potent *in vivo* anti-tumor efficacy, suggesting promising therapeutic strategies against a broad range of solid tumor or hematological malignancies, which warrants further clinical investigation. A clinical study to investigate the safety and efficacy of ATG-031 in cancer patients is being developed.

REFERENCES

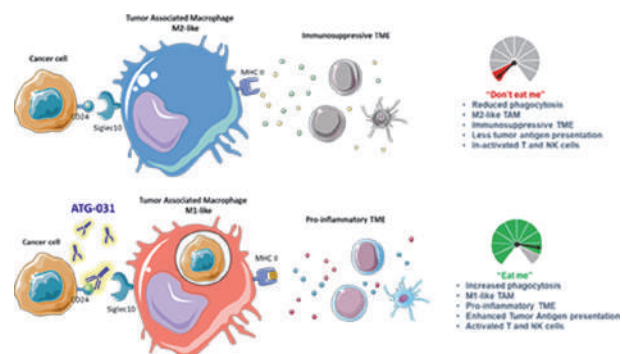
1. Logtenberg MEW, Scheeren FA, Schumacher TN. The CD47-SIRPα. Immune Checkpoint. *Immunity*. 2020 May 19;52(5):742–752
2. Barkal AA, Brewer RE, Markovic M, Kowarsky M, Barkal SA, Zaro BW, Krishnan V, Hatakeyama J, Dorigo O, Barkal LJ, Weissman IL. CD24 signalling through

macrophage Siglec-10 is a target for cancer immunotherapy. *Nature*. 2019 Aug;572(7769):392–396.

Ethics Approval This study was performed in strict accordance with institutional guidelines and approved by the Institutional Animal Care and Use Committee of the Shanghai Model Organisms Center, Inc. and the IACUC permit number was 2019-0011.



Abstract 482 Figure 1 ATG-031 showed potent anti-tumor efficacy. Immunofluorescence imaging of macrophage (green) mediated tumor cell (Nalm-6, red) induced by ATG-031 or IgG control. (B) Phagocytic index of macrophage. Monocyte-derived M2 macrophages were co-cultured with NALM-6 cells and phagocytosis was induced by ATG-031 or anti-CD47 (5F9). (C) Average tumor growth curves of mouse bearing MC38-hCD24 tumor cell. The mice were treated with 1mg/kg or 3mg/kg ATG-031. 3mg/kg of ATG-031 induced complete remission of tumor in 4 out of 8 mice. n=8 per group. CR, complete remission



Abstract 482 Figure 2 Schematic cartoon of the mechanism of action for ATG-031. Tumor associated macrophages were repolarized to pro-inflammation status when CD24/Siglec-10 interaction was blocked by ATG-031

<http://dx.doi.org/10.1136/jitc-2022-SITC2022.0482>

483

PRECLINICAL EVALUATION OF JTX-1484, AN ANTI-LILRB4 ANTAGONIST ANTIBODY, FOR REPROGRAMMING OF IMMUNOSUPPRESSIVE MYELOID CELLS

Heather Conurso, Amy Mueller, Jessica Jimenez, Lauren Badalucco, Kelly Aldridge, Pauline Sarraf, Michelle Priess, Vikki Spaulding, Sarah Jaffe, Prashanna Balaji Venkatasubramanian, Alexa Diiorio, Geneva Young, Kameron Mori, Karl Wetterhorn, Jeffrey Smith, Morgan Thompson, Jean-Christophe Pignon, Changyun Hu, Brandon Chin, Briana Murphy, Matthew Southard, Katalin Kis-Toth, Monica Gostissa, Dmitri Wiederschain, Andre da Cunha*. *Jounce Therapeutics, Cambridge, MA, United States*

Background Immune checkpoint therapy has achieved durable clinical responses, but only in a subset of cancer patients. Immunosuppressive myeloid cells, a heterogenous group of innate immune cells, have emerged as key contributors to resistance to T cell based immune checkpoint therapy. Leukocyte immunoglobulin-like receptor B4 (LILRB4), also known as immunoglobulin-like transcript 3 (ILT3), is an inhibitory receptor selectively expressed on myeloid cells, enriched in the tumor microenvironment and contributes to myeloid-driven immunosuppression. Recently, fibronectin has been identified as a functional ligand for LILRB4, and the LILRB4-fibronectin interaction was proposed as a stromal checkpoint suppressing myeloid cell anti-tumor activity. Targeting LILRB4 could represent a strategy to reprogram immunosuppressive myeloid cells and promote anti-tumor response. We developed JTX-1484, a highly selective, high-affinity humanized monoclonal antibody that binds to and antagonizes LILRB4 and blocks its interaction with fibronectin.

Methods A diverse panel of high affinity monoclonal antibodies that bind specifically to LILRB4 was generated. JTX-1484 activity alone or in combination with an anti-PD1 antibody was evaluated in vitro in different functional assays. Human primary myeloid-derived suppressor cells (MDSCs) were used in a T cell suppression assay and treated with JTX-1484. Primary monocyte-derived tolerogenic dendritic cells (tDCs) were utilized in mixed lymphocyte reactions with T cells and treated with JTX-1484 in combination with anti-PD1. JTX-1484's ability to block fibronectin inhibitory activity on tDCs and THP-1 cells was also tested. Finally, the pharmacodynamic effect of anti-LILRB4 treatment in human tumor samples was evaluated by assessing gene expression changes in an ex vivo histoculture system.

Results JTX-1484 reprogramed tDCs to a stimulatory phenotype as evidenced by increased pro-inflammatory cytokine production and increased ability to induce T cell activation in combination with anti-PD1. LILRB4 antagonism by JTX-1484 also reversed fibronectin-mediated inhibition of tDC activation and reduced MDSC-mediated T cell immunosuppression. Moreover, LILRB4 blockade in ex vivo human tumor samples induced pharmacodynamic responses consistent with increased immune activation and reduced myeloid immunosuppression.

Conclusions Results from our preclinical studies demonstrate that JTX-1484 is a highly specific and potent antagonist of LILRB4 that leads to myeloid cell reprogramming and more efficient T cell activation that could result in enhanced anti-tumor responses. JTX-1484 immunostimulatory properties towards myeloid cells could be complementary to immune checkpoint blockade therapy. Our data therefore support clinical development of JTX-1484. Indication selection will be guided by multiple factors including predictive biomarkers such as target and ligand abundance, as well as complementarity and combination potential with other therapies.

Ethics Approval Human blood and tumor samples were acquired from commercial providers and from the CHTN and NDRI networks respectively. Specimens were collected under each provider's human subject research institutional review board approved protocols and were fully anonymized or otherwise permanently de-identified to recipient investigators.

<http://dx.doi.org/10.1136/jitc-2022-SITC2022.0483>

484

BLOCKADE OF THE MYELOID CLEC-1 CHECKPOINT ENHANCES ANTITUMOR RESPONSES AND TUMOR ANTIGEN CROSS-PRESENTATION

¹Vanessa Gauttier*, ¹Marion Drouin, ¹Isabelle Girault, ¹Irène Baccelli, ¹Sabrina Pengam, ¹Emmanuelle Wilhelm, ²Javier Saenz, ¹Julien Taurelle, ²Emmanuel Merieau, ²Béangère Evrard, ¹Caroline Mary, ¹Géraldine Teppaz, ¹Ariane Desselle, ¹Virginie Thépénier, ¹Nicolas Poirier, ²Elise Chiffolleau. ¹OSE Immunotherapeutics, Nantes, France; ²Université Nantes, CHU, CR2TI – UMR1064, Nantes, France

Background Myeloid cells represent one of the most abundant immune cell types in solid tumors that impede antitumor immune responses. We previously reported that the orphan CLR CLEC-1 is expressed by dendritic cells (DCs) and macrophages (MPs). Single cell transcriptional analysis of the tumor microenvironment (TME) confirms the expression by myeloids especially cDC1, best professional antigen presenting cells and tumor-associated macrophages (TAM).

Methods Damaged CLEC-1 ligand expressing tumor cells were used to identify the ligand of CLEC-1 by co-immunoprecipitation. CLEC-1 mechanism deciphering was performed with Clec1a deficient mice, notably by isolating dendritic cells. Human CLEC-1 knock-in animals were challenged for antitumor responses, administered with antagonistic anti-human CLEC-1 monoclonal antibodies in hepatocellular carcinoma (Hepa1.6) and in colorectal cancer (MC38) preclinical models.

Results Furthermore, we showed that the CLEC-1 senses dead cells induced by programmed necrosis and identified this CLEC-1 protein ligand (CLEC-1 ligand) over-expressed in cancers. Mechanistically, we identified CLEC-1 as a sensor of tissue-damage which increases the cross-presentation of dead-cell tumor associated antigens by cDC1 without breaking established tolerance against natural antigens. Interestingly, we observed that CLEC-1 blockade as a monotherapy or combined with chemotherapy prolongs mice overall survival in hepatocellular and colon carcinoma models. We revealed that loss of CLEC-1 reduced the accumulation of immunosuppressive myeloid cells in tumors and invigorated the activation state of dendritic cells (DCs), thereby increasing T cell activation & response. Importantly, we generated anti-human CLEC-1 antagonist antibodies able to enhance anti-tumor immunity in CLEC-1 humanized mice.

Conclusions Altogether, our results demonstrate that CLEC-1 acts as an immune checkpoint in myeloid cells and support CLEC-1 as a novel target for cancer immunotherapy.

<http://dx.doi.org/10.1136/jitc-2022-SITC2022.0484>

485

FUNCTIONAL CHARACTERIZATION OF THE INHIBITORY ACTIVITY AND IDENTIFICATION OF NOVEL T-CELL RECEPTORS FOR THE TUMOR-ASSOCIATED MACROPHAGE RECEPTOR VSIG4

<http://dx.doi.org/10.1136/jitc-2022-SITC2022.0485>

¹Tim Eitas*, ¹Edward van der Horst, ¹Faith Finley, ¹Thomas Thisted, ¹Kanam Malhotra, ¹Arnab Mukherjee, ¹Zuzana Biesova, ¹Anokhi Cifuentes, ²Sandra Marder, ²Paul Helbling, ¹Robert Pierce. ¹*Sensei Biotherapeutics, Boston, MA, United States*; ²*Dualsystems Biotech AG, Schieren, Switzerland*

Background Tumor associated macrophages (TAMs) are important regulators of immunosuppression in the tumor microenvironment (TME) and are often associated with poor clinical responses in patients. VSIG4 (V-Set and Immunoglobulin domain containing 4) is a negative checkpoint regulator (NCR) and its expression has been well established on both tissue resident macrophages and TAM populations.¹⁻³ However, the inhibitory molecular mechanism of VSIG4 remains largely unknown¹⁻² and many therapeutic strategies targeting TAMs in general have been limited either by a lack of TME-specificity or high target abundance leading to target-mediated drug disposition (TMDD).⁴⁻⁵ The development of immunomodulatory antibodies that selectively target antigens in acidic environments, such as the TME, has the potential to increase tumor exposure and reduce toxicity.⁶

We have characterized endogenous expression patterns of VSIG4 and observed an absence of expression on peripheral immune cell populations but a significant induction on differentiated primary macrophages under conditions similar to the TME. Additionally, we have performed a proteomics screen for potentially novel T-cell receptor(s) that interact with VSIG4.

Methods Endogenous expression patterns of VSIG4 were characterized in primary human immune cell populations including whole blood, peripheral blood mononuclear cells (PBMCs), and polarized macrophage populations. The induction of VSIG4 expression in polarized macrophage populations was demonstrated by both flow cytometry and RNA expression analysis. A Ligand Receptor Capture-Trifunctional Chemoproteomic Reagents (LRC-TriCEPS)-based proteomics strategy was used to identify receptors on primary human T-cells that interact with recombinant VSIG4 protein.⁷

Results Our results show a robust upregulation of VSIG4 expression in polarized human macrophage populations. Additionally, we established multiple functional assays demonstrating VSIG4-mediated suppression of primary human T-cells. Finally, the LRC-TriCEPS-based proteomics screen yielded novel candidate receptors that interact with VSIG4.

Conclusions VSIG4 inhibits human T-cell activation in multiple assay formats and through numerous functional measurements. A group of T-cell receptors was found to be involved in novel interactions with VSIG4, and their potential roles in VSIG4-mediated regulation are currently being validated. Collectively, our work will lead to an enhanced mechanistic understanding of how VSIG4 suppresses T-cell activation and provide a strategy and tools for discovery of therapeutic relevant anti-VSIG4 antibodies.

REFERENCES

1. Liao *et al. Laboratory Investigation*. 2014; **94**: 706–715.
2. Zang *et al. J Clin Invest*. 2006; **116**: 2590–2593.
3. Helmy *et al. Cell*. 2006; **124**: 915–927.
4. Ries *et al. Cancer Cell*. 2014; **25**: 846–859.
5. Graversen *et al. Mol Ther*. 2012; **20**: 1550–1558.
6. Johnston *et al. Nature*. 2019; **574**: 565–570.
7. Frei *et al. Nat Biotechnol*. 2012; **30**: 997–1001.

486

COMPLEMENT DOWNREGULATION PROMOTES AN INFLAMMATORY SIGNATURE THAT RENDERS COLORECTAL CANCER SUSCEPTIBLE TO IMMUNOTHERAPY.

¹Silvia Guglietta*, ²Lukas Weber, ³Bruno Fosso, ³Marinella Marzano, ⁴Gary Hardiman, ⁵Monica Olcina, ⁶Mark Robinson, ¹Carsten Krieg. ¹Medical University of South Carolina, Charleston, SC, United States; ²Johns Hopkins Bloomberg School of Public Health, Baltimore, MD, United States; ³Consiglio Nazionale Ricerche, Bari, Italy; ⁴University of Belfast, Belfast, UK; ⁵University of Oxford, Oxford, UK; ⁶University of Zurich, Zurich, Switzerland

Background The role of inflammatory immune responses in colorectal cancer (CRC) development and response to therapy is a matter of intense debate. While inflammation is a known driver of CRC, inflammatory immune infiltrates are a positive prognostic factor in CRC and predispose to response to immune checkpoint blockade (ICB) therapy. Unfortunately, over 85% of CRC cases are primarily unresponsive to ICB due to the absence of an immune infiltrate and even the cases that show an initial immune infiltration can become refractory to ICB. The identification of therapy supportive immune responses in the field has been partially hindered by the sparsity of suitable mouse models to recapitulate the human disease. In this study, we aimed to understand how the dysregulation of the complement anaphylatoxin C3aR, observed in subsets of CRC patients, affects the immune responses, the development of CRC and response to ICB therapy.

Methods We used a comprehensive approach encompassing analysis of publicly available human CRC datasets, inflammation-driven and newly generated spontaneous mouse models of CRC, and multi-platform high dimensional analysis of immune responses using microbiota sequencing, RNASeq, and mass cytometry.

Results We found that patients' regulation of the complement C3aR is associated with epigenetic modifications. Specifically, down-regulation of *C3ar1* in human CRC promotes a tumor microenvironment characterized by the accumulation of innate and adaptive immune cells that support anti-tumor immunity. Using our novel spontaneous mouse model of CRC (APC^{Min/+}/C3aR^{-/-}) we showed that loss of C3aR resulted in enhanced immune infiltration in typically "cold" tumors and modified the intestinal microbiota. We also identified a species of *E. faecalis* that increased over time in the tumor microenvironment of APC^{Min/+}/C3aR^{-/-} mice. Notably, treatment with a-PD1 in APC^{Min/+}/C3aR^{-/-} but not APC^{Min/+} mice resulted in significant tumor reduction. Therefore, the lack of C3a in the colon activates a microbiota-mediated pro-inflammatory program, which promotes the development of tumors with an immune signature that renders them responsive to the ICB therapy.

Conclusions The complement system in the gastrointestinal tract is essential to avoid overt inflammation in health conditions. However, this regulatory mechanism may restrain the activation of immune responses during tumor development. Our findings reveal that C3aR may act as a previously unrecognized checkpoint to enhance anti-tumor immunity in CRC. C3aR can thus be exploited to overcome ICB resistance in a larger group of CRC patients.

Acknowledgements We would like to acknowledge the Italian Association of Cancer Research, the Umberto Veronesi foundation, the American Cancer Society and NIH P20GM130457 for supporting this study.

Ethics Approval All samples used in this study were obtained following individual informed consent and ethical approval by the National Research Ethics Service in the United Kingdom (ref 15/EE/0241).

<http://dx.doi.org/10.1136/jitc-2022-SITC2022.0486>

487 THE ROLE OF VSIG4 AS AN IMMUNO-REGULATORY PROTEIN IN CANCER

William Huang*, Michele Doucet, Rupashree Sen, Andrew Pardoll, Sudipto Ganguly. *Johns Hopkins University, Baltimore, MD, United States*

Background V-set and Ig domain-containing 4 (VSIG4; also known as CRIg) is a myeloid-restricted complement receptor indispensable for phagocytosis of C3-opsonized bacteria. Being a B7-family member, Vsig4 has also been described as a negative regulator of T cell activation. Murine Vsig4 expression is restricted to tissue-resident macrophages and notably absent in tumor-infiltrating macrophages. In contrast, human Vsig4 expression is more promiscuous- observed on circulating monocytes, dendritic cells, and macrophages within the ovarian tumor micro-environment (TME). Importantly, Vsig4 expression in the TME correlates with increased tumor burden and poor prognosis. Whether Vsig4 signals through a T cell counter-receptor is unknown. Similarly, the immuno-regulatory effects on tumors by non-infiltrating VSIG4⁺ tissue-resident macrophages have not been studied.

Methods Tumor growth inhibition was assessed *in vivo*. Peritoneal, splenic and intra-tumoral macrophages were analyzed by flow cytometry. Single-cell RNA sequencing was performed on human ovarian tumor tissue and on murine melanoma.

Results Vsig4 was detected on both resting and thioglycolate-elicited peritoneal macrophages as well as liver-resident Kupffer cells with little to no expression in splenic macrophages. *In vitro* differentiation of bone marrow precursors to M1 or M2 macrophages showed no differential expression of respective hallmark genes (NOS2 and Fizz-1) between wild-type and Vsig4^{-/-} precursors. Initially, our *in vivo* studies focused on the highly metastatic 4T1 model of breast cancer implanted orthotopically and found minimal Vsig4 expression (gene and protein) across different stages of tumor growth. However, when we implanted B16-F10 melanoma cells in VSIG4^{-/-} mice, we observed robust tumor growth inhibition relative to wild-type mice. A similar phenotype was seen in bone marrow chimeras (myeloablated wild-type recipients of Vsig4^{-/-} bone marrow), confirming the anti-tumor response was driven by the immune compartment. A dampened anti-tumor response in clodronate liposome-treated Vsig4^{-/-} mice confirmed that the phenotype was dependent on macrophages. Yet, conditional deletion of Vsig4 in macrophages (using a LysM-cre delete and Vsig4^{fl/fl} mice) did not phenocopy global knockouts when implanted with B16-F10 melanoma. *In vivo* Vsig4 expression kinetics revealed presence of Vsig4⁺ myeloid sub-populations in the bone marrow and liver of B16-F10 tumor-bearing mice with no early induction detected in the tumor or spleen.

Conclusions Vsig4 expression dynamics from myeloid progenitor to macrophage/ dendritic cell is being mapped. Transcriptomic/metabolic analyses of Vsig4⁺ myeloid populations from tumor-bearing mice will elucidate the temporal contribution of Vsig4 to immune regulation in cancer. Our goal is to develop Vsig4-targeting modalities targeting Vsig4 potentially in combination with PD-L1/1 and reset T-cell immunity in tumors.

Ethics Approval The study was approved by the Johns Hopkins OHSR-IRB (# IRB00287038). Participants gave informed consent before taking part.

All animal work was approved by the Animal Care and Use Committee (Protocol # MO22M67).

<http://dx.doi.org/10.1136/jitc-2022-SITC2022.0487>

488

GNUV201, A NOVEL HUMAN AND MOUSE CROSS-REACTIVE PD-1 MONOCLONAL ANTIBODY FOR CANCER IMMUNOTHERAPY

Haemi Kim, Kyoung-Jin Kim, Myeong Jin Yoon, Jenny Choih*, Eun Ji Cho, Hak-Jun Jung, Kwanghyun Lee, Jayoung Kim, Chae Gyu Park, Sungho Han, Donggoo Bae, Heungrok Park. *Genov, Seoul, Korea, Republic of*

Background Several PD-1 antibodies have been approved as anti-cancer therapies which work by blocking the interaction of PD-1 with its ligand PD-L1, thus restoring anti-cancer T cell activities. However, cross-reactive anti-PD-1 antibodies binding to both human and pre-clinically relevant animal models are still required to predict more precisely the efficacy and toxicity in humans, especially in various combination settings of anti-PD-1 with other treatments.

Methods Therefore, we have developed an anti-PD-1 named GNUV201, a highly selective and interspecies cross-reactive monoclonal antibody, with conventional hybridoma technology.

Results GNUV201 equally binds to mouse and human PD-1 (EC_{50} =32 pM and 28 pM, respectively), therefore successfully suppressed the growth of B16F10 (mouse melanoma) and MC38 (mouse colon cancer) in syngeneic mice models.

According to the results of co-crystal structure and alanine-scanning mutagenesis to examine the interaction mode between GNUV201 and human PD-1, the epitope recognized by GNUV201 is on the “FG loop” region of human PD-1, which is well conserved in both human and mouse PD-1, supporting GNUV201’s interspecies cross-reactivity; this position is distinct from those of Keytruda (“C’D loop”) and Opdivo (N-term). Notably, the structural feature in which the protruding epitope loop fits into GNUV201’s binding pocket supports the enhanced binding affinity due to slower dissociation (8.5 times slower than Keytruda in SPR). Furthermore, GNUV201 shows a stronger binding affinity at pH 6.0 ($K_D = 0.9$ nM at pH 6.0, 5.8 times smaller K_D than at pH 7.4), which mimics more closely the hypoxic and acidic tumor micro-environments (TME), especially due to further improved K_{off} (32.8 times slower dissociation than Keytruda in SPR). This phenomenon is not observed with other anti-PD-1 competitors, implying that GNUV201 achieves selective binding to and better occupancy on PD-1 in tumors compared to its marketed competitors. GNUV201 was also shown to completely block the interaction of hPD-1 with hPD-L1 *in vitro* at similar single digit nM levels compared with Keytruda and Opdivo, which results in enhanced T cell proliferation and cytokine (IL-2 and INF-g) secretion.

Conclusions In summary, even though similar *in vitro* efficacy of GNUV201, we can expect GNUV201 to be an excellent antibody candidate with superior target occupancy due to its slow dissociation and preferential binding in low pH tumor microenvironments and whose efficacy and toxicity in the human system can be predicted from preclinical study results due to its human-mouse cross-reactivity.

<http://dx.doi.org/10.1136/jitc-2022-SITC2022.0488>

489

NPX267, A FIRST-IN-CLASS MONOCLONAL ANTIBODY TARGETING KIR3DL3, BLOCKS HHLA2-MEDIATED IMMUNOSUPPRESSION AND POTENTIATES T AND NK CELL-MEDIATED ANTITUMOR IMMUNITY

¹McKenna Lamb*, ²Yao Wei, ²Xiaoxin Ren, ¹Rachel O'Connor, ¹Austin Dulak, ¹Matthew Rausch, ¹Jamie Strand, ¹Bijan Etemad-Gilbertson, ¹Riale Gilligan, ¹Scott Chappel, ³Tomonari Shigemura, ⁴David McDermott, ³Gordon Freeman, ²XingXing Zang. ¹NextPoint Therapeutics, Cambridge, MA, United States; ²Albert Einstein College of Medicine, Bronx, NY, United States; ³Dana-Farber Cancer Institute, Boston, MA, United States; ⁴Beth Israel Deaconess Medical Center, Boston, MA, United States

Background Killer cell immunoglobulin like receptor, three Ig domains and long cytoplasmic tail 3 (KIR3DL3) is a member of the killer cell Ig-like (KIR) receptor family and is expressed by both NK and T cells. KIR3DL3 has recently been shown to be a coinhibitory receptor for the B7 ligand, human endogenous retrovirus H long terminal repeat–associating protein 2 (HHLA2).^{1,2} KIR3DL3, expressed on T and NK cells in the tumor microenvironment, suppresses immune responses following engagement with HHLA2. Upon HHLA2-induced KIR3DL3 activation, SHP-1 and SHP-2 are recruited to KIR3DL3's cytoplasmic immunoreceptor tyrosine-based inhibitory motif (ITIM) and downstream activation signals are blunted. As a result, T and NK cell activity is suppressed. HHLA2 has limited expression in normal tissues, but is highly expressed in many cancers and is often associated with poor patient outcomes. In renal cell carcinoma (RCC), HHLA2 expression is often not co-expressed with PD-L1. However, co-expression of HHLA2 and PD-L1 in tumors from patients with RCC is associated with worse progression free survival that those with tumors exclusively expressing PD-L1. Thus, the KIR3DL3-HHLA2 axis represents a novel immune checkpoint pathway and blockade of KIR3DL3 signaling may be a promising strategy to promote antitumor immunity.³

Methods To explore the therapeutic potential of HHLA2-KIR3DL3 blockade, we generated NPX267, a first-in-class, monoclonal antibody that binds with high affinity to human KIR3DL3.

Results NPX267 blocks HHLA2 engagement with KIR3DL3 on primary human NK and T cells in a dose dependent fashion. The ability of NPX267 to block KIR3DL3-mediated suppression of T cell activation was assessed with a T cell reporter system and primary CD8⁺ T cell functional assays. KIR3DL3 blockade with NPX267 inhibited HHLA2-mediated suppression of T cell activation in a dose dependent manner. The anti-tumor activity of KIR3DL3 blockade with NPX267 was also demonstrated in NK-cell mediated cytotoxicity assays. NPX267 treatment augmented the ability of human NK cell lines and primary NK cells to kill HHLA2⁺ tumor cells in vitro. Finally, NPX267 blockade of HHLA2 mediated KIR3DL3 signaling enhanced anti-tumor immunity in humanized mouse models bearing HHLA2⁺ human tumors.

Conclusions Collectively, these data demonstrate that the KIR3DL3-HHLA2 pathway is a novel immune checkpoint axis that facilitates tumor escape by attenuating both innate and adaptive antitumor immune responses. NPX267, a first-in-class KIR3DL3 blocking antibody, potentiates anti-tumor immunity against HHLA2⁺ tumors and may represent a promising approach to treat certain cancers.

REFERENCES

1. Bhatt RS, Berjts A, Konge JC, *et al.* KIR3DL3 is an inhibitory receptor for HHLA2 that mediates an alternative immunoinhibitory pathway to PD1. *Cancer Immunol Res* 2021;**9**:156–169.

2. Wei Y, Ren X, Galbo PM, *et al.* KIR3DL3-HHLA2 is a human immunosuppressive pathway and a therapeutic target. *Science Immunol.* 2021;**6**: eab9792.
3. Ying H, Xu Y, Zhang X, *et al.* Human endogenous retrovirus-H long terminal repeat-associating 2: The next immune checkpoint for antitumor therapy. *EBioMedicine* 2022;**79**:103987.

<http://dx.doi.org/10.1136/jitc-2022-SITC2022.0489>

490

GALECTIN-9 DRIVES TIM-3+ NATURAL KILLER CELL DYSFUNCTION IN HEAD AND NECK SQUAMOUS CELL CARCINOMA

<http://dx.doi.org/10.1136/jitc-2022-SITC2022.0490>

¹Lazar Vujanovic*, ¹Juncheng Wang, ¹Housaiyin Li, ²Aditi Kulkarni, ²Jennifer Anderson, ¹Lidia Arantes, ¹Hridesh Banerjee, ¹Lawrence Kane, ³Xin Zhang, ¹Tullia Bruno, ¹Riyue Bao, ¹Robert Ferris. ¹University of Pittsburgh, Pittsburgh, PA, United States; ²UPMC Hillman Cancer Center, Pittsburgh, PA, United States; ³Xiangya Hospital, Changsha, China

Background Natural killer (NK) cells are innate cytotoxic and immunoregulatory lymphocytes that play a critical role in tumor immunosurveillance. Their activation states are regulated by an interplay of activating and inhibitory surface receptors, including T-cell immunoglobulin and mucin-domain containing molecule 3 (TIM-3), an immune checkpoint receptor (ICR) that is expressed on terminally-differentiated NK cells. The role TIM-3 plays in the context of NK cell-mediated anti-tumor response remains evasive, partly because TIM-3 has four known ligands: galectin-9, phosphatidylserine, HMGB1 and CEACAM-1.

Methods In the context of head and neck squamous cell carcinoma (HNSCC), single-cell RNA sequencing and flow cytometry were implemented to study the prevalence, phenotypes and functional differences of TIM-3+ NK cells in patient tumors and blood. *In vitro* killing and proliferation assays were used to evaluate whether the four TIM-3 ligands differentially modulate TIM-3+ NK cell functions and whether abrogation of TIM-3/ligand interaction is a valid therapeutic strategy to enhance NK cell-mediated anti-tumor effector mechanisms. Finally, TCGA survival analysis and digital spatial profiling were employed to study the potential impact of etiology-associated differences on HNSCC patient survival.

Results We demonstrate that TIM-3 is the dominant NK cell ICR, that it marks dysfunctional NK cells in tumors but not in circulation, and that galectin-9 is the only TIM-3 ligand that consistently suppresses NK cell cytotoxic and proliferative capacity. Galectin-9-induced effects on cytotoxicity can be abrogated using the clinical-grade anti-TIM-3 blocking antibody, MBG453. Clinically, high intratumoral TIM-3+ NK cell gene signature associates with worse outcome in HPV+, but not HPV- HNSCC patients. This may be due to higher intratumoral galectin-9 protein expression in HPV+ HNSCC lesions, as well as higher frequencies of circulating and tumor-infiltrating TIM-3+ NK cells in HPV+ patients.

Conclusions Our data stress the importance of TIM-3 in the context of NK cells and suggest that targeting the TIM-3/galectin-9 pathway may be a cogent immunotherapeutic strategy to reinvigorate NK cell effector function in HPV+ HNSCC patients.

Acknowledgements We thank Merida Serrano, Amy Cuda and Denise Kroll for assistance with patient sample procurement. This research utilized the Hillman Cancer Center Flow Cytometry Core Facility, supported in part by award P30 CA047904 (RLF). This research was supported in part by the University of Pittsburgh Center for Research Computing through the resources provided. Specifically, this work used the HTC cluster, which is supported by NIH award number S10OD028483.

Ethics Approval Peripheral blood and tumor tissues from treatment-naïve HNSCC patients were collected with their written consent in accordance with the Declaration of Helsinki, under the University of Pittsburgh Cancer Institute Review Board-approved protocol (99-069).

491

PRECLINICAL PHARMACOLOGY MODELING OF HX009, A CLINICAL STAGE FIRST-IN-CLASS PD-1/CD47 BSAB, FOR ANTI-LYMPHOMA APPLICATIONS

¹Xiaoyu An, ²Henry Li*, ²Hang Ke, ¹Lingxin Xiong, ²Faming Zhang, ¹Mingfa Zang, ¹Xiaolong Tu, ¹Jingjing Wang, ¹Demi Liu, ¹Cen Chen, ³Cunxiang Ju, ³Xianfei He, ²Lei Zhang. ¹Crown Bioscience Inc, San Diego, CA, United States; ²Hanx Pharmaceuticals, Inc., Wuhan, China; ³Shanghai Model Organisms Center, Inc., Shanghai, China

Background The important immune checkpoint inhibitors (ICIs), e.g. PD1/PD-L1 and CD47/SIRP α blockers, have yet to be successful for the majority of non-Hodgkin's lymphoma (NHL), albeit efficacious in NK/T-cell and Hodgkin's lymphoma, as well as in many solid tumors. CD47 targeting in the clinic, predominantly for lymphoma and AML remains challenging due to reported toxicities (e.g. anemia/thrombocytopenia) as well as insufficient efficacy. Many important lymphomas, e.g. T-cell lymphoma, relapsed/refractory DLBCL etc., remain to be unmet medical needs, warranting new treatment options, particularly immunotherapies. We hypothesized that the dual targeting both innate (CD47) and adoptive (PD-1) immune check points with a bi-specific antibody (BsAb) can significantly enhance efficacy, and that the hematological toxicity can be minimized through specific engineering.

Methods HX009, a 2x2 symmetric BsAb molecule targeting PD1/CD47, was designed and constructed by grafting a low affinity SIRP α to the 3' of Fc HX008 (anti-PD1 IgG1-Mab) frame with weakened CD47 binding. A series of *in vitro* characterizations on the target binding and functional blocking were performed, followed by *in vivo* pharmacology modeling using several preclinical lymphoma models (10mg/kg, twice weekly, i.p.), including subcutaneous xenograft (Karpas-299-T/Raji-B lymphoma), patient-derived lymphoma xenografts (PDXs), and humanized mouse syngeneic B-cell lymphoma A20 (HuGEMMTM PD1Xcd47). Tumor growth inhibition (TGI) was calculated by measuring tumor volume biweekly.

Results HX009 target binding, ligand blocking and biological effects were confirmed *in vitro*, with little binding to RBCs along as little hematological toxicity in the NHP studies due to the confirmed reduced affinity to CD47. All tested xenograft modeling using T/B- cell lymphoma CDXs and PDXs revealed strong anti-lymphoma activity by HX009, which was solely attributed to the CD47 targeting due to the lack of T-cell immunity in the xenografts. The humanized syngeneic mouse B-lymphoma A20 model with the presence of competent autologous immune-system revealed that both single targeting, either PD1 (HX008) or CD47 (SIRP α), had anti-tumor activity, while the dual targeting of both by HX009 caused synergistic anti-tumor activity. Finally, a panel of fully annotated lymphoma PDXs were tested in order to discover potential predictive biomarkers.

Conclusions HX009 demonstrated strong preclinical anti-lymphoma activity of HX009, confirming the contributions from both targeting MOAs (CD47/PD1), as well the superior activity of dual targeting as designed, validating our hypothesis. A Phase I/II study for this first-in-class BsAb is ongoing in patients with relapsed/refractory lymphoma, including both B and T cell subtypes (ClinicalTrials.gov Identifier: NCT05189093).

<http://dx.doi.org/10.1136/jitc-2022-SITC2022.0491>

492

SIRP α BLOCKADE RESULTS IN TUMOR INTRINSIC AND IMMUNE MICROENVIRONMENT EFFECTS RESULTING IN THE INHIBITION OF BREAST-TO-BRAIN METASTASIS

Elizabeth Stirling, Jessica Mackert*, Steven Bronson, Adam Wilson, Mitra Kooshki, Dawen Zhao, Pierre Triozzi, Glenn Lesser, David Soto-Pantoja. *Wake Forest School of Medicine, Winston-Salem, NC, United States*

Background Triple-negative breast cancer (TNBC) is a highly aggressive subtype of breast cancer characterized by a lack of specific targets and a 35% incidence of brain metastasis. There is no targeted treatment for managing brain metastasis associated with TNBC; therefore, new strategies are urgently needed to overcome disease mortality. The CD47/SIRP α signaling pathway is implicated in tumor progression due to bypassing innate and adaptive immune surveillance. Most strategies targeting this pathway focus on targeting the receptor CD47; however, targeting SIRP α as a potential strategy to mitigate metastatic tumor burden remains understudied.

Methods Breast cancer patient biopsies were stained with antibodies against SIRP α . A Real-Time Cell Analysis (RTCA) impedance assay was used to determine migration, proliferation, and microglia-mediated cancer cell clearance changes. Female BALB/C mice were used in a TNBC brain metastasis model by intracardiac injection of the 4T1-Br3-Luc cell line. Brain metastatic burden was measured by the *in vivo* imaging system (IVIS) and quantified by luciferase luminescence. Differences in protein expression were measured by proteomic digital spatial profiling (DSP) of brain lesions and immune infiltrated regions of interest (ROIs).

Results Immunohistochemical staining of patient biopsies revealed a 3.5-fold increase in SIRP α expression in metastatic lesions compared to the primary tumor (n=19; p \leq 0.0001). Additionally, there was an 84% increase in SIRP α in brain-trophic 4T1-Br3 TNBC cells compared to 4T1 parental cells (n=3; p \leq 0.05). RTCA impedance assay revealed that SIRP α blockade inhibits brain-trophic 4T1-br3 cell migration (24h; n=3; p \leq 0.05) and proliferation (48h; n=3; p \leq 0.05) and promotes microglia-mediated cancer cell clearance (n=3; p \leq 0.05). Furthermore, SIRP α blockade reduced metastatic brain lesion formation *in vivo* by approximately 90%, determined by IVIS imaging (n=4-7; p \leq 0.05). DSP of the brain lesions revealed that immune checkpoints cluster of differentiation 152 (CTLA4), programmed cell death protein 1 (PD-1), programmed death ligand-1 (PD-L1), and cluster of Differentiation 276 (CD276 or B7-H3) were significantly reduced in anti-SIRP α treated brain lesions (n=3-6; p \leq 0.05). Furthermore, spatial profiling revealed that SIRP α blockade promotes pro-inflammatory microglia polarization in brain lesions (n=3-6; p \leq 0.01). Additionally, the extracellular matrix protein fibronectin, which contributes to invasion, metastasis, and immune evasion, was reduced by 70% in anti-SIRP α -treated brain lesions (n=3-6; p \leq 0.05).

Conclusions These data suggest that SIRP α blockade modulates immune and TNBC cells to limit metastatic spread. Therefore, targeting SIRP α may be a new immunotherapeutic strategy to treat TNBC brain metastasis.

<http://dx.doi.org/10.1136/jitc-2022-SITC2022.0492>

493

PH-804, AN INTASYL SELF-DELIVERING RNAI COMPOUND THAT TARGETS TIGIT ENHANCES NK CELL CYTOTOXICITY TO TUMOR CELLS

Melissa Maxwell*, Dingxue Yan, Brianna Rivest, Andrew Boone, Shenghua Zhou, Benjamin Cuffio, James Cardia, Simon Fricker. *Phio Pharmaceuticals, Marlborough, MA, United States*

Background NK cells act as the body's first line of defense against cancer cells. They quickly recognize and kill tumor cells without prior exposure. Adoptive cell therapy (ACT) using NK cells shows promise against hematological cancers. Cytotoxic activity of these cells is restricted by inhibitory receptors that reduce NK cell-mediated cytotoxicity. Overcoming this inhibition would allow for a more potent antitumor response following ACT and potential application against solid tumors. We have developed a new class of stable, self-delivering RNAi compounds (INTASYL) that incorporate features of RNAi and antisense technology. INTASYL compounds demonstrate potent activity, stability, and are rapidly and efficiently taken up by cells. INTASYL PH-804 targeting the inhibitory receptor TIGIT enhances the cytotoxic activity of expanded human NK cells in vitro.

Methods Primary human CD56⁺ NK cells were expanded using the ImmunoCult™ NK Cell Expansion Kit from Stem-Cell Technologies. Following the 14-day expansion protocol, cells were collected, and the cell density was adjusted to 0.5 x 10⁶ cells/mL in culture media containing IL-2. Cells were seeded directly into 24-well plates containing PH-804 ranging in final concentration from 1 μM to 5 μM. Taqman gene expression assays were used to determine expression levels of TIGIT following the RNA-to-Ct 1-step protocol. In addition, cells were stained using fluorescently labeled antibodies for flow cytometry. Cytotoxic capabilities of the PH-804 transfected NK cells against the K562 (Chronic Myelogenous Leukemia) cancer cell line were tested in a DELFIA cell cytotoxicity assay.

Results Transfection with PH-804 results in consistent mRNA and protein silencing without negative impact on NK cell viability. For example, treatment with 5 μM PH-804 results in a 60% reduction in TIGIT mRNA. The reduction is seen at >7 days post-transfection and results in a 45% reduction in surface expression of TIGIT by flow cytometry. Silencing of TIGIT with PH-804 resulted in increased expression of markers of NK cell activation and increased cytotoxic capabilities of NK cells against K562 cancer cells in the DELFIA cell cytotoxicity assay.

Conclusions Here, we demonstrate the potential of PH-804 to improve NK cell potency in ACT. By treating NK cells with INTASYL targeting the inhibitory receptor TIGIT ex vivo, during NK cell expansion, the anti-tumor response of these cells was enhanced potentially resulting in a more effective cell therapy for solid tumors and hematological malignancies.

<http://dx.doi.org/10.1136/jitc-2022-SITC2022.0493>

494

CO-1: A NOVEL POTENT DUAL FUNCTION ANTI-CD47 ANTIBODY FOR CANCER THERAPY

Sittana Matar*, Seham Skah, Rolf Pettersen, Kjetil Hestdal, Nina Richartz. *Caedo Oncology, Oslo, Norway*

Background CD47 is a central part of the innate immune system through its interaction with signal regulatory protein alpha (SIRP α). This interaction is known as the “don't eat me” signal which inhibits cell phagocytosis by innate immune cells.^{1,2} Cancer cells often evade recognition by the hosts' immune cells through overexpression of CD47, and several anti-CD47 monoclonal antibodies (mAbs) are undergoing development to inhibit this interaction.³ Some anti-CD47 mAbs have been shown to have potential as treatment of human malignancy, but generally only in combination with other chemotherapeutic agents as their functionality primarily is due to the inhibition of the phagocytic signal.^{1,4} Here, we characterize CO-1, a novel bifunctional anti-CD47 mAb that is capable of eradicating cancer cells through direct induction of programmed cell death (PCD) as well as by enhancing cancer cell phagocytosis.

Methods The binding properties of CO-1 to a wide range of cancer cell lines derived from solid and hematological tumors was determined by incubating the cells to FITC-conjugated antibodies, followed by flow cytometry analysis. The induction of PCD after treatment with different anti-CD47 mAbs at different time points was determined by Annexin V staining.⁵

The enhancement of tumor cell phagocytosis induced by CO-1 was determined by co-culturing DiO-labelled RAW264.7 macrophages with CFSE-labelled target cell lines. Double-positive DiO-RAW264.7 and CFSE-target cells indicated phagocytosed cells.

Xenograft models were established by injecting lentivirally transduced cancer cells into NOD-*scid* IL2R γ^{null} (NSG) mice. The lentiviral vector contained sequences for firefly luciferase and enhanced green fluorescent protein.⁶

Results CO-1 binds to cancer cells with high efficiency and induces rapid (within 3 hours) and profound cell death in several cell lines derived from human hematological and solid tumors. No direct correlation was evident between CD47 expression and PCD response. In a xenograft model of B cell precursor acute lymphoblastic leukemia (BCP-ALL) in NSG mice, the mice were rapidly cured of their tumor even after only two injections of CO-1 as monotherapy. This demonstrates the PCD potency of CO-1 towards human tumor cells directly. Next, we determined the ability of CO-1 to block the “don't eat me” interaction and found that CO-1 potently and significantly enhanced tumor cell phagocytosis, even in cell lines that previously had responded less favorably with PCD to CO-1 treatment.

Conclusions CO-1 is a new and unique bifunctional anti-CD47 mAb that eradicates cancer cells by two mechanisms of action: 1) by direct induction of PCD, and 2) by enhancing cancer cell phagocytosis.

REFERENCES

1. J Huang, F Liu, C Li, X Liang, C Li, Y Liu, Z Yi, L Zhang, S Fu, Y Zeng. Role of CD47 in tumor immunity: a potential target for combination therapy. *Scientific Reports* 2022;**12**. 10.1038/s41598-022-13764-3.
2. S Kaur, JS Isenberg, DD Roberts. CD47 (Cluster of Differentiation 47). *Atlas Genet Cytogenet Oncol Haematol* 2021;**25**:83–102.
3. Z Jiang, H Sun, J Yu, W Tian, Y Song. Targeting CD47 for cancer immunotherapy. *J Hematol Oncol* 2021;**14**:180. 10.1186/s13045-021-01197-w.

4. Y Huang, Y Ma, P Gao, Z Yao. Targeting CD47: the achievements and concerns of current studies on cancer immunotherapy. *Journal of Thoracic Disease* 2017;**9**: E168–E174. 10.21037/jtd.2017.02.30.
5. I Vermees, C Haanen, H Steffens-Nakken, C Reutellingsperger. A novel assay for apoptosis: Flow cytometric detection of phosphatidylserine expression on early apoptotic cells using fluorescein labelled Annexin V. *Journal of Immunological Methods* 1995;**184**: 39–51. [https://doi.org/10.1016/0022-1759\(95\)00072-1](https://doi.org/10.1016/0022-1759(95)00072-1).
6. S Bomken, L Buechler, K Rehe, F Ponthan, A Elder, H Blair, CM Bacon, J Vormoor, O Heidenreich. Lentiviral marking of patient-derived acute lymphoblastic leukaemic cells allows in vivo tracking of disease progression. *Leukemia* 2013;**27**:718–721. 10.1038/leu.2012.206.

Ethics Approval The study was conducted under adherence with the Declaration of Helsinki. Animals were kept under appropriate housing conditions with food and water ad libitum. All animal experiments were approved by the Norwegian Food Safety Authorities.

<http://dx.doi.org/10.1136/jitc-2022-SITC2022.0494>

495

BYON4228, A PAN-ALLELIC SIRP α BLOCKING ANTIBODY WITH A FAVORABLE PRE-CLINICAL SAFETY PROFILE, ENHANCES ANTI-TUMOR IMMUNITY IN VITRO AND IN VIVO

¹Mary van Helden*, ¹Roel Arends, ¹Seline Zwarthoff, ¹Monique van der Vleuten, ¹Marc Paradé, ¹Karin de Laat-Arts, ²Hugo Olsman, ¹Ellen Mattaar, ¹Dirk Claudemans, ¹Daniëlle van Wijk, ¹Lilian Driessen-Engels, ¹Inge Reinieren-Beeren, ¹Paul Boersema, ¹Eva Hanckmann, ¹Gerard Rouwendal, ¹Ruud Ubink, ¹Miranda van der Lee, ¹Gijs Verheijden, ¹Wim Dokter, ¹Timo van den Berg. ¹*Byondis, Nijmegen, Netherlands*; ²*Sanquin Research, Amsterdam, Netherlands*

Background Preclinical data have established CD47-SIRP α interactions as a myeloid immune checkpoint in cancer, which is corroborated by preliminary evidence from the first clinical studies with CD47 blockers.

Methods However, the ubiquitously expressed CD47 mediates functional interactions with other ligands as well, and therefore targeting of the primarily myeloid cell-restricted inhibitory immunoreceptor SIRP α may represent a better strategy.

Results Here, we present preclinical results on a novel clinical candidate, BYON4228. BYON4228 is an antibody directed against SIRP α and recognizes both of the common allelic variants of human SIRP α which maximizes its potential clinical application in the broad human population. Notably, in contrast to several other anti-SIRP α antibodies in development, BYON4228 does not recognize the closely related T cell-expressed SIRP γ that has been reported to mediate interactions with CD47 as well, which are known to be instrumental in T cell extravasation and activation. BYON4228 binds to the N-terminal part of SIRP α and its epitope overlaps with the CD47-binding site. BYON4228 therefore prevents binding of CD47 to SIRP α and thus blocks inhibitory signaling through the CD47-SIRP α axis. Functional studies show that BYON4228 potentiates both macrophage- and neutrophil-mediated elimination of hematologic and solid cancer cells *in vitro* in the presence of several different tumor targeting antibodies like trastuzumab, rituximab, daratumumab and cetuximab, illustrating the broad potential clinical benefit and application of BYON4228. BYON4228 enhanced the efficacy of rituximab treatment *in vivo* when administered to human Non-Hodgkin lymphoma (NHL)-engrafted transgenic mice with a selective expression of huSIRP α_{BIT} on myeloid cells (huSIRP α_{BIT} -scid mice). Single intravenous infusion of up to 100 mg/kg BYON4228 to male and female cynomolgus monkeys was well tolerated and did not elicit any adverse effects.

Conclusions Collectively, this defines BYON4228 as a pan-allelic anti-SIRP α antibody without T cell SIRP γ recognition that promotes the destruction of antibody-opsonized cancer cells. Clinical studies are planned to start in 2022.

Ethics Approval Appropriate ethics approvals were present before commencing studies *in vivo*.

<http://dx.doi.org/10.1136/jitc-2022-SITC2022.0495>

496

HCB101: A SAFE AND EFFECTIVE LIGAND TRAP THERAPEUTIC TARGETING THE CD47-SIRPA SIGNALING PATHWAY FOR CANCER TREATMENT

Jiin-Tarng Wang, Chi-Ling Tseng, Han-Feng Teng, Pan-Hsien Kuo, Yun-Chih Cheng, Yi-Jing Chen, Yi-Hsuan Lu, Tsai-Kuei Shen, Hong-Fan Wang, Pei-Lun Tsai, Yu-Chen Wu, Chien-Hsin Ho, Wei-Tse Sun, Yen-Cheng Li, Yi-Hsuan Lee, Zong Sean Juo*. *HanchorBio Inc., Taipei, Taiwan*

Background Macrophages patrol intercellular spaces mainly through their receptor SIRPa, which interacts with CD47 on target cells. Such interaction elicits a 'do not eat' signal and spares the target cell from being phagocytosed. Many cancers take advantage of this mechanism via overexpressing CD47 to evade immune surveillance. Therefore, blocking SIRPa-CD47 interaction represents a promising approach for anti-cancer therapy. Numerous anti-CD47 antibodies and SIRPa fusion proteins have been developed with therapeutic potential, but their clinical progress was hindered by either severe side effects or lack of appreciable efficacy. To overcome this deficiency, we aim to produce a SIRPa-fusion biologic that exhibits superior efficacy against multiple hematological and solid malignancies while maintaining good safety profiles and protein stability.

Methods Using display technology combined with structure-guided protein engineering, we identified several SIRPa mutants that exhibited significant CD47-blocking activities and phagocytosis against tumor cells while minimizing side effects on CD47-expressing normal cells. To assess the impact of CD47 blockade on macrophages within the tumor microenvironment, these novel mutants were evaluated in multiple human tumor xenograft mouse models and compared with selected anti-CD47 monoclonal antibodies and/or SIRPa fusion proteins currently being investigated in clinical trials. The leading candidates were further analyzed for their respective CMC profiles to ensure good protein stability and straightforward manufacturability.

Results In comparison with prominent clinical candidates targeting the CD47 pathway (Magrolimab, TTI-622, ALX148, TJC4, IMM01), HCB101 demonstrated superior or compatible CD47-blocking activities; meanwhile, it triggered strong phagocytosis against tumor cells but not red blood cells. In all 7 human tumor xenograft NOD/SCID mouse models that we investigated, HCB101 consistently showed excellent efficacy against hematological and solid tumors as monotherapy, with tumor growth inhibition index (TGI) ranging from 60-100% at the dose of 0.5-10mg/kg over placebo. We observed an increase in the M1/M2 macrophage ratio and a reduction of CD24 expression in certain cases after the treatment with HCB101. This could partially account for its superior anti-tumor efficacy. There was no apparent adverse reaction observed during the exploratory cynomolgus monkey toxicology studies, suggesting a good safety profile of HCB101.

Conclusions Compared to relevant clinical candidates, HCB101 exhibits superior efficacy in 7 different CDX models of hematological and solid malignancies while maintaining good safety profiles. A highly effective blockade of the CD47-SIRPa pathway by HCB101 leads to robust pre-clinical results. Moreover, it exhibits outstanding protein stability and manufacturing characteristics for large-scale production. Clinical development of HCB101 is currently underway both as monotherapy and in combination.

<http://dx.doi.org/10.1136/jitc-2022-SITC2022.0496>

497

EVALUATION OF THE TIGIT+ IMMUNE SUBSET DEPLETION EFFECT OF THE ANTI-TIGIT ANTIBODY M6223

¹Chunxiao Xu*, ¹Sireesha Yalavarthi, ¹Clotilde Bourin, ¹Jacques Moisan, ²Andree Blaukat, ²Laura Helming. ¹EMD Serono, Billerica, MA, United States; ²The Healthcare Business of Merck KGaA, Darmstadt, Germany

Background T cell immunoreceptor with immunoglobulin and immunoreceptor tyrosine-based inhibitory motif domains (TIGIT) is an inhibitory receptor expressed on lymphocytes and has recently emerged as a target in cancer immunotherapy. M6223 is a fully human antagonistic anti-TIGIT antibody in immunoglobulin (Ig) G1 format with Fc-mediated effector function. Preclinical studies demonstrated that M6223 can induce an anti-tumor immune response by complementary mechanisms, including but not limited to: direct blockade of the TIGIT pathway; stimulation of costimulatory receptor CD226 dimerization/activation; and depletion of TIGIT+ immune subsets by Fc-mediated effector function. This study was designed to understand the mechanism of action of the depletion effect.

Methods The TIGIT+ immune subset depletion effect of M6223 in the tumor microenvironment (TME) was investigated in humanized TIGIT knock-in mice using a flow cytometry assay. The anti-tumor efficacy of two chimeric M6223 antibodies, one with an effector competent mouse IgG2c constant region (M6223-muIgG2c) and the other with an effector null mouse IgG1-D256A constant region (M6223-muIgG1), was investigated in syngeneic tumor models in humanized TIGIT knock-in mice.

Results M6223 dose-dependently depleted TIGIT+ immune subsets in the TME at day 1 post-treatment, but had no significant effect on total infiltrated CD8+ T cells and natural killer (NK) cells. The depletion effect gradually weakened over time but remained at day 7 and day 14. M6223 treatment stimulated CD8+ T cell and NK cell infiltration and boosted CD226 expression at day 7 and day 14 post treatment. The ratio of CD226 to TIGIT was significantly increased in immune subsets at all time points tested. Further studies demonstrated that only M6223 surrogate with effector function could deplete TIGIT+ immune subsets at day 1; the effector null version of M6223 slightly decreased TIGIT-expressing immune subsets on day 7 and day 14. In addition, this effector null surrogate version of M6223 did not have anti-tumor efficacy in syngeneic tumor models in humanized TIGIT knock-in mice.

Conclusions The results demonstrate that innate depletion of TIGIT+ immune subsets by Fc-mediated effector function plays an important role in anti-tumor immunity and suggest that immune pharmacodynamics in clinical trials should be closely monitored at early time points. Currently, M6223 is being evaluated in combination with avelumab as first-line maintenance therapy for advanced urothelial carcinoma in the phase 2 JAVELIN Bladder Medley umbrella trial (NCT05327530).

<http://dx.doi.org/10.1136/jitc-2022-SITC2022.0497>

498

PRECLINICAL CHARACTERIZATION OF OR502, AN ANTI-LILRB2 ANTIBODY THAT RESCUES INNATE AND ADAPTIVE IMMUNE RESPONSES FROM LILRB2 MEDIATED IMMUNE SUPPRESSION

Meghan Zuck*, Myriam Bouchlaka, Huyen Dinh, Kevin Green, Meilyn Sylvestre, Francisco Zapata, Ramya Chandrasekaran, Gajendra Naika, Lauren Loh, Ray Fox, Darbie Whitman, Tom Graddis, Kamal Puri, Peter Probst. *OncoResponse, Seattle, WA, United States*

Background The inhibitory receptor leukocyte immunoglobulin-like receptor subfamily B member 2 (LILRB2, ILT4) is expressed on immunosuppressive myeloid cells and expression correlates with poor survival in multiple cancers and contributes to anti-PD1 resistance. Interaction of LILRB2 with HLA class I ligands (e.g., HLA-G, HLA-A, etc.) mediates immune suppression by myeloid cells and promotes tumor immune evasion in the tumor microenvironment (TME). Blocking this interaction may enhance efficacy of T cell checkpoint inhibitors. Antibodies targeting LILRB2 are currently being evaluated in clinical trials for the treatment of cancer.

Methods Anti-LILRB2 antibodies were cloned from B cells derived from rabbits immunized with human LILRB2 recombinant protein. Clones were humanized after selection based on activity in a panel of functional and phenotypic assays using primary human macrophages and T cells. Humanized variants were screened for their ability to rescue T cell activity (proliferation and IFN- γ) from M2c macrophage-mediated suppression and enhance LPS-induced IFN- γ production by PBMCs. The top variants were also evaluated for cytokine release in whole blood. The pharmacokinetic profiles of lead LILRB2 antibodies were determined in humanized FcRn mice.

Results We have identified a panel of humanized anti-LILRB2 antibodies that specifically bind to human LILRB2-expressing cell lines and human myeloid cells without detectable binding to other LILRA or LILRB family members. These antibodies block LILRB2 interaction with HLA-G expressed on tumor cells. The lead antibody, OR502, enhanced LPS-induced IFN- γ production by PBMCs, and relieved M2c macrophage-mediated suppression of proliferation and IFN- γ secretion by anti-CD3-activated human CD8⁺ T cells in coculture assays. Furthermore, OR502 restored the ability of exhausted T cells to secrete IFN- γ in the presence of M2c macrophages and significantly enhanced the activity of pembrolizumab in combination studies. OR502-treatment did not trigger inflammatory cytokine release or activation of neutrophils in human whole blood. The pharmacokinetics of OR502 in humanized FcRn mice demonstrated a half-life of 6-10 days.

Conclusions We have identified a novel humanized anti-LILRB2 antibody, OR502, that restores innate and adaptive immune responses by modulating immunosuppressive myeloid cells. These data provide a strong rationale for further development of OR502 for cancer treatment.

<http://dx.doi.org/10.1136/jitc-2022-SITC2022.0498>

499

**THE SMALL MOLECULE PD-L1 INHIBITOR CCX559
PREFERENTIALLY ACCUMULATES IN TUMORS,
RESULTING IN DEPLETION OF CELL-SURFACE PD-L1 IN
A MURINE PRECLINICAL MODEL**

Kathleen Sullivan*, Linda Ertl, Zhenhua Miao, Pingchen Fan, Yibin Zeng, Carolyn Dunlap, Karen Ebsworth, Suprit Gupta, Shijie "Chris" Li, Ton Dang, Shichang Miao, Israel Charo, Thomas Schall, Penglie Zhang. *ChemoCentryx, San Carlos, CA, United States*

Background The small molecule CCX559 is a novel, highly potent inhibitor of human PD-L1 (hPD-L1) in development as an oral treatment for cancer patients.^{1,2} *In vitro* studies showed that CCX559 inhibits PD-L1 binding to PD-1 and induces PD-L1 internalization from the cell surface. To investigate the mechanism of action *in vivo*, we examined the effect of CCX559 distribution and clearance on tumor cell PD-L1 dynamics and anti-tumor activity.

Methods CCX559 was administered orally at the clinically relevant dose of 30 mg/kg once daily for 7 days to human PD-L1 knock-in mice bearing MC38 tumors (average volume 60-100 mm³). The MC38 cells were engineered to express hPD-L1, as CCX559 does not cross-react with mouse PD-L1. CCX559 levels in tumors and organs, including lung, liver, kidney, spleen, heart, and brain, were quantitated by mass-spectrum analysis at 1, 5 and 12 days after the last dose. Cell surface and intracellular PD-L1 were detected using flow cytometry and immunohistochemistry.

Results Dosing CCX559 for 7 days significantly reduced hPD-L1-MC38 tumor growth compared to vehicle control, and the reduction in tumor volume persisted post dosing until the end of study. The average CCX559 level on day 1 post dose was significantly higher in tumors than plasma and other organs (27.9 µg/g tissue vs. 0.007 – 1.4 µg/g). In tumors CCX559 induced hPD-L1 internalization into intracellular vesicles and reduced the cell surface level by over 90% compared to vehicle control. CCX559 levels dropped 98% in plasma, tumor and tissues by day 5 post dose, but the level in the tumors was still above the IC₉₀ for inhibiting PD-L1; consistent with this, intracellular PD-L1 was also observed. The drug was completely cleared by day 12 post dose, but tumor cell surface hPD-L1 in the CCX559 arm was only partially recovered compared to the vehicle control.

Conclusions In a preclinical model, higher levels of CCX559 were observed in tumors than in plasma and other organs. Cessation of dosing led to clearance of CCX559 within days, but recovery of tumor cell surface PD-L1 levels was delayed, perhaps as a result of higher CCX559 levels in the tumor. The *in vivo* properties of CCX559 suggest that PD-L1 inhibition in tumors may be achieved at relatively low drug levels in the periphery, thus mitigating potential risk of adverse events. No DLTs, treatment-related SAEs or severe (Grade 3 or higher) AEs have been reported in an ongoing first-in-human dose escalation trial with CCX559 (ACTRN12621001342808).

REFERENCES

1. Chris Li, *et al.* CCX559 is a potent orally-administered small molecule PD-L1 inhibitor that induces anti-tumor immunity. *Cancer Research* 2021;**81**(13_Suppl): Abstract nr 1274.
2. Gonzalo Tapia *et al.* Preliminary data from an ongoing phase 1 dose-escalation study of CCX559, an orally administered small molecule PD-L1 inhibitor, in patients with advanced solid tumors. *Journal of Clinical Oncology* 2022;**40**(16_Suppl): 2593.

<http://dx.doi.org/10.1136/jitc-2022-SITC2022.0499>

500

INV322, A TME SELECTIVE CD25 X CTLA4 BISPECIFIC ANTIBODY APPROACH FOR DEPLETION OF TUMOR RESTRICTED TREGS

¹Anna Ritter*, ¹Nicholas Marshal, ¹Dileep Pulukkunat, ¹Nikhil Pereira, ²Alexander Rakhmievich, ¹Joseph Gawdzik, ¹Jessica Wiwczar, ¹Jason Russell, ¹Laura McCormick, ¹Catherine Aversa, ²Paul Sondel, ¹Hilario Ramos, ¹Bonnie Hammer, ¹Daniel Pereira. ¹Invenra, Madison, WI, United States; ²University of Wisconsin, Madison, WI, United States

Background Tregs maintain immune homeostasis in healthy individuals by limiting excessive or aberrant immune responses to environmental or self-triggers. In the context of tumor immunity, Tregs are associated with increased tumor progression, poor patient prognosis, and limited responsiveness to immunotherapeutic approaches. Targeting of Tregs has shown promise in the clinic, though current approaches are limited by on-target, off-tumor induction of autoimmune related toxicities associated with global Treg blockade. To overcome these toxicities and improve efficacy, Invenra has generated INV322, a bispecific antibody designed to preferentially engage tumor microenvironment (TME) Tregs. By targeting Treg co-expressed targets, CD25 and CTLA-4 with lower-affinity monovalent interactions, INV322 is designed to drive avidity only in the presence of dual target engagement to support selective blockade of Treg function and depletion by Fc-mediated clearance.

Methods INV322 is a human-targeted bispecific antibody, engineered using Invenra's fully human B-Body[®] platform with a wild-type IgG1 for Fc-gamma-mediated effector function. Specificity of INV322 to CD25 and CTLA-4 was evaluated using both solid phase and cell-based read-outs. Potency of INV322 was evaluated by flow cytometry *in vitro* on overexpression cell lines and iTregs via NK-mediated cytotoxicity assays. A surrogate molecule, INV323, with specificity to murine CTLA-4 and CD25 was generated to evaluate *in vivo* potency in murine solid tumor models.

Results INV322 demonstrated selective lower-affinity monovalent binding to cells expressing CTLA-4 (single-digit-nM) and CD25 (triple-digit nM) independently. However, when bound to cells expressing both targets, these monovalent affinities result in combined avidity and result in improved sub-nM binding of INV322 to these cells. The strength of the avid binding was associated with improved Fc-mediated depletion as the potency of INV322 was increased on engineered lines expressing both targets compared with cell lines expressing single targets. *In vivo* evaluation of INV323 demonstrated Fc-dependent anti-tumor activity, and additive effects in combination with anti-PD-1 treatment after single – dose administration. The tumor-protective activity observed was associated with establishment of anti-tumor memory and correlated to Treg depletion and an increase in the T_{eff}:Treg ratio within the TME.

Conclusions INV322 is an innovative bispecific approach for the selective depletion of tumor resident Tregs. The unique binding profile is designed to direct selective engagement of Tregs within the TME, providing a novel avenue for potential improvement of therapeutic index and patient outcome as compared to current Treg modulating therapeutics. IND-enabling activities are underway with INV322.

Ethics Approval All animal studies were reviewed and approved under Invenra's IACUC protocol (I-RP-A-07).

<http://dx.doi.org/10.1136/jitc-2022-SITC2022.0500>

501

ANTI-PDL2 USES IL17-DRIVEN INTERFERON-GAMMA TO TREAT AGED BUT NOT YOUNG CUTANEOUS MELANOMA-BEARING MICE, AND TREATS OTHER TUMORS IN AN AGE- AND TME-DEPENDENT MANNER

¹Myrna Garcia, ¹Yilun Deng, ¹Clare Murray, ¹Carlos Ontiveros, ¹Alvaro Padron, ²Sladjana Skopelja-Gardner, ³Kah Teong Soh, ³Dhan Chand, ⁴Tyler Curiel*. ¹UT Health San Antonio, San Antonio, TX, United States; ²Dartmouth, Lebanon, NH, United States; ³Agenus, Lexington, MA, United States; ⁴Dartmouth Health, Lebanon, NH, United States

Background Immune checkpoint blockade (ICB) with α PD1, α PDL2, α CTLA4 and α Lag3 is FDA-approved but agents fail to treat up to ~80% of all cancers. PDL2 is a second PD1 ligand¹ but little is reported on α PDL2 cancer immunotherapy.² Age is the biggest risk for cancer, yet little few age effects on ICB are reported.³ We previously reported that α PD2 treats melanoma in aged but not young mice.⁴ Here we provide mechanistic insights, outcomes in other cancers and human data.

Methods We tested α PDL2 ICB and mechanisms in WT, IFN γ ^{KO} and IL17^{KO} mice in B16F10 (B16) and Nras mutated melanomas, ID8agg ovarian cancer and MB49 bladder cancer. We tested α PD-L2 in aged (18-33 months) and young (3-8 months) mice. Tumors were analyzed by flow cytometry plus UMAP. Human PBMC and tumor samples were from commercial and institutional sources. TCGA data were mined.

Results α PDL2 ICB was ineffective in young mice with transplanted SQ B16 or NRAS-mutated melanoma, but remarkably effective in both in aged. α PDL2 efficacy was host IFN γ -dependent as expected, but also unexpectedly host IL17-dependent, which induced IFN γ . α PDL2 promoted IFN γ production by CD8⁺, CD4⁺ and $\gamma\delta$ T cells and induced Treg fragility⁵ all in a host IL17-dependent manner. A cellular IL17 source for α PDL2 efficacy, mechanism for age-related IL17-driven IFN γ and contributions from Treg fragility are under study but not yet established. α PDL2 failed to treat transplanted orthotopic ovarian cancer in young or aged, but treated young mice bearing transplanted heterotopic, SQ bladder cancers, demonstrating α PDL2 is not efficacious only in aged or melanoma and that young skin is not necessarily hostile to α PDL2. TCGA data showed IL17 and PDL2 expression significantly increases by age in all cancers generally and specifically in melanomas. PDL2 protein increase by age was confirmed in human PBMC and primary tumors in lin^{DR}⁺CD141⁺cDC1 but not on cDC2, plasmacytoid DC or other myeloid cells, T cells or B cells by flow cytometry. Both TCGA and flow data sets corroborated mouse data.

Conclusions α PDL2 is effective in aged but not young melanoma-bearing hosts and requires IL17 for efficacy. IL-17 is necessary for improved IFN γ production which is a likely α PDL2 efficacy mechanism. α PDL2 is a promising ICB approach meriting additional studies of mechanisms and effects on distinct tumors and TME. As age effects were confirmed in humans, it could be especially useful in aged hosts, or selected ICB failures (e.g., α PDL1) as we previously reported.

Acknowledgements

Funding: This research was funded by the NIH M. G. (T32GM113896, TL1 TR002647), Y. (CPRIT Research Training Award [RP 170345] and Ovarian Cancer Research Alliance Ann and Sol Schreiber Mentored Investigator Award), C. M. and C.O. (T32GM113896) The Clayton Foundation (no grant number) and the NCI (CA204965, CA054515, CA231325) supported Curiel. This work was supported by the Flow Cytometry Shared Resource Facility, UL1 TR001120

REFERENCES

1. Latchman Y, Wood CR, Chernova T, Chaudhary D, Borde M, Chernova I, Iwai Y, Long AJ, Brown JA, Nunes R *et al*: PD-L2 is a second ligand for PD-1 and inhibits T cell activation. *Nat Immunol* 2001;**2**(3):261–268.
2. Tomihara K, Shin T, Hurez VJ, Yagita H, Pardoll DM, Zhang B, Curiel TJ, Shin T: Aging-associated B7-DC(+) B cells enhance anti-tumor immunity via Th1 and Th17 induction. *Aging Cell* 2012;**11**:128–138.
3. Garcia MG, Deng Y, Murray C, Reyes RM, Padron A, Bai H, Kancharla A, Gupta H, Shen-Orr S, Curiel TJ: Immune Checkpoint Expression and Relationships to Anti-PD-L1 Immune Checkpoint Blockade Cancer Immunotherapy Efficacy in Aged versus Young Mice. *Aging and Cancer* 2022, in press.
4. Garcia MG: Distinct efficacy and immunological responses to α PD-1, α PD-L1 and α PD-L2 immunotherapy in aged versus young hosts JITC 2021, 2021 SITC meeting abstracts.
5. Drerup JM, Deng Y, Pandeswara SL, Padron AS, Reyes RM, Zhang X, Mendez J, Liu A, Clark CA, Chen W *et al*: CD122-Selective IL2 complexes reduce immunosuppression, promote treg fragility, and sensitize tumor response to PD-L1 Blockade. *Cancer Res* 2020, **80**(22):5063–5075.

Ethics Approval This study obtained IACUC approval, from UTHSA (20180021AR)

<http://dx.doi.org/10.1136/jitc-2022-SITC2022.0501>

502

TRANSPLANT ONCOLOGY: UTILIZATION OF IMMUNOTHERAPY IN THE PERI-TRANSPLANT SETTING

¹Maen Abdelrahim*, ¹Abdullah Esmail, ²Ala Abudayyeh, ³Ashish Saharia, ³R Mark Ghobrial. ¹Houston Methodist Neal Cancer Center, Houston, TX, United States; ²MD Anderson Cancer Center, Houston, TX, United States; ³JC Walter Jr Center for Transplantation, Houston, TX, United States

Background Transplant oncology is an emerging concept of cancer treatment with a promising prospective outcome. The application of oncology, transplant medicine, and surgery to improve patients' survival and quality of life is the core of transplant oncology. Hepatobiliary malignancies have been treated by liver transplantation (LT) with significantly improved outcomes. The indications of LT for hepatobiliary malignancies have been slowly expanded over the years in a stepwise manner; however, they have only been shown to improve patient survival in the setting of limited systemic therapy options. Recently, the use of anti-programmed cell death protein 1 and programmed cell death ligand 1 (PD-1 and PD-L1) checkpoint inhibitors in the treatment of cancers have evolved rapidly and these therapies have been approved for the treatment of HCC. Immune checkpoint inhibitors have resulted in good clinical outcomes in pre-and post-transplant HCC patients, although, some reports showed that certain recipients may face rejection and graft loss.

Methods In this abstract, we aim to illustrate and summarize the utilization of immune checkpoint inhibitor therapies in pre-and post-liver transplants for HCC patients and discuss the assessment of immune checkpoint inhibitor regulators that might determine liver transplant outcomes.

Results The ICPI therapies have tolerable side effects and excellent responses in the treatment of cancer patients as well as pre-transplant patients in the bridging therapy setting. In contrast, for post-transplant patients in the palliative setting, the existing data have eliminated the contraindication of using ICPIs in liver transplant patients. However, the main concerns about organ rejection in liver transplant patients who will be treated with ICPIs are still the same in both pre-and post-transplant setting.

Conclusions The decision to administer ICPI treatment in liver transplant patients should be made on a case-by-case basis according to the goal of care and the availability and efficacy of other treatment options. Biopsies of liver allografts might be used to predict rejection and decide the proper ICPI class to be used based on PD-1/PDL-1 expression, however, larger and prospective studies are missing to support this conclusion. The role and type of immunosuppression in the setting of peri-transplant use of ICPI are not defined yet whether one kind can be safer than others is yet to be decided. ICPI treatment is an evolving and promising therapeutic option in oncology. Further investigations of these agents in the pre-and post-transplant settings are highly needed.

<http://dx.doi.org/10.1136/jitc-2022-SITC2022.0502>

Abstracts

503

CYTOTOXIC REVIVAL IS IMPLICATED IN RESPONSE TO NEOADJUVANT PD-1 BLOCKADE FOR HEAD AND NECK SQUAMOUS CELL CARCINOMA

¹Alexander Afeyan*, ¹Giacomo Oliveira, ²Ann Marie Egloff, ¹Zexiang Zeng, ³Rebecca Chernock, ¹Liye Zhou, ¹Cameron Messier, ¹Patrick Lizotte, ¹Jacquelyn Wolff, ¹Kathleen Pfaff, ¹Kari Stromhaug, ²Robert Haddad, ¹Glenn Hanna, ²Jonathan Schoenfeld, ²Laura Goguen, ²Donald Annino, ²Vickie Jo, ³Peter Oppelt, ³Patrik Pipkorn, ³Ryan Jackson, ³Sidharth Puram, ³Randal Paniello, ³Jason Rich, ¹Jason Webb, ¹Jose Zevallos, ³Mena Mansour, ¹Jingxin Fu, ⁴Gavin Dunn, ²Scott Rodig, ³Jessica Ley, ⁵Luc Morris, ⁵Lara Dunn, ¹Cloud Paweletz, ³Dorina Kallogjeri, ³Jay Piccirillo, ³Douglas Adkins, ¹Catherine Wu, ¹Ravindra Uppaluri. ¹Dana-Farber Cancer Institute, Boston, MA, United States; ²Brigham and Women's Hospital, Boston, MA, United States; ³Washington University School of Medicine, St. Louis, MO, United States; ⁴Massachusetts General Hospital, Saint Louis, MO, United States; ⁵Memorial Sloan Kettering Cancer Center, New York, NY, United States

Background Pre-operative immunotherapy results in pathologic tumor responses (pTR) for some patients with head and neck squamous cell carcinoma (HNSCC), but response mechanisms remain poorly defined.^{1,2} We evaluated T cell profiles and clonal dynamics associated with pTR in a phase II trial of two doses of neoadjuvant pembrolizumab.

Methods 29 patients with stage III/IV HPV-unrelated HNSCC were enrolled in a multicenter phase 2 clinical trial of anti-PD-1 antibody pembrolizumab (2 doses, Q3 weeks) as neoadjuvant immunotherapy over 5 weeks prior to surgery. pTR to PD-1 blockade was assessed based on histologic reduction of tumor cell-fraction, as previously published, with responders defined as pTR of >10%.¹ We profiled tumor-infiltrating lymphocytes (TILs) from 14 tumor biopsies from 4 Responders (Rs) and 4 Non-Responders (NRs), collected either before or after PD-1 blockade through single-cell RNA (scRNA-seq) and T-cell receptor sequencing (scTCR-seq). Quality and quantity of TILs were assessed with multiplex immunofluorescence. Data were validated via comparison with a similar cohort of 36 HNSCC patients receiving single-dose neoadjuvant pembrolizumab.¹

Results pTR was detected in surgical specimens from 15 patients (53%), with two-year overall survival (OS) and progression-free survival (PFS) rates of 92.2% (95% CI: 72.1-97.9) and 92.3% (95% CI: 72.6-98.0%), respectively. Single-cell analysis of CD8+ TILs identified 12 transcriptionally-defined clusters. The microenvironment of Rs compared to NRs showed higher pre-treatment frequencies of exhausted TILs (T_{Ex}-TILs) (p<0.0001, figure 1a), which were more clonally expanded and expressed a previously-defined gene signature associated with tumor-specificity.³ R T_{Ex}-TILs were dominated by T_{TE}-CTX, a subpopulation with characteristics of cytotoxicity and high expression of ZNF683, suggesting a tissue-resident memory (TRM) program.^{4,5} Multiplex immunofluorescence of pre-treatment biopsies confirmed that Rs were more highly infiltrated with CD3+ TILs with a TRM phenotype, identified through CD103 co-expression (figure 1b).⁴ 6 pTR following PD-1 blockade was associated with contraction of highly cytotoxic T_{TE}-CTX clones and likely unleashing of their antitumor activity (figure 1c). Within this timeframe, immunotherapy response was predominantly attributable to activity of pre-existing CD8+ TIL clones, while phenotypic revival of persisting clones and clonal replacement were modest. For NRs, the baseline microenvironment exhibited a relative absence of ZNF683+CTX+ TILs with post-therapy accumulation of extremely exhausted clones lacking evidence of post-therapy reinvigoration.

Conclusions A larger pre-treatment proportion of T_{Ex}-TILs retaining cytotoxic potential and a TRM signature are associated with pTR in HNSCC. Expanded T_{TE}-CTX clones were diminished in number after immunotherapy treatment, consistent with release of their anti-tumor activity and subsequent contraction due to antigen clearance.

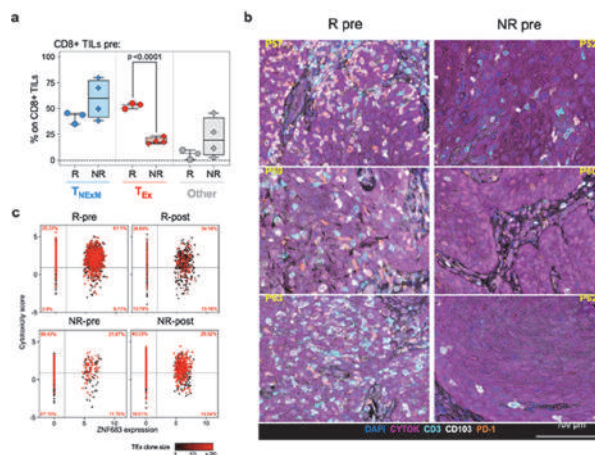
Acknowledgements This study was supported by the Alvin J. Siteman Cancer Center at Washington University School of Medicine and Barnes-Jewish Hospital in St. Louis, Missouri and the Clinical Trials Core. The Siteman Cancer Center is supported in part by the NCI Cancer Center. RU is funded by the National Cancer Institute, the National Institute for Dental and Craniofacial Research (NIH/NCI/NIDCR U01DE029188 and NIH/NIDCR R01DE027736) and a V Foundation Translational Research Award. Single-cell data acquisition was supported by Robert A. and Renee E. Belfer Foundation and Expect Miracles Foundation. Clinical trial support was through a Merck Investigator Studies Program award to R. Uppaluri/D.R. Adkins.

Trial Registration clinicaltrials.gov unique identifier: NCT02296684

REFERENCES

1. Uppaluri R, et al. Neoadjuvant and adjuvant pembrolizumab in resectable locally advanced, human papillomavirus-unrelated head and neck cancer: a multicenter, phase II Trial. *Clin. Cancer Res.* 2020; **26**:5140–5152.
2. Wise-Draper JM, et al. Phase II clinical trial of neoadjuvant and adjuvant pembrolizumab in resectable local-regionally advanced head and neck squamous cell carcinoma. *Clin Cancer Res.* 2022;**28**:1345–1352.
3. Oliveira G, et al. Phenotype, specificity and avidity of antitumor CD8+ T cells in melanoma. *Nature* 2021;**596**, 119–125.
4. Mackay LK, et al. Hobit and Blimp1 instruct a universal transcriptional program of tissue residency in lymphocytes. *Science* (80-). 2016; **352**:459–463.
5. Parga-Vidal L, et al. Hobit identifies tissue-resident memory T cell precursors that are regulated by Eomes. *Sci. Immunol* 2021;**6**.
6. Duhon T, et al. Co-expression of CD39 and CD103 identifies tumor-reactive CD8 T cells in human solid tumors. *Nat. Commun.* 2018;**9**.

Ethics Approval This study was approved by the Institutional Review Boards of Dana-Farber/Harvard Cancer Center (DFCI#16-385), Washington University (#201412118) and Memorial Sloan-Kettering Cancer Center (MSKCC) (#18-379).



Abstract 503 Figure 1 Dynamics of exhausted CD8 T cells expressing markers of cytotoxicity and a tissue-resident memory program in HNSCC tumors. a, Frequencies of principal phenotypes among CD8+ TILs collected from Responders (R, circles, n=3) or Non-Responders (NR, diamonds, n=4) at pre-treatment timepoints (Pre). Box plots – median percentage of TILs with phenotypes corresponding to CD8+ non-exhausted memory cell states (T_{NEM}, blue), exhausted states (T_{Ex}, red), or unclassified clusters (Other, grey). Whiskers: min-max values;

horizontal bars: medians. Boxes: 25th-75th percentiles. P values: significant comparisons (two-tailed Welch's t-test). b, Multiplexed Immunofluorescence of tumor biopsies collected prior to treatment from 3 Rs (left) and 3NRs (right) patients. The representative images demonstrate the pre-existing high levels of tissue resident memory-like (CD103+) and exhausted (PD1) TILs (CD3+) in Rs within the tumor bed, marked by expression of cytokeratin (Cytok). c, Bidimensional plot quantifying the expression ZNF683 expression (x axis) and cytotoxicity genes (summarized in a score [3], y axis) in CD8+ TILs with TEx-TCR clonotypes. Cells are colored according to the size of the TCR clonotype family they belong to. The percentage of cells in each quadrant is calculated based on thresholds representing the average values of variables (vertical and horizontal lines), as measured in the entire dataset of CD8+ TILs.

<http://dx.doi.org/10.1136/jitc-2022-SITC2022.0503>

PREPRINT

Abstracts

504

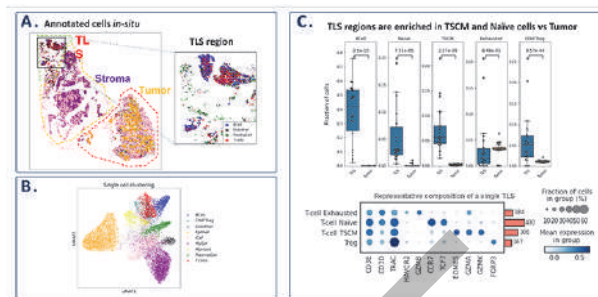
PVRIG, A NOVEL T CELL CHECKPOINT, IS PREFERENTIALLY EXPRESSED IN TLS ON STEM-LIKE MEMORY T CELLS, POTENTIALLY INHIBITING THEIR EXPANSION

¹Zoya Alteber, ¹Roy Granit, ¹Gady Cojocar, ¹Amit Novik, ¹Niv Sabath, ¹Assaf Wool, ¹Yossef Klinger, ²Yu Liang, ³Natalia Petrenko, ³Jiang He, ¹Pierre Ferre, ¹Yaron Turpaz, ¹Zurit Levin, ¹Eran Ophir*. ¹Compugen Ltd., Holon, Israel; ²Compugen USA Inc., South San Francisco, CA, United States; ³Vizgen Inc., Cambridge, MA, United States

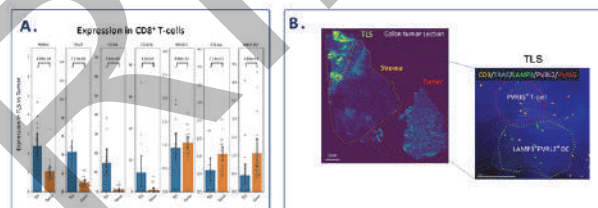
Background Tertiary lymphoid structures (TLS) recently emerged as an intra-tumoral niches of immune-cell aggregates with a predictive value for cancer immunotherapy responses.¹ LAMP3⁺DCs in the TLS were shown to interact and support the differentiation of stem-like CD8 T-cells into effector-like cells, that then expand in the tumor micro-environment (TME) and may exert anti-tumor responses.² We investigated the expression of DNAM-1 axis genes: PVRIG, TIGIT, DNAM-1 and their ligands PVRL2 and PVR in the TME.³
Methods MERFISH technology was employed to detect the expression of 350 distinct mRNA transcripts at sub-cellular resolution in CRC sections. Publicly available TME scRNA-seq datasets were analyzed for expression of PVRIG and PVRL2 across immune populations and validated by flow-cytometry. An extensive omics profiling was performed for patients with pre- and on-treatment biopsies from COM701 (anti-PVRIG antibody) and COM701+nivolumab Phase-1 study (NCT03667716).

Results Spatial distribution of gene transcripts allowed identifying localization of stem-like T-cells in TLS regions of two CRC patients (figure 1, p<0.001). While, CTLA-4, PD-1, and TIM3 were mainly expressed by tumor infiltrating T cells, PVRIG and other genes of DNAM-1 axis were also largely expressed in tumor bed, and even more intensely in TLS (p<0.05, figure 2). Furthermore, high resolution unsupervised scRNA gene co-expression analysis in the TME further validated that while PD-1 is strongly correlated with TIM3, CTLA-4, and other markers of exhausted T-cells, PVRIG uniquely clusters with markers of stem-like T-cells. The PVRIG protein expression was increased on CD28⁺ stem-like T-cells across indications (figure 3). RNA and protein expression data identified PVRL2, PVRIG ligand, preferentially expressed across DC-subtypes compared to PD-L1 and PVR (figure 4). PVRIG blockade could therefore enhance memory T-cell activation by DCs, resulting in their increased expansion and differentiation. Accordingly, COM701 monotherapy induced CD8⁺ T-cell numbers and immune activation in the TME of ovarian cancer patient (figure 5). Moreover, MSS-CRC patient with partial response to COM701+nivolumab, demonstrated an increase in TCR numbers, clonality, T-cell infiltration and activation in the TME (figure 6). Finally, preliminary analysis of serum from two patients clinically responding to COM701+nivolumab (RECIST criteria), revealed induction of activated-DC markers, compared to non-responders (figure 7).

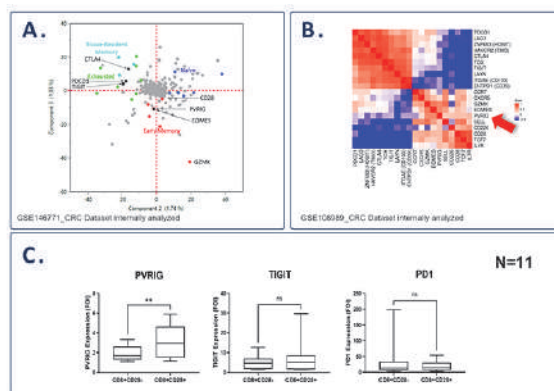
Conclusions By leveraging spatial and scRNA transcriptomics, we identified PVRIG⁺CD8⁺T-cells predominantly localized within TLS, interacting with PVRL2⁺LAMP3⁺DCs. PVRIG blockade could therefore enhance the differentiation and expansion of stem-like CD8⁺ T-cells into effector cells (figure 8). Accordingly, early clinical data shows increased T-cells infiltration and immune activation in patients treated with COM701 or COM701+nivolumab.



Abstract 504 Figure 1 Analysis of CRC samples by Vizgen allowed identification of Tertiary Lymphoid Structures. A. TLS region harbored a unique co-localization of B-cells, T-cell, Plasma and endothelial cells that are unique to these structures. B. UMAP showing the clustering of cell populations into distinct cell types based on MRFISH mRNA readouts. C. (Top) Boxplot demonstrating the cell composition in individual TLS structures or randomly sampled tumor regions. Tscm & naive T cells localize to TLS while exhausted T cells localize to tumor region. (Bottom) Dotplot showing the gene expression of selected cell-state markers in a single TLS.

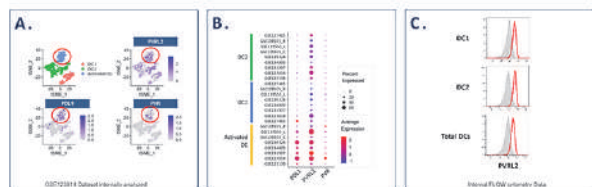


Abstract 504 Figure 2 DNAM-1 axis is dominantly expressed in TLS region. A. genes of the DNAM-1 axis, PVRIG, TIGIT, CD226, show dominant expression in TLS region, whereas other immune checkpoints, such as PD-1, CTLA4, TIM3 are expressed in the tumor bed. B. PVRIG expressing T cells intimately interacts with LAMP3⁺ PVRL2⁺ DC in the TLS of CRC patient.



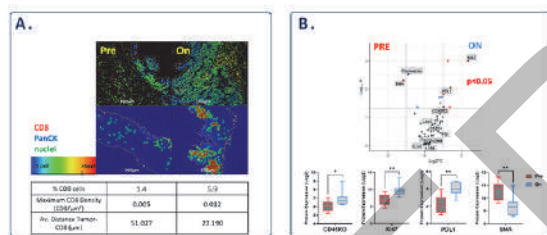
Abstract 504 Figure 3 PVRIG clusters with early differentiation/memory genes in the TME, unlike other immune checkpoints that cluster with exhausted genes, in CD8⁺ T cells. A. Unsupervised PCA analysis was performed on a scRNA expression matrix of TME CD8⁺ T cells, which includes all variable genes. Using cells as features and genes as entries, hierarchical co-expression pattern among genes known to be expressed on naive, memory, and exhausted CD8⁺ T-cells was performed. B. scRNA-Seq datasets were analyzed for co-expression pattern among 19 genes, including genes known to be expressed on naive (TCF7, IL7R, SELL), memory (GZMK, EOMES), and

exhausted (PDCD1, LAG3, HAVCR2) CD8 T cells. Average gene-gene correlation over all datasets was calculated. Representative CRC dataset of n=13 (CRC, NSCLC, HNSCC, Melanoma, Liver cancer) is presented. C. Samples (n=11) of CRC, ovarian and bladder cancer were dissociated to single cell suspensions and analyzed for gene expression by flow-cytometry. Paired T-test was used to compare between PVRIG expression among cell populations.

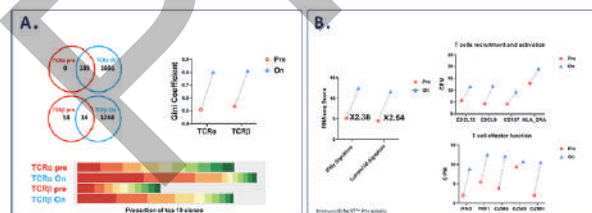


Abstract 504 Figure 4 PVR2 is dominantly expressed on dendritic cells in the TME.

A. tSNE map depicting the expression profile of PVR/PVR2/PD1 in major dendritic cell subsets in Basal Cell Carcinoma patients. B. Dot plots showing the percent of cells and average level of expression of PVR/PVR2/PD-1 in major dendritic cell subsets across multiple scRNA-seq cancer datasets. C. PVR2 protein expression across DC subsets in a representative ovarian cancer sample analyzed by flow-cytometry.

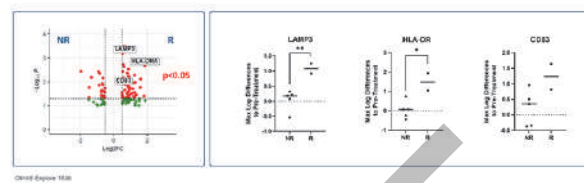


Abstract 504 Figure 5 COM701 Monotherapy induced immune activation in the TME of patient with ovarian cancer (radiologically defined as PD). Pre- and on-treatment biopsies from COM701 (anti-PVRIG antibody) treated patient with ovarian cancer were subjected to GeoMx[®] Immune Protein Assays, ROI selection was performed using DAPI, and mAbs detecting PanCK, CD8 and CD68. A. CD8 distribution in the TME post COM701 monotherapy. B. Protein expression in CD8 regions as was detected with Nanostring, DSP in the TME post COM701 monotherapy.

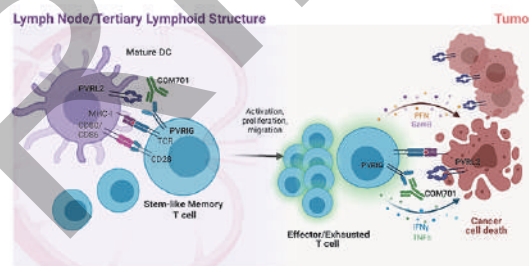


Abstract 504 Figure 6 Increased TME immune activation and TCR clonality in patient with MSS CRC with PR to COM701+nivolumab combination therapy. Pre- and on-treatment biopsies from COM701 (anti-PVRIG antibody)+ nivolumab treated patient with MSS-CRC were subjected to Personalis[®], ImmunoID NeXT analysis A. Increased number of clones and increased clonal expansion as was determined by Gini coefficient in the TME post COM701+nivolumab therapy. B. Increased

immune infiltration and activation in the TME post COM701+nivolumab therapy



Abstract 504 Figure 7 Combination of COM701+nivolumab Induced Markers of Activated DCs in Serum of Two Responding Patients. Serum of 7 patients from the nivolumab+COM701 dose escalation arm, were analyzed using Olink Explore 1536. For each patient, the maximal difference of log2 expression between all on-treatment time points and the pre-treatment value was calculated for each protein. Maximal log2 differences were compared by Student's t-test, with patients grouped based on response, RECIST criteria (responders (R): CR+PR vs. non responders (NR): SD+PD). Out of 10 proteins most significant for on-treatment up-regulation in responders, 3 are markers of activated DCs (LAMP3 ,HLA-DR and CD83).



Abstract 504 Figure 8 Summary. PVRIG-expressing stem-like memory T cells in LNs and TLS of cancer patients, are interacting PVR2+DCs. PVRIG blockade could therefore enhance the differentiation and expansion of stem-like memory CD8 T-cells into effector cells that proliferate and infiltrate tumor. In the tumor bed, PVRIG blockade could further potentiate anti-tumor responses by breaking the interaction between PVRIG+T cells and PVR2-expressing tumor cells.

REFERENCES

- Schumacher TN, Thommen DS. Tertiary lymphoid structures in cancer. *Science*. 2022;**375**(6576):eabf9419
- Magen A, Hamon P, Fiaschi N, Troncoso L, Humblin E, D'souza D, Dawson T, Park MD, Kim J, Hamel S, Buckup M. Intratumoral mregDC and CXCL13 T helper niches enable local differentiation of CD8 T cells following PD-1 blockade. *bioRxiv*. 2022
- Alteber Z, Kotturi MF, Whelan S, Ganguly S, Weyl E, Pardoll DM, Hunter J, Ophir E. Therapeutic targeting of checkpoint receptors within the DNAM1 axis. *Cancer Discovery*. 2021;**11**(5):1040–51.

<http://dx.doi.org/10.1136/jitc-2022-SITC2022.0504>

505

HIGH-DIMENSIONAL ANALYSES OF INTRATUMORAL MYELOID CELLS HIGHLIGHTS PRESENCE OF DISTINCT MYELOID CELL PHENOTYPES IN IMMUNE CHECKPOINT-SENSITIVE AND RESISTANT TUMORS

Swetha Anandhan*, Sangeeta Goswami, Shelley Herbrich, Yulong Chen, Padmanee Sharma. MD Anderson Cancer Center, Houston, TX, United States

Background Immune checkpoint therapy (ICT) has revolutionized cancer treatment, however, has produced around 20% durable clinical response rates.¹ Multiple studies demonstrate myeloid cell abundance and function in the tumor microenvironment (TME) correlates with poor outcome in ICT resistant cancers.^{2, 3} Despite the wealth of knowledge regarding the biology of these cells, our ability to distinguish immune-suppressive versus immune-stimulatory myeloid cells remains a major challenge and, thus, targeting myeloid cells has had limited clinical success. Our objective is to better understand the phenotype of these immunosuppressive myeloid cells to identify potential combination strategies to improve response to ICT.

Methods Comparative analyses of intratumoral myeloid cell subsets was performed in orthotopic murine models of ICT sensitive (B16F10 melanoma) and resistant (MT4 pancreatic) tumors at baseline and post ICT treatment (anti-PD-1 and/or anti-CTLA-4 antibodies) using single cell RNA sequencing (scRNAseq). To determine myeloid cell evolution with tumor progression, longitudinal scRNAseq was performed on MT4 tumors.

Results We observed two-fold higher abundance of macrophages and neutrophils in baseline MT4 tumors as compared to B16F10 tumors from our scRNAseq analysis (figure 1A-C). Overall, we identified 4 distinct macrophage subsets and 1 neutrophil subset (figure 1B). Mac_1 and mac_2 (MT4 macrophages) were the dominant macrophage clusters in MT4 tumors and while mac_1 expressed *mmp14*, *axl* and *maf3*; mac_2 had high expression of *vegfa*, *arg1*, *ccl24* and *fn1* (figure 1D). In contrast, mac_3 (B16F10 macrophages), the most abundant macrophage cluster in B16F10 tumors, expresses antigen presenting genes (*cd72*) and interferon-induced genes (*cxcl10*, *isg15*) (figure 1D). MT4 macrophages were significantly enriched TGF beta signaling, angiogenesis, hypoxia, glycolysis and B16F10 macrophages which enriched in oxidative phosphorylation and interferon gamma and alpha response pathways (figure 1E). The neutrophil subset was present specifically in MT4 tumors and expressed *cd24a*, *cxcl2*, *il1b* and *cd274* (figure 1D); consistent with the suppressive tumor-associated neutrophil (TAN) phenotype. Overall, at baseline, MT4 myeloid cells possess characteristics associated with T cell inhibition whereas B16F10 myeloid cells show T cell activating phenotypes. Post ICT treatment, macrophage subsets decreased moderately, however, MT4 TAN abundance increased, indicating possible compensatory resistance mechanisms (figure 1F). Longitudinal analyses indicated that neutrophil and macrophage subsets were abundant in early stage tumors and persisted during MT4 tumor progression (figure 1G).

Conclusions Distinct myeloid subsets are present in ICT sensitive and ICT resistant tumors. Myeloid targeting prior ICT treatment might be necessary to generate an effective immune response in resistant tumors. This study provides the foundation to identify novel myeloid specific targets in resistant solid tumors.

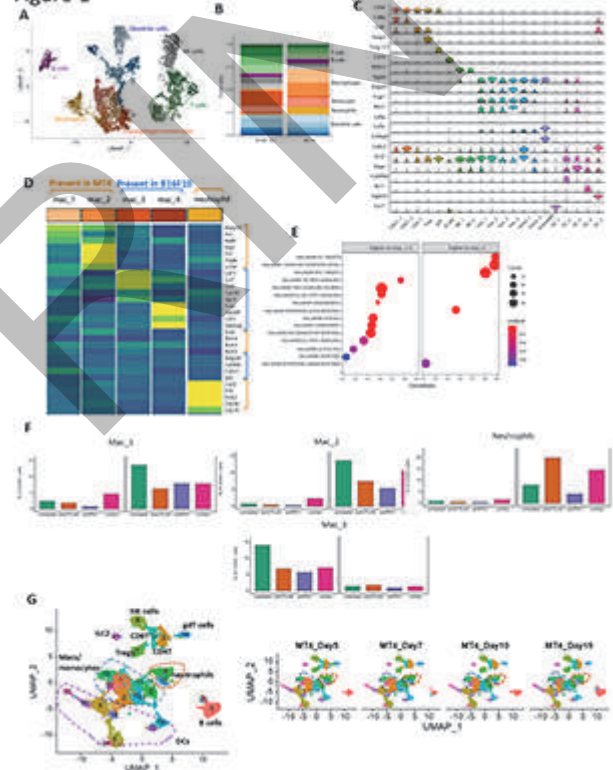
Acknowledgements This research is supported by Parker Institute for Cancer Immunotherapy (PICI)

REFERENCES

1. Pons-Tostivint E, Latouche A, Vaflard P, et al. Comparative analysis of durable responses on immune checkpoint inhibitors versus other systemic therapies: a pooled analysis of phase III Trials. *JCO Precision Oncology*, 2019(3): 1–10.
2. Zhang QW, Liu L, Gong CY, et al. Prognostic significance of tumor-associated macrophages in solid tumor: a meta-analysis of the literature. *PLoS One*, 2012. **7** (12):e50946.
3. Wang PF, Song SY, Wang TJ, et al., Prognostic role of pretreatment circulating MDSCs in patients with solid malignancies: A meta-analysis of 40 studies. *Oncoimmunology*, 2018. **7**(10): e1494113.

Ethics Approval All mice were housed in accordance with the Association for Assessment and Accreditation of Laboratory Animal Care and NIH standards. Experiments were conducted according to protocol 00000893-RN02 and approved by the University of Texas MD Anderson Cancer Center Institutional Animal Care and Use Committee.

Figure 1



Abstract 505 Figure 1 (A) Representation UMAP plot of intratumoral immune cell landscape in B16F10 and MT4 tumors. 3 tumors in each were pooled for internal control. All major immune cell subsets were identified. (B) Cluster frequency plots of each immune subset in B16F10 and MT4 tumors. (C) Characterization of immune subsets identified in figure 1A based on their marker gene expressions. (D) Heatmap of functional markers for the individual myeloid subsets providing phenotypic information. Expression levels are scaled between minimum and maximum expression for each gene across all clusters. (E) GSEA analysis of hallmark pathways enriched in mac_1 and mac_2 versus mac_3. (F) Cluster frequency plots of indicated myeloid subsets after treatment with ICT antibodies obtained from scRNAseq analyses. (G) Representative UMAP plots of intratumoral immune subsets collected from Day 5, 7, 10 and 15 of MT4 tumors. Highlighted regions in blue and brown indicate macrophage and neutrophil subsets, respectively.

<http://dx.doi.org/10.1136/jitc-2022-SITC2022.0505>

506 **FCγRIIB EXPRESSED ON CD8 T CELLS LIMITS RESPONSIVENESS TO PD-1 CHECKPOINT INHIBITION IN CANCER**

Kelsey Bennion*, Marvi Tariq, Megan Wyatt, Kirsten Baecher, Chrystal Paulos, Ragini Kudchadkar, Michael Lowe, Mandy Ford. *Emory University, Atlanta, GA, United States*

Background Immune checkpoint inhibition (ICI) using Fc-containing monoclonal antibodies has emerged as a powerful therapeutic approach to augment anti-tumor immunity. While ICI has drastically improved patient outcomes in melanoma, there is still variability in patient response.^{1, 2} We recently showed that FcγRIIB, the only inhibitory IgG-Fc receptor, is expressed on differentiated effector CD8 T cells in mice and humans^{3, 4}, raising the possibility that CD8 T cell responses may be directly modulated by checkpoint inhibitor binding to T cell-expressed FcγRIIB.

Methods Flow cytometric phenotyping was performed on PBMCs isolated from melanoma patients and healthy donors. For *in vitro* functional experiments, healthy human PBMCs were stimulated with CD3/28 Dynabeads and/or PMA/ionomycin. Effector function was assessed through intracellular cytokine staining. Anti-PD1 (clone J116) or anti-CTLA4 (clone BN13) were used where mentioned and the anti-PD1 F(ab) was generated from Nivolumab. *In vivo* experiments were performed in mice with B16-hgp100, B16-OVA, or LLC-OVA tumors. Where mentioned, WT OT-I, *Fcγr2b*^{-/-} OT-I, or WT pmel-17 CD8 T cells were adoptively transferred into these mice. For treatment, 250 μg of anti-PD1 (clone RMP1-14) and anti-FcγRIIB (clone 2.4G2) or isotype antibodies were administered for blockade experiments.

Results Here, we show that despite exhibiting strong proliferative and cytokine responses at baseline, human FcγRIIB⁺ CD8 T cells exhibited reduced responsiveness to both PD-1 and CTLA-4 checkpoint inhibition compared to FcγRIIB⁻ CD8 T cells *in vitro* (p<0.05). Moreover, frequencies of FcγRIIB⁺ CD8 T cells were reduced following treatment of human melanoma patients with nivolumab *in vivo* (p<0.05). This reduced responsiveness was FcγRIIB-dependent, because conditional genetic deletion of FcγRIIB on tumor-specific CD8 T cells improved response to checkpoint blockade in a B16 mouse melanoma model (p<0.01). The limited responsiveness of FcγRIIB⁺ CD8 T cells was dependent on an intact Fc region of the checkpoint inhibitor, in that treatment with Fc-devoid anti-PD-1 F(ab) fragments resulted in a significant increase in proliferation of FcγRIIB⁺ CD8 T cells, without altering the response of FcγRIIB⁻ CD8 T cells (p<0.05). Finally, blocking FcγRIIB in the context of PD-1 blockade significantly improved anti-tumor CD8 T cell responses in B16 melanoma and in Lewis lung cancer mouse models (p<0.05, p<0.001).

Conclusions These results illuminate an FcγRIIB-mediated, cell-autonomous mechanism of CD8 T-cell suppression which limits the efficacy of checkpoint inhibitors *in vivo*. The data presented here support the novel conclusion that CD8-expressed FcγRIIB is both a factor to consider in the development of therapeutic antibodies, and a new potential target for immunotherapeutic intervention.

REFERENCES

1. Lugowska I, Tetrycz P, Rutkowski P. Immunotherapy of melanoma. *Contemp Oncol (Pozn)*. 2018;**22**(1A):61–7. Epub 2018/03/05. doi: 10.5114/wo.2018.73889. PubMed PMID: 29628796.
2. Larkin J, Chiarion-Sileni V, Gonzalez R, Grob J-J, Rutkowski P, Lao CD, Cowey CL, Schadendorf D, Wagstaff J, Dummer R, Ferrucci PF, Smylie M, Hogg D, Hill A, Márquez-Rodas I, Haanen J, Guidoboni M, Maio M, Schöffski P, Carlino MS,

Lebbé C, McArthur G, Ascierto PA, Daniels GA, Long GV, Bastholt L, Rizzo JI, Balogh A, Moshyk A, Hodi FS, Wolchok JD. Five-Year Survival with Combined Nivolumab and Ipilimumab in Advanced Melanoma. *N Engl J Med*. 2019;**381**(16):1535–46. doi: 10.1056/NEJMoa1910836.

3. Morris AB, Farley CR, Pinelli DF, Adams LE, Cragg MS, Boss JM, Scharer CD, Fribourg M, Cravedi P, Heeger PS, Ford ML. Signaling through the Inhibitory Fc Receptor FcγRIIB Induces CD8(+) T Cell Apoptosis to Limit T Cell Immunity. *Immunity*. 2020;**52**(1):136–50 e6. Epub 2020/01/16. doi: 10.1016/j.immuni.2019.12.006. PubMed PMID: 31940267; PMCID: PMC7326381.
4. Farley CR, Morris AB, Tariq M, Bennion KB, Potdar S, Kudchadkar R, Lowe MC, Ford ML. FcγRIIB is a T cell checkpoint in antitumor immunity. *JCI Insight*. 2021;**6**(4). doi: 10.1172/jci.insight.135623.

Ethics Approval Patients undergoing treatment at Emory University Hospital for advanced stage II-IV melanoma between 2009 and 2019 were enrolled in an immune monitoring protocol approved by Emory University's Institutional Review Board (IRB #00046593). Healthy controls were enrolled after informed consent.

This study was also carried out in strict accordance with the recommendations in the Guide for the Care and Use of Laboratory Animals. The protocol (PROTO201700558) was approved by the Institutional Animal Care and Use Committee of Emory University. All surgery was performed under general anesthesia with maximum efforts made to minimize suffering.

<http://dx.doi.org/10.1136/jitc-2022-SITC2022.0506>

507

HIGH ENDOTHELIAL VENULES CONTROL THE JOURNEY OF STEM-LIKE CD8⁺ T CELLS FROM LYMPH NODE TO TUMOR DURING CANCER IMMUNOTHERAPY WITH COMBINED ANTI-PD-1 PLUS ANTI-CTLA-4 ANTIBODIES

Lucas Blanchard student*, Estefania Vina, Dorian Tarroux, Emma Lefrançois, Nathalie Ortega, Jean-Philippe Girard. CNRS-IPBS, University of Toulouse, Toulouse, France

Background Recent reports revealed that CD8⁺ T cell antitumor responses rely on a subset of stem-like CD8⁺ T cells during cancer immunity and immunotherapy. However, the origin of stem-like CD8⁺ T cells and the mechanisms controlling their trafficking are not well established. High endothelial venules (HEVs) are specialized blood vessels mediating lymphocyte trafficking in lymph nodes (LNs),^{1,2} and HEV-like blood vessels defined as tumor-associated HEVs (TA-HEVs) are important regulators of lymphocyte entry into tumors.³ Here, we investigated the role of LN-HEVs and TA-HEVs in the generation and migration of stem-like CD8⁺ T cells during spontaneous antitumor immunity and cancer immunotherapy.

Methods In mouse syngeneic tumor models, we applied multidisciplinary approaches (immunofluorescence, flow cytometry, short-term homing assays and *in vivo* imaging) to identify the adhesion pathways used by LN-HEVs and TA-HEVs for CD8⁺ T cell trafficking. Then, using *in vivo* function-blocking antibodies targeting LN-HEVs and/or TA-HEVs, we defined their respective roles in the recruitment of naive CD44⁺PD-1⁻ CD8⁺ T cells into tumor-draining lymph node and of CD44⁺PD-1⁺TCF-1^{high} stem-like CD8⁺ T cells into tumor. Lastly, we blocked the function of LN-HEVs and/or TA-HEVs during combined anti-PD-1 plus anti-CTLA-4 cancer immunotherapy to analyze their contributions in treatment-induced CD8⁺ T cell responses.

Results We found that naive and stem-like CD8⁺ T cells use distinct adhesion pathways to interact with LN-HEVs and TA-HEVs, respectively. Blocking naive CD8⁺ T cell adhesion to LN-HEVs and their subsequent entry into tumor-draining lymph node abrogated the generation of stem-like CD8⁺ T cells and prevented their accumulation in tumor, showing that peripheral and intratumoral responses are tightly related. In peripheral blood, circulating stem-like CD8⁺ T cells expressed adhesion molecules and chemokine receptors enabling interaction with TA-HEVs that mediated their entry into tumor. Finally, we found that checkpoint blockade therapy increased the number and activity of stem-like CD8⁺ T cells in tumor-draining lymph node and peripheral blood, suggesting that peripheral responses are involved during treatment. Accordingly, HEV-mediated trafficking in tumor, but also in tumor-draining lymph node, were required for expansion and differentiation of intratumoral stem-like CD8⁺ T cells during checkpoint blockade therapy.

Conclusions In this study, we unveil the dual role of HEVs in tumor and periphery for CD8⁺ T cell responses during cancer immunity and immunotherapy, and provide mechanistic insights on the importance of peripheral responses during checkpoint blockade therapy. Our findings also strongly support the use of combined anti-PD-1 plus anti-CTLA-4 cancer immunotherapy in the neoadjuvant setting.

Acknowledgements This work was supported by grants from Fondation ARC pour la Recherche sur le Cancer (PGA1 RF20180206911 to J-PG), Institut National du Cancer (INCa_2017-155 to J-PG). LB and EV were supported by fellowships from Fondation pour la Recherche Médicale

(ECO201806006827, FDT202106012889).

ECO202006011469,

and

REFERENCES

1. Mousion C, Girard JP. Dendritic cells control lymphocyte entry to lymph nodes through high endothelial venules. *Nature*. 2011;**479**:542–546.
2. Blanchard L, Girard JP. High endothelial venules (HEVs) in immunity, inflammation and cancer. *Angiogenesis*. 2021;**24**:719–753.
3. Asrir A*, Tardiveau C*, Coudert J*, Laffont R*, Blanchard L*, Bellard E, Veerman K, Bettini S, Lafouresse F, Vina E, Tarroux D, Roy S, Girault I, Molinaro I, Martins F, Scoazec JY, Ortega N, Robert C, Girard JP. Tumor-associated high endothelial venules mediate lymphocyte entry into tumors and predict response to PD-1 plus CTLA-4 combination immunotherapy. *Cancer Cell*. 2022;**40**:318–334. (* co-first authors)

Ethics Approval This study obtained ethical approvals by the French Ministry of Research and the FRBT (C2EA-01) animal care committee (Projects 2017112021529157v3 and 2019122019025727v3). (APAFIS#12256- and APAFIS#23416-)

<http://dx.doi.org/10.1136/jitc-2022-SITC2022.0507>

GENERALIZABILITY OF PREDICTIVE VERSUS PROGNOSTIC INDICATORS FROM PUBLISHED TRANSCRIPTOMIC ASSOCIATIONS WITH TUMOR RESPONSE TO IMMUNE CHECKPOINT INHIBITION

¹Dante Bortone, ²Anne Monette, ³Nicholas Tschernia, ⁴Alexandria Cogdill, ⁵Yana Najjar, ⁶Randy F Sweis, ⁷Sara Valpione, ⁸Erik Wennerberg, ⁹Praveen Bommareddy, ⁴Cara Haymaker, ¹⁰Uqba Khan, ¹¹Heather M McGee, ¹²Wungki Park, ¹³Houssein A Sater, ¹⁴Christine Spencer, ¹⁵Maria Ascierto, ¹⁶Valentin Barsan, ¹⁷Vinita Popat, ¹⁸Daniel Wells, ¹Steven Vensko, ¹Sarah Dexheimer, ¹⁹Vesteinn Thorsson, ^{14,20,21}Roberta Zappasodi, ^{4,10}Nils-Petter Rudqvist, ¹Benjamin Vincent*. ¹University of North Carolina at Chapel Hill, Chapel Hill, NC, United States; ²Jewish General Hospital, Montreal, Canada; ³National Cancer Institute, Bethesda, MD, United States; ⁴The University of Texas MD Anderson Cancer Center, Houston, TX, United States; ⁵UPMC Hillman Cancer Center, Pittsburgh, PA, United States; ⁶University of Chicago, Chicago, IL, United States; ⁷The Christie NHS Foundation Trust, Manchester, UK; ⁸Institute of Cancer Research, London, UK; ⁹Replimune Inc, Woburn, MA, United States; ¹⁰Weill Cornell Medicine, New York, NY, United States; ¹¹City of Hope, Duarte, CA, United States; ¹²Memorial Sloan Kettering Cancer Center, New York, NY, United States; ¹³Cleveland Clinic Florida, Stuart, FL, United States; ¹⁴Parker Institute for Cancer Immunotherapy, San Francisco, CA, United States; ¹⁵Providence Saint John's Cancer Institute, Santa Monica, CA, United States; ¹⁶Stanford University School of Medicine, Palo Alto, CA, United States; ¹⁷University of Texas Southwestern Medical Center, Dallas, TX, United States; ¹⁸Immunai, New York, NY, United States; ¹⁹Institute for Systems Biology, Seattle, United States; ²⁰Weill Cornell Medical College of Cornell University, San Francisco, CA, United States; ²¹Weill Cornell Graduate School of Medical Sciences, San Francisco, CA, United States

Background Clinically actionable biomarkers of immune checkpoint inhibitor (ICI) response are currently limited to specific mutation profiling, immunohistochemistry staining for PD-L1, and tumor mutational burden. Use of the latter two are challenging, as they are incompletely predictive and lack accepted standards for measurement and interpretation. Transcriptomic associations with response have been reported and may add critical information to an integrated biomarker strategy. There is a need for better understanding of the performance of potential biomarkers across multiple datasets and tumor tissue types.

Methods RNA sequencing FASTQ data files from 12 ICI trials¹⁻¹³ and 29 solid tumors in The Cancer Genome Atlas (TCGA)¹⁴ were processed using a standardized bioinformatics workflow for quality control, mapping, generation of gene expression matrices, and extraction of immunogenomics features. We evaluated 18^{2, 15-22} immunogenomics features that have been published or proposed to associate with clinical response to ICI therapy for correlation with response and survival across these datasets, estimating predictive information from the ICI trials and prognostic information from TCGA dataset results.

Results The MIRACLE score was associated with response and survival in most ICI studies, both overall and within melanoma trials (figures 1). Other immunogenomics features had both lower effect sizes of outcome associations and fewer cohorts in which their outcome associations were statistically significant. Features that were associated with outcome in the ICI studies were generally associated with survival in TCGA as well, whether evaluating all tumor tissue types (figure 2) or melanoma only (figure 3). In melanoma, the TIDE score was associated with response to ICIs, but not with overall survival in TCGA, though the effect size was small. Gene expression signatures built from responders versus non-responders in each trial did not yield generalizable associations with response across other trials. Harmonized gene expression data and immunogenomics features extracted in this project are available for review and further analysis in the CRI iAtlas platform (<https://cri-iatlas.org/>).

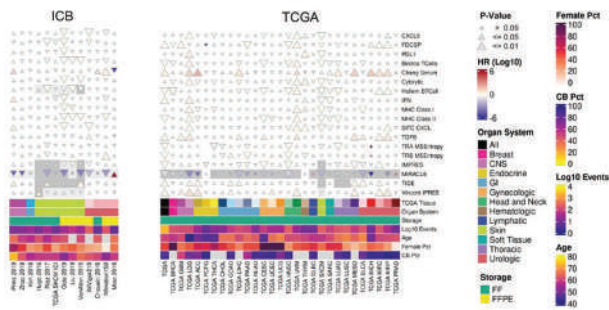
Conclusions The MIRACLE score performed best in both effect size and frequency of studies where its association with outcome was statistically significant. No features gave substantial predictive rather than prognostic information. We expect that integration of transcriptomic features with clinical features and DNA alterations will be required to provide predictive (rather than just prognostic) information. Methods that train models on prioritization of predictive information and generalizability across studies may be required for optimal biomarker development.

Acknowledgements We would like to thank SITC for funding for this work as part of the Sparkathon TimIOS collaborative project. We would also like to thank the authors of the published datasets we have used in the study.

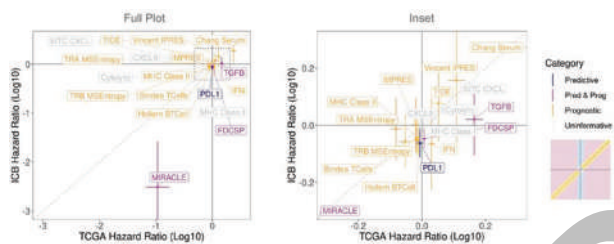
REFERENCES

1. Gide TN, et al. Distinct Immune Cell Populations Define Response to Anti-PD-1 Monotherapy and Anti-PD-1/Anti-CTLA-4 Combined Therapy. *Cancer Cell*, 2019;**35**(2):238–255 e6.
2. Hugo W, et al. Genomic and Transcriptomic Features of Response to Anti-PD-1 Therapy in Metastatic Melanoma. *Cell*, 2016;**165**(1): 35–44.
3. McDermott DF, et al. Clinical activity and molecular correlates of response to atezolizumab alone or in combination with bevacizumab versus sunitinib in renal cell carcinoma. *Nat Med*, 2018;**24**(6):749–757.
4. Balar AV, et al. Atezolizumab as first-line treatment in cisplatin-ineligible patients with locally advanced and metastatic urothelial carcinoma: a single-arm, multicentre, phase 2 trial. *Lancet*, 2017;**389**(10064): 67–76.
5. Rosenberg JE, et al. Atezolizumab in patients with locally advanced and metastatic urothelial carcinoma who have progressed following treatment with platinum-based chemotherapy: a single-arm, multicentre, phase 2 trial. *Lancet*, 2016;**387**(10031): 1909–20.
6. Liu D, et al. Integrative molecular and clinical modeling of clinical outcomes to PD1 blockade in patients with metastatic melanoma. *Nat Med*, 2019;**25**(12): 1916–1927.
7. Cloughesy TF, et al. Neoadjuvant anti-PD-1 immunotherapy promotes a survival benefit with intratumoral and systemic immune responses in recurrent glioblastoma. *Nat Med*, 2019. **25**(3): p. 477–486.
8. Riaz N, et al. Tumor and Microenvironment Evolution during Immunotherapy with Nivolumab. *Cell*, 2017;**171**(4): 934–949 e16.
9. Van Allen EM, et al. Genomic correlates of response to CTLA-4 blockade in metastatic melanoma. *Science*, 2015;**350**(6257): 207–211.
10. Zhao J, et al. Immune and genomic correlates of response to anti-PD-1 immunotherapy in glioblastoma. *Nat Med*, 2019;**25**(3): 462–469.
11. Kim ST, et al. Comprehensive molecular characterization of clinical responses to PD-1 inhibition in metastatic gastric cancer. *Nat Med*, 2018;**24**(9): 1449–1458.
12. Miao D, et al. Genomic correlates of response to immune checkpoint therapies in clear cell renal cell carcinoma. *Science*, 2018;**359**(6377): 801–806.
13. Choueiri TK, et al. Immunomodulatory activity of nivolumab in metastatic renal cell carcinoma. *Clin Cancer Res*, 2016;**22**(22): 5461–5471.
14. Cancer Genome Atlas Research N, et al. The Cancer Genome Atlas Pan-Cancer analysis project. *Nat Genet*, 2013. **45**(10): 1113–20.
15. Bindea G, et al. Spatiotemporal dynamics of intratumoral immune cells reveal the immune landscape in human cancer. *Immunity* 2013;**39**(4): 782–95.
16. Thorsson V, et al. The immune landscape of cancer. *Immunity* 2018;**48**(4): 812–830. e14.
17. Roufas C, et al. The expression and prognostic impact of immune cytolytic activity-related markers in human malignancies: a comprehensive meta-analysis. *Front Oncol* 2018;**8**: 27.
18. Hollern DP, et al. B Cells and T follicular helper cells mediate response to checkpoint inhibitors in high mutation burden mouse models of breast cancer. *Cell*, 2019;**179**(5): 1191–1206 e21.
19. Bortone DS, et al. Improved T-cell Receptor Diversity Estimates Associate with Survival and Response to Anti-PD-1 Therapy. *Cancer Immunol Res* 2021;**9**(1): 103–112.
20. Auslander N, et al. Robust prediction of response to immune checkpoint blockade therapy in metastatic melanoma. *Nat Med*, 2018;**24**(10): 1545–1549.
21. Turan T, et al. A balance score between immune stimulatory and suppressive microenvironments identifies mediators of tumour immunity and predicts pan-cancer survival. *Br J Cancer*, 2021;**124**(4): 760–769.
22. Jiang P, et al. Signatures of T cell dysfunction and exclusion predict cancer immunotherapy response. *Nat Med*, 2018;**24**(10): 1550–1558.

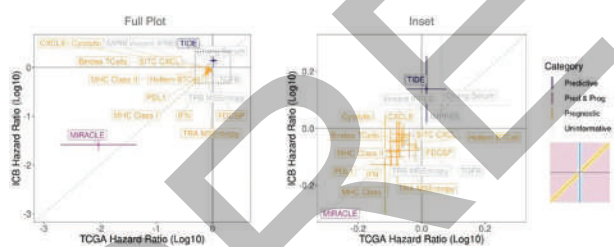
Abstracts



Abstract 508 Figure 1 Overall survival associations of selected immunogenomics features. Rows represent selected immunogenomics features and columns represent individual datasets. Results from ICI trials are shown in the left panel, and results from TCGA datasets are shown in the right panel. Row/column intersections represent effect size (triangle direction and color) and statistical significance (triangle size) of associations with overall survival. Column-side colorbars show various dataset features for comparison



Abstract 508 Figure 2 Predictive versus prognostic information content of selected immunogenomics features. X-axis represents the log10 hazard ratio with 95% confidence interval derived from TCGA data, and Y-axis represents log10 hazard ratio with 95% confidence interval derived from ICI data.



Abstract 508 Figure 3 Predictive versus prognostic information content of selected immunogenomics features, melanoma trials only. X-axis represents the log10 hazard ratio with 95% confidence interval derived from TCGA data, and Y-axis represents log10 hazard ratio with 95% confidence interval derived from ICI data.

<http://dx.doi.org/10.1136/jitc-2022-SITC2022.0508>

509

IMMUNE CHECKPOINT BLOCKADE BOOSTS ANTI-TUMOUR B CELL RESPONSES IN LUNG ADENOCARCINOMA

Jesse Boumelha*, Kevin Ng, Katey Enfield, Charles Swanton, George Kassiotis, Julian Downward. *The Francis Crick Institute, London, UK*

Background B cells are frequently found in the margins of solid tumours, where they are organized in tertiary lymphoid structures (TLS) that resemble antibody-producing germinal centres. The presence of TLS has been associated with improved patient outcome and response to immunotherapy, though the mechanisms underlying these associations remain unclear. Similarly, the contribution of B cells and TLS to anti-tumour immunity in non-small cell lung cancer (NSCLC) remains largely unexplored.

Methods We evaluated treatment-naive NSCLC cohorts to compare B cell and TLS gene signatures from human lung adenocarcinoma (LUAD) and squamous cell carcinoma (LUSC). Using a novel immunogenic mouse model of LUAD, we carried out lineage tracing, 3D immunofluorescence, and single-cell sequencing to characterise lung germinal centre and antibody responses during tumour progression and immunotherapy treatment.

Results B cell and TLS genes were significantly higher in LUAD compared to LUSC and correlated with improved survival. We therefore investigated the mechanistic basis of B cells in LUAD using a novel immunogenic KRAS-mutant lung cancer mouse model. Using serum transfer experiments, we demonstrated a highly protective role for tumour-binding class-switched antibodies. These germinal centre B cell responses and antibody quantity were increased after immunotherapy treatment or targeted KRAS inhibition. Interestingly, tumour-binding antibodies were demonstrated to be targeting re-expressed endogenous retroviral (ERV) antigens. Using single-cell BCR sequencing of immunotherapy-treated mice, we showed clonal expansion of B cells reactive to ERV antigens. Furthermore, ERVK-7 which encodes an endogenous retrovirus envelope glycoprotein was overexpressed in human LUAD and therefore may act as a relevant tumour antigen. Finally, we showed that combined treatment with CXCL13 and immune checkpoint blockade improved survival, suggesting that boosting local B cell responses can improve immunotherapy outcome.

Conclusions Our work describes a novel role for B cells in lung cancer and establishes that TLS directly contribute to anti-tumour immunity by producing class-switched protective antibodies. We demonstrate that selective boosting of anti-tumour B cells shows therapeutic potential in combination with immune checkpoint blockade.

Ethics Approval All animal experiments were approved by the ethics committee of the Francis Crick Institute and conducted according to local guidelines and UK Home Office regulations under the Animals Scientific Procedures Act 1986 (ASPA).

<http://dx.doi.org/10.1136/jitc-2022-SITC2022.0509>

510

A PD-L1 REPORTER CELL LINE BASED ON THE IMMUNE CHECKPOINT PROTEIN PROFILING OF ATCC CELL LINES FACILITATES CANCER IMMUNOTHERAPY DRUG SCREENING

Hyeyoun Chang*, Brian Della Fera, Haiyun Liu, Arunajyothi Bandla, Kevin Tyo, John Foulke, Luping Chen, Zhizhan Gu, Fang Tian. *ATCC (American Type Culture Collection), Gaithersburg, MD, United States*

Background The success of immune checkpoint inhibitors in the treatment of various types of cancers and their continued growth in the market have driven burgeoning interests in developing more drugs in this category. However, the intrinsic complexity of the immunological models and the variable drug responses among different cancer types have become the most prominent challenges.

Methods To facilitate large scale research projects and drug discovery of immune checkpoint inhibitors, we conducted a comprehensive protein profiling of ATCC's vast portfolio of human tumor and immune cell lines for several established and novel immune checkpoint molecules. Based on this protein profiling data, we generated an immune checkpoint reporter cancer cell line with high expression of endogenous programmed death-ligand 1 (PD-L1), a highly validated target for immune checkpoint inhibitor therapeutics. The reporter system contains a gamma interferon activation site (GAS)-response element upstream of the luciferase gene, preventing luciferase expression when PD-L1 binds to programmed death-1 (PD-1) that suppresses T cell-mediated antitumor activity. In the presence of a PD-1/PD-L1 inhibitor, a luciferase expression based bioluminescent signal is produced, which can be readily detected and quantitated to evaluate the efficacy, potency, and dynamics of the inhibitor.

Results Our data showed that the bioluminescence in the reporter cancer cells increased ~ 250 folds in a dose-dependent manner in response to interferon gamma stimulation, which mimics the signaling from activated CD8+ cytotoxic T cells. The bioluminescence increased ~100 folds in response to CD8+ primary T cell-conditioned media stimulation, and up to 5 folds in response to co-culture with CD8+ primary T cells in the presence of an anti-PD-L1 blocking antibody in a dose-dependent manner. The luciferase expression and endogenous PD-L1 expression were well maintained after the cell line had reached >30 population doubling level. These results highlight the robustness and responsiveness of the reporter system for the assessment of T cell-mediated immune responses triggered by PD-1/PD-L1 checkpoint inhibitors.

Conclusions This PD-L1 immune checkpoint reporter cancer cell line yields exceptional in vitro and ex vivo assay sensitivity and reproducibility, while simplifies the complex immunological model by providing physiologically relevant expression of PD-L1, in comparison to similar assays on the market with an artificial PD-L1 overexpression system.

<http://dx.doi.org/10.1136/jitc-2022-SITC2022.0510>

511

T CELL-INSTRUCTED INFLAMMATION DRIVES IMMUNE CHECKPOINT INHIBITOR THERAPY RESISTANCE

¹Nam Woo Cho*, ¹Sophia Guldberg, ²Eun Ji Kim, ¹Kamir Hiam-Galvez, ¹Katherine Wai, ¹Lauren Levine, ¹Rachel DeBarge, ¹Jacqueline Yee, ¹Naa Ashitey, ¹Matthew Spitzer. ¹Helen Diller Family Comprehensive Cancer Center, Parker Institute for Cancer Immunotherapy, Chan Zuckerberg Biohub, University of California, San Francisco, San Francisco, CA, United States; ²Unaffiliated, San Francisco, CA, United States

Background Resistance to immune checkpoint inhibitors (ICIs) is a significant barrier to improving cancer immunotherapy.¹ To this end, we interrogated ICI-induced inflammation. One type of inflammation, driven by nuclear factor- κ B (NF- κ B) activation in the tumor microenvironment (TME), can power tumor-promoting mechanisms including immunosuppression to limit ICI efficacy.² Conversely, the current paradigm predicts that another type of inflammation, characterized by T cell infiltration, improves ICI responsiveness.^{3,4} How these two units of inflammation can co-exist in the TME yet direct divergent responses to ICIs requires reconciliation. In particular, it is unknown whether conventional CD4 or CD8 T cells can themselves instruct NF- κ B inflammation in the TME, shaping the immunologic setpoint and, unexpectedly, limiting ICI efficacy.

Methods We generated new mouse syngeneic microsatellite instability-high (MSI-H) tumor models to study ICI response and resistance in the context of ample T cell inflammation. High-neoantigen-burden cell lines were implanted into syngeneic mice to assess responses to combination anti-PD-1 and -CTLA4 treatment.

Results Consistent with response in human tumors⁵, 50% of mouse MSI-H tumors were resistant to combination ICIs. Analysis of the TME in the resistant AT3 breast cancer model and responsive B16F10 melanoma model by mass cytometry revealed that ICIs increased tumor T cell infiltration in each model, but CD8 T cells in AT3 tumors assumed a non-cytotoxic but early-activated phenotype characterized by CD69 expression. T cell expansion in AT3 MSI-H tumors was accompanied by recruitment of T cell-suppressive polymorphonuclear myeloid-derived suppressor cells requiring cytokines G-CSF and CXCL1, absent in B16F10 tumors. Inhibition of the inflammatory NF- κ B circuit, which drives expression of these cytokines, via IL-1 receptor neutralization increased ICI efficacy against AT3 MSI-H tumors. Unexpectedly, in vivo depletion of T cells also abolished the NF- κ B circuit in AT3 MSI-H tumors, and activated CD8 T cells were sufficient to instruct tumor cells to increase G-CSF and CXCL1 expression. We found that TNF α , increased in T cells and neutrophils upon ICIs, perpetuated the NF- κ B circuit and contributed to ICI resistance in AT3 MSI-H tumors. Finally, analysis of single-cell RNA sequencing data from ICI-treated breast cancer patients revealed candidate human T cell correlates.

Conclusions We report a surprising, novel mechanism of ICI resistance whereby treatment-induced T cell infiltration and activation can paradoxically exacerbate a TNF α - and IL-1-dependent resistance circuit in tumors with active NF- κ B inflammation. Our findings refine the current models of ICI response and resistance with important therapeutic implications.

Acknowledgements We thank E. Engleman and J. Bluestone for cell lines. We thank A. Marson and T. Roth for CRISPR-Cas9 reagents, protocols and equipment. We thank the UCSF Clinical Cancer Genomics Laboratory, Molecular Oncology Initiative, and D. Raleigh for access to the UCSF cBioPortal dataset.

REFERENCES

1. P Sharma, S Hu-Lieskovan, JA Wargo, and A Ribas. Primary, Adaptive, and Acquired Resistance to Cancer Immunotherapy, *Cell*, Feb. 2017;**168**(4): 707–723, doi: 10.1016/j.cell.2017.01.017.
2. AC Betzler, et al. NF- κ B and its role in checkpoint control, *International Journal of Molecular Sciences* May 2020;**21**(11):3949, doi: 10.3390/IJMS21113949.
3. J Galon and D Bruni. Approaches to treat immune hot, altered and cold tumours with combination immunotherapies, *Nature Reviews Drug Discovery* 2018;**18**(3):197–218, Jan. 2019, doi: 10.1038/s41573-018-0007-y.
4. DT Le, et al. PD-1 blockade in tumors with mismatch-repair deficiency, *New England Journal of Medicine*, 2015;**372**(26):2509–2520, doi: 10.1056/nejmoa1500596.
5. F Petrelli, M Ghidini, A Ghidini, and G Tomasello. Outcomes following immune checkpoint inhibitor treatment of patients with microsatellite instability-high cancers: a systematic review and meta-analysis, *JAMA Oncology*, Jul. 2020;**6**(7):1068–1071, doi: 10.1001/JAMAONCOL.2020.1046.

<http://dx.doi.org/10.1136/jitc-2022-SITC2022.0511>

TIME-OF-DAY OF PEMBROLIZUMAB INFUSION AND CLINICAL OUTCOMES OF PATIENTS WITH NSCLC: TOO SOON TO PROMOTE MORNING INFUSIONS

^{1,2}Alessio Cortellini*, ³Adriana Barrichello, ³Joao Victor Alessi, ³Biagio Ricciuti, ³Victor Vatz, ⁴Thomas Newsom-Davis, ¹Joanne Evans, ³Giuseppe Lamberti, ³Federica Pecci, ⁵Patrizia Viola, ¹Antonio D'Alessio, ¹Claudia Fulgenzi, ³Mark Awad, ¹David Pinato. ¹Imperial College London, London, UK; ²University of L'Aquila, London, UK; ³Dana Farber Cancer Institute, Boston, MA, United States; ⁴Chelsea and Westminster Hospital, London, UK; ⁵Charing Cross Hospital, London, UK

Background Circadian oscillations in T-cell function may influence outcome from cancer immunotherapy.¹ Evidence for an association between time-of-day of immune checkpoint inhibitors (ICI) infusion on outcomes in patients with non-small cell lung cancer (NSCLC) is scanty.

Methods In this multicenter study, we retrospectively evaluated the association between time-of-day patterns of pembrolizumab infusion and outcomes in a cohort of patients with treatment-naïve metastatic NSCLC with PD-L1 expression $\geq 50\%$ treated from June 2016 to September 2021. Receipt of $\geq 20\%$ vs $< 20\%$ of infusions after the 16.30h cut off time ("late infusions") was set as threshold for analysis. In addition, we explored increasing thresholds for late infusions based on centre-specific distribution of cut-off times.

Results Overall 180/262 patients received ≥ 4 cycles and were eligible, 136 (75.5%) and 44 (24.5%) patients respectively received $< 20\%$ and $\geq 20\%$ of evening infusions. Evening infusions were associated with a lower number of cycles (median: 14 vs 8, $p=0.0002$). Following a propensity score matching (PSM) accounting for age, PD-L1-expression, ECOG-PS, bone metastases, smoking status and sex, 78 and 44 patients were matched from the $< 20\%$ and the $\geq 20\%$ evening infusions cohorts. Median OS and PFS of patients who received $\geq 20\%$ and $< 20\%$ of evening infusions were 27.8 vs 47.1 months ($p=0.11$) (figure 1A), and 6.6 vs 19.7 months ($p=0.056$) (figure 1B), respectively. Evening infusions did not affect the risk of death (HR 1.53, 95%CI: 0.88-2.76) or disease progression/death (HR 1.51, 95%CI: 0.95-2.42) at the multivariable analysis. When including the number of cycles in the PMS, patients who received $< 20\%$ and $\geq 20\%$ of evening infusions experienced similar OS and PFS estimates (figure 1C,D). The exploratory analyses of OS according to increasing quartiles using the 16.30h threshold and the centre-specific median time-of-day threshold across the entire population and the landmark population highlighted that both the receipt of 0% and 100% of evening and late infusions were associated with an increased risk of death (table 1), while after adjusting for the number of administered cycles, no proportion of late infusions was significantly associated to the risk of death.

Figure 2 provides a representation of the distribution of cycles across progressive thresholds for proportions of evening (16.30h threshold) and late (median time-of-day threshold) infusions according to incremental quartiles, highlighting duration of therapy as an inherent bias in retrospective analyses.

Conclusions Translational dynamic studies of peripheral T-cell immunity are warranted while prospective trials should be conducted before promoting morning infusion in clinic.

Acknowledgements The authors would like to acknowledge the infrastructure support provided by Imperial Experimental Cancer Medicine Centre, Cancer Research UK Imperial Centre and the Imperial College Healthcare NHS Trust Tissue Bank.

Antonio D'Alessio acknowledges the support received from the NIHR Imperial BRC, the European Association for the

Study of the Liver (Andrew Burroughs Fellowship) and Cancer Research UK (RCCPDB-Nov21/100008).

Biagio Ricciuti acknowledges the support received by the Society of Immunotherapy of Cancer-Astrazeneca Young Investigator Award.

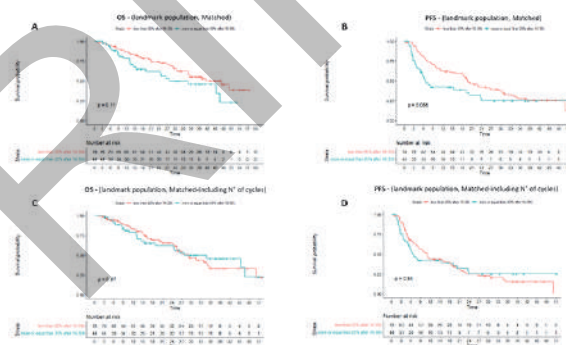
David J. Pinato acknowledges grant funding from the Wellcome Trust Strategic Fund (PS3416) and support from the Cancer Treatment and Research Trust (CTRT).

Alessio Cortellini acknowledges support by the NIHR Imperial BRC.

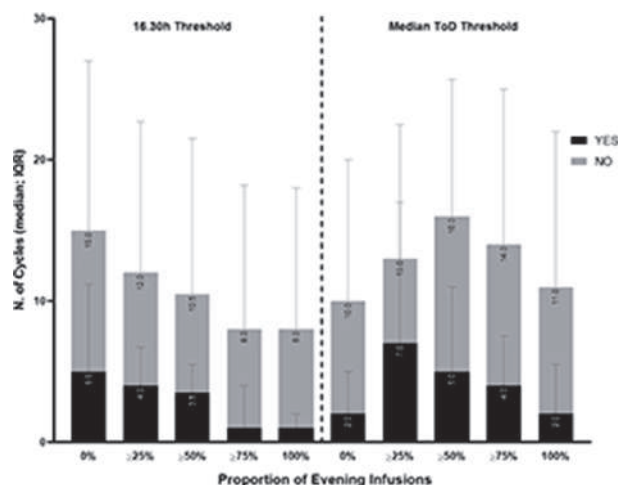
REFERENCE

1. Qian DC, Kleber T, Brammer B, *et al.* Effect of immunotherapy time-of-day infusion on overall survival among patients with advanced melanoma in the USA (MEMOIR): a propensity score-matched analysis of a single-centre, longitudinal study. *Lancet Oncol.* 2021 Dec;22(12):1777–1786. doi: 10.1016/S1470-2045(21)00546-5.

Ethics Approval The institutional review board for each institution granted approval to the study, which was conducted according to the ethical principles of the Declaration of Helsinki. (Central IRB ref.: 17/WA/0161/R18009).



Abstract 512 Figure 1 Kaplan-Meier survival estimates among the matched landmark population (=4 cycle) according to the receipt of $\geq 20\%$ or $< 20\%$ of evening infusions. Matching variables were: age, PD-L1 TPS, Eastern Cooperative Oncology Group Performance Status (ECOG-PS), bone metastases, smoking status and biological sex. (A) Overall survival (OS); (B) Progression Free Survival (PFS). Kaplan-Meier survival estimates among the matched landmark population (=4 cycle) according to the receipt of $\geq 20\%$ or $< 20\%$ of evening infusions, including the number of administered cycles in the matching procedure. (C) Overall survival (OS); (D) Progression Free Survival (PFS)



Abstract 512 Figure 2 Graphical representation of the distribution of median number of administered cycles across progressive thresholds for proportions of late infusions according to incremental quartiles. No infusions after 16.30h YES: 5 (IQR: 2-11.2), No infusion after 16.30h NO: 10 (IQR: 4-22); $\geq 25\%$ infusions after 16.30h: 4 (IQR: 2-6.7), $< 25\%$ infusions after 16.30h: 8 (IQR: 3-18.7); $\geq 50\%$ infusions after 16.30h: 3.5 (IQR: 2-5.5), $< 50\%$ infusions after 16.30h: 7 (IQR: 3-18); $\geq 75\%$ infusions after 16.30h: 1 (IQR: 1-4), $< 75\%$ infusions after 16.30h: 7 (IQR: 3-17.2); All infusions after 16.30h YES: 1 (IQR: 1-2), All infusions after 16.30h NO: 7 (IQR: 3-17). No infusions after median ToD YES: 2 (IQR: 1-5), No infusions after 16.30h NO: 8 (IQR: 3-18); $\geq 25\%$ infusions after median ToD: 7 (IQR: 3-17), $< 25\%$ infusions after 16.30h: 6 (IQR: 2-15.5); $\geq 50\%$ infusions after median ToD: 5 (IQR: 2-11), $< 50\%$ infusions after 16.30h: 11 (IQR: 3.2-20.7); $\geq 75\%$ infusions after median ToD: 4 (IQR: 2-7.5), $< 75\%$ infusions after 16.30h: 10 (IQR: 4-21); All infusions after median ToD YES: 2 (IQR: 1-5.5), All infusions after 16.30h: 9 (IQR: 4-20). IQR: inter-quartile range; ToD: time-of-day

Abstract 512 Table 1 Univariable and multivariable analysis of the risk of death according to incremental quartiles of evening infusions for each patients using the 16.30h threshold and centre-specific cut-offs (median time-of-day at each centre) among the whole study population and the landmark population. Increasing quartile of late infusions was first tested alone and then adjusted for the number of administered cycles. HR: hazard ratio; CI: confidence intervals

VARIABLE	Overall population		Landmark population (≥ 4 cycles)	
	HR (95% CI) for risk of death	HR (95% CI) for risk of death	HR (95% CI) for risk of death	HR (95% CI) for risk of death
0% of infusions after 16.30				
Yes vs No	1.69 (1.22-2.35)	1.37 (0.97-1.92)	1.42 (0.92-2.22)	1.33 (0.86-2.08)
N° of cycles (continuous)	-	0.91 (0.89-0.93)	-	0.93 (0.91-0.96)
25% of infusions after 16.30				
Yes vs No	1.71 (1.17-2.49)	1.03 (0.71-1.51)	1.34 (0.76-2.35)	0.79 (0.44-1.42)
N° of cycles (continuous)	-	0.91 (0.88-0.93)	-	0.93 (0.91-0.96)
50% of infusions after 16.30				
Yes vs No	1.80 (1.17-2.77)	0.97 (0.62-1.52)	1.98 (1.07-3.67)	1.13 (0.66-2.15)
N° of cycles (continuous)	-	0.91 (0.88-0.93)	-	0.93 (0.91-0.96)
75% of infusions after 16.30				
Yes vs No	3.17 (1.75-5.74)	1.82 (1.01-3.31)	1.43 (0.45-4.56)	0.78 (0.24-2.50)
N° of cycles (continuous)	-	0.91 (0.88-0.93)	-	0.93 (0.91-0.96)
100% of infusions after 16.30				
Yes vs No	4.81 (2.58-8.96)	2.83 (1.51-5.31)	1.88 (0.46-7.74)	1.08 (0.26-4.49)
N° of cycles (continuous)	-	0.91 (0.88-0.93)	-	0.93 (0.91-0.96)
0% of infusions after median time				
Yes vs No	1.85 (1.15-2.94)	0.94 (0.58-1.54)	1.37 (0.49-3.85)	0.81 (0.29-2.27)
N° of cycles (continuous)	-	0.91 (0.88-0.93)	-	0.93 (0.91-0.96)
25% of infusions after median time				
Yes vs No	1.09 (0.73-1.61)	1.06 (0.71-1.57)	1.27 (0.73-2.27)	1.05 (0.59-1.84)
N° of cycles (continuous)	-	0.91 (0.88-0.93)	-	0.93 (0.91-0.96)
50% of infusions after median time				
Yes vs No	1.63 (1.16-2.29)	1.12 (0.79-1.59)	1.52 (0.97-2.37)	1.09 (0.68-1.73)
N° of cycles (continuous)	-	0.91 (0.88-0.93)	-	0.93 (0.91-0.96)
75% of infusions after median time				
Yes vs No	2.04 (1.47-2.82)	1.24 (0.88-1.74)	1.81 (1.17-2.81)	1.13 (0.70-1.82)
N° of cycles (continuous)	-	0.91 (0.88-0.93)	-	0.93 (0.91-0.96)
100% of infusions after median time				
Yes vs No	2.14 (1.51-3.05)	1.19 (0.83-1.72)	1.00 (1.53-1.89)	0.58 (0.30-1.12)
N° of cycles (continuous)	-	0.91 (0.88-0.93)	-	0.93 (0.91-0.96)

<http://dx.doi.org/10.1136/jitc-2022-SITC2022.0512>

513 **OVERCOMING HEDGEHOG MEDIATED ANTI-PD-1 RESISTANCE IN MELANOMA THROUGH PROSTAGLANDIN INHIBITION**

Nicholas DeVito*, Y-Van Nguyen, Nagendra Yarla, Michael Plebanek, Balamayooran Theivanthiran, Michael Aksu, Vaibhav Jain, Brent Hanks. *Duke University, Durham, NC, United States*

Background Immunotherapy resistance correlates with mesenchymal transformation (MT),^{1, 2} however we are unable to therapeutically target this immune evasive phenotype. We have shown that in anti-PD-1 resistant melanomas, the Hedgehog (Hh) transcription factor Gli2 drives the upregulation of Wnt and prostaglandin synthesis, which promotes the recruitment of granulocytic myeloid-derived suppressor cells (PMN-MDSCs) leading to immune evasion and immunotherapy failure.^{3, 4} Hh activation has been described in immunotherapy resistance^{5, 6}, however targeting has focused on SMO inhibition, which is limited by noncanonical pathway activation.^{7, 8} Here, we demonstrate the utility of a Gli2 signature to predict anti-PD-1 immunotherapy failure and determine whether selective prostaglandin receptor inhibition (EP2i/EP4i) can overcome this resistance pathway in melanoma.

Methods Gli2 was constitutively activated (Gli2^{CA}) in a BRAF-V600EPTEN^{-/-} melanoma cell line by inducing an N-terminal truncating mutation. Multi-parameter flow cytometry, RNAseq, and scRNAseq were utilized to evaluate the impact of Gli2 activity and therapeutic treatments on the tumor immune microenvironment. Anti-PD-1, EP2i/EP4i, PORCNI (Wnt ligand inhibition), and PMN-MDSC ablation *in vivo* studies were performed in Gli2^{CA} and control tumors. Nanostring analysis was performed on clinical melanoma tumor specimens and bioinformatics studies were conducted using the TCGA and Hugo et al databases.²

Results Gli2^{CA} tumors display resistance to anti-PD-1, where flow cytometry revealed persistent exclusion of CD103⁺ antigen-presenting DCs, activated T and NK cells, and greater numbers of PMN-MDSCs compared to control tumors. Gli2 upregulates genes involved in prostaglandin synthesis and PGE2 production, which is ablated in Gli2-knockout melanomas. Treatment with EP2i/EP4i suppresses tumor growth, increasing levels of CD8⁺ T cells, NK cells, and cDC1s in Gli2^{CA} but not in control tumors; and this is further potentiated by anti-PD-1. EP2i/EP4i markedly reduces PMN-MDSCs in Gli2^{CA} tumors, and anti-Ly6G depletion of PMN-MDSCs had a similar impact on the immune microenvironment. scRNAseq showed enhanced NK cell activity with EP2i/EP4i over PORCNI in Gli2^{CA} tumors, and while both therapies reduced PMN-MDSC numbers, EP2i/EP4i also diminished suppressive markers. Gli2 and prostaglandin signatures correlate in the melanoma and colorectal TCGA. Importantly, a Gli2 signature predicts for anti-PD-1 resistance in a subset of melanoma patients.

Conclusions Gli2 drives the development of a tolerogenic tumor microenvironment during MT via Wnt and prostaglandin signaling, leading to anti-PD-1 failure through enhanced PMN-MDSC recruitment and activity. This state can be reversed with EP2i/EP4i in mouse models. These results suggest that a Gli2 signature may predict for EP2i/EP4i sensitivity in a subset of anti-PD-1 resistant melanomas.

REFERENCES

1. Bagaev A, et al. Conserved pan-cancer microenvironment subtypes predict response to immunotherapy. *Cancer Cell*, 2021.

2. Hugo W. et al. Genomic and Transcriptomic Features of Response to Anti-PD-1 Therapy in Metastatic Melanoma. *Cell* 2016;**165**(1): 35–44.
3. DeVito NC, et al. Pharmacological Wnt ligand inhibition overcomes key tumor-mediated resistance pathways to anti-PD-1 immunotherapy. *Cell Rep* 2021;**35**(5): 109071.
4. DeVito NC, SM, Nguyen Y, Plebanek M, Theivanthiran B, Liu F, Hanks BA. Hedgehog Signaling Drives Epithelial-to-Mesenchymal Transition, Immune Evasion, and Anti-PD-1 Resistance through Coordinated Upregulation of Wnt Ligands and PGE2 Synthesis. *Society for Immunotherapy in Cancer Annual Meeting*, 2021.
5. D'Angelo SP, et al. Pilot study of bempedegalesleukin in combination with nivolumab in patients with metastatic sarcoma. *Nat Commun* 2022;**13**(1): 3477.
6. Jiang J, et al. Pan-cancer analyses reveal that increased Hedgehog activity correlates with tumor immunosuppression and resistance to immune checkpoint inhibitors. *Cancer Med*, 2022;**11**(3): 847–863.
7. Pietrobono S, S Gagliardi, and B Stecca. Non-canonical Hedgehog Signaling Pathway in Cancer: Activation of GLI Transcription Factors Beyond Smoothed. *Front Genet*, 2019;**10**: 556.
8. De Jesus-Acosta A, et al. Phase 2 study of vismodegib, a hedgehog inhibitor, combined with gemcitabine and nab-paclitaxel in patients with untreated metastatic pancreatic adenocarcinoma. *Br J Cancer* 2020;**122**(4): 498–505.

Ethics Approval All appropriate ethics approvals were obtained. De-identified human data was obtained from publicly available resources (TCGA, Hugo et al databases). All patients from our internal dataset were collected under IRB protocol #Pro00059349, and animal experiments were conducted with IACUC approval #A114-21-05.

<http://dx.doi.org/10.1136/jitc-2022-SITC2022.0513>

514 TUMOR CONTEXT DICTATES RELIANCE ON TCF1 FOR RESPONSE TO IMMUNOTHERAPY

¹Giulia Escobar*, ¹Katherine Tooley, ¹Joan Pagès Oliveras, ¹Cheng Hanning, ¹Xue Chang, ¹Davide Mangani, ¹Hazel Natanael, ¹Carola Rutigliani, ²Luca Biasco, ¹Ana Carrizosa Anderson. ¹Brigham and Women's Hospital and Harvard Medical School, Boston, MA, United States; ²UCL Great Ormond Street Institute of Child Health, London, UK

Background Stem-like CD8 T cells that are regulated by the transcription factor TCF1 are key players in the response to immune checkpoint blockers (ICB). Recent findings indicate that the dependence on TCF1⁺ stem-like T cells for ICB efficacy may not be equal across patients and in different tumor contexts.

Methods Here we leveraged TCF1 conditional knock-out (TCF1-cKO) mice to investigate how TCF1 instructs the early fate and functions of CD8 cells upon ICB therapy in tumors that differ for immunogenicity and levels of tumor antigens expression.

Results Strikingly, we discovered that TCF1 expression in CD8 T cells is required for ICB efficacy in poorly immunogenic B16OVA melanomas but is dispensable in highly immunogenic MC38OVA colorectal tumors. Single-cell-RNA sequencing and immunophenotyping revealed defective priming and expansion of tumor-specific TCF1-cKO T cells in the tumor draining lymph-node (TDLN) of B16OVA- but not MC38OVA-bearing mice treated with ICB. In vitro, we found defective proliferation, reduced PD-1 and CD28 up-regulation and reduced phosphorylation of key molecules downstream the T cell receptor pathway when TCF1 cKO T cells were stimulated with low doses of antigens but not when stimulated with strong TCR signals. These data indicate that TCF1 poises T cells for optimal activation. Furthermore, transcriptional profiling of T cells in the TDLN further revealed the accumulation of a subset of tumor-specific naïve T cells poised to give rise to short-lived effectors in TCF1 cKO mice and thus is less suited to sustain anti-tumor responses in poorly immunogenic tumors where expansion of T cells retaining stem-like potential is required for durable anti-tumor responses. In tumors, single-cell-RNA sequencing and immunophenotyping showed that in MC38OVA tumors both WT and TCF1-cKO mice expanded a CD8 subset sharing a signature with transitory effector cells that mediate ICB efficacy in chronic viral infection models. Conversely, B16-OVA tumors retained a higher frequency of stem-like cells, failed to expand transitory effectors and accumulated Tox⁺ CD8 T cells, sharing a signature with CD8 cells expanded in non-responders to ICB. Importantly, loss of TCF1 was associated with reduced maintenance and proliferation of stem-like precursors and reduced expression of the Tox gene which was required for the survival of late effectors, altogether contributing to the failure of TCF1-cKO mice to sustain effective ICB responses.

Conclusions Our study highlights a role for TCF1 in the early stages of the CD8 T cell response with important implications for guiding the choice of optimal therapeutic interventions in tumors expressing low neoantigen levels.

<http://dx.doi.org/10.1136/jitc-2022-SITC2022.0514>

ASSESSING THE EFFECT OF POST-TRAUMATIC OSTEOARTHRITIS ON MURINE TUMOR GROWTH AND RESPONSIVENESS TO IMMUNE CHECKPOINT BLOCKADE

Elise Gray-Gaillard*, Younghwan Choi, Jin Han, Helen Nguyen, Katlin Stivers, Anna Ruta, Andrew Pardoll, Jennifer Elisseeff. *The Johns Hopkins University, Baltimore, MD, United States*

Background Immune checkpoint blockade (ICB) has revolutionized cancer treatment. The mechanisms of heterogeneous ICB responses (responder/non-responder), however, are poorly understood. Because of the increasing application of (neo)adjuvant ICB with tumor resection, the role of tissue injury caused by surgical procedures is a potential and usually overlooked factor in the generation of systemic anti-tumor immunity. Prior tissue injury has been shown to advance breast cancer progression.^{1,2} Whereas, the induction of senescent tumor cells and their senescence-associated secretory phenotype (SASP) within pancreatic cancer has been shown to remodel tumor vasculature, increasing ICB responsiveness.³ Thus, here we explore the role of cellular senescence induced by distant tissue damage on tumor growth. Anterior cruciate ligament (ACL) transection, a model of post-traumatic osteoarthritis, leads to senescent cell (SnC) accumulation in the joint and systemic SASP-mediated effects.⁴ We investigate the immunological and stromal changes arising with ACL injury and ICB within B16F10 murine melanoma, a classical non-responding model.

Methods ACL transection was performed prior to subcutaneous B16F10 inoculation. ICB treatment consisted of 4x intraperitoneal-injected 5mg/kg anti-PD1 monotherapy or anti-PD1/anti-CTLA4 combination therapy. Tumor growth was monitored via caliper measurements. Serum was collected after ICB treatment for cytokine array. Tumors were collected at termination for histological assessment. To elucidate changes in vascularization and senescence within tumors due to injury and/or treatment, we performed histological (H&E) and immunofluorescent staining of CD31 and p16, respectively. We quantified the change in tumor vessel number and size using QuPath and used HALO image analysis to quantify p16⁺ and CD31⁺ cells and their proximity.

Results ACL injury either 1- or 7-weeks prior to tumor injection significantly increased B16F10 responsiveness to ICB and survival. In tumors from ACL-injured mice treated with ICB, immunofluorescent staining showed significantly more p16⁺ SnCs and CD31⁺ cells, with a greater number of p16⁺ SnCs within 10µm of vasculature compared to controls. QuPath analysis of immunofluorescent-stained tumors from ACL-injured+ICB-treated mice uncovered a significantly higher frequency of large blood vessels (surface area >10000µm²) and H&E staining showed vessels had larger lumen. Cytokine array revealed increased serum-levels of pro-inflammatory cytokines and angiogenic factors in ACL-injured+ICB-treated mice.

Conclusions Our data demonstrate that ACL injury significantly increases ICB responsiveness in a classically non-responsive tumor model. ACL injury ameliorates tumor vascularization and increases the frequency of p16⁺ SnCs surrounding vasculature within ICB-treated tumors. The mechanism causing this effect is being elucidated. This study aims to develop predictive understanding of ICB responsiveness and provide mechanisms to sensitize non-responders.

REFERENCES

1. Koelwyn GJ, Newman AAC, Afonso MS, van Solingen C, Corr EM, Brown EJ, Albers KB, Yamaguchi N, Narke D, Schlegel M, Sharma M, Shanley LC, Barrett TJ, Rahman K, Mezzano V, Fisher EA, Park DS, Newman JD, Quail DF, Nelson ER, Caan BJ, Jones LW, Moore KJ. Myocardial infarction accelerates breast cancer via innate immune reprogramming. *Nat Med.* 2020;**26**:1452–1458.
2. Krall JA, Reinhardt F, Mercury OA, Pattabiraman DR, Brooks MW, Dougan M, Lambert AW, Bierie B, Ploegh HL, Dougan SK, Weinberg RA. The systemic response to surgery triggers the outgrowth of distant immune-controlled tumors in mouse models of dormancy. *Sci Transl Med.* 2018;**10**:eaan3464
3. Ruscetti M, Morris JP 4th, Mezzadra R, Russell J, Leibold J, Romesser PB, Simon J, Kulick A, Ho YJ, Fennell M, Li J, Norgard RJ, Wilkinson JE, Alonso-Curbelo D, Sridharan R, Heller DA, de Stanchina E, Stanger BZ, Sherr CJ, Lowe SW. Senescence-Induced Vascular Remodeling Creates Therapeutic Vulnerabilities in Pancreas Cancer. *Cell.* 2020;**181**:424–441.
4. Faust HJ, Zhang H, Han J, Wolf MT, Jeon OH, Sadtler K, Peña AN, Chung L, Maestas DR Jr, Tam AJ, Pardoll DM, Campisi J, Housseau F, Zhou D, Bingham CO 3rd, Elisseeff JH. IL-17 and immunologically induced senescence regulate response to injury in osteoarthritis. *J Clin Invest.* 2020;**130**:5493–5507.

Ethics Approval All animal studies were performed in accordance with approved Johns Hopkins University Animal Care and Use Committee protocol (Elisseeff, MO21M80).

<http://dx.doi.org/10.1136/jitc-2022-SITC2022.0515>

516

CLINICAL TIER GRADING OF CANCER STEM CELLS ACCORDING TO CLINICAL CHARACTERISTICS FOR IMMUNE CHECKPOINT INHIBITORS GUIDED BY MRNA STEMNESS INDEX

Priya Hays*. Hays Documentation Specialists, LLC, San Mateo, CA, United States

Background Cancer stem cells are cells in tumors that have self-renewing capabilities and proliferation, and are partly responsible for tumor growth, metastasis and drug resistance, and have been associated with multidrug resistance and epithelial-mesenchymal transition. Recent studies have shown that cancer stemness is capable of being targeted by immunotherapies.¹

mRNAsi, or mRNA stemness index, is a tool that has been developed to analyze prognostic significance for immunotherapy response for cancer stemness in lung adenocarcinoma, adrenocortical carcinoma and gastric cancer, among other carcinomas^{2,3,4} This abstract proposes to apply the prognostic signatures as determined by mRNAsi to create a clinical tier grading system that categorizes cancer stemness presenting characteristics based on studies by for ICI (nivolumab, (anti-PD-1) ipilimumab (anti-CTLA-4), pembrolizumab (anti-PD-L1), atezolizumab (anti-PD-L1)) treatment.⁵

Methods A literature search will be conducted using the keywords “cancer stem cells” OR “cancer stemness” AND “immunotherapies” AND “mRNAsi” AND “immune checkpoint inhibitors efficacy”. Additional keywords include “prognostic signatures” AND “metastasis” AND “clinical features” AND “clinical presentation.”

Results mRNAsi-guided tools determined differentially expressed genes in tumors and generated prognostic signatures which in turn reflected clinical characteristics that could be grouped into a tiered list, creating grading categories for ICI treatment efficacy (table 1). Low-risk and high-risk survival groups, tumor mutational burden, TNM pathological stages, overall survival were generated from prognostic gene signatures through mRNAsi. They also could predict 1-year, 3-year, and 5-year overall survival in certain cancers. Based on this clinical presentation, guidance for ICI therapy could be developed.

Conclusions A clinical tier grading list may be an effective way to guide oncologists in applying mRNAsi tools to cancer stemness for treatment through ICIs. Future studies could focus on stratifying patients through the prognostic signatures generated by these tools.

REFERENCES

1. Qin P, Li Q, Liu S, Ning N, Zhang X, Xu Y, Chang AE, Wicha MS. Targeting cancer stem cells using immunologic approaches. *Stem Cells*. 2015 July ; **33**(7): 2085–2092.
2. Li N, Li Y, Zheng P, Zhan Z. Cancer Stemness-Based Prognostic Immune-Related Gene Signatures in Lung Adenocarcinoma and Lung Squamous Cell Carcinoma. *Front. Endo*. 2021.
3. Mao D, Zhou Z, Song S, Li D, He Y, Wei Z, Zhang C. Identification of Stemness Characteristics Associated With the Immune Microenvironment and Prognosis in Gastric Cancer. *Front Onc* 2021.
4. Shi X, Liu Y, Cheng, S, Hu H, Zhang J, Wei M, Lin Zhao L, Xin S. Cancer stemness associate with prognosis and the efficacy of immunotherapy in adrenocortical carcinoma. *Front Onc*. 2021,
5. Santoro S. Clinical phenotype and management data in down syndrom regression disorder. *American College of Medical Genetics and Genomics Annual Meeting* 2022.

Abstract 516 Table 1 Clinical Tier Grading List According to Prognostic Signatures as Determined by mRNAsi (adapted from Shi 2021, Li 2021, Mao 2021, Santoro 2022)

Table 1 Clinical Tier Grading List According to Prognostic Signatures as Determined by mRNAsi (adapted from Shi 2021, Li 2021, Mao 2021, Santoro 2022)

	Tier 1	ICI Efficacy
Signature	Clinical Characteristics	
High-mRNAsi	High risk	Low
Low PD-L1	Low OS	
Low PD-1	High TMB	
Low CTLA-4		
	Tier 2	ICI Efficacy
Signature	Clinical Characteristics	
Low-mRNAsi	Low to moderate risk	High
High PD-L1	High OS	
High PD-1		
High CTLA-4		

<http://dx.doi.org/10.1136/jitc-2022-SITC2022.0516>

517

SPLENIC TUMOR-REACTIVE CD8⁺ T CELLS ARE ENDOWED WITH A UNIQUE POTENTIAL FOR EXPANSION AND ARE THE DOMINANT SOURCE OF SYSTEMIC ANTI-TUMOR IMMUNITY AFTER ICB THERAPY

Brendan Horton*, Duncan Morgan, J Love, Stefani Spranger. *Massachusetts Institute of Technology, Cambridge, MA, United States*

Background Expansion of systemic tumor-reactive T cells after immune checkpoint blockade (ICB) has been linked to successful tumor control, but regulators of systemic T cell expansion remain unknown. Using a murine lung cancer model, we previously demonstrated that flank tumors respond to ICB, while lung tumors do not. ICB-mediated control of flank tumors correlated with stronger expansion of systemic anti-tumor T cell responses, and the spleen, not tumor-draining lymph nodes (TdLNs), appeared to be the source of ICB-expanded tumor-reactive T cells.

Methods The murine KP lung cancer cell line was engineered to express the CD8⁺ T cell antigen SIY (KPSIY). Mice were inoculated subcutaneously to generate flank tumors or intravenously to generate lung tumors. For single cell sequencing experiments, endogenous SIY-reactive CD8⁺ T cells were isolated using fluorescence activated cell sorting (FACS) and RNA sequencing was performed using SeqWell. Mice expressing the transgenic 2C T cell receptor, specific for SIY, were used as T cell donors in adoptive transfer experiments.

Results KPSIY flank tumors generated higher numbers of splenic SIY-reactive CD8⁺ T cells than KPSIY lung tumors, and the spleen was the major site of SIY-reactive CD8⁺ T cell accumulation after ICB. Paired single cell RNA and TCR sequencing revealed extensive clonal expansion of SIY-reactive CD8⁺ T cells in flank tumor-bearing mice, including multiple recurrent TCR sequences shared between mice, that was significantly reduced in the lung tumor setting. To determine the influence of anatomic site on the response to ICB, we adoptively transferred naive 2C TCR-transgenic T cells to mice bearing KPSIY flank tumors. In vivo primed 2C T cells were FACS isolated from TdLNs or spleens and transferred into secondary tumor-bearing hosts prior to ICB treatment. Surprisingly, only 2C T cells isolated from spleens of primary tumor-bearing mice expanded in secondary hosts following ICB. Single cell sequencing of endogenous SIY-reactive CD8⁺ T cells confirmed distinct gene expression profiles between SIY-reactive T cells from TdLNs and spleens, and that tumor-infiltrating clonotypes were more prevalent in spleens of tumor-bearing mice than in TdLNs.

Conclusions The major source of systemic tumor-reactive CD8⁺ T cells after ICB in mice is the spleen, not the TdLN. The enhanced ability of splenic CD8⁺ T cells to expand after ICB therapy was driven by T cell-intrinsic differences which govern ICB responsiveness.

Ethics Approval The experiments in this abstract were approved by the Massachusetts Institute of Technology Committee on Animal Care, protocol number 0220-006-23, NIH assurance ID D16-00078.

<http://dx.doi.org/10.1136/jitc-2022-SITC2022.0517>

META-ANALYSIS ON IMMUNOTHERAPY-RELATED HYPERPROGRESSIVE DISEASE (HPD) INCIDENCE ACROSS TUMOR TYPES AND HPD DEFINITIONS

¹Min Jeong Kim*, ¹Seung Pyo Hong, ¹Yeonggyeong Park, ²Allison Belette, ³Chiwoo Song, ¹Youjin Oh, ⁴Sukjoo Cho, ¹Ilene Hong, ¹Young Kwang Chae. ¹Northwestern University Feinberg School of Medicine, Chicago, IL, United States; ²University of Texas Health Science Center, Houston, TX, United States; ³Nowon Eulji Medical Center, Eulji University, Seoul, Korea, Republic of; ⁴South Florida Morsani College of Medicine, Tampa, FL, United States

Background While reported in other types of systemic therapy as well, evidence for hyperprogressive disease (HPD) following onset of immunotherapy has increased in the past decade. Despite such growing evidence, the lack of a consensual definition precludes a better understanding of this phenomenon.

Methods A systematic literature search was done on PubMed, Embase, Web of Science, and Cochrane Database of Systematic Reviews based on a search algorithm that included key terms including immune checkpoint inhibitor, immunotherapy, and hyperprogress. Studies published until June 21, 2022 which used a definition based on tumor kinetics were included. All studies were categorized according to one of three definitions of HPD: A) RECIST-defined progressive disease (PD) and tumor growth rate (TGR) ratio $< u > > 2^1$ B) RECIST-based tumor growth kinetics (TGK) ratio $< u > > 2^2$, and C) RECIST-defined PD and $\Delta TGR > 50\%$.³ A generalized linear mixed-effects model was used, and multivariable analysis was conducted to explore differences in the incidence across tumor types and HPD definitions.

Results A total of 34 studies comprising 4117 patients and 5 different tumor types (renal cell carcinoma (RCC), mixed or other, hepatocellular carcinoma (HCC), non-small cell lung cancer (NSCLC), and advanced gastric cancer (AGC)) were included in the meta-analysis.⁴⁻³⁶ The overall pooled incidence of HPD was 12.40% (95% CI, 10.28 – 14.89%) and ranged from 0.0% to 36.73% (figure 1 and 2). Statistical heterogeneity was significant ($I^2 = 72.3\%$; $P < 0.01$). Patients diagnosed with AGC (odds ratio (OR), 10.83; 95% CI, 2.15-66.02; $P < .001$), HCC (OR, 7.99; 95% CI, 1.68-38.10; $P = .003$), NSCLC (OR, 7.14; 95% CI, 1.58-32.27; $P = .004$), and mixed or other (OR, 5.09; 95% CI, 1.12-23.12; $P = .03$) were more likely to experience HPD than patients with RCC. Across definitions, differences in the HPD incidence was significantly higher for definition B (OR, 1.81; 95% CI, 0.58-1.80; $P = .025$) compared to definition C.

Conclusions Significant differences in HPD incidence are observed across tumor types and HPD definitions. To better characterize these differences, further studies — as well as efforts to agree on a consensual definition — are warranted.

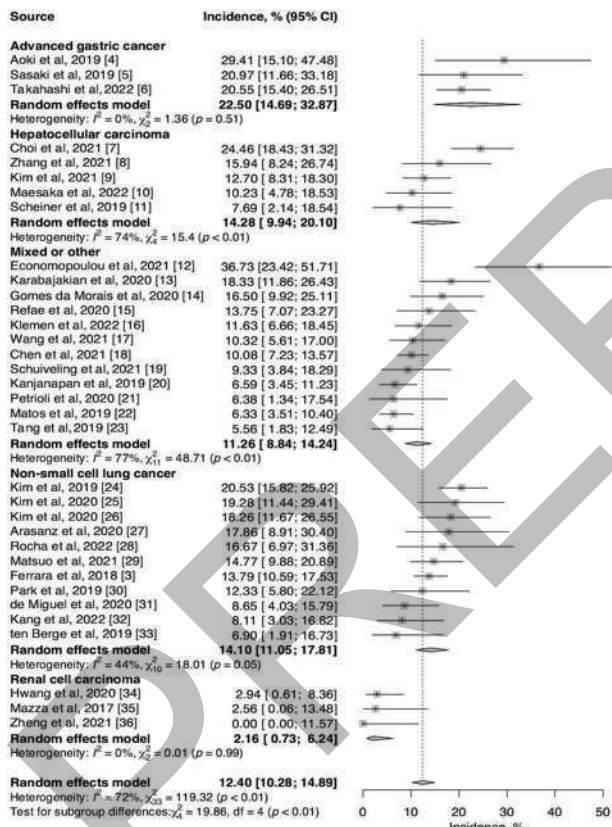
REFERENCES

1. Champiat S, Derle L, Ammari S, et al. Hyperprogressive Disease Is a New Pattern of Progression in Cancer Patients Treated by Anti-PD-1/PD-L1. *Clin Cancer Res Off J Am Assoc Cancer Res*. 2017;**23**(8):1920–1928. doi:10.1158/1078-0432.CCR-16-1741
2. Saada-Bouaid E, Defaucheux C, Karabajakian A, et al. Hyperprogression during anti-PD-1/PD-L1 therapy in patients with recurrent and/or metastatic head and neck squamous cell carcinoma. *Ann Oncol Off J Eur Soc Med Oncol*. 2017;**28**(7):1605–1611. doi:10.1093/annonc/mdx178
3. Ferrara R, Mezquita L, Texier M, et al. Hyperprogressive disease in patients with advanced non-small cell lung cancer treated with PD-1/PD-L1 inhibitors or with single-agent chemotherapy. *JAMA Oncol*. 2018;**4**(11):1543–1552. doi:10.1001/jamaoncol.2018.3676
4. Aoki M, Shoji H, Nagashima K, et al. Hyperprogressive disease during nivolumab or irinotecan treatment in patients with advanced gastric cancer. *ESMO Open*. 2019;**4**(3):e000488. doi:10.1136/esmoopen-2019-000488
5. Sasaki A, Nakamura Y, Mishima S, et al. Predictive factors for hyperprogressive disease during nivolumab as anti-PD1 treatment in patients with advanced gastric

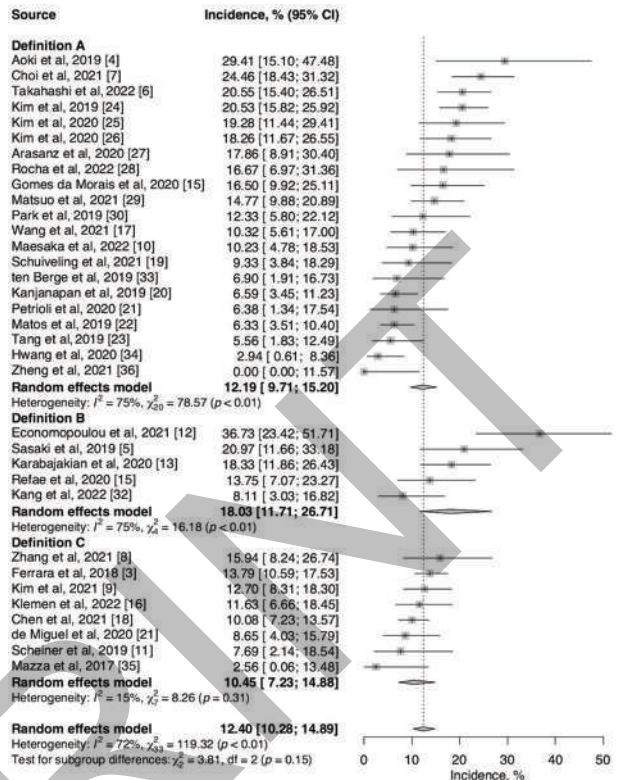
- cancer. *Gastric Cancer Off J Int Gastric Cancer Assoc Jpn Gastric Cancer Assoc*. 2019;**22**(4):793–802. doi:10.1007/s10120-018-00922-8
6. Takahashi Y, Sunakawa Y, Inoue E, et al. Real-world effectiveness of nivolumab in advanced gastric cancer: the DELIVER trial (JACCRO GC-08). *Gastric Cancer*. 2022;**25**(1):235–244. doi:10.1007/s10120-021-01237-x
7. Choi WM, Kim JY, Choi J, et al. Kinetics of the neutrophil-lymphocyte ratio during PD-1 inhibition as a prognostic factor in advanced hepatocellular carcinoma. *Liver Int Off J Int Assoc Study Liver*. 2021;**41**(9):2189–2199. doi:10.1111/liv.14932
8. Zhang L, Wu L, Chen Q, et al. Predicting hyperprogressive disease in patients with advanced hepatocellular carcinoma treated with anti-programmed cell death 1 therapy. *EClinicalMedicine*. 2021;**31**:100673. doi:10.1016/j.eclinm.2020.100673
9. Kim CG, Kim C, Yoon SE, et al. Hyperprogressive disease during PD-1 blockade in patients with advanced hepatocellular carcinoma. *J Hepatol*. 2021;**74**(2):350–359. doi:10.1016/j.jhep.2020.08.010
10. Maesaka K, Sakamori R, Yamada R, et al. Hyperprogressive disease in patients with unresectable hepatocellular carcinoma receiving atezolizumab plus bevacizumab therapy. *Hepatol Res*. 2022;**52**(3):298–307. doi:10.1111/hepr.13741
11. Scheiner B, Kirstein MM, Hucke F, et al. Programmed cell death protein-1 (PD-1)-targeted immunotherapy in advanced hepatocellular carcinoma: efficacy and safety data from an international multicentre real-world cohort. *Aliment Pharmacol Ther*. 2019;**49**(10):1323–1333. doi:10.1111/apt.15245
12. Economopoulou P, Anastasiou M, Papaxoinis G, et al. Patterns of response to immune checkpoint inhibitors in association with genomic and clinical features in patients with head and neck squamous cell carcinoma (HNSCC). *Cancers*. 2021;**13**(2):286. doi:10.3390/cancers13020286
13. Karabajakian A, Garrivier T, Crozes C, et al. Hyperprogression and impact of tumor growth kinetics after PD1/PDL1 inhibition in head and neck squamous cell carcinoma. *Oncotarget*. 2020;**11**(18):1618–1628. doi:10.18632/oncotarget.27563
14. Gomes da Moraes AL, de Miguel M, Cardenas JM, Calvo E. Comparison of radiological criteria for hyperprogressive disease in response to immunotherapy. *Cancer Treat Rev*. 2020;**91**:102116. doi:10.1016/j.ctrv.2020.102116
15. Refae S, Gal J, Brest P, et al. Hyperprogression under Immune Checkpoint Inhibitor: a potential role for germinal immunogenetics. *Sci Rep*. 2020;**10**(1):3565. doi:10.1038/s41598-020-60437-0
16. Klemen ND, Hwang S, Bradic M, et al. Long-term Follow-up and Patterns of Response, Progression, and Hyperprogression in Patients after PD-1 Blockade in Advanced Sarcoma. *Clin Cancer Res*. Published online January 19, 2022:OF1-OF9. doi:10.1158/1078-0432.CCR-21-3445
17. Wang Z, Liu C, Bai Y, et al. Redefine Hyperprogressive Disease During Treatment With Immune-Checkpoint Inhibitors in Patients With Gastrointestinal Cancer. *Front Oncol*. 2021;**11**. Accessed March 2, 2022. <https://www.frontiersin.org/article/10.3389/fonc.2021.761110>
18. Chen S, Gou M, Yan H, et al. Hyperprogressive Disease Caused by PD-1 Inhibitors for the Treatment of Pan-Cancer. *Dis Markers*. 2021;2021:e6639366. doi:10.1155/2021/6639366
19. Schuiveling M, Tonk E, Verheijden RJ, Suijkerbuijk KPM. Hyperprogressive disease rarely occurs during checkpoint inhibitor treatment for advanced melanoma. *Cancer Immunol Immunother Cll*. 2021;**70**(5):1491–1496. doi:10.1007/s00262-020-02716-3
20. Kanjanapan Y, Day D, Wang L, et al. Hyperprogressive disease in early-phase immunotherapy trials: Clinical predictors and association with immune-related toxicities. *Cancer*. 2019;**125**(8):1341–1349. doi:10.1002/ncr.31999
21. Petrioli R, Mazzei MA, Giorgi S, et al. Hyperprogressive disease in advanced cancer patients treated with nivolumab: a case series study. *Anticancer Drugs*. 2020;**31**(2):190–195. doi:10.1097/CAD.0000000000000864
22. Matos I, Martin-Liberal J, Garcia-Ruiz A, et al. Capturing hyperprogressive disease with immune-checkpoint inhibitors using RECIST 1.1 Criteria. *Clin Cancer Res Off J Am Assoc Cancer Res*. 2020;**26**(8):1846–1855. doi:10.1158/1078-0432.CCR-19-2226
23. Tang B, Chi Z, Sheng X, et al. Tumor growth rate as an early indicator of the efficacy of anti-PD-1 immunotherapy in advanced melanoma. *J Clin Oncol*. 2019;**37**(15_suppl):e21050–e21050. doi:10.1200/JCO.2019.37.15_suppl.e21050
24. Kim CG, Kim KH, Pyo KH, et al. Hyperprogressive disease during PD-1/PD-L1 blockade in patients with non-small-cell lung cancer. *Ann Oncol Off J Eur Soc Med Oncol*. 2019;**30**(7):1104–1113. doi:10.1093/annonc/mdz123
25. Kim SR, Chun SH, Kim JR, et al. The implications of clinical risk factors, CAR index, and compositional changes of immune cells on hyperprogressive disease in non-small cell lung cancer patients receiving immunotherapy. *BMC Cancer*. 2021;**21**(1):19. doi:10.1186/s12885-020-07727-y
26. Kim KH, Hur JY, Koh J, et al. Immunological Characteristics of Hyperprogressive Disease in Patients with Non-small Cell Lung Cancer Treated with Anti-PD-1/PD-L1 Abs. *Immune Netw*. 2020;**20**(6):e48. doi:10.4110/in.2020.20.e48
27. Arasanz H, Zuazo M, Bocanegra A, et al. Early Detection of Hyperprogressive Disease in Non-Small Cell Lung Cancer by Monitoring of Systemic T Cell Dynamics. *Cancers*. 2020;**12**(2):E344. doi:10.3390/cancers12020344
28. Rocha P, Ramal D, Ripoll E, et al. Comparison of Different Methods for Defining Hyperprogressive Disease in NSCLC. *JTO Clin Res Rep*. 2021;**2**(1):100115. doi:10.1016/j.jtocrr.2020.100115
29. Matsuo N, Azuma K, Kojima T, et al. Comparative incidence of immune-related adverse events and hyperprogressive disease in patients with non-small cell lung

Abstracts

- cancer receiving immune checkpoint inhibitors with and without chemotherapy. *Invest New Drugs*. 2021;**39**(4):1150–1158. doi:10.1007/s10637-021-01069-7
30. Park HJ, Kim KW, Won SE, *et al*. Definition, incidence, and challenges for assessment of hyperprogressive disease during cancer treatment with immune checkpoint inhibitors: a systematic review and meta-analysis. *JAMA Netw Open*. 2021;**4**(3):e211136. doi:10.1001/jamanetworkopen.2021.1136
31. Ayala de Miguel P, López Gallego J, Gorospe García I, *et al*. Hyperprogressive disease during treatment with immune checkpoint inhibitors in patients with advanced non-small cell lung cancer (NSCLC). *J Clin Oncol*. 2020;**38**(15_suppl):e21664–e21664. doi:10.1200/JCO.2020.38.15_suppl.e21664
32. Kang DH, Chung C, Sun P, *et al*. Circulating regulatory T cells predict efficacy and atypical responses in lung cancer patients treated with PD-1/PD-L1 inhibitors. *Cancer Immunol Immunother*. 2022;**71**(3):579–588. doi:10.1007/s00262-021-03018-y
33. ten Berge DMH, Hurkmans DP, den Besten I, *et al*. Tumour growth rate as a tool for response evaluation during PD-1 treatment for non-small cell lung cancer: a retrospective analysis. *ERJ Open Res*. 2019;**5**(4):00179–02019. doi:10.1183/23120541.00179-2019
34. Hwang I, Park I, Yoon SK, Lee JL. Hyperprogressive Disease in Patients With Urothelial Carcinoma or Renal Cell Carcinoma Treated With PD-1/PD-L1 Inhibitors. *Clin Genitourin Cancer*. 2020;**18**(2):e122–e133. doi:10.1016/j.clgc.2019.09.009
35. Mazza C, Arfi-Rouche J, Koscielny S, *et al*. Effect of nivolumab on tumor growth rate (TGR) in metastatic renal cell carcinoma (mRCC). *J Clin Oncol*. 2017;**35**(6_suppl):481–481. doi:10.1200/JCO.2017.35.6_suppl.481
36. Zheng B, Shin JH, Li H, Chen Y, Guo Y, Wang M. Comparison of Radiological Tumor Response Based on iRECIST and RECIST 1.1 in Metastatic Clear-Cell Renal Cell Carcinoma Patients Treated with Programmed Cell Death-1 Inhibitor Therapy. *Korean J Radiol*. 2021;**22**(3):366–375. doi:10.3348/kjr.2020.0404



Abstract 519 Figure 1 Forest Plot of HPD incidence across tumor types



Abstract 519 Figure 2 Forest Plot of HPD incidence across definitions

<http://dx.doi.org/10.1136/jitc-2022-SITC2022.0519>

520

PD-1 INHIBITS BYSTANDER T CELL ACTIVATION AND PROTECTS FROM ACTIVATION INDUCED CELL DEATH

Michael Sheng*, Catherine Le, Cordelia Dunai, Lam Khuat, Logan Vick, Kevin Stoffel, Arta Monjazeb, Craig Collins, Robert Canter, William Murphy. *University of California Davis, School of Medicine, Happy Valley, OR, United States*

Background Immune checkpoint inhibition (ICI) targeting PD-1/PDL-1 is being increasingly applied and for longer periods of time. Aside from rapid response to antigen stimulation, memory T cells can also be directly activated and perform effector functions via cytokine signaling alone in the presence of high concentrations of inflammatory or immunostimulatory cytokines due to expression of CD132/CD122 receptor complexes.¹⁻³ These ‘bystander-activated’ T cells can therefore amplify T cell effector responses particularly in aged individuals where a higher proportion of memory T cells exists.⁴ While the role of PD-1/PDL-1 on antigen-specific T cell responses has been extensively characterized, its role in bystander T cell responses is less clear.

Methods We examined the role of the PD-1/PD-L1 pathway during bystander activation using multiple mouse and human model systems. T cells from mice treated with high-dose (HD) rhIL-2 were evaluated for bystander activation using flow cytometry for NKG2D, CD69, granzyme B, CD25, Ki67, and PD-1 expression. Mouse T cells from control or TCR-transgenic OT-1 mice (which are specific for ovalbumin and thus not antigen-experienced) were stimulated in vitro with rhIL-2 or anti-CD3/28 to model bystander versus TCR-stimulated signaling. Activation, proliferative, and apoptotic responses (via annexin V staining) were assessed at various time-points. Effects of PD-1 blockade or loss was also assessed. We compared these results gating on PD1+ and PD1- T cell populations and subsequently repeated the same procedure using human T cells isolated from human PBMCs. We then assessed human T cells isolated from patients undergoing HD rhIL2 treatment for cancer, gating on PD1+ and PD-1- activated T populations.

Results Significantly reduced activation and proliferative responses were observed by activated PD-1+ bystander T cells compared to the PD-1- populations in both the mouse and human T cells following HD IL2 treatment in vitro or in vivo. PD-1- bystander-activated T cells also had increased apoptosis via activation induced cell death (AICD). Concurrent blockade or absence of PD-1 signaling in the mouse models resulted in greater activation responses comparable to PD-1- cells, but this also resulted in increased AICD and cell loss.

Conclusions The PD-1/PD-L1 pathway also inhibits antigen-nonspecific bystander-activated memory T cell responses and protects cells from AICD. While blockade of this pathway can result in increased bystander activation and effector functions, it also leads to increased AICD and T cell loss. These findings imply possible consequences of continuous PD-1 blockade application on the maintenance of the finite memory T-cell pool.

REFERENCES

1. Tough DF, Borrow P, Sprent J. Induction of bystander T cell proliferation by viruses and type I interferon in vivo. *Science*. 1996; **272**:1947–1950.
2. Whiteside SK, Snook JP, Williams MA, Weis J. Bystander T Cells: A Balancing Act of Friends and Foes. *Trends Immunol*. 2018; **39**:1021–1035.
3. Marice NJ, Taber AK, Prlc M. The Ugly Duckling Turned to Swan: A Change in Perception of Bystander-Activated Memory CD8 T Cells. *J Immunol*. 2021; **206**:455–462.
4. Farber DL, Yudanin A, Restifo NP. Human memory T cells: generation, compartmentalization and homeostasis. *Nat Rev Immunol*. 2014; **14**:24–35.

Ethics Approval All studies and protocols complied with ethical regulations and humane endpoints and were approved by University of California Davis (UCD) IACUC. Mice were housed in AAALAC-accredited animal facilities at UCD under specific-pathogen-free conditions.

For human blood samples, signed informed consent was obtained before enrollment. The study was approved by the Providence Health System Regional Institutional Review Board, Oregon.

<http://dx.doi.org/10.1136/jitc-2022-SITC2022.0520>

Abstracts

521

AK112, A TETRAVALENT BISPECIFIC ANTIBODY TARGETING PD-1 AND VEGF, ENHANCES BINDING AVIDITY AND FUNCTIONAL ACTIVITIES AND ELICITS POTENT ANTI-TUMOR EFFICACY IN PRE-CLINICAL STUDIES

Tingting Zhong, Zhaoliang Huang, Xinghua Pang, Chunshan Jin, Xinrong He, Yu Xia, Baiyong Li, Jing Min*, Akeso Biopharma Co., Ltd., Zhongshan, China

Background PD-1/PD-L1 inhibition immunotherapy holds great promise in cancer treatment. Combination treatment using anti-PD-1/PD-L1 agents with other immunotherapeutics brings additional benefits, such as preventing refractory effects towards PD-1/PD-L1 antibodies, and improving anti-tumor activities. Vascular endothelial growth factor (VEGF) is found to be frequently overexpressed in various solid tumors, which not only promotes tumor angiogenesis but also functions to suppress anti-tumor immune response.^{1, 2} Consequently, a novel anti-PD-1/VEGF bispecific antibody (AK112) was designed to inhibit PD-1-mediated immunosuppression and simultaneously block tumor angiogenesis in the tumor micro-environment (TME). The tetraivalent structure of AK112 allows formation of large complexes with dimeric VEGF, resulting in improved avidity to PD-1 and functional activities, which elicits potent anti-tumor efficacy in pre-clinical studies. **Methods** The antigen binding activity of AK112 with PD-1 and VEGF were assessed by ELISA, Fortebio and flow cytometry. The formation of AK112-VEGF complexes was detected by size-exclusion high-pressure liquid chromatography (SEC-HPLC). To determine if VEGF could enhance the avidity of AK112 to PD-1, the binding activity of AK112 with PD-1 was evaluated by Fortebio and flow cytometry in the presence of VEGF. The blockade of PD-1/PD-L1 signaling pathway was determined in luciferase reporter cell assay. The PD-1 internalization was determined by flow cytometry. In *in-vivo* pharmacology studies, the anti-tumor activity of AK112 was investigated in SCID/Beige mice implanted with HCC827 cells. **Results** AK112 could specifically bind to human PD-1 and VEGF with high affinity (table 1). Intriguingly, AK112 was found to form soluble complexes with VEGF by SEC-HPLC assay (figure 1). Notably, VEGF efficiently enhanced the binding of AK112 to PD-1 (table 2, figure 2), which led to increased PD-1 internalization (figure 3) and better potency on blockade of PD-1/PD-L1 signaling (figure 4). Moreover, AK112 demonstrated greater anti-tumor efficacy compared to Bevacizumab in mice (figure 5).

Conclusions AK112, a dual-blocking anti-PD-1/VEGF bispecific antibody, shows improved avidity to PD-1 in the presence of VEGF, and displays great anti-tumor efficacy in a mouse tumor model, supporting its clinical development for the treatment of human cancers.

REFERENCES

- Carmeliet P. VEGF as a key mediator of angiogenesis in cancer. *Oncology*. 2005;**69**(Suppl 3):4–10. doi: 10.1159/000088478. Epub 2005 Nov 21. PMID: 16301830.
- Ohm JE, Carbone DP. VEGF as a mediator of tumor-associated immunodeficiency. *Immunol Res*. 2001;**23**(2-3):263–72. doi: 10.1385/IR:23:2-3:263. PMID: 11444391.

Abstract 521 Table 1 Antigen binding activity of AK112 to PD-1 and VEGFA

Note: a, fusion protein of mouse Fc with human PD-1 extracellular domain or 6× histidine-tagged VEGFA protein was fixed onto the plates in the assays; b, 293T cells transfected with human PD-1 (293T-PD-1 cells) were used as target cells in the assay; c, biotinylated fusion protein of human Fc with human PD-1 extracellular domain or 6× histidine-tagged VEGFA protein was immobilized onto the sensor in the assays. NA, not applicable

Table 1 Antigen binding activity of AK112 to PD-1 and VEGFA

Antibody	EC50 (nM) of antigen binding activity			KD (M) of antigen binding affinity	
	ELISA ^a		FACS ^b	Fortebio ^c	
	PD-1	VEGFA	293T-PD-1 cells	PD-1	VEGFA
AK112	0.060	0.036	3.49	2.46E-10	3.30E-10
Bevacizumab	NA	0.035	NA	NA	6.64E-10
Nivolumab	0.044	NA	2.10	2.48E-10	NA

Note: a, fusion protein of mouse Fc with human PD-1 extracellular domain or 6× histidine-tagged VEGFA protein was fixed onto the plates in the assays; b, 293T cells transfected with human PD-1 (293T-PD-1 cells) were used as target cells in the assay; c, biotinylated fusion protein of human Fc with human PD-1 extracellular domain or 6× histidine-tagged VEGFA protein was immobilized onto the sensor in the assays. NA, not applicable.

Abstract 521 Table 2 Promoted binding avidity of AK112 to human PD-1

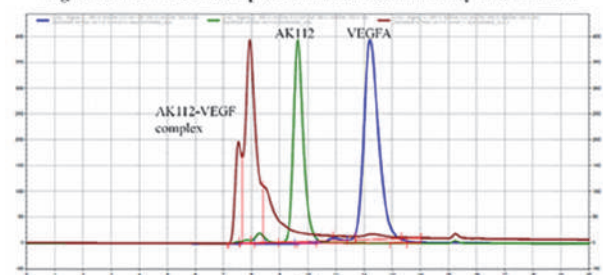
Promoted binding avidity of AK112 to human PD-1 in the presence of VEGFA. Note: a, antibodies with two-fold serial dilution from 50 nM to 1.56 nM; b, AK112 was pre-incubated with human VEGFA-his at same concentration and then diluted from 50 nM to 1.56 nM

Table 2. Promoted binding avidity of AK112 to human PD-1 in the presence of VEGFA.

Fixed antigen	Antibody ^a	VEGFA-his (nM)	KD (M)	kon (1/ms)	kdis (1/s)
PD1-his, 200 nM	AK105	0	4.11E-10	5.74E+05	2.36E-04
	AK112	0	7.15E-10	2.94E+05	2.10E-04
	AK112-VEGF ^b	50-1.56	3.83E-11	2.51E+05	9.62E-06

Note: a, antibodies with two-fold serial dilution from 50 nM to 1.56 nM; b, AK112 was pre-incubated with human VEGFA-his at same concentration and then diluted from 50 nM to 1.56 nM.

Fig 1. AK112-VEGFA complex formation determined by SEC-HPLC.

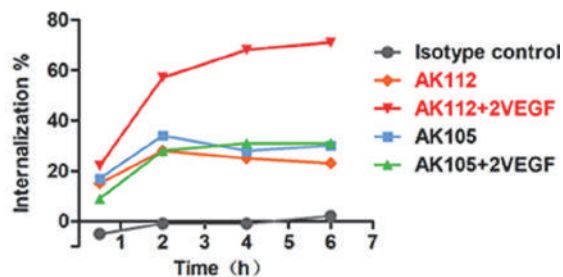


AK112 were premixed with 2× VEGFA and then analyzed on SEC-HPLC (Red color). AK112 alone (Green color) and VEGFA alone (Blue color) were included as reference.

Abstract 521 Figure 1 AK112 -VEGFA complex formation determined by SEC-HPLC

AK112 were premixed with 2× VEGFA and then analyzed on SEC-HPLC (Red color). AK112 alone (Green color) and VEGFA alone (Blue color) were included as reference.

Fig 2. Antigen binding activity of AK112 to PD-1 expressing cells.

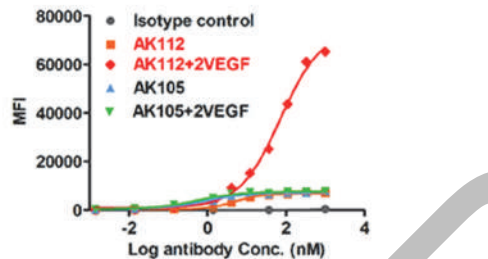


FACS binding curves of AK112 and AK105 with or without 2xVEGFA to PD-1 on PD-1 transfected Jurkat cells. Secondary antibody is mouse anti-Human IgG FC-Alexa Fluor 647. MFI, mean fluorescent intensity.

Abstract 521 Figure 2 Antigen binding activity to PD-1 expressing cells.

FACS binding curves of AK112 and AK105 with or without 2xVEGFA to PD-1 on PD-1 transfected Jurkat cells. Secondary antibody is mouse anti-Human IgG FC-Alexa Fluor 647. MFI, mean fluorescent intensity.

Fig 3. VEGFA effect on bioactivity of AK112 to enhance PD-1 internalization.

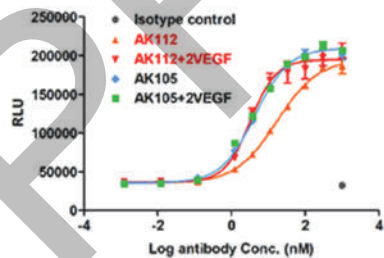


Cell surface PD-1 level on PD-1-expressing Jurkat cells were detected by FACS at different time points after AK112 and AK105 treatment with or without VEGFA. Internalization percentage was calculated from the decrease of surface PD-1 compared to its expression at 0 h.

Abstract 521 Figure 3 The bioactivity of AK112 to PD-1 Internalization.

VEGFA effect on bioactivity of AK112 to enhance PD-1 internalization. Cell surface PD-1 level on PD-1-expressing Jurkat cells were detected by FACS at different time points after AK112 and AK105 treatment with or without VEGFA. Internalization percentage was calculated from the decrease of surface PD-1 compared to its expression at 0 h.

Fig 4. Enhanced bioactivity of AK112 to block PD-1/PD-L1 signaling pathway in the presence of VEGFA.

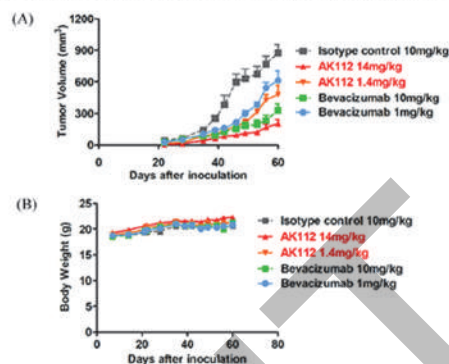


AK112 and anti-PD-1 antibody AK105 with or without 2xVEGFA blocked the interaction of PD-1 and PD-L1, leading to enhancement of luminescence in the co-culture of PD-L1 aAPC/CHO-K1 cells and PD-1 effector cells. Luminescence signals were detected by Steady-Glo Luciferase assay. RLU, relative light units.

Abstract 521 Figure 4 Bioactivity to block PD-1/PD-L1 signaling pathway.

Enhanced bioactivity of AK112 to block PD-1/PD-L1 signaling pathway in the presence of VEGFA. AK112 and anti-PD-1 antibody AK105 with or without 2xVEGFA blocked the interaction of PD-1 and PD-L1, leading to enhancement of luminescence in the co-culture of PD-L1 aAPC/CHO-K1 cells and PD-1 effector cells. Luminescence signals were detected by Steady-Glo Luciferase assay. RLU, relative light units.

Fig 5. AK112 inhibited tumor growth in SCID/Beige mice with subcutaneous HCC827 tumor.



Each mouse was inoculated subcutaneously at the right hind flank with HCC827 cells, PBMCs and AK112, Bevacizumab or Isotype control anti-HEL mixture on day 0. Different doses of antibodies were then continuously intravenously injected on day 7, 14, 21, 28, 35. Tumor volume (A) and body weight (B) were measured.

Abstract 521 Figure 5 The anti-tumor activity in mouse tumor model.

AK112 inhibited tumor growth in SCID/Beige mice with subcutaneous HCC827 tumor. Each mouse was inoculated subcutaneously at the right hind flank with HCC827 cells, PBMCs and AK112, Bevacizumab or Isotype control anti-HEL mixture on day 0. Different doses of antibodies were then continuously intravenously injected on day 7, 14, 21, 28, 35. Tumor volume (A) and body weight (B) were measured.

<http://dx.doi.org/10.1136/jitc-2022-SITC2022.0521>

Abstracts

522

CLINICAL AND MOLECULAR FEATURES OF ACQUIRED RESISTANCE TO IMMUNOTHERAPY IN NON-SMALL CELL LUNG CANCER

¹Danish Memon, ²Matthew Hellmann, ²Martin Miller*. ¹University of Cambridge, Cambridge, UK; ²AstraZeneca, New York, NY, United States

Background Although cancer immunotherapy with PD-(L)1 blockade is now routine treatment for patients with lung cancer, remarkably little is known about the molecular and cellular features of acquired resistance. This is partially due to the difficulty in obtaining pre- and post-treatment samples from patients that initially respond to immunotherapy but relapse with time. Studies from smaller cohorts in lung cancer have identified antigen presentation defects, alterations in interferon (IFN) signalling and neoantigen loss as potential mechanisms of immunotherapy resistance.

Methods To address the clinical and molecular landscape of acquired resistance to PD-(L)1 blockade in patients with NSCLCs, we examined the largest clinical cohort (n = 1,201) of acquired resistance to PD-(L)1 blockade in lung cancer to date paired with a systematic genomic and transcriptomic analysis in a subset of patients (n = 29) with pre- and post-treatment tissue samples available. Post-treatment samples were obtained following radiographic progression to PD-1 blockade. We also examined syngeneic lung and colorectal cancer murine model of acquired resistance to PD-1 blockade to validate relationships identified in human samples.

Results Of 1,201 NSCLC patients treated with PD-1 blockade at MSKCC, 243 (20%) achieved initial response. Many responding patients ultimately developed acquired resistance, with an estimated cumulative acquired resistance rate of 61% (95% CI 36% – 85%) at 5 years of follow up using a competing risk model (figure 1a). Post-progression overall survival was significantly longer in acquired resistance compared to primary progression (median 18.9 months vs 4.4 months, Log-rank p< 0.0001, figure 1b), suggestive of persistent, partially effective anti-tumor immune responses that permits prolonged survival even after the initial onset of AR.

In a subset of NSCLC patients (n=29) with available pre- and post-treatment samples (figure 1c), systematic immunogenomic analysis revealed that tumors with acquired resistance generally associated with enriched signals of inflammation (including IFN γ signaling and inferred CD8+ T cells) and could be separated into IFN γ upregulated and stable subsets. IFN γ upregulated tumors had putative routes of resistance with signatures of dysfunctional interferon signaling and mutations in antigen presentation genes (figure 1d).

Transcriptomic profiling of cancer cells from a murine model of acquired resistance to PD-1 blockade showed evidence of dysfunctional IFN signaling and acquired insensitivity to *in vitro* IFN γ treatment (figure 1e,f).

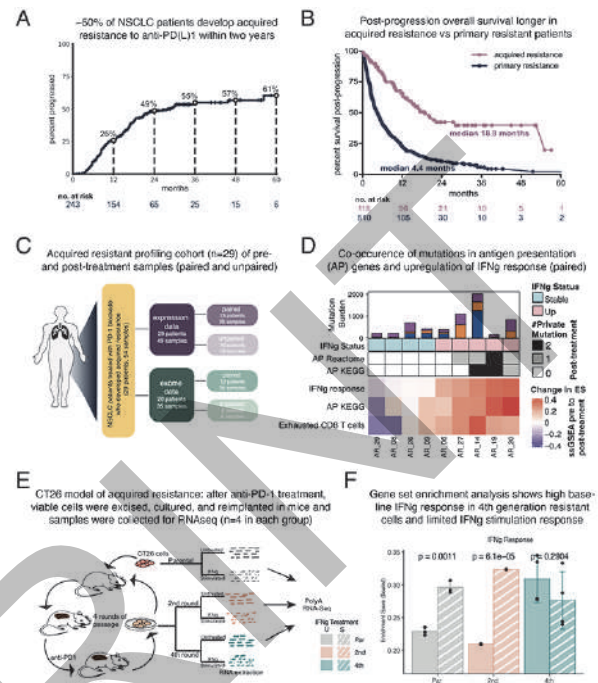
Conclusions We find evidence of ongoing but dysfunctional IFN response associated with acquired resistance to PD1 blockade in preclinical and clinical lung cancer data.

Acknowledgements All co-authors of our work in preprint: <https://www.biorxiv.org/content/10.1101/2021.07.21.452854v1.full>

Ethics Approval All work has been approved by MSKCC regulatory body and study has been performed with approved patient consent.

Consent All work has been approved by MSKCC regulatory body and study has been performed with approved patient consent.

Disclosures: Authors declare no competing financial interests. MLM and MH are both current employees of AstraZeneca, but this work is unrelated to AstraZeneca.



Abstract 522 Figure 1 Features of acquired resistance to PD1 in lung cancer

<http://dx.doi.org/10.1136/jitc-2022-SITC2022.0522>

523

SMALL CELL LUNG CANCER MOLECULAR SUBTYPES AND VULNERABILITY TO IMMUNE CHECKPOINT BLOCKADE

¹Barzin Nabet*, ¹Habib Hamidi, ¹Romain Banchereau, ²Stefanie Morris, ²Leah Adler, ¹Minu Srivastava, ¹Namrata Patil, ³Carl Gay, ⁴John Minna, ³John Heymach, ⁵Joseph Chan, ⁵Charles Rudin, ³Lauren Byers, ⁶Stephen Liu, ⁷Martin Reck, ¹David Shames. ¹Genentech, South San Francisco, CA, United States; ²Roche, Basel, Switzerland; ³MD Anderson Cancer Center, Houston, TX, United States; ⁴UT Southwestern Medical Center, Dallas, TX, United States; ⁵Memorial Sloan Kettering Cancer Center, New York, NY, United States; ⁶Lombardi Comprehensive Cancer Center, Washington, DC, United States; ⁷German Center of Lung Research, Ahrensburg, Germany

Background Extensive-stage (ES) small cell lung cancer (SCLC) disproportionately contributes to annual lung cancer-related deaths.^{1,2,3} Following the pivotal Phase III IMpower133 study, the PD-L1 inhibitor atezolizumab, combined with carboplatin and etoposide (CE), was the first immune checkpoint inhibitor approved for first-line treatment of ES-SCLC and is now a standard-of-care.⁴ In general, SCLC tumors are immunological deserts with limited tumor cell PD-L1 expression.^{5,6} Previous subtyping define SCLC tumors as neuroendocrine (NE) (ASCL1 or NEUROD1-driven) and non-neuroendocrine (nonNE) (POU2F3 or an Inflamed subtype).^{5,7,8,9} Subtyping approaches have been limited to small cohorts and cell lines, with associated clinical outcomes suggesting improved benefit of the inflamed subtype with immunotherapy.⁵

Methods We analyzed pre-treatment RNA-sequencing (RNA-seq) from 271 patient tumors from IMpower133. We applied nonnegative matrix factorization (NMF) to define SCLC classes within this dataset and correlated these new subtypes with clinical outcomes to atezolizumab+CE versus placebo+CE. We defined cell-intrinsic and -extrinsic hallmarks of each subtype with differential gene expression analyses.

Results We identify four subtypes that can be characterized by both cell-intrinsic and tumor microenvironmental features. The subtypes include NEUROD1-driven (NE-N, 31%), ASCL1-driven (NE-A, 33%), NE inflamed (NE-I, 14%), and nonNE inflamed (nonNE-I, 22%). Prior classification schema had one inflamed subgroup, whereas we identify two clusters with inflamed hallmarks. We observe both a NE-I and nonNE-I group with enrichment for T cells, B/plasma cells, antigen presentation machinery, and immune cell PD-L1 expression.

We find that while the NE-A and NE-N subtypes show similar atezolizumab+CE benefit compared to placebo, the inflamed subtypes have markedly distinct outcomes. The NE-I subtype shows a near doubling of median overall survival (OS) with atezolizumab+CE compared to placebo+CE (OS HR, 0.45 [0.22-0.89]), while the nonNE-I subtype shows no benefit despite hallmarks of lymphocyte inflammation and PD-L1 expression (OS HR, 1.02 [0.55-1.91]). The balance of T-effector to tumor-associated macrophage (TAM) signals distinguish these two inflamed subtypes (NE-I and nonNE-I). Tumors with high T-effector and high TAM signals have similar OS with atezolizumab+CE and placebo+CE (OS HR, 0.85 [0.53-1.37]), while tumors with high T-effector, but low TAM signals demonstrate markedly longer OS with atezolizumab+CE compared to placebo+CE (OS HR, 0.26 [0.12-0.57]).

Conclusions We further refine SCLC subtypes and describe a spectrum of heterogeneity. We identify two inflamed subtypes with distinct clinical outcomes to atezolizumab+CE therapy dependent on the balance of T-effector to TAM infiltration. These results demonstrate the potential for personalization of therapy for SCLC patients based on molecular subtypes.

Acknowledgements We thank the patients and their families. Medical writing assistance for this manuscript was provided by Michael J. Williams, PhD of Health Interactions and funded by F. Hoffmann-La Roche Ltd.

REFERENCES

1. Fruh M, De Ruyscher D, Popat S, Crino L, Peters S, Felip E, and Group EGW. Small-cell lung cancer (SCLC): ESMO Clinical Practice Guidelines for diagnosis, treatment and follow-up. *Ann Oncol* 2013 **24**(Suppl 6), vi99–105. 10.1093/annonc/mdt178.
2. Gazdar AF, Bunn PA, and Minna, JD. Small-cell lung cancer: what we know, what we need to know and the path forward. *Nat Rev Cancer*. 2017 **17**, 765. 10.1038/nrc.2017.106.
3. van Meerbeeck JP, FenonNEIL DA, and De Ruyscher DK. Small-cell lung cancer. *Lancet* 2011 **378**, 1741–1755. 10.1016/S0140-6736(11)60165-7.
4. Horn L, Mansfield AS, Szczesna A, Havel L, Krzakowski M, Hochmair MJ, Huemer F, Losonczy G, Johnson ML, Nishio M, et al. First-line atezolizumab plus chemotherapy in extensive-stage small-cell lung cancer. *N Engl J Med* 2018 **379**, 2220–2229. 10.1056/NEJMoa1809064.
5. Gay CM, Stewart CA, Park, EM, Diao L, Groves SM, Heeke S, Nabet BY, Fujimoto J, Solis LM, Lu W, et al. Patterns of transcription factor programs and immune pathway activation define four major subtypes of SCLC with distinct therapeutic vulnerabilities. *Cancer Cell* 2021 **39**, 346–360 e347. 10.1016/j.ccell.2020.12.014.
6. Liu SV, Reck M, Mansfield AS, Mok T, Scherpereel A, Reinmuth N, Garassino MC, De Castro Carpeno J, Califano R, Nishio M, et al. Updated overall survival and pd-1 subgroup analysis of patients with extensive-stage small-cell lung cancer treated with atezolizumab, carboplatin, and etoposide (IMpower133). *J Clin Oncol* 2021 **39**, 619–630. 10.1200/JCO.20.01055.
7. Carney DN, Gazdar AF, Bepler G, Guccion JG, Marangos PJ, Moody TW, Zweig MH, and Minna JD. Establishment and identification of small cell lung cancer cell lines having classic and variant features. *Cancer Res* 1985 **45**, 2913–2923.
8. Gazdar AF, Carney DN, Nau MM, and Minna JD. Characterization of variant subclasses of cell lines derived from small cell lung cancer having distinctive biochemical, morphological, and growth properties. *Cancer Res* 1985 **45**, 2924–2930.
9. Rudin CM, Poirier JT, Byers LA, Dive C, Dowlati A, George J, Heymach JV, Johnson JE, Lehman JM, MacPherson D, et al. Molecular subtypes of small cell lung cancer: a synthesis of human and mouse model data. *Nat Rev Cancer* 2019; **19**, 289–297. 10.1038/s41568-019-0133-9.

Ethics Approval The study protocol for IMpower133 was approved by the institutional review board or independent ethics committee for each study site and was performed in full accordance with the Guideline for Good Clinical Practice and the Declaration of Helsinki. All human tumor specimens in this study, and subsequent evaluations, were used in accordance with the informed consent agreements obtained from all subjects.

<http://dx.doi.org/10.1136/jitc-2022-SITC2022.0523>

524

SOLUBLE PROGRAMMED DEATH LIGAND 1 AS PROGNOSTIC BIOMARKER IN NON-SMALL CELL LUNG CANCER RECEIVING IMMUNE CHECK-POINT INHIBITORS – APPLICABILITY AND POTENTIAL CAVEATS

Line Nederby*, Sinne Brun, Torben Hansen, Christa Nyhus, Lisbeth Bertelsen, Rikke Andersen, Anders Jakobsen, Torben Hansen. *University Hospital of Southern Denmark, Vejle, Denmark*

Background Immune checkpoint inhibitors against programmed death protein 1 (PD-1) and programmed death ligand 1 (PD-L1) have improved the survival of non-small cell lung cancer (NSCLC) patients. A number of studies have analyzed the level of soluble PD-L1 (sPD-L1) as a prognostic marker, but the results are divergent and call for further investigations. We addressed this by looking at sPD-L1 in baseline samples of such patients. Moreover, we studied the dynamics of sPD-L1 in serum collected prior to the three subsequent cycles of treatment to determine if anti-PD-L1 therapy and anti-PD-1 treatments instigate changes in the level of sPD-L1.

Methods 79 patients with advanced or recurrent NSCLC were enrolled at the Department of Oncology, Vejle Hospital, Denmark. The patients were treated with pembrolizumab (n=73), nivolumab (n=3), and atezolizumab (n=3). Blood samples were collected at baseline and before the following three cycles of treatment. sPD-L1 was measured using the Simoa® PD-L1 Discovery Kit and the Simoa® HD-1 analyzer (Quanterix). The study was approved by the Regional Committee on Health Research Ethics for Southern Denmark, approval number S-20170063.

Results In baseline samples the median concentration of sPD-L1 was 52 pg/mL (95% CI=49-57). Based on baseline sPD-L1 level the cohort was divided in three groups: sPD-L1(low) (n=24, median 38 pg/mL), sPD-L1(medium) (n=31, median 53 pg/mL), and sPD-L1(high) (n=24, median 79 pg/mL). The median overall survival was 26 months in sPD-L1(low), 15 months in sPD-L1(medium), and 9 months in sPD-L1(high). The difference between these was statistically significant (p=0.04, logrank test). The dynamics of sPD-L1 differed between patients receiving anti-PD-1 and anti-PD-L1 treatment. In patients receiving anti-PD-1 therapy, the level of sPD-L1 remained stable from the baseline sample and over the course of three cycles. Notably, in patients treated with anti-PD-L1, sPD-L1 rose by 50-fold following the first cycle and the concentration remained at the same high level in the subsequent samples. However, spiking atezolizumab in serum from healthy donors and anti-PD-1 treated patients showed that atezolizumab did not result in assay interference, but caused lower levels of sPD-L1 as one would expect.

Conclusions sPD-L1 has potential as a prognostic marker in NSCLC receiving anti-PD-1 and anti-PD-L1 therapy. Moreover, the data imply that continuous measures of this antigen in patients in anti-PD-L1 therapy need to be interpreted with caution, as it is undecided whether the elevated levels observed are accurate. Currently, experiments are conducted in our lab to solve this issue.

Ethics Approval The study was approved by the Regional Committee on Health Research Ethics for Southern Denmark, approval number S-20170063. All participants provided written informed consent.

<http://dx.doi.org/10.1136/jitc-2022-SITC2022.0524>

526

MIR-15A AND MIR-15B MODULATE NATURAL KILLER AND CD8⁺T-CELL ACTIVATION AND ANTI-TUMOR IMMUNE RESPONSE BY TARGETING PD-L1 IN NEUROBLASTOMA

¹Kishore Challagundla*, ¹Anup Pathania, ²Philip Prathipati, ¹Srinivas Chava, ¹Omalla Olwenyi, ¹Oghenetajiri Smith, ³Subash Gupta, ¹Nagendra Chaturvedi, ¹Siddappa Byrareddy, ¹Don Coulter. ¹University of Nebraska Medical Center, Omaha, NE, United States; ²NIBIOHN, Ibaraki City, Japan; ³Banaras Hindu University, Varanasi, India

Background Neuroblastoma (NB) is an enigmatic and deadliest pediatric cancer to treat. The major obstacles to effective immuno-therapy treatments in NB are defective immune cells and the immune evasion tactics deployed by the tumor cells and the stromal microenvironment. Nervous system development during embryonic and pediatric stages is critically mediated by non-coding RNAs such as micro RNAs (miR). However, how miRs influence T and NK cell function and anti-tumor immune response in NB remains poorly understood.¹⁻³

Methods We explored the role of miRs in anti-tumor immune response via a range of data-driven workflows and in vitro & in vivo experiments. Using the TARGET, NB patient dataset (n=249), we applied the robust bioinformatic workflows incorporating differential expression, co-expression, survival, heatmaps, and box plots. We performed PD-L1 mRNA 3'-untranslated region sequence-specific luciferase activity and Ago2 RNA immunoprecipitation assays. NB cells expressing miR-15a/miR-15b were cocultured with CD8⁺T and NK cells and analyzed the activation and cytotoxicity against NB in vitro. Murine stable NB cells expressing miR-15a were subcutaneously injected into C57/BL6 mice and analyzed tumor size, tumor vasculature, and the activation and infiltration of tumoral CD8⁺T and NK cells. Further, surface PD-L1 was blocked using an anti-PD-L1 antibody and CD8⁺T, and NK cell-mediated anti-tumor responses were studied.

Results We initially demonstrated the role of miR-15a-5p (miR-15a) and miR-15b-5p (miR-15b) as tumor suppressors, followed by their negative association with stromal cell percentages and a statistically significant negative regulation of T and natural killer (NK) cell signature genes, especially CD274 (PD-L1) in stromal-low patient subsets. The NB phase-specific expression of the miR-15a/miR-15b-PD-L1 axis was further corroborated using the PDX (n=24) dataset. We demonstrated miR-15a/ miR-15b mediated degradation of PD-L1 mRNA through its interaction with the 3'-untranslated region and the RNA- induced silencing complex using sequence-specific luciferase activity and Ago2 RNA immunoprecipitation assays. In addition, we established miR-15a/miR-15b induced CD8⁺T and NK cell activation and cytotoxicity against NB in vitro. Moreover, the injection of murine cells expressing miR-15a reduced tumor size and tumor vasculature and enhanced the activation and infiltration of CD8⁺T and NK cells into the tumors in vivo. We further established that blocking the surface PD-L1 using an anti-PD-L1 antibody rescued miR-15a/ miR-15b induced CD8⁺T and NK cell-mediated anti-tumor responses.

Conclusions These findings demonstrate that miR-15a and miR-15b induce an anti-tumor immune response by targeting PD-L1 in NB.

Acknowledgements

Financial support: NIH/NCI grant CA197074; the Buffett Cancer Center/Child Health Research Institute/ Pediatric Cancer Research Group & the Department of Biochemistry & Molecular Biology at UNMC.

Dataset: Therapeutically Applicable Research to Generate Effective Treatments (TARGET) (<https://ocg.cancer.gov/programs/target>) initiative, phs000218.

PDXs: Childhood Cancer Repository of the COG and Solid Tumor Network of St. Jude Children's Research Hospital

REFERENCES

1. Challagundla KB, Wise PM, Neviani P, Chava H, Murtadha M, Xu T, Kennedy R, Ivan C, Zhang X, Vannini I, Fanini F, Amadori D, Calin GA, Hadjidanil M, Shimada H, Jong A, Seeger RC, Asgharzadeh S, Goldkorn A, Fabbri M. Exosome-mediated transfer of microRNAs within the tumor microenvironment and neuroblastoma resistance to chemotherapy. *Journal of the National Cancer Institute*. 2015;**107**(7).
2. Pathania AS, Prathipati P, Olwenyi OA, Chava S, Smith OV, Gupta SC, Chaturvedi NK, Byrareddy SN, Coulter DW, Challagundla KB. miR-15a and miR-15b modulate natural killer and CD8⁺T-cell activation and anti-tumor immune response by targeting PD-L1 in neuroblastoma. *Mol Ther Oncolytics*. 2022;**25**:308–29.
3. Pathania AS, Prathipati P, Pandey MK, Byrareddy SN, Coulter DW, Gupta SC, Challagundla KB. The emerging role of non-coding RNAs in the epigenetic regulation of pediatric cancers. *Seminars in Cancer Biology*. 2021. Epub 2021/04/29.

<http://dx.doi.org/10.1136/jitc-2022-SITC2022.0526>

527

SPATIAL PROTEOMIC AND TRANSCRIPTOMIC BIOMARKERS OF RESPONSE TO IMMUNE CHECKPOINT INHIBITORS IN OPERABLE LUNG CANCER

Jonathan Stauber, Corinne Ramos*, Adele Ponzoni, Amandine Gerstenberg. *ImaBiotech, Loos, France*

Background Non-small cell lung cancer (NSCLC) accounts for about 85% of all lung cancers. There is a strong rationale for incorporating immunotherapy into the treatment of early-stage NSCLC, given the breakthrough results with PD-1 checkpoint inhibitors in advanced-stage NSCLC. How immunotherapy should be implemented in patients who are operable is still unclear. Most of the efforts so far to identify clinically useful biomarkers do not preserve spatial information and leave us blind to the critical source of information revealed in the cell-to-cell biology of the tumor microenvironment (TME). In order to overcome these limitations, we used spatial biomarkers assays that preserve this critical information about which cells are influencing treatment response.

Methods Frozen sections from retrospectively collected surgically resected NSCLC (adenocarcinoma and squamous cell carcinoma) tumors treated with adjuvant pembrolizumab therapy were used. Patients were classified in two groups according to their Objective Response Rate (ORR): Complete Response (CR) and Progression Disease (PD) for spatial transcriptomic and proteomics assays. The statistical analysis was performed through the GeoMx[®] DSP analysis suite. Cell deconvolution using the SpatialDecon[®] algorithm (Nanostring[®]) was then used to estimate the cell-type abundance in the spatially-resolved region of interest. Results were validated with single cell proteomic spatial analysis using proprietary workflow to identify which cells are influencing the treatment response and how they are spatially distributed relative to each other.

Results A higher expression of the drug targets, PD1 (PDCD1) and PD-L1 (CD274), and genes related to T lymphocytes cytotoxicity (GZMB, CD8a) and activation (CD44, CD27, TNFRS9) were detected in the tumor microenvironment of the responder patient. The analysis of the non-responder patients highlighted the overexpression of inhibitory ligands CD86 and B7H3 (CD276). Interestingly, TIGIT, CTLA4 and TIM-3 were significantly overexpressed on the surface of the CD8a+ T cells. These results were validated by investigating the drug targets and immunosuppressive cells in the tumor microenvironment of patient samples that did not respond to immunotherapy.

Conclusions These findings highlight the relevance of considering a set of spatial biomarkers involved in immune suppression pathways to obtain a comprehensive portrait of the tumor microenvironment for personalized therapy selection. Our results suggest that for patients who did not respond to monotherapy, it would have been preferable to resort to a combined immune checkpoint inhibitors treatment strategy, aimed at the complete inhibition of all the immune-suppressive pathways.

<http://dx.doi.org/10.1136/jitc-2022-SITC2022.0527>

528

ACQUIRED RESISTANCE TO PD-(L)1 BLOCKADE IN PATIENTS WITH NON-SMALL CELL LUNG CANCER (NSCLC)

¹Biagio Ricciuti*, ¹Giuseppe Lamberti, ¹Joao Victor Alessi, ¹Federica Pecci, ¹Alessandro Di Federico, ²Xinan Wang, ¹Adriana Barrichello, ¹Victor Vaz, ¹Andy Pangilinan, ¹Danielle Haradon, ¹Lee Elinton, ³Mizuki Nishino, ³Scott Rodig, ³Lynette Sholl, ¹Mark Awad. ¹Dana-Farber Cancer Institute, Boston, MA, United States; ²Harvard TH Chan School of Public Health, Boston, MA, United States; ³Brigham and Women's Hospital, Boston, MA, United States

Background Although immune checkpoint inhibition (ICI) has improved survival in patients with non-small cell lung cancer (NSCLC), the majority of patients develop acquired resistance (AR) to ICI after an initial benefit.¹⁻² However, the mechanisms underlying AR to ICI in NSCLC are largely unknown.

Methods Comprehensive genomic profiling and HLA-I immunohistochemistry (IHC, by blinded pathology assessment) were performed on samples from patients with NSCLC treated with PD-(L)1 blockade at the Dana-Farber Cancer Institute and matched pre and post ICI tumor biopsies (figure 1). Acquired resistance was defined as the development of disease progression after an initial objective response, or stable disease ≥ 3 months with PD-(L)1 blockade.

Results Among 1823 patients with advanced NSCLC who received ICI, 60 developed acquired resistance to treatment and had matched pre- and post-ICI tissue samples.

Putative mechanisms of AR to PD-(L)1 blockade were identified in 56.7% (34/60) of cases (figure 2). Acquired mutations in *STK11* were identified in 8.3% of cases (N=5) resulting in homozygous loss in 2, due to acquired copy deletion. Acquired mutations in *KEAP1* and *SMARCA4* were noted in one (1.7%) and 3 patients (5%), respectively. Four patients (6.7%) developed acquired deleterious mutations in the beta 2-microglobulin (*B2M*) gene. Of these, one exhibited bi-allelic loss due to concurrent *B2M* copy deletion. Other acquired alterations implicated in resistance to ICI included homozygous loss in *JAK1* (N=1, 1.7%) and *APC* (N=1, 1.7%), and acquired activating *PI3KCA* mutation (N=1, 1.7%). In examining acquired copy number variations (CNVs), we found bi-allelic deletions in *CDKN2A/CDKN2B* in four cases (6.7%), and acquired heterozygous deletion in *CD274* (PD-L1) and *PDCD1LG2* (PD-L2) genes in four cases (6.7%), while high level *MDM2* and *MYC* amplifications were identified in 3 (5%) and 1 (1.7%) case, respectively. PD-L1 expression, tumor mutational burden, and total aneuploidy levels were not impacted by intervening ICI (figure 3). Among patients with tissue available for HLA-I IHC, we found a significant decrease in HLA-I expression by H-score at the moment of acquired resistance to ICI (median H-score decrease -10 [range: 0 to -220], P=0.03, figure 4).

In 2 independent control cohorts of patients with pre- and post-chemotherapy (N=41) or EGFR inhibitors (N=90) tumor genomic profiling, no acquired mutations in *STK11* or *B2M* were detected. Intervening chemotherapy and EGFR inhibition had no impact on HLA-I expression (figure 4).

Conclusions Mechanisms of AR to PD-(L)1 blockade are heterogeneous, and new therapeutic strategies are required to delay and overcome ICI resistance in patients with NSCLC.

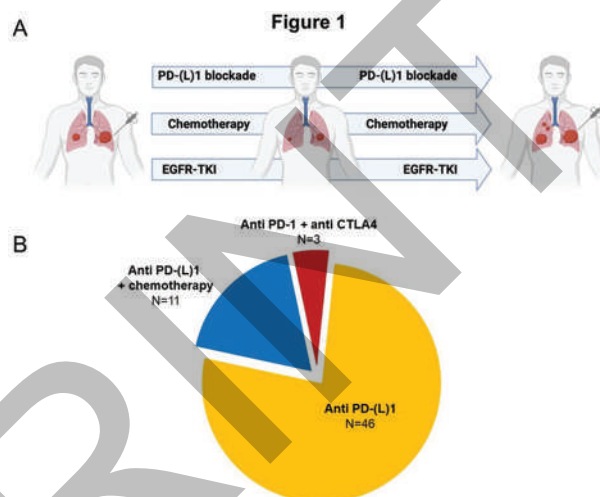
REFERENCES

- Schoenfeld AJ, Antonia SJ, Awad MM, Felip E, Gainor J, Gettinger SN, Hodi FS, Johnson ML, Leigh NB, Lovly CM, Mok T, Perol M, Reck M, Solomon B, Soria JC, Tan DSW, Peters S, Hellmann MD. Clinical definition of acquired resistance to immunotherapy in patients with metastatic non-small-cell lung cancer. *Ann Oncol*. 2021 Dec;32(12):1597-1607

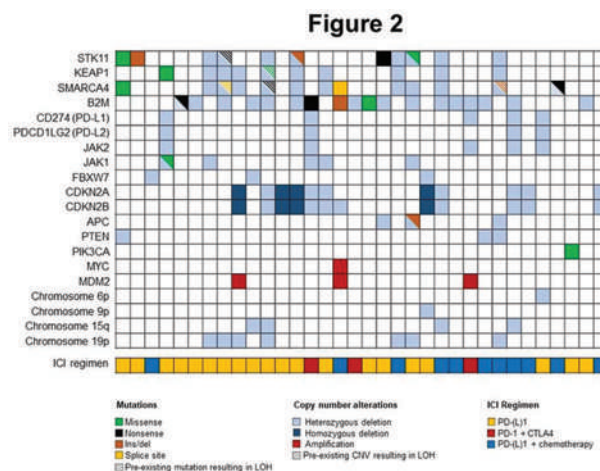
- Passaro A, Brahmer J, Antonia S, Mok T, Peters S. Managing resistance to immune checkpoint inhibitors in lung cancer: treatment and novel strategies. *J Clin Oncol*. 2022 Feb 20;40(6):598-610

Ethics Approval Patients at the Dana-Farber Cancer Institute who consented to institutional review board-approved protocols DF/HCC 02-180, 11-104, 13-364, and/or 17-000 which allowed for conducting translational research and tumor next-generation sequencing, respectively, were included.

Consent Not applicable



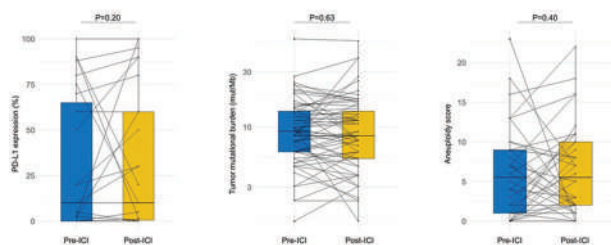
Abstract 528 Figure 1 (A) Study schema. Patients with NSCLC and matched pre and post PD-(L)1 blockade, chemotherapy (control cohort #1) and targeted therapy (EGFR inhibitors, control cohort #2) tumor biopsies were included in this study. (B) Distribution of immunotherapy regimens received by the 60 patients who developed acquired resistance to PD-(L)1 based therapies.



Abstract 528 Figure 2 Summary of the putative mechanisms of acquired resistance to PD-(L)1 blockade identified in this study.

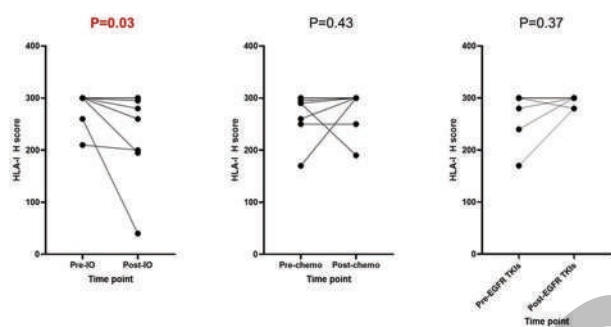
Abstracts

Figure 3



Abstract 528 Figure 3 PD-L1 expression on tumor cells, tumor mutational burden, and aneuploidy levels are not impacted by intervening PD-(L)1 blockade in NSCLC

Figure 4



Abstract 528 Figure 4 HLA-I expression by immunohistochemistry (IHC) significantly decreased in PD-(L)1 blockade resistant samples compared to baseline samples. In independent control cohorts of patients with pre- and post-chemotherapy or targeted therapy (EGFR inhibition) tumor biopsies, HLA-I expression did not change between baseline and resistant samples.

<http://dx.doi.org/10.1136/jitc-2022-SITC2022.0528>

529

REDUCED DENDRITIC CELL INFILTRATION IN ANTI-PD-1 RESISTANT HEAD AND NECK SQUAMOUS CELL CARCINOMA

¹Shin Saito*, ¹Hirofumi Shibata, ¹Liye Zhou, ²Katie Campbell, ³Ann Marie Egloff, ¹Ravindra Uppaluri. ¹Dana Farber Cancer Institute, Boston, MA, United States; ²University of California Los Angeles, Los Angeles, CA, United States; ³Brigham and Women's Hospital, Boston, MA, United States

Background Although immune checkpoint inhibitors have been approved for head and neck squamous cell carcinoma (HNSCC) patients, the majority do not respond, and further treatment optimization is required. Diverse anti-PD-1 resistance mechanisms have been proposed for this lack of benefit, which is inconsistent with the moderate tumor mutational burden and immune infiltration observed in HNSCC. Here we identified neoantigens and characterized dendritic cell (DC) infiltration in previously reported murine oral carcinoma (MOC) models with differential response to anti-PD-1, and we interrogated DC infiltration as a correlate of response in a neoadjuvant anti-PD-1 clinical trial.

Methods HNSCC MOC1 and its isogenic anti-PD-1 resistant MOC1-esc1 models were subjected to immunogenomic analysis. MOC1 and MOC1-esc1 expressed neoantigens that were defined using whole exome and RNA sequencing (RNASeq) data from cultured lines, and Class I presented neoantigens were predicted in silico (NetMHCpan4.0). MOC1 tumor infiltrating lymphocytes (TILs), following control, anti-PD-1 or anti-CTLA-4 treatment, were assayed for reactivity to synthesized predicted neoantigen peptides, and DC tumor infiltration was assessed by flow cytometry. Patient HNSCC tumor RNA-Seq data from our neoadjuvant pembrolizumab trial (NCT02296684) were interrogated, and response to neoadjuvant anti-PD-1 was classified based on pathological response in surgical specimens.

Results As we previously reported¹, MOC1 was anti-PD-1 responsive and MOC1-esc1 was resistant, while both lines were sensitive to anti-CTLA-4 therapy. Results from our immunogenomics pipeline identified 325 neoantigen candidates in MOC1 with a predicted Class I binding affinity (% rank) of less than 0.5. We tested 35 putative neoantigens for TIL immune reactivity to synthesized candidate neopeptide peptides using ELISPOT. MOC1 TIL had reactivity to mutant Yipf1 (mYipf1) neopeptide in addition to the endogenous retrovirus derived p15E antigen. Anti-PD-1 modestly increased while anti-CTLA-4 significantly increased MOC1 TIL reactivity to p15E and mYipf1 compared to control. Analysis of RNA-Seq data from MOC1 and MOC1esc1 showed a reduced conventional DC1 (cDC1) signature in MOC1esc1, and we confirmed this reduced infiltration by flow cytometry. Finally, in neoadjuvant anti-PD-1 HNSCC trial samples, a published DC signature [2] was found to be significantly higher in responder pretreatment biopsies compared to non-responders (p=0.016).

Conclusions We identified mYipf1 as a novel neoantigen in MOC1 and employed TIL response to mYipf1 or p15E peptides to measure MOC TIL anti-tumor activity. CTLA-4 directed antibodies enhanced TIL anti-tumor activity compared to anti-PD1 treatment. Reduced cDC1 infiltration and not lack of neoantigen expression may represent an anti-PD-1 resistance mechanism in HNSCC.

REFERENCES

1. Zhou L, Zeng Z, Egloff AM, Zhang F, Guo F, Campbell KM, *et al.* Checkpoint blockade-induced CD8+ T cell differentiation in head and neck cancer responders. *J Immunother Cancer.* 2022;**10**(1).
2. Böttcher JP, Bonavita E, Chakravarty P, Bles H, Cabeza-Cabrerizo M, Sammicheli S, *et al.* NK Cells Stimulate Recruitment of cDC1 into the Tumor Microenvironment Promoting Cancer Immune Control. *Cell.* 2018;**172**(5):1022–37.

Ethics Approval All patients provided informed consent prior to specimen donation.

Patient samples were analyzed under the auspices of Dana Farber Cancer Institute IRB approved protocol 18-092 (PI Uppaluri).

Animal studies were performed under Dana Farber Cancer Institute IACUC protocol 16-020 (PI Uppaluri).

<http://dx.doi.org/10.1136/jitc-2022-SITC2022.0529>

530

B7-H3 IS A CHECKPOINT IMMUNOTHERAPY TARGET IN ADVANCED PROSTATE CANCER HARBORING PTEN AND TP53 DEFECTS

Di Zhao*, Wei Shi, Yin Wang. *UT MD Anderson Cancer Center, Houston, TX, United States*

Background Prostate cancer is the most diagnosed cancer in men worldwide and the leading cause of cancer death in men worldwide. Genetic inactivation of *PTEN* and *TP53* are common in advanced prostate cancers. Checkpoint immunotherapy has yielded meaningful responses across many cancers but shown minimal activity in advanced prostate cancer. Prior studies showed that overexpression of immune checkpoint B7-H3 (CD276) correlates with the increased risks of clinical recurrence, disease spread, and poor outcomes in various cancer types, including prostate cancer. However, the roles of B7-H3 in prostate cancer development and its tumor microenvironment remain unclear, partially due to the lack of tissue-specific deletion mouse models. This gap in knowledge hinders the application of immunotherapy targeting B7-H3 in prostate cancers.

Methods To identify *PTEN*- and *p53*-associated immune checkpoints, we performed multi-omics analyses of expression patterns of 51 checkpoint molecules in human prostate cancer samples. Then, we generated a novel genetically engineered mouse model to elucidate the role of B7-H3 in tumor development and progression of *PTEN/p53*-deficient prostate cancer. We also performed unbiased immunoprofiling using Mass Cytometry (CyTOF) and Immunofluorescence to visualize B7-H3's impact on immune components in prostate tumors.

Results Our multi-omics analyses in human samples revealed that B7-H3 is one of the most significantly overexpressed immune checkpoints in prostate tumors containing *PTEN* and *TP53* genetic inactivation. Mechanistically, we found that the *PTEN*-AKT pathway co-operates with the *p53* pathway in modulating B7-H3 expression in cancer cells. In *Pten/Trp53* genetically engineered mouse (GEM) models, prostate-specific deletion of *Cd276* resulted in markedly delayed tumor progression. *Cd276* deletion also reversed the immunosuppression characterized by increased tumor-infiltrating lymphocytes.

Conclusions Our studies provide the genetic evidence for the tumor-promoting and immunosuppressive role of B7-H3 in prostate cancer and offer insights into combinatorial strategies for immunotherapy targeting B7-H3 in CRPC harboring *PTEN* and *TP53* defects.

<http://dx.doi.org/10.1136/jitc-2022-SITC2022.0530>

531

IDENTIFYING GENETIC FACTORS FOR RESISTANCE AND RESPONSE TO IMMUNE CHECKPOINT INHIBITORS (ICIS) IN ADVANCED NON-SMALL CELL LUNG CANCER (NSCLC) PATIENTS USING REAL-WORLD DATA

Neeraj Singh*, Smita Agrawal, Babu Narayanan. *ConcertAI, Bangalore, India*

Background ICIs are a promising class of drugs that have improved the treatment of a broad spectrum of cancers. Biomarkers such as high Tumor Mutation Burden (TMB), high PD-L1 expression, or high Microsatellite Instability (MSI) are predictive of improved response to ICIs.¹⁻³ However, not all patients with these biomarkers respond well to ICIs and some develop resistance over time. The underlying molecular mechanisms of resistance are poorly known. We leveraged our deeply curated real world clinico-genomics database (ConcertAI Genome360™) of NSCLC patients treated with ICIs to identify the drivers of resistance and response.

Methods This retrospective study used the ConcertAI Genome360™ NSCLC dataset. The eligible patients had advanced NSCLC treated with ICIs (N=2532). A subset of these patients also had high TMB/PD-L1/MSI (TPM) status (N=986). The following analysis was performed for both the TPM unselected and high TPM populations. The patients were subdivided into responder and non-responder cohorts based on their response to ICIs. For each patient in both cohorts, genes with pathogenic mutations, fusions and copy number changes were identified and enrichment analysis was performed between cohorts. Biomarkers with p value less than 0.05 were further considered for pathway analysis along with the immune signaling network to identify pathways and genes responsible for response and resistance to ICIs in spite of TPM high status.

Results We identified segments which predicted response or resistance to ICIs (table 1). TERT promoter mutations and loss of function (LOF) mutations in STAG2 promote high TMB and PD-L1 expression respectively.^{4,5} We also see them enriched in our overall responder cohort, however, the effect of STAG2 LOF mutations towards response to ICIs is seen even in the TPM high population indicating the effect is due to more than just upregulation of PD-L1. LOF mutations in ATM/ATR genes were also enriched in the overall responder cohort in-line with previous observations in murine cells.^{6,7} Gene amplifications in CDK12 and CEBPA genes were predictive of resistance to ICIs and interestingly, amplifications in CDK12 and RET were also highly predictive of resistance to ICIs in the TPM high cohort which was heavily biased towards response to therapy.

Pathway analysis on the combined results identified that genes in the cGAS-STING pathway are playing a vital role in determining response.

Conclusions Our analysis highlights some of the underlying mechanisms for response or resistance to ICIs which can provide clues for designing new combination trials for patients whose tumor progresses on ICIs.

REFERENCES

1. Xu Y, Wan B, Chen X, Zhan P, Zhao Y, Zhang T, Liu H, Afzal MZ, Dermime S, Hochwald SN, Hofman P, Borghaei H, Lin D, Lv T, Song Y; written on behalf of AME Lung Cancer Collaborative Group. The association of PD-L1 expression with the efficacy of anti-PD-1/PD-L1 immunotherapy and survival of non-small cell lung cancer patients: a meta-analysis of randomized controlled trials. *Transl Lung Cancer Res.* 2019 Aug;**8**(4):413–428.
2. Petrelli F, Ghidini M, Ghidini A, Tomasello G. Outcomes Following Immune Checkpoint Inhibitor Treatment of Patients With Microsatellite Instability-High Cancers:

A Systematic Review and Meta-analysis. *JAMA Oncol.* 2020 Jul **1**;6(7):1068–1071.

3. Palmeri M, Mehnert J, Silk AW, Jabbour SK, Ganesan S, Popli P, Riedlinger G, Stephenson R, de Meritens AB, Leiser A, Mayer T, Chan N, Spencer K, Girda E, Malhotra J, Chan T, Subbiah V, Groisberg R. Real-world application of tumor mutational burden-high (TMB-high) and microsatellite instability (MSI) confirms their utility as immunotherapy biomarkers. *ESMO Open.* 2022 Feb;**7**(1):100336.
4. Li H, Li J, Zhang C, Zhang C, Wang H. TERT mutations correlate with higher TMB value and unique tumor microenvironment and may be a potential biomarker for anti-CTLA4 treatment. *Cancer Med.* 2020 Oct;**9**(19):7151–7160.
5. Nie Z, Gao W, Zhang Y, Hou Y, Liu J, Li Z, Xue W, Ye X, Jin A. STAG2 loss-of-function mutation induces PD-L1 expression in U2OS cells. *Ann Transl Med.* 2019 Apr;**7**(7):127.
6. Hu M, Zhou M, Bao X, Pan D, Jiao M, Liu X, Li F, Li CY. ATM inhibition enhances cancer immunotherapy by promoting mtDNA leakage and cGAS/STING activation. *J Clin Invest.* 2021 Feb **1**;**131**(3):e139333.
7. Sheng H, Huang Y, Xiao Y, Zhu Z, Shen M, Zhou P, Guo Z, Wang J, Wang H, Dai W, Zhang W, Sun J, Cao C. ATR inhibitor AZD6738 enhances the antitumor activity of radiotherapy and immune checkpoint inhibitors by potentiating the tumor immune microenvironment in hepatocellular carcinoma. *J Immunother Cancer.* 2020 May;**8**(1):e000340.

Abstract 531 Table 1 Genomic segment of response towards ICIs treatment

Overall Cohort treated with ICI (N = 2532)			
Gene Name	Status	Response	p value
STAG2	LOF Mutations	Responder	0.001
NF1/2	LOF Mutations	Responder	0.015
ATM/ATR	LOF Mutations	Responder	0.031
RBM10	LOF Mutations	Responder	0.043
TERT	Promoter Mutation	Responder	0.048
CDK12	Amplification	Non-responder	0.011
CEBPA	Amplification	Non-responder	0.028
PDL1/MSI/TMB high cohort treated with ICI (N = 986)			
Gene Name	Status	Response	p value
STAG2	LOF Mutations	Responder	0.03
KRAS	GOF Mutations	Responder	0.041
CDK12	Amplification	Non-responder	0.003
RET	Amplification	Non-responder	0.017

<http://dx.doi.org/10.1136/jitc-2022-SITC2022.0531>

532

**ANTI-VISTA ANTIBODY HMBD-002 REPROGRAMS
TUMOUR ASSOCIATED MACROPHAGES AND PROMOTES
CYTOTOXIC T CELL RESPONSE**

Bhushan Dharmadhikari*, Dipti Thakkar, Olga Zharkova, Debleena Ray, Jason Lai, Konrad Paszkiewicz, Piers Ingram, Jerome Boyd-Kirkup. *Hummingbird Bioscience, Singapore, Singapore*

Background VISTA is an emerging, predominantly myeloid, immune checkpoint, and its blockade has shown benefit in multiple preclinical models of cancer as both a monotherapy and in combination with other immune checkpoint inhibitors (ICI) such as anti-PD1 and anti-CTLA-4. In some murine models of cancers, such as non-small cell lung cancer, clear-cell renal cell carcinoma and colorectal carcinoma, VISTA is expressed on both T cells and macrophages. Understanding the cell subset specific immunomodulatory functions of VISTA is important to inform patient selection, develop effective combination strategies, and identify biomarkers of response to anti-VISTA therapy.

Methods The murine colon cancer model, CT26, exhibits robust infiltrations of multiple immune cells into tumors, and has been reported to respond to VISTA blockade. This allows simultaneous investigation of VISTA-mediated immune modulation in multiple cell subsets. Here, HMBD-002, an IgG4 anti-VISTA antibody which does not deplete VISTA-expressing cells, was used to assess the functional role of VISTA blockade in the absence of Fc-mediated effects. CT26 tumor-bearing mice were treated with HMBD-002 and/or anti-PD1. Tumors were harvested and profiled via multicolor flow cytometry to determine underlying changes in the polarization and functional status of immune infiltrates associated with anti-tumor responses.

Results In CT26 tumors, VISTA expression was highest on macrophages followed by MDSCs, DCs and T cells. VISTA blockade polarized macrophages to an activated pro-inflammatory anti-tumor phenotype with significant increases in TNF α and MHCII expressing macrophage subsets. VISTA blockade also resulted in significant increases in tumor antigen gp70-specific CD8 T cells. A concurrent increase in CD8 T cell activation was seen with an upregulation of several cytotoxicity associated markers, including Granzyme B. However, no change in T cell exhaustion levels was observed. The combination of VISTA blockade with anti-PD1 treatment led to further increases in tumor antigen-specific CD8 T cells, significant decreases in T cell exhaustion levels and enhanced anti-tumor efficacy when compared to monotherapy anti-VISTA or anti-PD1 arms.

Conclusions Reprogramming of the tumor microenvironment by blockade of VISTA is associated with polarization of macrophages to an inflammatory phenotype and increases in both tumor antigen-specific CD8 T cells and their cytotoxic activity. Further, combining anti-VISTA with other immune checkpoint inhibitors that can reprogram exhausted T cells has the potential for synergistic activity.

Ethics Approval The study was approved by the Institutional Animal Care and Use Committee, approval number 2021/SHS/1660

<http://dx.doi.org/10.1136/jitc-2022-SITC2022.0532>

533

A TUMOR-LUNG NLRP3-TLR4 DISTANT SIGNALING AXIS DRIVES IMMUNOTHERAPY RESISTANCE VIA G-CSF-DEPENDENT EXPANSION OF CIRCULATING PD1⁺ PMN-MDSCS

Balamayooran Theivanthiran*, Nagendra Yarla, Tarek Haykal, Michael Plebanek, Y-Van Nguyen, Nicholas DeVito Brent Hanks. *Duke University, Durham, NC, United States*

Background The majority of solid tumor cancer patients do not benefit from current immunotherapy options due to the development of either primary or secondary resistance. We recently determined that the tumor-intrinsic NLRP3 inflammasome drives the recruitment of granulocytic myeloid-derived suppressor cells (PMN-MDSCs) and adaptive resistance to anti-PD-1 immunotherapy via a HSP70-TLR4 signaling axis. Prior studies have associated *TLR4* gain-of-function mutations with inferior clinical outcomes while pulmonary inflammation has been correlated with anti-PD-1 resistance. How lung-expressed TLR4 and lung-derived factors influence tumor immunity at distant sites remains poorly understood

Methods We engineered an inducible lung epithelial-specific TLR4 knock-out transgenic mouse model (SPC-TLR4^{-/-}) to investigate the impact of lung TLR4 on anti-PD-1 immunotherapy responses in BRAF^{V600E}CDKN2A^{-/-}PTEN^{-/-} (YUMM1) melanoma and EO771 breast cancer syngeneic tumor models. Genetic silencing of NLRP3 and HSP70 was performed in tumor models. Immunohistochemistry, qrt-PCR, Western blot analysis, and multi-parameter flow cytometry was used to characterize tumor NLRP3-lung TLR4 crosstalk and its impact on anti-tumor immunity. Baseline tumor specimens and plasma samples derived from 40 stage IV melanoma patients undergoing anti-PD-1 immunotherapy were interrogated for intrinsic NLRP3 inflammasome activation levels by NLRP3-ASC proximity ligation and HSP70 ELISA assays. Objective responses were assessed by computed tomography imaging at week 12 of therapy based on RECIST1.1 criteria

Results Anti-PD-1 immunotherapy expands circulating levels of PD-1⁺ PMN-MDSCs in mice harboring YUMM1 and EO771 breast cancer models. This was noted to correlate with elevated plasma levels of HSP70 and G-CSF. Both observations were ablated in mice harboring NLRP3^{-/-} tumors as well as in SPC-TLR4^{-/-} hosts. Further studies found lung epithelial HSP70-TLR4 signaling to induce G-CSF release in a Wnt5a-dependent manner. Pharmacologic inhibition of HSP70 suppresses lung epithelial Wnt5a and G-CSF expression and inhibits the accumulation of PD-1⁺ PMN-MDSCs in the circulation. Further studies demonstrate the distant lung TLR4-Wnt5a-G-CSF axis promotes PD-1⁺ PMN-MDSC accumulation and primary tumor progression. Baseline tumor NLRP3 inflammasome activity ($P = 0.0014$) and plasma HSP70 levels ($P = 0.0008$) in stage IV melanoma patients independently correlate with elevated circulating PMNs and disease progression during anti-PD-1 immunotherapy

Conclusions Together, these results describe a novel TLR4-Wnt5a-G-CSF signaling axis in the lung epithelium that induces the systemic expansion of PD-1⁺ PMN in response to activation of the tumor-intrinsic NLRP3 inflammasome. We conclude that this tumor-lung crosstalk supports primary tumor growth and contributes to anti-PD-1 immunotherapy resistance partially by serving as an anti-PD-1 antibody sink. Pharmacologic inhibition of NLRP3 and HSP70 represents promising strategies for overcoming anti-PD-1 resistance.

<http://dx.doi.org/10.1136/jitc-2022-SITC2022.0533>

534

SEX-LINKED DIFFERENCES IN OBESITY MARKEDLY IMPACT THE ANTI-TUMOR EFFICACY OF PD-1 BLOCKADE

¹Logan Vick*, ¹Ziming Wang, ¹Craig Collins, ¹Lam Khuat, ¹Cordelia Dunai, ¹Kevin Stoffel, ²Sai Yendamuri, ²Sarbajit Mukherjee, ²Spencer Rosario, ¹Robert Canter, ¹Arta Monjazeb, ¹William Murphy. ¹University of California, Davis, Sacramento, CA, United States; ²Roswell Park Comprehensive Cancer Center, Buffalo, United States

Background Immune checkpoint inhibitors (ICIs) particularly those targeting the PD-1/PD-L1 axis have markedly impacted cancer immunotherapy resulting in significant therapeutic responses across an increasingly wide variety of cancers. While obesity is often associated as a negative prognostic indicator in cancer and therapeutic outcomes, it has surprisingly been linked to greater anti-tumor efficacy and survival in multiple cancers following immune checkpoint blockade both in pre-clinical models and clinical outcomes. Clinical data have demonstrated that the increased clinical efficacy was only observed in high body mass index (BMI) males and not females, indicating that sex-linked differences of obesity as it pertains to immunotherapy may exist with regard to the “obesity paradox” in cancer immunotherapy.

Methods We assessed the effects of sex on obesity-associated immune checkpoint therapy responses using a diet induced obese (DIO) mouse model following placement on high fat diet (HFD) versus control diets for a period of several months. Mice then received tumors and the tumor-bearing male and female mice were treated by targeting PD-1/PDL-1 as a monotherapy. We then characterized the immune signature of the different cohorts before and after immunotherapy. To determine if hormonal pathways were indeed involved, we then assessed effects of anti-PD-1 therapy in ovariectomized DIO and lean tumor bearing mice. Stratification of immunotherapy outcomes in high versus low BMI male and female cancer patients was also assessed.

Results Tumor progression was observed greater in both male and female DIO mice compared to control diet recipients. Immunotherapy using anti-PD-1 resulted in significant anti-tumor effects in DIO male mice but not DIO female nor the lean male and female recipients. Ovariectomy of female mice resulted in markedly greater weight gain when placed on HFD as well as accelerated tumor growth but it also resulted in significant efficacy of anti-PD-1 monotherapy comparable to male DIO mice. Stratification of patient outcomes following checkpoint blockade for melanoma on both BMI and sex demonstrated that significant increases in survival and efficacy were only observed in high BMI male patients mirroring the effects observed in the mouse models.

Conclusions These data reveal potential implications in taking sex into account when using obesity as a predictive biomarker for effective use of ICI and provides potential insights on how to potentially improve immunotherapy efficacy by targeting hormonal pathways.

Ethics Approval All animal were housed in AAALAC-accredited animal facilities at University of California Davis and all animal protocols were approved by the University of California Davis Institutional Animal Care and Use Committee (IACUC). All studies maintained compliance with guidelines and regulation from the IACUC.

<http://dx.doi.org/10.1136/jitc-2022-SITC2022.0534>

535

HYDROXYCHLOROQUINE SYNERGIZES WITH ANTI-PD-1 IMMUNE CHECKPOINT BLOCKADE IN SQUAMOUS CARCINOMA OF THE HEAD AND NECK

¹Avani Vyas*, ¹Silvia Cruz-Rangel, ¹Nayel Khan, ¹Mikayla Bisignani, ¹Lidia Arantes, ²Nicole Schmitt, ¹Kirill Kiselyov, ¹Robert Ferris, ¹Umamaheswar Duvvuri. ¹University of Pittsburgh, Pittsburgh, PA, United States; ²Emory Department of Otolaryngology, Atlanta, GA, United States

Background The recent evidence shows that Programmed Death Ligand 1 (PD-L1) presentation on the plasma membrane is dynamically modulated by the delivery via the secretory pathway and withdrawal, recycling and degradation, which may involve endolysosomal pathway. PD-L1 is delivered to the plasma membrane via the secretory pathway which may involve lysosomal activity. Whereas the significance of this step is not completely understood, it provides a rationale for testing lysosomal inhibition as a means to regulate PD-L1. Limited, but intriguing, prior attempts yielded mixed results, suggesting that regulation of this process is complex. We hypothesized that inhibition of endolysosomal traffic would suppress PD-L1 plasma membrane presentation and synergize with anti-PD-1 immune checkpoint blockade.

Methods PD-L1 plasma membrane presentation was measured via flow cytometry using lysosomotropic drugs, apilimod or hydroxychloroquine (HCQ). Lysosomal exocytosis was measured using beta-hexosaminidase activity. PIKfyve knock down cells were created using CRISPR-Cas9 technique. We designed an *in vitro* assay to co-culture peripheral blood CD8+ T cells with human cancer cell lines. C57/Bl (4-week-old) mice were implanted subcutaneously with MOC-1 or UPCI: M4Tu lines on each flank and randomized. Treatments were administered two times a week intraperitoneally. The volume of the tumors was measured three times a week.

Results We find that *in vitro*, treatment with the PIKfyve inhibitor apilimod or suppresses plasma membrane presentation of PD-L1. Similarly, treatment with the lysosomal inhibitor hydroxychloroquine (HCQ) also reduced PD-L1 presentation, confirming endolysosomal involvement in PD-L1 handling. Using syngeneic mouse models of head and neck cancers, we find that HCQ synergizes with anti-PD-1 therapy, causing tumor growth inhibition of 80% and dramatically increased survival ($p < 0.001$, log-rank test). Treatment with HCQ promoted *in vitro* cancer cell cytotoxicity, suggesting that HCQ may directly promote CD8+ T cell activity.

Conclusions HCQ is a potent adjuvant for anti-PD-1 therapy, by mediating PD-L1 plasma membrane presentation on cancer cells and possibly mediating CD8+ T cell activation.

Ethics Approval The animals were handled and euthanized in accordance with Institutional Animal Care and Use Committee (IACUC) guidelines. Human blood samples were obtained from the University of Pittsburgh Medical Center in accordance with established University of Pittsburgh IRB guidelines. Written informed consent was obtained from all the patients before inclusion in the study.

<http://dx.doi.org/10.1136/jitc-2022-SITC2022.0535>

536

DECOUPLING CYTOTOXIC T LYMPHOCYTE AND EXHAUSTED T LYMPHOCYTE TRANSCRIPTOMIC SIGNATURES ENHANCES IMMUNE CHECKPOINT INHIBITORS RESPONSE PREDICTION IN MELANOMA

Binbin Wang, Kun Wang*, Eytan Ruppin, Peng Jiang. *National Cancer Institute, Rockville, MD, United States*

Background Cytotoxic T lymphocyte (CTL) plays a crucial role in anti-cancer immunity. Progression of CTL to exhausted T lymphocyte (ETL) cells that overexpress inhibitory receptors can substantially decrease effector cytokines production and diminish the cytolytic activity in tumor microenvironment (TME). However, while the activity levels of CTL and ETL are considered important determinants of Immune checkpoint inhibitor (ICI) response, it has been repeatedly observed that their predictive power of the latter is quite limited. Studying this conundrum on a large scale across the TCGA cohort, we find that ETL and CTL activity (estimated based on conventional gene signatures in the bulk tumor expression) is strongly positively correlated in most cancer types. We thus hypothesized that their limited predictive power may arise due to their high concordance in the bulk expression, such that their opposing associations with response effectively cancel each other.

Methods Aiming to better characterize these two CD8+ immune states as ICI response biomarkers, we analyzed several melanoma single cell expression datasets via an interaction linear regression model and identified 13 genes whose expression state decouples the CTLs and ETLs.

Results We further tested and validate this *decoupling signature* in several melanoma bulk expression ICI cohorts by first demonstrating that in high-decoupling-score patient groups, the correlation between ETL and CTL activities is indeed markedly lower than in the low-decoupling-score patient groups. Second, the performance of CTL activity in predicting ICI response is significantly better in the high-decoupling-score than that in the low one. Finally, importantly, in the high decoupling score, CTL activity is a better predictor of melanoma patients ICI response than state-of-art ICI prediction methods.

Conclusions These results demonstrate the utility of a new decoupling score for boosting the power of CTL activity in predicting ICI response in melanoma.

<http://dx.doi.org/10.1136/jitc-2022-SITC2022.0536>

537

LOCAL IMMUNOTHERAPY WITH INTASYL™ SELF-DELIVERING RNAI TARGETING CTLA-4 PROVIDES ROBUST TUMOR CONTROL IN VIVO

<http://dx.doi.org/10.1136/jitc-2022-SITC2022.0537>

Benjamin Cuiffo*, Melissa Maxwell, Dingxue Yan, Brianna Rivest, Andrew Boone, Shenghua Zhou, James Cardia, Simon Fricker. *Phio Pharmaceuticals, Marlborough, MA, United States*

Background Immune checkpoint inhibition (ICI) of CTLA-4 with ipilimumab has proven effective in improving clinical responses for patients with advanced melanoma or other approved indications in combination with nivolumab. However, systemic treatment with ipilimumab is associated with serious adverse events (SAEs) for many (>25%) patients that can be life-threatening and/or result in discontinuation of treatment. As such, balancing efficacy with associated toxicities remains a challenge in treating patients with ipilimumab.

Local intratumoral (IT) immunotherapy may enhance local activity and decrease systemic toxicity. Additionally, by using the tumor as its own vaccine, IT immunotherapy can ignite tumor-specific immune responses well beyond the local site of administration. While clinical testing of IT antibody therapies is underway, the high molecular weight properties of therapeutic antibodies may limit their local diffusion and retention time within tumors.

RNAi therapy is an emerging modality well-positioned to optimize local clinical application of ICI. We have previously demonstrated that self-delivering RNAi (INTASYL) therapeutic compounds built on proprietary INTASYL™ technology silence targets with high specificity and without need for specialized formulations or drug delivery systems and provide robust antitumor efficacy to both directly-treated and to non-directly treated distal tumors when delivered IT in vivo.

Here we present proof-of-concept (POC) in vivo data showing IT efficacy of a novel INTASYL targeting murine CTLA-4 (mCTLA-4; 27790) in two syngeneic mouse tumor models.

Methods CTLA4 mRNA silencing was validated in CHO K1 cells expressing murine CTLA-4 in vitro by RT-qPCR. For in vivo efficacy, Hepa1-6 or CT26 cells were implanted subcutaneously into the flanks of C57BL/6 or BALB/c mice, respectively. When tumors reached threshold volume (150 mm³), animals were randomized into treatment groups; treatments were administered on Days 1, 4, 7, 10 and 13. Vehicle (PBS), a chemically identical non-targeting control (NTC) INTASYL, or INTASYL 27790 at two dose concentrations were administered IT; anti-CTLA-4 monoclonal antibody (mAb; clone 9D9) was administered intraperitoneally (IP). Tumor volumes and body weights were recorded longitudinally.

Results mCTLA-4-targeting INTASYL 27790 provided concentration-associated silencing of mCTLA-4 in vitro. When administered IT, mCTLA-4-targeting INTASYL 27790 elicited robust dose-associated antitumor efficacy in both in vivo tumor models compared with vehicle- or NTC-treated tumors, comparable to that observed under systemic IP treatment with anti-CTLA4 mAb.

Conclusions These data show IT INTASYL targeting mouse CTLA4 elicits robust on-target dose concentration-associated antitumor efficacy in two syngeneic tumor models in vivo and provide POC for targeting CTLA-4 IT with INTASYL.

Ethics Approval Animal studies were performed at Pharma Models LLC, Marlborough, MA 01752, under standard protocol approved by their IACUC.

Clinical Trials Completed

538

COMPREHENSIVE SINGLE CELL TRANSCRIPTOMIC PROFILING OF UNTREATED RESECTABLE LUNG CANCERS

Sydney Connor*, Jijia Zhang, Justina Caushi, Boyang Zhang, Zhen Zeng, Khaled Sanber, Gavin Pereira, Valsamo Anagnostou, Ada Tam, Nicholas Ionta, Franck Housseau, Patrick Forde, Hongkai Ji, Andrew Pardoll, Kellie Smith. *Johns Hopkins School of Medicine, Baltimore, MD, United States*

Background Non-small cell lung cancer (NSCLC) is the leading cause of cancer-related deaths in men and women. The 5-year overall survival rate of metastatic NSCLC is an abysmal 21%, in part since >80% of lung cancers are diagnosed at an advanced stage.^{1,2} Encouragingly, neoadjuvant immune checkpoint blockade (ICB) plus chemotherapy is now approved as standard of care for resectable lung cancer.^{3,4} Because ICB success depends on an endogenous anti-tumor T cell response, it is critical that we understand the baseline functional biology of these T cells. To date, however, comprehensive studies of endogenous tumor-reactive TIL in operable NSCLC (Stage I-III) are lacking. Herein we present an integrated single cell immunogenomic profiling of 21 untreated tumor resections from patients who were surveilled for 1-5 years post-surgery.

Methods After acquiring written informed consent, PBMC and resected tissues were obtained from patients with Stage I-III NSCLC undergoing surgical resection. Tissues were enzymatically digested and viably frozen. Cryobanked tissues were thawed, T cells (CD3+CD45+) and non-T cells (CD3-) were sorted, and prepared for single cell RNA sequencing. Single Cell 5' V(D)J and 5' DGE kits (10X Genomics) were used to capture immune repertoire and gene expression information for the T cell fraction, DGE libraries were prepared for the non-T cell fraction.

Results Transcriptomic profiles were defined for CD3+ TIL from 21 untreated surgically-resected tumors (527,062 cells). Refined UMAP projection of CD8+ TIL (183,375 cells) uncovered 14 CD8+ T cell subsets. We observed four distinct tissue resident memory (TRM) clusters. This is notable, as our previous work defined the TRM subsets as being enriched in tumor-reactive TIL.^{5,6} Apropos of this notion, two of these TRM clusters were significantly enriched in the tumor tissue compared to adjacent normal lung and lymph node (adj.p-value=1.3x10⁻⁴ and 3.6x10⁻³), with one of these TRM clusters expressing high levels of markers previously shown to mark tumor-reactive TIL, including *HOBIT*, *CXCL13*, and *CD39* [5,7,8]. Further supporting our hypothesis that this cluster harbors tumor-reactive TIL, cross-reference with public TCR databases showed almost no overlap of the TCRs in this cluster with TCRs corresponding to virus-specific T cells, whereas 726 EBV- and 177 flu-specific TIL were readily detected within other TRM and T Effector clusters.

Conclusions This study is one of the first to evaluate the transcriptional programming of tumor-reactive TIL in treatment-naïve lung cancers. Understanding the baseline functional biology of these cells has significant implications for biomarker and novel therapy development for the treatment of lung cancers resistant to currently-approved therapies.

Trial Registration For the ICB treated NSCLC patients enrolled under NA_00092076 at JHU (NCT02259621), samples have already been collected, stored, and published.

REFERENCES

1. Hellmann MD, Chaft JE, William WN, *et al.* Pathological response after neoadjuvant chemotherapy in resectable non-small-cell lung cancers: proposal for the use of major pathological response as a surrogate endpoint. *Lancet Oncol.* 2014 Jan; **15**(1):e42–50.
2. Pataer A, Kalhor N, Correa AM, *et al.* Histopathologic response criteria predict survival of patients with resected lung cancer after neoadjuvant chemotherapy. *J Thorac Oncol.* 2012 May; **7**(5):825–32.
3. Forde PM, Chaft JE, Smith KN, *et al.* Neoadjuvant PD-1 Blockade in Resectable Lung Cancer. *N Engl J Med.* 2018. **378**(21):1976–1986.
4. Forde PM, Spicer J, Lu S, *et al.* Neoadjuvant Nivolumab plus Chemotherapy in Resectable Lung Cancer. *N Engl J Med.* 2022. **386**(21): 1973–1985.
5. Caushi JX, Zhang J, Ji Z, *et al.* Transcriptional programs of neoantigen-specific TIL in anti-PD-1-treated lung cancers. *Nature.* 2021. **596**(7870):126–132.
6. Danilova L, Anagnostou V, Caushi JX, *et al.* The Mutation-Associated Neoantigen Functional Expansion of Specific T Cells (MANAFEST) Assay: A Sensitive Platform for Monitoring Antitumor Immunity. *Cancer Immunol Res.* 2018. **6**(8): 888–899.
7. Wu F, Fan J, He Y, *et al.* Single-cell profiling of tumor heterogeneity and the microenvironment in advanced non-small cell lung cancer. *Nat Commun.* 2021. **12**(1): 2540.
8. Guo X, Zhang Y, Zheng L, *et al.* Global characterization of T cells in non-small-cell lung cancer by single-cell sequencing. *Nat Med.* 2018; **24**:978–985

Ethics Approval This study was approved by the Institutional Review Boards (IRB) at Johns Hopkins University (JHU), approval number IRB00100653 and NA_00092076.

Consent Written informed consent was obtained from all patients included in this study. A copy of the written consent is available for review by the Editor of this journal.

<http://dx.doi.org/10.1136/jitc-2022-SITC2022.0538>

541

MREGDC/T HELPER NICHES ENABLE LOCAL REACTIVATION OF CD8 T CELLS UPON PD-1 BLOCKADE

¹Assaf Magen*, ¹Pauline Hamon, ²Nathalie Fiaschi, ²Raquel Deering, ¹Sacha Gnjatic, ³Myron Schwartz, ¹Thomas Marron, ²Gavin Thurston, ¹Alice Kamphorst, ¹Miriam Merad. ¹Precision Immunology Institute, Icahn School of Medicine at Mount Sinai, New York, NY, United States; ²Regeneron, Tarrytown, NY, United States; ³Mount Sinai, New York, NY, United States

Background While T cell accumulation in tumors is associated with response to immune checkpoint blockade (ICB), many T cell-rich tumors fail to respond to ICB.

Methods Here we leveraged a large neoadjuvant PD-1 blockade trial in hepatocellular carcinoma (HCC) to search for correlates of ICB response within T cell-rich tumors.

Results Paired single-cell RNA and TCR sequencing of nearly one million immune cells revealed that anti-tumor responses to ICB correlated with significant clonal expansion of intratumoral CXCL13⁺CH25H⁺IL-21⁺TCF7⁺ CD4 T helper cells (CXCL13⁺ Th) and GranzymeK⁺PD-1⁺ CD8 effector-like T cells, whereas terminally exhausted CD39^{hi}TOX^{hi}PD-1^{hi} CD8 T cells dominated in non-responders. Most T cell clonotypes that expanded post-treatment were found in pre-treatment biopsies, suggesting local reactivation of antigen-experienced T cells by PD-1 blockade. Notably, PD-1⁺TCF-1⁺ CD8 T cells with features of progenitor-exhausted cells were found in tumors of responders and non-responders. Strikingly, tumors from responders were highly enriched in mregDCs, a DC state triggered by capture of tumor debris, which formed physically interacting cellular triads with CXCL13⁺ Th cells and PD-1⁺TCF1⁺ progenitor-like CD8 T cells. Receptor-ligand analysis revealed unique interactions within these triads that may promote the differentiation of progenitor-exhausted CD8 T cell into effector-like cells upon PD-1 blockade.

Conclusions These results suggest that discrete intratumoral niches that include mregDCs and CXCL13⁺ Th cells control the differentiation of tumor-specific progenitor-exhausted CD8 T cell clones into effective anti-tumor T cells in patients treated with ICB.

Trial Registration NCT03916627

Ethics Approval Samples of lymph node, tumor and non-involved adjacent liver were obtained from surgical specimens of patients undergoing resection at Mount Sinai Hospital (New York, NY) after obtaining informed consent in accordance with a protocol reviewed and approved by the Institutional Review Board at the Icahn School of Medicine at Mount Sinai (IRB Human Subjects Electronic Research Applications 18-00407) and in collaboration with the Biorepository and Department of Pathology.

The single-arm, open-label, phase 2 trial of HCC patients with resectable tumors was registered on ClinicalTrials.gov (NCT03916627, Cohort B). 21 patients were enrolled and received two cycles of Cemiplimab before surgical resection as described in (Marron et al., 2022a).

<http://dx.doi.org/10.1136/jitc-2022-SITC2022.0541>

B-CELL RECEPTOR (BCR) REPERTOIRE IS A DYNAMIC BIOMARKER OF SURVIVAL IN SARCOMA PATIENTS TREATED WITH NEOADJUVANT IMMUNE CHECKPOINT BLOCKADE (ICB)

Elise Nassif*, Bin Liu, Wei-Lien Wang, Alexander Lazar, Davis Ingram, Khalida Wani, Sheila Duncan, Taylor Tate, Grace Mathew, Shadara Crosby, Kenna Shaw, Monika Zelazowska, Barry Feig, Keila Torres, Kelly Hunt, B Ashleigh Guadagnolo, Andrew Bishop, Phillip Andrew Futreal, Jennifer Wargo, Neeta Somaiah, Kevin McBride, Christina Roland, Emily Keung. MD Anderson Cancer Center, Houston, TX, United States

Background Intratumoral B-cells are associated with improved survival with ICB in sarcomas.¹ We investigated the dynamics of intratumoral and peripheral BCR repertoires and their association with survival in dedifferentiated liposarcoma (DDLPS, n=17) and undifferentiated pleomorphic sarcoma (UPS, n=10) patients treated in a neoadjuvant ICB trial of nivolumab +/- ipilimumab.²⁻⁴

Methods Tumor and peripheral blood mononuclear cells (PBMCs) were collected at baseline and surgery. Intratumoral and peripheral BCR heavy (IgH) and light (IgL) chain repertoires were evaluated using bulk RNA sequencing and the TRUST4 algorithm.⁵ IgH and IgL repertoire diversity and clonality were assessed by inverse Simpson and Gini index, respectively. Comparisons of continuous variables were done using Wilcoxon Rank-Sum test. High and low categories were defined by median values. Comparisons of progression-free survival (PFS) and overall survival (OS) curves were performed by log-rank method. Correlations were assessed using Spearman's correlation.

Results Tumor transcriptomic data was available for 23 and 20 patients at baseline and surgery, respectively. PBMC transcriptomic data was available for 19 and 23 patients at baseline and surgery, respectively. BCR repertoire diversity increased with ICB, which was significant only in PBMCs (tumor: IgH $p=0.077$, IgL $p=0.11$; PBMC: IgH $p=0.0065$, IgL $p=0.029$; figures 1 and 2). Neither intratumoral nor peripheral BCR repertoire clonality was impacted by ICB treatment (figures 3 and 4). At baseline, patients with higher IgH BCR diversity had longer PFS (intratumoral: not reached [NR] vs 19 months, $p=0.15$; peripheral: NR vs 37 months, $p=0.25$). However, at surgery, patients with higher intratumoral IgH BCR diversity had shorter PFS (17 vs NR months, $p=0.024$), while peripheral BCR diversity was not associated with PFS ($p=0.98$). At baseline, patients with higher intratumoral IgH BCR clonality had longer PFS ($p=0.19$) and significantly longer OS ($p=0.022$) while neither intratumoral nor peripheral BCR clonality at surgery was associated with survival.

Conclusions ICB is associated with increases in intratumoral and peripheral BCR diversity but not with changes in clonality. Overall, neither the intratumoral IgL nor peripheral IgH and IgL BCR repertoires were associated with survival. Greater diversity of the intratumoral IgH repertoire was a favorable prognostic factor at baseline but a negative one after ICB. These findings warrant future investigations.

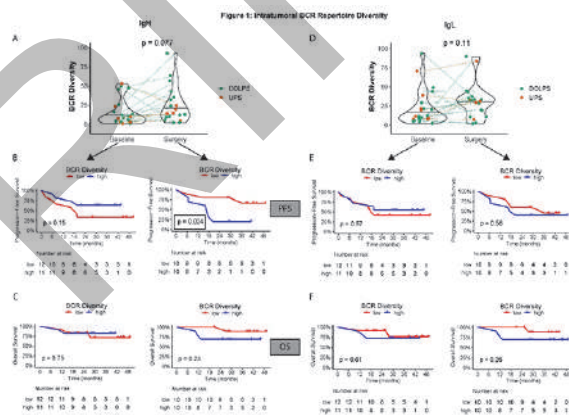
Acknowledgements This study was supported by Bristol Myers Squibb. EFN received support from Fondation pour la Recherche Medicale and Fondation Nuovo-Soldati. CLR received support from American College of Surgeons and Society of Surgical Oncology. EZK received support from NCI Early Surgeon Scientist Program.

Trial Registration NCT03307616

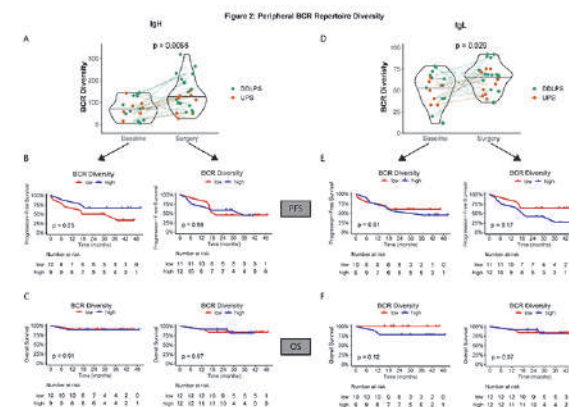
REFERENCES

1. Petitprez F, de Reynies A, Keung EZ, Chen TW, Sun CM, Calderaro J, et al. B cells are associated with survival and immunotherapy response in sarcoma. *Nature*. 2020;**577**(7791):556-60.
2. Keung EZ-Y, Nassif EF, Lin HY, Lazar AJ, Torres KE, Wang W-L, et al. Randomized phase II study of neoadjuvant checkpoint blockade for surgically resectable undifferentiated pleomorphic sarcoma (UPS) and dedifferentiated liposarcoma (DDLPS): Survival results after 2 years of follow-up and intratumoral B-cell receptor (BCR) correlates. *Journal of Clinical Oncology*. 2022;**40**(17_suppl):LBA11501-LBA.
3. Roland CL, Keung EZ-Y, Lazar AJ, Torres KE, Wang W-L, Guadagnolo A, et al. Preliminary results of a phase II study of neoadjuvant checkpoint blockade for surgically resectable undifferentiated pleomorphic sarcoma (UPS) and dedifferentiated liposarcoma (DDLPS). *Journal of Clinical Oncology*. 2020;**38**(15_suppl):11505.
4. Keung E, Nassif E, Lin H, Lazar A, Wang W-L, Parra E, et al. 379 Immune infiltrates are associated with clinical outcomes in patients with resectable soft tissue sarcoma (STS) treated with neoadjuvant immune checkpoint blockade (ICB). *Journal for ImmunoTherapy of Cancer*. 2021;**9**(Suppl 2):A410-A2.
5. Hu X, Zhang J, Wang J, Fu J, Li T, Zheng X, et al. Landscape of B cell immunity and related immune evasion in human cancers. *Nat Genet*. 2019;**51**(3):560-7.

Ethics Approval This study was approved by MD Anderson Cancer Center Institutional Review Board. IRB approval 2017-0143. All participants gave written informed consent.

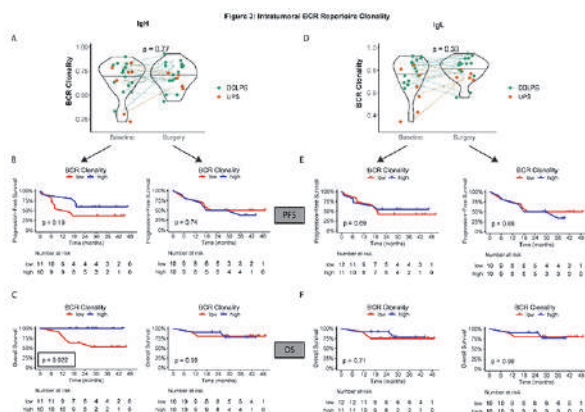


Abstract 542 Figure 1 Intratumoral BCR repertoire diversity A-B, Comparison of intratumoral BCR diversity at baseline and at surgery in heavy chains (A) and light chains (B), p-values are Wilcoxon tests. C-D, Kaplan-Meier survival curves of PFS by intratumoral diversity at baseline and at surgery in heavy chains (C) and light chains (D), p-values are log-rank tests. E-F, Kaplan-Meier survival curves of OS by intratumoral diversity at baseline and at surgery in heavy chains (C) and light chains (D), p-values are log-rank tests.

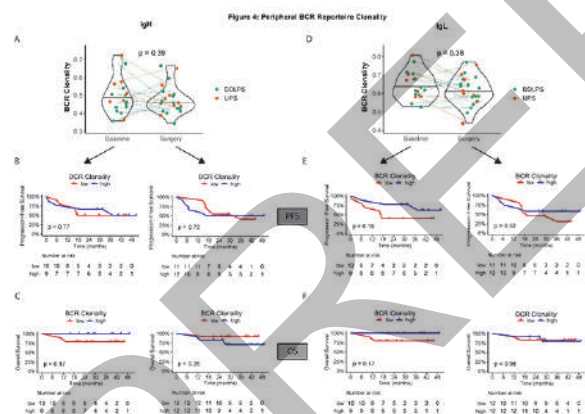


Abstract 542 Figure 2 Peripheral BCR repertoire diversity. A-B, Comparison of peripheral BCR diversity at baseline and at surgery

in heavy chains (A) and light chains (B), p-values are Wilcoxon tests. C-D, Kaplan-Meier survival curves of PFS by peripheral diversity at baseline and at surgery in heavy chains (C) and light chains (D), p-values are log-rank tests. E-F, Kaplan-Meier survival curves of OS by peripheral diversity at baseline and at surgery in heavy chains (C) and light chains (D), p-values are log-rank tests.



Abstract 542 Figure 3 Intratumoral BCR repertoire clonality. A-B, Comparison of intratumoral BCR clonality at baseline and at surgery in heavy chains (A) and light chains (B), p-values are Wilcoxon tests. C-D, Kaplan-Meier survival curves of PFS by intratumoral clonality at baseline and at surgery in heavy chains (C) and light chains (D), p-values are log-rank tests. E-F, Kaplan-Meier survival curves of OS by intratumoral clonality at baseline and at surgery in heavy chains (C) and light chains (D), p-values are log-rank tests.



Abstract 542 Figure 4 Peripheral BCR repertoire clonality. A-B, Comparison of peripheral BCR clonality at baseline and at surgery in heavy chains (A) and light chains (B), p-values are Wilcoxon tests. C-D, Kaplan-Meier survival curves of PFS by peripheral clonality at baseline and at surgery in heavy chains (C) and light chains (D), p-values are log-rank tests. E-F, Kaplan-Meier survival curves of OS by peripheral clonality at baseline and at surgery in heavy chains (C) and light chains (D), p-values are log-rank tests.

<http://dx.doi.org/10.1136/jitc-2022-SITC2022.0542>

543 **RESPONSE TO CHECKPOINT BLOCKADE IN HCC IS ASSOCIATED WITH IGG1 SKEWING**

¹Robert Sweeney*, ¹Edgar Gonzalez-Kozlova, ²Alexandra Tabachnikova, ³Christie Chang, ¹Laura Walker, ¹Assaf Magen, ¹Myron Schwartz, ¹Thomas Marron, ¹Miriam Merad, ¹Sacha Gnjatic. ¹Icahn School of Medicine at Mount Sinai, New York, NY, United States; ²Yale School of Medicine, New Haven, CT, United States; ³Stanford University School of Medicine, Stanford, CA, United States

Background Immune checkpoint blockade (ICB) is increasingly becoming the standard of care for many tumor types. Yet, useful predictive biomarkers for benefit from ICB are still lacking. Emerging literature has suggested the importance of intra-tumoral B cells in response to ICB; however, these studies fail to address the heterogeneity amongst B cells responses.¹⁻⁴ Here, we describe the largest single-cell RNA sequencing (scRNAseq) data set of B cells in treatment-naïve and ICB-treated hepatocellular carcinoma (HCC) patients and find specific B cell phenotypes that are highly associated with response to ICB.

Methods A cohort of 44 patients with early-stage HCC underwent surgical resection, of which, 26 patients received neoadjuvant anti-PD-1 treatment. Pre- and post-treatment blood and representative samples from resected tumor and adjacent uninvolved liver were collected fresh, and 10x scRNAseq was performed on the immune cell compartment. ELISA was performed on plasma from each patient to detect antibodies against a panel of 26 tumor antigens.

Results We identified three major subsets of B cells: naïve, memory (Bmems), and plasma cells (PCs), and identified different clusters within each subset with distinct transcriptional signatures. Bmem and PC clusters demonstrated differential expression of the immunoglobulin isotypes and subclasses, and we hypothesized that the B cell response in ICB responders might be skewed towards an IgG1 phenotype. Indeed, we observed that non-responders had a higher proportion of Bmems from clusters with the lowest IgG1 expression, while responders had an enrichment in Bmems originating from the cluster with the highest IgG1 expression. More strikingly, while we found an overall increase in PCs in responders compared to non-responders, there was a significantly higher enrichment of IgG1-high PC clusters in ICB responders compared to non-responders. Single-cell BCRseq on five patients (2 responders and 3 non-responders) revealed that the tumor-derived Bmems and PCs in responders were more clonally expanded than those from non-responders. Furthermore, we observed that while the clonally expanded B cells in non-responders were dominated by IgA or IgM isotypes, the clonally expanded B cells in responders were exclusively IgG1 or IgG3. Finally, we detected peripheral IgG antibodies against at least one tumor-antigen in our panel in 63% of the responders—which were mostly dominated by IgG1—whereas only 22% of non-responders had detectable IgG titers against any of the tumor antigens.

Conclusions HCC responders to ICB had B cell responses skewed towards an IgG1 phenotype, and the presence of anti-tumor IgG1 antibodies correlated with ICB response.

Acknowledgements This study was funded by Regeneron Pharmaceuticals. We thank all of the patients and their families for their involvement in this study.

Trial Registration NCT03916627

REFERENCES

1. Cabrita R, Lauss M, Sanna A, Donia M, Skaarup Larsen M, Mitra S, Johansson J, Phung B, Harbst K, Vallon-Christersson J, van Schoiack A, Lövgren K, Warren S,

Jirstrom K, Olsson H, Pietras K, Ingvar C, Isaksson K, Schadendorf D, Schmidt H, Bastholt L, Carneiro A, Wargo JA, Svane I, Jönsson G. Tertiary lymphoid structures improve immunotherapy and survival in melanoma. *Nature*. 2020;**577**(7791):561–565.

2. Griss J, Bauer W, Wagner C, Simon M, Chen M, Grabmeier-Pfistershammer K, Maurer-Granofszky M, Roka F, Penz T, Bock C, Zhang G, Herlyn M, Glatz K, Läubli H, Mertz K, Petzelbauer P, Wiesner T, Hartl M, Pickl W, Somasundaram R, Steinberger P, Wagner S. B cells sustain inflammation and predict response to immune checkpoint blockade in human melanoma. *Nat Commun*. 2019;**10**(1):4186

3. Helmink B, Reddy S, Gao J, Zhang S, Basar R, Thakur R, Yizhak K, Sade-Feldman M, Blando J, Han G, Gopalakrishnan V, Xi Y, Zhao H, Amaria R, Tawbi H, Cogdill AP, Liu W, LeBleu V, Kugeratski F, Patel S, Davies M, Hwu P, Lee J, Gerstenwald J, Lucci A, Arora R, Woodman S, Keung E, Gaudreau P, Reuben A, Spencer C, Burton E, Haydu L, Lazar AJ, Zappasodi R, Hudgens C, Ledesma D, Ong S, Bailey M, Warren S, Rao D, Krijgsman O, Rozeman E, Peeper D, Blank C, Schumacher T, Butterfield L, Zelazowska M, McBride K, Kalluri R, Allison J, Petitprez F, Fridman W, Sautès-Fridman C, Hachohen N, Rezvani K, Sharma P, Tetzlaff M, Wang L, Wargo J. B cells and tertiary lymphoid structures promote immunotherapy response. *Nature*. 2020;**577**(7791):549–555.

4. Petitprez F, de Reyniès A, Keung E, Chen TW, Sun C, Calderaro J, Jeng Y, Hsiao LP, Lacroix L, Bougouin A, Moreira M, Lacroix G, Natario I, Adam J, Lucchesi C, Laizet YH, Toulmond M, Burgess M, Bolejack V, Reinke D, Wani K, Wang W, Lazar A, Roland C, Wargo J, Italiano A, Sautès-Fridman C, Tawbi H, Fridman W. B cells are associated with survival and immunotherapy response in sarcoma. *Nature*. 2020;**577**(7791):556–560.

Ethics Approval This study was approved by Icahn School of Medicine at Mount Sinai's institutional review board, approval numbers 19-0246 and 19-06-061-05. All study participants gave informed consent before taking part in this study.

<http://dx.doi.org/10.1136/jitc-2022-SITC2022.0543>

544

COMPANION DIAGNOSTIC ASSAYS FOR PEMBROLIZUMAB IN PATIENTS WITH MSI-H/dMMR TUMORS

¹Aurelien Marabelle*, ²Jeff Cesario, ²Lixin Lang, ²Deepti Aurora-Garg, ²Siddhartha Krishan Mathur, ²Diane Levitan, ²Deb Card, ²Fan Jin, ²David Adelberg, ³Thierry André, ²Amy Wehn. ¹Gustave Roussy, Villejuif, France; ²Merck & Co., Inc., Rahway, NJ, United States; ³Sorbonne University and Saint Antoine Ho, Paris, France

Background Pembrolizumab is approved in the United States for unresectable or metastatic microsatellite instability-high (MSI-H)/mismatch repair-deficient (dMMR) solid tumors that progress after treatment. As part of a post-marketing commitment, we conducted a pan-tumor bridging study to determine MSI/MMR status for the purpose of developing 2 companion diagnostic assays. This bridging study was designed to evaluate clinical outcomes with second-line pembrolizumab and concordance with local enrollment assays. Concordance between the 2 companion diagnostic assays was also assessed.

Methods Patients with MSI-H/dMMR tumors, determined per local clinical trial assay (IHC, PCR, or NGS), who enrolled in the KEYNOTE-164 study (advanced colorectal cancer) or cohort K of the KEYNOTE-158 study (advanced non-colorectal cancer) were reevaluated for pembrolizumab efficacy (objective response rate [ORR] per RECIST v1.1) according to MSI/MMR status determined by companion diagnostic assays (Roche Tissue Diagnostics MMR RxDx Panel [RTD; IHC using MLH1, MSH2, MSH6, PMS2] and FoundationOne® CDx [NGS]). Agreement between the clinical trial assay and companion diagnostic assays was evaluated by overall percent agreement (OPA), positive percent agreement (PPA), and negative percent agreement (NPA) using the efficacy population; a supplemental population (KEYNOTE 158 cohorts A-J, KEYNOTE-177, and commercially procured tumor bank) was also used to assess NPA.

Results 444 patients with MSI-H/dMMR tumors per the clinical trial assay were analyzed for efficacy (n = 123, KEYNOTE-164; n = 321, KEYNOTE-158 cohort K). ORR is reported in table 1; responses were enriched in patients with MSI-H/dMMR tumors (RTD assay: 34.7%; FoundationOne CDx: 43.0%; clinical trial assay: 31.8%). When the clinical trial assay and RTD assay (n = 934) were compared, OPA was 90.9%, PPA was 72.0%, and NPA was 98.5%. When the clinical trial assay and FoundationOne CDx assay (n = 1174) were compared, OPA was 94.5%, PPA was 69.8%, and NPA was 99.3%. When the RTD and FoundationOne CDx assays (n = 662) were compared, OPA was 95.9%, PPA was 87.0%, and NPA was 97.1%.

Conclusions Although the RTD and FoundationOne CDx assays measure different analytes, they are comparable for the selection of patients with MSI-H/dMMR tumors likely to respond to pembrolizumab. Despite both companion diagnostic assays having lower concordance to the clinical trial assay, they demonstrated high concordance with each other and were able to better identify responders to pembrolizumab than the clinical trial assay.

Acknowledgements Medical writing and/or editorial assistance was provided by Holly C. Cappelli, PhD, CMPP, of ApotheCom (Yardley, PA, USA). This assistance was funded by Merck Sharp & Dohme LLC, a subsidiary of Merck & Co., Inc., Rahway, NJ, USA.

Ethics Approval The study protocol and all amendments were approved by the relevant institutional review board or ethics committee at each study site.

Consent All patients provided written informed consent to participate in the clinical trial.

Abstract 544 Table 1 ORR of Pembrolizumab-Treated Patients Based on MSI Status and Companion Diagnostic Assay or the Clinical Trial Assay

n/N (%)	RTD Assay	FoundationOne® CDx Assay	Clinical Trial Assay
MSI-H/dMMR	35/101 (34.7)	46/107 (43.0)	141/444 (31.8)
Non-MSI-H/pMMR	6/61 (9.8)	7/58 (12.1)	--
MSI/MMR status missing	100/282 (35.5)	88/279 (31.5)	--

<http://dx.doi.org/10.1136/jitc-2022-SITC2022.0544>

545

A PHASE II RANDOMIZED WINDOW OF OPPORTUNITY TRIAL EVALUATING CYTOTOXIC AND IMMUNOMODULATORY EFFECTS OF INTRATUMORAL INT230-6 (CISPLATIN, VINBLASTINE) IN EARLY STAGE BREAST CANCER: THE INVINCIBLE TRIAL

¹Angel Arnaut, ¹Susan Robertson, ¹Kianoosh Keyhanian, ¹Arif Awan, ²Gregory Pond, ³John Bartlett, ⁴Megan Hopkins, ⁴Linda Liao, ⁴Vida Talebian, ⁴Lazlo Radnyani, ⁵Lewis Bender*, ⁵Ian Walters, ¹Vanessa Lopez Ozuna, ⁴Melanie Spears. ¹Ottawa Hospital Research Institute, Ottawa, Canada; ²McMaster University, Hamilton, Canada; ³University of Edinburgh, Edinburgh, UK; ⁴Ontario Institute for Cancer Research, Toronto, Canada; ⁵Intensity Therapeutics, Westport, CT, United States

Background The majority of breast cancers are considered immunological quiescent and are therefore minimally responsive to immunotherapies. Local therapies that induce cell death and expose tumor antigens and potentially increase responsiveness to immunotherapies. We conducted a randomized, phase 2 presurgical window-of-opportunity trial with intratumoral (IT) INT230-6 (composed of a dispersion enhancer molecule (SHAO) in solution with drug agents vinblastine and cisplatin) designed to cause tumor necrosis by dispersion throughout the tumor and diffusion into cancer cells. The objective of the trial is to understand the effect of IT cytotoxic chemotherapy on the immune response within the tumor, microenvironment and blood in patients who are awaiting surgery for breast cancer.

Methods Women awaiting surgery for newly diagnosed intermediate or high-grade T1-T2 invasive breast cancers were recruited to the trial. Part I of the study randomized patients to 1-3 doses of INT230-6 injected weekly versus no treatment prior to surgery (2:1, open label) to evaluate safety, feasibility, and optimal drug dosing. Part II was a double-blinded randomized (2:1) trial where patients received one dose of INT230-6 versus saline injection. The primary objective was to assess the degree of tumor necrosis and to perform targeted sequencing and proteomic profiling in tumor samples from injected patients.

Results The study screened 95 patients, of which 87 enrolled. Mean age was 60 (range 40-77 yrs) and tumor size was 1.5-4.3 cm (mean = 2.4cm). The majority of the cancers were ductal histology (82%) and hormone (estrogen and/or progesterone) receptor positive (81%). The most common (>10%) AEs were injection site pain, injection site reaction and nausea/vomiting. INT230-6 induced up to 95% tumor necrosis in varying breast cancer subtypes and histologies, including invasive lobular carcinoma. Gene expression analysis showed significant differential gene expression between the baseline biopsy and surgical specimens. Pathway analysis identified genes associated with TCR signaling, B cells, T cells, chemokine signaling and NF- κ B signaling were significantly changed in the post treatment samples. There was a relative increase in CD4 and CD8 T cells and B and NK cells within the tumor and in the tumor microenvironment.

Conclusions This window of opportunity clinical trial demonstrates that INT230-6 injection is a novel and simple method to convert traditionally immune quiescent breast cancers into immunogenic tumors with minimal adverse effects and good tolerability. The results indicate a future potential for INT230-6 as an immunotherapeutic option in early stage breast cancer.

Trial Registration Phase 2 presurgical Window-Of-Opportunity trial for intratumoral (IT) INT230-6 (comprising VINblastine (VIN) Cisplatin (VIN)) evaluating clinical and BioLogical Effects in patients with early-stage operable Breast Cancer (the

INVINCIBLE trial- <https://clinicaltrials.gov/ct2/show/NCT04781725>).

Ethics Approval Ethics approval has been obtained at the Ottawa Hospital Research Institute 1.2 OHSN-REB Protocol Number: 20210002-01H.

<http://dx.doi.org/10.1136/jitc-2022-SITC2022.0545>

546

A PHASE I DOSE ESCALATION STUDY OF STEMVAC, A MULTI-ANTIGEN, MULTI-EPIOTOPE TH1 SELECTIVE PLASMID-BASED VACCINE, TARGETING STEM CELL ASSOCIATED PROTEINS IN PATIENTS WITH ADVANCED BREAST CANCER

¹Mary Disis*, ¹Ying Liu, ²Sasha Stanton, ¹William Gwin, ¹Andrew Coveler, ¹John Liao, ¹Jennifer Childs, ¹Denise Cecil. ¹UW Medicine Cancer Vaccine Institute, Seattle, WA, United States; ²Providence, Portland, OR, United States

Background Cancer stem cell or epithelial/mesenchymal transition antigens could have utility in vaccines for cancer treatment and prevention. We identified class II binding T-cell epitopes from non-mutated tumor antigens that selectively elicit a Th1 response. We constructed a 5 antigen (CD105-Yb-1-SOX2-CDH3-MDM2) multi-epitope plasmid-based vaccine; STEMVAC, and conducted a Phase I dose escalation study in patients with advanced breast cancer.

Methods Patients with advanced HER2 negative breast cancer previously treated and in remission were sequentially enrolled to 3 dose arms: 150, 300, or 600mcg of STEMVAC. Vaccines were given monthly intradermally for three doses with rhu-GM-CSF (100mcg) as adjuvant. Two booster immunizations (same dose) were given 3 and 6 months after the third vaccine. Primary endpoints were safety and immunogenicity. Secondary endpoints included persistence of the immune response after vaccination and assessment of potential stimulation of T-regulatory (Treg) cells or myeloid derived suppressor cells (MDSC) to the overexpressed non-mutated antigens expressed in STEMVAC. Antigen specific immunity was measured by IFN-gamma (g) and IL-10 ELISPOT. Immune cells were evaluated by flow cytometry.

Results Seventy-five percent of patients were hormone receptor positive and 25% triple negative (TNBC). Patient characteristics, including breast cancer subtype, did not vary significantly between doses (all $p > 0.1$). The vast majority of adverse events (AE), 98%, were grades 1/2. The most common AE were injection site reactions, flu-like syndrome, and transient leukopenia and lymphopenia. Arm 1 (150mcg) generated transient low levels of IFN-g secreting T-cells to a median of 1 antigen per patient and considered the least immunogenic dose. Arm 2 (300mcg) resulted in a mean response (sum of all antigens) of 1 antigen specific T-cell per 2500 (1:2500) PBMC at week 16 ($p < 0.05$ compared to baseline) which boosted to 1:1500 by week 60 ($p < 0.001$ compared to baseline). Immune responses for Arm 3 (600mcg) were statistically similar to Arm 2 at 16 weeks, but did not persist and could not be boosted. In Arm 2, booster immunizations increased the incidence and breadth of the immune response, with patients showing significant IFN-g secretion to a median of 4/5 antigens. At 16 weeks, there was no increase in antigen specific IL-10 secreting T-cells, Treg, or MDSC at any dose.

Conclusions STEMVAC selectively elicits high level persistent Type I T-cell responses at the 300mcg dose. Two Phase II studies are enrolling; adjuvant setting for TNBC (NCT05455658) and maintenance therapy with pembrolizumab in metastatic non-small cell lung cancer (NCT05242965).

Acknowledgements This work was supported by the Department of Defence Breast Cancer Program, VGG, and the Breast Cancer Alliance. We thank all our patient participants-we could not have completed this study without them.

Trial Registration NCT02157051

Ethics Approval The study was approved by the Fred Hutchinson Cancer Research Center Institutional Review Board

(#7396). All participants gave written informed consent before participation in the study.

<http://dx.doi.org/10.1136/jitc-2022-SITC2022.0546>

547

SAFETY AND EFFICACY OF DE-ESCALATED NEOADJUVANT CHEMOIMMUNOTHERAPY OF TRIPLE NEGATIVE BREAST CANCER (TNBC) USING CHEMOKINE-MODULATING REGIMEN (RINTATOLIMOD, IFN- α 2B, CELECOXIB)

Shipra Gandhi*, Mateusz Opyrchal, Cayla Ford, Ronald Slomba, Marie Quinn, Tracey O'Connor, Ellis Levine, Pawel Kalinski. *Roswell Park Comprehensive Cancer Center, Buffalo, NY, United States*

Background Pathologic complete response (pCR) or microinvasive residual disease (ypTmic), following neoadjuvant chemotherapy (NAC) of triple negative breast cancer (TNBC) predicts improved relapse-free and overall survival. Combination of NAC with pembrolizumab, the new standard of care, increases pCR rate from 40% to 65% but is associated with significant immune-related permanent toxicities. Production of chemokines CCL5, CXCL9, CXCL10 and CXCL11 in the tumor microenvironment (TME) is critical for the infiltration with CD8⁺ cytotoxic T-lymphocytes (CTLs), predicting higher probability of pCR.¹ Guided by our preclinical data that Chemokine-modulating (CKM) regimen, combining rintatolimod (TLR3 agonist), interferon (IFN)- α 2b and celecoxib (COX-2 inhibitor), selectively induces CTL-attractants but decreases Treg-attractants², we hypothesized that the combination of CKM with chemotherapy will promote CTL infiltration and result in higher pCR.

Methods In phase I study NCT04081389, 9 patients with stage I-III TNBC, median age 47 (37-55) years were treated with paclitaxel 80 mg/m² IV weekly for 12 weeks; CKM for first 3 weeks, days 1-3 (IV rintatolimod 200 mg daily and oral celecoxib 200 mg twice daily). IFN- α 2b was administered in an accelerated dose-escalation at 0 or 5 million units (MU)/m² [dose levels (DL) 1,2 respectively] in first 2 patients; 10 MU/m² [DL 3] in 4 patients and 20 MU/m² [DL 4] in 3 patients. CKM/Paclitaxel was followed by standard dose-dense doxorubicin and cyclophosphamide (AC) and surgery. Dose-limiting toxicity (DLT) was defined as grade 3 or higher toxicities within the first 3 weeks. Primary endpoint was safety and tolerability. Secondary endpoints included pCR rate. Tumor and blood biomarkers were analyzed in exploratory studies.

Results Treatment was well-tolerated with mostly grade 1 or 2 treatment-related adverse events (TRAEs) without DLTs or delayed or immune-related toxicities. Grade 3 TRAEs included neutropenia (3/9) attributed to CKM (1/9) or paclitaxel (3/9), pneumonia (1/9) and anemia (1/9) attributed to AC. Additional pneumonia and skin squamous cell carcinoma in situ were observed, unrelated to study treatment. Paclitaxel- or AC-related toxicities were not higher than expected. 5/9 (56%) patients attained pCR and 1 more patient attained ypTmic. CTL marker CD8 α was selectively elevated in post-CKM tumor biopsies (5 patients at DL3 and 4) but decreased in the post-CKM blood.

Conclusions The treatment was well tolerated, with promising clinical activity of pCR + ypTmic at 66%, comparable to pembrolizumab/NAC. Upcoming phase II study in early stage TNBC is planned to determine if CKM can be used as an alternative to pembrolizumab or to overcome pembrolizumab/NAC resistance.

Acknowledgements KL2TR001413, UL1TR001412, Roswell Park Alliance Foundation

Trial Registration NCT04081389

REFERENCES

1. Denkert C, Loibl S, Noske A, Roller M, Muller BM, Komor M, Budczies J, Darb-Esfahani S, Kronenwett R, Hanusch C, Torne CV, Weichert W, Engels K, Solbach C, Schrader I, Diemel M, von Minckwitz G. *J Clin Oncol*. 2010 Jan 1;**28**(1):105–13.
2. Muthuswamy R, Corman JM, Dahl K, Chatta GS, Kalinski P. Functional reprogramming of human prostate cancer to promote local attraction of effector CD8⁺ T-cells. *Prostate*. 2016 Sep; **76**(12): 1095–105.

Ethics Approval The study obtained ethics approval through Roswell Park institutional review board, and is registered under NCT04081389. The participants signed an informed consent before participating in this study.

<http://dx.doi.org/10.1136/jitc-2022-SITC2022.0547>

548

THE ONCOLYTIC VIRUS PELAREOREP IN COMBINATION WITH IMMUNE CHECKPOINT INHIBITOR ACTIVATES T-CELL FUNCTIONING IN EARLY BREAST CANCER PATIENTS – IMMUNOPHENOTYPE RESULTS FROM AWARE-1 STUDY

¹Thomas C Heineman*, ¹Houra Loghmani, ¹Richard Trauger, ²Fernando Salvador, ³Luis Manso, ⁴Tomás Pascual, ⁵Manel Juan, ^{4,5}Aleix Prat, ⁶Joaquín Gavilá, ¹Matt Coffey, ^{5E}Azucena González-Navarro. ¹Oncolytics Biotech Inc., San Diego, United States; ²SOLTI Breast Cancer Research Group, Barcelona, Spain; ³Hospital 12 de Octubre, Madrid, Spain; ⁴SOLTI/Hospital Clínic de Barcelona, Barcelona, Spain; ⁵Hospital Clínic de Barcelona/IDIBAPS, Barcelona, Spain; ⁶Instituto Valenciano de Oncología/SOLTI, Valencia, Spain

Background Pelareorep (pela) is an intravenously delivered unmodified oncolytic reovirus demonstrating anti-tumor activity through innate and adaptive immune responses.¹ Previous data from the window of opportunity AWARE-1 study demonstrated that pela, alone or in combination with atezolizumab (atezo), establishes a favorable immunologic response in tumors from HR+/HER2- early breast cancer (BC) patients.² Here, we report additional translational flow cytometry results from peripheral blood of patients participating in the AWARE-1 trial.

Methods Treatment naïve HR+/HER2- early BC patients were enrolled in two cohorts: Cohort 1 (C1)– pela + letrozole (n=10); and Cohort 2 (C2)– pela + letrozole + atezo (n=10). Pela was administered on days 1, 2 and 8, 9, while atezo was administered on day 3. Blood samples were collected pre-treatment and on days 3 and 21. In this context, we investigated the immune cell composition of peripheral blood using a multicolor flow cytometry to describe different subsets of immune cells.

Results Flow cytometry analysis showed a significant increase in natural killer cells on day 21 in C2 compared to C1 (≈ 2 -fold, p value=0.0166). No differences were observed in B cells, T cells, monocytes or neutrophils. Interestingly, a statistically significant decrease in CD4/CD8 ratio was observed when C2 was compared to C1 on day 21 after normalization with D3 (≈ 1.5 -fold, p value= 0.0142). Moreover, an increase in HLA-DR expression in CD8 population was detected in C2 vs C1 on day 21 (≈ 1.5 -fold, p value=0.0632). Regarding exhaustion markers, pela administration decreases CD39, LAG3 and TIM3 markers on day 3. However, low levels of these markers are only maintained at day 21 in patients who had received atezo on Day 3 (C2).

Conclusions These data suggest that combining pela with atezo may improve outcomes in HR+/HER2- BC by enhancing the cytotoxic and anti-tumor activity of T cells.

Trial Registration NCT04102618

REFERENCES

1. Samson A, Scott KJ, Taggart D, *et al.* Intravenous delivery of oncolytic reovirus to brain tumor patients immunologically primes for subsequent checkpoint blockade. *Sci Transl Med.* 2018;**10**(422):eaam7577. doi:10.1126/scitranslmed.aam7577
2. Manso L, *et al.* A window-of-opportunity study with atezolizumab and the oncolytic virus pelareorep in early breast cancer (AWARE-1). In: AACR Virtual Annual Meeting 2021; 2021 Apr 10-15; Virtual. AACR; 2021. Abstract CT191

Ethics Approval The study was approved by Hospital Clínic de Valencia Ethics Board and Agencia Española de Medicamentos y Productos Sanitarios (AEMPS) on February 8, 2019.

<http://dx.doi.org/10.1136/jitc-2022-SITC2022.0548>

549

BOOSTER VACCINATION OF A HER2 HELPER T-CELL VACCINE INCREASED HER2 IMMUNITY IN METASTATIC HER2 POSITIVE BREAST CANCER.

¹Sasha Stanton*, ²Jennifer Childs, ²Doreen Higgins, ³Angela Kask, ²Yi Yang, ²Mary Disis. ¹Earle A. Childs Research Institute, Portland, OR, United States; ²University of Washington, Seattle, WA, United States; ³Fred Hutchinson Cancer Research Center, Seattle, WA, United States

Background NCT00194714 vaccinated women with HER2+ metastatic breast cancer after first line therapy with a 3 epitope HER2 T-cell helper peptide vaccine. Patients received six vaccines with concurrent trastuzumab with median progression free survival of 17.7 months at 3 years and median overall survival of 86% at 4 years. Ten years later, 10 of the 22 patients were still living. We therefore determined whether HER2 immunity persisted and whether adding two booster vaccinations could boost that HER2-specific immunity.

Methods Ten eligible patients were contacted about the vaccine booster and four participated. All four patients received the six vaccine series between 2004 and 2006 and the booster vaccine series between 2017 and 2018. Patients received two booster vaccinations of the HER2 T-cell helper tri-peptide vaccine 6 months apart. Peripheral blood was collected prior to booster, 48 hours after each booster, and six months after the second booster to evaluate HER2 immunity by IFN-g ELISPOT. Pre-existing immunity was defined as mean antigen specific spots per well significantly higher than mean no antigen wells.

Results At the time of enrollment, two of the patients had progressive disease and two had no evidence of disease. The boosters were well tolerated with 28 AEs, 39% (11/28) related to the booster vaccines. The majority of AEs were grade 1 including injection site reactions in all four patients and flu like syndromes. The grade 2 toxicities included hypotension and dizziness after the vaccine. Prior to the booster vaccinations, two of the patients had pre-existing immunity to the 3 epitopes included in the vaccine and all four patients had pre-existing immunity to HER2 intracellular (ICD) and extracellular (ECD) peptide pools. After the boosters, all four patients had increased IFN-g T cell responses to the three pooled epitopes included in the vaccine with average precursor frequency prior to vaccination of 1:133,333 (range 0 to 61,539) increasing to 1:9381 after vaccination (range 1:53,333 to 1:4878, p=0.05). All four patients had augmented IFN-g immunity to the HER2 ICD peptide pool from baseline 1:2875 (range 1:400,000 to 1:1043) to 1:1851 (range 1:12,698 to 1:957, p=0.01). There was no significant augmentation in immunity to the HER2 ECD peptide pool from baseline (p=0.31).

Conclusions Patients receiving HER2 booster vaccines a decade after the initial vaccine series had augmented immune response to the immunizing epitopes and the HER2 ICD. Future studies will determine if boosters can improve long term disease control with vaccines.

Trial Registration Trial registration number NCT00194714

Ethics Approval This study had ethics approval from the Fred Hutchinson Institutional Review Board and all participants gave informed consent before taking part.

Consent No sensitive or identifiable information were used in this abstract.

<http://dx.doi.org/10.1136/jitc-2022-SITC2022.0549>

551 **INTRATUMORAL INFLUENZA VACCINE IN EARLY COLORECTAL CANCER**

Mikail Gögenur*, Mustafa Bulut, Senior Resident, Lukas Balsevicius, Anne-Marie Kanstrup Fiehn, Marianne Bøgevang Jensen, Nesibe Özgür Colak, Tobias Freyberg Justesen, Paulo Cesar Martins Urbano, Lasse Bremholm Hansen, Chief Surgeon, Ismail Gögenur. Zealand University Hospital, Køge, Denmark

Background Recurrence is the leading cause of increased morbidity and mortality after colorectal cancer surgery, with up to one-third of patients undergoing curatively intended surgery having a recurrence. The degree of tumor-infiltrating immune cells is crucial for the risk of recurrence, which is why interventions targeting the tumor and the local microenvironment are in increased focus. Intratumoral injection of the vaccine has in experimental studies shown to increase the proportion of infiltrating immune cells and lead to tumor shrinkage in both treated and untreated tumors. The purpose of this combined phase 1 and 2 study was to determine the safety of intratumoral influenza vaccine injection and whether it induces local and systemic elicitation of anti-tumor immune response.

Methods All patients with non-metastatic sigmoid and rectal cancer were eligible for inclusion. The intratumoral influenza vaccine was administered by an additional sigmoidoscopy 7-14 days before the scheduled surgery. The primary outcome was safety. The clinical outcome was evaluated as Mandard tumor regression grade (TRG) assessed by two independent pathologists. Translational outcomes included local and systemic immunological changes, analyzed via immunohistochemistry, and local mRNA gene expression.

Results Ten patients were included in the study, four with sigmoid cancer and six with rectum cancer. No serious adverse reactions or events occurred. TRG was rated as five in all patients, except one rated as four by a single pathologist. A significant increase of CD8⁺ but not CD3⁺ T cell count was noted based upon immunohistochemical staining. mRNA gene expression showed several differentially expressed genes when comparing pre vs. post vaccination specimens. Functional enrichment analysis showed significant suppression of pro-tumor inflammatory related pathways. Spatial analysis of protein expression revealed an increased expression of PD-1 in areas of CD8⁺ T cell infiltrated regions of the post-vaccination specimens compared with similar regions in pre-vaccination specimens.

Conclusions Intratumoral influenza vaccine is a safe intervention. The intervention did not lead to tumor regression, while immunohistochemistry and mRNA gene expression analyses revealed a significant increase in CD8⁺ T cell count and suppression of pro-tumor inflammation, suggesting that intratumoral influenza vaccine induces an anti-tumor response in the tumor microenvironment.

Trial Registration Trial registration on [clinicaltrials.gov](https://clinicaltrials.gov/ct2/show/study/NCT04591379): NCT04591379

Ethics Approval The study was approved by the regional ethics committee: SJ-834

<http://dx.doi.org/10.1136/jitc-2022-SITC2022.0551>

CHARACTERISTICS OF THE TUMOR MICROENVIRONMENT IN IDH1-MUTATED CHOLANGIOCARCINOMA PATIENTS FROM CLARIDHY TRIAL

¹H Duygu Saatcioglu, ²Juan Valle, ³Teresa Macarulla, ⁴Milind Javle, ⁵Do-Youn Oh, ⁶Lipika Goyal, ⁷Jake Conway, ⁷Janani Iyer, ⁷Fedaa Najdawi, ⁷Chintan Shah, ¹Camelia Gliser, ¹Susan Pandya, ¹Scott Daigle, ⁸Ghassan Abou-Alfa, ⁹Robin Kelley*. ¹Servier Pharmaceuticals, Boston, MA, United States; ²University of Manchester and Department, Manchester, UK; ³Hospital Universitario Vall d'Hebron, Barcelona, Spain; ⁴MD Anderson Cancer Center, Houston, TX, United States; ⁵Seoul National University College of Medicine, Seoul, Korea, Republic of; ⁶Massachusetts General Hospital Cancer Center, Boston, MA, United States; ⁷PathAI, Boston, MA, United States; ⁸Memorial Sloan Kettering Cancer Center, New York, NY, United States; ⁹University of California San Francisco, San Francisco, CA, United States

Background Somatic isocitrate dehydrogenase 1 mutations (*IDH1m*) convert α -ketoglutarate to the oncogenic metabolite R-2-hydroxyglutarate (2-HG). *IDH1m* are detected in approximately 13% of intrahepatic cholangiocarcinomas (CCAs).¹ Ivosidenib, an oral inhibitor of the *IDH1m* protein inhibits 2-HG and restores immune response in CCA.² We analyzed pre-treatment samples, using machine learning models to quantify histologic features of the CCA tumor microenvironment, enabling identification of correlates of *IDH1m* status, early disease progression (patients experienced progression or death within 1.54 months), and plasma 2-HG levels (median, 630 ng/ml).

Methods A set of H&E images, including from ClarIDHy³, a phase 3 placebo controlled clinical trial of ivosidenib in *IDH1m* CCA, were split into training/validation (n=200) and test sets for model development. Whole slide images were annotated by GI pathologists to identify and quantify more than 500 different human interpretable features (HIFs), including cell (cancer cell, lymphocyte, macrophage, plasma cell, fibroblast) and tissue (cancer epithelium, stroma, necrosis) features. Utilizing *IDH1m* and wild type (WT) screening samples, multivariate logistic regression models were trained to predict *IDH1m* status. P-values were calculated by univariate logistic regression and corrected for multiple comparisons via adjustment for FDR.

Results A HIF-based multivariate model discriminated between *IDH1m* and WT CCA (AUC, 0.83; 95% CI, 0.74-0.92). *IDH1m* was associated with a lower proportion of lymphocytes throughout the tumor (OR, 0.64; $P < 0.01$; FDR $P = 0.022$), and higher proportion of fibroblasts (OR, 1.8; $P < 0.01$; FDR $P = 0.023$) and lower proportion of plasma cells in the stroma (OR, 0.68; $P < 0.01$; FDR $P = 0.032$) (figure 1A). In a subset of samples, CD3 and CD8 staining showed reduced T-lymphocyte infiltration patterns in *IDH1m* (n=5) samples relative to *IDH1* WT (n=19) (figure 1B). Early disease progression of enrolled ClarIDHy patients (ivosidenib n=61, placebo n=38) was associated with a higher proportion of macrophages (OR, 1.70; $P < 0.01$; FDR $P = 0.08$) and a lower proportion of tumor infiltrating lymphocytes (OR, 0.63; $P < 0.01$; FDR $P = 0.08$), (figure 2A). When correcting for treatment effect, the proportion of lymphocytes in the tumor were still associated with improved PFS ($P = 0.011$). Consistent with previously published data², high 2-HG levels were associated with lower numbers of tumor infiltrating lymphocytes (OR, 0.63; $P = 0.011$; FDR $P = 0.08$) (figure 2B).

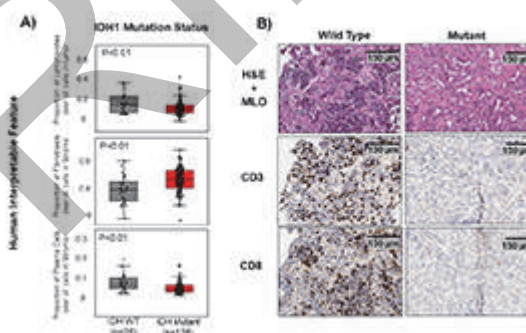
Conclusions Quantitative histologic evaluation suggests that pre-treatment *IDH1m* CCA samples have a colder tumor microenvironment relative to *IDH1* WT CCA, with an immunosuppressive tumor microenvironment being associated with

early progression. Results from this analysis support exploration of combination with immune checkpoint inhibitors. Trial Registration NCT02989857

REFERENCES

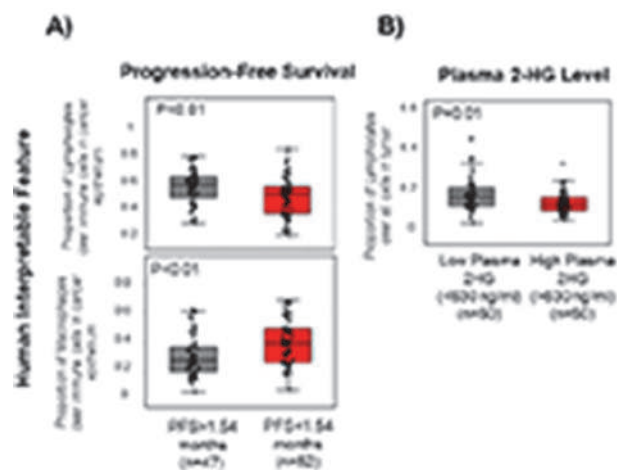
1. Boscoe AN, Rolland C, Kelley RK. Frequency and prognostic significance of isocitrate dehydrogenase 1 mutations in cholangiocarcinoma: a systematic literature review. *J Gastrointest Oncol.* 2019;**10**(4):751–765. doi: 10.21037/jgo.2019.03.10.
2. Wu MJ, Shi L, Dubrot J, et al. Mutant IDH Inhibits IFN γ -TET2 signaling to promote immunoevasion and tumor maintenance in cholangiocarcinoma. *Cancer Discov.* 2022;**12**(3):812–835. doi: 10.1158/2159-8290.CD-21-1077.
3. Abou-Alfa GK, Macarulla T, Javle MM, et al. Ivosidenib in *IDH1*-mutant, chemotherapy-refractory cholangiocarcinoma (ClarIDHy): a multicentre, randomised, double-blind, placebo-controlled, phase 3 study. *Lancet Oncol.* 2020;**21**(6):796–807. doi: 10.1016/S1470-2045(20)30157-1. Epub 2020 May 13. Erratum in: *Lancet Oncol.* 2020 Oct;**21**(10):e462.

Ethics Approval This study was done according to the International Conference on Harmonisation of Good Clinical Practice guidelines and the principles of the Declaration of Helsinki. Approval from the institutional review board and international ethics committee was obtained at each study site. Patients provided written, informed consent before participating in the study.



Abstract 552 Figure 1 Tumor microenvironment of *IDH1m* vs *IDH1* WT

Tumor microenvironment of *IDH1m* CCA compared to *IDH1* WT at screening. (A) 163 screening samples, including *IDH1m* (n=138) and *IDH1* WT (n=25) subjects were analyzed by machine learning of histological features. Samples deemed by a panel of GI pathologist to be extrahepatic as a best response were excluded from the analysis. *IDH1m* status in CCA was associated with lower proportions of lymphocytes in the tumor (Upper Row), higher proportions of fibroblasts in the stroma (Middle Row), and lower proportions of plasma cells in the stroma (Bottom Row). Tumor includes cancer epithelium and stroma tissues in the whole sections. Uncorrected P values are displayed on the Figures (B) Further analysis of a subset of screening samples (n=5 *IDH1m*, n=19 *IDH1* WT) by CD3 and CD8 staining was performed. Representative whole slide biopsy H&E images indicating lower proportions of lymphocytes in the *IDH1m* CCA tumor via machine learning-derived predictions (Upper Row; Lymphocytes are indicated with dark green marker overlay, MLO=Machine Learning Overlay, representative image for CD3 immunohistochemistry (Middle Row), and representative image for CD8 immunohistochemistry (Bottom Row).



Abstract 552 Figure 2 Differences in CCA tumor microenvironment. Differences in CCA tumor microenvironment based on early disease progression and pre-treatment plasma 2-HG levels. (A) Pre-treatment screening samples from 99 (ivosidenib cohort n=61, placebo cohort n=38) patients treated on the ClarIDHy study were analyzed for association with early disease progression, defined as experiencing progression or death within 1.54 months (47 days) (PFS<1.54 months) Early disease progression was associated with lower proportions lymphocytes over immune cells in cancer epithelium (Upper Row) and higher proportions of macrophages (Bottom Row) over immune cells in cancer epithelium (B) Plasma 2-HG levels were available for 100 IDH1m patients, with sample groups separated based on the median plasma 2-HG level (630 ng/ml). Higher plasma 2-HG levels were associated with lower proportions of lymphocytes in CCA tumor. Uncorrected P values are displayed on the Figures (A and B)

<http://dx.doi.org/10.1136/jitc-2022-SITC2022.0552>

Abstracts

553

DKN-01 AND TISLELIZUMAB AS A SECOND-LINE (2L) INVESTIGATIONAL THERAPY IN ADVANCED DKK1 HIGH GASTROESOPHAGEAL ADENOCARCINOMA (GEA): DISTINGUISH TRIAL

¹Samuel Klempner*, ²Jaffer Ajani, ³Joseph Chao, ⁴Hope Uronis, ⁵Cynthia Sirard, ⁶Michael Kagey, ⁷Jason Baum, ⁸Lilin Zhang, ⁹In-Ho Kim, ¹⁰Do-Youn Oh, ¹¹Byoung Yong Shim, ¹²Sun Jin Sym, ¹³Mohamad Sonbol, ¹⁴Mohamedtaki Tejani, ¹⁵Zev Wainberg, Devalingam Mahalingam, ¹⁶Keun-Wook Lee. ¹Massachusetts General Hospital, Boston, MA, United States; ²MD Anderson, Houston, TX, United States; ³City of Hope, Duarte, CA, United States; ⁴Duke University Medical Center, Durham, NC, United States; ⁵Leap Therapeutics, Inc., Cambridge, MA, United States; ⁶BeiGene, Beijing, China; ⁷The Catholic University of Korea, Seoul, Korea, Republic of; ⁸Seoul National University Hospital, Seoul, Korea, Republic of; ⁹Gachon University Gil Medical Center, Incheon, Korea, Republic of; ¹⁰Mayo Clinic Hospital, Phoenix, AZ, United States; ¹¹AdventHealth Cancer Institute, Orlando, FL, United States; ¹²University of California Los Angeles, Los Angeles, CA, United States; ¹³Northwestern University, Chicago, IL, United States; ¹⁴Seoul National University Bundang Hospit, Seoul, Korea, Republic of

Background Elevated tumoral DKK1 expression is seen in approximately one third of previously treated GEA and has been associated with more aggressive disease and shorter overall survival. DKN-01 (D) is a targeted anti-DKK1 mAb which has demonstrated improved clinical outcomes in previously treated GEA pts with elevated tumoral DKK1 expression when used in combination with an anti-PD1 antibody.

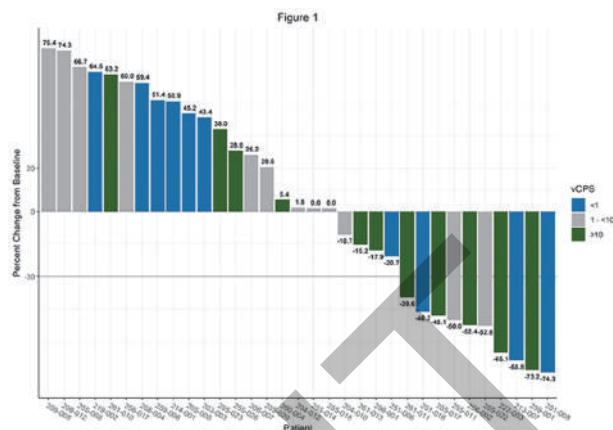
Methods DisTinguish (NCT04363801) is a Phase 2a single arm 2-part trial; Part A is reported separately; Part B investigated two dosing cohorts of D (300 mg and 600 mg) + tislelizumab (TS) as 2L therapy for DKK1-high GEA pts. Primary objective was to examine safety and tolerability and secondary objectives evaluated multiple efficacy endpoints including overall response rate (ORR) and disease control rate (DCR) in a modified intent to treat (mITT) population (>1 dose D).

Results 52 pts enrolled between 27 Oct 2020 and 7 Jun 2022; (D-300 mg, 24 pts; D-600 mg 28 pts). Median age was 63 (29, 76); 41 males (79%). 18 pts (35%) had gastroesophageal junction (GEJ) adenocarcinoma; 34 pts (65%) had gastric cancer (GC). 22 pts from US, 30 pts from Republic of Korea. 49 pts have PD-L1 visually-estimated combined positive score (vCPS) results: <1 n=13 (27%); 1-<10 n=22 (45%); ≥10 n=14 (29%). 38 pts with genomic profiling: Wnt activating mutations in 12 pts, no MSI-H. 4 pts were IO experienced. Median number of cycles 2 (1, 19). 12 pts remain on therapy. 19 pts (37%) experienced D-related adverse events (AE); 74% were G1/2. Most common regimen related AEs: fatigue, nausea, AST increased. 3 pts (6%) had serious D-related AEs [vomiting, fatigue, dehydration]. No G5 TRAEs. No D-related AE led to D-dose reduction or discontinuation. Preliminary ORR in response evaluable IO naive mITT (n=36) was 25% and DCR 44%. mITT ORR by vCPS (figure 1): <1: [n=11; PR-3 (27%), SD-1, PD-7]; 1-<10: [n=12; PR-1 (8%), SD-3, PD-8 (1 PD pt -> irPR)]; ≥10: [n=11; PR-5 (45%), SD-3, PD-3]. 6 of 9 responders remain on therapy, median DoR not reached. Median PFS: 1.4 mos (vCPS <1: 1.4 mos, 1-<10: 1.4 mos, ≥10: 2.9 mos).

Conclusions The combination of D + TS represents a well-tolerated, active chemotherapy-free combination in previously treated DKK1-high IO naïve GEA pts. Encouraging durable activity was observed particularly in DKK1 high/vCPS≥10 cohort: ORR 45%, DCR 73%. Updated ORR, DoR, PFS and additional correlative biomarker evaluation will be reported.

Acknowledgements Diane Piper and Mathis Thoma, Leap Therapeutics, Inc. biometrics support

Trial Registration NCT04363801



Abstract 553 Figure 1 Waterfall Plot by vCPS: IO naive mITT Population

<http://dx.doi.org/10.1136/jitc-2022-SITC2022.0553>

554

ARTIFICIAL INTELLIGENCE (AI)-POWERED IMMUNE PHENOTYPING OF ADVANCED OR METASTATIC UROTHELIAL CARCINOMA (AUC) CLINICAL TRIAL SAMPLES FROM HEMATOXYLIN AND EOSIN (H&E)-STAINED WHOLE SLIDE IMAGES (WSI)

¹Jake Conway*, ¹Limin Yu, ¹Yash Belhe, ¹Suyog Jain, ²Hans Grote, ¹Mary Lin, ¹Benjamin Trotter, ¹Darpan Sanghavi, ²Aslihan Gerhold-Ay, ³XiaoZhe Wang, ¹Sergine Brutus, ²Thomas Mrowiec. ¹PathAI, Boston, MA, United States; ²The Healthcare Business of Merck KGaA, Darmstadt, Germany; ³EMD Serono, Billerica, MA, United States

Background CD8 immune phenotype status is associated with response to anti-PD-L1 therapy in aUC. To assess the tumor microenvironment in aUC, we developed machine learning (ML)-based models to identify cell types and tissue regions in digitized H&E-stained WSI from the JAVELIN Bladder 100 trial, which showed that avelumab (anti-PD-L1) first-line maintenance plus best supportive care (BSC) significantly prolonged overall survival vs BSC alone in patients with aUC. ML-quantified features were used for subsequent slide-level immune phenotyping of these clinical trial samples.

Methods Models previously trained using samples from The Cancer Genome Atlas were refined using 25,926 tissue regions annotations and 183,259 cell type annotations on 704 formalin-fixed, paraffin-embedded, H&E-stained WSI scanned on MIRAX (40x) to identify artifacts, tissue regions (cancer, stroma, and necrosis), and cell types (cancer epithelial cells, lymphocytes, macrophages, fibroblasts, and granulocytes). Precision, recall, and F1 scores were calculated to evaluate model performance. Following pathologist guidelines, H&E slide-level digital immune phenotypes (excluded, inflamed, and desert) were determined using thresholds of lymphocyte area within stroma and proportion of lymphocytes vs all cells in cancer epithelium. The distribution of H&E slide-level digital immune phenotypes was calculated across samples in both trial arms, and the association between immune phenotype and CD8 score at the tumor core was determined using the Kruskal-Wallis and Mann-Whitney U tests.

Results Precision, recall, and F1 scores for model predictions were comparable to those of an average annotator across cell types. The model's concordance with consensus was also higher than that of an average human annotator (Cohen's kappa, 0.816 vs 0.680). Calculation of the distribution of H&E slide-level digital immune phenotypes across trial arms showed that most samples in each arm had an excluded immune phenotype, and a slightly higher proportion of samples in the BSC-only arm had an inflamed phenotype. Association between immune phenotype and the gold-standard CD8 immunohistochemistry (IHC) score at the tumor core showed that samples with the inflamed immune phenotype had higher CD8 scores at the tumor core than samples with the excluded immune phenotype (Mann-Whitney, $p < 0.026$).

Conclusions We show an AI-powered approach to determine slide-level immune phenotypes directly from digitized H&E-stained WSI of clinical aUC samples. An association between inflamed immune phenotypes and higher CD8 scores at the tumor core supports the potential use of this method as an alternative to CD8 IHC-based approaches to identify patients who may derive optimal benefit from anti-PD-L1 treatment.

Acknowledgements This research was supported by the healthcare business of Merck KGaA, Darmstadt, Germany (CrossRef Funder ID: 10.13039/100009945) as part of an alliance between the healthcare business of Merck KGaA, Darmstadt, Germany and Pfizer.

Trial Registration NCT02603432 (ClinicalTrials.gov)

Ethics Approval The trial protocol was approved by the independent ethics committee or institutional review board at each participating center.

<http://dx.doi.org/10.1136/jitc-2022-SITC2022.0554>

CLINICAL AND PHARMACODYNAMIC BIOMARKER RESULTS FROM PORTER, A MULTI-COHORT PHASE 1 PLATFORM TRIAL OF COMBINATION IMMUNOTHERAPY FOR METASTATIC CASTRATION-RESISTANT PROSTATE CANCER PATIENTS

¹Matthew Galsky*, ²Karen Autio, ³Kristopher Wentzel, ⁴Julie Graff, ⁵Terence Friedlander, ⁶Julie Densmore, ⁶Christopher Cabanski, ⁶Kristin Shotts, ⁶Tim Howes, ⁶Jia Yu, ⁶Elaine Eisenbeisz, ⁶Marko Spasic, ⁶Stephen Maddock, ⁶Diane DaSilva, ⁶Dinesh Kumar, ⁷Jonni Moore, ⁸Richard Schretzenmair, ⁸Jennifer Lata, ⁸Arron Xu, ⁸Emma Reuschel, ⁸Snehal Wani, ⁸Matthew Morrow, ⁸Jeffrey Skolnik, ⁶Sandra Santulli-Marotto, ⁶Lacey Padron, ⁶Lisa Butterfield, ⁶Theresa LaVallee, ⁶Samantha Bucktrout, ⁹Michael Yellin, ⁹Tibor Keler, ¹⁰Lisa Salvador, ¹¹Jill O'Donnell-Torney, ¹¹Vanessa Lucey, ⁶Justin Fairchild, ⁶Ute Dugan, ¹Nina Bhardwaj, ¹²Sumit Subudhi, ⁵Lawrence Fong. ¹Mount Sinai Medical Center, New York, NY, United States; ²Memorial Sloan Kettering Cancer Center, New York, NY, United States; ³The Angeles Clinic, Los Angeles, CA, United States; ⁴Oregon Health and Science University, Portland, OR, United States; ⁵University of California San Francisco, San Francisco, CA, United States; ⁶Parker Institute for Cancer Immunotherapy, San Francisco, CA, United States; ⁷University of Pennsylvania, Philadelphia, PA, United States; ⁸Inovio Pharmaceuticals, Plymouth Meeting, PA, United States; ⁹Celldex Therapeutics, Hampton, NJ, United States; ¹⁰Bristol Myers Squibb, Princeton, NJ, United States; ¹¹Cancer Research Institute, New York, NY, United States; ¹²MD Anderson, Houston, TX, United States

Background Immune checkpoint therapy has failed to demonstrate a survival benefit for patients with metastatic castration resistant prostate cancer (mCRPC). New immunotherapy combination strategies are required to improve clinical outcomes in heavily-pretreated mCRPC patients.

Methods This open-label exploratory platform trial tested the safety and activity of immunotherapy combinations in patients with mCRPC. Three cohorts were enrolled A) bempgaldesleukin/nivolumab, B) stereotactic body radiation therapy (SBRT)/CDX-301 (FLT3L)/poly-ICLC/nivolumab, and C) CDX-301/INO-5151 (DNA vaccine encoding PSA/PSMA/IL-12)/nivolumab. Each cohort enrolled up to 15 participants who had progressed on androgen deprivation therapy with a subset being chemo- and/or radiation-exposed. Primary endpoint: safety. Secondary endpoints: composite response rate (CRR, defined as PR/CR per PCWG-3 modified RECIST v1.1, confirmed PSA reduction >50%, or CTC change from 5 to 4 cells/7.5 mL of blood), disease control rate (DCR; SD \geq 6 mos), and time to radiographic PFS (rPFS). This study was not powered for comparison between cohorts.

Results Cohort A: CRR was 7% (1/14; 1 CTC response, no radiographic or PSA responses). DCR was 14% (2/14). Median rPFS was 2.8 months (95% CI: 2.0-7.3). Ten (71.4%) patients experienced a Grade 3-4 TRAE, including a Grade 5 TRAE of acute respiratory distress syndrome.

Cohort B: CRR was 33% (5/15; 1 PR, 1 CTC and 3 PSA responses, all in distinct patients). DCR was 27% (4/15). Median rPFS was 7.5 months (95% CI: 3.5-10.5). One (7%) patient experienced a Grade 3-4 TRAE.

Cohort C: CRR was 7% (1/14; 1 patient with both PR and PSA response). DCR was 14% (2/14). Median rPFS was 2.9 months (95% CI: 2.7-7.1). 2 (14%) patients experienced a Grade 3-4 TRAE.

Peripheral immune phenotyping analysis demonstrated distinct pharmacodynamic effects including increases in proliferating, activated T and NK cells following bempgaldesleukin treatment in cohort A. In cohorts B and C, the expansion of dendritic cells (DCs) and monocytes following FLT3L treatment was observed, as well as increases in serum proteins associated with DC activation/maturation. In cohort C, INO-5151 vaccination induced antigen-specific T cell responses. Elevated serum levels of PD-1 and IFN-gamma signaling

associated proteins were observed following nivolumab treatment in all cohorts.

Conclusions This platform study design demonstrated the feasibility and efficiency of iteratively testing distinct immunotherapy combinations with comprehensive biomarker assessment in patients with mCRPC. While neither cohort A nor C were expanded due to insufficient clinical activity, the clinical responses seen with SBRT/FLT3L/polyICLC/nivolumab suggest sufficient clinical benefit that may warrant additional investigation, particularly the contribution of radiation to the responses observed.

Acknowledgements We extend our gratitude to the patients, their families, the clinical investigators, and their site staff members who are making this trial possible. We would also like to thank Carri Browne at Parker Institute for Cancer Immunotherapy (PICI) for operations leadership of the trial. We thank Jay Campbell (CRI), Samik Upadhaya (CRI), Andres Salazar (Oncovir) and Silvia Boffo (BMS) for their contributions. We thank Bristol Myers Squibb (BMS), Celldex, Oncovir and Inovio for collaboration and study drugs. The study was funded by Cancer Research Institute, BMS and PICI.

Trial Registration NCT03835533

Ethics Approval This study was approved by OHRP/FDA Parent Organization Number, IOG0000432 with the IRB registration number IRB00000533.

Consent Written informed consent was obtained from the patient for publication of this abstract and any accompanying images. A copy of the written consent is available for review by the Editor of this journal.

<http://dx.doi.org/10.1136/jitc-2022-SITC2022.0555>

556

EXTRACELLULAR MATRIX (ECM) BIOMARKERS ARE ELEVATED IN ADVANCED RENAL CELL CARCINOMA (ARCC) AND PREDICTIVE OF RESPONSE TO NIVOLUMAB PLUS IPILIMUMAB (NIVO+IPI): ANALYSIS FROM CHECKMATE 214

¹Saurabh Gupta*, ¹Celine Han, ^{1,2}Bhakti Dwivedi, ¹Jun Li, ³Morten Karsdal, ⁴Robert Motzer, ³Nicholas Willumsen, ⁵David McDermott, ⁶Toni Choueiri. ¹Bristol Myers Squibb, Princeton, NJ, United States; ²Parexel, Princeton, NJ, United States; ³Nordic Bioscience, Herlev, Denmark; ⁴Memorial Sloan Kettering Cancer Center, New York, NY, United States; ⁵Beth Israel Deaconess Medical Center, Boston, MA, United States; ⁶Dana-Farber Cancer Institute, Harvard Medical School, Boston, MA, United States

Background Tumor fibrosis and cancer-associated fibroblast (CAF) activity is becoming a central aspect in cancer biology. The tumor microenvironment (TME) consists mainly of ECM, and biomarkers of tumor fibrosis activity can be quantified from small ECM fragments in serum. An unmet need exists to identify patients with aRCC who are most likely to benefit from treatment with NIVO+IPI.^{1,2} Therefore, we explored the prognostic and predictive potential of circulating ECM-associated biomarkers for the first time in patients with aRCC, using samples from the CheckMate 214 trial.

Methods Pretreatment serum was collected, and levels of 17 biomarkers associated with ECM formation, ECM degradation, or immune response (table 1) were assessed using immunoassay-based methods. Biomarker levels were compared between healthy volunteers and patients with aRCC. Associations with International Metastatic RCC Database Consortium (IMDC) risk score, sarcomatoid status, and objective response rate were evaluated. Prognostic and predictive associations were determined retrospectively from patients' progression-free survival (PFS) and overall survival (OS) outcomes.

Results Clinical (5-year follow-up) and biomarker data were evaluable in 1006 of 1082 treated patients (93%). Statistically significant differences ($P < 0.0001$) in all 17 biomarkers were observed between healthy individuals and patients with aRCC (table 2). Higher levels of the majority of the biomarkers (all except PRO-C23) were positively correlated with increasing IMDC score ($P < 0.01$), and 9 biomarkers (including PRO-C3, C6M, and TGFβ-LAP) were increased in patients with sarcomatoid histology ($P < 0.05$). CPA9-HNE and TGFβ-LAP levels were higher in patients who responded to NIVO+IPI ($P < 0.05$). In the overall population, higher levels of biomarkers such as C4M, C6M, PRO-C19, TGFβ-LAP, and TUM were associated with shorter PFS and OS ($P < 0.05$). When comparing treatment arms, higher levels of PRO-C19, PRO-C22, C4M, C6M, CPA9-HNE, VICM, TGFβ-LAP, and TUM were associated with improved PFS with NIVO+IPI ($P < 0.05$), which is indicative of predictive potential.

Conclusions Biomarkers of ECM formation, degradation, and TGFβ signaling were significantly increased in patients with aRCC compared with healthy individuals, which is indicative of high CAF activity. In patient with aRCC, high levels of ECM biomarkers were associated with poor OS and PFS outcomes. Patients with high ECM remodeling activity responded better to NIVO+IPI than to sunitinib. ECM biomarkers could potentially guide patient selection and/or stratification in future clinical trials. The predictive value of these biomarkers needs to be investigated in prospective clinical trials.

Acknowledgements We would like to thank the CheckMate 214 clinical study teams, as well as Oksana Palyha, Sai Vikram Vemula, Scott Chaslow, Han Chang, Abraham Apfel, Chung-Wei Lee, Jin Yao, Kimberly Gray, Megan Wind-Rotolo, and

Daniel Cohen. Editorial support was provided by Rowena Fung, MPhil, of Spark Medica Inc. Trial Registration Clinicaltrials. gov. NCT02231749.

REFERENCES

1. Motzer R *et al.* Nivolumab plus ipilimumab versus sunitinib in advanced renal-cell carcinoma. *N Engl J Med* 2018;**378**:1277–1290.
2. Motzer R *et al.* Biomarker analysis from CheckMate 214: nivolumab plus ipilimumab versus sunitinib in renal cell carcinoma. *J Immunother Cancer* 2022;**10**: e004316.

Ethics Approval The trial protocols were approved by site institutional review boards or independent ethics committees and conducted according to Good Clinical Practice guidelines, per the International Conference on Harmonisation. Patients provided written informed consent based on Declaration of Helsinki principles.

Abstract 556 Table 1 Descriptions of biomarkers assessed in this study

Symbol	Name	Biological process
ECM formation		
PRO-C3	N-terminal pro-peptide of type III collagen	Fibrinogenesis
PRO-C4	Internal epitope in the 7S domain of type IV collagen	Basement membrane remodeling
PRO-C5	N-terminal pro-peptide of type V collagen	Fibrinogenesis
PRO-C6	C-terminal NC-domain of type VIa3 collagen (endotrophin)	Pro-fibrotic signaling
PRO-C19	C-terminal of type XIX collagen, NC1 domain	FACIT remodeling
PRO-C20	C-terminal of type XX collagen, NC1 domain	FACIT remodeling
PRO-C22	C-terminal of type XXII collagen, NC1 domain	FACIT remodeling
PRO-C23	C-terminal of type XXIII collagen	Membrane protein shedding
PRO-C28	C-terminal of type XXVIII collagen	Fibrogenesis
ECM degradation		
C3M	MMP-degraded type III collagen	Interstitial matrix degradation and remodeling
C4M	MMP-degraded type IV collagen	Basement membrane degradation and remodeling
C6M	MMP-degraded type VI collagen	Interface matrix degradation
Inflammation		
VICM	MMP-degraded and citrullinated vimentin	Macrophage activity
C4G	Granzyme B-degraded type IV collagen	T-cell activity
CPa9-HNE	Neutrophil elastase degraded fragment of calprotectin	Neutrophil activity and NETosis
TGFβ-LAP	PLK-cleaved LAP fragment	Active TGFβ
Vascular remodeling		
TUM	MMP-mediated release of tumstatin	Signaling peptide of the basement membrane

ECM, extracellular matrix; FACIT, fibril-associated collagens with interrupted triple helices; HNE, human neutrophil elastase; LAP, latency-associated protein; MMP, matrix metalloproteinase; PLK, plasma kallikrein; TGFβ, transforming growth factor beta.

Abstract 556 Table 2 ECM biomarkers with significant differences ($P < 0.0001$) in baseline serum from healthy volunteers and patients with aRCC

Biomarker ^a	Healthy volunteers ^b			Patients with aRCC		
	n ^c	Median, ng/mL	SD	n ^c	Median, ng/mL	SD
PRO-C3	160	8.8	4.5	369	15.0	9.8
PRO-C4	30	3636.6	607.3	389	8400.2	1477.9
PRO-C5	160	406.3	156.2	174	1110.2	678.3
PRO-C6	160	6.6	3.6	968	14.2	8.1
PRO-C19	35	86.6	70.6	885	234.4	153.3
PRO-C20	627	4.4	1.1	672	6.8	2.4
PRO-C22	628	17.0	10.6	344	33.6	31.8
PRO-C23	142	1.6	2.6	740	3.6	3.6
PRO-C28	30	16.6	2.6	535	24.4	11.1
C3M	161	10.6	2.9	176	18.0	6.5
C4M	160	20.9	6.1	548	34.4	17.1
C6M	160	12.3	5.4	882	29.8	16.6
VICM	160	1.0	3.4	929	10.4	15.6
C4G	28	18.5	13.3	368	34.2	35.7
CPa9-HNE	161	11.0	78.4	566	307.5	175.7
TGFβ-LAP	29	0.1	0.3	859	2.6	3.2
TUM	30	0.7	0.4	573	2.8	1.2

^aP-values calculated by two-sample t-test, adjusted for multiple hypothesis testing. ^bProvided by Nordic Bioscience. ^cEvaluable individuals. aRCC, advanced renal cell carcinoma; ECM, extracellular matrix; HNE, human neutrophil elastase; LAP, latency-associated protein; SD, standard deviation; TGFβ, transforming growth factor beta; TUM, tumstatin; VICM, MMP-degraded and citrullinated vimentin.

<http://dx.doi.org/10.1136/jitc-2022-SITC2022.0556>

Abstracts

557

THE EPITOPE-ENHANCED TARP PEPTIDE CAN INDUCE SPECIFIC T CELLS THAT CAN RECOGNIZE WILD-TYPE TARP TETRAMER BY EITHER PEPTIDE OR PEPTIDE-PULSED DC VACCINATION IN PATIENTS WITH PROSTATE CANCER

¹Purevdorj Olkhanud, ²Refika Turnier, ²Kimberly Dunham, ¹Masaki Terabe, ¹Seth Steinberg, ¹Brenda Roberson, ¹Lauren Wood, ³David Stroncek, ¹Ira Pastan, ¹Jay Berzofsky, ¹Hoyoung Maeng*. ¹National Cancer Institute, Bethesda, MD, United States; ²Frederick National Laboratory, Frederick, MD, United States; ³NIH Clinical Center, Bethesda, MD, United States

Background TARP is expressed in >90% of prostate cancer throughout Gleason score and stages. Two TARP-targeting vaccines were developed at the NCI (figure 1). HLA-A*0201-restricted epitopes Wild Type 27-35 (TARP27-35WT) and Epitope-Enhanced 29-37(9V) (TARP29-37(9V)EE) of TARP were injected with an adjuvant or on autologous dendritic cells (DCs). Previously, the first-in-human clinical trial studying TARP-targeting vaccines in biochemically recurrent prostate cancer was reported.^{1, 2} This is a follow-up report focused on immunogenicity.

Methods TARP-specific T cell responses were assessed on study weeks 0, 12, 18, and 24 with vaccinations at weeks 3, 6, 9, 12, and 15 (Peptide vaccine=21, DC vaccine=20). PBMCs to assess the T cell response were collected and cryopreserved for batch testing. PSA was tested every 3 weeks. PSA-slope log was calculated using the MSKCC nomogram. Decreased PSA-slope log following vaccination at week 24 or week 48 was defined as the study-specific response as previously reported.

Thawed PBMCs were *in vitro* stimulated (IVS) with either TARP27-35WT, TARP29-37EE, or TARP29-37WT-pulsed monocytes in the presence of IL-7[1]. After 7 days of IVS, the cells were tested for tetramer-specific T cells by flow cytometry and for peptide-specific IFN-gamma response by ELISPOT.

Results Peptide-pulsed DC immunization induced tetramer-positive T cells at weeks 12, 18, and 24 post-immunization. The TARP29-37EE peptide performed as intended to induce specific T cells, the vast majority of which reacted equally well to the WT version of the EE sequence by 2-color flow cytometry. Only a small proportion reacted uniquely to EE, but not WT. This shows proof of the principle that EE-peptide can induce WT-specific T cells (figure 2).

In addition, all six patients who had the strongest IFN-gamma ELISPOT response to TARP27-35WT, TARP29-37EE, and TARP29-37WT peptides had decreased PSA-slope log at week 24 and/or 48 which corresponds to the study defined responses among 40 patients tested (figure 3). ELISPOT responses were more frequent in patients immunized with DC vaccines than in those with peptide/adjuvant vaccines.

Conclusions This first-in-human TARP vaccine study of peptide versus peptide-loaded DC platforms showed immunogenicity by peptide-HLA-tetramer assay and ELISPOT to detect IFN-gamma-producing cells. Importantly for proof-of-principle, the T cells recognizing the EE peptide immunogen recognized equally well the WT counterpart present in the tumor, as required for epitope-enhancement to be effective. The ability of high IFN-gamma ELISPOT response to the vaccine peptides to predict clinical responsiveness as measured by decreased PSA-slope log supports a protective role of antigen-specific T cells.

Acknowledgements The authors thank the patients and their families/caregivers for participating. This study was supported

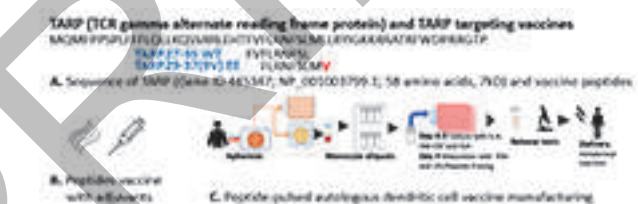
by the Center for Cancer Research/NCI intramural program. The authors appreciate the contributions of Dr. Anatoli Malyguine and Dr. Michael Davies who previously served at the Frederick National Laboratory for Cancer Research, and the members of NIH Clinical Center Pharmacy IDMRS (Investigational Drug Management and Research Section).

Trial Registration NCT00972309

REFERENCES

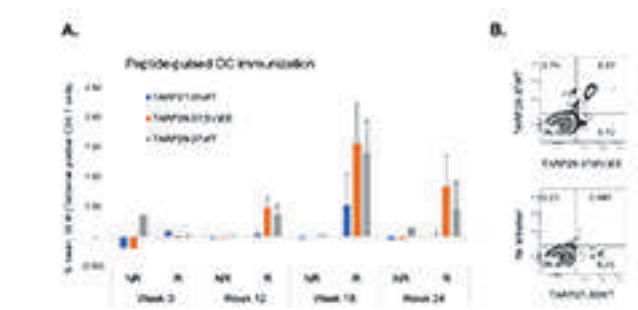
1. Wood LV, Fojo A, Roberson BD, Hughes MS, Dahut W, Gulley JL, Madan RA, Arlen PM, Sabatino M, Stroncek DF, Castiello L, Trepel JB, Lee MJ, Parnes HL, Steinberg SM, Terabe M, Wilkerson J, Pastan I, Berzofsky JA. TARP vaccination is associated with slowing in PSA velocity and decreasing tumor growth rates in patients with Stage D0 prostate cancer. *Oncoimmunology*. 2016;5(8):e1197459.
2. Maeng M, Moore B, Wood LV, Steinberg S, Mckinnon K, Terabe M, Okhanud P, Pastan I, Berzofsky JA. Cancer vaccine against prostate cancer antigen TARP induces antigen-specific CD8+ T cells with upregulation of activation marker PD1 in patients with decreased PSA velocity in D0 prostate cancer. *Journal for ImmunoTherapy of Cancer* Nov 2019, 7 (Suppl 1) 282; 332

Ethics Approval The study was approved (09C0139) by the Institutional Review Board of the National Cancer Institute/NIH. All participants were informed of the investigational nature of the study and provided written informed consent prior to enrollment.



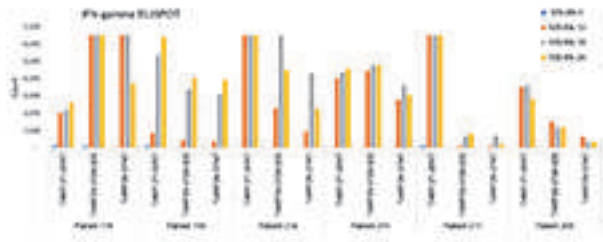
Abstract 557 Figure 1 Structure of TARP and peptides used in TARP vaccines

A) Structure of TARP; TARP peptides in the vaccines; B) peptide vaccine in ISA51 adjuvant; C) Manufacturing of TARP-DC vaccine.



Abstract 557 Figure 2 TARP-specific CD8 T cells were detected by tetramer.

A. PBMCs from patients immunized with peptide-pulsed DC were stained with either TARP27-35WT, TARP29-37EE, or TARP29-37WT-specific tetramers after 7 days of *in vitro* stimulation (IVS) (% Tetramer-positive CD8 T cells minus background; error bar = SEM). Note: TARP29-37WT was not used in the vaccine; R, responder; NR, nonresponder. B. Representative FACS plot of the tetramer staining; top, TARP29-37EE and TARP29-37WT co-stained, bottom, TARP27-35WT stained alone.



Abstract 557 Figure 3 The highest IFN-gamma ELISPOT responses against TARP peptide
Six patients with the highest IFN-gamma ELISPOT responses of PBMCs to one or both vaccine peptides at serial time points were all among the responders based on decrease in PSA-slope log at week 24 or 48. Patient's study number and stimulating peptides are indicated at the bottom. Colored bars represent different time points. Vertical axis is IFN-gamma ELISPOTs per 100,000 cells.

<http://dx.doi.org/10.1136/jitc-2022-SITC2022.0557>

PREPRINT

558

CTX130 ALLOGENEIC CRISPR-CAS9-ENGINEERED CHIMERIC ANTIGEN RECEPTOR (CAR) T CELLS IN PATIENTS WITH ADVANCED CLEAR CELL RENAL CELL CARCINOMA: RESULTS FROM THE PHASE 1 COBALT-RCC STUDY

¹Sumanta Pal*, ²Ben Tran, ³John Haanen, ⁴Michael Hurwitz, ⁵Adrian Sacher, ⁶Neeraj Agarwal, ⁷Nizar Tannir, ¹Elizabeth Budde, ²Simon Harrison, ³Sebastian Klobuch, ⁶Sagar Patel, ⁸Mary Lee Dequeant, ⁹Verena Karsten, ⁸Kaitlyn Cohen, ⁸Ellen Gurary, ⁸Henia Dar, ⁸Anna Ma, ⁸Anjali Sharma, ⁷Samer Srour. ¹City of Hope Comprehensive Cancer Center, Duarte, CA, United States; ²Peter MacCallum Cancer Centre, Melbourne, Australia; ³Netherlands Cancer Institute, Amsterdam, Netherlands; ⁴Yale School of Medicine, New Haven, CT, United States; ⁵Princess Margaret Cancer Centre, Toronto, Canada; ⁶University of Utah, Salt Lake City, UT, United States; ⁷The University of Texas, Houston, TX, United States; ⁸CRISPR Therapeutics, Boston, MA, United States; ⁹Formerly CRISPR Therapeutics, Boston, MA, United States

Background Clear cell renal cell carcinoma (ccRCC) is the most common subtype of renal tumors. Patients with ccRCC who fail checkpoint inhibitors (CPIs) and tyrosine kinase inhibitors (TKIs) have a poor prognosis. Preclinical studies identified substantial expression of CD70 in ccRCC tumor samples. Here, we report results from the Phase 1 dose-escalation study of CTX130™, a CD70-targeting allogeneic CAR T cell therapy in patients with ccRCC.

Methods COBALT-RCC (NCT04438083) is a Phase 1, open-label, multicenter, global study evaluating safety and efficacy of CTX130 in patients ≥18y with advanced (unresectable or metastatic), relapsed, or refractory (R/R) ccRCC and prior exposure to both CPIs and TKIs. Patients received standard lymphodepleting chemotherapy with fludarabine 30mg/m² and cyclophosphamide 500mg/m² for 3 days, followed by CTX130 infusion.

Results As of May 2, 2022, 14 patients with a median age of 64.5y (range, 54-77) were treated with CTX130. All patients had stage IV disease, and received a median of 3 (range, 1-6) prior treatments. Six patients had documented refractory disease at study entry. Median CD70 expression level on the tumors was 100% (range, 1-100%). Patients received CTX130 at dose levels (DLs) ranging from 3x10⁷ to 9x10⁸ CAR T cells. Overall, expansion occurred across all DLs. An emerging relationship between higher CAR T exposure and disease control was observed. CTX130 had an acceptable safety profile; there were no dose-limiting toxicities across all DLs. Seven (50%) patients experienced grade (Gr) 1-2 cytokine release syndrome (CRS); there was no Gr≥3 CRS. Three patients experienced serious adverse events (SAEs) related to CTX130; all were episodes of CRS. Three patients had SAEs of infections, all unrelated to CTX130, including a Gr5 pneumonia with Gr4 dyspnea resulting in death. No patients experienced immune effector cell associated neurotoxicity syndrome, graft versus host disease, or hemophagocytic lymphohistiocytosis. One patient (7.7%) had a durable complete remission (CR) maintained at 18+ months and 9 (69.2%) patients had stable disease (SD) with 4 patients (30.8%) in SD at 4 months. The disease control rate (CR + partial response + SD) was 76.9%.

Conclusions This first-in-human clinical trial exploring CD70 CAR T-cell therapy in ccRCC showed an excellent safety profile with no unexpected on-target off-tumor toxicities and encouraging antitumor activity. To our knowledge, this durable CR is the first to be achieved with allogeneic CAR T cell therapy in patients with R/R solid tumors and represents a proof-of-concept for further exploration of CD70-targeted CAR T cells in ccRCC and other CD70+ malignancies.

Trial Registration This study is registered at www.ClinicalTrials.gov. NCT04438083

Ethics Approval The study was performed in accordance with ethical principles that have their origin in the Declaration of Helsinki and are consistent with ICH Guidelines for GCP and applicable regulatory requirements. This study was approved by all participating Institutional Review Boards (IRBs). The Ethics Committee/IRB Approval Numbers/IDs for each participating institution are as follows: City of Hope (189473), Huntsman Cancer Institute (00133621), MD Anderson Cancer Center (2020-0151), Yale Cancer Center (20202730), Princess Margaret Cancer Centre (20-5071), Netherlands Cancer Institute (METC20.1170/M20CTX), and Peter MacCallum Cancer Centre (20/16). All participants provided informed consent before taking part in the study.

<http://dx.doi.org/10.1136/jitc-2022-SITC2022.0558>

559

BIOMARKER CORRELATES OF CLINICAL RESPONSE WITH FLT3L/NIVO BACKBONE TREATMENT IN THE MULTI-COHORT PHASE 1 PORTER PLATFORM TRIAL IN METASTATIC CASTRATION-RESISTANT PROSTATE CANCER PATIENTS

¹Kristin Shotts, ¹Timothy Howes*, ¹Jia Yu, ¹Julie Densmore, ¹Diane Da Silva, ¹Dinesh Kumar, ¹Sandra Santulli-Marotto, ¹Christopher Cabanski, ¹Elaine Eisenbeisz, ²Geoffrey Ivison, ²Aaron Mayer, ³Jonni Moore, ³Derek Jones, ⁴Kimberly Kraynyak, ⁴Alex Dolgoter, ⁵Richard Chen, ¹Lisa Butterfield, ¹Theresa LaVallee, ¹Samantha Bucktrout, ¹Lacey Padron, ¹Ute Dugan, ⁶Michael Yellin, ⁶Tibor Keler, ⁷Jill O'Donnell-Tormey, ¹Justin Fairchild, ⁸Lisa Salvador, ⁹Kristopher Wentzel, ¹⁰Lawrence Fong, ¹¹Sumit Subudhi, ¹²Nina Bhardwaj, ¹³Karen Autio, ¹²Matthew Galsky. ¹Parker Institute for Cancer Immunotherapy, San Francisco, CA, United States; ²Enable Medicine, Menlo Park, CA, United States; ³University of Pennsylvania, Philadelphia, PA, United States; ⁴Inovio Pharmaceuticals, Plymouth Meeting, PA, United States; ⁵Personalis, Menlo Park, CA, United States; ⁶Celldex Therapeutics, Hampton, NJ, United States; ⁷Cancer Research Institute, New York, NY, United States; ⁸Bristol Myers Squibb, Princeton, NJ, United States; ⁹The Angeles Clinic, Los Angeles, CA, United States; ¹⁰University of California San Francisco, San Francisco, CA, United States; ¹¹MD Anderson, Houston, TX, United States; ¹²Mount Sinai Medical Center, New York, NY, United States; ¹³Memorial Sloan Kettering Cancer Center, New York, NY, United States

Background Immune checkpoint therapy has not provided meaningful clinical benefit in patients with metastatic castration resistant prostate cancer (mCRPC). Biomarker-rich clinical trials offer the opportunity to identify molecular targets of response and resistance to potentially inform patient selection and novel combinations in future trials that improve anti-tumor responses in patients with mCRPC.

Methods Two cohorts of the biomarker-rich PORTER platform trial tested a backbone combination of CDX-301 [FLT3L] and nivolumab. Cohort B added treatments to enhance endogenous immunity (stereotactic body radiation therapy/polyICLC). Cohort C included INO-5151, DNA vaccine expressing PSA/PSMA/IL-12 DNA plasmids. Matched blood and tumor samples were collected longitudinally for extensive immune biomarker analyses using flow/mass and full spectrum flow cytometry, serum proteomics, DNA/RNA sequencing, and high-dimensional multiplex imaging. Immune cell composition and cell:cell interactions are being explored in the tumor microenvironment by CODEX imaging and correlated with peripheral biomarker findings of response. Candidate biomarkers were prioritized based on those that were associated with outcomes.

Results There were 7 participants (5 cohort B, 2 cohort C) with clinical benefit/response (rPR, DCR \geq 6 months, PSA and/or CTC response) and 22 non-responders.

Prior to treatment, responders had lower frequencies of both naïve CD4 Thelper and CD8 T cells in the periphery, but more proliferating PD-1+ CD4 Thelper cells and T cells with effector and/or memory phenotypes (Tbet+ CD8 and Eomes+ CD4 Thelper cells). Additionally, responders had lower peripheral naïve B cell percentages but higher percentages of Tbet+ and memory B cells.

Prior to and on treatment, higher levels of serum soluble proteins associated with cytotoxicity, inflammation, myeloid cell migration, cell adhesion, and immune response were observed in the responder group. LAMP3, a dendritic cell maturation marker, was elevated among patients with clinical benefit in cohort B.

Conclusions In this multi-cohort platform trial evaluating novel immunotherapy combination treatments in mCRPC, peripheral biomarkers associated with higher levels of proliferating, effector/memory B and T cells and inflammatory immune responses were found in patients with clinical benefit, both prior to and

on-treatment. Higher levels of LAMP3 protein in patients with clinical benefit from one cohort suggests a role for baseline and on-treatment differences in dendritic cell phenotypes. Further work to integrate these findings with tumor imaging and genomic data is ongoing. Overall, the joint analysis of the two cohorts involving FLT3L + nivolumab highlights the power of a platform study to rapidly identify common biomarkers of clinical response and/or resistance and simultaneously interrogate treatment effects of cancer-specific immunotherapy combinations.

Acknowledgements We extend our gratitude to the patients, their families, the clinical investigators, and their site staff members who are making this trial possible. We would also like to thank Carri Browne, Christopher Perry, and Lancelote Leong at Parker Institute for Cancer Immunotherapy (PICI) for operations leadership of the trial. We thank Maria Jaimes and Quentin Low from Cytex Biosciences for spectral flow method development and sample analysis. We thank Jay Campbell (CRI), Samik Upadhya (CRI), Andres Salazar (Oncovir) and Silvia Boffo (BMS) for their contributions. We thank Bristol Myers Squibb (BMS), Celldex, Oncovir and Inovio for collaboration and study drugs. The study was funded by Cancer Research Institute, BMS and PICI.

Trial Registration NCT03835533

Ethics Approval This study was approved by OHRP/FDA Parent Organization Number, IOG0000432 with the IRB registration number IRB00000533.

Consent Written informed consent was obtained from the patient for publication of this abstract and any accompanying images. A copy of the written consent is available for review by the Editor of this journal.

<http://dx.doi.org/10.1136/jitc-2022-SITC2022.0559>

Abstracts

560

MOLECULAR AND IMMUNOGENOMICS FEATURES ASSOCIATED WITH COMPLETE RESPONSE AND SURVIVAL AFTER NEOADJUVANT CHEMO-IMMUNOTHERAPY FOR MUSCLE-INVASIVE BLADDER CANCER

AB Wolfgang Beckabir*, Alec Wilkinson, Mark Woodcock, Mi Zhou, Hsing-Hui Wang, Karen McKinnon, Jonathan Serody, Tracy Rose, Matthew Milowsky, William Kim, Benjamin Vincent. *UNC-Chapel Hill, Chapel Hill, NC, United States*

Background Bladder cancer patients treated with immunotherapy have varied response and survival.¹⁻³ In the Phase II LCCC1520 trial, neoadjuvant chemo-immunotherapy (pembrolizumab with gemcitabine plus cisplatin) induced pathologic complete response (pCR) in 14 of 39 muscle-invasive bladder cancer patients.⁴ In this correlative analysis, we identify molecular features associated with pCR and survival in patients with and without pCR.

Methods Associations of TMB, tumor neoantigens, antigen presentation, immune checkpoint gene expression, immune gene signature expression, and TCR repertoire diversity with response and survival were evaluated pre-and post-treatment. Predicted neoantigens were identified using the Landscape of Effective Neoantigens Software.⁵ 25 patients with neoantigen data were divided into discovery (14 patients) and validation (11 patients) sets. Effective neoantigen count (ENC) was calculated by binning neoantigens by expression level score, binding affinity score, and normalized expression level, then identifying the subset in which neoantigen count was most strongly associated with pCR in the discovery set. Using elastic net modeling with 10-fold cross-validation, pCR was predicted from antigen presentation, immune checkpoint, and immune gene signature expression, TMB and ENC.

Results Pre-treatment features associated with pCR response included TMB ($p=0.015$) and PD-L1 expression ($p=0.008$); expression of antigen presentation genes TAP1 ($p=0.009$), TAP2 ($p=0.013$), B2M ($p=0.018$), and HLA-DRB1 ($p=0.011$); and signatures of T cell infiltration ($p=0.005$) and interferon gamma activation ($p=0.001$; figure 1). Pre-treatment TIGIT expression was associated with pCR ($p=0.018$), survival ($p=0.026$), and PD-1 expression ($p=3.3E-5$). Pre-treatment CD8+ TIGIT+ T cell percentage from flow cytometry was associated with complete response ($p=0.048$). ENC was calculated as the number of neoantigens with an expression level score above 90th percentile, a binding affinity below 90th percentile, and an upper quadrant normalized log₂ TPM expression above 40th percentile. Pre-treatment ENC was positively associated with complete response in the discovery ($p=0.036$) and validation sets ($p=0.042$, ROC-AUC = 0.867, ROC-AUC $p=0.021$; figure 2). The final elastic net model—comprised of HLA-DRB1 expression, Ayers_IFNG signature, and ENC—predicted complete response in the validation set ($p=0.017$, ROC-AUC=0.933, ROC-AUC $p=0.009$). Post-treatment ENC ($p=0.005$) and TAP1 ($p=0.003$) and TAP2 ($p=0.015$) expression were negatively associated with survival among patients without complete response (figure 3).

Conclusions We identify pre-treatment and post-treatment features associated with response and survival in the LCCC1520 trial of pembrolizumab with gemcitabine plus cisplatin neoadjuvant therapy for muscle-invasive bladder cancer. Key features of a predictive model included neoantigen and antigen presentation estimates. We propose that tumor antigen presentation is a major driver of response and survival with neoadjuvant chemo-immunotherapy.

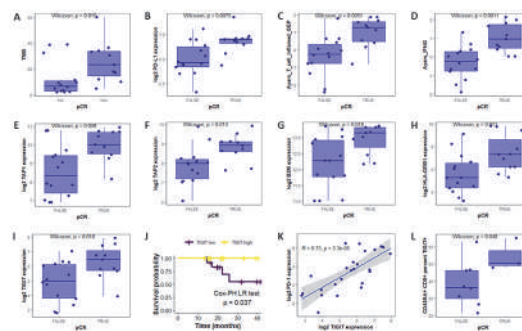
Acknowledgements Merck Sharp & Dohme, a subsidiary of Merck & Co, Kenilworth, NJ, USA (MSD) provided financial support for the LCCC1520 clinical trial as well as for correlative research in this study.

Trial Registration NCT02690558

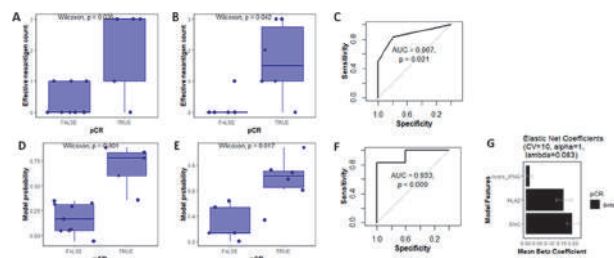
REFERENCES

1. Bellmunt J, de Wit R, Vaughn DJ, Fradet Y, Lee J-L, Fong L, Vogelzang NJ, Climent MA, Petrylak DP, Choueiri TK, Necchi A, Gerritsen W, Gurney H, Quinn DI, Culine S, Sternberg CN, Mai Y, Poehlein CH, Perini RF, Bajorin DF. Pembrolizumab as Second-Line Therapy for Advanced Urothelial Carcinoma. *N Engl J Med* 2017;**376**:1015–26. <https://doi.org/10.1056/NEJMoa1613683>.
2. Mariathasan S, Turley SJ, Nickles D, Castiglioni A, Yuen K, Wang Y, Kadel III EE, Koeppen H, Astarita JL, Cubas R, Jhunjhunwala S, Banchereau R, Yang Y, Guan Y, Chalouni C, Zhai J, Senbabaoglu Y, Santoro S, Sheinson D, Hung J, Giltman JM, Pierce AA, Mesh K, Lianoglou S, Riegler J, Carano RAD, Eriksson P, Höglund M, Somarriba L, Halligan DL, van der Heijden MS, Loriot Y, Rosenberg JE, Fong L, Mellman I, Chen DS, Green M, Derleth C, Fine GD, Hegde PS, Bourgon R, Powles T. TGF β attenuates tumour response to PD-L1 blockade by contributing to exclusion of T cells. *Nature* 2018;**554**:544–8. <https://doi.org/10.1038/nature25501>.
3. Balar AV, Galsky MD, Rosenberg JE, Powles T, Petrylak DP, Bellmunt J, Loriot Y, Necchi A, Hoffman-Censits J, Perez-Gracia JL, Dawson NA, van der Heijden MS, Dreicer R, Srinivas S, Retz MM, Joseph RW, Drakaki A, Vaishampayan UN, Sridhar SS, Quinn DI, Durán I, Shaffer DR, Eigel BJ, Grivas PD, Yu EY, Li S, Kadel EE, Boyd Z, Bourgon R, Hegde PS, Mariathasan S, Thåström A, Abidoye OO, Fine GD, Bajorin DF. Atezolizumab as first-line treatment in cisplatin-ineligible patients with locally advanced and metastatic urothelial carcinoma: a single-arm, multi-centre, phase 2 trial. *The Lancet* 2017;**389**:67–76. [https://doi.org/10.1016/S0140-6736\(16\)32455-2](https://doi.org/10.1016/S0140-6736(16)32455-2).
4. Rose TL, Harrison MR, Deal AM, Ramalingam S, Whang YE, Brower B, Dunn M, Osterman CK, Heiling HM, Bjurlin MA, Smith AB, Nielsen ME, Tan H-J, Wallen E, Woods ME, George D, Zhang T, Drier A, Kim WY, Milowsky MI. Phase II Study of Gemcitabine and Split-Dose Cisplatin Plus Pembrolizumab as Neoadjuvant Therapy Before Radical Cystectomy in Patients With Muscle-Invasive Bladder Cancer. *J Clin Oncol* 2021;**39**:3140–8. <https://doi.org/10.1200/JCO.21.01003>.
5. Vensko SP, Olsen K, Bortone DS, Smith CC, Chai S, Rubinsteyn A, Vincent BG. LENS – Landscape of Effective Neoantigens Software. *Cancer Biology*; 2022. <https://doi.org/10.1101/2022.04.01.486738>.

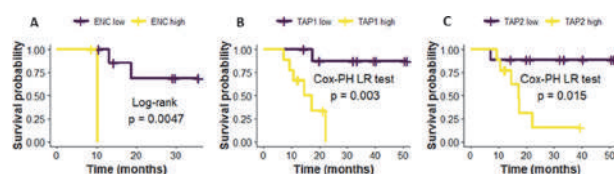
Ethics Approval The study was reviewed and approved by the institutional review boards at each participating institution and conducted in accordance with ethical principles per the Declaration of Helsinki.



Abstract 560 Figure 1 Pre-treatment features associated with complete response. Features associated with complete response include TMB (A) and PD-L1 expression (B); immunogenomic signatures Ayers_T_cell_inflamed_GEP (C) and Ayers_IFNG (D); and expression of antigen presentation genes TAP1 (E), TAP2 (F), B2M (G), and HLA-DRB1 (H). Pre-treatment TIGIT expression is associated with complete response (I), survival (J), and PD-1 expression (K). Pre-treatment CD8+ TIGIT+ T cell percentage from flow cytometry is associated with complete response (L).



Abstract 560 Figure 2 Effective neoantigen count predicts complete response. Pre-treatment effective neoantigen count is positively associated with complete response in the discovery (A) and validation sets (B,C). The final elastic net model predicts complete response in the discovery (D) and validation (E,F) sets. The final model features, which also have beta coefficient confidence intervals not spanning zero in 10-fold cross validation, are Ayers_IFNG, HLA2 (HLA-DRB1), and effective neoantigen count (G).



Abstract 560 Figure 3 Features associated with survival in patients without complete response. From post-treatment sequencing data, effective neoantigen count (A) and TAP1 (B) and TAP2 (C) expression are negatively associated with survival among patients without complete response.

<http://dx.doi.org/10.1136/jitc-2022-SITC2022.0560>

561

IMMUNE ACTIVATION AND CLINICAL RESPONSE FROM ENZALUTAMIDE (ENZA) ALONE OR WITH RADIUM223 (RA223) IN METASTATIC CASTRATION-RESISTANT PROSTATE CANCER (MCRPC)

<http://dx.doi.org/10.1136/jitc-2022-SITC2022.0561>

¹Peter Zang*, ²Tanya Dorff, ¹Zhang-Xu Liu, ¹Denice Tsao-Wei, ¹Susan Groshen, ¹Cheryl Kefauver, ²Czarina Patricio, ¹Anishka D'Souza, ¹Sarah Chevalier, ²Sumanta Pal, ¹Diane DaSilva, ¹Martin Kast, ¹David Quinn. ¹University of Southern California, Los Angeles, CA, United States; ²City of Hope, Duarte, CA, United States

Background We hypothesized that Ra223 in combination with enza would induce a higher degree of immune activation and clinical response than enzalutamide alone in patients with mCRPC.

Methods Patients were randomized 2:1 to Arm A (enza + Ra223) or Arm B (enza only). Blood was collected at start of treatment and evaluated by flow cytometry to measure immune activation or exhaustion after ≥ 3 months on study, and by Luminex for cytokines after 1 month on study. A Kaplan-Meier model was used to calculate survival data. Expression of immune correlates were log-transformed and analyzed with the Wilcoxon Rank Sum test to detect differences between the two arms.

Results A total of 28 patients were enrolled, whose median age was 68 (57 – 87). 6 are Hispanic (21%) and 2 each are African American or Asian (7%). Median duration of follow up was 8.3 (1.8 – 29.9) months (mo). 9 pts (36%) had visceral metastases. Arm A showed significantly greater increase in PD-L2 expression after treatment compared to Arm B ($p = 0.0026$). There was otherwise no significant difference between the two arms for flow cytometry markers. Cytokines remained low generally, except for IL10 and TNF α , elevated in 5 and 2 patients, respectively. 9 of 21 (48%) in Arm A had SD or PR as best RECIST response compared to 3 of 9 (33%) in Arm B. PSA response was not different between the arms. Arm A had PFS of 8.8 (3.6 – 29.9+) mo while PFS was 5.3 (3.4 – 12.2+) mo in Arm B. 4 (27%) patients in Arm A and 3 (50%) patients in Arm B stopped treatment due to disease progression. No grade 3 adverse events were observed in either arm and no unexpected toxicities occurred.

Conclusions Although Ra223 with enza did not show increased PD-L1 expression as seen in pre-clinical mouse models treated with Ra223, the combination did significantly induce PDL-2 expression in this study and raise the potential of improved treatment efficacy with the addition of an immune checkpoint inhibitor as suggested in these pre-clinical models.¹ Despite the lack of augmentation of humoral response, combination treatment paradoxically showed better clinical response, consistent with prior studies involving Ra223 and Sipleucel-T immunotherapy.²

Acknowledgements The authors thank Bayer for providing funding to perform the clinical trial.

Trial Registration NCT03344211

REFERENCES

1. Vardaki I, Corn P, Gentile E, *et al.* Radium-223 treatment increases immune checkpoint expression in extracellular vesicles from the metastatic prostate cancer bone microenvironment. *Clin Cancer Res* 2021; **27**: 3253–3264.
2. Marshall CH, Fu W, Wang H, *et al.* Randomized Phase II Trial of Sipuleucel-T with or without Radium-223 in Men with Bone-metastatic Castration-resistant Prostate Cancer. *Clin Cancer Res* 2021; **27**: 1623–1630.

Ethics Approval This study was approved by the IRB of the University of Southern California and the IRB of City of Hope.

562

TUMOR COLLECTION AND ESTABLISHMENT OF TUMOR-INITIATING CELL CULTURES TO SERVE AS THE ANTIGEN SOURCE FOR AV-OVA-1 DENDRITIC CELL VACCINES FOR PATIENTS WITH NEWLY DIAGNOSED ADVANCED OVARIAN CANCER

¹Ramez Eskander, ²Lisa Abaid, ³Bradley Corr, ⁴James Mason, ⁵Fabio Cappuccini, ⁶Richard Friedman, ⁷Rockelle Robles, ⁷Katrina Lopez, ⁷Gabriel Nistor, ⁷Robert Dillman*. ¹UC San Diego, San Diego, CA, United States; ²Hoag Hospital, Newport Beach, CA, United States; ³University of Colorado, Aurora, CO, United States; ⁴Scripps MD Anderson Cancer Center, La Jolla, CA, United States; ⁵UC Irvine, Irvine, CA, United States; ⁶Providence-St. Joseph Medical Center, Burbank, CA, United States; ⁷AIVITA Biomedical, Inc., Irvine, CA, United States

Background With standard therapy, which includes chemotherapy and aggressive surgical debulking, relative 5-year survival for newly diagnosed advanced epithelial ovarian cancer is only 30%. AV-OVA-1 is a personal vaccine consisting of autologous dendritic cells (DC) loaded ex vivo with autologous tumor antigens (ATA) from a lysate of irradiated cells from a short-term cell culture. After completion of primary chemotherapy, immunization with DC-ATA may improve survival. A multicenter, 2:1 double-blind randomized phase 2 clinical trial was designed to compare treatment with AV-OVA-1 to autologous monocytes (MC). One objective was to determine the feasibility of collecting fresh ovary cancer and establishing cell cultures to serve as the ATA source.

Methods Tumor samples were obtained during surgical debulking of patients with stage 3 or 4 ovary epithelial cancer. Fresh tumor was placed in media and shipped via transport kit per overnight courier to AIVITA where a cell suspension was placed into culture and incubated in serum-free medium with factors that favor survival and proliferation of stem cells and early progenitor cells, i.e, tumor initiating cells (TICS). The objective was to harvest a minimum of 1 million cells within 28 days, and preferably 10 million cells or more.

Results Patients were enrolled from five sites in California and one in Colorado. Tumors were collected between December 2017 and April 2021. 92 patients consented for tumor collection, but 12 were not malignant ovary, 4 withdrew consent, 3 had insufficient tissue to send, 1 had wrong stage; so, 72 malignant epithelial ovary tumors were placed into culture. 70/72 (97.2%) resulted in a successful cell culture; one could not be grown, one was contaminated. Of tumors submitted for patients who were subsequently randomized, 47/56 (84%) were in culture for 28 days or less, 4 (7%) were in culture for 29 to 35 days, and the remaining 5 were cultured 51, 52, 57, 62, and 67 days. All 56 cultures yielded at least 1 million cells; 48/56 (86%) yielded more than 10 million cells. The average number of irradiated cells per culture was 59.7 million (range 1.1 to 135 million); the median was 65.6 million (interquartile range 22.4 to 96.8 million).

Conclusions Self-renewing ovary TIC cultures were reliably and rapidly established for use as the antigen source for personal DC-ATA vaccines.

Trial Registration Clinicaltrials. gov NCT00331526

Ethics Approval This study was approved by the Western IRB, approval number 20171661; all participants gave written informed consent before taking part.

<http://dx.doi.org/10.1136/jitc-2022-SITC2022.0562>

Abstracts

563

A PHASE I CLINICAL TRIAL OF RADIATION THERAPY, DURVALUMAB AND TREMELIMUMAB IN RECURRENT GYNECOLOGIC CANCER

¹Larissa Lee, ²Panagiotis Konstantinopoulos, ²Ursula Matulonis, ²Joyce Liu, ²Neil Horowitz, ²Elizabeth Lee, ¹Martin King, ¹Kelly Fitzgerald*. ¹Brigham and Women's Hospital, Boston, MA, United States; ²Dana Farber Cancer Institute, Boston, MA, United States

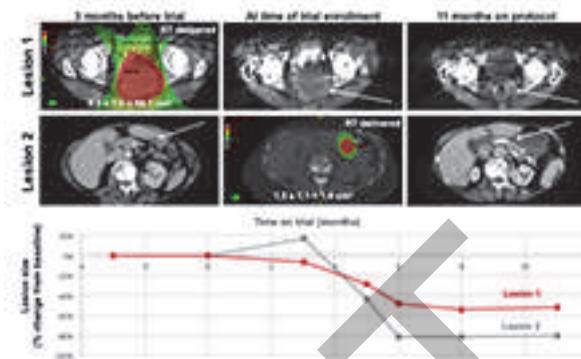
Background Dual immune checkpoint blockade (ICB) may synergize with palliative radiotherapy (RT) to improve response rates in patients with recurrent or metastatic gynecologic cancer. We conducted an open label prospective phase I trial to assess the safety and tolerability of ICB with RT to a single metastatic abdominopelvic site.

Methods Eligible patients included those with recurrent and/or metastatic gynecologic cancer of endometrial, ovarian, cervical, vaginal or vulvar origin without prior immunotherapy treatment. A safety lead-in cohort of patients (cohort A) was treated with durvalumab 1500 mg IV and palliative RT of 25 Gy in 5 fractions delivered to a single measurable lesion >1cm and <10cm in the abdomen or pelvis that was not previously irradiated. RT was initiated within 24 hours of immunotherapy. Durvalumab continued every 4 weeks up to one year or until disease progression. Following a toxicity assessment of cohort A, a second cohort (cohort B) received dual ICB with tremelimumab 75 mg IV given concurrently with the first 4 cycles of durvalumab. The primary endpoint was the rate of dose-limiting toxicities (DLT) in patients still on protocol 8 weeks after RT. Secondary endpoints included the overall response rate (ORR) in non-irradiated lesions.

Results 16 patients were enrolled, with 12 able to be assessed at the end of the 8-week DLT window, split evenly between the cohorts. There were 9 patients with ovarian, 2 with uterine, and 1 with cervical cancer. There were 0 DLTs in cohort A and 1 in cohort B (grade 3 pneumonitis possibly related to treatment). One patient with platinum resistant ovarian cancer in cohort B with two metastatic sites (a 8.3 x 7.0 cm pelvic lesion irradiated with 25 Gy/5 fractions 3 months prior to the study without initial shrinkage and a 1.3 x 1.1 cm peritoneal nodule irradiated on protocol) had a dramatic reduction in disease burden and no new lesions at 11 months of follow up (figure 1). No objective responses were observed in non-irradiated lesions in the remaining patients. The ORR for irradiated lesions was 50% for cohort A and 33% for cohort B.

Conclusions The combination of durvalumab, tremelimumab and RT to a single lesion had limited DLTs but no response in non-irradiated lesions in unselected patients with recurrent gynecologic malignancies. One patient with a previously irradiated lesion and another lesion irradiated on protocol experienced durable benefit in the setting of platinum resistant ovarian cancer.

Trial Registration Clinical trial information: NCT03277482



Abstract 563 Figure 1 Prolonged disease control in best responding patient. Patient 6B was initially diagnosed with FIGO Stage IIIC serous ovarian cancer in 2017 and underwent cytoreductive surgery plus neoadjuvant and adjuvant carboplatin/paclitaxel. She had no evidence of disease until 2020 when she recurred in the pelvis (lesion 1) and in a peritoneal implant on the lesser curvature of the stomach (lesion 2). She progressed in the pelvis on carboplatin and doxorubicin, then progressed again on paclitaxel. She received palliative RT of 25 Gy in 5 fractions to the large pelvic mass 3 months before trial enrollment. Lesion 1 remained stable, then she was enrolled on trial and received 25 Gy in 5 fractions to lesion 2 concurrently with durvalumab and tremelimumab. Both lesions shrank significantly and no new disease emerged.

<http://dx.doi.org/10.1136/jitc-2022-SITC2022.0563>

564

SAFETY AND CLINICAL ACTIVITIES OF THE ACID PH-SENSITIVE ANTI-CTLA-4 MAB ONC-392 IN OVARIAN CANCER PATIENTS

¹John Hays*, ²Tianhong Li, ²Hui Chen, ³George Zahrah, ³Richard Frank, ⁴John Hamm, ⁵Merry-Jennifer Markham, ⁵Thomas George, ⁶Eric Whitman, ⁷Mark Goldstein, ¹Kai He, ⁸Rohit Joshi, ⁹Dan Chen, ⁹Yang Liu, ⁹Pan Zheng, ¹David O'Malley. ¹The Ohio State University James Cancer Center, Columbus, OH, United States; ²UC Davis Cancer Center, Sacramento, CA, United States; ³Norwalk Health, Norwalk, CT, United States; ⁴Norton Healthcare, Louisville, KY, United States; ⁵University of Florida Cancer Center, Gainesville, FL, United States; ⁶Atlantic Health, Morristown, NJ, United States; ⁷Center for Cancer and Blood Disorders, Frederick, MD, United States; ⁸Cancer Research SA, Adelaide, Australia; ⁹OncoC4, Inc., Rockville, MD, United States

Background Despite extensive effort, no immunotherapy has been approved for ovarian cancer patients. Ovarian cancer patients who fail more than two lines of systemic therapies have very poor prognosis. ONC-392 is an acid pH-sensitive anti-CTLA-4 antibody that preserves CTLA-4 recycling and avoids lysosomal degradation. ONC-392 is more effective for immunotherapy but largely devoid of immunotherapy-related adverse events (irAE) in preclinical studies. Our previous dose escalation study has established an RP2D for monotherapy at 10.0 mg/kg.¹ Here we report safety and clinical response of ovarian cancer patients to monotherapy of ONC-392 at 10.0 mg/kg in dose finding and dose expansion studies (NCT04140526, Part A and Part C Arm L).

Methods Thirty four patients with advanced/metastatic ovarian cancer, including primary peritoneal cancer and fallopian tube cancer, who have progressive disease after prior systemic treatments, including chemotherapy, targeted therapy or checkpoint inhibitors have been enrolled. Four patients were enrolled in Part A monotherapy dose finding with defined doses. Thirty patients in expansion cohort had ONC-392 administered via IV infusion with starting two doses of 10.0 mg/kg, Q3W, followed by 6.0 mg/kg Q3W. The primary endpoints are safety and objective response rate (ORR) using RECIST 1.1 criteria.

Results Thirty-four patients have received 1-11 cycles of ONC-392 treatment. The safety data set consists of 32 patients. The median age is 67.5 (range 40-82), White/Asian/Black: 27/3/2, and 5 Hispanic. The median follow up is 17 weeks. Treatment related AEs (TRAEs) were observed in 26 (81%) patients. Grade 3 TRAEs were observed in 10 pts (31%): myocarditis (1), diarrhea (2), immune-mediated colitis or colitis (4), immune hepatitis (1). Grade 4 TRAE in 1 patient with hypotensive shock (3%). No grade 5 AE was observed. Among 26 evaluable patients, the CR/PR/SD/PD numbers are 1/3/15/7 (ORR=15%, DCR=73%) (figure 1).

Conclusions The safety profile of 10.0 mg/kg x 2, followed by 6.0 mg/kg Q3W is comparable to patients who received substantially lower doses other CTLA-4-targeting drug in the ovarian cancer patients. While the number of evaluable patients is small, the preliminary assessment suggests ONC-392 monotherapy has clinical activity among patients who has failed multiple lines of systemic therapy. The available data support continuous clinical testing of ONC-392 in ovarian cancer. A new Phase 2 study with combination of ONC-392 and pembrolizumab will initiated in Q32022 (ONC-392-004, MK3475-E24, GOG-3081).

Acknowledgements The study is sponsored by OncoC4, Inc.

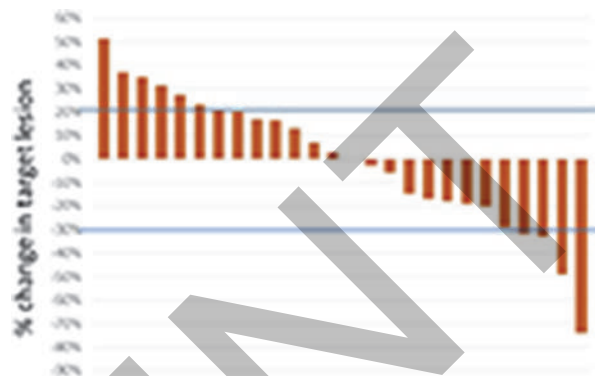
Trial Registration NCT04140526.

REFERENCE

1. Li T, Tang M, Kelly K, et al. First-in-human study of the first acid pH-sensitive and recycling CTLA-4 antibody that preserves the immune tolerance checkpoint to

avoid immunotherapy-related adverse events in cancer patients. *J Immunother Cancer*. 2021; 9(5 Suppl 2): A998.

Ethics Approval This study obtained ethic approval from WCG IRB with study #20193108 or the local institutional IRBs. All participants gave informed consent before taking part of the study.



Abstract 564 Figure 1 Best response with ONC-392 in ovarian cancer. Best response with ONC-392 monotherapy in ovarian cancer patients

<http://dx.doi.org/10.1136/jitc-2022-SITC2022.0564>

565

LEUKAPHERESIS TO OBTAIN MONOCYTES TO PRODUCE DENDRITIC CELLS FOR MANUFACTURING AV-OVA-1 PERSONAL VACCINES IN A RANDOMIZED PHASE II TRIAL IN PATIENTS WITH NEWLY DIAGNOSED ADVANCED OVARIAN CANCER

¹James Mason, ²Lisa Abaid, ³Bradley Corr, ⁴Ramez Eskander, ⁵Fabio Cappuccini, ⁶Richard Friedman, ⁷Rockelle Robles, ⁷Katrina Lopez, ⁷Gabriel Nistor, ⁷Robert Dillman*. ¹Scripps MD Anderson Cancer Center, La Jolla, CA, United States; ²Hoag Hospital, Newport Beach, CA, United States; ³University of Colorado, Aurora, CO, United States; ⁴UC San Diego, San Diego, CA, United States; ⁵UC Irvine, Irvine, CA, United States; ⁶Providence-St. Joseph Medical Center, Burbank, CA, United States; ⁷AIVITA Biomedical, Inc., Irvine, CA, United States

Background Despite standard therapy, which includes chemotherapy and aggressive surgical debulking, relative 5-year survival for newly diagnosed advanced epithelial ovarian cancer is only 30%. AV-OVA-1 is a personal vaccine consisting of autologous dendritic cells (DC) loaded ex vivo with autologous tumor antigens (ATA) from a lysate of irradiated tumor cells from short-term cell culture. After completion of primary chemotherapy, immunization with DC-ATA may improve survival. A multi-center, 2:1 double-blind randomized phase 2 clinical trial was designed to compare treatment with AV-OVA-1 to autologous monocytes (MC). One objective was to determine the feasibility of collecting sufficient MC from which to generate DC for pulsing with ATA from ovarian cancer tumor-initiating cells (TIC) to produce DC-ATA.

Methods Peripheral blood mononuclear cells (PBMC) were collected by leukapheresis per local standard operating procedures, then shipped by overnight courier to the AIVITA laboratory in Irvine, CA. The product was enriched for MC using the Elutra[®] Cell Separation System (Terumo, Lakewood, CO). If fewer than 450 million viable MC were available for cryopreservation, an additional leukapheresis was allowed. MC were cryopreserved in liquid nitrogen and subsequently thawed and incubated in media containing granulocyte-macrophage colony-stimulating factor and interleukin-4 to differentiate MC into DC. Batches of patient-specific AV-GBM-1 were produced by incubating autologous DC with a lysate of irradiated TICs, then aliquoted into individual doses.

Results Patients were enrolled from five sites in California and one in Colorado. PBMC were collected between December 2017 and April 2021. 47/50 patients (94%) had a successful PBMC collection, but four required a second procedure. An average of 1.90 billion monocytes (range 0.527 to 16.6 billion) were collected with an average of 1.55 billion monocytes cryopreserved (range 0.249 to 3.80), which subsequently could be thawed and differentiated into DC. For 29 patients treated with DC-ATA, an average of 648 million viable MC (range 336 to 1120) were differentiated into an average of 410 million DC (range 171 to 892) for incubation with ATA, which yielded an average of 78.6 million DC-ATA (range 16.0 to 270). This resulted in an average of 8.1 million DC-ATA cells per dose (range 2.0 to 27).

Conclusions Leukapheresis procedures reliably resulted in collection of sufficient numbers of monocytes to generate DC and large batches of personal AV-OVA-1 vaccines.

Trial Registration Clinicaltrials.gov NCT00331526

Ethics Approval This study was approved by the Western IRB, approval number 20171661; all participants gave written informed consent before taking part

<http://dx.doi.org/10.1136/jitc-2022-SITC2022.0565>

566

ENTPD1 AS PREDICTIVE MARKER OF TREATMENT RESPONSE TO GEMOGENOVATUCEL-T (VIGIL) IN NEWLY DIAGNOSED OVARIAN CANCER

¹Rodney Rocconi*, ²Laura Stanbery, ³Min Tang, ²Adam Walter, ⁴Bradley Monk, ⁵Thomas Herzog, ⁴Robert Coleman, ²Luisa Manning, ²Gladice Wallraven, ²Staci Horvath, ²Ernest Boggar, ⁶Neil Senzer, ⁷Scott Brun, ²John Nemunaitis. ¹University of Alabama at Birmingham; Infirmity Cancer Care, Mobile, AL, United States; ²Gradalis, Inc, Carrollton, TX, United States; ³Statbeyond, Carrollton, TX, United States; ⁴US Oncology, Phoenix, AZ, United States; ⁵University of Cincinnati, Cincinnati, OH, United States; ⁶Mary Crowley, Dallas, TX, United States; ⁷Gold Mast Consulting, Carrollton, TX, United States

Background Clinical cancer management with precision therapeutics is generally optimized with predictive molecular and phenotypic profiling. However, in ovarian cancer (OC) there has been limited clinical benefit demonstrated. Vigil (Gradalis, Dallas, TX) is a novel plasmid engineered autologous tumor cell immunotherapy designed to achieve a trifecta of immune anticancer activity using a unique bi-shRNA DNA based technology. The trifecta of systemic activity involves knock down of TGFβ1 and TGFβ2 which function as tumor suppressor cytokines, increased GM-CSF expression to enhance local immune function and presentation of personal clonal neoantigen epitopes via use of autologous cancer tissue. Phase 2b randomized double blind controlled study (VITAL) of Vigil involving newly diagnosed stage IIIB/IV OC patients undergoing frontline maintenance therapy revealed significant improvement in relapse free and overall survival (RFS/OS) in *BRCA1/2*wt, HRP patient subgroups. We explored molecular biomarker relationship to clinical benefit with NanoString assessment and comparison to RFS and OS.

Methods All patients enrolled on the VITAL study had RNA isolated from tumor tissue at time of procurement and submitted for NanoString® PanCancer Immuno-Oncology 360™ CodeSet using the nCounter® SPRINT platform. All 750 genes underwent a predefined statistical NanoString algorithm (NSA) to assess correlation with RFS and OS. First, a univariate Cox model was used to determine the gene Z-score for RFS and OS in Vigil treated patients at 1% significance. Next, a Cox proportional hazards model with interaction term was utilized to identify genes predictive of Vigil response in both Vigil and placebo treated patients. Patients were then dichotomized into high and low expression based on median gene expression and Kaplan Meier curves were generated. Finally, the *my.stepwise.coxph* function was used to select genes associated with RFS and OS in Vigil treated patients.

Results Using NSA, high expression of *ENTPD1/CD39* (the rate limiting enzyme in the adenosine pathway) was identified as a predictor of RFS (n=23 vs n=23; median not achieved vs 8.1 months, p=0.00007) and OS (n=23 vs n=23; median not achieved vs 41.4 months, p=0.013) benefit to Vigil irrespective of HRP status. Results further suggested additional benefit in HRP subset but were limited by small number of patients.

Conclusions NSA was successfully implemented and identified *ENTPD1/CD39* high expression correlated with RFS and OS benefit in OC treatment population to Vigil. Further consideration of NSA utilization to identify populations that would benefit from investigational targeted therapies is warranted. *ENTPD1* high may predict a more sensitive OC population to Vigil.

Trial Registration NCT02346747

<http://dx.doi.org/10.1136/jitc-2022-SITC2022.0566>

Abstracts

568

PHASE 2 TRIAL OF INDUCTION AND CONCOMITANT CTLA4 (IPILIMUMAB) AND PD-1 (NIVOLUMAB) IMMUNE CHECKPOINT BLOCKADE AND INTENSITY MODULATED RADIATION THERAPY (IMRT) IN HPV-POSITIVE OROPHARYNGEAL SQUAMOUS CELL CARCINOMA (HPV-OPSCC)

Maura Gillison*, Michelle Williams, Jason Johnson, Cheuk Leung, Jay Reddy, Adam Garden, Renata Ferrarotto, Frank Mott, Xiuning Le, Gary Gunn, Anna Lee, Clifton Fuller, Charles Lu, Amy Moreno, Katherine Hutcheson, Neil Gross, Miriam Lango, Ryan Goepfert, Jeffrey Myers, Ehab Hanna, Weihong Xiao, Bo Jiang, Nils-Petter Rudqvist, Jack Lee, Jack Phan. *The University of Texas MD Anderson Cancer Center, Houston, TX, United States*

Background PD-1 immune checkpoint blockade (ICB) improves survival versus chemotherapy in PD-L1 CPS \geq 1 recurrent or metastatic head and neck cancer. We evaluated the safety and efficacy of induction and concurrent CTLA4 and PD-1 ICB and IMRT in newly diagnosed HPV-OPSCC.

Methods PD-L1 CPS \geq 1, p16-positive + HPV RNA-Scope-positive, AJCC 8th edition T1-3N1-2 M0 or T3N0M0 OPSCC patients irrespective of smoking status received two, six-week cycles of ipilimumab (1 mg/kg) day 1 and nivolumab (3 mg/kg) on days 1, 15, and 29, and IMRT concurrent with cycle 2. IMRT was delivered in 4 weeks to pre-induction tumor volume (40-44 Gy) and one adjacent uninvolved nodal level (36 Gy). Post-induction volume was boosted to 50-66 Gy in 2 weeks. Response was evaluated by RECIST 1.1. Principal outcomes were FDG-PET complete response (PET-CR) at 6 months per Hopkins Criteria¹ and progression-free survival (PFS) at 2-years. Correlatives included histological (% tumor viability)² and molecular (plasma cfHPV clearance) responses after induction ICB.

Results Treated patients (35) were male (97%), median age 64 (49-78) years with stage T1(14), T2(16), T3(5) and N0(1), N1(33), N2(1) base of tongue (18) or tonsil (17) SCC. 66% had acute grade \geq 3 AEs (table 1). Five discontinued ICB due to toxicity (n=3), progression (n=1), or physician decision (n=1) and received concurrent platinum (n=3) or IMRT alone (n=2). PET-CR was 90% (29 of 32 evaluable). One of 3 patients without PET-CR progressed. After median follow-up of 14.9 months, 3 patients had local progression and were treated with surgery or SBRT. All patients are alive without cancer at last follow-up. Response to induction ICB was 14% (figure 1). Among 27 evaluable patients, histological response was 0% viability in 37% and <10% viability in 48% (figure 2). 96% had pathological treatment effect \geq 20% [2]. At baseline, 97% were positive and 74% quantifiable (\geq 16 copies/ml) by cfHPV. cfHPV clearance was 30% after induction ICB and 100% 4 weeks after IMRT. Compared to standard planning, RT volume to \geq 66 Gy and \geq 50 Gy was reduced by 21% (+/- 3%) and 36% (+/- 4%), and dose to ipsilateral parotid, spinal cord, larynx and esophagus was reduced by up to 50%.

Conclusions Patients with HPV-OPSCC treated with induction and concurrent CTLA4 and PD-1 ICB with dose-volume-adapted IMRT experienced a 6-month PET-CR of 90%, a 2-year PFS of 86%, and acute grade \geq 3 toxicity rate of 66%. Efficacy of induction ICB was supported by <10% tumor viability in 48% and cfHPV clearance in 30%.

Acknowledgements Funded by Cancer Prevention and Research Institute of Texas and Bristol-Myers-Squibb.

Trial Registration NCT03799445

REFERENCES

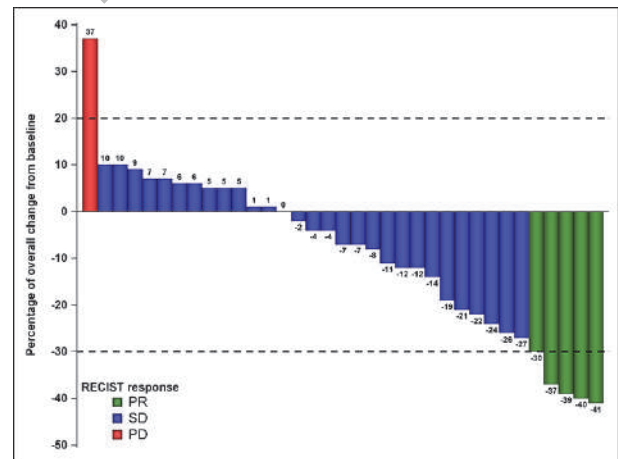
- Marcus C, et al. Head and neck PET/CT: therapy response interpretation criteria (Hopkins Criteria)-interreader reliability, accuracy, and survival outcomes. *J Nucl Med* 2014;**55**, 1411-6.
- Wise-Draper, et al. Phase II Clinical Trial of neoadjuvant and Adjuvant Pembrolizumab in Resectable Local-Regionally Advanced Head and Neck Squamous Cell Carcinoma. *Clin Cancer Res* 2022;**28**, 1345-1352.

Ethics Approval The study was approved by The University of Texas MD Anderson Cancer Center Institutional Review Board, approval numbers 2018-0381 and PA19-0470. All participants gave their informed consent prior to enrollment.

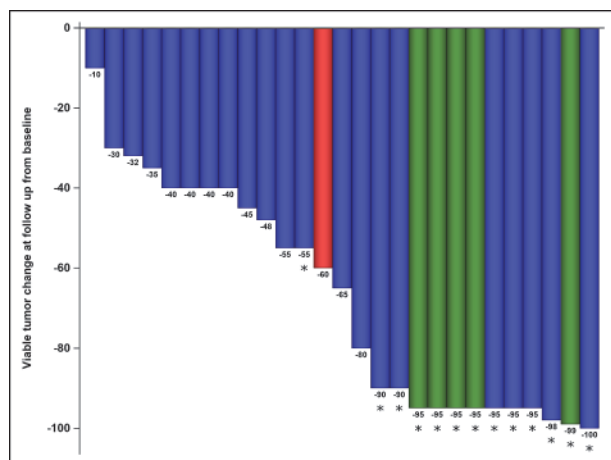
Abstract 568 Table 1 Grade=3 treatment related adverse events per CTCAE V4 that occurred after dose of ICB

Adverse Event	Grade 3		Grade 4	
	Count	%	Count	%
Dysphagia/Odynophagia	6	17		
Mucositis oral	5	14		
Aspiration pneumonia	4	11		
Lymphocyte count decreased	4	11		
Serum amylase increased	4	11		
Weight loss	4	11		
Fatigue*	3	9		
Pain (tongue, mouth, throat)	3	9		
Adrenal insufficiency*	1	3		
Alanine aminotransferase increased*	1	3		
Anorexia	1	3		
Diabetic ketoacidosis	1	3		
Hyperglycemia*	1	3		
Lipase increased*	1	3	1	3
Myositis*	1	3		
Pancreatitis*	1	3		
Rash maculo-papular*	1	3		

* attributable to ICB



Abstract 568 Figure 1 Waterfall plot of percent reduction in tumor volume by RECIST 1.1 after induction ICB



Abstract 568 Figure 2 Waterfall plot of percent reduction in tumor viability from baseline. Percent change in tumor viability (%) in core needle biopsy at baseline versus 3-5 weeks on induction ICB. Due to tumor viability of 90-100% at baseline, patients with =95% and =90% change in viability achieved complete (i.e., 0% viability) and major* (i.e., <10% viability) histological response, respectively. RECIST response, partial (green), stable (blue), progression (red)

<http://dx.doi.org/10.1136/jitc-2022-SITC2022.0568>

569

A CIVO INTRATUMOR MICRODOSE PHASE 0 TRIAL OF SUBASUMSTAT (TAK-981) IN COMBINATION WITH CETUXIMAB OR AVELUMAB REVEALS TYPE 1 INTERFERON INDUCTION AND IMMUNE ACTIVATION IN HEAD AND NECK CANCER PATIENTS

¹Jeffrey Houlton, ²Daniel Clayburgh, ²Ryan Li, ³Nathan Schauer, ³Marc Grenley, ³Connor Burns, ³Angela Merrell, ³Jason Frazier, ³Jonathan Derry, ³Emily Beirne, ³Wendy Jenkins, ⁴Allison Berger, ³Richard Klinghoffer*. ¹University of Washington, Seattle, United States; ²Oregon Health and Sciences University, Portland, OR, United States; ³Presage Biosciences, Seattle, WA, United States; ⁴Takeda Development Center Americas, Inc., Cambridge, MA, United States

Background Subasumstat (TAK-981) is an investigational drug designed to induce type I interferon (IFN) signaling via inhibition of the SUMO activating enzyme (SAE). In parallel to Phase I trials of intravenous (IV) dosing, we completed a Phase 0 intratumoral (IT) microdosing trial in head and neck cancer (HNC) using the Comparative In Vivo Oncology (CIVO) platform in order to understand effects of subasumstat within the native tumor microenvironment (TME). A major advantage of the CIVO platform is the ability to compare responses to up to 8 different drugs and combinations in the same human tumor. Here we present data from a Phase 0 trial evaluating TME responses to subasumstat alone or in combination with cetuximab or avelumab.

Methods We enrolled 12 patients with a confirmed diagnosis of HNC and planned surgical resection. Patients' surface accessible and ≥ 2 cm diameter tumors (either primary sites or metastatic to cervical lymph nodes or parotid) were injected with a 3, 5, or 8-needle CIVO device containing vehicle, subasumstat, cetuximab, avelumab, and combinations thereof co-formulated with a fluorescent tracking marker for injection site identification and visualization. Tumors were resected 24 to 96 hours after injection, processed, and analyzed at a central site using multiplex ISH / IHC and molecular profiling via GeoMx Digital Spatial Profiling (DSP). In each tumor, biomarker responses were resolved to individual injection sites, quantified, and compared by injection contents.

Results Consistent with our reports from the interim analysis of this study, subasumstat IT microdoses induced IFN signaling and activation of both innate immune cells and CD8+ T cells in the TME.¹

Combinations of subasumstat with avelumab or cetuximab led to enhanced and prolonged IFN signaling and increased expression of CD86 and granzyme B within the TME. GeoMx DSP revealed key similarities and differences between cetuximab and avelumab combination sites, including inflammatory markers, chemokines, and stromal markers.

Conclusions IT microdosing with CIVO provides early insights into investigational agents that can only be obtained in the native, intact TME. This is the first reported trial we know of where side-by-side evaluation of an investigational agent, two different biologics, and combinations thereof all in the same patient tumor was achieved. Results provide the first evidence in human tumors that subasumstat combinations can enhance immune cell activation in the TME. They also provide mechanistic rationale for further evaluating combinations of subasumstat with anti-EGFR antibodies and/or checkpoint blockade in human tumors.

Trial Registration NCT04065555: Intratumoral Microdosing of TAK-981 in Head and Neck Cancer

REFERENCE

1. Houlton J, Cash H, Xu H, Swiecicki PL, Casper K, Chinn SB, Clayburgh DR, Li RJ, Christian RJ, Halfpenny A, van Zante A, Hatton BA, Sottero K, Grenley MO, Burns C, Frazier J, Derry J, Kung G, Beirne E, Schauer NJ, Turner A, Jenkins W, Anderson K, Klinghoffer RA, Huszar D, Berger A, Kannan K. Abstract CT139: Intratumoral (IT) microdosing of the investigational SUMOylation inhibitor TAK-981 in a phase 0 CIVO trial demonstrates the reactivation of type I Interferon (IFN1) signaling in head and neck squamous cell carcinoma (HNSCC). *Cancer Res.* 2022; **82** (12_Supplement): CT139.

Ethics Approval This study obtained ethics approval from WIRB (1284928), the IRB Office at OHSU (MOD00033025), IRBMED at University of Michigan (HUM00177716), and the Human Research Protection Program at Northwell Health (20-0525). All participants gave informed consent before taking part in the study.

<http://dx.doi.org/10.1136/jitc-2022-SITC2022.0569>

570

CABOZANTINIB PLUS ATEZOLIZUMAB IN ADVANCED HEAD AND NECK CANCER PREVIOUSLY TREATED WITH PLATINUM-CONTAINING CHEMOTHERAPY: RESULTS FROM COHORT 17 OF THE COSMIC-021 STUDY

¹Sylvie Rottey*, ²Armando Santoro, ³Suzanne Arnold, ⁴Saad Khan, ⁵Allen Cohn, ⁶Bruno Fang, ⁷Svetlana Andrianova, ⁷Ramu Sudhagoni, ⁷Leleesha Samaraweera, ⁸Maria Gonzalez-Cao. ¹Ghent University Hospital, Gent, Belgium; ²Humanitas Cancer Center, Rozzano-Milan, Italy; ³University of Kentucky, Lexington, KY, United States; ⁴University of Texas, Dallas, TX, United States; ⁵Rocky Mountain Cancer Center, Denver, CO, United States; ⁶Regional Cancer Care Associates, East Brunswick, NJ, United States; ⁷Exelixis, Inc., Alameda, CA, United States; ⁸Dexeus University Hospital, Barcelona, Spain

Background Cabozantinib, a multiple receptor tyrosine kinase inhibitor, promotes an immune-permissive environment which might enhance activity of immune checkpoint inhibitors (ICI). COSMIC-021 (NCT03170960), a multicenter phase 1b study, is evaluating cabozantinib plus atezolizumab in advanced solid tumors; here we present outcomes in patients with platinum-pretreated advanced head and neck cancer (cohort 17).

Methods Patients with head and neck squamous cell carcinoma who had progressed during or following prior platinum-containing chemotherapy for advanced or metastatic disease were enrolled. Primary tumors in the oropharynx, oral cavity, hypopharynx, or larynx were allowed (nasopharynx was excluded). Up to two prior lines of systemic therapy were allowed. Prior ICI, EGFR-targeted therapy, and radiotherapy were permitted. Patients received cabozantinib, 40 mg PO QD, plus atezolizumab, 1200 mg IV Q3W. The primary endpoint was ORR per RECIST 1.1 as assessed by the investigator. Other endpoints included safety, DOR, PFS, and OS.

Results As of May 31, 2022, 30 patients were enrolled. Baseline characteristics were, median age, 62 y (range, 44-78); male, 83%; ECOG PS 0 and 1, 33% and 67%; HPV positive, negative, and unknown, 17%, 33%, and 50%; primary tumor in oropharynx, oral cavity, hypopharynx, and larynx, 40%, 33%, 10%, and 7%; lung, lymph node, and bone metastasis, 60%, 53%, and 10%; ≥ 3 metastatic sites, 43%; two lines of therapy for locally advanced or metastatic disease, 40%; median (range) number of prior lines of systemic therapy, 2.5 (1-10); prior ICI, 30%; prior radiation, 97%. The median follow-up was 25.9 mo. Clinical activity was observed with cabozantinib plus atezolizumab (table 1). Most common treatment-related adverse events (TRAEs) of any grade included fatigue (30%), stomatitis (30%), hypertension (27%), hypothyroidism (23%), nausea (23%), diarrhea (20%), decreased appetite (20%), and aspartate aminotransferase increased (20%); grade 3/4 TRAEs occurred in 47%. There were no grade 5 TRAEs.

Conclusions Cabozantinib plus atezolizumab demonstrated moderate clinical activity with manageable toxicity in patients with platinum-pretreated advanced head and neck cancer.

Trial Registration This study is registered with ClinicalTrials.gov (NCT03170960).

Ethics Approval The study Protocol (online only) was reviewed and approved by the institutional review board or ethics committee at participating sites. The study was conducted in accordance with the International Conference on Harmonisation Good Clinical Practice guidelines, the principles of the Declaration of Helsinki, and any local regulations.

Consent All patients provided written informed consent.

Abstract 570 Table 1

	Platinum-pretreated advanced head and neck cancer (N=30)
ORR, % (95% CI)	17 (6, 35)
Best overall response, n (%)	
Complete response (CR)	0
Partial response (PR)	5 (17)
Stable disease (SD)	13 (43)
Progressive disease	7 (23)
Missing/unable to evaluate	5 (17)
Disease control rate, % (95% CI)*	60 (41, 77)
Median DOR, mo (95% CI)	9.7 (2.8, NE)
Median PFS, mo (95% CI)	2.9 (1.7, 4.2)
Median OS, mo (95% CI)	9.2 (3.9, 16.3)

*CR + PR + SD.

<http://dx.doi.org/10.1136/jitc-2022-SITC2022.0570>

Abstracts

571

PENPULIMAB FOR RELAPSED/REFRACTORY (R/R) CLASSICAL HODGKIN'S LYMPHOMA (CHL): EXTENDED FOLLOW-UP OF THE MULTICENTER, SINGLE-ARM, PHASE 2 STUDY

¹Yujuan Song*, ²Keshu Zhou, ³Chuan Jin, ⁴Zhengzi Qian, ⁵Ming Hou, ⁶Lei Fan, ⁷Fei Li, ⁸Kaiyang Ding, ⁹Hui Zhou, ¹⁰Xiaoling Li, ¹¹Bing Chen, ¹²Xiuhua Sun, ¹³Xianmin Song, ¹⁴Ming Jiang, ¹⁵Qingyuan Zhang, ¹⁶Lihong Liu, ¹⁷Guohua Yu, ¹⁸Yu Hu, ¹⁹Zheng Zhao, ²⁰Ligen Liu, ²¹Hongwei Xue, ²²Jun Luo, ²³Bai He, ²⁴Zhifang Yao, ²⁴Fenghua Xu, ²⁴Min Zhao, ²⁴Baiyong Li, ²⁴Yu Xia, ¹Jun Zhu. ¹Peking University Cancer Hospital & Institute, Beijing, China; ²The Affiliated Cancer Hospital of Zhengzhou University and Henan Cancer Hospital, Zhengzhou, China; ³Cancer Hospital Affiliated to Guangzhou Medical University, Guangzhou, China; ⁴Tianjin Medical University Cancer Institute and Hospital, National Clinical Research Center of Cancer, Key Laboratory of Cancer Prevention and Therapy, the Sino-US Center for Lymphoma and Leukemia Rese, Tianjin, China; ⁵Qilu Hospital, Shandong University, Jinan, China; ⁶Shandong Provincial Key Laboratory of Immunohematology, Qilu Hospital, Shandong University, Jinan, China; ⁷The First Affiliated Hospital with Nanjing Medical University, Jiangsu Province Hospital, Collaborative Innovation Center for Cancer Personalized Medicine, Nanjing, China; ⁸The First Affiliated Hospital of Nanchang University, Nanchang, China; ⁹The First Affiliated Hospital of USTC, Division of Life Sciences and Medicine, University of Science and Technology of China, Hefei, China; ¹⁰Tumor Hospital of Xiangya School of Medicine of Central South University, Lymphoma & Hematology Department, China; ¹¹Liaoning Cancer Hospital and Institute, Shenyang, China; ¹²Nanjing Drum Tower Hospital, Clinical College of Nanjing Medical University, Nanjing, China; ¹³Second Affiliated Hospital of Dalian Medical University, Dalian, China; ¹⁴Shanghai First People's Hospital, Shanghai Jiaotong University, Shanghai, China; ¹⁵West China Hospital, Sichuan University, Chengdu, China; ¹⁶Heilongjiang Provincial Hospital, Harbin, China; ¹⁷The Fourth Hospital of Hebei Medical University, Shijiazhuang, China; ¹⁸Weifang People's Hospital, Weifang, China; ¹⁹Union Hospital, Tongji Medical College, Huazhong University of Science and Technology, Wuhan, China; ²⁰Shaanxi Provincial Cancer Hospital, Xi'an, China; ²¹Shanghai Tongren Hospital, Shanghai, China; ²²The Affiliated Hospital of Qingdao University, Qingdao, China; ²³The First Affiliated Hospital of Guangxi Medical University, Nanning, China; ²⁴The Third Affiliated Hospital of Suzhou University, The First People's Hospital of Changzhou, Changzhou, China; ²⁴Akeso Biopharma Co., Ltd., Zhongshan, China

Background Nearly all anti-PD-1 antibodies are of the IgG4 isotype which may possess residual crystallizable fragment (Fc) gamma receptor (FcγR) effector functions and are also associated with immune tolerance and escape due to instability of the CH3 domain and Fc-Fc interaction. Penpulimab is a novel IgG1 anti-PD-1 antibody that has a good stability and reduced host cell protein residue. Penpulimab was engineered to eliminate Fc-mediated effector function that compromises anti-tumor immune cell function. Penpulimab also showed numerous contacts with N58 glycosylation on the BC loop of PD-1 which may contribute to slower binding off-rate. In this trial, we examined the efficacy and safety of penpulimab in patients (pts) with R/R cHL. Here we report results from up to 30 months follow-up.

Methods AK105-201 (NCT03722147) is a multicenter, single-arm, open-label study of penpulimab in R/R cHL. Adult pts (≥18 years of age) received penpulimab 200 mg once biweekly until progression or unacceptable toxicities. Eligible pts had prior autologous stem cell transplant (ASCT) or at least 2 lines of prior chemotherapy. The primary endpoint was ORR based on the Lugano 2014 criteria as assessed by an independent review committee (IRC). Key secondary endpoints included complete response (CR) rate, progression-free survival (PFS), overall survival (OS), treatment-related adverse events (TRAEs) and immune-related adverse events (irAEs).

Results A total of 94 patients were enrolled. As of the data cutoff date (Dec 31, 2021), the median follow-up was 29.5 months. Median number of treatment cycles was 26.1 (range 2–36). 85 patients meted the definition of primary efficacy population-IRC. Efficacy data is presented in (table 1). TRAEs (with unlikely related events included) occurred in 98.9% of

pts (≥ G3 in 28.7% [27/94], treatment discontinuation in 6.4% [6/94]). Treatment related serious adverse event (SAEs) occurred in 12.8%. Most frequent TRAEs were hypothyroidism (33.0%), upper respiratory tract infection (26.6%), fever (24.5%), and ALT elevations (24.5%). Grade ≥3 TRAEs reported in ≥3 pts were platelet count decreased (3.2%), hyperlipemia (3.2%), rash (3.2%). In addition, 52 (55.3%) patients experienced an irAEs. The most frequent irAE was hypothyroidism (51.1%), and 4 (4.3%) patients developed grade 3 irAEs. No grade 4 or 5 irAEs were reported. No new safety signals were observed.

Conclusions Penpulimab was well tolerated, with a good safety profile in long-term use in R/R cHL pts. It demonstrated promising therapeutic activity and continued PFS and OS benefit.

Trial Registration NCT03722147

Ethics Approval The study was approved by relevant ethic committees and institutional review boards.

Consent Written informed consent was obtained from the patient for publication of this abstract and any accompanying images. A copy of the written consent is available for review by the Editor of this journal.

Abstract 571 Table 1 Efficacy data evaluated by IRC based on 2014 Lugano classification in the full analysis set (FAS; n=85)

	IRC-evaluated N=85
Confirmed ORR, n (%) (95% CI)	77 (90.6) (82.3, 95.8)
DCR, n (%) (95% CI)	83 (97.6) (91.8, 99.7)
CR, n (%)	42 (49.4)
PR, n (%)	35 (41.2)
SD, n (%)	6 (7.1)
PD, n (%)	2 (2.4)
Not evaluable, n (%)	0
TTR (month), median (range)	1.8 (1.4, 6.9)
PFS (month) ^a	
Median (95% CI)	33.2 (18.6, -)
12-mo rate (%) (95% CI)	76.9 (66.2, 84.6)
30-mo rate (%) (95% CI)	51.3 (39.0, 62.3)
OS (month) ^a	
Median (95% CI)	NR (NE, NE)
18-mo rate (%) (95% CI)	100.0 (100.0, 100.0)
36-mo rate (%) (95% CI)	96.1 (88.2, 98.7)

Abbreviations: CI, confidence interval; CR, complete response; DoR, duration of response; IRC: Independent Review Committee; NE, not evaluable; NR, not reached; ORR, objective response rate; OS, overall survival; PFS, progression-free survival; PR, partial response; SD, stable disease; TTR, time to tumor response.

^a Kaplan-Meier method; ^b some cases were censored.

<http://dx.doi.org/10.1136/jitc-2022-SITC2022.0571>

572

GUT MICROBIOTA TUNING PROMOTES TUMOR-ASSOCIATED ANTIGEN CROSS-PRESENTATION AND ENHANCES CAR T ANTITUMOR EFFECTS

Andrea Facciabene, Mireia Uribe-Herranz, Silvia Beghi, Marco Ruella, Kalpana Parvathaneni, Guido Ghilardi, Yung Gu Lee, Noelle Frey, John Scholler, Khatuna Gabunia, Research Specialist, Gary Wu, Elise Chong, David Porter, Carl June, Stephen Schuster, Vijay Bhoj*. *UPENN, Philadelphia, PA, United States*

Background CAR T cell therapy has shown impressive clinical responses in B cell lymphoma and leukemia, and to date, four CAR T therapies targeting CD19 have been approved by the Food and Drug Administration for the treatment of CD19-positive hematologic malignancies. Notwithstanding the encouraging results, a significant proportion of patients experience a lack of response or disease relapse. Recently several studies have shown the influence of commensal microbes on T cell function, specifically in the setting of checkpoint immunotherapy. We previously reported that gut microbiota perturbation by oral vancomycin, affects dendritic cell antigen presentation and cytokine secretion profile and affects the outcome of radiation and CAR-T therapies. Based on these data, in the present study we explore how modulation of the gut microbiota by vancomycin would influence the outcome of CART-19 therapy.

Methods We employed two murine tumor models, the hematopoietic CD19+ A20 lymphoma and the CD19+ B16 melanoma. We injected BALB/c or C57/black6 mice subcutaneously with 2×10^6 A20 or 1×10^5 CD19 positive B16 tumor cells. The same day we started treatment with oral vancomycin. Nineteen days after A20 inoculation or eleven days after CD19+ B16, mice were lymphodepletion with total body radiation (TBI). Two days later, CART-19 cells containing second generation fully murine CAR with a 4-1BB costimulatory domain were infused by tail vein. To validate the data in humans, we proceeded by: a. generating “human gut microbiota avatars”, antibiotics preconditioned recipient mice were engrafted with human gut microbiota and enrolled in similar experiments mentioned before, and b. evaluating CART-19 peak expansion on lymphoblastic leukemia patients receiving vancomycin.

Results In both models, mice receiving vancomycin in combination with CD19 directed CAR T cell therapy displayed increased tumor-associated antigens (TAAs) presentation and tumor control compared to CART-19 alone. Fecal microbiota transplant from human healthy donors to pre-conditioned mice recapitulated the results obtained in naïve gut microbiota mice. Lastly, B-cell acute lymphoblastic leukemia patients treated with CART-19 and exposed to oral vancomycin showed higher CART-19 peak expansion compared with matched unexposed patients.

Conclusions These results highlight the role of the gut microbiota on immunotherapy and suggest that the modulation of the gut microbiota using vancomycin affects the outcome of CAR T cell therapy.

Trial Registration NCT02030847

Ethics Approval This study was approved by the Internal Review Board at the Hospital of the University of Pennsylvania.

<http://dx.doi.org/10.1136/jitc-2022-SITC2022.0572>

BLOOD-BASED EXTRACELLULAR MATRIX BIOMARKERS ARE CORRELATED WITH PROGNOSTIC AND FIBROTIC-RELATED CLINICAL CHARACTERISTICS AND LIVER FUNCTION MARKERS IN PATIENTS WITH ADVANCED HEPATOCELLULAR CARCINOMA

<http://dx.doi.org/10.1136/jitc-2022-SITC2022.0574>

¹Jaclyn Neely*, ¹Jin Yao, ²Christina Jensen, ²Morten Karsdal, ²Nicholas Willumsen. ¹Bristol Myers Squibb, Lawrenceville, NJ, United States; ²Nordic Bioscience, Herlev, Denmark

Background Immune checkpoint inhibitors (ICI) have demonstrated clinical benefit in advanced hepatocellular carcinoma (aHCC). However, many patients do not respond to these therapies indicating a need for novel non-invasive biomarkers to monitor disease progression and predict treatment outcomes. HCC is a highly fibrotic disease with excessive extracellular matrix (ECM) and collagen remodeling and a reactive stroma that can affect T-cell infiltration and influence response to ICI. Fibrotic processes cause ECM remodeling, during which unique collagen fragments, like PRO-C3, are released into the blood and could be used as a non-invasive measure of the tumor fibrotic activity. Here we investigated if circulating ECM fragments are correlated with prognosis, fibrotic characteristics, and liver function in patients with aHCC.

Methods We performed the analysis on 602 patient sera specimens collected before treatment in the CheckMate 040 study (NCT01658878) of patients with advanced HCC. ELISA assays were used to measure ECM fragments related to fibroblast activity and collagen synthesis including pro-peptides of type III, IV, V, VI, XXVIII collagens (PRO-C3, PRO-C4, PRO-C5, PRO-C6, PRO-C28), cross-linked pro-peptide of type III collagen (PRO-C3X), alpha smooth muscle actin (α SMA) and ECM degradation fragments such as MMP-degraded type I, III, IV, V, VI collagens (reC1M, C3M, C4M, C5M, C6M, TUM), granzyme B-degraded type IV collagen (C4GzB), and citrullinated and MMP-degraded vimentin (VICM). ECM fragments were evaluated for their association with each other, liver function markers (Spearman's correlation, rho) and clinical characteristics (Kruskal-Wallis test).

Results Of the 15 ECM markers assessed, C3M and C4M (rho=0.82), C6M and TUM (rho=0.82), and PRO-C4 and PRO-C5 (rho=0.78) showed the highest correlation. Higher levels of the circulating collagens including PRO-C3 were associated with poor prognostic factors such as macrovascular invasion (p=4.8e-06) and ascites (p=4.1e-04), as well as poor overall survival. Similarly, PRO-C3 was also associated with fibrosis-related characteristics such as Child-Pugh score and class (p=5.4e-10 and p=5e-06 respectively) and OKUDA stage (p=4.3e-08). Circulating collagen fragments were positively correlated with C-reactive protein, alfa-fetoprotein, aspartate aminotransferase and negatively correlated with albumin levels. Collagen levels were distributed differentially based on viral etiology suggesting underlying biological differences in the TME.

Conclusions Quantifying circulating ECM fragments could enable non-invasive profiling of tumor stroma dynamics during the course of aHCC. Tumor stroma may influence response to ICI; therefore, these biomarkers may have prognostic and/or predictive potential. Further analysis is needed to determine the clinical utility of circulating ECM fragments and their impact on treatment outcomes in aHCC.

Acknowledgements We acknowledge CheckMate 040 investigators for providing patient samples for these correlative analyses.

576

COMPREHENSIVE SINGLE CELL SEQUENCING ANALYSIS OF PAIRED TISSUE AND BLOOD SAMPLES FROM HCC PATIENTS TREATED WITH NEOADJUVANT ANTI-PD-1 THERAPY REVEALS TREATMENT-INDUCED CLONAL T CELL DYNAMICS

¹Wei Wang, ¹Peter Hawkins, ¹Lianjie Li, ¹Nathalie Fiaschi, ²Assaf Magen, ¹Se Jeong, ¹Lauren Boucher, ¹Christina Adler, ¹Min Ni, ¹Nicola James, ²Myron Schwartz, ²Thomas Marron, ¹Elizabeth Miller, ¹Israel Lowy, ¹Yi Wei, ²Alice Kamphorst, ²Miriam Merad, ¹Gurinder Atwal, ¹Gavin Thurston, ¹Namita Gupta, ¹Raquel Deering*. ¹Regeneron Pharmaceuticals, Tarrytown, NY, United States; ²Mount Sinai School of Medicine, New York, NY, United States

Background While immune checkpoint blockade (ICB) therapy has provided benefit to many cancer patients, the characteristics of anti-tumor T cell responses in non-tumor tissues and in circulation are not fully understood. Neoadjuvant ICB therapy provides a unique opportunity to deeply characterize pre- and post-therapy biomarker samples and identify features of drug activity across matched patient tissues. In a single-arm, open label phase 2 study, 21 patients with resectable (stage Ib, II, and IIIb) hepatocellular carcinoma (HCC) were treated with anti-PD-1 antibody, cemiplimab, in the neoadjuvant setting. ¹Patients were treated with two cycles of cemiplimab (350 mg Q3W) prior to resection (median time to resection = 29 days), and 6/21 patients experienced pathologic response to therapy at the time of resection (Responders).

Methods Single cell RNA (scRNA) and T cell receptor (TCR) sequencing were performed on tumor, normal adjacent tissues (NAT), tumor draining lymph node (tdLN), and blood from 20/21 patients at the time of resection. Additionally, blood samples from all patients were analyzed by scRNA- and TCR-sequencing at baseline, during neoadjuvant therapy, at resection, and during adjuvant therapy. The characteristics of all tumor-expanded T cells were compared across tissues and longitudinally in the periphery.

Results We identified several populations of PD-1+ T cells that were enriched in patient tumors compared to other tissues. Responder tumors contained significantly more PD-1+ Effector T cells than Non-responders, and TCR clonality was greater in tumors of Responders. Using TCR sequence as a fingerprint, we tracked tumor TCR clones across tissues, including longitudinal blood samples. Interestingly, NAT and tdLN had more shared T cell clones with the tumors of Responders relative to Non-responders. The most clonally-expanded TCRs identified in Responders' resection tumors were present in baseline tumor biopsies. Additionally, tumor-expanded TCRs were found to be expanded in the circulation of Responders at baseline and multiple treatment timepoints, including just one week following initiation of anti-PD-1 therapy.

Conclusions Our analyses revealed significant tumor-expanded TCR sharing across the tdLN and NAT at the time of resection in patients who responded to neoadjuvant anti-PD-1 therapy. These clones were present in tumors at baseline, indicating that pre-existing T cell clones expanded in response to treatment and were also more expanded in circulation of Responders as early as one week into therapy. Our study suggests that tumor-expanded T cells are frequently found in the periphery, and peripheral expansion might correlate with response to neoadjuvant anti-PD-1 therapy.

Trial Registration NCT03916627

REFERENCE

1. Marron TU, et al. Neoadjuvant cemiplimab for resectable hepatocellular carcinoma: a single-arm, open-label, phase 2 trial. *Lancet Gastroenterol Hepatol* **7**, 219–229, doi:10.1016/S2468-1253(21)00385-X (2022).

Ethics Approval The study protocol and all amendments (available in the appendix pp 10–261) were approved by the institutional review board at Mount Sinai Hospital, and the study was done in accordance with the International Conference on Harmonisation of Technical Requirements for Pharmaceuticals for Human Use Good Clinical Practice guidelines. All patients provided written informed consent before enrolment.

<http://dx.doi.org/10.1136/jitc-2022-SITC2022.0576>

577

THE VARIATION OF T-CELL RECEPTORS (TCR) DIVERSITY AND GENOMIC HUMAN LEUKOCYTE ANTIGEN (HLA-I) AMONG NON-SMALL CELL LUNG CANCER (NSCLC) PATIENTS EXPRESSING HIGH PDL-1 ($\geq 50\%$) VERSUS THOSE WITH LOW OR NO PDL1 ($< 50\%$)

¹Aaron Beasley, ¹Anna Reid, ¹Leslie Calapre, ²Michael Millward, ¹Elin Gray, ¹Afaf Abed*.
¹Edith Cowan University, Joondalup, Australia; ²University of Western Australia, Perth, Australia

Background NSCLC patients with PDL1 $\geq 50\%$ are more likely to respond to single agent anti-PD1 comparing to those who are expressing PDL1 in less than 50% of their cancer cells. This suggest that there might be biological differences among high PDL1 ($\geq 50\%$) NSCLC comparing to low PDL1 ($< 50\%$) NSCLC. We aim to investigating the presence of differences between those two groups in terms of pre-treatment T-Cell Receptor (TCR) repertoire and genomic Human Leukocyte Antigen-I (HLA-I).

Methods We prospectively collected baseline blood from 90 NSCLC; 50 patients with high PDL1 and 40 patients with low PDL1. High quality DNA was extracted. Genomic HLA-I typing and TCR sequencing was performed. TCR diversity variables were represented by number of unique clones, evenness, Shannon diversity, clonality and convergence. TCR gene usage has been compared between both groups as well. Mann-Whitney test was used to perform the comparison analysis. HLA-I homozygosity at one or more loci versus maximal heterozygity was compared between the two groups using Fisher's exact test to calculate relative risk. HLA-A and -B supertypes was compared between the two groups as well. All analysis was conducted using GraphPad Prism version 9.3.1.

Results We had TCR results for 84 patients (47 high PDL1 and 37 low PDL1). We had to repeat the analysis for 6 patients. We found that patients with high PDL1 NSCLC are mole likely to have higher TCR evenness and lower clonality comparing to those with low or no PDL1 (median = 0.887 vs 0.845, $P=0.013$) and (median = 0.110 vs 0.155, $P=0.008$) respectively. No statistically significant results were found with other TCR variables. Moreover, certain TCR-genes are found more frequent among patients with high PDL1 comparing to those with low PDL1 like: TRBV3-1 ($P=0.012$), TRBV5-3 ($P=0.029$), TRBV9 ($P=0.029$), TRBV18 ($P=0.019$). Other TCR genes are found less frequent among patients with high PDL1 comparing to those with low PDL1 like: TRBV6-2 ($P=0.040$), TRBJ1-5 ($P=0.032$) and TRBJ2-7 ($P=0.049$). HLA typing was available for the 90 patients. No statistically significant result was found among both groups in terms of homozygosity versus heterozygosity. However, patients with high PDL1 are less likely to express HLA-A24 (RR=0.47, 95%CI 0.19-0.94, $P=0.027$) and more likely to express HLA-A03 (RR=1.87, 95%CI 1.24-2.98, $P=0.002$) on their cell surfaces.
Conclusions High PDL1 NSCLC is biologically differ from low or no PDL1 expressing NSCLC. This is reflected by their different response to immunotherapy treatment and confirmed by different pre-treatment TCR repertoire and HLA-I supertypes.

Ethics Approval Patients were recruited from two major teaching hos- pitals in Western Australia. All procedures were approved by the Human Research Ethics Committees at Edith Cowan University (ECU) (No. 18957) and Sir Charles Gairdner Hospital (No. 2013-246 and RGS0000003289) in compliance with the Declaration of Helsinki.

Consent All participants signed a consent form which is saved at ECU research database.

<http://dx.doi.org/10.1136/jitc-2022-SITC2022.0577>

578

FEASIBILITY OF EFTILAGIMOD ALPHA (SOLUBLE LAG-3 PROTEIN) COMBINED WITH STANDARD-OF-CARE-THERAPY IN ADVANCED NON-SMALL-CELL LUNG CANCER (NSCLC) ADENOCARCINOMAS. INITIAL RESULTS FROM INSIGHT-003

<http://dx.doi.org/10.1136/jitc-2022-SITC2022.0578>

¹Akin Atmaca, ²Daniel W Mueller, ¹Timursah Habibzade, ²Marina Schaaf, ²Jorge Klagges, ²Regina Eickhoff, ¹Elke Jaeger, ²Salah-Eddin Al-Batran, ¹Thorsten O Goetze*. ¹Krankenhaus Nordwest, Frankfurt a.M., Germany; ²Institut für Klinische Krebsforschung IKF am Krankenhaus Nordwest, Frankfurt a.M., Germany

Background Eftilagimod alpha (efti; IMP321) is a MHC II class agonist (soluble LAG-3 protein) which activates antigen-presenting cells followed by T-cell (CD4/CD8) activation. Data from the TACTI-002-trial (NCT03625323) and INSIGHT-004 of the current multiple-strata INSIGHT phase-I platform-study revealed that the combination of 30 mg efti subcutaneous (s.c.) with anti-PD-(L)1-checkpoint-inhibitor is well tolerated with encouraging efficacy especially in NSCLC. Stratum-C (INSIGHT-003) of the INSIGHT-study aims to evaluate the feasibility and tolerability of s.c. injections with efti combined with Standard-of-Care (SOC) chemo- and immuno-therapy in 1st-line NSCLC-patients (pts).

Methods In Stratum-C, pts with metastatic NSCLC adenocarcinomas are treated with: SOC-chemotherapy (carboplatin AUC5 / pemetrexed 500 mg/m² q3w for 4 cycles + 500 mg/m² q3w for maintenance) plus pembrolizumab 200 mg q3w combined with s.c. injections of efti (30 mg) (q2w for 24 weeks; thereafter q3w till week 52). Imaging is performed every 8 weeks and assessed locally. The primary endpoint is feasibility (defined by safety & tolerability) while secondary endpoints include objective response acc. to RECIST 1.1 and other efficacy parameters. In total 20 pts will be enrolled.

Results From 02Aug2021 till 22Jul2022, 14 pts have been enrolled. Median age is 66 years and 71.4% are male. Eleven (78.6 %) pts had PD-L1 TPS <50%. No occurrence of unacceptable toxicities (i.e., causally related to efti AND resulting in permanent discontinuation of combination-treatment before administration of two complete cycles). Two serious adverse events (1 thromboembolic event, grade 3; 1 bronchial infection grade, 3) were reported, both unrelated to efti. In total, 69 adverse events (grade 1-2: 29; grade 3: 38; grade 4: 2) were documented. The most frequent AEs were platelet-count decreased in three pts (21.4%, grade 1-3) and anemia (grade 2-3), white-blood-cell decreased (grade 3), and neutrophil-count decreased (grade 3-4) in four pts (28.6%). One grade 3 AE was considered related to efti (insomnia). 10/14 pts are currently evaluable for efficacy (four did not yet have any on-treatment tumor-staging): Seven (70 %) partial responses, two (20%) stable diseases, one (10%) progressive disease as best overall response acc to RECIST 1.1.

Conclusions To date, 30 mg efti combined with SOC appears to be feasible and safe with first promising signals of efficacy.

Acknowledgements We thank all the participating patients & their families.

We thank the dedicated clinical trial investigators & their team members.

Immutep, Berlin, Germany provided eftilagimod alpha and funding support for the study.

Ethics Approval The study was approved by 'Ethik-Kommission bei der Landesärztekammer Hessen' institution's Ethics Board, approval number 2019-1267-fAM. Participants gave informed consent before taking part.

Abstracts

579

NOVEL DIGITAL IMAGE APPROACH OF MULTIPLEX IMMUNOFLOUORESCENCE BASED PD-L1 EXPRESSION ENABLES THE STRATIFICATION OF ADVANCED NSCLC PATIENTS TREATED WITH DURVALUMAB

Nicolas Brieu*, Felix Segerer, Harald Hessel, Ashok Gupta, Ikbel Achour, Guenter Schmidt. AstraZeneca, Munich, Germany

Background Pathologist-based scoring of PD-L1 expression on tumor cells using IHC¹ has shown clinical utility in predicting favorable overall survival in advanced non-small cell lung cancer (NSCLC) patients treated with anti-PD-(L)1 therapies including durvalumab.²⁻³ Quantitative Continuous Scoring (QCS)⁴ enables the continuous measurement of the PD-L1 expression on single cells and the selection of the PD-L1 expression cutoff that best stratifies anti-PD-L1-treated patients with respect to prevalence and log-rank test p-value.⁵ We present here the extension of QCS to PD-L1 measured by multiplex immunofluorescence (mIF)⁶ to evaluate its ability to optimize patient stratification.

Methods Pre-treatment tumor samples from advanced NSCLC patients enrolled in durvalumab nonrandomized phase 1/2 trial (CP1108/NCT01693562)², were stained by mIF panel containing PD-L1.⁶ Similarly to IHC PD-L1 QCS, mIF PD-L1 QCS consists of two deep-learning models, first to segment epithelium regions and second to detect membrane, cytoplasm and nuclei of each epithelium cell, transferring for the second model annotations from IHC to mIF domain.⁷ The mIF images are normalized based on batch statistics prior to image analysis. PD-L1 expression is measured for each epithelium cell as the average of the PD-L1 signal in the segmented membrane. Cells with expression higher than an expression threshold (T_{PD-L1}) are considered positive. A slide is considered QCS-positive if it comprises a greater percentage of PD-L1 positive cells (QCS-score) than a cutoff value (CoV).

Results The QCS-scores are computed on 119 NSCLC patients treated with durvalumab. As a first proof of concept that QCS-scoring can replicate tumor proportion scoring (TPS), we optimize T_{PD-L1} as to maximize the correlation between QCS and TPS scores (figure 1). Second, we estimate for different combinations of (T_{PD-L1} , CoV) the log rank p-value associated with the stratification between patients with low and high QCS scores. A subregion of the parameter space was identified for which the stratification is significant ($p < 0.01$) with more than 50% prevalence in the positive subgroup (figure 2). The p-value is minimized ($p = 7.2 \cdot 10^{-5}$) for ($T_{PD-L1} = 37$, $CoV = 0.75\%$), yielding a median OS of 5.58 months and 13.44 months in the QCS negative and positive subgroups respectively, similar to those of IHC PD-L1 manual scoring with 25% cutoff.

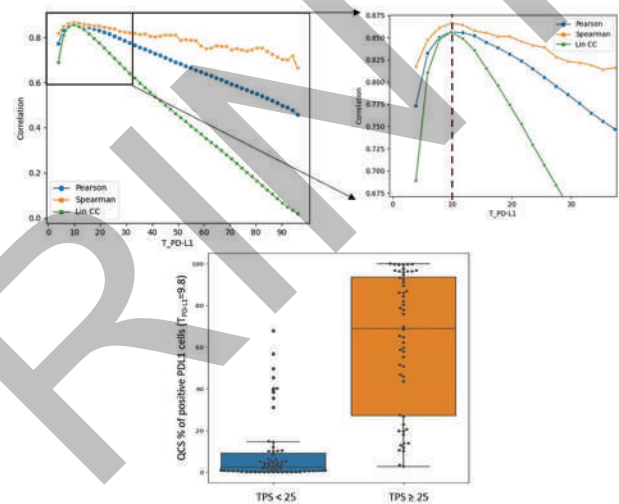
Conclusions The extension of QCS to mIF imaging provides opportunities to evaluate continuous PD-L1 expression of single tumor cells in relation to spatial distribution of other cells (e.g. PD1+ CD8+ T cells) and identify predictive biomarkers of tumor-immune cell interactions of anti-PD-(L)1 therapies.

Trial Registration CP1108/NCT01693562

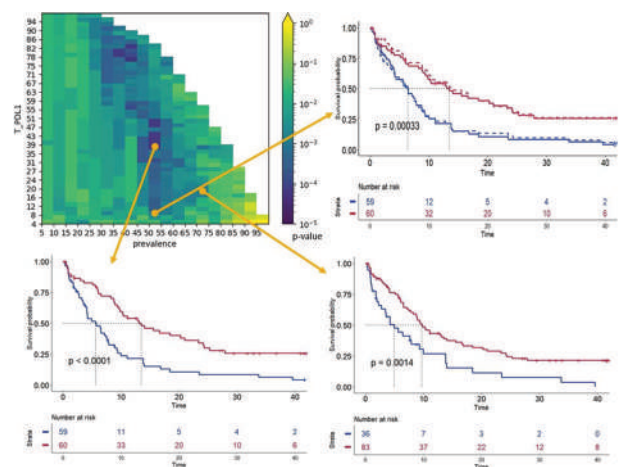
REFERENCES

1. Rebelatto M, et al. Development of a programmed cell death ligand-1 immunohistochemical assay validated for analysis of non-small cell lung cancer and head and neck squamous cell carcinoma. *Diagnostic Pathology* 2016 Oct 8;11(1):95.
2. Antonia S, et al. Clinical Activity, Tolerability, and Long-Term Follow-Up of Durvalumab in Patients With Advanced NSCLC *Journal of thoracic Oncology* 2019 Oct ; 14 (10):1794–1806

3. Rizvi NA, et al. Durvalumab With or Without Tremelimumab vs Standard Chemotherapy in First-line Treatment of Metastatic Non–Small Cell Lung Cancer. *JAMA Oncology* 2020;6(5) :661–674
4. Gustavson M, et al. Novel approach to HER2 quantification: digital pathology coupled with AI-based image and data analysis delivers objective and quantitative HER2 expression analysis for enrichment of responders to trastuzumab deruxtecan (T-DXd; DS-8201), specifically in HER2-low patients. *Cancer Res* 2021, 81 (4_Supplement): PD6–01.
5. Schmidt G, et al. Computational pathology delivers objective and quantitative PD-L1 expression analysis for enrichment of responders to durvalumab in non-small cell lung cancer (NSCLC), *J Immunother Cancer* 2021;9(Suppl 2):A1–A1054
6. Meinecke L, et al., Presence of TLS and combined high densities of PD-L1+ macrophages & CD8+ T cells predict long-term overall survival for patients with advanced NSCLC treated with durvalumab. *Cancer Res* 2022 82 (12_Supplement): 1235.
7. Brieu N, et al. Stain Isolation-based Guidance for Improved Stain Translation, Medical Imaging with Deep Learning (MIDL) 2022, <https://arxiv.org/abs/2207.00431>



Abstract 579 Figure 1 Correlation to pathologist-based TPS score Top: Lineplots of Pearson and Spearman correlations as well as of Lin correlation coefficient between the pathologist-based TPS scores and the QCS-based scores, computed for increasing expression threshold values (TPD-L1). The QCS shows maximum Pearson (0.856), Spearman (0.866) and Lin (0.856) correlations to the manual TPS score for TPD-L1 = 10. Bottom: QCS scores within the negative and positive patient subgroups as per pathologist assessment of IHC PD-L1 TPS.



Abstract 579 Figure 2 OS patient stratification Log rank p-values for OS stratification obtained by spanning the parameter space associated to the QCS, the higher CoV the lower the

prevalence of the positive patient subgroup. Top right: Kaplan Meier (KM) curves obtained with manual IHC PD-L1 TPS score at 25% cutoff (dashed line) and with median split for the QCS expression cut-off (TPD-L1=10) maximizing the correlation to TPS (full line). Bottom: KM curves of the QCS-based stratification as to minimize the p-value (TPD-L1=37) for a minimum prevalence of 50% (left) and as to maximize the prevalence (TPD-L1=18) (right).

<http://dx.doi.org/10.1136/jitc-2022-SITC2022.0579>

PREPRINT

HOST IMMUNE PROFILING IN FIRST-LINE IMMUNOTHERAPY TREATED ADVANCED STAGE NON-SMALL CELL LUNG CANCER: RESULTS FROM THE INSIGHT REGISTRY STUDY

¹Hefez Halawani, ²Eric Schaefer, ³Ray Page, ⁴Bassam Ghabach, ⁵Wallace Akerley*. ¹Christus St. Frances Cabrini, Alexandria, LA, United States; ²Highlands Oncology, Fayetteville, AR, United States; ³The Center For Cancer and Blood Disorder, Fort Worth, TX, United States; ⁴JPS Oncology and Infusion Center, Ft. Worth, TX, United States; ⁵Huntsman Cancer Institute, Salt Lake City, UT, United States

Background Immune checkpoint inhibitor therapies (ICI) have revolutionized the treatment of advanced stage non-small cell lung cancer (NSCLC) yielding 5 year-survival in ~30% for ICI treated patients and PD-L1 expression ($\geq 50\%$) with median survival of 26.3 months (m).¹ New treatment biomarkers have the potential to improve these results. Here we report the updated interim analysis results from the INSIGHT study, evaluating the extensively validated blood-based proteomic test, the Host Immune Classifier (HIC).²

Methods INSIGHT (NCT03289780) is a prospectively designed multicenter observational clinical study, having enrolled over 4,500 patients with NSCLC, across all stages and histologies. Pre-treatment blood samples were evaluated with the HIC test, which classifies patients as either HIC-Hot (HIC-H) or HIC-Cold (HIC-C). An interim analysis of exploratory endpoints was performed once patients had at least 12 months of follow up in the first 3,035 patients enrolled.

Results In the analysis population, 564 advanced stage (Stages IIIB & IV) patients were treated with a 1st line ICI containing regimen (ICI monotherapy [ICI-m] n=204 and ICI+Platinum based Chemotherapy [ICI+PC] n=360). Real-world median Overall Survival (mOS) for the ICI-m and ICI+PC cohorts was 12.9m and 13.0m, respectively. mOS for the ICI-m cohort stratified by the HIC test was 17.5m (HIC-H) vs. 5.6m (HIC-C), Hazard Ratio (HR): 0.49 (95% Confidence Interval [CI] 0.34-0.71), p-value=0.0001. Similarly, stratification of the ICI+PC cohort indicated that patients classified as HIC-H had a mOS of 17.1m vs. 8.2m in HIC-C (HR 0.53 [0.40-0.70]), p-value=<0.0001. Evaluation of the ICI-m treated patients with PD-L1 expression $\geq 50\%$ demonstrated a similar survival stratification, 16.4m vs 5.3m (HR 0.49 [0.32-0.76], p-value=0.001, Figure 1A) for HIC-H and HIC-C, respectively. However, in the ICI+PC PD-L1 high cohort, OS did not significantly differ between patients classified as HIC-H and HIC-C (Not Reached vs. 14.3, HR 0.49 [0.23-1.03], p value=0.06). Furthermore, the HIC test classifications were independent of PD-L1 expression (p-value=0.196) and remained an independent predictor of OS in ICI-treated patients, when covariates such PS and PD-L1 expression were adjusted for in a multivariate analysis (HR 0.54 [0.45-0.64], p-value=<0.0001).

Conclusions HIC-C patients with PD-L1 expression $\geq 50\%$ treated with ICI+PC had better survival than those treated with ICI-m (mOS 14.3m vs 5.3m) suggesting that a blood-based HIC test provides clinically meaningful information that may aid in selecting 1st line immunotherapy containing regimens. Additionally, in the real-world setting mOS of patients treated with ICI-m was reduced as compared to survival reported in registrational clinical trials (i.e. 26.3m).¹

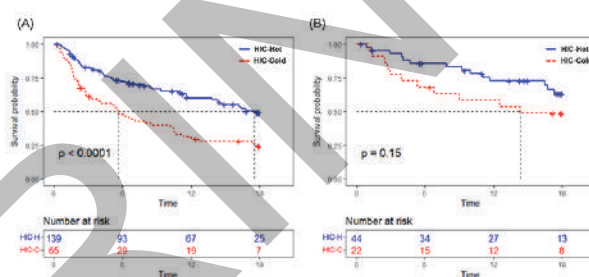
Acknowledgements The authors would like to thank the patients that have participated in the INSIGHT study and the INSIGHT Study Investigators

Trial Registration Clinicaltrial. gov: NCT03289780

REFERENCES

1. Reck M, Rodriguez-Abreu D, Robinson AG, et al. Five-year outcomes with pembrolizumab versus chemotherapy for metastatic non-small-cell lung cancer with PD-L1 Tumor Proportion Score $\geq 50\%$. *J Clin Oncol.* 2021;**39**(21):2339–2349.
2. Rich P, Mitchell RB, Schaefer E, et al. Real-world performance of blood-based proteomic profiling in first-line immunotherapy treatment in advanced stage non-small cell lung cancer. *J Immunother Cancer.* 2021;**9**(10).

Ethics Approval INSIGHT (NCT03289780) is an ongoing registry study involving over 30 academic and community oncology practices across the United States of America. The study has been reviewed and approved by an accredited central IRB (Advarra; formerly Quorum), as well as multiple local institutional review boards and conducted in accordance with the International Conference on Harmonization guidelines for Good Clinical Practice and the Declaration of Helsinki. All patients have provided written informed consent for participation.



Abstract 580 Figure 1 Overall survival stratification of patients with PD-L1 $\geq 50\%$ expression treated with either ICI-m (A) or ICI+PC (B). In patients treated with ICI-m, mOS differed significantly between HIC-H and HIC-C, HR 0.49 (CI 0.32-0.76), p-value = 0.001. Conversely, in patients with PD-L1 $\geq 50\%$ expression treated with ICI+PC, overall survival did not significantly differ between HIC-H and HIC-C, HR 0.49 (0.23-1.0), P-value = 0.06.

<http://dx.doi.org/10.1136/jitc-2022-SITC2022.0580>

581 **MATCHING-ADJUSTED INDIRECT TREATMENT COMPARISON OF TREMELIMUMAB + DURVALUMAB + CHEMOTHERAPY VS PEMBROLIZUMAB + CHEMOTHERAPY AND NIVOLUMAB + IPILIMUMAB + CHEMOTHERAPY FOR FIRST-LINE METASTATIC NSCLC**

¹Sukhvinder Johal*, ¹Miguel Miranda, ¹Tina Sarbajna, ¹Xiaojin Shi, ²Alastair Greystoke, ³Melissa Johnson. ¹AstraZeneca, Cambridge, UK; ²The Newcastle Hospitals NHS Foundation Trust, Newcastle, UK; ³Sarah Cannon Research Institute, Tennessee Oncology, PLLC, Nashville, TN, United States

Background Tremelimumab plus durvalumab and chemotherapy (T+D+CT), for first-line treatment of metastatic NSCLC, has been evaluated vs CT in a randomized phase III trial, POSEIDON (NCT03164616). In the absence of head-to-head studies, indirect treatment comparisons (ITCs) can be used to compare the efficacy of T+D+CT vs other currently approved agents including pembrolizumab plus CT (P+CT) and nivolumab plus ipilimumab plus CT (N+I+CT). However, given the potential differences in baseline characteristics between patient populations across studies, a standard ITC may be subject to bias and is therefore not necessarily the most appropriate method to derive comparative efficacy estimates. An anchored matching-adjusted indirect comparison (MAIC) is an alternative ITC method which attempts to adjust for cross-trial heterogeneity in patient populations using CT as the common comparator or anchor.

Methods Patient-level data from POSEIDON was weighted to match the baseline covariate distribution from the CheckMate 9LA trial, for both intention-to-treat (mixed histology) and non-squamous histology (NSQ) cohorts, and matched to the KEYNOTE-189 trial for the NSQ cohort. Overall survival (OS) was compared. Patient baseline characteristics and endpoints in POSEIDON were statistically tested to identify potential treatment effect modifiers (TEMs) which were subsequently clinically validated. Reweighting for POSEIDON was conducted in a pairwise manner against each comparator trial in turn using a propensity score weighting approach for the covariates that were identified as TEMs and were imbalanced across the trials. Hazard ratios (HRs) for OS were then re-estimated for POSEIDON using weighted Cox regression models and indirectly compared with those of CheckMate 9LA and KEYNOTE-189 using an ITC approach.

Results Covariates identified as TEMs through a series of interaction tests with treatment were race, histology and smoking status. For the mixed histology cohort, the estimated OS HR (95% CI) of T+D+CT vs N+I+CT after weighting was 0.89 (0.68, 1.16). For the NSQ cohort, the estimated OS HRs (95% CI) of T+D+CT vs P+CT and vs N+I+CT, were 0.96 (0.69, 1.35) and 0.76 (0.55, 1.07), respectively.

Conclusions The MAIC approach provides a method to generate comparative effectiveness estimates by accounting for heterogeneity in the baseline distribution of TEMs across trials. After adjusting for these differences between the considered trials, the OS HR point estimates were numerically in favour of treatment with T+D+CT vs N+I+CT in the mixed histology and NSQ populations and indicated similar OS with T+D+CT and P+CT in the NSQ population. This comparison supports T+D+CT as a potential new first-line treatment option for metastatic NSCLC.

Acknowledgements Editorial support for the development of this abstract, under the direction of the authors, was provided by Samantha Holmes of Ashfield MedComms (Macclesfield, UK), an Inizio company, and was funded by AstraZeneca.

Trial Registration Clinicaltrials. gov: NCT03164616; NCT03215706; NCT02578680

Ethics Approval All studies were performed in accordance with applicable local regulations with approval from independent ethics committees or institutional review boards. These were large international, multicenter trials and there are too many ethics approvals to feasibly list these details for each site. All patients provided written informed consent for participation.

<http://dx.doi.org/10.1136/jitc-2022-SITC2022.0581>

PATIENT-REPORTED OUTCOMES WITH CEMIPIMAB VERSUS CHEMOTHERAPY IN ADVANCED NON-SMALL CELL LUNG CANCER (ANSCLC): EASTERN COOPERATIVE ONCOLOGY GROUP (ECOG) PERFORMANCE STATUS SUBGROUPS IN EMPOWER-LUNG 1

¹Saadettin Kilickap*, ²Ahmet Sezer, ³Mahmut Gümüş, ⁴Igor Bondarenko, ⁵Mustafa Ozguroglu, ⁶Miranda Gogishvili, ⁷Xuanyao He, ⁷Giuseppe Gullo, ⁷Petra Rietschel, ⁷Ruben Quek. ¹Istinye University Faculty of Medicine, Istanbul, Turkey; ²Başkent University, Adana, Turkey; ³Istanbul Medeniyet University, Istanbul, Turkey; ⁴Dnipropetrovsk Medical Academy, Dnipro, Ukraine; ⁵Istanbul University-Cerrahpaşa, Istanbul, Turkey; ⁶University Clinic Ltd, Tbilisi, Georgia; ⁷Regeneron Pharmaceuticals, Inc., Tarrytown, NY, United States

Background Subgroup analysis of EMPOWER-Lung 1, a 1:1 randomized, open-label Phase 3 study, showed improvements in overall survival (OS) and progression-free survival with cemiplimab monotherapy (CEMI, n=283) versus platinum-doublet chemotherapy (CHEMO, n=280) in patients with an ECOG performance status (PS) score 0 and 1 (OS: PS 0: hazard ratio [HR] 0.77, 95% confidence interval [CI] 0.41, 1.44; PS 1: HR 0.54, 95% CI 0.38, 0.76) in patients with aNSCLC with programmed cell death-ligand 1 \geq 50%.¹ Post-hoc analyses evaluated patient-reported outcomes (PROs) in both ECOG PS subgroups.

Methods PROs were assessed at baseline and Day 1 of each treatment cycle for the first 6 cycles, and then on Day 1 of every third cycle using the European Organization for Research and Treatment of Cancer Quality of Life-Core 30 (QLQ-C30) and Lung Cancer Module (QLQ-LC13) questionnaires. Higher scores indicate better functioning and global health status (GHS)/quality of life (QoL), or worse symptom severity. Mixed-model repeated-measures analyses were performed to compare overall change from baseline scores between the two treatment arms while controlling for baseline characteristics. Time to definitive clinically meaningful deterioration (TTD) per 10-point threshold was analyzed using a stratified log-rank test and proportional hazards model.²

Results Baseline PRO scores were broadly similar between treatment arms. Statistically significant difference in overall change from baseline in GHS/QoL favoring CEMI versus CHEMO occurred in the ECOG PS score 1 subgroup (mean treatment difference 5.03, 95% CI 1.90, 8.15, $P=0.0017$). CEMI also resulted in statistically significant favorable differences in both ECOG subgroups in overall change from baseline in physical and social functioning; fatigue, nausea/vomiting, and constipation symptoms per QLQ-C30; and peripheral neuropathy and alopecia symptoms per QLQ-LC13. There was a statistically significant delay in TTD in physical functioning in the ECOG PS score 1 subgroup, favoring CEMI (HR 0.59, 95% CI 0.37, 0.95, $P=0.028$). Statistically significant delays in TTD favoring CEMI occurred in both ECOG subgroups in social functioning, fatigue and nausea/vomiting symptoms per QLQ-C30; peripheral neuropathy and alopecia symptoms per QLQ-LC13. When comparing between arms, no analyses yielded statistically significant PRO results favoring CHEMO for any QLQ-C30 or QLQ-LC13 scale.

Conclusions In this post-hoc analysis of patients with aNSCLC across both ECOG PS subgroups, CEMI resulted in significant overall improvement and delayed TTD relative to CHEMO in multiple patient-reported cancer-related and lung cancer-specific functions and symptoms. Positive PRO results further support the favorable benefit-risk profile of CEMI versus CHEMO in aNSCLC in both PS subgroups.

Acknowledgements This study was funded by Regeneron Pharmaceuticals, Inc. Medical writing support and typesetting were

provided by John G Facciponte, PhD, of Prime, Knutsford, UK, funded by Regeneron Pharmaceuticals, Inc., and Sanofi. Trial Registration NCT03088540

REFERENCES

1. Sezer A, Kilickap S, Gümüş M, et al. *Lancet*. 2021;**397**(10274):592–604.
2. Sezer A, Gümüş M, Bondarenko I, et al. Patient-reported Outcomes of Cemiplimab versus Chemotherapy in Advanced NSCLC: PD-L1 Level Subgroups in EMPOWER-Lung 1. Poster P1.15-13. To be presented at the International Association for the Study of Lung Cancer (IASLC), August 6–9, 2022, Vienna, Austria.

Ethics Approval The protocol and all amendments were approved by the appropriate institutional review board or independent ethics committee at each participating study site. The study was conducted in accordance with the principles of the Declaration of Helsinki and the International Conference on Harmonization Good Clinical Practice guidelines.

Consent Written informed consent was obtained for publication of this abstract.

<http://dx.doi.org/10.1136/jitc-2022-SITC2022.0582>

583

QUANTITATIVE COMPUTATIONAL ASSESSMENT OF PD-L1 ENABLES ROBUST PATIENT SELECTION FOR BIOMARKER-INFORMED ANTI-PD-L1 TREATMENT OF NSCLC PATIENTS

¹Jan Lesniak*, ¹Markus Schick, ¹Thomas Kunzke, ¹Pallavi Sontakke, ¹Thomas Padel, ¹Anatoliy Shumilov, ¹Farzad Sekhavati, ¹Christian Sachs, ¹Federico Pollastri, Ansh Kapil, ¹Masters of Informatics, ¹Nicolas Brieu, ²Carl Barrett, ¹Hadassah Sade, ¹Guenter Schmidt, ²Ross Stewart. ¹AstraZeneca Computational Pathology GmbH, Munich, Germany; ²AstraZeneca Early Oncology, Gaithersburg, MD, United States

Background Immune checkpoint inhibitors (ICIs) targeting PD-1 or its ligand PD-L1 have shown clinical activity in patients with metastatic non-small cell lung cancer (mNSCLC). However, only subgroups of mNSCLC patients respond to ICI, while their robust and accurate identification using PD-L1 as a biomarker remains challenging. Typically, PD-L1 expression is assessed by pathologist scoring of immunohistochemically (IHC) stained tissue, e.g. using the tumor proportion score (TPS). However, this manual process is subjective and semi-quantitative. To this end, we aim to develop robust quantitative continuous scoring of PD-L1 expression via IHC (PD-L1 QCS), relying on digitized image analysis, with the aim of improving robustness of patient selection.

Methods QCS of PD-L1 (Ventana SP263) on digitized whole slide images (WSI) is approached by segmenting the tumor epithelium within a given region of interest. Here, a deep learning (DL) region segmentation model is applied which was enriched with additional training data; expanding previous work.^{1,2} A second DL model segments individual tumor cells and their membranes. By applying color deconvolution, the resulting Optical Density (OD) provides a continuous measurement of PD-L1 intensity on each cell membrane. The percentage of positive cells is derived by thresholding the OD, whereas the specific cut-point for stratification was obtained by optimizing on an exploratory cohort (samples from 163 mNSCLC patients treated with anti-PD-L1; NCT01693562) and validated for its robustness using an independent cohort (samples from 252 patients treated with anti-PD-L1; NCT02453282), for which IHC staining and WSI scanning were completed at a contract research organization (CRO).^{3,4}

Results On the exploratory cohort, pathologist TPS correlated favorably against PD-L1 QCS (Spearman $R=0.86$), confirming the validity of image analysis. PD-L1 QCS yielded a group of responders to anti-PD-L1 treatment with a significantly increased median overall survival (mOS) by 9.2 months (log-rank $p=0.0017$, HR=0.54, prevalence=46%). On the independent validation cohort, this finding was confirmed with an mOS increase of 9.9 months (log-rank $p=0.0001$, HR=0.55, prevalence=40%), although IHC for the second cohort was completed in a different laboratory and slides digitized with a different scanner.

Conclusions We describe a computational pathology approach for precise quantification of PD-L1 expression and selection of mNSCLC patients for anti-PD-L1 treatment using the Ventana SP263 assay. Importantly, we successfully validated the performance of our PD-L1 QCS solution in two independent clinical trial datasets, which were processed by different CROs using different scanners revealing broad applicability and thereby underscoring the potential of PD-L1 QCS to transform pathology.

Trial Registration NCT01693562, NCT02453282

REFERENCES

1. Gustavson M, et al. Abstract PD6-01: Novel approach to HER2 quantification: Digital pathology coupled with AI-based image and data analysis delivers objective and quantitative HER2 expression analysis for enrichment of responders to trastuzumab deruxtecan (T-DXd; DS-8201), specifically in HER2-low patients. *Cancer Research*. 2021;**81**(P4_Supplement):PD6-01.
2. Sade H, et al. Abstract 468: Quantitative assessment of IHC using computational pathology allows superior patient selection for biomarker-informed patients. *Cancer Research*. 2022; **82** (12_Supplement):68.
3. Antonia SJ, et al. Clinical activity, tolerability, and long-term follow-up of durvalumab in patients with advanced NSCLC. *Journal of Thoracic Oncology*. 2019;**14** 10:1794–1806.
4. Rizvi NA, et al. Durvalumab with or without tremelimumab vs standard chemotherapy in first-line treatment of metastatic non-small cell lung cancer: the MYSTIC phase 3 randomized clinical trial. *JAMA Oncology*. 2020;**6** 5:661–674.

Ethics Approval Clinical studies NCT01693562 and NCT02453282, from which data in this report were obtained, were carried out in accordance with the Declaration of Helsinki and GoodClinical Practice guidelines. The study protocols, amendments, and participant informed consent documents were approved by the appropriate institutional review boards.

<http://dx.doi.org/10.1136/jitc-2022-SITC2022.0583>

584

EVALUATION OF A COMPOSITE IMMUNOTHERAPY SIGNATURE IN NON-SMALL CELL LUNG CANCER PATIENTS TREATED WITH ATEZOLIZUMAB

¹Khaled Tolba, ²David Gandara, ¹Meagan Montesion, ³Barzin Nabet, ³Minu Srivastava, ¹Lee Albacker, ⁴Mary Redman, ⁵David Kozono, ³Craig Cummings, ⁶Roy Herbst, ³David Shames, ¹David Fabrizio*. ¹Foundation Medicine, Cambridge, MA, United States; ²UC Davis, Sacramento, CA, United States; ³Genentech, South San Francisco, CA, United States; ⁴Fred Hutchinson Cancer Research Center, Seattle, WA, United States; ⁵Brigham and Women Hospital, Harvard, Boston, MA, United States; ⁶Yale University, New Haven, CT, United States

Background Immune checkpoint inhibitors have transformed the care of NSCLC, however many patients do not respond and current biomarkers have limited predictive value. While current guidelines recommend that patients with advanced NSCLC undergo large panel NGS to guide treatment selection, most of the genomic data generated are rarely utilized for therapeutic decision making in the absence of an actionable driver mutation. In this work, we validated a composite IO biomarker that integrates multiple genomic features readily available on large-panel NGS to predict response to ICI in NSCLC patients.

Methods OAK is a phase III trial that randomized 1250 patients with advanced stage NSCLC who progressed on initial platinum therapy to receive atezolizumab (Atezo) or docetaxel until disease progression (1). 239 participants with Foundation Medicine tissue NGS were included and 180 were WT for EGFR, ALK, ROS1, BRAF, MET and RET, of whom 86 received Atezo while 94 received docetaxel. We tested the predictive value of 7 biomarkers that had been trained previously on a subset of squamous lung patients treated with immunotherapy and were part of the Lung-MAP clinical trial, including TMB < 10, 10-19 and ≥ 20 Mut/Mb; PD-L1 IHC <1%, 1-49% and ≥ 50%; mutations or loss of ARID1A, KEAP1, STK11, CDKN2A; and altered DDR defined as functional loss of one or more of these 7 genes: ATM, BRCA2, BRIP1, MRE11, POLE, MSH2 and PARP1. A nominal system included binning scores based on individual biomarker positivity of 0-2, 3-4 or 5-8 (IO signature low, medium, high). We used a Cox proportional hazards regression model to investigate the effect of individual covariates and three composite bins on OS of the two treatment arms.

Results Individual biomarker analysis showed that TMB ≥ 20 exerted the greatest effect on OS in Atezo-treated patients (HR= 0.4, P = 0.07). Altered DDR, PD-L1 >50% and STK11 loss numerically impacted OS but did not reach statistical significance due to small sample size. High IO signature correlated with improved OS within the Atezo-treated patients, yielding a median OS of 23 months vs. 7 months (HR=0.38; 95% CI, 0.18-0.81) between high vs. low, as well as a median OS of 23 months vs. 10 months between Atezo and docetaxel treated patients within the high IO signature subpopulations (HR=0.68; 95% CI, 0.34-1.3).

Conclusions Our data suggest that Composite IO signature might be more accurate and informative than a single biomarker in guiding ICI treatment selection in NSCLC.

Trial Registration OAK Trial NCT02008227

REFERENCE

1. Achim Rittmeyer, Fabrice Barlesi, Daniel Waterkamp, Keunchil Park, Fortunato Ciardiello, Joachim von Pawel, Shirish M Gadgil, Toyooki Hida, Dariusz M Kowalski, Manuel Cobo Dols, Diego L Cortinovis, Joseph Leach, Jonathan Polikoff, Carlos Barrios, Fairooz Kabbinavar, Osvaldo Arén Frontera, Filippo De Marinis, Hande Tuma, Jong-Seok Lee, Marcus Ballinger, Marcin Kowanetz, Pei He, Daniel S Chen, Alan Sandler, David R Gandara. Atezolizumab versus docetaxel in

patients with previously treated non-small-cell lung cancer (OAK): a phase 3, open-label, multicentre randomised controlled trial. *The Lancet* 2017;**389**(10066).

Ethics Approval All patients signed informed consent prior to publication of the original study manuscript at the Lancet in 2017.

<http://dx.doi.org/10.1136/jitc-2022-SITC2022.0584>

585

PHASE 1 DOSE ESCALATION TRIAL OF THE SELECTIVE A2B ADENOSINE RECEPTOR ANTAGONIST PBF-1129 IN PATIENTS WITH METASTATIC NON-SMALL CELL LUNG CANCER (MNSCLC)

¹Dwight Owen*, ¹Lai Wei, ¹Mikhail Dikov, ¹Shankar Suman, ¹Ruohan Wu, ¹Joseph Amann, ¹Catherine Schweitzer, ¹Sarah Ferguson, ¹Michael Smith, ²Julio Castro, ¹Erin Bertino, ¹Peter Shields, ¹Kai He, ¹Carolyn Presley, ¹Gregory Otterson, ¹David Carbone. ¹The Ohio State University, Columbus, OH, United States; ²Palobiofarma S.L., Barcelona, Spain

Background Adenosinergic signaling has recently emerged as a powerful regulator within the tumor microenvironment (TME). Preclinical studies on interference with adenosine generation or signaling through A2A and A2B adenosine receptors (A2BAR) have been shown to relieve immunosuppression by reducing stress in the TME by decreasing expression of key adenosine-generating enzymes. A2BAR blockade enhances anti-tumor immunity through a reduction in myeloid-derived suppressor cell differentiation and an enhancement of the capacity of dendritic cells to evoke anti-tumor T cell responses. We conducted a phase 1 dose escalation trial of PBF-1129, a first in class selective A2BAR inhibitor in patients with mNSCLC who progressed on chemotherapy and immune checkpoint inhibitors (ICI).

Methods NCT03274479 was a single site dose escalation phase 1 trial. Patients received escalating doses of PBF-1129 orally daily (80 mg, 160 mg, 240 mg, 360 mg) until disease progression or intolerance. Primary objective was safety and tolerability as defined by occurrence of dose limiting toxicities (DLT) and to determine maximum tolerated dose (MTD). PK, ORR, PFS, OS were secondary endpoints.

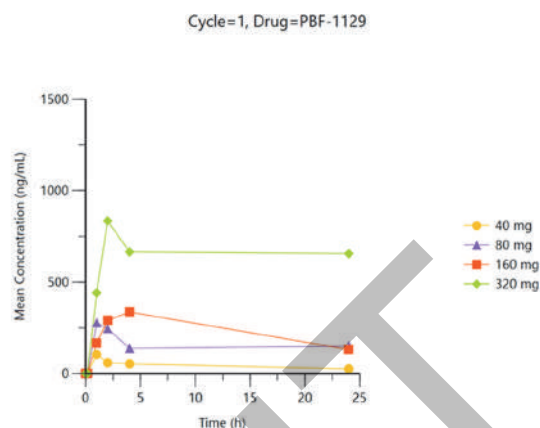
Results 21 patients (9 female), median age 61 years (range 49-75) were enrolled. 12 patients with adenocarcinoma, 7 with squamous, 1 with adenosquamous and 1 NOS. Median line of therapy was 4th (range 3-6). All patients received prior PD-1/L1 therapy and chemotherapy; 4 pts received prior anti-CTLA-4. PD-L1 expression negative in 6 pts, positive in 12 and unknown in 3 pts. No DLTs were observed at any dose level. No MTD was identified. Grade ≥ 3 treatment-related adverse events (TRAEs) occurred in 3 patients including lymphocytopenia (n=2), hyponatremia (n=1), hypertension (n=1), and encephalopathy (n=1). Most frequent TRAEs of any grade were lymphocytopenia (n=8, 38%), vomiting (n=8, 38%), anorexia (n=6, 29%), and fatigue (n=6, 29%). 18 patients were evaluable for response, best response of stable disease was observed in 3 pts; median PFS 1.5 months (95% CI 1.0, 1.9), median OS 4.6 months (95% CI: 2.1, 5.2). PK analysis revealed a dose-dependent exposure increase, with median C(max) ranging from 150ng/ml at the 40mg dose to 800ng/ml at the 320mg dose, together with a moderate half-life above 10h (figure 1). The 320mg is able to maintain PBF-1129 free concentrations above the IC(50) against the adenosine A2b receptor for 24h.

Conclusions PBF-1129 was safe and tolerable in patients with heavily pretreated mNSCLC although limited single agent activity was observed. RP2D was identified as 360 mg orally daily. A trial of PBF-1129 given in combination with ICI is planned (NCT05234307).

Trial Registration NCT03274479

Ethics Approval The study was approved by the OSU institution's Ethics Board (#2018C0019)

Consent All study participants granted a written informed consent prior to treatment initiation.



Abstract 585 Figure 1 PBF11-29 pharmacokinetics Mean Concentrations of PBF-1129 Following Once Daily Oral Administration of PBF-1129

<http://dx.doi.org/10.1136/jitc-2022-SITC2022.0585>

Abstracts

586

DURVALUMAB (D) ± TREMELIMUMAB (T) + PLATINUM-EPOSIDO (EP) IN EXTENSIVE-STAGE SMALL-CELL LUNG CANCER (ES-SCLC): RNA SEQUENCING ANALYSIS TO EXPLORE CANONICAL MARKERS OF IO ACTIVITY IN CASPIAN

¹Mingchao Xie, ¹Priti Chugh, ¹Cathy O'Brien, ¹Zhongwu Lai, ¹Ross Stewart, ²Luis Paz-Ares, ³Jonathan Goldman, ⁴Marina Garassino, ⁵Charles Rudin, ¹J Carl Barrett, ¹Yashaswi Shrestha*. ¹AstraZeneca, Waltham, United States; ²Hospital Universitario 12 de Octubre, Madrid, Spain; ³David Geffen School of Medicine at UCLA, Los Angeles, CA, United States; ⁴Istituto Nazionale dei Tumori, Milan, Italy; ⁵Memorial Sloan Kettering Cancer Center, New York, NY, United States

Background In the Phase 3 CASPIAN study, first-line D+EP significantly improved overall survival (OS) vs EP in patients with ES-SCLC, and OS benefit was sustained at >3 years of median follow-up (HR 0.71 [95% CI 0.60–0.86]; nominal p=0.0003; median OS [mOS] 12.9 vs 10.5 months). Although not statistically significant, a numerical improvement in OS was observed with D+T+EP vs EP, which continued at >3 years of median follow-up (HR 0.81 [95% CI 0.67–0.97]; nominal p=0.0200; mOS 10.4 vs 10.5 months). Various biomarkers of immune checkpoint inhibitor activity have been identified previously, including CD8A, CD4, CTLA-4, and FOXP3 (a regulatory T-cell marker), although such biomarkers are not well characterized in SCLC. In this exploratory analysis using RNA sequencing (RNAseq) data from CASPIAN, we explored the association of these canonical biomarkers with OS in patients with ES-SCLC.

Methods In CASPIAN, treatment-naïve patients with ES-SCLC received 4 cycles of D+EP or D+T+EP followed by maintenance D; or up to 6 cycles of EP. RNAseq data were generated from FFPE tumor samples collected at screening. Data cutoff: Mar 22, 2021.

Results 57/268 (21.3%) patients in the D+EP arm, 60/268 (22.4%) patients in the D+T+EP arm, and 47/269 (17.5%) patients in the EP arm had RNAseq data (biomarker-evaluable population; BEP). In the BEP, mOS was 11.8 months in the D+EP arm, 11.9 months in the D+T+EP arm, and 9.1 months in the EP arm (HR for D+EP vs EP: 0.61 [95% CI 0.40–0.92]; HR for D+T+EP vs EP: 0.53 [95% CI 0.35–0.81]). In both the D+EP and D+T+EP arms, mOS was higher in the CD8A-high vs -low expression group (table 1). In the D+T+EP arm only, mOS was higher in the CD4-, CTLA-4-, or FOXP3-high vs -low expression groups (table 1).

Conclusions These exploratory data on the association of CD8A, CD4, CTLA-4, and FOXP3 with outcomes in CASPIAN provide insights into the mechanism and biology of IO in ES-SCLC and support their further exploration as biomarkers in this setting. Pre-existing cytotoxic T cells may be an important factor for durvalumab to extend anti-tumor activity, and tremelimumab may enhance T-cell activation by overcoming sequestration of CD28 ligands by regulatory T cells. The RNAseq BEP was ~20% of the CASPIAN intention-to-treat population, so these findings should be regarded as hypothesis generating.

Acknowledgements Medical writing support for the development of this abstract, under the direction of the authors, was provided by Helen Kitchen of Ashfield MedComms (Macclesfield, UK), an Inizio company, and was funded by AstraZeneca.

Trial Registration Clinicaltrials. gov, NCT03043872 (Release date February 6, 2017)

Ethics Approval The study was done in accordance with applicable local regulations with approval from independent ethics

committees or institutional review boards. CASPIAN was a large international, multicenter trial and there are too many ethics approvals to feasibly list these details for each site. All patients provided written informed consent for participation.

Abstract 586 Table 1

		D+EP		D+T+EP		EP	
		High*	Low*	High*	Low*	High*	Low*
CD8A	mOS, months (95% CI; n)	17.9 (11.3-NE; 13)	10.6 (6.9-14.6; 46)	25.9 (11.4-NE; 19)	10.0 (7.2-12.6; 41)	9.1 (6.3-16.0; 11)	8.9 (7.3-11.4; 36)
	HR (95% CI) high vs low	0.52 (0.24-1.13)		0.45 (0.23-0.84)		0.89 (0.45-1.77)	
CD4	mOS, months (95% CI; n)	11.3 (6.6-17.9; 12)	12.0 (8.1-15.9; 45)	29.0 (6.6-NE; 14)	10.4 (7.7-14.8; 46)	11.3 (7.9-15.9; 15)	8.2 (6.1-11.2; 32)
	HR (95% CI) high vs low	1.24 (0.63-2.45)		0.42 (0.19-0.90)		0.68 (0.36-1.26)	
FOXP3	mOS, months (95% CI; n)	11.5 (6.6-14.9; 15)	11.8 (7.3-16.6; 42)	30.8 (7.5-NE; 13)	10.4 (8.6-14.1; 47)	12.4 (7.3-19.8; 13)	8.3 (6.8-11.2; 34)
	HR (95% CI) high vs low	1.12 (0.59-2.14)		0.51 (0.25-1.05)		0.66 (0.35-1.28)	
CTLA-4	mOS, months (95% CI; n)	11.5 (6.6-21.3; 13)	11.8 (7.3-14.9; 44)	28.4 (7.7-NE; 18)	10.3 (8.6-14.1; 42)	10.9 (6.3-15.9; 10)	8.4 (7.3-11.4; 37)
	HR (95% CI) high vs low	0.84 (0.42-1.70)		0.48 (0.25-0.93)		0.78 (0.38-1.58)	

*High expression = top quartile; low expression = other three quartiles
NE, not estimable

<http://dx.doi.org/10.1136/jitc-2022-SITC2022.0586>

587

AMADEUS TRIAL: TUMOR AGNOSTIC PRE- AND ON-TREATMENT BIOMARKERS OF RESPONSE TO NIVOLUMAB PLUS IPILIMUMAB CORRELATE WITH ON-TREATMENT TUMORAL T CELL INFILTRATION

¹Farah Alayli*, ¹Kwame Okrah, ²Apostolia Tsimberidou, ³Alexandra Drakaki, ⁴Danny Khalil, ⁵Saad Khan, ⁶Stephen Hodi, ⁷David Oh, ¹Meelad Amouzgar, ¹Shikha Guatam, ¹Robin Kageyama, ¹Shannon Pfeiffer, ¹Stefanie Meier, ¹Christopher Cabanski, ¹Diane Da Silva, ¹Dinesh Kumar, ¹Sandra Santulli-Marotto, ⁷Michael Tetzlaff, ²Wai Chin Foo, ⁴Travis Hollman, ⁴Yanyun Li, ⁴Mathew Adamow, ⁴Philip Wong, ¹Marko Spasic, ⁸Richard Chen, ¹Samantha Bucktrout, ¹Justin Fairchild, ¹Lisa Butterfield, ¹Theresa LaVallee, ¹Lacey Padron, ⁹Lisa Salvador, ¹⁰Jill O'Donnell-Tormey, ¹Ute Dugan, ²Padmanee Sharma. ¹Parker Institute for Cancer Immunotherapy, San Francisco, United States; ²The University of Texas MD Anderson Cancer Center, Houston, TX, United States; ³University of California, Los Angeles, Los Angeles, United States; ⁴Memorial Sloan Kettering Cancer Center, New York, United States; ⁵Stanford University, Stanford, United States; ⁶Dana-Farber Cancer Institute, Boston, United States; ⁷University of California, San Francisco, San Francisco, United States; ⁸Personalis Inc., Menlo Park, CA, United States; ⁹Bristol Myers Squibb, Princeton, NJ, United States; ¹⁰Cancer Research Institute, New York, United States

Background Although immune checkpoint inhibitors (ICI) are efficacious in some patients with cancer, many do not benefit. Identifying pre- and on-treatment biomarkers correlating with clinical outcomes is essential for better treatment strategies. High pre- and on-treatment recruitment of CD8+ T cells into the tumor are associated with improved outcomes following ICI therapy. We report orthogonal biomarker results from the AMADEUS study, an all-comer solid tumors trial, in which patients were treated with nivolumab (NIVO) with or without ipilimumab (IPI) based on the proportion of pretreatment tumoral CD8+ T cells.

Methods AMADEUS is a prospective, non-randomized, multi-center study that enrolled 79 patients with various metastatic solid tumors. The frequency of pretreatment tumoral CD8+ T cells was measured by a CLIA-certified immunohistochemistry (IHC) assay. Patients with $\geq 15\%$ tumoral CD8 received NIVO monotherapy (CD8 high) and those with $< 15\%$ tumoral CD8 received NIVO+IPI (CD8 low). Pre- and on-treatment tumor and blood samples were collected for longitudinal multi-omic biomarker analysis. Bulk RNA/DNA sequencing and high dimensional imaging technologies were used to analyze the tumor biopsies. Peripheral blood analyses included mass cytometry time of flight (CyTOF) for broad immune profiling, and a high parameter flow cytometry panel for T cell specific phenotypic evaluation.

Results In the CD8 low arm, on-treatment conversion from CD8 low to high ($\geq 15\%$) was associated with a trend towards improved clinical benefit ($p = 0.0582$), whereas pretreatment tumoral CD8 T cell frequency was not correlated with clinical benefit. Analysis of tumor bulk mRNA sequencing yielded pan-tumor gene signatures of response and resistance to NIVO+IPI. Responders had elevated expression of genes relating to IFN γ and JAK/STAT signaling, whereas glycolysis pathway genes and MYC targets dominated in the non-responders. Analysis of pretreatment peripheral blood immune cell populations demonstrated a significantly higher frequency of T cells with a stem cell progenitor-like phenotype (TCF1+) ($p = 0.0179$) in the non-responders compared to the responders. On-treatment, elevated frequencies of circulating gdT cells, NK cells, as well as enhanced activation and proliferation of effector and central memory conventional T cells were associated with response to ICI therapy.

Conclusions In this study, increased tumoral infiltration of CD8+ T cells on-treatment ($\geq 15\%$) was associated with a trend towards improved clinical benefit ($p = 0.0582$). Using multi-omic analysis of pre- and on-treatment tissue and blood

samples, we identified additional composite tumor agnostic biomarkers correlating with response. These biomarkers warrant further investigation for patient stratification and identification of novel drug targets to overcome ICI resistance.

Acknowledgements We extend our gratitude to the patients, their families, the clinical investigators, and their site staff members who made this trial possible. We would also like to thank Fizza Hussain and Carri Browne at Parker Institute for Cancer Immunotherapy (PICI) for operations leadership of the trial. We thank Bristol Myers Squibb (BMS) for collaboration and study drugs. The study was funded by Cancer Research Institute (CRI), BMS, and PICI.

Trial Registration ClinicalTrials.gov (NCT03651271)

Ethics Approval The study was approved by MD Anderson Cancer Center IRB, Approval Number: 2017-0446

Consent All participants provided written informed consent before enrollment

<http://dx.doi.org/10.1136/jitc-2022-SITC2022.0587>

Abstracts

588 PHASE IB STUDY OF THE P38 INHIBITOR ARRY-614 WITH NIVOLUMAB, IPILIMUMAB OR NIVOLUMAB +IPILIMUMAB IN ADVANCED SOLID TUMORS

¹Ryan Augustin*, ²Andrew Poklepovic, ³Xin Gao, ¹William Gooding, ¹Sarah Brodeur, ¹Julie Urban, ¹Amy Rose, ¹Amy Goodman, ¹Darcy Ploucha, ¹Roby Thomas, ¹Dan Zandberg, ¹John Kirkwood, ¹Yana Najjar, ¹Divakar Davar, ¹Liza Villaruz, ¹Jan Beumer, ¹Riyue Bao, ¹Jason Luke. ¹UPMC Hillman Cancer Center, Pittsburgh, PA, United States; ²VCU Massey Cancer Center, Richmond, VA, United States; ³MGH Cancer Center, Boston, MA, United States

Background The p38 mitogen-activated protein kinase (MAPK) pathway limits dendritic cell priming and we have discovered a novel tumor-intrinsic immune-exclusion role for p38 MAPK across multiple tumor types. ARRY-614 (pexmetinib) is a p38 MAPK inhibitor that enhances immune-checkpoint blockade (ICB) in murine models. Here we report on the safety and anti-tumor activity of ARRY-614 with nivolumab (N), ipilimumab (I), or N+I in human subjects with advanced solid tumors.

Methods Subjects received daily, oral ARRY-614 (de-escalated from 800 to 200mg) with N (480 mg), I (3 mg/kg), or N+I (1 mg/kg) on either 28- or 21-day cycles. The primary objective was safety and tolerability of ARRY-614 with N, I, or N+I and selection of the recommended phase II dose (RP2D) using a Bayesian dose-finding strategy. Preliminary anti-tumor activity per RECISTv1.1 or irRECIST were secondary objectives.

Results Twenty-eight subjects were recruited (n=15 with N; including NSCLC, GEJ, RCC and mesothelioma; n=13 with I or N+I; all melanoma). Most were male (71.4%) with median age 67, three prior therapy lines, and 93% previously exposed to PD(L)1 (all meeting SITC PD(L)1 resistance definition)[1]. Treatment-related adverse events (TRAEs) were documented in all 28 subjects with 17.2% TRAEs reported as clinically significant, 9.2% grade 3, and 7.0% deemed immune-related adverse events (irAE). Eight subjects experienced dose-limiting toxicities (DLT) including rash, colitis, atrial fibrillation, hypotension, dyspnea, anaphylaxis, and visual disturbances; all in patients receiving a starting dose \geq 400mg ARRY-614 and equally distributed in N vs N+I cohorts. The RP2D is 200 mg ARRY-614 with ICB and preliminary ARRY-614 PK assessment suggesting a dose-exposure relationship with DLT via area under the curve. Response was evaluable in 20 subjects (eight were nonevaluable due to toxicity or early progression) with three confirmed PRs and nine SD/irSD (figure 1). Median duration of response is not reached with two PR ongoing more than 1.5 years (NSCLC: PDL1 0%, TMB 5.4 muts/Mb, prior chemotherapy + anti-PD1 / RCC: prior TKI, IL2, multiple PD(L)1 combinations). Six-month progression-free survival was achieved in six subjects including two patients with SD/irSD reaching >12 months (and three with continued benefit despite early drug cessation due to irAE; figure 2). Length of prior treatment time on most recent anti-PD(L)1 therapy did not associate with outcome. Immune monitoring and pharmacodynamic assessments are in progress.

Conclusions Inhibition of the p38 MAPK pathway with ARRY-614 is well tolerated at 200mg in combination with ICB, eliciting durable responses and disease control in poor risk and PD(L)1-refractory subjects.

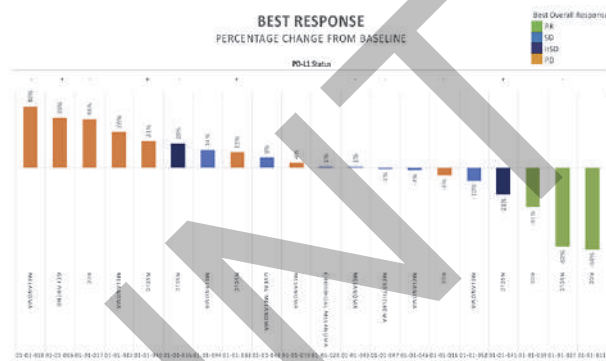
Trial Registration NCT04074967

REFERENCE

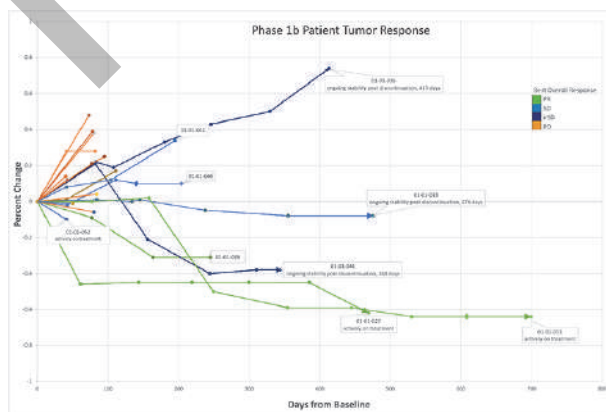
1. Kluger HM, Tawbi HA, Ascierto ML, Bowden M, Callahan MK, Cha E, Chen HX, Drake CG, Feltquate DM, Ferris RL, Gulley JL, Gupta S, Humphrey RW, LaVallee

TM, Le DT, Hubbard-Lucey VM, Papadimitrakopoulou VA, Postow MA, Rubin EH, Sharon E, Taube JM, Topalian SL, Zappasodi R, Sznol M, Sullivan RJ. Defining tumor resistance to PD-1 pathway blockade: recommendations from the first meeting of the SITC Immunotherapy Resistance Taskforce. *J Immunother Cancer*. 2020 Mar;**8**(1):e000398.

Ethics Approval This phase Ib study obtained prior ethics approval from the University of Pittsburgh Institutional Review Board (IRB: HCC#19-097). All participants gave informed consent prior to enrolling in this study.



Abstract 588 Figure 1 Best overall response. Waterfall plot depicting best overall response in all twenty evaluable subjects. (PR, partial response; SD, stable disease, irSD, immune-related stable disease; PD, progressive disease)



Abstract 588 Figure 2 Subject tumor response over time. Spider plot depicting subject tumor response from baseline over time. (PR, partial response; SD, stable disease, irSD, immune-related stable disease; PD, progressive disease)

<http://dx.doi.org/10.1136/jitc-2022-SITC2022.0588>

589

XEVINAPANT PLUS NIVOLUMAB IN PATIENTS WITH ADVANCED SOLID TUMORS WHO PROGRESSED ON PRIOR ANTI-PD-1/PD-L1 TREATMENT: RESULTS OF A DOSE-OPTIMIZATION, EXPLORATORY PHASE 1B/2 TRIAL

¹Emiliano Calvo Aller, ²Glenn Hanna*, ³Maria Vieito Villar, ⁴Caroline Even, ⁵Victor Moreno, ⁶Chul Kim, ⁷Shuchi Gulati, ⁸Daniel Morgensztern, ⁹Ana Acuna-Villaorduna, ¹⁰Philippe Cassier, ¹¹Dennie Jones, ¹²Florilene Bouisset, ¹²Daniela Sahlender, ¹²Elisabeth Rouits, ¹²Dany Spaggiari, ¹²Lars Damstrup, ¹³Carlos-Alberto Gomez-Roca. ¹START Madrid-CIOCC, Centro Integral Oncológico Clara Campal, Madrid, Spain; ²Dana-Farber Cancer Institute, BOSTON, MA, United States; ³Hospital Universitari Vall d'Hebron, Barcelona, Spain; ⁴Institut Gustave Roussy, Villejuif, Val de Marne, France; ⁵Hospital Universitario Fundación Jimenez Diaz, Madrid, Spain; ⁶Georgetown University – Lombardi Comprehensive Cancer Center, Washington, DC, DC, United States; ⁷University of Cincinnati, Cincinnati, OH, United States; ⁸Washington University, School of Medicine, St. Louis, MO, United States; ⁹Montefiore Medical Center PRIME, Bronx, NY, United States; ¹⁰Centre Léon Bérard, Lyon, Rhone, France; ¹¹University of Florida, Gainesville, FL, United States; ¹²Debiopharm International SA, Lausanne, Switzerland; ¹³Institut Claudius Regaud, Toulouse, Haute Garonne, France

Background Anticancer agents that render cancer cells susceptible to apoptosis and increase antitumor immunity may enhance clinical responses to immune checkpoint inhibitors. In this phase 1b/2 trial, we investigated the antitumor activity and safety of xevinapant, a first-in-class, potent, oral, small-molecule inhibitor of apoptosis proteins inhibitor which restores cancer cell sensitivity to apoptosis, in combination with the anti-PD-1 antibody nivolumab.

Methods Eligible patients had histologically confirmed advanced or metastatic solid tumors that progressed on prior anti-PD-1/PD-L1 treatment, including small cell lung cancer (cohort 1), squamous cell carcinoma of the head and neck (cohort 2), gastrointestinal cancers with known microsatellite-high (MSI-H)/mismatch repair deficiency (MMRd) or other DNA-damage response (DDR) abnormalities (cohort 3), or platinum-resistant epithelial ovarian, endometrial, primary peritoneal or cervical cancer (with known MSI-H/MMRd, *BRCA1/2* mutations, or other DDR abnormalities; cohort 4). In the dose-escalation part of the trial (part A), patients received xevinapant 150 or 200 mg/day on days 1-10 and days 15-24 plus nivolumab 240 mg on days 1 and 15 of a 28-day cycle. The primary objective of part A was to determine the recommended phase 2 dose (RP2D). In the phase 2 basket trial (part B), patients received xevinapant plus nivolumab at the RP2D; the primary endpoint was objective response rate (ORR).

Results Eleven patients were enrolled in part A; 3 patients received xevinapant 150 mg/day and 8 received 200 mg/day. No dose-limiting toxicities during the observation period (28 days) or grade ≥ 3 treatment-related adverse events (TRAEs) were reported. The RP2D was established as xevinapant 200 mg/day (days 1-10 and 15-24) plus nivolumab 240 mg (days 1 and 15) per 28-day cycle.¹ In part B, 35 patients (n=8 cohorts 1-3, n=11 cohort 4) received xevinapant plus nivolumab at the RP2D. Most patients (60.0%) had stage IV disease and all patients had received prior chemotherapy treatment. At data cutoff (April 6, 2022), the ORR was 2.9%, with 1 partial response (cohort 4; endometrial cancer); 15 patients (42.9%) had stable disease. Thirty-four patients (97.1%) had discontinued treatment; the most common reason was disease progression (26 patients; 74.3%). Median PFS across cohorts was 1.9 months (95% CI, 1.7-2.7); median OS was 11.7 months (95% CI, 6.0-15.9). TRAEs occurred in 30 patients (85.7%); grade ≥ 3 TRAEs in 9 patients (25.7%). No treatment-related deaths were reported.

Conclusions Xevinapant plus nivolumab had a tolerable safety profile in patients with heavily pretreated solid tumors but limited clinical activity in this immunotherapy-refractory population.

Acknowledgements This trial was sponsored by Debiopharm. Medical writing support was provided by Sophie Saunders of ClinicalThinking and was funded by the healthcare business of Merck KGaA, Darmstadt, Germany (CrossRef Funder ID: 10.13039/100009945).

Trial Registration NCT04122625 (ClinicalTrials.gov)

REFERENCE

1. Azaro Pedrazzoli AB, Moreno V, Gomez-Roca CA, et al. Safety and efficacy of Debio 1143, an antagonist of inhibitor of apoptosis proteins (IAPs), in combination with nivolumab in a phase Ib/II trial in patients (pts) failing prior PD-1/PD-L1 treatment. *Ann Oncol* 2020;**31**(Suppl 4):Abstract 560P.

Ethics Approval The trial protocol was approved by the independent ethics committee or institutional review board at each participating center.

<http://dx.doi.org/10.1136/jitc-2022-SITC2022.0589>

590

METAGENOMIC SEQUENCING REVEALS UNIQUE GUT MICROBIAL FEATURES ASSOCIATED WITH TERTIARY LYMPHOID STRUCTURES IN RESPONSE TO IMMUNE CHECKPOINT BLOCKADE IN SOLID CANCERS

¹Manoj Chelvanambi*, ¹Nathaniel Deboever, ¹Elise Nassif, ¹Ashish Damania, ¹Lili Chen, ¹Cheuk Leung, ¹Emily Keung, ¹Chia-Chin Wu, ¹Russell Witt, ¹Michael White, ¹Sarah Johnson, ¹Matthew Wong, ¹Aditya Mishra, ¹Matthew Lastrapes, ¹Neeta Somaiah, ¹Humam Kadara, ¹Sreyashi Basu, ¹James Allison, ¹Padmanee Sharma, ¹Kevin McBride, ²Wolf Fridman, ¹John Heymach, ¹Boris Sepesi, ¹Nadim Ajami, ¹Christina Roland, ¹Jennifer Wargo, ¹Tina Cascone. ¹UT MD Anderson Cancer Center, Houston, TX, United States; ²Centre de Recherche des Cordeliers, Paris, France

Background Immune checkpoint blockade (ICB) therapy has significantly improved clinical outcomes; however, a significant proportion of patients fail to develop durable responses.¹ Therefore, novel targetable biomarkers are needed. Our group has previously shown that the composition of the gut microbiome and presence of intratumoral tertiary lymphoid structures (TLS) can influence response to ICB.²⁻⁴ Here, we study three randomized phase II neoadjuvant ICB trials [melanoma (MEL; NCT02519322; n=23), non-small-cell lung cancer (NSCLC; NCT03158129; n=31)⁵ and sarcoma (SARC; NCT02301039; n=17)] to investigate the relationship and interplay between these two established determinants of response.

Methods Patients were defined as responders (R) or non-responders (NR) based on major pathologic response (MPR; MEL and NSCLC-viable \leq 10%; SARC-hyalinization \geq 30%). Transcriptional profiles of tumor specimen collected pre-ICB (MEL and SARC) and post-ICB (MEL, SARC and NSCLC) were used to score and dichotomize patients (by median) based on a TLS gene signature (*LTA*, *LTB*, *TNFSF14*, *CXCL13*, *CCL18*, *CCL19*, *CCL21*, *CD79B*, *CR2*, *PAX54A1*, *MZB1*). Paired baseline stool samples were profiled via metagenomic sequencing to characterize the composition and the molecular and metabolic function using MetaPhlAn 3.0 and HUMAnN 3.0, respectively.

Results There were 21 R overall (NSCLC n=9; MEL n=9; SARC n=3). TLS signature was significantly higher in R vs NR on-treatment with ICB ($p=0.032$; unpaired t-test). Longitudinal evaluation of transcriptional profiles showed increased expression of the TLS signature with treatment in R ($p=0.032$; paired t-test) but not in NR ($p>0.99$; paired t-test). Following patient dichotomization by TLS score, analysis of baseline microbiome profiles revealed the presence of unique TLS-associated gut microbiome signatures, including enrichment of specific taxa such as *Holdemanella* and *Lactococcus* (ANCOM-BC; $p<0.0001$). Further analysis of Kyoto Encyclopedia of Genes and Genomes (KEGG) pathways in baseline stool metagenomes suggested enhanced function of membrane transport proteins ($q=0.006$) in TLS^{high} patients and increased carbohydrate metabolism ($q=0.04$) in TLS^{low} patients.

Conclusions Our data suggest that unique gut microbiome features are associated with TLS in the context of treatment with ICB in solid cancers. Future mechanistic and translational studies will seek to validate and parlay these novel findings into microbiome-based treatments to induce TLS and/or augment the efficacy of ICB in solid tumors.

Trial Registration NCT02519322, NCT03158129, NCT02301039

REFERENCES

1. Korman AJ, SC Garrett-Thomson, and N Lonberg. The foundations of immune checkpoint blockade and the ipilimumab approval decennial. *Nat Rev Drug Discov*, 2022. **21**(7): 509–528.

2. Gopalakrishnan V, et al. Gut microbiome modulates response to anti-PD-1 immunotherapy in melanoma patients. *Science*, 2018. **359**(6371): 97–103.
3. Helmink BA, et al. B cells and tertiary lymphoid structures promote immunotherapy response. *Nature*, 2020;**577**(7791): 549–555.
4. Baruch EN, et al. Fecal microbiota transplant promotes response in immunotherapy-refractory melanoma patients. *Science*, 2021. **371**(6529): 602–609.
5. Cascone T, et al. Neoadjuvant nivolumab or nivolumab plus ipilimumab in operable non-small cell lung cancer: the phase 2 randomized NEOSTAR trial. *Nat Med*, 2021;**27**(3): 504–514.

Ethics Approval Patients were treated at the University of Texas MD Anderson Cancer Center and had tumor samples collected and analyzed under Institutional Review Board (IRB)-approved protocols (Melanoma: 2015-0041, 2012-0846, LAB00-063 and PA17-0261; NSCLC: 2016-0982; Sarcoma: 2017-0143)

<http://dx.doi.org/10.1136/jitc-2022-SITC2022.0590>

591 IMMUNOGENICITY OF DURVALUMAB: ANALYSIS OF POOLED PAN-TUMOR DATA

¹Anthony El-Khoueiry*, ²Diansong Zhou, ³Mustafa Ozguroglu, ⁴Melissa Johnson, ⁵Ghassan Abou-Alfa, ²Mallory Makowsky, ²Lee Krug, ²Ashok Gupta, ²Cecil Chen. ¹University of Southern California, Los Angeles, CA, United States; ²AstraZeneca, Waltham, MA, United States; ³Istanbul University-Cerrahpasa, Istanbul, Türkiye; ⁴Sarah Cannon Research Institute, Nashville, TN, United States; ⁵Memorial Sloan Kettering Cancer Center, New York, NY, United States

Background Durvalumab, an immune checkpoint inhibitor (ICI) targeting PD-L1, has demonstrated clinical activity with or without tremelimumab, a CTLA-4 inhibitor, in Phase 3 studies in multiple tumor types.¹⁻³ The occurrence of anti-drug antibodies (ADA) could potentially negatively impact ICI safety and efficacy.⁴ This analysis assessed the immunogenicity of durvalumab using pooled pan-tumor data.

Methods Durvalumab immunogenicity was assessed using pooled data from 18 clinical studies of 7826 participants with lung cancer (MYSTIC, ATLANTIC, NEPTUNE, Study 6, ARCTIC, PACIFIC), hepatocellular carcinoma (HIMALAYA, Study 22), bladder cancer (DANUBE, Study 10), head and neck cancer (KESTREL, HAWK, CONDOR, EAGLE, Study 11), gastric or gastroesophageal junction adenocarcinoma (Study 21) or advanced solid tumors (Study 1108, Japan Study 2). ADA and neutralizing ADA (nAb) to durvalumab were detected using validated solution-phase bridging electrochemiluminescence immunoassays. Impact of durvalumab ADA on safety was assessed using pan-tumor data from the pool of 18 studies. Impact of ADA on durvalumab pharmacokinetics was assessed using a pooled dataset from Study 1108, PACIFIC, ATLANTIC, CASPIAN, POSEIDON, HIMALAYA, and Study 22. Due to differences in cancer settings of the studies, the impact of durvalumab ADA on efficacy was not assessed.

Results The proportion of durvalumab ADA-positive participants at any visit (ADA prevalence) was 6.2% with durvalumab monotherapy (D), 6.8% with T75+D, and 7.3% with T300+D (STRIDE) (table 1). The proportion of treatment-emergent ADA-positive participants (ADA incidence) was low and similar across data pools: 2.7% with D, 3.4% with T75+D, and 2.8% with T300+D (table 1). Median ADA titers were ≤16 across all ADA categories in all pools (table 1). The proportion of transiently ADA-positive participants out of those with ADA prevalence was 32/191 with D, 22/146 with T75+D, and 3/26 with T300+D. The proportion of participants who tested positive for durvalumab nAb at any visit was 0.5% with D, 0.6% with T75+D, and 1.4% with T300+D (table 1). Incidence of infusion-related reactions was low in ADA-positive participants across treatment regimens (1% with D, and 0% with T75+D and T300+D); there was no marked impact of durvalumab ADA presence on categorical AE data (table 2). Durvalumab ADA presence did not have a clinically meaningful impact on durvalumab exposure metrics.

Conclusions Although incidences of ADA vary greatly among ICI⁴, analysis of this large, multi-study, pooled pan-tumor dataset demonstrates that durvalumab has a low-risk immunogenicity profile as monotherapy or in combination with tremelimumab. Immunogenicity of durvalumab appeared to have no marked impact on safety or exposure.

Acknowledgements Medical writing support, under the direction of the authors, was provided by Claire Tinderholm, PhD, of CMC Connect, McCann Health Medical Communications, with funding from AstraZeneca, in accordance with Good Publications Practice (GPP3) guidelines.

Trial Registration MYSTIC: NCT02453282

ATLANTIC: NCT02087423

NEPTUNE: NCT02542293

Study 6: NCT02000947

ARCTIC: NCT02352948

PACIFIC: NCT02125461

HIMALAYA: NCT03298451

Study 22: NCT02519348

DANUBE: NCT02516241

Study 10: NCT02261220

KESTREL: NCT02551159

HAWK: NCT02207530

CONDOR: NCT02319044

EAGLE: NCT02369874

Study 11: NCT02262741

Study 21: NCT02340975

Study 1108: NCT01693562

Japan Study 2: NCT01938612

CASPIAN: NCT03043872

POSEIDON: NCT03164616

REFERENCES

1. Abou-Alfa GK, Lau G, Kudo M, *et al.* Tremelimumab plus durvalumab in unresectable hepatocellular carcinoma. *NEJM Evid.* 2022. Doi: <https://doi.org/10.1056/EVIDo2100070>.
2. Oh D-Y, He AR, Qin S, *et al.* Durvalumab plus gemcitabine and cisplatin in advanced biliary tract cancer. *NEJM Evid.* 2022. Doi: <https://doi.org/10.1056/EVIDo2200015>.
3. Goldman JW, Dvorkin M, Chen Y, *et al.* Durvalumab, with or without tremelimumab, plus platinum-etoposide versus platinum-etoposide alone in first-line treatment of extensive-stage small-cell lung cancer (CASPIAN): updated results from a randomised, controlled, open-label, phase 3 trial. *Lancet Oncol.* 2021;22:51-65.
4. Enrico D, Paci A, Chaput N, Karamouza E, Besse B. Antidrug antibodies against immune checkpoint blockers: impairment of drug efficacy or indication of immune activation? *Clin Cancer Res.* 2020;26:787-792.

Ethics Approval The trial protocol was approved by local institutional review boards.

Abstract 591 Table 1 Summary of ADA responses to durvalumab

Table 1. Summary of ADA responses to durvalumab

Parameter	D pan-tumor pool ¹ (N=4045)	T75+D pan-tumor pool ¹ (N=3319)	T300+D HCC pool ² (N=462)
ADA-evaluable participants, n (%)	3069 (75.9)	2152 (64.8)	354 (76.6)
ADA positive at any visit (ADA prevalence), n (% of ADA evaluable)	191 (6.2)	146 (6.8)	26 (7.3)
Median of maximum titer (range)	4.0 (1-1024)	2.0 (1-128)	2.0 (1-16)
Treatment-emergent ADA positive (ADA incidence), n (% of ADA evaluable)	84 (2.7)	74 (3.4)	10 (2.8)
Median of maximum titer (range)	4.0 (1-1024)	4.0 (1-128)	6.0 (1-16)
Transiently ADA positive, n (% of ADA evaluable)	32 (1.0)	22 (1.0)	3 (0.8)
Median of maximum titer (range)	4.0 (1-128)	4.0 (1-32)	1.0 (1-16)
nAb positive at any visit, n (% of ADA evaluable)	16 (0.5)	12 (0.6)	5 (1.4)
Median of maximum titer (range)	16.0 (1-1024)	8.0 (2-128)	4.0 (1-16)

ADA prevalence includes pre-treatment ADA present at baseline. Transient ADA positivity was defined as ≥1 post-baseline ADA-positive measurement and if ≤2, less than 16 weeks between the first and last not ADA positive at the last assessment.

¹Participants with various tumor types from studies (HIMALAYA, Study 22, MYSTIC, ATLANTIC, Study 1108, ARCTIC, PACIFIC, HAWK, CONDOR, EAGLE, Japan Study 2, DANUBE, KESTREL) who have received at least one dose of durvalumab monotherapy at 10 mg/kg Q2W (or equivalent) or 20 mg/kg Q2W (or equivalent) for any line of therapy.

²Participants with various tumor types from studies (HIMALAYA, Study 22, MYSTIC, NEPTUNE, Study 6, ARCTIC, CONDOR, EAGLE, Study 10, Japan Study 2, Study 11, Study 21, DANUBE, KESTREL) who have received at least one dose of durvalumab at 20 mg/kg Q2W (or equivalent) in combination with tremelimumab 1 mg/kg Q2W (or equivalent) for any line of therapy.

³Participants with HCC from HIMALAYA and Study 22 who have received at least one dose of durvalumab at 1500 mg Q2W (or equivalent) in combination with tremelimumab 300 mg x 1 dose (or equivalent).

ADA, anti-drug antibody; D, durvalumab; HCC, hepatocellular carcinoma; nAb, neutralizing antibody; T75+D, tremelimumab 1 mg/kg Q2W + durvalumab; T300+D (Single Tremelimumab Regular Interval Durvalumab; STRIDE), tremelimumab 300 mg x 1 dose + durvalumab, Q2W, every 3 weeks.

Abstracts

Abstract 591 Table 2 Summary of safety data by ADA status

Table 2. Summary of safety data by ADA status

ADA category, n (%)	D pan-tumor pool* (N=4045)		T75+D pan-tumor pool [†] (N=3319)		T300+D HCC pool [‡] (N=462)	
	ADA+	ADA-	ADA+	ADA-	ADA+	ADA-
ADA-evaluable participants	191	2878	146	2006	26	328
Any AE	184 (96.3)	2762 (96.0)	138 (94.5)	1944 (96.9)	25 (96.2)	322 (98.2)
Any durvalumab-related AE	122 (63.9)	1806 (62.8)	102 (69.9)	1506 (75.1)	19 (73.1)	259 (79.0)
Grade 3/4 AE	97 (50.8)	1166 (40.5)	76 (52.1)	1067 (53.2)	12 (46.2)	166 (50.6)
Grade 3/4 durvalumab-related AE	29 (15.2)	339 (11.8)	34 (23.3)	473 (23.6)	6 (23.1)	85 (25.9)
Serious AE	81 (42.4)	909 (31.6)	59 (40.4)	855 (42.6)	9 (34.6)	123 (37.5)
Serious durvalumab-related AE	20 (10.5)	178 (6.2)	23 (15.8)	362 (18.0)	1 (3.8)	50 (15.2)
Any AESI/AEPI	129 (67.5)	1846 (64.1)	106 (72.6)	1528 (76.2)	21 (80.8)	283 (86.3)
Any durvalumab-related AESI/AEPI	93 (48.7)	1219 (42.4)	82 (56.2)	1245 (62.1)	17 (65.4)	235 (71.6)
AE leading to durvalumab discontinuation	20 (10.5)	222 (7.7)	23 (15.8)	286 (14.3)	2 (7.7)	31 (9.5)
Durvalumab-related AE leading to durvalumab discontinuation	14 (7.3)	109 (3.8)	14 (9.6)	181 (9.0)	1 (3.8)	21 (6.4)
AE leading to death	7 (3.7)	106 (3.7)	4 (2.7)	90 (4.5)	2 (7.7)	10 (3.0)
Durvalumab-related AE leading to death	0	10 (0.3)	0	10 (0.5)	0	3 (0.9)
Infusion-related reaction	2 (1.0)	4 (0.1)	0	2 (<0.1)	0	1 (0.3)

*Participants with various tumor types from studies (HIMALAYA, Study 22, MYSTIC, ATLANTIC, Study 1108, ARCTIC, PACIFIC, HAWK, CONDOR, EAGLE, Japan Study 2, DANUBE, KESTREL) who have received at least one dose of durvalumab monotherapy at 10 mg/kg Q2W (or equivalent) or 20 mg/kg Q4W (or equivalent) for any line of therapy.
[†]Participants with various tumor types from studies (HIMALAYA, Study 22, MYSTIC, NEPTUNE, Study 6, ARCTIC, CONDOR, EAGLE, Study 10, Japan Study 2, Study 11, Study 21, DANUBE, KESTREL) who have received at least one dose of durvalumab at 20 mg/kg Q4W (or equivalent) in combination with tremelimumab 1 mg/kg Q3W (or equivalent) for any line of therapy.
[‡]Participants with HCC from HIMALAYA and Study 22 who have received at least one dose of durvalumab at 1500 mg Q4W (or equivalent) in combination with tremelimumab 300 mg x 1 dose (or equivalent).
 ADA, anti-drug antibody; AE, adverse events; AEPI, adverse events of potential interest; AESI, adverse event of special interest; D, durvalumab; HCC, hepatocellular carcinoma; T75+D, tremelimumab 1 mg/kg Q3W + durvalumab; T300+D (Single Tremelimumab Regular Interval Durvalumab, STRIDE), tremelimumab 300 mg x 1 dose + durvalumab, Q3W, every X weeks.

<http://dx.doi.org/10.1136/jitc-2022-SITC2022.0591>

592

PHASE 1/2A STUDY OF THE NOVEL NONFUCOSYLATED ANTI-CTLA-4 MONOCLONAL ANTIBODY BMS-986218 ± NIVOLUMAB IN ADVANCED SOLID TUMORS: PART 1 RESULTS

¹Claire Friedman*, ²Richard Carvajal, ³Diwakar Davar, ⁴Eduardo Castanon, ⁵Paolo Ascierto, ⁶Emiliano Calvo, ⁷Mark O'Hara, ⁸Steven Powell, ⁹Ronnie Shapira-Frommer, ¹⁰Elena Garralda, ¹¹Daniel John Renouf, ¹²Ruth Perets, ¹³Mona Yunan, ¹³Palanikumar Ravindran, ¹³Amy Hammell, ¹³Shaun O'Brien, ¹³Ke Xu, ¹³Nicholas Wilson, ¹³Amy Jhatakia, ¹³Anandaroop Mukhopadhyay, ¹⁴Martin Gutierrez. ¹Memorial Sloan Kettering Cancer Center, New York, NY, United States; ²Columbia University Irving Medical Center, New York, NY, United States; ³University of Pittsburgh Medical Center, Pittsburgh, PA, United States; ⁴Clinica Universidad de Navarra, Pamplona, Spain; ⁵Istituto Nazionale Tumori IRCCS Fondazione G. Pascale, Milan, Italy; ⁶START Madrid-CIOCC. Centro Integral Oncológico Clara Campal, Madrid, Spain; ⁷University of Pennsylvania, Philadelphia, PA, United States; ⁸Sanford Cancer Center, Sioux Falls, SD, United States; ⁹Sheba Medical Center, Ramat Gan, Israel; ¹⁰Vall d'Hebron University Hospital, Barcelona, Spain; ¹¹BC Cancer, The University of British Columbia, Vancouver, Canada; ¹²Rambam Health Care Campus, Technion – Israel Institute of Technology, Haifa, Israel; ¹³Bristol Myers Squibb, Princeton, NJ, United States; ¹⁴John Theurer Cancer Center, Hackensack University Medical Center, Hackensack, NJ, United States

Background BMS-986218 is a nonfucosylated human IgG1 anti-cytotoxic T-lymphocyte antigen (CTLA)-4 monoclonal antibody with optimized CD16 FcγR binding that enhances T-cell priming and mitigates T-regulatory cell-mediated suppression in the tumor microenvironment. In preclinical models, BMS-986218 increased the proportion of antigen-specific CD8 + effector T cells vs ipilimumab in peripheral blood.¹ We present safety, efficacy, and pharmacodynamic data from the dose-escalation part of the first-in-human study of BMS-986218 ± nivolumab in patients with advanced solid tumors (NCT03110107).

Methods Patients with advanced solid tumors, disease progression on ≥ 2 lines of therapy (≥ 1 line for patients with melanoma), and Eastern Cooperative Oncology Group performance status 0–1 were included. Patients received BMS-986218 as monotherapy (2–200 mg Q4W or 20–50 mg Q2W) or as combination therapy (BMS-986218 20–70 mg Q4W plus nivolumab 480 mg Q4W). The primary endpoint was safety and tolerability. Secondary endpoints included preliminary efficacy and characterization of BMS-986218 ± nivolumab pharmacokinetics and immunogenicity.

Results In total, 155 patients were treated on dose escalation; 107 with monotherapy and 48 with combination (table 1). Any-grade and grade 3/4 treatment-related adverse events (TRAEs) were reported in 58% and 18% of monotherapy patients, respectively. The most common grade 3/4 TRAE was diarrhea (5%). Any-grade and grade 3/4 TRAEs were reported in 60% and 27% of combination patients, respectively. The most common 3/4 TRAEs were colitis (6%) and increased amylase (6%). TRAEs leading to treatment discontinuation were reported in 11% of monotherapy patients and 15% of combination patients. A grade 5 TRAE of pneumonitis was reported in the monotherapy group at the 7-mg Q4W dose level. Partial responses with durations of 1.9–10.3 months were observed with monotherapy and combination therapy in patients with microsatellite-stable colorectal, pancreatic, gastric, and breast cancer. Analysis of peripheral cytokine levels (interferon-γ, CXCL9, and CXCL10) showed increases with increasing BMS-986218 dose in the monotherapy and combination groups (figure 1). Additional preclinical and clinical results will be presented.

Conclusions BMS-986218 demonstrated a tolerable safety profile and preliminary antitumor activity as monotherapy and in combination with nivolumab across various tumor types,

including tumors with high unmet need or that are traditionally immune checkpoint inhibitor-insensitive. These results support further investigation of nonfucosylated anti-CTLA-4 therapies. The dose expansion part of the BMS-986218 ± nivolumab study and a phase 1/2 study evaluating anti-CTLA-4 nonfucosylated probody (BMS-986288; NCT03994601) ± nivolumab are ongoing.

Acknowledgements Claire Friedman is supported in part by a Cancer Center Support Grant of the NIH/NCI (Grant No. P30CA008748). Editorial support was provided by Rowena Fung, MPhil, of Spark Medica Inc.

Trial Registration Clinicaltrials.gov NCT03110107

REFERENCES

- Loffredo J, et al. Non-fucosylated anti-CTLA-4 antibody enhances vaccine-induced T cell responses in a non-human primate pharmacodynamic vaccine model. *J Immunother Cancer*. 2017;5(Suppl 2):Abstract P55.

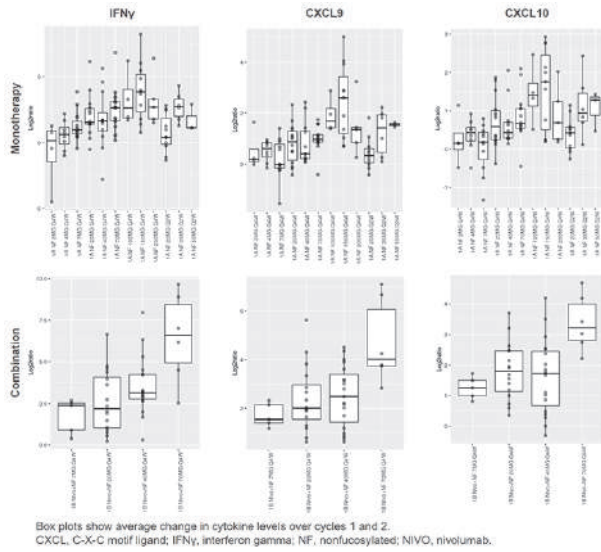
Ethics Approval The trial protocol was approved by the institutional review boards or independent ethics committees of each study site and was conducted according to Good Clinical Practice guidelines, per the International Conference on Harmonisation. Patients provided written informed consent based on the principles of the Declaration of Helsinki.

Abstract 592 Table 1 Patient demographics and characteristics

Parameter, n (%)	Monotherapy (N = 107)	Combination therapy (N = 48)
Age, median years (range)	61.0 (24–85)	61.5 (39–81)
Sex		
Male	54 (50)	26 (54)
Female	53 (50)	22 (46)
ECOG PS		
0	38 (36)	16 (33)
1	69 (64)	32 (67)
Tumor types		
CRC	24 (22)	16 (33)
Pancreatic cancer	16 (15)	16 (33)
Lung cancer	6 (6)	3 (6)
Breast cancer	5 (5)	0 (0)
Melanoma	5 (5)	0 (0)
Gastric cancer	4 (4)	5 (10)
Other ^a	46 (43)	7 (15)
Not reported	1 (1)	1 (2)
Prior systemic therapy		
Any	101 (94)	45 (94)
1	28 (26)	16 (33)
2	9 (8)	9 (19)
3	21 (20)	11 (23)
≥ 4	43 (40)	9 (19)

^aIncludes bladder, non-small cell lung, ovarian, prostate, and urothelial cancers, pancreatic adenocarcinoma, renal cell carcinoma, squamous cell carcinoma of the head and neck, and other.
CRC, colorectal cancer; ECOG PS, Eastern Cooperative Oncology Group performance status.

Abstracts



Abstract 592 Figure 1 Change in peripheral interferon- γ , CXCL9, and CXCL10 levels by BMS 986218 dose in the monotherapy and combination groups.

<http://dx.doi.org/10.1136/jitc-2022-SITC2022.0592>

594

DOSE ESCALATION OF NEXT GENERATION ANTI-CTLA-4 ANTIBODY ONC-392 IN COMBINATION WITH FIXED DOSE OF PEMBROLIZUMAB IN PATIENTS WITH ADVANCED SOLID TUMORS

¹Siwen Hu-Lieskovan*, ²Kai He, ³Mei Tang, ⁴Dan Chen, ⁴Yang Liu, ⁴Pan Zheng, ⁵Tianhong Li. ¹University of Utah Huntsman Cancer Institute, Salt Lake City, UT, United States; ²The Ohio State University Cancer Center, Columbus, OH, United States; ³Greater Baltimore Medical Center, Baltimore, MD, United States; ⁴OncoC4, Inc., Rockville, MD, United States; ⁵University of California at Davis, Sacramento, CA, United States

Background Combination of CTLA-4 and PD-1/PD-L1 targeting antibodies are effective cancer immunotherapy with great potential, but the high risk of severe toxicity limits clinical development. Our preclinical studies suggest that acid pH-sensitive anti-CTLA-4 antibodies that preserve CTLA-4 recycling by avoiding lysosomal degradation are more effective for immunotherapy while largely devoid of immunotherapy-related adverse events (irAE) when used in combination with anti-PD-1 antibodies. We previously showed the recommended phase II dose (RP2D) of ONC-392 monotherapy is 10mg/kg IV Q3W.¹ In the current study, we evaluated the safety and tolerability of ONC-392 in combination with pembrolizumab.

Methods ONC-392-001 (NCT04140526) Part B is a dose finding study of ONC 392 at 3 mg/kg (cohort 1) or 6 mg/kg (cohort 2) in combination with a fixed dose of pembrolizumab 200 mg, IV, Q3W. We enrolled patients with advanced/metastatic solid tumors whose disease had progressed on standard of care (SOC) therapies and pembrolizumab was approved as SOC. The primary endpoints are safety, tolerability and RP2D of ONC-392 in combination with pembrolizumab (RP2D-C).

Results Cohort 1 enrolled 7 patients and cohort 2 enrolled 6 patients, including 4 NSCLC, 5 melanoma, 1 each with cervical, TNBC, HCC and CuSCC. Patient characteristics are listed in table 1. Eleven patients had prior anti-PD-1/PD-L1 and 5 melanoma patients had prior ipilimumab. The mean cycles of treatment are 5.7 cycles (1-13) in 5.2 months and 4.5 cycles (1-9) in 4.1 months in cohort 1 and 2, respectively. None of the 13 pts experienced dose limiting toxicity (DLT) in the DLT period. Treatment related AEs (TRAEs) were observed in 11 (85%) patients without Grade 4 or 5 TRAEs. Grade 3 TRAEs were observed in 5 pts (38.5%) (3/7 in cohort 1 and 2/6 in cohort 2): infusion reaction (2) and immune-mediated colitis (3). Three patients (23%) had Gr 3 irAEs in the form of immune colitis or colitis. The RP2D-C is determined to be 6.0 mg/kg ONC-392+ 200 mg of pembrolizumab Q3W. Two confirmed PR (TNBC and cervical cancer, ORR=29%, DOR>6 months) and 4 SD in cohort 1, and 3 SD and 1 PD in cohort 2 were observed (figure 1).

Conclusions ONC-392 combination with pembrolizumab is safe and clinically active. The rate of irAE is low relative to drugs of the same class. These results support the feasibility to significantly increase drug exposure for full immunotherapeutic potential of anti-CTLA-4 and anti-PD-1 combination therapy.

Acknowledgements This study is sponsored by OncoC4, Inc with the support of NCI SBIR grant R44CA250824.

Trial Registration NCT04140526.

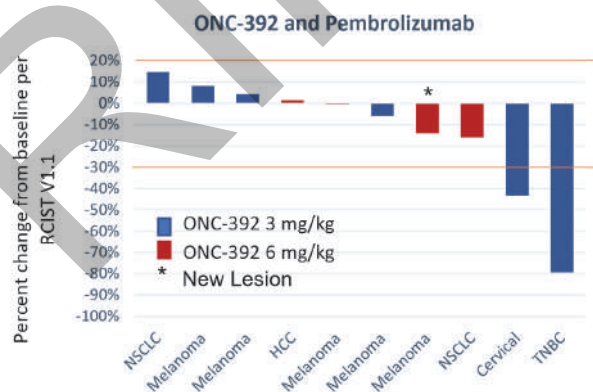
REFERENCE

- Li T, Tang M, Kelly K, et al. First-in-human study of the first acid pH-sensitive and recycling CTLA-4 antibody that preserves the immune tolerance checkpoint to avoid immunotherapy-related adverse events in cancer patients. *J Immunother Cancer*. 2021; **9** (5 Suppl 2): A998.

Ethics Approval This study obtained ethic approval from WCG IRB with study #20193108. All participants gave informed consent before taking part of the study.

Abstract 594 Table 1 Patient characteristics and safety profile in Part B of ONC-392-001 study. Patient characteristics and safety profile

	ONC-392 + Pembrolizumab		ONC-392 + Pembrolizumab		Total
	3mg/kg +	6mg/kg +	3mg/kg +	6mg/kg +	
N	7	6	7	6	13
Gender (F/M)	3F, 4M	3F, 3M			
White/others	7 White	6 White			
Median age (range)	62 (48-83)	66 (59-72)			
ECOG score:					
0	2	4			
1	5	2			
Prior lines of systemic treatment, Median (range)	4 (1-6)	3 (1-14)			
Lines	4 (1-6)	3 (1-14)			
Prior PD-1/L1	6	6			
Prior CTLA-4	2	3			
			3mg/kg +	6mg/kg +	
N			7	6	13
Tx cycles, mean (range)			5.7 (1-13)	4.5 (1-9)	1-13 (ongoing)
Tx duration in Months, mean (range)			5.2 (1-10)	4.1 (1-7)	1-13 (ongoing)
Any TEAE			7 (100%)	6 (100%)	13 (100%)
Gr ≥ 3			5 (71%)	3 (50%)	8 (61%)
Leading to study drug d/c			2 (29%)	0	2 (15%)
Any TRAE			6 (86%)	5 (83%)	11 (85%)
Gr = 3			3 (43%)	2 (33%)	5 (38%)
Leading to study drug d/c			1 (14%)	0	1 (8%)
Gr = 3 irAE			2 (29%)	1 (17%)	3 (23%)
DLT			0	0	0



Abstract 594 Figure 1 The best overall response in Part B of ONC-392-001

<http://dx.doi.org/10.1136/jitc-2022-SITC2022.0594>

Abstracts

595

FLT3L-PRIMED *IN SITU* VACCINATION AND PEMBROLIZUMAB INDUCE SYSTEMIC TUMOR REGRESSIONS OF BULKY TUMORS IN PATIENTS WITH LYMPHOMAS AND ER/PR+ BREAST CANCER

¹Thomas Marron*, ¹Julie Fasano, ¹Deborah Doroshov, ¹Dana Ostrowski, ¹Joan Sorich, ¹Martine Van-Voorhuysen, ¹Jennifer Coffey, ¹Erin Moshier, ²Andres Salazar, ³Michael Yellin, ¹Marshall Posner, ¹Joseph Sparano, ¹Jonah Shulman, ¹Paula Klein, ¹Hanna Irie, ¹Seunghye Kim-Schulze, ¹Sacha Gnjatic, ¹Miriam Merad, ¹Joshua Brody, ¹Haley Labo. ¹Icahn School of Medicine at Mount Sinai, New York, NY, United States; ²Oncovir, Washington DC, United States; ³Celldex, Hampton, NJ, United States

Background Most patients fail to respond to checkpoint blockade, partly due to a lack of preexisting anti-tumor immunity. Cancer vaccines aim to induce *de novo* anti-tumor immune responses against tumor neoantigens. We previously described an *in situ* vaccine approach combining intratumoral (IT) Flt3L, low dose irradiation (XRT), and IT polyICLC to, respectively, mobilize, antigen-load, and activate IT DC1 in patients with advanced stage indolent non-Hodgkin’s lymphoma (iNHL), yielding partial and complete remissions lasting months to years. Pre-clinical modeling revealed this combination induced tumoral PD-L1 expression, potentially explaining resistance, and addition of PD-1 blockade to the vaccine improved cure rates.¹

Methods In this Phase 1/2 trial, patients with iNHL, metastatic breast cancer (MBC) or head and neck squamous cell carcinoma (HNSCC) received local XRT on Days 1-2, IT Flt3L to the same tumor for 9 days, followed by 8 IT injections of poly-ICLC over 6 weeks. On Day 23 patients received their first of 8 doses of intravenous (IV) pembrolizumab q3wk (figure 1).

Phase 1 enrolled 6 patients to assess safety. In Phase 2, tumor-specific cohorts are enrolling, each with a Simon’s Two-Stage design (figure 2). Here, we report interim results from the first 10 patients.

Results Between April 2019 and July 2022, 10 patients were enrolled; 6 with MBC, 3 with iNHL and one patient with HNSCC have completed their first disease response assessment. All patients experienced TRAEs, mostly low-grade injection-site reactions and flu-like symptoms related to poly-ICLC. Two patients experienced Grade 3 TRAE, one experienced self-resolving grade 3 fever after poly-ICLC, another experienced grade 3 pembrolizumab-related colitis. Of ten evaluable patients, 1 patient had a CR, 2 achieved partial response, one had SD, and six had PD. One patient with ER/PR+ breast cancer had received 12 prior lines of therapy with non-response to two prior chemotherapies, achieved PR—with all residual hypermetabolism likely related to scar tissue—without evidence of new or recurrent disease at 6 months, including regression of (distant) bulky left adrenal metastasis (figure 3) and other metastatic sites.

Conclusions *In situ* vaccination with Flt3L, XRT, poly-ICLC and pembrolizumab is well tolerated, with early signs of efficacy in patients with relapsed/refractory NHL and MBC, warranting expansion of this approach. Analysis of biopsies and blood from patients to define determinants of response to this *in situ* vaccine approach is ongoing.

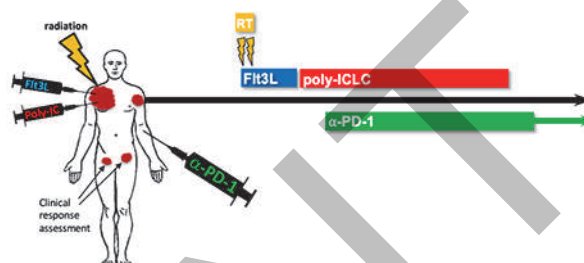
Trial Registration NCT03789097

REFERENCE

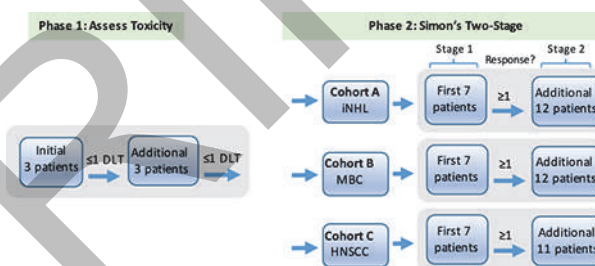
1. Hammerich, L. *et al.* Systemic clinical tumor regressions and potentiation of PD1 blockade with *in situ* vaccination. *Nat Med* 2019;**25**:814–824, doi:10.1038/s41591-019-0410-x.

Ethics Approval This trial is approved by the Mount Sinai Institutional Review Board (Study ID #: GCO# 19-0477/HS18-01154), all participants provided informed consent before taking part in this trial.

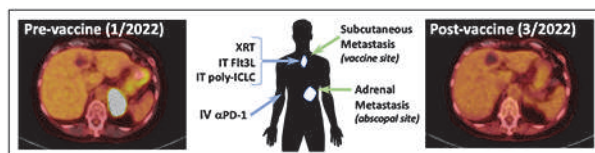
Consent All participants provided informed consent before taking part in this trial, and provided consent for sharing of de-identified information regarding their clinical responses to therapy.



Abstract 595 Figure 1 Trial Schema



Abstract 595 Figure 2 Statistical design



Abstract 595 Figure 3 Patient with ER/PR+ MBC demonstrating resolution of superficial suprasternal lesion (vaccine site), as well as other superficial satellite lesions, and a large left adrenal metastasis (abscopal site). Patient in near CR at present.

<http://dx.doi.org/10.1136/jitc-2022-SITC2022.0595>

596

RESULTS FROM A PHASE 1 STUDY OF CDX-1140, A FULLY HUMAN ANTI-CD40 AGONIST MONOCLONAL ANTIBODY (MAB), IN COMBINATION WITH PEMBROLIZUMAB

¹Rachel Sanborn*, ²Nashat Gabrail, ³Benedito Carneiro, ⁴Mark O'Hara, ⁵Rodolfo Bordoni, ⁶Michael Gordon, ⁷Danny Khalil, ⁸Ralph Hauke, ⁹Cherie Taglienti, ⁹Mark Rogalski, ⁹Rachel Styles, ⁹Diego Alvarado, ⁹Deena Maurer, ⁹Linda Crew, ⁹Tibor Keler, ⁹Michael Yellin. ¹Earle A. Chiles Research Institute, Providence Cancer Institute, Portland, OR, United States; ²Gabrail Cancer Center, Canton, OH, United States; ³Legorreta Cancer Center at Brown University, Lifespan Cancer Institute, Providence, RI, United States; ⁴Hospital of the University of Pennsylvania, Philadelphia, PA, United States; ⁵Georgia Cancer Specialists, Marietta, GA, United States; ⁶HonorHealth Research Institute, Scottsdale, AZ, United States; ⁷Memorial Sloan Kettering Cancer Center, New York, NY, United States; ⁸Nebraska Cancer Specialists, Omaha, NE, United States; ⁹Celldex Therapeutics, Inc., Hampton, NJ, United States

Background CD40 agonist mAbs can enhance the efficacy of checkpoint blockade in preclinical models and can functionally revive PD-1^{hi} exhausted T cells. This Phase 1 study examined safety, clinical activity, and pharmacodynamics of CDX-1140 as monotherapy or in combination with other agents (NCT03329950). We now report the completed results from Part 3 of the study, combination with anti-PD-1 mAb pembrolizumab.

Methods Patients with advanced solid tumors and documented disease progression on a single prior anti-PD-1/L1 based regimen were enrolled. In dose-escalation (DE) cohorts, CDX-1140 was administered at 0.72 mg/kg and 1.5 mg/kg. Expansion cohorts (EX) in non-small cell lung cancer (NSCLC) and squamous cell carcinoma of head and neck (SCCHN) evaluated CDX-1140 1.5 mg/kg. Treatment was q3w co-administered with pembrolizumab 200 mg in both DE and EX.

Results 10 patients were treated in DE (renal cell carcinoma n=2, SSCHN n=2, n=1 for NSCLC, endometrial cancer, MSI^{hi}-CRC, ocular melanoma, esophageal adenocarcinoma, MSI^{hi}-cholangiocarcinoma) and 15 patients treated in EX; NSCLC (n=9) and SCCHN (n=6). The median number of prior regimens was 3. Treatment was generally well tolerated, with most treatment-related AEs (TRAE) being grade 1 or 2. The most frequent TRAE at the CDX-1140 1.5 mg/kg dose level (n=21) were arthralgia (62%), fatigue (62%), nausea (48%), diarrhea (48%), vomiting (43%), myalgia (43%), fever (38%), chills (38%), AST increase (38%), bilirubin increase (24%), ALT increase (19%), and cytokine release syndrome (CRS) (19%). Across Part 3, there was 1 complete response (CR) in a patient with oropharyngeal cancer (HPV⁺ and PD-L1 status unknown); 9 additional patients had stable disease (SD), including 4 with SCCHN and 4 with NSCLC. The patient achieving CR received 4 prior regimens (including chemotherapy, pembrolizumab, and cetuximab), discontinued study therapy after 2 doses due to arthralgia (grade 3) and CRS (grade 2), and initially demonstrated a partial response that evolved into CR, with the response ongoing at 12+ months without further anti-tumor treatment. Of the 4 SCCHN with SD, 2 had target lesions shrinkage (-15% and -18%) and 2 had no change. One NSCLC patient has SD for 10+ months with a nadir in target lesions of -15%. Part 3 biomarker data will be presented.

Conclusions CDX-1140 in combination with pembrolizumab had an acceptable safety profile. Evidence of clinical benefit was most evident in patients with SCCHN, all of whom had progressive disease on prior anti-PD-1/L1 based therapies. Further studies are warranted.

Trial Registration NCT03329950

Ethics Approval The study was reviewed and approved by the following institutional review boards:

Providence Health & Services Institutional Review Board for Earle A. Chiles Research Institute/Providence Cancer Institute; approval number/ID: PHS IRB #2017000532

WCG-IRB for Gabrail Cancer Center, Georgia Cancer Specialists, HonorHealth Research Institute, and Nebraska Cancer Specialists; approval number/ID: 20172645

Rhode Island Hospital IkrB#1 for Legorreta Cancer Center at Brown University/Rhode Island Hospital/Lifespan Cancer Center; approval number/ID: LS-P-Camp

Office of Regulatory Affairs of the University of Pennsylvania for Hospital of the University of Pennsylvania; approval number/ID: UPCC 18917

Memorial Sloan Kettering Cancer Center Institutional Review Board/Privacy Board; approval number/ID: 18-225

Participants gave informed consent before taking part in the study.

<http://dx.doi.org/10.1136/jitc-2022-SITC2022.0596>

PRELIMINARY SAFETY, EFFICACY AND PHARMACOKINETIC RESULTS OF THE EP4 ANTAGONIST INV-1120 FROM A FIRST-IN-HUMAN STUDY IN SUBJECTS WITH ADVANCED SOLID TUMORS

<http://dx.doi.org/10.1136/jitc-2022-SITC2022.0597>

¹John Sarantopoulos, ²Amita Patnaik, ³Zhaopie Zeng, ³Johannes Nippgen, ³Yongkui Sun, ³Yi Zhu*. ¹Mays Cancer Center, San Antonio, TX, United States; ²South Texas Accelerated Research Therape, San Antonio, TX, United States; ³Shenzhen Ionova Life Science Co., Ltd, Shenzhen, China

Background INV-1120 is a highly selective, small-molecule antagonist of the E-type prostanoid receptor 4 (EP4) for prostaglandin E2 (PGE2), an immunosuppressive mediator of tumor immune microenvironment. Objectives of this first in human study were to assess safety, tolerability, pharmacokinetics (PK), pharmacodynamics (PD), maximum tolerated dose (MTD) and recommended phase 2 dose of INV-1120.

Methods Dose-escalation was based on the traditional “3+3” dose-escalation design in sequential escalating dose cohorts (15, 30, 60, 100, 150, 200, 250, 300 mg). Dose limiting toxicity (DLT) evaluation period was 28 days. Efficacy evaluation was performed every 8 weeks by RECIST 1.1. Blood samples were collected for pharmacokinetic characterization of the treatment.

Results Twenty-four patients were enrolled and treated with single-agent INV-1120 in 6 dose cohorts (15 mg, n=3; 30 mg, n=3; 60 mg, n=6; 100 mg, n=3; 150mg, n=3; 200 mg, n=6). The median age is 58.0 with the range from 20 to 80. 10 patients are male and 14 are female. Tumor types include colorectal cancer (8), lung cancer (4), parotid adenocarcinoma (2), sarcoma (2) and others (8). 7 patients had received prior CPI therapy.

There were two DLTs, one at 60 mg (grade 2 duodenal ulcer) and one at 200 mg (grade 2 duodenitis).

At least 1 TEAE was reported in 24 patients (100%). The most common TEAEs (all grades) were diarrhea (6 subjects, 25.0%), nausea (6, 25.0%), anemia (6, 25.0%), and fatigue (5, 20.8%). Drug-related TEAEs occurred in 13 patients (54.2%) and grade ≥ 3 treatment related TEAEs occurred in one patient (4.2%). Five patients (20.8%) were discontinued or interrupted for treatment due to TEAEs, and two of them due to TEAEs that were unrelated to study drug treatment.

Twenty-one patients were evaluable for efficacy as of the cut-off date of May 30, 2022. Stable disease was observed in 9 of 21(42.9%) patients. Among the 9 patients with stable disease, 5 had treatment duration ≥ 18 weeks.

INV-1120 was rapidly absorbed across all doses, and time to maximum drug concentration was observed at ~ 2 hours postdose. The exposure of INV-1120 appeared to increase with dose from 15 mg to 100/150 mg and plateaued thereafter. There is no PD markers data available currently.

Conclusions Single agent INV-1120 was generally well tolerated and showed prolonged stable disease. Preclinical data showing the efficacy synergy when INV-1120 combining with anti PD-1 support phase Ib protocol amendment about INV-1120 in combination with anti PD-1, and the dose escalation of the combination study will explore INV 1120 at 60, 100 and 150mg QD.

Trial Registration Clinical trial registry number: NCT04443088.

Ethics Approval

Ethics statement: This study was approved by IntegReview IRB.

598

**FIRST IN HUMAN STUDY OF S-488210/S-488211, A
CANCER PEPTIDE VACCINE, IN PATIENTS WITH
ADVANCED SOLID TUMOURS**

¹Mark Linch*, ¹Paramvir Sawhney, ¹Jasmin Waterhouse, ¹Kayani Mahaz, ¹Anuradha Jayaram, ¹Dionysis Papadatos-Pastos, ²Takahiro Hasegawa, ²Ide Nobuyuki, ²Takayuki Kanazawa, ²Tomohiko Harada. ¹University College London Hospital, London, UK; ²Shionogi & Co., Ltd, Osaka, Japan

Background S-488210/S-488211 is a cancer peptide vaccine composed of 5 human leukocyte antigen (HLA)-A*02:01-restricted epitope peptides derived from 5 cancer-testis antigens: DEPDC1, MPHOSPH1, URLC10, CDCA1 and KOC1. These antigens were shown to be highly and differentially expressed in a range of solid tumours. A vaccine composed of HLA-A*24:02 restricted epitopes of the same antigens previously demonstrated safety and immunogenicity. This study aimed to evaluate the safety and immunological responses of S-488210/S-488211 in patients with HLA-A*02:01, the most prevalent HLA subtype in Europe and the US.

Methods An open-label, single centre, first-in-human phase I study (NCT04316689) was conducted. Eligible patients had unresectable recurrent or metastatic malignancies of the lung, oesophagus, mesothelium, head and neck or urinary tract and had exhausted conventional treatment options. Patients who were HLA-A*02:01 positive, performance status 0-1 and had a lymphocyte count $\geq 10\%$ received S-488210/S-488211 (1 mg of each of 5 peptides mixed with Montanide ISA 51 VG) subcutaneously weekly for 4 weeks, then every 2 weeks for up to 8 weeks. The primary objective was to evaluate the safety and tolerability with adverse events classified by CTCAE version 4.03. The secondary objective was to evaluate cytotoxic T lymphocyte (CTL) induction rate during treatment, defined as the proportion of patients who showed increased CTL activity for ≥ 1 peptide. An exploratory objective was to assess disease control rate (DCR; CR+PR+SD) at 12 weeks.

Results 7 patients were enrolled between 30/7/19 and 9/7/21. One patient did not receive treatment due to a decline in performance status and was excluded from the safety analysis. Median age was 57, 5/6 patients were male and 5/6 were white. All patients experienced at least 1 adverse event (AE), most commonly a Grade 1 injection site reaction. There were 2 Grade 3 treatment-related AEs (hypertension and injection site reaction), neither of which met the dose-limiting toxicity criteria. There were no treatment-related serious AEs. 3/6 patients received the full planned treatment (9 doses) and 3/6 patients were withdrawn due to disease progression or death. The CTL induction rate was 100% in the 5 evaluable patients and was highest for the DEPDC1 (100%), MPHOSPH1 (60%) and URLC10 (40%) peptides. The DCR at 12 weeks was 16.7% (1/6 patients with SD).

Conclusions S-488210/S-488211 was generally well tolerated and led to a robust CTL response in a range of solid tumours. S-488210/S-488211 is being taken forward in a phase 2 study in combination with PD-L1 blockade.

Acknowledgements Ricky Yang and Chi Yee Chung provided and cared for study patients

Trial Registration NCT04316689

Ethics Approval The study was approved by Ethical Committee on Clinical Trial of Shionogi (held on 27 Oct 2018)

<http://dx.doi.org/10.1136/jitc-2022-SITC2022.0598>

599 **MECHANISM OF ACTION FOR OT-101 TGF- β IMMUNOTHERAPY**

Vuong Trieu*, Osmond D'Cruz. *Oncotelic, Agoura Hills, CA, United States*

Background OT-101 is being developed as immunotherapy for a broad range of cancers. Cancers overexpress TGF- β , which suppresses host innate immune response to the cancers. Treatment with OT-101 lifts the TGF- β cloaking effect and allows innate or therapeutic immunity to attack and eliminate the cancers. OT-101 completed phase 2 for pancreatic cancer and melanoma and phase 2 in glioblastoma with robust efficacy and safety.

Methods Pharmacokinetic analysis of OT-101/trabedersen for P001 study was assessed over the first two cycles of 7- or 4-day intravenous infusions, separated by 7- or 10-day treatment-free interval, respectively, at doses of 40, 80, 140, 160, 190, 240, 250, and 330 mg/m²/day to demonstrate dose exposure response. Xenograft studies were performed across immunocompetent mice (C57Bl6), humanized immune mice (SCID), and T-cell deficient immune mice (nude) to demonstrate immune cell responses.

Results The median AUC_{last} was 232 ug*h/mL (29.7-834) across the three tumor types (pancreatic cancer (PC), melanoma (Mel), and colorectal cancer (CRC)). OT-101 PK is dose proportional ($p < 0.0001$). The PK is highly variable between patients with the AUC_{last} of 140 mg/m² spanning the range of observed values for the four dose levels examined for 4 days on 10 days off schedule (140, 190, 250, 330). Patients with AUC > median exhibited improved PFS for Mel and CRC but not for PC with median PFS of 67 vs. 49 days, $p = 0.005$, 84 vs. 40 days, $p = \text{ns}$, and 55 vs. 56 days, $p = \text{ns}$, respectively. More than half of the OT-101 treated PC patients went into long term disease control (21 of 37 pts, 55%) allowing them to enter into subsequent chemotherapy which has an unexpected benefit of more than doubling their median OS, 9.3 vs. 2.6 mos, $p < 0.0001$. Among those who underwent subsequent chemotherapy, high AUC was associated with improved OS, 9.6 vs. 2.4 mos, $p = 0.0006$. Animal xenograft studies demonstrated robust immune cell infiltration of the tumors. Synergy demonstrated when OT-101 combined with immunotherapy or chemotherapy.

Conclusions Suppression of the TGF- β resulted in conversion of cold to hot tumors with dose dependent relationship. The synergy between OT-101 chemotherapy is similar to OT-101 immunotherapy suggesting that chemotherapy is inducing immune responds amplified with prior treatment of OT-101. OT-101 is currently being combined with IL2, PD-1, and PDL-1 agents in multiple phase 2 trials.

Trial Registration NCT00844064- Safety and Tolerability of AP 12009, Administered I.V. in Patients With Advanced Tumors Known to Overproduce TGF-beta-2

<http://dx.doi.org/10.1136/jitc-2022-SITC2022.0599>

600

POST-HOC ANALYSIS FROM TWO PHASE I/II NY-ESO-1-TCR T-CELL THERAPY CLINICAL TRIALS IN PATIENTS WITH ADVANCED SARCOMA (SS OR MRCLS) DEMONSTRATES RESPONSE ACROSS A RANGE OF NY-ESO-1 EXPRESSION

¹Erika Klohe, ¹Sunil Suchindran, ¹Gurpreet Kapoor, ¹Jimson D'Souza, ¹Ellie Corigliano, ²Dejka Araujo, ³Sandra D'Angelo*. ¹GlaxoSmithKline, Collegeville, PA, United States; ²University of Texas MD Anderson Cancer Center, Houston, TX, United States; ³Memorial Sloan Kettering Cancer Center, New York, NY, United States

Background An investigational use only immunohistochemical (IHC) clinical trial assay was used to prospectively identify NY-ESO-1-positive patients for eligibility in two phase I/II pilot clinical trials. NY-ESO-1 T-cell receptor (TCR) T-cell therapy was investigated in NY-ESO-1 expressing HLA-A*02:01, 05, or 06 positive patients with either metastatic or locally advanced synovial sarcoma (SS) (NCT01343043)¹, or advanced myxoid round cell liposarcoma (MRCLS) (NCT02992743).² Post-hoc analyses on both studies investigated the relationship of NY-ESO-1 expression levels in patients with response and no response as per RECIST1.1 (investigator assessed) to NY-ESO-1 TCR T-cell therapy.

Methods NY-ESO-1 expression was determined by total tumor percent staining at stain intensities 0, 1+, 2+, 3+ (TP-score) as assessed by a board-certified pathologist. Eligible SS patients were enrolled into study cohorts with differing cut-off criteria for NY-ESO-1 expression levels (table 1). MRCLS patients were enrolled into study cohorts using a single cut-off for NY-ESO-1 expression levels ($\geq 2+$, TP $\geq 30\%$). SS and MRCLS eligible patients received different dose lymphodepleting regimens (LDR) of fludarabine and cyclophosphamide depending on trial and cohort (table 1).^{3,4} For the present NY-ESO-1 expression analysis, the distribution of the NY-ESO-1 TP-score is displayed as boxplots allowing simultaneous visual comparisons of the range of expression across response, indication, and LDR. In addition, an exploratory cut-off of $\geq 50\%$ was used to evaluate responses. All analyses are exploratory and descriptive.

Results All MRCLS patients and most SS patients expressed NY-ESO-1 as predominately moderate/strong (2+/3+) in $\geq 50\%$ tumor cells.⁵ A pooled ORR assessment at $\geq 50\%$ threshold was 33%. Responders and non-responders were observed across a range of NY-ESO-1 TP-scores in SS from $\geq 1\%$ to 100% and in MRCLS $\geq 50\%$ to 100% (figure 1). Of the six patients with threshold $\leq 30\%$; there were two SS responders expressing TP-score at 30% and one at 10% (figure 1, table 1).

Conclusions NY-ESO-1 expression as a biomarker of patient selection is a relevant approach for use with NY-ESO-1 TCR T-cell therapy. Observed range of response may be supportive of a cut-off in SS of less than 50% TP-score given that three patient responders had low to moderate ($< 50\%$ TP-score) NY-ESO-1 expression, and that MRCLS cut-off was set at $\geq 30\%$. Further exploration of TP-score is underway in a current phase II trial of NY-ESO-1 TCR T-cell therapy (NCT03967223).

Acknowledgements Medical writing support was provided by Scion, and was funded by GSK.

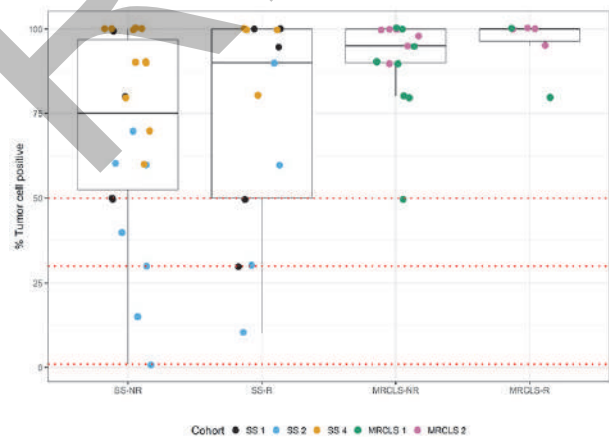
Trial Registration NCT01343043; NCT02992743

REFERENCES

1. ClinicalTrials.gov. A pilot study of genetically engineered NY-ESO-1 specific NY-ESO-1^{c259T} in HLA-A2+ patients with synovial sarcoma (NY-ESO-1). <https://clinicaltrials.gov/ct2/show/NCT01343043>.

- ClinicalTrials.gov. Letetresgene autoleucel engineered T cells in NY-ESO-1 positive participants with advanced myxoid/round cell liposarcoma. <https://clinicaltrials.gov/ct2/show/NCT02992743>.
- Gyurdieva A, Zajic S, Chang Y-F, et al. Modeling the efficacy of NY-ESO-1 TCR T cells (letetresgene autoleucel; GSK3377794) in patients with synovial sarcoma: correlations of response with transduced cell kinetics and biomarkers. <https://sitc.sitcancer.org/2020/abstracts/titles/index.php?filter=GSK3377794>.
- D'Angelo SP, Druta M, Tine BAV, et al. Primary efficacy and safety of letetresgene autoleucel (lete-cel; GSK3377794) pilot study in patients with advanced and metastatic myxoid/round cell liposarcoma (MRCLS). *J Clin Oncol*. 2022;**40**:11500.
- Klohe E, Gyurdieva A, Kapoor G, Kim J, Corigliano E. (P 145) NY-ESO-1 expression profiling and prevalence assessment of tumor biopsies from Phase I/II TCR T cell therapy clinical trials in advanced synovial sarcoma or myxoid round cell liposarcoma. <https://www.eventscribe.net/2021/CTOS/fs/Popup.asp?Mode=posterinfo&PosterID=422735>.

Ethics Approval NCT01343043: The study was conducted in accordance with ICH Good Clinical Practice (GCP), all applicable subject privacy requirements, and the guiding principles of the current version of the Declaration of Helsinki. NCT02992743: The investigator ensured this study was conducted in full compliance with the principals of the "Declaration of Helsinki" or with the laws and regulations of the country in which the research is conducted, whichever, affords the greater protection to the subject. The study fully adhered to the principles outlined in "Guideline for Good Clinical practice" ICH Tripartite Guideline (January 1997) or with local law if it affords greater protection to the subject.



Abstract 600 Figure 1 NY-ESO-1 TP-score across SS and MRCLS treated patient cohorts and TP-score cut-offs ($\geq 1\%$, $\geq 30\%$, $\geq 50\%$) MRCLS, myxoid round cell liposarcoma; NR, non-responders; R, responders; SS, synovial sarcoma

Abstracts

Abstract 600 Table 1 Summary of NY-ESO-1 scoring algorithms and Lymphodepletion regimens by cohort

Ver 1 26/07/22 CDX Deep Dive 466/469 SITC 2022 Abstract

Study	Cohort (number of patients)	R and NR (number of patients)	Scoring algorithm for NY-ESO-1 expression	Drug	Dose
NCT02892743	MRCLS 1 (n=10)	R (n=2) NR (n=8)	IHC intensity score ≥2+, TP ≥30%	Fludarabine	90 mg/m ² (30 mg/m ² x 3 days)
				Cyclophosphamide	1800 mg/m ² (600 mg/m ² x 3 days)
	MRCLS 2 (n=10)	R (n=4) NR (n=6)		Fludarabine	120 mg/m ² (30 mg/m ² x 4 days)
				Cyclophosphamide	2700 mg/m ² (900 mg/m ² x 3 days)
NCT01343043	SS 1 (n=9)	R (n=5) NR (n=4)	IHC intensity score ≥2+, TP ≥50%	Fludarabine	120 mg/m ² (30 mg/m ² x 4 days)
				Cyclophosphamide	3600 mg/m ² (1800 mg/m ² x 2 days)
	SS 2 (n=11)	R (n=4) NR (n=7)		Fludarabine	120 mg/m ² (30 mg/m ² x 4 days)
				Cyclophosphamide	3600 mg/m ² (1800 mg/m ² x 2 days)
	SS 4 (n=15)	R (n=4) NR (n=11)		Fludarabine	90 mg/m ² (30 mg/m ² x 3 days)
				Cyclophosphamide	1800 mg/m ² (600 mg/m ² x 3 days)

IHC, immunohistochemistry; LD, lymphodepletion; MRCLS, mixed round cell liposarcoma; NR, non-responders; R, responders; SS, synovial sarcoma

Scion

Page 1

<http://dx.doi.org/10.1136/jitc-2022-SITC2022.0600>

601

BIOMARKER CORRELATES OF LETETRESGENE AUTOLEUCEL (LETE-CEL; GSK3377794) RESPONSE IN PATIENTS WITH ADVANCED MYXOID/ROUND CELL LIPOSARCOMA (MRCLS)

¹Gurpreet Kapoor*, ¹Stefan Zajic, ¹Sunil Suchindran, ¹Jaegil Kim, ¹Uma Saxena, ¹Aishwarya Bhaskar, ¹Heather Kaczynski, ¹Michael Nathenson, ¹Jimson D'Souza, ¹Benjamin Rich, ²Sandra D'Angelo, ³Mihaela Druta, ⁴Brian Van Tine, ⁵Neeta Somaiah, ⁶David Lieber, ⁷Scott Schuetze, ¹Ioanna Eleftheriadou. ¹GlaxoSmithKline, Collegeville, PA, United States; ²Memorial Sloan Kettering Cancer Center, New York, NY, United States; ³H. Lee Moffitt Cancer Center, Tampa, FL, United States; ⁴Washington University in St. Louis, MO, United States; ⁵University of Texas MD Anderson Cancer Center, Houston, TX, United States; ⁶The Ohio State University, Columbus, OH, United States; ⁷University of Michigan, Ann Arbor, MI, United States

Background NCT02992743 is an open-label pilot study of lete-cel, a New York esophageal squamous cell carcinoma 1 (NY-ESO-1)-specific autologous T-cell therapy, expressing a high-affinity T-cell receptor (TCR) that recognizes the NY-ESO-1 antigen epitope in complex with specific human leukocyte antigen (HLA) alleles of group A*02. Lete-cel exhibited anti-tumor activity and an acceptable safety profile in patients with advanced MRCLS¹ Previously, the association of T-cell kinetics with response and elevated inflammatory cytokines levels has been shown in responders.² This abstract presents additional data on potential biomarkers of response and non-response to lete-cel in patients with advanced MRCLS.

Methods Twenty patients with advanced MRCLS received either reduced-dose (Cohort 1 [C1]; n=10; 30 mg/m² fludarabine for 3 days + 600 mg/m² cyclophosphamide for 3 days) or standard-dose (Cohort 2 [C2]; n=10; 30 mg/m² fludarabine for 4 days + 900 mg/m² cyclophosphamide for 3 days) lymphodepletion prior to lete-cel infusion (median transduced T-cell dose = 4.6 × 10⁹). Key eligibility criteria were: ≥18 years of age; HLA-A*02:01 and/or 05 and/or 06; advanced or metastatic NY-ESO-1-positive MRCLS (≥30% of cells 2+/3+ by immunohistochemistry); prior anthracycline treatment; and measurable disease. Investigator-assessed objective response rate by Response Evaluation Criteria in Solid Tumors (RECIST) v1.1 was the primary efficacy endpoint. For T-cell kinetics, a quantitative polymerase chain reaction assay was used to assess transgene vector copies in DNA from peripheral blood mononuclear cells collected longitudinally during the trial. Serum cytokines were measured by Meso Scale Discovery platform. Whole-transcriptome sequencing was performed on pre- and post-infusion tumor samples. Statistical methods specific to data modalities were used for post-hoc correlative analyses.

Results T-cell persistence at Week 4 was significantly higher ($P=0.0067$) in responders (n=5) than in non-responders (n=13). Lete-cel peak cell expansion was associated with maximum levels of interferon- γ (IFN- γ ; $r=0.56$, $P=0.03$) and interleukin-15 (IL-15; $r=0.55$, $P=0.02$) post-infusion. Preliminary gene expression data from the tumors collected at baseline showed enrichment of metabolic pathways in responders and epithelial-mesenchymal transition and fibroblast activation in non-responders.

Conclusions These data suggest that higher lete-cel persistence and the association of lete-cel expansion with cytokine upregulation post-infusion, as well as tumor-intrinsic transcriptional features, may have a role in lete-cel response in patients with advanced MRCLS.

Acknowledgements Editorial support in the form of copyediting was provided by Scion and was funded by GSK. This study (208469; NCT02992743) was funded by GSK.

Trial Registration NCT02992743

REFERENCES

1. D'Angelo SP, et al. Primary efficacy and safety of letetresgene autoleucel (lete-cel; GSK3377794) pilot study in patients with advanced and metastatic myxoid/round cell liposarcoma (MRCLS). *J Clin Oncol*. 2022;**40** (16_suppl):11500.
2. Kapoor GS, et al. Biomarker correlates of response in patients with advanced myxoid/round cell liposarcoma (MRCLS) treated with NY-ESO-1 TCR T cells (Lete-tresgene autoleucel). *J Immunother Cancer*. 2021;**9** (Suppl 2):A424.

Ethics Approval The study protocol and patient informed consent documentation were approved by center Institutional Review Boards (or Independent Ethics Committees and other site-level committees, as deemed appropriate by the institution).

Consent The study protocol and patient informed consent documentation were approved by center Institutional Review Boards (or Independent Ethics Committees and other site-level committees, as deemed appropriate by the institution).

<http://dx.doi.org/10.1136/jitc-2022-SITC2022.0601>

602

MASS SPECTROMETRY-BASED PROTEIN BIOMARKER ANALYSIS IN CHEMOIMMUNOTHERAPY COMBINATIONS IDENTIFIES UNIQUE IMMUNE SIGNATURES IN PANCREATIC CANCER

Marco Tognetti, Nigel Beaton*, Kamil Sklodowski, Roland Bruderer, Lukas Reiter. *Biognosys, Schlieren, Switzerland*

Background Although the combination of chemotherapy with immunotherapy has led to significant improvements in the treatment of some solid tumors, metastatic pancreatic ductal adenocarcinoma (mPDAC) prognosis has remained largely unaffected by such approaches. Recently, PRINCE, a randomized phase 2 clinical study, reported significantly improved 1-year overall survival (OS) for mPDAC patients treated with nivolumab (nivo)/chemo compared to historical control¹ but not for sotigalimab (sotiga)/chemo or the sotiga/nivo/chemo combination. However, the study identified potential improvement to treatment outcome with patient stratification.² Here, we report an unbiased mass spectrometry (MS)-based proteomics profiling of a subset of plasma samples from the PRINCE trial.

Methods Plasma proteomic profiling was conducted on PRINCE nivo/chemo and sotiga/chemo longitudinal samples (n = 211, 62 individuals) using Biognosys ultradeep plasma workflow. Briefly, plasma samples were depleted, digested to tryptic peptides, measured by MS/MS and quantified using Spectronaut (Biognosys). Data was investigated for both protein and peptide biomarker with an emphasis on baseline biomarkers associated with clinical outcomes.

Results Plasma profiling identified 1,662 proteins and 17,451 modified peptides across the cohorts. First, we developed a model that identified the pharmacodynamic effects of treatment in individual patients. In accordance with the PRINCE study and among the major model contributors, sotiga/chemo increased proteins associated with innate immunity and chemokines (including CCL15) while proteins aiding in T cell activation and immune cell migration increased with nivo/chemo (including CXCL7 and CD115). Second, we looked for markers in the pretreatment plasma samples that could predict OS. Overall, we found 25 predictive markers (p < 0.05), with only six shared among the two arms, including Attractin and CD58. Among the seven predictive biomarkers specific to nivo/chemo, we found MEGF10 and GALNT1, which are suggested to play a role in neoantigen generation.[3] For sotiga/chemo, we found 12 predictive biomarkers including IGF2, CD304, and periostin (known to support immune responses). Third, we expanded our predictive biomarker search to the identified peptides, an analysis that is currently only possible using an unbiased mass spectrometry-based approach. Using such an approach we were able to identify predictive peptides, likely cleavage products, as well as predictive post-translational modifications.

Conclusions Herein we demonstrate the value of both an unbiased approach, as well as the use of peptide level data for novel biomarker identification. We identify numerous proteins and peptides that have the potential to be used for better patient treatment stratification in the case of mPDAC and immunotherapy.

Acknowledgements We extend our gratitude to the patients, their families, the clinical investigators, and their site staff members who are making this trial possible. We would also like to thank Elizabeth Christopher, Sultan Nawabi, Deena M. Maurer, Jia Xin Yu, Lacey J. Padron, Theresa M. LaVallee,

and Diane Da Silva at Parker Institute for Cancer Immunotherapy (PICI).

Trial Registration NCT03214250

REFERENCES

1. Von Hoff D, *et al.* Increased Survival in Pancreatic Cancer with nab-Paclitaxel plus Gemcitabine. *N Engl J Med.* 2013;**369**:1691–1703.
2. Padrón LJ, *et al.* Sotigalimab and/or nivolumab with chemotherapy in first-line metastatic pancreatic cancer: clinical and immunologic analyses from the randomized phase 2 PRINCE trial. *Nat Med.* 2022;**28**:1167–1177.
3. Rodriguez E, *et al.* The tumour glyco-code as a novel immune checkpoint for immunotherapy. *Nat Rev Immunol.* 2018;**18**(3):204–211.

<http://dx.doi.org/10.1136/jitc-2022-SITC2022.0602>

603

A RANDOMIZED, PLACEBO-CONTROLLED, FIRST IN HUMAN PHASE I SINGLE ASCENDING DOSE (SAD) AND MULTIPLE ASCENDING DOSE (MAD) STUDY IN HEALTHY MALE VOLUNTEERS OF THE IMMUNOSTIMULANT 7HP349

¹Lionel Lewis*, ²William Schary, ²Siddhartha De, ²Peter Vanderslice, ³Ronald Biediger, ⁴Yared Hailemichael, ³Darren Woodside, ⁵William Overwijk, ⁶Frank Lee, ²Upendra Marathi. ¹Hills Pharma & The Geisel School of Medicine at Dartmouth, Lebanon, NH, United States; ²Hills Pharma LLC Texas Heart Institute, Houston, TX, United States; ³Texas Heart Institute, Houston, TX, United States; ⁴MD Anderson Cancer Center, Houston, TX, United States; ⁵Nextar, Houston, TX, United States; ⁶Frontage Clinical Services, Sacausus, NJ, United States

Background 7HP349 is a first in class allosteric agonist of integrins $\alpha 4\beta 1$ and $\alpha L\beta 2$ which promotes both T-cell extravascular trafficking and antigen priming. In B16 and CT26 syngeneic models 7HP349 monotherapy has anti-tumor efficacy and enhanced anti-CTLA-4 and anti-PD-1 tumoricidal effects. 7HP349 has a very safe acute and chronic preclinical toxicity profile. We undertook a placebo-controlled Phase I SAD and MAD study with the objectives of determining (i) the safety and tolerability of oral 7HP349 (ii) the optimal pharmacokinetic dose (OPD).

Methods Four cohorts (1-4) of healthy male volunteers (n=8; 6 active; 2 placebo) received single oral 7HP349/placebo doses of 50, 100, 200 or 300 mg after a standard breakfast. Two further cohorts [5&6 (n=8)] received 100 or 300 mg 7HP349/placebo daily for five days. Subjects were monitored for clinical and laboratory adverse events (AEs) during and up to 7 days post single dose and during and up to 10 days post multiple dosing and graded using 5.0 CTCAE criteria. Pharmacokinetic samples were collected pre-treatment and up to 96h post single and the last multiple dose. 7HP349 plasma concentrations were measured by LC-MS/MS, PK data was analyzed non-compartmentally.

Results Forty-eight healthy male volunteers median age 32 (range 21-44 y) were enrolled in the study, 36 received 7HP349 and 12 placebo. No 7HP349 related SAEs or clinical AEs were noted. Treatment emergent, reversible, non-clinically significant safety lab abnormalities were: SAD cohort 100 mg Gr 1. amylase/lipase n= 1/6; SAD Cohort 200 mg Gr 1 isolated ALT n=1/6 and Gr 1 amylase/lipase n=1/6; SAD Cohort 300 mg isolated Gr 1 ALT =1/6; MAD cohort 100 mg Gr 1 isolated ALT n=1/8 ; MAD cohort 300 mg Gr 1 AST/ALT & Gr 1 amylase/lipase n=1/8 and Gr 1 AST/ALT n=1/6. Similar out of range lab values were seen in a minority of placebo-treated subjects (1-2/12). 7HP349 mean PK parameters [(n=6; (±SD)] are detailed in table 1.

Conclusions Oral 7HP349 at single and multiple doses (daily x 5) up to 300 mg was safe and very well tolerated. 7HP349 mean terminal $T_{1/2}$ ranged from 20.6-34.6 h, with no accumulation and non-linear PK at the highest doses. Planned studies combining 7HP349 dosed at 100 mg and 300 mg/day x 5 (at a monotherapy safety margin of >10x) have the potential to augment immune checkpoint blockade without additional toxicity.

Acknowledgements This clinical study was supported by NCI SBIR grant number R44CA250646

We wish to thank all study subjects for participating in this study

Trial Registration NCT04508179

Ethics Approval Ethics approval for this study was obtained from the Frontage Clinical Services utilized IRB. All study

participants gave written informed consent prior to taking part in any study procedures

Abstract 603 Table 1 7HP349 mean pharmacokinetic parameters by study cohort

Cohort # & dose	T _{max} (h)	C _{max} (ng/ml)	T _{1/2elim} (h)	AUC _{0-∞} (ng·h/ml)	R _{max} (AUC)
1. SAD-50 mg	2.5 (1-6)	10.2 (± 8.2)	8.9	34.2 (± 22.0)	
2. SAD-100 mg	2 (1-2)	36.1 (± 16.4)	20.6 (± 15.0)	164.4 (± 113.4)	
3. SAD-200 mg	2 (2)	165.6 (± 61.8)	34.6 (± 20.7)	753.1 (± 239.7)	
4. SAD-300 mg	2 (1-6)	321.0 (± 121.8)	29.7 (± 15.4)	1346.3 (± 316.1)	
5. MAD-100 mg Day 1	2 (1-6)	43.0 (± 31.8)	NC	105.3 (± 38.8)	
MAD-100 mg Day 5	2 (1-4)	20.3 (± 9.9)	16.3 (± 15.2)	109.8 (± 64.4)	0.79 (± 0.37)
6. MAD-300 mg Day 1	1.5 (0.5-4)	237.3 (± 194.7)	NC	961.6 (± 533.7)	
MAD-300 mg Day 5	1.5 (1-4)	222.2 (± 143.6)	22.7 (± 6.9)	1238.5 (± 747.8)	1.04 (± 0.27)

* n = median (range). NC = not calculable because of second dose was administered at 24h post first dose

<http://dx.doi.org/10.1136/jitc-2022-SITC2022.0603>

604

FIRST-LINE AVELUMAB TREATMENT IN PATIENTS WITH METASTATIC MERKEL CELL CARCINOMA: 4-YEAR FOLLOW-UP FROM THE JAVELIN MERKEL 200 TRIAL

¹Sandra D'Angelo*, ²Celeste Lebbé, ³Laurent Mortier, ⁴Andrew Brohl, ⁵Nicola Fazio, ⁶Jean-Jaques Grob, ⁷Natalie Prinzi, ⁸Glenn Hanna, ⁹Jessica Hassel, ¹⁰Felix Kiecker, ¹¹Anja von Heydebreck, ¹¹Gülseren Güzel, ¹²Paul Nghiem. ¹Memorial Sloan Kettering Cancer Center; and Department of Medicine, Weill Cornell Medical College, New York, NY, United States; ²Université Paris Cité, Dermato-Oncology, CIC AP-HP Hôpital Saint Louis, Paris, France; ³CARADERM; and University of Lille, INSERM U1189, Lille Hospital-Claude Huriez Hospital, Lille Cedex, France; ⁴Moffitt Cancer Center, Tampa, FL, United States; ⁵European Institute of Oncology, IEO, IRCCS, Milan, Italy; ⁶Aix-Marseille University, Marseille, France; ⁷Fondazione IRCCS Istituto Nazionale dei Tumori, Milan, Italy; ⁸Dana-Farber Cancer Institute, Boston, MA, United States; ⁹University Hospital Heidelberg, Heidelberg, Germany; ¹⁰Charité Universitätsmedizin Berlin, Campus Charité Mitte, Berlin, Germany; ¹¹The Healthcare Gusiness of Merck KGaA, Darmstadt, Germany; ¹²University of Washington Medical Center at South Lake Union, Seattle, WA, United States

Background Prior to the approval of immune checkpoint inhibitors, patients with metastatic Merkel cell carcinoma (mMCC), a rare and aggressive neuroendocrine skin carcinoma, had a poor prognosis (5-year overall survival [OS] rate of approximately 17%). Avelumab, an anti-PD-L1 antibody, has been approved in multiple countries for the treatment of mMCC based on the results of the phase 2 JAVELIN Merkel 200 trial (NCT02155647). In the primary analysis of part B of the trial, which investigated avelumab as first-line (1L) treatment for mMCC and was reported after 15 months of follow-up in all patients, the objective response rate was 39.7%, the durable (≥ 6 months) response rate was 30.2%, and median OS was 20.3 months. Here, we report findings after 4 years of follow-up.

Methods Eligible patients had histologically confirmed stage IV mMCC and had received no prior systemic therapy. Patients received avelumab 10 mg/kg intravenously every 2 weeks as monotherapy until confirmed disease progression, unacceptable toxicity, or withdrawal of consent. Here, patient disposition and long-term OS were analyzed.

Results A total of 116 patients received 1L avelumab treatment. At data cutoff (February 2, 2022), median follow-up was 54.3 months (range, 48.0-69.7 months) and 72 patients (62.1%) had died. At last follow-up, 7 patients (6.0%) remained on treatment and were progression-free, 22 patients (19.0%) had discontinued treatment but remained in follow-up, and 87 patients (75.0%) had discontinued from the trial. Reasons for treatment discontinuation were disease progression in 54 (46.6%), adverse event in 27 (23.3%), withdrawal of consent in 6 (5.2%), death in 5 (4.3%), loss to follow-up in 1 (0.9%), and other reasons in 16 (13.8%). Median OS was 20.3 months (95% CI, 12.4-42.0 months) and OS rates (95% CIs) after 2, 3, and 4 years were 49% (40%-58%), 44% (34%-53%), and 38% (29%-47%), respectively. Median OS was 38.7 months (95% CI, 11.3 months to not estimable) in patients with PD-L1+ tumors (n=21) and 16.1 months (95% CI, 9.6-42.0 months) in patients with PD-L1- tumors (n=87). Overall, 48 patients (41.4%) had received ≥ 1 subsequent anticancer drug therapy, most commonly etoposide (20 [17.2%]), carboplatin (18 [15.5%]), and avelumab (post-trial; 14 [12.1%]).

Conclusions Avelumab 1L monotherapy in patients with mMCC resulted in a 4-year OS rate of 38%. OS rates were numerically higher than those seen in historical studies of 1L chemotherapy. These results further support the use of avelumab as a standard-of-care treatment for patients with mMCC.

Acknowledgements This trial was sponsored by the healthcare business of Merck KGaA, Darmstadt, Germany (CrossRef Funder ID: 10.13039/100009945) as part of an alliance between the healthcare business of Merck KGaA, Darmstadt, Germany and Pfizer. Medical writing support was provided by Eleanor Bishop of ClinicalThinking and was funded by the healthcare business of Merck KGaA, Darmstadt, Germany and Pfizer.

Trial Registration NCT02155647 (ClinicalTrials.gov)

Ethics Approval The trial protocol was approved by the independent ethics committee or institutional review board at each participating center

<http://dx.doi.org/10.1136/jitc-2022-SITC2022.0604>

605

NEOADJUVANT VIDUTOLIMOD (VIDU) AND NIVOLUMAB (NIVO) RESULTS IN MPR AND IMMUNE ACTIVATION IN HIGH-RISK RESECTABLE MELANOMA (MEL): FINAL PHASE II CLINICAL TRIAL RESULTS

¹Arivarasan Karunamurthy, ¹Joe-Marc Chauvin, ¹Robert Morrison, ¹Yulong Bai, ¹Jie Sun, ¹Hong Wang, ¹Douglas Hartman, ²Julie Stein, ¹Christopher Deitrick, ¹Riyue Bao, ¹Jagjit Singh, ¹Quanquan Ding, ¹Wentao Gao, ¹Drew Hurd, ¹Ornella Pagliano, ¹Amy Rose, ¹Yana Najjar, ¹Jason Luke, ³David Mauro, ³Arthur Krieg, ³James Wooldridge, ³Dmitri Bobilev, ¹John Kirkwood, ²Janis Taube, ¹Hyun Jung Park, ¹Hassane Zarour, ¹Diwakar Davar*. ¹University of Pittsburgh Medical Center Hillman Cancer Center, Pittsburgh, PA, United States; ²Johns Hopkins University, Baltimore, MD, United States; ³Checkmate Pharmaceuticals, Cambridge, MA, United States

Background Neoadjuvant PD-1 blockade produces major pathological responses (MPR) in ~30% of patients (pts) with high-risk resectable MEL with durable relapse-free benefit, and increased circulating activated CD8+ T cells.^{1,2} Vidutolimod (vidu) comprises a CpG-A oligodeoxynucleotide packaged within a virus-like particle (VLP) and is designed to activate tumor-associated plasmacytoid dendritic cells (pDC) via TLR9, inducing an IFN-rich tumor microenvironment and anti-tumor CD8+ T cell responses. Vidu/anti-PD-1 resulted in durable tumor responses in PD-1 refractory MEL.³ This phase II study evaluated the pathological, clinical and immunological activities of neoadjuvant vidu/nivo in high-risk stage III B/C/D resectable MEL.

Methods Vidu/nivo was administered over 7 weeks (vidu 10mg IT Q1W x7, nivo 240mg Q2W x3) pre-surgery. Post-surgery, vidu/nivo (vidu SC 5mg, nivo 480mg Q4W) was continued for 48 weeks. Primary endpoints included MPR rate, and incidence of DLT. Secondary endpoints were radiographic response, relapse-free survival (RFS), distant metastasis-free survival (DMFS) and overall survival (OS). Pathological response assessment was performed to evaluate % residual volume of tumor (RVT) per consensus criteria⁴⁻⁶ by 3 blinded dermatopathologists: 0% (pCR); 0%50% (pNR). Radiographic response assessed using RECIST v1.1. Serial blood, tumor and stool were collected for correlative analyses.

Results 31 pts were enrolled, of whom 30 evaluable for per-protocol (PP) analyses as 1 pt progressed pre-surgery. No DLTs were observed. 8 Gr3 TRAE, including hypertension (7/8) and colitis (1/8) were observed; no delays in surgery occurred. ORR by BICR was 45% (all) and 47% (PP). In PP population, MPR was observed in 57% (17/30) including 47% pCR (14/30) and 10% pMR (3/30). With median follow-up of 26.5 months, median RFS was not reached (table 1). Post-treatment, MPR was associated with increased CD8+ tumor infiltrating lymphocytes (p<0.0001), and peripheral immune activation and pDC activation by multiparameter flow cytometry (p < 0.001). Spatial investigation of immune cell infiltrates by mIHC revealed significantly immune cell infiltrates (p<0.05) and higher pDC (p=0.053) within tumor (but not stroma) of MPRs post-treatment (figure 1a,b). Deconvoluted RNAseq confirmed these findings compared to a control cohort of PD-1 treated MEL.

Conclusions Neoadjuvant vidu/nivo has minimal tox and demonstrated promising activity with 47% pCR rate and 57% MPR rate. MPR was associated with improved 1-/2- year RFS (94%/88%), and 1-/2- year DMFS (94%/94%) and 2-year OS (100%). MPR is associated with pDC and immune infiltrate (figure 1c). Further evaluation of this combination is ongoing in an ongoing randomized phase II trial (EA6194, NCT04708418).

Acknowledgements We thank and Checkmate Pharmaceuticals for funding and vidutolimod.

This research was supported in part by the University of Pittsburgh Center for Research Computing through the resources provided. Specifically, this work used the HTC cluster, which is supported by NIH award number S10OD028483.

This research was supported by the Melanoma Research Foundation Breakthrough Consortium (MRFBC) Award (Davar, Stein); NIH R01 CA257265 (Zarour, Davar); and NIH P50 CA254865 (Zarour).

Trial Registration Clinical trial information: NCT03618641.

REFERENCES

1. Amaria RN, Reddy SM, Tawbi HA, et al. Neoadjuvant immune checkpoint blockade in high-risk resectable melanoma. *Nat Med*. 2018 Nov;24(11):1649–1654.
2. Huang AC, Orlowski RJ, Xu X, et al. A single dose of neoadjuvant PD-1 blockade predicts clinical outcomes in resectable melanoma. *Nat Med*. 2019 Mar;25(3):454–461. doi: 10.1038/s41591-019-0357-y.
3. Ribas A, Medina T, Kirkwood JM, et al. Overcoming PD-1 Blockade Resistance with CpG-A Toll-Like Receptor 9 Agonist Vidutolimod in Patients with Metastatic Melanoma. *Cancer Discov*. 2021 Dec 1;11(12):2998–3007. doi: 10.1158/2159-8290.CD-21-0425.
4. Tetzlaff MT, Messina JL, Stein JE, et al. Pathological assessment of resection specimens after neoadjuvant therapy for metastatic melanoma. *Ann Oncol*. 2018 Aug 1;29(8):1861–1868.
5. Cottrell TR, Thompson ED, Forde PM, et al. Pathologic features of response to neoadjuvant anti-PD-1 in resected non-small-cell lung carcinoma: a proposal for quantitative immune-related pathologic response criteria (irPRC). *Ann Oncol*. 2018 Aug 1;29(8):1853–1860. doi: 10.1093/annonc/mdy218.
6. Stein JE, Soni A, Danilova L, et al. Major pathologic response on biopsy (MPRbx) in patients with advanced melanoma treated with anti-PD-1: evidence for an early, on-therapy biomarker of response. *Ann Oncol*. 2019 Apr 1;30(4):589–596. doi: 10.1093/annonc/mdz019.

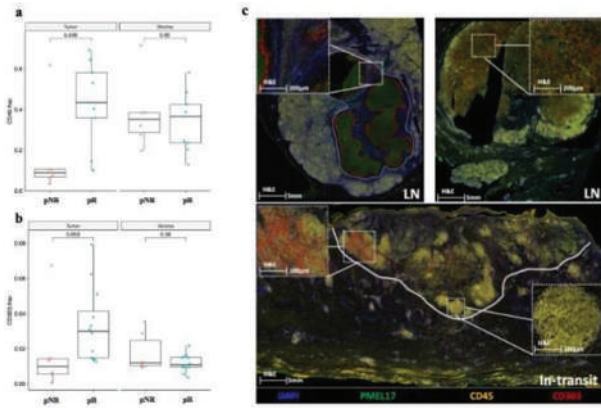
Ethics Approval The study was approved by University of Pittsburgh's Institutional Review Board, approval number MOD19040237-002.

Consent Written informed consent was obtained from the patient for publication of this abstract and any accompanying images. A copy of the written consent is available for review by the Editor of this journal.

Abstract 605 Table 1 Breakdown of pathologic response categories and associated survival

Pathologic Response Breakdown – % (N, 95% CI)	Median RFS (months)	Landmark Survival		
		1-/2-year RFS	1-/2-year DMFS	1-/2-year OS
MPR including pCR and pMR in 57% (17/30, 95% CI 37-75%)	Unreached	94%/88%	94%/94%	100%/100%
pCR in 10% (3/30, 95% CI 2-27%)	23.0 months	100%/33%	100%/33%	100%/100%
pNR in 33% (10/30, 9% CI 17-53%)	6.0 months	40%/40%	40%/40%	60%/60%

Abstracts



Abstract 605 Figure 1 Multiplex IHC (mIHC) Analysis of Post-treatment Samples by GeoMx Spatial Analysis

<http://dx.doi.org/10.1136/jitc-2022-SITC2022.0605>

606

BIOMARKER ANALYSES OF BASELINE TUMOR SPECIMENS AND ON-TREATMENT CHANGES IN SERA SAMPLES OF PATIENTS ENROLLED IN THE RELATIVITY-047 TRIAL TO CHARACTERIZE LAG-3 BIOLOGY

¹Sonia Dolfi*, ¹Tracy Tang, ²Georgina Long AO, ³Paolo Ascierto, ⁴F Stephen Hodi, ⁵Evan Lipson, ⁶Dirk Schadendorf, ¹John Wojcik, ¹Jennifer Postelnek, ¹Yu Wang, ¹Anne Marie Sobiesk, ¹Kaushal Mishra, ¹Sarah Keidel, ¹Karen Miller-Moslin, ⁷Hussein Tawbi, ¹Charlie Garnett-Benson. ¹Bristol Myers Squibb, Princeton, NJ, United States; ²Melanoma Institute Australia, The University of Sydney; Royal North Shore Hospital; Mater Hospital, Wollstonecraft, Australia; ³Istituto Nazionale Tumori IRCCS Fondazione G. Pascale, Milan, Italy; ⁴Dana-Farber Cancer Institute, Boston, MA, United States; ⁵Bloomberg-Kimmel Institute for Cancer Immunotherapy, Johns Hopkins Sidney Kimmel Comprehensive Cancer Center, Baltimore, MD, United States; ⁶University Hospital Essen, and German Cancer Consortium, Essen, Germany; ⁷University of Texas MD Anderson Cancer Center, Houston, TX, United States

Background The phase 2/3 RELATIVITY-047 clinical trial (NCT03470922) in patients with previously untreated metastatic or unresectable melanoma met its primary endpoint of improved progression-free survival with a combination of nivolumab plus relatlimab (NIVO+RELA) compared with NIVO monotherapy.¹ To better understand the biology underlying combined programmed death-1 (PD-1) and lymphocyte-activation gene 3 (LAG-3) inhibition, a series of exploratory biomarker analyses was performed. Analyses included longitudinal changes in immunomodulatory cytokines, free soluble LAG-3 (sLAG-3), and selected immune-cell markers within tumor biopsies collected at baseline.

Methods Peripheral blood serum samples collected prior to treatment, and prior to study drug during week 4 and week 8 of treatment, were evaluated for changes in inflammatory cytokines including interferon gamma (IFN γ) and sLAG-3. Baseline tumor samples were collected prior to treatment and were analyzed by immunohistochemistry for LAG-3 (17B4), CD8 (C8/144B), and tumor cell programmed death-ligand 1 (PD-L1) expression (Agilent/Dako PD-L1 28-8 IHC pharmDx).^{1–3} Correlative analyses were performed.

Results Four weeks after treatment initiation, IFN γ levels increased over baseline in both treatment arms (table 1), but increases were significantly larger with NIVO+RELA than with NIVO (fold change 2.17 and 1.54, respectively; $P < 0.0001$). Eight weeks after treatment initiation, sLAG-3 levels were modestly increased with NIVO (fold change 1.12; $P < 0.001$), and significantly decreased with NIVO+RELA (fold change 0.60; $P < 0.001$) (table 2), suggesting RELA-specific target engagement in the combination arm. No significant correlation was observed between baseline sLAG-3 and tissue-based LAG-3 expression in pretreatment tumors (Spearman's $r = 0.21$). In baseline tumor biopsies, LAG-3 showed moderate correlation with PD-L1 expression ($r = 0.53$) (figure 1). The majority of LAG-3-negative tumors (<1%) were also PD-L1 negative (<1%). PD-L1 expression varied among LAG-3-expressing tumors, with differences observed in the range of PD-L1 expression (high vs low) across LAG-3 subgroups. CD8 levels correlated more strongly with LAG-3 than with PD-L1. Furthermore, patients whose tumors had higher LAG-3 expression ($\geq 1\%$ and $\geq 5\%$) had numerically higher median progression-free survival and objective response rates in both the NIVO+RELA and NIVO arms.

Conclusions These exploratory analyses support the hypothesis that NIVO+RELA enhances immune activation compared with NIVO alone, and that LAG-3 may be a promising biomarker of tumor inflammation. Although LAG-3 alone may not be a useful predictive biomarker for selection of patients with

melanoma for NIVO+RELA vs NIVO regimens, further work is required to assess the clinical utility of LAG-3, likely as part of a composite biomarker of immunotherapy susceptibility.

Acknowledgements Editorial support was provided by Sandra J Page, PhD, of Spark Medica Inc.

Trial Registration Clinicaltrials. gov. NCT03470922.

REFERENCES

1. Tawbi HA *et al.* Relatlimab and nivolumab versus nivolumab in untreated advanced melanoma. *N Engl J Med.* 2022;**386**:24–34.
2. Johnson L *et al.* Development of a LAG-3 immunohistochemistry assay for melanoma. *J Clin Pathol.* 2022;clinpath-2022-208254. doi:10.1136/clinpath-2022-208254.
3. Szabo PM *et al.* Development and performance of a CD8 gene signature for characterizing inflammation in the tumor microenvironment across multiple tumor types. *J Mol Diagn.* 2021;**23**:1159–1173.

Ethics Approval All trial investigators received approval from their respective institutional review boards. The trial was conducted in accordance with the International Council for Harmonisation Good Clinical Practice guidelines, and all patients provided written informed consent before participation. An independent data monitoring committee provided oversight to assess the efficacy and safety profile of relatlimab and nivolumab.

Abstract 606 Table 1 Serum IFN γ increases after treatment with NIVO+RELA and NIVO.

Arm	Baseline		Week 4 ^a		Week 8 ^b		
	n	n	Fold change	P ^c	n	Fold change	P ^c
NIVO+RELA	344	320	2.17	<0.001	274	1.99	<0.001
NIVO	342	315	1.54	<0.001	273	1.51	<0.001

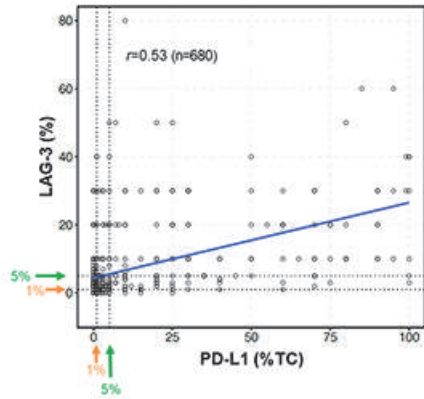
^aWeek 4 corresponded to treatment cycle 2, day 1; ^bWeek 8 corresponded to treatment cycle 3, day 1; ^cP-values were estimated from linear mixed models that evaluated changes in log_e-transformed IFN γ values from baseline. IFN γ , interferon gamma; NIVO, nivolumab; RELA, relatlimab.

Abstract 606 Table 2 Soluble LAG-3 changes after treatment with NIVO+RELA and NIVO.

Arm	Baseline		Week 4 ^a		Week 8 ^b		
	n	n	Fold change	P ^c	n	Fold change	P ^c
NIVO+RELA	324	299	0.98	<0.001	238	0.60	<0.001
NIVO	322	283	1.15	<0.001	244	1.12	<0.001

^aWeek 4 corresponded to treatment cycle 2; ^bWeek 8 corresponded to treatment cycle 3; ^cP-values were estimated from linear mixed models that evaluated changes in log_e-transformed soluble LAG-3 values from baseline. LAG-3, lymphocyte-activation gene 3; NIVO, nivolumab; RELA, relatlimab.

Abstracts



Blue line represents linear regression analysis. Arrows show cutoffs used for LAG-3 and PD-L1 subgroups. %TC, percentage of viable tumor cells with cell membrane PD-L1 expression; LAG-3, lymphocyte-activation gene 3; PD-L1, programmed death ligand 1; r , Spearman's correlation coefficient.

Abstract 606 Figure 1 Correlation between LAG-3 and PD-L1 expression by immunohistochemistry.

<http://dx.doi.org/10.1136/jitc-2022-SITC2022.0606>

607

MCGRAW TRIAL: EVALUATION OF THE SAFETY AND EFFICACY OF AN ORAL MICROBIOME INTERVENTION (SER-401) IN COMBINATION WITH NIVOLUMAB IN FIRST LINE METASTATIC MELANOMA PATIENTS

¹Isabella Glitza Oliva*, ²Omid Hamid, ³Patrick Ott, ⁴Genevieve Boland, ⁴Ryan Sullivan, ⁵Kenneth Grossmann, ⁶Christopher Desjardins, ⁶Nathan Hicks, ⁶Brian Weiner, ⁷Farah Alayli, ⁷Farah Alayli, ⁷Christine Spencer, ⁷Shikha Guatam, ⁷Christopher Loo, ⁷Benjamin Kamphaus, ⁷Julie Densmore, ⁷Christopher Cabanski, ⁷Diane Da Silva, ¹Jennifer Wargo, ⁷Justin Fairchild, ⁷Marko Spasic, ⁶John Aunins, ⁶Kelly Brady, ¹Elizabeth Burton, ⁶Jennifer Wortman, ⁷Theresa LaVallee, ⁶Mathew Henn, ¹Hussein Tawbi. ¹The University of Texas MD Anderson Cancer Center, Houston, TX, United States; ²Angeles Clinic and Research Institute, Los Angeles, CA, United States; ³Dana-Farber Cancer Institute, Boston, MA, United States; ⁴Mass General Cancer Center, Boston, MA, United States; ⁵Huntsman Cancer Institute, Salt Lake City, UT United States; ⁶Seres Therapeutics, Cambridge, MA, United States; ⁷Parker Institute for Cancer Immunotherapy, San Francisco, CA, United States

Background While anti-PD-based therapy is an approved first-line treatment for patients with advanced, surgically unresectable metastatic melanoma (MM), many do not benefit. Abundance of *Ruminococcaceae* and other microbes in cancer patients' gut microbiome has been associated with improved anti-PD1 efficacy. Thus, combination approaches to overcome anti-PD1 primary resistance with gut microbiome modulation are being explored. In this trial, SER-401, an investigational microbiome therapeutic enriched in *Ruminococcaceae* and other spore-forming microbes, was evaluated in combination with nivolumab in first line MM patients.

Methods MCGRAW is a multi-center, randomized, blinded, and placebo-controlled phase 1b study in patients with advanced melanoma. Patients were randomized 2:1 to the SER-401 active or placebo arm, respectively, and stratified by baseline stool *Ruminococcaceae* abundance. Patients received an oral vancomycin preparative regimen+SER-401 (active arm), versus no antibiotics+placebo (placebo arm). One week later, all patients received nivolumab 480 mg Q4W. The primary endpoint was safety. Secondary endpoints were SER-401 microbiome engraftment, ORR, DCR, PFS, and change in frequency of tumoral CD8+ T cells on-treatment. The study was not powered for comparison between arms. Baseline and on-treatment stool samples were collected for microbiome analysis, tumor and blood samples were collected for exploratory biomarker analysis.

Results Fourteen patients were randomized (N=8 active, N=6 placebo). Grade 3-4 TRAEs were observed in 0 and 1 (17%) participants in the SER-401/nivolumab and placebo/nivolumab arms, respectively. In the vancomycin+SER-401/nivolumab arm, ORR was 25.0% (95% CI: 3-65) and DCR was 37.5% (95% CI: 9-76). In the no antibiotics+placebo/nivolumab arm, ORR was 66.7% (95% CI: 22-96) and DCR was 83.3% (95% CI: 36-99). Overall, microbiome engraftment was observed in the active arm but did not reach optimal kinetics or magnitude in many patients. Differences in the fecal microbial and metabolic profiles of responders and non-responders were observed to be prior to initial nivolumab administration. Additional orthogonal biomarker analyses revealed further differences between the responders and non-responders, with the CR patient in the active arm having a distinct profile both at screening and on-treatment.

Conclusions This study demonstrated that SER-401 and anti-PD1 are a safe combination in MM patients, however DCR was lower in the active arm versus control, perhaps related to the antibiotic preparative regimen. Enrollment challenges and sub-optimal SER-401 engraftment resulted in early termination of the study. Despite these limitations, our integrative clinical

and biomarker analysis provides information regarding the link between the gut microbiome, peripheral immune cell populations, and the tumor microenvironment during nivolumab therapy with or without SER-401.

Acknowledgements We extend our gratitude to the patients, their families, the clinical investigators, and their site staff members who made this trial possible. We would also like to thank Sultan Nawabi at Parker Institute for Cancer Immunotherapy (PICI) for operations leadership of the trial. The study was funded by Seres Therapeutics.

Trial Registration ClinicalTrials.gov (NCT03817125)

Ethics Approval The MCGRAW study was approved by WCG IRB (previously known as WIRB) protocol # 20182747

Consent All participants provided written informed consent before enrollment

<http://dx.doi.org/10.1136/jitc-2022-SITC2022.0607>

Abstracts

608

PREDICTING PRIMARY RESISTANCE AND EXPLORING MECHANISMS IN PATIENTS WITH ADVANCED MELANOMA TREATED WITH IMMUNE CHECKPOINT INHIBITORS (ICIS)

¹Georgina Long AO*, ²Tracy Tang, ²Abraham Apfel, ²David Paulucci, ²Scott Chasalow, ²Daniel Tenney, ²Gina Fusaro, ³Dirk Schadendorf, ⁴Hussein Tawbi, ⁵F Stephen Hodi, ²Pratik Thakkar, ⁶James Larkin, ⁷Jedd Wolchok, ²Megan Wind-Rotolo, ²Shu-Pang Huang, ⁸Peter Mohr, ⁹Caroline Robert, ¹⁰Christoph Hoeller, ¹¹Jean-Jacque Grob, ¹²Helen Gogas, ¹³Jeffrey Weber, ²Han Chang, ²Rebecca Moss. ¹Melanoma Institute Australia, The University of Sydney; Royal North Shore Hospital; Mater Hospital, Wollstonecraft, Australia; ²Bristol Myers Squibb, Princeton, NJ, United States; ³University Hospital Essen, Essen, Germany; ⁴University of Texas MD Anderson Cancer Center, Houston, United States; ⁵Dana-Farber Cancer Institute, Boston, MA, United States; ⁶Royal Marsden Hospital, London, UK; ⁷Memorial Sloan Kettering Cancer Center; Weill Cornell Medicine; Parker Institute for Cancer Immunotherapy, New York, NY, United States; ⁸Elbekliniken Buxtehude, Buxtehude, Germany; ⁹Institut Gustave-Roussy, Villejuif-Paris, France; ¹⁰Medical University of Vienna, Vienna, Austria; ¹¹APHM and Aix-Marseille University, Marseille, France; ¹²National and Kapodistrian University of Athens, Athens, Greece; ¹³NYU Langone Health, New York, NY, United States

Background Despite significant improvements in treatment outcomes with ICIs, deeper understanding is needed to improve outcomes for patients with melanoma who experience no clinical benefit from ICI therapy and exhibit early disease progression (primary resistance).¹ We analyzed clinical and translational factors using data from 9 BMS-sponsored clinical trials of nivolumab (NIVO), ipilimumab (IPI) and their combination in patients with advanced cutaneous melanoma (CheckMate 003, 037, 038, 064, 066, 067, 069, 511, 742) to predict resistance to ICIs and explore underlying mechanisms.

Methods Analyses of pre-treatment clinical covariates and biomarkers (determined by tumor immunohistochemistry, whole exome DNA sequencing, RNA sequencing, and serum cytokine analysis) were performed in patients with melanoma who received NIVO, IPI or NIVO+IPI and were evaluable for resistance. Several methods were used to develop and test models predicting ICI primary resistance, defined as death due to disease or best overall response of progressive disease (excluding pseudoprogression) before the first radiographic scan (≤ 13 weeks of treatment). Model performance was assessed using cross-validated area under the receiver operating characteristic curve (AUROC) and bootstrap bias-adjusted calibration metrics. Additionally, we evaluated individual biomarker associations with primary resistance.

Results Across 1803 patients from 9 clinical trials, 1638 were evaluable for cutaneous melanoma primary resistance and 585 (36%) met the criteria. A multivariable logistic regression model for predicting primary resistance yielded an AUROC of 0.78 ($R^2=0.29$) and included 17 commonly available clinical factors and PD-L1 (table 1). External validation using data from an independent study yielded an AUROC of 0.70 ($R^2=0.17$). Higher levels of acute phase cytokines and expression of genes associated with suppressive tumor microenvironment or stromal factors, including epithelial-mesenchymal transition, cancer-associated fibroblasts, transforming growth factor beta, and angiogenesis, were associated with increased risk of primary resistance. In contrast, higher levels of tumor mutational burden, PD-L1, CD8, mutations in MAPK-pathway genes, and immune gene signature scores were associated with decreased risk (figure 1, table 2).

Conclusions This exploratory analysis of clinical and translational factors in patients with advanced cutaneous melanoma identified associations with primary resistance to NIVO, IPI, or NIVO+IPI, with the best model yielding an AUROC of 0.78. Factors associated with primary resistance included

higher levels of prognostic cytokines, gene expression indicating an immune suppressive tumor microenvironment, lower levels of anti-tumor immunity, and lack of MAPK-pathway mutations. These findings are supportive of future clinical trial stratification of patients and mechanistic studies targeting the biology of primary resistance to ICI therapy.

Acknowledgements We would like to thank Jasmine Rizzo, John Loffredo, Darin Dobler, Amanda Scoffield, James Winters, Corey Ritchings, and Kenzie MacIsaac for supporting efforts. Editorial support was provided by Sandra Page, PhD, of Spark Media Inc.

Trial Registration Clinicaltrials.gov. NCT00730639, NCT01721746, NCT01621490, NCT01783938, NCT01721772, NCT01844505, NCT01927419, NCT02714218, NCT02905266.

REFERENCE

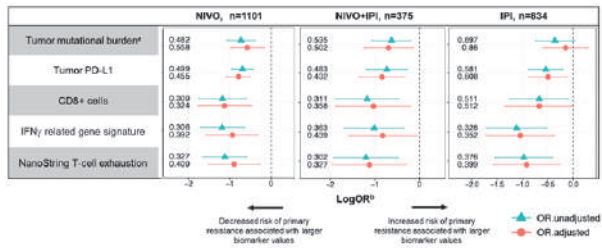
1. Hodi FS, et al. TMB and inflammatory gene expression associated with clinical outcomes following immunotherapy in advanced melanoma. *Cancer Immunol Res.* 2021;9:1202–1213.

Ethics Approval The trial protocols were approved by site institutional review boards or independent ethics committees and conducted according to Good Clinical Practice guidelines, per the International Conference on Harmonisation. Patients provided written informed consent based on Declaration of Helsinki principles.

Abstract 608 Table 1 Ranking of variable importance, as assessed by Wald tests of overall effects, for the factors included in the multivariable logistic regression model predicting primary resistance.

Factor ^a	χ^2	DF	P
Treatment arm	80.9	3	< 0.001
PD-L1 expression on tumor cells ^b	36.7	2	< 0.001
Log (LDH) ^b	25.3	3	< 0.001
Absolute neutrophil count ^b	22.1	3	< 0.001
Absolute lymphocyte count ^b	18.4	3	< 0.001
Platelets	13.1	1	< 0.001
Metastatic stage	12.9	3	0.005
Liver metastases	8.3	1	0.004
Region	9.3	2	0.009
Age ^b	7.1	3	0.070
BRAF V600 status	4.2	1	0.040
Days between advanced melanoma diagnosis and treatment	4.0	1	0.045
BMI	2.1	1	0.145
Sex	1.9	1	0.166
Antacids	0.9	1	0.356
HGB	0.6	1	0.444
Tumor burden	0.3	1	0.562
ECOG	0.3	1	0.564

^aFactors ranked by χ^2 -DF. ^bPossible non-linear associations allowed via restricted cubic regression splines. BMI, body mass index; BRAF, B-Raf proto-oncogene serine/threonine kinase; DF, degrees of freedom; ECOG, Eastern Cooperative Oncology Group; HGB, hemoglobin; ICI, immune checkpoint inhibitor; LDH, lactate dehydrogenase; PD-L1, programmed death ligand 1; χ^2 , chi-squared statistic from overall Wald test for each factor.



^aTumor mutational burden was defined as the total number of nonsynonymous, somatic, missense mutations. ^bAnalysis performed using translational factor values as continuous variables. Blue triangles show unadjusted OR \pm 95% CI; red circles show OR \pm 95% CI after adjusting for study ID, baseline tumor burden, Eastern Cooperative Oncology Group score, melanoma subtypes, region, age, gender, history of liver metastases, cancer M stage, baseline lactate dehydrogenase status, absolute lymphocyte count, absolute neutrophil count, platelets, and white blood cell count. ORs were scaled to compare two biomarker scores differing by the interquartile range. CD8, cluster of differentiation 8; ICI, immune checkpoint inhibitor; IFN γ , interferon gamma; IPI, ipilimumab; LogOR, natural log of OR; NIVO, nivolumab; OR, odds ratio for primary resistance; PD-L1, programmed death ligand 1.

Abstract 608 Figure 1 Common translational biomarkers were negatively associated with primary resistance to ICIs in patients with advanced cutaneous melanoma.

Abstract 608 Table 2 Additional translational factors associated with primary resistance to ICIs in patients with advanced or metastatic melanoma.

Factor	Evaluable patients (n)	Expression in patients with primary resistance	P
MAPK pathway mutations ^a (<i>BRAF</i> , <i>NRAS</i> , <i>NF1</i>)	515	Decreased	< 0.001
Select gene sets associated with primary resistance ^b	425		
HALLMARK_EMT		Increased	< 0.001
CAF		Increased	< 0.001
Stromal		Increased	< 0.001
HALLMARK_ANGIOGENESIS		Increased	< 0.001
TGF- β response signature		Increased	< 0.001
IFN γ -signature		Decreased	< 0.001
B cells		Decreased	< 0.001
Serum cytokine levels ^c	1709		
CRP		Increased	\leq 0.05
IL-10		Increased	\leq 0.05
IL-8		Increased	\leq 0.05
ICAM-1		Increased	\leq 0.05
EN-RAGE		Increased	\leq 0.05

^aLogistic regression *P*-value reported for patients who received NIVO or NIVO+IPI (n=515). No clear association was found in the IPI-treated cohort (n=217). ^bGene set enrichment *P*-values FDR-adjusted for multiple comparisons. ^cCytokines selected from a panel of 50 serum factors. Logistic regression *P*-values are reported for patients who received NIVO monotherapy and are FDR-adjusted for multiple comparisons. *BRAF*, B-Raf proto-oncogene serine/threonine kinase; CAF, cancer-associated fibroblast; CRP, C-reactive protein; EMT, epithelial-mesenchymal transition; EN-RAGE, S100 calcium binding protein A12; FDR, false discovery rate; ICAM-1, intercellular adhesion molecule 1; ICI, immune checkpoint inhibitor; IFN γ , interferon gamma; IL-8, interleukin 8; IL-10, interleukin 10; MAPK, mitogen-activated protein kinase; *NF1*, neurofibromin 1; *NRAS*, NRAS proto-oncogene GTPase; PD-L1, programmed death ligand 1; TGF- β , gene signature related to transforming growth factor beta response.

<http://dx.doi.org/10.1136/jitc-2022-SITC2022.0608>

609

NITRIC OXIDE DEPENDENT IMPROVED RELAPSE FREE SURVIVAL TO IPIILIMUMAB THERAPY IN MELANOMA PATIENTS

¹Joseph Markowitz*, ¹Saurabh Garg, ²James Sun, ¹Youngchul Kim, ¹Junmin Whiting, ¹Jose Conejo-Garcia, ³Mitch Phelps, ⁴Jeffrey Weber, ¹James Mule. ¹Moffitt Cancer Center & Research Institute, Tampa, FL, United States; ²Case Western Reserve University, Cleveland, OH, United States; ³The Ohio State University, Columbus, OH, United States; ⁴Perlmutter Cancer Center, New York University Langone Health, New York, NY, United States

Background Though FDA-approved for use after surgery for stage III/IV melanoma in the adjuvant setting, ipilimumab (anti-CTLA-4) and interferon- α are not typically used because of the improved toxicity profile and relapse-free survival (RFS) benefits seen with anti-PD-1-based regimens in this patient population. However, it is important to study samples derived from anti-CTLA-4 treated patients from the mechanistic perspective to understand its contribution to ipilimumab/nivolumab therapy and to study single agent CTLA4 therapy in the adjuvant cases of BRAF wild-type patients who were re-resected and previously received anti-PD-1 therapy. Recently published data from our group indicated that nitric oxide (NO) increased in immune effector cells among patients treated with longer RFS, whereas NO also increased in immune suppressor cells among patients with shorter RFS. Given this unexpected dichotomy, we measured the posttranslational modification in the immune cells that is a direct result of increased NO levels on the interferon response protein STAT1 important for response to anti-CTLA-4 therapy/interferon responsiveness. Nitration is a stable post-translational modification of NO metabolism and STAT1 is nitrated at the same position (Y701) as it is phosphorylated.

Methods Peripheral blood mononuclear cells (PBMCs) collected from 35 patients at day 0 and day 155 of ipilimumab therapy were analyzed for phosphorylated STAT1 (pSTAT1; using flow cytometry) and nitrated STAT1 at position 701 (nSTAT1; using liquid chromatography with tandem mass spectrometry). Patients were divided into groups based on RFS post ipilimumab therapy.

Results Pre- and post-therapy PBMCs were available from 35 patients with stage III/IV melanoma. The median patient age was 58 years (range, 21-78 years), and 63% of patients were male. pSTAT1 levels had the least variability in the tercile of patients with the longest RFS ($P=0.002$). Higher pSTAT1 levels in PBMCs were associated with worse RFS before ($P = 0.007$) and after therapy ($P = 0.036$) with ipilimumab. Expectedly, pSTAT1 levels in PBMCs increased following ipilimumab therapy. Patients whose STAT1 remained nitrated had decreased RFS, but intriguingly, increases in nitration of STAT1 following ipilimumab therapy was associated with favorable outcomes ($P=0.01$).

Conclusions These data suggest that interferon responsiveness is regulated by changes in nitration of STAT1. Nitration of Y701 on STAT1 may regulate excessive interferon responses by limiting pSTAT1 phosphorylation for successful ipilimumab-based therapy in melanoma and deserves further study in the adjuvant and metastatic settings.

Acknowledgements K08CA252164 to J.M.; Career Enhancement Project under P50CA168536 to J.M; Flow cytometry core and Biostatistics & Bioinformatics core under Moffitt's Cancer Center Support Grant P30-CA076292.

Trial Registration NCT00084656

Ethics Approval The study was approved by Moffitt Cancer Center Scientific Review Committee. The University of South Florida IRB determined that the study was non human

subjects research as the PBMC specimens were deidentified prior to this research activity.

<http://dx.doi.org/10.1136/jitc-2022-SITC2022.0609>

610

IMMUNE BIOMARKER ANALYSIS OF RP1 IN COMBINATION WITH NIVOLUMAB IN PATIENTS WITH ADVANCED SOLID TUMORS

¹Kevin Harrington*, ²Pablo Nendares, ¹Isla Leslie, ³Ari VanderWalde, ⁴Tawnya Bowles, ⁵Joseph Sacco, ⁵Anna Olsson-Brown, ⁶Jiixin Niu, ⁷Katy Tsai, ⁸Jason Chesney, ⁹Bartosz Chmielowski, ¹⁰Adel Samson, ⁴Terence Rhodes, ¹¹Gino In, ¹²Anna Pavlick, ¹³Trisha Wise-Draper, ¹⁴Miguel Sanmamed, ¹⁵Laxminarasimha Donthireddy, ¹⁵Yawei Zhang, ¹⁵Jeannie Hou, ¹⁵Praveen Bommarreddy, ¹⁵Robert Coffin, ¹⁶Mark Middleton, ¹⁷Mohammed Milhem. ¹Royal Marsden NHS Foundation Trust & ICR, Sutton, UK; ²The Institute of Cancer Research, London, UK; ³West Cancer Center and Research Institute, Germantown, TN, United States; ⁴Intermountain Medical Center, Murray, UT, United States; ⁵Clatterbridge Cancer Centre, Liverpool, UK; ⁶Banner MD Anderson Cancer Center, Gilbert, AZ, United States; ⁷Helen Diller Family Comprehensive Cancer, San Francisco, CA, United States; ⁸James Graham Brown Cancer Center, Louisville, KY, United States; ⁹University of California Los Angeles, Los Angeles, CA, United States; ¹⁰University of Leeds, Leeds, UK; ¹¹Norris Comprehensive Cancer Center, Los Angeles, CA, United States; ¹²Weill Cornell Medical College, New York, NY, United States; ¹³University of Cincinnati, Cincinnati, OH, United States; ¹⁴Clinica Universidad de Navarra, New Haven, CT, United States; ¹⁵Replimune Inc, Woburn, MA, United States; ¹⁶Churchill Hospital, Oxford, UK; ¹⁷Holden Comprehensive Cancer Center, Iowa City, IA, United States

Background RP1 is a novel, enhanced potency, oncolytic version of HSV-1 engineered to express human GM-CSF and GALV-GP R-.¹ RP1 + anti-PD1 therapy combination has resulted in deep and durable responses, including in melanoma patients who have previously failed prior anti-PD1 therapy.² Here we present biomarker data from the ongoing clinical trial of RP1 + nivolumab (nivo).

Methods Tumor biopsies were taken pre-treatment and at 43 days after the first dose of RP1. The tumor immune microenvironment (TIME) was analyzed IHC for CD8 (SP57 clone, Ventana) and PD-L1 (PD-L1 IHC 28-8 pharmDx by Agilent) and by gene expression analysis using the NanoString IO360 panel. The tumor inflammation signature score (TIS) was also calculated using an 18 gene signature.³ Systemic anti-tumor immunity was assessed using PBMCs by sequencing the CDR3 regions of human TCR β chains using the immunoSEQ assay. Correlation analysis of baseline tumor PD-L1 and CD8 status versus clinical response was also performed.

Results A consistent increase in CD8 and PD-L1 expression in the tumor was observed in most of the tested biopsies (30/44), which generally appeared to be co-located. These increases were observed both in superficial lesions and visceral tumors, including in the liver. A notable reversal of CD8 T cell exclusion was observed in a melanoma patient who failed prior ipilimumab and nivo treatment. Clinical responses were independent of baseline CD8 T cell infiltration, PD-L1 expression levels, and prior anti-PD-1 therapy. Gene expression analyses of tumor biopsies (n=11) demonstrated significant increases in the expression levels of genes associated with innate and adaptive immune activation and genes previously reported to be associated with responsiveness to anti-PD1 therapy, particularly CD8, CXCL9, CD27, and TIGIT, as well as consistent increases in TIS. TCR sequencing of PBMCs revealed expansion of pre-existing T cell clones and the appearance of new clones with 20-80% of these changes being newly detected clones. Expansion of new clones (n=170) was observed in a melanoma patient who had a complete response.

Conclusions The biomarker data indicate broad immune activation by RP1 + nivo. Clinical responses are independent of baseline PD-L1 expression and associated with increases in gene signatures associated with cytotoxic T, NK, and Th1 cells. The data indicate the potential for broad utility of RP1

in a range of tumor types, including in patients with primary or acquired resistance to immune checkpoint blockade.

Trial Registration NCT03767348

REFERENCES

1. Thomas S, Kuncheria L, Roulstone V, Kyula JN, Mansfield D, Bommarreddy PK, Smith H, Kaufman HL, Harrington KJ, Coffin RS. Development of a new fusion-enhanced oncolytic immunotherapy platform based on herpes simplex virus type 1. *J Immunother Cancer*. 2019;**7**(1):214.
2. Milhem M, Vanderwalde V, Bowles T, Sacco J, Niu J, Tsai K, Chesney J, Chmielowski B, Samson A, Rhodes T, In G, Pavlick A, Wise-Draper T, Sanmamed M, Bommarreddy P, Zhu J, Coffin R, Harrington K, and Middleton M. Updated results from the skin cancer cohorts from an ongoing phase 1/2 multicohort study of RP1, an enhanced potency oncolytic HSV, combined with nivolumab (IGNYTE). *Journal of Clinical Oncology*. 2022;**40**(16_suppl):9553-9553
3. Ayers M, Luceceford J, Nebozhyn M, Murphy E, Loboda A, Kaufman DR, Albright A, Cheng JD, Kang SP, Shankaran V, Piha-Paul SA, Yearley J, Seiwert TY, Ribas A, McClanahan TK. IFN- γ -related mRNA profile predicts clinical response to PD-1 blockade. *J Clin Invest*. 2017;**127**(8):2930-2940.

Ethics Approval The study was approved by the institutional review board or the local ethics committee at each participating site. Informed consent was obtained from patients before participating in the trial.

<http://dx.doi.org/10.1136/jitc-2022-SITC2022.0610>

611

BIODISTRIBUTION AND SHEDDING ANALYSIS FOLLOWING TREATMENT WITH RP1 ONCOLYTIC IMMUNOTHERAPY IN THE SKIN CANCER PATIENTS FROM THE IGNYTE CLINICAL TRIAL

¹Mohammed Milhem, ²Ari VanderWalde, ³Tawnya Bowles, ⁴Joseph Sacco, ⁴Anna Olsson-Brown, ⁵Jiaxin Niu, ⁶Katy Tsai, ⁷Jason Chesney, ⁸Bartosz Chmielowski, ⁹Adel Samson, ³Terence Rhodes, ¹⁰Gino In, ¹¹Anna Pavlick, ¹²Trisha Wise-Draper, ¹³Miguel Sanmamed, ¹⁴Alireza Kalbasi, ¹⁴Colin Love, ¹⁴Aaron Clack, ¹⁴Jeannie Hou, ¹⁴Praveen Bommarreddy*, ¹⁴Robert Coffin, ¹⁵Mark Middleton, ¹⁶Kevin Harrington. ¹Holden Comprehensive Cancer Center, Iowa City, IA, United States; ²West Cancer Center and Research Institute, Germantown, TN, United States; ³Intermountain Medical Center, Murray, UT, United States; ⁴Clatterbridge Cancer Centre, Liverpool, UK; ⁵Banner MD Anderson Cancer Center, Gilbert, AZ, United States; ⁶Helen Diller Family Comprehensive Cancer, San Francisco, CA, United States; ⁷James Graham Brown Cancer Center, Louisville, KY, United States; ⁸University of California Los Angeles, Los Angeles, CA, United States; ⁹University of Leeds, Leeds, UK; ¹⁰Norris Comprehensive Cancer Center, Los Angeles, CA, United States; ¹¹Weill Cornell Medical College, New York, NY, United States; ¹²University of Cincinnati, Cincinnati, OH, United States; ¹³Clinica Universidad de Navarra, New Haven, CT, United States; ¹⁴Replimune Inc, Woburn, MA, United States; ¹⁵Churchill Hospital, Oxford, UK; ¹⁶Royal Marsden NHS Foundation Trust, Sutton, UK

Background RP1 is HSV1-based oncolytic immunotherapy expressing GM-CSF and the fusogenic GALV-GP R- protein. We present biodistribution and shedding data from the melanoma (n=30) and NMSC patients (n=31) of an ongoing clinical trial of RP1 + nivolumab (nivo).

Methods RP1 was injected into lesions (10⁶ PFU/mL, then 10⁷ PFU/mL Q2W) for up to 8 cycles. Injected lesions were covered with occlusive dressings. Blood, urine and swabs from dressing exteriors, tumor surface, oral mucosa, and areas of suspected herpetic origin were collected. RP1 DNA presence was assessed using qPCR and infectivity by TCID50.

Results RP1 DNA was detected in blood from 32.1% patients and 11.0% of blood samples. Highest levels were detected at 6 hrs. A sub-set of patients showed continued DNA until the next injection, with kinetics indicating RP1 replication. RP1 DNA was undetectable in all urine samples. Additionally, 50.9% of patients and 22.7% of swabs were positive from injection sites, with approximately 20% of patients positive at the next injection, also indicating RP1 replication. 20.5% of patients and 6.2% of samples tested positive for RP1 DNA on the dressing exterior between 24 hrs and the next dose, at low levels compared to injection sites. RP1 DNA was detected at low levels on the oral mucosa (15.1% of patients or 1.9% of samples). During the safety follow-up period, RP1 DNA was only detected on the injected lesion surface and not other sites, with 5.5% and 3.8% of patients positive at 30 and 60 days after the last RP1 dose respectively. Swabs positive for RP1 DNA were assessed for infectious virus by TCID50, and all were negative. No RP1 DNA was detected in swabs from potentially herpetic lesions, with no reports of herpetic infection in patient's caregivers.

Conclusions All positive samples showed only residual RP1 DNA rather than RP1 itself. RP1 DNA was detected on injected tumor surfaces at higher levels compared to other sites for up to 15 days (time of next dose), and then at diminishing levels up to 60 days from last dose. DNA levels at other sites were much lower and transient. In blood, RP1 DNA was detected in a quantity and with kinetics indicative of virus replication in a sub-set of patients, as expected based on the mechanism of action of RP1. Overall, the data suggest that the possibility of RP1 transmission to contacts is minimal, with no evidence of transmission reported.

Trial Registration NCT03767348

Ethics Approval The study was approved by the institutional review board or the local ethics committee at each participating site. Informed consent was obtained from patients before participating in the trial.

<http://dx.doi.org/10.1136/jitc-2022-SITC2022.0611>

612

PERIPHERAL IMMUNE SIGNATURE OF RESPONSIVENESS TO ADOPTIVE CELL THERAPY WITH EX VIVO EXPANDED TILS USING HIGH DIMENSIONAL SINGLE CELL ANALYSIS

Cecilie Oelvang Madsen*, Marta Velasco Santiago, Troels Holz Borch, Inge Marie Svane, Morten Hansen. *The National Center of Cancer Immune Therapy (CCIT-DK), Herlev, Denmark*

Background Adoptive cell therapy (ACT) with *ex-vivo* expanded tumor infiltrating lymphocytes (TILs) has shown remarkable results in patients with metastatic melanoma (MM).^{1, 2} There is a crucial need for noninvasive biomarkers for screening patients which could improve the selection of patients responsive to therapy. Most studies have until now investigated phenotype, numbers, and persistence of infused TILs, while the role of peripheral immune cell in this process is still poorly understood. Here, we sought to elucidate potential peripheral immune signatures before and early on-treatment to predict patients with clinical outcome of ACT-TIL therapy, as well as characterize its impact on circulating immune cells.

Methods Here we retrospectively analyzed peripheral blood mononuclear cells (PBMCs) and serum on-treatment changes from 45 patients with MM treated at our cancer center in one of three clinical trials: Study I (NCT00937625),³ Study II (NCT02379195),⁴ and Study III (NCT02354690).⁵ Three multicolor flow cytometry panels were developed, two focused on T cells and one designed to measure all major mononuclear subsets and their characteristics. Data were evaluated by algorithm-based clustering and manual gate-setting of major immune cell subsets. Multiplex Luminex and ELISA was used to analyze serum samples to further reveal specific cytokine profiles of responsiveness to TIL therapy.

Results Higher frequency of CD8⁺ effector memory (EM) T cells was the only subset characterizing a peripheral immune signature of responsiveness pre-TIL. However, post-TIL therapy multiple immune subsets were associated with clinical outcome. Non-responders were characterized by mobilization of monocytic and NK subsets at the expense of CD4⁺ T cells and several subsets of dendritic cells (DCs). While major pro-inflammatory cytokines, IL-6 and IL-8, decreased post-TIL in responding patients they persisted in non-responding patients. In contrast, responders post-TIL therapy was characterized by higher frequency of both cDC2s and pDCs, CD4⁺ T cells and a subpopulation of CD4⁺ EM T cells expressing CD28, CD29, CD95, and PD-1.

Conclusions While TIL therapy encompasses adoptive transfer of *ex-vivo* expanded preexisting TILs such therapy seems to modify both lymphoid and myeloid cell populations in peripheral blood. This indicates that early on-treatment peripheral immune signature of responsiveness to TIL therapy is characterized by higher frequency of CD4⁺ T cells and subsets of DCs, and a decrease in inflammatory cells and their mediators.

Trial Registration NCT00937625, NCT02379195, NCT02354690

REFERENCES

1. Rosenberg, Steven A, *et al.* Durable Complete Responses in Heavily Pretreated Patients with Metastatic Melanoma Using T-Cell Transfer Immunotherapy. *Clinical cancer research*. 2011;**17**(13):4550-4557.
2. Dafni, U, *et al.* Efficacy of adoptive therapy with tumor-infiltrating lymphocytes and recombinant interleukin-2 in advanced cutaneous melanoma: a systematic review and meta-analysis. *Annals of Oncology*. 2019;**30**(12):1902-1913.
3. Andersen, Rikke, *et al.* Long-Lasting Complete Responses in Patients with Metastatic Melanoma after Adoptive Cell Therapy with Tumor-Infiltrating Lymphocytes

and an Attenuated IL2 Regimen TIL Therapy for Melanoma Patients with Attenuated IL2 Dose. *Clinical cancer research*. 2016;**22**(15):3734-3745.

4. Andersen R, *et al.* T cells isolated from patients with checkpoint inhibitor-resistant melanoma are functional and can mediate tumor regression. *Annals of Oncology*. 2018;**29**(7):1575-1581.
5. Borch, Troels Holz, *et al.* Clinical efficacy of T-cell therapy after short-term BRAF-inhibitor priming in patients with checkpoint inhibitor-resistant metastatic melanoma. *Journal for ImmunoTherapy of Cancer*. 2021;**9**(7).

Ethics Approval The Ethical Committee of the Capital region of Denmark, the Danish Data Protection Agency and the Danish Medical Agencies approved Study I (NCT00937625: EudraCT no. 2008-008141-20), Study II (NCT02379195: EudraCT no. 2014-001420-29), and Study III (NCT02354690: EudraCT no. 2014-001419-38).

<http://dx.doi.org/10.1136/jitc-2022-SITC2022.0612>

613 **NEOADJUVANT SEMA4D BLOCKADE WITH NIVOLUMAB ALTERS SUPPRESSIVE MYELOID CELLS WHILE ELEVATING B CELL AND CD26^{hi} T CELL INFILTRATION IN THE TUMORS OF PATIENTS WITH RESECTABLE STAGE III MELANOMA**

¹Brian Olson*, ²Crystal Mallow, ²Christine Reilly, ¹Jacklyn Hammons, ¹Jayden Kim, ¹Brian Burns, ¹Agnes Harutyunyan, ²Elizabeth Evans, ²Terrence Fisher, ²Maurice Zauderer, ¹Keith Delman, ¹Melinda Yushak, ¹Ali Mokhtari, ¹Douglas Parker, ¹Chrystal Paulos, ¹Gregory Lesinski, ¹Michael Lowe. ¹Emory University, Atlanta, GA, United States; ²Vaccinex, Inc., Rochester, NY, United States

Background Semaphorin 4D (SEMA4D) modulates suppressive myeloid cells to promote infiltration of effector immune populations into the tumor microenvironment (TME). When combined with immune checkpoint blockade (ICB), SEMA4D blockade limits tumor progression in preclinical models. We have shown that pepinemab (a SEMA4D-blocking Ab) can be safely combined with ICB in the neoadjuvant setting, and we hypothesize it will enhance immune infiltration in TME and benefit patients with resectable stage III melanoma.

Methods Patients with resectable stage III melanoma received neoadjuvant nivolumab alone, pepinemab/nivolumab, pepinemab/ipilimumab, or pepinemab/nivolumab/ipilimumab for six weeks followed by surgical resection (NCT03769155). A control cohort underwent surgery without neoadjuvant therapy. Full clinical data from this trial will be presented at ESMO 2022. Peripheral blood was drawn at three time points: a) pre-treatment, b) two weeks into treatment, and c) at time of surgery. High dimensional immune analysis was performed on tissue and blood using 32-color flow cytometry. Pretreatment archival tissue was also used in conjunction with on study surgical resection tissue to evaluate spatial distribution of immune populations using multiplex immunohistochemistry. Finally, pharmacodynamics of SEMA4D blockade by pepinemab was tested using flow-based saturation assays.

Results Pepinemab treatment significantly increased tumor-infiltrating B cells (CD19+) and CD4+ T cells in surgical tissue of patients also given nivolumab (alone or with ipilimumab). A striking increase in a sub-population of proliferating (Ki67+) CD4+ T cells expressing the costimulatory molecule CD26 was also detected in patients receiving pepinemab-containing regimens (as compared to those receiving nivolumab alone). Intriguingly, tertiary lymphoid structures (TLS) comprised of a rich density of B and T cells were found in the tumor bed of patients given the tripartite therapy, as illuminated by spatial distribution of these immune populations using multiplex IHC. Patients experiencing a major pathologic response to pepinemab and nivolumab (with or without ipilimumab) had increased frequencies of tumor-infiltrating B cells and CD4+CD26^{hi} T cells and elevated M1/M2 macrophage ratio. Multiplex IHC results, biomarker analysis, and peripheral blood analysis will be updated at presentation.

Conclusions Neoadjuvant pepinemab with nivolumab (alone or with ipilimumab) modulates immune responses in tumors from patients with resectable melanoma, particularly those with major pathologic responses. Mechanistically, this therapy may act in part by fostering interactions between B and T cell populations within TLS in tumors, with concurrent modulation of myeloid cells. Given the encouraging clinical activity and tolerability of these regimens, the addition of pepinemab has the potential to augment the activity of ICB in advanced melanoma.

Trial Registration Information regarding this clinical trial is available at www.clinicaltrials.gov, NCT03769155.

Ethics Approval The study was approved by Emory University's Institutional Review Board, approval number IRB00104273.

<http://dx.doi.org/10.1136/jitc-2022-SITC2022.0613>

614

MICROBIOME MODIFICATION WITH FECAL MICROBIOTA TRANSPLANT FROM HEALTHY DONORS BEFORE ANTI-PD1 THERAPY REDUCES PRIMARY RESISTANCE TO IMMUNOTHERAPY IN ADVANCED AND METASTATIC MELANOMA PATIENTS

¹Bertrand Routy, ²John Lenehan, ²Brendan Daisley, ¹Meriem Messaoudene, ²Kait Al, ¹Corentin Richard, ³Wilson Miller, ¹Rahima Jamal, ²Scott Ernst, ²Diane Logan, ¹Karl Belanger, ⁴Luara Martinez- Gili, ⁴Benjamin Mullish, ⁴Panteleimon Takis, ⁵Cecilia Hermosilla Samayoa, ²Marina Ninkov, ⁶Seema Nair Parvathy, ³Caroline Lambert, ¹Arielle Elkrief, ¹Rejean Lapointe, ²Mansour Haeryfar, ²Jeremy Burton, ⁶Michael Silverman, ²Saman Maleki*. ¹CRCHUM, Montreal, Canada; ²Western University, London, Canada; ³McGill University, Montreal, Canada; ⁴Imperial College London, London, UK; ⁵McGill, Montreal, Canada; ⁶St. Joseph's Hospital, London, Canada

Background Microbiome-based interventions with fecal microbiota transplant (FMT) from treatment responders (R) have shown promising results in re-sensitizing anti-PD-1-refractory melanoma patients to anti-PD1 therapy. However, it is not currently known whether FMT can be used to prevent primary resistance. Here, we report results from the first phase I clinical trial (NCT03772899) that combines FMT with anti-PD1 therapy in anti-PD1-naïve melanoma patients.

Methods Twenty patients with advanced disease were treated with FMT with capsules from healthy donors one week before the standard of care anti-PD-1. A total of three donors were used. Fecal microbiota was profiled with 16S rRNA and metagenomics sequencing. ¹H-NMR/SMoESY was used to measure plasma metabolites, and flow cytometry was performed on PBMCs. Additionally, FMT in avatar murine models was performed.

Results The median age was 75.5 years, and eight were female. The median follow-up time was 12.2 months. No unexpected toxicities or grade 3/4 toxicities were observed with FMT. Grade 3 immune-related adverse events included nephritis, pneumonitis, and vasculitis. ORR was 65% (13/20), of which 3 were CR. Clinical benefit rate (includes SD lasting > 6 months) was 75% (15/20). There was no correlation between outcomes/toxicities and donors. Microbiome profiling revealed positive engraftment of all patients one week after FMT; however, sustainable engraftment was only observed in R at one month and maintained at three months. At the taxa level, R had enrichment of *Eubacterium rectale*, *Eubacterium ramuleus*, and *Firmicutes* while a loss of *Hungatella*. Metabolomics analysis uncovered that succinate levels were lower in R at baseline. A significant fold change increase in plasma propionate between pre- and post-FMT was observed in R but not non-responders (NR). Immune profiling showed an increase in conventional effector CD8⁺ T-cells and an increase in CD38⁺CD8⁺ Mucosa-associated invariant T (MAIT) cells in R compared to NR post-FMT. Avatar mouse models in germ-free and antibiotic-treated mice confirmed our clinical observations in that pre-FMT stool from both NR and R patients did not induce a response to anti-PD1 therapy. However, the post-FMT stool from R or FMT using donor feces sensitized B16-OVA and MCA-205 tumors to anti-PD1. Post FMT alpha diversity in responder mice correlated with increased intratumor memory CD8⁺ T-cells, TIM3⁺ T-cells, and stronger anti-PD-1 response.

Conclusions Our findings show that combining FMT from healthy donors with anti-PD1 potentially reduces primary resistance to immunotherapy. Successful engraftment of donor microbiota in patients correlated with better outcomes, and this was corroborated by translational experiments.

Acknowledgements This work was funded by the Lotte and John Hecht memorial foundation, an impact grant from the Canadian Cancer Society, medical oncology research funds at Western University, and the London Health Sciences Foundation.

Trial Registration NCT03772899

Ethics Approval This study was approved by the Ethics Research Board (REB) at Western University, CHUM hospital, and The Jewish General Hospital. REB # 113131

All participants signed informed consent before participating in the trial.

<http://dx.doi.org/10.1136/jitc-2022-SITC2022.0614>

615 **REPEAT DOSING OF ONCOLYTIC ADENOVIRUS ONCOS-102 IS ASSOCIATED WITH ENHANCED AND PERSISTENT IMMUNE RESPONSES AND IMPROVED SYSTEMIC ACTIVITY IN ANTI-PD-1 RESISTANT/REFRACTORY (R/R) MELANOMA**

¹Alexander Shoushtari*, ²Lone Ottesen, ²Victor Levitsky, ²Thomas Birkballe Hansen, ³Thomas Hornyak, ⁴Anthony Olszanski, ⁵Martha Nyakas, ⁶Jedd Wolchok. ¹Memorial Sloan Kettering Cancer Center, New York, NY, United States; ²Targovax Asa, Lysaker, Norway; ³University of Maryland Cancer Center, Baltimore, MD, United States; ⁴Fox Chase Cancer Center, Philadelphia, PA, United States; ⁵Oslo University Hospital, Oslo, Norway

Background Defining the optimal dosing-schedule is critical for the development of novel immunotherapeutic combinations. We recently completed phase 1/2 testing of ONCOS-102, a GM-CSF-encoding oncolytic adenovirus (Ad5/3-D24-GMCSF) in two different dosing schedules in combination with pembrolizumab (pem) in patients (pts) with unresectable, stage III-IV, anti-PD-1 resistant/refractory melanoma (NCT03003676). Here, we report tumor viral exposure, comparative, longitudinal gene expression analysis of tumor samples, safety, and detailed analysis of local and systemic effects on tumor lesions according to dosing schedule.

Methods In study Part 1, pts (n=9) received sequential treatment comprising three priming injections of ONCOS-102 (3x1011 VP/injection, intra-tumoral) at every 3 days during the first week of treatment followed by i.v. pem administration (10 mg/kg) every 3 weeks from day 22 for 6 months. In study part 2, pts (n=12) received concomitant treatment with three priming injections of ONCOS-102 during the first week and at day 15 and then ONCOS-102+pem every 3 weeks from day 22. Injected and non-injected target lesion response was assessed, and tumor biopsies were collected at baseline, day 22 and 64. Total RNA sequencing with differential gene expression analysis was conducted on samples from 17 pts. AEs were assessed according to CTCAE.

Results 35% (7 of 20) of evaluable patients achieved RECIST v1.1 objective response. ORR was similar in the two cohorts: 38% (3 of 8 patients) in Part 1 and 33% (4 of 12 patients) in Part 2, despite evidence of more advanced disease in Part 2. Fifty-two individual target lesions (TL) were assessed for response; 16 injected (I)-TL and 36 non-injected (NI)-TL. In I-TL, 25% completely regressed. In NI-TL, $\geq 30\%$ shrinkage was observed in 1 of 8 (12.5%) in Part 1 vs 7 of 28 (25%) in Part 2.

Greater persistence of ONCOS-102 DNA in the tumor through day 64 was observed in Part 2. This correlated with an increased expression of immune-related genes particularly at day 64.

The most frequently reported TEAEs were pyrexia (48%), chills (43%), hypertension (43%), nausea (33%), and alanine aminotransferase increase (33%) with similar incidence, and severity in both parts.

Conclusions Repeat dosing concomitantly with pembrolizumab demonstrated greater viral persistence in the tumor and a trend for upregulation of immune-related genes at Day 64, with no added toxicity concerns beyond pyrexia and local injection site events. Persisting immune activation and substantial tumor shrinkage in non-injected lesions supports the extended (Part 2) dosing regimen for further clinical development.

Trial Registration NCT03003676

Ethics Approval The study obtained ethics approval in the US by:

1. Memorial Sloan Kettering Cancer Center Institutional Review Board/Privacy Board
1275 York-Avenue, New York 10065
Name of committee chair: R. Michael Tuttle, MD.
Protocol # 16-1107
2. Fox Chase Cancer Center WCG IRB
101939 Ave SE/Suite 120, Puyallup, WA 98374
Name of committee chair: Dawn Flitcraft
FCCC Study # 17-1083
3. University of Maryland Institutional Review Board
22 S. Greene Street, Baltimore, Maryland 21201
Name of committee chair: Mark Mishra, MD
HP-00078557/17121GCCC and in Norway by
4. REK sør-øst A
Gullhaugveien 1-3, 0484 Oslo
Name of committee chair:
Knut Engedal
All participants gave informed consent before taking part.

<http://dx.doi.org/10.1136/jitc-2022-SITC2022.0615>

616 UNDERSTANDING MOLECULAR CONSEQUENCES OF IMMUNOTHERAPY ON THE GERMINAL CENTER AXIS

¹Sabrina Solis*, ¹Tomoaki Muramatsu, ¹Sophie Gray-Gaillard, ¹Ramin Herati. ¹NYU Langone Health, New York, NY, United States

Background Checkpoint inhibitor (CPI) antibodies induce blockade of CTLA-4 and PD-1 to reinvigorate the immune system to induce tumor cell clearance. Despite the success of CPI in cancer treatment, CPIs often result in toxicity due to immune related adverse events (irAEs).¹ Both mechanistic understanding and predictive biomarkers for irAEs is lacking. It is necessary to characterize the effect of CPI on the immune system to reduce therapeutic toxicity and improve patient outcomes.

CD4 T follicular helper cells (Tfh) strongly express PD-1 and CTLA-4, yet little is known about the effects of CPI on these cells. Tfh provide help to antibody producing B cells within germinal centers in lymphoid tissue.² Although this is an essential mechanism of adaptive immunity, several groups have shown hyperactivity in Tfh drives germinal center activity, resulting in increased help to autoreactive B cells and the generation of disease-causing autoantibodies.^{3, 4, 5} In the context of CPI, Tfh dysfunction may also drive the induction of autoantibodies and associated irAEs.

Methods Using flow cytometry and scRNAseq, we are analyzing PBMC samples from the Checkmate-238 clinical trial in which patients with resected stage III or IV melanoma received either α PD-1 or α CTLA-4 monotherapy.⁶ Patients had blood drawn on the same day as the first immunotherapy infusion (baseline) and two weeks post-baseline.

Tfh may be key to understanding irAE, but the study of Tfh in humans is challenging as these cells are commonly found in germinal centers of lymph nodes. To overcome this, our group has shown that circulating Tfh cells (cTfh) are recent emigrants from the lymph node and can be used to study cellular dynamics.⁷

Results In this study, α CTLA-4-treated patients developed irAE at higher rates than α PD-1-treated patients, with 46% of α CTLA-4 patients developing Grade 3 or 4 irAE compared to 14% of α PD-1 patients.⁶ We are interested in determining if the higher rate of irAE associated with α CTLA-4 was correlated to cTfh responses. Indeed, in flow cytometry studies, our lab identified a dramatic induction of activated cTfh following α CTLA-4 but not α PD-1 therapy, with a median fold-change of 7.5 within two weeks after baseline in α CTLA-4 patients but no difference in α PD-1 patients (figure 1).

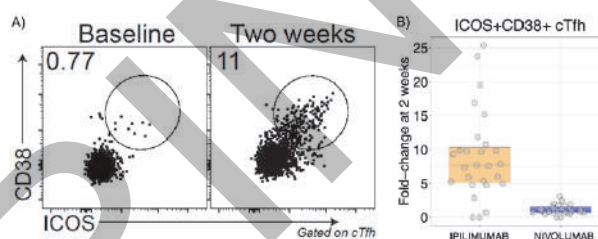
Conclusions The greater influx of cTfh and higher incidence of severe irAEs suggest that α CTLA-4 therapy may predispose patients to dysregulated Tfh proliferation and induction of autoantibody responses.

REFERENCES

1. Kennedy LB, Salama AKS. A review of immune-mediated adverse events in melanoma. *Oncol Ther* [Internet]. 2019;**7**(2):101–20.
2. Ma CS, Deenick EK, Batten M, Tangye SG. The origins, function, and regulation of T follicular helper cells. *The Journal of experimental medicine* [Internet]. 2012;**209**(7):1241–53.
3. Shiao Y, Lee C, Hsu Y, Huang S, Lin C, Li L, Fann CS–, Tsai C, Tsai S, Chiu H. Ectopic and high CXCL13 chemokine expression in myasthenia gravis with thymic lymphoid hyperplasia. *Journal of neuroimmunology* [Internet]. 2010;**221**(1):101–6.
4. Ma J, Zhu C, Ma B, Tian J, Baidoo SE, Mao C, Wu W, Chen J, Tong J, Yang M, Jiao Z, Xu H, Lu L, Wang S. Increased frequency of circulating follicular helper T cells in patients with rheumatoid arthritis. *Clinical & developmental immunology* [Internet]. 2012;**2012**:827480–7.

5. Zhu C, Ma J, Liu Y, Tong J, Tian J, Chen J, Tang X, Xu H, Lu L, Wang S. Increased frequency of follicular helper T cells in patients with autoimmune thyroid disease. *The journal of clinical endocrinology and metabolism* [Internet]. 2012;**97**(3):943–50.
6. Weber J, Mandala M, Del Vecchio M, Gogas HJ, Arance AM, Cowey CL, Dalle S, Schenker M, Chiarion-Sileni V, Marquez-Rodas I, Grob J, Butler MO, Middleton MR, Maio M, Atkinson V, Queirolo P, Gonzalez R, Kudchadkar RR, Smylie M, Meyer N, Mortier L, Atkins MB, Long GV, Bhatia S, Lebbé C, Rutkowski P, Yokota K, Yamazaki N, Kim TM, de Pril V, Sabater J, Qureshi A, Larkin J, Ascierto PA. Adjuvant nivolumab versus ipilimumab in resected stage III or IV melanoma. *The New England journal of medicine* [Internet]. 2017;**377**(19):1824–35.
7. Herati RS, Muselman A, Vella L, Bengsch B, Parkhouse K, Del Alcazar D, Kotzin J, Doyle SA, Tebas P, Hensley SE, Su LF, Schmadler KE, Wherry EJ. Successive annual influenza vaccination induces a recurrent oligoclonotypic memory response in circulating T follicular helper cells. *Science immunology* [Internet]. 2017;**2**(8)

Ethics Approval These samples were obtained through a collaboration with Jeffrey Weber, MD, PhD at NYU Langone Health. As we are blinded and not provided details on samples this study is exempt from IRB approval.



Abstract 616 Figure 1 α CTLA-4 Induces Robust cTfh Response Compared to α PD-1 (A) Flow cytometry analysis illustrates robust induction of cTfh following α CTLA-4 monotherapy at 2 weeks post baseline (B) 7.5 fold change within two weeks after baseline of cTfh for ipilimumab (α CTLA-4) treated patients and no fold change for nivolumab (α PD-1) treated patients

<http://dx.doi.org/10.1136/jitc-2022-SITC2022.0616>

617 **NEOADJUVANT INTRATUMORAL TAVO-EP (PLASMID IL-12 ELECTRO GENE TRANSFER) IN COMBINATION WITH NIVOLUMAB; PRELIMINARY CLINICAL AND BIOMARKER DATA IN PATIENTS WITH OPERABLE LOCOREGIONALLY ADVANCED MELANOMA**

¹Ahmad Tarhini*, ¹Zeynep Eroglu, ¹Amod Sarnaik, ¹Jonathan Zager, ¹Ricardo Gonzalez, ¹Deannyan De Aquino, ¹Edith Abraham, ¹Justin Martin, ¹Allison Richards, ¹Yian Ann Chen, ¹Denise Kalos, ²Jessica Lloyd, ²Jonathan Hanna, ²Erica Browning, ²David Canton, ¹Kenneth Tsai, ¹Jane Messina, ¹Pei-Ling Chen, ¹Vernon Sondak. ¹Moffitt Cancer Center & Research Inst., Tampa, FL, United State; ²OncoSec, San Diego, CA, United States

Background Intratumoral (IT) treatment with TAVO-EP (tavokinogene telseplasmid delivered by electroporation) results in localized expression of IL-12 in the tumor microenvironment. This study (NCT04526730) was designed to evaluate neoadjuvant TAVO-EP in combination with nivolumab followed by surgery and adjuvant nivolumab in patients with operable, locoregionally advanced melanoma.

Methods The neoadjuvant phase comprised up to 3 x4-week cycles of TAVO-EP on days 1, 8 and 15 (optional) concurrently with 480 mg nivolumab I.V. on day 8 of each cycle. Surgery followed and adjuvant nivolumab was initiated after recovery from surgery for up to one year. Longitudinal samples of tumor biopsies, PBMCs, serum, PAXgene® blood DNA/RNA, and fecal material were collected at screening, C1D8, C2D1, pre-surgery and during adjuvant phase. Patients provided an IRB-approved (Advarra-IRB Pro00041794) informed consent and were treated at Moffitt Cancer Center.

Results Ten patients (6 female, 4 male, 1 black, 9 white, 10 cutaneous primary including 1 acral), age 58–88, were treated. Five had Stage IIIB (4N1c, 1N2b), 3 IIIC (1N3b, 1N3c, 1N1c) and 2 IV (M1a). Treatment was well tolerated. Highest-grade treatment-related events to date were limited to one Gr3 hyponatremia possibly related to nivolumab. One patient is currently in the neoadjuvant phase. Among the nine patients who completed the neoadjuvant phase, median number of neoadjuvant cycles was 3; 2 patients received 2 cycles due to near complete clinical response. Preoperative response rate (RECIST, unconfirmed) was 7/9 (77.8%; 95%CI 40.0–97.2); 1PD, 1SD, 4CR, 3 PR. One patient with PR declined surgery. Among 8 patients who had surgery to date, 1 pathologic non-response (Surgery at 4 weeks after initiating treatment due to clinical progression), 1 pathologic major response (pMR; ≤10% viable tumor), 6 pathologic complete response (pCR). The overall pMR rate was 7/8 (87.5%; 95%CI 47.4–99.7), all with no disease recurrence to date, at a median follow up from the date of surgery of 7.08 months (range 0.2–17.5).

Transient on-treatment changes in systemic peripheral immune subsets were identified. At C2D1 (week 5), peripheral proliferating CD8+PD-1+ T cells were significantly increased. In addition, memory precursor effector cells (mPECs; CD8 +KLRG1-CD127+) were transiently upregulated at same time-point, while short-lived effector cells (SLECs; CD8+KLRG1 +CD127-) were significantly reduced. These peripheral T cell changes coincided with increased intratumoral CD8+ TIL.

Conclusions Neoadjuvant IT TAVO-EP in combination with nivolumab exhibited promising clinical activity and a favorable safety profile. There was evidence of significantly enhanced immune activation supporting the proposed immune mechanisms. Analyses of additional biomaterials are underway.

Acknowledgements We are grateful to the participating patients and their family members as well as all research staff supporting the conduct of the clinical trial.

Trial Registration NCT04526730

Ethics Approval All participating patients in this investigator-initiated clinical provided an IRB-approved (Advarra IRB Pro00041794) written informed consent and were treated at Moffitt Cancer Center.

<http://dx.doi.org/10.1136/jitc-2022-SITC2022.0617>

618

DIETARY FIBER INTAKE IS ASSOCIATED WITH INCREASED TERTIARY LYMPHOID STRUCTURES IN DEDIFFERENTIATED LIPOSARCOMA FOLLOWING IMMUNE CHECKPOINT BLOCKADE

Raymond Traweek*, Russell Witt, Elise Nassif, Nadim Ajami, Aditya Mishra, Ashish Damania, Manoj Chelvanambi, Wei-Lien Wang, Alexander Lazar, Emily Keung, Keila Torres, Christopher Scally, Xiaotao Zhang, Carrie Daniel-MacDougall, Jennifer Wargo, Neeta Somaiah, Christina Roland. MD Anderson Cancer Center, Houston, TX, United States

Background Recent evidence suggests that dietary fiber intake is associated with improved clinical and pathologic response to anti-PD-1 therapy,¹ though this relationship is unclear in soft-tissue sarcoma. We evaluated the impact of dietary fiber intake on survival and the immune microenvironment in patients with surgically resectable dedifferentiated liposarcoma (DDLPS) and extremity/truncal undifferentiated pleomorphic sarcomas (UPS) treated with neoadjuvant immune checkpoint blockade (ICB) (NCT03307616).²

Methods Adult patients with treatment-naïve or locally recurrent resectable retroperitoneal DDLPS (n=17) or UPS (n=10) were randomized to receive either neoadjuvant nivolumab or nivolumab/ipilimumab, with UPS patients receiving concurrent radiation. Fecal and tumor samples were collected at baseline, after 1 cycle of ICB, and at surgery; dietary habits (NCI Dietary Screener Questionnaire [NCI-DSQ]) were collected at baseline. Fiber intake was derived from responses to the NCI-DSQ. Tumor infiltration by immune cells was assessed by multiplex immunofluorescence and presence of tertiary lymphoid structures (TLS) was assessed by immunohistochemistry of CD20 and CD21. Fecal microbiomes were profiled via metagenomic sequencing, MetaPhlan 3 and differential abundance analysis was performed using Analysis of Compositions of Microbiomes with Bias Correction (ANCOM-BC).³ Log-rank tests were used to compare survival curves. Wilcoxon rank sum tests were used to compare continuous variables between groups.

Results Median fiber intake was 16 g/day (IQR 13.6-18.4) and similar between the two histologic subtypes (p=0.27). Patients who consumed more (≥ 16 g/day) fiber had significantly improved overall survival when compared to patients who consumed less (p=0.025, Figure 1). Dietary fiber intake was significantly greater in DDLPS patients with a higher density of intratumoral cytotoxic T cells (CD3+CD8+/CD3+) at baseline (p=0.0088, Figure 2a). The presence of TLS at surgery was significantly associated with improved overall survival in DDLPS patients (p=0.031, Figure 2b), and fiber intake was significantly greater in patients with intratumoral TLS following ICB (p=0.0012, Figure 2c). Fiber intake was significantly higher in DDLPS patients who either gained or retained the TLS signature over their treatment course (p=0.0047). Multiple Firmicutes spp. were observed to be significantly associated with fiber intake and the presence of TLS at surgery (q<0.05) over the treatment duration.

Conclusions This study demonstrates that dietary fiber is associated with increased cytotoxic T cell infiltration and TLS formation in DDLPS treated with neoadjuvant ICB. Dietary fiber intake may represent a modifiable factor to improve response to ICB, and the stability of certain fecal microbial taxa may be clinically beneficial.

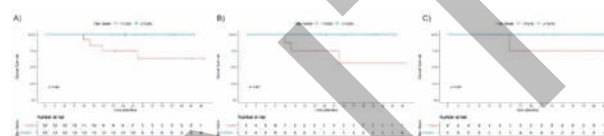
Acknowledgements RST received support from the National Institute of Health (T32CA009599)

Trial Registration ClinicalTrials.gov Identifier: NCT03307616

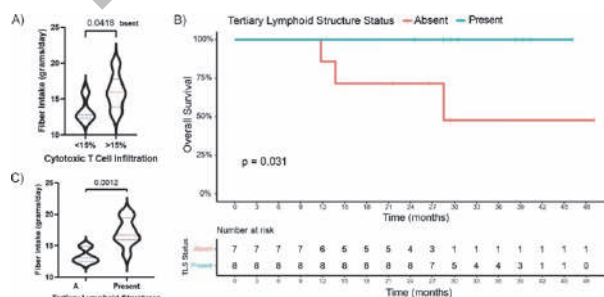
REFERENCES

1. Spencer CN, et al. Dietary fiber and probiotics influence the gut microbiome and melanoma immunotherapy response. *Science*. 2021;**374**(6575): p. 1632–1640.
2. Keung EZ-Y, et al. Randomized phase II study of neoadjuvant checkpoint blockade for surgically resectable undifferentiated pleomorphic sarcoma (UPS) and dedifferentiated liposarcoma (DDLPS): Survival results after 2 years of follow-up and intratumoral B-cell receptor (BCR) correlates. *Journal of Clinical Oncology*. 2022;**40**(17_suppl): p. LBA11501-LBA11501.
3. Lin H and SD Peddada. Analysis of compositions of microbiomes with bias correction. *Nat Commun*.2020;**11**(1):3514.

Ethics Approval This study was approved by University of Texas MD Anderson Cancer Center's Ethics Board, approval number 2017-0143.



Abstract 618 Figure 1 Impact of dietary fiber on survival in resectable retroperitoneal dedifferentiated liposarcoma (DDLPS) and undifferentiated pleomorphic sarcomas (UPS). A) Kaplan-Meier curves of overall survival (OS) in DDLPS and UPS patients who had higher (≥ 16 g/day, n = 17) and lower (< 16 g/day, n = 8) fiber intake from date of first dose to death. B) Kaplan-Meier curves of OS in DDLPS patients who had higher (≥ 16 g/day, n = 8) and lower (< 16 g/day, n = 8) fiber intake from date of first dose to death. C) Kaplan-Meier curves of OS in UPS patients who had higher (≥ 16 g/day, n = 5) and lower (< 16 g/day, n = 4) fiber intake from date of first dose to death. Abbreviations: OS, overall survival; DDLPS, dedifferentiated liposarcoma; UPS, undifferentiated pleomorphic sarcoma



Abstract 618 Figure 2 Association of fiber with the immune microenvironment in retroperitoneal dedifferentiated liposarcoma. A) Fiber intake (g/day) of samples with higher ($> 15\%$) density of intratumoral cytotoxic T cells (n = 12) and lower ($< 15\%$) density of intratumoral cytotoxic T cells (n = 3) at baseline as assessed by multiplex immunofluorescence. B) Kaplan-Meier curves of OS in DDLPS patients who had TLS (n = 8) and those who did not have TLS (n = 7) at surgery from date of first dose to death. C) Fiber intake (g/day) of samples with TLS (n = 8) and those without TLS (n = 7) at surgery. Abbreviations: OS, overall survival; DDLPS, dedifferentiated liposarcoma; TLS, tertiary lymphoid structure.

<http://dx.doi.org/10.1136/jitc-2022-SITC2022.0618>

619 **TEBENTAFUSP INDUCED T AND B CELL EPITOPE SPREAD IN PATIENTS WITH ADVANCED MELANOMA**

Alexander Greenshields Watson, Camille Britton-Rivet, Sarah Stanhope, Laura Collins, Koustubh Ranade, Adel Benlahrech*. *Immucore Ltd, Abingdon, UK*

Background ImmTAC[®] molecules are TCR-CD3 bispecific fusion proteins that can redirect and activate polyclonal T cells to kill tumors. Tebentafusp, which targets gp100 (gp100 × CD3), is the first ImmTAC to demonstrate overall survival benefit and is approved for the treatment of metastatic uveal melanoma¹ in HLA-A*02:01+ patients. We explored whether tebentafusp can induce new T and B cell responses to tumor antigens other than gp100, a phenomenon termed epitope spread.

Methods TCRseq was performed on pre- and post-treatment PBMC samples from tebentafusp-treated patients with advanced malignant melanoma (N=10 from NCT01211262). T cell repertoire breadth was assessed using Simpson clonality index (SCI). A proteome array with 22,976 human proteins was used to assess changes in serum antibody profiles on tebentafusp treatment (N=29 from NCT02570308). Immunohistochemistry (N=36) and RNAseq (N=35) were used to analyze paired baseline and on-treatment tumor biopsies.

Results Substantial T cell clonal expansion and diversification were observed upon treatment with tebentafusp. A median of 56 (range 11-216) T cell clones per patient were expanded after 5-8 doses of tebentafusp, of which 25 (range 0-46) were new clones undetected at baseline. Patients with greater than 1 year overall survival (OS, N = 4) exhibited a focused T cell repertoire at baseline (median SCI=0.08) compared to patients with shorter than 6 months OS (N = 6, median SCI=0.02, p=0.009), which increased in diversity on tebentafusp in patients with long OS but not short OS (median 44% on-treatment decrease in SCI from baseline in patients with long OS compared to a median of 15% on-treatment increase in SCI in patients with short OS, p=0.038).

B cell responses were also induced upon treatment with tebentafusp. B cells were recruited to the tumor microenvironment after 3 doses of tebentafusp, with evidence of new tertiary lymphoid structures. On-treatment B cell levels in biopsies correlated with better OS (hazard ratio HR=0.3, p=0.016) and tumor shrinkage (odds ratio OR=0.06, p=0.007). Serum IgG repertoire profiling showed a median of 42 auto-antibody specificities (range 16-114) per patient at baseline, which increased to 106 (range 32-261) after 4 doses of tebentafusp. Tebentafusp induced antibodies against multiple proteins including p53, the uveal melanoma driver CYSLTR2 and numerous cancer testis antigens. Antibodies were also induced against novel somatic mutants in 2 patients.

Conclusions By inducing T cell repertoire expansion and diversification and antibodies against multiple tumor antigens, tebentafusp is the first TCR-CD3 bispecific to demonstrate T and B cell epitope spread.

Trial Registration A Study of the Intra-Patient Escalation Dosing Regimen With IMCgp100 in Patients With Advanced Uveal Melanoma

ClinicalTrials.gov Identifier: NCT02570308

Study to Assess the Tolerability of a Bispecific Targeted Biologic IMCgp100 in Malignant Melanoma

IMCgp100-01 study: NCT01211262

Ethics Approval The study was approved by each site's Institutional Review Board. An independent data monitoring committee (IDMC) was also established to provide oversight of safety and efficacy considerations and give advice and recommendations regarding steps to ensure both patient safety and the ethical integrity of the study.

Consent Written informed consent was provided by all study participants.

<http://dx.doi.org/10.1136/jitc-2022-SITC2022.0619>

REFERENCE

1. Nathan P *et al.* *N Engl J Med.* 2021;1196–1206.

620

MOLECULAR FEATURES IN TUMORS AT TIME OF PROGRESSION ON TEBENTAFUSP ASSOCIATED WITH OVERALL SURVIVAL (OS)

Laura Collins, Alexander Greenshields Watson, Shaad Abdullah, Sarah Stanhope, Koustubh Ranade, Emma Leach, Emma Leach*. *Immunocore Ltd, Abingdon, UK*

Background Tebentafusp, a TCR bispecific (gp100xCD3) fusion protein (ImmTAC) that targets gp100 in the context of HLA-A*02:01 and activates T cells to kill tumor cells, was approved for the treatment of unresectable or metastatic uveal melanoma (mUM), with many patients demonstrating OS benefit despite radiographic progression.^{1,2} We explored molecular features of the tumor and its micro-environment at clinically confirmed progression, and their association with OS on tebentafusp.

Methods NCT02570308 was conducted in HLA-A*02:01 2L+ patients with advanced mUM. Tumor biopsies (N=14) collected soon after progression on tebentafusp were analyzed by immunohistochemistry (IHC) and RNAseq. Presence of HLA-A and B2M on tumor cells was analyzed by IHC with expression at any intensity quantified. Presence of necrosis was determined by hematoxylin and eosin staining, and CD163+ melanophages by IHC. K-M analysis landmarked to 90 days from initiation of treatment was used for OS.

Results Median OS in the 14 pts with biopsies collected at the time of progression was 22 months, and patients were treated with tebentafusp for 1 day-22 months beyond progression.

Expression of PMEL (gp100) was high at the time of progression and not associated with OS. The degree of necrosis or presence of melanophages in the tumor microenvironment was also not associated with OS.

RNAseq analysis revealed that higher levels of the antigen presentation machinery, presence of PRDM1 expressing effector CD3 T cells, expression of genes required in the necroptosis and apoptosis pathways, and the IFN-inducible transcription factor IRF1 were associated with long OS. In contrast, higher expression of the cell cycle gene CDC45 and the tumor metabolism gene HPDL were associated with short OS. (table 1).

Membrane bound HLA-A was strongly correlated with B2M expression on tumor cells (R-squared = 0.68, p = 2.8e-9), consistent with the requirement of B2M for stability of cell surface HLA. Lack of membrane-bound HLA-A and B2M was associated with short OS, consistent with the requirement of cell surface HLA for antigen presentation.

Conclusions Tebentafusp has demonstrated OS benefit even in patients with progressive disease. Based on tumor biopsies at time of progression, long OS was associated with higher levels of antigen presentation machinery, expression of apoptosis and necroptosis pathways, presence of effector memory T cells and activation of the interferon pathway. These observations provide mechanistic insight into how some patients can derive benefit from tebentafusp despite radiographic progression.

Trial Registration NCT02570308

REFERENCES

- Nathan P. *et al.* Overall Survival Benefit with Tebentafusp in Metastatic Uveal Melanoma. *NEJM.* 2021;**385**:1196–1206
- Joshua A.M., *et al.* Overall Survival Benefit from Tebentafusp in Patients with Best Response of Progressive Disease. *JCO.* 2021;**39**(15_suppl):9509–9509.

Ethics Approval Written informed consent was provided by all study participants. The study was approved by each site’s

Institutional Review Board. An independent data monitoring committee (IDMC) was also established to provide oversight of safety and efficacy considerations and give advice and recommendations regarding steps to ensure both patient safety and the ethical integrity of the study.

Abstract 620 Table 1

Gene	Median OS in low subgroup, months	Median OS in high subgroup, months	Hazard ratio (95% C.I.)
Target gp100	13	20	0.8 (0.24 - 2.59)
Antigen presentation machinery			
• Membrane HLA-A (IHC)	9	38	0.3 (0.08 - 1)
• B2M (RNA)	7	38	<0.01 (NC)
• TAPBP	8	39	<0.01 (NC)
• PSMB8	10	37	0.3 (0.07 - 0.94)
Apoptosis pathway: GZMB, PRF1	8	39	<0.01 (NC)
Necroptosis pathway: RIPK3, MLKL	8	39	<0.01 (NC)
PRDM1, CD3D/E/G T cells	8	39	<0.01 (NC)
IRF1	8	39	<0.01 (NC)
CDC45	38	11	6.7 (1.29 - 34.29)
HPDL	40	11	12.4 (1.47 - 104.59)

†NC = not calculable

<http://dx.doi.org/10.1136/jitc-2022-SITC2022.0620>

Clinical Trials In Progress

621 ATEZOLIZUMAB AND BEVACIZUMAB PRE-LIVER TRANSPLANTATION FOR PATIENTS WITH HEPATOCELLULAR CARCINOMA BEYOND MILAN CRITERIA: TRIAL IN PROGRESS

¹Maen Abdelrahim*, ¹Abdullah Esmail, ²Ashish Saharia, ³Gonzalo Sapisochin, ³Grainne Kane, ²Sudha Kodali, ²David Victor, ¹Kirk Heyne, ²Rafik Ghobrial. ¹Houston Methodist Neal Cancer Center, Houston, TX, USA; ²JC Walter Jr Center for Transplantation, Houston, TX, USA; ³University Health Network, Toronto, Canada

Background Hepatocellular carcinoma (HCC) represents the second most common cause of cancer-related death and accounts for over 80% of primary liver cancers worldwide. However, in 90% of patients, HCC occurs in the setting of cirrhosis where optimal management remains liver transplantation (LT) with 5-year survival rates of approximately 80%. Therapeutic blockade of PD-L1 binding by atezolizumab has been shown to enhance the magnitude and quality of tumor-specific T cell responses, resulting in improved anti-tumor activity. Bevacizumab is a recombinant humanized monoclonal IgG1 antibody that binds to and inhibits the biologic activity of human vascular endothelial growth factor (VEGF) in vitro and in vivo assay systems. We hypothesize that atezolizumab and bevacizumab can appropriately bridge patients with HCC beyond MC to transplantation and not increase the risk of 1-year post-transplant rejection. To test this hypothesis, patients with HCC beyond Milan Criteria (in brief, 5 – 10 cm), who are transplant-eligible will be treated with 6 months of neoadjuvant/downstaging atezolizumab plus bevacizumab while receiving standard of care transarterial chemoembolization (TACE). The proposed clinical trial will evaluate the feasibility of using a combination of the chemotherapeutic interventions atezolizumab and bevacizumab in a group of patients with HCC who have tumors beyond the Milan Criteria in order to bridge them to liver transplantation.

Methods This is a Phase II multi-site study, a site in the US and a site in Canada. Combined enrollment from these sites will be up to 30 patients. Atezolizumab will be administered as a 1200mg intravenous infusion followed by bevacizumab 15mg/kg on the same day. The regimen will be administered every three weeks for up to 8 cycles (or 6 months) in pre-Liver Transplantation patients with HCC. The primary objective of this study is to assess the feasibility and safety of transplantation post atezolizumab/bevacizumab for patients with HCC beyond Milan criteria. The secondary endpoints include ORR of participants who enroll in the study, DFS at 1-year in participants who undergo a liver transplant, defined as time to disease recurrence or death, whichever is earlier, from time of liver transplant, and OS in patients from the time of study enrollment to death from any cause as well as from the time of transplant to death from any cause. An interim analysis will be performed is to assess the feasibility and safety after 20 patients become evaluable. The study is open with 30 patients enrolled at the time of submission. Clinical trial information: NCT05185505.

<http://dx.doi.org/10.1136/jitc-2022-SITC2022.0621>

622

A PHASE 1 STUDY EXPLORING THE SAFETY AND TOLERABILITY OF THE SMALL-MOLECULE PD-L1 INHIBITOR, INCB099318, IN PATIENTS WITH SELECT ADVANCED SOLID TUMORS

¹David Pinato*, ²Ruth Plummer, ³Martin Gutierrez, ⁴Jeffrey Yachnin, ⁵Aglaia Schiza, ⁶Martin Hojgaard, ⁷Knut Smeland, ⁸William Edenfield, ⁹Hans Prenen, ¹⁰Lars Ny, ¹¹Alan Anthoney, ¹²Nuria Kotecki, ¹³Stefan Symeonides, ¹⁴Louis Viviers, ¹⁴Jeannie Daniel, ¹⁴Jennifer Pulini, ¹⁵Udai Banerji. ¹Imperial College Healthcare NHS Trust, London, UK; ²Newcastle Hospital NHS Foundation Trust, Newcastle-upon-Tyne, UK; ³Hackensack University Medical Center, Hackensack, NJ, USA; ⁴Karolinska University Hospital, Solna, Sweden; ⁵Uppsala Universitet, Uppsala, Sweden; ⁶Rigshospitalet Copenhagen University Hosp, Copenhagen, Denmark; ⁷Oslo University Hospital, Oslo, Norway; ⁸Prisma Health Cancer Institute, Greenville, SC, USA; ⁹University Hospital Antwerp, Antwerp, Belgium; ¹⁰Sahlgrenska University Hospital, Gothenburg, Sweden; ¹¹St. James University Hospital, Leeds, UK; ¹²Intitut Jules Bordet, Brussels, Belgium; ¹³University of Edinburgh, Edinburgh, UK; ¹⁴Incyte Corporation, Wilmington, DE, USA; ¹⁵The Royal Marsden Hospital NHS Trust, London, UK

Background INCB099318 is an orally administered small-molecule inhibitor of programmed cell death ligand 1 (PD-L1). This is an ongoing phase 1, open-label, multicenter study.

Methods Eligible patients are aged ≥ 18 years with advanced solid tumors and Eastern Cooperative Oncology Group performance status of 0–1. Patients had disease progression after treatment with available therapies or were ineligible for or without access to standard treatment. The study is conducted in 2 parts: in part 1, a Bayesian optimal interval design is being used to identify the maximum tolerated dose (MTD) of INCB099318. In part 2, selected doses will be expanded for patients who are immunotherapy-naive with various tumor types. The primary endpoints are safety and tolerability measured by monitoring frequency and severity of adverse events (AEs) and to determine a pharmacologically active dose and/or MTD. Antitumor activity is assessed using Response Evaluation Criteria in Solid Tumors (RECIST) v1.1.

Results As of April 22, 2022, 32 patients received INCB099318 in part 1 in 6 dose-escalation cohorts ranging from 100 mg twice daily (bid) to 600 mg bid; median age was 60 years (range, 34–78), 56.3% were women, 81.3% were white, 56.3% had ≥ 2 lines of previous therapy, and 15.6% had prior exposure to immunotherapy. Eleven patients (34.4%) discontinued treatment, 10 of whom discontinued for disease progression. Treatment-emergent AEs (TEAEs) occurring in $>20\%$ of patients were fatigue and nausea. Seven serious TEAEs (SAEs) occurred in 5 patients (15.6%) and consisted of abdominal pain, cerebrovascular accident, migraine, neck pain, pleural infection, pneumonia, and sepsis (n=1 each). Three grade ≥ 3 treatment-related TEAEs occurred in one patient (abdominal pain, fatigue, and insomnia). No dose-limiting toxicities occurred. Several responses have been observed, and updated results will be presented.

Conclusions INCB099318 was generally well tolerated at total daily doses up to 600 mg bid. Unlike with the first-generation oral PD-L1 inhibitor, INCB086550, no dose-limiting immune-mediated peripheral neuropathy has occurred with INCB099318 to date. Preliminary safety warrants continued investigation and further development. Dose escalation is ongoing, and dose expansion is planned to further characterize the safety, tolerability, pharmacokinetics, pharmacodynamics, and antitumor activity of INCB099318.

Trial Registration NCT04272034

Ethics Approval This study was reviewed and approved by the institutional review boards of the participating institutions. Approval numbers are: Comité d'éthique Institut Jules Bordet

(Belgium), CE3326; Ethics Committee Research UZ/KU Leuven (Belgium), S65537; Ethisch Comité UZA/Antwerpen (Belgium), 2021-0592-Edge 001759; Medical Ethics Committee UZ Brussel – VUB (Belgium) EC-2021-285; UZ Gent Ethische Commissie (Belgium), BC-10108 CE3326; National Videnskabetisk komite (Denmark), 2110272; HUS Hospital District of Helsinki and Uusimaa (Finland), HUS/2452/2021; REK South-East Kulmu A (Norway), 253989; Linköping Department Medicine EC (Sweden), 2021-02574; NHS Fast Track REC (United Kingdom), 21/FT/0058; WIRB (USA), 20201315; Vanderbilt IRB (USA), 211153; WCG IRB (USA), 20201315, 1300136, 1308493. All patients provided written informed consent.

<http://dx.doi.org/10.1136/jitc-2022-SITC2022.0622>

623

TRIAL IN PROGRESS: A PHASE 1 FIRST-IN-HUMAN STUDY OF HMBD-002, AN IGG4 MONOCLONAL ANTIBODY TARGETING VISTA, AS A MONOTHERAPY AND COMBINED WITH PEMBROLIZUMAB IN PATIENTS WITH ADVANCED SOLID MALIGNANCIES

¹Tom Haber*, ¹Jessica Symons, ¹Bhushan Dharmadhikari, ¹Thomas Müller, ¹Dipti Thakkar, ²Jordi Ahnert Rodon, ³Joshua Gruber, ⁴Melinda Telli, ⁵Monica Mita, ⁵Alain Mita, ⁶Meera Patel, ⁶Daniel Wang, ⁷Joseph Kim, ²Shalini Yadav, ²Padmanee Sharma, ¹Leah DiMascio, ¹Eric Rowinsky, ¹Piers Ingram, ¹Jerome Boyd-Kirkup. ¹Hummingbird Bioscience, Houston, TX, USA; ²The University of Texas MD Anderson Cancer Center, Houston, TX, USA; ³UT Southwestern Medical Center, Dallas, TX, USA; ⁴Stanford University School of Medicine, Stanford, CA, USA; ⁵Cedars-Sinai Medical Center, Los Angeles, CA, USA; ⁶Baylor College of Medicine, Houston, TX, USA; ⁷Yale School of Medicine, New Haven, CT, USA

Background V-domain Ig Suppressor of T-cell Activation (VISTA) is an immune-checkpoint regulator predominantly expressed on myeloid cells. The presence of VISTA has been shown to promote tumorigenesis and induce an immunosuppressive environment within the tumor microenvironment (TME). Moreover, VISTA's upregulation has been associated with acquired resistance to anti-CTLA-4 and anti-PD-1/PD-L1 therapies. Therefore, VISTA represents a promising therapeutic target. HMBD-002 has been designed as a non-depleting, IgG4 monoclonal-antibody with high affinity and specificity to VISTA across species (human, cynomolgus monkey, and rodent). In preclinical studies, HMBD-002 significantly inhibited tumor growth, both as a monotherapy and in combination with pembrolizumab, while decreasing infiltration of suppressive-myeloid cells within the TME and thus increasing T-cell activity. In addition to VISTA expression on pro-inflammatory immune cells, examination of VISTA expression across cancer types has revealed that several malignancies, particularly triple-negative breast cancer (TNBC) and non-small cell lung cancer (NSCLC), express high levels of VISTA, thereby providing a rationale for exploring these indications in early clinical studies.

Methods This phase 1/2, open-label, multi-center, first-in-human trial is evaluating HMBD-002 as a monotherapy and in combination with pembrolizumab in patients with advanced solid tumors and is conducted in two parts. The dose-escalation cohorts (Part 1), follow a standard 3 + 3 study design, with adaptive dose-escalation increments, and weekly dosing for HMBD-002, to identify the maximum tolerated (or tested) dose (MTD) of HMBD-002 as a monotherapy, and in combination with pembrolizumab (pembrolizumab to be dosed Q3W), and to recommend doses for subsequent disease-directed studies (i.e. RP2D) as well as to determine safety, PK, and ADA. In the dose-expansion stage at the RP2D (Part 2), the antitumor activity of HMBD-002 alone or combined with pembrolizumab will be evaluated in patients with TNBC and NSCLC. Combination therapy will also be evaluated in additional VISTA-expressing malignancies. Biomarker analyses are exploratory endpoints in this clinical study and are assessed for treatment-induced immunological changes both systemically and within the TME. Longitudinal blood samples and pre and on-treatment tumor tissue samples will be assessed using CyTOF, multiplex-cytokine analysis, VISTA & PD-L1 IHC, and gene-expression profiling. Identification of immunological parameters associated with HMBD-002 monotherapy and combination therapy may provide insight into markers associated with the biological activity of HMBD-002. Exploratory correlative analyses with clinical outcomes may lead to the

identification of predictive biomarkers of clinical benefit with HMBD-002.

Clinical trial information NCT05082610

Acknowledgements Research Funding: Cancer Prevention and Research Institute of Texas (CPRIT) Grant DP190027, and Hummingbird Bioscience Inc., Houston TX, USA & Singapore
Ethics Approval The study obtained approval from the following institutional review boards: MDACC- (ID/2021-0434), Yale (ID/20214330), Stanford (ID/63175), Cedars-Sinai (ID/STUDY00001841), UTSW Medical Center (ID/STU-2021-1161), BAYLOR COLLEGE OF MEDICINE (ID/H-51228).

All participants in the trial gave informed consent before taking part in the trial.

<http://dx.doi.org/10.1136/jitc-2022-SITC2022.0623>

624

A PHASE I/II STUDY EVALUATING THE SAFETY AND EFFICACY OF A NOVEL LONG-ACTING INTERLEUKIN-7, NT-I7, FOR PATIENTS WITH NEWLY DIAGNOSED HIGH-GRADE GLIOMAS AFTER CHEMORADIOTHERAPY

¹Omar Butt*, ¹Yu Tao, ¹Jiayi Huang, ¹Jingquin Luo, ¹Alice Zhou, ¹Christopher Abraham, ¹Ruth Katumba, ²Se Hwan Yang, ²Byung Lee, ¹Michael Rettig, ¹George Anstas, ¹Tanner Johanns, ¹Milan Chheda, ³Jian Campian. ¹Washington University, Saint Louis, MO, USA; ²NeoImmuneTech, Rockville, MD, USA; ³Mayo Clinic, Rochester, MN, USA

Background Standard of care after surgery for high-grade gliomas (HGG), including glioblastoma (GBM) and anaplastic astrocytoma, is radiation therapy (RT) and temozolomide (TMZ). Unfortunately, lymphopenia commonly occurs after treatment, leading to decreased survival.^{1,2} Concentrations of interleukin-7 (IL-7), a T-cell homeostatic cytokine, are inappropriately low in patients with HGG.³ Our previous work, using murine glioma models, demonstrated that NT-I7 (efineptakin alfa), a long-acting recombinant human IL-7, corrects lymphopenia and improves survival.⁴ Here we examine survival, safety, and change in absolute lymphocyte counts (ALCs) following administration of NT-I7 after concurrent RT/TMZ in patients with newly diagnosed HGG.

Methods Key inclusion criteria for this Phase I/II study included ALC \geq 600 cells/mm³. NT-I7 was administered intramuscularly within 2 weeks after completion of concurrent RT/TMZ and then every 12 weeks for up to 4 doses. The primary objective of the Phase I portion was to determine safety and the maximum tolerated dose (MTD) of NT-I7 using a 2-dose accelerated phase, followed by a 3+3 design. The Phase II portion (ongoing) is a double-blind, randomized study of 20 HGG patients (10 per arm) to compare ALC changes after administration of either NT-I7 at the MTD or placebo. Exploratory objectives include immune profiling and survival analysis.

Results Phase I completed accrual with results as follows: 19 patients enrolled (17 GBM, median age 58.0 years [25-78], median baseline ALC 1000 cells/mm³ [400-2,000], median baseline dexamethasone use 0 mg/day [0-12], cut-off date 7/15/22). Twelve patients (63%) were MGMT promotor unmethylated, as unmethylation is associated with worse survival. The median number of NT-I7 doses administered was 2 [2-4]. NT-I7 was well-tolerated with grade 1/2 injection site reactions (42%) the most common treatment-related adverse event (TRAE). The MTD was 720 mcg/kg due to two grade 3 dose-limiting toxicities at 960 mcg/kg (elevated alanine aminotransferase and back pain). Dose-dependent increases in ALC were observed at 4 weeks (1.3-4.1 times of baseline level), persisting up to 12 weeks. Median progression-free survival (mPFS) was 19.1 months (95%CI: 15.1-NA) and median overall survival (mOS) was 22 months (95%CI: 20.7-NA) in methylated GBM. For the harder-to-treat unmethylated GBM patients, mPFS was 11.2 months (95%CI: 5.4-22.4) and mOS was 16 months (95%CI: 12.3-24.3). Immune profiling of peripheral blood is ongoing.

Conclusions NT-I7 is well tolerated and is associated with an increase in ALC in HGG patients after chemoradiotherapy. Phase II accrual and immune profiling are ongoing.

Acknowledgements Funding by NeoImmuneTech, Inc. and Site-man Investment Program, Siteman Cancer Center

Trial Registration Clinical Trial ID: NCT03687957

REFERENCES

1. Mendez JS, Govindan A, Leong J, Gao F, Huang J, Campian JL. Association between treatment-related lymphopenia and overall survival in elderly patients

with newly diagnosed glioblastoma. *J Neurooncol.* 2016;**127**(2):329–35. doi: 10.1007/s11060-015-2037-1. Epub 2016 Jan 4. PMID: 26725885; PMCID: PMC4783226.

2. Campian JL, Piotrowski AF, Ye X, Hakim FT, Rose J, Yan XY, Lu Y, Gress R, Grossman SA. Serial changes in lymphocyte subsets in patients with newly diagnosed high grade astrocytomas treated with standard radiation and temozolomide. *J Neurooncol.* 2017;**135**(2):343–351. doi: 10.1007/s11060-017-2580-z. Epub 2017 Jul 29. PMID: 28756593.
3. Campian JL, Ye X, Gladstone DE, Ambady P, Nirschl TR, Borrello I, Golightly M, King KE, Holdhoff M, Karp J, Drake CG, Grossman SA. Pre-radiation lymphocyte harvesting and post-radiation reinfusion in patients with newly diagnosed high grade gliomas. *J Neurooncol.* 2015;**124**(2):307–16. doi: 10.1007/s11060-015-1841-y. Epub 2015 Jun 13. PMID: 26070554; PMCID: PMC4696006.
4. Campian JL, Ghosh S, Kapoor V, Yan R, Thotala S, Jash A, Hu T, Mahadevan A, Rifai K, Page L, Lee BH, Ferrando-Martinez S, Wolfarth AA, Yang SH, Hallahan D, Chheda MG, Thotala D. Long-Acting Recombinant Human Interleukin-7, NT-I7, Increases Cytotoxic CD8 T Cells and Enhances Survival in Mouse Glioma Models. *Clin Cancer Res.* 2022;**28**(6):1229–1239. doi: 10.1158/1078-0432.CCR-21-0947. PMID: 35031547.

Ethics Approval Each site's respective institutional review board approved the study.

Consent Written informed consent was obtained from each participant prior to any trial related activities.

<http://dx.doi.org/10.1136/jitc-2022-SITC2022.0624>

625

**A PHASE 1 SINGLE ASCENDING DOSE STUDY
EVALUATING THE SAFETY, TOLERABILITY, AND
PHARMACODYNAMIC EFFECTS OF MDK-703, AN IL-7
MIMETIC WITH EXTENDED HALF-LIFE**

¹Richard Friend, ²Bryan Baxter, ²Inkyung Angie Park, ²Steven Cwirla, ²Ronald Barrett*.
¹Nucleus Network Pty Ltd, Herston, QLD, Australia; ²Medikine, Menlo Park, CA, USA

Background There has been historical interest in applying IL-7 as an immunotherapeutic in oncology. Efforts to develop derivatives of IL-7 have been hampered by short half-life and immunogenicity, which has the potential to neutralize native IL-7. MDK-703 is an IL-7 mimetic peptide fused to an immunoglobulin Fc-domain. MDK-703 behaves like IL-7 in human immune cells *in vitro* and in humanized mice and non-human primates studies. In addition to increasing the total number of CD8+ and CD4+ T cells, MDK-703 increases the number of memory T cells, particularly the T stem cell memory (Tscm) subpopulation. In addition, MDK-703 had a negligible-to-no impact on the expansion of CD4+ T regulatory and natural killer (NK) cells. Because the IL-7 mimetic peptide in MDK-703 is structurally unrelated to IL-7, it is unlikely to generate anti-drug antibodies (ADAs) that neutralize native IL-7.

Methods This Phase 1, randomized, placebo-controlled, single-blind, single ascending dose study evaluates the safety, tolerability, pharmacokinetics, and pharmacodynamics of MDK-703 in healthy adult volunteers. Three sequential cohorts of 10 subjects (8 MDK-703; 2 Placebo) will be studied. The primary outcome measure is the assessment of adverse events after a single injection of MDK-703 over 8 weeks. Pharmacodynamic measures include assessment of blood cells by complete blood counts, including lymphocytes, and immunophenotyping of T-cells, including memory cell subpopulations. Blood cytokine/chemokines and T-cell receptor repertoire will also be measured, along with the presence of ADAs and NAbs against MDK-703 and IL-7.

Results As of July 28, 2022, the first cohort of subjects has been dosed. It is expected that preliminary data for three ascending dose cohorts will be available in November 2022 (Clinical trial information: NCT05366634)

<http://dx.doi.org/10.1136/jitc-2022-SITC2022.0625>

626

TRIAL IN PROGRESS: AN INTRAVENOUSLY ADMINISTERED SECOND-GENERATION STING AGONIST, BI 1703880 WITH A NOVEL LEAD-IN DESIGN IN COMBINATION WITH EZABENLIMAB

¹Kevin Harrington*, ²Elizabeth Dowling, ³Robert Latek, ³Michael Schmohl, ⁴Patricia Lorusso. ¹The Royal Marsden NHS Foundation Trust, Sutton, UK; ²Boehringer Ingelheim Pharmaceuticals Inc, Ridgefield, CT, USA; ³Boehringer Ingelheim International GmbH, Ingelheim, Germany; ⁴Yale Cancer Center, New Haven, CT, USA

Background The prognosis for cancer patients diagnosed with advanced-stage disease or who have experienced disease progression is poor. STING (stimulator of interferon genes) is an intracellular nucleic acid sensor, which has a key role in innate immunity and detects the presence of cytosolic cyclic dinucleotides indicative of pathogen invasion and cellular disruption. BI 1703880 is a synthetic second-generation STING agonist, which induces a type 1 interferon response and transient secretion of interferon β and proinflammatory cytokines. Interferon receptor signaling upregulates PD-L1 expression, which reduces T-cell functionality and facilitates immune evasion through interaction with PD-1, suggesting that the combination of BI 1703880 with an anti-PD-1 antibody, such as ezabenzimab, may synergize to overcome tumor resistance.

Methods The 1480-0001 study is a first-in-human Phase Ia, open-label, dose-escalation trial of BI 1703880 monotherapy and in combination with ezabenzimab. In this innovative trial design, all patients will receive intravenous BI 1703880 as monotherapy followed by BI 1703880 in combination with ezabenzimab. The primary objective is to characterize the dose-toxicity curve for escalating doses of BI 1703880 in combination with ezabenzimab. Secondary objectives are to determine the safety profile of escalating doses of BI 1703880 (dose-limiting toxicities), to characterize its pharmacokinetics and pharmacodynamics, and to assess efficacy.

The lead-in dose escalation of BI 1703880 will be tested through six consecutive cohorts (figure 1) guided by a Bayesian 5-parameter logistic regression model with fitted overdose control. This will determine the maximum tolerated dose estimate. BI 1703880 will be administered intravenously for up to 18 cycles, or unacceptable toxicity or disease progression, at increasing dose levels (figure 2). Patients can continue to receive treatment if there is clinical benefit. Ezabenzimab 240 mg will be administered intravenously from Cycle 2 (figure 2). Approximately 36 patients will be enrolled.

Key eligibility criteria include an advanced, unresectable and/or metastatic malignant solid tumor, Eastern Cooperative Oncology Group performance score of 0–1, exhausted established treatment options and at least one lesion amenable to pre- and on-treatment biopsy.

Peripheral and tumor biomarkers will be analyzed to assess the BI 1703880 mode of action. Peripheral cytokine analysis will supplement clinical safety profiles for informing dose escalation decisions, since cytokine release syndrome is a potential risk for STING agonists.

Acknowledgements The authors meet criteria for authorship as recommended by the International Committee of Medical Journal Editors (ICMJE). The authors did not receive payment related to the development of the abstract. William Townley, MRes, of MediTech Media provided writing and editorial support which was contracted and funded by Boehringer Ingelheim International GmbH (BI). BI was given the opportunity to review the abstract for medical and scientific accuracy as well as intellectual property considerations. The 1480-000-1 study was supported and funded by BI.

Trial Registration EudraCT: 2022-000298-22



Abstract 626 Figure 1



Abstract 626 Figure 2

<http://dx.doi.org/10.1136/jitc-2022-SITC2022.0626>

627

ORAL ADMINISTRATION OF MRX0518 IN TREATMENT-NAÏVE CANCER PATIENTS IS ASSOCIATED WITH COMPOSITIONAL TAXONOMIC AND METABOLOMIC CHANGES INDICATIVE OF ANTI-TUMORIGENIC EFFICACY

¹Mark Lythgoe*, ¹Benjamin Mullish, ²Adam Frampton, ³Paola Dama, ¹Emily Pickford, ¹Laura Tookman, ¹Paula Cunnea, ¹Christina Fotopoulou, ⁴Ian Jeffery, ⁴Gayle Fyvie, ⁴Alexander Stevenson, ¹Jonathan Krell. ¹Imperial College London, London, UK; ²University of Surrey, Guildford, UK; ³University of Sussex, Brighton, UK; ⁴AD Pharma, Leeds, UK

Background Live biotherapeutic products (LBPs) are promising novel anti-cancer therapies. Their mechanism of action has not yet been fully elucidated but is thought to be partly due to compositional changes in the gut microbiome and metabolomic profile. There is particular interest in the anti-cancer efficacy of microbial fermentation products, including short chain fatty acids (SCFAs), including butyrate and propionate.

MRx0518 is a novel, gut microbiome-derived LBP, consisting of a single strain of *Enterococcus gallinarum*, which has demonstrated potent anti-tumorigenic efficacy preclinically.¹ We have previously shown MRx0518 therapy is associated with significant anti-tumorigenic genomic, cytokine and immune modulatory changes in treatment-naïve cancer patients.^{2,3} Here, we report compositional taxonomic and metabolomic changes following MRx0518 treatment.

Methods NCT03934827 is a Phase 1B single-centre study in patients with histologically confirmed cancer undergoing surgical resection. Patients receive 1 capsule of MRx0518 (1x10¹⁰-1x10¹¹CFU) BID from inclusion until surgery (maximum 28 days therapy). Exploratory outcomes included microbiome analysis of longitudinal faecal samples, with 16S rRNA gene sequencing, and investigation of metabolomic changes in SCFAs in plasma samples, by liquid chromatography-mass spectrometry.

Results 17 patients received 7-28 days of MRx0518 therapy. Significantly (P=0.0001) increased levels of MRx0518 16S rRNA levels were detected in all faecal samples at time of therapy cessation (Visit 6). 30-days after treatment stoppage (Visit 8), levels of MRx0518 16S rRNA were undetectable. MRx0518 therapy was associated with a small but significant increase in beta-diversity. Post-therapy samples showed significant microbiota changes, with a visual trend (non-statistical) back towards baseline profile at 6-month follow-up (Visit 9). Significant (P<0.05) taxa changes in *Bacteroides* at Visit 6, and Lachnospiraceae, Clostridium sensu, Enterocloster, *Ruminococcaceae*, and *Anaerobutyricum* at Visit 8, were identified.

Analysis of plasma metabolomics on paired pre- and post-treatment samples, at 30-days, demonstrated a significant reduction (P<0.05) in levels of acetic acid, with positive trends (non-significant) identified in 2-methyl butyric acid, butyrate and propionate. Sub-analysis of subjects (n=11) who received MRx0518 for >15 days showed significant (P<0.05) post-treatment increases in 2-methyl butyrate, butyrate, propionate and valerate, with a concordant significant reduction in acetic acid levels.

Conclusions MRx0518 therapy is associated with significant compositional taxonomic changes and alterations in SCFA, indicative of anti-cancer efficacy. This effect is more pronounced in patients who receive treatment for longer periods. Changes in SCFAs, such as butyrate and propionate, may contribute to the anti-cancer efficacy of MRx0518. Further investigation is required to link post-treatment metabolomic changes to taxonomic changes in the gut microbiome.

Trial Registration NCT03934827

REFERENCES

1. Lauté-Caly DL, Raftis EJ, Cowie P, *et al.* The flagellin of candidate live biotherapeutic *Enterococcus gallinarum* MRx0518 is a potent immunostimulant. *Scientific Reports*. 2019;**9**(1):1–14. doi:10.1038/s41598-018-36926-8
2. Lythgoe M, Stebbing J, Pickford E, *et al.* 805 Safety and emerging evidence of immune modulation of the live biotherapeutic MRx0518 in the neoadjuvant setting for patients awaiting surgical removal of solid tumours. *Journal for ImmunoTherapy of Cancer*. 2020;**8**(Suppl 3):A854–A854. doi:10.1136/jitc-2020-sitc2020.0805
3. Lythgoe M, Adriani M, Stebbing J, *et al.* 543P Neoadjuvant MRx0518 treatment is associated with significant gene and metagene signature changes in solid tumours. *Annals of Oncology*. 2021;**32**:S607. doi:10.1016/j.annonc.2021.08.1065

Ethics Approval This study has been approved by the UK Research Ethics Committee (East of England – Cambridge East Research Ethics Committee – C/35/2017). All patients gave informed consent for participation in this research.

Consent Written informed consent was obtained from the patient for publication of this abstract and any accompanying images. A copy of the written consent is available for review by the Editor of this journal.

<http://dx.doi.org/10.1136/jitc-2022-SITC2022.0627>

628

TRIAL IN PROGRESS: PHASE I DOSE-ESCALATION STUDY OF VSV-GP (BI 1831169) MONOTHERAPY AND WITH EZABENLIMAB (BI 754091) IN PATIENTS WITH LOCALLY ADVANCED OR METASTATIC SOLID TUMORS

¹Mercedes Porosnicu*, ²Anne-Marie Quinson, ³Abi MacKay, ⁴Stephan Luecke, ⁵Ulrich M Lauer. ¹Wake Forest School of Medicine, Winston Salem, NC, USA; ²Boehringer Ingelheim Pharmaceuticals Inc, Ridgefield, CT, USA; ³Boehringer Ingelheim Ltd, Bracknell, UK; ⁴Boehringer Ingelheim Pharma GmbH and Co.KG, Biberach, Germany; ⁵University Hospital Tübingen, Tübingen, Germany

Background Patients with locally advanced or metastatic cancer have poor prognosis despite treatment advancements. VSV-GP (BI 1831169) is a chimeric vesicular stomatitis virus (VSV) with its neurotropic glycoprotein (G) replaced by the non-neurotropic glycoprotein (GP) of the lymphocytic choriomeningitis virus. This live, recombinant oncolytic virus has demonstrated preclinical efficacy as a viral-based immunotherapy due to its interferon-dependent tumor specificity and stimulation of anti-tumor immune activity. Co-administration of ezabenlimab (BI 754091), a PD-1 targeting checkpoint inhibitor, may enhance antitumor efficacy. The potential synergism of VSV-GP and ezabenlimab will be explored in this first-in-human trial.

Methods This Phase I, open-label, dose-escalation trial will assess the safety, tolerability and early efficacy of VSV-GP given intratumorally (IT), intravenously (IV) or both, as a monotherapy (Part 1) and in combination with ezabenlimab (Part 2) in patients with locally advanced, metastatic or relapsed/refractory solid tumors who previously received or are not candidates for available standard treatment. Key objectives are to determine the maximum tolerated dose (MTD) and recommended Phase 2 dose (RP2D).

Part 1 is a dose-escalation and expansion study of VSV-GP monotherapy administered in four 21-day cycles starting at 5×10^7 median tissue culture infectious dose (TCID₅₀) in Arm A (IT) and at the next tolerated dose level in Arm B (IV) and Arm C (IT + IV). Part 2 is a dose-escalation study of VSV-GP in combination with ezabenlimab. The starting dose of VSV-GP will be one dose level less than the monotherapy RP2D in the corresponding Part 1 arm (IT [Arm D], IV [Arm E], IT + IV [Arm F]) (figure 1). Dose finding will be guided by the Bayesian Optimal Interval design (BOIN).

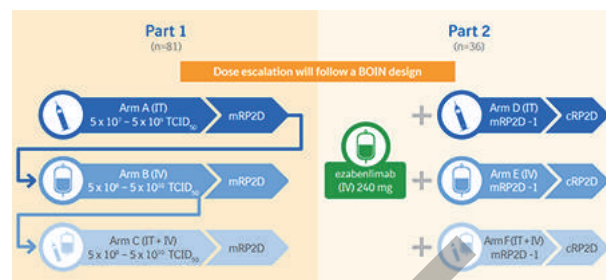
Primary endpoints include the number of patients experiencing dose-limiting toxicities (DLTs [Part 1/2]) and objective response according to Intratumoral RECIST (itRECIST; Part 1). Secondary endpoints are safety-based (on-treatment DLTs and adverse events). Patients are being recruited. Updates will be provided at the time of presentation.¹

Acknowledgements The authors meet criteria for authorship as recommended by the International Committee of Medical Journal Editors (ICMJE). The authors did not receive payment related to the development of the abstract. Devon Else, BSc, of MediTech Media provided writing and editorial support which was contracted and funded by Boehringer Ingelheim International GmbH (BI). BI was given the opportunity to review the abstract for medical and scientific accuracy as well as intellectual property considerations. The 1456.1 study was supported and funded by BI.

Trial Registration NCT05155332

REFERENCE

1. Porosnicu M, et al. Phase I study of VSV-GP (BI 1831169) as monotherapy or combined with ezabenlimab in advanced and refractory solid tumors. *Future Oncol.* 2022;**18**:2627–2638.



Abstract 628 Figure 1

<http://dx.doi.org/10.1136/jitc-2022-SITC2022.0628>

Abstracts

629

NEOADJUVANT NIVOLUMAB COMBINED WITH CCR2/5 INHIBITOR OR ANTI-IL-8 ANTIBODY IN NON-SMALL CELL LUNG CANCER AND HEPATOCELLULAR CARCINOMA

¹Nicholas Venturini*, ¹Thomas Marron, ²Maria Casanova-Acebes, ¹John Mandeli, ¹Deborah Doroshov, ¹Natalie Lucas, ¹Kathy Wu, ¹Olivia Hapanowicz, ¹Paula King, ¹Pauline Hamon, ¹Jessica Le Berichel, ¹Diane Del Valle, ¹Clotilde Hennequin, ¹Seunghye Kim-Schulze, ¹Sacha Gnjatic, ¹Miriam Merad, ¹Zhen Zhao, ¹Stephen Ward, ¹Maria Isabel Fiel, ¹Mary Beasley, ¹Edward Kim, ¹Kirema Garcia-Reyes, ¹Udit Chaddha, ¹Timothy Harkin, ¹David Yankelevitz, ¹Ganesh Gunasekaran, ¹Parissa Tabrizian, ¹Myron Schwartz, ¹Andrew Kaufman, ¹Daniel Nicastri, ¹Andrew Wolf, ¹Raja Flores. ¹Icahn School of Medicine at Mount Sinai, New York, NY, USA; ²Centro Nacional de Investigaciones Oncológicas, Madrid, Spain

Background Immune checkpoint blockade (ICB) has revolutionized cancer treatment; however, most patients fail to achieve the full clinical benefit of ICB. Although anti-PD-1 agents are FDA-approved for non-small cell lung cancer (NSCLC) and hepatocellular carcinoma (HCC), only a minority of patients respond clinically.^{1,2} This limited response is likely due, in part, to immunosuppressive factors within the tumor microenvironment (TME). Myeloid cells, specifically monocyte-derived macrophages (mo-Macs) and immature granulocytes (iPMNs), make up the majority of leukocytes in the TME and suppress anti-tumor immunity; pre-clinical work has revealed that tumor-derived CCR2 ligands and interleukin-8 (IL-8) play a key role in recruiting mo-Macs and iPMNs, respectively, to the TME.³⁻⁷ Disrupting these signaling pathways appears to potentiate the role of PD-1 blockade in mouse models, although only modest clinical benefit has been demonstrated to date in metastatic cancer models. In this “window-of-opportunity” trial, patients will receive neoadjuvant nivolumab monotherapy or neoadjuvant nivolumab in conjunction with a CCR2/5 inhibitor or an anti-IL8 antibody prior to surgical resection, providing a unique opportunity to elaborate the specific effects of these agents on the TME and to identify factors that may allow clinicians to better predict response in the future.

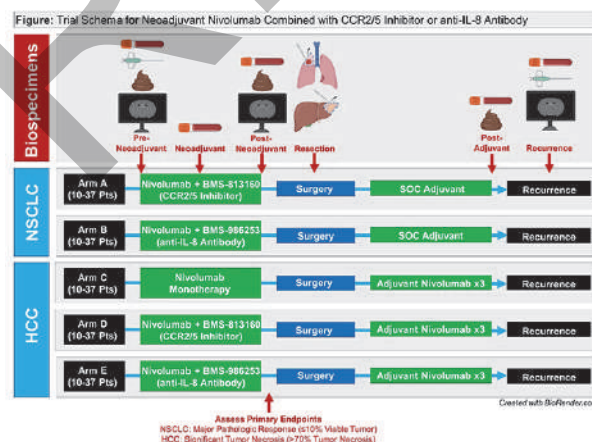
Methods This phase IIa multi-cohort, two-stage trial was designed to assess the clinical efficacy of BMS-813160 (CCR2/5 inhibitor) and BMS-986253 (anti-IL8 antibody) in patients with resectable NSCLC and HCC. The trial contains 2 cohorts (NSCLC and HCC) consisting of 5 arms (figure 1); arms A and B will enroll patients with NSCLC and arms C, D, and E will enroll patients with HCC. Patients will be treated with neoadjuvant nivolumab either alone (arm C) or in combination with BMS-813160 (arms A and D) or BMS-986253 (arms B and E). The patients will then undergo surgical resection, followed by standard-of-care adjuvant therapy in the NSCLC cohort or adjuvant nivolumab therapy in the HCC cohort. The primary endpoint for the NSCLC cohort is major pathologic response, defined as ≤10% viable tumor at time of surgery. The primary endpoint for the HCC cohort is significant tumor necrosis, defined as >70% tumor necrosis at time of surgery. The secondary endpoints are time to surgery, safety and tolerability, radiographic response, progression-free survival, and overall survival. Tissue, blood, and stool will be collected prior to treatment and at the time of surgery. Deep immune monitoring will be performed using multiplex and single-cell analysis platforms to define the immunodynamic effects of the therapies.

Trial Registration NCT04123379

REFERENCES

1. Forde PM, Chaft JE, Smith KN, Anagnostou V, Cottrell TR, Hellmann MD, *et al.* Neoadjuvant PD-1 blockade in resectable lung cancer. *New England Journal of Medicine.* 2018;**378**(21):1976–86.
2. El-Khoueiry AB, Sangro B, Yau T, Crocenzi TS, Kudo M, Hsu C, *et al.* Nivolumab in patients with advanced hepatocellular carcinoma (Checkmate 040): An open-label, non-comparative, phase 1/2 dose escalation and expansion trial. *The Lancet.* 2017;**389**(10088):2492–502.
3. Casanova-Acebes M, Dalla E, Leader AM, LeBerichel J, Nikolic J, Morales BM, *et al.* Tissue-resident macrophages provide a pro-tumorigenic niche to early NSCLC cells. *Nature.* 2021;**595**(7868):578–84.
4. Lesokhin AM, Hohl TM, Kitano S, Cortez C, Hirschhorn-Cymerman D, Avogadri F, *et al.* Monocytic CCR2+ myeloid-derived suppressor cells promote immune escape by limiting activated CD8 T-cell infiltration into the tumor microenvironment. *Cancer Research.* 2012;**72**(4):876–86.
5. Schlecter E, Stojanovic A, Eisen C, Quack C, Falk CS, Umansky V, *et al.* Tumor-infiltrating monocytic myeloid-derived suppressor cells mediate CCR5-dependent recruitment of regulatory T cells favoring tumor growth. *The Journal of Immunology.* 2012;**189**(12):5602–11.
6. Hegde S, Leader AM, Merad M. MDSC: Markers, development, states, and undressed complexity. *Immunity.* 2021;**54**(5):875–84.
7. Teijeira A, Garasa S, Gato M, Alfaro C, Migueliz J, Cirella A, *et al.* CXCR1 and CXCR2 chemokine receptor agonists produced by tumors induce neutrophil extracellular traps that interfere with immune cytotoxicity. *Immunity.* 2020;**52**(5).

Ethics Approval This trial obtained approval from the Icahn School of Medicine at Mount Sinai Institutional Review Board (#18-2375); all patients gave informed consent before participating in this trial.



Abstract 629 Figure 1: Trial Schema

<http://dx.doi.org/10.1136/jitc-2022-SITC2022.0629>

631

PHASE I DOSE ESCALATION STUDY IN PATIENTS WITH ADVANCED SOLID TUMORS WITH ANV419, A NOVEL FUSION PROTEIN SELECTIVE FOR IL-2R β / γ

¹Christoph Bucher, ²Guzman Alonso, ³Juanita Lopez, ⁴Emiliano Calvo, ⁵Markus Joerger, ³Vicky Sanchez Perez, ⁴Elena Corral, ¹Daniela Di Blasi*, ¹Kirsten Richter, ¹Christoph Huber, ¹Julie Mouton, ¹Silvio Costanzo, ¹Sangeeta Jethwa, ²Elena Gerralda, ⁶Heinz Läubli. ¹Anaveon AG, Basel, Switzerland; ²Vall d'Hebron, Barcelona, Spain; ³Royal Marsden, London, UK; ⁴START Madrid-CIOCC, Madrid, Spain; ⁵Kantonsspital St. Gallen, St. Gallen, Switzerland; ⁶University Hospital, Basel, Switzerland

Background ANV419 is a fusion protein of an anti-IL-2 antibody and human-IL-2 with selective signaling through IL-2R β / γ thus limiting the side effects of activating the IL-2R α / β / γ ANV419 is investigated in a phase I dose finding study in patients with advanced solid tumors (ANV419-001).

Methods The primary objective of ANV419-001 is safety and tolerability of ANV419. Secondary objectives include response rate (RECISTv1.1), pharmacokinetic and pharmacodynamic evaluation. ANV419 is administered as a 15 minutes intravenous infusion Q2W. As of 29th June 2022, 26 patients with Eastern Cooperative Oncology Group (ECOG) Performance Status 0 or 1 and a range of primary tumor types with multiple previous lines of therapy have been enrolled and dosed in 9 cohorts up to 243 μ g/kg.

Results ANV419 was generally well tolerated across multiple cycles, with no dose-limiting toxicities (DLTs) up to and including 243 μ g/kg. The most frequent ANV419 related adverse events (AEs), reported in at least 10% of patients, were chills, fever, fatigue, nausea, vomiting, cytokine release syndrome (CRS) and increased liver function tests, mainly Grade 1 and Grade 2. All drug related events were responsive to supportive care therapy and reversible.

A dose proportional increase in ANV419 plasma concentration results in an increased estimated half-life up to 28 hours at higher doses.

In this study, IL-6, IL-8, TNF- α , and IFN- γ levels (10-Plex Panel) were transiently increased at high doses (108 and 243 μ g/kg), 4 hours after infusion.

Pharmacodynamic evaluation of ANV419 on day 4 post-dosing (cycle 1 and 2) showed a selective and dose dependent proliferation of CD8⁺ T and NK cells, with a lower increase of proliferating Tregs. As typical for IL-2 related lymphocyte sequestration, a transient dose dependent lymphopenia was observed in all patients lasting up to at least 72 hours after ANV419 infusion, followed by a dose dependent increasing lymphocyte counts up to 5.4-fold of baseline. Lymphocyte numbers keep increasing over multiple cycles up to 3.8-fold after 2 cycles (243 μ g/kg). In 21 patients with at least one post-baseline tumor response assessment, 52% of patients (n=11) achieved a response of SD or PR, with 10 SD, 1 PR and 10 PD.

Conclusions ANV419 maintains a favorable safety profile, while inducing a systemic inflammatory response in cancer patients with preferential proliferation of effector cells compared to high dose of IL-2. Dose escalation is ongoing. The preliminary efficacy data shows a potential for ANV419 as therapeutic option for patients with progressing/relapsing cancer. Updated data will be shared at the meeting.

Trial Registration NCT04855929

Ethics Approval The study ANV419-001 has been approved by the following Ethics committee:

- HM Hospitals Drug Research Ethics Committee (CEIm) (ID: 20.12.1736-GHM)

- EKNZ – Ethikkommission Nordwest und Zentralschweiz (ID 2021-00911)

- London – Surrey Borders Research Ethics Committee (ID: 21/LO/0213)

Written consent was obtained from all patients prior taking part into this study.

Consent Written informed consent was obtained from the patient for publication of this abstract.

<http://dx.doi.org/10.1136/jitc-2022-SITC2022.0631>

632

CLINICAL UPDATE FROM A PHASE 1, FIRST-IN-HUMAN, OPEN-LABEL SINGLE AGENT STUDY OF SUPLEXA THERAPEUTIC CELLS IN PATIENTS WITH METASTATIC SOLID TUMOURS AND HAEMATOLOGIC MALIGNANCIES

¹Rohit Joshi*, ²Jeffrey Goh, ²Warren Joubert, ³Vineet Kwarta, ³Meena Okera, ³Sarwan Bishnoi, ⁴Jim Lederer, ⁴Frank Borriello, ⁴Sharon Gargosky. ¹*Cancer Research South Australia, Adelaide, Australia*; ²*Gallipoli Research Foundation, Brisbane, Australia*; ³*Cancer Research South Australia (CRSA), Adelaide, Australia*; ⁴*Alloplex Biotherapeutics Inc, Woburn, MA, USA*

Background SUPLEXA is a first-in-class, autologous, adoptive immunotherapy; prepared from patients' PBMCs it contains NK cells, NKT-like, gd T cells, and ab T cells of both the CD8⁺ and CD4⁺ variety primed for broad tumor cytolytic activity.

Methods This is a FIH Phase 1, non-comparative, open-label, basket-design study NCT05237206. The study is enrolling up to 40 participants in Australia in 2 cohorts: 1. Solid tumours cohort that includes subjects with histologically or cytologically or radiographically confirmed and 2. a haematologic malignancies cohort including subjects with histologically or cytologically confirmed multiple myeloma, lymphoma, and chronic lymphocytic leukemia. Primary objective is to assess safety and tolerability of SUPLEXA and the secondary objective is to assess the efficacy. All eligible subjects will receive a minimum 7.5×10^9 cumulative dose of SUPLEXA therapeutic cells. Each treatment is administered at least 1 week apart at Day 1 (baseline), Week 1, Week 2 and possibly more depending on manufacturing yield. The first 3 subjects in each cohort will be enrolled in a staggered manner, at least 1 week apart; these subjects will be evaluated for safety and if no safety concerns are identified, all remaining subjects will be enrolled. All subjects will be evaluated for DLTs, 1 week after the 1st dose and 2nd dose (prior to administration of 2nd dose and 3rd dose, respectively).

Results As of submission, 10 patients (8 female and 2 male; age 34-75years) have been enrolled. Cancer types have included squamous cell, ovarian, bladder, urothelial and pancreatic cancers. SUPLEXA therapy was successfully manufactured for all patients to receive the minimum course of 7.5×10^9 SUPLEXA cells. Treatment has been well tolerated with no study related SAEs or discontinuations. No clinical observations have been noted with clinical chemistry, hematology, urinalysis, or other serology, nor with ECG or other assessments. Of note there has been a mild transient observation of odour for 24hrs post infusion as commonly expected from the DMSO cellular cryopreservative used. Data for the first 3 participants has been reviewed by the DSMB and the study is now fully opened to enrolment.

Conclusions Trial is proceeding well with an excellent tolerability profile and ease of administration for the patients. Additional safety and efficacy data will be forthcoming.

Acknowledgements Daniel Clark, Kelly Mead, Stephanie Kosmala

Trial Registration NCT05237206

Ethics Approval Ethics approval received from Belberry HREC

<http://dx.doi.org/10.1136/jitc-2022-SITC2022.0632>

633

A PHASE 1, FIRST IN HUMAN (FIH) STUDY OF AUTOLOGOUS MACROPHAGES CONTAINING AN ANTI-HER2 CHIMERIC ANTIGEN RECEPTOR (CAR) IN PARTICIPANTS WITH HER2 OVEREXPRESSING SOLID TUMORS

¹Kim Reiss*, ²Naoto Ueno, ³Yuan Yuan, ⁴Melissa Johnson, ⁵E Claire Dees, ³Joseph Chao, ⁶Mathew Angelos, ⁷Ramona Swaby, ⁷Daniel Cushing, ⁷Amy Ronczka, ⁷Thomas Condamine, ⁷Debra Barton, ⁷Michael Klichinsky, ⁵Yara Abdou. ¹University of Pennsylvania Abramson Cancer, Philadelphia, PA, USA; ²The University of Texas MD Anderson Cancer Center, Houston, TX, USA; ³City of Hope Cancer Center, Duarte, CA, USA; ⁴Sarah Cannon Research Institute, Nashville, TN, USA; ⁵University of North Carolina Lineberger, Chapel Hill, NC, USA; ⁶Abramson Cancer Center, Philadelphia, PA, USA; ⁷Carisma Therapeutics, Philadelphia, PA, USA

Background Macrophages are phenotypically plastic cells that are abundant in the solid tumor microenvironment (sTME) and can promote tumor growth (M2) or enhance anti-tumor immunity (M1). Macrophage function can be redirected by CAR expression to selectively target and phagocytose antigen overexpressing cancer cells. CAR macrophages can reprogram the sTME and present neoantigens to T cells, leading to epitope spreading and anti-tumor immune memory.¹ HER2 overexpression promotes tumorigenesis in many solid tumors (table 1). CT-0508 is comprised of autologous monocyte-derived proinflammatory macrophages expressing an anti-HER2 CAR. Pre-clinical studies showed that CT-0508 induced targeted cancer cell phagocytosis while sparing normal cells, decreased tumor burden, prolonged survival, and was safe and effective in humanized xenograft mouse models of human HER2 overexpressing ovarian cancer. In immunocompetent mouse models of HER2 overexpressing solid tumors, syngeneic anti-HER2 CAR-M mediated tumor control and improved overall survival as compared to untreated or control untransduced macrophage (UTD) treated mice. Notably, anti-HER2 CAR-M treatment led to significant activation of the sTME, with notable infiltration of CD8+ and CD4+ T cells, NK cells, dendritic cells, and an increase in activated CD8+ tumor infiltrating lymphocytes. Anti-HER2 CAR-M were evaluated in a PD1 blockade resistant syngeneic model – mice that received both therapies had improved tumor control, overall survival, and TME activation as compared to either treatment alone, indicating synergy and the capacity for CAR-M to sensitive solid tumors to checkpoint blockade.

Methods This Phase 1, FIH study is evaluating safety, tolerability, cell manufacturing feasibility, trafficking, TME activation, and preliminary evidence of efficacy of investigational product CT-0508 in 18 participants with locally advanced (unresectable)/metastatic solid tumors overexpressing HER2. Pts previously treated with anti-HER2 therapies are eligible. Filgrastim mobilizes autologous hematopoietic progenitor cells for monocyte collection by apheresis. CT-0508 is manufactured, prepared, and cryopreserved from mobilized peripheral blood monocytes. Group 1 participants (n = 9; enrollment complete) received CT-0508 infusion split over Days 1, 3, and 5. Group 2 participants (n = 9) will receive CT-0508 single infusion on D1. Additional study cohorts include: CT-0508 co-administered with pembrolizumab and CT-0508 monotherapy administered intraperitoneally in participants with peritoneal predominant disease. Correlative assessments include pre and post-treatment biopsies and blood samples for safety (immunogenicity), trafficking (PCR, RNA scope), CT-0508 persistence in blood and tumor, target antigen engagement, TME modulation (single cell RNA sequencing), immune response (TCR sequencing) and others.

Trial Registration NCT04660929

REFERENCE

1. Klichinsky M, Ruella M, Shestova O. *et al.* Human chimeric antigen receptor macrophages for cancer immunotherapy. *Nat Biotechnol.* 2020;**38**:947–953.

Ethics Approval This study has been approved by each participating site: University of Pennsylvania Abramson Cancer Center IRB approval #844106, University of North Carolina Lineberger Cancer Center IRB approval #20201732, City of Hope Cancer Center IRB approval #20201732, The University of Texas MD Anderson Cancer Center IRB approval #2021-0327, Sarah Cannon Research Institute IRB #20201732. All participants gave their informed consent before taking part in the study.

Abstract 633 Table 1: HER2 Overexpression Across Tumor Types

Table 1: HER2 Overexpression Across Tumor Types

Tumor	HER2 Overexpression (%)
Bladder	8 - 70
Salivary duct / mucoepidermoid	30 - 40 / 17.6
Gastric	7 - 34
Ovarian / Cervical / Uterine	26 / 2.8 - 3.9 / 3
Breast	11 - 25
Esophageal	12 - 14
Gallbladder / Cholangiocarcinoma	9.8 - 12.8 / 6.3 - 9
Colorectal	1.6 - 5
Testicular	2.4

<http://dx.doi.org/10.1136/jitc-2022-SITC2022.0633>

634

A PHASE 1, FIRST-IN-HUMAN (FIH) CLINICAL TRIAL OF THE ANTI-HER2 CAR MACROPHAGE CT-0508 IN PARTICIPANTS WITH HER2 OVEREXPRESSING SOLID TUMORS

¹Kim Reiss*, ²Yuan Yuan, ³Naoto Ueno, ⁴Melissa Johnson, ⁵E Claire Dees, ⁶Mathew Angelos, ²Joseph Chao, ⁶Saar Gill, ⁹Olga Shestova, ⁵Jonathan Serody, ²Saul Priceman, ⁷Amy Ronczka, ⁷Rehman Qureshi, ⁷Poonam Sonawane, ⁷Daniel Cushing, ⁷Debra Barton, ⁷Michael Klichinsky, ⁷Thomas Condamine, ⁷Ramona Swaby, ⁵Yara Abdou. ¹Abramson Cancer Center Univ of Penn, Philadelphia, PA, USA; ²City of Hope Cancer Center, Duarte, CA, USA; ³The Univ of Texas MD Anderson Cancer Center, Houston, TX, USA; ⁴Sarah Cannon Research Institute Cancer Center, Nashville, TN, USA; ⁵University of North Carolina Lineberger Comprehensive Cancer, Chapel Hill, NC, USA; ⁶Univ of Pennsylvania Abramson Cancer Center, Philadelphia, PA, USA; ⁷Carisma Therapeutics, Philadelphia, PA, USA

Background In pre-clinical studies, CAR macrophages (CAR-M) phagocytose tumor cells, activate the tumor micro-environment (TME), recruit T cells, and induce anti-tumor T cell immunity. CT-0508 is a first-in-class CAR-M product comprised of autologous monocyte-derived macrophages expressing an anti-HER2 CAR. Here we present preliminary clinical results from the CT-0508 Phase 1 FIH study.

Methods This multi-center, open-label study is evaluating CT-0508's safety, tolerability, and manufacturing feasibility in 18 participants with advanced solid tumors overexpressing HER2 with progression on prior therapies. Monocytes are isolated from mobilized apheresis products, differentiated into macrophages, and engineered with an anti-HER2 CAR. Group 1 participants (n = 9) receive a fractionated dose on days 1, 3, 5 and Group 2 participants (n = 9) receive the full dose on day 1. CT-0508 is administered without preparative chemotherapy. Serial blood samples and biopsies (baseline and 2 post-treatment) are collected to investigate safety, pharmacokinetics, and mechanism of action.

Results Nine participants (6F/3M) have been treated, comprising breast (4), esophageal (2), cholangiocarcinoma, ovarian, and parotid gland cancers, with a median age of 58. Participants had received a median of 3 (range, 2-11) prior lines of therapy; 8 had received prior anti-HER2 therapy. CT-0508 was successfully manufactured and well tolerated with no dose-limiting toxicities. Three related SAEs occurred in 2 participants: grade 1 CRS with hospitalization for monitoring and grade 2 infusion reaction that resolved within 1 hour were reported in one participant. Grade 2 CRS with fever and hypoxia occurred in another participant and resolved within ~ 72 hours. Five additional participants experienced Grade 1-2 CRS and/or infusion reactions with rapid resolution. There were no major organ toxicities and no on-target off-tumor toxicities. Post-infusion cytokines were transiently elevated in most participants enrolled in group 1 and were self-limiting. Four of 7 participants evaluated had stable disease. CT-0508 was transiently detectable in the blood and was detected in the TME 8 days and 4 weeks after infusion. CT-0508 modulated the TME, leading to myeloid cell activation, T cell infiltration, activation, and proliferation. TCR sequencing demonstrated newly expanding T cell clones in the blood post-treatment that accumulated within the TME, suggesting expansion of tumor-reactive T cells upon CT-0508 infusion. Data from participants enrolled in group 1 will be presented.

Conclusions CT-0508 was safe and feasible to manufacture. Early correlative data demonstrate trafficking, TME modulation, and induction of anti-tumor T cell immunity. The study is actively enrolling.

Trial Registration NCT04660929

REFERENCE

1. Klichinsky M, Ruella M, Shestova O. *et al.* Human chimeric antigen receptor macrophages for cancer immunotherapy. *Nat Biotechnol.* 2020;**38**:947–953.

Ethics Approval This study has been approved by each participating site: University of Pennsylvania Abramson Cancer Center IRB approval #844106, University of North Carolina Lineberger Cancer Center IRB approval #20201732, City of Hope Cancer Center IRB approval #20201732, The University of Texas MD Anderson Cancer Center IRB approval # 2021-0327, Sarah Cannon Research Institute IRB #20201732. All participants gave their informed consent before taking part in the study.

<http://dx.doi.org/10.1136/jitc-2022-SITC2022.0634>

635

KEYNOTE-495/KEYIMPACT: UPDATED ANALYSIS OF A BIOMARKER-DIRECTED, RANDOMIZED, PHASE 2 TRIAL OF PEMBROLIZUMAB-BASED COMBINATION THERAPY FOR NON-SMALL CELL LUNG CANCER

¹Roy Herbst*, ²Wei-Sen Lam, ³Matthew Hellmann, ⁴Matthew Gubens, ⁵Charu Aggarwal, ⁶Daniel Shao Weng Tan, ⁷Enriqueta Felip, ⁸Joanne Chiu, ⁹Jong-Seok Lee, ¹⁰James Chih-Hsin Yang, ¹¹Edward Garon, ¹²Giovanna Finocchiaro, ¹³Myung-Ju Ahn, ¹⁴Alexander Luft, ¹⁵Gregory Landers, ¹⁶Andrea Basso, ¹⁶Hua Ma, ¹⁶Julie Kobie, ¹⁶John Palcza, ¹⁶Razvan Cristescu, ⁴Lawrence Fong, ¹⁶Alexandra Snyder, ¹⁶Jianda Yuan, ¹⁷Martin Gutierrez. ¹Yale Cancer Center, Yale School of Medicine, New Haven, CT, USA; ²Fiona Stanley Hospital and Western Australia Country Health Service, Perth, Australia; ³Memorial Sloan Kettering Cancer Center, New York, NY, USA; ⁴UCSF Helen Diller Family Comprehensive Cancer Center, San Francisco, CA, USA; ⁵Perelman School of Medicine, University, Philadelphia, PA, USA; ⁶National Cancer Centre Singapore, Singapore, Singapore; ⁷Vall d'Hebron University Hospital, Vall, Barcelona, Spain; ⁸University of Hong Kong, Queen Mary Hosp, Pok Fu Lam, Hong Kong; ⁹Seoul National University Bundang Hospital, Seongnam, Republic of Korea; ¹⁰National Taiwan University Hospital and, Taipei City, Taiwan; ¹¹David Geffen School of Medicine at UCLA, Los Angeles, CA, USA; ¹²IRCCS Humanitas Research Hospital, Milan, Italy; ¹³Samsung Medical Center, Sungkyunkwan Uni, Seoul, Republic of Korea; ¹⁴Leningrad Regional Clinical Hospital, Saint Petersburg, Russian Federation; ¹⁵The Oncology Centre, KwaZulu-Natal, South Africa; ¹⁶Merck and Co., Inc., Rahway, NJ, USA; ¹⁷Hackensack University Medical Center, Hackensack, NJ, USA

Background The group sequential, adaptively randomized, open-label, phase 2 KEYNOTE-495/KeyImPaCT trial (NCT03516981) demonstrated the feasibility of using prospective T-cell-inflamed gene expression profile (Tcell_{inf}GEP) and tumor mutation burden (TMB) dual biomarker status to assess the clinical activity of first-line pembrolizumab-based combination therapies in advanced non-small-cell lung cancer (NSCLC). Here, we present updated efficacy data relative to prespecified biomarker-defined subgroups for each treatment arm.

Methods Patients with previously untreated stage IV NSCLC were categorized by Tcell_{inf}GEP and TMB dual biomarker status (Tcell_{inf}GEP^{low}TMB^{non-high}, Tcell_{inf}GEP^{low}TMB^{high}, Tcell_{inf}GEP^{non-low}TMB^{non-high}, Tcell_{inf}GEP^{non-low}TMB^{high}) then randomly assigned 1:1:1 to receive pembrolizumab (200 mg IV Q3W) plus the multikinase inhibitor (targeting VEGFRs 1-3, FGFRs 1-4, PDGFRα, RET, and KIT) lenvatinib (20 mg oral QD), CTLA-4 inhibitor quavonlimab (75 mg IV Q6W), or LAG-3 inhibitor favezelimab (initially 200 mg and then 800 mg IV Q3W). Adaptive randomization based on objective response rate (ORR) was employed, and frequent interim analyses were performed to quantify efficacy and assess for futility. The primary end point of investigator-assessed ORR per RECIST v1.1 was assessed using prespecified efficacy thresholds for each biomarker-defined subgroup: an ORR of >5% within the Tcell_{inf}GEP^{low}TMB^{non-high} subgroup, >20% within the Tcell_{inf}GEP^{low}TMB^{high} subgroup and Tcell_{inf}GEP^{non-low}TMB^{non-high} subgroup, and >45% within the Tcell_{inf}GEP^{non-low}TMB^{high} subgroup evaluated using a Bayesian posterior probability. Secondary end points included progression-free survival (PFS) per RECIST v1.1, overall survival (OS), and safety.

Results At data cutoff (March 21, 2022), 243 patients had been treated (pembrolizumab+lenvatinib, n=80; pembrolizumab+quavonlimab, n=82; pembrolizumab+favezelimab 200 mg, n=30; pembrolizumab+favezelimab 800 mg, n=51). Efficacy data are presented in table 1. ORR with pembrolizumab+lenvatinib in the Tcell_{inf}GEP^{non-low}TMB^{non-high} subgroup met the prespecified efficacy threshold. The safety profile of each treatment arm was consistent with the known safety profile of each combination.

Conclusions Pembrolizumab-based combination therapy continued to show promising antitumor activity and durable response in the Tcell_{inf}GEP^{non-low}TMB^{high} subgroup across all combinations. Response in the Tcell_{inf}GEP^{non-low}TMB^{non-high} subgroup treated with pembrolizumab+lenvatinib met the prespecified efficacy threshold. Although response in the pembrolizumab+favezelimab arm did not reach the efficacy bar, there was a trend toward improved ORR in the Tcell_{inf}GEP^{non-low}TMB^{high} subgroup versus the other 3 biomarker-defined subgroups; median PFS and OS were also numerically longer in the Tcell_{inf}GEP^{non-low}TMB^{high} subgroup compared with the other 3 biomarker-defined subgroups. Prospective assessment of dual biomarkers, as performed in this study, may help identify patients with NSCLC most likely to respond to pembrolizumab-based combination therapies.

Acknowledgements Medical writing and/or editorial assistance was provided by Mehak Aggarwal, PharmD, and Holly C. Cappelli, PhD, CMPP, of ApotheCom (Yardley, PA, USA). This assistance was funded by Merck Sharp & Dohme LLC, a subsidiary of Merck & Co., Inc., Rahway, NJ, USA.

Trial Registration NCT03516981

Consent The study protocol and all amendments were approved by the institutional review board or ethics committee at each institution. All patients provided written informed consent

Abstract 635 Table 1 Efficacy by treatment and dual biomarker status

Arm	End point	Tcell _{inf} GEP ^{low} TMB ^{non-high}	Tcell _{inf} GEP ^{low} TMB ^{high}	Tcell _{inf} GEP ^{non-low} TMB ^{non-high}	Tcell _{inf} GEP ^{non-low} TMB ^{high}	Total
Pembrolizumab+ lenvatinib	ORR, % (95% CI) [n/N]	12 (2-21) [3/25]	33 (10-65) [4/12]	61 (21-84) [9/22]	57 (34-78) [12/21]	35 (28-46) [28/80]
	Median PFS, months (95% CI)	5 (2-9)	14 (1-NR)	8 (4-21)	18 (6-22)	8 (6-12)
	Median OS, months (95% CI)	18 (5-20)	19 (4-NR)	21 (12-NR)	23 (17-NR)	19 (16-23)
Pembrolizumab+ quavonlimab	ORR, % (95% CI) [n/N]	12 (2-20) [3/26]	31 (9-61) [4/13]	14 (3-35) [3/22]	32 (30-74) [11/21]	20 (17-22) [21/82]
	Median PFS, months (95% CI)	3 (2-6)	3 (1-17)	6 (2-13)	17 (10-NR)	6 (3-10)
	Median OS, months (95% CI)	12 (8-20)	24 (8-NR)	19 (8-NR)	28 (17-NR)	20 (14-26)
Pembrolizumab+ favezelimab 200 mg	ORR, % (95% CI) [n/N]	0 (0-28) [0/11]	33 (4-78) [2/6]	25 (3-65) [2/8]	50 (15-85) [3/5]	23 (7-30) [7/30]
	Median PFS, months (95% CI)	2 (2-2)	8 (2-NR)	2 (1-6)	6 (0-NR)	2 (2-6)
	Median OS, months (95% CI)	9 (4-NR)	21 (2-NR)	13 (1-NR)	NR (13-NR)	15 (9-25)
Pembrolizumab+ favezelimab 800 mg	ORR, % (95% CI) [n/N]	N/A*	27 (6-61) [3/11]	14 (3-35) [3/22]	50 (26-74) [9/18]	29 (17-44) [15/51]
	Median PFS, months (95% CI)	N/A*	4 (2-12)	3 (2-8)	13 (4-NR)	6 (3-8)
	Median OS, months (95% CI)	N/A*	26 (3-NR)	11 (5-16)	NR (13-NR)	16 (12-NR)

*Not applicable; this group did not proceed because of the lack of clinical activity in this subgroup observed at the 200-mg dose of favezelimab. NR, not reached.

<http://dx.doi.org/10.1136/jitc-2022-SITC2022.0635>

636

A PHASE 1, OPEN-LABEL, DOSE ESCALATION AND EXPANSION STUDY OF CUE-102 MONOTHERAPY IN HLA-A*0201 POSITIVE PATIENTS WITH WT1-POSITIVE RECURRENT/METASTATIC CANCERS

¹Steven Margossian*, ²John Powderly, ³Nashat Gabrail, ⁴Yvonne Saenger, ⁵J Eva Selfridge, ⁶Nataliya Uboha, ⁷Jun Gong, ⁸Brian Van Tine, ⁹Olatunji Alese, ¹⁰Dae Won Kim, ¹¹Wen Ma, ¹¹Tanios Bekaii-Saab, ¹¹Jeremy Jones, ¹²Angela Alistar, ¹Laura Agensky, ¹Apollina Goel, ¹Reena Lynam, ¹Raymond Moniz, ¹Steve Quayle, ¹Cynthia Rajan, ¹⁵Kenneth Pienta, ¹Matteo Levisetti. ¹Cue Biopharma Inc., Boston, MA, USA; ²Carolina BioOncology, Huntersville, NC, USA; ³Gabrail Cancer Center, Canton, OH, USA; ⁴Albert Einstein Cancer Center, Bronx, NY, USA; ⁵UH Cleveland, Cleveland, OH, USA; ⁶Carbone Cancer Center, Madison, WI, USA; ⁷Cedar Sinai, Los Angeles, CA, USA; ⁸Washington University, St Louis, MO, USA; ⁹Emory University, Atlanta, GA, USA; ¹⁰H. Lee Moffitt Cancer Center, Tampa, FL, USA; ¹¹Mayo Clinic, Rochester, MN, USA; ¹²Carol G. Simon Cancer Center, Winston Salem, NJ, USA; ¹⁵Johns Hopkins University School of Med, Cambridge, MD, USA

Background Immuno-STATsTM are modular fusion proteins designed for the selective activation of tumor-antigen specific CD8+ T cells. CUE-102, the second Immuno-STAT in clinical trials, is composed of a human leukocyte antigen (HLA) complex, HLA-A*0201, a peptide epitope derived from the Wilms Tumor 1 (WT1) protein, and 4 molecules of reduced affinity human interleukin-2 (IL-2), and is designed to bind, expand, and activate WT1-specific CD8+ T cells for the treatment of WT1-positive cancers. In pre-clinical studies, CUE-102 elicits selective expansion of WT1-specific cytotoxic CD8+ T-cells in vitro and in vivo.¹

Methods CUE-102-01 is a phase 1, open-label, 2-part, multicenter study evaluating the safety, tolerability, pharmacokinetics (PK), pharmacodynamics (PD), immunogenicity, and preliminary antitumor activity of CUE-102 monotherapy administered every three weeks in HLA-A*0201 positive patients with WT1 positive recurrent/metastatic Colorectal, Gastric/Gastroesophageal Junction (GEJ), Pancreatic and Ovarian cancer who have failed conventional therapies. Part A is a dose escalation phase following 3+3 design rules with a Bayesian Logistic Regression Model (BLRM) overlay. Dose levels that exhibit an immune response may be expanded to further characterize activity and toxicity. Part B is a dose expansion/confirmation phase in patients with colorectal cancer.

The primary objectives of Part A are to evaluate dose-limiting toxicities and maximum tolerated dose during the first cycle of treatment, to evaluate the pharmacokinetics (PK) of CUE-102, and to establish a recommended Phase 2 dose. Secondary objectives of Parts A and B include evaluating the safety and tolerability of CUE-102 using NCI CTCAE v5.0; preliminary antitumor activity by RECIST 1.1 including objective response rate (ORR), duration of response (DOR), durable stable disease (DSD) (SD \geq 6 weeks), clinical benefit rate (CBR), progression-free survival (PFS); overall survival (OS); the potential for CUE-102 mediated immune response; and the potential immunogenicity of CUE-102. Exploratory objectives include evaluation of biomarkers of activity and immune effects, and preliminary antitumor activity by iRECIST.

Eligible patients must have locally advanced/nonresectable or metastatic disease, an ECOG status of 0 or 1, life expectancy > 12 weeks and measurable disease by RECIST 1.1 criteria. Patients with colorectal and cisplatin-sensitive ovarian cancer must have documented disease progression to 2 prior systemic treatment regimens (CUE-102 will be \geq 3rd line therapy); patients with Gastric/GEJ, pancreatic and cisplatin-resistant ovarian cancer must have documented disease progression to 1 prior systemic treatment regimens (CUE-102 will be \geq 2nd line therapy).

Results Trial is currently open and enrolling as of June 14, 2022.

Acknowledgements The authors would like to thank all the patients who are participating in this study. The study is sponsored by Cue Biopharma.

Trial Registration ClinicalTrials.gov NCT05360680

REFERENCE

1. Zhang C, Girgis N, Merazga Z. *et al.* CUE-102 selectively activates and expands WT1-specific T cells for the treatment of patients with WT1+ malignancies. *JITC*. 2021;9(Suppl 3):A749–A749

Ethics Approval This study was approved by Ethics and Institutional Review Boards (IRBs) at all study sites. IRB reference numbers: WIRB 1331836 (Carolina BioOncology), WIRB 1335388 (Gabrail Cancer Center)

<http://dx.doi.org/10.1136/jitc-2022-SITC2022.0636>

637 PHASE IIA COMBINING NEO-201 WITH PEMBROLIZUMAB IN ADULTS WITH CHEMO-RESISTANT SOLID TUMORS

¹Princess Mark-Adjeli*, ¹Christina Annunziata, ¹Christopher Cole, ²Maria Pia Morelli, ¹Ann McCoy, ³Massimo Fantini, ³Sharon Mavroukakis, ³Anjum Zaki, ³Kwong Tsang, ³Philip Arlen. ¹National Cancer Institutes, Bethesda, MD, United States; ²MD Anderson, Houston, TX, United States; ³Precision Biologics, Inc., Bethesda, MD, United States

Background NEO-201 is a humanized IgG1 monoclonal antibody which binds to Core 1 and/or extended Core 1 O-glycans expressed by human solid and blood tumors as well as by human neutrophils. NEO-201 reacts against colon, pancreatic, non-small cell lung, head and neck, cervical, uterine and breast cancer, but it does not bind to most normal tissues. NEO-201 kills tumor cells via antibody dependent cell mediated cytotoxicity and complement dependent cytotoxicity. NEO-201 also binds to circulating regulatory T cells (Tregs). The low response rates and resistance to PD-1/PD-L1 blockade in solid cancers may be due to the activity of Tregs in the tumor microenvironment. Based on these data we hypothesize that combining NEO-201 with pembrolizumab for the treatment of solid tumors may overcome resistance to checkpoint inhibitors by depleting Tregs.

Methods The Clinical Trial NCT03476681 is open and recruiting patients at National Institutes of Health (USA).

Eligibility Criteria A. Subjects must be over 18 years old and have histologically or cytologically confirmed recurrent, locally advanced unresectable or metastatic Non-Small Cell Lung Cancer, Cervical Cancer, Head and Neck Squamous Cell Carcinoma, Uterine Carcinoma who have progressed during or after front-line standard of care treatment, including chemotherapy and/or targeted therapy.

B. At least 10% of tumor cells expressing NEO-201 target antigen on immunohistochemistry.

C. Patient is not a candidate for potentially curative surgery or radiation

Given that NEO-201 has not been previously administered with pembrolizumab, a safety lead-in will be conducted in three to six subjects who will receive NEO-201 at 1.5 mg/kg IV every 2 weeks, and pembrolizumab 400 mg IV every 6 weeks. The safety lead-in course will be 42 days in length and consist of 1 dose of pembrolizumab and 3 doses of NEO-201. Once safety is established, 21–31 subjects would be enrolled in the four disease groups. Primary and secondary objectives include determining Objective Response Rate and Progression Free Survival, characterizing the pharmacokinetics of NEO-201 in combination with pembrolizumab, exploring the effects of the combination on functions and phenotypes of immune subsets, modulation of serum levels of cytokines and soluble factors.

Trial Registration NCT03476681

Ethics Approval This study was approved by NCI Institutional Review Board (protocol code NCT03476681, first approved 03/26/2018; latest update 01/08/2020)

<http://dx.doi.org/10.1136/jitc-2022-SITC2022.0637>

638

COMMANDER-001: A PHASE 1/2, FIRST-IN-HUMAN, MULTICENTER, OPEN LABEL STUDY OF SQZ-EAPC-HPV AS MONOTHERAPY AND WITH PEMBROLIZUMAB IN PATIENTS WITH HPV16+ RECURRENT, LOCALLY ADVANCED, OR METASTATIC SOLID TUMORS (TRIAL IN PROGRESS)

¹Meredith Pelster*, ²Michael Gordon, ³Justin Moser, ³Trisha Wise-Draper, ⁴Jong Chul Park, ⁵Wade Iams, ⁶Ricardo Zwirter, ⁶Julia Jennings, ⁶Nathan Miselis, ⁶Rui Ru Ji, ⁶Scott Loughhead, ⁶Howard Bernstein, ⁶Armon Sharei, ⁷Antonio Jimeno. ¹*Sarah Cannon Research Institute, Nashville, TN, USA;* ²*HonorHealth Research and Innovation Inst, Scottsdale, AZ, USA;* ³*University of Cincinnati Medical Center, Cincinnati, OH, USA;* ⁴*Massachusetts General Hospital, Boston, MA, USA;* ⁵*Vanderbilt University Medical Center, Nashville, TN, USA;* ⁶*SQZ Biotechnologies, Watertown, MA, USA;* ⁷*Colorado University Cancer Center, Aurora, CO, USA*

Background Antigen-specific CD8+ T cells are critical for mounting a potent immune response against tumors. Creation of T cell responses requires 3 key signals from antigen presenting cells (APCs): (signal 1) the peptide-MHC complex binding to the T cell receptor, (signal 2) costimulatory molecules that bind to T cell stimulatory domains, and (signal 3) inflammatory cytokines binding to receptors on T cells. To create enhanced APCs (eAPCs) from peripheral blood mononuclear cells (PBMCs), we used the Cell Squeeze[®] technology to deliver mRNAs encoding HPV16 E6 and E7 antigens (signal 1), CD86 (signal 2), and membrane-bound IL-2 and IL-12 cytokines (signal 3). Co-localizing these signals on the eAPC surface may enable more potent T cell stimulation and limit off-target effects from systemic exposure to signal 2 and 3. SQZ-eAPC-HPV is an improved 2nd generation product, with no HLA restrictions, that builds on the clinical and manufacturing experience with the 1st generation SQZ-PBMC-HPV product. This approach may enable rapid implementation across many tumor types as it facilitates exchange of mRNA to encode for other antigens or T cell activation signals.

Methods Trial Design: COMMANDER-001 is open for enrollment to patients (pts) with HPV16 driven recurrent, locally advanced, or metastatic solid tumors and includes dose escalation for eAPC monotherapy and in combination with pembrolizumab (pembro) (Part 1), and a lead-in where eAPC is given prior to treatment with pembro (Part 2). Part 1A will assess 3 eAPC monotherapy cohorts using a Bayesian optimal interval design enrolling 3 – 12 pts per cohort. After establishing a safe and tolerable dose (RP2D), Part 1B will assess the RP2D with pembro 200mg q3 weeks (w). Part 2 will explore giving 2 doses of eAPC before the pt receives pembro. Pts will receive eAPC q3w for up to 1 year or until available eAPC is exhausted. Pembro will be given for up to 2 years. Eligible pts will undergo 1 leukapheresis. Manufacturing takes <24 hours and the vein-to-vein time for the 1st dose is expected to be ~1 week. Preconditioning is not required, and the study will be primarily conducted out-patient.

Trial Registration NCT05357898

Ethics Approval The study is registered on clinicaltrials.gov and was approved by the Ethics Board of all institutions listed as recruiting.

<http://dx.doi.org/10.1136/jitc-2022-SITC2022.0638>

639

BASECAMP-1: LEVERAGING HLA LOSS OF HETEROZYGOSITY IN SOLID TUMORS BY NGS TO IDENTIFY PATIENTS WITH RELAPSED SOLID TUMORS FOR FUTURE CEA AND MSLN LOGIC-GATED TMOD™ CAR T-CELL THERAPY

¹Diane Simeone*, ²Maria Pia Morelli, ³J Randolph Hecht, ⁴Sandip Patel, ⁵Marwan Fakhri, ⁶Kedar Kirtane, ¹Theodore Welling, ¹Sally Lau, ⁷Yi Lin, ⁸Mitesh Borad, ³Edward Garon, ³Sarah Larson, ⁴Shumei Kato, ⁴Peter Vu, ⁶Frederick Locke, ⁶Dae Won Kim, ¹⁰John Sunwoo, ³David Miklos, ¹⁰Matthew Frigault, ¹⁰Marcela Maus, ¹¹Sarah Nikiforow, ¹¹Caron Jacobson, ¹³Kirstin Liechty, ¹²Armen Mardiros, ¹³Ariane Lozac’hmeur, ¹³Karl Beutner, ¹²John Welch, ¹⁴Eric Ng, ¹²William Go, ¹⁵David Maloney, ²Scott Kopetz, ⁷Julian Molina. ¹New York University Langone Health, New York, NY, USA; ²University of Texas MD Anderson Cancer, Houston, TX, USA; ³University of California at Los Angeles, Los Angeles, CA, USA; ⁴University of California San Diego, La Jolla, CA, USA; ⁵City of Hope, Duarte, CA, USA; ⁶H. Lee Moffitt Cancer Center, Tampa, FL, USA; ⁷Mayo Clinic, Rochester, MN, USA; ⁸Mayo Clinic Cancer Center, Scottsdale, AZ, USA; ⁹Stanford University School of Medicine, Palo Alto, CA, USA; ¹⁰Massachusetts General Cancer Center, Boston, MA, USA; ¹¹Dana-Farber Cancer Institute, Boston, MA, USA; ¹²A2 Biotherapeutics, Inc., Agoura Hills, CA, USA; ¹³Tempus, Chicago, IL, USA; ¹⁴A2 Biotherapeutics, Agoura Hills, CA, USA; ¹⁵Fred Hutchinson Cancer Research Center, Seattle, WA, USA

Background Solid tumors comprise >90% of cancers. Non-small cell lung cancer (NSCLC), metastatic colorectal cancer (CRC), and pancreatic cancer are the leading causes of cancer-related mortality (5-year overall survival: 26%, 15%, and 11%, respectively).¹

Chimeric antigen receptor (CAR) T-cell therapy has demonstrated clinical efficacy in hematologic malignancies.^{2,3} However, translating engineered T-cell therapies to solid tumors has proven to be challenging due to a lack of tumor-specific targets that can discriminate cancer cells from normal cells. Previous studies using carcinoembryonic antigen (CEA) T-cell receptors and mesothelin (MSLN) CARs resulted in dose-limiting on-target, off-tumor toxicities.^{4,5}

To create a therapeutic safety window, Tmod CAR T-cell therapy utilizes dual-signaling receptors to create a robust logic gate capable of killing tumor cells, while leaving healthy cells intact.^{6,7}

The 2 receptors in Tmod CAR T-cell therapy comprise an activator that recognizes an antigen on the surface of tumor cells that may also be present on normal cells, such as CEA and MSLN, and a blocker that recognizes a second surface antigen from an allele lost only in tumor cells (figure 1).^{8,9}

Human leukocyte antigen (HLA) loss of heterozygosity (LOH) offers a definitive tumor versus normal discriminator target for CAR T-cell therapy.¹⁰ The frequency of HLA LOH among advanced NSCLC, CRC, and pancreatic cancers in the Tempus real-world dataset is 16.3% with a range of 15.6%-23.1%.¹¹ LOH can be reliably detected using the Tempus xT-Onco next-generation sequencing (NGS) assay.^{12,13} Different activator/blocker combinations can be engineered with the Tmod platform technology and may be applied to T cells and natural killer cells in autologous and allogeneic settings.

BASECAMP-1 is a currently enrolling observational study with key objectives: 1) To identify patients with somatic HLA LOH eligible for Tmod CAR T-cell therapy, and 2) Subsequent apheresis and manufacturing feasibility for the future EVEREST CEA or MSLN Tmod CAR T-cell studies.

Methods BASECAMP-1 (NCT04981119) patient eligibility has 2 parts (figure 2): 1) Patients will be initially screened to identify germline HLA-A*02 heterozygosity by central NGS. If HLA-A*02 heterozygosity is confirmed, primary archival tumor tissue will be analyzed for somatic mutations by xT-Onco NGS testing; 2) If the tumor demonstrates HLA-A*02:01 LOH and the patient is eligible after screening, the

patient will undergo apheresis. Banked T cells will be available for the autologous EVEREST Tmod CAR T-cell therapy interventional study to reduce waiting time at relapse.

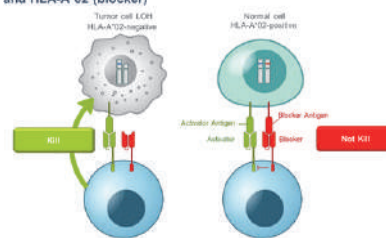
Trial Registration ClinicalTrials.gov, NCT04981119

REFERENCES

1. American Cancer Society. *Cancer Facts & Figures 2022*. Atlanta: American Cancer Society; 2022.
2. Locke F, Miklos D, Jacobson C, et al. Axicabtagene ciloleucel as second-line therapy for large B-cell lymphoma. *N Engl J Med*. 2022;**386**(7):640-654.
3. Maude S, Laetsch T, Buechner J, et al. Tisagenlecleucel in children and young adults with B-cell lymphoblastic leukemia. *N Engl J Med*. 2018;**378**(5):439-448.
4. Parkhurst M, Yang J, Langan R, et al. T cells targeting carcinoembryonic antigen can mediate regression of metastatic colorectal cancer but induce severe transient colitis. *Mol Ther*. 2011;**19**(3):620-626.
5. Haas AR, Tanyi JL, O'Hara MH, et al. Phase I study of lentiviral-transduced chimeric antigen receptor-modified T cells recognizing mesothelin in advanced solid cancers. *Mol Ther*. 2019;**27**(11):1919-1929.
6. Hamburger A, DiAndreth B, Cui J, et al. Engineered T cells directed at tumors with defined allelic loss. *Mol Immunol*. 2020;**128**:298-310.
7. DiAndreth B, Hamburger AE, Xu H, Kamb A. The Tmod cellular logic gate as a solution for tumor-selective immunotherapy. *Clin Immunol*. 2022;**241**:109030.
8. Sandberg ML, Wang X, Martin AD, et al. A carcinoembryonic antigen-specific cell therapy selectively targets tumor cells with HLA loss of heterozygosity in vitro and in vivo. *Sci Transl Med*. 2022;**14**(634):eabm0306.
9. Tokatlian T, Asuelime GE, Mock JY, et al. Mesothelin-specific CAR-T cell therapy that incorporates an HLA-gated safety mechanism selectively kills tumor cells. *J Immunother Cancer*. 2022;**10**(1):e003826.
10. Hwang MS, Mog BJ, Douglass J, et al. Targeting loss of heterozygosity for cancer-specific immunotherapy. *Proc Natl Acad Sci U S A*. 2021;**118**(12):e2022410118.
11. Simeone DM, Hecht JR, Patel SP, et al. BASECAMP-1: Leveraging human leukocyte antigen (HLA) loss of heterozygosity (LOH) in solid tumors by next-generation sequencing (NGS) to identify patients with relapsed solid tumor for future logic-gated Tmod CAR T-cell therapy. Poster presented at: ASCO Annual Meeting; June 3-7, 2022; Chicago, IL. Abstract #TPS2676.
12. Perera J, Mapes B, Lau D, et al. Detection of human leukocyte antigen class I loss of heterozygosity in solid tumor types by next-generation DNA sequencing. *J Immunother Cancer*. 2019, **7**(suppl 1):P103.
13. Hecht JR, Kopetz S, Patel SP, et al. Next generation sequencing (NGS) to identify relapsed gastrointestinal (GI) solid tumor patients with human leukocyte antigen (HLA) loss of heterozygosity (LOH) for future logic-gated CAR T therapy to reduce on target off tumor toxicity. *J Clin Oncol*. 2022;**40**(4_suppl):190-190.

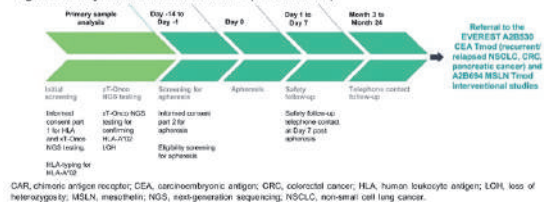
Ethics Approval The study was approved by site IRBs

Figure 1. Logic-gated CAR T with the goal to reduce toxicity: CEA and MSLN (activators) and HLA-A*02 (blocker)



Abstract 639 Figure 1

Figure 2. Study schema for BASECAMP-1 (NCT04981119)



CAR, chimeric antigen receptor; CEA, carcinoembryonic antigen; CRC, colorectal cancer; HLA, human leukocyte antigen; LOH, loss of heterozygosity; MSLN, mesothelin; NGS, next-generation sequencing; NSCLC, non-small cell lung cancer.

Abstract 639 Figure 2

<http://dx.doi.org/10.1136/jitc-2022-SITC2022.0639>

640

COMBINATORIAL CHEMOIMMUNOTHERAPY BASED ON THE ANTIBODY-CYTOKINE FUSION PROTEIN L19TNF UNLEASHES POTENT ANTI-TUMOR IMMUNITY AGAINST TREATMENT-REFRACTORY GLIOBLASTOMA

¹Thomas Look, ²Emanuele Puca, ²Riccardo Stucchi, ²Roberto De Luca, ²Dario Neri, ¹Michael Weller, ²Teresa Hemmerle*, ¹Tobias Weiss. ¹Universitätsspital Zürich, Zürich, Switzerland; ²Philogen S.p.A., Otelfingen, Switzerland

Background Glioblastoma is a poorly immunogenic brain tumor and treatment options at recurrence after standard of care chemoradiation are very limited. Several immunotherapeutic strategies, including immune checkpoint inhibition and peptide vaccination, have failed to improve the survival of patients. Except from potentially regorafenib, no other agent has demonstrated superior activity to the alkylating chemotherapeutic lomustine. Here, we investigate a new combination treatment based on lomustine and on the tumor-targeting antibody-cytokine fusion protein L19TNF in preclinical glioma models and in patients with recurrent glioblastoma.

Methods Orthotopic immunocompetent mouse glioma models were used to study the anti-tumor activity of L19TNF in combination with (i) anti-PD1 antibody, (ii) bevacizumab, (iii) L19IL2, or (iv) lomustine. Tumor growth was monitored by MRI as well as survival. Single-cell RNA-sequencing, Flow cytometry and microscopy were used to characterize tumor-infiltrating-immune cells. MHC immunoaffinity purification and mass spectrometry were used to investigate the MHC immunopeptidome. Genetic mouse models enabled to study immune-dependent effects. Subsequently, the most efficient treatment combination, L19TNF plus lomustine, was translated to patients with recurrent glioblastoma within a phase I/II clinical trial (NCT04573192). The study has been approved by the Swiss national authority (Swissmedic reference number 2020DR1125) and the ethic committee (BASEC number 2020-02413).

Results The combination treatment based on lomustine and L19TNF cured the majority of immunocompetent orthotopic glioma-bearing mice, whereas other mono- or combination therapies had only limited anti-glioma activity. The investigation of the mechanisms of action revealed that lomustine plus L19TNF led to intratumoral necrosis, DNA damage and triggered a strong local anti-tumor immune response with increased MHC-I expression, presentation of neoepitopes and increased abundance of tumor-infiltrating lymphoid cells. In the first patients treated within a phase I/II clinical trial, the treatment was well tolerated, and durable objective tumor responses as well as disease stabilizations could be observed, even in patients with unmethylated MGMT promoter.

Conclusions The combination of L19TNF and lomustine is demonstrating promising anti-glioma activity. Additional patients are currently being recruited within a phase I/II clinical trial for patients with glioblastoma at first progression.

Trial Registration NCT04573192

Ethics Approval The study was approved by the Swiss national authority (Swissmedic reference number 2020DR1125) and the ethic committee (BASEC number 2020-02413)

<http://dx.doi.org/10.1136/jitc-2022-SITC2022.0640>

641

STRONG IMMUNE RESPONSE TO THERAPEUTIC VACCINATION WITH EO2401 MICROBIOME DERIVED THERAPEUTIC VACCINE + NIVOLUMAB: INTERIM REPORT OF THE EOGBM1-18/ROSALIE STUDY

¹Ana Maia*, ²Hélène Toussaint, ²Joao Gamelas Magalhaes, ³David Reardon, ⁴Ahmed IDBAIH, ⁵Maria Vieito, ⁶Ghazaleh Tabatabai, ⁷Agostina Stradella, ⁸François Ghiringhelli, ⁹Michael C Burger, ¹⁰Iris Mildenerger, ¹¹Ulrich Herrlinger, ¹²Macarena Gonzalez, ⁸Alice Hervieu, ⁷Marta GilMartin, ⁶Mirjam Renovanz, ⁴Mehdi Touat, ³Patrick Y Wen, ¹²Antje Wick, ²Laurent Chene, ¹Cécile Gouttefangeas, ²Christophe Bonny, ³Jan Fagerberg, ¹²Wolfgang Wick. ¹Eberhard-Karls-University Tuebingen, Germany; ²Enterome, Paris, France; ³Dana-Farber Cancer Institute, Boston, MA, USA; ⁴Hôpital Universitaire La Pitié-Salpêtrière, Paris, France; ⁵Hospital Universitari Vall d'Hebron, Barcelona, Spain; ⁶Universitätsklinikum Tübingen, Tübingen, Germany; ⁷Institut Catala D'Oncologia Hospital, Barcelona, Spain; ⁸Centre Georges-François Leclerc, Dijon, France; ⁹Universitätsklinikum Frankfurt Goethe, Frankfurt, Germany; ¹⁰Medizinische Fakultät Mannheim, Mannheim, Germany; ¹¹Universitätsklinikum Bonn, Bonn, Germany; ¹²Universitätsklinikum Heidelberg Cancer, Heidelberg, Germany

Background EO2401 is a therapeutic vaccine designed to activate memory commensal specific T-cells that are cross-reacting against validated tumor associated antigens (TAAs). EO2401 includes synthetically produced HLA-A2 peptides with molecular mimicry to TAAs (IL13R α 2, BIRC5 and FOXM1) upregulated in glioblastoma, and the CD4 helper peptide UCP2.

Methods Patients with glioblastoma at first progression after radiotherapy/temozolomide received EO2401 with nivolumab (EN), or EN with bevacizumab within trial EOGBM1-18 (NCT04116658). Blood collection was performed at baseline and then every two or four weeks. Immune responses were investigated either directly on cryopreserved PBMCs without stimulation (ex vivo), or after 12 days in vitro stimulation (IVS) using tetramer staining, IFN γ ELISpot and intracellular cytokine staining. The study was approved by all participating institution's Ethics Boards.

Results Immune monitoring in EO2401 vaccinated patients demonstrates the ability of bacterial peptides to induce a strong CD8+ T cell response with cross-reactivity against human selected TAAs. Immune response against the 3 microbiome-derived peptides is demonstrated for 28 of 29 investigated patients using ELISpot after IVS. Post vaccination frequency of CD8+ T cells against bacterial peptide after IVS is extremely high, with a median of 5.5% of specific CD8+ T cells for EO2316 (max 18%), 16% for EO2317 (max 46%) and 14% (max 40%) for EO2318. Cross-reactivity against the pool of human peptides is demonstrated in 27/28 patients using ELISpot after IVS and validated using tetramer staining against BIRC5 and FOXM1. Polyfunctionality of CD8+ T cells effectors is supported by frequent expression of CD107a as well as IFN- γ and TNF- α production after stimulation. Ex vivo, CD8+ T cells against at least one of the EO2401 peptides are detected in 26/28 evaluable patients with some patients exhibiting up to 5% of circulating specific CD8+ T cells. Memory specific CD8+ T cells response are found as early as two weeks after the first vaccination and maintenance of a strong and stable immune response could be detected for more than 10 months. CD4+ T cell response against the UCP2 helper peptide is demonstrated using IFN- γ ELISpot after IVS.

Conclusions EO2401 vaccine demonstrates ability to generate fast and durable immune responses in patients treated with EO2401/nivolumab +/- bevacizumab. Activation of specific T cells cross-reacting against commensal antigens and TAAs is thereby validated as an efficient approach to activate strong

immune responses in a difficult to treat tumor with low neo-antigen expression and poor T cell priming.

Trial Registration NCT04116658

Ethics Approval This study has obtained an ethics approval (Dana Farber Cancer Institute IRB: iRIS number 438532) and all participants gave informed consent before taking part.

<http://dx.doi.org/10.1136/jitc-2022-SITC2022.0641>

642

EO2401 MICROBIOME DERIVED THERAPEUTIC VACCINE + NIVOLUMAB, WITH/WITHOUT STANDARD CONTINUOUS, OR LOW-DOSE SYMPTOM DIRECTED, BEVACIZUMAB, IN RECURRENT GLIOBLASTOMA: PHASE 1–2 EOGBM1–18/ROSALIE STUDY

¹David Reardon*, ²Ahmed Idhah, ³Maria Vieito, ⁴Ghazaleh Tabatabai, ⁵Agostina Stradella, ⁶Francois Ghiringhelli, ⁷Michael Burger, ⁸Iris Mildemberger, ⁴Ulrich Herrlinger, ³Macarena González, ⁵Marta GilMartin, ⁴Mirjam Renovanz, ⁹Mehdi Touat, ¹Patrick Wen, ⁴Antje Wick, ¹⁰Cecile Gouttefangeas, ¹⁰Ana Maia, ¹¹Christophe Bonny, ¹¹Jan Fagerberg, ¹²Wolfgang Wick. ¹Dana-Farber Cancer Institute, Boston, MA, USA; ²Sorbonne Université, AP-HP, ICM, Hôpital Universitaire La Pitié-Salpêtrière, Paris, MA, France; ³Hospital Universitari Vall d'Hebron, Barcelona, Spain; ⁴Universitätsklinikum, Tübingen, Germany; ⁵Institut Catala D'Oncologia, Hospital Duran i Reynals, Barcelona, Spain; ⁶Centre Georges-François Leclerc, Dijon, France; ⁷Universitätsklinikum Frankfurt Goethe-Universität, Frankfurt, Germany; ⁸Medizinische Fakultät, Mannheim, Germany; ⁹Hôpital Universitaire La Pitié-Salpêtrière, Paris, France; ¹⁰Department of Immunology, Eberhard-Karls-University, Tuebingen, Germany; ¹¹Enterome, Paris, France; ¹²Universitätsklinikum Heidelberg and German Cancer Research Center, Heidelberg, Germany

Background EO2401 was designed to activate memory T cells cross-reacting with tumor associated antigens. EO2401 includes synthetically produced HLA-A2 peptides with molecular mimicry to antigens (IL13R α 2, BIRC5 and FOXM1) upregulated in glioblastoma, and the CD4 helper peptide UCP2.

Methods Patients with glioblastoma at first progression after radiotherapy/temozolomide received EO2401 (300 μ g/peptide, q2w x4 then q4w) with nivolumab (3 mg/kg q2w; EN-regimen), or EN with bevacizumab (10 mg/kg q2w; ENB-regimen). In study part 2, low-dose bevacizumab (LDB) (5 mg/kg q2w up to 6 doses) could be used as symptom directed treatment of edema. The study, NCT04116658, was approved by all participating institution's Ethics Boards.

Results Part 1 included 40 patients (EN = 29, ENB = 11). Part 2 enrolled 36 patients treated with EN, and the possibility of symptom directed LDB. In study part 3, 15 further patients are to be treated with ENB (enrollment ongoing).

EN and ENB were well tolerated with EO2401 associated tox limited to local administration site reactions (45% of patients; events 70% Grade 1, 26% Grade 2, and 4% Grade 3). The frequency and severity of nivolumab-/bevacizumab-tox was consistent with historical single-agent data.

Immune monitoring demonstrated positive responses against the 3 microbiome-derived peptides for 28 of 29 patients investigated ex vivo or after in vitro stimulation (IVS). For some patients, positive response was already detected two weeks after the first vaccination and was maintained for more than 10 months. Cross-reactivity against the pool of 3 human target peptides was demonstrated in 27 of 28 patients using IFN- γ ELISpot assay.

For part 1, median progression-free survival (mPFS), and median survival for EN (n=29, median follow-up 14.0 months) were 1.8 and 10.6 months. Patients on ENB (n=11, median follow-up 9.6 months) had mPFS of 5.5 months and 9 patients were alive (7-12.4 months). Objective Response Rate (ORR)/Disease Control Rate (DCR) (ORR + stable disease) for EN and ENB were 10%/34% and 55%/82%.

Median treatment duration for EN in part 1 was 8.9 weeks (2 of 29 on treatment), while it was 12.0 weeks (21 of 36 on treatment) in part 2. Overall, in part 2, 13 patients (36%) received LDB.

Conclusions EO2401 was well tolerated and generated fast and durable immune responses in most patients. Addition of standard bevacizumab to EN improved PFS and ORR/DCR. Symptom directed LDB supported longer treatment durations.

Updated safety, immunogenicity, and efficacy data from all parts of the trial will be presented.

Trial Registration NCT04116658

Ethics Approval This study has obtained an ethics approval (Dana Farber Cancer Institute IRB: iRIS number 438532) and all participants gave informed consent before taking part.

<http://dx.doi.org/10.1136/jitc-2022-SITC2022.0642>

643

SPATIAL-TRANSCRIPTOMIC ANALYSIS OF NEOADJUVANT CHECKPOINT IMMUNOTHERAPY IN RECURRENT GLIOBLASTOMA

¹Michael Schachter*, ²Lu Sun, ¹Wesley Kwong, ¹Samantha Liang, ¹Sandra Santulli-Marotto, ¹Lacey Kitch, ²Willy Hugo, ²Robert Prins, ¹Dinesh Kumar. ¹Parker Institute for Cancer Immunotherapy, Castro Valley, CA, USA; ²David Geffen School of Medicine at UCLA, Los Angeles, CA, USA

Background Glioblastomas (GBMs) are a prevalent form of brain tumor with median overall survival of 1-1.5 years, and inevitable recurrence after initial surgical resection and chemotherapy. Less than half of patients are eligible for surgery at recurrence.¹ In many other cancers, checkpoint immunotherapies are efficacious, but GBMs resist treatment. Multiple resistance mechanisms may be at play and overcoming them is essential to improve immunotherapy response. The high heterogeneity of GBM, both in cellular phenotype and immune landscape, likely contributes to resistance. Although the GBM tumor-immune transcriptome is well-studied, spatial organization is an open frontier.

Methods Spatial transcriptomic samples were analyzed from a two-arm randomized trial for recurrent GBM patients (NCT04201873). One arm received neoadjuvant and adjuvant PD-1 mAb (“neoadjuvant” group), while the other received placebo (“placebo” group). Both groups received adjuvant autologous tumor lysate-pulsed DC vaccination. Tissue samples (N=10) were taken from on-study surgical resection, with 4 patients in the neoadjuvant group, 6 in placebo. The Visium spatial assay was applied to produce 3,140 +/- 969 transcriptomic “spots” per sample, 31,395 in total. Gene signature analysis quantified each spot’s tumor-immune composition. Signatures were obtained from MSigDB Hallmarks, ImSig,² and Neftel et. al.³ AUCell⁴ was used to score signatures at each spot.

Results Analysis of glioma subtype signatures showed mesenchymal scores (MES1 and MES2) highly correlated [Pearson coefs. > 0.77], while astrocyte (AC), oligodendrocyte precursor (OPC), and neural precursor (NPC1 and NPC2) scores formed a second correlated group [Pearson coefs. > 0.5]. There was no discernable difference in correlation structure between neoadjuvant and placebo patients.

MES1-high spots had a characteristic signature of high macrophage, hypoxia, angiogenesis, glycolysis, interferon-gamma response, TGF-beta, and TNF-alpha scores [Pearson coefs. > 0.5]. AC, OPC and NPC-high spots correlated weakly to immune and vascular signatures [Pearson coefs. < 0.35]. Microglia did not correlate highly to other scores [Pearson coefs < 0.35].

Differential expression showed negative log fold-change (logFC) in glioma subtype scores for neoadjuvant patients, for all types except NPC2 [Wilcoxon tests, p < 0.001]. Negative logFC was observed for macrophages, TNF-alpha, hypoxia, and proliferation, but positive logFC for T-cells and microglia.

Conclusions Spatial-transcriptomic analysis suggests that patients treated with neoadjuvant immunotherapy have lower mesenchymal subtype scores, with lower proliferation, but higher T-cell scores. Subsequent analysis will relate neoadjuvant immunotherapy with spatial heterogeneity of T-cells, myeloid subtypes, glioma subtypes, and vascularization, to understand resistance mechanisms.

Trial Registration NCT04201873

REFERENCES

1. Birzu C, French P, Caccese M, Cerretti G, Idbaih A, Zaganel V, & Lombardi G. Recurrent glioblastoma: from molecular landscape to new treatment perspectives. *Cancers*. 2020;**13**(1):47.
2. Ajit J Nirmal, Tim Regan, Barbara B Shih, David A Hume, Andrew H Sims and Tom C. Immune Cell Gene Signatures for Profiling the Microenvironment of Solid Tumors. *Freeman Cancer Immunol Res*. 2018;**6**(11):1388–1400; DOI: 10.1158/2326-6066.CIR-18-0342
3. Neftel C, Laffy J, Filbin, MG, HaraT, Shore ME, Rahme GJ, and Suvà, ML (2019). An integrative model of cellular states, plasticity, and genetics for glioblastoma. *Cell*, **178**(4), 835–849.
4. Aibar S, Bravo Gonzalez-Blas C, Moerman T, Huynh-Thu V, Imrichova H, Hulselmans G, Rambow F, Marine J, Geurts P, Aerts J, van den Oord J, Kalender Atak Z, Wouters J, Aerts S (2017). SCENIC: Single-Cell Regulatory Network Inference And Clustering. *Nature Methods*. 2017;**14**:1083–1086.

<http://dx.doi.org/10.1136/jitc-2022-SITC2022.0643>

Abstracts

644 MAJOR PATHOLOGIC RESPONSE AFTER A SINGLE RADIOTHERAPY FRACTION + A SINGLE PEMBROLIZUMAB DOSE GIVEN PREOPERATIVELY IN PATIENTS WITH CT1N0 TRIPLE NEGATIVE BREAST CANCER (TNBC) – PRELIMINARY RESULTS OF A PHASE 1B/2 STUDY (NCT04454528)

Julia Tchou*, Amy Clark, Neil Taunk, Gary Freedman, Nucleus Xu, Andy Minn, Angela Bradbury, Angela Demichele Gross, Susan Domchek, Hayley Knollman, Rachel Jankowitz, Payal Shah, Oluwadamilola Fayanju, Anupma Nayak, Joseph Fraietta, Alexander Huang. *University of Pennsylvania, Wayne, PA, USA*

Background Pembrolizumab (Pembro) was recently approved for use in combination with neoadjuvant chemotherapy for the treatment of cT2-4N0-2 or T1cN1-2 triple negative breast cancer (TNBC).¹ For patients with early stage (e.g. cT1N0) disease, this regimen may be excessive.² We hypothesize that a single 7 Gy radiotherapy (RT) fraction directed at the tumor combined with a single Pembro dose given preoperatively (preop) in patients with early stage breast cancer is feasible and may result in pathologic response.

Methods Patients with cT1N0 TNBC or other subtypes and without a history of ipsilateral breast/chest wall RT or conditions that preclude Pembro treatment are eligible to enroll in this 21-day window of opportunity 3-armed study. Patients either receive RT, Pembro, then surgery; or Pembro, RT, then surgery; or Pembro only in arm 1, 2, or 3, respectively. The primary endpoints were feasibility and tolerability. The secondary endpoints were % change in tumor infiltrating lymphocytes (TILs) and pathologic response. A major pathologic response is defined as <10% residual invasive tumor in post-treatment resected tissues. All patients underwent standard of care adjuvant therapy following surgery.

Results Patients' clinical characteristics are summarized in Table 1. An initial 6 patients (phase 1b; 4 in arm 1 and 2 in arm 2) completed preop treatment with none experiencing >grade 2 skin toxicity or surgery delay (defined as >14 days), thus establishing feasibility. Study is expanded to phase 2 in which patients are assigned 1:1:1 into arms 1, 2, and 3 according to subtype. Comparison of pre- and post-treatment tissues demonstrated that ΔTILs increased significantly in TNBC (21 ±15%, n=9) than in other subtypes (1±2%, n=3†), p=0.049. Major pathologic response (PR) was observed in 3 of 9 TNBC (33%) (2 in arm 1; 1 in arm 2) including 1 with complete PR (arm 1).

Conclusions For the first time to our knowledge, a major PR was observed in TNBC after a single RT + 1 Pembro infusion given preop. Comprehensive digital spatial profiling of the pre- and post-treatment tumor microenvironment to identify potential biomarkers associated with PR is underway. Results of this proof-of-concept study may provide the rationale to evaluate the effectiveness of de-escalating preoperative combination immunotherapy in select patients in future studies.

Trial Registration NCT04454528

REFERENCES

1. Maity A, Mick R, Huang AC, et al. A phase I trial of pembrolizumab with hypofractionated radiotherapy in patients with metastatic solid tumours. *British journal of cancer*. 2018;**119**(10):1200–1207.
2. Huang AC, Orlowski RJ, Xu XW, et al. A single dose of neoadjuvant PD-1 blockade predicts clinical outcomes in resectable melanoma. *Nat Med*. 2019;**25**(3):454–+.

Ethics Approval Our study has received approval from our Clinical Trials Scientific Review and Monitoring Committee

(protocol no. UPCC 04119) and our institutional review board (protocol no. 833464). All participants have provided informed consent.

Abstract 644 Table 1 Study cohort clinical characteristics Stratified by pathologic response

	Overall	TNBC non-major PR	TNBC Major PR	p-value
N	11†	6	3	
Age median (range)	54(34-68)	54(34-68)	67(45-63)	
Race				
Caucasian	7	3	2	
Black	4	3	1	
Subtype				
HR+HER2-	2†	-	-	
HR+HER2+	1	-	-	
TNBC	9	6	3	
Arm				
1	6	2	2	
2	3	2	1	
3	3†	2	0	
Tumor Size in mm, median (range)				
Pre-treatment	12(2-38)	13(10-16)	6(1-13)	
Post-treatment	7(0-29)	10(7-21)	1(0-3)	
Post-treatment %Tumor Size ↓, mean (SD)	15±13	*43±15	*87±12	*0.003
Pathologic response (PR)				
none	5	2	0	
Partial	4	4	0	
Major	3	0	3	
†1 patient had left TNBC and right HR+HER2- BC; PR - pathologic response				

<http://dx.doi.org/10.1136/jitc-2022-SITC2022.0644>

645

PHASE I STUDY OF ADOPTIVE T CELL THERAPY FOLLOWING HER2-PULSED DENDRITIC CELL VACCINE AND PEPINEMAB/TRASTUZUMAB IN PATIENTS WITH METASTATIC HER2-POSITIVE BREAST CANCER (MBC)

¹Hyo Han*, ²Elizabeth Evans, ²Terrence Fisher, ¹Hatem Soliman, ¹Hung Khong, ¹Aixa Soyano, ¹Ricardo Costa, ¹Loretta Loftus, ¹Kimberley Lee, ¹Avan Armaghani, ¹Hien Liu, ¹Frederick Locke, ¹Alexandria Shrewsbury, ¹Jessica Malka, ¹Lavakumar Karyampudi, ²Maurice Zauderer, ¹Brian Czerniecki. ¹Moffitt Cancer Center, Tampa, FL, USA; ²Vaccinex, Inc., Rochester, NY, USA

Background Despite major improvement of overall survival of HER2+ MBC with effective HER2 targeted therapies, many patients experience significant toxicities and develop progressive disease during treatment. Therefore, new and more effective therapeutic options are needed. This novel approach will evaluate whether the combination of three immunotherapies in addition to trastuzumab: dendritic cell (DC) vaccination, anti-SEMA4D blocking antibody (pepinemab) and CD4+ T cell adoptive transfer can lead to improved outcomes for patients with MBC refractory to HER2-targeted agents.

BC have been considered as immunologically cold which is attributed to immune evasion and suppression of host effector immune cells homing into tumor bed. Progressive loss of Th1 immunity against HER2 oncodriver correlates with poor prognosis. HER2 peptide pulsed type I dendritic cells (HER2-DC1) restored anti-HER2 CD4+ Th1 immune response and improved pathologic complete response (pCR) in HER2+ BC.¹

Antibodies to SEMA4D have been shown to modulate the TME by increasing effector cell infiltration and reducing immunosuppression.¹ In preclinical studies, treatment with anti-SEMA4D and HER2-DC1 in mice bearing established HER2+ tumors improved DC homing, expansion of CD4+ T cells, and complete tumor regression, compared to treatment with anti-SEMA4D or HER2-DC1 alone. Further, subsequent expansion and adoptive transfer of CD4+ T cells induced synergistic anti-tumor activity by activating CD8+ T mediated cytotoxicity. Pepinemab was well-tolerated^{2,3} and showed signs of anti-tumor activity in immunotherapy-resistant, PD-L1 negative/low non-small cell lung cancer patients when combined with checkpoint inhibitor (avelumab).³

Methods This open label Phase 1 study is enrolling up to 28 patients with HER2+ MBC. Patients will be treated with 6 weekly injections of dendritic cell (DC1) vaccines in combination with trastuzumab and pepinemab. We hypothesize these therapies may elicit CD4+ HER2-specific T cell responses. HER2-specific T cells will be expanded ex vivo and subsequently infused to patients following lymphodepletion with cyclophosphamide. Trastuzumab and pepinemab will be given as maintenance in addition to booster DC1 vaccines.

Patients (ECOG 0,1) must have had disease progression while on trastuzumab for the treatment of HER2+ MBC and received no more than 3 lines of therapy in the setting of metastatic disease. Dose escalation will consist of 3-6 patients each with increasing amounts of transferred CD4+ T cells, followed by dose expansion of 10 patients at the MTD. The primary objective is safety and tolerability; secondary objectives will include evaluation of T cell immunity and immune subsets, efficacy, PK/PD/ADA of pepinemab, and biomarker assessments.

Trial Registration NCT05378464

REFERENCES

1. Lowenfeld L, Mick R, Datta J, Xu S, Fitzpatrick E, Fisher CS, Fox KR, DeMichele A, Zhang PJ, Weinstein SP, Roses RE, Czerniecki BJ. Dendritic Cell Vaccination Enhances Immune Responses and Induces Regression of HER2pos DCIS Independent of Route: Results of Randomized Selection Design Trial. *Clin Cancer Res.* 2017;**23**(12):2961–2971.
2. Patnaik A, Weiss GJ, Leonard JE, Rasco DW, Sachdev JC, Fisher TL, Winter LA, Reilly C, Parker RB, Mutz D, Blydorn L, Tolcher AW, Zauderer M, Ramanathan RK. Safety, Pharmacokinetics, and Pharmacodynamics of a Humanized Anti-Sema-4D Antibody, in a First-In-Human Study of Patients with Advanced Solid Tumors. *Clin Cancer Res.* 2016;**22**(4):827–36.
3. Shafiq MR, Fisher TL, Evans EE, Leonard JE, Pastore DRE, Mallow CL, Smith E, Mishra V, Schröder A, Chin KM, Beck JT, Baumgart MA, Govindan R, Gabrail NY, Spira AI, Seetharamu N, Lou Y, Mansfield AS, Sanborn RE, Goldman JW, Zauderer M. A Phase Ib/II Study of Pepinemab in Combination with Avelumab in Advanced Non-Small Cell Lung Cancer. *Clin Cancer Res.* 2021;**27**(13):3630–3640.

Ethics Approval This study was approved by Advarra; approval number IRB# 00000971

<http://dx.doi.org/10.1136/jitc-2022-SITC2022.0645>

646

NEOADJUVANT IMMUNOTHERAPY COMBINING MAVEROPEPIMUT-5 (MVP-S) WITH LETROZOLE DECREASES KI67 AND INCREASES TH1 IMMUNE RESPONSE IN HORMONE RECEPTOR POSITIVE (HR+) EARLY-STAGE BREAST CANCER (ESBC)

¹Sasha Stanton*, ²Lisa MacDonald, ²Stephan Fiset, ²Heather Hirsch, ²Kabir Mody, ²Jeremy Graff, ²Aurelio Lobo, ²Danielle Lanroue, ²Heather Torrey, ³Nicole Moxon, ³Staci Mellinger, ³Tracy Kelly, ¹David Page, ¹Kristina Young, ¹Earle A. Chiles Research Institute, Portland, OR, USA; ²IMV Inc., Dartmouth, Canada; ³Providence Portland Cancer Institute, Portland, OR, USA

Background HR+ ESBC is associated with a suboptimal pathologic complete response rate (pCR, ~10%) following neoadjuvant cytotoxic chemotherapy. A genomic analysis among Ki67-high HR+ tumors identified 8-fold upregulation of BIRC5 (survivin), a gene commonly overexpressed in several cancers that regulates apoptosis and cell cycle progression and that is associated with poor clinical outcome. Maveropepimut-5 (MVP-S) is an immune-educating therapy including 5 HLA-restricted peptides from survivin leveraging the lipid-based DPX delivery platform. Treatment with MVP-S and intermittent, low-dose cyclophosphamide (CPA) has shown tumor infiltration of survivin-specific T cells in ovarian cancer. The goal of this study is to determine if MVP-S can be safely administered and whether MVP-S can instigate a survivin-specific immune response in this patient population.

Methods NCT04895761 is a phase I trial evaluating the safety and immunologic effects of neoadjuvant MVP-S plus letrozole. Three postmenopausal patients with T1c+ HR+HER2- breast cancer with Ki67>10% have been enrolled to arm A and received two doses of MVP-S and 7 weeks of neoadjuvant letrozole prior to surgery. The systemic type I survivin-specific immune response was measured by IFN- γ ELISPOT using the pooled peptides in MVP-S. Changes in tumor infiltrating lymphocytes (TILs) and Ki67 were determined. TILs were evaluated by hemoxylin and eosin staining (H&E) per Salgado *et al.*¹

Results Three patients have tolerated letrozole and MVP-S well without dose reductions or delays in surgery. All toxicities related to MVP-S were grade 1 injection site reactions including pruritis, induration, and erythema, occurring in all three patients. All toxicities related to letrozole are expected including hot flashes and joint pains. All three patients had at least a 50% decrease in Ki67 between biopsy and surgery, from median 24% (range 12% to 43%) before treatment to median 6% (range 5% to 10%) after treatment. All patients had pre-treatment TIL of 5-10%. One patient had patchy infiltrate of TIL up to 40% in the tumor after treatment but the other two had no increase in TIL by H&E. One patient had 8-fold increase of survivin-specific circulating IFN- γ T cells at surgery. One patient did not have a significant increase over baseline and the third patient was not evaluable.

Conclusions Combining MVP-S and letrozole is safe and well tolerated to date as neoadjuvant therapy in HR+ early-stage breast cancer. This neoadjuvant regimen decreased Ki67 in all patients. One patient had significantly increased survivin-specific IFN- γ T cells and one had increased TILs in the tumor.

Trial Registration Clinic trials. gov is NCT04895761

REFERENCE

1. Salgado, R. *et al.* The evaluation of tumor-infiltrating lymphocytes (TILs) in breast cancer: recommendations by an International TILs Working Group 2014. *Ann Oncol.* 2015;**26**:259–271, doi:10.1093/annonc/mdu450.

Ethics Approval Study consent and protocol were approved by the Providence Cancer Institute IRB board and all patient were given informed consent before participating in the study. **Consent** No identifying information is included in this abstract.

<http://dx.doi.org/10.1136/jitc-2022-SITC2022.0646>

647

PHASE I STUDIES OF AGENT-797, A NOVEL ALLOGENEIC INVARIANT NATURAL KILLER T (iNKT) CELL THERAPY, FOR THE TREATMENT OF PATIENTS WITH SOLID TUMORS OR MULTIPLE MYELOMA

¹Don Stevens, ²Clifton Mo, ³Benjamin Garnezy, ¹John Hamm, ⁴Benedito Carneiro, ⁵Breelyn Wilky, ⁶Rachel Sanborn, ⁷Anthony El- Khouery, ⁸Alexa Buffa, ⁹Sonia De Munari, ⁹Burcu Yigit, ⁹Marco Purbhoo, ⁹Mark Exley, ¹⁰David Einstein*. ¹Norton Cancer Institute, Louisville, KY, USA; ²Dana-Farber Cancer Institute, Boston, MA, USA; ³Sarah Cannon Cancer Institute Nashville, Nashville, TN, USA; ⁴Lifespan Cancer Institute, Providence, RI, USA; ⁵University of Colorado Cancer Center, Aurora, CO, USA; ⁶Earle A. Chiles Research Institute, Portland, OR, USA; ⁷USC Norris Comprehensive Cancer Center, Los Angeles, CA, USA; ⁸Agenus Inc, Lexington, MA, USA; ⁹MINK Therapeutics, Lexington, MA, USA; ¹⁰Beth Israel Deaconess Medical Center, Boston, MA, USA

Background AgenT-797, is an allogeneic CD1d-restricted T cell population (iNKT) that responds to lipid antigenic stimulation with potent cytokine secretion. iNKTs promote innate and adaptive immunity, home to critical organs (e.g., liver/lung/bone marrow), suppress myeloid-derived suppressor cells, and recondition the tumor microenvironment. AgenT-797 is a scalable, off-the-shelf therapy that retains potent cytotoxicity after cryopreservation and can be administered without lymphodepletion. This analysis represents data from 2 ongoing phase 1 studies of agenT-797 in patients with relapsed/refractory (r/r) multiple myeloma (MM) (NCT04754100) and agenT-797 alone or combined with pembrolizumab or nivolumab in r/r solid tumors (NCT05108623).

Methods Patients with r/r solid tumors and measurable disease per RECIST 1.1 received either agenT-797 monotherapy at 4.3×10^6 cells/kg or 1.4×10^7 cells/kg or in combination with pembrolizumab or nivolumab. Patients with r/r multiple myeloma received agenT-797 at 1.4 or 4.3×10^6 cells/kg or 1.4×10^7 cells/kg after having failed at least three prior treatments (proteasome inhibitor, immunomodulatory agent and anti-CD38 antibody). Dose-escalation followed a 3+3 scheme and endpoints included safety, persistence of agenT-797, anti-tumor activity measured as duration of response, progression-free survival, and time to response. Adverse events (AEs) were reported per CTCAE v5.0 and dose limiting toxicities (DLTs) were evaluated.

Results Enrollment commenced May 2022; as of July, thirteen patients with r/r solid tumors (median age 62y, range 46-92) were treated with a single dose of agenT-797 as a monotherapy (cervical, gastric, breast, pancreas, thymoma, GU, others) or in combination with approved anti-PD-1 (NSCLC, RCC, SCC). In r/r multiple myeloma, four patients (median age 55y, range 50-72) with ECOG 0 and median 5 prior lines of therapy were treated with a single dose of agenT-797, without lymphodepletion in two escalating cohorts. No DLTs were observed. Tolerability was favorable with no cytokine release syndrome (CRS), neurotoxicity, or severe immune-related AEs. No patients experienced treatment-related serious adverse events nor AEs \geq grade 3. Enrollment is ongoing with early observations including reduction of liver mets and SD>3 (Rectal) and >50% reduction of tumor cells in bone marrow with SD>10 (multiple myeloma).

Conclusions AgenT-797 is a novel iNKT cell potential therapy for patients with solid tumor cancers and hematologic malignancies. Updated data on safety, efficacy, and translational analyses, including persistence, serum biomarkers, and alloimmunity, will be presented.

Trial Registration NCT04754100; NCT05108623

<http://dx.doi.org/10.1136/jitc-2022-SITC2022.0647>

AUTOLOGOUS MACROPHAGE-BASED IMMUNOTHERAPY INDUCES A PRO-INFLAMMATORY STATE IN GBM TUMOR MICROENVIRONMENT – (TEM-GBM)

<http://dx.doi.org/10.1136/jitc-2022-SITC2022.0648>

¹Gaetano Finocchiaro*, ¹Bernhard Gentner, ²Marica Eoli, ¹Francesca Farina, ¹Alessia Capotondo, ²Elena Anghileri, ¹Matteo Barcella, ³Valentina Brambilla, ²Maria Grazia Bruzzone, ¹Matteo Carrabba, ²Valeria Cuccarini, ⁴Giorgio D'Alessandris, ²Francesco Di Meco, ¹Valeria Ferla, ⁵Alberto Franzin, ²Paolo Ferroli, ¹Filippo Gagliardi, ²Federico Legnani, ³Stefania Mazzoleni, ¹Pietro Mortini, ¹Matteo Maria Naldini, ⁴Alessandro Olivi, ⁴Roberto Pallini, ²Monica Patanè, ²Rosina Paterra, ²Bianca Pollo, ¹Marco Saini, ¹Silvia Snider, ³Andrew Zambanini, ¹Naldini Luigi, ³Carlo Russo, ¹Fabio Ciceri. ¹San Raffaele Hospital, Milan, Italy; ²Istituto Neurologico Carlo Besta, Milan, Italy; ³Genentia Science, Milan, Italy; ⁴Policlinico Gemelli, Rome, Italy; ⁵Fondazione Poliambulanza, Brescia, Italy

Background The dynamic regulation of the tumor microenvironment (TME) is a key mechanism driving clinical outcome with immunotherapies. The presence of different macrophage phenotypes in the TME may either promote tumor growth (M2) or phagocytose cancer cells and remodel the TME (M1). Influencing macrophage polarization may be an important target for immunotherapy.

Methods Temferon is an autologous HSC-based platform that delivers targeted IFN α into the TME via Tie-2 expressing monocytes, with transcriptional & post-transcriptional control mediated by miRNA target sequences. Temferon is being administered in a Phase 1/2a clinical trial in 21 newly diagnosed glioblastoma (GBM) patients with unmethylated MGMT promoter.

Results As of July 2022, 4 escalating doses of Temferon (0.5–3.0x10⁶/kg) were tested across 17 patients assigned to 6 cohorts. Current total follow-up from Temferon infusion is 7–749 days (3–28 months after 1st Surgery). Seven recurrent tumors were resected and where enough fresh material was available gene-marked cells were identified in the CD45+ tumor infiltrate in 2/2 specimens (3%–5%). scRNA analysis of the myeloid TME compartment (n=4 Temferon patients) detected a broad induction of an IFN, TNF/NF κ B and hypoxia response relative to n=6 standard-of-care treated patients and unveiled an overrepresentation of pro-inflammatory macrophage clusters. Strikingly, this closely resembled the microenvironmental changes observed in a murine GBM model treated with IFN gene therapy (Birocchi, *Sci Transl Med*, 2022), where a shift in the M2 to M1 macrophage balance was associated with tumor responses. Notably, the highest proportion of pro-inflammatory macrophages was detected in a stable lesion biopsied from a patient that had a contemporaneous progressing lesion, which instead contained the lowest pro-inflammatory macrophage quantity. Analysis of the T cell compartment (scRNAseq+TCRseq) of the stable lesion highlights the presence of specific CD8+ T cells clones characterized by an effector phenotype with an inflammatory profile (IFN α /g response, TNF α signaling).

Conclusions These data support the hypothesis that Temferon, by acting on the M1-M2 balance, favors a pro-inflammatory state that, as predicted by preclinical studies, induces an immune system reset that may favor containment of GBM growth.

Ethics Approval The TEM-GBM Clinical Trial (NCT03866109) has been reviewed and approved by the Italian Competent Regulatory Authority, AIFA, on 26/09/2018. The Coordinating Ethical Committee, San Raffaele Hospital (Milan), approved the study on 12/07/2018 and then on 11/10/2018.

649

PHASE 1/2 STUDY OF AGENT-797, AN ALLOGENEIC INVARIANT NATURAL KILLER T (iNKT) CELL THERAPY, IN SUBJECTS WITH MODERATE TO SEVERE ACUTE RESPIRATORY DISTRESS SYNDROME (ARDS) SECONDARY TO SARS-COV-2 (COVID-19)

<http://dx.doi.org/10.1136/jitc-2022-SITC2022.0649>

¹Marco Purbhoo, ¹Burcu Yigit, ¹Xavier Michelet, ¹Rachel Smith, ¹Darrian Moskowitz, ²Maurice Kirby, ²Alexa Buffa, ¹Sonia De Munari, ²Waldo Ortuzar Feliu, ³Koen Van Besien, ⁴Don Stevens, ¹Mark Exley, ⁵Terese Hammond*. ¹*MiNK Therapeutics, Lexington, MA, USA;* ²*Agenus Inc, Lexington, MA, USA;* ³*Weill Cornell Medicine, New York, NY, USA;* ⁴*Norton Cancer Center, Louisville, KY, USA;* ⁵*Providence Saint John's Health Center, Santa Monica, CA, USA*

Background AgenT-797 is a novel allogeneic iNKT cell therapy demonstrating activity in malignancies and serious viral infections (i.e., SARS-CoV-2). In response to inflammatory injury, iNKTs home to critical organs, including lungs, dampen proinflammatory cytokines and protect epithelial tissues. iNKTs drive response through activation of innate and adaptive immunity, recruitment/trans-activation of NK, B, and T cells, and myeloid cells via contact and soluble mediators. iNKTs represent a novel and attractive potential immunotherapy for viral ARDS. This analysis presents results from an ongoing phase 1/2 study of agenT-797 in mechanically ventilated patients with moderate to severe ARDS secondary to COVID-19; NCT04582201.

Methods As of February 2022, patients on mechanical ventilation with confirmed moderate to severe (Berlin Definition) ARDS, secondary to COVID-19 were treated with a single infusion of agenT-797 at 100, 300, or 1000 x 10⁶ iNKT cells. Primary endpoint was safety and secondarily, time to extubation, prevention of secondary infections, persistence and alloimmunity were evaluated. Clinical benefit was defined as improvement/resolution of viral ARDS evaluated as time to extubation and survival at 30 days post-infusion.

Results Twenty evaluable patients were treated with agenT-797 with a median age of 66 years (range 26-77; 85% ≥65y). Patients enrolled early in pandemic (pre-vaccines) and were heavily pre-treated with remdesivir, steroids and/or tocilizumab. No dose-limiting toxicities were observed. Tolerability was favorable with no cytokine release syndrome (CRS), neurotoxicity, or severe immune-related AEs. One SAE was deemed possibly related to agenT-797 (Dyspnea, Grade 4). The most frequent AEs deemed possibly related was pyrexia (grade 1; n=6). Survival was 70% (14/20) in this predominantly elderly, mechanically ventilated population. Early signals of reduction in ARDS symptoms, rapid extubation, and reduction in secondary infections were observed.

Agent-797 was detected in peripheral blood up to day 6 post-infusion, consistent with a rapid translocation from blood to tissue. Spikes in the blood during D1 and D2 showed a dose-proportional relationship, however, increased dose did not lead to prolonged peripheral persistence. Additional translational and biomarker evaluation is underway.

Conclusions In patients with severe viral ARDS secondary to SARS-COV-2, agenT-797 demonstrated encouraging survival and disease mitigating benefit with a favorable tolerability profile. The deep and broad activity observed is likely attributed to iNKT cells' ability to promote viral clearance, home to the lungs, and reduce inflammation. These findings support the potential for a variant-agnostic therapy for patients with viral ARDS, a condition for which there are currently no effective therapies.

Trial Registration NCT04582201

650

PELAREOREP COMBINED WITH ATEZOLIZUMAB AND CHEMOTHERAPY DEMONSTRATES ENCOURAGING RESULTS AS FIRST-LINE TREATMENT IN ADVANCED OR METASTATIC PANCREATIC DUCTAL ADENOCARCINOMA (PDAC) PATIENTS – INTERIM RESULTS FROM THE GOBLET STUDY

<http://dx.doi.org/10.1136/jitc-2022-SITC2022.0650>

¹Dirk Arnold, ¹Maike Collienne, ²Alexander Stein, ³Guy Ungerechts, ²Eray Goekkurt, ⁴Jack Chater, ⁵Houra Loghmani, ⁵Matt Coffey, ⁵Richard Trauger, ⁶Uwe Martens, ⁵Thomas Heineman*. ¹Asklepios Tumorzentrum Hamburg, Hamburg, Germany; ²Hematology-Oncology Practice Eppendorf, Hamburg, Germany; ³University Hospital Heidelberg, Heidelberg, Germany; ⁴Klinikum Chemnitz gGmbH, Chemnitz, Germany; ⁵Oncolytics Biotech, Calgary, Canada; ⁶SLK-Kliniken Heilbronn GmbH, Heilbronn, Germany

Background Pelareorep (pela) is an intravenously administered, non-genetically modified oncolytic reovirus that selectively kills tumor cells and activates both innate and adaptive immune responses. In prior clinical trials, pela was shown to prime tumors for checkpoint inhibition by enhancing infiltration of lymphocytes into tumors and increasing PD-L1 expression. The GOBLET basket study was designed to assess the safety and efficacy of pela in combination with atezolizumab (atezo) +/- chemotherapy in multiple gastrointestinal cancer indications (PDAC, 1L MSI-H colorectal cancer, 3L MSS colorectal cancer, 2L anal carcinoma). Here we report the interim results for patients with advanced/metastatic PDAC.

Methods GOBLET is a phase 1/2 Simon two-stage study. PDAC patients enrolled in GOBLET are treated with pela, atezo and gemcitabine/nab-paclitaxel. They must have locally advanced/metastatic unresectable disease evaluable by RECIST v1.1, be ≥ 18 years old and have an ECOG score ≤ 1 . The first stage enrolled 12 evaluable PDAC patients (evaluable patients must have at least one post-baseline tumor assessment). The primary objectives are safety and efficacy by investigator-assessed objective response rate (ORR). The protocol-specified Stage 1 success criterion for PDAC is ≥ 3 confirmed responses. In addition, blood samples collected at baseline (cycle 1 day 1 [c1d1]) and c2d1 of the 28-day treatment cycle will undergo T-cell receptor sequencing (TCR-seq) to assess treatment effect on the T-cell repertoire.

Results No safety signals have been observed in patients treated with pela, atezo and gemcitabine/nab-paclitaxel. Seven of 10 evaluable patients to date (28 July 2022) had a partial response at week 8 or later (3 confirmed, 4 currently unconfirmed), and 2 had stable disease for an objective response rate (ORR) of 70% and a clinical benefit rate (CBR) of 90%. TCR-seq revealed an expansion of T-cell clones, a decrease in clonal diversity, and an increase in T-cell fraction from c1d1 to c2d1 in all three patients for whom data are available. Updated tumor response and TCR-seq results will be presented.

Conclusions Consistent with previous studies in PDAC and other indications, pela in combination with chemotherapy and a checkpoint inhibitor is well-tolerated. The primary efficacy success criterion was met, and the high ORR and CBR observed in this study are very encouraging in comparison to tumor response rates observed in prior first-line PDAC treatment studies. The changes in T-cell repertoire observed in the first three patients are consistent with previous pelareorep/checkpoint inhibitor studies and will be further evaluated as possible biomarkers for response to therapy.

Trial Registration (Eudra-CT: 2020-003996-16)

Ethics Approval The study was approved by the ethic committee of Hamburg on February 22, 2021.

651 PHASE 2 TRIAL OF AGEN1423, AN ANTI-CD73-TGF β -TRAP BIFUNCTIONAL ANTIBODY, IN COMBINATION WITH BALSTILIMAB, WITH OR WITHOUT CHEMOTHERAPY IN SUBJECTS WITH ADVANCED PANCREATIC CANCER

²Joseph Grossman, ²Jaymin Patel, ²Bonnie Bullock, ²Benjamin Morin, ²Lilian Gaynor, ³Manuel Hidalgo, ¹Bruno Bockorny*. ¹Beth Israel Deaconess Medical Center, Boston, MA, USA; ²Agenus Inc., Lexington, MA, USA; ³Cornell University, New York, NY, USA

Background Immunotherapy has made relatively few inroads in pancreatic ductal adenocarcinoma (PDAC) due to its non-redundant mechanisms of resistance, underscoring the need to target alternative immune pathways using a multi-faceted approach. Transforming growth factor-beta (TGF β) plays an important role in mediating primary resistance to programmed cell death protein/ligand 1(PD-1)/PD-(L)1 blockade. Active adenosine signaling and high basal CD73 expression (an enzyme involved in adenosine metabolism), represent another established resistance mechanism in PDAC and other solid tumors. AGEN1423 is a bifunctional humanized immunoglobulin (IgG1) antibody designed to target both CD73 and TGF β with a unique mechanism of action featuring (1) preferential localization within the tumor microenvironment (TME) via its CD73 targeting moiety; (2) ability to reduce the concentration of adenosine in the TME by blocking CD73 enzymatic activity; and (3) inhibition the immunosuppressive effect of TGF β via intracellular trapping. A Phase 1 dose escalation study of AGEN1423 monotherapy was already conducted in patients with advanced solid tumors. Collectively, AGEN1423 is a promising therapeutic investigational candidate designed to address two unique immunosuppressive resistance mechanisms in PDAC simultaneously.

Methods This open-label, two-cohort Phase 2 clinical trial was designed to assess the safety and efficacy of AGEN1423 plus balstilimab with or without chemotherapy in advanced PDAC. Eligible patients include individuals ≥ 18 years with histologically or cytologically confirmed metastatic or locally advanced PDAC, Eastern Cooperative Oncology Group performance status of 0 or 1 and adequate organ and bone marrow function. In cohort 1, twelve patients with advanced PDAC with progression after ≥ 1 prior lines of therapy will be enrolled to receive AGEN1423 30mg/kg plus balstilimab 3mg/kg on day 1 of a 14-day cycle. In cohort 2, twelve patients with metastatic PDAC following disease progression on fluorouracil-based therapy will be enrolled to receive AGEN1423 30mg/kg plus balstilimab 3mg/kg on days 1 and 15 of a 28-day cycle in combination with gemcitabine 1000 mg/m² plus nab-paclitaxel 125 mg/m² on days 1, 8 and 15 of a 28-day cycle. The primary endpoint is to assess the objective response rate (ORR) according to RECISTv1.1. Secondary endpoints include disease control rate (stable disease or a complete or partial response), overall survival and progression-free survival, and to evaluate safety and tolerability. Biopsies will be obtained at baseline and on-treatment for multiplex immunohistochemistry and additional genomic analyses to better understand changes in the tumor microenvironment following AGEN1423 and balstilimab treatment. Recruitment is anticipated to commence in Q3 2022.

<http://dx.doi.org/10.1136/jitc-2022-SITC2022.0651>

652

A PHASE 1 DOSE ESCALATION STUDY OF GCC19CART A NOVEL COUPLEDCAR[®] THERAPY FOR SUBJECTS WITH METASTATIC COLORECTAL CANCER

<http://dx.doi.org/10.1136/jitc-2022-SITC2022.0652>

¹Naifei Chen, ²Chengfei Pu, ¹Lingling Zhao, ³Ning Li, ¹Chang Wang, ⁴Yusheng Huang, ³Suxia Luo, ⁵Xun Li, ⁴Zhenzhou Yang, ⁶Jun Bie, ²Ruihong Zhu, ²Xi Huang, ²Haiyang Tang, ¹Tingting Liang, ¹Yizhuo Wang, ²Beibei Jia, ²Dongqi Chen, ²Eugene Kennedy, ²Zhao Wu, ³Yongping Song, ²Lei Xiao, ¹Jiuwei Cui, ²Lei Xiao*, ²Victor Lu*. ¹The First Bethune Hospital of JLU, Changchun, China; ²Innovative Cellular Therapeutics, Shanghai, China; ³Henan Cancer Hospital, Zhengzhou, China; ⁴The Second Affiliated Hospital of CQMU, Chongqing, China; ⁵The First Hospital of Lanzhou University, Lanzhou, China; ⁶Nanchong Central Hospital, Nanchong, China

Background Chimeric antigen receptor (CAR) T-cell therapy has shown remarkable clinical efficacy in hematologic malignancies but limited success in solid tumors. GCC19CART, the first clinical candidate from the CoupledCAR[®] solid tumor platform, is designed to overcome the limitations of conventional CAR T-cells in solid tumor malignancies by pairing solid tumor CAR T-cells with CD19 targeting CAR T-cells to amplify proliferation and activation of the solid tumor CAR T component. GCC19CART targets guanylate cyclase-C (GCC) which is expressed in the metastatic lesions of 70%-80% of subjects with colorectal cancers. A Phase 1 investigator-initiated clinical trial is underway in China for patients with relapsed or refractory metastatic colorectal cancer who have received at least 2 prior lines of therapy. Based on a data cut-off on December 13, 2021, 21 subjects have been enrolled in 2 dose escalation groups at 5 hospitals in China.

Methods Subjects are screened for GCC expression by immunohistochemistry. Eligible subjects undergo leukapheresis, a single dose of lymphodepleting chemotherapy (fludarabine 30mg/m² and cyclophosphamide 300mg/m²) 3 days prior to infusion, and then administration of a single infusion of GCC19CART at one of two preassigned doses: 1x10⁶ or 2x10⁶ CAR T-cells/kg. Endpoints are safety and preliminary evidence of efficacy as determined by CT or PET/CT per RECIST 1.1 or PERCIST 1.0. All responses were confirmed by an independent third-party imaging contract research organization (CRO).

Results 13 subjects have been enrolled to dose level 1 (1x10⁶ cells/kg) and 8 subjects have been enrolled to dose level 2 (2x10⁶ cells/kg). The most common adverse events were cytokine release syndrome (CRS) in 21/21 subjects (Grade 1 19/21 (90.48%) or Grade 2 2/21 (9.52%)) and diarrhea in 21/21 subjects (Grade 1 6/21 (28.57%) Grade 2 5/21 (23.81%) Grade 3 9/21 (42.86%) or Grade 4 1/21 (4.76%)). Neurotoxicity was observed in 2/21 (9.52%) subjects at Grade 3 or 4 and resolved with corticosteroids. The combined overall response rate (ORR) for both dose levels was 28.6% (6/21). For dose level 1, the overall response rate (ORR) per RECIST 1.1 was 15.4% (2/13). Two subjects demonstrated a partial response (PR) while 3 additional subjects had partial metabolic response (PMR) on PET/CT with stable disease (SD) or progressive disease (PD) per RECIST 1.1. For dose level 2, The ORR per RECIST 1.1 was 50% (4/8). 4 subjects demonstrated a PR (3 at month 1, 1 at month 3 after being SD at month 1) and 2 additional subjects had PMR on PET/CT with SD per RECIST 1.1.

Conclusions GCC19CART demonstrated meaningful dose dependent clinical activity and an acceptable safety profile in relapsed or refractory metastatic colorectal cancer. This trial is ongoing and updated data will be presented. A United States based Phase 1 trial of GCC19CART is anticipated for mid-2022.

653

APN401, A NOVEL EPIC-BASED ANTI-CANCER CELL THERAPY, CASE REPORT: CBL-B SILENCED, AUTOLOGOUS PBMCS INDUCED STABLE DISEASE IN AN APPENDIX CARCINOMA PATIENT

¹Romana Gugenberger*, ¹Alexander Dohnal, ²Andreas Tanzmann, ²Beate Pribitzer, ²Felix Batrina, ²Stefan Bunka, ²Sophia Spagl, ²Manuela Branka, ¹Sarah Bischof, ¹Kathrin Thell, ¹Mario Kuttke, ¹Maria Urban, ¹Hannes Muehleisen, ¹Bernhard Peball, ²Markus Raderer, ²Gerald Prager, ²Nina Worel. ¹*invlOs GmbH, Vienna, Austria*; ²*Medical University of Vienna, Vienna, Austria*

Background While the immune system of cancer patients is generally capable of generating tumor-specific effector cells, their function is impaired due to immune checkpoint control. We and others have shown that the E3 ubiquitin ligase Cbl-b (Casitas B-lineage lymphoma-b) functions as a master checkpoint and plays a central role in suppressing both adaptive and innate anti-tumor responses. Thus, by blocking Cbl-b function, immune effector functions against tumor cells may be restored. We have developed a novel way to transiently silence Cbl-b in a patient's peripheral blood mononuclear cells (PBMCs), named APN401, an autologous cell therapy. The use of an innovative closed cell processing Enhancement Platform for immune Cells (EPiC) enables manufacturing of high numbers of modified PBMCs for APN401 in a short processing time and allows for same-day out patient therapy.

Methods In our ongoing phase 1b trial, a 59-year-old white male patient with appendix carcinoma was treated with APN401, a drug product composed of a suspension of his own viable PBMCs. Those PBMCs were transfected *ex vivo* with a small interfering ribonucleic acid (siRNA) in order to reduce Cbl-b expression by using the innovative EPiC manufacturing process, comprising (I) purification of PBMCs from leukapheresis products, (II) electroporation of PBMCs to incorporate Cbl-b siRNA and (III) final PBMC formulation for re-infusion. The entire manufacturing process requires less than 6 hours and is approved by the national competent authorities for a same-day out patient therapy in a phase 1b trial. The trial is evaluating clinical outcome, safety, activity, and potency of the drug product; in addition, specific biomarkers are being analyzed.

Results This case report is part of an open-label, multi-center, dose escalation and expansion clinical trial evaluating three dose levels of APN401 using a 3+3 design in advanced solid tumor patients. The first cohort of the phase 1b study demonstrated feasibility, safety and tolerability for the lowest dose level (infused cell number: 5.0×10^6 PBMCs/kg). The patient with appendix carcinoma presented stable disease after APN401 treatment. Subsequent biomarker analyses revealed increased IL-2 levels indicating potency and an elevated CD8/CD4 ratio suggesting potential cytotoxic efficacy. In stimulation assays with HLA-1 restricted viral or tumor antigens, increased IFN γ levels were detected as surrogate markers for improved immunity and tumor reactivity.

Conclusions Our findings highlight that APN401, an autologous cell therapy based on selective Cbl-b silencing, may be a safe, potent, and effective immunotherapy for solid tumors.

Ethics Approval The study is approved by Medical University of Vienna institution's independent Ethics Board, approval number 1778/2020.

<http://dx.doi.org/10.1136/jitc-2022-SITC2022.0653>

654 **PERSONALISED TUMOUR-TRAINED LYMPHOCYTES DERIVED FROM REGIONAL LYMPH NODES FOR TREATMENT OF COLORECTAL CANCER**

Anne-Laure Joly*, Sofia Berglund, Erwan Le Maitre, Ana Lukic, Luigi Notari, Ola Nilsson, Guro Gafvelin, Hans Grönlund. *Karolinska Institutet, Stockholm, Sweden*

Background Adoptive T cell therapy as a treatment for solid tumours is gaining increasing interest. Cancer neoantigens as targets for such therapy is also gaining recognition. Personalised tumour trained lymphocytes (pTTL) is a novel autologous T cell therapy targeting patient-specific neoantigens. A phase I/II First in Human (FIH) clinical trial of pTTL in Stage IV colorectal cancer (CRC) patients will be initiated in the near future.

Methods pTTL is produced through *in vitro* expansion of T cells derived from regional lymph nodes (RLNs). The T cells derived from RLNs, nodes in anatomical proximity of the tumour, contain a pool of naive and antigen-experienced T cells enriched for tumour-antigen specificity. This enriched population is stimulated during pTTL production with an array of neoantigen epitopes individually designed using PIOR[®], an in house-developed software for neoantigen detection and selection. Selected neoantigens are linked to paramagnetic particles using EpiTCer[®] technology. The resulting EpiTCer[®] particles are used to stimulate the RLN T cells via phagocytosis and presentation of the neoantigen epitopes by antigen-presenting cells. This process is HLA-independent. Each pTTL product is unique due to the personalised nature of cellular and molecular players (cancer characteristics, immune cell properties and neoantigens are specific to one single individual).

In the planned FIH trial patients with Stage IV CRC which have either no remaining relevant standard care therapies or which are in a scheduled break in such therapy can be included. pTTL will be administered as a single dose monotherapy after chemotherapy-based preconditioning with cyclophosphamide and fludarabine. The primary endpoint of the trial is safety of pTTL. Biomarker analysis of pTTL persistence and characteristics will also be central in trial assessments, and clinical outcome and response will be evaluated.

Results Clinical results are not yet available. We here present central pTTL product characteristics. We have found that pTTL can be manufactured with a high rate of success despite the patient-specific nature of each product. The majority of the cells in pTTL are T cells, with small proportions of remaining NK and B cells originating from the RLN. The CD4 and CD8 T cell ratio are variable. Main pTTL characteristics include a significant proportion of memory T cells and phenotypic markers indicating maintained functionality such as limited levels of Temra (late stage memory cells re-expressing CD45RA) and CD57+ T cells, and maintained expression of CD28. TCRseq data have shown increased clonality in pTTL compared to RLNs, indicating antigen-specific expansion.

Trial Registration EUDRA CT #2022-000394-96

Ethics Approval The trial have been approved by the Swedish Ethical Review Authority, Approval # 2022-01842-01

Consent Written informed consent will be requested from study participants in future, but no study subjects have yet been included.

<http://dx.doi.org/10.1136/jitc-2022-SITC2022.0654>

655

PIVOTAL SCREENING AND PROPOSED TREATMENT ALGORITHM FOR IMMUNE CHECKPOINT INHIBITOR-INDUCED CARDIO/MYOTOXICITIES IN NEOADJUVANT-TREATED RECTAL CANCER PATIENTS: EXPERIENCE FROM THE CHINOREC TRIAL

¹Johannes Laengle*, ¹Jutta Bergler-Klein, ¹Simon Hametner, ¹Ellen Gelpi, ¹Irene Kuehrer, ¹Branka Petricevic, ¹Askin Kulu, ²Clemens Bittermann, ¹Anton Stift, ²Friedrich Laengle, ¹Klaus Machold, ¹Stephan Bluemel, ¹Michael Bergmann. ¹Medical University of Vienna, Vienna, Austria; ²State Hospital Wiener Neustadt, Vienna, Austria

Background Myotoxicities (myositis, myocarditis or rhabdomyolysis) are rare (incidence 0.21%) but potentially life-threatening immune-mediated adverse reactions (IMARs) of immune checkpoint inhibitors (ICI), such as ipilimumab (IPI) or nivolumab (NIVO), with a case fatality rate (CFR) of up to 40%. The true incidence is likely to be underestimated and may not be representative for neoadjuvant treatment approaches in gastrointestinal (GI) cancers, especially in combination with chemoradiotherapy (CRT). Currently the summary of product characteristics (SmPC) does not suggest any pre-emptive screening and surveillance for myotoxicities.

Methods The CHINOREC study (NCT04124601) is an ongoing prospective, randomized, open-label, multicenter, phase II investigator-initiated trial (IIT). Patients with locally advanced rectal cancer (LARC) receive either neoadjuvant CRT (50 Gy + capecitabine 1650 mg/m²/d PO) alone or in combination with a single dose of IPI 1 mg/kg IV and 3 cycles of NIVO 3 mg/kg IV Q2W, with subsequent surgical resection in a curative intend. Patients are continuously screened at baseline and throughout the whole study period for cardio/myotoxicity biomarkers, such as creatine kinase (CK), creatine kinase muscle-brain (CK-MB), myoglobin (MB), troponin T (TnT) and N-terminal prohormone brain natriuretic peptide (NT-proBNP).

Results From 06/2020-03/2022, 24 patients were randomized to the CRT+IPI/NIVO arm. Out of these, 4 patients (16%) developed a biopsy-proven myositis, of whom 2 (8%) were symptomatic (1 patient with a grade 4 SAE). All patients were promptly initiated with medical interventions in a step-up approach, starting at the first time of elevated cardio/myotoxicity biomarkers (regardless of symptoms). Patients received prednisolone 1-2 mg/kg with concomitant intravenous immunoglobulin (IVIG) 2 g/kg. If myotoxicity biomarkers did not improve, patients received plasma exchange (PLEX) and if further ineffective, infliximab 5 mg/kg IV. To this date all patients have resolved back to normal CK and MB levels. Although all myositis patients had strikingly elevated TnT (median peak 330 ng/L, 95% CI 39-3097) and NT-proBNP levels (median peak 655 pg/mL, 95% CI 507-1161) myocardial involvement/overlap could not be proven by cardiac magnetic resonance imaging (MRI), transthoracic echocardiogram (TTE), electrocardiography (ECG) and/or coronary computed tomography angiography (CTA). However, myocardial biopsies were not performed due to safety concerns.

Conclusions Patients receiving neoadjuvant ICI with CRT should be closely monitored by myotoxicity biomarkers for potentially severe ICI-induced myositis to initiate early counter treatment in a step-up approach. Highly elevated TnT values were observed despite the lack of myocarditis in cardiac diagnostic work-up. As treatment for ICI-induced myositis will concomitantly treat potential cardiotoxicity, myocardial biopsy may be debatable.

Acknowledgements This is an investigator-initiated trial (IIT), which received a research grant and the study medications from Bristol-Myers Squibb (BMS).

Trial Registration NCT04124601

Ethics Approval The study protocol was verified by the "Ethics Committee of the Medical University of Vienna" (EC No. 2040/2019).

Consent Written informed consent was obtained from the patient for publication of this abstract. A copy of the written consent is available for review by the Editor of this journal.

<http://dx.doi.org/10.1136/jitc-2022-SITC2022.0655>

EXPLORATORY PLATFORM TRIAL TO EVALUATE IMMUNOTHERAPY COMBINATIONS WITH CHEMOTHERAPY FOR THE TREATMENT OF PATIENTS WITH PREVIOUSLY UNTREATED METASTATIC PANCREATIC ADENOCARCINOMA (REVOLUTION)

¹Jaclyn Lyman*, ²Eileen O'Reilly, ³Zev Wainberg, ⁴George Fisher, ⁵Robert Wolff, ⁶Andrew Ko, ⁷Mark O'Hara, ⁸Harshabhad Singh, ⁹Ravi Amaravadi, ⁹Alec Kimmelman, ⁶Eric Collison, ²Danny Khalil, ¹Rosemarie Schmidberger, ¹Christopher Cabanski, ¹Stephen Maddock, ¹Marko Spasic, ¹Deena Maurer, ¹Diane Da Silva, ¹Christopher Perry, ¹Jia Xin Yu, ¹Lacey Padrón, ¹Samantha Bucktrout, ¹⁰Lisa Butterfield, ¹Ramy Ibrahim, ¹Justin Fairchild, ¹Theresa LaVallee, ¹¹Thomas Lillie, ¹²William Hoos, ¹³Silvia Boffo, ¹Ute Dugan, ¹⁴Jill O'Donnell-Tormey, ⁷Robert Vonderheide. ¹Parker Institute for Cancer Immunotherapy, San Francisco, CA, USA; ²Memorial Sloan Kettering Cancer Center, New York, NY, USA; ³University of California, Los Angeles, Los Angeles, CA, USA; ⁴Stanford University, San Francisco, CA, USA; ⁵MD Anderson Cancer Center, Houston, TX, USA; ⁶University of California, San Francisco, San Francisco, CA, USA; ⁷University of Pennsylvania, Abramson Cancer Center, Philadelphia, PA, USA; ⁸Dana-Farber Cancer Institute, Boston, MA, USA; ⁹New York University School of Medicine, Perlmutter Cancer Center, New York, NY, USA; ¹⁰Parker Institute for Cancer Immunotherapy, San Francisco, CA, USA; ¹¹PsiOxus Therapeutics, Ltd, Abingdon, UK; ¹²1440 Foundation, Scotts Valley, CA, USA; ¹³Bristol Myers Squibb, Princeton, NJ, USA; ¹⁴Cancer Research Institute, New York, NY, USA

Background Metastatic pancreatic adenocarcinoma (mPDAC) remains notoriously treatment-refractory, particularly to immunotherapy; however, recent promise has been demonstrated with chemoimmunotherapy combinations.^{1,2} REVOLUTION is an adaptive platform trial, designed to further these advancements by assessing the safety and antitumor activity of parallel, novel chemoimmunotherapy combinations in patients with untreated mPDAC. Coupled with deep immune biomarker profiling, this approach will enable rapid insights from each combination, generating data to be leveraged for future cohorts. REVOLUTION also builds upon the collaborative framework between academic, nonprofit and industry partners, laid by the PRINCE trial.¹

Methods REVOLUTION is an open-label, non-randomized, exploratory platform trial. Each cohort utilizes a Simon two-stage design: Stage 1 enrolling n=15 patients, expansion to Stage 2 (an additional n=15 patients) based on the totality of safety, efficacy and biomarker analyses.

Key inclusion criteria histologically or cytologically confirmed, treatment-naïve, recurrent or de novo mPDAC, measurable by RECIST 1.1. Primary endpoints: safety, as assessed by the incidence and severity of adverse events. Secondary endpoints: ORR (per RECIST 1.1), DCR, DOR, PFS, and OS. Exploratory endpoints: pharmacodynamics and association of tumor, blood, and stool biomarkers with clinical activity.

Three cohorts are underway, all using a backbone of standard-of-care gemcitabine/nab-paclitaxel (gem/nP).

Cohort A: nivolumab + ipilimumab + gem/nP. We hypothesize chemotherapy will induce antigen release, ipilimumab will enhance T cell activation, proliferation and tumor infiltration, and nivolumab will overcome immunosuppression while re-invigorating therapeutically relevant T cells.

Cohort B: high-dose hydroxychloroquine (HCQ), an autophagy inhibitor, + ipilimumab + gem/nP. The same mechanisms of action for chemotherapy and ipilimumab as Cohort A are hypothesized, with HCQ augmenting T cell priming and cytotoxicity by upregulating MHC-1.³

Cohort C: NG-350A, an intravenously administered adenovirus that selectively replicates in tumor cells and expresses a fully human agonistic CD40 monoclonal antibody, + ipilimumab + gem/nP. The same mechanisms of action for chemotherapy and ipilimumab as Cohorts A and B are hypothesized, with NG-350A re-programming the tumor microenvironment,

activating antigen-presenting cells, and facilitating immune priming.⁴

In accordance with recent findings, all current cohorts are also testing a novel dosing schedule of ipilimumab (2 doses at 1 mg/kg, Q6W).⁵

Results Cohorts A and B are fully enrolled for Stage 1 and accumulating data to support an expansion decision. Cohort C is in development.

Acknowledgements We extend our gratitude to the patients and their families, as well as the clinical investigators and their site teams for making this trial possible. We also thank Jay Campbell and Samik Upadhaya at Cancer Research Institute for their collaboration. The study is funded by Cancer Research Institute, 1440 Foundation, Bristol Myers Squibb and PsiOxus Therapeutics, Ltd. Study drug is supplied by Bristol Myers Squibb and PsiOxus Therapeutics, Ltd.

Trial Registration NCT04787991

REFERENCES

1. O'Hara MH, O'Reilly EM, Varadhachary G, Wolff RA, Wainberg ZA, Ko AH, et al. CD40 agonist monoclonal antibody APX005M (sotigalimab) and chemotherapy, with or without nivolumab, for the treatment of metastatic pancreatic adenocarcinoma: An open-label, multicentre, phase 1B study. *Lancet. Oncol.* 2021;**22**(1):118–31.
2. Padrón LJ, Maurer DM, O'Hara MH, O'Reilly EM, Wolff RA, Wainberg ZA, et al. Sotigalimab and/or nivolumab with chemotherapy in first-line metastatic pancreatic cancer: Clinical and immunologic analyses from the Randomized Phase 2 prince trial. *Nat. Med.* 2022;**28**(6):1167–77.
3. Yamamoto K, Venida A, Yano J, Biancur DE, Kakiuchi M, Gupta S, et al. Autophagy promotes immune evasion of pancreatic cancer by degrading MHC-I. *Nature.* 2020;**581**:100–105.
4. Rosen LS, Camidge DR, Khalil D, Lillie T, Carter J, Krige D, et al. 1011P FORTITUDE phase I study of NG-350A, a novel tumour-selective adenoviral vector expressing an anti-CD40 agonist antibody: Monotherapy dose escalation results. *J. Clin. Oncol.* 2022;**40**(16_suppl):2559–2559.
5. Postow MA, Goldman DA, Shoushtari AN, Warner AB, Callahan MK, Mometz P, et al. A phase II study to evaluate the need for > two doses of nivolumab + ipilimumab combination (combo) immunotherapy. *J. Clin. Oncol.* 2020;**38**(15_suppl):10003–10003.

Ethics Approval This study is approved by the WCG IRB, reference number 20203790.

<http://dx.doi.org/10.1136/jitc-2022-SITC2022.0656>

657

NT-17, A LONG-ACTING IL-7, PLUS PEMBROLIZUMAB FAVORS CD8 T-CELL INFILTRATION IN LIVER METASTASES OF HEAVILY PRE-TREATED, IMMUNOLOGICALLY COLD, MSS-COLORECTAL AND PANCREATIC CANCER

¹Aung Naing*, ²Sara Ferrando-Martinez, ²Michael Ware, ¹Cara Haymaker, ²Allison Bierly, ²Jack Goon, ³Marya Chaney, ²Swati Dhar, ⁴Chan-Young Ock, ⁵Siyung Lee, ⁴Kyunghyun Paeng, ⁵Taeseob Lee, ²Tolani Adebajo, ²Se Hwan Yang, ²Byung Ha Lee, ⁶Richard Kim. ¹MD Anderson Cancer Center, Houston, TX, USA; ²NeolImmuneTech, Inc., Rockville, MD, USA; ³Merck and Co., Inc., Kenilworth, NJ, USA; ⁴Lunit, Inc., Seoul, Republic of Korea; ⁵Geninus, Inc., Seoul, Republic of Korea; ⁶Moffitt Cancer Center, Tampa, FL, USA

Background Checkpoint inhibitors (CPI) have null objective response (ORR) and dismal disease control rates (DCR) in microsatellite-stable colorectal (MSS-CRC) and pancreatic cancer (PaC), due to low mutation burden and sparse T-cell infiltration. Liver metastases are common in these indications and are harder to infiltrate, further reducing the efficacy of immunotherapy. NT-17 (efineptakin alfa) in combination with pembrolizumab has been shown to increase T-cell infiltration. This study explores the ability of NT-17 and pembrolizumab to support T-cell infiltration in subjects with liver metastasis as a correlate of clinical efficacy.

Methods Open-label, phase 2a study in subjects with relapsed/refractory (r/r) CPI-naïve MSS-CRC and PaC. Subjects received NT-17 at 1200 µg/kg every 6 weeks (Q6W) plus pembrolizumab at 200 mg Q3W. Antitumor activity was assessed by RECIST v1.1 and iRECIST. Pre-treatment and on-treatment biopsies were analyzed by Lunit SCOPE IO, an artificial intelligence-powered H&E analyzer, and immunohistochemistry. For exome sequencing analysis, single nucleotide variants and indels were detected and filtered by GATK Mutect2.

Results As of April 29, 2022, 53 subjects were evaluable. 67.9% of subjects had ≥2 prior therapies; 73.6% had liver metastasis and median tumor mutation burden (TMB; n=18) was 3.22 mutations/megabase. ORR was 3.8% per RECIST and 9.4% per iRECIST. Total density of tumor-infiltrating lymphocytes (TIL) significantly increased on-treatment, despite low TMB. Subjects with metastasis to sites other than the liver had 28.6% iORR and 71.4% iDCR, a remarkable result considering the lack of response with anti-PD(L)1 monotherapy, and significantly higher overall survival (OS; p=0.0241). However, NT-17 and pembrolizumab still demonstrated benefit for patients with liver metastasis; with an iDCR of 25.6%. CD8 T-cell infiltration increased with treatment regardless of tissue location, including liver biopsies (p=0.0032). Lymphoid aggregates containing CD8+TCF1+ lymphocytes, suggestive of tertiary lymphoid structures, were observed on-treatment (n=14) in both liver and non-liver biopsies, including all 3 patients with objective response. Moreover, CD8+ T-cell infiltration was directly associated with OS (p=0.0002), suggesting that NT-17 plus pembrolizumab increases intratumoral TIL density and CD8 T-cell infiltration in primary and metastatic locations to mediate clinical benefit.

Conclusions NT-17 plus pembrolizumab shows remarkable efficacy in immunologically cold CPI-naïve r/r MSS-CRC and PaC in the absence of liver metastasis. Furthermore, this combination also increases T-cell infiltration in immune-excluded liver biopsies, favoring a hot tumor microenvironment that contributes to the overall high iDCR observed in these hard-to-treat CPI-resistant indications.

Acknowledgements The authors thank ICON for their partnership in conducting this trial.

Trial Registration NCT04332653

Ethics Approval The trial was approved by MD Anderson IRB, Advarra IRB, Mary Crowley IRB, and Integ Review IRB.

<http://dx.doi.org/10.1136/jitc-2022-SITC2022.0657>

A PHASE 2 STUDY TO ASSESS THE SAFETY, EFFICACY OF FLX475 COMBINED WITH PEMBROLIZUMAB IN PATIENTS WITH ADVANCED OR METASTATIC GASTRIC CANCER

¹Paul Rhee*, ²Do-Youn Oh*, ³Min Hee Ryu, ⁴Jun-Eul Hwang, ⁵Jaeyong Cho, ⁶Daeyoung Zang, ⁷Sang Cheul Oh, ⁸Jeeyun Lee, ⁹Keun-Wook Lee, ¹⁰Sun Young Rha, ¹¹Byoung Yong Shim, ¹²William Ho, ¹Taewan Kim, ¹Eunhye Baek, ¹Seungjae Baek, ¹³Michael Chisamore. ¹Hanmi Pharmaceutical Co., Ltd., Seoul, Republic of Korea; ²Seoul National University Hospital, Seoul, Republic of Korea; ³Asan Medical Center, Seoul, Republic of Korea; ⁴Chonnam National University Hwasun Hospital, Gwangju, Republic of Korea; ⁵Gangnam Severance Hospital, Seoul, Republic of Korea; ⁶Hallym University Medical Center, Anyang-si, Republic of Korea; ⁷Korea University Guro Hospital, Seoul, Republic of Korea; ⁸Samsung Medical Center, Seoul, Republic of Korea; ⁹Seoul National University Bundang Hospital, Seongnam, Republic of Korea; ¹⁰Yonsei University College of Medicine, Seoul, Republic of Korea; ¹¹St. Vincent's Hospital, Suwon, Republic of Korea; ¹²RAPT Therapeutics, South San Francisco, CA, USA; ¹³Merck and Co., Inc., Kenilworth, NJ, USA

Background Regulatory T-cells (T_{reg}) maintain homeostasis and self-tolerance, but can also suppress anti-tumor immunity in the tumor microenvironment (TME), correlating with poor clinical outcomes. C-C chemokine receptor type 4 (CCR4), the cognate receptor of the secreted proteins C-C motif chemokine ligand 17 (CCL17), and 22 (CCL22), is the predominant chemokine receptor on human T_{reg} and is responsible for migration and accumulation of T_{reg} in the TME.^{1, 2, 3} FLX475 is an orally available and selective small-molecule antagonist of CCR4 which demonstrated potent inhibition of CCL17- and CCL22-induced CCR4-mediated chemotaxis, an increase in the intratumoral T_{eff}/T_{reg} ratio, and anti-tumor efficacy as a single agent and in combination with checkpoint inhibitors.⁴ Given the proposed mechanism of action, a Phase 2 study investigating the safety, efficacy of FLX475 in combination with pembrolizumab in patients with advanced or metastatic gastric cancer is being conducted.

Methods This is a Phase 2, open-label study to assess the safety and efficacy of FLX475 in combination with pembrolizumab in patients with advanced or metastatic gastric cancer. Patients were treated across 2 cohorts administered with 100mg PO QD of FLX475 and 200mg IV Q3W of pembrolizumab. In cohort 1, checkpoint inhibitor (CPI) naïve Epstein-Barr Virus (EBV)-negative gastric cancer patients who have progressed on at least 2 prior systemic treatments for advanced or metastatic gastric cancer were enrolled, and in cohort 2, CPI-naïve EBV-positive gastric cancer patients who had at least 1 prior systemic treatment for advanced or metastatic gastric cancer were enrolled.

Results Initial analysis of cohorts was performed when the first 10 patients of each cohort completed 4 cycles or after 2nd response assessment (Cut-off date: 11 Oct 2021 (cohort 1), 15 Apr 2022 (cohort 2)). Overall, FLX475 in combination with pembrolizumab was well-tolerated, with no new safety signal detected. The most common treatment-emergent adverse events (all grade) occurred in more than 20% of patients across cohorts were QTc prolongation, pruritus, anaemia, headache, abdominal pain, fatigue, and aspartate aminotransferase increased. There were no responses observed in the EBV-negative cohort of 10 patients. However, 6 partial responses (ORR: 60.0%, all confirmed) from EBV-positive cohort were reported. Pharmacokinetic data demonstrated that majority of patients achieved the target minimum FLX475 exposure level of 130 ng/mL after 1 week of dosing. Pharmacodynamic biomarker changes were observed in tumor demonstrating biological activity of FLX475.

Conclusions FLX475 in combination with pembrolizumab was well-tolerated and exhibited promising anti-tumor efficacy in patients with advanced or metastatic EBV-positive gastric cancer.

Acknowledgements Thanks to the patients, and to their families and caregivers for allowing us to be part of the journey.

RAPT Therapeutics, Inc., South San Francisco, CA, USA is providing FLX475 for the study.

Merck Sharp & Dohme LLC, a subsidiary of Merck & Co., Inc., Rahway, NJ, USA is providing pembrolizumab for the study.

Trial Registration ClinicalTrials.gov Identifier: NCT04768686

REFERENCES

1. Talay O, et al. Potent and selective C-C chemokine receptor (CCR4) antagonists potentiate anti-tumor immune responses by inhibiting regulatory T cells (Treg). *J Immunother Cancer*. 2017;**5**(Suppl 2):P467 (SITC 2017)
2. Curiel, Tyler J, et al. Specific recruitment of regulatory T cells in ovarian carcinoma fosters immune privilege and predicts reduced survival. *Nature medicine*. 2004;**10**(9):942–949
3. Nakayama et al. Selective induction of Th2-attracting chemokines CCL17 and CCL22 in human B cells by latent membrane protein 1 of Epstein-Barr virus. *J Virol*. 2004;**78**(4):1665–74
4. Marshall LA, Marubayashi S, Jorapur A, et al. Tumors establish resistance to immunotherapy by regulating Treg recruitment via CCR4. *Journal for Immunotherapy of Cancer*. 2020;**8**:e000764

Ethics Approval This study has been approved by the Institutional Review Board at each investigational site.

<http://dx.doi.org/10.1136/jitc-2022-SITC2022.0658>

659

COM701 PLUS NIVOLUMAB DEMONSTRATES PRELIMINARY ANTITUMOR ACTIVITY AND IMMUNE MODULATION OF TUMOR MICROENVIRONMENT IN PATIENTS WITH METASTATIC MSS-CRC AND LIVER METASTASES

¹Drew Rasco, ²Ecaterina Dumbrava, ³Manish Sharma, ⁴Dale Shepard, ⁵Daniel Vaena, ⁶Gini Fleming, ⁷Bartosz Chmielowski, ⁸Erika Hamilton, ⁹Ryan Sullivan, ¹Kyriakos Papadopoulos, ¹Amita Patnaik, ¹¹Eran Ophir, ¹¹Gady Cojocar, ¹²Chet Bohac, ¹²Adeboye Adewoye, ¹³Manish Patel, ²Michael Overman*. ¹START-San Antonio, San Antonio, TX, USA; ²MDACC, Houston, TX, USA; ³START-Midwest, Grand Rapids, MI, USA; ⁴Cleveland Clinic, Cleveland, OH, USA; ⁵West Cancer Center, Memphis, TN, USA; ⁶University of Chicago, Chicago, IL, USA; ⁷University of California, Los Angeles, Los Angeles, CA, USA; ⁸Sarah Cannon Research Institute/TN Onc, Nashville, TN, USA; ⁹Massachusetts General Hospital, Boston, MA, USA; ¹¹Compugen Ltd, Holon, Israel; ¹²Compugen USA Inc., South San Francisco, CA, USA; ¹³Florida Cancer Ctr., Sarasota, FL, USA

Background COM701 a novel, 1st in-class, humanized IgG4 monoclonal antibody binds with high affinity to PVRIG, blocking its interaction with its natural ligand PVRL2 expressed in tumor cells and antigen-presenting-cells. We have reported antitumor and pharmacodynamic activity of COM701.¹ Anti-PD1/L1 therapies have limited to no activity in MSS-CRC. Therefore, novel ICI are urgently needed for the treatment of pts with MSS-CRC particularly pts with liver metastasis. We present preliminary clinical and translational results of the combination in pts with MSS-CRC.

Methods This is a phase I clinical trial of COM701 and nivolumab. Key objectives were safety/tolerability [primary], preliminary antitumor activity, immune-related changes [secondary/exploratory]. Key inclusion criteria: Age \geq 18 yrs, histologically/cytologically confirmed advanced malignancy who have exhausted all available standard therapy or not a candidate for standard therapy, MSS-CRC determination per local testing. Pre- and on-treatment biopsies were obtained and analyzed by IHC for PDL1, CD8 expression and omics profiling.

Results Twenty two pts were enrolled: 2 pts combination dose-escalation [COM701 0.3,1mg/kg + nivolumab 360 mg] both IV Q3W and 20 pts dose-expansion cohort [COM701 20mg/kg + nivolumab 480mg IV Q4W]. Age \leq 65 17/22, [77%], male 16/22 [73%], median [Min, Max] of 3 (2, 10) prior lines of therapy, 17/22 [77%] had liver metastases. Overall, ORR 9% (2/22 pts, PRs); ORR 12% [2/17] in pts with liver metastases [1 PR, PFS 44 weeks; 1 PR, PFS 16 weeks due to brain metastasis, however, response of target and non-target lesions still maintained]; DCR (CR+PR+SD) 27% (6/22). No new safety findings are reported. In 13 paired biopsy samples, 9 demonstrated induction in PD-L1 expression (mean 16.3+/-7% PD-L1 CPS-score increase, $p < 0.05$), suggesting TME immune-modulation following treatment. In pts with PR or SD $>$ 6months greater induction in PD-L1 expression was seen (49.7+/-14.9%). CD8 T-cell quantification was available in 12 paired biopsies with increase $>$ 1% in 8 pts (mean% CD8 increase of 9.1+/-4.4% , $p = 0.08$), with substantial increases in responders (36.5% and 44.7% CD8 increase). In responding pts IFN γ signature up-regulation, increased T-cell clonality and specific clonal expansion, were demonstrated between baseline and on-treatment biopsies.

Conclusions COM701 + nivolumab demonstrates preliminary antitumor activity in pts with heavily pretreated metastatic MSS-CRC with 12% ORR in pts with liver metastases [typically unresponsive to ICI]. TME immune modulation observed in the majority of pts, substantial in responders, suggests unique potential of COM701 in less inflamed tumors such as

MSS-CRC. The combination warrants further development. Datacut June 17, 2022.

Acknowledgements The study is sponsored by Compugen Ltd and is in collaboration with Bristol Myers Squibb.

Trial Registration NCT03667716

REFERENCE

1. Vaena, DA, Fleming, GF, Chmielowski B *et al* COM701 with or without nivolumab: Results of an ongoing phase 1 study of safety, tolerability, and preliminary antitumor activity in patients with advanced solid malignancies (NCT03667716). *Journal of Clinical Oncology* 2021;**39**:15_suppl, 2504–2504.

Ethics Approval The study obtained ethics approval from all participating clinical trial sites. All study participants gave informed consent before taking part.

- o 0001: M0D00985865 [SCRI]
- o 0002: START2018.06 [START-San Antonio]
- o 0003: 20181858 [West Cancer Center]
- o 0004: 19-238 [Cleveland Clinic]
- o 0005: 18-0806-CR003 [Uni Chicago]
- o 0006: 18-555 [MGH]
- o 0007: CUMC-AAAR9998 [Columbia University]
- o 0010: 18-001383 [UCLA]
- o 0012: 2018-0891 [MDACC]
- o 0013: STMW2019.01 [Florida Cancer Center]

<http://dx.doi.org/10.1136/jitc-2022-SITC2022.0659>

Abstracts

660

CLINICOPATHOLOGIC CHARACTERISTICS OF PATIENTS WITH METASTATIC COLORECTAL CANCER WITH MOLECULAR RESPONSES FOLLOWING TREATMENT WITH AN INDIVIDUALIZED NEOANTIGEN VACCINE REGIMEN

¹Chih-Yi Liao*, ²Benny Johnson, ³Alexander Spira, ⁴David Carbone, ⁵Brian Henick, ²Michael Overman, ¹Blase Polite, ⁴Sameek Roychowdhury, ⁶Amit Mahipal, ⁶Daniel Ahn, ⁷Melissa Johnson, ⁸Desiree Schenk, ⁸Kyoungwha Bae, ⁸Matthew Davis, ⁸Karin Jooss, ⁸Andrew Ferguson, ⁹Benjamin Solomon. ¹University of Chicago, Chicago, IL, USA; ²The University of Texas MD Anderson, Houston, TX, USA; ³Virginia Cancer Specialists, Fairfax, VA, USA; ⁴The Ohio State University Medical Center, Columbus, OH, USA; ⁵Columbia University Medical Center, New York, NY, USA; ⁶Mayo Clinic, Rochester, MN, USA; ⁷Sarah Cannon Research Institute, Nashville, TN, USA; ⁸Gritstone bio, Inc., Emeryville, CA, USA; ⁹Peter MacCallum Cancer Centre, Melbourne, Australia

Background Individualized neoantigen cancer vaccines aim to benefit patients by generating strong, durable neoantigen-specific CD8 T cells. Previous data showed extended overall survival (OS) in patients with metastatic colorectal cancer (CRC) who achieved a molecular response (MR) versus those who did not after individualized neoantigen vaccination in combination with nivolumab and ipilimumab.¹ We report updated OS and analysis of clinicopathologic features of patients achieving a MR.

Methods Patients with metastatic CRC, non-small cell lung cancer, or gastroesophageal adenocarcinoma who had received routine chemotherapy were treated in a Phase 1/2 first-in-human study (NCT03639714). The vaccine regimen consisted of sequential administrations of chimpanzee adenovirus and self-amplifying mRNA (samRNA) vectors encoding 20 patient-specific neoantigens in combination with nivolumab (IV 480 mg Q4W) and ipilimumab (SC 30 mg).

Results Thirteen of 29 patients treated had CRC. Six of these 13 had stable disease (SD) and 7 had progressive disease (PD) per RECIST v1.1. Six patients achieved a MR defined as \geq -30% reduction in ctDNA. Patients with a MR had prolonged overall survival (OS) compared to patients without a MR (see Table 1). MR was not associated with primary tumor location, presence of liver metastases, or RAS mutations and patients with a MR were not enriched for higher tumor mutation burden (TMB), PD-L1, or T cell inflamed gene expression profiles (GEP), and had similar baseline ctDNA values based on variant allele frequency (VAF) (p-value=0.18) (table 1).

Conclusions Patients who achieved MR had extended OS compared with those patients without MR. Patients with a MR were not enriched based on primary or metastatic tumor site or known correlates of response to checkpoint inhibitors. The lower baseline VAF observed in patients with a MR may be reflective of VAF in early metastatic disease. A subsequent, ongoing randomized study is evaluating individualized neoantigen vaccine in the 1L maintenance setting (NCT05141721).

Acknowledgements We thank patients and their families for participating in this clinical study and Bristol-Myers Squibb for supply of nivolumab and ipilimumab.

Trial Registration NCT03639714

REFERENCE

1. Catenacci *et al.* Clinical outcomes and immune responses in a phase I/II study of personalized, neoantigen-directed immunotherapy in patients with advanced MSS-CRC, GEA and NSCLC. European Society of Medical Oncology Annual Meeting 2021. <https://doi.org/10.1016/j.annonc.2021.08.1345>

Ethics Approval This study was reviewed and approved by institutional review boards at participating clinical sites and all

patients gave informed consent before taking part in this clinical study.

Abstract 660 Table 1 Clinicopathologic features associating with molecular response.

	Overall Survival (median in months)	Primary Tumor Location	Presence of liver lesions	Median TMB (mutations per megabase, range)	PD-L1	T cell inflamed GEP based on RNAseq (z-score)	Baseline ctDNA (mean VAF, range)	SD per RECIST v1.1
MR (n=6)	Median: NR 12-mo: 67%	Colon: 2 Rectum: 3 Both: 1	4	2.9 (2.1-6.6)	<1%: 4 NE: 2	IFNG: -0.18 (-0.44-2.69) CD8A: 635 (390-1113) CXCL9: 100 (12-4402)	3.2% (0.2-10.4)	5
No MR (n=7)	Median: 7.8 12-mo: 0%	Colon: 5 Rectum: 1 Both: 1	6	3.6 (2.5-17.6)	<1%: 5 NE: 2	IFNG: -0.32 (-0.56-0.46) CD8A: 532 (241-1901) CXCL9: 176 (25-436)	6.4% (0.0-17.4)	1

<http://dx.doi.org/10.1136/jitc-2022-SITC2022.0660>

661

INITIAL RESULTS FROM A PHASE 1A/B STUDY OF IK-175, AN ORAL AHR INHIBITOR, AS A SINGLE AGENT AND IN COMBINATION WITH NIVOLUMAB IN PATIENTS WITH ADVANCED SOLID TUMORS AND UROTHELIAL CARCINOMA

¹David Aggen*, ²Meredith McKean, ³Nehal Lakhani, ⁴Babar Bashir, ⁵Jean Hoffman-Censits, ⁶Omar Alhalabi, ⁷Elizabeth Guancial, ⁸Isaac Bowman, ⁹Alan Tan, ¹⁰Trupti Lingaraj, ¹⁰Marissa Timothy, ¹⁰Nerymar Ortiz-Otero, ¹⁰Wilmin Bartolini, ¹⁰Katherine Kacena, ¹⁰Karim Malek, ¹⁰Sergio Santillana, ¹¹Jason Luke. ¹Memorial Sloan Kettering Cancer Center, New York, NY, USA; ²Tennessee Oncology, Nashville, TN, USA; ³START Midwest, Grand Rapids, MI, USA; ⁴Thomas Jefferson University, Philadelphia, PA, USA; ⁵Johns Hopkins, Baltimore, MA, USA; ⁶MD Anderson Cancer Center, Houston, TX, USA; ⁷Florida Cancer Specialists, Sarasota, FL, USA; ⁸Banner Health, Gilbert, AZ, USA; ⁹Rush University, Chicago, IL, USA; ¹⁰Ikena Oncology, Boston, MA, USA; ¹¹University of Pittsburgh, Pittsburgh, PA, USA

Background Aryl Hydrocarbon receptor (AHR) is a transcription factor activated by binding to ligands, including kynurenine, causing expression of immune modulating genes leading to immunosuppression. IK-175 is an oral, selective, small molecule being developed as a potential first-in-class AHR inhibitor to overcome the immunosuppressive effects driving resistance to PD-1/L1 inhibitors. Computational and tissue-based analyses revealed urothelial cancer as having high levels of AHR signaling and nuclear protein localization.

Methods Dose escalation patients with advanced solid tumors received escalating daily doses of IK-175 as monotherapy or in combination with nivolumab 480 mg IV every 4 weeks (mTPI-2 design). Expansion cohorts of both treatment arms enrolled heavily pretreated urothelial carcinoma patients, who have progressed within 12 weeks of last dose of PD-1/L1 inhibitors (Simon 2-stage design). Expansion cohorts were enriched to include AHR+ patients determined by immunohistochemistry using a cutoff of 65% cells with 2+/3+ staining. Study objectives included evaluation of safety, pharmacokinetics, pharmacodynamics, MTD, RP2D and antitumor activity (RECIST 1.1) of IK-175 in both arms.

Results As of June 24, 2022, 43 patients were evaluated: 26 monotherapy (from 200 to 1600mg PO daily) and 17 combination (800 and 1200mg PO daily). Median age was 70 years (range 28-82), 28/43 (65%) patients received ≥ 3 lines of prior therapy including CPIs. 4/11 monotherapy and 3/11 combination urothelial cancer patients had AHR+ tumors. In both treatment arms, MTD was not reached and 1200mg PO QD was the selected IK-175 expansion dose based on the totality of the data. Most common treatment-related adverse events (TRAEs) in monotherapy were nausea and rash with 3 patients (12%) reporting \geq Grade3 TRAEs (nausea, proteinuria, and adrenal insufficiency). Most frequent TRAEs in combination arm were fatigue and dysgeusia with 1 patient (6%) reporting \geq Grade3 TRAEs (immune-related arthritis). Other suspected immune-related AEs included adrenal insufficiency, proteinuria, rash, and myopathy. In dose escalation, 3/13 response-evaluable patients in monotherapy and 2/5 in combination had prolonged stable disease (range 16-74 weeks). Preliminary assessment of antitumor activity in 20 response-evaluable urothelial carcinoma patients in both treatment arms showed 3 confirmed partial responses, having DoR up to 11.7 months and ongoing. Updated results, immune monitoring, and biomarker analysis will be presented.

Conclusions In this initial analysis, IK-175 was well tolerated and showed encouraging antitumor activity in eligible urothelial cancer patients in both monotherapy and combination arms. Based on the objective responses observed in stage 1 of

both cohorts, investigation of AHR inhibition with IK-175 in urothelial carcinoma is ongoing.

Trial Registration NCT04200963

Ethics Approval This trial was approved by all participating IRBs.

<http://dx.doi.org/10.1136/jitc-2022-SITC2022.0661>

663

PHASE 2 MULTI-COHORT CLINICAL STUDY EVALUATING DISITAMAB VEDOTIN ALONE AND IN COMBINATION WITH PEMBROLIZUMAB IN PATIENTS WITH HER2-EXPRESSING UNRESECTABLE OR METASTATIC UROTHELIAL CARCINOMA (RC48G001, TRIAL IN PROGRESS)

¹Matthew Galsky*, ²Peter O'Donnell, ³Earle Burgess, ⁴Michiel Van der Heijden, ⁵Laurence Krieger, ⁶Andrea Necchi, ⁷Evan Yu, ⁸Nobuaki Matsubara, ⁹Matthew Campbell, ¹⁰Saikrishna Gadde, ¹¹Jeanny Aragon-Ching, ¹²Vadim Koshkin, ¹³Wei Zhang, ¹³Kevin Sokolowski, ¹⁴Thomas Powles. ¹Icahn School of Medicine at Mount Sinai, New York, NY, USA; ²University of Chicago, Chicago, IL, USA; ³Atrium Health Levine Cancer Institute, Charlotte, NC, USA; ⁴The Netherlands Cancer Institute, Amsterdam, Netherlands; ⁵Genesis Care, North Shore, Sydney, Australia; ⁶Vita-Salute San Raffaele University, Milan, Italy; ⁷University of Washington, Seattle, WA, USA; ⁸National Cancer Center Hospital East, Chiba, Japan; ⁹MD Anderson Cancer Center, Houston, TX, USA; ¹⁰University of Tennessee Medical Center, Knoxville, TN, USA; ¹¹Inova Schar Cancer Institute, Fairfax, VA, USA; ¹²University of California San Francisco, San Francisco, CA, USA; ¹³Seagen Inc., Bothell, WA, USA; ¹⁴Barts Health NHS Trust, London, UK

Background Urothelial carcinoma (UC) is the 10th most diagnosed cancer worldwide, with a mortality rate of 1.9 per 100,000.¹ Nearly 50% of patients cannot tolerate the standard cisplatin-based first-line (1L) chemotherapy, which presents a strong need to improve outcomes in both 1L and later lines of therapy.

Human epidermal growth factor receptor 2 (HER2) overexpression has been reported in multiple malignant tumors, including UC, and may be associated with poor outcomes.² No HER2-directed therapies are currently approved for the treatment of urothelial carcinoma.

Disitamab vedotin (DV; RC48-ADC) is an investigational antibody–drug conjugate comprised of a novel HER2-directed monoclonal antibody, disitamab, conjugated to monomethyl auristatin E (MMAE) via a protease-cleavable linker. DV elicits antitumor activity through multimodal mechanisms of action including MMAE-directed cytotoxicity, bystander effect, and immunogenic cell death.³ DV is conditionally approved in locally advanced unresectable or metastatic urothelial carcinoma (LA/mUC) and gastric cancer in China and was granted Breakthrough Therapy designation by the FDA.⁴

Methods RC48G001 (NCT04879329) is a phase 2, multi-cohort, open-label, multicenter trial to evaluate DV in patients with HER2-expressing LA/mUC.

Patients are enrolled in 3 cohorts based on prior treatment and tumor HER2 expression by immunohistochemistry (IHC) and gene amplification (via in situ hybridization [ISH]), assessed centrally. Cohorts A and B are enrolling patients who have received prior systemic therapy (1 or 2 lines, including platinum-containing chemotherapy) and whose tumors are HER2-positive (IHC 3+, or 2+ and ISH-positive) or HER2-low (IHC 2+ and ISH-negative, or IHC 1+), respectively. Cohort C is enrolling first-line treatment-naïve patients in the LA/mUC setting, whose tumors have HER2-positive or HER2-low expression.

Cohorts A and B will evaluate DV as monotherapy (intravenous [IV] administration, once every 2 weeks [Q2W]). Cohort C will evaluate DV (IV, Q2W) +/- pembrolizumab (IV, Day 1 of each 6-week cycle).

Patients in all cohorts must have measurable disease per Response Evaluation Criteria in Solid Tumors (RECIST) v1.1 and an Eastern Cooperative Oncology Group Performance Status of 0-1 in Cohorts A and B, and 0-2 in Cohort C.

The primary endpoint is confirmed objective response rate (cORR) assessed by blinded independent central review

(BICR). Secondary endpoints include cORR by investigator assessment, overall survival, duration of response, progression-free survival, disease control rate per RECIST v1.1 by BICR and investigator assessment, safety, and pharmacokinetic parameters.

Enrollment for all cohorts is ongoing in North America and Europe, and planned in Latin America, Asia-Pacific, and Israel.

Trial Registration NCT04879329

REFERENCES

1. Ferlay J, Ervik M, Lam F, Colombet M, Mery L, Piñeros M, Znaor A, Soerjomataram I, Bray F. Global cancer observatory: cancer today. *International agency for research on cancer*. 2020. Gco.iarc.fr/today, accessed 18JUL22
2. Zhao J, Xu W, Zhang Z, Song R, Zeng S, Sun Y, Xu C. Prognostic role of HER2 expression in bladder cancer: a systemic review and meta-analysis. *Int Urol Nephrol*. 2015;**47**:87–94.
3. Li L, Xu M-Z, Wang L, Jiang J, Dong L-H, Chen F, Dong K, Song H-F. Conjugating MMAE to a novel anti-HER2 antibody for selective targeted therapy. *Eur Rev Med Pharmacol Sci*. 2020;**24**:12929–12937
4. Deeks E-D. Disitamab Vedotin: First Approval. *Drugs*. 2021;**81**(16):1929–1935

Ethics Approval The trial is being conducted in compliance with the Declaration of Helsinki and International Conference on Harmonization Guidelines for Good Clinical Practice. All patients, or their legal representatives, provided informed consent. All participating sites have been approved by a corresponding institutional review board or independent ethical committee per the participating institution.

<http://dx.doi.org/10.1136/jitc-2022-SITC2022.0663>

664

A PHASE I TRIAL OF TREMELIMUMAB, DURVALUMAB (MEDI4736) AND BELINOSTAT IN *ARID1A* MUTATED CANCERS WITH FOCUS ON UROTHELIAL CARCINOMA (RESOLVE)

Sumati Gupta*, Benjamin Maughan, Manish Kohli, Bradley Cairns, Umang Swami, Neeraj Agarwal. *Huntsman Cancer Institute, University of Utah, Salt Lake City, UT, USA*

Background *ARID1A* loss by mutation or deletion is the most common chromatin remodeling genomic alteration in cancer and occurs in about a fourth of all urothelial carcinoma (UC). Histone deacetylase inhibition (HDACi) has clinical benefit in *ARID1A* mutated UC.¹ *ARID1A* loss in cancer confers vulnerability to immune checkpoint inhibition (ICI) due to its association with microsatellite instability, high tumor mutational burden, increased expression of programmed death-ligand 1, and immune-active tumor microenvironment.² *ARID1A* mutation and inflammatory tumor microenvironment are associated with prolonged survival in metastatic UC treated with ICI.³ The combination of HDACi plus ICI may enhance anti-tumor activity,⁴ especially when used in a phased manner.⁵ RESOLVE is a phase 1 study to study the dosing, safety, and efficacy of a phased regimen of tremelimumab and durvalumab (dual ICI) in combination with belinostat (HDACi) in advanced cancers with *ARID1A* loss, with a focus on UC.

Methods We are currently enrolling patients in this phase 1 open-label, dose-escalation, and safety-evaluating study of a phased triplet combination in a single cohort of patients with locally advanced or metastatic UC with *ARID1A* mutation. The primary objectives are to assess the recommended phase II dose of belinostat in combination with tremelimumab and durvalumab in advanced solid tumors harboring *ARID1A* mutations and to assess the ongoing safety of the combination. The secondary objective is to determine the efficacy of the triplet combination in patients with locally advanced or metastatic UC with *ARID1A* mutation.

Patients are treated with a fixed-dose intravenous regimen of tremelimumab 300 mg once with durvalumab 1500 mg on the first day of the first cycle. Belinostat is administered intravenously starting at cycle 2 in combination with durvalumab 1500 mg every three weeks for 6 cycles. This is followed by a maintenance phase of durvalumab 1500 mg every four weeks for a total treatment period of up to two years. Phase 1A begins with a single patient dose acceleration of belinostat from a dose of 750 mg/m² to 1000 mg/m² daily for five days, then administered every three weeks, with the expansion of cohort enrollment at the maximum-tolerated dose in phase 1B portion of the study. Patients with unresectable locally advanced or metastatic UC (variant histology is allowed) that harbor *ARID1A* loss of function genomic alterations are eligible for the study. Tissue and peripheral blood are collected at baseline, treatment, and progression for correlative studies. (NCT05154994)

Acknowledgements We acknowledge Acrotech and Astra Zeneca for supporting this trial.

Trial Registration NCT05154994

REFERENCES

1. Gupta S, Albertson DJ, Parnell TJ, Butterfield A, Weston A, Pappas LM, et al. Histone deacetylase inhibition has targeted clinical benefit in *ARID1A* mutated advanced urothelial carcinoma. *Mol Cancer Ther.* 2018.
2. Hu G, Tu W, Yang L, Peng G, Yang L. *ARID1A* deficiency and immune checkpoint blockade therapy: From mechanisms to clinical application. *Cancer Letters.* 2020;**473**:148–55.
3. Goswami S, Chen Y, Anandhan S, Szabo PM, Basu S, Blando JM, et al. *ARID1A* mutation plus CXCL13 expression act as combinatorial biomarkers to predict

responses to immune checkpoint therapy in mUCC. *Sci Transl Med.* 2020;**12** (548).

4. Borcoman E, Kamal M, Marret G, Dupain C, Castel-Ajgal Z, Le Tourneau C. HDAC Inhibition to Prime Immune Checkpoint Inhibitors. *Cancers.* 2021;**14**(1):66.
5. Hull EE, Montgomery MR, Leyva KJ. HDAC Inhibitors as Epigenetic Regulators of the Immune System: Impacts on Cancer Therapy and Inflammatory Diseases. *Biomed Res Int.* 2016;**2016**:8797206.

Ethics Approval This clinical trial is approved by the University of Utah Institutional Review Board (IRB 143952).

<http://dx.doi.org/10.1136/jitc-2022-SITC2022.0664>

665

JAVELIN BLADDER MEDLEY: A PHASE 2 TRIAL OF AVELUMAB IN COMBINATION WITH OTHER ANTITUMOR DRUGS AS FIRST-LINE MAINTENANCE THERAPY FOR ADVANCED UROTHELIAL CARCINOMA

¹Jean Hoffman-Censits, ²Petros Grivas, ³Thomas Powles, ⁴Danko Martincic, ⁵Jessica Hawley, ⁶Karin Tyröller, ⁷Sonja Seeberger, ⁷Silke Guenther, ⁷Natalia Jacob, ⁷Keyvan Tadjalli Mehr*, ⁸Noah Hahn. ¹The Sidney Kimmel Comprehensive Cancer Center at Johns Hopkins, Johns Hopkins Medical Institutions, Baltimore, MA, USA; ²University of Washington, Fred Hutchinson Cancer Center, Seattle, WA, USA; ³Barts Cancer Institute, Experimental Cancer Medicine Centre, Queen Mary University of London, St Bartholomew's Hospital, London, UK; ⁴Beacon Cancer Care, Coeur d'Alene, ID, USA; ⁵Division of Medical Oncology, University of Washington, Fred Hutchinson Cancer Research Center, Seattle Cancer Care Alliance, Seattle, WA, USA; ⁶EMD Serono, Billerica, MA, USA; ⁷The Healthcare Business of Merck KGaA, Darmstadt, Germany; ⁸Johns Hopkins University, Johns Hopkins Greenberg Bladder Cancer Institute, Baltimore, MD, USA

Background In the JAVELIN Bladder 100 trial (NCT02603432), avelumab (anti-PD-L1) first-line (1L) maintenance + best supportive care (BSC) significantly prolonged overall survival (OS) and progression-free survival (PFS) vs BSC alone in patients with advanced urothelial carcinoma (UC) that had not progressed with 1L platinum-based chemotherapy. Results led to the approval of avelumab 1L maintenance therapy in various countries worldwide and inclusion in international treatment guidelines. We hypothesized that avelumab-based combinations may further improve outcomes in this setting. The JAVELIN Bladder Medley trial will investigate such combinations as 1L maintenance therapy for advanced UC.

Methods JAVELIN Bladder Medley (NCT05327530) is a phase 2, randomized, multicenter, open-label, parallel-arm, umbrella trial. Eligible patients aged ≥ 18 years should have unresectable locally advanced or metastatic UC that has not progressed (complete or partial response, or stable disease) after 4-6 cycles of 1L chemotherapy (gemcitabine + cisplatin or carboplatin) and ECOG PS 0-1. After 4-10 weeks from end of chemotherapy, 252 patients will be randomized 1:2:2:2 to avelumab 800 mg every 2 weeks as monotherapy (control) or combined with sacituzumab govitecan (anti-Trop2/topoisomerase inhibitor conjugate) 10 mg/kg on days 1 and 8 of 21-day cycles, M6223 (anti-TIGIT) 1600 mg every 2 weeks, or NKTR-255 (IL-15 agonist) 3 μ g/kg every 4 weeks. Randomization is stratified by presence of visceral metastases at start of 1L chemotherapy. Treatment will continue until progression, unacceptable toxicity, withdrawal of consent, or initiation of a new anticancer treatment. Data from the control group may be extended by combining with external data from the avelumab arm of the JAVELIN Bladder 100 trial. Primary endpoints are PFS based on investigator assessment (RECIST 1.1) and safety/tolerability of the combination regimens. Secondary endpoints include OS, objective response and duration of response based on investigator assessment (RECIST 1.1), and pharmacokinetics. The trial opened in June 2022 with sites planned to recruit in the US, Europe, Asia, and Australia.

Acknowledgements This trial is sponsored by the healthcare business of Merck KGaA, Darmstadt, Germany (CrossRef Funder ID: 10.13039/100009945) as part of an alliance between the healthcare business of Merck KGaA, Darmstadt, Germany and Pfizer. Medical writing support was provided by Sophie Saunders of ClinicalThinking and was funded by the healthcare business of Merck KGaA, Darmstadt, Germany and Pfizer.

Trial Registration NCT05327530 (ClinicalTrials.gov)

Ethics Approval The trial protocol was approved by the independent ethics committee or institutional review board at each participating center.

<http://dx.doi.org/10.1136/jitc-2022-SITC2022.0665>

666

PHASE 2, SINGLE ARM STUDY OF CG0070 COMBINED WITH PEMBROLIZUMAB IN PATIENTS WITH NON-MUSCLE INVASIVE BLADDER CANCER (NMIBC) UNRESPONSIVE TO BACILLUS CALMETTE-GUERIN (BCG)

¹Roger Li*, ²Gary Steinberg, ³Edward Uchio, ⁴Donald Lamm, ⁵Shah Paras, ⁶Ashish Kamat, ⁷Trinity Bivalacqua, ⁸Vignesh Packiam, ⁹Michael Chisamore, ¹⁰John McAdory, ¹⁰Paola Grandi, ¹⁰Nataliya Hnat, ¹⁰James Burke. ¹H. Lee Moffitt Cancer Center and Research, Tampa, FL, USA; ²NYU Langone Health, New York, NY, USA; ³University of California, Irvine, CA, USA; ⁴BCG Oncology, Phoenix, AZ, USA; ⁵Mayo Clinic, Rochester, MN, USA; ⁶The University of Texas MD Anderson, Houston, TX, USA; ⁷University of Pennsylvania, Philadelphia, PA, USA; ⁸University of Iowa, Iowa City, IA, USA; ⁹Merck and Co., Inc., Kenilworth, NJ, USA; ¹⁰CG Oncology, Irvine, CA, USA

Background CG0070, is an Ad5-based oncolytic vaccine engineered to express GM-CSF and replicate selectively in tumor cells with mutated or deficient RB. The CG0070 mechanism of action includes cell lysis and immunogenic cell death which is enhanced in the presence of GM-CSF. In an open label ph. 2 study, an overall CR rate of 62% and a CR at 12 months (m) of 29% have been observed in patients with high risk NMIBC previously treated with BCG.

IV pembrolizumab, was recently approved by the FDA for patients with BCG-unresponsive CIS (with or without papillary tumors) with an overall complete RR of 41% and a 12 m CR rate of ~20%.

This ph. 2 study will assess the potential synergy of the two agents in the treatment of BCG-unresponsive NMIBC.

Methods 35 pts with BCG-unresponsive CIS with or without concurrent Ta or T1 disease will be treated with intravesical CG0070 (1x10¹² vp) in combination with pembrolizumab at a dose of 400 mg IV q6 weeks. CG0070 will be administered weekly x 6 as induction followed by weekly x 3 maintenance instillations at months 3, 6, 9, 12, and 18. Patients with persistent CIS or HG Ta at 3 m may receive re-induction with weekly x 6 of CG0070. Pembrolizumab will be administered up to 24 m. Assessment of response will include q 3 m cystoscopy with biopsy of areas suspicious for disease, urine cytology, CTU/MRU, and mandatory bladder mapping biopsies at 12 m. Recurrence of HG disease will be enumerated as disease recurrence.

The primary endpoint of the study is CR at 12 m. Secondary endpoints will include CR at any time, progression free survival, duration of response, cystectomy free survival and the safety.

Results Enrollment has been completed. Based on follow up thus far, CR rate of 92% (22/24) at 3 m has been observed. All patients in CR at 3 m remain in CR at downstream time-points including: 14/16 at 6 m, 9/11 at 9 m, and 6/8 at 12 m. Treatment related AE are consistent with those observed in studies of each agent alone.

Conclusions This initial data on the efficacy and safety of CG0070 plus pembrolizumab for the treatment of BCG unresponsive NMIBC is encouraging. Data on efficacy and safety for all enrolled patients, N=35, as well as biomarker (CAR, E2F, and PDL1) assessment will be presented at the time of the conference.

Trial Registration NCT04387461

Ethics Approval CENTRAL IRB Castle: Protocol Number: CORE-001 (CG2003C)

Sponsor CG Oncology, Inc

Study Title A Phase 2, Single Arm Study of CG0070 Combined with Pembrolizumab in Patients with Non- Muscle Invasive Bladder Cancer (NMIBC) Unresponsive to Bacillus Calmette-Guerin (BCG)

Study Materials Reviewed and Approved by Castle IRB:

- Clinical Study Protocol CORE-001 (CG2003C) Summary of Changes, Version: Amendment 4, 24JAN 2022
- Clinical Study Protocol CORE-001 (CG2003C), Version: Amendment 4, 24 JAN 2022
- Investigator's Brochure Pembrolizumab Risk Language, Version: Edition 03 SEP 2021
- Investigator's Brochure Pembrolizumab, Version: Edition 21, 02 SEP 2021
- Master Informed Consent Form Template, Version: 5, 04 FEB 2022
- Patient Educational Slide Deck

Sites Approved by Castle IRB as part of this submission:

- CORE-001-BCG Oncology (Donald Lamm, MD)
- CORE-001-Chesapeake Urology Research Associates (Rian Dickstein, MD)
- CORE-001-Genesis Research, LLC 1 (Richard David, MD)
- CORE-001-Keystone Urology Specialists (Paul Sieber, MD)
- CORE-001-Spokane Urology (Shane Pearce, MD)

<http://dx.doi.org/10.1136/jitc-2022-SITC2022.0666>

667

A PHASE 1, MULTIPLE-DOSE STUDY TO EVALUATE THE SAFETY AND TOLERABILITY OF XMAB[®]819 (ENPP3 X CD3) IN SUBJECTS WITH RELAPSED OR REFRACTORY CLEAR CELL RENAL CELL CARCINOMA (RCC)

¹Sumanta Pal*, ²Sreeni Yalamanchili, ²Huajiang Li, ²Jitendra Kanodia, ²Raphael Clynes, ²Zequan Tang, ³Benjamin Garmez. ¹City of Hope Comprehensive Cancer Center, Duarte, CA, USA; ²Xencor, Inc., San Francisco, CA, USA; ³Tennessee Oncology, Nashville, TN, USA

Background Despite multiple advances in the treatment of metastatic RCC based on VEGF-directed therapies and immune checkpoint inhibitors (ICIs), few patients are ultimately cured. Therapies exploiting novel targets are greatly needed. A detailed antigen screen identified ENPP3 (Ectonucleotide pyrophosphatase/phosphodiesterase family member 3) as having consistent high expression in RCC (among other histologies), and low expression in adjacent normal tissue. ENPP3 is a transmembrane ectoenzyme, thought to be involved in hydrolysis of extracellular nucleotides. XmAb819 is an affinity-tuned 2+1 (high-avidity bivalent ENPP3 binding with low-affinity monovalent CD3 binding) bispecific antibody that was engineered for preferential engagement of high ENPP3-expressing cancer cells relative to low ENPP3-expressing normal cells, with the goal of preferentially inducing T-cell-mediated killing of the cancer cells. In addition, the expression of ENPP3 in healthy human tissues is generally low and typically localized apically which is likely to make it inaccessible to XmAb819 and/or T cells.

Methods This is a US based, multicenter, open-label, multiple-dose study designed in 2 parts with up to 95 participants: Part A dose escalation, to establish a priming dose, step-up priming dose(s), a cohort limit dose, and the dosing schedule; and Part B dose expansion, to further evaluate safety and tolerability, as well as provide an initial evaluation of efficacy for the relevant dose regimens established in Part A. The primary objectives are safety and tolerability, and to identify the doses and schedule for expansion. XmAb819 will be administered weekly by IV dosing on Day 1 of each priming dose(s) and Days 1, 8, and 15 for the cohort limit dose of each 21-day cycle. All eligible subjects will have relapsed or refractory RCC and have undergone disease progression on standard-of-care therapies including combination of immune checkpoint inhibitors followed by targeted therapies or immune checkpoint inhibitors plus anti-vascular endothelial growth factor agents in combination or sequentially.

Enrollment has been initiated.

Trial Registration NCT05433142. Research Sponsor: Xencor, Inc.

Ethics Approval This study was approved wcg IRB; IRB Tracking Number 20221085.

<http://dx.doi.org/10.1136/jitc-2022-SITC2022.0667>

668

A PHASE 2 STUDY OF VUDALIMAB, A PD-1 X CTLA-4 BISPECIFIC ANTIBODY, PLUS CHEMOTHERAPY OR TARGETED THERAPY IN PATIENTS WITH MOLECULARLY DEFINED SUBTYPES OF METASTATIC CASTRATION-RESISTANT PROSTATE CANCER

¹Mark Stein*, ²Oscar Goodman, ³Tanya Dorff, ⁴Vivek Narayan, ⁵Jose Avitia, ⁶Rana McKay, ⁷Luke Nordquist, ⁸Matthew Rettig, ⁹Michael Schweizer, ¹⁰Roby Thomas, ¹¹Michael Silverman, ¹²Li Yao, ¹²Raphael Clynes, ¹²Jolene Shorr. ¹Columbia University Irving Medical Cntr, New York City, NY, USA; ²Comprehensive Cancer Centers of Nevada, Las Vegas, NV, USA; ³City of Hope Comprehensive Cancer Center, Duarte, CA, USA; ⁴Hospital of University of Pennsylvania, Philadelphia, PA, USA; ⁵New Mexico Oncology Hematology Consult, Albuquerque, NM, USA; ⁶University of California, San Diego, La Jolla, CA, USA; ⁷Urology Cancer Center, Omaha, NE, USA; ⁸VA Greater Los Angeles Healthcare System, Los Angeles, CA, USA; ⁹University of Washington/Fred Hutchinson, Seattle, WA, USA; ¹⁰University of Pittsburgh Medical Center, Pittsburgh, PA, USA; ¹¹BioStratigics, Ltd, Marblehead, MA, USA; ¹²Xencor, Inc, Monrovia, CA, USA

Background Immune checkpoint inhibitor (ICI) monotherapy generally has shown limited clinical benefit in unselected patients with metastatic castration-resistant prostate cancer (mCRPC); thus, strategies to improve response and/or identify patients more likely to respond to treatment are being investigated. Combination anti-PD-1/CTLA-4 therapy has shown better outcomes than either therapy alone. Altering the tumor microenvironment to promote antitumor immunity by combining ICIs with chemotherapy or targeted agents also has potential to increase clinical benefit. Finally, tumors with selected molecular characteristics, including those associated with aggressive variant disease, CDK12 inactivation, and microsatellite instability high (MSI-H) status, have shown increased sensitivity to ICIs. Vudalimab (XmAb20717) is a humanized bispecific monoclonal antibody that simultaneously targets PD-1 and CTLA-4 and binds preferentially to PD-1/CTLA-4 dual-positive cells. In a Phase 1 study, vudalimab monotherapy was generally well-tolerated and associated with complete and partial responses in patients with multiple tumor types, including mCRPC.¹ This Phase 2 study is designed to evaluate the safety and antitumor activity of vudalimab in combination with other anticancer agents or alone in mCRPC patients with and without specific tumor molecular subtypes.

Methods This multicenter, open-label study is being conducted at approximately 20 sites in the United States. Patients with mCRPC that progressed following treatment with ≥ 2 lines of therapy are enrolled into parallel cohorts based on the presence or absence of molecular abnormalities from prior sequencing reflecting the metastatic state: aggressive variant (Cohort 1), homologous recombination deficient or CDK12 mutation positive PARP inhibitor progressor (Cohort 2) or PARP inhibitor naïve (Cohort 3), MSI-H or mismatch repair deficient (Cohort 4), and no targetable mutation (Cohort 5). Patients receive vudalimab 10 mg/kg intravenously every 2 weeks plus either carboplatin AUC 4/cabazitaxel 20 mg/m² (or docetaxel 60 mg/m², if chemotherapy naïve) every 3 weeks (Cohorts 1, 2, 5; n=20 each) or olaparib 300 mg 2x/day (Cohort 3; n=20), or as monotherapy (Cohort 4; n=5). The study includes review of data from a subset of combination chemotherapy patients by a safety review committee. The primary objective of the study is to evaluate the safety/tolerability of treatment based on adverse events. Secondary objectives include evaluating objective response (RECIST 1.1, as modified by PCWG3), radiographic progression-free survival, and PSA response. Exploratory objectives include assessing pharmacodynamic activity in peripheral blood and tumor, and

correlations of response with cohort-specific molecular tumor characteristics.

Results Enrollment is underway, and initial safety data review has been completed. Preliminary safety and activity data will be presented.

Trial Registration NCT05005728

REFERENCE

1. Shum E, Reilley M, Najjar Y, et al. Preliminary clinical experience with XmAb20717, a PD-1 x CTLA-4 bispecific antibody, in patients with advanced solid tumors. *J Immunother Cancer*. 2021;**9**: doi: 10.1136/jitc-2021-SITC2021.523.

Ethics Approval The study was approved by each institution's IRB.

<http://dx.doi.org/10.1136/jitc-2022-SITC2022.0668>

669

USE OF HPV16 CIRCULATING TUMOR DNA DETECTED IN LIQUID BIOPSIES TO PREDICT RESPONSE IN PATIENTS WITH ADVANCED HPV16-POSITIVE CERVICAL CANCER

Paula Bousquet, Milena Blaga, Berit Nicolaisen, Karsten Bruins Slot, Agnete Fredriksen, Karoline Schjetne*. *Nykode Therapeutics, Oslo, Norway*

Background Circulating tumor DNA (ctDNA) can potentially provide a valuable tumor-specific and non-invasive biomarker for longitudinal monitoring of a patient's response to therapy. We aimed to quantify HPV16 ctDNA in patients with advanced cervical cancer and explore the potential use of ctDNA to predict on treatment clinical responses to VB10.16 in combination with atezolizumab.

Methods This open-label, single-arm, Phase 2a trial was conducted in patients with HPV16-positive recurrent or metastatic cervical cancer. Patients received multiple doses of the therapeutic DNA vaccine VB10.16 in combination with the PD-L1 inhibitor atezolizumab.

Blood specimens were collected at baseline and every 9 weeks during treatment to quantitatively determine the HPV16 E7 viral DNA in plasma by duplex digital PCR (dPCR).

The primary endpoint of the trial was the objective response rate assessed by an independent central review using RECIST version 1.1 criteria. HPV16 ctDNA was correlated with the defined clinical response as an exploratory endpoint. The study was approved by the national regulatory authorities and Independent Ethic Committees (NCT04405349).

Results Of the 39 patients included in the efficacy population of this interim analysis, 21 had detectable HPV16 ctDNA samples at baseline. The presence of ctDNA at baseline was not associated with clinical benefit. However, early reduction of HPV16 ctDNA after treatment start correlated with clinical response and prolonged progression-free survival ($p < 0.0021$). Patients who had a clearance of HPV ctDNA to levels below the detection limit, all achieved some level of clinical benefit (DCR 100%). In contrast, on-treatment increases in HPV16 ctDNA was associated with poor clinical outcomes and a shortened time to progression, indicating that on-treatment changes in HPV16 ctDNA levels may predict responses to treatment with VB10.16 and atezolizumab in cervical cancer.

Conclusions Analysis of liquid biopsies in patients with HPV16-positive recurrent or metastatic cervical cancer, treated with VB10.16 in combination with atezolizumab indicate that monitoring HPV16 ctDNA may predict clinical outcome and duration of response in a HPV16-specific therapy setting.

Trial Registration NCT04405349

Ethics Approval The study was approved by the national regulatory authorities and Independent Ethic Committees (NCT04405349).

<http://dx.doi.org/10.1136/jitc-2022-SITC2022.0669>

670

CORRELATION OF DURABILITY OF RESPONSE WITH BEST RESPONSE OR EARLY DISCONTINUATION: A POST HOC ANALYSIS OF THE GARNET ENDOMETRIAL CANCER COHORTS

¹Lucy Gilbert*, ²Kathleen Moore, ³Vanessa Samouëlian, ⁴Cara Mathews, ⁵Maria-Pilar Barretina-Ginesta, ⁶Janet Rader, ⁷Anna Tinker, ⁸Adriano Gravina, ⁹Joanna Pikiel, ¹⁰Grace Antony, ¹⁰Eleftherios Zografos, ¹⁰Jennifer Veneris, ¹¹Ana Oaknin. ¹McGill University Health Centre, Montreal, Quebec, Canada; ²University of Oklahoma HSC, Oklahoma City, OK, USA; ³Centre Hospitalier de l'Uni de Montréal, Montréal, Canada; ⁴Women and Infants Hospital of RI, Providence, RI, USA; ⁵Medical School University of Girona, Girona, Spain; ⁶Medical College of Wisconsin, Milwaukee, WI, USA; ⁷University of British Columbia, Vancouver, Canada; ⁸Ist Na Tumori Fondazione G. Pascale, Naples, Italy; ⁹Regional Center of Oncology, Gdansk, Gdansk, Poland; ¹⁰GSK, Hertfordshire, UK; ¹¹Hospital Universitari Vall d'Hebron, Barcelona, Spain

Background The potential benefits of immunotherapy following discontinuation for reasons other than progressive disease (PD) are not well described. Furthermore, some patients may benefit from remaining on immunotherapy beyond 2 years. We evaluated ORR and DOR in subgroups of patients with endometrial cancer (EC) per reason for treatment discontinuation and duration of treatment ≥ 2 years.

Methods GARNET is a multicenter, open-label, single-arm phase 1 study. Patients were assigned to cohort A1 (mismatch repair deficient [dMMR]/microsatellite instability-high [MSI-H] EC) or A2 (MMR proficient [MMRp]/microsatellite stable [MSS] EC) based on immunohistochemistry assessment. Patients received 500 mg of dostarlimab IV Q3W for 4 cycles, then 1000 mg Q6W until PD, discontinuation, or withdrawal; treatment could be considered beyond 2 years following discussion between sponsor and investigator. Primary endpoints were ORR, DOR, and safety. Subgroups in this post hoc analysis were thus: patients who discontinued treatment due to PD, those who discontinued for reasons other than PD, patients who remained on treatment for ≥ 2 years, and patients who discontinued before 2 years.

Results 299 patients with dMMR and MMRp EC were included in the efficacy-evaluable population. 88 patients discontinued for reasons other than PD, 164 discontinued for PD, and 47 remain on treatment (table 1). The median duration of follow-up was 27.7 months, and median DOR (mDOR) was not reached (NR) for patients who discontinued for reasons other than PD; 75% (18/24) of responders remain in response. mDOR was 9.8 months for patients discontinuing due to PD and was NR for those who remain on treatment; 90.9% (40/44) of responders who remain on treatment remain in response.

Nearly 52% of patients with complete response, partial response (PR), or stable disease (SD) remained on treatment for ≥ 2 years (46 of 89 responders). Of those patients who were on treatment for ≥ 2 years, 59.6% had PR and 8.5% had SD as their best response. 25% of patients (12/47) who remained on treatment for ≥ 2 years had MMRp/MSS tumors.

Safety has been previously reported.¹

Conclusions Patients demonstrated durable responses to treatment when they discontinued for reasons other than PD. Meaningful durability (≥ 2 years) was observed even in patients with SD and PR. Biomarkers of durable responses to immunotherapy are needed.

Trial Registration NCT02715284

REFERENCE

1. Oaknin A, Pothuri B, Gilbert L, et al. Dostarlimab in advanced/recurrent (AR) mismatch repair deficient/microsatellite instability-high or proficient/stable (dMMR/

MSI-H or MMRp/MSS) endometrial cancer (EC): The GARNET study. *J Clin Oncol*. 2022;40(16_suppl):5509–5509.

Ethics Approval This study was approved by Western Institutional Review Board, #20160056.

Abstract 670 Table 1

	Patients who discontinued for reasons other than PD ^a N=88	Patients remaining on treatment N=47	Patients who discontinued after PD N=164
Median duration of follow-up, months	27.7	30.7	44.2
ORR, n (%; 95% CI)	24 (27.3; 18.3–37.8)	44 (93.6; 82.5–98.7)	21 (12.8; 8.1–18.9)
BOR, n (%)			
CR	7 (8.0)	19 (40.4)	1 (0.6)
PR	17 (19.3)	25 (53.2)	20 (12.2)
SD	11 (12.5)	2 (4.3)	37 (22.6)
PD	33 (37.5)	1 (2.1)	105 (64.0)
NE	20 (22.7)	0	1 (0.6)
Median DOR (range), months ^b	NR (21.5–NR)	NR (NR–NR)	9.8 (6.5–13.7)
	Remained on treatment ≥ 2 years ^c N=47	Treated < 2 years ^c N=252	All patients with endometrial cancer N=299
Median duration of follow-up, months	36.0	19.3	29.1
ORR, n (%; 95% CI)	42 (89.4; 76.9–96.5)	47 (18.7; 14.0–24.0)	89 (29.8; 24.6–35.3)
BOR, n (%)			
CR	14 (29.8)	13 (5.2)	27 (9.0)
PR	28 (59.6)	34 (13.5)	62 (20.7)
SD	4 (8.5)	46 (18.3)	50 (16.7)
PD	1 (2.1)	138 (54.8)	139 (46.5)
NE	0	21 (8.3)	21 (7.0)
Median DOR (range), months ^b	NR (38.9–NR)	21.5 (12.8–NR)	NR (38.1–NR)

^aReasons for discontinuation other than PD include adverse event (n=45), clinical criteria (n=25), patient request (n=11), and other (n=7). Other includes 5 patients who died of disease progression, which is a limitation of the statistical analysis, with a negative bias.
^bLimited to those patients in response.
^cIncludes patients still on treatment.
 BOR, best overall response; CR, complete response; DOR, duration of response; DOT, duration of treatment; NE, not evaluable; NR, not reached; ORR, objective response rate; PD, progressive disease; PR, partial response; SD, stable disease.

<http://dx.doi.org/10.1136/jitc-2022-SITC2022.0670>

671

A PHASE 1 ADOPTIVE CELL THERAPY USING DRUG-ENHANCED, TUMOR-INFILTRATING LYMPHOCYTES, DETIL-0255, IN ADULTS WITH ADVANCED MALIGNANCIES

<http://dx.doi.org/10.1136/jitc-2022-SITC2022.0671>

¹Eugenia Girda*, ²Emese Zsiros, ³John Nakayama, ⁴Sarah Whelan, ⁴Srinand Nandakumar, ⁴Seema Rogers, ⁴Beverly Benson, ⁴Michael Lotze, ⁴Robert Brown, ⁵Robert Wenham. ¹Rutgers Cancer Institute of New Jersey, New Brunswick, NJ, USA; ²Roswell Park Comprehensive Cancer Center, Buffalo, NY, USA; ³Allegheny Health Network, Pittsburgh, PA, USA; ⁴Nurix Therapeutics, Inc., San Francisco, CA, USA; ⁵Moffitt Cancer Center, Tampa, FL, USA

Background Tumor-infiltrating lymphocytes (TIL) are a heterogeneous population of T cells that recognize multiple endogenous tumor antigens but may have developed an exhausted phenotype due to the tumor microenvironment. While existing TIL therapies produce durable responses in patients with melanoma, cervical, and head and neck cancers, poor *in vitro* cell expansion, limited short-lived *in vivo* persistence, and diminishing potency restrict this approach's broader application. DeTIL-0255 (drug-enhanced TIL [DeTIL]) is an autologous adoptive cell therapy (ACT) derived from a patient's tumor and expanded *ex vivo* with NX-0255, a small-molecule inhibitor of the E3 ligase, Casitas B-lineage lymphoma proto-oncogene B (CBL-B). CBL-B is expressed in T cells, where it functions as a regulator of immune cell activation, in part by requiring CD28 co-stimulation in addition to T cell receptor activation. Desirable properties enhanced by DeTIL-0255 compared with TIL include increased number of stem-like CD39⁺/CD69⁺, and CD8⁺ T cells associated with persistence, as well as enhanced cytolytic function. ACT with T cells expanded *ex vivo* using NX-0255 demonstrated increased anti-tumor activity, longer survival, increased stem-like phenotype, and persistence of tumor antigen-specific T cells in mouse tumor models. Adoptive cell transfer of DeTIL-0255 may, therefore, exhibit broader functional activity than conventional TIL, potentially conferring improved anti-tumor activity and response.

Methods NX-DeTIL-0255-201 is a Phase 1 multicenter, open-label study of DeTIL-0255 administered with systemic high-dose IL-2 following nonmyeloablative lymphodepleting chemotherapy in patients with advanced gynecological malignancies for whom standard therapy with proven clinical benefit does not exist, is no longer effective, or is inappropriate. Primary objectives are to evaluate safety, tolerability, and preliminary antitumor activity of DeTIL-0255. A safety run-in will consist of 3 to 6 patients treated with DeTIL-0255 and evaluated for dose-limiting toxicity (DLT). The DLT period starts with DeTIL-0255 infusion and ends after 28 days. The safety run-in will investigate DeTIL-0255 at a dose range of 1 to 150 x 10⁹ CD3⁺ T cells (exact dose varying based on expansion potential of DeTIL-0255 from tumor biopsies). Following the safety run-in, cohort expansion will further evaluate the safety and antitumor activity of DeTIL-0255 in patients with recurrent/persistent platinum-resistant epithelial ovarian cancer, cervical carcinoma, and endometrial cancer. Key eligibility criteria include measurable disease, a resectable lesion for TIL harvest, ≥2 prior lines of therapy, and an Eastern Cooperative Oncology Group performance status 0 or 1. The study is expected to enroll ~54 patients in ~10 sites across the United States. NCT05107739

Trial Registration NCT05107739

Ethics Approval The study obtained institutional review board (s) approval, and participants gave informed consent before taking part.

672

PHASE I CLINICAL TRIAL OF AUTOLOGOUS T-CELLS GENETICALLY ENGINEERED WITH A CHIMERIC RECEPTOR TO TARGET THE FOLLICLE-STIMULATING HORMONE RECEPTOR (FSHR) IN PATIENTS WITH RECURRENT OVARIAN CANCER (OVCA)

¹Robert Wenham*, ²Marco Davila, ¹Daniel Abate-Daga, ¹Melissa McGettigan, ¹Xuefeng Wang, ¹Theresa Boyle, ³Pamela Garzone, ³Amit Kumar, ¹Jose Conejo-Garcia. ¹Moffitt Cancer Center, Tampa, FL, USA; ²Roswell Park Cancer Center, Buffalo, NY, USA; ³Anixa Biosciences Inc., San Jose, CA, USA

Background Epithelial OVCA remains a highly fatal disease. FSHR is a tissue specific antigen expressed in >55% of high-grade epithelial OVCAs of different histological types. No significant FSHR expression is found in non-ovarian healthy tissues in women (figure 1). The treatment of OVCA patient derived xenografts with FSHCER T (FSH-Chimeric Endocrine Receptor + T-Cell (CER T)) cells (figure 2) in controlled, paired, mice was shown to effectively redirect the cytotoxic activity of T cells against patient-derived FSHR+ ovarian carcinomas (figure 3).¹ We hypothesize targeting FSHR in women with FSHR+ OVCA will result in improved response rates due to engraftment, expansion, and survival of these adoptively transferred FSHCER T cells and will have acceptable toxicity.

Methods This is an open phase 1 dose-escalation study (NCT05316129) in high-grade epithelial OVCA to assess the safety of autologous T cells genetically modified to express CER targeting FSHR. Primary objective is to assess the safety of the intraperitoneal (IP) and intravenous (IV) infusions of FSHCER T cells with or without prior cyclophosphamide plus fludarabine. Secondary objectives include antitumor efficacy, persistence of transferred FSHR T cells, expansion of endogenous tumor-targeted cells, and to compare IP and IV routes of administration.

A screening part of the study will examine archived tissue from patients with recurrent platinum resistant or refractory OVCA following 2-8 prior lines of chemotherapy. Those who demonstrate positive or indeterminate FSHR Expression by an RNA Salivary Targeted Expression Panel (STEP) will be eligible to screen for the treatment dose-escalation portion. Additional criteria include measurable or evaluable disease; performance status 0-2; adequate bone marrow, renal, and hepatic function; and eligibility for IP catheter placement.

If a patient is unable to be treated in the IP arm, the patient may be treated in the IV arm in the lowest unfilled cohort for that arm. Cohorts of 3 to 6 patients will be infused with escalating doses of FSHCER T cells to establish the maximum tolerated dose (MTD) with 6 planned dose levels: 1×10^5 , 3×10^5 , 1×10^6 , 3×10^6 , and 1×10^7 FSHCER T cells/kg. If the MTD is not established after 3×10^6 , then next cohorts will receive conditioning cytoxan/fludarabine 5 days before starting T-cell infusion at dose levels 1×10^6 , 3×10^6 and 1×10^7 FSHCER T cells/kg. Following determination of MTD, an expansion phase will be initiated.

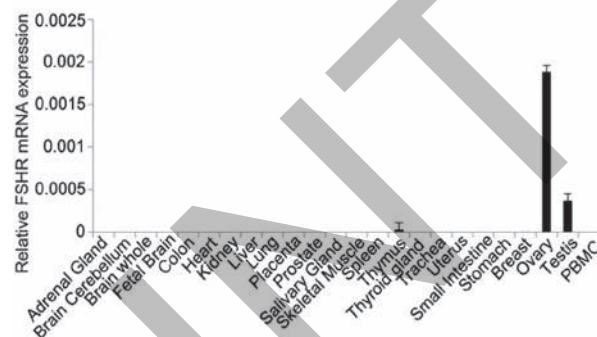
Acknowledgements We wish to acknowledge Carrie Thomas, Keri Erb, Tam Jackson, Allison Murphy, Van Barnes, Kumar Karyampudi, Samantha Demmi, Denise Dorman, Cheryl Cox, Tanner Pearson, Brook Olmo, and many others on the teams at both Moffitt Cancer Center and Anixa Biosciences involved in cell therapies and clinical trial development and execution who have helped to enable this study.

Trial Registration NCT05316129

REFERENCE

1. Perales-Puchalt A, Svoronos N, Rutkowski MR, Allegrezza MJ, Tesone AJ, Payne KK, Conejo-Garcia JR. Follicle-Stimulating Hormone Receptor Is Expressed by Most Ovarian Cancer Subtypes and Is a Safe and Effective Immunotherapeutic Target. *Clin Cancer Res.* 2017;**23**(2):441–453. doi:10.1158/1078-0432.CCR-16-0492

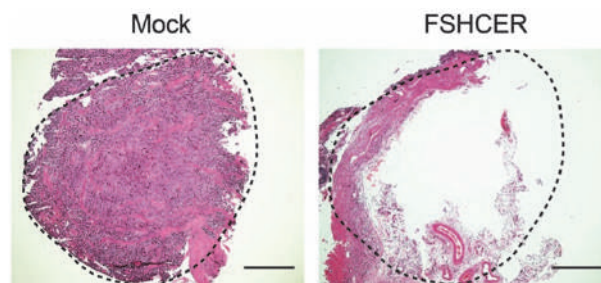
Ethics Approval This study was approved by Moffitt Scientific Review #21113 and Advarra Institutional Review Board #0000971. Patients give informed consent before participation.



Abstract 672 Figure 1 Normalized real-time quantitative-PCR of FSHR expr
Normalized real-time quantitative-PCR of FSHR expression in human healthy tissues.



Abstract 672 Figure 2 FSHCER construct for expression in T cells.



Abstract 672 Figure 3 Patient-derived ovarian cancer xenografts could be effectively targeted with FSH-expressing chimeric receptors. Hematoxylin-Eosin staining of ovarian PDX tumor grown in NOD-SCID mice ovary treated with either FSHCER ("case" mouse) or mock ("control" mouse) transduced autologous HUMAN FSHCER T cells (106 total; >70%GFP+).

<http://dx.doi.org/10.1136/jitc-2022-SITC2022.0672>

673

EFFICACY AND SAFETY OF ZIMBERELIMAB (GLS-010) MONOTHERAPY IN PATIENTS WITH RECURRENT OR METASTATIC CERVICAL CANCER: A MULTICENTER, OPEN-LABEL, SINGLE-ARM, PHASE II STUDY

¹Xiaohua Wu*, ¹Lingfang Xia, ²Jing Wang, ³Chunyan Wang, ⁴Qingming Zhang, ⁵Jianqing Zhu, ⁶Qunxian Rao, ⁷Huijun Cheng, ⁸Zheng Liu, ⁹Yongmei Yin, ¹⁰Xiaohong Ai, ¹¹Kurban Gulina, ¹²Hong Zheng, ¹³Xiaoyong Luo, ¹⁴Baoping Chang, ¹⁵Li Li, ¹⁶Haiyan Liu, ¹⁷Yunxia Li, ¹⁸Ge Lou, ¹⁹Qi Zhou, ²⁰Yanling Zhu, ²¹Zemin Xiao, ²²Jiandong Tong, ²³Ke Wang, ²³Jie Chen, ²⁴Xia Wang, ²⁵Lijie Song, ²⁶Zhixia Wei, ²⁷Yijing Ye, ²⁸Jiman Zhu. ¹Fudan University Shanghai Cancer Center, Shanghai, China; ²Hunan Cancer Hospital, The Affiliated Cancer Hospital of Xiangya School of Medicine, Central South University, Changsha, China; ³Liaoning Cancer Hospital and Institute, Shenyang, China; ⁴Gansu Provincial Cancer Hospital, Gansu Provincial Academic Institute for Medical Research, Lanzhou, China; ⁵Cancer Hospital of the University of Chinese Academy of Sciences, Hangzhou, China; ⁶Sun Yat-sen Memorial Hospital, Sun Yat-sen University, Guangzhou, China; ⁷Henan Cancer Hospital, Zhengzhou, China; ⁸Handan Central Hospital, Handan, China; ⁹The First Affiliated Hospital of Nanjing Medical University, Nanjing, China; ¹⁰The First Affiliated Hospital Of University Of South China, Hengyang, China; ¹¹The Affiliated Cancer Hospital of Xinjiang Medical University, Urumqi, China; ¹²Beijing Cancer Hospital, Beijing, China; ¹³The Affiliated Luoyang Central Hospital of Zhengzhou University, Luoyang, China; ¹⁴The First Affiliated Hospital of Henan University of Science and Technology, Luoyang, China; ¹⁵Guangxi Medical University Affiliated Tumor Hospital, Nanning, China; ¹⁶The Second Affiliated Hospital of Shandong First Medical University, Taian, China; ¹⁷General Hospital of Ningxia Medical University, Yinchuan, Yinchuan, China; ¹⁸Harbin Medical University Cancer Hospital, Harbin, China; ¹⁹Chongqing University Cancer Hospital, Chongqing, China; ²⁰Xuzhou Tumor Hospital, Xuzhou, China; ²¹The First People's Hospital of Changde City, Changde, China; ²²Affiliated Hospital of Yangzhou University, Yangzhou, China; ²³Tianjin Medical University Cancer Institute and Hospital, Tianjin, China; ²⁴The Affiliated Hospital of Xuzhou Medical University, Xuzhou, China; ²⁵The First Affiliated Hospital of Zhengzhou University, Zhengzhou, China; ²⁶Hainan Cancer Hospital, Haikou, China; ²⁷Zhongshan City People's Hospital, Zhongshan, China; ²⁸Guangzhou Gloria Biosciences Co., Ltd., Beijing, China

Background Cervical cancer is the fourth most common cancer affecting women globally, but treatment options and outcomes for patients with recurrent or metastatic disease remain limited. Zimberelimab is a novel, fully human anti-PD-1 monoclonal antibody with high affinity and selectivity for PD-1. The objective of this study (ClinicalTrials.gov identifier: NCT03972722) was to evaluate zimberelimab, a novel, anti-programmed cell death protein 1 monoclonal antibody, in patients with programmed death ligand-1-positive recurrent or metastatic cervical cancer that had progressed after first- or subsequent-line platinum-containing standard chemotherapy.

Methods In this single-arm, phase II study, eligible patients in 27 Chinese sites were assigned to receive intravenous zimberelimab 240 mg as monotherapy every 2 weeks until confirmed disease progression, death, intolerable adverse effects, or withdrawal from the study. The primary endpoint was the objective response rate (ORR) assessed per Response Evaluation Criteria in Solid Tumors (version 1.1) by an independent review committee. Secondary endpoints included duration of response (DoR), disease control rate (DCR), progression-free survival (PFS), overall survival (OS), and safety.

Results Ninety participants were included in the full analysis set, with a median follow-up of 11.5 months. Complete and partial responses were achieved by 4 and 21 patients, respectively, corresponding to an ORR of 27.8% (95% confidence interval [CI], 18.85 to 38.22; $P < .0001$ vs historical controls). Median OS and DoR were not reached during the study: 12-month OS rates were 54% (95% CI, 41 to 66) and 6-month DoR rates were 84% (95% CI, 58 to 95). Median PFS was 3.7 months and the 12-month PFS rate was 15% (95% CI, 2 to 42). Treatment-related adverse events (TRAEs) occurred in 78.1% of participants, with hypothyroidism (25.7%) and anemia (19.0%) being the most frequently

reported. Grade ≥ 3 TRAEs occurred in 22.9% of participants.

Conclusions Zimberelimab monotherapy demonstrated durable antitumor activity and an acceptable safety profile in patients with recurrent or metastatic cervical cancer that had progressed after first- or subsequent-line platinum-containing standard chemotherapy. Further investigation of zimberelimab in patients with cervical cancer is warranted.

Trial Registration NCT03972722

Ethics Approval This phase II, single-arm, open-label study (NCT03972722) enrolled patients at 27 sites in China. The study was approved by the ethics committee at each participating center and was conducted in accordance with the Declaration of Helsinki and Good Clinical Practice for Drug Trials. All participants provided signed informed consent before any study procedure.

<http://dx.doi.org/10.1136/jitc-2022-SITC2022.0673>

674

IMMUNOCERV, AN ONGOING PHASE II TRIAL COMBINING PDS0101, AN HPV-SPECIFIC T CELL IMMUNOTHERAPY, WITH CHEMOTHERAPY AND RADIATION FOR TREATMENT OF LOCALLY ADVANCED CERVICAL CANCERS

<http://dx.doi.org/10.1136/jitc-2022-SITC2022.0674>

Kyoko Yoshida-Court, Olsi Gjyshi, Madison O'Hara, Lilie Lin, Anuja Jhingran, Melissa Joyner, Tatiana Cisneros Napravnik, Erica Lynn, Lauren Colbert, Jagannadha K Sastry, Ann Klopp*. MD Anderson Cancer Center, Houston, TX, USA

Background Human Papillomavirus (HPV) cancers are uniquely antigenic with a ubiquitous and essential expression of the viral proteins E6 and E7. Radiation therapy is essential in treating locally advanced HPV-associated cancers, including cervical cancers. Radiation therapy (RT) may synergize with immunotherapy to stimulate T-cell mediated anti-tumor effects by increasing T-cell flux in tumors and promoting pathways that result in increased antigen presentation. To evaluate this, we are conducting a single-arm phase II trial combining PDS0101, an E6/7 HPV16 T-cell activating immunotherapy delivered subcutaneously, combined with the standard of care chemoradiation for patients with locally advanced squamous cell cervical cancer with either lymph node metastasis or tumors of >5 cm.

Methods 17 patients of a planned 35 have enrolled in the study. Patients receive 5 doses of PDS0101 starting 10 days before RT, then on Days 7, 28, and 49 (\pm 5 days) during the 7-week course of treatment and again after chemoradiation is complete at Day 170 (\pm 14 days). To date, eight patients have completed treatment and were evaluated with a post-treatment Positron Emission Tomography (PET) scan to assess the response. Tumor specimens were collected at baseline and end of treatment and were evaluated for changes in T-cell activation.

Results Seven of 8 patients (87.5%) enrolled on IMMUNOCERV demonstrated a complete response (CR) on PET at 3 months. For comparison, 40 of 54 (74.1%) patients treated on a prospective tissue collection protocol with standard of care chemoradiation had a CR on PET after 3 months. The observed 1-year disease-free survival rate for IMMUNOCERV patients is 85.7%, and the 1-year overall survival is 100%. The percentage of polyfunctional CD8⁺ T-cells expressing granzyme B and Ki67 increased from baseline to end of treatment (38.5% vs. 65.4%, $p = 0.0253$). There were also enhanced signals in the single function CD8⁺ T-cells (granzyme B, Ki67, and CD69). However, there were no significant changes in these markers for patients treated with a prospective tissue collection protocol. Toxicity attributable to PDS0101 included self-limited Grade 1 and 2 local injection site reactions in 7 patients (3 Grade 1 and 4 Grade 2).

Conclusions In an ongoing trial, PDS0101 HPV-specific immunotherapy is safe and well tolerated in combination with chemoradiation. The combination treatment appears to result in an expansion of intratumoral activated T-cells expressing granzyme B. Further analysis will determine if the combination results in sufficiently high disease-free survival rates in patients with locally advanced cervical cancer.

Acknowledgements We thank PDS biotechnology (Dr. F. Bedu-Addo, Dr. L. Wood) for providing PDS0101.

Trial Registration NCT04580771

Ethics Approval All patients were enrolled under a protocol approved by the UT M.D. Anderson Cancer Center Institutional Review Board (MDACC 2019-1260) and written informed consent were obtained from all patients.

675 **TACTI-003: A RANDOMIZED PHASE IIB STUDY OF EFTILAGIMOD ALPHA (SOLUBLE LAG-3 PROTEIN) AND PEMBROLIZUMAB AS FIRST-LINE TREATMENT OF PATIENTS WITH RECURRENT OR METASTATIC HEAD AND NECK SQUAMOUS CELL CARCINOMA**

¹Irene Brana*, ²Valeriy Cheshuk, ³Claus Andrup Kristensen, ⁴Maria Eugenia Ortega, ⁵Brieuc Sautois, ⁶Antonio López-Pousa, ⁷Judith Christian, ⁸Willem Lybaert, ⁹Julio Peguero, ¹⁰John Park, ¹¹Robert Metcalf, ¹²Lisle Nabell, ¹³Bernard Doger de Spéville, ¹⁴Jordi Rubió Casadevall, ¹⁵Ainara Soria Rivas, ¹⁶Martin Forster, ¹⁷Frederic Triebel. ¹Vall d'Hebron Institute of Oncology, Barcelona, Spain; ²ARENSIA Exploratory Medicine LLC, Kyiv, Ukraine; ³Rigshospitalet, Copenhagen, Denmark; ⁴Hospital Universitario Miguel Servet, Zaragoza, Spain; ⁵Centre Hospitalier Universitaire (CHU), Liège, Belgium; ⁶Hospital de la Santa Creu i de Sant Pau, Barcelona, Spain; ⁷Nottingham University Hospitals, NHS, Nottingham, UK; ⁸VITAZ, Sint-Niklaas, Belgium; ⁹Oncology Consultants, P.A, Houston, TX, USA; ¹⁰Macquarie University Hospital, NSW 2109, Australia; ¹¹The Christie NHS Foundation Trust, Manchester, UK; ¹²University of Alabama at Birmingham UAB, Birmingham, AL, USA; ¹³START Madrid, Madrid, Spain; ¹⁴Institut Català d'Oncologia – Hospital, Girona, Spain; ¹⁵Hospital Universitario Ramón y Cajal, Madrid, Spain; ¹⁶UCL Cancer Institute; University College London Hospitals NHS Foundation – The Harley Street Clinic, London, UK; ¹⁷Immutep S.A. S., Chatenay Malabry, France

Background Eftilagimod alpha (efti) is a soluble LAG-3 protein targeting a subset of MHC class II molecules that mediate antigen-presenting cell (APC) and then CD8 T-cell activation. Data from a non-randomized, phase II trial of efti plus pembrolizumab (TACTI-002) showed encouraging antitumor activity and manageable safety when given as second-line treatment of patients with recurrent or metastatic head and neck squamous cell carcinoma (RM-HNSCC). TACTI-003 (NCT04811027) is a multicenter, open-label, randomized phase IIb trial to investigate efti plus pembrolizumab in the first line setting for RM-HNSCC.

Methods A total of 154 patients (pts) are currently being recruited into two cohorts (A+B). In cohort A, pts with tumors that are CPS \geq 1 will be randomly assigned 1:1 to receive either efti (30 mg subcutaneously Q2W for initial 6 months, thereafter Q3W) plus pembrolizumab (400 mg intravenously Q6W) for up to two years or pembrolizumab alone. Randomization will be stratified by CPS (1-19 vs. \geq 20) and ECOG PS (0 vs. 1). Pts with tumors that are CPS $<$ 1 will receive efti plus pembrolizumab (cohort B). Imaging will be performed every 9 weeks. The primary endpoint (EP) is the objective response rate (ORR) by RECIST1.1. Secondary EPs include overall survival, ORR according to iRECIST, time to and duration of response, disease control rate, progression-free survival, the occurrence of anti-efti -specific antibodies, safety, and quality of life. Exploratory endpoints comprise biomarkers.

Acknowledgements · We thank all the participating patients & their families.

· We thank the dedicated clinical trial investigators & their team members.

· Merck Sharp & Dohme LLC, a subsidiary of Merck & Co., Inc., Rahway, NJ, USA provided pembrolizumab for the study.

· Sponsored by Immutep.

Trial Registration The trial identifiers are IMP321-P022 (Sponsor code), Keynote-PNC-34 (MSD code), 2021-000055-39 (EudraCT) and NCT04811027 (ClinicalTrials.gov).

Ethics Approval This has been approved by relevant Competent Authorities, Ethics Committees, and Institutional Review Boards.

<http://dx.doi.org/10.1136/jitc-2022-SITC2022.0675>

676

A PHASE 2 STUDY OF EVORPACEPT (ALX148) IN COMBINATION WITH PEMBROLIZUMAB AND CHEMOTHERAPY IN PATIENTS WITH ADVANCED HEAD AND NECK SQUAMOUS CELL CARCINOMA (HNSCC); ASPEN-04

¹Ezra Cohen*, ²Kevin Harrington, ³Jean-Pascal Machiels, ⁴Sjoukje Oosting, ⁵Bhumsuk Keam, ⁶Beatriz Cirauqui, ⁷Annette Lim, ⁸Keun-Wook Lee, ⁹Tim Welliver, ⁹Christine Ju, ⁹Feng Jin, ⁹Alison Forgie, ⁹Jaume Pons, ⁹Sophia Randolph, ⁹Athanasios Tsiatis. ¹University of California San Diego, La Jolla, CA, USA; ²The Royal Marsden Hospital, Sutton, UK; ³Cliniques Universitaires Saint-Luc, Brussels, Belgium; ⁴University Medical Center Groningen, Groningen, Netherlands; ⁵Seoul National University Hospital, Seoul, Republic of Korea; ⁶Institut Catala d'Oncologia Badalona, Barcelona, Spain; ⁷Peter MacCallum Cancer Centre, Parkville, Australia; ⁸Seoul National University College, Seoul, Republic of Korea; ⁹ALX Oncology Inc, South San Francisco, CA, USA

Background Anticancer immunity relies on the release of tumor antigens and subsequent activation of both the innate and adaptive immune systems. After cytotoxic chemotherapy induces neoantigen release, myeloid checkpoint inhibitors have been shown to help potentiate innate immune cell activity including antigen presentation. CD47, a marker of self, interacts with SIRPα on myeloid immune cells and can be upregulated by cancer cells to evade immune responses. Evorpaccept is a high affinity CD47-blocking fusion protein with an inactive Fc region designed to safely enhance standard anticancer therapeutics. Pembrolizumab, a T cell checkpoint inhibitor, represents a standard treatment option for patients with previously untreated recurrent/metastatic (R/M) HNSCC, both as a monotherapy and in combination with 5FU + platinum. Through increased activation of the immune system, the combination of evorpaccept + pembrolizumab + 5FU/platinum might have greater anti-tumor activity in R/M HNSCC than standard therapeutic approaches. This combination approach could be especially beneficial to R/M HNSCC patients with low PD-L1 expression, where anti-PD-(L)1 therapy historically has diminished efficacy. The combination of evorpaccept + pembrolizumab + 5FU/platinum has undergone preliminary testing in the Phase 1 ASPEN-01 study,¹ demonstrating tolerability and clinical response. In previously untreated patients with R/M HNSCC treated with evorpaccept + pembrolizumab + 5FU/platinum regardless of PD-L1 expression, objective responses including complete response were demonstrated.

Methods ASPEN-04 (figure 1) is an ongoing non-comparative, open-label, randomized Phase 2 global study for patients with metastatic or unresectable recurrent HNSCC who have not yet received first-line treatment. After an initial safety lead-in cohort, ~162 patients will be randomized using a 2:1 allocation to receive evorpaccept + pembrolizumab + chemotherapy (5FU + either cisplatin or carboplatin) or pembrolizumab + chemotherapy, regardless of PD-L1 expression. Minimization factors used to randomize patients include geography, PD-L1 combined positive score, and human papilloma virus (HPV) (p16) status. Patients in the evorpaccept treatment arm will receive evorpaccept 45 mg/kg IV Q3W. All patients will receive pembrolizumab 200 mg IV Q3W (maximum of 35 cycles) and standard administration of 5FU and platinum agents. The co-primary endpoints in this trial are 12-month overall survival rate and objective response rate using RECIST v1.1. Key secondary endpoints include duration of response, progression-free survival, overall survival, and safety. Exploratory endpoints will characterize pharmacodynamic properties.

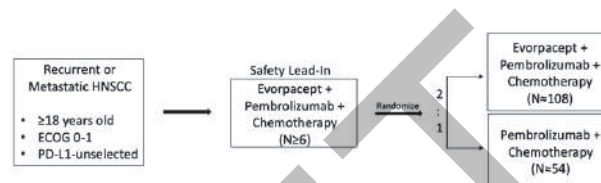
Acknowledgements We would like to thank all the participating patients, their families, and site research teams.

Trial Registration ClinicalTrials.gov identifier, NCT04675333

REFERENCE

1. Keun-Wook Lee, Hyun Cheol Chung, Tae Min Kim, *et al.* Evorpaccept (ALX148), a CD47 Myeloid Checkpoint Inhibitor, in Patients with Head and Neck Squamous Cell Carcinoma (HNSCC) and with Gastric/Gastroesophageal Cancer (GC); ASPEN-01. Poster presented at: Society for Immunotherapy of Cancer Annual Meeting; November 2021.

Ethics Approval The study was approved by all participating institutions' Ethics and/or Review Boards.



Abstract 676 Figure 1 ASPEN-04 study schema

<http://dx.doi.org/10.1136/jitc-2022-SITC2022.0676>

677

A PHASE 2, OPEN-LABEL, MULTICENTER STUDY OF INCAGN01876 (ANTI-GITR AGONIST) IN COMBINATION WITH RETIFANLIMAB (ANTI-PD-1) IN RECURRENT OR METASTATIC HEAD AND NECK SQUAMOUS CELL CARCINOMA

¹Rom Leidner*, ²Robert Haddad, ³Nawel Bourayou, ³Sonia Ioannidis, ³Feng Zhou, ³Zhiwan Dong, ⁴Ezra Cohen. ¹Earle A. Childs Research Institute, Portland, OR, USA; ²Dana Farber Cancer Institute, Boston, MA, USA; ³Incyte Biosciences International Sàrl, Wilmington, DE, USA; ⁴University of California San Diego, La Jolla, CA, USA

Background Although anti-programmed cell death (PD)-ligand (L)1 therapies have improved clinical outcomes in patients with PD-L1+ recurrent or metastatic head and neck squamous cell carcinoma (r/m HNSCC), many patients do not respond or develop resistance. Reactivation of antitumor immune responses through a combination of co-inhibitory and co-stimulatory pathways may offer improved patient outcomes. Engagement of the glucocorticoid-induced tumor necrosis factor receptor family-related protein (GITR) promotes effector T-cell proliferation and activation while inhibiting regulatory T cells. In preclinical cancer models, the combination of PD-1 blockade and anti-GITR agonist monoclonal antibodies has led to long-term survival. Preliminary clinical data suggest that combined blockade using anti-PD-(L)1 and anti-GITR antibodies has an acceptable safety profile and antitumor activity in solid tumors including HNSCC. Therefore, this study aims to assess the safety, efficacy, pharmacokinetics, and pharmacodynamics of INCAGN01876 (anti-GITR agonist) in combination with retifanlimab (anti-PD-1) in patients with r/m HNSCC with GITR+ tumors whose disease has progressed on or after prior systemic treatment.

Methods This open-label, multicenter, single-arm, phase 2 clinical study (NCT05359692) will enroll approximately 50 patients into part 1 (safety lead-in; n≤12) and part 2 (expansion; n≤38). In part 1, patients will receive intravenous (IV) INCAGN01876 at 2 dose levels (300 or 600 mg) every 2 weeks (q2w) plus IV retifanlimab 500 mg every 4 weeks (q4w). Dose escalation will follow the BOIN design algorithm until identification of a pharmacologically active dose or the maximum tolerated dose, or the maximum dose of 600 mg q2w is reached. Part 2 will enroll up to 32 anti-PD-(L)1 treatment-experienced and 6 anti-PD-(L)1-naive patients. Patients will receive IV INCAGN01876 at the recommended phase 2 dose in combination with IV retifanlimab 500 mg q4w for up to 2 years. The primary endpoints are the safety and tolerability of INCAGN01876 in combination with retifanlimab (part 1) and the objective response rate determined by investigator assessment per Response Evaluation Criteria in Solid Tumors (RECIST v1.1) in all patients previously treated with anti-PD-(L)1 therapy (parts 1 and 2). Secondary endpoints include duration of response, disease control rate, progression-free survival according to RECIST v1.1, and safety and tolerability of INCAGN01876 in combination with retifanlimab in anti-PD-(L)1-naive and previously treated patients. Exploratory endpoints include pharmacokinetics, pharmacodynamics, and overall survival assessments of INCAGN01876 in combination with retifanlimab.

Trial Registration Clinicaltrials.gov identifier NCT05359692

Ethics Approval The study protocol was approved by institutional review boards or independent ethics committees at participating centers.

<http://dx.doi.org/10.1136/jitc-2022-SITC2022.0677>

678

A PHASE 2 STUDY OF EVORPACEPT (ALX148) IN COMBINATION WITH PEMBROLIZUMAB IN PATIENTS WITH ADVANCED HEAD AND NECK SQUAMOUS CELL CARCINOMA (HNSCC); ASPEN-03

¹Kevin Harrington*, ²Ezra Cohen, ³Bhumsuk Keam, ⁴Jean-Pascal Machiels, ⁵Sjoukje Oosting, ⁶Brett Hughes, ⁷Jong Chul Park, ⁸Tim Welliver, ⁸Christine Ju, ⁹Feng Jin, ⁸Alison Forgie, ⁸Jaume Pons, ⁸Sophia Randolph, ⁸Athanasios Tsiatis. ¹The Royal Marsden Hospital, Sutton, UK; ²University of California San Diego, La Jolla, CA, USA; ³Seoul National University Hospital, Seoul, Republic of Korea; ⁴Cliniques Universitaires Saint-Luc, Brussels, Belgium; ⁵University Medical Center Groningen, Groningen, Netherlands; ⁶Royal Brisbane and Women's Hospital, Brisbane, Australia; ⁷Massachusetts General Hospital Cancer Ce, Boston, MA, USA; ⁸ALX Oncology Inc, South San Francisco, CA, USA

Background Both innate and adaptive immune responses are important components of anticancer immunity. CD47 is a marker of self that interacts with SIRPα on myeloid immune cells, inhibiting their function. CD47 is upregulated by tumors to evade immune responses and its expression is associated with poor prognosis. Evorpaccept is a high affinity CD47-blocking fusion protein with an inactive Fc region designed to be safely combined with and to enhance the efficacy of standard anticancer therapeutics. Pembrolizumab inhibits PD-1/PD-L1 signaling, which is a T cell immune checkpoint, and pembrolizumab has demonstrated anti-tumor efficacy through activation of tumor-infiltrating lymphocytes. Evorpaccept used in combination with pembrolizumab has the potential to augment both innate and adaptive anti-tumor immune responses. Pembrolizumab as a single agent is a standard treatment option for patients with previously untreated recurrent or metastatic (R/M) HNSCC with PD-L1-positive (combined positive score [CPS] ≥1) tumors. The combination of evorpaccept + pembrolizumab has shown acceptable tolerability and preliminary efficacy in patients with advanced HNSCC in ≥2nd line in the ongoing Phase 1 ASPEN-01 study.¹ Patients who had not received prior checkpoint inhibitor treatment and who were treated with evorpaccept + pembrolizumab regardless of PD-L1 expression level (n=10) experienced a 40% objective response rate (ORR) and 22.1 months median overall survival (OS), comparing favorably with historical controls.

Methods ASPEN-03 (figure 1) is an ongoing non-comparative, open-label, randomized Phase 2 global study of evorpaccept + pembrolizumab or pembrolizumab alone in patients with metastatic or unresectable recurrent, PD-L1-positive (CPS ≥1) HNSCC who have not yet received first-line treatment. After an initial safety lead-in cohort, ~177 patients will be randomized 2:1 to receive evorpaccept + pembrolizumab or pembrolizumab alone. Minimization factors used to randomize patients include geography, CPS, and human papilloma virus (HPV) (p16) status. Patients in the evorpaccept + pembrolizumab treatment arm will receive evorpaccept 45 mg/kg IV Q3W. All patients will receive pembrolizumab 200 mg IV Q3W (maximum of 35 cycles). The co-primary endpoints in this trial are 12-month overall survival (OS) rate and ORR using RECIST v1.1. Key secondary endpoints include duration of response, progression-free survival, OS, and safety. Exploratory endpoints will characterize pharmacodynamic properties.

Acknowledgements We would like to thank all the participating patients, their families, and site research teams.

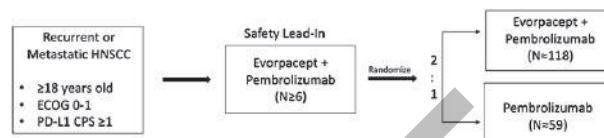
Trial Registration ClinicalTrials.gov identifier, NCT04675294

REFERENCE

1. Keun-Wook Lee, Hyun Cheol Chung, Won Seog Kim, *et al.* ALX148, a CD47 blocker, in combination with standard chemotherapy and antibody regimens in patients with gastric/gastroesophageal junction (GC) cancer and head and neck

squamous cell carcinoma (HNSCC); ASPEN-01. Poster presented at: Society for Immunotherapy of Cancer Annual Meeting; November 2020.

Ethics Approval The study was approved by all participating institutions' Ethics and/or Review Boards.



Abstract 678 Figure 1 ASPEN-03 study schema

<http://dx.doi.org/10.1136/jitc-2022-SITC2022.0678>

679

NT-I7 FOR THE TREATMENT OF LOCALLY RECURRENT SQUAMOUS CELL CARCINOMA OF HEAD AND NECK UNDERGOING SALVAGE SURGERY: A CLINICAL TRIAL IN PROGRESS

¹Hyunseok Kang*, ¹Matthew Spitzer, ¹Mi-Ok Kim, ¹Patrick Ha, ¹Daniel Johnson, ²Byung Ha Lee, ²Se Hwan Yang. ¹University of California, San Francisco, San Francisco, CA, USA; ²NeolImmune Tech, Inc, Rockville, MD, USA

Background The current standard of care for recurrent/metastatic squamous cell carcinoma of head and neck (SCCHN) includes immune checkpoint inhibitors, which have demonstrated survival benefit. However, overall response rate remains around 10-15% and almost 40% of patients do not benefit from the therapy. We have identified low baseline absolute lymphocyte count (ALC) as a predictive biomarker associated with a lower likelihood of response to immune checkpoint inhibitors.¹Patients with higher ALC tend to respond better to immune checkpoint inhibitors, but a majority of patients tend to have low baseline ALC from previous radiation.² The cytokine interleukin-7 (IL-7) promotes the proliferation and survival of naïve and memory T-cells, without inducing proliferation of immunosuppressive regulatory T-cells. Administration of IL-7 induces T-cell expansion without evidence of hyperinflammation or acute cytokine storm in murine preclinical models; however, this approach was limited by the short half-life of IL-7. NT-I7 (efineptakin alfa) is a fusion product of IL-7 with a human Fc domain and a longer half-life. NT-I7 has demonstrated an excellent safety profile and the ability to significantly and persistently expand peripheral ALC [SFM1] in phase 1/2 studies. This is a window of opportunity study of a single dose of NT-I7 in patients with locally recurrent squamous cell carcinoma of head and neck undergoing salvage surgery (NCT04588038).

Methods Patients with recurrent SCCHN (SCC of oral cavity, oropharynx, hypopharynx and larynx) undergoing curative intent salvage surgery are eligible. Patients will receive a single intramuscular injection of NT-I7 up to 2 weeks prior to planned surgery, after pre-treatment core biopsies are collected. Surgical specimens will be collected at the time of surgery for analysis of tumor infiltrating lymphocytes[HL1] and immune cell subsets. Peripheral blood will be collected pre-treatment, at the time of surgery and post-operatively (36 days after surgery). The primary objective is to establish the safety and feasibility of administering a pre-operative dose of NT-I7 in this population. Secondary[ALB2] objectives are (1) to determine changes in ALC in peripheral blood, (2) to examine changes in tumor infiltrating lymphocytes (TILs) [SFM3] , (3) to evaluate changes in immune subsets in peripheral blood after a single injection of NT-I7 and (4) to assess exploratory biomarkers for pharmacodynamic (PD) activity in peripheral blood and/or tumor tissue[SFM4] . Baseline biopsy and surgical specimens will be compared to describe and compare TILs. The study plans to enroll 10 patients and is currently on-going.

Trial Registration NCT04588038

REFERENCES

1. Ho WJ, Yarchoan M, Hopkins A, Mehra R, Grossman S, Kang H. Association between pretreatment lymphocyte count and response to PD1 inhibitors in head and neck squamous cell carcinomas. *J Immunother Cancer*. 2018;**6**(1):84.
2. Campian JL, Sarai G, Ye X, Marur S, Grossman SA. Association between severe treatment-related lymphopenia and progression-free survival in patients with newly diagnosed squamous cell head and neck cancer. *Head & neck*. 2014;**36** (12):1747–1753.

Ethics Approval This study was approved by the University of California San Francisco IRB (#20-31673).

<http://dx.doi.org/10.1136/jitc-2022-SITC2022.0679>

680

A PHASE 1B OPEN-LABEL, SINGLE-ARM DOSE EXPANSION STUDY OF IK-175, AN ORAL AHR INHIBITOR, IN COMBINATION WITH NIVOLUMAB IN PATIENTS WITH PRIMARY PD-1 INHIBITOR RESISTANT ADVANCED HEAD AND NECK CANCER

Trupti Lingaraj*, Marissa Timothy, Nerymar Ortiz-Otero, Wilmin Bartolini, Katherine Kacena, Karim Malek, Sergio Santillana. *Ikena Oncology, Boston, MA, USA*

Background Despite recent advances with immunotherapy in head and neck squamous cell carcinoma (HNSCC), many patients progress and develop resistance to checkpoint inhibitors. Aryl hydrocarbon receptor (AHR) is a ligand-activated nuclear transcription factor that regulates the activity of multiple innate and adaptive immune cells. Kynurenine, a ligand generated from tryptophan by IDO1 and TDO2, binds AHR and leads to a net immunosuppressive tumor microenvironment. HNSCC has been found to have high prevalence of nuclear AHR protein expression, indicative of active AHR signaling, making AHR an attractive therapeutic target. IK-175 is an oral selective, small molecule that is being developed as potential first-in-class AHR inhibitor for the treatment of cancer. Given the role of AHR in mediating immunosuppression, IK-175 may overcome the immunosuppressive effects driving resistance to PD-1 inhibitors in HNSCC and improve the clinical activity of nivolumab.

Methods This is a phase 1b, open-label, multicenter, dose-expansion study of IK-175 in combination with nivolumab in adult patients with primary programmed cell death-1 (PD-1) inhibitor resistant metastatic or locally incurable, recurrent head and neck squamous cell carcinoma (HNSCC). IK-175 is administered orally at a dose of 600mg QD (Cohort 1) or 450mg q12h (Cohort 2) in 28 day-cycles in combination with nivolumab (480 mg q4w on Day 1 of every cycle). AHR nuclear localization is being studied as a potential predictive biomarker in patients with HNSCC. The study will enroll unselected HNSCC patients as well as an enriched population that includes patients with AHR + tumors as determined by immunohistochemistry. Key eligibility criteria include patients with histologically confirmed advanced HNSCC that have progressed within 12 weeks of initiation of a PD-1 inhibitor, whether administered alone or in combination with chemotherapy. The primary objectives are to determine the safety, tolerability, and preliminary antitumor activity (ORR, DCR, and DOR) of IK-175 in combination with nivolumab. Secondary objectives are to evaluate the pharmacokinetics of IK-175 and its active metabolites and to assess additional parameters of preliminary antitumor activity (PFS). Key exploratory objectives are to evaluate pharmacodynamic effects on paired tumor biopsies and peripheral immune cells, to assess candidate baseline biomarkers, and correlative analyses of tumor AHR nuclear localization with disease response. Estimated enrollment is approximately 54 patients; the study started in July 2022.

Trial Registration NCT05472506

Ethics Approval The study was approved by Advarra Central IRB, approval number MOD01366597

<http://dx.doi.org/10.1136/jitc-2022-SITC2022.0680>

681

**A PHASE 1 STUDY OF CUE-101, A NOVEL HPV16 E7-
PHLA-IL2-FC FUSION PROTEIN, AS MONOTHERAPY AND
IN COMBINATION WITH PEMBROLIZUMAB IN PATIENTS
WITH RECURRENT/METASTATIC HPV16+ HEAD AND
NECK CANCER**

¹Christine Chung*, ²Dimitrios Colevas, ³Douglas Adkins, ⁴Jong Chul Park, ⁵Cristina Rodriguez, ⁶Michael Gibson, ⁷Ammar Sukari, ⁸Barbara Burtness, ⁹Faye Johnson, ¹⁰Ricklie Julian, ¹¹Nabil Saba, ¹²Lara Dunn, ¹³Tanguy Seiwert, ¹⁴Francis Worden, ¹⁵Rami Haddad, ¹⁶Nashat Gabrail, ¹⁷Julie Bauman, ¹⁸Laura Agensky, ¹⁸Apollina Goel, ¹⁸Reena Lynam, ¹⁸Steven Margossian, ¹⁸Raymond Moniz, ¹⁸Steve Quayle, ¹⁸Cynthia Rajan, ¹³Kenneth Pienta, ¹⁸Matteo Levisetti, ⁴Sara Pai. ¹H. Lee Moffitt Cancer Center, Tampa, FL, USA; ²Stanford University School of Medicine, Stanford, CA, USA; ³Washington University School of Medicine, St Louis, MO, USA; ⁴Massachusetts General Hospital, Boston, MA, USA; ⁵University of Washington, Seattle, WA, USA; ⁶Vanderbilt University Medical Center, Nashville, TN, USA; ⁷Karmanos Cancer Center, Detroit, MI, USA; ⁸Yale School of Medicine, New Haven, CT, USA; ⁹The University of Texas MD Anderson, Houston, TX, USA; ¹⁰University of Arizona Cancer Center, Tucson, AZ, USA; ¹¹Emory University, Atlanta, GA, USA; ¹²Memorial Sloan Kettering Cancer Center, New York, NY, USA; ¹³Johns Hopkins University, Baltimore, MD, USA; ¹⁴University of Michigan, Ann Arbor, MI, USA; ¹⁵Affiliated Oncologists, LLC, Chicago Ridge, IL, USA; ¹⁶Gabrail Cancer and Research Center, Canton, OH, USA; ¹⁷George Washington University Cancer Center, Tucson, DC, USA; ¹⁸Cue Biopharma Inc, Boston, MA, USA

Background Immuno-STATs™ are modular fusion proteins designed for the selective delivery of IL-2 to tumor-antigen specific CD8+ T cells. CUE-101, the first Immuno-STAT in clinical trials, is composed of a human leukocyte antigen (HLA) complex, HLA-A*0201, a peptide epitope derived from the HPV16 E7 protein, and 4 molecules of reduced affinity human interleukin-2 (IL-2) designed to bind, expand, and activate HPV16-specific CD8+ T cells for the treatment of HPV16+ cancers.

Methods CUE-101-01 is a first-in-human study in patients with HLA-A*0201 genotype and HPV16+ recurrent/metastatic head and neck squamous cell carcinoma (R/M HNSCC). R/M HNSCC patients refractory to ≥ 1 platinum- or checkpoint-inhibitor-based systemic therapies received CUE-101 monotherapy. Patients with previously untreated PD-L1+ (CPS ≥ 1) R/M HNSCC received CUE-101 and pembrolizumab 200 mg. Therapy was administered every 3 weeks until disease progression or unacceptable toxicity. Escalating doses of CUE-101 monotherapy or in combination with pembrolizumab were evaluated, followed by expanded enrollment at the recommended phase 2 dose (RP2D). Objectives included evaluation of safety, pharmacokinetics (PK), pharmacodynamics (PD), and antitumor activity.

Results As of July 25, 2022, 62 patients have received CUE-101 ranging from 0.06 to 8 mg/kg/dose. The most common adverse events included fatigue (46%), anemia (24%), chills (24%), and hyponatremia (22%). In the monotherapy dose escalation portion, a MTD was not identified, and 4 mg/kg was chosen as the RP2D based on PK, PD, and preliminary clinical activity. CUE-101 dose escalation from 1 to 4 mg/kg in combination with pembrolizumab 200 mg has been completed with no DLTs observed and expansion of CUE-101 at 4 mg/kg with pembrolizumab is ongoing. PK data demonstrate dose-dependent increases in drug exposure that are sustained upon repeat dosing. PD data demonstrate selected expansion of HPV-16 E7₁₁₋₂₀-specific CD8+ T cells in the peripheral blood. Of the 19 evaluable patients treated with CUE-101 monotherapy at the RP2D of 4 mg/kg, 1 patient experienced partial response (PR) and 7 stable disease (SD) for ≥ 12 weeks. Of the 10 evaluable patients treated with CUE-101 plus pembrolizumab, 3 patients experienced PR (2 confirmed) and 2 patients SD for ≥ 12 weeks.

Conclusions CUE-101 has a manageable safety profile and demonstrates activity alone and in combination with pembrolizumab.

Acknowledgements The authors would like to thank all the patients who are participating in this study. The study is sponsored by Cue Biopharma, in collaboration with Merck Sharp & Dohme LLC, a subsidiary of Merck & Co., Inc., Rahway, NJ, USA and support from LG Chem, Ltd., Seoul, South Korea.

Trial Registration ClinicalTrials.gov NCT03978689

Ethics Approval This study was approved by Ethics and Institutional Review Boards (IRBs) at all study sites. IRB reference numbers: Advarra Pro00037736 (Moffitt Cancer Center), IRB 52744 (Stanford University School of Medicine), HRPO# 201905108 (Washington University School of Medicine), DF/HCC IRB# 19-374 (Massachusetts General Hospital), WIRB STUDY00008948 (University of Washington, Seattle), IRB 191714 (Vanderbilt University Medical Center Vanderbilt-Ingram Cancer Center),

2019-087 Karmanos Cancer Institute, WIRB 2000026098 (Yale Cancer Center), 2019-0578 (The University of Texas MD Anderson Cancer Center), WIRB 1908869642 (University of Arizona Cancer Center), WIRB IRB00112341 (Winship Cancer Institute/Emory University), IRB 20-073 (Memorial Sloan Kettering Cancer Center), IRB00255391 (Johns Hopkins University School of Medicine), IRB(IRBMED) HUM00165746 (University of Michigan Comprehensive Cancer Center), IRB0001113 (US Oncology Inc./Affiliated Oncologists, LLC), WCG IRB00000533 (Gabrail Cancer Center), IRB000001113 (George Washington University Cancer Center).

<http://dx.doi.org/10.1136/jitc-2022-SITC2022.0681>

682

CHANGING THE RADIATION AND IMMUNE-ONCOLOGY PARADIGM WITH THE RADIOENHANCER NBTXR3: OVERCOMING RESISTANCE TO ANTI-PD-1 BLOCKADE FROM THE BENCH TO THE CLINIC

¹Ari Rosenberg*, ²Jessica Frakes, ³Jiixin Niu, ⁴Jared Weiss, ²Jimmy Caudell, ⁵Patricia Said, ⁵Pavel Tyan, ⁵Sebastien Paris, ⁶Tanguy Seiwert, ⁴Colette Shen, ⁵Sergio Szyldergemajn, ⁵Omar Vivar, ⁵Leonard Farber. ¹University of Chicago, Chicago, IL, USA; ²Moffitt Cancer Center, Tampa, FL, USA; ³Banner MD Anderson Cancer Center, Gilbert, AZ, USA; ⁴University of North Carolina, Chapel Hill, NC, USA; ⁵Nanobiotix, Paris, France; ⁶Johns Hopkins Medicine, Baltimore, MD, USA

Background Numerous recent studies have assessed the future direction of radiation oncology. Now more than ever there is a need to examine the changing landscape of novel agents and approaches that improve radiation efficacy as well as amplify the immune response with certain therapies. Immune checkpoint inhibitors (ICIs) have led to improved treatment outcomes in a variety of cancers, however many patients exhibit resistance. Overcoming this resistance is a major challenge in immuno-oncology. Radiation therapy (RT) has emerged as a promising combination with ICIs since it may act in some settings to produce an immunomodulatory effect. NBTXR3, a radioenhancer, is injected one time intratumorally and activated by RT. NBTXR3 increases RT energy deposition inside tumor cells, subsequent tumor cell death, and tumor antigen release and thus in combination with ICI may overcome resistance.

Methods Pre-Clinical: Abscopal assays were conducted in immunocompetent mice. Anti-PD-1 sensitive or resistant lung tumor cell lines were injected in both flanks. Intratumoral injection of NBTXR3 (or vehicle) followed by RT was performed in right flank (primary) tumors only. Some mice also received anti-PD-1 injections. Tumor growth was monitored, and tumor immune cell infiltrates analyzed by immunohistochemistry (IHC).

Clinical A multicenter phase I trial [NCT03589339] is evaluating NBTXR3/RT/anti-PD-1 in 3 cohorts of patients with advanced solid tumors eligible for anti-PD-1: 1) Locoregional recurrent or recurrent and metastatic HNSCC, 2) Lung metastases, or 3) Liver metastases. NBTXR3 was administered by intratumoral injection. Stereotactic body RT (SBRT) was delivered at tumor-site selective doses per standard practice.

Results Pre-clinical studies demonstrated that NBTXR3/RT induces an immune response not observed with RT alone and enhances systemic control. IHC showed significant increase of CD8+ T-cell infiltrates in both NBTXR3/RT treated, and untreated tumors. Furthermore, NBTXR3/RT/anti-PD-1 improved local and systemic control in mice bearing anti-PD-1 resistant lung tumors, produced long-term memory, and reduced spontaneous lung metastases.

NBTXR3 intratumoral injection was feasible and safe. Preliminary signs of efficacy were observed in patients treated with NBTXR3/RT/anti-PD-1 including in patients refractory to anti-PD-1. Responses in distal, non-irradiated lesions were also observed in patients with resistance to anti-PD-1.

Conclusions With demonstrated radioenhancement as well as immune system priming, NBTXR3 positions itself to be a paradigm shift catalyst in the treatment of cancers in a variety of clinical settings- definitive, palliative, and metastatic. These data support further development of NBTXR3 in combination with anti-PD-1 as well as other ICIs.

Trial Registration NCT03589339

<http://dx.doi.org/10.1136/jitc-2022-SITC2022.0682>

683

CD8 T CELL REPERTOIRE ANALYSIS OF PATIENTS WITH RESECTABLE HEAD AND NECK CANCER ENROLLED IN A PHASE II NEOADJUVANT STUDY OF α -PD1 ADMINISTERED ALONE OR IN COMBINATION WITH α -CTLA4 OR α -LAG3

¹Patricia Santos, ¹Aditi Kulkarni, ²Housaiyin Li*, ¹Jie Chen, ¹Lazar Vujanovic, ¹Seungwon Kim, ¹Umamaheswar Duvvuri, ¹Dan Zandberg, ¹Robert Ferris. ¹UPMC Hillman Cancer Center, Pittsburgh, PA, USA; ²University of Pittsburgh, Pittsburgh, PA, USA

Background Head and neck squamous cell carcinomas (HNSCC) are caused by alcohol and/or tobacco-derived exposure to carcinogens or by malignant transformation following oncogenic HPV infection. Standard of care regimen for HNSCC involve surgical resection followed by radiation or chemoradiation. Recently, monoclonal antibodies against immune checkpoint inhibitors (ICI) have been approved for patients with unresectable or metastatic disease.¹ However, response rate for ICI remains low in HNSCC and other solid tumors (20-40%).² Thus, there is a need to better understand the mechanisms involved in heterogeneous responses to ICI and to identify new targets that may sensitize HNSCC to combinatorial treatments. As part of a Phase II study examining the safety and tolerability of α -PD1 administered alone or in combination with α -CTLA4 or α -LAG3, the alterations in T cell receptor (TCR) clonotypes and changes in transcription profiles in CD8 T cells from blood and tumor following mono- and combinatorial immune checkpoint blockade (ICB) in treatment naïve HNSCC patients were analyzed.

Methods Subjects with resectable, stage III/IVa HNSCC were stratified based on HPV, PD-L1, and LAG3 status and randomized into 3 treatment arms: α -PD1 alone, α -PD1+ α -CTLA4, or α -PD1+ α -LAG3 prior to surgical resection. Blood and tumor samples were collected at baseline and on the day of surgery (21-35 days after ICB) and processed to generate single cell suspensions as previously described.³ FACS-sorted CD45+CD3+ cells were used to generate single cell RNA (scRNA) 5' gene expression libraries and TCR libraries using 10x Genomics workflow. Libraries were sequenced and data was processed using Cellranger 5.0.0 (10x Genomics). Data analysis was performed using R (v4.2.0) packages Seurat (v4.1.1), scRepertoire (v1.6.0) and Immunarch (v0.6.9).

Results To date, 34/60 patients have been enrolled in the trial. Based on scRNA data available from accrued patients (n=25), the proportion of CD8 T cells in the tumor increased after treatment in patients randomized to α -PD1+ α -CTLA4 arm. Patients treated with α -PD1+ α -LAG3 show an increase in CD8 TCR repertoire diversity as measured by Gini-Simpson index and had more TCR clones occupying 50% of the repertoire in post-treatment tumors compared to baseline. Overlap analysis on the number of TCR clones shared between post-treatment versus baseline did not show any significant differences across treatment arms. Trial accrual is still in progress and further analysis is currently ongoing to 1) correlate these data with clinical outcomes and 2) further investigate changes in transcriptional profiles of expanded clones in tumors across different treatment arms and by response.

Acknowledgements This research was funded by BMS CA223049 (RLF), P50 CA097190 (RLF), R01 CA206517 (RLF), and R01 DE031947 (RLF, LV). This research was supported in part by the University of Pittsburgh Center for Research Computing through the resources provided by using the HTC cluster, supported by NIH award number S10OD028483. This research utilized the UPMC Hillman

Cancer Center Flow Cytometry Core Facility, supported in part by award P30 CA047904 (RLF).

Trial Registration NCT04080804

REFERENCES

1. Johnson DE, *et al.* Head and neck squamous cell carcinoma. *Nat Rev Dis Primers.* 2020;**6**(1):92.
2. Doroshow DB, *et al.* PD-L1 as a biomarker of response to immune-checkpoint inhibitors. *Nat Rev Clin Oncol.* 2021;**18**(6):345–362.
3. Kurten CHL, *et al.* Investigating immune and non-immune cell interactions in head and neck tumors by single-cell RNA sequencing. *Nat Commun.* 2021;**12**(1):7338.

Ethics Approval This study was approved by University of Pittsburgh's Institutional Review Board; approval number HCC 18-139/CA224-056.

<http://dx.doi.org/10.1136/jitc-2022-SITC2022.0683>

684

NBTR3 ACTIVATED BY RADIOTHERAPY IN COMBINATION WITH NIVOLUMAB OR PEMBROLIZUMAB IN PATIENTS WITH ADVANCED CANCERS: RESULTS FROM AN ONGOING DOSE ESCALATION PHASE I TRIAL (STUDY 1100)

¹Colette Shen*, ²Jessica Frakes, ³Jiaxin Niu, ¹Jared Weiss, ²Jimmy Caudell, ⁴Tanguy Seiwert, ⁵Patricia Said, ⁵Mickael Guedj, ⁵Pavel Tyan, ⁵Omar Vivar, ⁵Sergio Szyldergemajn, ⁵Leonard Farber, ⁶Ari Rosenberg. ¹University of North Carolina, Chapel Hill, NC, USA; ²Moffitt Cancer Center, Tampa, FL, USA; ³Banner MD Anderson Cancer Center, Gilbert, AZ, USA; ⁴Johns Hopkins Medicine, Baltimore, MD, USA; ⁵Nanobiotix, Paris, France; ⁶University of Chicago, Chicago, IL, USA

Background Immune checkpoint inhibitors (ICIs) have changed how cancer patients are treated, still, most patients ultimately develop resistance. Overcoming or preventing this resistance is a major clinical challenge. NBTR3, when injected intratumorally, has been shown preclinically to enhance RT energy deposition, subsequent tumor cell death, and tumor antigen release to effectively expand T-cell repertoire. NBTR3/RT thus has the potential to trigger both a local and a systemic immune response to help improve ICI treatment.

Methods Study 1100 is a phase I dose escalation/expansion trial [NCT03589339] evaluating NBTR3 activated by stereotactic body radiotherapy (SBRT) and followed by anti-PD-1 therapy (either nivolumab or pembrolizumab) in 3 cohorts of patients (pts) with advanced solid tumors. Pts are either resistant to prior ICI or naïve. Escalation cohorts were defined by site of injection: head & neck (H&N) lesions, lung, or liver metastases. SBRT was delivered as per standard practice. The primary objective of the escalation phase was to determine the NBTR3/RT/anti-PD-1 recommended phase 2 dose for each cohort. Secondary objectives were feasibility, safety, and anti-tumor efficacy (objective responses).

Results 28 patients have been treated in the dose escalation phase in two escalating dose-levels for each cohort: 11 H&N, 10 lung, and 7 liver. Median age was 66.5 years. Two DLTs occurred in 1 pt at the first dose level in the H&N cohort. Grade ≥ 3 NBTR3-related AEs occurred in 4 (14.3%) pts. SBRT+ ICI safety profile was in line to previously reported. Among 20 pts evaluable for efficacy, overall tumor responses were observed in 8/20 (40%) with disease control observed in 15/20 (75%) respectively, including durable complete responses. Objective tumor responses were observed in patients resistant to prior ICI. Updated safety and efficacy results will be presented.

Conclusions NBTR3/RT/anti-PD-1 is feasible, predictable and safe in pts with recurrent HNSCC, lung, or liver metastases. The RP2D was defined. This new treatment shows promising early signs of efficacy. Subgroup analyses are ongoing and might help improve further results in specific populations. Overall, these results support evaluation of NBTR3/RT/anti-PD-1 in the ongoing enlarged expansion phase.

Trial Registration NCT03589339

<http://dx.doi.org/10.1136/jitc-2022-SITC2022.0684>

685 PRELIMINARY RESULTS OF MT-401 IN POST-TRANSPLANT MRD⁺ AML PATIENTS

¹Mythili Koneru*, ¹Juan Vera, ²Shukaib Arslan, ³Hongtao Liu, ⁴Margarida Magalhaes-Silverma, ⁵Nelli Bejanyan, ⁶Antonio DiStasi, ⁷Betul Oran, ⁸Jingmei Hsu, ¹Robin McCallum, ¹Silvia Quintero, ¹Gerald Garrett, ¹Karrie Wang, ¹Eric Smith, ¹Tsvetelina Hoang, ¹Tara Shahim, ¹Jeannette Crisostomo, ¹Anna Wilga-Savitski, ¹Jennifer Pickering, ¹Laura Angelo, ¹Anastasiya Smith. ¹Marker Therapeutics, Houston, TX, USA; ²City of Hope, Los Angeles, CA, USA; ³University of Chicago, Chicago, IL, USA; ⁴University of Iowa, Iowa City, IA, USA; ⁵Moffitt, Tampa, FL, USA; ⁶University of Alabama, Birmingham, AL, USA; ⁷MDACC, Houston, TX, USA; ⁸Cornell, New York City, NY, USA

Background Measurable residual disease (MRD) testing has become more prevalent in AML. MRD positivity is associated with increased relapse risk and shorter survival in AML, and currently, there no approved therapies for these patients. Zedenoleucel (also known as MT-401) is a non-genetically modified allogeneic multi-tumor associated antigen (mTAA)-specific T cell therapy with selectivity to multiple tumor antigens, specifically preferentially expressed antigen in melanoma (PRAME), Wilms' tumor 1 (WT1), New York esophageal 1 (NY-ESO-1) and Survivin.

Methods A multicenter Phase 2 study (ARTEMIS) evaluating the safety, tolerability and efficacy of zedenoleucel in patients with AML, including MRD⁺patients, post-HSCT is ongoing. The study explores this therapy in patients with no active disease [in complete remission (CR) and MRD⁻] or in patients with active disease (frank relapse or MRD⁺). Patients may receive up to 3 consecutive infusions of zedenoleucel as a monotherapy (50-200 × 10⁶ cells every 2 weeks) at weeks 0, 2 and 4 during the Intervention Period, and enter Follow-up at Week 8. Primary endpoints include various safety measurements. Efficacy evaluations occur at weeks 8, 12, 18, 24, 48 and yearly for 4 years using ELN recommendations for standard AML response criteria. MRD testing was done by flow cytometry or molecular testing (e.g. RT-PCR).

Results No concerning safety signals arose, including any dose-limiting toxicities in safety lead-in patients. The MRD⁺patients had a variety of genetic mutations/abnormalities. One patient with NPM1 mutation converted from MRD⁺ to MRD⁻ at week 8 evaluation. Another patient with RUNX1 genetic abnormality showed a decrease in MRD by PCR from a starting baseline of 0.8093% to resolution via peripheral blood at approximately 32 weeks post-treatment with MT-401. T cell composition of the product consisted of 71% CD4⁺ and 24% CD8⁺ T cells. T cell receptor (TCR) analysis identified 3,117 antigen-specific clones (881 Survivin, 783 NY-ESO-1, 750 PRAME, 709 WT1). Immune monitoring of this patient using biomarker analysis showed T cell specificity not only for the targeted antigens but also for non-targeted antigens over time, thereby demonstrating epitope spreading. Interestingly, the tumor antigen composition by RNASeq identified an antigen expression profile that changes over time and inversely correlates with the presence of antigen-specific T cells, demonstrating the interplay of tumor cell immunogenicity and antigen-specific T cells.

Conclusions The preliminary ARTEMIS results showed that administration of MT-401 converted MRD⁺patients to MRD⁻ indicating that early intervention with MT-401 administration at MRD⁺ stage in post-transplant AML can be beneficial.

Ethics Approval Ethics approval has been obtained by the Western IRB and participants gave informed consent before taking part. IRB tracking number is 20192173.

Consent Written informed consent was obtained from the patient for publication of this abstract and any accompanying

images. A copy of the written consent is available for review by the Editor of this journal.

<http://dx.doi.org/10.1136/jitc-2022-SITC2022.0685>

686

MECHANISM OF ACTION OF LAVA-051, A BISPECIFIC V γ 9V δ 2 T-CELL ENGAGER (BSTCE), CONFIRMED IN THE CLINICAL SETTING

¹Roeland Lameris, ²Jurjen Ruben, ²Rob Roovers, ¹Arnon Kater, ²Thilo Riedl, ²Victoria Iglesias, ³Annemiek Broijl, ²Ilse Tuinhof, ²Sanjana Umarale, ²Anton Adang, ¹Tanja de Gruijl, ²Paul Parren, ²Benjamin Winograd*, ⁴Hans Van der Vliet. ¹Amsterdam UMC, Amsterdam, Netherlands; ²LAVA Therapeutics N.V, Utrecht, Netherlands; ³Erasmus MC, Rotterdam, Netherlands

10.1136/jitc-2022-SITC2022.1

Amsterdam UMC, LAVA Therapeutics N.V., Amsterdam, Netherlands

Background LAVA-051, a CD1d-targeting first-in-class bispecific single domain antibody (27 kDa), was brought into the clinic based on its high potency antitumor activity through dual engagement of V γ 9V δ 2-T and iNKT cells, and a low risk of cytokine release syndrome (CRS).

Methods A phase 1 study using LAVA-051 is ongoing in patients with relapsed/refractory MM or CLL to determine the recommended phase 2 dose (RP2D). This study has been approved by relevant ethics committees (NCT04887259). A panel of specific pharmacodynamic assays is included to determine the pattern of change in the binding of LAVA-051 to patients' peripheral blood V γ 9V δ 2-T cells (i.e. V γ 9V δ 2-TCR occupancy) and in the frequency and activation status of V γ 9V δ 2-T and iNKT cells in circulation. Data presented are focused on the comparison of clinical to pre-clinical observations.

Results LAVA-051 triggers V γ 9V δ 2-T and iNKT cell mediated pro-inflammatory cytokine production, proliferation and anti-tumor activity in *in vitro* and *ex vivo* assays using patient CD1d⁺ AML, CLL and MM cells. In addition, LAVA-051 induced a strong anti-tumor effect *in vivo* in a CDX model using NSG mice with intermittent dosing. In a non-human primate (NHP) model utilizing a cross-reactive CD1d-V γ 9 bsTCE there was clear observation of V γ 9V δ 2-T cell engagement as reflected by a (temporary) decrease in circulating V γ 9V δ 2-T cells after dosing and concomitant upregulation of the activation marker CD69. As of July 2022, doses up to 100x the starting dose have been evaluated as safe in the clinical setting with 8 patients treated in total; importantly no CRS was observed. A similar temporary decrease in V γ 9V δ 2-T cells with consistent upregulation of activation markers (CD25 and CD69) as was seen in the NHP study has been observed in the clinic. In the NHP model, dose-dependent binding of the bsTCE to peripheral blood V γ 9-T cells was observed up to several days after injection. Similarly in the clinic, V γ 9V δ 2-TCR occupancy was shown to increase with higher dose cohorts with a current maximum of 20.9% receptor occupancy after dosing (45 μ g). The frequency and activation status of iNKT cells has been assessable in the clinic and will continue to be evaluated with escalating doses.

Conclusions LAVA-051 has demonstrated on-mechanism pharmacodynamics in the clinic, reflective of pre-clinical findings. The differentiating importance of these pharmacodynamic parameters with any correlating preliminary antitumor activity will be further elucidated in determining the RP2D and schedule; updated comparative data will be presented at the congress.

Trial Registration NCT04887259

Ethics Approval This study has been approved by relevant ethics committees in the Netherlands, Spain and Italy

(EUDRACT: 2020-004583-26). Informed consent was obtained from all patients prior to their participation.

<http://dx.doi.org/10.1136/jitc-2022-SITC2022.0686>

687

PROTEOMIC PROFILING IN BLOOD IDENTIFIES NOVEL PRETREATMENT AND MECHANISTIC MARKERS RELATED TO INFLAMMATORY ADVERSE EVENTS IN RELAPSED/REFRACTORY LARGE B-CELL LYMPHOMA AFTER AXICABTAGENE CILOLEUCEL

¹Kelly Speth, ¹Gayatri Tiwari, ¹Sabina Adhikary*, ¹Qinghua Song, ¹Justin Chou, ²Frederick Locke, ³Caron Jacobson, ⁴David Miklos, ⁵Olalekan Oluwole, ⁶Marie José Kersten, ⁷Max Topp, ¹Jenny Kim, ¹Adrian Bot. ¹Kite, a Gilead Company, Santa Monica, CA, USA; ²Moffitt Cancer Center, Tampa, FL, USA; ³Dana-Farber Cancer Institute, Boston, MA, USA; ⁴Stanford University School of Medicine, Stanford, CA, USA; ⁵Vanderbilt University Cancer Center, Nashville, TN, USA; ⁶Amsterdam UMC, University of Amsterdam, Amsterdam, Netherlands; ⁷Universitätsklinikum Würzburg, Würzburg, Germany

Background Axicabtagene ciloleucel (axi-cel) is an autologous anti-CD19 CAR T-cell therapy approved for patients with relapsed/refractory (R/R) large B-cell lymphoma (LBCL) and follicular lymphoma. In the ZUMA-1 pivotal study, Grade ≥ 3 cytokine release syndrome (CRS) and neurological events (NE) were observed in 13% and 28% of patients, with median time to onset of any grade at 2 and 5 days, respectively.¹ Using conventional low-throughput platforms (eg, multiplex ELISA), pretreatment markers, including serum levels of LDH, IL-6, and IL-15, demonstrated a positive association with Grade ≥ 3 CRS and/or NE.² We sought to explore biological mechanisms and novel markers underlying the development of early-onset (within 5 days post-CAR T-cell infusion) Grade ≥ 3 CRS and NE using high-throughput Olink[®] proteomic profiling.

Methods Serum samples collected prior to conditioning chemotherapy (baseline) and immediately prior to CAR T-cell therapy (Day 0) for 142 patients with R/R LBCL treated in ZUMA-1 Phase 2 Cohorts 1, 2, and 4 were analyzed by Olink[®] panels comprising 1,458 markers. Association between marker expression and early Grade ≥ 3 toxicity was evaluated using Wilcoxon test and logistic regression. Weighted gene coexpression network analysis (WGCNA)³ was performed to identify highly coexpressed protein clusters, which were used for gene ontology (GO) analysis for biological interpretation. Machine learning methods were used to select features and build classifiers.

Results Twenty-four patients (17%) experienced Grade ≥ 3 CRS and/or NE within 5 days post-CAR T-cell infusion. Univariate and WGCNA analyses demonstrated that clusters of pretreatment markers were associated with these toxicities; these clusters correlated positively with poor prognosis factors (eg, International Prognostic Index and baseline tumor burden). GO analysis applied to these clusters showed enrichment of proteins involved in metabolic processes and leukocyte activation. Machine learning demonstrated excellent performance (mean AUC > 0.80 in both training and testing runs) of groups of Olink[®] markers in classifying patients with early high-grade toxicity. Further, we observed that IL-1/IL-6 pathway markers (eg, IL-1A and OSMR) were useful in identifying Grade ≥ 3 CRS, while inflammatory endothelial markers (eg, ACE2, CEACAM1, ICAM2, and ADAM15) could classify patients with both Grade ≥ 3 CRS and NE upon axi-cel treatment.

Conclusions Our proteomic analysis supports the relevance of previously described markers. In addition, we have identified potential markers that are mechanistically involved in the development of high-grade toxicity. Safety of CAR T-cell therapy may be improved by optimization of product or conditioning regimen to reduce adverse event-dependent proinflammatory activities while maintaining efficacy.

KS and GT contributed equally.

REFERENCES

1. Neelapu SS, Locke FL, Bartlett NL, *et al.* Axicabtagene ciloleucel CAR T-cell therapy in refractory large B-cell lymphoma. *N Engl J Med.* 2017;**377**(26):2531–2544.
2. Locke FL, Rossi JM, Neelapu SS, *et al.* Tumor burden, inflammation, and product attributes determine outcomes of axicabtagene ciloleucel in large B-cell lymphoma. *Blood Adv.* 2020;**4**(19):4898–4911.
3. Langfelder P, Horvath S. WGCNA: an R package for weighted correlation network analysis. *BMC Bioinformatics.* 2008;**9**:559.

Ethics Approval The study was approved by the institutional review board at each study site and was conducted in accordance with the Good Clinical Practice guidelines of the International Conference on Harmonization. All the patients provided written informed consent.

<http://dx.doi.org/10.1136/jitc-2022-SITC2022.0687>

688

PREDICTION OF HCC RESPONSE TO NEOADJUVANT IMMUNOTHERAPY USING MULTIPARAMETRIC MAGNETIC RESONANCE IMAGING: A PRELIMINARY STUDY

¹Octavia Bane*, ¹Enamul Bhuiyan, ¹Paul Kennedy, ¹Muhammed Shareef, ¹Pauline Hamon, ¹Mark Buckup, ¹Sacha Gnjatic, ²Stefanie Hectors, ²Hung Kam Cheung, ²Elizabeth Miller, ¹Maria Isabel Fiel, ¹Stephen Ward, ¹Myron Schwartz, ¹Thomas Marron, ¹Miriam Merad, ¹Bachir Taouli. ¹Icahn School of Medicine at Mount Sinai, New York, NY, USA; ²Regeneron, Tarrytown, NY, USA

Background Despite advances in therapy, the prognosis of hepatocellular carcinoma (HCC) remains poor. The introduction of biologic drugs, including immune check-point inhibitors, has revolutionized HCC treatment. However, only a portion of patients with HCC respond to immunotherapy and predicting response is an unmet need. In this preliminary study, we assessed the value of quantitative multiparametric MRI (mpMRI) for predicting HCC response to neoadjuvant immunotherapy.

Methods In this prospective IRB-approved single-center study, we included 17 patients (M/F 14/3, mean age 65y) with resectable HCC who underwent mpMRI including T1 mapping, 3D MR elastography (MRE), diffusion-weighted imaging (DWI), and dynamic contrast-enhanced (DCE)-MRI with a hepatobiliary contrast agent (gadoteric acid, Eovist/Primovist, Bayer), at pre-treatment and after completion of anti PD-1 immunotherapy (cemiplimab) as part of a trial. All patients underwent surgical resection. HCC lesions were identified by an experienced radiologist and regions of interest were placed to measure tumor native and post-contrast T1 measured during hepatobiliary phase (T1-HBP), tumor stiffness (TS), apparent diffusion coefficient (ADC), and perfusion parameters. The reference standard was the histopathologic percentage of necrosis. Patients with significant tumor necrosis (STN ≥50%) were considered responders. MRI parameters were compared between responders and non-responders by Mann-Whitney U test, and their diagnostic performance to predict response to treatment was assessed by ROC analysis.

Results 17 HCC lesions (6.4±4.9 cm, range 2.0-19.0 cm) were resected in 17 patients. At pre-treatment MRI, tumor native T1 and upslope from DCE-MRI were prolonged in responders compared to non-responders, and predicted response with good diagnostic performance (table 1; T1 AUC(CI)=0.82 (0.58-0.99), upslope AUC(CI)=0.80(0.58-0.99). The other parameters had no value in predicting response to immunotherapy (AUC range 0.52-0.68). Tumor native T1 and T1-HBP increased with degree of tumor necrosis at resection (%).

Conclusions Our results demonstrate the potential utility of native T1 and upslope measured with DCE-MRI for predicting HCC response to neoadjuvant immunotherapy. These findings require validation in an independent study.

Acknowledgements Regeneron Pharmaceuticals, Inc. funded the study. We would like to thank our clinical coordinators, Jordan Cuevas and Jenna Korotkin for helping with patient consent and for maintaining the study database. Enamul H. Bhuiyan gratefully acknowledges Professor Steven Sourbron, The University of Sheffield for his generosity to provide updated PMI software.

Trial Registration Neoadjuvant Cemiplimab for the Treatment of Resectable NSCLC, HCC, and HNSCC clinicaltrials.gov identifier NCT03916627

Ethics Approval The study obtained continuing approval from the IRB at Mount Sinai through 01/19/2023, for Regeneron Pharmaceuticals, Inc. Protocol # R2810-ONC-1866/PI:

Marron/BRANY File # 19-06-061-05. All participants signed informed consent.

Abstract 688 Table 1 Comparison of mpMRI (pretreatment) parameters (tumor size, tumor native T1, tumor HBP T1, arterial plasma flow Fa; venous plasma flow Fp, total plasma flow Ft, arterial flow fraction ART, mean transit time MTT, extra cellular volume Ve, uptake fraction fi, uptake rate ki, time-to-peak TTP and upslope, apparent diffusion coefficient ADC, true diffusion coefficient D, pseudo diffusion coefficient D* and perfusion fraction PF) and their corresponding AUC for prediction of histopathologically assessed tumor response as significant tumor necrosis (STN = 50%) . Parameters with highest AUCs and significant p-values are shown in bold.

Table 1: Comparison of mpMRI (pretreatment) parameters (tumor size, tumor native T1, tumor HBP T1, arterial plasma flow Fa; venous plasma flow Fp, total plasma flow Ft, arterial flow fraction ART, mean transit time MTT, extra cellular volume Ve, uptake fraction fi, uptake rate ki, time-to-peak TTP and upslope, apparent diffusion coefficient ADC, true diffusion coefficient D, pseudo diffusion coefficient D* and perfusion fraction PF) and their corresponding AUC for prediction of histopathologically assessed tumor response as significant tumor necrosis (STN ≥ 50%) . Parameters with highest AUCs and significant p-values are shown in bold.

Parameters	Significant tumor necrosis (STN)	Non-STN	p**	AUC	p*	95% CI
Tumor native T1 (ms)	726.01±58.51	652.56±75.39	0.037	0.82	0.035	0.58-0.99
Tumor HBP T1 (ms)	622.47±69.64	589.03±62.83	0.462	0.62	0.421	0.31-0.93
Tumor stiffness, TS (kPa)	6.57±2.78	4.89±1.41	0.350	0.65	0.315	0.31-0.93
Extracellular volume, Ve (%)	49.29±29.13	42.05±21.34	1.00	0.50	1.00	0.18-0.81
Mean transit time, MTT (s)	21.39±6.19	20.91±11.21	0.591	0.59	0.546	0.30-0.87
Uptake fraction, fi (%)	1.76±1.17	1.51±1.33	0.156	0.56	0.688	0.27-0.85
Uptake rate ki, (min ⁻¹)	2.69±2.41	1.80±1.80	0.404	0.64	0.366	0.33-0.94
Arterial flow, Fa (ml/100ml/min)	98.04±56.40	120.76±46.97	0.216	0.70	0.191	0.39-0.99
Venous flow, Fp (ml/100ml/min)	36.33±46.43	10.99±16.63	0.462	0.62	0.421	0.30-0.94
Total flow Ft, (ml/100ml/min)	134.37±62.92	131.76±51.43	0.961	0.52	0.92	0.17-0.86
Arterial flow fraction, ART (%)	76.59±26.78	90.93±16.37	0.525	0.68	0.228	0.42-0.94
Time-to-peak, TTP (s)	65.53±16.56	46.03±21.45	0.149	0.73	0.132	0.48-0.97
Upslope (mM/min)	0.004±0.001	0.008±0.003	0.048	0.80	0.049	0.58-0.99
Apparent diffusion coefficient, ADC (10 ⁻³ mm ² /s)	1.36±0.24	1.42±0.30	0.660	0.58	0.615	0.28-0.87
Perfusion fraction, PF (%)	0.31±0.05	0.36±0.11	0.660	0.59	0.546	0.31-0.86

<http://dx.doi.org/10.1136/jitc-2022-SITC2022.0688>

Abstracts

689

PRELIMINARY RESULTS OF A PILOT STUDY OF INTRATUMORAL INJECTION OF AUTOLOGOUS DENDRITIC CELLS AFTER HIGH-DOSE CONFORMAL EXTERNAL BEAM RADIOTHERAPY IN UNRESECTABLE PRIMARY LIVER CANCERS

¹Lionel Kankeu Fonkoua*, ¹Panwen Wang, ¹Christopher Hallemeier, ¹Thomas Atwell, ¹Nguyen Tran, ²Amit Mahipal, ¹Elham Babadi, ¹Svetlana Bornschlegl, ¹Anatilde Gonzalez Guerrero, ¹Kodi Martinez, ¹Gabrielle McCoy, ¹Kevin Regan, ¹Zuoyi Shao, ¹Henan Zhang, ¹Junwen Wang, ¹Ying Li, ¹Allan Dietz, ¹Haidong Dong, ¹Yi Lin, ¹Sean Park, ¹Lewis Roberts. ¹Mayo Clinic, Rochester, MN, USA; ²Case Western Reserve University, Cleveland, OH, USA

Background Survival outcomes for patients with unresectable primary liver tumors (hepatocellular carcinoma [HCC] and intrahepatic cholangiocarcinoma [iCCA]) remain dismal, despite available locoregional and systemic treatment options. This pilot study aims to evaluate the safety and tolerability of intratumorally delivered autologous dendritic cell (DC) vaccine after external beam radiotherapy (EBRT) in unresectable HCC and iCCA. We hypothesize that *in situ* DC-mediated tumor vaccination via radiation-induced immunogenic cell death, will elicit tumor-specific immunity and improve clinical outcomes.

Methods Enrolled subjects undergo leukapheresis for DC manufacturing prior to EBRT administration as per standard of care for unresectable localized HCC/iCCA. After EBRT, 7 monthly ultrasound-guided intratumoral injections of mature DC (30-60 million cells) are administered (figure 1). An adjuvant booster (Plevnar vaccine) is given with the first 3 injections. The primary endpoint is the incidence of significant toxicity, and secondary endpoints include objective response rate (ORR) and survival. Pre/post-treatment peripheral blood samples are collected for immune correlative studies, including multiparametric flow cytometry and single-cell RNA sequencing.

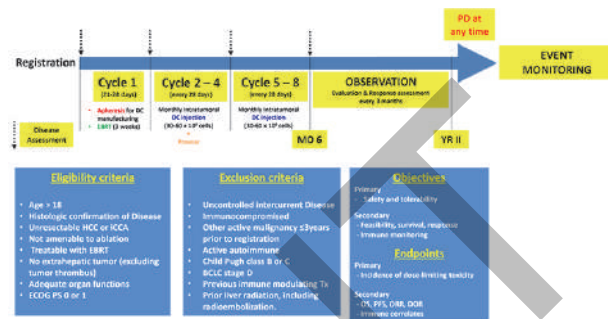
Results As of July 28, 2022, eight subjects have enrolled (5 HCC; 3 iCCA) with five (3 HCC; 2 iCCA) having completed the protocol and three (2 HCC; 1 iCCA) currently in active phase. DC manufacturing success has been 100% and the maximal dose of 60×10^6 DC appears to be tolerated without autoimmunity or grade ≥ 3 adverse events (AEs), with the exception of one subject with grade 3 hyperbilirubinemia. The most common AEs include limited injection site pain and nausea. Early response data from the five subjects who have completed the protocol is encouraging with ORR of 60% (n=3, all partial response). One responder with iCCA has an ongoing response at 2 years (figure 2), and another HCC subject had stable disease for over one year. Preliminary cellular immunophenotyping and T cell receptor (TCR) clonotyping/profiling has revealed both the emergence of new TCR clones and expansion of existing TCR clones, including clones with tumor reactive and cytotoxic profile, suggesting this combination could enhance tumor reactive cytotoxic T cell response (figure 3). However, many of the TCR clones also have early exhaustion signal with upregulation of multiple checkpoint receptors. Thus, incorporating immune checkpoint inhibition (ICI) may help further enhance the cytotoxic functions of these TCR clones.

Conclusions Despite being preliminary, data from subjects treated to date suggest a favorable safety profile, encouraging signs of efficacy and induction of tumor-specific immunity which could be further enhanced by the addition of ICI.

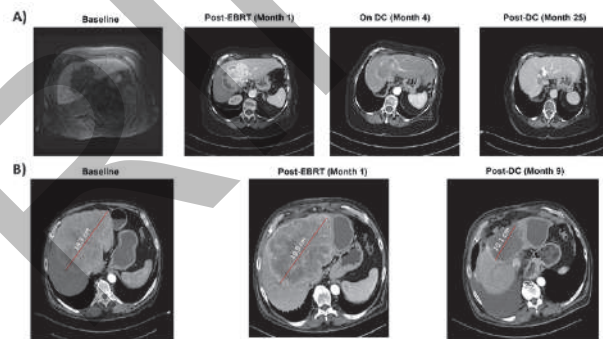
Acknowledgements This study has received funding and support from the Mayo Clinic Immuno-Oncology Project,

Conquer Cancer Foundation of ASCO, Mayo Clinic Hepatobiliary SPORE, and the Bristol Myers Squibb Foundation. Trial Registration NCT03942328

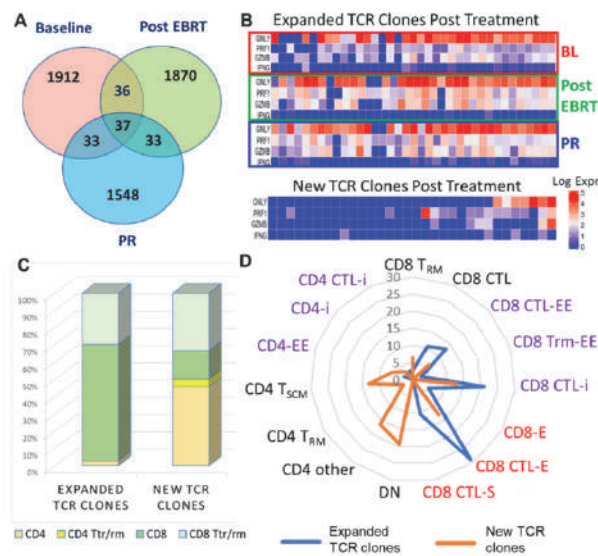
Ethics Approval This study was approved by the Mayo Clinic Ethics & Institutional Review Board (IRB# 16-0096335).



Abstract 689 Figure 1 NCT03942328 study schema.



Abstract 689 Figure 2 Representative images of treated patients. Patients with iCCA (A) and HCC (B) treated with EBRT and intratumoral DC injection on NCT03942328 study. Reduction in tumor size, corresponding to partial response is seen and is ongoing at 25 months and 9 months post-enrollment, respectively.



Abstract 689 Figure 3 TCR repertoire changes with EBRT and DC. (A) The number of unique and shared TCR clones from baseline (BL) to post-EBRT and after DC, at the time of partial response (PR) are shown.

(B) Heatmap of for TCR clones' RNA expression are show here for cytotoxic functions: GNLY, PRF1, GZMB; and for cytokine IFNG. Most of the TCR clones that are expanded with treatment have increased expression for cytotoxicity and IFNG (top 3 panels). In contrast, few new TCR clones post treatment have cytotoxic or IFNG expression (bottom panel). (C) While majority of the expanded clones are CD8, new TCR clones post-treatment are both CD4 and CD8, with a much smaller percentage having tissue/tumor origin. (D) Majority of the expanded TCR clones post- treatment have inhibited (-I, one or more checkpoints expressed), early exhausted (-EE), exhausted (-E) or senescent (-S) transcriptome. In contrast, new TCR clones post treatment have more stem memory and tissue derived resident memory profile.

<http://dx.doi.org/10.1136/jitc-2022-SITC2022.0689>

PREPRINT

690

CORRELATES OF POOR RESPONSE TO NEOADJUVANT ANTI-PD-1 THERAPY IN HEPATOCELLULAR CARCINOMA (HCC) INCLUDE WNT PATHWAY ACTIVATION AND LOSS OF HLA EXPRESSION

¹Kunal Kundu, ¹Nathalie Fiaschi, ¹Wei Wang, ¹Baijun Kou, ²Assaf Magen, ²Pauline Hamon, ²Sacha Gnjatic, ²Myron Schwartz, ²Alice Kamphorst, ²Thomas Marron, ²Miriam Merad, ¹Chunguang Guo, ¹Gavin Thurston, ¹Namita Gupta, ¹Kamil Cygan*. ¹Regeneron Pharmaceuticals, Tarrytown, NY, USA; ²Icahn School of Medicine at Mount Sinai, New York, NY, USA

Background Although anti-PD-1/PD-L1 therapy has improved patient outcomes in the past decade, only a subset of patients shows clinical benefit.¹ Furthermore, many responders develop acquired resistance after initial responses.² Therefore, understanding baseline correlates of response and mechanisms of resistance is necessary for improving anti-PD-1/PD-L1 efficacy. In a neoadjuvant Phase 2 study (NCT03916627), patients with resectable hepatocellular carcinoma (HCC) were treated with cemiplimab, a PD-1 antibody. Pathologic Tumor Necrosis (PTN) of at least 50% at resection was used as the exploratory endpoint. Here we review possible biomarkers to identify responders and explore potential underlying mechanisms of resistance.

Methods Tumor samples collected at baseline and time of resection were analyzed by multiplex immunohistochemistry. Nucleic acid isolates from tumor, adjacent normal tissue, and matched blood were analyzed by RNA and whole exome DNA sequencing. OptiType was used to infer HLA haplotype. Loss of heterozygosity (LOH) was calculated by a custom workflow.

Results At baseline, higher levels of tumor-infiltrating T cells were present in Responders with PTN (N=5) compared with Non-responders to cemiplimab (N=15). The trend was consistent and amplified when measured at resection. However, clinical responses were also observed in patients with low levels of baseline T cell infiltration. Clinical efficacy was associated with presence of HLA-A*24:02 allele (N=5; 4 Responders and 1 Non-responder). Response to cemiplimab was independent of baseline tumor mutation burden, underlying viral etiology, or PD-L1 expression in the tumor. WNT pathway activating mutations, a previously reported mechanism of immunotherapy resistance,³ were enriched in Non-responders (6 Non-responders vs. 1 Responder; mutations in 4 baseline and 5 resection samples) and correlated with low CD8 T cell infiltration at baseline and low CD8 and CD4 T cell infiltration at resection. Loss of WNT pathway mutations were observed on treatment in one Responder and one Non-responder. The Responder displayed LOH at the HLA locus during treatment and subsequently relapsed. On-treatment acquired WNT pathway mutations were identified in 3 out of 7 patients that relapsed.

Conclusions Preliminary analyses suggest that high levels of baseline tumor-infiltrating T cells is associated with clinical response to cemiplimab in HCC. The presence of WNT pathway activating mutations is indicative of low T cell infiltration and may be a potential negative predictor of clinical benefit with cemiplimab. One patient showed LOH at the HLA locus associated with clinical progression, suggesting potential alternative disease escape. Additional mechanisms of resistance are under investigation.

Trial Registration ClinicalTrials.gov identifier (NCT number): NCT03916627

REFERENCES

- [1] Ventola CL. Cancer Immunotherapy, Part 3: Challenges and Future Trends. *P T*. 2017;**42**(8):514–521.
- [2] Persa OD, Schatton K, Rübber A, Berking C, Erdmann M, Schlaak M, Mauch C, Steeb T. Risk Factors for Relapse after Intentional Discontinuation of Immune Checkpoint Inhibitors in Melanoma Patients. *J Immunother*. 2021;**44**(6):239–241. doi: 10.1097/CJI.0000000000000375.
- [3] Chehrizi-Raffle A, Dorff TB, Pal SK, Lyou Y. Wnt/ β -Catenin Signaling and Immunotherapy Resistance: Lessons for the Treatment of Urothelial Carcinoma. *Cancers (Basel)*. 2021;**13**(4):889. doi: 10.3390/cancers13040889.

Ethics Approval Samples were obtained from specimens of patients undergoing resection at Mount Sinai Hospital (New York, NY) after obtaining informed consent in accordance with a protocol reviewed and approved by the Institutional Review Board at the Icahn School of Medicine at Mount Sinai (RUTH Human Subjects Electronic Submission System 18-00407 and 20-04150) and in collaboration with the Biorepository and Department of Pathology.

<http://dx.doi.org/10.1136/jitc-2022-SITC2022.0690>

691

IMMUNE PRESSURE IN AN ADVANCED HEPATOCELLULAR CANCER PATIENT FOLLOWING TREATMENT WITH PERSONALIZED NEOANTIGEN DNA VACCINE (GNOS-PV02) IN COMBINATION WITH PLASMID IL-12 (pIL12) AND ANTI-PD1 (PEMBROLIZUMAB)

¹Mark Yarchoan*, ²Edward Gane, ³Renzo Perales, ³Alfredo Perales-Puchalt, ⁴Gabor Bartha, ³Sarah Rochestie, ³Neil Cooch, ³Joann Peters, ³Ildiko Csiki, ³Jian Yan, ³Niranjan Sardesai. ¹The Johns Hopkins Hospital, Baltimore, MD, USA; ²The University of Auckland, Auckland, New Zealand; ³Genoos Therapeutics, Plymouth Meeting, PA, USA; ⁴Personalis, Inc, Menlo Park, CA, USA

Background Tumor immune editing and escape are key mechanisms of cancer progression and metastatic dissemination. However, immune editing in response to therapeutic cancer vaccines has been challenging to demonstrate in patients. Neoantigens derived from tumor-specific mutations are promising targets for immunotherapy. They can be incorporated in personalized cancer vaccines (PCV) to prime T cell activation. Here, we report evidence of immune editing in a patient treated with a therapeutic neoantigen DNA PCV from the ongoing GT-30 advanced hepatocellular carcinoma single-arm open-label multi-center phase Ib/IIa trial.

Methods A 74 yo white male, having progressed on multiple prior lines of therapy including ablation, TACE and lenvatinib, was enrolled in the GT-30 study. Following WES and transcriptome analysis of the primary liver tumor biopsy, a DNA PCV encoding 29 neoantigens (GNOS-PV02) was manufactured. GNOS-PV02 (1mg) and pIL12 (0.3mg) were administered intradermally Q3w x 4 doses; Q9w thereafter. Pembrolizumab 200mg IV was administered Q3w. Treatment response was evaluated Q9w by RECIST 1.1. Pre-treatment and on-treatment biopsy samples and periodic blood samples were evaluated retrospectively for neoantigen repertoire, immune responses and ctDNA.

Results GNOS-PV02+pIL12+pembrolizumab treatment resulted in a partial response, with target lesion reduction of -36% at w9 deepening to -59% at w54 by RECIST1.1. TCR/TIL analysis of w9 biopsy versus screening biopsy samples revealed the expansion and infiltration of multiple new T-cell clones post-vaccination. PBMC analysis by IFNg ELISpot detected strong T-cell response to 4/29 vaccine epitopes. Flow cytometry analysis showed antigen-specific, activated (CD69+, Ki67+) CD8 and CD4 T-cells at high frequency. A new, distal adrenal lesion was detected at w18 that increased in size by w54. Sequencing of the adrenal lesion at w54 identified 25 neoantigens, including 16 shared with the primary liver lesion. However all 4 of the vaccine epitopes with strongest ELISpot responses were absent in the adrenal lesion, consistent with neoantigen loss resulting from immune editing and subsequent clonal escape. ctDNA analysis was consistent with complete response of the liver-specific tumor clone by w21 persisting through w57 but showed an increasing frequency of the adrenal specific tumor ctDNA over time.

Conclusions We documented evidence of PCV immune pressure induced clonal escape via the emergence and growth of a new distal lesion despite the primary lesion showing continued and deepened response. Such ongoing analysis of immune response and ctDNA for monitoring tumors offers a means to dynamic cancer therapy, whereby therapeutic vaccines with evolved neoantigen panels may be designed against new, or newly unresponsive, lesions.

Trial Registration NCT04251117

Ethics Approval For GT-30 trial, the protocols were approved by Johns Hopkins Medicine Review Boards (CR00039002/IRB00227771), Icahn School of Medicine-Program for the Protection of Human Subjects (20-00076 GCO#1), and Northern A Health and Disability Ethics committee (Ethics ref: 20/NTA), respectively. Written informed consent was obtained from each patient prior to the patient participating in the trial.

<http://dx.doi.org/10.1136/jitc-2022-SITC2022.0691>

692

CIRCULATING TUMOR DNA ANALYSIS OF ADVANCED HEPATOCELLULAR CANCER (HCC) PATIENTS TREATED WITH NEOANTIGEN TARGETED PERSONALIZED CANCER DNA VACCINE (GNOS-PV02) IN COMBINATION WITH PLASMID IL-12 (PIL12) AND ANTI-PD1 (PEMBROLIZUMAB)

¹Renzo Perales, ¹Alfredo Perales-Puchalt, ²Gabor Bartha, ²Joseette Northcott, ²Richard Chen, ²John Lyle, ²Dan Norton, ¹Neil Cooch, ³Edward Gane, ⁴Mark Yarchoan, ⁵Thomas Marron, ¹Sarah Rochestie, ¹Joann Peters, ¹Ildiko Csiki, ¹Jian Yan*, ¹Niranjan Sardesai. ¹*Geneos Therapeutics, Plymouth Meeting, PA, USA*; ²*Personalis, Inc, Menlo Park, CA, USA*; ³*The University of Auckland, Auckland, New Zealand*; ⁴*The Johns Hopkins Hospital, Baltimore, MD, USA*; ⁵*The Tisch Cancer Institute, New York, NY, USA*

Background Recent advances in circulating tumor DNA (ctDNA) analysis have enabled the non-invasive detection of mutations that lead to resistance mechanisms and therapeutic and disease monitoring in cancer patients. Improvements in whole exome sequencing with high sensitivity and specificity has made it feasible to interrogate a large number of genes simultaneously. We sought to evaluate the clinical utility of ctDNA analysis for longitudinal tracking of cancer neoantigen targets and for monitoring of disease status in advanced cancer patients being treated with aDNA personalized cancer vaccine (PCV). Our results also inform the kinetics of somatic variants included in the PCV (neoantigen vaccine targets) as well as the larger set of all variants identified in the tumor (MRD targets).

Methods Patients with unresectable or metastatic HCC with progression on, or intolerance to, first-line therapy with tyrosine kinase inhibitors were enrolled into the Phase Ib/IIa GT-30 study [NCT04251117]. Tumors were biopsied for exome and transcriptome sequencing and a patient-specific neoantigen DNA vaccine (GNOS-PV02) was designed. Patients were treated with GNOS-PV02 (1mg) and DNA plasmid encoded IL-12 (0.34mg) in combination with pembrolizumab (200mg). Treatment response was evaluated by RECIST 1.1. Prospectively collected pre- and post-treatment samples from 17 patients were batched and analyzed by personalized ctDNA assays. Somatic mutation calls were made using Personalis ACE[®] exome data from tumor tissue biopsies. Capture probe panels were designed for the two sets of targets. ctDNA was extracted from the plasma samples; up to 50ng was used as input for deep sequencing. Advanced noise suppression, mutation calling, aggregate tumor tracking and MRD calling was performed using NeXT ctDNA technology.

Results Pre-treatment ctDNA magnitude varied widely across patients for both neoantigen targets and MRD targets. Although analyzed retrospectively, changes in ctDNA magnitude over time correlated well with disease status in most patients. ctDNA broadly tracked with MRI scans for monitoring objective responses (CR and PR). In patients with tumor recurrence and/or emergence of de novo metastatic lesions, an increase in target copy number or mean tumor molecules/ml was detected prior to confirmation by MRI. Patient level data from the ongoing GT-30 clinical trial will be discussed at the meeting.

Conclusions Our analysis indicated that ctDNA can be a useful tool for monitoring disease in a patient specific manner. The ease of sample handling and analysis, and rapid availability of data, could enable the use of ctDNA monitoring to allow real time clinical treatment decision making for personalized cancer immunotherapy.

Trial Registration NCT04251117

Ethics Approval For GT-30 trial, the protocols were approved by Johns Hopkins Medicine Review Boards (CR00039002/IRB00227771), Icahn School of Medicine-Program for the Protection of Human Subjects (20-00076 GCO#1), and Northern A Health and Disability Ethics committee (Ethics ref: 20/NTA), respectively. Written informed consent was obtained from each patient prior to the patient participating in the trial.

<http://dx.doi.org/10.1136/jitc-2022-SITC2022.0692>

693

PERSONALIZED DNA NEOANTIGEN VACCINE (GNOS-PV02) IN COMBINATION WITH PLASMID IL-12 AND PEMBROLIZUMAB AS SECOND-LINE (2L) TREATMENT FOR ADVANCED HEPATOCELLULAR CARCINOMA (HCC)

¹Edward Gane*, ²Mark Yarchoan, ³Thomas Marron, ⁴Sarah Rochestie, ⁴Renzo Perales, ⁴Neil Cooch, ⁴Jian Yan, ⁴Joann Peters, ⁵David Weiner, ⁴Ildiko Csiki, ⁴Alfredo Perales-Puchalt, ⁴Niranjan Sardesai. ¹The University of Auckland, Auckland, New Zealand; ²The Johns Hopkins Hospital, Baltimore, MD, USA; ³The Tisch Cancer Institute, New York, NY, USA; ⁴Geneos Therapeutics, Plymouth Meeting, PA, USA; ⁵The Wistar Institute, Philadelphia, PA, USA

Background Hepatocellular carcinoma (HCC) is a low TMB tumor with largely immune-excluded phenotype. Anti-PD1 monotherapy for 2L HCC has response rates of 12-18%. Therapeutic cancer vaccines targeting neoantigens can generate tumor-specific T-cell immunity, potentially enhancing responses to anti-PD1 therapy. GNOS-PV02 is a personalized cancer DNA vaccine encoding up to 40 patient-specific neoantigens. GT-30 trial is an ongoing single-arm open-label multi-center phase Ib/IIa study to evaluate safety, immunogenicity, and efficacy of GNOS-PV02 administered in combination with plasmid-encoded IL-12 (pIL12) and pembrolizumab.

Methods Patients with unresectable or metastatic HCC and progression or intolerance on first-line therapy with tyrosine kinase inhibitors (sorafenib or lenvatinib) are enrolled. Tumors are biopsied for exome and transcriptome sequencing, peripheral blood is collected for germline sequencing, and a patient-specific vaccine is designed, optimized and manufactured, all in 6-8 weeks. GNOS-PV02 (1mg) and pIL12 (0.34mg) are administered via intradermal injection and electroporation Q3w x 4 doses, Q9w thereafter. Pembrolizumab 200mg is administered IV Q3w. Treatment response is evaluated Q9w by RECIST 1.1. Blood samples are collected pre-treatment, Q3w until w12, then Q12w for immunological analyses. Tumor biopsy is obtained at w9 for TME assessment.

Results As of cutoff date of June 30, 2022, 24 patients were enrolled with median age 66.5 years (range 40-78 years). There were no DLTs, GNOS-PV02+pIL12 related SAEs, or Grade 3 or 4 AEs reported. Two cases of hypothyroidism and immune nephritis, likely immune-mediated were noted, however no increase in irAEs or SAEs was seen with the combination therapy relative to previously known pembrolizumab monotherapy data. ORR (mITT) per RECIST 1.1 was 29.2% (7/24). Disease control rate was 54.2% (13/24) consisting of 2 CR, 5 PR, 6 SD, 10 PD. One patient early-terminated due to a non-treatment-related SAE six days after their sole PCV dose and was deemed unevaluable but included in the mITT analysis. One patient with a radiological PR after five PCV doses achieved secondary resectability, and discontinued therapy to pursue resection without disease recurrence. Novel and expanded T cell clones, predominantly CD8+ with activated phenotype, were identified in all evaluated patients via pre-/post-vaccination analysis of TCR repertoire in peripheral blood and tumor tissue. These clones trafficked to the TME by w9, potentially mediating the observed tumor regressions.

Conclusions GNOS-PV02 + INO-9012 combined with pembrolizumab in the 2L setting was well tolerated and induced tumor-neoantigen-directed CD8+ T cells and TILs. Data to date suggest clinical benefit relative to PD1 monotherapy in patients with advanced HCC.

Trial Registration NCT04251117

Ethics Approval For GT-30 trial, the protocols were approved by Johns Hopkins Medicine Review Boards (CR00039002/IRB00227771), Icahn School of Medicine-Program for the

Protection of Human Subjects (20-00076 GCO#1), and Northern A Health and Disability Ethics committee (Ethics ref: 20/NTA), respectively. Written informed consent was obtained from each patient prior to the patient participating in the trial.

<http://dx.doi.org/10.1136/jitc-2022-SITC2022.0693>

694

AN OPEN-LABEL PHASE I DOSE-ESCALATION CLINICAL TRIAL TO EVALUATE THE SAFETY, TOLERABILITY, PHARMACOKINETIC PROFILE AND PRELIMINARY EFFICACY OF VG161 IN PATIENTS WITH ADVANCED PRIMARY LIVER CANCER

<http://dx.doi.org/10.1136/jitc-2022-SITC2022.0694>

¹Yinan Shen*, ²Guoming Shi, ¹Xingmei Liang, ¹Xinyan Jin, ¹Youlei Wang, ¹Guyue Wei, ²Yi Chen, ²Xiaoyong Huang, ²Jiacheng Lu, ³Huiqun Xia, ³Miao Xiao, ³Shah Rahimian, ³Ronghua Zhao, ¹Yuwei Li, ¹Danni Lin, ¹Tian Fang, ¹Wei Chen, ¹Tao Ma, ¹Xueli Bai, ¹Tingbo Liang. ¹The First Affiliated Hospital, ZJU, Hangzhou, China; ²Zhongshan Hospital, Fudan University, Shanghai, China; ³Virugin Biotech, Vancouver, Canada

Background VG161 is a novel HSV-1 oncolytic virus expressing IL-12, IL-15, IL-15 receptor alpha subunit isoform 1 (IL-15R α), and a PD-1/PD-L1 blocking peptide (TF-Fc). This is to report the preliminary clinical and translational data from 11 efficacy evaluable patients.

Methods In this multicenter phase I trial, we enrolled 11 patients with advanced primary liver cancer refractory to standard therapy including immune checkpoint inhibitor (ICI). VG161 was administrated by imaging guided intra-tumoral injection. Based on preclinical NOAEL, the initial dose level was 1×10^8 PFU/subject, followed with 4 cohorts (1×10^8 , QD for D1 and D2; 1×10^8 , QD for D1-3; 1.3×10^8 , QD for D1-3; and 1.7×10^8 , QD for D1-3). Fast titration design was used for the first 2 cohorts and followed by standard 3 + 3 design. For PK and viral shedding, virus DNA was measured in blood, urine, oral and injection site swabs by a validated PCR test. Changes of cytokines and lymphocyte subsets in blood was also measured. Antitumor activity was assessed by RECIST1.1 and iRECIST. Overall survival (OS) was recorded.

Results Eleven patients (aged from 43-74, 9 males and 2 females; 8 HCC and 3 ICC) were enrolled between April 2021 and January 2022. By 10 May 2022, all patients had at least one tumor assessment. No dose limiting toxicity (DLT) was observed. The most common treatment related adverse event (TRAE) was fever (100%). No dose limiting toxicity (DLT) was observed. One serious adverse events (SAEs), Grade 2 sub-facial paralysis (33.3%) was seen in 1 patient, which is related to study drug, no immune-related adverse events (irSAEs) occurred. One ICC patient in 3rd cohort (9%) had immune partial response (iPR) with PFS of 5.3 month based on both iRECIST and RECIST 1.1. Another 2 patients with HCC in the 1st and 2nd cohort had prolonged PFS of 3.7 and 11.5 months respectively. The levels of each T cell immune-related parameter including PD-L1, PD-1, CD69 and CD8+Ki67^{high} of subjects in each cohort showed an increasing trend after VG161 administration. To date, the median follow-up time is 7.8(2.3-15.6), significantly prolonged OS was seen in 5 patients received ICI after the trial ($p=0.025$).

Conclusions Image guided IT injection of VG161 up to 3 times of 1.7×10^8 PFU/subject was safe and well tolerated, with no unexpected viral spread or shedding. The efficacy of prolonged PFS in 3 patients and PR in 1 patient is encouraging and needs to be further investigated. Clinical trial information: NCT04806464.

Trial Registration NCT04806464

Ethics Approval The study was approved by the Ethics Committee of the First Affiliated Hospital, School of Medicine, Zhejiang University, approval number 20191101.

Consent Written informed consent was obtained from the patient for publication of this abstract and any accompanying images. A copy of the written consent is available for review by the Editor of this journal.

695

IMMUNE CORRELATES ASSOCIATED WITH CLINICAL BENEFIT IN PATIENTS WITH IMMUNE CHECKPOINT REFRACTORY HPV-ASSOCIATED MALIGNANCIES TREATED WITH TRIPLE COMBINATION IMMUNOTHERAPY

<http://dx.doi.org/10.1136/jitc-2022-SITC2022.0695>

Meghali Goswami*, Julius Strauss, Yo-Ting Tsai, Caroline Jochems, Jennifer Marte, James Gulley, Jeffrey Schlom, Renee Donahue. *National Cancer Institute, Bethesda, MD, USA*

Background Globally more than 600,000 cases of HPV-associated cancers occur annually. Approximately 15-20% of cases respond to PD-(L)1 inhibitors, and approximately 30%, including 10% of immune checkpoint inhibitor (ICI) refractory patients, respond to bintrafusp alfa, a bifunctional fusion protein targeting TGF- β and PD-L1. Thus, for most patients who are ICI refractory, there is no effective therapy. Preclinical studies have shown that the triple combination of bintrafusp alfa, M9241, a tumor-targeting IL-12 immunocytokine, and PDS0101, a therapeutic vaccine targeting HPV-16, resulted in maximal tumor reduction. A phase II trial (NCT04287868) evaluating this triple therapy has shown a manageable safety profile and preliminary evidence of clinical activity in ICI refractory HPV-associated cancers, with 45% of patients having disease reduction, including 27% with objective responses.

Methods Peripheral blood from patients with ICI refractory HPV-associated malignancies (n=27) treated with the triple therapy was analyzed prior to and 2 weeks post first treatment (a timepoint prior to restaging) for multiple serum cytokines and soluble factors, complete blood counts, and 158 immune cell subsets. HPV-16 specific T-cells were assessed before and during treatment in a subset of patients (n=14). Immune parameters were evaluated for changes with therapy and compared between patients deriving clinical benefit (with a best overall response of stable disease, partial response, or complete response) versus those with progressive disease (PD).

Results The triple therapy promoted a pro-inflammatory serum cytokine and factor milieu, and significantly increased NK cells (p=0.002) and decreased conventional dendritic cells (cDCs, p=0.001), plasmacytoid DCs (p=0.011), CD4+ T-cells (p=0.008), CD8+ T-cells (p=0.004), T-regulatory-cells (p=0.002), and B-cells (p=0.042). HPV-16 specific T-cells were increased >2 fold after therapy in 11/14 patients evaluated. Before therapy, patients developing clinical benefit from the triple therapy had significantly higher levels of CD8+ naïve T-cells (p=0.037), trends of higher CD8:MDSC ratios (p=0.098), and significantly lower levels of cDCs (p=0.019) and classical monocytes (p=0.049), than patients developing PD. A greater early increase (2 weeks after one treatment cycle) in soluble granzyme B (p=0.004), TNF α (p=0.013), and monocytes (p=0.025), and less of a decrease in cDCs (p=0.006) associated positively with clinical benefit, while trends of an increase in the neutrophil to lymphocyte ratio (p=0.073) associated inversely.

Conclusions These studies interrogating the peripheral immune add insight into the combined mechanism of action of bintrafusp alfa, M9241, and PDS0101 in patients with HPV-associated cancers, and provide valuable information to identify ICI refractory patients potentially more likely to benefit from immunotherapy.

Ethics Approval All patients gave written informed consent for participation. This study was approved by the National Cancer Institute's Institutional Review Board. The trial registration number is NCT04287868.

696

ABATACEPT FOR IMMUNE CHECKPOINT INHIBITOR ASSOCIATED MYOCARDITIS (ATRIUM): A PHASE 3, INVESTIGATOR-INITIATED, RANDOMIZED, DOUBLE BLIND, PLACEBO-CONTROLLED TRIAL

¹Kerry Reynolds*, ¹Meghan Mooradian, ¹Daniel Zlotoff, ²Paul Ridker, ¹Tomas Neilan, On Behalf Of The ATRIUM Investigators. ¹Massachusetts General Hospital, Boston, MA, USA; ²Brigham and Women's Hospital, Boston, MA, USA

Background Patients with myocarditis secondary to treatment with an immune checkpoint inhibitor (ICI) represent a poor prognosis population with a high unmet clinical need. Data from multiple independent international cohorts have shown that the rate of major adverse cardiac events (MACE) with ICI myocarditis despite administration of corticosteroids ranges from 25-50%. Abatacept is a selective co-stimulation modulator that inhibits T cell activation by binding to CD80 and CD86, thereby blocking its interaction with CD28. In case reports, abatacept has been used to treat ICI myocarditis. The use of abatacept in ICI myocarditis is supported by animal models of ICI myocarditis, with the administration of abatacept leading to a reduction in cardiac immune activation and increased survival.

Methods The abatacept for immune checkpoint inhibitor associated myocarditis (ATRIUM) trial is designed as a phase 3, investigator-initiated, randomized, double-blind, placebo-controlled study to evaluate the efficacy and safety of abatacept compared to placebo in 390 hospitalized participants with ICI associated myocarditis. Hospitalized participants diagnosed with ICI-related myocarditis, aged ≥ 18 years, with serum evidence of ongoing myocardial injury (troponin ≥ 5 times the upper limit normal), and treated, or with intent to treat, with 1000 mg of solumedrol/day are eligible. Participants will receive either abatacept (10 mg/kg) or placebo given IV followed by study drug infusion/placebo again at 24 hours and on day 14 with an optional 4th dose on day 28. The primary aim is to test whether abatacept, as compared to placebo, is associated with a reduction in MACE among participants hospitalized with myocarditis secondary to an ICI. The primary outcome, MACE, is a composite of cardiovascular death, non-fatal sudden cardiac arrest, cardiogenic shock, significant ventricular arrhythmias, significant bradyarrhythmias, or incident heart failure. Each component of the primary composite end point will be evaluated individually as a secondary endpoint, as are troponin levels, rates of deep venous thrombosis and pulmonary embolism, and incidence rates of treatment-related adverse events. Exploratory outcomes focus on cancer outcomes, healthcare utilization, quality of life, and correlative studies.

This study is recruiting at time of submission. Clinical trial information: NCT05335928.

Trial Registration

NCT05335928

Ethics Approval The clinical trial protocol has been approved by the Mass General Brigham Institutional Review Board (Protocol #:2021P003690) and all participants will provide informed consent before taking part.

<http://dx.doi.org/10.1136/jitc-2022-SITC2022.0696>

697

A PHASE 1 STUDY OF AMG 119, A DLL3-TARGETING, CHIMERIC ANTIGEN RECEPTOR (CAR) T CELL THERAPY, IN RELAPSED/REFRACTORY SMALL CELL LUNG CANCER (SCLC)

¹Lauren Byers*, ¹John Heymach, ¹Don Gibbons, ¹Jianjun Zhang, ²Alberto Chiappori, ³Erik Rasmussen, ³Benjamin Decato, ³Marie-Anne Smit, ³Nooshin Hashemi Sadraei. ¹MD Anderson Cancer Center, Houston, TX, USA; ²Moffitt Cancer Center, Tampa, FL, USA; ³Amgen Inc., Thousand Oaks, CA, USA

Background AMG 119 is a CAR-T cell therapy that targets delta-like ligand 3 (DLL3), an inhibitory Notch ligand that is expressed on the surface of most SCLC cells. In preclinical studies, AMG 119 specifically lysed DLL3-expressing SCLC cell lines and inhibited tumor growth in SCLC xenograft models.¹

Methods Primary objectives of this open-label, phase 1 study are to determine the safety, tolerability, and optimum cell dose of AMG 119 in adults with relapsed/refractory SCLC who progressed after ≥ 1 platinum-based chemotherapy regimen. Safety, efficacy, pharmacokinetics, and biomarkers were assessed.

Results At data cutoff, 5 adult subjects (median age: 59 years [range, 33-64], ECOG status: 0-1, ≥ 1 prior line of anticancer therapy) had received at least 1 intravenous infusion of AMG 119 as part of cohort 1 (n = 3; 3×10^5 cells/kg) or cohort 2 (n = 2; 1×10^6 cells/kg) in the dose exploration phase. One subject in cohort 1 and both subjects in cohort 2 were re-treated with a second dose.

Post-infusion, a grade 1 treatment-related adverse event (TRAE) was noted in 1 subject (seizure), grade 2 TRAEs in 2 subjects (anemia and supraventricular tachycardia), and a grade 3 TRAE in 1 subject (pneumonitis; cohort 1). No dose-limiting toxicities or grade 4/5 TRAEs were observed.

Among evaluable subjects (n=4), a confirmed partial response (PR) was seen in 1 subject (cohort 2) 1.1 months after the first dose. Two subjects had stable disease, including 1 subject who experienced a 16% decrease in sum of the target lesions from baseline. One subject had progressive disease. Median progression-free survival was 3.7 months (range, 1.1-6.7) and median overall survival was 7.4 months (range, 4.6-18.9).

AMG 119 exhibited peak expansion 1-3 weeks after infusion; CAR-T cells were detectable up to 86 days in both cohorts. A preliminary dose-response relationship was observed with higher CAR-T cell expansion (~ 14 -fold increased C_{max} and AUC_{0-28d}) in the subject with confirmed PR compared with the nonresponder (cohort 2). DLL3 expression was detected by immunohistochemistry on $>85\%$ of tumor cells in all evaluable subjects at all assessed timepoints. Changes in serum/whole blood markers were consistent with a pharmacodynamic response. The subject who achieved PR exhibited a rapid decline in total circulating tumor cell levels within 7 days of treatment initiation.

Conclusions AMG 119, the first CAR-T cell therapy for SCLC, was associated with a manageable safety profile and promising anti-tumor activity. Enrollment is currently paused but may resume.

Acknowledgements The authors would like to acknowledge Vijay Upreti, Di Zhou, Beate Sable, and Amrita Pati (all Amgen) for their contributions to this study and abstract.

Trial Registration NCT03392064

REFERENCE

1. Byers LA, Chiappori A, Damiette Smit MA. Phase 1 study of AMG 119, a chimeric antigen receptor (CAR) T cell therapy targeting DLL3, in patients with relapsed/refractory small cell lung cancer (SCLC). *J Clin Oncol*. 2019;**37**:15_suppl. doi:10.1200/JCO.2019.37.15_suppl.TPS8576.

Ethics Approval This human study was approved by the Moffitt Cancer Center's Institutional Review Board (IRB Approval Number 00000971) and MD Anderson Cancer Center's Institutional Review Board (Ethics Board Approval Number: 2017-1072).

<http://dx.doi.org/10.1136/jitc-2022-SITC2022.0697>

698

A PHASE 2 STUDY OF DURVALUMAB COMBINED WITH CHEMOTHERAPY AND STEREOTACTIC BODY RADIOTHERAPY (SBRT) IN PATIENTS WITH OLIGOMETASTATIC NON-SMALL CELL LUNG CANCER (NSCLC) (SABRCURE TRIAL)

¹Ming Chen*, ²Honglian Ma, ²Xianghui Du, ²Yujin Xu, ²Yongling Ji, ²Zhengbo Song, ¹Sun Yat-sen University Cancer Center, Guangzhou, China; ²Zhejiang Cancer Hospital, Hangzhou, China

Background Immunotherapy +/- chemotherapy is currently the standard of care for metastatic NSCLC, but strategies to expand the benefit are still needed. Oligometastatic NSCLC is a state of limited disease in which widespread metastasis has not yet evolved. Locally radiotherapy achieves prolonged progression-free survival and overall survival in a small proportion of well selected oligometastatic NSCLC patients¹. Preliminary evidence suggests high dose fractionated radiotherapy, such as SBRT, in combination with systemic immunotherapy has a synergistic effect and may enhance survival². Durvalumab (PD-L1 antibody) is approved as consolidation therapy for unresectable, locally advanced NSCLC who have not progressed following chemoradiotherapy. These findings support further investigation of durvalumab + SBRT combinations in oligometastatic NSCLC who received standard systematic therapy.

Methods SABRCURE is an open-label, phase 2 study evaluating the efficacy and safety of durvalumab combined with SBRT and chemotherapy in oligometastatic stage IV NSCLC. Key eligibility criteria include no more than 5 metastatic lesions in up to 3 organs, EGFR/ALK/ROS1 wild type, no previous systemic therapy or brain metastases. Forty patients will be enrolled and receive durvalumab 1500mg + platinum-doublet chemotherapy every 3 weeks for 4 cycles, and then durvalumab 1500mg every 4 weeks monotherapy until disease progression or up to 24 months. Patient without progression after 4 cycles durvalumab + chemotherapy will receive stereotactic body radiotherapy. SBRT will be started within 2 weeks after chemotherapy completion and administered to primary lesion and all known metastatic lesions, with a total dose of 50-60Gy in ≤10 fractions. The primary endpoint is progression free survival (PFS) per RECIST v1.1. Secondary end points are objective response rate (ORR), overall survival (OS), safety and treatment failure pattern. This study was funded by AstraZeneca China.

Trial Registration NCT04255836

REFERENCES

1. Gomez DR, Tang C, Zhang J, *et al.* Local consolidative therapy vs. maintenance therapy or observation for patients with oligometastatic non-small-cell lung cancer: long-term results of a multi-institutional, phase II, randomized study. *J. Clin. Oncol.* 2019;**37**(18):1558.
2. Azghadi S, Daly ME. Radiation and immunotherapy combinations in non-small cell lung cancer. *Cancer Treatment and Research Communications.* 2021;**26**:100298.

Ethics Approval This study was approved by Cancer Hospital of the University of Chinese Academy of Sciences Ethics Committee.

Consent Written informed consent was obtained from the patient for publication of this abstract.

<http://dx.doi.org/10.1136/jitc-2022-SITC2022.0698>

699

INTERIM RESULTS FROM A PHASE IB, FIRST-IN-HUMAN STUDY OF A NOVEL COMPLEMENT FACTOR H INHIBITOR (GT103) IN PATIENTS WITH REFRACTORY NON-SMALL CELL LUNG CANCER (NSCLC)

¹Jeffrey Clarke*, ¹Thomas Stinchcombe, ¹Jeffrey Crawford, ²Hirva Mamdani, ¹Lin Gu, ¹Neal Ready, ¹Andrew Nixon, ¹Stephen Baleviic, ¹Michael Campa, ¹Liz Gottlin, ¹Ryan Bushey, ¹James Herndon, ¹Scott Antonia, ³Edward Patz, ⁴George Simon. ¹Duke University Medical Center, Durham, NC, USA; ²Maranos Cancer Institute, Detroit, MI, USA; ³Grid Therapeutics; Duke University, Durham, NC, USA; ⁴H Lee Moffitt Cancer Center, Tampa, FL, USA

Background Complement factor H (CFH) modulates immune self-recognition and complement mediated cytotoxicity by regulating the alternative pathway of the complement cascade. Overexpression of CFH can facilitate immune evasion and is associated with poor prognosis in NSCLC. Discovery of CFH autoantibodies in patients with early-stage lung cancer led to the development of GT103, a first-in-class IgG3 monoclonal antibody inhibitor of CFH which has demonstrated preclinical anti-tumor activity.

Methods We conducted a multi-institutional, first-in-human, phase Ib study of GT103 in patients with advanced, refractory NSCLC. A standard '3+3' dose escalation schema was utilized with four dose levels of GT103 (0.3, 1, 3, 10 mg/kg) administered IV every 3 weeks until disease progression or unacceptable toxicity. The dose limiting toxicity (DLT) observation period included cycle 1 and radiographic disease assessment using RECIST 1.1 was performed before every third cycle. Three additional patients were enrolled at the highest dose level to confirm the maximum tolerated dose. We present the interim results of the dose escalation portion of the trial.

Results Twenty-one patients were enrolled and received protocol treatment. Median age was 63 years (range 50-78). All 21 patients had stage 4 disease, 81% had received prior immunotherapy, 8 patients (38%) had known brain metastases, and a majority of patients had adenocarcinoma histology (67%). Median number of prior lines of therapy was 3 (range 2-8). DLT was observed in 2 patients; one patient at the 0.3 mg/kg dose level experiencing grade 3 acute kidney injury and one patient at 1 mg/kg dose level experiencing grade 2 colitis. No DLT was observed at the 3 and 10 mg/kg dose levels. Six patients (28%) experienced grade 2 or higher treatment-related adverse events. In addition to DLTs, treatment related grade 2-3 adverse events included grade 2 anorexia (n=1), grade 2 colitis (n=1), grade 2 and grade 3 lymphopenia (n=2), grade 2 creatinine increase (n=1), and grade 2 psoriasis flare (n=1). Stable disease was demonstrated in 5/21 (24%) patients and no objective responses were seen. The median progression-free survival observed was 42 days (95% CI: 40-NE) and the median number of cycles of treatment received was 2 (range 1-8). Updated pharmacokinetic data and correlative analyses of circulating biomarkers will be presented at time of the meeting.

Conclusions GT103 was well tolerated during dose escalation including at the 10 mg/kg level and demonstrated an acceptable safety profile in refractory NSCLC population. A separate phase 2 study of combination GT103 with anti-PD1 therapy is planned in NSCLC.

Acknowledgements The authors appreciate the efforts of the Data and Safety Monitoring Board members: Dr. Mary Redman, Dr. Shirish Gadgeel, and Dr. Martin Edelman.

Trial Registration ClinicalTrials.gov Identifier: NCT04314089

Ethics Approval All participants underwent informed consent and the study was approved by Duke University IRB with approval number Pro00104564.

<http://dx.doi.org/10.1136/jitc-2022-SITC2022.0699>

700

LUCA-MERIT-1: FIRST-IN-HUMAN OPEN LABEL DOSE CONFIRMATION TRIAL EVALUATING SAFETY, TOLERABILITY, AND EFFICACY OF BNT116 ALONE AND IN COMBINATIONS IN PATIENTS WITH ADVANCED NON-SMALL CELL LUNG CANCER

¹Patrick Forde, ²Akin Atmaca, ³Neru Munshi*, ⁴Malgorzata Kaczorowska, ⁴Patrick Brueck, ⁴Thomas Schell, ⁴Oezlem Tuereci, ⁴Ugur Sahin. ¹Johns Hopkins University, Baltimore, MD, USA; ²Krankenhaus Nordwest, Frankfurt a.M., Germany; ³BioNTech US, Cambridge, MA, USA; ⁴BionTech SE, Mainz, Germany

Background Lung cancer is the leading cause of cancer deaths worldwide.¹ The diagnosis of non-small cell lung cancer (NSCLC) is often made when the disease is already advanced or metastatic (Stage IIIB/IV).² The approved Programmed Cell Death protein 1/Programmed Cell Death Ligand 1 (PD-1/PD-L1) inhibitors have demonstrated substantial anti-tumor activity; however, a majority of patients do not respond to therapy or only respond for a limited time.³⁻⁷ BNT116 is an intravenously (IV) administered cancer immunotherapy consisting of a mixture of six liposomally formulated ribonucleic acids (RNA) each of which encodes for a different tumor-associated antigen. BNT116 alone or in combination with either docetaxel or the PD-1 inhibitor cemiplimab (Libtayo[®]) may have synergistic anti-tumor effects, thus potentially addressing the unmet medical need of these cancer patients.

Methods The trial comprises four cohorts, each with a single-step dose confirmation using a 3+3 design in both monotherapy and in combinations followed by an expansion phase including up to 20 patients in each cohort. Depending on the cohort, patients with histologically confirmed unresectable or metastatic NSCLC, measurable disease by Response Evaluation Criteria in Solid Tumors (RECIST) 1.1 and the ability to tolerate additional PD-1 inhibitor therapy are included. In all cohorts, the first dose of BNT116 is given at 60 µg total RNA (Cycle 1 Day 1 [C1 D1]). Depending on Safety Review Committee decisions, all subsequent doses of 90 µg total RNA are given once weekly for the initial 7 weeks followed by every 3-week (Q3W) dosing on Day 1 of each cycle. Cemiplimab (350 mg) may be added at the discretion of the investigator in Cohort 1 after the second cycle. Patients in cohort 2 and 4 receive cemiplimab starting with C1 D1. Docetaxel will be administered at the approved dose of 75 mg/m² IV Q3W on Day 2 of each cycle (Cohort 3). Primary endpoints are occurrence of dose limiting toxicities and adverse events coded using MedDRA[®] assessed according to National Cancer Institute – Common Terminology Criteria for Adverse Events v5.0. Secondary endpoints are related to clinical activity, e.g., tumor assessments, as per RECIST 1.1.

The first patient was dosed in JUL 2022, with enrolment expected for approximately 12 months.

The study was approved by IRB/IEC, approval numbers: 2022-03/1691 (Turkey), OGYÉI/6962-9/2022 (Hungary), and US and Spain (approval numbers for the later were not provided).

Acknowledgements This trial is sponsored by BioNTech SE. The authors would like to acknowledge Suma Guttal for medical writing support.

Trial Registration IND 27908, EudraCT: 2021-004739-94, NCT05142189

REFERENCES

1. American Cancer Society 2020. About lung cancer. <https://www.cancer.org/content/dam/CRC/PDF/Public/8703.00.pdf>.

2. Morgensztern D, Ng SH, Gao F, *et al.* Trends in stage distribution for patients with non-small cell lung cancer: A National Cancer Database Survey. *J Thorac Oncol.* 2010;**5**(1):29–33.
3. Opdivo[®] PI 2019 (Prescribing information) https://www.accessdata.fda.gov/drug-satfda_docs/label/2019/125554s070lbl.pdf.
4. Keytruda[®] PI 2019 (Prescribing information) https://www.accessdata.fda.gov/drug-satfda_docs/label/2019/125514s040lbl.pdf.
5. Tecentriq[®] PI 2019 (Prescribing information) https://www.accessdata.fda.gov/drug-satfda_docs/label/2019/761034s019lbl.pdf.
6. Imfinzi[®] PI 2019 (Prescribing information) https://www.accessdata.fda.gov/drug-satfda_docs/label/2018/761069s002lbl.pdf.
7. Libtayo[®] PI 2021 (Prescribing information) https://www.accessdata.fda.gov/drug-satfda_docs/label/2021/761097s007lbl.pdf

Ethics Approval The study was approved by IRB/IEC, approval numbers: 2022-03/1691 (Turkey), OGYÉI/6962-9/2022 (Hungary), and US and Spain (approval numbers for the later were not provided).

<http://dx.doi.org/10.1136/jitc-2022-SITC2022.0700>

701

BRIGHTPLEX® TCE AND BRIGHTPLEX® MDSC ASSAYS COMBINATION IMPROVES ADVANCED NSCLC PATIENTS' STRATIFICATION UNDER ANTI-PD1/L1 IMMUNOTHERAPY IN THE PIONEER PROJECT

¹Lamia Ghezali, ¹Marcellin Landri, ¹Florence Monville, ¹Vanina Leca, ¹Théo Vasse, ¹Chafik Hamdad, ¹Margaux Mercadal, ¹Laurent Vanhille, ¹Alboukadel Kassambara, ¹Thomas Sbrarato, ²Maryannick Le Ray, ³Marie Roumieux, ²Richard Malkoun, ⁴Noémie Resseguier, ⁵Amaud Boyer, ⁶Clarisse Audigier-Valette, ⁷Stephanie Martinez, ⁸Hervé Pegliasco, ⁹Patrice Ray, ¹⁰Lionel Falchero, ¹¹Antoine Serre, ¹²Nicolas Cloarec, ¹³Louisiane Lebas, ¹⁴Stéphane Hominal, ¹⁵Patricia Barré, ¹⁶Sarah Zahi, ¹⁷Ahmed Frikha, ¹⁸Pierre Bory, ¹⁹Lilian Laborde, ²⁰Julien Mazières, ¹⁹Virginie Martin, ²⁰Julien Mazières, ²¹Maurice Pérol, ⁴Laurent Greillier, ²²Fabrice Barlesi, ¹Jacques Fieschi*. ¹Veracyte, Marseille, France; ²APHM, Marseille, France; ³Aix Marseille Université, Marseille, France; ⁴Aix Marseille Université, APHM, Marseille, France; ⁵Hôpital Saint-Joseph, Marseille, France; ⁶Centre Hospitalier Sainte-Musse, Toulon, France; ⁷Centre Hospitalier d'Aix-en-Provence, Aix-en-Provence, France; ⁸Hôpital Européen, Marseille, France; ⁹CHU de Nîmes, Nîmes, France; ¹⁰Hôpital Nord-Ouest, Villefranche-sur-Saône, France; ¹¹Institut Cancerologie du Gard, Oncogard, Nîmes, France; ¹²Centre hospitalier Henri Duffaut, Avignon, France; ¹³Centre Hospitalier du Val d'Arriège, St Jean de Verges, France; ¹⁴Centre Hospitalier Annecy Genevois, EPAGNY-METZ TESSY, France; ¹⁵Centre Hospitalier Jean Rougier, Cahors, France; ¹⁶Centre Hospitalier de Montauban, Montauban, France; ¹⁷Polyclinique Maynard, Bastia, France; ¹⁸Centre Hospitalier de Bastia, Bastia, France; ¹⁹Institut PAOLI-CALMETTES, Marseille, France; ²⁰Hopitaux de Toulouse, Toulouse, France; ²¹Centre Leon Berard, Lyon, France; ²²Gustave Roussy, Aix Marseille Université, Villejuif, France

Background Immune Checkpoint Inhibitors (ICIs) are associated with long-term survival in ~20% of advanced NSCLC patients while biological mechanisms triggering resistance are not fully elucidated. Myeloid-Derived Suppressor Cells (MDSC) might however play a key role. The PIONEER project (NCT03493581, ANR-17-RHUS-0007) aims to predict the response/resistance to PD1/L1 ICIs in advanced NSCLC patients through comprehensive agnostic multiparametric biomarker assessment. Here, the combination of both lymphoid and myeloid lineages infiltration in the tumor is evaluated on tissue collected at diagnosis to predict outcome.

Methods Tumor samples from 60 advanced NSCLC patients, all ECOG PS0/1, treated with standard PD1/L1 monotherapy as ≥2nd line of treatment were studied. PD1/L1 ICIs Overall Response Rate was assessed by RECIST 1.1. Multiplex IHC assay Brightplex® TCE (former Immunoscoring® CR T cells exhaustion) quantifies T-lymphocytes allowing tumor stratification into 4 groups: Hot, Parenchyma Hot, Cold and tumors with Stromal TILs. ¹Brightplex® MDSC assay quantifies myeloid cells (monocytes, neutrophils and other granulocytes), Monocytic- (M-) and PolyMorphoNuclear- (PMN-) MDSC. Correlation analyses: spearman non-parametric test. Association between biomarkers: Fisher's exact test. Samples' classification: unsupervised neural-network-based machine learning algorithm Self-Organizing Maps (SOM). Statistical significance of overall (OS) and progression-free survival (PFS) differences between groups: log-rank test.

Results Patients were mainly male (60%), smokers (98.33%), <70yrs (71.66%), median PFS was 3.9 months. Across the 60 tumors, M-MDSC were not correlated to any other cell type while PMN-MDSC were negatively correlated to Monocytes (R=-0.28) and highly correlated to granulocytes (R=0.85), even more when removing neutrophils (R=0.93). SOM clustering on myeloid cells alone did not allow any patients stratification regarding PFS nor OS. Considering previously described patient groups through Brightplex® TCE [1], the 20 "Hot tumors", with high T-cells infiltration initially presenting the best PFS (median PFS=8.1months) were split into 2 groups. Patients' subgroup with high PMN-MDSC and granulocytes tumor infiltration included no responder and had poor

survival: 20% PFS at 20months vs 70% (p=0.035) in patients with low-infiltrated tumors, which included the 3 responders. Interestingly, in the 17 "Cold tumors", high infiltration of PMN-MDSC and granulocytes also identified 5 patients with worse prognostic: at 2.5 months, only 20% PFS vs 58% in the low-density group (NS) (table 1).

Conclusions Brightplex® TCE and MDSC assays in combination allowed the stratification of advanced NSCLC patients in 5 subgroups, among which two subgroups with poor outcome and no responder, representing 45% of the total population that would likely not benefit from anti-PD1/L1 monotherapy.

Acknowledgements This work is supported by French National Research Agency (ANR-17-RHUS-0007), a partnership of AMU, APHM, AstraZeneca, Centre Léon Bérard, CNRS, Veracyte, ImCheck Therapeutics, Innate Pharma, Inserm, Institut Paoli Calmettes and sponsored by APHM. Drug supply is funded by AstraZeneca. Special thanks to patients and families.

Trial Registration

NCT03493581 REFERENCES

1. Leca V, Kassambara A, Ghezali L. Spatial distribution of infiltrating T lymphocytes with Immunoscoring® CR T cells exhaustion test helps stratification of NSCLC patients treated with PD1/PDL1 inhibitors in the PIONEER project. *JITC*. 2021;9

Ethics Approval The study is conducted in accordance with Good Clinical Practice and the French applicable regulatory requirements (Public Health Code, article L.1121-1/La loi n° 2012-300 du 5 mars 2012 relative aux recherches impliquant la personne humaine (dite loi Jardé), the applicable subject privacy requirements, and the ethical principles that are outlined in the Declaration of Helsinki. The study was approved by the French Ethic Committee, CPP Ouest II – Angers, ref. CPP: 2028/08, Ref ANSM (French competent authority) 2018020500208, 2018072600120, 2019083000148. Freely given written informed consent was signed and obtained from each individual participating in the study, before any study specific procedure was undertaken and after the provision of information about the study by the investigator during a physician-patient consultation and sufficient time for reflection.

Abstract 701 Table 1 Advanced NSCLC stratification according to tumor infiltration by T-lymphocytes, PMN-MDSC+Granulocytes and correlation to survival

Spatial TILs classification according to Brightplex® TCE assay [1]	Hot tumors ¹		Cold tumors ¹	
	n = 20 Median PFS: 8.1 months 20 months OS: 70% Responders: n = 3		n = 17 Median PFS: 1.7 months 20 months OS: 23% Responders: n = 0	
PMN-MDSC and Granulocytes infiltration status according to Brightplex® MDSC assay	High	Low	High	Low
	n = 10 20 months PFS: 20% 20 months OS: 35% Responders: n = 0	n = 10 20 months PFS: 70% 20 months OS: 100% Responders: n = 3	n = 5 2.5 months PFS: 20% 2.5 months OS: 40% Responders: n = 0	n = 12 2.5 months PFS: 58% 2.5 months OS: 83% Responders: n = 0

1: Spatial distribution of infiltrating T lymphocytes with Immunoscoring® CR T Cells Exhaustion test helps stratification of NSCLC patients treated with PD1/PDL1 inhibitors in the PIONEER project, Leca et al., SITC 2021

<http://dx.doi.org/10.1136/jitc-2022-SITC2022.0701>

Abstracts

702

TERTIARY LYMPHOID STRUCTURES (TLS) OBSERVED IN NON-SMALL CELL LUNG CANCER (NSCLC) TUMORS TREATED WITH PULSED ELECTRIC FIELDS

¹Jeff Iding, ²Paul VanderLaan, ³Marcelo Jimenez, ³José Fernández García-Hierro, ⁴Javier Flandes Aldeyturriaga, ³Erik HFM van der Heijden, ⁶Calvin SH Ng, ⁶Rainbow WH Lau, ³Maria Ludeña, ⁴Rafael Carías, ⁴Oderay Cedeño, ⁷Alicia Moreno-Gonzalez, ⁷Beryl Hatton, ⁷William Krinsky*. ¹MedStar Health and affiliated hospitals, Baltimore, MD, USA; ²Board-Certified Anatomic Pathologist, Boston, MA, USA; ³Hospital Universitario de Salamanca, Salamanca, Spain; ⁴Hospital Universitario Fundación Jiménez, Madrid, Spain; ⁵Radboudumc, Nijmegen, Netherlands; ⁶The Chinese University of Hong Kong, Hong Kong, China; ⁷Galvanize Therapeutics, San Carlos, CA, USA

Background Tertiary lymphoid structures (TLS) may develop in non-lymphoid tissues in response to a variety of different stimuli and can serve as foci for generating anti-tumor immunity.¹ TLS formation is emerging as a strong prognostic and predictive biomarker² associated with patient survival benefits in NSCLC.^{3,4} Pulsed Electric Fields (PEF) have been reported to induce an immunogenic form of cell death and thus may enhance adaptive immunity in the setting of cancer. The treat-and-resect INCITE ES study enrolled adults with suspected or confirmed NSCLC stage IA2-IB (>1 to ≤4 cm) and without a history of treatment for cancer within the previous two years. **Methods** The INCITE ES study design includes both control and treatment groups with 8 enrolled control group subjects and 30 enrolled treatment group subjects. Treatment group subjects received PEF (Aliya™ System, GTI-00018 investigational device; Galvanize Therapeutics, San Carlos, CA) either percutaneously or endoscopically at time of biopsy prior to surgical resection. Blood, bronchoalveolar lavage (BAL) when applicable, and tissue samples were collected over the course of the study for appropriate pre- and post-PEF comparison.

Serial histologic sections were obtained from an initial cohort of 12 patients (n=1 control, n=11 treatment group) on the day of surgery 17-21 days post-PEF delivery, stained for standard H&E as well as duplex stained for pan-cytokeratin (panCK) and CD20, and reviewed by an independent pathologist.

Results TLS were identified and characterized according to their maturity and localization within or adjacent to the tumor (see criteria in Table 1). Intratumor TLS were observed admixed among tumor cells or within the invasive margin (figures 1 to 5), including within the cellular depletion zone induced by PEF (figures 6 and 7). Independent of tumor morphology, a significant quantity of 49.8 ± 55.8 TLS per tumor was observed post-PEF (n=11, average \pm S.D.). TLS across treated tumors showed varying proportions of mature vs. immature TLS, using the criteria in Table 1. No TLS were identified in the available pre-PEF biopsy specimens (figures 2 and 8). TLS density was greater in PEF specimens compared to the non-treated control, where only three immature TLS were observed (figure 9).

Conclusions This initial cohort suggests that PEF may induce the formation of TLS within the tumor, including proximal to the PEF delivery zone. The observed density and detection of mature TLS may suggest ongoing immune activity. As such, PEF has the potential to induce or enhance an immune response irrespective of tumor morphology.

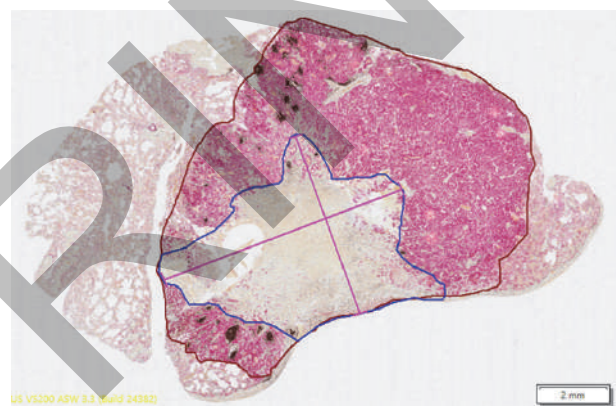
Trial Registration The study is registered on clinicaltrials.gov (NCT04732520).

REFERENCES

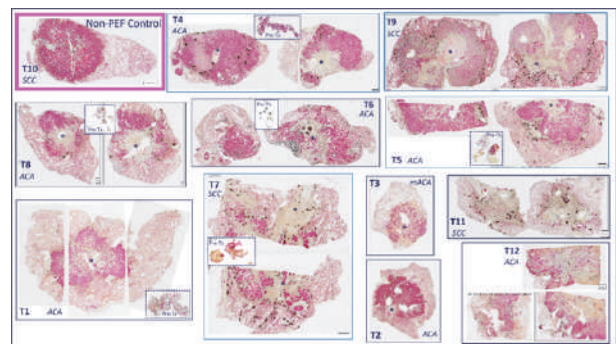
1. Schumacher TN, Thommen DS. Tertiary lymphoid structures in cancer. *Science*. 2022;**375**(6576):eabf9419.

2. Petitprez F, de Reynies A, Keung E. B cells are associated with survival and immunotherapy response in sarcoma. *Nature*. 2020;**577**(7791):556–560.
3. Sautès-Fridman C, Petitprez F, Calderaro J. Tertiary lymphoid structures in the era of cancer immunotherapy. *Nat Rev Cancer*. 2019;**19**:307–325.
4. Cottrell TR, Thompson ED, Forde PM. Pathologic features of response to neoadjuvant anti-PD-1 in resected non-small-cell lung carcinoma: a proposal for quantitative immune-related pathologic response criteria (irPRC). *Ann Oncol*. 2018;**29**(8):1853–1860.

Ethics Approval This abstract discusses the INCITE ES clinical study. Participants gave informed consent before taking part in the study. The study obtained ethics approval from the Ethics Committee for Research with Drugs (CEIm) of the Salamanca Health Area (Salamanca, Spain, reference 20/1615 (E.C.P.S.), Committee on Research Involving Human Subjects (CMO) of Radboud University Medical Center (Nijmegen, the Netherlands, NL76406.091.21), and the Joint Chinese University of Hong Kong – New Territories East Cluster Research Ethics Committee (Hong Kong SAR, reference 2021.294-T).

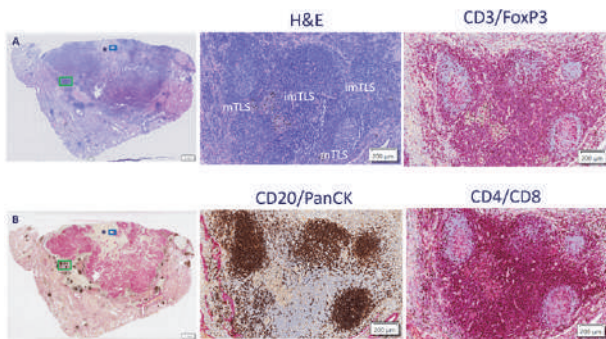


Abstract 702 Figure 1 Example of outlined resected tumor region and CDZ post-PEF. Tumors were resected post PEF delivery and underwent immunostaining. The duplex staining with PanCK (pink) identifies epithelial cells and CD20+ B cells (brown). Areas of dense pink coloration are tumor and the remaining tissue is non-cancerous lung parenchyma. The residual tumor area is outlined in maroon to the leading tumor edge adjacent to non-cancerous lung parenchyma. The PEF-induced cellular depletion zone (CDZ) is outlined in blue. On average, the CDZ measures 0.9 ± 0.3 cm (longest dimension) by 0.6 ± 0.2 cm (longest perpendicular dimension) after a single PEF delivery (n=9).

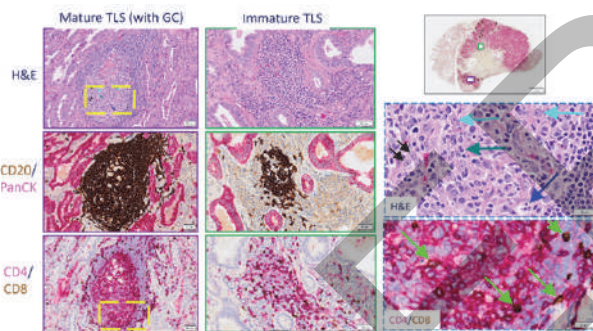


Abstract 702 Figure 2 Compilation of resected NSCLC tumors from INCITE ES study. Tumors underwent duplex PanCK and CD20+ staining. One non-treatment control specimen resected 35 days post biopsy is included (T10). Tumors after a single delivery of PEF energy were resected 17 to 21 days after PEF. Inset images are of pre-PEF biopsy specimens with duplex stain, when available. Colored asterisk (*) in each image denotes the estimated location of the cellular depletion

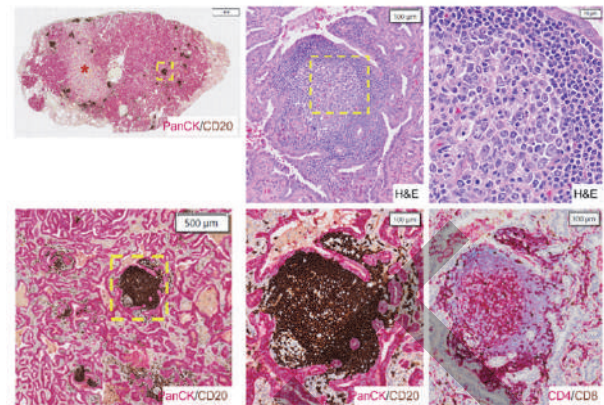
zone. Acronyms ACA, mACA, and SCC indicate tumor histopathology adenocarcinoma, mucinous adenocarcinoma, and squamous cell carcinoma, respectively.



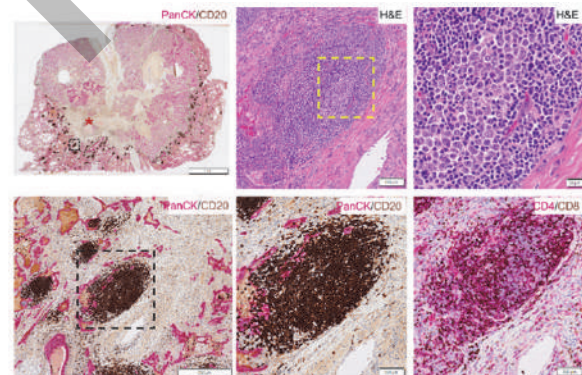
Abstract 702 Figure 3 TLS in tumor periphery 19 days after a single PEF delivery. Representative H&E and IHC images of a right upper lobe tumor. Characterization of the TLS indicates presence of CD20+ B cells (brown), CD3+ T-cells (red), FoxP3+ regulatory T-cells (Tregs, brown), CD4+ helper T-cells (red) and cytotoxic CD8+ T-cells (brown). Higher magnification images of the area denoted by the green box in A and B show two mTLS and two immature imTLS. Asterisks (*) in images shown in A and B denote the estimated location of the cellular depletion zone.



Abstract 702 Figure 4 Mature and immature TLS in a tumor post-PEF energy delivery. Representative H&E and IHC images of a left lower lobe tumor. Purple-outlined (left column) and green-outlined (middle column) boxes representing mature TLS (mTLS) and immature TLS (imTLS), respectively, are higher power magnification of the specimen sampled at approximately 7 o'clock and 12 o'clock, respectively, in the wide field view (upper right). Both mTLS and imTLS are identified by a collection of dense, small CD20+ B cells (brown, middle row), generally juxtaposed with T cell aggregate (CD4+ helper T-cells (red) and cytotoxic CD8+ T-cells (brown), bottom row). The mTLS contains a germinal center (GC) discernable via H&E. The center of the GC is shown in the right column (yellow-dashed outline represents area of higher magnification) to identify dendritic cells (black arrows) and CD8+ T-cells (bright green arrows). Mature CD20+ B cells within the GC exhibit the characteristic morphology of proliferating centroblasts (cyan arrows) and centrocytes (dark green arrow). A GC may also contain tingible body macrophages (dark blue arrow) licensed for phagocytosis by follicular dendritic cells within the germinal center.

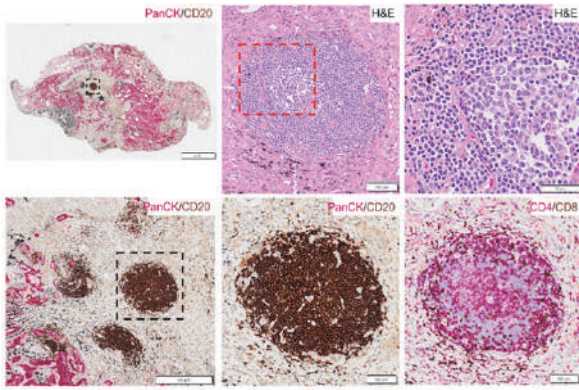


Abstract 702 Figure 5 Representative mature TLS located intratumorally post-PEF. Images were captured from duplex PanCK and CD20, duplex CD4 and CD8, and H&E-stained tissue sections of tumor T4. The whole tissue from the resection sample is shown with red asterisk (*) denoting the estimated location of the cellular depletion zone and the yellow dashed box indicating the mTLS within the tumor bed that is shown at higher magnification as indicated in subsequent image panels. The mTLS contains a germinal center (GC) discernable via H&E. The high magnification image of the region denoted by the dashed yellow box in the H&E image demonstrates mature CD20+ B cells within the GC exhibiting the characteristic morphology of proliferating centroblasts and centrocytes. Accumulation of CD4+ and CD8+ T cells can be seen within and surrounding the mTLS.

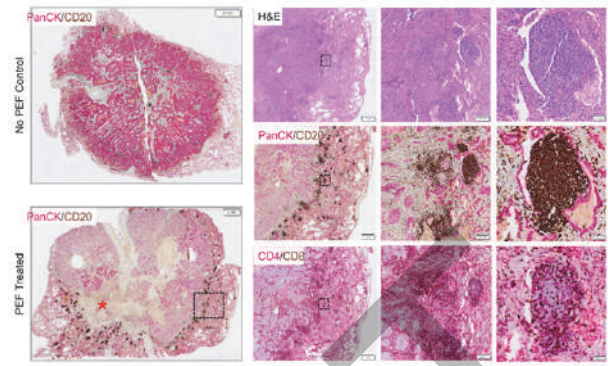


Abstract 702 Figure 6 A mature TLS located at the CDZ-lung parenchyma interface. Images were captured from duplex PanCK and CD20, duplex CD4 and CD8, and H&E-stained tissue sections of tumor T9. The whole tissue from the resection sample is shown with the red asterisk (*) denoting the estimated location of the CDZ and the black dashed box indicating the mTLS that is shown at higher magnification as indicated in subsequent image panels. The mTLS contains a germinal center (GC) discernable via H&E. The high magnification image of the region denoted by the dashed yellow box in the H&E image demonstrates mature CD20+ B cells within the GC exhibiting the characteristic morphology of proliferating centroblasts and centrocytes. Accumulation of CD4+ and CD8+ T cells can be seen within and surrounding the mTLS.

Abstracts

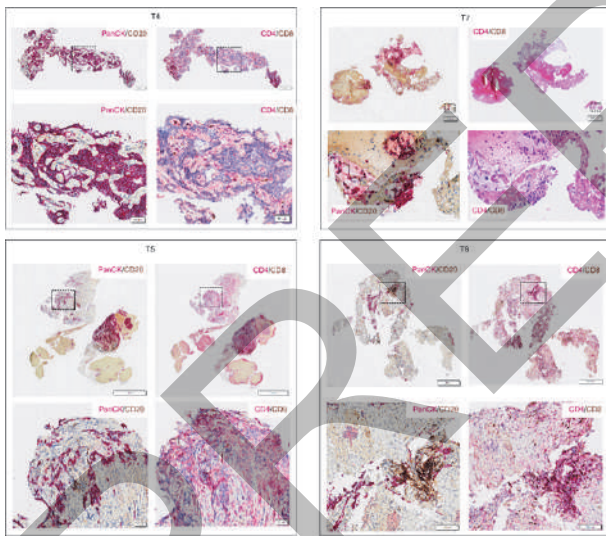


Abstract 702 Figure 7 A mature TLS located within the cellular depletion zone (CDZ). Images were captured from duplex PanCK and CD20, duplex CD4 and CD8, and H&E-stained tissue sections of tumor T6. The whole tissue from the resection sample is shown with the black asterisk (*) denoting the estimated location of the CDZ and the black dashed box indicating the mTLS within the CDZ that is shown at higher magnification as indicated in subsequent image panels. The mTLS contains a germinal center (GC) discernable via H&E. The high magnification image of the region denoted by the dashed red box in the H&E image demonstrates mature CD20+ B cells within the GC exhibiting the characteristic morphology of proliferating centroblasts and centrocytes. Accumulation of CD4+ and CD8+ T cells can be seen within and surrounding the mTLS.



Abstract 702 Figure 9 TLS accumulation in PEF-treated tumor and control tumor. Non-PEF control (T10) and a PEF-treated (T9) demonstrating the accumulation of TLS at the tumor periphery in the PEF-treated sample. Images were captured from duplex PanCK and CD20, duplex CD4 and CD8, and H&E-stained tissue sections. The whole tissue from the resection sample is shown with the red asterisk (*) denoting the estimated location of the CDZ in the PEF-treated sample, and the black dashed box indicating an imTLS that is shown at the invasive tumor margin at higher magnification as indicated in subsequent image panels (right). Accumulation of CD4+ and CD8+ T cells can be seen within and surrounding the imTLS.

<http://dx.doi.org/10.1136/jitc-2022-SITC2022.0702>



Abstract 702 Figure 8 Representative pre-PEF tumor biopsy specimens. Images were captured from duplex PanCK and CD20 and duplex CD4 and CD8 stained tissue sections of tumors T4, T5, T7, and T8. The black dashed box indicates the region of the tissue at shown at higher magnification in the lower panels for each sample. While some CD20+ staining is evident in the pre-treatment biopsy from sample T8, this did not meet the criteria for being considered a TLS.

703

FIRST-LINE TUMOR TREATING FIELDS (TTFIELDS; 150 KHZ) THERAPY PLUS PEMBROLIZUMAB FOR ADVANCED OR METASTATIC INTRATHORACIC NON-SMALL CELL LUNG CANCER: THE PHASE 2 EF-36/KEYNOTE B36 PILOT STUDY

¹Rupesh Kotecha*, ²Corey Langer, ³Vinicius Ernani, ⁴Anne Tsao. ¹Miami Cancer Institute, Miami, FL, USA; ²Hospital of University of Pennsylvania, Philadelphia, PA, USA; ³Mayo Clinic Arizona, Phoenix, AZ, USA; ⁴MD Anderson Cancer Center, Houston, TX, USA

Background Tumor Treating Fields (TTFields) therapy is a loco-regional treatment modality approved for glioblastoma and malignant pleural mesothelioma. Effectiveness of TTFields (150 kHz) therapy plus pemetrexed in recurrent non-small cell lung cancer (NSCLC) was previously demonstrated in a phase 1/2 study. TTFields therapy plus standard of care (SOC; docetaxel or immune checkpoint inhibitors) vs SOC alone is currently being evaluated in the large phase 3 LUNAR study (NCT02973789). Given that preclinical data show that TTFields induce immunogenic cell death and enhance efficacy of PD-1 inhibitors, investigation of this combination in a clinical population is warranted.

Methods EF-36/KEYNOTE B36 (NCT04892472) is a multi-center, phase 2, open-label study evaluating efficacy and safety of TTFields (150 kHz) therapy plus pembrolizumab for first-line treatment of advanced NSCLC. The study was approved by the institutional review board/ethics committee as required for each participating site. Patients (≥ 22 years) with Eastern Cooperative Oncology Group performance status 0–1 and treatment-naïve advanced or metastatic intrathoracic, PD-L1 positive (tumor proportion score [TPS] $\geq 1\%$) NSCLC are eligible. Patients with epidermal growth factor receptor-sensitizing mutations or anaplastic lymphoma kinase translocation NSCLC are ineligible. Patients stratified by PD-L1 expression (TPS $\geq 50\%$ vs TPS 1–49%) will receive TTFields therapy ≥ 18 h/day, via the NovoTTF-200T System, with pembrolizumab 200 mg intravenously every 3 weeks (Q3W), until disease progression per Response Evaluation Criteria in Solid Tumors v1.1. Follow-up is Q3W, with computerized tomography (CT) scans Q9W. Primary endpoint is objective response rate (ORR). Secondary endpoints include overall survival (OS), progression-free survival (PFS), duration of response, disease control rate, and safety. ORR, OS, and PFS in patients with TPS $\geq 50\%$ and TPS 1–49% are also secondary endpoints. The device manufacturer will provide patients and caregivers with technical and lifestyle integration training, and guidance on preventing and managing skin effects, via Device Support Specialists and field personnel. Usage information from the device is provided to physicians to aid discussions with patients and maximize usage. This novel support framework helps ensure patients can confidently operate the NovoTTF-200T System and integrate TTFields therapy into daily life, improving usage duration and optimizing patient outcomes. A sample size of 66 is required to achieve 80% power to detect ORR of 40% at 1-sided alpha level 0.1, using 1-sample exact test for proportion, considering $< 10\%$ loss to follow-up. Recruitment is ongoing; planned interim analysis will occur after enrollment of 15 patients with ≥ 1 follow-up CT scan.

Trial Registration NCT04892472

Ethics Approval The study was approved by the institutional review board/ethics committee as required for each participating site

<http://dx.doi.org/10.1136/jitc-2022-SITC2022.0703>

704

PHASE I STUDY OF TISLELIZUMAB IN COMBINATION WITH BEVACIZUMAB AND PEMETREXED IN FIRST-LINE TREATMENT FOR ADVANCED ELDERLY NON-SQUAMOUS NON-SMALL CELL LUNG CANCER: TRIAL IN PROGRESS

Xiubao Ren, Liang Liu*. *Tianjin Medical University Cancer Institute and Hospital, Tianjin, China*

Background Lung cancer has higher incidence and mortality in the elderly population, although substantial evidence confirms the efficacy of PD-1/L1 inhibitors in combination with chemotherapy for advanced non-small cell lung cancer (NSCLC) regardless of PD-L1 expression. However, efficacy and safety of immunotherapy in elderly NSCLC remains unclear, with most evidence is sourced from subgroup analysis of prospective clinical trials.¹ Elderly lung cancer patients often have more underlying diseases and function of major organs decreases with ageing,² safety is certainly a key factor that must be carefully considered when these patients receive treatment because of poor tolerability. Therefore, we designed the study of tislelizumab in combination with pemetrexed and bevacizumab for the treatment of elderly non-squamous NSCLC. To improve safety and tolerability, we remove the more toxic platinum from the chemotherapy regimen, and the anti-angiogenic agent bevacizumab, with relatively mild adverse effect, was added to avoid decreased efficacy. This study aims to explore the efficacy and safety of this treatment regimen in elderly NSCLC patients.

Methods This open-label, single arm, phase I clinical study is enrolling patients aged ≥ 65 years with histologically or cytologically confirmed, untreated IIIB/IIIC/IV (according to AJCC 8th) non-squamous NSCLC. Patients must have measurable disease per RECIST v1.1; ECOG PS of 0 or 1; without harboring EGFR-sensitizing mutation or ALK and ROS1 gene translocation; no active autoimmune disease, bleeding risk, or coagulation disorders. Patients will receive 4 cycles of pemetrexed (500mg/m², d1) Q3W and tislelizumab (200mg, d4) Q3W in combination with bevacizumab (7.5mg/kg, d1) Q3W followed by tislelizumab (200mg, d1) Q3W and bevacizumab (7.5mg/kg, d1) Q3W, until disease progression, unacceptable AEs, investigator/patient decision or 2 years. The primary endpoint is objective response rate (ORR) by RECIST v1.1. Secondary endpoints include overall survival (OS), progress-free survival (PFS), duration of response (DOR), health-related quality of life (HRQoL) and safety. HRQoL is assessed using EORTC QLQ-C30 questionnaires; AEs are graded according to NCI CTCAE v5.0. This study will enroll 30 patients and enrollment is ongoing.

Trial Registration ClinicalTrials.gov NCT05273814

REFERENCES

1. Fang Yang, Svetomir NM, Julian RM, *et al.* Association of Sex, Age, and Eastern Cooperative Oncology Group Performance Status with Survival Benefit of Cancer Immunotherapy in Randomized Clinical Trials: A Systematic Review and Meta-analysis. *JAMA Netw Open.* 2020;**3**:e2012534.
2. Vera C, Direndra H, Encarnação T, *et al.* Characterization and management of elderly and very elderly patients with non-small cell lung cancer. *Clin Respir J* 2020;**14**:683–686.

Ethics Approval The study was approved by Tianjin Medical University Cancer Institute & Hospital Ethics Board, approval number E20210962A.

<http://dx.doi.org/10.1136/jitc-2022-SITC2022.0704>

705

PHASE 2 STUDY OF SEA-CD40 COMBINATION THERAPIES IN ADVANCED MALIGNANCIES (SGNS40-002, TRIAL IN PROGRESS)

¹April Salama*, ²Meredith McKean, ³Thaddeus Beck, ⁴Omid Hamid, ⁵Sandeep Mashru, ⁶Sapna Patel, ⁷Timothy Kuzel, ⁸Michael Castine, ⁹Vincent Ma, ¹⁰Keenan Fenton, ¹⁰Jonathan Hayman, ¹¹Adil Daud. ¹Duke Cancer Institute, Durham, NC, USA; ²Sarah Cannon Research Institute, Nashville, TN, USA; ³Highlands Oncology, Springdale, AR, USA; ⁴The Angeles Clinic and Research Institute, a Cedars-Sinai Affiliate, Los Angeles, CA, USA; ⁵Kaiser Permanente, Portland, OR, USA; ⁶MD Anderson Cancer Center, Houston, TX, USA; ⁷Rush Medical College, Chicago, IL, USA; ⁸Hematology Oncology Clinic, Baton Rouge, LA, USA; ⁹University of Wisconsin Carbone Cancer Center, Madison, WI, USA; ¹⁰Seagen Inc., Bothell, WA, USA; ¹¹University of California, San Francisco Medical Center, San Francisco, CA, USA

Background While immunotherapy has improved outcomes for patients with metastatic non-small cell lung cancer (NSCLC) and melanoma, most progress despite standard treatment. Therefore, treatments with the potential to enhance the efficacy of existing immunotherapy-based regimens are being actively examined to further improve outcomes in these diseases.

CD40 is a tumor necrosis factor receptor expressed on multiple immune cell populations as well as on tumor cells. CD40 activation drives B- and T-cell activation to evoke tumor-specific cytotoxic T-cell responses. SEA-CD40 is an investigational, receptor-agonistic, nonfucosylated, humanized IgG1 monoclonal antibody (mAb) directed to CD40. SEA-CD40 binds with high affinity to FcγRIIIa and CD40, resulting in enhanced effector function and CD40 agonism, allowing amplification of immune stimulation and antitumor activity.

Preclinical studies have shown that SEA-CD40 combined with chemotherapy and pembrolizumab resulted in significant antitumor activity. This combination regimen has also demonstrated a tolerable safety profile, encouraging antitumor activity, and evidence of persistent immune activation in an ongoing phase 1 study (SGNS40-001, NCT02376699). Given the preclinical and clinical data supporting SEA-CD40 combined with pembrolizumab and/or chemotherapy, further investigation into additional diseases is warranted.

Methods SGNS40-002 (NCT04993677) is a phase 2, open-label, multicenter trial designed to assess the antitumor activity, safety, and tolerability of SEA-CD40 in combination with pembrolizumab and/or chemotherapy in adults (≥18 years) with NSCLC or melanoma. Five indication-specific cohorts will explore 2 different regimens: cohorts 1–3 will receive SEA-CD40 with pembrolizumab while cohorts 4 and 5 will receive SEA-CD40, pembrolizumab, carboplatin, and pemetrexed.

Cohort 1 will enroll patients with relapsed or refractory metastatic melanoma (≤3 prior lines of therapy, including an anti-programmed death/ligand 1 (PD-1/PD-L1) mAb within 90 days), cohort 2 will enroll patients with metastatic uveal melanoma, and cohort 3 will enroll patients with metastatic PD-1/PD-L1-naïve melanoma. Patients in cohorts 2 and 3 must have no prior therapy for advanced disease except adjuvant/neoadjuvant therapy. Cohorts 4 and 5 will include patients with NSCLC with a PD-L1 tumor proportion score of 1–49% or <1%, respectively.

The primary endpoint is investigator-assessed confirmed objective response rate per Response Evaluation Criteria in Solid Tumors Version 1.1 (RECIST v1.1). Secondary endpoints include incidence of adverse events; laboratory abnormalities; treatment interruptions, reductions or discontinuations; disease

control rate; duration of response; progression-free survival; and overall survival. Exploratory endpoints include pharmacokinetic parameters, antidrug antibodies, biomarkers of response, and patient-reported quality of life. Enrollment is ongoing in North America and Europe.

Trial Registration NCT04993677

Ethics Approval Institutional review boards or independent ethics committees of participating sites approved the trial, which will be conducted in compliance with the Declaration of Helsinki and International Conference on Harmonization Guidelines for Good Clinical Practice. All patients will provide written informed consent.

Consent All patients will provide written informed consent.

<http://dx.doi.org/10.1136/jitc-2022-SITC2022.0705>

706

NOUS-PEV, A NOVEL PERSONALIZED VIRAL-BASED PRIME/BOOST CANCER IMMUNOTHERAPY TARGETING PATIENT-SPECIFIC NEOANTIGENS: INTERIM RESULTS FROM THE FIRST SUBJECTS IN THE PHASE 1B STUDY

¹Oliver Bechter*, ²Juan Martin-Liberal, ³Anna D'Alise, ³Guido Leoni, ³Gabriella Cotugno, ³Loredana Siani, ³Rosa Vitale, ³Valentino Ruzza, ³Elisa Micarelli, ³Irene Garzia, ⁴Thea Faivre, ⁴Sven Gogov, ⁴Patricia Delaite, ⁵Stefano Colloca, ⁵Maria Ambrosio, ⁵Rossella Merone, ³Elisa Scarselli, ⁶Stefan Symeonides. ¹Leuven Cancer Institute, Leuven, Belgium; ²Catalan Institute of Oncology, Barcelona, Spain; ³Nouscom Srl, Rome, Italy; ⁴Nouscom AG, Basel, Switzerland; ⁵Reithera Srl, Roma, Italy; ⁶Edinburgh Cancer Centre, Edinburgh, UK

Background NOUS-PEV is a vector based personalized cancer vaccine, expressing about 60 patient specific neoantigens identified by next generation sequencing (NGS). Vaccination consists of Great Ape Adenoviral (GAd) prime followed by Modified Vaccinia Ankara (MVA) boosts. The study is a dose-confirmation and cohort expansion, phase 1b, first in human (FIH) trial (NCT04990479) evaluating safety, tolerability, immunogenicity and preliminary anti-tumour activity of NOUS-PEV in combination with the PD-1 blocking antibody pembrolizumab.

Methods The study is enrolling treatment-naïve subjects with unresectable stage III/IV cutaneous melanoma and/or PD ligand 1 (PD-L1) \geq 50% stage IV non-small cell lung cancer. Following pembrolizumab induction treatment (3 cycles), the vaccines are administered intramuscularly: the GAd priming dose concomitantly with pembrolizumab at week 10 (4th pembrolizumab infusion) followed by 3 boosts of MVA, each 3 weeks apart. Baseline and on treatment tumor biopsies are collected at screening and post 1st MVA, respectively. PBMC are collected at baseline, post pembrolizumab, and post each vaccination for evaluation of immune response. Clinical response is evaluated according to RECIST v1.1 by CT scan according to standard of care.

Results All vaccines were made and administered on time to the three melanoma subjects in the dose-confirmation cohort. As of June 2022, the median follow-up is 6.9 months (range 3.0-11.5). No dose limiting toxicities (DLTs) were observed, and the treatment was safe and no NOUS-PEV related AEs $>$ Grade 1 were observed, allowing the enrollment of subjects in the expansion cohort.

In the first subject, the first CT scan before vaccination showed initial SD with dynamic of growth in target lesion size, that then reverted after NOUS-PEV administration, resulting in a confirmed PR deepening over time. The second subject had a PR already at the first CT scan, further deepened after the vaccination. The third subject had PD at the first scan before vaccination and discontinued based on the confirmatory scan.

Vaccine-induced immunogenicity was demonstrated by *ex vivo* interferon-gamma ELISpot in 2 evaluable subjects who showed clinical response, with detection of potent neoantigen specific immune response to multiple neoantigens in the peripheral blood and induction of both CD4 and CD8 T cell responses. NGS analysis of baseline and on-treatment biopsies showed an increased T cell infiltrate, with expansion and diversification of the TCR repertoire post treatment.

Conclusions NOUS-PEV in combination with anti-PD1 is safe and well tolerated. Data show that vaccination elicits a robust immune response which correlates with preliminary clinical activity.

Trial Registration NCT04990479

Ethics Approval The study was approved by UZ Leuven Ethics Committee (Study Reference S64578) and by Research Ethics Committee of Fundacion Jimenez Diaz, Madrid

<http://dx.doi.org/10.1136/jitc-2022-SITC2022.0706>

707

A PHASE 1, OPEN-LABEL, DOSE FINDING STUDY OF NI-1801, A BISPECIFIC MESOTHELIN X CD47 ENGAGING ANTIBODY, IN PATIENTS WITH MESOTHELIN EXPRESSING SOLID CANCERS

¹Emanuela Romano, ²Jacques Medioni, ³Thibault De La Motte Rouge, ⁴Nicolas Fischer, ⁵Clélia Bardonneau, ⁶Walter Ferlin, ⁴Dirk Hose, ⁴Anja Seckinger*, ⁵Matteo Simonelli, ⁶Giuseppe Curigliano. ¹Institut Curie, Paris, France; ²Hôpital Européen Georges Pompidou, Paris, France; ³Centre Eugène Marquis, Rennes, France; ⁴Light Chain Bioscience – Novimmune SA, Geneva, Switzerland; ⁵IRCCS Humanitas Research Hospital, Milan, Italy; ⁶European Institute of Oncology, IRCCS, Milan, Italy

Background Mesothelin (MSLN) is highly expressed in many solid tumors while expression in normal tissue is limited, thus representing an attractive target for immunotherapeutic approaches. NI-1801 is a fully human IgG1 bispecific antibody based on the kl-body format.^{1,2} NI-1801 targets MSLN with a high-affinity arm coupled to a low affinity-optimized CD47-blocking arm. This unbalanced affinity enables the selective CD47-blockade on MSLN-expressing cells. Additionally, NI-1801 contains an unmodified IgG1 Fc and can therefore mediate effector functions. *In vitro*, NI-1801 induces antibody-dependent cellular phagocytosis (ADCP) and antibody-dependent cell-mediated cytotoxicity of MSLN-positive cancer cells. ADCP is negligible or unaffected by a CD47-sink effect mimicked by CD47-expressing red blood cells. NI-1801 does not induce *in vitro* hemagglutination or platelet aggregation. *In vivo*, NI-1801 inhibits tumor growth in xenograft models. NI-1801 was well tolerated and demonstrated favorable PK in multiple non-human primate studies.

Methods Study LCB-1801-001 (NCT05403554) is a first-in-human clinical trial of NI-1801 in patients with MSLN-expressing solid malignancies. Part A (dose escalation) evaluates the safety and tolerability of NI-1801, to determine the maximum tolerated dose (MTD) and the non-tolerated toxic dose. The decision to include additional patients as well as dose escalation decisions are made at the discretion of the Safety Review Committee (SRC). Inpatient dose escalation is permitted by SRC approval. Part B (cohort expansion) will further evaluate the safety and efficacy in up to 20 additional subjects to determine the recommended Phase 2 dose. Expansion may occur at the MTD established in Part A, or at an alternative tolerable dosing schedule, based on review of safety and PK/PD data by the SRC. Treatments are administered intravenously in 28-day cycles for up to 6 months until disease progression, unacceptable toxicity, or investigator/patient decision to withdraw. Treatment can extend for patients without disease progression. The starting dose is 15 mg (fixed dose). Subsequent doses are given QW in Cycles 1/2 and Q2W in Cycles 3-6. LCB-1801-001 study enrolls patients since April 2022 and is ongoing in France and Italy. Adverse events are assessed according to CTCAE v5, tumor response is determined according to RECIST 1.1. Key inclusion criteria include (1) histologically or cytologically confirmed diagnosis of epithelial ovarian cancer (high-grade serous or endometroid), triple-negative breast cancer, or non-squamous non-small cell lung cancer, (2) advanced, metastatic, or recurrent disease, and (3) MSLN expression with staining intensity of $\geq 2+$ as per immunohistochemistry in $\geq 60\%$ of tumor cells.

REFERENCES

- [1] Fischer N, Elson G, Magistrelli G, Dheilly E, Fouque N, Laurendon A, Gueneau F, Ravn U, Depoisier JF, Moine V, Raimondi S, Malinge P, Di Grazia L, Rousseau F, Poitevin Y, Calloud S, Cayatte PA, Alcoz M, Pontini G, Fagète S, Broyer L, Corbier M, Schrag D, Didelot G, Bosson N, Costes N, Cons L, Buatois V, Johnson Z, Ferlin W, Masternak K, Kosco-Vilbois M. Exploiting light chains for the scalable

generation and platform purification of native human bispecific IgG. *Nat Commun.* 2015;6:6113

- [2] Hatterer E, Chauchet X, Richard F, Barba F, Moine V, Chatel L, Broyer L, Pontini G, Bautzova T, Juan F, Calloud S, Bosson N, Charreton M, Masternak K, Buatois V, Shang L. Targeting a membrane-proximal epitope on mesothelin increases the tumoricidal activity of a bispecific antibody blocking CD47 on mesothelin-positive tumors. *MAbs.* 2020;12:e1739408.

Ethics Approval Ethics approval was obtained from corresponding ethics committees (Committee for Protection of Persons for Sud Méditerranée III, MEDAECPP-2021-09-0021 _ 2021-003808-40; Comitato Etico Degli IRCCS Istituto Europeo Di Oncologia E Centro Cardiologico Monzino, IEO 1632 – RE3604/Em. 001). Participants give informed consent before taking part.

<http://dx.doi.org/10.1136/jitc-2022-SITC2022.0707>

MEDI1191 (IL-12 MRNA) INDUCES PERIPHERAL AND INTRATUMORAL IMMUNOSTIMULATORY EFFECT IN PATIENTS WITH CUTANEOUS OR SUBCUTANEOUS (C/SC) LESIONS

¹Michael Abadier*, ¹Emily Jennings, ¹Jim Eyles, ¹Philip Martin, ¹Fernanda Pilataxi, ¹Yuling Wu, ¹Xiaoru Chen, ¹Analia Azaro, ¹Benjamin Ridgway, ¹Marc Phillips, ²Benedito Carneiro, ³Omid Hamid, ⁴Thomas Marron, ⁵Dmitriy Zamarin, ⁶Eduardo Castañón, ⁷Sandip Patel, ⁸Elena Garralda, ⁹Vivek Subbiah, ¹⁰Anthony El-Khoueiry, ¹Paula Fraenkel, ¹Nicholas Durham. ¹AstraZeneca, Waltham, MA, USA; ²Legorreta Cancer Center at Brown University, Providence, RI, USA; ³The Angeles Clinic and Research Institute, Los Angeles, CA, USA; ⁴Icahn School of Medicine at Mount Sinai, New York, NY, USA; ⁵Memorial Sloan Kettering Cancer Center, New York, NY, USA; ⁶Clinica Universidad de Navarra, Navarra, Spain; ⁷University of California San Diego, La Jolla, CA, USA; ⁸Vall d'Hebron Institute of Oncology, Barcelona, Spain; ⁹MD Anderson Cancer Center, Houston, TX, USA; ¹⁰USC Norris Comprehensive Cancer Center, Los Angeles, CA, USA

Background MEDI1191 is an investigational therapy composed of mRNA encoding bioactive interleukin-12 (IL-12p70) in a lipid nanoparticle optimized for intratumoral injection. We hypothesized that intratumoral injection of MEDI1191 will reprogram the immunosuppressed tumor microenvironment (TME) and increase cytotoxic T-cell recruitment, proliferation and activation.

Methods In an ongoing phase 1 dose escalation study (NCT03946800), patients with C/SC lesions received 0.1-12 μ g MEDI1191 sequentially (Part 1A) or concurrently (Part 1B) with intravenous durvalumab (1500 mg).¹ Clinical samples were collected to monitor changes in peripheral cytokines, circulating tumor (ct) DNA, peripheral and tumoral gene signatures and T cell infiltration.

Results Peripheral blood cytokine analysis revealed increased serum IL-12 levels in 27/29 (93%) patients post first injection and was associated with ≥ 2 -fold increase in serum IFN- γ in 24/29 (83%) patients. The IFN-inducible chemokines (CXCL9, CXCL10 and CXCL11) in periphery were detected at the protein and transcriptomic levels. In 11 patients whose blood samples underwent bulk RNA sequencing, markers of activated peripheral T cells were detectable over time with increased mean fold change of GZMB, IFNG and IL12RB1 gene expression in patients with partial response (PR, n=1) or stable disease (SD, n=5) patients. Pre-treatment expression of the genes encoding key mediators of cytotoxic T-cell function were potential predictors of response as observed by significantly higher expressions of peripheral IL12RB1 and IFNG genes at baseline in PR/SD patients.

Using immunohistochemistry (IHC), we observed ≥ 2 -fold increase in CD8 T cells (8/17, 47%) and Ki-67+CD3+ T-cells (7/17, 41%) in tumor biopsies 15 days post first injection. Patients with increased intratumoral CD8 T cells by IHC and RNA sequencing showed higher tumoral GZMB and IFNG gene expression. In 9 patients with evaluable tumor biopsies at baseline and post-treatment, we observed an increase in antitumor gene signatures, including activated CD8 (7/9, 78%), activated NK (7/9, 78%), M1 macrophages (7/9, 78%) and IFN- γ signaling (8/9, 89%). Consistent with IL-12's role as a central mediator of Th1 cell development, we observed an increase in Th1 signature and STAT4 gene (6/9, 67%). Analysis of ctDNA in plasma of 17 patients demonstrated $>50\%$ reduction in mutant allele frequency in 2/3 patients who developed PR.

Conclusions Intratumoral injection of MEDI1191 induces pharmacodynamic changes within the TME such as increase in activated T cell infiltration and upregulation of anti-tumor gene signatures. There was an associated immunomodulatory

effect in the periphery, including elevated IL-12, IFN- γ and activated T-cells.

Trial Registration NCT03946800

REFERENCE

- [1] Benedito A Carneiro, Dmitriy Zamarin, Thomas Marron, Inderjit Mehmi, Sandip P Patel, Vivek Subbiah, Anthony El-Khoueiry, David Grand, Kirema Garcia-Reyes, Sanjay Goel, Phillip Martin, Jixin Wang, Yuling Wu, Steven Eck, Benjamin Ridgway, Nairouz Elgeioushi, Jim Eyles, Nicholas Durham, Analia Azaro, Omid Hamid. First-in-human study of MEDI1191 (mRNA encoding IL-12) plus durvalumab in patients (pts) with advanced solid tumors [abstract]. In: Proceedings of the American Association for Cancer Research Annual Meeting 2022; 2022 Apr 8-13. Philadelphia (PA): AACR; Cancer Res 2022;82(12_Suppl):Abstract nr CT183.

Ethics Approval The IRB/IEC responsible for each site reviewed and approved the final study protocol, including the final version of the ICF and any other written information and/or materials to be provided to the subjects. Institutional Review Boards, Mount Sinai Health System, New York (Board Number 19-00279).

<http://dx.doi.org/10.1136/jitc-2022-SITC2022.0708>

709

PHASE II STUDY TO ASSESS THE SAFETY AND EFFICACY OF THE CLEVER-1 ANTIBODY BEXMARILIMAB IN COMBINATION WITH PD-1 BLOCKADE IN PATIENTS WITH ADVANCED SOLID TUMORS – BEXCOMBO

¹Petri Bono*, ²Juho Jalkanen, ³Inka Pawlitzky, ³Marie-Louise Fjaellskog, ³Cecilia Ahlin. ¹University of Helsinki, Helsinki, Finland; ²Faron Ltd, Turku, Finland; ³Faron, Boston, MA, USA

Background Clever-1 is an immunosuppressive scavenger receptor expressed on tumor associated macrophages¹⁻². High levels of Clever-1 are associated with poor survival, T-cell exclusion and dysfunction, and immunotherapy resistance³⁻⁷. Bexmarilimab (Bex) is a novel humanized anti-CLEVER-1 IgG4-antibody that induces IFN- γ upregulation, which is required for PD-L1 upregulation and response to PD-1 blockade⁸. Bex is currently evaluated as monotherapy in a phase I/II study (MATINS; NCT03733990) in patients with advanced solid tumors and in combination with standard of care in patients with hematological malignancies (BEXMAB; NCT05428969). Preliminary data show well tolerated safety profile and promising clinical activity with disease control rates up to 40% translating into enhanced survival⁹. In addition, early analyses suggest that lower levels of proinflammatory cytokines at base line or higher CLEVER-1 expression in tumor can predict for a superior clinical outcome. The BEXCOMBO study will assess the safety and efficacy of Bex in combination with PD-1 blockade in 1st line setting in patients with advanced solid tumors expressing CLEVER-1 and with modest response to PD-1 blockade. It is anticipated that the induction of IFN- γ production by Bex will result in enhanced clinical efficacy from PD-1 blockade in patients lacking pre-existing immune activation.

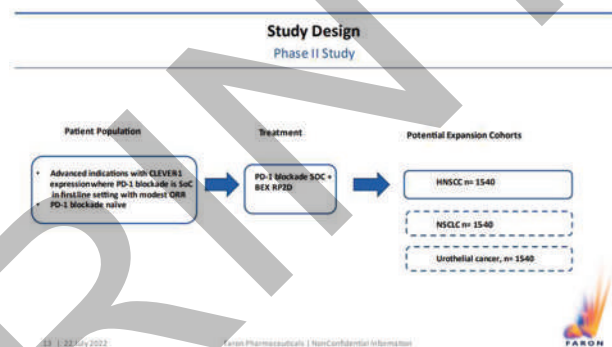
Methods BEXCOMBO is a single arm multicentre clinical study with an adaptive design (figure 1). The study uses a Simon's 2-stage design (Stage 1 n=15; Stage 2 n=40 for each indication). Study treatment will be initiated in patients with advanced head and neck squamous cell (HNSCC) with the potential to open patient cohorts with advanced urothelial carcinoma and non-small cell lung cancer (NSCLC) or other indications based on emerging translational and clinical data. Patient selection based upon lower baseline levels of proinflammatory cytokines or higher levels of CLEVER-1 expression will be considered if supported by translational data. Patients will be treated at the Recommended Phase 2 Dose of Bex in combination with standard of care PD1 blockade until progression or unacceptable toxicity. The primary endpoints are objective response rate based on Response Evaluation Criteria in Solid Tumors version 1.1 (RECIST v1.1) and duration of response. Key secondary endpoints include time to response by RECIST 1.1, disease control rate, progression-free survival, overall survival, safety and CLEVER-1 and PD-L1 expression levels in tumor biopsy; as well as IFN γ and TNF α levels in serum.

REFERENCES

1. Kzhyshkowska J. Multifunctional receptor stabilin-1 in homeostasis and disease. *Scientific World Journal*. 2010;10. DOI:10.1100/tsw.2010.189.
2. Palani S *et al*. Stabilin-1/CLEVER-1, a type 2 macrophage marker, is an adhesion and scavenging molecule on human placental macrophages. *Eur J Immunol* 2011;41. DOI:10.1002/eji.201041376.
3. Hollmén M *et al*. New tools to prevent cancer growth and spread: a 'Clever' approach. *Br. J. Cancer*. 2020;123. DOI:10.1038/s41416-020-0953-0.
4. Tervahartiala M *et al*. Immunological tumor status may predict response to neoadjuvant chemotherapy and outcome after radical cystectomy in bladder cancer. *Sci Rep* 2017;7. DOI:10.1038/s41598-017-12892-5.

5. Lin SY *et al*. Identification of STAB1 in Multiple Datasets as a Prognostic Factor for Cytogenetically Normal AML: Mechanism and Drug Indications. *Mol Ther – Nucleic Acids* 2019;18. DOI:10.1016/j.omtn.2019.09.014.
6. Karikoski M *et al*. Clever-1/stabilin-1 controls cancer growth and metastasis. *Clin Cancer Res* 2014;20. DOI:10.1158/1078-0432.CCR-14-1236.
7. Viitala M *et al*. Immunotherapeutic blockade of macrophage clever-1 reactivates the CD8 β T-cell response against immunosuppressive tumors. *Clin Cancer Res* 2019;25. DOI:10.1158/1078-0432.CCR-18-3016.
8. Virtakoivu R *et al*. Systemic Blockade of Clever-1 Elicits Lymphocyte Activation Alongside Checkpoint Molecule Downregulation in Patients with Solid Tumors: Results from a Phase I/II Clinical Trial. *Clin Cancer Res* 2021;27. DOI:10.1158/1078-0432.CCR20-486.
9. Bono P *et al*. Promising clinical benefit rates in advanced cancers alongside potential biomarker correlation in a phase I/II trial investigating Bexmarilimab, a novel macrophage-guided immunotherapy. Poster presented at ASCO 2022.

Ethics Approval This study will be sent to all participating sites review boards and local ethics committees for approval.



Abstract 709 Figure 1 Clinical Trial Design

<http://dx.doi.org/10.1136/jitc-2022-SITC2022.0709>

710

SAFETY AND SURVIVAL RESULTS FROM A PHASE 1/2 TRIAL OF INTRATUMORAL AGENT INT230-6 (CISPLATIN VINBLASTINE) INDUCES IMMUNOLOGICAL CANCER CELL DEATH ALONE OR WITH PEMBROLIZUMAB IN PATIENTS WITH REFRACTORY, METASTATIC CANCERS

¹Jacob Thomas*, ¹Anthony El-Khoueiry, ¹Diana Hanna, ²Anthony Olszanski, ³Nilofer Azad, ⁴Giles Whalen, ⁵Matthew Ingham, ⁶Luis Camacho, ⁷Franco Abbate, ⁸Lewis Bender, ⁷Ian Walters, ⁹Lillian Siu. ¹University of Southern California, Los Angeles, CA, USA; ²Fox Chase Cancer Center, Philadelphia, PA, USA; ³Johns Hopkins University, Chevy Chase, MD, USA; ⁴UMASS Memorial, Worcester, MA, USA; ⁵Columbia University Irving Cancer Ctr, New York, NY, USA; ⁶Houston Methodist, Houston, TX, USA; ⁷Intensity Therapeutics, Westport, CT, USA; ⁸Intensity Therapeutics, Inc., Westport, CT, USA; ⁹Princess Margaret Cancer Center, Toronto, Canada

Background Study IT-01, KN-A10: INT230-6 is a new product with a unique dual anti-cancer mechanism. The drug is comprised of cisplatin and vinblastine co-formulated with a molecule that enables drug dispersion throughout an injected tumor and diffusion into cancer cells. The drug directly kills cancer and activates an immune response. Results from a neo-adjuvant breast cancer study confirms that a single injection induces necrosis in up to 95% of a tumor and recruits TILs.¹

Methods INT230-6 intratumoral (IT) treatments are Q2W up to 5 followed by maintenance dosing Q9W. Dose is set by the tumor's longest diameter or volume. Pembrolizumab is 200mg IV Q3W in the INT230-6 combination arm. Biopsies from the injected tumor at pretreatment and day 28 are sent for immunohistochemistry analysis. Endpoints are safety and exploratory efficacy by overall survival.

Results Sixty-four subjects received INT230-6 alone (median 4 prior treatments). Thirty received INT230-6 + pembrolizumab (median 3 prior). There were 652 image-guided INT230-6 IT injections (378 to visceral tumors eg lung, liver, pancreas) median 5 injections, range (1,50). Doses ranged from 0.14 up to 175mL (87.5 mg of cisplatin, 17.5mg vinblastine – much higher than typical IV doses). The INT230-6 arm enrolled 19 cancer types; the PEM combination recruited primarily colon, pancreatic, TNBC or bile duct cancers. IHC results show marked reduction in DAPI of proliferating cancer cells with influx of CD4 and CD8 T-cells. Non-injected visceral tumors shrank in several INT230-6 monotherapy subjects. Due to drug absorption or immune influx RECIST is not ideal for use with INT230-6 (ASCO2022). Overall survival is preferred. The estimated median OS (mOS) was 361 days for INT230-6; the mOS for the combination has not been reached (173 days of median follow-up). Pharmacokinetics shows >95% of the active agents remain in the injected tumor at 1 hour² compared to IV. The most common (>20%) treatment-related adverse events (TRAEs) for INT230-6 alone/combination were localized pain (59%/50%), nausea (39%/13%), fatigue (28%/20%) and vomiting (23%/20%). The incidence of grade 3 TRAEs for the INT230-6 and combination arms were 10% and 20%. One combination patient had a grade 4 neutrophil decrease that quickly resolved. No patient discontinued therapy due to treatment toxicities.

Conclusions Intratumoral injections of large drug volumes into visceral tumors was feasible and well-tolerated. Biopsies confirmed immunological cell death. OS was compelling for this heavily pretreated population lacking standard therapeutic options. INT230-6 may offer a well-tolerated treatment for refractory patients and is entering randomized controlled trials.

Trial Registration [Intensity-IT-01, Merck-KN-A10] NCI#03058289

REFERENCES

1. Arnaout A. INVINCIBLE TRIAL: Intratumoral INT230-6 in Breast Cancer; ASCO 2022 Abstract 605; ClinicalTrials.gov [Internet]. Bethesda (MD): U.S. National Library of Medicine. 2000 – 2022. Available from: <http://clinicaltrials.gov/show/NCT00417417>ClinicalTrials.gov Identifier: NCT00417417.
2. Owelien, Historical PK data from IV administration. *J. Cancer Res.* 1977;8.

Ethics Approval The protocol was approved by an institutional review board, independent ethics committee, or research ethics board at each institution. All subjects or their legally acceptable representative provided written informed consent before screening. The study was designed, undertaken, and reported in accordance with the Declaration of Helsinki, and is registered with clinicaltrials.gov with registration no. NCT03058289.

<http://dx.doi.org/10.1136/jitc-2022-SITC2022.0710>

711

INTERIM RESULTS OF A PHASE 2 STUDY OF NIVOLUMAB AND RELATLIMAB IN ADVANCED MISMATCH REPAIR DEFICIENT (dMMR) CANCERS RESISTANT TO PRIOR PD-(L)1 INHIBITION

Katherine Bever*, Hao Wang, Jennifer Durham, Colleen Apostol, Nilofar Azad, Ilene Browner, Stephanie Gaillard, Daniel Laheru, Valerie Lee, William Sharfman, Mark Yarchoan, Qingfeng Zhu, Robert Anders, Andrew Pardoll, Suzanne Topalian, Nicolas Llosa, Elizabeth Jaffee, Dung Le. *Johns Hopkins University, Baltimore, MD, USA*

Background Cancers deficient in DNA mismatch repair (dMMR) are highly immunogenic but exhibit variable benefit from immune checkpoint inhibitors targeting programmed cell death-1 (PD-1)/PD-1 ligand (PD-L1). Other immune checkpoints are upregulated in these tumors and may be acting in parallel, in particular, lymphocyte activation gene 3 (LAG-3) which mediates exhaustion of activated T cells. The clinical relevance of the LAG-3 pathway has recently been demonstrated in 1L advanced melanoma (Tawbi NEJM 2022). We hypothesized that the addition of a LAG-3 blocking antibody (relatlimab) to a PD-1i (nivolumab) may overcome resistance to PD-(L)1 blockade in advanced dMMR tumors.

Methods Patients with advanced dMMR cancers that progressed during or within 6 months of PD-(L)1 inhibitor-containing therapy and after at least 12 weeks of therapy, and met other eligibility criteria were enrolled. Patients were treated with relatlimab 160 mg + nivolumab 480 mg (Cohort 1) every 4 weeks until intolerance or progression. Biopsies were obtained at baseline and on-treatment. The primary endpoint of the study is objective response rate according to RECIST 1.1. The outcomes of patients enrolled on Cohort 1 as of April 2022 are reported herein.

Results 15 patients were enrolled on Cohort 1 between November 2018 and April 2022. Of 13 patients evaluable for response (median follow up=12.4 months), partial response by RECIST 1.1 was observed in 1 patient with small bowel adenocarcinoma at 17 months (response duration of 11+ months), and 1 patient with colorectal cancer achieved a complete response at 18 months. An additional 5 patients achieved a best response of stable disease (SD), including one patient with 24% reduction in SLD ongoing at 41+ months. Treatment related adverse events (trAEs) occurred in 6 patients (40%) and were all G1-2 in severity. One patient discontinued treatment due to trAE (G2 oral pain/mucositis). Updated results will be presented at the time of the conference.

Conclusions Relatlimab + nivolumab is well tolerated and results in response or prolonged disease stability in some patients with advanced dMMR cancers that progressed on anti-PD-(L)1 therapy. Correlative analysis is ongoing to evaluate markers predictive of clinical benefit.

Acknowledgements Funding for this study was obtained through a grant from Bristol Myers Squibb. We gratefully acknowledge the patients who participated in this study and their families.

Trial Registration Clinical trial information: NCT03607890.

Ethics Approval This study was approved by the Johns Hopkins Medicine Institutional Review Board (IRB00173534). Written informed consent was obtained from participants prior to their participation.

<http://dx.doi.org/10.1136/jitc-2022-SITC2022.0711>

712 **RETROSPECTIVE TUMOR MICROENVIRONMENT ANALYSIS FROM A PERSONALIZED NEOTCR-T CELL THERAPY CLINICAL TRIAL AND ITS POTENTIAL APPLICATIONS FOR OFF-THE-SHELF HPV TCRS**

Eric Stawiski*, Chad Smith, Tyler Borrmann, Zheng Pan, Stefanie Mandl, Vinnu Bhardwaj.
PACT Pharma, South San Francisco, CA, USA

Background We have developed a state-of-the-art approach to validate predicted neoepitopes (neoEs) and their cognate T cell receptors (neoTCRs) by capturing neoepitope-specific T cells from peripheral blood. This neoTCR discovery and validation process is being applied in a phase I clinical trial (NCT03970382) evaluating personalized neoTCR-T cell therapy to treat patients across eight solid tumor types. We have since expanded our mission to discover off-the-shelf TCRs against recurrent epitopes including HPV+ cancers. The tumor microenvironment (TME) has been shown to critically influence responses to immunotherapy making it paramount to explore in the context of adoptive cell therapy.

Methods Using bulk RNA-seq data from biopsies, we examined the TME of both our clinical cohort (n=137) as well as TCGA H&N samples (n=485). To do this we measured 29 gene expression signatures that capture specific aspects of largely pro or anti-tumor infiltrates that were previously described as being predictive to response to immunotherapy. These signatures were used for K-means clustering with 4 distinct subsets, Immune Enriched (IE), Depleted (D), Fibrotic (F), Immune Enriched/Fibrotic (IE/F) across 6 different cancer types.

Results TME subtypes were predictive of response to ICI in a previously published Melanoma data set (p=0.04).¹ Screening biopsies from patients enrolled in our clinical trial consisted of 22% D, 30% F, 23% IE and 25% IE/F (n=137) across 6 solid tumor types. Amongst samples screened for autologous TCRs (n=64), TME subtype did not affect our ability to isolate TCRs from patients with a median of 2 TCRs for D and IE, 3 for F and 0 for IE/F (ranges 0-10) (p-value = 0.62). We observed a significant positive correlation between ovarian TCR capture and MHCII presentation as well as Treg and Th2 Trafficking (p<0.001), which may be general markers for inflammation. Amongst samples that were ultimately dosed with autologous TCRs, 2/3 had unfavorable TME's (D=7, F=3). TCGA H&N samples that were HPV- (n=414) had 19% IE, 21% IE/F, 28% D, and F 31%. In contrast HPV+ cancers (n=71) showed a significant enrichment for IE samples (61%) and depletion of D and F subtypes (16% and 5% respectively).

Conclusions Retrospective analysis shows no correlation with TME subtype and our ability to isolate autologous TCRs from those patients. The current trial shows lower levels of immunotherapy favorable subtypes. In contrast HPV+ cancers show high levels of immunotherapy responsive subtypes suggesting it may be a favorable cancer indication for adoptive cell therapy.

REFERENCE

1. Bagaev A, Kotlov N, Nomie K, Svekolkin V, Gafurov A, Isaeva O, Osokin N, Kozlov I, Frenkel F, Gancharova O, Almog N, Tsiper M, Ataullakhanov R, Fowler N. Conserved pan-cancer microenvironment subtypes predict response to immunotherapy. *Cancer Cell*. 2021;**39**(6):845-865

<http://dx.doi.org/10.1136/jitc-2022-SITC2022.0712>

713

THE PRAME OPPORTUNITY – HIGH PEPTIDE COPY NUMBERS, HOMOGENOUS EXPRESSION AND HIGH PREVALENCE TO ADDRESS A BROAD PATIENT POPULATION ACROSS DIFFERENT SOLID CANCERS WITH TCR-BASED THERAPEUTICS

¹Cedrik Britten*, ²Dejka Araujo, ³Linus Backert, ⁴Carsten Bokemeyer, ⁵Richard Carvajal, ⁶Manik Chatterjee, ⁷Asim Dash, ³Lena Freudenmann, ³Jens Fritsche, ³David Fuhrmann, ³Valentina Goldfinger, ⁸Tobias Holderied, ³Franziska Hoffgaard, ³Jens Hukelmann, ²Amir Jazaeri, ²Ahmed Kaseb, ³Florian Köhler, ³Daniel Kowalewski, ³Jason Luke, ²Van Morris, ⁷Shivani Mukhi, ³Martina Ott, ⁵Ran Reshef, ³Michael Römer, ³Lida Rostock, ³Swapna Satam, ⁷Arun Satelli, ³Christoph Schröder, ⁷Merline Thambi, ²Apostolia Tsimberidou, ³Maïke Wagner, ¹⁰Martin Wermke, ³Heiko Schuster, ²Oliver Schoor, ¹Toni Weinschenk. ¹Immatics N.V., Tuebingen, Germany; ²MD Anderson Cancer Center, Houston, TX, USA; ³Immatics Biotechnologies GmbH, Tuebingen, Germany; ⁴University Medical Center Hamburg-Eppend, Hamburg, Germany; ⁵Columbia University, New York, NY, USA; ⁶University Hospital Würzburg, Würzburg, Germany; ⁷Immatics US, Inc., Houston, TX, Germany; ⁸University Hospital Bonn, Bonn, Germany; ⁹University of Pittsburgh, Pittsburgh, PA, USA; ¹⁰University Hospital Dresden, Dresden, Germany

Background Several peptide-HLA targets for T cell receptor (TCR)-based immunotherapies are currently being evaluated in the field, however, many are limited by their overall low prevalence, low copy numbers or relevant expression in healthy tissues. A T cell target with nearly ideal properties has high, homogenous and prevalent expression across multiple cancers in the absence of significant safety/toxicity liabilities. Here, we describe the in-depth characterization of an HLA-A*02:01-presented peptide derived from the cancer germline antigen preferentially expressed antigen in melanoma (PRAME) that opens an avenue of new opportunities for patients with solid cancers which we aim to leverage by two distinct TCR-based therapeutic modalities, TCR-engineered T cells (ACTengine[®] IMA203) and TCR Bispecifics (TCER[®] IMA402).

Methods PRAME target peptide presentation and mRNA expression in tumor and normal tissues was assessed by quantitative mass spectrometry (MS) and transcriptomics. *In situ* hybridization was used to analyze target homogeneity. We compare target prevalences based on IMADetect[®] qPCR testing of screening biopsies from clinical trial patients with prevalences based on a PRAME target tailored, MS-based mRNA expression threshold applied to a large RNA sequencing dataset.

Results PRAME RNA expression is elevated across many tumor types and only minimal in some normal tissues except testis. As demonstrated by MS, RNA expression does not translate into relevant peptide presentation on normal tissues. Peptide copy numbers range from 100 to 1,000 peptide copies per cell (target density) in the majority of tumor tissues as measured by highly sensitive MS-based AbsQuant[®] technology. Histologic analysis of PRAME RNA in different solid tumors demonstrates homogenous expression of PRAME with a high frequency of positive tumors cells. PRAME shows a prevalence between 80-100% in uterine and ovarian carcinoma, sarcoma subtypes, cutaneous and uveal melanoma and high prevalence in many other solid cancer types, such as cholangiocarcinoma, lung, kidney, breast, head and neck, esophageal, bladder and hepatocellular carcinoma. Prevalence numbers obtained during patient screening in our clinical trials match predicted prevalences. Interim phase 1a data from the IMA203 TCR-T trial (cut-off Oct 05, 2021) showed clinical responses in head and neck carcinoma, synovial sarcoma, uveal melanoma, and cutaneous melanoma.

Conclusions Here, we demonstrate comprehensive target characterization and validation data supporting the nearly ideal

target properties of PRAME that can be exploited for the benefit of patients: PRAME is highly cancer-associated, homogeneously expressed, presented at high target density, highly prevalent across many solid cancers and clinically validated, underlining its potential to reach a large cancer patient population.

Trial Registration NCT03686124

Ethics Approval The study was approved by the institutional review board/ethics committee as required for each participating site.

<http://dx.doi.org/10.1136/jitc-2022-SITC2022.0713>

714

ATOR-1017, A 4-1BB ANTIBODY, DEMONSTRATES PROMISING SAFETY AND PROOF OF MECHANISM IN A FIRST-IN-HUMAN STUDY IN PATIENTS WITH ADVANCED SOLID MALIGNANCIES

¹Ana Carneiro*, ²Sumeet Ambarkhane, ²Karin Enel Smith, ³Gustav Ullenhag, ²Lena Schulz, ²Tova Landstrom, ²Peter Ellmark, ²Malin Carlsson, ⁴Jeffrey Yachnin. ¹Skåne University Hospital, Lund, Sweden; ²Alligator Bioscience AB, Lund, Sweden; ³Uppsala University Hospital, Uppsala, Sweden; ⁴Karolinska Universitetssjukhuset, Solna, Sweden

Background ATOR-1017 is a human Fcγ-receptor cross-linking dependent IgG4 4-1BB (CD137) agonist. ATOR-1017 activates T cells and natural killer cells in the tumor environment, leading to immune-mediated tumor cell killing.

Methods In this first-in-human, dose escalation, multicenter, phase 1 study, adult patients with solid tumors refractory to standard therapy were enrolled in single patient cohorts for doses up to 40 mg, and thereafter in cohorts of 3-6 patients. Intra-patient dose escalation is allowed. ATOR-1017 is administered intravenously as monotherapy (as flat dose) every three weeks until disease progression or unacceptable toxicity. The primary objectives are assessment of safety (maximum tolerated dose (MTD), adverse events (AEs), dose-limiting toxicities (DLT)), and determination of recommended phase 2 dose. Secondary and exploratory objectives include pharmacokinetics (PK), immunogenicity, efficacy (by iRECIST), and Pharmacodynamic (PD) biomarkers.

Results At cut off date 14 June 2022, 25 patients (20 females/5 males), with median age 57 years (34-76), median of 3 (1-9) prior lines of chemotherapy and/or median 1 (1-3) lines of immunotherapy, 21 (84%) with disease stage IV at entry had been treated. Ten dose levels were evaluated; 0.38mg, 1.5mg, 5mg, 15mg, 40mg, 100mg, 200mg, 360mg, 600mg, and 900mg. Treatment-related AEs (TRAEs) were reported in 13 patients (52%); most common (≥10%) were fatigue (16%) and neutropenia (12%). Five patients experienced a grade 3-4 TRAE; neutropenia (n = 2), febrile neutropenia (n = 1), non-cardiac chest pain (n = 1), increased liver enzymes (n = 1) and leukopenia/thrombocytopenia (n = 1). No patients discontinued due to TRAEs, no DLTs were observed, and MTD has not been reached. Three patients remained on treatment and 22 had discontinued treatment [(confirmed disease progression (n = 12), clinical deterioration (n = 6), withdrawal of consent (n = 1), death due to disease progression (n = 2), investigator's decision (n=1)]. The median time on treatment was 12.1 weeks (range 5.3-67.3). A dose-proportional pharmacokinetics was observed. PD biomarkers demonstrated activation of peripheral CD8 T cells and a dose-dependent increase in soluble 4-1BB confirming biological activity and proof-of-mechanism. Stable disease was observed in 13 patients (52%), which lasted longer than 6 months for 6 (24%) patients (of which 2 had ovarian cancer).

Conclusions ATOR-1017 demonstrated excellent safety at doses up to 900 mg, together with a favorable PK profile, confirmation of biologic activity and signs of clinical benefit. These data warrant further development of ATOR-1017, a 4-1BB agonistic antibody, in combination with other therapeutic approaches in solid tumors.

Acknowledgements We acknowledge the patients, their families, as well as the research staff who contributed to the study.

Trial Registration ClinicalTrials.gov Identifier: NCT04144842

Ethics Approval Name of the ethics committee(s): Swedish Ethical Review Authority (Etikprövningsmyndigheten)

The number/ID of the approval(s): Registration no – 2019-03820

All patients provided written informed consent prior to study participation.

<http://dx.doi.org/10.1136/jitc-2022-SITC2022.0714>

715

EMERGING RESULTS FROM THE USE OF AN ONCOLYTIC ADENOVIRUS ARMED WITH TNFA AND IL-2 (TILT-123) IN DIFFERENT PHASE I SOLID TUMOR CLINICAL TRIALS

¹Victor Cervera-Carrascon, ²Inge Svane, ³Katriina Peltola, ⁴Tuomo Alanko, ⁴Riitta Korpisaari, ⁵Susanna Juteau, ⁴Marjut Jaakkola, ⁴Jorma Sormunen, ⁴Juha Kononen, ²Eva Ellebaek Steensgaard, ²Tine Monberg, ²Marco Donia, ⁶Amir Khammari, ⁶Brigitte Dreno, ¹Joao Santos, ¹Suvi Sorsa, ¹Riikka Havunen, ¹Akseli Hemminki. ¹TILT Biotherapeutics Ltd, Helsinki, Finland; ²CCIT, Herlev, Denmark; ³Comprehensive Cancer Centre, Helsinki, Finland; ⁴Docrates Cancer Centre, Helsinki, Finland; ⁵Helsinki University Hospital, Helsinki, Finland; ⁶CRCINA Inserm, CHU Nantes, Nantes, France

Background After the first Immune Checkpoint Inhibitor (ICI) was approved (ipilimumab, 2011 for cancer therapy, the list of indications routinely treated with ICIs keeps increasing. In this new era of cancer immunotherapy, the major drawback of the approach is the difficulty in delivering long term benefits to a larger portion of patients. Different forms of immunotherapy used in solid tumor cancer patients seem to work better in immunologically hot tumors. To that extent, TILT-123 (an Oncolytic Adenovirus armed with TNFa and IL-2) was designed to stimulate the immune system within the tumor to enable subsequent forms of immunotherapy. After discovery and preclinical testing, the therapy was taken into clinical trials in 2020. Two years after, four Phase I clinical trials are ongoing where TILT-123 is being tested to determine its safety as monotherapy (NCT04695327), together with adoptive cell therapy using tumor-infiltrating lymphocytes (NCT04217473), and ICIs (NCT05271318, NCT05222932).

Methods These phase I open-label, dose-escalation clinical trials, have the primary endpoint of establishing safety of the treatments in patients with injectable advanced refractory and recurrent solid tumors, that cannot be treated with curative intent. Safety is evaluated based on the occurrence of adverse events, impact on vital signs and safety laboratory tests. Additionally, secondary endpoints relative to the trials include efficacy of the approaches and mechanistic analyses based on biological samples, including studies on the presence and persistence of virus in different fluids and tissues, as well as, the proteomic and transcriptomic changes seen in tumors after therapy. Antitumor efficacy, according to RECIST 1.1/iRECIST/PET criteria, has been recorded in different patients.

Results Interim safety data emerging from patients treated with TILT-123 (n=18 patients), provided confidence to continue dose escalation as the investigational medicinal product did not cause dose limiting toxicities. The most frequent treatment related adverse events, as judged by investigators, were fever, nausea, chills and fatigue, typically low grade according to the CTCAE v5.0. Systemic antitumor efficacy according to RECIST 1.1/iRECIST/PET criteria has been seen in several patients. Biological sample analyses demonstrate the remodeling of the tumor microenvironment towards an antitumor status, when studying the T cell presence and the immune signature within the tumor.

Conclusions Preliminary data emerging from Phase I clinical trials using TILT-123, point to an adequately safe approach able to induce antitumor activity, both as monotherapy and in combination. Dose escalation continues in pursuit of a recommended dose to use in Phase II clinical trials.

Acknowledgements The clinical trials reported above were made possible due to the magnificent teamwork from the trial sites and the willingness of patients to collaborate in this research. Authors are thankful to the entire Cancer Gene Therapy Group of University of Helsinki for their valuable support. Funded by TILT Biotherapeutics Ltd.

Trial Registration NCT04695327, NCT04217473, NCT05271318, and NCT05222932

Ethics Approval TILT-T115: This study was approved by the Finnish National Committee on Medical Research Ethics (TUKIJA); approval number HUS/1804/2020

TILT-T215: This study was approved by the Danish National Committee on Health Research Ethics (NVK); approval number 1905760

TILT-T563: This study was approved by the Finnish National Committee on Medical Research Ethics (TUKIJA); approval number TUKIJA/405/2021

TILT-T776: This study was approved by the Finnish National Committee on Medical Research Ethics (TUKIJA); approval number TUKIJA/366/2021

<http://dx.doi.org/10.1136/jitc-2022-SITC2022.0715>

716

AURELIO-04: A PHASE 2, OPEN-LABEL, SINGLE-ARM, MULTICENTER STUDY TO DETERMINE THE EFFICACY AND SAFETY OF SOT101 IN COMBINATION WITH PEMBROLIZUMAB IN PATIENTS WITH SELECTED ADVANCED SOLID TUMORS

¹Stephane Champiat*, ¹Aurelien Marabelle, ²Diwakar Davar, ³Peter Grell, ¹Kaissa Ouali, ¹Anna Patrikidou, ⁴Andreu Schoenenberger, ⁴Lenka Palova Jelinkova, ⁴Irena Adkins, ⁵Sascha Tillmanns, ⁵Joachim Kiemle-Kallee, ⁵Richard Sachse, ⁶Elena Garralda. ¹Gustave Roussy, Villejuif, France; ²University of Pittsburgh, Pittsburgh, PA, USA; ³Masaryk Memorial Cancer Institute, Brno, Czech Republic; ⁴SOTIO Biotech a.s., Prague, Czech Republic; ⁵SOTIO Biotech AG, Basel, Switzerland; ⁶Vall d'Hebron Institute of Oncology, Barcelona, Spain

Background SOT101 (INN: nanrilkefusp alfa), a fusion protein of IL-15 and the IL-15 receptor α sushi+ domain, was investigated in AURELIO-03 (NCT04234113), a phase 1 dose-escalation study, as monotherapy and in combination with pembrolizumab. In that trial, combination had a favorable safety profile and MTD was not reached up to the recommended phase 2 dose (RP2D) for monotherapy. Maximum activation of natural killer cells was observed already at low dose levels, maximum CD8⁺ T cell activation was reached from 9 to 12 μ g/kg, no relevant effect on T regulatory cells was observed. Therefore, 12 μ g/kg SOT101 was selected as combination RP2D. Encouraging efficacy signals were observed, even in immune checkpoint inhibitor (CPI)-relapsed patients. For combination therapy, the majority of patients had clinical benefit.^{1,2} Study AURELIO-04 (NCT05256381) aims to further evaluate the efficacy of SOT101 in combination with pembrolizumab in selected solid tumor indications.

Methods AURELIO-04 is a phase 2 single-arm study in:

- Non-small cell lung cancer after a CPI and/or platinum regimen, with no EGFR or ALK aberration
- Unresectable or metastatic MSI-H/dMMR colorectal cancer
- First-line cutaneous squamous cell carcinoma not curable by surgery or radiation and second-line after a CPI regimen
- Hepatocellular carcinoma after a CPI regimen
- Metastatic castrate-resistant prostate cancer (mCRPC) after docetaxel
- Ovarian cancer after a platinum regimen

Main inclusion criteria are measurable disease as per RECIST 1.1, accessible tumor tissue, ECOG PS 0-1, adequate organ function, no prior IL-2 or IL-15 therapy. For mCRPC, a defined number of patients with non-measurable disease is allowed.

Patients will receive 12 μ g/kg SOT101 s.c. on days 1, 2, 8, and 9 in combination with 200 mg pembrolizumab i.v. on day 1 every 3 weeks until disease progression or unacceptable toxicity.

Primary endpoint is overall response rate (ORR) per RECIST 1.1. Key secondary endpoints include efficacy

parameters such as progression-free survival, frequency and severity of treatment-emergent adverse events, pharmacokinetics (PK) including population PK, pharmacodynamics, and immunogenicity parameters.

Approximately 55 patients per indication will be enrolled. No formal testing of statistical hypotheses is planned, analyses will be descriptive. Considering benchmark ORRs, a futility analysis is planned for each indication separately. Exploratory analyses include immune and molecular biomarkers.

Recruitment started in June 2022.

REFERENCES

1. Champiat S, Marabelle A, Galvao V, *et al.* SOT101, an IL-2/IL-15 R β superagonist, in combination with pembrolizumab in patients with advanced solid tumors: Interim safety and efficacy results from the AURELIO-03 dose escalation trial. Presented at: American Association for Cancer Research Annual Meeting 2022; April 8-13, 2022; New Orleans, LA.
2. Garralda E, Naing A, Galvao V, *et al.* Interim safety and efficacy results from AURELIO-03, a phase 1 dose escalation study of the IL-2/IL-15R β receptor superagonist SOT101 as a single agent and in combination with pembrolizumab in patients with advanced solid tumors. Presented at: American Society of Clinical Oncology Annual Meeting 2022; June 3-7, 2022; Chicago, IL.

Ethics Approval The study was approved by Advarra Institutional Review Board approval number Pro00062123. Participants give informed consent before taking part

<http://dx.doi.org/10.1136/jitc-2022-SITC2022.0716>

717

INTERIM CLINICAL UPDATE OF THE PHASE 1B TRIAL OF ATRC-101 AS MONOTHERAPY OR IN COMBINATION WITH PEMBROLIZUMAB FOR SELECT ADVANCED SOLID TUMORS

¹Bartosz Chmielowski*, ²John Weroha, ³Susanna Ulahannan, ⁴John Powderly, ⁵Frances Valdes-Albini, ⁶Tanios Bekaii-Saab, ⁷Deborah Doroshov, ⁸Alejandro Recio-Boiles, ⁹Jordan Berlin, ¹⁰Yan Xing, ¹¹Sudha Khurana, ¹¹Jonathan Benjamin, ¹²Steven Isakoff, ¹³Benjamin Weinberg. ¹University of California Los Angeles, Los Angeles, CA, USA; ²Mayo Clinic College of Medicine and Sci, Rochester, MN, USA; ³OU Health Stephenson Cancer Center, OKC, OK, USA; ⁴Carolina BioOncology Institute, Huntersville, NC, USA; ⁵University of Miami, Miami, FL, USA; ⁶Mayo Clinic Comprehensive Cancer Center, Phoenix, AZ, USA; ⁷Icahn School of Medicine at Mount Sinai, New York, NY, USA; ⁸The University of Arizona Cancer Center, Tucson, AZ, USA; ⁹Vanderbilt University Medical Center, Nashville, TN, USA; ¹⁰City of Hope Comprehensive Cancer Center, Duarte, CA, USA; ¹¹Atreca, Inc., San Carlos, CA, USA; ¹²Massachusetts General Hospital, Boston, MA, USA; ¹³Georgetown University Medical Center, Washington, DC, USA

Background ATRC-101 is an engineered, fully human, monoclonal antibody identified via the Atreca discovery platform that targets a novel tumor-specific ribonucleoprotein complex.

Methods ATRC-101-A01 is a Phase 1b dose escalation and expansion trial of ATRC-101 administered to participants with select solid tumors as monotherapy every 3 (Q3W-Mono) or 2 (Q2W-Mono) weeks and in combination with pembrolizumab (Q3W-Pembro). Participants in Q3W-Pembro must have had suboptimal response to prior/ongoing anti-PD-1/PD-L1 and deemed to potentially benefit from addition of ATRC-101. Objectives include safety (primary), pharmacokinetics, immunogenicity, recommended dose for expansion, and anti-tumor activity (RECIST v1.1). Biomarker analyses include immunohistochemical staining for target expression and CD8⁺ T cell infiltration in baseline and on-treatment tumor biopsies. For participants described herein, target expression was analyzed retrospectively.

Results As of data cut-off (February 15, 2022), 50 heavily pre-treated participants (median prior lines of therapy 5, range 1–11) received ≥1 dose of ATRC-101 (Q3W-Mono, n=37; Q2W-Mono, n=9; Q3W-Pembro, n=4). ATRC-101 was administered at 0.3 mg/kg (n=3), 1 mg/kg (n=6), 3 mg/kg (n=12), 10 mg/kg (n=13), and 30 mg/kg (n=16). Tumor types included colorectal (n=24), breast (n=8), ovarian (n=7), non-small cell lung (NSCLC, n=5), melanoma (n=3), head and neck squamous cell (n=2), and urothelial (n=1).

Dose escalation has been completed for Q3W-Mono and is ongoing for other cohorts. To date, no dose-limiting toxicities have been reported and no maximum tolerated dose identified. The dose for ongoing cohorts is 30 mg/kg.

Treatment-emergent adverse events (TEAEs) are summarized in Table 1. None resulted in treatment discontinuation or dose reduction. Grade ≥3 TEAEs occurred in 13 (26%) participants. Grade ≥3 TEAEs considered by investigators as related to ATRC-101 occurred in 3 (6%) participants (tumor pain, headache, small intestinal obstruction).

There was one partial response (NSCLC) in Q3W-Mono (30 mg/kg) and one complete response (melanoma) in Q3W-Pembro (10 mg/kg). The latter participant had previously progressed during treatment with nivolumab. An additional 5 participants experienced stable disease (SD) as best response, with reductions in target lesions. Target expression, as detected retrospectively by immunohistochemical analysis of screening tumor biopsies, was associated with achievement of SD or better and with reduction in the sum of diameters of target lesions.

Conclusions ATRC-101, without and with pembrolizumab, has been well tolerated and has demonstrated anti-tumor activity among target expressers. Enrollment in specific expansion cohorts now requires pretreatment tumor biopsies demonstrating ATRC-101 target expression (H-score ≥50) by immunohistochemistry. Updated data will be presented at the meeting.

Trial Registration NCT04244552

Ethics Approval This trial was approved by the institutional review board or ethics committee as required for each participating site.

Abstract 717 Table 1 Cumulative safety data as of February 15, 2022

Table 1: Cumulative safety data as of February 15, 2022

ATRC-101 dose, mg/kg	Q3W-Mono					Q2W-Mono			Q3W-Pembro	
	0.3	1	3	10	30	1	3	10	10	30
n	3	3	9	7	15	3	3	3	3	1
Number of cycles	11	7	37	18	47	8	14	8	12	3
Participants with ≥1 TEAE, n (%)	3 (100)	3 (100)	9 (100)	7 (100)	13 (86.7)	3 (100)	3 (100)	3 (100)	3 (100)	1 (100)
Participants with ≥2 Grade ≥3 TEAE, n (%)	1 (33.3)	1 (33.3)	3 (33.3)	2 (28.6)	0	1 (33.3)	0	1 (33.3)	0	0
Participants with ≥3 Grade ≥3 treatment-related TEAE, n (%)	0	0	2 (22.2) ¹	1 (14.3) ²	0	0	0	0	0	0

1. Preferred terms for Grade ≥3 treatment-related TEAE – tumor pain and headache.
 2. Preferred term for Grade ≥3 treatment-related TEAE – small-intestinal obstruction.
 Q3W-Mono = ATRC-101 monotherapy every 3 weeks cohort; Q2W-Mono = ATRC-101 monotherapy every 2 weeks cohort; Q3W-Pembro = ATRC-101 every 3 weeks + pembrolizumab cohort; TEAE = treatment-emergent adverse event.

<http://dx.doi.org/10.1136/jitc-2022-SITC2022.0717>

718

PRELIMINARY RESULTS OF GII-101-P101 (KEYNOTE-B59): GI-101 (CD80-IGG4 FC-IL2V) AS A SINGLE AGENT AND IN COMBINATION WITH PEMBROLIZUMAB IN PATIENTS WITH ADVANCED AND/OR METASTATIC SOLID TUMORS

¹Byoung Chul Cho*, ¹Sang Shin, ²Jae Lyun Lee, ³Byoung Shim, ⁴Hyo Lee, ⁵Nari Yun, ⁵Mina Ham, ⁵YunHee Jeong, ⁵Wooyul Lee, ⁵Hyunjin Kang, ⁵Jisoo Kim, ⁵Myoung Ho Jang. ¹Severance Hospital, Seoul, Korea, Republic of; ²Asan Medical Center, Seoul, Korea, Republic of; ³St. Vincent's Hospital, Seoul, Korea, Republic of; ⁴Chungnam National University Hospital, Daejeon, Korea, Republic of; ⁵GI Innovation, Seoul, Korea, Republic of

Background GI-101 is a novel bispecific fusion protein containing CD80 and interleukin-2 variant, designed to boost immune cell proliferation including cytotoxic T and NK cells without increasing Treg cell. A first-in-human study was performed to evaluate safety and efficacy of GI-101 as a monotherapy and in combination with pembrolizumab.

Methods Patients (pts) with advanced/metastatic solid tumors that have progressed on standard of care (SOC), or for whom no SOC exists, or SOC was deemed not appropriate, received escalating doses of GI-101 monotherapy or GI-101 in combination with 200 mg pembrolizumab intravenously every 3 weeks. The primary objective was to assess safety, tolerability and maximum tolerated dose and/or RP2D utilizing a conventional 3+3 design.

Results 25 pts received GI-101 monotherapy (n=16) or in combination with pembrolizumab (n=9) between Aug 2021 and July 2022. The median number of prior systemic therapies was 3 [1–6] and 64% of pts were previously treated with immunotherapy. No dose-limiting toxicities up to 0.15 mg/kg were reported with planned dose level of 0.002~0.6 mg/kg. Treatment-related adverse events (TRAEs) occurred in 11 (69%) and 5 (56%) pts in the single and combination cohorts, respectively. Three pts experienced Grade 3+ TRAEs (19%) with GI-101 monotherapy and no Grade 3+ TRAEs were reported with combination. Anti-tumor activities were seen both in single agent and in combination. One confirmed partial response (PR), among 16 pts, in metastatic urothelial carcinoma with a time to progression of 121 days was observed with GI-101 monotherapy. The patient previously experienced immunotherapy with best response of progressive disease. Additionally, two ongoing pts were observed PRs in combination cohorts among nine pts [one confirmed PR in non-small cell lung cancer (NSCLC) and 1 unconfirmed PR in metastasis of unknown origin]. The NSCLC patient had acquired resistance to previous immunotherapies with best response of PR and stable disease (SD), respectively. In single and combination cohorts of diverse tumor types, five and three pts had SDs. Median duration of treatment was 61 (15–171+) days. Systemic exposure to GI-101 increased with dose-escalation with half-life of 7.5~10.1 hours, resulting in a dose-dependent increase in NK and CD8+ T cells, without significant impact on Treg cells in peripheral blood.

Conclusions GI-101 was well tolerated as monotherapy and in combination with pembrolizumab in pts with previously treated, advanced solid tumors. Preliminary anti-tumor activity was seen both in monotherapy and in combination with pembrolizumab. The dose-escalation is currently ongoing to identify RP2D.

Trial Registration Clinical trial identification: NCT04977453

<http://dx.doi.org/10.1136/jitc-2022-SITC2022.0718>

719

PHASE 1 STUDY OF THE PORCUPINE (PORCN) INHIBITOR RXC004 IN COMBINATION WITH THE PD-1 INHIBITOR NIVOLUMAB IN PATIENTS WITH ADVANCED SOLID TUMORS

¹Natalie Cook, ²Sarah Blagden, ³Juanita Lopez, ⁴Debashis Sarker, ⁵Alastair Greystoke, ⁶Saira Bashir, ²Aglaia Skolariki, ²Salma ElBadri, ⁴Cienne Morton, ⁶Ana OrtegoFranco, ³Shybi MohamedKhan, ⁷Catherine Eagle, ⁷Eimear Flanagan, ⁷Louise Goodwin, ⁷Caroline Phillips, ⁷Jane Robertson*, ⁷Craig Tilston, ⁷Helen Timmis, ⁸Simon Woodcock, ⁵Ruth Plummer. ¹University of Manchester, The Christie, Manchester, UK; ²Oxford University Hospitals, Oxford, UK; ³Royal Marsden Hospital, London, UK; ⁴Guy's Hospital NHS Trust, London, UK; ⁵The Freeman Hospital, Newcastle-upon-Tyne, UK; ⁶University of Manchester, The Christie, Manchester, UK; ⁷RedX Pharma Plc, Alderley Edge, UK; ⁸RedX Pharma, Alderley Edge, UK

Background Tumour-derived Wnt-ligand signalling leads to a reprogramming of the immune microenvironment and is implicated in intrinsic and adaptive resistance to Immune Checkpoint Inhibitor (ICI) therapy. Specifically, Wnt-ligand signaling is correlated with reduced CD8+ve T-cell infiltration,¹ and ICI resistance² in multiple cancers.³ Inhibition of Wnt-ligand signalling can enhance ICI efficacy by (i) reversing dendritic cell tolerization, (ii) decreasing generation of Treg cells, and (iii) reducing the recruitment of myeloid-derived suppressor cells in tumor models.⁴

RXC004 is a novel small molecule inhibitor of PORCN, a protein-serine-O-palmitoyltransferase [5]. PORCN is essential for post-translational modification of Wnt ligands which is required for downstream Wnt signaling. RXC004 thus has potential for monotherapy efficacy in Wnt-ligand driven tumors i.e. cancers with RNF43 mutations or R-Spondin fusions, or with high Wnt-ligand activity. Furthermore, RXC004 can reverse immune evasion in mouse models,⁵ and may therefore restore ICI sensitivity in ICI resistant tumors when co-administered.

This abstract reports the second module of a multi-modular adaptive design protocol (NCT03447470). The first module was previously reported⁶ and the recommended Phase 2 dose (RP2D) for RXC004 monotherapy was 2mg QD.

Methods This was an open label, 3+3 dose escalation study. Following a single dose with a 7-day washout, patients received RXC004 QD in 28-day cycles, and nivolumab 480mg i.v every 4 weeks.

The primary objectives were to assess safety and tolerability and define a RP2D of RXC004 to combine with ICIs. Secondary objectives were Pharmacokinetics (PK) and RECIST response. Exploratory objectives included changes in circulating immune subsets by flow cytometry, and cytokines by a bead-based multiplexed immunoassay.

Results Between 24/03/2021 and 30/06/2022, 14 patients with unselected advanced solid tumors received RXC004 at doses of 1mg and 1.5mg QD, in combination with nivolumab.

The AE profile for the combination was broadly similar to RXC004 monotherapy. The most common treatment-related AEs were nausea, dysgeusia, fatigue, anorexia and weight loss. No grade 4/5 AEs, bone events or immune-related AEs were reported.

RXC004 PK exposure in the combination did not exceed the 2mg QD monotherapy exposure. Disease control was observed in some patients in the 1.5mg QD combination cohort.

Conclusions In patients with unselected cancers, RXC004 was safe and tolerated at doses up to 1.5mg QD in combination with standard dose nivolumab. The RP2D was 1.5mg QD.

RXC004+ICI combinations will now be investigated in selected patients with Wnt-ligand driven tumors. Trial Registration EudraCT No: 2017-000720-98

REFERENCES

1. Spranger S, Bao R, Gajewski TF. Melanoma-intrinsic β -catenin signalling prevents anti-tumour immunity. *Nature*. 2015;**523**(7559):231–5. doi: 10.1038/nature14404. Epub 2015 May 11. PMID: 25970248.
2. Abril-Rodriguez *et al*. PAK4 inhibition reverses immune cell exclusion and overcomes resistance to checkpoint blockade therapy. *Journal for Immunotherapy of Cancer*. 2018;**6**(suppl 1):O39
3. Luke JJ, Bao R, Sweis RF, Spranger S, Gajewski TF. WNT/ β -catenin Pathway Activation Correlates with Immune Exclusion across Human Cancers. *Clin Cancer Res*. 2019;**25**(10):3074–3083. doi: 10.1158/1078-0432.CCR-18-1942. Epub 2019 Jan 11. PMID: 30635339
4. DeVito NC, Sturdivant M, Thievanthiran B, Xiao C, Plebanek MP, Salama AKS, Beasley GM, Holtzhausen A, Novotny-Diermayr V, Strickler JH, Hanks BA. Pharmacological Wnt ligand inhibition overcomes key tumor-mediated resistance pathways to anti-PD-1 immunotherapy. *Cell Rep*. 2021;**35**(5):109071. doi: 10.1016/j.celrep.2021.109071. PMID: 33951424;
5. Phillips C. *et al*. Wnt/ β -Catenin pathway inhibitor RXC004 enhances the immunity of pre-clinical models of cancer. *Cancer Res*. 2019;**79**(13_Supplement):506
6. Cook N. *et al* Phase I study of the porcupine (PORCN) inhibitor RXC004 in patients with advanced solid tumours *Annals of Oncology*. 2021;**32**(suppl_5): S583-S620. 10.1016/annonc/annonc699

Ethics Approval This study was approved by West Midlands-Edgbaston Research Ethics Committee and Health Research Authority in UK; approval number 222362 (IRAS ID).

<http://dx.doi.org/10.1136/jitc-2022-SITC2022.0719>

ENHANCING THE ANTI-TUMOR IMMUNITY AND THERAPEUTIC POTENTIAL OF ICT01, A BUTYROPHILIN3A-TARGETED, γ 982 T CELL-ACTIVATING MONOCLONAL ANTIBODY, WITH LOW DOSE IL-2 IN PATIENTS WITH ADVANCED SOLID TUMORS: THE EVICTION-2 TRIAL

<http://dx.doi.org/10.1136/jitc-2022-SITC2022.0720>

¹Johann De Bono*, ²Stephane Champiat, ²Francois-Xavier Danlos, ³Martin Wermke, ⁴Volker Kunzmann, ⁵Aude de Gassart, ⁵Emmanuel Valentin, ⁶Marina Iche, ⁵Maelle Mairesse, ⁵Patrick Brune, ⁷Daniel Olive, ⁵Paul Frohna. ¹Institute for Cancer Research and Royal Marsden, London, UK; ²Gustave Roussy, Villejuif, France; ³Universitaetsklinikum Carl Gustav Carus Dresden, Dresden, Germany; ⁴University Hospital Würzburg, Würzburg, Germany; ⁵ImCheck Therapeutics, Marseille, France; ⁶Life Consulting, Argenteuil, France; ⁷Centre de Recherche en Cancérologie de Marseille, Marseille, France

Background ICT01 is an anti-BTN3A mAb that selectively activates γ 982 T cells to orchestrate a robust antitumor immune response of the innate and adaptive immune systems that leads to solid tumor infiltration of activated γ 982 T cells, CD8 T cells, and NK cells. (EVICTION trial (NCT04243499); SITC 2021, #503) However, the pharmacodynamic effects of ICT01 are dependent on an adequate population of γ 982 T cells, which is lacking in most advanced cancer patients. ICT01 plus low-dose SC (LDSC) IL-2 has been shown to safely and selectively increase the number of γ 982 T cells, without Treg expansion, in non-human primates.

Methods EVICTION-2 (NCT05307874) is a phase I/IIa basket trial including Bayesian dose escalation across 8 dose cohorts that is being conducted at 4 clinical sites in the UK, France and Germany. ICT01 is administered IV on day 1 of each Q3W cycle (1, 5, 20 or 75mg) and LDSC IL-2 (1 or 2 MIU/m²) on days 1-5 of the first 3 cycles to patients with colorectal (CRC), ovarian (OV), prostate, or pancreatic cancer. Efficacy evaluable patients are defined as receiving ≥ 3 cycles with a \geq Wk 8 RECIST assessment. Blood samples are collected for immunophenotyping by flow cytometry and cytokine analysis (IFN γ , TNF α , IL-1b/2/4/6/8/10/12/13) on days 1, 5, 8 and 15 of each cycle. Tumor biopsies (baseline, Day 28) for flow cytometry, IHC, and Nanostring profiling. Patients are monitored during the first 21-day cycle for DLTs and a safety review committee determines if dose escalation can continue.

Results Cohort 1 (n=2) received 1 MIU/m² IL-2 + 1 mg ICT01 with rapid activation and complete migration of γ 982 T cells within 30 minutes post ICT01 without any DLTs. This was followed by an absolute increase of γ 982 T cells that peaked on day 15 of 52K (CRC pt; 7.5x increase; 12% of total T cells) and 236K (OV pt; 2.2x increase; 43% of total T cells). γ 982 T cells returned to baseline in the CRC pt, while the OV patient had ~300K at the time of C2, which was well tolerated. Additionally, rapid activation and migration of CD4 and CD8 T cells, NK cells, and granulocytes were observed on day 1. Cytokine, biopsy and RECIST results will be presented. Dose escalation to 5mg ICT01+ 1 MIU/m² IL-2 and 1 mg ICT01 +2MIU/m² IL-2 is ongoing.

Conclusions LDSC IL-2 plus ICT01 safely and significantly increase the number of activated γ 982 T cells with broad immune activation.

Trial Registration clinicaltrials.gov NCT05307874

Ethics Approval France Committee for Personal Protection (CPP)

Consent Written informed consent was obtained from the patient for publication of this abstract and any accompanying images. A copy of the written consent is available for review by the Editor of this journal.

721

PIXATIMOD (P) IN COMBINATION WITH NIVOLUMAB (N) +/- LOW-DOSE CYCLOPHOSPHAMIDE (CY) IN ADVANCED CANCERS: A PHASE IIA BASKET TRIAL

¹Diwakar Davar*, ²Hong Wang, ¹Sarah Behr, ¹Aubrey Murano, ¹Sarah Johnson, ¹Amy Rose, ³Darryn Bampton, ³Keith Dredge, ¹Hassane Zarour, ¹John Rhee, ¹Liza Villaruz, ¹Yana Najjar, ¹Jason Luke. ¹UPMC Hillman Cancer Center, Pittsburgh, PA, USA; ²University of Pittsburgh, Pittsburgh, PA, USA; ³Zucero, Brisbane, Australia

Background Immune checkpoint inhibitors (ICI) directed against PD-(L)1 are associated with improved response rates in melanoma (MEL), and squamous/non-squamous non-small cell lung cancer (NSCLC).¹⁻⁴ Conversely, anti-PD(L)1 blockade is minimally efficacious in microsatellite stable (MSS) colorectal carcinoma (CRC). Pixatimod (P) is a heparan sulfate (HS) mimetic that is a cholestanol-sulfotetrasaccharide conjugated small molecule compound with unique NK- and T cell-dependent immunomodulatory properties. P does not possess CpG ODN motifs and hence does not activate TLR9 directly. Rather, P increases CpG ODN accumulation in lysosomal compartment of DCs, leading to enhanced production of IL-12 and NK cell activation.⁵ Preclinically, in combination with anti-PD-1, P led to increased infiltration of both central and effector memory CD4 and CD8 T cells in a IL-12 and TLR9 dependent fashion in multiple tumor modes.⁵⁻⁹ Low dose Cy has immunostimulatory and antiangiogenic properties and has synergy with CpG,^{10, 11} and PD-1 ICI.¹² In MSS mCRC, P/N demonstrated objective response rate (ORR) 12% in a Phase Ib study.¹³

We hypothesized that P and nivolumab (N) combination may overcome resistance in PD-1 relapsed/refractory (R/R) tumors; and that the addition of Cy may facilitate P+N activity in MSS CRC.

Methods This is a nonrandomized, open-label, multicohort, phase IIA study (NCT05061017) evaluating several pixatimod combinations in 3 cohorts (figure 1). The recommended phase 2 dose (RP2D) of P is 25mg IV Q1W and N is dosed at 480mg IV Q4W. Immunomodulatory dose of Cy is 50 mg twice daily, 1-week-on, 1-week-off.

P+N+low-dose Cy will be evaluated in PD-1 naïve MSS CRC (cohort 1). P+N will be evaluated in PD-1 R/R melanoma (cohort 2) and NSCLC (cohort 3). In 1st stage of each cohort, 9-13 patients will be enrolled. If ≥ 1 response(s) are seen, 8-14 additional patients will be enrolled in the 2nd stage.

The primary endpoint in this Simon two-stage trial is objective response rate (ORR) using RECIST v1.1. Key secondary endpoints include ORR by iRECIST, median and landmark survival (PFS, OS) and safety. Exploratory endpoints will characterize pharmacokinetics, immune contexture, immunophenotypic analyses and gut microbiome pre- and post-treatment blood, tumor and stool samples.

Acknowledgements We would like to thank all the participating patients, and their families.

We would like to thank the research staff of the Hillman Cancer Center's (HCC) Immunotherapy and Drug Development Center (IDDC).

Trial Registration Clinical trial information: NCT05061017.

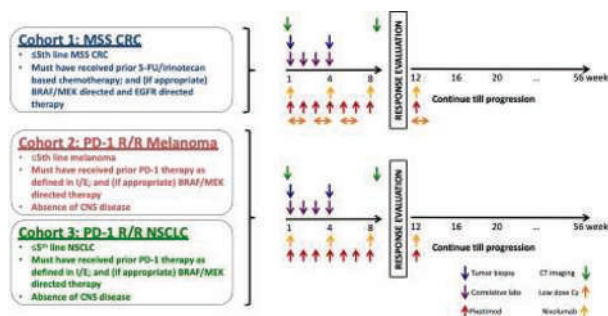
REFERENCES

1. Borghaei H, Paz-Ares L, Horn L, Spigel DR, Steins M, Ready NE, et al. Nivolumab versus Docetaxel in Advanced Nonsquamous Non-Small-Cell Lung Cancer. *N Engl J Med.* 2015;**373**(17):1627-39.
2. Brahmer J, Reckamp KL, Baas P, Crino L, Eberhardt WE, Poddubskaya E, et al. Nivolumab versus Docetaxel in Advanced Squamous-Cell Non-Small-Cell Lung Cancer. *N Engl J Med.* 2015;**373**(2):123-35.

3. Robert C, Long GV, Brady B, Dutriaux C, Maio M, Mortier L, et al. Nivolumab in previously untreated melanoma without BRAF mutation. *N Engl J Med.* 2015;**372**(4):320-30.
4. Robert C, Schachter J, Long GV, Arance A, Grob JJ, Mortier L, et al. Pembrolizumab versus Ipilimumab in Advanced Melanoma. *N Engl J Med.* 2015;**372**(26):2521-32.
5. Brennan TV, Lin L, Brandstadter JD, Rendell VR, Dredge K, Huang X, et al. Heparan sulfate mimetic PG545-mediated antilymphoma effects require TLR9-dependent NK cell activation. *J Clin Invest.* 2016;**126**(1):207-19.
6. Barash U, Lapidot M, Zohar Y, Loomis C, Moreira A, Feld S, et al. Involvement of Heparanase in the Pathogenesis of Mesothelioma: Basic Aspects and Clinical Applications. *J Natl Cancer Inst.* 2018;**110**(10):1102-14.
7. Boyango I, Barash U, Naroditsky I, Li JP, Hammond E, Ilan N, et al. Heparanase cooperates with Ras to drive breast and skin tumorigenesis. *Cancer Res.* 2014;**74**(16):4504-14.
8. Katz A, Barash U, Boyango I, Feld S, Zohar Y, Hammond E, et al. Patient derived xenografts (PDX) predict an effective heparanase-based therapy for lung cancer. *Oncotarget.* 2018;**9**(27):19294-306.
9. Ostapoff KT, Awasthi N, Cenik BK, Hinz S, Dredge K, Schwarz RE, et al. PG545, an angiogenesis and heparanase inhibitor, reduces primary tumor growth and metastasis in experimental pancreatic cancer. *Mol Cancer Ther.* 2013;**12**(7):1190-201.
10. Huang XM, Zhang NR, Lin XT, Zhu CY, Zou YF, Wu XJ, et al. Antitumor immunity of low-dose cyclophosphamide: changes in T cells and cytokines TGF-beta and IL-10 in mice with colon-cancer liver metastasis. *Gastroenterol Rep (Oxf).* 2020;**8**(1):56-65.
11. Leong WJ, Ames RY, Haverkamp JM, Torres L, Kline J, Bans A, et al. Low-dose metronomic cyclophosphamide complements the actions of an intratumoral C-class CpG TLR9 agonist to potentiate innate immunity and drive potent T cell-mediated anti-tumor responses. *Oncotarget.* 2019;**10**(68):7220-37.
12. Italiano A, Bessedes A, Pulido M, Bompas E, Piperno-Neumann S, Chevreau C, et al. Pembrolizumab in soft-tissue sarcomas with tertiary lymphoid structures: a phase 2 PEMBROSARC trial cohort. *Nat Med.* 2022;**28**(6):1199-206.
13. Kuo JC, Bampton D, Lemech C, Brown M, Stanley A, Chojnowski G, et al. Preliminary results from a phase 1b study of pixatimod (PG545) in combination with nivolumab in patients with advanced solid tumors with an expansion cohort in patients with metastatic pancreatic cancer. *Ann Oncol.* 2018;2018.

Ethics Approval The study was approved by University of Pittsburgh's Institutional Review Board, approval number MOD21060203-002.

Consent Written informed consent was obtained from the patient for publication of this abstract and any accompanying images. A copy of the written consent is available for review by the Editor of this journal.



Abstract 721 Figure 1 Clinical Trial Schema for Phase IIA Study Evaluating Pixatimod and Nivolumab +/- Low-dose Cy in MSS CRC, PD-1 R/R Melanoma and PD-1 R/R NSCLC

<http://dx.doi.org/10.1136/jitc-2022-SITC2022.0721>

722

CBL-B SILENCED, AUTOLOGOUS PBMCS AS A NOVEL ANTI-CANCER THERAPY USING THE CLOSED CELL PROCESSING PLATFORM EPIC – A PHASE 1B TRIAL WITH APN401

¹Romana Gugenberger*, ¹Alexander Dohnal, ¹Kathrin Thell, ¹Sarah Bischof, ¹Mario Kuttke, ¹Bernhard Peball, ¹Hannes Muehleisen, ¹Maria Urban, ²Andreas Tanzmann, ²Beate Pribitzer, ²Felix Batrina, ²Stefan Bunka, ²Sophia Spagl, ²Manuela Branka, ²Markus Raderer, ²Gerald Prager, ²Thorsten Fuereder, ²Nina Worel. ¹invIOs GmbH, Vienna, Austria; ²Medical University of Vienna, Vienna, Austria

Background Tumor-specific immune cells possessing effector functions to infiltrate and eradicate tumors circulate in peripheral blood and can infiltrate tumors but are impaired in their effector functions due to immune checkpoint control by Cbl-b (Casitas B-lineage lymphoma-b). Further, tumor antigen (TA) expression and recognition is limited in time and magnitude due to frequent alterations in the TA repertoire and low abundance of TA-specific immune cells within a patient's peripheral blood mononuclear cells (PBMCs). Here, we present a clinical trial of an autologous cell therapy APN401 that blocks Cbl-b in patient PBMCs using a rapid manufacturing process with the goal of enhancing immune effector functions and cytotoxicity against tumor cells. For this, we have developed the closed cell processing Enhancement Platform for immune Cells (EPiC). This platform enables manufacturing of high numbers of PBMCs with transiently silenced Cbl-b in a short processing time for the drug product (DP) APN401. In a first clinical phase 1b multiple dose study, APN401 showed clinical safety and tolerability in patients with advanced solid tumors (NCT02166255).

Methods The APN401 DP is manufactured by the 3-step EPiC process comprising (I) purification of PBMCs from leukapheresis products, (II) electroporation of PBMCs to incorporate Cbl-b siRNA and (III) final PBMC formulation for re-infusion. The final DP is specified for release according to GMP standards specific for ATMPs. The entire process requires less than 6 hours and is approved by the national competent authorities for a same-day out patient therapy in a phase 1b trial. This clinical trial is designed as an open-label, multi-center, dose escalation and expansion study and is performed in two parts. In Part A the maximum tolerated dose (MTD) will be determined, evaluating three dose levels of APN401. Key eligibility criteria include patients with advanced solid tumors for whom standard therapies have failed. Part B is an expansion study at the MTD with 15 patients for each of three specific tumor types – lung cancer, colorectal cancer and squamous cell carcinoma of the head and neck.

Results The ongoing phase 1b Part A study demonstrates the feasibility of APN401 autologous cell therapy through releasing 14 manufacturing batches (mean manufacturing dose: 5.3×10^9 PBMCs) of Cbl-b silenced patient PBMCs. Safety and tolerability have been shown for the first dosing cohort (infused cell number: 5.0×10^6 PBMCs/kg). Dose escalation is ongoing, and patients are being enrolled in the second dosing cohort (1.5×10^7 PBMCs/kg).

Ethics Approval The study is approved by Medical University of Vienna institution's independent Ethics Board, approval number 1778/2020.

<http://dx.doi.org/10.1136/jitc-2022-SITC2022.0722>

723

A PHASE 1, FIRST-IN-HUMAN, OPEN-LABEL, MULTICENTER STUDY OF INCA32459, A BISPECIFIC ANTI-PD1 AND ANTI-LAG-3 ANTIBODY, IN PATIENTS WITH SELECT ADVANCED MALIGNANCIES

¹Sarina Piha-Paul*, ²Nawel Bourayou, ³Richard Schaub, ³Yan-ou Yang, ³Wendy Wei, ³Patrick Mayes, ⁴Tara Gangadhar. ¹The University of Texas MD Anderson Cancer Center, Houston, TX, USA; ²Incyte Biosciences International Sàrl, Wilmington, DE, USA; ³Incyte Corporation, Wilmington, DE, USA; ⁴Abramson Cancer Center of the University of Pennsylvania, Philadelphia, PA, USA

Background Anti-programmed cell death (PD)-ligand (L1) therapies have improved clinical outcomes in patients with various cancers.¹ However, many patients either do not respond or develop resistance, partly due to additional immune checkpoint receptors including lymphocyte activation gene-3 (LAG-3), which is frequently co-expressed with PD-1 on tumor-infiltrating lymphocytes.^{2, 3} Combined anti-PD-1 and anti-LAG-3 therapy has demonstrated improvements in clinical outcomes compared with anti-PD-1 alone.⁴ Co-targeting PD-1 and LAG-3 with a bispecific antibody has the potential to demonstrate enhanced clinical activity compared with individual monoclonal antibodies by achieving synergistic blockade. Therefore, this study aims to assess the safety, tolerability, pharmacokinetics, pharmacodynamics, and preliminary clinical efficacy of INCA32459, a bispecific anti-PD-1 × anti-LAG-3 antibody, in patients with advanced malignancies.

Methods This first-in-human, multicenter, open-label, dose-escalation, dose-expansion phase 1 clinical study will enroll approximately 120 patients into separate dose-escalation (n≈40) and dose-expansion phases (n≈80; figure 1). Patients with select advanced malignancies will be eligible to participate in the dose-escalation phase and will receive intravenous INCA32459 starting at dose level 1 every 3 weeks. Dose escalation will proceed according to a protocol-defined statistical hybrid design⁵ to assess the safety and tolerability of INCA32459 and determine the maximum tolerated dose and/or the recommended doses for expansion. The dose-expansion phase will consist of 2 tumor-specific cohorts. Cohort 1 will enroll patients with unresectable or metastatic melanoma who have experienced disease progression after standard therapy (n≈40). Cohort 2 will enroll patients with recurrent or metastatic PD-L1+ (combined positive score ≥1) squamous cell carcinoma of the head and neck who have experienced disease progression after standard therapy (n≈40). Treatment will be administered in 3-week cycles up to a maximum duration of 2 years. The primary endpoints are safety and tolerability as assessed by occurrence of dose-limiting toxicities and incidence of treatment-emergent adverse events (TEAEs), including overall TEAEs and TEAEs that lead to treatment interruption or withdrawal. Secondary endpoints include objective response rate, disease control rate, and duration of response as determined by investigator assessment according to Response Evaluation Criteria in Solid Tumors (RECIST) v1.1 or Lugano criteria (for patients with B-cell lymphomas); pharmacokinetic parameters; and PD-1 receptor occupancy in peripheral blood samples.

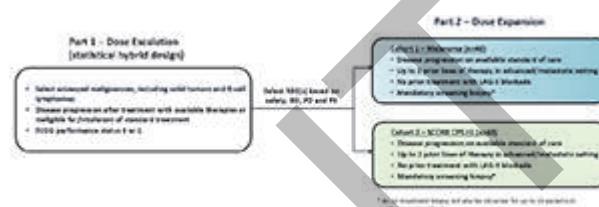
Trial Registration ClinicalTrials.gov registration pending

REFERENCES

1. Sun L, Zhang L, Yu J, et al. Clinical efficacy and safety of anti-PD-1/PD-L1 inhibitors for the treatment of advanced or metastatic cancer: a systematic review and meta-analysis. *Sci Rep.* 2020;**10**(1):2083.
2. Gros A, Robbins PF, Yao X, et al. PD-1 identifies the patient-specific CD8⁺ tumor-reactive repertoire infiltrating human tumors. *J Clin Invest.* 2014;**124**(5):2246-2259.

3. Long L, Zhang X, Chen F, et al. The promising immune checkpoint LAG-3: from tumor microenvironment to cancer immunotherapy. *Genes Cancer.* 2018;**9**(5-6):176-189.
4. Tawbi HA, Schadendorf D, Lipson EJ, et al. Relatlimab and nivolumab versus nivolumab in untreated advanced melanoma. *N Engl J Med.* 2022;**386**(1):24-34.
5. Liao JJZ, Zhou F, Zhou H, et al. A hybrid design for dose-finding oncology clinical trials. *Int J Cancer.* 2022. doi: 10.1002/ijc.34203. Online ahead of print.

Ethics Approval The study protocol was approved by institutional review boards or independent ethics committees at participating centers.



Abstract 723 Figure 1 Study schema

CPS, combined positive score; ECOG, Eastern Cooperative Oncology Group; LAG-3, lymphocyte activation gene-3; PD, pharmacodynamics; PK, pharmacokinetics; RDE, recommended dose for expansion; RO, receptor occupancy; SCC/HCN, squamous cell carcinoma of the head and neck.

<http://dx.doi.org/10.1136/jitc-2022-SITC2022.0723>

Abstracts

724

A PHASE I STUDY OF HCW9218, A BIFUNCTIONAL TGF- β ANTAGONIST/IL-15 PROTEIN COMPLEX, IN ADVANCED SOLID TUMORS

¹Melissa Geller*, ¹Manish Patel, ²Hing Wong, ²Peter Rhode, ²Philip Arlen, ²Pallavi Chaturvedi, ²Jack Egan, ²Giles Leclerc, ¹Martin Felices, ¹Shannon Lunn, ¹Bethany Hanke, ¹Deepa Kolseri, ¹Rose Wangen, ¹Jeffrey Miller. ¹University of Minnesota, St. Paul, MN, USA; ²HCW Biologics, Miramar, FL, USA

Background HCW9218 is a bifunctional protein complex comprising dimeric extracellular domains of the human transforming growth factor beta (TGF- β) receptor II and human interleukin-15 (IL-15). HCW9218 acts to (1) stimulate immune effector cells and (2) sequester soluble immunosuppressive TGF- β .^{1, 2} The primary objective of this Phase I first-in-human clinical trial is to determine the maximum tolerated dose of HCW9218 in advanced solid tumors.

Methods HCW9218 is administered subcutaneously in the outpatient setting once every 3 weeks for a minimum of two cycles. HCW9218 dose range was established through extensive nonclinical studies using the MABEL approach. Patients' assigned dose levels range from 0.25 mg/kg (DL1) to 1.2 mg/kg (DL4). Correlative analyses include HCW9218 immunogenicity and pharmacokinetic profiles, serum cytokine levels and lymphocyte number, phenotype and function.

Results Since 4/2022, three patients have been dosed. Patient #1 had a recurrent GI stromal tumor, received one dose but elected to discontinue due to metastatic bone pain. He experienced an injection site reaction lasting >72 hours requiring dose expansion to 3 subjects. Patient #2 had recurrent colon cancer, received 2 doses and discontinued due to unrelated grade 3 ascites requiring paracentesis and disease progression. Patient #3 had recurrent ovarian cancer and has received 2 doses to date. There has been one grade 3 adverse event (AE). The most common AEs have been grade 1-2 injection site reactions. Unexpectedly, patients at the DL1 level exhibit consistent and robust immune activity for at least 2 weeks after a single dose (figure 1). PBMNC and serum were collected prior to dose 1, and at 2 to 15 days after dosing. All subjects had a robust increase in NK cell proliferation (81% Ki-67⁺ by day 8 after dosing vs. 12.6% pre-dosing), which corresponded to an increased mean percent of NK cells to 34% of lymphocytes (12.6% pre-dosing). These responses were sustained through day 15, a biologic effect beyond that previously observed for other IL-15 agonists. By day 14, 44% of NK cells were CD56^{bright}. Additionally, there was a modest increase in Ki-67⁺ CD8⁺ T cells at day 8. No treatment-mediated effects were seen on serum IL-1 α , IL-1 β , IL-6, IFN- γ or TNF α , whereas levels of TGF- β 1 and TGF- β 2 were reduced (as expected) and MCP-1 was elevated. Preliminary pharmacokinetic analysis showed a C_{max} at 20-73h post-dosing and half-life of ~78h.

Conclusions HCW9218 safely and robustly expands NK cells after a single dose and escalation continues as planned to DL2 (0.5 mg/kg).

Trial Registration NCT05322408

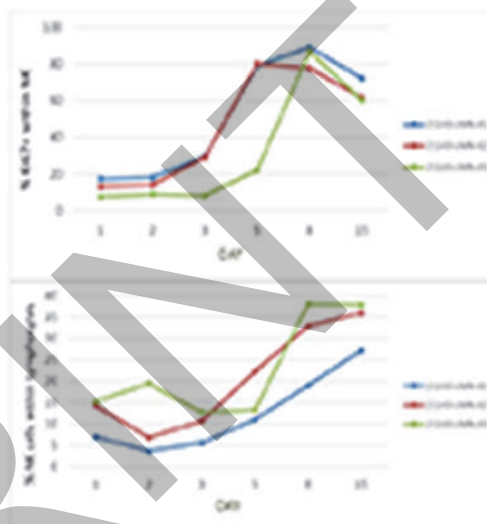
REFERENCES

1. Liu B, Zhu X, Kong L, et al. Bifunctional TGF-beta trap/IL-15 protein complex elicits potent NK cell and CD8(+) T cell immunity against solid tumors. *Mol Ther*. 2021;**29**:2949–62.
2. Chaturvedi P, George V, Shrestha N, et al. Immunotherapeutic HCW9218 augments anti-tumor activity of chemotherapy via NK cell-mediated reduction of therapy-induced senescent cells. *Mol Ther*. 2022;**30**:1171–87.

Ethics Approval This study was approved by the University of Minnesota's Institutional Review Board; approval number: 00015102. All participants gave informed consent before taking part in this clinical trial.

Consent Written informed consent was obtained from the patients for publication of this abstract and any accompanying images. A copy of the written consent is available for review by the Editor of this journal.

Figure 1



Abstract 724 Figure 1 NK cell proliferation following administration of HCW9218

Following subcutaneous administration of 0.25 mg/kg of HCW9218 there is robust proliferation of NK cells measured by Ki67, with maximum levels seen on Day 8 (81%) which corresponds to a mean of 34% of the lymphocytes.

<http://dx.doi.org/10.1136/jitc-2022-SITC2022.0724>

725

PHASE I SAFETY AND PRELIMINARY EFFICACY OF PM8002 IN SUBJECTS WITH ADVANCED SOLID TUMORS, A BISPECIFIC ANTIBODY TARGETING PD-L1 AND VEGF-A

¹Ye Guo, ²Suxia Luo, ³Yanru Qin, ⁴Yongmei Yin, ⁵Guiling Li, ⁶Jingfen Wang, ⁷Yongsheng Li, ⁸Jun Guo, ⁹Feng Zhang, ⁹Yi Huang, ¹⁰Hong Luo, ¹¹Dongqing Lv, ¹²Cheng Ying, ¹³Chunyan Wang, ¹⁴Chuan-Chu Chou*, ¹⁴Chundan Gong, ¹⁴Ruixia Chang, ¹⁴Jing Liu, ¹⁴Guoqiang Hu. ¹Shanghai East Hospital, Shanghai, China; ²Henan Cancer Hospital, Zhengzhou, China; ³The First Affiliated Hospital, Zhengzhou, China; ⁴Jiangsu Province Hospital, Nanjing, China; ⁵Union Hospital Tongji Medical College, Wuhan, China; ⁶Linyi Cancer Hospital, Linyi, China; ⁷Chongqing University Cancer Hospital, Chongqing, China; ⁸Peking University Cancer Hospital and Inst, Beijing, China; ⁹Hubei Cancer Hospital, Wuhan, China; ¹⁰Chongqing Cancer Hospital, Chongqing, China; ¹¹Taizhou Hospital of Zhejiang Provinc, Taizhou, China; ¹²Jilin Cancer Hospital, Jilin, China; ¹³Liaoning Cancer Hospital, Shenyang, China; ¹⁴Biotheus Inc., Westfield, NJ, USA

Background PD-L1 and VEGF play important roles in immune escape and tumor angiogenesis and thus enhance cancer growth and metastasis. PM8002 is a bispecific antibody targeting PD-L1 and VEGF-A. Here we present the results from a Phase I first-in-human dose-escalation and ongoing expansion study of PM8002 in advanced solid tumors.

Methods This study includes a standard 3+3 dose escalation stage (Part A: single dosing of 1, 3, 10, 20, 30, and 45 mg/kg for 3-week DLT evaluation, then administration Q2W if the subject did not experience DLT) followed by dose expansion (Part B). Primary endpoints include safety and tolerability for Part A, and ORR per RECIST 1.1 for Part B. Secondary endpoint includes pharmacokinetics (PK).

Results As of June 15, 2022, a total of 59 subjects had received at least one dose of PM8002, including 18 subjects in Part A (3 subjects per 1, 3, 10, 20, 30 and 45 mg/kg dose-levels), and 41 subjects in Part B (1mg/kg Q2W [n=1], 10mg/kg Q2W [n =1], 20mg/kg Q2W [n=18], 20mg/kg Q3W [n=4] and 30mg/kg Q3W [n=17]). In part A, no DLTs were observed and MTD was not reached. Of the 59 subjects, the median duration of PM8002 exposure was 8.1 weeks (range, 3.0–29.0 weeks). Any-grade TRAEs occurred in 40 subjects (67.8%), with 9 subjects (15.3%) reported with ≥ Grade 3 TRAEs. 9 subjects (15.3%) discontinued PM8002 administration due to TRAEs. The most common TRAEs were proteinuria (18.6%), thrombocytopenia (11.9%), aspartate aminotransferase increase (10.2%). Any-grade irAEs occurred in 24 subjects (40.7%), with 4 subjects (6.8%) reported with ≥ Grade 3 irAEs. PK analysis showed a linear dose-exposure relationship with PM8002 dosing from 1 to 45 mg/kg. $T_{1/2}$ varied from 4.2–8.9 days. Peripheral PD-L1 receptor occupancy exceeded 95% in the 10 mg/kg and higher dose groups. In part B, 30 subjects completed at least one efficacy evaluation. The ORR per RECIST 1.1 by investigator was 20%, with 6 PRs in subjects with ovarian cancer (n=1, 20mg/kg Q2W), colorectal cancer (n=1, 10mg/kg Q2W), renal cell carcinoma (n=3, 30mg/kg Q3W) and NSCLC (n=1, 20mg/kg Q2W). Fifteen subjects achieved best responses of stable disease, with a total DCR of 70%. 20 mg/kg Q2W and 30 mg/kg Q3W were recommended as the RP2D for further clinical study.

Conclusions PM8002 showed an acceptable safety profile and encouraging antitumor activity in refractory solid tumors. Phase II clinical trials with PM8002 as a monotherapy or in combination with chemotherapy are ongoing for multiple indications.

Acknowledgements We would like to thank the trial patients and their families for the contribution to this clinical trial. This trial was funded by Biotheus Inc.

Trial Registration ChiCTR. org.cn: ChiCTR2000040552

Ethics Approval This study was approved by the Ethics Committee for Drug Clinical Trials, Shanghai East Hospital.

<http://dx.doi.org/10.1136/jitc-2022-SITC2022.0725>

726

PHASE I RESULTS OF FT516, AN OFF-THE-SHELF, IPSC-DERIVED NK CELL THERAPY EXPRESSING A HIGH-AFFINITY, NON-CLEAVABLE CD16 (HNCD16) COMBINED WITH AVELUMAB IN PATIENTS WITH ADVANCED SOLID TUMORS

¹Martin Gutierrez*, ²Manish Patel, ³Feng Liu, ³Peter Szabo, ³Bob Valamehr, ³Yu-Way Chu, ³Brandon Beagle, ³Jeffrey Chou, ⁴David Hong. ¹Hackensack University Medical Center, John Theurer Cancer Center, Hackensack, NJ, USA; ²University of Minnesota. Masonic Cancer Center, Rochester, MN, USA; ³Fate Therapeutics, Inc., San Diego, CA, USA; ⁴MD Anderson Cancer Center, Houston, TX, USA

Background FT516 is an allogeneic, off-the-shelf natural killer (NK) cell cancer immunotherapy derived from a clonal master induced pluripotent stem cell (iPSC) line expressing hnCD16 to optimize antibody-dependent cellular cytotoxicity (ADCC) when combined with monoclonal antibodies (mAbs). A Phase I dose-escalation study of FT516 in combination with rituximab for patients with B-cell lymphomas has shown favorable safety and anti-tumor activity.¹ We report results from a Phase I dose-escalation study of FT516 in combination with avelumab for patients with advanced solid tumors.

Methods Patients initially received 2 treatment cycles, with the option for 2 additional cycles, each cycle consisting of 3 days of outpatient conditioning chemotherapy (cyclophosphamide 500 mg/m² and fludarabine 30 mg/m²) followed by 3 once-weekly doses of FT516 with subcutaneous IL-2 (6 MIU). Avelumab 800 mg was administered every 2 weeks until progression. FT516 dose escalation was based on 3+3 design. Endpoints included safety, tolerability, and anti-tumor activity.

Results As of a data cutoff of 16 May 2022, 12 patients (non-cutaneous melanoma [6], cutaneous melanomas [4], non-small cell lung cancer and triple-negative breast cancer [1 each]) with a median of 3 prior therapies were treated, including 11 patients who received prior anti-PD-(L)1 therapy. Doses of 90 million (n=3), 300 million (n=3), or 900 million (n=6) FT516 cells/dose were administered. No dose-limiting toxicities, graft vs. host disease, neurotoxicity, FT516-related Grade \geq 3 adverse events (AEs), or FT516-related serious AEs were reported. Grade 1 cytokine release syndrome was reported in 1 patient. Tumor burden reduction was observed in 6 patients, with a median peak reduction of 12.9% (range 3.5, 50); 1 patient with cutaneous melanoma refractory to 2 prior anti-PD-1 containing regimens achieved and maintained partial response per iRECIST through 6.2 months after initiation of treatment, and 6 patients had stable disease per iRECIST with median duration of disease control of 4.9 (range 3.8, 10.9) months.

Conclusions Up to 900 million FT516 cells administered with IL-2 in multiple doses and multiple cycles in combination with avelumab are safe and tolerable, with evidence of anti-tumor activity following failure of prior anti-PD-(L)1 therapy. These data support the development of next-generation iPSC-derived NK cells engineered with additional synthetic functional elements designed to enhance anti-tumor activity in solid tumors.

REFERENCE

1. Patel K, Bachanova V, Goodman A, et al. Phase I Study of FT516, an Off-the-Shelf iPSC-Derived NK Cell Therapy, in Combination with Rituximab in Patients with Relapsed/Refractory B-Cell Lymphoma. *Blood*; 2021;**138**, s1:3873.

Ethics Approval This study is being conducted in accordance with the Declaration of Helsinki and was approved by all Institutional Review Boards from each clinical site participating

in the study. Specific approval numbers can be provided upon request.

<http://dx.doi.org/10.1136/jitc-2022-SITC2022.0726>

727

INTERIM PHASE I CLINICAL DATA OF FT538, AN OFF-THE-SHELF, MULTIPLEXED-ENGINEERED, iPSC-DERIVED NK CELL THERAPY, COMBINED WITH MONOCLONAL ANTIBODIES IN PATIENTS WITH ADVANCED SOLID TUMORS

¹Martin Gutierrez*, ²Melissa Johnson, ³David Sommerhalder, ⁴Wells Messersmith, ⁵Haeseong Park, ⁶Muhammad Furqan, ⁷Jason Chesney, ⁸Ryan Bjordahl, ⁹Lingmin Zeng, ¹⁰Peter Szabo, ¹¹Yu-Waye Chu, ¹²Brandon Beagle, ¹³Bob Valamehr, ¹⁴Jeffrey Chou, ¹⁵David Hong. ¹Hackensack University Medical Center, John Theurer Cancer Center, Hackensack, NJ, USA; ²Sarah Cannon Research Institute, Tennessee Oncology, Nashville, TN, USA; ³NEXT Oncology, San Antonio, TX, USA; ⁴University of Colorado Cancer Center, Aurora, CO, USA; ⁵Alvin J Siteman Cancer Center, Washington University in Saint Louis, Saint Louis, MO, USA; ⁶University of Iowa Hospitals and Clinics, Holden Comprehensive Cancer Center, Iowa City, IA, USA; ⁷University of Louisville, James Graham Brown Cancer Center, Louisville, KY, USA; ⁸Fate Therapeutics, Inc., San Diego, CA, USA; ⁹MD Anderson Cancer Center, Houston, TX, USA

Background Clonal induced pluripotent stem cell (iPSC) lines serve as a renewable source for mass production of immune cells, enabling engineered cell therapies to be administered off-the-shelf in multi-dose regimens to patients, including in combination with other anti-cancer agents. In preclinical solid tumor models, iPSC-derived natural killer (NK) cells have been observed to synergize with monoclonal antibodies (mAbs), including anti-PD-1/L1 checkpoint blockade and antibody-dependent cellular cytotoxicity (ADCC)-competent mAbs, resulting in greater anti-tumor activity. FT538, a first-of-kind, multiplexed-engineered NK cell therapy generated from a clonal master engineered iPSC line, incorporates 3 synthetic elements for enhanced innate immunity: (1) high-affinity 158V, non-cleavable CD16 Fc receptor that maximizes ADCC; (2) IL-15/IL-15 receptor fusion that promotes cytokine-autonomous persistence; (3) CD38 knockout that provides improved metabolic fitness and resistance to oxidative stress within the tumor microenvironment.¹ We intend to report initial clinical data from a Phase I study of FT538 combined with mAbs in patients with advanced solid tumors.

Methods FT538-102 is a Phase I dose-escalation study (ClinicalTrials.gov: NCT05069935) investigating FT538 combined with anti-PD-1/L1 or ADCC-competent mAbs in advanced solid tumors. Treatment consists of two, 29-day treatment cycles, each consisting of 3 days outpatient conditioning chemotherapy (cyclophosphamide 500 mg/m² and fludarabine 30 mg/m²), followed by 3 outpatient once-weekly doses of FT538; mAbs are administered at standard dose and schedule. Key study endpoints include determining the recommended Phase II dose, safety and tolerability, anti-tumor activity, pharmacokinetics, and anti-product immunogenicity of FT538.

Dose escalation is based on a modified toxicity probability interval algorithm dose-escalation design with a starting dose level of 100 million FT538 cells/dose in combination with avelumab or pembrolizumab in PD-L1-expressing solid tumors; trastuzumab in HER2-expressing tumors; or cetuximab in colorectal cancer, squamous head and neck or lung cancers, or epidermal growth factor receptor-mutated lung cancer.

Results As of 14 July 2022, 7 patients were treated at the first dose level of 100 million FT538 cells/dose combined with avelumab (3), trastuzumab (1), or cetuximab (3). No dose-limiting toxicities, and no events of any grade of cytokine release syndrome, immune effector cell-associated neurotoxicity syndrome, or graft vs. host disease, were reported. No FT538 treatment-related Grade \geq 3 adverse events (AEs), or serious AEs were observed. Dose escalation is ongoing.

Conclusions Interim clinical data, including safety and tolerability and initial anti-tumor activity, from the ongoing Phase I dose-escalation study of FT538 combined with anti-PD-1/L1 or ADCC-competent mAbs in advanced solid tumors will be presented at the conference.

REFERENCE

1. Woan KV, Kim H, Bjordahl R, *et al.* Harnessing features of adaptive NK cells to generate iPSC-derived NK cells for enhanced immunotherapy. *Cell Stem Cell.* 2021;**28**(12):2062–2075.e5. doi:10.1016/j.stem.2021.08.013

Ethics Approval This study is being conducted in accordance with the Declaration of Helsinki and was approved by all Institutional Review Boards from each clinical site participating in the study. Specific approval numbers can be provided upon request.

<http://dx.doi.org/10.1136/jitc-2022-SITC2022.0727>

728

PHASE 1 STUDY OF P-MUC1C-ALLO1 ALLOGENEIC CAR-T CELLS IN PATIENTS WITH EPITHELIAL-DERIVED CANCERS

¹Jason Henry*, ²David Oh, ³Jeff Eskew, ⁴Joaquina Baranda, ⁵Ildefonso Ismael Rodriguez Rivera, ⁶Ecatarina Dumbrava, ⁷Ezra Cohen, ⁸Rajesh Belani, ⁹Joanne McCaigue, ⁸Devon Shedlock, ⁸Julia Coronella, ⁸Christopher Martin, ⁸Hamid Namini, ⁸Ann Murphy, ⁸Eric Ostertag. ¹Sarah Cannon Research Institute, Denver, CO, USA; ²University of California, San Francisco, CA, USA; ³Poseida Therapeutics, Kansas City, MO, USA; ⁴University of Kansas Cancer Center, Kansas City, KS, USA; ⁵NEXT Oncology, San Antonio, TX, USA; ⁶MD Anderson Cancer Center, Houston, TX, USA; ⁷University of California, San Diego, La Jolla, CA, USA; ⁸Poseida Therapeutics, Inc, San Diego, CA, USA

Background There is an urgent unmet medical need for patients with advanced unresectable and/or metastatic carcinomas. Mucin 1 (MUC1) is a well-characterized heterodimeric glycoprotein that is overexpressed on many epithelial-derived tumors and consists of non-covalently linked N-terminal (MUC1-N) and C-terminal (MUC1-C) monomers. The MUC1-C epitope is selectively seen in epithelial-derived solid tumors such as breast, colorectal, ovarian, gastric, lung carcinoma and others. MUC1-C is also expressed broadly and accessibly throughout tumor tissue due to the loss of cell polarity, one of the hallmarks of tumorigenesis. P-MUC1C-ALLO1 is a fully allogeneic CAR-T targeting the MUC1-C epitope and is manufactured using non-viral transposon-based integration (piggyBac[®] DNA Delivery System) that results in a highly enriched T stem cell memory (T_{SCM}) product. It contains 3 transgenes: an anti-MUC1-C humanized scFv-based CAR, a DHFR drug selection gene to improve product homogeneity, and an iCasp9-based safety switch gene to allow for rapid ablation of the CAR-T if required. The cells are gene edited using the Cas-CLOVER™ Site-Specific Gene Editing System to eliminate expression of endogenous T cell receptors in all cells via knockout of the T cell receptor beta chain 1 gene to prevent graft-vs-host (GvH) response, and the β 2-microglobulin gene to eliminate expression of MHC class I to attenuate host-vs-graft responses. Preclinical efficacy was observed with P-MUC1C-ALLO1 in murine models of triple negative breast cancer and ovarian cancer, providing rationale for this first-in-human (FIH) Phase 1 trial.

Methods This is a Phase 1, multi-center, open-label, FIH, 3+3 design to evaluate P-MUC1C-ALLO1 in patients with advanced or metastatic epithelial-derived cancers measurable by RECIST 1.1 and refractory/ineligible to standard of care therapy. Up to 100 patients will be enrolled into 4 arms of single and cyclic administrations using two different lymphodepletion (LD) regimens (cyclophosphamide/fludarabine \pm rituximab). Planned dose escalation in each arm ranges from 0.75 to 15×10^6 cells/kg.

Primary objectives for this study include defining maximum tolerated dose (MTD), evaluation of overall safety and tolerability, preliminary efficacy, and disease response. Exploratory endpoints will include MUC1-C tumor expression and correlation to response, P-MUC1C-ALLO1 cell kinetics, and biomarker analysis including MUC1 related tumor markers CA15-3 and CA27-29 and CTCs.

Results To date, three patients have been treated with P-MUC1C-ALLO1 (esophageal adenocarcinoma, colorectal adenocarcinoma, and breast cancer). P-MUC1C-ALLO1 treatment to date has been well tolerated, with no dose limiting toxicities, CRS, or GvH disease observed. This study continues to recruit subjects and updated data will be presented.

Trial Registration NCT05239143

Ethics Approval Ethics approvals have been obtained from the clinical sites enrolling patients: Sarah Cannon Research Institute Denver CO (IORG0010151); NEXT Oncology San Antonio TX (IORG0005674); University of California, San Francisco, CA (IORG0000135)

<http://dx.doi.org/10.1136/jitc-2022-SITC2022.0728>

729

TARGETING EPIDERMAL GROWTH FACTOR RECEPTOR (EGFR)-EXPRESSING SOLID TUMORS WITH AFM24, A NOVEL CD16A BISPECIFIC INNATE CELL ENGAGER: COMPREHENSIVE CORRELATIVE SCIENCE FINDINGS FROM A PHASE 1 STUDY

¹Gabriele Hintzen*, ¹Susanne Wingert, ¹Michael Emig, ²Pilar Nava-Parada, ¹Kerstin Pietzko, ¹Laura Kohlhas, ¹Uwe Reusch, ³Melissa Berrien-Elliott, ³Todd Fehniger, ³Mark Foster, ⁴Paolo Nuciforo, ⁵Ester Castillo Andreo, ¹Sina Staebler, ¹Paulien Ravenstijn, ¹Bettina Rehbein, ¹Erich Rajkovic, ¹Arndt Schottelius, ¹Joachim Koch. ¹Affimed GmbH, Heidelberg, Germany; ²Affimed Inc, New York, NY, USA; ³Washington University, Missouri, USA; ⁴Vall d'Hebron University Hospital, Barcelona, Spain; ⁵Cancer Genomics Group, Vall d'Hebron Institute of Oncology, Vall d'Hebron University Hospital, Barcelona, Spain

Background AFM24 is an innate cell engager that binds both EGFR on tumor cells and CD16A on natural killer (NK) cells and macrophages. The primary mechanism of action is the induction of antibody-mediated cellular cytotoxicity and antibody-mediated cellular phagocytosis towards EGFR-positive tumor cells, independent of EGFR mutational status. This innovative, targeted approach utilizes patient's own innate immunity and redirects NK cells and macrophages to tumors. **Methods** An ongoing Phase 1/2a study (NCT04259450) is evaluating the safety and efficacy of AFM24 in patients with metastatic, treatment-refractory tumors known to express EGFR and has completed dose-escalation. The longitudinal effects on the immune system were examined to confirm the pharmacodynamic (PD) activity of AFM24.

Patients received AFM24 intravenously at 14–720 mg once weekly in 28-day cycles until disease progression, intolerable toxicity, investigator discretion, or patient withdrawal. Extensive correlative science analysis included profiling of pharmacokinetics, PD activity, anti-drug antibodies and CD16A receptor occupancy (CD16ARO). Comprehensive analyses of peripheral blood (PB) leukocytes and tumor biopsies were performed.

Results In total, 35 patients were treated with AFM24; tumor types included colorectal (19/35; 13 KRAS and/or NRAS and/or BRAF mutants), non-small cell lung cancer (8/35; 7 EGFR mutant) and others (8/35). A favorable safety profile in all cohorts was revealed, and an approximate half-life of 11 days was established. An exposure-response model correlating plasma concentration of AFM24 with CD16ARO demonstrated that AFM24 binds to NK cells in circulating blood, approaching a plateau at 480 mg. Mass cytometry revealed enhanced expression of activation marker CD69 on NK cells even at low doses (14–80 mg), which coincided with a transient loss of NK cells from the PB, possibly indicating migration of NK cells to the tumor. Cytotoxic CD8 T cells showed a continuous increase of Ki-67 expression in the periphery, indicating crosstalk with the adaptive immune system. T cells in the tumor bed also substantially increased. Tumor EGFR expression was maintained during treatment.

Conclusions This analysis supports the PD activity of AFM24; NK cell changes in PB suggest that AFM24 activates and redirects NK cells from PB to EGFR-positive tissue. T cells are activated within the periphery, and T cell numbers increase in tumors, which may indicate stimulation of anti-cancer activity of the adaptive immune system as an indirect effect of AFM24. Clinical and correlative science from the escalation phase of the study supports further investigation of AFM24 anti-tumor activity in EGFR-expressing tumor-specific cohorts.

Acknowledgements Editorial assistance was provided by Meridian HealthComms Ltd, funded by Affimed.

Trial Registration NCT04259450

Ethics Approval The study will be conducted in accordance with ICH GCP, the Declaration of Helsinki, the European Union Clinical Trials Directive 2001/20/EC, the GCP Directive 2005/28/EC, the requirements of local IRB/EC, and the US Code of Federal Regulations, Title 21 CFR Part 50. The principles of informed consent in the Declaration of Helsinki and GCP guidelines will be implemented before any protocol-specific procedures or interventions are carried out.

<http://dx.doi.org/10.1136/jitc-2022-SITC2022.0729>

Abstracts

731

A FIRST-IN-HUMAN TRIAL OF AN INTEGRIN BETA-6 TARGETED ANTIBODY-DRUG CONJUGATE (ADC), SGN-B6A, IN PATIENTS WITH ADVANCED SOLID TUMORS: INTERIM RESULTS OF A PHASE 1 STUDY (SGNB6A-001)

¹Antoine Hollebecque*, ²Juanita Lopez, ³Sarina Piha-Paul, ⁴Afshin Dowlati, ⁵Amita Patnaik, ⁶Vladimir Galvao, ⁷Bruno Buckorny, ⁸Kartik Sehgal, ⁹Edwin Kingsley, ¹⁰Rachel Sanborn, ¹¹Solange Peters, ¹²Yan Sun, ¹²Gabriela Patilea-Vrana, ¹²Natalya Nazarenko, ¹³Emiliano Calvo. ¹Institut Gustave Roussy, Villejuif, France; ²The Royal Marsden Hospital (Surrey), London, UK; ³The University of Texas, Houston, TX, USA; ⁴Case Western Reserve University, Cleveland, OH, USA; ⁵START San Antonio, San Antonio, TX, USA; ⁶Vall d'Hebron Institute of Oncology, Barcelona, Spain; ⁷Beth Israel Deaconess Medical Center, Boston, MA, USA; ⁸Dana-Farber Cancer Institute, Boston, MA, USA; ⁹Comprehensive Cancer Centers of Nevada, Las Vegas, NV, USA; ¹⁰Earle A. Childs Research Institute, Portland, OR, USA; ¹¹Centre Hospitalier Universitaire Vaudois, Lausanne, Switzerland; ¹²Seagen Inc., Bothell, WA, USA; ¹³START Madrid-CIOCC, Madrid, Spain

Background Integrin beta-6 plays a role in tumor pathogenesis and invasiveness, and is correlated with poor outcomes in several cancers, making it a therapeutic target of interest.^{1,2} SGN-B6A is an investigational vedotin ADC comprised of an integrin beta-6-directed monoclonal antibody conjugated to monomethyl auristatin E (MMAE) via a protease-cleavable linker. SGN-B6A elicits antitumor activity through MMAE-mediated cytotoxicity, bystander effect, and immunogenic cell death.³ Herein, we present the first clinical data in Part A (dose escalation) of a Phase 1 clinical trial evaluating SGN-B6A.

Methods SGNB6A-001 (NCT04389632) is a Phase 1, open-label, multicenter dose-escalation/expansion study evaluating the safety, pharmacokinetics, and antitumor activity of SGN-B6A (confirmed objective response per Response Evaluation Criteria in Solid Tumors v1.1) in adults with advanced solid tumors.

Part A is enrolling patients with histologically or cytologically confirmed metastatic or unresectable solid tumors, relapsed or refractory disease or intolerance to standard-of-care therapies. Data for continuous weekly dosing (Days 1, 8, and 15 in a 21-day cycle [Q1W]) and intermittent dosing (Days 1 and 8 in a 21-day cycle [2Q3W]) are presented in this abstract.

Results As of 10 May 2022, 30 patients in Q1W (0.8, 1.0, and 1.2 mg/kg) and 18 patients in 2Q3W (1.2 or 1.25 mg/kg) received SGN-B6A. Baseline demographics are outlined in Table 1.

In Q1W, 1 dose limiting toxicity (DLT) of stomatitis (5.9%) was reported at the 1.2 mg/kg dose level (n=17; Table 2). The most common treatment-related adverse events (TRAEs) in Q1W across all doses (n=30) were fatigue (26.7%), peripheral sensory neuropathy (23.3%), alopecia (20%) and decreased appetite (20%). The most common Grade ≥ 3 TRAE reported across all dose groups was neutropenia (10%).

In 2Q3W (n=18), two patients experienced DLTs (diarrhea, neutropenia, and rash maculo-papular [5.6%]). The most common TRAEs were alopecia, diarrhea, and peripheral sensory neuropathy (16.7% each), and the most common Grade ≥ 3 TRAEs were diarrhea, hyperglycemia, and neutropenia (11.1%).

Objective responses were observed in Q1W and 2Q3W in several tumor types including non-small cell lung, head and neck squamous cell, esophageal, and cutaneous squamous cell cancer, starting at 1.2 mg/kg. Detailed efficacy results will be presented.

Conclusions SGN-B6A at both dosing schedules demonstrated an acceptable safety profile, with more favorable tolerability at 2Q3W (table 2). Preliminary antitumor activity has been observed starting at 1.2 mg/kg. Enrollment in Part B (dose expansion) is ongoing.

Trial Registration NCT04389632

REFERENCES

- Li F, Shang Y, Shi F, Zhang L, Yan J, Sun Q, She J. Expression of Integrin β6 and HAX-1 Correlates with Aggressive Features and Poor Prognosis in Esophageal Squamous Cell Carcinoma. *Cancer Management and Research*. 2020;**12**:9599-9608
- Elayadi A, Samli K-N, Prudkin L, Liu Y-H, Bian A, Xie X-J, Wistuba I.I, Roth J.A, McGuire M.J, Brown K.C. A Peptide Selected by Biopanning Identified the Integrin αvβ6 as a Prognostic Biomarker for Non-small Cell Lung Cancer. *Cancer Res*. 2007;**67**:(12)
- Klussman K, Tenn E-M, Higgins S, Mazahreh R, Snead K, Hamilton J, Grogan B, Sigurdsson J, Cao A, Gardai S, Liu B. Vedotin ADCs Induce ER Stress and Elicit Hallmarks of ICD Across Multiple Cancer Indications. *J Immunother Cancer*. 2020;**8**(Suppl 3):A1-A559

Ethics Approval The trial is being conducted in compliance with the Declaration of Helsinki and International Conference on Harmonization Guidelines for Good Clinical Practice. All patients, or their legal representatives, provided informed consent. All participating sites have been approved by a corresponding institutional review board or independent ethical committee per the participating institution.

Abstract 731 Table 1 Baseline demographics
Summary of baseline demographics of all patients treated in Q1W and 2Q3W

Table 1	SGNB6A					
	Q1W			2Q3W		
	0.8 mg/kg (n=10)	1.0 mg/kg (n=10)	1.2 mg/kg (n=10)	Total (n=30)	1.2 mg/kg (n=18)	1.25 mg/kg (n=18)
Median Age (yr), range (yr)	60 (51, 64)	70 (26, 70)	58 (26, 81)	62 (26, 84)	58 (41, 76)	65 (37, 76)
Sex, n (%)						
Male	6	2 (20)	9 (90)	17 (57)	5 (28)	4 (89)
Female	4 (40)	8 (80)	1 (10)	13 (43)	13 (72)	9 (91)
Disease Diagnosis, n (%)						
Head and Neck Squamous Cell Cancer	0	0	3 (30)	3 (10)	4 (22)	3 (33)
Breast Cancer	2 (20)	4 (40)	4 (40)	10 (33)	4 (22)	0
Non-small Cell Lung Cancer	0	1 (10)	3 (30)	4 (13)	2 (11)	4 (44)
Esophageal Cancer	0	1 (10)	3 (30)	4 (13)	2 (11)	3 (33)
Ovarian Cancer	2 (20)	1 (10)	0	3 (10)	0	0
Cutaneous Squamous Cell Cancer	0	0	3 (30)	3 (10)	0	0
Cervix Cervicoid Adenocarcinoma	1 (10)	1 (10)	0	2 (7)	0	0
Bladder Cancer	0	0	1 (10)	1 (3)	0	0
Cervical Cancer	0	0	1 (10)	1 (3)	0	0

Abstract 731 Table 2 Adverse events and dose limiting toxicities
Summary of the most common treatment-related adverse events (all grades) and dose limiting toxicities for all patients treated in Q1W and 2Q3W

Table 2	SGNB6A					
	Q1W			2Q3W		
	0.8 mg/kg (n=10)	1.0 mg/kg (n=10)	1.2 mg/kg (n=10)	Total (n=30)	1.2 mg/kg (n=18)	1.25 mg/kg (n=18)
Treatment-related Adverse Events, n (%)						
Fatigue	1 (10)	2 (20)	5 (50)	8 (27)	1 (6)	1 (11)
Peripheral Sensory Neuropathy	1 (10)	1 (10)	5 (50)	7 (23)	3 (17)	0
Alopecia	1 (10)	1 (10)	4 (40)	6 (20)	2 (11)	0
Decreased appetite	0	2 (20)	4 (40)	6 (20)	3 (17)	0
Diarrhea	0	1 (10)	3 (30)	4 (13)	2 (11)	2 (22)
Dose Limiting Toxicities, n (%)						
Diarrhea	0	0	0	0	3 (17)	1 (6)
Neutropenia	0	0	0	0	1 (6)	0
Rash maculo-papular	0	0	0	0	1 (6)	0
Stomatitis	0	0	1 (10)	1 (3)	0	0

<http://dx.doi.org/10.1136/jitc-2022-SITC2022.0731>

732

FIRST-IN-HUMAN TRIAL TO EVALUATE SAFETY, PK/PD AND INITIAL CLINICAL ACTIVITY OF NM21-1480, AN AFFINITY-BALANCED PD-L1X4-1BBXHS TRISPECIFIC ANTIBODY: RESULTS OF PHASE 1 DOSE ESCALATION

²Jason Luke, ³Melissa Johnson, ⁴Shirish Gadgil, ⁵Alexander Spira, ⁶James Yang, ⁷Jennifer Johnson, ⁸Taryn Losch-Beridon, ⁸Daniel Snell, ⁸Stefan Warmuth, ⁸Maureen Cleaver, ⁸Elmar vom Baur, ⁸David Urech, ⁸Peter Lichtlen, ¹David Hong*. ¹Investigational Cancer Therapeutics, The University of Texas MD Anderson Cancer Center, Houston, TX, USA; ²Cancer Immunotherapeutics Center, UPMC Hillman Cancer Center, University of Pittsburgh, Pittsburgh, PA, USA; ³Department of Medicine, Sarah Cannon Research Institute, Nashville, USA, Nashville, TN, USA; ⁴Department of Internal Medicine, Henry Ford Cancer Institute, Henry Ford Health System, Detroit, MI, USA; ⁵Virginia Cancer Specialists, Fairfax, VA, USA; ⁶National Taiwan University and Department of Oncology, National Taiwan University Hospital, Taipei City, Taiwan, Republic of China; ⁷Sidney Kimmel Cancer Center, Thomas Jefferson University, Philadelphia, PA, USA; ⁸Numab Therapeutics AG, Wädenswil Switzerland, Wädenswil, Switzerland

Background NM21-1480 is a tri-specific Fc-lacking antibody that agonizes 4-1BB and blocks PD-L1/PD-1 signaling, designed to restrict activation of the 4-1BB pathway to the tumor microenvironment.¹ NM21-1480 contains an ultra-potent PD-L1 blocking moiety and an affinity-balanced 4-1BB binding moiety to assure maximal activity on both pathways over a broad dose range. Here we report the results of the Phase 1 dose-escalation part of the ongoing First-in-Human Phase 1/2a clinical trial with NM21-1480.

Methods Patients with metastatic or unresectable solid tumors not eligible for standard therapy received flat-dose NM21-1480 (0.15–800mg) intravenously every 2 weeks until disease progression or unacceptable toxicity. Primary endpoints were dose-limiting toxicities (DLTs) and adverse events (AEs). Secondary endpoints included pharmacokinetic (PK) parameters and anti-drug antibody (ADA) assessments. Pharmacodynamic (PD) biomarkers and antitumor activity (RECIST1.1) were assessed as exploratory endpoints.

Results 26 patients with various primary solid tumors were enrolled (median age: 63 years). Patients had previously received a median (range) of 3.5 (1–10) treatments; 62% of whom had prior anti-PD-(L)1 immunotherapy. As per 14 July 2022 patients received a median (range) of 4 (1–19) biweekly NM21-1480 infusions. Full peripheral receptor occupancy at trough level was observed at the dose of 24mg or above. Maximum tolerated dose was not reached; 1 patient experienced a DLT. The most common ($\geq 10\%$ of patients) treatment-related AEs (all grades; Grades 3–4) were infusion-related reactions (27% (11% at 800mg dose); 0%), fatigue (12%; 0%) and transaminase elevations (12%; 4%) according to CTCAEv5.0. One patient each experienced treatment-related Grade-3 transaminase elevations and adrenal insufficiency, respectively; no treatment-related adverse event higher than Grade 3 occurred. In the 24mg-800mg dose range, disease control, i.e., at least stable disease at first assessment at 8 weeks, occurred in 12/21 patients (57%). One patient demonstrated an unconfirmed partial response at Week 16. PD activity on PD-L1 blockade as well as 4-1BB signaling was observed and remained stable at a broad dose range (24–800mg). Based on the totality of the data derived from safety/immunogenicity, PK/PD and clinical activity, the 800mg flat dose of NM21-1480 has been selected for further clinical evaluation.

Conclusions NM21-1480 demonstrated biological activity associated with a manageable safety profile. Encouraging early clinical activity across different dose levels was observed in a heavily pretreated population with advanced solid tumors,

including those resistant to prior immunotherapy or typically less sensitive to ICIs. Enrollment into expansion cohorts will start in the second half of 2022.

Acknowledgements We thank the patients and all involved site personnel for their participation in this trial. The authors thank Dr. Mario Sznol (Yale Cancer Center, Yale School of Medicine, New Haven, USA), Dr. Ignacio Melero (Department of Immunology and Immunotherapy, Clínica Universidad de Navarra, Pamplona, Spain), Dr. Robert L. Ferris (UPMC Hillman Cancer Center, Pittsburgh, USA), Dr. Matthew Galsky (Icahn School of Medicine at Mount Sinai, New York, USA) and Dr. Miguel F. Sanmamed (Departments of Oncology and Immunology, Clínica Universidad de Navarra, Pamplona, Spain) for their valuable contributions. This trial was funded by Numab Therapeutics AG.

Trial Registration ClinicalTrials.gov; trial number: NCT04442126

REFERENCE

1. Warmuth S *et al.* Engineering of a trispecific tumor-targeted immunotherapy incorporating 4-1BB co-stimulation and PD-L1 blockade. *Oncoimmunology*. 2021;**10**(1):e2004661

Ethics Approval This trial is undertaken following full approval of the final protocol, amendments, informed consent form, applicable recruiting materials, and subject compensation programs by the Independent Ethics Committee/Institutional Review Board.

Consent Written informed consent, in accordance with principles that originated in the Declaration of Helsinki 2013, current ICH guidelines including ICH-GCP E6(R2), applicable regulatory requirements, and sponsor policy, was provided by the patients.

<http://dx.doi.org/10.1136/jitc-2022-SITC2022.0732>

733

A PHASE 2 STUDY OF VUDALIMAB (XMAB®20717), AN ANTI-PD-1/CTLA-4 BISPECIFIC ANTIBODY, IN PATIENTS WITH SELECTED GYNECOLOGICAL MALIGNANCIES AND HIGH-RISK METASTATIC CASTRATION-RESISTANT PROSTATE-CANCER

¹June Hou*, ²Oscar Goodman, ³David Berz, ⁴Li Yao, ⁴Nital Soni. ¹Columbia University Irving Medical Center, New York, NY, United States; ²Comprehensive Cancer Centers of Nevada, Las Vegas, NV, USA; ³Valkyrie Clinical Trials, Los Angeles, CA, USA; ⁴Xencor, Inc., Monrovia, CA, USA

Background Vudalimab (XmAb20717) is a humanized bispecific monoclonal antibody that simultaneously targets PD-1 and CTLA-4 and binds preferentially to PD-1/CTLA-4 dual-positive cells. In a Phase 1 study, vudalimab was generally well-tolerated and associated with complete and partial responses in various solid tumor types, including ovarian cancer and metastatic castration-resistant prostate cancer (mCRPC).¹ These tumor types typically are not responsive to single-agent immune checkpoint inhibitor (ICI) therapy but have shown better outcomes in studies in which anti-PD-1 and CTLA-4 therapies have been combined. This Phase 2 study is designed to evaluate the safety and antitumor activity of vudalimab in selected gynecological oncologic indications and high-risk mCRPC.

Methods This is a multicenter, two-stage, open-label study being conducted in the United States. Patients with histologically confirmed platinum-resistant high-grade serous ovarian cancer; chemotherapy relapsed or refractory clear cell ovarian, endometrial, or peritoneal cancer; ICI-refractory microsatellite stable (MSS) endometrial cancer (EC); previously treated recurrent or metastatic cervical cancer; or high-risk mCRPC will be enrolled into parallel cohorts. Patients must have measurable disease by response evaluation criteria in solid tumors (RECIST) 1.1. Prior treatment with anti-PD-1 and PDL-1/PDL-2 therapy is excluded, except for patients with MSS EC and cervical cancer; prior anti-CTLA-4 treatment is excluded for all patients. Vudalimab will be administered intravenously every 3 weeks at a fixed dose of 1000 mg (1200 mg for patients \geq 80 kg). Antitumor effects will be evaluated using RECIST 1.1; additionally, disease assessment via bone scans and PSA will be performed in patients with mCRPC. Safety and tolerability will be assessed based on treatment-emergent adverse events. Pharmacodynamic effects in peripheral blood and tumor, and potential biomarkers associated with clinical response will be explored. In Stage 1 (n = 10/cohort), a primary endpoint of objective response rate (ORR) \geq 20% at 12 weeks (based on investigator review) will determine which cohorts advance into Stage 2 (n = 20/cohort), where primary and secondary endpoints of ORR (based on independent central review) and duration of response, respectively, will be determined for the combined number of patients enrolled into Stages 1 and 2 (n = 30). Enrollment has been initiated.

Trial Registration NCT05032040

REFERENCE

- [1] Shum E, Reilley M, Najjar Y, et al. 523 Preliminary clinical experience with XmAb20717, a PD-1 x CTLA-4 bispecific antibody, in patients with advanced solid tumors. *Journal for ImmunoTherapy of Cancer*. 2021;9: doi: 10.1136/jitc-2021-SITC2021.523

Ethics Approval The study was approved by each institution's IRB.

<http://dx.doi.org/10.1136/jitc-2022-SITC2022.0733>

734

A PHASE 1 STUDY EXPLORING THE SAFETY AND TOLERABILITY OF THE SMALL-MOLECULE PD-L1 INHIBITOR, INCB099280, IN PATIENTS WITH SELECT ADVANCED SOLID TUMORS

¹Hans Prenen*, ²Thierry Lesimple, ³Marie Robert, ⁴Brant Delafontaine, ⁵Jean-Pascal Machiels, ⁶Tarek Meniawy, ⁷Eric Van Cutsem, ⁸Nuria Kotecki, ⁹Sarina Piha-Paul, ¹⁰Michael Schweizer, ¹¹Shirish Gadgeel, ¹²Jeannie Daniel, ¹²Louis Viviers, ¹²Jason Howe, ¹³Antoine Italiano. ¹University Hospital Antwerp, Antwerp, Belgium; ²CLIP2 and ARPEGO Networks, Rennes, France; ³Unicancer Group ICO René Gauducheau Site, CLIP2 and ARPEGO Networks, Saint-Herblain, France; ⁴Drug Research Unit Ghent, UZ Ghent, Ghent, Belgium; ⁵Cliniques Universitaires Saint-Luc, UCLo, Brussels, Belgium; ⁶Linear Clinical Research and University, Nedlands, Western Australia, WA, Australia; ⁷University Hospitals Gasthuisberg, Leuven, Leuven, Belgium; ⁸Institut Jules Bordet, Brussels, Belgium; ⁹University of Texas MD Anderson Cancer, Houston, TX, USA; ¹⁰University of Washington and Fred Hutch, Seattle, WA, USA; ¹¹Henry Ford Cancer Institute/Henry Ford Health, Detroit, MI, USA; ¹²Incyte Corporation, Wilmington, DE, USA; ¹³Early Phase Trials Unit, Institut Bergon, Bordeaux, France

Background INCB099280 is an orally administered, small-molecule inhibitor of programmed cell death ligand 1 (PD-L1). This is an ongoing, phase 1, open-label, multicenter study.

Methods Eligible patients are aged ≥ 18 years with advanced solid tumors and an Eastern Cooperative Oncology Group performance status of 0–1. Patients had disease progression after treatment with available therapies or were ineligible for or without access to standard treatment. The study is being conducted in two parts: in part 1, a Bayesian optimal interval design is being used to identify the maximum tolerated dose (MTD) of INCB099280; in part 2, two doses have been expanded for patients with various tumor types who were immunotherapy-naïve. The primary endpoints are (1) safety and tolerability as measured by monitoring frequency/severity of adverse events (AEs) and (2) determining a pharmacologically active dose and/or MTD. Anti-tumor activity is assessed using Response Evaluation Criteria in Solid Tumors (RECIST) v1.1.

Results As of April 22, 2022, 73 patients had received INCB099280 at total daily doses ranging from 100 to 800 mg. Among all patients, median (range) age was 62 (21–82) years, 60.3% were women, 57.5% were white, 43.8% had gastrointestinal malignancies, 56.2% had ≥ 2 prior lines of therapy, and 6.8% had prior exposure to an immune checkpoint inhibitor. 46 patients (63.0%) discontinued treatment, 38 of whom discontinued for disease progression. Treatment-emergent AEs (TEAEs) occurring in $>20\%$ of patients were decreased appetite, fatigue, nausea, anemia, diarrhea, asthenia, and vomiting. Serious TEAEs (SAEs) occurred in 21 patients (28.8%); SAEs occurring in >1 patient were pneumonia and sepsis (n=3 each) and anemia, dyspnea, and urinary tract infection (n=2 each). Grade ≥ 3 treatment-related TEAEs occurred in 5 patients (6.8%): asthenia, fatigue, elevated lipase, decreased appetite, hypophagia, and confusional state (n=1 each). One patient had a protocol-defined dose-limiting toxicity (DLT; 600-mg once-daily group; unable to receive $\geq 75\%$ of the prescribed dose owing to vomiting). The 600-mg once-daily dose was expanded in 9 patients with no further DLTs. Several responses have been observed, and updated results will be presented.

Conclusions INCB099280 was generally well tolerated at total daily doses up to 800 mg. Unlike with the first-generation oral PD-L1 inhibitor INCB086550, no dose-limiting immune-mediated peripheral neuropathy has occurred to date with INCB099280. Preliminary efficacy indicates anti-tumor activity.

Continued investigation and further development are warranted.

Trial Registration NCT04242199

Ethics Approval This study was reviewed and approved by the institutional review boards of the participating institutions. Approval numbers are: WIRB (USA), 20202491; University of Texas, MD Anderson Cancer Center (USA), 2020-0082; Alfred HREC (Australia), HREC/60995/Alfred-2020; Bellberry (Australia), HREC2020-05-463; EudraCT EC (Belgium), 2019-004967-35 (Ref#, 5407); EudraCT EC (France), 2019-004967-35 (FR EC, 20.10.09.40853). All patients provided written informed consent.

<http://dx.doi.org/10.1136/jitc-2022-SITC2022.0734>

Abstracts

735

A PHASE 1/2 STUDY OF REGN7075 (EGFRxCD28 COSTIMULATORY BISPECIFIC ANTIBODY) IN COMBINATION WITH CEMIPIMAB (ANTI-PD-1) IN PATIENTS WITH ADVANCED SOLID TUMORS: INITIAL DOSE-ESCALATION RESULTS

¹Melissa Johnson*, ²Nehal Lakhani, ³Eugenia Girda, ⁴Anthony Olszanski, ⁵Lawrence Fong, ⁶Hyunsil Han, ⁶Kerry Casey, ⁶Siyu Li, ⁶Jennifer Visich, ⁶Dmitris Skokos, ⁶Frank Seebach, ⁶Israel Lowy, ⁶Matthew Fury, ⁶Melissa Mathias, ⁷Neil Segal. ¹Sarah Cannon Research Institute, Nashville, TN, USA; ²START Midwest, Grand Rapids, MI, USA; ³Rutgers Cancer Institute of New Jersey, New Brunswick, NJ, USA; ⁴Fox Chase Cancer Center, Philadelphia, PA, USA; ⁵University of California, San Francisco, CA, USA; ⁶Regeneron Pharmaceuticals, Inc., Tarrytown, NY, USA; ⁷Memorial Sloan Kettering Cancer Center, New York, NY, USA

Background There is a need to develop novel immunotherapeutic approaches to enhance responses to immune checkpoint blockade. REGN7075 is a human costimulatory bispecific antibody designed to bridge epidermal growth factor receptor (EGFR)-expressing tumor cells with CD28-positive T cells to support further T-cell activation by endogenous tumor antigens [1, 2] (figure 1). We initiated a first-in-human, open-label, Phase 1/2 dose-escalation and expansion study evaluating the safety, tolerability, pharmacokinetics, and preliminary antitumor activity of REGN7075 (EGFRxCD28) in combination with cemiplimab (anti-PD-1) in patients with advanced solid tumors (figure 2; NCT04626635).

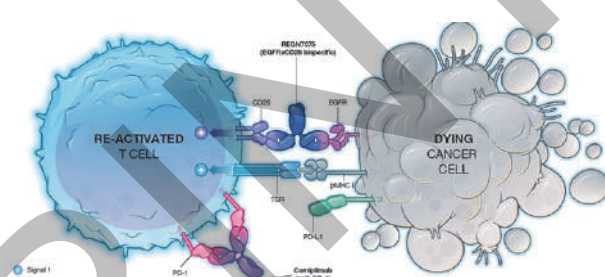
Methods We report preliminary results of the dose-escalation phase (Bayesian optimal interval design; Part 1), in which heavily pre-treated patients with advanced solid tumors will receive a lead-in of REGN7075 monotherapy every week for 3 weeks, followed by combination therapy with cemiplimab 350mg every 3 weeks. Planned dose levels (DL) of REGN7075 are 0.03, 0.1, 0.3, 1, 3, 10, 30, 100, 300, and 900mg. Primary objective is to assess safety and tolerability of REGN7075 in combination with cemiplimab.

Results As of the data cutoff date (May 6, 2022), 18 patients (median age, 53.5 years, 56% female) were treated in the dose-escalation phase (table 1), up to the 30mg DL for REGN7075 in combination with cemiplimab. Most patients (67%) were treated for microsatellite stable colorectal cancer. No patients experienced dose-limiting toxicities; maximum tolerated dose was not reached. Table 2 summarizes treatment-emergent adverse events (TEAEs) and treatment-related adverse events (TRAEs). The most frequent TEAEs (any grade) were increases in aspartate aminotransferase (AST), constipation, and fatigue (33% [n=6] each). The most frequent TRAEs (any grade) were fatigue (17% [n=3]), increases in AST, diarrhea, hypothyroidism, pyrexia, and rash (11% [n=2] each). One patient developed cytokine release syndrome which was characterized by isolated grade 1 fever without hypotension nor hypoxia. Five recorded deaths were not during study treatment and not attributed to study drug(s). Ongoing PK evaluation suggests possible target-mediated effects. T cell activation-associated cytokines were detected in monotherapy lead-in and combination dosing. Of all patients treated, 1 patient who received 1mg REGN7075 with cemiplimab for cervical cancer achieved an ongoing partial response.

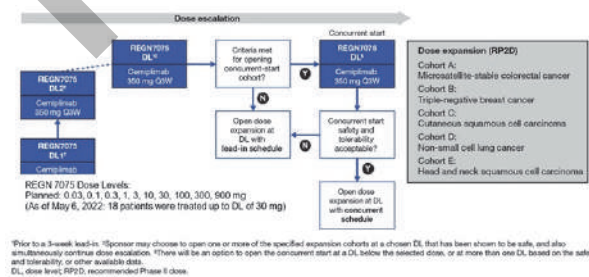
Conclusions In this dose-escalation study, REGN7075 was safely administered up to the 30mg dose level in combination with cemiplimab without dose-limiting toxicities. Early data indicates that novel agent REGN7075 was generally well tolerated, with preliminary potential anti-tumor activity. Biomarker studies are ongoing. Clinical trial enrollment is ongoing; we are currently evaluating the 100mg cohort.

Acknowledgements This study was funded by Regeneron Pharmaceuticals, Inc. Medical writing support and typesetting was provided by John G Facciponte, PhD, of Prime, Knutsford, UK, funded by Regeneron Pharmaceuticals, Inc. **Trial Registration** NCT04626635

Ethics Approval The protocol and all amendments were approved by the appropriate institutional review board or independent ethics committee at each participating study site. The study was conducted in accordance with the principles of the Declaration of Helsinki and the International Conference on Harmonization Good Clinical Practice guidelines. **Consent** Written informed consent was obtained from the patient for publication of this abstract and any accompanying images. A copy of the written consent is available for review upon request.



Abstract 735 Figure 1 Mechanism of action for REGN7075 (EGFRxCD28 costimulatory bispecific antibody)



Abstract 735 Figure 2 Study design

Abstract 735 Table 1 Demographics and baseline characteristics

	Total (N=18)
Age (years)	53.5 (47-65)
Median (Q1-Q3)	
Sex, n (%)	
Male	8 (44%)
Female	10 (56%)
ECOG, n (%)	
0	8 (44%)
1	10 (56%)
Cancer diagnosis, n (%)	
Colorectal cancer, microsatellite stable	12 (67%)
Pancreatic carcinoma	3 (17%)
Cervical carcinoma	2 (11%)
Prostate adenocarcinoma	1 (6%)

Abstract 735 Table 2 Summary of treatment-emergent adverse events (TEAE) and treatment-related adverse events (TRAE)

TEAE	Total (N=18)	
	All grades	Grades 3-5
Number of patients with any TEAE, n (%)	17 (94%)	7 (39%)
Most common TEAEs (in >10% of patients)		
Aspartate aminotransferase increased	6 (33%)	0
Constipation	6 (33%)	1 (6%)
Fatigue	6 (33%)	0
Diarrhea	5 (28%)	0
Vomiting	5 (28%)	0
Blood bilirubin increased	4 (22%)	1 (6%)
Nausea	4 (22%)	0
Abdominal distension	3 (17%)	0
Abdominal pain	3 (17%)	0
Alanine aminotransferase increased	3 (17%)	0
Arthralgia	3 (17%)	0
Cough	3 (17%)	0
Hypomagnesemia	3 (17%)	0
Anemia	2 (11%)	0
Back pain	2 (11%)	0
Blood alkaline phosphatase increased	2 (11%)	1 (6%)
Blood creatinine increased	2 (11%)	0
Decreased appetite	2 (11%)	0
Dehydration	2 (11%)	0
Dry skin	2 (11%)	0
Hypothyroidism	2 (11%)	0
Nasal congestion	2 (11%)	0
Pruritus	2 (11%)	0
Pyrexia	2 (11%)	0
Rash maculo-papular	2 (11%)	0
TRAE		
Number of patients with any TRAE for either REGN7075 (including lead-in period) and/or cemiplimab, n (%)	14 (78%)	0
Most common TRAEs (in >10% of patients)		
Fatigue	3 (17%)	0
Aspartate aminotransferase increase	2 (11%)	0
Diarrhea	2 (11%)	0
Hypothyroidism	2 (11%)	0
Pyrexia	2 (11%)	0
Rash maculo-papular	2 (11%)	0

<http://dx.doi.org/10.1136/jitc-2022-SITC2022.0735>

736

A CLINICAL STAGE ENGINEERED TOXIN BODY (ETB) TARGETING PD-L1 (MT-6402) INDUCES PERIPHERAL PHARMACODYNAMIC RESPONSES UNIQUE FROM PD-L1 MONOCLONAL ANTIBODIES

Swati Khanna, Rachael Orlandella, Elizabeth Saputra, Sydney Matthews, Lydia Navarrete-Galvan, Sara LeMar, Joseph Dekker*, Eric Poma, Chris Moore. *Molecular Templates Inc., Austin, TX, USA*

Background PD-L1 targeting mAbs have had success in the clinic for a variety of solid tumors and specific patient subsets. To date, all PD-L1 mAbs rely on blocking the PD-1/PD-L1 axis through steric hindrance for their activity. MT-6402 is a clinical stage ETB that binds to PD-L1, triggers receptor internalization, and induces cell death of PD-L1+ cells through ribosomal destruction. MT-6402 represents a wholly novel approach to targeting PD-L1 expressing immune and tumor cells built upon the clinical hypothesis that elimination rather than blocking of PD-L1+ tumor and immune cells could transform immune tolerant tumor microenvironments (TME) to immune augmenting phenotypes. To this end, MT-6402 also carries a CMVpp65 peptide capable of HLA-A*02 restricted antigen presentation designed to redirect CMV-specific cytotoxic T cells to tumor tissue. Thus far, MT-6402 has completed three dosage cohorts (n=16) in a phase 1 dose escalation trial. Here we show changes in serum vascular endothelial growth factor (VEGF) correlate with peripheral reductions in monocyte derived suppressor cells (MDSCs), both biomarkers of potential TME alterations and a unique peripheral effect not seen with α PD-L1 blocking mAbs.

Methods Peripheral blood mononuclear cells (PBMC) from MT-6402-dosed patients were stained with surface antibodies and acquired on a flow cytometer to identify CD11b+CD14+HLA-DR-/low Monocytic MDSCs. Luminex was used to quantify VEGF concentrations in patient matched serum.

Results A sawtooth pattern of peripheral VEGF levels emerged in 5/7 patients with higher pre-dose VEGF levels (>125pg/ml) following multiple doses of MT-6402 and indicative of a tumor remodeling response. A gradual VEGF increase in cohort 1 cycle 1 correlated with peripheral MDSC extravasation into tissue or TME. For cohorts 2 and 3, an inverse relationship between VEGF concentrations and MDSC frequencies emerged, where spikes in MDSCs correlated to sharp reductions in serum VEGF levels. Overall, PBMC phenotyping and cytokine data demonstrated an inverse correlation of MDSC frequencies and VEGF concentrations across dosage cohorts.

Conclusions PD-L1 expression on tumor and immune cells have non-redundant contributions to the maintenance of the TME and disease progression. Current PD-L1 antibodies physically inhibit PD-L1 and PD-1 interaction but do not fully inhibit PD-L1+ immune cell functions that contribute to TME maintenance (i.e., cytokine/chemokine secretion). Unlike PD-L1 antibodies, MT-6402 was designed to destroy PD-L1+ immune cells in a target-specific manner. We demonstrate here that MDSCs are depleted in the periphery of patients treated with MT-6402 and that this depletion appears related to peripheral changes in VEGF and alterations of the TME.

Trial Registration NCT04795713

Ethics Approval This study was conducted in compliance with current Good Clinical Practice (GCP) standards as defined by the International Council for Harmonization of Technical Requirements for Pharmaceuticals for Human Use (ICH) Guideline for GCP, all applicable national, state, and local laws and regulations, and the applicable Institutional Review

Board/Independent Ethics Committee (IRB/IEC) and other institutional requirements.

Consent Written informed consent was obtained from the patient for publication of this abstract and any accompanying images. A copy of the written consent is available for review by the Editor of this journal.

<http://dx.doi.org/10.1136/jitc-2022-SITC2022.0736>

737

INTERIM RESULTS OF A FIRST-IN-HUMAN PHASE 1 DOSE-ESCALATION TRIAL OF TAK-102, A GLYPICAN-3 TARGETED ARMORED CHIMERIC ANTIGEN RECEPTOR T-CELL IMMUNOTHERAPY IN PATIENTS WITH ADVANCED SOLID TUMORS

¹Takafumi Koyama*, ¹Toshio Shimizu, ²Toshihiko Doi, ¹Noboru Yamamoto, ¹Shunsuke Kondo, ³Abood Okal, ³Aman Singh, ³Janet Markman, ⁴Takeori Akaike, ⁴Hideaki Kagehara, ²Yasutoshi Kuboki. ¹National Cancer Center Hospital, Tokyo, Japan; ²National Cancer Center Hospital East, Kashiwa, Japan; ³Takeda Development Center Americas, Inc., Waltham, MA, USA; ⁴Takeda Pharmaceutical Company Limited, Osaka, Japan

Background Glypican 3 (GPC3) is a member of the glypican family of heparan sulfate (HS) proteoglycans that are attached to the cell surface by a glycosylphosphatidylinositol (GPI) anchor. High GPC3 expression rates are present in numerous cancer types with high unmet medical needs, including hepatocellular carcinoma, squamous non-small cell lung cancer, upper gastrointestinal cancers, cervical cancer, and undifferentiated sarcomas. TAK-102 is a GPC3-targeted, interleukin (IL)-7- and CC chemokine ligand 19 (CCL19)-expressing autologous chimeric antigen receptor (CAR) T-cell immunotherapy. The addition of IL-7 and CCL19 to the construct is expected to support the expansion of memory subsets and persistence of CAR T cells. This is hypothesized to help overcome the challenges associated with an immunosuppressive tumor microenvironment, one of the foremost pathogenic mechanisms likely limiting the activity of non-armored CAR T-cell therapies in solid tumors. In vivo antitumor activity of TAK-102 was confirmed in NOD scid gamma mice engrafted with GPC3-positive human HepG2 cells.

Methods The first-in-human, Phase 1 dose-escalation study is evaluating TAK-102 in patients with GPC3-expressing solid tumors who are refractory or intolerant to standard treatments. TAK-102 is administered via a single infusion on 3 dose cohorts after lymphodepleting chemotherapy (fludarabine and cyclophosphamide): Cohort 1 (starting cohort), 1×10^7 CAR+ cells/body; Cohort 2, 1×10^8 CAR+ cells/body; Cohort 3, 1×10^9 CAR+ cells/body. Objectives include evaluation of safety, dose-limiting toxicity (DLT), recommended Phase 2 dose, cellular kinetic (CK) parameters, pharmacodynamic (PD) effects, and antitumor activity based on RECIST 1.1.

Results As of March 25, 2022, 4 patients were enrolled and infused with TAK-102 (Cohort 1: 3 patients, one each with gastric neuroendocrine carcinoma, liposarcoma, and hepatocellular carcinoma; Cohort 2: 1 patient with liposarcoma). No DLT, cytokine release syndrome, or neurotoxicity were observed in any of the patients. Two patients, one with hepatocellular carcinoma and the other with liposarcoma, achieved stable disease (SD). There was a dose-dependent increase in expansion and persistence based on peripherally measured TAK-102 transgene levels. Peripheral blood CK also trended with some of the cytokines' kinetics, including interferon- γ , IL-12/-23p40, and IL-10. Pre-/post-treatment paired tumor biopsies from a patient with hepatocellular carcinoma who was administered TAK-102 showed significant increase in endogenous T-cell infiltration and activation markers (CD69, granzyme B). The observed SD and accompanying changes in relevant tumor biomarker levels (alpha-fetoprotein, lactate dehydrogenase) are encouraging.

Conclusions TAK-102 is an autologous GPC3-targeted IL-7/CCL19 armored CAR T-cell immunotherapy. Preliminary data show an encouraging safety profile and CK/PD results. The dose-escalation study is ongoing (NCT04405778).

Acknowledgements The authors would like to thank all patients who participated in this study and their families, as well as all the investigators and site staff who made the study possible.

Trial Registration www.clinicaltrials.gov; NCT04405778

Ethics Approval The study was approved by National Cancer Center Institution's Ethics Board on 27 May 2020.

<http://dx.doi.org/10.1136/jitc-2022-SITC2022.0737>

738

INTERIM DOSE ESCALATION OF DAVOCETICEPT, A CONDITIONAL CD28 COSTIMULATOR AND DUAL CHECKPOINT INHIBITOR, IN COMBINATION WITH PEMBROLIZUMAB IN ADVANCED MALIGNANCIES (NEON-2)

¹Nehal Lakhani*, ²Amita Patnaik, ³Meredith McKean, ⁴Justin Gainor, ⁵Cathy Vo Buu, ⁵Amanda Enstrom, ⁵Rupert Davies, ⁵Stacey Dillon, ⁵Hany Zayed, ⁶Michael Chisamore, ⁷James Michael Pluda, ⁵Allison Naumovski, ⁵Stanford Peng. ¹START Midwest, Grand Rapids, MI, USA; ²START San Antonio, San Antonio, TX, USA; ³Sarah Cannon Research Institute and TN Onc, Nashville, TN, USA; ⁴Massachusetts General Hospital, Boston, MA, USA; ⁵Alpine Immune Sciences, Seattle, WA, USA; ⁶Merck and Co., Kenilworth, NJ, USA; ⁷ICON Clinical Research, Blue Bell, PA, USA

Background PD-1/PD-L1 inhibitors (PD-(L)1i) have improved outcomes for many patients with advanced malignancies; however, most do not respond, or fail to achieve durable anti-tumor immunity. PD-1-mediated inhibition of T-cell effector function works primarily by inactivating the CD28 costimulatory signal. While PD-(L)1i can remove such inhibition, active CD28 costimulation is likely still required for optimal T-cell activation. Davoceticept is a variant CD80 vIgD-Fc fusion protein, engineered to provide PD-L1-dependent CD28 costimulation, while inhibiting PD-1 and CTLA-4. In NEON-1 (NCT04186637), davoceticept monotherapy was well-tolerated up to 10mg/kg, Q3W, and showed evidence of clinical activity in papillary renal cell carcinoma (RCC). A davoceticept + PD-1i approach is supported by preclinical models where combination treatment yielded tumor volume reductions beyond those seen with either monotherapy. Further, PD-1 inhibition may up-regulate PD-L1 in the tumor and sensitize it to PD-L1-dependent CD28 costimulation by davoceticept.

Methods NEON-2 is an open-label dose escalation and expansion study of davoceticept + pembrolizumab in adults with advanced solid tumors or lymphoma (NCT04920383). Eligibility includes tumors for which single agent PD-(L)1i are standard of care, are refractory/resistant to standard therapies, or have no standard or curative treatments available. The study employs a standard 3+3 dose-escalation design with 2 schedules of intravenous (IV) davoceticept: Q1W and Q3W. Pembrolizumab is given per label at 400mg IV Q6W. Study objectives include evaluation of safety and tolerability, identification of the recommended phase 2 dose(s) (RP2D), pharmacokinetic, pharmacodynamic, exploratory biomarker analyses, and preliminary efficacy.

Results As of June 2022, 19 subjects have been treated with davoceticept in dose escalation at 0.1 and 0.3mg/kg, Q1W and Q3W. Seven subjects experienced a total of 9 Grade 3+ treatment-related adverse events, including one Grade 5 cardiogenic shock in the 0.3mg/kg, Q3W cohort. Gr3+ immune-related adverse events were more common in subjects receiving 0.3 vs. 0.1mg/kg regimens of davoceticept, at 27.3% and 12.5%, respectively. Of 14 evaluable subjects, 1 confirmed partial response has been observed in a nivolumab-experienced subject with clear cell RCC. Additionally, tumor reductions have been noted in a second ongoing RCC subject, and in subjects with prostate cancer and serous peritoneal carcinoma. Fifty percent of evaluable subjects achieved a best response of stable disease.

Conclusions The davoceticept + pembrolizumab combination has demonstrated preliminary anti-tumor activity in clear cell RCC, potentially by reversing resistance to PD-(L)1i. Dose escalation efforts will resume at 0.1mg/kg, Q1W and Q3W. Tumor-specific expansion cohorts will open once the RP2D/schedule of the combination treatment is identified.

Trial Registration NCT04920383

Ethics Approval This study received ethics approval from the WCG IRB (Sarah Cannon; ID 20211877), Salus IRB (START Texas; ID START2021.28, START Midwest; ID STMW2021.18), and Mass General Brigham IRB (Massachusetts General Hospital; ID 2021P002079). All study subjects provided their informed consent to participate in this study.

<http://dx.doi.org/10.1136/jitc-2022-SITC2022.0738>

739

A PHASE 1B/2, OPEN-LABEL, SAFETY, TOLERABILITY AND EFFICACY STUDY OF NC410 PLUS PEMBROLIZUMAB FOR PARTICIPANTS WITH IMMUNE CHECKPOINT INHIBITOR (ICI) REFRACTORY, OR MSS/MSI-LOW ICI NAÏVE ADVANCED OR METASTATIC SOLID TUMORS

¹Han Myint, ²Eric Christenson*, ³Siqing Fu, ⁴Martin Gutierrez, ⁵Ashley Martz, ⁵Stephanie Zeidan, ⁵Megan Nelson, ⁵Alina Barbu, ⁵Aaron Morawski, ⁵Chelsea Zhou, ⁵Zachary Cusumano, ⁵Rachel O'Neill, ⁵Ron Copeland, ⁵Dallas Flies, ⁵Solomon Langermann, ⁶Julia Cohen, ²Dung Le. ¹NextCure Inc, Beltsville, MD, USA; ²Johns Hopkins Hospital, Baltimore, MD, USA; ³MD Anderson Cancer Center, Houston, TX, USA; ⁴John Theurer Cancer Center, Hackensack, NJ, USA; ⁵NextCure, Beltsville, MD, USA; ⁶Merck, West Point, PA, USA

Background The tumor extracellular matrix (ECM) functions as a physical barrier to immune cell infiltration and acts to directly inhibit immune cells by interacting with the inhibitory receptor, Leukocyte Associated Immunoglobulin-Like Receptor-1 (LAIR-1). Several recent publications on pre-clinical studies have demonstrated this inhibition can be reversed by NC410, a recombinant form of the LAIR-2 protein, a naturally produced soluble decoy that normally functions to compete with LAIR-1 binding. NC410 is composed of LAIR-2 protein fused to a human Fc domain of the immunoglobulin (Ig) subtype IgG1.¹ More recently, in vivo modeling studies demonstrate that treatment with PD(L)-1 blockade in a murine lung model drives enhanced collagen production due to an increase in TGF- β signaling, resulting in resistance to treatment targeting the PD-L1 pathway. Genetically driven overexpression of LAIR-2, in this model was able to overcome resistance, sensitize tumors to PD(L)-1 blockade, reduce tumor growth, and increase local immune cell activation.² Extensive preclinical testing by NextCure and collaborators has demonstrated that the combination of NC410, and anti-PD(L)-1 leads to consistent reduction of tumor burden and enhanced survival in several animal models. A clinical trial of NC410 Phase 1 monotherapy in participants with advanced or metastatic solid tumors is currently on-going. Preliminary clinical and biomarker data has been presented,³ supporting immune activation and mechanism of action proposed for NC410.

Methods This is an open-label, non-randomized, Phase 1b/2 study to determine the safety and tolerability of NC410 when combined with Pembrolizumab. This study will also assess the clinical benefit of combination therapy in participants with advanced unresectable and/or metastatic ICI refractory solid tumors (CRC MSI-H, Gastric including GE junction, Esophageal, Endometrial, and H&N cancer) in Cohort 1, and ICI Naïve, Microsatellite Stable or Microsatellite Instability Low (MSS/MSI-low) solid tumors (CRC, Gastric including GE junction and Ovarian) in Cohort 2. Key eligibility criteria include measurable disease based on RECIST v1.1 and being able to provide tissue samples at screening. Participants will receive pembrolizumab 400 mg on Day 1 of each 42-day cycle. NC410 will be given on Days 1, 15 and Day 29 of each 42-day cycle. Objective response rate (ORR) based on RECIST v1.1 will be the primary endpoint, while duration of response (DoR), disease control rate (DCR), progression-free survival (PFS), and overall survival will be evaluated as secondary endpoints. Several biomarker effects of NC410 in combination with pembrolizumab in peripheral blood and tumor tissue will be assessed.

REFERENCES

1. Ramos MIP, Tian L, de Ruiter EJ, *et al.* Cancer immunotherapy by NC410, a LAIR-2 Fc protein blocking human LAIR-collagen interaction. *Elife*. 2021;**10**: e62927. Published 2021 Jun 14. doi:10.7554/eLife.62927
2. Peng DH, Rodriguez BL, Diao L, *et al.* Collagen promotes anti-PD-1/PD-L1 resistance in cancer through LAIR1-dependent CD8+ T cell exhaustion. *Nat Commun*. 2020;**11**(1):4520. Published 2020 Sep 9. doi:10.1038/s41467-020-18298-8
3. Myint H, Tian L, Shaik J, *et al.* NC410, a fusion protein of LAIR-2 (Leukocyte Associated Immunoglobulin-like Receptor) with human IgG1 Fc, is safe & tolerable with evidence of immune modulation in subjects with advanced solid tumors. *Journal for ImmunoTherapy of Cancer*. 2021;**9**:doi: 10.1136/jitc-2021-SITC2021.487

Ethics Approval This study has been approved by the IRB of all the participating institutions, and all participants have given informed consent before taking part in the study.

<http://dx.doi.org/10.1136/jitc-2022-SITC2022.0739>

740

A FIRST-IN-HUMAN TRIAL OF HSTC810 (ANTI-BTN1A1 AB), A NOVEL IMMUNE CHECKPOINT WITH A MUTUALLY EXCLUSIVE EXPRESSION WITH PD-1/PD-L1, IN PATIENTS WITH RELAPSED/REFRACTORY SOLID TUMORS

¹Soohyeon Lee*, ²Sangjoon Shin, ³Lynn Howie, ⁴Hyunjin Jung, ^{3,4}Steven Yoo, ⁵David Hong. ¹Korea University Anam Hospital, Seoul, Korea, Republic of; ²Yonsei Cancer Center, Seoul, Korea, Republic of; ³STCube Pharmaceuticals, Inc, Gaithersburg, MD, USA; ⁴STCube, Inc, Seoul, Korea, Republic of; ⁵MD Anderson Cancer Center, Houston, TX, USA

Background Butyrophilin 1A1 (BTN1A1) is a novel immune checkpoint with a mutually exclusive expression with PD-1/PD-L1 and may offer a promising therapeutic target for tumors that are anti-PD-1/PD-L1 antibody refractory. BTN1A1 was identified as a potential stress-inducible candidate immune checkpoint using the STCube *in vivo* immune checkpoint target discovery platform. Murine studies demonstrated that the anti-BTN1A1 antibody exhibited antitumor activity as a single agent as well as when combined with anti-PD-1/PD-L1 or radiation therapy. A humanized anti-BTN1A1 antibody, hSTC810, was developed and evaluated in immunologically cold A549 tumors that are unresponsive to anti-PD-L1 treatment. hSTC810-treated mice exhibited significantly reduced tumor volumes relative to hlgG4-treated control animals without any treatment-related toxicity. Humanized STC810 is currently being evaluated in a first in human study to identify hSTC810's maximally tolerated dose (MTD) and initial safety profile for patients with advanced solid tumors.

Methods A Phase I clinical study using a standard 3 + 3 escalation design to explore safety, tolerability, dose-limiting toxicities (DLTs), pharmacokinetics, define a recommended phase II dose (RP2D) and to evaluate preliminary efficacy in patients with advanced solid tumors is currently enrolling (NCT05231746). The study is a multi-site, non-randomized, open-label study with subjects ages >18 to be enrolled with various advanced solid tumors. Eligible patients receive hSTC810 intravenously (0.3mg/kg-15 mg/kg) once every 2-weeks as a single agent until disease progression or lack of tolerability. Dose expansion cohorts are planned at RP2D to further assess safety, pharmacokinetics (PK), pharmacodynamics and immunohistochemistry in pre-and post-treatment tumor tissue samples.

Results To date, 13 patients have been enrolled, and 2 dose levels have been completed. No DLTs have been observed and enrollment continues. Subject enrollment in the dose escalation cohorts is expected to be completed in the fourth quarter of 2022.

Conclusions Interim clinical data, including safety and tolerability and initial anti-tumor activity, from the ongoing Phase 1 dose-escalation study of STCube's hSTC810 in advanced solid tumors will be presented at the conference.

Trial Registration NCT05231746

Ethics Approval The study obtained ethics approval from Korea University Anam Hospital (2022AN008) and the other all participating institutions and a statement that participants gave informed consent before taking part.

Consent Written informed consent was obtained from the patient for publication of this abstract and any accompanying images. A copy of the written consent is available for review by the Editor of this journal.

<http://dx.doi.org/10.1136/jitc-2022-SITC2022.0740>

741

FIRST IN HUMAN PHASE I TRIAL OF DT-9081, A SELECTIVE EP4 RECEPTOR ANTAGONIST IN PATIENTS WITH RECURRENT AND OR METASTATIC SOLIDS TUMORS

¹Jean-Pierre Delord, ²Christophe Le Tourneau, ³Nuria Kotecki, ⁴Patricia Zerr, ⁴Claire Jouffroy Zeller, ⁴Samira El Farouk, ⁴Asmaa Boudribila, ⁵Jean-Pascal Machiels*. ¹*Institut Claudius Regaud, IUCT-Oncopole, Toulouse, France;* ²*Department of Drug Development and Inn, Paris, France;* ³*Institut Jules Bordet, Brussels, Belgium;* ⁴*Domain Therapeutics, Strasbourg, France;* ⁵*Cliniques Universitaires Saint Luc, Brus, Brussels, Belgium*

Background Overexpression of Prostaglandin E2 (PGE2) in tumour tissues suppresses anti-tumour immunity in the tumour microenvironment and can lead to disease progression. DT-9081 is small molecule, orally administered, highly selective antagonist of prostaglandin E receptor 4 (EP4R) developed to overcome the immune-suppressive effects of PGE2, and to reverse the resistance to immune checkpoint blockers. DT-9081 has recently demonstrated significant anti-tumor activity in vivo as monotherapy and in combination with immunotherapeutic agents in several mouse tumor models.

Methods This first-in-human phase 1, multicentre, open label trial is evaluating the safety, tolerability, pharmacokinetics (PK), pharmacodynamics (PD), and preliminary efficacy of DT-9081 in adult's patients with recurrent and/or metastatic solid tumours who failed standard of care therapies (EudraCT Number 2022-000092-40) Patients will be dosed orally once daily. The schedule might be adjusted in case of toxicities or based on PK parameters.

This Phase 1 consists of 2 parts. The first part will consist in an initial dose-escalation phase using a 3+3 design up to 6 dose escalation cohorts at increasing levels are planned. The primary objectives will be to determine the dose-limiting toxicities, maximal tolerated dose, and the toxicity profile (NCI CTCAE v5.0) to establish the recommended phase II dose (RP2D) as single agent. Adjustment of the doses will be based on toxicities, pharmacokinetics data and pharmacodynamics effects of DT-9081.

The second part will be an expansion phase at the RP2D in a homogeneous patient population to validate the dose/schedule of administration as well as to assess preliminary efficacy of DT-9081 according to RECIST1.1.

Ethics Approval UNDER REVIEW

<http://dx.doi.org/10.1136/jitc-2022-SITC2022.0741>

742

A MULTICOHORT PHASE 1B STUDY (STELLAR-002) OF XL092 IN COMBINATION WITH IMMUNOTHERAPY IN PATIENTS WITH ADVANCED SOLID TUMORS

¹Bradley Mcgregor*, ¹Toni Choueiri, ²Neil Shah, ³Aung Bajaj, ⁴Jad Chahoud, ⁵Bert O'Neil, ⁶Joel Michalski, ⁷Benjamin Garmez, ⁸Lixian Jin, ⁹Usman Aziz, ⁹Fiona Xu, ²Robert Motzer. ¹Dana-Farber Cancer Institute, Boston, MA, USA; ²Memorial Sloan Kettering Cancer Center, New York, NY, USA; ³Arizona Oncology, Tucson, AZ, USA; ⁴Moffitt Cancer Center, Tampa, FL, USA; ⁵Indiana University, Indianapolis, IN, USA; ⁶Nebraska Cancer Specialists, Omaha, NE, USA; ⁷Sarah Cannon Research Institute, Nashville, TN, USA; ⁸Bristol Myers Squibb, Lawrenceville, NY, USA; ⁹Exelixis, Inc., Alameda, CA, USA

Background XL092 is a novel, oral inhibitor of multiple receptor tyrosine kinases including MET, VEGFR2, AXL, and MER, which are implicated in tumor growth, metastasis, angiogenesis, and immune modulation. XL092 has a half-life of ~21h, convenient for daily dosing and managing tolerability. Preclinical studies of XL092 plus an immune checkpoint inhibitor (ICI) showed antitumor activity in tumor models. STELLAR-002 will evaluate the safety and clinical activity of XL092 alone and in combination with nivolumab ± ipilimumab in patients with advanced solid tumors. Presented here is the study design which includes a dose-escalation stage in solid tumors and a cohort-expansion stage in genitourinary cancers.

Methods This multicenter phase 1b, open-label study (NCT05176483) will enroll patients with unresectable advanced or metastatic solid tumors. The dose-escalation stage will determine recommended doses of XL092 (orally) in combination with nivolumab ± ipilimumab (intravenously) for the cohort-expansion stage. Dose escalation will enroll a total of ~24 patients into two cohorts using a rolling 6 design: Cohort A, XL092 + nivolumab (360 mg Q3W); Cohort B, XL092 + nivolumab (3 mg/kg Q3W × 4, then 480 mg Q4W) + ipilimumab (1 mg/kg Q3W × 4). The cohort-expansion stage will include six tumor-specific cohorts: clear cell renal cell carcinoma (ccRCC), first-line therapy; ccRCC, second-line therapy after one prior ICI regimen; metastatic castration-resistant prostate cancer (mCRPC), second-line therapy after one prior novel hormonal therapy; urothelial carcinoma (UC), second-line therapy after prior platinum-based regimen and ICI-naïve; UC, ICI-experienced, up to 2 prior lines of systemic therapy with prior platinum-based regimens allowed; non-clear cell RCC, first-line therapy. Cohort-specific randomization will include XL092 alone or in combination with nivolumab ± ipilimumab to evaluate the contribution of the individual agents to the combination regimens. Thirty patients will be enrolled in each XL092 alone arm and 40 patients in each combination arm. Preliminary efficacy, safety, and pharmacokinetics of XL092 alone or in combination with ICI will be assessed in each cohort. Primary endpoints include objective response rate per RECIST v1.1 by investigator, progression-free survival per Prostate Working Group 3 criteria by blinded review (mCRPC cohort only), and safety. The study is enrolling patients.

Trial Registration Trial registry is ClinicalTrials.gov NCT05176483

Ethics Approval The study will adhere to the principles outlined in "Guideline for Good Clinical Practice" (GCP) and remain consistent with the most recent version of the Declaration of Helsinki.

Consent Patients will be required to provide written informed consent.

<http://dx.doi.org/10.1136/jitc-2022-SITC2022.0742>

743

PHARMACOKINETIC AND PHARMACODYNAMIC PROFILE OF A FIRST-IN-HUMAN STUDY WITH MDNA11, AN ENGINEERED LONG-ACTING BETA-ONLY IL-2 AGONIST

¹Minh To*, ¹Nina Merchant, ¹Melissa Coello, ¹Carole Galligan, ¹Kritika Mehta, ²Victoria Atkinson, ¹Martin Bexon, ³Jim Coward, ⁴Jenny Lee, ⁵Charlotte Lemech, ⁶Peter Lloyd, ⁷Jesus Antras, ⁸Arash Yavari, ¹Fahar Merchant. ¹Medicenna Therapeutics, Toronto, Canada; ²Gallipoli Medical Research Foundation, Woolloongabba, Australia; ³ICON Cancer Centre, South Brisbane, Australia; ⁴Chris O'Brien Lifehouse, Camperdown, Australia; ⁵Scientia Clinical Research, Randwick, NSW, Australia; ⁶KinDyn Consulting Ltd, Wamham, West Sussex, UK; ⁷Princess Margaret Hospital, Toronto, Canada; ⁸University of Oxford, Oxford, UK

Background MDNA11 is an engineered beta-only IL-2 albumin fusion protein with enhanced affinity and signalling via IL2-Rβγ (CD122/CD132) and no binding to IL-2Rα (CD25). Consequently, MDNA11 preferentially stimulates immune effector cells to elicit effective tumor regression both, as monotherapy and in combination with immune checkpoint inhibitors in mouse syngeneic cancer models.¹ The ABILITY (A Beta-only IL-2 ImmunoTherapY) trial is a first-in-human phase 1/2 study evaluating the safety, tolerability, pharmacokinetics (PK), pharmacodynamic (PD) effects, and preliminary clinical activity of MDNA11 as monotherapy and in combination with an immune checkpoint inhibitor in patients with advanced solid tumors (NCT05086692).

Methods The ABILITY study comprises a dose-escalation monotherapy phase in a modified 3+3 Q2W design followed by monotherapy and combination expansion at the recommended phase 2 dose (RP2D) in specific-tumor cohorts. Key eligibility criteria are locally advanced or metastatic unresectable solid tumors with no more than 4 prior lines of therapy and measurable disease per RECIST v1.1. Dose levels (DL) 1-3 were administered at a fixed dose of 3, 10 or 30 ug/kg, respectively. A step-up dosing (SUD) strategy was implemented starting at DL4 in which patients received 2 priming doses of 30 ug/kg followed by a target dose of either 60 ug/kg (DL-4) or 90 ug/kg at DL-5 (enrolment initiated).

Results PK analysis showed dose-dependent increase in exposure as anticipated, with no evidence of anti-drug antibodies (ADA) based on consistent PK profile following each of 3 repeat dose administrations. Lymphocyte counts increased with each repeat dose administration and to date, there is no evidence of eosinophilia, associated with vascular leak syndrome (VLS) commonly observed with high dose IL-2. Immune profiling showed several-fold increases in Ki67 expression by peripheral CD8+ T and NK cell without stimulation of immune suppressive Tregs. Accordingly, CD8+ T and NK cell counts increased with each repeat dose (Q2W) of MDNA11 without eliciting any significant increase in Treg number. Increase in activation markers were also noted on CD8+ T cells without elicitation of similar markers on Tregs. Transient increase in some cytokines was observed. Analysis of paired biopsies is underway to examine local changes in the tumor micro-environment.

Conclusions Cumulative PD readouts to date are consistent with the anticipated pharmacological effect of MDNA11 demonstrating dose dependent activation of various biomarkers on effector cells without concomitant stimulation of immune suppression. Updated PK, PD and ADA data will be presented as dose escalation continues.

Acknowledgements We thank the patients participating in the ABILITY study.

REFERENCE

1. Merchant R, Galligan C, Munegowda M, Pearce LB, Lloyd P, Smith P, Merchant F, To MD, Fine-tuned long-acting interleukin-2 superkine potentiates durable immune responses in mice and non-human primate. *J Immunother Cancer*. **10**(1): e003155

Ethics Approval The study was approved by each institution's Ethic Board.

<http://dx.doi.org/10.1136/jitc-2022-SITC2022.0743>

744

INTERIM SINGLE-AGENT SAFETY AND ANTI-TUMOR ACTIVITY FROM DOSE ESCALATION PHASE OF ABILITY STUDY ON MDNA11, A LONG-ACTING BETA-ONLY IL-2 AGONIST

¹Minh To, ¹Fahar Merchant*, ²Victoria Atkinson, ¹Martin Bexon, ³Jim Coward, ⁴Jenny Lee, ⁵Charlotte Lemech, ⁶Jesus Antras, ⁷Peter Lloyd, ⁸Arash Yavari, ¹Melissa Coello, ¹Nina Merchant. ¹Medicenna Therapeutics, Toronto, Canada; ²Gallipoli Medical Research Foundation, Woollongabba, Australia; ³ICON Cancer Centre, South Brisbane, Australia; ⁴Chris O'Brien Lifehouse, Camperdown, Australia; ⁵Scientia Clinical Research, Randwick, NSW, Australia; ⁶Princess Margaret Hospital, Toronto, Canada; ⁷KinDyn Consulting Ltd, Wamham, West Sussex, UK; ⁸University of Oxford, Oxford, UK

Background High dose (HD) IL-2 has shown durable tumor response in a subset of metastatic melanoma and renal cell carcinoma (RCC), but its clinical utility is limited by need for frequent administration, undesirable activation of immune suppressive Tregs, and severe toxicities. MDNA11 is an albumin-fused long-acting engineered IL-2 agonist with enhanced affinity for IL-2R β with no binding to IL-2R α , enabling Q2W administration, limiting Treg activation while potentiating anti-tumor CD8⁺ T and NK cells and reducing toxicities.¹

Methods The objective of the dose-escalation phase of the ABILITY (A Beta-only IL-2 ImmunoTherapy) study is to determine the safety and tolerability, define the recommended phase-2 dose (RP2D), and assess preliminary tumor response of MDNA11 in patients with advanced solid tumors. In this modified 3+3 dose escalation, patients received a fixed dose of 3 (dose level 1 or DL1), 10 (DL2) or 30 (DL3) μ g/kg by intravenous (IV) infusion on a Q2W schedule. Step-up dosing (SUD) is implemented starting at DL4 where patients received 2 priming doses at 30 μ g/kg (Q2W) prior to escalation to the target dose (Q2W) of 60 μ g/kg (DL4) or 90 μ g/kg (DL5; enrolling). Primary endpoints include incidence, nature and severity of adverse events (AEs). Secondary endpoints include assessment of pharmacokinetics, pharmacodynamics and tumor response per RECISTv1.1.

Results As of July 21, 2022, 14 patients have been dosed with MDNA11 (DL1 = 1, DL2 = 3, DL3 = 4, DL4 = 6). Tumor types enrolled were melanoma (n=7), RCC (n=1), pancreatic ductal adenocarcinoma (n=2), sarcoma (n=2), squamous cell carcinoma (n=1) and gastro-esophageal adenocarcinoma (n=1). PK analysis showed dose-dependent increase in MDNA11 exposure. MDNA11 has been well tolerated with no dose-limiting toxicities observed at up to DL4. The most common drug-related AEs were infusion related reactions (71%), pyrexia (35%), diarrhea (28%) and nausea (28%), and with a majority of these being Grade 1 or 2 and lasted less than 24 hours. Tumor responses were evaluated in 10 patients and 4 patients had not reached their first assessment. Single-agent activity based on RECISTv1.1 included stable disease (SD) observed in patients with melanoma (n=1), sarcomas (n=2) and pancreatic cancer (n=1).

Conclusions MDNA11 is well tolerated with no DLTs up to target dose of 60 μ g/kg (DL4) and enrolment for 90 μ g/kg (DL5) has initiated. There is dose-dependent increase in plasma exposure and evidence of single-agent anti-tumor activity in 4 of 10 (SD) patients.

Acknowledgements We would like to thank the patients for participating in the ABILITY study.

Trial Registration NCT05086692

REFERENCE

1. Merchant R, Galligan C, Munegowda M, Pearce LB, Lloyd P, Smith P, Merchant F, To MD, Fine-tuned long-acting interleukin-2 superkine potentiates durable

immune responses in mice and non-human primate. *J Immunother Cancer* **10**(1): e003155.

Ethics Approval The study was approved by each institution's Ethic Board.

<http://dx.doi.org/10.1136/jitc-2022-SITC2022.0744>

745

IMP-MEL: A PHASE 1 FIRST-IN-HUMAN DOSE-FINDING STUDY OF A NOVEL INVARIANT NATURAL KILLER T-CELL AGONIST (INKT) IMM60 IN ADVANCED MELANOMA AND NON-SMALL-CELL LUNG CANCER (NSCLC)

¹Nicholas Coupe, ²Ian Walters*, ²Justin Fairchild, ³Matthew Parkes, ³David Thompson, ²Robert Kramer, ³Uzi Gileadi, ³Mark Middleton. ¹Oxford University Hospitals, Oxford, UK; ²Portage BioTech, Westport, CT, USA; ³University of Oxford, Oxford, UK

Background Invariant natural killer T-cells (iNKTs) share features of innate cells (NK-like) and T-cells. The importance of this relatively rare lymphocyte subset has generated increased interest due to its dual ability to have a direct cytotoxic effect on CD1d-expressing tumors and its ability to induce long-lasting antitumor CD8 T-cell responses mediated by cross priming and licensing of dendritic cells. Various clinical approaches involving the use of allogeneic iNKT cells are in development; here we describe an initial clinical study with IMM60, a synthetically derived agonist of iNKT cells which is formulated in a liposome (PORT-2). In preclinical studies, IMM-60 treatment results in maturation of DCs and B cells and potent stimulation of iNKT cell-derived IFN-g. In efficacy studies, IMM60 demonstrated monotherapy activity in PD-1 resistant models, (e.g., B16-F10), and upregulation of PD-L1 expression on cancer cells as a consequence of its priming effect.

Methods IMP-MEL is an open-label first-in-human phase 1/2 study, currently enrolling adult subjects with advanced NSCLC and melanoma. IMM60-containing liposomes were administered IV Q3W at 3 escalating dose levels for 6 doses. The study seeks to assess the safety and efficacy of IMM-60 alone, as well as in combination with a PD-1 inhibitor. Pharmacodynamic analyses were performed, including circulating cytokines and flow cytometry.

Results Six patients with advanced melanoma (n=3) or NSCLC (n=3) have been enrolled in the monotherapy dose cohorts, having a median of 4.5 prior therapies (min 2, max 5). The drug was well tolerated with no treatment-related SAEs or Grade 3-5 adverse events to date. Cytokine analysis and flow cytometry of pre- and on-study blood samples revealed evidence of iNKT activation as well as NK and dendritic cell activation. [MP1] One patient achieved >50% reduction in select target and non-target lesions. The MTD has not been reached.

Conclusions This trial provides early proof of concept for using a small molecule iNKT agonist to promote both innate and adaptive immune responses. PORT-2 (liposomal IMM60) is well tolerated at 1 and 3 mg/m². Pharmacodynamic measurements support a broad immune mechanism. Once the Phase 2 dose is defined the trial is designed to accrue six Phase 2 arms testing PORT-2 alone or combined with a PD-1 inhibitor, compared to PD-1 inhibitor monotherapy. Further data on pharmacokinetics and biopsy analyses will be presented.

Ethics Approval This University of Oxford study has received ethical approval by a UK Research Ethics Committee, approval number 20/SC/0367. All participants provided informed consent before taking part in this clinical trial.

<http://dx.doi.org/10.1136/jitc-2022-SITC2022.0745>

AFM24 AND ATEZOLIZUMAB COMBINATION IN PATIENTS WITH ADVANCED EPIDERMAL GROWTH FACTOR RECEPTOR-EXPRESSING (EGFR⁺) SOLID TUMORS: INITIAL RESULTS FROM THE PHASE 1 DOSE-ESCALATION STUDY

¹Omar Saavedra Santa Gadea*, ²Daniela Morales-Espinosa, ³Juanita Lopez, ⁴Eric Christenson, ⁵Anthony El-Khoueiry, ⁶Andrés Cervantes, ²Christa Raab, ²Ulrike Gärtner, ²Kerstin Pietzko, ²Laura Kohlhas, ²Daniel Schütz, ²Gabriele Hintzen, ²Paulien Ravenstijn, ²Michael Emig, ⁷Pilar Nava-Parada. ¹Vall D'Hebron University Hospital, Barcelona, Spain; ²Affimed GmbH, Heidelberg, Germany; ³Royal Marsden Hospital, London, UK; ⁴John Hopkins University Hospital, Baltimore, MD, USA; ⁵University of Southern California, Los Angeles, CA, USA; ⁶Hospital Clínico, University of Valencia, Valencia, Spain; ⁷Affimed Inc., New York, NY, USA

Background AFM24 is an innate cell engager binding EGFR on tumor cells, and CD16A on natural killer cells and macrophages; AFM24 activates and redirects these cells to EGFR⁺ tumors to enhance antibody-dependent cellular cytotoxicity and antibody-dependent phagocytosis, respectively. Atezolizumab, a PD-L1 inhibitor, has been approved in patients with solid tumors. Combining AFM24 with atezolizumab may synergistically enhance the innate and adaptive immune responses, respectively, to target EGFR⁺ tumors.

Methods AFM24-102 (NCT05109442) is a Phase 1/2a open-label, non-randomized, multicenter, dose escalation, and expansion study evaluating AFM24 in combination with atezolizumab in patients with selected EGFR⁺ advanced solid malignancies whose disease has progressed after treatment with previous anticancer therapies. Phase 1 will follow a 3+3 design to establish the maximum tolerated dose or recommended phase 2 dose of AFM24; patients will receive AFM24 IV QW at an escalating dose per cohort and 840 mg atezolizumab IV once fortnightly in a 4-week cycle until disease progression, intolerable toxicity, termination by the investigator, or patient withdrawal. Secondary endpoints include pharmacokinetic, pharmacodynamic, and immunogenicity analysis. A starting dose of 160 mg QW of AFM24 was selected based on data from an ongoing Phase 1/2a first-in-human trial of AFM24 monotherapy.

Results Four patients have been enrolled in the first dose cohort, with three completing the safety lead-in phase and receiving 160 mg AFM24 and atezolizumab. Patients are female with gastric (n=1) or pancreatic (n=3) adenocarcinomas (median [range] age was 60 years [50–73], number of prior therapies was 3.5 [3–4], with 90% EGFR expression [70–100%] by immunohistochemistry). All patients have European Cooperative Oncology Group scores of 0–1. Adverse events (AEs) (n≥2) included lymphopenia, anemia, neutropenia, and infusion-related reactions. No dose-limiting toxicities (DLTs) occurred. Serious AEs likely related to AFM24 treatment were one Grade 2 IRR and one Grade 1 medication error. In the patient with gastric cancer and skin metastases, who had rapidly progressed following four prior lines of therapy, including a PD-L1 inhibitor, an ongoing partial response has been confirmed after two cycles of AFM24 treatment. A still ongoing stable disease of 4+ months and symptomatic improvement has been observed in a patient with pancreatic adenocarcinoma that had rapid disease progression after three lines of previous therapy.

Conclusions AFM24 at 160 mg in combination with atezolizumab was adequately tolerated. No DLTs were reported. Clinical activity was observed in two patients. Dose escalation is proceeding at 480 mg and enrollment has begun.

Acknowledgements Editorial assistance was provided by Meridian HealthComms Ltd, funded by Affimed.

Trial Registration NCT05109442

Ethics Approval The study is being conducted in accordance with ICH GCP, the Declaration of Helsinki, the European Union Clinical Trials Directive 2001/20/EC, the GCP Directive 2005/28/EC, the requirements of local IRB/EC, and the US Code of Federal Regulations, Title 21 CFR Part 50. The principles of informed consent in the Declaration of Helsinki and GCP guidelines are being implemented before any protocol-specific procedures or interventions are carried out.

<http://dx.doi.org/10.1136/jitc-2022-SITC2022.0746>

747

A PHASE 1 TRIAL OF IO-202, AN ANTAGONIST ANTIBODY TARGETING MYELOID CHECKPOINT LILRB4 (ILT3), AS MONOTHERAPY AND IN COMBINATION WITH PEMBROLIZUMAB IN ADULT PATIENTS WITH ADVANCED RELAPSED OR REFRACTORY SOLID TUMORS

¹Aung Naing, ²John Powderly, ³Meredith Pelster, ⁴Alexander Spira, ⁵Reva Schneider, ⁶Paul Woodard, ⁶Luke Chung, ⁶Elizabeth Wieland, ⁶Sydney Ray, ⁶Kyu Hong, ⁶Tao Huang, ⁶X Charlene Liao, ⁶Hong Xiang, ⁷Heinz-Josef Lenz, ⁶Wen Hong Lin*. ¹MD Anderson Cancer Center, Houston, TX, USA; ²Carolina BioOncology Institute, Huntersville, NC, USA; ³Sarah Cannon Research Institute at Tennessee Oncology, Nashville, TN, USA; ⁴Virginia Cancer Specialists, Fairfax, VA, USA; ⁵Mary Crowley Cancer Institute, Dallas, TX, USA; ⁶Immuno-Onc, Palo Alto, CA, USA; ⁷USC Norris Comprehensive Cancer Center, Los Angeles, CA, USA

Background Most patients with advanced solid tumors relapse after T-cell checkpoint blockade despite of immunotherapy becoming the mainstream with the approvals of T-cell checkpoint inhibitors. Myeloid checkpoint inhibition is a new approach to immunotherapy.

Leukocyte immunoglobulin-like receptor subfamily B member 4 (LILRB4) is a myeloid checkpoint with its expression restricted to monocytes or monocyte-derived cells^{1,2,3} and in normal antigen presenting cells. LILRB4 functions as a negative regulator of immunity through interaction with its ligands, apolipoprotein E and fibronectin^{1,2,4,5,6}. Blockade of LILRB4 has the potential to enhance anti-tumor T cell activities.

IO-202 is a IgG1 monoclonal antibody that binds to LILRB4 to block ligand interactions and inhibits the function of LILRB4. In vitro, IO-202 treatment of immune cells increases pro-inflammatory responses and enhances antigen presenting cell phenotypes. IO-202 has been studied at a first-in-human, phase 1 study in acute myeloid leukemia and chronic myelomonocytic leukemia patients (IO-202-CL-001) up to 30 mg/kg IV Q2W with no observed dose limiting toxicity (DLT), which provided sufficient data supporting the starting dose of 250 mg.

Methods This trial (NCT05309187) is a Phase 1, dose-escalation, dose-expansion, safety, and pharmacokinetic (PK) evaluation of IO-202 alone and plus pembrolizumab in patients with advanced solid tumors. Up to 36 patients will be enrolled in the dose-escalation portion (Part 1) and up to 168 patients will be enrolled in the dose-expansion portion (Part 2). IO-202 will be administered IV Q3W, with a 21-day DLT evaluation period. In Part 1, patients will be treated with increasing doses of IO-202 alone and plus pembrolizumab using the modified Toxicity Probability Interval method; the combination cohorts will start once the 1st monotherapy dose has cleared the DLT window and be conducted independently. In Part 2, patients will be treated with IO-202 RP2D plus pembrolizumab 200 mg IV Q3W.

The primary objective is to assess safety and tolerability of IO-202 alone and plus pembrolizumab in patients with advanced solid tumors, to estimate the maximal tolerated dose or maximum administered dose and select the recommended phase 2 dose (RP2D). Secondary objectives include characterizing PK for IO-202 alone or plus pembrolizumab; and assessing efficacy of IO-202 plus pembrolizumab in various solid tumors. Biomarker evaluation includes changes in immune cell markers, LILRB4 expression and receptor occupancy.

Statistical analyses will be descriptive. Tabulations will be produced for appropriate disposition, demographics, baseline characteristics, safety, PK, pharmacodynamic, and clinical activity parameters. To date, one patient has been treated with IO-202 without DLT.

Trial Registration NCT05309187

REFERENCES

- 1) Chang C, Ciubotariu R, Manavalan J, et al. Tolerization of dendritic cells by T (S) cells: the crucial role of inhibitory receptors ILT3 and ILT4. *Nat Immunol.* 2002;**3**:237–243.
- 2) Deng M, Gui X, Kim J. et al. LILRB4 signalling in leukaemia cells mediates T cell suppression and tumour infiltration. *Nature.* 2018;**562**:605–609.
- 3) John S, Chen H, Deng M, et al. A novel anti-LILRB4 CAR-T cell for the treatment of monocytic AML. *Mol Ther.* 2018;**26**(10):2487–2495.
- 4) Cella M, Döhning C, Samaridis J, Dessing M, Brockhaus M, Lanzavecchia A, Colonna M. A novel inhibitory receptor (ILT3) expressed on monocytes, macrophages, and dendritic cells involved in antigen processing. *J Exp Med.* 1997;**185**(10):1743–51.
- 5) Kim-Schulze S, Scotto L, Vlad G, et al. Recombinant Ig-like transcript 3-Fc modulates T cell responses via induction of Th anergy and differentiation of CD8 + T suppressor cells. *J Immunol.* 2006;**176**(5):2790–8.
- 6) Paavola K, Roda JM, Lin VY, et al. The fibronectin-ILT3 interaction functions as a stromal checkpoint that suppresses myeloid cells. 2021; **9**:1283–1297.

Ethics Approval The trial has been approved by the Advarra IRB on January 18, 2022, with the Advarra IRB ID of Pro00060224. All the subjects will give informed consent before being enrolled into this trial and any study related procedures.

<http://dx.doi.org/10.1136/jitc-2022-SITC2022.0747>

A PHASE 1/2, OPEN-LABEL, DOSE-ESCALATION, SAFETY AND TOLERABILITY STUDY OF NC762 IN SUBJECTS WITH ADVANCED OR METASTATIC SOLID TUMORS

<http://dx.doi.org/10.1136/jitc-2022-SITC2022.0748>

¹Han Myint, ²Satish Shah*, ³Martin Gutierrez, ⁴Emese Zsiros, ⁵Megan Nelson, ⁶Stephanie Zeidan, ⁷Nadia Myrthil, ⁸Aaron Morawski, ⁹Alina Barbu, ¹⁰Jahangheer Shaik, ¹¹Chelsea Zhou, ¹²Chrysi Kanellopoulou, ¹³Ron Copeland, ¹⁴Zachary Cusumano, ¹⁵Dallas Flies, ¹⁶Solomon Langemann, ¹⁷Patricia Lorusso, ¹⁸Kunle Odunsi. ¹NextCure Inc, Beltsville, MD, USA; ²Pennsylvania Cancer Specialists, Gettysburg, PA, USA; ³John Theurer Cancer Center, Hackensack, NJ, USA; ⁴Roswell Park Comprehensive Cancer Center, Buffalo, NY, USA; ⁵NextCure, beltsville, MD, USA; ⁶Yale Cancer Center, New Haven, CT, USA; ⁷UFC Comprehensive Cancer Center, Chicago, IL, USA

Background NC762 is a humanized IgG1κ monoclonal antibody that targets human B7-H4 (B7 homolog 4), a transmembrane protein, associated with the B7 family of molecules known for their immunomodulatory functions. While limited expression is observed on healthy tissue, B7-H4 is commonly expressed by several tumor types including ovarian, lung, renal, melanoma, prostate, pancreatic, and breast cancers and is often correlated with poor clinical outcome. Given differential expression of B7-H4 in healthy and cancerous tissue, B7-H4 presents itself as an attractive candidate for a targeted therapeutic monoclonal antibody (mAb) for oncology.

Preclinical data demonstrated that binding of NC762 to tumors expressing B7-H4 results in inhibition of tumor growth in vivo. The inhibitory effect on tumor growth is not dependent upon T cells and does not appear to be a predominant antibody-dependent cellular cytotoxicity (ADCC) mechanism. However, NC762 has been Fc engineered to enhance binding to CD16a and does demonstrate increased anti-tumor activity in the presence of NK cells.

Methods This is a multi-center, first in human, phase 1/2, open-label, single-armed study to determine the safety and tolerability, MTD, and pharmacologically active dose for NC762, as well as to assess preliminary efficacy, and explore predictive and pharmacodynamic biomarkers in subjects with advanced or metastatic solid tumors. The 3+3 dose escalation design in 5 cohorts is to establish recommended phase 2 dose (RP2D) (NCT04875806). Phase 1b and 2 study will select for patients expressing B7-H4+ in specific tumor types including ovarian.

Results As of 07/20/2022, a total of 14 patients (Median age 69; 5F, 9M) with 5 tumor types, have been enrolled, treated, and completed the DLT period. Median line of prior therapies was six. NC762 (up to 10mg/kg), was well tolerated, with no safety concerns, no infusion-related toxicities, nor any reported DLT. Clinical benefit is seen from the lowest dose cohorts with a few stable diseases beyond six months. PK and potential pharmacodynamic biomarkers continue to be evaluated as the phase 1 study continues to enroll and will be presented.

Conclusions Preliminary evaluation of NC762 in subjects with advanced or metastatic solid tumors appears to be safe and well-tolerated. Further evaluation will be performed with the final cohort at 20mg/kg and simultaneous expansion of 10mg/kg in B7-H4+ advanced solid tumors to confirm these initial findings.

Trial Registration NCT04875806

Ethics Approval This study has been approved by the IRB of all the participating institutions, and all participants have given informed consent before taking part in the study.

Consent Written informed consent was obtained from the patient for publication of this abstract and any accompanying images. A copy of the written consent is available for review by the Editor of this journal.

749

USE OF POSITRON EMISSION TOMOGRAPHY FOR THE DIAGNOSIS OF IMMUNE CHECKPOINT INHIBITOR MYOCARDITIS

Nicolas Palaskas*, Yang Lu, Rebecca Caldwell, Praise Oderinde, Gaspar Pina, Abdelrahman Ali, Khatera Shah, Cezar Iliescu, Syed Wamique Yusuf, Efstratios Koutroumpakis, Shaden Khalaf, Ihab Hamzeh, Bilal Siddiqui, Sumit Subudhi, Anita Deswal. *The University of Texas MD Anderson Cancer Center, Houston, TX, USA*

Background Myocarditis from immune checkpoint inhibitor (ICI) therapy has a reported mortality of 25 to 50%.¹ The gold standard for myocarditis diagnosis is endomyocardial biopsy (EMB).¹ The feasibility and diagnostic accuracy of fluorodeoxyglucose positron emission tomography (FDG PET) computed tomography (CT) has not been extensively evaluated compared to EMB in ICI myocarditis.

Methods This was a prospective observational study conducted at MD Anderson Cancer Center between March 2021 and May 2022. Patients were eligible if age ≥ 18 years, ICI was administered in single or combination therapy, and there was clinical or diagnostic suspicion of myocarditis. All patients had an EMB with at least 4 samples of the right ventricular septal wall. Prior to imaging with FDG PET CT, patients followed a 72-hour low carbohydrate, high fat diet. Sensitivity, specificity, positive predictive value (PPV), and negative predictive value (NPV) of FDG PET CT were calculated.

Results There were 10 patients enrolled with FDG PET CT performed. The demographics were 68.9 years (median), 70% male, 70% Caucasian and 30% Hispanic. The most common malignancies were genitourinary (30%), melanoma (30%), lung (20%), liver (10%), and papillary thyroid (10%). The ICI use was 40% programmed cell death 1 (PD-1) inhibitor, 30% programmed cell death ligand 1 (PD-L1) inhibitor, and 30% combination PD-1 and cytotoxic T-lymphocyte-associated protein 4 (CTLA-4) inhibition. The sensitivity of FDG PET CT was 75%, specificity 67%, PPV 60%, and NPV 80% (table 1). The time from admission to imaging with FDG PET CT was median 11 days. The time from admission to EMB was median 1 day. Reasons for delay in FDG PET CT included plasmapheresis being administered with glucose infusion (50%), inability to adhere to dietary protocol (20%), and clinical instability (20%) for imaging. One of the three patients EMB and FDG PET CT positive for ICI myocarditis had imaging uptake in the septal wall. Two patients FDG PET CT positive and EMB negative had imaging uptake in the lateral left ventricular wall and apex. Two of the FDG PET CT noted skeletal muscle FDG avidity and these patients had concomitant myositis.

Conclusions The feasibility of performing FDG PET CT is limited due to the use of plasmapheresis and the dietary protocol necessary for imaging. There is reasonable sensitivity and specificity for FDG PET CT in ICI myocarditis. There may be a role for identification of concomitant immune related adverse events also with the diagnosis of myositis.

Trial Registration NCT05062395

REFERENCE

1. Palaskas N, Lopez-Mattei J, Durand JB, Iliescu C, Deswal A. Immune Checkpoint Inhibitor Myocarditis: Pathophysiological Characteristics, Diagnosis, and Treatment. *J Am Heart Assoc.* 2020;**9**(2):e013757. doi: 10.1161/JAHA.119.013757. Epub 2020 Jan 21. PMID: 31960755; PMCID: PMC7033840.

Ethics Approval The protocol was approved by the institutional review board 4.

Consent Written informed consent was obtained from the patients prior to enrollment in the study. A copy of the written consent is available for review by the Editor of this journal.

Abstract 749 Table 1 FDG PET CT compared to EMB for the diagnosis of ICI myocarditis

Comparison of FDG PET CT to EMB		FDG PET CT	
		Positive	Negative
EMB	Positive	3	1
	Negative	2	4

<http://dx.doi.org/10.1136/jitc-2022-SITC2022.0749>

750

TWT-101: A FIRST-IN-CLINIC, PHASE 1/2 STUDY OF CFI-402411, A HEMATOPOIETIC PROGENITOR KINASE-1 (HPK1) INHIBITOR, AS A SINGLE AGENT AND IN COMBINATION WITH PEMBROLIZUMAB IN SUBJECTS WITH ADVANCED SOLID MALIGNANCIES

¹Kyriakos Papadopoulos, ²Siqing Fu, ³Erika Hamilton, ⁴Alexander Spira, ⁵Scott Laurie, ⁶Judy Wang, ⁷Brigitte Ma, ⁸Anna Spreafico, ⁹Manish Sharma, ¹⁰Quincy Chu, ¹¹Mark Bray, ¹¹Glenn Michelson, ¹¹Dih-Yih Chen, ¹¹Linh Nguyen, ¹¹Emily Roberts-Thomson, ¹²Omid Hamid*. ¹START, San Antonio, San Antonio, TX, USA; ²MD Anderson Cancer Center, Houston, TX, USA; ³SCRITennessee Oncology, Nashville, TN, USA; ⁴Virginia Cancer Specialists, Fairfax, VA, USA; ⁵The Ottawa Hospital Cancer Center, Ottawa, Canada; ⁶Florida Cancer Specialists/SCRIT, Sarasota, FL, USA; ⁷The Chinese University of Hong Kong, Sha Tin, Hong Kong; ⁸Princess Margaret Cancer Centre, Toronto, Canada; ⁹START Midwest, Grand Rapids, MI, USA; ¹⁰Cross Cancer Institute, Edmonton, Canada; ¹¹Treadwell Therapeutics, Toronto, Canada; ¹²The Angeles Clinic and Research Inst., Los Angeles, CA, USA

Background CFI-402411 is a potent inhibitor of HPK1 (Hematopoietic progenitor kinase 1), a protein serine/threonine kinase that negatively-regulates T-cell activation. Following T-cell receptor engagement, HPK1 phosphorylates SLP-76, to down-regulate signals required for T-cell activation and proliferation^{1,2}. CFI-402411 is expected to relieve HPK1-mediated inhibition of T-cell activation, facilitating an anti-tumor immune response.

Methods In this ongoing phase 1 study, part A evaluates CFI-402411 daily dose in dose escalation cohort (3+3 design) and dose expansion, part B evaluates CFI-402411 in combination with pembrolizumab in dose escalation (BOIN design) and dose expansion in pembrolizumab eligible tumors. Dose limiting toxicity (DLT) is any grade ≥ 3 toxicity in the first cycle of therapy (21d cycles). Starting dose was 80mg.

Results As of 14 May 2022 (data cutoff), 25 and 9 patients (pts) enrolled to A and B respectively. Median age was 62 (30-79). Median cycles of treatment were 3 (range: 0-20). Majority of patients were male (A, 60% and B, 78%). Median prior regimens were 2 (range: A, 1-4; B, 1-3). 6pts (A, 24%) and 5pts (B, 56%) received prior anti-PD-1/anti-PD-L1 inhibitor. Diagnoses in ≥ 2 pts for A: colorectal (6pts), pancreatic (5pts); for B: small cell lung cancer (2pts). 8 dose levels (80 to 800 mg) have been studied in A, 2 dose levels (60 and 80 mg) in B. TEAEs occurring in $\geq 40\%$ of A pts: diarrhea (n=17, 68%), nausea (n=11, 44%), decreased appetite (n=10, 40%); and B: vomiting (n=4, 44%). 19pts (76%) in A and 6pts (67%) in B experienced CFI-402411 related AEs. Immune-related AEs were reported in 1pt (A; 4% [ALT and AST increase]) and 2pts (B; 22% [febrile illness, flu-like symptoms]). Grade ≥ 3 AEs and serious AEs occurred in 14pts (56%) and 10pts (40%) in A; and 3pts (33%) and 4pts (44%) in B. DLTs occurred in 2pts (A [800mg]: diarrhea, spinal cord compression) and 1pt (B [80mg+pembro]: flu-like symptoms). No novel toxicity signals were seen. Disease control rates were 24% in A (6/25) and 44% in B (4/9). One B patient (11%), squamous head and neck cancer (H&N) previously treated with pembrolizumab, has confirmed partial response (PR) and remains on treatment, 8 cycles. An additional H&N patient treated with monotherapy CFI-402411 achieved unconfirmed PR after data cut.

Conclusions CFI-402411 is a well-tolerated, potent inhibitor of HPK1 with a manageable AE profile and initial evidence of activity. RP2D and additional safety and efficacy data will be reported at conference presentation.

Acknowledgements Treadwell Therapeutics would like to thank both the patients and the research staff at enrolling centers who have helped to bring this novel therapy to the clinic. Trial Registration NCT04521413

REFERENCES

1. Hu MQ. Human HPK1, a novel human hematopoietic progenitor kinase that activates the JNK/SAPK kinase cascade. *Genes & Development*. 1996;**10**:2251–2264.
2. Lasserre RC-G. Release of serine/threonine-phosphorylated adaptors from signaling microclusters down-regulates T cell activation. *Immuno Res*. 2011;**295**:839–853.

Ethics Approval This study obtained ethics approvals at the following ethics/IRB's;

- Papadopoulos, KP; Advarra IRB ID: Pro00051609
Fu, S; University of Texas MD Anderson Cancer Center Office of Human Subject Protection IRB ID 2020-0678
Hamilton, E; Advarra IRB ID: Pro00051611
Spira, A; Advarra IRB ID: Pro00043629
Laurie, S; Ontario Cancer Research Ethics Board, CTO Project ID 3320
Wang, J; Advarra IRB ID: Pro00051611
Ma, B; Joint Chinese University of Hong Kong-New Territories East Cluster Clinical Research Ethics Committee CREC Ref. No. : 2020.367-T
Spreafico, A; Ontario Cancer Research Ethics Board, CTO Project ID 3320
Sharma, M; Advarra IRB: ID Pro00051609
Chu, Q; Health Research Ethics Board of Alberta Ethics ID: HREBA.CC-20-0504_REN1
Hamid, O; WCG, IRB: IRB Tracking Number: 2020236
As evidenced by verified clinical database information all subjects gave informed consent before taking part in this clinical trial.

<http://dx.doi.org/10.1136/jitc-2022-SITC2022.0750>

751

PMC-309, A HIGHLY SELECTIVE ANTI-VISTA ANTIBODY REVERSES IMMUNOSUPPRESSIVE TME TO IMMUNE-SUPPORTIVE TME

Cheon Ho Park, Sang Soon Byun*, Ki Dae Kim*, Hye Rim Han*, Weon Sup Lee. *PharAbcine Inc., Daejeon, Korea, Republic of*

Background The tumor microenvironment (TME) consists of blood & lymphatic vessels, stromal cells, and immune cells such as lymphocytes, macrophages, and APC cells. V-domain immunoglobulin suppressor of T cell activation (VISTA) is highly expressed in myeloid-derived cells and its blockade enhances antitumor immunity in multiple tumor models. Therefore, anti-VISTA agents may provide additional cancer immunotherapy and may work synergistically with PD1/PDL1 targeting drugs.

Methods Target cell analysis: human peripheral blood mononuclear cells (PBMC) containing lymphocyte and myeloid lineage cells were used for target cell analysis with flow cytometry.

T cell activity (ex vivo): human PBMC was employed for the evaluation of T cell activity (IRB #1041107-201703-BR-002-02) and CD3+ T cells and CD14+ monocytes were isolated from human PBMC and co-cultured in a 2.5 mg/ml anti-CD3 antibody-coated plate for 6 days in the presence of PMC-309 or other drugs. Culture media were harvested and evaluated the secreted levels of IFN- γ by ELISA.

MDSC suppression activity (ex vivo): MDSCs cells (5×10^4 cells) were cultured with CD3+ T cells (2×10^5 cells) in the presence of anti-CD3/28 bead with 10, 30, 100 μ g/ml of PMC-309, or 100 μ g/ml of anti-PD1, anti-PDL1, and anti-CTLA4 and for 3 days. IFN-g production was measured by ELISA.

In vivo study: MC38 bearing human VISTA knock-in (KI) mice were employed for the assessment of anti-tumor activity of PMC-309.

The tumor infiltrated immune cells: Immune cells in the TME were evaluated by immunohistochemistry (IHC) or flow cytometry (FACS) analysis.

Results PMC-309 binding to VISTA expressing cells is highly selective and the selectivity is maintained even in the low pH conditions that mimic TME. PMC-309 enhances the secretion of IFN-gamma, TNF-alpha, and IL-2 in T cell and monocyte co-culture settings. In addition, PMC-309 promoted monocyte differentiation into M1 macrophage that stimulates proinflammatory cytokine secretion of T cells. For the in vivo study, PMC-309 was intravenously administrated in VISTA-KI mice. The tumor growth rate was suppressed accompanied by a synergistic effect with an anti-PD1 antibody. The anti-tumor activity was associated with enhanced T cell activation, increased secretion of pro-inflammatory cytokines, and increased penetration of cytotoxic T cells, but lowering immune-suppressive MDSC cells into TME as demonstrated with IHC analysis.

Conclusions PMC-309 increased the number of T cell infiltration while a decrease of MDSCs in the TME. PMC-309 in combination with chemotherapy or other IO drugs could address highly medical unmet needs from patients with drug resistance to currently available IO treatment options.

<http://dx.doi.org/10.1136/jitc-2022-SITC2022.0751>

753

A PHASE 1B/2 STUDY OF A NOVEL ANTI-CTLA-4 NEOBODY™ ADG116 MONOTHERAPY AND IN COMBINATION WITH TORIPALIMAB (TORI; ANTI-PD-1 ANTIBODY) IN PATIENTS WITH ADVANCED/METASTATIC SOLID TUMORS

¹John Park, ²Matthew Hsien, ³Gary Richardson, ⁴Anthony Tolcher, ⁵Hong Jae Chon, ⁶Sang Joon Shin, ⁷Ho Yeong Lim, ⁸Anis Hamid, ⁹Daneng Li, ¹⁰Kristine Shi, ¹¹Songmao Zheng, ¹²Guizhong Liu, ¹³Ai Li, ¹⁴Lvyu Zhu, ¹⁵Ruby Dai, ¹⁶Wei Peng, ¹⁷Dana Lowe, ¹⁸Peter Luo, ¹⁹Jiping Zha*. ¹Macquarie University, Sydney, Australia; ²National Cancer Centre, Singapore, Hospital Crescent, Singapore; ³Cabrini Health, Melbourne, Australia; ⁴Next Oncology, San Antonio, TX, USA; ⁵CHA Bundang Medical Center, Seoul, Korea, Republic of; ⁶Severance Hospital, Yonsei University, Seoul, Korea, Republic of; ⁷Samsung Medical Center, Seoul, Korea, Republic of; ⁸City of Hope Comprehensive Cancer Center, Duarte, CA, USA; ⁹Adagene, San Diego, CA, USA

Background The anti-CTLA-4 immuno-oncology therapy (IO) is limited in clinical efficacy due to its on-target toxicities. ADG116 is a fully human IgG1 monoclonal antibody that targets a unique and highly conserved epitope of CTLA-4. ADG116 enables a controlled T cell activation via partial CD80/86 ligand blockade and promotes strong Treg depletion in the tumor microenvironment via enhanced ADCC. In pre-clinical studies, ADG116 has been shown to be more potent and better tolerated than ipilimumab. We believe ADG116 can offer a better therapeutic window for this class of molecules, especially when combined with anti-PD-1 therapies.

Methods ADG116 monotherapy [10 dose levels from 0.003 to 15 mg/kg (mpk)] and ADG116 (3 or 6 mpk) plus Tori (240 mg) combination therapy were administered Q3W intravenously. The primary endpoints are safety and tolerability; the secondary endpoints are PK, ORR per RECIST 1.1, and PFS.

Results As of July 14, 2022, 45 patients (pts) were treated with ADG116 monotherapy, among which 3, 4, 6, 18, and 3 pts received 1, 3, 6, 10, and 15 mpk dose, respectively. The median age was 62; 62% received ≥ 3 prior lines of therapies, and 31% progressed after prior IO therapies. Only 1 DLT [Grade (G) 4 hyperglycemia] was observed (10 mpk), and MTD was not reached. Only 3 pts showed G3 or above treatment-related AEs (TRAEs); common TRAEs (>10%) consisted of diarrhea, pruritis, and fatigue. Disease control rate is 35% across doses of ≥ 1 mg/kg (range 30-80%). An initial partial response was observed from a patient with Kaposi's sarcoma (15 mpk). Dose expansion is ongoing at 10 mpk.

Nine pts received ADG116/Tori combination therapy. The median age was 59; 11% received > 3 prior lines of therapies, and none had prior IO therapies. At 6 mpk ADG116/Tori, two pts developed DLTs (2/3; G3 myocarditis & G3 diarrhea). At 3 mpk ADG116/Tori, 1 DLT (1/6, G3 diarrhea) was observed, and five pts are still on treatment (2-5 cycles). One pt with recurrent platinum-refractory HNSCC has a confirmed complete response (CR) and is still on the study (cycle 5). Detailed safety and efficacy data from this study will be reported.

Conclusions ADG116 monotherapy has cleared multiple dose levels including 15 mpk, a dose higher than any reported anti-CTLA-4 class agents in the repeat dose setting. ADG116 (3 mpk)/Tori (240mg) Q3W continuous dosing showed a manageable safety profile and encouraging efficacy including CR, supporting its further clinical evaluation.

Acknowledgements We would like to acknowledge the editorial support from Ami Celeste Knoefler

Trial Registration Clinical trial identification: NCT04501276

Ethics Approval The study obtained ethics approvals from the following Ethics Committee(s)/Institutional Review Board(s), the number/ID of the approval(s),

1. Macquarie University HREC; ID: 520-2166-4335-513
2. National Health Group Central IRB; ID: 2021/00824
3. Bellberry HREC; ID: 2020-04-397-AA
4. Salus IRB; ID: IORG0005674
5. CHAMG IRB; ID: 2021-10-064-001-HE001
6. Yonsei University Health System IRB; ID: 2021-2495-002/4-2021-1454
7. Samsung Medical Center IRB; ID: 2021-09-053-001
8. WCG IRB; ID: 2021-4916

All participants of this clinical study gave informed consent before taking part.

Consent Written informed consent was obtained from patients for publication of this abstract and any accompanying images. A copy of the written consent is available for review by the Editor of this journal.

<http://dx.doi.org/10.1136/jitc-2022-SITC2022.0753>

754

A PHASE 1/2 STUDY OF ASP1570 IN PARTICIPANTS WITH LOCALLY ADVANCED OR METASTATIC SOLID TUMORS WHO HAVE PROGRESSED ON, OR ARE INELIGIBLE FOR, ALL AVAILABLE STANDARD THERAPIES

¹Manish Patel*, ²David Park, ³Stefano Tarantolo, ⁴Afshin Dowlati, ⁵Daniel Olson, ⁶Yuichiro Kaneko, ⁷Mei Tang, ⁷Serguei Soukharev, ⁶Masaomi Takizawa, ⁶Yohei Okada, ⁷Christine Fredericks, ⁷Derek Smith, ⁷Teresa Flegel, ⁷Tsubasa Watanabe, ⁷Sue Lee, ⁸Jason Luke. ¹Florida Cancer Specialists/Sarah Cannon Research Institute, Sarasota, FL, USA; ²St Jude Crosson Cancer Institute, Fullerton, CA, USA; ³Midwest Cancer Center, Omaha, NE, USA; ⁴University Hospitals Seidman Cancer Center and Case Western Reserve University, Cleveland, OH, USA; ⁵University of Chicago Comprehensive Cancer Center, Chicago, IL, USA; ⁶Astellas Pharma, Inc., Northbrook, IL, USA; ⁷Astellas Pharma Global Development, Inc., Northbrook, IL, USA; ⁸UPMC Hillman Cancer Center, Pittsburgh, PA, USA

Background Cancer immunotherapies target immune checkpoints and have been transformative in the treatment practices of oncology. However, only a subset of all patients in most cancer types effectively respond to these therapies. It has been established that approximately 60% to 70% of patients who receive anti-programmed cell death protein-1 (anti-PD-1) or anti-cytotoxic T-lymphocyte-associated antigen 4 (CTLA4) do not respond to treatment.¹ Furthermore, acquired resistance is common, causing some patients who initially responded to the therapy to later experience disease progression. Therefore, there is a significant opportunity for immunotherapy expansion in cancer treatment.

Diacylglycerol kinase (DGK) is a large enzyme family of 10 mammalian isoenzymes that catalyzes the conversion of diacylglycerol (DAG) to phosphatidic acid (PA). In T cells, DGK (such as DGK ζ) inhibits DAG-mediated signals following T-cell receptor engagement by catalyzing the conversion of DAG to PA.² Even when PD-1 is blocked by anti-PD-1 antibodies, there may be partial inactivation by DGK. Therefore, DGK inhibitors have the potential to enhance DAG downstream signaling, leading to T-cell activation regardless of the PD-1 signal. ASP1570 is a novel inhibitor against DGK ζ and has the potential to enhance DAG downstream signaling which can activate T cells regardless of PD-1 signaling and lead to tumor killing. ASP1570 restored T-cell functions suppressed by multiple immunosuppressive signals (PD-1, transforming growth factor beta, prostaglandin E2, and adenosine) and induced tumor growth inhibition in mice models of MC38 (anti-PD1 sensitive) and B16-F1 (tumor-infiltrating lymphocyte poor, anti-PD-1 insensitive). Taken together, ASP1570 treatment as a single agent and/or in combination with anti-PD-1 therapy for locally advanced or metastatic solid tumors may result in clinical benefit.

Methods This is a phase 1/2, open-label, multicenter, multiple-dose, dose-escalation/expansion study of ASP1570 in participants with locally advanced or metastatic solid tumors. The study will enroll approximately 168 participants into 2 phases, dose escalation and dose expansion, to assess safety, tolerability, efficacy, pharmacokinetics, and pharmacodynamics (figure 1). The study will consist of the following periods: screening, treatment with ASP1570 daily oral dosing in 21-day cycles, end of treatment, follow-up (safety and survival follow-up), and end of study (figure 2). The study is open for enrollment.

Acknowledgements We thank the patients, investigators, and study teams for being involved in this study. Editorial support was provided by OPEN Health and funded by Astellas Pharma, Inc. This study is funded by Astellas Pharma, Inc.

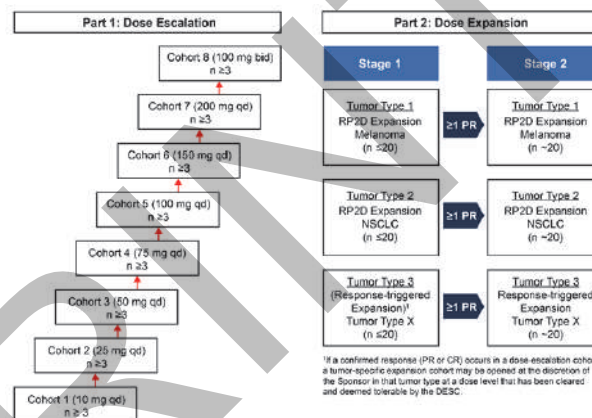
Trial Registration NCT05083481

REFERENCES

1. Simeone E, Ascierto PA. Anti-PD-1 and PD-L1 antibodies in metastatic melanoma. *Melanoma Manag.* 2017;**4**:175–178.
2. Zhong XP, Guo R, Zhou H, Liu C, Wan CK. Diacylglycerol kinases in immune cell function and self-tolerance. *Immunol Rev.* 2008;**224**:249–264.

Ethics Approval This study received IRB approval from Advarra (Pro00055357), and all participants must provide informed consent before taking part.

Consent Written informed consent was obtained from the patient for publication of this abstract and any accompanying images. A copy of the written consent is available for review by the Editor of this journal.



Abstract 754 Figure 1 Study Design Schema



Abstract 754 Figure 2 Study Visit Schema

<http://dx.doi.org/10.1136/jitc-2022-SITC2022.0754>

755

RESULTS OF A PHASE I TRIAL OF FT500, A FIRST-IN-CLASS, OFF-THE-SHELF, iPSC-DERIVED NK CELL THERAPY COMBINED WITH PD-1/PD-L1 CHECKPOINT BLOCKADE THERAPY AND IL-2 IN PATIENTS WITH ADVANCED SOLID TUMORS

<http://dx.doi.org/10.1136/jitc-2022-SITC2022.0755>

¹Sandip Patel, ²Manish Patel, ³Martin Gutierrez, ⁴Marlisa Anderson, ⁴Peter Szabo, ⁴Bob Valamehr, ⁴Yu-Way Chu, ⁴Brandon Beagle, ⁴Jeffrey Chou, ⁵David Hong*. ¹University of California, San Diego, La Jolla, CA, USA; ²University of Minnesota, Rochester, MN, USA; ³Hackensack University Medical Center, Hackensack, NJ, USA; ⁴Fate Therapeutics, Inc., San Diego, CA, USA; ⁵The University of Texas MD Anderson Cancer Center, Houston, TX, USA

Background FT500, an allogeneic natural killer (NK) cell cancer immunotherapy derived from a clonal induced pluripotent stem cell (iPSC) line, is available off-the-shelf for on-demand administration to patients in multi-dose regimens. In preclinical studies, FT500 has been shown to recruit and activate T cells, increasing response to checkpoint inhibition for enhanced inflammatory cytokine production and tumor elimination. We report results from a Phase I clinical trial of patients with classical Hodgkin lymphoma (cHL) or non-small cell lung cancer (NSCLC) who were relapsed/refractory to prior anti-PD-1/L1 immune-checkpoint inhibitor (ICI) therapy and received FT500 combined with ICI therapy and IL-2.

Methods Treatment consisted of 2 days of outpatient conditioning chemotherapy (cyclophosphamide 300 mg/m² and fludarabine 25 mg/m²), followed by two 29-day cycles of 3 once-weekly doses of 300 million FT500 cells/dose with subcutaneous IL-2 (6 MIU), and nivolumab, pembrolizumab, or atezolizumab administered at standard dose and schedule. Key endpoints included safety, tolerability, and anti-tumor activity.

Results As of 09 May 2022 data cutoff, 5 patients with cHL and 7 patients with NSCLC, with a median of 10 and 3 prior therapies, respectively, were treated. No events of cytokine release syndrome, neurotoxicity, or graft-versus-host disease were observed. Most common treatment-emergent adverse events (AEs) included lymphopenia and anemia. No FT500-related serious AEs were reported; only 1 Grade \geq 3 FT500-related AE of lymphopenia was reported. For cHL, objective response by RECIL was reported in 4 patients (1 complete, 1 partial, 2 minor), with median peak tumor burden reduction of 24.9% (range 10.2, 72.4) and median response through 7.9 months (range 4.1, 12.0) from initiation of treatment, including an ongoing complete response subsequently lost to follow-up at 8.7 months. For NSCLC, tumor burden reduction was observed in 3 patients, with median peak reduction of 9.8% (range 6.3, 40); 1 patient refractory to 2 prior ICI-containing regimens had an ongoing partial response by iRECIST through 12.6 months from initiation of treatment, and 3 had stable disease with median duration of disease control of 7.7 months (range 3.4, 8.6).

Conclusions Six doses of 300 million FT500 cells with IL-2 and concurrent ICI therapy is safe and tolerable, with evidence of durable anti-tumor activity observed in heavily pretreated patients resistant to anti-PD1/L1 therapy. These results support the development of next-generation iPSC-derived NK cells engineered with synthetic functional elements designed to synergize with ICI therapy and enhance anti-tumor activity in solid tumors.

Ethics Approval This study is being conducted in accordance with the Declaration of Helsinki and was approved by all Institutional Review Boards from each clinical site participating in the study. Specific approval numbers can be provided upon request.

756

INCLINE-101, A PHASE 1/2, OPEN LABEL, DOSE ESCALATION AND EXPANSION STUDY OF TAC-001 (A TLR9 AGONIST CONJUGATED TO A CD22 ANTIBODY) IN PATIENTS WITH SELECT ADVANCED OR METASTATIC SOLID TUMORS

¹Cesar Perez*, ²Jason Henry, ³Timothy Humphries, ⁴Sunnie Kim, ⁵Adi Diab, ⁶Ons Harrabi, ⁶Feng Jin, ⁶Hong Wan, ⁶Candy Bermingham, ⁷Anthony El-Khoueiry. ¹SCR1 at Florida Cancer Specialists, Lake Nona, FL, USA; ²SCR1 at HealthONE, Denver, CO, USA; ³Linear Clinical Research Ltd, Nedlands, WA, 6009, Australia; ⁴University of Colorado Cancer Center, Aurora, CO, USA; ⁵MD Anderson Cancer Center, Houston, TX, USA; ⁶Tallac Therapeutics, Burlingame, CA, USA; ⁷Norris Comprehensive Cancer Center, USC, Los Angeles, CA, USA

Background Enrichment of memory B cells, plasma cells and tertiary lymphoid structure is a positive prognostic factor in patients with a variety of solid tumors.¹⁻³ Toll-like receptor 9 (TLR9) agonists generate both innate and adaptive immune responses. TLR9 activation in B cells has been shown to induce expression of co-stimulatory molecules, enhanced cross-presentation leading to T cell activation and proliferation, cytokine, chemokine and immunoglobulin secretion. Designed for systemic administration, TAC-001 is a Toll-like Receptor Agonist Antibody Conjugate (TRAAC) comprised of a potent and differentiated TLR9 agonist (T-CpG) conjugated to an antibody against CD22, a receptor restricted to B cells, including tumor-infiltrating B cells. In preclinical models, TAC-001 has demonstrated single agent anti-tumor activity in checkpoint inhibitor resistant and refractory tumor models, accompanied by increased B cell infiltration, T cell effector functions and modulation of suppressive myeloid cells within the tumor microenvironment.⁴ INCLINE-101 is a Phase 1/2 study designed to evaluate the safety, efficacy, pharmacokinetics (PK) and biomarkers of TAC-001 in patients with select advanced or metastatic solid tumors.

Methods TAC-001 is being evaluated in an open-label, non-randomized, dose-escalation (Phase 1) study in patients with select advanced or metastatic solid tumors, and dose-expansion (Phase 2) in patients with select tumor types (NCT05399654). Eligible patients in Phase 1 must have histologically or cytologically-documented advanced, metastatic, unresectable or recurrent breast cancer, cervical squamous cell carcinoma, cholangiocarcinoma, colorectal carcinoma, cutaneous melanoma, endometrial carcinoma, gastro-esophageal adenocarcinoma, head and neck squamous cell carcinoma, hepatocellular carcinoma, Merkel cell carcinoma, non-small cell lung cancer, ovarian cancer, renal cell carcinoma, or urothelial carcinoma that have progressed on or are intolerant to standard therapy, including checkpoint inhibitor therapy if appropriate. Phase 1 study will explore ascending dose levels of TAC-001 monotherapy administered intravenously every 2 weeks and utilize the Bayesian Optimal Interval (BOIN) design in order to identify the maximum tolerated dose (MTD) or maximum administered dose (MAD), and recommended Phase 2 dose (RP2D). Once RP2D is determined, the Phase 2 expansion in four specific tumor-type cohorts is planned. A 2-stage design will be utilized for Phase 2, and the Clopper-Pearson method to compute exact confidence limits for the response rates will be employed. The primary endpoints are safety and preliminary efficacy (overall response rate, duration of response, clinical benefit rate) per RECIST v1.1 and iRECIST. Additional endpoints include PK, immunogenicity, progression free survival, overall survival, and changes in relevant biomarkers. INCLINE-101 is enrolling in the USA and Australia.

Trial Registration NCT05399654

REFERENCES

1. Griss J, Bauer W, Wagner C, *et al.* B cells sustain inflammation and predict response to immune checkpoint blockade in human melanoma. *Nat Commun.* 2019;**10**(1):4186.
2. Helmink, B.A., Reddy, S.M., Gao, J. *et al.* B cells and tertiary lymphoid structures promote immunotherapy response. *Nature* 2020;**577**:549–555.
3. Kroeger DR, Milne K, Nelson BH. Tumor-Infiltrating Plasma Cells Are Associated with Tertiary Lymphoid Structures, Cytolytic T-Cell Responses, and Superior Prognosis in Ovarian Cancer. *Clin Cancer Res.* 2016;**22**(12):3005–3015.
4. Kuo TC, Harrabi O, Chen A, Sangalang ER, Doyle L, Fontaine D, Li M, Han B, Pons J, Sim J, Wan H. TAC-001, a toll-like receptor 9 (TLR9) agonist antibody conjugate targeting B cells, promotes anti-tumor immunity and favorable safety profile following systemic administration in preclinical models. *Cancer Res* 2021;**81**(13_Supplement):1721.

Ethics Approval The study has received ethics approval from the WCG IRB (tracking number 20222058, study numbers 1334808 and 1334807) and Bellberry Human Research Ethics Committee (application number 2022-04-408).

<http://dx.doi.org/10.1136/jitc-2022-SITC2022.0756>

757

A PHASE 1/1B DOSE ESCALATION AND COHORT EXPANSION STUDY OF MGC018 IN COMBINATION WITH LORIGERLIMAB IN PATIENTS WITH ADVANCED SOLID TUMORS (AST)

¹John Powderly*, ²Patrick Kaminker, ²Enxu Zhao, ²Denise Casey, ³Eugene Shenderov. ¹Carolina BioOncology Institute, Huntersville, NC, USA; ²MacroGenics, Inc., Rockville, MD, USA; ³Johns Hopkins Medicine, Baltimore, MD, USA

Background The immune checkpoint molecule B7-homolog 3 (B7-H3) is highly expressed in multiple solid tumors with limited expression in normal tissue, may play an immune suppressive role, and favors cancer growth. MGC018 is an investigational anti-B7-H3 IgG1 antibody-drug conjugate with a duocarmycin-based DNA-alkylating payload that can damage DNA in both dividing and nondividing cells, causing cell death.¹ As previously presented, Phase 1 testing of single-agent MGC018 (NCT03729596) demonstrated an acceptable safety profile with manageable toxicity in 115 patients and 25% objective response rate (ORR) among 32 evaluable patients in the NSCLC and mCRPC cohorts.^{2,3} Lorigerlimab is an investigational bispecific, Fc-bearing (IgG4) DART[®] molecule that blocks PD-1 with enhanced CTLA-4 blockade on dual PD-1/CTLA-4-expressing tumor-infiltrating lymphocytes within the tumor microenvironment, and reduced CTLA-4 blockade in normal tissues.⁴ Phase 1 testing of single-agent lorigerlimab (NCT03761017) demonstrated acceptable safety in 43 patients with advanced solid tumors and encouraging antitumor activity.⁵ Coblockade of PD-1 and CTLA-4 with lorigerlimab combined with targeted delivery of a cytotoxic payload via MGC018 may improve antitumor activity in B7-H3+ cancers.

Methods This is a Phase 1/1b, open-label, multicenter, dose-escalation, and cohort-expansion study of MGC018+lorigerlimab in patients with relapsed/refractory, unresectable, locally advanced/metastatic solid tumors, including mCRPC, melanoma, pancreatic cancer, HCC, ovarian cancer, and RCC for whom there is no available therapy. Eligibility criteria include ECOG performance status ≤ 2 and having archival tumor or fresh biopsy specimens for B7-H3 and PD-L1 immunohistochemistry (IHC) analysis, although IHC results will not be used for patient selection. The primary objective is evaluation of safety/tolerability, dose-limiting toxicities, and the maximum-tolerated dose or maximum-administered dose for MGC018+lorigerlimab. Secondary objectives include assessment of pharmacokinetics, immunogenicity, and antitumor activity (ORR, DoR, progression-free survival, overall survival) of MGC018+lorigerlimab. MGC018 and lorigerlimab are administered as sequential infusions on Day 1 of each 28-day cycle, for up to 26 cycles. Dose escalation follows a 3+3 design with MGC018 escalating from 1.0-3.0 mg/kg and lorigerlimab fixed at 6 mg/kg. Cohort expansion of MGC018+lorigerlimab follows a Simon's 2-stage design for each tumor-specific cohort. Safety assessments are based on AEs, graded by NCI CTCAE v5.0, occurring from the first dose until 30 days after the last dose or until starting another anti-cancer therapy. Tumor assessments are performed every 8 weeks for the first 6 months, then every 12 weeks until progressive disease. Response evaluation is determined using RECIST v1.1 or PCWG3 (for mCRPC). Enrollment ongoing.

Trial Registration Clinicaltrials.gov NCT05293496

REFERENCES

1. Scribner JA, Brown JG, Son T, *et al.* Preclinical development of MGC018, a duocarmycin-based antibody-drug conjugate targeting B7-H3 for solid cancer. *Mol Cancer Ther.* 2020;**19**(11):2235–2244.

2. Jang S, Powderly JD, Spira AI, *et al.* Phase 1 dose escalation study of MGC018, an anti-B7-H3 antibody-drug conjugate (ADC), in patients with advanced solid tumors. *J Clin Oncol.* 2021;**39**(suppl 15):Abstract #2631.
3. Shenderov E, Mallesara GHG, Wysocki PJ, *et al.* MGC018, an anti-B7-H3 antibody-drug conjugate (ADC), in patients with advanced solid tumors: preliminary results of phase I cohort expansion. *Ann Oncol.* 2021;**32**(suppl 5):S657–S658, Abstract #620P.
4. Bereznoy A, Sumrow BJ, Stahl K, *et al.* Development and preliminary clinical activity of PD-1-guided CTLA-4 blocking bispecific DART[®] molecule. *Cell Rep Med.* 2020;**1**(9):100163.
5. Sharma M, Sanborn RE, Cote GM, *et al.* A phase 1, first-in-human, open-label, dose escalation study of MGD019, an investigational bispecific PD-1 x CTLA-4 DART[®] molecule in patients with advanced solid tumors. *Ann Oncol.* 2020;**31**(suppl 4):S704–S705, Abstract #10200.

Ethics Approval Trial conduct was in accordance with Good Clinical Practice and Principles in the Declaration of Helsinki. An independent ethics committee approved the protocol at each participating site. All patients provided written informed consent.

<http://dx.doi.org/10.1136/jitc-2022-SITC2022.0757>

758

A PHASE 1 DOSE ESCALATION AND EXPANSION STUDY OF THE ANTI-CD200R1 ANTIBODY 23ME-00610 IN PATIENTS WITH ADVANCED SOLID MALIGNANCIES

¹Drew Rasco*, ²Albiruni Razak, ³Maïke Schmidt, ³Sariah Kell, ³Dylan Glatt, ³Erin Belshaw, ³Sophia Majeed, ⁴Shivaani Kummar. ¹START San Antonio, San Antonio, TX, USA; ²Princess Margaret Cancer Centre, Toronto, Canada; ³23andMe, South San Francisco, CA, USA; ⁴Oregon Health and Sciences University, Portland, OR, USA

Background 23ME-00610 is a first-in-class, fully humanized monoclonal antibody that inhibits the CD200R1 immune checkpoint, a promising immuno-oncology target identified by the 23andMe genetic database.¹ 23ME-00610 binds with high affinity ($K_D < 0.1$ nM) to CD200R1 on immune cells and has been shown to block immunosuppressive signaling and enhance T cell-mediated killing of tumor cells that express its only known ligand in humans, CD200, in preclinical studies.² We hypothesize that blocking CD200R1 with 23ME-00610 will reverse immune cell tolerance in the microenvironment of tumors that are reliant on the CD200R1 pathway, leading to immune-mediated disease control.

Methods The safety and preliminary antitumor activity of 23ME-00610 is being evaluated in a Phase 1 dose escalation and expansion study in adults with locally advanced unresectable, or metastatic solid malignancies who have progressed on standard therapies with an ECOG score of 0 or 1; adolescents at least 12 years, weighing at least 40 kg with a Lansky play scale score of at least 50 will be included in the expansion phase. The primary objectives in the dose escalation phase are determination of the maximum tolerated dose (MTD)/recommended phase 2 dose (RP2D), and safety and tolerability, measured by the incidence and severity of dose-limiting toxicities, treatment-emergent adverse events (AEs) and withdrawals due to AEs. Secondary objectives include pharmacokinetics, immunogenicity, and preliminary antitumor activity of 23ME-00610. The monotherapy activity of 23ME-00610 will be evaluated in indication-specific expansion cohorts (N~15/cohort), which include clear cell renal cell carcinoma; epithelial ovarian, fallopian tube or primary peritoneal carcinoma; neuroendocrine cancer; and microsatellite instability-high (MSI-H) or tumor mutational burden-high (TMB-H) cancers that have progressed on standard therapies. A cohort of adolescents with locally advanced unresectable, or metastatic solid malignancies will also be enrolled. These indications were selected based on the expression of CD200R1 and its ligand, CD200, T cell markers, and immune characteristics that may increase likelihood of response to CD200R1 inhibition. The primary objective of the expansion phase is objective response rate (ORR) based on RECIST 1.1. The pharmacodynamic profile of 23ME-00610, including markers of CD200R1 engagement, will be evaluated. Germline genotypic information collected from participants will be used to correlate genetic variants and polygenic risk scores with safety and efficacy outcomes. The statistical analyses will primarily be descriptive. Participants reflecting the characteristics for the indication-specific cohorts with regards to age, sex, race, and ethnicity, including those from the Black, Latinx/Hispanic and Indigenous communities, will be prioritized for enrollment.

Acknowledgements Dr. Jennifer Low and Dr. Adrian Jubb for providing guidance and review of the study design. Dr. Robin Bliss for providing statistics support.

Trial Registration www.clinicaltrials.gov; NCT05199272

REFERENCES

1. Fang X, Chung W, Fenaux J, Chen A, Batada N, Schmidt M, Majeed SR, Kumar S, and Pitts S. Discovery of CD200R1 as a Novel Immuno-oncology Target Using Pleiotropic Signals From 23andMe's Genetic and Health Survey Database. AACR Annual Meeting 2022.
2. Fenaux J, Huang Y, Melero C, Chung W, Lee S, Ayupova D, Poggio M, Glatt D, Yi Z, Lay C, Schmidt M, Majeed SR, Fuh G, Chen A, and Kumar S. 23ME-00610 is a first-in-class monoclonal antibody that targets the CD200R1 immune checkpoint to enhance T cell-mediated antitumor activity. AACR Annual Meeting 2022.

Ethics Approval The study obtained approval from the following ethics committees/institutional review boards (approval IDs are in parentheses): Advarra IRB (Pro00062976), Salus IRB (START2021.35), MD Anderson OHRP IRB (2021-0888), Oregon Health & Science University IRB (STUDY00023966) and Ontario Cancer Research Ethics Board (3953). All study participants must provide informed consent prior to taking part in the study.

<http://dx.doi.org/10.1136/jitc-2022-SITC2022.0758>

PHASE 1B STUDY OF LNS8801 IN COMBINATION WITH PEMBROLIZUMAB IN PATIENTS WITH SECONDARY RESISTANCE TO IMMUNE CHECKPOINT INHIBITORS

¹Jordi Rodon*, ²Marya Chaney, ³Justine Cohen, ⁴Tina Garyantes, ⁵Jessica Lin, ⁶Patricia Lorusso, ⁷Alain Mita, ⁸Monica Mita, ⁹Carolyn Muller, ¹⁰Christopher Natale, ¹¹Marlana Orloff, ¹²Kyriakos Papadopoulos, ¹³Sapna Patel. ¹MD Anderson Cancer Center, Houston, TX, USA; ²Merck and Co., Inc., Kenilworth, NJ, USA; ³University of Pennsylvania, Philadelphia, PA, USA; ⁴Linnaeus Therapeutics, Haddonfield, NJ, USA; ⁵Mass General Hospital Cancer Center, Boston, MA, USA; ⁶Yale Cancer Center, New Haven, CT, USA; ⁷Cedars Sinai Medical Center, Los Angeles, CA, USA; ⁸University of New Mexico Cancer Center, Albuquerque, NM, USA; ⁹Sidney Kimmel Cancer Center, Philadelphia, PA, USA; ¹⁰START San Antonio, San Antonio, TX, USA

Background LNS8801 is an oral, selective, small molecule agonist of the G-protein coupled estrogen receptor (GPER). LNS8801 treatment results in reduced c-Myc protein levels in cancer cells, inhibition of proliferation, suppression of invasion, and enhancement of immune recognition. In preclinical models, LNS8801 has demonstrated increased activity in combination with immune checkpoint inhibitors (ICIs). In the first-in-human dose escalation study, LNS8801 was safe and tolerable alone and in combination with pembrolizumab in patients with advanced solid tumors (NCT04130516).

Methods Patients who have secondary resistance to ICIs (CR/PR/>16w of SD followed by progression) and have measurable disease are enrolling in a Phase 1b cohort and receive LNS8801 (125 mg, QD, PO) and pembrolizumab (200 mg, Q3W, IV) (NCT04130516). The primary objective is safety and tolerability assessed according to NCI CTCAE v5.0. Secondary endpoints include pharmacokinetic, pharmacodynamics, objective response rate (ORR) and disease control rate (DCR, CR+PR+SD) per RECIST v1.1, and assessment of biomarkers including germline GPER genotype at the single nucleotide polymorphism (SNP) rs11544331.

Results As of 7/15/22, patients with secondary resistance to ICIs (n=18) were treated with LNS8801 and pembrolizumab, including those who entered the study directly after confirmed progression on ICIs (n=16). Cancer types include lung (n=5), cutaneous melanoma (n=2), mesothelioma (n=2), neuroendocrine, colorectal, vaginal, nasopharyngeal, uterine, pancreatic cancer, uveal melanoma, small-cell cervical, and sarcoma. 7 of 18 patients had AEs possibly related to study drugs (n=6 with grades 1-2 and n=4 with grade 3), with colitis, dyspnea, and fatigue appearing in more than 1 patient. Of the 15 patients evaluable for efficacy, 3 had partial responses and 6 had stable disease, resulting in an ORR of 20% and DCR of 60%. All patients with partial responses had confirmed progression on ICIs immediately prior to entering the study. 4 patients continued on treatment for >6 months. Germline GPER genotype of C/C at SNP rs11544331 was associated with improved outcomes in patients treated with LNS8801.

Conclusions The combination of LNS8801 and pembrolizumab demonstrates encouraging anti-tumor activity in patients with secondary resistance to ICIs, including patients who enrolled immediately after confirmed progression on ICIs. The combination is tolerable without unanticipated toxicities. Germline GPER genotype is a promising predictive biomarker that could be used to select patients in future studies. These data support further development of LNS8801 in combination with pembrolizumab as a therapeutic approach to treat patients with secondary resistance to ICIs.

Trial Registration NCT04130516

Ethics Approval LNS-101 uses Western Institutional Review Board (WIRB) as a central IRB for this study. WIRB serves as

the IRB for Cedars-Sinai Medical Center, the University of New Mexico, University of Pennsylvania, and Thomas Jefferson University. WIRB also serves as the IRB for the Yale University School of Medicine–Yale Cancer Center, but this site must be responsible for submissions due to institutional policies. Three sites do not use WIRB as the central IRB. South Texas Accelerated Research Therapeutics (START) is required to use Advarra IRB due to institutional policies, Massachusetts General Hospital is required to use their local IRB due to institutional policies, and MD Anderson Cancer Center is required to use their local IRB due to institutional policies.

Participants gave informed consent before taking part.

<http://dx.doi.org/10.1136/jitc-2022-SITC2022.0759>

760

A PHASE I/II TRIAL INVESTIGATING SAFETY AND EFFICACY OF AUTOLOGOUS TAC T CELLS TARGETING HER2 IN RELAPSED OR REFRACTORY SOLID TUMORS

¹Benjamin Schlechter*, ²Daniel Olson, ³Samuel Saibil, ⁴Mridula George, ¹Riemke Bouvier, ⁵Jessica McKinley, ²Brooke Pieke, ⁶Jill Geisburger, ⁷Nathan Ternus, ⁷Kara Moss, ⁷Deyaa Adib, ⁵Ecatarina Dumbrava. ¹Dana Farber Cancer Institute, Boston, MA, USA; ²University of Chicago, Chicago, IL, USA; ³Princess Margaret Cancer Center, Toronto, Canada; ⁴Rutgers University, New Brunswick, NJ, USA; ⁵MD Anderson Cancer Center, Houston, TX, USA; ⁶Princess Margaret Cancer Center – UHN, Toronto, Canada; ⁷Triumvira Immunologics, Austin, TX, USA

Background Despite recent therapeutic developments for patients with advanced, metastatic, unresectable HER2 positive (HER2+) solid tumors, significant unmet medical needs still exist, especially in tumors other than breast and gastric cancers and in patients with HER2-low expression. The T cell antigen coupler (TAC) technology is a novel approach to modifying T cells, allowing them to recognize and treat HER2 + solid tumors. Mechanistically, the TAC receptor redirects T cells to tumor cells, and upon recognition, co-opts the natural T cell receptor (TCR) signaling action to yield safe anti-tumor responses. In preclinical studies, TAC T cells led to complete tumor clearance in various human HER2+ mouse models, without any TAC-related toxicities, and results superior to a similar 2nd generation chimeric antigen receptor (CAR) T cell.

In this ongoing clinical trial (NCT04727151), subjects undergo leukapheresis, bridging therapy while their TAC T cells are engineered (if needed), lymphodepletion chemotherapy (LDC), and finally TAC01-HER2 infusion.

Methods Dose escalation in Phase 1 is investigating the safety and tolerability of TAC01-HER2 single doses of 0.08, 0.3 (starting dose), 0.8, 3, 8 x 10⁶ cells/kg in adult subjects with HER2+ solid tumors (1+, 2+ or 3+ by immunohistochemistry) who have progressed after ≥2 lines of systemic therapy. Dose limiting toxicities (DLTs) are being assessed up to 28 days after TAC01-HER2 infusion.

In Phase 2, dose expansion groups will further evaluate the safety, efficacy, and pharmacokinetics of the optimal TAC01-HER2 dose in HER2+ breast and other HER2+ tumor types, including: lung, pancreatic, colorectal, gastric, endometrial, and ovarian.

As of 20 July 22, eight subjects have been treated in Cohorts 1 and 2, with no DLTs or events of special interest, such as cytokine release syndrome or immune effector cell-associated neurotoxicity syndrome, being observed. Four subjects had 8 serious adverse events; all unrelated to TAC01-HER2 infusion and attributed to LDC or underlying malignancies. Preliminary safety results indicate single TAC01-HER2 treatments in a heavily pre-treated population have been well-tolerated, with the most frequent adverse events (AEs) being cytopenias related to LDC. Continued dose escalation of TAC01-HER2 is ongoing.

Following completion of each dose level, a Data Safety Monitoring Committee has met to review all AEs to approve or deny escalation to the next highest dose level

<http://dx.doi.org/10.1136/jitc-2022-SITC2022.0760>

761

PHARMACOKINETIC AND PHARMACODYNAMIC DATA FROM A PHASE 1 STUDY OF CI-8993 ANTI-VISTA ANTIBODY IN PATIENTS WITH ADVANCED SOLID TUMORS

¹Randolph Noelle*, ²Melissa Johnson, ³Jordi Rodon, ⁴Marjorie Zauderer, ¹Lionel Lewis, ⁵Mariano Severgnini, ⁵Jefferson Parker, ⁵Maureen Lane, ⁵Reinhard von Roemeling, ⁶Alex Martin, ⁷Michael Molloy, ⁵Robert Martell, ⁸Tong Dai. ¹*Geisel School of Medicine at Dartmouth, Hanover, NH, USA;* ²*Tennessee Oncology, Nashville, TN, USA;* ³*MD Anderson Cancer Center, Houston, TX, USA;* ⁴*Memorial Sloan Kettering Cancer Center, New York, NY, USA;* ⁵*Curis Inc, Lexington, MA, USA;* ⁶*Curis Inc/Tufts Medical Center, Lexington, MA, USA;* ⁷*ImmuNext Inc, Lebanon, NH, USA;* ⁸*Roswell Park Comprehensive Cancer Center, Buffalo, NY, USA*

Background V-domain Ig suppressor of T-cell activation (VISTA) is a novel negative checkpoint ligand that suppresses T cell activation forcing cells into a quiescent state. In pre-clinical studies anti-VISTA monotherapy has been shown to promote anti-tumor immunity. The impact of anti-VISTA therapy within the tumor microenvironment (TME) resulted in upregulated antigen-presentation pathways, reduced myeloid mediated immune suppression, enhanced lymphocyte infiltration and, with the promotion of co-stimulatory genes, reduced regulators of T cell quiescence and reduced tumor growth. In this work, we present pharmacokinetic (PK) data, and describe pharmacodynamic (PD) changes in the immune system in patient samples from the Phase 1 CI-8993-101 study, open label, dose escalation study (NCT04475523) administering an IgG1 anti-VISTA antibody (CI-8993) to patients with solid tumors.

Methods Patients were enrolled into cohorts that are structured to receive step-dosing regimens before administering a single ‘full dose’ of CI-8993. Cytokine release related toxicities were successfully managed with initial step-dosing and corticosteroids. The CI-8993 full doses ranged from 0.15 mg/kg to 0.6mg/kg in three separate cohorts. Immune-related PD, and PK analyses were performed on blood/serum from 17 patients at time points following step-dose, and full dose administration of CI-8993.

Results Data indicates a rapid, but transient, increase in cytokines and chemokines (e.g., IL6, IL18, IP10, MCP1) ($P \leq 0.05$). Soluble markers (TNF α and MIP1 β) present differences between cohorts 4 hours after treatment ($P \leq 0.05$) without a clear dose-response relationship. We observed changes in neutrophils and activated monocytes populations after 24 hours of initial treatment ($P \leq 0.05$). Activated T cells (CD8+CD69+), decreased CD16 on NK cells, and increased HLDR expression on monocytes were observed between cohorts ($P \leq 0.05$). A greater than dose-proportional exposure increased with higher doses of CI-8993.

Conclusions CI-8993 was well tolerated and no DLTs were observed in the cohorts studied. An increase in pro-inflammatory cytokines, and anti-cancer immune cell phenotypes was observed. The lack of a dose-response effect in cytokine concentrations between cohorts is likely related to the higher step-dose regimen in cohort 3 (0.6mg/kg) that is dampening the cytokine release following the first full dose. The increase in pro-inflammatory phenotypes and soluble mediators post-treatment suggests an early immune response with different anti-tumoral mechanisms. Saturation PK indicates a favorable drug bioavailability at higher doses with an increased half-life. This suggests the ability to saturate the VISTA sink consistent with pre-clinical studies.¹ Further evaluation of the immune system and PK properties of CI-8993 will be performed as we continue enrollment to determine the RP2D.

Trial Registration NCT04475523

REFERENCE

1. Wichmann CW, Burvenich IJG, McDonald AF, Scott FE, Guo N, Rigopoulos A, Soikes R, Angelides S, von Roemeling R, Scott AM. Preclinical evaluation of anti-VISTA antibody CI-8993 in a syngeneic huVISTA-KI model. SITC Abstract 2021: #324

Ethics Approval Yes, this study has obtained ethical approval and participants have given full consent

<http://dx.doi.org/10.1136/jitc-2022-SITC2022.0761>

762

FIRST-IN-HUMAN PHASE 1A STUDY OF NG-641, A TUMOUR-SELECTIVE VECTOR EXPRESSING A FAP-TAC BISPECIFIC ANTIBODY AND IMMUNE ENHANCER MODULE, IN PATIENTS WITH METASTATIC/ADVANCED EPITHELIAL TUMOURS (STAR)

¹George Simon*, ²Vivek Subbiah, ³Lee Rosen, ⁴Heinz-Josef Lenz, ⁵Haeseong Park, ⁶Minesh Patel, ⁶David Miles, ⁶Stephanie Wallis, ⁶Vladimir Evilevitch, ⁶David Krige, ⁶Mark Powell, ⁶Tom Lillie. ¹H Lee Moffitt Cancer Center, Tampa FL and Advent Health Research Institute, Celebration, Tampa, FL, USA; ²MD Anderson Cancer Center, Houston, TX, USA; ³UCLA Medical Center, Los Angeles, CA, USA; ⁴USC Norris Comprehensive Cancer Center, Los Angeles, CA, USA; ⁵Washington University, St. Louis, MO, USA; ⁶PsiOxus Therapeutics Ltd, Abingdon, Oxford, UK

Background NG-641 is a tumour-selective adenoviral vector that expresses a fibroblast activation protein-directed bi-specific T-cell activator antibody (FAP-Tac) and potent immune cell enhancers (CXCL9/CXCL10/IFN α). FAP-Tac targets killing of immunosuppressive cancer-associated fibroblasts, while immune enhancers recruit and activate immune cells (e.g. CD8+ T cells and dendritic cells). NG-641 is stable in the bloodstream and has low immunogenicity, allowing for IV delivery. We report first-in-human dose-escalation results for this novel immunotherapy.

Methods STAR (NCT04053283) is a Phase 1 study of NG-641 in patients with metastatic/advanced epithelial tumours and no standard treatments. The primary objective was safety and tolerability of IV NG-641 monotherapy (one cycle with single doses on Days 1, 3 and 5; five increasing dose levels). Preliminary anti-tumour activity was a secondary objective.

Results As of June 2022, 20 heavily pre-treated patients (median 60 years; 55% male) with metastatic/advanced epithelial tumours (35% colorectal; 15% pancreatic; 10% liver) received NG-641. DLTs of hypertension and dyspnoea occurred in one patient at Dose Level [DL] 2. The first patient at DL5 (1×10^{12} vp on Day 1 and 1×10^{13} vp on Days 3 and 5) experienced a DLT of Grade 3 CRS following an innate response to viral particles. The NG-641 MTD was thus determined to be 6×10^{12} vp as part of a “low-high-high” dosing regimen. Overall, the NG-641 safety profile was consistent with acute reactions to viral particles, with no evidence of transgene-related toxicity (table 1). Dose-dependent, specific and sustained increases in serum IL-12, IFN γ and IL-17a were detected from ~Wk2-12 (last measurement). Similar elevations did not occur with the unarmed parent vector, suggesting a transgene driven effect. No systemic FAP-Tac transgene protein was detected at any dose level indicating a lack of spill over from tumour into systemic circulation. Among evaluable patients, increases in tumour CD8+ T-cell infiltration were seen in 3/7 patients, including one patient with pancreatic cancer and one with colorectal cancer. No objective responses occurred but 2/3 patients at DL3 had stable disease (DL4 under assessment).

Conclusions NG-641 demonstrated manageable tolerability, with no evidence of systemic transgene-related toxicity. The MTD of NG-641 was 6×10^{12} vp when given in a “low-high-high” dosing regimen. Consistent with the encoded immunostimulatory transgenes, NG-641 led to specific and sustained cytokine responses, without systemic spill over of transgene products from the tumour microenvironment. These results suggest that NG-641 drives local immunological tumour changes without systemic toxicity. A further trial (NEBULA, NCT05043714) examining NG-641 with nivolumab is ongoing.

Acknowledgements This study was funded by PsiOxus Therapeutics Limited. Medical writing support: Sandra Borkowska-Heurtaux, PhD, of PsiOxus Therapeutics Limited.

Trial Registration NCT number: NCT04053283

Ethics Approval This study was approved by UT MD Anderson Cancer Center IRB (Protocol 2019-0636)

UCLA Institutional Review Board (IRB#21-000275)
University of Southern California Institutional Review Board (Proposal #HS-19-00696)

Ochsner Health System Institutional BioSafety Committee (Protocol 2019.02)

WIRB/Wcg IRB (Tracking number 20190830; Washington University in St. Louis; Moffitt – Advent Health)

Consent All patients provided informed consent before taking part in this study.

Abstract 762 Table 1 Safety of NG-641 monotherapy (Dose Levels 1–4)

Type of event n (%) patients	Overall n=19	Dose Level 1 ^[a] n=4	Dose Level 2 ^[b] n=8	Dose Level 3 ^[c] n=3	Dose Level 4 ^[d] n=4
Most common TEAEs					
Decreased appetite	9 (47)	3 (75)	3 (38)	2 (67)	1 (25)
Pyrexia	8 (42)	1 (25)	3 (38)	2 (67)	2 (50)
Chills	8 (42)	3 (75)	3 (38)	2 (67)	0
Proteinuria	7 (37)	2 (50)	5 (63)	0	0
Fatigue	7 (37)	1 (50)	3 (38)	2 (67)	1 (25)
Any Grade ≥ 3 TEAE	7 (37)	0	4 (50)	1 (33)	2 (50)
Any TE-SAEs	9 (47)	3 (75)	4 (50)	1 (33)	1 (25)
Any treatment-related SAE	6 (32)	3 (75)	3 (38)	0	0
DLTs	1 (5) [two DLTs in a single patient] [e]	0	1 (13)	0	0

Abbreviations: DLT=dose limiting toxicity; TEAE= treatment emergent adverse event; SAE=serious adverse event; TE-SAE= treatment emergent serious adverse event
[a] Dose level 1= 1×10^{11} vp on Days 1, 3 and 5
[b] Dose level 2= 1×10^{12} vp on Days 1, 3 and 5
[c] Dose level 3= 1×10^{12} vp on Day 1; followed by 3×10^{12} vp on Days 3 and 5
[d] Dose level 4= 1×10^{12} vp on Day 1; followed by 6×10^{12} vp on Days 3 and 5
[e] Grade 3 hypertension and dyspnoea

<http://dx.doi.org/10.1136/jitc-2022-SITC2022.0762>

763

PHASE 1/2 DOSE ESCALATION AND DOSE EXPANSION STUDY OF TRANSCON TLR7/8 AGONIST ALONE OR IN COMBINATION WITH PEMBROLIZUMAB IN PATIENTS WITH LOCALLY ADVANCED OR METASTATIC SOLID TUMOR MALIGNANCIES: INITIAL RESULTS FROM DOSE ESCALATION

¹Diwakar Davar*, ²Morteza Aghmesheh, ³Alain Algazi, ⁴David Bajor, ⁵Vinod Ganju, ⁶Douglas Laux, ⁷Alexander Spira, ⁸Elizabeth Ahern, ⁹Jaspreet Grewal, ¹⁰Jamie Rand, ¹¹Randy Sweis, ¹²Jens-Jakob Karlsson, ¹²Mette Kriegbaum, ¹³Yang Wu, ¹³Tuan-Anh Tran, ¹³Stina Singel, ¹⁴Nashat Gabrail. ¹University of Pittsburg Medical Center, Pittsburgh, PA, USA; ²Southern Medical Day Care Centre, Wollongong, Australia; ³University of California San Francisco, San Francisco, CA, USA; ⁴University Hospitals Cleveland Medical, Cleveland, OH, USA; ⁵Peninsula and Southeast Oncology, Frankston, Australia; ⁶University of Iowa Hospital and Clinics, Iowa City, IA, USA; ⁷Virginia Cancer Specialists, Fairfax, VA, USA; ⁸Monash Health, Clayton, Australia; ⁹Norton Cancer Institute, Louisville, KY, USA; ¹⁰City of Hope, Duarte, CA, USA; ¹¹University of Chicago Medicine, Chicago, IL, USA; ¹²Ascendis Pharma A/S, Copenhagen, Denmark; ¹³Ascendis Pharma, Inc., Palo Alto, CA, USA; ¹⁴Gabrail Cancer Center, Canton, OH, USA

Background Resiquimod is a potent TLR7/8 agonist where systemic tolerability limits clinical use. TransCon TLR7/8 Agonist is an investigational prodrug of resiquimod with sustained release intended for intratumoral administration. It has the potential to overcome shortcomings of existing treatments by providing prolonged high local concentrations of resiquimod, promoting potent anti-tumoral responses while reducing systemic drug exposure and treatment related adverse events (TRAEs).¹ The primary objectives of the transcendIT-101 phase 1/2 trial are to evaluate safety and tolerability, and define the maximum tolerated dose and recommended phase 2 dose (RP2D) of TransCon TLR7/8 Agonist, alone or in combination with pembrolizumab.

Methods In dose escalation (3+3 design), patients aged ≥ 18 with advanced solid tumors receive TransCon TLR7/8 Agonist (dose levels: 0.3 and 0.5 mg/injected lesion) as monotherapy or in combination with pembrolizumab. Monotherapy patients receive dosing every 3 weeks (q3w). Combination therapy patients receive staggered dosing in cycle 1 where pembrolizumab is administered 7 days after TransCon TLR7/8 Agonist, then same-day dosing q3w at subsequent cycles. In expansion cohorts, TransCon TLR7/8 Agonist and pembrolizumab are administered same day q3w starting at cycle 1 day 1. Disease is assessed every 9 weeks using Response Evaluation Criteria in Solid Tumors version 1.1, supplemented by pathology, as available. Safety, pharmacokinetics (PK), and pharmacodynamics (PD) are evaluated.

Results As of 27th May 2022, 19 patients enrolled into dose escalation: 9 to monotherapy (3 at 0.3 mg, 6 at 0.5 mg) and 10 to combination therapy (3 at 0.3 mg, 7 at 0.5 mg). All 22 TRAEs were grade 1 or 2 (12 at 0.3 mg, 10 at 0.5mg) with most common TRAEs related to injection site reactions (59%) followed by fever (9%). Preliminary PK results showed low systemic resiquimod C_{max} , with mean systemic resiquimod half-life of 9 days, and no PK interaction with pembrolizumab. PD data from tumor biopsies were consistent with sustained intratumoral upregulation of type I interferon and TLR pathway genes that were comparable across the two dose levels. Preliminary antitumor efficacy was observed, including 1 confirmed partial response (melanoma, monotherapy at 0.3 mg).

Conclusions The transcendIT-101 trial indicates TransCon TLR7/8 Agonist has a well-tolerated safety profile as monotherapy and in combination with pembrolizumab. Results from PD studies demonstrated target engagement that correlates

with observed antitumor activity. While enrollment continues, data support 0.5 mg/injected lesion as the projected RP2D.

Trial Registration NCT04799054

REFERENCE

1. Zuniga LA, Leßmann T, Holten-Andersen L, et al. Intratumoral delivery of TransCon™ TLR7/8 Agonist provides potent anti-tumor activity as a monotherapy and in combination with IL-2 while minimizing systemic cytokine induction. Society for Immunotherapy of Cancer 2019. Nov 6-10, 2019. National Harbor, MD. Poster 676.

Ethics Approval The study protocol was approved by the institutional review board at each participating center. All the patients provided written informed consent.

<http://dx.doi.org/10.1136/jitc-2022-SITC2022.0763>

764

FIRST-IN-HUMAN, DOSE ESCALATION AND EXPANSION STUDY OF MT-6402, A NOVEL ENGINEERED TOXIN BODY (ETB) TARGETING PD-L1, IN PATIENTS WITH PD-L1 EXPRESSING RELAPSED/REFRACTORY ADVANCED SOLID TUMORS: INTERIM DATA

¹Brian Van Tine*, ²Eugene Ahn, ³John Powderly, ⁴Herbert Duvivier, ⁵Drew Rasco, ⁶Rebecca Redman, ⁷Steven Powell, ⁸Agnes Rethy, ⁸Chris Moore, ⁸Amy Yuet, ⁸Rachael Orlandella, ⁸Swati Khanna, ⁹David Spigel, ⁸Angela Georgy, ⁸Joseph Dekker. ¹Washington University in St. Louis, St Louis, MO, USA; ²Cancer Treatment Centers of America, Chicago, IL, USA; ³Carolina BioOncology Institute, Huntersville, NC, USA; ⁴CTCA-Atlanta, Atlanta, GA, USA; ⁵START, San Antonio, TX, USA; ⁶University of Louisville, Louisville, KY, USA; ⁷Sanford Cancer Center, Sioux Falls, SD, USA; ⁸Molecular Templates, Inc., Austin, TX, USA; ⁹Sarah Cannon Research Institute, Nashville, TN, USA

Background MT-6402 is a unique, potent PD-L1-targeted engineered toxin body capable of directly killing PD-L1 expressing tumor and immune cells by internalization of a de-immunized Shiga-like toxin A subunit (SLTA), which results in permanent SLTA-mediated ribosomal inactivation. Targeting PD-L1 expressing tumor cells may directly drive tumor regression, whereas targeting of PD-L1 expressing immune cells (IC) may release immunosuppression and drive immune recognition of the tumor. MT-6402 also delivers an HLA-A*02 restricted cytomegalovirus (CMV) class I antigen into PD-L1 expressing cells (antigen seeding) that can be recognized by existing CMV-specific cytotoxic T cells.

Methods A first-in-human dose escalation and expansion study (QW in 4-week cycles) was initiated in 2021.

Results 18 patients with PD-L1-expressing advanced solid tumors received ≥ 1 dose of MT-6402. 14 patients were eligible for Dose Limiting Toxicity (DLT) assessment in Cohorts 1 through 4. MT-6402 was well tolerated and no DLT was observed in Cohorts 1 and 3 (16 $\mu\text{g}/\text{kg}$ and 32 $\mu\text{g}/\text{kg}$, respectively). 1 DLT of a Grade (G)2 maculopapular rash occurred in Cohort 2 (24 $\mu\text{g}/\text{kg}$). There was no G4 or G5 adverse events (AEs) or treatment-related discontinuations in the first 3 cohorts. Immune-related AEs of Infusion-related reaction (G1 and G2) and cytokine-release syndrome (G1 and G2) occurred, generally lasting 1-2 days.

2 patients in Cohort 1 had stable disease for 8 months. A significant reduction in CD14+ monocytes was observed after each administration, indicating HLA-independent pharmacodynamic effect. Dose dependent reduction of monocytes was observed across 3 cohorts and correlated with CCL2 and IL-8 modulation. PD-L1-negative peripheral monocytes and dendritic cell populations were spared, indicating on-target removal. Most patients display CD8 T cell expansion/activation and IL-2 and TNF α cytokine release, consistent with removal of PD-1/PD-L1 interaction.

One patient with high PD-L1 expression and osseous metastases who is HLA-A*02/CMV+ showed complete CMV-specific T-cell extravasation by C1D8, persisting until C6, and serum cytokine signatures consistent with antigen dependent responses and T cell mobilization. This patient had reduced tracer uptake of metastatic bone lesions with resolution of 3 lesions. 3 additional HLA-A*02/CMV+ patients with low PD-L1 expression followed a similar trend of extravasation of peripheral CMV-specific T cells.

Conclusions These results describe a novel approach to checkpoint modulation by MT-6402 with a potential to alter tumor immunophenotype particularly in patients with HLA-A*02/CMV positivity. Dose escalation is ongoing. These results provide compelling rationale for continued development of MT-

6402, including in the R/R setting, possibly in combination with PD-1 inhibitors.

Trial Registration NCT04795713

Ethics Approval This study was conducted in compliance with current Good Clinical Practice (GCP) standards as defined by the International Council for Harmonisation of Technical Requirements for Pharmaceuticals for Human Use (ICH) Guideline for GCP, all applicable national, state, and local laws and regulations, and the applicable Institutional Review Board/Independent Ethics Committee (IRB/IEC) and other institutional requirements.

Consent Written informed consent was obtained from the patient for publication of this abstract and any accompanying images. A copy of the written consent is available for review by the Editor of this journal.

<http://dx.doi.org/10.1136/jitc-2022-SITC2022.0764>

766

PHASE I/II EVALUATION OF THE COMBINATION OF ENTINOSTAT, M9241 AND BINTRAFUSP ALFA IN PATIENTS WITH ADVANCED HPV RELATED MALIGNANCIES

¹Julius Strauss*, ¹Charalampos Floudas, ¹Danielle Pastor, ¹Jason Redman, ²Deneise Francis, ²Elizabeth Lamping, ¹Lisa Cordes, ¹Jennifer Marte, ¹Renee Donahue, ¹Caroline Jochems, ¹Sofia Gameiro, ¹Jeffrey Schlom, ¹James Gully. ¹Center for Immuno-Oncology, NCI, Bethesda, MD, USA; ²Office of Research Nursing, NCI, Bethesda, MD, USA

Background More than 630,000 cases of HPV related cancer (e.g. cervical, oropharyngeal, anal) occur worldwide annually. Unfortunately, only about 15-20% of cases respond to PD-(L) 1 inhibitors alone. Recent data with the triple combination of PDS0101 (a therapeutic vaccine targeting HPV 16 E6/E7), M9241 (a tumor-targeting IL-12 immunocytokine), and bintrafusp alfa (a bifunctional fusion protein targeting TGF- β and PD-L1) have shown early clinical activity in advanced checkpoint refractory HPV related cancers, with 45% of patients having disease reduction, including 27% with objective responses.¹ In addition, preclinical studies have shown that the triple combination of entinostat (histone deacetylase inhibitor), M9241, and bintrafusp alfa may also have promising anti-tumor activity in checkpoint refractory disease.

Methods 7 patients with advanced checkpoint refractory HPV positive cancers who had been previously treated with PDS0101, M9241 and bintrafusp alfa (NCT04287868) and progressed went on to be treated with the combination of entinostat, M9241, and bintrafusp alfa (NCT04708470). These patients received bintrafusp alfa at 300 mg IV q 2weeks, entinostat 3 mg po weekly including a 1 week lead in of entinostat alone, and M9241 at either 4 mcg/kg SC q 2 weeks or 8 mcg/kg SC q 4weeks (based on dose escalation cohort). Pts receiving M9241 at 8 mcg/kg did not receive entinostat on the week of M9241 treatment but did on all other weeks.

Results 7 patients with advanced checkpoint refractory HPV positive cancers (5 oropharyngeal, 1 anal, 1 neuroendocrine rectal) who had progressed on PDS0101, M9241 and bintrafusp alfa went on to receive entinostat, M9241, and bintrafusp alfa. After switching to the entinostat based triple combination, 2/7 patients had grade 3 treatment related AEs including grade 3 anemia in one patient and grade 3 leukopenia/lymphopenia in another. Otherwise, there were no grade 3 or greater treatment related AEs observed in patients switching to the entinostat based triple combination. 3/7 (43%) patients (2 oropharyngeal, 1 anal) have had tumor reduction of 28.8%, 38.3% and 42.6% by RECIST after switching to the entinostat based triple combination.

Conclusions Escalating doses of the triple combination of entinostat, M9241 and bintrafusp alfa continue to be evaluated in an ongoing phase I/II trial (NCT04708470). To date the triple combination appears to have a manageable safety profile along with encouraging clinical activity in patients with advanced checkpoint refractory HPV related cancers including in pts who have previously progressed on PD(L)1 inhibitor then on PDS0101, M9241 and bintrafusp alfa.

Trial Registration NCT04708470

REFERENCE

1. Strauss J, et al. Phase II evaluation of the combination of PDS0101, M9241, and bintrafusp alfa in patients with HPV 16+ malignancies. *J Clin Oncol.* 2022;**40** (suppl 16; abstr 2518).

Ethics Approval Ethics approval for NCT04708470 was obtained from the National Institutes of Health IRB (Ref #

551458). Participants gave informed consent prior to participating.

<http://dx.doi.org/10.1136/jitc-2022-SITC2022.0766>

767

SAFETY AND PRELIMINARY EFFICACY OF MRNA-2752, A LIPID NANOPARTICLE ENCAPSULATING MRNAS ENCODING HUMAN OX40L/IL-23/IL-36 γ FOR INTRATUMORAL (ITU) INJECTION, AND DURVALUMAB (IV) IN TNBC, HNSCC, AND MELANOMA

¹Daniel Olson, ²Adil Daud, ³Ronnie Shapira-Frommer, ⁴Antonio Jimeno, ⁵Patrick Reagan, ⁶Shivaani Kummur, ⁷Raghad Abdul-Karim, ⁸Salomon Stemmer, ⁹Meredith McKean, ¹⁰Ravit Geva, ¹¹Ruth Perets, ¹²Manish Patel, ¹³Thomas Marron, ¹⁴Shilpa Gupta, ¹⁵Anupam Desai, ¹⁶Jeffrey Weber, ¹⁷Kim Margolin, ¹⁸Jong Chul Park, ¹⁹Sima Zacharek, ¹⁹Andressa Sodre Laino, ¹⁹Joshua Frederick, ¹⁹Oleg Milberg, ¹⁹Lili Zhu, ¹⁹Kinjal Mody, ¹⁹Natalia Lopez, ¹⁹Praveen Aanur, ¹⁹Robert Meehan, ¹⁹Lisa Johansen, ¹⁹Sara Lavoie, ¹⁹Khanh Do, ¹⁹Ryan Sullivan, ¹⁹Randy Sweis*. ¹University of Chicago, Chicago, IL, USA; ²University of California San Francisco, San Francisco, CA, USA; ³Sheba Medical Center, Ramat Gan, Israel; ⁴University of Colorado, Aurora, CO, USA; ⁵University of Rochester, Rochester, NY, USA; ⁶Oregon Health and Science University, Portland, OR, USA; ⁷Henry Ford Hospital, Detroit, MI, USA; ⁸Rabin Medical Center, Tel Aviv, Israel; ⁹Sarah Cannon Research Institute, Nashville, TN, USA; ¹⁰Sourasky Medical Center, Tel-Aviv, Israel; ¹¹Rambam Medical Center and Technion, Haifa, Israel; ¹²SCRI-Florida Cancer Specialists, Sarasota, FL, USA; ¹³Icahn School of Medicine at Mount Sinai, New York, NY, USA; ¹⁴The Cleveland Clinic Foundation, Cleveland, OH, USA; ¹⁵Beth Israel Deaconess Medical Center, Boston, MA, USA; ¹⁶NYU Langone Health, New York, NY, USA; ¹⁷Saint John's Cancer Institute, Santa Monica, CA, USA; ¹⁸Massachusetts General Hospital, Boston, MA, USA; ¹⁹Moderna Inc., Cambridge, MA, USA

Background mRNA-2752 is a first-in-class mRNA-based therapeutic agent encoding T cell co-stimulator OX40L, and pro-inflammatory cytokines IL-23 and IL-36 γ . Preclinical data demonstrated activity in a range of tumor microenvironments (TMEs), including immune checkpoint inhibitor (CPI)- refractory cancer models, and synergy when combined with α -PD-L1 antibodies. Data from the dose escalation phase of the study was previously reported and the recommended mRNA-2752 dose for expansion (RDE) was up to 8mg ITu.

Methods We evaluated the safety and efficacy of ITu mRNA-2752 administered as monotherapy (Arm A; previously reported ASCO 2020) and in combination with the PD-L1 inhibitor durvalumab (Arm B) in patients (pts) with tumors that were palpable or accessible with image guidance. Here we report preliminary data for the expansion cohorts in TNBC, CPI-refractory melanoma, and HNSCC. Biomarker analyses included IHC/F-IHC of immune status markers and whole transcriptome assessments of paired tumor biopsies. Protein quantification of IL-23, IL-36 γ and other pro-inflammatory cytokines were performed in plasma and tumors.

Results As of 01JUL 2022, 88 pts were treated, 69 in Arm B with mRNA-2752 dosed by tumor size ranging from 0.25-8 mg. The most common treatment related adverse events occurring in \geq 10% of pts in Arm B included grade 1/2 injection site erythema/pain/swelling, fever, chills, fatigue, nausea, and flushing. Grade 3 events included injection site pain/erythema, and fever. There were no grade 4/5 related events. Objective responses were observed in immune refractory tumors by RECIST and iRECIST, including a confirmed PR in a PD-L1 low TNBC and confirmed iCR in an immune checkpoint-refractory melanoma pt, respectively. Biomarker analyses of plasma and tumor show mRNA-2752 treatment was associated with elevated pro-inflammatory cytokines, including IL-23, IL-36 γ , IFN γ , and TNF α . F-IHC of paired tumor biopsies showed increase in proliferating CD8+ T cells. Transcriptional profiling of the TME demonstrates a pronounced immune response including dendritic cell recruitment and T cell activation, which remained elevated in longitudinal samples. The greatest increases in immune response and markers of cytolytic activity were observed in pts deriving clinical benefit.

Conclusions ITu mRNA-2752 + IV durvalumab is safe, tolerable, and shows preliminary efficacy in immune refractory tumors, including TNBC and melanoma. Biomarker analyses indicate mRNA-2752 drives cytokine responses. Consistent with the expected mechanism of action, a productive and sustained inflammatory response is observed in the TME in response to treatment, including signatures of increased innate and adaptive immune cell abundance and effector response.

Acknowledgements We thank AstraZeneca for provision of durvalumab for this study.

Trial Registration NCT03739931

Ethics Approval This study was approved by participating Institutions' Ethics Board and conducted according to the principles of ICH GCP. Participants gave informed consent before taking part.

Consent Written informed consent was obtained from the patient for publication of this abstract and any accompanying images. A copy of the written consent is available for review upon request.

<http://dx.doi.org/10.1136/jitc-2022-SITC2022.0767>

768

PERIPHERAL PHARMACODYNAMIC (PD) EFFECTS OF OCIPERLIMAB (OCI) IN COMBINATION WITH TISELIZUMAB (TIS) IN PATIENTS WITH ADVANCED SOLID TUMORS: ADVANTIG-105 PHASE 1 DOSE-ESCALATION STUDY

¹Wei Tan*, ²Yang Shi, ²Han Yan, ²Zhirong Shen, ³Nageshwar Budha, ³Ahsan Rizwan, ¹Ruiqi Huang, ³Hao Zheng, ¹Rang Gao, ⁴Sophia Frentzas, ⁵Steven Kao, ⁶Tarek Meniawy, ²Yun Zhang. ¹BeiGene (Shanghai) Co., Ltd., Shanghai, China; ²BeiGene (Beijing) Co., Ltd., Beijing, China; ³BeiGene (USA) Co., Ltd., San Mateo, CA, USA; ⁴Monash Health, Melbourne, Australia; ⁵Chris O'Brien Life House, Sydney, Australia; ⁶Linear Clinical Research and University of Western Australia, Nedlands, Western Australia, WV, Australia

Background OCI is a humanized monoclonal antibody (mAb) against T-cell immunoreceptor with immunoglobulin and immunoreceptor tyrosine-based inhibitory motif domains (TIGIT) with high affinity and specificity, enabling Fc-mediated effector functions that induce antibody-dependent cellular cytotoxicity.¹ The Phase 1/1b open-label AdvanTIG-105 trial was designed to assess the safety and efficacy of OCI plus TIS (an anti-programmed cell death protein 1 mAb) in patients with advanced solid tumors (NCT04047862).² In the dose-escalation part, the combination was well tolerated, and preliminary antitumor responses were observed. Here, we report PD biomarker data from peripheral blood.

Methods Eligible patients had locally advanced/metastatic, unresectable solid tumors previously treated with standard systemic therapy or for which treatment was not available/tolerated, ECOG PS ≤ 1 and had received no prior anti-TIGIT therapy. Patients received five escalating doses of OCI (50–1800mg) intravenously (IV) on Cycle (C) 1 Day (D) 1 and TIS 200mg IV was initiated on C1D8. If tolerated, patients received OCI (50–1800mg) plus TIS 200mg on D29 (C2D1) and every three weeks thereafter until discontinuation. Peripheral blood samples were collected to monitor changes in total and TIGIT-expressing immune cell subsets pre- and post-treatment. Meso Scale Discovery V-plex panels were used to assess cytokine/chemokine release in plasma samples. Wilcoxon signed-rank test compared pre- and post-treatment cytokine/chemokine levels; p values are descriptive.

Results At data cutoff (09/01/2021), 32 patients had received ≥ 1 dose of OCI plus TIS. Total peripheral regulatory T cells (Tregs) decreased following OCI monotherapy (at C1D2 and C1D8) with doses of 900mg and 1800mg (not dose proportional), but not 450mg; the decrease was maintained with subsequent combination with TIS (at C1D15 and C2D1). CD4+ and CD8+ T-cell populations were not impacted at any OCI dose. TIGIT downregulation was observed on Tregs, CD4+, and CD8+ T cells at C1D8 with multiple OCI doses (not dose proportional); the reduction was sustained after combination with TIS. Plasma IL12/23p40 ($p < 0.001$), CCL4 ($p < 0.05$), and CXCL10 ($p < 0.05$) were notably induced post-OCI (C1D8), and further elevated following combination with TIS ($p < 0.001$, $p < 0.001$, and $p < 0.0001$, respectively) at C2D1. Plasma IFN γ and TNF α increased post-OCI at C1D8 and were dramatically induced post-combination at C2D1 ($p < 0.0001$ and $p < 0.001$, respectively).

Conclusions OCI, with or without TIS, led to Treg reduction at higher doses, TIGIT downregulation, and proinflammatory cytokine/chemokine release, reflecting the potential mechanism of action of OCI as an Fc-competent anti-TIGIT mAb.

Acknowledgements This study was sponsored by BeiGene, Ltd. Medical writing support, under the direction of the authors, was provided by Sophie Cook, PhD, of Ashfield MedComms, an Inizio company, and was funded by BeiGene, Ltd.

Trial Registration NCT04047862

REFERENCES

1. Chen X, Xue L, Ding X, *et al.* A Fc-competent anti-human TIGIT blocking antibody BGB-A1217 elicits strong immune responses and potent anti-tumor efficacy in pre-clinical models. *J Cancer Res.* 2021 Abstract 1854;81(13 Supplement):1854–54
2. Frentzas S, Meniawy T, Kao S, *et al.* AdvanTIG-105: Phase 1 dose-escalation study of anti-TIGIT monoclonal antibody ociperlimab (BGB-A1217) in combination with tislelizumab in patients with advanced solid tumors. *J Clin Oncol.* 2021;15:2583.

Ethics Approval The protocol, informed consent forms, any information given to the patients, and relevant supporting information were submitted, reviewed, and approved by the Institutional Review Board and Independent Ethics Committee before this study was initiated. This study was conducted in full conformance with the International Council for Harmonization E6 guideline for Good Clinical Practice, the International Council for Harmonization E2A guideline for Clinical Safety Data Management, and the principles of the Declaration of Helsinki or the laws and regulations of the country in which the research was conducted.

<http://dx.doi.org/10.1136/jitc-2022-SITC2022.0768>

769

RESULTS FROM AN ONGOING OPEN-LABEL, MULTICENTER, PHASE 1 TRIAL OF CCX559, AN ORALLY ADMINISTERED SMALL MOLECULE PD-L1 INHIBITOR, IN PATIENTS WITH ADVANCED SOLID TUMORS

²Gonzalo Tapia-Rico, ³Joanne Lundy, ⁴Gary Richardson, ¹Niky Zhao, ¹Karen Ebsworth, ¹Huibin Yue, ¹Shichiang Miao, ¹Emil deGoma, ¹Rita Jain, ¹Thomas Schall, ¹Kathleen Sullivan, ¹Penglie Zhang, ⁵Paul de Souza, ¹Emil deGoma*. ¹ChemoCentryx, San Carlos, CA, USA; ²Icon Cancer Centre, Adelaide, Australia; ³PASO Medical, East Bentleigh, Australia; ⁴Cabrini Research, Melbourne, Australia; ⁵Western Sydney University, Campbelltown, Australia

Background The novel small molecule CCX559 is a highly potent and selective PD-L1 inhibitor that induces dimerization and internalization of cell-surface PD-L1. CCX559, when orally administered in animal models, demonstrated anti-tumor efficacy, including the ability to induce complete responses.¹ Initial results from a phase 1 study of CCX559 indicated on-target pharmacodynamic (PD) effects consistent with PD-L1 inhibition, including peripheral T cell activation and stimulation of cytokines.^{2,3}

Methods This phase 1, first-in-patient, dose-escalation trial is evaluating safety, tolerability, pharmacokinetics (PK), PD, and preliminary anti-tumor activity of CCX559 in patients with advanced solid tumors. CCX559 is dosed orally once daily in repeated 21-day cycles with a starting dose level of 30 mg. PBMC and plasma samples are collected from patients over the first 2 cycles of treatment for PD assessments, including quantification of T cell proliferation and measurement of plasma cytokines and chemokines. Principal component analysis (PCA) was used to identify patient clusters with discrete cytokine/chemokine profiles.

Results As of July 12, 2022, a total of 17 patients were dosed with CCX559, including 13 patients across the 120 mg and 180 mg dose groups. No DLTs, treatment-related SAEs, or severe (Grade 3 or higher) treatment-related AEs were reported. The observed PK exposures were generally dose-proportional from 30 mg to 180 mg and in line with projections based on nonclinical data.

PD assays were performed with samples from the 30 mg (n=1), 60 mg (n=1), 120 mg (n=8) and 180 mg (n=2) cohorts. Patients in all four cohorts showed 1.5-fold or greater increases in peripheral CD4 and CD8 T cell proliferation starting in the first cycle (21 days) of treatment, as measured by Ki67 positivity. In patients treated with CCX559 120 mg or 180 mg, plasma levels of IFN γ , IFN γ -stimulated factors CXCL10 and CXCL11, and soluble PD-L1 were significantly increased ($p < 0.05$) during the first treatment cycle, and changes in these factors were positively correlated with each other. PCA of the 120 mg cohort showed that patients with increased IFN γ -stimulated factors formed a cluster with a differentiated global cytokine/chemokine response, including upregulation of CXCL13, CXCL8, and IL-1 β .

Conclusions Interim results from the phase 1 dose-escalation trial of CCX559 indicate on-target PD effects consistent with PD-L1 inhibition. Peripheral IFN γ -stimulated responses were observed in the 120 mg and 180 mg cohorts, consistent with the expected activity profile for immune checkpoint inhibitors. Additional PD data, together with the safety and PK profile, will be presented.

Trial Registration ANZCTR registration
ACTRN12621001342808

REFERENCES

1. Li C, et al. CCX559, A Potent, Orally-Administered Small Molecule PD-L1 Inhibitor That Induces Anti-Tumor Immunity. In: Proceedings of the American Association for Cancer Research Annual Meeting 2021; 2021 Apr 10-15 and May 17-21. Philadelphia (PA): AACR; *Cancer Res.* 2021;**81**(13_Suppl):Abstract nr 1274.
2. Tapia-Rico G, et al. Preliminary data from an ongoing phase 1 dose-escalation study of CCX559, an orally administered small molecule PD-L1 inhibitor, in patients with advanced solid tumors. *J Clin Oncol.* 2022;**40**(16_Suppl):2593–2593.
3. Herbst RS, et al. Predictive Correlates Of Response To The Anti-PD-L1 Antibody MPDL3280A In Cancer Patients. *Nature.* 2014;**515**(7528):563–567. doi:10.1038/nature14011.

Ethics Approval This study was approved by the central Human Research Ethics Committee Bellberry Limited; approval numbers 2021-04-374, 2021-04-374-AB, 2021-04-374-AC, and 2021-04-374-AD.

<http://dx.doi.org/10.1136/jitc-2022-SITC2022.0769>

SAFETY, EFFICACY, AND PHARMACOKINETIC RESULTS FROM A PHASE I FIRST-IN-HUMAN STUDY OF ABBV-151 WITH OR WITHOUT ANTI-PD1 MAB (BUDIGALIMAB) IN PATIENTS WITH LOCALLY ADVANCED OR METASTATIC SOLID TUMORS

¹Anthony Tolcher*, ²Desamparamos Roda-Perez, ³Kai He, ⁴Victor Moreno, ⁵Carlos Gomez-Roca, ⁶Jean-Pascal Machiels, ⁷Albiruni Razak, ⁸Mohammad Sahtout, ⁹Xiaowen Guan, ⁸Stacy Jaryno-Daly, ⁸Rachel Leibman, ⁸Martha Blaney, ⁸James O'Brien, ⁹Patricia Lorusso, ¹⁰John Powderly, ¹¹Talia Golan, ¹²Kathy Miller, ¹³Jordi Bruix. ¹*NEXT Oncology, San Antonio, TX, USA*; ²*The Institute of Cancer Research, London, UK*; ³*The James Cancer Hospital, Columbus, OH, USA*; ⁴*START Madrid-FJD, Madrid, Spain*; ⁵*Institut Claudius Regaud/IUCT Oncopole, Marseille, France*; ⁶*Institut Roi Albert II Cancer Centre, Brussels, Belgium*; ⁷*Princess Margaret Cancer Center, Toronto, Canada*; ⁸*AbbVie, Inc., North Chicago, IL, USA*; ⁹*Yale Cancer Center, Yale University, New Haven, CT, USA*; ¹⁰*Carolina Biooncology Institute, Huntersville, NC, USA*; ¹¹*Sheba Medical Center, Tel-Hashomer, Israel*; ¹²*Indiana University School of Medicine, Indianapolis, IN, USA*; ¹³*Hospital Clinic Barcelona, Barcelona, Spain*

Background Glycoprotein-A repetitions predominant (GARP) is expressed on regulatory T-cells and modulates release of active transforming growth factor β 1 (TGF β 1), an immunosuppressive cytokine. ABBV-151 is a first-in-class monoclonal antibody (mAb) that binds to the GARP-TGF β 1 complex, blocking the release of active TGF β 1. Preclinical data demonstrate that blocking GARP-TGF β 1 and programmed cell death protein-1 (PD-1) improves antitumor efficacy compared with anti-PD-1 alone. Combining ABBV-151 with the anti-PD-1 mAb budigalimab may enable increased antitumor efficacy by reducing the immunosuppressive effects of TGF β 1. Herein, we report preliminary safety, efficacy, and pharmacokinetic (PK) results from a first-in-human, phase 1 study (NCT03821935) assessing ABBV-151 \pm budigalimab in adult patients (\geq 18 years) with locally advanced/metastatic solid tumors. Results from the all-comer dose escalation (ESC) phase and two cohorts from the dose expansion (EXP) phase are available: anti-PD-1/PD-ligand (L)1 naïve hepatocellular carcinoma (HCC) and anti-PD-1/PD-L1 relapsed/refractory urothelial cancer (UC).

Methods ESC patients must be refractory/intolerant to existing effective therapies; EXP cohorts have tumor-specific eligibility requirements. The primary ESC endpoint is the recommended phase II dose of ABBV-151 \pm budigalimab. The primary EXP endpoint is preliminary efficacy of ABBV-151 + budigalimab, assessed by objective response rate per Response Evaluation Criteria in Solid Tumors (RECIST) version 1.1.

Results As of June 2022, 157 patients have been enrolled, 57 in ESC (23 ABBV-151 monotherapy; 34 combination therapy) and 100 in EXP (including 36 UC; 12 HCC). As of January 2022, safety data were available for 129 patients. Any-grade adverse events (AEs) were reported in 119/129 (92%) patients. Most commonly: fatigue (28%), pruritus (27%), and nausea (22%). Grade 3-4 AEs occurred in 66/129 (51%) patients, with drug-related grade 3-4 AEs in 18/129 (14%) patients. ABBV-151 showed dose proportional PK. No antitumor responses were reported for the ABBV-151 monotherapy ESC cohorts. In the combination ESC cohorts, there were 4 confirmed responses, 1 unconfirmed response, and 4 patients had stable disease (SD) \geq 6 months. In the anti-PD-1/PD-L1 relapsed/refractory UC EXP cohort, there were 5 confirmed responses, 1 unconfirmed response, and 5 patients had a best response of SD. In the anti-PD-1/PD-L1 naïve HCC EXP cohort, there were 5 confirmed responses, including one response per immune RECIST, and 3 patients had a best response of SD.

Conclusions ABBV-151 \pm budigalimab showed a manageable safety profile in patients with advanced solid tumors. Preliminary efficacy results demonstrate durable antitumor activity with ABBV-151 + budigalimab, including in anti-PD-1 relapsed/refractory UC and in anti-PD-1 naïve HCC.

Acknowledgements AbbVie and the authors thank all the trial investigators and the patients who participated in this clinical trial. Medical writing support was provided by Rebecca L. Crepeau, PhD, from Aptitude Health, Atlanta, GA, USA and funded by AbbVie.

Trial Registration NCT03821935

Ethics Approval The study was approved by the Advarra Ethics Board, under the license number IRB00000971.

<http://dx.doi.org/10.1136/jitc-2022-SITC2022.0770>

771

A PHASE 1, FIRST IN HUMAN, OPEN-LABEL, DOSE ESCALATION AND DOSE EXPANSION STUDY OF TST005 IN PATIENTS WITH LOCALLY ADVANCED OR METASTATIC SOLID TUMORS

¹Lei Chen, ²Anthony Tolcher*, ³Nashat Gabrail, ⁴Minal Barve, ⁵Xiaohua WU, ⁵Jian Zhang, ¹Michael Shi, ¹Chuan Qi, ¹Steven Yu, ¹Jenny Yao, ¹Jianming Wang, ¹Christopher Cavanaugh. ¹TRANSCENTA, Shanghai, China; ²NEXT Oncology, San Antonio, TX, USA; ³Gabrail Cancer, Canton, OH, USA; ⁴Mary Crowley Cancer Research Centers, Dallas, TX, USA; ⁵Fudan University Shanghai Cancer Center, Shanghai, China

Background Anti-programmed death 1/ligand 1 (PD-1/PD-L1) therapies have been established as standard treatment for multiple tumor types. However, the key challenge of these therapies is resistance caused by immunosuppressive factors in the tumor microenvironment (TME). TGF- β is a multi-functional cytokine that is involved in the tight regulation of either anti-tumor immunity or tumor immunosuppression. TGF- β promotes an immune exclusion TME thus renders PD-L1 blockade ineffective. Therefore, dual targeting PD-L1 and TGF- β represents a rational synergistic strategy to enhance clinical outcome relative to each agent alone. TST005 is a novel bi-functional fusion protein combining a high affinity PD-L1 monoclonal antibody (mAb) in a fragment crystallizable (Fc) silenced immunoglobulin G1 (IgG1) backbone and a differentiated transforming growth factor beta (TGF- β) trap with improved stability. This study will investigate TST005's safety, tolerability and preliminary anti-tumor activity in solid tumors.

Methods This Phase 1, first in human (FIH) study is an open-label, multicenter trial that consists of a dose escalation phase in patients with advanced solid tumors who has failed prior therapy followed by a dose expansion phase in human papillomavirus (HPV) related malignancies that is not amenable to surgery and have received prior standard therapy(ies). The primary objectives are to evaluate the safety and tolerability and determine the maximum tolerated dose or recommended Phase 2 dose(s) of TST005. Secondary objectives include pharmacokinetic, pharmacodynamic and preliminary anti-tumor activity of TST005. The dose escalation phase comprises five dose cohorts: accelerated titration of 1 subject in the starting dose cohort (1 mg/kg), and then four dose cohorts (3 mg/kg, 10 mg/kg, 20 mg/kg, 30 mg/kg) following classic 3+3 design. No more than one prior immune checkpoint inhibitor (ICI) treatment is allowed for eligible subjects. In the dose expansion phase, up to 30 patients with locally advanced or metastatic HPV+ malignancies, including cervical cancers, P16+ Oropharyngeal cancers, and other tumors that are known HPV+, and who are ICI treatment naive will be enrolled. Subjects will receive TST005 intravenous infusion every 3 weeks (Q3W) until disease progression per RECIST v1.1 and/or immune RECIST or unacceptable toxicity. Subjects may continue to receive TST005 beyond RECIST v1.1 defined progression at the discretion of the Investigator. This study is ongoing at 4 sites in the US and China. As of the 30 June, 2022, the first two dose cohorts evaluation has been completed and no DLT was observed. Clinical trial information: NCT04958434. Study Sponsor: Suzhou Transcenta Therapeutics Co., Ltd.

Ethics Approval The study obtained sites' IRB approval for as listed below. All participants gave informed consent before taking part.

- Salus IRB (NXSAT20.69)
- Advarra IRB (SSU00157936)
- Mary Crowley Medical Research Center IRB (21-37)
- Shanghai Cancer Center IRB (2112248-1-2203)

Consent Written informed consent was obtained from the patient for publication of this abstract and any accompanying images. A copy of the written consent is available for review by the Editor of this journal.

<http://dx.doi.org/10.1136/jitc-2022-SITC2022.0771>

A PHASE 1/2 DOSE ESCALATION/EXPANSION STUDY EVALUATING THE SAFETY, PHARMACOKINETICS, PHARMACODYNAMICS, AND ANTITUMOR ACTIVITY OF E-602, A BI-SIALIDASE FUSION PROTEIN, IN ADVANCED CANCER (GLIMMER-01)

¹Manish Sharma*, ²Deanne Lathers, ³Melissa Johnson, ⁴Jason Luke, ⁵Igor Puzanov, ⁶Brendan Curti, ⁷Christopher Chen, ⁸Anthony El-Khoueiry, ⁹Brian Henick, ¹⁰Margaret Callahan, ¹¹Mario Sznol, ¹²Sandip Patel, ²Dawn Wilson, ²Melissa Ricker, ²Lizhi Cao, ²Pushpa Jayaraman, ²Jenny Che, ²Li Peng, ²David Feltquate, ²Deanne Lathers, ¹³Anthony Tolcher. ¹START Midwest, Grand Rapids, MI, USA; ²Palleon Pharmaceuticals, Waltham, MA, USA; ³Sarah Cannon Research Institute, Nashville, TN, USA; ⁴University of Pittsburgh Medical Center, Pittsburgh, PA, USA; ⁵Roswell Park Comprehensive Cancer Center, Buffalo, NY, USA; ⁶Providence Cancer Institute, Portland, OR, USA; ⁷Stanford University Medical University, Palo Alto, CA, USA; ⁸University of Southern California, Los Angeles, CA, USA; ⁹Columbia University Medical Center, New York, NY, USA; ¹⁰Memorial Sloan Kettering Cancer Center, New York, NY, USA; ¹¹Yale Cancer Center, New Haven, CT, USA; ¹²University of California, La Jolla, CA, USA; ¹³NEXT Oncology, San Antonio, TX, USA

Background E-602 is a novel, first-in-class fusion protein of engineered human sialidases, neuraminidase (Neu)2, and the human IgG1 Fc region. The sialidase moieties of E-602 cleave terminal sialic acid residues from sialoglycans on diverse immune cell subsets and tumor cells. Sialoglycans are immunosuppressive in cancer, associated with poorer outcomes across numerous tumor indications, and have emerged as a critical glyco-immune checkpoint. In preclinical studies, sialidase-mediated cleavage of terminal sialic acids improves antitumor immunity by restoring the immune function of exhausted-like T cells and enhancing dendritic cell priming and naïve T cell activation.¹ In multiple syngeneic mouse tumor models, sialidase treatment has demonstrated antitumor activity as monotherapy¹ and additive antitumor activity when combined with anti-programmed death-1 (PD-1)/programmed death-ligand 1 (PD-L1) blockade. E-602 has a wide safety margin, is not an immune agonist and does not stimulate cytokine activation in an in vitro PBMC cytokine release assay.^{1,2} In humans, E-602, via desialylation of tumor cells and immune cells, is expected to have antitumor activity either as monotherapy or in combination with an anti-PD-1 agent.

Methods A Phase 1/2, first-in-human, open label, dose escalation and expansion study of E-602 administered as monotherapy and in combination with an anti-PD-1 agent is ongoing to evaluate the safety, pharmacokinetics, pharmacodynamics, and antitumor activity in participants with advanced cancers. Phase 1 of the study consists of 4 planned dose escalation cohorts of E-602 monotherapy and 2 planned dose escalation cohorts of E-602 in combination with an anti-PD-1 agent. Phase 1 is treating eligible participants with advanced melanoma, ovarian, non-small cell lung, colorectal, pancreatic, breast, gastric/esophagogastric junction, head and neck, or urothelial cancers. Utilizing a modified 3+3 study design in Phase 1, the safety of the dose regimens is under evaluation to identify the maximum tolerated dose and/or recommended Phase 2 dose. Additional participants (backfill) may be enrolled in the Phase 1 cohorts to obtain additional safety, pharmacokinetic or pharmacodynamic data. Phase 2 will include up to 3 disease indications, evaluating E-602 as monotherapy and/or in combination with an anti-PD-1 agent utilizing a Simon's minimax 2-stage design. Pre and on-treatment biopsies to further explore the pharmacodynamic effects of E-602 are required for the Phase 1 backfill and Phase 2 participants.

Acknowledgements The authors would like to thank the clinical trial participants and their families for their willingness to participate in the study.

Trial Registration The study is registered on clinicaltrials.gov as NCT05259696.

REFERENCES

1. Peng L, Cao L, Nerle S, et al. Development and engineering of human sialidase for degradation of immunosuppressive sialoglycans to treat cancer. *J Immunother Cancer*. 2021;**9**(Suppl 2):A1–A1054.
2. Cao L, Che J, Chesney A, et al. Assessment of the safety, pharmacokinetics, and pharmacodynamics of a first-in-class cancer drug candidate E-602, a sialoglycan degrader, in non-human primates [abstract]. *Cancer Res*. 2022;**82**(12_Suppl): Abstract nr LB203.

Ethics Approval The study is approved by the Advarra institutional Ethics Board, approval number Pro00058627 and participants gave informed consent before taking part.

<http://dx.doi.org/10.1136/jitc-2022-SITC2022.0772>

773

A PHASE 1B/2, OPEN-LABEL, DOSE ESCALATION AND EXPANSION STUDY OF AN ANTI-CTLA-4 NEOBODY™ ADG116 IN COMBINATION WITH PEMBROLIZUMAB (ANTI-PD-1 ANTIBODY) IN PATIENTS WITH ADVANCED/METASTATIC SOLID TUMORS: A PRELIMINARY UPDATE

¹Anthony Tolcher, ²John Powderly, ³Kristine Shi, ³Songmao Zheng, ³Guizhong Liu, ³Jin Shang, ³Xinwei Wang, ³Wenda Li, ³Dana Lowe, ⁴Michael Chisamore, ³Peter Luo, ³Jiping Zha*. ¹*Next Oncology, San Antonio, TX, USA;* ²*Carolina Biooncology Institute, Huntersville, NC, USA;* ³*Adagene, San Diego, USA;* ⁴*Merck, Kenilworth, NJ, USA*

Background CTLA-4 as an immunotherapeutic target that has been challenged with limited single agent efficacy and high-grade toxicities in the clinic. ADG116 is a fully human anti-CTLA-4 IgG1 monoclonal antibody that targets a unique and a highly conserved epitope of CTLA-4 using the NEObody™ technology platform. ADG116 enables a safer T cell activation via partial CD80/86 ligand blockade and enhances the Treg depletion in the tumor microenvironment via a stronger ADCC. Preclinical studies demonstrated that ADG116 is more potent and better tolerated than ipilimumab. In a Phase 1 dose escalation study, single agent ADG116 has been well-tolerated up to 10 mg/kg when dosed intravenously, once every 3 weeks (Q3W); target lesion size reduction and stable diseases were observed in multiple heavily pre-treated patients including those bearing “cold” tumors.¹ We propose that ADG116 in combination with pembrolizumab may enhance clinical antitumor activity through a simultaneous blockade of the PD-1/PD-L1 and CTLA-4 pathways while still maintaining a favorable safety profile.

Methods This is a Phase 1b/2, open label, multicenter, dose escalation and dose expansion study of ADG116 in combination with pembrolizumab in patients with advanced/metastatic solid tumors. During dose escalation, ADG116 and pembrolizumab are administered intravenously, Q3W. Primary endpoints are safety and tolerability. Secondary endpoints are PK, ORR per RECIST 1.1, and PFS.

Results As of June 30, 2022, 4 patients have been treated by ADG116 (3 mg/kg) + pembrolizumab (200 mg) combination therapy. Patients were 69 (47-74) years-old [median (range)] and have been heavily pre-treated before enrollment: all 4 (100%) had prior chemotherapy, 1 (25%) radiation therapy, 1 (25%) hormonal therapy; 2 (50%) received ≥ 3 prior lines of therapies, but none had been treated with an anti-PD-1/PD-L1, or an anti-CTLA-4 therapy. ADG116 + Pembro combination showed a manageable safety profile with no DLTs. Most common treatment-related adverse events were Grade 1 nausea (50%) and pruritis (50%). One Grade 3 AE (dehydration) was observed after repeated dosing in Cycle 3 (C3D12). Additional safety and efficacy data will be reported.

Conclusions The current safety data supports the regimen of ADG116 (3 mg/kg)/pembrolizumab (200 mg), Q3W for dose expansion, which is a higher dose than that approved for ipilimumab (1 mg/kg) when in combination with nivolumab for several cancer indications. Additional repeat dosing data are being generated to inform the safety, tolerability, and activity of ADG116 in combination with the anti-PD-1 therapy.

Acknowledgements We would like to acknowledge the editorial support from Ami Celeste Knoefler

Trial Registration Clinical trial identification NCT04501276

REFERENCE

1. G Richardson, A Tolcher, *et al* and P Luo. Phase I dose-finding study of a novel anti-CTLA-4 antibody ADG116 as monotherapy in patients with advanced solid

tumors. *Annals of Oncology*. 2021;**32**(Suppl 7):S1436-S1437 [https://www.annals-oncology.org/article/S0923-7534\(21\)04692-5/fulltext](https://www.annals-oncology.org/article/S0923-7534(21)04692-5/fulltext)

Ethics Approval The study obtained ethics approvals from the following Ethics Committee(s)/Institutional Review Board(s), the number/ID of the approval(s):

1. Salus IRB; ID: IORG0005674
2. Advarra IRB; ID: IORG0000635

All participants of this clinical study gave informed consent before taking part.

Consent Written informed consent was obtained from patients for publication of this abstract and any accompanying images. A copy of the written consent is available for review by the Editor of this journal.

<http://dx.doi.org/10.1136/jitc-2022-SITC2022.0773>

A PHASE 1 STUDY EXPLORING THE SAFETY AND TOLERABILITY OF THE SMALL MOLECULE PD-1 INHIBITOR, INCB086550, IN PATIENTS WITH SELECT ADVANCED TUMORS

¹Christophe Le Tourneau*, ²Sarina Piha-Paul, ³Hans Prenen, ⁴Brant Delafontaine, ⁵David Pinato, ⁶Armando Santoro, ⁷Rebecca Kristeleit, ⁸Kristen Spencer, ⁹Tara Gangadhar, ¹⁰Howard Burris, ¹¹Nuria Kotecki, ¹²Bristi Basu, ¹³Donna Graham, ¹⁴Anna Maria Di Giacomo, ¹⁵Solmaz Sahebjam, ¹⁶Massimo Di Nicola, ¹⁷Carlos Gomez-Roca, ¹⁸Pascale Tomasini, ¹⁹Paolo Ascierto, ²⁰Giuseppe Curigliano, ²¹Thomas Karasic, ²²Ryan Geschwindt, ²³Jeannie Daniel, ²⁴Eric Van Cutsem. ¹Institut Curie, Paris, France; ²University of Texas, Houston, TX, USA; ³Universitair Ziekenhuis – Antwerpen, Antwerp, Belgium; ⁴Drug Research Unit Ghent, Ghent, Belgium; ⁵Imperial College London, London, UK; ⁶Humanitas University, Rozzano-Milan, Italy; ⁷Guy's and St Thomas NHS Foundation Trust, London, UK; ⁸Perlmutter Cancer Center of NYU, Langone health and NYU Grossman School of Medicine, New York, NY, USA; ⁹Abramson Cancer Center, Philadelphia, PA, USA; ¹⁰Tennessee Oncology, Nashville, TN, USA; ¹¹Institut Jules Bordet, Brussels, Belgium; ¹²University of Cambridge, Cambridge, UK; ¹³The Christie NHS Foundation Trust, Manchester, UK; ¹⁴University of Siena, Siena, Italy; ¹⁵Moffitt Cancer Center, Tampa, FL, USA; ¹⁶Fondazione IRCCS Istituto Nazionale Tumori, Milan, Italy; ¹⁷Assistance Publique Des Hôpitaux de Marseille, Marseille, France; ¹⁸Istituto Nazionale Tumori, Milan, Italy; ¹⁹European Institute of Oncology, Milan, Italy; ²⁰Perelman School of Medicine, Philadelphia, PA, USA; ²¹Incyte Corporation, Wilmington, DE, USA; ²²University Hospitals Gasthuisberg, Leuven, Belgium

Background INCB086550 is an orally administered small-molecule inhibitor of programmed cell death ligand 1 (PD-L1). This is an ongoing phase 1, open-label, multicenter study.

Methods Eligible patients are aged ≥ 18 years with advanced solid tumors and Eastern Cooperative Oncology Group performance status of 0–1. Patients had disease progression after treatment with available therapies or were ineligible for or without access to standard treatment. Part 1 uses a modified 3+3 dose-escalation design to identify a maximum tolerated dose (MTD) of INCB086550. Multiple doses are expanded in additional cohorts: part 2 cohort A (tumors that progressed on previous PD-1 treatment), part 2 cohort B (immunotherapy-naïve), part 3 (high microsatellite instability [MSI-H] or deficient mismatch repair), and part 4 (human papilloma virus-positive tumors). The primary endpoints were safety and tolerability measured by monitoring frequency and severity of adverse events (AEs) and to determine a pharmacologically active dose and/or MTD. Tumor response was evaluated per RECIST v1.1 or RANO.

Results As of April 1, 2022, 138 patients received INCB086550 treatment at doses ranging from 100 mg once daily to 800 mg twice daily (bid); median age was 65 years (range, 31–86), 60.9% were women, 80.4% were white. 78 patients (56.5%) had ≥ 2 lines of prior therapy. The most common tumor types were colorectal (13.8%), cervical (10.9%), and anal (10.9%). 121 patients (87.7%) discontinued treatment, 90 of whom discontinued for disease progression. Treatment-emergent AEs (TEAEs) occurring in $>20\%$ of patients were fatigue, nausea, decreased appetite, constipation, vomiting, and diarrhea. Serious TEAEs (SAEs) occurred in 50 patients (36.2%); SAEs occurring in >2 patients were small intestinal obstruction, abdominal pain, intestinal obstruction, and pneumonia. No dose-limiting toxicities (DLTs) occurred. Grade ≥ 3 treatment-related AEs occurred in 18 patients (13.0%), with aspartate aminotransferase increased, fatigue, immune-mediated neuropathy, and rash reported in >1 patient (n=2 each). Sponsor-defined immune-related TEAEs occurred in 41 patients (29.7%), 22 (15.9%) of which were peripheral neuropathies. Stepdown/intermittent dose regimens did not mitigate events of immune-mediated peripheral neuropathy. 16 patients (11.6%) had TEAEs that led to discontinuation of

INCB086550. Two patients (1.4%) achieved a complete response (squamous cell anal cancer, 400 mg bid; MSI-H colorectal cancer, 400 mg bid); 10 patients overall (7.2%) achieved partial response.

Conclusions No DLTs occurred. Encouraging antitumor activity has been observed. INCB086550 has a safety profile consistent with monoclonal antibody immune checkpoint inhibitors, except for an observed increased rate of immune-mediated peripheral neuropathy.

Trial Registration NCT04629339

Ethics Approval This study was reviewed and approved by the institutional review boards of the participating institutions. Approval numbers are: EC/FAHMP (Belgium), P/2020-149; ARS/RHA (Regional Health Authority) (France), 2018-2610; AIFA (Italy), 133700; IRAS (UK), 282291; REC (UK), 20/LO/1001; (USA), RM 598, 1254008, 2018-0765, MOD00971017, 20182238, 1291221. All patients provided written informed consent.

<http://dx.doi.org/10.1136/jitc-2022-SITC2022.0774>

775

INITIAL RESULTS FROM DOSE ESCALATION OF A PHASE 1/2 FIRST-IN-HUMAN, OPEN LABEL STUDY OF AU-007, A MONOCLONAL ANTIBODY THAT BINDS TO IL-2 AND PREVENTS ITS BINDING TO CD25, IN PATIENTS WITH SOLID TUMORS

¹James Vasselli*, ²Paul de Souza, ³Sophia Frentzas, ⁴Andrew Weickhardt, ¹Timothy Wyant, ¹Jenny Tang, ⁵Lori Richards, ¹Aron Knickerbocker, ⁶Inbar Amit, ⁶Yanay Ofra. ¹Aulos Bioscience, San Francisco, CA, USA; ²Southside Cancer Care, Campbelltown, Australia; ³Monash Cancer Center, Melbourne, Australia; ⁴Austin Health, Heidelberg, VT, Australia; ⁵Aulos Biosciences, Oakland, CA, USA; ⁶Biologic Design, Rehovot, Israel

Background AU-007 is a computationally designed monoclonal antibody that binds IL-2 on its CD25 binding epitope. AU-007 bound IL-2 (A/IL-2) cannot bind to trimeric (CD25, CD122, CD132) IL-2 receptors (IL-2R) on Tregs and vascular endothelium, but leaving IL-2's binding to dimeric IL-2Rs (CD122, CD132) on T effector and NK cells unhindered. Therefore AU-007 redirects endogenous or exogenous IL-2 (aldesleukin) towards T effector and NK cell activation, while diminishing Treg activation and vascular leak. Unique in the IL-2 field, AU-007 can bind and redirect endogenous IL-2 generated from A/IL-2 driven T cell expansion in vivo, converting a Treg-mediated autoinhibitory loop into an immunostimulating loop. Additionally, A/IL-2 is expected to substantially prolong the 90-minute T_{1/2} of IL-2, potentially allowing the use of endogenous IL-2 (as A/IL-2) alone to initiate an anti-tumor response. In non-human primates, AU-007 bound IL-2 with a similar affinity to human IL-2 and increased IL-2 serum concentrations in a dose-dependent manner while demonstrating an excellent safety profile.

Methods Phase 1 of this Phase 1/2 study (NCT05267626) consists of 3 dose escalation arms. Each Arm begins with one 1+2 escalation cohort followed by 3+3 escalation cohorts. In Arm 1A, escalating doses of monotherapy AU-007 (Q2W) are evaluated in sequential cohorts. In Arm 1B, AU-007 (Q2W) is evaluated in combination with a single low-dose of aldesleukin with the first AU-007 dose. The AU-007 dose will be fixed with escalating aldesleukin doses in sequential cohorts. In Arm 1C, AU-007 is evaluated in combination with escalating low-doses of aldesleukin, both given Q2W. The AU-007 and aldesleukin dose and schedule for Phase 2 cohort expansion in selected solid tumor types will be based on safety, objective signs of efficacy and PD parameters including increases of IL-2 concentration (as A/IL-2), total lymphocytes, CD8+ T cells, IFN- γ , and soluble CD25.

Results As of July 2022, two patients enrolled into dose escalation Arm 1A, 1 patient on 0.5 mg/kg (First In Human starting dose) and one patient into the second cohort (1.5 mg/kg). AU-007 was well tolerated with no drug related adverse events in the ongoing dose escalation.

Conclusions At this early data cut, AU-007 monotherapy given 0.5 mg/kg Q2W or 1.5 mg/kg Q2W was safe and well tolerated. Data from additional patients are expected to be presented in the poster.

Trial Registration NCT05267626

Ethics Approval HREC: Monash Health Human Research Ethics Committee CT-2021-CTN-03938-1

All of the participants in this study gave informed consent before taking part in the study.

<http://dx.doi.org/10.1136/jitc-2022-SITC2022.0775>

Abstracts

776

ITIL-306-201: A MULTICENTER, FIRST-IN-HUMAN PHASE 1A/1B STUDY OF ITIL-306, AN ENGINEERED AUTOLOGOUS TUMOR-INFILTRATING LYMPHOCYTE (TIL) CELL THERAPY PRODUCT, IN ADULTS WITH ADVANCED SOLID TUMOR

¹Jeffrey Ward*, ¹Armin Ghobadi, ²John Liao, ³Adam Schoenfeld, ²Scott Tykodi, ⁴Yizhou Jiang, ⁴John Le Gall, ⁴Ruben Alvarez-Rodriguez, ⁴Marika Sherman, ⁴Tiffany Singson, ⁴Jeffrey Mc Leroy. ¹Washington University School of Medicine and Siteman Cancer Center, Saint Louis, MO, USA; ²University of Washington and Fred Hutchinson Cancer Center, Seattle, WA, USA; ³Memorial Sloan Kettering Cancer Center, New York, NY, USA; ⁴Instil Bio, Inc., Dallas, TX, USA

Background Pioneering work in advanced melanoma has prompted investigation of TIL cell therapy in other immunogenic solid tumor indications.¹⁻³ Although TILs encompass a broad diversity of antitumor reactivities with an unrestricted T-cell receptor (TCR) repertoire, their activity may be limited in certain tumors.⁴ Addition of synthetic costimulation improves T-cell functional activity while maintaining the diverse antigen specificity of TILs (figure 1).⁵ In a murine model with a human solid tumor xenograft, the anti-folate receptor alpha (FR α) costimulatory antigen receptor (CoStAR) significantly enhanced T-cell proliferation, persistence, and antitumor activity without exogenous IL-2 support, resulting in enhanced tumor control and prolonged survival.⁶ ITIL-306 is an engineered autologous TIL cell therapy that supplements native TCR-specific antigen recognition with synthetic costimulation upon engagement with FR α . ITIL-306-201 is a multicenter, single-arm, phase 1a/1b dose escalation and expansion study evaluating the safety and feasibility of ITIL-306 in adult patients with advanced epithelial ovarian cancer (EOC), non-small cell lung cancer (NSCLC), and renal cell carcinoma (RCC) who relapsed from or are refractory to ≥ 1 prior line of systemic therapy.

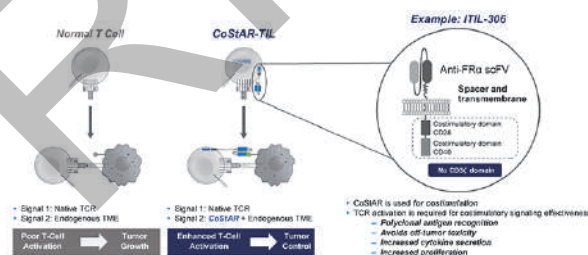
Methods Eligible patients are aged ≥ 18 years with histologically confirmed EOC, NSCLC, or RCC that has progressed during or after ≥ 1 prior line of systemic standard-of-care therapy, have ECOG performance status 0-1, and have viable tumor tissue that is suitable to resect with ≥ 2 grams for TIL harvest. Patients will be enrolled in phase 1a (dose escalation in a standard 3+3 design; n \approx 6-18) or 1b (expansion; n \approx 15 in each of 3 cohorts, 1 for each tumor type; Figure 2). Following tumor resection for TIL harvest, patients must have ≥ 1 remaining measurable lesion per RECIST v1.1.⁷ Patients will receive a reduced dose of lymphodepleting chemotherapy followed by a single, intravenous fixed-dose of ITIL-306 in phase 1a (1 of 3 dose levels) or 1b (dose selected in the phase 1a portion) and no post-infusion IL-2. The phase 1a primary endpoint is incidence of dose-limiting toxicities. The phase 1b primary endpoint is frequency and severity of treatment-emergent adverse events (AEs), serious AEs, and AEs of special interest. Secondary endpoints include manufacturing success rate, objective response rate per modified RECIST v1.1,⁷ disease control rate, best overall response, time to response, duration of response, progression-free survival, and overall survival. Key exploratory endpoints include association of biomarkers with response (eg, tumor FR α expression) and characterization of ITIL-306 activation, trafficking, persistence, and phenotype. The study is open (NCT05397093).

Acknowledgements Medical writing support was provided by Christopher Waldapfel, PharmD, of Instil Bio, Inc. and Jennifer Yang, PhD, of Nexus Global Group Science, with funding from Instil Bio, Inc.

REFERENCES

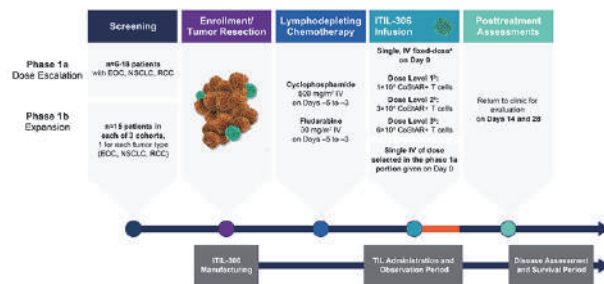
1. Dafni U, Michielin O, Lluemas SM, et al. Efficacy of adoptive therapy with tumor-infiltrating lymphocytes and recombinant interleukin-2 in advanced cutaneous melanoma: a systematic review and meta-analysis. *Ann Oncol.* 2019;**30**(12):1902–1913.
2. Andersen R, Westergaard MCW, Kjeldsen JW, et al. T-cell responses in the micro-environment of primary renal cell carcinoma-implications for adoptive cell therapy. *Cancer Immunol Res.* 2018;**6**(2):222–235.
3. Creelan B, Wang C, Teer J, et al. Abstract CT056: Durable complete responses to adoptive cell transfer using tumor infiltrating lymphocytes (TIL) in non-small cell lung cancer (NSCLC): a phase I trial. *Cancer Research.* 2020;**80**(16 supplement):CT056–CT056.
4. Rohaan MW, van den Berg JH, Kvistborg P, et al. Adoptive transfer of tumor-infiltrating lymphocytes in melanoma: a viable treatment option. *J Immunother Cancer.* 2018;**6**(1):102.
5. Sukumaran S, Kalaitidou M, Mojadidi M, et al. Costimulatory antigen receptor (CoStAR): a novel platform that enhances the activity of tumor infiltrating lymphocytes (TILs). *J Immunother Cancer.* 2021;**9**(Suppl 2):198.
6. Moon O, Qu Y, King, MG, et al. *J Clin Oncol.* 2022;**40**(16_suppl):2535.
7. Eisenhauer EA, Therasse P, Bogaerts J, et al. New response evaluation criteria in solid tumours: Revised RECIST guideline (version 1.1). *Eur J Cancer.* 2009;**45**(2):228–47.

Ethics Approval All patients will provide written informed consent. The study will be approved by the Institutional Review Board/Independent Ethics Committee at each site and conducted in accordance with the Good Clinical Practice Guidelines of the International Council for Harmonisation.



Abstract 776 Figure 1 CoStAR Platform Overview

The novel CoStAR platform is engineered to enhance TIL functional activity. Similar to unmodified T cells, CoStAR TILs require specific antigen recognition via the native TCR for activation. CoStAR ligand engagement also provides T cells with synthetic costimulatory signals that enhance antitumor responses. Therefore, CoStAR-expressing T cells supplement tumor-specific antigen recognition via TCR with a robust costimulatory signal delivered via CoStAR. CoStAR, costimulatory antigen receptor; FR α , folate receptor alpha; scFv, single-chain variable fragment; TCR, T-cell receptor; TIL, tumor-infiltrating lymphocyte; TME, tumor microenvironment.



Abstract 776 Figure 2 ITIL-306-201 Phase 1a/1b Treatment Schema ITIL-306-201 is a phase 1a/1b dose escalation and expansion study evaluating the safety and feasibility of ITIL-306 in adult patients with advanced EOC, NSCLC, and RCC who relapsed from or are refractory to ≥ 1 prior line of systemic standard-of-care therapy.

^a Enrollment at the next dose level will be based on the incidence of dose-limiting toxicities observed within each dose level. Enrollment into

dose levels will continue sequentially until a maximum-tolerated dose is reached, or all dose levels have been tested. If the dose-limiting toxicity threshold is not met at the highest dose level, then dose level 3 will be selected for testing in phase Ib.

^b ± 20% target dose.

EOC, epithelial ovarian, fallopian tube, and peritoneal carcinomas; IV, intravenous; NSCLC, non-small cell lung cancer; RCC, renal cell carcinoma; TIL, tumor-infiltrating lymphocyte.

<http://dx.doi.org/10.1136/jitc-2022-SITC2022.0776>

PREPRINT

777

INITIAL CLINICAL CHARACTERIZATION OF NOVEL PROXIMAL BIOMARKERS FOR NX-1607, A FIRST-IN-CLASS ORAL CBL-B INHIBITOR, IN PATIENTS WITH ADVANCED MALIGNANCIES

¹Sarah Whelan*, ¹Christopher Karim, ¹Jordan Ye, ¹Timothy Ingallinera, ¹Ganesh Cherala, ¹Katherine Jameson, ²Anja Williams, ³Adam Sharp, ⁴Matthew Krebs, ⁵Simon Pacey, ⁶Sarah Blagden, ⁷Ruth Plummer, ⁸Daniel Hochhauser, ⁹Jeff Evans, ¹⁰Johann De Bono, ¹Janine Powers. ¹Nurix Therapeutics, Inc., San Francisco, CA, USA; ²Sarah Cannon Research Institute UK, London, UK; ³Royal Marsden NHS Foundation Trust, Sutton, UK; ⁴The Christie NHS Foundation Trust, Manchester, UK; ⁵University of Cambridge, Cambridge, UK; ⁶University of Oxford, Oxford, UK; ⁷Newcastle University Centre for Cancer, Newcastle-upon-Tyne, UK; ⁸University College Hospital, London, UK; ⁹CR-UK Beatson Institute, Glasgow, UK; ¹⁰Institute of Cancer Research, London, UK

Background Casitas B-lineage lymphoma proto-oncogene B (CBL-B) is an E3 ubiquitin ligase expressed in multiple immune cell lineages and is a master regulator of the immune response. NX-1607 is a first-in-class oral small molecule inhibitor of CBL-B that has demonstrated potent anti-tumor activity in animal models by reversing T cell dysfunction and overcoming suppressive signaling in the tumor microenvironment.¹ Nurix has identified and characterized novel proximal biomarkers of CBL-B inhibition that correlate with anti-tumor activity in syngeneic tumor models. Assays for these biomarkers characterize the activity of NX-1607 in a first-in-human clinical trial (NCT05107674).

Methods Agnostic screening campaigns utilizing flow cytometry protein phosphorylation signals and mass spectrometry-based methods to measure direct ubiquitination substrates identified multiple proprietary proximal biomarkers of CBL-B inhibition in activated T cells. Validation of these biomarkers in mouse and non-human primate (NHP) *in vivo* models, coupled with allometric scaling of pharmacokinetic (PK) profiles, were used to inform clinical dose selection. PK and pharmacodynamic (PD) data are currently being monitored in a Phase I trial with daily oral dosing in 21-day cycles.

Results Phosphorylated hematopoietic lineage cell-specific protein 1 (pHS1), a regulator of T cell-receptor signaling, was identified as a robust and reproducible biologically relevant proximal biomarker for monitoring pharmacologic inhibition of CBL-B in whole blood. Validation of proximal biomarkers *in vivo* demonstrated target engagement with dose-dependent increases of pHS1 in CD8+ T cells in both mice and NHP dosed orally with NX-1607. As of June 16, 2022, 10 patients have enrolled on study at 4 ascending oral dose levels (5, 15, 25 and 50 mg once daily). Dose-proportional increases of pHS1-expressing T cells were observed in cycle 1. Preliminary PK data suggest a half-life of 4 to 9 hours and dose-proportional exposures with no apparent accumulation. Together these data are consistent with preclinical human dose projections and compare to pHS1 levels associated with anti-tumor activity in mouse models.

Conclusions NX-1607 is a first-in-class oral CBL-B inhibitor displaying linear PK, dose-dependent target engagement as measured by the validated proximal biomarker, pHS1, and downstream signals of T cell engagement. PK and PD data derived from non-clinical and clinical studies have shown remarkable concordance with biomarker levels observed in the clinic corresponding to those levels associated with potent anti-tumor activity observed in mouse models. The study continues to enroll, and updated PK and PD data will be presented.

Trial Registration NCT05107674

REFERENCE

1. Rountree R, Cohen F, Tenn-McClellan A, et al. Small molecule inhibition of the ubiquitin ligase CBL-B with NX-1607 results in potent T and NK cell mediated anti-tumor response. *Cancer Res.* 2021;**81**(Suppl. 13; poster #1595).

Ethics Approval The study obtained ethics committee(s) approval, and participants gave informed consent before taking part.

<http://dx.doi.org/10.1136/jitc-2022-SITC2022.0777>

778

BOTENSILIMAB, A NOVEL INNATE/ADAPTIVE IMMUNE ACTIVATOR, PLUS OR MINUS BALSTILIMAB (ANTI-PD-1) IN "COLD" AND I-O REFRACTORY METASTATIC SOLID TUMORS

¹Breelyn Wilky*, ²Anthony El-Khoueiry, ³Andrea Bullock, ⁴Apostolia Tsimberidou, ⁵Daruka Mahadevan, ⁶Kim Margolin, ⁷Jonathan Trent, ⁸Bruno Bockorny, ⁹Justin Moser, ⁷Peter Hosein, ⁹Marwan Fakih, ¹⁰Benjamin Schlecter, ²Jacob Thomas, ¹¹Ani Balmanoukian, ¹²Rachel Sanborn, ¹³Ghassan Abou-Alfa, ¹⁴Gary Schwartz, ²Diana Hanna, ¹⁵Waldo Ortuzar Feliu, ¹⁵Joseph Grossman, ¹⁵Katherine Rosenthal, ¹⁵James Godwin, ¹⁵Jaymin Patel, ¹⁵Bonnie Bullock, ¹⁶Justin Stebbing, ¹⁵Bhupendra Rawal, ¹⁵Hunter Cole, ¹⁵Chloe Delepine, ¹⁵Jacky Chow, ¹⁵Ross Walker, ¹⁵Chris MacDermaid, ¹⁵Dhan Chand, ⁸Michael Gordon, ²Heinz-Josef Lenz, ¹⁷Steven O'Day. ¹University of Colorado Cancer Center, Aurora, CO, USA; ²University of Southern California Norris Comprehensive Cancer Center, Los Angeles, CA, USA; ³Beth Israel Deaconess Medical Center, Boston, MA, USA; ⁴The University of Texas MD Anderson Cancer Center, Houston, TX, USA; ⁵The University of Texas Health Sciences Center at San Antonio, San Antonio, TX, USA; ⁶Providence Saint John's Cancer Institute, Santa Monica, CA, USA; ⁷Sylvester Comprehensive Cancer Center, University of Miami, Miami, FL, USA; ⁸HonorHealth Research and Innovation Institute, Scottsdale, AZ, USA; ⁹City of Hope Comprehensive Cancer Center, Duarte, CA, USA; ¹⁰Dana-Farber Cancer Institute, Boston, MA, USA; ¹¹The Angeles Clinic and Research Institute, Los Angeles, CA, USA; ¹²Earle A. Chiles Research Institute, Providence Cancer Institute, Portland, OR, USA; ¹³Memorial Sloan Kettering Cancer Center, New York, NY, USA; ¹⁴Herbert Irving Comprehensive Cancer Center, Columbia University School of Medicine, New York, NY, USA; ¹⁵Agenus, Lexington, MA, USA; ¹⁶Agenus and Imperial College London, Lexington, MA, USA; ¹⁷Agenus and Providence Saint John's Cancer Institute*, Lexington, MA, USA

Background Botensilimab (BOT) promotes optimized T cell priming, activation and memory formation by strengthening antigen presenting cell/T cell co-engagement. As an Fc-enhanced next-generation anti-CTLA-4 antibody, BOT also promotes intratumoral Treg depletion and reduces complement fixation. We present results from patients with metastatic solid tumors treated with BOT±balstilimab (BAL; anti-PD-1) in an expanded phase IA/B study; NCT03860272.

Methods Patients received either BOT monotherapy at 0.1-3 mg/kg every 3 weeks (Q3W), BOT monotherapy 1 or 2mg/kg every 6 weeks (Q6W), BOT 0.1-2mg/kg Q6W+BAL 3 mg/kg every 2 weeks, or a fixed-dose of BOT 150mg Q6W+BAL 450mg Q3W. Unconfirmed responses are included. Of the 44 BOT monotherapy patients, 13 crossed over to combination.

Results 142 patients (98 combination, 44 monotherapy [13 crossover]) were evaluable for efficacy/safety (treated as of April 7, 2022 with ≥1 Q6W tumor-imaging assessment). Patients had immunologically cold and/or immunotherapy resistant tumors and were heavily pretreated: 61% received ≥3 prior lines of therapy including 34% prior immunotherapy. Median follow-up was 6.1 months.

Disease-specific combination therapy cohorts are being expanded with BOT at 1 or 2mg/kg or 150mg+BAL (including 4 crossover patients): (1) microsatellite stable (MSS) colorectal cancer (n=44, ORR 25%), (2) platinum resistant ovarian cancer (n=18, ORR 28%), (3) sarcoma (n=12, ORR 42%), and (4) PD-(L)1 relapsed/refractory non-small cell lung cancer (n=3, ORR 67%).

The ORR was 22% (22/98; 3 CR/19 PR) with median duration of response [DOR] not reached (range, 1.4+ to 19.5+ months) in all combination patients (BAL+BOT 0.1-2 mg/kg or 150 mg); 13/22 responses are ongoing. In addition, 15% (2/13) monotherapy patients achieved PR after crossing over to combination therapy. The ORR was 11% (5/44; 1 CR/4 PR) in all monotherapy patients (BOT 0.1-3 mg/kg). Responses were independent of PD-L1 expression and tumor mutation burden. Further evaluation of biomarkers is ongoing including paired biopsies (before/during treatment).

Grade 1/2, 3 or 4 treatment-related adverse events (TRAE) occurred in 88%, 29%, 2% respectively. Diarrhea/colitis (19%) was the only grade 3/4 TRAE occurring in ≥5% of patients. There were no cases of hypophysitis or myocarditis. Pneumonitis occurred in 4 patients (3%). Two patients had grade 5 TRAEs (enterocolitis, colonic perforation).

Conclusions BOT±BAL demonstrates remarkable activity in heavily pretreated patients with solid tumors historically unresponsive to immunotherapy. The safety profile is consistent with the mechanism of action of BOT. Randomized studies in MSS CRC, pancreatic cancer, and melanoma are planned to open this year.

Trial Registration NCT03860272

<http://dx.doi.org/10.1136/jitc-2022-SITC2022.0778>

779

A PHASE I, DOSE ESCALATION AND EXPANSION STUDY OF PT199, A NEXT GENERATION CD73 MONOCLONAL ANTIBODY, ADMINISTERED ALONE AND IN COMBINATION WITH A PD-1 INHIBITOR IN ADULT PATIENTS WITH ADVANCED SOLID TUMORS

Ramzi Melhem*, Harold Wright, Hui Zou, Claudia Ramos, Jack Li, Ming Wang. *Phanes Therapeutics, San Diego, CA, USA*

Background PT199 is an anti-CD73 monoclonal antibody (mAb) with a differentiated mechanism of action. PT199 is designed to counter the adenosine-mediated immunosuppressive tumor microenvironment, rendering antitumor immune cells more responsive to checkpoint immunotherapies, such as PD-1/PD-L1 inhibitors. PT199 fully inhibits both soluble and membrane-bound CD73, unlike some other CD73 inhibitors which may inhibit only one form of enzyme or exhibit incomplete inhibition. Moreover, at higher concentrations no loss of inhibition or “hook effect” is observed with PT199, unlike with some other CD73 inhibitors in clinical development. Hence, PT199 addresses the limitations of current CD73 inhibitors and is expected to increase antitumor immune activation, especially in combination with PD-1 pathway inhibition, and thus offers a new treatment option for cancer patients.

Methods This study is evaluating the safety, tolerability, pharmacokinetics, pharmacodynamics, and preliminary efficacy of PT199 alone and in combination with a PD-1 inhibitor, in patients with locally advanced or metastatic solid tumors that have progressed after all available standard therapy or for which standard therapy has proven to be ineffective, intolerable, or is considered inappropriate. Approximately 32-38 patients will be enrolled. The study consists of 3 parts: Monotherapy Dose Escalation, Combination Therapy Dose Escalation, and Combination Dose Expansion. The dose escalation study of PT199 will be guided by a standard 3+3 dose escalation study design to determine the maximum tolerated dose (MTD) and/or the dose recommended for dose expansion (DRDE). The MTD and/or DRDE will be further evaluated in a dose expansion cohort and a recommended phase II dose (RP2D) may be determined based on the totality of the safety, pharmacokinetics (PK), pharmacodynamics (PD), and efficacy data obtained from both dose escalation and expansion cohorts. Each enrolled patient will receive PT199 as a monotherapy (10, 20, or 30 mg/kg QW) as an intravenous infusion continuously in 21-day cycles or in combination with a PD-1 inhibitor.

Results The primary endpoints are Dose Limiting Toxicity and MTD, if reached, and RP2D of PT199 as a single agent and/or in combination with a PD-1 inhibitor. PD assessments will include measurements of CD73 enzyme activity and cytokines in serum and CD73/PD-L1 expression in tumor tissues.

Conclusions The study is currently enrolling. Preliminary safety and efficacy data is anticipated the middle of next year.

Trial Registration NCT05431270

Ethics Approval The study obtained ethics approval through a central IRB (Advara IRB: Pro00063442). All participants have given informed consent before taking part in this trial.

<http://dx.doi.org/10.1136/jitc-2022-SITC2022.0779>

780

SRK-181, A LATENT TGF β 1 INHIBITOR: SAFETY, EFFICACY, AND BIOMARKER RESULTS FROM THE DOSE ESCALATION PORTION OF A PHASE I TRIAL (DRAGON TRIAL) IN PATIENTS WITH ADVANCED SOLID TUMORS

¹Timothy Yap*, ²Justin Gainor, ³Meredith McKean, ³Melissa Johnson, ⁴Bruno Bockorny, ⁵Minal Barve, ⁶Randy Sweis, ⁷Ulka Vaishampayan, ⁸Ahmad Tarhini, ⁹Deepak Kilari, ¹⁰Yawen Ju, ¹⁰Si-Tuen Lee-Hoeflich, ¹⁰Stephen DeWalt, ¹⁰Lan Liu, ¹⁰Nisha Shah, ¹⁰Ann Marie Kennedy, ¹⁰Lu Gan. ¹The University of Texas MD Anderson Cancer Center, Houston, TX, USA; ²Massachusetts General Hospital Harvard Medical School, Boston, MA, USA; ³Sarah Cannon Research Institute, Nashville, TN, USA; ⁴Beth Israel Deaconess Medical Center, Boston, MA, USA; ⁵Mary Crowley Cancer Research, Dallas, TX, USA; ⁶University of Chicago, Chicago, IL, USA; ⁷University of Michigan, Ann Arbor, MI, USA; ⁸Moffitt Cancer Center, Tampa, FL, USA; ⁹Medical College of Wisconsin, Milwaukee, WI, USA; ¹⁰Scholar Rock, Inc., Cambridge, MA, USA

Background Transforming growth factor-beta 1 (TGF β 1) plays an important role in mediating the primary resistance to PD-1/PD-L1 [PD-(L)1] blockade. SRK-181 is a fully human, selective anti-latent TGF β 1 IgG4 monoclonal antibody under investigation as a monotherapy or in combination with anti-PD(L)1 therapy in patients with solid tumors. Compared to broad TGF β inhibitors, SRK-181 was observed to have improved safety profile (no cardiotoxicities) in four-week GLP nonclinical toxicology studies.

Methods The DRAGON trial (NCT04291079) is an ongoing open-label, phase 1 study. Part A followed a 3+3 dose escalation design to evaluate SRK-181 in patients with advanced solid tumors at 80-3000mg every three weeks (q3w) and 2000mg q2w in Part A1, and SRK-181+anti-PD-(L)1 in patients who did not respond to prior anti-PD-(L)1 therapy at 240-2400mg q3w in Part A2. In Part B (expansion phase), SRK-181 (1500mg q3w or 1000mg q2w)+anti-PD-(L)1 are administered in anti-PD-(L)1-resistant patients with non-small cell lung cancer (NSCLC), urothelial carcinoma, melanoma, clear cell renal cell carcinoma (ccRCC) or other advanced solid tumors. The level of circulatory TGF β 1 was assessed as a target engagement biomarker.

Results As of 2 June 2022, Part A1 and Part A2 enrolled 19 and 15 patients, respectively, with median prior lines of therapies of 4 (range 1-10). No dose limiting toxicity (DLT) were observed in Part A. In Part A1, the most common treatment-related AEs (TRAEs, >10%) of any grade were fatigue (16%, n=3), decreased appetite and nausea (each: 11%, n=2). Eight patients had stable disease (SD) as best response (3/colorectal, 3/ovarian, 1/pancreatic, and 1/testicular). The three patients with ovarian cancer were stable for 25 to 42 weeks. In Part A2, the TRAEs (>10%) of any grade were pruritus, rash and rash maculo-papular (each: 20%, n=3), diarrhea (13%, n=2). One confirmed RECIST1.1 partial response (PR) was observed at 800mg in a patient with anti-PD-1 resistant RCC who stayed on study for 30 weeks. Nine patients had best response of SD and five of them were stable for more than 16 weeks (2/head and neck, 1/melanoma, 1/skin squamous cell carcinoma, 1/RCC). SRK-181 treatment resulted in increased levels of circulatory TGF β 1, which suggested target engagement. Part B enrollment is ongoing.

Conclusions As of 2 June 2022, SRK-181 has been tolerated as monotherapy and in combination with anti-PD-(L)1. No DLT was observed up to 3000mg q3w/2000mg q2w as monotherapy and up to 2400mg q3w as combination treatment. Early evidence of efficacy was observed with prolonged stable disease and a confirmed PR.

<http://dx.doi.org/10.1136/jitc-2022-SITC2022.0780>

DELTA-2: A PHASE 1, OPEN-LABEL, MULTICENTER STUDY OF ITIL-168, AN AUTOLOGOUS TUMOR-INFILTRATING LYMPHOCYTE (TIL) CELL THERAPY, WITH PEMBROLIZUMAB IN PATIENTS WITH ADVANCED SOLID TUMORS

¹Oladapo Yeku*, ²Daniel Olson, ³Jeffrey Ward, ⁴Sandip Patel, ⁵Jeff Aycock, ⁵Amber Donahue, ⁵Yizhou Jiang, ⁵John Le Gall, ⁵Zachary Roberts, ⁵Rubén Alvarez-Rodríguez, ⁵Judy Seng, ⁵Tong Shen, ⁵Nishi Kothari. ¹Massachusetts General Hospital, Harvard Medical School, Boston, MA, USA; ²The University of Chicago Medical Center, Chicago, IL, USA; ³Washington University School of Medicine and Siteman Cancer Center, Saint Louis, MO, USA; ⁴University of California San Diego, La Jolla, CA, USA; ⁵Instil Bio, Inc., Dallas, TX, USA

Background Despite the benefits of immune checkpoint inhibitors (ICIs) in solid tumors, additional treatment options are needed for patients with primary or acquired resistance.¹ TILs are present in various solid tumors, and TIL therapy has demonstrated efficacy and durable responses in some advanced solid tumors due to its antitumor reactivity and broad T-cell repertoire.²⁻⁴ Additionally, preclinical data suggest ICIs may further support the persistence of TILs in immunogenic tumors.⁵ Here, we describe a study that will explore the safety, feasibility, and preliminary efficacy of an autologous TIL therapy, ITIL-168, in combination with pembrolizumab in patients with cervical cancer (CC), head and neck squamous-cell carcinoma (HNSCC), or non-small cell lung cancer (NSCLC).

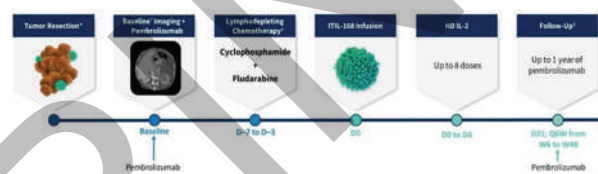
Methods DELTA-2 (NCT05393635) is an ongoing phase 1, multicenter, multicohort, open-label trial evaluating ITIL-168 with pembrolizumab in previously treated patients with advanced solid tumors. Patients will be enrolled in 1 of 3 cohorts (n≈9-15 patients per cohort): advanced CC (Cohort 1), HNSCC (Cohort 2), or NSCLC (Cohort 3). Eligible patients must have progressed during or following ≥1 prior line of chemotherapy along with an ICI. EGFR mutations or ALK translocations in NSCLC are included in Cohort 3, and patients are required to have progressed on targeted therapy but not ICI. Eligibility criteria across all cohorts include ECOG PS ≤1, adequate organ function, resectable tumor lesion(s), and ≥1 remaining measurable lesion per RECIST v1.1 post-tumor resection. Bridging therapy is allowed but must be discontinued at least 2 weeks or 5 half-lives before baseline imaging. Patients with prior cell therapy treatment, symptomatic and/or untreated central nervous system metastases, or requiring chronic steroids are ineligible. Treatment will include lymphodepleting chemotherapy (the dosage of cyclophosphamide and fludarabine will be adjusted based on cohort and patient comorbidities) followed by a single infusion of ITIL-168 and up to 8 doses of high-dose IL-2 (figure 1). Patients will receive pembrolizumab at baseline before ITIL-168 infusion, day 21 postinfusion, and then every 6 weeks for ≤48 weeks or until disease progression or intolerable toxicity. An interim and a primary analysis for each cohort will be conducted. The primary endpoint is the frequency and severity of ITIL-168 treatment-emergent adverse events (AEs) per Common Terminology Criteria for AEs version 5.0. Secondary endpoints include manufacturing success rate, objective response rate per modified RECIST v1.1, duration of response, progression-free survival, and overall survival. The study opened in July 2022 and is currently recruiting patients.

Acknowledgements Medical writing support was provided by Christopher Waldapfel, PharmD, of Instil Bio, Inc. and Lauryn Samelko, PhD, and Phylcia Aaron, PhD, of Nexus Global Group Science, with funding from Instil Bio, Inc.

REFERENCES

1. Nordstrom BL, Hamilton M, Collins JM, *et al.* Treatment patterns and outcomes following disease progression on anti-PD-1 therapies for advanced melanoma. *Future Oncol.* 2022;**18**:1343–1355.
2. Gooden MJ, de Bock GH, Leffers N, Daemen T, Nijman HW. The prognostic influence of tumour-infiltrating lymphocytes in cancer: a systematic review with meta-analysis. *Br J Cancer.* 2011;**105**(1):93–103.
3. van den Berg JH, Heemskerk B, van Rooij N, *et al.* Tumor infiltrating lymphocytes (TIL) therapy in metastatic melanoma: boosting of neoantigen-specific T cell reactivity and long-term follow-up. *J Immunother Cancer.* 2020;**8**:e000848.
4. Borch TH, Andersen R, Ellebaek E, *et al.* Future role for adoptive T-cell therapy in checkpoint inhibitor-resistant metastatic melanoma. *JITC.* 2020;**8**:e000668.
5. Donia M, Kjeldsen JW, Andersen R, *et al.* PD-1+ polyfunctional T cells dominate the periphery after tumor-infiltrating lymphocyte therapy for cancer. *Clin Cancer Res.* 2017;**23**:5779–5788.

Ethics Approval All patients will provide written informed consent. The study will be approved by the Institutional Review Board/Independent Ethics Committee at each site and conducted in accordance with the Good Clinical Practice Guidelines of the International Council for Harmonisation.



Abstract 781 Figure 1 DELTA-2 Treatment Schema

DELTA-2 is a phase 1 trial evaluating the safety, feasibility, and preliminary efficacy of ITIL-168 in combination with pembrolizumab in patients with select advanced solid tumors with progressive disease during or after 1 prior line of treatment.

*Tumor resection occurs within 30 days after patient consent, followed by optional bridging therapy.

†Baseline visit occurs within 14 days prior to lymphodepleting chemotherapy, followed by pembrolizumab (200 mg).

‡Cohorts 1/3 will receive lymphodepleting chemotherapy on days –7 to –3; Cohort 2 will receive lymphodepleting chemotherapy on days –5 to –3.

§Pembrolizumab is administered once on day 21 (200 mg), followed by every 6 weeks from weeks 6 to 48 (400 mg).

D, day; HD, high-dose; IL-2, interleukin-2; Q6W, every six weeks; W, week.

<http://dx.doi.org/10.1136/jitc-2022-SITC2022.0781>

782

INTRATUMORAL SOTIGALIMAB WITH PEMBROLIZUMAB ACTIVATES ANTIGEN-PRESENTING CELLS AND INDUCES LOCAL AND DISTANT ANTI-TUMOR RESPONSES IN FIRST-LINE METASTATIC MELANOMA: RESULTS OF A PHASE I/II STUDY

<http://dx.doi.org/10.1136/jitc-2022-SITC2022.0782>

Salah-Eddine Bentebibel*, Daniel Johnson, Barbara Pazdrak, Daniel McGrail, Srisuda Lecagoonporn, Cara Haymaker, Dzifa Y Duose, Khalida Wani, Heather Sonnemann, Houssein Safa, Jared K Burks, Patrick Hwu, Cho Sunghnam, Chantale Bernatchez, Suhendan Ekmekcioglu, Gregory Lizée, Adi Diab. *The University of Texas MD Anderson, Houston, TX, USA*

Background Checkpoint inhibitors (CPI) provide significant clinical benefits for patients with metastatic melanoma (MM). However, the majority of patients do not respond or develop resistance after initial tumor regression. In this ongoing phase I/II study, we assessed intratumoral sotigalimab, a CD40 agonistic antibody in combination with systemic pembrolizumab in CPI treatment naïve MM.

Methods As of May 15, 2022, thirty-two patients were enrolled. Patients received sotigalimab every 3 weeks for a total of 4 doses. The primary objectives include safety and tolerability, determination of the recommended phase 2 dose (RP2D), and assessment of the overall response rate (ORR) by RECIST v1.1. Biomarker analyses of blood and tumor samples were performed to measure immune activation using imaging mass cytometry, TCR sequencing, and a cross-cohort comparison of gene expression data (sotigalimab plus pembrolizumab versus anti-PD-1 monotherapy). Single-nucleus ATAC and RNA sequencing are being performed to determine cell-type-specific chromatin accessibility and transcriptional profiles associated with clinical response.

Results The combination therapy has been well-tolerated, and there were no study discontinuations or death due to treatment-related adverse events, most common treatment-related adverse events were injection-site reactions. Efficacy analysis of thirty patients with disease evaluations demonstrated an ORR of 50% in distant lesions and a disease control rate of 67%. The ORR at the RP2D of 10 mg is 55% (12/22). Responses were observed in PD-L1 negative patients and those with elevated LDH. Multi-omics analysis of peripheral blood mononuclear cells and tumor biopsies demonstrate that sotigalimab effectively engaged CD40 pathway. In comparison to anti-PD-1 monotherapy, the combination therapy significantly increased expression of genes associated with antigen presentation and effector T-cells in local lesions accompanied by an increase in T cell activation genes at distant lesions. Additionally, combination therapy resulted in an increase in clonality with expansion of new clones shared between local and distant lesions. All these immunologic changes were correlated with clinical response. Findings were recapitulated in B16 melanoma pre-clinical model, which demonstrated that intratumoral CD40 activation synergizes with systemic anti-PD-1 therapy and suppress tumor growth. Therapeutic efficacy was associated with increases in intratumoral conventional type 1 dendritic cells (cDC1), CD8⁺ T cells, and an increased ratio of intratumoral CD8⁺ T cells to myeloid-derived suppressor cells.

Conclusions This combination therapy is well tolerated and has a notable clinical response rate, accompanied by broad innate and adaptive immune activation at both local and distant lesions. More biomarker and clinical response data are anticipated in November.

Trial Registration NCT02706353

Ethics Approval The study was approved by FDA and the Institutional Review Board

783

TRIAL IN PROGRESS: A PHASE 1/2 OPEN-LABEL STUDY (IOV-GM1-201) OF TALEN-MEDIATED PD-1-INACTIVATED AUTOLOGOUS TUMOR-INFILTRATING LYMPHOCYTES (TIL; IOV-4001) IN PATIENTS WITH ADVANCED MELANOMA AND NSCLC

¹Allison Betof*, ²Trisha Wise-Draper, ³Kai He, ⁴Amod Sarnaik, ⁵Jonathan Thompson, ⁶Friedrich Finckenstein, ⁶Parameswaran Hari, ⁶Madan Jagasia, ⁶Anjali Desai, ⁶Akiko Suzuki, ⁶Xiao Wu, ⁷Jason Chesney. ¹Memorial Sloan Kettering Cancer Center, New York, NY, USA; ²University of Cincinnati Cancer Center (UCCC), Cincinnati, OH, USA; ³Ohio State University, Columbus, OH, USA; ⁴H. Lee Moffitt Cancer Center, Tampa, FL, USA; ⁵Medical College of Wisconsin, Froedtert Hospital Cancer Center, Milwaukee, WI, USA; ⁶Iovance Biotherapeutics, Inc., San Carlos, CA, USA; ⁷James Graham Brown Cancer Center, University of Louisville, Louisville, KY, USA

Background Adoptive cell therapy with TIL has demonstrated efficacy in patients with advanced solid tumors, both as monotherapy in melanoma,¹ NSCLC,² and cervical cancer,³ and in combination with anti-PD-1 therapy in melanoma, head and neck cancer, and cervical cancer.⁴ IOV-4001 is a TALEN®-mediated *PDCD-1* knockout autologous TIL cell therapy product. Preclinical studies suggest that PD-1 inactivation by *PDCD-1* gene knockout may enhance TIL cell therapy efficacy, with similar quality attributes and phenotypes to those of non-edited TIL.⁵

Methods This first-in-human phase 1/2, open-label, non-randomized, multicenter study (NCT05361174; open to enrollment) will enroll ~53 adult patients. During the phase 1 portion, enrollment and dose level decisions will be based on emerging safety and tolerability data in a 28-day dose-limiting toxicity (DLT) observation period.

Cohort 1 will include patients with unresectable/metastatic melanoma that has progressed during/within 12 weeks of last anti-PD-1/PD-L1 dose (patients must have also received a BRAF ± MEK inhibitor if *BRAF V600* mutation-positive). Cohort 2 will include patients with advanced NSCLC who have received ≤3 prior therapies and whose disease progressed either: (1) during/within 12 weeks after last anti-PD-1/PD-L1 dose (patients without oncogene driver mutations) or (2) during/after ≥1 targeted therapy and either platinum doublet chemotherapy or during/within 12 weeks after last anti-PD-1/PD-L1 dose (patients with oncogene-driven tumors). Patients must have ECOG performance status ≤1, ≥1 resectable lesion(s) (≥1.5 cm), ≥1 remaining RECIST-measurable lesion(s) and recovered from prior surgery/anticancer treatment-related adverse events (AEs; grade ≤1). IOV-4001 is generated from resected tumor in a centralized GMP process. The regimen includes nonmyeloablative lymphodepletion, IOV-4001 infusion, and a short course of high-dose IL-2.

The primary endpoints of phases 1 and 2 are safety (DLTs and AEs) and objective response rate per RECIST v1.1, respectively. Secondary endpoints include complete response rate, duration of response, disease control rate, progression-free survival, overall survival, feasibility, and additional safety.

Trial Registration NCT05361174

REFERENCES

1. Sarnaik AA, et al. Lifileucel, a Tumor-Infiltrating Lymphocyte Therapy, in Metastatic Melanoma. *J Clin Oncol*. 2021;**39**(24):2656–2666.
2. Schoenfeld AJ, et al. First phase 2 results of autologous tumor-infiltrating lymphocyte (TIL; LN-145) monotherapy in patients with advanced, immune checkpoint inhibitor-treated, non-small cell lung cancer (NSCLC). SITC 2021.
3. Jazaeri AA, et al. Safety and efficacy of adoptive cell transfer using tumor infiltrating lymphocytes (LN-145) for treatment of recurrent, metastatic, or persistent cervical carcinoma. ASCO 2019.

4. O'Malley D, et al. Phase 2 efficacy and safety of autologous tumor-infiltrating lymphocyte (TIL) cell therapy in combination with pembrolizumab in immune checkpoint inhibitor-naïve patients with advanced cancers. SITC 2021.
5. Natarajan A, et al. Preclinical activity and manufacturing feasibility of genetically modified *PDCD-1* knockout (KO) tumor infiltrating lymphocyte (TIL) cell therapy. AACR 2022.

Ethics Approval The study was approved by the institutional review board at each site and was conducted in accordance with the Declaration of Helsinki and Good Clinical Practice guidelines of the International Conference on Harmonization. **Consent** All patients provided written informed consent.

<http://dx.doi.org/10.1136/jitc-2022-SITC2022.0783>

784

IMMUNE PROFILING OF PATIENTS WITH ADVANCED MELANOMA INTRATUMORALLY TREATED WITH CV8102 AS A SINGLE-AGENT OR IN COMBINATION WITH ANTI-PD-1 ANTIBODIES – RESULTS OF A PHASE I TRIAL EXPANSION

¹Marina Gonzalez, ¹Peter Wengenmayer, ²Igor Samoylenko, ³Sebastian Ochsenreither, ⁴Erika Richtig, ⁵Ioannis Thomas, ⁶Michael Erdmann, ⁷Celeste Lebbe, ⁸Juan Martin-Liberal, ⁹Patrick Terheyden, ¹⁰Artem Poltoratskiy, ¹¹Marina Sekacheva, ¹²Yuliya Semiletova, ¹³Thomas Eigentler, ¹Beate Schmitt-Bormann, ¹Dominik Vahrenhorst, ¹Sarah-Katharina Kays, ¹³Tobias Seibel, ¹Gianluca Quintini, ¹Birgit Scheel, ¹Martin Falk, ¹Ulrike Gnad-Vogt, ¹Paula Codo*. ¹CureVac AG, Frankfurt am Main, Germany; ²N.N. Blokhin Cancer Research Center, Moscow, Russian Federation; ³Charité Comprehensive Cancer Center, Berlin, Germany; ⁴Medical University of Graz, Graz, Austria; ⁵University Clinic Tübingen, Tübingen, Germany; ⁶University Hospital Erlangen, Erlangen, Germany; ⁷Hôpital Saint Louis, Paris, France; ⁸Catalan Institute of Oncology (ICO), Barcelona, Spain; ⁹University of Lübeck, Lübeck, Germany; ¹⁰National Medical Research Oncology Center n.a. N.N. Petrov, Saint Petersburg, Russian Federation; ¹¹Sechenov University, Moscow, Russian Federation; ¹²Clinic of advanced medical technologies n. a. Nicolay I. Pirogov, Saint Petersburg, Russian Federation; ¹³Charité Medical University, Berlin, Germany

Background CV8102 is a non-coding, non-capped RNA complexed with a carrier peptide activating the innate (via TLR7/8, RIG-I) and adaptive immune system.^{1, 2} An ongoing expansion of a phase I trial is investigating the intratumoral (i.t.) administration of CV8102 in patients with advanced cutaneous melanoma (cMEL), either as a single agent or in combination with systemic anti-PD-1 antibody therapy. In the initial dose escalation part, the recommended dose for subsequent cohort expansion and phase II was defined as 600 mg. Here we report preliminary immune profiling results.

Methods For the expansion cohorts, 30 anti-PD-1 refractory Melanoma patients received CV8102 in combination with Pembrolizumab or Nivolumab and 10 patients as single agent. Eight i.t. injections of CV8102 were administered over a 12-week period, with optional continuation in case of clinical benefit.

Blood samples for flow cytometry-based immune cell phenotyping and next-generation RNA sequencing (RNAseq) were collected at baseline and multiple time points during the treatment period. For characterization of the tumor microenvironment (TME), core needle biopsies of injected and/or non-injected lesions were taken before, during and after treatment. Changes on various tumor-infiltrating immune cells were assessed by multiplex immunofluorescence (MultiOmyx TM) and immune-related gene expression profiling using nCounter® Pan Cancer IO360 TM panel (NanoString).

Results Blood RNAseq analysis showed increase in several transcripts related to systemic immune response activation like interferon alpha and gamma after the first dose.

Paired serial biopsies showed changes in the TME, not only in the immune cell infiltration but also in gene expression profiling.

Comprehensive results of blood RNAseq, immune cell phenotyping, and tissue analysis for the expansion cohorts will be presented, including examples of individual patients.

Conclusions Intratumoral injection of CV8102 activated several pathways of immune response detectable in peripheral blood after the first dose and showed immunological changes in the tumor microenvironment, with increased parameters of immune infiltration in a group of patients.

Trial Registration NCT03291002

REFERENCES

- [1] Ziegler A, Soldner C, Lienenklaus S, Spanier J, Trittel S, Riese P, Kramps T, Weiss S, Heidenreich R, Jasny E, Guzmán CA, Kallen KJ, Fotin-Mlecsek M, Kalinke U. A New RNA-Based Adjuvant Enhances Virus-Specific Vaccine Responses by Locally Triggering TLR- and RLH-Dependent Effects. *J Immunol.* 2017;**198**(4):1595–1605. doi: 10.4049/jimmunol.1601129
- [2] Heidenreich R, Jasny E, Kowalczyk A, Lutz J, Probst J, Baumhof P, Scheel B, Voss S, Kallen KJ, Fotin-Mlecsek M. A novel RNA-based adjuvant combines strong immunostimulatory capacities with a favorable safety profile. *Int J Cancer.* 2015;**137**(2):372–84. doi: 10.1002/ijc.29402.

Ethics Approval The study was approved by central or local ethics committees depending on the country:

In Germany: Central Ethics Committees in Tuebingen, Germany under 785/2016AMG1.

In France: COMITE DE PROTECTION DES PERSONNES SUD-EST I under 2019-49, approval dated 17-May-2019.

In Spain: CEC COMITÉ DE ÉTICA DE INVESTIGACIÓN CLÍNICA CON MEDICAMENTOS del Hospital Universitari Vall d'Hebron, Barcelona, approval date 28-Nov-2019 under the EUdRaCT number.

In Austria: Central Ethics Committee in Graz under 31-426 ex 18/19 approved on 19-Sep-2019.

In the Russian Federation: ETHICS COMMITTEE AT FSBI "NMRC OF ONCOLOGY n.a. N.N. BLOKHIN" OF THE MINISTRY OF HEALTHCARE OF THE RUSSIAN FEDERATION, INTERDISCIPLINARY ETHICS COMMITTEE of Omsk Region, Local Ethics Committee at FSAEI HE "I.M. Sechenov First MSMU" of the Ministry of Healthcare of Russia (Sechenov University, Extract from Minutes □ 03-21 of the scheduled meeting of the Local Ethics Committee dated 03 February 2021), BIOMEDICAL ETHICS COMMITTEE at N.I. PIROGOV CLINIC OF HIGH MEDICAL TECHNOLOGIES (IN-PATIENT AND OUTPATIENT FACILITIES), ST. PETERSBURG STATE UNIVERSITY (EXTRACT FROM MINUTES □ 02/21 of the meeting of the Biomedical Ethics Committee), Ethics Committee at Federal State Budgetary Institution "National Medical Research Center of Oncology named after N. N. Petrov" of the Ministry of Health of the Russian Federation (Extract No. 5/130 from the Minutes of the regular session No. 8 of the Ethics Committee).

Consent Written informed consent from the patient was obtained for publication of this abstract and any accompanying images. A copy of the written consent is available for review by the Editor of this journal.

<http://dx.doi.org/10.1136/jitc-2022-SITC2022.0784>

785

A PHASE I STUDY OF INTRALYMPHATIC (IL) ADMINISTRATION OF IPILIMUMAB (IPI) WITH INTRAVENOUS NIVOLUMAB (NIVO) USING THE SOFUSA® DOSECONNECT™ DEVICE IN PATIENTS WITH ADVANCED MELANOMA

Anastasios Dimou*, Vera Suman, Kristina Denic, Lisa Kottschade, Heather Montane, Heidi Finnes, Kristina Franta, Jill Schimke, Yiyi Yan, Robert McWilliams, Matthew Block, James Jakub, Joel Reid, Svetomir Markovic. *Mayo Clinic, Rochester, MN, USA*

Background Pre-clinical studies of Sofusa® DoseConnect™ (DC) have shown that IL infusion of antineoplastic medications results in higher lymph node concentrations, more efficient tumor growth inhibition and less systemic exposure when compared to conventional systemic administration. We conducted a Phase I clinical trial to assess the safety of IL infusion of ipilimumab with DC followed by nivolumab IV in patients with advanced melanoma.

Methods A 3+3 phase I clinical trial was conducted to assess the safety of IL infusion of IPI by DC over 12-24 hours followed by NIVO 3 mg/kg IV among patients with advanced melanoma. A maximum of four 21 day cycles were administered. Cycle 1 IPI was administered by DC; cycles 2-4 IPI were administered at 1 mg/kg IV. Dose levels (DL) of cycle 1 IPI included: DL1: 1 mg/kg; DL-1: 0.75 mg/kg; and DL-2: 0.5 mg/kg. All DL were given at 0.5 mL/hour. Dose limiting toxicities included the following if they were at least possibly related to DC: inability to administer at least 75% of the protocol-specified dose due to DC dislodgement, \geq grade 4 hematologic toxicity, \geq grade 3 non-hematologic toxicity or \geq grade 3 infusion site reaction or infusion related reaction that does not resolve to Grade 0-1 within 2 weeks. IPI pharmacokinetics were characterized in all patients who participated in the study.

Results Six patients (3 males and 3 females) were enrolled in this trial at DL1. The median number of prior therapies for metastatic disease was 1 (range 1-3). The most common sites of metastatic disease were distant lymph nodes and lung. No dose limiting toxicities were observed. Cycle 1 toxicities reported included grade 2 hypophysitis (N=1) and grade 2 abdominal pain (N=1). No adjustments to the DC flow rate were required. Two severe, DC unrelated, immune-related toxicities were reported: grade 3 maculopapular rash and grade 3 colitis (same patient, cycle 1 causing discontinuation). Four patients progressed on treatment (1-cycle 2; 3-cycle 4). One patient completed 4 cycles of treatment. The mean IPI serum concentrations at the end of the infusion and 15 days after the DC infusion in Cycle 1 were 4.13 ug/mL and 4.88 ug/mL, respectively.

Conclusions IL administration of IPI with the DC device on the first cycle was well tolerated with no dose limiting toxicities. Safety and secondary efficacy of IL infusion of IPI through all 4 cycles will be assessed next.

Trial Registration ClinicalTrials.gov: NCT04967196

Ethics Approval This study was performed in line with the principles of the Declaration of Helsinki. Approval was granted by the Ethics Committee of Mayo Clinic.

Consent Informed consent was obtained from all individual participants included in this study.

<http://dx.doi.org/10.1136/jitc-2022-SITC2022.0785>

786

INTRATUMORALLY ADMINISTERED CV8102 IN PATIENTS WITH ADVANCED SOLID TUMORS: PRELIMINARY RESULTS FROM ONGOING EXPANSION PART IN STUDY 008

¹Thomas Eigentler*, ²Igor Samoylenko, ³Sebastian Ochsenreither, ⁴Erika Richtig, ⁵Ioannis Thomas, ⁶Michael Erdmann, ⁷Celeste Lebbe, ⁸Juan José Soto-Castillo, ⁹Patrick Terheyden, ¹⁰Artem Poltoratskiy, ¹¹Marina Sekacheva, ¹²Yuliya Semiletova, ¹³Janina Henze, ¹³Beate Schmitt-Bormann, ¹³Paula Codó, ¹³Martin Falk, ¹³Ulrike Gnad-Vogt. ¹Charité Medical University, Berlin, Germany; ²N.N. Blokhin Cancer Research Center, Moscow, Russian Federation; ³Charité Comprehensive Cancer Center, Berlin, Germany; ⁴Medical University of Graz, Graz, Austria; ⁵University Medical Center Tübingen, Tübingen, Germany; ⁶University Hospital Erlangen, Erlangen, Germany; ⁷Hôpital Saint Louis, Paris, France; ⁸Catalan Institute of Oncology Hospitalet, Barcelona, Spain; ⁹University of Lübeck, Lübeck, Germany; ¹⁰National Medical Research Oncology Center n.a. N.N. Petrov, Saint Petersburg, Russian Federation; ¹¹Sechenov University, Moscow, Russian Federation; ¹²Clinic of advanced medical technologies n. a. Nicolay I. Pirogov, Saint Petersburg, Russian Federation; ¹³Curevac AG, Frankfurt, Germany

Background CV8102 is a non-coding, non-capped RNA complexed with a carrier peptide activating the innate (via TLR7/8, RIG-I) and adaptive immune system. An ongoing phase I trial (CV-8102-008) is investigating intratumoral administration of CV8102 either as a single agent or in combination with systemic anti-PD-1 antibodies in patients with advanced cutaneous melanoma (cMEL), squamous cell carcinoma of the skin (cSCC) or head and neck (hnSCC) and adenoid cystic carcinoma (ACC). Recruitment of the expansion part in melanoma patients is completed and preliminary results from this part are reported here.

Methods Study CV-8102-008 is an open-label, cohort-based, dose escalation and expansion phase I study. Eight intratumoral injections of CV8102 are being administered initially over a 12-week period. The trial consists of two parts, a dose escalation part and an expansion part. Primary objective of the expansion part is to obtain additional safety data as well as initial estimates of efficacy in patients with advanced melanoma in a single agent cohort and patients with advanced melanoma patients refractory to anti-PD-1 therapy receiving CV8102 in combination with anti-PD-1 antibodies. In the expansion part, CV8102 was administered at a dose level of 600µg which has been determined as recommended phase 2 dose during the dose escalation part.

Results As of January 2022 10 patients have been treated with CV8102 as a single agent and 30 patients have received CV8102 in combination with anti-PD-1 antibodies within the expansion part. Most frequent treatment emergent adverse events were mild to moderate fever, chills and asthenia. Regression of injected and distant noninjected lesions was observed (including 4 PR per RECIST 1.1. in the combination cohort). Preliminary safety and efficacy as well as selected biomarker results from the expansion cohorts will be presented.

Conclusions The acceptable safety profile already observed during the dose escalation part could be confirmed in the expansion part. Preliminary evidence of clinical efficacy in the expansion cohorts was seen in combination with anti-PD-1-antibodies.

Trial Registration NCT03291002

Ethics Approval The study was approved by central or local ethics committees depending on the country.

In Germany: Central Ethics Committees in Tuebingen, Germany under 785/2016AMG1.

In France: COMITE DE PROTECTION DES PERSONNES SUD-EST I under 2019-49, approval dated 17-May-2019.

In Spain: CEC COMITÉ DE ÉTICA DE INVESTIGACIÓN CLÍNICA CON MEDICAMENTOS del Hospital Universitari Vall d'Hebron, Barcelona, approval date 28-Nov-2019 under the EUdRaCT number.

In Austria: Central Ethics Committee in Graz under 31-426 ex 18/19 approved on 19-Sep-2019.

In the Russian Federation: ETHICS COMMITTEE AT FSBI "NMRC OF ONCOLOGY n.a. N.N. BLOKHIN" OF THE MINISTRY OF HEALTHCARE OF THE RUSSIAN FEDERATION, INTERDISCIPLINARY ETHICS COMMITTEE of Omsk Region, Local Ethics Committee at FSAEI HE "I.M. Sechenov First MSMU" of the Ministry of Healthcare of Russia (Sechenov University, Extract from Minutes □ 03-21 of the scheduled meeting of the Local Ethics Committee dated 03 February 2021), BIOMEDICAL ETHICS COMMITTEE at N.I. PIROGOV CLINIC OF HIGH MEDICAL TECHNOLOGIES (IN-PATIENT AND OUTPATIENT FACILITIES), ST. PETERSBURG STATE UNIVERSITY (EXTRACT FROM MINUTES □ 02/21 of the meeting of the Biomedical Ethics Committee), Ethics Committee at Federal State Budgetary Institution "National Medical Research Center of Oncology named after N. N. Petrov" of the Ministry of Health of the Russian Federation (Extract No. 5/130 from the Minutes of the regular session No. 8 of the Ethics Committee).

Consent Written informed consent from the patient was obtained for publication of this abstract and any accompanying images. A copy of the written consent is available for review by the Editor of this journal.

<http://dx.doi.org/10.1136/jitc-2022-SITC2022.0786>

DELTA-1: A GLOBAL, MULTICENTER, PHASE 2 STUDY OF ITIL-168, AN UNRESTRICTED AUTOLOGOUS TUMOR-INFILTRATING LYMPHOCYTE (TIL) CELL THERAPY, IN ADULT PATIENTS WITH ADVANCED CUTANEOUS MELANOMA

¹Brian Gastman*, ²Amod Sarnaik, ³Donald Lawrence, ⁴Anthony Olszanski, ⁵Bartosz Chmielowski, ⁶Jose Lutzky, ⁷Marcus Butler, ⁸Omid Hamid, ⁹Pippa Corrie, ¹⁰Evidio Domingo-Musibay, ¹¹Sajeve Thomas, ¹²Fiona Thistlethwaite, ¹³Gregory Daniels, ¹⁴Thomas Evans, ¹⁵Andrew Furness, ¹⁶Geoffrey Gibney, ¹⁷Mark Harries, ¹⁸Theresa Medina, ¹⁹Daniel Olson, ²⁰Lalit Pallan, ²¹Eric Whitman, ²²Melissa Wilson, ²³Jeff Aycocock, ²³Robert Hawkins, ²³Yizhou Jiang, ²³Audrey Kennedy, ²³Paul Robbins, ²³Zachary Roberts, ²³John Le Gall. ¹Cleveland Clinic, Cleveland, OH, USA; ²Moffitt Cancer Center, Tampa, FL, USA; ³Massachusetts General Hospital, Harvard Medical School, Boston, MA, USA; ⁴Fox Chase Cancer Center, Philadelphia, PA, USA; ⁵University of California Los Angeles, Los Angeles, CA, USA; ⁶University of Miami, Miami, FL, USA; ⁷Princess Margaret Cancer Centre, Ontario, Canada; ⁸The Angeles Clinic and Research Institute, A Cedars-Sinai Affiliate, Los Angeles, CA, USA; ⁹Cambridge University Hospitals NHS Foundation Trust, Cambridge, UK; ¹⁰University of Minnesota, Masonic Cancer Center, Minneapolis, MN, USA; ¹¹Orlando Health Cancer Institute, Orlando, FL, USA; ¹²The Christie NHS Foundation Trust and University of Manchester, Manchester, UK; ¹³University of California San Diego, Moores Cancer Center, La Jolla, CA, USA; ¹⁴University of Glasgow, Beatson West of Scotland Cancer Centre, Glasgow, UK; ¹⁵The Royal Marsden NHS Foundation Trust, London, UK; ¹⁶MedStar Georgetown University Hospital, Washington, DC, USA; ¹⁷Guy's and St. Thomas' NHS Foundation Trust, London, UK; ¹⁸University of Colorado, Denver, CO, USA; ¹⁹University of Chicago, Chicago, IL, USA; ²⁰University Hospitals Birmingham NHS Foundation Trust, Birmingham, UK; ²¹Atlantic Health System, Morristown, NJ, USA; ²²St. Luke's University Health Network, Easton, PA, USA; ²³Instil Bio, Inc., Dallas, TX, USA

Background Investigational autologous TIL cell therapies have shown promise in patients with advanced cutaneous melanoma and persistent disease after checkpoint inhibitor therapy, a population with a high unmet medical need.^{1,2} Made from autologous digested and cryopreserved tumor, ITIL-168 is a TIL cell therapy manufactured to offer an unrestricted T-cell receptor repertoire. DELTA-1 (NCT05050006) is a global, multicenter, phase 2 study evaluating efficacy and safety of ITIL-168 in patients with cutaneous melanoma relapsed or refractory to a PD-1i, patients intolerant to a PD-1i, and patients with stable disease on a PD-1i.

Methods Adult patients with histologically confirmed advanced cutaneous melanoma and ECOG performance status 0-1 will be enrolled in 1 of 3 cohorts. Cohort 1 (n≈80) will include patients who relapsed after or were refractory to ≥1 prior line of systemic therapy, including a PD-1i and, if *BRAF*-mutated, a BRAFi ± MEKi. Cohorts 2 and 3 (n≈25 each) will include patients intolerant to PD-1i and those with stable disease after ≥4 doses of PD-1i, respectively. After tumor harvest, patients must have ≥1 measurable lesion per RECIST 1.1. Noncutaneous melanoma, certain prior therapies, and patients with symptomatic and/or untreated central nervous system metastases are ineligible. Patients will receive 5 days of lymphodepleting chemotherapy (cyclophosphamide ×2 days overlapping with fludarabine ×5 days) followed by a single ITIL-168 infusion and supportive IL-2. The primary endpoint is objective response rate (ORR) per central review. Secondary endpoints include duration of response, progression-free survival, overall survival, disease control rate, TIL persistence, and safety. Hypothesis testing of ORR will be performed for cohort 1. The primary analysis will occur ≥6 months after the first posttreatment disease assessment of patients in the cohort 1 modified intent-to-treat population. Enrollment has expanded into Canada and Europe.

Acknowledgements Medical writing support was provided by Christopher Waldapfel, PharmD, of Instil Bio, Inc. and

Phylicia Aaron, PhD, of Nexus Global Group Science, with funding from Instil Bio, Inc.

REFERENCES

1. Schadendorf D, van Akkoi ACJ, Berking C, *et al.* Melanoma. *Lancet.* 2018;**392** (10151):971-984.
2. Borch TH, Anderson R, Ellebaek E, *et al.* Future role for adoptive T-cell therapy in checkpoint inhibitor-resistant metastatic melanoma. *J Immunother Cancer.* 2020;**8** (2):e000668.

Ethics Approval All patients will provide written informed consent. The study will be approved by the Institutional Review Board/Independent Ethics Committee at each site and conducted in accordance with the Good Clinical Practice Guidelines of the International Council for Harmonisation.

Consent N/A; the abstract does not contain sensitive or identifiable patient information.

<http://dx.doi.org/10.1136/jitc-2022-SITC2022.0787>

788

A PHASE 1B STUDY TO EVALUATE THE SAFETY, TOLERABILITY, PHARMACOKINETICS AND ANTI-TUMOR ACTIVITY OF NEOADJUVANT USE OF PH-762 ADMINISTERED INTRATUMORALLY IN SUBJECTS WITH ADVANCED MELANOMA

¹Simon Fricker*, ²Caroline Robert, ³François-Xavier Danloss, ³Emilie Routier, ¹Benjamin Cuiﬀo, ¹James Cardia. ¹Phio Pharmaceuticals, Marlborough, MA, USA; ²Gustave and Paris-Saclay University, Villejuif-Paris, France; ³Gustave Roussy, and Paris-Saclay Univers, Paris, France

Background Immunotherapy with antibodies targeting PD-1 and CTLA-4 has shown significant benefit in late-stage melanoma. However, as response is limited to approximately 60%, and with emergence of resistance, further improvements in therapeutic options are still required. Two approaches for improving the outcome of immunotherapy with checkpoint inhibitors are neoadjuvant treatment and local intratumoral (IT) injection. Neoadjuvant immunotherapy can induce significant pathological responses that seem to be associated with a decrease in the risk of relapse. Currently there is no neoadjuvant standard of care for patients with resectable, advanced melanoma. IT immunotherapy uses the tumor as its own vaccine to activate the immune system, priming an anti-tumor immune response and minimizing systemic exposure and off-target toxicities. PH-762 is a potent RNAi molecule targeting PD-1 that contains structural and chemical modifications conferring rapid and efficient tissue uptake suitable for IT administration. In pharmacology studies PH-762 provided robust silencing of PD-1 associated with T cell activation, and dose-dependent inhibition of tumor growth in *in vivo* syngeneic tumor models with on-target PD-1 silencing-associated with immunostimulatory effects in the tumor microenvironment.

Methods The primary objective of this first-in-human study is to evaluate the safety of neoadjuvant use of PH-762 administered by IT injection. Secondary objectives include PK after IT injection, potential immunologic and pathologic tumor responses, and determination of the recommended Phase 2 dose. Subjects must have histologically confirmed stage IIIB/IIIC/IIID or IV oligometastatic cutaneous melanoma with at least one resectable lesion that is large enough to allow IT injection, and that can undergo repeated biopsy. Subjects with brain metastases, leptomeningeal disease, uveal melanoma, and auto-immune disease are excluded. PH-762 is administered IT into one designated tumor lesion once weekly for 4 weeks prior to surgical excision at 5-6 weeks after the initial injection. The dose of PH-762 is normalized to tumor volume to ensure an equivalent local dose (tumor tissue concentration). Post tumor excision, subjects are followed-up for 6 weeks. Primary endpoint is determination of a safe dose of PH-762 assessed by incidence of dose limiting toxicities (DLT) prior to tumor resection. Bayesian optimal interval (BOIN) design will be employed to evaluate escalating doses of PH-762 with up to 5 dose levels in cohorts of 3 or more subjects. Tumor changes will be evaluated per RECIST criteria (version 1.1 and iRECIST adapted for IT therapy) and pathological response. Secondary endpoints include immunological response in tumor tissue and blood. The first cohort has been enrolled.

Trial Registration EudraCT number 2021-002859-10

Ethics Approval Approval was provided by: Comite de Protection de Personnes Sud Mediterranee III, 2021.12.04 bis _21.04174.000055

<http://dx.doi.org/10.1136/jitc-2022-SITC2022.0788>

LIFILEUCEL TIL CELL MONOTHERAPY IN PATIENTS WITH ADVANCED MELANOMA AFTER PROGRESSION ON IMMUNE CHECKPOINT INHIBITORS (ICI) AND TARGETED THERAPY: POOLED ANALYSIS OF CONSECUTIVE COHORTS (C-144-01 STUDY)

¹Amod Sarnaik*, ²Karl Lewis, ³Harriet Kluger, ⁴Omid Hamid, ⁵Eric Whitman, ⁶Sajeve Thomas, ⁷Martin Wermke, ⁸Mike Cusnir, ⁹Evidio Domingo-Musibay, ¹⁰Giao Phan, ¹¹John Kirkwood, ¹²Jessica Hassel, ¹³Marlana Orloff, ¹⁴James Larkin, ¹⁵Jeffrey Weber, ¹⁶Andrew Furness, ¹⁷Nikhil Khushalani, ¹⁸Theresa Medina, ¹⁹Friedrich Finckenstein, ²⁰Madan Jagasia, ²¹Parameswaran Hari, ²²Giri Sulur, ²³Wen Shi, ²⁴Xiao Wu, ²⁵Jason Chesney. ¹H. Lee Moffitt Cancer Center, Tampa, FL, USA; ²University of Colorado Cancer Center-Anschutz Medical Campus, Aurora, CO, USA; ³Yale School of Medicine and Smilow Cancer Center, Yale New Haven Hospital, New Haven, CT, USA; ⁴The Angeles Clinic and Research Institute, a Cedars Sinai Affiliate, Los Angeles, CA, USA; ⁵Atlantic Health System Cancer Care, Morristown, NJ, USA; ⁶Orlando Health Cancer Institute, Orlando, FL, USA; ⁷Technical University Dresden, NCT/UCC Early Clinical Trial Unit, Dresden, Germany; ⁸Mount Sinai Medical Center, Miami Beach, FL, USA; ⁹University of Minnesota, Masonic Cancer Center, Minneapolis, MN, USA; ¹⁰Virginia Commonwealth University, Massey Cancer Center, Richmond, VA, USA; ¹¹UPMC Hillman Cancer Center, Pittsburgh, PA, USA; ¹²Skin Cancer Center, University Hospital Heidelberg, Heidelberg, Germany; ¹³Thomas Jefferson University, Sidney Kimmel Cancer Center, Philadelphia, PA, USA; ¹⁴The Royal Marsden Hospital NHS Foundation Trust, London, UK; ¹⁵Laura and Isaac Perlmutter Cancer Center, NYU Langone Medical Center, New York, NY, USA; ¹⁶Iovance Biotherapeutics, Inc., San Carlos, CA, USA; ¹⁷UofL Health – Brown Cancer Center, University of Louisville, Louisville, KY, USA

Background Despite improved outcomes in advanced (unresectable or metastatic) melanoma, many patients progress after ICI,¹⁻³ and have low response rates to subsequent therapy.⁴⁻⁷ Lifileucel, a one-time autologous TIL cell therapy, demonstrated an investigator-assessed ORR of 36% in Cohort 2 (C2), which enrolled 66 patients who progressed post-ICI and appropriate targeted therapy.^{8,9} We now report outcomes of 153 patients enrolled across C2 and C4 (NCT02360579), representing the largest phase 2 study of cell therapy in melanoma.

Methods Eligibility criteria were identical for C2 and C4. Patients had ≥1 lesion(s) resected (~1.5 cm in diameter post-resection) and shipped to a central GMP facility for 22-day lifileucel manufacturing. All patients received a nonmyeloablative lymphodepletion (NMA-LD) regimen, a single lifileucel infusion, and up to 6 doses of high-dose IL-2. Primary endpoint was IRC-assessed ORR (RECIST v1.1).

Results The full analysis set included 153 patients (C2: n=66; C4: n=87) treated with lifileucel, with a median of 3 prior lines of therapy (range: 1-9) and substantial baseline disease burden (>3 target and non-target lesions: 76%; median target lesion SOD: 97.8 mm; LDH >ULN: 54%). ORR was 31% (95% CI: 24.1%-39.4%) (C2: 35%; C4: 29%), with 8 CRs and 40 PRs (figure 1). At median study follow-up of 27.6 months, median DOR was not reached (NR). Forty-two percent of responses extended ≥18 months, and 40% (19/48) of responses were ongoing at time of datacut (figure 2). In multivariable analyses adjusted for ECOG PS, elevated LDH and target lesion SOD >median were independently correlated with ORR ($p=0.008$); normal LDH and SOD < median were associated with higher odds of response than either (OR=2.08) or both (OR=4.42) risk factors. The median OS was 13.9 months (95% CI: 10.6-17.8). In an analysis of survival by response at first assessment (1.5 months post-lifileucel infusion), median OS in responders was NR (95% CI: 22.5 months-NR). The most common (≥30%) G3/4 TEAEs were thrombocytopenia (77%), anemia (50%), and febrile neutropenia (42%). TEAEs were consistent with known safety profiles of NMA-LD and IL-2, and their incidence decreased within

the first 2 weeks post-lifileucel infusion, characteristic of one-time treatment.

Conclusions Lifileucel demonstrated clinically meaningful and durable activity (ORR: 31%; mDOR: NR) in heavily pre-treated patients with advanced melanoma and high tumor burden after ICI (and targeted therapy, where appropriate). Favorable safety profile and sustained responses support the potential benefit of one-time lifileucel TIL cell therapy as a novel treatment option for patients without approved therapies post-ICI.

Acknowledgements Medical writing support was provided by Second City Science, with funding from Iovance Biotherapeutics.

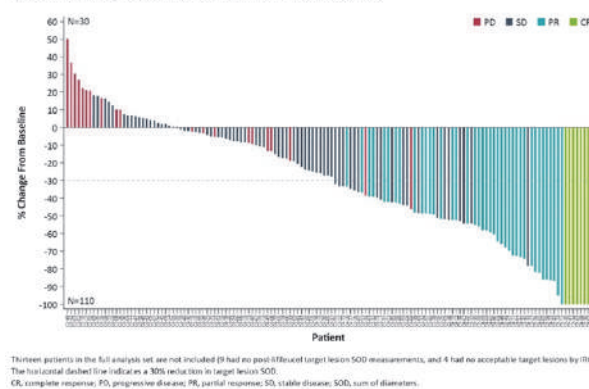
Trial Registration NCT02360579

REFERENCES

1. Long GV, Robert C, Butler MO, et al. Standard-dose pembrolizumab plus alternate-dose ipilimumab in advanced melanoma: KEYNOTE-029 cohort 1C, a phase 2 randomized study of two dosing schedules. *Clin Cancer Res.* 2021;**27**:5280–5288.
2. Tawbi HA, Schadendorf D, Lipson EJ, et al. Relatlimab and nivolumab versus nivolumab in untreated advanced melanoma. *N Engl J Med.* 2022;**386**:24–34.
3. Postow MA, Goldman DA, Shoushtari AN, et al. Adaptive dosing of nivolumab + ipilimumab immunotherapy based upon early, interim radiographic assessment in advanced melanoma (The ADAPT-IT study). *J Clin Oncol.* 2022;**40**:1059–1067.
4. Ribas A, Puzanov I, Dummer R, et al. Pembrolizumab versus investigator-choice chemotherapy for ipilimumab-refractory melanoma (KEYNOTE-002): A randomised, controlled, phase 2 trial. *Lancet Oncol.* 2015;**16**:908–918.
5. Weichenthal M, Ugurel S, Leiter UM, et al. Salvage therapy after failure from anti-PD-1 single agent treatment: A study by the German ADOReg melanoma registry. *J Clin Oncol.* 2019;**37**(suppl 15):9505.
6. Weber JS, D'Angelo SP, Minor D, et al. Nivolumab versus chemotherapy in patients with advanced melanoma who progressed after anti-CTLA-4 treatment (CheckMate 037): A randomised, controlled, open-label, phase 3 trial. *Lancet Oncol.* 2015;**16**:375–384.
7. Goldinger SM, Buder-Bakhaya K, Lo SN, et al. Chemotherapy after immune checkpoint inhibitor failure in metastatic melanoma: A retrospective multicentre analysis. *Eur J Cancer.* 2022;**162**:22–23.
8. Sarnaik AA, Hamid O, Khushalani NI, et al. Lifileucel, a tumor-infiltrating lymphocyte therapy, in metastatic melanoma. *J Clin Oncol.* 2021;**39**:2656–2666.
9. Larkin J, Sarnaik A, Chesney JA, et al. Lifileucel (LN-144), a cryopreserved autologous tumor infiltrating lymphocyte (TIL) therapy in patients with advanced melanoma: Evaluation of impact of prior anti-PD-1 therapy. *J Clin Oncol.* 2021;**39**(suppl 15):abstract 9505.

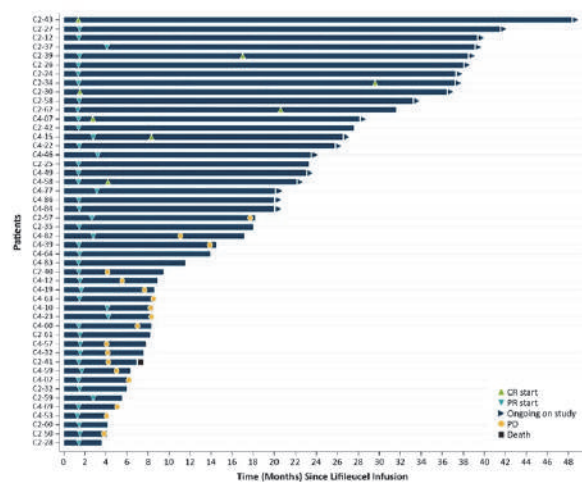
Ethics Approval The study was approved by the institutional review board at each site and was conducted in accordance with the Declaration of Helsinki and Good Clinical Practice guidelines of the International Conference on Harmonisation. All patients provided written informed consent.

Figure 1. Best percentage change from baseline in target lesion SOD



Abstract 789 Figure 1 Best percentage change from baseline in target lesion SOD

Figure 2. Time to first response, duration of response, and time on efficacy assessment for confirmed responders (PR or better)



Abstract 789 Figure 2 Time to first response, duration of response, and time on efficacy assessment for confirmed responders (PR or better)

<http://dx.doi.org/10.1136/jitc-2022-SITC2022.0789>

Abstracts

790

PHASE I CLINICAL TRIAL ON INTRATUMORAL ADMINISTRATION OF AUTOLOGOUS CD1c (BDCA-1)⁺/CD141 (BDCA-3)⁺ MYELOID DENDRITIC CELLS PLUS IPIILIMUMAB AND AS01_B IN COMBINATION WITH INTRAVENOUSLY ADMINISTERED NIVOLUMAB

¹Jens Tijtgat*, ¹Julia Katharina Schwarze, ¹An-Sofie Vander Mijnsbrugge, ¹Steven Raeymaeckers, ¹Ivan Van Riet, ²Xenia Geeraerts, ²Latoya Stevens, ²Sandra Tuyaerts, ¹Bart Neyns. ¹UZ Brussel, Jette, Belgium; ²Vrije Universiteit Brussel, Jette, Belgium

Background The presence of CD1c (BDCA-1)⁺ (cDC2) and CD141 (BDCA-3)⁺ (cDC1) conventional dendritic cells (myDC) in the tumor microenvironment (TME) is a necessary prerequisite to induce an effector CD8⁺ T cell response and for response to immune checkpoint blockade (ICB).¹⁻⁴ AS01_B is an adjuvant component of a commercialized prophylactic shingles vaccine which induces adaptive immunity through recruitment and activation of cDC1 and cDC2.⁵⁻⁶ Previously, intratumoral (IT) administration of ipilimumab and autologous myDC has shown promising antitumoral activity.⁷

Methods In this phase Ib clinical trial, patients with metastatic melanoma refractory to ICB and BRAF/MEK inhibitors (in case of BRAF V600-mutant melanoma) were recruited. Patients underwent a leukapheresis followed by immunomagnetic bead isolation of CD1c (BDCA-1)⁺/CD141 (BDCA-3)⁺ myDC. Patients received an intravenous (IV) administration of low dose nivolumab (10mg d1 and q2w) plus an IT administration of ipilimumab 10 mg (d1 and q2w). The isolated myDC were injected (palpation or ultrasound-guided) as a single injection into a metastatic lesion on day 2; together with AS01_B 0.5 ml (d2 and q2w). Response assessment was performed by PET/CT q12w. Blood and tissue samples were collected each treatment cycle. Translational research including gene expression profiling, TCR analysis and multiplex immunohistochemistry is ongoing. (figure 1)

Results Between July 2021 and May 2022, 8 patients were recruited (all female) with a median age of 63 years (range 33-83). All patients had been treated with ICB as well as BRAF/MEK inhibitors when applicable. Median number and range of treatment administrations was 4 (range 1-7) for IT and 4.5 (range 1-15) for IV. Three patients remained on treatment at data cutoff date. Median PFS was 10.1 weeks (95% CI 5.193-15.007), median OS has not been reached. One patient obtained a complete remission on PET/CT 6 months after the start of study treatment. One patient obtained a pathological complete response 4 weeks after start of study treatment. One patient obtained a complete remission of injected lesions but progressed in non-injected lesions. Three patients died due to progressive disease. Treatment was well tolerated. There were no unexpected adverse events. One patient had G3 pyrexia, leading to prolongation of hospital stay with 1 day.

Conclusions In this clinical trial, IT injection of CD1c (BDCA-1)⁺/CD141 (BDCA-3)⁺ myDC in combination with repeated IT administration of ipilimumab and AS01_B and systemic low dose nivolumab has shown promising early results and no unexpected safety signals, deserving further clinical investigation. Translational investigations are ongoing.

Trial Registration Clinicaltrials. gov: NCT03707808

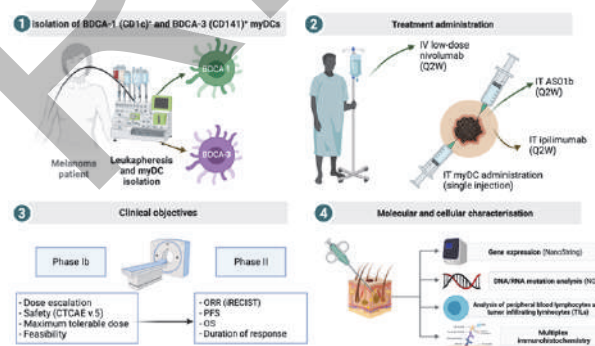
REFERENCES

1. Broz, M.L., *et al.* Dissecting the tumor myeloid compartment reveals rare activating antigen-presenting cells critical for T cell immunity. *Cancer Cell.* 2014;**26**:638–652.

2. Roberts, E.W., *et al.* Critical Role for CD103(+)/CD141(+) Dendritic Cells Bearing CCR7 for Tumor Antigen Trafficking and Priming of T Cell Immunity in Melanoma. *Cancer Cell.* 2016;**30**:324–336.
3. Spranger, S, Dai, D, Horton, B. & Gajewski, T.F. Tumor-Residing Batf3 Dendritic Cells Are Required for Effector T Cell Trafficking and Adoptive T Cell Therapy. *Cancer Cell.* 2017;**31**:711–723 e714.
4. Binnewies, M, *et al.* Unleashing Type-2 Dendritic Cells to Drive Protective Antitumor CD4(+) T Cell Immunity. *Cell.* 2019;**177**:556–571 e516.
5. Didierlaurent A.M, *et al.* Enhancement of adaptive immunity by the human vaccine adjuvant AS01 depends on activated dendritic cells. *J Immunol.* 2014;**193** (4):1920–30.
6. Bosteels C, *et al.* CCR2- and Flt3-Dependent Inflammatory Conventional Type 2 Dendritic Cells Are Necessary for the Induction of Adaptive Immunity by the Human Vaccine Adjuvant System AS01. *Front Immunol.* 2020;**11**:606805.
7. Schwarze J.K, *et al.* Intratumoral Combinatorial Administration of CD1c (BDCA-1) (+) Myeloid Dendritic Cells Plus Ipilimumab and Avelumab in Combination with Intravenous Low-Dose Nivolumab in Patients with Advanced Solid Tumors: A Phase IB Clinical Trial. *Vaccines (Basel).* 2020;**8**(4).

Ethics Approval Clinical trial protocol was approved by the medical ethics committee of Universitair Ziekenhuis Brussel and by the Belgian Federal Agency for Medicines and Health Products. Patients have signed an informed consent for participation in this clinical trial.

Consent Written consent of participating patients was obtained for publication of anonymized patient data. A copy of the written consent is available for review by the Editor of this journal.



Abstract 790 Figure 1 Schematic overview of clinical trial (Created in Biorender.com)

<http://dx.doi.org/10.1136/jitc-2022-SITC2022.0790>

Combination Immunotherapies

791 IMMUNE CHECKPOINT BLOCKADE ENHANCES CYCLOPHOSPHAMIDE INDUCED ANTI-TUMOR IMMUNITY IN A PRECLINICAL MELANOMA MODEL

Mariam George*, Allison Betof, Taha Merghoub, Linda Hamadene, Daniel Hirschhorn, Alan Houghton, Jedd Wolchok. *Memorial Sloan Kettering Cancer Center, New York, NY, USA*

Background Immune Checkpoint Blockade (ICB) with anti-programmed cell death protein (PD)-1 and anti-cytotoxic T lymphocyte associated protein (CTLA)-4 have had immense success in cancer treatment. However, primary and acquired resistance to these therapies limits their clinical benefit. Accumulating evidence indicates that chemotherapeutic agents such as Cyclophosphamide (CTX) can induce anticancer immunity and improves the efficacy of ICBs when used in combination. A combination strategy to reorchestrate the anti-tumor immune response could magnify the clinical benefit of ICBs. CTX is an alkylating chemotherapeutic agent which is directly tumoricidal and induces immunomodulatory properties. CTX preferentially depletes T cell subsets (such as T regulatory cells) and leads to homeostatic proliferation of T cells. We hypothesized that the addition of ICBs to CTX treatment will augment the immunomodulatory changes induced by CTX including but not limited to the homeostatic proliferation of T cells which will reset the T cell receptor (TCR) repertoire to favor tumor antigen-specific T cells. The murine melanoma tumor model, B16-F10, is known to be refractory to treatment with ICBs, particularly anti-PD-1, as it only modestly slows tumor growth.

Methods Mice were given a single dose of CTX one day prior to starting an ICB (anti-PD-1 and/or anti-CTLA-4) regimen.

Results The treatment slows tumor progression of B16-F10 compared to CTX or ICB alone and significantly prolongs the survival of mice. Further, the combination of CTX with anti-PD-1 and anti-CTLA-4 increased the number of activated and proliferating CD8+ tumor infiltrating lymphocytes (TILs). This increase in cytotoxic T cells was accompanied by a decrease in Tregs, which further augments the tumor control. Additionally, we observed a significant increase in a highly cytolytic population of CD4+ CD8+ double positive TILs. The depletion of CD8+ cells but not CD4+ cells abrogates the therapeutic effect of the triple combination suggesting that the anti-tumor effect is CD8+ T cell dependent. The tumor control effect of the triple combination (CTX+ anti- PD-1 + anti-CTLA-4) extends to other murine tumor models namely, MC38 (colon adenocarcinoma) and 4T1 (mammary carcinoma).

Conclusions Our results suggest that the combination of CTX with ICBs, anti- PD-1 and anti-CTLA-4, is a potent combinatorial approach that can prime an anti-tumor response and promote robust control of tumor growth. These findings form the basis for further investigations in understanding the mechanisms of combinatorial cancer therapies in tumor models that are refractory to ICB therapies and can inform the design of future therapeutic interventions that combine ICB with chemotherapy.

<http://dx.doi.org/10.1136/jitc-2022-SITC2022.0791>

792

NATURAL KILLER T CELL IMMUNOTHERAPY COMBINED WITH FUSOGENIC ONCOLYTIC VIRUS AND PD-1 BLOCKADE ENHANCES SURVIVAL IN A MOUSE MODEL OF SPONTANEOUS LUNG ADENOCARCINOMA

Jordan Lukacs*. *Dalhousie University, Halifax, Canada*

Background Non-small cell lung cancer (NSCLC) is a leading cause of cancer deaths, with a 5-year survival rate of 19%. Improvements in treatment are crucial for reducing both morbidity and mortality. In this study, we examined the therapeutic benefit of combining oncolytic vesicular stomatitis virus (VSV) expressing reovirus-derived fusion-associated small transmembrane (FAST) proteins (p14 or p15), PD-1 checkpoint blockade, and natural killer T (NKT) cell immunotherapy in a genetic mouse model of lung adenocarcinoma.

Methods Mice containing a tamoxifen-inducible Cre recombinase gene driven by the (Club cell-secretory protein) CCSP promoter, were crossed with mice containing a Lox-Stop-Lox KRAS^{G12D} mutation and a floxed p53 allele. CCSP-KP mice were treated with VSV-GFP, VSV-p14, or VSV-p15 on days 40, 42, and 44, followed on day 45 by treatment with α -galactosylceramide-loaded dendritic cells to activate NKT cells. Anti-PD-1 (ip. 300 μ g) was given once a week for a total of 4 doses (days 48, 55, 62, and 69). MTT assays were performed to examine the oncolytic potential of the VSV-FAST constructs (VSV-p14, -p15, -p14delta, -p14endop15, -p10 ARV, -p10 NBV) in comparison to UV-inactivated VSV and VSV-GFP controls in murine (LLC, CMT-167) and human lung cancer cell lines (A549).

Results MTT cell viability assays demonstrate that VSV-FAST constructs VSV-p14, -p15, and chimeric -p14endop15 have increased tumor cell killing ability when compared to VSV-GFP in both mouse and human lung cancer cells. CCSP-KP mice receiving combinatorial treatment of VSV-p14 or VSV-p15, NKT cell activation, and PD-1 blockade exhibited increased overall survival in comparison with untreated or VSV-GFP combination therapy treated mice CCSP-KP mice. Furthermore, signs of morbidity (heavy or labored respirations, hunched posture, weight loss, etc.) were considerably delayed in treated mice.

Conclusions Our study demonstrates that VSV-FAST constructs are effective at killing lung cancer cells and when combined with NKT cell immunotherapy and immune checkpoint blockade, can prolong survival in a mouse model of NSCLC.

Acknowledgements BJ is funded by a CIHR operating grant (PJT-153285), JDL is funded by CIBC via the BHCRI CRTP 2020-21 Award, a DMRF 2020-22 I3V Graduate Studentship, and a BHCRI DMRF 2022-24 Rosetti Scholarship.

Ethics Approval This study was approved by the Dalhousie University Committee on Laboratory Animals; approval number 20-100.

<http://dx.doi.org/10.1136/jitc-2022-SITC2022.0792>

793

TREATMENT OF ANTI-SIRP α IN COMBINATION WITH ANTI-TAA EXERTS SUPERIOR ANTI-TUMOR ACTIVITY

Xiaofeng Niu, Chunlian Wang, Jinfeng Zhao, Haiying Wang, Li Zhang, Jiahui Hu, Jingfeng Yu, Yefeng Lu, Xiaoli Guo, Haixia Jiang, Rui Gao, Zhihao Wu, Yangsheng Qiu, Quan Qiu, Zheng Song, Dawei Sun, Hongtao Lu*. *Elpscience Biopharma, Shanghai, China*

Background Signal-regulatory protein alpha (SIRP α), is an inhibitory receptor expressed on myeloid cells and dendritic cells. Ligation of CD47 to SIRP α delivers a “don’t eat me” signal to suppress phagocytosis. Tumor cells frequently overexpress CD47 to evade macrophage-mediated destruction. Currently, agents targeting CD47 have proceeded to clinical trials and demonstrated promising anti-tumor results. However, these agents have been associated with hemolytic anemia and thrombocytopenia. In addition, universal expression of CD47 causes antigen sink, which leads to reduced efficacy. We therefore consider targeting CD47 receptor SIRP α to achieve improved efficacy with better safety profile. We have developed a pan-allele anti-SIRP α competitive functional antibody ES004-B5 that potently potentiates antibody dependent cellular phagocytosis (ADCP) activity of antibodies against tumor associated antigens (TAAs) *in vitro* and *in vivo*.

Methods Pan-allele SIRP α reactivities, SIRP family homologue binding properties, and cross-species reactivity were evaluated by ELISA and FACS. Antigen binding affinity was determined by surface plasmon resonance system (Biacore). Blocking activity was determined by competition assay and SHP-1 recruitment assay. *In vitro* functional activity was determined by phagocytosis assay. The impact on T cell function was evaluated by mixed lymphocyte reaction (MLR). *In vivo* efficacy was evaluated in a syngeneic mouse tumor model with human CD47/human SIRP α double knock-in mice. Epitope analysis was performed by competitive ELISA and hydrogen deuterium exchange mass spectrometry (HDX-MS). Lead clone was humanized via CDR grafting and back mutation screening. Non-human primates (NHPs) models were used to assess the safety and pharmacokinetics of the humanized candidate.

Results ES004-B5 recognizes pan-allele human SIRP α with high affinity, and cross reacts well with cynomolgus SIRP α . It binds a unique epitope on SIRP α that is distinct from known competitor molecules. Although ES004-B5 binds to SIRP γ expressed on T cell surface, it doesn’t cause negative impact on T cell activation. ES004-B5 potently blocks CD47-SIRP α interaction as well as CD47 mediated SHP-1 recruitment to phosphorylated SIRP α intracellular tail. Through blocking CD47-induced inhibitory “don’t eat me” signals, ES004-B5 potently potentiates ADCP activity of anti-TAA antibodies like rituximab and cetuximab. In a syngeneic mouse tumor model, the combination of ES004-B5 plus anti-Claudin18.2 significantly inhibited tumor growth *in vivo*. ES004-B5 has favorable pharmacokinetics and safety profile in NHPs.

Conclusions In summary, the functional anti-SIRP α mAb ES004-B5 has great potential to be used in combinations with multiple anti-TAA antibodies in cancer treatment. We are currently advancing the development of ES004-B5 into clinical candidate.

<http://dx.doi.org/10.1136/jitc-2022-SITC2022.0793>

794

TKM-011, ANTI-CD20 ANTIBODY CONFERS MULTI-PROPERTIES AGAINST BURKITT'S LYMPHOMA IN COMPARABLE EFFICACY TO RITUXIMAB AND OBINUTUZUMAB

Jutatip Panaampon*, Seiji Okada. Kumamoto University, Kumamoto, Japan

Background Burkitt's lymphoma (BL), an aggressive non-Hodgkin B-cell lymphoma needs an intensive chemotherapy regimen for the treatment. Immunotherapy plays significant roles in the treatment of BL. Rituximab (RTX) treatment regimens display the correlation with a positive prognosis. Yet, there is the subset of patients failed to respond to RTX treatment or became the resistance to RTX treatment. Newer generation of monoclonal anti-CD20 antibodies such as Obinutuzumab (OBI) have shown to inhibit B cell malignancies. TKM-011, the novel anti-CD20 antibody that binds to different CD20 epitope has been established. In this study, we studied the efficacy of TKM-011, RTX, and OBI against BL cell lines both *in vitro* and *in vivo*.

Methods We screened the antibody-dependent cytotoxicity (ADCC) and antibody-dependent cell phagocytosis (ADCP) by using the luciferase effector bioassay-based Jurkat cells with the expression of Fc receptor to evaluate ADCC and ADCP activities of RTX, TKM-011, and OBI. Raji and Ramos cell lines were used as the target cells. Flowcytometric analysis was performed to confirm ADCC by using KHYG-1 (CD16⁺) and N6 (CD16 transduced KHYG-1) NK cell lines. In order to determine ADCP, we generated monocyte-derived macrophages from healthy donors and performed ADCP assay. Moreover, we also tested the efficacy of these antibodies *in vivo* model by using Raji cells xenografted-immunodeficient mice.

Results TKM-011 exerted ADCC and ADCP activities in the similar levels compared to that of RTX and OBI. Moreover, TKM-011 also showed a potent CDC activity against BL cells. By performing MTT assay, all 3 antibodies presented an induction of cell death. The results of an *in vivo* experiment demonstrated an equivalent inhibitory level of tumor growth by the three tested antibodies.

Conclusions TKM-011 shows multi-activities against BL cell lines. The efficacy of TKM-011 reaches the level of standard RTX antibody. Considering the different binding epitopes in CD20, TKM-011 can be an alternative antibody therapy for the treatment of BL.

<http://dx.doi.org/10.1136/jitc-2022-SITC2022.0794>

795

STAT3 SIGNALING AS A CHECKPOINT FOR TLR9-DRIVEN EPIGENETIC REPROGRAMMING OF ACUTE MYELOID LEUKEMIA INTO ANTIGEN-PRESENTING CELLS

<http://dx.doi.org/10.1136/jitc-2022-SITC2022.0795>

Dongfang Wang, Priyanka Duttgupta, Yu-Lin Su, Haiqing Li, Mingye Feng, Bin Zhang, Ya-Huei Kuo, Guido Marcucci, Marcin Kortylewski*. Beckman Research Institute at City of Hope, Duarte, CA, USA

Background Cultured AML blasts can differentiate into antigen-presenting cells, however, stimulating leukemic cell differentiation and immunogenicity in patients has not translated into therapeutic effects. We previously demonstrated that eliminating STAT3 signaling in *Cbfb/MYH11/Mpl* (CMM) leukemia using siRNA or decoy DNA strategies permits TLR9-induced AML cell differentiation and thereby leads to potent adaptive immune responses and leukemia regression.^{1,2}

Methods Here, we interrogated cellular and molecular underpinnings of leukemic cells differentiation following STAT3-inhibition and TLR9-activation (STAT3i/TLR9a).

Results Our whole genome and single-cell transcriptomic analyses combined with immunophenotyping revealed that the combined STAT3i/TLRa had a dramatic effect on CMM cell differentiation. The treatment induced heterogenous leukemia cell clusters at different stages of myeloid cell differentiation towards macrophage and antigen-presenting cell phenotype. These were characterized by decreasing gene signatures of proliferation/survival genes with appearance of signature of leukocyte activation, antigen presentation, and in case of more differentiated AML-derived clusters, type I and type II IFNs. The more differentiated clusters 6, 12 and 15 were characterized by markers of antiviral/antimicrobial responses with pronounced expression of type I and II IFNs. The transcriptional profiling of CMM cells isolated from mice treated using inducible STAT3 gene silencing or decoy STAT3 in combination with TLR9 stimulation, revealed the increased expression of genes regulating myeloid cell differentiation such as *Irf8*, *Cebpa*, and *Cebpe* with decreased expression of leukemia-promoting *Runx1*. The combination treatment also increased expression of genes regulating antigen-presentation such as *Gadd45A*, *Ciita*, *Il12a*, and *Ifng* in leukemic cells. We further confirmed that IRF8 expression is required for AML cell differentiation as shown by conditional *Irf8* silencing. The AML cell reprogramming was likely regulated epigenetically as indicated by the reduced gene methylation profile of crucial myeloid cell differentiation genes such as *Irf8*. These changes were associated with reduced expression of DNMT1 and DNMT3ab, known STAT3 target genes.

Conclusions Our studies suggest that eliminating STAT3 checkpoint allows for TLR9-mediated reprogramming of leukemic cells into antigen-presenting cells capable of stimulating adaptive T cell immune responses against AML. Furthermore, these findings support further development of CpG-STAT3 inhibitors as a new bi-functional agent for AML immunotherapy.

Acknowledgements This project was supported by the National Cancer Institute of the National Institutes of Health under award number R01CA213131 to M.K.

REFERENCES

1. Hossain DMS, Dos Santos C, Zhang Q, Kozłowska A, Liu H, Gao C, Moreira D, Swiderski P, Jozwiak A, Kline J, *et al.* Leukemia cell-targeted STAT3 silencing and TLR9 triggering generate systemic antitumor immunity. *Blood*. 2014;**123**:15–25. PMID: PMC3879904
2. Zhang Q, Hossain DMS, Duttgupta P, Moreira D, Zhao X, Won H, Buettner R, Nechaev S, Majka M, Zhang B, *et al.* (2016). Serum-resistant CpG-STAT3 decoy for targeting survival and immune checkpoint signaling in acute myeloid leukemia. *Blood*. 2016;**127**:1687–1700. PMID: PMC4817311

796

REPURPOSING NSAIDS FOR CANCER IMMUNOTHERAPY: MECHANISMS BEYOND COX INHIBITION

¹Gang Zhou*, ¹Nada Aboeella, ¹Md Gazi, ²Gary Piazza. ¹Augusta University, Augusta, GA, USA; ²Auburn University, Auburn, AL, USA

Background Adoptive cell therapy (ACT) using genetically modified T cells has evolved into a promising treatment option for patients with cancer. However, even for the best-studied and clinically validated CD19-targeted chimeric antigen receptor (CAR) T-cell therapy, many patients face the challenge of lack of response or disease relapse. There is increasing need to improve the efficacy of ACT so that durable, curative outcomes can be achieved in a broad patient population.

Methods Here we investigated the impact of non-steroidal anti-inflammatory drugs (NSAIDs) on the efficacy of ACT in multiple preclinical models. Mice with established B-cell lymphoma received various combinations of preconditioning chemotherapy, infusion of suboptimal dose of tumor-reactive T cells, and administration of either indomethacin (indo, a COX-inhibitory NSAID) or ADT-030 (a non-COX-inhibitory novel NSAID). Donor T cells used in the ACT models included CD4+ T cells expressing a tumor-specific T cell receptor (TCR) and T cells engineered to express CD19CAR. Mice were monitored for tumor growth and survival. The effects of indo on donor T cell phenotype and function were evaluated. The molecular mechanisms by which the selected NSAID shapes the outcome of ACT were investigated.

Results ACT coupled with indo administration led to improved tumor growth control and prolonged mouse survival. Indo did not affect the activation status and tumor infiltration of the donor T cells. Moreover, the beneficial effect of indo in ACT did not rely on its inhibitory effect on the immunosuppressive COX2/PGE2 axis. Instead, indo-induced oxidative stress boosted the expression of death receptor 5 (DR5) in tumor cells, rendering them susceptible to donor T cells expressing TNF-related apoptosis-inducing ligand (TRAIL). Furthermore, the ACT-potentiating effect of indo was diminished against DR5-deficient tumors, but was amplified by donor T cells engineered to overexpress TRAIL.

Conclusions Our results demonstrate that the pro-oxidative property of NSAIDs can be exploited to enhance death receptor signaling in cancer cells, providing rationale for combining NSAIDs with genetically modified T cells to intensify tumor cell killing through the TRAIL-DR5 axis.

Ethics Approval All animal experiments and procedures were performed in accordance with the institutional protocol and were approved by the Institutional Animal Care and Use Committee (IACUC) of Augusta University.

<http://dx.doi.org/10.1136/jitc-2022-SITC2022.0796>

797

REAL-WORLD TREATMENT DURATION OF ATEZOLIZUMAB+CARBOPLATIN+ETOPOSIDE AMONG OLDER PATIENTS WITH EXTENSIVE-STAGE SMALL CELL LUNG CANCER (ES-SCLC) AND THE IMPACT OF PERFORMANCE STATUS AND BRAIN METASTASES

¹Husam Albarmawi*, ²Scott Robinson, ²Kevin Dietz, ²Kris Norris, ¹Nindhana Paranthaman, ¹Sarika Ogale, ²Taylor Schwartz. ¹Genentech, South San Francisco, CA, USA; ²Inovalon, Bowie, MD, USA

Background Previous real-world studies of first-line (1L) atezolizumab+carboplatin+etoposide for ES-SCLC in the US community oncology setting showed similar treatment durations (medians: 4.9;5.7 months) as in the IMpower133 trial (median: 4.7 months) although the real-world populations had higher proportions of patients with poor ECOG performance status (PS) and brain metastases.^{1,2} This study measured treatment duration in an older ES-SCLC population initiating 1L atezolizumab+carboplatin+etoposide and the impact of ECOG PS and brain metastases at baseline on treatment duration.

Methods This retrospective cohort study utilized the 100% sample of Medicare Fee-For-Service enrollment and Parts A/B claims from January 1, 2018 to June 30, 2021. Beneficiaries with ≥ 2 claims with an ICD-10-CM code for lung cancer and claims for atezolizumab+carboplatin+etoposide were identified. Index was 1L treatment initiation occurring between October 11, 2018 to December 31, 2019. ECOG PS at baseline was approximated using a claims-based measure that classifies individuals as good (ECOG 0-1) or fair/poor (ECOG ≥ 2) based on healthcare utilization in the 12-month pre-index period.³ Baseline brain metastases were identified from diagnosis to 30 days post-index based on ICD-10-CM codes. 1L treatment duration was measured from index to a gap in treatment claims of ≥ 60 days, initiation of a new anti-cancer regimen or death. Kaplan-Meier curves were utilized to examine the differences for patients stratified by brain metastases (Y/N) and binary ECOG PS.

Results A total of 2,470 patients older than 65 years (median age: 73 years) were included in the study with a median follow-up of 8.4 months. 62% had a proxy for fair/poor ECOG PS and 22% had baseline brain metastases. Median 1L duration for the full cohort was 5.4 months (95% CI: 5.2-5.6). Median 1L treatment duration was 5.1 months for patients with poor/fair ECOG PS (95% CI: 5.1-5.3) and 5.8 months (95% CI: 5.6-6.0) for patients with good ECOG PS (figure 1) (Log-Rank $p < 0.0001$). Median 1L treatment duration for patients with brain metastases was 5.0 months (95% CI: 4.6-5.3) and 5.5 months (95% CI: 5.3-5.7) for patients without brain metastases (figure 2) (Log-Rank $p = 0.2488$).

Conclusions Despite the older age of the study population and the worse baseline ECOG PS and brain metastases status, 1L treatment duration with atezolizumab+carboplatin+etoposide was similar to those observed in IMpower133 and in previous real-world community oncology studies. Based on descriptive comparisons, treatment duration was longer in patients with a proxy for good ECOG PS (statistically significant) and patients without brain metastases (not statistically significant).

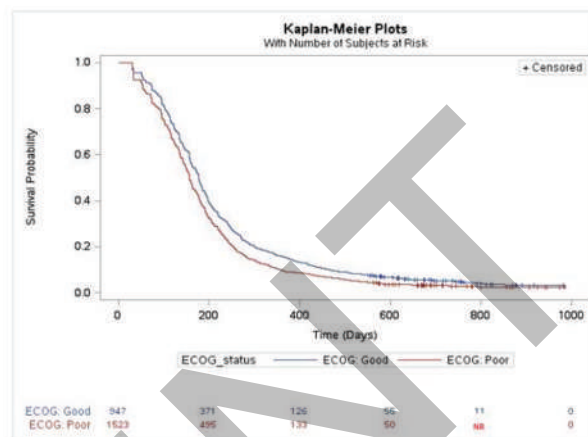
Acknowledgements Shambhavi Kumar for statistical analysis.

REFERENCES

1. Nadler, Eric S, et al. Real-world evidence of cancer immunotherapy (CIT) combination treatment in first-line (1L) extensive-stage small cell lung cancer (ES-SCLC). 2021;8561-8561.
2. Tsui DCC, et al. 1650P Adoption and early clinical outcomes of atezolizumab (atezo)+ carboplatin and etoposide (CE) in patients with extensive-stage small cell

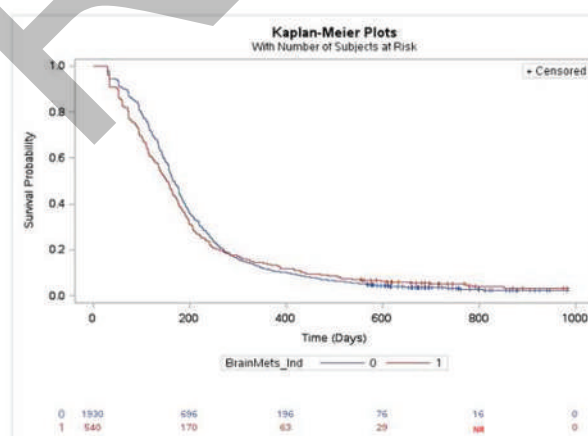
lung cancer (ES-SCLC) in the real-world (RW) setting. *Annals of Oncology*. 2021;**32**:S1164.

3. Sheffield, Kristin M, et al. Development and validation of a claims-based approach to proxy ECOG performance status across ten tumor groups. *Journal of Comparative Effectiveness Research*. 2018;**7**(3):193-208.



Notes: NR: No record - counts less than 11 are suppressed

Abstract 797 Figure 1 Unadjusted time to the end of 1L treatment for patients with ES-SCLC initiating on carboplatin + etoposide + atezolizumab, by ECOG status (Good vs. Poor/Fair).



Notes: NR: No record - counts less than 11 are suppressed

Abstract 797 Figure 2 Unadjusted time to the end of 1L treatment for patients with ES-SCLC initiating on carboplatin + etoposide + atezolizumab, by brain metastases at baseline (Yes/No)

<http://dx.doi.org/10.1136/jitc-2022-SITC2022.0797>

Abstracts

798

REAL-WORLD OVERALL SURVIVAL AMONG PATIENTS RECEIVING FIRST-LINE (1L) PEMBROLIZUMAB IN THE TREATMENT OF RECURRENT/METASTATIC HEAD AND NECK SQUAMOUS CELL CARCINOMA (R/M HNSCC) IN THE UNITED STATES

<http://dx.doi.org/10.1136/jitc-2022-SITC2022.0798>

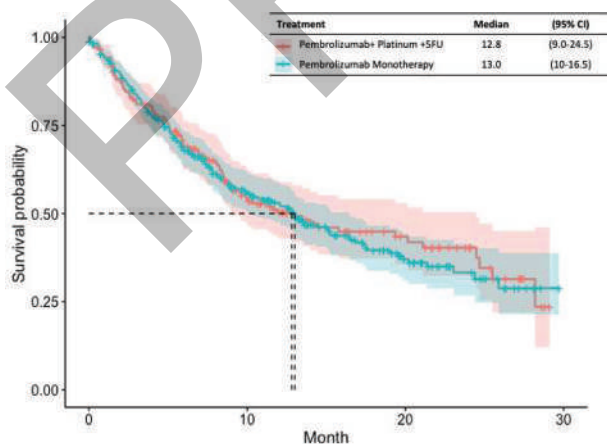
Christopher Black*, Liya Wang, Karthik Ramakrishnan, Gleicy Hair, Daisuke Goto. Merck and Co., Inc., Rahway, NJ, USA

Background KEYNOTE-048 has demonstrated extended survival benefit of pembrolizumab in 1L R/M HNSCC. This study aims to assess real-world overall survival (rwOS).

Methods A retrospective cohort study was conducted using the Flatiron Health Advanced Head and Neck database. The study cohort included adult R/M HNSCC patients, who initiated 1L pembrolizumab monotherapy (P) or combination with chemotherapy (P+C) between 07/01/19 – 6/30/21 with follow-up until 12/31/21. Patients were excluded if they received prior platinum treatment ≤ 6 months of 1L pembrolizumab therapy, had other primary cancers before R/M HNSCC diagnosis, or were treated with a clinical study drug. rwOS was assessed using Kaplan-Meier methods, and a multivariate Cox proportional hazard model assessed the effects of age (≥ 75 vs < 75), gender, race, primary tumor site, staging at diagnosis, HPV status, smoking, ECOG PS, and CPS score.

Results A total of 513 patients initiated 1L pembrolizumab therapy, [P (n=337), P+C (n=176)]. The median rwOS was 13.0 months (95%CI 10.0-15.3) for P and 12.8 months (95% CI 9.0-21.1) for P+C (figure 1), consistent with the results of the KEYNOTE-048 trial [P: 11.5 months (10.3 – 13.5) P+C: 13.0 months (10.9 – 14.7)]. Survival rates at 24 months (P: 33.3% (26.2 – 40.6) and P+C: 40.3% (31.3- 49.2) were greater in the real-world compared to KEYNOTE-048. The Cox proportional- hazards model found that older age (≥ 75 years vs < 75) and higher ECOG PS (2+ vs 0-1) were unfavorable predictors of rwOS survival (HR=1.4 , 95% CI 1.03-1.90, HR: 1.5, 95%CI 1.08-2.1). This analysis further showed no significant differences in rwOS between P and P+C populations.

Conclusions Overall survival among patients treated with pembrolizumab in the real-world were consistent with results from KEYNOTE-048. We found that age and ECOG were predictive of rwOS even after removing the effects of other common predictors, such as race, HPV status, and staging at diagnosis.



Abstract 798 Figure 1
Real-World Overall Survival of Pembrolizumab Regimens

799

REAL-WORLD USE OF PEMBROLIZUMAB COMBINATION REGIMENS IN FIRST-LINE RECURRENT/METASTATIC HEAD AND NECK SQUAMOUS CELL CARCINOMA

Christopher Black*, Liya Wang, Karthik Ramakrishnan, Daisuke Goto. *Merck and Co., Inc., Rahway, NJ, USA*

Background Based on KEYNOTE-048 results, pembrolizumab was approved for use as monotherapy and in combination with platinum+5FU in the first-line (1L) treatment of patients with recurrent or metastatic head and neck squamous cell carcinoma (R/M HNSCC). Taxanes can help expand the available treatment options in the 1L R/M HNSCC, in place of 5-FU. NCCN guidelines recommend pembrolizumab + platinum + taxane as another treatment option for R/M HNSCC patients. This study assessed the real-world treatment patterns of patients receiving pembrolizumab combination regimens in 1L R/M HNSCC.

Methods This retrospective cohort study assessed data from a US based de-identified EHR-derived database (Flatiron Health Advanced H&N database) of patients initiating pembrolizumab + platinum + taxane or platinum + 5-FU regimens between 07/01/19 – 6/30/21 with follow-up until 12/31/21. Real-world time on treatment (rwToT) was defined as length of time between first and last documented administration date pembrolizumab and assessed using Kaplan-Meier method.

Results A total of 225 patients received pembrolizumab combination therapy (Platinum+5-FU:176, Platinum+Taxane:49). Patient characteristics (age, gender, ECOG PS) were similar; differences were noted in oropharyngeal HPV+ cancer (50.0% vs 75.0%), and% treated at an academic center (6.3% vs 34.7%) between pembrolizumab with platinum + 5-FU and platinum + taxane, respectively (table 1). Carboplatin use was similar among pembrolizumab + platinum + 5-FU (84.8%) and platinum + taxane (87.8%) patients, where paclitaxel was the most used taxane (87.8%). Patients remained on treatment longer with pembrolizumab + platinum + taxane compared to pembrolizumab + platinum + 5-FU .

Conclusions Substituting 5-FU with a taxane resulted in a longer median rwToT of 2.4 months. These results support guideline recommendations for the pembrolizumab + platinum + taxane combination as another treatment option for 1L R/M HNSCC patients.

Abstract 799 Table 1

	Pembrolizumab+Platinum+5-FU (N = 176)	Pembrolizumab+Platinum+Taxane (N = 49)
Discontinued, N (%)	132 (75.0)	28 (57.1)
Median Follow Up, months (range)	8.5 (0.1 - 29.1)	8.3 (0.0 - 29.2)
Median ToT, months (95% CI)	5.0 (3.9 - 6.0)	7.4 (4.2 - 20.0)
On-treatment rate (95% CI)		
6 months	42.3% (34.8 - 49.7)	55.8% (40.5 - 68.6)
12 months	20.2% (14.0 - 27.3)	36.8% (21.0 - 52.7)
18 months	16.3% (10.5 - 23.3)	36.8% (21.0 - 52.7)
24 months	14.3% (8.3 - 21.7)	27.6% (10.5 - 47.9)

Real-World Time on Treatment Results

<http://dx.doi.org/10.1136/jitc-2022-SITC2022.0799>

CLINICOPATHOLOGICAL AND MOLECULAR PREDICTIVE FACTORS OF SURVIVAL IN NON-SMALL CELL LUNG CANCER PATIENTS TREATED WITH FIRST-LINE IMMUNOTHERAPY WITH OR WITHOUT CHEMOTHERAPY: A SYSTEMATIC REVIEW AND META-ANALYSIS

Alessandro Di Federico*, Francesco Gelsomino, Andrea De Giglio, Francesca Sperandi, Barbara Melotti, Andrea Ardizzone. *IRCCS Azienda Ospedaliero-Universitaria Di Bologna, Bologna, Italy*

Background The majority of advanced non-small cell lung cancer (NSCLC) patients derives modest benefit from immunotherapy (IO) alone. For some of them, adding chemotherapy (CT) may significantly improve the outcomes, but the reliability of PD-L1 expression as the only biomarker to identify patients that might need concomitant CT is unsatisfactory.^{1,2}

Methods A systematic research of articles using PubMed/MEDLINE, and the Cochrane Database of Systematic Reviews and Central Register of Controlled Trials was performed, last updated April 11th, 2022. Abstract from main oncology congresses were also searched, including ASCO 2022. Eligible studies were randomized controlled clinical trials (RCT) investigating IO, alone or combined with CT, versus CT alone in previously untreated advanced NSCLC patients. The objective was to detect clinicopathological and molecular predictive factors of survival (progression-free survival and overall survival). Study characteristics and outcome estimates (hazard ratio and 95% CI) were extracted. Random-effects meta-analyses were performed to investigate IO alone versus CT, and IO plus CT versus CT. Random-effects meta-regression analyses were performed to provide a comparison of IO alone versus IO plus CT.

Results a total of 14367 patients with advanced NSCLC in 25 RCT was included (table 1).³⁻⁴⁸ Squamous histology, male gender, current/former smoker status, PD-L1 expression $\geq 50\%$, and high TMB correlated with improved survival with IO alone compared to CT. Conversely, female gender, absence of smoking history, negative PD-L1 expression, and low TMB correlated with unsatisfactory outcomes with IO alone versus CT (figure 1), but not with IO plus CT versus CT (figure 2). IO plus CT improved survival versus IO alone in female patients [HR for PFS: 1.65, 95% CI, 1.25-2.18, $p=0.0004$; HR for OS: 1.31, 95% CI, 1.01-1.71, $p=0.044$], never smokers [HR for PFS: 3.59, 95% CI, 1.62-7.94, $p=0.0016$; HR for OS: 1.28, 95% CI, 0.95-1.72, $p=0.10$], in those having a PD-L1 expression $\geq 1\%$ [HR for PFS: 1.88, 95% CI, 1.55-2.28, $p<0.0001$; HR for OS: 1.28, 95% CI, 1.11-1.48, $p=0.0007$] or a low TMB [HR for PFS: 2.08, 95% CI, 1.61-2.70, $p<0.0001$; HR for OS: 1.43, 95% CI, 1.12-1.82, $p=0.004$], and in patients with central nervous system metastasis [HR for PFS: 1.51, 95% CI, 1.01-2.25, $p=0.045$; HR for OS: 1.32, 95% CI, 0.85-2.06, $p=0.22$] (figure 3).

Conclusions Certain clinicopathological and molecular features may add predictive value to PD-L1 expression in the selection of the most appropriate first-line treatment for advanced NSCLC patients.

REFERENCES

1. Di Federico A, De Giglio A, Parisi C, Gelsomino F, Ardizzone A. PD-1/PD-L1 inhibitor monotherapy or in combination with chemotherapy as upfront treatment for advanced NSCLC with PD-L1 expression $\geq 50\%$: Selecting the best strategy. *Crit Rev Oncol Hematol*. 2021;160. doi:10.1016/j.critrevonc.2021.103302
2. Gelsomino F, Facchinetti F, Sisi M, Zielli T, Tiseo M, Ardizzone A. PD-L1 $\geq 50\%$ lung cancer refractory to PD-1 inhibition: the role of salvage chemo-immunotherapy combination. *Immunotherapy*. 2021 Apr;13(5):363-369. doi: 10.2217/imt-2020-0280. Epub 2021 Feb 3. PMID: 33533279.

3. Ren S, Chen J, Xu X, et al. Camrelizumab Plus Carboplatin and Paclitaxel as First-Line Treatment for Advanced Squamous NSCLC (Camel-Sq): A Phase 3 Trial. *J Thorac Oncol*. 2022;17(4):544-557. doi:10.1016/j.jtho.2021.11.018
4. Carbone DP, Reck M, Paz-Ares L, et al. First-Line Nivolumab in Stage IV or Recurrent Non-Small-Cell Lung Cancer. *N Engl J Med*. 2017;376(25):2415-2426. doi:10.1056/NEJMoa1613493/SUPPL_FILE/NEJMoa1613493_DISCLOSURES.PDF
5. Borghaei H, Pluzanski A, Caro RB, et al. Abstract CT221: Nivolumab (NIVO) + ipilimumab (IPI) as first-line (1L) treatment for patients with advanced non-small cell lung cancer (NSCLC) with brain metastases: Results from CheckMate 227. *Cancer Res*. 2020;80(16_Supplement):CT221-CT221. doi:10.1158/1538-7445.AM2020-CT221
6. Hellmann MD, Paz-Ares L, Bernabe Caro R, et al. Nivolumab plus Ipilimumab in Advanced Non-Small-Cell Lung Cancer. *N Engl J Med*. 2019;381(21):2020-2031. doi:10.1056/NEJMoa1910231/SUPPL_FILE/NEJMoa1910231_DATA-SHARING.PDF
7. Paz-Ares LG, Ramalingam SS, Ciuleanu TE, et al. First-Line Nivolumab Plus Ipilimumab in Advanced NSCLC: 4-Year Outcomes From the Randomized, Open-Label, Phase 3 CheckMate 227 Part 1 Trial. *J Thorac Oncol*. 2022;17(2):289-308. doi:10.1016/j.jtho.2021.09.010
8. Hellmann MD, Ciuleanu T-E, Pluzanski A, et al. Nivolumab plus Ipilimumab in Lung Cancer with a High Tumor Mutational Burden. *N Engl J Med*. 2018;378(22):2093-2104. doi:10.1056/NEJMoa1801946/SUPPL_FILE/NEJMoa1801946_DISCLOSURES.PDF
9. Paz-Ares L, Ciuleanu TE, Cobo M, et al. First-line nivolumab plus ipilimumab combined with two cycles of chemotherapy in patients with non-small-cell lung cancer (CheckMate 9LA): an international, randomised, open-label, phase 3 trial. *Lancet Oncol*. 2021;22(2):198-211. doi:10.1016/S1470-2045(20)30641-0
10. Reck M, Ciuleanu TE, Cobo M, et al. First-line nivolumab plus ipilimumab with two cycles of chemotherapy versus chemotherapy alone (four cycles) in advanced non-small-cell lung cancer: CheckMate 9LA 2-year update. *ESMO Open*. 2021;6(5). doi:10.1016/j.esmoop.2021.100273/ATTACHMENT/6DA1AD81-B43A-4503-BA0B-7BFA0079C4AE/MMC2.PDF
11. Paz-Ares L, Ciuleanu T-E, Cobo M, et al. 980 First-line nivolumab (NIVO) + ipilimumab (IPI) + 2 cycles chemotherapy (chemo) vs 4 cycles chemo in advanced non-small cell lung cancer (aNSCLC): Association of blood and tissue tumor mutational burden (TMB) with efficacy in CheckMate 9LA. *J Thorac Oncol*. 2021;16(4):S750-S751. doi:10.1016/S1556-0864(21)01940-7
12. Sezer A, Kilickap S, Gümüş M, et al. Cemiplimab monotherapy for first-line treatment of advanced non-small-cell lung cancer with PD-L1 of at least 50%: a multicentre, open-label, global, phase 3, randomised, controlled trial. *Lancet*. 2021;397(10274):592-604. doi:10.1016/S0140-6736(21)00228-2
13. Gogishvili M, Melkadze T, Makhharadze T, et al. LBA51 EMPOWER-Lung 3: Cemiplimab in combination with platinum doublet chemotherapy for first-line (1L) treatment of advanced non-small cell lung cancer (NSCLC). *Ann Oncol*. 2021;32:S1328. doi:10.1016/j.annonc.2021.08.2130
14. Zhou C, Wang Z, Sun Y, et al. Sugemalimab versus placebo, in combination with platinum-based chemotherapy, as first-line treatment of metastatic non-small-cell lung cancer (GEMSTONE-302): interim and final analyses of a double-blind, randomised, phase 3 clinical trial. *Lancet Oncol*. 2022;23(2):220-233. doi:10.1016/S1470-2045(21)00650-1
15. Langer CJ, Gadgeel SM, Borghaei H, et al. Carboplatin and pemetrexed with or without pembrolizumab for advanced, non-squamous non-small-cell lung cancer: a randomised, phase 2 cohort of the open-label KEYNOTE-021 study. *Lancet Oncol*. 2016;17(11):1497-1508. doi:10.1016/S1470-2045(16)30498-3
16. Awad MM, Gadgeel SM, Borghaei H, et al. Long-Term Overall Survival From KEYNOTE-021 Cohort G: Pemetrexed and Carboplatin With or Without Pembrolizumab as First-Line Therapy for Advanced Nonsquamous NSCLC. *J Thorac Oncol*. 2021;16(1):162-168. doi:10.1016/j.jtho.2020.09.015
17. Gandhi L, Rodríguez-Abreu D, Gadgeel S, et al. Pembrolizumab plus Chemotherapy in Metastatic Non-Small-Cell Lung Cancer. *N Engl J Med*. 2018;378(22):2078-2092. doi:10.1056/NEJMoa1801005/SUPPL_FILE/NEJMoa1801005_DISCLOSURES.PDF
18. Rodríguez-Abreu D, Powell SF, Hochmair MJ, et al. Pemetrexed plus platinum with or without pembrolizumab in patients with previously untreated metastatic nonsquamous NSCLC: protocol-specified final analysis from KEYNOTE-189. *Ann Oncol*. 2021;32(7):881-895. doi:10.1016/j.annonc.2021.04.008
19. Gadgeel SM, Rodríguez-Abreu D, Felip E, et al. Abstract LB-397: Pembrolizumab plus pemetrexed and platinum vs placebo plus pemetrexed and platinum as first-line therapy for metastatic nonsquamous NSCLC: analysis of KEYNOTE-189 by STK11 and KEAP1 status. *Cancer Res*. 2020;80(16_Supplement):LB-397. doi:10.1158/1538-7445.AM2020-LB-397
20. Gadgeel S, Rodríguez-Abreu D, Felip E, et al. KRAS mutational status and efficacy in KEYNOTE-189: Pembrolizumab (pembro) plus chemotherapy (chemo) vs placebo plus chemo as first-line therapy for metastatic non-squamous NSCLC. *Ann Oncol*. 2019;30:xi64-xi65. doi:10.1093/annonc/mdz453.002
21. Paz-Ares L, Luft A, Vicente D, et al. Pembrolizumab plus Chemotherapy for Squamous Non-Small-Cell Lung Cancer. *N Engl J Med*. 2018;379(21):2040-2051. doi:10.1056/NEJMoa1810865/SUPPL_FILE/NEJMoa1810865_DATA-SHARING.PDF

22. Paz-Ares L, Vicente D, Tafreshi A, et al. A Randomized, Placebo-Controlled Trial of Pembrolizumab Plus Chemotherapy in Patients With Metastatic Squamous NSCLC: Protocol-Specified Final Analysis of KEYNOTE-407. *J Thorac Oncol.* 2020;15(10):1657-1669. doi:10.1016/j.jtho.2020.06.015/ATTACHMENT/DB543C43-C5A7-4C49-B4C1-0B54A4FAA2A0/MMC2.PDF

23. Reck M, Rodriguez-Abreu D, Robinson AG, et al. Pembrolizumab versus Chemotherapy for PD-L1-Positive Non-Small-Cell Lung Cancer. *N Engl J Med.* 2016;375(19):1823-1833. doi:10.1056/NEJM0A1606774/SUPPL_FILE/NEJM0A1606774_-DISCLOSURES.PDF

24. Reck M, Rodriguez-Abreu D, Robinson AG, et al. Five-Year Outcomes With Pembrolizumab Versus Chemotherapy for Metastatic Non-Small-Cell Lung Cancer With PD-L1 Tumor Proportion Score \geq 50. *J Clin Oncol.* 2021;39(21):2339-2349. doi:10.1200/JCO.21.00174

25. Mok TSK, Wu YL, Kudaba I, et al. Pembrolizumab versus chemotherapy for previously untreated, PD-L1-expressing, locally advanced or metastatic non-small-cell lung cancer (KEYNOTE-042): a randomised, open-label, controlled, phase 3 trial. *Lancet.* 2019;393(10183):1819-1830. doi:10.1016/S0140-6736(18)32409-7

26. Herbst RS, Lopes G, Kowalski DM, et al. LBA4 Association of KRAS mutational status with response to pembrolizumab monotherapy given as first-line therapy for PD-L1-positive advanced non-squamous NSCLC in Keynote-042. *Ann Oncol.* 2019;30:xi63-xi64. doi:10.1093/annonc/mdz453.001

27. Cho BC, Lopes G, Kowalski DM, et al. Abstract CT084: Relationship between STK11 and KEAP1 mutational status and efficacy in KEYNOTE-042: pembrolizumab monotherapy versus platinum-based chemotherapy as first-line therapy for PD-L1-positive advanced NSCLC. *Cancer Res.* 2020;80(16_Supplement):CT084-CT084. doi:10.1158/1538-7445.AM2020-CT084

28. Herbst RS, Lopes G, Kowalski DM, et al. Association between tissue TMB (tTMB) and clinical outcomes with pembrolizumab monotherapy (pembro) in PD-L1-positive advanced NSCLC in the KEYNOTE-010 and -042 trials. *Ann Oncol.* 2019;30:v916-v917. doi:10.1093/annonc/mdz394.077

29. Garassino M, Rodriguez-Abreu D, Gadgeel S, et al. OA04.06 Evaluation of TMB in KEYNOTE-189: Pembrolizumab Plus Chemotherapy vs Placebo Plus Chemotherapy for Nonsquamous NSCLC. Published online 2019. doi:10.1016/j.jtho.2019.08.427

30. Herbst RS, Giaccone G, de Marinis F, et al. Atezolizumab for First-Line Treatment of PD-L1-Selected Patients with NSCLC. *N Engl J Med.* 2020;383(14):1328-1339. doi:10.1056/NEJM0A1917346

31. West H, McCleod M, Hussein M, et al. Atezolizumab in combination with carboplatin plus nab-paclitaxel chemotherapy compared with chemotherapy alone as first-line treatment for metastatic non-squamous non-small-cell lung cancer (IMPowder130): a multicentre, randomised, open-label, phase 3 trial. *Lancet Oncol.* 2019;20(7):924-937. doi:10.1016/S1470-2045(19)30167-6

32. Jotte R, Cappuzzo F, Vynnychenko I, et al. Atezolizumab in Combination With Carboplatin and Nab-Paclitaxel in Advanced Squamous NSCLC (IMPowder131): Results From a Randomized Phase III Trial. *J Thorac Oncol.* 2020;15(8):1351-1360. doi:10.1016/j.jtho.2020.03.028

33. Nishio M, Barlesi F, West H, et al. Atezolizumab Plus Chemotherapy for First-Line Treatment of Nonsquamous NSCLC: Results From the Randomized Phase 3 IMPowder132 Trial. *J Thorac Oncol.* 2021;16(4):653-664. doi:10.1016/j.jtho.2020.11.025

34. Socinski MA, Jotte RM, Cappuzzo F, et al. Atezolizumab for First-Line Treatment of Metastatic Nonsquamous NSCLC. *N Engl J Med.* 2018;378(24):2288-2301. doi:10.1056/NEJM0A1716948/SUPPL_FILE/NEJM0A1716948_DISCLOSURES.PDF

35. West HJ, McClelland M, Cappuzzo F, et al. Clinical efficacy of atezolizumab plus bevacizumab and chemotherapy in KRAS- mutated non-small cell lung cancer with STK11, KEAP1, or TP53 mutations: subgroup results from the phase III IMPowder150 trial. *J Immunother Cancer.* 2022;10(2). doi:10.1136/JITC-2021-003027

36. Rizvi N, Cho BC, Reinmuth N, et al. OA04.07 Mutations Associated with Sensitivity or Resistance to Immunotherapy in mNSCLC: Analysis from the MYSTIC Trial. *J Thorac Oncol.* 2019;14(10):S217. doi:10.1016/j.jtho.2019.08.428

37. Yang Y, Wang Z, Fang J, et al. Efficacy and Safety of Sintilimab Plus Pemetrexed and Platinum as First-Line Treatment for Locally Advanced or Metastatic Nonsquamous NSCLC: a Randomized, Double-Blind, Phase 3 Study (Oncology pProgram by InnovENT anti-PD-1-11). *J Thorac Oncol.* 2020;15(10):1636-1646. doi:10.1016/j.jtho.2020.07.014/ATTACHMENT/A450760A-EFAF-4CFA-AC80-66972EBF946D/MMC3.PDF

38. Yang Y, Sun J, Wang Z, et al. Updated Overall Survival Data and Predictive Biomarkers of Sintilimab Plus Pemetrexed and Platinum as First-Line Treatment for Locally Advanced or Metastatic Nonsquamous NSCLC in the Phase 3 ORIENT-11 Study. *J Thorac Oncol.* 2021;16(12):2109-2120. doi:10.1016/j.jtho.2021.07.015/ATTACHMENT/DD298D6B-F7AA-48D6-8288-DDA53C31BB1/MMC2.XLSX

39. Lu S, Wang J, Yu Y, et al. Tislelizumab Plus Chemotherapy as First-Line Treatment for Locally Advanced or Metastatic Nonsquamous NSCLC (RATIONALE 304): A Randomized Phase 3 Trial. *J Thorac Oncol.* 2021;16(9):1512-1522. doi:10.1016/j.jtho.2021.05.005

40. Sugawara S, Lee JS, Kang JH, et al. Nivolumab with carboplatin, paclitaxel, and bevacizumab for first-line treatment of advanced nonsquamous non-small-cell lung cancer. *Ann Oncol.* 2021;32(9):1137-1147. doi:10.1016/j.

ANNONC.2021.06.004/ATTACHMENT/OED241FD-B8B6-487E-83CB-4F8075F02C58/MMC1.PDF

41. Powell SF, Rodriguez-Abreu D, Langer CJ, et al. Outcomes With Pembrolizumab Plus Platinum-Based Chemotherapy for Patients With NSCLC and Stable Brain Metastases: Pooled Analysis of KEYNOTE-021, -189, and -407. *J Thorac Oncol.* 2021;16(11):1883-1892. doi:10.1016/j.jtho.2021.06.020

42. Johnson ML, Cho BC, Luft A, et al. Durvalumab + tremelimumab + chemotherapy as first-line treatment for mNSCLC: results from the phase 3 POSEIDON study. Presented at: International Association for the Study of Lung Cancer 2021 World Conference on Lung Cancer; September 8-14, 2021; Virtual. Abstract PL02.01.

43. Zhou C, Wu L, Fan Y. Sintilimab Plus Platinum and Gemcitabine as First-Line Treatment for Advanced or Metastatic Squamous NSCLC: Results From a Randomized, Double-Blind, Phase 3 Trial (ORIENT-12). *J Thorac Oncol.* 2021 Sep;16(9):1501-1511. doi: 10.1016/j.jtho.2021.04.011. Epub 2021 May 25. PMID: 34048947.

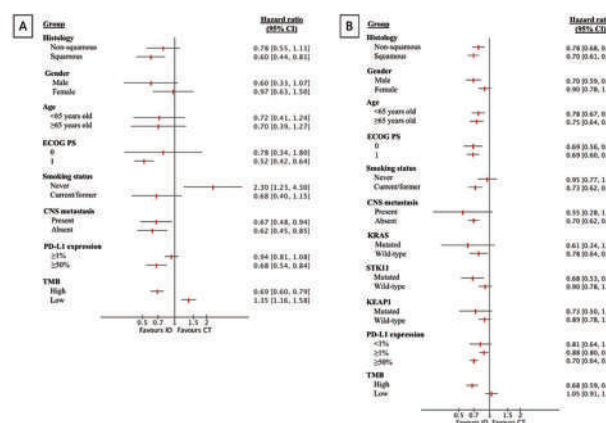
44. Wang J, Lu S, Yu X, et al. Tislelizumab Plus Chemotherapy vs Chemotherapy Alone as First-line Treatment for Advanced Squamous Non-Small-Cell Lung Cancer: A Phase 3 Randomized Clinical Trial. *JAMA Oncol.* 2021 May 1;7(5):709-717. doi: 10.1001/jamaoncol.2021.0366. PMID: 33792623; PMCID: PMC8017481.

45. Zhou C, Wang Z, Sun M, et al. A protocol pre-specified interim overall survival (OS) analysis of GEMSTONE-302: A phase 3 study of sugemalimab (suge) versus placebo plus platinum-based chemotherapy (chemo) as first-line (1L) treatment for patients (pts) with metastatic non-small cell lung cancer (NSCLC). https://doi.org/10.1200/JCO.2022.40.16_suppl.9027. 2022;40(16_suppl):9027-9027. doi:10.1200/JCO.2022.40.16_SUPPL.9027

46. Paz-Ares LG, Ciuleanu T-E, Cobo-Dols M, et al. First-line (1L) nivolumab (NIVO) + ipilimumab (IPI) + 2 cycles of chemotherapy (chemo) versus chemo alone (4 cycles) in patients (pts) with metastatic non-small cell lung cancer (NSCLC): 3-year update from CheckMate 9LA. https://doi.org/10.1200/JCO.2022.40.17_suppl.LBA9026. 2022;40(17_suppl):LBA9026-LBA9026. doi:10.1200/JCO.2022.40.17_SUPPL.LBA9026

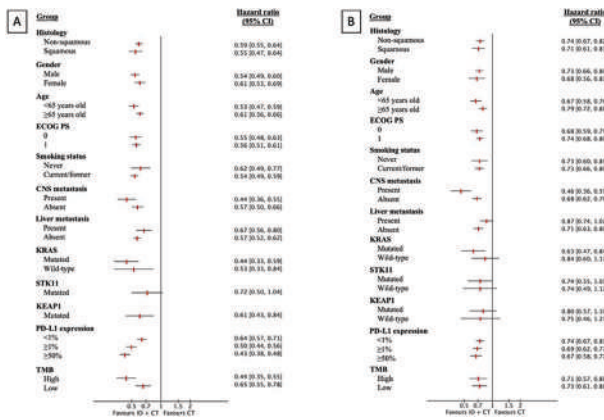
47. Brahmer JR, Lee J-S, Ciuleanu T-E, et al. Five-year survival outcomes with nivolumab (NIVO) plus ipilimumab (IPI) versus chemotherapy (chemo) as first-line (1L) treatment for metastatic non-small cell lung cancer (NSCLC): Results from CheckMate 227. https://doi.org/10.1200/JCO.2022.40.17_suppl.LBA9025. 2022;40(17_suppl):LBA9025-LBA9025. doi:10.1200/JCO.2022.40.17_SUPPL.LBA9025

48. Wang J, Wang Z, Wu L, et al. Final progression-free survival, interim overall survival, and biomarker analyses of CHOICE-01: A phase III study of toripalimab versus placebo in combination with first-line chemotherapy for advanced NSCLC without EGFR/ALK mutations. https://doi.org/10.1200/JCO.2022.40.36_suppl.362936. 2022;40(36_suppl):362936-362936. doi:10.1200/JCO.2022.40.36_SUPPL.362936

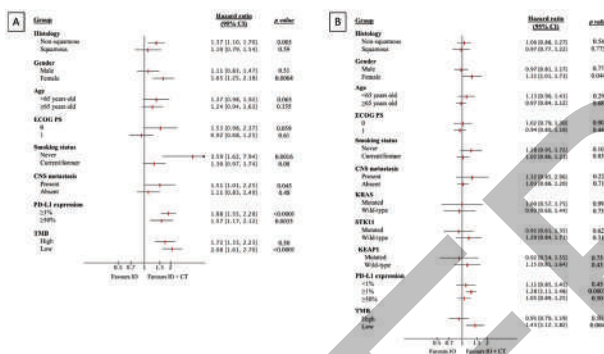


Abstract 800 Figure 1 IO versus CT
 Graphical representation of the PFS (A) and OS (B) of patients treated with IO versus CT resulting from the meta-analysis in each group. PFS: progression-free survival; OS: overall survival; IO: immunotherapy; CT: chemotherapy; CNS: central nervous system; PD-L1: programmed death-ligand 1; ECOG PS: eastern cooperative group performance status; TMB: tumor mutation burden.

Abstracts



Abstract 800 Figure 2 IO plus CT versus CT
Graphical representation of the PFS (A) and OS (B) of patients treated with IO plus CT versus CT resulting from the meta-analysis in each group.
PFS: progression-free survival; OS: overall survival; IO: immunotherapy; CT: chemotherapy; CNS: central nervous system; PD-L1: programmed death-ligand 1; ECOG PS: eastern cooperative group performance status; TMB: tumor mutation burden.



Abstract 800 Figure 3. IO versus IO plus CT
Graphical representation of the PFS (A) and OS (B) of patients treated with IO versus IO plus CT resulting from the meta-regression analysis in each group.
PFS: progression-free survival; OS: overall survival; IO: immunotherapy; CT: chemotherapy; CNS: central nervous system; PD-L1: programmed death-ligand 1; ECOG PS: eastern cooperative group performance status; TMB: tumor mutation burden.

Abstract 800 Table 1. Included trials

Trial	Phase	Histology	No. intervention/control	Arms of treatment
Camel-Sq	III	Squamous	192/196	Camrelizumab + carboplatin + paclitaxel vs carboplatin + paclitaxel
CheckMate 026	III	Squamous & non-squamous	211/212	Nivolumab vs platinum-based CT Part 1a: nivolumab + ipilimumab vs nivolumab vs platinum-based CT Part 1b: nivolumab + ipilimumab vs nivolumab + platinum-based CT vs platinum-based CT
CheckMate 227	III	Squamous & non-squamous	Part 1a: 396/396/397 Part 1b: 187/177/166	Nivolumab + ipilimumab + platinum-based CT vs nivolumab + platinum-based CT vs platinum-based CT
CheckMate 9LA	III	Squamous & non-squamous	361/358	Nivolumab + ipilimumab + platinum-based CT vs platinum-based CT
CHOICE-01*	III	Squamous & non-squamous	309/156	Toripalimab + platinum-based CT vs platinum-based CT
EMPOWER Lung 1	III	Squamous & non-squamous	283/280	Camrelizumab vs platinum-based CT
EMPOWER Lung 3*	III	Squamous & non-squamous	312/154	Camrelizumab + platinum-based CT vs platinum-based CT
GEMSTONE-302	III	Squamous & non-squamous	320/159	Sugemalimab + platinum-based CT vs platinum-based CT
Keynote 021	II	Non-squamous	60/63	peniciclovir + carboplatin + paclitaxel vs carboplatin + paclitaxel
Keynote 024	III	Squamous & non-squamous	154/151	Ipilimumab vs platinum-based CT
Keynote 042	III	Squamous & non-squamous	637/637	Ipilimumab vs platinum-based CT
Keynote 139	III	Non-squamous	410/206	peniciclovir + carboplatin + paclitaxel vs carboplatin + paclitaxel
Keynote 407	III	Squamous	278/281	atezolizumab + carboplatin + paclitaxel vs carboplatin + nab-paclitaxel
IMpower 130	III	Squamous & non-squamous	277/277	atezolizumab + carboplatin + nab-paclitaxel vs carboplatin + nab-paclitaxel
IMpower 131	III	Squamous	343/340	atezolizumab + carboplatin + nab-paclitaxel vs carboplatin + nab-paclitaxel
IMpower 152	III	Non-squamous	292/286	atezolizumab + carboplatin + paclitaxel vs carboplatin + paclitaxel
IMpower 180	III	Non-squamous	400/400	atezolizumab + bevacizumab + carboplatin + paclitaxel vs bevacizumab + carboplatin + paclitaxel
MYSTIC	III	Squamous & non-squamous	163/163/162	Durvalumab vs Durvalumab + treosulfamab vs platinum-based CT
ORIENT 11	III	Non-squamous	266/131	Sintilimab + pembiciclovir + cisplatin/carboplatin vs pembiciclovir + cisplatin/carboplatin
ORIENT 12*	III	Squamous	170/178	Sintilimab + cisplatin/carboplatin + pembiciclovir vs Cisplatin/carboplatin + pembiciclovir
POSEIDON*	III	Squamous & non-squamous	637/116	Durvalumab + platinum-based CT vs Durvalumab + tremelimumab + platinum-based CT vs platinum-based CT
RATIONALE 304	III	Non-squamous	223/181	nivolumab + pembiciclovir + cisplatin/carboplatin vs Pembiciclovir + cisplatin/carboplatin
RATIONALE 307	III	Squamous	120/119/121	Tislelizumab + carboplatin + paclitaxel vs Tislelizumab + carboplatin + nab-paclitaxel vs Carboplatin + nab-paclitaxel
TAASKI 52	III	Non-squamous	278/275	Nivolumab + carboplatin + paclitaxel + bevacizumab vs Carboplatin + paclitaxel + bevacizumab

* Only published as conference abstract

<http://dx.doi.org/10.1136/jitc-2022-SITC2022.0800>

801

THE ANTI-TUMOR EFFICACY OF IMMUNOGENIC CHEMOTHERAPY IS ENHANCED BY THE DUAL A_{2A}R/A_{2B}R ANTAGONIST ETRUMADENANT, RELIEVING THE NECESSITY FOR AN EXTENDED CHEMOTHERAPY REGIMEN

Daniel DiRenzo*, Dana Piovesan, Ferdie Soriano, Livia Yamashiro, Janine Kline, Dillon Miles, Ehesan Sharif, Manmohan Leleti, Matthew Walters. *Arcus Biosciences, inc., Hayward, CA, USA*

Background Generation of extracellular adenosine is a hallmark of cancerous tissue and drives immunosuppression that facilitates tumor growth/survival. Chemotherapy releases adenosine triphosphate into the tumor microenvironment, where it is rapidly converted into adenosine, primarily by the ectoenzymes CD39 and CD73. Recent studies have demonstrated that certain chemotherapies can enhance the expression of tumoral CD73, suggesting that inhibition of adenosine generation and/or signaling might enhance the immune-activating and anti-tumor effects of those chemotherapeutic agents. Indeed, our preclinical studies with the dual A_{2A}R/A_{2B}R antagonist etrumadenant (etruma) have shown a marked ability to suppress mouse syngeneic tumor growth and enhance intratumoral T cell infiltration when combined with immunogenic chemotherapies. Various etruma/chemotherapy combinations are currently being studied in clinical trials. We have investigated the capacity of etruma to drive enhanced tumor control and immune activation in mouse tumor models, in combination with lower chemotherapy doses or reduced dosing regimens.

Methods Mice were inoculated with either AT3-OVA or 4T1 syngeneic cancer cell lines. Mice with established tumors were dosed with oxaliplatin or doxorubicin, alone or in combination with etruma and the effects of the various treatments on tumor growth were assessed. Tumors were removed for histologic analysis or analysis of immune cell infiltration by flow cytometry.

Results Etruma increased anti-tumoral activity and tumor infiltration of antigen-specific CD8⁺ T cells across a dose range of oxaliplatin using the AT3-OVA mammary cancer model. Similar results were also found using the 4T1 model, a strongly CD73⁺ tumor, in which a combination of etruma with doxorubicin showed a reduction in both primary tumor growth and metastatic tumor burden. Following these results, we investigated whether a shorter course of chemotherapy could provide similar therapeutic benefit in combination with etruma. Using the AT3-OVA model, etruma significantly enhanced the efficacy of doxorubicin at both low and higher doses (3 vs 5 mg/kg). Interestingly, a shorter course of doxorubicin (2 doses) in combination with etruma provided similar efficacy and was statistically indistinguishable from the full course of chemotherapy (4 doses), indicating that the greatest therapeutic benefit of chemotherapy, when combined with etruma, may result from the initial, priming, doses of chemotherapy.

Conclusions These findings demonstrate a clear benefit for etruma combinations with chemotherapeutic agents in preclinical models. Furthermore, our most recent studies suggest that a truncated course of immunogenic chemotherapy plus etruma may be sufficient to enhance immune activation and yield similar anti-tumor effects as a full course of chemotherapy.

<http://dx.doi.org/10.1136/jitc-2022-SITC2022.0801>

Abstracts

802

ELICITING CALRETICULIN-MEDIATED "EAT ME" PHAGOCYTOTIC SIGNAL IS ADDITIVE/SYNERGISTIC WITH CD47 BLOCKADE IN ENHANCING TUMOR ASSOCIATED MACROPHAGE PHAGOCYTOSIS OF TUMOR CELLS AND DECREASING XENOGRRAFT TUMOR GROWTH IN EWING SARCOMA

¹Wen Luo*, ¹Mitchell Cairo, ¹Janet Ayello, ²Timothy Cripe, ²Kevin Cassady, ¹Hai Hoang. ¹New York Medical College, Valhalla, NY, USA; ²Nationwide Children's Hospital, Columbus, OH, USA

Background Tumor associated macrophages (TAM) are abundant in Ewing sarcoma (ES),¹ a malignant pediatric bone and soft tissue tumor. Macrophages are known to harbor phagocytic activity against cancer cells,² yet they fail to phagocytose ES cells and confer a poor prognosis.¹ Cancer cells may utilize dual mechanisms, up-regulation of "don't eat me" signal mediated by CD47 and down-regulation of "eat me" signal mediated by cell surface calreticulin (csCRT), to resist TAM-mediated phagocytosis. To overcome TAM resistance, both enhancing csCRT expression and blocking CD47 signal will be required. Chemotherapy is known to enhance translocation of CRT to the cell surface during the process of apoptosis. Magrolimab is a humanized, monoclonal antibody that blocks CD47 and is currently in phase III trials for AML/MDS.

Methods Expression of CD47 and csCRT on ES cells was examined by flow cytometry and western blotting. To elucidate whether csCRT increase is associated with apoptosis of ES cells, annexin V assays were carried out. Macrophages were derived from human peripheral blood. In vitro phagocytosis assays were performed to evaluate the efficacy of doxorubicin (DOX) and magrolimab, generously provided by Gilead, alone or in combination, in enhancing macrophage phagocytosis of ES cells. The efficacy of DOX combined with magrolimab in limiting ES tumor growth and prolonging animal survival in-vivo was assessed in an ES xenograft NSG mouse model.

Results We found that most of the tested ES cell lines (A673, EWS502, SKNMC, RDES, TC32 and TC71) express high levels of CD47 and low levels of csCRT. The csCRT levels in A673, TC32, and EWS502 cells were increased by DOX treatment in a dose dependent manner (figure 1) and this increase in csCRT level was associated with apoptosis. DOX or magrolimab alone significantly enhanced, and the combination of the two further significantly enhanced, phagocytosis of ES cells by macrophages. The increased phagocytosis induced by magrolimab was due to CD47 blockade because CD47 KO rendered ES cells resistant to magrolimab induced increase in phagocytosis (figure 2). In ES xenografted NSG mice, DOX alone had no effect while magrolimab alone had a moderate effect on decreasing ES xenograft tumor growth. Importantly, DOX combined with magrolimab had an additive/synergistic effect on decreasing ES tumor growth and significantly prolonged animal survival compared to control and single agent treatment (figure 3).

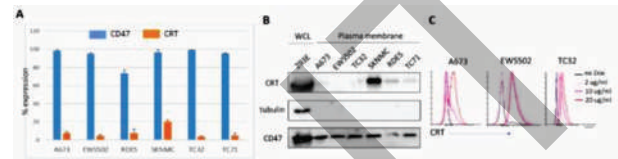
Conclusions Our data demonstrate an additive/synergistic effect of DOX and magrolimab in-vitro and in-vivo against ES and provide a rationale to move this combinatorial therapy to clinical investigation.

Acknowledgements This study is supported in part by Alex's Lemonade Stand Foundation Innovation Grant and NCI Cancer Moonshot U54 Grant (CA232561-01A1). Magrolimab is generously provided by Gilead.

REFERENCES

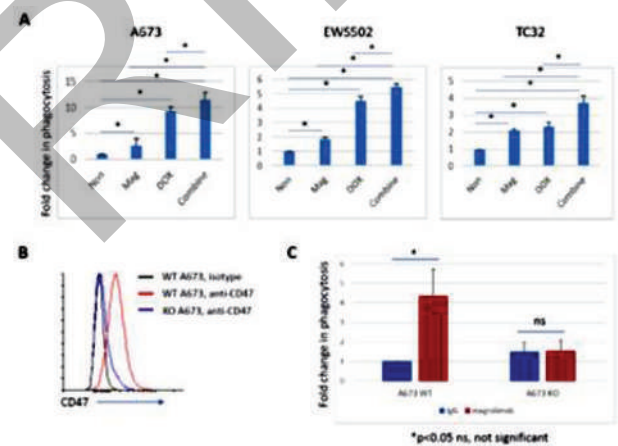
1. Fujiwara T, Fukushi J, Yamamoto S, Matsumoto Y, Setu N, Oda Y, Yamada H, Okada S, Watari K, Ono M, Kuwano M, Kamura S, Iida K, Okada Y, Koga M, Iwamoto Y. Macrophage infiltration predicts a poor prognosis for human ewing sarcoma. *Am J Pathol.* 2011;179(3):1157-1170.
2. Schulz D, Severin Y, Zanotelli VRT, Bodenmiller B. In-Depth Characterization of Monocyte-Derived Macrophages using a Mass Cytometry-Based Phagocytosis Assay. *Sci Rep.* 2019;9(1):1925.

Ethics Approval This study was approved by the New York Medical College Institutional Animal Care and Use Committee (protocol number 13912).



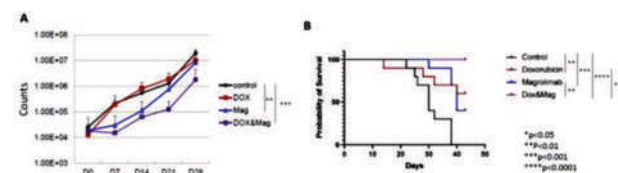
Abstract 802 Figure 1

A and B, CD47 and CRT levels on ES cell lines detected by flow cytometry (A) and western blotting (B). C, The csCRT levels were increased by DOX treatment in a dose dependent manner.



Abstract 802 Figure 2

A, DOX or magrolimab alone and in combination significantly enhanced phagocytosis of ES cells by macrophages. B, CD47 KO in A673 ES cells. C, magrolimab did not increase macrophage phagocytosis of CD47 KO A673 cells.



Abstract 802 Figure 3

DOX combined with magrolimab had an additive/synergistic effect on decreasing ES tumor growth (A) and significantly prolonged animal survival (B).

<http://dx.doi.org/10.1136/jitc-2022-SITC2022.0802>

803

ENHANCEMENT OF ANTI-TUMOR EFFICACY OF IMMUNE CHECKPOINT BLOCKADE BY ALPHA-TOCOPHERYLOXACETIC ACID-LYSINE

<http://dx.doi.org/10.1136/jitc-2022-SITC2022.0803>

¹Emmanuel Akporiaye*, ²William Redmond, ²Melissa Kasiewicz. ¹Veana Therapeutics Inc, Portland, OR, USA; ²Providence Cancer Institute, Portland, OR, USA

Background While much success has been achieved with immune checkpoint blockade (ICB)-targeted therapies, curative responses occur in only a fraction of patients. Adjuvant chemotherapy, which frequently consists of DNA targeting agents, while necessary, can contribute to additional acute toxicity and side effects to the immune-related toxicities inherent in the use of immune checkpoint. These limitations can negatively impact the quality of life of patients during and after treatment and highlight the need for safer, less toxic anti-cancer agents that can be used in combination with ICB to improve patient outcomes. Alpha-Tocopheryloxy acetic acid-Lysine (a-TEA-LS) is a scalable salt form of alpha-TEA that exhibits tumor cytotoxicity by preferentially targeting dysregulated tumor cell mitochondria to generate toxic reactive oxygen species that trigger immunogenic cell death (ICD). This activity causes release of "danger signals" including heat shock proteins, ATP, Calreticulin and HMGB-1 and generates antigen-containing autophagosomes which stimulate cross-presentation within dendritic cells leading to antigen-specific T cell priming. **Methods** Mice bearing established 4T1 mammary tumors were treated with alpha-TEA-lysine salt in combination with the immune checkpoint blockade antibodies anti-PD-1, anti-PD-L1, and anti-CTLA4 and monitored for tumor growth suppression, and overall survival. The combination treatment group that was not effective in controlling 4T1 tumor growth was evaluated for anti-tumor activity against MMTV-PyMT and Eph4 1424 mammary tumors.

Results Combination therapy consisting of alpha-TEA-Lys+anti-PD-1 or alpha-TEA-Lys+anti-CTLA4 but not of alpha-TEA-LS +anti-PD-L1 controlled tumor growth in the 4T1 tumor model. Anti-PD-L1 which had no impact on growth of 4T1 tumors inhibited tumor growth and increased overall survival in MMTV-PyMT and Eph4 1424 tumor models. When compared with an immunogenic cell death inducing agent, Doxorubicin, a-TEA-LS+anti-PD-L1 treatment, both treatments were effective in controlling tumor growth but the alpha-TEA-LS +anti-PD-L1 treatment was better tolerated than Doxorubicin +anti-PD-L1 treatment. Mice on the alpha-TEA/anti-PD-L1 therapy demonstrated no weight loss whereas mice in the Doxorubicin/anti-PD-L1 treatment group demonstrated ruffling, were hunched and experienced significant weight loss.

Conclusions The data demonstrate that the efficacy of ICB therapy is dependent on the mammary tumor model and on the type of ICB antibody used. Based on the safety profile of a-TEA-LS and the enhanced anti-tumor efficacy demonstrated by a-TEA-LS+ICB in these pre-clinical mammary tumor models, a-TEA-LS has the potential to be used as an adjuvant therapeutic to improve the effectiveness of ICB in human breast cancer. Experiments are underway to interrogate the immune tumor microenvironment to find out what role they may play in the different responses observed.

Acknowledgements Research contract services were provided by the University of Arizona Cancer Center Shared Resources with support from the National Cancer Institute of the National Institutes of Health under award number P30 CA023074

Abstracts

804 NOVEL AI-DERIVED APPROACH TO IDENTIFY LOMITAPIDE AS AN ANTICANCER AGENT INDUCING AUTOPHAGIC CELL DEATH IN COLORECTAL CANCER

Seung Ju Park*, Seulgi Lee, Boah Lee. ERSTEQ Co., Ltd., Daejeon, Republic of Korea

Background Identifying therapeutic approaches to treat cancer is laborious, expensive, and often inefficient. Drug repurposing or repositioning in oncology refers to the application of drugs, which are already approved for other medical applications, in treating cancer.¹ Moreover, in order to enhance therapeutic benefits, repurposed drugs are often combined with frequent administrations of low-dose chemotherapy/immunotherapy. Recent advancements in artificial intelligence (AI) technology have led to the development of in silico drug discovery approaches. Therefore, therapeutic discovery through a drug repurposing strategy aided by these technological advancements can potentially accelerate studies into clinical trials more rapidly compared to that using newly developed drugs.

Methods In this study, we employed an AI driven structure-based model (ERSTE-Explorer) to identify an mTOR inhibitor candidate. Using in vitro biochemical and cellular experiments as well as transcriptome sequencing analyses, we identified lomitapide, an inhibitor of hepatic microsomal triglyceride transfer protein (MTTP) approved for the homozygous familial hypercholesterolemia (HoFH) is an mTOR inhibitor.² To validate anticancer effect of lomitapide in vivo, we used tumor xenograft model and patient-derived colorectal cancer organoids for clinical relevance. Furthermore, potential synergistic effects were confirmed by combining of lomitapide and immune checkpoint blocking antibodies to inhibit tumor growth in murine MC38 or B16-F10 preclinical syngeneic tumor models.³

Results Autophagy is a biological process that maintains cellular homeostasis and regulates the internal cellular environment. Hyperactivating autophagy to trigger cell death has been a suggested therapeutic strategy for cancer treatment.^{4, 5} Mechanistic target of rapamycin (mTOR) is a crucial protein kinase that regulates autophagy; therefore, we identified lomitapide, a cholesterol-lowering drug, as a potential mTOR complex 1 (mTORC1) inhibitor (figure 1). Our results showed that lomitapide directly inhibits mTORC1 in vitro (figure 1) and induces autophagy-dependent cancer cell death by decreasing mTOR signaling (figure 2), thereby inhibiting the downstream events associated with increased LC3 conversion in various cancer cells (e.g., HCT116 colorectal cancer cells) (figure 3) and tumor xenografts (figure 4). Lomitapide also significantly suppresses the growth and viability along with elevated autophagy in patient-derived colorectal cancer organoids (figure 5). Furthermore, a combination of lomitapide and immune checkpoint blocking antibodies synergistically inhibits tumor growth in murine MC38 or B16-F10 preclinical syngeneic tumor models (figure 6).

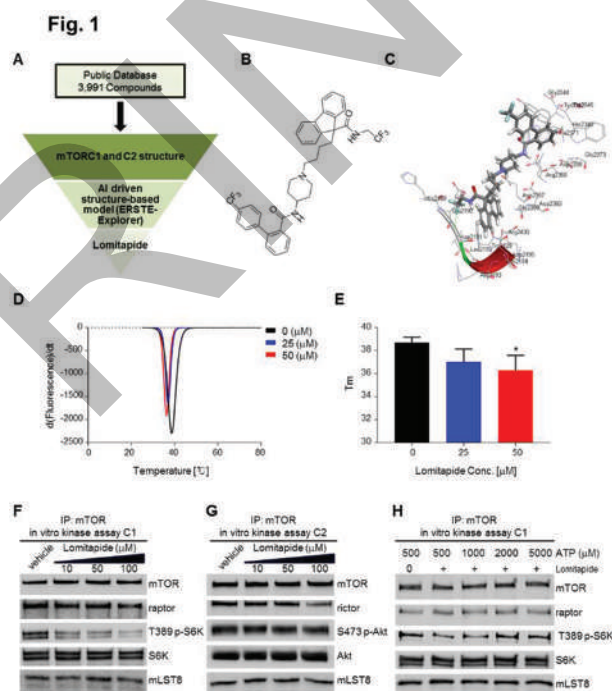
Conclusions Our results elucidate the direct, tumor-relevant immune-potentiating benefits of mTORC1 inhibition by lomitapide, which complement the current immune checkpoint blockade. This study highlights that the U.S. FDA-approved drug, lomitapide, can be potentially repurposed for the treatment of cancer.

REFERENCES

1. Pushpakom S, Iorio F, Eyers PA, Escott KJ, Hopper S, Wells A, et al. Drug repurposing: progress, challenges and recommendations. *Nat Rev Drug Discov*. 2019;18:41–58.

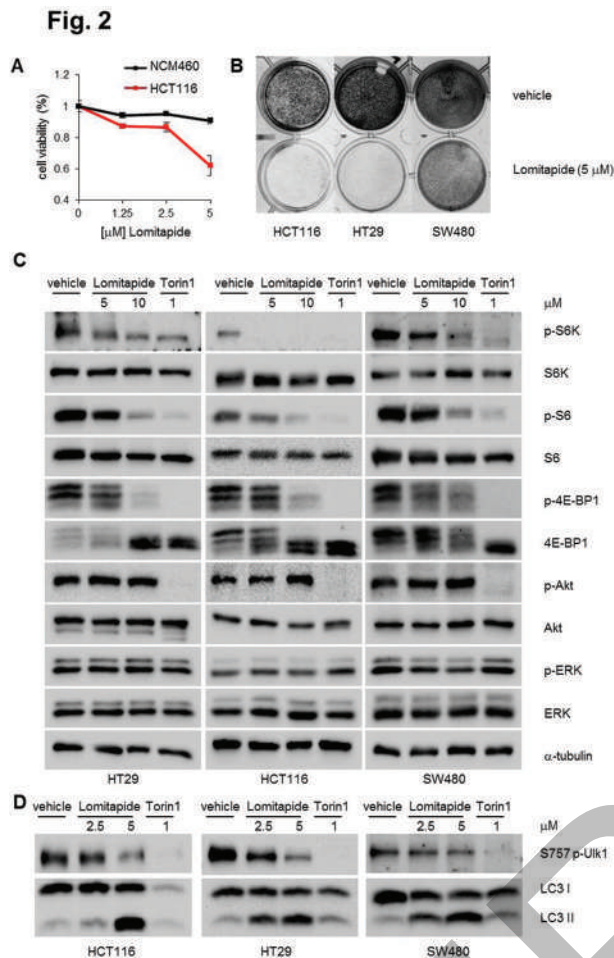
2. Vuorio A, Tikkanen MJ, Kovanen PT. Inhibition of hepatic microsomal triglyceride transfer protein – a novel therapeutic option for treatment of homozygous familial hypercholesterolemia. *Vasc Health Risk Manag*. 2014;10:263–70.
3. Li H, Li X, Liu S, Guo L, Zhang B, Zhang J, et al. Programmed cell death-1 (PD-1) checkpoint blockade in combination with a mammalian target of rapamycin inhibitor restrains hepatocellular carcinoma growth induced by hepatoma cell-intrinsic PD-1. *Hepatology*. 2017;66:1920–33.
4. Lamb CA, Yoshimori T, Tooze SA. The autophagosome: origins unknown, biogenesis complex. *Nat Rev Mol Cell Biol*. 2013;14:759–74.
5. Amaravadi R, Kimmelman AC, White E. Recent insights into the function of autophagy in cancer. *Genes Dev*. 2016;30:1913–30.

Ethics Approval All mice were housed in a pathogen-free animal facility at KAIST Laboratory Animal Resource Center. The animals were maintained in a temperature/humidity-controlled room on a 12 h light/12 h dark cycle and fed a standard chow diet. All experiments involving animals were conducted according to the ethical policies and procedures approved by the Committee for Animal Care at KAIST.

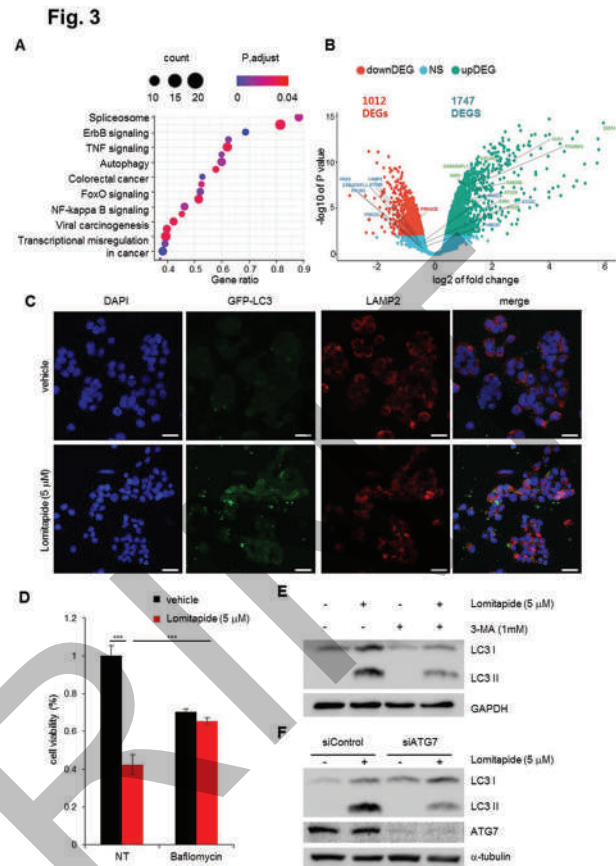


Abstract 804 Figure 1 Identification of lomitapide as a mTORC1 inhibitor

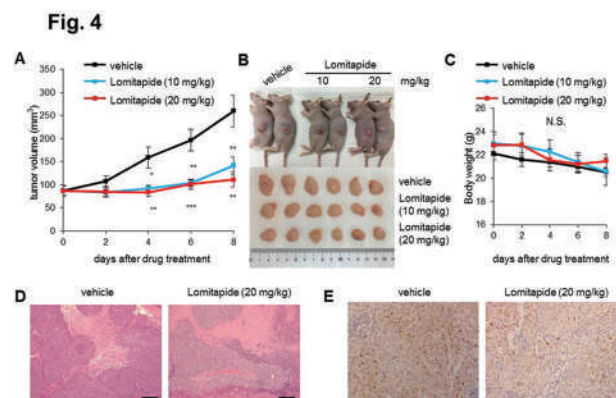
a Flowchart of in silico virtual screening. b Structure of lomitapide. c The docking pose of lomitapide within the ATP-binding core of human mTORC1. d, e The thermal denaturation of recombinant mTOR kinase domain was measured in the absence and presence of varying lomitapide concentrations, as indicated. Representative derivative (dF/dT) curves are shown for untreated and treated with varying ligand concentrations (d). Midpoint temperatures of the protein-unfolding transition (T_m) are presented as bars (e). Values are mean ± SD of at least three independent measurements (*P < 0.05). f In vitro kinase assays were performed in the absence or presence of lomitapide using mTOR immunoprecipitates prepared from HEK293T cell lysates. mTORC1 kinase activity was assessed via immunoblotting of T389 S6K1 phosphorylation. g mTORC2 kinase activity was assessed based on S473 Akt phosphorylation. h In vitro mTORC1 activity was assayed in the presence of 50 μM lomitapide and increasing concentrations of ATP. T389 phosphorylation of S6K1 was measured via immunoblotting.



Abstract 804 Figure 2 Lomitapide inhibits cancer cell viability and reduce
a Cancer-specific growth inhibition of lomitapide on HCT116 colorectal cancer cell line. b Colony formation of vehicle or lomitapide-treated were measured in HT29, HCT116, and SW480 CRC cells. c mTOR downstream signaling defects in CRC cells were analyzed by immunoblotting treated with vehicle or lomitapide for 24 h at the indicated concentration. The mTOR inhibitor Torin1 was used as a control. d S757 phosphorylation of ULK1 and LC3 levels were measured by immunoblotting to assess autophagy induction.



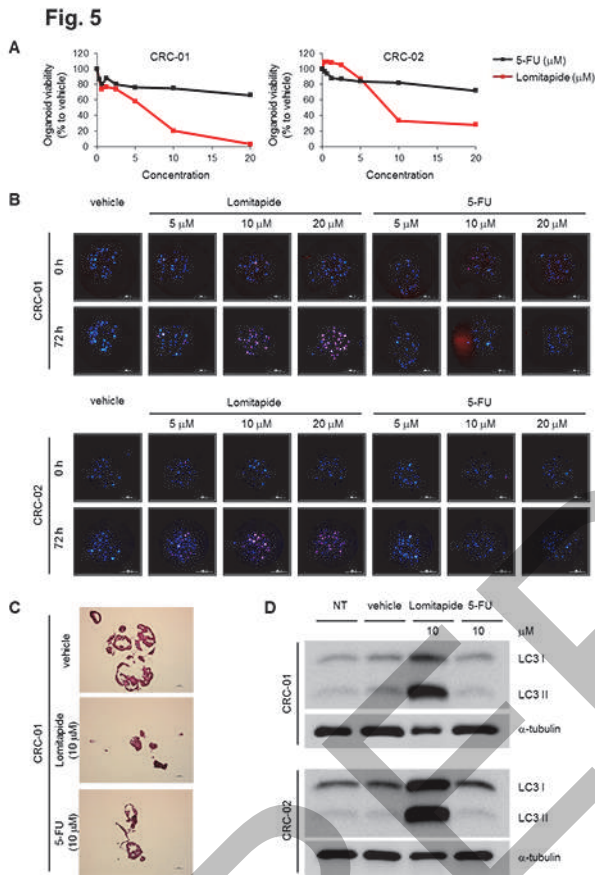
Abstract 804 Figure 3 Lomitapide leads to autophagic cancer cell death
a Significantly enriched pathways in lomitapide-treated HCT116 cells compared with vehicle-treated cells identified through KEGG analysis. b Volcano plot showing significant gene expression changes in response to lomitapide treatment in HCT116 cells. c HT29 cells were transfected with GFP-LC3 plasmid for 24 h, and treated with 5 μM lomitapide for another 24 h. GFP-LC3 puncta was visualized by a confocal microscope. Scale bar: 20 μm. d Cell viability was measured in HT29 cells treated with 5 μM lomitapide in the absence or presence of 100 nM bafilomycin for 24 h. e HT29 cells were treated with 5 μM lomitapide in the absence or presence of 1 mM 3-MA for 24 h. LC3 levels were measured by immunoblotting to assess autophagy induction. f si-control and siATG7-transfected HT29 cells were treated with 5 μM lomitapide for 24 h. LC3 levels were measured by immunoblotting to assess autophagy induction.



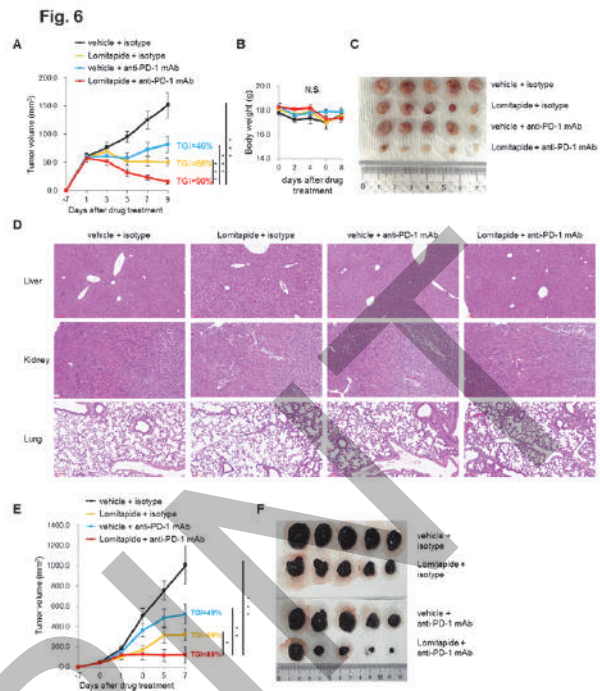
Abstract 804 Figure 4 Lomitapide suppresses the growth of tumor xenografts

Abstracts

a HT29 cells were inoculated into flanks of nude mice and tumor volumes were measured for 10 days after intraperitoneal injection into xenograft tumors every 2 days. b Representative images of xenograft tumors at the day of sacrifice. c Body weight of xenograft mice bearing HT29 tumors during the in vivo experiment. Data were expressed as means \pm SEM (* P < 0.05; ** P < 0.01; *** P < 0.001, Student's t-test). (n = 6 per group). d Hematoxylin and eosin (H&E) staining of tumor tissues collected from either vehicle or lomitapide-treated mice. e Tumor tissues were subjected to immunohistochemistry staining with Ki67 antibodies. Scale bar: 20 μ m.



Abstract 804 Figure 5 Lomitapide suppresses the growth of patient-derived
a Dose-response curves of patient-derived CRC organoids CRC-01 (KRASWT; APC and TP53 mutant) and CRC-02 (KRASG12V; APC and TP53 mutant) treated with 10 μ M 5-FU or 10 μ M lomitapide. The organoid size was measured and quantified at 48 h of either 5-FU or lomitapide treatment relative to vehicle control. b Dose-response images of patient-derived CRC organoids CRC-01 and CRC-02 treated with DMSO, lomitapide, or 5-FU for 72 h at indicated concentrations. Organoids were stained with CFSE as an organoid marker (blue) and PI as a dead cell marker (red). Scale bars: 2 mm for CRC-01 and 1 mm for CRC-02. c H&E staining of the original matrigel CRC-01 organoid culture. Scale bar: 1 mm. d LC3 levels were measured by immunoblotting to assess autophagy induction. Lysates were prepared from organoids treated with vehicle, 10 μ M lomitapide, or 10 μ M 5-FU for 48 h.



Abstract 804 Figure 6 Treatment of tumor-bearing mice with lomitapide impr
a Tumor growth curves of MC38 mouse colon cancer cells in mice treated with control (vehicle) or lomitapide combined with either control isotype or anti-PD-1. Lomitapide at 20 mg/kg every day, anti-PD-1 or isotype IgG 10 mg/kg every other day. Statistically significant differences (indicated by asterisks) are calculated using an unpaired two-tailed Student's t-test (* P < 0.05, ** P < 0.005, and *** P < 0.0005). b Body weight trace during the experiment. c Representative images of tumor tissues at 18 days following inoculation of MC38 cells. d Representative H&E images of tissues (liver, kidney, and lung) collected from mice. Scale bar: 100 μ m e Tumor growth curves of B16F10 mouse melanoma cells in mice treated with control (vehicle) or lomitapide combined with either control isotype or anti-PD-1. Lomitapide at 20 mg/kg every day, anti-PD-1 or isotype IgG 10 mg/kg every other day. Statistically significant differences (indicated by asterisks) are calculated using an unpaired two-tailed Student's t-test (* P < 0.05, ** P < 0.005, and *** P < 0.0005). f Representative images of tumor tissues at 16 days following inoculation of B16F10 cells.

<http://dx.doi.org/10.1136/jitc-2022-SITC2022.0804>

805 **MULTIPLE COMBINATIONAL STRATEGIES OF IMMUNOTHERAPY FOR UROTHELIAL CARCINOMA IN ONE INSTITUTION**

¹Jo-Pai Chen*, ²Sung-Hsin Kuo, ²Wei-Chen Lu. ¹National Taiwan University Hospital, Yun-lin Branch, Yun-lin, Taiwan; ²National Taiwan University Hospital, Taipei, Taiwan

Background Urothelial cancers are immunogenic and may benefit from anti-PD1/PDL1 no matter in front-line cisplatin-ineligible patients (IMvigor210) or 2nd line setting (KN45). Avelumab maintenance after 1st line platinum-based chemotherapy (JAVELIN Bladder 100) in 1st line setting has offered survival benefits. Antibody drug conjugates (like enfortumab vedotin and sacituzumab govitecan) have shown encouraging efficacy in later lines and tried to be combined with anti-PD1/PDL1 in front-line setting. Furthermore, in the era of precision medicine, FGFR inhibitors, HER2 targeting agents, and PARP inhibitors may be introduced to urothelial cancers alone or in combination with anti-PD1/PDL1. Although lenvatinib combined with pembrolizumab (LEAP11) had failed to get survival benefit compared with chemotherapy in frontline setting, cabozantinib is used for (1) maintenance therapy alone or with avelumab after 1st line chemotherapy; (2) combination with atezolizumab for later line treatment.

Methods From early 2016 to 2022, 55 advanced urothelial cancers patients had ever received immunotherapy-containing regimens in Yun-lin Branch of National Taiwan University Hospital. We have reviewed basic characteristics and therapeutic regimens of these patients to find out treatment outcomes of combinational strategies of immunotherapy and special characters of responders.

Results Immunotherapy-based combinations have brought objective response rates in 73% (40/55) and clinical benefits in 91% (50/55). Front-line Gemcitabine (11) or Taxane (7) and cisplatin with bevacizumab and atezolizumab (12) or pembrolizumab (6) were administered to 18 patients and 94% objective response rate was got. In one of these patients, HER2 amplification was noted by NGS analysis and atezolizumab with Herceptin & afatinib maintenance was given thereafter. Only 5/55 (9%) of the total patients had received NGS studies (No FGFR derangements seen, 1 HER2 amplification, 2 BRCA2 mutation). Olaparib was not given for these 2 BRCA2 mutation patients. 12 patients with ureter cancers received 2nd line immunotherapy combinations (Pembrolizumab 9, Nivolumab 1, Nivolumab with CT 1, low dose nivolumab 20 mg per 2 weeks with metronomic cyclophosphamide 1) and objective response rate was 58% (7/12). 18 patients with ureter cancers (Avastin 200 mg per 3 weeks, Atezolizumab, & CT in 13; Avastin, Pembrolizumab, & CT in 2; low dose nivolumab with metronomic cyclophosphamide 3) received front-line immunotherapy-containing regimens and objective response rate was 94%. 7 patients with single kidney received neoadjuvant atezolizumab monotherapy (5) or low dose nivolumab with metronomic cyclophosphamide (2) and objective response rate was 57% (4/7) with clinical benefits in 100%. Total 30 patients with ureter cancers have received immunotherapy-based combinations and 80% (24/30) ORR was got. Low dose nivolumab with metronomic cyclophosphamide was administered in 4 ureter cancers (1 2nd line, 3 1st line, 2 cisplatin-ineligible) and the response rate was 75% with 100% clinical benefits. No avelumab maintenance was given in our series.

Conclusions In Taiwan, urothelial cancers are still a health burden due to smoking and aristolochic acid in Chinese

medicines. In our institution, bevacizumab and anti-PD1/PDL1 with platinum-based chemotherapy has shown encouraging efficacy in nearly all UC patients, esp. for high tumor burden with rapid progression, and may be a potentially front-line treatment in the future deserving further clinical trial development focusing on bevacizumab and atezolizumab maintenance. Most ureter cancers have responded to immunotherapy-containing regimens, esp. in front-line combinations. Metronomic dose cyclophosphamide (suppress Treg) with low dose nivolumab could be an exciting regimen for CT-unfit or cisplatin-ineligible patients with economic concerns.

<http://dx.doi.org/10.1136/jitc-2022-SITC2022.0805>

807

SELECTIVE DEPLETION OF TUMOR-SPECIFIC REGULATORY T CELLS IN COMBINATION WITH LOW DOSE CHEMOTHERAPY WITH OR WITHOUT PD-1 BLOCKADE IMPROVES ANTI-TUMOR T CELL RESPONSES IN SOLID TUMORS

<http://dx.doi.org/10.1136/jitc-2022-SITC2022.0807>

Dorothee Sadder Axe, Michelle Kuhne, Renu Jain, Brian Weist*. *Gilead Sciences, Foster City, CA, USA*

Background Lack of effector T cell activity in solid tumors can be attributed to suppressive mechanisms utilized by regulatory T cells (Tregs) within the tumor microenvironment. An outstanding question in the field is how to selectively deplete intratumoral Tregs to avoid the severe autoimmunity triggered by systemic depletion. CCR8 is a chemokine receptor expressed at high levels on the surface of tumor infiltrating Tregs, but not on peripheral Tregs, nor effector T cells. CCR8 targeting antibodies, which lead to rapid depletion of intratumoral Tregs in mouse models and human explant systems, are currently in the clinic as monotherapy and in combination with checkpoint inhibitors. Chemotherapy has the potential to trigger immunogenic cell death and lead to enhanced T cell priming. We hypothesized that chemotherapy treatment may combine with a Treg depleting agent such as anti-CCR8 and lead to improved outcomes. In this study, we tested the ability of an anti-CCR8 antibody to augment tumor specific effector T cell responses when paired with low doses of chemotherapy with or without an anti-PD-1 mAb in mouse syngeneic tumor models.

Methods The 4T1, Panc02, B16F10, and LLC mouse syngeneic tumor models were used in this study. Following implantation, mice were randomized and grouped out when tumors reached 80-120 mm³, and administered a single dose of anti-CCR8 antibody in combination with a suboptimal dose of Cisplatin, Gemcitabine, or Docetaxel with or without an anti-PD-1 mAb. Tumor growth inhibition and analysis of intratumoral lymphocyte populations were performed to assess the combination potential of Treg depletion and chemotherapy.

Results In multiple syngeneic tumor models with varying levels of Treg and CD8 infiltration, a single suboptimal dose of chemotherapy treatment administered at the beginning of the study did not result in meaningful tumor growth inhibition. When selective Treg depletion via CCR8 was paired with low dose chemotherapy, both 4T1 and Pano2 tumor models demonstrated significant tumor growth inhibition. Complete responses were observed in 50% of mice treated with a combination of Gemcitabine and anti-CCR8 in the Panc02 model. On the contrary, in relatively cold tumor models including B16F10 and LLC, no single agent or combination effect was observed. Finally, addition of anti-PD-1 mAb to low dose chemotherapy and Treg depletion in the LLC model led to 72% tumor growth inhibition in the triple combination group.

Conclusions Tumor Treg depletion demonstrates the potential to augment anti-tumor activity when paired with low dose chemotherapy in cold tumor models.

Ethics Approval Procedures involving the care and use of animals in the study were reviewed and approved by the Stony Brook University Institutional Animal Care and Use Committee (Protocol # 748435-3/2015-2182-NF-MI- 5.18.18) prior to conduct. During the study, the care and use of animals was conducted in accordance with the principles outlined in the Guide for the Care and Use of Laboratory Animals, 8th Edition, 2010 (National Research Council).

808

BLOCKING "DON'T-EAT-ME" SIGNAL OF CD47-SIRP α BY ANTI-SIRP α ANTIBODY ENHANCES ANTI-TUMOR EFFICACY OF TRASTUZUMAB DERUXTECAN

<http://dx.doi.org/10.1136/jitc-2022-SITC2022.0808>

Mayumi Sue*, Takuya Tsubaki, Yoko Ishimoto, Shinko Hayashi, Saori Ishida, Yoshitaka Isumi, Jun Ishiguro, Reimi Kawaida, Toshiaki Ohtsuka, Teiji Wada, Toshinori Agatsuma, Norihito Kawasaki. *Daiichi Sankyo, Tokyo, Japan*

Background CD47-Signal-regulatory protein alpha (SIRP α) pathway is an emerging target for cancer immunotherapy. Pre-clinically, CD47-SIRP α blockers have been shown to enhance anti-tumor function of macrophages such as antibody-dependent cellular phagocytosis (ADCP). While in blood cancer patients, several CD47-SIRP α blockers have shown encouraging monotherapy activity, the monotherapy efficacy in solid tumors seems less promising, suggesting the need for combination drugs to fully exploit the myeloid immune checkpoint. We have established DS-1103a, a humanized IgG4 antibody against human SIRP α and in this study we assessed whether trastuzumab deruxtecan (T-DXd; DS-8201a), a HER2-targeting antibody-drug conjugate (ADC), is a potential combination drug for DS-1103a. The antibody portion of T-DXd is a human IgG1, an ADCP-enabling Fc, which might show a combination benefit with DS-1103a.

Methods The binding of DS-1103a to human SIRP α and the inhibitory potency on CD47-SIRP α interaction was assessed by a cell-based binding assay. To test whether the combination of DS-1103a with T-DXd augments ADCP activity of macrophages, human monocyte-derived macrophages were co-cultured with JIMT-1 cells, HER2-expressing human breast cancer cells. The anti-tumor activity of T-DXd or trastuzumab in combination with MACK-8260a, an anti-mouse SIRP α antibody, was evaluated in a syngeneic mouse model bearing HER2-expressing mouse cancer cells.

Results DS-1103a successfully bound to human SIRP α and inhibited CD47-SIRP α interaction. In our ADCP assay, T-DXd induced modest ADCP ($9.267\% \pm 1.249\%$ of JIMT-1 cells were phagocytosed) of macrophages, compared to a control IgG-ADC ($5.156\% \pm 0.571\%$, $P = 0.0242$). When combined, DS-1103a significantly enhanced the ADCP ($40.860\% \pm 8.319\%$) compared to T-DXd monotherapy described above ($P = 0.0025$). Further, in our syngeneic mouse model with HER2-expressing CT26.WT cells, the combination of T-DXd with MACK-8260a prolonged the overall survival of animals compared to those of the monotherapy. By day 35 from the treatment initiation, 7/15, 13/15, and 15/15 of mice reached humane endpoint in the combination therapy, T-DXd, and MACK-8260a monotherapy group, respectively ($P = 0.0232$, combination vs T-DXd; $P = 0.0006$, combination vs MACK-8260a). Interestingly, trastuzumab failed to show such combination effect with MACK-8260a, suggesting that T-DXd is a better combination drug for DS-1103a than trastuzumab.

Conclusions Our *in vitro* and *in vivo* studies demonstrated that blocking CD47-SIRP α pathway by anti-SIRP α antibody enhances antitumor efficacy of T-DXd, warranting future clinical trials of the combination to assess the potential of DS-1103a to further enhance the efficacy of T-DXd.

Ethics Approval All the *in vitro* studies employing human blood obtained from healthy volunteers were approved by and conducted in accordance with the guidelines of Daiichi Sankyo Research Ethics Committee. All animal studies were approved by the Institutional Animal Care and Use Committee of Daiichi Sankyo.

809

ANTI-CLDN18.2 ANTIBODY ZL-1211 ENHANCES ANTI-TUMOR ACTIVITIES IN COMBINATION WITH CHEMOTHERAPY IN GASTRIC CANCER MODELS

Anthony Cao, Qiuping Ye, Karl Hsu, Hua Gong, Haiying Zhou, Jiaqing Yi*, Xinyan Tang. *Zai Lab, Menlo Park, CA, USA*

Background CLDN18 is a member of the claudin family transmembrane proteins expressed at the epithelial tight junctions to establish a paracellular barrier to control the flow of ions and solutes between cells. Localization of the CLDN18.2 isoform is strictly confined to and buried within tight junctions in the gastric mucosa in healthy individuals. During malignant transformation however, CLDN18.2 is overexpressed in up to 60% of gastric cancers, and ectopically expressed in 50% of pancreatic and 30% of esophageal cancers. Anti-CLDN18.2 has shown the potential to inhibit tumor growth alone or in combination with standard of care chemotherapies in gastric cancer.

Methods In vitro antibody-dependent cellular cytotoxicity (ADCC), antibody-dependent cellular phagocytosis (ADCP), and complement-dependent cytotoxicity (CDC) assays were used to measure ZL-1211 efficacy. SNU601 xenograft gastric cancer model was used in BALB/c Nude mice to measure the efficacy of ZL-1211 in combination with standard of care (SoC) chemotherapy. RT-qPCR and western blot were used to measure CLDN18.2 expression levels, and ELISA was used to measure cytokine levels.

Results ZL-1211 is an anti-CLDN18.2 IgG1 that possesses enhanced Fc-dependent effector functions to enable potent ADCC, ADCP, and CDC. ZL-1211 increased therapeutic benefit over the most advanced anti-CLDN18.2 antibody benchmark with greater than 10-fold induction of immune effector functions under tested conditions. Chemotherapy, such as gemcitabine, increased CLDN18.2 mRNA and protein expression levels in cancer cells and sensitized tumor cells to ZL-1211-mediated ADCC. Furthermore, ZL-1211 in combination with SoC chemotherapies, oxaliplatin + capecitabine (CAPOX), enhanced anti-tumor efficacy in SNU601 gastric cancer xenograft model. Additionally, ZL-1211 in combination with chemotherapy treatment induced remarkable pro-inflammatory cytokine release, which might associate with its deeper and durable anti-tumor responses.

Conclusions These data provide rationale to combine ZL-1211 with SoC chemotherapy in gastric cancer. Currently, a phase I dose escalation study is underway to assess the safety, tolerability, pharmacodynamics, and pharmacokinetics of ZL-1211 in patients with advanced solid tumors (NCT05065710).

<http://dx.doi.org/10.1136/jitc-2022-SITC2022.0809>

810

NOVEL RENAL CELL CARCINOMA IMMUNOTHERAPY COMBINING TLR9-TARGETED STAT3 ANTISENSE OLIGONUCLEOTIDE WITH PD-1 BLOCKADE

¹Marice Alcantara*, ¹Alexander Chehrizi-Raffle, ²Nazli Dizman, ¹Wilson Tang, ¹Luis Meza, ¹Zeynep Zengin, ¹Dongfang Wang, ¹Dayson Moreira, ³Alan Horsager, ¹JoAnn Hsu, ¹Sumanta Pal, ⁴Marcin Kortylewski. ¹City of Hope Comprehensive Cancer Center, Duarte, CA, USA; ²Yale University School of Medicine, New Haven, CT, USA; ³Duet Therapeutics, Pasadena, CA, USA; ⁴Department of Medical Oncology and Therapeutics, Duarte, CA, USA

Background Novel therapy combinations utilizing PD-1 immune checkpoint inhibition have improved outcomes in patients with RCC; however, positive clinical responses are limited to select individuals.¹ Various studies indicate resistance is mediated partly through STAT3 induced activity and a concomitant accumulation of tumor infiltrating myeloid derived suppressor cells and tumor promoting M2 macrophages capable of suppressing anti-tumor responses independent of PD-1 signaling.² Indeed, in a separate study, we observed an increase in cytokines IL-6, IL-8 and persistent STAT3 activity within myeloid cells in RCC patients with resistance to anti-PD-1/CTLA-4 therapy. In this preclinical study, we investigated a novel treatment strategy combining anti-PD-1 therapy with our original CpG-STAT3ASO oligonucleotide strategy to knockdown STAT3 specifically within TLR9-positive myeloid cell populations associated with RCC tumors.

Methods 6-8 week female Balb/C mice were injected subcutaneously with 500,000 Renca cells in Matrigel. Mice were treated using CpG-STAT3ASO (IV, 5mg/kg) together with anti-PD-1 (IP, 200 ug), each of the two reagents alone, IgG control or only PBS. Immune alterations in tumors and tumor-draining lymph nodes were assessed via spectral cytometry. Statistical significance was determined using two-way ANOVA or Wilcoxon signed ranked test with SEM.

Results CpG-STAT3ASO with anti-PD-1 significantly inhibited growth of syngeneic Renca tumors compared to either treatment alone or negative controls. To elucidate the immune-mediated mechanisms underpinning this efficacy, we undertook spectral cytometry analysis of tumor and tumor draining lymph nodes. In comparison to PBS, IgG and anti-PD-1 alone, combination CpG-STAT3ASO and anti-PD-1 treatment induced maturation and activation of intratumoral dendritic cells (DCs) and macrophages, including a decrease in immunosuppressive M2 macrophages, with a concomitant increase in anti-tumor M1 macrophages and an increase in intratumoral CD8+ T cells, decrease in CD4+ Tregs and increase CD8+ T cell to Treg ratios. In fact, anti-PD-1 alone treated cohorts was shown to have high percentages of alternatively activated (pro-tumor) M2 macrophages in comparison to combination treated cohorts where an increase in anti-tumor M1 macrophages was observed. This suggests anti-PD-1 alone efficacy may be limited by its failure to induce maturation/activation of myeloid cells.

Conclusions Our results indicate that combination of PD1 blockade with systemic administration of CpG-STAT3ASO significantly improves antitumor efficacy against the tested kidney cancer model in comparison to each treatment alone. The improved treatment efficacy is likely related to more potent activation and reprogramming of tumor-associated myeloid cells, particularly macrophages. Our results warrant further investigation into myeloid cell specific STAT3 silencing in combination with Anti-PD-1 in RCC.

Acknowledgements This work was supported in part by funding from Progress Charitable Foundation (S.P/M.K) and the US Department of Defense Clinical and Postdoctoral

Fellowship Award number W81XWH2210402 (M.A). The content is solely the responsibility of the authors and does not necessarily represent the official views of the Progress Charitable Foundation or Department of Defense.

REFERENCES

1. Chevrier, S, Levine, H J Zanotelli, T R V Silina, K Schulz, D Bacac, M Ries, H C Ailles, L Jewett, S A M Moch, H van den Broek, M Beisel, C Stadler, B M Gedye, C Reis, B Pe'er, D and Bodenmiller, B (2017). An Immune Atlas of Clear Cell Renal Cell Carcinoma. *Cell*, 169(4), 736–749
2. Guo, C Yang, G Khun, K Kong, X Levy, D Lee, P and Melamed, J (2009). Activation of Stat3 in renal tumors. *Am J Transl Res*, 1 (3), 283-290

Ethics Approval All protocols in this study were approved by City of Hope Institutional Animal Care and Use Committee (IACUC protocol 10015)

<http://dx.doi.org/10.1136/jitc-2022-SITC2022.0810>

811 PD1 AND LAG3 SYNERGIZE ON CD8⁺ T CELLS TO HINDER IFN γ -DEPENDENT ANTI-TUMOR IMMUNITY

Lawrence Andrews*, Carly Cardello, Jian Cui, Creg Workman, Dario Vignali. *University of Pittsburgh, Pittsburgh, PA, USA*

Background Overcoming immune-mediated resistance to PD1 blockade remains a challenge, however enhanced efficacy has now been demonstrated in metastatic melanoma patients with a combinatorial regimen of nivolumab and relatlimab, an anti-LAG3 targeting antibody recently FDA approved. Despite this success, little is known about how PD1 and LAG3 synergize to hinder anti-tumor immunity, particularly on CD8⁺ T cells, which is the dominant LAG3-expressing intratumoral population signifying highly dysfunctional exhausted T (T_{EX}) cells regulated by the transcription factor TOX.

Methods To understand the cellular and mechanistic basis for PD1/LAG3 synergy, conditional knock-in mice “surgically dissect” *Pdcd1* and/or *Lag3* floxed alleles restricted to CD8⁺ T cells expressing E81^{Cre,GFP}. These mice were crossed with the pMEL transgene to assess PD1 and/or LAG3-sufficient or deficient gp100-specific CD8⁺ T cell populations adoptively transferred into mice harboring a B16-gp100-overexpressing tumor. Single-cell RNAseq analysis was performed, identifying both effector and IFN γ -stimulated genes up-regulated in PD1/LAG3-deficient pMEL. The IFN γ signaling pathway was further interrogated by retroviral transduced knockdown of IFN γ R in pMEL.

Results While little therapeutic benefit was observed with a prophylactic adoptive transfer (AT; d-1) of wild-type CD8⁺ pMEL cells into mice, there was reduced B16-gp100 tumor growth in mice receiving PD1-deficient CD8⁺ pMEL cells, which was further enhanced in mice receiving PD1/LAG3-deficient CD8⁺ pMEL cells with long-term tumor-free survival. Likewise, therapeutic AT (d6) of PD1/LAG3-deficient CD8⁺ pMEL cells showed initial therapeutic benefit, with enhanced survival, that was not demonstrated with AT of PD1 or LAG3-deficient, or wild-type, counterparts.

PD1/LAG3-deficient CD8⁺ T cells were shown to be more proliferative and more functional, with increased IFN γ and GzmB observed by flow cytometry. Interestingly, PD1 and LAG3 were demonstrated to synergize together to modulate the T_{EX} program by restraining the expression of TOX and promoting a more terminally-exhausted phenotype defined by expression of TIM3 and Ly108.

As this population was shown to be transcriptionally distinct by transcriptomic analysis, we interrogated whether enhanced IFN γ signaling was responsible for the phenotypes observed. Retroviral knockdown of IFN γ R reversed the therapeutic benefit observed with AT of PD1/LAG3-deficient pMEL. In addition, other IFN-responsive genes upregulated in PD1/LAG3-deficient pMEL, such as CCL5, were reduced with IFN γ R knockdown.

Conclusions Overall PD1 and LAG3 limit antitumor immune effects as PD1/LAG3-deficient pMEL AT resulted in reduced tumor growth and enhanced survival due to increased functionality, dependent on IFN γ signaling. These results provide mechanistic insight for the success seen with the clinical development of anti-LAG3 agents in combination with anti-PD1.

<http://dx.doi.org/10.1136/jitc-2022-SITC2022.0811>

812

DEVELOPMENT OF BCMA-TARGETED IMMUNOTHERAPY USING VACCINE-INDUCED ANTIGEN-SPECIFIC MEMORY CD8⁺ T CELLS FOR TREATING PATIENTS WITH MULTIPLE MYELOMA

Joeeun Bae*, Derin Keskin, Yueyi Huang, Sean Rowell, Sarah Nikiforow, Gerry MacDonald, Jerome Ritz, Nikhil Munshi, Kenneth Anderson. *Dana Farber Cancer Institute, Boston, MA, USA*

Background Multiple myeloma (MM) is a largely incurable cancer of the plasma cells. Despite remarkable recent advances in treatment using novel therapeutics, MM remains incurable. Previously, we reported a vaccination strategy that induced antigen-specific memory CD8⁺ T lymphocytes (CTL) against XBP1 (X-box binding protein 1), CD138 (Syndecan-1) and CS1 (SLAMF7), which are highly expressed in MM cells. Clinical trials on patients with smoldering MM have proven this multi-peptide vaccine's safety and immunogenicity, and larger clinical trials are ongoing. We further developed a translational research strategy to combine vaccination with the *ex vivo* expansion and infusion of vaccine-induced antigen-specific memory T cells. As a first step, we focused on targeting the B cell maturation antigen (BCMA), as it is specifically and highly expressed on the MM cells, and developed a protocol to efficiently isolate and expand BCMA-specific memory CTL *ex vivo*.

Methods In conjunction with our proposed immunogenic heteroclitic BCMA peptide-based vaccine, we have developed a protocol to efficiently isolate and expand the antigen-specific memory CD8⁺ CTL *ex vivo* as a supplemental immunotherapy against MM.

Results We developed a feasible and efficient method to secure antigen-specific T cells following the induction of MM-specific CTL using immunogenic heteroclitic BCMA₇₂₋₈₀ (YLMFLLRKI) peptide. The resulting CD8⁺ CTL show specific upregulation of various costimulatory molecules including CD28, 4-1BB, CD40L and OX40. Among the different conditions we evaluated, anti-CD3/CD28 (clinical grade) stimulation produced the greatest expansion of BCMA-specific CTL within 2 weeks and specifically induced the proliferation of antigen-specific central memory CTL (47% with anti-CD3/CD28 treatment vs. 6% without anti-CD3/CD28). To further enhance the efficacy of the final cell product, functionally active BCMA-specific IFN-γ⁺ CTL were sorted and expanded with anti-CD3/CD28, IL-2 (200 units/ml) and IL-15 (10 ng/ml). Under the conditions, we found a significant and continuous expansion (day 3: 2-fold, day 14: 22-fold, day 21: 55-fold) of BCMA-specific CTL with high Th1 cytokine (IL-2, TNF-α) production and anti-tumor activity (CD107a upregulation) against MM, which were both the BCMA epitope-specific and HLA-A2-restricted.

Conclusions BCMA-specific CD8⁺ CTL can be effectively expanded using clinical grade anti-CD3/CD28 and IL-2/IL-15 to yield MM-specific memory CTL with robust poly-functional anti-tumor activities. These results provide the framework for combining BCMA-peptide vaccination and the specific cellular therapy using the vaccine-induced IFN-γ⁺ memory T cells to further enhance anti-MM immunity and improve MM patient outcome.

<http://dx.doi.org/10.1136/jitc-2022-SITC2022.0812>

813 **CANCER VACCINE TRIPLE SYNERGISTIC COMBINATION
IMMUNOTHERAPY ENHANCES ANTI-CANCER EFFICACY**

^{1,2}Jay Berzofsky*, ²William Becker, ²Purevdorj Olkhanud. ¹NIH, Bethesda, MD, USA; ²National Cancer Institute, Bethesda, MD, USA

Background The discovery of checkpoint inhibitors (CPIs) has revolutionized cancer treatment, but many cancers remain resistant. In many cases, resistant tumors are considered “cold” because they lack infiltrating T cells that can be reinvigorated by the CPIs. Cancer vaccines may overcome this resistance by inducing the needed T cell immune response against the tumor. Conversely, cancer vaccines may not be effective alone if immunoregulatory mechanisms inhibit the immune response. Overcoming such regulatory mechanisms by CPIs or other immunomodulatory agents can improve vaccine efficacy. Thus, these complementary therapies can synergize

Methods Here we used a B6 mouse tumor model, TC1, expressing HPV16 E6 and E7 oncogenes, and utilized a vaccine consisting of an E7 synthetic long peptide 43-77 combined with alpha-galactosylceramide (a potent NKT cell agonist) and GM-CSF as adjuvants. We examined combinations of CPIs with the vaccine for increased efficacy in control of TC1 tumor growth.

Results We found triple synergy among the E7 vaccine, anti-TIGIT, and anti-PD-L1, more effective than any pairwise combination. Further, whereas the protection was dependent on CD8 T cells, depletion of CD4 T cells surprisingly improved the vaccine response, suggesting it was removing a suppressive CD4 T cell. Experiments are in progress to determine whether this putative suppressive cell is a Foxp3+ Treg cell. The triple therapy enhanced the number of E7-specific T cells infiltrating the tumors by tetramer staining. Further, the triple therapy was effective, although slightly less so, in aged mice as in young mice, suggesting it may be effective in older humans in whom cancer is more frequent.

Conclusions These studies show proof-of-concept for use of a synergistic combination of cancer vaccine immunotherapy to generate tumor-specific T cells and multi-checkpoint inhibitor therapy to overcome resistance in order to inhibit tumor growth and improve survival in mouse cancer models that is translatable to human cancer patients.

Ethics Approval This study was approved by the NCI Animal Care and Use Committee under ACUC Protocol METB-033.

<http://dx.doi.org/10.1136/jitc-2022-SITC2022.0813>

814

DT-9081, A SELECTIVE EP₄ RECEPTOR ANTAGONIST WHICH SYNERGIZES WITH IMMUNE CHECKPOINT INHIBITORS TO INDUCE COMPLETE RESPONSES IN SYNGENEIC MURINE CANCER MODELS

¹Anne-Laure Blayo*, ¹Claire Jouffroy-Zeller, ¹Nathalie Lenne, ²Imane Nafia, ¹Patricia Zerr, ¹Stéphan Schann*, ¹Xavier Leroy*. ¹Domain Therapeutics, Illkirch, France; ²Explicyte Immuno-Oncology, Bordeaux, France

Background Elevated levels of Prostaglandin E₂ (PGE₂), an eicosanoid synthesized by the cyclooxygenase-2 (COX-2), exert strong immunosuppressive effects in the tumor microenvironment (TME). COX-2-positive solid tumors have the ability to use this pathway as a resistance mechanism, especially to escape from the host immune system, thus limiting the anti-tumor effects of immune checkpoint inhibitors (ICI). These immunosuppressive effects are largely mediated by the EP₄ receptor, expressed on multiple immune cells. DT-9081, a selective EP₄ receptor antagonist, has been designed to counteract the PGE₂-immunosuppressive effects in the TME and to synergize with ICI.

Methods DT-9081 has been evaluated in 2 syngeneic murine cancer models in combination with ICI. DT-9081 was first tested at 30 and 60 mg/kg, as single agent or in combination with anti-CTLA-4 antibody, in the CT26 colorectal cancer model. DT-9081 was then tested at 30 mg/kg as single agent, or at 3, 10 or 30 mg/kg in combination with an anti-PD-1 in the MCA205 sarcoma model. In both studies, tumor growth, survival and type of response were evaluated. Complete responders were additionally submitted to a tumor rechallenge study to evaluate the immune system memory.

Results In the CT26 colorectal cancer model, combination of DT-9081 at both doses with anti-CTLA-4 antibody enabled a significant tumor growth inhibition and a noticeable increase in survival as compared to the anti-CTLA-4 antibody treatment alone. Moreover, 3 and 2 complete responses over 10 mice were observed in the groups treated with 30-mg/kg and 60-mg/kg DT-9081 in combination with the anti-CTLA-4 antibody, compared to none in the anti-CTLA-4 antibody treatment alone group.

In the MCA205 sarcoma model, combination of DT-9081 at the 3 tested doses with anti-PD-1 antibody enabled significant tumor growth inhibition and increase in survival, with a maximum anti-tumor efficacy from 10-mg/kg DT-9081. 5, 9 and 10 complete responses over 15 mice were observed in the groups treated with 3-, 10- and 30-mg/kg DT-9081, respectively, in combination with the anti-PD-1 antibody, compared to a single one in the anti-PD-1 antibody treatment alone group.

Complete responders from both studies were additionally assessed to address their response to a new challenge with the corresponding tumor cells. No tumor growth was observed indicating a long lasting tumor immune control.

Conclusions DT-9081 demonstrates strong anti-tumor effects in multiple syngeneic mouse tumor models, and synergizes with immune checkpoint inhibitors to induce long lasting complete responses. DT-9081 has completed regulatory development and will enter in clinical development by the end of 2022.

<http://dx.doi.org/10.1136/jitc-2022-SITC2022.0814>

815 **CRB-601, A SELECTIVE INTEGRIN $\alpha\text{V}\beta\text{8}$ BLOCKING ANTIBODY, EXHIBITS POTENT ANTI-TUMOR ACTIVITY IN ANTI-PD-1 RESISTANT MODELS**

Daqing Wang*, Vaishali Shinde, Maneesh Singh, Rachael Brake, Andrew Kolodziej. *Corbus Pharmaceuticals, Norwood, MA, USA*

Background Transforming growth factors-beta (TGF β) is a promising immunotherapeutic target in cancer given its association with increased signaling in the tumor microenvironment (TME) immune exclusion, resistance to checkpoint inhibitors (CPI), and poor clinical outcomes. TGF β is expressed as a latent form (L-TGF β) and presented on cell surfaces by L-TGF β binding proteins (e.g. GARP and LTPB1) as part of the large latent complex (LLC) whereupon it is activated by binding to integrins. Integrin $\alpha\text{V}\beta\text{8}$ binds to and activates L-TGF β , specifically the TGF β 1 and TGF β 3 isoforms. Corbus Pharmaceuticals is developing a humanized monoclonal antibody, CRB-601, that binds with high specificity and affinity to integrin $\alpha\text{V}\beta\text{8}$ and blocks its critical interaction with L-TGF β .

Methods Mice bearing subcutaneously implanted murine colon carcinoma MC38 or orthotopically implanted murine breast cancer EMT6 and 4T1 were treated with $\alpha\text{V}\beta\text{8}$ -blocking antibody CRB-601, anti-mouse PD-1 or the combination. These models demonstrate differential sensitivity to CPI treatment and are thought to reflect an immune inflamed (MC38), excluded (EMT6) or desert (4T1) tumor immune phenotypes. To determine the impact of disease establishment on sensitivity of these models to CRB-601 treatment both early (tumor volume = 50-80 mm³) and late (tumor volume > 200 mm³) intervention studies were conducted. Tumor growth, immune cell populations, and biomarkers of response (e.g. TGF β levels) were evaluated.

Results CRB-601 as a single agent, significantly inhibited growth of both MC38 and EMT6 models in both early and late intervention studies. In combination with anti-PD-1, CRB-601 not only enhanced anti-PD-1 therapy efficacy in early- and late-stage immune inflamed MC38, but also overcame resistance to PD-1 therapy in late-stage immune excluded EMT6 model. Notably, in the 4T1 model, an anti-PD-1 resistant desert tumor, combination therapy with CRB-601 and anti-PD-1 resulted in significant tumor growth inhibition even though there was negligible effect of each single agent. Analysis of tumor infiltrating lymphocytes in treated EMT6 tumors, showed TME remodeling, marked by increased infiltration of T cells, NK cells and M1-like macrophages in animals receiving CRB-601 or the combination. Biomarkers of response were consistent with Integrin $\alpha\text{V}\beta\text{8}$ target engagement.

Conclusions CRB-601 is a potent and selective integrin $\alpha\text{V}\beta\text{8}$ blocking monoclonal antibody that can overcome tumor immune exclusion and enhance the activity of immune checkpoint inhibitors *in vivo*. Investigational New Drug (IND) enabling studies are currently underway.

<http://dx.doi.org/10.1136/jitc-2022-SITC2022.0815>

816

BLOCKADE OF SIRP α ON MACROPHAGES TO ENHANCE CAR T ACTIVITY AGAINST GLIOBLASTOMA

Rebecca Brock*, Alesandra Echeandia-Marrero, Matthew Dysthe, Robin Parihar, Nabil Ahmed, Meenakshi Hegde. *Baylor College of Medicine, Houston, TX, USA*

Background The tumor microenvironment in glioblastoma (GBM) is highly immune suppressive, largely due to tumor-associated macrophages (TAMs) signaling. TAMs utilize several checkpoint inhibitors including SIRP α to regulate T cell function through the induction of apoptotic signaling and reduced activation. These also pose a challenge for engineered T cell therapies such as chimeric antigen receptor (CAR) T cells. While previous work has investigated blockade of either SIRP α or its ligand CD47, showing a temporal increase in trafficking of endogenous T cells to the tumor, understanding of the potential impact of such treatments on CAR T cells is lacking. We hypothesize that blocking the interaction of SIRP α with CD47 can improve the trafficking and functional activity of CAR T cells against glioblastoma.

Methods HER2-specific second generation CAR T cells were generated from primary human T cells using a retroviral transduction method. Primary human monocytes were harvested from peripheral blood and differentiated in vitro using M-CSF and IL-4 into M2-skewed macrophages. Macrophages, HER2+ GBM cell lines, and CAR Ts were co-cultured together with and without an anti-human SIRP α blocking monoclonal antibody. Cell surface expression of phenotypic macrophage markers, T cell activation markers, and SIRP α were assessed at baseline and post-treatment by flow cytometry. Supernatant from co-cultures was assessed for the presence of chemokines and cytokines using a custom multiplex panel and analyzed for differences in immunosuppressive signaling. CAR T cytolytic activity was determined by live-cell imaging using GFP-containing LN229-GBM.

Results We observed that TAM-like macrophages altered the cytokine release in CAR T and GBM co-cultures, promoted tumor cell growth, and increased CAR T apoptotic signaling resulting in delayed tumor cell lysis. In the presence of a SIRP α blocking antibody, we noted decreased surface expression of endogenous SIRP α and increased expression of M1-related marker CD86 on the macrophages at 24 hours of co-culture. The expression of several chemokines including MCP-1 was increased. At high ratios of CD28 ζ CAR T cells, down-regulation of SIRP α induced by the antibody blockade was not sustained.

Conclusions Macrophages cultured with GBM cells in vitro can alter the immune milieu, leading to CAR T cell apoptosis and hinder tumor-directed cytotoxicity. Blockade of SIRP α favorably alters the cytokine and chemokine production and may facilitate lymphocyte trafficking while reducing inhibitory receptor expression on macrophages. However, these effects can be countered by potent pro-inflammatory CAR T cell signaling, underscoring the need for more robust SIRP α disruption strategies.

Ethics Approval This study was approved by Baylor College of Medicine's Ethics Board; approval number H-15280.

<http://dx.doi.org/10.1136/jitc-2022-SITC2022.0816>

Abstracts

817 ENGINEERED TOXIN BODY TARGETING CTLA-4 (MT-8421) DEPLETES TREGS IN THE TUMOR MICROENVIRONMENT AND SYNERGIZES WITH α PD-1 TO ENHANCE T CELL IMMUNITY

Lauren Byrne, Swati Khanna*, Rebecca Martin, Caleigh Howard, Lilia Rabia, Michaela Sousares, Jay Zhao, John Majercak, Eric Poma, Chris Moore. *Molecular Templates Inc., Austin, TX, USA*

Background Despite being approved for clinical use over a decade ago, CTLA-4 mAbs remain encumbered by a narrow therapeutic window and relatively severe adverse event (AE) profile. Increasing data support that CTLA-4 mAb efficacy is primarily driven by depletion of CTLA-4+ T regulatory cells (Tregs) in the tumor microenvironment (TME), while AEs have been linked to an overzealous peripheral T cell response mediated by prolonged CTLA-4 blockade. It has been postulated that a more selective approach directly targeting TME-associated Treg cell depletion, while reducing peripheral T cell effects, might improve the tolerability of this class of immune checkpoint inhibitors, yet no CTLA-4 targeted mAb has achieved this. MT-8421 is a potent CTLA-4-targeted engineered toxin body (ETB) that can preferentially deplete high CTLA-4 expressing Tregs in the TME while sparing low CTLA-4 expressing peripheral T cells. In addition, MT-8421 was well-tolerated in a non-GLP non-human primate (NHP) study at doses hundreds-fold higher (450ng/mL) than the IC50 on CTLA-4 expressing cells. Here we demonstrate that MT-8421 synergizes with α PD-1 mAb in a Treg/T cell primary cell co-culture to stimulate T cell proliferative responses through direct Treg cell depletion.¹ Results from animal models including a GLP-NHP study will be described.

Methods T cells and Tregs were isolated from PBMCs of healthy donors and were stained to track T cell proliferation. T cells were co-cultured with autologous Tregs at various ratios. Anti-CD3/CD28 was used to drive proliferation of T cells in the presence of 4,000ng/mL of MT-8421, inactive MT-8421, or α PD-1 mAb (20 μ g/mL) to test for monotherapy activity. In addition, cells were treated with α PD-1 mAb followed by MT-8421 to evaluate combination effects. After 4 days, cells were stained with surface antibodies and analyzed by flow cytometry.

Results Co-cultures treated with MT-8421 alone demonstrated release of Treg-mediated CD8 T cell suppression compared to the untreated or inactive MT-8421. In addition, while α PD-1 treatment alone expectedly increased CD4+ and CD8+ T cell proliferation, when followed by MT-8421 treatment, the effects on T cell proliferation were greater than with either treatment alone.

Conclusions MT-8421 is a novel approach to CTLA-4 targeting: a potent depletion of TME CTLA-4+ Tregs without long-lasting CTLA-4 blockade in the periphery. This approach may allow for enhanced efficacy over current antibody approaches through the elimination of Tregs in the TME. The lack of prolonged peripheral CTLA-4 blockade may reduce toxicity as seen with antibody approaches to CTLA-4. Clinical studies are expected to start in 2023.

REFERENCE

1. Sarkar A, Martin R, Byrne LR, Howard C, Khanna S, Rabia LA, Adhikari D, Sousares MM, Aldana A, Robinson GL, Zhao J, Moore CB, Iberg A. A CTLA-4 targeted ETB for Treg depletion shows favorable preclinical efficacy and safety. *Cancer Research* 2022; **82**:12 supplement, 3538–3538.

<http://dx.doi.org/10.1136/jitc-2022-SITC2022.0817>

818

COMBINATION THERAPY WITH ANTI-PD1 AND ANTI-LAG3 LEADS TO UNIQUE PERIPHERAL AND INTRATUMORAL CD8+ T CELLS SIGNATURES IN PATIENTS WITH METASTATIC MELANOMA

Trial Registration ClinicalTrials. gov NCT03743766.

<http://dx.doi.org/10.1136/jitc-2022-SITC2022.0818>

¹Anthony Cillo*, ¹Carly Cardello, ¹Lilit Karapetyan, ¹Feng Shan, ²Cindy Sander, ²Elizabeth Rush, ³Aofei Li, ³Arivarasan Karunamurthy, ¹Sheryl Kunning, ¹John Kirkwood, ¹Tullia Bruno, ¹Dario Vignali. ¹University of Pittsburgh, Pittsburgh, PA, USA; ²UPMC Hillman Cancer Center, Pittsburgh, PA, USA; ³University of Pittsburgh Medical Center, Pittsburgh, PA, USA

Background CD8+ T cell exhaustion, characterized by co-expression of multiple inhibitory receptors, limits antitumor immunity. Combination therapy with anti-PD1 and anti-LAG3 synergistically improves CD8+ T cell function in murine models of cancer and has recently demonstrated improved progression-free survival versus anti-PD1 alone in metastatic melanoma. However, the mechanisms underlying improved efficacy of this combination therapy have yet to be fully elucidated.

Methods A phase 2 clinical study was designed to assess the antitumor efficacy of anti-PD1 or anti-LAG3 alone versus anti-PD1 with anti-LAG3 in combination in patients with advanced melanoma naïve to prior immunotherapy. Peripheral blood mononuclear cells (PBMC) and tumor biopsies were obtained prior to and at four weeks following therapy. Single-cell RNA-seq (scRNAseq) was performed using 5'-based chemistry (10X Genomics) on live FACS-sorted immune cells from blood and tumors. scRNAseq data was normalized across patients using scVI, and CD8+ T cells from PBMC and tumors were bioinformatically isolated for detailed analyses. miloR was used to identify CD8+ T cell transcriptional signatures that would distinguish effects associated with each treatment arm.

Results We identified a total of 33,646 CD8+ T cells from PBMC and tumor infiltrating leukocytes (TIL) from 22 patients. Using miloR to define subpopulations of CD8+ TIL, we found that each treatment arm led to a distinct CD8+ T cell transcriptional signature at just four weeks post-treatment. Using a gene set derived from genes upregulated in CD8+ TIL following combination therapy, we found that melanoma patients from The Cancer Genome Atlas with high enrichment of this anti-PD1 plus anti-LAG3 combination signature had improved overall survival (HR=0.39, p<0.001), indicating that this signature is associated with antitumor immunity. We also found that CD8+ T cells from PBMC of patients receiving combination therapy had higher levels of T cell receptor (TCR) and interferon gamma (IFN γ) signaling, suggestive of peripheral signatures of pharmacodynamic response to combination therapy. Notably, TCR and IFN γ signaling were correlated between CD8+ T cells in PBMC and TIL at week 4 (rho=0.67, p=0.020 for TCR; rho=0.59, p=0.046 for IFN γ), demonstrating that peripheral CD8+ T cells may serve as a surrogate for intra-tumoral responses.

Conclusions The anti-PD1, anti-LAG3, and anti-PD1 plus anti-LAG3 treatment arms each led to unique CD8+ TIL signatures. A transcriptional signature derived from combination therapy was associated with favorable prognosis in patients from an independent cohort. Functional signatures expressed by CD8+ T cells in PBMC were reflective of signatures occurring within tumors during therapy.

Acknowledgements We thank all members of the Vignali, Bruno, and Kirkwood labs for helpful discussions. We also thank our funding sources, the University of Pittsburgh Skin SPORE and Bristol-Myers Squibb. Finally, we thank Bristol-Myers Squibb for providing drug for this study.

819

INTRATUMORAL ADMINISTRATION OF HIGH-CONCENTRATION NITRIC OXIDE AND ANTI PD-1 TREATMENT LEADS TO HIGHER TUMOR REGRESSION RATES AND PROLONGED SURVIVAL IN CT26 TUMOR-BEARING MICE

¹Hila Confino*, ¹David Greenberg, ¹Selena Chaisson, ¹Jedidiah Mercer Monson, ²Steve Lisi, ¹Amir Avniel, ³Ido Wolf, ¹Yana Epshtein. ¹*Beyond Cancer, Beyond Air Inc., Rehovot, Israel;* ²*Beyond Cancer, Beyond Air Inc., Garden City, NY, USA;* ³*Tel Aviv Sourasky Medical Center, Tel Aviv Yafo, Israel*

Background Immune checkpoint inhibitors have shown dramatic activity transforming clinical oncology.¹ Yet, their activity is limited to a subset of highly sensitive tumors (e.g., melanoma). Even then response is observed in only 50% of patients.²

Nitric Oxide (NO) is a signaling molecule in multiple diseases, including cancer and has been shown to activate anti-tumor immune responses.³ Previously, we reported that treatment of CT26 tumor-bearing mice with high-concentration NO (UNO) stimulated anti-tumor immune responses leading to the rejection of a secondarily-induced tumor. More specifically, a significant increase of tumor-infiltrating T-cells and blood and spleen B and T-cells were observed 14-21 days post-UNO treatment.

In this study we investigated the ability of UNO to improve the efficacy of anti-PD-1 antibody.

Methods Day zero, 5.0×10^6 CT26 cells were injected to the right flank of Balb/c mice (n=15-16 per group). Day six, CT26 cells were injected to the contralateral flank and anti-PD1 injections (5mg/kg mouse, q2d, x 5) commenced.

Day eight, tumors (average size $71.9 \pm 37.2 \text{mm}^3$) were treated intratumorally with UNO (50,000 ppm, 5 or 10 minutes, flow rate ~ 0.2 liter per minute). Post-treatment tumor volume and survival were monitored thereafter.

Results Complete regression of the primary tumor occurred in 9/15 (60%) of mice treated with combination 10-minute NO and anti-PD-1, post-treatment day 26. This compared to 4/16 (25%) of controls treated with anti-PD-1 alone (p=0.13) and 0/15 (0%) treated with UNO alone (p=0.0027).

Survival was drastically increased in the 10-minute UNO/anti-PD-1 combination arm compared to anti-PD-1 alone (p<0.05), post-treatment day 32.

Secondary, contralateral flank tumor take in the anti-PD-1 alone arm was 21.4% but reduced by 38% to 13.3% in the 10-min combination arm and reduced by 67% to 7.14% in the 5-min combination arm, post-treatment day 19.

Survival was significantly improved for both the 5- and 10-minute combination arms compared to the 5- and 10-minute UNO controls (p=0.02 and p<0.0001, respectively).

Conclusions Combination of UNO with anti-PD-1 significantly improved outcomes compared with UNO or anti-PD-1 alone. A strong possibility is that high-concentration NO assists the immune system in overcoming anti-PD-1 resistance. Thus, the combination of high-concentration NO and immune checkpoint inhibitors such as anti-PD-1 can be a breakthrough therapy with important clinical implications.

REFERENCES

1. Pardoll DM. The blockade of immune checkpoints in cancer immunotherapy. *Nat Rev Cancer* 2012; **12**(4):252–264. <https://www.ncbi.nlm.nih.gov/pmc/articles/PMC4856023/>

2. Schoenfeld AJ, Hellmann MD. Acquired resistance to immune checkpoint inhibitors. *Cancer Cell* 2020; **37**(4):443–455. <https://www.ncbi.nlm.nih.gov/pmc/articles/PMC7182070/>
3. Khan FH, Dervan E, Bhattacharyya DD, McAuliffe JD, Miranda KM, Glynn SA. The role of nitric oxide in cancer: master regulator or not? *Int J Mol Sci* 2020; **21**(24):9393–9423. <https://www.ncbi.nlm.nih.gov/pmc/articles/PMC7763974/>

<http://dx.doi.org/10.1136/jitc-2022-SITC2022.0819>

820

LINEAR DNA AMPLICONS AS A NOVEL ANTIVIRAL AND CANCER VACCINE STRATEGY

¹Luigi Aurisicchio*, ²Antonella Conforti, ³Mirco Compagnone, ¹Erika Salvatori, ¹Lucia Lione, ¹Eleonora Pinto, ⁴Clay Shorrock, ⁴James Hayward, ⁴Brian Viscount, ³Fabio Palombo, ⁴Yuhua Sun, ⁴Ben Minghwa Liang. ¹Takis Srl, Rome, Italy; ²Evvivax Srl, Rome, Italy; ³Neomatrix Srl, Rome, Italy; ⁴ADNAS, Stony Brook, NY, USA

Background DNA-based vaccines represent a simple, safe and promising strategy for harnessing the immune system to fight infectious diseases as well as various forms of cancer and thus are considered an important tool in the cancer immunotherapy toolbox. Nonetheless, the manufacture of plasmid DNA vaccines has several drawbacks, including long lead times and the need to remove impurities from bacterial cultures. Here we report the development of polymerase chain reaction (PCR)-produced amplicon expression vectors as DNA vaccines and their *in vivo* application to elicit antigen-specific immune responses in animal cancer models.¹

Methods Plasmid DNA and amplicon expression was assessed both *in vitro*, by Hela cells transfection, and *in vivo*, by evaluating luciferase expression in mice through optical imaging. Immunogenicity induced by DNA amplicons was assessed by vaccinating mice, cats and ferrets against SARS-CoV-2 Spike protein. Similarly, amplicons encoding a tumor-associated antigen (Telomerase Reverse Transcriptase, TERT) and neoantigens were tested to evaluate the antitumoral effect of DNA amplicons in murine cancer models in combination with immune-checkpoint inhibitors (ICIs).

Results Amplicons encoding Spike Receptor Binding Domain (RBD) were strongly immunogenic in all models and were able to confer antiviral effects. DNA vaccines encoding tumor-associated-antigens, such as telomerase reverse transcriptase or neoantigens expressed by murine tumor cell lines were able to elicit antigen-specific immune responses and proved to significantly impact tumor growth when administered in combination with ICIs.

Conclusions These results strongly support the further exploration of the use of PCR-based amplicons as an innovative immunotherapeutic approach to viral diseases and cancer treatment.

REFERENCE

1. Conforti A, et al. Linear DNA amplicons as a novel cancer vaccine strategy. *J Exp Clin Cancer Res* 2022 Jun 6; **41**(1):195. doi: 10.1186/s13046-022-02402-5.

Ethics Approval All animal experiments were performed according to the guidelines for the care and use of laboratory animals and were approved by the ethical committee of the Italian Ministry of Health, with authorization #1166/2020-PR

<http://dx.doi.org/10.1136/jitc-2022-SITC2022.0820>

821 THE POTENTIAL CLINICAL USAGE OF FC-OPTIMIZED ANTI-CCR8 THERAPEUTIC ANTIBODIES AS A MONOTHERAPY OR COMBINED WITH OTHER PROMISING IMMUNE-MODULATING AGENTS BEYOND PD-1/L1

¹Shuang Dai, ¹Weifeng Huang, ¹Longjun Yan, ¹Shaogang Peng, ¹Shihui Zhou, ²Zhijun Yuan, ²Chao Wang, ²Chuan-Chu Chou*, ²Andy Tsun, ¹Tianhang Zhai. ¹Biotheus (Suzhou) Co., Ltd., Suzhou, China; ²Biotheus Inc., Zhuhai, China

Background FOXP3⁺ Regulatory T cells (Tregs) play a critical role in mediating tolerance to self-antigens but can repress anti-tumor immunity through multiple mechanisms. TGF- β is a potent immunosuppressive cytokine that acts as an essential factor during the differentiation of Treg cells. Therefore, targeted depletion of tumor-promoting Tregs is warranted to promote effective anti-tumor immunity while preserving peripheral homeostasis. CCR8 is a chemokine receptor that has recently been identified as a specific marker for tumor-infiltrating Tregs. Preclinical mouse tumor models have shown that the depletion of CCR8⁺ Tregs by anti-CCR8 monoclonal antibodies (mAbs) and Fc γ R engagement, but not ligand blockade, enables effective and long-lasting anti-tumor immunity in combination with PD-1 blockade. Several ADCC function-enhanced anti-CCR8 mAbs have been approved for clinical study both as a monotherapy and combined with PD-1 blockade. However, whether ADCC function enhancement would further potentiate anti-CCR8-mediated Treg depletion is still unknown. Here, we reveal an Fc-optimized anti-CCR8 mAb, which shows stronger ADCC and ADCC function than a wild-type IgG1 control. To explore potential combination strategies in the clinic, we also investigated the synergistic potential of combining the anti-CCR8 mAb with an anti-PD-L1 mAb fused to the extracellular domain of the human TGF- β receptor II (TGF β RII) via a flexible linker, to neutralize TGF- β (anti-PD-L1- β trap).

Methods Effector function-optimized anti-CCR8 mAbs were generated by the mutation of Fc residues plus expression in a *fut8*^{-/-} CHO cell line. ADCC and ADCC function was detected in both luciferase reporter cell line and primary cells. *In vivo* efficacy studies using anti-muCCR8-mG2a combined with an anti-PD-L1- β trap was conducted in a CT-26 colon carcinoma model.

Results Fc-optimized anti-CCR8 mAb showed stronger ADCC and ADCC function than the version containing wildtype IgG1 Fc in *in vitro* assays. The combination of anti-CCR8 mAb and anti-PD-L1- β trap more effectively controlled *in vivo* tumor growth compared to both monotherapies. We hypothesize that this potent anti-tumor immune response is propagated by the synergy of activating tumor infiltrating lymphocytes and the depletion of tumor-infiltrating Treg cells.

Conclusions We successfully generated an Fc-optimized anti-CCR8 mAb with both ADCC and ADCC enhancement. We also highlight the potential clinical combination benefit of anti-CCR8 mAbs with agents simultaneously blocking the PD1/L1 and TGF- β pathways.

Ethics Approval All mice were maintained under specified pathogen-free conditions, and all studies were approved by the Animal Care and Use Committee of HUST-Suzhou Institute for Brainmatics.

<http://dx.doi.org/10.1136/jitc-2022-SITC2022.0821>

822

OVERCOMING THE SUPPRESSIVE TUMOR MICROENVIRONMENT WITH A LIVE BACTERIAL IMMUNOTHERAPY

<http://dx.doi.org/10.1136/jitc-2022-SITC2022.0822>

Andrew Scott, Matthieu Besneux, Oluwatobiloba Oke, Mary Chol, Claudia Prevosto, Nicholas Glanville, Livija Deban*. *Prokarium Limited, London, UK*

Background Tumor-infiltrating myeloid cells suppress anti-tumor immunity within the tumor microenvironment (TME) through direct and indirect inhibitory mechanisms. However, inherent myeloid plasticity offers the opportunity for treatments to reprogramme these cells. One class of agents with potential to reprogramme myeloid cells are bacteria and their products, which act locally on suppressive cell populations, but also induce long-lasting systemic reprogramming of myeloid cells, a process termed trained immunity. Prokarium is developing a live attenuated *Salmonella enterica* serovar Typhi strain (ZH9) to be the next cancer immunotherapy and sought to establish whether *Salmonella* reprograms myeloid cells and enhances anti-tumor immune function.

Methods The effects of *Salmonella* on established suppressive myeloid cell phenotypes was assessed by flow cytometry staining, cytokine release and T cell suppression assays using M2 polarised human macrophages. The effects of *Salmonella* on unpolarised myeloid cells was investigated after oral *Salmonella* infection of healthy mice by phenotyping splenic myeloid cells using flow cytometry and assessing their cytokine production after *ex vivo* re-stimulation. Anti-tumor activity of *Salmonella* treatment was measured in syngeneic subcutaneous colon (MC38) and experimental metastasis (4T1) models. Finally, potential synergy with established therapies was assessed utilising a co-culture system of human monocyte-derived M2 macrophages treated with *Salmonella* and autologous T cells, with or without checkpoint inhibitor antibodies.

Results *Salmonella* treatment repolarized human M2 macrophages towards an anti-tumor phenotype, upregulating costimulatory molecules, increasing secretion of pro-inflammatory cytokines and relieving suppression of co-cultured T cells. Oral *Salmonella* treatment of mice induced long-term phenotypic and functional myeloid changes, including upregulation of costimulatory and MHC molecules on systemic dendritic cells, monocytes and macrophages, and increased responsiveness of CD11c+ splenocytes to secondary stimuli, suggesting *Salmonella* also affects unpolarised myeloid cells. Oral treatment with *Salmonella* as a monotherapy was able to suppress tumour growth in subcutaneous and experimental metastasis models, indicating this *Salmonella*-induced myeloid phenotype may translate to changes in the myeloid compartment of the TME. Finally, *Salmonella* complemented other cancer therapies both *in vitro* and *in vivo*. *In vitro*, *Salmonella*-trained human monocytes overcame the suppressive phenotype induced by subsequent culture in M2-polarizing conditions to synergize with checkpoint inhibitors in driving T-cell proliferation. *In vivo*, oral *Salmonella* treatment synergized with anti-PD-L1 in suppressing growth of subcutaneously implanted MC38 tumors.

Conclusions *Salmonella* immunotherapy can both reverse established suppressive myeloid phenotypes and systemically prime myeloid cells, likely rendering them resistant to immunosuppression in the TME and ultimately leading to improved efficacy of existing cancer immunotherapies.

Ethics Approval All animal studies were conducted under authority of United Kingdom Animals (Scientific Procedures) Act 1986 project license number PP8366809.

823

IMM20059, A NOVEL ANTI-EPN1 ANTIBODY, IN COMBINATION WITH ATEZOLIZUMAB SIGNIFICANTLY ENHANCES TUMOR REGRESSION IN THE B16.F10 SYNGENEIC MELANOMA MODEL COMPARED TO ANTI-PD-L1 MONOTHERAPY

John Dowling*, Pavel Nikitin, Cezary Swider, Chris Nicolescu, Halley Shukla, Jamie Bingaman-Steele, Nirja Patel, Eden Sikorski, Benjamin Harman, Jillian DiMuzio, Karen Lundgren, Yumi Ohtani, Michael Morin, Matthew Robinson, Fang Shen. *Immunome, Inc., Exton, PA, USA*

Background Immune checkpoint inhibitors (ICI), such as anti-PD-L1 and anti-PD-1 antibodies, have exhibited remarkable efficacy in the clinic. However only a small subset of patients will ultimately respond to therapy and there is a dire need for expanding the patient population who will benefit from ICI treatments. Immunome's proprietary platform allows the interrogation of the memory B cell population for potential therapeutic antibodies, including those that may enhance ICI responses.

Methods In this study, IMM20059, an antibody discovered using Immunome's proprietary platform, is assessed for target specificity using immunoprecipitation/mass spectrometry (IP/MS), surface plasmon resonance (SPR), and epitope mapping. Tumor cell binding is evaluated via flow cytometry. Anti-tumor efficacy of IMM20059 in combination with anti-PD-L1 is evaluated in the syngeneic B16.F10 melanoma model in C57BL/6 mice and intra-tumoral chemokines are assessed by Luminex.

Results IMM20059 selectively binds to the N-terminal domain of epsin 1 (EPN1), an adapter protein involved in clathrin-mediated endocytosis, as compared to other epsin family members. Although expressed in multiple tissues, EPN1 is specifically upregulated in multiple cancer types, including lung, breast, and prostate cancers. Strikingly, while this expression is largely restricted to the intracellular compartment in normal cells, EPN1 appears to be ectopically expressed on the cell surface in multiple cancer cell lines, allowing for tumor specific targeting. The selectivity of IMM20059 and surface expression of EPN1 was confirmed by knockout of EPN1 and competition with recombinant protein. IMM20059 cross reacts with murine EPN1, exhibits a favorable pharmacokinetic profile *in vivo*, and exhibits a good tolerability profile in C57BL/6 mice. In the B16.F10 melanoma syngeneic model, combination treatment of IMM20059 and anti-PD-L1 (Atezolizumab) induced significant tumor regression compared to IMM20059 or Atezolizumab treatment alone, suggesting a combinatorial effect between the two pathways. Furthermore, this combination treatment significantly enhanced production of intratumoral chemokines, including MIP-1 α , MIP-1 β , and RANTES.

Conclusions This study suggests that EPN1 is a promising tumor target. Combination treatment of IMM20059 and anti-PD-L1 could enhance the efficacy of anti-PD-L1 therapy by boosting intratumoral chemokines and attracting immune cells to the immunologically cold tumor microenvironment.

<http://dx.doi.org/10.1136/jitc-2022-SITC2022.0823>

824

NX-1607, A SMALL MOLECULE INHIBITOR OF THE CBL-B E3 UBIQUITIN LIGASE, PROMOTES T AND NK CELL ACTIVATION AND ENHANCES NK-MEDIATED ADCC IN A MOUSE LYMPHOMA TUMOR MODEL

Marilena Gallotta*, Jennifa Gosling, Austin Tenn-McClellan, Serena Ranucci, Jose Gomez Romo, Frederick Cohen, Gwenn Hansen, Arthur Sands, Cristiana Guiducci, Ryan Rountree. *Nurix Therapeutics, San Francisco, CA, USA*

Background The E3 ubiquitin ligase Casitas B-lineage lymphoma B (CBL-B) is expressed in leukocytes and regulates signaling pathways in T and NK cells, significantly limiting their antitumor effector function. In T cells CBL-B attenuates activation initiated by TCR engagement, in part by mediating the requirement for CD28 co-stimulation, thus setting the threshold for T cell activation. In NK cells, CBL-B functions downstream of TAM receptors and negatively regulates cytokine production and cytotoxicity.

Methods Here we describe the effects of NX-1607, an orally bioavailable intramolecular glue inhibitor of CBL-B, on primary human T and NK cells and assess NX-1607 in combination with Rituximab in a murine xenograft model of Non-Hodgkin's Lymphoma (NHL).

Results Previously, we showed that NX-1607 enhances IL-2 and IFN- γ secretion in human T cells following TCR stimulation. Regulatory T cells (Tregs) produce multiple cytokines in the tumor microenvironment (TME) that work to counteract the antitumor response by suppressing T-cell activation. Proliferation of CD4⁺ effector T cells activated by anti-CD3/CD28 was suppressed when cultured 1:1 with Tregs or TGF- β . Addition of NX-1607 recovered the proliferative capacity of CD4⁺ effector T cells to levels equivalent to that of anti-CD3/CD28 stimulation alone. Therefore, in addition to enhancing T-cell activation, NX-1607 renders T cells resistant to Treg and TGF- β -mediated suppression.

In an *in vitro* ADCC assay, addition of NX-1607 significantly enhanced TNF- α and IFN- γ production in human primary NK cells. The efficacy of NX-1607 in combination with Rituximab was evaluated in a Raji NHL model where Raji cells were administered by IV to establish disseminated tumors followed by treatment with NX-1607 (30 mg/kg QD) and/or Rituximab (10 mg/kg). Both NX-1607 and Rituximab given as monotherapy provided a significant survival benefit. Combination of NX-1607 and Rituximab significantly enhanced tumor growth inhibition and stable rejections when compared to single agent activity. Importantly, the survival benefit provided by NX-1607 was abrogated by depletion of NK cells. Therefore, NX-1607 augments NK cell activity both in human NK cells and in mouse tumor models.

Conclusions These studies provide insight into the antitumor activity of this novel, small molecule inhibitor of CBL-B, demonstrating that NX-1607 enhances both innate and adaptive immune responses, both of which are important for overcoming a suppressive TME. These studies also provide support for clinical development of NX-1607 as a monotherapy or in combination with antibody therapeutics to enhance ADCC antitumor effects. We have initiated a clinical trial with NX-1607 in patients with advanced solid tumors NX-1607-101 (NCT05107674).

<http://dx.doi.org/10.1136/jitc-2022-SITC2022.0824>

826

IL7R TME EXPRESSION CORRELATES WITH IMMUNOTHERAPY RESPONSE AND IS ASSOCIATED WITH T-CELL STEMNESS WITH DECREASED APOPTOSIS

Nicolas Poirier*, Isabelle Girault, Aurore Morello, Justine Durand, Margaux Seite. *OSE Immunotherapeutics, Nantes, France*

Background Anti-PD(L)1 therapy can reinvigorate exhausted Tcells by inducing a proliferative burst of PD1+TCF7+ stem-like Tcells but, Tcells rapidly undergo exhaustion and death, limiting efficacy of therapy. IL7 induces survival and homeostatic proliferation of Tcells. IL7R is associated with memory-stem-like Tcells subset but, the effect of IL7 on cancer-specific TILs remains unknown. We studied gene expression of the IL7/IL7R pathway on single cell transcriptomic analysis in multiple datasets of anti-PD1/PDL1 responder's and non-responders' patients.

Methods RNAseq of bulk tumor and scRNAseq of TILs and tumor-specific clonotypes datasets were analyzed prior checkpoint inhibitors treatment from different clinical studies representing a total of 1036 patients for RNAseq analysis and 39 patients for scRNAseq analysis: Melanoma (aPD1+/-aCTLA4), TNBC (Chemotherapy+PDL1), NSCLC (aPD1) and Ovary (*Ex vivo* aPD-1 response).

Results IL7R and IL7R pathways gene expression on tumor bulk is significantly correlated with better OS or PFS across multiple cancers, as analyzed by PanCancer TCGA and iATLAS datasets ($p < 0.02$; $p < 0.0001$). In Melanoma, NSCLC, Ovarian, TNBC, HNSCC and/or Kidney cancers, we demonstrated a significant higher expression of IL7R and/or IL7R pathway signatures of future ICI responders versus non-responders and confirmed this data by scRNAseq analysis specifically on TILs and tumor-specific Tcell clonotypes.¹⁻⁵ TILs over-expressing IL7R show upregulation of genes related to stemness and downregulation of genes related to exhaustion. In addition, IL7R^{High} TILs are less apoptotic and express significant higher level of BCL2 anti-apoptotic molecule. As TCF7 gene is described as key marker for stemness and anti-PD(L)1 response, we also analysed impact of IL7R+/-TCF7 expression. TCF7 or IL7R expression only are not sufficient to predict ICI response, while the coexpression is predictive to ICI response in Melanoma. scRNAseq and FACs analyses of chronically stimulated human Tcells *in vitro* show that IL7 significantly promotes long-term survival (up to 5 weeks) and proliferation of stem-like Tcells (TCF7+Tcells), whereas IL2 or IL15 promotes proliferation of Tcells with exhausted phenotype dying after >10 days of culture.

Ex-vivo, IL7 fused to an anti-PD1 mAb reinvigorates TILs (IFN γ secretion) in human 3D-tumoroids from both anti-PD1 sensitive or not patients.

Conclusions Altogether, our data show that IL7R pathway expression in TILs and tumor-specific Tcell clonotypes are predictive of long-term ICI clinical response. Redirecting IL7 on PD1+Tcells provides stemness, proliferative and survival signals to tumor-specific Tcells capable to induce durable response.

REFERENCES

1. Sade-Feldman M, Yizhak K, Bjorgaard SL, Ray JP *et al.* Defining T cell states associated with response to checkpoint immunotherapy in melanoma. *Cell* 2018 Nov 1; **175**(4):998–1013.e20.
2. Zhang Y, Chen H, Mo H, Hu X *et al.* Single-cell analyses reveal key immune cell subsets associated with response to PD-L1 blockade in triple-negative breast cancer. *Cancer Cell* 2021 Dec 13; **39**(12):1578–1593.e8

3. Caushi JX, Zhang J, Ji Z, Vaghiasia A *et al.* Transcriptional programs of neoantigen-specific TIL in anti-PD-1-treated lung cancers. *Nature* 2021 Aug; **596**(7870):126–132.
4. Duraiswamy J, Turrini R, Minasyan A, Barras D *et al.* Myeloid antigen-presenting cell niches sustain antitumor T cells and license PD-1 blockade via CD28 costimulation. *Cancer Cell* 2021 Dec 13; **39**(12):1623–1642.e20.
5. Andreatta M, Corria-Osorio J, Müller S. *et al.* Interpretation of T cell states from single-cell transcriptomics data using reference atlases. *Nat Commun* 2021; **12**, 2965.

<http://dx.doi.org/10.1136/jitc-2022-SITC2022.0826>

827 THE ROLE OF COMBINATION IMMUNE CHECKPOINT INHIBITORS AS SALVAGE THERAPY FOR PD-1/PD-L1-RESISTANT MERKEL CELL CARCINOMA

Tarek Haykal*, Georgia Beasley, April Salama, Brent Hanks. *Duke University, Durham, NC, United States*

Background Merkel cell Carcinoma (MCC) is a rare but aggressive cutaneous neuroendocrine malignancy that often presents as locally advanced or metastatic disease. MCC has a high risk of relapse, morbidity, and mortality that can be challenging to manage. The PD-1/PD-L1 inhibitors, pembrolizumab and avelumab, have recently been shown to benefit approximately 50% of metastatic MCC patients, indicating that a significant fraction of these patients are in need of alternative therapeutic options. There is currently no standard salvage treatment regimen for anti-PD-1-refractory MCC patients. We sought to explore our clinical experience at Duke University with combination immune checkpoint inhibitors (ICIs), ipilimumab and nivolumab, after progression on PD-1/PD-L1 inhibitors for patients with metastatic or locally advanced MCC.

Methods A comprehensive electronic database search was conducted for all metastatic and locally advanced MCC patients that were treated with PD-1/PD-L1 therapies between years 2015 and 2022, at Duke University. Patients that were treated with combination ICIs were included. Patients treated with surgery, radiation, and chemotherapy were not excluded. The primary outcome was objective response rates (ORR), as assessed by utilizing Response Evaluation Criteria in Solid Tumors (RECISTv1.1) as well as immune-related Response Evaluation Criteria in Solid Tumors (irRECIST). Secondary outcomes were progression free survival (PFS), overall survival (OS), and immune-related adverse events (irAEs) at the longest follow-up.

Results Our search yielded 6 patients with metastatic or locally advanced MCC that were treated with ipilimumab and nivolumab after progression on PD-1/PD-L1 inhibitor therapies. The patients' mean age was 69.6 years with a male percentage of 66.66%. ORR was 50%, where 2 patients had a complete response and one had a partial response. Of the other 50% of patients, 2 patients had progression of disease and one had stable disease at their week 12 restaging scans. Mortality rate was 50% and all deaths were cancer-related. Median PFS was 7 months and median OS was 13 months. 50% of patients suffered an irAE while 33% experienced a grade 3 or higher irAE.

Conclusions Our study highlights that the use of combination ICIs with ipilimumab and nivolumab as salvage therapy for patients with metastatic or locally advanced MCC resistant to PD-1/PD-L1 therapy can be effective and is relatively well-tolerated. These data indicate that this treatment regimen is worthy of further exploration in a larger cohort of MCC patients.

<http://dx.doi.org/10.1136/jitc-2022-SITC2022.0827>

828 **COMBINATION OF FLT3L AND STING AGONISM SENSITIZES NON-T CELL-INFLAMED TUMORS TO CHECKPOINT BLOCKADE THERAPY**

Emily Higgs*, Thomas Gajewski. *University of Chicago, Chicago, IL, United States*

Background STING agonists have been pursued as a strategy to trigger innate immune activation within the tumor microenvironment, which can lead to adaptive immunity and tumor regression in mice. However, clinically activity of STING agonists has been less impressive. We hypothesized that a low response rate clinically could be because most patients have non-T cell-inflamed (cold) tumors. We hypothesized that non-T cell-inflamed tumors may lack the required CD103⁺dendritic cell (DC) subset for T cell priming, thus failing to make the bridge to adaptive immunity. To investigate this notion, we turned to a B-catenin-driven genetically engineered mouse melanoma model, which is non-inflamed and known to lack CD103⁺ DCs. We evaluated whether recruitment of CD103⁺ DCs via Flt3L might cooperate with a STING agonist to promote tumor control, alone or in combination with checkpoint blockade antibodies.

Methods We used the BRAF-activated, PTEN-deleted, B-catenin-stabilized (BPC) genetic melanoma model. Our laboratory previously showed that these tumors lack spontaneous CD103⁺ DC and T cell infiltration and have low expression of the chemokines known to recruit these cells, which closely resembles the biology of many non-T cell-inflamed human cancers. To recruit and activate CD103⁺ DCs to these tumors, we injected intratumoral Flt3L alone, the STING agonist DMXAA alone, and both in combination.

Results Intratumoral DMXAA injection led to significant increases in CD8⁺ T cells in BPC tumors five days post injection. However, the CD103⁺ DC numbers in these tumors were not increased. Moreover, T cells recruited following DMXAA treatment were unable to control tumors alone or with anti-PD-L1 + anti-CTLA-4. This led us to adopt an additional strategy aimed at promoting CD103⁺ DC accumulation directly. A single injection of Flt3L was able to drive CD103⁺ DC accumulation in BPC tumors. However, Flt3L alone or with a subsequent DMXAA injection had minimal effects on tumor growth. Excitingly, Flt3L and DMXAA injection followed by anti-PD-L1 + anti-CTLA-4 mAb therapy led to significant tumor control.

Conclusions Injection of Flt3L + DMXAA supported intratumoral accumulation of both CD8⁺ T cells and CD103⁺ DCs. This enabled subsequent therapeutic activity of anti-CTLA-4 + anti-PD-L1 mAb therapy in this very challenging cold tumor model. Inasmuch as tumors in this model fail to respond to vaccination, adoptive T cell therapy, and checkpoint blockade strategies, the activity of this regimen is highly significant. Clinical investigation of intratumoral Flt3L + STING agonists should be prioritized for future study in anti-PD-1-refractory patients.

Ethics Approval This study obtained ethics approval by the Institutional Animal Care and Use Committee (IACUC) at the University of Chicago as outlined in the animal protocol #71621. The IBC protocol number is IBC1309(3).

<http://dx.doi.org/10.1136/jitc-2022-SITC2022.0828>

829

IN SITU VACCINATION UTILIZING INTRATUMORAL ELECTROPORATION OF PLASMIDS EXPRESSING IL-12 AND CD40 LIGAND (CD154) HAS EFFICACY AGAINST MURINE TUMORS

<http://dx.doi.org/10.1136/jitc-2022-SITC2022.0829>

Gregory Ho*, Steven Fiering. *Dartmouth College, Lebanon, NH, United States*

Background Although the human body generates tumor-specific T cells, tumor-mediated immunosuppression protects tumors from antitumor immunity. Any immunotherapy must overcome this local/systemic immunosuppression. One strategy is *in situ* vaccination (ISV), where an immunostimulant is applied directly to an established tumor to disrupt the local immunosuppression, generating a robust local antitumor immunity, slowing or potentially eliminating the treated tumor. In addition, the rapid expansion of tumor-specific T cells induces antitumoral effects on distant, non-treated tumors known as the abscopal effect. While there are many therapeutic options under development for ISV, the optimal combination of immunostimulants needed for different tumor types remains unclear. Reported here are studies to express specific proteins by plasmid electroporation as ISV therapy.^{1,2} Previous studies have reported the benefit of expressing different molecules from plasmids in tumors, particularly IL-12, which has also been tested in phase II clinical trials.³ CD154 expression, (ligand for CD40), can mature antigen-presenting cells, lead to changes in cytokine expression, and support antigen presentation. We find that intratumoral CD154 electroporation has potent local antitumor effects and those effects are increased when CD154 is combined with IL-12. Presented studies will include abscopal effects on established but untreated tumors.

Methods Plasmids encoding for either CD154, IL-12, or control (Bgeo) were transformed into competent *E.coli* and inoculated into LB Miller cultures. Plasmid DNA was isolated and purified using Qiagen Plasmid Mega kit. Mice were anesthetized and injected with 2×10^5 B16F10 cells into the right flank intradermally prior to electroporation treatment into C57BL6 mice. 50ug of each plasmid was injected intratumorally twice one week apart. Immediately following injection, mice were electroporated for 6 pulses at 1500v/cm for 6 pulses at 100us durations using BTX Harvard Gemini X2 electroporator.

Results We find that intratumoral CD154 electroporation has potent local antitumor effects and those effects are increased when CD154 is combined with IL-12. With the addition of the IL-12 plasmid, we are able to generate significant abscopal effects on established, untreated tumors.

Conclusions The addition of CD40 ligand expression in combination with IL-12 induces a tumor clearance on the treated tumor. CD154 and IL-12 plasmid electroporation combination therapy provides superior protection on the treated tumor, in addition to providing protection on distant, untreated tumors.

REFERENCES

1. Lucas ML, Heller L, Coppola D & Heller R. IL-12 plasmid delivery by in Vivo electroporation for the successful treatment of established subcutaneous B16.F10 melanoma. *Molecular Therapy* 2002;5(6), 668–675. <https://doi.org/10.1006/mthe.2002.0601>
2. Daud AI, DeConti RC, Andrews S, Urbas P, Riker AI, Sondak VK, ... Heller R. Phase I trial of interleukin-12 plasmid electroporation in patients with metastatic melanoma. *Journal of Clinical Oncology* 2008;26(36):5896–5903. <https://doi.org/10.1200/JCO.2007.15.6794>
3. Algazi A, Bhatia S, Agarwala S, Molina M, Lewis K, Faries M, ... Daud AI. Intratumoral delivery of tavokinogene telseplasmid yields systemic immune responses in metastatic melanoma patients. *Annals of Oncology*, 2020;31(4):532–540. <https://doi.org/10.1016/j.annonc.2019.12.0084>

Abstracts

830 TARGETING B CELL SUPPRESSION TO IMPROVE THE EFFICACY OF IMMUNOTHERAPIES IN BRAIN CANCER

¹David Hou*, ²Brandyn Castro, ¹Andrew Zolp, ¹Mark Dapash, ¹Victor Arrieta, ³Jana Biermann, ³Johannes Melms, ¹Maciej Lesniak, ³Benjamin Izar, ¹Jason Miska, ³Junfei Zhao, ¹Catalina Lee-Chang. ¹Northwestern University, Chicago, IL, United States; ²University of Chicago, Chicago, IL, United States; ³Columbia University, New York, NY, United States

Background Immunotherapy is a promising approach to treat brain tumors, but several factors, especially the suppressive tumor microenvironment (TME), make translation of immunotherapies difficult. Studies in several other solid tumors have revealed the accumulation of germinal-center-like B-cells as a critical survival predictor of immune-checkpoint-blockade (ICB) therapy, suggesting a central of B-cell immunity in driving ICB therapeutic impact.^{1,2} However, the harsh TME of brain tumors such as glioblastoma (GBM) suppress B-cell activity. We seek to better understand mechanisms of TME-driven immunosuppression and leverage B-cell immunity to enhance immunotherapy effectiveness in brain tumors.

Methods Single-cell and single-nuclei transcriptomic sequencing were used to analyze human GBM and melanoma brain metastasis tumor samples, as well as CT2A murine glioma models. Spatial multiplex analysis and single-cell transcriptomic analysis were used to characterize B-cell interactions within the TME of GBM samples to identify pathways of B-cell immunosuppression.

Results We characterized tumor infiltrating B-cells as activated but suppressed, with expression of coinhibitory checkpoint molecules such as CD22, CD72, and CD32 that inhibit effector functions such as plasmablast differentiation and antibody production (figure 1). Single-cell transcriptomic and spatial multiplex analysis highlighted the TGF- β receptor 2 (TGFBR2) as a key regulator of tumor B-cell suppression with tumor associated myeloid cells (TAMCs) and tumor cells being main producers of TGF- β 1 cytokine (figure 2). TGF- β 1 signaling directly inhibited B-cell proliferation and plasmablast differentiation, and induced expression of checkpoint molecules *in vitro*. Murine and tumor models with conditional knock-outs of TGFBR2 or TGF- β 1, showed significant increased efficacy of PD1 blockade compared to wild type controls (figure 3). The TME of these animals had expanded germinal-center-like proliferating intratumoral B-cells, production of tumor-reactive antibodies, and T-cell activation, and these animals showed increased survival. We also blocked α V β 8 integrin, which has tumor-B-cell specificity and activates TGF- β 1, and found that our treatment promoted PD1 blockade efficacy and long-term survival benefit. Combining α V β 8 and PD1 blockade eradicated gliomas in nearly 60% of treated mice and promoting immunological memory against tumor rechallenge (figure 4). This robust therapeutic effect depended on B-cell immunity as mice lacking B-cells (B-cell deficiency or intratumoral B-cell depletion using rituximab) failed to prevent tumor growth. After dual treatment, analysis of the TME showed robust cellular proliferation and differentiation into plasmablasts and effector T-cells (figure 5).

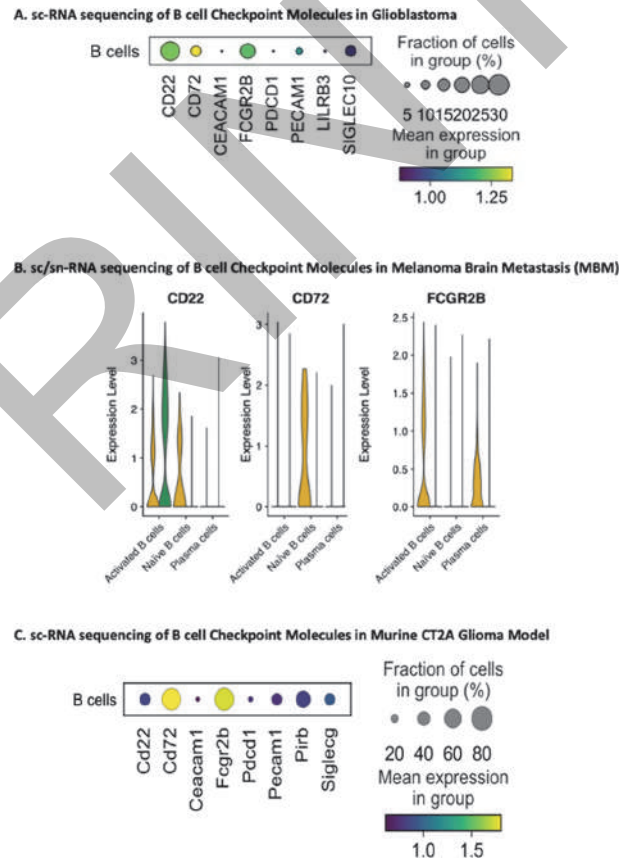
Conclusions Our results highlight the importance of B-cells in anti-tumor response, and that promoting Bcell function is a novel approach to boosting the effects of checkpoint blockade in brain tumors.

REFERENCES

1. Griss J, Bauer W, Wagner C, Simon M, Chen M, Grabmeier-Pfistershammer K, Maurer-Granofszky M, Roka F, Penz T, Bock C, Zhang G, Herlyn M, Glatz K,

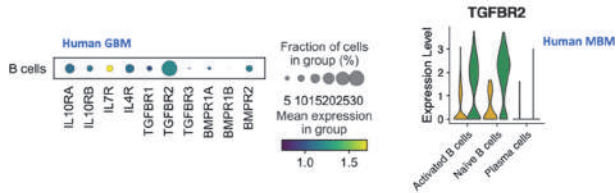
Laubli H, Mertz KD, Petzelbauer P, Wiesner T, Hartl M, Pickl WF, Somasundaram R, Steinberger P, Wagner SN. B cells sustain inflammation and predict response to immune checkpoint blockade in human melanoma. *Nat Commun.* 2019;**10** (1):4186. Epub 2019/09/15. doi: 10.1038/s41467-019-12160-2. PubMed PMID: 31519915; PMCID: PMC6744450.

2. Helmink BA, Reddy SM, Gao J, Zhang S, Basar R, Thakur R, Yizhak K, Sade-Feldman M, Blando J, Han G, Gopalakrishnan V, Xi Y, Zhao H, Amaria RN, Tawbi HA, Cogdill AP, Liu W, LeBleu VS, Kugeratski FG, Patel S, Davies MA, Hwu P, Lee JE, Gershenwald JE, Lucci A, Arora R, Woodman S, Keung EZ, Gaudreau PO, Reuben A, Spencer CN, Burton EM, Haydu LE, Lazar AJ, Zappasodi R, Hudgens CW, Ledesma DA, Ong S, Bailey M, Warren S, Rao D, Krijgsman O, Rozeman EA, Peeper D, Blank CU, Schumacher TN, Butterfield LH, Zelazowska MA, McBride KM, Kalluri R, Allison J, Petitprez F, Fridman WH, Sautes-Fridman C, Hacohen N, Rezvani K, Sharma P, Tetzlaff MT, Wang L, Wargo JA. B cells and tertiary lymphoid structures promote immunotherapy response. *Nature.* 2020;**577** (7791):549–55. Epub 2020/01/17. doi: 10.1038/s41586-019-1922-8. PubMed PMID: 31942075.

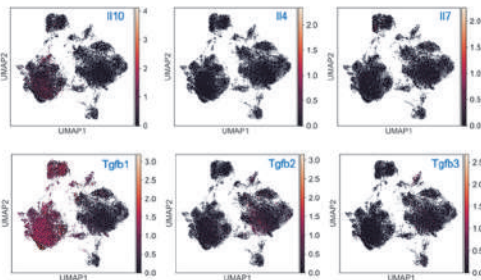


Abstract 830 Figure 1 Single cell RNA analysis of Tumor B cells Single cell (sc) and single nuclei (sn) RNA sequencing for inhibitory checkpoint molecules on tumor infiltrating B cells in (A) human glioblastoma (GBM), (B) melanoma brain metastases (MBM), and (C) murine CT2A glioma model. All models show elevated expression of coinhibitory checkpoint molecules CD22, CD72, and CD32

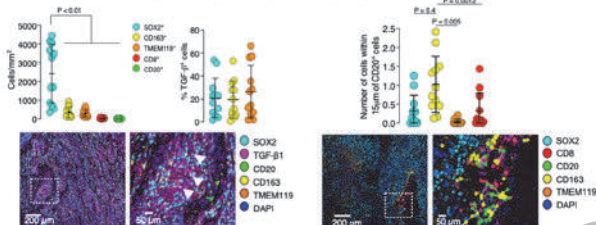
A. sc-RNA sequencing of Inhibitory Receptors on B cells in GBM (Left) and Melanoma Brain Metastasis (Right)



B. sc-RNA sequencing of Inhibitory Cytokines in GBM



C. Spatial Multiplex Analysis of TGF-β1 Expression in GBM

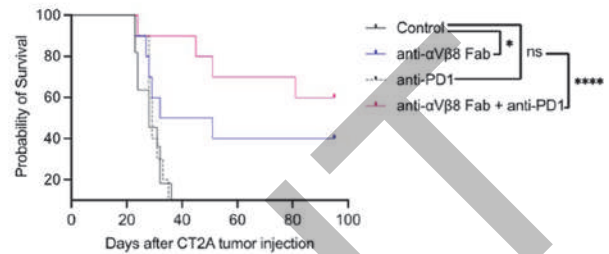


Abstract 830 Figure 2 TGFβ1-TGFβ-R2 Pathway Mediates B cell Suppression

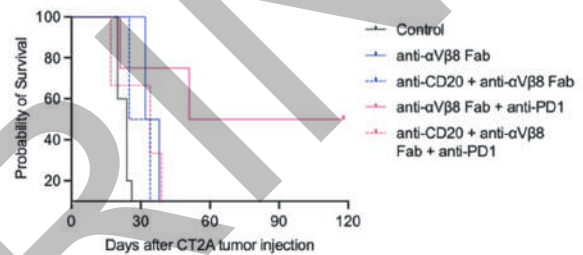
(A) Tumor B cells express high levels of TGFβ-R2 in both GBM (left) and MBM (right) samples as well as murine CT2A model. (B) scRNAseq shows that the TME of GBM has high levels of TGFβ1 cytokine. (C) Spatial multiplex analysis shows TAMCs and tumor cells are key producers of TGFβ1 in the TME

(A) We generated conditional knockouts of TGFβ-R2 from B cells. These animals had an improved response to PD1 therapy ($p < 0.01$). (B) Wild type mice with CT2A-TGFβ1KO tumors had improved survival compared to those with CT2A-wild type tumors ($p < 0.5$). B cells in these mice also had improved proliferation and function

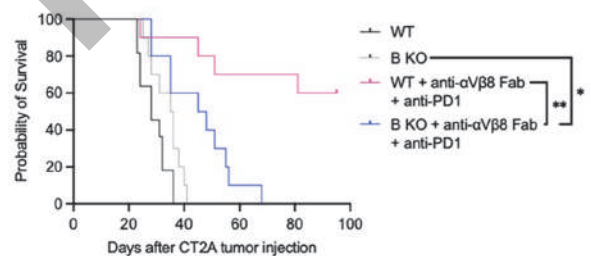
A. Survival of CT2A Glioma Bearing Mice Treated with Dual αVβ8 and PD1 Blockade



B. Effects of Rituximab B cell Depletion on Anti-tumor Memory Response



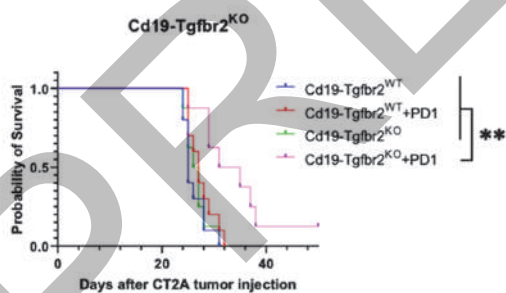
C. Effects of Dual αVβ8 and PD1 Blockade on B cell KO Mice



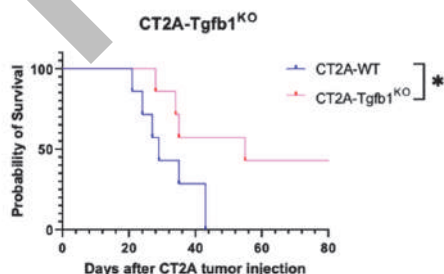
Abstract 830 Figure 4 αVβ8 Integrin Blockade Improves PD1 Blockade Efficacy

(A) CT2A bearing mice were treated with dual or single αVβ8 and PD1 blockade. Dual treated animals showed significantly improved survival benefit ($n = 10$ animals/group, $p < 0.0001$). (B) Animals were re-challenged with CT2A tumors in the contralateral hemisphere. Those that also received B cell depletion via rituximab were not able to mount a memory response. (C) Dual αVβ8 and PD1 blockade did not exhibit the same therapeutic benefit in B cell KO mice compared to wild type mice ($p < 0.01$).

A. Survival of CD19(cre)-TGFBR2(flox) bearing CT2A Gliomas Treated with PD1 Blockade

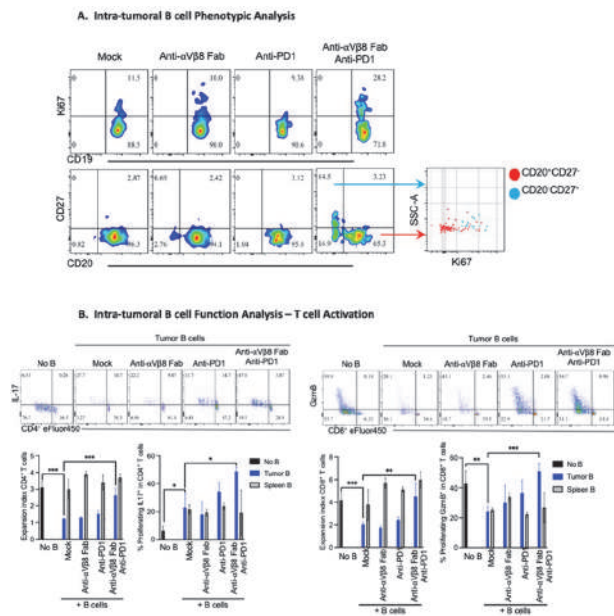


B. Survival of wild-type mice bearing CT2A-TGFβ1KO Gliomas



Abstract 830 Figure 3 Inhibiting TGFβ Signaling on B cells Increases Survival

Abstracts



Abstract 830 Figure 5 Dual aVb8 and PD1 blockade Improves B cell Functionality

(A) Phenotypic analysis of B cells after treatment show increased proliferation and plasmablast differentiation. (B) Functional analysis of B cells show increased activation and proliferation of CD4 and CD8 T cells as determined via induction of IL17 and granzyme B

<http://dx.doi.org/10.1136/jitc-2022-SITC2022.0830>

831

TARGETING TUMOR OXIDATIVE METABOLISM TO OVERCOME HYPOXIA-INDUCED IMMUNOTHERAPY RESISTANCE IN PROSTATE CANCER

¹Priyamvada Jayaprakash*, ¹Michael Curran, ¹Brittany Morrow, ¹Joseph Marszalek, ¹Krithikaa Rajkumar Bhanu, ¹Meghan Rice, ¹Jason Gay, ¹Christopher Vellano, ²Benjamin Cowen, ²Dean Welsh. ¹The University of Texas MD Anderson Cancer Center, Houston, TX, United States; ²Immunomet, Houston, TX, United States

Background Immunotherapy is successful in “hot” tumors with pre-existing immune infiltrates. However, “cold” tumors like prostate cancers remain unresponsive.^{1,2,3} Murine prostate tumors harbor hypoxic regions, islands of immune privilege, excluding T cells while promoting recruitment and suppressive polarization of myeloid-derived suppressor cells (MDSC). Targeting hypoxia using the hypoxia-activated prodrug, TH-302 (Evofofosamide) reduced MDSC driven suppression, enhanced T cell function, improving sensitivity to immune checkpoint blockade (ICB).⁴ In a Phase I clinical trial, combining Evofofosamide with Ipilimumab (anti CTLA-4) elicited both objective responses and prolonged disease stabilization in late-stage “cold” tumor patients. However, Evofofosamide reduces, but does not eliminate hypoxia and patients resistant to Evofofosamide/Ipilimumab combination exhibited hyper-metabolic tumors.⁵ Targeting tumor oxidative metabolism reduced hypoxia and improved sensitivity to PD-1 blockade.^{6,7} We hypothesized that targeting tumor oxidative metabolism using mitochondrial complex I inhibitors might diminish tumor hypoxia, and act synergistically with Evofofosamide to sensitize unresponsive tumors to immunotherapy. Since oxidative phosphorylation (OxPhos) is also crucial to T cell function, we tested multiple doses of two complex I inhibitors to determine a regimen with optimal capacity to compromise tumor oxygen metabolism while sparing T cell metabolic fitness.

Methods Utilizing the transplantable TRAMP-C2 prostate tumor model, we investigated the capacity of two complex I inhibitors to reduce tumor oxidative metabolism, diminish myeloid suppressive capacity and improve T cell immunity, alone and in combination with Evofofosamide and ICB. We assessed tumor burden, evaluated immune composition using flow cytometry and characterized metabolism using Seahorse XFe96 analyzer.

Results While Evofofosamide or OxPhos inhibition alone did little to inhibit prostate cancer progression, combination acted synergistically to reduce tumor burden and augment tumor-specific CD8 and CD4 effector T cell proliferation. Complex I inhibition reduced TRAMP-C2 tumor cell proliferation and MDSC suppressive polarization, but improved function of previously activated T cells. Consequently, neither prior, nor concurrent, complex I inhibition diminished efficacy of CTLA-4/PD-1 blockade in TRAMP-C2. Used in combination, complex I inhibition and ICB promoted tumor-infiltrating T cell proliferation, activation and cytotoxicity while reducing dysfunction/exhaustion markers.

Conclusions Tumor hypoxia and associated immune suppressive programming can be reduced through both restoration of oxygen supply through vascular remodeling (i.e. Evofofosamide) and limitation of tumor oxygen metabolism (e.g. complex I inhibition). OxPhos inhibition selectively inhibits tumor and myeloid function, while sparing T cell function and responsiveness to ICB. Coordinated remodeling of tumor oxygen metabolism with existing drugs can compromise hypoxia-associated T cell suppression without compromising intrinsic T cell metabolic potential.

REFERENCES

1. Curran MA, Montalvo W, Yagita H, and Allison JP. PD-1 and CTLA-4 combination blockade expands infiltrating T cells and reduces regulatory T and myeloid cells within B16 melanoma tumors. *Proc Natl Acad Sci U S A* 2010; **107**(9): 4275–80.
2. Wolchok JD, Kluger H, Callahan MK, Postow MA, Rizvi NA, Lesokhin AM, *et al.* Nivolumab plus ipilimumab in advanced melanoma. *N Engl J Med* 2013; **369**(2): 122–33.
3. Kwon ED, Drake CG, Scher HI, Fizazi K, Bossi A, van den Eertwegh AJ, *et al.* Ipilimumab versus placebo after radiotherapy in patients with metastatic castration-resistant prostate cancer that had progressed after docetaxel chemotherapy (CA184-043): a multicentre, randomised, doubleblind, phase 3 trial. *Lancet Oncol*. 2014;**15**(7):700–12.
4. Jayaprakash P, Ai M, Liu A, Budhani P, Bartkowiak T, Sheng J, *et al.* Targeted hypoxia reduction restores T cell infiltration and sensitizes prostate cancer to immunotherapy. *J Clin Invest*. 2018; **128** (11): 5137–5149.
5. Hegde A, Jayaprakash P, Couillaud CA, Piha-Paul S, Karp D, Rodon J, *et al.* A Phase I Dose-Escalation Study to Evaluate the Safety and Tolerability of Evofofosamide in Combination with Ipilimumab in Advanced Solid Malignancies. *Clin Cancer Res*. 2021; **27**(11): 3050–3060.
6. Najjar YG, Menk AV, Sander C, Rao U, Karunamurthy A, Bhatia R, *et al.* Tumor cell oxidative metabolism as a barrier to PD-1 blockade immunotherapy in melanoma. *JCI Insight*. 2019; **4**(5): e124989.
7. Scharping NE, Menk AV, Whetstone RD, Zeng X, Delgoffe GM. Efficacy of PD-1 Blockade is potentiated by metformin-induced reduction of tumor hypoxia. *Cancer Immunol Res*. 2017; **5**(1):9–16.

Ethics Approval All animal studies were approved by the MD Anderson Cancer Center Institutional Animal Care and Use Committee (IACUC, Houston, Texas) under protocol 00001378-RN00/1.

<http://dx.doi.org/10.1136/jitc-2022-SITC2022.0831>

832

ANTIGEN SPREAD MEDIATED BY ONCOLYTIC ADENOVIRUS DELTA-24-RGDOX DURING INTRATUMORAL ADOPTIVE T CELL THERAPY IN IMMUNOCOMPETENT MICE WITH DISSEMINATED TUMORS

<http://dx.doi.org/10.1136/jitc-2022-SITC2022.0832>

Hong Jiang*. MD Anderson Cancer Center, Houston, TX, United States

Background Tumor relapse due to antigen escape is an essential problem in adoptive T cell therapy (ACT) with limited antigen targets, such as CAR T cells. This is especially true for solid tumors since they are more heterogeneous than hematological malignancies. Moreover, systemically delivered T cells infiltrate poorly into the solid tumors and are susceptible to the immune suppressive tumor microenvironment (TME) (“cold tumor”). On the other hand, oncolytic viruses, such as oncolytic adenovirus Delta-24-RGDOX developed by our group, can turn “cold tumor” into immune active “hot tumor” and induce immune response against a variety of tumor-associated antigens (TAAs). Thus, we hypothesize that Delta-24-RGDOX potentiates the effect of ACT through activating TME and antigen spread.

Methods We used B16-OVA-C57BL/6 subcutaneous (s.c.)/s.c. melanoma model¹ to assess systemic therapeutic effect in disseminated tumors. gp100-TCR CD8+ T cells were injected into the first tumor, followed by three injections of Delta-24-RGDOX into the same tumor. Leukocytes from the tumors were profiled for surface markers with flow cytometry. Activity of splenocytes against specific TAAs and tumor cells was measured with ELISA.

Results Delta-24-RGDOX injections following gp100-TCR CTLs in the first tumor increased total CD8+ leukocyte presence within both tumors. Further analysis revealed that treatments with either agents or combination dramatically downregulated CD62L whose expression kept at low levels in adopted gp100-TCR and endogenous OVA-specific CTLs. Moreover, although Delta-24-RGDOX significantly upregulated PD-1, TIM3 and LAGs in CD8+ leukocytes, its effect on these immune inhibitors was different in gp100-TCR or OVA-specific CTLs. The overall levels of these inhibitors in OVA-specific CTLs were remarkably higher than in gp100-TCR CTLs or CD8+ leukocytes. The virus slightly increased the inhibitors in the gp100-TCR CTLs from the treated tumor and decreased the inhibitors in the gp100-TCR CTLs from the untreated tumor. Importantly, PD-1 levels in OVA-specific CTLs were significantly downregulated in OVA-specific CTLs from both treated and untreated tumors although the other two inhibitors kept at a steady lower level. As a result, Delta-24-RGDOX drastically increased the density of OVA-specific CTLs in both tumors and the combination synergistically enhanced the effect. Consistently, the splenocytes from the combination group showed significant stronger response against other TAAs (OVA and TRP2) than gp100, leading to higher activity against tumor cells.

Conclusions Our data demonstrate that localized treatment with intratumoral ACT followed by Delta-24-RGDOX enhances global immune activation and antigen spread to expand antitumor T cell repertoire, leading to efficacious systemic anti-tumor immunity.

REFERENCE

1. Jiang H, et al. Localized Treatment with Oncolytic Adenovirus Delta-24-RGDOX Induces Systemic Immunity against Disseminated Subcutaneous and Intracranial Melanomas. *Clin Cancer Res*, 2019. **25**(22): 6801–6814.

833 **BLOCKADE OF HUMAN LILRB4/ILT3 INHIBITS THE FORMATION OF LUNG METASTASIS IN MELANOMA MODEL**

¹Darya Khantakova*, ¹Martina Molgora, ²Julie Roda, ²Geoffrey Stone, ¹Susan Gilfillan, ¹Tihana Trsan, ¹Marina Cella, ²Alan Kutach, ²Daniel Kaplan, ²Jer-Yuan Hsu, ¹Marco Colonna. ¹Washington University School of Medicine, St. Louis, MO, United States; ²NGM Biopharmaceuticals, South San Francisco, CA, United States

Background Targeting the immunosuppressive tumor microenvironment to enhance or recover anti-tumor functions is a promising strategy to favor tumor regression and response to checkpoint immunotherapy. LILRB4 is an inhibitory immune receptor, also named ILT3, that is primarily expressed in myeloid cells. We previously showed with *in vitro* assays that ILT3 is highly expressed in tumor-associated macrophages (TAMs) and binds fibronectin (Fn), which is ubiquitously expressed in the extracellular matrix and enriched in various primary tumor tissues and metastatic sites.¹ Therefore, targeting ILT3 can be a promising therapeutic strategy to reprogram TAMs and promote tumor control.

Methods Transgenic mice (LILR-T) that carry the human LILR cluster comprising the ILT3 gene were generated. A recombinant anti-human ILT3 monoclonal antibody (an NGM831 surrogate antibody) that blocks the interaction between ILT3 and Fn was produced. The anti-tumor efficacy and immune profile were investigated in the B16 lung metastasis model in LILR-T mice treated with anti-ILT3 antibody.

Results Analysis of ILT3 expression in the LILR-T mouse showed a consistent expression pattern with that in humans across different tissues. We found that ILT3 blockade has beneficial effects on anti-tumor immune responses in B16 lung metastasis *in vivo* and promotes metastasis control.

Conclusions These results suggest that ILT3 blockade could be an effective approach to reprogram tumor myeloid infiltrates and promote tumor control. Our study further elucidates the role of ILT3 in the tumor immune cell composition.

REFERENCE

1. Paavola KJ, *et al.* The Fibronectin-ILT3 interaction functions as a stromal checkpoint that suppresses myeloid cells. *Cancer Immunol. Res.* 2021;**9**, 1283–1297.

<http://dx.doi.org/10.1136/jitc-2022-SITC2022.0833>

Abstracts

834 INTEGRIN $\alpha\text{v}\beta\text{8}$ INHIBITOR IMPROVES IMMUNE CHECKPOINT THERAPY IN ADVANCED OVARIAN CANCER MODEL AND ITS ACTIVITY CAN BE MONITORED IN BLOOD

¹Natalia Reszka-Blanco*, ¹Megan Krumpoch, ¹Huidong Chen, ¹Lia Luus, ¹Michaela Mentzer, ¹Aleksey Molodtsov, ¹Adrian Ray, ¹Vinod Yadav, ²Matthew Clark, ²Ian Gerken, ²Justin Snider, ¹Blaise Lippa, ¹Bruce Rogers, ¹Gerard Bain. ¹Morphic TX, Waltham, MA, United States; ²Labcorp Drug Development, Ann Arbor, MI, United States

Background Ovarian cancer (OC) is the most lethal gynecologic malignancy. Despite the initial high response rate to chemotherapy, most patients relapse. Immunotherapy offers potential for long-term remission but single checkpoint inhibition benefits less than 15% of patients. Growing evidence suggests that immune-checkpoint blockade (ICB) is enhanced when combined with therapies that target tumor tolerance. Transforming growth factor beta (TGF- β) is associated with resistance to immunotherapy and tumor tolerance. Integrin $\alpha\text{v}\beta\text{8}$ controls cell-type-specific activation of TGF- β and $\alpha\text{v}\beta\text{8}$ antagonism promotes anti-tumor immunity leading to tumor regression in ICB refractory tumors.^{1,2} We explored the impact of $\alpha\text{v}\beta\text{8}$ inhibition to restore ICB response in a murine ovarian carcinoma model and performed blood cytokine profiling to search for pharmacodynamic markers of response to treatment.

Methods Bioinformatic analysis on bulk and single-cell levels of public OC datasets was performed to evaluate ITGB8 and TGF- β -related gene signatures. qPCR was used for the detection of TGF- β and ITGB8 expression in ID8, a murine ovarian carcinoma model (ID8-Luc-mCh-Puro.TD1). ID8 tumors unresponsive to PD-1/L1 inhibition were established to mimic advanced-stage disease. The efficacy of $\alpha\text{v}\beta\text{8}$ mAbs in combination with PD-L1 blockade was evaluated. Mice were evaluated for survival for 65 days. Blood samples were harvested before treatment and on days 1, 8 and 14. Plasma was analyzed via Luminex for a total of 30 cytokines. Transcriptomic analyses of MC38 and EMT6 mouse tumors were performed by bulk RNA seq.

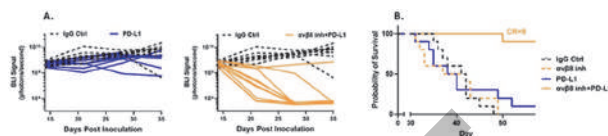
Results In high-grade serous OC, ITGB8 expression is associated with shorter overall survival and increased gene signatures of TGF- β 1/3 pathways. The ID8 murine ovarian carcinoma model is unresponsive to PD-1/L1 inhibition and expresses *Itgb8* together with TGF- β 1/3. The combination of $\alpha\text{v}\beta\text{8}$ and PD-L1 mAbs led to complete tumor regression in 9/10 mice relative to 0/10 in the PD-L1 group, resulting in superior survival ($P=0.0001$) (Fig 1 A, B). The combination therapy led to upregulation of blood granzyme B ($P=0.05$), IL-27 ($P=0.03$), and IL-1a ($P=0.008$) at 14-day post-treatment and transient upregulation of CCL3 ($P<0.0001$) and CCL7 ($P=0.0005$) at 8-day post-treatment. Cross-analysis of tumor tissues from the colon and breast syngeneic models after treatment showed similar transcript upregulation for cytokines.

Conclusions Inhibition of $\alpha\text{v}\beta\text{8}$ renders advanced ID8 tumors sensitive to immune checkpoint therapy, leading to tumor eradication and superior survival. These data provide evidence that a treatment modality targeting $\alpha\text{v}\beta\text{8}$ -mediated TGF- β 1/3 pathways may enhance patients' sensitivity to checkpoint therapies. Plasma blood-based biomarkers serve as a non-invasive method for response assessment to $\alpha\text{v}\beta\text{8}$ -based therapy.

REFERENCES

1. Reszka-Blanco NJ, Yadav V, Krumpoch M, Cappellucci L, Cui D, Dowling JE, et al. Inhibition of integrin $\alpha\text{v}\beta\text{8}$ enhances immune checkpoint induced anti-tumor

- immunity by acting across immunologic synapse in syngeneic models of breast cancer. *AACR; Cancer Res* 2021;**81**(13_Suppl): Abstract nr 1559
2. Dodagatta-Marri E, Ma H-Y, Liang B, Li J, Meyer DS, Chen S-Y, et al. Integrin $\alpha\text{v}\beta\text{8}$ on T cells suppresses anti-tumor immunity in multiple models and is a promising target for tumor immunotherapy. *Cell Report*. 2021; **36**(1): 109309



Abstract 834 Figure 1 Efficacy of $\alpha\text{v}\beta\text{8}$ inhibitor (mAb clone C6D4) combined with PD-L1 (clone 10F.9G2) against an advanced syngeneic model of ovarian carcinoma, ID8. (A) The combination of $\alpha\text{v}\beta\text{8}$ mAb (7 mg/kg three times weekly for 3 weeks) and PD-L1 mAb (10 mg/kg twice weekly for 2 weeks) was efficacious in the checkpoint-resistant ID8 model and resulted in superior tumor regression. Shown are spaghetti plots for each individual mouse in each treatment group. Tumor burden measurements performed weekly by bioluminescence imaging (BLI). (B) Kaplan-Meier curves presenting time to progression. $\alpha\text{v}\beta\text{8}$ and PD-L1 mAb markedly improved survival over monotherapy with either $\alpha\text{v}\beta\text{8}$ or PD1 mAb. Statistics by log-rank test. CR-complete responders

<http://dx.doi.org/10.1136/jitc-2022-SITC2022.0834>

835

AZD4820 ONCOLYTIC VACCINIA VIRUS ENCODING IL-12 MEDIATES ANTI-TUMOR ACTIVITY THROUGH ONCOLYSIS AND TUMOR-SPECIFIC IMMUNITY

¹Cheyne Kurokawa, ¹Sonia Agrawal, ¹Abhisek Mitra, ¹Elena Galvani, ¹Shannon Burke, ¹Ankita Varshine, ¹Raymond Rothstein, ²Johann Foloppe, ²Nathalie Silvestre, ²Eric Quemeneur, ¹Puja Sapra, ¹Carl Barrett, ¹Scott Hammond, ¹Jason Laliberte, ¹Nicholas Durham, ¹Michael Oberst*, ¹Maria Broggi. ¹Astrazeneca, Gaithersburg, MD, United States; ²Transgene, Illkirch-Graffenstaden, France

Background While vaccinia virus (VACV) has demonstrated robust oncolytic activity, we sought to enhance therapeutic efficacy by engineering VACV to express interleukin-12 (IL-12), a potent NK and T cell activating cytokine that reprograms the tumor immune microenvironment. AZD4820 is an oncolytic VACV engineered to express IL-12 with viral thymidine kinase and ribonucleotide reductase deleted to enhance tumor cell-specific replication. We evaluated the oncolytic activity of AZD4820 and enhancement of anti-tumor immunity in combination with immune checkpoint inhibitors (ICIs).

Methods The oncolytic activity of VACV was evaluated in 47 primary patient derived xenograft (PDX) models representing 9 tumor indications. Replication, oncolytic activity, and IL-12 transgene production of AZD4820 was evaluated in cultured human tumor cell lines, normal human cells, primary human dissociated tumor cells (DTCs) and tumor tissue slice cultures (TSCs). The anti-tumor activity and mechanism of action for AZD4820 was evaluated in syngeneic rat tumor models, as well as MC38 and CT26 syngeneic mouse tumor models with or without ICI targeting PD-L1. Specific anti-tumor immunity in the CT26 model was assessed in mice treated with AZD4820 alone or in combination with anti-PD-L1 mAb by interferon- γ (IFN γ) ELISpot assays after stimulating splenocytes with tumor-specific peptides.

Results Oncolytic VACV demonstrated anti-tumor activity (disease stabilization, partial or complete responses) in 35 of 47 PDX models tested. AZD4820 was highly oncolytic in human tumor cells relative to normal cells, both *in vitro* (EC₅₀ range 0.0005 to 0.86) and *in vivo*. To evaluate AZD4820 in human tumor samples, we showed that AZD4820 resulted in production of IL-12 in DTCs (19/19 samples) and TSCs (22/22 samples). A surrogate virus expressing murine IL-12 demonstrated anti-tumor activity in both the MC38 and CT26 syngeneic models. In the CT26 syngeneic tumor model, delivery of AZD4820 significantly upregulated IFN γ relative to control VACV-Luciferase treated mice. In this study, 6/10 mice had a complete response following treatment with AZD4820, while the control VACV-Luciferase treated mice had 0/10 complete responders. Next, we demonstrated in the CT26 tumor model that treatment with AZD4820 in combination with an anti-PD-L1 blocking antibody augmented tumor-specific T cell immunity relative to monotherapies.

Conclusions AZD4820 is an oncolytic VACV expressing IL-12 *in vitro* and *in vivo* which replicates preferentially in tumor cells compared to normal cells. A surrogate of AZD4820 demonstrated activity in pre-clinical syngeneic mouse tumor models in combination with anti-PD-L1 mAb, supporting its use in combination with ICIs in patients with cancer.

<http://dx.doi.org/10.1136/jitc-2022-SITC2022.0835>

836

ACTIVATING THE ANTIGEN PRESENTING CELLS TO IMPROVE VIROTHERAPY EFFICACY IN DIFFUSE MIDLINE GLIOMAS

¹Sara Labiano*, ¹Reyes Hernández-Osuna, ¹Virginia Laspidea, ¹Marc Garcia-Moure, ¹Javier Marco-Sanz, ¹Iker Ausejo, ¹Montserrat Puigdelloses, ²Oren Becher, ¹Ana Patiño-García, ³Candelaria Gomez-Manzano, ³Juan Fueyo, ¹Marta Alonso. ¹University of Navarra, Pamplona, Spain; ²Mount Sinai Kravis Children's Hospital, New York, NY, United States; ³MD Anderson Cancer Center, Houston, TX, United States

Background Within Diffuse Midline Gliomas, Diffuse Intrinsic Pontine Glioma (DIPG) is the principal cause of non-accidental pediatric deaths. Although gold-standard treatments have improved, the outcome for children with DIPGs remains poor pointing to the need for alternative therapies. In this sense, we have previously demonstrated that the oncolytic adenovirus Delta-24-RGD (which has already shown safety and feasibility in DIPG patients) is able to recruit T cells into the tumor. However, such as T-lymphocyte infiltration rapidly acquires an exhausted phenotype that prevents from achieving long-term anti-tumor responses. Therefore, we decided to improve this therapy by combining the Delta-24-RGD with the activation of the costimulatory receptor CD40, which is known to increase antigen presentation and enable T-cell priming.

Methods To determine anti-tumor efficacy, we treated immunocompetent and immunodeficient mice bearing orthotopic DIPG tumors with an intratumoral injection including the Delta-24-RGD and a CD40 agonistic monoclonal antibody. Survival and toxicity were monitored after treatment and the changes in the tumor immune microenvironment were analyzed by flow cytometry, immunofluorescence, and RNA sequencing. Long-term survivors were rechallenged with primary tumor cells to study the development of anti-tumor immunological memory.

Results The combination therapy is safe and extends survival of immunocompetent treated mice as compared to single treatments or non-treated mice, resulting in 40% of complete responses. In addition, mice that rejected the tumor were able to control the growth of a rechallenge with the primary cells indicating the development of long-term anti-tumor immunity. This, together with the lack of effect observed in immunodeficient mice evidences a key role of the adaptive immune system in the anti-tumor response. We found that the combination remodels the tumor context towards a proinflammatory scenario with an increase of proinflammatory chemokines, proliferating T lymphocytes and activated dendritic cells, which express high levels of the CD40 receptor. In addition, the blocking of CSF1R (mainly expressed by microglia/macrophages) avoids the recruitment of dendritic cells into the tumor and abrogates the anti-tumor effect observed upon the combination of Delta-24-RGD and anti-CD40.

Conclusions Our results show that the combination of Delta-24-RGD with the stimulation of CD40 is safe, has a potent and long-term anti-tumor effect and promotes a proinflammatory tumor microenvironment. We believe that these results can be translational and open the door for a future innovative clinical trial.

Ethics Approval The study was approved by the University of Navarra's Ethics Committee for Animal Experimentation (CEEAA), approval number 068-20

<http://dx.doi.org/10.1136/jitc-2022-SITC2022.0836>

837

REDIRECTING IL-7-INDUCED BYSTANDER TUMOR-INFILTRATING LYMPHOCYTES BY BISPECIFIC T-CELL ENGAGER AUGMENTS ANTITUMOR RESPONSE

¹Kun-Joo Lee student*, ²Nara Tae, ¹Yeon-Woo Kang, ¹Dain Moon, ¹Youngsik Oh, ¹Ji-Hae Kim, ³Minji Lee, ²Ha Won Song, ²Sun Shim Choi, ³Donghoon Choi, ²Dae Hee Kim, ¹Seung-Woo Lee*. ¹Pohang University of Science & Technology (POSTECH), Pohang, Republic of Korea; ²Kangwon National University, Chuncheon, Republic of Korea; ³Research Institute of NeolImmuneTech, Pohang, Republic of Korea

Background rhIL-7-hyFc (efineptakin alfa, NT-17) is a long-acting form of recombinant human IL-7 and is currently under clinical trials for various cancers in combination with immune checkpoint inhibitors (ICI). We have previously shown that rhIL-7-hyFc monotherapy increases tumor-infiltrating lymphocytes (TILs); however, the majority of CD8⁺ TILs is PD-1⁻ bystander T cells that lack tumor-specific activity.¹ Therefore, we hypothesized that bispecific T-cell engagers (TCE) composed of two single-chain variable fragments simultaneously targeting CD3 ϵ and tumor antigens, including PD-L1, can redirect and activate IL-7-induced bystander TILs to kill tumor cells resulting in enhanced antitumor response

Methods We conducted scRNA-seq paired with TCR-seq of CD8⁺ TILs isolated from tumors after rhIL-7-hyFc treatment to evaluate transcriptomic changes of both tumor-reactive and bystander T cells. We generated various TCEs targeting mouse or human CD3 ϵ and tumor antigens. The efficacy of antitumor responses by combination treatment of rhIL-7-hyFc and TCE was evaluated in immunogenic and non-immunogenic murine tumor models. To address the activation of bystander TILs, we analyzed the expression of effector molecules and cytotoxicity of PD-1⁻ CD8⁺ TILs after co-culturing with TCE and tumor cells. We determined the antitumor response of bystander CD8⁺ T cells with an adoptive transfer experiment in RAG1^{-/-} mice.

Results scRNA-seq analysis of CD8⁺ TILs revealed that rhIL-7-hyFc attenuates the dysfunctional (or exhaustion) process of tumor-reactive cells and recruits bystander cells with the characteristics of cytokine-primed central memory phenotype. TCE can activate CD8⁺ T cells when it simultaneously binds to tumor antigen. The combination of rhIL-7-hyFc and TCE enhanced the antitumor responses by upregulating CD8⁺ TILs in MC38, B16F10, and CT-26 models. In addition, IL-7-induced bystander CD8⁺ TILs are TCR-activated to gain a cytotoxic activity to tumor cells. Lastly, we observed the antitumor response of IL-7-primed bystander CD8⁺ T cells when redirected in vivo by TCE in RAG1^{-/-} mice.

Conclusions Our data suggest that bispecific T-cell engagers are promising candidates to augment the antitumor activity of rhIL-7-hyFc by redirecting bystander CD8⁺ TILs

REFERENCE

1. Kim JH Kim, YM Kim, D Choi, SB Jo, HW Park, SW Hong, *et al*, Hybrid Fc-fused interleukin-7 induces an inflamed tumor microenvironment and improves the efficacy of cancer immunotherapy, *Clinical & Translational Immunology* 2020;**9** :9:1–16.

Ethics Approval All animal experiments were performed in accordance with National Institutes of Health guidelines for the care and approved by the Institutional Animal Care and Use Committee of the POSTECH (POSTECH-2022-0052).

<http://dx.doi.org/10.1136/jitc-2022-SITC2022.0837>

838

COMBINATION MRX0518 AND ANTI-PD-1 OVERCOMES CHECKPOINT INHIBITOR RESISTANCE VIA MYELOID MODULATION

¹June Li*, ¹Karen Millerchip, ¹Carlos Ramos, ¹Edwin Parra, ¹Luisa Solis, ²Alex Stevenson, ²Aurelie Couturier, ²Gayle Fyvie, ³Michael Chisamore, ⁴Rahul Parikh, ⁵Eric Bernicker, ⁶Diwakar Davar, ⁷Arvind Chaudhry, ¹Nizar Tannir, ¹Shubham Pant, ¹Cara Haymaker. ¹The University of Texas MD Anderson Cancer Center, Houston, TX, United States; ²4D Pharma Research Ltd., Leeds, UK; ³Merck & Co., Inc., Kenilworth, NJ, United States; ⁴University of Kansas Medical Center Research Institute, Kansas City, KS, United States; ⁵The Methodist Hospital Research Institute, Houston, TX, United States; ⁶UPMC, Pittsburgh, PA, United States; ⁷Medical Oncology Associates, Spokane, WA United States

Background The gut microbiome is a known modulator of response to checkpoint inhibitors.¹⁻⁴ MRx0518 is a strain of *Enterococcus gallinarum* that was isolated from a healthy human fecal sample. Administration of MRx0518 in pre-clinical cancer models results in anti-tumor effects and immune system modifications potentially contributing to therapeutic effects of checkpoint inhibitors. We hypothesized that a PD-1 checkpoint inhibitor in combination with MRx0518 would decrease suppressive myeloid cells and increase T-cell activation

Methods

Study design: Patients who had developed resistance to checkpoint inhibitors received MRx0518 (1×10^{10} to 1×10^{11} CFU) PO BID and 200mg pembrolizumab IV Q3W for up to 2 years or disease progression. Responders are defined as patients achieving clinical benefit (CR, PR or SD \geq 6months per RECIST v1.1).

Flow cytometric analysis: PBMCs from baseline (BL) and cycle 4 day 1 (C4D1) were subjected to immune profiling. Normal donor (ND, n=9) PBMCs serve as controls for non-responder (NR, n=33) and responder (R, n=11) BL samples.

Circulating biomarker assay: Cytokines were assessed in plasma collected at BL (n=27) and C4D1 (n=27) using a kit from Meso Scale Discovery.

Statistical tests: Non-parametric ANOVA and Mann-Whitney test or Wilcoxon matched-pairs signed rank test were utilized for flow cytometry data and paired T-test for cytokine analysis.

Results At BL, expression of HLA-DR on mDC is reduced and the frequency of HLA-DR negative monocytes is increased in patients ($p < 0.05$) suggesting a higher degree of suppressive myeloid cells prior to combination therapy. Expression of PD-L1 and PD-L2 on mDC and monocytes is higher in patients at BL ($p < 0.05$). Checkpoint receptor expression and activation markers on T cells (both CD4+ and CD8+) is higher in patients at BL, including CTLA4 ($p < 0.01$), PD-1 ($p < 0.05$), Tim3 ($p < 0.05$), OX40 ($p < 0.001$) and Ki67 ($p < 0.05$). CTLA4, PD-1, and Tim3 ($p < 0.05$) expression on NK cells are higher in patients at BL. Overall, the circulating immune microenvironment is immuno-suppressed in patients at BL irrespective of subsequent clinical outcome.

Upon treatment, HLA-DR+ myeloid cells are increased, PD-L1 expression on HLA-DR+ myeloid cells is consistently reduced, and the frequency of CD8+ T cells is increased in R patients ($p < 0.05$). IL-6 and MIP-1 α are increased in circulation in NR upon treatment ($p < 0.05$).

Conclusions Immune activation was recovered in R patients with MRx0518 and anti-PD-1 combination therapy. Immune changes associated with improved outcome include: 1) increased expression of HLA-DR and decreased PD-L1 expression on myeloid cells and 2) increased CD8+ T-cell frequencies in circulation.

Acknowledgements Study is funded through the 4D Pharma strategic alliance with MD Anderson Cancer Center. We appreciate the support of all the patients and their families for their participation in the study.

Trial Registration ClinicalTrials.gov Identifier: NCT03637803

REFERENCES

1. Gopalakrishnan V, Helmink BA, Spencer CN, Reuben A and Wargo JA. The influence of the gut microbiome on cancer, immunity, and cancer immunotherapy. *Cancer Cell* 2018; **33**: 570–580.
2. Routy B, Chatelier EL, Derosa L *et al.* Gut microbiome influences efficacy of PD-1-based immunotherapy against epithelial tumors. *Science* 2018; **359**: 91–97.
3. Baruch F, Youngster I, Ben-Betzalel G *et al.* Fecal microbiota transplant promotes response in immunotherapy-refractory melanoma patients. *Science* 2021; **371**: 602–609.
4. Davar D, Dzutsev A, McCulloch J *et al.* Fecal microbiota transplant overcomes resistance to anti-PD-1 therapy in melanoma patients. *Science* 2021; **371**: 595–602.

Ethics Approval This study was written and conducted in accordance with the principles from the Declaration of Helsinki. Written informed consent was provided by all study participants or their legal representatives. The study was approved by the University of Texas MD Anderson Cancer Center's Institutional Review Board.

<http://dx.doi.org/10.1136/jitc-2022-SITC2022.0838>

839

SELECTIVE TARGETING OF GARP-LTGF β AXIS IN THE TUMOR MICROENVIRONMENT AUGMENTS PD-1 BLOCKADE VIA ENHANCING CD8 $^+$ T CELL ANTI-TUMOR IMMUNITY

¹Anqi Li*, ¹Yuzhou Chang, ¹No-Joon Song, ¹Xingjun Wu, ¹Dongjun Chung, ²Brian Riesenber, ¹Maria Velegraki, ¹Hyunwoo Kwon, ¹Karthik Chakravarthy, ¹Chelsea Bolyard, ¹Yi Wang, ¹Qin Ma, ¹Zihai Li. ¹The Ohio State University, Columbus, OH, United States; ²University of North Carolina, Chapel Hill, NC, United States

Background Immune checkpoint blockade (ICB) targeting programmed cell death protein 1 (PD-1) and its ligand has revolutionized cancer immunotherapy. Unfortunately, while some cancer patients experience robust and lasting remission following treatment, most fail to respond clinically. Accumulation of transforming growth factor β (TGF β) in the tumor microenvironment (TME) can induce an immunosuppressive milieu and therapeutic resistance. TGF β drives cancer immune evasion by inducing regulatory T cells (Tregs) and limiting CD8 $^+$ T cell function within the TME. Glycoprotein-A repetitions predominant (GARP; encoded by *LRRC32*) is a cell surface docking receptor for all isoforms of latent TGF β (LTGF β) and is expressed by effector Tregs, cancer cells, and platelets.

Methods We studied the role of *LRRC32* expression in human cancer patients by mining the existing bulk transcriptomic databases. Then, we generated, characterized, and humanized an anti-GARP monoclonal antibody (called 'PIIO-1'). Lastly, anti-tumor efficacy and its underline mechanism was investigated by murine tumor models.

Results We found that the overexpression of *LRRC32* in human cancers correlates with unfavorable immune TME and poor responsiveness to ICB, indicating that targeting GARP may improve cancer immunotherapy. Therefore, we established our anti-GARP antibody PIIO-1 with a unique characterization that specifically binds to the ligand-interacting domain of free GARP and blocks the recognition by all LTGF β isoforms. PIIO-1 antibody does not induce thrombocytopenia in our human *LRRC32* knock-in mice due to the lack of recognition of GARP-LTGF β complex on platelets. It obtains the anti-tumor efficacy against both GARP $^+$ and GARP $^-$ tumors in a mono- or combo- therapeutic strategies with PD-1 blockade. Mechanistically, PIIO-1 preferentially distributes to the TME and dLNs and inhibits canonical TGF β pathway in their infiltrating immune cells. In addition, PIIO-1 treatment prevents CD8 $^+$ T cell exhaustion and improves its migration into TME in a CXCR3-dependent manner.

Conclusions GARP overexpression in cancer patients contributes to immune suppression as well as ICB resistance. Targeting GARP by using PIIO-1 antibody blocks LTGF β activation *in vivo* effectively and safely. PIIO-1 is responsible for the improvement of function and trafficking in tumor-infiltrating CD8 $^+$ T cells and synergizing anti-PD-1 efficacy. Therefore, PIIO-1 is potent for the clinical development of cancer immunotherapy.

<http://dx.doi.org/10.1136/jitc-2022-SITC2022.0839>

840

TRIPLE-DRUG ORAL IMMUNOTHERAPY TARGETING MYELOID CELLS FOR TREATMENT OF METASTATIC OSTEOSARCOMA EVALUATED IN SPONTANEOUS CANINE MODEL

¹Cheryl London, ²Dan Regan*, ²Lyndah Chow, ²Kristen Weishaar, ³Heather Gardner, ²Doug Thamm, ²Steven Dow. ¹Tufts University Veterinary College, Grafton, MA, United States; ²Colorado State University, Ft Collins, CO, United States; ³Tufts University, Grafton, CO, United States

Background We reported recently in a spontaneous canine model of metastatic osteosarcoma (OS) that oral treatment with two repurposed agents targeting monocyte migration (losartan) and MDSC and Tregs (toceranib) induced partial responses in 4/16 dogs (25%) with another 4 dogs experiencing durable stable disease (SD), for a clinical benefit rate of 50%. In the current study, we evaluated the utility of incorporating ladarixin (an orally bioavailable allosteric CXCR1/2 antagonist) into the losartan/toceranib regimen in 15 dogs with OS metastatic to the lungs.

Methods The effects of treatment on lung metastases, circulating cytokine concentrations, and gene expression profiles in PBMC were assessed in this new study. Studies are also ongoing to determine whether this same approach has activity in the adjuvant setting in dogs with appendicular OS treated prior to and continuously following amputation, in lieu of standard cytotoxic adjuvant chemotherapy. To date, 18 animals have been enrolled in the adjuvant trial, and analysis of the impact on MFI and OST are ongoing as data matures.

Results Of enrolled dogs with greater than 60 days of follow up, 1 dog underwent a complete response (400+ days) and another 4 dogs experienced PR, for an objective response rate of 36%; another 5 dogs exhibited durable SD, for an overall clinical benefit rate of 71%. The 3-drug protocol was generally well-tolerated, with no adverse events other than those associated with toceranib alone (gastrointestinal signs). Transcriptomic analysis of PBMCs from 8 dogs on days 0 and 14 using Nanostring revealed significant downregulation of 30 immune genes, including IRF2, IRF8, CTLA4, NFKB, and CCR2, and upregulation of 176 genes, including IL21, CCL19, B7-H3, IL17A/B. Pathway analysis demonstrated significant downregulation of IFN- γ and IFN- α response pathways, and upregulation of β -catenin signaling pathways.

Conclusions In summary, these findings in a canine spontaneous osteosarcoma model indicate that the combined losartan/ladarixin/toceranib immunotherapy protocol is biologically active and can effectively modify the immune suppressive tumor microenvironment to generate spontaneous antitumor activity in dogs with advanced OS lung metastases.

<http://dx.doi.org/10.1136/jitc-2022-SITC2022.0840>

841 **XTX202, A TUMOR-SELECTIVE PROTEIN-ENGINEERED IL-2, EXHIBITED ENHANCED ANTI-TUMOR ACTIVITY IN COMBINATION WITH CHECKPOINT INHIBITION IN MICE**

Wilson Guzman*, Uli Carl Bialucha, Hanumantha Rao Madala, Haley Duprey, Manoussa Fanny, Stephanie Hsiao, Parker Johnson, Jake Taylor, Rebekah O'Donnell, Magali Pederzoli-Ribeil, Benjamin Nicholson, Jennifer O'Neil, Caitlin O'Toole. *Xilio Therapeutics, Waltham, MA, United States*

Background High-dose recombinant human interleukin-2 (IL-2, aldesleukin) is approved for the treatment of renal cell carcinoma (RCC) and melanoma based on durable responses. However, use of aldesleukin is limited due to treatment-related life-threatening toxicities. With the goal of overcoming these toxicities and improving the therapeutic index of IL-2, we employed protein engineering (Geographically Precise Solutions) to generate XTX202, a masked, non-alpha tumor-selective IL-2. XTX202 is designed to bias its binding towards beta/gamma IL-2 receptors and be pharmacologically inactive until unmasked by proteases that are enriched in the tumor microenvironment, resulting in activation and IL-2 signaling.

Methods The *in vitro* bioactivity of masked and proteolytically unmasked XTX202 was compared using STAT-5 phosphorylation in human CD8+T (CD8) and regulatory T (Treg) cells. Dissociated cells from primary human tumor tissues or patient plasma were incubated with XTX202, and % of cleaved XTX202 was measured by Western blot. Tumor growth was monitored after treatment with XTX202 alone and in combination with checkpoint inhibition in human FcRn transgenic mice bearing syngeneic MB49 tumors.

Results XTX202 has attenuated IL-2 receptor signaling in CD8 and Treg cells, as compared to its unmasked control XTX200. Upon activation by proteases, XTX202 had comparable activity in CD8 and Treg cells to that of its unmasked control XTX200. Unlike recombinant IL-2, unmasked XTX202 has similar potency on CD8 and Treg cells, rather than higher potency on Treg cells. XTX202 was cleaved by a broad range of human primary solid tumors (29-100% of samples tested were cleaving XTX202). XTX202 was not significantly activated by plasma from healthy control donors, and RCC patients. *In vivo* data indicated that single-agent dosing with XTX202 resulted in anti-tumor activity in the MB49 murine bladder carcinoma model. Combining XTX202 with checkpoint inhibition further enhanced the anti-tumor activity.

Conclusions XTX202, a tumor-selective IL-2, was proteolytically activated by a broad range of solid primary human tumors and minimally cleaved in plasma. In the syngeneic mouse bladder MB49 model, XTX202 as a single agent showed significant tumor-growth inhibition, and no evidence of toxicity or peripheral immune activation was observed, thus demonstrating tumor-selective activity in this model. The combination of XTX202 with immune checkpoint blockade demonstrated further enhancement in the anti-tumor activity in MB49 tumor bearing mice. Clinical testing of XTX202 is ongoing (NCT05052268).

Ethics Approval All animal procedures were either approved by an Institutional Animal Care and Use Committee and conducted in accordance with the National Institutes of Health Guide for the Care and Use of Laboratory Animals.

<http://dx.doi.org/10.1136/jitc-2022-SITC2022.0841>

Abstracts

842

DEVELOPMENT OF A MULTIPLEX TEST FOR PREDICTING RESPONSE TO COMBINED IMMUNOTHERAPIES IN PATIENTS WITH METASTATIC MELANOMA

¹Gabriele Madonna, ²Pedro Machado Almeida*, ¹Mariaelena Capone, ¹Vito Vanella, ¹Lucia Festino, ²Antonio Sorrentino, ²Marco Cassano, ²Benjamin Pelz, ²Diego Dupouy, ¹Paolo Ascierto. ¹Istituto Nazionale Tumori IRCCS Fondazione "G. Pascale", Napoli, Italy; ²Lunaphore Technologies, Tolochenaz, Switzerland

Background In recent years, advanced melanoma treatment has improved dramatically thanks to the advent of immunotherapy. Particularly immune checkpoint inhibitors (ICI), in some patients, have demonstrated to improve long-term outcomes associated with limited toxicity. However, only a small population of patients achieve a durable response to therapy, owing to the lack of clinically validated predictive biomarkers (reviewed in¹). The availability of improved predictive biomarkers may allow the identification of patients who will most benefit from ICI treatment and those who may be susceptible to immune-related adverse events. This difficulty in obtaining clinically relevant predictive biomarkers underscores the complexity of the immune system and the heterogeneity of the tumor microenvironment. In the present study, we take the first steps towards stratification of advanced melanoma patients who received a combination of ICI. We studied the predictive value of a multi-parameter spatial signature composed of lymphocyte-activation gene-3 (LAG-3), programmed death-ligand 1 (PD-L1) and cluster of differentiation 8 (CD8) in a retrospective cohort of patients with metastatic melanoma treated with a combination of ICI.

Methods In this retrospective study, from the biobank of the Istituto Nazionale Tumori IRCCS Fondazione G. Pascale, we recovered FFPE skin metastasis samples obtained from 10 melanoma patients with AJCC 8th edition stage IV² subsequently treated with combined ICI, enrolled from September 2016 to November 2017. According to the Response Evaluation Criteria in Solid Tumors (RECIST 1.1),^{3,4} patients achieved response to the treatment, while 6 patients were non-responders. A single FFPE tumor tissue of each patient was stained using LabSat[®] platform (Lunaphore Technologies) performing a Tyramide Signal Amplification multiplex immunohistochemistry staining for PD-L1, CD8, and LAG-3 expression, followed by DAPI counterstaining and whole slide fluorescent scanning. Single cell segmentation, phenotyping and quantification were performed in QuPath (0.3.0). The workflow is depicted in figure 1.

Results Responder patients showed a statistically significant increase in CD8+ single-positive cell frequency compared to non-responders (figure. 2A and 2C). Non-responder patients displayed a statistically significant increase of PD-L1+ single-positive cell frequency, as well as statistically significant increased frequency of double CD8+PD-L1+ positive cells, previously found to be a poor prognostic in multiple cancer types,^{4,5} and triple positive cells (figure 2B and 2C).

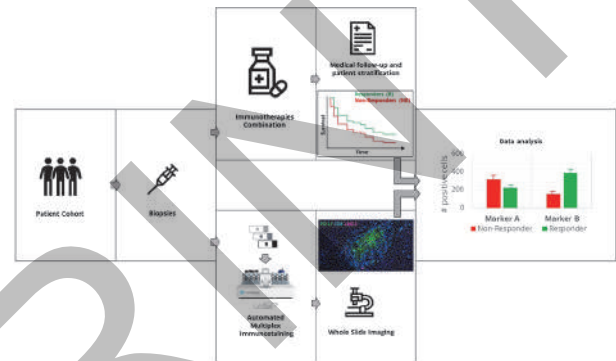
Conclusions We show here preliminary evidence of the predictive value of a spatial biomarker signature in patients who underwent combined ICI therapy for advanced melanoma. To further demonstrate clinical relevance, a more detailed analysis using larger retrospective and prospective cohorts is ongoing.

REFERENCES

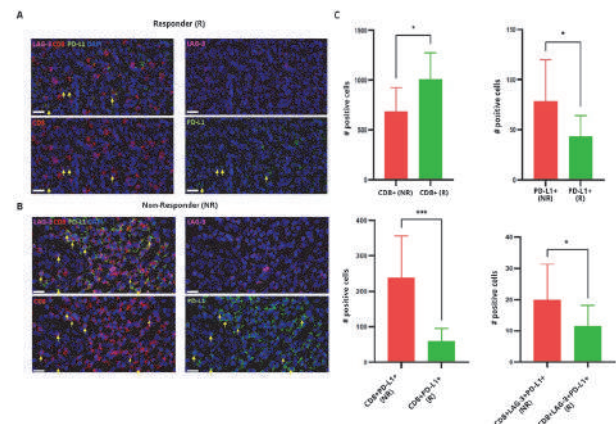
1. Garutti M, Bonin S, Buriolla S, Bertoli E, Pizzichetta MA, Zalaudek I, et al. Find the Flame: Predictive Biomarkers for Immunotherapy in Melanoma. *Cancers* 2021;13:1819.
2. Gershenwald JE, Scolyer RA. Melanoma Staging: American Joint Committee on Cancer (AJCC) 8th Edition and Beyond. *Ann. Surg. Oncol.* 2018; 2105–10.

3. Eisenhauer EA, Therasse P, Bogaerts J, et al. New response evaluation criteria in solid tumors: revised RECIST guideline (version 1.1) *Eur J Cancer.* 2009;45:228–247.
4. Brochez L, Meireson A, Chevolet I, Sundahl N, Ost P, Kruse V. Challenging PD-L1 expressing cytotoxic T cells as a predictor for response to immunotherapy in melanoma. *Nat Commun* 2018;9:2921.
5. Zhang L, Chen Y, Wang H, Xu Z, Wang Y, Li S, et al. Massive PD-L1 and CD8 double positive TILs characterize an immunosuppressive microenvironment with high mutational burden in lung cancer. *J Immunother Cancer* 2021;9:e002356.

Ethics Approval This study was conducted in accordance with the guidelines of the Declaration of Helsinki, and approved by the Institutional Review Board of the Istituto Nazionale Tumori IRCCS Fondazione "G. Pascale" (Naples, Italy) (protocol code 33/17oss, approved on 10 January 2018).



Abstract 842 Figure 1 Visual representation of the study presented here. A cohort of 10 advanced melanoma patients underwent biopsies of skin metastasis (left panels). The cohort then followed a full course of combined immune-checkpoint inhibitor immunotherapies (upper middle panels). Based on their clinical response to the combined treatment, the cohort was subdivided in Responders (R) and Non-Responders (NR) (note: disease free survival chart for representation purpose only, not based on real data analysis from this our study). In parallel (bottom middle panels), a single FFPE tissue sample slide from tissue collected prior the start of the treatment underwent automated multiplex immunohistochemistry staining for LAG-3, programmed death-ligand 1 (PD-L1) and cluster of differentiation 8 (CD8) on a LabSat[®] (Lunaphore) instrument. All samples underwent whole slide imaging (WSI). Finally, a retrospective data analysis quantified the number of positive cells for given markers from the WSI to determine relevant biomarkers discriminating R to NR patients. This strategy is now being scaled up with a larger cohort and a larger panel of markers.



Abstract 842 Figure 2 Multiplex staining and quantification on advanced melanoma (A-B) Representative region of interest of Tyramide Signal Amplification multiplex immunohistochemistry staining for lymphocyte-activation

gene-3 (LAG-3, magenta), programmed death-ligand 1 (PD-L1, green), cluster of differentiation 8 (CD8, red) and DAPI (blue) on FFPE melanoma skin metastasis samples obtained from patients prior to their first cycle of combined immune checkpoint inhibitors (ICI) treatment. Three patients were classified as Responder (R) (A) and three as Non-Responder (NR) (B) based on their response evaluation criteria. Scale bar: 20 μ m. Yellow arrows (A-B) indicates examples of double-positive CD8+PD-L1+ cells, prominently present in NR patients (B-C). (C) Quantification of the number of CD8+ (upper left), PD-L1+ (upper right), CD8+PD-L1+(bottom left) and CD8+LAG-3+PD-L1+ (bottom right) cells from R and NR patients. * $p < 0.05$, *** $p < 0.001$, Unpaired t-test

<http://dx.doi.org/10.1136/jitc-2022-SITC2022.0842>

PREPRINT

843

LAG3 BLOCKADE IN COMBINATION WITH GITR IMPROVES ANTI-TUMOR IMMUNE RESPONSES IN A PRECLINICAL MELANOMA MODEL

¹Rachana Maniyar*, ²Roberta Zappasodi, ¹Yuval Elhanati, ¹Samantha St Jean, ¹Sebastian Carrasco, ¹Benjamin Greenbaum, ¹Jedd Wolchok, ¹Taha Merghoub. ¹Memorial Sloan Kettering Cancer Center, New York, NY, United States; ²Weill Cornell Medical Center, New York, NY, United States

Background Immune checkpoint blockade (ICB) therapies anti-PD1 and anti CTLA-4 have had tremendous successes in clinic. However, many patients are either inherently resistant or acquire resistance to these therapies. Appropriately activating co-stimulation pathways of T cells together with blocking immune checkpoints can provide substantial anti-tumor responses. Glucocorticoid induced TNFR Related protein (GITR), is a costimulatory molecule whose engagement with agonist antibodies leads to proliferation, cytokine production and survival of cytotoxic T cells, and destabilization and depletion of suppressive T regulatory cells in the tumor microenvironment, making it an attractive target for cancer immunotherapy. GITR agonism as a monotherapy in murine models of advanced melanoma leads to increased effector T cell dysfunction with a marked upregulation in expression of exhaustion markers PD-1 and Lag3, making them rational targets to combine with GITR agonism.

Methods C57BL/6 mice were implanted with B16-F10 melanoma and were treated with a single dose of GITR Agonism with or without anti Lag3 on Day 7 post tumor implant, followed by anti Lag3 every 3 days. Spectral flow cytometry and immunohistochemistry was used to study immune cell repertoires. Splenic B cell repertoire was studied using BCR IgH sequencing.

Results We show that combining GITR agonism with Lag3 ICB therapy, leads to better tumor control, and improved survival in mice with advanced ICB resistant B16 melanoma. Additionally, mice treated with GITR agonism monotherapy show a marked increase in activated B cells infiltrating the tumor microenvironment. This infiltration is further increased when GITR agonism is combined with Lag3 blockade therapy. These tumor-infiltrating B cells are highly activated with an increased expression of activation markers CD86, MHC-II, and CD38. The spleens from mice treated with GITR agonism in combination with Lag3 blockade demonstrate increased hyperplasia, and an increase in size and number of germinal centers. B cell receptor sequencing from the spleens of these mice revealed an increased clonality and reduced entropy in mice treated with GITR agonism + Lag3 blockade therapy.

Conclusions Increased B cell activity observed in these mice warrants further investigation into the role and mechanism of action of a GITR/Lag3 combination therapy. Our results suggest that combining GITR agonism with Lag3 blockade is a safe and potent therapeutic strategy to overcome ICB resistance in mice with advanced melanoma.

Ethics Approval This study was approved by the Institutional Animal Care and Use Committee (IACUC) and Memorial Sloan Kettering Cancer Center

<http://dx.doi.org/10.1136/jitc-2022-SITC2022.0843>

844

COMBINED IMMUNOTHERAPY EFFICACY ON A MULTIFOCAL HEPATOCELLULAR CARCINOMA MODEL BASED ON HYDRODYNAMIC ONCOGENE TRANSFER

¹Maria Ochoa*, ²Sandra Sanchez-Gregorio, ³Alvaro Teijeira, ³Saray Garasa, ²Carlos De Andrea, ²Maria Villalba, ³Inaki Etxeberria, ³Ignacio Melero. ¹CIBERONC, Pamplona, Spain; ²Clinica Universidad de Navarra, Pamplona, Spain; ³CIMA Universidad de Navarra, Pamplona, Spain

Background Immunotherapy based on checkpoints inhibitors has become a conventional treatment of advanced hepatocellular carcinoma (HCC) and is under clinical investigation as a strategy to improve the efficacy of locoregional interventions such as transarterial chemoembolization and radiofrequency. In advanced disease, the combination of nivolumab and ipilimumab has resulted in more frequent and durable objective responses as compared to nivolumab monotherapy. Important aspects are pending for these developments, such as reliable and predictive preclinical models, as well as biomarker discovery.

Methods A model based on mice bearing multifocal HCC as a result of hydrodynamic gene transfer to hepatocytes of c-myc and CRISPR/CAS9 disruption of p53 was used. This model was sophisticated to induce coexpression of luciferase, EGFP and the melanosomal antigen gp100 to permit incisive immunological mechanistic experimentation. This genetic approach attains traceability of the tumor and sufficient levels of antigenicity in order to test immunotherapy agents such as anti-CTLA-4, antiPD-1 and anti-CD137 monoclonal antibodies, IL-2 or adoptive Pmel-1 CD8⁺ T cell therapy and their combinations. Survival assays, as well as multiplex immunofluorescence and intravital microscopy were performed to study the efficacy and mechanism of action of the therapies.

Results In this tumor setting, combinations of anti-CTLA-4 + anti-PD1 mAbs attained partial efficacy that was markedly augmented by combination with either recombinant IL-2 or an anti-CD137 mAb to deploy triplet regimens. As shown by multiplex tissue immunofluorescence and intravital microscopy, treatments enhanced T-cell infiltration and antitumor immune responses.

Conclusions We provide a relatively simple, reproducible and reliable spontaneous HCC mouse model that enabled us to test various immunotherapies. With it, we have investigated clinically feasible combinatorial regimens including triplets.

Ethics Approval All animal procedures were approved by the animal experimentation ethics committee of the regional government of Navarra (protocol 108-19).

<http://dx.doi.org/10.1136/jitc-2022-SITC2022.0844>

845 IDENTIFYING PATIENT SUBSETS FOR CTLA4 AND GITR DEPLETION STRATEGIES IN POORLY T CELL INFILTRATED TUMORS

Arjun Mittal*, Jason Luke, Riyue Bao. *University of Pittsburgh, Pittsburgh, PA, United States*

Background Many combination immunotherapies have been investigated however identifying subsets of patients who will benefit from each combination has been challenging. While immunotherapy combinations have to date centered on therapeutic targets on immune cells, the expression of immunooncology (IO) targets on cancer cells has not been well studied. We investigated the gene expression landscape across human solid tumors for seven existing IO targets (CTLA4, GITR, CSF1R, IDO1, LAG3, TIM3, and FOXP3) in conjunction with PDL1 to evaluate tumor-intrinsic patterns and potential for IO combinations in specific patient populations.

Methods We used a hierarchical approach on samples from the Cancer Genome Atlas (TCGA). Normalized RNAseq data was converted to quartile rank to define patient populations of PDL1 high/low in combination with high/low from one of the IO targets. Genes differentially expressed between groups were identified by limma voom (fold change >1.5, FDR 0.05). Upstream regulators were predicted by causal networks from Ingenuity Pathway Analysis (z-score >1.95).

Results Patients with PDL1 high expression showed high expression in all seven genes, and those of PDL1 low showed low expression in all genes, consistent with the literature. We identified a unique subset of patients in the PDL1 low setting, however, that demonstrated high CTLA4 or GITR expression, composing 14% and 21% of all tumor samples, respectively. Subsequent analysis of the CTLA4-high/PDL1-low subset indicated that high CTLA4 expression in PDL1 low tumors may represent an intermediate-T cell-inflamed tumor microenvironment (TME) with activated upstream regulators of Type-I IFN γ pathways (IFNG, AHR, TNF, STAT1, NFKB1, IFNA1), which comprised 12% of cervical squamous cell carcinoma, 15% of head and neck squamous cell carcinoma, and 17% of liver hepatocellular carcinoma. Analysis surrounding GITR suggested that high GITR expression in PDL1 low tumors may also represent an intermediate-T cell-inflamed TME. 14% of skin cutaneous metastatic melanoma, 20% of liver hepatocellular carcinoma, 20% of sarcoma, and 11% of testicular germ cell tumor samples fell in GITR-high/PDL1-low group and demonstrated intermediate activation of IFNG, TNF, CD28, AHR, NFKB1, and MYD88. These analyses were not impacted when adjusted by tumor mutational burden across cancer types.

Conclusions High CTLA4 or GITR in the context of low PDL1 may represent an intermediate-T cell-inflamed TME and/or tumor cell-intrinsic expression. Stratification of tumors by T cell-inflamed gene signature, or PDL1 status, as well as expression of a specific therapeutic target may identify patient populations who could benefit from CTLA4 or GITR depletion strategies in IO combination therapies.

<http://dx.doi.org/10.1136/jitc-2022-SITC2022.0845>

846

TRASTUZUMAB, AN ANTI-HER2 ANTIBODY MODULATES CYTOTOXICITY AGAINST CHOLANGIOCARCINOMA (CCA) VIA MULTIPLE MECHANISMS

Seiji Okada*, Jutatip Panaampon. Kumamoto University, Kumamoto, Japan

Background Trastuzumab (Tras) monoclonal antibody targets the extracellular domain of human epidermal growth factor receptor 2 (HER2). FDA approved Tras for the treatment of HER2 positive breast cancer. Cholangiocarcinoma (CCA) is a cancer forms in the bile ducts. Several CCAs are multifocal and cannot be completely removed by surgery and are incurable. Combination of gemcitabine and cisplatin is a standard first line therapy for patients with advanced CCA. Nowadays, the precision medicine and immunotherapy has been playing remarkable roles for cancer treatment. In this study, we found that HER2 expression is relatively high in CCA PDX and cell lines from Thailand. We hypothesized and speculated that Trastuzumab could be a promising antibody immunotherapy for CCAs.

Methods We examined surface HER2 expression on 5 CCA cell lines (M213B, D068, D113, RBE, YSCCC) and patient-derived cell (PDC) by Flowcytometry. We defined the activities of antibody-dependent cytotoxicity (ADCC) and antibody-dependent cell phagocytosis (ADCP) by using FcR-bearing recombinant Jurkat T cell expressing firefly luciferase gene under the control of NFAT response elements. ADCC was then confirmed by using CD16-transduced NK cell line (KHYG-1) and NK cells from a healthy donor. Rabbit and human serum were administered to test CDC activity of Tras. To clarify ADCP activity, we used mouse peritoneal macrophages and monocyte-derived macrophages from healthy donor as effector cells. Moreover, we performed MTT assay to investigate the direct effect of Tras. Finally, we evaluated the efficacy of Tras *in vivo* xenograft and PDX model.

Results Flowcytometric analysis and immunohistochemistry revealed high expression of HER2 in CCA cells. Tras conferred ADCC, ADCP, CDC, and direct effect to induce CCA cell death. Tras demonstrated potent *in vivo* inhibitory effect using PDX model.

Conclusions

Tras indicates multi-activities against CCA. Tras can be considered as a promising antibody immunotherapy for the treatment of HER2 expressing CCA.

Ethics Approval The use of human materials is approved by Kumamoto University's ethical committee (ID: 30-78-20-20201119). Animal experiments are approved by Kumamoto Univeristy's animal ethics committee (ID: A2021-053)

<http://dx.doi.org/10.1136/jitc-2022-SITC2022.0846>

847

CF33-CD19T ONCOLYTIC VIRUS (ONCARLYTICS) IN COMBINATION WITH OFF-THE-SHELF ALLOGENEIC CYCART-19 T CELLS TARGETING DE NOVO CD19+ SOLID TUMORS

¹Anthony Park*, ¹Isabel Monroy, ¹Colin Cook, ²Shuyang He, ²Kathy Karasiewicz, ³Monil Shah, ³Nimali Withana, ³Leslie Chong, ²Robert Hariri, ¹Yuman Fong, ¹Saul Priceman. ¹City of Hope, Duarte, CA, United States; ²Celularity, Warren, NJ, United States; ³Imugene, Sydney, Australia

Background Autologous chimeric antigen receptor (CAR) T cell therapy has shown impressive clinical responses against CD19+ B-cell hematological malignancies and is being actively explored in the treatment of solid tumors. However, several barriers have precluded therapeutic responses in solid tumors, including limited tumor-restricted CAR targets and the immunosuppressive tumor microenvironment. We have recently reported the successful combination immunotherapy using a novel chimeric vaccinia-based oncolytic virus (OV), called onCARlytics (Imugene Limited), that is engineered to express a non-signaling, truncated CD19 (CD19t) antigen for tumor-selective delivery, enabling de novo targeting of tumor cells by autologous CD19-CAR T cells. One of the field's unanswered questions is whether treatment-naïve allogeneic CAR T cells are superior to cancer patient-derived T cells for product manufacturing to improve overall responses against solid tumors.

Methods Here, we evaluated this combination strategy using two allogeneic CAR T cell products generated from peripheral blood mononuclear cells (PBMC) and placental T cells, respectively. PBMC-derived CAR-T cells were manufactured from normal, healthy donors. CYCART-19 (Celularity, Inc.) cells were derived from postpartum human placental T cells that are genetically modified to express the CD19 CAR followed by CRISPR-Cas9-mediated knockout of the endogenous TCR and expanded to produce multiple doses of allogeneic "off the shelf" treatment. For preclinical testing, we utilized *in vitro* co-culture assays. We evaluated tumor cell killing and T cell activation using flow cytometry and cytokine assays. Xenograft mouse models were used to evaluate anti-tumor activity of the combination *in vivo*.

Results CYCART-19 T cells induced potent cytolytic activity against solid tumor cells infected with onCARlytics. Interestingly, while we observed comparable anti-tumor activity between PBMC-derived CD19-CAR T cells and CYCART-19, significant differences in cytokine secretion were detected. This warrants the possibility that the placental-derived CAR T product may elicit reduced CRS potential in patients with maintained or improved efficacy. This combination approach demonstrated impressive *in vivo* anti-tumor response in human tumor xenograft models.

Conclusions In summary, our results have demonstrated that further development of this combination immunotherapy for the potential treatment of a wide array of solid tumors is warranted.

<http://dx.doi.org/10.1136/jitc-2022-SITC2022.0847>

848

IMPACT OF IMMUNOTHERAPY TIME-OF-DAY INFUSION ON OVERALL SURVIVAL IN PATIENTS WITH METASTATIC RENAL CELL CARCINOMA

¹Jimmy Patel*, ¹Amber Draper, ²Yena Woo, ²Layla Dhabaan, ¹Preteesh Patel, ¹Ashesh Jani, ¹Bradley Carthon, ¹Viraj Master, ¹Haydn Kissick, ¹Mehmet Bilen, ¹Zachary Buchwald, ¹David Qian. ¹Emory Winship Cancer Institute, Atlanta, GA, United States; ²Emory University, Atlanta, GA, United States

Background Our prior study demonstrated that the time-of-day of immune checkpoint inhibitor (ICI) infusion influences clinical outcomes including overall survival (OS) for Stage IV melanoma patients. Similar results have subsequently been shown in lung cancer. In this study, we hypothesized that the time-of-day of ICI infusion may impact OS for patients with stage IV renal cell carcinoma (RCC).

Methods The treatment records of all patients with stage IV RCC who underwent ICI therapy within a multi-center academic hospital system between 2015 and 2020 were reviewed. Association between OS and proportion of ICI infusions received prior to 13:00 (cutoff to denote morning infusions) was evaluated using Cox proportional hazards regression.

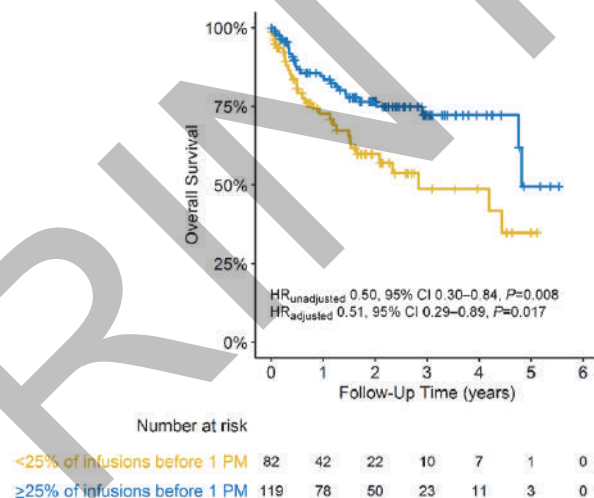
Results In this study, there were 201 patients with stage IV RCC (28% female) who were administered ICIs and followed over a median of 18 months (IQR 5–30). Median age at the time of starting ICI treatment was 63 years (IQR 56–70). Initial ICI agents consisted of pembrolizumab (8%), nivolumab (61%), and dual nivolumab/ipilimumab (31%); table 1. The 119 patients (59%) who received at least a quarter of their ICI infusions in the morning had significantly longer OS (median 58 vs. 34 months, HR 0.51, 95% CI 0.29–0.89, $P=0.017$), independent of age, sex, RCC histology, liver and brain metastases, pre-treatment LDH, and choice of initial ICI; table 2, figure 1.

Conclusions Patients with metastatic RCC may benefit from earlier time-of-day ICI infusions. Our findings are consistent with established mechanisms of chrono-immunology, as well as with preceding analogous studies in melanoma and lung cancer. Additional prospective randomized trials are warranted.

Abstract 848 Table 2 Multivariable cox proportional hazards regression

Table 2. Multivariable Cox proportional hazards regression

	OS Hazard Ratio	95% CI	P-value
≥25% ICI infusions prior to 13:00	0.51	(0.29–0.89)	0.017
Male (vs. Female)	0.91	(0.49–1.69)	0.771
Age (each year)	1.02	(0.98–1.03)	0.647
ECOG 1 (vs. 0)	1.21	(0.66–2.23)	0.531
ECOG 2+ (vs. 0)	2.68	(1.28–5.58)	0.009
Clear cell histology (vs. non-clear cell)	0.56	(0.31–1.00)	0.051
Brain metastasis	0.53	(0.20–1.44)	0.214
Liver metastasis	1.82	(1.02–3.23)	0.042
LDH high (vs. normal)	2.75	(1.29–5.85)	0.009
LDH unknown (vs. normal)	1.27	(0.68–2.39)	0.457
Initial nivolumab (vs. pembrolizumab)	0.80	(0.27–2.37)	0.683
Initial ipi/nivo (vs. pembrolizumab)	0.74	(0.23–2.37)	0.609



Abstract 848 Figure 1 Kaplan-Meier overall survival

<http://dx.doi.org/10.1136/jitc-2022-SITC2022.0848>

Abstract 848 Table 1 Patient characteristics

Table 1. Patient characteristics

	≥25% ICI infusions prior to 13:00 N=119 (%)	<25% ICI infusions prior to 13:00 N=82 (%)	P-value
Sex			0.92
Female	32 (28)	23 (28)	
Male	87 (72)	59 (72)	
Age at ICI initiation			0.08
≤50	19 (16)	14 (17)	
51-60	21 (18)	28 (34)	
61-70	45 (38)	25 (30)	
71-80	27 (23)	12 (15)	
≥81	7 (5)	3 (4)	
ECOG			0.66
0	53 (44)	33 (40)	
1	47 (39)	32 (39)	
≥2	19 (14)	17 (15)	
RCC histology			0.60
Clear cell	86 (72)	56 (68)	
Papillary	5 (4)	5 (6)	
Chromophobe	2 (2)	1 (1)	
Collecting duct	4 (3)	0 (0)	
Sarcomatoid	1 (1)	2 (2)	
Other	15 (13)	13 (17)	
Mixed	6 (5)	5 (6)	
Brain metastasis			0.02
No	109 (92)	65 (79)	
Yes	10 (8)	17 (21)	
Liver metastasis			0.72
No	86 (73)	62 (76)	
Yes	33 (27)	20 (24)	
Pre-treatment LDH			0.32
≤280	64 (54)	42 (51)	
>280	13 (11)	15 (18)	
Unknown	42 (35)	25 (31)	
Initial ICI regimen			0.37
Nivolumab	71 (59)	52 (63)	
Nivolumab + Ipilimumab	41 (34)	22 (27)	
Pembrolizumab + Axitinib	7 (7)	8 (10)	

849

NT-I7, A NOVEL LONG-ACTING INTERLEUKIN-7, IMPROVES ENGRAFTMENT OF PATIENT IMMUNE CELLS AND EFFICACY OF ANTI-PD-1 THERAPY IN A PRECLINICAL HUMANIZED MELANOMA MODEL

¹Yee Peng Phoon*, ¹Kang Kai, ²Alexandra Wolfarth, ²Sara Ferrando-Martinez, ²Byung Ha Lee, ¹Brian Gastman. ¹Cleveland Clinic, Cleveland, OH, United States; ²NeolImmuneTech, Inc., Rockville, MD, United States

Background Although immune checkpoint inhibitors (ICIs) have led to significant massive improvements in melanoma survival, half of these patients fail to benefit, necessitating the discovery of novel strategies. There is a pivotal need for the development of preclinical models to evaluate 'next-generation' immunotherapies prior to clinical investigation.

In this study, we developed and optimized our all-autologous humanized melanoma mouse model for the study of NT-I7 (efineptakin alfa), a long-acting recombinant human IL-7. Because NT-I7 has been shown to enhance T cell proliferation and survival in both humans and mice, we hypothesized NT-I7 would both improve the engraftment of patient immune cells and the efficacy of anti-PD-1 therapy in our humanized mouse model.

Methods Both tumor cells and peripheral blood lymphocytes (PBLs) were collected from melanoma patients to establish our autologous humanized melanoma mouse model. Tumor-bearing NSG mice were infused with matched melanoma PBLs prior to receiving 10 mg/kg NT-I7. Optimization of the model was performed and evaluated by measuring engraftment of the patient immune cells via flow cytometry and comparing tumor growth. The optimized autologous melanoma model was then used to test the efficacy of NT-I7 combined with anti-PD-1 therapy.

Results NT-I7 was well tolerated in the preclinical humanized melanoma mouse model. The optimal dosing of NT-I7 was determined to be two subcutaneous injections of 10 mg/kg NT-I7 1-2 weeks apart after infusing unexpanded PBLs. NT-I7 dramatically increased engraftment of patient PBLs in the spleen and infiltration of the tumor, with a majority of T cells being CD4⁺. NT-I7 also enhanced the anti-tumor response with decreased tumor growth compared to vehicle control. In combination with anti-PD-1, NT-I7 continued to boost immune cell engraftment, with a majority of T cells still being CD4⁺. While NT-I7 and anti-PD-1 displayed a similar modest anti-tumor effect as monotherapies, combination treatment significantly decreased tumor growth compared to control.

Conclusions Our all-autologous humanized melanoma mouse model allows us to evaluate novel immunotherapies in the context of matched patient immune and tumor cells. NT-I7 dramatically improves engraftment of patient PBLs. When combining NT-I7 and anti-PD-1 therapy, tumor control was significantly improved. In sum, we have developed a platform to feasibly design NT-I7 combination therapies to identify optimal strategies that can be translated into clinical investigations.

Ethics Approval All human tissue was obtained at the Cleveland Clinic under a protocol approved by the institutional review board with written informed consent obtained from each patient. Animal studies were performed in accordance with the guidelines of and approved by the Institutional Animal Care and Use Committee at the Cleveland Clinic.

<http://dx.doi.org/10.1136/jitc-2022-SITC2022.0849>

850

INTERIM RESULTS FOR PHASE 1B DOSE EXPANSION OF MTL-CEBPA IN COMBINATION WITH PEMBROLIZUMAB IN PATIENTS WITH ADVANCED SOLID TUMOUR MALIGNANCIES

¹Ruth Plummer, ²Mikael Sodergren*, ³Brid Ryan, ³Ilian Tachkov, ³Vikash Reebye, ⁴Tim Meyer, ²David Pinato, ⁵Debashis Sarker, ⁶Bristi Basu, ⁷Sarah Blagden, ⁸Natalie Cook, ⁹Jeff Evans, ¹⁰Jeffrey Yachnin, ¹¹Cheng-Ean Chee, ¹²Daneng Li, ¹³Anthony El-Khoueiry, ¹⁴Maria Diab, ¹⁵Kai-Wen Huang, ²Antonio D'Alessio, ²Claudia Fulgenzi, ¹⁶Marcus Noel, ¹⁷Bridget Keenan, ¹⁸Devalingam Mahalingam, ³Nina Raulf, ³Rose Hogson, ³Choon Ping Tan, ²Joanna Nicholls, ³Alison Adderkin, ³Julia Vassiliadou, ³Robert Habib, ¹⁹John Rossi, ³Nagy Habib. ¹Newcastle University, Newcastle-upon-Tyne, UK; ²Imperial College London, London, UK; ³MiNA Therapeutics Ltd, London, UK; ⁴University College London, London, UK; ⁵Kings College London, London, UK; ⁶University of Cambridge, Cambridge, UK; ⁷University of Oxford, Oxford, UK; ⁸The Christie NHS Foundation Trust, Manchester, UK; ⁹University of Glasgow, Glasgow, UK; ¹⁰Karolinska University Hospital, Stockholm, Sweden; ¹¹National University Cancer Institute, Singapore, Singapore; ¹²City of Hope Comprehensive Cancer Center, Duarte, CA, United States; ¹³University of Southern California, Los Angeles, CA, United States; ¹⁴Emory University, Atlanta, GA, United States; ¹⁵National Taiwan University Hospital, Taipei, Taiwan; ¹⁶Medstar Georgetown University Hospital, Washington, WA, United States; ¹⁷University of California San Francisco, San Francisco, CA, United States; ¹⁸Northwestern University, Chicago, IL, United States; ¹⁹Beckman Research Institute, City of Hope, CA, United States

Background Most cancer patients do not benefit from currently approved immune checkpoint inhibitors (ICI), suggesting that additional immunomodulation is required to improve outcomes. MTL-CEBPA is a novel immunotherapy targeting the myeloid cell lineage that has shown promising clinical activity in hepatocellular carcinoma, and preclinical activity in models of solid tumour cancers in combination with ICIs. We previously reported dose escalation data for MTL-CEBPA in combination with ICI from TIMEPOINT, an ongoing multi-centre phase 1/1b study (NCT-04105335) evaluating the safety, PK, immunomodulation and clinical activity of MTL-CEBPA in combination with pembrolizumab in patients with anti-PD(L)1 naïve advanced solid tumours for whom no standard therapy is available.¹

Methods In the dose expansion part of TIMEPOINT, patients were treated at RP2D 130mg/m² MTL-CEBPA QW for 3 consecutive weeks and 1 week off (28-day cycle) and 200mg pembrolizumab Q3W. Analysis was undertaken of plasma cytokine and complement profiles; gene expression (qPCR and Nanostring I/O 360) and immune landscape (multiplex IHC) from core tumour biopsies taken at baseline and cycle 2. Adverse events (AEs) were assessed by CTCAEv5.0. Clinical activity was assessed by RECIST v1.1/iRECIST.

Results At data cut-off 15 March 2022, 50 patients across a wide range of tumour types reported to have primary resistance to anti-PD(L)1 therapy have been enrolled. Patient demographics, clinical characteristics are in table 1. The most frequent AEs in at least 5 patients (10%) are listed in table 2. 20 patients (40%) experienced an AE Gr ³3, 1 pt (2%) had a Gr4 AE, and there were no Gr 5 AEs. 7 pts (14%) had a SAE, however there were no AEs leading to dose modification or treatment discontinuation of MTL-CEBPA. Pharmacokinetic profile of MTL-CEBPA was not affected by pembrolizumab. Cytokine/complement analysis did not suggest cytokine release syndrome. Paired tumour biopsies during treatment suggested significant increase in Immunosign21 (figure 1) and proliferation of granzyme-producing T cells. 4 (10%) patients had confirmed PR (table 1). A 30-year-old NET patient with primarily lung involvement (failed 3 prior lines of therapy) achieved PR (43% reduction) in cycle 4, associated with a transformation from cold to hot TME (Immunosign21 from 2/21 to 19/21).

Conclusions MTL-CEBPA in combination with pembrolizumab is safe and well tolerated, with encouraging early signs of activity in heavily pre-treated patients across multiple tumour types. Treatment was associated with intratumoural changes supporting the hypothesis of immunomodulation by MTL-CEBPA and further investigation in combination with ICI is warranted.

REFERENCE

1. Plummer R, Sodergren M, Pinato D, et al. 515 A phase 1 study of myeloid modulating agent MTL-CEBPA in combination with pembrolizumab in adult patients with advanced solid tumours *Journal for ImmunoTherapy of Cancer* 2021;**9**:doi: 10.1136/jitc-2021-SITC2021.515.

Ethics Approval The study was approved by the North East – Newcastle & North Tyneside 2 Research Ethics Committee, approval number 19/NE/0312.

Abstract 850 Table 1 Demographics, clinical characteristics and clinical response

	Phase 1a (Escalation) n=10 (n=9 Eval for RECIST)	Phase 1b (Expansion) n=40 (n=31 Eval for RECIST)	All Patients n=50 (n=40 Eval for RECIST)
Age (Mean/Median)	47.5/50.5	60.4/62.5	57.8/58.5
Gender (M/F%)	30/70	35/65	34/66
ECOG (0/1%)	60/40	42.5/57.5	46/54
Median Prior Lines of Therapy	2	3	3
Tumour types	Colorectal (n=9), Pancreatic (n=9), Ovarian(n=8), Cholangiocarcinoma (n=7), Breast (n=4), Others* (n=13)		
RECIST response	2 (22%) (1 x Ovarian; 1 x Mesothelioma)	2 (6.5%) (1 x Intrah. Cholangioca; 1 x Neuroendocrine)	4 (10%)
Stable Disease (SD)	3 (33.3%)	8 (25.8%)	11 (27.5%)
Progressive Disease (PD)	4 (44.4%)	21 (67.7%)	25 (62.5%)

Table 1. Demographics, clinical characteristics and clinical response
Other category contains epithelioid mesothelioma, thymic cancer metastatic, hepatocellular carcinoma, eccrine carcinoma, adenocarcinoma, lung neoplasm malignant, extrahepatic cholangiocarcinoma, neuroendocrine tumour, leiomyosarcoma, malignant peritoneal neoplasm, anal squamous cell carcinoma and mesothelioma

Abstract 850 Table 2 Most common AEs in order of decreasing incidence in at least 5 patients (10%)

TEAE (MedRA PT)	All Patients (n=50)	All Patients CTC Gr >=3 (n=50)
Anaemia	17 (34%)	1 (2%)
Fatigue	17 (34%)	1 (2%)
Abdominal pain	14 (28%)	2 (4%)
ALT increased	12 (24%)	1 (2%)
AST increased	12 (24%)	2 (4%)
Decreased appetite	11 (22%)	0
Nausea	11 (22%)	0
Back pain	9 (18%)	0
Constipation	9 (18%)	0
Diarrhoea	9 (18%)	0
GGT increased	8 (16%)	2 (4%)
Vomiting	8 (16%)	1 (2%)
AP increased	7 (14%)	1 (2%)
Arthralgia	6 (12%)	0
Cough	6 (12%)	0
Lethargy	6 (12%)	0
Abdominal pain upper	5 (10%)	1 (2%)
Hyponatraemia	5 (10%)	1 (2%)
Lower respiratory tract infection	5 (10%)	0

Table 2. Most common AEs in order of decreasing incidence in at least 5 patients (10%)

Abstracts

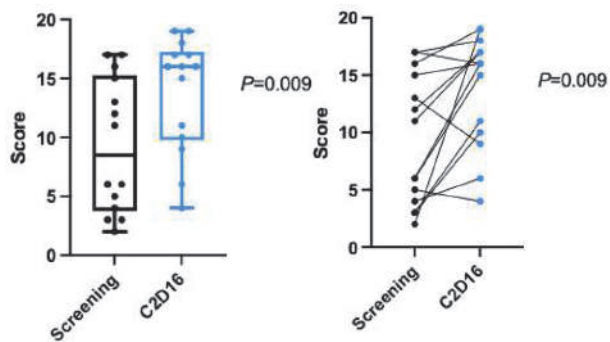


Figure 1. Change in Immunosign21 score (Veracyte) following combination treatment with MTL-CEBPA and pembrolizumab

Abstract 850 Figure 1 Change in Immunosign21 score (Veracyte) following combination treatment with MTL-CEBPA and pembrolizumab

<http://dx.doi.org/10.1136/jitc-2022-SITC2022.0850>

851

VOYAGER V1 (VV1) ONCOLYTIC VIRUS COMBINED WITH IMMUNE CHECKPOINT THERAPY BOOSTS CTL RESPONSES TO MULTIPLE TUMOR ANTIGENS AND CORRESPONDINGLY DEEPENS TUMOR RESPONSES IN MURINE MODELS OF MELANOMA, LUNG AND COLON CANCER

¹Priyanka Ram, ¹Navpreet Tung, ¹Himani Sharma, ¹Ben Fulton, ²Kah-Whye Peng, ²Stephen Russell, ¹Markus Mohrs, ¹Gavin Thurston, ¹Christos Kyratsous, ¹Alina Baum, ¹Jessica Kirshner, ¹John Lin, ¹Saida Dadi-Mehmetaj*. ¹Regeneron Pharmaceuticals, Tarrytown, NY, United States; ²Vyriad, Rochester, MN, United States

Background There is a need for novel immunotherapies to address patient populations resistant or refractory to immune checkpoint inhibitors (CPI). VV1 is an oncolytic vesicular stomatitis virus engineered to express interferon beta (IFN β) to enhance anti-tumor immune responses and tumor selectivity. Phase 1 studies demonstrated VV1 anti-tumor activity in certain clinical settings either alone or in combination with a CPI. The current preclinical study aimed to identify dosing and scheduling regimens that maximize the efficacy of VV1 in combination with CPIs.

Methods Immune-competent mice bearing syngeneic tumor models MC38 (colorectal), B16F10 (melanoma) and CMT64 (lung adenocarcinoma) tumors were dosed to test combinations of VV1 delivered intravenously with anti-PD-1 and anti-CTLA4 antibodies. Treatment was started once tumors were established, and T cell responses in the tumor and peripheral lymphoid organs were analyzed using flow cytometry and ELISPOT assays.

Results Potent anti-tumor efficacy was observed following intratumoral or intravenous administration of VV1 combined with anti-CTLA4 and anti-PD-1. A comparison of single dose versus repeat administration of anti-CTLA4 in combination with VV1 plus continuous anti-PD-1 showed that a single dose was sufficient to maximally enhance the depth and durability of tumor response. This effect was observed consistently in multiple tumor models, including anti-PD-1 sensitive (MC38) or anti-PD-1 resistant tumor models (B16F10 and CMT64). Remarkably, the triple combination boosted T cell priming against the B16F10 and CMT64 neo-antigen peptides in TILs and tumor-draining lymph nodes. ELISPOT and multimer staining showed that, in contrast to doublet therapy using virus and a single CPI, triplet combination therapy strongly boosted CTL responses against a broad array of B16F10 and CMT64 neoepitopes, detected both in the tumor and in tumor-draining lymph nodes. This was associated with increased infiltration of CD8 T cells in the tumor, but the number of regulatory T cells was not impacted, indicating that the enhancing effect of anti-CTLA4 was not a consequence of Treg depletion.

Conclusions Intratumoral or intravenous VV1 virotherapy combined with anti-CTLA4 and anti-PD-1 checkpoint antibodies synergistically enhances tumor control in multiple syngeneic mouse tumor models. The triple combination seems to promote a tumor-vaccination effect, by inducing a polyclonal anti-tumor T cell response and boosting anti-tumor CTL responses. This triplet combination approach will soon be evaluated clinically in patients with advanced melanoma (after progression on an anti-PD1) and first line NSCLC patients. (ClinicalTrials.gov Identifier: NCT04291105).

<http://dx.doi.org/10.1136/jitc-2022-SITC2022.0851>

INVESTIGATING THE FUNCTIONAL ROLE OF GPNMB IN GLIOBLASTOMA AND THE TUMOR IMMUNE MICROENVIRONMENT AND ITS TARGETED ELIMINATION USING CAR-Ts

¹Neil Savage*, ²Franz Zemp, ³Nick Mikolajewicz, ³Hong Han, ¹Chitra Venugopal, ¹Chirayu Chokshi, ¹Nazanin Tatari, ⁴Thomas Kislinger, ³Jason Moffat, ²Doug Mahoney, ¹Sheila Singh. ¹McMaster University, Hamilton, Canada; ²University of Calgary, Calgary, Canada; ³University of Toronto, Toronto, Canada; ⁴Princess Margaret Hospital, Toronto, Canada

Background Glioblastoma (GBM) is the most common primary malignant brain tumor in adults. Due to GBM displaying extreme heterogeneity and immune suppression, prognosis remains dismal. Glycoprotein nonmetastatic melanoma protein B (GPNMB) has previously been identified as a clinically relevant target in GBM while being absent in normal brain tissues and shown to be active in the tumor immune microenvironment.^{1,2} Chimeric Antigen Receptor T-cells (CAR-Ts) fail clinical trials because multiple antigens will be required to eliminate all GBM subpopulations.^{3,4} We previously proved CD133 to be an effective CAR-T target in GBM models.⁵

Methods Immunohistochemistry was performed on patient derived xenograft (PDX) brains and tissue microarrays of 16 patient matched primary/recurrent GBMs as well as 23 normal organ tissues. Whole cell proteomics was performed on 43 matched primary/recurrent GBM samples. Flow cytometry measured surface expression levels of CD133 and GPNMB to confirm CAR-T accessibility. CRISPR/Cas9 was used to eliminate expression in GBM lines to measure proliferation and mouse survival times. GPNMB knockout clones were generated in GL261 and engrafted in immunocompetent mice to examine single cell transcriptomes using scRNAseq at endpoint. A second-generation CAR-T was developed to target GPNMB-expressing populations, and efficacy was interrogated using standard *in vitro* assays and PDX models.

Results GPNMB detected in residual tumors of PDX brains treated with CD133 CAR-Ts revealed it as a targetable subpopulation. Tissue microarrays and proteomics found GPNMB to be upregulated in recurrent GBMs compared to primary ($p=0.0349$ and $p=0.0033$ respectively), particularly in macrophage populations while being absent in normal tissues. Eliminating GPNMB in cell lines decreased proliferation ($P\leq 0.001$) and prolonged survival times in all mouse models ($P\leq 0.01$) indicating its functional relevance. GPNMB knockout clones displayed downregulation of hallmark signalling pathways of GBM such as PDGFR, TGF-beta, Integrins and Stats, as well as decreased innate/adaptive immune activation. CAR-T cytotoxicity and activation was observed *in vitro* and *in vivo* resulting in decreased tumor burden ($P\leq 0.001$) and increased survival times ($P\leq 0.001$). Ultimately a CD133+ population was observed in residual tumors of GPNMB treated mice at endpoint. Surface expression of CD133 and GPNMB revealed co-expression and distinct populations.

Conclusions We show GPNMB influences tumor intrinsic biology of GBM and is active in the tumor immune microenvironment. By targeting GPNMB along with CD133, combinatorial therapeutic regimens could target the cancer stem cell hierarchy and its supportive niche. We therefore plan to administer both CAR-T cells to provide better cytotoxic coverage and increase efficacy.

REFERENCES

1. Kuan Chien-Tsun, Kenji Wakiya, Jeannette M Dowell, James E Herndon, David A Reardon, Michael W Graner, Gregory J Riggins, Carol J Wikstrand, and Darell D

- Bigner. Glycoprotein nonmetastatic melanoma protein B, a potential molecular therapeutic target in patients with glioblastoma multiforme. *Clinical Cancer Research* 2006;**12**(7): 1970–82. <https://doi.org/10.1158/1078-0432.ccr-05-2797>
2. Feng X, Zhang L, Ke S, Liu T, Hao L, Zhao P, Tu W, & Cang S. High expression of GPNMB indicates an unfavorable prognosis in glioma: Combination of data from the GEO and CGGA databases and validation in tissue microarray. *Oncology Letters*, 2020;**20**(3), 2356–2368. <https://doi.org/10.3892/ol.2020.11787>
3. Brown Christine E, Brenda Aguilar, Renate Starr, Xin Yang, Wen-Chung Chang, Lihong Weng, Brenda Chang, *et al.* Optimization of IL13R η 2-targeted chimeric antigen receptor T cells for improved anti-tumor efficacy against glioblastoma. *Molecular Therapy* 2018;**26**(1): 31–44. <https://doi.org/10.1016/j.ymthe.2017.10.002>
4. Goff Stephanie L, Richard A Morgan, James C Yang, Richard M Sherry, Paul F Robbins, Nicholas P Restifo, Steven A Feldman, *et al.* Pilot trial of adoptive transfer of chimeric antigen receptor–transduced T cells targeting EGFRvIII in patients with glioblastoma. *Journal of Immunotherapy* 2019;**42**(4) :126–35. <https://doi.org/10.1097/cji.0000000000000260>
5. Vora Parvez, Chitra Venugopal, Sabra Khalid Salim, Nazanin Tatari, David Bakhshinyan, Mohini Singh, Mathieu Seyfrid, *et al.* The rational development of CD133-targeting immunotherapies for glioblastoma. *Cell Stem Cell* 2020;**26**(6). <https://doi.org/10.1016/j.stem.2020.04.008>

Ethics Approval Human GBM samples were obtained from consenting patients, as approved by the Hamilton Health Sciences/McMaster Health Sciences Research Ethics Board(#07-366). All animal work was conducted by Animal Research Ethics Board (AREB)-approved Protocols (AUP#19-01-01).

<http://dx.doi.org/10.1136/jitc-2022-SITC2022.0852>

853

NOVEL CEAXCD47 (NILK-2401) AND CEAXCD3 (NILK-2301) KL BISPECIFIC ANTIBODIES FOR MULTIMODAL IMMUNOTHERAPY OF CEA-EXPRESSING SOLID CANCER

¹Anja Seckinger*, ²Vanessa Buatois, ²Valéry Moine, ²Lise Nouveau, ²Bruno Daubeuf, ²Sara Majocchi, ²Ulla Ravn, ²Nicolas Bosson, ²Krzysztof Masternak, ²Yves Poitevin, ²Giovanni Magistrelli, ²Pauline Malinge, ²Limin Shang, ²Nicolas Fischer, ¹Klaus Strein, ²Walter Felin, ¹Dirk Hose. ¹LamKap Bio, Pfaeffikon SZ, Switzerland; ²Light Chain Bioscience – Novimmune SA, Geneva, Switzerland

the project by the Commission Cantonale d'Expérimentation Animale (CCEA; GE83 and GE134).

<http://dx.doi.org/10.1136/jitc-2022-SITC2022.0853>

Background We present here our novel macrophage-directed CEAXCD47 bispecific antibody (bsAb) NILK-2401 alone and in combination with the CEAXCD3 T-cell retargeting bsAb NILK-2301 for multimodal treatment of CEA-expressing solid malignancies, e.g., gastrointestinal or lung carcinomas.

Methods BsAbs are generated using LCB's fully human $\kappa\lambda$ body platform based on a common heavy chain and on one κ and one λ light chain, determining specificity and affinity. Binding, inhibition of CD47-SIRP α interaction, antibody-dependent cellular phagocytosis (ADCP) and antibody-dependent cellular cytotoxicity (ADCC) were assessed *in vitro* using colorectal (n=3), lung (n=2), and gastric (n=2) cancer cell lines. Human monocyte-derived macrophages (MDMs) or peripheral blood mononuclear cells (PBMCs) were used as effector cells. Combination activity ("mixed killing assay") of NILK-2401 and NILK-2301 was assessed by flow cytometry, incubating both effector cell populations with tumor cells. *In vitro* safety data include binding to other CEACAM-members, ADCP of CEA-negative cells (n=3), cytokine release in whole blood, erythrophagocytosis, and platelet activation. *In vivo*, NSG-mice were co-engrafted SC with PBMCs, MDMs, and LS-174T tumor cells, and exposed to 10 mg/kg NILK-2401 IV once weekly vs. control. Pharmacokinetics and tolerability were assessed in cynomolgus monkeys and Tg32 human FcRn mice.

Results NILK-2401 has a functional IgG1 Fc part and shows low nM binding-affinity to CEA and high nM binding-affinity to CD47, enabling tumor specific blockade of the CD47-SIRP α interaction. Elimination of CEA-expressing cell lines by ADCP and ADCC is induced, including CEA-high (e.g., MKN-45) and low expressing cell lines (e.g., LS-174T). Killing activity was CEA-dependent as no phagocytosis of CD47-positive but CEA-negative cells, including red blood cells, was observed. Likewise, no platelet activation occurred. In the mixed killing assay, NILK-2301 plus NILK-2401 combination showed an additive effect, both increasing maximum activity (Emax) and necessitating lower doses of the T-cell bsAb to reach Emax. E.g., Emax of 30% killing (NILK-2301 alone) was increased in combination with NILK-2401 at 0.1/1/10 $\mu\text{g}/\text{mL}$ to 40%, 80%, and 80%, respectively. *In vivo*, NILK-2401 delayed tumor growth vs. mean of control in 100% (15/15) of mice and prevented establishment of detectable tumors (i.e., $>50\text{mm}^3$, d23 post co-graftment) in 53% (8/15). In cynomolgus and Tg32 mice, doses of 0.5 and 20 mg/kg NILK-2401 (single IV dose) were well tolerated.

Conclusions NILK-2401 bsAb is active as single agent with limited potential side effects due to the tumor-targeted blockade of CD47. NILK-2401 plus NILK-2301 combination treatment significantly increases activity, without overlapping safety profiles. GMP drug substance has been produced for both molecules.

Ethics Approval Animal experiments were approved by the animal research committee of Geneva canton and experiments performed in accordance with the Swiss Federal Veterinary Office guidelines. This included submission and approval of

854

**HPK1 INHIBITION RELIEVES SUPPRESSION
DOWNSTREAM OF TCR ACTIVATION TO DRIVE
ENHANCED CYTOKINE PRODUCTION AND ANTIGEN-
SPECIFIC KILLING, AN EFFECT THAT IS FURTHER
ENHANCED BY IMMUNE CHECKPOINT BLOCKADE**

Rajesh Singh*, Bindi Patel, Rameshwari Rayaji, Sachie Marubayashi, Sean Cho, Stefan Garrido-Shaqfeh, Joseph Kulusich, Cesar Meleza, Nidhi Tibrewal, Joice Thomas, Pradeep Nareddy, Ehesan Sharif, Sharon Zhao, Dave Green, Manmohan Leleti, Jay Powers, Matt Walters, Daniel DiRenzo. *Arcus Biosciences, Hayward, CA, United States*

Background T cell activation is critical in the initiation and potentiation of anti-tumor immune responses. Hematopoietic Progenitor Kinase 1 (HPK1) is a member of the MAP4K family whose activity restrains T cell activation through phosphorylation of SLP-76 (pSLP-76) at Serine 376, leading to disassembly of the TCR complex. Mouse genetic deletion and kinase dead mutants of HPK1 have been shown to enhance T cell activity and combine with immune checkpoint inhibition. Therefore, we sought to demonstrate that inhibitors of HPK1 activity can increase T cell activation, drive antigen-specific cancer cell killing, and combine with immune checkpoint blockade to amplify anti-tumor T cell responses. Herein, we describe the characterization of novel inhibitors of HPK1 and assess their effects on T cell activation in combination with PD-1 blockade.

Methods Measurement of pSLP-76 using a flow cytometry-based assay was employed to assess HPK1 activity in human and mouse whole blood. Jurkat cells, human CD8⁺ T cells and PBMCs were activated using anti-CD3/CD28 stimulation, CEF peptide pools, or Staphylococcal enterotoxin A (superantigen), in the presence of HPK1 inhibitors; levels of IL-2, IFN- γ and TNF- α were assayed in supernatants by cytokine bead array. Mouse OT-1 splenocytes were stimulated with SIINFEKL peptide and co-cultured with E.G7-OVA cells to assess cytokine production and target cell killing.

Results HPK1 inhibitors exhibited a potent, concentration-dependent reduction in pSLP-76, with a concurrent increase in IL-2 secretion in both Jurkat and human CD8⁺ T cells. Human T cells also demonstrated increased IFN- γ and TNF- α secretion as well as a greater percentage of activated CD69⁺ cells with HPK1 inhibition. These increases in T cell activation were mirrored in antigen-specific OT-1 T cell assays, in which HPK1 inhibition enhanced IFN- γ production in response to OVA peptide and greater killing of E.G7-OVA cancer cells. Similarly, antigen-recall assays demonstrated that inhibition of HPK1 increased IFN- γ production from human PBMC stimulated with CEF peptide and combined with PD-1 blockade to further enhance cytokine production. Consistent with these results, HPK1 inhibition and PD-1 blockade increased cytokine secretion in superantigen-stimulated human PBMC individually and further enhanced cytokine production in combination. Taken together, these data demonstrate that the combined activity of HPK1 inhibition with checkpoint therapy may yield greater anti-tumor T cell activity.

Conclusions These data demonstrate that pharmacological inhibition of HPK1 amplifies antigen-specific T cell activation alone or in combination with immune checkpoint blockade and provide a strong mechanistic rationale for targeting HPK1 to amplify anti-tumor immune responses.

<http://dx.doi.org/10.1136/jitc-2022-SITC2022.0854>

855

DIACYLGLYCEROL KINASE ALPHA AND ZETA DUAL INHIBITORS ENHANCE T CELL RESPONSES AND PROMOTE ROBUST AND DURABLE ANTI-TUMOR T CELL IMMUNITY

Marcos Steinberg*, Darina Spasova, Danelle Eto, AnneMarie Pferdekamper, Phuong Nguyen, Brian Le, Zachary Naiman, Susan Murphy, Maricel Gozo, James Skipper, Taylor Ismaili, Xikui Liu, Sunil Sahdeo, Xiao Hu, Isharat Yusuf, Kristen Taylor Meadows, Laura Carter. *Gossamer Bio, Inc., San Diego, CA, United States*

Background Diacylglycerol kinases (DGK) convert diacylglycerol (DAG) into phosphatidic acid which limits DAG-induced propagation of T cell activation.¹ T cells predominantly express DGK alpha and DGK zeta isoforms (DGKalpha/zeta),² and deletion of either enhances T cell activation and function.^{3,4} DGKalpha/zeta are overexpressed in tumor infiltrating T cells and may limit the anti-tumor activity of these cells.⁵ Thus, inhibition of DGKalpha/zeta is a potential therapeutic avenue to enhance T cell anti-tumor responses. We demonstrate that inhibition of DGKalpha/zeta with novel dual DGKalpha/zeta inhibitors (DGKi) enhances anti-tumor T cell activity.

Methods The role of DGKalpha/zeta in T cell activation was studied using wildtype and CRISPR-knockout T cells. *In vitro* studies assessing the effect of DGKi were conducted using various mouse and human T cell functional assays. T cell exhaustion studies were performed in T cells from lymphocytic choriomeningitis virus (LCMV) clone 13-infected mice. *In vivo* activity of DGKi was assessed by measuring T cell activation in OT-I mice challenged with OVA-peptides. Efficacy studies and memory rechallenge experiments were performed in the MC38 syngeneic tumor model.

Results CRISPR knockout studies characterizing the role of DGKalpha/zeta on T cells demonstrated that both isoforms regulate T cell activation and function. DGKi enhanced IFN gamma production by human melanoma-specific T cells stimulated with the weak affinity MART1 antigen. Similarly, treatment of mouse OT-I cells with DGKi enhanced responses to low-affinity OVA-peptides and OT-I-mediated cytotoxicity of MC38-OVA tumor cells. Treatment of exhausted CD8 T cells with DGKi reverted exhaustion caused by chronic LCMV infection, and enhanced T cell function with PDL1 blockade. DGKi rescued cytokine release from T cells suppressed by adenosine, TGF beta or PGE₂ treatment. Oral administration of DGKi resulted in dose-dependent increase in T cell activation in mice. Furthermore, DGKi in combination with anti-PD-1 therapy was efficacious in the MC38 model with complete tumor regressions in treated animals. These mice eradicated tumors upon rechallenge with MC38 cells two months later, demonstrating durable anti-tumor memory responses.

Conclusions We demonstrate that DGKalpha/zeta negatively regulates T cell activity. Dual DGKalpha/zeta inhibition restores T cell responses to weak tumor antigens, overcomes cell exhaustion, and enhances CD8 T cell cytotoxic activity. *In vivo* efficacy data demonstrates that DGKi in combination with anti-PD-1 antibody therapy promotes robust anti-tumor responses and generates durable T cell memory. These data support dual DGKalpha/zeta inhibition in combination with anti-PD-1 antibodies as a therapeutic approach for cancer treatment.

REFERENCES

1. Mérida I, Avila-Flores A, Merino E. Diacylglycerol kinases: at the hub of cell signalling. *Biochem J*. 2008; **409**(1):1–18.

2. Krishna S, Zhong X. Role of diacylglycerol kinases in T cell development and function. *Crit Rev Immunol*. 2013; **33**(2):97–118.
3. Guo R, Wan C-K, Carpenter JH, et al. Synergistic control of T cell development and tumor suppression by diacylglycerol kinase alpha and zeta. *Proc Natl Acad Sci U S A*. 2008; **105**(33):11909–14.
4. Riese MJ, Grewal J, Das J, et al. Decreased diacylglycerol metabolism enhances ERK activation and augments CD8+ T cell functional responses. *J Biol Chem*. 2011; **286**(7):5254–65.
5. Prinz PU, Mendl AN, Masouris I, et al. High DGK- α and disabled MAPK pathways cause dysfunction of human tumor-infiltrating CD8+ T cells that is reversible by pharmacologic intervention. *J Immunol*. 2012; **188**(12):5990–6000.

Ethics Approval All animal studies were approved and conducted in accordance with the Explora IACUC Program of Veterinary Care.

<http://dx.doi.org/10.1136/jitc-2022-SITC2022.0855>

856

SNS-101, A HIGHLY PH-SELECTIVE VISTA:PSGL-1 INHIBITORY ANTIBODY, POTENTIATES ANTI-PD-1 SENSITIVITY, EXPANDS MEMORY T-CELLS AND ENHANCES TUMOR INFILTRATION OF CD8 T-CELLS

Thomas Thisted, Tim Eitas, Kanam Malhotra, Yuliya Kleschenko, Faith Finley, Zhi-Gang Jiang, Arnab Mukherjee, Zuzana Biesova, Anokhi Cifuentes, Robert Pierce, Edward van der Horst*. *Sensei Biotherapeutics, Boston, MA, United States*

Background VISTA (V-domain Ig suppressor of T-cell activation) is a negative checkpoint regulator (NCR), highly expressed on myeloid cells.¹ PSGL-1 on T-cells has been identified as a novel NCR that limits survival and promotes T-cell exhaustion.² Recently, VISTA was reported to bind PSGL-1 and suppress T-cell activity exclusively under acidic conditions (~pH 6 in lymph nodes or the tumor microenvironment).^{3, 4} Although VISTA inhibition demonstrated excellent therapeutic combinability with other modalities targeting NCRs (e.g. CTLA-4, PD-1/PD-L1),⁵ clinical development of anti-VISTA antibodies has been challenging due to: 1) high clearance via target-mediated drug disposition (TMDD) by VISTA⁺ neutrophils and monocytes at physiologic pH; and 2) cellular activation and cytokine release syndrome (CRS) at sub-therapeutic doses by engagement of VISTA in the blood.⁶

We developed SNS-101, a human monoclonal IgG1 antibody specific for the protonated, active form of VISTA, which is designed to disrupt the immunosuppressive VISTA:PSGL-1 interaction, avoid TMDD and mitigate potential CRS.

Methods The binding potential of SNS-101 to VISTA⁺ cells was determined in human and non-human primate (NHP) whole-blood by flow cytometry. The effect of SNS-101 on human monocytes and T-cells was evaluated *in vivo* in human CD34⁺ cord blood cell reconstituted BRGSF mice, which develop both human lymphoid and myeloid compartments. The pharmacokinetic (PK) profile was assessed in NHPs. Anti-tumor efficacy was assessed in VISTA-KI mice implanted with the syngeneic tumor model, MC38, and tumor-infiltrating T-cells were analyzed by flow cytometry.

Results SNS-101 did not bind to human or NHP VISTA⁺ monocytes, neutrophils and natural killer cells. In humanized BRGSF mice, SNS-101 induced significant expansion of CD4 and CD8 central memory (CCR7⁺CD45RA⁻), and naïve (CCR7⁺CD45RA⁺) CD8 T-cells, respectively, but had no significant impact on monocyte activation. PK studies in NHPs showed linear elimination kinetics. Conversely, a non-pH-sensitive antibody bound VISTA⁺ immune cells, induced monocyte activation followed by a decrease in cell numbers and was rapidly cleared in NHPs. Anti-tumor efficacy studies in MC-38 demonstrate that SNS-101 enhanced anti-PD-1 response and dose-dependently increased tumor-infiltrating CD8 T-cells.

Conclusions Our results demonstrate that SNS-101 exhibits linear elimination kinetics in NHPs, overcoming TMDD-induced PK limitations observed with other anti-VISTA antibodies. Importantly, SNS-101 induced expansion of naïve and memory T-cell phenotypes *in vivo* without activation or depletion of monocytes, differentiating it from non-pH-selective VISTA antibodies. In the MC-38 syngeneic tumor model, SNS-101 demonstrated significant enhancement of anti-tumor effects in combination with anti-PD-1 antibodies through an increase in CD8⁺ T-cells.

REFERENCES

1. Yuan L, Tatineni J, Mahoney KM, *et al.* VISTA: a mediator of quiescence and a promising target in cancer immunotherapy. *Trends Immunol.* 2021; **42**:209–227.

2. Tinoco R, Carrette F, Barraza ML, *et al.* PSGL-1 is an immune checkpoint regulator that promotes T cell exhaustion. *Immunity.* 2016; **44**:1190–1203.
3. Johnston RJ, Su LJ, Pinckney J, *et al.* VISTA is an acidic pH-selective ligand for PSGL-1. *Nature* 2019; **574**:565–570.
4. Wu H, Estrella V, Beatty M, *et al.* T-cells produce acidic niches in lymph nodes to suppress their own effector functions. *Nat Commun.* 2020; **11**:4113.
5. Gao J, Ward JF, Pettaway CA, *et al.* VISTA is an inhibitory immune checkpoint that is increased after ipilimumab therapy in patients with prostate cancer. *Nat. Med.* 2017; **23**:551–555.
6. Curis Corporate Presentation Jan 2022 [<http://investors.curis.com/events-and-presentations?item=100>]

<http://dx.doi.org/10.1136/jitc-2022-SITC2022.0856>

857 IDENTIFYING NOVEL IMMUNOTHERAPY TARGETS UNDER THE PRESSURE OF INHIBITORY CYTOKINE TGF- β

1

¹Liangzhe Wu*, ¹Nicholas Gascoigne, ¹Ling Wu, ¹Vivian Tan, ²Manoj Krishnan, ²Unnikrishnan Unniyampurath, ¹Benson Chua. ¹National University of Singapore, Singapore, Singapore; ²Duke-NUS, Singapore, Singapore

Background T cell function is under regulation by some suppressive signals such as anti-inflammatory cytokines and immune checkpoint molecules in order to maintain self-tolerance and immune cells homeostasis. Transforming growth factor β 1 (TGF- β 1) is a pleiotropic cytokine which participates to orchestrate the negative regulation of T cell activity and is produced in large quantities within tumor microenvironment that ultimately promotes neoplastic progression, notably by suppressing the host's T-cell immunosurveillance.^{1,2} Cancer immunotherapy with aims to re-activate tumour-induced exhaustive T cells to fight against cancer cells is a hot and promising field of cancer therapy in recent years. However, despite some positive results in the past years, success of immune checkpoint blockade therapies in clinic is still limited. These have suggested that albeit several key immune checkpoint genes have been identified, there is still an urgent and unmet medical need to discover new inhibitory genes.

Methods mRNA sequencing of human CD8+ T cells, either with or without TGF- β treatment, was performed and compared for novel immunosuppressive genes discovery.

CRISPR-Cas9 validation system was followed and applied in both Jurkat T cell line and primary T cells to investigate the knockout effect of the gene candidates in terms of T cell effector function, proliferation, cytotoxicity and in vivo anti-cancer ability.

Results Among the mRNA sequencing list, two genes – show the significant inhibitory effect to T cells. After being knocked out, T cell function would be impressively rescued in terms of cytokine secretion, proliferation, and target cell killing. In vivo study also demonstrated that adoptive transferred T cells with these genes knock out enhance the anti-cancer effect in terms of controlling tumor size and improving survival rate. On the other hand, these two genes also showed the ability to affect Treg polarization. With these genes knock out, CD4+ T cells tended to less likely to polarize to Treg population under polarizing conditions.

Conclusions Two genes, a regulator of G protein and a F actin-binding protein, are discovered to be novel T cell inhibitory genes and showed their potential to become the immunotherapy gene targets.

Acknowledgements Thanks to Prof. Nicholas Gascoigne and all the members in the NRG lab.

REFERENCES

1. David CJ, Massagué J. Contextual determinants of TGF β action in development, immunity and cancer. *Nat Rev Mol Cell Biol.* 2018;**19**(7):419–35.
2. Yang L, Pang Y, Moses HL. TGF-beta and immune cells: an important regulatory axis in the tumor microenvironment and progression. *Trends Immunol.* 2010;**31**(6):220–7.

Ethics Approval Animal Protocols were approved by NUS IACUC (R20-1118)

Use of human primary T cells was approved by institutional review board (IRB) (H-19-026)

<http://dx.doi.org/10.1136/jitc-2022-SITC2022.0857>

858 **HBM7008 (B7H4x4-1BB HBICE[®]) SYNERGIZES HBM7004 (B7H4xCD3 HBICE[®]) FOR SOLID TUMOR THERAPY**

Xiaodong Wu*, Yongqiang Wang, Gezi Jia, Bing Huang, Yunxing Yang, Yun He, Yiping Rong. Harbour BioMed Co., Ltd., Shanghai, China

Background B7H4 is a member of B7-family and its expression is not detected or barely detected in healthy tissues but highly expressed in multiple solid tumors. Thus, B7H4 is a good tumor associated antigen (TAA) for tumor therapy, especially used for construction of T cell engagers. CD3 T cell engager has shown promising efficacy in hematologic malignancies. However, the outcomes for solid tumors are still disappointing. One possible impediment to the efficacy could be that CD3 signal alone may cause rapid T cell exhaustion and apoptosis. 4-1BB(CD137) costimulation along with CD3 signal can significantly enhance T cell proliferation, cytotoxicity, as well as counteract T cell exhaustion and cell death. Combination B7H4xCD3 with B7H4x4-1BB T cell engagers may be a promising strategy for solid tumor therapy.

Methods Both B7H4xCD3 and B7H4x4-1BB bispecific antibodies were developed from Harbour BioMed heavy chain only antibodies (HCAb) based bispecific immune cell engager (HBICE[®]) platform. HBM7004 (B7H4xCD3 HBICE[®]) is composed of a bivalent B7H4 VH domain (2+1 format) to increase avidity driven cytotoxicity, and monovalent CD3 Fab domain with reduced activity to decrease systemic toxicity. *In vitro* cytotoxicity of HBM7004 was tested on multiple B7H4 positive tumor cell lines. HBM7008 (B7H4x4-1BB HBICE[®]) is composed of anti-B7H4 IgG1 and anti-4-1BB HCAb variable domains appended at C-terminus of Fc fragment (2+2 format). The synergistic effect of combination of HBM7004 and HBM7008 was studied in a series of assays.

Results HBM7004 (B7H4xCD3) showed potent *in vitro* efficacy to multiple tumor cell lines at high effector T cell: target cell (E: T) ratio. 2+1 HBICE[®] format showed much higher efficacy than monovalent B7H4 HBICE[®]. When the cytotoxicity assay was conducted in the co-culture with low E:T ratio, which mimicked the status in tumor microenvironment as measured by immunohistochemistry staining of T cell infiltration, HBM7004 could not kill the tumor cells. Combination with HBM7008 (B7H4x4-1BB) could restore HBM7004 cytotoxicity at low E:T ratio. It significantly reduced T cell apoptosis and increased T cell division, thus maintained T cell numbers after long-term co-culture with tumor cells. In addition to HBM7008 (B7H4x4-1BB), combination of HBM7004 with HER2x4-1BB HBICE[®] also had synergistic effect on killing SKBR3 cells which is B7H4 and HER2 double positive, indicating flexible combination approaches.

Conclusions Combination with HBM7008 (B7H4x4-1BB) could provide a secondary signal for T cell activation and significantly increase the efficacy of HBM7004 by reducing T cell apoptosis and increasing T cell division, providing a promising therapy solution for solid tumor therapy.

Ethics Approval The cancer tissue microarray was purchased from Fanpu Biotech, Inc. The company ensured ethical approval from the patients, and patient consent for publication.

<http://dx.doi.org/10.1136/jitc-2022-SITC2022.0858>

859

COMBINATION OF HER2 ADC AND LEMZOPARLIMAB ELICITS ENHANCED EFFICACY IN BOTH HER2 HIGH-AND LOW-EXPRESSING BREAST AND GASTRIC CANCERS

Yanni Zhang*, Yu Pang, Ao Li, Ke Xu, Ming Yang, Zhengyi Wang, Andrew Zhu. *I-Mab biopharma, Shanghai, China*

Background Lemzoparlimab (also known as TJC4) is a differentiated anti-CD47 antibody with novel epitope and RBC sparing properties. Previous data has shown that CD47 is upregulated preferentially in HER2-expressing cells and dual blockade of CD47 and HER2 increased tumor attack. The combination of lemzoparlimab with HER2 ADC maybe a promising therapy for treating HER2 positive patients. Here, we report the enhanced anti-tumor efficacy of the combination of lemzoparlimab with HER2 ADC in cell derived xenograft (CDX) and patient derived xenograft (PDX) breast and gastric cancer models.

Methods Breast and gastric cancer cell lines with different expression levels of HER2 and CD47 quantified by flow cytometry were selected for this study. *In vitro* cytotoxicity of RC48 (Disitamab Vedotin), alone or in combination with lemzoparlimab was evaluated in co-culture of human PBMC with tumor cell lines. *In vivo* activity of RC48 or in-house produced DS8201 analogue in combination with lemzoparlimab were investigated in CDX (HER2 0/1+/3+ by IHC) and PDX (HER2 2+ by IHC) models. Tumor infiltrating leukocytes (TILs) were analyzed by flow cytometry. The expressions of CD47 and CD68 in tumor were measured by immunohistochemistry.

Results In combination with lemzoparlimab *in vitro*, RC48-mediated cytotoxicity against both BT-474 and MCF-7 cells was enhanced, while the increase in cytotoxicity was more prominent in HER2-low MCF-7 cells than HER2-high BT474 cells. *In vivo* combination treatment of DS8201 analogue or RC48 with lemzoparlimab exhibited stronger anti-tumor efficacy compared with monotherapy in both CDX and PDX models with different levels of HER2 expression. The synergistic efficacy by combination treatment was more pronounced in tumor with HER2-low expression than that with HER2-high expression. Treatment effect in tumor microenvironment by RC48 and lemzoparlimab was further investigated. Compared to RC48 monotherapy, RC48 combined with lemzoparlimab significantly up-regulated the percentage of activated and total NK cells, CD68⁺ macrophages and the ratio of M1/M2 macrophage in TILs ($p < 0.05$ in all comparisons). In addition, the CD47 expression in tumor cells was also increased by the combination treatment.

Conclusions This study demonstrated the synergistic effect of combining CD47 blocker and HER2 ADC in tumors with different levels of HER2 expression. Lemzoparlimab potentiated HER2 ADC mediated tumor killing by modulating NK cells and macrophage activity to increase cytotoxicity and phagocytosis. These data support future clinical investigation of lemzoparlimab and HER2 ADC combination in HER2 positive patients, especially those with HER2-low expressing tumors.

<http://dx.doi.org/10.1136/jitc-2022-SITC2022.0859>

860

IN VIVO EFFECTIVENESS OF TUMOR TREATING FIELDS (TTFIELDS) CONCOMITANT WITH IMMUNE CHECKPOINT INHIBITORS IN NON-SMALL CELL LUNG CANCER (NSCLC)

Yiftah Barsheshet*, Tali Voloshin, Boris Brant, Gadi Cohen, Lilach Avigdor, Roni Blatt, Shay Cahal, Tharwat Haj Khalil, Efrat Zemer-Tov, Rom Paz, Anat Klein-Goldberg, Catherine Tempel-Brami, Sara Jacobovitch, Alexandra Volodin, Tal Kan, Bella Koltun, Cfir David, Adi Haber, Moshe Giladi, Uri Weinberg, Yoram Palti. *Novocure Ltd, Haifa, Israel*

Background Tumor Treating Fields (TTFields) are electric fields that disrupt cellular processes critical for cancer cell division and tumor progression. Recently, cancer cell death following delivery of TTFields has been shown to stimulate anti-tumor immunity and promote maturation of dendritic cells. The efficacy of TTFields concomitant with anti-PD-1 was previously shown *in vivo*, and is currently under clinical investigation. Here, we investigated whether concomitant treatment with TTFields and the anti-PD-1 and anti-CTLA-4 combination can improve therapeutic efficacy.

Methods Lung tumor-bearing mice were treated with TTFields (150 kHz, continuously for 10 days), with the anti-PD-1 and anti-CTLA-4 combination (3 i.p. injections, one every 72 h), or with the two modalities together. At the end of treatment, tumor volume was measured, tumor single-cell suspensions were generated, and tumor-infiltrating lymphocytes (TILs) were characterized by flow cytometry using fluorochrome-conjugated anti-mouse antibodies for lineage defining factors. Furthermore, TILs were isolated using mouse pan T magnetic beads, and IFN- γ levels were examined. Blood and spleen were examined for changes in effector memory cells.

Results The combined treatment of TTFields and anti-PD-1/anti-CTLA-4 led to a significant decrease in tumor volume as compared to untreated control mice, as well as relative to mice treated with only one of the modalities. In addition, a significant increase in the number of tumor infiltrating immune cells, specifically cytotoxic T-cells, was observed in the TTFields plus anti-PD-1/anti-CTLA-4 group. Correspondingly, cytotoxic T-cells isolated from these tumors have shown higher levels of IFN- γ production relative to untreated mice. The levels of splenic and blood effector memory cytotoxic T-cells were elevated following TTFields with anti-PD-1/anti-CTLA-4 relative to control and TTFields alone, and were similar to those induced by anti-PD-1/anti-CTLA-4 alone.

Conclusions Our results suggest that combining TTFields with the immune checkpoint inhibitors combination anti-PD-1/anti-CTLA-4 may enhance antitumor immunity relative to each modality alone.

<http://dx.doi.org/10.1136/jitc-2022-SITC2022.0860>

861 **COMBINED IRREVERSIBLE ELECTROPORATION AND LOCAL CD40 AGONISM STIMULATE NEOANTIGEN SPECIFIC SYSTEMIC IMMUNE RESPONSES THAT INHIBIT LIVER METASTASIS IN AN ORTHOTOPIC PANCREATIC CANCER MODEL**

¹Jayanth Shankara Narayanan*, ¹Rebekah White, ¹Tomoko Hayashi, ¹Dennis Carson, ²Stephen Schoenberger. ¹University of California San Diego, La Jolla, CA, United States; ²La Jolla Institute of Immunology, La Jolla, CA, United States

Background Pancreatic ductal adenocarcinoma (PDAC) has a poor prognosis, and most patients present with either locally advanced or metastatic disease. Irreversible Electroporation (IRE) is a non-thermal method of ablation, used clinically in locally advanced PDAC, but most patients eventually develop distant recurrence. We have previously shown that IRE alone is capable of generating protective, neoantigen-specific immunity. Here we aim to generate meaningful therapeutic immune effects by combining IRE with local (intratumoral) delivery of CD40 agonistic antibody (CD40Ab)

Methods KPC46 organoids were generated from a tumor-bearing male *Kras^{LSL-G12D}-p53^{LSL-R172H}-Pdx-1-Cre* (KPC) mouse. Orthotopic tumors were established in the pancreatic tail of B6/129 F1J mice via laparotomy (KPC46O). Candidate neoantigens were identified by mutanome profiling of tumor. Tumors were monitored by ultrasound, and when they reached 4-5 mm, mice were randomized to either sham laparotomy, IRE alone, CD40Ab alone, or IRE followed immediately by CD40Ab injection. Metastatic disease and immune infiltration in the liver were analyzed 14 days post-procedure using flow cytometry and multiplex immunofluorescence assay with spatial analysis.

Results Sham-treated KPC46O mice showed a median survival of 14 days post-procedure due to rapid development of metastasis and increasing tumor burden. IRE or CD40Ab alone improved the median survival to 21 and 24 days, respectively, but significantly ($p < 0.01$) lower than the median survival of >35 days achieved by the combination of IRE+CD40Ab. CD40Ab had a significant effect on metastatic disease with average liver weights significantly lower in the IRE+CD40Ab group than the Sham group ($p < 0.01$) or IRE alone ($p < 0.05$). Immunohistochemistry of metastatic nodules in the liver revealed a significantly ($p < 0.01$) higher infiltration of CD8+ T-cells in the IRE+CD40Ab group than the other groups. Multiplex immunofluorescence imaging also revealed a 4-6-fold increase in the density of CD80+CD11c+ activated dendritic cells ($p < 0.05$), which were spatially distributed throughout the tumor unlike the sham group, where they were restricted to the periphery. In contrast, CD4+FoxP3+ T-regulatory cells ($p < 0.05$) and Ly6G+ MDSCs ($P < 0.01$) were reduced and restricted to the tumor periphery in the IRE+CD40Ab group. T-cells from the IRE+CD40Ab group recognized more peptides ($65 \pm 9.3\%$) representing candidate neoantigens than did T-cells from IRE or Sham groups suggesting the dendritic cell activation and improved antigen presentation caused by IRE+CD40Ab treatment leads to wider tumor neoantigen recognition.

Conclusions IRE can induce local tumor regression and generate neoantigen-specific immune responses. Addition of CD40Ab to IRE improved neoantigen recognition, thereby generating a strong systemic anti-tumor T-cell response that inhibited metastatic disease progression.

<http://dx.doi.org/10.1136/jitc-2022-SITC2022.0861>

ADMINISTRATION OF INTRATUMORAL HU14.18-IL2 IMMUNOCYTOKINE AND LOCAL RADIATION THERAPY TO ACTIVATE IMMUNE REJECTION OF SPONTANEOUS CANINE MELANOMA

¹Mark Albertini*, ¹Cindy Zuleger, ¹Erik Ranheim, ²Oyewale Shiyambola, ¹Andrew Kosharek, ¹Paul Sondel, ²Zachary Morris, ¹Jens Eickhoff, ¹Michael Newton, ¹Irene Ong, ¹Rene Welch Schwartz, ¹Rubi Hayim, ¹Sarah Adrianowycz, ¹Rachel Uyebara, ¹Ilene Kurzman, ¹Michelle Turek, ¹David Vail. ¹University of Wisconsin, Madison, WI, United States; ²Stanford University School of Medicine, Stanford, CA, United States

Background Canine malignant melanoma provides a clinically relevant, large animal model to study the GD2-reactive hu14.18-IL2 immunocytokine (IC) as it is similar to human melanoma and expresses GD2. Murine preclinical studies have shown that intratumoral (IT) injection of IC (IT-IC) in combination with local radiation therapy (RT) can convert the injected tumor into an effective *in situ* tumor vaccine. We previously reported that IT-IC at 12 mg/m² on 3 consecutive days is well tolerated in tumor-bearing dogs.

Methods Twelve dogs (6 dogs/arm) with locally advanced or metastatic melanoma were randomized to receive a single 8 Gy fraction (Arm A) or three 8 Gy fractions delivered over 1 week (Arm B) to the primary site and regional lymph nodes (when clinically involved) with the single or last fraction 5 days prior to IT-IC at 12 mg/m² on 3 consecutive days. Tumor biopsies and peripheral blood mononuclear cells (PBMC) were obtained for immune monitoring at pre-treatment and various times post-treatment.

Results All 12 dogs completed protocol treatment and none experienced significant or unexpected adverse events. Antitumor activity includes 3 dogs with partial response at day (D) 30 and 4 dogs with mixed responses. Eleven dogs ultimately experienced progressive disease and 1 is currently alive in immune partial response 5 months post treatment initiation. Hematoxylin and eosin (H&E) stains of 5 serial biopsies (pre-treatment, D1, D10, D17, D24) show a variably timed increase in intratumoral lymphocytic inflammation post-therapy in 6/6 dogs in Arm A while 4/6 also show at least focal tumor necrosis post-treatment. In 2/6 dogs in Arm B, a clear increase in intratumoral lymphoid infiltrate occurred post-treatment. However, 5/6 of Arm B dogs also showed tumor necrosis with 2/6 with no viable tumor by D24. Immunohistochemistry (IHC) staining for CD3, CD8, and FOXP3 (pre-treatment, D1, D10, D17) show the large majority of intratumoral lymphoid cells to be CD3+ T cells, with only a minority staining for CD8 or FOXP3. A 9-marker multi-color immunophenotyping panel for flow cytometry (CD3, CD5, CD4, CD8, CD14, CD21, CD25, FoxP3, and PD-1) was optimized using cryopreserved healthy canine PBMC and will be used to assay PBMC from pre and post-treatment timepoints for the protocol treatment dogs.

Conclusions IT-IC in combination with local RT in canine melanoma is safe and has antitumor activity with potential to inform clinical development of IT-IC in melanoma patients.

Acknowledgements This material was supported by Merit Review Award I01 BX003916 from the Biomedical Laboratory Research and Development Service of the United States (U.S.) Department of Veterans Affairs, P50026787 (NIH/NIDCR), the University of Wisconsin Carbone Cancer Center (UWCCC) Support Grant (P30 CA014520, NIH/HHS), the Barbara A. Suran Comparative Research Endowment, melanoma research gifts to the UWCCC, and use of facilities at the William S. Middleton Memorial Veterans Hospital, Madison, WI. The contents do not represent the views of the U.S. Department

of Veterans Affairs or the United States Government. The hu14.18-IL2 IC was provided by Apeiron Inc. of Vienna Austria. This animal protocol was reviewed and approved by the following: School of Veterinary Medicine Institutional Animal Care and Use Committee (IACUC), Protocol ID V006037, and William S. Middleton Memorial Veterans Hospital IACUC, Protocol ID MRA0001-1. Consent forms for each part of the study and language in the ACORP state that "The owner must provide written, informed consent prior to enrolling the dog in the study."

Ethics Approval Our animal protocol was reviewed and approved by the following: School of Veterinary Medicine Institutional Animal Care and Use Committee (IACUC), Protocol ID V006037. William S. Middleton Memorial Veterans Hospital IACUC, Protocol ID MRA0001-1. We have consent forms for each part of the study and language is included in the ACORP that "The owner must provide written, informed consent prior to enrolling the dog in the study."

<http://dx.doi.org/10.1136/jitc-2022-SITC2022.0862>

866

POTENTIATING RADIOTHERAPY-INDUCED ABS COPAL IMMUNITY BY ATR ABROGATION AND CTLA-4 BLOCKADE IN COLORECTAL CANCER

<http://dx.doi.org/10.1136/jitc-2022-SITC2022.0866>

¹Rodney Cheng-En Hsieh*, ²Ricardo Alexandre De Azevedo, ²Pham Hong Anh Cao, ²Arthur Liu, ²Akash Boda, ²Michelle Winkler, ²Broderick Turner, ²Michael Curran. ¹Chang Gung Memorial Hospital, Taoyuan City, Taiwan; ²MD Anderson Cancer Center, Houston, TX, United States

Background Although radiotherapy has been widely adopted in localized colorectal cancer (CRC) treatment, its therapeutic efficacy for distal, non-irradiated tumors remains limited. Ataxia telangiectasia and Rad3- related (ATR) kinase has recently been identified as a key mediator in post-irradiation cancer immune evasion.¹ Here, we aimed to explore the systemic antitumor efficacy of ATR abrogation in combination with radiotherapy and immune checkpoint inhibition.

Methods We assessed the antitumor immune responses of focal radiotherapy, ATR abrogation, and CTLA-4 blockade by using microsatellite instability-high (MSI-H) MC38 and microsatellite stable (MSS) CT26 murine syngeneic CRC models. Flow cytometry, immunoblot, and gene knockdown were adopted to investigate the post-irradiation immune responses.

Results Ionizing radiation triggered the elevation of anti-phagocytic checkpoints, CD47 and PD-L1, in both MC38 and CT26 cells. ATR inhibition or short hairpin RNA knockdown (shATR) prevented RT-induced CD47 and PD-L1 upregulation and sensitized tumor cells to phagocytic clearance by bone marrow-derived antigen-presenting cells (APCs). We observed significantly improved complete response (CR) rates in both irradiated and abscopal tumors and prolonged survival in C57BL/6J mice bearing bilateral MC38-OVA tumors treated with unilateral radiotherapy, an ATR inhibitor, and anti-CTLA-4 antibodies, in comparison to untreated controls or mice undergoing mono- or dual therapies. In the irradiated tumor microenvironment, radiotherapy followed by ATR inhibition and CTLA-4 blockade significantly improved tumor antigen cross-presentation in APCs, increased NK and tumor-specific CD8 T cell infiltration, and decreased regulatory T lymphocyte accumulation. Concordantly, BALB/c mice bearing bilateral shATR-CT26 tumors treated with unilateral fractionated radiotherapy and anti-CTLA-4 antibodies had significantly higher CR rates in both irradiated and abscopal tumors and improved survival, compared with those bearing wild type CT26 tumors. Furthermore, a cecal orthotopic MC38 tumor model consistently demonstrated superior systemic antitumor efficacy of radiotherapy, ATR inhibition, and CTLA-4 blockade combinatorial therapy. Re-implantation of MC38 cells was performed in mice with complete remission of both irradiated and abscopal tumors, and the rechallenged tumors were rejected in all mice in the triple therapy group.

Conclusions Abrogation of ATR potentiates the systemic antitumor immune responses of radiotherapy and CTLA-4 blockade in both MSI-H and MSS murine CRC models.

REFERENCE

1. Hsieh RC, Krishnan S, Wu RC, *et al.* ATR-mediated CD47 and PD-L1 up-regulation restricts radiotherapy-induced immune priming and abscopal responses in colorectal cancer. *Sci Immunol* 2022, **7**(72):eabl9330.

Ethics Approval All animal experiments were performed in compliance with the approved protocol (00001378-RN01/RN02) by the Institutional Animal Care and Use Committee at MD Anderson Cancer Center.

867

DECIPHERING OF RADIOTHERAPY-INDUCED IMMUNOMODULATION EFFECT SYNERGIZED WITH IMMUNOTHERAPY IN HEPATOCELLULAR CARCINOMA BY SPATIAL MULTI-OMICS PROFILING

¹Mai Chan Lau*, ²Lisda Suteja, ³Lawrence Cheung, ¹Jeffrey Lim, ¹Chun Jye Lim, ¹Xinru Lim, ⁴Neslihan Kaya, ¹Jiang Feng Ye, ¹Felicia Wee, ⁵Han Chong Toh, ⁵Su Pin Choo, ³Suat Ying Lee, ⁵Joycelyn Jie Xin Lee, ²Jin Liu, ⁶Tony Kiat Hon Lim, ⁷Weiwei Zhai, ⁵David Tai, ¹Joe Poh Sheng Yeong. ¹Institute of Molecular and Cell Biology, Singapore, Singapore; ²Duke-NUS Medical School, Singapore, Singapore; ³Singapore General Hospital, Singapore, Singapore; ⁴Genome Institute of Singapore, Singapore, Singapore; ⁵National Cancer Centre Singapore, Singapore, Singapore; ⁶Singapore General Hospital, Singapore, Singapore; ⁷Chinese Academy of Sciences, Beijing, China

Background Multiple clinical trials have shown an overall improved response rate in hepatocellular carcinoma (HCC) by combining radiotherapy (RT) with immunotherapy (IO), however, treatment rates remain low and unpredictable.¹ The sub-optimal outcomes are largely due to the lack of knowledge of the underlying immunomodulation effect and an effective treatment-response biomarker. Previous studies using tissue-based assays like multiplexed immunofluorescence (mIF) have demonstrated that cellular spatial organization within the tumor microenvironment represents a critical factor influencing anti-tumor immunity.^{2, 3} Hence, we sought to characterize the in-situ molecular immune response of RT-treated HCC tissues, to advance our understanding of RT-induced immunomodulation effect and its synergistic benefits with IO.

Methods Using an HCC cohort treated with Yttrium-90 (Y90)-radioembolization (locoregional RT) and anti-PD-1 combination therapy,¹ we profiled the FFPE tissues collected at baseline and post-Y90 from 4 responders and 8 non-responders using NanoString's Digital Spatial Profiler (DSP), 10× Genomics Visium technology, and mIF. In DSP profiling, two types of regions of interest (ROIs) were selected by a pathologist: (1) geometric ROIs far from Y90 beads, and (2) contiguously micro-dissected ROIs contouring the Y90 beads; Visium data contains spatially barcoded spots (figure 1).

Results Tumor Immune Dysfunction and Exclusion (TIDE)⁴ analysis using DSP geometric ROIs showed a counter-intuitively decrease of IO-responsiveness (i.e., higher TIDE scores) in responders post-RT. Immune analysis using DSP micro-dissected ROIs revealed that RT might have induced a systemic increase in T-cell exclusion and decrease in T-cell dysfunction in the non-responders, but opposite trends in the responders (figure 2). A possibly RT-induced systemic increase in CD274 (ligand of PD-1) expression was seen in the responders ($P_{\text{treatment}} < 0.001$, $P_{\text{distance-to-Y90-beads}} = 0.04$). Analysis using the higher-spatial-resolution Visium data showed a systemic increase in cytotoxic T-cell abundance in the non-responders post-RT where the cells were spread over the tissues (figure 3). mIF analysis showed a specific subset of T-cells, CD38⁺CD8⁺, in the responders preferentially interacted with the tumor cells ($P_{\text{cell-to-tumor distance}} = 0.08$), an effect possibly induced by RT ($P_{\text{cell-to-Y90-bead distance}} < 0.001$) (figure 4).

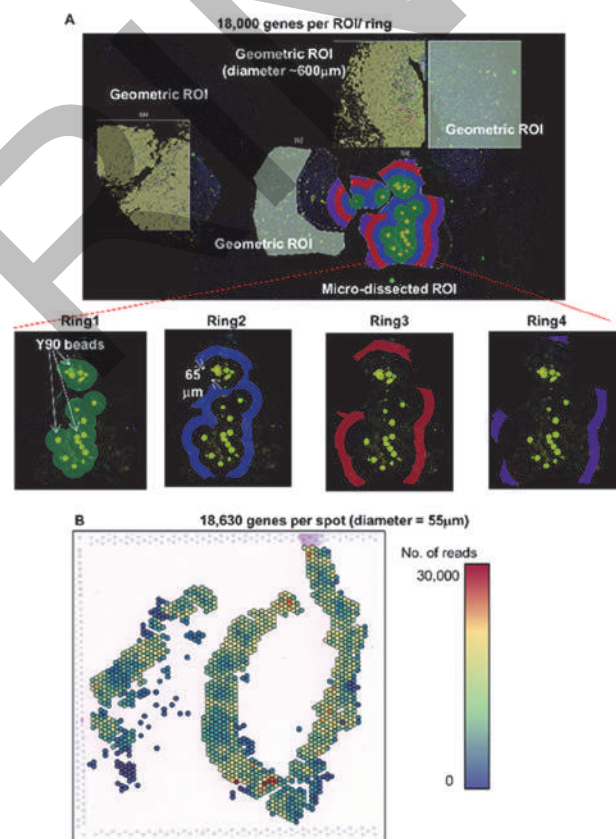
Conclusions TIDE, a transcriptomic-based IO-biomarker mainly tested in melanoma, is not directly applicable to HCC. Spatial multi-omics analysis enables identification of RT-specific immunomodulation effects that synergized with IO in HCC, including the systemic increase in T-cell dysfunction and CD274 expression. To explain for the systemic increase of cytotoxic T-cells in non-responders, further investigation on the tumor-specificity by cell-to-cell proximity analysis is needed.

Trial Registration NCT03033446

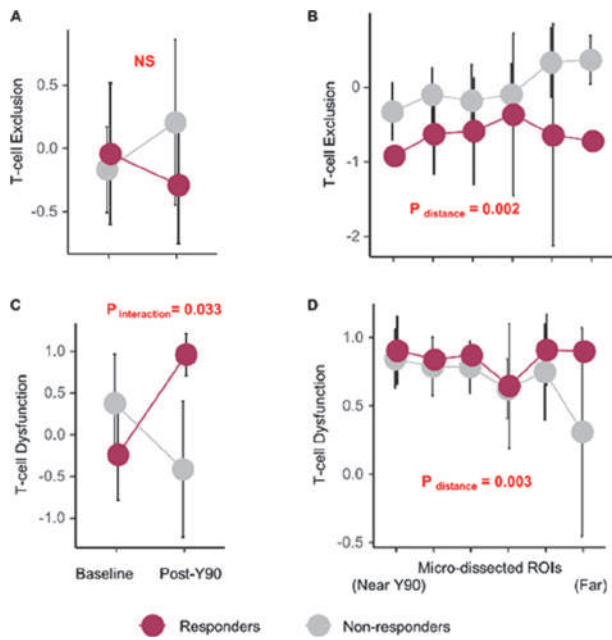
REFERENCES

1. Tai D, Loke K, Gogna A, Kaya NA, Tan SH, Hennedige T, *et al.* Radioembolisation with Y90-resin microspheres followed by nivolumab for advanced hepatocellular carcinoma (CA 209–678): a single arm, single centre, phase 2 trial. *The Lancet Gastroenterology & Hepatology*. 2021. doi: [https://doi.org/10.1016/S2468-1253\(21\)00305-8](https://doi.org/10.1016/S2468-1253(21)00305-8).
2. Barua S, Fang P, Sharma A, Fujimoto J, Wistuba I, Rao AUK, *et al.* Spatial interaction of tumor cells and regulatory T cells correlates with survival in non-small cell lung cancer. *Lung Cancer*. 2018;**117**:73–9. Epub 2018/02/08. doi: [10.1016/j.lungcan.2018.01.022](https://doi.org/10.1016/j.lungcan.2018.01.022). PubMed PMID: 29409671; PubMed Central PMCID: PMC6294443.
3. Väyrynen JP, Haruki K, Lau MC, Väyrynen SA, Ugai T, Akimoto N, *et al.* Spatial organization and prognostic significance of NK and NKT-like cells via multimarker analysis of the colorectal cancer microenvironment. *Cancer Immunol Res*. 2022;**10**(2):215–27. Epub 2021/12/24. doi: [10.1158/2326-6066.Cir-21-0772](https://doi.org/10.1158/2326-6066.Cir-21-0772). PubMed PMID: 34937729; PubMed Central PMCID: PMC8816895.
4. Jiang P, Gu S, Pan D, Fu J, Sahu A, Hu X, *et al.* Signatures of T cell dysfunction and exclusion predict cancer immunotherapy response. *Nature Medicine*. 2018;**24**(10):1550–8. Epub 2018/08/22. doi: [10.1038/s41591-018-0136-1](https://doi.org/10.1038/s41591-018-0136-1). PubMed PMID: 30127393; PubMed Central PMCID: PMC6487502.

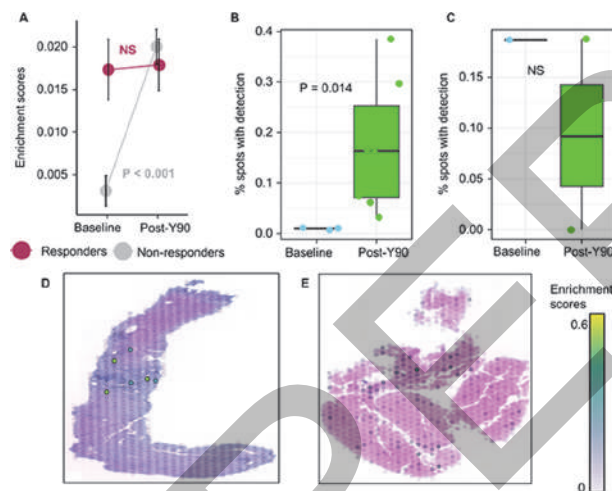
Ethics Approval Singhealth CIRB 2016/2613



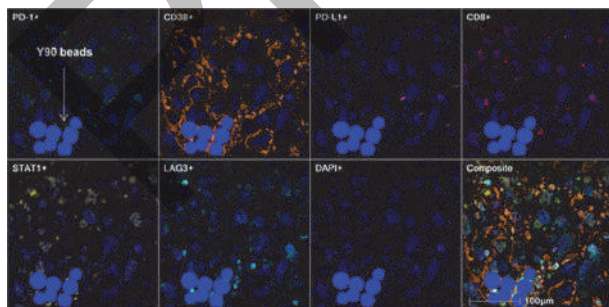
Abstract 867 Figure 1



Abstract 867 Figure 2



Abstract 867 Figure 3



Abstract 867 Figure 4

<http://dx.doi.org/10.1136/jitc-2022-SITC2022.0867>

868 **CD122-DIRECTED IL-2/ANTI-IL-2 COMPLEXES MASSIVELY EXPAND STEM-LIKE TUMOR-SPECIFIC T CELLS AND ENHANCE ABCOPAL RESPONSES TO RADIATION AND ANTI-PD-1**

Kateryna Onyshchenko*, Ren Luo, Liqun Wang, Gabriele Niedermann. *University Hospital Freiburg, Freiburg im Breisgau, Germany*

Background Early clinical trials have provided evidence for RT-induced systemic effects in conjunction with aPD-1 or IL-2 in metastatic patients, but strong abscopal responses are clinically rare. Dual combinations of aPD-1 with more effective and less toxic IL-2 derivatives, e.g., CD122-directed pegylated IL-2, are also currently under investigation. Whether a combination of RT, aPD-1, and CD122-directed IL-2/anti-IL-2 complexes (IL-2c) can increase abscopal effects against established non-irradiated tumors is unknown. Also, in-depth analyses of the differentiation of tumor-specific CD8⁺ T cells have not yet been reported for aPD-1/IL-2c. We investigated how adding IL-2c to hRT/aPD1 affects tumor-specific CD8⁺ T cell differentiation and the potential of this triple combination to enhance the abscopal effect compared to the respective dual treatments.

Methods Mice bearing bilateral tumors were treated with two fractions of 8 Gy (C51 colon carcinoma model) or 12 Gy (B16 melanoma model); aPD1 was given weekly; IL-2c was given for five consecutive days. CD8 T cell-depleting and CXCR3-blocking antibodies were used to determine if the therapeutic effects depend on CD8⁺ and CXCR3⁺ T cells. Differentiation stages of tumor-specific CD8⁺ T cells in tumor-draining lymph nodes, spleen, blood, and tumors were determined flow cytometrically using MHC-I tetramers and various antibodies.

Results The abscopal effect was significantly stronger in triple-treated mice compared to mice treated with RT/aPD1 (C51 model: $p < 0.01$; B16 model: $p < 0.05$), RT/IL-2c (C51 model: $p < 0.01$; B16 model: $p < 0.001$) or aPD1/IL-2c (C51 model: $p < 0.0001$, B16 model: $p < 0.01$). Moreover, triple therapy improved survival and resulted in complete cures of 3/12 mice in the C51 model and 2/12 mice in the B16 model. These anti-tumor effects were associated with dramatic expansion of tumor-specific CD8⁺ T cells. Undifferentiated stem-like and effector-like but not terminally differentiated exhausted cells particularly strongly increased. Moreover, IL-2c induced CXCR3 mainly on non-terminally differentiated CD8⁺ T cells. Both CD8⁺ (C51 model: $p < 0.0001$; B16 model: $p < 0.01$) and CXCR3⁺ (C51 model: $p < 0.0001$) T cells were crucial for the RT-induced abscopal effect upon RT/aPD-1/IL-2c treatment.

Conclusions RT/aPD-1/IL-2c triple treatment resulted in superior local and systemic expansion of tumor-specific CD8⁺ T cells with stem- and effector-like phenotypes. Also, IL-2c strongly increased CXCR3⁺ CD8⁺ T cells that were associated with pronounced abscopal responses in models with an established metastasis resistant to aPD-1/IL-2c and only transiently responding to RT/aPD-1 or RT/IL-2c. Therefore, such triple combinations appear promising for clinical evaluation in metastatic patients.

Ethics Approval All animal experiments were approved by the Regierungspräsidium Freiburg, Germany (registration numbers: G18/066, G20-016).

<http://dx.doi.org/10.1136/jitc-2022-SITC2022.0868>

869

NBTXR3-ENHANCED PROTON BEAM IMMUNORADIOTHERAPY RESHAPES TUMOR IMMUNE MICROENVIRONMENT AND IMPROVES ABCOPAL EFFECT IN AN ANTI-PD1-RESISTANT LUNG CANCER

¹Yun Hu*, ²Sebastien Paris, ¹Narayan Sahoo, ¹Genevieve Bertolet, ¹Qi Wang, ¹Qianxia Wang, ¹Hampartsoum Barsoumian, ²Jordan SILVA, ¹Ailing Huang, ¹Claudia Kettlun Leyton, ¹Tiffany Voss, ¹Ethan Hsu, ¹Fatemeh Masrourpour, ¹Carola Leuschner, ¹Nahum Puebla Osorio, ¹Quynh Nguyen, ¹Saamil Gandhi, ¹Jing Wang, ¹Maria Cortez, ¹James Welsh. ¹MD Anderson Cancer Center, Houston, TX, United States; ²Nanobiotix, Paris, France

Background Proton beam therapy (PBT) has frequently yielded superior results to conventional X-ray therapy. However, combination of PBT with checkpoint inhibitors is rarely reported for treating metastatic cancers. NBTXR3 is a radioenhancer with immunomodulatory capacities able to restore efficacy of anti-PD1 (aPD1) in a model resistant to this treatment with conventional X-ray therapy. Therefore, we hypothesized that addition of NBTXR3 to localized PBT combined with aPD1 could enhance the systemic antitumor immune response in aPD1-resistant lung cancer in mice.

Methods Five groups of 8 mice each were inoculated with 5×10^4 aPD1-resistant 344SQR murine lung cancer cells in each hind leg, 4 days apart, to establish 'primary' (right, to-be-irradiated) and 'secondary' (left, not-to-be-irradiated) tumors. aPD1 (200 μ g) was intraperitoneally administered on days 7, 10, 14, 21, 28, 35, and 42. Primary tumors were intratumorally injected with NBTXR3 on day 7, followed by 12 Gy PBT on days of 8 and 9 (24 Gy total). The immune microenvironment of both irradiated and unirradiated tumors was analyzed through NanoString and single cell sequencing. On day 76, the right flank of the survivor mice treated with NBTXR3+PBT+aPD1 was rechallenged with 5×10^4 344SQR cells.

Results The therapies of PBT, PBT+aPD1, NBTXR3+PBT, and NBTXR3+PBT+aPD1 each resulted in significantly delayed growth in both primary and secondary tumors relative to control. In addition, adding NBTXR3 to both PBT and PBT+aPD1 significantly retarded the progress of the two tumors. Remarkably, the combination therapy of NBTXR3+PBT+aPD1 achieved 37.5% survival rate and the lowest number of lung metastases. Moreover, the survivor mice maintained potent antitumor immunological memory, effectively rejecting tumor re-challenge. NanoString analysis of immune-related genes revealed that the triple therapy (NBTXR3+PBT+aPD1) significantly upregulated the activities of a wide range of antitumor immune pathways in the two tumors. Single cell analysis demonstrated that both PBT+aPD1 and NBTXR3+PBT+aPD1 increased tumor infiltration by NKT cells, innate lymphoid cells, and CD8⁺ T cells, CD4⁺ T cells, and gamma delta T cells, as well as promoted cytotoxic lymphocyte activation. Lastly, PBT-mediated immunoradiotherapy enriched specific TCR repertoires that may target tumor antigens.

Conclusions PBT combined with aPD1 was able to potently activate systemic antitumor immunity and effectively control both irradiated and unirradiated tumors. In this context, the addition of NBTXR3 to PBT+aPD1 significantly improved treatment efficacy through modulating the tumor immune microenvironment.

Ethics Approval All mouse studies were approved by the Institutional Animal Care and Use Committee of MD Anderson Cancer Center.

<http://dx.doi.org/10.1136/jitc-2022-SITC2022.0869>

870 **HIGH-DOSE RADIATION IS REQUIRED FOR EFFECTIVE COMBINATION WITH TUMOR-SPECIFIC VACCINATION IN A PROSTATE CANCER MODEL**

Hemanth Potluri*, Carolina Ferreira, Joseph Grudzinski, Christopher Massey, Reinier Hernandez, Jamey Weichert, Douglas McNeel. *UW-Madison, Madison, WI, United States*

Background The approval of Sipuleucel-T demonstrates the value of antigen-specific vaccination approaches for prostate cancer. We have studied a DNA vaccine specific for the ligand-binding domain of the androgen receptor (pTVG-AR) as a more scalable vaccination approach, though its efficacy is limited by the immunosuppressive prostate microenvironment. Radiation has been shown to sensitize poorly responsive tumors to immunotherapy. Our group has developed a compound, NM600, that is selectively retained by tumors following intravascular delivery, and is therefore capable of delivering radiation systemically to metastases (targeted radionuclide therapy, TRT). In this study, we evaluated whether TRT or external beam radiation therapy (EBRT) in combination with pTVG-AR could improve anti-tumor efficacy by increasing antigen-specific CD8+ T cell tumor infiltration in a murine prostate cancer model.

Methods 6-week old male C57Bl/6 mice were implanted subcutaneously with TRAMP-C1 cells. pTVG-AR or empty vector were administered weekly from the day after tumor implantation. Mice were then given an intravenous injection of 50 ("low-dose") or 250 μ Ci ("high dose") ^{90}Y -NM600, estimated to deliver a dose of 1-2 Gy or 5-6 Gy to 300 mm^3 tumors, respectively. EBRT was delivered to flank tumors in a single fraction of 6-12 Gy. Groups of mice (n=5) were euthanized at several timepoints for flow cytometry analysis of the tumors. Separate cohorts (n=7) were followed for tumor growth.

Results Single-dose TRT did not have greater anti-tumor efficacy when used in combination with vaccine, regardless of TRT dose or the schedule of the vaccine. Combination treatment did not increase CD8+ T cell infiltration. However, TRT administered twice three weeks apart, in combination with pTVG-AR, significantly slowed tumor growth, unlike fractionated TRT alone (p=0.01). Combination-treated mice did not have greater infiltration of memory CD8+ T cells or T cells more responsive to antigen-specific stimulation. However, PD-1 expression was lower on infiltrating CD8+T cells (p=0.047) and PD-L1 expression was lower on dendritic cells (p=0.004). We then used EBRT to evaluate whether these differences might be dose-dependent. We found that vaccination combined with 12 Gy of EBRT, but not 6 Gy or 8 Gy, elicited a significantly improved anti-tumor response compared with EBRT alone (p<0.001).

Conclusions These data suggest that doses of RT in excess of 8 Gy, higher than what can be delivered by single treatment with ^{90}Y -NM600, may be necessary to optimally combine with antigen-specific vaccines in this model. Further work will explore the mechanism of this potential dose threshold.

Acknowledgements This work was supported by the National Institutes of Health (TL1 TR002375, P30 CA014520, P01 CA250972), the Prostate Cancer Foundation, and by the Department of Defense Prostate Cancer Research Program (W81XWH-19-1-0227 and W81XWH-19-1-0285).

<http://dx.doi.org/10.1136/jitc-2022-SITC2022.0870>

871 **IRRADIATION POTENTIATES NK CELLS FOR SURVEILLANCE AGAINST PARENTAL AND CANCER STEM CELLS OF HEPATOCELLULAR CARCINOMA THROUGH LFA-1/ICAM-1 AXIS**

¹Tung Uong Nguyen Thanh*, ¹Huy Nguyen Phuoc Quang, ²Mee Sun Yoon. ¹Chonnam National University, Hwasun, Republic of Korea.; ²Chonnam National University Hwasun Hospital, Hwasun, Republic of Korea

Background Radiation therapy (RT) is considered an effective local treatment for downstage or definitive therapy of inoperable localized hepatocellular carcinoma (HCC). However, the potential synergistic effect of RT in combination with local tumor irradiation, immune cytokines, and allogeneic NK cells has not been explored in metastatic liver cancer. In this study, we evaluated the efficacy of combination therapy in both localized and metastatic human liver cancer models.

Methods *Ex vivo* expansion of NK cells from human peripheral blood mononuclear cells was performed by co-culture with irradiated K562 cells. HepG2/HepG2-Luciferase and Hep3B cells were injected into the right lobe of the liver or intraperitoneally injected into NOD-SCID IL2 receptor gamma chain knockout (NSG) mice. A 2 Gy RT was delivered to the peritoneum or liver tumor of NSG mice. A 12 Gy local RT was applied to the HCC subcutaneous tumor. HCC tumor spheres were generated to evaluate the function of combination treatment against liver cancer stem cells (CSCs). Finally, HepG2 and Hep3B ICAM-1 knockout (KO) cells were generated using CRISPR/CAS9 to clarify the role of the LFA-1/ICAM-1 axis in combination therapy.

Results Allogeneic NK cells enhanced recognition and conjugation of irradiated liver cancer cells through the LFA-1(lymphocyte function-associated antigen 1)/ICAM-1(intercellular adhesion molecule-1) axis. In addition, combination with RT and IL-15 also increased allogeneic NK cells' degranulation ability against ICAM-1 positive HCC cell lines. Knock-out ICAM-1 in HepG2 cells significantly reduced the lysis and cytokine release ability of NK cells. The combination therapy significantly improved therapeutic efficacy over the monotherapies against localized liver tumors in subcutaneous (HepG2) and orthotopic (HepG2 and Hep3B) mice models. Interestingly, expanded NK cells pretreated with LFA-1 inhibitor before infusion failed to enhance the therapeutic efficacy against Hep3B tumors compared to RT treatment alone. Knockout ICAM-1 in HepG2 also prevented the combination therapy in controlling tumor growth in the xenografted model. In the metastasis model, the combination therapy enhanced the recognition and lysis of EPCAM+CD133+CD24 + CSCs by NK cells, which led to the improving survival of the mice. Moreover, the deficiency of ICAM-1 in the HepG2 and Hep3B tumor spheres also reduced the cytolysis ability of expanded NK cells. The LFA-1/ICAM-1 axis also correlated with better prognosis in patients with metastasis from the PANCAN database.

Conclusions Our data suggested that combination therapy enhances the ability of allogeneic NK cells to recognize and eliminate both parental and liver CSCs through LFA-1/ICAM-1.

Ethics Approval All animal procedures and experiments were approved by the Institutional Animal Care and Use Committee of Chonnam National University (CNU IACUC-H-2019-7).

<http://dx.doi.org/10.1136/jitc-2022-SITC2022.0871>

872 LIPOSOMAL DOXORUBICIN ENHANCES THE RADIATION-INDUCED ABCOPAL EFFECT BY PROMOTING THE RELEASE OF TUMOR CELL MITOCHONDRIAL DNA

Liquan Wang*, Ren Luo, Kateryna Onyshchenko, Gabriele Niedermann. *University of Freiburg, Freiburg, Germany*

Background Localized radiotherapy (RT) can cause a T cell-mediated abscopal effect on non-irradiated tumor lesions, particularly in combination with immune checkpoint blockade (ICB). By using syngeneic tumor models, we studied whether adding low-dose doxorubicin to RT and α PD-1 can enhance the RT-induced abscopal effect.

Methods In mice bearing bilateral subcutaneous tumors, the primary tumor was irradiated with 2×12 Gy (B16-CD133 melanoma model) or 3×8 Gy (MC38 colon carcinoma model). Liposomal doxorubicin (4 mg/kg) was given i.v. once together with RT; α PD1 was given weekly. Tumor growth and survival of mice were determined (5–9 mice per group). Depleting antibodies were used to elucidate whether the abscopal effect depended on CD8⁺ T cells. Tumor-specific CD8⁺ T cells were determined flow cytometrically using MHC tetramers and various antibodies. Mitochondrial DNA (mtDNA) was depleted in tumor cells with Zalcitabine. *In vitro*, extracellular (e)ATP release by tumor cells was determined by CellTiter-Glo[®] 2.0. Tumor cell production of type I Interferon (IFN β 1) was measured by ELISA with/without incubation with cGAS-STING pathway inhibitors. CXCL10, cytosolic genomic DNA (gDNA), and cytosolic mtDNA were measured by qPCR.

Results Abscopal tumor control was as follows: RT/ α PD-1/doxorubicin > doxorubicin/ α PD-1 ($p < 0.01$) \approx RT/doxorubicin ($p < 0.01$) \approx RT/ α PD-1 ($p < 0.05$) (B16 melanoma model); RT/ α PD-1/doxorubicin > RT/ α PD-1 ($p < 0.01$) \approx RT/doxorubicin ($p < 0.001$) \approx doxorubicin/ α PD-1 ($p < 0.01$) (MC38 colon carcinoma model). Experiments with various inhibitors of the cGAS/STING pathway showed that liposomal doxorubicin induced type I IFN through the cGAS/STING pathway ($p < 0.05$ with vs. without inhibitors). In mtDNA-depleted tumor cells, doxorubicin induced less cytosolic mtDNA ($p < 0.001$) (but not less cytosolic genomic DNA), less IFN β 1 secretion ($p < 0.05$), less eATP release ($p < 0.0001$), and less CXCL10 ($p < 0.0001$) than in non-mtDNA-depleted tumor cells. Triple therapy with RT, α PD-1, and liposomal doxorubicin induced more mature dendritic cells ($p < 0.05$) and more tumor-specific CD8⁺ T cells ($p < 0.01$) compared to RT/ α PD-1 and doxorubicin/ α PD-1 therapy. When CD8⁺ T cells were depleted or mtDNA-depleted tumor cells were implanted, the doxorubicin-induced enhancement of the abscopal effect was abolished ($p < 0.05$).

Conclusions Single low-dose liposomal doxorubicin can substantially enhance the RT-induced abscopal effect in conjunction with α PD-1. mtDNA leakage induced by doxorubicin appears crucial for the doxorubicin-enhanced RT-induced abscopal effect. These findings may be helpful for the planning of clinical radiochemoimmunotherapy trials in (oligo) metastatic patients.

Ethics Approval All animal experiments were approved by the animal care committee of the Regierungspräsidium Freiburg (registration number: G18-066).

<http://dx.doi.org/10.1136/jitc-2022-SITC2022.0872>

873

RADIATION-INDUCED DYNAMIC ALTERATIONS IN PD-1/PD-L1 ACTIVITY AND RELEVANT IMMUNE CELL PROFILES DEPENDING ON TREATMENT RESPONSE STATUS IN MOUSE TUMOR MODELS

¹Yi Na Yoon*, ²Yu Jin Lim, ¹Jae-Sung Kim. ¹*Korea Institute of Radiological & Medical Sciences, Seoul, Republic of Korea;* ²*Kyung Hee University College of Medicine, Seoul, Republic of Korea*

Background In order to assess the immunologic effects of anti-cancer treatment and their therapeutic implications, we investigated the dynamic changes in programmed death-1 (PD-1)/programmed death ligand-1 (PD-L1) expression patterns caused by radiotherapy (RT).

Methods In the CT26 mouse model, local RT with 2 Gy × 5 or 7.5 Gy × 1 was treated on the tumors. Tumors were excised and analyzed at certain time points depending on radiation response status: baseline, early (immediately after RT), middle (beginning of tumor reduction), late (stable state with RT impact), and progression (tumor regrowth). The activity of PD-1/PD-L1 and associated immune cell profiles were quantitatively measured.

Results RT potentiated PD-L1 expression levels in tumor cells from the middle to the late phase, which thereafter dropped to the equivalent PD-L1 levels to baseline in the progression phase. The fractionated RT treatment resulted in a lower degree of tumor regression than the 7.5 Gy regimen, although the frequency of PD-L1⁺ myeloid-derived suppressor cells remained greater. In the progression phase, the frequency of PD-1⁺ and interferon (IFN)- γ ⁺ CD8 T cells was increased, meanwhile the mean fluorescence intensity (MFI) values of IFN- γ started to drop. The proportion of PD-1⁺CD8⁺ T cells in the spleen was dramatically increased and maintained longer with 2 Gy × 5. Further, we confirmed that RT promoted the overall transcription levels of immune-related genes in the transcriptome data, supporting previously confirmed sequential patterns.

Conclusions According to time-course radiation responses, the dynamic changes in PD-1/PD-L1 activity were analyzed. The sequential patterns and dose-fractionation effects should be considered to determine relevant radioimmunotherapy regimens.

Consent Written informed consent was obtained from the patient for publication of this abstract and any accompanying images. A copy of the written consent is available for review by the Editor of this journal.

<http://dx.doi.org/10.1136/jitc-2022-SITC2022.0873>

874

OPTIMIZING A COMBINATION RADIO-IMMUNOTHERAPY REGIMEN IN A PRECLINICAL MODEL OF TREATMENT-RESISTANT, HIGH-RISK NEUROBLASTOMA

Lauren Zebertavage*, Amy Erbe, Taylor Aiken, Allison Schopf, Megan Nielsen, Sydney Katz, Zachary Morris, Alexander Rakhmievich, Paul Sondel. *University of Wisconsin, Madison, WI, United States*

Background Neuroblastoma (NBL), a cancer derived from neural crest precursor cells, is the most common extra-cranial solid tumor in children, with a median age of diagnosis of 22 months. Patients diagnosed with NBL are segmented into prognostic categories with ~50% categorized as high-risk (HR). Of these patients, ~40% are refractory to, or relapse following, initial treatment; there are currently no effective treatment options for these patients once they have failed salvage therapy of chemotherapy combined with α GD2 therapy (dinutuximab). Our group has previously published work developing a combination adaptive and innate immunotherapy regimen, "CAIR", to treat a murine model of treatment-resistant, HR-NBL.^{1,2} CAIR utilizes α GD2 immunocytokine (hu14.18-IL2), radiotherapy (RT), α CD40, CpG, and α CTLA4 but questions remain about the relative contribution of each component. In this study, we tested if our model of HR-NBL is resistant to salvage therapy of temozolomide and irinotecan (TEM+IRI) and α GD2-based therapy and if components of our effective CAIR therapy can be removed, in order to determine their necessity.

Methods To establish 9464D-GD2 as a model for treatment-resistant, HR-NBL, tumor-bearing mice were treated with TEM+IRI and/or hu14.18-IL2. To establish the necessity of each component of CAIR, mice bearing 9464D-GD2 tumors were treated with CAIR (12Gy RT, α CD40, α CTLA4, CpG, and hu14.18-IL2) or variations of CAIR subtracting one component.

Results Salvage therapy of TEM+IRI and/or hu14.18-IL2 extended the survival of mice ($p < 0.03$) but did not result in 9464D-GD2 tumor cures. Adding RT (12Gy, SARRP) improved survival ($p < 0.0001$), but not more than RT alone ($p = 0.29$), and still did not cure tumors.

Removing RT or hu14.18-IL2 from CAIR dramatically shortened survival ($p < 0.0001$) and yielded few tumor cures (1/16, 0/16 versus 13/30). Conversely, removing α CD40, α CTLA4, or CpG did not alter survival ($p = 0.81$, $p = 0.85$, $p = 0.70$) relative to CAIR, and resulted in similar rates of tumor cures (8/16, 9/21, 7/16 versus 13/30). Removing two of the "expendable" components (α CD40, α CTLA4, CpG) generally reduced efficacy, with only CAIR subtracting CpG and α CTLA4 (RT, hu14.18-IL2, and α CD40) curing a similar number of mice as CAIR (3/16 versus 13/30, survival $p = 0.12$).

Conclusions Here we demonstrate that 9464D-GD2 tumors behave similarly to human HR-NBLs that fail to be cured by salvage therapy. In contrast, these tumors can be cured by both CAIR therapy and by several versions of a reduced CAIR therapy (CAIR subtracting α CD40, α CTLA4, or CpG). We are now exploring the role of each component of CAIR in anti-tumor immune responses in this immunologically cold model.

REFERENCES

1. Voeller J, Erbe A, Slowinski J, et al. Combined innate and adaptive immunotherapy overcomes resistance of immunologically cold syngeneic murine neuroblastoma to checkpoint inhibition. *J Immunother Cancer*. 2019;7:344.

2. Aiken T, Erbe A, Zebertavage L, et al. Mechanism of effective combination radio-immunotherapy against 9464D-GD2, an immunologically cold murine neuroblastoma. *J Immunother Cancer*. 2022;10:e004834.

Ethics Approval The study was approved by the University of Wisconsin's School of Medicine and Public Health Institutional Animal Care and Use Committee (IACUC), protocol: M005984.

<http://dx.doi.org/10.1136/jitc-2022-SITC2022.0874>

875 **TARGETING CCR8-EXPRESSING TUMOR INFILTRATING TREGS IN COMBINATION WITH RADIOTHERAPY ENHANCES ANTI-TUMOR IMMUNITY**

Yurun Zhang*, Vikash Bhagwandin, Sandra Hatcher, Ziyun Ding, Liang Tang, Ricky Sharma, Sophia Pfister. *Varian, a Siemens Healthineers Company, Los Altos, CA, United States*

Background Tumor infiltrating Tregs (TITRs) negatively regulates anti-tumor immunity and promotes tumor progression. Increased level of TITRs has also been associated with poor prognosis in multiple cancer types which led to identification of several TITR specific therapeutic targets. Chemokine receptor CCR8 is highly enriched in the TITR population. Depletion of TITR via anti-CCR8 antibody resulted in potent anti-tumor efficacy as single agent in checkpoint inhibitor responsive syngeneic models.¹ At Varian, immune profiling of *ex vivo* irradiated human head and neck tumors showed decreased viability in CD4⁺ and CD8⁺ T cells but not in the TITR population, which suggest depleting TITR as a therapeutic strategy to improve efficacy of radiotherapy (RT). Here, we hypothesized that combining anti-CCR8 with RT improves anti-tumor response via TITR depletion.

Methods To investigate the therapeutic potential of combining anti-CCR8 with RT, female Balb/c mice were orthotopically implanted with 4T1-Luc2-1A4 cells in mammary fat pad followed by focal radiation. Implanted mice were irradiated at 0 or 10 Gy on day 7 post-implantation. Anti-mouse CCR8 depleting antibody (BioLegend) or isotype control was administered intraperitoneally at 10 mg/kg on day 7, 10, and 14 post-implantation. Tumor measurements were taken three times per week for 47 days for efficacy evaluation. On day 15 post-implantation, treated and non-treated tumors were harvested for flow cytometric and bulk-RNA sequencing analyses.

Results Combining anti-CCR8 treatment with 10 Gy radiation significantly improved anti-tumor efficacy compared with anti-CCR8 treatment alone or radiation treatment alone. One day following completion of anti-CCR8 treatment, we observed increased percentage of CD8⁺ T cells ($p < 0.01$) and decreased percentage of TITRs ($p < 0.05$) in anti-CCR8-treated and irradiated tumors versus anti-CCR8 treatment alone. Tumor CD8⁺ T cells also demonstrated increased expression of activation marker CD39 ($p < 0.01$) in anti-CCR8 plus RT treated tumors. At the transcriptional level, combination of anti-CCR8 with radiation upregulated pathways associated with TNF- α and IFN- γ response in comparison to single-agent treatment, suggesting activation of anti-tumor immunity via enhanced T cell activation. Furthermore, anti-CCR8 plus RT significantly prolonged survival of tumor-bearing mice (78% alive) compared with anti-CCR8 treatment alone (11% alive).

Conclusions Our preclinical data demonstrate high therapeutic potential of combining anti-CCR8 depleting antibody with radiotherapy to trigger synergistic enhancement of immune response in tumors that are refractory to immune checkpoint blockade. In conclusion, targeting CCR8-expressing TITRs in combination with radiotherapy displayed superior anti-tumor activity and prolonged survival than single-agent treatment alone.

REFERENCE

1. Campbell JR, et al. Fc-Optimized Anti-CCR8 Antibody Depletes Regulatory T Cells in Human Tumor Models. *Cancer Res.* 2021;**81**(11):2983–2994.

Ethics Approval De-identified human head and neck squamous cell carcinoma samples were obtained from Cooperative Human Tissue Network (CHTN) under a CHTN IRB-approved protocol, in accordance with the Department of Health and Human Services regulations for the protection of human subjects (45 CFR Part 46).

<http://dx.doi.org/10.1136/jitc-2022-SITC2022.0875>

876 **VOLUMETRIC MUSCLE LOSS INJURY IMPACTS MURINE TUMOR GROWTH AND RESPONSE TO IMMUNE CHECKPOINT BLOCKADE THERAPY**

Anna Ruta*, Jordan Garcia, Locke Davenport Huyer, Joscelyn Mejias, Kavita Krishnan, Helen Nguyen, Elise Gray-Gaillard, Jin Han, Andrew Pardoll, Jennifer Elisseeff. *Johns Hopkins University, Baltimore, MD, United States*

Background Tumor resection and subsequent surgical reconstruction is a prevalent, often effective, treatment approach for many operable solid cancers. Unfortunately, post-operative surgical trauma and tissue injury induce major physiological stressors (i.e. acute inflammation and subsequent wound-healing) that can contribute to cancer progression, recurrence and metastatic spread. In this study, we investigate whether effectively treating distal tissue injuries with biologically-derived wound-healing therapeutics can help mitigate injury-induced accelerated tumor progression. Given the numerous clinical trials underway that couple surgical intervention with (neo)adjuvant immune checkpoint blockade (ICB) treatment, we further explore whether physiological stress due to tissue injury can impact tumor responsiveness to ICB therapy.

Methods A concurrent biological insult murine model was established in which a bilateral volumetric muscle loss (VML) injury, consisting of a 3x4mm excisional defect performed in the quadriceps muscles, is followed by subcutaneous inoculation of syngeneic cancer cells on the flank (CT26 colon carcinoma and B16F10 melanoma, 100,000 cells/mouse). Wound-healing was promoted by directly implanting a porcine-derived decellularized extracellular matrix (ECM) scaffold into the muscle injury site. The ICB treatment regimen consisted of either aPD1 (5mg/kg, RMP1-14) monotherapy or aPD1/aCTLA4 (5mg/kg, 9H10) combination therapy delivered via intraperitoneal injection for 4 total doses. Tumor size was measured every 2-3 days with predetermined survival criteria of tumor volume >1500mm³. The immunological landscape of tumors and draining lymph nodes was assessed via high-parameter flow cytometry, transcriptional analysis (RT-qPCR, bulk RNA sequencing) and immunofluorescence staining of paraffin-embedded tissue sections.

Results VML injury accelerated CT26 and B16F10 tumor growth in comparison to the non-injured control group. However, treatment of the VML injury site with pro-regenerative ECM scaffold slowed tumor progression to match the non-injured baseline. Tumors harvested from mice with ECM-treated muscle injuries displayed an elevated type 2 immune signature, marked by CD206+ M2 macrophages and interleukin (IL)-4 production by CD4+ T cells and myeloid cells. Lastly, mice with concurrent VML injury exhibited impaired response to ICB treatment measured by faster tumor growth and shortened overall survival.

Conclusions Physiological stress induced by tissue injury can impact tumor growth kinetics, immunological phenotype of tumor microenvironment, and responsiveness to ICB therapy. Treatment of injury site with wound-healing biomaterials may offer a novel approach to reducing exacerbated tumor outcomes. Further studies will help discern the immunological mechanisms that connect concurrent tissue injury and tumor insults.

Ethics Approval All animal studies were performed in accordance with approved Johns Hopkins University Animal Care and Use Committee protocol (Elisseeff, MO21M80).

<http://dx.doi.org/10.1136/jitc-2022-SITC2022.0876>

877

BLOCKING SOLUBLE TNF α SENSITIZES HER2-POSITIVE BREAST CANCER TO TRASTUZUMAB THROUGH MUC4 DOWNREGULATION AND SUBVERTS IMMUNOSUPPRESSION

¹Sofia Bruni*, ²Mara De Martino, ¹Florencia Mauro, ¹Maria Mercogliano, ¹Cecilia Proietti, ¹Rosalía Cordo-Russo, ¹Patricia Elizalde, ¹Roxana Schillaci. ¹Instituto de Biología y Medicina Experimental (IBYME-CONICET), Buenos Aires, Argentina; ²Department of Radiation Oncology, Weill Cornell Medical College, New York, NY, United States

Background Trastuzumab resistance is an important clinical issue. Although a plethora of resistance mechanisms have been characterized, few have been shown to be actionable. We have demonstrated that soluble TNF α isoform (sTNF α) upregulates mucin 4 (MUC4) expression, which shields the trastuzumab epitope on HER2, hindering its therapeutic effect *in vitro* and *in vivo*.^{1,2} Since the success of trastuzumab treatment relies on immune response, we addressed the role of MUC4 on modulating the tumor immune infiltrate to foster immune evasion in sTNF α -induced trastuzumab-resistant HER2-positive (HER2 +) breast cancer.

Methods *De novo* trastuzumab-resistant JIMT-1 and KPL-4 cell lines were engineered to express a doxycycline-inducible MUC4 shRNA (JIMT-1-shMUC4 and KPL-4-shMUC4, respectively). Female nude mice bearing these s.c. tumors (~100 mm³), were treated i.p with IgG or trastuzumab (5mg/kg), a dominant negative (DN) sTNF α inhibitor (10 mg/kg) or trastuzumab+DN (n=4-6 per group). After 3 weeks of treatment, tumor-infiltrating immune cells were studied by immunofluorescence and flow cytometry. For macrophage and NK cell depletion, clodronate or anti-asialo GM1 was used, respectively. ADCP was studied using parental JIMT-1 cells pre-cultured for 48h with DN (10 μ g/ml) or vehicle and then co-cultured with human macrophages for 1.5 h. A cohort of 91 HER2+ breast cancer patients treated with trastuzumab was used to correlate tumor MUC4 expression with tumor-infiltrating lymphocytes (TILs).

Results Upon MUC4 silencing through doxycycline induction, trastuzumab antitumor effect was reinstated (80% or 85% tumor growth inhibition, JIMT-1-shMUC4 or KPL-4-shMUC4, respectively; p<0.0001). The addition of DN did not further decrease tumor burden. In the absence of doxycycline, trastuzumab+DN inhibited tumor growth and modified the immunosuppressive tumor milieu, increasing M1-like macrophage polarization (p<0.01) and NK cell degranulation (p<0.01). In MUC4-silenced tumors, trastuzumab treatment alone mimics this tumor infiltrate. Depletion experiments revealed a cross-talk between macrophages and NK cells necessary for trastuzumab+DN antitumor effect. When MUC4 was silenced, trastuzumab antitumor effect was lost upon macrophage depletion, but it was preserved when NK cells were absent. Furthermore, JIMT-1 cells pre-treated with DN were more susceptible to trastuzumab-dependent cellular phagocytosis (p<0.05). Finally, MUC4 expression in HER2+ breast cancer negatively correlated with TILs (p=0.004), reflecting “immune desert” tumors.

Conclusions In all, we conclude that sTNF α isoform blockade is able to tackle MUC4 expression and, together with trastuzumab, triggers an effective antitumor immune response that relies on M1-macrophage-NK cell collaboration. These findings provide rationale to pursue sTNF α blockade combined with trastuzumab or trastuzumab drug-conjugates for MUC4+ and HER2+ breast cancer patients to overcome trastuzumab resistance.

REFERENCES

1. Mercogliano MF, De Martino M, Venturutti L, et al. TNF α -Induced Mucin 4 Expression Elicits Trastuzumab Resistance in HER2-Positive Breast Cancer. *Clin Cancer Res* 2017 23:636–48.
2. Bruni S, De Martino M, Mauro FL, et al. Soluble TNF α induced mucin 4 is a mediator of trastuzumab resistance and of an immunosuppressive tumor microenvironment in HER2+ breast cancer. *J. Immunotherapy Cancer* 7, 2019;283:039. doi:10.1186/s40425-019-0764-0

Ethics Approval Patient samples were collected with the patient's informed consent and with Helsinki approval from Hospital Fernández (CEI # 201629) and Henry Moore Institute of Oncology, (Buenos Aires, Argentina) and from Hospital Oncológico Provincial de Córdoba (Cordoba, Argentina). All animal studies were conducted in accordance with the highest standards of animal care as outlined by the NIH Guide for the Care and Use of Laboratory Animals and were approved by the Institutional Animal Care and Use Committee (IACUC) of IBYME.

<http://dx.doi.org/10.1136/jitc-2022-SITC2022.0877>

878 **BET INHIBITION SENSITIZES IMMUNOLOGICALLY-COLD RB-DEFICIENT PROSTATE CANCER TO IMMUNE CHECKPOINT BLOCKADE VIA DNA DAMAGE-INDUCED STING/NF- κ B/TYPE I IFN SIGNALING**

¹Kiranj Chaudagar, ²Marguerite Li*, ²Christina Hong, ¹Srikrishnan Rameshbabu, ¹Raymond Chen, ²Alison Thomas, ²Brian Olson, ¹Akash Patnaik. ¹University of Chicago, Chicago, IL, United States; ²Emory University, Atlanta, GA, United States

Background Non-T cell-inflamed immunologically “cold” tumor microenvironments (TME) are associated with poor responsiveness to immune checkpoint blockade (ICB), and can be sculpted by tumor cell genomics. We have previously described how Retinoblastoma (Rb) tumor suppressor loss of function, one of the most frequent alterations in human cancer and associated with lineage plasticity, poor prognosis and therapeutic outcomes, promotes an immunosuppressive TME *in vitro* and *in vivo*. Here, we evaluated how inhibition of the bromodomain and extraterminal (BET) domain family can reverse the consequences of Rb loss to enhance the efficacy of ICB.

Methods Wild-type or Rb-deficient murine MycCaP tumor cells were evaluated *in vitro* and *ex vivo* for how BET inhibition (BETi) alters DNA damage and type I IFN signaling pathways by qRT-PCR, Western blot, ELISA, and ImageStream analysis. Tumor-bearing animals were treated with BETi (alone or with STING or NF- κ B inhibition), and immune infiltration into the TME was evaluated by flow cytometry. Anti-tumor responses to BETi was evaluated in the presence or absence of T cell and/or macrophage depletion. Finally, BETi was combined with PDL1 blockade, with or without androgen deprivation therapy (ADT), and anti-tumor responses were evaluated in the presence or absence of STING/NF- κ B blockade.

Results BETi was found to increase tumor cell-intrinsic DNA damage, which induced STING/NF- κ B signaling and type I IFN expression and T cell migration in Rb-deficient tumor cells, in part due to increased baseline STING expression following Rb loss. *In vivo* BETi treatment increased T cell infiltration into the TME and suppressed Rb-deficient tumor growth that were T cell- and macrophage-dependent as well as STING/NF- κ B-dependent. BETi alone increased PD-1 expression on tumor-infiltrating T cells and PD-L1 expression on suppressive M2 and MDSC populations *in vivo*, resulting in increased susceptibility to combined BETi and PDL1 blockade in Rb-deficient tumors *in vivo*. Finally, ADT further enhanced the efficacy of BETi and ICB in a STING/NF- κ B-dependent fashion.

Conclusions These data demonstrate that BETi increases immune infiltration into the immunologically-cold Rb-deficient TME via activation of tumor cell-intrinsic STING/NF- κ B activation and type I IFN signaling within tumor cells. This results in differential macrophage and T cell-mediated inhibition of Rb-deficient prostate tumor growth and sensitization of Rb-deficient prostate cancer to ICB. This provides the mechanistic rationale to test combinations of ADT, BETi and ICB in clinical trials of Rb-deficient hormone-sensitive metastatic prostate cancer.

<http://dx.doi.org/10.1136/jitc-2022-SITC2022.0878>

879

REVERSAL OF LACTATE AND PD-1-MEDIATED MACROPHAGE IMMUNOSUPPRESSION CONTROLS GROWTH OF PTEN/P53-DEFICIENT PROSTATE CANCER

¹Akash Patnaik*, ¹Kiranj Chaudagar, ¹Hanna Hieromnimon, ²Taghreed Hirz, ²Shenglin Mei, ²David Sykes. ¹University of Chicago, Chicago, IL, United States; ²Massachusetts General Hospital, Boston, MA, United States

Background There has been renewed interest in immunotherapy for the treatment of advanced prostate cancer (PC), partly based on the anti-tumor immune activation that occurs with ADT, and partly based on the clinical responses to immune checkpoint inhibitors (ICI) targeting CTLA-4 and PD-1/PD-L1 in other cancers.¹⁻³ However, only 10-25% of metastatic castrate-resistant prostate cancer (mCRPC) patients respond to ICI, with a lack of durable benefit in the majority of patients.⁴⁻⁵ PTEN LOF alterations, which occur in approximately 50-75% of mCRPC patients, are associated with poor prognosis, development of metastases,⁶⁻⁸ and immunosuppressive tumor microenvironment.⁹⁻¹¹ Given the aggressive natural history and poor therapeutic outcomes of PTEN-mutant advanced PC to standard-of-care hormonal therapies,⁶ chemotherapies¹² and ICI,¹⁰ a deeper understanding of immune evasion mechanisms is critical for the discovery of new therapeutic strategies to effectively treat this molecular subset of AVPC.

Methods Prostate-specific PTEN/p53-deficient genetically engineered mice (GEM) (40) were screened for autochthonous prostate tumor development and monitored for response to therapy by ultrasound and MRI, respectively. Following the development of 150-200 mm³ solid tumors, the mice were treated with either androgen deprivation therapy (degarelix), PI3K inhibitor (copanlisib), or PD-1 antibody, as single agents or their combinations. Harvested tumors following *in vivo* treatment underwent flow cytometry, or utilized for *ex vivo* studies on single cell suspensions or sorted TAM. Single cell RNAseq on human metastatic bone and lymph node samples were performed using established methods.¹³

Results We performed co-clinical trials in prostate-specific PTEN/p53-deficient genetically engineered mice, and discovered that recruitment of PD-1-expressing tumor-associated macrophages (TAM) thwarts androgen deprivation therapy (ADT)/PI3K inhibitor (PI3Ki) combination-induced tumor control. Strikingly, we observed TAM-dependent ~3-fold increased anti-cancer response with ADT/PI3Ki/PD-1 antibody (aPD-1) combination. Mechanistically, decreased lactate production from PI3Ki-treated tumor cells suppressed histone lactylation within TAM, resulting in their phagocytic activation, which was augmented by ADT/aPD-1 treatment and attenuated by feedback activation of Wnt/ β -catenin-pathway. Furthermore, single-cell RNA-sequencing analysis in mCRPC patient biopsy samples revealed a direct correlation between high glycolytic activity and TAM phagocytosis suppression.

Conclusions Our findings demonstrate that immunometabolic strategies to reverse lactate and PD-1-mediated TAM immunosuppression by PI3Ki and aPD-1, respectively, in combination with ADT, controls tumor growth and warrants further clinical investigation in PTEN/p53-deficient mCRPC.

REFERENCES

1. Wolchok JD, Chiarion-Sileni V, Gonzalez R, Rutkowski P, Grob JJ, Cowey CL, et al. Overall survival with combined nivolumab and ipilimumab in advanced melanoma. *N Engl J Med* 2017;**377**(14):1345–56. doi: 10.1056/NEJMoa1709684.
2. Sharma P, Allison JP. Dissecting the mechanisms of immune checkpoint therapy. *Nat Rev Immunol* 2020;**20**(2):75–86. doi: 10.1038/s41577-020-0275-8.

3. Gamat M, McNeel DG. Androgen deprivation and immunotherapy for the treatment of prostate cancer. *Endocr Relat Cancer* 2017;**24**(12):T297–T310. doi: 10.1530/ERC-17-0145.
4. Antonarakis ES, Piulats JM, Gross-Goupil M, Goh J, Ojamaa K, Hoimes CJ, et al. Pembrolizumab for treatment-refractory metastatic castration-resistant prostate cancer: multicohort, open-label phase II KEYNOTE-199 Study. *J Clin Oncol* 2020;**38**(5):395–405. doi: 10.1200/JCO.19.01638.
5. Sharma P, Pachynski RK, Narayan V, Flechon A, Gravis G, Galsky MD, et al. Initial results from a phase II study of nivolumab (NIVO) plus ipilimumab (IPI) for the treatment of metastatic castration-resistant prostate cancer (mCRPC; CheckMate 650). *Journal of Clinical Oncology* 2019;**37**:142.
6. Jamaspishvili T, Berman DM, Ross AE, Scher HI, De Marzo AM, Squire JA, et al. Clinical implications of PTEN loss in prostate cancer. *Nat Rev Urol* 2018;**15**(4):222–34. doi: 10.1038/nrurol.2018.9.
7. Wang S, Gao J, Lei Q, Rozengurt N, Pritchard C, Jiao J, et al. Prostate-specific deletion of the murine Pten tumor suppressor gene leads to metastatic prostate cancer. *Cancer Cell* 2003;**4**(3):209–21. doi: 10.1016/s1535-6108(03)00215-0.
8. Robinson D, Van Allen EM, Wu YM, Schultz N, Lonigro RJ, Mosquera JM, et al. Integrative Clinical Genomics of Advanced Prostate Cancer. *Cell* 2015;**162**(2):454. doi: 10.1016/j.cell.2015.06.053.
9. Di Mitri D, Mirenda M, Vasilevska J, Calciniotto A, Delaleu N, Revandkar A, et al. Re-education of Tumor-Associated Macrophages by CXCR2 Blockade Drives Senescence and Tumor Inhibition in Advanced Prostate Cancer. *Cell Rep* 2019;**28**(8):2156–68. e5. doi: 10.1016/j.celrep.2019.07.068. gene leads to metastatic prostate cancer. *Cancer Cell* 2003;**4**(3):209–21 doi: 10.1016/s1535-6108(03)00215-0.
10. Cetintas VB, Batada NN. Is there a causal link between PTEN deficient tumors and immunosuppressive tumor microenvironment? *J Transl Med* 2020;**18**(1):45. doi: 10.1186/s12967-020-02219-w.
11. Peng W, Chen JQ, Liu C, Malu S, Creasy C, Tetzlaff MT, et al. Loss of PTEN Promotes Resistance to T Cell-Mediated Immunotherapy. *Cancer Discov* 2016;**6**(2):202–16. doi: 10.1158/2159-8290.CD-15-0283.
12. Toso A, Revandkar A, Di Mitri D, Guccini I, Proietti M, Sarti M, et al. Enhancing chemotherapy efficacy in Pten-deficient prostate tumors by activating the senescence-associated antitumor immunity. *Cell Rep* 2014;**9**(1):75–89. doi: 10.1016/j.celrep.2014.08.044.
13. Kfoury Y, Baryawno N, Severe N, Mei S, Gustafsson K, Hirz T, et al. Human prostate cancer bone metastases have an actionable immunosuppressive microenvironment. *Cancer Cell* 2021;**39**(11):1464–78 e8. doi: 10.1016/j.ccell.2021.09.005.

Ethics Approval Murine experiments were performed in accordance with NIH guidelines and protocol approved by the Institutional Animal Care and Use Committee (IACUC) at University of Chicago (ACUP 72483-12). Bone metastatic PC samples were collected and handled in accordance to the protocol approved by the Institutional Review Board (IRB, Dana Farber/Harvard Cancer Center protocol 13-416 and Partners protocol 2017P000635/PHS). For metastatic lymph nodes of PC patients, baseline biopsies were collected and processed as mentioned in the investigator-initiated, IRB-approved clinical trial (IRB-18-0154 of Chicago, NCT03572478) of rucaparib in combination with nivolumab, co-sponsored by Clovis Oncology and Bristol Myers Squibb.

<http://dx.doi.org/10.1136/jitc-2022-SITC2022.0879>

880 **ACTIVATION OF STAT3 SIGNALING IS ASSOCIATED WITH RESISTANCE TO IMMUNE CHECKPOINT INHIBITORS IN PATIENTS (PTS) WITH METASTATIC RENAL CELL CARCINOMA (MRCC)**

¹Alexander Chehrizi-Raffle*, ¹Marice Alcantara, ²Nazli Dizman, ¹Wilson Tang, ¹Luis Meza, ²Zeynep Zengin, ¹Dongfang Wang, ¹Dayson Moreira, ¹Daniela Castro, ¹Ameish Govindarajan, ³Alan Horsager, ¹JoAnn Hsu, ¹Sumanta Pal, ¹Marcin Kortylewski. ¹City of Hope Comprehensive Cancer Center, Duarte, CA, United States; ²Yale University School of Medicine, New Haven, CT, United States; ³Duet Biotherapeutics, Pasadena, CA, United States

Background Frontline nivolumab plus ipilimumab (N+I) has dramatically improved outcomes in mRCC pts. Nevertheless, only a minority of pts achieve an objective response to therapy. We investigated whether serum cytokine dynamics in pts receiving N+I can elucidate immunotherapy resistance mechanisms. We also evaluated targeted STAT3 inhibition combined with anti-PD-1 in a preclinical model.

Methods Pts who received N+I as first-line treatment of mRCC with baseline and week 12 (+/- 4 weeks) blood samples were identified using an institutional database. Spectral cytometry was used to investigate alterations in immune populations, and the Human Cytokine 30-plex protein assay (Invitrogen) was used to measure circulating cytokines. viSNE projection of peripheral blood analyzed using spectral cytometry was investigated for expression of PD-L1 and STAT3 activation. For studies utilizing syngeneic mouse models of RCC, 6-8 week female Balb/C mice were injected subcutaneously with 500,000 RENCA cells resuspended in a 1:1 ratio of 1x PBS and Matrigel. Mice were treated with either PBS, IgG, CpG-STAT3ASO (a novel oligonucleotide-based TLR9 activator and STAT3 inhibitor), anti-PD-1, or CpG-STAT3ASO plus anti-PD-1. Immune alterations in tumor were assessed via flow cytometric analysis of tumor and in tumor draining lymph nodes. Statistical significance was determined using two-way ANOVA or Wilcoxon signed ranked test with SEM.

Results We evaluated 37 mRCC pts (30:7 M:F) who received N+I, most of whom had clear cell histology (89%) and were IMDC intermediate-risk (76%). Sixteen pts (43%) achieved an objective response, all of which were partial responses. A significant increase in plasma concentrations of cytokines IL-6 ($p=0.0046$), IL-8 ($p=0.0174$), IP-10 ($p=0.0067$), IL-2R ($p=0.0174$), and IL-1RA ($p=0.0079$) as well as high pSTAT3 levels were observed in pts who did not respond to N+I. In our syngeneic mouse models, the anti-PD-1 plus CpG-STAT3ASO cohort demonstrated significant tumor growth inhibition vs PBS ($p=0.0006$), anti-PD-1 ($p=0.0285$), and CpG-STAT3ASO ($p=0.0353$) cohorts along with a 4-fold decrease in mean tumor growth when compared to the PBS cohort.

Conclusions Pts unresponsive to N+I exhibited significant increases in cytokines stimulating STAT3 signaling (IL-6, IL-8, and IL-2R) as well as higher levels of active pSTAT3. In addition, our preclinical models indicate that administering anti-PD-1 plus CpG-STAT3ASO leads to significant tumor growth restriction compared to either agent alone. Taken together, these findings suggest that STAT3 activation may be a key mediator of tumor immune evasion and support further exploration of targeting STAT3 in tumor-associated myeloid cells in combination with anti-PD-1 therapy in mRCC.

Ethics Approval The protocol was approved by the institutional scientific review committee, data safety monitoring board, and the institutional review board at the City of Hope Comprehensive Cancer Center. The study conformed with the

amended Declaration of Helsinki and the International Conference on Harmonization Guidelines.

<http://dx.doi.org/10.1136/jitc-2022-SITC2022.0880>

881

SIGNIFICANT THERAPEUTIC EFFECTS OF ANTI-ROR1 CAR NK AGAINST NEUROBLASTOMA BY ONCOLYTIC VIRUS ARMORED WITH IL-21 *IN-VITRO* AND *IN-VIVO*

¹Yaya Chu*, ¹Meijuan Tian, ²Uksha Saini, ²Dean Lee, ²Timothy Cripe, ²Elaine Mardis, ³Gregory Behbehani, ⁴Stanley Riddell, ²Kevin Cassady, ¹Mitchell Cairo. ¹New York Medical College, Valhalla, NY, United States; ²Nationwide Children's Hospital, Columbus, OH, United States; ³The Ohio State University, Columbus, OH, United States; ⁴Fred Hutchinson Cancer Research Center, Seattle, WA, United States

Background Metastatic and relapsed/refractory neuroblastoma (NB) has very poor diagnosis.¹ Novel therapies are desperately needed.² ROR1 is overexpressed in a variety of human cancers including NB.³⁻⁵ Our group has successfully expanded peripheral blood NK cells (exPBNCs) and modified exPBNC cells to express chimeric antigen receptor (CAR).⁶ Oncolytic herpes simplex viruses (oHSVs) have been safely used in clinical trials for a wide range of cancers.⁷ IL-21 sustained the survival and increased the cytotoxicity of NK cells.⁸ We sought to determine the anti-tumor effect of anti-ROR1 CAR engineered exPBNC cells (CAR-exPBNCs) against ROR1⁺ NB and if the anti-tumor efficacy can be improved by oHSV engineered to express human IL21.

Methods NK cells were expanded and electroporated with anti-ROR1-CAR mRNA. oHSV C134 was modified to express hIL-21 gene (C021). In-vitro cytotoxicity and cytokines levels of CAR-exPBNCs against NB cell lines were examined as we previously described (2). In-vivo hIL21 secretion and anti-tumor effect of CAR-exPBNCs with or without the C021 was examined utilizing human NB xenografted NSG mice.

Results NK cells were significantly expanded by co-culture with irradiated K562-mbIL21 cells at 14 days (>2000 folds), and expanded NK cells were isolated with more than 95% purity. Anti-ROR1-CAR was expressed on >90% of exPBNC cells after CAR mRNA electroporation. CAR-exPBNC cells had significantly enhanced in-vitro cytotoxicity compared to Mock-exPBNC against ROR1+ SKNBE(2)N, CHLA-255, and SKNFI NB cells at different E:T ratios (p<0.001) regardless of MYCN amplification status. Expression of CD107a and IFN-g were significantly increased in CAR-exPBNC cells compared to Mock-exPBNC (p<0.05). CyTOF analysis showed that phosphorylation of STAT5 was enhanced in CAR-exPBNC when targeting NB as compared to exPBNC cells. In-vivo study showed that CAR-exPBNC significantly extended mice survival in human NB xenografted NSG mice (p<0.01) (figure 1). Furthermore, the combination of C021 and CAR-exPBNC significantly enhanced the killing of NB with significantly enhanced secretion of IFN-g, granzyme B and perforin and significantly enhanced expression of NK activating marker CD25 (all p<0.05) compared to controls. Our in-vivo animal study showed that NB infected with C021 secreted hIL21 and the combination of C021 and CAR-exPBNC cells reduced tumor burden in human NB xenografted NSG mice compared to the untreated group (p<0.05) and the CAR exPBNCs-treated group (P=0.056) (figure 2).

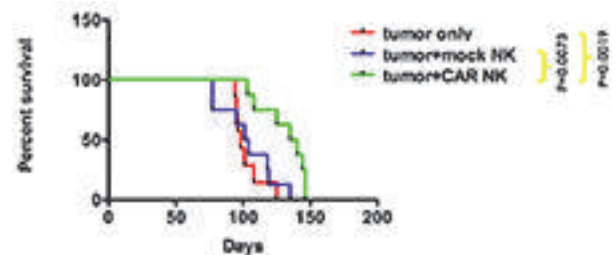
Conclusions Our data demonstrate the significant anti-tumor efficacy of combining C021 with anti-ROR1 CAR-exPBNCs to therapeutically target NB in-vitro and in-vivo. (Funded by U54 CA232561).

REFERENCES

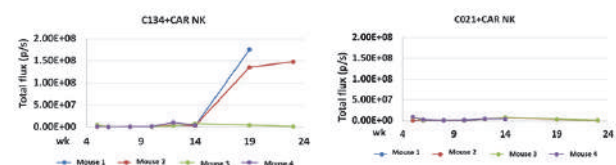
1. Ambros PF, Ambros IM, Brodeur GM, Haber M, Khan J, Nakagawara A, et al. International consensus for neuroblastoma molecular diagnostics: report from the International Neuroblastoma Risk Group (INRG) biology committee. *Br J Cancer*. 2009;100(9):1471-82. Epub 2009/04/30. doi: 6605014 [pii]. 10.1038/sj.bjc.6605014. PubMed PMID: 19401703; PubMed Central PMCID: PMC2694415.

- Chu Y, Nayyar G, Jiang S, Rosenblum JM, Soon-Shiong P, Safrit JT, et al. Combinatorial immunotherapy of N-803 (IL-15 superagonist) and dinutuximab with ex vivo expanded natural killer cells significantly enhances in vitro cytotoxicity against GD2(+) pediatric solid tumors and in vivo survival of xenografted immunodeficient NSG mice. *J Immunother Cancer*. 2021;9(7). Epub 2021/07/11. doi: 10.1136/jitc-2020-002267. PubMed PMID: 34244307; PubMed Central PMCID: PMCPCMC8268924.
- Matsuda T, Nomi M, Ikeya M, Kani S, Oishi I, Terashima T, et al. Expression of the receptor tyrosine kinase genes, Ror1 and Ror2, during mouse development. *Mech Dev*. 2001;105(1-2):153-6. Epub 2001/06/29. doi: S0925477301003835 [pii]. PubMed PMID: 11429290.
- Zhang S, Chen L, Wang-Rodriguez J, Zhang L, Cui B, Frankel W, et al. The onco-embryonic antigen ROR1 is expressed by a variety of human cancers. *Am J Pathol*. 2012;181(6):1903-10. PubMed PMID: 23041612.
- Hudecek M, Lupo-Stanghellini MT, Kosasih PL, Sommermeyer D, Jensen MC, Rader C, et al. Receptor affinity and extracellular domain modifications affect tumor recognition by ROR1-specific chimeric antigen receptor T cells. *Clin Cancer Res*. 2013;19(12):3153-64. Epub 2013/04/27. doi: 1078-0432.CCR-13-0330 [pii]. 10.1158/1078-0432.CCR-13-0330. PubMed PMID: 23620405; PubMed Central PMCID: PMC3804130.
- Chu Y, Hochberg J, Yahr A, Ayello J, van de Ven C, Barth M, et al. Targeting CD20+ Aggressive B-cell Non-Hodgkin Lymphoma by Anti-CD20 CAR mRNA-Modified Expanded Natural Killer Cells In Vitro and in NSG Mice. *Cancer Immunol Res*. 2015;3(4):333-44. Epub 2014/12/11. doi: 10.1158/2326-6066.CIR-14-0114. PubMed PMID: 25492700.
- Ghonime MG, Saini U, Kelly MC, Roth JC, Wang PY, Chen CY, et al. Eliciting an immune-mediated antitumor response through oncolytic herpes simplex virus-based shared antigen expression in tumors resistant to viroimmunotherapy. *J Immunother Cancer*. 2021;9(10). Epub 2021/10/03. doi: 10.1136/jitc-2021-002939. PubMed PMID: 34599026; PubMed Central PMCID: PMCPCMC8488720.
- Skak K, Frederiksen KS, Lundsgaard D. Interleukin-21 activates human natural killer cells and modulates their surface receptor expression. *Immunology*. 2008;123(4):575-83. Epub 2007/11/17. doi: 10.1111/j.1365-2567.2007.02730.x. PubMed PMID: 18005035; PubMed Central PMCID: PMCPCMC2433320.

Ethics Approval NSG mice were bred, treated, and maintained in the animal facility of New York Medical College with NYMC International Animal Care and Use Committee approved protocols. The animal experiments were conducted in accordance with the recommendations of the Guide for Care and Use of Laboratory Animals.



Abstract 881 Figure 1 Anti-ROR-1 CAR NK significantly prolonged the survival of NSG mice xenografted with human NB cells



Abstract 881 Figure 2 C021+CAR-NK appeared to have a better anti-tumor effect than C134+CAR-NK in human NB xenografted NSG mice

<http://dx.doi.org/10.1136/jitc-2022-SITC2022.0881>

882 USING ONCOGENIC PATHWAY AGONISM TO SENSITIZE RAS MUTANT CANCERS TO IMMUNOTHERAPY

¹Alvaro De Mingo Pulido, ²Charles Adelman, ¹Kim Nguyen, ¹Cynthia Dixey, ¹Francisca Beato, ¹Karol Prieto, ¹Marco Napoli, ¹Elsa Flores, ¹Karen Mann, ¹Jason Fleming, ¹Kenneth Tsai*. ¹H. Lee Moffitt Cancer Center, Tampa, FL, United States; ²MD Anderson, Houston, TX, United States

Background Overall, 30% of human cancers are driven by mutant RAS proteins. While immunotherapy is effective for NRAS-mutant melanoma, no options exist for resistant disease, and mutant KRAS-driven lung and pancreatic carcinomas are much less responsive. Oncogenic pathways are key targets for inhibition. However, pathway agonism has not been explored as a therapeutic approach. BRAF-mutant melanomas respond to BRAF inhibitors (BRAFi) due to decreased ERK signaling. They can recover signaling by acquiring activating RAS/MEK mutations, but exhibit decreased proliferation in the absence of inhibitor, suggesting that supraphysiologic ERK signaling also compromises fitness. Therefore, we observed that increasing ERK hyperactivation in RAS-mutant cancers might elevate ERK signaling, inducing senescence, and creating an inflammatory tumor microenvironment (TME)

Methods BRAFi have been used to study senescence by different assays. *In vivo* assays were performed in C57/Bl6 treated with BRAFi with/without anti-PD1 therapy to study tumor progression. Tumors single cell suspension was used for immunophenotyping by Flow Cytometry and scRNASeq data

Results We have shown that 15/21 RAS-mutant cancer cell lines undergo senescence following exposure to all FDA-approved BRAF inhibitors. Simultaneous MEK or ERK inhibition allows the cells to recover proliferation, and a BRAFi which does not induce ERK activation fails to have any effect, showing that ERK hyperactivation is the key driver of this response. Furthermore, our extensive preliminary data in two novel genomically-characterized, high TMB immunocompetent models of NRAS-mutant melanoma and KRAS-mutant pancreatic adenocarcinoma support our *in vitro* findings. Both murine models have shown that anti-PD1 therapy is more efficacious when mice are additionally treated with BRAFi. Molecular profiling of the TME reveals the expression of cytokines related to senescence and marked infiltration of activated CD8+ T-cells. To implement effective immunotherapies, we have analyzed the expression of different immune-checkpoint molecules and we have observed a high expression of LAG3 and TIM3 in the melanoma NRAS-mutant model treated with BRAFi. We will further analyze the effect of those checkpoints in combination with BRAFi to potentiate the anti-tumoral responses and tumor regression

Conclusions Oncogenic pathway agonism is a novel, effective, and untested strategy to induce proliferation arrest and sensitization to immunotherapy. The impact of this data is in the ability to broadly sensitize RAS-mutant cancers to immunotherapy in the settings of de-novo and acquired resistance. The direct connection between a tumor cell signaling vulnerability to immunotherapy response is a major point of novelty and provides a clear rationale for pursuing combined targeted and immunotherapy

<http://dx.doi.org/10.1136/jitc-2022-SITC2022.0882>

883

MCLA-145, AN ANTI CD137×PD-L1 BISPECIFIC ANTIBODY, INDUCES T CELL ACTIVATION AND PROLIFERATION IN EX VIVO MODELS OF HEPATOCELLULAR CARCINOMA

¹Jyaysi Desai*, ¹Lissane Noordam, ¹Patrick Boor, ²Rachid Bouzid, ²Diana Mittag, ²Paul Tacken, ²Jeroen Lammerts van Bueren, ²Cecile Guijen, ¹Jaap Kwekkeboom, ¹Dave Sprengers, ¹Sonja Buschow. ¹Erasmus Medical Center, Rotterdam, Netherlands; ²Merus N.V., Utrecht, Netherlands

Background Costimulatory molecules, such as CD137 (4-1BB), have emerged as promising targets for cancer immunotherapy. Despite promising results in animal tumor models, clinical trials with CD137 agonists have had limited success due to both dependency on FcγR-mediated clustering and dose limiting hepatotoxicity. Merus has developed an Fc-silenced Bionics[®] CD137×PD-L1 antibody, MCLA-145, whose stimulatory activity is correlated with PD-L1-mediated CD137 clustering which is designed to be preferentially confined to the PD-L1 expressing tumor microenvironment. The aim of this study was to characterize the mechanism of action of MCLA-145 in resected hepatocellular carcinoma (HCC), a heterogenous solid tumor with limited therapeutic options. We studied target expression and *ex vivo* responses in human HCC tumor-infiltrating lymphocytes (TIL).

Methods Lymphocytes and myeloid cells isolated from resected HCC (n=10) tumors (TIL), paired tissues adjacent to tumor (TFL) and peripheral blood were characterized for CD137, PD-1 and PD-L1 expression by flow cytometry. Additionally, TIL proliferation upon either anti-CD3/CD28 stimulation or autologous B cell blasts electroporated with tumor-associated antigens (TAA) glypican-3 (GPC3) and/or melanoma-associated antigen (MAGE)-C2 stimulation was assessed *ex vivo* in presence of MCLA-145, its bivalent monospecific parental mAbs, the bivalent mAbs urelumab (anti-CD137) or atezolizumab (anti-PD-L1) or isotype control.

Results Compared to lymphocytes derived from adjacent tissues and blood, CD137 and PD-1 expression was found to be highest in TIL, and specifically on activated regulatory T cells. CD137 was also found to be expressed on myeloid cells such as tissue resident Kupffer cells and granulocytes. PD-L1 was mainly found to be expressed on CD3⁻ cells. Treatment with MCLA-145 led to increased proliferation, as measured by Ki67 staining, of HCC-derived CD8⁺ TILs, compared to isotype control treatment. Expression of CD137 was significantly increased on these proliferating CD8 T cells upon the treatment with MCLA-145. Additionally, MCLA-145 enhanced CD8⁺ TIL proliferation more potently compared to its bivalent monospecific parent mAbs or Urelumab.

Conclusions Bionics[®] antibody MCLA-145 has the capacity to enhance activation and proliferation of tumor-derived CD8 + T cells in the PD-L1 expressing tumor microenvironment of HCC *ex vivo*, warranting further evaluation in HCC.

Ethics Approval Ethical approval (METC) for this study has been obtained.

<http://dx.doi.org/10.1136/jitc-2022-SITC2022.0883>

884

PERK INHIBITOR HC-5404 DEMONSTRATES IMMUNE-ACTIVATION AND ANTI-TUMOR EFFICACY IN COMBINATION WITH ANTI-PD1 IMMUNE CHECKPOINT INHIBITOR ANTIBODY

Anissa SH Chan*, Jeremy Drees, Yunfang Li, Takashi Kangas, Weiyu Zhang, Maria Fumagalli, Iman Dewji, Xiaohong Qiu, Nick Collette, Ben Harrison, Ashley LaCayo, Veronica Calvo Vidal, Crissy Dudgeon, Michael Stokes, Eric Lightcap, David Surguladze, Nandita Bose. *HiberCell, Inc., Roseville, MN, United States*

Background Protein kinase R-like endoplasmic reticulum kinase (PERK) is part of the unfolded protein response that facilitates cellular adaptation to ER stress. PERK is activated in cancer cells by accumulation of misfolded proteins in the ER, enabling adaptation and survival. PERK signaling has also recently been implicated in maintaining immunosuppressive functions of myeloid-derived suppressor cells (MDSCs) through inhibition of a type 1 interferon response¹ and macrophages through metabolic and epigenetic modification.² We are developing HC-5404, a highly selective and potent first-in-class, first-in-human PERK inhibitor that is currently in a phase 1 trial for solid tumors (NCT04834778). HC-5404 has demonstrated single agent and combinatorial efficacy in multiple solid tumor xenograft models. In this study, we sought to investigate the immunomodulatory effects of HC-5404 by evaluating efficacy and correlative immune effects of HC-5404 combined with an anti-murine-PD-1 immune checkpoint inhibitor (ICI) antibody.

Methods C57BL/6 mice were subcutaneously inoculated with syngeneic MB49 bladder cancer cells, and treatment started on day 8 post cell inoculation. A group of animals (n=10/group) received either vehicle, HC-5404 (PO, BID), anti-PD-1 antibody RMP1-14 (IB, every 3 days), or the combination of both. At various timepoints, flow cytometry was performed on blood or single cell suspensions from tumors or lymph nodes (n=6) of treated mice. MDSCs derived from human cord blood or mouse bone marrow were co-cultured with purified T-cells in the presence of HC-5404 *in vitro*, and proliferation was evaluated.

Results HC-5404 treatment alone showed only a modest anti-tumor effect (32% TGI), the addition of HC-5404 to aPD-1 provided combination antitumor benefits (75% TGI) and significantly improved the effects of aPD-1 alone (53% TGI). HC-5404 + aPD-1 efficacy was correlated with increased expression of type 1 interferon receptor (IFNAR1) and increased surface calreticulin on tumor cells. Additionally, IFNAR1 was also significantly increased on PMN-MDSCs and tumor-associated macrophages (TAM). TAMs also showed increased PD-L1 with combination treatment. Additionally, combination treatment increased the frequency of CD8 T-cells in the tumor along with increased expression of activation marker CD69 on T-cells in the tumor draining lymph node. Notably, the effect of HC-5404 on IFNAR1 was also detected on monocytes in peripheral blood, demonstrating surface expression of IFNAR1 as a potential biomarker for HC-5404 activity. MDSCs also showed a reduced inhibition of T-cells in the presence of HC-5404 *in vitro*.

Conclusions Collectively, these data demonstrate the efficacious and immuno-stimulatory effects of HC-5404 coadministered with anti-PD1 mAb and outline its potential application in ICI-treated cancers.

REFERENCES

1. Mohamed E, *et al.* The unfolded protein response mediator perk governs myeloid cell-driven immunosuppression in tumors through inhibition of STING signaling. *Immunity*. 2020;**52**(4): 668–682. e667.
2. Raines LN, *et al.* PERK is a critical metabolic hub for immunosuppressive function in macrophages. *Nat Immunol* 2022;**23**(3): 431–445.

Ethics Approval All *in vivo* experimental procedures were done in accordance with the NIH Guide for Care and Use of Animals and were approved by the Institutional Animal Care and Use Committee of University of Minnesota. IACUC protocol 2009A38458

<http://dx.doi.org/10.1136/jitc-2022-SITC2022.0884>

885

ENHANCING IMMUNE CHECKPOINT INHIBITOR EFFICACY WITH ANTI-ANGIOGENICS IN OVARIAN CANCER

Sarah Gitto*, Sergey Medvedev, Veethika Pandey, Dalia Omran, Matthew Anderson, Lauren Schwartz, Fiona Simpkins, Daniel Powell. *University of Pennsylvania, Philadelphia, PA, United States*

Background Clinical data from our group supports that ovarian cancer (OC) patients respond better to immune checkpoint blockade (ICB) when targeting both PD-1 and CTLA4 compared to anti-PD-1 alone (33% v. 10%, respectively),¹ yet there is still room to improve dual-ICB response. Bevacizumab is approved as a front-line therapy for OC and targets vascular endothelial growth factor A (VEGF-A). VEGF has been shown to have both anti-tumor and immunomodulatory effects as it induces macrophage infiltration and M2 polarization² and directly suppresses T-cell activation, proliferation, and cytotoxic activity.^{3,4} Here we aim to determine if priming the immunosuppressive tumor microenvironment (TME) with anti-VEGF enhances the response of T-cell stimulating ICB.

Methods We developed a patient avatar model by administering *ex vivo* expanded tumor infiltrating lymphocytes (TILs) into immunodeficient mice harboring a patient-matched, patient-derived xenograft (PDX).^{5,6} Autologous TIL reactivity was validated by flow cytometry and ELISA. Preclinical *in vivo* studies were performed to evaluate if the efficacy of dual-ICBs (nivolumab and ipilimumab) could be enhanced through priming with anti-VEGF (bevacizumab). *Ex vivo* culture systems using donor ascites specimens and viable tumor slices were evaluated to further evaluate this combination in OC.

Results Six distinct PDX/TIL models were developed. Co-culture of TILs with autologous tumor cells resulted in HLA-dependent IFN γ production by TILs with a parallel impact on TIL activation phenotype. In response to IFN γ , PD-L1 expression was increased on tumor cells, suggesting antitumor activity might be improved via PD-1 blockade.⁵ As proof-of-concept, anti-PD-1 efficacy was tested in PDX/TIL models (n=3).⁵ Anti-PD-1 reduced tumor burden and increased survival in two models compared to TIL treatment alone. Next, we tested the hypothesis that the efficacy of dual-ICBs could be enhanced through TME priming with anti-VEGF (n=3). Results revealed increased efficacy of dual-ICB with anti-VEGF priming in 2 models. Immunohistochemistry and flow cytometry analysis support that the TILs in the combination ICB +/- anti-VEGF have increased anti-tumor activity.

To better delineate the activity of dual-ICB and anti-VEGF in an intact TME, *ex vivo* cultures were used. OC ascites significantly increased the secretion of T-cell effector and myeloid cell associated immunosuppressive molecules in response to ICB treatment, and CD11b+ tumor associated macrophages (TAMs) significantly reduced T-cell activation. In tumor slice cultures, combination treatment with dual-ICB and anti-VEGF reduced overall tumor burden.

Conclusions This data supports the notion that, in addition to the effect of anti-VEGF priming, modulation of the immunosuppressive myeloid population may further enhance ICB efficacy.

Acknowledgements We would like to thank the National Center for Advancing Translational Sciences of the National Institutes of Health (award number TL1TR001880), the Rivkin Center for Ovarian Cancer, the Ovarian Cancer Research Alliance, and the Penn Ovarian Cancer Translational Center of

Excellence for funding this research. We would like to acknowledge the UPenn Stem Cell and Xenograft, Histology, and Human Immunology cores. We also thank Benjamin Ferman for his technical support for in vivo studies. Finally, we would like to acknowledge the patients who volunteered to donate their tissue to the Ovarian Cancer Biotrust Collection.

REFERENCES

1. Zamarin, D, *et al.* Randomized phase II trial of nivolumab versus nivolumab and ipilimumab for recurrent or persistent ovarian cancer: an NRG oncology study. *J Clin Oncol* 2020;**38**, 1814–1823, doi:10.1200/JCO.19.02059.
2. Roland CL, *et al.* Inhibition of vascular endothelial growth factor reduces angiogenesis and modulates immune cell infiltration of orthotopic breast cancer xenografts. *Mol Cancer Ther* 2009;**8**, 1761–1771, doi:10.1158/1535-7163.MCT-09-0280.
3. Gavalas NG, *et al.* VEGF directly suppresses activation of T cells from ascites secondary to ovarian cancer via VEGF receptor type 2. *Br J Cancer* 2012;**107**, 1869–1875, doi:10.1038/bjc.2012.468.
4. Voron T, *et al.* VEGF-A modulates expression of inhibitory checkpoints on CD8+ T cells in tumors. *J Exp Med* 2015;**212**, 139–148, doi:10.1084/jem.20140559.
5. Gitto SB, *et al.* An autologous humanized patient-derived-xenograft platform to evaluate immunotherapy in ovarian cancer. *Gynecol Oncol* 2020;**156**, 222–232, doi:10.1016/j.ygyno.2019.10.011.
6. Gitto SB, George E, Medvedev S, Simpkins F. & Powell DJ, Jr. Humanized patient-derived xenograft models of ovarian cancer. *Methods Mol Biol* 2022;**2424**, 255–274, doi:10.1007/978-1-0716-1956-8_17.

Ethics Approval Surgical or biopsy samples were obtained with informed consent from the Hospital of the University of Pennsylvania in accordance with the IRB (#702679). PDX studies were carried out in accordance with animal ethics guidelines approved by the University of Pennsylvania IACUC (#806002) protocol and in the regulations of the Association for Assessment and Accreditation of Laboratory Animal Care (AAALAC).

Consent Written informed consent was obtained from the patients for the collection and use of de-identified biospecimens in this research. A copy of the written consent is available for review by the Editor of this journal.

<http://dx.doi.org/10.1136/jitc-2022-SITC2022.0885>

886 **COMBINED ALLOGENEIC NK CELL AND HERZUMA® IS EFFECTIVE IN HER2-LOW BREAST CANCER PRECLINICAL MODEL BY ENHANCING ANTIBODY-DEPENDENT CELLULAR CYTOTOXICITY**

¹Yong Moon*, ²Mithun Gosh, ¹Hee-Jung An, ¹Tae Hoen Kim, ²Sa Deok Hong, ²Nar Bahadur Katuwal, ¹Minsil Kang. ¹CHA Bundang Medical Center, Seongnam, Republic of Korea; ²The Graduate School, CHA University, Seongnam, Republic of Korea

Background Trastuzumab has shown significant improvements in the overall survival in patients with HER2-positive breast cancer. But HER2 is expressed at varying levels in breast cancer patients, therefore, only a fraction with robust HER2 overexpression is beneficial from trastuzumab therapy. However, the efficacy of trastuzumab in HER2-low expressing breast cancer, which is defined as immunohistochemistry 1+ or 2+ and lack of HER2 amplification by in situ hybridization, is not reported yet. Therefore, to enhance the effects of trastuzumab in HER2-low expressing breast cancers, we investigated a novel combination of Herzuma® (a trastuzumab biosimilar), paclitaxel and allogeneic Natural Killer (NK) cells in the HER2-low breast cancer preclinical models.

Methods Two breast cancer cell lines, BT-474 (HER2-low, by western blot) and SKBR3 (HER2-high, by western blot) were used for in-vitro study. Cytotoxicity was analyzed by flow cytometry (CFSE, 7AAD) after co-culture, where cancer cells were used as target (T) cell and allogeneic NK cells as effector (E) cell at various E:T ratio in the presence or absence of Herzuma®. Antibody-dependent cellular cytotoxicity (ADCC) activity was analyzed by evaluating interaction of Herzuma® and FCγIII (CD16) of NK cells. Lastly, HER2-low breast cancer patients-derived tumor xenograft (PDX) model was used for in vivo efficacy test. When tumor size reached to 100mm³, mice were randomly divided in 4 groups (control, Herzuma® + paclitaxel, NK, Herzuma® + paclitaxel + NK) and treated.

Results Cytotoxicity assay demonstrated that dead target cells were only increased in the combined Herzuma® and NK therapy as compared to NK monotherapy in both cell lines (BT474, SKBR3) at various E:T ratio. To confirm the above-mentioned cytotoxic effect of the combination therapy is an ADCC effect, we conducted co-culture using HER2-low BT474 cells after blocking the CD16 of NK cells. Dead target cells were not increased in the combined Herzuma® and NK therapy group after CD16 blocking, whereas similar cytotoxic effects were observed in NK monotherapy and combination therapy respectively, suggesting the above-mentioned cytotoxic effect resulted from ADCC. Finally, the in-vivo study using HER2-low breast cancer PDX model showed that the NK therapy in combination with Herzuma® and paclitaxel group significantly inhibited the tumor growth as compared to combined Herzuma® and paclitaxel group or control ($p=0.003$, vs control; $p=0.01$, vs Herzuma® + paclitaxel).

Conclusions The combination of allogeneic NK therapy, Herzuma® and paclitaxel showed synergistic anticancer activity in HER2-low breast cancer preclinical model. This combination merits further clinical investigation in HER2-low breast cancer patients.

Acknowledgements The study was funded by CELLTRION PHARM, Inc. (Chungcheongbuk-do, Republic of Korea)

Ethics Approval IACUC190139

<http://dx.doi.org/10.1136/jitc-2022-SITC2022.0886>

887

MULTIMODAL GLIOMA IMMUNOTHERAPY COMBINING TLR9-TARGETED STAT3 ANTISENSE OLIGODEOXYNUCLEOTIDES WITH PD1-SPECIFIC IMMUNE CHECKPOINT BLOCKADE

Marcin Kortylewski*, Chia-Yang Hung*. Beckman Research Institute, City of Hope, Duarte, CA, United States

Background Malignant gliomas (MG) are rapidly fatal despite multimodal treatments including radiation therapy, used to treat nearly all MG patients, or even the emerging cellular immunotherapies. Therapeutic resistance in glioma is related to tolerogenic STAT3 activity in both glioma cancer stem cells (GSCs) and in the tumor-associated myeloid immune cells, such as macrophages and microglia, which dominate MG microenvironment.^{1,2} We previously demonstrated that STAT3 activity in GSCs and tumor-associated myeloid cells can be targeted using Toll-like Receptor-9 (TLR9)-targeted oligonucleotide therapeutics such as siRNA or antisense oligonucleotides (ASO).^{2,3}

Methods Here, we describe development of a new TLR9-targeted and double-stranded STAT3 antisense oligonucleotide (CpG-STAT3dsASO) with optimized efficacy and safety for glioma immunotherapy.

Results Compared to our benchmark ASO oligonucleotides, the LNA-modified CpG-STAT3dsASO showed enhanced target gene knockdown in human and in mouse glioma cells and also in TLR9⁺ immune cells, such as macrophages and microglia. When tested against orthotopic model of human U251 glioma, intracranial injections of CpG-STAT3dsASO (1 mg/kg/q2w) inhibited tumor growth and significantly extended survival of immunodeficient NSG mice compared to benchmark oligonucleotide. Next, we tested CpG-STAT3dsASO against syngeneic GL261 model in immunocompetent mice. Our results demonstrated that CpG-STAT3dsASO was more effective but also significantly better tolerated than single-stranded CpG-STAT3ASO when injected intracranially, without evidence of severe acute neural toxicities within tested dosing. All tested CpG-STAT3ASO variants induced maturation/activation of intratumoral DCs, macrophages and microglia, while reducing numbers of tumor-associated M2 macrophages and resting microglia as assessed using flow cytometry. Importantly, CpG-STAT3ASO treatments improved the ratio of intratumoral CD8 T cells to Tregs. To elucidate changes in the glioma microenvironment related to STAT3-inhibition/TLR9-activation, we performed an initial single-cell RNAseq analysis of transcriptomic profiles in immune cell subsets isolated from tumors after treatment using CpG-STAT3dsASO^{LNA}. Our analysis indicated the reprogramming of tumor-associated myeloid cell populations within treated glioma with an increased ratio of CD8:regulatory T cells. Our results also suggested the elevation of several immune checkpoint molecules on tumor-infiltrating T cells likely as a result of IFN signaling. Importantly, our preliminary experiments demonstrated a synergy between systemic PD1 inhibition with low-dose (0.25 mg/kg) CpG-STAT3dsASO local therapy. While, neither of treatments alone was curative, the combination anti-PD1/CpG-STAT3dsASO therapy resulted in complete rejection of orthotopic GL261 tumors in the majority of treated mice (figure 1).

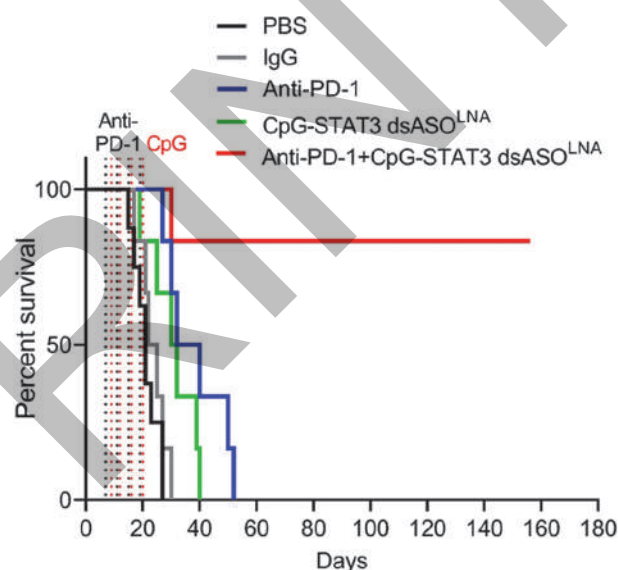
Conclusions We believe that further development of CpG-STAT3dsASO will pave way to clinical translation of this strategy to immunotherapy of malignant glioma.

Acknowledgements This work was supported in part by the National Cancer Institute/National Institutes of Health awards

number R01CA215183 (M.K.) and P30CA033572 (COH). The content is solely the responsibility of the authors and does not necessarily represent the official views of the National Institutes of Health.

REFERENCES

1. Herrmann A, Cherryholmes G, Schroeder A, Phallen J, Alizadeh D, Xin H, Wang T, Lee H, Lahtz C, Swiderski P, et al. TLR9 is critical for glioma stem cell maintenance and targeting. *Cancer Res* 2014;**74**:5218–5228.
2. Moreira D, Adamus T, Zhao X, Su Y-L, Zhang Z, White SV, Swiderski P, Lu X, DePinho RA, Pal SK, et al. STAT3 inhibition combined with CpG immunostimulation activates antitumor immunity to eradicate genetically distinct castration-resistant prostate cancers. *Clin. Cancer Res.* 2018;**24**:5948–5962.
3. Adamus T, Hung C-Y, Yu C, Kang E, Hammad M, Flores L, Nechaev S, Zhang Q, Gonzaga JM, Muthaiyah K, et al. Glioma-targeted delivery of exosome-encapsulated antisense oligonucleotides using neural stem cells. *Mol. Ther. Nucleic Acids.* 2022;**27**: 611–620.



Abstract 887 Figure 1 Combination of CpG-STAT3dsASO with PD1 blockade in GBM model

C57BL/6 mice with established orthotopic GL261 gliomas were injected twice weekly using intraperitoneal injections of 200 µg of PD1-specific or control antibodies, using intratumoral/IC injections of 0.25 mg/kg of LNA-modified CpG-STAT3dsASO or both treatments combined; shown is the Kaplan-Meier survival curve (n=6-7/group).

<http://dx.doi.org/10.1136/jitc-2022-SITC2022.0887>

888 **SYNERGISTIC EFFICACY OF THE BRM/BRG1 ATPASE INHIBITOR, FHD-286, AND ANTI-PD-1 ANTIBODY IN MOUSE SYNGENEIC TUMOR MODELS**

¹Kana Ichikawa*, ¹Ammar Adam, ²Hsin-Jung Wu, ¹David Lahr, ³Lan Xu, ¹Brandon Antonakos, ¹Liv Johannessen, ¹Steven Bellon, ¹Ryan Kruger, ¹Richard Centore, ¹Martin Hentemann. ¹*Foghorn Therapeutics, Cambridge, MA, United States*; ²*Blueprint Medicines, Cambridge, MA, United States*; ³*Ikena Oncology, Boston, MA, United States*

Background The BAF family of chromatin remodeling complexes are critical regulators of chromatin accessibility and gene expression, and BRM and BRG1 (also known as SMARCA2 and SMARCA4), the catalytic subunits of BAF, provide the enzymatic activity required for chromatin remodeling activity. We have previously identified and characterized a series of novel dual inhibitors of the BRM/BRG1 ATPases, and FHD-286, a potent and selective BRM/BRG1 inhibitor, is currently under clinical investigation for the treatment of metastatic uveal melanoma and advanced hematological malignancies (NCT04879017 and NCT04891757). BAF chromatin remodeling complex activities are implicated in many immunologic responses, and previous studies have shown the involvement of PBAF in the regulation of antitumor immunity.¹

Methods Given the recent reports correlating SMARCA4 deficiency and ICI response,² we explored the combination of BRM/BRG1 ATPase inhibition and anti-PD-1 antibody in syngeneic mouse models from various lineages and with different sensitivities to checkpoint inhibition.

Results The combination of FHD-286 and anti-PD-1 antibody provided synergistic efficacy and survival benefit compared to anti-PD-1 alone in A20, CT26, and the immunologically barren B16F10 melanoma model. FHD-286 increased MHCI expression on B16F10 cells, and increases in IFN γ and Th1-type chemokine CXCL10 levels were observed in immunocompetent mice following treatment, suggesting that combinatorial activity may result from effects on both the tumor and the immune system.

Conclusions FHD-286 has the potential to sensitize tumor to immune-checkpoint inhibition and represents a novel combination approach for cancer immunotherapy.

REFERENCES

1. Pan D, *et al.* A major chromatin regulator determines resistance of tumor cells to T cell-mediated killing. *Science*. 2018; **359**:770–775.
2. Zhou M, *et al.* Emerging role of SWI/SNF complex deficiency as a target of immune checkpoint blockade in human cancers. *Oncogenesis*. 2021; **10**:3.

<http://dx.doi.org/10.1136/jitc-2022-SITC2022.0888>

889

IOA-244 IS A NON-ATP-COMPETITIVE, HIGHLY SELECTIVE, TOLERABLE PHOSPHOINOSITIDE 3-KINASE DELTA INHIBITOR THAT DIRECTLY TARGETS SOLID TUMOURS AND BREAKS IMMUNE TOLERANCE

¹Giusy Di Conza*, ¹Lars Van der Veen, ²Chiara Tarantelli, ²Francesco Bertoni, ³Amy Fraser, ³Pritom Shah, ⁴Simon Tiede, ⁴Laura Tesmer, ⁴Gerhard Hummer, ⁵Oscar Vadas, ¹Michael Lahn, ⁶Nomanbhoy Tyzoonn, ¹Zoe Johnson. ¹*Onctura SA, Geneva, Switzerland*; ²*Institute of Oncology Research, Faculty of Biomedical Sciences, USI, Bellinzona, Switzerland*; ³*Cancer Research Horizon, London, UK*; ⁴*Max Planck Institute of Biophysics, Frankfurt, Germany*; ⁵*University of Geneva, Geneva, Switzerland*; ⁶*Activix, La Jolla, CA, United States*

Background Phosphoinositide 3-kinase delta (PI3Kd) inhibitors are used to treat lymphomas but safety concerns and limited target selectivity complicate their wider application. More recently, the potential for PI3Kd inhibition in solid tumours has become appreciated, through both the modulation of T cell responses and direct anti-tumor activity. Here we report the exploration of IOA-244/MSK2360844, a non-ATP-competitive PI3Kd inhibitor, for the treatment of solid tumors.

Methods To harness the differentiation of IOA-244 from other PI3Kd inhibitors, we have performed molecular dynamic and protein dynamic studies, as well as in-cell kinase assay where we compared structural and selectivity features of IOA-244 with other inhibitors. Then, to investigate the tumor intrinsic and extrinsic properties of IOA-244, we performed patient-derived xenograft models, in vitro proliferation assay and in vivo syngenic tumor models. Here, we tested IOA-244 in monotherapy or in combination with checkpoint blockade inhibitors.

Results Molecular dynamics and protein dynamics studies highlighted that, opposite to other inhibitors, IOA-244 binding to PI3Kd causes a bending of the C-terminal α 12 helix inwards towards the ATP binding pocket, overall resulting in the stabilisation of the inactive form of PI3Kd. Based on this unique binding mode, IOA-244 showed very selectivity when tested against a large set of other kinases, enzymes and receptors. IOA-244 inhibited the *in vitro* growth of cancer cells expressing high levels of PI3Kd, as well as of patient-derived xenografts of melanoma and mesothelioma, suggesting that there are cancer cell-intrinsic effects of IOA-244. Importantly, IOA-244 inhibits T_{reg} proliferation while having limited anti-proliferative effects on conventional CD4⁺ T cells and no effect on CD8⁺ T cells, highlighting immune-modulatory properties that can be exploited in solid tumors. Indeed, in CT26 colorectal and LL2 lung cancer model IOA-244 sensitised the tumours to anti-PD(L)-1 treatment, with similar activity in the Pan-02 and A20 syngenic mouse models. In these models IOA-244 also reshaped the tumour-infiltrating cells, favouring infiltration of CD8 and NK cells, while decreasing suppressive cells. IOA-244 presented no significant safety concerns in animal and *in vitro* toxicology studies and is currently in clinical Phase I evaluation for lymphoma and solid tumors. In this study, IOA-244 treatment in cancer patients showed unprecedented tolerability and clinical benefit, particularly in patients with metastatic uveal melanoma.

Conclusions In conclusion, thanks to its unique structural and selectivity features, IOA-244 represent a first in class PI3Kd inhibitor, with an exceptional safety profile.

<http://dx.doi.org/10.1136/jitc-2022-SITC2022.0889>

890

USING INTRATUMOR MICRODEVICES TO IDENTIFY HIGHLY SYNERGISTIC COMBINATIONS BETWEEN TARGETED AGENTS AND IMMUNOTHERAPIES IN BREAST CANCER

Oliver Jonas*. *Brigham and Women's Hospital, Boston, MA, United States*

Background Targeted therapies in cancer aim to block specific molecular pathways that are constitutively activated and are crucial for tumor cell growth and survival, but they also elicit immune responses. This raises the possibility that these treatments may be combined with immunotherapy to induce synergistic anti-tumor effects that improve treatment outcomes. How to rationally prioritize combinations of targeted agents with immunotherapies among the many possible options, represents a major unmet need in clinical oncology.

Methods We have developed a novel *in situ* approach that provides a phenotypic measurement of single and combinatorial drug effect directly within the tumors of patients or animal models. The approach uses implantable microdevices (IMD), which are loaded with nano-doses of up to 20 approved and experimental agents, and releases these treatments into confined and non-overlapping regions of the tumor where each treatment interacts with the native tumor microenvironment (TME) for multiple days. Upon retrieval of the IMD with surrounding tissue, a spatial analysis tissue phenotyping pipeline is employed to define the effect of each treatment on tumor and TME cells.^{1,2} For each treatment, a specific response and resistance phenotype is described which leads to the identification of an immune-modulating agent which combines synergistically with the targeted therapy.

Results We have employed this combined IMD – spatial analysis platform to identify three novel and highly synergistic combinations in breast cancer models, including inhibitors of CDK4/6, HDAC and BCL-2, as well as anti-PD1, anti-CSF1R and anti-CD40 treatments.

Conclusions The approach is currently being used in multiple clinical studies, which provides a platform for validating the biomarkers and resistance signatures in patients.

REFERENCES

1. Jonas O, *et al.* An implantable microdevice to perform high-throughput in vivo drug sensitivity testing in tumors. *Sci Transl Med.* 2015 Apr 22;**7**(284):284ra57.
2. Tatarova Z, *et al.* A multiplex implantable microdevice assay identifies synergistic combinations of cancer immunotherapies and conventional drugs. *Nat Biotechnol.* 2022 Jul 4.

Ethics Approval The study has obtained the required ethics approvals.

<http://dx.doi.org/10.1136/jitc-2022-SITC2022.0890>

891 IMMUNE RELATED VULNERABILITIES OF NON-NEUROENDOCRINE SMALL CELL LUNG CANCER

Ryan Kowash*, Mingrui Zhu, Benjamin Drapkin, John Minna, Luc Girard, Esra Akbay. *UT Southwestern Medical Center, Dallas, TX, United States*

Background Small Cell Lung Cancer (SCLC) is primarily a neuroendocrine (NE) cancer, however there is a subtype of SCLC that displays non-neuroendocrine (non-NE) phenotype. This subtype displays a unique immune and metabolic signature. Specifically, immune related vulnerabilities of this subtype are increases in expression of MHC-I and natural killer (NK) cell activating ligands. We discovered that there are additional immune modulators differentially produced in this subtype such as *NT5E*. *NT5E* encodes for CD73. CD73 acts as an ectoenzyme and is involved in adenosine production within the tumor microenvironment. Accumulation of adenosine limits the function of T and NK cells. Our recent studies suggest targeting CD73 in combination with immune checkpoint blockade results in an additive effect through decreased adenosine production in Non Small Cell Lung Cancer. However, the role of CD73 is yet to be explored in SCLC.

Methods We analyzed expression of *NT5E* for both SCLC cell lines and patient derived xenograft (PDX) models. Expression of CD73 at the protein level was validated in mouse and human cell line models. Mouse and human SCLC cell lines were used in co-culture experiments. Syngeneic mouse models were utilized for *in vivo* experiments. Flow cytometry was used to analyze changes in the tumor microenvironment.

Results Non-NE SCLC cell lines and PDX's express significantly higher levels of CD73 compared to NE models. Co-cultures of tumor cells with NK cells demonstrated that SCLC's with increased NK cell activating ligands display increased response to NK cell killing. Blockade of CD73 further enhanced activation of cytotoxic T cells in peripheral blood mononuclear cell (PBMC) co-cultures. When combined with immune checkpoint blockade treatment, syngeneic tumor growth was inhibited in mice. Combination treatment resulted in significantly increased activated T cells and NK cells within the tumor microenvironment as well as changes in myeloid cell populations.

Conclusions Our results argue that increased NK cell activating ligands and CD73 inhibition is a potential therapeutic target for non-NE SCLC. Increased NK cell activating ligands makes non-NE SCLC more susceptible to NK cell killing compared to NE SCLC. CD73 inhibition in combination with immune checkpoint blockade resulted in decreased tumor growth. This response was attributed to increased T cell and NK cell populations within the tumor microenvironment.

Acknowledgements Mingrui Zhu, Luc Girard, John Minna, Benjamin Drapkin, Esra A Akbay

<http://dx.doi.org/10.1136/jitc-2022-SITC2022.0891>

892

THE NOVEL TELOMERASE-DIRECTED TELOMERE-TARGETED ANTICANCER AGENT 6-THIO-DG (THIO) DEMONSTRATES POTENT ACTIVITY AND INDUCES ANTITUMOR IMMUNITY IN HEPATOCELLULAR CARCINOMA (HCC) MODELS

¹Ilgen Mender, ¹Silvia Siteni, ²Mihail Obrocea, ²Vlad Vitoc, ²Sergei Gryaznov*, ¹Jerry Shay. ¹UT Southwestern, Dallas, TX, United States; ²Maia Biotechnology, Inc., Chicago, IL, United States

Background HCC is one of the leading causes of cancer-related deaths worldwide. Low response rates with current treatments for HCC demonstrate an urgent unmet need for more effective systemic therapies. However, development of novel treatments for HCC has been challenging due to a lack of functionally druggable targets. The nucleoside prodrug analogue THIO is a first-in-class telomerase-directed, telomere-targeted, anticancer agent that has shown potent activity in other tumor types, including colorectal, lung, melanoma, and brain cancer models. In cancer cells, THIO is converted into the corresponding 5'-triphosphate, which is efficiently incorporated into telomeres by telomerase, activating DNA damage responses and pro-apoptotic pathways. We hypothesized that telomerase-targeting agents may be effective in HCC given the high rate of mutations in the telomerase reverse transcriptase (hTERT) promoter. Moreover, since >90% of HCCs reactivate telomerase to drive escape from senescence-induced growth arrest, treatment with THIO or second-generation telomere-targeted analogues is likely highly selective for telomerase-positive cancer cells relative to nonmalignant hepatocytes.

Methods Activity of THIO and second-generation analogues was evaluated in vitro using telomerase-positive HCC cells and in vivo using syngeneic mouse models of aggressive HCC. HCC cells treated with or without THIO were analyzed for cell proliferation and stained with markers of replicative stress or cell cycle arrest, followed by confocal microscopy and/or flow cytometry. Immunophenotyping of tumor-infiltrating T cells in mice treated with THIO was performed by measuring the frequencies of MDSCs (Ly6C+Ly6G-), NK cells (NK1+), CD4 T cells (Ki67+/CD4+), and CD8 T cells (Ki67+/CD8+). Antitumor activity was assessed by serial measurements of tumor volume in mice sequentially treated with therapeutically relevant doses of THIO ± checkpoint inhibitors compared to control mice and mice treated with checkpoint inhibitors alone.

Results THIO treatment induced replicative stress, followed by cell cycle arrest and apoptosis in telomerase-reactivated HCC cells. In syngeneic mouse models of aggressive HCC, treatment with THIO activated pathways associated with innate and adaptive immunity (eg, cGAS-STING pathway and infiltration of CD8+ T cells into the tumor microenvironment) and altered the immune-suppressive tumor microenvironment. THIO treatment enhanced the response to checkpoint inhibitors, yielding complete responses in some HCC model systems with no dose-limiting toxicities. Similar results were observed with second-generation THIO analogues.

Conclusions Results of this study indicate that THIO, a first-in-class telomerase-directed, telomere-targeted agent, and its analogues may enhance the overall therapeutic efficacy of current immune checkpoint inhibitor-based treatments for HCC.

Acknowledgements Medical writing and editorial support was funded by MAIA Biotechnologies and provided by Anuradha

Kumari, PhD, and Melanie Styers, PhD, of BluPrint Oncology Concepts, LLC.

Ethics Approval All in vivo studies were approved by the animal ethics committee of UT Southwestern, Dallas, Texas.

<http://dx.doi.org/10.1136/jitc-2022-SITC2022.0892>

893

MYELOID DERIVED SUPPRESSIVE CELLS ATTENUATE THE ANTI-TUMOR EFFICACY OF ANDROGEN DEPRIVATION THERAPY AND TARGETED RADIONUCLIDE THERAPY IN A MURINE PROSTATE CANCER MODEL

Anusha Muralidhar*, Carolina Ferreria, Reinier Hernandez, Jamey Weichert, Douglas McNeel. *University of Wisconsin-Madison, Madison, WI, United States*

Background Androgen deprivation therapy (ADT) is the cornerstone treatment for recurrent prostate cancer. ADT is also routinely used in combination with external beam radiation therapy (EBRT) for localized prostate cancer, and the combination results in a high rate of cure for low-risk disease. However, for metastatic castration-resistant prostate cancer (mCRPC), EBRT is typically only used in the palliative setting, because of the inability to radiate all sites of disease. We have developed an alkyl phosphocholine compound, NM600, that is selectively retained by multiple tumor types following systemic delivery. ^{90}Y -NM600 is being explored as a means of targeted radionuclide therapy (TRT) to irradiate all sites of metastases specifically and simultaneously in different tumor models, and a treatment that might modulate the tumor immune microenvironment. We hypothesized that ADT with TRT should be effective in the treatment of metastatic prostate cancer and tested this approach in a relevant murine tumor model.

Methods 6-week-old male FVB mice were implanted subcutaneously with MycCaP tumor cells. Mice were given a single intravenous injection 250 μCi of ^{90}Y -NM600, estimated to deliver 16 Gy to 0.2 cm^3 tumors, in combination with ADT (degarelix). The sequence of administration was evaluated for effect on tumor growth, and groups of mice were euthanized at different time points to characterize the tumor-infiltrating immune populations by flow cytometry.

Results ADT delivered prior to TRT resulted in a significantly greater anti-tumor response and overall survival than if delivered after TRT. Similar studies performed in immunodeficient NRG mice demonstrated no difference with respect to the treatment sequence, suggesting this difference was immunologically mediated. Flow cytometry analysis revealed that CD4+ and CD8+ T cells persisted in the ADT prior to TRT group while they were significantly reduced in the other sequence. CD11b+Gr-1+ myeloid derived suppressor cells (MDSCs) were significantly increased in tumors following TRT prior to ADT treatment and retained immune suppressive function. Depletion of MDSC led to greater anti-tumor response following either treatment sequence.

Conclusions The combination of ADT and TRT significantly delayed tumor growth and improved anti-tumor responses in a murine model of prostate cancer, however this was dependent on the order of administration. This was found to be due to one treatment sequence leading to an increase in infiltrating MDSC. Current studies are investigating the mechanism of these findings.

<http://dx.doi.org/10.1136/jitc-2022-SITC2022.0893>

894

A NOVEL ONCOLYTIC IMMUNOTHERAPY, VET3-TGI, OVERCOMES TGFB1 MEDIATED IMMUNOSUPPRESSION, AUGMENTS TYPE-1 IMMUNE RESPONSE, AND DISPLAYS POTENT THERAPEUTIC ACTIVITY IN MULTIPLE MOUSE TUMOR MODELS

Ravikumar Muthuswamy*, Steve Thorne, Carly Carter, Ming Zhang, Dan Byrd. *Kalivir Immunotherapeutics, Pittsburgh, PA, United States*

Background TGFB1 mediated immune resistance is one of the major mechanisms of immune suppression utilized across multiple tumor types. Immune resistance imparted by TGFB1 is mediated through its pleiotropic effects on vasculature, fibrogenesis and regulatory/effector immune cells within the tumor microenvironment. Blockade of TGFB1 (TGFBi) will likely improve response to immunotherapy. IL-12 is a cytokine that through IFN γ induction, promotes type 1 inflammatory response, M1 macrophages and effector CD8 T cell response. Combining TGFB1 blockade with IL-12 may maximize therapeutic benefits through simultaneously reducing immunosuppression and enhancing anti-tumor immune response. Current studies have developed a vaccinia-based immunotherapy, combining enhanced systemic virus delivery to CXCR3 ligand rich tumors and locally expressed IL-12 and TGFBi within the tumor microenvironment, for efficient control of multiple tumor models.

Methods An oncolytic vaccinia virus expressing CXCR3, IL-12 and a TGFB1 antagonizing mini-monomer was constructed (VET3-TGI) and the expression and function of the transgenes were confirmed. Using *in vivo* mouse RENCA, EMT-6 and MC38 tumor models, the functionality and therapeutic efficacy of VET-TGI were tested with comparison to control virus. Post mortem analysis was used to analyze the impact of VET3-TGI on immune/stromal/endothelial milieu of the tumors and to determine toxicity profile.

Results VET3-TGI infected cells expressed CXCR3 and showed enhanced migration to CXCR3 ligands *in vitro* and improved systemic delivery to tumors expressing CXCR3 ligands *in vivo*, even in the face of pre-existing anti-viral immunity. IL-12 expression and TGFBi blockade of TGFB1 mediated suppression of CD8 T cell proliferation were confirmed *in vitro*. *In vivo* mouse studies using EMT6, RENCA and MC38 tumor models demonstrated potent therapeutic activity, including 100% CRs, even at doses several logs below equivalent clinical doses and in multiple models. Mechanism of activity studies suggested that the therapeutic efficacy of VET3-TGI is associated with considerable modification of the tumor microenvironment. In addition, preliminary toxicity studies demonstrated the safety of VET3-TGI in mouse models.

Conclusions VET3-TGI demonstrated an ability to reduce immunosuppression and dramatically enhance antitumor immune response leading to safe and potent therapeutic activity in multiple mouse tumor models. This data led to the selection of VET3-TGI as our lead clinical candidate. A human version of the virus is currently undergoing clinical manufacture and toxicology testing.

Ethics Approval Animal studies were approved by IACUC, Hilltop animal center

<http://dx.doi.org/10.1136/jitc-2022-SITC2022.0894>

895

ENHANCED ANTI-TUMOR EFFICACY BY COMBINATION OF CHECKPOINT IMMUNOTHERAPY AND ANTIBODY-DRUG CONJUGATES UTILIZING THE TOPOISOMERASE I INHIBITOR LINKER-PAYLOAD AZ'0133

<http://dx.doi.org/10.1136/jitc-2022-SITC2022.0895>

Bilal Omar*, Steve Arbitman, Kalyani Daita, Ana Paucarmayta, Huiyanangel Chow, Judith Anderton, Raymond Rothstein, Allison Gerber, Kathy Mulgrew, Leslie Wetzel, Edward Rosfjord, Nadia Luheshi, Krista Kinneer, Scott Hammond. *AstraZeneca, Gaithersburg, MD, United States*

Background Recent clinical trials highlight the potential therapeutic benefit from combining checkpoint immunotherapies (IO) with antibody drug conjugates (ADC) incorporating different cytotoxic warheads. We hypothesize that diverse ADC warheads modulate different aspects of tumor immune biology.

Methods Antibodies specific for tumor antigens B7-H4 and other model antigens were conjugated to either topoisomerase inhibitor linker-payload AZ141470133 (AZ'0133) or microtubule inhibitor warhead monomethyl auristatin E (MMAE), and their biologic effects on immune-related endpoints in vitro and anti-tumor activity in vivo in mouse models were determined.

Results In vitro studies demonstrated that AZ'0133-ADCs increases the immunogenicity of tumor cells and enhances the activation and maturation of dendritic cells (DC) to an equal to or greater extent compared to MMAE-ADCs. Treatment of human tumor cell lines with B7-H4-AZ'0133 or another model antigen targeting-AZ'0133 ADC increased cell surface expression of MHC class I to a greater extent than the same ADCs conjugated to MMAE. Surface expression of TIGIT ligand PVR/CD155 was exclusively increased by the model antigen targeting-AZ'0133 ADC but not with the same antibody conjugated to MMAE. PD-L1, Nectin-2, MHC class II, and immunogenic cell death markers calreticulin and phosphatidylserine were increased by both AZ'0133- and MMAE-ADCs. Co-culture of immature DCs with tumor cell lines in the presence of model antigen targeting AZ'0133-ADCs induced expression of DC maturation markers and CTLA-4 ligands CD80 and CD86 as well as Nectin-2. The same ADC conjugated to MMAE upregulated only CD80 and decreased TIM-3 expression on DC.

In immunocompetent mouse models, the combination of anti-PDL1 with either AZ'0133- or MMAE-ADCs drove enhanced anti-tumor activity versus monotherapy controls. In a CT26 syngeneic model expressing mouse B7-H4, the combination of anti-PD-L1 with either a mouse cross-reactive anti-B7-H4 MMAE or anti-B7-H4-AZ'0133 ADC reduced tumor growth rates and increased overall survival versus monotherapy controls. In a CT26 model overexpressing a different human model tumor antigen, the combination of anti-PD-L1 with either an AZ'0133 conjugated-ADC or the same antibody conjugated to MMAE, reduced the rate of tumor growth and improved survival as compared to monotherapy controls. In both models, growth rate inhibition and survival benefit were comparable for the combination of anti-PD-L1 with either AZ'0133- or MMAE-ADCs.

Conclusions AZ'0133 and MMAE ADCs both combine with anti-PD-L1 to enhance anti-tumor activity in vivo. In vitro, whilst both classes of ADC induce immunogenicity and immune activation, they have differing impacts on T cell checkpoint ligand expression.

Ethics Approval All studies involving animals were approved by the Institutional Animal Care and Use Committee at AstraZeneca under protocol number AUP-21-05.

896

ONCOLYTIC HERPES SIMPLEX VIRUS IMMUNO-VIROTHERAPY IN COMBINATION WITH TIGIT IMMUNE CHECKPOINT BLOCKADE TO TREAT GLIOBLASTOMA

¹Eleni Panagiotti, ¹J Kelley*, ²William F Goins, ³Keith Ligon, ¹Karen Dixon, ¹Ana Anderson, ¹Vijay Kuchroo, ¹Antonio Chiocca. ¹Brigham and Women's Hospital, Boston, MA, United States; ²University of Pittsburgh, Pittsburgh, PA, United States; ³Dana Farber Cancer Institute, Boston, MA, United States

Background Glioblastoma Multiforme (GBM) is an aggressive primary brain tumor and represents the most fatal type of malignant cancer. Despite rigorous clinical research efforts there is minimal improvement in GBM patient outcomes. Oncolytic herpes simplex virus 1 (oHSV-1) is emerging as a promising approach to promote anti-tumor responses in GBM patients. In this study, we hypothesized that intratumoral administration of a novel HSV-1 based oncolytic virus (HSV-1 rQNestin34.5v2) will result in synergy when combined with anti-TIGIT checkpoint blockade therapy. We investigated the antitumor efficacy of this combination in immunocompetent syngeneic murine glioma models that exhibit different genetic alterations and tumor mutations.

Methods HSV-1 based oncolytic virus (HSV-1 rQNestin34.5v2), currently investigated in a phase I clinical trial for recurrent glioblastoma (ClinicalTrials.gov: NCT03152318) was employed, that maintains a copy of the HSV-1- ICR34.5 gene, which is responsible for HSV-1 neurovirulence under transcriptional control of the tumor-specific promoter nestin to drive robust tumor-selective replication. Syngeneic GL261, CT-2A, IDH1 mutant and IDH1 wild type orthotropic glioma mouse models were used to evaluate immunotherapeutic and antitumor responses. Immune cell signatures at the tumor microenvironment and in the peripheral blood involved at the treatment response were assessed by multiparameter flow cytometry analysis.

Results HSV-1 rQNestin34.5v2 exhibited robust ability to infect murine glioma cells *in vitro* triggering cytotoxicity. Infection stimulated immunogenic cell death in glioma cells as evidenced by extracellular release of damage-associated molecular patterns (DAMPs) and proinflammatory cytokines. *In vitro* screens for upregulation of immune checkpoint molecules following infection with HSV-1 rQNestin34.5v2 identified CD155/CD112/TIGIT and PD-L1/PD1 axes as promising targets for combination therapies. TIGIT was found to be overexpressed in tumor infiltrating NK, CD4 and CD8 T cells suggesting systemic therapy with TIGIT blockade antibodies could have therapeutic utility in combination with HSV-1 rQNestin34.5v2 in GBM. Intratumoral administration HSV-1 rQNestin34.5v2 resulted in the development of a proinflammatory environment as shown by decreased CX3CR1 expression on tumor infiltrating NK cells. Benefit in overall survival was not observed by systemic anti-TIGIT monotherapy. Combination treatment with intratumoral HSV-1 rQNestin34.5v2 administration exhibited modest therapeutic effect with a cure rate 12% in mice bearing intracranial CT-2A tumors. Long term CT-2A tumor survivor mice were effectively protected by rechallenge with autologous CT-2A cells indicating the development of long lasting tumor specific immunity.

Conclusions Our findings show that the combination of HSV-1 rQNestin34.5v2 virotherapy with anti-TIGIT checkpoint blockade immunotherapy represents a promising strategy to overcome primary resistance to immune checkpoint inhibitors in GBM.

Ethics Approval All animal experiments and procedures described in this study were approved by Brigham and Women's Institutional Animal Care and Use Committee.

<http://dx.doi.org/10.1136/jitc-2022-SITC2022.0896>

897

PARTNERS FOR BISPECIFICS: COMBINATORIAL APPROACHES TO AUGMENT T-CELL FUNCTION AND MITIGATE EXHAUSTION

Nora Philipp*, Marion Subklewe, Amelie Muth, Michael Von Bergwelt-Baildon, Veit Bücklein. University Hospital, LMU Munich, Munich, Germany

Background T-cell engaging bispecific antibody molecules (BsAb) redirect T cells towards antigen-expressing cells and have shown efficacy in various B-cell malignancies.¹⁻³ The CD19xCD3 BsAb blinatumomab was the first in class to be approved in the setting of R/R BCP-ALL with a response rate of 43%.⁴ Evaluating mechanisms of resistance to bispecifics has been hampered by a lack of an appropriate model to mimic the clinical application of continuous BsAb exposure over several weeks to months. We developed an *in vitro* model system to simulate the clinical administration of blinatumomab as continuous infusion over 28 days and demonstrated that continuous exposure to a BsAb induces T-cell exhaustion.⁵ To identify partners for bispecifics to mitigate exhaustion, a diverse toolbox of off-the-shelf immunomodulating agents was evaluated. Using our *in vitro* model system, we explored the potential of BsAb treatment in combination with i) the tyrosine kinase inhibitor dasatinib, ii) the immunomodulator lenalidomide and iii) aPD-1/aPD-L1 checkpoint blockade to enhance T-cell function (figure 1).

Methods Healthy donor T cells were cocultured with CD19⁺ OCI-Ly1 cells and continuously stimulated with a CD19xCD3 BsAb alone or in combination with dasatinib (12.5 nM), lenalidomide (10 µg/ml), nivolumab (10 µg/ml) or atezolizumab (10 µg/ml) for 28 days. Every 7 days, T cells were isolated and characterized in functional assays: (1) Expression of inhibitory receptors (IRs; PD-1, Tim-3, LAG-3), (2) BsAb-mediated cytotoxicity against hCD19-Ba/F3 cells after 72h, (3) T-cell expansion as fold change of CD2⁺ counts, (4) BsAb-mediated cytokine secretion measured via intracellular staining or in supernatants.

Results Dasatinib reduced IR co-expression and led to an increased proliferative and cytotoxic potential of T cells after 14 days of BsAb stimulation. Furthermore, it strongly increased granzyme B expression and secretion of IL-2 and IFN-g. Lenalidomide did not affect IR co-expression, but increased cytotoxicity of T cells after 14 and 21 days of BsAb stimulation. Additionally, it increased IL-2 and IFN-g secretion. Interestingly, both nivolumab and atezolizumab did not enhance T-cell function, suggesting a minor role of the PD-1/PD-L1 axis in the induction of exhaustion in our model system.

Conclusions Together, our findings highlight that T-cell function during BsAb stimulation *in vitro* strongly improves by combinatorial treatment with dasatinib or lenalidomide. Albeit checkpoint inhibitors can boost T-cell responses, they could not ameliorate BsAb-induced T-cell exhaustion. Our data supports combinatorial approaches of BsAbs and small molecules to achieve durable T-cell responses in patients.

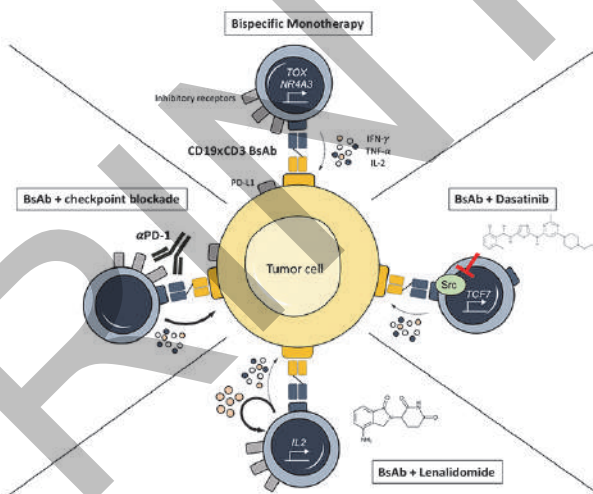
REFERENCES

1. Kantarjian H, Stein A, Gokbuget N, et al. Blinatumomab versus chemotherapy for advanced acute lymphoblastic leukemia. *The New England Journal of Medicine*. 2017;**376**(9):836–847.
2. Goldstein RL, Goyos A, Li CM, et al. AMG 701 induces cytotoxicity of multiple myeloma cells and depletes plasma cells in cynomolgus monkeys. *Blood Adv*. 2020;**4**(17):4180–4194.
3. Hutchings M, Morschhauser F, Iacoboni G, et al. Glofitamab, a novel, bivalent CD20-targeting T-cell-engaging bispecific antibody, induces durable complete remissions in relapsed or refractory B-cell lymphoma: a phase I trial. *Journal of*

Clinical Oncology : Official Journal of The American Society of Clinical Oncology. 2021;**39**(18):1959–1970.

4. Zugmaier G, Gokbuget N, Klinger M, et al. Long-term survival and T-cell kinetics in relapsed/refractory ALL patients who achieved MRD response after blinatumomab treatment. *Blood*. 2015;**126**(24):2578–2584.
5. Philipp N, Kazerani M, Nicholls A, et al. T-cell exhaustion induced by continuous bispecific molecule exposure is ameliorated by treatment-free intervals. *Blood*. 2022;online ahead of print

Ethics Approval Peripheral blood (PB) were collected from healthy donors (HDs) after written informed consent was received in accordance with the Declaration of Helsinki and approval was granted by the Institutional Review Board of the Ludwig-Maximilian-Universitaet (Munich, Germany; ID 216-08).



Abstract 897 Figure 1 Partners for Bispecifics

<http://dx.doi.org/10.1136/jitc-2022-SITC2022.0897>

898

TRIPLE THERAPY (BINIMETINIB, BEVACIZUMAB, PEMBROLIZUMAB) MODULATES THE TUMOR IMMUNE MICROENVIRONMENT IN MICROSATELLITE STABLE COLORECTAL CANCER PDXS IN A HUMANIZED MICE MODEL

Julie Lang*, Adrian Dominguez, Matthew Lewis, Sarah Hartmann, Jordi Lanis, Hannah Strassburger, Wells Messersmith, S Lindsey Davis, Alexis Leal, Sunnie Kim, Tyler Friedrich Kimberly,, Christopher Lieu, Todd Pitts. *University of Colorado Denver AMC, Aurora, CO, United States*

Background Single-agent checkpoint blockade inhibitors have shown great promise in recent years but has unfortunately been limited to a subset of tumor types. The tumor mutation burden as well as the tumor microenvironment are two key important features that distinguish immunogenic, from non-immunogenic tumors. There is currently a massive effort, including a wide range of strategies, turning tumors from cold to hot including combining with small molecule inhibitors.

For colorectal (CRC) cancers, anti-PD1 therapies have proven to be successful in the clinic for microsatellite instable (MSI-high) tumors but have no efficacy in the majority of patients with CRC that have microsatellite stable (MSS) cancers. Our primary goal is to determine if the addition of binimetinib (small molecule MEK inhibitor) and bevacizumab (anti-VEGF therapeutic antibody) increases the response rate of metastatic microsatellite stable colorectal cancer to pembrolizumab in humanized patient-derived xenografts (hPDXs) of CRC. We will also identify immune and pathway modulation in MSS CRC hPDXs treated with the combination of MEK, VEGF, and immune checkpoint inhibitors.

Methods In six independent experiments, we implanted distinct MSS CRC PDXs, that were recently isolated from patients on a matching clinical trial, into the flanks of humanized BRGS (BALB/c, Rag2^{-/-}, IL2RgC^{-/-}, NOD^{SIRPα}) mice that had been engrafted with human hematopoietic stem cells at birth. For each PDX we generated humanized mice cohorts treated with vehicle, binimetinib, binimetinib/pembrolizumab combination, or binimetinib/pembrolizumab/bevacizumab/DC101. The human immune system in the immune organs and tumors were interrogated by flow cytometry to assess changes in the cellular composition and the activation state of the immune system as a result of treatments, and the expression of immune-related molecules were assessed on the tumor cells.

Results There were no significant differences in primary tumor growth in all treated models. However, immune modulation was observed in TILs in which we measured increased activated T cells (DR+, effector memory, TIM-3+), GrB+CD8+ and IFNγ+CD8+ T cells. We also observed increased TNFα and IFNγ and decreased T regulatory (FoxP3+CD25+) CD4+ T cells in the pembrolizumab/binimetinib and triple combination groups. Immune infiltrates were unique for the various PDXs.

Conclusions In this preclinical examination of combination MEK, VEGF, and PD-1 inhibition in CRC hPDXs no significant differences in tumor growth were noted, but immune modulation in TILs and tumor were observed suggesting potential immune modulation of the tumor microenvironment that may lead to greater susceptibility to immune checkpoint inhibition in patients with MSS mCRC.

Ethics Approval The human cord blood samples were generously provided as de-identified donors from Clinimmune Cord Blood Bank (Aurora, CO). All procedures and mouse husbandry were performed in accordance with IACUC protocols

approved by the University of Colorado Denver Institutional Animal Care and Use Committee in the Office of Laboratory of Animal Resources (OLAR), a facility approved by the American Association for Laboratory Animal Care.

<http://dx.doi.org/10.1136/jitc-2022-SITC2022.0898>

899

BET INHIBITORS SYNERGIZE WITH ANTI-PD1 BY ENHANCING TCF7 ACCESSIBILITY IN LEUKEMIA-DERIVED TERMINALLY EXHAUSTED CD8⁺ T CELLS

Kyle Romine, Hyun-jun Cho, Yoko Kosaka, Patrick Flynn, Kaelan Byrd, Jesse Coy, Matthew Newman, Jamie Scott, Andrew Adey, Evan Lind*. OHSU, Portland, OR, United States

Background Our lab and others have shown that a proportion of blood and bone marrow specimens from AML patients have an immunosuppressive microenvironment and have hallmarks of immune exhaustion: increased frequencies of regulatory T cells (Tregs)¹ and myeloid-derived suppressor cells (MDSCs),² decreased T-cell proliferation,³ elevated expression of immune checkpoint molecules⁴ and increased TEx vs. TPEX⁵⁻⁷ populations. Importantly, a subset of these patient samples containing dysfunctional T cells can be rescued by ICB[3]. We have identified the same immune-related features, in a mouse model of AML. BET inhibitors (BETi) have been shown to positively affect CD8⁺ T cells, indirectly via reduction of PD-L1 expression on myeloid cells^{8,9} and directly by inhibition of chronic TCR activation genes, increasing stem-cell like memory CD8⁺ T cells.^{10,11} We hypothesized that BETi may synergize with anti-PD1 therapy in AML through promoting T cell stemness.

Methods Our AML mouse model bears FLT3-ITD and deletion of TET2 restricted to the myeloid lineage (LysM-CRE). For *in vitro* studies, splenocytes were stimulated with anti-CD3 and either JQ1, anti-PD1 or both and proliferation and differentiation status were assessed by flow cytometry. For *in vivo* studies, treatment consisted of 2 weeks. s3-ATAC-seq; Cells were prepared as described.¹² Libraries were sequenced on a NextSeq 2000. Data was then analyzed and visualized using the ArchR. GSE Accession: GSE205386.

Results We show that inhibitors which target bromodomain and extra-terminal domain (BET) proteins rescue T cell exhaustion. *Ex vivo* treatment of cells from AML mice and AML patients with BET inhibitors (BETi) reversed CD8⁺ T cell exhaustion by restoring proliferative capacity and expansion of the more functional TPEX (figure 1). This reversal is enhanced by combined BETi and anti-PD1 treatment. BETi synergized with anti-PD1 *in vivo*, resulting in the reduction of circulating leukemia cells, enrichment of CD8⁺ T cells in the bone marrow, and increased expression of *Tcf7*, *Slamf6*, and *Cxcr5* in CD8⁺ T cells (figure 2). Finally, we profiled the epigenomes of *in vivo* JQ1 treated AML-derived CD8⁺ T cells by single-cell ATAC seq and find that JQ1 increases *Tcf7* accessibility specifically in TEx cells, suggesting that BETi likely mechanistically acts by relieving repression of progenitor programs in TEx CD8⁺ T cells and maintaining a pool of anti-PD1 responsive CD8 T cells (figure 3).

Conclusions Using an AML mouse model that exhibits leukemia-induced immune exhaustion, we demonstrate the pre-clinical efficacy of combining BETi and anti-PD1 therapy in the treatment of AML.

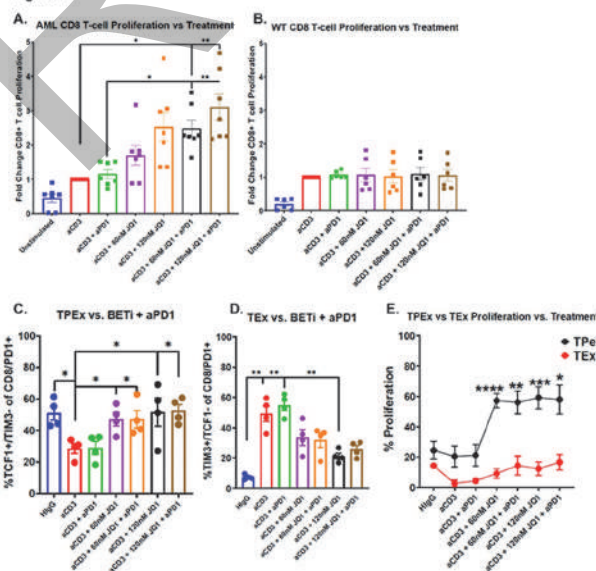
REFERENCES

1. Szczepanski MJ, Szajnik M, Czystowska M, et al. Increased frequency and suppression by regulatory T cells in patients with acute myelogenous leukemia. *Clin Cancer Res* 2009;**15**(10):3325–32 doi: 10.1158/1078-0432.CCR-08-3010.
2. Wang L, Jia B, Claxton DF, et al. VISTA is highly expressed on MDSCs and mediates an inhibition of T cell response in patients with AML. *Oncoimmunology* 2018;**7**(9):e1469594 doi: 10.1080/2162402X.2018.1469594.
3. Lambie AJ, Kosaka Y, Laderas T, et al. Reversible suppression of T cell function in the bone marrow microenvironment of acute myeloid leukemia. *Proc Natl Acad Sci U S A* 2020;**117**(25):14331–41 doi: 10.1073/pnas.1916206117.

4. Williams P, Basu S, Garcia-Manero G, et al. The distribution of T-cell subsets and the expression of immune checkpoint receptors and ligands in patients with newly diagnosed and relapsed acute myeloid leukemia. *Cancer* 2019;**125**(9):1470–81 doi: 10.1002/cncr.31896.
5. Noviello M, Manfredi F, Ruggiero E, et al. Bone marrow central memory and memory stem T-cell exhaustion in AML patients relapsing after HSCT. *Nat Commun* 2019;**10**(1):1065 doi: 10.1038/s41467-019-08871-1.
6. Tan J, Chen S, Lu Y, et al. Higher PD-1 expression concurrent with exhausted CD8⁺ T cells in patients with de novo acute myeloid leukemia. *Chin J Cancer Res* 2017;**29**(5):463–70 doi: 10.21147/j.issn.1000-9604.2017.05.11.
7. Tan J, Yu Z, Huang J, et al. Increased PD-1+Tim-3+ exhausted T cells in bone marrow may influence the clinical outcome of patients with AML. *Biomark Res* 2020;**8**:6 doi: 10.1186/s40364-020-0185-8.
8. Hogg SJ, Vervoort SJ, Deswal S, et al. BET-bromodomain inhibitors engage the host immune system and regulate expression of the immune checkpoint ligand PD-L1. *Cell Rep* 2017;**18**(9):2162–74 doi: 10.1016/j.celrep.2017.02.011.
9. Zhu H, Bengsch F, Svoronos N, et al. BET Bromodomain Inhibition Promotes Anti-tumor Immunity by Suppressing PD-L1 Expression. *Cell Rep* 2016;**16**(11):2829–37 doi: 10.1016/j.celrep.2016.08.032.
10. Kagoya Y, Nakatsugawa M, Yamashita Y, et al. BET bromodomain inhibition enhances T cell persistence and function in adoptive immunotherapy models. *J Clin Invest* 2016;**126**(9):3479–94 doi: 10.1172/JCI86437.
11. Milner JJ, Toma C, Quon S, et al. Bromodomain protein BRD4 directs and sustains CD8 T cell differentiation during infection. *J Exp Med* 2021;**218**(8) doi: 10.1084/jem.20202512.
12. Mulqueen RM, Pakholok D, O'Connell BL, et al. High-content single-cell combinatorial indexing. *Nat Biotechnol* 2021;**39**(12):1574–80 doi: 10.1038/s41587-021-00962-z.

Ethics Approval IACUC protocol TR01_IP00000907

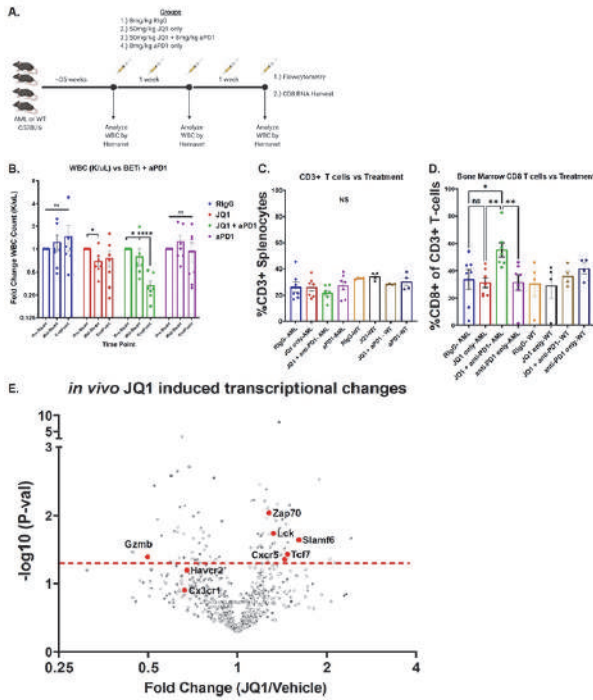
Figure 1.



Abstract 899 Figure 1 BETi partially rescues T cell function in vitro. Splenocytes were isolated from 7 AML (a) or 6 WT mice (b), stained with CFSE, and cultured for 72 hours without TCR stimulation (HlgG), anti-CD3 alone, anti-CD3 with anti-PD1 or titrations of anti-CD3 with JQ1 or anti-CD3 with both JQ1 and anti-PD1. Cells were stained and analyzed by flow cytometry. Plots represent the fold-change in proliferation in CD8⁺ T cells, as measured by percent CFSE diluted relative to anti-CD3 stimulated alone. Significance determined by Kruskal-Wallis multiple comparisons T-tests. Effect of BETi, anti-PD1, or BETi + anti-PD1 treatment on the percent of TPEX CD8⁺ T cells (c) and TEx CD8⁺ T cells (d) after culturing for 72 hours as previously in a-b. Significance determined by Kruskal-Wallis multiple comparisons T-tests. Splenocytes from 4 AML mice were stained with CFSE and plated for 72 hours without TCR stimulation (HlgG), anti-CD3 alone, anti-CD3 with anti-PD1 and titrations of anti-CD3 with JQ1 or anti-CD3 with both JQ1 and anti-PD1. Proliferation of TPEX (black) and TEx (red) CD8⁺ T cells from AML mice was assessed by flow cytometry (e). Significance determined by Kruskal-Wallis multiple comparisons t-tests.

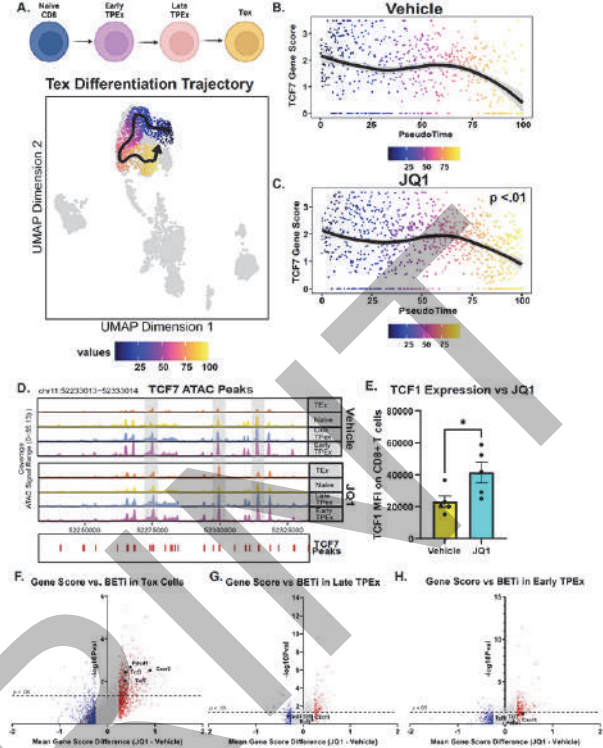
Abstracts

Figure 2.



Abstract 899 Figure 2 In vivo treatment with BETi and anti-PD1 a.) Schematic detailing in vivo BETi + anti-PD1 treatment strategy and functional readouts of efficacy. b.) Mice treated with RlgG, JQ1, JQ1 with anti-PD1, or anti-PD1 alone were bled periodically over a two-week period and assessed for WBC. Data displays fold-change WBC (k/μL) normalized per mouse in comparison to pre-treatment bleed WBC. Significance determined by one-way ANOVA. Timepoints are Pre-Blood, Mid-bleed (day 7), Endpoint (day 14). c, d.) Bone marrow cells were isolated from treated AML and WT mice and assessed by flow cytometry. Graph denotes %CD3+ T cells in the bone marrow (c) and %CD8+ T cells in the bone marrow as a percent of all T cells (d). Significance derived from combining two experimental replicates and determined by one-way ANOVA. e.) CD8+ T cells were isolated from JQ1-treated and RlgG-treated AML mice and RNA harvested and analyzed by Nanostring. Volcano plot shows the fold-change in normalized transcript levels of JQ1-treated mice vs RlgG treated AML mice vs. $-\log_{10}$ P-value as determined by multiple t-tests. Hits of interest are highlighted in red. Dashed red line denotes significance threshold (0.05).

Figure 3.



Abstract 899 Figure 3 ATAC-seq of CD8 T cells from animals treated with BETi

a.) (Top) cartoon schematic describing the cell types fit to the differentiation trajectory (bottom). Colors represent pseudotime values throughout TEX differentiation. b-c.) Pseudotime trajectory plot with corresponding TCF7 gene score throughout TEX differentiation for b.) Vehicle treated cells and c.) JQ1 treated cells. Vertical red dashed marks the third quartile throughout pseudotime (late TPEX/Early Tex) and the horizontal red dashed line markers the TCF7 accessibility at pseudotime 100. Significance was calculated by mann-whitney T-test comparing the aggregate TCF7 gene scores for each cell throughout pseudotime in vehicle and JQ1 treated groups. d.) Schematic of the ATAC signal peaks vs treatment and cluster which were generated in ArchR. (Top) Vehicle treated Tex, Naive, Late TPEX, and early Tex cells. (Bottom) Matching clusters for JQ1 treated cells. Grey boxes highlight greatest differential peaks in the Tex cells between Vehicle and JQ1 treated cells. e.) A portion of splenocytes derived from the vehicle or JQ1 treated AML mice were analyzed by flow cytometry. Data represents TCF1 median fluorescence intensity of TCF1 on all CD8+ T cells. Significance determined by Mann-Whitney T-test. f-h.) Volcano plot describing the mean difference in gene scores (JQ1 – Vehicle) from f.) Tex cells only (Cluster 5), g.) late TPEX cells only (Cluster 7), and h.) early TPEX cells only (Cluster 8). Significance calculated via multiple corrected t-tests. Genes with a mean difference $>.25$ are highlighted in red and genes $< -.25$ are highlighted in blue. Genes of interest (Tcf7, Tcf3, Pcdcl1, and Cxcr3) are highlighted in black. The dashed horizontal line marks the significance cutoff. Genes below the line are not significant.

<http://dx.doi.org/10.1136/jitc-2022-SITC2022.0899>

900

DECREASING TOXICITY OF IMMUNOCYTOKINES BY TRANSIENT AND SELECTIVE INHIBITION OF THEIR INTRACELLULAR SIGNALING ACTIVATION

¹Sheila Dakhel Plaza*, ¹Giulia Rotta, ¹Samuele Cazzamalli, ¹Ettore Gilardoni, ¹Riccardo Stucchi, ²Christian Pellegrino, ¹Jacqueline Mock, ¹Roberto De Luca, ³Emanuele Puca, ³Dario Neri. ¹Philochem AG, Otelfingen, Switzerland; ²University Hospital Zurich, Zurich, Switzerland; ³Philogen S.p.A, Otelfingen, Switzerland

Background The use of cytokine-based therapeutics has traditionally been limited by systemic toxicity, but it is now becoming evident that it may be possible to circumvent this problem in a number of ways. Tumor-targeting antibody-cytokine fusions proteins (also called “immunocytokines”) typically allow to administer lower dosages of the payload as a result of the selective localization at the site of disease, thus, improving the therapeutic index. A second aspect relates to the non-linearity of cytokine-mediated toxicity and to the possibility of progressively increasing payload concentration in the tumor. At the clinical level, undesired side effects are often seen when the concentration of cytokines in blood exceeds a certain threshold. In most cases, adverse events disappear when cytokines are cleared from circulation.

Methods Here, we describe an innovative approach to transiently inhibit off-target toxicity of targeted-cytokines, while maintaining their antitumor activity. L19-TNF and L19-IL12 are two clinical-stage tumor-targeted antibody-cytokine fusion proteins that display potent activity by triggering the receptor-interacting serine/threonine-protein kinase 1 (RIPK1) and Janus Kinase 2 (JAK2) intracellular signaling pathways, respectively. Interestingly, small molecule inhibitors and immunocytokines based on antibody fragments have similar half-lives in blood, but only the immunocytokine accumulates at the tumor site for longer periods.

Results In a first study, GSK'963, a potent small molecule inhibitor of RIPK1, was tested in tumor-bearing mice with the aim to reduce acute systemic toxicity associated with TNF signaling. Transient inhibition of RIPK1 allowed the administration of TNF doses, which would otherwise be lethal. The protective effect of GSK'963 did not affect the selective localization of the immunocytokine to tumors. Moreover, L19-murTNF, when given in combination with GSK'963, was still able to induce tumor necrosis and to exert its potent anti-cancer effects. In a second study, tumor-bearing mice receiving L19-murIL12 were pretreated with Ruxolitinib (Jakafi®), a commercially available JAK2 inhibitor. The addition of Ruxolitinib could significantly improve the tolerability profile without affecting the anti-cancer properties of the immunocytokine. The safety profile was monitored following the body-weights of the animals and by measuring the interferon- γ (IFN γ) levels in blood at early time points after the intravenous injection of L19-murIL12.

Conclusions Our results are of clinical relevance, as patients treated with targeted cytokines L19-TNF and L19-IL12 could potentially benefit from judicious combinations treatments using GSK'963 or Ruxolitinib respectively.

<http://dx.doi.org/10.1136/jitc-2022-SITC2022.0900>

901

INHIBITION OF GAS6/MERTK SIGNALING BY NOVEL MERTK ANTIBODY, 20A77, EXERTS SIGNIFICANT ANTI-TUMOR EFFICACY WITH LITTLE RETINAL DEGENERATION IN MICE

Atsushi Sawada*, Masayoshi Toyoura, Aki Takaiwa, Toshikazu Inoue, Koji Nakamura. *Chiome Bioscience Inc., Tokyo, Japan*

Background Mer Receptor Kinase (MerTK) is a member of TAM (Tyro-3, AXL, MerTK) family of receptor tyrosine kinase and known as a macrophage receptor that mediates the efferocytosis. MerTK interacts with apoptotic cells through its ligands, Gas6 or protein S, and promotes the polarity of tumor-associated macrophages toward M2 phenotype.¹ Recent studies have revealed that MerTK signaling is involved in the immune suppression in the tumor microenvironment and specific inhibition of MerTK signaling suppressed tumor progression.²⁻⁴ On the other hand, MerTK also plays an essential role in homeostasis of the retina through its ligands, Tubby and Tulp1 and the mutations in these genes cause retinal degeneration.⁵⁻⁹ Thus, blockage of MerTK signaling have a potential risk for the retinal toxicity.

Methods Anti-MerTK monoclonal antibodies which recognized both with mouse and human antigen were established by immunization of recombinant human MerTK proteins in MerTK deficient mice. Isolated antibodies were analyzed their blocking activity against Gas-6 induced MerTK auto-phosphorylation by using MerTK-expressing cell-based assay. These antibodies were also analyzed their Inhibition activity of Tulp1-MerTK binding. The anti-tumor activity of isolated antibodies, 20A77 and 24A1, was evaluated in mouse colorectal CT26 bearing syngeneic mice model as monotherapy and in combination with anti-PD-1 antibody. In addition, retinal deficiency of 20A77 treated mice was analyzed histologically.

Results The isolated antibodies, 20A77 and 24A1, specifically recognized with both mouse and human MerTK and inhibited Gas6-dependent MerTK auto phosphorylation. In contrast, these antibodies didn't inhibit the Tulp1-MerTK binding. The treatment of either 20A77 or 24A1 antibody into CT26 bearing mice resulted in the reduction of the tumor growth. Tumor Infiltrated Lymphocyte (TIL) analysis revealed that the ratio of M1 polarized macrophage was increased in 20A77 treated mice. Moreover, the combination of anti-MerTK and anti-PD-1 antibody treatment indicated enhanced anti-tumor responses than any of single-agents of antibody treatment. Lastly, we analyzed the histological defect in the eyes of 20A77 treated mice. No deficiency of retina was detected in medical effective dose of 20A77 treated mice. However, increased amount of 20A77 treatment caused retinal degeneration.

Conclusions Novel anti-MerTK antibody, 20A77, which selectively inhibited GAS6-mediated MerTK signaling showed significant anti-tumor activity without retinal degeneration in a mouse model. Our results suggest that the strategy for ligand-selective inhibition of MerTK signaling by the specific antibody could become a novel treatment option with lower retinal toxicity for solid tumors.

REFERENCES

1. Zizzo G, Hilliard BA, Monestier M, Cohen PL. Efficient clearance of early apoptotic cells by human macrophages requires M2c polarization and MerTK induction. *J Immunol.* 2012;**189**(7):3508–3520.
2. Zhou, et al. Blockade of the phagocytic receptor MerTK on tumor-associated macrophages enhances P2X7RDependentSTING Activation by Tumor-Derived cGAMP. *Immunity.* 2020;**52**:357–373.

3. Lin, et al. MerTK-mediated efferocytosis promotes immune tolerance and tumor progression in osteosarcoma through enhancing M2 polarization and PD-L1 expression. *Oncimmunology.* 2022;**11**: 1:e2024941 (12 pages).
4. Davra V, Kumar S, Geng K, et al., Axl and Mertk receptors cooperate to promote breast cancer progression by combined oncogenic signaling and evasion of host antitumor immunity. *Can Res.* 2021;**81**(3):698–712.
5. D'Cruz PM, Yasumura D, Weir J et al. Mutation of the receptor tyrosine kinase gene MERTK in the retinal dystrophic RCS rat. *Hum Mol Genet.* 2000;**9**:645–651
6. Gal A, Li Y, Thompson DA et al. Mutations in MERTK, the human orthologue of the RCS rat retinal dystrophy gene, cause retinitis pigmentosa. *Nat Genet.* 2000;**26**:270–271.
7. Duncan JL, LaVail MM, Yasumura D, Yasumura D, Matthes MT et al. An RCS-like retinal dystrophy phenotype in mer knockout mice. *Invest Ophthalmol vis Sci.* 2003;**44**:826–838.
8. Sayama A, Okado K, Nakamura K et al. UNC569-induced morphological changes in pigment epithelia and photoreceptor cells in the retina through MerTK inhibition in mice. *Toxicol Pathol.* 2018;**46**(2):193–201.
9. Caberoy NB, Zhou Y and Li W. Tubby and tubby-like protein 1 are new MerTK ligands for phagocytosis. *EMBO J.* 2010;**29**:3898–3910.

Ethics Approval This study was approved by the internal animal ethics board of Chiome Bioscience Inc, approval number A2018-005, A2018-015, A2019-010 and A2019-016.

<http://dx.doi.org/10.1136/jitc-2022-SITC2022.0901>

902

NKX019, AN OFF-THE-SHELF CD19 CAR-NK CELL, MEDIATES IMPROVED ANTI-TUMOR ACTIVITY AND PERSISTENCE IN COMBINATION WITH CD20-DIRECTED THERAPEUTIC MABS

Mira Tohmé*, Tina Davis, Max Zhang, Hadia Lemar, Bao Duong, Joanne Tan, James Trager. *Nkarta Therapeutics, South San Francisco, CA, United States*

Background NKX019 is an investigational CD19-targeting chimeric antigen receptor (CAR) natural killer (NK) cell therapy with engineered persistence for treating B cell malignancies. NKX019 exhibits more rapid cytotoxic kinetics than CD19-directed CAR T cells, and lower production of cytokines associated with cytokine release syndrome (CRS).¹ The safety and clinical activity of NKX019 are currently being evaluated in a phase I [GM1] clinical study [NCT05020678]. Recent studies^{2,3} have shown that combining NK cell therapies with monoclonal antibodies (mAbs) may improve targeted NK cell activation and overcome some of the disadvantages associated with the stand-alone use of therapeutic mAbs. CD20-targeted mAbs such as rituximab (RTX) and obinutuzumab (OBI), can mediate antibody-dependent cellular cytotoxicity (ADCC), a key effector mechanism of NK cells. RTX also activates some levels of caspase-dependent direct cell death (DCD). OBI is engineered to induce improved DCD and ADCC mechanisms.⁴ Antigen escape is reported in 30–95% of relapses after CD19-directed CAR T cell therapy in B cell –acute lymphoblastic leukemia (B-ALL).⁵ Here, we describe the potential advantage of using NKX019 in combination with [GM2] RTX or OBI to reduce relapse following monotherapy with either agent alone by targeting both CD19⁺ and CD20⁺ malignant B cells.

Methods NK cells, isolated from healthy PBMCs, were expanded and engineered to express a CD19-targeted CAR and membrane-bound interleukin 15 to generate NKX019. NKX019 cells were cryopreserved and freshly thawed for experimental use. NKX019 mediated-cytotoxicity was assessed in both 4-Hour (4H) and extended assays in the presence or absence of anti-CD20 mAbs, RTX or OBI, using CD19⁺ and CD20⁺ expressing tumor B cell lines: Raji (lymphoblast-like), DOHH-2 (follicular lymphoma) and EHEB (B-Lymphoblastoid) cells. A non-glycosylated version of RTX (RTX mutant) with compromised ADCC function was used to evaluate ADCC-mediated vs ADCC-independent activity of NKX019.

Results NKX019 in combination with RTX or OBI demonstrated increased activity and persistence against tumor B cell lines in a 4H kill assay and in tumor rechallenge experiments. NKX019 in combination with RTX demonstrated an enhanced cytotoxicity against EHEB lymphoblastoid cell line in a manner consistent with ADCC. OBI demonstrated increased activity in comparison to RTX, as a single agent and in combination with NKX019 cells.

Conclusions This study demonstrates increased activity and persistence of NKX019 when used in combination with approved CD20-targeted mAbs, RTX and OBI, against B cell malignancies. A first-in -human Phase I clinical trial of NKX019 in combination with RTX is planned.

REFERENCES

1. Morisot N, Wadsworth S, Davis T, *et al.* 127 Preclinical evaluation of NKX019, a CD19-targeting CAR NK cell. *J ImmunoTherapy Cancer*. 2020;**8**(suppl 3):A78.
2. Goodridge J, Mahmood S, Zhu H, *et al.* FT596: translation of first-of-kind multi-antigen targeted off-the-shelf CAR-NK cell with engineered persistence for the treatment of B cell malignancies. *Blood*. 2019;**134**(suppl 1):301.
3. Cichocki F, Bjordahl R, Gaidarova S, *et al.* iPSC-derived NK cells maintain high cytotoxicity and enhance in vivo tumor control in concert with T cells and anti-PD-1 therapy. *Sci Transl Med*. 2020;**12**(568):eaaz5618.

4. Luo C, Wu G, Huang X, *et al.* Efficacy and safety of new anti-CD20 monoclonal antibodies versus rituximab for induction therapy of CD20+B-cell non-Hodgkin lymphomas: a systematic review and meta-analysis. *Sci Rep*. 2021;**11**(1):3255.
5. Spiegel JY, Patel S, Muffly L, *et al.* CAR T cells with dual targeting of CD19 and CD22 in adult patients with recurrent or refractory B cell malignancies: a phase 1 trial. *Nat Med*. 2021;**27**(8):1419–1431.

<http://dx.doi.org/10.1136/jitc-2022-SITC2022.0902>

Abstracts

903 APR-246 INDUCES AN INCREASE IN TUMOR IMMUNOGENICITY IN A P53 INDEPENDENT MANNER

¹Divya Venkatesh*, ¹Judith Michels, ¹Cailin Lu, ¹Sadna Budhu, ¹Mariam George, ¹Ouathek Ouerfelli, ²Lars Abrahamson, ³Roberta Zappasodi, ³Jedd Wolchok, ³Taha Merghoub. *Memorial Sloan Kettering Cancer Center (MSKCC), New York, NY, United States*; ²Apria Therapeutics, Solna, Sweden; ³MSKCC and Weil Cornell Medicine (WCM), New York, NY, United States

Background Immunotherapy has made a significant impact in treating cancer, yet more than 40% of the patients remain unresponsive or have a short-lived response to therapy. Rationally designed combinations of targeted therapies with immune modulators have the potential to enhance therapeutic efficacy[1, 2]. As p53 is also well known to differentially modulate the immune system[3], it is an attractive target to be used in combination with immunotherapy. Thus, we evaluated the immunogenic potential of APR-246, a targeted therapy that activates p53[4]. In addition, APR-246 can also elicit p53-independent effects mainly through the induction of endoplasmic reticulum stress and oxidative stress in several preclinical tumor models[5]. As these cellular stressors as well as p53 are capable of enhancing the immunogenicity of tumor cells[6, 7], we hypothesized that agents that stabilize p53 such as APR-246 may also increase the tumor antigenicity.

Methods We designed a set of *in vitro* and *in vivo* assays to evaluate the ability of targeted therapies to elicit an immunogenic response in tumor cells. Here, we use the preclinical melanoma cell line B16-F10 as a model since it is highly metastatic and responds poorly to immunotherapy alone[8, 9].

Results When we treated B16-F10 cells with APR-246 either in culture *in vitro* or implanted as a tumor in C57BL/6J mice *in vivo*, we observed an increase in MHC expression. Further, when mice were immunized with APR-246-treated B16-F10 cells and then implanted with healthy untreated melanoma cells, they had prolonged tumor free survival. Additionally, in our *in vitro* co-culture assays, APR-246 treatment enabled tumor cells to activate antigen-specific cytotoxic T cells when mediated by antigen presenting cells. Therefore, we hypothesized that APR-246 has the potential to mechanistically combine with immune modulation owing to its immunogenic potential. Thus, we rationally designed a treatment regimen to further enhance the tumor immunogenic effects elicited by APR-246. When APR-246 treatment was combined with the TLR4 agonist, Monophosphoryl lipid A (MPL) and a CD40 agonist antibody, we observed significant delay in the growth of B16 tumor in mice. Importantly, using CRISPR generated B16 p53 KO cells, we have identified that these immunogenic effects of APR-246 are observed independently of p53, albeit slightly reduced.

Conclusions Based on our findings, we propose that the combination of APR-246 with immunomodulatory agents may be effective in treating cancers irrespective of their p53 mutation status.

Note: D.V. and J.M contributed equally to this work.

REFERENCES

1. Esfahani K, Roudaia L, Buhlaiga N, Del Rincon SV, Papneja N, Miller WH. A review of cancer immunotherapy: from the past, to the present, to the future. *Current Oncology*. 2020;**27**(12). doi: 10.3747/co.27.5223.
2. Zappasodi R, Merghoub T, Wolchok JD. Emerging concepts for immune checkpoint blockade-based combination therapies. *Cancer Cell*. 2018;**33**(4):581–98. doi: 10.1016/j.ccell.2018.03.005. PubMed PMID: 29634946.
3. Lowe J, Shatz M, Resnick MA, Menendez D. Modulation of immune responses by the tumor suppressor p53. *BioDiscovery*. 2013;**8**:e8947.
4. Zhang Q, Bykov VJN, Wiman KG, Zawacka-Pankau J. APR-246 reactivates mutant p53 by targeting cysteines 124 and 277. *Cell Death Dis*. 2018;**9**(5):439. Epub

2018/04/20. doi: 10.1038/s41419-018-0463-7. PubMed PMID: 29670092; PubMed Central PMCID: PMC5906465.

5. Perdrix A, Najem A, Saussez S, Awada A, Journe F, Ghanem G, *et al*. PRIMA-1 and PRIMA-1(Met) (APR-246): From Mutant/Wild Type p53 Reactivation to Unexpected Mechanisms Underlying Their Potent Anti-Tumor Effect in Combinatorial Therapies. *Cancers (Basel)*. 2017;**9**(12):172. doi: 10.3390/cancers9120172. PubMed PMID: 29258181.
6. Kotsafti A, Scarpa M, Castagliuolo I, Scarpa M. Reactive Oxygen Species and Antitumor Immunity-From Surveillance to Evasion. *Cancers (Basel)*. 2020;**12**(7):1748. doi: 10.3390/cancers12071748. PubMed PMID: 32630174.
7. Lorenzo-Herrero S, Sordo-Bahamonde C, González S, López-Soto A. Immunosurveillance of cancer cell stress. *Cell Stress*. 2019;**3**(9):295–309. doi: 10.15698/cst2019.09.198. PubMed PMID: 31535086.
8. Ralli M, Botticelli A, Visconti IC, Angeletti D, Fiore M, Marchetti P, *et al*. Immunotherapy in the treatment of metastatic melanoma: current knowledge and future directions. *J Immunol Res*. 2020;**2020**:9235638. doi: 10.1155/2020/9235638. PubMed PMID: 32671117.
9. Trojaniello C, Vitale MG, Scarfato L, Esposito A, Asciero PA. Melanoma immunotherapy: strategies to overcome pharmacological resistance. *Expert Review of Anti-cancer Therapy*. 2020;**20**(4):289–304. doi: 10.1080/14737140.2020.1745634.

Ethics Approval All mice were maintained and treated in accordance with the NIH and American Association of Laboratory Animal Care regulations. All murine treatments and procedures were approved by the MSKCC Institutional Animal Care and Use Committee (IACUC).

<http://dx.doi.org/10.1136/jitc-2022-SITC2022.0903>

904

LDH INHIBITION IMPROVES RESPONSE TO CTLA-4 BLOCKADE BY ENHANCING EFFECTOR T CELL ACTIVITY AND IMPAIRING REGULATORY T CELL SUPPRESSION

¹Svena Verma*, ¹Inna Serganova, ²Sadna Budhu, ¹Lauren Dong, ²Levi Mangarin, ²Myat Ko, ²Ronald Blasberg, ¹Roberta Zappasodi, ²Jedd Wolchok, ²Taha Merghoub., ¹Weill Cornell Medicine, New York, NY, United States; ²Memorial Sloan Kettering, New York, NY, United States

Background Tumor reliance on glycolysis is not only a hallmark of cancer, but also a mechanism of resistance to immunotherapy due to lactate-mediated immune suppression and competition for glucose between T cells and glycolytic tumor cells within the tumor microenvironment.^{1,2} We have shown that CTLA-4 blockade is more effective in glycolysis-low tumors, or tumors lacking functional lactate dehydrogenase A (LDH-A), primarily due to functional destabilization of regulatory T cell suppression.³ LDH inhibitors (LDHi) have been reported to inhibit tumor glucose uptake and slow tumor cell proliferation in pre-clinical models of cancer.⁴ However, the optimal conditions for pharmacologic inhibition of LDH in combination with immunotherapy to maximize anti-tumor immune and therapeutic responses require further study.

Methods B16F10-bearing C57BL/6 mice were treated daily with LDHi GNE-140 (oral gavage) and/or biweekly with anti-CTLA-4 (intraperitoneal injection) and tumor volume was measured twice per week. Bioactivity of LDHi was confirmed by quantification of lactate and LDH enzymatic activity in sera and tumors, as well as immunoblotting for LDHA protein levels. In separate experiments, tumors were harvested after 3 administrations of anti-CTLA-4 and processed for flow cytometric analysis of tumor-infiltrating lymphocytes to assess infiltration, activation, and function. Glucose uptake was assessed in tumor and T cells by fluorescent glucose analog GlucoseCy3.

Results At baseline, tumor cells express higher levels of LDHA and consume more glucose than tumor-infiltrating T cells, creating a therapeutic window for tumor-specific targeting of glycolysis. Serum LDH and lactate levels correlate with primary tumor burden, as well as tumor LDH levels. LDHi relies on the adaptive immune system and the overexpression of tumor LDH to delay melanoma growth. Inhibiting LDH in combination with CTLA-4 blockade is more effective in controlling tumor progression compared to CTLA-4 blockade alone, and this combination promotes effector T cell infiltration and activation while functionally destabilizing regulatory T cells. Treatment with LDHi reduces tumor cell glucose uptake while facilitating increased glucose uptake by tumor-infiltrating T cells.

Conclusions CTLA-4 blockade with LDHi enhances effector T cell function while impairing regulatory T cell suppression. LDH inhibition is an effective strategy to reduce tumor cell glucose uptake, therefore increasing tumor glucose availability and facilitating an increase in tumor-infiltrating T cell glucose uptake. Serum LDH may serve as a biomarker for clinical response to LDHi. This study provides a rationale for combining immune checkpoint blockade with inhibitors of glycolysis for patients with highly glycolytic cancers.

REFERENCES

1. Hanahan D & Weinberg R A. Hallmarks of cancer: the next generation. *Cell*. 2011;**144**:646–674.
2. Zappasodi R, Merghoub T & Wolchok JD. Emerging concepts for immune checkpoint blockade-based combination therapies. *Cancer Cell*. 2018; **34**:690.
3. Zappasodi R, et al. CTLA-4 blockade drives loss of Treg stability in glycolysis-low tumours. *Nature*. 2021;**591**:652–658.

4. Boudreau A, et al. Metabolic plasticity underpins innate and acquired resistance to LDHA inhibition. *Nat Chem Biol*. 2016;**12**:779–786.

<http://dx.doi.org/10.1136/jitc-2022-SITC2022.0904>

905

BROAD ANTI-TUMOR ACTIVITY OF A POTENT AND SELECTIVE SMALL MOLECULE ANTAGONIST OF PD-L1 ABSK043 IN COMBINATION WITH OTHER AGENTS IN PRECLINICAL MODELS

Haiyan Ying*, Yongxian Zhang, Fei Yang, Wenqun Xin, Jie Wang, Jie Zhang, Zhui Chen.
Abbisko Therapeutics, Shanghai, China

Background Immunotherapy has revolutionized cancer treatment in the last decade. Several monoclonal PD-1 and PD-L1 antibodies have been approved for various cancers. Unlike antibodies, small molecules may offer potential advantages in oral dosing, adjustable control of drug exposure, improved tumor penetration and many other aspects. Therefore, small molecule antagonist which can efficiently abolish interaction of PD-1 and PD-L1 may render a novel and alternative treatment approach with potentially improved clinical benefits. ABSK043, an oral small molecule antagonist of PD-L1 discovered by us, has entered into clinical Phase I in 2021. Preclinically, ABSK043 has shown significant tumor growth inhibition as a single agent in multiple models. To explore potential synergy of ABSK043 with other therapeutic agents, *in vivo* combination experiments were conducted.

Methods For *in vivo* studies, the tumor (MC38-human PDL1 knock in)-bearing syngeneic mice were treated with ABSK043 and other agents. In addition, we also developed a humanized bladder cancer model using the RT112/84 cell line. Mice were injected intravenously with human PBMC from healthy volunteer, and injected subcutaneously into flank with cancer cells.

Results ABSK043 demonstrated strong *in vivo* synergy with several therapeutic agents such as carboplatin, a key component of the widely used CRC standard-of care chemotherapy treatment regimen, as well as other target therapy or immunology agents.

Conclusions Taken together, these data for the first time demonstrated broad combination synergy of a small molecule PD-L1 antagonist with other agents and provided basis for potential clinical evaluation of these combination treatment for cancer patients.

<http://dx.doi.org/10.1136/jitc-2022-SITC2022.0905>

906

TELOMERE DYSFUNCTION MEDIATES ANTI-TUMOR IMMUNITY IN SMALL CELL LUNG CANCER

Mingrui Zhu*, Buse Eglenen-Polat, Matthew Bender, Ilgen Mender, Silvia Siteni, Benjamin Drapkin, Jerry Shay, Esra Akbay. *UT Southwestern Medical Center, Dallas, TX, United States*

Background Small cell lung cancer (SCLC) is a pulmonary neuroendocrine cancer with very poor prognosis and limited effective therapeutic options. Chemotherapy is used as first-line treatment for this highly proliferative cancer. High telomerase activity was observed in SCLC which may contribute to active proliferation. 6-thio-2-deoxyguanine(6T-dG) is a novel telomere-specific nucleoside precursor recognized by telomerase. It is incorporated into *de novo* synthesized telomeres and lead to telomere dysfunction. It specifically affects cells with high telomerase activity such as cancer cells. Here we induced telomere dysfunction in SCLC by 6T-dG to investigate the effects on tumor growth and the tumor microenvironment.

Methods We first evaluated the anti-tumor effect of 6T-dG on SCLC by cell viability assay and colony formation *in vitro*. Then the effect was examined *in vivo* by mouse allografts or xenografts. Post-treatment tumor microenvironment was characterized by flow cytometry and *in vitro* co-culture assay was performed to set up mechanistic study on drug-evoked immunity. For therapeutic studies 6T-dG was combined with other current treatments for SCLC to assess its therapeutic potential.

Results 6T-dG induces DNA damage in SCLC and inhibited tumor progression both *in vitro* and *in vivo*. Cancer cells with higher telomerase activity were more vulnerable to the inhibition. Flow cytometry analysis of 6T-dG treated mouse tumors revealed changes in the tumor microenvironment such as infiltration and activation of cytotoxic lymphocytes while reducing infiltration of immune-suppressive myeloid cells and T regulatory cells. 6T-dG also works synergistically with common clinical treatment of SCLC such as immune checkpoint blockade (ICB) in mouse allograft model.

Conclusions Inducing telomere dysfunction impairs tumor progression by eliminating cancer cells with high telomerase activity and triggers anti-tumor immunity in SCLC. Inhibiting telomerase activity is a promising therapeutic strategy as single agent or synergistically with immunotherapy in SCLC.

<http://dx.doi.org/10.1136/jitc-2022-SITC2022.0906>

907 **BLOCKADE OF VEGF, ANGIOPOIETIN-2, AND PD1 REPROGRAMS DYSFUNCTIONAL ENDOTHELIAL CELLS IN GLIOBLASTOMA TO QUASI-ANTIGEN-PRESENTING CELLS**

¹Zohreh Amoozgar*, ²Jun Ren, ²Nancy Wang, ²Patrik Andersson, ²Gino Ferraro, ²Shanmugarajan Krishnan, ²Pin-Ji Lei, ²Sonu Subudhi, ¹Kosuke Kawaguchi, ³Rong En Tay, ¹Igor Gomes-Santos, ¹Peigen Huang, ⁴Hye-Jung Kim, ¹Dai Fukumura, ¹Rakesh Jain. ¹MGH, Harvard Medical School, Boston, MA, United States; ²MGH, Boston, MA, United States; ³Singapore Immunology Network, Singapore, Singapore; ⁴DFCI, Harvard Medical School, Boston, MA, United States

Background Glioblastoma (GBM) is the most aggressive and deadly primary tumor. Endothelial cells (ECs) in GBM vessels form a barrier between circulating immune cells and parenchymal tissue. ECs in GBM are dysfunctional,^{1, 2} conferring resistance to immunotherapy. Anti-VEGF-induced vascular normalization is insufficient to fully restore the EC function. Our studies and others have shown that antiangiogenic agents inhibiting VEGF signaling can transiently restore normal vascular function^{1, 2} and thus significantly increase infiltration of cytotoxic T cells (CTLs)^{3, 4} However, CTL accumulation in the tumor bed is necessary but not sufficient for the therapeutic response. Sustained activation of CTLs by antigen-presenting cells is a key step for effective antitumor responses.

Methods Using three orthotopic preclinical GBMs, ex vivo and in vitro studies, we investigated whether reprogramming the dysfunctional GBM ECs upregulates receptors on ECs that promote CTL trafficking, reprogrammed ECs present tumor antigens to CTLs, and this antigen presentation results in generation of an active tumor-immune niche in GBM.

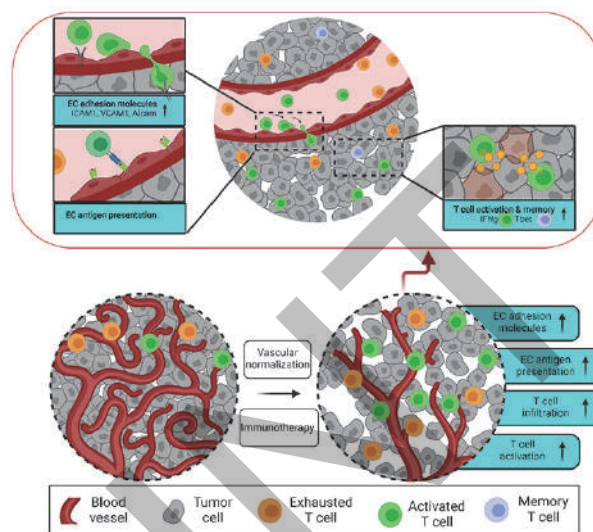
Results Concomitant blockade of Ang2, VEGF using a bispecific antibody (A2V), and aPD1 reprograms dysfunctional endothelial cells to quasi-antigen presenting cells and upregulates receptors required for cytotoxic T lymphocyte entry into the tumor. Blocking VEGF, Ang2, and PD1 induces durable anti-tumor T cell response in preclinical GBM models. Upregulation of the transcription factor T-bet is both necessary and sufficient for generating resident memory T cells elicited by this therapeutic regimen (figure 1).

Conclusions Collectively, our data (i) provide heretofore unknown insights into targeting Ang2 as a shared resistance pathway for both aVEGF and aPD1 in experimental GBM models, (ii) demonstrate a strategy to reprogram ECs to activate and promote CTL recruitment into GBMs followed by retaining intratumoral T cells, (iii) offer a possible solution to overcome GBM resistance to aVEGF and aPD1, and (iv) provide mechanistic insights into how T cell memory forms after aPD1+A2V therapy. Multiple strategies to combine aPD1 and aVEGF are currently being evaluated in clinical trials for non-CNS tumors, and our study provides a foundation for testing the combination of a more effective vascular normalizer A2V in combination with α PD1/PD-L1 in GBM patients where aPD1 monotherapy and in combination with aVEGF+aPD1 have failed in all randomized clinical trials.

REFERENCES

1. Wirsching HG, P Roth, and M Weller. A vasculature-centric approach to developing novel treatment options for glioblastoma. *Expert Opin Ther Targets* 2021;**25**(2): 87–100.
2. Fukumura D, et al., Enhancing cancer immunotherapy using antiangiogenics: opportunities and challenges. *Nat Rev Clin Oncol* 2018;**15**(5):325–340.
3. Lee WS, et al. Combination of anti-angiogenic therapy and immune checkpoint blockade normalizes vascular-immune crosstalk to potentiate cancer immunity. *Experimental & Molecular Medicine* 2020;**52**(9): 1475–1485.
4. Huang Y, et al, Vascular normalizing doses of antiangiogenic treatment reprogram the immunosuppressive tumor microenvironment and enhance immunotherapy. *Proc Natl Acad Sci U S A* 2012;**109**(43): 17561–6.

Ethics Approval All participants agree to the submission



Abstract 907 Figure 1

<http://dx.doi.org/10.1136/jitc-2022-SITC2022.0907>

908 TUMOR-INTRINSIC P38 SIGNALING AS A THERAPEUTIC TARGET TO OVERCOME NON-T CELL-INFLAMED TUMORS AND IMMUNOTHERAPY RESISTANCE

¹Rebekah Dadey*, ²Shannon Winski, ²Patrice Lee, ²Sarah Brodeur, ¹Tullia Bruno, ¹Heath Skinner, ¹Robert Ferris, ¹Jason Luke, ¹Riyue Bao. ¹University of Pittsburgh, Pittsburgh, PA, United States; ²Pfizer, Boulder, CO, United States

Background We previously identified WNT/ β -catenin (CTNNB1) and an atlas of molecular alterations that drive the non-T cell-inflamed phenotype and immune-checkpoint inhibitor (ICI) resistance across cancers. To refine our analysis, we have subsequently separated tumor types by clinically relevant stratifications, such as human papilloma virus (HPV) in head and neck squamous cell carcinoma (HNSCC), to identify immune-exclusion mechanisms associated with specific patient populations. P38 MAPK is a known regulator of dendritic cells (DCs) and myeloid cells however a tumor-intrinsic immunomodulatory role has not been previously described.

Methods Using the T cell-inflamed gene expression signature we previously defined, we integrated tissue RNAseq from 395 HPV- HNSCCs in The Cancer Genome Atlas (TCGA) with single-cell RNAseq from two independent HNSCC studies. We detected differentially expressed genes in non-T cell-inflamed versus inflamed tumors by limma voom (v3.36) in concert with causal network prediction, followed by validation in two independent HNSCC cohorts. scRNAseq data was processed by Cellranger (v6) and Seurat (v3.99). We quantified pathway expression levels in tumor cells, DCs, macrophages, and other main cell types in the tumor microenvironment. Single-cell pathway comparisons were further conducted using generalized linear mixed-effects models (GLMM) and protein-protein interaction networks constructed by STRING. Pharmacologic inhibition of p38 MAPK was explored in combination with ICI in two syngeneic murine models. Patients with ICI refractory tumors were treated with p38 inhibitor plus ICI.

Results We identified 67 pathways as activated in non-T cell-inflamed tumors from the HPV- cohort of HNSCC, 59 of which were independently validated. This included CTNNB1 from our prior work and p38 MAPK, the therapeutic target in our ongoing clinical trial (NCT04074967). CTNNB1 and p38 pathway molecules both showed inverse correlation with CD8A protein abundance from the Clinical Proteomic Tumor Analysis Consortium. We observed a significant enrichment of pathway expression only in tumor cells ($p < 0.05$) from both HNSCC scRNAseq studies and dominantly in non-T cell-inflamed tumors. Using an accumulative scoring system integrating bulk tissue and single cell sequencing data, we prioritized seven pathways as strongly connected in non-inflamed tumors, with the top regulators as CTNNB1 and p38, among others. EMT6 and CT26 syngeneic murine models demonstrated improved survival with the addition of p38 inhibitor to ICI relative to ICI monotherapy. Major and durable clinical responses have been observed in patients with anti-PD1 refractory tumors.

Conclusions p38 is a novel tumor-intrinsic mechanism that drives immune exclusion. P38 inhibition enhances ICI and can overcome anti-PD1 resistance in patients.

Ethics Approval Our study gained approval from IRB, HCC#19-097. Any/all participants in human studies gave informed consent before participating.

<http://dx.doi.org/10.1136/jitc-2022-SITC2022.0908>

909

OVERCOMING RESISTANCE TO NK-MEDIATED LYSIS IN ENZALUTAMIDE-RESISTANT PROSTATE CANCER CELLS

Madeline Dahut*, Kristen Fousek, Lucas Horn, Haiyan Qin, Jeffrey Schlom, Claudia Palena.
National Cancer Institute, Bethesda, MD, United States

Background Enzalutamide, a next-generation hormonal agent, is approved for the treatment of metastatic castration-resistant prostate cancer (CRPC). Although treatment with enzalutamide results in initial clinical benefit in men with CRPC, resistance to therapy and disease progression are ultimately observed in the majority of patients. Several mechanisms of resistance have been described in this context, including reactivation of androgen receptor (AR) signaling via gene amplification, splice variants or mutations, activation of the glucocorticoid receptor (GR), and tumor cell plasticity. Our laboratory and others have shown that tumor cell plasticity, a phenomenon characterized by the acquisition of mesenchymal markers and the loss of epithelial features by carcinoma cells, can drive tumor resistance to immune effector cell lysis; however, the link between enzalutamide resistance, tumor cell plasticity, and resistance to immune-mediated lysis has not been yet investigated. In this study, we interrogated enzalutamide-resistant prostate cancer models for their susceptibility to NK-mediated cell lysis, and evaluated approaches to enhance immune-mediated lysis of prostate cancer cells that are resistant to enzalutamide.

Methods Models of enzalutamide-resistant prostate cancer were developed by long-term exposure of LNCAP and MDA-PCa 2b human prostate cancer cells to enzalutamide in culture. Resistant and parental cells were comparatively evaluated for phenotypic features via RT-PCR, ELISA, western blot, immunofluorescence, and RNAseq analysis. Sensitivity to NK-cell mediated cytotoxicity was evaluated with NK cells isolated from peripheral blood from healthy donors. Xenografts established in NSG MHCII-deficient mice were characterized for phenotypic markers and potential therapeutic targets.

Results Our findings demonstrated that LNCAP and MDA-PCa 2b cells resistant to enzalutamide had acquired a phenotype consistent with the occurrence of an epithelial-mesenchymal switch. In addition, enzalutamide-resistant cells had significantly decreased sensitivity to NK cell-mediated lysis. RNAseq and PCR analyses demonstrated a significant upregulation of estrogen receptor alpha (ESR1) in enzalutamide-resistant cells. Treatment with fulvestrant, a selective estrogen receptor degrader (SERD) was able to increase sensitivity to NK killing while decreasing mesenchymal tumor features and increasing expression of epithelial E-cadherin. In vivo data confirmed the ability of fulvestrant to increase epithelial tumor features in LNCAP enzalutamide-resistant xenografts.

Conclusions Our data indicates that blockade of estrogen receptor signaling in enzalutamide-resistant prostate cancer cells can revert mesenchymal tumor features resulting in increased sensitivity to immune attack. Future studies will evaluate combination of fulvestrant or other estrogen antagonists with NK-based immunotherapy in models of enzalutamide-resistant prostate cancer.

<http://dx.doi.org/10.1136/jitc-2022-SITC2022.0909>

910 **STING AGONISM OVERCOMES STAT3-MEDIATED IMMUNOSUPPRESSION AND ADAPTIVE RESISTANCE TO PARP INHIBITION IN OVARIAN CANCER**

¹Liya Ding*, ¹Qiwei Wang, ²Antons Martincuks, ¹Michael Kearns, ¹Tao Jiang, ¹Ziyang Lin, ¹Xin Cheng, ¹Changli Qian, ¹Hye-Jung Kim, ³Inga-Maria Launonen, ³Anniina Färkkilä, ¹Thomas Roberts, ¹Joyce Liu, ¹Panagiotis Konstantinopoulos, ¹Ursula Matulonis, ²Hua Yu, ¹Jean Zhao. ¹Dana-Farber Cancer Institute, Boston, MA, United States; ²City of Hope National Medical Center, Duarte, CA, United States; ³University of Helsinki, Helsinki, Finland

Background PARP inhibition (PARPi) has demonstrated potent therapeutic efficacy in patients with BRCA-mutant ovarian cancer.¹ However, acquired resistance to PARPi remains a major challenge in the clinic.^{2,3}

Methods PARPi-resistant ovarian cancer mouse models were generated by long-term treatment of olaparib in syngeneic Brca1-deficient ovarian tumors. STAT3-mediated immunosuppression was investigated *in vitro* by co-culture experiments and *in vivo* by analysis of immune cells in the TME of human and mouse PARPi-resistant tumors. Whole genome transcriptome analysis was performed to assess the anti-tumor immunomodulatory effect of STING (stimulator of interferon genes) agonists on myeloid cells in the TME of PARPi-resistant ovarian tumors. A STING agonist was used to overcome STAT3-mediated immunosuppression and acquired PARPi resistance in syngeneic and PDX models of ovarian cancer.

Results In this study, we uncover an adaptive resistance mechanism to PARP inhibition mediated by tumor associated macrophages (TAMs) in the tumor microenvironment (TME). Markedly increased populations of pro-tumor macrophages are found in BRCA-deficient ovarian tumors that rendered resistance to PARPi in both murine models and patients. Mechanistically, PARP inhibition elevates the STAT3 signaling pathway in tumor cells, which in turn promotes pro-tumor polarization of TAMs. STAT3 ablation in tumor cells mitigates polarization of pro-tumor macrophages and increases tumor infiltrating T-cells upon PARP inhibition. These findings are corroborated in patient-derived, PARPi-resistant BRCA1-mutant ovarian tumors. Importantly, STING agonists reshape the immunosuppressive TME by reprogramming myeloid cells and overcome the TME-dependent adaptive resistance to PARPi in ovarian cancer. This effect is further enhanced by addition of PD-1 blockade.

Conclusions We elucidate an adaptive immunosuppression mechanism rendering resistance to PARPi in BRCA1-mutant ovarian tumors. This is mediated by enrichment of pro-tumor TAMs propelled by PARPi-induced STAT3 activation in tumor cells. We also provide a new strategy to reshape the immunosuppressive TME with STING agonist and overcome acquired PARPi resistance in ovarian cancer (figure 1).

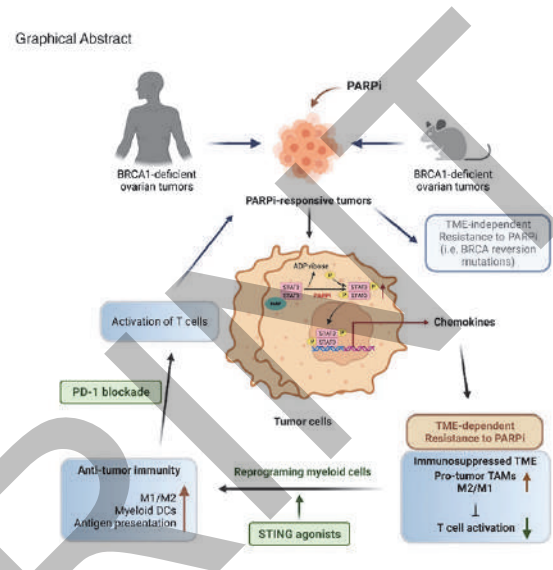
Acknowledgements This research is supported by Ovarian Cancer Research Alliance (OCRA), Susan Smith Women's Cancers program at DFCI, and National Institutes of Health (NIH)/National Cancer Institute (NCI).

REFERENCES

1. Ding L, Kim HJ, Wang Q, *et al.* PARP Inhibition Elicits STING-dependent antitumor immunity in brca1-deficient ovarian cancer. *Cell Rep* 2018;**25**(11):2972–80.
2. Pettitt SJ, Frankum JR, Punta M, *et al.* Clinical BRCA1/2 reversion analysis identifies hotspot mutations and predicted neoantigens associated with therapy resistance. *Cancer Discovery* 2020;**10**(10):1475.
3. PARP1 Suppresses the Transcription of PD-L1 by Poly(ADP-Ribosyl)ating STAT3. *Cancer Immunol Res* 2019;**7**(1):136–49.

Ethics Approval Immunofluorescent staining and analysis of ovarian tumor sections from female ovarian cancer patients were conducted according to a City of Hope Institutional

Review Board approved protocol. All the animal experiments described in this study were performed according to animal protocols approved by the DFCI Institutional Animal Care and Use Committee (IACUC).



Abstract 910 Figure 1 Graphical Abstract Overcoming TME-dependent adaptive resistance to PARPi in BRCA1-deficient ovarian cancer with STING agonist treatment. Over a course of PARPi treatment, BRCA1-deficient ovarian tumors develop TME-dependent or -independent adaptive resistance to PARPi therapy. PARPi induces STAT3 signaling in the tumor cells, which in turn polarizes macrophages towards pro-tumor M2-like TAMs and contributes to TME-dependent PARPi resistance in ovarian cancer. Treatment with a STING agonist can reshape the immunosuppressive TME to an anti-tumor status by reprogramming myeloid cells, re-sensitizing the resistant tumors to PARPi therapy in BRCA1-deficient ovarian cancer

<http://dx.doi.org/10.1136/jitc-2022-SITC2022.0910>

ANTI-VEGF THERAPY IMPROVES EGFR-VIII-CAR-T CELL DELIVERY AND EFFICACY IN SYNGENEIC GLIOBLASTOMA MODELS IN MICE

Xinyue Dong, Jun Ren, Zohreh Amoozgar*, Meenal Datta, Somin Lee, Sylvie Roberge, Mark Duquette, Dai Fukumura, Rakesh Jain. MGH, Harvard Medical School, Boston, MA, United States

Background Chimeric antigen receptor (CAR)-T cells have revolutionized treatment of multiple types of hematological malignancies, but have shown limited efficacy in patients with glioblastoma (GBM) or other solid tumors. This may be largely due to the immunosuppressive tumor microenvironment (TME) that compromises the delivery and anti-tumor activity of CAR-T cells. We previously showed that blocking VEGF (vascular endothelial growth factor) signaling can normalize tumor vessels in murine and human tumors, including GBM, breast, liver, and rectal carcinomas. Moreover, we demonstrated that vascular normalization can improve the delivery of CD8+ T cells and efficacy of immunotherapy in breast cancer models in mice. In fact, the US FDA has approved 7 different combinations of anti-VEGF drugs and immune-checkpoint blockers for liver, kidney, lung and endometrial cancers in the past 3 years.¹⁻²⁵ Here we tested the hypothesis that anti-VEGF therapy can improve the delivery and efficacy of CAR-T cells in immunocompetent mice bearing orthotopic GBM tumors

Methods We engineered two syngeneic mouse GBM cell lines (CT2A and GSC005) to express EGFRvIII – one of the most common neoantigens in human GBM – and CAR T cells to recognize EGFRvIII. We tested our CAR T cells in orthotopic GBMs for their efficacy in recognizing, and killing tumor cells, and the survival advantage when tumor vessels are normalized.

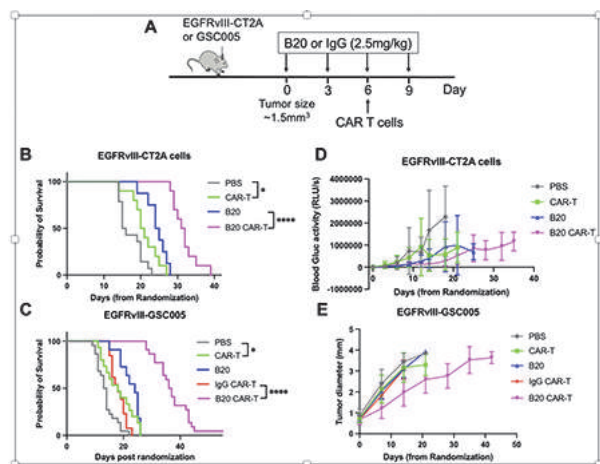
Results We found that treatment with the anti-mouse VEGF antibody (B20) improved CAR-T cell infiltration and distribution throughout the GBM TME, delayed tumor growth, and prolonged survival of GBM-bearing mice compared to EGFRvIII-CAR-T cell therapy alone (figure 1).

Conclusions Our study provides a strategy to overcome major challenges in CAR-T cell therapy in GBM by: (i) increasing the CAR-T cell infiltration, intratumoral distribution, and activation in murine GBM models, and (ii) reprogramming TME by increasing the number and activation of endogenous effector T cells, resulting in improved anti-tumor efficacy of CAR-T therapy in two GBM mouse models. Given that anti-VEGF therapies have been approved for a number of solid tumors, including GBM, our study provides mechanistic insights and compelling preclinical data in support of testing the combination of vascular normalizing agents and CAR-T therapies in GBM patients. Furthermore, this approach may also improve CAR-T therapy of other solid tumors that share similar TME features as well as for other cell-based therapies using autologous or allogenic immune cells (e.g., NK cells, macrophages).

REFERENCES

1. Young RM, Engel NW, Uslu U, Wellhausen N & June CH. Next-Generation CAR T-cell Therapies. *Cancer Discov* 2022;**12**:1625–1633, doi:10.1158/2159-8290.Cd-21-1683.
2. Rafiq S, Hackett CS & Brentjens RJ. Engineering strategies to overcome the current roadblocks in CAR T cell therapy. *Nat Rev Clin Oncol* 2020;**17**, 147–167, doi:10.1038/s41571-019-0297-y.
3. Brown CE, et al. Regression of glioblastoma after chimeric antigen receptor T-Cell Therapy. *N Engl J Med* **375**, 2561–2569, doi:10.1056/NEJMoa1610497 (2016).
4. O'Rourke DM, et al. A single dose of peripherally infused EGFRvIII-directed CAR T cells mediates antigen loss and induces adaptive resistance in patients with recurrent glioblastoma. *Sci Transl Med* 2017;**9**, doi:10.1126/scitranslmed.aaa0984.

5. Good CR, et al. An NK-like CAR T cell transition in CAR T cell dysfunction. *Cell* 2021;**184**, 6081–6100.e6026, doi:10.1016/j.cell.2021.11.016.
6. Johnson L A, et al. Rational development and characterization of humanized anti-EGFR variant III chimeric antigen receptor T cells for glioblastoma. *Sci Transl Med* 2015;**7**, 275ra222, doi:10.1126/scitranslmed.aaa4963.
7. Huang Y, et al. Vascular normalizing doses of antiangiogenic treatment reprogram the immunosuppressive tumor microenvironment and enhance immunotherapy. *Proc Natl Acad Sci U S A* 2012;**109**:17561–17566, doi:10.1073/pnas.1215397109.
8. Fukumura D, Kloepper J, Amoozgar Z, Duda DG & Jain RK. Enhancing cancer immunotherapy using antiangiogenics: opportunities and challenges. *Nat Rev Clin Oncol* 2018;**15**:325–340, doi:10.1038/nrclinonc.2018.29.
9. Shrimali RK, et al. Antiangiogenic agents can increase lymphocyte infiltration into tumor and enhance the effectiveness of adoptive immunotherapy of cancer. *Cancer Res* 2010;**70**, 6171–6180, doi:10.1158/0008-5472.Can-10-0153.
10. Amoozgar Z, et al. Targeting Treg cells with GITR activation alleviates resistance to immunotherapy in murine glioblastomas. *Nat Commun* 2021;**12**, 2582, doi:10.1038/s41467-021-22885-8.
11. Ma L, et al. Enhanced CAR-T cell activity against solid tumors by vaccine boosting through the chimeric receptor. *Science* 2019;**365**:162-168, doi:10.1126/science.aav8692.
12. Marsh J, Mukherjee P & Seyfried TN. Akt-dependent proapoptotic effects of dietary restriction on late-stage management of a phosphatase and tensin homologue/tuberous sclerosis complex 2-deficient mouse astrocytoma. *Clin Cancer Res* 2008;**14**, 7751–7762, doi:10.1158/1078-0432.ccr-08-0213.
13. Saha D, Martuza RL & Rabkin SD. Oncolytic herpes simplex virus immunovirotherapy in combination with immune checkpoint blockade to treat glioblastoma. *Immunotherapy* 2018;**10**, 779–786, doi:10.2217/imt-2018-0009.
14. Kloepper, J, et al. Ang-2/VEGF bispecific antibody reprograms macrophages and resident microglia to anti-tumor phenotype and prolongs glioblastoma survival. *Proc Natl Acad Sci U S A* 2016;**113**:4476–4481, doi:10.1073/pnas.1525360113.
15. Seano G, et al. Solid stress in brain tumours causes neuronal loss and neurological dysfunction and can be reversed by lithium. *Nat Biomed Eng* 2019;**3**, 230–245, doi:10.1038/s41551-018-0334-7.
16. Gibson VB, et al. A novel method to allow noninvasive, longitudinal imaging of the murine immune system in vivo. *Blood* 2012;**119**:2545–2551, doi:10.1182/blood-2011-09-378356.
17. Aldape K, et al. Challenges to curing primary brain tumours. *Nat Rev Clin Oncol* 2019;**16**:509–520, doi:10.1038/s41571-019-0177-5.
18. Jain RK. Antiangiogenesis strategies revisited: from starving tumors to alleviating hypoxia. *Cancer Cell* 2014;**26**:605–622, doi:10.1016/j.ccell.2014.10.006.
19. Martin JD, Seano G & Jain RK. Normalizing Function of Tumor Vessels: Progress, Opportunities, and Challenges. *Annu Rev Physiol* 2019;**81**:505–534, doi:10.1146/annurev-physiol-020518-114700.
20. Liu CJ, et al. Treatment of an aggressive orthotopic murine glioblastoma model with combination checkpoint blockade and a multivalent neoantigen vaccine. *Neuro Oncol* 2020;**22**:1276–1288, doi:10.1093/neuonc/noaa050.
21. Saha D, Martuza RL & Rabkin SD. Macrophage polarization contributes to glioblastoma eradication by combination immunovirotherapy and immune checkpoint blockade. *Cancer Cell* 2017;**32**:253–267.e255, doi:10.1016/j.ccell.2017.07.006.
22. Akbari P, et al. Directing CAR T cells towards the tumor vasculature for the treatment of solid tumors. *Biochim Biophys Acta Rev Cancer* 2022;**1877**:188701, doi:10.1016/j.bbcan.2022.188701.
23. Lanitis E, et al. VEGFR-2 redirected CAR-T cells are functionally impaired by soluble VEGF-A competition for receptor binding. *J Immunother Cancer* 2021;**9**, doi:10.1136/jitc-2020-002151.
24. Bocca P, et al. Bevacizumab-mediated tumor vasculature remodelling improves tumor infiltration and antitumor efficacy of GD2-CAR T cells in a human neuroblastoma preclinical model. *Oncoimmunology* 2021;**7**, e1378843, doi:10.1080/2162402X.2017.1378843.
25. Martinez Bedoya D, Dutoit V & Migliorini D. Allogeneic CAR T Cells: An Alternative to Overcome Challenges of CAR T Cell Therapy in Glioblastoma. *Front Immunol* 2021;**12**:640082, doi:10.3389/fimmu.2021.640082.



Abstract 911 Figure 1 Anti-VEGF treatment improves the efficacy of EGFRVIII-CAR-T

(A) Schematic representation of experimental setup to evaluate the effect of PBS, CAR-T, B20, IgG + CAR-T and B20 + CAR-T on the survival of GSC005 and C2TA GBM-bearing mice. (B) and (C) Median survival and tumor growth kinetics for CT2A tumors [PBS (n=22, 15.5 days), CAR-T (n=14, 20.5 days), B20 (n=8, 24.5 days), B20 + CAR-T (n=19, 32 days)]. (D) and (E) Median survival and tumor growth kinetics for GSC005 tumors [PBS (n=12, 13.5 days), CAR-T (n=17, 18.5 days), B20 (n=10, 24 days), IgG + CAR-T (n=13, 18 days), B20 + CAR-T (n=21, 37 days)]. Error bars show median ± SEM. Statistical analysis was performed using one-way ANOVA test. *p < 0.05, ****p < 0.001

<http://dx.doi.org/10.1136/jitc-2022-SITC2022.0911>

912

EPIGENETIC REMODELING ENHANCES THERAPEUTIC RESPONSES TO STING AGONISM *IN VIVO*

¹Rana Falahat*, ¹Anders Berglund, ¹Patricio Perez-Villarroel, ¹Shari Pilon-Thomas, ²Glen Barber, ¹James Mule. ¹Moffitt Cancer Center, Tampa, FL, United States; ²University of Miami, Miami, FL, United States

Background Despite evidence of therapeutic activity in preclinical models, STING activating agents have shown limited efficacy in early phase clinical trials. This discrepancy in outcomes suggests that in addition to antigen presenting cells, targeting STING pathway could be also functionally relevant in tumor cells with well documented epigenetically driven STING suppression.^{1, 2} In this study, we determined if reversal of tumor cell-intrinsic STING silencing using a DNA methyltransferase inhibitor can improve the efficacy of a STING agonist in mouse models of melanoma.

Methods Using genome-wide methylation profiling, we assessed methylation levels of STING in B16-F10 and Yumm1.7 mouse melanoma cell lines before and after treatment with 5-aza-2'-deoxycytidine (5AZADC). We also evaluated their activation of STING following stimulation with the STING agonist ADU-S100. Using B16-F10 and Yumm1.7 models in STING-deficient and STING-sufficient hosts, we next assessed the effect of 5AZADC treatment on the efficacy of ADU-S100. Additionally, we performed mechanistic studies using T-cell depletion experiments as well as phenotypic and gene expression profiling.

Results While we observed hypermethylation of STING in both B16-F10 and Yumm1.7 cell lines, their treatment with 5AZADC resulted in a decrease in STING methylation levels. We also found reconstitution of STING protein expression in 5AZADC-pretreated cell lines as well as up to a 46-fold increase in induction of IFN- β ($p < 0.001$) and a 4.5-fold increase in MHC class I surface expression ($p < 0.01$) compared to untreated controls following stimulation with ADU-S100. In tumor-bearing mice, while treatment with a combination of 5AZADC and ADU-S100 resulted in a marked increase in *Irfn1* transcripts within tumors ($p < 0.001$), it significantly delayed tumor growth ($p < 0.05$). Antibody-mediated depletion studies in mice receiving the combination therapy further indicated that this antitumor activity depends on the generation of functional tumor antigen-specific CD8⁺ T cells ($p < 0.001$); however, tumor growth remained unaltered by the depletion of CD4⁺ T cells.

Conclusions We have shown that although epigenetic silencing of STING in melanoma cells can confer resistance to STING agonist therapy, a rational combination of a clinically available DNA methylation inhibitor with a STING agonist can reverse this silencing and lead to robust antitumor responses in the setting of two STING^{low} murine models of melanoma. Therefore, identification and pharmacologic restoration of tumor cell-intrinsic STING defects through epigenetic reprogramming might be critical for the successful use of STING agonists in the clinic.

Acknowledgements This work was supported by the Moffitt Cancer Center Flow Cytometry and Molecular Genomics Core Facilities, all comprehensive cancer center facilities designated by the National Cancer Institute (P30-CA076292). This work was funded by the NCI-NIH (P30 CA076292, and P50 CA168536), CJG Fund, Chris Sullivan Fund, V Foundation, and the Dr. Miriam and Sheldon G. Adelson Medical Research Foundation.

REFERENCES

1. Falahat R, Perez-Villarroel P, Mailloux AW, Zhu G, Pilon-Thomas S, Barber GN, Mulé JJ. STING signaling in melanoma cells shapes antigenicity and can promote antitumor T-cell activity. *Cancer Immunol Res* 2019;**7**(11):1837–48.
2. Falahat R, Berglund A, Putney RM, Perez-Villarroel P, Aoyama S, Pilon-Thomas S, Barber GN, Mulé JJ. Epigenetic reprogramming of tumor cell-intrinsic STING function sculpts antigenicity and T cell recognition of melanoma. *PNAS* 2021;**118**(15):e2013598118.

<http://dx.doi.org/10.1136/jitc-2022-SITC2022.0912>

913 **TRANSLATIONAL ANALYSIS OF ADVANCED METASTATIC BLADDER CANCER PATIENTS TREATED WITH IO COMBINATION MAVEROPEPIMUT-S, CYCLOPHOSPHAMIDE, AND PEMBROLIZUMAB**

Heather Torrey*, Walead Ebrahimizadeh, Valarmathy Kaliaperumal, Aurelio Lobo, Barry Kennedy, Tran Ngo, Lisa MacDonald, Stephan Fiset, Jeremy Graff, Heather Hirsch. *IMV inc., Dartmouth, Canada*

Background Maveropepimut-S (MVP-S, formerly DPX-Survivac) is comprised of immunogenic T cell peptides from the cancer antigen, survivin, as well as a universal T helper peptide, A16L, and the innate immune activator, poly-dIdC, packed within the proprietary DPX[®] lipid-in-oil delivery platform. When combined with intermittent low-dose cyclophosphamide (CPA), and the immune checkpoint inhibitor, pembrolizumab, the proprietary DPX lipid-in-oil delivery platform elicits a sustained immune response that has been associated with clinical benefit in multiple tumor types. Here, we present translational analyses of immune cell infiltration and peripheral, cell-mediated immunity in advanced metastatic bladder cancer subjects (n=19) from this Phase 2 trial, NCT03836352.

Methods Survivin specific immune response was measured in PBMCs by IFN- γ ELISPOT (n=14) and MHC-Tetramer assay (n=13). Multiplex immunofluorescence (mIF) (n=5) was performed by Precision for Medicine. PD-L1 status (n=13) was analyzed using the 22C3 IHC assay at Covance. Gene expression analysis was performed using the NanoString IO360 panel (n=11).

Results Analysis of PBMCs by IFN- γ ELISPOT or MHC-tetramer assay demonstrates antigen-specific cell response in 71.4% (10/14) of evaluable patients, and in all five patients with measurable tumor responses. Baseline profiling of RNA signatures suggests that levels of B, T, and NK cells are higher in tumors of responding patients similar to previous MVP-S trials (DeCidE¹; NCT02785250). Preliminary mIF also shows that one complete responder (RECISTv1.1) has a higher density of infiltrate, including CD8⁺ cells, at baseline. Grouped analysis of five on-treatment samples suggests higher immune resistance pathways such as TGF and CD71⁺ early erythroid cells, in non-responding patients, which has been linked to immune tolerance and suppression of T cells.¹ mIF of five paired pre- and on-treatment biopsies reveals higher levels of FoxP3⁺ (T_{regs}) in post-treatment tumour of non-responders whereas the reverse is observed in tissue of responders. PD-L1 staining of pre-treatment tumor tissue by IHC, shows (4/4) of evaluable responding patients had a CPS score of $\geq 1\%$.

Conclusions The combination of MVP-S, CPA, and anti-PD-1 therapy provides a renewed approach directly targeting the TAA survivin and imposing a limit on immune suppression with CPA along with checkpoint inhibition. The data herein show that the treatment of advanced metastatic bladder cancer with MVP-S plus CPA in combination with pembrolizumab elicits a strong survivin-specific immune cell response in addition to the clinical response as reported previously (AACR 2022). Taken together, the translational data demonstrate that this novel immune oncology approach leads to immune education that is correlated with improved disease control.

REFERENCE

1. Grzywa TM, Sosnowska A, Rydzynska Z, et al. Potent but transient immunosuppression of T-cells is a general feature of CD71⁺ erythroid cells. *Commun Biol* 2021;4:1384. doi: 10.1038/s42003-021-02914-4.

Ethics Approval WIRB (20183396); Cedars-Sinai Medical Center Institutional Review Boards (Pro00057155); The University of Texas MD Anderson Cancer Center Institutional Review Board (IRB 2) (2019-0135); Ochsner Clinic Foundation Institutional Review Board (2019 084); University of Louisville IRB # 1 – Biomedical (19.045); WCG IRB (20183396); Wilima Osler Health System Research Ethics Board (18-0064); Ontario Cancer Research Ethics Board (OCREB) (1732); Comité d'éthique de la recherche du CHU de Québec – Université Laval (MP-20-2019-4582*);

<http://dx.doi.org/10.1136/jitc-2022-SITC2022.0913>

914

REGULATING NEGATIVE IMMUNE REGULATORS TO ENHANCE IMMUNE CHECKPOINT BLOCKADE ANTITUMOR POTENTIAL

Yared Hailemichael*, Glenn Winn, Michael Davies. *The University of Texas MD Anderson Cancer Center, Houston, TX, United States*

Background Understanding the exact immunobiology of immune checkpoint blockade (ICB)-related relapse would be essential to augmenting ICB-induced antitumor immunity and overcoming resistance. In response to ICB, a specific and effective immune response is induced. However, the levels of distinct immune cell subsets and the specific signals that draw them into a tumor microenvironment (TME) following broad application of cancer immunotherapies such as immune checkpoint blockade (ICB) remain poorly characterized. We previously showed that lymphocyte function associated antigen-1 (LFA-1) activation is critical for converting CD8 T cell exclusionary tumor microenvironment (TME) and allowing enhanced ICB-induced tumor control.^{1,2} Whereas very late antigen-4 (VLA-4) activation did not contribute to anti-CTLA-4 therapy antitumor response. Here, we evaluated the effect of integrin a4b7 blocker as a strategy to overcome immune resistance in the setting of combination immunotherapy (anti-CTLA-4, anti-PD-1 and/or anti-Lag-3).

Methods To evaluate synergy between ICB (anti-CTLA-4 and anti-PD-1 or anti-PD-1 and anti-Lag-3) and VLA-4 integrin blocker, once mice with B16 melanoma, Lewis lung carcinoma (LLC) or pancreatic adenocarcinoma (PAN-02) had developed tumors of approximately 20mm², they were treated with either IgG control, VLA-4 blocker, ICB, or combination of both therapies together.

Results We observed no difference in therapeutic benefit between a4b7 blocker and IgG control (p<0.05) in all tumor models. Interestingly, we observed that a4b7 integrin blocker demonstrated therapeutic synergy with anti-CTLA-4 and anti-PD-1 but not anti-PD-1 and anti-Lag-3. Likewise, a4b7 integrin blocker in combination with anti-CTLA-4 and anti-PD-1 significantly enhanced antitumor response in PAN-02 (p<0.001) and LLC tumor (p<0.001) models. Initial immune infiltrates analysis shows improved antitumor response corresponded with increase in CD8+ T_{eff}/T_{reg}, CD4+ T_{eff}/T_{reg} ratios at the TME.

Conclusions Our preliminary results from treatment of mice implanted with tumor and receiving combination checkpoint blockade therapies suggest that a4b7 could potentially enhance intratumoral CD8+ effector T cell/T_{reg} ratios to establish antitumor immunity.

REFERENCES

1. Hailemichael Y, et al. Cancer vaccine formulation dictates synergy with CTLA-4 and PD-L1 checkpoint blockade therapy. *The Journal of Clinical Investigation* 2018;**128**:1338–1354.
2. Hickman A. et al. LFA-1 activation enriches tumor-specific T cells in a cold tumor model and synergizes with CTLA-4 blockade. *The Journal of clinical investigation* 2022.

<http://dx.doi.org/10.1136/jitc-2022-SITC2022.0914>

915 **TARGETING LSD1 RESCUES MHC-I ANTIGEN PRESENTATION AND OVERCOMES RESISTANCE TO PD-L1 BLOCKADE THERAPY IN SMALL CELL LUNG CANCER**

Evelyn Nguyen*, Andrew Chow, Charles Rudin, Triparna Sen, Hirokazu Taniguchi. *Memorial Sloan Kettering Cancer Center, New York, NY, United States*

Background Small cell lung cancer (SCLC) is an immunosuppressive tumor with modest clinical response to immune checkpoint blockade (ICB). Repression of major histocompatibility class I (MHC-I) molecules represents a potential mechanism driving ICB resistance in SCLC. Lysine-specific demethylase 1 (LSD1) has been regarded as a promising therapeutic target in SCLC. Our study investigated immunomodulatory functions of LSD1 in regulating MHC-I antigen presentation pathway (APP) in SCLC.

Methods We employed the inhibitor ORY-1001 and RNA interference to assess changes in MHC-I expression in SCLC cell lines by flow cytometry. We then performed RNA-seq to characterize whole transcriptomic changes in SCLC cells following LSD1 inhibition. To explore effects of targeting LSD1 on T cell cytotoxicity, we co-cultured SCLC presenting endogenous peptides with pre-activated cognate CD8⁺ T cells. Finally, we treated immunocompetent mice bearing syngeneic SCLC tumors with ORY-1001 and/or anti-PD-L1 to evaluate tumor growth and characterize intratumor immune activities.

Results We found that targeted inhibition of LSD1 in SCLC restores MHC-I cell surface expression and transcriptionally activates genes encoding the antigen presentation pathway. LSD1 inhibition further activates interferon signaling, induces tumor-intrinsic immunogenicity, and sensitizes SCLC cells to MHC-I-restricted T cell cytotoxicity. Combination of LSD1 inhibitor with ICB augments the antitumor immune response in refractory SCLC models. Together, these data define a role for LSD1 as a potent regulator of MHC-I antigen presentation and provide rationale for combinatory use of LSD1 inhibitors with ICB to improve therapeutic response in SCLC.

Conclusions Epigenetic silencing of MHC-I in SCLC contributes to its poor response to ICB. Our study identifies a previously uncharacterized role for LSD1 as a regulator of MHC-I antigen presentation in SCLC. LSD1 inhibition enables MHC-I-restricted T cell cytotoxicity, induces immune activation, and augments the antitumor immune response to ICB in SCLC.

Ethics Approval All animal experiments were approved by and used in accordance with animal care guidelines from the Memorial Sloan Kettering Cancer Center (MSKCC) Animal Care and Use Committee.

<http://dx.doi.org/10.1136/jitc-2022-SITC2022.0915>

916

**ACQUIRED RESISTANCE TO IMMUNE CHECKPOINT
BLOCKADE BY PHENOTYPIC PLASTICITY OF MELANOMA**

¹Emily Robitschek*, ²Arnab Mehta, ³Jia-Ren Lin, ⁴Dennie Frederick, ⁵Alvin Shi, ⁶Ana Larque, ²Benchun Miao, ⁷Rumya Raghavan, ²Tatyana Sharova, ²John Shin, ⁵Manolis Kellis, ⁴Nir Hacohen, ²Keith Flaherty, ²Genevieve Boland, ¹Ivan Chebib, ¹David Liu, ²Ryan Sullivan. ¹Dana Farber Cancer Institute, Boston, MA, United States; ²Massachusetts General Hospital, Boston, MA, United States; ³Harvard Medical School, Boston, MA, United States; ⁴Broad Institute of MIT and Harvard, Cambridge, MA, United States; ⁵Massachusetts Institute of Technology, Boston, MA, United States; ⁶Hospital Clinic Barcelona, Barcelona, Spain; ⁷Broad Institute of Harvard and MIT, Cambridge, MA, United States

Background The vast majority of immunotherapy resistant tumors do not harbor obvious resistance mutations and little remains known about alternative mechanisms of adaptive resistance.

Methods We present a patient with Stage III melanoma treated with adjuvant Pembrolizumab (Pembro) who developed progressive disease three months after starting therapy. The patient was started on a trial of Pembrolizumab (Pembro) and Entinostat, a histone deacetylase inhibitor (HDACi), and had a mixed response. Progressive lesions were palliatively resected and found to have distinct histologies of either melanoma or pleomorphic rhabdomyosarcoma. Six tumors were analyzed with whole exome sequencing, bulk RNA-seq, and CyCIF (cyclic immunofluorescence). Quality-control, calling of somatic mutations and copy number alterations, and inference of phylogenetic relationships were performed.

Results Sequenced tumors shared 1007 SNV (single nucleotide variant) mutations and clonal loss of heterozygosity (LOH) of 1p, 4, 6q, 9, 18, 21q, and 22q confirming a common ancestor clone with homozygous deletion of CDKN2A and driver mutations in NRAS, NF1 (bi-allelic), CDK12, and SMARCA4. Genomic features unique to the melanoma phenotype included a clonal LOH of chromosome 11, while the rhabdomyosarcomas shared clonal LOH of chromosome 19. Phylogenetic analysis revealed an early split between histologic melanomas and rhabdomyosarcoma subtypes. We further uncovered enriched expression signatures for myogenesis, epithelial mesenchymal transition (EMT) and several immune signatures enriched in rhabdomyosarcoma samples relative to melanoma samples. CyCIF imaging confirmed the mutual exclusivity of the melanoma and rhabdomyosarcoma phenotypes, elevated levels of M2 macrophages in rhabdomyosarcoma samples, and high NGFR signaling in post combination treatment tumors.

Conclusions Our data suggest phenotypic switching as a form of immune evasion. The majority of lesions biopsied to be rhabdomyosarcomas initially emerged (radiographically) as progressive lesions on adjuvant Pembro. These lesions were resistant (stable/progressive disease) to Pembro/Entinostat, while other disease lesions responded, suggesting that the phenotype switch to rhabdomyosarcoma from an initial melanoma ancestral clone was associated with ICB resistance. Other resistant lesions had a melanoma phenotype, and our analysis revealed that the genomic divergence between the melanoma and rhabdomyosarcoma phenotypes occurred prior to Pembro/Entinostat treatment, suggesting alternative mechanisms of treatment resistance. While unlikely that a HDACi led to the phenotypic conversion of pre-existing tumor lesions, its role in selection or enrichment of phenotypically switched cells is undetermined. The higher NGFR signal post Pembro/Entinostat treatment could represent a concurrent therapeutic resistance mechanism. More broadly, detailed integrated clinical/genomic longitudinal studies within individual patients can shed light

on the evolution and underlying mechanisms of clinical therapeutic resistance.

Ethics Approval The work described herein was approved by the Dana Farber Harvard Cancer Center IRB, protocol #11-181, to which the patient signed informed consent.

Consent The work described herein was approved by the Dana Farber Harvard Cancer Center IRB, protocol #11-181, to which the patient signed informed consent.

<http://dx.doi.org/10.1136/jitc-2022-SITC2022.0916>

917

REVERSING THE IMMUNE-EXCLUDED (“COLD”) TUMOR IMMUNE MICROENVIRONMENT IN ORAL SQUAMOUS CELL CARCINOMA

Yewen Shi, Alanis Rodriguez-Rosario, Tongxin Xie, Frederico Gleber-Netto, Curtis Pickering, Abdullah Osman, Andrew Sikora, Jeffrey Myers, Roberto Rangel*. *MD Anderson Cancer Center, Houston, TX, United States*

Background The tumor immune microenvironment (TIME), plays a major role in oral squamous cell carcinoma (OSCC) resistance to therapy, including immunotherapy. Many OSCC are considered poorly immunogenic tumors or “immune deserts” which lack immune infiltration, evade immune recognition and suppress immune system activation, all of which have been associated with early disease relapse and poor prognosis in OSCC patients. Somatic *TP53* mutations, the most common genetic alterations in 75% to 85% of OSCCs. The loss or mutation of *TP53* in a cancer can affect the recruitment and activity of myeloid and T cells, thereby enabling immune evasion and tumor progression. Here we generated a set of syngeneic mouse oral cancer cell lines (ROCs) from mice exposed to 4-nitroquinoline-1 oxide, a carcinogen that acts as a tobacco mimetic and causes DNA damage. The syngeneic murine ROC cell lines were tumorigenic, with different immune landscapes and response to immunotherapy.

Methods Orthotopic tongue injections were performed to (i) characterize tumor growth rate (ii) the TIME landscape by immunohistochemistry (IHC); and (iii) immunotherapy drug studies. We inactivated mutant p53 expression by shRNA, profile gene expression changes by RNAseq, and validated these findings by quantitative PCR, ELISA, co-culture and flow cytometry studies. Tumor response was achieved by combined therapy and TIME changes were evaluated by opal multiplex IHC.

Results We used the ROC1 cell line to investigate the effect of mutant p53 in the modulation of cell-intrinsic factors that shape the tumor immune landscape and affect sensitivity to immunotherapy. We observed that a carcinogen-induced *p53* mutation promoted a cold TIME enriched with immunosuppressive M2 macrophages highly resistant to ICI therapy. *p53*-mutated cold tumors failed to respond to combination ICI treatment; however, the combination of a programmed cell death protein 1 (PD-1) inhibitor and stimulator of interferon genes (STING) agonist restored responsiveness.

Conclusions Our syngeneic OSCC models provide an experimental system, which can be used to understand the interplay between cell-intrinsic genetic changes and immunosuppressive mechanisms that promote tumor progression, and serve as a translationally-relevant platform for evaluating immunotherapy combinations to improve treatment strategies for OSCC

<http://dx.doi.org/10.1136/jitc-2022-SITC2022.0917>

TREATMENT-RELATED ADVERSE EVENT (TRAE)-RELATED DISCONTINUATION RATE OF IMMUNOTHERAPY ALONE (IO-ONLY) COMPARED TO IMMUNOTHERAPY COMBINED WITH CHEMOTHERAPY (CHEMO-IO): A META-ANALYSIS

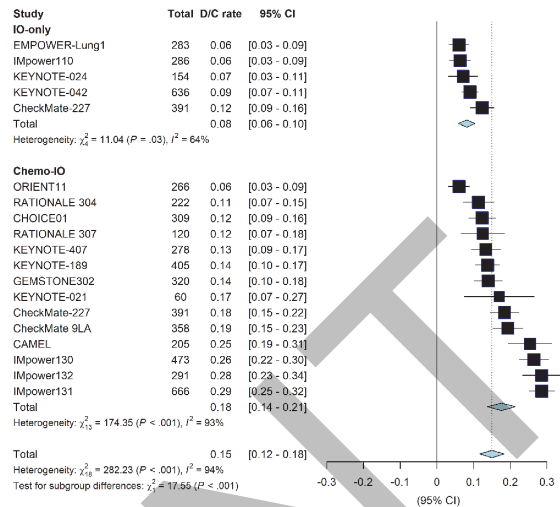
¹Seunghwan Shin, ²Sumin Lee, ¹Huijeong Kim, ¹Chiyeon Oum, ¹Soolck Cho, ¹Yoojoo Lim, ¹Ken Nesmith*, ¹Chan-Young Ock. ¹Lunit Inc., Seoul, Korea; ²Korea University, College of Pharmacy, Sejong, Korea

Background Chemo-IO is generally known to have better efficacy than IO-only, despite a higher incidence of TRAEs. The incidence of treatment discontinuation related to TRAE is generally related to uncontrollable TRAE. However, differences in TRAE-related treatment discontinuation rates between the two treatments has not been well studied. In this study, we compared the discontinuation rates of the two treatments for first-line treatment of NSCLC and other cancer types.

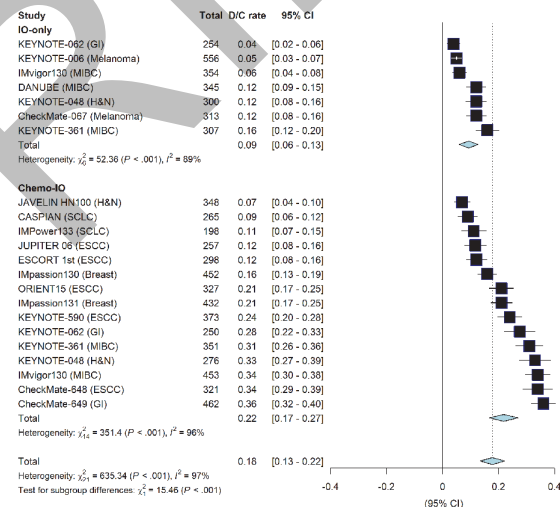
Methods We searched PubMed, Embase, and the Web of Science databases for eligible articles that include prospective phase III randomized controlled trial data of first-line treatments using IO-only or chemo-IO. IO-only was defined as a single immunotherapy drug or a combination of immunotherapy drugs, and chemo-IO was defined as a combination of immunotherapy and other chemotherapy drugs. The analysis was performed separately for NSCLC and other cancer types because most of the first-line trials with immunotherapy were published in NSCLC. We found 19 and 22 trials encompassing 6,114 and 7,492 patients in NSCLC and other cancer types, respectively. The data for discontinuation rate due to TRAEs and their 95% confidence intervals (CIs) were extracted.

Results Although there was heterogeneity of specific drugs in both the IO-only and chemo-IO groups, overall, IO-only showed a significantly lower TRAE-related discontinuation rate than chemo-IO. For NSCLC, we found that IO-only had a lower TRAE-related discontinuation rate (8.13%, 95% CI 5.90-10.36) than chemo-IO (17.54%, 95% CI 13.75-21.34) (figure 1). IO-only also showed a lower TRAE-related discontinuation rate (9.32%, 95% CI 5.94-12.69) compared to chemo-IO (21.78%, 95% CI 16.56-26.98) in other cancer types (figure 2). Clinical trials of NSCLC patients showed that there were differences in TRAE-related discontinuation rates associated with specific drugs in both IO-only (p=0.02) and chemo-IO (p<0.001), as well as in other cancer types trials (IO-only : p=0.01, chemo-IO: p<0.001).

Conclusions Compared to IO-only, chemo-IO showed a higher treatment discontinuation rate due to TRAEs. Since TRAE-related discontinuation may lead to suboptimal treatment outcomes, further study to discover the novel biomarker that dictates who could achieve durable response from IO-only, without early treatment discontinuation should be warranted.



Abstract 918 Figure 1 TRAE-related discontinuation rate in first-line NSCLC trials



Abstract 918 Figure 2 TRAE-related discontinuation rate in other cancer types

<http://dx.doi.org/10.1136/jitc-2022-SITC2022.0918>

COVID and Immunotherapy

919 ACUTE RESPIRATORY FAILURE AND THE RISK IMMUNOTHERAPY RELATED PNEUMONITIS DURING THE COVID PANDEMIC

Scott Amrhein*, Andrew Faucheu, Lara Khoury, John Kalada, Greg Russell, Thomas Lycan. Wake Forest University School of Medicine, Winston-Salem, NC, United States

Background Immune checkpoint inhibitors are a newer modality of systemic cancer-directed therapy that is often more tolerable and has broader eligibility criteria than traditional cytotoxic chemotherapy. Unfortunately, pneumonitis is a feared complication of these drugs in around 5% of all patients, including a rare risk of death. Per professional guidelines, there are no pathognomonic features in radiology, clinical history, or laboratory testing to confirm pneumonitis. The global COVID-19 pandemic and the widespread utilization of these drugs have complicated this diagnostic challenge. We sought to develop a systematic method to measure the incidence of different etiologies of acute respiratory failure in the current landscape.

Methods We developed a novel patient registry from a retrospective cohort of patients treated with an immune checkpoint inhibitor for cancer and then presented to the hospital after the onset of the COVID19 pandemic in this region. We created a novel case report template in REDCap that collected all relevant data from clinical documentation, imaging reports, and laboratory values during the hospitalization and follow-up. The template prompted the physician reviewer to attribute the respiratory failure based on diagnostic criteria from professional guidelines.

Results Our retrospective cohort was made up of 110 patients who had 304 separate hospitalizations between March 2020 and June 2022. Nearly half of these encounters (n = 138, 45%) had a respiratory complaint noted on admission, and an additional 36 encounters (11%) had respiratory testing at any point during their hospitalization. Respiratory complaints were most commonly due to bacterial pneumonia (n = 52, 30.2%), COPD exacerbations (n = 20, 11.6%), pleural effusions (n = 18, 10.5%), malignant obstruction (n = 18, 10.5%), multiple etiologies (n = 16, 9.3%), other etiologies (n = 16, 9.3%), checkpoint inhibitor pneumonitis (n = 3, 2%) and COVID19 pneumonia (n = 2, 1%).

Conclusions Our analysis found that respiratory evaluations occurred in most hospitalizations among patients receiving an immune checkpoint inhibitor for cancer. Although the current widespread use of these drugs and the COVID19 pandemic have altered the diagnosis and management of respiratory failure patients with cancer, most cases were still due to bacterial infections or malignant progression. Our study also provides proof-of-concept for a novel case report template form that can systematically collect and categorize data from these complicated hospitalizations.

<http://dx.doi.org/10.1136/jitc-2022-SITC2022.0919>

920

ALTERATION OF T CELL RESPONSES AGAINST SARS-COV-2 OMICRON VARIANT AFTER VACCINATION WITH MRNA BOOSTER IN LUNG CANCER PATIENTS

Karthik Chakravarthy*, No-Joon Song, Chelsea Bolyard, Kelsi Reynolds, Kevin Weller, Sarah Reisinger, Yi Wang, Anqi Li, Mark Rubinstein, Peter Shields, Zihai Li. *The Ohio State University, Columbus, OH, United States*

Background The severe acute respiratory syndrome coronavirus 2 (SARS-CoV-2) Omicron variant has demonstrated high transmissibility and possesses several spike protein mutations that allow for evasion of previously established immunity.¹ mRNA vaccines against the spike protein of the ancestral strain of the virus have been reported to induce robust T cell immunity against the omicron variant when examined in healthy individuals.² However, the effectiveness of the booster vaccine doses in late-stage lung cancer patients undergoing active anti-PD-1/PD-L1 agent immunotherapy has yet to be investigated.³

Methods To address this question, we assessed both CD8+ and CD4+ T cell responses using a modified activation-induced marker (AIM) assay that was performed on peripheral blood mononuclear cells (PBMCs), which was coupled with high dimension spectral flow cytometry analyses. The PBMCs were obtained using cryopreserved blood samples collected from The COVID-19 Vaccine Study of Infections and Immune REspoNse (SIIREN) trial, and a total of 51 patient samples (20 non-cancer patients and 31 lung cancer patients) were assessed.

Results Our observations included that booster vaccines induced CD8+ T cell response in both non-cancer subjects and lung cancer patients against ancestral strain and omicron variant, while only marginal induction or trend was detected for CD4+ T cells in normal subjects. Pertinent results also consisted of identification of distinct subpopulation dynamics involving varying degrees of differentiation of antigen-specific CD8+ and CD4+ T cells in lung cancer patients compared to non-cancer subjects, thus demonstrating evidence of dysfunction. Another noteworthy finding included the observation of sex biased T cell responses with female lung cancer patients demonstrating more efficient antigen-specific T cell responses compared to males.

Conclusions We conclude that lung cancer patients in our study cohort have substantial qualitative deviation in their T cell response to mRNA vaccine from the normal individuals. This altered response may be a consequence of altered T cell differentiation states, resulting in the high degree of heterogeneity of AIM+ T cells identified in booster vaccinated individuals. Moreover, the dampened T cell response to omicron in cancer patients could implicate that less protection was established by vaccination for lung cancer patients, especially given that humoral response is also reduced in cancer patients.⁴ This further highlights the need for heightened protective measures for cancer patients to minimize the risk of breakthrough infection with the omicron and other future variants of SARS-CoV-2.⁵

Acknowledgements We thank individuals who participated in sample collection, preparation, and preservation/storage, including Jamie Hamon, Donna Bucci, Mohamed Yusuf, Robert Davenport, and Taylor Chatlos from Pelotonia Institute for Immuno-Oncology and Immune Monitoring and Discovery Platform of the Pelotonia Institute for Immuno-Oncology. Additional gratitude is extended toward the Wherry lab, including Mathew Divij for providing detailed protocol for AIM assay and discussion.

REFERENCES

1. Hu J. Increased immune escape of the new SARS-CoV-2 variant of concern Omicron. *Cell Mol Immunol.* 2022;**19**:293–295.
2. Liu Y. Robust induction of B cell and T cell responses by a third dose of inactivated SARS-CoV-2 vaccine. *Cell Discov.* 2022;**8**:10.
3. Naranbhai V. T cell reactivity to the SARS-CoV-2 Omicron variant is preserved in most but not all individuals. *Cell.* 2022;**185**:1041–1051.
4. Fendler A. COVID-19 vaccines in patients with cancer: immunogenicity, efficacy and safety. *Nat Rev Clin Oncol.* 2022.
5. Mair MJ. Enhanced SARS-CoV-2 breakthrough infections in patients with hematologic and solid cancers due to Omicron. *Cancer Cell.* 2022.

Ethics Approval All samples and clinical data were collected from patients who consented to the research study and were enrolled under an approved IRB protocol (2021C0041). An Institutional Review Board responsible for human subjects research at The Ohio State University reviewed this research project and found it to be acceptable, according to applicable state and federal regulations and University policies designed to protect the rights and welfare of research participants.

<http://dx.doi.org/10.1136/jitc-2022-SITC2022.0920>

922

EFFECT OF COVID-19 VACCINATION STATUS ON ADVERSE EVENTS AND OUTCOMES IN ADVANCED NON-SMALL CELL LUNG CANCER (ANSCLC) PATIENTS TREATED WITH IMMUNOTHERAPIES

Rohini George*, Babu Narayanan, Smita Agrawal. ConcertAI LLC, Bengaluru, KS, India

Background Immunotherapy is one of the most prominent therapies for NSCLC patients. While there is a lot of promise, adverse events (AEs) due to immunotherapies are a concern. Entering the era of COVID-19, the interaction of COVID-19 vaccination status with immunotherapy is not fully understood.¹⁻² As most newly diagnosed NSCLC patients will be vaccinated, understanding this interaction is important for managing their treatment. This study aims at determining whether COVID-19 vaccination status has any significant effect on AEs and outcomes of aNSCLC patients treated with immunotherapies in 1st line.

Methods This retrospective study leverages ConcertAI's NSCLC Patient360™ dataset, a deeply curated real-world oncology dataset with patients from across the United States. aNSCLC patients who started 1st line treatment containing an immunotherapy at least 30 days after their last COVID-19 vaccine were included in the vaccine-primed cohort (N=138). 1st line treatment in these patients started between January 2021 – April 2022. Similarly, a cohort of vaccine-naïve patients was created by including all patients in the dataset who received their 1st line immunotherapy treatment between January 2019 – April 2020 (N=1537) to ensure none of them received COVID-19 vaccine prior to immunotherapy treatment. Descriptive analysis on these cohorts showed no significant differences in terms of age, race, gender and treatment patterns. AEs for each patient during the course of 1st line immunotherapy treatment were identified. These AEs were categorised into 5 levels (table 1). To normalise the effect of length of treatment, AE/time on immunotherapy was calculated. Progression-Free Survival (PFS) and Overall Survival (OS) from start of L1 was also compared between the two cohorts.

Results 56% vaccine-naïve and 54% vaccine-primed patients had an AE while on immunotherapy. The distribution of severity of AEs between the two cohorts was also quite similar (table 2). Although the AE/time was higher in the vaccine-naïve cohort (p-value=0.03) (figure 1), this effect was mostly driven by 41 (2.6%) outlier patients who had many AEs in a very short span of time after starting immunotherapy. We believe such outliers were not seen in the vaccine-primed cohort primarily due to its smaller sample size. OS and PFS were similar between the two cohorts (figures 2 and 3).

Conclusions COVID-19 vaccination status does not affect frequency or severity of immunotherapy related AEs or have a significant impact on patients' outcomes. As more data becomes available on the vaccine-primed cohort the impact on rarer patient sub-populations can be evaluated

Acknowledgements The author would like to thank the following people from the Data Science Solutions team for help in generating accurate OS and PFS plots

Andrew Noble, Judith Mueller, Rahul Das, Jericho Cain, Somasekhar Suryadevara – Data Science Solutions Concert AI USA and Rishi Jajoo formerly at ConcertAI

REFERENCES

1. Mei Q, Hu G, Yang Y, et al Impact of COVID-19 vaccination on the use of PD-1 inhibitor in treating patients with cancer: a real-world study. *Journal for ImmunoTherapy of Cancer* 2022;10:e004157. doi: 10.1136/jitc-2021-004157.

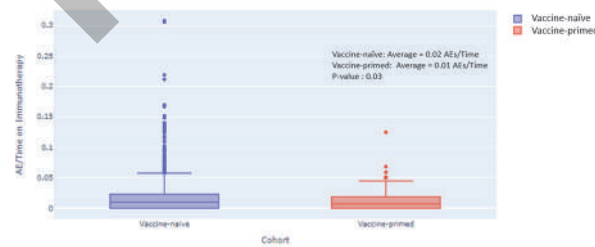
2. Brest P, Mograbi B, Hofman P, et al. COVID-19 vaccination and cancer immunotherapy: should they stick together?. *Br J Cancer* 2022;126, 1–3. <https://doi.org/10.1038/s41416-021-01618-0>

Level	Name	Examples
1	Minor medical intervention	Vitamin A deficiency, Hypocalcemia
2	Major medical intervention	Anemia, Neutropenia, Polyneuropathy
3	Hospital admission or similar	Renal failure, Dyspnea, Pulmonary embolism
4	Life threatening events	Leading to emergency room visit
5	Death	Death

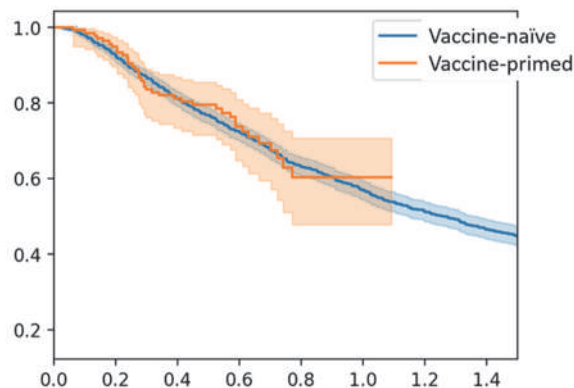
Abstract 922 Table 1 Categorization of level of AEs based on the level of medical intervention required

Level	Vaccine-naïve	Vaccine-primed
# of patients with adverse events within Line 1	865 (56%)	75 (54%)
# of adverse events	2332	166
1 Minor medical intervention	398 (17%)	38 (22%)
2 Major medical intervention	920 (39%)	70 (42%)
3 Hospital admission or similar	770 (33%)	49 (30%)
4 Life threatening events	241 (10%)	11 (7%)
5 Death	3 (0%)	

Abstract 922 Table 2 The distribution of frequency and severity of AEs between the vaccine-naïve and vaccine-primed cohorts

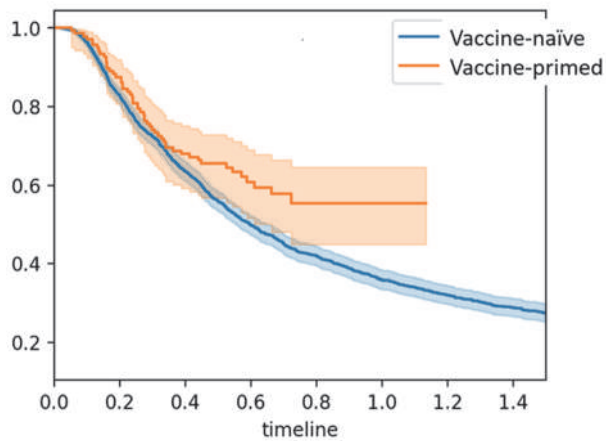


Abstract 922 Figure 1 Distribution of AEs/Time for the vaccine-naïve vs vaccine-primed cohorts



Abstract 922 Figure 2 Overall survival of vaccine naïve vs vaccine primed patients from start of first line of therapy. Median survival for Vaccine-naïve = 1.27 year and was not reached for the vaccine-primed cohort. P-value = 0.84

Abstracts



Abstract 922 Figure 3 Progression free survival of vaccine naïve vs vaccine primed patients. Median PFS for Vaccine-naïve = 0.6 year and was not reached for the vaccine-primed cohort. P-value = 0.02

<http://dx.doi.org/10.1136/jitc-2022-SITC2022.0922>

PREPRINT

923

DEEP SINGLE-CELL, PROTEOGENOMIC INSIGHTS FROM SARS-COV-2 INFECTED LUNG TISSUES

¹Arutha Kulasinghe*, ²Chin Wee Tan, ²Ning Liu, ¹James Monkman, ³Emily Killingbeck, ³Youngmi Kim, ³Liuliu Pan, ¹Tony Blick, ²Dharmesh Bhuvra, ²Kristen Feher, ³Michael Leon, ³Mark Gregory, ¹Kirsty Short, ¹Fernando Guimaraes, ³Michael Rhodes, ¹Gabrielle Belz, ²Melissa Davis. ¹The University of Queensland, Brisbane, Australia; ²WEHI, Melbourne, Australia; ³Nanostring Technologies, Seattle, WA, United States

Background The severe acute respiratory syndrome coronavirus 2 (SARS-CoV-2) that emerged in late 2019 has spread globally, causing a pandemic of respiratory illness designated coronavirus disease 2019 (COVID-19) and is likely to lead to complexities in treating thoracic malignancies. Patients with lung cancer are at an increased risk of becoming infected with the SARS-CoV-2 virus and experience higher morbidity and mortality than the general population. However, little is known about the host tissue and cellular responses associated with SARS-CoV-2 infection, symptoms, and disease severity.

Methods Here, we use the Nanostring GeoMX Digital Spatial Profiler (DSP) and CoxMX Spatial Molecular Imager (SMI) technology to determine tissue signatures, and spatially resolved quantitative single-cell proteogenomic changes driven by SARS-CoV-2 infection. This dual approach was used to generate an in-depth picture of the pulmonary transcriptional and proteomic landscape of COVID-19, pandemic H1N1 and uninfected control patients.¹ Rapid autopsy COVID-19 lung samples were collected across two independent cohorts of patients, and tissue microarrays (TMAs) were prepared. For GeoMx, n=10 COVID-19, n=10 pH1N1 and n=5 normal control tissues were compared. For CosMx, n=19 COVID-19 cores in technical replicates, and n=20 normal control tissues were compared. Tissue-based gene signatures were subsequently tested in the peripheral samples from COVID-19 patients.

Results SARS-CoV-2 viral presence was confirmed by RNA-seq and integrated to inform region of interest and cell types involved in infection. Analysis of the Nanostring GeoMx data revealed tissue signatures associated with SARS-CoV-2 infection, including Type 1 IFN, blood coagulation, hypoxia and angiogenesis. Analysis of the Nanostring CosMx data enabled single cell typing and mapping of tissue-specific signatures to cellular compartments of interest (e.g. macrophages, fibroblasts) and investigation of complex cell population heterogeneity and interactions. All these while preserving spatial context and highlighted differential cell type distribution in the lungs of COVID-19 patients compared to non-infected controls. Our tissue-based Type 1 IFN signatures, when tested in the blood, were found to be predictive of disease severity in COVID-19 patients when measured within the first few days of symptom onset.

Conclusions Here, we've used innovative, cutting-edge spatial transcriptomics approaches to delineate tissue signatures and cellular profiles unique to COVID-19 and common across acute respiratory distress syndrome. These data will aid in understanding the proteogenomic landscape of SARS-CoV-2 infected lung tissues and form new knowledge for the impact on thoracic malignancies, and treatments such as immunotherapy. Moreover, the study demonstrates how tissue-based findings can be rapidly developed into signatures tested in non-invasive samples.

REFERENCE

1. Arutha Kulasinghe *et al.* Profiling of lung SARS-CoV-2 and influenza virus infection dissects virus-specific host responses and gene signatures. *European Respiratory Journal* 2022.

Ethics Approval Autopsy and biopsy materials were obtained from the Pontificia Universidade Catolica do Parana PUCPR the National Commission for Research Ethics (CONEP) under ethics approval numbers: protocol number 3.944.734/2020 (for COVID-19 group), and 2.550.445/2018 (for H1N1 and Control group). All methods were carried out following relevant guidelines and regulations. Families permitted the post-mortem biopsy of COVID-19 and H1N1pdm09 samples and conventional autopsy for the cases of the Control group. The study was also approved under University of Queensland and Queensland University of Technology Human Research Ethics Committee (HREC) ratification.

<http://dx.doi.org/10.1136/jitc-2022-SITC2022.0923>

924

BARCODE ENABLED ANTIGEN MAPPING (BEAM) AND SINGLE-CELL SEQUENCING ENABLES NEXT-GENERATION SYSTEMS IMMUNOLOGY ANALYSIS OF THE POST-COVID-19 IMMUNE LANDSCAPE

Peter Finnegan*, Bruce Adams, Daniel Reyes, Sean Marrache, Payam Shahi, FuNien Tsai, Thomas Vollbrecht, Micheal Stubbington. *10x Genomics, Walnut Creek, CA, United States*

Background The adaptive immune system identifies foreign antigens based on a series of highly specific interactions involving multiple immune cell types. Identifying the exact mechanisms of said interactions can be difficult to achieve using bulk sequencing methods due to poor resolution. Single cell sequencing offers the ability to match a specific antigen to an immune cell receptor sequence at the cellular level.

Methods We used Barcode Enabled Antigen Mapping (BEAM) and Single Cell Immune Profiling technology to profile hundreds of thousands of human peripheral blood mononuclear cells (PBMCs) from a donor following their recovery from COVID-19. These cells were screened for potential binding interactions with multiple antigens from SARS-CoV-2 and other viral pathogens. Sequencing data were also generated for gene expression and paired sequences for both BCRs and TCRs.

Results The combination of these two techniques allowed us to identify a number of antigen-specific clonotypes of T cells and B cells. The high throughput of the experiment allowed us to gain understanding on a global scale of the state of the immune system following recovery from a COVID-19 infection, as well as to identify potentially rare clonotypes that may not have been discerned from a smaller sample size.

Conclusions This experiment demonstrates the ability of BEAM to both profile the entire immune system at the cellular level at a given point in time as well as distinguish specific antigen-receptor interactions with the same resolution. Insights provided by similar experiments could be invaluable in the creation of precision cell therapies for use in cancer treatment, as well as the development of vaccines and analysis of allergic and autoimmune responses.

<http://dx.doi.org/10.1136/jitc-2022-SITC2022.0924>

Data Sharing, Handling and Access

925 PHENOCOMB, A TOOL FOR EVALUATING COMPLEX PHENOTYPES IN HIGH-DIMENSION CYTOMETRY DATASETS

¹Ann Strange*, ²David Woods, ¹Brian Thompson, ¹Carol Amato, ¹Paulo Burke. ¹CU Anschutz, Aurora, CO, United States; ²University of Colorado School of Medicine, Aurora, CO, United States

Background Modern cytometry can simultaneously measure dozens of markers, empowering investigation of complex phenotypes. However, manual gating relies on previous biological knowledge, and clustering/dimension-reduction tools fail to capture discrete phenotypes. Consequently, complex phenotypes with potential biological importance are often overlooked. To address this, we developed PhenoComb, an R package that allows agnostic exploration of complex phenotypes by assessing the frequencies of all marker combinations in cytometry datasets.

Methods PhenoComb uses signal intensity thresholds to assign markers to discrete states (e.g. negative, low, high). As PhenoComb works in a memory-safe manner, time and disk space are the only constraints to the number of markers and discrete states that can be evaluated. Next, the number of cells per sample from all possible marker combinations are counted and frequencies assessed. PhenoComb provides several approaches to perform statistical comparisons, evaluate the relevance of phenotypes, and assess the independence of identified phenotypes. PhenoComb also allows users to guide analysis by adjusting several function arguments such as identifying parent populations of interest, filtering low-frequency populations, and defining a maximum marker complexity. PhenoComb is compatible with local computer or server-based use.

Results In testing of PhenoComb's performance on synthetic datasets, computation on 16 markers was completed in the scale of minutes and up to 26 markers in hours. We applied PhenoComb to two publicly available datasets: an HIV flow cytometry dataset (12 markers and 421 samples) and the COVIDome CyTOF dataset (40 markers and 99 samples). In the HIV dataset, PhenoComb identified immune phenotypes associated with HIV seroconversion, including those highlighted in the original publication. In the COVID dataset, we identified several immune phenotypes with altered frequencies in infected individuals relative to healthy individuals.

Conclusions PhenoComb is a unique and powerful tool for agnostically assessing phenotypes. By more fully utilizing the high-dimension data in single cell datasets, PhenoComb empowering exploratory data analysis and discovery of phenotypes for further characterization. PhenoComb is publicly available at <https://github.com/SciOmicsLab/PhenoComb>.

<http://dx.doi.org/10.1136/jitc-2022-SITC2022.0925>

926

EVALUATING DIVERSE DECONVOLUTION METHODS FOR TUMOR SPATIAL TRANSCRIPTOMIC DATASETS

Guangyuan (Frank) Li*, Amir Bayegan, Joon Sang Lee, Donald Jackson, Jack Pollard. *Sanofi US, Cincinnati, OH, United States*

Background Spatial transcriptomics technology may improve our ability to understand the organization of tumor microenvironment (TME) and uncover the recurrent interaction patterns across diverse cell types. While naturally complementing traditional scRNA-Seq, recent popular spatial platforms (such as 10x visium) fail to achieve single-cell resolution and require deconvolution methods to calculate the underlying cell type distributions. There are dozens of spatial deconvolution methods whereas systematic benchmarks comparing the methods are lacking.

Methods Here we present a comprehensive evaluation of 3 widely-used and top-performing deconvolution methods, DeconRNASeq, CARD, Cell2location, as well as 3 label transfer methods that assign a single cell type to one spot. We benchmarked these tools in four publicly available human breast cancer datasets by measuring the correspondence (spearmanr, pearsonr and F1-score) between inferred cell type proportions and normalized expressions of canonical marker genes at each spatial spot.

Results Cell2location consistently performs best. We further showed deconvolution methods that are particular designed for spatial context (CARD, Cell2location) achieved significantly better results compared to bulk deconvolution (DeconRNASeq) and label transfer methods (ingest, Seurat, Scanorama), suggesting the explicit modeling of spatial correlations and consideration of technical artifacts between sequencing technologies are crucial. Furthermore, when pairing with clinically unmatched scRNA reference, the deconvolution performance is largely on par with the available matched reference for non-tumor cells, indicating that publicly available scRNA data can serve as reference for spatial deconvolution.

Conclusions Taken together, our study suggests that methods such as Cell2location with either matched or unmatched references will give actionable deconvolution in spatial studies in tumor tissues.

<http://dx.doi.org/10.1136/jitc-2022-SITC2022.0926>

927

STREAMLINING CANCER IMMUNOTHERAPY RESEARCH WITH THE CRI IATLAS DATA RESOURCE AND WEB PORTAL

¹Vésteinn Thorsson*, ¹Carolina Heimann, ²Andrew Lamb, ¹David Gibbs, ³Dante Bortone, ³Sarah Dexheimer, ³Steven Vensko, ²Yooree Chae, ¹Ilya Shmulevich, ³Benjamin Vincent, ²James Eddy. ¹Institute for Systems Biology, Seattle, WA, United States; ²Sage Bionetworks, Seattle, WA, United States; ³University of North Carolina at Chapel Hill, Chapel Hill, NC, United States

Background With the increased volume of genomics data from studies involving treatment with immune checkpoint inhibition (ICI) and other immunotherapies, researchers remain unable to make full use of results due to lack of comprehensive access to data or the ability to compare outcomes across datasets. The Cancer Research Institute (CRI) iAtlas¹ (www.cri-iatlas.org) is a comprehensive web platform for interactive data exploration and discovery in immuno-oncology, originating in a study by The Cancer Genome Atlas (TCGA).¹⁻³ iAtlas provides topic-oriented analysis modules, each generating visualizations and statistics for studying interactions between tumors and the immune microenvironment (figure 1).

Methods Immunogenomic features from 15 ICI trials encompassing 1,142 samples were processed with a standardized bioinformatics workflow⁴ and incorporated into iAtlas, augmenting the 11,535 patient samples from TCGA¹⁻³ and the Pan-Cancer Analysis of Whole Genomes⁵ consortia. A compendium of in-development immunotherapy drug targets⁶ and results of a study of germline genetic contribution to immune response in cancer⁷ were included. For efficient access, all data were incorporated into a relational database, and programmatic access was made available through an application programming interface (API) (figure 2). The set of available iAtlas modules was vastly extended, and numerous improvements were made to the codebase. Users can now define sample cohorts and sample groups based on any available categorical or numerical variable.

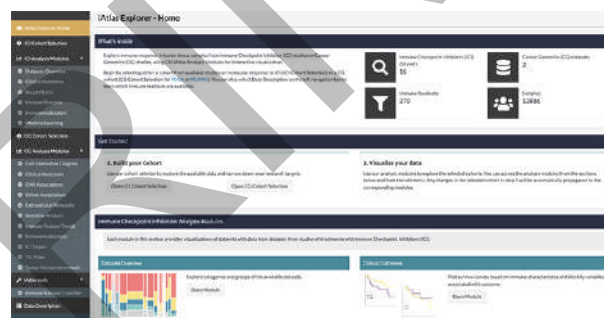
Results iAtlas provides 17 interactive analysis modules (table 1) to explore immune-cancer interactions, immunotherapy treatment, and outcomes in 12,677 patient samples. Six modules are dedicated to ICI studies: dataset overview, immune readouts, immunomodulators, clinical outcome, regression analysis, and a machine learning module to enable identification of factors associated with response to therapy (figure 3). We added modules to explore how germline variation and copy number alterations relate to immune response, and how receptor-ligand interactions mediate interactions among tumor and immune cells (figure 4). Docker images using Common Workflow Language descriptors are provided so that researchers can run iAtlas workflows on their own data. Computational notebooks are provided to illustrate and explain iAtlas code, plots, and functionality and to facilitate integration of iAtlas data with data sourced from a researcher's own study.

Conclusions iAtlas serves as a repository and resource for harmonized data on immune response in cancer and response to immunotherapy. iAtlas enables researchers to readily test hypotheses and access data through multiple modalities: an interactive web portal, data download, tools,⁸ and computational workflows and notebooks.

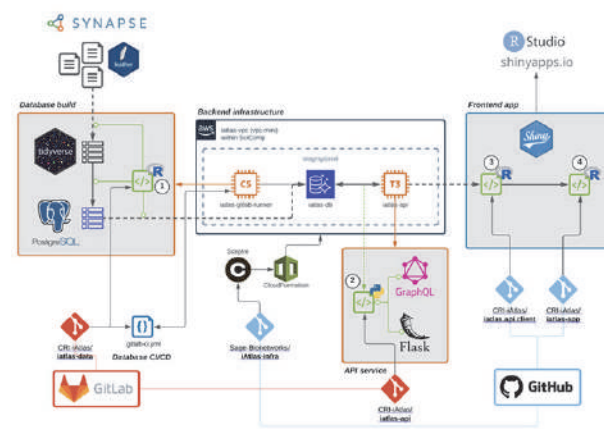
Acknowledgements This work is supported by the Cancer Research Institute. We thank Allison Kudla, Institute for Systems Biology, for generating the illustration used in the Cell-Interaction Diagram module and for web design and implementation.

REFERENCES

1. Eddy JA, Thorsson V, Lamb AE, Gibbs DL, Heimann C, Yu JX, et al. CRI iAtlas: an interactive portal for immuno-oncology research. *F1000Research* 2020;**9**:1028. <https://doi.org/10.12688/f1000research.25141.1>.
2. Hutter C, Zenklusen JC. The cancer genome atlas: creating lasting value beyond its data. *Cell* 2018;**173**:283–5. <https://doi.org/10.1016/j.cell.2018.03.042>.
3. Thorsson V, Gibbs DL, Brown SD, Wolf D, Bortone DS, Ou Yang T-H, et al. The immune landscape of cancer. *Immunity* 2018;**48**:812–830.e14. <https://doi.org/10.1016/j.immuni.2018.03.023>.
4. Bortone DS, Vensko SP, Dexheimer S, Thorsson V, Zappasodi R, Rudqvist N-P, Vincent, BG et al. Generalizability of predictive versus prognostic indicators from published transcriptomic associations with tumor response to immune checkpoint inhibition. SITC Annual Meeting 2022, submitted.
5. ICGC/TCGA Pan-Cancer Analysis of Whole Genomes Consortium. Pan-cancer analysis of whole genomes. *Nature* 2020;**578**:82–93. <https://doi.org/10.1038/s41586-020-1969-6>.
6. Upadhaya S, Hubbard-Lucey VM, Yu JX. Immuno-oncology drug development forges on despite COVID-19. *Nat Rev Drug Discov* 2020;**19**:751–2. <https://doi.org/10.1038/d41573-020-00166-1>.
7. Sayaman RW, Saad M, Thorsson V, Hu D, Hendrickx W, Roelands J, et al. Germline genetic contribution to the immune landscape of cancer. *Immunity* 2021;**54**:367–386.e8. <https://doi.org/10.1016/j.immuni.2021.01.011>.
8. Gibbs DL. Robust classification of immune subtypes in cancer. *bioRxiv* 2020:2020.01.17.910950. <https://doi.org/10.1101/2020.01.17.910950>.



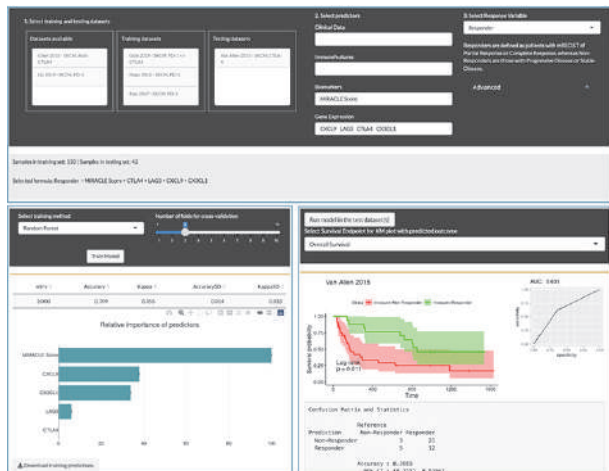
Abstract 927 Figure 1 CRI iAtlas Explorer Entry into exploration of immune response in cancer with iAtlas. Researchers start by defining cohorts and sample groups, and can then explore and visualize results using any of 17 analysis modules (left navigation bar, and bottom right of image).



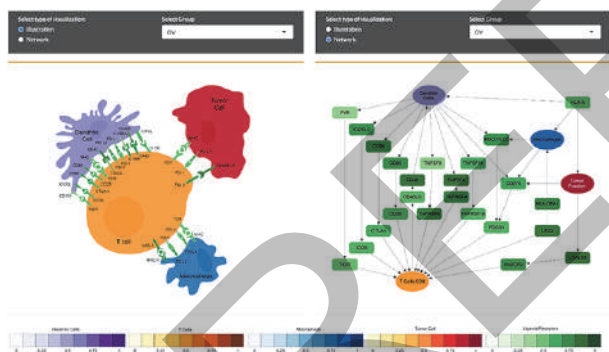
Abstract 927 Figure 2 iAtlas 2.0 infrastructure The infrastructure underlying the iAtlas web application (top right) has four main components: 1. R scripts to (i) download data files from Synapse; (ii) extract tables from files and perform any transformations to fit database schema; and (iii) build PostgreSQL database tables, which are stored in Aurora DB. 2. Python package that implements a GraphQL API service using Flask; GraphQL query requests are resolved to SQL database queries using SQLAlchemy. 3. R package that implements a GraphQL API client to retrieve data (and transform JSON responses into tables) within the app, or as part of a regular R session. 4. Shiny/R app

Abstracts

code, including a set of reusable Shiny modules in the iAtlas.modules R package; app is hosted using shinyapps.io and deployed manually using the rconnect package



Abstract 927 Figure 3 iAtlas ICI Machine Learning Module To identify factors that may be associated with response to Immune Checkpoint Inhibition (ICI), users choose test and training sets, factors of interest, and the response variable (top). After selection of the modeling method (here, Random Forest – other choices are Elastic Net, Logistic regression and Gradient Boosting) and parameters, the model can be trained (bottom left) and statistics are reported after running on the test set (bottom right)



Abstract 927 Figure 4 Interactions in the Tumor Immune Microenvironment In this iAtlas analysis module, Cell-Interaction Diagram, the estimated levels of cells and associated ligands and receptors that bind are shown within a selected group of samples, in this case ovarian (OV) tumor samples in the TCGA. Users can elect to show interactions superimposed on an illustration (left) or on a node-edge network diagram (right). A related module, Extracellular Networks, infers from data the likely ligand-receptor-mediated cellular interactions in the microenvironment and displays those as a node-edge network diagram.

Abstract 927 Table 1 Interactive analysis modules available in iAtlas

Data Source	Module Name	Module Description
Immune Checkpoint Inhibition	Datasets Overview	Explore categories and groups of the available datasets.
	Clinical Outcomes	Plot survival curves based on immune characteristics and identify variables associated with outcomes.
	Hazard Ratio	Create Cox Proportional Hazard Regression Models and visualize Hazard Ratio in a heatmap and a forest plot.
	Immune Features	See how immune readouts vary across your groups and ICI datasets.
	Immunomodulators	Explore the expression of genes that code for immunomodulating proteins, including checkpoint proteins.
	Machine Learning	Train and run multivariable models with cross-validation on ICI genomics and immunogenomics data.
	Cell-Interaction Diagram	Explore cell and protein abundance on an illustration.
	Clinical Outcomes	Quantify the relationship between immune response and disease outcome, in terms of either overall survival (OS) or progression free interval (PFI).
	CNV Associations	Explore associations of microenvironment with gene copy number.
	Driver Associations	Explore associations of microenvironment with cancer driver mutations.
	Extracellular Networks	Explore the extracellular networks modulating tumoral immune response.
	Germline Analysis	Explore the germline genetic contribution to the immune landscape of cancer.
	Immune Feature Trends	Visualize how immune readouts vary across sample groups.
	Immunomodulators	Explore the expression of genes that code for immunomodulating proteins, including checkpoint proteins.
Cancer Genomics	IO Targets	Explore the expression of genes that code for immunological (IO) targets.
	TIL Maps	Explore the characteristics of maps of tumor infiltrating lymphocytes obtained from analysis of H&E images.
	Tumor Microenvironment	Explore the immune cell proportions in sample groups.

<http://dx.doi.org/10.1136/jitc-2022-SITC2022.0927>

928 STANDARDIZING THE ANALYSIS OF SPATIAL IMAGING FEATURES IN TUMOR SAMPLES

¹Jason Weirather*, ¹Ian Dryg, ¹Madison Turner, ¹Ann-Elizabeth Le, ¹Anne Carlisle, ¹Kathleen Pfaff, ¹F Stephen Hodi, ²Scott Rodig. ¹Dana-Farber Cancer Institute, Boston, MA, United States; ²Brigham and Women's Hospital, Boston, MA, United States

Ethics Approval The HTAN study is approved by the DFCI Institutional Review Board as protocol 18-452.

<http://dx.doi.org/10.1136/jitc-2022-SITC2022.0928>

Background The analysis of cellular imaging data produces annotations of image regions, derived features, and cellular annotations that are the basis for quantitative reports. This data can come from different instruments and annotations applied to regions of interest (ROI); annotations of this data require can arrive in many different formats, and these formats require standardization so they can be analyzed using a common syntax. Our software package, Pythologist (<https://github.com/dfci/pythologist>), provides the functionality for extracting spatial and cellular features from analyzed images.^{1,2} Here we demonstrate how this software can be used to standardize the process of investigating and generating reports from annotated tumor samples.

Methods Multiplex-Immunofluorescence images from FFPE were analyzed by the DFCI Center for Immuno-Oncology as part of the Human Tumor Atlas Network (HTAN) to study the tumor immune microenvironment of cancers. We analyze samples stained by two panels: 1) a checkpoint specific panel measuring Tumor (SOX10 or Cytokeratin), CD8, PD-1, PD-L1, and FOXP3, and 2) a macrophage specific panel includes CD3, CD68, PD-L1, CD163, and Ki-67 in addition to the Tumor marker. Cellular features were annotated by InForm software, and region annotations were manually drawn, these include: cell segmentation, processed image regions, drawn tumor regions, and cellular annotations produced in InForm. A subset of cases were analyzed for cell density and percent cellularity measures in the context of the full-ROI but also within the tumor and invasive margin compartments. Furthermore, spatial features including cell-proximity, cell-cell-contacts, and nearest-neighbor distances are extracted and reported through the same tool.

Results As a vignette to demonstrate how this software package can be used to generate reports, two colorectal samples where the manually-annotated invasive margin annotations were available are analyzed. Within these two samples, treating all regions of interest as a single image, a greater density of CD8+ T cells (535 and 506 cells/mm²) are adjacent to the tumor region (within ~40um from the outside of the tumor region) compared to those CD8+ T cells within the tumor region (101 and 370 cells/mm²).

Conclusions Spatially informed annotations, enable us to examine cell populations in these different contexts. By standardizing imaging data annotation formats our tool provides a common platform for generating reports from the analyzed data. These capabilities provide a straight-forward approach to analyzing and visualizing tumor samples and provide insights into meaningful spatial contexts by performing hypothesis driven analyses of the tumor-immune microenvironment.

Acknowledgements This work is supported through the Human Tumor Atlas Network, grant U2CCA233195, and the Dana-Farber Cancer Institute Center for Immuno-Oncology

REFERENCES

1. Griffin Gabriel K, et al. Spatial Signatures Identify Immune Escape via PD-1 as a Defining Feature of T-Cell/Histiocyte-Rich Large B-Cell Lymphoma. *Blood*, 2021;137:(10)1353–1364. <https://doi.org/10.1182/blood.2020006464>.
2. Patel Sanjay S, et al. The Microenvironmental Niche in Classic Hodgkin Lymphoma Is Enriched for CTLA-4- Positive T-Cells That Are PD-1-Negative. *Blood*, 2019, <https://doi.org/10.1182/blood.2019002206>.

929

THE DATA MANAGEMENT AND RESOURCE SHARING CENTER FOR THE CANCER MOONSHOT IMMUNO-ONCOLOGY TRANSLATIONAL NETWORK

¹Alan Hutson*, ¹Himangi Marathe, ¹Martin Morgan, ²Kunle Odunsi, ¹Song Liu. ¹Roswell Park Comprehensive Cancer Center, Buffalo, NY, United States; ²University of Chicago, Chicago, IL, United States

Background Background: Despite regulatory approval and advancements of immune-based interventions over the last decade, significant obstacles remain to be overcome before the full potential of immunotherapy can be realized to improve outcomes for cancer patients [1,3]. The NCI Cancer Moonshot Immuno-Oncology Translational Network (IOTN) was established in 2018 with the overarching goal of improving the efficacy, durability, and safety of immunotherapy across the spectrum of human cancers, as well as developing immunoprevention approaches that will prevent cancers before they occur.^{1,2}

Methods The IOTN consortium, consisting of 29 research project awards spanning 33 institutions, conducts translational research focused on four thematic areas: Immunotherapy, Immuno-Engineering to improve immuno-therapy (i3), Mitigating immune related adverse events (irAE) and Immuno-Prevention.^{2, 3} At each stage of the IOTN's translational studies, the Data Management Resource Sharing Center (DMRC) serves as an administrative and analytic hub, focusing on lowering barriers for access to analytic expertise, improving network productivity, maintaining a high standard for data collection and management, and fostering a collaborative and supportive research community.

Results The DMRC has developed centralized infrastructures to enhance the IOTN's research output, including a collection of publicly accessible and scalable resource sharing catalogs for Data, Model, Software and Clinical Trials.⁴ In addition to supporting intra-network collaboration, the DMRC engaged cross-moonshot communication by hosting and coordinating a number of meetings and workshops, including the inaugural Cancer Moonshot Collaborative Meeting and monthly NCI Cancer Moonshot Seminar Series.^{5, 6} The DMRC in collaboration with SITC has organized the highly popular SITC-NCI webinar series on "Computational Science in Immuno-Oncology", fostering collaboration, communication and outreach to the broader communities.⁷

Conclusions The IOTN's consortium structure, strengthened by the DMRC's centralized management, analytical, and data integration supports, has facilitated effective intra- and inter-moonshot communication and enabled collaborative translational studies.

Acknowledgements This work was supported by IOTN Moonshot grant U24CA232979-01

REFERENCES

1. Jacks T, Jaffee E and Singer D. Blue Ribbon Panel Co-Chairs (2016) Cancer Moonshot Blue Ribbon Panel Report. *National Cancer Institute*, Bethesda, MD.
2. Adult Immunotherapy Network Fact Sheet [https://www.cancer.gov/research/key-initiatives/moonshot-cancer-initiative/implementation/adult-immunotherapy-network/fact-sheet.pdf]
3. Annapragada A, Sikora A, Bollard C, *et al.* Cancer Moonshot Immuno-Oncology Translational Network (IOTN): accelerating the clinical translation of basic discoveries for improving immunotherapy and immunoprevention of cancer. *J Immunother Cancer* 2020;**8**:e00079.
4. Immuno-Oncology Translational Network. IOTN Resource Sharing Catalogs. 2022. Available from: https://www.iotnmoonshot.org/en/resources/all-resources/.
5. National Cancer Institute. Cancer Moonshot Workshop Highlights Advances – National Cancer Institute 2020. Available from: https://www.cancer.gov/news-events/cancer-currents-blog/2020/cancer-moonshot-nci-workshop-advances-collaboration.

6. National Cancer Institute. Cancer MoonshotSM Seminar Series [online workshop series], September 24, 2020-May 26, 2022: National Cancer Institute; 2021. Available from: https://www.cancer.gov/research/key-initiatives/moonshot-cancer-initiative/seminar-series.
7. 18. Society for Immunotherapy of Cancer. SITC-NCI Computational Immunology Webinar Series [online workshop series], May 11, 2021-December 17, 2022: Society for Immunotherapy of Cancer (SITC) in partnership with the National Cancer Institute (NCI); 2021 Available from: https://www.sitcancer.org/education/computational.

<http://dx.doi.org/10.1136/jitc-2022-SITC2022.0929>

Education and Treatment Management

<http://dx.doi.org/10.1136/jitc-2022-SITC2022.0930>

930

PROVIDER INSIGHTS ON MANAGING PATIENTS ON IMMUNOTHERAPY, BARRIERS TO CLINICAL TRIALS, AND BIOMARKER TESTING PREFERENCES

¹Tariqa Ackbarali*, ²Joel Neal, ³Yelena Janjigian, ⁴Michael Overman. ¹PlatformQ Health, Lake Worth, FL, United States; ²Stanford Cancer Institute, Stanford, CA, United States; ³Memorial Sloan Kettering Cancer Center, New York, NY, United States; ⁴MD Anderson Cancer Center, Houston, TX, United States

Background With the advent of immunotherapies for a plethora of solid tumors, the standard of care has dramatically shifted. Approved and investigational options shaping the treatment paradigm for cancer include immune checkpoint inhibitors (ICIs), antibody-drug conjugates, CAR-T cell therapies, and treatments with tumor-infiltrating lymphocytes. As data from numerous clinical trials are reported, new indications are approved, and emerging combinations with checkpoint inhibitors show promise, the immunotherapy landscape continues to morph and evolve.

Methods A 2-part educational series was broadcast live-online in January 2022 and remains on-demand through January 2023 at OMedLive.com. The series was provided in collaboration with the Society for Immunotherapy in Cancer (SITC) and was divided into 2 sessions; the first of which focused on update and emerging approaches in small cell lung cancer and non-small cell lung cancer. The second session highlighted updated in gastroesophageal junction cancer (GEJ) and colorectal cancer (CRC). Knowledge and competence questions were administered pre-, immediate post-, and 2 mos. post-activity. Data from these questions were analyzed to determine engagement and clinical impact.

Results Interim outcomes of the series are reported as of July 2022 from 496 learners; 62% of whom were physicians, nurse practitioners, physician assistants, and pharmacists. The series has impacted care for 2,860 patients currently receiving immunotherapy for either lung cancer, GEJ, or CRC. Statistically significant improvements in knowledge and competence were observed across all nine assessment questions. Provider insights were captured related to biomarker practices and challenges/barriers experienced when managing patients on immunotherapy. The most commonly ordered immunotherapy-related biomarker was PD-L1 (50%) with the least commonly ordered being tumor mutational burden (21%). At baseline, only 56% of providers utilized biomarkers to drive treatment planning; however, following engagement in the educational series this % increased to 68%. The greatest challenges for providers managing patients on ICIs were 'patient ability to afford therapy' (28%), 'adherence to treatment schedules' (18%), and 'patient understanding of treatment options' (11%). Barriers to patient enrollment in immunotherapy clinical trials were noted by providers as 'lack of immunotherapy trials at my institution/in my geographic region' (35%), 'patient interest' (25%), and 'eligibility requirements' (14%).

Conclusions The educational series was successful in improving knowledge and competence immediate post-sessions. Provider practice patterns and perceptions of challenges were insightful for further educational opportunities for providers as well as patients.

Acknowledgements The educational series was supported by educational grants from Genentech, Merck & Co., Inc., and Regeneron.

931 **TARGETING THE LYMPHOCYTE-ACTIVATION GENE-3 (LAG-3) IMMUNE CHECKPOINT IN PATIENTS WITH CANCER: AWARENESS AND CONFIDENCE AMONG ONCOLOGY HEALTHCARE PROFESSIONALS (HCP)**

¹Marie Becker*, ¹Timothy Quill, ²Tian Zhang, ³Evan Lipson. ¹*Clinical Care Options, LLC, Reston, VA, United States*; ²*UT Southwestern Medical Center, Dallas, TX, United States*; ³*Johns Hopkins University, Baltimore, MD, United States*

Background Over the last decade, immune checkpoint inhibitors targeting CTLA-4 and PD-(L)1 have revolutionized the care of patients with melanoma and many other tumor types. Recently, the immunoregulatory pathway comprised of LAG-3 and its ligands became the third immune checkpoint pathway for which blockade demonstrated benefit in a phase III clinical trial (RELATIVITY-047).¹ We explored oncology HCP familiarity with anti-LAG-3 mechanism of action, FDA-approved indications, and identification and management of associated adverse events.

Methods Between March and July 2022, we conducted an educational activity series for oncology HCPs. Each activity included 1) an interactive lecture led by a clinical investigator with expertise in the efficacy and safety of targeting LAG-3 in patients with melanoma and other cancers, and 2) polling questions designed to assess key aspects of HCP knowledge of LAG-3 and LAG-3-directed therapies.

Results 338 HCPs participated in 8 live and 1 online on-demand activities. Awareness of the role of LAG-3 and the rationale for combining a LAG-3 inhibitor with a PD-1 inhibitor was low at baseline with only 29% (37/126) of learners correctly identifying that the LAG-3 and PD-1 pathways are non-redundant, improving to 86% (115/134) after the lecture. A similarly low percentage of HCPs (21%, 28/132) could identify the FDA-approved indication for relatlimab (anti-LAG-3) plus nivolumab (anti-PD-1) (patients with advanced melanoma regardless of line of therapy or LAG-3 expression level) at baseline, improving to 85% (116/136) after the lecture. A majority of HCPs (83%, 99/119) reported low confidence to identify and appropriately manage adverse events associated with anti-LAG-3 combination therapy (baseline 2.42 on scale of 1-7, improving to 4.9 after the lecture). Participation in this educational activity improved HCP knowledge of the role of LAG-3 and of approved indications for anti-LAG-3 therapy. Self-reported confidence in managing adverse events associated with relatlimab plus nivolumab was also improved through education.

Conclusions HCP knowledge and confidence regarding the clinical utility of targeting LAG-3 with anti-LAG-3 therapies is low. Educational activities designed to address these deficiencies would be of clear benefit to HCPs treating patients with advanced melanoma and potentially other cancers. A detailed analysis of HCP trends will be presented.

REFERENCE

1. Tawbi HA, Schadendorf D Lipson EJ, et al. Relatlimab and nivolumab versus nivolumab in untreated advanced melanoma. *New Engl J Med.* 2022;**386**:24–34.

<http://dx.doi.org/10.1136/jitc-2022-SITC2022.0931>

932

IMMUNOTHERAPY EFFICACY AND TOLERABILITY IN ADVANCED HEPATOCELLULAR CARCINOMA (HCC) IN A DIVERSE AND UNDERSERVED POPULATION IN THE UNITED STATES – IMPORTANCE OF BASELINE LIVER FUNCTION AND SCREENING

¹Fernand Bteich*, ²Kush Desai, ²Chenxin Zhang, ²Charlotte Mcguckin, ³John Yan, ²Sharmin Sultana, ²Lawrence Leung, ¹Andreas Kaubisch, ⁴Milan Kinkhabwala, ⁴Sarah Bellemare, ²Adebola Adedimeji, ⁵Clara Tow, ¹Yvonne Saenger. ¹Montefiore Medical Center, Albert Einstein Cancer Center, Bronx, NY, United States; ²Albert Einstein College of Medicine, Bronx, NY, United States; ³Montefiore Medical Center, Bronx, NY, United States; ⁴Montefiore Einstein Center for Transplantation, Bronx, NY, United States; ⁵Montefiore Comprehensive Liver Program, Bronx, NY, United States

Background Incidence of hepatocellular cancer (HCC) in the Bronx in 2019 was 61% higher than New York State as a whole.¹ The advent of immune checkpoint inhibitors (ICI) has changed HCC therapy. ICI efficacy has not been extensively studied in underserved populations often excluded from clinical trials.

Methods 183 patients treated with nivolumab (n = 118), pembrolizumab (n = 22), nivolumab with ipilimumab (n = 4), atezolizumab (n = 6) and atezolizumab with bevacizumab (n = 33) between 2017 and 2021 (data cut-off) at the Montefiore-Einstein Cancer Center were identified based on electronic medical record (EMR) review. Kaplan Meier and Chi-squared analysis were performed.

Results

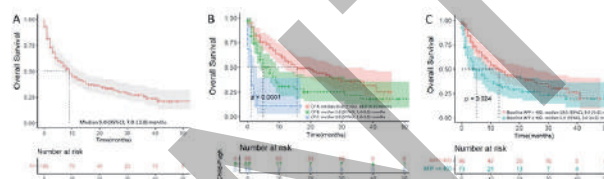
Racial and ethnic composition was: 42.1% Hispanic, 21.3% Black, 13.1% White, 4.9% Asian and 18.6% unknown. Hepatitis C and alcoholism were more commonly the sole cause of liver disease relative to the SEER database (13.7% vs 4.7% and 39.3% vs 8.2% respectively).² 64.33% of patients were diagnosed with HCC upon symptomatic presentation rather than by screening. Child-Pugh score at start of ICI was: A (51.4%), B (36.1%), and C (10.4%). (table 1). Median overall survival (mOS) after immunotherapy initiation was 9.0 (95% CI, 7.0-13.0) months. Child-Pugh A, B, and C patients had a mOS of 16.0, 5.0, and 1.0 months respectively (p=0.003). mOS was longer when pre-treatment AFP was <400 (13.0 vs 6.0 months; p=0.024) (figure 1). Patients diagnosed based on screening had prolonged mOS from diagnosis relative to those presenting with symptomatology (58.0 vs 16.0 months; p=0.004). 145 patients were evaluated on follow-up imaging. Disease control rate (DCR) was 39.3%. 8 patients (5.52%) had a complete response (CR). Patient achieving disease control were more likely to be diagnosed based on screening than were progressing patients (p=0.045), and all patients with Child-Pugh C cirrhosis progressed. There was no difference in survival when data were stratified by etiology of cirrhosis or race/ethnicity. 50 patients (27.3%) reported any immune related adverse event (irAE). 8 patients (4.4%) experienced grade ≥3 irAEs. One patient died of perforated immune colitis.

Conclusions In an underserved population of patients in the Bronx, enriched for alcoholism and hepatitis C, ICI to treat HCC yielded a DCR of 39.3%, mOS of 9 months, and toxicity in line with published reports.³ Etiology of cirrhosis did not predict benefit of immunotherapy, but baseline liver function and diagnosis made based on screening correlated with mOS and disease control. These results highlight a need for earlier HCC diagnosis and immunotherapy administration.

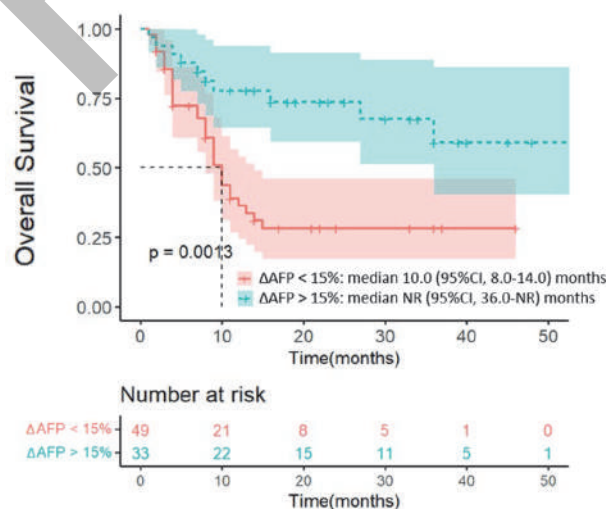
REFERENCES

1. New York State Cancer Registry. Cancer Incidence and Mortality in New York State, 1976–2014. Available from: <http://www.health.ny.gov/statistics/cancer/registry/> (Accessed: July 27, 2022).
2. Brar G, et al. Hepatocellular Carcinoma Survival by Etiology: A SEER-Medicare Database Analysis. *Hepatol Commun* 2020;**4**(10): 1541–1551.
3. Scheiner B, et al. Programmed cell death protein-1 (PD-1)-targeted immunotherapy in advanced hepatocellular carcinoma: efficacy and safety data from an international multicentre real-world cohort. *Aliment Pharmacol Ther* 2019;**49**(10):1323–1333.

Ethics Approval The study was approved by the Albert Einstein College of Medicine institution's Ethics Board, approval number 2021-13514.

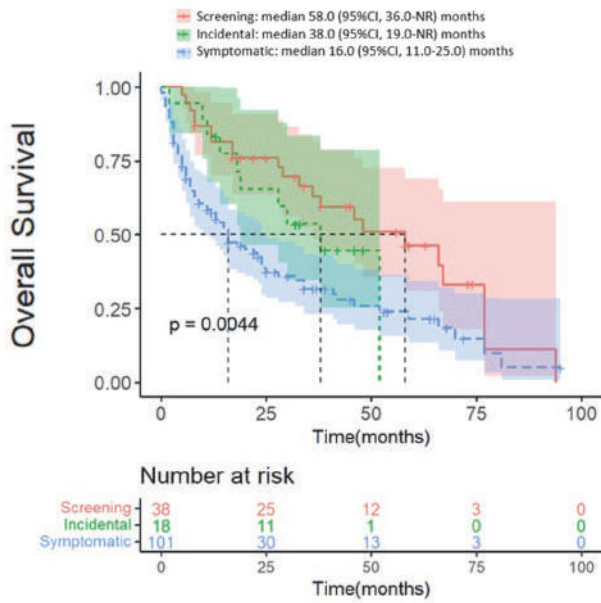


Abstract 932 Figure 1 Kaplan-Meier analysis of overall survival in HCC patients in The Bronx treated with ICI. Survival rates are shown for: A. All patients. B. Patients stratified by Child-Pugh score at initiation of ICI. C. Patients stratified by baseline serum AFP prior to ICI therapy. Survival is presented as the median (95% confidence interval). AFP, a-fetoprotein protein; CP, Child-Pugh; ICI, immune checkpoint inhibitor



Abstract 932 Figure 2 AFP Response Correlates with Overall survival. Kaplan-Meier analysis of overall survival is shown stratified by AFP response at 3 months

Abstracts



Abstract 932 Figure 3 Overall survival based on HCC presentation. Survival is shown from time of diagnosis, stratified by cancer presentation; found at screening, incidentally, or based on symptoms

Abstract 932 Table 1 Patient characteristics. HBV, chronic hepatitis B; HCV, chronic hepatitis C; NAFLD, nonalcoholic fatty liver disease; CLIP score, Cancer of the Liver Italian Program score; AFP, a-fetoprotein protein

		N(%)
Gender - no. (%)	Male	131 (71.6)
	Female	52 (28.4)
Race/ethnicity - no. (%)	Black, not Hispanic	39 (21.3)
	Hispanic	77 (42.1)
	White, not Hispanic	24 (13.1)
	Asian, not Hispanic	9 (4.9)
	Unknown	34 (18.6)
	Median age at diagnosis (range)	65 (19-87)
Etiology - no. (%)	Viral	89 (48.6)
	HBV	16 (8.8)
	HCV	72 (39.3)
	HBV/HCV	1 (0.5)
	Nonviral	94 (51.4)
	Alcohol abuse	25 (13.7)
	NAFLD	15 (8.2)
	Multi-factorial	35 (19.1)
	Alcohol/HBV	4 (2.2)
	Alcohol/HCV	30 (16.4)
	HCV/NAFLD	1 (0.5)
Rare/Unknown etiologies	19 (10.4)	
Method of diagnosis - no. (%)	Screening	38(20.8)
	Incidental	18(9.8)
	Symptomatic	101(55.2)
	Unknown	26(14.2)
HIV Status - no. (%)	Negative	170 (92.9)
	Positive	13 (7.1)
Child Pugh Score - no. (%), at immunotherapy	A	94 (51.4)
	B	66 (36.1)
	C	19 (10.4)
	Unknown	2 (1.1)
CLIP Score - no. (%), at immunotherapy	0	17 (9.3)
	1	53 (29.0)
	2	37 (20.2)
	3	37 (20.2)
	4	22 (12.0)
	5 to 6	10 (5.4)
	Unknown	7 (3.8)
AFP - no. (%), baseline	<400	96 (52.4)
	≥400	73 (39.9)
	Unknown	14 (7.7)
First immunotherapy agent(s) received - no. (%)	Atezolizumab	6 (3.3)
	Atezolizumab + bevacizumab	33 (18.0)
	Nivolumab	118 (64.5)
	Ipilimumab + nivolumab	4 (2.2)
	Pembrolizumab	22 (12.0)

<http://dx.doi.org/10.1136/jitc-2022-SITC2022.0932>

933

REAL-WORLD TREATMENT PATTERNS AND CLINICAL OUTCOMES IN PATIENTS WITH METASTATIC NSCLC AFTER RECEIVING FIRST-LINE PEMBROLIZUMAB WITH PEMETREXED/PLATINUM CHEMOTHERAPY IN THE US ONCOLOGY NETWORK

¹Jerome Goldschmidt, ²Srinivas Annavarapu, ²Divea Venkatesetty, ³Melissa Santorelli, ³Thomas Burke*, ⁴Nathan Pennell. ¹The US Oncology Network, Blacksburg, VA, United States; ²Ontada, Irving, TX, United States; ³Merck & Co., Inc., Rahway, NJ, United States; ⁴Cleveland Clinic, Cleveland, OH, United States

Background Pembrolizumab-pemetrexed-platinum is a standard of care in previously untreated metastatic non-squamous non-small cell lung cancer (NSCLC) based on significantly longer overall survival (OS) compared to pemetrexed-platinum in the Keynote 189 clinical trial.¹ In Keynote 189, 77% of patients received maintenance pemetrexed after induction while real-world studies in the United States (US) using the Flatiron Health database observed only 44-48% of patients received pemetrexed beyond cycle 4.²⁻⁴ This study aimed to further describe treatment patterns and clinical outcomes in metastatic non-squamous NSCLC patients receiving first-line pembrolizumab-platinum-pemetrexed in the US community oncology setting.

Methods First-line metastatic non-squamous NSCLC patients without actionable alterations (ECOG 0-2, known PD-L1 expression) starting pembrolizumab-platinum-pemetrexed between May 10, 2017, and August 31, 2020, within The US Oncology Network, were retrospectively identified and described using structured data. Patients who completed the 4-6 induction cycles without disease progression and continued pembrolizumab, with or without maintenance pemetrexed, were further examined using chart review. Continuation pembrolizumab patients were followed until earliest of August 31, 2021, last visit, or date of death. Patient characteristics and treatment patterns were summarized using descriptive statistics. Real-world time on treatment and OS were evaluated using Kaplan-Meier (KM) methods.

Results In the induction cohort (figure 1, n=751), 532 patients completed induction (71%) and among them, 50% (266/532) received continuation pembrolizumab with maintenance pemetrexed based on review of the structured data. The median (95% confidence interval [CI]) times on pembrolizumab and pemetrexed treatments were 5.1 (4.6-5.7) months and 4.2 (3.5-4.6) months from start of induction, respectively. In the continuation pembrolizumab cohort (figure 1, n=241), the median (95% CI) OS was 20.3 (13.8-26.2) months from start of continuation pembrolizumab. In the continuation pembrolizumab cohort, 64% received maintenance pemetrexed and 36% received pembrolizumab alone. Patients receiving maintenance pemetrexed were more commonly <75 years of age, male, PD-L1 <1%, and had more metastatic sites than those receiving pembrolizumab alone (table 1). Reasons for pemetrexed discontinuation were most frequently noted as progressive disease (38%) and toxicity (29%) in patients who received maintenance pemetrexed and partial response (68%) and completion of planned therapy (53%) in patients who received pembrolizumab alone.

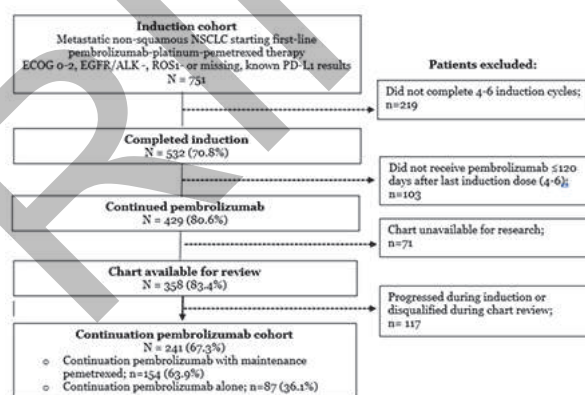
Conclusions Reasons for pemetrexed discontinuation and patient characteristics varied for patients receiving continuation pembrolizumab with maintenance pemetrexed relative to those receiving continuation pembrolizumab alone. More information is needed to understand clinical decision making around pemetrexed discontinuation in the real-world community oncology

setting, extension to other clinical settings, and associated impact on clinical outcomes.

REFERENCES

1. Gadgeel S, Rodríguez-Abreu D, Speranza G, et al. Updated Analysis From KEYNOTE-189: pembrolizumab or placebo plus pemetrexed and platinum for previously untreated metastatic nonsquamous non-small-cell lung cancer. *J Clin Oncol*. 2020 May 10;**38**(14):1505–1517.
2. Gandhi L, Rodríguez-Abreu D, Gadgeel S, et al. KEYNOTE-189 investigators. pembrolizumab plus chemotherapy in metastatic non-small-cell lung cancer. *N Engl J Med*. 2018 May 31;**378**(22):2078–2092.
3. Velcheti V, et al. Real-world outcomes of first-line pembrolizumab plus pemetrexed-carboplatin for metastatic non-squamous NSCLC at US oncology practices. *Sci Rep* 2021;**11**:9222.
4. Bayo K, Aggarwal H, Han Y, et al. Real World Data on Maintenance Therapy Utilization and Overall Survival Among Advanced Non-Small Cell Lung Cancer Patients Treated with Pemetrexed in combination with Pembrolizumab and Platinum Chemotherapy in the US. 2020 North America Conference on Lung Cancer, October 16-17, 2020. Virtual Conference.

Ethics Approval The study was approved by US Oncology, Inc. Institutional Review Board, approval number 21-017E-2021-02-01-01.



Abstract 933 Figure 1 Construction of study sample

Abstracts

Abstract 933 Table 1 Characteristics of patients in the continuation pembrolizumab cohort by maintenance pemetrexed exposure

Variable	Pembrolizumab + maintenance pemetrexed	Pembrolizumab alone
Total patient count	154	87
Median age at diagnosis (Min, Max)	68 (33,85)	69 (52,88)
Age group, N (%)		
<75 years	122 (79.2%)	58 (66.7%)
≥75 years	32 (20.8%)	29 (33.3%)
Gender, N (%)		
Male	82 (53.2%)	39 (44.8%)
Smoking history, N (%)		
Never smoker	15 (9.7%)	12 (13.8%)
Current or former smoker	121 (78.6%)	65 (74.7%)
Not documented	18 (11.7%)	10 (11.5%)
Practice location, N (%)		
Midwest	40 (26.0%)	22 (25.3%)
Northeast	13 (8.4%)	1 (1.1%)
South	45 (29.2%)	30 (34.5%)
West	56 (36.4%)	34 (39.1%)
ECOG performance score, N (%)		
0-1	109 (70.8%)	66 (75.9%)
2	14 (9.1%)	11 (12.6%)
Not documented	31 (20.1%)	10 (11.5%)
PD-L1 expression, N (%)		
Tumor proportion score ≥1%	90 (58.4%)	63 (72.4%)
Tumor proportion score <1%	62 (40.3%)	23 (26.4%)
Not documented	2 (1.3%)	1 (1.2%)
Charlson comorbidity score, N (%)		
0	84 (54.5%)	49 (56.3%)
1-2	64 (41.6%)	34 (39.1%)
3+	6 (3.9%)	4 (4.6%)
Count of metastatic site(s) at index, N (%)		
1	33 (21.4%)	26 (29.9%)
2	66 (42.9%)	36 (41.4%)
3	36 (23.4%)	18 (20.7%)
4+	19 (12.3%)	7 (8.0%)

<http://dx.doi.org/10.1136/jitc-2022-SITC2022.0933>

934

IMMUNOTHERAPY-BASED STRATEGIES FOR ADVANCED NON–SMALL CELL LUNG CANCER: IDENTIFYING AND REDUCING CLINICIAN KNOWLEDGE GAPS WITH ONLINE EDUCATION

¹Elizabeth Heller*, ¹Keira Smith, ¹Eden Maack, ¹Lyn Brook, ¹Sarah Williams, ²Beth Sandy. ¹i3 Health, Rochelle Park, NJ, United States; ²Abramson Cancer Center University of Pennsylvania, Philadelphia, PA, United States

Background Research indicates that some of the continuing burden of advanced non–small cell lung cancer (NSCLC) may be attributed to the difficulty for the multidisciplinary team in maintaining a working knowledge of emerging data and recommendations that can inform clinical decision making, particularly surrounding the use of immunotherapy. This study was conducted to investigate whether an online, case-based continuing medical education (CME)/nursing continuing professional development (NCPD)–approved activity could address gaps in clinicians’ knowledge regarding recent advances in immunotherapy and the need for personalized care of patients with advanced NSCLC without driver mutations.

Methods Ticiana Leal, MD, and Beth Sandy, MSN, CRNP, presented a video viewpoint strategy session titled *Harnessing Immunotherapy-Based Strategies for Advanced Non–Small Cell Lung Cancer*. This CME/NCPD-approved activity was made available online starting on April 6, 2022. Learners participated in a 1.25-hour session that explained the latest guidance on patient selection, efficacy, safety, and supportive care strategies for NSCLC immunotherapy. Learners completed a repeated-pairs pre- and post-activity assessment consisting of case-based questions that gauged their ability to apply emerging data to clinical decision making. Baseline knowledge gaps and subsequent learning gains were calculated based on percentages of learners obtaining correct responses on the pre- and post-activity assessments. Significance was assessed using a chi-squared test of independence. In addition, learners reported self-perceived gains in confidence and competence using 5-point Likert scale questions.

Results As of July 27, 2022, 189 clinicians had completed the activity for credit. Baseline assessment data revealed gaps in knowledge regarding patient selection criteria, emerging actionable targets, and management of treatment-related adverse events. Learners scored an average of 34% on pretest topics; after completing the activity, the posttest average rose to 86%. The activity resulted in significant gains in knowledge and competence related to these topics, with $P < 0.0001$ for all learning gains (table 1, figure 1–3). Upon completion of the activity, 88% of learners self-reported that knowledge acquired from this activity would be utilized to improve the outcomes of their patients, and 86% of learners self-reported that after the activity, they felt more confident in treating patients with advanced NSCLC.

Conclusions These data indicate that a substantial knowledge gap exists regarding the latest developments in the treatment of advanced NSCLC. They also demonstrate that online, case-based CME/NCPD-approved activities can result in statistically significant improvements in clinicians’ knowledge of therapeutic advances and management of treatment-related adverse events for patients with advanced NSCLC receiving immunotherapy.

Acknowledgements This activity was supported by an independent educational grant from Merck.

Abstract 934 Table 1

Learner Competence

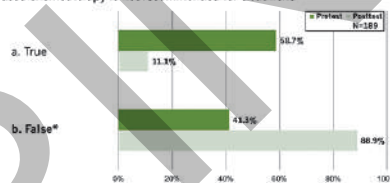
Case-based topic	Knowledge gap	Learning gain
Immunotherapy treatment selection for advanced NSCLC	58.73%	3.5% (p<.001)
Adverse event monitoring for immunotherapy combinations	64.55%	28.3% (p<.001)
Management of immune-related adverse events	73.54%	34.0% (p<.001)

NSCLC = non-small cell lung cancer.

Immunotherapy Treatment Selection for Advanced NSCLC

Case 1: Ms. PL is a 68-year-old never-smoker with advanced squamous NSCLC. Testing has revealed programmed death ligand 1 (PD-L1) expression of 51% and no actionable oncogenes.

Because this patient has lower than 1% PD-L1 expression, pembrolizumab plus platinum-based chemotherapy is not recommended for treatment.

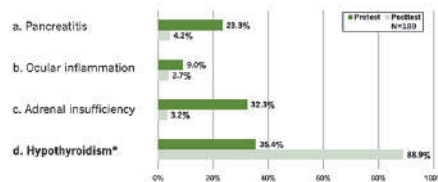


Abstract 934 Figure 1

Adverse Event Monitoring: Immunotherapy Combinations

Case 2: Mr. GG is a 58-year-old man with non-squamous NSCLC about to begin treatment with atezolizumab/bevacizumab/carboplatin/paclitaxel.

Which common immune-mediated adverse event is he most likely to experience?

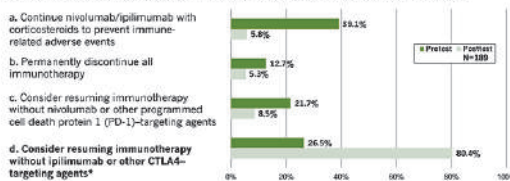


Abstract 934 Figure 2

Management of Immune-Related Adverse Events

Case 3: Mr. GN is a 48-year-old man with metastatic non-squamous NSCLC. He was being treated in the first-line setting with nivolumab/ipilimumab and was having a partial response when he experienced grade 3 colitis. Treatment was discontinued. He was hospitalized, but his colitis responded quickly to methylprednisolone.

Mr. GN asks if he can resume treatment with nivolumab/ipilimumab. Which of the following would be an appropriate next course of action after complete resolution of symptoms?



Abstract 934 Figure 3

<http://dx.doi.org/10.1136/jitc-2022-SITC2022.0934>

Abstracts

935 A CASE REPORT OF PEDIATRIC ADENOVIRAL REACTIVATION AFTER CAR T-CELL THERAPY

Jimmy Maiarana*, Saara Kaviani, Jim Connelly, Carrie Kitko, Richard Ho. *Vanderbilt University, Nashville, TN, United States*

Background The patient is an 11-year-old male with pre-B acute lymphoblastic leukemia (ALL) in second relapse 15 months after a hematopoietic stem cell transplant (HSCT) who presented for anti-CD19 CAR T-cell therapy with tisagenlecleucel. Tumor burden prior to therapy revealed ~60% bone marrow involvement by leukemia without CNS disease. He received Fludarabine/Cyclophosphamide for lymphodepletion followed by CAR T-cell infusion on D0 (Image 1). He developed grade 1 CRS, grade 1 neurotoxicity for which he received Tocilizumab and 10 days of dexamethasone, and carHLH (grade 3 transaminitis, hyperferritinemia, coagulopathy) for which he received 5 days of Anakinra (figure 1). He developed abdominal pain and tenesmus that progressed to hematochezia on D+12. CT abdomen revealed bowel wall thickening and mucosal hyperenhancement suggestive of pancolitis. Stool viral panel and Clostridium difficile were negative. He was empirically treated for typhlitis with Zosyn and switched to Cefepime/Flagyl without improvement. Fecal Adenovirus resulted positive while CMV and enterovirus were negative. Blood Adenovirus was detected at <190 copies/mL. Endoscopy showed crypt epithelial apoptosis with scattered atrophy and loss. Colonic biopsy was positive for Adenovirus. The patient slowly improved and discharged on D+36.

Methods Adenovirus infection leads to significant morbidity and mortality among pediatric HSCT patients.¹⁻³ After infection, adenovirus persists in mucosal lymphocytes but competent host immunity prevents viral expansion in gut epithelial cells [4]. When host immunity is compromised, viral reactivation can lead to adenoviremia resulting in enteritis, hepatitis, and death.^{2,5} Historically, supportive care has been used with cidofovir reserved for fulminant disease. Recently, viral specific T-cells (VSTs) have shown promise.⁶

A recent study noted that adenovirus was the most common identifiable pathogen in a cohort of pediatric patients receiving CAR T-cells.⁷ However, previous studies have not identified it as a common cause of post-CAR infections.⁸ Pre-infusion disease burden, lymphodepleting regimens, carHLH, neutropenia duration, hypogammaglobulinemia, high grade CRS, and previous HSCT have been identified as risk factors for infections.⁷⁻⁹

We propose three contributors to adenoviral reactivation in the gut during CAR T-cell treatment (Image 2):

1. Pre-infusion lymphodepletion destroys gut mucosal lymphocytes, spreading viral particles to host epithelial cells and reactivating infection.
2. CAR T-cell expansion leads to generalized immune dysregulation/contraction during CRS and HLH/MAS
3. Immune blockade blunts immune regulation.

Conclusions Adenovirus should be considered in patients who develop gastrointestinal symptoms (abdominal pain, diarrhea, tenesmus, hematochezia) after CAR infusion. Further research is needed to identify those at risk for severe disease who may warrant additional treatment.

REFERENCES

1. Ali S, Krueger J, Richardson SE, Sung L, Waespe N, Renzi S, et al. The yield of monitoring adenovirus in pediatric hematopoietic stem cell transplant patients. *Pediatric Hematology and Oncology*. 2019 Apr 3;**36**(3):161-72.

2. Fisher BT, Boge CLK, Petersen H, Seif AE, Bryan M, Hodinka RL, et al. Outcomes of human adenovirus infection and disease in a retrospective cohort of pediatric hematopoietic cell transplant recipients. *J Pediatric Infect Dis Soc*. 2019 Sep 25;**8**(4):317-24.

3. Feghoul L, Chevret S, Cuiet A, Dalle JH, Ouachée M, Yacouben K, et al. Adenovirus infection and disease in paediatric haematopoietic stem cell transplant patients: clues for antiviral pre-emptive treatment. *Clinical Microbiology and Infection*. 2015 Jul;**21**(7):701-9.

4. Lion T. Adenovirus persistence, reactivation, and clinical management. *FEBS Letters*. 2019 Dec 8;**593**(24):3571-82.

5. Lion T. Adenovirus infections in immunocompetent and immunocompromised patients. *Clinical Microbiology Reviews*. 2014 Jul;**27**(3):441-62.

6. Rubinstein JD, Zhu X, Leemhuis T, Pham G, Ray L, Emberesh S, et al. Virus-specific T cells for adenovirus infection after stem cell transplantation are highly effective and class II HLA restricted. *Blood Advances*. 2021 Sep 14;**5**(17):3309-21.

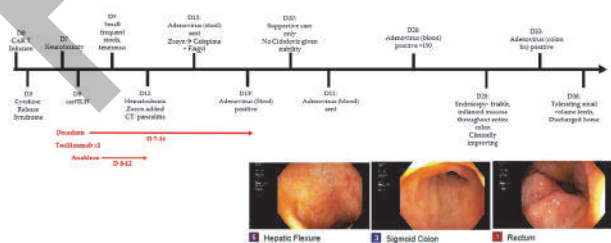
7. Maron GM, Hijano DR, Epperly R, Su Y, Tang L, Hayden RT, et al. Infectious complications in pediatric, adolescent and young adult patients undergoing CD19-CAR T cell therapy. *Frontiers in Oncology*. 2022 Mar 9;12.

8. Vora SB, Waghmare A, Englund JA, Qu P, Gardner RA, Hill JA. Infectious complications following cd19 chimeric antigen receptor T-cell therapy for children, adolescents, and young adults. *Open Forum Infect Dis*. 2020 May;**7**(5):ofaa121.

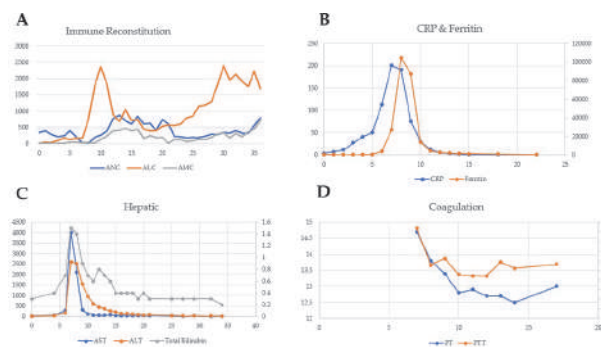
9. Maude SL, Laetsch TW, Buechner J, Rives S, Boyer M, Bittencourt H, et al. Tisagenlecleucel in children and young adults with B-cell lymphoblastic leukemia. *New England Journal of Medicine*. 2018 Feb;**378**(5):439-48.

Consent Written informed consent was obtained from the patient for publication of this abstract and any accompanying images. A copy of the written consent is available for review by the Editor of this journal.

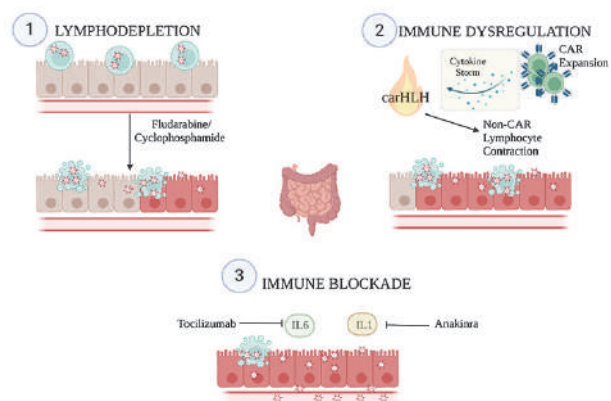
Patient Timeline



Abstract 935 Image 1 Patient timeline with endoscopic findings Hospital course (black), immune modulation (red), and associated endoscopy showing inflammatory changes at the hepatic flexure, sigmoid colon, and rectum



Abstract 935 Figure 1 Laboratory trends Laboratory values over time for immune reconstitution (A), inflammatory markers (B), hepatic toxicity (C), and coagulopathy (D). Absolute Neutrophil Count (ANC), Absolute Lymphocyte Count (ALC), Absolute Monocyte Count (AMC), C-reactive protein (CRP), Aspartate Aminotransferase (AST), Alanine Aminotransferase (ALT), Prothrombin Time (PT), Partial Thromboplastin Time. Days (x axis). Cell counts in cells/microliter, CRP in mg/L, Ferritin in ng/mL, AST and ALT in IU/L, Total bilirubin in mg/dL, PT and PTT in seconds.



Abstract 935 Figure 2 Contributors of adenoviral reactivation Lymphodepletion (1), carHLH (2), and immune modulation (3) as potential contributors to adenoviral reactivation

<http://dx.doi.org/10.1136/jitc-2022-SITC2022.0935>

Abstracts

936

ASSESSING EDUCATIONAL NEEDS FOR IMMUNE-RELATED ADVERSE EVENTS CURRICULUM IN CLINICAL PRACTICE

Gong He*, Austin Wesevich, Pankti Reid. *University of Chicago, Chicago, IL, United States*

Background Immune checkpoint inhibitors (ICIs) are increasingly used to treat cancer but can lead to immune-related adverse events (irAEs) such as hepatitis, pneumonitis, or thyroiditis. While ICIs and irAEs are typically managed in an outpatient setting by oncologists, 11% of patients receiving ICIs require hospital admission for irAEs.¹ While rheumatologists' irAE management knowledge and skills have been assessed in prior studies,² clinicians within oncology and hospital medicine have been understudied despite their relevance to the care of patients with irAEs.

Methods In June and July 2022, we administered a web-based survey to University of Chicago (UChicago)-affiliated oncology providers: oncology fellows and attendings, oncology nurse practitioners (NPs) and physician assistants (PAs). We also surveyed UChicago hospitalists and medicine residents and community oncologists practicing in Chicago. We assessed current knowledge, prior experience, provider confidence, and current educational resource utilization regarding irAE diagnosis and management. We also surveyed how receptive our participants would be to future educational resources dedicated to irAE evaluation and therapy. Linear regression and logistic regression were utilized to analyze relationships between different variables.

Results In total, we had a 37% response rate (171/467): highest for UChicago-affiliated oncology providers (55-59%) (table 1). Oncology attendings and fellows scored the highest on knowledge-based questions (67-68%). Higher levels of ICI and irAE experience over the past year were associated with higher levels of knowledge (OR 1.5, $p < 0.002$). Confidence levels were also significantly associated with higher knowledge and more ICI and irAE experience ($p < 0.001$). Almost all participants surveyed (93%) were receptive to using an online irAE resource with delineated guidelines, patient handouts, and frequently asked questions regarding irAEs. Oncology fellows and NPs/PAs were also more interested in online CME-accredited irAE sessions dedicated to irAEs than medicine residents and hospitalists (83% versus 65%).

Conclusions The knowledge gaps across various groups of providers caring for patients with irAEs reflect a significant need to develop an effective didactic program aimed at enhancing knowledge and confidence for irAE evaluation and treatment. Our results support the development of an online curriculum with interactive online modules to provide case-based and simulated experiential didactics that will lead to increased knowledge and confidence in caring for patients with irAEs.

REFERENCES

1. Ahern E, Allen M, Schmidt A, Lwin Z, Hughes B. Retrospective analysis of hospital admissions due to immune checkpoint inhibitor-induced immune-related adverse events (irAE). *Asia Pac J Clin Oncol*. 2021;**17**:e109–e116.
2. Maltez N, Abdullah A, Fifi-Mah A, Hudson M, Jamal S. Checking in with immune checkpoint inhibitors: Results of a needs assessment survey of Canadian rheumatologists. *J Cancer Sci Therap*. 2019;**2**:12

Abstract 936 Table 1 Response rates by respondent type

	Medicine Resident	Oncology Fellow	Oncology NP/PA	Oncology Attending	Community Oncologist	Hospitalist	Total
Surveyed	119	18	51	74	144	61	467
Responded	51	10	30	41	11	28	171
Response Rate	43%	56%	59%	55%	8%	46%	37%

<http://dx.doi.org/10.1136/jitc-2022-SITC2022.0936>

937

POST-IMMUNOTHERAPY SURVIVORSHIP IN ADVANCED MELANOMA (AMEL): ROUTINE VERSUS SYMPTOM-BASED IMAGING SURVEILLANCE, A RETROSPECTIVE REVIEW IN A LARGE INTEGRATED HEALTHCARE NETWORK, KAISER PERMANENTE NORTHERN CALIFORNIA (KPNC)

Juraj Kavcansky*, Richie Xu, Lue-Yen Tucker, Jahan Tavakoli, Alexander Menter, Thach-Giao Truong. *Kaiser Permanente, Oakland, CA, United States*

Background Best practice in surveillance imaging for survivors after immune checkpoint inhibitors (CPI) remain poorly defined for stage 3-4 aMEL; KPNC oversees care for 4 million patients and has 300 new diagnoses of aMEL per year. Follow-up after CPI is coordinated in KPNC via care pathways using national guidelines.

Methods We report a retrospective study of patients treated between 2014 and 2018 for aMEL with CPI. Data was obtained by chart review. Patients were included who received anti-PD1, anti-CTLA4, or combination; had ≥ 1 dose of any-line palliative (pTX) or adjuvant therapy (adjTX); and had ≥ 1 year of follow-up after treatment, and imaging response (SD/PR/CR) or ≥ 6 months without recurrence if after adjTX. Symptomatic versus asymptomatic progression was defined by evidence of documentation of symptoms at time of imaging. Events from patients who had >1 line of CPI therapy were counted separately. Log-rank test was used to determine Kaplan-Meier survival estimates, and rates were calculated per 100 person-months.

Results 176 patients met inclusion criteria. These patients underwent 191 lines of therapy (69 adjTx and 122 pTX). Progression after therapy occurred in 29 lines of treatment (42%) after adjTX, of these 62% were symptomatic. 51 (41.8%) patients relapsed after pTX and 44% were symptomatic. Comparing asymptomatic and symptomatic progression, there were no differences in risk of relapse after adjTX ($p=0.14$) or pTX ($p=0.73$). Within adjTX, patients with asymptomatic recurrences had lower all-cause mortality (ACM) than those with symptoms (Relative Risk (RR) 0.6 [0.0-1.3] vs 1.9 [0.8-3.0], $p=0.03$) and lower melanoma-specific mortality (MSM) (RR 0.2 [0.0-0.6] vs 1.2 [0.3-2.1], $p=0.03$ for MSM). No differences were detected for ACM and MSM for patients receiving in pTX with asymptomatic versus symptomatic recurrence (ACM RR 1.9 (1.0-2.9) in asymptomatic recurrence vs 2.8 (1.4-4.2) in symptomatic, $p=0.15$ for ACM and; MSM RR 1.6 (0.7-2.4) vs 2.4 (1.2-3.7), $p=0.12$ for MSM). There were differences in ACM ($p=0.02$) and MSM survival ($p=0.01$) in adjTX but not in pTX (ACM $p=0.90$; MSM $p=0.79$).

Conclusions Our study finds identification of asymptomatic relapse has survival benefit in the curative setting but not for aMEL treated with palliative intent. This finding is likely because curative therapy can be offered if relapse is identified early for resectable disease. Our study findings suggests a symptom-based imaging surveillance strategy similar to that used in histologies with effective systemic therapy is effective (e.g. lymphoma, breast cancer) could potentially be used for melanoma. Prospective study is needed to further guide clinical practice.

<http://dx.doi.org/10.1136/jitc-2022-SITC2022.0937>

Immune Cell Types and Biology

939 AUGMENTATION OF CD8 T CELL MEMORY VIA CDK4/6 INHIBITION CAN BE SEQUENTIALLY COMBINED WITH PD-1 BLOCKADE TO AVOID TOXICITIES

Lestat Ali, Ana Garrido-Castro, Sara Tolaney, Stephanie Dougan*. Dana-Farber Cancer Institute, Boston, MA, United States

Background CDK4/6 inhibitors are approved to treat breast cancer and are in trials for other malignancies. We examined CDK4/6 inhibition in mouse and human CD8 T cells during early stages of activation. Mice receiving tumor-specific CD8 T cells treated with CDK4/6 inhibitors displayed increased T cell persistence and immunologic memory. CDK4/6 inhibition upregulated *Mxd4*, a negative regulator of *Myc*, in both mouse and human CD8 T cells. Silencing of *Mxd4* or *Myc* in mouse CD8 T cells demonstrated the importance of this axis for memory formation. We used single cell transcriptional profiling and TCR clonotype tracking to evaluate recently activated human CD8 T cells in breast cancer patients before and during treatment with either palbociclib or abemaciclib. CDK4/6 inhibitor therapy in humans increases the frequency of CD8 memory precursors and downregulates their expression of MYC target genes, suggesting that CDK4/6 inhibitors in cancer patients may augment long-term protective immunity (Heckler and Ali et al. Cancer Discovery 2021).

Methods We will present unpublished data on samples collected from a Phase I trial of combination ribociclib with PD-1 blockade (NCT03294694). Unfortunately, combination of CDK4/6i and PD-1 blockade leads to high rates of adverse events, as seen in several clinical trials. To better understand the mechanism of action of CDK4/6i versus PD-1 blockade on tumor-specific CD8 T cells, we performed single-cell RNA-sequencing and T-cell receptor clonotype tracking of breast and ovarian cancer patients treated with the CDK4/6 inhibitor ribociclib and PD-1 blockade.

Results We confirmed our observation of increased memory skewing of peripheral CD8 T cells, and we identified TCR clonotypes that matched tumor-infiltrating T cells. We highlight evidence of two orthogonal treatment-associated phenomena: expansion of T cell effector populations and promotion of T cell memory formation. Augmentation of the antitumor memory pool by ribociclib boosts the efficacy of subsequent PD-1 blockade in a mouse models of melanoma and breast cancer.

Conclusions We therefore demonstrate that PD-1 blockade and CDK4/6 inhibition augment nonoverlapping features of CD8 T cell activation in metastatic cancer, pointing toward sequential therapy as a potentially safe and synergistic strategy in patients.

Ethics Approval For breast and ovarian cancer patients, we obtained written informed consent from the patients, and the studies were conducted in accordance with the Declaration of Helsinki and the Belmont Report. Patient peripheral blood samples were obtained via Dana-Farber Cancer Institute Institutional Review Board protocols 18-258, 13-364, and/or 17-024. Animals were housed at the Dana-Farber Cancer Institute and were maintained according to protocols approved by the DFCI IACUC (#14-019 and #14-037).

<http://dx.doi.org/10.1136/jitc-2022-SITC2022.0939>

940

SIRNA SCREEN OF UPREGULATED GENES IDENTIFIES TARGETS FOR A MULTIANTIGEN POLYPEPTIDE VACCINE TO PREVENT HNSCC

¹FNU Alka*, ²James Annis, ¹Brady Bernard, ¹Sasha Stanton. ¹Earl A. Chiles Research Institute, Portland, OR, United States; ²Blackhat Limited, Seattle, WA, United States

Background Oral Dysplasia (OD) is a precursor lesion for developing head and neck squamous cell carcinoma (HNSCC). The risk of developing HNSCC from OD is 12% in 2 years. In HNSCC, presence of tumor-specific type I T-cells predict improved progression free survival compared to the patients with tumor that do not have tumor-specific Th1 T-cells. We therefore sought to identify candidate antigens overexpressed in both OD and HNSCC as targets for a vaccine that can both treat and prevent HNSCC.

Methods Selected target genes were overexpressed in human OD and HNSCC and were selected from curated open access GEO data sets. Functionally relevant candidate genes were selected as targets that were necessary for survival using high-throughput siRNA screen. We evaluated the effect of 3 pooled siRNA per target in 3 human HPV negative HNSCC cell lines (FaDu, SSC15, SCC25) and 1 hyperplastic keratinocyte (NOK) as compared to the non-malignant human gingival fibroblast (HGF) cell line. We prioritized candidate antigens whose loss induced $\geq 50\%$ decreased viability in HNSCC cell lines and OD but not in non-malignant gingival cell line.

Results We identified 46 targets that were overexpressed greater than 2-fold in both OD and HNSCC but not in normal tissue, from 2 OD and 5 HNSCC datasets including 206 normal samples, 66 OD samples, and 198 HNSCC samples. To increase the number of candidate antigens, a literature search of gene expression studies, not included in public data set was performed including four studies with 58 normal samples, 21 OD samples, 179 HNSCC. 80 genes that were highly overexpressed in OD and HNSCC and overexpressed in greater than 75% of datasets were selected for the siRNA screen. 17 candidate antigens that reduced viability $>50\%$ in 2 or more HNSCC cell lines were selected: COL1A1, COL1A2, COL4A1, LOXL2, JUN, WDR66, POSTN, TNC, HOXB7, WDR72, TENM3, FN1, PDPN, SERPINE1, INDO, IFI6, ACTN1. All these 17 genes have known roles in HNSCC tumor progression.

Conclusions We have identified 17 candidate antigens that are functionally relevant to survival in OD and HNSCC. Future studies will evaluate if these candidate antigens are immunogenic in OD and HNSCC by evaluation if autoantibodies to these targets are present in the serum of OD and HNSCC patients but not in normal controls. These antigens will be used to design an MHC class II multiantigen polypeptide vaccine.

<http://dx.doi.org/10.1136/jitc-2022-SITC2022.0940>

941

BOTENSILIMAB MODULATES INNATE AND ADAPTIVE GENE EXPRESSION PROGRAMS RESULTING IN SUPERIOR IMMUNE STIMULATION RELATIVE TO A FIRST-GENERATION ANTI-CTLA-4 ANTIBODY

<http://dx.doi.org/10.1136/jitc-2022-SITC2022.0941>

¹Shanmugarajan Krishnan*, ¹Jacky Chow*, ¹Kah Teong Soh, ¹Kayla Ostergard, ¹Christopher MacDermaid, ²Marc Van Dijk, ¹Dennis Underwood, ¹Dhan Chand, ¹Caillin Joyce. ¹Agenus Inc., Lexington, MA, United States; ²Mink Therapeutics, Lexington, MA, United States

Background Botensilimab is a next-generation fragment crystallizable (Fc)-enhanced anti-cytotoxic T-lymphocyte antigen 4 (CTLA-4) antibody that promotes optimized T cell priming, activation, memory formation, and intratumoral regulatory T cell depletion. In patients with advanced solid tumors, botensilimab alone and in combination with balstilimab (anti-programmed cell death protein 1 [PD-1] antibody) demonstrated durable clinical responses in nine different immunotherapy-resistant or poorly immunogenic tumor types. We hypothesize that botensilimab engages multiple immune cell types, including macrophages, dendritic cells (DCs) and natural killer (NK) cells through its enhanced Fc region, to drive deep and broad clinical responses. Here, we applied high-resolution single-cell profiling to demonstrate the differentiated molecular mechanisms of botensilimab relative to a first-generation IgG1 (non-Fc-enhanced) anti-CTLA-4 antibody (bot-IgG1).

Methods Human *ex vivo* peripheral blood mononuclear cells were stimulated with staphylococcus enterotoxin antigen followed by treatment with botensilimab, bot-IgG1 or an IgG1 Fc-enhanced isotype control. Secreted cytokines and single-cell measurements of RNA and protein were evaluated over multiple time points and across various immune cell populations. Treatment-specific changes were evaluated within and across donors.

Results Enhanced interleukin-2 (IL2) secretion in botensilimab-treated cultures relative to bot-IgG1 or isotype control was confirmed across donors. To identify the upstream mechanisms of botensilimab-induced immune activation, RNA and protein expression patterns were interrogated at different time points leading up to maximum IL2 secretion. Sub-clustering of myeloid cells revealed monocyte-, macrophage-, and DC-like populations. Within the myeloid fraction, botensilimab increased the frequency of DCs relative to monocytes and macrophages, and upregulated innate immune signaling pathways distinct from that of first-generation IgG1 anti-CTLA-4. Notably, botensilimab increased the frequency of leukocyte immunoglobulin like receptor B1 (LILRB1 or ILT2)-expressing myeloid cells. Sub-clustering of lymphocytes revealed CD4, CD8, Treg, NK, NKT, and B cell-like populations. Botensilimab increased activation and effector gene expression, including granzyme B and tumor necrosis factor receptor superfamily 9 (TNFRSF9; CD137) in lymphocyte subsets superior to that observed with an IgG1 anti-CTLA-4.

Conclusions The differentiated ability of botensilimab to reshape myeloid transcriptional programs is consistent with its clinical activity in poorly immunogenic tumors where improved antigen presentation or cross-priming could potentiate responses. Increased expression of LILRB1 and TNFRSF9 in botensilimab-treated immune subsets supports the combination strategies with AGEN1571 (anti-ILT2) and AGEN2373 (anti-CD137) currently under clinical investigation.

Ethics Approval This study was approved by WCG IRB Ethics Board; approval number 120160614.

942

FLOW CYTOMETRY IMMUNOPHENOTYPING OF NECK LYMPH NODES SAMPLED BY FINE NEEDLE ASPIRATION (FNA) IN PATIENTS SUFFERING FROM ADVANCED CUTANEOUS SQUAMOUS CELL CARCINOMA: A PILOT STUDY

Vilma Lagebro*, Krzysztof Piersiala, Gregori Margolin, Susanna Kumlien Georén, Lars-Olaf Cardell. *Karolinska Institutet, Stockholm, Sweden*

Background Cutaneous Squamous cell cancer (cSCC) is one of the most common forms of cancer and has the highest incidence increase in Sweden. cSCC has a good prognosis, however around 5% develops advanced cSCC which is difficult to treat. Check point inhibitor (CPI) treatment is promising, but many patients do not show long-lasting remission. Therefore, we need to understand how the CPI modulation works to increase its clinical benefit.

Methods We analysed the lymphocyte phenotypes in peripheral circulation (PBMC), unfixed tumour tissue and sentinel lymph node samples from advanced cSCC patients with flow cytometry. The sentinel nodes were of particular interest since they are rarely analysed in this context but are essential for a well-functioning anticancer immune response. The lymphocytes were phenotypically characterized and analysed with the focus on activation markers and CPI expression.

Results In this pilot, we analysed samples from six patients. Sentinel node samples had a higher percentage of CD4+ T cells compared to PBMC. Furthermore, the number of activated CD4+CD69+ T cells was higher in sentinel nodes (32.4%) compared to PBMC (1.1%). A smaller amount of CD4+ cells in sentinel node expressed PD-1 compared to CD4+ cells in the tumour samples. CTLA-4 was expressed on CD4+ cells in sentinel nodes at low levels compared to the tumour samples.

Conclusions Our results confirm that the sentinel node is rich in highly activated cells that express immune checkpoint molecules. Further experiments are needed to investigate how the systemic treatment with immune checkpoint inhibitors influence the phenotypes and function of lymphocytes in sentinel nodes. In this project, we are going to look into correlation between flow cytometry findings (activation level, expression of CPI molecules) and clinical outcome of our patients (locoregional control, survival, response to the treatment). In the future, this could also help us discover biomarkers predicting response to CPI treatment. Furthermore, the results might also strengthen the role of flow cytometry analysis in clinical assessment and staging of cSCC patients.

Ethics Approval All procedures performed in studies involving human participants were in accordance with the ethical standards of the institutional and/or national research committee and with the 1964 Helsinki declaration and its later amendments or comparable ethical standards. Informed consent was obtained from all individual participants included in the study. Regional Ethics Committee Approval: 2019-03518.

<http://dx.doi.org/10.1136/jitc-2022-SITC2022.0942>

943

HARNESSING ANTI-TUMOR METABOLIC SENSING SWITCH GPR84 ON MACROPHAGES FOR CANCER IMMUNOTHERAPY

Gang Xin, Ruohan Zhang, Bao Zhao, Cankun Wang, Wantong Li, Qin Ma, Nuo Sun, Haitao Wen, William Carson, Zihai Li, Anjun Ma, Jianying Li*. *Ohio State University, Columbus, OH, United States*

Background Immune checkpoint blockade (ICB) has shown tremendous clinical success, but this clinical response is limited to a small proportion of patients, and one of the major resistance mechanisms is the macrophage enriched in the immunosuppressive tumor microenvironment (TME).¹⁻³ Majorities of tumor-associated macrophages (TAMs) are associated with enhanced pro-tumorigenesis activity, significantly impairing T cell function and facilitating tumor escape from immune checkpoint blockade therapy.⁴⁻⁶ Due to the plasticity of macrophages, excitement has been growing for the possibility of reshaping these pro-tumorigenic TAMs toward the anti-tumorigenic phenotype to enhance immunity against cancer.^{7, 8} Emerging evidence reveals that free fatty acids (FFAs) accumulated in TME are critical in determining macrophage function. Though a majority of studies highlight the impact of metabolic processes, fatty acids also serve as vital signaling molecules for regulating immune response, however the molecular mechanism remains elusive.

Methods By an unbiased analysis of single-cell transcriptome data from multiple tumor models, we discovered that anti-tumorigenic TAMs uniquely express elevated levels of a fatty acid receptor, G-protein-coupled receptor 84 (GPR84). To determine the role of GPR84 in TAM-mediated immunity against cancer, we have established new mice with myeloid-specific deletion of GPR84 (*Gpr84^{flox/flox} LysM^{Cre}*) and evaluated the GPR84 agonist 6-OAU using the MC38 tumor model.

Results Herein, the bioinformatics analysis of the clinical patient sample finds that GPR84 enriched TAM is associated with enhanced anti-tumor function. Furthermore, genetic ablation of GPR84 will impair the pro-inflammatory phenotype and enhance the anti-inflammatory phenotype. In contrast, GPR84 activation by 6-OAU subverts TAM-mediated immunosuppression via enhanced NF- κ B activity. Moreover, 6-OAU treatment significantly retards tumor growth and increases the anti-tumor efficacy of anti-PD-1 therapy.

Conclusions Overall, we identify a previously unappreciated fatty acid receptor, GPR84, as an important metabolic sensing switch for orchestrating anti-tumorigenic macrophage polarization. Pharmacological agonists of GPR84 hold great promise to reshape and reverse the immunosuppressive TME, and thereby restore responsiveness of cancer to overcome resistance to immune checkpoint blockade. Overall, GPR84, a not fully understood fatty acid receptor, can repolarize the TAM towards the antitumor phenotype and enhance the anti-PD1 response, which is a promising potential therapeutic target.

Acknowledgements Words cannot express my gratitude to my mentors: Dr. Gang Xin and Dr. Qin Ma for their invaluable patience and feedback. I also could not have undertaken the bioinformatics journey without Anjun Ma, Cankun Wang, Ruohan Zhang, and Yao Chen, who generously provided their knowledge and expertise. Additionally, this endeavor would not have been possible without the generous cooperation of Dr. Zihai Li's lab, Dr. Haitao Wen's lab, and Dr. William E. Carson's lab.

REFERENCES

1. Tang J, et al. Trial watch: The clinical trial landscape for PD1/PDL1 immune checkpoint inhibitors. *Nat Rev Drug Discov*, 2018;**17**(12): 854–855.
2. Wein L, et al. Checkpoint blockade in the treatment of breast cancer: current status and future directions. *Br J Cancer* 2018;**119**(1): 4–11.
3. Jalalvand MF Darbeheshti, and N Rezaei. Immune checkpoint inhibitors: review of the existing evidence and challenges in breast cancer. *Immunotherapy* 2021;**13**(7): 587–603.
4. DeNardo DG, and B Ruffell. Macrophages as regulators of tumour immunity and immunotherapy. *Nat Rev Immunol*, 2019;**19**(6): 369–382.
5. Pan Y, et al. Tumor-Associated Macrophages in Tumor Immunity. *Front Immunol*, 2020. **11**: 583084.
6. Zeng D, et al. Macrophage correlates with immunophenotype and predicts anti-PD-L1 response of urothelial cancer. *Theranostics* 2020;**10**(15): 7002–7014.
7. Poh AR and M Ernst. Targeting macrophages in cancer: from bench to bedside. *Front Oncol*, 2018;**8**: 49.
8. Pathria P, TL Louis and JA Varner. Targeting tumor-associated macrophages in cancer. *Trends Immunol*, 2019;**40**(4): 310–327.

<http://dx.doi.org/10.1136/jitc-2022-SITC2022.0943>

944

TARGETING OF NOTCH LIGAND JAGGED2 IN LUNG CANCER CELLS DRIVES ANTI-TUMOR IMMUNITY VIA NOTCH-INDUCED FUNCTIONAL REPROGRAMMING OF TUMOR-ASSOCIATED MACROPHAGES

¹J Mandula, ¹Rosa Sierra-Mondragon, ¹Darwin Chang*, ¹Rachel Jimenez, ²Eslam Mohamed, ¹Jimena Trillo, ¹Alyssa Obermayer, ¹Carlos Moran-Segura, ¹Das Satyajit, ¹Julio Vazquez-Martinez, ¹Timothy Shaw, ¹Jose Conejo-Garcia, ¹Paulo Rodriguez. ¹H. Lee Moffitt Cancer Center, Tampa, FL, United States; ²California Northstate University, Elk Grove, CA, United States

Background Signaling through the Notch family of receptors after engagement with ligands, Jagged (JAG1-2) or Delta-like ligands (DLL1-4), promotes the development and progression of several tumors and modulates anti-tumor immunity. However, whether expression of Notch ligands in tumor cells impacts anti-tumor immunity remains practically unknown. Herein, we sought to determine the impact of the expression of Notch ligands, Jagged1 and Jagged2, on lung tumors in the modulation of anti-tumor immunity.

Methods We evaluated the correlation between JAG1-2 expression in lung tumors along with clinical outcome and intratumoral T-cell infiltration. Furthermore, we eliminated Jagged forms in murine lung tumors via Crispr-based approaches followed by studies identifying the tumor immune-landscape and functional changes in T-cells and macrophages.

Results Analyses of the TCGA lung adenocarcinoma datasets showed that augmented expression of JAG2 in tumors, but not JAG1, correlated with reduced patient survival. Additionally, tumor tissue microarray-based studies showed a correlation between lower Jagged2 levels in lung cancer cells and increased intra-tumor T-cell frequency. Consistently, elimination of *Jag2*, but not *Jag1*, in murine lung cancer cells activated anti-tumor T-cell immunity and delayed tumor growth in mice. Elimination of T-cells restored growth of *Jag2*^{KO} tumors *in vivo*. Moreover, analysis via single-cell RNA sequencing (scRNAseq) and flow cytometry indicated the expansion of effector T-cells and, perhaps more importantly, a subset of macrophages in *Jag2*^{KO} tumors. The expanded subset of macrophages in *Jag2*^{KO} tumors displayed a further differentiated phenotype, exhibited increased antigen presentation, and consequently promoted lymphocyte-driven anti-tumor immunity. Moreover, transfer of macrophages from *Jag2*^{KO} tumors into wild-type tumors reduced growth in immunocompetent mice but not in *Rag1*^{KO} mice. Prevention of macrophage expansion using anti-CSF1 receptor blockade, treatment with clodronate, or ablation of *Ccr2* rescued growth in *Jag2*^{KO} tumors and blocked intra-tumoral accumulation of T-cells. Mechanistically, *Notch1/2* signaling on macrophages promoted *Irf4*-dependent immunostimulatory reprogramming. Subsequent knockout of *Irf4* in myeloid populations abrogated the development of this subset of macrophages and reinstated growth of *Jag2*^{KO} tumors.

Conclusions Our findings demonstrate an underlying, pivotal role for Jagged2 in lung tumor cells in directing immune evasion. Our experiments provide mechanistic opportunities to reprogram immunosuppressive myelopoiesis *in vivo* for the benefit of cancer immunotherapy.

<http://dx.doi.org/10.1136/jitc-2022-SITC2022.0944>

945

OVERLAPPING AND DISTINCT PATTERNS OF LILRB RECEPTORS SUPPORT COMPLEMENTARY TARGETING APPROACH IN CANCER

Jeffrey Smith, Amy Mueller, Vikki Spaulding, Michelle Priess, Krithi Bala, Andrew Dunn, Sarah Jaffe, Morgan Thompson, Jean-Christophe Pignon, Alexa Diorio, Andre Cunha, Heather Conurso, Kristin O'Malley, Olivia Petrillo, Prashanna Balaji Venkatasubramanian, Geneva Young, Christina Meyer, Michael Meehl, Katalin Kis-Toth, Monica Gostissa, Dmitri Wiederschain, Ben Umiker, Yasmin Hashambhoy-Ramsay*. *Jounce Therapeutics, Cambridge, MA, United States*

Background Leukocyte immunoglobulin-like receptors (LILRBs) are cell surface immunoinhibitory proteins that have been recently recognized as therapeutic targets of interest in immuno-oncology. LILRB1, LILRB2 and LILRB4 among them are broadly expressed on myeloid cells; however, their individual expression patterns have been difficult to define due to high sequence homology. To devise rational treatment options, it is important to develop a better understanding of LILRB1, LILRB2 and LILRB4 specific expression patterns as well as functional overlap and differences, as suggested by their diverse ligand binding partners. Here we characterize expression of these receptors on human immune cells in tumor and blood samples across different cancer indications. In addition, we performed pharmacodynamic analysis and unbiased clustering after individual LILRBs (1,2 or 4) were blocked in primary human tumor ex vivo systems to understand the roles of these receptors in complex cellular environments.

Methods Cell-specific anchoring across multiple single cell RNAseq data sets was performed to characterize temporal and spatial LILRB gene expression on individual cells. Proteins were detected on human tumor specimens using ligand, cell type and LILRB-specific IHC antibodies. LILRB protein levels on immune cells from dissociated human tumors and peripheral blood mononuclear cells (PBMCs) were quantified using flow cytometry. Fresh treatment-naïve human tumor samples were treated with anti-LILRB1, anti-LILRB2, anti-LILRB4 or isotype control antibodies and gene expression analysis was performed on treated samples.

Results LILRBs (1,2,4) are expressed on myeloid cells but distinct expression patterns also emerge. LILRB1 is expressed by T, B and NK cells; LILRB4 is highly expressed on plasmacytoid dendritic cells (pDCs) and a subset of conventional DCs (cDC2); LILRB2 is prominently expressed on immunosuppressive macrophages as well as monocytes, and within that population, intermediate monocytes display higher levels of LILRB2 than classical monocytes. In complex ex vivo systems, treatment with blocking anti-LILRB molecules induced both overlapping and distinct patterns of gene expression changes.

Conclusions LILRB1, LILRB2 and LILRB4 each display unique cell-specific expression patterns and blocking their ligand binding activity in ex vivo systems suggests that they have non-redundant functions. Thus, context-dependent inhibition of one or more of these molecules can contribute to the optimal activation of anti-tumor immunity.

Ethics Approval Human blood and tumor samples were acquired from commercial providers and from the CHTN and NDRI networks respectively. Specimens were collected under each provider's human subject research institutional review board approved protocols and were fully anonymized or otherwise permanently de-identified to recipient investigators.

<http://dx.doi.org/10.1136/jitc-2022-SITC2022.0945>

946

DISSECTING MYELOID CELL-MEDIATED MECHANISMS OF RESISTANCE TO IMMUNE CHECKPOINT BLOCKADE IN BLADDER CANCER

Michelle Tran*, Adam Farkas, Kristin Beaumont, Amir Horowitz, John Sfakianos, Matthew Galsky, Nina Bhardwaj. *Icahn School of Medicine at Mount Sinai, New York, NY, United States*

Background PD-(L)1 immune checkpoint blockade (ICB) therapy yields objective responses in 15-25% of patients with bladder cancer (BC), suggesting that tumor-associated resistance mechanisms undermine their efficacy.¹⁻⁶ We previously identified two gene signatures derived from pre-treatment tumor tissue independently associated with ICB outcomes in BC patients: 1) a signature enriched in adaptive immune response genes and associated with better ICB outcomes named the “adaptive immune response signature” and 2) a signature enriched in innate immune and inflammation genes and associated with worse ICB outcomes labelled the “pro-tumorigenic inflammation signature”.⁷ The adaptive immune response: pro-tumorigenic inflammation score ratio, named the 2IR score, was highly correlated with ICB response and validated in an independent cohort.

Methods Single-cell RNA sequencing (scRNAseq) was performed on BC tumors (n=26) and normal-adjacent tissue (n=3) to resolve the cellular composition underlying the 2IR score. Ingenuity Pathway Analysis was applied to predict upstream ligands skewing MΦ phenotypes and such ligands were tested for their effects on healthy donor peripheral blood monocytes differentiated with (G)M-CSF. Patient plasma was assessed for pro-inflammatory cytokines across disease stage using O-Link Proteomics and Enzyme-Linked Immuno-Sorbent Assay.

Results From our scRNAseq, we discovered the adaptive immune response and pro-tumorigenic inflammation signatures were enriched in distinct MΦ subsets we labelled immunostimulatory (is)MΦs and pro-tumorigenic (pt)MΦs, respectively. ptMΦs upregulated inflammatory markers: SPP1, TREM1, and CLEC5A; expressed pro-angiogenic and hypoxic programs; and downregulated antigen presentation machinery. ptMΦs were enriched in tumor versus normal-adjacent tissue, which was confirmed by flow cytometry on additional patients. From our screen of predicted upstream ligands, lipopolysaccharide (LPS) induced the highest amount of ptMΦs (p<.05), as defined by Clec5a and Trem1 surface expression, in GM-CSF-induced MΦs, while IL-1β induced the most for M-CSF-induced MΦs (p<.005). ptMΦs also upregulated SPP1 on a transcriptional level. Inflammatory cytokines (e.g. IL-1β, IL-6, IL-8) as well as macrophage-colony stimulating factor (CSF-1) were elevated in the plasma of advanced stage BC patients as compared to early stage and healthy donors.

Conclusions From our BC scRNAseq cohort, we discovered a pro-tumorigenic inflammatory MΦ subset underlying a gene signature previously linked to ICB resistance in bladder cancer. We recapitulated these MΦs using blood monocytes differentiated with G(M)-CSF and skewed with LPS/IL-1β. We also found inflammatory cytokines associated with these MΦs were elevated in the peripheral blood of advanced patients. Together, these findings identify a distinct MΦ transcriptional state that may underlie tumor-promoting inflammation and ICB resistance and be therapeutically modulated to overcome ICB resistance.

REFERENCES

1. Sharma P, et al. Nivolumab in metastatic urothelial carcinoma after platinum therapy (CheckMate 275): a multicentre, single-arm, phase 2 trial. *The Lancet Oncology* 2017;**18**, 312–322 .
2. Rosenberg JE, et al. Atezolizumab in patients with locally advanced and metastatic urothelial carcinoma who have progressed following treatment with platinum-based chemotherapy: A single-arm, multicentre, phase 2 trial. *The Lancet* 2016;**387**:1909–1920.
3. Bellmunt J, et al. Pembrolizumab as second-line therapy for advanced urothelial carcinoma. *New England Journal of Medicine* 2017;**376**:1015–1026.
4. Patel MR, et al. Avelumab in metastatic urothelial carcinoma after platinum failure (JAVELIN Solid Tumor): pooled results from two expansion cohorts of an open-label, phase 1 trial. *The Lancet Oncology* 2018;**19**:51–64.
5. Powles T, et al. Efficacy and safety of durvalumab in locally advanced or metastatic urothelial carcinoma: Updated results from a phase 1/2 open-label study. *JAMA Oncology* 2017;**3**:1–10.
6. Powles T, et al. MPDL3280A (anti-PD-L1) treatment leads to clinical activity in metastatic bladder cancer. *Nature* 2014;**515**:558–562.
7. Wang L, et al. Myeloid Cell-associated Resistance to PD-1/PD-L1 Blockade in Urothelial Cancer Revealed Through Bulk and Single-cell RNA Sequencing. *Clinical Cancer Research* 2021;1–15, doi:10.1158/1078-0432.ccr-20-4574.

Ethics Approval The study was approved by Mount Sinai Institution's Ethics Board, approval number 10-1180.

Consent Participants gave informed consent before taking part in the study.

<http://dx.doi.org/10.1136/jitc-2022-SITC2022.0946>

947 QUIESCENT CANCER CELLS RESIST T CELL ATTACK BY FORMING AN IMMUNOSUPPRESSIVE NICHE

Judith Agudo*, Pilar Baldominos. Dana-Farber Cancer Institute, Boston, MA, United States

Background Triple Negative Breast Cancer (TNBC) is the most aggressive form of breast cancer and lacks expression of hormone receptors and HER2, preventing its treatment with targeted therapies. Until recently, chemotherapy was the only systemic therapy for these patients, limiting their options. Recently, two phase III clinical trials showed that immune checkpoint blockade (ICB) in combination with chemotherapy resulted in improved progression-free survival in metastatic PD-L1-positive TNBC, which led to approval of these regimens as a first line treatment.^{1,2} Thus, immunotherapy is currently a promising approach for TNBC, however, only a fraction of patients benefits from it. An outstanding question is what mechanisms lead to resistance to these therapies.

Methods We investigated resistance to T cell killing in breast cancer cells that unequivocally expressed the targeted antigen by using the Green Fluorescent Protein (GFP) as a visible tumor neo-antigen. This was possible by exploiting our GFP-specific CD8+ T cells called Jedi.³

To understand how T cell infiltration and function was decreased in specific regions of the tumor, we used single cell RNA-sequencing (scRNA-seq) with precise spatial resolution. We adapted a technique involving photo-labelling, FACS-sorting and scRNA-seq⁴ to large breast tumors, which we named Photo-conversion of Areas to Dissect Micro-Environments (PADME-seq).

Results By isolating antigen (GFP) positive breast cancer cells that survived during attack by CD8+ Jedi T cells, we uncovered quiescence as their principal feature. Quiescent cancer cells (QCCs) were found forming clusters with reduced immune infiltration and demonstrated a higher tumorigenic potential. By employing PADME-seq, we profiled cells infiltrating clusters of QCCs and, in parallel, cells in other regions. This enabled, for the first time, a comparison of intra-tumor infiltrates from functionally distinct niches within the same tumor mass by scRNA-seq. We uncovered that QCCs form a niche that contains immune-suppressive fibroblasts, dysfunctional dendritic cells, and highly exhausted T cells. Such ecosystems were orchestrated by a distinct quiescent population of cancer cells through activation of a hypoxia-induced program.

Conclusions QCCs constitute immunotherapy-resistant reservoirs by orchestrating a local hypoxic immune-suppressive milieu that blocks T-cell function. Eliminating QCCs holds the promise to counteract resistance to immunotherapy and prevent disease recurrence in TNBC.

REFERENCES

1. P Schmid, *et al.* Atezolizumab and nab-paclitaxel in advanced triple-negative breast cancer. *N. Engl. J. Med.* 2018, doi:10.1056/NEJMoa1809615.
2. J Cortes, *et al.* Pembrolizumab plus chemotherapy versus placebo plus chemotherapy for previously untreated locally recurrent inoperable or metastatic triple-negative breast cancer (KEYNOTE-355): a randomised, placebo-controlled, double-blind, phase 3 clinical trial. *Lancet* 2020;**396**:1817–1828.
3. J Agudo, *et al.* GFP-specific CD8 T cells enable targeted cell depletion and visualization of T-cell interactions. *Nat. Biotechnol.* 2015;**33**:1287–1292.
4. C Medaglia, *et al.* Spatial reconstruction of immune niches by combining photoactivatable reporters and scRNA-seq. *Science* 2017; 358(80):1622–1626.

<http://dx.doi.org/10.1136/jitc-2022-SITC2022.0947>

948

DEVELOPING ENGINEERED ANIMAL MODELS TO INVESTIGATE TUMOR-SPECIFIC T CELL RESPONSES AND IMMUNE-RELATED ADVERSE EVENTS AFTER IMMUNOTHERAPY

Martina Damo, Noah Hornick, Nikhil Joshi*. *Yale School of Medicine, New Haven, CT, United States*

Background The rise of immune checkpoint blocking therapies (ICBs) as treatments across multiple cancer types has revealed a previously underappreciated role for the immune response in the natural regulation of cancer development. ICBs potentiate the functions of anti-tumor CD8 T cells, leading to durable tumor regression, yet, ICB treatment (particularly combination ICB) is associated with frequent and poorly-understood immune related adverse events (irAEs), which has limited the broader use of combination ICB. Thus, it is important to better understand how ICBs impact T cell responses in both tumor and non-tumor contexts, and these differ.

Methods A major gap in the field remains the availability of animal models that faithfully recapitulate the immune-tumor microenvironment associated with different types of human cancers, and models that recapitulate the disease biology of irAEs. Our laboratory previously developed the iNversion INducible Joined neoAntigen (NINJA) model, which allows for tight spatial and temporal regulation of the induction of an known neoantigen. Using NINJA, my lab has now developed autochthonous genetically engineered mouse cancer models for studying anti-tumor T cell responses and models for studying the mechanisms by which ICBs break peripheral T cell tolerance and result in irAEs. We use paired single cell-RNAseq (scRNAseq) and T cell receptor (TCR) seq to validate that our NINJA models faithfully recapitulate the responses of T cells participating in human irAEs and in human cancer. Moreover, because T cells recognize the same antigen across all our models, tumor-specific and disease-causing CD8 and CD4 T cells can be directly compared.

Results In a model of skin-antigen induction, we identified recruitment of CD11c+ CD11b+ CD14+ CD16+ PD-L1+ myeloid cells in response to effector CD8 T cell infiltration, but not disease—unless mice are also treated with anti-PD-1 antibodies—suggesting that skin myeloid cells prevent disease pathology via the PD-1 pathway. Analyses of the CD8 T cells showed a PD-1-blockade induced upregulation of CD103 and Granzyme A, but otherwise minimal transcriptional impact. By contrast, protein-level increases in effector cytokines and degranulation were associated with blockade, as was migration into the epidermis and tissue destruction. Similar clonal CD8 T cell expansion and increased effector gene expression was seen in skin irAE patients.

Conclusions These data highlight that NINJA serves as platform for understanding mechanisms that lead to irAEs in different tissues, which could be used to testing interventions to prevent ICB-induced disease. Ongoing work focuses on elucidating the role of PD-1/PD-L1 in skin-myeloid cell-mediated suppression of skin-specific CD8 T cells.

<http://dx.doi.org/10.1136/jitc-2022-SITC2022.0948>

949

INOVATIVE *IN VIVO* (*IN OVO*) CAM MODEL TO PREDICT EFFICACY AND MODE OF ACTION OF A NEW ANTITUMOR VACCINE STC-1010 ON HUMAN COLORECTAL ADENOCARCINOMA

<http://dx.doi.org/10.1136/jitc-2022-SITC2022.0949>

¹Yan Wang, ²Corinne Tortorelli, ¹Arnaud Peyronnier, ²Benoit Pinteur, ²Lionel Chalus, ²Paul Bravetti, ¹Jean Viallet, ³François Ghiringhelli. ¹Inovotion, La Tronche, France; ²Brenus Pharma, ISSOIRE, France; ³Centre Georges François Leclerc, Dijon, France

Background Colorectal cancer (CRC) is the second-most deadly cancer. Therapeutic resistance to immuno-oncology drives the need for new treatments. Stimulated tumor cell (STC) vaccine (Brenus Pharma) is composed of selected tumor cell lines, stimulated to overexpress tumor-associated or tumor-specific antigens and neoantigens including resistance factors. Haptenization of these proteins forms an immunogenic complex which stimulate the immune system to recognize and target the patient's tumor cells expressing same resistance factors. We report *in vivo* results of STC-1010 vaccine, on human CRC adenocarcinoma from HT29 cell using chorioallantoic membrane (CAM) assay developed by Inovotion in immune reactive model.

Methods This study was carried out in 2 steps: Firstly, three batches of naïve chicken embryos were stimulated by injections of STC1010 at Embryo Development Day (EDD) 11 and EDD13. At EDD18 of each batch, chicken peripheral blood mononuclear cells (PBMCs) were collected and used as anti-tumor reagent to treat respectively, at EDD 11, EDD 13 and EDD16 chicken embryos xenografted with HT29 cells. Activation of PBMCs was evaluated by IL2 and IL12 secretion quantified by ELISA. At EDD18, i.e., 9 days post-graft, *in ovo* anti-tumor efficacy was evaluated by tumor weight, metastatic invasion (qPCR analysis of human Alu sequence in lower CAM) and quantification of tumor-infiltrating by CD8, CD4, IFN-gamma, Perforin and TNF-alpha.^{1,2}

Results Compared to negative control, STC-1010 vaccine induced: 1) significant increase of IL-12 and IL-2 secretion in peripheral blood during the generation of all three batches of PBMCs, confirming previous results (IL-12: +52%, p=0.0003 ; IL-2: +482%, p=0.0033); 2) a significant expression of IFN-gamma in tumor (+130,83%, p=0.0185); 3) a tendency to increase infiltrating cells: CD4+: +79,2%, CD8+: +29,4% , Perforin: +105,5%, TNFα : +78,63% confirmed by immunohistochemistry and translated into 4) a significant increase of tumor necrosis (p = 0.0267); and 5) a tendency of metastasis regression (-49%); with 6) no embryonic toxicity/mortality (daily evaluation of embryonic viability) induced by STC-1010.

Conclusions This *in ovo* study confirms efficacy of the STC-1010 observed in previous CRC syngeneic models and gives more insight about STC mechanism of action with the activation and maturation of dendritic cells, induction of CD8+ and LTh1 against tumor as the main driver of the response, all without toxicity.

Inovotion's CAM model could be used for indication screening and as a pre-proof-of-concept before syngeneic model study.

REFERENCES

1. Wang Y, Rousset X, Prunier C, Garcia P, Dosda E, Leplus E and Jean Viallet. PD-1/PD-L1 checkpoint inhibitors are active in the chicken embryo model and show antitumor efficacy *in ovo*. *Cancers*. 2022;**14**(13):3095.
2. Garcia P, Wang Y, Viallet J, Macek Jilkova Z. The chicken embryo model: a novel and relevant model for immune-based studies. *Front Immunol*. 2021 Nov 19;**12**:791081.

950

TNFR2 HUGEMM™ MURINE MODEL FOR EVALUATION OF HTNF α -HTNFR2 SIGNALING EFFECT ON INDUCED REGULATORY T CELL DIFFERENTIATION

Demi Liu, Xuefei Yan. *Crownbio, Beijing, China*

Background Peripheral induced regulatory T cells (iTreg) play an important role for immune homeostasis. Dysregulation of iTreg differentiation is frequently associated with autoimmune diseases or tumors. Tumor necrosis factor (TNF) α is a pleiotropic cytokine with multiple biological function. Some studies suggest that mouse TNF α inhibits the differentiation of iTregs via TNFR2, providing TNF α -TNFR2 as an attractive target for drug development, for potential control of various diseases including malignant tumors and autoimmune diseases. However, whether human TNF α -TNFR2 signaling pathway plays similar role on iTreg differentiation remains unknown. Moreover, no optimal animal model is currently available for candidate drug evaluation targeting human TNF α -TNFR2. In this study, a humanized TNFR2 mouse model (TNFR2 HuGEMM) was developed to evaluate the effect of human TNFR2 agonist or antagonist on iTreg differentiation, which may be useful in the development of immunotherapies to treat tumors or autoimmune diseases, respectively.

Methods A humanized TNFR2 mouse model (HuGEMM) in C57BL/6 background was generated by replacing the extracellular domain of mouse TNFR2 with its human counterpart. Naïve CD4⁺ T cells were isolated from the splenocytes of homozygous TNFR2 HuGEMM. To validate the signal transduction function of this humanized chimeric TNFR2 upon human TNF α stimulation and its effect on iTreg differentiation, the isolated naïve mouse CD4⁺ cells were cultured under iTreg differentiation condition with mouse cytokines in the presence or absence of human TNF α . To test the effect of human TNF α -TNFR2 signaling on iTreg function, standard Treg suppression was performed.

Results The expression of humanized chimeric TNFR2 in mouse CD4⁺ T cells were determined by flow cytometry. Exogenous human TNF α significantly inhibited iTreg differentiation but had no effect on iTreg function in the suppression of naïve mouse CD3⁺ T cell proliferation.

Conclusions This study provided a novel and useful murine model to evaluate the drug candidate targeting hTNF α -hTNFR2 signaling pathway. *In vitro* iTreg differentiation assay can be used to evaluate the drug candidate's effect on hTNF α -hTNFR2 signaling. These data also suggest that TNF α -TNFR2 signaling plays an important inhibitory role on iTreg differentiation, while it has no obvious effect on iTreg suppressive function on T cell proliferation.

<http://dx.doi.org/10.1136/jitc-2022-SITC2022.0950>

951 SPATIAL ATLASES OF IMMUNOLOGICAL DEVELOPMENT WITHIN THE LYMPH NODE

Tyler Hether*, Stephanie Zimmerman, Zachary Lewis, Shanshan He, Liang Zhang, Kathy Ton, Liuliu Pan, Wei Yang, Stefan Phelan, Charles Glaser, Andy Nam, Emily Brown, Michael Patrick, Gary Geiss, Sarah Church, Michael Rhodes, Yan Liang, Jason Reeves, Joseph Beechem. *NanoString Technologies, Inc., Seattle, WA, United States*

Background Immunological mechanisms regulating detection and clearance of cancer, including CTLA-4 and PD-L1, were discovered by studying the natural physiological processes regulating immune cell maturation, attenuation, and dissemination throughout the body. Single-cell atlases mapping immune cells provide hints to these aspects of immunology but lack essential spatio-temporal relationships between cells. With the advent of spatial 'omics we can resolve thousands of RNA or more than 60 protein molecules simultaneously *in situ*, enabling direct insight into the dynamics occurring as immune cells mature and migrate through tissue.

Methods We profiled lymph node samples using complementary spatial 'omics platforms: the GeoMx® Digital Spatial Profiler and the CosMx™ Spatial Molecular Imager. With GeoMx, we profiled whole transcriptomes from 5 patients focusing on key structures within the lymph node including the germinal center, mantle zones, medulla, and paracortex. With CosMx, we examine one FFPE lymph node with clear germinal center zonation, analyzing 1000 genes and 55 proteins across serial sections covering >100mm² and >1.4 million cells/section. We used a novel, semi-supervised clustering algorithm to map cells to CosMx from lymph node scRNAseq.

Results Across structures profiled with GeoMx we observed 11,316 genes above background in >10% of tissue regions profiled. We identified 2,618 genes (FDR<0.05) associated with distinct functional regions, and 928 significant pathways (FDR<0.05). Profiling with CosMx identified 27 cell types, 6 of which were not captured in the dissociated reference. Integrating results from GeoMx and CosMx, we observed 643 pathways enriched (FDR<0.05) in dark (n=283) and light (n=206) zones of the germinal center or at their interface (n=154), as well as 139 key ligand-receptor interactions driving such pathways. For example, we found co-stimulation of CD28 was enriched within the light zone (FDR<7.5e-06, GeoMx). CosMx confirmed that CD86 ligands within light zone B cells were significantly colocalized with the CD28 receptors of the T_H cells of the germinal center (FDR<1.5e-05). We also found IL18 signaling between macrophages and B cells within the germinal center (FDR<5.6e-09), which was confirmed with protein profiling with CosMx.

Conclusions The spatial ecosystem provided by the GeoMx and CosMx platforms captures an unprecedented view into architecture, hard-to-profile cells, and immunological processes happening within tissue. These findings shed light on novel interactions happening at key immunological interfaces, which can be compared to immune infiltrate into tumors to identify perturbed interactions active during tumor immune escape.

<http://dx.doi.org/10.1136/jitc-2022-SITC2022.0951>

952

THE TEMPORAL CONTRIBUTION OF INTERFERON- γ IN DRIVING T-CELL EXHAUSTION AND RESPONSE TO IMMUNE CHECKPOINT BLOCKADE

¹Vaishali Aggarwal*, ²Chang Liu, ¹Lawrence Andrews, ¹Madhu Malinee, ¹Carly Cardello, ¹Creg Workman, ¹Dario Vignali. ¹University of Pittsburgh, Pittsburgh, PA, United States; ²Nanjing University, Pittsburgh, PA, United States

Background Immune checkpoint blockade (ICB) therapies have revolutionized treatment for cancer patients, yet minority do not respond, highlighting the importance of understanding therapeutic resistance. Interferon-gamma (IFN γ) drives protective T cell responses and augments anti-tumor immunity yet also promotes T cell exhaustion during tumor progression. Such dichotomy exhibited by IFN γ impacts immunotherapeutic responses. However, whether IFN γ continues to modulate immune responses on exhausted T (T_{EX}) cells remains unanswered. Our lab has been extensively studying lineage plasticity of T_{EX} cells by lineage-tracing lymphocyte activation gene-3 (LAG3)-expressing cells in the context of anti-tumor responses. We hypothesize that understanding the temporal expression profile of IFN γ on T_{EX} cells will help address mechanistic insights into diverse responses to ICB.

Methods To evaluate the pleiotropic role of IFN γ , we established two unique murine models, one assessing temporal tamoxifen induced global transcriptional expression of *Ifn γ* on LAG3-expressing cells (*Lag3*^{iCreERT2} *Ifn γ* ^{YFP} *Rosa26*^{LSL-tdTomato}). This allows the immune cell-specific contribution of IFN γ on progenitor T_{EX} and terminal T_{EX} cells to be assessed. The second model temporally induces genetic deletion of *Ifn γ* on LAG3-expressing cells (*Lag3*^{iCreERT2} *Ifn γ* ^{L/L} *Rosa26*^{LSL-tdTomato}). Melanoma (B16F10) and adenocarcinoma (MC38) models were used to evaluate tumor growth and survival kinetics, T_{EX} cell profile and response to ICB therapy.

Results Assessing the transcriptional profile of *Ifn γ* shows that IFN γ is expressed by LAG3-expressing cells as early as D7, a progenitor T_{EX} state, with NK and NKT cells as major contributors. Expression of IFN γ is maintained through a terminally exhausted state (D23), with CD8⁺ T cells as the major IFN γ -producing cells. Our *Lag3*^{iCreERT2} *Ifn γ* ^{L/L} *Rosa26*^{LSL-tdTomato} model system, allows to examine the pleiotropic effects of IFN γ in early immune responses as well as T cell exhaustion (early vs terminal). Early temporal deletion of IFN γ (D5~D7) potentiates tumor growth in MC38 model with no survival advantage with anti-PD1. This suggests that during initial antigen exposure, IFN γ is necessary for reinvigoration of anti-tumor response and deletion of *Ifn γ* augments T cell exhaustion. However, with later time-point deletion (D11~D13), we observed 50% survival advantage with anti-PD1 ICB, which suggests modulating tumor microenvironment in a time-dependent manner is the key to augmenting ICB response.

Conclusions This study highlights the distinct temporal response patterns and exhaustion profile with deletion of *Ifn γ* from pre-exhausted to terminally exhausted LAG3+ cells. IFN γ production at early time points (D5~D7) is a key mediator of anti-tumor immunity while the deletion of *Ifn γ* at terminal points (D11~D13) highlights better ICB response.

Acknowledgements This study was supported by the NIH – P01 AI108545 to D.A.A.V., A.H.S., and E.J.W.

<http://dx.doi.org/10.1136/jitc-2022-SITC2022.0952>

Abstracts

953 TREATMENT WITH SQ3370, A DOXORUBICIN-BASED THERAPEUTIC, CORRESPONDS WITH IMMUNOMODULATION OF THE TUMOR MICROENVIRONMENT

Masa Aleckovic*, Sangeetha Srinivasan, Jesse McFarland, Leslie Priddy, Matthew Tso, Jose Mejia Oneto. *Shasqi Inc, San Francisco, CA, United States*

Background The CAPAC platform uses click chemistry to activate potent anti-cancer drugs specifically at the tumor while minimizing systemic toxicity. SQ3370, the lead investigational asset, consists of 1) tetrazine-modified biopolymer injected into the tumor protodrug; 2) intravenously administered protodrug of doxorubicin (Dox). Active Dox is released in the tumor through an efficient chemical reaction between the biopolymer and protodrug. SQ3370 enables a 19-fold increase over the conventional Dox dose in mice with minimal systemic toxicity.¹ Moreover, SQ3370-treated tumor-bearing mice show improved survival, T-cell infiltration, and a robust anti-tumor response against both biopolymer-injected and non-injected lesions,² suggesting SQ3370 promotes anti-tumor immune activation.

SQ3370 is currently in a Phase I clinical trial in patients with advanced solid tumors (NCT04106492). The on-going dose escalation phase has shown no dose limiting toxicity thus far. No acute cardiotoxicity has been observed with Dox levels >12-times the molar equivalent dose of conventional Dox treatment.

We performed in-depth evaluation of tumor immune infiltration after SQ3370 treatment using syngeneic tumor models and correlated findings with data obtained from clinical samples from patients treated with SQ3370. Based on these data, we present a mechanism-of-action for SQ3370 and propose rationale for combination therapies of SQ3370 with immunotherapies.

Methods SQ3370 treatment is described in figure 1. Immuno-competent mice were inoculated with B16-F10 or MC38 tumor cells. SQL70 was given intratumorally; SQP33 was given intravenously as five daily doses. Tumors used for immune analysis were harvested 2 weeks after the last SQP33 dose and were assessed by flow cytometry and multiplex immunofluorescent analysis. Patient samples were assessed by multiplex immunohistochemistry (tumor biopsies) and CyTOF analyses (blood cells).

Results SQ3370 treatment induced immune activation in patient tumor biopsies despite assessment of a diverse, heavily pre-treated population. Similarly, SQ3370 promoted immune activation in preclinical models. The data are consistent with immunogenic cell death and characterized by activation of T-cell responses.

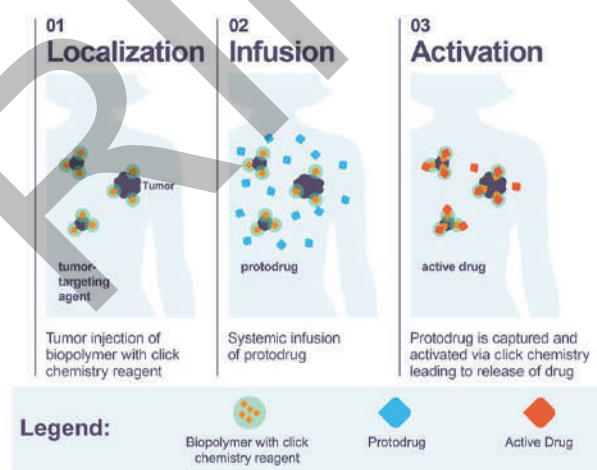
Conclusions SQ3370, CAPAC's lead candidate, improves safety and efficacy as compared to conventional Dox. It also activates an anti-tumor immune response through induction of immunogenic cell death and modulates adaptive and innate immune cell populations. Consistency between immune responses observed in clinical samples and mouse syngeneic tumor models underlines the translatability of the SQ3370 preclinical data and suggests a window of opportunity for combination strategies with immunotherapies.

Acknowledgements This work was supported by Shasqi and the National Institutes of Health.

REFERENCES

1. Wu K, Yee NA, Srinivasan S, Mahmoodi A, Zakharian M, Oneto JM, Royzen M. Click activated prodrugs against cancer increase the therapeutic potential of chemotherapy through local capture and activation. *Chem Sci*. 2021;**12**:1259–71.
2. Srinivasan S, Yee NA, Wu K, Zakharian M, Mahmoodi A, Royzen M, Mejia Oneto JM. SQ3370 activates cytotoxic drug via click chemistry at tumor and elicits sustained responses in injected and non-injected lesions. *Adv Ther*. 2021;**4**:2000243.

Ethics Approval Animal studies were approved by the Institutional Animal Care and Use Committee (IACUC) of respective vendors. Study protocol number SP17-010-139B was carried out at Explora BioLabs operating several Office for Laboratory Animal Welfare (OLAW) Animal Welfare Assurance Statements #D16-00743) with Association for Assessment and Accreditation of Laboratory Animal Care (AAALAC) accreditation and United States Department of Agriculture (USDA) license #93-R-0512. Study protocol number CA-SHAS-1 was carried out at Washington Biotechnology Inc. Operating under OLAW Assurance Statement #D16-00616. The clinical trial was approved by the US Federal Food and Drug Administration (FDA), IND #137024.



Abstract 953 Figure 1 The CAPACTM platform (1) SQL70 biopolymer is locally injected at the tumor area and (2) SQP33 protodrug is infused systemically. (3) SQP33 protodrug is activated by SQL70 biopolymer at the tumor site through a rapid covalent reaction between tetrazine and trans-cyclooctene moieties, followed by chemical rearrangement to release active Dox

<http://dx.doi.org/10.1136/jitc-2022-SITC2022.0953>

954

SQ2270, A NOVEL MMAE-BASED THERAPEUTIC, PROMOTES TUMOR GROWTH INHIBITION AND EXTENSIVE IMMUNE CELL INFILTRATION IN THE RENCA CANCER MODEL

Masa Aleckovic*, Sangeetha Srinivasan, Jesse McFarland, Leslie Priddy, Matthew Tso, George Coricor, Jose Mejia Oneto. *Shasqi Inc, San Francisco, CA, United States*

Background The CAPAC™ platform aims to help patients beat cancer by activating powerful therapies at the tumor site while minimizing systemic exposure. The click chemistry-based technology is highly modular and can be applied to a broad range of cancer drugs whose use is limited by toxicity.

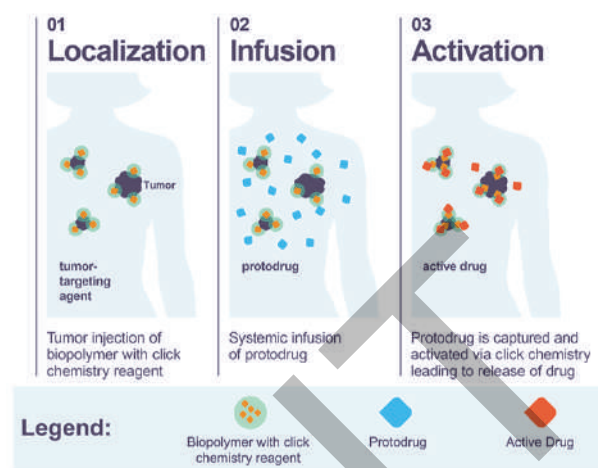
The platform consists of an intratumorally injected biopolymer and an intravenously administered prodrug. Efficient reaction between the biopolymer and prodrug releases the active drug in situ. SQ3370, the lead asset, uses a Doxorubicin prodrug and is being evaluated in a Phase 1 clinical trial in solid tumors (NCT04106492).

We've developed a new prodrug of monomethyl auristatin E (MMAE) and demonstrated its antitumor efficacy when combined with the biopolymer in two tumor models. Here, we performed analyses of immune infiltration into syngeneic tumors that were treated with this novel therapeutic, SQ2270. **Methods** SQ2270 treatment is described in figure 1. Immunocompetent mice were inoculated with RENCA tumor cells. The biopolymer was given intratumorally and MMAE prodrug was given intravenously. Control groups— vehicle and MMAE (1 mg/kg), were treated intravenously. After 2 weeks, tumors were harvested, and immune infiltration was assessed by flow cytometry and immunofluorescent (IF) analyses. Tumor histology was evaluated by H&E staining.

Results SQ2270 and MMAE control significantly inhibited growth of RENCA tumors compared to vehicle ($p < 0.0001$). Histological analysis indicated increased stromal cell infiltration, extracellular matrix deposition, and presence of large phagocytic cells in SQ2270- and MMAE-treated tumors. Flow cytometry indicated >110-fold increase in CD45+ cells fraction of SQ2270-treated tumors compared to vehicle (41% vs 0.4%, $p = 0.01$). MMAE, on the other hand, expanded the CD45+ fraction in tumors by 27-fold (10% vs 0.4%, $p = 0.0004$). SQ2270-treated tumors showed significant increases in several immune populations compared to vehicle, including CD3+, CD8+ (including activated and PD-1+) and CD4+ T-cells, NKT-cells, and activated NK cells. MMAE-treated tumors exhibited less pronounced increases. IF analysis supported these findings, showing increased frequencies of total and Granzyme B-positive CD8+ T-cells in SQ2270-treated tumors compared to controls.

Conclusions SQ2270, CAPAC's novel MMAE-based candidate, is a potent anticancer therapeutic. Here, we show that it also activates an anti-tumor immune response through an extensive immune cell infiltration. Several immune cell types infiltrate the SQ2270-treated tumors where they become activated, including cytotoxic CD8+ T-cells.

Ethics Approval These studies, project numbers SQONCO22-001 and SQONCO22-002, were approved by the Institutional Animal Care and Use Committee (IACUC) of the vendor, following the guidance of Association for Assessment and Accreditation of Laboratory Animal Care (AAALAC), accreditation number 001738.



Abstract 954 Figure 1 The CAPAC Platform (1) Biopolymer click reagent (e.g., SQL70 biopolymer) is locally injected at the tumor area. (2) Prodrug, an attenuated therapy activated by click chemistry, is infused systemically. (3) Prodrug is captured by its click chemistry partner through a rapid covalent reaction between tetrazine and TCO moieties, followed by localized release of the active drug

<http://dx.doi.org/10.1136/jitc-2022-SITC2022.0954>

955

GINGIVO-BUCCAL ORAL CANCER: INFERRING PROGNOSIS FROM IMMUNE CONTEXTURES OF TUMOR AND SURROUNDING MARGIN

¹Ankita Chatterjee*, ²Partha Majumder, ²Ankita Chatterjee, ²Nidhan Biswas, ²Arindam Maitra, ²Arnab Ghosh. ¹NIBMG, Kolkata, India; ²National Institute of Biomedical Genomic, Kalyani, India

Background Interactions between cancer and immune cells create a tumor-promoting or tumor-rejecting environment and correlate with prognosis for many cancers. The variability of immune contextures among oral squamous cell carcinoma of gingivobuccal region (OSCC-GB) patients and their relationship with prognosis are largely unknown.

Methods In this study we estimated the immune infiltration in the tumor, surrounding surgical negative margins and adjacent normal tissues of 43 treatment naïve OSCC-GB patients, using bulk RNA-sequencing and immunohistochemistry. Prognosis of each patient was followed-up for at least two years. Immune subtypes were inferred from gene expression data. Association of patient subtypes and disease prognosis was studied.

Results Using expressions of 544 immune related genes (IRGs) we identified a subgroup of patients with poor prognosis (high recurrences and deaths). High expression levels of three genes – CD73, ITGA3, and ITGA6 – were associated with poor overall survival and higher recurrence. Patients with good prognosis had (a) in their tumors, a high proportion of CD4+ and CD8+ T cells, B cells, NK cells, M1 macrophages, higher TCR and BCR repertoire diversity and cells positive for immune checkpoint markers, and (b) their surgical negative margins were enriched with resting memory-T and dendritic cells.

Conclusions Better prognosis in OSCC-GB is associated with appropriate immune contextures and a subgroup, with high expression of immune checkpoint genes, may further benefit from immunotherapy.

Acknowledgements Amrita Chaudhary², Arnab Ghosh¹, Patta-theyil Arun², Geetashree Mukherjee², Indu Arun ², Arindam Maitra ¹, Nidhan Biswas ¹, Partha P. Majumder,^{1,3}.

¹ National Institute of Biomedical Genomics, Kalyani, India.

² Tata Medical Centre, Kolkata, India.

³ Indian Statistical Institute, Kolkata, India.

Ethics Approval Ethical approval was obtained from the Tata Medical Institution, Kolkata, from where patients were recruited in the study.

Consent "Written informed consent was obtained from the patient for publication of this abstract and any accompanying images. A copy of the written consent is available for review by the Editor of this journal."

<http://dx.doi.org/10.1136/jitc-2022-SITC2022.0955>

956

SPATIAL CLUSTERING REVEALS IMMUNE HUB INTERACTION WITH RESERVOIR OF STEM-LIKE CD8 T CELLS AND PREDICTS IMMUNOTHERAPY RESPONSE IN LUNG CANCER PATIENTS

<http://dx.doi.org/10.1136/jitc-2022-SITC2022.0956>

¹Jonathan Chen*, ¹Linda Nieman, ¹Maxwell Spurrell, ¹Mari Mino-Kenudson, ¹Justin Gainor, ²Nir Hacohen, ¹Jonathan Chen., ¹Massachusetts General Hospital, Boston, United States; ²Broad Institute, Cambridge, MA, United States

Background Immunologic tumor control involves coordination of multiple cell types, but the organization of these interactions in human tumors is poorly understood. We recently reported that immunogenic tumors contain spatially-localized multicellular immunity hubs characterized by expression of interferon-stimulated genes, including *CXCL10/CXCL11* (T cell attracting chemokines), and the presence of *IFNG*+ T cells.¹ This suggested a positive feedback loop where T cell-derived IFN γ stimulates production of CXCR3 ligands, thereby attracting more T cells. However, we did not know (1) whether these hubs predict response to immunotherapy and (2) how hubs intersect with the various CD8 T cell states which play central roles in anti-tumor immunity.

Methods To understand the composition of this immunity hub and its potential association with immunotherapy response, we performed multiplex RNA FISH to visualize hub components in NSCLC tissue from 68 patients prior to PD1-blockade. Cells were segmented and phenotyped automatically. We additionally imaged serial sections with a second panel for markers of CD8 T cell state. We then computationally registered sequential images, integrating our panels. To identify hubs in an unbiased manner, we employed kmeans clustering.

Results We found that the presence of the immunity hub is predictive of subsequent response to PD1-blockade. Image registration revealed that hubs are enriched for CD8 T cells in multiple states, confirming their role as key sites of anti-tumor T cell activity. Furthermore, immunity hubs in responders contained more activated CD8 T cells and *IFNG*+ cells than those in nonresponders. To determine how hub heterogeneity may influence hub functions, we subclustered hubs by phenotypic composition. This analysis uncovered a 'hybrid hub' subclass that spatially overlaps with structures containing stem-like TCF7+ CD8 T cells, resembling the interfollicular zone of lymph nodes. The presence of a single hybrid hub was strongly associated with RECIST response ($p = 0.0005$), found in 85% of responders and only 24% of non-responders. Hybrid hubs also showed a striking association with patient PFS ($p = 0.0014$).

Conclusions Our study provides insight into the multicellular networks that underlie anti-tumor immunity. Immunity hubs are predictive of response to immunotherapy in human lung cancer and organize intratumoral CD8 T cell activity. Moreover, hybrid hubs may represent an active intra-tumoral niche for tumor-specific stem-like T cells that sustain anti-tumor immunity. These multicellular networks are excellent candidates for biomarker development and targets for immunotherapy.

REFERENCE

1. Pelka K, et al. Spatially organized multicellular immune hubs in human colorectal cancer. *Cell* 2021;184:4734–4752.e20.

Ethics Approval This study was approved by the Massachusetts General Hospital Institutional Review Board as a discard tissue protocol (#2019P002829).

957

ASSESSMENT OF THE SPATIAL DISTRIBUTION AND CELL-TO-CELL INTERACTIONS INTO THE TUMOR MICRO-ENVIRONMENT, WITHIN AND BETWEEN SERIAL SLIDES STAINED WITH BRIGHTPLEX[®], A SEQUENTIAL CHROMOGENIC MULTIPLEX ASSAY

¹Aurelie Collignon*, ¹Alboukadel Kassambara, ¹Alex Trinh, ¹Maité Chamourin, ¹Georgia Culley, ¹Marion Olive, ¹Clemence Jaume, ¹Assil Benchaaben, ²Jerome Galon, ¹Jacques Fieschi. ¹Veracyte, Marseille, France; ²Inserm, Paris, France

Background Tumor-infiltrating immune cells play an important role against cancer and are critical to control tumor growth and spread. Immunotherapy and immune checkpoint inhibitors, which aim to reinvigorate exhausted T cells have revolutionized cancer therapy. Despite inducing long-term response in many cancer types, these therapies remain ineffective for most patients.

A better understanding of tumor microenvironment and in particular the presence of immune cells and other stromal cells, along with their abundance, distribution and interactions with other immune/or tumor cells, may help to better stratify patients and understand mechanisms of resistance to immunotherapy. Indeed, the distribution of T cells in tumor could be associated to favorable prognosis in different cancers and the relationship between cells could be linked to patient outcome. For instance, the presence of macrophages close to tumor cells in non-small cell lung cancer or the proximity of regulatory T cells (Treg) cells to cytotoxic CD8⁺ T-cells in gastric cancer are associated with worse outcome.

Methods The analysis of the spatial distribution of immune and non-immune cells and of their proximity in the tumor microenvironment seems relevant to understand response to immunotherapy. Here, we propose a new tool allowing the assessment of 3 spatial parameters: 1) Evaluation of cell-to-cell proximity metrics between 2 different populations or within the same population (clustering), 2) Interaction of two cell populations using nearest neighbor distance measurement (G-function) and 3) Spatial cell distribution highlighting hot spots (Kernel's heatmap).

Brightplex[®] is a chromogenic multiplex immunohistochemistry technology allowing the detection of several biomarkers on a single FFPE slide to identify and quantify complex cell populations such as T-cells expressing immune checkpoints, M1 and M2 macrophages, Treg cells and myeloid-derived suppressor cells. Following staining and digitization, images are fused to create a virtual multi-channel image where cells of interest are detected by digital pathology (DP). With Brightplex and DP, we have developed a workflow to assess the spatial distribution and potentially cell-to-cell interactions within a slide or between two or three adjacent slides stained with different multiplex panels. Following cell detection, spatial analysis is performed using spatstat module on R-studio software.

Integrated to Immunogram, this new tool could help clinical researchers to understand tumor landscape, predict response to treatment and patient outcome.

<http://dx.doi.org/10.1136/jitc-2022-SITC2022.0957>

959

PD-1 AND ICOS CO-EXPRESSION IDENTIFIES TUMOR-REACTIVE CD4 T CELLS IN HUMAN SOLID TUMORS

Rebekka Duhen, Olivier Fesneau, Kimberly Samson, Alexandra Frye, Michael Beymer, Venkatesh Rajamanickam, David Ross, Eric Tran, Brady Bernard, Andrew Weinberg, Thomas Duhen*. *EACRI | Providence Cancer Institute, Portland, OR, United States*

Background CD4 T helper (Th) cells play a key role in orchestrating immune responses, but the identity of the CD4 Th cells involved in the immune response against cancer remains to be defined.

Methods To better define the composition of the CD4 Th cells infiltrating human solid tumors, we analyzed the phenotype of CD4 T cells in 22 patients with head and neck squamous cell carcinoma and 16 patients with microsatellite stable colorectal cancer by high dimensional flow cytometry. In addition, we determined their spatial location and cellular interactions in the tumor microenvironment by multiplex IHC to understand their role in the anti-tumor immune response. We also assessed the capacity of the CD4 Th cell populations sorted and expanded based on the expression of PD-1 and ICOS to recognize tumor-associated antigens and tumor-specific neoantigens. Finally, we investigated whether the presence of PD-1+ICOS+ CD4 Th cells in the tumor was associated with disease-free survival in HNSCC patients.

Results Following t-SNE analysis, we identified a subset of CD4 Th cells distinct from FOXP3+ regulatory T cells that co-expressed PD-1 and ICOS. This cell population, which was present in the tumor but absent in the periphery, exhibited features of chronic stimulation and displayed characteristics of tissue resident memory T cells. PD-1+ICOS+ tumor-infiltrating (TIL) CD4 Th cells were located primarily in the tumor stroma in proximity to MHC class II+ cells and were proliferating, suggesting local antigen recognition. Interestingly, both PD-1+ICOS+ CD4 Th cells and CD39+CD103+ tumor-reactive CD8 T cells were enriched for cells secreting CXCL13, a chemokine involved in the recruitment of B cells. PD-1+ICOS+ CD4 Th TIL were shown to recognize both tumor-associated antigens and tumor-specific neoantigens, which were distinct from the epitopes recognized by the CD8 T cells from the same patients. Finally, higher frequencies of PD-1+ICOS+ CD4 Th TIL in patients with HNSCC was associated with better disease-free survival.

Conclusions Our findings provide an approach for isolating tumor-reactive CD4 Th TIL directly ex vivo that will help define their role in the anti-tumor immune response and potentially improve future adoptive T-cell therapy approaches.

Ethics Approval All surgical tumor samples and blood samples used in this study were taken from individuals treated at the Providence Cancer Center. All patients signed written informed consent approved by the Providence Portland Medical Center Institutional Review Board (IRB protocol n0. 06-108A) and the study was conducted in accordance with the ethical standards established by the Declaration of Helsinki.

<http://dx.doi.org/10.1136/jitc-2022-SITC2022.0959>

960

TT-816, A NOVEL SMALL MOLECULE IMMUNE CHECKPOINT INHIBITOR TARGETING CANNABINOID CB₂ RECEPTOR, STIMULATES INNATE AND ADAPTIVE IMMUNITY FOR CANCER THERAPY

Peidong Fan*, Elfatih Elzein, Lina Yao. *Teon Therapeutics, Inc., Redwood City, CA, United States*

Background The endocannabinoid system is widely expressed in the human body, including the innate and adaptive immune system, where endocannabinoids, Δ^9 -tetrahydrocannabinol and synthetic ligands regulate immune response. The effects of endocannabinoids on immune regulation are primarily mediated by G-protein coupled cannabinoid CB₂ receptors (CB₂R) via several mechanisms, including development, migration, proliferation and effector functions. The upregulated expression of CB₂R and elevated levels of endocannabinoids have been observed in a variety of tumor microenvironments and are associated with the aggressiveness of cancer.

Methods Membranes prepared from CHO-K1 cells stably expressing human CB₂R were used for receptor binding assays in the presence of TT-816 and [³H]CP-55,940, and for GTP γ S binding assay in the presence of TT-816, 10 μ M GDP and 0.3 nM [³⁵S]GTP γ S. cAMP assay was performed by incubating the CHO-K-1 cells for 30 min with TT-816, 25 μ M forskolin and 12 nM CP-55,940, or with TT-816 and 5 μ M forskolin. NK cell function was determined by co-culturing TT-816 pretreated NK cells with K562 cancer cells for 24 hours. The mixed lymphocyte reaction assay was conducted by co-culturing human CD4+ T cells with monocyte-derived dendritic cells. Cell viability was measured by FACS and IFN- γ by MSD.

Results TT-816 is a competitive and selective CB₂R antagonist. It bound to human CB₂R with an IC₅₀ 26.2 nM, showing greater than 380-fold selectivity over cannabinoid CB₁ receptors. The ability of TT-816 to inhibit the constitutive activity of CB₂R was characterized in both GTP γ S and cAMP assays. TT-816 concentration-dependently inhibited the basal GTP γ S binding response, antagonized CB₂R agonist-mediated cAMP production and enhanced the forskolin response on basal cAMP level. Consistent with its inhibition of CB₂R function, TT-816 inhibited the growth of human breast, colorectal and lung cancer cells. In addition, TT-816 concentration-dependently enhanced the functions of NK cells, dendritic cells and T cells. It increased NK cell killing of the human cancer cells and IFN- γ production, significantly stimulated the expression of CD86, HLA-DR, IL-12 and TNF- α in monocyte-derived dendritic cells, and enhanced CD4+ T cell proliferation and IFN- γ production in a mixed lymphocyte reaction assay.

Conclusions TT-816 is a novel, oral small molecule immune checkpoint inhibitor that selectively blocks CB₂R on cancer cells and immune cells. Preclinical data have demonstrated that it stimulates antitumor innate and adaptive immune response and inhibits cancer cell proliferation. TT-816 is currently undergoing phase 1 clinical trials for the treatment of a broad range of solid tumors.

<http://dx.doi.org/10.1136/jitc-2022-SITC2022.0960>

961

TUMOR-INFILTRATING MUCOSAL-ASSOCIATED INVARIANT T CELLS (MAIT) FROM PATIENTS WITH PANCREATIC CANCER RECOGNIZE SHARED TUMOR ANTIGENS IN AN MR1-RESTRICTED FASHION

¹Jéssica Kamiki*, ¹Patrícia António, ¹Rodrigo Eduardo, ¹Sara Cascais, ¹Bernardo Marinheiro, ¹Andreia Maia, ¹Eric De Sousa, ¹Joana Lérias, ¹Carolina Gorgulho, ¹Mireia Castillo-Martin, ¹Markus Buechler, ¹Antonio Beltran, ¹Carlos Carvalho, ²Ridong Chen, ²Sam Jeong, ¹Markus Maeurer. ¹Champalimaud Foundation, Lisbon, Portugal; ²Human Cell Inc., Napperville, IL, United States

Background Pancreatic adenocarcinoma (PDAC) is one of the most lethal cancers with a 5-year survival rate of 10%.¹ Standard chemotherapeutics have failed to produce relevant increased survival for patients with pancreatic cancer.² Cellular immunotherapies are a viable option to achieve anti-tumor directed clinically relevant treatment modalities.

Mucosal-associated invariant T-cells (MAIT) are defined by the restricted usage of the invariant V α 7.2 T-cell receptor (TCR) α -chain combined with different TCR β -chains that bridge innate and adaptive immune responses. MAIT produce pro-inflammatory cytokines^{3,4} and are present in primary and metastatic cancer lesions.^{4,5} MAIT may contribute to control malignant cells by either MR1-restricted recognition of cancer cells and/or by production of anti-cancer directed cytokines induced by tumoral-associated bacterial species. A set of bacterial species has been associated with improved survival in patients with PDAC.^{6,7} We studied the role of MAIT in tumor-infiltrating lymphocytes (TIL) from patients with PDAC. **Methods** MAIT were identified in PDAC specimens by immunohistology. Freshly harvested tumor specimen allowed to expand TILs from patients with PDAC and to selectively isolate MAIT by immunomagnetic sorting. MR1-restricted recognition and cancer specificity was tested in an autologous tumor cell recognition model- blocked by antibodies against MR1 and in a MR1+ allogeneic tumoral cell line via MR1-siRNA downregulation defined by IFN- γ production. Phenotypic and functional analysis of MAIT was carried out by flow cytometry and ELISAs. Deep TCR-sequencing of tumor tissue and TIL was performed to gauge TCR diversity and spatial transcriptomics to localize V α 7.2 cells associated with MR1 and immune effector gene expression.

Results PDAC lesions are positive for MR1 and V α 7.2+ cells defined by immunohistology and spatial transcriptomics. MAIT were isolated and found to be specifically reactive against autologous tumor determined by IFN- γ and IL-17A production. The majority of MAIT resided in the effector-memory pool (CD45-CCR7-) and tested positive for CD8, CD161 and CD26. Reactivity against a panel of candidate bacteria associated with patient survival was confirmed by cytotoxicity and a CD107a degranulation assay.

Conclusions MAIT infiltrate into PDAC lesions, they recognize the tumor in a MR1-restricted fashion defined by IFN- γ release and cytokine production could be augmented by a defined set of bacterial species. MAIT represent biologically relevant immune cells that may aid to kill cancer cells. Anti-tumor directed TCRs can be used as a molecular blueprint to construct anti-cancer directed transgenic immune cells restricted by commonly shared MR1.

Acknowledgements The work was sponsored by the Champalimaud Foundation and assisted by the Champalimaud Biobank and Vivarium.

REFERENCES

1. Yao W, Maitra A, Ying H. Recent insights into the biology of pancreatic cancer. *EBioMedicine*. 2020
2. Sideras K, Braat H, Kwekkeboom J, van Eijck CH, Peppelenbosch MP, Sleijfer S, et al. Role of the immune system in pancreatic cancer progression and immune modulating treatment strategies. *Cancer Treat Rev* 2014;**40**(4):513–22.
3. Toubal A, Nel I, Lotersztajn S, Lehuen A. Mucosal-associated invariant T cells and disease. *Nat Rev Immunol*. 2019;**19**(10):643–57.
4. Lukasiak Z, Elewaut D, Venken K. Mait cells come to the rescue in cancer immunotherapy? *Cancers (Basel)*. 2020;**12**(2):1–19.
5. Vacchini A, Chancellor A, Spagnuolo J, Mori L, De Libero G. MR1-Restricted T Cells Are Unprecedented Cancer Fighters. *Front Immunol*. 2020;**11**(April):1–8.
6. Aykut B, Pushalkar S, Chen R, Li Q, Abengozar R, Kim JI, et al. The fungal microbiome promotes pancreatic oncogenesis via activation of MBL. *Nature*. 2019; 264–7.
7. Pushalkar S, Hundeyin M, Daley D, Zambirinis CP, Kurz E, Mishra A, et al. The pancreatic cancer microbiome promotes oncogenesis by induction of innate and adaptive immune suppression. *Cancer Discov*. 2018;**8**(4):403–16.

Ethics Approval This study was approved by the Champalimaud Foundation Ethics Committee and by Ethics Research Committee of NOVA Medical School of NOVA University of Lisbon.

Consent For each patient, written informed consent and approval by the Ethical Committee of the Champalimaud Foundation will be obtained. The study will be in compliance with the Declaration of Helsinki.

<http://dx.doi.org/10.1136/jitc-2022-SITC2022.0961>

Abstracts

962

IFI16 PROMOTES IMMUNE RESPONSES THROUGH IFN- γ PATHWAY ACTIVATION IN METASTATIC CUTANEOUS MELANOMAS

¹Yuta Kobayashi*, ¹Matias Bustos, ²Qiang Yu, ¹Dave Hoon. ¹Saint John's Cancer Institute, Santa Monica, CA, United States; ²Genome Institute of Singapore, Biopolis, Singapore

Background IFN- γ -inducible protein 16 (IFI16) is known to initiate STING pathway cascade, which leads to the downstream activation of various cytokines and chemokines that play important roles in enhancing tumor microenvironment immune responses. IFI16 activates STING signaling through the cooperation with cyclic GMP-AMP synthase (cGAS) through the detection of cytoplasmic DNA. Recently, we have shown that IFI16-dependent STING signaling upregulates effective anti-HER2 cellular immune responses in HER2 (+) breast cancer.¹ The aim of this study was to assess the role of *IFI16* levels with immune responses in metastatic cutaneous melanomas.

Methods Cutaneous melanoma datasets for mRNA expression were obtained from TCGA SKCM, GTEx, GSE7553, GSE15605, and GSE46517. The fraction of tumor-infiltrated immune cells (TIIC) was estimated by CIBERSORT. Patients from TCGA were divided into high- and low-*IFI16* mRNA level groups, based on the highest and lowest quartiles. Extraction of Expression Module (EEM) analysis was performed. Correlations between variables were calculated with the Mann-Whitney U test with FDR corrections.

Results *IFI16* mRNA levels were significantly upregulated in metastatic cutaneous melanomas (AJCC III/IV, n = 193) compared to normal skin (figure 1A, p < 0.0001), but significantly downregulated in metastatic versus primary melanomas in GSE7553 dataset (figure 1B, p = 0.016). High levels of *IFI16* were significantly associated with poor prognosis in stage III/IV melanoma patients (figure 1C, p < 0.0001). The analysis of TIIC showed that M1 macrophage subset levels were significantly higher in the high-*IFI16* vs low-*IFI16* group (figure 1D, p = 0.0028). IFN- γ score was significantly higher in the high- vs low-*IFI16* group in TCGA (figure 1E, p = 0.00051), GSE46516 (p = 0.00068), and GSE15605 (p = 0.026). EEM analysis showed that the activity scores of IFN- γ response were significantly higher in high-*IFI16* vs low-*IFI16* groups (p = 0.0048). Furthermore, data integration from EEM and differential expressed genes analysis identified 34 immune-related genes, of which chemokines *CXCL10* and *CXCL11* were significantly upregulated by the IFN- γ response pathway. The elevated *CXCL10* and *CXCL11* are known to enhance tumor immune microenvironment activity. *CXCL10* and *CXCL11* were significantly higher in high-*IFI16* group in both the TCGA (figure 1F, p < 0.0001, p < 0.0001, respectively) and GSE46517 (p = 0.00016, p = 0.00062, respectively).

Conclusions High-*IFI16* mRNA levels may represent predictive biomarkers of good prognosis in metastatic melanomas, whereby *IFI16* mRNA levels were associated with significant immune responses through the upregulation of the IFN- γ pathway, M1 macrophage subset, and *CXCL10/CXCL11*.

Acknowledgements This work was supported by Dr. Miriam and Sheldon G. Adelson Medical Research Foundation (D.S.B.H).

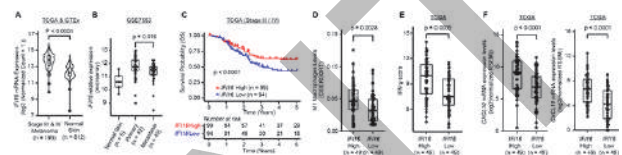
REFERENCE

1. Ong LT, Lee WC, Ma S, Oguz G, Niu Z, Bao Y, Yusuf M, Lee PL, Goh JY, Wang P et al. IFI16-dependent STING signaling is a crucial regulator of anti-HER2

immune response in HER2+ breast cancer. *Proc Natl Acad Sci U S A* 2022;119(31):e2201376119.

Ethics Approval This study followed the principles in the Declaration of Helsinki. All human samples and clinical information for this study were obtained according to the protocol guidelines approved by Providence SJHC under SJHC Joint Institutional Review Board (IRB): IRB: JWCI-18-0401) and IRB: MORD-RTPCR-0995.

Consent Written informed consent was obtained from the patient for publication of this abstract. A copy of the written consent is available for review by the Editor of this journal.



Abstract 962 Figure 1 IFI16 expression in metastatic cutaneous melanomas

A. IFI16 mRNA levels in tumor tissues (TCGA SKCM dataset) and normal skin tissues (GTEx dataset). B. IFI16 mRNA levels in normal skin, primary tumors, and metastatic tumors (GSE7553). C. Kaplan-Meier curves for melanoma patients of AJCC stage III&IV according to IFI16 mRNA expression in TCGA dataset. D. Infiltration levels of M1 macrophages estimated by CIBERSORT using TCGA dataset. E. IFN- γ signature score in TCGA. F. CXCL10, and CXCL11 mRNA expression levels in TCGA

<http://dx.doi.org/10.1136/jitc-2022-SITC2022.0962>

963

SIGNIFICANTLY DIFFERENT IMMUNE MICROENVIRONMENT BETWEEN TRIPLE-NEGATIVE BREAST CANCER WITH AND WITHOUT NEOADJUVANT CHEMOTHERAPY THROUGH MULTIPLEX IMMUNOHISTOCHEMISTRY

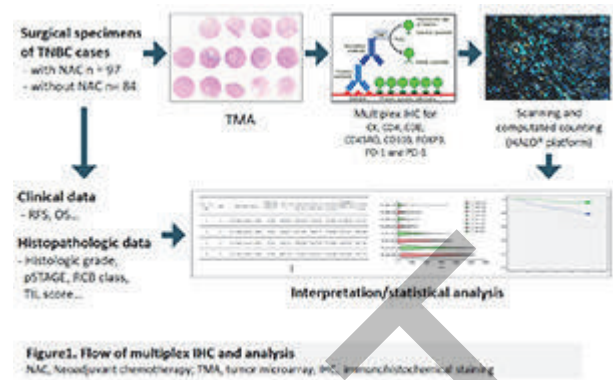
¹Miseon Lee*, ²Hyun Lee, ³Gyungyub Gong, ³Hee Jin Lee. ¹Seoul St. Mary's Hospital College of medicine, Seoul, Korea, Republic of; ²NeogenTC corp., Gyeonggi-do, hanam-si, Korea, Republic of; ³University of Ulsan College of Medicine, Seoul, Korea, Republic of

Background Understanding the tumor immune microenvironment in triple-negative breast cancer (TNBC) is essential for the development of successful immunotherapy. Although neoadjuvant chemotherapy (NAC) for TNBC is increasing, studies about the difference in tumor immune microenvironment with or without NAC and the association with clinical data are lacking.

Methods We made tumor microarray for 181 TNBC surgical specimens [84 cases (46.4%) without NAC and 97 cases (53.6%) with NAC] and performed multiplex immunohistochemistry (pan-cytokeratin, CD4, CD8, CD45RO, FOXP3, PD-1, PD-L1, and CD103) (figure 1). In cases without NAC, 23 patients (27.4%) were in stage I and 61 (72.6%) in II or III. In the cases with NAC, the residual cancer burden (RCB) class was 20 (20.6%) in 0, 5 (5.2%) in I, 51 (52.6%) in II, and 21 (21.6%) in III.

Results Tumors without NAC had significantly higher amounts of CD4+, CD8+, CD103+, CD45RO+, FOXP3+, or PD-1+ with CK- cells per area compared to tumors with NAC (p-value range: <0.001 ~ 0.001). In the Kaplan-Meier survival analysis of patients without NAC, disease-free survival (DFS) was significantly better in the group with higher amount of CK-CD4+PD-1+CD45RO+CD103+ (p=0.023), CK-CD4+PD-1-CD45RO+CD103+ (p=0.018), CK-CD8+PD-1+CD45RO+CD103+ (p=0.023), CK-CD8+PD-1-CD45RO+CD103+ (p=0.023), CK-CD8+PD-1-CD45RO-CD103+ (p=0.023), CK-CD8+ (p= 0.024), CK-CD8+PD-1+CD45RO+CD103-(p=0.023), and CK-CD8+PD-1-CD45RO+CD103-(p=0.024) per area than the median value. In tumors with NAC, the DFS was significantly better in the group with a higher amount of CK-CD8+PD-1+CD45RO-CD103+ (p=0.020) and CK-CD8+PD-1+CD45RO-CD103- (p=0.042) per area than the median. In the multivariable analysis of tumors without NAC, the high histologic grade was a significant prognostic factor of unfavorable DFS [Hazard ratio (HR), 0.029; 95% confidence interval (CI), 0.004 to 0.217; p=0.001] and a higher amount of CK-CD8+ per area than median value was a significant prognostic factor of favorable DFS (HR, 0.094; 95% CI, 0.014 to 0.613; p=0.013). In tumors with NAC, a higher amount of CK-CD8+PD-1+CD45RO-CD103+ per area than median value (HR, 0.398; 95% CI, 0.192 to 0.825; p=0.015) and low RCB class (class 0 vs. class III; HR, 0.097; 95% CI, 0.023 to 0.418; p=0.002, class II vs. III; HR, 0.192; 95% CI, 0.085 to 0.433; p< 0.001) were significantly favorable prognostic factors of DFS.

Conclusions In TNBC, the tumor immune microenvironment between tumors without NAC and tumors with NAC was significantly different, and the immune phenotype with a clinically significant effect was distinct. A deeper understanding of the difference in the tumor immune microenvironment between TNBC with and without NAC will help develop successful immunotherapy.



Abstract 963 Figure 1 Flow of multiplex IHC and analysis

<http://dx.doi.org/10.1136/jitc-2022-SITC2022.0963>

DYNAMIC IMMUNE LANDSCAPES DURING MELANOMA PROGRESSION REVEAL A ROLE FOR ENDOGENOUS OPIOIDS IN DRIVING T CELL DYSFUNCTION

¹Davide Mangani*, ²Linglin Huang, ³Meromit Singer, ²Ruitong Li, ¹Rocky Barilla, ¹Giulia Escobar, ¹Katherine Tooley, ¹Hanning Cheng, ³Conor Delaney, ³Kathleen Newcomer, ⁴Jackson Nyman, ⁴Nemanja Marjanovic, ¹James Nevin, ⁵Orit Rozenblatt-Rosen, ¹Vijay Kuchroo, ⁵Aviv Regev, ¹Ana Anderson. ¹Evergrande Center for Immunologic Diseases, Ann Romney Center for Neurologic Diseases, Harvard Medical School and Mass General Brigham, Boston, MA, 02115, USA, Boston, MA, United States; ²Department of Biostatistics, Harvard T.H. Chan School of Public Health, Boston, MA, 02115, USA, Boston, MA, United States; ³Dana-Farber Cancer Institute, Boston, MA 02215, USA, Boston, MA, United States; ⁴Klarman Cell Observatory, Broad Institute of Harvard and MIT, Cambridge, MA, USA, Cambridge, MA, United States; ⁵Klarman Cell Observatory, Broad Institute of Harvard and MIT, Cambridge, MA, USA ; Genentech, South San Francisco, CA, USA., Cambridge, MA, United States

Background Immune checkpoint blockade (ICB) therapies aimed at invigorating the anti-tumor immune response have achieved unprecedented responses in several tumor types, including melanoma.^{1,2} Despite this great success, approximately 50% of melanoma patients either fail to respond or develop resistance to ICB.³ As the immune response becomes progressively disabled as tumors advance, achieving a better understanding of the immunosuppressive mechanisms that take hold during tumor progression is needed to identify novel therapeutic targets and extend the benefit of immunotherapy to more patients

Methods We performed an unsupervised examination of the immune infiltrate of B16F10 melanoma tumors over the course of tumor progression using single-cell RNAseq. At each time point we harvested tumors of different sizes to enable parsing of changes associated with tumor size and time from implant separately. We investigated dynamic changes in composition of the tumor infiltrate and in genes and pathways expressed in CD8⁺ T cells over the course of tumor progression

Results We uncovered an unexpected role for endogenous opioid signaling in the development of CD8⁺ T cell dysfunction during melanoma progression. The endogenous opioid-polypeptide hormone pro-enkephalin (*Penk*) was progressively up-regulated in CD8⁺ T cells that transitioned from the effector to terminally exhausted T cell state with tumor progression. We applied gain- and loss-of-function approaches to test the role of *Penk* in tumor antigen-specific responses. Adoptive transfer of OT-I CD8⁺ T cells transduced with a lentiviral vector to over-express *Penk* had reduced cytolytic capacity and secretion of effector cytokines (IFN γ , TNF α) and failed to control the growth of B16F10-OVA compared to WT OT-I cells. Conversely, CRISPR-Cas9-mediated knock-out of *Penk* in OT-I cells led to enhanced tumor control. Further, *Penk* deficiency in CD8⁺ Pmel T cells that recognize the mouse homologue of the human premelanosome protein, overcame the poor ability of Pmel T cells to exert tumor control. Notably, *Penk*-deficient CD8⁺ T cells exhibited increased cytolytic potential and effector function, without acquiring features of terminal dysfunction as determined by TOX, Eomes, and TIM3 expression. Lastly, treatment of established B16F10 melanoma with an inhibitor of opioid signaling significantly improved tumor growth control

Conclusions Our data reveal an unexpected role for endogenous opioids in driving T cell dysfunction, thereby linking analgesic pathways and the dampening of T cell functionality in cancer. Finally, our findings have high clinical relevance as patients with advanced tumors are often treated with opioids,

which may ultimately limit anti-tumor CD8⁺ T cell responses and ICB efficacy

REFERENCES

1. Robert C, Schachter J, Long GV, Arance A, Grob JJ, Mortier L, Daud A, Carlino MS, McNeil C, Lotem M, Larkin J, Lorigan P, Neyns B, Blank CU, Hamid O, Mateus C, Shapira-Frommer R, Kosh M, Zhou H, Ibrahim N, Ebbinghaus S, Ribas A; KEYNOTE-006 investigators. Pembrolizumab versus ipilimumab in advanced melanoma. *N Engl J Med*. 2015 Jun 25;**372**(26):2521–32. PMID: 25891173.
2. Wolchok JD, Chiarion-Sileni V, Gonzalez R, Rutkowski P, Grob JJ, Cowey CL, Lao CD, Wagstaff J, Schadendorf D, Ferrucci PF, Smylie M, Dummer R, Hill A, Hogg D, Haanen J, Carlino MS, Bechter O, Maio M, Marquez-Rodas I, Guidoboni M, McArthur G, Lebbé C, Ascierto PA, Long GV, Cebon J, Sosman J, Postow MA, Callahan MK, Walker D, Rollin L, Bhone R, Hodi FS, Larkin J. Overall survival with combined nivolumab and ipilimumab in advanced melanoma. *N Engl J Med*. 2017 Oct 5;**377**(14):1345–1356. PMID: 28889792
3. Huang AC, Zappasodi R. A decade of checkpoint blockade immunotherapy in melanoma: understanding the molecular basis for immune sensitivity and resistance. *Nat Immunol*. 2022 May;**23**(5):660–670. PMID: 35241833

<http://dx.doi.org/10.1136/jitc-2022-SITC2022.0964>

965

DEFICIENCY OF METABOLIC REGULATOR PKM2 ACTIVATES THE PENTOSE PHOSPHATE PATHWAY TO GENERATE TCF1+ PROGENITOR CD8 T CELLS TO IMPROVE EFFICACY OF PD-1 CHECKPOINT BLOCKADE

Geoffrey Markowitz*, Yi Ban, Diamile Tavarez, Michael Crowley, Liron Yoffe, Mitchell Martin, Tito Sandoval, Dingcheng Gao, Juan Cubillos-Ruiz, Timothy McGraw, Nasser Altorki, Vivek Mittal. *Weill Cornell Medicine, New York, NY, United States*

Background TCF1^{high} progenitor CD8+ T cells have been shown to mediate the efficacy of PD-1 checkpoint blockade.¹⁻³ However, the mechanisms that govern generation of TCF1^{high} cells are poorly understood.

Methods We sequenced bulk RNA from tumor-infiltrating lymphocytes to identify differentially expressed genes based on tumor progression. We utilized *in vitro* co-cultures of tumor-specific T cells tumor cells to examine differentiation, effector function, and metabolism of T cells with different genetic and pharmacologic manipulations by flow cytometry, metabolic flux analyses, and metabolomic profiling. We performed *in vivo* adoptive transfers of control and genetically manipulated tumor-specific T cells into tumor-bearing mice from both a non-small cell lung cancer and a melanoma model to examine effects of genetic manipulation on differentiation and effector function, as well as to determine tumor burden and overall mouse survival both in the treatment-naïve and anti-PD-1 treated contexts.

Results RNA Sequencing demonstrated a metabolically active response in tumor-infiltrating CD8+ T cells isolated from large and late-stage tumors. Using a genetic screen targeting glycolytic enzymes up-regulated in tumor-infiltrating CD8+ T cells, we demonstrate that PKM2 deficiency (PKM2^{KO}) enriched for TCF1^{high} progenitor cells (figure 1). Antigen-specific PKM2^{KO} CD8+ T cells from draining lymph nodes and tumors exhibited a central memory-like phenotype (figure 2) with reduced effector cytokine production, increased CD44/CD62L expression, and increased TCF1 and Eomes in non-small cell lung cancer and melanoma. Adoptive transfer of PKM2^{KO} CD8+ T cells in combination with PD-1 blockade impaired tumor growth and improved survival (figure 3). PKM2^{KO} CD8+ T cells showed reduced glycolytic flux and accumulation of glycolytic intermediates with concomitant increases in pentose phosphate pathway (PPP) metabolites. Importantly, small molecule agonism of PPP was sufficient to skew activated CD8+ T cells towards the TCF1^{high} population (figure 4).

Conclusions Here we show that targeting glycolytic flux by deletion of pyruvate kinase muscle 2 (PKM2) results in elevated pentose phosphate pathway activity, leading to generation of an altered differentiation state responsive to PD-1 blockade. Our study demonstrates a novel metabolic reprogramming that contributes to a memory-like T cell state amenable to checkpoint blockade.

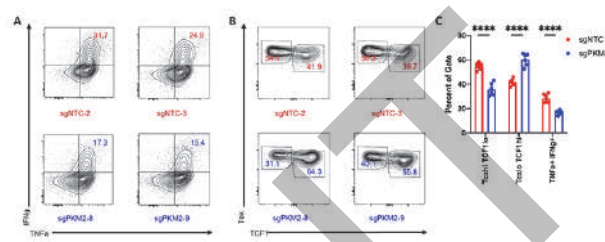
Acknowledgements This work was supported by NIH grants T32 CA203702 and KL2-TR-002385 to GJM, and funds from the Neuberger Berman Foundation Lung Cancer Research Center to NKA and VM.

REFERENCES

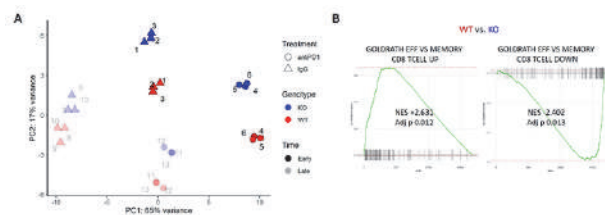
- Escobar G, Mangani D & Anderson AC. T cell factor 1: A master regulator of the T cell response in disease. *Sci Immunol* 2020;**5**.
- Siddiqui I, et al. Intratumoral Tcf1 + PD-1 + CD8 + T Cells with stem-like properties promote tumor control in response to vaccination and checkpoint blockade immunotherapy. *Immunity* 2019;**50**:195–211.e110.
- Kurtulus S, et al. Checkpoint blockade immunotherapy induces dynamic changes in PD-1-CD8+ Tumor-Infiltrating T Cells. *Immunity* 2019;**50**:181–194.e186.

- Luckey CJ, et al. Memory T and memory B cells share a transcriptional program of self-renewal with long-term hematopoietic stem cells. *Proc Natl Acad Sci USA* Feb 2006;**28**:103(9):3304–9.

Ethics Approval All animal work was performed in accordance with an animal protocol approved by the institutional Animal Care and Use Committee at Weill Cornell Medical College (Protocol number 0806-762A).

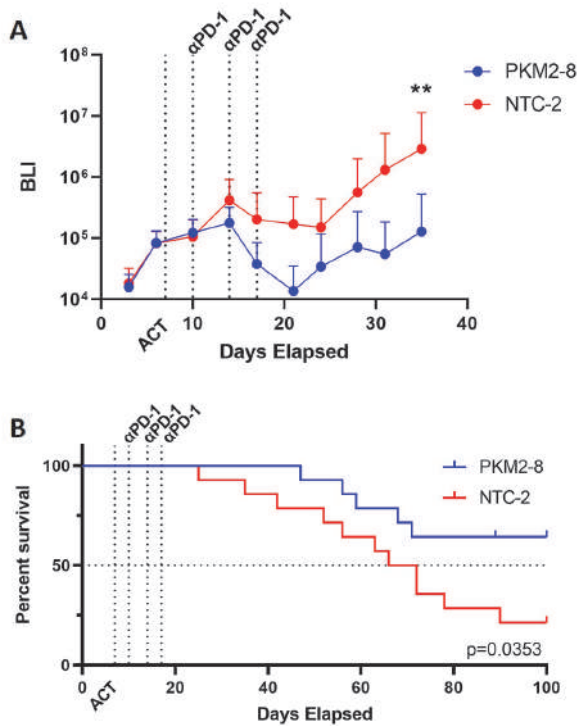


Abstract 965 Figure 1 Flow cytometry analysis of OT-I+ Thy1.1+ T cells co-cultured with HKP1-ova-GFP tumor cells. Activated T cells were electroporated with guides targeting PKM2 (sgPKM2) or non-targeting controls (sgNTC), and co-cultured with tumor cells for 4 days. a, Representative contour plots for IFN γ and TNF α staining in T cells electroporated with two non-targeting control guides (red, sgNTC-2 and sgNTC-3) and two guides targeting PKM2 (blue, sgPKM2-8 and sgPKM2-9) after 4 days of co-culture. b, Representative contour plots for Tox and TCF1 staining in T cells electroporated with two non-targeting control guides (red, sgNTC-2 and sgNTC-3) and two guides targeting PKM2 (blue, sgPKM2-8 and sgPKM2-9) after 4 days of co-culture. c, Quantification of populations of T cells electroporated with sgNTC (red) and sgPKM2 (blue) after 4 days of co-culture. **** $p < 0.0001$

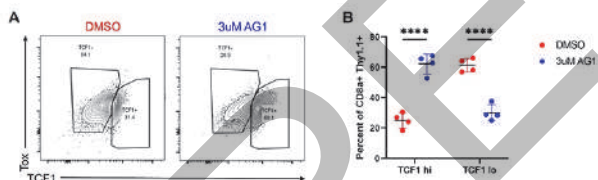


Abstract 965 Figure 2 Transcriptomic analysis of adoptively-transferred T cells. Adoptive co-transfers of activated OT-I+ Thy1.1+ PKM2WT (NTC-2, red) or PKM2KO (PKM2-8, blue) CD8+ T cells distinguished by Thy1.1 zygosity were performed into lymphodepleted C57Bl/6 mice 7 days after implantation of HKP1-ova-GFP tumors. 3 doses of either IgG control or anti-PD-1 were administered on days 10, 14, and 17 after orthotopic implantation. T cells were subsequently sorted back from tumors based on Thy1.1, phenotyped by flow cytometry, and underwent bulk RNA sequencing. a, Principal component analysis of bulk RNA sequencing data with mouse batch effects removed. b, Gene set enrichment analyses by Luckey et al⁴ examining signatures for effector and memory cells in PKM2WT compared with PKM2KO.

Abstracts



Abstract 965 Figure 3 Activated OT-I+ Thy1.1+ PKM2WT (NTC-2, red) or PKM2KO (PKM2-8, blue) CD8+ T cells were adoptively transferred into lymphodepleted C57Bl/6 mice 7 days after orthotopic implantation of HKP1-ova-GFP tumors. 3 doses of anti-PD-1 were administered on days 10, 14, and 17 after tumor implantation. Bioluminescence imaging to measure tumor burden (a) and overall mouse survival monitoring (b) were performed. ** p<0.01



Abstract 965 Figure 4 Flow cytometry analysis of activated OT-I+ Thy1.1+ T cells treated with either DMSO control (red) or 3μM glucose-6-phosphate dehydrogenase agonist AG1 (blue) and co-cultured with HKP1-ova-GFP tumor cells. T cells were activated for 24 hours, treated with DMSO or AG1 for another 24 hours, then co-cultured with HKP1-ova-GFP tumor cells at a 5:1 effector:target ratio for 4 days with continuing DMSO or AG1 treatment. a, Representative contour plots for Tox and TCF1 staining in T cells treated with DMSO (left) or AG1 (right), with gates for populations with differential TCF1 expression. b, Quantification of populations from (a) as percent of cultured CD8+ Thy1.1+ T cells in DMSO (red) and AG1 (blue) treated co-cultures. **** p<0.0001

<http://dx.doi.org/10.1136/jitc-2022-SITC2022.0965>

966

MULTISPECTRAL IMMUNOHISTOCHEMISTRY REVEALS AN IMMUNOSUPPRESSIVE TUMOUR MICROENVIRONMENT IN ESOPHAGEAL ADENOCARCINOMA

¹Charles Rayner*, ¹Tyler Wooldridge, ¹Sunny Sunshine, ²Izhar Bagwan*, ²Shaun Preston, ¹Hardev Pandha, ²Nima Abbassi-Ghadi, ¹Nicola Annels. ¹University of Surrey, Guildford, UK; ²Royal Surrey NHS Foundation Trust, Guildford, UK

Background Esophageal cancer – of which adenocarcinoma (EAC) is the predominant type in the UK – is a highly aggressive malignancy, with 5-year survival rates of approximately 15%.¹ Surgically resectable disease is treated with neo-adjuvant chemo+/-radiotherapy. The recent publication of Checkmate-577 supports the use of anti-PD-1 immunotherapy in EAC post chemoradiotherapy and surgery.² Beyond CD8⁺ T cells and PD-1/PD-L1 expression, the immune tumour microenvironment of EAC is poorly understood. Further research is required to understand the immune phenotype of the EAC microenvironment and how this could be modulated to improve outcomes.

Methods Treatment naïve patients who had undergone esophago-gastrectomy at the Royal Surrey County Hospital, Guildford, United Kingdom, for esophageal adenocarcinoma, between April 2009 and March 2020 were identified through analysis of a retrospectively collected database. Formalin fixed paraffin embedded (FFPE) tissue was retrieved for multispectral immunohistochemical analysis. Adjacent normal and tumour tissues were stained with primary antibodies for CD68, CD57, CD8, CD4, FoxP3, Granzyme B, PDL1 and pancytokeratin. Cell populations and spatial relationships were analysed using the Phenoimager HT (Akoya Biosciences) and QuPath.³

Results A total of 44 patients were identified. Significantly increased populations in tumours compared to normal tissue were seen for CD68⁺ (p<0.0001), FoxP3⁺ (p=0.0001) and PDL1⁺ (p<0.0001) cells. Geographical distribution analysis of these cells showed that the increases seen were mainly in the stromal compartment of the invasive margin of the tumour rather than the tumour core. Spatial relationship analysis demonstrated a survival benefit for those that had an increased median distance from tumour cells (PanCK⁺ (p=0.002)) CD8⁺ (p=0.0469) or CD4⁺ (p<0.0001) cells to CD68⁺ cells.

Conclusions Our results demonstrate that the immune tumour microenvironment of EAC appears to be an immunosuppressive phenotype. Increases in cell types associated with a pro-tumour microenvironment but no significant alteration in cytotoxic cell phenotypes (CD8⁺, CD57⁺, Granzyme B⁺) suggests that in order to improve response rates in EAC, immunotherapeutic strategies need to focus on decreasing immunosuppressive cells, as well as recruiting cytotoxic cells into the tumour microenvironment. Further works needs to be undertaken to fully understand the phenotype of macrophages seen in the TME of EAC.

REFERENCES

1. Pennathur A, Gibson MK, Jobe BA, Luketich JD. Oesophageal carcinoma. *The Lancet*. 2013;**381**(9864):400–12
2. Kelly RJ, Ajani JA, Kuzdzal J, Zander T, Van Cutsem E, Piessen G, et al. Adjuvant Nivolumab in Resected Esophageal or Gastroesophageal Junction Cancer. *New England Journal of Medicine*. 2021;**384**(13):1191–203.
3. Bankhead P, Loughrey MB, Fernández JA, et al. QuPath: Open source software for digital pathology image analysis. *Sci Rep*. 2017;**7**(1):16878.

Ethics Approval Formalin fixed paraffin embedded (FFPE) tissue was retrieved for immunohistochemical analysis with ethical approval (ethical reference 19/NS/0196, IRAS 270878).

<http://dx.doi.org/10.1136/jitc-2022-SITC2022.0966>

967

UNFAVORABLE NEOANTIGEN ARCHITECTURES BLUNT ANTI-TUMOR T CELL RESPONSES IN A MOUSE MODEL OF LUNG ADENOCARCINOMA

Malte Roerden*, Kim Nguyen, Nory Klop-Packel, Christopher Copeland, Nishant Singh, Michael Birnbaum, Stefani Spranger. *Massachusetts Institute of Technology, Cambridge, MA, United States*

Background Intra-tumoral heterogeneity (ITH) can limit effective anti-tumor immune responses despite the presence of immunogenic neoantigens. Yet, there is little mechanistic insight into how ITH blunts anti-tumor T cell responses or how clonal and sub-clonal neoantigens define immunologically unfavorable neoantigen architectures, preventing the rational design of neoantigen-targeting immunotherapy approaches for heterogeneous tumors.

Methods Using lentiviral transduction, we expressed single or multiple neoantigens with different levels of immunogenicity in a transplantable, syngeneic mouse model of lung adenocarcinoma (driven by an oncogenic Kras^{G12D} mutation and a deletion of p53). Modeling ITH-associated clonal and sub-clonal neoantigen expression, we systematically analyzed the impact of neoantigen architectures on neoantigen-specific T cell responses and overall immune-mediated tumor control.

Results Clonal co-expression of multiple neoantigens by tumor cells had distinct, converse effects on neoantigen-specific T cell responses dependent on neoantigen immunogenicity. Clonal expression of a poorly immunogenic (weak) neoantigen together with a highly immunogenic (strong) neoantigen, resulted in stronger T cell responses toward both antigens. The synergistic effect extended to increased neoantigen-specific in-vivo killing capacity and improved tumor control. In contrast, clonal co-expression of multiple strong neoantigens had detrimental effects on neoantigen-specific T cell responses, with immunogenic competition weakening the response against each individual neoantigen. Analysis of cross-presenting dendritic cells (cDC1) in the tumor-draining lymph node implicated differential T cell priming as a pivotal mechanism for these converse effects. When modeling sub-clonal tumors, the observed synergistic effects on T cell responses were less profound. Expression of multiple strong neoantigens on the other hand continued to impair anti-tumor immunity. Unfavorable neoantigen architectures were able to hinder immune-mediated tumor control even in tumors with a highly immunogenic clonal neoantigen trunk.

Conclusions Neoantigen architecture and ITH can be beneficial or detrimental for T cell responses. In tumors with high ITH, synergistic effects are reduced while detrimental effects may persist, providing a rationale for the higher immunogenicity of clonal tumors compared to their sub-clonal counterparts. These findings have strong implications for the design of immunotherapy approaches, including but not limited to cancer vaccines.

Acknowledgements This work was supported by a Postdoctoral Fellowship by the German Research Foundation (RO 6575/1-1).

Ethics Approval All mouse experiments were approved by MIT's Committee on Animal Care (CAC) – DHHS Animal Welfare Assurance # D16-00078

<http://dx.doi.org/10.1136/jitc-2022-SITC2022.0967>

968

IMPROVED ANTITUMORAL ACTIVITY OF ANTIGEN-SPECIFIC CD8+T CELLS IN COMPARISON TO UNSPECIFIC ACTIVATED CD8+T CELLS IN A 2D T CELL KILLING ASSAY TARGETING HER2+ BREAST CANCER

Ina Rohleff, Matthias Bleisch, Kanstantsin Lashuk, Julia Schueler*. *Charles River Laboratories, Freiburg, Germany*

Background Breast cancer is one of the leading causes of death in women worldwide. Hence, it is important to develop and improve (immuno)therapies for breast cancer patients. Adoptive T-cell therapy with autologous CD8⁺T cells is a promising method that has already succeeded in melanoma patients. Unfortunately, there is almost no information about the use in breast cancer patients.

Methods We developed an in vitro protocol to generate antigen-specific CD8⁺T cells by priming on the HER2+ breast cancer cell line JIMT-1. Subsequently, these primed CD8⁺T cells were tested in a 2D immune cell killing assay in a life cell imaging device in combination with an endpoint viability assay. The activity was compared with unspecific CD8⁺T cells activated by phytohemagglutinin (PHA) or α CD2/ α CD3/ α CD28 beads. All T cells were tested as monotherapy and in combination with pembrolizumab (anti-PD1 antibody).

Results The antigen specific CD8+T cells displayed a significantly improved killing potential of JIMT-1 cells compared to unspecifically activated or non-activated CD8+T cells. Along these lines, those cells showed the highest TNF-alpha secretion and expression of CD69 (determined by flow cytometry, FC) among all T cell lines. The use of complete peripheral blood monocytes (PBMC) instead of isolated CD8+T cells did not influence the activity against JIMT-1 significantly. Combination treatment with pembrolizumab did not increase the antitumoral activity, which was in line with the fact that PD-1 expression did not increase across the different settings. Testing of different donors revealed a donor dependent degree of killing, however in all donors the activity pattern was the same with antigen specific CD8+T cells being the most active. A direct comparison of fresh vs frozen immune cells from the same donors indicated no significant differences in the killing activity of unspecifically activated CD8+T cells. However, there were substantial differences in antigen-specific immune cells: the killing potential of the freshly isolated immune cells was significantly higher than of the frozen.

Conclusions In summary, we have developed a protocol to produce antigen-specific tumor-infiltrating CD8⁺T cells primed to the heterologous JIMT-1 breast cancer cell line. The antigen-specific CD8⁺T cells showed an increased killing potential over non-specific CD8⁺T cells. The 2D immune cell killing assay proved to be robust and amendable for mid throughput screening. The impact of donor variability and fresh vs frozen immune cells must be further evaluated. In the future, this assay will be used to screen novel drugs in combination with antigen-specific CD8⁺T cells to select the most promising candidates.

<http://dx.doi.org/10.1136/jitc-2022-SITC2022.0968>

969

NEXT-GENERATION IMMUNOTHERAPY USING PATIENT-DERIVED APC

Zhen Bian*, Lei Shi, Harry Stylli, Yuan Liu, Jane Zen. *Karnelian X, Inc, Atlanta, GA, United States*

Background Immune cell-based therapies with monocytes-derived macrophages and/or dendritic cells (DC), both phagocytic antigen-presenting cells (APCs), have arisen to be a powerful branch of immunotherapy against cancer. The promises of phagocytic APCs are their abilities to not only initiate phagocytosis towards cancer cells (to “eat off” tumor) but also, more importantly, to mediate antigen presentation to activate tumor-specific adaptive immunity, including tumoricidal T cells and long-lasting anticancer antibodies. However, the absence of technology that robustly drives monocytes from cancer patients to differentiate into proinflammatory DC/macrophage-like, effective APCs hinder the clinical application of APC therapy.

Results We through a proprietary process created a unique cellular agent (termed Karnelian X) that robustly differentiate monocytes from cancer patients (cancer monocytes, cMo) to be potent antigen presenting cells (termed kAPC) that have profoundly enhanced phagocytic capability and, most importantly, antigen presentation machinery, resulting in enhanced uptake and presentation of tumor neoantigens that activate tumor-specific CD4 and CD8 T cells derived from patients TIL (tumor-infiltrating lymphocytes) or the patients peripheral T cells. The expanded tumor-specific CD8 T cells are highly tumoricidal demonstrated in both murine and human tumors, whereas the CD4 T cells contribute memory and supports that create a favorable environment for CD8 T cell, NK cell and other anticancer activation and expansion.

Conclusions We believe kAPC and Neo-T are novel drug vectors with unique features.

Ethics Approval All experiments using animals and procedures of animal care and handling were carried out following protocols approved by the Institutional Animal Care and Use Committee (IACUC) of the T3 lab at the Georgia Institute of Technology. Patient and healthy donor's peripheral blood mononuclear (PBMC) were provided by the Cooperative Human Tissue Network or purchased from StemCell Technology. All of the samples were anonymized

http://dx.doi.org/10.1136/jitc-2022-SITC2022_0969

970 EXHAUSTED T CELLS ARE CHARACTERIZED BY INAPPROPRIATE LIPID ACCUMULATION

<http://dx.doi.org/10.1136/jitc-2022-SITC2022.0970>

¹Kellie Spahr*, ²Nicole Scharping, ¹Greg Delgoffe. ¹University of Pittsburgh, Pittsburgh, PA, United States; ²University of California – San Diego, San Diego, CA, United States

Background The efficacy of immunotherapy depends on the presence and persistence of functional immune cells within the tumor. While tumor-specific T cells can be activated and infiltrate the tumor microenvironment, they are quickly rendered dysfunctional by the combination of chronic antigen stimulation, hypoxia, and nutrient stress that creates a uniquely immune-suppressive environment. Thus, T cell dysfunction remains a significant hurdle for immunotherapeutic success. We have shown T cell exhaustion and metabolic dysfunction are driven by mitochondrial stress.¹ These features evoke an image of weak, starving T cells that are unable to sufficiently fuel their effector function. However, we and others have observed that CD8+ T cells accumulate large lipid stores as they progress towards exhaustion.² What remains unclear is whether lipid accumulation in these cells contributes to their dysfunction or represents an untapped source of carbon that may be the key to their reinvigoration.

Methods Using an *in vitro* model of T cell exhaustion developed in our lab, we evaluated the effect of perturbing lipid metabolism by inhibiting synthesis or promoting catabolism.³ We also used CRISPR-Cas9 deletion of the mitochondrial citrate transporter, SLC25A1, to assess the effect of perturbing lipid synthesis on tumor-infiltrating T cell exhaustion. Cognitively mismatched SLC25A1 deficient and control OT-I T cells were co-transferred into mice bearing ovalbumin-expressing B16F10 melanoma tumors. We immunophenotyped CD8+ T cells for markers of terminal exhaustion, cytokine production, and lipid accumulation.

Results Here we sought to define the role lipid metabolism plays in the progression of CD8+ T cell exhaustion. Inhibition of citrate transport from the mitochondria via SLC25A1 in CD8+ T cells resulted in reduced lipid accumulation and expression of inhibitory receptors, PD-1 and Tim-3, known to be upregulated on exhausted T cells. We also observed increased production of inflammatory cytokines IFN γ and TNF in response to TCR restimulation after chronic antigen exposure.

Conclusions Taken together, our results indicate a role for mitochondrial citrate flux in the accumulation of cytosolic lipids and progression of CD8+ T cell exhaustion. We propose that as exhausted T cells experience mitochondrial stress and perform less oxidative phosphorylation, they shuttle excess citrate to the cytosol where it fuels production of acetyl-CoA and de novo fatty acid synthesis. This pathway may be targeted to delay exhaustion or reinvigorate exhausted T cells within tumors. These data provide new insight into the mechanisms of T cell exhaustion and may inform future immunotherapeutic development.

REFERENCES

1. Scharping NE, Rivadeneira DB, Menk AV, Vignali PDA, Ford BR, Rittenhouse NL, *et al.* Mitochondrial stress induced by continuous stimulation under hypoxia rapidly drives T cell exhaustion. *Nat Immunol.* 2021;**22**:205–15.
2. Manzo T, Prentice BM, Anderson KG, Raman A, Schalck A, Codreanu GS, *et al.* Accumulation of long-chain fatty acids in the tumor microenvironment drives dysfunction in intrapancreatic CD8+ T cells. *J Exp Med.* 2020;217.
3. Scharping NE, Menk AV, Moreci RS, Whetstone RD, Dadey RE, Watkins SC, *et al.* The tumor microenvironment represses T cell mitochondrial biogenesis to drive intratumoral T cell metabolic insufficiency and dysfunction. *Immunity.* 2016;**45**:374–88.

971 **VISTA REGULATES THE DIFFERENTIATION AND FUNCTION OF MYELOID-DERIVED SUPPRESSOR CELLS**

¹Keman Zhang*, ²Amin Zekeri, ³Juan Dong, ²Sarah Stone, ²Li Wang. ¹Cleveland Clinic Foundation, Lerner Research Institute, Cleveland, OH, United States; ²Lerner Research Institute, Cleveland, OH, United States; ³Hong Kong-Shenzhen Hospital, Shenzhen, China

Background Previous studies show that VISTA is a critical immune-checkpoint protein controlling the maturation of myeloid antigen-presenting cells in response to TLR signaling that in turn stimulates T cell activation. The role of VISTA in the differentiation and function of myeloid-derived suppressor cells (MDSCs) remains incompletely understood.

Methods Wild type and VISTA knockout mouse bone marrow monocytes were purified and myeloid-derived suppressor cells (MDSC) were cultured and purified. Total RNAs were isolated and cDNAs were made to examine the genes expression. Whole cell lysates were prepared and proteins level were determined by Western blot. MDSC cells were analysed in tumor models by flow cytometry.

Results Here, by studying BM-derived MDSCs and tumor-associated MDSCs, we have discovered that ablation of VISTA significantly reduces the expression of Arg1 and iNOS, as well as diminishing the inhibitory effects of MDSC on T cell activation. Mechanistically, VISTA directly controls the signaling of monocytes in response to inflammatory stimuli including GM-CSF and IL-6.

Conclusions Our studies uncover VISTA as an important regulator of MDSC differentiation and suggest that targeting VISTA may alleviate MDSC-mediated immunosuppression.

<http://dx.doi.org/10.1136/jitc-2022-SITC2022.0971>

972

ENRICHMENT OF ATYPICAL MEMORY DOUBLE NEGATIVE (CD27⁻ IgD⁻) TUMOUR INFILTRATING B CELLS FOLLOWING NEOADJUVANT CHEMOTHERAPY FOR EARLY-STAGE BREAST CANCER

¹Esme Carpenter*, ²Thanussuyah Alaguthurai, ²Farhana Hossain, ¹Rosalind Graham, ¹Helen Kakkassery, ¹Sean Keane, ¹Sheeba Irshad. ¹King's College London, London, UK; ²Guy's and St Thomas NHS Foundation Trust, London, UK

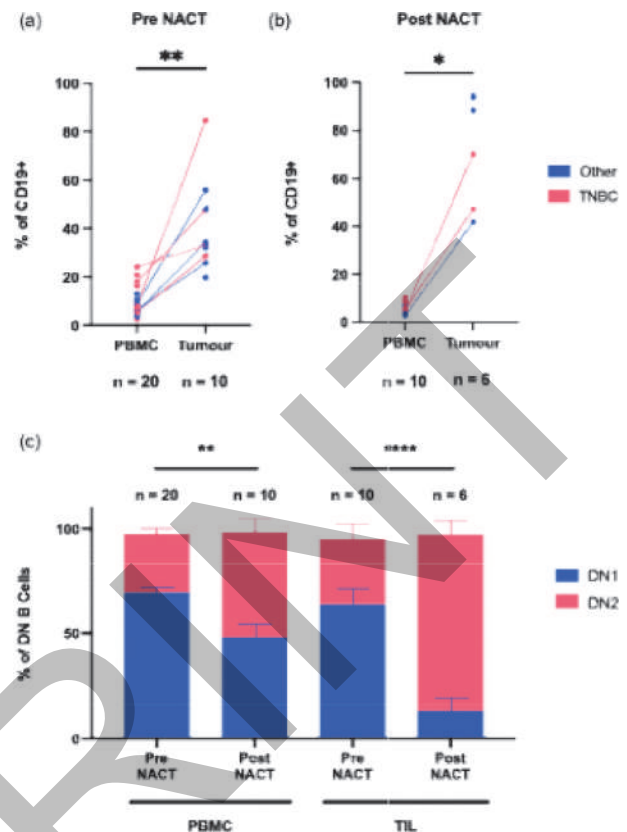
Background Humoral immune responses have previously been associated with improved outcomes, with B cell infiltrates able to independently predict pathologic complete response to neoadjuvant chemotherapy (NACT). B cells represent a diverse population of cells and the complex interplay between specific B cell subsets in the context of chemotherapy treated breast cancers remains unclear. Here, we investigate the dynamic changes in the B cell immune landscape before and after NACT treatment across different breast cancer subtypes.

Methods Treatment naïve, mid-treatment and post-NACT breast tumour tissue samples were dissociated into single cells, stained with two panels of B cell-specific antibodies recognising a total of 24 target proteins, and analysed by flow cytometry. In addition, PBMC before and after NACT were also profiled. B cell subsets were classified as either naïve (CD27⁻IgD⁺), class-switched memory (CD27⁺IgD⁻), unswitched memory (CD27⁺IgD⁺) or double negative (DN) (CD27⁻IgD⁻). DN B cells were further characterised into DN1 (CXCR5⁺CD21⁺) and DN2 (CXCR5⁻CD21⁻) subsets. *In vitro* co-cultures of breast cancer cell line spheroid and PBMC were carried out.

Results In both treatment naïve and chemotherapy treated samples, we observed a significant expansion in the DN B cell population within the tumour microenvironment (TME) compared to the periphery. DN B cells represented on average 40.96% of B cells in treatment naïve tumours vs 9.48% in PBMC ($p < 0.0001$), and 71.80% vs 6.34% of B cells in post-NACT tumour vs PBMC samples respectively ($p < 0.05$) (figure 1). Interestingly, in treatment naïve PBMC and tumour tissue samples, the largest proportion of the DN subset consisted of DN1 cells, 69.35% and 64.11% respectively. In contrast, following NACT, DN2 cells constituted the majority of the DN population both within the TME (86.30%) and in the periphery (50.44%) (figure 1). Although the specific functions of these B cell subsets remain unclassified, deeper phenotyping suggests DN1 cells more closely resemble the phenotype of class-switched memory cells, whilst DN2 cells are thought to have antibody-secreting properties and more closely resemble the plasmablast phenotype. scRNA sequencing of B cells pre and post NACT is currently underway.

Conclusions To our knowledge, this work is the first to identify an expanded population of DN B cells in breast tumour tissue and highlights the requirement for further investigation into these cells to decipher their role in the context of chemotherapy treatment and resistance in breast cancer.

Ethics Approval Written informed consent was obtained from all individuals in accordance with the Declaration of Helsinki under the following research ethics committee; London-Chelsea approved study (REC ID 13/LO/1248).



Abstract 972 Figure 1 Expansion of DN B cells in early breast cancers

The DN B cell population is elevated in the TME of breast cancer patients compared to the periphery, in both treatment naïve (a) and post-NACT (b) samples. Significance was assessed using paired t test with * $p < 0.05$. (c) There is a phenotypic change in DN B cells in the TME upon chemotherapy treatment from predominantly DN1 cells pre-NACT to predominantly DN2 cells post-NACT. Significance was assessed using 2way ANOVA with * $p < 0.05$

<http://dx.doi.org/10.1136/jitc-2022-SITC2022.0972>

973 **EXTRAFOLLICULAR EXPANSION AND DIFFERENTIATION OF B CELLS DRIVES ANTI-TUMOR RESPONSES IN METASTATIC CANCER**

¹Noor Nader*, ²Dongyan Liu, ¹Hye Mi Kim, ¹Ayana Ruffin, ¹Sheryl Kunning, ¹Xiaron Zhang, ¹Daniel Dunlap, ¹Roy Semaan, ¹Rajeev Dhupar, ¹Adam Soloff, ¹Tullia Bruno. ¹University of Pittsburgh, Pittsburgh, PA, United States; ²Tsinghua University, Beijing, China

Background Recent studies have demonstrated that B cell infiltration in patients with primary tumors is associated with increased survival and superior response to immune checkpoint blockade (ICB). Further, B cells play a significant role in the tumor microenvironment, such as the production of tumor-specific antibodies, antigen presentation, modulation of the cellular immune response by the production of specific cytokines, and formation of tertiary lymphoid structures (TLS). One knowledge gap in the field is determining how B cells function within microenvironments that don't have TLS, specifically in metastatic spaces that occur because of a primary tumor. Malignant pleural effusions (MPEs) are metastatic microenvironments that are marked by the accumulation of interstitial fluid and the infiltration of tumor and immune cells into the pleural space of the lung of patients with advanced disease. Currently, there is no treatment for patients with MPE; thus, there is a need to improve our understanding of the complete MPE microenvironment. B cells highly infiltrate MPE, and antibody accumulation is significant in this space. Thus, our studies have geared to functionally interrogate MPE B cells to better understand how to target B cells in metastatic disease.

Methods We aimed to assess B cell subsets in MPEs and correlated these subsets with the initial primary tumors of origin for patients with benign and MPE fluids. Specifically, we compared the infiltration of memory and naïve B cells within these patients, antibody isotype and production in the paired fluids, antigen specificity of the antibodies, and differentiation of B cells in the presence or absence of MPE fluid. When cellularly possible, we also interrogated antigen presentation by B cells subsets to CD4+ and CD8+ T cells.

Results We observed increased levels of naïve B cells in MPE compared to benign fluids and a high level of double negative 3 (DN3) memory B cells, suggesting potential extrafollicular B cell differentiation in the MPE microenvironment. Furthermore, we quantified tumor antigen-specific IgG antibodies in MPE fluid and matched plasma reactive to extracellular antigens of breast and lung tumor cell lines. Moreover, we determined that MPE-associated B cells are often superior to professional antigen-presenting cells (APCs) at educating CD4 + T cells.

Conclusions Understating B cell composition and function in metastatic spaces is critical for engineering future immunotherapies. Here we highlight B cells in metastasis as a potential immunotherapeutic target given increased extrafollicular B cell expansion and differentiation into tumor antigen-specific plasmablast in MPE.

<http://dx.doi.org/10.1136/jitc-2022-SITC2022.0973>

974

REGULATORY B CELLS PRODUCING IL-10 ARE INCREASED IN HUMAN TUMOUR DRAINING LYMPH NODES

¹Krzysztof Piersiala*, ²Pedro Farrajota Neves da Silva, ¹Vilma Lagebro, ¹Gregori Margolin, ¹Susanna Kumlien Georén, ¹Lars Olaf Cardell. ¹Karolinska Institute, Stockholm, Sweden; ²Karolinska University Hospital, Stockholm, Sweden

Background The contribution of different immune cell subsets, especially T cells, in anti-tumour immune response is well established. In contrast to T cells, the anti-tumour contribution of B cells has been scarcely investigated. B-cells are often overlooked, even though they are important players in a fully-integrated immune response and constitute a substantial fraction of tumour draining lymph nodes (TDLNs) known also as Sentinel Nodes.

Methods Samples including TDLNs, non-TDLNs and metastatic lymph nodes (LNs) from 23 patients with oral squamous cell carcinoma (OSCC) were analyzed by multicolour flow cytometry with a focus on B cells populations.

Results TDLNs were characterized by a significantly higher proportion of B cells compared with nTDLNs ($p=0,0112$). TDLNs associated B cells contained high percentages of naïve activated B cells, in contrary to nTDLNs which contained significantly higher percentages of memory B cells. Patients having metastases in TDLNs showed a significantly higher presence of B regulatory cells among TDLNs associated B cells ($p=0,0008$) compared with N0 patients. B cells derived from TDLNs were characterized by significantly higher expression of an immunosuppressive cytokine – IL-10 compared with non-TDLNs ($p=0,0077$).

Conclusions Our data indicate that B cells in human TDLNs differ from B cells in nTDLNs and exhibit more naïve and immunosuppressive phenotypes. We identified a high accumulation of regulatory B cells within TDLNs which may be a potential obstacle in achieving response to novel cancer immunotherapies in HNSCC. Elevated levels of regulatory B cells in TDLNs are associated with the advancement of the disease. Detailed knowledge of pre-existing antitumor immune response in human TDLNs is needed in order to fully understand the mode of action of ICI agents and potentially solve tumour and host-dependent mechanisms leading to resistance towards ICIs.

Ethics Approval All procedures performed in studies involving human participants were in accordance with the ethical standards of the institutional and/or national research committee and with the 1964 Helsinki declaration and its later amendments or comparable ethical standards. Informed consent was obtained from all individual participants included in the study. Regional Ethics Committee Approval: 2019-03518.

<http://dx.doi.org/10.1136/jitc-2022-SITC2022.0974>

975

CHARACTERIZATION OF SIGNALING AND METABOLIC DIFFERENCES BETWEEN $\gamma\delta$ AND $\alpha\beta$ CAR T CELLS

Xiomar Bustos*, Daniel Abate-Daga, Leticia Tordesillas. *H. Lee Moffitt Cancer Center & Research, Tampa, FL, United States*

of Laboratory Animals manual published by the National Institutes of Health.

<http://dx.doi.org/10.1136/jitc-2022-SITC2022.0975>

Background $\gamma\delta$ T cell-based immunotherapies have emerged as an alternative to the traditional $\alpha\beta$ T cell-based products. For example, our group has shown that $\gamma\delta$ CAR T cells can reduce tumor burden and mitigate tumor-induced bone deterioration in a preclinical model of bone metastatic prostate cancer. In the present study, we investigated the signaling events triggered by a second-generation CAR (originally designed for $\alpha\beta$ T cells) in $\gamma\delta$ T cells, to test the hypothesis that CAR-induced signaling varies depending on the T cell subset. The ultimate goal of our study is to gain mechanistic insight into the biology of $\gamma\delta$ T cells and to inform future CAR design for improved $\gamma\delta$ -based adoptive cell therapies.

Methods We designed our analysis as a side-by-side comparison of phosphorylation events, resulting from CAR activation, between $\gamma\delta$ and $\alpha\beta$ T cells. These were expanded in parallel from a healthy donor and transduced with a retroviral vector (MSGV1) to express a second-generation anti-PSCA CAR (PSCA-8t28z). CAR-T cells were then cocultured independently with metabolically labelled C4-2B-PSCA tumor cells, for 1 hour, and protein phosphorylation was quantified using Liquid Chromatography–Tandem Mass Spectrometry (LC/MS-MS). Statistically significant differences in phosphorylation were defined using a Welch's *t*-test (fold-change ≥ 1.5 and *p*-value < 0.05). Using Qiagen's Ingenuity Pathway Analysis software, we identified canonical pathways that were significantly over-represented in the population of proteins that displayed differential phosphorylation in $\gamma\delta$ CAR T cells relative to $\alpha\beta$. We used the SeaHorse XF kits for Glycolytic Rate Assay and T Cell Metabolic Profiling for functional characterization of the metabolic properties of CAR-T cells. Finally, flow cytometry was used to analyze Glut-1 expression (anti-Glut1, clone 202915), glucose intake (2NBDG), mitochondrial mass (Mito-Tracker Green), and mitochondrial membrane polarization (TMRE).

Results We identified 323 phosphorylation events that were differentially abundant between T cell subsets. Within this group, glycolysis and gluconeogenesis were within the top overrepresented canonical pathways. Stimulated $\gamma\delta$ T cells showed significantly lower glycolytic rate compared to $\alpha\beta$. CAR expression was accompanied by higher glycolytic rate and expression of Glut-1 receptor in both T-cell types. Finally, oxidative phosphorylation (OXPHOS) was lower in $\gamma\delta$ CAR T cells, potentially related to their also lower mitochondrial mass.

Conclusions CAR-induced signaling varies among T cell subsets, and $\gamma\delta$ T cells display lower glycolytic and OXPHOS rates upon activation. Ongoing efforts are focused on delineating molecular causes and functional consequences of the metabolic differences between $\alpha\beta$ and $\gamma\delta$ T cells.

Acknowledgements This work has been supported in part by the Bioinformatics, the Proteomics, and the Flow Cytometry Core Facilities at the Moffitt Cancer Center, an NCI designated Comprehensive Cancer Center (P30-CA076292). We would also like to thank Dr. Paulo Rodriguez, and Dr. Gina DeNicola for their input in the analysis of the results.

Ethics Approval All animal experiments were performed under University of South Florida IACUC approval (R1762; R7429) and in accordance with the Guidelines for the Care and Use

976 **T-CELL METABOLIC ACTIVITY IS IMPACTED BY THE NUTRIENT COMPOSITION WITHIN THE TUMOR MICROENVIRONMENT**

Jesse Bucksot*, Dorys Lopez-Ramos, Tushar Pandey, Anuja Antony, Joseph Peterson, Daniel Cook. *SimBioSys, Inc., Chicago, IL, United States*

Background Immunotherapy use is increasing across cancer types, however, how the nutrient microenvironment affects immune cell activity is not fully understood.¹ We addressed this challenge using a novel framework combining nutrient distributions within a tumor, single cell RNA-seq data, and genome-scale metabolic modeling² to understand how immune cell cytotoxic potential varies within tumor microenvironments.

Methods We constructed 3D nutrient composition atlases of over 1200 breast cancer tumors using the SimBioSys Tumor-Scope software. We then constructed a genome-scale metabolic model of tumor infiltrating T-cells based on single cell RNA-sequencing data from over 5000 single T-cells from breast cancer patients. We simulated this T-cell metabolic model across the range of nutrient compositions present in our tumor atlases to understand how nutrient availability affects the cytotoxic potential of T-cells.

Results Our results demonstrated that the local nutrient composition has a dramatic impact on T cell functionality, with fundamental cellular behaviors being significantly impaired by a reduction in key nutrients such as glucose and oxygen. Additionally, the degree of impairment varies between the various types of T cells. For example, proliferative T cells are relatively insensitive to hypoxia, but very sensitive to reduced glucose, which may be related to the increase in IO response that we observe in tumors with a greater degree of hypoxia.

Conclusions Overall, we found that the nutrient composition of the tumor microenvironment has a strong influence on T-cell activity, especially in hypoxic tumor regions.

REFERENCES

1. Makowski L, Chaib M, Rathmell JC. Immunometabolism: From basic mechanisms to translation. *Immunol Rev.* 2020;**295**(1):5–14. doi:10.1111/imr.12858
2. Harcombe WR, Riehl WJ, Dukovski I, et al. Metabolic resource allocation in individual microbes determines ecosystem interactions and spatial dynamics. *Cell Rep.* 2014;**7**(4):1104–1115. doi:10.1016/j.celrep.2014.03.070

<http://dx.doi.org/10.1136/jitc-2022-SITC2022.0976>

977

HIGHLY CYTOTOXIC RESILIENT CD8⁺ T CELLS AVOID EXHAUSTION BY LOWERING ROS THROUGH ME1 UPREGULATION

¹Joanina Gicobi*, ¹Haidong Dong, ²Cindy Liu. ¹Mayo Clinic Graduate School of Biomedical Sciences, Rochester, MN, United States; ²Department of Urology, Mayo Clinic, Rochester, MN, United States

Background Cytotoxic T cells are indispensable in protecting the organism from malignant disease. Even though they are prone to be exhausted in patients with large tumor burden, some of them can regain their antitumor activity upon immune checkpoint inhibitor (ICI) therapy and reject large tumors or metastatic malignancies. Our knowledge to these “rebound” effector T cells is limited. Recently, resilient T cells have been perceived to explain the presence of highly cytotoxic T cells that are less exhausted and rebound in responses to ICI therapy, however the phenotypic and functional characters of resilient T cells have not been clearly defined.

Methods CD8⁺ T cells were isolated from PBMCs and stained with TMRM. They were then sorted into Low and High $\Delta\psi_m$ cells. Following activation with or without other experimentation, we conducted killing assays, metabolic assays, flow cytometry, Bulk RNA sequencing, western blot, qPCR etc.

Results We found ICI-therapy responsive CX3CR1⁺ CD8⁺ T cells are endowed with low mitochondrial potential ($\Delta\psi_m$). The frequency of CX3CR1⁺ CD8⁺ T cells with low $\Delta\psi_m$ increased in patients with metastatic malignancies who have better clinical outcomes in responses to ICI therapy and radiation therapy. Further characterization of CD8⁺ T cells with low $\Delta\psi_m$ revealed that they are highly cytotoxic and produce less ROS (reactive oxygen species) but express more ME1 (malic enzyme 1). Interestingly, overexpression of ME1 reduced ROS in CD8⁺ T cells and augmented tumoricidal activity of CD8⁺ T cells. Importantly, enhanced expression of ME1 in T cells isolated from patients improved cytotoxic T cell responses to ICI treatment in vitro.

Conclusions Our study suggests that not all highly cytotoxic CD8⁺ T cells are exhausted but some of them are functionally resilient in patients with advanced cancers. Modification of ME1 expression in T cells could be a new method to avoid T cell exhaustion and to improve the efficacy of cancer immunotherapy.

Ethics Approval Study approval. “Healthy Donor” human blood leukocytes were acquired from anonymous donors who had consented for blood donation at the Blood Transfusion Center at Mayo Clinic. All donors and patients provided signed informed written consent; the study was approved by the Mayo Clinic Rochester IRB and was conducted according to Declaration of Helsinki principles.

<http://dx.doi.org/10.1136/jitc-2022-SITC2022.0977>

978 **DENDRITIC CELL-INTRINSIC PTPN22 NEGATIVELY REGULATES ANTI-TUMOR IMMUNITY**

Santiago Acero-Bedoya*, Thomas Gajewski, Emily Higgs. *University of Chicago, Chicago, IL, United States*

Background Checkpoint blockade immunotherapies have revolutionized cancer treatment, yet only a subset of patients benefit. Individuals with a loss-of-function single nucleotide polymorphism in the gene encoding PTPN22 are at increased risk for autoimmune disease and display a lower incidence of certain cancers. Studies in PTPN22 knockout (KO) mice have established it as a negative regulator of T cell responses in autoimmune and cancer models. However, these studies have not defined the cell lineage-intrinsic roles of PTPN22 in distinct immune cell compartments, and the potential role of PTPN22 in dendritic cells remains undefined.

Methods We developed a novel dendritic cell (DC) PTPN22 conditional KO (cKO) mouse model that enables specific deletion in CD11c⁺ cells. Using the B16.SIY melanoma model, tumor growth and immune profiles of tumors and tumor-draining lymph nodes (tdLNs) were analyzed. CD8⁺ T cells were depleted to establish their necessity using an anti-CD8b monoclonal antibody. Antigen-specific T cell priming was tested by IFN- γ ELISpot analysis on the spleens of tumor-bearing mice. Lastly, the MC38.SIY cell line was used to establish the applicability in different cancer models.

Results Deletion of PTPN22 in DCs resulted in augmented tumor control. At endpoint, total CD8⁺ T cells, but not CD4⁺ T cells or Tregs, were increased in the tumors of CD11c⁺ PTPN22 cKO mice. Moreover, CD8⁺ T cells demonstrated increased activation and memory markers at day 10 in the tdLN and in day 27 tumor-infiltrating lymphocytes. Depleting CD8⁺ T cells eliminated the tumor growth control in this model, suggesting a reliance on the DC-CD8⁺ T cell axis. Accordingly, day 7 tumor-bearing mice revealed an increased frequency of IFN- γ -producing T cells in the presence of tumor antigen SIY, indicating improved CD8⁺ T cell priming. Further, spectral analysis of tumor antigen-specific T cells in the tdLN also showed a significant increase of CD8⁺ SIY⁺ T cells displaying elevated activation and memory markers. Analysis of DCs in the tdLN similarly revealed an overall increase attributed to an increase of CD103⁺, but not CD11b⁺, DCs displaying increased activation and proliferation markers. Together, the number of tumor-infiltrating CD8⁺ T cells and CD103⁺ DCs correlated with decreased tumor volumes. Lastly, PTPN22 cKO mice similarly showed greater tumor control of the colon cancer line MC38.SIY.

Conclusions We show that deletion of PTPN22 in DCs is sufficient to drive a tumor antigen-specific T cell response resulting in enhanced tumor control. This work highlights the potential to modulate anti-tumor immunity through the manipulation of DC signaling.

Ethics Approval This study obtained ethics approval by the Institutional Animal Care and Use Committee (IACUC) at the University of Chicago as outlined in the animal protocol #71621.

<http://dx.doi.org/10.1136/jitc-2022-SITC2022.0978>

979

COMPOUND SCREEN IDENTIFIES INHIBITOR OF APOPTOSIS PROTEINS (IAP) ANTAGONIST AS AN INDUCER OF T CELL PROLIFERATION AFTER CROSS-PRESENTATION BY DENDRITIC CELLS

Esmee Hoefsmit*, Paula van Royen, Disha Rao, Johanna Stunnenberg, Petros Dimitriadis, Cor Liefink, Ben Morris, Elisa Rozeman, Irene Reijers, Ruben Lacroix, Huma Shehwana, Maarten Ligtenberg, Roderick Beijersbergen, Daniel Peeper, Christian Blank. *Netherlands Cancer Institute, Amsterdam, Netherlands*

Background Cross-presentation of tumor antigens by dendritic cells (DCs) is crucial to prime and (re-) stimulate CD8⁺ T cells. This process is important in initiating and maintaining an anti-tumor response. Previously, we found that tumor presence of conventional type 1 DCs (cDC1), a subtype that excels at cross-presentation, correlates with response to neoadjuvant immune checkpoint blockade (ICB) in melanoma. This led us to hypothesize that patients failing to respond to ICB could benefit from enhanced cross-presentation of tumor antigens.

Methods A cross-presentation assay to screen over 5,500 compounds for improvement of CD8⁺ T cell proliferation after cross-presentation of tumor antigens by DCs was established. For this purpose, bone marrow derived GM-CSF DCs were cultured in the presence of irradiated B16F10-OVA^{B2m^{-/-}} tumor cells, CpG ODN class B and naïve CTV-labelled CD8⁺T cells that have a TCR specificity for OVA₂₅₇₋₂₆₄ (SIINFEKL) in the context of H2-k^b (OT-I TCR). In this setting, tumor antigens (OVA) that have been processed into SIINFEKL peptide and are presented in the context of H2-k^b by the DCs can induce CD8⁺ t cell proliferation and activation.

Results A total 145 compounds were identified that significantly improved T cell proliferation after cross-presentation of tumor antigens by DCs. Subsequently, we selected compounds that also increased IFN-γ production. A total of 11 compounds were confirmed to significantly enhance CD8⁺ T cell proliferation and IFN-γ production. A particular strong effect was observed for AZD5582, an antagonist of inhibitor of apoptosis proteins (IAPs) cIAP1, cIAP2 and XIAP. AZD5582 treatment led to DC activation of the non-canonical nuclear factor kappa B (NF-κB) pathway, enhanced antigen import from endolysosomes into the cytosol and increased expression of genes involved in cross-presentation. Furthermore, it upregulated expression of CD80, CD86, MHC class II, CD70 and secretion of TNF by DCs. This enhanced DC activation and maturation program was observed also in tumor-bearing mice upon AZD5582 treatment, culminating into an increased frequency of systemic tumor antigen-specific CD8⁺ T cells.

Conclusions We identified several compounds that enhance T cell proliferation after cross-presentation. Addition of the identified AZD5582 to (combinations of) ICB might improve outcome in unfavorable patients.

Ethics Approval The protocol and amendments of the OpA-CIN-neo and PRADO trial were reviewed and approved by the appropriate review boards and ethics committees of each institute. All participating patients provided written informed consent before enrollment.

All animal procedures were approved by the Animal Welfare Committee of the Netherlands Cancer Institute, in accordance with institutional and national guidelines.

<http://dx.doi.org/10.1136/jitc-2022-SITC2022.0979>

980

IN-DEPTH CHARACTERIZATION OF CDC1 EX VIVO AND IN VITRO MODELS: DEVELOPMENT AND COMPARISON OF CONVENTIONAL DENDRITIC CELL CULTURE SYSTEMS FOR INDUSTRY

Anna Licht*, Tamera Ashworth, Laura L Goodfield, Hannah Gardner, Johanna Lahdenranta, Philip Brandish, Kevin McDonnell, Nicholas Keen. *Bicycle Therapeutics, Lexington, MA, United States*

Background Conventional dendritic cells (cDC) are innate immune cells specialized in antigen sampling and subsequent cross-presentation to immune cells, and are critical for an effective anti-tumor immune response. The relatively rare subset cDC type I (cDC1) has been associated with human cancer patient survival, and strategies aimed at increasing their abundance and activation in the tumor microenvironment (TME) are of interest. It is a challenge to use these rare cells in screening assays as they constitute less than 0.05% of cells in the blood and are difficult to isolate with high viability and purity.

Methods We compared two systems that generate a mixed culture containing cDC1 cells from human CD34+ hematopoietic stem cells (HSC) isolated from cord blood. In the first system, we developed a scalable in vitro differentiation method that expands and differentiates the CD34+ HSC to generate cDC1s over the course of 3.5 weeks. The second system utilized a humanized mouse model. Mice engineered to express human GM-CSF and IL-3 to support the myeloid compartment were engrafted with human CD34+ HSC and boosted twice with Flt3L-IgG. Femurs were taken at day 10 for bone marrow extraction and subsequent cDC1 culture.

Results The human CD34+ HSC and cytokine treatments in these methods yield an increase in number of cDC1 cells in a mixed cellular population. The cDC1 cells are phenotypically and functionally similar to those in the blood; they express high levels of CD141 and Clec9a, and respond to activating stimuli such as poly(I:C). The ex vivo cDC1 system using bone marrow from humanized mice is highly reproducible across laboratory operators and with multiple cord blood donors, and it is less laborious than the in vitro differentiation assay. A single operator can process 4 to 5 mouse femur pairs at one time to collect on average enough cells for 15 test compounds at a 5-pt dose curve with controls. Multicolor flow cytometry was used to further phenotype and assess functionality of other cell types present in the ex vivo culture.

Conclusions Both systems demonstrate that HSC-derived cDC1 cultures can be reliably generated with cDC1 phenotype and functionality, and may be used for screening assays in industry settings. The ex vivo system allows for a faster and higher throughput but requires supply of humanized mice.

<http://dx.doi.org/10.1136/jitc-2022-SITC2022.0980>

981 PERITUMORAL STROMAL REMODELING LICENSES CDC1 THROUGH CD40 TO ELICIT T-CELL INFLAMMATION

¹Athanasios Papadas*, ¹Alexander Cicala, ¹Alejandro Rizo, ²Chelsea Hope, ³Katerina Politi, ²Christian Capitini, ²Kristina Matkowskyj, ⁴Scott Abrams, ¹Fotis Asimakopoulos. ¹UCSD, San Diego, CA, United States; ²UW-Madison, Madison, WI, United States; ³Yale, New Haven, CT, United States; ⁴Roswell Park, Rochester, NY, United States

Ethics Approval The study was approved by UCSD IACUC #S19109.

<http://dx.doi.org/10.1136/jitc-2022-SITC2022.0981>

Background T-cell-inflamed tumor microenvironments (TME) are pre-requisite for immunotherapy efficacy; however, the drivers for promoting T cell priming and infiltration within the TME remain incompletely understood. Conventional type I dendritic cells (cDC1) are indispensable for anti-tumor immunity. Several key studies have documented the paradoxical localization of cDC1 within tumor stroma. We hypothesized that conserved provisional matrix signals emanating from peritumoral stroma remodeling play an unrecognized role in this paradox and license cDC1 to promote T-cell repriming and tumor entry.

Methods We performed multiplex IHC in human lung cancer biopsies using antibodies against anti-VCAN proteolysis neoepitope DPEAAE, cDC1 (XCR1⁺), CD8⁺ and CD4⁺ T cells. Multiparametric flow cytometry was used to characterize stroma-licensed cDC1. Therapeutic anti-PD1 antibodies were used in a preclinical model of lung cancer (LLC).

Results We found that in human T-cell inflamed cancers, even though T cells penetrated the tumor core, cDC1 remained confined within tumor-adjacent stroma recurrently demonstrating versican (VCAN) proteolysis, an extracellular matrix modification typically associated with provisional matrix remodeling in embryonic development and wound healing. VCAN proteolysis releases a bioactive N-terminal fragment, versikine. Using multi-parametric flow cytometry, we found that versikine-exposed cDC1, but not cDC2 or monocyte-derived (Mo)-DC, overexpressed CD40 whereas all three DC subtypes overexpressed PD-L1. Moreover, cDC1, but not other tumor DC subtypes, expanded in absolute numbers in versikine-replete tumors. Versikine sensitized refractory LLC tumors to anti-PD1 immunotherapy and produced a survival benefit in vivo, suggesting that versikine overcomes immune checkpoint inhibitor resistance. Human lung cancers demonstrated a predominant localization of CD4⁺ and CD8⁺ T cells within peritumoral stroma. Consistent with CD40-mediated cDC1 licensing models, we observed enhanced antigen-specific T cell responses using the model antigen OVA in versikine-replete TME.

Conclusions Peritumoral stroma has traditionally been viewed as an immune barrier. Our data provide an alternative view and demonstrate that peritumoral stroma mimicking embryonic or wound provisional matrix remodeling instead promotes cDC1 abundance and activation. "Stroma-licensed" cDC1 may represent a conserved homeostatic response against nascent tumors during immune surveillance ("elimination" and "equilibrium"). Progressive loss of stromal proteolytic remodeling (e. g., versikine loss) and transition into stromal fibrosis are associated with immunoediting "escape". Stroma-licensed cDC1 overexpress CD40 and localize near stromal CD4⁺ and CD8⁺ T cells, raising the possibility that CD4 T-cells may provide CD40L-CD40-mediated "help" in stromal locations. These data provide novel insights into the role of stroma in regulating the nature of the T-cell-inflamed TME and may permit optimized designs for T-cell penetration into solid tumors.

Acknowledgements Supported through grants R01CA252937 and R01CA230275 and the Robert J. Shillman Foundation.

982

CDC1 CELLS ARE REQUIRED TO SUSTAIN CD8 T CELL STEMNESS IN CANCER AND FOR THE SUCCESS AT THE ONSET OF VARIOUS IMMUNOTHERAPIES.

Alvaro Teijeira*, Carlos Luri, Saray Garasa, Assunta Cirella, Ignacio Melero. *CIMA, Universidad de Navarra, Pamplona, Spain*

Background cDC1 cells are a subset of antigen presenting cells highly specialized in cell-associated antigen crosspresentation.¹ The presence of this DC population in human cancer correlates with good patient prognosis and response to immunotherapy.² Mice that are ontogenically deficient in cDC1 or crosspresenting mechanisms fail to effectively prime antitumor immune responses and therefore show poor response to immunotherapy.³⁻⁶ The mechanisms by which cDC1 support immunity during immunotherapy mediated responses have not been well defined.

Methods Using XCR-1-DTR venus mice we were able to track and deplete at will cDC1 cells at different time points during immunotherapy. Tumor growth studies were performed with different types of immunotherapies (adoptive T cell transfer, anti-PD-1, anti-CD13 and anti-CTLA-4 mAbs). Flow cytometry and multiplex immunofluorescence were used to characterize CD8 T cell responses and intravital imaging was used to track the behavior of cDC1 and antitumor CD8 T cells.

Results The presence of cDC1 cells was an absolute requirement at the onset of immunotherapy for most of the therapies tested but once the first dose of immunotherapy their absence had lesser impact on the antitumor response. We observed that immunotherapy affected cDC1 migratory capacities and interaction with anti-tumor T cells and that cDC1 were important to maintain a pool of TCF7⁺ CD8 cells in the TDLN and to some extent in the tumor preventing T cell exhaustion during immunotherapy.

Conclusions cDC1 presence is important during the onset of various immunotherapies to maintain CD8 T cell stemness and as a consequence to allow tumor rejection. However once immunotherapy has already been established cDC1 requirement is less pronounced.

REFERENCES

1. Bottcher JP and Reis e Sousa C. The role of type 1 conventional dendritic cells in cancer immunity. *Trends Cancer* 2018;**4**:784–792.
2. Barry KC, Hsu J, Broz ML, Cueto FJ, Binnewies M, Combes AJ, Nelson AE, Loo K, Kumar R, Rosenblum MD, Alvarado MD, Wolf DM, Bogunovic D, Bhardwaj N, Daud AI, Ha PK, Ryan WR, Pollack JL, Samad B, Asthana S, Chan V, and Krummel MF. A natural killer-dendritic cell axis defines checkpoint therapy-responsive tumor microenvironments. *Nat Med* 2018;**24**: 1178–1191.
3. Salmon H, Idoyaga J, Rahman A, Leboeuf M, Remark R, Jordan S, Casanova-Acebes M, Khudoynazarova M, Agudo J, Tung N, Chakarov S, Rivera C, Hogstad B, Bosenberg M, Hashimoto D, Gnjatich S, Bhardwaj N, Palucka AK, Brown BD, Brody J, Ginhoux F and Merad M. Expansion and Activation of CD103(+) dendritic cell progenitors at the tumor site enhances tumor responses to therapeutic PD-L1 and BRAF inhibition. *Immunity* 2016;**44**:924–938.
4. Sanchez-Paulete AR, Cueto FJ, Martinez-Lopez M, Labiano S, Morales-Kastresana A, Rodriguez-Ruiz ME, Jure-Kunkel M, Azpilikueta A, Aznar MA, Quetglas JI, Sancho D and Melero I. Cancer immunotherapy with immunomodulatory anti-CD137 and Anti-PD-1 monoclonal antibodies requires BATF3-dependent dendritic cells. *Cancer Discov* 2016;**6**: 71–79.
5. Hildner K, Edelson BT, Purtha WE, Diamond M, Matsushita H, Kohyama M, Calderon B, Schraml BU, Unanue ER, Diamond MS, Schreiber RD, Murphy TL and Murphy KM. Batf3 deficiency reveals a critical role for CD8alpha+ dendritic cells in cytotoxic T cell immunity. *Science* 2008;**322**: 1097–1100.
6. Theisen DJ, Davidson JT, Briseno CG, Gargaro M, Lauron EJ, Wang Q, Desai P, Durai V, Bagadia P, Brickner JR, Beatty WL, Virgin HW, Gillanders WE, Mosammaparast N, Diamond MS, Sibley LD, Yokoyama W, Schreiber RD, Murphy TL and Murphy KM. WDFY4 is required for cross-presentation in response to viral and tumor antigens. *Science* 2018. **362**: 694–699.

Ethics Approval All animal experimentation have been approved by the institutional animal research ethics committee and the regional government.

<http://dx.doi.org/10.1136/jitc-2022-SITC2022.0982>

Rosy Liao*, Anika Thomas-Toth, Joshua McKeever, Andrew Koh, James LaBelle. *University of Chicago, Chicago, IL, United States*

Background The specific BCL-2 small molecule inhibitor venetoclax has been shown to effectively induce apoptosis in a wide range of malignancies either alone and in combination with other drugs. Based upon these results, there has been considerable growth in its use in clinical studies used alone and in combination with chemotherapy and immune-based therapies. Lymphocytes, and T cells in particular, rely heavily on BCL-2 for survival and function. This has been determined largely by genetic deletion or overexpression of BCL-2 in murine models. However, the adaptive effects of short or long-term small molecule BCL-2 family blockade on surviving immune cell subsets and their function is not fully understood. In the current work, we aimed to better understand the effect of long-term systemic treatment with venetoclax on regulatory T (Treg) cells, which are relatively apoptotically resistant to specific BCL-2 drugging compared to other T cells. We found that venetoclax altered surviving global T cell signaling and induced Treg cells towards a T_H17-like Treg (Tr17) via PI3K pathway activation and FOXO1 inhibition.

Methods Normal and MC38-bearing C57BL/6 FOXP3^{ires-GFP} mice were treated systemically with venetoclax for 14 days followed by phenotypic, functional, apoptotic, and genetic (RNA sequencing, ATAC seq, etc.) evaluation of Tregs isolated from immune organs and tumor infiltrating lymphocytes from these animals.

Results We show that venetoclax treatment resulted in Treg cell plasticity resulting in the conversion of a subset of canonical Tregs to a Tr17-like cell in normal and tumor-bearing mice. Venetoclax induced Tr17-like cells which were found to express increased IL-17A and IFN γ . RNA expression profiling of treated Tregs indicated that the PI3K pathway is activated. PI3K pathway activation was consistently also found in CD8⁺ and conventional CD4⁺ T cells (Tcons), similar to our recently reported observations in homeostatically expanding naive T cells from stem cell transplanted animals treated with venetoclax.¹ PI3K activation in Tregs resulted in inhibition of FOXO1 through phosphorylation at Ser256, leading to exclusion of FOXO1 from the nucleus. This resulted in transcriptional activation of a Th17-associated genetic program through ROR γ t upregulation in Tregs, but not Tcons, and as confirmed by altered genome wide accessibility patterns in treated Tregs.

Conclusions Our results indicate that long-term BCL-2 blockade by venetoclax results in Treg plasticity towards a Th17-like functional state through PI3K activation. We believe that this phenomenon may be beneficial for recently reported immune-mediated anti-tumor effects as a result of venetoclax therapy.

REFERENCE

1. Ludwig LM, Hawley KM, Banks DB, Thomas-Toth AT, Blazar BR, McNerney ME, et al. Venetoclax imparts distinct cell death sensitivity and adaptivity patterns in T cells. *Cell Death & Disease*. 2021;**12**(11):1–13.

Ethics Approval All animal experiments were approved by and performed in accordance with the guidelines and regulations set forth by the Institutional Animal Care and Use Committee of the University of Chicago. ACUP # 72295

984 MEK1 WITHIN EXTRACELLULAR VESICLES INHIBITS TUMOR GROWTH BY PROMOTING ANTI-TUMOR IMMUNITY

¹Jack Bui*, ¹Stephen Searles, ¹Jarrold Yee, ¹Preston Lee, ¹Christine Caron, ¹Calvin Lee, ²Irina Matei, ²David Lyden. ¹University of California, San Diego, La Jolla, CA, United States; ²Weill Cornell Medicine, New York, NY, United States

Background All cells have the capability to produce and release extracellular vesicles (ECVs), small vesicles that have similar topology to the cell and can deliver diverse cargo to mediate cell-cell communication. ECVs derive from the late endosomal pathway and contain bioactive cargo that can include lipids, nucleic acids (both RNA and DNA), and proteins. Once released into the extracellular space, ECVs can bind to and enter other cells, resulting in the physical transfer of bioactive cargo between cells, leading to functional changes in the target cell. Cancer cells secrete more ECVs than non-transformed cells. Tumor-derived (TD) ECVs can affect numerous cell types, including other cancer cells in an autocrine/paracrine manner and non-cancer host cells exerting both pro- and anti-tumor effects on immunity.

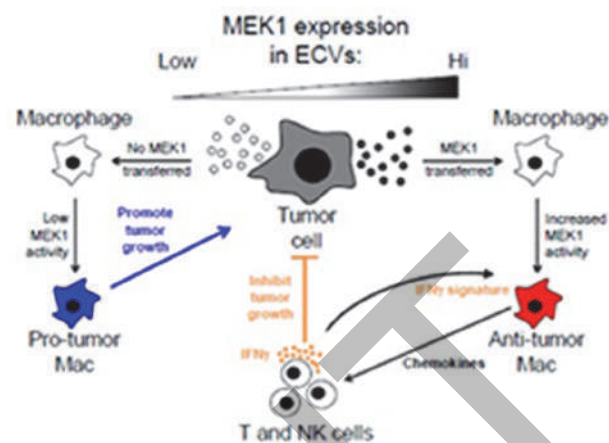
Methods To identify ECV proteins that could modulate immune responses, we have used a model of regressor and progressor cell lines that undergo immune rejection or progressive growth, respectively. We isolated ECVs from these cultured cell lines and performed proteomic analysis of the ECVs to identify unique proteins in ECVs secreted by regressor versus progressor cell lines. Having identified MEK1 as a unique protein in regressor-derived ECVs, we developed a model system to test the effect of MEK1-containing ECVs on tumor immunity.

Results We found that the signaling molecule MAP2K1 (MEK1) was enriched in ECVs secreted by regressor versus to progressor cells. ECVs engineered to have levels of MEK1 similar to regressor ECVs could inhibit tumor growth. In labeling experiments, ECVs were found to be taken up by tumor macrophages, delivering MEK1 into the cytoplasm, resulting in upregulation of certain genes such as chemokines. In tumors expressing MEK1 in ECVs, the microenvironment was enriched in cytolytic lymphocytes, resulting in induction of genes in the interferon gamma (IFN γ) pathway. Blocking IFN γ , MEK1 inhibition, or lack of adaptive immunity prevented the effect of MEK1-containing ECVs. Our results support a mechanism by which MEK1 protein within certain ECVs is delivered to tumor macrophages to promote adaptive immune responses against the tumor via IFN γ (figure 1).

Conclusions We conclude that MEK1 activity within exosomes and macrophages promote tumor immunity. These results suggest that the delivery of MEK1 to tumor-associated macrophages, either by ECVs, nanoparticles, or some other means, could be a useful strategy to treat cancer. On the other hand, the use of systemic MEK1 inhibitors in patients could reduce anti-tumor immunity. Therefore, targeting MEK1 inhibition to tumor cells could spare its putative immune suppressive effects.

Acknowledgements We acknowledge funding and conceptual support from The Hartwell Foundation.

Ethics Approval Animal studies were approved by the UCSD IACUC under protocol S06201.



Abstract 984 Figure 1 Model of how MEK1-ECVs activate tumor immunity
Tumor cells secreting ECVs that contain high levels of MEK1 can deliver MEK1 to macrophages, resulting in production of chemokines and recruitment of IFN γ -producing lymphocytes, leading to tumor growth inhibition

<http://dx.doi.org/10.1136/jitc-2022-SITC2022.0984>

985 **INHIBITION OF FIBROBLAST GROWTH FACTOR RECEPTOR 4 (FGFR4) SIGNALING ACTIVATES TUMOR INTERFERON (IFN) SIGNALING IN HEPATOCELLULAR CARCINOMA (HCC)**

Nannan Zhang*, Zhui Chen, Bin Shen, Zhixuan Zhu, Jueping Shi, Jiacheng Zhang, Pan Liang, Jie Wang. *Abbisko Therapeutics, Shanghai, China*

Background Hepatocellular carcinoma (HCC) is the most common primary liver cancer. Deregulation of FGF19-FGFR4 signaling has been found in HCC and several FGFR4 inhibitors have shown preliminary efficacy in patients with FGF19 overexpression. The combination of FGFR4 inhibitors with anti-PD-(L)1 antibodies is also under clinical investigation. However, the role of FGFR4 inhibition in tumor microenvironment (TME) remains to be elucidated. ABSK011 is a potent, selective FGFR4 inhibitor that has demonstrated strong antitumor activity in preclinical models and advanced into phase 1b clinical trials. In this study, we investigated the role of ABSK011 in TME of FGF19 overexpressed HCC models, and especially its crosstalk with interferon (IFN) pathway and antitumor immunity *in vitro* and *in vivo*.

Methods We evaluated the effects of ABSK011 in multiple FGF19 overexpressed HCC cell lines and *in vivo* models by RNA sequencing, quantitative PCR, flow cytometry and immunohistochemistry (IHC).

Results RNA sequencing revealed that IFN pathway was consistently enriched after treatment with ABSK011 across various HCC models. Quantitative PCR analysis showed that ABSK011 upregulated mRNA expression of several key genes related to IFN pathway, including *IRF1*, *IFIT1* and *CXCL10*, both in cell lines and tumor models. Furthermore, expression of surface PD-L1 on HCC cells were significantly increased and reached the plateau with the treatment of ABSK011 at the concentration higher than 0.1 μ M. In addition, we found that ABSK011 increased CD8⁺ T cell infiltration in humanized HCC mouse models.

Conclusions These preclinical data demonstrated that ABSK011 treatment increased IFN related response as well as CD8⁺ T cell infiltration in FGF19 overexpressed HCC models, supporting the combination of FGFR4 inhibitor and immune checkpoint molecules such as anti-PD-(L)1 antibodies to achieve enhanced antitumor activity.

<http://dx.doi.org/10.1136/jitc-2022-SITC2022.0985>

986

LOCAL AND LYMPHOID IMMUNE SURVEILLANCE MECHANISMS IN "EXCEPTIONAL SURVIVORS" OF STAGE IV BREAST CANCERS FOLLOWING STANDARD OF CARE CHEMO- AND TARGETED THERAPIES

¹Helen Kakkassery*, ²Thanussuyah Alaguthurai, ¹Rosalind Graham, ¹Esme Carpenter, ²Farhana Hossain, ¹Sean Keane, ¹Sheeba Irshad. ¹King's College London, Ilford, UK; ²Guy's and St Thomas NHS Foundation Trust, London, UK

Background Breast cancer patients with metastatic disease can exhibit rapid disease progression, disease stabilisation or partial responses of varying duration. However, for reasons that are not fully elucidated, a small fraction of patients will elicit an exceptional durable response to standard anti-cancer treatments or survive significantly longer than patients with clinically comparable tumours. Here, we investigate the drivers of immune surveillance mechanisms of long-term survivors of metastatic breast cancers.

Methods Peripheral blood mononuclear cells (PBMCs) from long-term survivors of metastatic breast cancer patients alongside matched control cohorts of stage IV rapid progressors and typical responders, early breast cancer patients and healthy volunteers were isolated. High-dimensional flow cytometry and proteomic analysis of the PBMCs across these groups was performed. In vitro activation of candidate immune cell types isolated from PBMCs was conducted for downstream proteomics analysis of activated phenotypes.

Results Principle Components Analysis (PCA) showed distinct segregation of the exceptional survivors from the other control groups with an immune signature in exceptional survivors constituting of activated NK, CD8 T cells and gd T cells pointing towards higher innate immunogenicity in these individuals. Specifically, although these metastatic exceptional responder patients possessed comparable NK cell frequencies, the proportion of NKG2D⁺CD56^{dim}CD16⁺ NK cells were significantly enriched compared to the typical responders. Additionally, proportions of CD8⁺ central memory (CD45RA⁻ CD27⁺) and effector memory (CD45RA⁻ CD27⁻) Vd1 and Vd2 gd T cells, were also seen to be significantly increased. Moreover, proteomics analysis on PBMCs of the responders revealed proteins involved in cell cycle progression and cell proliferation such as RBBP7, KCTD10 and PTH2 were elevated in the exceptional responders compared to the typical responders. Functional in vitro validation of these findings by analysing the proteome of activated immune effector cells along with scRNA sequencing of lymph node and tumour tissue is currently underway.

Conclusions To our knowledge, this work is the first to explore in depth the immune signatures in the peripheral blood of exceptional survivors with metastatic breast cancer. Elucidating the immunological reasons for favourable atypical responses alongside functional tumour microenvironment analysis offers unique insights for predictive biomarker identification and discovery of axes that could be exploited therapeutically to benefit those with less favourable responses.

Ethics Approval Written informed consent was obtained from all individuals in accordance with the Declaration of Helsinki under the following research ethics committee; London-Chelsea approved study (REC ID 13/LO/1248).

<http://dx.doi.org/10.1136/jitc-2022-SITC2022.0986>

Abstracts

987

COMPREHENSIVE IMMUNOPHENOTYPING AND GENOMICS FROM SINGLE BLOOD TUBE FOR T-CELL DYNAMICS IN CLINICAL TRIALS

Manling Ma-Edmonds*, Gregg Masters, Omar Jabado, Lisa Grimm, Mahesh Bachu, Matthew Loya, Gabrielle Suppa, Jordan Blum, David Soong, Han Si, Brandon Higgs, Nicole Bottrel, Erin Henitz, Christopher Chiu, Kate Sasser, Mark Fereshteh. *Genmab, Princeton, NJ, United States*

Background Analysis of peripheral whole blood is a cornerstone of investigational therapeutic development. Phase I/II trials request multiple blood draws from patients to understand pharmacokinetics and pharmacodynamics; in cases where they are experiencing severe disease, reducing draw volumes is desirable. Long distances between collecting hospitals and bio-analytical labs risks sample degradation. To conserve patient whole blood samples, we coupled deep immunophenotyping and transcriptomic workflows using a single, cryopreserved tube as input (figure 1). This method allowed characterization of T-cell immune state by flow cytometry, TCR diversity and transcriptomics in a global clinical trial of Non-Hodgkin Lymphoma (NHL).

Methods Peripheral blood mononuclear cells (PBMC) were collected from NHL patients ($n = 165$; NCT03625037) and age matched normal healthy volunteer donors ($n = 24$). PBMC extraction was performed in three central labs located in Europe, Asia, and North America. A T-cell focused, 16-parameter flow cytometry panel was performed on PBMCs and then RNA was purified from the remaining cells in the tube. T-cell receptor β sequencing (TCRseq) using a multiplex PCR (Illumina) and transcriptomics using EdgeSeq (HTG Molecular) was performed. In parallel, patient whole blood samples were assessed by flow cytometry in the central labs. Data from all three platforms was integrated and analyzed with linear models in R.

Results We compared immunophenotyping from patient whole blood (overnight shipped) to cryopreserved PBMCs from the same blood draw; the viable cell percentage of PBMCs after thawing averaged 55%. T-cell populations in high viability PBMC samples ($>70\%$) were correlated to whole blood estimates (average Spearman's ρ of 0.7). Samples with viability $>30\%$ retained correlation across the immune subsets of interest (T naïve, effector, central memory and regulatory). Our flow cytometry workflow consumed 1M cells, 70% of patients profiled had sufficient sample remaining for TCR and transcriptomic assays (500k+ cells; average RNA yield of 350ng).

Combining TCR and transcriptomics with flow cytometry enables a composite picture of T-cell activity. Statistical analysis revealed $CD4^+$ naïve proportions were the primary driver of TCR diversity. Top genes associated with diversity were *CD69*, a well-known activation marker, *DUSP10/MKP5*, an immune regulator¹ and *GPR183/EBI2* an oxysterol receptor with a role in lymphoid development.^{2,3}

Conclusions This streamlined workflow is amenable to global clinical trials with long shipping distances and reduces blood draw requirements. Integration of flow cytometry, TCR diversity and the transcriptome allows a deeper understanding of T-cell activity that can support mechanism of action analyses.

Acknowledgements Tiffany Vines, Yong Lee, Fouad Janat, Byron Lawson, Rafael Maynez, Michael Ball and Ed Galan from HTG Molecular for their scientific and technical support.

Li Fan, Bradley Forman, Alex Wolicki, and Denise Gallagher for scientific expertise and technical support.

Trial Registration GEN3013 Trial in Patients With Relapsed, Progressive or Refractory B-Cell Lymphoma (NCT03625037)

REFERENCES

1. Zhang Y, Blattman JN, Kennedy NJ, Duong J, Nguyen T, Wang Y, Davis RJ, Greenberg PD, Flavell RA, Dong C. Regulation of innate and adaptive immune responses by MAP kinase phosphatase 5. *Nature* 2004 Aug 12;430(7001):793–7.
2. Li J, Lu E, Yi T, Cyster JG. EBI2 augments Tfh cell fate by promoting interaction with IL-2-queenching dendritic cells. *Nature* 2016 May 5;533(7601):110–4.
3. Emgård J, Kammoun H, García-Cassani B, Chesné J, Parigi SM, Jacob JM, Cheng HW, Evren E, Das S, Czarnewski P, Sleiers N, Melo-Gonzalez F, Kvedaraite E, Svensson M, Scandella E, Hepworth MR, Huber S, Ludewig B, Peduto L, Villablanca EJ, Veiga-Fernandes H, Pereira JP, Flavell RA, Willinger T. Oxysterol Sensing through the Receptor GPR183 promotes the lymphoid-tissue-inducing function of innate lymphoid cells and colonic inflammation. *Immunity* 2018 Jan 16;48(1):120–132.

Ethics Approval The protocol and informed consent were approved by an independent ethics committee or institutional review board before initiation. The trial was done in accordance with the International Conference on Harmonization Good Clinical Practice Guidelines, Declaration of Helsinki, and all applicable regulatory requirements. All patients gave written informed consent.

Consent Written informed consent was obtained from the patient for publication of this abstract and any accompanying images. A copy of the written consent is available for review by the Editor of this journal.

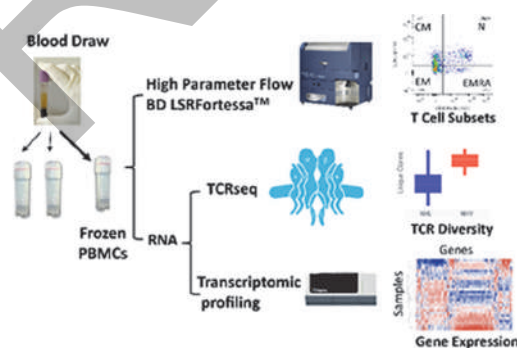


Figure 1: Combined phenotyping and genomic workflow for single-tube PBMC analysis

Abstract 987 Figure 1 Combined phenotyping and genomic workflow for single-tube PBMC analysis

<http://dx.doi.org/10.1136/jitc-2022-SITC2022.0987>

988

B-CELL RECEPTOR (BCR) REPERTOIRE AND ANTIBODY RECOGNITION ANALYSIS OF MELANOMA PATIENTS TREATED WITH NEOADJUVANT IMMUNE CHECKPOINT BLOCKADE (ICB)

Monika Zelazowska*, Somnath Paul, Joshua Plummer, Manoj Chelvanambi, Beth Helmink, Russell Witt, Michael White, Shalaka Lotlikar, Melissa Simper, Sarah Johnson, Alexandra Hebertson, Bin Liu, Jennifer Wargo, Kevin McBride. *The University of Texas MD Anderson Cancer Center, Houston, TX, United States*

Background Enriched B cell signature is correlated with positive outcome of immune checkpoint blockade (ICB) therapy in melanoma¹ and other cancers.² B cells have the capability to engage and activate other immune effector cells by recognition and further presentation of tumor antigens. B cells can also secrete an array of cytokines that modulate tumor microenvironment (TME) driving anti-tumor response. Though the mechanism through which B cells contribute to the treatment outcome is still not completely understood, we hypothesize that the BCR and antibodies produced by tumor-residing B cells play an important role in immunotherapy response by recognizing tumor.

Methods Immunoglobulin sequences from intratumoral B cells were reconstructed from single-cell RNAseq data using VDJ Puzzle algorithm.³ Additionally, single B cells were sorted from melanoma tumor tissue and/or adjacent lymph nodes. DNA sequences encoding antibody heavy and light chains were recovered by RT-PCR. Reconstructed immunoglobulin sequences were annotated and analyzed using NCBI IgBlast⁴ or IMG/HighV-QUEST.⁵ The hallmarks of antigen recognition like somatic hypermutation (SHM), isotype switching, and clonal expansion were analyzed based on heavy chain sequences. Simultaneously, selected Ig transcripts were cloned into expression vectors enabling the production of tumor-derived human recombinant monoclonal antibodies (rmAbs) in mammalian expression system. Antibodies were subsequently purified and tested for tumor and/or cell line binding. A subset of which are being subjected to antigen identification analysis.

Results We successfully utilized our workflow pipeline (figure 1) to generate human rmAbs from tumors of 10 melanoma patients; 6 responders, 2 partial responders and 2 nonresponders. In total, we have been cloning hundreds of antibodies, over 600 from complete and partial responders, and almost a hundred from nonresponders. We observed expansion of selected clones and acquisition of SHM in a manner consistent with an immune selection process. We find a large number of antibodies bind tumor tissue or related cell lines and antigen identification is ongoing.

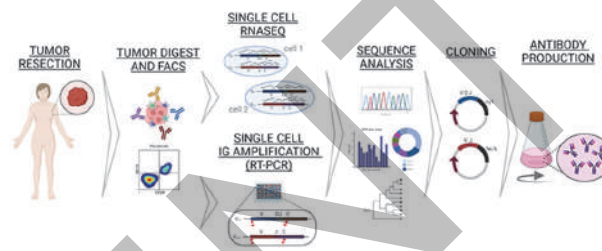
Conclusions Ig sequence analysis indicates that the B cells in TME participate in antigen-driven selection process and a large percentage of the antibodies recognize antigens from the tumor or related cell lines. We conclude that the expanded B cell signature is recognizing and being selected for by tumor antigens. The utilization of single-cell RNAseq and single-cell Ig isolation in patients with response to ICB therapy can be used to identify and clone antibodies associated with tumor samples. This method has potential to identify unique tumor antigens and offer novel therapies.

REFERENCES

1. Helmink, BA, *et al.* B cells and tertiary lymphoid structures promote immunotherapy response. *Nature* 2020;**577**(7791): 549–555.
2. Petitprez F, *et al.* B cells are associated with survival and immunotherapy response in sarcoma. *Nature* 2020;**577**(7791): 556–560.
3. Rizzato S, *et al.* B-cell receptor reconstruction from single-cell RNA-seq with VDJpuzzle. *Bioinformatics* 2018;**34**(16): 2846–2847.

4. Ye J, *et al.* IgBLAST: an immunoglobulin variable domain sequence analysis tool. *Nucleic Acids Res* 2013;**41**:W34–40.
5. Alamyar E, *et al.* IMG(T(R)) tools for the nucleotide analysis of immunoglobulin (IG) and T cell receptor (TR) V-(D)-J repertoires, polymorphisms, and IG mutations: IMG(T/V)-QUEST and IMG(T/HighV)-QUEST for NGS. *Methods Mol Biol* 2012;**882**:569–604.

Ethics Approval These patients were treated at the University of Texas MD Anderson Cancer Center and had tumor samples collected and analyzed under Institutional Review Board (IRB)-approved protocols (2015-0041, 2012-0846, LAB00-063 and PA17-0261).



Abstract 988 Figure 1 Schematic workflow
A section of a tumor is digested and stained with specific antibodies to identify subsets of B cells. Ig transcripts are recovered from single-sorted cells via RNAseq or RT-PCR. Variable domains of heavy and light chains are either synthesized or amplified and cloned into expression vectors for subsequent expression in mammalian cells. Figure created with BioRender.com

<http://dx.doi.org/10.1136/jitc-2022-SITC2022.0988>

0989

A LUCIFERASE-BASED METHOD TO ASSESS ANTIGEN-SPECIFIC T CELL RESPONSES AND ANTIGEN PRESENTATION TO EVALUATE IMMUNOMODULATORY CHECKPOINTS AND THERAPEUTICS

Jimena Alvarez Freile*, Yuzhu Qi, Lisa Jacob, Maria Franceskin Lobo, Harm Jan Lourens, Gerwin Huls, Edwin Bremer. *Universitair Medical Centrum Groningen (UMCG), Groningen, Netherlands*

Background Targeted reactivation of the immune system, e.g. using immune checkpoint inhibitors (ICI), has shown great potential in the treatment of cancer. However, *in vitro* tools to rapidly investigate the impact of checkpoints in the context of specific T cell receptor (TCR) activation as well therapeutic effects of ICI treatment are lacking. Here, we have developed a simple method using the human papilloma virus 16 (HPV-16) E7-peptide (HLA-A2*02:01) and corresponding antigen-specific NFAT-luciferase model to assess antigen presentation and antigen-specific T cell responses and evaluate the impact of immunosuppressive factors and therapeutics that target such factors.

Methods HPV-16_E7₁₁₋₂₀ peptide was used as model antigen.¹ Jurkat NFAT-luciferase cell line or isolated primary T cells were modified with a previously reported TCR recognizing the E7₁₁₋₂₀ peptide.² HLA-A2+/- cancer cells were pulsed and incubated with Jurkat/T cells, with and without the E7₁₁₋₂₀-TCR. To study E7 presentation endogenously, CaSki cells were used. For the luciferase-based assay, T cell activation was correlated with the luminescence read out. For primary T cells, CD25/CD69 expression (Flow Cytometry), cytokine production (ELISA) and clustering (microscopy) were evaluated. As proof of concept for monitoring immunomodulatory events, cells were also treated with TGF-beta or modified to overexpress inhibitory immune checkpoints (e.g., HLA-G, VISTA).

Results Upon E7₁₁₋₂₀ pulsing of HLA-A2+ cells, an E:T ratio dependent increase in luminescence compared to non-pulsed cells (2-25 fold-increase) was observed upon coculture with Jurkat E7₁₁₋₂₀-TCR but not with parental Jurkat cells. Analogous experiments with CaSki yielded 30% increase in luminescence, demonstrating that the method is valid for measuring endogenous E7₁₁₋₂₀ processing and MHC presentation. Both HLA-A2+ pulsed cells and CaSki triggered specific T cell activation, illustrated by 5-20 fold-increase in MFI values for CD25 and CD69 expression and T cell clustering. For cytokine production, only the combination peptide: E7₁₁₋₂₀-TCR + pulsed cells, whereas for CaSki only higher IFN γ production was observed. Overexpression of inhibitory molecules, such as HLA-G and VISTA, had a significant negative impact on TCR-induced luminescence compared to EV or non-treated cells. Moreover, treatment with immunosuppressive cytokines such as TGF-beta significantly impacted on luminescence.

Conclusions The MHC-I-specific Jurkat E7₁₁₋₂₀-TCR NFAT-luciferase system presented here can be used as an alternative method for the rapid evaluation of antigen-specific T cell responses *in vitro*. This method may be used as a rapid tool to study the impact of the TME or novel ICI in triggering effective T cell responses within the immune-oncology field.

REFERENCES

1. Riemer AB, *et al.* A conserved E7-derived cytotoxic T lymphocyte epitope expressed on human papillomavirus 16-transformed HLA-A2+ epithelial cancers. *J Biol Chem.* 2010;**285**(38):29608–29622.

2. Jin BY, Campbell TE, Draper LM, Stevanovic S, Weissbrich B Yu, *et al.* Engineered T cells targeting E7 mediate regression of human papillomavirus cancers in a murine model. *JCI Insight* 2018. pmid:29669936

<http://dx.doi.org/10.1136/jitc-2022-SITC2022.0989>

990

HETEROGENEITY IN GLIOBLASTOMA TUMOR MICROENVIRONMENT: STRATEGIES FOR CANCER-ASSOCIATED FIBROBLAST TARGETING

Jonathan Stauber, Corinne Ramos*, Sandra Delebecq, Adele Ponzoni, Lisa Guzzi.
ImaBiotech, Loos, France

Background Glioblastoma (GBM) is the most common and aggressive form of brain tumor, characterized by a poorly accessible microenvironment that render it notoriously hard to treat. The insufficient treatment success is, in large parts, due to its tremendous molecular heterogeneity, which affects the overall prognosis and response to therapies. The significant intra- and inter-tumor microenvironment (TME) composition heterogeneity plays a crucial role in GBM progression. Mostly due to this high, multifactorial immunosuppression occurring in the microenvironment, the efficacy of immunotherapy in GBM is low. Focusing on characterizing the components of different TMEs to evaluate their molecular and cellular component heterogeneity has a significant advantage to target group of cancer patients that would normally be resistant to immunotherapy.

Methods Deep spatial transcriptomics profiling was performed on non-treated glioblastoma human tissue microarrays (TMA) using NanoString's *GeoMx* Digital Spatial Profiler (DSP). 6 tumor tissues from 6 different patients were hybridized and analyzed with the Whole Transcriptomic Atlas (WTA) panel that includes 18,000 genes. Three regions of interest (ROIs) were selected per tissue sample. All the statistical analysis were performed with *GeoMx*[®] DSP Analysis Suite. Cell deconvolution using the *SpatialDecon*[®] algorithm (*Nanostring*[®]) was then performed to estimate mixed cell type abundance in the spatially-resolved gene expression defined segments.

Results Spatial transcriptomic analyses revealed that glioblastoma tumors varied dramatically in their global gene expression profiles and suggested the existence of differential gene expression among the tumors highlighting the inter-tumors heterogeneity of glioblastoma. Interestingly, different areas of the same tumor did not display distinct molecular profiles. Upregulation of stromal collagen genes was significantly detected in some patient specifically the fibrillar collagens type I, III and VI. Those findings indicated excessive collagen depositions in the surrounding of the tumor for some patient characteristic of tumor progression and involvement of cancer associated fibroblasts (CAFs) in the dysregulated collagen turnover leading to tumor fibrosis.

Conclusions As a cold tumor, malignant glioma has strong immunosuppression and immune escape characteristics. The TME provides the "soil" for the survival of malignant tumors, and recent studies have highlighted a major role for cancer-associated fibroblasts (CAFs) in promoting immunotherapy resistance by excluding T cells from tumors in the TME. Here the spatial transcriptomic analyses allowed a better phenotypical stratification of the cancer patient. In some, targeting CAFs would improve the TME and enhance the efficacy of immunotherapy.

<http://dx.doi.org/10.1136/jitc-2022-SITC2022.0990>

991

AB598, A THERAPEUTIC ANTI-HUMAN CD39 ANTIBODY, BINDS AND INHIBITS CD39 ENZYMATIC ACTIVITY *IN VIVO* TO PROMOTE ANTI-TUMOR IMMUNITY

Kaustubh Parashar, Julie Clor, Amy Anderson, Urvi Vani, Jaskirat Singh, Enzo Stagnaro, Ferdie Soriano, Angelo Kaplan, Janine Kline, Lisa Seitz, Stephen Young, Nigel Walker, Matthew Walters, Ester Fernandez-Salas, Christine Bowman*. *Arcus Biosciences, Hayward, CA, United States*

Background AB598 is being developed as a novel cancer immunotherapy which potently binds and inhibits CD39 enzymatic activity. CD39 catalyzes the conversion of extracellular adenosine triphosphate (ATP) into adenosine monophosphate (AMP), resulting in decreased amounts of immunostimulatory ATP and increased levels of immunosuppressive adenosine in the tumor microenvironment (TME). By blocking CD39 in the TME, local levels of ATP increase, leading to myeloid cell activation and improved tumor control. AB598 is highly potent and specific, binding and inhibiting human CD39 with sub-nanomolar potency. AB598 binds and inhibits both human and cynomolgus monkey CD39 but not murine CD39, presenting a challenge for studying CD39 inhibition in an immune-competent syngeneic tumor model.

Methods Human CD39 knock-in (hCD39KI) mice were employed to examine the preclinical anti-tumor efficacy of AB598 in animals with a fully competent immune system. The use of a murine model with natural expression and distribution of human CD39, targetable by AB598, allowed for a more physiological assessment of CD39 inhibition in solid tumors compared to the alternative use of human cancer cells growing in immuno-deficient mice. Combination of CD39 inhibition with chemotherapy was explored. A murinized version of AB598, ch39_mIgG2a, which contains a murine Fc silent domain was used for *in vivo* studies.

Results Real-time measurement of ATP showed the ability of oxaliplatin to induce ATP release in MC38 tumor cells *in vitro*. In a hCD39KI mouse MC38 tumor model, ch39_mIgG2a in combination with oxaliplatin significantly inhibited tumor growth compared to treatment with either single agent. The combination was well tolerated and no decreases in body weight were observed. Analysis of cytokines in the periphery resulted in no significant increases after ch39_mIgG2a administration. Analysis of tumors from both MC38 and 4T1 models revealed substantial inhibition of intratumoral CD39 enzymatic activity in ch39_mIgG2a-treated mice. Tumor draining lymph nodes in the MC38 model showed a decrease in cell surface CD39 in ch39_mIgG2a mice, a finding supported by peripheral receptor occupancy studies. Relative percentages of the immune cells in the lymph nodes were unaffected, suggesting internalization or downregulation, not cellular depletion, as the mechanism for the decrease in cell-surface CD39.

Conclusions Our results indicate the superb ability of AB598 to inhibit enzymatic activity and tumor growth *in vivo* and provide a rationale for the combination of CD39 inhibition with ICD-inducing chemotherapy in the clinic.

<http://dx.doi.org/10.1136/jitc-2022-SITC2022.0991>

992

INTRATUMORAL S100A8-TO-CD8 RATIO IN INFLAMED MERKEL CELL CARCINOMA TUMORS CORRELATES WITH RESPONSE TO PD-1 PATHWAY BLOCKADE

<http://dx.doi.org/10.1136/jitc-2022-SITC2022.0992>

¹Shira Tabachnick-Cherny*, ¹Thomas Pulliam, ¹Haroldo Rodriguez Chevez, ²Kimberly Smythe, ¹Rima Kulikauskas, ¹Kristina Lachance, ²Daniel Hippe, ¹Paul Nghiem. ¹University of Washington, Seattle, WA, United States; ²Fred Hutchinson Cancer Center, Seattle, WA, United States

Background PD-(L)1 blockade has changed the landscape for advanced Merkel cell carcinoma (MCC) as over 50% of patients initially respond to therapy. There are no clinically useful approaches to assess a patient's likelihood of response to PD-1 blockade. Understanding the underlying biology of anti-PD(L)1 responses and identifying predictive biomarkers can inform future combination therapies for patients that do not benefit from treatment. MCC is caused by the Merkel cell polyomavirus in ~80% of cases with the remaining cases being due to extensive UV exposure. Both of these processes are highly immunogenic due to viral oncoprotein expression or UV-neoantigens, respectively. Historically, studies have focused on adaptive immunity, and little is known about innate immunity in MCC which may play an important role in immune evasion. Myeloid cells are heterogeneous and have been shown to play a suppressive role in many cancer types. We sought to investigate the link between tumor-infiltrating myeloid cells and outcomes to PD-(L)1 blockade.

Methods Identification of myeloid subtypes in MCC tumors was determined by single-cell RNA sequencing (scRNAseq) of dissociated tumor samples obtained from 9 patients. Following unsupervised clustering based on differential gene signatures, we selected major markers expressed in the myeloid subtypes in MCC (CD14, CD163, S100A8) and a cytotoxic T cell marker (CD8) for multiplex immunohistochemistry (m-IHC) analysis of 51 pre-treatment patients' tumors.

Results scRNAseq analysis discovered tumor associated macrophages in MCC tumors that express hallmarks of monocytic myeloid derived suppressor cells (M-MDSCs)¹: the surface molecules CD14⁺CD11b⁺HLA-DR^{lo/-} and upregulated S100A8 and S100A9 genes. Initial m-IHC analysis comparing pre-treatment tumors of 32 responders and 18 non-responders did not show differences between the response groups. However, after classifying tumors by CD8 infiltration status (intratumoral CD8⁺ cells/1mm – Hot score: CD8 > 60, Cold score: CD8 < 60), we observed higher ratios of S100A8-to-CD8 in patients with hot tumors that did not respond to PD-(L)1 blockade treatment (p=0.046).

Conclusions S100A8 is associated with a tumor promoting effect and is a potential prognostic biomarker for advanced melanoma.² Our data suggests a correlation of S100A8-expressing cells in MCC tumors with response to treatment, as the ratio of S100A8-to-CD8 is higher in inflamed tumors that did not respond to immunotherapy. Future approaches to target M-MDSCs, or S100A8 directly might modify the ratio of S100A8-to-CD8 and potentially improve patient responses to PD-(L)1 blockade treatment.

REFERENCES

1. Veglia F, Sanseviero E & Gabrilovich DI. Myeloid-derived suppressor cells in the era of increasing myeloid cell diversity. *Nat Rev Immunol* 2021;**21**:485–498
2. Wagner NB, Weide B, Gries M, et al. Tumor microenvironment-derived S100A8/A9 is a novel prognostic biomarker for advanced melanoma patients and during immunotherapy with anti-PD-1 antibodies. *JITC* 2019;**7**:343.

Ethics Approval The study was approved by Fred Hutchinson Cancer Center Ethics Board, approval number 6585.

993

INTERACTPRINT PREDICTS CLINICALLY MEANINGFUL INTERACTIONS BETWEEN CANCER EPITHELIAL CELLS AND IMMUNE CELLS: LESSONS FROM A SINGLE-CELL BREAST CANCER ATLAS

¹Lily Xu, ¹Kaitlyn Saunders, ²Hildur Knutsdottir, ¹Kenian Chen, ³Julia Maués, ³Christine Hodgdon, ⁴Evanthia Roussos Torres, ¹Sangeetha Reddy, ¹Lin Xu, ¹Isaac Chan*. ¹University of Texas Southwestern Medical Center, Dallas, TX, United States; ²Johns Hopkins University Whitting School of Engineering, Baltimore, MD, United States; ³GRASP Cancer, Baltimore, MD, United States; ⁴Keck School of Medicine, University of Southern California, Los Angeles, CA, United States

Background While immunotherapy has revolutionized the treatment of many solid tumors, the efficacy of immunotherapy regimens is comparatively lower in breast cancer. Immunotherapy efficacy is often negatively correlated with intratumor heterogeneity. Novel breast cancer immunotherapy approaches should leverage how intratumor heterogeneity affects immune cells in the tumor microenvironment. However, current definitions of heterogeneity in breast cancer have limited resolution. Single-cell RNA-seq (scRNA-seq) provides an unprecedented opportunity to further define cancer epithelial cell heterogeneity and identify how it influences immune interactions.

Methods We generated a novel dataset of 236,363 cells from 119 primary breast tumors biopsied from 88 patients taken from 8 publicly available datasets, currently the largest published scRNA-seq dataset in breast cancer. To define cancer epithelial cell heterogeneity, we performed unsupervised and supervised clustering based on molecular subtype and clinical target expression of all cancer epithelial cells. This identified 10 gene elements (GEs), which reflect molecular features that vary between cancer epithelial cells. Receptor-ligand pairing analysis determined how cells that highly express each GE interact with immune cells. We developed InteractPrint, a score which predicts the predominant tumor-interacting immune cells based on GE composition of a patient's tumor.

Results In our dataset, 20% of samples were HER2+, 46% HR+, and 32% TNBC. This dataset was statistically powered to characterize cancer epithelial cell heterogeneity. For the 10 GEs, we predicted interactions with immune cells. GEs with predicted NK cell interactions were resistant to NK cell cytotoxicity. In a spatial transcriptomics dataset, GEs with predicted T cell interactions demonstrated colocalization with CD8+ T cells. To infer GE-immune interactions at the patient level, we developed InteractPrint and assessed its accuracy in predicting response to anti-PD-1 therapy. Across two trials and clinical subtypes, T cell InteractPrint demonstrated significant improvement over PD-L1 in predicting response to anti-PD-1 therapy. In an scRNA-seq dataset of samples from patients treated with pembrolizumab, we observed AUC of 81% for T cell InteractPrint versus 54% for PD-L1. In patients treated with paclitaxel + pembrolizumab in the I-SPY2 trial, we observed AUC of 84% for T cell InteractPrint versus 73% for PD-L1.

Conclusions We defined intratumor heterogeneity and leveraged it to predict immune cell interactions within a patient's tumor. We developed T cell InteractPrint which captures heterogeneity in cancer epithelial and CD8+ T cell interactions and is predictive of anti-PD-1 therapy response at higher AUC than PD-L1. This provides a path forward for the interpretation of intratumor heterogeneity in a clinically meaningful way.

<http://dx.doi.org/10.1136/jitc-2022-SITC2022.0993>

994

INVESTIGATING THE ABILITY OF TUMOR CELL-DERIVED TYPE I INTERFERON TO POTENTIATE ANTI-OVARIAN CANCER IMMUNE RESPONSES

Fiona Chatterjee*, Ellen Duong, Arijun Bhutkar, Stefani Spranger. *Massachusetts Institute of Technology, Cambridge, MA, United States*

Background Ovarian cancer is the fifth leading cause of cancer-related death in women in the United States.¹ The standard of care for ovarian cancer remains surgical debulking and chemotherapy. While this treatment is effective initially, most patients experience relapse within five years of initial diagnosis, and recurrent tumors are often chemotherapy-resistant.²⁻⁴ Ovarian cancer generally induces extremely poor immune responses (characterized by poor effector immune cell infiltration and a lack of innate immune activation), and thus, efforts to induce robust anti-tumor immunity will require potent activation of the innate immune system.⁵ The period between the end of chemotherapy and disease recurrence, often termed first remission, presents a unique opportunity to induce anti-tumor immune responses to delay or even prevent tumor regrowth. Recent work in our lab has demonstrated that inducing tumor cell-derived type I interferon (IFN-I) can rescue dysfunctional anti-tumor immune responses by activating a specific dendritic cell subset that subsequently activates CD8⁺ T cells.⁶ In this project, we aim to investigate how tumor cell-derived IFN-I induction impacts anti-ovarian cancer immunity.

Methods To model first remission and the subsequent tumor regrowth, we inoculated syngeneic ovarian cancer cells into the intraperitoneal spaces of mice, which resulted in the development of solid metastatic tumors and ascites. We utilized two cell lines: BPPNM, driven by *Brca1*^{-/-} *p53*^{-/-R172H} *Pten*^{-/-} *Nf1*^{-/-} and *Myc*^{OE}, to model homologous recombination-deficient (HR-deficient) tumors and CPAK, driven by *Ccne1*^{OE} *p53*^{-/-R172H} *Akt2*^{OE} and *Kras*^{G12V}, to model homologous recombination-proficient (HR-proficient) tumors.⁷ Interferon beta and interferon-stimulated gene transcript levels were assessed by qPCR. Dendritic cell and T cell infiltration were assessed by flow cytometric analysis of BPPNM and CPAK tumors 14 days after injection into wildtype mice.

Results BPPNM tumor cells, which are HR-deficient, expressed higher levels of interferon beta and downstream signaling target transcripts compared to CPAK tumor cells, which are HR-proficient. Flow cytometry immunophenotyping of BPPNM and CPAK tumors revealed that BPPNM tumors were more infiltrated by DC1, DC2, ISG⁺ DC, CD8⁺ T cells, and CD4⁺ T cells. Finally, wildtype C57BL/6 mice implanted with BPPNM tumors displayed extended survival compared to mice implanted with CPAK tumors.

Conclusions Our data suggest that ovarian cancer cells with the ability to produce IFN-I induce more potent anti-tumor immune responses. Understanding how to induce IFN-I production in HR-proficient ovarian cancer could not only improve our knowledge of interactions between ovarian cancer cells and immune cells but also lead to novel therapeutic strategies for ovarian cancer.

Acknowledgements We would like to thank MIT's Department of Comparative Medicine and the Koch Institute's Swanson Biotechnology Core Facility. This work was supported by Break Through Cancer.

REFERENCES

1. Siegel RL, Miller KD, Fuchs HE & Jemal A. Cancer Statistics, 2021. *CA Cancer J Clin* 71, 7-33.

2. Gavalas NG, Karadimou A, Dimopoulos MA, & Bamias A. Immune response in ovarian cancer: how is the immune system involved in prognosis and therapy: potential for treatment utilization. *Clin Dev Immunol* 2010; 791603.
3. Coleman RL, Monk BJ, Sood AK & Herzog TJ. Latest research and treatment of advanced-stage epithelial ovarian cancer. *Nat Rev Clin Oncol* 2013; 10:211–224.
4. Bowtell DD, *et al.* Rethinking ovarian cancer II: reducing mortality from high-grade serous ovarian cancer. *Nat Rev Cancer* 2015;15, 668–679.
5. Fucikova J, *et al.* Immunological configuration of ovarian carcinoma: features and impact on disease outcome. *J Immunother Cancer* 2021; 9.
6. Duong E, *et al.* Type I interferon activates MHC class I-dressed CD11b(+) conventional dendritic cells to promote protective anti-tumor CD8(+) T cell immunity. *Immunity* 2022;55, 308–323, e309.
7. Iyer S, *et al.* Genetically defined syngeneic mouse models of ovarian cancer as tools for the discovery of combination immunotherapy. *Cancer Discov* 2021;11, 384–407.

Ethics Approval All mouse experiments were approved by MIT's Committee on Animal Care (CAC) – PHS Animal Welfare Assurance # D16-00078 (A3125-01).

<http://dx.doi.org/10.1136/jitc-2022-SITC2022.0994>

995

V DOMAIN IMMUNOGLOBULIN SUPPRESSOR OF T CELL ACTIVATION (VISTA) RE-PROGRAMS MACROPHAGE BIOLOGY AND PROMOTES PHAGOCYTOSIS AND M2C-DIFFERENTIATION

¹Yusheng Lin candidate*, ¹Ghizlane Choukrani, ²Lena Dubbel, ²Lena Rockstein, ¹Jimena Freile, ¹Yuzhu Qi, ¹Harm Jan Lourens, ¹Nienke Visser, ¹Valerie Wiersma, ³Hao Zhang, ¹Emanuele Ammatuna, ¹Tom Meerten, ¹Gerwin Huls, ¹Edwin Bremer. ¹University Medical Center Groningen, Groningen, Netherlands; ²Carl von Ossietzky Universität Oldenburg, Oldenburg, Germany; ³Jinan University Medical College, Guangzhou, China

Background VISTA is an established T cell immune checkpoint. However, its role in innate immunity is less established, with VISTA regulating cytokine production and chemotaxis by myeloid cells. The role of VISTA in macrophage biology and effector functions such as phagocytosis has not been delineated. Here, we investigated the impact of VISTA on phagocytosis and macrophage polarization.

Methods The frequency of CD14⁺ monocytes expressing VISTA was determined in peripheral blood mononuclear cells (PBMC) from 37 healthy donors by flow cytometry. Macrophages, differentiated from VISTA overexpressed THP-1 cells and cord blood CD34⁺ cell-derived monocytes, were used in phagocytosis assay using B-cell lymphoma target cells opsonized with rituximab. PBMC-derived macrophages were used to assess the correlation between phagocytosis and VISTA expression. qRT-PCR and flow cytometry were performed to analyze the impact of VISTA on other checkpoints and M1/M2-like macrophage biology. Enzyme-linked immunosorbent assay was performed to evaluate cytokine secretion of macrophages.

Results VISTA surface expression was identified on CD14⁺ monocytes of 28 of the 37 healthy donors. On PBMC-derived macrophages, VISTA expression was higher in M2-like macrophages than in M0- or M1-like macrophages, and positively correlated with phagocytic activity in M2-like macrophages. Endogenous VISTA expression on monocytes coincided with the expression on CD3⁺ T lymphocytes, whereas absence of VISTA on monocytes coincided with the absence on T lymphocytes. Ectopic expression of VISTA in THP-1 cells facilitated differentiation towards macrophage lineage upon PMA treatment. Additionally, VISTA elicited transcriptional and functional changes in THP-1 and CD34⁺ cell-derived macrophages, increasing M2-like macrophage-related gene expression, while decreasing SIRP α , HLA-ABC, and M1-like macrophage-related gene expression. Further, ectopic VISTA augmented phagocytosis of cancer cells, with a marked decrease in IL-1beta secretion and a significant increase in IL-10 secretion.

Conclusions Collectively, our findings reveal that VISTA expression associates with M2-like activation of macrophages with a high phagocytic capacity, suggesting a role for VISTA in macrophage-mediated immune suppression.

<http://dx.doi.org/10.1136/jitc-2022-SITC2022.0995>

996

FUNCTIONAL AND TRANSCRIPTOMIC PROFILING OF MYELOID CELLS IN PEDIATRIC SOLID TUMORS TO INFORM NEXT GENERATION IMMUNOTHERAPY

¹Sabina Kaczanowska, ²Francesca Buffa, ¹Rosandra Kaplan, ¹Cristina Contreras*. ¹National Cancer Institute, Bethesda, MD, United States; ²University of Oxford, Oxford, UK

Background Monocytes are innate immune cells recognized for their ability to play both tumor permissive and surveillant roles in cancer. The heterogeneity of monocyte function can be guided by tumor-derived factors. Phenotypic and transcriptional alterations in circulating monocytes and other myeloid-derived cells in patients with solid tumors have been reported and associated with clinical outcomes. However, specific monocyte functions and their perturbations in the setting of solid malignancies have not been well explored.

Methods Primary monocytes isolated from healthy donors and pediatric patients with sarcoma were used to examine the production of reactive oxygen species (ROS) via staining with 2',7'-dichlorofluorescein diacetate (DCFDA). Monocyte-mediated phagocytosis of tumor cells was tested by co-culture with the HuO9-H3 human osteosarcoma cell line. Functional populations from healthy donor monocytes were sorted by FACS and bulk RNA-seq was performed on the sorted samples for transcriptomic profiling.

Results We found that monocytes are functionally heterogeneous and identified populations of low and high ROS production as well as phagocytic and non-phagocytic cells. Phagocytosis was dysregulated in patients when compared to healthy donors. In addition, phagocytosis significantly increased when tumor cells were pre-incubated with anti-CD47, a blocker of the "do not eat me" signal on tumor cells (53.16% vs 12.06%, $p=0.0456$). We successfully enriched for these functional populations from three healthy donors by FACS. Pathway enrichment analysis revealed key inflammatory processes increased in phagocytic cells such as GM-CSF, VEGF and PDGF signaling. Of note, phagocytic monocytes of tumor cells blocked with anti-CD47 had downregulated inflammatory signaling and increased anti-inflammatory PPAR signaling, compared to those from the isotype control. In addition, phagocytic cells had higher expression of MHC class II surface receptors than nonphagocytic cells suggesting an activation of antigen presentation.

Conclusions Myeloid ROS production and phagocytosis can provide circulating markers of tumor microenvironment activity. Phagocytosis of tumor cells triggers transcriptional changes in monocytes related to inflammatory and antigen presentation responses. Such changes are dampened when levels of phagocytosis were increased by the addition of anti-CD47, highlighting the importance of evaluating the delicate balance between pro- and anti-tumoral myeloid function. The incorporation of functional selection with -omic characterization provides insights into our understanding of monocyte-function in solid malignancies, which will in turn inform the design of myeloid-mediated therapies.

Acknowledgements This work was supported in part by US National Institutes of Health grants ZIA BC 011332 and ZIA BC 011855 as well as NCI cancer moonshot. Additional support was provided through the NIH Oxford-Cambridge Scholars Program.

Ethics Approval This study is exempt research as determined by NIH Institutional Review Board.

<http://dx.doi.org/10.1136/jitc-2022-SITC2022.0996>

T CELL IMMUNOTHERAPIES TRIGGER NEUTROPHILS TO ELIMINATE HETEROGENOUS TUMORS

¹Sadna Budhu, ²David Redmond, ¹Jacob Ricca, ¹Billel Gasmı, ¹Mathieu Gigoux, ¹Cailian Liu, ¹Yanyun Li, ¹Czrina Cortez, ¹David Schroder, ¹Arshi Arora, ¹Travis Hollman, ¹Lukas Kraehenbuehl, ¹Hyejin Choi, ¹Sara Schad, ¹Isabell Schulze, ³Rebekka Duhen, ³Andrew Weinberg, ¹Andrew Chow, ⁴Mikala Egeblad, ¹Katherine Panageas, ²Gabrielle Rizzuto, ¹Olivier de Henau, ¹Aliya Holland, ⁴Jean Albregues, ¹Linda Hamadane, ⁴David Ng, ⁴Xue-Yan He, ¹Jedd Wolchok, ¹Taha Merghoub, ¹Daniel Hirschhorn*. ¹MSKCC, New York, NY, United States; ²Weill Cornell Medical School, New York, NY, United States; ³Earle A. Childs Research Institute, Portland, OR, United States; ⁴Cold Spring Harbor Laboratory, Cold Spring Harbor, NY, United States; ⁵UCSF, San Francisco, CA, United States

Background Immune surveillance can eliminate developing cancers at the early stages of malignant transformation. The selective pressure that the immune system imposes on tumor cells, however, can “edit” tumors, yielding immune escape variants. Many tumors contain clones that cease to express antigenic proteins. Intra-tumoral antigenic heterogeneity is an important mechanism by which progressing tumors become refractory to standard immunotherapeutic interventions. This is particularly problematic for interventions that target a single antigen, such as adoptive T cell therapies and CAR T cells.

Current immunotherapies in the clinic consist of strategies that mobilize the adaptive compartment of the immune system. The most common approaches include immune checkpoint blockade with antibodies, infusion of ex vivo educated or genetically modified tumor-specific T cells, and therapeutic anti-tumor vaccination. Moreover, a wave of agents that target tumor necrosis factor receptor (TNFR) superfamily members expressed by activated T cells, such as glucocorticoid induced TNF receptor (GITR), 4-1BB and OX40 are being further investigated.

The role of neutrophils in tumor promotion versus tumor elimination is not well understood. The pro-tumorigenic role of neutrophils in chronic inflammation has been described. Higher neutrophil-to-lymphocyte ratios are associated with deleterious outcomes in patients receiving immune checkpoint blockade. Moreover, neutrophil effector mechanisms such as the formation of NETs can promote metastases and can shield tumors from effector T cell elimination. In other models, however, neutrophils and NETs can directly kill cancer. The role of neutrophils as potential effectors in the context of immunotherapies that target T cells remains incompletely defined.

Methods We applied a combination therapy consisting of cyclophosphamide (CTX), CD4⁺ T cells specific for the melanoma antigen Trp1 (Trp1 cells), and an anti-OX40 agonist or anti-CTLA-4 antagonist antibodies to mice bearing advanced antigenically heterogeneous melanomas.

Results Complete eradication of heterogeneous melanomas was observed in mice treated with the combination therapy. Surprisingly, regressing tumors were heavily infiltrated with neutrophils with a distinct anti-tumorigenic phenotype and neutrophil depletion abrogated tumor eradication. Upon closer examination, we observed that inducible nitric oxide synthase expressed by neutrophils was necessary for heterogeneous tumor elimination. In support of these findings, extensive neutrophil activation in biopsies of melanoma patients treated with immune checkpoint blockade. Moreover, our findings uncover a novel interplay between T cells mediating the initial anti-tumor immune response, and neutrophils mediating the destruction of tumor antigen loss variants.

<http://dx.doi.org/10.1136/jitc-2022-SITC2022.0997>

998

NEUTROPHIL SUBSETS IN HEAD AND NECK CANCER

¹Sandra Ekstedt*, ¹Krzysztof Piersiala, ²Magnus Starkhammar, ²Gregori Margolin, ¹Susanna Kumlien Georén, ¹Lars Olaf Cardell. ¹Karolinska Institutet, Sollefnuna, Sweden; ²Karolinska University Hospital, Solna, Sweden

Background The neutrophil is the first cell recruited to the site of inflammation in HNSCC.¹ Neutrophils have been perceived as a relatively homogenous cell type. However, our group has demonstrated that neutrophils can be divided into different subsets.²⁻⁵ and we have identified a subset that can migrate into the tumour in HNSCC patients.⁶ HNSCC may promote a shift towards more activated neutrophil subsets and the neutrophils may thereafter migrate to the lymph nodes.

Methods Thanks to our unique access to unfixed samples of lymph nodes and tumour biopsies of patients with oral HNSCC we were able to identify neutrophil subsets in each tissue and compare them to neutrophils found in the blood. The tissue, homogenized to a single cell suspension, and blood were analyzed with flow cytometry.

Results There are more CD16^{High}CD62L^{High} Neutrophils in the blood compared to lymph nodes and the tumour tissue. The neutrophils subset CD16^{High}CD62L^{dim} neutrophils are found mainly in the lymph node of the cancer patients and the subset CD16^{dim}CD62^{dim} is almost only present in the tumour site. In healthy lymph nodes is the dominant subset CD16^{High}CD62L^{High}.

Conclusions Our study suggests that neutrophil subsets have different functions and play role in HNSCC.

REFERENCES

1. Decker AS, Pylaeva E, Brenzel A, Spyra I, Droege F, Hussain T, *et al.* Prognostic Role of Blood NETosis in the Progression of Head and Neck Cancer. *Cells* 2019;**8**(9).
2. Pillay J, Kamp VM, van Hoffen E, Visser T, Tak T, Lammers JW, *et al.* A subset of neutrophils in human systemic inflammation inhibits T cell responses through Mac-1. *The Journal of Clinical Investigation* 2012;**122**(1):327–36.
3. Ekstedt S, Stenberg H, Tufvesson E, Diamant Z, Bjermer L, Kumlien Georen S, *et al.* The potential role of CD16(high) CD62L(dim) neutrophils in the allergic asthma. *Allergy* 2019;**74**(11):2265–8.
4. Ekstedt S, Tufvesson E, Bjermer L, Kumlien Georen S, Cardell LO. A new role for "eat me" and "don't eat me" markers on neutrophils in asthmatic airway inflammation. *Allergy*. 2020.
5. Ekstedt S, Saffholm J, Georen SK, Cardell LO. Dividing neutrophils in subsets reveals a significant role for activated neutrophils in the development of airway hyperreactivity. *Clinical and Experimental Allergy: Journal of the British Society for Allergy and Clinical Immunology*. 2019;**49**(3):285–91.
6. Millrud CR, Kagedal A, Kumlien Georen S, Winqvist O, Uddman R, Razavi R, *et al.* NET-producing CD16(high) CD62L(dim) neutrophils migrate to tumor sites and predict improved survival in patients with HNSCC. *International Journal of Cancer*. 2017;**140**(11):2557–67.

Ethics Approval All procedures performed in studies involving human participants were in accordance with the ethical standards of the Swedish national research committee and with the 1964 Helsinki declaration and its later amendments or comparable ethical standards. Informed consent was obtained from all individual participants included in the study. Ethics Committee Approvals: 2015/1650-31/2 and 2019-03518.

<http://dx.doi.org/10.1136/jitc-2022-SITC2022.0998>

999

INVESTIGATING THE IMMUNOMODULATORY ROLE OF INNATE LYMPHOID CELLS IN EPITHELIAL OVARIAN CARCINOMA

Douglas Chung*, Kathrin Wamer, Jehan Vakharia, SeongJun Han, Maryam Ghaedi, Carlos García-Batres, Nicolas Jacquilot, Azin Sayad, Sarah Ferguson, Pamela Ohashi. Princess Margaret Cancer Center, Toronto, Canada

Background Innate lymphoid cells (ILCs) are an emerging family of effector cells that mostly reside within non-lymphoid peripheral tissues and orchestrate innate and adaptive immunity in response to infections.¹ ILCs play an important role in cancer including its ability to directly kill cancer cells and promote anti-tumour immunity within the tumour microenvironment (TME).² In addition to these classical pro-inflammatory functions of ILCs, our group and others have identified a subset of immunoregulatory ILCs (ILCregs) in various diseases including cancer.³ We previously found a CD56⁺ ILCreg population that suppressed T cells in slow growing ex vivo tumour-infiltrating lymphocyte (TIL) cultures.⁴ The objective of this study is to identify markers that distinguish immunoregulatory and non-immunoregulatory ILCs straight from primary tumours and uncover its role within the TME of epithelial ovarian carcinoma (EOC).

Methods Women with suspected EOC were recruited and consented pre-operatively at the Gynecology Cancer Clinic at Princess Margaret Hospital. Surgical resections were processed and analyzed by flow cytometry and single-cell RNA sequencing (scRNA-seq). In vitro stimulation of peripheral blood CD56⁺ ILCs were performed over 7 days in IL-15 with 50% ascites supernatant.

Results We identified subsets of intratumoural ILCs including ILC1s, ILC2s, ILC3s, and CD56⁺ ILCs within lineage negative populations. Interestingly, a population of CD56⁺ GZMB⁻ ILCs exhibited distinct tissue-resident-like properties including expression of tissue-retention marker CD69 and reduced expression of tissue-egress marker CD49e. Interestingly, transcriptomic profile of CD56⁺GZMB⁻CD49e⁻ ILCs from our scRNA-seq dataset (n=3) had similar gene expression as intraepithelial ILC1s (ieILC1) from other studies.⁵ These ieILC1-like cells were associated with poor recurrent free survival and reduced granzyme B expression in CD8⁺ TILs. Moreover, ieILC1-like phenotypes can be induced from peripheral blood CD56⁺ cells using ascites supernatant from patients with EOC. Finally, ieILC1-like cells from primary tumours expressed gene signatures that have been previously upregulated in ILCregs and regulatory T cells (Tregs), suggesting that these populations may have immunoregulatory properties. Ongoing work is being done to identify whether ieILC1-like cells directly suppress T cells in vitro, and uncover mechanisms of immunosuppression.

Conclusions Our findings suggest that ieILC1-like CD56⁺ cells are negatively associated with prognosis of EOC and may play a unique role in modulating the tumour microenvironment. Further investigation into the biology of ILCs in human tumours may provide novel therapeutic targets for ovarian carcinoma and beyond.

REFERENCES

1. Sonnenberg GF, Artis D. Innate lymphoid cells in the initiation, regulation and resolution of inflammation. *Nat Med* 2015;**21**:698–708.
2. Jacquilot N, Seillet C, Vivier E, Belz GT. Innate lymphoid cells and cancer. *Nat Immunol*. 2022; **23**: 371–379.
3. Chung DC, Jacquilot N, Ghaedi M, Warner K, Ohashi PS. Innate lymphoid cells: Role in immune regulation and cancer. *Cancer*. 2022; **14**(9): 2071.

4. Crome SQ, Nguyen LT, Lopez-Verges S, Yang SYCC, Martin B, Yam JY, Johnson DJ, Nie J, Pniak M, Yen PH, *et al.* A distinct innate lymphoid cell population regulates tumor-associated T cells. *Nat Med* 2017; **23**: 368–375.
5. Collins PL, Cella M, Porter SI, Li S, Gurewitz GL, Hong HS, Johnson P, Oltz EM, Colonna M. Gene regulatory programs conferring phenotypic identities to human NK cells. *Cell*. 2019;**176**: 348–360.

Ethics Approval This study was conducted according to principles in the Declaration of Helsinki. The Research Ethics Board (REB) of the University Health Network (UHN) approved of this study. Fresh tissue was prepared from pre-operatively consented patients with EOC who were undergoing standard-of-care surgical procedures (UHN REB 10-0335).

<http://dx.doi.org/10.1136/jitc-2022-SITC2022.0999>

1000

MELANOMA LYMPH NODE METASTASES ARE ASSOCIATED WITH HYPOXIA AND IMMUNOLOGIC DYSFUNCTION

¹Dustin McCurry*, ²Christopher Deitrick, ²Yan Zang, ²Arivarasan Karunamurthy, ²Theresa Whiteside, ²Diwakar Davar, ²Hassane Zarour, ²Jason Luke, ²John Kirkwood, ²Riyue Bao, ²Yana Najjar. ¹University of Texas MD Anderson Cancer Center, Houston, TX, United States; ²UPMC Hillman Cancer Center, Pittsburgh, PA, United States

Background Deranged cellular metabolism is a hallmark of cancer and the hypoxic tumor microenvironment (TME) is associated with T-cell dysfunction. We have shown that in melanoma patient samples, high tumor cell oxidative stress is associated with T-cell dysfunction, intratumoral hypoxia, and worse clinical outcomes. Less is known about the impact of tumor cells on the environment of sentinel lymph nodes (SLN), though recent studies have implicated SLN as critical sites in the efficacy of the anti-tumor immune response. Thus, we sought to assess the impact of melanoma SLN metastasis on intra-nodal immune cell composition and hypoxia.

Methods We identified 87 patients with primary melanoma who had undergone SLN biopsy. Tumor FFPE slides were stained and imaged using Vectra OPAL panels (immune: CD3, FOXP3, CD8, CD68; tumor: SOX10; checkpoint receptor/ligands: PD-1, PD-L1, IDO [indoleamine 2,3-dioxygenase]; hypoxia: HIF-1a [Hypoxia-inducible factor 1-alpha], CAIX [carbonic anhydrase IX]). 732 regions of interest (ROIs) were selected from 47 patients who had a positive SLN, and 426 ROIs from 40 patients with a negative SLN. 20X images were analyzed for cell segmentation by StarDist, and phenotyping by Random Forests machine learning models. Images from adjacent tumor sections were co-registered using SimpleITK to enable spatial evaluation of markers across panels. Cell density and distances in tumor, tumor/stroma boundary (+/-50um), and stroma were compared between groups using linear mixed-effects models (LMM). The study was approved by the University of Pittsburgh's Institutional Review Board.

Results Within tumor infiltrated sentinel lymph nodes, areas of SOX10+ metastatic melanoma were enriched for CAIX, a marker of hypoxia. IDO, an immunosuppressive enzyme which is upregulated in hypoxic conditions, was more frequently expressed within the surrounding stroma (CD3-SOX10-) of tumor infiltrated nodes compared to negative nodes ($p < 0.0001$). The immune composition of CD68+ myeloid cells, FOXP3+ T-cells, and CD8+ T-cells was similar in infiltrated and non-infiltrated nodes. Consistent with other reports of immune dysfunction within tumor infiltrated nodes, the frequency of PD-1+CD8+ cells was significantly enriched compared to negative lymph nodes ($p < 0.01$).

Conclusions Infiltration of tumor draining lymph nodes by metastatic melanoma is associated with markers of immunologic dysfunction and intranodal hypoxia. This constellation of features recapitulates the hypoxic primary tumor microenvironment. Studies are underway to evaluate the potential of oxidative balance within melanoma SLN as a prognostic biomarker.

Ethics Approval The study was approved by the University of Pittsburgh's Institutional Review Board.

<http://dx.doi.org/10.1136/jitc-2022-SITC2022.1000>

1001

IMMUNOPHENOTYPING OF BRAIN TUMORS IDENTIFIES INTERFERON ENRICHED PHAGOCYTES IN HUMAN GLIOMAS

¹Pravesh Gupta*, ¹Minghao Dang, ¹Dapeng Hao, ¹Krishna Bojja, ¹Tuan Tran, ¹Huma Shehwana, ¹Carlos Kamiya-Matsuoka, ¹Jianzhuo Li, ¹Alessandra Audia, ¹Cynthia Kassab, ¹Martina Ott, ¹Joy Gumin, ¹Sanaalarab Alenazy, ²Alicia Goldman, ²Sameer Seth, ²Atul Maheshwari, ¹Veerakumar Balasubramanian, ³Brian Vaillant, ¹John de Groot, ⁴Antonio Lavarone, ¹Frederick Lang, ¹Nicholas Navin, ⁵Amy Heimerger, ¹Linghua Wang, ¹Krishna Bhat. ¹University of Texas MD Anderson Cancer Center, Houston, TX, United States; ²Baylor College of Medicine, Houston, TX, United States; ³The University of Austin, Austin, TX, United States; ⁴Columbia University Medical Center, Herbert Irving Comprehensive Cancer Center, New York, NY, United States; ⁵Feinberg School of Medicine, Northwestern University, Chicago, IL, United States

Background Gliomas are recalcitrant brain tumors. Anti-glioma immunity and immunopathogenic responses are critical contributors for better survival of isocitrate dehydrogenase-mutant (IDH^{mut}) over wild-type (IDH^{wt}) gliomas. Despite this correlative pattern of immunity and survival, an unbiased understanding of cell-type specific transcriptomic and epigenomic states of glioma-derived myeloid cells beyond immunosuppressive paradigms remains elusive.

Methods To this end, we performed single-cell RNA-sequencing (scRNA-seq) on 140,000 tumor-associated immune cells from eighteen IDH mutation classified primary (N=8) and recurrent (N=10) human gliomas and three non-glioma brains (NGBs). We performed unsupervised clustering and cell annotation based on overlapping canonical lineage and signal dependent transcription factors. Gene ontology and gene set enrichment analyses were performed to define functional states of glioma associated myeloid cells.

Results Our analyses revealed twelve myeloid cell types across glioma subgroups. We noted abundant microglial cells in IDH^{mut} than IDH^{wt} gliomas. Concomitantly, continuum of microglia and macrophage phenotypes were observed in IDH^{wt} glioma, which exhibit more severe tumor pathologies. Strikingly, we identified a hybrid microglia/macrophage cell subset with enriched interferon module inferred from our gene ontology analyses. These hybrid phagocytes were significantly increased in recurrent IDH^{wt} gliomas. As tissue macrophages exhibit multifaceted polarization in response to microenvironmental cues, we clarify the existence of microglia/macrophage functional states beyond M1/M2 paradigms exemplified by the presence of palmitic-, oleic- acid, and glucocorticoid responsive polarized states. Specifically, certain microglia and monocyte-derived subpopulations were associated with antigen presentation gene modules, akin to cross-presenting dendritic cells. Furthermore, immune related gene ontology analysis identified enriched antigen presentation and phagocytosis gene modules in distinct microglia-like clusters. Importantly, the phagocytic immunomodulator; Triggering Receptor Expressed on Myeloid Cells 2 (TREM2) was upregulated in these microglia-like cells. Contrary to tumor promoting role of TREM2 myeloid cells in non-brain cancers, we identify TREM2 axis as a regulator of antigen presentation. Additionally, single cell- Assay for Transposase-Accessible Chromatin using sequencing (sc-ATAC-seq) on ~40,000 tumor-associated microglia revealed genes associated with IFN-gamma/IL-12/IL-10 pathway were negatively regulated in IDH^{mut}/IDH^{wt} microglia compared to homeostatic microglia in NGBs.

Conclusions In summary, our study sculpts transcriptional and epigenomic details and re-defines glioma-specific immune contexture for downstream immunogenomics applications. We specifically reveal interferon and TREM2 nodes on microglia-

like phagocytic cells as clinically tractable anti-glioma immunotherapy target.

<http://dx.doi.org/10.1136/jitc-2022-SITC2022.1001>

1002

CIRCULATING MYELOID STATES INDUCED WITH ANTI-PD-1 AND GM-CSF COMBINATION THERAPY ARE ASSOCIATED WITH TREATMENT RESISTANCE IN HUMAN BILIARY CANCER

¹Bridget Keenan*, ¹Elizabeth McCarthy, ¹Arielle Ilano, ¹Diamond Luong, ¹Hai Yang, ¹Li Zhang, ¹Kathryn Allaire, ¹Zenghua Fan, ²Tony Li, ²David Lee, ¹Yang Sun, ¹Alexander Cheung, ¹Hewitt Chang, ¹Brandon Chen, ¹Brenna Sheldon, ¹Robin Kelley, ¹Chun Jimmie Ye, ¹Lawrence Fong. ¹University of California San Francisco, San Francisco, CA, United States; ²University of Washington, Seattle, WA, United States

Background Advanced biliary tract cancers (BTC) have a poor prognosis and low rates of response to immune checkpoint inhibition (CPI), with overall response rates ranging from 3–13%.^{1–3} The BTC tumor microenvironment contains immunosuppressive immune populations, desmoplastic stroma, and a paucity of tumor infiltrating effector T cells^{4,5}, but the role of circulating immune cells in response and resistance to CPI is less well-characterized. We aimed to explore circulating immune cells from BTC patients treated with CPI to understand immunotherapy response and resistance.

Methods We used multiplexed multi-omic single cell RNA sequencing and cell surface proteomics (CITEseq) to profile >400,000 circulating immune cells in BTC patients receiving anti-PD-1 with and without GM-CSF as part of a phase II clinical trial (NCT02703714)⁶, as well as from age and gender-matched healthy donors. We also evaluated a subset of tumor tissues from BTC patients to investigate the spatial organization of immune cell populations.

Results Using CITEseq, we identified several unique CD14⁺ monocyte sub-populations in BTC patients' circulation compared to healthy donors. In the circulation of patients with BTC tumors that are CPI-resistant, there was an increased frequency of "CD14_{CTX}", a monocyte sub-population expressing high levels of immunosuppressive cytokines and chemotactic molecules, following anti-PD-1 monotherapy. CD14_{CTX} can directly suppress CD4⁺ T cells and induce SOCS3 expression in CD4⁺ T cells, rendering them functionally unresponsive. Analogous tumor-associated macrophage populations could also be found within tumor tissues. Consistent with the pleiotropic effects of GM-CSF, we saw changes in the frequency and genomic programs of multiple myeloid populations, including dendritic cells and monocytes, when GM-CSF was combined with anti-PD-1. Within one week of GM-CSF combination therapy, monocyte-derived dendritic cells were induced in the circulation of BTC patients and associated with pro-inflammatory signals, including upregulation of MHC I and II in monocytes and dendritic cells.

Conclusions These results demonstrate the capacity of CPI plus GM-CSF combination therapy to induce monocyte states that both foster and inhibit adaptive immunity. Monocytes arising after anti-PD-1 treatment induced T cell paralysis in a subset of patients with CPI-resistant tumors, as a distinct mode of tumor-mediated immunosuppression. GM-CSF demonstrated the potential to enhance both pro-inflammatory and antigen-processing and presentation-related programs within myeloid cells. These results highlight the importance of identifying pharmacodynamic markers of immune response and targets for combination immunotherapy to overcome CPI resistance in BTC.

Trial Registration NCT02703714

REFERENCES

1. Ueno M, *et al.* Nivolumab alone or in combination with cisplatin plus gemcitabine in Japanese patients with unresectable or recurrent biliary tract cancer: a non-

randomised, multicentre, open-label, phase 1 study. *Lancet Gastroenterol Hepatol* 2019;**4**:611–621.

2. Piha-Paul SA, *et al.* Efficacy and safety of pembrolizumab for the treatment of advanced biliary cancer: Results from the KEYNOTE-158 and KEYNOTE-028 studies. *Int J Cancer* 2020.
3. Kim RD, *et al.* A Phase 2 multi-institutional study of nivolumab for patients with advanced refractory biliary tract cancer. *JAMA Oncol* 2020;**6**: 888–894.
4. Rizvi S, Khan SA, Hallemeier CL, Kelley RK & Gores GJ. Cholangiocarcinoma – evolving concepts and therapeutic strategies. *Nat Rev Clin Oncol* 2018;**15**, 95–111.
5. Zhang M, *et al.* Single cell transcriptomic architecture and intercellular crosstalk of human intrahepatic cholangiocarcinoma. *Journal of Hepatology* 2020.
6. Kelley RK, *et al.* Phase II trial of pembrolizumab (PEM) plus granulocyte macrophage colony stimulating factor (GM-CSF) in advanced biliary cancers (ABC). *Journal of Clinical Oncology* 2018;**36**, 386–386.

Ethics Approval Peripheral blood mononuclear cells were obtained from patients (per UCSF institutional review board (IRB) #15-18420) from the clinical trial #NCT02703714. Tumor samples were collected from patients biopsied as part of the clinical trial and from patients undergoing standard-of-care resections and consented under the UCSF Hepatobiliary Tissue Bank and Registry (IRB #12-09576). Healthy donor PBMCs were collected from age and gender-matched healthy donors as part of the Cancer Immunotherapy Biobanking protocol and the Immune Cell Census (IRB #15-16385 and #19-27147, respectively). Informed consent was obtained from all patients for participation in the listed trials and for use of blood and tumor samples in research studies.

Consent None of the patient data in this abstract is identifiable; IRB information included as above.

<http://dx.doi.org/10.1136/jitc-2022-SITC2022.1002>

1003

MACROPHAGE ADHESION TO TUMOR CELLS POSITIVELY IMPACTS TUMOR GROWTH

¹Jovan Nikolic, ²Joseph Ackerman, ¹Sarah Taherally, ³Thierry Rose, ¹Ouardia Ait-Mohamed, ²Martine Ben Amar, ¹Jean-François Joanny, ¹Philippe Benaroch*. ¹Institut Curie, Paris, France; ²Ecole Normale Supérieure, Paris, France; ³Institut Pasteur, Paris, France

Background Myeloid cells are major players of the tumor microenvironment contributing to immune evasion mechanisms and providing pro-tumorigenic effects. Here we aim to analyze at the physical and molecular level, how myeloid cells can impact tumor growth and fate.

Methods Combining quantitative cell biology with the derivation of physical modeling of tumor growth, allow us to extract key parameters and make predictions that are testable both, by simulations *in silico* and by *in vitro* experiments.

Results We set up an *in vitro* system to follow the growth of tumor spheroids in 3D by real-time microscopy over long periods of time. Importantly, we replicate in this system the strong positive effect of alveolar macrophages on tumor growth and the poor effect of monocytes. From the quantifications and growth curves obtained, we derived mathematical modeling of spheroid growth in 2 and 3D. The semi-continuous model we developed makes use of a particle-based model which allows the treatment of proliferating cells in physical interactions. This model, tested in simulations, fits well with the data obtained in the absence or presence of macrophages. The model predicted that adhesion forces between tumor cells and macrophages are key in the pro-tumoral effect observed. Among the integrins potentially mediating these forces, CD11c stands out as a key candidate since it is expressed by alveolar macrophages but not by monocytes. Anti-CD11c blocking antibodies indeed diminish cell-to-cell adhesion forces as measured by a rupture force assay, prevent spheroid nucleation, and impair spheroid growth.

Conclusions Our results establish that adhesion of macrophages to tumor cells can have a direct impact on tumor growth by modifying key physical parameters. These findings may lead to the identification of new approaches targeting myeloid cells to counteract their pro-tumoral activity within the tumor microenvironment.

Acknowledgements Grants to PB and J-FJ were provided by ITMO PCSI and ITMO MCMP. PB also received grants from Chercher Trouver foundation, PSL/Qlife, Emergent Curie project.

<http://dx.doi.org/10.1136/jitc-2022-SITC2022.1003>

1004

SIGNALING PATHWAYS INDUCING TUMORICIDAL PHAGOCYTOSIS IN PANCREATIC CANCER

¹Li Qiang*, ¹Stephanie Dougan, ¹Samantha Liu, ²Gabrielle Ro, ³Michael Dougan, ¹Lestat Ali, ¹Patrick Lenehan, ¹Felix Hambitzer. ¹Dana-Farber Cancer Institute, Harvard Medical School, Boston, MA, United States; ²University of Utah, Salt Lake City, UT, United States; ³Massachusetts General Hospital, Boston, MA, United States

Background Macrophages can be repolarized to promote tumor destruction, particularly by triggering tumoricidal phagocytosis of cancer cells. Despite the increasing interest in monoclonal antibody therapies targeting tumor antigens to drive cancer cell elimination via phagocidal macrophages, we still face tremendous challenges in developing adequate therapeutics due to lack of knowledge of the signaling pathways that induce phagocidal macrophages. Our previous work showed that cIAP1/2 antagonism and T cell derived cytokines promote anti-tumor immunity by reprogramming tumoricidal macrophages to phagocytose live tumor cells.

Methods Here we performed transcriptional analysis on both macrophages and tumor cells treated with cIAP1/2 antagonism or vehicle and identified candidate positive and negative regulators of phagocytosis. We are demonstrating how these receptors-ligand pairs on macrophages and tumor cells are induced and the mechanisms by which they effect tumor cell destruction. We also performed an in vitro CRISPR screen on tumor cells cocultured with macrophages, treated with cIAP1/2 antagonism or vehicle, recovered the DNA of phagocytosed tumor cells from within macrophages and compared to non-phagocytosed tumor cells to discover mediators of resistance or sensitivity to both baseline phagocytosis (efferocytosis) and cIAP1/2 antagonism induced phagocytosis. Our screen revealed a striking lack of dependence on MHC class I for tumors treated in vivo. Genes involved in phagocytosis resistance instead converged on regulation of the cytoskeleton and *other candidates which we have now validated in single gene knockout tumor cells and will be discussed*. This study will provide critical insights on tumoricidal macrophages, uncover the key pathways reprogramming these myeloid cells, and decipher the essential tumor-intrinsic pathways resulting in sensitivity and resistance to anti-tumor phagocytosis.

<http://dx.doi.org/10.1136/jitc-2022-SITC2022.1004>

1005

PD-L1 KNOCKOUT NATURAL KILLER CELLS AS A CELLULAR PRODUCT FOR THERAPEUTIC USE IN COMBINATION WITH HUMANIZED ADCC-COMPETENT ANTI-PD-L1

¹Taylor Croom-Perez*, ²Jeremiah Oyer, ¹Md Faqur Hasan, ¹Thomas Dieffenthaler, ¹Liza Robles-Carrillo, ²Aliqa Copik. ¹University of Central Florida, Orlando, FL, United States; ²University of Central Florida, College of Medicine, Orlando, FL, United States

Background Immunotherapeutic strategies, such as checkpoint blockade of PD-1/PD-L1, have become a focal point of immunotherapy in oncology. Recent studies highlight the importance of Natural Killer (NK) cells in the success of these immunotherapies and adoptive NK cellular therapy is being explored to enhance response to these treatments. Antibodies targeting PD-L1 are mostly Fc silent but some, such as Avelumab, can engage FcγR (CD16) receptor on NK cells resulting in killing cancer cells via antibody-dependent cellular cytotoxicity (ADCC). PM21-particle expanded NK (PM21-NK) cells are an optimal NK cell product to consider for a combination strategy as these NK cells lack PD-L1 but can induce PD-L1 on tumors cells. Previous reports, however, have shown that PD-L1 can be induced on NK cells. This could potentially lead to fratricide of NK cells in the presence of Fc-competent, PD-L1 targeting antibodies and mitigate their cytotoxic response. This study determined if PD-L1 can be induced on PM21-NK cells and what effect PD-L1 engagement had on their activity and potential for fratricide in both WT and PD-L1 knockout PM21-NK cells.

Methods CRISPR-based Knockout (KO) of PD-L1 in PM21-NK cells was performed and efficiency was determined after overnight incubation of WT or PD-L1 KO PM21-NK cells with cytokines to induce PD-L1 expression. Cancer cells were incubated with NK cells in the presence of non-competent or Fc-competent α-PD-L1 and cytotoxicity was measured using a kinetic live-cell imaging assay. NK cell fratricide was measured in cultures of WT or PD-L1 KO PM21-NK cells induced for PD-L1 expression with non-competent or Fc-competent α-PD-L1.

Results PM21-NK cells were found to express low levels of PD-L1 (< 20%) after exposure to various cancer cell line monolayers or K562 co-culture. Exposure to SKOV-3 spheroids or to a cytokine combination of IL12, IL15, and IL18 led to a significant induction in PD-L1 in WT PM21-NK cells (> 80%). PD-L1 knockout prevented the induction of PD-L1 on NK cells after cytokine exposure and enhanced cytotoxicity. Fratricide was decreased and cytotoxicity increased in PD-L1 KO PM21-NK cells in combination with Fc-competent α-PD-L1.

Conclusions Knockout of PD-L1 in *ex vivo* expanded PM21-NK cells prevented the induction of PD-L1 on NK cells without negative effects on cytotoxicity. PD-L1 KO PM21-NK cell cytotoxicity was further enhanced in combination with Fc-competent α-PD-L1 compared to WT NK cells. PD-L1 knockout PM21-NK cells are a potential cell product for therapeutic use in combination with PD-L1 targeting antibodies.

Acknowledgements We would like to thank the FL DOH (Grant #9JK04); Kiadis Pharma, a Sanofi company; and the UCF Preeminent Postdoctoral Program for funding and Max-Cyte for providing instrument for initial testing.

<http://dx.doi.org/10.1136/jitc-2022-SITC2022.1005>

1006

SINGLE-CELL FUNCTIONAL GENOMICS OF NATURAL KILLER CELL EVASION IN BLOOD CANCERS

¹Olli Dufva*, ¹Sara Gandolfi, ¹Jani Huuhtanen, ²Olga Dashevsky, ¹Khalid Saeed, ¹Jay Klievink, ¹Petra Nygren, ¹Jonas Bouhlal, ³Jenni Lahtela, ³Anna Näätänen, ³Bishwa Ghimire, ³Tiina Hannunen, ³Pekka Ellonen, ¹Hanna Duàn, ¹Jason Theodoropoulos, ¹Essi Laajala, ⁴Jouni Härkönen, ⁵Petri Pölonen, ⁴Merja Heinäniemi, ²Shizuka Yamano, ²Ryosuke Shirasaki, ²David Barbie, ⁶Jennifer Roth, ²Rizwan Romee, ²Michal Sheffer, ⁷Harri Lähdesmäki, ⁸Dean Lee, ²Ricardo De Matos Simoes, ¹Matti Kankainen, ²Constantine Mitsiades, ¹Satu Mustjoki. ¹University of Helsinki, Helsinki, Finland; ²Dana-Farber Cancer Institute, Boston, MA, United States; ³Institute for Molecular Medicine Finland, Helsinki, Finland; ⁴University of Eastern Finland, Helsinki, Finland; ⁵St. Jude Children's Research Hospital, Memphis, TN, United States; ⁶Broad Institute of MIT and Harvard, Cambridge, MA, United States; ⁷Aalto University, Espoo, Finland; ⁸Nationwide Children's Hospital, Columbus, OH, United States

Background Natural killer (NK) cells are emerging as a promising therapeutic option in cancer. To better understand how cancer cells evade NK cells, we studied interacting NK and blood cancer cells using single-cell and genome-scale functional genomics screens.

Methods We performed multiplexed single-cell RNA-seq (scRNA-seq) on co-cultures of NK cells and 26 cell lines representing diverse blood cancers. Using screens of pooled DNA-barcoded cell lines (PRISM), we quantified the sensitivity of over 60 blood cancer cell lines and integrated the results with CCLE multi-omics to uncover molecular correlates of tumor cell susceptibility to NK cells. We performed 12 genome-scale CRISPR loss-of-function and gain-of-function screens of cancer-cell intrinsic NK cell resistance mechanisms across 7 blood cancer cell lines. Finally, we investigated the mechanisms-of-action of 65 genome-scale screen hits using CRISPR screens with scRNA-seq readout in both tumor and NK cells.

Results At single-cell resolution, interaction of NK and cancer cells induced distinct activation states in both cell types depending on the cancer cell lineage and molecular phenotype. NK cells transitioned either into an activated state characterized by *4-1BB*, *GITR*, *TIM-3*, and *TIGIT* or a state marked by type I interferon signature. Tumor cells responded to NK cell attack by activating interferon gamma (IFN γ) signaling, inducing MHC class I. The activation states correlated with sensitivity to NK cells, ranging from more sensitive myeloid to more resistant B-lymphoid cancers. Molecular correlates of increased sensitivity included expression of activating receptor ligands *NCR3LG1*, *PVR*, and *ULBP1* and mutations in the NF- κ B regulator *TRAF3*. CRISPR screens uncovered cancer cell-intrinsic genes driving sensitivity and resistance, including antigen presentation and death receptor signaling mediators and adhesion molecules. The screens identified new blood cancer-specific NK cell inhibitory regulators (*SELPLG*, *SPN*, and *MYB*) and genes previously underappreciated in NK cell evasion, including protein fucosylation and transcriptional regulators (e.g. *GFI1B*). CRISPR screens with scRNA-seq readout identified MHC-I, IFN γ , and NF- κ B regulation as underlying mechanisms. Cancer cell knockout of positive regulators of NK cell response (*CD58*, *NCR3LG1*) induced an inactive NK cell state, providing experimental evidence how cancer cell-intrinsic genetic alterations can shape the molecular profile of attacking immune cells to promote immune evasion.

Conclusions By integrating diverse functional genomics screens and patient genomic profiles, we provide a comprehensive landscape of potential biomarkers and functionally validated genetic mechanisms which influence how NK cells recognize and kill malignant cells. The results offer a roadmap to

facilitate development of NK-cell based immunotherapy for blood cancers and beyond.

Ethics Approval The study was approved by the Helsinki University Hospital ethics committee, (permit number 303/13/03/01/2011), and abided by the principles of the Declaration of Helsinki.

<http://dx.doi.org/10.1136/jitc-2022-SITC2022.1006>

1007

MICROGLIA RECRUIT AND ACTIVATE NATURAL KILLER CELLS TO CONTROL TUMOR PROGRESSION IN BREAST CANCER BRAIN METASTASIS

Timothy McMullen*, Aaron Longworth, Dennis Ma, Devon Lawson, Katrina Evans.
University of California, Irvine, Irvine, CA, United States

Background Metastatic brain tumors are incurable, rapidly fatal, and five times more common than primary glial or meningeal tumors of the central nervous system (CNS). Up to 30% of metastatic breast cancer patients will develop brain metastasis as a complication of their disease. This represents a significant clinical problem for the 1 in 8 women who will receive a diagnosis of invasive breast cancer during her lifetime. Natural Killer (NK) cells are cytotoxic lymphocytes with strong *in vivo* anti-tumor activity, a native ability to cross the BBB, and a demonstrated role in regulation of metastasis in peripheral organs. NK cells perform critical roles in antitumor immunosurveillance via the expression of germline-encoded activation and inhibition receptors on the cell membrane. These receptors recognize ligands on both normal and transformed cells, and ultimately determine whether an NK cell will be stimulated to kill a neoplastic cell or inhibited from killing a healthy cell. Notably, NK cells are under investigation in clinical trials as both drug targets and adoptive cell therapies.

Methods We have performed single-cell RNA sequencing (scRNA-seq) in conjunction with a fluorescent cytokine screen to determine the cytokine secretion profile of microglia under tumor-bearing conditions. We have also carried out NK cell-depletion experiments using intraperitoneal injections of i.p. injections of anti-Asialo GM1 IgG to determine the functional significance of NK cells in the response to breast cancer brain metastasis.

Results Our scRNA-seq data and cytokine screen suggest that NK cell activation and recruitment to the brain in BCBM depends on the secretory action of microglia. Furthermore, we observe a complete lack of NK cell infiltration in microglia-knockout mice harboring breast cancer brain metastasis. We confirm with selective antibody-mediated NK cell depletion that NK cells are critical for preventing the outgrowth of disseminated tumor cells in the brain. However, we also observe NK cell dysfunction within the microenvironment of brain metastasis—a clear obstacle to the development of NK cell-based therapies for intracranial metastatic lesions.

Conclusions Microglia appear to play a necessary role in the recruitment of NK cells to the brain under metastatic conditions. An improved understanding of the native functional status of NK cells in the context of brain metastasis, including their interactions with microglia, will inform the development of neuroprotective anti-metastatic therapies aimed at modulating and potentiating the anti-tumor action of both native and adoptive NK cells.

Ethics Approval All experiments were approved by IACUC at the University of California, Irvine

<http://dx.doi.org/10.1136/jitc-2022-SITC2022.1007>

1008

CROSS-SPECIES CHARACTERIZATION OF SPLENIC NATURAL KILLER (NK) CELLS REVEALS ORGAN-SPECIFIC HETEROGENEITY WITH IMPLICATIONS FOR CANCER IMMUNOTHERAPY

Khurshid Iranpur*, Aryana Razmara, Sylvia Cruz, Marshall Lammers, Cyrus Sholevar, Robert Rebhun, Michael Kent, William Culp, Richard Bold, Sean Judge, William Murphy, Robert Canter, Lauren Farley*. *University of California Davis Health, Sacramento, CA, United States*

Background Natural killer (NK) cell immunotherapy is a promising modality for cancer immunotherapy, but questions of optimal donor characteristics for in vivo persistence, engraftment, and effector function remain. Splenic NK cells have been poorly characterized in humans and dogs. Although they are not readily available as a source for adoptive immunotherapy, we hypothesized that splenic NK harbor unique phenotype and function which can inform optimal NK immunotherapy.

Methods Matched NK cells were isolated from spleen and blood of 4 human and 3 dog patients undergoing surgery. Immune phenotype, proliferation, viability, and apoptosis were assessed pre and post 14 days of co-culture with irradiated clone9 K562 feeders. Differential gene expression was assessed using 3'-Tag-RNA-sequencing.

Results NK cell frequencies in resting human spleen were significantly lower compared to PBMCs per live CD45+ cells ($9.4 \pm 0.3\%$ vs. $16.7 \pm 8.8\%$, $P=0.05$) whereas the frequencies of NKT, CD3+, and CD8+ were not significantly different ($P>0.05$ all). Phenotypically, TIGIT expression was higher in resting human spleen NK compared to PBMCs ($39.8 \pm 2.4\%$ vs. $19.0 \pm 8.6\%$), as was CD69 ($23.8 \pm 8.7\%$ spleen vs. $14.4 \pm 7.6\%$ PBMCs). Across both dog and human, spleen cells expanded more significantly than PBMCs with human showing 266-fold versus 105-fold expansion. In human, maximal expansion was also greater for spleen NK cells ($690 \pm 1080 \times 10^6$) compared to PBMC NKs ($111 \pm 165 \times 10^6$), although not statistically significant. Similar results were obtained with dog NK expansions. Purity of human NK cells at day 14 was similar for spleen and PBMC-expanded NK cells at $>90\%$, and both groups showed similar Ki67 (70-90%) and Granzyme B (97-100%). In killing assays against human sarcoma targets (SAOS2, A673), there was greater cytotoxicity with spleen-expanded NK cells compared to PBMC-expanded at 10:1 E:T (40-50% vs. 30-35%). Day 14 spleen-expanded NK cells from dog showed greater killing compared to PBMC-expanded against osteosarcoma and melanoma targets at 10:1 E:T (45% vs. 25%). At day 14, there was no difference in apoptosis between human spleen and PBMC-expanded NK cells. Sequencing results showed an upregulation of genetic pathways associated with persistence and metabolic fitness for both human and dog spleen-expanded NK cells at day 14.

Conclusions NK cells derived from spleen appear to show greater activation and expansion compared to PBMC-derived in human and dog subjects with no difference in apoptosis. Further characterization of NK cells from the spleen may provide novel insights into mechanisms to overcome barriers to successful NK immunotherapy for solid tumors in both human and canine models.

<http://dx.doi.org/10.1136/jitc-2022-SITC2022.1008>

1009

KNOCKOUT OF THE INHIBITORY RECEPTOR TIGIT ENHANCES ANTI-TUMOR RESPONSE OF *EX VIVO* EXPANDED NK CELLS AND PREVENTS FRATRICIDE WITH THERAPEUTIC Fc-COMPETENT TIGIT ANTIBODIES

Md Faqrul Hasan*, Tayler Croom-Perez, Jeremiah Oyer, Thomas Dieffenthaler, Liza Robles-Carrillo, Alicja Copik. *University of Central Florida, Orlando, FL, United States*

Background Antibody blockade of the Natural Killer cells (NK cells) and T cell inhibitory receptor TIGIT has been shown to enhance tumor control and survival in preclinical mouse models and early clinical trials; however, there is a lack of understanding of the effect of TIGIT engagement on anti-tumor functions of activated primary human NK cells. Additionally, the majority of TIGIT antibodies in clinical development have a humanized IgG, which induces antibody-dependent cellular cytotoxicity (ADCC) and likely contributes to their efficacy. However, the potential consequences of these Fc-competent antibodies when binding NK cells, such as fratricide, have not been well characterized. Fratricide could deplete NK cells upon treatment, a detrimental effect to the overall efficacy since NK cells play a critical role in the success of checkpoint blockade immunotherapies. Recent efforts have focused on developing adoptive NK cell therapy and combinatorial immune-oncology therapies in order to enhance response. Adoptive transfer of TIGIT KO NK cells could provide a treatment strategy to mitigate potential negative effects of TIGIT blockade on NK cells. In this study, TIGIT knockout in *ex vivo* PM21-particle expanded human NK cells was performed and the effect on anti-tumor activity alone or in combination with Fc-competent TIGIT antibody blockade was evaluated and compared to WT NK cells.

Methods CRISPR was used to make a targeted TIGIT knockout (KO) in *ex vivo* PM21-particle expanded NK cells (PM21-NK cells). TIGIT KO NK cells were compared to wild type (WT) NK cells to determine changes cytotoxicity, ADCC, and IFN γ , TNF α , and the degranulation marker CD107a expression. Glycolytic rate and mitochondrial stress were measured. TIGIT KO or WT PM21-NK cells were combined with Fc-competent or non-Fc-competent anti-TIGIT and fratricide and cytotoxicity were measured.

Results TIGIT KO PM21-NK cells showed improved killing compared to WT against 3D spheroids from multiple cancer cell lines. ADCC increased proportionally in TIGIT KO NK cells. TIGIT KO PM21-NK cells had increased CD107a surface expression after cancer spheroid exposure and increased basal glycolytic rate after stimulation. TIGIT Knockout prevented Fc-competent anti-TIGIT driven NK cell fratricide and prevented decrease in NK cell cytotoxicity when combined with Fc-competent anti-TIGIT.

Conclusions Knockout of TIGIT in *ex vivo* expanded PM21-NK cells resulted in NK cells with improved anti-tumor activity and metabolic fitness. TIGIT KO prevented ADCC driven NK cell fratricide and inhibition of cytotoxicity when combined with Fc-competent anti-TIGIT. TIGIT KO PM21-NK cells are a potential cellular product for therapeutic use in combination with TIGIT blockade.

Acknowledgements We would like to thank the FL DOH (Grant #9JK04); Kiadis Pharma, a Sanofi company; and the UCF Preeminent Postdoctoral Program for funding and Max-Cyte for providing instrument for initial testing.

<http://dx.doi.org/10.1136/jitc-2022-SITC2022.1009>

1010

A SINGLE-CELL TRANSCRIPTOMIC ATLAS OF HUMAN NK CELLS TO GUIDE CANCER IMMUNOTHERAPY

¹Ryan King*, ^{2,3}Azim Amirabad, ¹Amir Bayegan, ¹Joachim Theilhaber, ¹Nicole Acuff, ^{1,4}Shannon McGrath, ¹Xiangming Li, ^{2,5}Franck Rapaport, ^{1,6}Jack Pollard, ¹Donald Jackson. ¹Sanofi, Cambridge, MA, United States; ²Digital Data Science, Cambridge, MA, USA; ³Current Affiliation: Johnson and Johnson, Cambridge, MA, USA; ⁴Current Affiliation: Moderna Clinical Biomarker Lab, Cambridge, MA, USA; ⁵Current Affiliation: Sanofi Precision Medicine and Computational Biology, Cambridge, MA, USA; ⁶Current Affiliation: Moderna Oncology, Cambridge, MA, US

Background Natural killer (NK) cell can serve as an effective anti-cancer treatment,^{1,2} and enhancing NK function has been shown to enhance patient outcomes.^{1,2} Therefore, insight into NK cell states and subtypes may lead to new treatment options. Initial characterization of NK cells relied on flow cytometry with surface markers dividing NK cells into less mature CD56^{bright} NKs and more mature CD56^{dim} NKs.⁴ More recently, single-cell RNAseq profiling has enabled deeper characterization and revealed three novel subtypes: cytokine-induced memory-like (CIML), adaptive, low ribosomal, and type I IFN responding NKs, which enhanced the previously known CD56^{bright}, CD56^{dim}, and CD56^{dim} CD57⁺ subtypes.⁵ Here, we extend this single cell subtyping by building a cancer-focused NK cell Atlas that integrates 25 public datasets from multiple types of cancers and delineates both the subtypes and states of the NK cells.

Methods Single cell sequencing datasets were downloaded from the studies listed in [table 1]. NK cells were identified using the HaiTam cell type prediction algorithm v1.⁶ Harmony v0.1.0⁷ was used for batch correction and ACTIONet v3.0.0⁸ was used for data integration and cell state identification. Cell state abundance comparisons were performed using 1-way ANOVA with Dunnett's post hoc test.

Results We generated an Atlas of 89,704 NK cells from 281 donors in 21 cancer focused studies, 3 studies using healthy donors, and 1 study of ulcerative colitis [table 1]. We identified 12 unique NK cellular states in our Atlas [figure 1]. Some states recapitulated known NK subtypes such as CIMLs and type 1 IFN responders. By contrast, CD56^{dim} NKs were represented by 2 cellular states and CD56^{bright} NKs were represented by 3 states. We found that one of these CD56^{bright} states is more abundant in blood from renal cell cancer patients than in blood from healthy donors (2.1-fold change; $p < 0.02$). Compared to other CD56^{bright} states, this overrepresented state expresses higher levels of the cytotoxic gene *GZMK* and of migratory markers *CD44*, *CXCR3* and *SELL*.

Conclusions Our Atlas describes 12 NK cell states reflecting maturation, activation, and exhaustion in cancer. These states provide a framework for assessing co-expression of targets for NK modulators and for understanding the effects of treatments on NK cells.

REFERENCES

1. Chu J, Gao F, Yan M, Zhao S, Yan Z, Shi B, Liu Y. Natural killer cells: a promising immunotherapy for cancer. *eBioMedicine* 2020;**59**:102975.
2. Suen W, Lee W, Leung K, Pan X, Li G. Natural Killer Cell-Based Cancer Immunotherapy: A Review on 10 Years Completed *Clinical Trials*. 2018;**36**:431–457.
3. Abou-El-Enin M, Bauer G, Medcalf N, Volk H, Reinke P. Putting a price tag on novel autologous cellular therapies. *Cytotherapy* 2016;**18**:1056–1061.
4. Moretta L. Dissecting CD56dim human NK cells. *Blood* 2010; **116**:3689–3691.
5. Smith L, Kennedy P, Stacey K, Worboys J, Yarwood A, Seo A, Solloa W, Mistretta B, Chatterjee S, Gunaratne P, Allette K, Wang Y, Smith M, Sebra R, Mace E, Horowitz A, Thomson W, Martin P, Eyre S, Davis D. Diversity of peripheral blood human NK cells identified by single-cell RNA sequencing. *Blood Adv* 2020;**4**:1388–1406.
6. Talk2data [https://talk2data.bioturing.com/predict]

7. Korsunsky I, Millard N, Fan J, Slowikowski K, Zhang F, Wei K, Baglaenko Y, Brenner M, Loh P, Raychaudhuri S. Fast, sensitive and accurate integration of single-cell data with Harmony. 2019;**16**:1289–1296.
8. Mohammadi S, Velderrain J, Kellis M. A multiresolution framework to characterize single-cell state landscapes. *Nature Communications* 2020;**11**:5399.

Name	Study ID	Donors	NK cells	Disease Focus
Discovery of specialized NK cell populations infiltrating human melanoma metastases	GSE139249	5	20,737	Cancer
Mapping the immune environment in clear cell renal carcinoma by single-cell genomics	PMID33504936	7	8,510	Cancer
Heterogeneity of human bone marrow and blood natural killer cells defined by single-cell transcriptome	GSE130430	9	8,114	Healthy
Immune Landscape of Viral- and Carcinogen-Driven Head and Neck Cancer	GSE139324	36	7,824	Cancer
Single-cell RNA sequencing demonstrates the molecular and cellular reprogramming of metastatic lung adenocarcinoma	GSE131507	34	7,309	Cancer
Diversity of peripheral blood human NK cells identified by single-cell RNA sequencing	GSE144191	2	6,346	Healthy
High-Dimensional Single-Cell Analysis Identifies Organ-Specific Signatures and Conserved NK Cell Subsets in Humans and Mice	GSE119562	6	5,001	Healthy
A molecular cell atlas of the human lung from single-cell RNA sequencing	EGAS00001004344	3	4,584	Cancer
Peripheral T cell expansion predicts tumour infiltration and clinical response	GSE139555	12	4,019	Cancer
Heterogeneity and clonal relationships of adaptive immune cells in ulcerative colitis revealed by single-cell analyses	GSE125527	20	3,045	Auto-immune
A pan-cancer blueprint of the heterogeneous tumor microenvironment revealed by single-cell profiling	PMID32561858	31	2,337	Cancer
High systemic and tumor-associated IL-8 correlates with reduced clinical benefit of PD-L1 blockade - blood-tumor	GSE145281	8	1,956	Cancer
Single cell transcriptomes from human kidneys reveal the cellular identity of renal tumors	PMID30093597	11	1,854	Cancer
Single-cell RNA sequencing reveals compromised immune microenvironment in precursor stages of multiple myeloma	GSE124310	31	1,827	Cancer
Dissecting intratumoral myeloid cell plasticity by single cell RNA-seq	GSE117570	4	846	Cancer
Acquired cancer resistance to combination immunotherapy from transcriptional loss of class I HLA	GSE117988	2	817	Cancer
Regenerative lineages and immune-mediated pruning in lung cancer metastasis	GSE123904	13	755	Cancer
Single cell transcriptomic architecture and intercellular cross-talk of human intrahepatic cholangiocarcinoma	GSE138709	5	740	Cancer
Phenotype molding of stromal cells in the lung tumor microenvironment	E-MTAB-6149	7	711	Cancer
Landscape and Dynamics of Single Immune Cells in Hepatocellular Carcinoma 10x - GSE140228	GSE140228	6	646	Cancer
Chromatin mapping and single-cell immune profiling define the temporal dynamics of ibrutinib response in CLL	GSE111014	4	645	Cancer
Single-cell RNA landscape of intratumoral heterogeneity and immunosuppressive microenvironment in advanced osteosarcoma	GSE152048	11	534	Cancer
Clonal replacement of tumor-specific T cells following PD-1 blockade - BCC	GSE123814	7	199	Cancer
Single-Cell transcriptome analysis revealed the heterogeneity and microenvironment of gastrointestinal stromal tumors GSE162115	GSE162115	2	103	Cancer
Multimodal Analysis of Composition and Spatial Architecture in Human Squamous Cell Carcinoma	GSE144236	5	45	Cancer

Abstract 1010 Figure 1 UMAP of the cellular states in the NK atlas. Each unique cellular state identified in this study has a unique color assigned to it and has been plotted in the UMAP.

Abstracts

Name	Study ID	Donors	NK cells	Disease Focus
Discovery of specific NK cell populations in circulating human melanoma metastases	GSE118749	5	30,357	Cancer
Mapping the human myeloid compartment in the tumor microenvironment by single-cell genomics	RR1035671957	7	8,517	Cancer
Longevity of human TCR α and TCR β chains in thymus and blood is determined by distinct thymic phases	GSE118410	9	11,114	Healthy
Immune response of human T cells against Epstein-Barr virus and B-cell disease	GSE118794	37	7,074	Cancer
Single-cell RNA sequencing reveals the molecular and cellular programming of metastatic lung adenocarcinoma	GSE118947	24	7,247	Cancer
Discovery of peripheral blood human NK cells with elevated expression of CD160 signaling	GSE118747	7	6,747	Healthy
High-dimensional single-cell analysis of the human spleen, thymus and gut tissues	GSE118821	8	5,001	Healthy
A molecular atlas of the human lung from single-cell RNA sequencing	RR1035671954	4	4,884	Cancer
Reference T cell atlas from single-cell transcriptomic analysis of human lymphocytes	GSE118822	12	4,014	Cancer
Development and differentiation of adult human natural killer cells	GSE118823	10	3,047	Auto-immune
A gene set for diagnosis of the human germline tumor microenvironment revealed by single-cell profiling	RR1035671958	57	2,537	Cancer
Highly specific and narrow gene set of 8 genes defines human T cells in the blood of T1D patients	GSE118791	8	1,917	Cancer
Single-cell transcriptomic tumor microenvironment reveals the cellular diversity of tumor stroma	RR1035671957	17	1,654	Cancer
Single-cell RNA sequencing reveals transcriptional heterogeneity of human natural killer cells	GSE118792	11	1,629	Cancer
Discovering transcriptional modules in single-cell RNA-seq	GSE118793	4	176	Cancer
Assessment of gene expression in combination immunotherapy from transcriptome coverage data	GSE118794	4	137	Cancer
Massive loss of tissue and immune-mediated grafting in allogeneic transplantation	GSE118795	15	758	Auto-immune
Transcriptomic analysis of human natural killer cells in the lung tumor microenvironment	GSE118796	8	740	Cancer
Phenotypic and functional analysis of human natural killer cells in the lung tumor microenvironment	RR1035671959	7	711	Cancer
Genotypes and functions of human natural killer cells in the lung tumor microenvironment	GSE118797	8	646	Cancer
Human natural killer cell transcriptome in the lung tumor microenvironment	GSE118798	4	625	Cancer
Single-cell RNA sequencing of human natural killer cells reveals a transcriptional program for cytotoxicity	GSE118799	17	771	Cancer
Genetic heterogeneity of human natural killer cells in the lung tumor microenvironment	GSE118800	7	749	Cancer
Single-cell transcriptomic analysis of human natural killer cells in the lung tumor microenvironment	GSE118801	7	700	Cancer
High-resolution analysis of transcriptional and spatial architecture in human thymus T cell development	GSE118802	5	75	Cancer

Abstract 1010 Figure 2 Public studies used to construct the NK atlas. The names of each dataset used are listed along with identifiers and disease focus.

<http://dx.doi.org/10.1136/jitc-2022-SITC2022.1010>

1011

ANTIBODY TARGETING NKG2D LIGANDS MICA/B TO UNLEASH ANTI-TUMOR IMMUNITY OF NK AND ILC1 CELLS

¹Sizhe Liu*, ¹Tyler Smith, ²Lisha Zhu, ³Payal Dhar, ¹Jennifer Wu. ¹Northwestern University, Chicago, IL, United States; ²University of Chicago, Chicago, IL, United States; ³Northwestern University (*currently affiliated with BMS), Chicago, IL, United States

Background Natural Killer (NK) cells, the founding member of innate lymphoid cells (ILCs), contribute to tumor control via direct cytotoxicity and secretion of immune-modulatory cytokines and chemokines. Despite well-characterized roles of NK cells, the involvement of other ILC family members in cancer is less understood. Recent reports indicate that solid tumors are populated by heterogeneous ILC subsets.¹ The implication of such heterogeneity for anti-tumor immunity is not entirely clear.

MICA/B serve as ligands for the activating receptor NKG2D on NK and CD8+ T cells. Yet tumor-shed soluble MICA/B are shown to mediate immune suppression via multiple mechanisms.² We designed a MIC-targeting antibody B10G5 which was shown to enhance anti-tumor immunity of NK and CD8+ T cells in a murine prostate cancer model recapitulating MIC shedding (TRAMP/MICB).^{3,4} In this study we performed single-cell characterization of intra-tumoral ILCs from untreated and B10G5-treated TRAMP/MICB mice (figure 1) to better understand the effects of B10G5 on tumor immune contexture.

Methods We performed single-cell RNA sequencing of CD45+ immune cells from pooled tumors of TRAMP/MICB mice. The samples represent well-differentiated tumors of untreated mice (n = 7), poorly-differentiated tumors of untreated mice (n= 4), and tumors of B10G5-treated mice (n= 3) respectively. CD3-NK1.1+ cells were further sub-clustered into NK and ILC1 subsets, denoted based on their phenotypical and functional profiles. We also measured cytotoxicity of PBMCs from healthy donors stimulated with MIC/B10G5 complexes *in vitro* using calcein release assay.⁵

Results TRAMP/MICB tumors were infiltrated by functionally heterogeneous NK and ILC1 subsets. The subsets exhibited distinct expression of genes related with cytotoxicity (*GZMB*, *PFR1*, *TNFSF10*) and immunomodulation (*IFN γ* , *XCL1*, *CCL5*), suggesting their capacity to engage in both cytotoxicity and immune modulation via diverse pathways. Notably, NK cells had higher perforin (*PFR1*) expression, whilst ILC1s exclusively expressed the death ligand TRAIL (*TNFSF10*). B10G5 treatment led to NK enrichment and increased heterogeneity of type I ILCs. Lastly, we showed that sMIC/B10G5 complexes enhanced cytotoxicity of PBMCs from healthy donors against tumor cells *in vitro*.

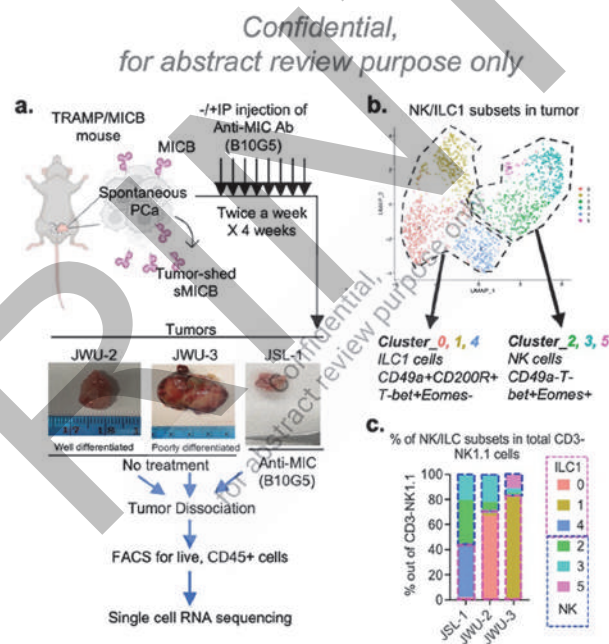
Conclusions Our data elucidated the functional heterogeneity of type I ILCs in prostate tumor microenvironment in a murine model, which has not been previously characterized. Moreover, we showed that targeting MIC with B10G5 could increase heterogeneity of type I innate lymphoid cells *in vivo*, which potentially contribute to better overall anti-tumor responses.

REFERENCES

1. Simoni Y, Fehlings M, Kløverpris HN, McGovern N, Koo SL, Loh CY, Lim S, Kurioika A, Fergusson JR, Tang CL, Kam MH. Human innate lymphoid cell subsets possess tissue-type based heterogeneity in phenotype and frequency. *Immunity* 2017 Jan 17;46(1):148–61.
2. Zhang J, Basher F, Wu JD. NKG2D ligands in tumor immunity: two sides of a coin. *Frontiers in Immunology* 2015 Mar 4;6:97.

3. Liu G, Lu S, Wang X, Page ST, Higano CS, Plymate SR, Greenberg NM, Sun S, Li Z, Wu JD. Perturbation of NK cell peripheral homeostasis accelerates prostate carcinoma metastasis. *The Journal of Clinical Investigation* 2013 Oct 1;123(10):4410–22.
4. Zhang J, Liu D, Li G, Staveley-O'Carroll KF, Graff JN, Li Z, Wu JD. Antibody-mediated neutralization of soluble MIC significantly enhances CTLA4 blockade therapy. *Science Advances* 2017 May 17;3(5):e1602133.
5. Neri S, Mariani E, Meneghetti A, Cattini L, Facchini A. Calcein-acetyoxymethyl cytotoxicity assay: standardization of a method allowing additional analyses on recovered effector cells and supernatants. *Clinical Diagnostic Laboratory Immunology*. 2001 Nov 1;8(6):1131–5

Ethics Approval STU0020734 was approved by Northwestern University's Ethics Board. Healthy volunteers have given informed consent before taking part.



Abstract 1011 Figure 1 Single cell characterization of ILCs from TRAMP/MICB tumors

a, schematic describing sample preparation for scRNA-seq of immune cells from TRAMP/MICB tumors. **b,** UMAP plots visualizing sub-clusters of CD3-NK1.1+ cells pooled from all samples. **c,** percentage of each NK or ILC1 subset out of total CD3-NK1.1+ cells in each sample

<http://dx.doi.org/10.1136/jitc-2022-SITC2022.1011>

1012 FIBROBLAST ACTIVATION PROTEIN REGULATES HUMAN NATURAL KILLER CELL MIGRATION

¹Rachael Maynard*, ¹Allison Fitzgerald, ¹Apsra Nasir, ¹Eric Glasgow, ¹Sandra Jablonski, ²Pieter Van Der Veken, ¹Gray Pearson, ³Emily Mace, ¹Louis Weiner. ¹Georgetown University Medical Center, Washington, DC, United States; ²University of Antwerp, Wilrijk, Belgium; ³Columbia University Irving Medical Center, New York, NY, United States

Background Natural killer (NK) cells play a crucial role in both physiologic and pathologic conditions, including cancer. A number of strategies have been employed to utilize the cytolytic properties of NK cells in the treatment of cancer.^{1,2} One hurdle to the efficacy of NK-cell based therapy is NK cell infiltration into tumors.³ The mechanisms NK cells employ for physical migration are not well described.^{4,5} We recently found that fibroblast activation protein (FAP) is expressed by human NK cells. FAP is a type-II transmembrane serine protease previously thought to primarily be expressed in reactive stromal fibroblasts. FAP plays a role in tissue remodeling and extracellular matrix digestion to facilitate cell migration.⁶

Methods FAP expression was examined on NK cells by both western blot and immunofluorescence. Compound 60 (CDP60) was used as a specific pharmacological inhibitor of FAP in these assays.

Results We have confirmed that fibroblast activation protein (FAP) is expressed by human NK cells, using both western blot and immunofluorescence. To examine the role of FAP in NK cells we find that following inhibition of FAP activity, NK cells demonstrate decreased migration in 3D culture systems, as well as decreased extravasation from the blood vessels of zebrafish.

Conclusions Future studies include generating an FAP knock-out NK cell line to verify the role of FAP in NK cells identified using CPD60. These findings suggest that FAP is responsible for NK cell migration and may provide a potential novel mechanism to regulate this process. This role in migration can potentially be exploited to enhance NK cell migration into tumors.

Acknowledgements The Lombardi Comprehensive Cancer Center's Shared Resources, including Flow Cytometry Shared Resource and Microscopy and Imaging Shared Resource

REFERENCES

1. Fayette J, Lefebvre G, Posner M R, Bauman J, Salas S, Even C, Saada-Bouزيد E, Seiwert T, Colevas D, Calmels F, Zerbib R, Boyer Chammard A, Cohen R. Results of a phase II study evaluating monalizumab in combination with cetuximab in previously treated recurrent or metastatic squamous cell carcinoma of the head and neck (R/M SCCHN). *Ann Oncol*. 2018;**37**:4:29.
2. Sarhan D, Brandt L, Felices M, Guldevall K, Lenvik T, Hinderlie P, Curtsinger J, Warlick E, Spellman S R, Blazar B R, Weisdorf D J, Cooley S, Vallera D A, Onfelt B, Miller J S. 161533 TriKE stimulates NK-cell function to overcome myeloid-derived suppressor cells in MDS. *Blood Adv*. 2018;**2**:1459–1469.
3. Zhang Q, Zhang H, Ding J, Liu H, Lu M, Miao Y, Li L, Zheng J. Combination therapy with EPCAM-CAR-NK-92 cells and regorafenib against human colorectal cancer models. *J Immunol Res* 2018;**2018**:4263520.
4. Wennerberg E, Kremer V, Childs R, Lundqvist A. CXCL10-induced migration of adoptively transferred human natural killer cells toward solid tumors causes regression of tumor growth in vivo. *Cancer Immunol Immunother* 2014;**64**:225–235.
5. Kameritsch P, Renkawitz J. Principles of Leukocyte Migration Strategies. *Trends Cell Biol*. 2020;**30**:818–832.
6. Fitzgerald A, Weiner LM. The role of fibroblast activation protein in health and malignancy. *Cancer metastasis reviews* 2020;**39**:783–803.

<http://dx.doi.org/10.1136/jitc-2022-SITC2022.1012>

1013 **PROGNOSTIC VALUE OF NATURAL KILLER CELL ACTIVITY AND DERIVED NEUTROPHILS-TO-LYMPHOCYTES RATIO IN NON-SMALL CELL LUNG CANCER PATIENTS RECEIVING IMMUNE CHECKPOINT INHIBITORS**

Line Nederby*, Sara Wen, Christa Nyhus, Lisbeth Bertelsen, Rikke Andersen, Anders Jakobsen, Torben Hansen. *Vejle Hospital, University Hospital of Southern Denmark, Vejle, Denmark*

Background Even though immune checkpoint inhibitors have improved the survival of non-small cell lung cancer (NSCLC) patients, their prognosis is still poor. Natural Killer (NK) cells are lymphocytes with distinct anti-cancer properties, and NK cell activity (NKA) may have a prognostic role. Similarly, derived Neutrophils-to-lymphocyte ratio (dNLR) has been suggested as a prognostic biomarker in cancer patients.

Methods Patients with advanced or recurrent NSCLC eligible for anti-PD-1/PD-L1 treatment were enrolled at the Department of Oncology, Vejle Hospital, Denmark. Blood was sampled at baseline and immediately before the following three cycles of therapy. Interferon gamma (IFN γ) as a surrogate for NKA was measured using the NK Vue[®] assay (NKMAX, Seongnam-si, South Korea). Normal levels of IFN γ were considered as >250 pg/mL. Neutrophils and leukocytes were quantified by XN-9000 (Sysmex, Kobe, Japan). dNLR was calculated as (neutrophils/(leukocytes-neutrophils)) and dNLR<3 was considered normal. The study was approved by the Regional Committee on Health Research Ethics for Southern Denmark, approval number S-20170063.

Results Baseline level of NKA had no prognostic impact for overall survival (OS) (p=0.1279, NKA-normal n=45 vs NKA-low n=27, logrank). Longitudinal sampling allowed us to determine if dynamics in NKA were of prognostic value. For this purpose, patients were grouped as follows: NKA-low group had NKA <250 pg/mL at all available time-points (n=13), NKA-mixed group had NKA of varying levels (n=34), and NKA-high group had NKA >250 pg/mL at all available time-points (n=29). A logrank test revealed a significant difference between the groups in terms of OS (p=0.0002). Compared to the NKA-high group, the NKA-low group had a poor prognosis with a hazard ratio (HR) of 3.690 (p=0.001). After adjusting for dNLR, histology and performance status it remained an independent prognostic factor (HR=3.581, p=0.005). Interestingly, while dNLR also had prognostic impact for overall survival (OS) (p=0.0274, dNLR<3 n=57 and dNLR>3 n=18, logrank) and dNLR>3 was a prognostic marker for poor OS in univariate analysis (HR=1.908, p=0.03), this was lost in multivariate analysis taking NKA, histology, and performance status into account (HR=1.364, p=0.451).

Conclusions NKA dynamics, and not dNLR, was an independent prognostic marker for OS in NSCLC patients receiving anti-PD-1/PD-L1 treatment. These findings highlight the value of not restricting biomarker evaluation to immune cell enumeration, but rather looking at the ability of these cells to carry out vital immune functions.

Ethics Approval The study was approved by the Regional Committee on Health Research Ethics for Southern Denmark, approval number S-20170063. All participants provided written informed consent.

<http://dx.doi.org/10.1136/jitc-2022-SITC2022.1013>

1014

COMPLEMENT C3 DEFICIENCY INCREASES THE ANTI-TUMOR IMMUNITY OF NK CELLS AND CONTROLS TUMOR GROWTH

Girdhari Lal, Pradipta Pal*, Sourav Paul, Heikrujam Thoihen Meitei, Praneet Wahi, Arvind Sahu. *National Centre for Cell Science, Pune, India*

Background Natural killer cells play an important role in controlling tumor growth. On the other hand, the complement system is known for its protective function in infection and for maintaining cellular homeostasis. It is reported that the complement system promotes tumor growth and metastasis. However, the role of complement and its importance in the anti-tumor function of NK cells is not clearly understood.

Methods Mouse melanoma cell B16F10 was subcutaneously injected in C57BL/6 mice or C3^{-/-} mice, and the growth of the tumor was monitored. The cellular phenotyping of immune cells in the tumor and secondary lymphoid tissues were analyzed using flow cytometry.

Results The transplantation of B16F10 cells in the C3^{-/-} mice showed a significantly reduced tumor growth compared to wild-type mice. Immunohistological analysis of tumor showed increased infiltration of NK cells and CD8 T cells in the C3^{-/-} mice as compared to C3^{+/+} mice. Under the homeostatic condition, analysis of spleen and lymph nodes of C3^{-/-} and C3^{+/+} mice did not show any change in either the frequency or the absolute number of total CD4 T cells, CD8 T cells, NK cells, and NKT cells. However, CD4⁺ T cells and CD8⁺ T cells from C3^{-/-} mice secreted significantly higher IFN-g than C3^{+/+} mice and the splenic NK cells from C3^{-/-} mice showed a significantly increased cytotoxic activity compared to C3^{+/+} mice. Further, hepatic NK cells in the C3^{-/-} mice showed significantly lower NKG2A inhibitory receptors, resulting in reduced NKG2D to NKG2A ratio (activating/inhibitory ratio) of molecules per NK cell compared to wild-type NK cells. As expected, NK cells isolated from tumor-bearing C3^{-/-} mice showed a robust cytotoxic activity compared to the tumor-bearing C3^{+/+} mice. Interestingly, C3^{-/-} NK cells showed increased secretion of pro-inflammatory cytokines such as GM-CSF and IFN-g when re-stimulated with IL-2, IL-15, or IL-18 compared to C3^{+/+} NK cells. Depleting NK cells in C3^{-/-} mice with anti-NK1.1 mAb significantly prevented the reduction of tumor growth as compared to isotype control IgG mAb.

Conclusions Our data suggest that complement C3 deficiency alters the effector and cytotoxic function of NK cells, and thereby deficiency of C3 promotes anti-tumor immunity and controls tumor growth. Our data suggest that interfering with the complement system gives a new therapeutic advantage in controlling tumor growth.

Acknowledgements PP received a Senior Research Fellowship from the Department of Biotechnology, Government of India. GL received grants (EMR/2016/007108 and DST/SJF/LSA-01/2017-18) from the Science and Engineering Research Board, Department of Science and Technology, Ministry of Science and Technology, Government of India. A.S. is a J. C. Bose National Fellow. His laboratory is supported by project grant BT/PR28506/MED/29/1307/2018 from the Department of Biotechnology, New Delhi, India.

<http://dx.doi.org/10.1136/jitc-2022-SITC2022.1014>

1015 NATURAL KILLER CELLS IN IMMUNOTHERAPY-INDUCED MHC-I TUMOR ESCAPE

Eric Miao, Jennifer Poursine-Laurent, Kathleen Sheehan, Robert Schreiber, Wayne Yokoyama, Sytse Piersma*. *Washington University in St. Louis, St Louis, MO, United States*

Background Cancer immunotherapy including immune checkpoint blockade (ICB) has been successful in inducing durable responses in a variety of cancers. However, a proportion of patients who receive ICB undergo tumor relapse, putatively as result of tumor escape. A potential tumor escape mechanism is mutation of the antigen processing and presentation pathway, resulting in decreased surface major histocompatibility complex class I (MHC-I) levels. These escaped tumor cells then become invisible to CD8 T cells, which are central in the anti-tumor immune response to ICB therapy. Indeed, this type of tumor escape has been observed in relapsed patients in longitudinal studies in which mutations in *B2M* (encoding b₂-microglobulin), an essential component of classical and non-classical MHC-I, have been detected. As a result, *B2M*-deficient tumor cells lack cell surface MHC-I expression that should result in activating natural killer (NK) cells through a mechanism termed “missing-self”. Yet, the NK cell response does not appear to be strong enough to clear escaped tumor cells in all patients, as mutations in the antigen processing and presentation machinery are detected in relapsed patients. It is unclear why NK cells are unable to eliminate escaped MHC-I-deficient tumors and whether NK cells can be harnessed to prevent emergence of these escaped tumors.

Methods To address these prominent questions, we developed a methylcholanthrene-induced mouse tumor model in which *B2m* loss can be induced with tamoxifen. The selected *B2m* inducible knockout tumor (named BIKOT) lines were validated to lose surface MHC-I in response to tamoxifen administration by oral gavage in vivo.

Results To investigate MHC-I escape in the context of ICB therapy, we treated BIKOT-challenged mice with anti-PD1 and anti-CTLA4. Consistent with established MCA tumor models, tumors grew out progressively in untreated mice, while tumors in ICB-treated mice initially grew out after which they regressed until completely receded. The combination of sub-optimal tamoxifen administration with ICB resulted in initial control of tumor outgrowth, which was followed by progressive outgrowth between week 2-3 in a proportion of animals suggesting immune escape. Indeed, relapsed tumors displayed loss of surface MHC-I.

Conclusions Taken together these preliminary data strongly suggest that the novel inducible MHC-I-deficient tumors are uniquely suited to investigate how tumors can escape T-cell recognition in face of a functional NK cell response, and furthermore provide a platform for development of NK cell-targeting therapeutics that aim to prevent tumor immune escape.

Acknowledgements This work was supported by Grant # IRG-21-133-64 from the American Cancer Society.

Ethics Approval This study was approved by Washington University in St. Louis institution's Ethics Board; approval number 21-0090

<http://dx.doi.org/10.1136/jitc-2022-SITC2022.1015>

1016

IL-2 EXPANDED TUMOR INFILTRATED NATURAL KILLER (TINK) CELLS FROM CANINE SARCOMAS POSSESS POTENT ANTI-TUMOR CYTOTOXICITY

¹Weiqing Jing*, ¹Himaly Shinglot, ¹Juliana Chi Kei Ng, ¹Ali Zhang, ²Bernard Seguin, ³Jeffrey Bryan, ⁴Timothy Fan, ⁵Jennifer Wu, ¹Seth Pollack. ¹*Northwestern Medicine, Chicago, IL, United States*; ²*Colorado State University, Fort Collins, CO, United States*; ³*University of Missouri, Columbia, MO, United States*; ⁴*University of Illinois at Urbana-Champaign, Urbana, IL, United States*; ⁵*Northwestern University, Chicago, IL, United States*

Background Tumor infiltrating NK (TINK) cells are present and linked to prognosis in many solid tumors.¹ While these cells may have potent antitumor effector function, they are thought to be dysfunctional in the tumor microenvironment (TME).² Because it is difficult to culture potent TINKs from human tumors, relatively little is known about their interactions with various TME components or their potential for therapeutic applications. Here we report reproducible culture of highly potent TINKs from naturally occurring canine sarcomas for use in modeling the human TME.

Methods Canine sarcoma tumor specimens were cut into fragments and cultured individually in 24-well plates with medium supplemented with 6000 IU/ml of rhIL-2. Expanded wells were maintained separately and autologous tumors were cultured separately. Expanded TINKs and TILs were characterized by flow cytometry and co-cultured with autologous and allogeneic tumor cells at a E:T ratio of 5:1; cytotoxicity of TILs was monitored by tumor confluence in the Incucyte system.

Results Ninety-six individual fragments were derived from soft tissue sarcomas (STS) and 120 fragments were derived from osteosarcoma. 88 (92%) of fragments from STS tumors and 23(19%) from Osteosarcoma were expanded sufficiently for additional analysis. While most TINKs and TILs were able to kill autologous tumor and resulted in increased Granzyme B expression, we surprisingly found that the number of TINKs (NKp46+) was positively correlated with tumor killing, with pure cultures of NKp46+ cells resulting in complete and efficient tumor elimination. Furthermore, the percentage of CD5 + T cells was negatively correlated with tumor killing. By flow cytometry, we found that NKp46+ TINKs were CD5(dim) TCRαβ- TCRγδ- CD4- B220- CD1d-, with some NKp46+ subpopulations co-expressing CD3 or CD8. Compared with the less potent TIL cultures composed of mainly CD5+ T cells, NKp46+ TINKs secreted significantly higher T1 cytokines (IFN-γ, TNF-α and GM-CSF) after co-cultured with tumor. Tumor stimulation preferentially activated the secretion of TNF-α over IFN-γ from TINKs, with concentration levels of TNF-α about 20 folds higher than IFN-γ, suggesting important role of TNF-α in TINK mediated tumor killing.

Conclusions Our results demonstrated that functional TINKs can be efficiently expanded from canine sarcoma tumor tissue with little NK cell infiltration seen by immunohistochemistry. Future studies using canine TINKs will explore therapeutic potential for targeting, manipulating, and transferring these cells in human.

Acknowledgements This work was supported by the Northwestern University – Flow Cytometry Core Facility supported by Cancer Center Support Grant (NCI CA060553), the Analytical bioNano Technology Core supported by the Soft and Hybrid Nanotechnology Experimental (SHyNE) Resource (NSF ECCS-2025633). CD1d tetramer was acquired from the NIH Tetramer Facility.

REFERENCES

1. Cózar B, Greppi M, Carpentier S, Narni-Mancinelli E, Chiossone L, Vivier E. Tumor-infiltrating natural killer cells. *Cancer Discov.* 2021;**11**(1):34–44.
2. Nersesian S, Schwartz SL, Grantham SR, MacLean LK, Lee SN, Pugh-Toole M, Boudreau JE. NK cell infiltration is associated with improved overall survival in solid cancers: a systematic review and meta-analysis. *Transl Oncol.* 2021;**14**(1):100930.

<http://dx.doi.org/10.1136/jitc-2022-SITC2022.1016>

1017

A TUMOR MODEL IN THE HUMANIZED IMMUNO-RECONSTITUTED HIL15 TRANSGENIC MICE REVEALED THE IMPACT OF OTHER IMMUNE COMPONENTS ON THE DEVELOPMENT AND FUNCTION OF NK CELLS AGAINST MALIGNANCIES

Li Yang*, Chunlei Dai, Hongmei Xu, Hui Qi, Xuzhen Tang, Qingyang Gu, Qunsheng Ji.
WuXi AppTec, Shanghai, China

Background The roles of natural killer (NK) cells, in the process of immunosurveillance and elimination against malignancies, have been increasingly interesting in the space of immuno-oncology. The utilization of humanized mice, reconstituted with human immune cells, improves the translational relevance of animal models in this field. However, it remains a challenge for the effective reconstitution of human NK cells in mice, due to the lack of human cytokines which are essential for the development of NK. Typically, IL-15 humanization could promote the differentiation, function, and survival of NK in such models. Nevertheless, few studies have been conducted to evaluate the impact of IL-15 humanization on a wider range of human immune cell lineages in a comprehensively immuno-reconstituted system.

Methods To understand this, we conducted a study comparing the reconstitution of human NK alone or in a mixture with the autologous PBMC, in the hIL-15-expressing NOD-scid IL2Rg null mice. NCI-H929 human myeloma was established in each mouse, for the evaluation of anti-tumor efficacy by the immunotherapies targeting NK-mediated cell killing. The frequencies of human immune cells in both the circulation and the tumor microenvironment were evaluated by flow cytometry.

Results As a result, the mixed system of NK/PBMC reconstitution achieved a better reconstitution rate of NK cells compared to the NK-alone system. But the anti-tumor efficacy by anti-CD47 or anti-CD38, in contrast to the higher NK frequency, appeared to be poorer in the NK/PBMC-mixed system. To investigate the underlying mechanism, we analyzed the phenotyping of each immune sub-lineages and found an extremely high frequency of hCD4+ cell in the NK/PBMC mixed system.

Conclusions One possible reason for the inversion between NK frequency and drug efficacy might be the enrichment of hCD4+ sub-lineages including Treg, which were promoted by IL-15, suppressed the NK effector function, and compromised the relevant immuno-therapy. Further studies could be suggested including a deeper look into the phenotyping of TILs, combining with a Treg targeting therapy like anti-CTLA4, and studying the mechanism of interaction between Treg and NK. In summary, given the complexity with the function of various immune components co-existing in the system, an appropriate method of immune reconstitution is critical for the evaluation of cancer immuno-therapies utilizing humanized models.

<http://dx.doi.org/10.1136/jitc-2022-SITC2022.1017>

1018

**MULTIFUNCTIONAL NATURAL KILLER CELL ENGAGER
RELEASING CXCL10 AUGMENTS NATURAL KILLER CELL
RECRUITMENT AND ANTI-TUMOR EFFICACY AGAINST
GLIOBLASTOMA**

Xue Yao*, Sandro Matosevic. *Purdue University, Lafayette, IN, United States*

Background The effectiveness of natural killer (NK) cell-based immunotherapy against solid tumors is limited by the inadequate infiltration of NK cells into the tumors and the heterogeneous immunosuppressive tumor microenvironment (TME), suggesting that a multi-specificity of targeting mechanisms is needed to achieve durable responses.

Methods We isolated and phenotyped tumor-infiltrating NK cells and peripheral blood (PB) NK cells from glioblastoma multiforme (GBM) patients for the expression of chemokine receptor CXCR3. The effect of exogenous CXCL10 on NK cell migration and functions was also established. We further investigated the regulation of the CXCR3-CXCL10 axis on NK cells and tumor cells by establishing CXCR3-knockdown primary NK cells and CXCL10-overexpressing GBM cells. Based on these findings, we designed and synthesized a novel natural killer cell engager (NKCE), which not only targets NKp46 on NK cells and IL13Ra2 on tumor cells but also specifically releases CXCL10 at the tumor sites while sustaining NK cell activation via interleukin (IL)-15.

Results CXCR3 was highly expressed on NK cells in PB from either GBM patients or healthy donors. Although low numbers of tumor-infiltrating NK cells in patients were observed, CXCR3 expression was up-regulated on these cells. CXCL10 induced NK cell migration via CXCR3 but did not affect NK cell functions. Simultaneously, CXCL10 overexpression showed no effect on tumor growth but resulted in enhanced NK cell migration into tumor sites and, in turn, improved the anti-tumor activity of NK cells. Furthermore, our novel NKCE activated NK cells by binding NKp46 and recognized GBM tumor cells via IL13Ra2, thus promoting the contact between NK cells and tumor cells. The engager's CXCL10-releasing domain, which is activated in the local TME, promotes the specific increase in CXCL10 concentration and, in turn, NK cell homing in the TME.

Conclusions The CXCR3-CXCL10 axis contributes to the recruitment of NK cells to GBM. Our novel NKCE within a locally-cleavable CXCL10 domain induced NK cell migration and boosted NK cell anti-tumor activity against solid tumors. Such a multi-specific approach not only activates NK cells locally but promotes their recruitment and retention in the TME.

<http://dx.doi.org/10.1136/jitc-2022-SITC2022.1018>

1019 CSF1R⁺PD-L1⁺ TUMOR-ASSOCIATED MACROPHAGES TRIGGER MAIT CELL DYSFUNCTION AT THE HCC INVASIVE MARGIN

¹Benjamin Ruf*, ²Matthias Bruhns, ²Sepideh Babaei, ¹Noemi Kedei, ¹Chi Ma, ¹Lichun Ma, ¹Mahler Revsine, ¹Bernd Heinrich, ¹Varun Subramanyam, ¹Jonathan Qi, ¹Simon Wabitsch, ¹Benjamin Green, ¹Kylynda Bauer, ¹Yuta Myojin, ¹Mohamed-Reda Benmebarek, ¹Layla Greten, ¹Justin McCallen, ¹Patrick Huang, ¹Marie Pouzolles, ¹David Kleiner, ¹William Telford, ¹Kimia Dadkhah, ¹Allison Ruchinskas, ¹Merrill Stoffroff, ³Jiman Kang, ³Kesha Oza, ⁴Mathuros Ruchirawat, ³Alexander Kroemer, ¹Xin Wang, ²Manfred Claassen, ¹Firouzeh Korangy, ¹Tim Greten. ¹National Institutes of Health (NIH), Bethesda, MD, United States; ²University Hospital Tübingen, Tübingen, Germany; ³MedStar Georgetown University Hospital, Washington, DC, United States; ⁴Chulabhorn Research Institute, Bangkok, Thailand

Background Hepatocellular Carcinoma (HCC) is considered a prototype of inflammation-derived cancer arising from chronic liver injury. The cellular composition of the HCC tumor immune microenvironment (TiME) has a major impact on cancer biology as the TiME influences tumor initiation, progress, and response to therapy. Mucosal-associated invariant T (MAIT) cells can represent the most abundant T cell subtype in the human liver and are assigned crucial roles in regulating immunity and inflammation in the context of infection, albeit their role in HCC remains elusive.

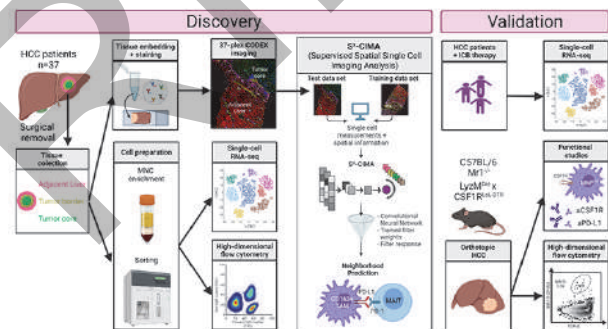
Methods Study design is displayed in figure 1. High-dimensional flow cytometry (n=37) and scRNA sequencing (n=8) was used to analyze MAIT cell phenotypic changes in patient tissue samples. Highly-multiplexed immunofluorescence microscopy was used to quantify immune cell infiltration in paired human HCC samples. We developed and validated a 37-plex antibody panel and applied CODEX technology to simultaneously profile in situ expression of 37 proteins at sub-cellular resolution in n=15 HCC patient samples using whole slide scanning. We established an image analysis pipeline using a machine learning (ML) algorithm (S³-CIMA) to quantify the MAIT cell interaction network at the HCC invasive front. Murine models of orthotopic HCC using transgenic mouse strains were used for *in vivo* validation, a co-culture system using sorted MAITs from primary human liver cancer tissue was established to gain further mechanistic insight.

Results Hepatic MAIT cells in n=37 patient samples are characterized by impaired infiltration (p<0.001) into tumor lesions, increasing dysfunction (e.g. upregulation of PD-1 (p<0.05) & reduced IFN-γ (p<0.01) within the HCC TiME and show previously underappreciated heterogeneity as seen by scRNA-seq. CODEX imaging revealed the distinct cellular composition of the MAIT neighborhood in human HCC tissue. This allowed for in-depth characterization of cellular interaction networks underlying the MAIT cell dysfunction in HCC. S³-CIMA, a novel ML method, to analyze our spatially resolved immune cell atlas of human liver cancer identified interactions of CSF1R⁺PD-L1⁺ tumor-associated macrophages (TAMs) and MAIT cells localized in the adjacent (non-tumor) liver as key regulatory elements of MAIT cell dysfunction. Finally, perturbation of this detrimental cell-cell interaction using PD-L1 and CSF1R blocking strategies or depletion of TAMs using *Lysm^{Cre} x Csf1^{LSL-DTR}* transgenic mice increased MAIT cell infiltration (p<0.05) into murine HCC lesions and reinvigorated the cytotoxic MAIT cell phenotype (p<0.01).

Conclusions This work provides evidence that MAIT antitumor immunity and response to ICB therapies relies on organized, spatially nuanced interactions between MAITs and PD-L1⁺CSF1R⁺ TAMs within the tumor immune microenvironment.

Acknowledgements B.R. was supported by the International Liver Cancer Association (ILCA) Fellowship Award 2021, M. B. was funded by the Deutsche Forschungsgemeinschaft (DFG, German Research Foundation) under Germany's Excellence Strategy – EXC number 2064/1. S.B. was funded by the Deutsche Forschungsgemeinschaft (DFG, German Research Foundation) under Germany's Excellence Strategy – EXC number 2180. N.K. was supported by the Intramural Research Program of the NIH, NCI (ZIC BC 011434). S.W. was funded by the Deutsche Forschungsgemeinschaft (WA-4610/1-1), A.K. acknowledges funding support from the National Institute of Allergy and Infectious Diseases (R01AI132389; R21AI130800). X.W.W. was supported by the Intramural Research program of the NIH, NCI (ZIA BC 010313). T.F.G. was supported by the Intramural Research Program of the NIH, NCI (ZIA BC 011345).

Ethics Approval All patients gave informed consent for collection of clinical information, tissue acquisition under the Institutional Review Board (IRB)-approved protocol IRB #2017-0365 and the material transfer agreement (M.T.A. #43655-18) between the GUH and the U.S. National Cancer Institute (NCI).



Abstract 1019 Figure 1 Study design

<http://dx.doi.org/10.1136/jitc-2022-SITC2022.1019>

1020

TARGETING TIM-3 ON T REGULATORY CELLS MAKE NONRESPONSIVE COLD MELANOMA, MORE RESPONSIVE TO IMMUNE MEDIATED TUMOR CONTROL

<http://dx.doi.org/10.1136/jitc-2022-SITC2022.1020>

¹Hridesh Banerjee*, ²Hector Rosado, ¹Benjamin Murter, ¹Lawrence Kane. ¹University of Pittsburgh, Pittsburgh, PA, United States; ²UPMC Medical School, Pittsburgh, PA, United States

Background Cold Tumor mouse model study are useful, as a few category of human tumor in breast, brain, prostate, pancreas and ovary are Cold and resistant to Immune checkpoint inhibitors (ICIs) based therapeutic treatments. one of the widely studied model in mouse for cold tumor is B16F10 melanoma, and this model is known to be non-responsive to checkpoint inhibitor therapy. while T regulatory cells have been known to play a major role in cancer immunosuppression, targeting T reg cells directly has been a challenge, due to their role in immune homeostasis. we use TIM-3 expressing Tregulatory cells as a significant proportion of Treg cells in various mouse and human tumor model are known to be expressing TIM-3 and this expression is far restricted to the site of Tumor.¹⁻⁴

Methods C57BL 6 mice were injected with Tumor cells subcutaneously, followed by tracking of Size of tumors and also immuno typing of tumor and lymphoid organ. for Treg specific targeting TIM-3 conditional Knockout mouse were generated and Bred to FoxP3 ERT2 Cre model to induce time dependent knocking out of T regulatory cellTIM-3. efficiency of Knock out in various organ and tumor was confirmed by Flow cytometry.

Results MC38(immune responsive) and B16F10(non immune responsive), tumors are both delayed in progression of tumor when Treg cells are incapable of inducing TIM-3.

Frequency of Tregulatory cells goes down in tumors of TIM-3 conditional knockout mouse.

CD8 exhaustion kinetics in TIM-3 Knockout mouse is delayed and knockout mouse survive longer after tumor induction.

Delay in B16F10 melanoma may be a indicative of better immune response in TIM-3 Knockout mice.

Conclusions Targeting TIM-3 in Combination therapy, with their Role in Treg specificity may be a viable and effective strategy. Inability of Treg cells to persist in tumors in absence of TIM-3, indicate to the fact that TIM-3 may be playing a role in survival of Treg cells in tumor microenvironment, and a possibility of role of TIM-3 in T reg cells traffic in tumors can also be not ruled out.

surprisingly along with our previously published Data on MC38 where we have shown that T cell exhaustion kinetics gets delayed , we see the same trend in cold tumor model, B16 F10. suggestive of a possibility of these tumor being more responsive to immune therapy.

REFERENCES

1. Banerjee H, Kane LP. Immune regulation by Tim-3. *F1000Res* 2018;**7**:316. doi: 10.12688/f1000research.13446.1.
2. Kataoka S, Manandhar P, Lee J, Workman CJ, Banerjee H, Szymczak-Workman AL, Kvorjak M, Lohmueller J, Kane LP. The costimulatory activity of Tim-3 requires Akt and MAPK signaling and its recruitment to the immune synapse. *Sci Signal*. 2021;**14**(687):eaba0717. doi: 10.1126/scisignal.aba0717.
3. Kane LP. Regulation of Tim-3 function by binding to phosphatidylserine. *Biochem J*. 2021;**478**(22):3999–4004. doi: 10.1042/BCJ20210652.
4. Banerjee H, Nieves-Rosado H, Kulkarni A, Murter B, McGrath KV, Chandran UR, Chang A, Szymczak-Workman AL, Vujanovic L, Delgoffe GM, Ferris RL, Kane LP. Expression of Tim-3 drives phenotypic and functional changes in Treg cells in secondary lymphoid organs and the tumor microenvironment. *Cell Rep*. 2021;**36**(11):109699. doi: 10.1016/j.celrep.2021.109699.

1021

A PAN-CANCER SIGNATURE IDENTIFIES TUMOR-REACTING CD8⁺ TILS AND REVEALS THEIR FUNCTIONAL HETEROGENEITY

¹Christopher Chamberlain*, ¹Arianna Draghi, ¹Shawez Khan, ²Katja Harbst, ¹Mario Presti, ¹Aimilia Schina, ¹Agnete Witness Præst Jensen, ¹Anne-Christine Kiel Rasmussen, ¹Torben Lorentzen, ¹Jakob Vasehus Schou, ²Göran Jönsson, ¹Inge Svane, ¹Marco Donia. ¹Copenhagen University Hospital, Herlev, Denmark; ²Lund University, Lund, Sweden

Background Identification of CD8⁺ tumor-reactive tumor-infiltrating lymphocytes (TILs) is a key focus for understanding TIL:tumor interactions in the tumor microenvironment and improving adoptive cell therapies. Current methods concentrate on the detection of TILs endowed with tumor-specific T cell receptors (TCRs) and largely overlook their functional profiles. In addition, analyses of actively tumor-reacting TIL function are often analyte limited and may not reflect the heterogeneity of TIL responses to stimulation. Therefore, we set out to identify tumor-reacting CD8⁺ TILs and thoroughly characterize their functional profiles at the single-cell level pan-cancer.

Methods Minimally *in vitro* cultured TILs and matching autologous tumor cell lines (TCLs) were derived from metastatic melanoma (n=6), renal cell carcinoma (n=3), sarcoma (n=2), colorectal cancer (n=1), and ovarian cancer (n=1) patient samples. Bulk TILs were cocultured with their wildtype or a major histocompatibility complex I and II deficient control TCL, sorted for CD8⁺ (fluorescence-activated cell sorting), and then underwent single-cell RNA sequencing (scRNAseq, 10xGenomics 5' v2/3' v3.1) to form a discovery dataset. Publicly available scRNAseq datasets (n=25, 12 histologies) of fresh tumor biopsies were obtained from online databases (Gene Expression Omnibus, Genome Sequence Archive, European Genome-phenome Archive) or the authors directly and merged into a singular validation dataset. Cell Ranger and Seurat were used for data processing and analysis.

Results Distinct clusters of tumor-reacting CD8⁺ TILs could be easily bioinformatically identified using known reactivity markers. A tumor-reacting CD8⁺ TIL signature (TR8S) derived via comparison to non-reacting cells clearly differentiated tumor-reacting and non-reacting CD8⁺ bulk TILs for all samples and histologies. Deeper characterization of TR8S^{hi} cells revealed diverse sub-populations with distinct and heterogeneous functional profiles, many of which could be re-identified in the validation dataset. In particular, an XCL1^{hi}XCL2^{hi} cluster and a separate CCL3^{hi}CCL4^{hi} cluster dominated the reacting population. The majority of tumor-reacting CD8⁺ TIL sub-populations were shared across tumor histologies.

Conclusions Our results indicate that the TR8S is an effective pan-cancer tool for identifying and characterizing actively tumor-reacting CD8⁺ TILs. Furthermore, our data highlight the complexity of the actively tumor-reacting CD8⁺ TIL population and that deeper investigation of their functional abilities is warranted. Specifically, the prevalence of distinct clusters may have predictive/prognostic strength and could direct future immunotherapies.

Acknowledgements The authors sincerely thank all the patients who consented to the use of their samples for this study. The following funding sources are thanked for their continuous support: Lundbeck Foundation (grants R233-2016-3728, R286-2018-991, R307-2018-3636), The Danish Cancer Society (grants R180-A11339, R184-A11806, R204-A12535), Independent Research Fund Denmark (8045-00067B), Danish National Board of Health (4-1612-236/8, Empowering Cancer Immunotherapy in Denmark), and Herlev and Gentofte

Hospital Research Council (Clinician-Scientist grant to MD). All physicians, surgeons, and technicians involved in patient enrolment and sample procurement are thanked for their efforts. The authors of the public scRNAseq data used are thanked for sharing the data either directly or via public databases.

Ethics Approval Fresh tumour material from patients with cancer was acquired via surgical resection or needle biopsy in the context of standard treatment or enrolment in clinical trials (Ethical approval references: H-20070020, H-19076238, Data Protection approval P-2021-303) at the National Center for Cancer Immune Therapy (CCIT-DK), Department of Oncology, Copenhagen University Hospital, Herlev, Denmark. All procedures were performed in compliance with the clinical protocols approved by the Ethics Committee of the Capital Region of Denmark and national regulations for biomedical research.

<http://dx.doi.org/10.1136/jitc-2022-SITC2022.1021>

1022

TUMOR-INFILTRATING CXCR6-EXPRESSING TISSUE-RESIDENT MEMORY HPV-SPECIFIC CD8⁺ T CELLS ARE TERMINALLY EXHAUSTED IN HPV-ASSOCIATED HEAD AND NECK SQUAMOUS CELL CARCINOMA

Yang Cheng*, Kathleen Atkinson, Talia Saal, Jean Campbell, Sara Pai. *Massachusetts General Hospital, Boston, MA, United States*

Background Tissue-resident memory T cells (T_{RM}) are important for controlling both infection and tumor growth. We performed comprehensive immunophenotyping of HPV-specific and non-HPV-specific viral bystander (EBV, CMV, IAV, and SARS2-CoV2) CD8⁺ T_{RM} cells in HPV-associated HNSCCs.

Methods We assessed HPV-specific and non-HPV-specific viral bystander CD8⁺ T cell frequency and functional states in the primary tumor, tumor-involved lymph node (LN), and peripheral blood mononuclear cells (PBMC) from 34 HPV-associated HNSCC patients. CD8⁺ T cells were isolated and probed by 89 different pMHC tetramers across three HLA alleles (A*02:01, A*01:01 and A*24:02) using multiplexed combinatorial peptide-MHC (pMHC) tetramer staining and spectral flow cytometry. To interrogate HPV-specific responses, we analyzed 61 HPV16 E6 and E7 epitopes. To compare non-HPV bystander virus-specific T cells, we investigated 11 bystander virus (EBV, CMV and IAV) and 17 SARS2-CoV-2 (spike protein) epitopes. Tetramer⁺ CD8⁺ T cells were immunophenotyped by co-staining 20 cellular markers to probe T cell exhaustion and tissue resident phenotypes.

Results 76.4% (26 of 34) of HPV-associated HNSCCs had detectable HPV-specific T cells within their tissue and 82% (28 of 34) had bystander virus-specific T cells. Overall, we identified 26 HPV- (10 HPV16-E6 and 16 HPV16-E7), 11 bystander (non-HPV) virus-, and 8 SARS-CoV-2 spike-specific CD8⁺ T cell populations. We observed a broader HPV epitope repertoire within LN and PBMC as compared to tumors. However, the frequency of HPV-specific T cells infiltrating the tumor was significantly higher compared to the LN and PBMC. Within the tumor, 13 HPV- (6 HPV16-E6 and 7 HPV16-E7), 6 bystander (non-HPV) virus-, and 3 SARS-CoV-2 spike-specific CD8⁺ T cell populations were identified. The frequency of tumor-infiltrating HPV-specific T cells ranged from 0.02-3.01% for E6, 0.013-10.9% for E7, 0.013-1.93% for bystander (non-HPV) virus-specific T cells, and 0.014-11.5% for SARS-CoV-2 spike-specific T cells. High-dimensional analysis identified four distinct T_{RM} subsets. Tumor-infiltrating HPV-specific T cells were enriched for two CXCR6⁺ T_{RM} subsets that were also PD-1^{hi}TIM-3⁺, suggesting they were terminal exhausted. In contrast, tumor- and LN-infiltrating bystander non-HPV-specific T cells were CXCR5⁺PD-1^{int} T_{RM} and not exhausted.

Conclusions We report a high frequency of HPV and bystander viral epitopes within HPV-associated HNSCCs, and identified two distinct CXCR6⁺ terminal exhausted HPV-specific T_{RM} subsets within the tumor. Spatial localization of these two distinct CXCR6⁺ terminally exhausted T_{RM} to myeloid populations in the primary tumor and tumor draining lymph nodes are ongoing to better understand tumor-specific T cell priming within these two sites.

<http://dx.doi.org/10.1136/jitc-2022-SITC2022.1022>

1023

THE SIGNAL STRENGTH OF SIGNAL 2 AND 3 DURING T CELL PRIMING AFFECT THE FUNCTIONAL FATE OF AN ANTI-TUMOR T CELL RESPONSE

Duncan Morgan, Vidit Bhandarkar, Emi Lutz, K Wittrup, Stefani Spranger, Teresa Dinter*. *Massachusetts Institute of Technology, Cambridge, MA, United States*

Background Fate decision in CD8⁺ T cells refers to the process of differentiation that occurs when a naïve T cell enters into effector, memory, exhausted, or other states. Multiple models of fate decision have been proposed, but the exact determinants of T cell fate are unknown. Evidence in LCMV and cancer models support the notion that signals during T cell priming are especially important in deciding T cell fate and that fate decisions are made early in the priming process. Priming interactions are highly complex, requiring the integration of multiple signals. Each of these signals can vary in strength and it is the sum of these signals that decides the T cell response. Thus, it is unsurprising that we currently do not know the combinatorial specificities and molecular underpinnings of priming interactions. Understanding the factors that drive these different fates could be therapeutically harnessed to reduce exhaustion phenotypes and increase effector functions and memory potential of CD8⁺ T cells in cancer.

Methods We used therapeutic interventions as a tool to alter the signals received by a T cell during priming and characterized the impact on T cell fate. Using a BRAF^{V600E}PTEN^{-/-} melanoma cell line that expresses the SIYRYYGL (SIY) model antigen, we implanted tumors and provided therapy during priming. We surveyed the effects of checkpoint blockade therapy (anti-PD1 and anti-CTLA4), costimulatory agonists (anti-CD40 and anti-41BB), and Type-I Interferon (IFN α and IFN β) on tumor-reactive CD8⁺ T cell phenotypes at early timepoints during priming via flow cytometry and single-cell RNA sequencing.

Results All treatments resulted in an increase of effector-like (TCF1⁺TIM3⁺) tumor-reactive T cells. Interestingly however, each intervention induced differential expression of a specific set of transcription factors. For example, expression of Eomes is significantly increased upon IFN β treatment at both protein and RNA level, while it is decreased in T cells exposed to agonistic anti-CD40. Analysis of single-cell RNA sequencing of tumor-reactive CD8⁺ T cells revealed unsupervised clustering of cells based on the therapeutic intervention administered during priming. Tumor outgrowth and phenotypic studies at later timepoints indicated that CD8⁺ T cells primed with therapeutic intervention adopt different cell fates.

Conclusions Priming signals are crucial determinants of T cell fate. Changing the signals received by a CD8⁺ T cell during priming results in an altered phenotypic and transcriptional profile early during priming. These early transcriptional changes appear to generate different CD8⁺ T cell fates, providing an opportunity to improve anti-tumor immunity in a neoadjuvant setting.

Acknowledgements MIT Frontier Research Grant

Ethics Approval All mouse experiments in this study were approved by MIT's Committee on Animal Care (CAC) – DHHS Animal Welfare Assurance # D16-00078

<http://dx.doi.org/10.1136/jitc-2022-SITC2022.1023>

1024

ILLUMINATING STEM MEMORY T CELL (TSCM) HETEROGENEITY IN HUMAN CANCER: CHARACTERIZATION OF A UNIQUE CD45RO+ TSCM POPULATION IN HUMAN OVARIAN CANCER

Erica Brown*, Monika Eiva, Veethika Pandey, Alexander Benton, Stacy Thomas, Wenzhao Meng, Aaron Rosenfeld, Eline Luning Prak, Daniel Powell. *University of Pennsylvania, Philadelphia, PA, United States*

Background Stem memory T cells (Tscm) are a unique T cell subset positioned between naïve and central memory (CM) T cells, that express the surface markers CCR7, CD45RA and CD95, and are CD45RO negative.¹ Tscm cells can self-renew, are multipotent, and appear to be critical for effective anti-tumor immunity, but little is known about Tscm immunobiology in human tumors.¹⁻⁴ Most studies examining canonical Tscm cells are performed using mouse models, expanded tumor-infiltrating lymphocytes (TILs), or peripheral blood T cells, and few studies examine Tscm-like cells directly from human tumors, despite evidence for their crucial role in solid tumor immunotherapeutic treatment.²⁻⁶

Methods Therefore, we hypothesized that Tscm cells in human ovarian cancer exist and explored Tscm heterogeneity in ovarian cancer tumor digests using flow and mass cytometry. This investigation resulted in the identification of a novel CD45RO + expressing Tscm subset, which was further interrogated using FACS sorted TIL populations to assess self-renewal capabilities and effector function. Additionally, bulk RNA-seq and TCR sequencing were completed on sorted TIL populations to examine the RO+ Tscm subset.

Results Like canonical CD45RO- (RO-) Tscm cells, the RO+ subset can self-renew and is maintained by the homeostatic cytokines IL-7 and IL-15; however, RNA-seq, TCR sequencing, and functional assessment of the RO+ Tscm population position it as a unique subset between RO- Tscm and CM T cell subsets. RNA-seq revealed that RO+ Tscm cells are transcriptionally distinct from other subsets, exhibiting intermediate expression of naïve and effector associated genes. TCR sequencing indicates that the RO+ subset shares a high degree of clones with downstream memory populations and has an intermediate clonality relative to canonical RO- Tscm and CM populations. Notably, our results demonstrate that RO+ Tscm cells exhibit greater effector potential than the RO- Tscm subset, with RO+ Tscm cells producing more IFN γ upon stimulation. These results, paired with the observation that RO+ Tscm cells express CD137, a biomarker of tumor-specificity, more frequently than other differentiation subsets, indicate that this subset may have enhanced anti-tumor capabilities.

Conclusions In conclusion, we (1) demonstrate that a heterogeneous Tscm population exists in human ovarian cancer and (2) identify a distinct RO+ Tscm subset that appears to be transcriptionally, phenotypically, and functionally intermediate between canonical RO- Tscm and CM populations. Importantly, we show that the RO+ Tscm subset is multipotent and exhibits effector-like attributes, making it a desirable target for future research in the setting of cancer immunotherapy.

Acknowledgements The authors acknowledge the Penn Ovarian Cancer Research Center Tumor BioTrust collection, including Dalia K. Omran and Euihye Jung, for providing patient samples. The authors also thank Takuya Ohtani for training and running mass cytometry samples. Finally, the authors thank Jonathan Schug, Shilpa Rao and Olga Smirnova of the UPenn Next-Gen Sequencing Core (NGSC) and John Tobias of the

UPenn Molecular Profiling Facility for their aid in RNA-seq experimentation and bioinformatics analysis.

REFERENCES

1. Gattinoni L, Lugli E, Ji Y, Pos Z, Paulos CM, Quigley MF, Restifo NP. A human memory T cell subset with stem cell-like properties. *Nature medicine* 2011;**17**(10),1290–1297.
2. Gattinoni L, Speiser DE, Lichterfeld M, Bonini C. T memory stem cells in health and disease. *Nature Medicine* 2017;**23**(1):18–27.
3. Krishna S, Lowery FJ, Copeland AR, Bahadiroglu E, Mukherjee R, Jia L, Rosenberg, SA. Stem-like CD8 T cells mediate response of adoptive cell immunotherapy against human cancer. *Science* 2020;**370**(6522):1328–1334.
4. Biasco L, Izotova N, Rivat C, Ghorashian S, Richardson R, Guvenel A, Amrolia PJ. Clonal expansion of T memory stem cells determines early anti-leukemic responses and long-term CAR T cell persistence in patients. *Nature Cancer* 2021;**2**(6):629–642.
5. Jansen CS, Prokhnjevka N, Master VA, Sanda MG, Carlisle JW, Bilen MA, Kissick H. An intra-tumoral niche maintains and differentiates stem-like CD8 T cells. *Nature* 2019;**576**(7787):465–470.
6. Siddiqui I, Schaeuble K, Chennupati V, Marraco SAF, Calderon-Copete S, Ferreira DP, Held W. Intratumoral Tcf1+ PD-1+ CD8+ T cells with stem-like properties promote tumor control in response to vaccination and checkpoint blockade immunotherapy. *Immunity* 2019;**50**(1):195–211.

Ethics Approval Viably frozen, human high-grade serous ovarian tumor or ascites samples were purchased from the University of Pennsylvania (UPenn) Ovarian Cancer Research Center (OCRC) Tumor BioTrust Collection. All donor samples used in this study were de-identified and approved for use by the UPenn Institutional Review Board (IRB 702679, UPCC 17909).

<http://dx.doi.org/10.1136/jitc-2022-SITC2022.1024>

1025

SINGLE CELL EVALUATION OF COSTIMULATORY AND COINHIBITORY RECEPTORS AND THEIR LIGANDS ACROSS SOLID TUMOR INDICATIONS

Shawn Fahl*, Kerri Colwell, Cavin Ott, Casey Smith, Kayla Williams, Alex Moore. *Discovery Life Sciences, Huntsville, AL, United States*

Background Costimulatory and coinhibitory receptors on T-cells are key mediators of the overall immune response, and the clinical success of checkpoint inhibitor therapies has proven the therapeutic benefits of targeting these pathways. Viable, cryopreserved dissociated tissue provides an opportunity to understand the dynamic expression patterns of these receptor/ligand sets at the single-cell level, providing insights into the differential expression of each receptor/ligand pair across different cancer indications as a means to target new therapeutic interventions.

Methods The study compared expression patterns from two cohorts composed of indications that are clinically approved for checkpoint inhibitor therapy versus indications that are not currently approved for checkpoint therapy. We performed bulk RNA sequencing on both cohorts to understand the global expression of costimulatory and coinhibitory receptors, and their ligands, within the tumor microenvironment. Furthermore, we developed a flow cytometry panel that allows for efficient screening of these receptor/ligand sets on the major cellular subsets (tumor cells, T-cells, B-cells, myeloid cells) within the tumor microenvironment. These data sets were initially evaluated for the expression patterns of PD1/PDL1/PDL2 as the standard for immunomodulatory receptors, and to evaluate the accuracy and sensitivity of the methods for the evaluation of receptor/ligand expression. In addition, we evaluated the expression patterns of two less well-characterized immunomodulatory receptors sets: TIGIT/PVR/PVRL2/CD226 and CD160/HVEM/BTLA/LIGHT to provide new insight into the expression patterns of these potential receptor/ligand sets and to better understand their value as therapeutic targets for specific cancer indications.

Results The protocols developed for this study were able to provide a clear and detailed picture of the receptor-ligand expression patterns across different cancer indications. Consistent with previous reports, PD1 expression was high on T-cell subsets, but low on the other lymphoid subsets within the tumor microenvironment. PDL1, on the other hand, was more differentially expressed on tumor cells across patient samples and was also expressed on myeloid cell populations. The expression patterns for the TIGIT and CD160 receptors and their associated ligands demonstrate the distinct differences in expression patterns across cancer indications.

Conclusions Given the varied and distinct expression patterns observed in different cancer indications, it is clear that the successful targeting of immune modulatory therapeutics will require an understanding of the expression of individual receptors and ligands at the single-cell level. This study demonstrates the utility of dissociated tumor cells as a tool to provide detailed insight into, and an understanding of the receptor-ligand expression of different cancer indications.

<http://dx.doi.org/10.1136/jitc-2022-SITC2022.1025>

1027

CHRONIC ANTIGEN IN SOLID TUMORS DRIVES A DISTINCT PROGRAM OF T CELL RESIDENCE

¹Noah Gavil*, ¹Milcah Scott, ¹Eyob Weyu, ¹Olivia Smith, ¹Stephen O'Flanagan, ¹Sathi Wijeyesinghe, ¹Sahar Lotfi-Emran, ²Stephen Shiao, ¹Vaiva Vezys, ¹David Masopust. ¹University of Minnesota, Minneapolis, MN, United States; ²Cedars-Sinai Medical Center, Los Angeles, CA, United States

Background Resident-memory T cells (T_{RM}) permanently reside in tissues, surveying local environments without recirculating. Surface protein expression (e.g. CD69, CD103) and transcriptional signatures from infection models are used as surrogate markers of T cell residency. Across numerous solid tumor types, T_{RM} -like phenotypes have been identified and correlated with improved prognosis and responsiveness to immunotherapy. However, the migration properties of CD8⁺tumor infiltrating lymphocytes (TILs) have not been well described, and the reliability of healthy tissue T_{RM} markers for correlating with CD8⁺ TIL migration properties remains unknown.

Methods In this study, we employed parabiosis migration assays in the context of both acute viral infection and a mouse model of breast cancer. In combination, this system allowed us to simultaneously track both virus-specific memory T cells and tumor-specific T cells.

Results Our migration assays demonstrated that both virus-specific, bystander and tumor-specific CD8⁺ TILs can be resident. Canonical markers of T_{RM} , including CD69, correlated with tissue residence in healthy mammary tissue, but failed to discriminate between resident cells and recent migrants in tumors. Instead, the expression of markers associated with chronic T cell stimulation (PD-1, CD39, Tim-3) identified a population of resident, tumor-specific cells. We further observed that after tumor entry, Tcf-1⁺PD-1^{lo} tumor-specific T cells progressively acquired the expression of inhibitory receptors, such as Tim-3, correlating with the phenotypes that represented tumor retention and residence.

Conclusions Thus, T_{RM} exist within tumors, durable intratumoral residence was not informed by common markers associated with pathogen-specific T_{RM} that have been described in healthy tissue, but tumor-specific T cells become resident upon tumor antigen recognition and the subsequent upregulation of CD39 and Tim-3. Together with high-dimensional, single-cell transcriptomics, we propose an integrated view of tumor immunosurveillance in which tissue environments and antigen-specific recognition drive distinct residence programs.

Ethics Approval All mice used in experiments were 5–15 weeks of age and used in accordance with the Institutional Animal Care and Use Committees guidelines at the University of Minnesota.

<http://dx.doi.org/10.1136/jitc-2022-SITC2022.1027>

1028

IL-12 AND IL-27 UPREGULATE CD39 EXPRESSION ON CD8⁺ T-CELLS AND DIFFERENTIALLY AFFECT CD39⁺CD8⁺ T-CELL EFFECTOR FUNCTION

Lara Gerhardt*, Rene Figueredo, Saman Maleki. *Western University, London, ON, Canada*

Background Tumor-specific CD8⁺ T-cells play a critical role in tumor control, as demonstrated by the success of immune checkpoint inhibitors and adoptive cell therapy. Studies of mice and human tumor-infiltrating lymphocytes (TILs) demonstrate that tumor-specific CD8⁺ TILs can be defined by CD39 expression on their surface. CD39 is commonly considered an immunosuppressive enzyme, as it depletes ATP. However, CD39 is also associated with mitigating activation-induced cell death and mediating leukocyte trafficking. It is, however, unclear whether CD39 expression on tumor-specific T-cells can be regulated by putative anti-tumor factors such as pro-inflammatory cytokines similar to the phenotype and anti-tumor properties of CD8⁺ TILs. IL-12 and IL-27 have established roles in promoting effector T-cell differentiation, expansion, and cytotoxic activity. Both cytokines are implicated in the upregulation of CD39 by T regulatory cells, suggesting they may regulate CD39 expression in other cell types, including tumor-specific CD8⁺ T-cells. We hypothesize that IL-12 and IL-27 induce CD39 upregulation on CD8⁺ T-cells, modulating their anti-tumor properties.

Methods An engineered immunogenic, syngeneic neuroblastoma (neuro-2a) mouse model was used for *in vitro* and *in vivo* experiments. CD8⁺ T-cells or bulk splenocytes isolated from naïve or neuro-2a vaccinated mice were stimulated *in vitro* using anti-CD3/CD28 Dynabeads and IL-2 ± IL-12 or IL-27. Flow cytometry was used to determine the phenotype of CD8⁺ T-cells and assess effector activity. Additionally, we inhibited IL-12 activity *in vivo* to study the effect on CD8⁺ TIL expression of CD39. An isotype control antibody was administered to a separate group to act as a control.

Results Our *in vitro* results demonstrate that CD8⁺ T-cells stimulated in the presence of IL-12 or IL-27 had higher expression of CD39 compared to stimulated controls. In addition, we found a higher frequency of CD39⁺CD8⁺ T-cells expressing IFN γ and CD107a than CD39⁻ counterparts. Finally, blocking IL-12 activity *in vivo* reduced CD39⁺CD8⁺ TIL frequency compared to the isotype control group.

Conclusions Our results establish that IL-12 and IL-27 induce CD39 expression on CD8⁺ T-cells and blocking IL-12 reduced CD39⁺CD8⁺ TIL frequency. Furthermore, CD39 expression is associated with improved effector CD8⁺ T-cell function. Future experiments will assess the functionality of CD39⁺CD8⁺ T-cells using *ex vivo* cytotoxicity assays. Data generated in this study will provide novel information on the mechanism of CD39 induction and its effect on CD8⁺ T-cell function, which can be exploited to improve future cancer therapies.

<http://dx.doi.org/10.1136/jitc-2022-SITC2022.1028>

1029 **ENGINEERING OF T CELLS WITH CCR10 FOR ENHANCED TRAFFICKING OF ADOPTIVE CELL THERAPY**

²Hee Jin Lee, ²Gyung Yub Gong, ³Kwang Hee Kim, ¹Jong Moo Hong*. ¹University of Ulsan College of Medicine, Seoul, South Korea, Republic of; ²Asan Medical Center, Seoul, South Korea, Republic of; ³NeogenTC Crop, Seoul, South Korea, Republic of

Background Trafficking T cells into tumor microenvironments is critical to the success of cancer immunotherapy, such as adoptive cell transfer therapy. Chemokines and their receptors play an important role in inducing trafficking and homing of T cells. They activate integrin for T cell adhesion to endothelial cells and help T cells traffic through chemotaxis in microenvironment of cancer. Therefore, the introduction of chemokine receptors that react with tumor-derived chemokines could improve the effectiveness of adoptive T cells. CCR10 is a chemokine receptor for CCL28, which is a high-ranking chemokine secreted from tumor tissue. We engineered T cells with CCR10 to improve trafficking of T cells.

Methods Cloning was performed using vectors containing NY-ESO-1 and HLA-A*02:01 specific (1G4) TCR and CCR10. Transduction of Jurkat cells-NFAT-luciferase (TCR KO) and peripheral blood mononuclear cells (PBMC) was performed after the production of the lentivirus using a lenti-x-293T cell. A375 cell line, which expresses HLA-A*02:01 and NY-ESO-1, was selected as a target. CCL28 was overexpressed in A375 cell line, and transwell migration assay was performed using CCR10-1G4 TCR-T and 1G4 TCR-T. 1G4 TCR reactivity was measured using luciferase after NY-ESO-1 peptide pulsing in T2 cell.

Results Transduction efficiency of the 1G4 TCR and CCR10 on post-transduction day 7 was more than 90% each in Jurkat and 40% each in CD8+ PBMC. However, when we used the vector containing 1G4 TCR and CCR10 together with T2A linker, the expression efficiency of CCR10 was 30% to 40% in Jurkat and 10% to 20% in CD8+ PBMC. Transwell migration assay was performed using mock Jurkat, CCR10-Jurkat, 1G4 TCR-Jurkat, and CCR10 1G4 TCR-Jurkat. Compared to mock or 1G4-Jurkat, CCR10-Jurkat or CCR10-1G4 TCR-Jurkat had increased migration by more than 10% during 4 h migration period. In addition, migration of CCR10 1G4 TCR-Jurkat increased according to incubation time when transwell assays were performed for 4, 8, and 16 hours. The reactivity of CCR10 1G4 TCR-Jurkat was measured using luciferase. The RLU of the T2 cells without pulsing the NY-ESO-1 peptide was below detection level. When reacted with T2 cells pulsed NY-ESO-1 peptide by diluting 10 times from 1ug to 0.001ug, RLU was 3.40E+04, 5.44E+04, 6.16E+04, and 7.24E+04, respectively.

Conclusions CCR10 engineered TCR-T showed increased in vitro trafficking efficacy. Further studies with application of CCR10 to other T cell therapies would improve quality of adoptive T cell therapy.

<http://dx.doi.org/10.1136/jitc-2022-SITC2022.1029>

1030

PSGL-1-DEFICIENCY SUPPRESSES TUMOR GROWTH OF ORTHOTOPIC PANCREATIC DUCTAL ADENOCARCINOMA TUMORS AND ENHANCES IMMUNE CELL INFILTRATION AND CD8⁺ T CELL RESPONSES

Jennifer Hope*, Yijuan Zhang, Ashley Palete, Hannah Faso, Sreeja Roy, Dennis Otero, Swetha Maganti, Cosimo Comisso, Linda Bradley. *Sanford Burnham Prebys Medical Discovery Institute, La Jolla, CA, United States*

Background Pancreatic ductal adenocarcinoma (PDAC) is an aggressive, poorly immunogenic cancer that is increasing in incidence. PDAC tumors are highly refractory to all currently available treatments including existing immune checkpoint blockade (ICB) therapies, demonstrate limited CD8⁺ T cell infiltration. Patient prognosis is poor with a 5-year overall survival rate of only 11%. As such, there is a critical need to develop novel approaches to improve patient outcomes. We previously demonstrated that deficiency of P-selectin glycoprotein 1 (PSGL-1) promotes enhanced CD8⁺ T cell responses that clear chronic LCMV Cl13 virus infection and inhibit the growth of PD-1 blockade resistant melanoma. Here we evaluated if targeting PSGL-1 similarly promotes CD8⁺ T cell responses to PDAC tumors to inhibit growth and metastases.

Methods 2.5x10⁴ KPC.4662 tumor cells suspended in Matrigel were injected orthotopically into the pancreas tail in 6-8 week old C57BL/6 (wildtype control) and PSGL-1^{-/-} male or female mice. PDAC tumors were collected on day 28 post-injection and assessed by flow cytometry and histology. For evaluation of metastatic potential, 2x10⁵ KPC.4662 tumor cells suspended in 1X PBS were injected intravascularly into the tail vein of control and PSGL-1^{-/-} mice. Lung metastases were assessed on day 17 post-injection.

Results At 28 days post orthotopic tumor cell injection, KPC.4662 tumor burden was reduced on average by 45% (0.74±0.27g vs 0.41±0.24g) in PSGL-1^{-/-} mice compared to control mice. Moreover, fewer mice developed non-primary tumor metastases in the intraperitoneal cavity, liver, and lungs. To assess if PSGL-1^{-/-} mice had the capability to reduce metastatic burden, KPC.4662 cells were injected intravascularly and tumor development in the lungs was assessed on day 17. PSGL-1^{-/-} reproducibly developed fewer tumors in the lungs compared to control mice as determined by histological examination. Immune infiltration (CD45⁺ cells) was markedly increased (10% vs 24%) in orthotopic tumors from PSGL-1^{-/-} mice, including an increase in Thy⁺T cells (3.1% vs 9.4%). Flow cytometry and immunofluorescence staining confirmed a significant increase in tumor-infiltrating CD8⁺ T cells in PDAC tumors from PSGL-1^{-/-}. Importantly, PSGL-1^{-/-} CD8⁺ T cells were less functionally exhausted.

Conclusions In the absence of PSGL-1, we observe significantly reduced growth of primary orthotopic PDAC tumors and decreased metastases. These findings were associated with increased CD45⁺ immune cell infiltration in the tumors and notably, increased CD8⁺ T cell effector responses. PSGL-1 therefore represents a novel target for promoting immune responses to PDAC tumors.

Ethics Approval These animal studies were conducted at Sanford Burnham Prebys with the approval of the Sanford Burnham Prebys IACUC.

<http://dx.doi.org/10.1136/jitc-2022-SITC2022.1030>

¹Katie Hurst, ¹Brian Riesenberger, ¹Elizabeth Hunt*, ²Alex Andrews, ²Megan Tennant, ¹Evelyn Gandy, ³Peng Gao, ²Lauren Ball, ¹Emily Wallace, ¹David Corcoran, ¹Jessica Thaxton. ¹University of North Carolina Chapel Hill, Chapel Hill, NC, United States; ²Medical University of South Carolina, Charleston, SC, United States; ³Northwestern University, Chicago, IL, United States

Background Reshaping metabolism improves T cell tumor control¹⁻³, but direct enzymatic targets that restrict antitumor bioenergetics are poorly defined. Acetyl CoA Carboxylase (ACC) induces carboxylation of cytosolic Acetyl CoA to form Malonyl CoA, a metabolite that restricts the well-defined T cell antitumor program of β oxidation of fatty acids (FAO).⁴⁻⁵ Here we tested whether ACC inhibition (ACCi) could act as a molecular switch in CD8 T cells to program lipid catabolism and metabolic efficacy for tumor control.

Methods ACCi-treated T cells were collected and submitted for metabolomics, lipidomics, proteomics, and RNA-sequencing. Seahorse XF Real-Time ATP Rate and Seahorse XF Mito Stress Tests using T cells treated with the ACC1/2 inhibitor ND-646 were performed using the Seahorse XFe96 Analyzer. Spectral flow cytometry was used for T cell phenotyping, using cells stained with 18 fluorophore-conjugated antibodies. To assess ACCi T cell antitumor capability, B16F1-OVA melanomas were established subcutaneously by injecting 2.5×10^5 cells into the right flank of female C57BL/6. After 10 days of tumor growth, 5×10^5 OT-1 T cells conditioned with vehicle or ACCi were infused into tumor-bearing mice. Tumor growth was measured every other day and survival was monitored.

Results Using the compound ND-646 (ACCi), we assessed the effects of ACC inhibition on CD8+ T cell metabolism, lineage, and tumor fate in mouse and human cells. Through metabolomics and metabolic analysis using Seahorse Bioanalysis, we show that ACCi remodels CD8 T cell metabolism, driving FAO and enhancing mitochondrial spare respiratory capacity (SRC) as a result of sustained fatty acid import. Through phenotypic analysis using spectral flow cytometry and RNA-sequencing, we found that alongside this metabolic reprogramming, ACCi also induced transcriptional and functional traits associated with robust tumor control, including sustained production of mitochondrial ATP, allowing for persistent protein and cytokine synthesis. This phenotypic remodeling induced by ACCi resulted in the generation of T cells with prolonged survival and tumor control capabilities.

Conclusions The data indicate that ACC is a molecular switch that impairs FAO in CD8 T cells, driving metabolic, phenotypic, and transcriptional remodeling that confers T cell longevity and robust anti-tumor capabilities. Targeting ACC is an avenue to program therapeutic efficacy of T cells for solid tumors.

REFERENCES

1. Buck MD, O'Sullivan D, Pearce EL. T cell metabolism drives immunity. *J Exp Med*. 2015;**212**(9):1345–1360
2. Pearce EL, Walsh MC, Cejas PJ, et al. Enhancing CD8 T-cell memory by modulating fatty acid metabolism. *Nature*. 2009;**460**(7251):103–107.
3. van der Windt GJ, O'Sullivan D, Everts B, et al. CD8 memory T cells have a bioenergetic advantage that underlies their rapid recall ability. *Proc Natl Acad Sci U S A*. 2013;**110**(35):14336–14341.
4. Hardie DG, Pan DA. Regulation of fatty acid synthesis and oxidation by the AMP-activated protein kinase. *Biochemical Society Transactions* 2002;**30**:1064–70
5. Pietrocola F, Galluzzi L, Bravo-San Pedro José M, Madeo F, Kroemer G. Acetyl Coenzyme A: a central metabolite and second messenger. *Cell Metabolism* 2015;**21**:805–21

1032 UNCOUPLING CD39 AND T CELL ANTIGEN SPECIFICITY
IN BRAIN TUMORS

Sierra Kleist, Shawn Musial, Hanna Degefu, Pamela Rosato, Jordan Isaacs*. *Dartmouth College, Lebanon, NH, United States*

Background Tumor-infiltrating lymphocytes have long been thought to encompass a repertoire recognizing primarily tumor antigens. However, our lab and others have found that tumor-infiltrating CD8+ T cells include a population with viral-specificity which can often outnumber tumor-reactive cells. Thus, identifying markers of tumor-reactive T cells are critical for developing ways to target this sub-population and boost anti-tumor immunity. Work to this end has defined CD39 and CD103 as putative markers of tumor-reactive T cells in several solid tumors. CD39+ CD8+ T cells have impaired cytokine production and increased expression of inhibitory receptors, while CD39- CD8+ T cells lack hallmarks of chronic antigen stimulation, highlighting their bystander role.

Methods In contrast, we unexpectedly found that CD39 is highly expressed on functional virus-specific CD8+ T cells in healthy brain compared to other non-lymphoid tissues examined. These findings prompted us to investigate whether the established CD39 antigen-specificity paradigm held true in brain tumors. To test this, we established a mouse model of glioblastoma (GBM) and melanoma brain metastasis harboring virus-specific memory T cells, similar to the observations found in humans.

Results Surprisingly, we found that CD39 expression was uniformly high on all CD8+ T cells in both brain tumor models, including on virus-specific T cells which also co-expressed CD103. Moreover, these CD39+ antiviral T cells remained functionally active and could mediate local inflammation upon recognition of cognate antigen. In contrast, in a mouse model of primary melanoma, bystander virus-specific T cells did not express CD39 while the bulk CD8+ population, including tumor-reactive T cells, expressed high CD39 as has been demonstrated clinically.

Conclusions Our ongoing studies aim to elucidate the functional role of CD39 in T-cell mediated immunity of brain tumors. Overall, these data suggest that CD39 may not stratify tumor-reactive CD8+ T cells in brain tumors as has been demonstrated in other solid tumors. Thus, therapeutic approaches to target CD39/CD103+ T cells or restore anti-tumor immunity through CD39 blockade may have different clinical implications in tumors of the central nervous system.

<http://dx.doi.org/10.1136/jitc-2022-SITC2022.1032>

1033

STEM-LIKE CD8 T-CELLS RESIDING IN ANTIGEN PRESENTING IMMUNE NICHES ARE PROGNOSTIC FOR LOCAL CONTROL IN BRAIN METASTASES AND ARE SUSTAINED FOLLOWING RADIATION THERAPY

¹Caroline Jansen*, ¹Prasanthi Chappa, ¹Nataliya Prokhnevskaya, ¹Maria Cardenas, ²Roshan Prabhu, ¹Jim Zhong, ¹Kimberly Hoang, ¹Subir Goyal, ¹Suzanna Logan, ¹Jeffrey Olson, ¹Edjah Nduom, ¹Luke del Balzo, ³Kirtesh Patel, ²Stuart Burri, ⁴Anthony Asher, ⁵Scott Wilkinson, ⁵Ross Lake, ¹Kristin Higgins, ¹Preteesh Patel, ¹Vishal Dhare, ¹Mylin Torres, ⁵Adam Sowalsky, ¹Mohammad Khan, ¹Haydn Kissick, ¹Zachary Buchwald. ¹Emory University, Decatur, GA, USA; ²Atrium Health, Charlotte, NC, USA; ³Yale, Atlanta, GA, USA; ⁴Atrium Health, Charlotte, NC, USA; ⁵National Cancer Institute, Bethesda, MD, USA

Background While tumor infiltrating T-cells have a prognostic benefit in many tumor types¹⁻⁸, the prognostic role of infiltrating immune cells is in patients with brain metastases (BrM) is poorly understood. While patients with 1-2 BrM are treated with resection and stereotactic radiosurgery (SRS), intracranial failure is common, and prognostic biomarkers are needed. Our group recently reported the T-cell response in renal tumors is beneficial for patient outcomes. This response is supported by TCF1+ stem-like CD8 T-cells residing in dense regions of closely clustered antigen presenting cells within the tumor known as the immune niche.⁹ Notably, these stem-like T cells are critical for a robust anti-PD-1 response. Here, we wished to determine whether: 1) TCF1+ stem-like CD8 T-cells are present, residing in immune niches, in BrM?, (2) the density of these niches is associated with patient outcomes? and (3) stem-like CD8 T-cells and immune niches persist following SRS?

Methods Tumor tissue was collected from 146 patients with BrM undergoing surgery at two clinical centers. Samples were analyzed by flow cytometry, single cell RNA sequencing, and immunofluorescence. Imaging data was analyzed using custom quantitative pipelines. Together, this allowed for evaluation of the BrM immune microenvironment at baseline or following pre-operative SRS.

Results We describe the presence of TCF1+ stem-like CD8 T-cells in BrM (figure 1A-B), regardless of histology, these stem-like cells reside in dense, antigen-presenting immune niches (figure 1C-D). We find that higher density of these immune niches in BrM correlates with improved local control of BrM (figure 1E). Pre-operative SRS did not decrease immune niche density (figure 1F-G), nor significantly alter the stem-like signature of this population of T-cells. Finally, we also find that a longer time from SRS to resection may lead to increased CD8+ T-cell density in BrM (figure 1H).

Conclusions We have shown that stem-like T-cells are present in BrM in immune niches. The density of this intratumoral immune organization is associated with improved patient outcomes regardless of primary tumor origin. These findings recapitulate the previously reported phenomena of immune organization in tumor tissue, underscoring the trans-tumor/trans-tissue importance of this biology in the anti-tumor immune response. Finally, this niche is maintained following SRS suggesting it is a relatively radioresistant compartment. This has significant implications for combinatorial strategies of immunotherapy and SRS for BrM.

Acknowledgements We would like to acknowledge NCI grant 1-F30-CA-243250 (to C.S. Jansen), the Yerkes NHP Genomics Core which is supported in part by NIH P51 OD011132, the Emory Flow Cytometry Core supported by the National Center for Georgia Clinical & Translational Science Alliance of the National Institutes of Health under award number

UL1TR002378, the Intramural Research Program of the NIH, National Cancer Institute and the Emory University Integrated Cellular Imaging Microscopy Core of the Winship Cancer Institute of Emory University and NIH/NCI under award number 2P30CA138292-04.

REFERENCES

1. Azimi F, et al. Tumor-infiltrating lymphocyte grade is an independent predictor of sentinel lymph node status and survival in patients with cutaneous melanoma. *J Clin Oncol* 2012;**30**(21):2678–83. Epub 2012/06/20. doi: 10.1200/jco.2011.37.8539. PubMed PMID: 22711850.
2. Galon J, et al. Type, density, and location of immune cells within human colorectal tumors predict clinical outcome. *Science*. 2006;**313**(5795):1960–4. Epub 2006/09/30. doi: 10.1126/science.1129139. PubMed PMID:17008531.
3. Mlecnik B, et al. Integrative analyses of colorectal cancer show immunoscore is a stronger predictor of patient survival than microsatellite instability. *Immunity*. 2016;**44**(3):698–711. Epub 2016/03/18. doi: 10.1016/j.immuni.2016.02.025. PubMed PMID: 26982367.
4. Mlecnik B, et al. Histopathologic-based prognostic factors of colorectal cancers are associated with the state of the local immune reaction. *J Clin Oncol* 2011;**29**(6):610–8. Epub 2011/01/20. doi:10.1200/JCO.2010.30.5425. PubMed PMID: 21245428.
5. Pagès F, et al. Immune infiltration in human tumors: a prognostic factor that should not be ignored. *Oncogene* 2009;**29**:1093. doi:10.1038/onc.2009.416.
6. Peranzoni E, et al. Macrophages impede CD8 T-cells from reaching tumor cells and limit the efficacy of anti-PD-1 treatment. *Proceedings of the National Academy of Sciences of the United States of America* 2018;**115**(17):E4041–E50. Epub 2018/04/11. doi: 10.1073/pnas.1720948115. PubMed PMID: 29632196.
7. Savas P, et al. Single-cell profiling of breast cancer T-cells reveals a tissue-resident memory subset associated with improved prognosis. *Nat Med*. 2018;**24**(7):986–93. Epub 2018/06/27. doi: 10.1038/s41591-018-0078-7. PubMed PMID: 29942092.
8. Tosolini M, et al. Clinical impact of different classes of infiltrating T cytotoxic and helper cells (Th1, th2, treg, th17) in patients with colorectal cancer. *Cancer Res* 2011;**71**(4):1263–71. Epub 2011/02/10. doi: 10.1158/0008-5472.Can-10-2907. PubMed PMID: 21303976.
9. Jansen CS, et al. An intra-tumoral niche maintains and differentiates stem-like CD8 T-cells. *Nature*. 2019;**576**(7787):465–70. doi: 10.1038/s41586-019-1836-5.

Ethics Approval Samples are collected under an approved IRB protocol (00001896).

Consent All patients provided informed consent.

<http://dx.doi.org/10.1136/jitc-2022-SITC2022.1033>

1034

ANALYSIS OF FACTORS ASSOCIATED LESS DIFFERENTIATED T CELLS IN BREAST CANCER FOR IMPROVEMENT OF ADOPTIVE T CELL THERAPY

¹Jeong-Han Seo, ¹Hyeonjin Lee, ²Gyungyub Gong, ²Hee Jin Lee, ³Sung Wook Jung*.
¹NeogenTC Corp, Seoul, South Korea, Republic of; ²Asan Medical Center, Seoul, South Korea, Republic of; ³University of Ulsan College of Medicine, Seoul, South Korea, Republic of

Background The survival and proliferative potential of T cells *in vivo* is related to the differentiation status of T cells. Less differentiated cells show prolonged survival duration and effective anti-tumor response for adoptive T cell therapy. To improve *in vivo* sustainability of adoptive T cell therapy, we analyzed factors associated with less differentiated T cells in breast cancer.

Methods We performed a single cell RNA (scRNA) sequence of CD45+ immune cells from 21 breast cancers. Basic analysis was performed using the Seurat package, and immune cells were clustered through UMAP. CD8+ cluster was defined using CD3E, CD8A, and CD8B markers. Differentially expressed genes between differentiated and less differentiated cells were assessed in 3 conditions [SELL-CCR7- (Tem) vs. SELL+CCR7+ (early memory T cell); CD39+CD69+ (terminally differentiated T cell) vs. CD39-CD69- (Tscm phenotype); KLRG1+CD127- (terminal effector cells) vs. KLRG1-CD127+ (pre-memory cell phenotype)]. Genes related to transcription factor and metabolic genes and epigenetic pathways were identified. We also derived data from 5 breast cancer scRNA datasets identified in the NCBI-Gene Expression omnibus and performed the same process as above.

Results 29,102 CD8+ T cells from 6 datasets were analyzed (GSE141665, n=1,767; GSE114724, n=8,400; GSE161529, n=3,023; GSE176078, n=8,036; GSE110686, n=1,214; in house, n=6,662). Based on the 3 conditions in each dataset, up-regulated genes were classified by comparing more and less differentiated phenotypes, and the identified genes were annotated as transcription factors, metabolic genes, and epigenetic genes (transcription factors, n=138, 128, 246, 452, 35, and 546; metabolic genes, n=324, 230, 700, 1,224, 63, and 1,262; epigenetic genes, n=24, 34, 53, 106, 7, and 546 for each dataset, respectively). Total 486 genes, which were up-regulated in less differentiated CD8+ T cells, were obtained by sorting two or more overlapping conditions among the 3 conditions in each dataset (GSE141665, n=141; GSE114724, n=154; GSE161529, n=305; GSE176078, n=840; GSE110686, n=22; in house, n=974). Among 486 genes obtained from 6 datasets, 17 genes including *FOS*, *JUNB*, and *LEF1* were present in all datasets.

Conclusions By combining 21 tumor samples and 5 public datasets, we identified 17 up-regulated genes, which are transcription factors or genes associated with metabolic and epigenetic pathways, in less differentiated CD8+ T cells. Further studies modulating these genes may suggest the possibility of returning terminally differentiated T cells to less differentiated status to improve the T cell therapy.

Ethics Approval The study was approved by the Institutional Review Board of Asan Medical Center, approval number IRB 2016-0935.

<http://dx.doi.org/10.1136/jitc-2022-SITC2022.1034>

1035 **HIGH-DIMENSIONAL IMMUNE PROFILING OF PERIPHERAL EPSTEIN-BARR VIRUS-SPECIFIC T CELLS IN NASOPHARYNGEAL CARCINOMA**

¹Nandita Kumar*, ²Hugh MacMillan, ³Joe Poh Sheng Yeong, ⁴Melvin Chua, ⁴Amit Jain, ²Evan Newell. ¹University of Washington, Seattle, WA, USA; ²Fred Hutchinson Cancer Research Center, Seattle, WA, USA; ³Agency for Science, Technology and Research, Singapore, Singapore; ⁴National Cancer Centre Singapore, Singapore, Singapore

Background Nasopharyngeal carcinoma (NPC) is an EBV-driven cancer endemic to East and Southeast Asia with poor survival rates and limited treatment options. While EBV infection plays a key role in NPC pathogenesis, little is known about EBV-specific T cells in the context of immune response to NPC. We, therefore, interrogated the role of EBV-specific T cell responses in NPC immunopathology with the goal of better understanding how the tumor evades immune targeting and identifying new targets for immunotherapy.

Methods We profiled the phenotypes and antigenicity of EBV-specific CD8 T-cells in NPC patient peripheral blood mononuclear cells (PBMCs) from a 51-patient new diagnosis Singaporean NPC cohort using a combined mass cytometry (CyTOF) and multiplexed peptide-MHC tetramer panel. UMAP and clustering analyses were performed to analyze these highly dimensional data and then phenotypic clusters were correlated to patient clinical parameters to identify clinically relevant, NPC-associated EBV-specific phenotypes. Additionally, we performed single-cell multi-omics sequencing (10X Genomics/CITE-seq) on NPC patient PBMCs to dissect the role of peripheral T cells with NPC-associated phenotypes on tumor pathogenesis.

Results We identified that peripheral EBV-specific CD8 T cells in NPC patients are phenotypically distinct from other antigen-specific T cells and differentially express activation, exhaustion, and homing markers, such as CD38, HLA-DR, CD39, and CD103. We found that the frequencies of EBV-specific T cells with these phenotypes are correlated with clinical parameters (i.e., EBV-DNA titer, tumor volume, stage etc.), and observed similar correlations with bulk CD8 T cells with these phenotypes. Finally, we assessed differential gene expression profiles of CD8 T cells with surface expression of NPC-associated phenotypic markers.

Conclusions Overall, we show that the phenotypic profiles of peripheral EBV-specific T cells may be reflective of NPC anti-tumor immune responses, and these phenotypic profiles could potentially be used as biomarkers for immunotherapeutic response.

Ethics Approval All patient samples were obtained from patients who provided informed consent at the National Cancer Centre Singapore, and de-identified patient information from this cohort was obtain through approval by the institutional review board at the Fred Hutchinson Cancer Research Center (IR File#: 6007-1053).

<http://dx.doi.org/10.1136/jitc-2022-SITC2022.1035>

1036

RON KINASE AS POTENTIAL IMMUNOTHERAPEUTIC TARGET FOR AUGMENTING T CELL ACTIVITY IN BREAST CANCER METASTASIS

Alicia Lai*, Alana Welm. *Huntsman Cancer Institute, Salt Lake City, UT, USA*

Background Metastatic breast cancer is the overwhelming cause of mortality among all breast cancers. Harnessing the immune system to eliminate metastasis is appealing because it does not require knowledge of the “drivers” of heterogeneous tumors or specific targeted-therapies. T cells play critical roles in anti-tumor immunity, but they are often dysfunctional in cancer patients. How T cells become dysfunctional during tumor progression is still controversial and requires further investigation. Our lab identified host expression of the receptor tyrosine kinase Ron as a potential target for breast cancer immunotherapy. We discovered that a specific Ron isoform, short-form Ron (sfRon), plays a key role in regulating the anti-tumor immune response. Importantly, genetic deletion of sfRon (Ron SF^{-/-}) in the mouse host nearly eliminates outgrowth of established lung micro-metastases through potent activation of T cell-mediated anti-tumor immune responses. We sought to test the hypothesis that sfRon expression in T cells regulates their function and that inhibiting Ron kinase activity is a viable therapeutic strategy to augment T cell activity against metastasis.

Methods To investigate sfRon in the suppression of anti-tumor immunity, we conducted single-cell RNA sequencing on immune cells isolated from lungs of wild type and Ron SF^{-/-} mice 2 or 4 weeks after tumor injection via tail-vein. To study whether sfRon controls T cell function, T cells from wild type or Ron SF^{-/-} mice were cultured *ex vivo* and T cell activation and exhaustion were examined. Additionally, specific T cell receptors were ectopically expressed on T cells and stimulated with corresponding peptides to assess immune modulatory responses. To examine the effector functions, CD8 T cells were stimulated with either specific peptide or co-cultured with antigen-expressing tumor cells and subjected to IFN γ detection by flow cytometry or ELISA. To examine the function of helper T cells, peptide-stimulated CD4 T cells were subjected to intracellular detection of IFN γ , IL4, IL17A, and IL10, which represent helper effector subsets Th1, Th2, Th17, and iTreg, respectively.

Conclusions Our results showed that expression of sfRon causes defects in T cell recruitment into the metastatic site, and deletion of sfRon maintains T cell homeostasis and prevents T cell anergy caused by overactivation. These data strongly advance the field on the mechanism by which sfRon suppresses T cell responses and sheds light on new therapeutic strategies focusing on Ron kinase inhibitors for the prevention and treatment of metastatic breast cancer.

Ethics Approval All animal procedures were reviewed and approved by the University of Utah Institutional Animal Care and Use Committee; protocol number: 21-06006.

<http://dx.doi.org/10.1136/jitc-2022-SITC2022.1036>

1037

SINGLE CELL EVALUATION OF ANTIGEN SPECIFICITY, CLONAL DYNAMICS AND TRANSCRIPTIONAL SIGNATURES OF CD8+ T CELLS IN HEAD AND NECK SQUAMOUS CARCINOMA

Housaiyin Li*, Patricia Santos, Aditi Kulkarni, Alok Joglekar, Lazar Vujanovic, Robert Ferris. University of Pittsburgh, Pittsburgh, PA, USA

Background Head and neck squamous cell carcinoma (HNSCC) is caused by high tobacco and alcohol consumption and/or human papillomavirus (HPV) associated.¹⁻³ Anti-PD-1 immunotherapy only benefits 15-20% of HNSCC patients^{4, 5} Thus, there is a need to identify mechanisms involved in resistance to immune checkpoint blockade. Several studies have described the transcriptional phenotypes of tumor infiltrating lymphocytes (TIL) and correlated it with clinical response to ICB.⁶⁻⁸ It has also been shown that majority of neoantigen-specific CD8+ T cells from the tumor have an exhausted-like phenotype⁹⁻¹¹, but specific targetable epitopes and whether anti-viral T cells dominate in HPV-associated HNSCC immunotherapy have not been determined. Collectively, these studies do not address neoantigen and HPV-antigen specificities of evaluated T cells and their transcriptional and functional status in the HNSCC TME, nor whether these cells re-circulate and demonstrate restoration of function once in the peripheral circulation.

Methods Single cell suspensions were prepared from tumor and blood of 21 treatment-naïve HNSCC patients. T cells were FACS-sorted using barcoded mAbs (CITE-seq) and used to generate single cell RNA sequencing (scRNA), T cell receptor (TCR) and ADT libraries using 10x Genomics workflow. A cell-based method for epitope discovery (SABRs) was used to characterize antigen specificity of selected CD8+ TILs.¹²

Results Clonal expanded CD8 T cells in the tumor express high levels of T cell exhaustion markers (PDCD1, HAVCR2, ENTPD1, LAG3). GSEA analysis show that highly expanded CD8+ TILs share gene signatures with neoantigen-specific CD8+ TILs identified from other cancers. There was no significant overlap observed between TCRs of CD8 T cells with high expression of immune checkpoint receptors in the tumor with peripheral blood CD8+ T cells. TCR analysis show that T cell clones shared between tumor and peripheral blood are found in a cluster of CD8 T cells with an effector memory phenotype expressing distinct granzyme expression in activated versus exhausted tumor reactive cells.

Conclusions In this study, we'd like to evaluate 1). Antigen specificities and transcriptional phenotypes of CD8+ T cells. We found that potential tumor reactive cells express high checkpoints, implying most of tumor reactive cells are dysfunctional within tumor. 2). Clonal dynamics of tumor reactive cells. We observed low clonal overlap between peripheral and tumor resident TCRs, suggesting tumor resident population expanded locally. Shared T cell clones between peripheral CD8+ T cells in effector memory population may reflect an active recruitment and/or exchange of T cells between periphery and tumor.

Acknowledgements This research was funded by R01 CA206517 (RLF), P50 CA097190 (RLF), and R01 DE031947 (RLF, LV). This research was supported in part by the University of Pittsburgh Center for Research Computing through the resources provided by using the HTC cluster, supported by NIH award number S10OD028483. This research utilized the UPMC Hillman Cancer Center Flow Cytometry Core Facility, supported in part by award P30 CA047904 (RLF).

REFERENCES

1. Bray F, et al. Global cancer statistics 2018: GLOBOCAN estimates of incidence and mortality worldwide for 36 cancers in 185 countries. *CA Cancer J Clin* 2018;**68**(6):394–424.
2. Powell SF, et al. The Key Differences between Human Papillomavirus-Positive and -Negative Head and Neck Cancers: Biological and Clinical Implications. *Cancers (Basel)*, 2021;**13**(20).
3. Chaturvedi AK, et al. Human papillomavirus and rising oropharyngeal cancer incidence in the United States. *J Clin Oncol* 2011;**29**(32):4294–301.
4. Cramer JD, et al. The changing therapeutic landscape of head and neck cancer. *Nat Rev Clin Oncol*, 2019. **16**(11):669–683.
5. Ferris RL, et al. Nivolumab for Recurrent Squamous-Cell Carcinoma of the Head and Neck. *N Engl J Med*, 2016;**375**(19):1856–1867.
6. Liu B, et al. Temporal single-cell tracing reveals clonal revival and expansion of precursor exhausted T cells during anti-PD-1 therapy in lung cancer. *Nat Cancer* 2022;**3**(1):108–121.
7. Bassez A, et al. A single-cell map of intratumoral changes during anti-PD1 treatment of patients with breast cancer. *Nat Med* 2021;**27**(5):820–832.
8. Zhang Y, et al. Single-cell analyses reveal key immune cell subsets associated with response to PD-L1 blockade in triple-negative breast cancer. *Cancer Cell*, 2021;**39**(12):1578–1593 e8.
9. Zheng C, et al. Transcriptomic profiles of neoantigen-reactive T cells in human gastrointestinal cancers. *Cancer Cell* 2022;**40**(4):410–423 e7.
10. Oliveira G, et al. Phenotype, specificity and avidity of antitumour CD8(+) T cells in melanoma. *Nature* 2021;**596**(7870):119–125.
11. Caushi JX, et al. Transcriptional programs of neoantigen-specific TIL in anti-PD-1-treated lung cancers. *Nature* 2021;**596**(7870):126–132.
12. Joglekar AV, et al. T cell antigen discovery via signaling and antigen-presenting bifunctional receptors. *Nat Methods* 2019;**16**(2):191–198.

Ethics Approval Peripheral blood and tumor tissues from treatment-naïve HNSCC patients were collected with their written consent in accordance with the Declaration of Helsinki, under the University of Pittsburgh Cancer Institute Review Board-approved protocol (99-069).

<http://dx.doi.org/10.1136/jitc-2022-SITC2022.1037>

1038 **LOSS OF PD-1 SIGNALS IMPROVES CD8+ TIL FUNCTION IN A CELL INTRINSIC AND CELL EXTRINSIC MANNER**

¹Samuel Markson*, ¹Kristen Pauken, ¹Vikram Juneja, ²Osmaan Shahid, ¹Kelly Burke, ¹Jared Rowe, ¹Jacklyn Long, ¹Megan Fung, ²Jacob Lubber, ¹Jennifer Judge, ¹Alison Ringel, ¹Marcia Haigis, ²Meromit Singer, ¹Arlene Sharpe. ¹Harvard Medical School, Boston, MA, USA; ²Dana-Farber Cancer Institute, Boston, MA, USA

Background Blockade of PD-1 or its ligand PD-L1 has led to improved clinical outcomes in diverse cancer types, and has been approved by the FDA for use in over 20 different advanced stage cancers. Though PD-1 pathway inhibitors show great promise, the mechanisms contributing to protective anti-tumor immunity following loss of PD-1 signaling remain incompletely understood.

Methods To elucidate the cell intrinsic consequences of PD-1 loss, as well as the impact of this loss on neighboring PD-1-expressing cells, we developed an inducible PD-1 knockout (KO) model whereby PD-1 could be deleted on roughly half of the CD8⁺ T cell population.

Results Using paired single cell RNA seq and TCR seq, we found that PD-1-expressing CD8⁺ T cells in the tumor received much of the same therapeutic benefit as those T cells lacking PD-1. Thus, many of the anti-tumoral changes that occurred in the CD8⁺ TIL population were not dependent on a cell intrinsic loss of PD-1, but instead were shared between cells that do or do not express PD-1.

Conclusions These data suggest that PD-1 inhibitors can act beyond each individual cell that they contact to promote a heightened anti-tumor state, and can impact T cell functions independent of direct PD-1 blockade.

Acknowledgements This work was supported by NIH P50 CA101942 and P01 AI56299.

<http://dx.doi.org/10.1136/jitc-2022-SITC2022.1038>

1040

A POPULATION OF ECTOENZYME EXPRESSING T-CELLS WITH AN IMMUNOSUPPRESSIVE PHENOTYPE ARE ASSOCIATED WITH CHECKPOINT IMMUNOTHERAPY RESISTANCE IN METASTATIC MELANOMA PATIENTS

¹David Woods*, ¹Carol Amato, ¹Ann Strange, ¹Brian Thompson, ²Jeffrey Weber, ²Ankita Mitra. ¹University of Colorado School of Medicine, Aurora, CO, USA; ²New York University Langone, New York, NY, USA

Background Therapies targeting T-cell checkpoints have resulted in anti-tumor responses leading to FDA approval of multiple immunotherapies for metastatic melanoma and an expanding list of other malignancies. Despite having unprecedented efficacy, PD1 and CTLA4 antagonist antibodies still fail to benefit many patients. Critically, an understanding of mechanisms of resistance to immunotherapies is lacking. We recently identified and validated a novel population of peripheral blood T-cells predictive of resistance in nivolumab (α PD1) treated metastatic melanoma patients. This population is defined by the marker set CD3+CD4+CD127-GARP-CD38+CD39+. Based on the co-expression of CD38 and CD39, we have termed the population ectoenzyme expressing T-cells (T_{eee}).

Methods We utilized high-dimension flow cytometry to assess T_{eee} frequencies in adjuvant immunotherapy treated metastatic melanoma patient peripheral blood samples. To characterize the phenotype of T_{eee} , we utilized flow cytometry and CITE-Seq on melanoma patient tumor specimens. We also evaluated the presence and phenotype of T_{eee} in several 1 syngeneic murine tumor models.

Results We found that T_{eee} were of low frequency in demographic matched healthy donors and increased in both resected ($p=0.018$) and active disease metastatic melanoma patients ($p=0.003$). Circulating T_{eee} frequencies positively correlated with frequencies of Tregs ($R^2=0.4367$, $p<0.0001$), MDSCs ($R^2=0.2706$, $p=0.0004$) and M2-like monocytes ($R^2=0.1514$, $p=0.0109$). Increases in circulating T_{eee} were associated with relapse in resected melanoma patients treated with adjuvant combination ipilimumab (α CTLA4) and nivolumab ($p=0.0213$). Human tumors showed high frequencies of T_{eee} in tumor infiltrate. We also demonstrated the existence of this population in MC38 and YUMM mouse tumor models. Intratumor frequencies of T_{eee} positively correlated with tumor volume ($R^2=0.96$, $p=0.0006$) and inversely correlated with overall immune infiltrate ($R^2=0.3198$, $p=0.0280$). Our characterization of this population showed an enhanced adenosine generating phenotype (i.e. CD73^{high}, CD26^{low}), a terminal exhaustion phenotype (i.e. TOX^{high}, TCF1^{low}), expression of inhibitory receptors (e.g. CTLA4, TIM3) and ligands (e.g. PDL1, B7-H4), and expression of immunosuppressive cytokines (e.g. IL-8, TGF β). Supporting a mechanistic relationship to resistance, T_{eee} suppressed autologous T-cell proliferation ($p=0.0278$) and inflammatory function.

Conclusions We have identified a novel population of ectoenzyme expressing T-cells associated with immunotherapy resistance in metastatic melanoma patients. This population of cells had phenotypes associated with immune suppression and suppressed autologous T-cells *in vitro*. Collectively, our data support evaluation of targeting T_{eee} to augment the efficacy of immunotherapy.

Ethics Approval Study was approved by IRB at CU Anschutz and NYU Langone.

<http://dx.doi.org/10.1136/jitc-2022-SITC2022.1040>

1041 **PIK3IP1/TRIP IMMUNE REGULATION ON CD8⁺ T CELLS RESTRICTS ANTI-TUMOR IMMUNITY**

Benjamin Murter*, Hridesh Banerjee, Sean Robinson, Andrea Szymczak-Workman, Lawrence Kane. *University of Pittsburgh, Pittsburgh, PA, USA*

Background The signaling pathways involving phosphoinositide-3-kinases (PI3Ks) are highly conserved and tightly regulated to influence the activation, proliferation, and survival of all cell types. PI3K signaling plays a major role in T cell responses to antigen due to its position directly downstream of T cell receptor (TCR)/CD28 ligation.^{1, 2} Our lab has shown that the cell surface protein TrIP (Transmembrane Inhibitor of PI3K, gene name: *Pik3ip1*) has a distinctly high expression on T cells and is capable of regulating PI3K signaling in T cells, acting as a negative regulator of T cell immune responses.^{3, 4} These studies revealed that CD4⁺ T cells lacking TrIP expression exhibit a more Th1 inflammatory phenotype compared to WT T cells, both *in vivo* and *in vitro*.³ These data have led us to propose that TrIP restricts the inflammatory activity of T cells, including CD8⁺ T cells, and that targeting/knockout of this negative regulator may promote anti-tumor immunity.

Methods Using a novel conditional TrIP knockout mouse model developed in house, we have performed syngeneic tumor challenges in CD8⁺ T cell-specific TrIP knockout mice (TrIP^{fl/fl}E8i^{cre}). We have also characterized the tumor immune infiltrate of these mice to understand the impact of T cell-specific TrIP deficiency on the immune landscape.

Results Our data show that CD8⁺ T cell-specific TrIP knockout mice (TrIP^{fl/fl}E8i^{cre}) are resistant to growth of syngeneic tumors. In addition to increased tumor resistance, we have also found that tumors harvested from our TrIP^{fl/fl}E8i^{cre} knockout mice contain twice as many infiltrating T cells compared to their WT counterparts. We also found that CD8⁺ T cells are the major drivers of this infiltration, and importantly don't display any increase in exhaustion.

Conclusions We describe data demonstrating that TrIP, a relatively novel PI3K inhibitor uniquely expressed on the surface of T cells, plays a significant role in the antitumor immune activity of CD8⁺ T cells. Our CD8⁺ T cell-specific TrIP knockout mice are resistant to tumor challenge and show more robust tumor CD8⁺ T cell infiltrate. We are hoping for future/ongoing adoptive transfer experiments will help elucidate if TrIP knockout promotes infiltration/proliferation/survival within the TME. Nevertheless, we propose TrIP as an exciting novel immunotherapeutic target worthy of further investigation.

REFERENCES

1. Okkenhaug K, Turner M, Gold MR. PI3K Signaling in B Cell and T Cell Biology. *Front Immunol* 2014;**5**:557. doi:10.3389/fimmu.2014.00557
2. Kane LP, Weiss A. The PI-3 kinase/Akt pathway and T cell activation: pleiotropic pathways downstream of PIP3. *Immunol Rev* 2003;**192**:7–20. doi:10.1034/j.1600-065X.2003.00008.x
3. Uche UU, Piccirillo AR, Kataoka S, et al. PIK3IP1/TrIP restricts activation of T cells through inhibition of PI3K/Akt. *J Exp Med*. 2018;**215**:3165–3179. doi:10.1084/jem.20172018
4. DeFrances MC, Debelius DR, Cheng J, Kane LP. Inhibition of T-cell activation by PIK3IP1. *Eur J Immunol* 2012;**42**:2754–2759. doi:10.1002/eji.201141653

<http://dx.doi.org/10.1136/jitc-2022-SITC2022.1041>

THE DUAL FUNCTION OF THE ADENOSINE PATHWAY IN THE LIPOSARCOMA TUMOR MICROENVIRONMENT

¹Jacqueline Oliva*, ¹Younghee Lee, ²Rebeca Rodriguez, ¹Katarzyna Tomczak, ¹Davis Ingram, ¹Xiao Zhou, ¹Vinod Ravi, ¹Anthony Conley, ¹John Livingston, ¹Joseph Ludwig, ¹Neeta Somaiah, ¹Cara Haymaker. ¹University of Texas MD Anderson Cancer Center, Houston, TX, USA; ²Wellesley College, Houston, TX, USA

Background Single agent anti-PD1 therapy has shown limited clinical benefit in liposarcoma, but combination with anti-CTLA-4 demonstrated a higher response rate.¹⁻³ In the MDACC study NCT02815995, combining anti-CTLA4 and anti-PDL1 across multiple soft-tissue sarcomas increased CD73, PD-1, and OX40 expression in T cells early on treatment. The adenosine pathway, which includes CD73 and the A2A receptor, induces immunosuppression^{4,5} and protects from antitumoral responses.^{6, 7} This pathway is related to immune therapy resistance⁸⁻¹¹, metastasis, and poor prognosis.¹²⁻¹⁵ Conversely, CD73+ T cells have long-lived memory and higher proliferation and survival, suggesting a dual role of the pathway.¹⁶⁻¹⁸ We hypothesized that adenosine would negatively correlate with TIL expansion and function.

Methods Surgically resected liposarcoma samples (n=41), are divided for fresh tissue phenotyping by flow cytometry, TIL expansion, and quantification of tissue adenosine, cytokines, and adipokines. The phenotypic analysis included: CD73, A2aR, PD-1, Tim3, CTLA-4, LAG3, OX40, ICOS and 41BB markers. TIL 3.0 expansion protocol¹⁹ was performed, and expanded TIL were assessed for cytotoxicity by IFN-g production and metabolic state (ROS, mitochondrial activity) by flow cytometry.

Results We found high heterogeneity in the frequency of CD45+ cells (0-88.3%), CD4+ and CD8+ TIL infiltrate, and expression of PD-1 (0.66-59.60% and 0.99-76.6% respectively), CD73 (CD4+ 0- 40.97%, CD8+ 0-34.04%), and A2AR (mean CD4+ 0-0.6%, CD8+ 0-17.96%), with no co-expression of CD73 and A2AR. Interestingly adenosine concentration was highly variable (0-84.05 nmol/g tissue) but did not correlate with TIL phenotype or tissue cytokines. Tumors were rich in growth factors and chemokines but lacked a pro-inflammatory profile. The success of TIL expansion was 50% (n=24 cases) in samples with a count of 300 CD3+ events in the fresh tissue by flow analysis. The frequency of CD8 +CD73+ TIL was significantly higher in cases with successful TIL expansion (p=0.041). The expanded TIL phenotype showed CD73 expression (range: CD4+ 0.67-29 % and CD8 + 0.85-13.9%) and upregulation of A2AR (range: 0.2-15.40% and 1.44-87.6%). IFN-g production was related to intrinsic metabolic profiles by mitochondrial mass and ROS production (n=8).

Conclusions A heterogeneous adenosine landscape was found in liposarcoma. A2AR but not CD73 correlated with mitochondrial dysfunction and reduced cytotoxicity. Conversely CD73+ TIL were more likely to expand. Our results indicate a dichotomy in two key members in the adenosine pathway in liposarcoma and suggest that CD73 might play a positive role in TIL function.

Acknowledgements Patients and their families.

CCSG Metabolomics Core (Grant P30CA016672)

Philanthropy support provided by a generous donation by the William Oates family

REFERENCES

1. Klaver Y, et al. Differential quantities of immune checkpoint-expressing CD8 T cells in soft tissue sarcoma subtypes. *J Immunother Cancer* 2020;**8**(2).

- Livingston JA, et al. Role of chemotherapy in dedifferentiated liposarcoma of the retroperitoneum: defining the benefit and challenges of the standard. *Sci Rep*, 2017;**7**(1):11836.
- D'Angelo SP, et al. Nivolumab with or without ipilimumab treatment for metastatic sarcoma (Alliance A091401): two open-label, non-comparative, randomised, phase 2 trials. *Lancet Oncol* 2018;**19**(3):416-426.
- Jin D, et al. CD73 on tumor cells impairs antitumor T-cell responses: a novel mechanism of tumor-induced immune suppression. *Cancer Res* 2010;**70**(6):2245-55.
- Allard B, et al. The adenosine pathway in immuno-oncology. *Nat Rev Clin Oncol* 2020;**17**(10):611-629.
- Mastelic-Gavillet, B., et al., Adenosine mediates functional and metabolic suppression of peripheral and tumor-infiltrating CD8(+) T cells. *J Immunother Cancer* 2019;**7**(1):257.
- Ohta A, et al. A2A adenosine receptor protects tumors from antitumor T cells. *Proc Natl Acad Sci U S A* 2006;**103**(35):13132-7.
- Zhou L, et al. The distinct role of CD73 in the progression of pancreatic cancer. *J Mol Med (Berl)* 2019;**97**(6):803-815.
- Wu R, et al. Effects of CD73 on human colorectal cancer cell growth in vivo and in vitro. *Oncol Rep* 2016;**35**(3):1750-6.
- Chen S et al. CD73 expression on effector T cells sustained by TGF-beta facilitates tumor resistance to anti-4-1BB/CD137 therapy. *Nat Commun* 2019;**10**(1):150.
- Cekic C et al. Myeloid expression of adenosine A2A receptor suppresses T and NK cell responses in the solid tumor microenvironment. *Cancer Res* 2014;**74**(24):7250-9.
- Turcotte M et al. CD73 is associated with poor prognosis in high-grade serous ovarian cancer. *Cancer Res* 2015;**75**(21):4494-503.
- Panigrahi S, et al., CD8(+) CD73(+) T cells in the tumor microenvironment of head and neck cancer patients are linked to diminished T cell infiltration and activation in tumor tissue. *Eur J Immunol* 2020;**50**(12):2055-2066.
- Gao Z.W, et al. CD73 promotes proliferation and migration of human cervical cancer cells independent of its enzyme activity. *BMC Cancer* 2017;**17**(1):135.
- Koszalka P, et al. Targeted disruption of cd73/ecto-5'-nucleotidase alters thromboregulation and augments vascular inflammatory response. *Circ Res* 2004;**95**(8):814-21.
- Capone M, et al. Frequency of circulating CD8+CD73+T cells is associated with survival in nivolumab-treated melanoma patients. *J Transl Med* 2020;**18**(1):121.
- Roseblatt MV, et al. Ecto-5'-Nucleotidase (CD73) Regulates the Survival of CD8 + T Cells. *Front Cell Dev Biol* 2021;**9**:647058.
- Fang F, et al. The cell-surface 5'-nucleotidase CD73 defines a functional T memory cell subset that declines with age. *Cell Rep* 2021;**37**(6):109981.
- Tavera RJ, et al. Utilizing T-cell Activation Signals 1, 2, and 3 for Tumor-infiltrating Lymphocytes (TIL) Expansion: The Advantage Over the Sole Use of Interleukin-2 in Cutaneous and Uveal Melanoma. *J Immunother* 2018;**41**(9):399-405.

Ethics Approval This study was written and conducted in accordance with the principles from the Declaration of Helsinki. Written informed consent was provided by all study participants or their legal representatives. The study was approved by the University of Texas MD Anderson Cancer Center's Institutional Review Board.

<http://dx.doi.org/10.1136/jitc-2022-SITC2022.1042>

1043

HIGH VISTA EXPRESSION ON TUMOR-INFILTRATING LYMPHOCYTES IS PROGNOSTIC OF POOR SURVIVAL IN PATIENTS WITH ENDOMETRIAL CANCER

¹Sachin Patnaik*, ¹Cassandra Gilmour, ²Stefanie Avril, ¹Andreie Branicky, ¹Ajay Zalavadia, ¹Judith Drazba, ¹Li Wang. ¹Cleveland Clinic Foundation, Cleveland, OH, USA; ²University Hospitals Cleveland, Cleveland, OH, USA

Background Immune checkpoint inhibitor therapy has become an effective treatment option for many types of cancers. By enhancing the function of anti-tumor T cells, inhibitors targeting PD1, PDL1, and CTLA4 have shown durable clinical results and increased patient survival. However, the response rate to these checkpoint blockades is generally limited to 30-40% of patients, with the majority failing to respond. This suggests the need to investigate other targets for immunotherapy. One promising candidate is V-domain Immunoglobulin Suppressor of T cell Activation (VISTA), an immune checkpoint protein expressed on several lymphocyte and myeloid lineages, including regulatory T cells, cytotoxic T cells, monocytes, and myeloid-derived suppressor cells. VISTA has been found to potently impair anti-tumor immunity by negatively regulating the activation and function of tumor-reactive T cells. Targeting VISTA has therefore been the focus of several preclinical and clinical studies, with current anti-VISTA antibodies in development as well as in clinical trial. Our study explores the association of VISTA expression on tumor-infiltrating lymphocytes (TILs) with patient outcomes in endometrial cancer.

Methods Pretreatment tissue samples were collected from 121 women diagnosed with endometrial cancer at University Hospitals Cleveland, Cleveland, Ohio, between 2006 and 2012. Tumor microarray (TMA) sections of 4 micron thickness were fixed for multiplex immunohistochemistry using clinically established protocols and stained with a panel of PanCK, CD3, FOXP3, VISTA, TIGIT, and DAPI. TMA measurements were quantified to determine patient subpopulations based on protein expression. Using these data, Kaplan-Meier curves were constructed to analyze overall survival and recurrence-free survival for different groups based on checkpoint protein expression levels in immune cell subsets. Follow-up time for survival outcomes was from 2006 to 2018.

Results We found that the high expression of VISTA on TILs correlates to worse overall survival as well as worse recurrence-free survival. In contrast, TIGIT expression on TILs is not a prognostic factor.

Conclusions Our data elucidate VISTA's importance as a prognostic immune marker for poorer outcomes in patients with endometrial cancer. These results also demonstrate the value of exploring VISTA as a potential immunotherapy target for improving survival.

Ethics Approval Our studies have been approved by the Ethics Committee of the Cleveland Clinic Foundation.

<http://dx.doi.org/10.1136/jitc-2022-SITC2022.1043>

1044

PROTEASOME MEDIATED PROTEIN CATABOLISM FUELS ANTITUMOR IMMUNITY

¹Brian Riesenber*, ¹Elizabeth Hunt, ²Megan Tennant, ¹Katie Hurst, ²Alex Andrews, ²Lee Leddy, ²David Neskey, ²Elizabeth Hill, ³Guillermo Rangel Rivera, ³Chrystal Paulos, ⁴Peng Gao, ¹Jessica Thaxton. ¹University of North Carolina, Chapel Hill, NC, USA; ²Medical University of South Carolina, Charleston, SC, USA; ³Emory University, Atlanta, GA, USA; ⁴Northwestern University, Chicago, IL, USA

Background The solid tumor microenvironment (TME) exposes CD8 T cells to metabolic stressors including nutrient and oxygen deprivation coupled with persistent antigen stimulation which work in concert to inhibit cell function.¹⁻⁵ Importantly, successful immunotherapy is predicated on CD8 T cells overcoming these hurdles to maintain proliferation and protein secretion. While recent advances in single cell RNA and ATAC sequencing have allowed for identification of genetic and epigenetic traits associated with enhanced antitumor T cell function⁶⁻⁷, little is known about the mechanisms responsible for controlling the translation of these instructions into effector functions. In this study, we sought to identify the mechanisms responsible for allowing sustained protein translation in the TME.

Methods Protein synthesis was monitored using a flow cytometry-based approach whereby the fluorescent analogue of methionine, L-homopropargylglycine (L-HPG), is incorporated into new forming polypeptide chains and quantified by flow cytometry through Click-IT chemistry.⁸⁻¹¹ Optimal antitumor T cells were generated via cytokine conditioning with IL-15 and then subjected to a series of *in vitro* tumor-T cell coculture systems and *in vivo* tumor growth experiments. Proteasome activity was monitored using a fluorescent activity probe via flow cytometry and pharmacologic intervention using the proteasome inhibitor MG-132 paired with metabolomics. Proteasome stimulator Cyclosporine A was used to validate our findings.

Results Using both human and mouse tumors we found that protein translation is repressed in T cells by the solid TME through activation of the unfolded protein response element p-eIF2a due to competition for glucose. Reprogramming T cells away from glucose dependency alleviated p-eIF2a mediated translation attenuation allowing for sustained translation under TME stress. Using metabolic and pharmacological approaches, we discovered that optimal antitumor T cells mitigate p-eIF2a through enhanced proteasome activity, protecting from translation attenuation enabling sustained cytokine synthesis in solid tumors that resulted in enriched tumor control. Additionally, we found the ability to access protein degradation via the proteasome complex was associated with metabolic programs previously linked to optimal antitumor immunity such as glutathione metabolism and gluconeogenesis.¹²

Conclusions These findings suggest that stress mediated attenuation of translation represents a cellular checkpoint which must be overcome for optimal tumor immunity. Our findings demonstrate protein degradation is a critical component of T cell tumor control and strategies that relieve the misfolded protein burden could be avenues to supplement current immunotherapy approaches.

REFERENCES

1. Wherry EJ. T cell exhaustion. *Nat Immunol* 2011;**12**(6):492–9.
2. Bian Y, Li W, Kremer DM, et al. Cancer SLC43A2 alters T cell methionine metabolism and histone methylation. *Nature* 2020;**585**(7824):277–82.
3. Chang CH, Qiu J, O'Sullivan D, et al. Metabolic Competition in the Tumor Microenvironment Is a Driver of Cancer Progression. *Cell* 2015;**162**(6):1229–41.

4. Thevenot PT, Sierra RA, Raber PL, et al. The stress-response sensor chop regulates the function and accumulation of myeloid-derived suppressor cells in tumors. *Immunity* 2014;**41**(3):389–401.
5. Brand A, Singer K, Koehl GE, et al. LDHA-Associated Lactic Acid Production Blunts Tumor Immunosurveillance by T and NK Cells. *Cell Metab* 2016;**24**(5):657–71.
6. Miller BC, Sen DR, Al Abosy R, et al. Subsets of exhausted CD8(+) T cells differentially mediate tumor control and respond to checkpoint blockade. *Nat Immunol* 2019;**20**(3):326–36.
7. Shin HM, Kim G, Kim S, et al. Chromatin accessibility of circulating CD8+ T cells predicts treatment response to PD-1 blockade in patients with gastric cancer. *Nature Communications* 2021;**12**(1):975.
8. Araki K, Morita M, Bederman AG, et al. Translation is actively regulated during the differentiation of CD8(+) effector T cells. *Nat Immunol* 2017;**18**(9):1046–57.
9. Graczyk D, White RJ, Ryan KM. Involvement of RNA Polymerase III in Immune Responses. *Mol Cell Biol* 2015;**35**(10):1848–59.
10. Lai CP, Kim EY, Badr CE, et al. Visualization and tracking of tumour extracellular vesicle delivery and RNA translation using multiplexed reporters. *Nat Commun* 2015;**6**:7029.
11. Best MD. Click chemistry and bioorthogonal reactions: unprecedented selectivity in the labeling of biological molecules. *Biochemistry* 2009;**48**(28):6571–84.
12. Ma R, Ji T, Zhang H, et al. A Pck1-directed glycogen metabolic program regulates formation and maintenance of memory CD8(+) T cells. *Nat Cell Biol* 2018;**20**(1):21–27.

Ethics Approval Patients undergoing surgical removal of tumors granted consent via MUSC Biorepository surgical consent forms. This work was determined by MUSC Institutional Review Board to be exempt under protocol Pro00050181. Tissue samples were de-identified. Studies were conducted in accordance with the Declaration of Helsinki, International Ethical Guidelines for Biomedical Research Involving Human Subjects (CIOMS), Belmont Report, or U.S. Common Rule. All animal experiments were approved by both the Medical University of South Carolina (MUSC) Institutional Animal Care and Use Committee and the University of North Carolina at Chapel Hill (UNC) Division of Comparative Medicine. Mice were maintained by the Division of Laboratory Animal Resources at MUSC and Division of Comparative Medicine at UNC.

<http://dx.doi.org/10.1136/jitc-2022-SITC2022.1044>

1045

HIGH DIMENSIONAL PROFILING OF MERKEL CELL POLYOMAVIRUS-SPECIFIC T CELLS IN RESPONSE TO ANTI-PD-1 IMMUNOTHERAPY

¹Heeju Ryu*, ¹Timothy Bi, ¹Korok Sarkar, ²Candice Church, ¹Nirasha Ramchurren, ²Thomas Pulliam, ¹Steven Fling, ²Paul Nghiem, ¹Evan Newell. ¹Fred Hutchinson Cancer Center, Seattle, WA, USA; ²University of Washington, Seattle, WA, USA

Background Merkel cell carcinoma (MCC) is an aggressive skin cancer often associated with clonal integration of Merkel cell polyomavirus (MCPyV) and expression of T antigen oncoproteins in 80% of cases with the remainder of cases caused by UV mutations.^{1,2} PD-1 blockade is effective in treating both etiologies of MCC patients, however, only ~60% of patients respond.³ MCPyV-specific T cells are implicated in immunotherapeutic responses⁴, yet further qualitative and quantitative analysis of those cells among responders and non-responders is needed.

Methods We analyzed MCPyV-specific T cells in blood from responders (CR, n=13) and non-responders (n=6 for partial responses, PR; n=5 for stable and progressive disease, SD/PD) before, during and after anti-PD-1 immunotherapy (from trial NCT02267603) using a mass cytometry (CyTOF)-based multiplexed peptide-MHC tetramer staining approach. This allowed us to simultaneously assess 76 MCPyV epitopes and 34 control epitopes derived from viruses such as CMV, EBV, Flu, and HSV, in parallel with 34 cellular phenotyping markers of differentiation, trafficking, and exhaustion. We also performed deep TCR sequencing of sorted T cell populations from the blood samples to track T cell clonotypes between the periphery and tumor.

Results Combinatorial tetramer staining with CyTOF allowed us to detect T cells specific for 11 previously reported and 5 novel MCPyV-specific epitopes. Frequencies of MCPyV-specific cells were higher in patients with CR (mean = 0.103% of CD8⁺ T cells) than those with PR (mean = 0.021%; P=0.007) and SD/PD (mean = 0.003%; P<0.0001) at the baseline, and decreased over the course of immunotherapy in patients with CR. Strikingly, the phenotypes of MCPyV-specific CD8⁺ T cells were enriched for an activated/exhausted (CD71⁺PD-1⁺CD39⁺) phenotype. Those cells also highly expressed cutaneous lymphocyte-associated antigen (CLA), a marker of skin trafficking, and CD103, a marker of tissue-recirculating cells. Informed by these phenotypes, high-dimensional profiling of bulk CD8⁺ T cells revealed correlations of the frequencies of CD39⁺ cells co-expressing CLA or CD103 with both the baseline tumor burden and magnitude of clinical outcome. TCR sequencing was used to assess clonal sharing between tumor infiltrating T cells and these subpopulations of CD8⁺ T cells from blood.

Conclusions Although these findings need to be confirmed in an independent cohort, our high-dimensional analysis and immune profiling of MCC patients suggest that MCPyV-specific cells and CD39⁺ cells co-expressing CLA or CD103 in blood are enriched for tumor-reactive TCRs and potentially useful as blood-based biomarkers of response to immunotherapy or for novel cellular therapeutic strategies.

Trial Registration ClinicalTrials.gov NCT02267603

REFERENCES

1. Feng H, Shuda M, Chang Y, Moore PS. Clonal integration of a polyomavirus in human Merkel cell carcinoma. *Science* 2008;**319**(5866):1096–100.
2. Goh G, Walradt T, Markarov V, Blom A, Riaz N, Doumani R, Stafstrom K, Moshiri A, Yelistratova L, Levinsohn J, Chan T. A., Nghiem P., Lifton R. P., Choi J. Mutational landscape of MCPyV-positive and MCPyV-negative Merkel cell carcinomas with implications for immunotherapy. *Oncotarget* 2016;**7**:3403–3415.

3. Nghiem PT, Bhatia S, Lipson EJ, Kudchadkar RR, Miller NJ, Annamalai L, Berry S, Chartash EK, Daud A, Fling SP, Friedlander PA, Kluger HM, Kohrt HE, Lundgren L, Margolin K, Mitchell A, Olencki T, Pardoll DM, Reddy SA, Shantha EM, Sharfman WH, Sharon E, Shemanski LR, Shinohara MM, Sunshine JC, Taube JM, Thompson JA, Townson SM, Yearley JH, Topalian SL, Cheever MA. PD-1 Blockade with Pembrolizumab in Advanced Merkel-Cell Carcinoma. *N Engl J Med* 2016;**374**(26):2542–52.
4. Miller NJ, Church CD, Dong L, Crispin D, Fitzgibbon MP, Lachance K, Jing L, Shinohara M, Gawwoidis I, Willimsky G, McIntosh M, Blankenstein T, Koelle DM, Nghiem P. Tumor-Infiltrating Merkel Cell Polyomavirus-Specific T Cells Are Diverse and Associated with Improved Patient Survival. *Cancer Immunol Res* 2017;**5**(2):137–147.

Ethics Approval The samples were provided by Cancer Immunotherapy Trails Network (trial registration: ClinicalTrials.gov NCT02267603) and the analysis was performed according to the IRB file/approval number IR File #10686.

<http://dx.doi.org/10.1136/jitc-2022-SITC2022.1045>

1046

TARGETING NOVEL PATHWAYS IN CHRONICALLY ACTIVATED T CELLS PREVENTS FUNCTIONAL EXHAUSTION

Justyna Rzepecka*, Andrew Hall, Mark Barbour, Emma Mallon, Marija Bedaj, Lucia Janicova, Xabier Cortes-Lavaud, Frances Acklam, Joanne Hay, Hayley Gooding, Darryl Turner, Preeti Singh, Aaron Crawford. *Concept Life Sciences, Edinburgh, UK*

Background In cancer, persistent antigenic challenge leads to T cells acquiring a hyporesponsive cell state, also referred to as T cell exhaustion. We have previously demonstrated that human CD3⁺ T cells repeatedly stimulated *in vitro*, via their TCR, develop phenotypical characteristics of exhausted T cell found *in vivo*, including increased expression of inhibitory receptors PD-1, TIM-3 and LAG-3 and diminished responsiveness to dendritic cell activation and cancer cell cytotoxicity. We showed that PD-1 blockade with nivolumab and treatment with an IKZF3 inhibitor, lenalidomide, reinvigorated the exhausted T cells. We next wished to evaluate if blocking of IKZF3 during the development of T cell exhaustion could protect them from acquiring the exhausted phenotype.

Methods Human CD3⁺ T cells, isolated from healthy PBMC donors, were repeatedly stimulated with anti-CD3/anti-CD28 coated beads to mimic chronic antigenic challenge. The stimulations were conducted in the presence or absence of lenalidomide. T cells, both CD4⁺ and CD8⁺, were assessed for changes in expression of inhibitory receptors and cytokine release was quantified. Following the final round of TCR stimulation, T cells were co-cultured with allogeneic dendritic cells to determine if their functionality has been altered by lenalidomide treatment. T cell proliferation and IFN-g release were assessed as well as changes in inhibitory receptor expression at the end of the co-culture.

Results We demonstrated that lenalidomide had no impact on T cell viability or CD4⁺/CD8⁺ ratio in repeatedly stimulated cultures. Lenalidomide did however affect inhibitory receptor expression and impacted cytokine secretion from chronically stimulated T cells. Lenalidomide led to increased PD-1 expression on CD8⁺ T cells and LAG-3 expression on CD4⁺ T cells whereas TIM-3 expression was downregulated on both T cell subsets in the presence of compound. Lenalidomide enhanced production of cytokines in repeatedly stimulated T cells. To assess if lenalidomide-driven changes had any impact on T cell functionality, we cultured lenalidomide-treated and untreated repeatedly activated T cells with allogeneic dendritic cells. Whilst repeatedly stimulated T cells not exposed to lenalidomide showed diminished ability to proliferate and secrete IFN-g, consistent with their exhausted cell state, lenalidomide treated T cells displayed increased IFN-g secretion suggesting that lenalidomide protected repeatedly stimulated T cells from acquiring an exhausted phenotype.

Conclusions The *in vitro* assays described herein offer the opportunity to investigate the effect of candidate therapeutics, including combination therapies, on exhausted T cell development and function.

<http://dx.doi.org/10.1136/jitc-2022-SITC2022.1046>

1047 FROM EXHAUSTION TO MEMORY: ALTERING T CELL FATE IMPROVES IMMUNOTHERAPEUTIC RESPONSES TO CANCER

Nicole Scharping*, Allison Cafferata, Maximilian Heeg, Quynhanh Nguyen, Ananda Goldrath. *University of California San Diego, San Diego, CA, USA*

Background In cancer, CD8⁺ T cells have the power to target and kill tumor cells with precision but often fail due to chronic activation from the immunosuppressive tumor micro-environment (TME), differentiating into a dysfunctional cell state known as exhaustion. In healthy tissues, T cells differentiate into tissue-resident memory cells (T_{RM}) in response to infection, which remain lodged in tissues to provide protection from reinfection. When T_{RM} cells are found in patient tumors, they correlate with improved responses to immunotherapy and patient outcomes. Understanding how to manipulate T cell fates to avoid exhaustion and favor T_{RM} characteristics could benefit cancer immunotherapy.

Methods To explore differences between these cell states, we screened the core T_{RM} gene expression signatures for genes downregulated as T cells differentiate to terminal exhaustion. Targets were then overexpressed in antigen-specific T cells and adoptively transferred into tumor-bearing mice for analysis.

Results We found many genes related to protein regulation were identified, including multiple E3 ubiquitin ligases with not well-described targets. When these genes are individually overexpressed in tumor-specific T cells, we found the transduced T cells express less inhibitory receptors and showed enhanced anti-tumor function: increased accumulation in the TME, upregulation of T_{RM} markers, and polyfunctional cytokine production, which resulted in controlled tumor growth and increased mouse survival in multiple cancer models.

Conclusions These results highlight the understudied field of negative regulation of T cell function by protein degradation in T cell differentiation fate and function, and uncovers potential gene targets for immunocellular therapies to favor functional T cell fates in cancer.

<http://dx.doi.org/10.1136/jitc-2022-SITC2022.1047>

1048

INTERPLAY OF IL-12 AND IFNG TO INDUCE T_{REG} FRAGILITY WITHIN THE TUMOR MICROENVIRONMENT

<http://dx.doi.org/10.1136/jitc-2022-SITC2022.1048>

Ellen Scott*, Angela Gocher, Creg Workman, Dario Vignali. *University of Pittsburgh, Pittsburgh, PA, USA*

Background Immune cells play an integral role in the prevention as well as the progression of cancers. Within the T cell compartment, regulatory T cells (T_{regs}) suppress the anti-tumor T cell response through use of direct and indirect mechanisms.^{1,2} However, under some circumstances T_{regs} can lose their suppressive activity while retaining expression of their master transcription factor, Foxp3, a phenomenon our lab has termed T_{reg} fragility.³ A hallmark of T_{reg} fragility is production of IFN γ , a pleiotropic cytokine necessary for response to cancer immunotherapies such as anti-PD1.⁴ However, it is unknown the exact mechanism that leads to T_{reg} fragility as well as the consequences of T_{reg}-produced IFN γ . By using a novel transgenic mouse with a conditional deletion of IL-12Rb2 (*Il12rb2.Thy1.1^{L/LhNGFR} Foxp3^{Cre.YFP}*) in T_{regs} we were able to test the effect of IL-12 signaling on T_{reg} function and response to different immunotherapies during tumor progression.

Methods We inoculated wildtype mice with MC-38 adenocarcinoma or B16 melanoma and determined the amount of IL-12 and IFN γ induced by different immunotherapies. We also inoculated mice with a T_{reg}-specific IL12R deletion with MC-38 or B16 and characterized the effect of IL-12R loss on T_{reg} function after immunotherapy treatment by measuring tumor growth and flow cytometric analyses of intratumoral T_{regs}.

Results We have found that anti-PD1 therapy is able to cause modest increases in IFN γ and IL-12 levels within the tumor. In contrast, when using an IL-12 inducing therapy (anti-CD40 agonism) there was a larger amount of IL-12 intratumorally along with very large increases of IFN γ levels in both tumors and serum of wildtype mice. However, when mice with IL-12R deficient T_{regs} were treated with either of these therapies, tumor growth was not affected. Additionally, flow cytometric analyses of these mice after anti-CD40 agonist treatment suggests that these T_{regs} are still sensitive to fragility induction.

Conclusions These data suggest that IL-12 is not necessary for the induction of T_{reg} fragility. More specifically, these data may indicate that the increase in IFN γ that is induced by immunotherapy may circumvent the IL-12 signaling loss in our mouse model and induce T_{reg} fragility. While the mechanism of how IL-12 is effecting these changes still unknown, this evidence suggests that IL-12 can indirectly induce fragility in T_{regs} and therefore augment the TME and the response to immunotherapy.

REFERENCES

1. Scott EN, Gocher AM, Workman CJ, Vignali DAA. Regulatory T cells: barriers of immune infiltration into the tumor microenvironment. *Front Immunol* 2021;**12**:702726.
2. Vignali DAA, Collison LW, Workman CJ. How regulatory T cells work. *Nat Rev Immunol*. 2008;**8**(7):523–32.
3. Overacre-Delgoffe AE, Chikina M, Dadey RE, Yano H, Brunazzi EA, Shayan G, et al. Interferon- γ Drives Treg Fragility to Promote Anti-tumor Immunity. *Cell* 2017;**169**(6):1130–1141.e11.
4. Gocher AM, Workman CJ, Vignali DAA. Interferon- γ : teammate or opponent in the tumour microenvironment? *Nat Rev Immunol* 2022 Mar;**22**(3):158–72.

Ethics Approval All mice were co-housed in the University of Pittsburgh Animal Facility under SPF conditions. All experiments strictly adhered to the University of Pittsburgh Animal Care and Use Committee requirements.

1049

RECONSTRUCTION OF GENE REGULATORY NETWORKS DISSECTS TRANSCRIPTIONAL CONTROL OF INTRATUMORAL REGULATORY T CELLS

¹Feng Shan*, ¹Anthony Cillo, ¹Carly Cardello, ¹Daniel Yuan, ¹Sheryl Kunning, ¹Jian Cui, ¹Robert Ferris, ¹Tullia Bruno, ¹Creg Workman, ²Panayiotis Benos, ¹Dario Vignali. ¹University of Pittsburgh, Pittsburgh, PA, USA; ²University of Florida, Gainesville, FL, USA

Background Regulatory T cells (T_{reg}) -targeted therapy exhibit clinical benefit and has been reported as a promising strategy. However, many gaps remain in our understanding of T_{reg} biology within the context of tumor microenvironment (TME). The autoimmune toxicity and restricted efficacy are major limitations of T_{reg} therapies in the clinic, when T_{reg} depletion occurred not only in the tumor but in other organ systems, or concurrent downregulation of antitumor effector T cells.^{1, 2}

Methods We profiled 51,195 single-cell transcriptomes of CD4⁺ T cells in tumors and peripheral blood from patients with head and neck squamous cell carcinomas (HNSCC)³, in inflamed tonsil tissues and in healthy peripheral blood. Canonical genes, gene sets and RNA Velocity⁴ were used to define cell states of T_{reg}. Cibersortx⁵ and bulk RNA sequencing data in The Cancer Genome Atlas were used to infer the association between the enrichment of T_{reg} subpopulations and progression-free survival of patients with solid tumors. SCENIC⁶ and Causal mixed graphical modeling⁷ were used to reconstruct the gene regulatory network (GRN). Knockout of *BATF* with CRISPR-Cas9⁸ in conjunction with bulk RNA sequencing, immunophenotyping and in vitro functional assays were used to interrogate the roles of *BATF* in human activated T_{reg}.

Results We identified an activated subpopulation of T_{reg} expressing multiple tumor necrosis factor receptor (TNFR) genes, including *OX40* and *4-1BB*, which is highly enriched in solid TME compared with non-tumor tissues. These TNFR-activated T_{reg} were associated with worse prognosis across solid tumors. Notably, we found *BATF* is a central component of a GRN that controls the transcriptional signature of TNFR-activated T_{reg}. Consistent with single-cell analyses, *BATF* was co-expressed with *4-1BB*, *OX40*, *CD96* and *CD39* that highly enriched in HNSCC intratumoral T_{reg} at protein level. CRISPR-editing results revealed an enhancement of immunosuppression in *BATF* KO T_{reg} and activation in *BATF* KO T_{reg} accompanied with increased expression of genes including *4-1BB*, *OX40*, *ICOS*, *LAG3* and *neuropilin-1*, indicating that *BATF* functions as a transcriptional nexus in human activated T_{reg} that essential for T_{reg} activation, function and stability.

Conclusions We identify a unique intertumoral subpopulation of T_{reg} characterized by *BATF*-driven expression of tumor necrosis factor receptor family expression and associated with survival across solid tumors, suggesting a possibility to target suppressive intratumoral T_{reg} without causing overt autoimmunity in normal tissues. A deeper understanding of transcriptional network in T_{reg} biology will provide novel mechanisms for immunotherapies in cancer, but also for T_{reg} engineering in autoimmunity.

Acknowledgements We thank the Vignali, Bruno and Benos Labs for all their constructive comments and feedback.

REFERENCES

1. Zappasodi R, Sirard C, Li Y, Budhu S, Abu-Akeel M, Liu C, et al. Rational design of anti-GITR-based combination immunotherapy. *Nature Medicine* 2019;**25**(5):759–66.
2. Jacobs JF, Punt CJ, Lesterhuis WJ, Suttmuller RP, Brouwer HM, Scharenborg NM, et al. Dendritic cell vaccination in combination with anti-CD25 monoclonal

antibody treatment: a phase I/II study in metastatic melanoma patients. *Clin Cancer Res* 2010;**16**(20):5067–78.

3. Cillo AR, Kürten CHL, Tabib T, Qi Z, Onkar S, Wang T, et al. Immune Landscape of Viral- and Carcinogen-Driven Head and Neck Cancer. *Immunity* 2020;**52**(1):183–99.
4. Bergen V, Lange M, Peidli S, Wolf FA, Theis FJ. Generalizing RNA velocity to transient cell states through dynamical modeling. *Nature Biotechnology* 2020;**38**(12):1408–14.
5. Newman AM, Steen CB, Liu CL, Gentles AJ, Chaudhuri AA, Scherer F, et al. Determining cell type abundance and expression from bulk tissues with digital cytometry. *Nature Biotechnology* 2019;**37**(7):773–82.
6. Van de Sande B, Flerin C, Davie K, De Waegeneer M, Hulselmans G, Aibar S, et al. A scalable SCENIC workflow for single-cell gene regulatory network analysis. *Nature Protocols* 2020;**15**(7):2247–76.
7. Sedgewick AJ, Buschur K, Shi I, Ramsey JD, Raghu VK, Manatakis DV, et al. Mixed graphical models for integrative causal analysis with application to chronic lung disease diagnosis and prognosis. *Bioinformatics* 2019;**35**(7):1204–12.
8. Schumann K, Raju SS, Lauber M, Kolb S, Shifrut E, Cortez JT, et al. Functional CRISPR dissection of gene networks controlling human regulatory T cell identity. *Nature Immunology* 2020;**21**(11):1456–66.

Ethics Approval All patients provided informed written consent, and this study was approved by our Institutional Review Board (University of Pittsburgh Cancer Institute, Tissue Collection Protocol 99-069).

<http://dx.doi.org/10.1136/jitc-2022-SITC2022.1049>

1050

SINGLE CELL TRANSCRIPTOME AND EPIGENOME PROFILING REVEALS THE DIVERSITY OF T CELL STATES IN *EX VIVO* GROWN TUMOR-INFILTRATING LYMPHOCYTES FROM MALIGNANT PLEURAL MESOTHELIOMA

Katarzyna Tomczak*, Carlos Ramos, Nathaniel Deboever, Nicolas Zhou, Jacqueline Liszeth Oliva, Chang-Jiun Wu, Chad Strange, Annikka Weissferdt, David Rice, Reza Mehran, Jianjun Zhang, Mehmet Altan, Anne Tsao, Boris Sepesi, Cara Haymaker. *University of Texas MD Anderson Cancer Center, Houston, TX, United States*

Background Malignant pleural mesothelioma (MPM) is a rare and aggressive cancer associated with exposure to asbestos that lacks effective treatment options.¹ Immunotherapy approaches remain challenging with a current paucity of knowledge on the tumor-infiltrating lymphocyte (TIL) landscape.² We aimed to generate a reference transcriptomic and epigenomic atlas of MPM T cell subpopulations that could inform on cellular features and states of propagated *ex vivo* cells to allow new immunotherapy design.

Methods TIL were expanded utilizing the MDACC ‘TIL 3.0’ method from surgically managed MPM patients (n=8, 6/8 cases received chemotherapy with treatment ending an average of 82 days prior to surgery).³ Cells were processed for 10x Genomics 5’ single cell (sc) RNA- and scATAC-seq profiling. Analysis was performed using 10x Genomics cell ranger pipelines. Downstream analysis was performed in R utilizing Seurat and Signac packages, following Monocle3 trajectory analysis.⁴⁻⁶ The significant expression of key defining genes was used to label cell states. Wilcoxon Sum Ranking test was applied for determination of statistical significance of genes (adjusted p-value significance: 0≤*** <0.001≤** <0.01).

Results Profiling revealed 18 clusters: one CD4+ T cell cluster (CD4-CD40LG), twelve clusters representing different CD8+ states (CD8-CD27, CD8-MIF, CD8-ZNF683, two MAIT, IL9R-Tcells, five CD8-MKI67 and CD8-TOX), four gamma-delta T cell clusters (γδ-TRDC), and one unique cluster (MALAT1). scATAC-seq analysis of the MPM TIL paired with their transcriptomic clusters validated the presence of existing cell states with trajectory analysis confirming the separation of the distinct cell states. Activation and inhibitory markers showed heterogenous pattern. Upregulation of activation markers OX40 (*TNFRSF4****) and ICOS*** was present in CD4-CD40LG and OX40 (*TNFRSF4****) marker in IL9R-Tcells. Moreover, CD4-CD40LG showed high upregulation of CTLA4*** and GITR (*TNFRSF18****), whereas, among CD8+ subsets, GITR *** expression was observed only in γδ-TRDC and IL9R-Tcells. γδ-TRDC also displayed heterogenous upregulation of other inhibitory markers as TIGIT, LAG3 and TOX. Progenitor exhausted state transcription factor TCF7*** was only observed in CD8-CD27 and across CD8-MK67 populations. Transcription factors *PRDM1****, *MAF**** promoting T cell exhaustion were present within MALAT1 cluster.

Conclusions As expected, CD8+ TIL states predominated the grown TIL products. The expression of signature genes suggested presence of several activated and proliferating CD8+ states, tissue resident memory CD8+, an effector CD4+ state and a γδ+ T-cell state. The presence of inhibitory receptors is heterogenous and informs the dysfunctional states of cells, which may be of use for design of novel immunotherapy strategies.

Acknowledgements Study was supported in part by the Ronald E. and Reba M. Kennedy Endowment for lung cancer research, the Aileen M. Dillon and Lee M. Bourg mesothelioma fund and the Fleming Endowed Fund. We would like

to thank patients and their families for participation in this study.

REFERENCES

1. Bibby AC, Tsim S, Kanellakis N, Ball H, Talbot DC, Blyth KG, Maskell NA, Psalidas I. *Eur Respir Rev* 2016;**25**:472–86.
2. Gray SG, Mutti L. *Transl Lung Cancer Res*. 2020;**9**:S100–S119.
3. Tavera RJ, Forget MA, Kim YU, Sakellariou-Thompson D, Creasy CA, Bhatta A, Fulbright OJ, Ramachandran R, Thorsen ST, Flores E, Wahl A, Gonzalez AM, Toth C, Wardell S, Mansaray R, Radvanyi LG, Gombos DS, Patel SP, Hwu P, Amaria RN, Bernatchez C, Haymaker C. *J Immunother*. 2018;**41**:399–405.
4. Hao Y, Hao S, Andersen-Nissen E, Mauck WM, Zheng S, Butler A, Lee MJ, Wilk AJ, Darby C, Zager M, Hoffman P, Stoeckius M, Papalexi E, Mimitou EP, Jain J, Srivastava A, Stuart T, Fleming LM, Yeung B, Rogers AJ, McElrath JM, Blish CA, Gottardo R, Smibert P, Satija R. *Cell*. 2021;**184**:3573–87.
5. Stuart T, Srivastava A, Madad S, Lareau CA, Satija R. *Nat Methods*. 2021;**18**:1333–41.
6. Qiu X, Mao Q, Tang Y, Wang L, Chawla R, Pliner HA, Trapnell C. *Nat Methods*. 2017;**14**:979–982.

Ethics Approval This study was written and conducted in accordance with the principles from the Declaration of Helsinki. Written informed consent was provided by all study participants or their legal representatives. The study (LAB08-0380) was approved by the University of Texas MD Anderson Cancer Center’s Institutional Review Board.

<http://dx.doi.org/10.1136/jitc-2022-SITC2022.1050>

1051 RADIATION DOSE-RELATED TEMPORAL CHANGES IN STING-ASSOCIATED IMMUNE GENES IN MURINE CD8 T CELLS

Ana Torres*, Amanda Shea, Wonjong Jin, Caroline Kerr, Kaleb Schroeder, Paul Clark, Zachary Morris. University of Wisconsin-Madison, Madison, WI, USA

Background Systemic lymphopenia from radiation results in poor outcomes for patients. Clinical interventions can reduce lymphopenia; however, more efficient treatments could drastically improve patient outcomes, particularly when receiving immunotherapeutic treatments. Interactions of T cells, radiation, and the tumor microenvironment remain largely unknown, and in this study, we examined modulation of CD8 T cell transcriptional activity after radiation at various doses and time points.

Methods Five spleens of C57BL/6 mice were disaggregated into single cell suspensions and positively sorted with a CD8 T cell isolation kit. The CD8⁺ cell suspensions were expanded *in vitro* for 9 days with CD3/CD28 plate-bound stimulation and then left unirradiated (0Gy control) or administered 2Gy, 8Gy, 12Gy, or 20Gy. At 24-, 48-, and 72-hours post-irradiation, the cells were collected for RNA, followed by expression analysis using qPCR. Fold-change (with relation to 0Gy) expression data were compared among multiple cohorts using a two-way ANOVA with a post hoc Tukey test.

Results We identified several immune genetic changes in irradiated CD8 T cells compared to unirradiated controls. *Ifn- γ* , a direct stimulator of type 1 IFN response, expression was highest at 72 hours post radiation, with all doses exhibiting >10-fold increases ($p < 0.006$). *Irf3*, a transcription factor of type 1 interferons, was increased in 8Gy, 12Gy, and 20Gy conditions, and expression levels were highest 48 hours post radiation in the 8Gy condition ($p = 0.0009$). *Trex1*, a potential negative regulator of STING-response, increased in a dose dependent manner with the highest expression being a 14-fold increase at 48 hours post radiation (p -values for all conditions < 0.0001 , except 2Gy ns). Interestingly, *Ifn- β* , a Type 2 interferon response and activated T cell interferon, was also increased ($p < 0.0001$) at 8Gy 48 hours post radiation. *Pd-L1* and *Mhc-1* expression both increased at all radiation doses with highest expression at 48 hrs (*Mhc-1*: 2-10 fold increase; *Pd-L1*: 2-7 fold increase).

Conclusions Radiation dose-related and temporal changes in transcription of various immune genes (*Ifn- γ* , *Irf3*, *Trex1*, *Ifn- β* , *Pd-L1*, *Mhc-1*) suggests CD8 T cells play a role in activation, maintenance, and regulation of immune response, at least partially via the STING pathway. Changes included actionable targets such as *Pd-L1* and *Mhc-1* that could inform timing of immunotherapies to patients such as immune checkpoint inhibitors and CAR-T cells.

Ethics Approval All animal experiments were performed with the approval of UW Madison Institutional Animal Care and Use Committee (IACUC). PI Zachary Morris M005670. No human materials were used in the experiment described. All experiments were conducted under BSL-1 conditions with the approval of the UW Institutional Safety Board (B00000510).

<http://dx.doi.org/10.1136/jitc-2022-SITC2022.1051>

1052

TISSUE-SPECIFIC INTERFERON-GAMMA DRIVES REGULATORY T-CELLS TO RESTRAIN DC1-MEDIATED PRIMING OF CYTOTOXIC T-CELLS AGAINST LUNG CANCER

¹Maria Zagorulya*, ¹Leon Yim, ¹Duncan Morgan, ²Austin Edwards, ¹Elen Torres-Mejia, ¹Noor Momin, ¹Chloe McCreery, ¹Izabella Zamora, ¹Brendan Horton, ¹K Wittrup, ¹J Love, ¹Stefani Spranger. ¹Massachusetts Institute of Technology, Cambridge, MA, United States; ²University of California San Francisco, San Francisco, CA, United States

Background Although failure to respond to checkpoint blockade immunotherapies is frequently associated with a lack of T-cell infiltration into the tumor, clinical data suggests that in patients with lung cancer, T-cell-inflamed tumors can also be resistant to therapy.¹ Work by us identified that checkpoint blockade immunotherapy resistance in T-cell-inflamed lung cancer is driven by lung cancer-specific CD8⁺ T-cell dysfunction, characterized by reduced cytolytic capacity and established during priming in the mediastinal lymph nodes (mLN).² In this study, we sought to uncover lung-specific mechanisms that blunt priming of anti-tumor cytotoxic T-cell responses.

Methods To study T-cell priming against lung cancer, we implanted a syngeneic lung cancer cell line (KP) orthotopically in the lungs or subcutaneously in the flanks of C57BL/6 mice. Immune subsets were profiled using flow cytometry, immunofluorescence staining and RNA-sequencing. Immunological mechanism was dissected using adoptive T-cell transfers, bone marrow chimeras and *ex vivo* co-cultures.

Results Both lung and flank KP tumors resulted in type-1-conventional dendritic cell (DC1)-dependent expansion of tumor-reactive T-cells, however, CD8⁺ T-cells primed in response to lung tumors in the mLN failed to upregulate key markers of effector CD8⁺ T-cell differentiation, namely CD25 and Granzyme B. Comparing DC1 from tumor-draining inguinal (iLN) and mLN revealed equivalent antigen load, but reduced expression of CD80, CD86 and IL-12 on mLN-derived DC1. Regulatory T-cell (Treg) depletion rescued both stimulatory molecule expression on DC1 and cytotoxic T-cell priming in the tumor-draining mLN, suggesting that lung CD8⁺ T-cell dysfunction required the local presence of Treg during priming. *Ex vivo* co-cultures validated that DC1 and Treg were required and sufficient to induce dysfunctional CD8⁺ T-cells. This immunosuppression was spatially coordinated within tissue-specific LN microniches and required antigen-specific contact between DC1 and Tregs, as abrogating MHCII-dependent Treg:DC1 interactions restored DC1 capacity to prime cytotoxic T-cell responses against lung tumors. The lung-specific suppression was associated with clonally expanded CXCR3⁺ T_H1-like effector Tregs, which were induced upon interferon sensing in the mLN. Consequently, interferon-gamma neutralization early during tumor induction could prevent the immunosuppression and restore cytotoxic T-cell priming in the mLN. Similarly, in cancer patients, interferon-sensing CXCR3⁺ Tregs but not CD8⁺/Treg ratios correlated with resistance to checkpoint blockade immunotherapy.

Conclusions Our work suggests that the functional quality of Tregs, specifically the interferon-induced CXCR3⁺ T_H1-like effector state, rather than Treg quantity, is instrumental in restraining tumor-reactive T-cell responses and represents a critical barrier to productive anti-tumor immunity.

Acknowledgements This work was supported by the Pew Stewart scholarship, the Koch Institute Frontier Research program, the Ludwig Center at MIT and the MIT School of Science Fellowship in Cancer Research.

REFERENCES

1. Doroshov DB, Sanmamed MF, Hastings K, Politi K, Rimm DL, Chen L, Melero I, Schalper KA, and Herbst RS. Immunotherapy in non-small cell lung cancer: facts and hopes. *Clin Cancer Res* 2019;**25**:4592–602.
2. Horton BL, Morgan DM, Momin N, Zagorulya M, Torres-Mejia E, Bhandarkar V, Wittrup KD, Love JC, Spranger S. Lack of CD8(+) T cell effector differentiation during priming mediates checkpoint blockade resistance in non-small cell lung cancer. *Sci Immunol.* 2021;**6**:eabi8800.

Ethics Approval All mouse experiments in this study were approved by MIT's Committee on Animal Care (CAC) – DHHS Animal Welfare Assurance £ D16-00078.

<http://dx.doi.org/10.1136/jitc-2022-SITC2022.1052>

1053

IDENTIFICATION OF DISTINCT IMMUNE LANDSCAPES OF INFILTRATING T CELLS IN COLON CANCER USING MULTIPLEX IMMUNOFLUORESCENCE STAINING

¹Hehuan Zhu*, ¹Jessica Roelands, ²Eiman Ahmed, ¹Imke Stouten, ¹Rachel Hoorntje, ¹Ronald Vlierberghe, ¹Marieke Ijsselstein, ¹Noel Miranda, ¹Rob Tollenaar, ²Wouter Hendrickx, ²Davide Bedognetti, ¹Peter Kuppen. ¹Leiden University Medical Center, Leiden, Netherlands; ²Sidra Medicine, Doha, Qatar

Background The immune system recognizes foreign microorganisms as "non-self" and reacts to destroy these disease-causing agents, playing a similar role in protecting the body from malignancies. The spatial distribution of T cell subsets in tumor tissues, like colon cancer, may provide information on the role of the immune system in tumor development. To gain novel insights into different types of T cells including cytotoxic T (Tc) cells, helper T (Th) cells, and regulatory T (Treg) cells, a seven-color multiplex immunofluorescence (mIF) panel was used to study the number and spatial distribution of these T cell subsets in a panel of colon tumors.

Methods We simultaneously assessed CD3, CD8, Foxp3, Ki67, Granzyme B and pan cytokeratin in ninety colon cancer cases using a tyramide signal amplification based mIF approach. Using dedicated image analysis software, we analyzed the multiple cell phenotypes and their spatial distribution inside tumor stromal and epithelial regions of interest. Moreover, in a previous study, next-generation sequencing was performed on the same samples, resulting in consensus clustering based on the immunologic constant of rejection (ICR) genes,¹ segregating colon cancer patients in three different groups: ICR low, medium and high. Statistical analyses were conducted to determine associations between the density of T cell subsets and their spatial location.

Results All T cell subtypes were more prevalent in the stromal fraction than in the epithelial fraction, but the proportion of Ki-67+ or Granzyme B+ T cells was significantly higher in the tumor epithelium than in the tumor stroma. In both tumor epithelium and tumor stroma, T cell densities were significantly higher in those with high ICR than in those with low ICR. Meanwhile, the median distance between immune cells and epithelial cells was significantly smaller in ICR-high than in ICR-low. Interestingly, patients with an ICR high/Th cells high experienced improved overall survival ($p = 0.016$).

Conclusions In this study, we quantified the spatial distribution of T cell subsets and highlight the tumor infiltration of Th cells, which can improve the prognostic value of T cell immune signatures in colon cancer.

REFERENCE

1. Roelands J, Decock J, Boughorbel S, *et al.* A collection of annotated and harmonized human breast cancer transcriptome datasets, including immunologic classification. *F1000Research*. 2017;6:296.

<http://dx.doi.org/10.1136/jitc-2022-SITC2022.1053>

MYELOID AND T CELL SUBSETS DEFINED IN BLADDER CANCER USING SINGLE-CELL RNA SEQUENCING AND PAIRED PROTEIN PROFILING

<http://dx.doi.org/10.1136/jitc-2022-SITC2022.1054>

¹Viktor Sincic*, ²Ashfaq Ali, ¹Alar Aab, ¹Thoas Fioretos, ¹Carl Borrebaeck, ¹Fredrik Liedberg, ¹Kristina Lundberg. ¹Lund University, Lund, Sweden; ²National Bioinformatics Infrastructure Sweden, Lund, Sweden

Background Muscle-invasive bladder cancer (MIBC) has a 5-year survival of only 50% despite preoperative chemotherapy and radical cystectomy. For non-muscle-invasive bladder cancer (NMIBC), the 5-year survival rate is > 80%, but the local recurrence rate is very high. Immune checkpoint inhibitors can drastically increase survival, however only a fraction of bladder cancer patients is currently responding. We have performed single-cell RNA sequencing (scRNAseq) of tumor-infiltrating immune cells from NMIBC and MIBC biopsies as well as full-length scRNAseq with parallel protein profiling of T cells in MIBC, to pinpoint novel targets for immunomodulatory therapy.

Methods Tumor biopsies obtained from untreated patients with MIBC (N= 14) and NMIBC (N=4) were mechanically and enzymatically digested into single cell suspensions and either CD45⁺ or CD3⁺ cells were sorted. Parallel protein assessment (index sorting) was performed for CD3⁺ cells. In total, 30 000 CD45⁺ and 4061 CD3⁺ cells were processed according to the 10x Genomics and Smart-seq3 protocols, respectively.

Results Approximately 1600 and 4000 genes per cell were detected using the 10x and Smart-seq3 methodologies, respectively. The transcriptomic immune cell landscape in NMIBC and MIBC was delineated and within the myeloid compartment, e.g. SPP1⁺ tumor associated macrophages (TAMs) were identified and shown to correlate with response to checkpoint blockade in the IMvigor210 cohort.¹ Within the T-cell compartment, populations including cytotoxic CD4⁺ and CD8⁺ T cells and exhausted CD8⁺ T cells were identified and their transcriptional profiles were defined. Of note, using protein-level data from the index sorting, two populations of cytotoxic CD4⁺ T cells with remarkable similarity to CD8⁺ counterparts were identified. Furthermore, CD56⁺ T cells were found to differentially populate certain T cell clusters, including Treg and cytotoxic T cell clusters.

Conclusions Our results provide new insights into the myeloid and lymphocyte compartment in the microenvironment of bladder cancer. This understanding can give clues for designing novel treatment strategies.

REFERENCE

1. Mariathasan S, Turley SJ, Nickles D, Castiglioni A, Yuen K, Wang Y, *et al.* TGFB attenuates tumour response to PD-L1 blockade by contributing to exclusion of T cells. *Nature* 2018;**554**(7693):544–8. Epub 2018/02/15. doi:10.1038/nature25501. PubMed PMID: 29443960; PubMed Central PMCID: PMC6028240.

Ethics Approval The study was approved by the Research Ethics Board of Lund University (Dnr 2017/269 and 2018/963) and Stockholm University (Dnr 2020-05559). Written informed consent was obtained from the patients for publication of the results.

Consent Written informed consent was obtained from the patient for publication of this abstract and any accompanying images. A copy of the written consent is available for review by the Editor of this journal.

1055 IMMUNE CELL SUBTYPES ASSOCIATED WITH THE LEVEL OF TUMOR-INFILTRATING LYMPHOCYTES IN BREAST TUMOR MICROENVIRONMENT

¹Su Min Cha*, ^{1,2}Jeong-Han Seo, ^{2,3}Jung-Wook Park, ²Hee Jae Lee, ^{1,2}Hee Jin Lee.
¹University of Ulsan College of Medicine, Seoul, South Korea, Republic of; ²NeogenTC Corp., Seoul, South Korea, Republic of; ³Sungkyunkwan University, Seoul, South Korea, Republic of

Background The level of tumor-infiltrating lymphocytes (TILs) is a predictive and prognostic factor for improved clinical outcomes in breast cancer. To identify immune cell subtypes associated with the level of TILs, we compared composition of immune cells between breast cancers with high or low level of TILs using single cell RNA sequencing (scRNA-seq).

Methods The scRNA-seq was performed with dissociated and CD45+ sorted cells from 21 breast tumor tissues. Among them, 12 samples with high TIL ($\geq 40\%$, n=6) or low TIL ($\leq 2\%$, n=6) were compared. Standard procedures were performed by the Seurat package in R. T cells, B cells, monocytes, and dendritic cells (DCs) were separated using the Azimuth package. Differentially expressed genes (DEGs) were computed according to the level of TILs for pathway analysis using ReactomePA package (p value < 0.05, abs(log2 fold change) ≥ 1).

Results The proportion of T cells (60.6% vs 41.8%) and B cells (9.8% vs 3.9%) in the high TIL group were higher than the low TIL group. Monocytes (16.3% vs 29.3%) and DCs (4.6% vs 4.5%) in the high TIL group were lower or not different. In each immune cell type, cell subtypes and clusters were compared by proportion in the high and low TIL groups. T cell subtypes showed no difference between the high and low TIL groups. However, B cells, monocytes, and DCs had different composition of cell subtypes between the high and low TIL groups [B intermediate (22.2% vs 35.8%), B memory (14.2% vs 36.6%), plasmablast (57.1% vs 19.1%), cDC2 (54.5% vs 66.7%), pDC (39.0% vs 27.8%), and 4 monocyte clusters (11.1% vs 19.6%, 12.7% vs 20.1%, 18.8% vs 13.8%, and 14.9% vs 7.5%)]. DEGs derived from differential subtypes between the high and low TIL groups were used for pathway analysis. Upregulated pathways including interleukin and interferon signaling pathways in the high TIL group were shared by several immune subtypes.

Conclusions Composition of immune cell subtypes and their signaling pathways were different between breast cancers with the high or low level of TILs. Further researches for better understanding and modulation of immune cell subtypes associated with high level of TILs are needed to heighten the level of TILs in breast cancer microenvironment.

<http://dx.doi.org/10.1136/jitc-2022-SITC2022.1055>

Immune-Stimulants and Immune Modulators

1056

ZG033, A NOVEL CD137 AGONIST, INDUCES SUPERIOR ANTI-TUMOR ACTIVITY WITHOUT HEPATOTOXICITY RELY ON FC-MEDIATED CROSSLINKING

¹Liansheng Cheng, ¹Wenting Liu*, ¹Dayan Zhang, ¹Xiaoli Zeng, ²Guodong Shen. ¹Hefei Hankemab Biotechnology Co., LTD, Hefei, Anhui, China; ²The First Affiliated Hospital of University of Science and Technology of China, Hefei, Anhui, China

Background CD137 (TNFRSF9, 4-1BB) is a member of the tumor necrosis factor receptor superfamily that functions as a costimulatory molecule of immunocytes. Agonistic antibodies against CD137 have shown promising therapeutic activity in mouse tumor models. However, molecules in clinical development have shown limitations due to either dose-dependent severe liver toxicity or modest antitumor activity. We developed ZG033, a fully human IgG4 agonist of CD137 that engages with an exclusive epitope, to achieve a better efficacy and safety profile for immunotherapy.

Methods The biophysical properties and activities were determined using multiple *in vitro* assays, including enzyme-linked immunosorbent assay (ELISA), surface plasmon resonance (SPR), cell-based and reporter gene assays. *In vivo* antitumor activities were assessed in human 4-1BB transgenic mice transplanted with human colon cancer cell line MC38. The pharmacokinetic (PK) behavior and safety profiles of ZG033 were characterized in cynomolgus monkeys.

Results ZG033 is a safe and potent antibody injection associated with a differentiated pharmacology and toxicology profile. The structure of the ZG033/CD137 complex was determined by X-ray crystallography. The Fab of ZG033 binds CD137 at an obvious competitive epitope with the CD137 ligand, which differs from the currently known agonist antibodies of CD137. The residues T61A and I64R play a vital role in the formation of the complex, which was demonstrated by affinity assays. The binding affinity to human 4-1BB of ZG033 determined by surface plasmon resonance (SPR) was moderate (KD=10 nM). ZG033 increased CD137-driven NFκB reporter gene activation and the production of IFN-γ by human T cells in an FcγR-dependent manner. In human 4-1BB transgenic mice, ZG033 showed robust single-agent antitumor activity and induced durable antigen-specific immunological memory that prevented the tumor formation in the rechallenged mice. To determine the safety of ZG033, we incubated ZG033 with peripheral blood mononuclear cells (PBMCs) from healthy donors (n=4) and proved that it does not induce nonspecific production of proinflammatory cytokines. The results in 5-week I.V. repeated-dose (3, 10 and 30 mg/kg) and single-dose toxicity studies (60 and 180 mg/kg) suggested that ZG033 was well tolerated in cynomolgus monkeys with no abnormal hepatic or renal function and hematological index.

Conclusions These data demonstrate that ZG033 acts as an FcγR crosslinking-dependent CD137 agonist that displays a favorable safety profile and has potential in either mono- or combinational immunotherapies.

<http://dx.doi.org/10.1136/jitc-2022-SITC2022.1056>

1057

HBM7008, A FIRST-IN-CLASS BISPECIFIC ANTIBODY TARGETING BOTH B7-H4 AND 4-1BB, EXHIBITS ROBUST ANTI-TUMOR IMMUNITY AND LOW TOXICITY THROUGH B7-H4-DIRECTED 4-1BB ACTIVATION

Bing Huang*, Fangfang Du, Xiaocheng Lv, Jianxun Zhao, Fei Chen, Zailian Lu, Yang Zhang, Victor Chen, Xin Gan, Jiujiao Zhao, Yun He, Xiaodong Wu, Yiping Rong. *Harbour BiMed Co., Ltd, Shanghai, China*

Background 4-1BB is an immune costimulatory receptor. Anti-4-1BB agonistic monoclonal antibodies have high potential of therapeutic efficacy in cancers. However, 4-1BB agonistic antibody urelumab shows dose-limiting hepatotoxicity in clinical trials. B7-H4 is a member of the B7 superfamily. It shows limited expression in most normal tissues but high expression on the surface of tumor cells in breast, ovarian, and endometrial cancers. B7-H4 also inhibits the proliferation and activation of T cells. Blockade of B7-H4 demonstrates some efficacy in mouse models. To overcome the hepatotoxicity of systemically active 4-1BB agonist and to improve the anti-tumor activity of B7-H4 antagonist, HBM7008, a B7-H4x4-1BB bispecific antibody specifically activated in tumor microenvironment, has been developed.

Methods B7-H4 expression of multiple tumor tissues was evaluated by immunohistochemistry staining. Anti-B7-H4 fully human IgG antibodies and anti-4-1BB fully human heavy chain only antibodies (HCAb) were generated from H2L2 and HCAb Harbour Mice[®], respectively. HBM7008 was developed from Harbour BioMed HCAb based bispecific immune cell engager (HBICE[®]) platform. It is composed of anti-B7-H4 IgG1 monoclonal antibody and anti-4-1BB HCAb variable domain fused at the C-terminus of heavy chain constant region with LALA (L234A and L235A) mutations. Its proposed mechanism of action and nonclinical pharmacology were characterized by a series of *in vitro* and *in vivo* assays.

Results B7-H4 showed high prevalence of expression on breast, ovarian, cervical, endometrial cancers, and squamous non-small-cell lung carcinoma. HBM7008 can bind to B7-H4 and 4-1BB simultaneously. HBM7008 robustly induced T cell activation *in vitro* in a B7-H4-dependent manner with activity comparable to that of urelumab. HBM7008 demonstrated potent antitumor activity with complete response and resistance to tumor rechallenge in a mouse model. It also increased proliferation of tumor infiltrating lymphocyte (TIL) cytotoxic CD8+ T and effector memory CD8+ T cells. HBM7008 is a first-in-class bispecific T cell engager targeting both B7-H4 and 4-1BB and enhances T cell function by dual mechanisms: (1) blockade of the B7-H4 mediated T cell inhibition and (2) activation of 4-1BB+ T cells only in a B7-H4 cross-linking dependent manner. In a good laboratory practice-compliant non-human primate 4-week repeat dose toxicity study, HBM7008 was well tolerated up to 100 mg/kg with no discernable drug-related toxicity.

Conclusions HBM7008 demonstrated comparable biological activity to urelumab and improved safety profile characterized by *in vitro* functional assays, *in vivo* antitumor efficacy model, and TIL analysis. These preclinical data support the clinical investigation of HBM7008 for the treatment of cancers.

Ethics Approval The cancer tissue microarray was purchased from Fanpu Biotech, Inc. The company ensured ethical approval from the patients, and patient consent for publication. The anti-tumor efficacy and pharmacodynamics studies in mice were approved by the internal ethics board of the respective contract research organization (CRO). The good laboratory

practice-compliant toxicity studies in non-human primate were approved by Ethics Board of an appropriate contract research organizations (CROs).

<http://dx.doi.org/10.1136/jitc-2022-SITC2022.1057>

1058

YH32364 (ABL104), A NOVEL EGFR/4-1BB BISPECIFIC ANTIBODY EXHIBITS POTENT ANTITUMOR EFFICACY WITH AN EXCELLENT SAFETY PROFILE

¹Eunjung Lee*, ²Hyejin Chung, ²Yangsoon Lee, ¹Young Bong Park, ¹Eun-Jung Lee, ¹Hyunmo Koo, ¹Mikyeong Ju, ¹Ju Young Park, ¹Sujin Ahn, ¹Junhwan Kim, ²Kyeongso Park, ²Wonjun Son, ²Jaehyun Eom, ²Hanbyul Lee, ²Jaeho Jung, ²Jonghwa Won, ¹Se-Woong Oh. ¹Yuhan Corporation, Seoul, South Korea, Republic of; ²ABL Bio Inc., Gyeonggi-do, South Korea, Republic of

Background Epidermal growth factor receptor (EGFR) is a key factor in cellular proliferation, differentiation, and survival, which has been considered as a main target in the treatment of malignancies. Although treatment with EGFR-targeted therapy and chemotherapy improved outcomes for EGFR overexpressing cancer, its clinical application is limited due to drug resistance. Therefore, there is an urgent *unmet medical need for new* therapies that can *overcome drug resistance*, particularly for EGFR overexpressing cancer. Combination with immunotherapy would be one of the new treatment options to resolve drug resistance. 4-1BB (CD137) is a key costimulatory receptor expressed on activated T cells and natural killer (NK) cells, which is a promising therapeutic target in cancer. A novel YH32364 (ABL104) has been generated to overcome the challenges with EGFR-drug resistance via tumor-directed 4-1BB agonism and EGFR signal blocking.

Methods YH32364 is EGFR/4-1BB-bispecific antibody with an engineered IgG1 isotype. Its activity was determined using cell-based 4-1BB bioassay and co-culture assay with human peripheral blood mononuclear cells (hPBMC). *In vivo* antitumor efficacy of YH32364 and the infiltrated-immune cells into tumor were assessed in h4-1BB knock-in (KI) mice models. Three-week repeated dose toxicity study of YH32364 for dose range finding (DRF) was conducted in cynomolgus monkeys at the dose of 30 and 100 mg/kg.

Results YH32364 binds to EGFR and 4-1BB with high affinity. YH32364 not only blocked EGFR signaling of tumor cells, but also activated T cells as indicated by IFN- γ secretion, leading to tumor cell lysis in co-culture assay using hPBMC and EGFR-expressing tumor cells. YH32364 exhibited superior efficacy on tumor regression and anti-tumor immunity in MC38/hEGFR-bearing h4-1BB KI mouse models, compared to the equimolar dosing of cetuximab. *In 3-week* toxicity study in monkey, there were no YH32364-related toxicological findings including skin toxicity, mortality, body weight, hematology, clinical chemistry etc., indicating a favorable safety profile.

Conclusions YH32364 exhibited potent *in vitro* and *in vivo* efficacy and it was well tolerated and safe potentially due to tumor-localized T cell activation. These results suggest that YH32364 could be a promising therapeutic for EGFR-overexpressing cancer patients, especially with EGFR drug resistance.

<http://dx.doi.org/10.1136/jitc-2022-SITC2022.1058>

1059

ON203: A NEW ANTIBODY TARGETING THE OXIDIZED FORM OF MACROPHAGE MIGRATION INHIBITORY FACTOR (OXMIF) EXERTS ANTITUMORIGENIC ACTIVITY AND MODULATES THE TUMOR MICROENVIRONMENT

Barbara Maurer, Irina Mirkina, Julia Mayer, Christine Landinger, Alexander Schinagl, Michael Thiele, Randolph Kerschbaumer*. *OncOne Research and Development GmbH, Vienna, Austria*

Background Immunotherapy success in solid cancers is largely dependent on the tumor microenvironment (TME) and its modulation is central to improve clinical outcomes. One of the key players regulating the TME is the macrophage migration inhibitory factor (MIF), which contributes to an immunosuppressive environment. MIF induces polarization of macrophages to the M2 subtype, suppresses cytotoxic T cells and correlates with poor response to immune checkpoint therapy. MIF expression is associated with tumor aggressiveness, metastasis, and disease progression, but due to its ubiquitous nature is considered an elusive target for therapeutic intervention. In contrast, the disease-related structural isoform of MIF, termed oxMIF, is specifically present in solid tumor tissue. We now determined the antitumorigenic and TME-modifying potential of the new oxMIF-specific antibody ON203.

Methods In 3D tumoroids retaining an intact TME, which were isolated from colorectal carcinoma patients, tumor cell killing (high-content 3D computational bioimaging) and TME modulation (immune cell composition and activation, secretome analysis) induced by ON203 were analyzed. *In vivo* tumor penetration was assessed by infrared-labeled ON203 injected in tumor-bearing mice. Efficacy was assessed in human cancer cell-line (PC3) xenografted mice and ON203's effects on tumor cell proliferation, vascularization and infiltrating immune cells were evaluated by immunohistochemistry.

Results Four out of five ON203-treated, freshly isolated tumoroids from colorectal carcinoma patients responded with significant tumor cell death. In the responding tumoroids a clear immunomodulatory effect on the tumor-associated immune cells was detected: ON203 activated NK and NKT cells (upregulation of Granzyme B and CD107a) and supported M1 polarization, correlating with reduced IL-10 levels in the secretome of ON203-responding tumoroids.

ON203 accumulated and retained in the tumor tissue *in vivo* and treatment of immunocompromised mice xenografted with human PC3 tumors led to significantly reduced tumor volumes. Tumor cell proliferation (assessed by Ki67 staining quantification) and tumor vessel density (CD31 staining quantification) were strongly decreased and currently ongoing analysis of tumor-infiltrating immune cells by immunohistochemistry and flow cytometry will provide further insights on the immunomodulatory therapeutic effects of ON203.

Conclusions The anti-oxMIF antibody ON203 demonstrated antitumorigenic effects by (i) reducing tumor cell proliferation, (ii) reducing angiogenesis and intravasation and (iii) by modulating the TME towards immunosupportive functions. In the upcoming clinical Phase 1 trial ON203's safety, tolerability, pharmacokinetics, and pharmacodynamics in patients with solid tumors will be analyzed to evaluate its potential as a standalone or combinatorial therapy with immune checkpoint inhibitors, kinase inhibitors or antiangiogenic agents.

<http://dx.doi.org/10.1136/jitc-2022-SITC2022.1059>

1060

EVOLVE™: A NOVEL COSTIMULATORY T CELL ENGAGER PLATFORM ENGINEERED FOR THE TREATMENT OF IMMUNE SUPPRESSIVE TUMORS

Jeremy Myers*, Mohosin Sarkar, Abudukadier Abulizi, Eric Tam, Guixian Jin, Xingyue An, Evelyn Teran, Shu Shien Chin, Danielle Klaskin, Nana Adjoa Pels, Maria Hackett, Oksana Sergeeva, Hayden Karp, Julio Rodriguez, Sonali Dhindwal, Changqing Yuan, Zengzu Lai, Jennifer Zeiger, Amber Fearnley, Louis Matis, Jay Fine. *EvolImmune Therapeutics, Branford, CT, USA*

Background CD3-bispecifics are antibody-based therapies that can simultaneously bind to a tumor cell surface antigen and T cells to establish a synapse between the tumor and T cell and activate T cell to induce specific killing of the tumor cell. CD3-bispecifics have demonstrated clinical success in B cell acute lymphoblastic leukemia and follicular lymphoma with approvals of that blinatumomab (Blinicyto®) and mosunetuzumab (Lunsumio®) that target B cell lineage antigens CD19 and CD20, respectively. However, clinical progress in deploying CD3-bispecifics for positive patient outcomes in solid tumors has been slow, due to tumor microenvironmental factors such as induction of T cell exhaustion, as well as the potential of CD3-bispecifics to mediate T cell anergy and dysfunction in the absence of adequate costimulation.

Methods Here we describe the development and preclinical validation of the EVOLVE platform, a tumor-targeted biologic that induces the formation of a synthetic synapse that simultaneously activates the T cell receptor complex and the CD2 receptor to optimize CD8 T cell effector phenotype and improve tumor cell killing *ex vivo* and *in vivo*, compared to matched CD3-bispecifics.

Results We demonstrate that CD2 costimulation is superior to other forms of T cell costimulation in its ability to promote cytolytic costimulation, T cell cytokine production and T cell expansion. Furthermore, CD2 receptor expression is markedly elevated in tumor infiltrating lymphocytes across a broad set of tumor types, relative to the CD28 and 4-1BB costimulatory receptors. EVOLVE-mediated T cell activation is conditionally dependent on tumor antigen binding and can be tuned to promote optimal costimulation without increasing cytokine release relative to matched CD3-bispecifics. We also demonstrate the modular nature of the EVOLVE platform across diverse tumor antigens including B7H4 (VTCN1), the B cell lymphoma antigen CD20 and a novel squamous tumor antigen ULBP2.

Conclusions Our data highlight the broad applications of the EVOLVE platform to improve CD8 T cell-mediated anti-tumor immunity and suggest its potential as an emerging, first-in-category immunotherapeutic strategy to address unmet medical needs in oncology.

<http://dx.doi.org/10.1136/jitc-2022-SITC2022.1060>

1061

CLN-617 IS AN INTRATUMORALLY INJECTED AND LOCALLY RETAINED FUSION OF IL-2 AND IL-12 THAT DRIVES SYSTEMIC ANTI-TUMOR ACTIVITY

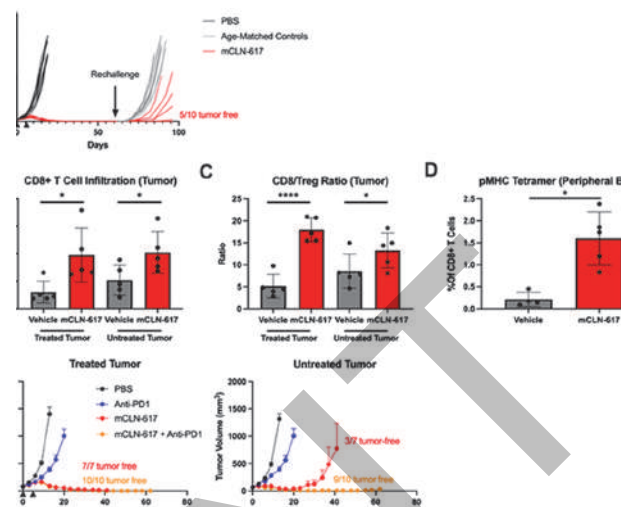
¹Mehta Naveen*, ¹Kavya Rakhra, ¹Kristan Meetze, ¹Irina Shapiro, ²Karl Wittrup, ¹Patrick Baeuerle, ¹Jennifer Michaelson. ¹Cullinan Oncology, Inc., Cambridge, MA, USA; ²Massachusetts Institute of Technology, Cambridge, MA, USA

Background IL-2 and IL-12 synergistically trigger the stimulation and proliferation of T and NK cells to mediate anti-tumor immunity. Although aldesleukin (recombinant IL-2 for high-dose infusion) has been approved for the treatment of melanoma and renal cell carcinoma, adoption has been hindered by frequent grade 3 and 4 severe adverse events. No IL-12 therapy has been approved yet due to dose-limiting toxicities. CLN-617 is comprised of IL-2, leukocyte-associated immunoglobulin-like receptor 2 (LAIR2), human serum albumin (HSA), and IL-12, and is designed for intra-tumoral (IT) administration. Upon injection, tumor retention is enabled by LAIR2, which binds to collagen, and by HSA, which increases the molecular weight, to reduce toxicity and enhance efficacy.

Methods Proteins were expressed in HEK293 or CHO cells. Collagen binding was measured by ELISA. Cytokine bioactivity was evaluated by treating PBMCs with CLN-617 followed by flow cytometry and protein microarray analysis. In vivo studies were conducted in B16F10 and MC38 murine syngeneic tumor models. Cytokine concentrations were determined by Mesoscale Discovery, and immunophenotyping was performed in blood and digested tissue samples.

Results CLN-617 triggered signal transducer and activator of transcription 4 and 5 (STAT4 and STAT5) signaling pathways in T cells and NK cells *in vitro* comparable to recombinant IL-2 and IL-12. When a murine surrogate of CLN-617 (mCLN-617) was injected IT in MC38 tumors, IT concentrations of mCLN-617 were >20x serum concentrations. In the checkpoint-refractory B16F10 and MC38 tumor models, mCLN-617 demonstrated 95% tumor growth inhibition and 100% CRs, respectively. All mice cured of their primary MC38 tumors were either protected from re-challenge or showed delayed tumor growth kinetics (figure 1A). In mice bearing two MC38 tumors, only one of which was treated IT, the number of CD8+ T cell infiltrates more than doubled (figure 1B) and the CD8+ to T regulatory cell ratio increased to >10 (figure 1C) in both treated and distal untreated tumors. The frequency of tumor-specific T cells in the periphery increased >7-fold (figure 1D). 100% of treated tumors and 90% of untreated tumors were eliminated when mCLN-617 was combined with an anti-PD1 antibody (figure 1E), demonstrating a robust abscopal response.

Conclusions Fusion to LAIR2 and HSA enables well-tolerated and effective IT delivery of IL-2 and IL-12 in a single multi-functional molecule. Despite local administration and retention, CLN-617 mobilizes systemic immunity to drive abscopal responses. CLN-617 is currently in IND-enabling studies.



Abstract 1061 Figure 1 CLN-617 drives memory responses and systemic immunity. A) MC38 tumors were treated IT with mCLN-617. Surviving mice were re-challenged with MC38 tumors after two months. B-D) Mice were implanted with two MC38 tumors, and one was treated IT. Treated and untreated tumors (B,C) as well as peripheral blood (D) were evaluated by flow cytometry. E) In a dual flank MC38 tumor model, one tumor was treated with mCLN-617 IT with or without systemic anti-PD1 administered intraperitoneally. For B-D, statistics were analyzed by t-test, *p<0.05 ****p<0.0001

<http://dx.doi.org/10.1136/jitc-2022-SITC2022.1061>

1062

ES009, A LILRB2-SPECIFIC BLOCKING ANTIBODY, REPROGRAMS MYELOID CELLS INTO PRO-INFLAMMATION PHENOTYPE AND POTENTIATES T CELL ACTIVATION

Xiaofeng Niu, Chunnian Wang, Jinfeng Zhao, Jiahui Hu, Yanfen Hu, Jun Sun, Xiaoyan Zheng, Yuting Qiu, Zhihao Wu, Yangsheng Qiu, Quan Qiu, Hongtao Lu*. *Elpscience Biopharma, Shanghai, China*

Background The ITIM-containing inhibitory receptor leukocyte immunoglobulin-like receptor B 2 (LILRB2, also known as ILT4) is predominantly expressed on myeloid-lineage cells, including monocytes, macrophages, dendritic cells and granulocytes, and is emerging as a key immune checkpoint for tumor immunotherapy. Human LILRB2 broadly binds to multiple ligands including classical MHC-I, HLA-G, angiopoietin-like (ANGPTL) family members, myelin-associated glycoprotein (MAG), and contributes to immune suppression in the tumor microenvironment (TME). Accumulating evidence has demonstrated that blocking LILRB2 reprograms tumor-associated myeloid cells and promotes anti-tumor efficacy in combination with PD-1 antibody in clinical setting. In this study, we seek to further investigate LILRB2 biology and have developed a LILRB2 blocking antibody called ES009 with high affinity and specificity that potently reprograms myeloid cells into pro-inflammation phenotype and potentiates T cell activation.

Methods LILR family homologue binding properties were evaluated by ELISA and FACS. Antigen binding affinity was determined by surface plasmon resonance system (Biacore). Blocking activity was determined by competition assay. Functional activity was evaluated by *in vitro* monocyte activation assay, dendritic cell (DC) differentiation assay, macrophage polarization assay, M2 macrophages-T cells (M2-T) co-culture assay, and an *ex vivo* study with malignant ascites in ovarian cancer patients. Epitope analysis was performed by competitive ELISA and hydrogen deuterium exchange mass spectrometry (HDX-MS). Lead clone was humanized via CDR grafting and back mutation screening.

Results ES009 specifically recognizes human LILRB2 with high affinity. It binds to a unique epitope on LILRB2 that is distinct from known competitor molecules. ES009 potently blocks LILRB2 binding to multiple HLA ligands (HLA-A2, HLA-G) as well as non-HLA ligands (ANGPTL1, ANGPTL2, ANGPTL4, ANGPTL7, MAG). Through blocking ligand interaction and receptor activation, ES009 can promote human monocytes and human monocytes derived DCs into a pro-inflammatory status, reprogram human monocyte derived M2 macrophages into pro-inflammatory M1 phenotype, and restore T cell activity from M2 macrophage-mediated suppression. Most importantly, in an *ex vivo* study, ES009 demonstrated very potent ability in reprogramming primary macrophages from malignant ascites of ovarian cancer patients into a pro-inflammatory status.

Conclusions In summary, the anti-LILRB2 mAb ES009 has demonstrated great potential in the reversion of immune suppression in the TME, leading to promotion of anti-tumor immunity. We are currently advancing the development of ES009 into a clinical candidate.

<http://dx.doi.org/10.1136/jitc-2022-SITC2022.1062>

1063 ANTI-4-1BB X PD-1, A BISPECIFIC ANTI-CANCER THERAPEUTICS

Byoung S Kwon, Hanna Lee*, Jin Sung Park, SeungHee Han, Sungmin Park, Sun Woo x Im, HyunTae Son, Joseph H Jeong. *Eutilex Co. Ltd., Seoul, South Korea, Republic of*

Background 4-1BB and Programed cell death protein-1(PD-1) are both T cell costimulatory receptors/immune checkpoint regulators. 4-1BB/4-1BBL provides stimulatory signals while PD-1/PD-L1, suppressive ones to T lymphocytes. Various forms of agonists to 4-1BB or blockers to PD-1 have shown a potent anti-cancer activity by modulating mainly CD8⁺ T cells. Thus, synergistic or additive anti-cancer effect may be achieved by combining the agonists to 4-1BB and blockers to PD-1.

Methods We have tested various combinations of antibodies and proteins with consideration of overall size of the therapeutic candidates. To obtain molecularly-evolved PD-1 we first used the 3D complex between PD-1 and PD-L1 to select the major contributing PD-1 amino acids, a library targeting selected amino acids and random mutations were constructed and screened using yeast surface display. To demonstrate functions of EU505, Cell binding assay, 4-1BB bioassay and cytotoxicity assay have been conducted. Furthermore, 4-1BB/PD-1 double Knock-in(DKI) mouse and humanized mouse tumor models were used to evaluate the inhibitory activity of EU505.

Results The best anti-cancer activities were obtained by combination of an agonistic anti-4-1BB antibody and soluble PD-1 that binds to PD-L1 with high affinity. we confirmed that EU505 binds both targets independently at the same time. The result of 4-1BB bioassays, a biologically relevant MOA-based assay, showed that potent PD-L1-dependent T cell activation with EU505. *In-vitro* killing assays showed that EU505 selectively activated T cells which in turn killed high PD-L1-expressing cells, but not low-PD-L1-expressing ones. EU505 demonstrated much stronger tumor-killing effect compared with each component alone when we tested against human PD-L1-expressing tumor cells in a 4-1BB/PD-1 DKI mouse model and humanized mouse model. Furthermore, it was observed that number of effector CD8⁺ T cells increased in the peripheral blood upon EU505 injection and consequently tumor size was reduced.

Conclusions EU505, a promising anti-cancer drug, appears to enhance CD8⁺ T cell infiltration and activate T cells *in situ* at the tumor sites by binding two different targets of 4-1BB and PD-L1 simultaneously.

<http://dx.doi.org/10.1136/jitc-2022-SITC2022.1063>

1064

EXERCISE INDUCED HORMONE IRISIN INHIBITS INTEGRIN α V-TGF- β AXIS IN TUMOR MICROENVIRONMENT TO IMPROVE CD8⁺ T CELL MEDIATED TUMOR CONTROL

No-Joon Song*, Yuzhou Chang, Anqi Li, Yi Wang, Kelsi Reynolds, Kevin Weller, Chelsea Bolyard, Gang Xin, Qin Ma, Zihai Li. *The Ohio State University, Upper Arlington, OH, USA*

Background It has been reported multiple times that exercise can prevent cancer development, help anti-tumor therapies, and lower relapse rate after successful cancer treatment. However, an underlying molecular mechanism for these beneficial effects remained elusive. Recent studies revealed that cytotoxic immune cell populations contribute to exercise mediated effects, and exercise induced hormones including insulin, cortisol, testosterone, and epinephrine have been studied in this context, especially related to CD8⁺ T cell function. Exercise also induces secretion of another myokine irisin, which was originally discovered in 2012. Role of irisin has been primarily studied in metabolic disease including obesity and diabetes. However, the role of irisin in tumor immunology has not been studied.

Methods To address this point, multiple pre-clinical tumor models including colon, skin, bladder, and lung cancer were utilized. After tumor implantation, irisin was intraperitoneally injected for every 2 days starting at day 7. Tumor growth was monitored to check anti-tumoral effect of irisin. To address immunological changes within the tumor microenvironment (TME), high-dimensional flow cytometry panels were applied and analyzed. To confirm our findings, publicly available scRNA-seq data sets were re-analyzed and web-based TCGA database was utilized for further validation.

Results Irisin displayed anti-tumoral activity when tested in multiple pre-clinical models. High-dimensional flow cytometry analysis revealed that irisin treatment reduced accumulation of regulatory T cells (Tregs) in TME. Suppressible marker expressions in Tregs were also decreased and led to better CD8⁺ T cell function with evidence of less dysfunctional signature. Integrin α v-TGF- β axis was identified for responsible mechanism, and myeloid cell specific knockout of integrin α v further confirmed importance of this pathway. Our findings were validated using publicly available scRNA-seq, spatial-transcriptomics, and TCGA data sets. Integrin α v was specifically expressed in myeloid cells, and TGF- β signaling pathway was higher in integrin α v adjacent spots. Also, overall survival rate and immunotherapy response rate was lower in patients with high expression of integrin complex and TGF- β . This was experimentally validated in pre-clinical model by combining irisin with PD-1 blocking antibody; the combination group exhibited better tumor control.

Conclusions We conclude that irisin treatment reduced tumor growth in multiple tumor models and this outcome was mediated by T cells. Integrin α v-TGF- β axis in the TME was responsible for this effect, and blocking this pathway exhibited better tumor control. Re-analysis of publicly available data sets further validated importance of this signaling pathway, implying therapeutic potential of irisin in treating cancer.

<http://dx.doi.org/10.1136/jitc-2022-SITC2022.1064>

1065

ACTM-838, A MICROBIAL-BASED IMMUNOTHERAPY THAT ENRICHES IN SOLID TUMORS AFTER IV DOSING, REVERSES THE IMMUNOSUPPRESSIVE TME TO PROMOTE DURABLE ANTI-TUMOR IMMUNITY, ALONE AND IN COMBINATION WITH ANTI-PD1 IN MICE

Akshata Udyavar*, Hailey He, John Brandenburg, Julie Janes, Oanh Pham, Sara Tribble, Ryan Daroy, Keith Cheung, Haixing Kehoe, Bret Peterson, Emily Miyashita-Lin, Omkar Joshi, Nick Eisele, Christopher Thanos, Chan Whiting. *Actym Therapeutics, Hayward, CA, USA*

Background Effective treatment of metastatic cancers requires reversal of the immunosuppressive tumor microenvironment (TME) and priming a broad repertoire of tumor-specific CD8 + T cells. ACTM-838 is an attenuated, precision genome-engineered, *S.Typhimurium*-Attenuated Cancer Therapy (STACT) strain carrying a DNA plasmid that encodes payloads consisting of IL-15plex and engineered, constitutively active STING (eSTING). ACTM-838 is designed to colonize the TME and deliver payloads to phagocytic APCs, inducing a durable anti-tumor immune response, after IV dosing.

Methods STACT was developed through genome editing of the parental strain, VNP20009. Single payload (IL-15plex or eSTING) STACT strains and ACTM-838 were bacto-fected into immune cell lines and primary immune cells. Uptake, payload expression and activity were measured *in vitro* using ELISAs, MSD, and flow cytometry. ACTM-838 was evaluated in multiple murine tumor models for efficacy as a monotherapy or in combination with anti-PD1 antibodies. Modulation of immune responses in the TME and payload effects were assessed using IHC, RNAseq, flow cytometry and ELISA. ACTM-838 tolerability studies were performed in NHPs and mice.

Results Expression of encoded IL-15plex and eSTING payloads led to IFN- γ expression and IL-15 secretion in cell lines and primary M2 macrophages. Furthermore, primary human M2 macrophages polarized toward a novel, co-stimulatory and phagocytic M1/M2 hybrid phenotype. ACTM-838 preferentially colonizes tumors in mice upon IV administration and is well tolerated in NHPs, with enhanced safety compared to VNP20009 in mice. ACTM-838 is selectively taken up by phagocytic APCs *in vitro* and by tumor-resident APCs *in vivo*. ACTM-838 treatment showed dose- and payload-dependent anti-tumor efficacy in an anti-PD1 refractory, myeloid rich and T cell excluded, orthotopic EMT6 mouse model as a single agent, and induced a durable anti-tumor CD8+ T cell-dependent memory response upon tumor re-challenge. ACTM-838 induced profound immune reprogramming and remodeling of the TME through increased myeloid cell activation and CD8+ T cell infiltration. Synergistic combination anti-tumor activity was observed when dosed with anti-PD1.

Conclusions ACTM-838 delivers IL-15plex + eSTING payloads to phagocytic APCs in the TME after systemic administration, leading to potent immune reprogramming. Indeed, myeloid cell repolarization, T-cell activation and recruitment promotes durable anti-tumor efficacy as a monotherapy and in combination with anti-PD1. IV-delivered ACTM-838 possesses a compelling safety profile in mice and primates, and is currently in IND-enabling, preclinical development.

Ethics Approval All animals were used according to protocols approved by an Institutional Animal Care and Use Committee and maintained in specific pathogen-free conditions in a AAA-LAC accredited barrier facility.

<http://dx.doi.org/10.1136/jitc-2022-SITC2022.1065>

1066

PHARMACOLOGIC INHIBITION OF DGK α ACTIVATES T CELLS AND ENHANCES ANTI-TUMOR IMMUNITY

Adele Wang*, Lance Stapleton, Jean-Philippe Belzie, Weimei Xing, Gladys Muiru, Dmytro Kornyyev, Edward Hsieh, Albert Licican, Pamela Toy, Mengshu Xu, Kei Kim, Jacob Lee, Michelle Kuhne, Latesh Lad. *Gilead Sciences, Inc., Foster City, CA, USA*

Background Immunotherapies blocking checkpoint receptors on T cells have demonstrated impressive activity in cancer patients, however, a significant population of patients do not respond to these therapies or develop acquired resistance over time. Therefore, alternate approaches to enhance T cell immunity are needed to broaden and deepen the current clinical response rates in patients. A potential promising approach is to target intracellular negative regulators of T cell receptor (TCR) signaling. Diacylglycerol (DAG) is a key second messenger that links TCR signal strength to the intensity and duration of signaling by the RAS-extracellular signal-regulated kinase (ERK)- and protein kinase C (PKC)-dependent pathways. Diacylglycerol kinase α (DGK α) is an intracellular lipid kinase that is enriched in T cells and functions as a key negative regulator of TCR signaling by catalyzing the conversion of DAG to phosphatidic acid (PA), thus attenuating DAG-mediated signaling. Inhibition of DGK α maintains levels of DAG following TCR stimulation and potentiates T cell activation. Here we describe a potential first-in-class, potent, highly selective and orally bioavailable inhibitor of DGK α .

Methods The proximal activity and specificity of Gilead's inhibitor for enhancing the main TCR-driven transcriptional nodes was measured in Jurkat cell lines containing a luciferase reporter under the control of NFAT, NF- κ B, or AP-1. To assess anti-tumor activity of the inhibitor in vitro, a three-dimensional GFP-expressing human breast tumor spheroid co-culture assay with CD8⁺ T cells was established. Tumor lysis was determined by assessing the reduction of GFP signal and supernatants were collected to measure IFN- γ and granzyme B production. In parallel, to further confirm the activation of T cells by the inhibitor, splenocytes from OT-I mice were stimulated and supernatants were collected for IL-2 quantification. Furthermore, Gilead's inhibitor was evaluated in multiple mouse tumor models to assess anti-tumor efficacy as monotherapy and in combination with checkpoint antibodies.

Results Gilead's DGK α inhibitor enhanced DAG-mediated TCR signaling pathways (AP-1 and NF- κ B), leading to augmented T cell activation, as measured by increased IL-2, IFN- γ and granzyme B secretion, that resulted in increased T cell-dependent killing of tumor cells in vitro. In colorectal (CT26 and MC38) and melanoma (B16F10) mouse tumor models, the inhibitor demonstrated tumor growth inhibition as a monotherapy and improved the efficacy of α -PD-1 and α -CTLA-4.

Conclusions Specific inhibition of DGK α by Gilead's inhibitor enhances effector T cell function, leading to robust tumor growth inhibition in mouse tumor models as a monotherapy and potentiating the activity of checkpoint blockade.

<http://dx.doi.org/10.1136/jitc-2022-SITC2022.1066>

1067

SYNERGISTIC COMBINATION OF NATURAL KILLER CELL ENGAGERS (NKEs) WITH PROINFLAMMATORY CYTOKINES

Tian Zhang*, Matthew Faber, Erik Pong, Ke Liu, Matthew Bernett, Christine Bonzon, Juan Diaz, Dong Hyun Nam, Kendra Avery, Jing Qi, Rumana Rashid, Rena Bahjat, John Desjarlais, Katrina Bykova. *Xencor Inc., Monrovia, CA, USA*

Background While promoting antigen-dependent T cell responses has proven successful in a subset of patients and in certain tumors, the emergence of resistance and tumor heterogeneity with respect to MHC class I expression suggests additional approaches be considered. Expanding the anti-tumor response to include natural killer (NK) cell activation could broaden the clinical impact against tumors with heterogeneous MHC I status. Our aim was to develop a new format capable of stimulating both the innate and adaptive arms of immunity, to induce direct tumor elimination while also eliciting multicellular responses to promote durable tumor control. NK cells' intrinsic anti-tumor activity and low toxicity profile make them an attractive effector cell population for immunotherapy. We designed tumor antigen targeted NK cell engaging antibodies (NKEs) that synergistically activate NK cells via NKG2D or Nkp46 agonism with simultaneous engagement of Fc gamma receptors via the Fc domain. In addition to stimulating NK cells, NKG2D targeting NKEs also provide co-stimulation to CD8 T cells.

Methods Expanding on Xencor's XmAb protein engineering platform, we developed tumor-targeted NKE molecules agonizing multiple activation pathways including NKG2D or Nkp46, together with FcγRIIIa engagement through the intrinsic Fc domain interaction. Functional activity of these novel NKE molecules was evaluated through assessment of anti-tumor cytotoxicity, production of proinflammatory cytokines, and activation of NK and T cells.

Results Co-engagement of activating receptors, NKG2D or Nkp46, with FcγRIIIa enhanced production of IFNγ and increased cytotoxicity towards tumor cells. These activities were further enhanced in the presence of proinflammatory cytokines, including IL-15. One of the challenges associated with targeting multiple receptors expressed on effector cells is a potential induction of effector cell fratricide. To address this, we tuned NKG2D and FcγR affinities to balance the desired anti-tumor activity with the off-target activity against effector cells. In a parallel approach, we developed NKEs targeting NKG2D ligands MICA/B. MICA/B NKEs activate effector cells by co-targeting a tumor associated antigen and MICA/B on the surface of target cells, facilitating their interaction with NKG2D on effector cells. MICA/B NKEs showed potent anti-tumor activity in vitro and induced production of IFNγ by effector cells.

Conclusions XmAb NKE molecules designed to activate NK and T cells show potent tumor cell lysis and cytokine production activities that are further enhanced in the presence of proinflammatory cytokines. Future directions include evaluation of in vivo activity and establishment of safety profile.

<http://dx.doi.org/10.1136/jitc-2022-SITC2022.1067>

1068

A ROR1 SPECIFIC CD3 BISPECIFIC T-CELL ENGAGER ENGINEERED FOR SOLID TUMORS WITH AN EXPANDED THERAPEUTIC WINDOW

Brian Rabinovich*, Xueyuan Zhou, Jeffrey Takimoto, Paul Song, Evren Alici, Nikhita Khanna. *Fuse Biotherapeutics, Winchester, MA, USA*

Background T cell engagers (TCEs) activate T cells by bridging the CD3 complex to a tumor associated antigen (TAA). TCEs have shown clinical efficacy for hematological malignancies and hold promise for solid-tumors. Dose limiting toxicities, including Cytokine Release Syndrome (CRS) and Tumor Lysis Syndrome (TLS) remain major concerns.

Methods We engineered two ROR1 specific TCEs with properties to increase the size of their therapeutic windows using a unique ROR1 specific VHH from *Camelus bactrianus* (clone 5A1) that contains a non-canonical disulfide-bond between CDR1 and CDR3 and ROR1 specific valency that (1) decouples cytotoxicity from cytokine release and (2) facilitates the discrimination between ROR1 cell surface density on normal versus tumor cells.

Results When 5A1 was paired with an anti-CD3 Fab in two orientations that include a half-life extending Fc domain, we were able to establish a T cell/tumor synapse that resulted in sufficient activation to induce degranulation/tumor-killing at TCE concentrations of 10-30 pM (EC50 ~ 150-200 nM). In contrast, expression of CD69, CD25 and IFN γ , the latter of which is directly upstream of CRS, was not observed until the concentration of TCEs reached ~1 nM (EC50 ~ 5-10 nM). Compared to the non-decoupling control TCE, 5A1 TCEs demonstrated 3.5-4.5 fold greater decoupling. In the context of JeKo1 CD19+/ROR1+ tumor targets, the 5A1 TCEs were 6-7.5 fold better decoupled compared to blinatumomab. We also observed an EC50-cytotoxicity for blinatumomab of below 100 fM, suggesting that the risk of both CRS and TLS are multiple folds higher than for 5A1 TCEs. Compared to the non-decoupling control TCE, the 5A1 TCEs mediated superior cytotoxicity/serial killing at an effector to target ratio (E:T) as low as 1:16, more consistent with solid-tumors. The 5A1 TCEs were also utilized ROR1 specific binding valency to discriminate between cell surface densities of ROR1 typical to tumor cells (>15k molecules/cell) versus normal cells (generally <10,000 molecules/cell). The concentration of TCEs required for maximum IFN γ release and killing of tumor cells registered in the pM range, as opposed to the supraphysiologic nM/uM range that was insufficient to induce more than 25% and 35% of IFN γ release and cytotoxicity, respectively, on cells expressing <10,000 molecules of ROR1.

Conclusions We hypothesize, that our ROR1 TCEs will provide a superior therapeutic index and safety profile associated with reduced risks of CRS and TLS, the capacity to dose higher, avoid continuous infusion and potentially mediate better efficacy in solid tumors.

<http://dx.doi.org/10.1136/jitc-2022-SITC2022.1068>

1069

OX40/CD137 DUAL AGONISM POTENTIATES ANTI-TUMOUR IMMUNITY BY DRIVING FUNCTIONAL REPROGRAMMING AND INSTABILITY OF REGULATORY T (T_{REG}) CELLS

¹Charlotte Imianowski, ¹Paula Kuo, ²Edmund Poon, ²Matthew Lakins, ²Michelle Morrow, ¹Rahul Roychoudhuri*. ¹University of Cambridge, Cambridge, UK; ²F-Star Therapeutics Ltd, Cambridge, UK

Background Immunomodulatory therapies targeting the effector T (T_{eff}) cell inhibitory signalling pathways PD-1/PD-L1 and CTLA-4 induce striking objective clinical responses in patients with certain cancer types, but are ineffective at inducing durable responses in a majority of patients.¹ CD4⁺ regulatory T (T_{reg}) cells, dependent on the transcription factor Foxp3, powerfully suppress T_{eff} cells and prevent immune-mediated rejection of tumours.^{2,3} Low T_{reg} to T_{eff} cell ratios in humans are associated with favourable survival in multiple cancer types and murine models show that ablation of T_{reg} cells results in activation of CD4⁺ or CD8⁺ T_{eff} cells and rejection of tumours. T_{reg} cells therefore represent an attractive target for immunostimulatory therapy.

FS120 is a novel tetravalent bispecific antibody targeting OX40 and CD137 (4-1BB), both tumour necrosis factor (TNF) receptor superfamily members which are expressed on activated and memory T-cell subsets, T_{reg} and NK cells. Pre-clinically, an FS120 mouse surrogate antibody has demonstrated significant anti-tumour immunity in syngeneic tumour models.⁴ FS120 is currently being evaluated in a Phase 1 trial (NCT04648202) which aims to identify a well-tolerated and pharmacologically active dose of FS120 for exploration as monotherapy, and in combination with anti-PD-1.⁵

Methods We elucidate mechanisms of action of OX40/CD137 dual agonist therapy with a mouse-specific FS120 surrogate molecule, using syngeneic tumour models, in conjunction with genetic T_{reg} lineage tracing, high-dimensional flow cytometry, transcriptome analyses and functional studies.

Results FS120 treatment invokes profound anti-tumour immune responses resulting in substantially reduced growth of syngeneic MC38 colorectal adenocarcinoma tumours. FS120 treatment induces two distinct phenomena within tumours: 1) T_{reg} lineage instability, marked by accumulation of 'ex-T_{reg}' cells from T_{reg} progenitors, which gain the ability to express IFN- γ and TNF- α , and 2) T_{reg} functional reprogramming, where Foxp3⁺ T_{reg} cells are induced to produce effector cytokines IFN- γ and TNF- α . The ability of FS120 surrogate to drive T_{reg} instability and functional reprogramming are not shared by anti-PD-1 therapy, suggesting a mode of therapeutic efficacy distinct from anti-PD-1. Accordingly, FS120 treatment synergises with PD-1 checkpoint blockade therapy to induce profound anti-tumour responses.

Conclusions Treatment with FS120 surrogate causes lineage instability and functional reprogramming of T_{reg} cells, resulting in their ability to produce effector cytokines and drive tumour regression. This mode of action is distinct from anti-PD-1 therapy. These findings support a combination therapy approach exploiting the distinct anti-tumour immune activities of FS120 and anti-PD-1 in cancer patients.

REFERENCES

1. Postow MA, Callahan MK, Wolchok JD. Immune Checkpoint Blockade in Cancer Therapy. *Journal of clinical oncology: official journal of the American Society of Clinical Oncology* 2015;**33**:1974–1982. doi:10.1200/JCO.2014.59.4358.
2. Roychoudhuri R, Eil RL, Restifo NP. The interplay of effector and regulatory T cells in cancer. *Current opinion in immunology* 2015;**33**:101–111. doi:10.1016/j.coi.2015.02.003.

3. Quezada SA, Peggs KS, Simpson TR, Allison JP. Shifting the equilibrium in cancer immunoediting: from tumor tolerance to eradication. *Immunological reviews* 2011;**241**:104–118. doi:10.1111/j.1600-065X.2011.01007.x.
4. Gaspar M, Pravin J, Rodrigues L, Uhlenbroich S, Everett KL, Wollerton F, Morrow M, Tuna M, Brewis N. CD137/OX40 Bispecific Antibody Induces Potent Antitumor Activity that Is Dependent on Target Coengagement. *Cancer Immunol Res* 2020;**8**(6):781–793. doi:10.1158/2326-6066.CIR-19-0798
5. Papadopoulos K, Yap TA, Piha-Paul SA, Lorusso P, Hu-Lieskovan S, Shepherd CJ, Marshall S, Holz J-B, Poon E, Grabowska UB, Kayitalire LA. First-in-human phase I study of FS120, an OX40/CD137 tetravalent bispecific antibody, in patients with advanced malignancies. *Annals of Oncology*. doi:10.1016/j.annonc.2021.08.1417

<http://dx.doi.org/10.1136/jitc-2022-SITC2022.1069>

1070

HEXABODY-CD27 ENHANCES T-CELL ACTIVATION, PROLIFERATION, CYTOKINE SECRETION AND CYTOTOXIC ACTIVITY INDEPENDENTLY OF FC GAMMA RECEPTOR-MEDIATED CROSSLINKING

²Kristina Nürmberger, ²Andrea Imlé, ²Aras Tokar, ¹Kristin Strumane, ²Sina Fellermeier-Kopf, ¹Andreea Ioan-Facsinay, ²Alexander Muik, ²Mustafa Diken, ¹Frank Beurskens, ¹Rob De Jong, ²Sebastian Kreiter, ¹David Satijn, ²Friederike Gieseke, ¹Janine Schuurman, ³Tahamtam Ahmadi, ²Oezlem Tuereci, ³Kate Sasser, ¹Esther Breijl, ²Ugur Sahin, ¹Isil Altinas*. ¹Genmab B.V., Utrecht, Netherlands; ²BioNTech SE, Mainz, Germany; ³Genmab US, Inc., Plainsboro, NJ, USA

Background Clustering of CD27 on the plasma membrane of T cells induces T-cell activation, proliferation, and differentiation. Therefore, this costimulatory receptor represents a target for cancer immunotherapy. Multiple monoclonal antibodies (mAbs) targeting CD27 are being explored in the clinic, which require Fc gamma receptor (FcγR)-mediated crosslinking to induce CD27 agonism. HexaBody-CD27 (GEN1053/BNT313) is a novel anti-CD27 mAb with an IgG Fc domain engineered to induce CD27 agonist activity independently of FcγR-bearing cells, which may be scarce in tumors. The Fc domain was further modified to silence Fc-mediated antibody effector functions, with the aim to prevent T-cell depletion. Here we present preclinical characterization of the mechanism of action of HexaBody-CD27.

Methods Target binding characteristics and functional activity of HexaBody-CD27 were analyzed *in vitro* using flow cytometry, cell-based reporter assays and primary human lymphocyte assays. The capacity of HexaBody-CD27 to induce tumor-infiltrating lymphocyte (TIL) proliferation was assessed *ex vivo* using non-small cell lung cancer (NSCLC) tissue resected from patients. HexaBody-CD27 activity *in vivo* was investigated in human CD27 knock-in mice that were immunized with ovalbumin and treated with HexaBody-CD27 by characterizing peripheral blood and splenic T cells using flow cytometry.

Results HexaBody-CD27 exhibited dose-dependent CD27 agonist activity in reporter assays, independent of crosslinking via FcγR-expressing cells. In contrast, agonist activity of benchmark anti-CD27 antibody analogs was dependent on FcγR-mediated crosslinking. HexaBody-CD27 did not functionally engage with FcγRs, and membrane-bound HexaBody-CD27 was unable to bind C1q, confirming functional silencing of the IgG Fc domain. *In vitro*, HexaBody-CD27 enhanced activation, proliferation, and proinflammatory cytokine secretion of TCR-stimulated human CD4⁺ and CD8⁺ T cells as well as CD8⁺ T-cell mediated cytotoxic activity towards cognate antigen-expressing tumor cells. In TIL assays with human NSCLC tumor tissue, HexaBody-CD27 promoted expansion of CD8⁺ T cells. In human CD27 knock-in mice, HexaBody-CD27 enhanced expansion and IFN-γ secretion of antigen-specific CD8⁺ T cells. No decrease in percentages of circulating or splenic T cells was detected *in vivo* after treatment with HexaBody-CD27, whereas treatment with a benchmark anti-CD27 mAb analog resulted in a marked reduction of T cells.

Conclusions HexaBody-CD27 has a functionally inert Fc domain and exhibits FcγR-crosslinking-independent CD27 agonist activity, a unique mechanism of action that distinguishes HexaBody-CD27 from benchmark mAbs targeting CD27. In preclinical studies *in vitro* and *in vivo*, HexaBody-CD27 increased T-cell activation, proliferation, cytokine secretion, and cytotoxic activity. A first-in-human clinical trial has been initiated to evaluate HexaBody-CD27 in patients with advanced solid tumors (NCT05435339).

Ethics Approval The use of resected tumor tissue was approved by BioNTech SE's Ethics Board, approval number 837.309.12 (8410-F).

All mouse studies were performed at Crown Bioscience Inc. in China. Animals were housed and handled in accordance with good animal practice as defined by the regulations of the Association for Assessment and Accreditation of Laboratory Animal Care (AAALAC).

<http://dx.doi.org/10.1136/jitc-2022-SITC2022.1070>

1071

AUTOLOGOUS TUMOR CELL IMMUNOTHERAPEUTIC PLATFORM INDUCES STRESS-CORRELATED IMMUNOGENIC CELL DEATH LEADING TO IMMUNE ACTIVATION WITHIN THE DRAINING LYMPH NODES

¹Christopher Cultrara*, ¹Kenneth Kirby, ¹Essam Elrazaq, ¹Christopher Uhl, ¹Amelia Zellander, ²Lorenzo Galluzzi, ¹Mark Exley, ¹Jenny Zilberberg. ¹Imvax, Philadelphia, PA, USA; ²Weill Cornell, New York, NY, USA

Background Imvax is developing a novel personalized immunotherapeutic platform combining irradiated patient-derived tumor cells and insulin-like growth factor type-1 receptor antisense oligonucleotide (IMV-001) in biodiffusion chambers (BDC; 0.1-micron pores). The combination product IGV-001 was recently evaluated in a newly diagnosed glioblastoma (GBM) phase 1b clinical trial¹. Median overall survival of highest exposure IGV-001-treated ‘Stupp-eligible’² patients (n=10) was 38.2 months compared with 16.2 months in recent standard-of-care-treated patients (P=0.044)¹ [NCT02507583]. Imvax also reported anti-tumor activity of IGV-001 in the GL261-luc GBM murine model³. Here, we show that IGV-001 is associated with activation of stress-related pathways and the release of immunogenic cell death (ICD) molecules capable of stimulating myeloid and T cell subsets with potential anti-tumor activity in the draining lymph nodes (DLN) proximal to the BDCs.

Methods GL261-IGV-001 was formulated and BDCs were incubated at 37°C and 5% CO₂ for 48h. Supernatants were analyzed for extracellular ATP (eATP) and high mobility group box 1 (HMGB1) protein as indicators of ICD, along with flow cytometric analysis of viability, surface calreticulin exposure, and reactive oxygen species (ROS). Stress-related pathways were analyzed by immunoblotting. DLN from mice receiving GL261-IGV-001 and s.c. tumor-challenge were isolated for immunophenotyping.

Results GL261-IGV-001 cells in BDCs showed significant increase in cell death in vitro (>80%, P<0.001) after 48h incubation. eATP was present after cell preparation. HMGB1 was present in BDCs containing dying cells, while surface calreticulin was undetectable. Immunoblot analysis showed induction of the integrated stress response pathway via eif2 α activation and upregulation of the ATF4-CHOP axis. ROS levels were elevated after 24h with subsequent activation of the JNK pathway and downregulation of the anti-apoptotic marker BCL-2. Importantly, similar levels of cell death were observed in in vivo implanted BDCs. Phenotyping analyses showed increased CD45⁺CD11b⁺CD11c⁺MHCII⁺ DCs in the DLN compared to the contralateral control site without BDC (P<0.001). Likewise, the percentage of effector (P<0.001) and effector memory (P<0.0001) in CD4⁺ T cells and effector memory CD8⁺ T cells (P=0.006) were also higher in the DLN, as were CD8⁺Tim3⁺, CD8⁺PD1⁺, and CD4⁺PD1⁺ T cells (P=0.03, P=0.0024, P<0.0001, respectively).

Conclusions Cell death in IGV-001 correlated with the detection of ICD damage-associated molecular patterns (eATP and HMGB1), was characterized by stress-mediated activation of apoptosis pathways, and induced immune responses detected in the DLNs. These data suggest a potential mechanism of action of IGV-001 in GBM via ICD.

REFERENCES

1. Andrews DW, Judy KD, Scott CB, Garcia S, Harshyne LA, Kenyon L, Talekar K, Flanders A, Atsina KB, Kim L, Martinez N, Shi W, Werner-Wasik M, Liu H, Prosniak M, Curtis M, Kean R, Ye DY, Bongiorno E, Sauma S, Exley MA, Pigott K,

Hooper DC. Phase Ib Clinical Trial of IGV-001 for Patients with Newly Diagnosed Glioblastoma. *Clin Cancer Res* 2021;**27**:1912–1922. doi:10.1158/1078-0432.CCR-20-3805.

2. Stupp R, Mason WP, van den Bent MJ, Weller M, Fisher B, Taphoorn MJ, Belanger K, Brandes AA, Marosi C, Bogdahn U, Curschmann J, Janzer RC, Ludwin SK, Gorlia T, Allgeier A, Lacombe D, Cairncross JG, Eisenhauer E, Mirmanoff RO, European Organisation for R, Treatment of Cancer Brain T. Radiotherapy G, National Cancer Institute of Canada Clinical Trials, G. Radiotherapy plus concomitant and adjuvant temozolomide for glioblastoma. *N Engl J Med* 2005;**352**:987–996. doi:10.1056/NEJMoa043330.
3. Zilberberg J, Zellander A, Kirby K, Uhl C, Cultrara C, Scott C, Andrews D, Exley M. 218 Autologous glioblastoma tumor cells and an antisense oligonucleotide against insulin-like growth factor type 1 receptor protect against tumor challenge and generate T cell anti-tumor responses. *Journal for ImmunoTherapy of Cancer* 2021;**9**:A231–A231. doi:10.1136/jitc-2021-SITC2021.218.

<http://dx.doi.org/10.1136/jitc-2022-SITC2022.1071>

1072

INTRAVENOUS BCG ADMINISTRATION IN MICE STIMULATES NK AND T CELL-MEDIATED ANTITUMOR IMMUNITY IN THE LUNG AND OVERCOMES RESISTANCE TO IMMUNOTHERAPY

<http://dx.doi.org/10.1136/jitc-2022-SITC2022.1072>

Eduardo Moreo Lapieza*, Santiago Uranga, Carlos Martín, Nacho Aguiló. *University of Zaragoza, Zaragoza, Spain*

Background Intravesical administration of the tuberculosis vaccine Bacillus Calmette-Guérin (BCG) was the first immunotherapy to be approved by the FDA and is still nowadays the treatment of choice for a subset of non-muscle invasive bladder cancer patients. Intravenous (IV) administration of BCG has been recently reported to be highly effective at preventing tuberculosis infection in macaques by inducing strong T cell responses in the lung¹, as well as to alter myelopoiesis, generating "trained" macrophages which confer protection against tuberculosis infection in the lung². Therefore, in this work we set out to characterize the therapeutic application of IV BCG in mouse models of lung cancer.

Methods We used mouse models of tumors growing in the lung based on IV inoculation of B16-F10 melanoma and LLC lung carcinoma tumor cells to study the therapeutic effect of IV BCG. We performed immune cell profiling by flow cytometry to study the mechanism of action, as well as functional assays such as NK and T cell cytotoxicity assays.

Results First, we observed that therapeutic IV BCG administration extended mice survival in models of B16-F10 lung metastasis and orthotopic LLC lung tumors (figure 1). Immune cell depletion studies revealed that NK cells and CD4⁺ and CD8⁺ T cells were required for IV BCG efficacy against lung tumors (figure 2). IV BCG induced a tumor-specific CD8⁺ T cell response in the lung in a process relying on type 1 conventional dendritic cells (cDC1s). Mechanistically, BCG stimulated lung NK cells (figure 3A), which participated in the recruitment of cDC1s to the tumor (figure 3B) and initiated tumor-specific T cell responses (figure 3C) by favoring the loading of cDC1s with tumor-associated material by killing tumor cells in a perforin-dependent manner (figure 4). Remarkably, IV BCG reduced tumor growth in B16-F10 and LLC lung tumors in which MHC-I expression was ablated (figure 5). Finally, we observed that IV BCG upregulated PD-L1 in multiple immune cells in the tumor microenvironment (TME), suggesting the generation of an inflamed TME. Combination of IV BCG and antiPD-L1 antibodies further increased mouse survival in mouse models of lung tumors, which were otherwise resistant to checkpoint blockade as a monotherapy (figure 6).

Conclusions Here we describe a therapy based on IV BCG administration which enabled antitumor immunity in the lung by coordinating multiple immune cell populations, including both T and NK cells as well as *Batf3*-dependent cDC1s. Remarkably, IV BCG sensitized lung tumors to antiPD-L1 checkpoint blockade therapy.

REFERENCES

1. Darrah PA, et al. Prevention of tuberculosis in macaques after intravenous BCG immunization. *Nature* 2020;**577**:95–102.
2. Kaufmann E, et al. BCG Educates Hematopoietic Stem Cells to Generate Protective Innate Immunity against Tuberculosis. *Cell* 2018;**172**:176–190.e19.

Ethics Approval Experimental work was conducted in agreement with European and national directives for protection of experimental animals and experimental procedures were approved by the Ethics Committee for Animal Experiments of University of Zaragoza (PI46/18, PI33/15 PI50/14).

1073 **COSTIMULATORY CD28 TRISPECIFIC ANTIBODIES
TARGETING PDL1 AND PDL2 ENHANCE T CELL
ACTIVATION IN SOLID TUMORS**

Veronica Zeng*, Juan Diaz, Jing Qi, Thuy Truong, Matthew Dragovich, Rumana Rashid, Christine Bonzon, Panida Lertkiatmongkol, Ruschelle Love, Michael Hackett, Kendra Avery, Norman Barlow, John Desjarlais, Michael Hedvat, Gregory Moore. *Xencor, Inc., Monrovia, CA, USA*

Background T cells in the tumor micro-environment require TCR/MHC engagement and co-stimulatory receptor engagement to achieve optimal activation. Tumor cells lack expression of CD28 ligands, so we hypothesized that activation of CD28 signaling at the T cell/tumor cell interface could enhance anti-tumor activity. We designed PDL1 x PDL2 x CD28 trispecific antibodies that conditionally costimulate CD28 only in the presence of PDL1 or PDL2 expression, and TCR engagement. As PD1 signaling has been shown to directly inhibit CD28 costimulation, this novel bispecific modality has potential to promote CD28 costimulation while simultaneously preventing the suppression of the same signal. Furthermore, since CD3 bispecific T cells engagers are known to indirectly promote PDL1 expression, PDL1 x PDL2 x CD28 trispecific antibodies can potentially be applied in combination to CD3-bispecific T cell engagers to enhance their activity.

Methods We developed a CD28 antibody that is agonistic only under the context of TCR engagement. We paired this CD28 binding domain with PDL1 and PDL2 Fab binding domains that share a common light chain to generate PDL1 x PDL2 x CD28 trispecifics monovalent for each of the three antigens. We optimized the affinity for each of the antigens for potent blockade of PDL1 and PDL2 and enable CD28 costimulation across a range of PDL1 and PDL2 cell surface densities. Cell based assays with different TCR engagement modalities were utilized to describe the function of trispecifics including, CD3-stimulated T cells cocultured with cancer cell lines, CMV+ T cells recognizing cancer cells expressing pp65-derived NLV peptide, and Mixed Lymphocyte Reactions. Cell based assays measured IL2 and IFN γ release, T cell proliferation and cancer-cell death as readouts for activity.

Results PDL1 x PDL2 x CD28 trispecifics block PDL1 and PDL2 binding to PD1 in both solid phase and cell-based assays. PDL1 and PDL2 blockade led to enhanced cytokine secretion from human mixed lymphocyte reactions. Target cell expression of either PDL1 or PDL2 was shown to be sufficient to promote CD28 co-stimulation leading to acute IL2 release of cocultures of CD3-stimulated PBMC with cancer cell lines. In a more physiologically relevant model of TCR engagement, PDL1 x PDL2 x CD28 trispecifics enhanced T cell activation in a CMV-recall assay. When in combination with CD3-targeted T cell engagers, PDL1 x PDL2 x CD28 trispecifics enhanced T cell proliferation and TDCC activity.

Conclusions Data warrant further development of PDL1 x PDL2 x CD28 trispecifics for treatment of solid tumors.

<http://dx.doi.org/10.1136/jitc-2022-SITC2022.1073>

1074

A NOVEL FULLY HUMAN CD28 ANTIBODY THAT CROSS-REACTS WITH CTLA-4 AND MOUSE CD28 FOR POTENTIAL APPLICATIONS IN CANCER IMMUNOTHERAPY

¹Abdullah Elsayed*, ¹Frederik Peissert, ¹Louis Plüss, ²Franziska Ulrich, ¹Emanuele Puca, ¹Roberto De Luca, ²Cornelia Halin, ³Dario Neri. ¹Philochem AG, Otelfingen, Switzerland; ²Swiss Federal Institute of Technology, Zurich, Switzerland; ³Philogen Spa, Otelfingen, Switzerland

Background T cell activation is initiated through engaging T cell receptor (TCR)/CD3 complex upon recognizing antigenic peptides presented by major histocompatibility complex (pMHC).^{1,2} However, TCR/CD3 complex alone is not sufficient for full T cell activation. In fact, the absence of an additional signal induces T cell exhaustion and thus impaired activation of T cells.³ CD28 is a crucial co-stimulatory receptor that enhances T cell proliferation, survival and production of key cytokines such as IL-2, IFN- γ , and TNF- α .⁴⁻⁷ Despite the potential key role of CD28 in cancer immunotherapy, there have been safety concerns following the TeGenero disaster in 2006.⁸ Here we describe the generation of a fully human anti-CD28 antibody named “VE19ZH”. VE19ZH features a unique combination of desirable properties in comparison to other currently available mAbs such as TGN1412.

Methods We isolated a new fully human antibody (VE19ZH) against human CD28 by phage display technology. Binding was validated by flow cytometry on primary human T cells. The co-stimulatory effect in combination with anti-CD3 (OKT3) was assessed *in vitro* by proliferation of human PBMCs and cytokine release. To rule out the undesirable super-agonistic effect observed by TGN1412, VE19ZH was tested for its capability to activate human PBMCs in the absence of TCR/CD3 signaling. Cross-reactivity against CTLA-4 and mouse CD28 were evaluated by ELISA and flow cytometry. Finally, the binding epitope of VE19ZH was revealed using PepSpot™ technology.

Results VE19ZH is a fully human antibody that binds selectively to both human and murine CD28. VE19ZH IgG₄ exhibited a strong and significant co-stimulatory effect on human PBMCs when combined with anti-human CD3 (OKT3). Unlike TGN1412, VE19ZH did not activate T cells without TCR/CD3 signaling. In addition, VE19ZH was shown to bind to CTLA-4. VE19ZH binds to an epitope similar to the natural ligand (CD80/CD86) as revealed by PepSpot™ technology. *In vitro* killing activity was validated using BiTE formats and showed synergism with low concentrations of CD3 bispecifics.

Conclusions VE19ZH is a promising module for cancer immunotherapy with unique properties: (i) Fully human mAb for minimal immunogenicity (ii) Potent co-stimulator for full T cell activation (iii) Conventional agonist of CD28 and not super-agonistic like TGN1412 (iv) cross reacts with mouse CD28 for better assessment in immunocompetent mouse models (v) Binds to human CTLA-4 for potential checkpoint inhibition. The potential of VE19ZH to boost T cell response via CD28 activation and CTLA-4 blockade is currently being investigated *in vitro* and *in vivo*.

REFERENCES

1. Davis MM, Bjorkman PJ. T-cell antigen receptor genes and T-cell recognition. *Nature* 1988;**334**(6181):395–402.
2. La Gruta NL, *et al*, Understanding the drivers of MHC restriction of T cell receptors. *Nat Rev Immunol* 2018;**18**(7):467–478.

3. Mueller DL, Jenkins MK, Schwartz RH. Clonal expansion versus functional clonal inactivation: a costimulatory signalling pathway determines the outcome of T cell antigen receptor occupancy. *Annu Rev Immunol*, 1989;**7**:445–80.
4. Jenkins MK, *et al*. CD28 delivers a costimulatory signal involved in antigen-specific IL-2 production by human T cells. *J Immunol* 1991;**147**(8):2461–6.
5. June CH, *et al*. T-cell proliferation involving the CD28 pathway is associated with cyclosporine-resistant interleukin 2 gene expression. *Mol Cell Biol* 1987;**7**(12):4472–81.
6. Martin PJ, *et al*. A 44 kilodalton cell surface homodimer regulates interleukin 2 production by activated human T lymphocytes. *J Immunol* 1986;**136**(9):3282
7. Weiss A, Manger B, Imboden J. Synergy between the T3/antigen receptor complex and Tp44 in the activation of human T cells. *J Immunol* 1986;**137**(3):819–25.
8. Suntharalingam G, *et al*. Cytokine storm in a phase 1 trial of the anti-CD28 monoclonal antibody TGN1412. *N Engl J Med* 2006;**355**(10):1018–28.

<http://dx.doi.org/10.1136/jitc-2022-SITC2022.1074>

1075

HBM1020 IS A FULLY HUMAN NOVEL ANTI-B7H7 ANTIBODY WITH EXCELLENT PRECLINICAL EFFICACY AND SAFETY PROFILE

Xiaodong Wu*, Yongqiang Wang, Jonna Liu, Xiaocheng Lv, Fei Chen, Izzie Wang, Jiujiao Zhao, Yiping Rong. *Harbour BiMed Co., Ltd, Shanghai, China*

Background Immunotherapeutic targeting immune checkpoints such as programmed death-1 receptor (PD-1)/PD1 ligand (PD-L1) and cytotoxic T-lymphocyte antigen-4 (CTLA4) offer effective treatment alternatives to traditional cancer therapies. However, a considerable proportion of patients remains unresponsive to treatment indicating that a more complex immune inhibitory tumor microenvironment is involved. B7H7 is a novel B7 family member and reported to be highly expressed on a variety of human cancers such as colon, kidney, bladder, lung cancers; and is associated with metastatic disease and poor survival. B7H7 can inhibit T cell and NK cell activation and its co-inhibitory function makes it a new checkpoint and candidate for cancer immunotherapy other than PD-L1 or other immune checkpoints.

Methods Fully human Anti-B7H7 antibodies were generated from H2L2 Harbour Mice® transgenic platform. The binding and blocking activities were tested by fluorescence-activated cell sorting (FACS) method. *In vitro* function of the antibodies was tested for their abilities to activate T cell and NK cell. *In vivo* efficacy was tested on multiple NOD-Prkdc^{em26Cd52}Il2r-g^{em26Cd22}/NjuCrI (NCG) mouse models engrafted human PBMC tumor. The dose range-finding (DRF) tox study was evaluated on a non-human primates (NHP) 4-week repeat-dose toxicity study.

Results HBM1020, a fully human anti-B7H7 antibody, bound specifically to cell lines that over-express either human B7H7 or cynomolgus monkey B7H7, as well as human tumor cell lines that express endogenous B7H7, with high selectivity against other B7 family members. HBM1020 blocked the interaction between B7H7 and its receptors and potently promoted T cell activation and NK cell cytotoxicity *in vitro*. Furthermore, HBM1020 showed potent anti-tumor activity in multiple murine tumor models. In DRF 4-week repeat-dose NHP toxicity study (20, 60, 147 mg/kg), HBM1020 was well tolerated up to 147 mg/kg dosed weekly (total 5 doses) with no notable test article-related adverse finding but increased anti-KLH IgG and IgM after KLH immunization at ≥ 60 mg/kg.

Conclusions HBM1020 is a fully human novel anti-B7H7 antibody with potent activity on T cell activation, NK cell cytotoxicity, excellent *in vivo* anti-tumor efficacy, and excellent safety profile. HBM1020 may present a promising novel anti-tumor agent as monotherapy and/or combination therapy with currently established immune-oncology agents.

Ethics Approval The anti-tumor efficacy studies in mice were approved by the internal ethics board of the respective contract research organization (CRO). The dose-range finding toxicity studies in non-human primates were approved by Ethics Board of an appropriate contract research organizations (CROs).

<http://dx.doi.org/10.1136/jitc-2022-SITC2022.1075>

1076

ANCHORED IMMUNOTHERAPY WITH INTRATUMORALLY ADMINISTERED ALUMINUM HYDROXIDE-TETHERED IL-12 INDUCES POTENT ANTI-TUMOR IMMUNE RESPONSE

¹Sailaja Battula, ¹Gregory Papastoitsis, ¹Howard Kaufman, ²K Wittrup, ¹Michael Schmidt*. ¹Ankyra Therapeutics, Lexington, MA, USA; ²Massachusetts Institute of Technology, Cambridge, MA, USA

2. Wittrup KD, Kaufman HL, Schmidt MM, Irvine DJ. Intratumorally anchored cytokine therapy. *Expert Opin Drug Del* 2002;1–8.

<http://dx.doi.org/10.1136/jitc-2022-SITC2022.1076>

Background Interleukin-12 (IL-12) is a potent cytokine that can promote innate and adaptive anti-cancer immunity, but its clinical development has been limited by toxicity when delivered systemically.¹ Intratumoral (IT) administration can expand the therapeutic window of IL-12 and other cytokines but is in turn limited by rapid clearance from the tumor, thereby reducing efficacy, necessitating frequent administration, and increasing systemic accumulation. We recently described an approach called ‘anchored immunotherapy’² in which an engineered IL-12 variant is complexed with the vaccine adjuvant aluminum hydroxide (alum) to form a locally retained cytokine depot that induces potent therapeutic activity in syngeneic murine tumors after only 1 or 2 IT injections. Here, we provide additional characterization of the retention kinetics and mechanism of action of alum-complexed IL-12.

Methods Human or murine IL-12 was genetically fused to a phosphorylated alum-binding peptide (IL-12-ABP) and mixed with aluminum hydroxide to form the therapeutic complexes ANK-101 (human) or mANK-101 (mouse). Local retention and biodistribution of labeled mANK-101 after IT administration in syngeneic murine tumors was measured by IVIS and SPECT imaging. Intratumoral immune changes were detected by flow cytometry, IHC, Nanostring, and scRNA-seq to characterize mANK-101’s mechanism of action. Safety of ANK-101 was assessed in cynomolgus macaques after subcutaneous injection. Statistical comparisons between groups were performed using one-way ANOVA.

Results ANK-101 induces IFN γ expression from human PBMCs, purified T-cells, and NK-cells with similar potency as native IL-12. Following IT administration in murine tumor models, mANK-101 complexes are retained locally for multiple weeks while unanchored IL-12-ABP protein is cleared within hours as detected by IVIS or SPECT imaging. This extended retention leads to prolonged expression of IFN γ and other pro-inflammatory cytokine and chemokines for >1 week. We hypothesized that this would result in improved CD8+ T cell recruitment, which was tested by intratumoral immunophenotyping by IHC and flow cytometry. We found that mANK-101 treatment led to robust CD8 T-cell infiltration and an increased CD8/Treg ratio that correlated with anti-tumor efficacy. Gene expression and scRNA-seq analyses suggested a profound remodeling of the tumor microenvironment after mANK-101 treatment with T-cell and NK-cell activation, shifts to pro-inflammatory myeloid cell phenotypes, and increased markers of antigen presentation and co-stimulation. Subcutaneous administration of ANK-101 in cynomolgus macaques was well tolerated.

Conclusions Anti-tumor activity of locally retained IL-12/alum is mediated by recruitment and activation of lymphocytes and myeloid immune cells. Anchored immunotherapy may represent a general approach to improve the therapeutic potential of immuno-oncology agents.

REFERENCES

1. Lasek W, Zagodzdzon R, Jakobisiak M. Interleukin 12: still a promising candidate for tumor immunotherapy?. *Cancer Immunol Immunother* 2014;**63**:419–435.

1077

DEVELOPMENT OF A MOLECULAR TARGETED CYTOKINE THAT SPECIFICALLY EXPANDS VGAMMA9VDELTA2 T CELLS AND POTENTIATES ANTI-TUMOR ACTIVITY

Bryan Becklund*, Kaitlyn Robinson, Kyle Jones, Angelica Sanabria, Elisebeth Torretti, Andrew Eckles, Abraham Hussain, Sae Jeong Ahn, Rajay Pandit, Florian Sulzmaier, John Timmer, Brendan Eckelman. *Inhibrx, La Jolla, CA, USA*

Background Vgamma9Vdelta2 (Vg9Vd2) T cells are an ideal target for cancer immunotherapy due to their ability to recognize stress-related ligands from transformed cells and eliminate them with broad, potent cytotoxicity.¹ One limitation restraining the ability of Vg9Vd2 T cells from eliminating tumors is that they are a rare population in peripheral blood. Efforts to expand Vg9Vd2 T cells *in vivo* have typically relied on treatment with bisphosphonates and low-dose interleukin-2 (IL-2). This combination is limited by rapid clearance of the molecules, competition for IL-2 and dose-limiting toxicities.² Using our molecular targeted cytokine (MTC) platform, we developed an alternative strategy to specifically expand Vg9Vd2 T cells utilizing a detuned IL-2 variant targeted to the Vg9Vd2 T cell receptor.

Methods Human IL-2 was engineered to eliminate CD25 binding and have reduced affinity for CD122.³ A high-affinity single-domain antibody specific to the Vg9-subunit of the Vg9Vd2 T cell receptor targets this cytokine to cells expressing the target antigen and thereby restricts IL-2 activity to Vg9Vd2 T cells. The ability of this Vg9Vd2-targeted MTC (anti-Vg9xIL2-X) to selectively bind and activate Vg9Vd2 T cells was assessed *in vitro* utilizing human PBMCs from healthy donors and dissociated tumor cells (DTCs) from various indications. IL-2 signaling and cell proliferation were analyzed by flow cytometry. Cancer-specific target cell killing was determined by coculturing Vg9Vd2 T cells with labeled tumor cells or healthy B cells. Expansion of Vg9Vd2 T cells *in vivo* was analyzed in NSG-B2M KO mice engrafted with human PMBCs.

Results Anti-Vg9xIL2-X bound Vg9Vd2 T cells and activated STAT5 signaling in a target-dependent manner. Treatment with anti-Vg9xIL2-X led to a dramatic increase in proliferation and accumulation of Vg9Vd2 T cells in healthy human PBMCs and DTCs. Anti-Vg9xIL2-X-driven expansion of Vg9Vd2 T cells increased expression of cytotoxic effector molecules, including IFN γ and granzyme-B, leading to potent *in vitro* anti-tumor activity across numerous cancer cell types. The killing activity was selective for transformed cells as healthy cells were largely spared. Treatment with anti-Vg9xIL2-X also improved antibody dependent target cell killing by Vg9Vd2 T cells. Finally, dosing of human PBMC-engrafted mice with anti-Vg9xIL2-X was well-tolerated and resulted in an increased prevalence and specific expansion of Vg9Vd2 T cells.

Conclusions Utilizing our MTC platform, we have developed a targeted cytokine that specifically activates and expands Vg9Vd2 T cells. By restraining IL-2 activity to this subset, we hope to limit IL-2-mediated toxicity and enhance Vg9Vd2 T cell anti-tumor activity across numerous cancer types.

REFERENCES

1. Yazdanifar M, Barbarito G, Bertaina A, Airoidi I. $\gamma\delta$ T Cells: The Ideal Tool for Cancer Immunotherapy. *Cells*. 2020;**9**:1305.
2. Hoeres T, Smetak M, Pretscher D, Wilhelm M. Improving the Efficiency of V γ 9V δ 2 T-Cell Immunotherapy in Cancer. *Front Immunol* 2018;**9**:800.
3. Sulzmaier F, Kinkead H, Polovina A, Kern N, Sanabria A, Macedo C, et al. 722 INBRX-121 is an Nkp46-targeted detuned IL-2 with antitumor activity as a monotherapy or in combination with multiple cancer immunotherapy modalities. *J Immunother Cancer*. 2021;**9**:A751–A751.

Ethics Approval All animal studies were conducted in accordance with AAALAC regulations and were approved by the IACUC for Explora BioLabs (#SP17-010-013).

<http://dx.doi.org/10.1136/jitc-2022-SITC2022.1077>

1078

CONDITIONALLY ACTIVATABLE INTERFERON-ALPHA 2B IMPROVES TOLERABILITY AND EXHIBITS PREFERENTIAL ACTIVITY IN TUMORS

Alexey Berezhnoy*, Hsin Wang, Nicole Lapuyade, Na Cai, Carol LePage, Michael Winter, Michael Krimm, Kenneth Wong, Robert Dunn II, Sean McAlister, Leila Boustany, Madan Paidhungat, Marcia Belvin, Erwan Le Scolan, Dylan Daniel. *CytoX Therapeutics, South San Francisco, CA, USA*

Background Despite its potential, the toxicity of interferon alpha has limited its clinical use. CytomX proprietary Probody® Therapeutics (Pb-Tx) technology allowed us to create a conditionally active IFN- α 2b (Pb-IFN- α 2b) with minimal activity in its prodrug form. The prodrug is activated in the tumor microenvironment (TME), leading to preferential activity in the TME but not in healthy tissues. Pb-IFN- α 2b demonstrated a substantially enhanced tolerability profile compared to standard IFN therapy without compromising its antitumor effects.

Methods The Pb-Tx platform technology attenuates activity of a molecule by blocking its active regions through affinity or steric interference. Such blockade, termed masking, is reversed upon proteolytic cleavage of a linker between the molecule and the mask by tumor associated proteases.

Results Pb-IFN- α 2b demonstrated considerable reduction (1000-fold or more) of interferon signaling in vitro and significantly reduced immune cell activation. Exposure to viable tumor tissues or tumor-associated proteases in vitro fully restored its bioactivity, including the ability of Pb-IFN to stimulate tumor-infiltrating immune cells.

Antitumor activity of the Pb-IFN- α 2b in xenograft studies is equal to or greater than Peg-IFN- α 2b. In syngeneic mouse tumor models, Pb-IFN demonstrated significant antitumor activity that was further enhanced by PD-(L)1 blockade. Activation of lymphocytes by the molecule was observed in tumors but not in secondary lymphoid organs.

Toxicology studies performed in hamsters demonstrated enhanced tolerability of the molecule compared to its unmasked control. In addition, Pb-IFN- α 2b suppressed growth of hamster melanoma tumor model RPMI1846 at dose levels that were above the tolerated dose of the unmasked control.

Biomarkers of IFN signaling were greatly attenuated in non-human primates compared to the unmasked control. In cynomolgus monkey, Pb-IFN- α 2b demonstrated linear pharmacokinetics, extended half-life, and was well tolerated at weekly doses up to 60 mg/kg.

Conclusions Pb-IFN- α 2b shows improved tolerability and antitumor activity in preclinical studies compared to traditional IFN treatment. These data support Probody cytokine therapeutics as a promising addition to current immunotherapy regimens, potentially expanding their benefits to patients with typically unresponsive tumors.

Ethics Approval All animal experiments were reviewed and approved by CytomX's Institutional Animal Care and Use Committee (IACUC Protocol AP303).

<http://dx.doi.org/10.1136/jitc-2022-SITC2022.1078>

1079

LAG3-TARGETED IL15/IL15R α -FC (LAG3 X IL15) FUSION PROTEINS FOR PREFERENTIAL TIL EXPANSION VIA CIS DELIVERY OF IL15 TO LAG3+ CELLS

Matthew Bernett*, Suzanne Schubert, Michael Hackett, Lukasz Ochyl, Lizett Scott, Christine Bonzon, Rumana Rashid, Kendra Avery, Nicole Rodriguez, Irene Leung, Norman Barlow, Rena Bahjat, Umesh Muchhal, John Desjarlais. *Xencor, Inc., Monrovia, CA, USA*

Background Therapeutic approaches utilizing IL2 or IL15 have suffered from low tolerability, fast clearance, and limited therapeutic window due to extensive activity on peripheral T and NK cells. Conversely, selective targeting of tumor-reactive lymphocytes (TIL) may improve tolerability and anti-tumor activity while simultaneously improving drug PK. We hypothesized that we could selectively target tumor-reactive TILs by combining a reduced potency IL15/IL15R α heterocomplex with an immune checkpoint(CP)-targeting arm to bias binding and activation to CP-positive TILs, potentially improving therapeutic index. Lymphocyte activation gene 3 (LAG3) was chosen as the CP targeting-arm due to its frequent co-expression with PD1, bias to CD8+ T cells, ability to easily combine with anti-PD1 agents, and recent promising results with anti-LAG3 agents in the clinic.

Methods First, potency-reduced IL15/IL15R α were created by engineering amino acid substitutions in IL15 – at the IL2R β / γ c interface – that reduced in vitro potency by at least 1000-fold. We then designed LAG3 x IL15 fusion proteins containing single-chain IL15/IL15R α and LAG3-targeting arms attached to a heterodimeric-Fc region, relying on targeting avidity (in cis) to recover potency on LAG3+ cells. In vitro proliferation of lymphocytes in human PBMCs, stimulated with sub-optimal concentrations of anti-CD3 to induce LAG3 expression, was monitored by CFSE dilution or by counting Ki67+ cells after incubation with LAG3 x IL15. In vivo activity was evaluated using a humanized mouse tumor model. Lead LAG3 x IL15 were evaluated in non-human primates (NHP).

Results LAG3 x IL15 showed >500-fold selectivity compared to a non-targeted IL15 in an in vitro proliferation assay of lymphocytes stimulated for induced LAG3 expression. In vitro potency was greatest on effector memory CD8 T cells. LAG3 x IL15 were 3-fold more potent on CD8 T cells compared to CD4 T cells and had very weak activity on NK cells, consistent with minimal LAG3 expression on this population. In mouse tumor models, LAG3 x IL15 had single-agent anti-tumor activity and promoted significantly increased numbers of T cells. Moreover, LAG3 x IL15 combined productively with anti-PD1 to promote additional anti-tumor activity and T cell expansion. In NHP, LAG3 x IL15 has superior PK compared to native IL15-Fc and showed selective targeting of LAG3+ peripheral T cells.

Conclusions LAG3 x IL15 shows a promising profile of selective delivery to LAG3+ cells with minimal peripheral activity and may help to preferentially expand LAG3+ TIL in patients with cancer, while potentially avoiding systemic toxicity due to off-target activation and expansion of peripheral lymphocytes.

<http://dx.doi.org/10.1136/jitc-2022-SITC2022.1079>

1080

USING SITE-SPECIFIC CHEMICAL CONJUGATION TO GENERATE SUPERIOR HALF-LIFE EXTENDED OR PD-1-TARGETED FORMATS OF A POTENT IL-18 VARIANT RESISTANT TO IL-18 BINDING PROTEIN

Jean Carralot*, Camille Delon, Rubén Alvarez Sanchez, Roy Meoded, Philipp Moosman, Kea Martin, Arnaud Goepfert, Andrew Chi, Vijaya Pattabiraman, Bertolt Kreft. *Bright Peak Therapeutics, Basel, Switzerland*

Background Interleukin-18 (IL-18) is a pro-inflammatory cytokine able to trigger both innate as well as adaptive immune responses. IL-18 is a potent amplifier of IFN γ signaling which induces pleiotropic Th1 responses, making it an attractive cytokine for cancer immunotherapy. However, the clinical efficacy of wild-type (wt) IL-18 was limited, potentially due to the upregulation IL-18 binding protein (IL-18BP). IL-18BP is a secreted IFN γ -induced antagonist that binds IL-18 with high affinity, prevents its interaction with the IL-18 receptor, and neutralizes IL-18 activity. Hence, we aimed to generate a potent IL-18BP-resistant IL-18 "payload" that can be turned into optimal therapeutic formats with superior pharmacologic properties or leverage synergistic mechanisms of action (MOA).

Methods By introducing of a minimal set of mutations we generated an optimized human IL-18 that, compared to wt-IL-18, shows enhanced potency and significant resistance to IL-18BP. We further engineered the enhanced IL-18 variant to create a versatile "payload" that can be chemically conjugated in a site-specific manner. Conjugation to polyethylene glycol (PEG) resulted in a half-life extended agent, while conjugation to an anti-PD-1 antibody yielded a PD1-IL18 immunocytokine (IC) allowing exploitation of synergistic MOAs. We then characterized the pharmacologic and anti-tumor properties of these two therapeutic formats *in vitro* and *in vivo*.

Results Compared to wt-IL-18, the conjugatable payload is 300-fold more potent and >600-fold less sensitive to IL-18BP inhibition. Conjugation to a 30 kDa PEG yields a molecule with significantly improved PK properties in mice that is able to strongly activate CD8 $^{+}$ T and NK cells and to potently trigger the release of pro-inflammatory cytokines. PEGylated IL-18 showed strong anti-tumor efficacy which was enhanced in combination with an anti-PD-1 antibody. For the PD1-IL18 IC, the basic properties of the anti-PD-1 antibody and the cytokine payload were largely preserved after chemical conjugation. The PD1-IL18 IC exhibited potent antitumor activity *in vivo* inducing complete responses in the large majority of animals.

Conclusions We generated a potent and IL-18BP-resistant IL-18 payload that can be chemically conjugated to distinct chemical or biological entities in a site-specific manner to generate unique IL-18-based therapeutic formats with desirable pharmacological properties. Both the PEGylated half-life extended IL-18 and the PD1-IL18 IC are well tolerated, show encouraging efficacy in pre-clinical models, and have the potential to be next-generation enhanced IL-18 therapeutics.

<http://dx.doi.org/10.1136/jitc-2022-SITC2022.1080>

1081

EXENOKINE-2: A HALF-LIFE EXTENDED NO- α -IL-2 WITH IMPROVED PRECLINICAL PHARMACOLOGICAL PROPERTIES SUPPORTS FIRST-IN-HUMAN CLINICAL DEVELOPMENT

¹Lili Cheng*, ¹Fan Ye, ¹Sandra Chen, ¹Jianing Huang, ¹Jenny Jiang, ¹Henry He, ¹Shirley Shi, ¹Mingxing Yang, ¹Qiang Fu, ¹Ark Xia, ¹Yudan Hong, ¹Wang Xin, ¹Karen Yuan, ²Hongchuan Liu, ²Hui Feng, ¹Eugene Liu, ¹Ziyang Zhong. ¹Anwita Biosciences, San Carlos, CA, USA; ²Junshi Pharma, Shanghai, China

Background IL-2 is a critical cytokine driving immune mediated killing of tumor cells by stimulating both the innate and adaptive immune cells. High-dose IL-2 (aldesleukin) has been approved for the treatment of metastatic melanoma and metastatic renal cell carcinoma, however, the practical use of aldesleukin in the clinic is limited. The short half-life of aldesleukin necessitates a frequent and burdensome treatment schedule for patients. In addition, binding to IL-2R α on endothelial cells and type 2 innate lymphoid cells is thought to induce severe adverse events associated with vascular leak syndrome. Furthermore, the efficacy of aldesleukin is compromised due to strong activation of immunosuppressive regulatory T cells (Treg) expressing the high-affinity IL-2R $\alpha\beta\gamma$. To overcome the major limitations of wild-type (WT) IL-2, Exenokine-2 (Exn-2), a fusion protein comprised of a no- α -IL-2 linked to a humanized anti-human serum albumin (HSA) single domain antibody (sdAb), was designed using Anwita's discovery platform technology.

Methods Binding affinities were determined using Bio-Layer Interferometry. *In vitro* potency was assessed using a human primary immune cell-based pSTAT5 assay. *In vivo* efficacies were assessed in MC38 and B16F10 syngeneic as well as N87 and Raji xenograft mouse models.

Results The no- α -IL-2 in Exn-2 is a chimera between IL-2 and IL-15 cytokines. The lack of binding with IL-2R α resulted in limited activation of Treg while retaining the high potency on NK cells and CD8⁺ T cells. The addition of an anti-HSA sdAb in Exn-2 resulted in prolonged systemic exposure with a 30-fold longer half-life in mice as compared to WT IL-2. In syngeneic mouse tumor models, Exn-2 showed strong dose-dependent antitumor efficacy as a single agent with up to 95% reduction in tumor growth, as well as an enhanced efficacy with a high rate up to 66% of complete response when combined with an anti-PD-1 monoclonal antibody. In xenograft models of gastric cancer and lymphoma, Exn-2 significantly potentiated the antitumor activity of Trastuzumab and Rituximab, respectively, demonstrating clinical potential as a combination therapy with ADCC-competent antibodies. In cynomolgus monkeys, Exn-2 was well tolerated and induced robust and sustained expansions of lymphocytes and CD8⁺ T cells while showing negligible effects on eosinophils and Tregs.

Conclusions Collectively, *in vivo* efficacies from mouse tumor models as well as the desired pharmacodynamic effects and safety profile observed in cynomolgus monkeys support the first-in-human clinical development of Exn-2. IND-enabling studies for Exn-2 is nearing completion, with GMP lot production completed for the Phase 1 study.

Ethics Approval The protocol of animal studies has been reviewed and approved by IACUC

<http://dx.doi.org/10.1136/jitc-2022-SITC2022.1081>

1082

IL-27 EXPRESSED IN THE TUMOR MICROENVIRONMENT IS CORRELATED WITH PD-L1 LEVELS AND CAN INDUCE PD-L1 EXPRESSION ON IMMUNE AND TUMOR CELLS

Karin Golan*, Ricard Masia, Yu Yang, Yue Ren, Kerry White, Benjamin Lee, Vito Palombella, Jonathan Hill. *Surface Oncology, Cambridge, MA, USA*

Background Interleukin (IL)-27 is a heterodimeric cytokine expressed by myeloid cells that is known to reduce the intensity and duration of immune responses. IL-27 signaling via IL-27RA receptor augments the expression of co-inhibitory molecules (PD-L1, LAG-3, TIM-3, and TIGIT) on immune cells and reduces proinflammatory cytokines in the tumor microenvironment. Blocking IL-27 activity by SRF388, a first-in-class monoclonal antibody, enhances immune function and demonstrates monotherapy activity in patients with cancer (NCT04374877). This study further characterizes the expression of IL-27 in primary solid tumors.

Methods Gene expression profiles from published datasets were analyzed to identify *IL27* and *IL27RA* transcripts. Immunohistochemistry (IHC) and flow cytometry were used to quantify IL-27, PD-L1, and IL-27RA expression in primary tumors. IL-27 levels were measured in cell culture media of primary tumor cells and activated peripheral blood mononuclear cells (PBMCs) by ELISA.

Results Primary tumor samples showed IL-27 expression by IHC within morphologically defined tumor-associated macrophages (TAMs) in several cancers, including lung, liver, renal, gastric, and head and neck. This is consistent with single-cell RNA-seq transcriptional data showing predominant expression in macrophages from several tumor types. Interestingly, IL-27⁺ TAMs are localized in the vicinity of PD-L1-expressing cells in gastric, lung, and liver tumors, where the highest IL-27⁺ TAM density is associated with the highest expression of PD-L1. Expression of IL-27RA in tumor tissues was also explored by IHC. IL-27RA expression was identified on tumor cells in several cancers and included examples where tumor cell expression of the receptor was maintained at sites of lymph node metastasis. In vitro cultures of activated PBMCs showed that IL-27 increased PD-L1 expression on immune cells, an effect that was further amplified in the presence of dissociated primary tumors co-cultured with activated PBMCs. IL-27 levels were higher in co-cultures of activated PBMCs and dissociated primary tumors than in cultures of PBMCs alone. Finally, IL-27 was shown to upregulate PD-L1 expression on tumor cell lines that express IL-27RA.

Conclusions IL-27 is expressed by TAMs and plays a role in immune suppression. IL-27⁺ cells are found in close proximity to PD-L1⁺ cells in patient tumors, and IL-27 can regulate levels of PD-L1 expression in immune cells and tumor cell lines, suggesting cross-talk between these molecules to diminish immune activation within the tumor microenvironment. Combined blockade of IL-27 and PD-(L)1 to enhance antitumor immune responses is currently being evaluated in clinical trials.

<http://dx.doi.org/10.1136/jitc-2022-SITC2022.1082>

1083

AB821 IS A CD8+ T CELL SELECTIVE IL-21 WITH ENHANCED BIOAVAILABILITY THAT MEDIATES POTENT ANTI-TUMOR ACTIVITY, CYTOTOXICITY, AND EXPANSION OF MEMORY CD8+ T CELLS

¹Renee Greer, ¹Henry Nguyen, ¹Paul Mesko, ¹Ruth Lan, ¹Wei Wei Prior, ²Hussein Sultan, ¹Meghana Sukthankar, ¹Irene Ni, ¹S Michael Chin, ¹Kelly Moynihan, ³Ton Schumacher, ²Robert Schreiber, ¹Andy Yeung, ¹Ivana Djuretic*. ¹Asher Biotherapeutics Inc., South San Francisco, CA, USA; ²Washington University, St. Louis, MO, USA; ³The Netherlands Cancer Institute, Amsterdam, Netherlands

Background IL-21 is a clinically validated cytokine that showed monotherapy activity in melanoma¹ and renal cell carcinoma². Further clinical development of IL-21 was discontinued, likely due to limitations such as short half-life and poor bioavailability, a result of IL-21's low molecular weight and highly positive charged nature, respectively. The pleiotropic effects of IL-21 may have also limited its effectiveness in the clinic. While IL-21 can activate STAT3 in CD8+ T cells to promote anti-tumor immunity, STAT3 activation in NK cells and myeloid cells may be associated with toxicity and immunosuppression, respectively^{3,4}. To maximize the potential of IL-21, we developed AB821, a cis-targeted IL-21 that selectively activates CD8+ T cells and exhibits improved bioavailability.

Methods AB821 was generated by fusing a CD8 targeting antibody to an IL-21 mutein which has attenuated binding to IL-21 receptor and a reduced positive charge profile. AB821 and its murine surrogate, muAB821, were characterized alongside WT IL-21 in multiple in vitro and in vivo studies.

Results In STAT3 assays with human PBMCs, whereas IL-21 indiscriminately activated CD8+ T cells and non CD8 cells with almost equivalent potency, AB821 demonstrated high potency of 0.5nM on CD8+ T cells and 1000-fold selectivity over other IL-21 target cell types such as B cells, NK cells and CD4+ T cells. Selective activation of STAT3 in CD8+ T cell was also observed following AB821 dosing in cynomolgus monkeys. Besides selectivity, AB821 showed enhanced in vivo exposure with reduced non-specific consumption compared to WT IL-21. Functionally, AB821 largely recapitulated the gene expression signatures of WT IL-21 in both resting and antigen-activated CD8+ T cells. Notably, AB821 induced minimal gene expression changes in resting CD8+ T cells but synergized with antigen stimulation and induced a larger set of genes in activated CD8+ T cells, consistent with IL-21's primary role in the context of antigen activation. Furthermore, in hematopoietic stem cell-humanized mice, a single dose of AB821 resulted in a persistent increase in Granzyme B+ CD8+ T cells and marked increases in the memory compartment. Finally, muAB821 demonstrated remarkable monotherapy activity in multiple tumor models, with muAB821 significantly outperforming mouse IL-21. Furthermore, muAB821 showed synergistic anti-tumor activity with anti-PD1 antibody in multiple PD1-resistant tumors.

Conclusions AB821 is a next-generation IL-21 with superior anti-tumor activity and enhanced bioavailability over WT IL-21. AB821 promotes cytotoxicity and memory CD8+ T cells in the context of antigen activation and synergizes with PD1 blockade in PD1-resistant tumors. Clinical development of AB821 is planned.

REFERENCES

1. Petrella T, Mihalciou C, Monzon J, *et al.* Final Efficacy Results of a Randomized Phase II Study of Recombinant Interleukin-21 Compared to Dacarbazine in Patients with Recurrent or Metastatic Melanoma. *J Oncol Res Treat* 2019;**4**:132

2. Schmidt H, Brown J, Mouritzen U, *et al.* Safety and Clinical Effect of Subcutaneous Human Interleukin-21 in Patients with Metastatic Melanoma or Renal Cell Carcinoma: A Phase I Trial. *Clin Cancer Res* 2010;**16**(21):5312–5319.
3. Skak K, Frederiksen K, Lundsgaard D. Interleukin-21 activates human natural killer cells and modulates their surface receptor expression. *Immunology* 2008;**123**(4):575–583
4. Brandt K, Bulfone-Paus S, Foster D, Rückert R. Interleukin-21 inhibits dendritic cell activation and maturation. *Blood* 2003;**102**(12):4090–4098;

Ethics Approval All procedures performed on the animals were in accordance with regulations and established guidelines and were reviewed and approved by the Explora's Institutional Animal Care and Use Committee

Consent No patient's data is presented in this abstract

<http://dx.doi.org/10.1136/jitc-2022-SITC2022.1083>

Abstracts

1084

NTX-0250, A MULTIMODAL MRNA-BASED IMMUNOTHERAPY, ERADICATES LARGE ESTABLISHED TUMORS IN A STRINGENT MOUSE MODEL OF HPV16-DRIVEN CANCER

¹Ole Haabeth*, ²Diane DaSilva, ¹Colin McKinlay, ¹Weiqun Liu, ¹Edward Lemmens, ¹Christopher Rae, ¹Adrienne Sallets, ¹Daniel Frimansson, ¹Sangeeta Nath, ¹Nicole Peck, ¹Ou Li, ¹Nicole Fay, ²Ruben Prins, ¹Meredith Leong, ²W Martin Kast, ¹Samuel Deutsch. ¹Nutcracker Therapeutics, Emeryville, CA, USA; ²Norris Comprehensive Cancer Center, University of Southern California, Los Angeles, CA, USA

Background Human papillomavirus (HPV) is a contagious cause of anogenital and oropharyngeal cancers developing from persistently infected and subsequently transformed basal keratinocytes of mucosal epithelium. More than 90% of cervical cancers and pre-cancerous cervical intraepithelial neoplasia (CIN) are linked to infections with high-risk HPV, with more than 50% of cancers linked to HPV16.^{1,2} At least 25% of women with high-grade CIN lesions progress to in situ or invasive cancer, if untreated.³ Current treatments for high-grade CIN can remove abnormal tissue but do not address underlying HPV infection, and 15% of women treated develop residual or recurrent high-grade CIN or cervical cancer.⁴ Long-term efficacy may require induction of tumor-specific T cell responses combined with alleviated local immune suppression and increased tumor immune cell infiltration. Multimodal mRNA-based immunotherapies that deliver both antigens and immunomodulators in a single drug product represent a promising new approach for treatment of CIN and cervical cancer that can address current disease as well as the underlying cause (HPV infection). Here we report on pre-clinical efficacy of NTX-0250, a nanoparticle-formulated, multi-component mRNA drug that co-delivers a novel HPV16 antigen design with two potent immunomodulators.

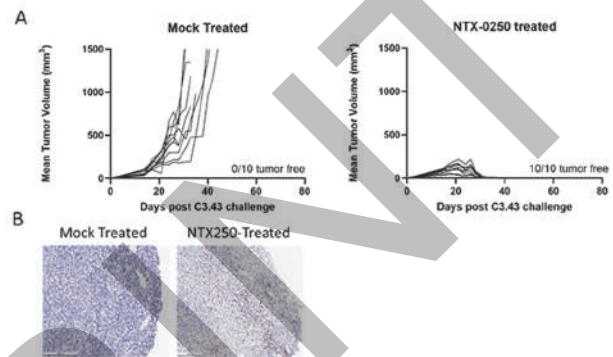
Methods To test efficacy, we utilized the well-established, clinically relevant, C3.43 tumor model (5). C3.43 is a progressive subclone of C3, HPV16-transformed B6 mouse embryo cell line that expresses HPV16 E6 and E7 antigens under the natural promoter.⁵ Therapeutic efficacy of NTX-0250 was assessed in mice with large (>120mm³) C3.43 tumors. HPV16-specific T cells were assessed by flow cytometry on peripheral blood mononuclear cells (PBMCs). Mechanistic studies were performed by post-treatment tumor microenvironment characterization. To assess translational potency of NTX-0250, induction of HPV-specific T cell responses in cynomolgus monkeys was measured by flow cytometry and IFN γ ELISpot on PBMCs

Results In tumor challenged mice, administration of NTX-0250 induces complete regression of large tumors resulting in long-term, tumor-free survival of 100% of treated animals (figure 1A). Complete responses are accompanied by strong tumor immune infiltration of CD8+, CD4+ APCs and NK cells and upregulation of IFN γ in the tumor microenvironment (figure 1B). In cynomolgus monkeys, administration of NTX-0250 induces strong HPV16-specific responses (figure 2). **Conclusions** Here we report for the first time robust pre-clinical efficacy of a multimodal, mRNA-based therapeutic combining antigen- and immunomodulator-encoding mRNAs in a novel nanoparticle formulation. NTX-0250 treatment resulted in complete regression of large established murine tumors and robust induction of HPV-specific T cell responses in non-human primates.

REFERENCES

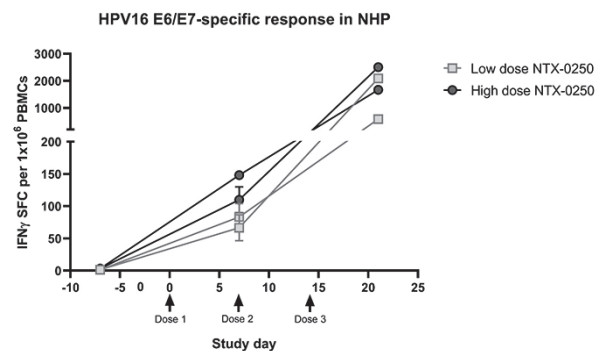
1. https://www.who.int/health-topics/cervical-cancer#tab=tab_1

- da Silva RL, da Silva Batista Z, Bastos GR, *et al.* Role of HPV 16 variants among cervical carcinoma samples from Northeastern Brazil. *BMC Women's Health* 2020;**20**:162.
- Tao L, Han L, Li X, *et al.* Prevalence and risk factors for cervical neoplasia: a cervical cancer screening program in Beijing. *BMC Public Health* 2014;**14**:1185.
- Risk of recurrent high-grade cervical intraepithelial neoplasia after successful treatment: a long-term multi-cohort study. Mariëlle Kocken 1, Theo J M Helmerhorst, Johannes Berkhof, Jacqueline A Louwers, Mariëlle A E Nobbenhuis, Aagje G Bais, Cornelis J A Hogewoning, Afra Zaal, René H M Verheijen, Peter J F Snijders, Chris J L M Meijer. *Lancet Oncol* 2011;**12**(5):441–50
- Feltkamp MC, Smits HL, Vierboom MP, *et al.* Vaccination with cytotoxic T lymphocyte epitope-containing peptide protects against a tumor induced by human papillomavirus type 16-transformed cells. *Eur J Immunol* 1993;**23**:2242–9.



Abstract 1084 Figure 1 NTX-0250 induces complete regression of large tumors in mice

A) 10 C57/BL6 mice per group were inoculated with 1×10^6 C3.43 cells in the subcutaneous compartment. NTX-0250 or Mock-treatment, was initiated when tumors were >120mm³ (18 after tumor inoculation). Mice received 3 doses of 1.5 μ g NTX-0250 with 7 days interval. Tumor growth was monitored for 90 days. B) Representative immunohistochemistry staining of C3.43 tumors 3 days post treatment with vehicle control (Mock treated) or NTX-0250. Slides were stained for infiltrating CD8+ T cells (Brown).



Abstract 1084 Figure 2 NTX-0250 induces robust HPV16-specific responses in NHPs.

Cynomolgus monkeys (n=2) were immunized three times with low or high dose of NTX-0250. Induction of HPV16 E6 and E7-specific T cell responses were measured by IFN γ ELISpot after one and three doses.

<http://dx.doi.org/10.1136/jitc-2022-SITC2022.1084>

1085

THE NAD⁺ DEPENDENT DEACETYLASE SIRT2 IS A NEGATIVE REGULATOR OF THE JAK/STAT PATHWAY IN EFFECTOR T CELLS

¹Imene Hamaidi*, ²Lin Zhang, ¹Pingyan Cheng, ¹Min-Hsuan Wang, ¹Erika Johnson, ¹Bin Fang, ¹Sungjune Kim. ¹Moffitt Cancer Center, Tampa, FL, USA; ²Medical University Cancer Institute, Tianjin, China

Background The Janus kinase (JAK)-signal transducer and activator of transcription (STAT) pathway plays critical roles in orchestrating the immune system through cytokine receptors by modulating T cell polarization and effector functions. Cytokine binding to the cognate receptors activates JAKs that phosphorylates STATs which in turn translocate to the nucleus in order to activate or suppress the transcription of genes. This pathway is regulated by an array of regulator proteins, determining the initiation, duration, and termination of the signaling. However, the roles of these protein regulators other than phosphorylation-dephosphorylation remain unclear.

Sirt2 is an (NAD⁺)-dependent histone deacetylase with conflicting reports on its tumor suppressor or oncogenic roles. We previously showed that Sirt2 is a suppressor of T cell metabolism that deacetylates key metabolic targets and negatively impacts their enzymatic activity. Accordingly, Sirt2 deficient T cells exhibited a hyper-metabolic status with a profound upregulation of glycolysis.

Methods The role of Sirt2 in T cell immune response was investigated using RNA-sequencing, CFSE proliferation assay, DAPI/AnnexinV staining, IFN- γ ELISpot assay, intracellular staining of effector molecules and LDH cytotoxicity assay in Wild-type and Sirt2 knockout mice. Sirt2 interactome was identified via mass spectrometry (MS) and immunoprecipitation/Wb analyses. Phosphorylation and acetylation of JAK/STAT effector molecules following cytokine stimulation were assessed by Wb. Pharmacologic inhibition of Sirt2 in human T cells was achieved using Thiomyristoyl, a Sirt2 selective inhibitor.

Results Sirt2 expression is induced following T cell activation. Our molecular studies revealed that Sirt2 directly interacts with JAK1/2/3 and STAT1/3/5 and negatively impacting their acetylation status.

Strikingly Sirt2 inhibition resulted in increased phosphorylation of JAK1/2/3 and STAT3/5 following IL2 stimulation and increased phosphorylation of JAK1/2 and STAT1 following IFN- γ stimulation in murine and human T cells.

Accordingly, RNA-sequencing analysis revealed upregulation of IL-2 signaling and IFN- γ response with Sirt2 deficiency in activated T cells.

As a consequence of enhanced JAK/STAT activation, Sirt2 deficient T cells displayed enhanced T cell proliferation and effector functions.

Conclusions Our findings indicate Sirt2 as a suppressor of JAK/STAT pathways and show that protein acetylation plays an important role in the modulation of cytokine signaling and T cell fate. Therefore, Sirt2 constitutes a potential target to manipulate the immune response and to treat immune-related diseases or enhance antitumor immunity.

Acknowledgements This work was supported in part by K08 CA194273, ACS IRG-17-173-22, NCI Cancer Center Support Grant (P30-CA076292) and the Moffitt Foundation.

<http://dx.doi.org/10.1136/jitc-2022-SITC2022.1085>

1086

NKTR-288, A POLYMER-CONJUGATED INTERFERON GAMMA MUTEIN FOR THE TREATMENT OF SOLID TUMORS

¹Damon Hamel*, ²Marlene Hennessy, ³Sarah Ingersoll, ¹Olga Zemka, ¹Phi Quatch, ¹Rhoneil Pena, ¹Thomas Chang, ²David Doherty, ⁴Guifen Xu, ¹Arkopal Choudhury, ¹Danni Yu, ⁴Werner Rubas, ¹Christie Fanton, ¹Brian Vuilleminot, ¹Saul Kivimaa, ¹Takahiro Miyazaki, ¹Jonathan Zalevsky. ¹Nektar Therapeutics, San Francisco, CA, USA; ²Exelixis, Alameda, CA, USA; ³Amgen, South San Francisco, CA, USA; ⁴Sutro BioPharma, South San Francisco, CA, USA

Background Interferon gamma (IFN γ) cytokine induces cellular antigen presentation and has great potential in cancer treatment through enhancement of tumor antigen specific cytotoxic T cell response. However, the unfavorable pharmacokinetics (PK) and the pleiotropy of native IFN γ have limited its therapeutic potential. NKTR-288 is a polymer-conjugated IFN γ mutein, designed to improve exposure by increasing hydrodynamic radius and reducing receptor and heparin binding affinity to provide optimized on-target pharmacodynamics (PD). Here, we report on the discovery of NKTR-288 and investigate its pharmacological properties.

Methods Binding of NKTR-288 to interferon gamma receptor 1 (IFNGR1) and heparin was measured by surface plasmon resonance. The biological activity of NKTR-288 was measured by pSTAT1 induction in tumor cell lines and primary myeloid cells in vitro and in vivo. PK/PD was measured in nonhuman primates (NHP), and human xenograft mouse models. Anti-tumor efficacy and enhancement of checkpoint blockade was measured in the mouse syngeneic B16F10 tumor model using a mouse IFN γ polymer conjugate as a surrogate for NKTR-288.

Results NKTR-288 has increased hydrodynamic radius to slow renal clearance and binds to IFNGR1 and heparin with reduced affinity compared to recombinant IFN γ 1b, thereby reducing clearance due to target-mediated drug deposition. In vitro, NKTR-288 maintains the maximum potential (E $_{max}$) for pSTAT1 induction on target cells. In vivo, NKTR-288 shows durable exposure in tumor bearing mice (half-life [T $_{1/2}$] 18.2 to 24.2 hr) and NHP (T $_{1/2}$ 31.6 to 37.3 hr) and is well tolerated at pharmacologically active doses. NKTR-288 has a desirable PK/PD profile that can attain greater induction and duration of MHCI than can be achieved with the native cytokine. NKTR-288 also upregulates PD-L1 in tumor tissue supporting combination therapy with checkpoint inhibitors. In a syngeneic tumor model, a surrogate mouse conjugate exhibited significant anti-tumor efficacy (57% TGI), and increased efficacy when combined with anti-PD-1 (73% TGI) or anti-PD-L1 (68% TGI). Treatments were well tolerated and tumor growth inhibition was immune system mediated, requiring T cells.

Conclusions NKTR-288 is a novel IFNGR agonist with optimized pharmacological properties for tolerable and sustained induction of tumor antigen presentation, potentially increasing tumor cytotoxic T cell response, immune infiltration, and TME modification. As evidence, a mouse surrogate conjugate demonstrated T cell-mediated anti-tumor activity, and enhanced checkpoint blockade efficacy in a low-MHCI “cold” tumor model. These results highlight the potential of NKTR-288 as a novel cytokine immunotherapy in cancer patients, with the potential to enhance PD-1/PD-L1 checkpoint blockade efficacy and broaden the responsive patient population.

Ethics Approval Animal studies were performed under protocols approved by the Institutional Animal Care and Use Committee of Nektar Therapeutics and the Canadian Council on

Animal Care. All studies met the ethical and humane criteria for transportation, housing, and care established by the US NIH guidelines or Canadian animal care regulators.

<http://dx.doi.org/10.1136/jitc-2022-SITC2022.1086>

1087 **ADDITION OF IL-2 OVERCOMES LUNG TUMOR RESISTANCE TO IL-12 BY COORDINATING CYTOTOXIC AND REGULATORY T CELL RESPONSES**

Brendan Horton*, Maria Zagorulya, Noor Momin, Yash Agarwal, K Wittrup, Stefani Spranger. *Massachusetts Institute of Technology, Cambridge, MA, USA*

Background IL-12 is a pleiotropic cytokine with potent T cell stimulatory ability that can induce tumor regression in pre-clinical models. Translation of IL-12 has been hampered by high toxicity and a lack of efficacy. While many efforts have been made to engineer IL-12 to be less toxic and more effective, our understanding of resistance to IL-12 is limited due to a lack of appropriate model systems. We have identified a model of IL-12-resistant lung cancer that allows us to probe mechanisms of IL-12 response and resistance.

Methods We utilized the syngeneic, transplantable murine lung cancer KP cell line to analyze the response to extended half-life IL-12 or IL-2 fused to murine serum albumin (IL12-MSA, MSA-IL2). Expression of the CD8⁺ T cell antigen SIY in KP cells (KPSIY) allowed the tracking of antigen-specific anti-tumor immune responses.

Results IL12-MSA induced significant tumor control and improved survival of mice with subcutaneous KP flank tumors. However, mice inoculated intravenously with KP cells to form metastatic lung tumors derived no survival benefit from IL12-MSA. Using KPSIY cells, we determined that successful IL12-MSA immunotherapy in the flank setting involved significant expansion and effector differentiation of SIY-reactive CD8⁺ T cells in the tumor-draining lymph node (TdLN), and the depletion of CD4⁺ regulatory T cells (T_{reg}) from the tumor microenvironment. In the lung tumor setting, however, T cells were unresponsive to IL12-MSA, as SIY-reactive T cells did not expand in lung TdLNs and did not upregulate the effector molecules CD25, GzmB, and TIM-3. Using fluorescently labeled IL12-MSA, we found significantly reduced IL-12 binding by SIY-reactive CD8⁺ T cells and T_{reg} in the lung tumor setting, explaining the lack of IL12-MSA efficacy against lung tumors. However, combined MSA-IL2 and IL12-MSA improved lung tumor control and synergistically enhanced CD8⁺ T cell activation. In lung tumors and lung TdLNs, the addition of MSA-IL2 increased the binding of IL12-MSA by T_{reg}, suggesting that IL-2 sensitized lung tumors to IL-12 through a coordinated enhancement of tumor-reactive CD8⁺ T cell activation with a concomitant inhibition of T_{reg}.

Conclusions Resistance to IL-12 can be mediated by tumor-reactive T cells with low IL-12 receptor expression, therefore IL-12 receptor expression should be considered when administering IL-12-based therapies. IL-2 can sensitize T cell responses to IL-12 through a feed-forward mechanism of CD8⁺ T cell activation and concurrent T_{reg} inhibition.

Ethics Approval The experiments in this abstract were approved by the Massachusetts Institute of Technology Committee on Animal Care, Protocol Number 0220-006-23, NIH Assurance Number D16-00078.

<http://dx.doi.org/10.1136/jitc-2022-SITC2022.1087>

1088

A HIGHLY POTENT ANTI-LAG-3-IL-2C THAT SELECTIVELY TARGETS TUMOR-SPECIFIC CD8⁺ T CELLS

Zoey Huang, Jianing Huang, Fan Ye*, Sandra Chen, Danny Huang, Michael Hua, Ella Li, Jenny Jiang, Hanna Lin, Shirley Shi, Bella Yue, Henry He, Mingxing Yang, Qiang Fu, Ziyang Zhong. *Anwita Biosciences, San Carlos, CA, USA*

Background Interleukin 2 (IL-2) is an essential link in immune activation and heavily contributes to tumor eradication. Clinically, IL-2 has shown impressive efficacy in various tumor types. However, the abundant and ubiquitous expression of IL-2 receptors made IL-2 pleiotropic and hence limits its application as the sole agent for immunotherapy. LAG-3 emerged as the next-generation inhibitory immune checkpoint (ICP) following CTLA-4, PD-1, and PD-L1. Simultaneous blockade of LAG-3 and PD-1 has shown favorable clinical outcomes in PD-1/PD-L1 resistant melanoma patients. In addition to its ICP role, the expression pattern of LAG-3 has made it an appealing target to be used in combination with IL-2 as a bifunctional fusion protein for tumor immunotherapy as LAG-3 is highly expressed on tumor-specific CD8⁺ T cells. A LAG-3⁺-T-cell-targeting IL-2 has strong anti-tumor efficacy and minimal systemic toxicity, as well as the compatibility to be combined with PD-1 blockade. We herein proposed the use of an α LAG-3-IL-2c fusion protein which consists of a LAG-3 binding domain and IL-2c, a chimeric molecule that contains a fragment from IL-15 and does not bind to IL-2 receptor alpha, to achieve the aforementioned purpose.

Methods The *in vitro* potency was determined with pSTAT5 signaling assay and human PBMC proliferation assay. The *in vivo* efficacy was evaluated in syngeneic CT26 mouse model with a surrogate molecule. A humanized α LAG-3-IL-2c fusion protein was tested on hLAG-3-knocked-in (KI) mice with MC-38 model, as well as in combination with mesothelin-targeted CAR-T on NSG mice with N87 gastric cancer xenograft model.

Results α LAG-3-IL-2c induced a greater pSTAT5 activation signal in LAG-3⁺ T cells than in LAG-3⁻ T cells. Additionally, α LAG-3-IL-2c enhanced *in vitro* proliferation in LAG-3⁺ T cells compared to untargeted IL-2c by approximately 1000 folds. Furthermore, among the LAG-3⁺ cell population, α LAG-3-IL-2c expanded CD8⁺ T cells to a greater extent compared to CD4⁺ T cells. In the syngeneic CT26 model and hLAG-3 KI model, α LAG-3-IL-2c induced a much stronger anti-tumor response compared to LAG-3 mAb, IL-2c, or LAG-3 mAb in combination with IL-2c. Moreover, α LAG-3-IL-2c showed enhanced intratumoral CD8⁺ T cells proliferation and anti-tumor efficacy in a CART model, demonstrating the promising usage of α LAG-3-IL-2c to combine with CART therapy.

Conclusions Altogether, these results indicate that α LAG-3-IL-2c is a potent tumor-infiltrating CD8⁺ T agonist without notable peripheral toxicity.

Ethics Approval The protocol of animal studies has been reviewed and approved by IACUC.

<http://dx.doi.org/10.1136/jitc-2022-SITC2022.1088>

1089

IMMUNOPHERESIS®: A NOVEL IMMUNOTHERAPY PLATFORM FOR EXTRACORPOREAL REMOVAL OF SOLUBLE TARGET MOLECULES IN ONCOLOGY

Steven Josephs, Robert Segal, Steve Prince, Mathew Ong, Amir Jafri, Lawrence Florin, Victoria Manax, Michael Matho, Sameera Bilgrami, Annette Marleau*. *Immunicom, Inc., San Diego, CA, USA*

Background Immunopheresis® is a novel immunotherapeutic approach for treating cancer that employs Immunicom, Inc.'s proprietary technology platform for extracorporeal removal of soluble target molecules from plasma. The technology platform consists of patent-protected apheresis columns containing an affinity matrix to which customized ligands are coupled for capturing one or more cytokines, cytokine receptors and/or growth factors. The lead product, the LW-02 Column, selectively removes soluble tumor necrosis factor receptors (sTNF-Rs) from plasma, which are shed by tumors to neutralize TNF- α and evade its anti-tumor activities. Performance of the LW-02 Column demonstrates the effective and selective target molecule capture that is achievable using the Immunopheresis platform.

Methods The LW-02 Column comprises a trimeric single-chain TNF- α molecule covalently conjugated to an agarose bead matrix to form a proprietary high affinity resin. Laboratory performance testing of the LW-02 Column includes: 1) Capture efficiency and binding capacity for sTNF-Rs (sTNF-R1 and sTNF-R2) measured using MSD assays; 2) Leaching of ligand from the affinity matrix evaluated using MSD assays; 3) Potential off-target binding assessed by measuring plasma protein profiles and cytokine concentrations pre- and post-column exposure using HPLC and immunoassays

Results In laboratory testing, the LW-02 Column has a capture efficiency of >80% removal of both sTNF-R1 and sTNF-R2, during recirculation of 1L test plasma through the column to model a clinical apheresis procedure. The column binding capacity exceeds the sTNF-R quantities that are typically present in cancer patients' plasma (approximately 30 micrograms total). The quantities of TNF- α ligand that leach from the affinity matrix (equivalent to < 1 microgram per procedure) are significantly lower than TNF- α levels reported to cause clinical adverse events. The LW-02 Column exhibits selectivity for sTNF-Rs with negligible off-target binding of cytokines, immunoglobulins, or other plasma components.

Conclusions LW-02 Column Immunopheresis has a highly specific and selective mechanism of action and offers a novel subtractive therapy approach for treating cancer that avoids the typical toxicities associated with systemic drug therapy. Clinical performance of the LW-02 Column is currently being monitored as part of three ongoing clinical trials as monotherapy or as an adjunct to chemo- or immunotherapy for various solid tumors. The technology platform is being leveraged with novel high-affinity capture ligands to address other clinically relevant target molecules in immuno-oncology.

<http://dx.doi.org/10.1136/jitc-2022-SITC2022.1089>

1090

OVERCOMING SYSTEMIC TOXICITY OF IL-12-BASED IMMUNOTHERAPY BY TUMOR-TARGETING AND IL-12 ATTENUATION

Jihoon Chang*, Donggeon Kim, Dahea Lee, Dongsu Kim, Soomin Ryu, Byoung Lee. *Kanaph Therapeutics, Seoul, Korea, Republic of*

Background Cytokines are well-known immunomodulators. Thanks to recent success of immune checkpoint inhibitors there is a renewed interest in cytokines as a promising cancer immunotherapy option. Several inflammatory cytokines including IL-12 showed potent anti-tumor activities but severe immune adverse events when administered systemically greatly hindered using them as anti-tumor agents.

Methods Previously (SITC 2020) we showed that IL-12 activity was reduced by our introduced mutation (termed as mut1) if measured by pSTAT4 AlphaLISA assay. But when it was treated in human immune cells IFN γ production was not reduced as expected. Thus, we further attenuated IL-12 activities by protein engineering and created our candidate molecule KNP-101.

Results We showed that KNP-101 maintained potent anti-tumor activities in vivo but gained greatly improved toxicity profiles. When we measured pSTAT4 signals, KNP-101 showed about 30-fold attenuation in IL-12 activities compared with rIL-12. IFN γ production from human PBMC was also reduced. Although the IL-12 activity was weakened in order to reduce its systemic toxicity, our KNP-101 mouse surrogate still maintained good anti-tumor potency in various mouse syngeneic models with a single intravenous injection as low as 2 μ g/head. In combination with anti-PD-L1, KNP-101 surrogate showed a synergistic anti-tumor effect and further FACS analysis of tumor infiltrated lymphocytes demonstrated that the effects were mediated by immune cell infiltration. Importantly, in CD1 naive mouse toxicity test, KNP-101 surrogate was tolerable up to 50 μ g/head and no survival issue was observed. However, that was not the case with the control group, non-tumor-targeting null/IL-12 showing survival issues with all tested dose levels. Compared with the control, KNP-101 surrogate also showed much safer profiles in terms of organ weight and serum chemistry such as ALT level. We also performed similar toxicity study in tumor-bearing mice. KNP-101 surrogate again showed a very safe profiles being tolerable up to 500 μ g/head and no survival issue. Noticeably, when serum IFN γ was measured in tumor-bearing mice, our KNP-101 surrogate induced far less IFN γ in serum compared to null/IL-12 suggesting that systemic toxicity was greatly reduced.

Conclusions Together, we demonstrated that systemic toxicity of IL-12 cytokine therapy can be overcome by tumor-targeting and IL-12 attenuation. Our KNP-101 has a wider therapeutic window by maintaining potent anti-tumor activities and showing much improved safety profiles. We hope that KNP-101 can benefit patients in the future who suffer from primary and acquired resistance of the current anti-PD-1/PD-L1 treatments.

<http://dx.doi.org/10.1136/jitc-2022-SITC2022.1090>

1091

CGC-601, A NOVEL $\beta\gamma$ -ONLY IL-2 VARIANT, ENHANCES MODERATE IMMUNE ACTIVATION WITHOUT TREG EXPANSION, AND EXHIBITS A SUPERIOR SAFETY EVIDENCE IN VIVO

Lei Zhao*, Rong Wang, Chuan Feng, Yongji Jiang, Patrick Liu, Yuan Liu. Cure Genetics Co., LTD, Suzhou, China

Background IL-2 was first approved by FDA for the solid tumor treatment. However, the therapeutic window of IL-2 (low dose suppresses immune system by Treg activation and high dose represents toxicity) limited its clinical use. The major dose-limiting toxicity IL-2 is vascular leak syndrome (VLS). The mechanism of VLS is mainly considered as the direct interaction of IL-2 with IL-2R α expressed on endothelial cells *in vivo*^{1, 2} or by over-stimulation of immune cells.^{3, 4} To get rid of the IL-2R α interaction, non- α IL-2 muteins were designed to deplete the Treg expansion which may contributes to its anti-tumor efficacy (figure 1). However, they still remain the risk of overstimulated immune response.

Here, we introduce our IL-2 variant, CGC-601, which abolished its binding to IL-2R α , while obtained a structural twist on four α -helix (figure 2). This brand new molecule was designed as a non-suppressive and moderate immune agonist, through the strategy of de-coupling the IL-2 binding pattern to "beta-gamma".

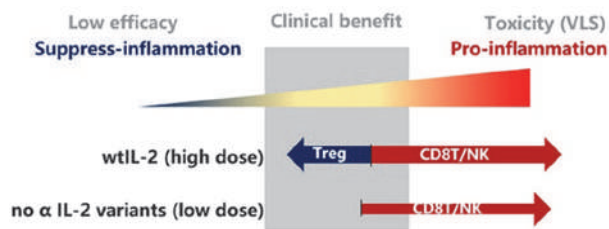
Results CGC-601 does not bind to IL-2R α or IL-2R β alone, while only binds to $\beta\gamma$ complex with the similar affinity to wtIL-2 in a "fast-on, fast-off" feature (figure 3). Moreover, CGC-601 shows a low Treg response and mild CD8 T and NK activation in human PBMC (figure 4). For T cell expansion, upon 50nM treatment, CGC-601 holds a similar T cell expansion capacity with rhIL-2 (figure 5A). Meanwhile, CGC-601 expands both CD8 T cells and NK cells, but Treg expansion dramatically constrained after PBMC *ex vivo* expansion (figure 5B). Thus, compare with rhIL-2, CGC-601 gives "young" and less differentiated T cells after expansion (figure 6).

In the toxicity test, CGC-601 dose as high as 30 mg/kg, mice stay in good health conditions, while 10 mg/kg rhIL-2 showed a severe weight loss and a reduced activity since Day 3, suggesting CGC-601 has a much safer profile than rhIL-2 (figure 7A). Pulmonary edema is significantly reduced even CGC-601 dose reached 30mg/kg (figure 7B). CGC-601 treatment did not elevate serum IL-5 levels 6 hrs after the first dose (Fig. 7C). CGC-601 prefers C8 T cells and NK cells expansion, on the contrary, CGC-601 does not expand Tregs *in vivo* (figure 8).

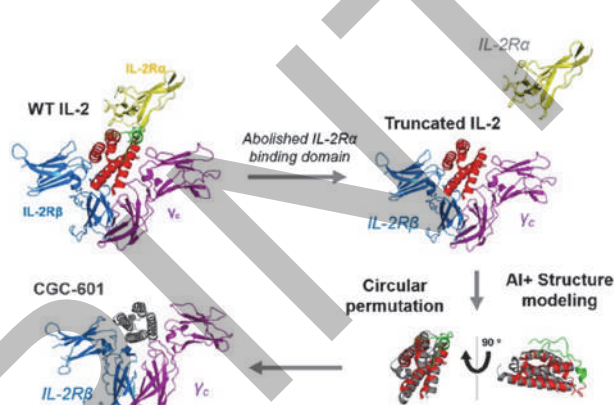
Conclusions CGC-601 with a unique $\beta\gamma$ -only binding property, promotes moderate CD8 T and NK expansion and diminishes immunosuppressive Tregs *in vivo*, has a great potential in immune-stimulation indications. CGC-601's safety evidence sets up a platform allowing multiple application scenarios (figure 9).

REFERENCES

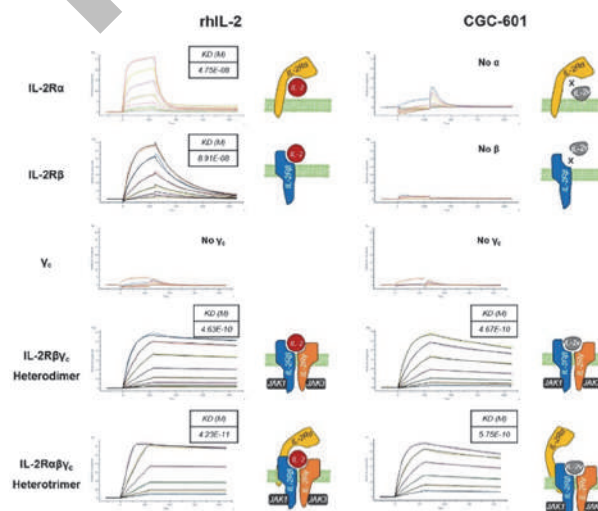
1. Boyman O, et al. Selective stimulation of T cell subsets with antibody-cytokine immune complexes. *Science*. 2006;**311**:1924–1927.
2. Krieg C, et al. Improved IL-2 immunotherapy by selective stimulation of IL-2 receptors on lymphocytes and endothelial cells. *Proc Natl Acad Sci U S A*. 2010;**107**:11906–11911.
3. Li Y, et al. Regulatory T cells control toxicity in a humanized model of IL-2 therapy. *Nat Commun*. 2017;**8**:1762.
4. Shanafelt AB, et al. A T-cell-selective interleukin 2 mutein exhibits potent antitumor activity and is well tolerated *in vivo*. *Nat Biotechnol*. 2000;**18**:1197–1202.



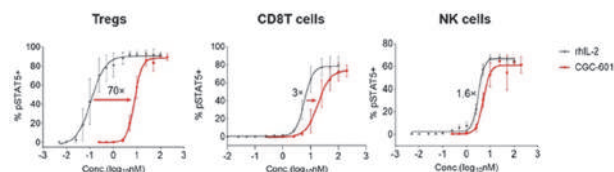
Abstract 1091 Figure 1 Schematic of IL-2 and no- α IL-2 variants in immuno-regulation



Abstract 1091 Figure 2 The design of CGC-601

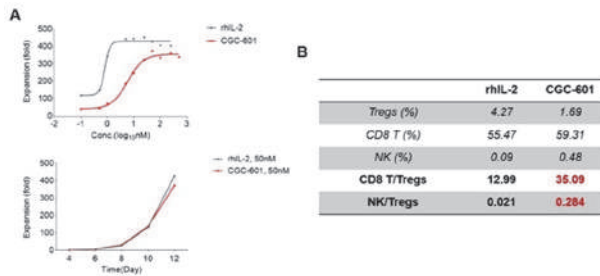


Abstract 1091 Figure 3 CGC-601 has a distinct IL-2 receptor binding profile

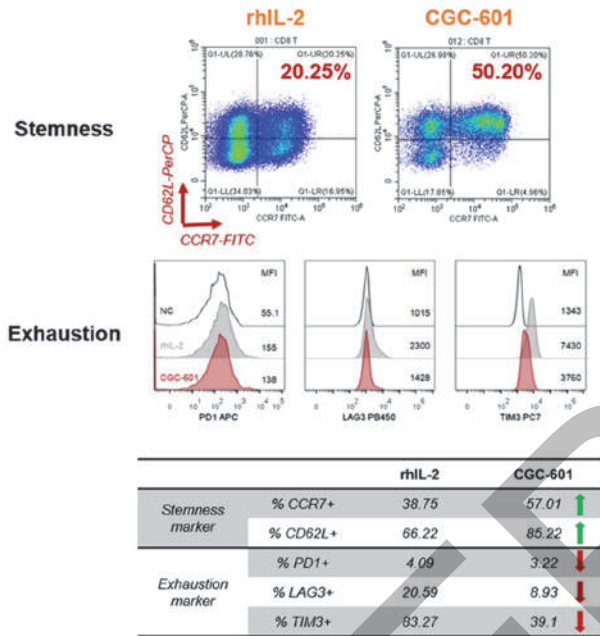


Abstract 1091 Figure 4 CGC-601 has a no IL-2R $\alpha\beta\gamma$ preferable signaling activation

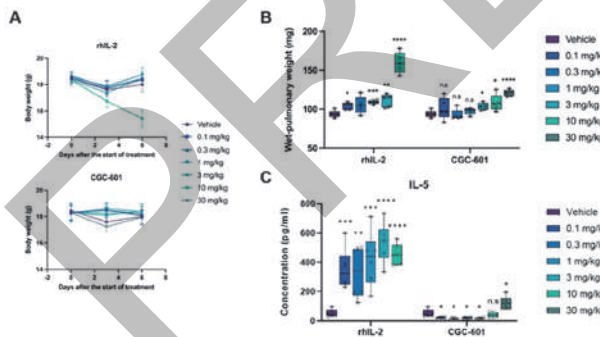
Abstracts



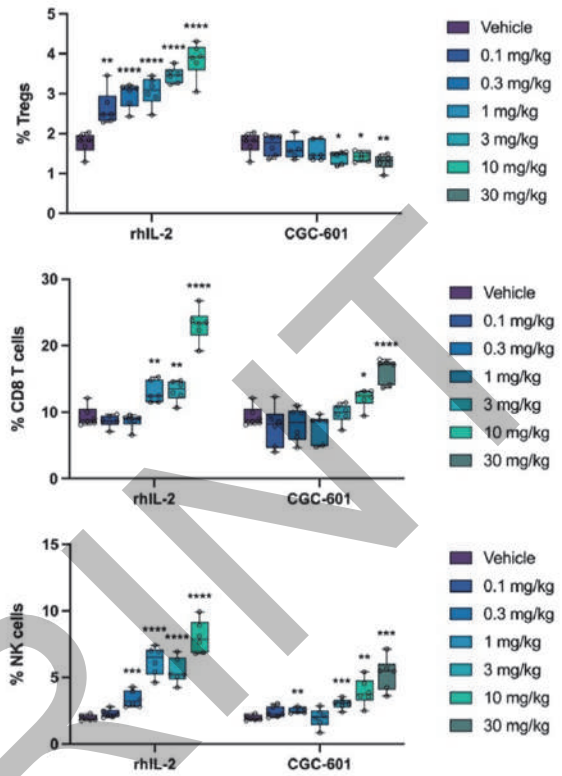
Abstract 1091 Figure 5 CGC-601 retains T cell proliferation activity



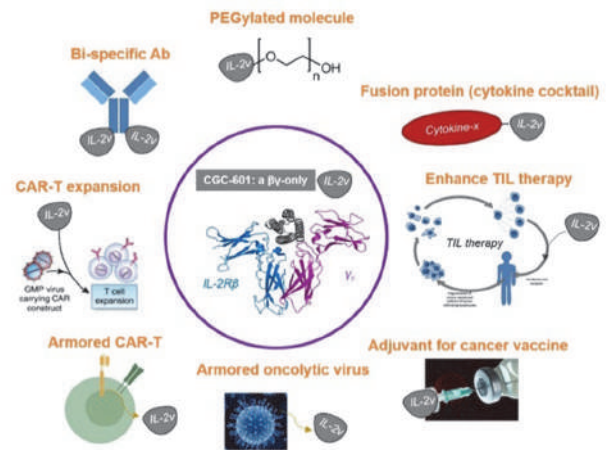
Abstract 1091 Figure 6 CGC-601 presents a high potential in T cell expansion



Abstract 1091 Figure 7 CGC-601 exhibits an excellent in vivo safety profile



Abstract 1091 Figure 8 CGC-601 effectively expand CD8 T and NK cells, but not Tregs in vivo



Abstract 1091 Figure 9 CGC-601 sets up a platform allowing multiple application scenarios

1092

THE CD8+ T CELL SELECTIVITY OF AB248 IS ESSENTIAL FOR OPTIMAL ANTI-TUMOR ACTIVITY AND SAFETY IN NONCLINICAL MODELS

¹Kelly Moynihan*, ¹Danielle Pappas, ²Hussein Sultan, ¹Terrence Park, ¹Manu Kumar, ¹Ruth Lan, ¹Irene Ni, ¹Jessie Chen, ¹Michael Chin, ³Ton Schumacher, ¹Andy Yeung, ²Robert Schreiber, ¹Ivana Djuretic. ¹Asher Biotherapeutics, South San Francisco, CA, USA; ²Washington University in St. Louis, St. Louis, MO, USA; ³The Netherlands Cancer Institute, Amsterdam, Netherlands

Background AB248 is a fusion of an affinity-attenuated IL-2 mutein and an antibody targeting CD8+ T cells designed to overcome the limitations of wild-type IL-2 and second-generation IL-2R β agonists, “not- α ” IL-2 and IL-15 variants. Like “not- α ” IL-2, AB248’s IL-2 mutein does not bind IL-2R α and thus avoids IL-2R α -associated vascular leak syndrome (VLS) and preferential Treg activation in nonclinical models. Further, the IL-2 mutein in AB248 has reduced IL-2R β affinity, and its cis-targeting to CD8+ T cells enables AB248 to avoid the biased expansion of IL-2R β ^{high} NK cells and IL2R β -mediated activation of Tregs associated with untargeted IL2R β agonists. Thus, AB248’s design enables robust IL-2 pharmacology on CD8+ T cells, key effectors with IL-2-based therapy¹⁻², while avoiding cell types that may promote toxicity or oppose anti-tumor activity. Here, the mechanisms by which AB248 achieves enhanced nonclinical activity and safety profiles over untargeted IL-2-based therapies are elucidated.

Methods In vitro activation and cytokine release assays were performed on human immune cells. Tumor immune profiling including scRNAseq was performed in mice treated with AB248’s surrogate, muAB248. Cynomolgus monkeys were dosed with AB248.

Results We previously showed that IL-2 and “not- α ” IL-2 triggered antigen-independent cytokine release from PBMCs in vitro, which was mitigated by the depletion CD56+ cells, which are largely NK cells, and that AB248 avoided this non-selective cytokine release. Studies with sorted PBMC subsets further interrogated this observation and demonstrated the necessity of dual IL-2R α and IL-2R β affinity reduction as well as CD8+ T cell cis-targeting to avoid antigen-independent cytokine release. Strong anti-tumor activity was elicited by muAB248 in multiple murine models without body weight loss. In contrast, “not- α ” IL-2 could not achieve meaningful activity without accompanying NK cell-dependent weight loss. Bypassing the NK cell sink was also important for optimal expansion of intratumoral CD8+ T cells. Comprehensive analysis following treatment with muAB248 demonstrated profound impacts to the tumor immune infiltrate, including activation of unique CD8+ T cell clusters by muAB248 compared to “not- α ” IL-2, which may explain muAB248’s superior anti-tumor activity. In cynomolgus monkeys, repeated doses of AB248 that selectively expanded CD8+ T cells >20-fold were well tolerated, without evidence of cytokine release syndrome or VLS.

Conclusions AB248 exhibited strong anti-tumor activity in mice, profound pharmacodynamic effects in primates, and a favorable nonclinical safety profile. CD8+ T cell restriction was essential for optimal anti-tumor activity and safety in non-clinical models. Collectively, this data demonstrates AB248’s differentiation from broadly acting IL-2-based therapies and supports AB248’s clinical development.

REFERENCES

1. Rakhmilevich AL, North RJ. Elimination of CD4+ T cells in mice bearing an advanced sarcoma augments the antitumor action of interleukin-2. *Cancer Immunol Immunother.* 1994;**38**(2):107–112.
2. Sun Z, Ren Z, Yang K, et al. A next-generation tumor-targeting IL-2 preferentially promotes tumor-infiltrating CD8+ T-cell response and effective tumor control. *Nat Commun.* 2019;**10**(1):3874.

<http://dx.doi.org/10.1136/jitc-2022-SITC2022.1092>

1093

A NOVEL IL12-BASED IMMUNOCYTOKINE TARGETING FIBROBLAST ACTIVATION PROTEIN (FAP) FOR THE TREATMENT OF CANCER

¹Lisa Nadal, ¹Frederik Peissert, ¹Abdullah Elsayed, ²Tobias Weiss, ²Thomas Look, ²Michael Weller, ³Geny Piro, ³Carmine Carbone, ³Giampaolo Tortora, ¹Mattia Matasci, ¹Nicholas Favalli, ¹Riccardo Corbellari, ¹Cesare Di Nitto, ¹Eleonora Prodi, ⁴Chiara Libbra, ⁴Simone Galeazzi, ⁴Claudiopietro Carotenuto, ⁵Cornelia Halin, ¹Emanuele Puca, ⁴Dario Neri, ¹Roberto De Luca*. ¹Philochem AG, Otelfingen, Switzerland; ²University Hospital Zurich, Zurich, Switzerland; ³Catholic University of the Sacred Heart, Rome, Italy; ⁴Philogen S.p.A, Siena, Italy; ⁵ETH Zurich, Zurich, Switzerland

Background Fibroblast Activation Protein (FAP) has been described as the “next billion-dollar nuclear theranostics target”¹, since more than 28 different tumor types have successfully been imaged in patients with radiolabeled FAP ligands. ²⁻³ FAP can be found in the tumor microenvironment (TME) of most malignant solid tumors, while being absent in most healthy tissues. Thus, it is an attractive target for both imaging and therapeutic applications. Monoclonal antibodies targeting TME antigens have been considered for the delivery of bioactive payloads, such as proinflammatory cytokines. Antibody-cytokine fusions (also called immunocytokines) may exploit the tumor-homing properties of the antibody moiety, in order to concentrate the cytokine payload at the site of disease and enhance the therapeutic index.⁴ Interleukin-12 (IL12) have been extensively studied in oncology. IL12 strongly promotes NK cells, CD4+ and CD8+ T cells to produce interferon-gamma (IFN-g), one of the most relevant mediators of anti-cancer immunity.⁵

Methods In this work, we describe the generation of a novel anti-FAP antibody, called 7NP2. The tumor recognition properties of the antibody were validated by immunofluorescence procedures performed on cancer biopsies from human patients. A fusion protein consisting of the 7NP2 antibody linked to interleukin-12 was generated and the anti-cancer activity of the murine surrogate product (named mL12-7NP2) was evaluated in mouse models. To prepare for future clinical trials, a fusion protein consisting of human IL12 linked to the 7NP2 antibody was further investigated in a toxicology study in *Cynomolgus* monkeys.

Results Biodistribution analysis in tumor bearing mice confirmed the ability of the product to selectively localize to solid tumors while sparing healthy organs. Encouraged by these results, therapy studies were conducted *in vivo*, showing a potent anti-tumor activity in immunocompetent and immunodeficient mouse models of cancer, both as single agent and in combination with immune checkpoint inhibitors. The fully human product was tolerated when administered to non-human primates.

Conclusions The results obtained in this work provided a rationale for future clinical translation activities using IL12-7NP2.

REFERENCES

1. Calais J. FAP: The next billion dollar nuclear theranostics target?. *Journal of Nuclear Medicine* 2020;**61**(2). doi:10.2967/jnumed.119.241232.
2. Kratochwil C, et al. 68Ga-FAPi PET/CT: Tracer uptake in 28 different kinds of cancer. *Journal of Nuclear Medicine* 2019;**60**(6). doi: 10.2967/jnumed.119.227967.
3. Backhaus P, et al. Translational imaging of the fibroblast activation protein (FAP) using the new ligand [68Ga]Ga-OncoFAP-DOTAGA. *European Journal of Nuclear Medicine and Molecular Imaging* 2022;**49**(6). doi:10.1007/s00259-021-05653-0.
4. Neri D. Antibody–Cytokine Fusions: Versatile Products for the Modulation of Anti-cancer Immunity. *Cancer Immunology Research* 2019. doi: 10.1158/2326-6066.CIR-18-0622.
5. Puca E, et al. The antibody-based delivery of interleukin-12 to solid tumors boosts NK and CD8+ T cell activity and synergizes with immune checkpoint inhibitors. *International Journal of Cancer* 2019. doi:10.1002/ijc.32603.

Ethics Approval Mouse experiments were performed under a project license (license number 04/2018) granted by the Veterinärämamt des Kantons Zürich, Switzerland, in compliance with the Swiss Animal Protection Act (TSchG) and the Swiss Animal Protection Ordinance (TSchV).

Procedures on *Cynomolgus* monkeys (including housing, health monitoring, restraint, dosing, etc) and ethical revision were performed according to the current Italian legislation (Legislative Decree March 4th, 2014 n. 26) enforcing the 2010/63/EU Directive on the protection of animals used for biomedical research.

<http://dx.doi.org/10.1136/jitc-2022-SITC2022.1093>

1094

FAVORABLE PRECLINICAL EFFICACY AND SAFETY PROFILE OF AVB-001 A NOVEL IL-2 CELL-BASED IMMUNOTHERAPY THAT ERADICATES OVARIAN CANCER IN MOUSE TUMOR MODELS AND SUPPORTS FIRST IN HUMAN CLINICAL DEVELOPMENT

¹Guillaume Carmona*, ²Amanda Nash, ¹Ryan Newman, ¹Jake Schladenhauffen, ²Maria Jarvis, ²Samira Aghlari-Fotovat, ²Sudip Mukherjee, ²Andrea Hernandez, ²Andrew Hecht, ³Peter Rios, ²Shirin Nouraein, ⁴Rahul Sheth, ⁵Weiyi Peng, ³Jose Oberholzer, ⁴Amir Jazaeri, ²Omid Veisheh. ¹Avenge Bio, Natick, MA, USA; ²Rice University, Houston, TX, USA; ³Celltrans, Chicago, IL, USA; ⁴University of Texas MD Anderson Cancer, Houston, TX, USA; ⁵University of Houston, Houston, TX, USA

Background Aldesleukin, recombinant human IL-2 has been approved by the FDA for the treatment of melanoma and renal cancer. However, effective cytokine therapy is limited by its short half-life in circulation and the severe adverse effects associated with high systemic exposure when administered iv. To overcome these limitations, Avenge Bio has developed a localized cytokine delivery LOCOcyte™ platform comprised of polymer encapsulated epithelial cells that produce potent immune effector molecules for loco-regional delivery with temporal regulation. AVB-001 is engineered to produce native IL-2, for the treatment of ovarian cancer.

Methods Safety, PK and PD testing of AVB-001 using a combination of rodent and NHP animal models.

Results Tumor-adjacent local administration of AVB-001 demonstrated that mIL-2 local concentration (intraperitoneal space) was 100x higher than the systemic concentration (blood) demonstrating the ability of the LOCOcyte™ platform to deliver native cytokines in vivo and create a high locoregional concentration of cytokines with limited peripheral exposure. Additional studies in mice demonstrated dose-dependent levels of IL-2 in the IP cavity in mice. Treatment of solid tumors using a single administration of AVB-001 demonstrated complete responses as monotherapy and provided sustained eradication of peritoneal tumors in ID8 ovarian cancer mouse model. Our data in mice confirmed that AVB-001 leads to a local increase in activation and proliferation of cytotoxic T-cells within the IP space in comparison to sham mice. In addition, in MC38 colorectal cancer rechallenge model it was observed that a single local administration of AVB-001 leads to complete tumor eradication as a single agent and was accompanied by systemic antitumor immune responses. A single administration of AVB-001 in NHP led to therapeutic levels of IL-2 in the IP cavity and produced local and systemic T-cell biomarker profiles that predict efficacy. In safety assessments of AVB-001, no signs of cytokine storm and vascular leak syndrome and no evidence of adverse pathologic effects on local or systemic tissue were observed with administration of AVB-001 expressing up to 16.7 µg hIL-2/kg in mice and 12.8 µg hIL-2/kg in NHP giving a sufficient safety window for the planning of our first clinical study.

Conclusions It was demonstrated that the AVB-001 is dose adjustable, safe and efficacious in preclinical animal models. Avenge Bio aims to pursue a Phase 1 First in Human study of AVB-001 in ovarian cancer patients. The LOCOcyte™ platform enables delivery of a diverse set of cytokines alone or in combination which is presently being explored.

<http://dx.doi.org/10.1136/jitc-2022-SITC2022.1094>

Abstracts

1095

IL-12-BASED CYTOKINE FACTORIES MODULATE TUMOR MICROENVIRONMENT TO ERADICATE PANCREATIC TUMORS IN MICE AND ARE WELL TOLERATED IN NON-HUMAN PRIMATES

¹Amanda Nash*, ¹Samira Aghlari-Fotovat, ¹Andrea Hernandez, ²Sofia Ghani, ²Ira Joshi, ²Douglas Ira, ²Peter Rios, ¹Omid Veisheh. ¹Rice University, Houston, TX, USA; ²Cell Trans Inc, Chicago, IL, USA

Background Pancreatic cancer is often diagnosed at advanced stages and responds poorly to chemotherapy.¹ Because high tumor T cell infiltration corresponds with better clinical outcomes in pancreatic cancer patients, immunotherapy has gained significant interest for treatment. IL-12 is a proinflammatory cytokine that activates CD8+ T cells and NK cells.² Unfortunately, systemic high dose IL-12 administration led to severe toxicities in clinical trials which limited further development of this cytokine as a cancer therapeutic. To address this limitation, we developed an implantable cytokine delivery platform for local administration of IL-12. These cytokine factories, composed of genetically engineered cells encapsulated in biocompatible polymers, allow for safe and controlled dosing *in vivo*.

Methods

Cytokine PK Studies Supernatant from individual capsules were assayed at 1-, 2-, 4-, or 24-hours using ELISA (n=6).

Mouse Studies For IP tumors, 1e6 pan02 cells were injected in the IP space of mice. Cytokine factories were implanted 7 days post tumor injection.

Primate Studies Cytokine factories were administered to cynomolgus macaques (n=1). Complete blood count and blood chemistry analysis were performed for 28 days after administration.

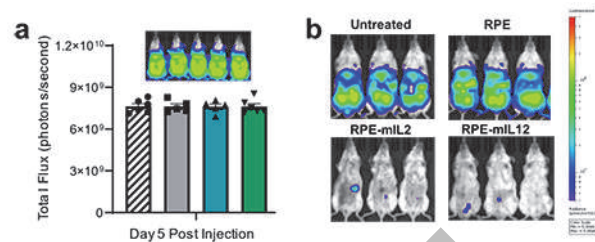
IVIS Imaging Mice were injected in the IP space with D-luciferin (300 µg/mL, PerkinElmer). Photographs and luminescent images were acquired 10 minutes after injection.

Results Local administration of IL-12-based cytokine factories caused reduction of pan02 tumor burden by 80% after 1 week of treatment in mice (figure 1). Single cell RNAseq of the tumor adjacent immune cells showed 2x more T cells in IL-12 treated mice than untreated mice suggesting immune cell infiltration. Importantly, the IL-12 dose was well tolerated in all mice for 180 days. In efforts to evaluate the translatability of this platform, we further tested IL-12-based cytokine factories in a non-human primate. The cytokine factories produced a high local IL-12 concentration without substantial leakage into the systemic circulation and were well tolerated by the primates as shown by the lack of fever or weight loss, as well as the lack of renal or liver toxicity.

Conclusions Our findings highlight the therapeutic potential of IL-12 treatments when administered locally via cytokine factories in preclinical animal models. Further, these findings provide rationale for future clinical testing of cytokine factories in a wide range of metastatic cancers in humans.

REFERENCES

1. Choudhry H, Helmi N, Abdulaal WH, Zeyadi M, Zamzami MA, Wu W, Mahmoud MM, Warsi MK, Rasool M, Jamal M.S, Prospects of IL-2 in Cancer Immunotherapy. *Biomed Res Int* 2018;**2018**: 9056173.
2. McDermott DF, Atkins MB. Interleukin-2 therapy of metastatic renal cell carcinoma—predictors of response. *Semin Oncol* 2006;**33**:583–587.



Abstract 1095 Figure 1 IL-12 cytokine factories reduce mice pancreatic tumor burden a) Total flux calculated from IVIS imaging prior to treatment with RPE-mIL2, RPE-mIL12, RPE only, or untreated (n=5). b) Representative IVIS images of each treatment group 5 days post treatment.

<http://dx.doi.org/10.1136/jitc-2022-SITC2022.1095>

1096

MWTX-330, AN IL-12 INDUKINE MOLECULE, SELECTIVELY ACTIVATES TUMOR INFILTRATING LYMPHOCYTES AND REPROGRAMS THE TUMOR MICROENVIRONMENT IN MURINE SYNGENEIC TUMOR MODELS

Christopher Nirschl*, Heather Brodtkin, Connor Dwyer, Daniel Hicklin, Nesreen Ismail, Celesztina Domonkos, Cynthia Seidel-Dugan, Philipp Steiner, Zoe Steuert, Jenna Sullivan, William Winston, Andres Salmeron. *Werewolf Therapeutics, Watertown, MA, USA*

Background Cytokines are powerful modulators of the immune system, making them a promising target for novel cancer immunotherapies. IL-12 is a pleotropic cytokine that acts on various immune cell populations, including professional APCs as well as adaptive and innate effector cells. Furthermore, recombinant IL-12 generates robust anti-tumor activity in murine models. However, its clinical use has been impeded by a poor pharmacokinetic profile and severe, sometimes fatal, adverse events following systemic administration. mWTX-330 is a selectively inducible IL-12 containing pro-drug (INDUKINE™ molecule) that is comprised of chimeric IL-12 (human p40, mouse p35) linked to a half-life extension domain and an inactivation domain by protease cleavable linkers. Following systemic administration, the inactivation domain keeps the molecule inactive in the periphery, while selective processing of the linkers in the tumor microenvironment results in the local release of chimeric IL-12.

Methods Mice bearing syngeneic tumors were treated with mWTX-330, and tumor growth and body weight were monitored over time. In some experiments tissues were harvested at various timepoints, and analyzed by flow cytometry, NanoString analysis, or other downstream techniques.

Results mWTX-330 generated robust anti-tumor immunity in multiple syngeneic tumor models, including MC38, CT26, B16-F10, and EMT-6. Antibody based depletion of the CD8+ T cells resulted in a loss of late tumor control, while depletion of CD8+ T cells, CD4+ T cells, and NK cells resulted in a complete loss of tumor control following mWTX-330 treatment. Furthermore, mWTX-330 treated mice that rejected primary tumors were protected against later rechallenge with the same tumor cell line. Systemic mWTX-330 treatment selectively activated tumor infiltrating immune cells, with little evidence of immune cell activation in the peripheral blood or secondary lymphoid tissues. Likewise, mWTX-330 was better tolerated than chimeric IL-12, while maintaining efficacy at a similar dose, resulting in a significant expansion of the therapeutic window due to the INDUKINE design of this molecule. Additionally, mWTX-330 treatment increased the frequency of polyfunctional CD8+ T cells, skewed CD4+ non-Tregs towards a TH1 phenotype, robustly drove NK cell production of effector cytokines within the tumor and triggered a metabolic re-invigoration of effector cells.

Conclusions These data highlight the preclinical potency and selective inducibility of mWTX-330 in various murine syngeneic tumor models. More importantly, they demonstrate the feasibility of the INDUKINE approach to address the clinical roadblocks seen with IL-12 therapy and support the ongoing clinical development of our IL-12 INDUKINE molecule containing a fully human payload, WTX-330.

<http://dx.doi.org/10.1136/jitc-2022-SITC2022.1096>

1097

MDK1654: A BRANCHED SYNTHETIC PEPTIDE THAT ACTIVATES BOTH THE IL-7 RECEPTOR AND THE $\beta\gamma$ C FORM OF THE IL-2/15 RECEPTOR

Inkyung Angie Park*, Steven Cwirla, Alice Bakker, Ronald Barrett, Michael Needels, Praechompoo Pongtornpipat, Blake Williams, Prarthana Joshi, William Dower. *Medicine, Menlo Park, CA, USA*

Background Derivatives of IL-2, IL-15, and IL-7 are in clinical development as immuno-oncology agents. IL-2 and IL-15 stimulate proliferation and enhance the function of effector T cells and natural killer cells, whereas IL-7 acts on naïve and memory T cells and is crucial for persistent effector T cell generation. Combining these complementary effects on immune cells may offer benefits over either mechanism alone. We have previously described small synthetic peptidyl agonists (PEPTIKINES), unrelated to IL-2, IL-15, or IL-7, that selectively activate either IL-2/15R $\beta\gamma$ c or IL-7R $\alpha\gamma$ c.

Methods Here we report the creation and pharmacology of a synthetic branched peptide, MDK1654, comprised of three peptide ligands binding to IL-7R α , IL-2/15R β , and γ c separately and linkers that are engineered to provide appropriate spatial orientation of the ligands. The *in vitro* pharmacology of MDK1654 was compared to non-alpha IL-2/15 or IL-7 mono-specific PEPTIKINES by signaling and immune cell proliferation.

Results MDK1654 can activate both IL-2/15R $\beta\gamma$ c and IL-7R $\alpha\gamma$ c signaling pathways as measured by phosphorylation of STAT5 and showed full agonist activity for both receptors with EC₅₀s <10 nM in naturally γ c-expressing TF-1 cells engineered to overexpress either IL-2R β or IL-7R α .

In *ex vivo* studies with PBMCs from 5 healthy donors, MDK1654 exhibited additive and complementary effects of IL-2/15R $\beta\gamma$ c and IL-7R $\alpha\gamma$ c signaling among various lymphocyte subpopulations. The mono-specific non-alpha IL-2/15 and IL-7 PEPTIKINES produced signaling patterns in lymphocyte subsets similar to those induced by IL-2v (a “non-alpha” mutant of IL-2) and IL-7, respectively. In the resting PBMCs, MDK1654 induced pSTAT5 and cell proliferation response profiles in CD8, CD4, and naïve and memory subpopulations similar to the IL-7 PEPTIKINE, including expansion of T_{scm} cells. In PBMCs activated with anti-CD3 antibody, a treatment known to increase IL-2/15R β expression, MDK1654 behaved similarly to the non-alpha IL-2/15 PEPTIKINE in most cell populations except for the T_{scm} population. NK cells were expanded by MDK1654 and the non-alpha IL-2/15 PEPTIKINE but not by the IL-7 PEPTIKINE.

Conclusions These data indicate that MDK1654 mimics the effect of the non-alpha binding form of IL-2/15 or IL-7, depending on the cell type. To our knowledge, this is the first demonstration of a synthetic peptide with agonist activity for two different cytokine receptors and offers an exciting new modality for cancer immunotherapy.

<http://dx.doi.org/10.1136/jitc-2022-SITC2022.1097>

1098

TARGETING WILDTYPE IL-2 TO CD8 T CELLS INDUCES POTENT ANTI-TUMOR IMMUNE RESPONSES AND DECREASES IL-2 MEDIATED TOXICITY

Selvi Ramasamy*, Joanathan Nardozi, Shannon Boi, Joanna Swain, Anthony Coyle, Stefano Gulla. *Repertoire Immune Medicine, Cambridge, MA, USA*

Background High dose IL-2 treatment in metastatic renal cell carcinoma and metastatic melanoma patients induced complete remission in 5%–10% of patients without recurrence for over 25 years and potentially cured 70% of these patients.¹ Although FDA approved for treatment of metastatic melanoma and renal cell carcinoma, the clinical utility of high-dose IL-2 is limited by significant multisystem toxicity, treatment-related mortalities in up to 4% of patients, and a lack of response in some patients. As a pleiotropic cytokine, IL-2 not only boosts the desired proliferation and effector function of T and NK cells, but also enhances detrimental immune suppression by expanding high affinity IL-2R($\alpha\beta\gamma$) expressing T_{reg} cells. Contributing to its toxicity, IL-2 also activates innate lymphoid cells (ILC) and IL-2R α^+ endothelial cells to cause vascular leak syndrome. A key challenge in developing IL-2 as a safe and efficacious cancer therapeutic is uncoupling its efficacy from its toxicity. Here, we present data to support that this could be achieved by linking wildtype IL-2 to an anti-CD8 antibody and selectively delivering IL2 to CD8 T cells.

Methods We separately linked wild type human IL-2 to anti-murine and anti-human CD8 or untargeted RSV antibodies for studies in murine and human systems, respectively. *In vitro* pharmacology was studied with mouse splenocytes and human PBMC. *In vivo* pharmacodynamics, efficacy, and toxicity were assessed in naive mice, B16F10 and MC38 syngeneic tumor models.

Results Incubating respective CD8-IL2s with mouse splenocytes and human PBMC selectively loaded IL2 on CD8 T cells. This resulted in potent pSTAT5 activation downstream of the IL-2R and CD8 T cell expansion compared to incubating with untargeted IL-2 antibody fusions. CD8-IL2 localization is driven by CD8 antibody affinity where as untargeted IL2 localization is driven by IL-2 affinity for its receptors. In naive mice, CD8-IL2 preferentially expanded CD8 T cells over T_{reg} and NK cells. In contrast, untargeted IL-2 primarily expanded high-affinity IL-2R positive T_{reg} and NK cells. In B16F10 syngeneic tumor bearing mice, untargeted IL-2 induced a dose dependent increase in inflammatory cytokines responsible for high toxicity and body weight loss. In contrast, treatment with CD8-IL2 significantly reduced toxicities but potently inhibited B16F10 and MC38 syngeneic tumor growth.

Conclusions Our data supports that selective targeting of IL-2 to CD8⁺ T cells minimizes exposure of other cell types to IL2 and reduce IL2 mediated toxicity. CD8-IL2 is expected to be a safe and effective cancer immunotherapy.

REFERENCE

1. Rosenberg SA. IL-2: the first effective immunotherapy for human cancer. *J Immunol.* 2014;**192**(12):5451–58

Ethics Approval All experimental animal procedures were approved by the Institutional Ethics Review Board.

<http://dx.doi.org/10.1136/jitc-2022-SITC2022.1098>

1099 ANV419 IS A NOVEL CD122-BIASED IL-2/ANTI-IL-2 FUSION PROTEIN SHOWING INCREASED EFFICACY IN COMBINATION WITH CHECKPOINT INHIBITORS AND TREATMENTS ACTING THROUGH ANTIBODY DEPENDENT CELLULAR CYTOTOXICITY

Christoph Huber*, Kirsten Richter, Laetitia Petersen, Nicole Egli, Patrizia Murer. *Anaveon AG, Basel, Switzerland*

Background ANV419 is an antibody-cytokine fusion protein with natural affinity to the heterodimeric IL-2R β / γ , but no affinity for IL-2R α / β / γ . As a result, ANV419 preferentially stimulates CD8 T cells and NK cells over regulatory T cells. ANV419 is currently being investigated in a phase I dose finding study in patients with solid tumors. The goal of this study is to evaluate the activity of ANV419 on NK and CD8 T cells and investigate the potential synergy of ANV419 with complementary immune-activating mechanisms. We also evaluated pharmacological combination partners enhancing the therapeutic potential of ANV419.

Methods The signaling properties of ANV419 were compared to recombinant hIL-2 and hIL-15 in human PBMCs. NK cell killing was analyzed in combination with trastuzumab. Mechanistic studies were performed to test the combination of ANV419 with checkpoint inhibitors using the H22 syngeneic tumor mouse model. The impact of checkpoint inhibitor combination on safety was tested in human whole blood.

Results To assess the impact of ANV419 treatment, human PBMCs were analyzed. NK and CD8 T cells showed comparable STAT5 phosphorylation kinetics upon treatment with ANV419, hIL-2 and hIL-15. Combination of ANV419 with the antibody-dependent cellular cytotoxicity (ADCC) inducing anti-HER2 antibody trastuzumab showed additive effects in NK cell killing compared to single trastuzumab treatment supporting clinical combination of ANV419 with treatments promoting NK cell mediated killing.

To assess the role of ANV419 in indications where T cells are involved in tumor resolution, ANV419 combination with the checkpoint inhibitors anti-PD1 or anti-CTLA4 was tested and showed additive effects in inducing tumor growth retardation in mice bearing H22 tumors compared to mice treated with single agents. Analysis of tumor infiltrating lymphocytes indicated intra-tumoral accumulation of NK and CD8 T cells. Treatment of whole blood with a combination of ANV419 and pembrolizumab (anti-PD1) or ipilimumab (anti-CTLA4) induced only slightly increased cytokine secretion compared to ANV419 alone and is therefore considered to have a reasonable safety profile.

Conclusions The data presented here further elucidate the *in vitro* and *in vivo* effects of ANV419 and support the rationale for clinical development in indications where NK and CD8 T cells are involved in tumor resolution as well as in combination with ADCC inducing treatments or checkpoint inhibitors.

<http://dx.doi.org/10.1136/jitc-2022-SITC2022.1099>

1100

IL-15 ENHANCES CYTOTOXICITY OF SIPULEUCEL-T FROM METASTATIC CASTRATION-RESISTANT PROSTATE CANCER PATIENTS BY ACTIVATING CD8+ T AND NK EFFECTOR CELLS

Muhammad Saeed*, Kevin Kim, Russell Pachynski. *Washington University School of Medicine, Saint Louis, MO, USA*

Background Prostate cancer is the most commonly diagnosed non-skin cancer in men, and metastatic castration-resistant prostate cancer (mCRPC) represents the most lethal form of the disease. Sipuleucel-T (sip-T) is an autologous active cellular immunotherapy approved by FDA for patients with mCRPC and has been shown effective in improving overall survival (OS) among individuals with mCRPC. To date, detailed analysis of the sip-T product has not been studied using an advanced mass cytometry approach. Here, we present high dimensional data describing the phenotype of sip-T in detail. Furthermore, we show the effects of IL-15 on the anti-tumor efficacy of sip-T using in vitro and in vivo studies.

Methods We performed a comprehensive assessment of sip-T (n=13 samples) from 10 patients with mCRPC, using high-throughput mass cytometry (CyTOF) comprised of 37 different antibodies/markers. Furthermore, we performed CyTOF on control and IL-15 stimulated sip-T and identified changes in leukocyte subsets as well as markers of activation and exhaustion. Finally, we examined the effects of IL-15 on cytotoxicity of sip-T against human prostate cancer cells (LNCaP and DU145) using in vitro cytotoxicity assays and in vivo studies in NSG mice.

Results CyTOF analysis revealed that CD3+ T-cells (including CD4+ and CD8+) constituted the highest proportion (median, range: 63%, 9-89%) of unstimulated sip-T, followed by CD19+ B-cells (4%, 1-82%), CD3-CD14-CD56+ natural killer (NK) cells (4%, 1-18%), and CD3-CD19-CD56-HLA-DR+CD11c+CD14+ monocytes (1%, 1-37%). Following sip-T stimulation with IL-15, a significant expansion and activation (increase in IFN γ +, CD95+, CD107+, and CD69+ cells) of CD8+ T-cell and NK cell populations was seen. A significant increase in signature cytokines (e.g. IFN γ and granulysin) in cell supernatants was also seen after IL-15 stimulation. Furthermore, IL-15 stimulated sip-T showed significantly higher cytotoxicity of LNCaP and DU145 cells in vitro. Adoptive transfer of IL-15 stimulated sip-T into LNCaP-bearing NSG mice resulted in significantly reduced tumor growth compared with those receiving untreated sip-T. Evaluation of tumor-infiltrating lymphocytes revealed a significant expansion of CD8 T-cell/NK populations and reduction in exhausted (PD1+, TIM3+) T-cell/NK cells in the IL-15-sip-T group compared to controls.

Conclusions This is the first comprehensive study to evaluate the composition of sip-T from mCRPC patients using high dimensional CyTOF analysis, and serves as an important reference source for further modification and improvement of sip-T efficacy. Furthermore, our data is the first to show that the addition of IL-15 to sip-T could potentially enhance the efficacy of sip-T in mCRPC patients.

<http://dx.doi.org/10.1136/jitc-2022-SITC2022.1100>

1101

ASKG315 – AN IL-15 PRODRUG WITH ANTIBODY-LIKE PK, ENHANCED SAFETY AND EXPANDED THERAPEUTIC WINDOW

¹Chunxiao Yu*, ¹Kurt Shanebeck, ²Jieye Sun, ²Chao Wang, ¹Shiguang Yu, ¹Jeannie Luiz, ¹Ray Chuang, ¹Ming Li, ²Yong Wen, ¹Jeff Lu, ¹Yuefeng Lu. ¹AskGene Pharma Inc., Camarillo, CA, USA; ²Aosaikang Biotherapeutics Co Ltd, Nanjing, China

Background AskGene has established a proprietary cytokine prodrug platform (Smartkine[®]) to achieve its overarching objective of modulating immune reactions at a disease site in a selective and controlled manner. Cytokines are potent molecules, yet their broad application as therapeutics has been hampered due to short PK, severe systemic toxicity, and narrow therapeutic window. To improve the therapeutic potential of cytokines, AskGene has developed several cytokine prodrugs using its proprietary SmartKine[®] platform. To our knowledge, ASKG315 is the first IL-15 prodrug moving into clinical development.

Methods The in vitro activities of ASKG315 were evaluated using reporter assay and PBMC-based assays. The anti-tumor activities were tested in human PBMC-engrafted tumor xenograft models. The PK/PD properties and safety profiles of ASKG315 were assessed in non-human primates (NHPs) following three IV injections every two weeks.

Results ASKG315 showed minimal activity prior to protease-dependent activation and significantly enhanced activity after protease-dependent activation in vitro. It selectively stimulated NK cells and CD8+ T cells in vitro. In in vivo efficacy studies, ASKG315 at 0.3 mg/kg showed similar potency and better safety compared to a reference IL-15 molecule (unmasked) at 0.5 mg/kg, suggesting that ASKG315 had an expanded therapeutic window. These results also showed that, compared to the reference molecule, ASKG315 had similar or higher immune stimulation in the tumor while having significantly reduced immune stimulation in the periphery. In NHPs, ASKG315 demonstrated prolonged and antibody-like PK profiles. It selectively induced proliferation of NK cells and CD8+ T cells while showing minimal effect on CD4+ T cells in vivo. In addition, ASKG315 was well tolerated at the highest dosage tested in NHPs, with no cytokine release syndrome (CRS) and minimal immune reaction at injection sites.

Conclusions Activated ASKG315 showed selective stimulation for NK cells and CD8+ T cells in vitro and in vivo. ASKG315 in vivo showed less periphery immune activation and higher anti-tumor activity compared to the reference molecule. In addition, it had extended antibody-like PK in NHPs and was well tolerated at the highest dosage tested in the GLP safety study. It also showed a significantly expanded therapeutic window. A first-in-human (FIH) study for ASKG315 is expected to start in the second half of 2022.

Ethics Approval The uses of the animals in the in vivo studies were approved by the ethics committees of the CROs who performed the studies.

<http://dx.doi.org/10.1136/jitc-2022-SITC2022.1101>

1102

A SINGLE SPARK CAN START A PRAIRIE FIRE – RE-THINK THE COMBINATION STRATEGY AND CLINICAL SETTING OF IL-12 WITH ANTI-PD-1

¹Pei-Yi Tsou, ¹Wan-Ying Lin, ¹Meng-Na Lee*, ²San-chi Chen. ¹Libo Pharma Corp., New Taipei City, Taiwan; ²Taiwan Veterans General Hospital, Taipei, Taiwan

Background Immune-checkpoint inhibitors have become the standard therapy in many types of cancers. The combination of anti-PD-1 and anti-CTLA4 demonstrated better anti-tumor response, but toxicity is a concern. Cytokines including IL-2, IL-12, IL-15, IL-21 that target immune cells have been developed to enhance immune response against tumors. IL-12, a multifunctional and potency cytokine, regulates both innate and adaptive immunity. IL-12 is considered to: (1) promote the proliferation and survival of T cell; (2) upregulate the chemokine and adhesion molecule to facilitate lymphocyte trafficking; (3) and trigger the T cell:DC crosstalk in combination with aPD1 treatment which might could potently enhance antitumor immunity. Therefore, this study aims to explore the synergistic anti-tumor immune response of IL-12 and anti-PD-1.

Methods Demonstrate the combination tumor growth inhibition effect in 11 (MBT-2, MC38, CT-26, B16F10, 4T1, RENCA, B16F10, Hepa1-6, EMT-6, LL/2, J558) syngeneic mice tumor bearing model. Dose dependent effect, dosing sequential effect, and immunophenotyping in tumor microenvironment (TME) is conducted in CT26 and MC38 tumor bearing model. Mixed lymphocyte reaction (MLR) assay of Keytruda and human recombinant IL-12 (rHu-IL12) combination is conducted for *in vitro* lymphocyte proliferation and activation assessment.

Results MBT-2, MC38, EMT-6, Hepa 1-6, and J558 is moderate to high responding to mIL-12 monotherapy (TGI 30 ~ 90%); CT-26 and 4T1 is slight responding to mIL-12 monotherapy (TGI 10 ~ 20%); LL/2, RENCA and B16F10 is non-responding to mIL-12 monotherapy. Anti-PD-1 combine with mIL-12 has permissive effect in MC38 (TGI 70% vs. 70% vs. 95%) and J558 (TGI 10% vs. 30% vs. 30%); has synergetic effect in CT26 (TGI 20% vs. 25% vs. 60%); and indifference in B16F10 and 4T1. Immunohistochemical and flow cytometric analyses confirmed that CD8+ T cells accumulate at the tumor margin and infiltrate the tumor mass in response to the combination therapy, resulting in favorable effector and regulatory T-cell ratios (12.33% : 4.64% to 18.40% : 2.03%), M1/M2 ratios (0.07%:0.08% vs. 0.1%:0.01%). In the MLR assay, rHu-IL12 could enhance the T cell proliferation combined with Keytruda; the T cell activation biomarker (CD25, CD69, HLA-DR) is also induced higher in rHu-IL12 combination group.

Conclusions Systemic mIL-12 administration could show the robust tumor growth inhibition effect under specific TME setting, and reshape the tumor microenvironment even at extremely low concentration (20~50ng/mice). It gives us a hint to re-think the clinical setting and combination strategy of rHu-IL12 with anti-PD-1.

<http://dx.doi.org/10.1136/jitc-2022-SITC2022.1102>

1103

HALF-LIFE EXTENDED, CONDITIONALLY ACTIVE IFNA PRODRUG INDUCES TUMOR-SELECTIVE ACTIVATION AND POTENT ANTITUMOR RESPONSE

Alice Yam*, Kshama Doshi, Krishna Bajjuri, Millicent Embry, Frank Xiao, Grace Lee, Stephanie Armstrong, Daniel Calarese, Xiaofan Li, Gang Yin, Kristin Bedard, Trevor Hallam. *Sutro Biopharma, South San Francisco, CA, USA*

Background Type-1 Interferons (IFN) are known to elicit both direct antitumor effects as well as modulate tumor microenvironment (TME) to induce antitumor immune responses. Combination of IFNa with PD-1 blockade has shown promising outcomes in patients with melanoma. However, clinical use of currently marketed IFNa products is limited due to poor systemic tolerability. Using our breakthrough XpressCF+TM cell-free technology we have developed a conditionally active IFNa-2b prodrug designed to widen the therapeutic window by virtue of limited systemic activation and preferential tumor-selective activation.

Methods IFNa-2b was prodrugged via site-specific conjugation of releasable polyethylene glycol (PEG) molecules, enabling both half-life extension (HLE) and tumor-selective demasking of the interferon molecules. PEG molecules were attached via a tumor selective linker, taking advantage of specific protease enrichment in the TME across a broad range of cancer indications. The size of PEG and sites of conjugation were chosen to enable an optimal balance of HLE, prodrug attenuation, demasking and potency of released catabolite.

Results In-vitro human IFNa-2b prodrug (IFNa-2b-prodrug) was greater than 1000-fold attenuated compared to recombinant IFNa-2b, thus supporting reduced systemic activation. However, on release of PEG activity of the catabolite is fully restored and comparable to wild-type protein. Site-specific PEG conjugation also conferred significant HLE supporting less frequent systemic administration. In mouse xenograft model MDA-MB-231 grown in immunocompromised mice, IFNa-2b-prodrug induced greater antitumor activity compared to control IFNa-2b variant with a non-releasable PEG mask. At equivalent doses, antitumor activity of the prodrug was significantly greater in mice engrafted with human peripheral blood mononuclear cells. This suggests IFNa-2b-prodrug elicits antitumor response both via direct action on tumor cells and by engaging the immune system. Mouse surrogate for IFNa-2b-prodrug induced potent tumor growth inhibition in both immunogenic and less immunogenic syngeneic tumor models. Response in syngeneic models was associated with increased expression of cytotoxic effector molecules in TME. Finally, we used hamsters to assess tolerability and showed that single dose of IFNa-2b-prodrug is well tolerated up to 45 mg/kg with no body weight loss and minimal liver enzyme induction. In contrast, both HLE-IFNa-2b variant and IFNa-2b-prodrug masked with a more permissible PEG linkage, exhibited poor tolerability associated with significant systemic activation.

Conclusions In summary, these preclinical data suggest this novel HLE, tumor-selective human IFNa-2b prodrug has the potential to improve therapeutic index of IFNa therapies. Moreover, the results also support further development of this molecule as a single agent and in a combination setting.

<http://dx.doi.org/10.1136/jitc-2022-SITC2022.1103>

1104

A SAFE AND HIGHLY POTENT PD-1-IL-2 FUSION (AWT020) THAT DECOUPLES THE EFFICACY AND TOXICITY OF IL-2 THERAPY

¹Fan Ye*, ¹Zoey Huang, ¹Lili Cheng, ¹Jianing Huang, ¹Sandra Chen, ¹Michael Hua, ¹Danny Huang, ¹Ella Li, ¹Jenny Jiang, ¹Hanna Lin, ¹Xin Wang, ¹Bella Yue, ¹Shirley Shi, ¹Henry He, ¹Karen Yan, ²Binfeng Lu*, ¹Ziyang Zhong. ¹Anwita Biosciences, Mountain View, CA, USA; ²University of Pittsburgh, Pittsburgh, PA, USA

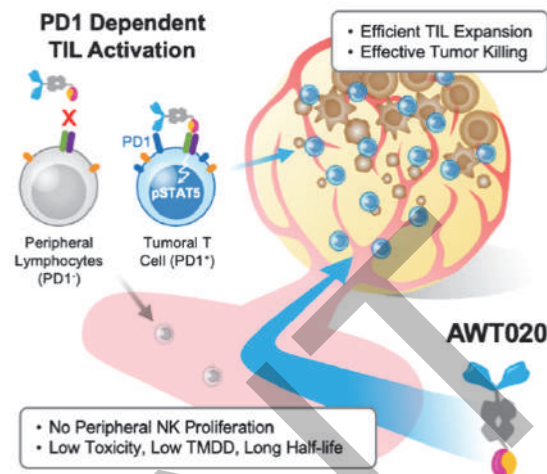
Background Interleukin 2 (IL-2) is a pivotal immune agonist for tumor immunotherapy that has demonstrated its clinical efficacies in melanoma and renal cell carcinoma. Nevertheless, its pleiotropic effect has led to severe side effects and its anti-tumor activity is compromised by its activation of regulatory T cells. In contrast, the PD-1 blockade-based cancer immunotherapy has good safety profiles by targeting and sustaining the activity of tumor-antigen specific T cells within cancer tissues. To take advantage of the complementary antitumor activity of PD-1 monoclonal antibody (mAb) and IL-2, a bifunctional fusion protein composed of PD-1 mAb and IL-2c mutein (AWT020) is designed to enhance the therapeutic efficacy while reducing the IL-2 related toxicity (figure 1).

Methods The in vitro activity of AWT020 was verified using STAT5 signaling assays and human PBMC proliferation assays. A mouse surrogate of AWT020 (mAWT020) was tested in multiple syngeneic tumor models including colon carcinoma models (MC38 and CT26), melanoma model (B16F10), and breast carcinoma model (EMT6). The tolerability, pharmacokinetics (PK), and pharmacodynamics (PD) of AWT020 were accessed in cynomolgus monkeys.

Results AWT020 stimulated much greater pSTAT5 activation and proliferation in PD-1⁺ T cells than PD-1⁻ T cells. The high specificity of AWT020 on PD1⁺ T cells not only minimizes the systematic toxicity but also improved the anti-tumor efficacy. In PD-1 resistant B16F10 and EMT6 models, mAWT020 achieved >90% TGI, while in CT26 tumor, mAWT020 treatment achieved 70% complete response (CR). In MC38 model, mAWT020 achieved 100% CR with a single dose at 0.3 mg/kg. Cell phenotyping studies showed that mAWT020 specifically and significantly expands tumor-infiltrating CD8⁺ T cells but has minimal effects on peripheral T cells and NK cells. Global gene expression profiling studies showed that mAWT020 significantly elevated expression levels of Cd3d, Cd3e, Cd8a, Il2r α , Cxcr3, Cxcr6, Zap70, Lck, and Pdc1 inside tumor tissues, indicating a specific expansion and activation of T cells. Single dose study at up to 10 mg/kg in cynomolgus monkeys showed that AWT020 was well tolerated, with good exposure and long half-life.

Conclusions The high target specificity of AWT020 significantly mitigates the IL-2 related adverse side effects and allows it to be dosed at a much higher level compared to IL-2 therapy, achieving full blockade of PD-1 and optimal activation of intratumoral CD8⁺ T cells.

Ethics Approval The protocol of animal studies has been reviewed and approved by IACUC.



Abstract 1104 Figure 1 MOA of AWT020
AWT020 is highly specific to tumor infiltrated T cells

<http://dx.doi.org/10.1136/jitc-2022-SITC2022.1104>

Woong Hee Yoon*, Junhyeok Heo, Daeun Kim, Geona Kim, Kyungmi Han, Jun-Young Lee. *Selexcine, Seoul, Korea, Republic of*

Background SLC-3010 is a noncovalent conjugate of IL-2 and anti-IL-2 antibody (TCB2) that can preferentially stimulate CD8 T cells and NK cells over Tregs. It is achieved by blocking the binding of IL-2 to the IL-2R α , which is predominantly expressed on the Tregs. Previously we have reported that SLC-3010 exhibited strong anti-tumor activity in various mouse tumor models.¹ Notably, the dissociated TCB2 persisted in serum for several weeks despite the clearance of SLC-3010 within 72 h. We hypothesized that the dissociated TCB2 can intercept the endogenous IL-2, thereby suppressing the Tregs while stimulating the CD8 T cells and NK cells. Such versatility was termed as the triple action, and the proof-of-concept studies were conducted. GLP toxicity and pharmacodynamic studies were also performed, which provided promising results for the safety and efficacy.

Methods GMP batch of SLC-3010 was manufactured at GenScript Probio. POC studies for the triple action were performed in mice either by administrating the anti-mouse IL-2 antibody (S4B6, functional substitute of TCB2 in mice) after the SLC-3010 to measure the Treg suppression, and by injecting the TCB2 several weeks ahead of IL-2 to validate the re-conjugation of TCB2 with the endogenous IL-2. GLP PK, PD, and toxicology assessments were conducted in mice or cynomolgus monkeys after i.v. injecting various doses of SLC-3010 or TCB2.

Results The potency of the dissociated TCB2 to enable the additional anti-cancer mechanisms was studied in mice. Co-treatment of SLC-3010 and S4B6 reduced the number of Tregs and Foxp3 expression, which is a functional indicator of Treg. In addition, TCB2 remained for weeks and reinitiated the immunostimulatory function upon the IL-2 encounter. GLP PK and PD studies in the cynomolgus monkeys demonstrated the selective expansion of CD8 T cells and NK cells. Adverse effects were unobserved in all dose groups of mice and monkeys in the pathological aspects. Half-lives of SLC-3010 were approximately 14 and 8 hours in mice and monkeys, respectively.

Conclusions

- SLC-3010 is a noncovalent conjugate of IL-2 and TCB2, of which nature enables the “triple action” including the selective stimulation of anti-cancer immunity, disruption of Treg homeostasis, and re-boosting the immune system through the conjugation with the endogenous IL-2.
- Favorable GLP toxicity results provided a large safety margin, with the NOAEL being over 30 folds greater than the initial dose (DL1) of the phase 1 clinical trial.

Acknowledgements We thank to the Pohang Institute of Science and Technology (POSTECH) for generously providing the research facilities. We are also grateful for Dr. Jae-Ho Cho for the scientific collaboration and the support.

REFERENCE

1. Lee JY, Lee E, Hong SW, *et al.* TCB2, a new anti-human interleukin-2 antibody, facilitates heterodimeric IL-2 receptor signaling and improves anti-tumor immunity. *Oncoimmunology*. 2020;**9**:e1681869.

1106 **HZ-S506, A SELECTIVE AND ORALLY BIOAVAILABLE
HPK1 DEGRADER, IS EFFICACIOUS AS A SINGLE AGENT
OR IN COMBINATION WITH PD-1 ANTIBODY**

Yizhe Wu*, Xinglu Zhou, Tingting Jin, Xinxin Jin, Yizhe Wu. *Hangzhou HeaZen, Hangzhou, China*

Background Hematopoietic Progenitor Kinase 1 (HPK1/ MAP4K1) has been demonstrated to restrain T cell activation through phosphorylation of SLP-76 at Serine 376 leading to TCR signal blocking. The negative feedback role of HPK1 in TCR signaling makes it a promising target for immunooncology therapy. Several HPK1 inhibitors have entered into phase 1 clinical trial. However, the HPK1 selectivity against other MAP4Ks family protein is still challenging, which may lead to the weakening of HPK1-targeted therapy. Recently, PROTeolysis TArgeting Chimera (PROTAC) is a bifunctional molecule that can bring the target protein and E3 enzyme closer for ubiquitination labeling, and the target protein can be degraded by UPS system. Therefore, in theory, it can reduce the generation of drug resistance and avoid the problem of off target inhibition to further enhance subtype selectivity.

Methods HZ-S506 was discovered based on our team's unique DaTProD[®] platform. Western blot and HPK1 biochemical assay were used to analyze HPK1 degradation and inhibition. T cell activation and SLP-76 phosphorylation were also conducted. The in-vivo anti-tumor efficacy was assessed in C57BL/c mice which were engrafted with CT-26 cell line.

Results We found that HZ-S506 potently inhibited HPK1 kinase activity ($IC_{50} = 4.6$ nM) under K_m concentration of ATP, and it also had good selectivity against other MAP4K family members. HZ-S506 catalyzed the degradation of HPK1 in Jurkat and PBMC ($DC_{50} < 10$ nM). HZ-S506 treatment of Jurkat T cell demonstrated robust HPK1 degradation without significant downregulation of other off-target proteins in the proteomics experiment. HZ-S506 had stimulatory effect on immune response by increasing in IL-2 production ($EC_{50} = 279.1$ nM) in Jurkat cell with stimulation with anti-CD3 and anti-CD28, which was more significantly more potent. Treatment with HZ-S506 also can overcome PGE2 mediated immune-suppression. Interestingly, HZ-S506 possessed excellent pharmacokinetic properties, the exposure of which is higher than its parent inhibitor (~2 folds). In efficacy studies, HZ-S506 exhibited anti-tumor activity CT26 tumor model as single agent and in combination with an anti-PD1 antibody, demonstrated robust anti-tumor activities of anti-PD1 efficacy in 4T1 and MC38 syngeneic tumor models.

Conclusions In summary, HZ-S506 is a potent and selective degrader of HPK1 with good ADME properties and efficacy. These results support further development of HZ-S506 as a single-agent or combinational therapy with the current checkpoint inhibitors.

Acknowledgements Prof. Xiaowu Dong (Institute of Drug Discovery and Design, College of Pharmaceutical Sciences, Zhejiang University, Hangzhou 310058, P. R. China)

Ethics Approval All animal studies were performed in strict accordance with the institutional guidelines as defined by the Institutional Animal Care and Use Committee (IACUC), approved by the Animal Care and Use Committee, Zhejiang University Laboratory Animal Center (Hangzhou, China), approval ID: 20210068. All participants gave informed consent before taking part.

<http://dx.doi.org/10.1136/jitc-2022-SITC2022.1106>

1107

ANTI-HVEM MAB THERAPY IMPROVES ANTITUMORAL IMMUNITY BOTH *IN VITRO* AND IN A NOVEL MICE MODEL EXPRESSING HUMAN HVEM AND BTLA MOLECULES USING HVEM EXPRESSING TUMORS

¹Demerle Clemence, ¹Laurent Gorvel, ²Marielle Mello, ³Sonia Pastor, ³Clara Degos, ²Ana Zarubica, ²Frederic Fiore, ³Geoffrey Guittard, ⁴Bernard Malissen, ²Herve Luche, ⁵Jacques Fieschi-Meric, ⁶Laurent Greillier, ⁷Fabrice Barslesi, ¹Daniel Olive*. ¹Institute Paoli Calmettes, Marseille, France; ²CIPHE, Marseille, France; ³Cancer Research Center Marseille, Marseille, France; ⁴Centre d'Immunologie de Marseille-Luminy, Marseille, France; ⁵Veracyte, Marseille, France; ⁶Assistance Publique- Hopitaux Universitaires de Marseille, Marseille, France; ⁷Gustave Roussy, Paris, France

Background TNFRSF-14/HVEM is a molecule that is the ligand for BTLA and CD160 immune co-inhibitory molecules as well as viral proteins. Its expression is dysregulated with an overexpression in tumors and a connection with tumors of adverse prognosis

Methods We developed models expressing huBTLA and huHVEM in C57/bl6 mice as well as mAbs that completely prevent the interactions of HVEM with its ligands. We also generated mutants of HVEM devoid of the binding sites for BTLA and CD160 binding

Results Here, we show that anti-HVEM18-10 increases primary human alpha beta T cells activity alone (Cis-activity) or in presence of HVEM expressing lung or colorectal cancer cells in vitro (Trans-activity). HVEM18-10 synergizes with anti-PDL1 antibody to activate T cells in presence of HVEM⁺PDL-1⁺tumors, but is sufficient to trigger T cell activation in presence of PD-L1⁺cells. In order to better understand HVEM18-10 effect in vivo and especially CIS and TRANS effects, we developed cutting edge Human BTLA expressing mouse model (BTLA hu KI) and a mouse model expressing both human BTLA and human HVEM (BTLA^{huKI}/HVEM^{huKI} or DKI). *In vivo* pre-clinical experiments performed in both mouse models showed that HVEM18-10 treatment was efficient to decrease human HVEM⁺ tumor growth. This effect was more pronounced in DKI mice and linked to an increase in CD8⁺cytotoxic T cells tumor infiltration. Interestingly, in both settings, tumor free mice appeared (\pm 20%) and did not develop tumors upon re-challenge, therefore showing a marked T cell memory effect.

Conclusions Altogether, our preclinical models validate anti-HVEM18-10 as a promising antibody to use in clinics alone or in combination with existing therapies such as anti-PD-L1.

Trial Registration The study presented here is part of the clinical trial PIONeeR BioMarqueurs registered under the number NCT03493581 and part of the RHU PIONeeR ANR-17-RHUS-0007.

Ethics Approval Animal housing and experimental procedures have been conducted according to the French and European Regulations (Parlement Européen et du Conseil du 22 Septembre 2010. Décret n°2013-118 du 1er Février 2013 relatif à la protection des animaux utilisés à des fins scientifiques). All animal procedures (including surgery, anesthesia and euthanasia as applicable) used in the current study have been submitted to the Institutional Animal Care and Use Committee of CIPHE approved by French authorities (CETEA DSV -APAFIS#6151- 201607202339418-V5).

<http://dx.doi.org/10.1136/jitc-2022-SITC2022.1107>

1108 **SCREENING FOR IMMUNE RESPONSE INDICATORS AFTER P53 GENE TRANSFER AND CABAZITAXEL TREATMENT IN HUMAN PROSTATE CARCINOMA *IN VITRO***

¹Nadine Assis*, ²Bryan Strauss. ¹Universidade de São Paulo, São Paulo, Brazil; ²Instituto do Câncer do Estado de São Paulo, São Paulo, Brazil

Background Prostate cancer is among the most common cancers in men worldwide¹ and despite current treatment options, patients with metastatic disease have a five-year survival rate of only 31% in the United States.² Taxane chemotherapy is the standard of care for metastatic Castration-Resistant Prostate Cancer (mCRPC) with cabazitaxel as second-line treatment, however, it causes grade ≥ 3 adverse effects such as neutropenia, leukopenia and anemia.³ Our group has previously shown that p53 gene transfer sensitized prostate cancer cells to cabazitaxel, permitting the application of lower drug doses, thus avoiding toxicity, while still achieving complete inhibition of tumor progression in a mouse model.⁴ Integrating our encouraging results with recent findings on the relevance of p53 reinstatement in initiating an anti-tumor immune response^{5,6} here we present data related to the validation of experimental conditions, examination of cell death and gene expression analysis of indicators of immune response in human mCRPC cells *in vitro*.

Methods PC3 human carcinoma cells were transduced with AdRGD-PG-p53, AdRGD-PG-eGFP or AdRGD-PG-Luc non-replicative serotype 5 adenoviral vectors and treated with the 25% inhibitory concentration (IC₂₅) of cabazitaxel. Flow cytometry was used for assessment of vector transduction efficiency after transduction with the GFP vector as well as evaluation of hypodiploid cell population after p53 gene transfer and treatment with low-dose cabazitaxel, which was complemented with MTT assay for determination of cell viability. Screening for indicators of immune response was performed by quantitative PCR for genes involved in recognition of tumor cells by immune cells, IFN signaling and antigen processing and presentation in the tumor cells after combined treatment.

Results Combined treatment led to an approximately 50% reduction in cell viability, showing a potentiation of the cytotoxic effects of each treatment alone. Induction of p53-target genes (e.g. CDKN1A, HDM2 and NOXA1) was confirmed together with the modulation of genes of immune activation pathways (e.g. TLR3, IRF1, ISG15 and TAP1). Genes involved in the recently described Viral Mimicry Response (e.g. HERV-E and DNMT1) were also shown to be modulated, mainly as a result of p53 restoration in our model.

Conclusions Both cabazitaxel treatment and p53 gene transfer were shown to display important reduction in viability of PC3 cells, especially when combined. Modulation of important immune response mediators, at least at the mRNA level, encourages us to proceed to protein and immunology assays.

Acknowledgements This work has been supported by the São Paulo Research Foundation (FAPESP). We thank Fernanda Antunes and Nayara Gusmão Tessarollo for technical assistance.

REFERENCES

1. Sung H, Ferlay J, Siegel RL, Laversanne M, Soerjomataram I, Jemal A, Bray F. Global Cancer Statistics 2020: GLOBOCAN Estimates of Incidence and Mortality Worldwide for 36 Cancers in 185 Countries. *CA Cancer J Clin.* 2021;**71**(3):209–249.
2. Siegel RL, Miller KD, Fuchs HE, Jemal A. Cancer statistics, 2022. *CA Cancer J Clin.* 2022;**72**(1):7–33.

3. de Bono JS, Oudard S, Ozguroglu M, Hansen S, Machiels JP, Kocak I, Gravis G, Bodrogi I, Mackenzie MJ, Shen L, Roessner M, Gupta S, Sartor AO, TROPIC Investigators. Prednisone plus cabazitaxel or mitoxantrone for metastatic castration-resistant prostate cancer progressing after docetaxel treatment: a randomised open-label trial. *Lancet.* 2010;**376**(9747):1147–54.
4. Tamura RE, Lana MG, Costanzi-Strauss E, Strauss BE. Combination of cabazitaxel and p53 gene therapy abolishes prostate carcinoma tumor growth. *Gene Ther.* 2020;**27**(1-2):15–26.
5. Guo G, Yu M, Xiao W, Celis E, Cui Y. Local Activation of p53 in the Tumor Microenvironment Overcomes Immune Suppression and Enhances Antitumor Immunity. *Cancer Res.* 2017;**77**(9):2292–2305.
6. Zhou X, Singh M, Sanz Santos G, Guerlavais V, Carvajal LA, Aivado M, Zhan Y, Oliveira MMS, Westerberg LS, Annis DA, Johnsen JL, Selivanova G. Pharmacologic Activation of p53 triggers viral mimicry response thereby abolishing tumor immune evasion and promoting antitumor immunity. *Cancer Discov.* 2021;**11**(12):3090–3105.

<http://dx.doi.org/10.1136/jitc-2022-SITC2022.1108>

1109 **PROGESTERONE IMPACTS THE GROWTH AND IMMUNE CELL INFILTRATION OF MURINE MAMMARY GLAND TUMORS**

¹Laurny Werner*, ¹Eilidh Chowanec, ¹Julio Tinoco, ¹Harmony Saunders, ¹Dominika Helm, ¹Sean Holloran, ¹Richard Hastings, ¹Junping Wei, ²Gangjun Lei, ²Xiao-Yi Yang, ¹Mary Markiewicz, ¹Prabhakar Chalise, ³Justin Balko, ²Zachary Hartman, ¹Christy Hagan. ¹University of Kansas Medical Center, Kansas City, KS, USA; ²Duke University School of Medicine, Durham, NC, USA; ³Vanderbilt University Medical Center, Nashville, TN, USA

Background Clinical studies have linked usage of progestins (synthetic progesterone) to breast cancer risk. However, little is understood regarding the role of native progesterone (P4), signaling through the progesterone receptor (PR), in breast tumor formation. Recently, we demonstrated that P4 treatment or PR overexpression can drive changes in immune cell populations in the murine mammary gland and that PR overexpression leads to increased development of mammary gland tumors in mice. Given these findings, we sought to investigate whether P4 impacts tumor growth and immune cell infiltration of mammary gland tumors.

Methods To evaluate the effect of P4 on PR+ mammary gland tumor growth, orthotopic syngeneic mammary gland tumors were utilized. Briefly, mice were implanted with P4 (30mg) or placebo pellets and were injected with mammary gland tumor cells. After 28 days, tumors were excised and immunophenotyping was performed via flow cytometry. To determine the effect of anti-progestin treatment on mammary gland tumor growth and immune cell infiltration, two syngeneic mammary gland tumor models were used, in which mice were implanted with onapristone (30mg) or placebo pellets followed by mammary gland tumors. After 28 days, tumors were excised and immunophenotyping was performed via flow cytometry. The experiment was repeated in SCID mice to determine if effects of onapristone were immunologically mediated.

Results In syngeneic mammary gland tumor models, P4 promoted tumor growth and impacted immune cell infiltration of PR+ mammary gland tumors. Numbers of tumor-infiltrating dendritic cells were decreased and exhausted T cells and regulatory T cells were increased with P4 treatment in PR+ tumors. Onapristone treatment led to significantly decreased tumor volumes in two syngeneic mammary gland tumor models and reversed the effect that P4 had on tumor-infiltrating regulatory T cells. To determine if inhibition of tumor growth by onapristone was immunologically mediated, SCID mice bearing PR+ mammary gland tumors were treated with onapristone. Results revealed a decreased ability of onapristone to inhibit tumor growth in SCID mice compared to immunocompetent mice, suggesting that inhibition of tumor growth is, in part, immunologically mediated.

Conclusions These findings offer a novel mechanism of P4-driven mammary gland tumor development and provide rationale in investigating the usage of anti-progestin therapies to promote immune-mediated elimination of mammary gland tumors.

<http://dx.doi.org/10.1136/jitc-2022-SITC2022.1109>

1110 EFFECT OF SUB-ABLATIVE HYPERTHERMIA ON PD-1/PD-L1 AXIS MODULATION IN THE TUMOR MICROENVIRONMENT

Md Raihan Chowdhury, Mohamed Farghaly Ramadan, Vassiliki Boussiotis, Muneeb Ahmed, Marwan Moussa*. Beth Israel Deaconess Medical Center, Boston, MA, USA

Background Lack of intratumoral immune checkpoint receptor (ICR) expression results in resistance to immune check point inhibitors (ICIs), limiting their clinical efficacy in many patients. Here we investigate the modulatory effect of percutaneous sub-ablative hyperthermia (SA-HT) on PD-1/PD-L1 axis as a potential strategy to modulate ICR expression towards ICI responsiveness.

Methods A three phase experiment was performed. In phase 1, an *in-vitro* experiment was performed using breast adenocarcinoma R3230 cells, exposed to variable thermal doses (41, 43 and 45 all ± 1 °C) for variable durations (5- 60 min, 5 times). Cells were propagated, and supernatant and cells were collected at 0-11d (6 times) post-treatment. Soluble PD-L1 (sPD-L1) in supernatant was analyzed using ELISA. In phase 2, 3 cell lines of different species and cell type (R3230/rat, Hepa 1-6/mouse and HeLa/human) were treated with effective thermal doses (41°C x 60 mins (HT41), 43°C x 30 mins (HT43) & 45°C x 15 mins (HT45)), informed by phase 1 results. Propagated cells were collected up to 14d post-treatment and evaluated for c-Met (a potent PD-L1 regulator) and PD-L1 expression by flow cytometry. Finally, a phase 3 *in-vivo* validation was performed by using 6 Fisher rats with 10-12 mm R3230 tumors, randomized to hyperthermia (HT; SA-HT @ 45°C x 15 mins) (n=3) or control (n=3). Animals were sacrificed at 7d and tumors harvested for FC.

Results In phase 1, specific SA-HT doses demonstrated effective PD-L1 modulation. Specifically, sPD-L1 demonstrated significant decrease in comparison to control at days 2, 4 and 7-9 at a treatment of HT45, HT43 and HT41, respectively, $p < 0.05$ for all. In phase 2, response to SA-HT varied by tumor type. R3230 cells demonstrated downregulation of cMet/PD-L1 in HT45 at 7 days of post treatment ($p < 0.05$). However, HeLa cells demonstrated upregulation of cMet/PD-L1 in HT43 and HT45 treated cells at 7 days post treatment ($p < 0.03$) compared to control. Moreover, Hepa 1-6 cells demonstrated upregulation of cMet/PD-L1 in HT41 at day 16, but downregulation in HT45 at days 7 & 14, when compared to control ($p < 0.05$ for all). Interestingly, all treatment groups demonstrated significant correlation of cMet and PD-L1 expression. In phase III, HT45 resulted in increased intratumoral CD8/PD-1⁺ cells, and upregulation of cMet⁺ and PanCK/PD-L1⁺ cells compared to sham, $p < 0.05$.

Conclusions Sub-ablative hyperthermia effectively modulates PD-1/PD-L1 axis and may be a viable adjuvant against ICI resistance. Furthermore, SA-HT PD-L1 modulation may vary based on tumor type and strongly correlates with intratumoral cMET expression.

<http://dx.doi.org/10.1136/jitc-2022-SITC2022.1110>

1111 IMMUNE MODULATION OF MELANOMA BRAIN METASTASES BY IRAK-4 INHIBITION

Christina Von Roemeling, Erica Matich, Tyler Elliot, Vincent Archibald, Duane Mitchell, Kelena Klippel, Vrunda Trivedi, Lan Hoang-Minh, Bently Doonan*. *University of Florida, Gainesville, FL, USA*

Background Melanoma brain metastases (MBM) remain the primary driver of melanoma associated mortality. With improved survival from current therapy, the rate of MBM is expected to rise and it is already estimated that up to 60% of patients with metastatic disease will develop MBM during the course of their disease.¹ With dual agent immunotherapy or dual RAF/MEK targeted therapy, the intracranial response rate can reach 50%.² This leaves half of patients in a position of either partial, temporary, or no response to treatment in their area of highest risk disease. Additionally, these sites lose response to both immunotherapy and targeted therapy sooner than areas of peripheral disease.³ Novel strategies are needed to improve the treatment of MBM patients. We propose the targeting of IRAK-4 as a mechanism of immune modulation in combination with immune checkpoint inhibition in MBM.

Methods We analyzed human MBM samples for expression of IRAK-4 and components of the inflammatory myddosomal pathway of activation through advanced immunohistochemistry (IHC) and protein array. We then modeled MBM in aggressive, PD-1 refractory mouse MBM model system B16.F10. Following implantation of B16.F10 tumor both intracranially and into the flank of C57BL6 mice we treated mice with the oral IRAK-4 inhibitor CA-4948 with or without anti-PD-1 mAb therapy or vehicle control. Mice were treated for 7 days and then the tumor microenvironment of both intracranial and flank tumors was analyzed through IHC and flow cytometry.

Results We show here human MBM samples express high level of IRAK-4 and downstream target proteins in the NF-KB pathway of activation. We additionally show oral CA-4948 is capable of rapid passage across the blood brain barrier and reaches therapeutically significant levels. We further show the addition of the novel oral IRAK-4 inhibitor CA-4948 to immune checkpoint inhibition has a tumor growth restriction capacity through downregulation in MAPK, NF-KB, and pERK and this results in a survival advantage of combination treatment. We also show the combination has a secondary effect of enhanced T cell activation and T cell infiltration in MBM tumors.

Conclusions Though IRAK-4 sits on the pathway of innate inflammation and suppression acts to restrict inflammation, this actually enhances anti-tumor T cell activity unlike traditional anti-inflammatory agents like steroids. We posit IRAK-4 inhibition as a mechanism of restoring the inflammatory balance in MBM to improve immune checkpoint inhibition. We propose the further investigation of IRAK-4 inhibition with combination immunotherapy approaches in MBM patients.

REFERENCES

1. Liu H, *et al.* Predictive value of a nomogram for melanomas with brain metastases at initial diagnosis. *Cancer Med* 2019;**8**(18):7577–7585.
2. Acharya S, *et al.* Distant intracranial failure in melanoma brain metastases treated with stereotactic radiosurgery in the era of immunotherapy and targeted agents. *Adv Radiat Oncol* 2017;**2**(4):572–580.
3. Sloot S, *et al.* Improved survival of patients with melanoma brain metastases in the era of targeted BRAF and immune checkpoint therapies. *Cancer* 2018;**124**(2):297–305.

Ethics Approval All animal studies have been performed with the approval of the University of Florida Institutional Animal Care and Use Committee (IACUC) Study #201910960.

<http://dx.doi.org/10.1136/jitc-2022-SITC2022.1111>

1112 **PARP INHIBITION INCREASES IN THE SUPPRESSIVE CAPACITY OF TUMOR-ASSOCIATED TREGS IN A BRCA1-DEFICIENT MODEL OF OVARIAN CANCER**

Daniel Falcon*, Ichiko Kinjyo, Sarah Adams. *University of New Mexico, Albuquerque, NM, USA*

Background Emerging evidence indicates that tumor-directed anticancer agents have immunomodulatory effects that contribute to therapeutic outcomes. Targeted therapy by inhibition of poly(ADP-ribose) polymerase (PARPi) has had a profound effect on disease outcomes in ovarian cancer. The cytotoxic effects of PARPi are attributed to inhibition of single-stranded DNA repair pathways resulting in accumulation of DNA-damage in BRCA-deficient cells. While PARP is commonly associated with DNA repair, it has also been linked to a variety of other processes including cell division and inflammation. Published data using PARP1-KO mice suggests that PARP impairs circulating regulatory T cell (Treg) function through modulation of FoxP3, however, the impact on tumor-associated Tregs is unclear. As in many cancers, Tregs accumulate in the ovarian cancer tumor microenvironment (TME) and represent a key mechanism of immune escape. With growing interest in testing combinations of PARPi and immunotherapy, we sought to examine the impact of PARPi on peripheral and tumor-associated Tregs.

Methods To isolate viable Tregs we used FoxP3-eGFP co-expressing transgenic mice. Female mice (8-10 wk) were challenged with BRCA1-deficient ID8 cells (i.p.) and treated daily with ABT-888 (40 mg/kg) for six weeks. Tumor-associated Tregs were sorted from total peritoneal cells pre-enriched for CD4+ T cells. In separate experiments, peripheral Tregs were sorted from CD4+ spleen and lymph node cells and pre-treated with ABT-888 for 24 hours prior to use. Standard proliferation assays using naïve T cells were used to assess Treg suppressive function. Flow cytometry was used to measure cell divisions and expression of FoxP3 and CTLA-4.

Results Ex-vivo treatment of Treg from non-treated, tumor-naïve mice showed that ABT-888 pre-treatment significantly reduced the suppressive capacity of Tregs in a dose-dependent manner ($P < 0.05$). Similarly, ABT-888 treatment resulted in decreased expression of FoxP3 and CTLA-4 in a dose-dependent manner ($P < 0.05$). Conversely, tumor-associated Tregs from PARPi-treated mice had superior suppressive capacity compared to those from non-treated mice ($P < 0.05$). No differences between treated and non-treated groups were observed in Tregs isolated from the spleen.

Conclusions Taken together these data highlight the immunomodulatory effects of PARPi on tumor-associated Tregs. Here we present evidence that PARPi treatment promotes the suppressive capacity of Tregs in the TME and also identify a potential interaction between PARPi and response to immunotherapy in BRCA-deficient ovarian cancer. Future studies will include PARP inhibitors with varying degrees of DNA trapping ability as well as non-BRCA mutated tumors.

<http://dx.doi.org/10.1136/jitc-2022-SITC2022.1112>

1113 **EPIGENETIC MODIFICATIONS INFLUENCE IMMUNE REGULATORY PATHWAYS IN MURINE AND HUMAN NEUROBLASTOMA AND MELANOMA TUMOR MODELS**

Arika Feils*, Lizzie Frankel, Ankita Shahi (De), Alina Hampton, Paul Sondel, Amy Erbe.
University of Wisconsin-Madison, Madison, WI, USA

Background Immunotherapy for the treatment of various cancers has substantially improved the clinical outcome for many patients. Yet, some cancers classified as immunologically “cold”, including high-risk neuroblastoma (HR-NBL) and melanoma (MEL), still have a poor response to immunotherapeutic intervention. These tumors are characterized by low tumor mutation burden, poor immune infiltrate, and/or low MHC I expression. As a potential route of immune escape, these cold NBL/MEL tumors may have induced epigenetic modifications to regulate expression of MHC I/II. Here, we investigated the ability of epigenetic modifiers (EMs), including inhibitors of DNA methyltransferases (DNMTs), histone deacetylases (HDACs), and histone methyltransferases (HMTs), to restore MHC I/II expression in murine and human NBL/MEL models.

Methods To determine the doses of various EM inhibitors (EMis) (n=8), human and murine NBL/MEL cell lines (n=14) were treated with various concentrations of EMis and monitored for proliferation and apoptosis via an Incucyte. Optimal doses were then used to treat NBL/MEL cells with single-agent EMis, or combinations, +/- IFN γ . Following treatment, cells were assessed by qPCR and flow cytometry for changes in MHC I/II, PD-L1, and other genes [e.g., antigen presenting machinery (APM)].

Results With increased doses of EMis, we observed reduced proliferation and increased apoptosis across the NBL/MEL cell lines. Using doses of EMis that we found did not alter proliferation or apoptosis (in an effort to focus on the potential immune modulation), we found that certain combinations of EMis with IFN γ restored MHC I/II surface expression. Accordingly, we observed increased transcription of genes involved in the APM and chemokines known to influence immune cell infiltration, following guadecitabine (DNMTi) and entinostat (HDACi) treatment. Moreover, the combination of guadecitabine and entinostat resulted in co-expression of MHC I and MHC II on several of the cell lines tested.

Conclusions These findings suggest that certain combinations of EMis may allow us to turn these cold NBL/MEL tumors “hot” by reversing the loss of MHC I/II. By combining guadecitabine and entinostat with current immunotherapeutic regimens, there is potential to reinvigorate the activity of T cells in the anti-tumor response through T cell engagement with MHC I/II. Future studies are aimed to investigate the *in vivo* ability of guadecitabine and entinostat to restore MHC I/II expression.

<http://dx.doi.org/10.1136/jitc-2022-SITC2022.1113>

1114 IMMUNOTHERAPEUTIC ACTIVITY OF OX425 AGAINST PD-1 RESISTANT HR⁺HER2⁻ BREAST CANCER

¹Claudia Galassi, ²Wael Jdey, ¹Lorenzo Galluzzi*, ¹Weill Cornell Medicine, New York, NY, USA; ²Onxeo, Paris, France

Background Hormone receptor (HR)⁺ breast cancer is a cold tumor that responds poorly to immune checkpoint blockers targeting PD-1^{1,2}, calling for the development of therapeutic strategies that inflame the HR⁺ tumor microenvironment to restore PD-1 sensitivity. OX425 is a second-generation poly (ADP)-ribose polymerase 1 (PARP1)-targeting decoy oligonucleotide (ODN) that drives PARP1 hyperactivation coupled to exhaustion of the DNA damage response, ultimately killing cancer (but not normal) cells as a function of metabolic breakdown.³ PARP1-targeting decoy ODNs have been shown to mediate multiple immunostimulatory effects, standing out as promising combinatorial partners for PD-1 blockers in cold tumors.³

Methods We harnessed a unique endogenous mouse model that recapitulates key immunobiological features of human HR⁺HER2⁻ breast cancer, as driven by subcutaneous, slow-release medroxyprogesterone acetate (MPA) pellets combined with 7,12-dimethylbenz[a]anthracene (DMBA) gavage⁴, to investigate the therapeutic efficacy of OX425 delivered intraperitoneally 1X or 2X per week at 100 or 500 µg/mouse, optionally combined with a mouse PD-1 inhibitor (delivered intraperitoneally in 2 doses of 200 µg/mouse 3 days apart from each other). Tumor growth, mouse-adapted RECIST score assessments, progression-free survival, overall survival and other clinically relevant parameters were monitored until ethical endpoint.

Results OX425 at the highest dose (500 µg/mouse 2X per week) was associated with weight loss across treated mice (irrespective of PD-1 blockage) and premature mortality in 10% of the mice, calling for dose reduction to 100 µg/mouse 2X per week. At all other administration schedules, OX425 was well tolerated, effective at controlling tumor growth and extending overall survival in mice bearing MPA/DMBA-driven carcinomas (which are intrinsically resistant to PD-1, similar to HR⁺ breast cancer in women).^{1,2,4} Blocking PD-1 increased the therapeutic activity of OX425 when delivered 2X per week at 100 µg/mouse as it inhibited the development of secondary tumors.

Conclusions OX425 at doses < 500 µg/mice 2X per week is well tolerated in mice and mediates single-agent immunotherapeutic activity in models of PD-1-resistant HR⁺HER2⁻ breast cancer, with a potential for synergy with PD-1. Further investigation of the immunostimulatory and therapeutic properties of OX425 is warranted.

REFERENCES

1. Emens LA. Breast Cancer Immunotherapy: Facts and Hopes. *Clin Cancer Res*. 2018;**24**(3):511–520.
2. Rugo HS, Delord JP, Im SA, Ott PA, Piha-Paul SA, Bedard PL, Sachdev J, Le Tourneau C, van Brummelen EMJ, Varga A, Salgado R, Loi S, Saraf S, Pietrangelo D, Karantza V, Tan AR. Safety and antitumor activity of pembrolizumab in patients with estrogen receptor-positive/human epidermal growth factor receptor 2-negative advanced breast cancer. *Clin Cancer Res* 2018;**24**(12):2804–2811.
3. Wael Jdey, Chloe Doizelet, Claudia Galassi, Christelle Zandanel, Veronique Trochon-Joseph, Vincent Hayes, Marie-Christine Lienafa, Giulia Petroni, Lorenzo Galluzzi. Anticancer effects of PARP1 hyperactivation by a decoy oligodeoxynucleotide in vitro and in vivo. *Journal of Clinical Oncology*. 2022;**40**: e15060. doi:10.1200/JCO.2022.40.16_suppl.e15060.
4. Buqué A, Bloy N, Perez-Lanzón M, Iribarren K, Humeau J, Pol JG, Levesque S, Mondragon L, Yamazaki T, Sato A, Aranda F, Durand S, Boissonnas A, Fucikova J, Senovilla L, Enot D, Hensler M, Kremer M, Stoll G, Hu Y, Massa C, Formenti SC, Seliger B, Elemento O, Spisek R, André F, Zitvogel L, Delaloge S, Kroemer G,

Galluzzi L. Publisher Correction: Immunoprophylactic and immunotherapeutic control of hormone receptor-positive breast cancer. *Nat Commun*. 2020;**11**(1):4787.

Ethics Approval This study was approved by Weill Cornell Medicine IACUC.

<http://dx.doi.org/10.1136/jitc-2022-SITC2022.1114>

1115

T-DXd INCREASES IMMUNE CELL INFILTRATION AND ENHANCES ACTIVITY OF IMMUNE CHECKPOINT BLOCKADE IN MURINE TUMOR MODELS

¹Liam Jenkins*, ¹Matt Wilson, ²Jerome Mettetal, ²Theresa Proia. ¹AstraZeneca UK Ltd, Cambridge, UK; ²AstraZeneca Pharmaceuticals LP, Waltham, MA, USA

Ethics Approval All animal studies were performed in accordance with AstraZeneca IACUC policies.

<http://dx.doi.org/10.1136/jitc-2022-SITC2022.1115>

Background The combination of antibody-drug conjugates (ADCs) and immunotherapeutic agents has gained attention due to impressive activity demonstrated in bladder and triple-negative breast cancer. Trastuzumab deruxtecan (T-DXd) is an ADC composed of an anti-HER2 antibody, a cleavable tetrapeptide-based linker, and a cytotoxic topoisomerase I inhibitor approved for HER2+ metastatic breast and gastric cancer. T-DXd has been shown to induce PD-L1 and MHC-I upregulation and demonstrated activity in combination with immune checkpoint inhibitors.^{1,2} We report the result of mechanistic studies of the immune response profile to T-DXd and immune checkpoint inhibitor combinations, utilizing an MMAE containing ADC as a comparator.

Methods Human PBMCs were treated with DXd, MMAE, T-DXd, and T-MMAE (trastuzumab-vc-MMAE) with and without CD3/CD28, and viability measured. Supernatant for co-culture assays was collected from human cancer cell lines treated *in vitro* with T-DXd or T-MMAE. *In vivo*, BALB/c mice bearing human HER2 expressing EMT6 tumors were treated with T-DXd or T-MMAE +/- anti-PD-L1 mAb and evaluated for pharmacodynamic changes and efficacy.

Results *In vitro*, treatment of human PBMCs with free DXd caused anti-proliferative effects (IC₅₀ = 0.06uM); however, conjugation of DXd to trastuzumab (T-DXd IC₅₀ = 60ug/mL) mitigated the anti-proliferative effects and was comparable to T-MMAE (IC₅₀ = 12ug/mL). Incubation of human macrophages with supernatant collected from T-DXd treated, but not T-MMAE treated cancer cells resulted in greater than 1.5-fold increase in HLA-DR and CD86 expression, without notable increases in CD163 expression. *In vivo*, both compounds exhibited anti-tumor activity in a human HER2-EMT6 tumor model, with treatment resulting in tumor growth inhibition (TGI) of 25.7% (*P* = 0.001) for T-DXd, and 11.6% (*P* = 0.123) for T-MMAE. In combination with anti-PD-L1 treatment, T-DXd (TGI = 55.4%, *P* <0.001) but not T-MMAE (TGI = 10.8%, *P* = 0.280) significantly delayed tumor growth compared to anti-PD-L1 monotherapy (TGI = 16.5%, *P* = 0.063). Flow cytometric analysis of T-DXd-treated tumors revealed a significant increase in total CD45⁺ cells (1.9-fold, *P* = 0.028) and CD8⁺ T cells (2.8-fold, *P* = 0.018) that was not observed in T-MMAE-treated tumors. T-DXd treatment also promoted a significant increase in tumoral abundance of macrophages (2.2-fold, *P* = 0.001), Th cells (2.2-fold, *P* = 0.028) and Tregs (2.6-fold, *P* = 0.018).

Conclusions These data demonstrate that T-DXd treatment enhances the immunogenicity of human cancer cell lines, promotes tumoral immune cell infiltration, and can be effectively combined with immune checkpoint blockade to enhance anti-tumor immune responses.

REFERENCES

1. Iwata TN, Ishii C, Ishida S, Ogita Y, Wada T, Agatsuma T. A HER2-Targeting Antibody-Drug Conjugate, Trastuzumab Deruxtecan (DS-8201a), Enhances Antitumor Immunity in a Mouse Model. *Mol Cancer Ther*. 2018;**17**(7):1494–1503. doi: 10.1158/1535-7163.MCT-17-0749. Epub 2018 Apr 27. PMID: 29703841.
2. Iwata TN, Sugihara K, Wada T, Agatsuma T. [Fam-] trastuzumab deruxtecan (DS-8201a)-induced antitumor immunity is facilitated by the anti-CTLA-4 antibody in a mouse model. *PLoS One*. 2019;**14**(10):e0222280. doi: 10.1371/journal.pone.0222280. PMID: 31574081; PMCID: PMC6772042.

1116

OXPHOS INHIBITION OFFSETS THE METABOLIC ADVANTAGE OF PANCREATIC CANCER AND PROMOTES A PRO-INFLAMMATORY TUMOR MICROENVIRONMENT

Madeline Steiner*, Arthur Liu, Sayan Alekseev, Charlotte Dahlem, Michael Curran. MD Anderson Cancer Center, Houston, TX, USA

Background Cancer cells must reprogram their metabolic state to adapt to the heightened energy demands needed for tumorigenesis.¹ Aberrant tumor metabolism rapidly exhausts the tumor microenvironment of oxygen and key nutrients, creating a hypoxic, immunosuppressive landscape that limits T cell infiltration and renders immunotherapy ineffective.² We have previously shown that targeted hypoxia reduction restores effector T cell infiltration and sensitizes tumors to anti-CTLA-4/anti-PD-1 blockade.³ Inhibitors of tumor oxidative metabolism (OxPhos) are also promising strategy to offset the tumor metabolic advantage over the immune system by reducing the oxygen utilization of tumor cells and combating tumor hypoxia. Metformin, a mitochondrial complex I inhibitor, has been reported to improve tumor control when combined with PD-1 blockade by alleviating tumor hypoxia and improving T cell activation.⁴ While targeting tumor oxidative metabolism has shown promising results, studies have mainly focused on the impacts of complex I inhibition, leaving the impact of inhibition on downstream components of the electron transport chain poorly understood.

Methods Napyradiomycin A1 (OxPhos complex I and II inhibitor), α TOS (OxPhos complex II inhibitor) and Atovaquone (OxPhos complex III inhibitor) were used to assess the differential impact of OXPHOS inhibition on mT4-2D PDAC tumor cells (derived from *Kras*^{+G12D}*TP53*^{+R172H}*Pdx1-Cre* (KPC) organoid cultures) (5) versus on T cells *in vitro* and *in vivo*.

Results We found that MT4-2D cancer cells treated with OxPhos complex II/III inhibitors *in vitro* showed no significant decrease in viability or proliferative capacity, however Atovaquone treatment decreased mitochondrial respiration potential based on reduced MitoRed staining in treated cells. We also found Ovalbumin-specific CD8⁺ T cells treated with Atovaquone during activation *in vitro* showed no significant reduction of T cell activation markers (CD44 and 4-1BB), as well as a minimal increase in T cell exhaustion marker expression (PD-1 and LAG3). Additionally, complex III inhibition during CD8⁺ T cell activation did not adversely impact IFN- γ production. OxPhos inhibitor treatment *in vivo* reduced the frequency of MDSCs within the tumor microenvironment and elicited increased CD8⁺ T cell infiltration.

Conclusions Here we show that inhibition of the complex II/III components of the mitochondrial OxPhos chain has the potential to offset the tumor metabolic advantage of the murine pancreatic cancer cell line MT4-2D. We found that these complex II/III inhibitors limit the metabolic fitness of MT4-2D while minimally compromising the activation state and function of cytotoxic T cells. Additionally, OxPhos inhibition repolarized the immunosuppressive tumor microenvironment, showing favorable potential for synergy with immune checkpoint blockade.

REFERENCES

1. Warburg O. On the origin of cancer cells. *Science*. 1956;123.3191: 309–314.
2. Liu A, Curren MA. Tumor hypermetabolism confers resistance to immunotherapy. *Seminars in cancer biology*. Academic Press. 2020;65.
3. Jayaprakash, et al. Targeted hypoxia reduction restores T cell infiltration and sensitizes prostate cancer to immunotherapy. *J Clin Invest* 2018;128(11):5137–5149.

4. Scharping Nicole E, et al. Efficacy of PD-1 blockade is potentiated by metformin-induced reduction of tumor hypoxia metformin improves PD-1 blockade immunotherapy. *Cancer immunology research* 2017;5.1:9–16.
5. Boj SF, Hwang C-I, Baker LA, et al. Organoid models of human and mouse ductal pancreatic cancer. *Cell* 2015;160:324–38. doi:10.1016/j.cell.2014.12.021

<http://dx.doi.org/10.1136/jitc-2022-SITC2022.1116>

Abstracts

1117 A PATIENT-DERIVED TUMOR ORGANOID PLATFORM TO INVESTIGATE RADIATION-INDUCED NEOANTIGEN EXPOSURE

¹Samantha Van Nest*, ¹Jared Capuano, ¹Tuo Zhang, ¹Bhavneet Bhinder, ¹Xi Zhou, ¹Adriana Irizarry, ¹Laura Martin, ¹Silvia Formenti, ¹Olivier Elemento, ²Nils-Petter Rudqvist, ¹Sandra Demaria. ¹Weill Cornell Medicine, New York, NY, USA; ²The University of Texas MD Anderson Cancer Center, Houston, TX, USA

Background The level of expression of a mutation-associated neoantigen (MANA) is a critical determinant of effective T cell priming.¹ Thus, interventions that increase the expression of a protein containing a MANA could increase responses to immune checkpoint inhibitors (ICI), especially for tumors with relatively low mutation burden like microsatellite stable (MSS) colorectal cancer (CRC).¹ We have shown that radiation therapy (RT) upregulates the expression of genes containing MANA in a preclinical model, resulting in enhanced presentation of the derived MANA.² We also found expansion of CD8 T cells against a MANA upregulated in expression by RT in a lung cancer patient with complete response to RT +ipilimumab.³ Here we set out to test if MANA upregulation is a common response of human tumors to RT.

Methods Patient-derived tumor organoids (PDO) from colorectal (CRC) (n=3) (figure 1a) and lung (n=4) cancer were characterized for radiation response⁴ (figure 1b). PDOs were then irradiated with doses of 5-8 Gy daily for 3 days (RT) or left untreated (UT) and RNAseq performed 24h post-RT. Differentially expressed genes were identified using DESeq2 differential expression analysis. Ingenuity Pathway Analysis (IPA) was used to identify pathways modulated by RT.

Results In the CRC PDO, 2034 and 362 genes were found to be concordantly upregulated and downregulated, respectively, by RT (figure 1c). Upregulated genes were associated with p38 MAPK signaling and innate immune signaling pathways (figure 1d). This RT-modulated gene set was used to interrogate predicted MANA dataset from CRC patients [1]. We found that ≥1 MANA-encoding gene was predicted to be significantly upregulated by RT in 263/266 patients from the TCGA COADREAD MSS cohort (figure 2a). The median number/patient of upregulated MANA was 11 (range 0-79), while for downregulated MANA it was 0 (range 0-15, figure 2b). In the lung PDO, 439 and 117 genes were found to be concordantly upregulated and downregulated, respectively, by RT. Upregulated genes were largely associated with DNA damage response pathways. We found that ≥1 MANA-encoding gene was predicted to be significantly upregulated by RT in 29/35 patients from a lung cancer dataset.⁵ The median number/patient of upregulated MANA was 3 (range 0-25), while for downregulated MANA it was 0 (range 0-14).

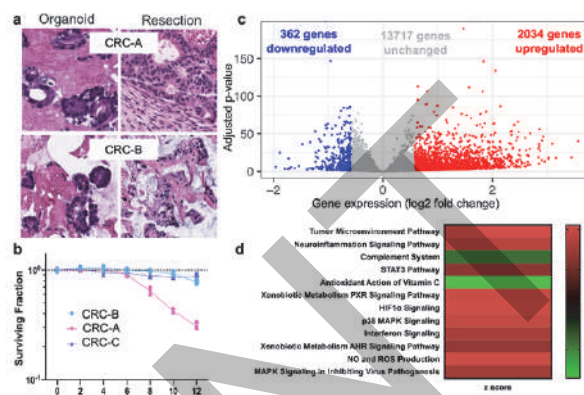
Conclusions Our data support the novel concept that RT can uncloak neoantigens in tumors like MSS CRC where low neoantigen expression may preclude effective T cell priming and contribute to ICI resistance.

Acknowledgements The authors are grateful for the financial support of The NIH (R01CA198533, SD) and from the AACR (21-40-12-VANN, SV).

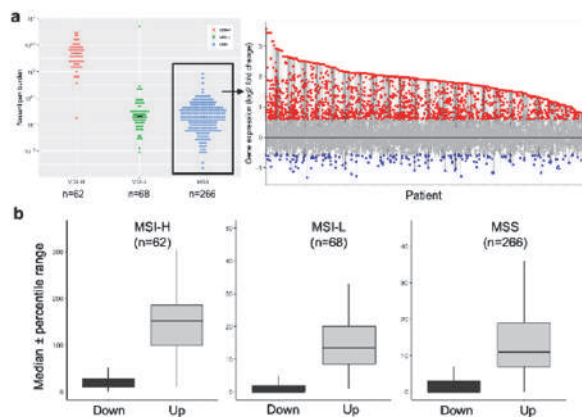
REFERENCES

- Westcott PMK, Sacks NJ, Schenkel JM, et al. Low neoantigen expression and poor T-cell priming underlie early immune escape in colorectal cancer. *Nat Cancer*. 2021;2:1071–1085.
- Lhuillier C, Rudqvist NP, Yamazaki T, et al. Radiotherapy-exposed CD8+ and CD4+ neoantigens enhance tumor control. *J Clin Invest*. 2021;131(5):E138740.
- Formenti SC, Rudqvist NP, Golden E et al. Radiotherapy induces responses of lung cancer to CTLA-4 blockade. *Nat Med*. 2018;24(12):1845–1851.

- Martin ML, Adileh M, Hsu KS et al. Organoids reveal that inherent radiosensitivity of small and large intestinal stem cells determines organ sensitivity. *Cancer Res*. 2020;80(5):1219–1227.
- Rizvi NA, Hellmann MD, Snyder A et al. Cancer immunology. Mutational landscape determines sensitivity to PD-1 blockade in non-small cell lung cancer. *Science*. 2015;348(6230):124–8.



Abstract 1117 Figure 1 a. Representative H&E images showing morphological similarity between carcinoma cells in the original resection and organoid culture for two CRC PDOs. b. Radiation response for each CRC organoid studied. Surviving fraction was evaluated based on ATP levels as measured using the CellTiter-Glo Assay, in irradiated compared to unirradiated PDO samples at 1 week following exposure to single radiation doses between 2 Gy and 12 Gy.⁴ c. Volcano plot showing 2,034 genes upregulated (red), 362 genes downregulated (blue) and 13,717 genes unchanged (grey) concordantly in all three PDOs at 24 hours following RT (5Gy x 3). Differential expression analysis was applied to a pooled dataset of three CRC PDOs, each with n=4 biological replicates per treatment condition. Cutoffs corresponding to a fold change in gene expression of 1.5 and adjusted p-value of 0.05 as determined from DESEQ2 were used to define the threshold between genes that are unchanged vs modulated by RT. d. Ingenuity Pathway Analysis (IPA) identified a total of 79 pathways enriched (-log(p-value)>2) by RT in the transcriptome, in all three CRC PDOs. Twelve representative pathways are shown.



Abstract 1117 Figure 2 a. Neoantigen burden associated with MSI-H (n=62), MSI-L (n=68) and MSS (n=266) patient subsets in the TCGA COADREAD cohort as reported by Westcott et al.¹ and overlay of the RT-modulated gene set derived from CRC PDOs with MANA encoding genes on a patient-by-patient basis for the MSS subset. Only neoantigens with binding affinity (IC50)<500 nM and upper quartile normalized FPKM>0 are included. b. Box plots (outliers removed) showing the median and percentile range of MANA predicted to be upregulated (Up) and downregulated (Down) for MSI-H, MSI-L, and MSS patient subsets.

upregulated and downregulated based on the PDO-derived RT-modulated gene set.

<http://dx.doi.org/10.1136/jitc-2022-SITC2022.1117>

PREPRINT

1118 IMMUNOLOGICALLY RELEVANT EFFECTS OF PT-112 ON CANCER CELL MITOCHONDRIA

¹Takahiro Yamazaki*, ¹Lorenzo Galluzzi, ²Christina Yim, ²Tyler Ames, ¹Weill Cornell Medical College, New York, NY, USA; ²Promontory Therapeutics Inc., New York, NY, USA

Background PT-112 is a novel platinum-pyrophosphate conjugate¹ under clinical development for cancer therapy.²⁻⁵ Besides mediating cytostatic and cytotoxic effects in numerous human and mouse cancer cells, PT-112 elicits various danger signals that are linked to immunogenic cell death (ICD), such as calreticulin exposure, as well as ATP and HMGB1 secretion.^{3,6,7} Accordingly, mouse cancer cells succumbing to PT-112 *in vitro* efficiently protect immunocompetent, tumor-naïve mice from challenge with living cancer cells of the same type.^{6,7} Moreover, PT-112 synergizes with PD-1 or PD-L1 blockade to control mouse tumors developing in immunologically competent hosts.^{6,7} In some tumor models, robust type I interferon (IFN) signaling is required for ICD⁸⁻¹⁰ However, the role of type I IFN signaling in the immunogenicity of PT-112 remains unclear.

Methods We used wild-type, mitochondrial DNA (mtDNA) depleted (ρ^0), as well as *Casp2*^{-/-} and *Casp3*^{-/-} mouse TS/A cells.¹¹ ELISA, flow cytometry and immunofluorescence microscopy were employed to monitor type I IFN levels, reactive oxygen species (ROS) generation, mitochondrial polarization, cell death, and cytosolic dsDNA accumulation driven by PT-112 and underlying regulatory mechanisms.

Results In cultured TS/A cells, PT-112 induced mitochondrial dysfunction, as demonstrated by ROS generation and mitochondrial hyperpolarization, as well as cytosolic accumulation of dsDNA that was abrogated in ρ^0 TS/A cells. Type I IFN secretion by wild-type TS/A responding to PT-112 was not observed. Both *Casp2* and *Casp3* deletion provided TS/A cells with some protection from PT-112-driven ROS generation and mitochondrial hyperpolarization, but only *Casp3* deletion afforded robust protection against the acute cytotoxicity of PT-112. Importantly, both *Casp2* and *Casp3* deletion augmented cytosolic dsDNA accumulation driven by PT-112.

Conclusions PT-112 causes pronounced mitochondrial dysfunction in cancer cells coupled with cytosolic mtDNA accumulation, which generally leads to type I IFN secretion.⁸ PT-112-driven caspase activation, however, possibly prevents mtDNA-driven type I IFN secretion, likely reflecting CGAS cleavage by active CASP3¹² and/or the rapid CASP3-dependent transition of dying cancer cells into metabolically inert corpses.^{13,14} In line with this possibility, both *Casp2*^{-/-} and *Casp3*^{-/-} TS/A cells exhibited increased cytosolic mtDNA accumulation upon PT-112 treatment. As PT-112 is a potent inducer of ICD in vaccination assays^{6,7} CASP3 activation elicited during the cytotoxic response to PT-112 may not influence the ability of PT-112 to drive prophylactic anticancer immunity in tumor-naïve hosts. Additional studies with established tumor models are needed to clarify the impact of caspases on the immunogenicity of PT-112 in clinically relevant settings.

REFERENCES

1. Ames T, Slusher B, Wozniak K, et al. Findings across pre-clinical models in the development of PT-112, a novel investigational platinum-pyrophosphate anti-cancer agent. *European Journal of Cancer* 2016;**69**:S153.
2. Ames TD, Sharik ME, Rather GM, et al. Translational research of PT-112, a clinical agent in advanced phase I development: evident bone tropism, synergy *In vitro* with bortezomib and lenalidomide, and potent efficacy in the V κ *MYC mouse model of multiple myeloma. *Blood* 2017;**130**(Supplement 1):1797–1797.
3. Buque A, Rodriguez-Ruiz ME, Fucikova J, Galluzzi L. Apoptotic caspases cut down the immunogenicity of radiation. *Oncoimmunology* 2019;**8**(11):e1655364.

4. De Giovanni C, Nicoletti G, Landuzzi L, Palladini A, Lollini PL, Nanni P. Bioprofiling TS/A. Murine mammary cancer for a functional precision experimental model. *Cancers (Basel)*. 2019;**11**(12).
5. Karp DD, Camidge DR, Bryce AH, Jimeno J, Infante JR. A phase I study of PT-112 in advanced solid tumors. *Journal of Clinical Oncology*. 2017;**35**(15_suppl):2519–2519.
6. Karp DD, Camidge DR, Infante JR, Ames TD, Jimeno JM, Bryce AH. PT-112: A well-tolerated novel immunogenic cell death (ICD) inducer with activity in advanced solid tumors. *Annals of Oncology*. 2018;**29**(suppl_8).
7. Karp DD, Camidge DR, Infante JR, et al. Phase I study of PT-112, a novel pyrophosphate-platinum immunogenic cell death inducer, in advanced solid tumours. *EClinicalMedicine* 2022;**49**:101430.
8. Ning X, Wang Y, Jing M, et al. Apoptotic caspases suppress type I interferon production via the cleavage of cGAS, MAVS, and IRF3. *Mol Cell* 2019;**74**(1):19–31 e17.
9. Rodriguez-Ruiz ME, Buque A, Hensler M, et al. Apoptotic caspases inhibit abscopal responses to radiation and identify a new prognostic biomarker for breast cancer patients. *Oncoimmunology* 2019;**8**(11):e1655964.
10. Sistigu A, Yamazaki T, Vacchelli E, et al. Cancer cell-autonomous contribution of type I interferon signaling to the efficacy of chemotherapy. *Nat Med* 2014;**20**(11):1301–1309.
11. Yamazaki T, Ames TD, Galluzzi L. Abstract B199: Potent induction of immunogenic cell death by PT-112. *Cancer Immunology Research* 2019;**7**(2 Supplement): B199.
12. Yamazaki T, Buque A, Ames TD, Galluzzi L. PT-112 induces immunogenic cell death and synergizes with immune checkpoint blockers in mouse tumor models. *Oncoimmunology* 2020;**9**(1):1721810.
13. Yamazaki T, Kirchmair A, Sato A, et al. Mitochondrial DNA drives abscopal responses to radiation that are inhibited by autophagy. *Nat Immunol*. 2020;**21**(10):1160–1171.
14. Zitvogel L, Galluzzi L, Kepp O, Smyth MJ, Kroemer G. Type I interferons in anti-cancer immunity. *Nat Rev Immunol* 2015;**15**(7):405–414.

<http://dx.doi.org/10.1136/jitc-2022-SITC2022.1118>

1119

GLUTAMINE ANTAGONIST PRODRUG JHU083 REPROGRAMS IMMUNOSUPPRESSIVE TUMOR-ASSOCIATED MACROPHAGES TO DRIVES TUMOR IMMUNITY IN UROLOGIC CANCERS

¹Monali Prahara^{*}, ¹Fan Shen, ¹Thomas Nirschl, ¹Alee Lee, ¹Xiaoxu Wang, ¹Liang Zhao, ²Alok Singh, ¹Debebe Theodoros, ¹Laura Sena, ¹Elizabeth Thompson, ¹Ada Tam, ¹Srinivasan Yegnasubramanian, ¹Edward Pearce, ¹Robert Leone, ¹Jesse Alt, ¹Rana Rais, ¹Barbara Slusher, ¹Andrew Pardoll, ³Jonathan Powell, ¹Jelani Zarif. ¹*Johns Hopkins School of Medicine, Baltimore, MD, USA*; ²*University of Pennsylvania, Philadelphia, PA, USA*; ³*Calico Labs, South SF, CA, USA*

Background Tumor metabolism is emerging as a regulator of immune mediated anti-tumor responses. Previously, we reported increased infiltration of immunosuppressive tumor associated macrophages (TAMs) with disease progression in prostate adenocarcinoma.¹ Glutamine metabolism has been implicated in immunosuppressive TAMs as well as mCRPC² and radioresistant urothelial carcinoma³. To harness the potent anti-tumor effects of 6-Diazo-5-oxo-L-norleucine (DON) which targets glutamine utilizing enzymes and to mitigate known significant toxicities, we here use a novel pro-drug moiety of DON, i.e., JHU083. We hypothesize that JHU083 will enhance anti-tumor immunity by simultaneously targeting both TAMs and cancer cells.

Methods Using a scRNA-seq dataset from prostate cancer bone metastatic patients we investigated the importance of glutamine metabolism in TAMs in the tumors.⁴ We utilized a novel pro-drug JHU083 to treat two urological syngeneic immunogenic mouse tumor models *in vivo*; B6CaP (prostate cancer) and MB49 (bladder cancer). We studied the direct effect on tumor cells, as well as the required immune compartment for drug efficacy *in vivo* using antibody targeted depletions or adoptively transferred treated TAMs. Moreover, we used RNA-sequencing, multi-parameter flow cytometry and targeted LC-MS/MS metabolic profiling to characterize the effect of JHU083 on sorted TAMs transcriptional programming, proteomic expression profiles and metabolite flux *in vivo*. Lastly, we assessed the functional phagocytotic capacity of TAMs with flow cytometry and IF microscopy.

Results Enriched expression of glutamine utilizing enzymes was observed in increased TAMs in the tumor relative to benign tissue from patient samples. JHU083 showed significant tumor regression in both urologic cancer models. Using *in vivo* depletion of CD4 or CD8 T cells, or adoptively transferring previously *in-vivo* JHU083 treated TAMs we established a direct anti-tumor role of TAMs. These TAMs were inflammatory. Strikingly, in the TME we also observed an metabolic flux of glycolytic metabolites which corresponded with increased of Glut1 and Hexokinase II in their protein expression indicating metabolic reprogramming towards glycolytic phenotype. Importantly, JHU083-treated TAMs showed significantly increased phagocytic activity, providing direct evidence of functional reprogramming.

Conclusions We found that JHU083 has two distinct functions *in vivo*; first, it directly impairs cancer cells which are glutamine dependent and second, it reprograms TAMs from an immunosuppressive to an inflammatory state. These macrophages convert to a highly glycolytic state, have increased TNF production, and have improved phagocytic activity against tumor cells. As urologic cancers are heavily infiltrated with immunosuppressive TAMs, JHU083 is an excellent pre-clinical candidate.

Acknowledgements This work was supported by the Bloomberg-Kimmel Institute for Cancer Immunotherapy, (J.C.Z.),

Prostate Cancer Foundation Young Investigator award (J.C.Z.), National Institutes for Health, United States/National Cancer Institute, United States K22 CA237623 award (J.C.Z.), Maryland Cigarette Restitution Fund grant FHB33CRF (J.C.Z.) and NIH R01CA229451 (B.S.S). Immunohistochemistry and Next generation sequencing studies were performed with the help of the Sidney Kimmel Comprehensive Cancer Center's Oncology Tissue, Tumor microenvironment core and Imaging Services Core and the Experimental and Computational Genomics Core (ECGC), which is supported by NIH/NCI Cancer Center Support Grant P30CA006973. The authors would like to thank Dr. Tamara L. Lotan for her pathology annotation of murine tumor samples.

REFERENCES

1. Zarif Jelani C, *et al.* Mannose receptor-positive macrophage infiltration correlates with prostate cancer onset and metastatic castration-resistant disease. *European Urology Oncology* 2019;**2**:429–436.
2. Zacharias, Niki Marie, *et al.* Metabolic differences in glutamine utilization led to metabolic vulnerabilities in prostate cancer. *Scientific Reports* 2017;**7**:1–11.
3. Zhou, Qun, *et al.* LincRNA-p21 suppresses glutamine catabolism and bladder cancer cell growth through inhibiting glutaminase expression. *Bioscience Reports*. 2019;**39**: BSR20182372.
4. Kfoury, Youmna, *et al.* Human prostate cancer bone metastases have an actionable immunosuppressive microenvironment. *Cancer Cell*. 2021;**39**:1464–1478.

<http://dx.doi.org/10.1136/jitc-2022-SITC2022.1119>

1120

NEOADJUVANT *IN SITU* INTRATUMORAL VACCINATION WITH EMPTY COWPEA MOSAIC VIRUS NANOPARTICLES IS EFFECTIVE AGAINST CANINE MAMMARY CANCER

¹Daniel Alonso-Miguel*, ¹Guillermo Valdivia, ²Barbara Zimmermann, ¹Lucía Lucia Barreno, ¹Angela Alonso-Diez, ¹Maria Dolores Perez-Alenza, ³Veronique Beiss, ¹María Suárez-Redondo, ⁴Nicole Steinmetz, ⁵Steven Fiering, ²Johannes Vom Berg, ¹Laura Laura Peña, ⁵Hugo Arias-Pulido. ¹Complutense University of Madrid, Madrid, Spain; ²University of Zurich, Schlieren, Switzerland; ³Case Western Reserve University Schools, Cleveland, USA; ⁴University of California San Diego, Cleveland, CA, USA; ⁵Geisel School of Medicine at Dartmouth, Lebanon, NH, USA

Ethics Approval The study was approved by the Animal Experiment Ethics Committee (Study #04/2018)

<http://dx.doi.org/10.1136/jitc-2022-SITC2022.1120>

Background Approved anti-PD-1/PD-L1 immunotherapy has demonstrated clinical benefits for breast cancer (BC) mostly in triple-negative breast cancer (TNBC) patients. Developing effective immunotherapies for breast cancer is slow in part due to the lack of appropriate models to evaluate novel agents. In this study, we evaluated efficacy, safety, and effect on survival of neoadjuvant *in situ* intratumoral immunotherapy with noninfectious empty cowpea mosaic virus (eCPMV) nanoparticles in spontaneous canine mammary cancer (CMC) patients. CMC shares clinical, pathologic, biologic, and immune similarities to human BC.

Methods Eighteen companion CMC patients were enrolled in the study approved by the Ethics Committee (Study #04/2018). Dogs with poor prognosis received adjuvant medical therapy (oral metronomic cyclophosphamide and firocoxib). Seven dogs received surgery, and eleven dogs received neoadjuvant *in situ* intratumoral eCPMV immunotherapy (0.2 mg per injection in the target tumor) at day 0 (D0) and at D6-D9, surgery at D12-D17, and adjuvant medical therapy. Efficacy was evaluated by tumor growth inhibition (TGI), safety by hematologic, and biochemistry changes in blood, and patient outcome by survival analysis. eCPMV-induced changes in blood cells were analyzed by flow cytometry.

Results Two neoadjuvant *in situ* intratumoral eCPMV injections generated tumor reduction of injected tumors in all patients by surgery day without systemic adverse events. TGI ranged from 6% to 63%. Remarkably, TGI was also observed in non-injected lesions (abscopal effect) both in the ipsilateral (TGI=1% to 96%) and contralateral (TGI=10% to 78%) mammary chains. Efficacy was independent of tumor size, clinical stage, histopathologic grade, and tumor receptor status (eight cases were luminal A, one luminal B, and two TN). Values stayed within normal range for hematocrit and hemoglobin and biochemistry (total proteins, glucose, creatine, alanine aminotransferase, and urea), confirming that eCPMV immunotherapy is not toxic. eCPMV injections induced a significant increase in the number of mature and immature blood neutrophils at D6-D9 ($p < 0.05$ for both relative to D0). Flow cytometry of circulating immune cells identified minor fluctuations induced by eCPMV injections in various immune cell subsets (not significant). eCPMV-treated patients had a statistically significant ($p = 0.006$) improved overall survival compared to patients not treated with eCPMV.

Conclusions Neoadjuvant *in situ* intratumoral eCPMV immunotherapy demonstrated anti-tumor efficacy and improved survival in CMC patients without systemic adverse effects. This novel immunotherapy could be a groundbreaking immunotherapy for CMC patients and a potential future immunotherapy for human BC patients beyond the current TNBC subtype.

Acknowledgements We would like to thank all canine owners who were very generous and supportive of the present study and the personnel of the Veterinary Teaching Hospital Complutense for their help and support.

1121

TIGILANOL TIGLATE IS A NATURALLY OCCURRING SMALL MOLECULE ONCOLYTIC THAT EFFECTIVELY ABLATES TUMORS VIA INTRATUMOURAL INJECTION AND CAN ENHANCE RESPONSE TO IMMUNE CHECKPOINT BLOCKADE

¹Jason Cullen*, ¹Pei-Yi Yap, ¹Blake Ferguson, ¹Zara Bruce, ²Motoko Koyama, ¹Herlina Handoko, ³Jacinta Simmons, ¹Jenny Johns, ¹Marjorie D'Souza, ¹Natasa Broit, ⁴Praphaporn Stewart, ⁴Daniel Shelley, ⁴Tracey McMahon, ⁵Steven Ogbourne, ⁶Yi Chieh Lim, ⁷Giovanni Appendino, ⁵Victoria Gordon, ⁵Paul Reddell, ¹Glen Boyle, ¹Peter Parsons. ¹QIMR Berghofer Medical Research Institute, Brisbane, Australia; ²Fred Hutchinson Cancer Research Center, Seattle, WA, USA; ³Queensland University of Technology, Brisbane, Australia; ⁴University of the Sunshine Coast, Sippy Downs, Australia; ⁵QBiotics Group Ltd., Brisbane, Australia; ⁶Danish Cancer Society Research Center, Copenhagen, Denmark; ⁷Università del Piemonte Orientale, Novara, Italy

Background Tigilanol Tiglate (TT) is a novel small molecule under development for local treatment of solid tumours via intratumoral (I.T.) injection. TT is a protein kinase C (PKC)/C1 domain activator that disrupts tumour vasculature, leading to haemorrhagic necrosis of the lesion.¹ Strikingly, in both preclinical syngeneic mouse models and cutaneous/subcutaneous tumours presenting in the veterinary clinic, I.T. injection of TT results in complete and enduring ablation of target tumours in >70% of patients.^{1,2,3} TT has completed a Phase I/IIa dose-escalation trial in humans (ACTRN12614000685617), with strong evidence of local anticancer efficacy and signs of abscopal effects in some patients.⁴ However, the underlying mechanism of action (MOA) of TT, together with its immunotherapeutic potential in oncology, is not fully understood.

Methods A combination of microscopy, immunofluorescence, immunoblotting, subcellular fractionation, intracellular ATP assays, LDH release assays and mixed lymphocyte reactions were used to probe the MOA of TT *in vitro*. TT-mediated damage associated molecular pattern (DAMP) release/externalization was assessed using luciferase (ATP), ELISA (HMGB1), flow cytometry and immunohistochemical (calreticulin) approaches. *In vivo* experimentation with TT utilized CT-26 and B16-F10-OVA tumor bearing mice, with or without anti-PD1/anti-CTLA4 treatment.

Results Our data demonstrates that therapeutic concentrations of TT induce death of cancer and endothelial cell lines, both *in vitro* and *in vivo*, via oncosis. Whilst largely PKC-independent, PKC/C1 domain signaling appears necessary for timely oncolysis *in vitro* and efficacious tumor ablation *in vivo*. Our results also show that TT binds to ER membranes, causing ER stress with subsequent activation of the integrated stress response. This is followed by mitochondrial membrane potential loss, ATP depletion, organelle swelling, oncosis and terminal necrosis. We also found that TT treatment promoted the release/externalization of DAMPs (HMGB1, ATP, calreticulin) from cancer cells *in vitro* and *in vivo*, characteristics indicative of immunogenic cell death (ICD). Confirmation of ICD *in vivo* was obtained through rechallenge experiments using CT-26 tumour bearing mice, which also demonstrated that TT promoted the development of tumour-specific T cells. In addition to stimulating immune cell infiltration into tumours, TT significantly improved treatment response in the B16-F10-OVA mouse melanoma model when combined with immune checkpoint blockade.

Conclusions These data indicate that TT is an oncolytic small molecule with the potential to enhance responses to immunotherapy. TT is currently undergoing Phase I/II trials in head and neck cancers (ACTRN12619001407189), soft tissue

sarcomas, Stage III melanoma in-transit (NCT05234437) and non-resectable Stage IIIB to IV M1c melanoma (TT/pembrolizumab combination: NCT04834973).⁵

REFERENCES

1. Boyle GM, D'Souza MMA, Pierce CJ, Adams RA, Cantor AS, Johns JP, Maslovskaya L, Gordon VA, Reddell PW, Parsons PG. Intra-Lesional Injection of the Novel PKC Activator EBC-46 Rapidly Ablates Tumors in Mouse Models. *PLOS ONE* 2014;**9**:e108887.
2. Cullen JK, Boyle GM, Yap PY, Elmlinger S, Simmons JL, Broit N, Johns J, Ferguson B, Maslovskaya LA, Savchenko AI, Mirzayans PM, Porzelle A, Bernhardt PV, Gordon VA, Reddell PW, Pagani A, Appendino G, Parsons PG, Williams CM. Activation of PKC supports the anticancer activity of tigilanol tiglate and related epoxytiglanes. *Sci Rep* 2021;**11**:207.
3. De Ridder TR, Campbell JE, Burke-Schwarz C, Clegg D, Elliot EL, Geller S, Kozak W, Pittenger ST, Pruitt JB, Riehl J, White J, Wiest ML, Johannes CM, Morton J, Jones PD, Schmidt PF, Gordon VA, Reddell PW. Randomized controlled clinical study evaluating the efficacy and safety of intratumoral treatment of canine mast cell tumors with tigilanol tiglate (EBC-46). *J Vet Intern Med* 2021;**35**:415–429.
4. Panizza BJ, de Souza P, Cooper A, Roohullah A, Karapetis CS, Lickliter JD. Phase I dose-escalation study to determine the safety, tolerability, preliminary efficacy and pharmacokinetics of an intratumoral injection of tigilanol tiglate (EBC-46). *Ebiomedicine* 2019;**50**:433–441.
5. QBiotics Group Ltd. website. <https://qbiotics.com/>

Ethics Approval All animal procedures were approved in accordance with NHMRC guidelines (Australian Code for the Care and Use of Animals for Scientific Purposes 8th Edition, 2013; National Health and Medical Research Council of Australia) by the QIMR Berghofer Animal Ethics Committee: A0106-042M, A0404-606M and A01047M.

<http://dx.doi.org/10.1136/jitc-2022-SITC2022.1121>

1122

RADIOTHERAPY-ACTIVATED NBTXR3 NANOPARTICLES INDUCE INTERFERON BETA SECRETION BY CANCER CELLS

Jordan Da Silva*, Sebastien Paris. *Nanobiotix, Paris, France*

Background The first-in-class radioenhancer NBTXR3 is composed of hafnium oxide nanoparticles, design to be delivered to patients by a single intratumor injection. When exposed to radiotherapy (RT), NBTXR3 nanoparticles increase radiation dose deposition from within the cancer cells. Results from a phase II/III clinical trial in patients with locally advanced Soft Tissue Sarcoma demonstrated significant superiority and clinical benefits of NBTXR3 activated by RT compared to RT alone, with a very good safety profile. Several preclinical studies have established the immunomodulatory capacities of NBTXR3 (e.g., increase of CD8 infiltrates in tumors, restoration of anti-PD1 sensitivity, induction of abscopal effect, etc.). Nonetheless, few data are currently available to understand the biological mechanisms triggered by NBTXR3+RT at the cancer cell level which could explain these results. Here, we investigated the impact of NBTXR3 activated by RT (NBTXR3+RT) on the interferon beta (IFN-beta) secretion by cancer cells.

Methods The impact of NBTXR3 activated by radiotherapy on IFN-beta production by cancer cells was evaluated by ELISA assay in the supernatant of CT26.WT cells (a murine colorectal cancer cell line). Six-wells plates containing plated cells were treated (or not) with 400µM of NBTXR3. The following day, cells were irradiated (or not) by a single dose of 4Gy. After 3 days, supernatants were collected, and the IFN-beta secretion was analyzed by ELISA assay. The efficacy of each treatment modality on cell viability was also measured by MTT assay.

Results ELISA analyses showed no effect of NBTXR3 without RT. In contrast, RT alone induced a significant increase of IFN-beta secretion. Interestingly, NBTXR3+RT significantly increased IFN-beta secretion by treated cells, compared to RT alone. MTT assay also show the superior capacity of NBTXR3+RT to destroy cancer cells, compared to RT alone.

Conclusions It has been previously reported that NBTXR3 +RT (3 fractions of 4Gy) produced a significant abscopal effect in competent mice bearing CT26.WT tumors. Our in vitro data show that NBTXR3+RT can significantly enhance the secretion of IFN-beta by these cells, with only a single dose of 4Gy. These results suggest that the immunomodulatory capacities of NBTXR3+RT measured in vivo could be explained, at least in part, by a greater secretion of IFN-beta, a cytokine known to play a central role in the priming of immune response.

<http://dx.doi.org/10.1136/jitc-2022-SITC2022.1122>

1123 **PRECLINICAL ACTIVITY AND SAFETY PROFILE OR JANX008, A NOVEL EGFR-TARGETING TUMOR-ACTIVATED T CELL ENGAGER FOR TREATMENT OF SOLID TUMORS**

Shahram Salek-Ardakani*, Thomas DiRaimondo, Natalija Budimir, Lina Ma, Simon Shenhav, Vanessa Cicchini, Hua Wu, Renee Jovic, Fabreze Roup, Calvin Cambell, Carolina Caffaro, Hans Aerni, Ugur Eskioçak, Wayne Godfrey, Charles Winter, Marc Nasoff, Neil Gibson, David Campbell. *Janux Therapeutics, San Diego, CA, USA*

Background Epidermal growth receptor (EGFR) is the most expressed membrane oncogenic protein in human cancers. KRAS and BRAF mutations are significant drivers of resistance to EGFR-targeted therapies. Unlike other treatments, EGFR-targeting, CD3 bispecific T cell engagers (TCEs) can potentially retain activity against tumors bearing resistance mutations. However, cytokine release syndrome (CRS), on-target off-tumor toxicities, and poor pharmacokinetics (PK) properties present significant clinical limitations for these potent immunomodulators. To overcome these challenges, Janux has developed JANX008, an EGFR- and CD3-targeted tumor-activated T cell engager (TRACTr). JANX008 is a humanized trispecific protein that contains EGFR- and CD3-binding domains, an albumin binding domain to extend circulating half-life, and two different peptide masks fused to the molecule through tumor protease cleavable linkers. One peptide mask inhibits EGFR engagement on target cells, and the other inhibits CD3 engagement on T cells. Once the cleavage sequences undergo proteolysis by tumor proteases, the EGFR and CD3 masks are released, and the resulting active molecule can bind EGFR and CD3 on target cells.

Methods Peptide masks against EGFR- and CD3-binding domains were identified via phage display. The efficiency of the masks was evaluated using human EGFR and CD3 ELISAs. JANX008-induced cleavage-dependent T cell killing was evaluated in human PBMC/tumor cell co-culture assays. Antitumor efficacy of JANX008 was tested in multiple preclinical models, including EGFR antibody-resistant KRAS- and PIK3CA-mutant mouse colon cancer model (HCT116) and a fully human primary colorectal cancer (CRC) tumoroid system. The pharmacokinetic and safety profile of JANX008 was evaluated in non-human primate studies.

Results JANX008 target engagement was cleavage-dependent, where masking reduced EGFR and CD3 binding by >300x and >1,000x, respectively. JANX008 exhibited potent cleavage- and dose-dependent activity in multiple preclinical models, including EGFR antibody-resistant tumor and T cell co-culture assays, humanized mouse CRC model, and a human primary CRC tumoroids with an intact tumor microenvironment. JANX008 showed a significantly enhanced safety profile in NHPs compared to non-masked EGFR-TCE, including decreased CRS-associated cytokines and healthy tissue toxicities at high exposures. Clinical chemistry, hematology, and pathology measurements supported No-Observed-Adverse-Effect-Level ≥ 0.6 mg/kg/dose. Finally, the cleavable albumin-binding domain extended the half-life of JANX008 to ~94h, relative to the ~1.3h half-life of non-masked TCE, supporting its weekly clinical dosing.

Conclusions Preclinical data demonstrate key characteristics of JANX008, including cleavage-dependent activity, half-life extended PK, the potential for superior safety, and manufacturability properties that could mitigate significant limitations of TCEs and support JANX008 clinical development.

Acknowledgements We acknowledge Marque Todd for providing insightful comments and help with the design and interpretation of NHP safety studies.

Ethics Approval All animal experiments were approved by the Institutional Animal Use and Care Committee of the institutions conducting the studies and in compliance with the Animal Welfare Act, the Guide for the Care and Use of Laboratory Animals, and the Office of Laboratory Animal Welfare.

<http://dx.doi.org/10.1136/jitc-2022-SITC2022.1123>

1124

INTRATUMORAL ADMINISTRATION OF VAX014 COOPERATES WITH CHECKPOINT BLOCKADE TO REPROGRAM TUMOR IMMUNE MICROENVIRONMENTS AND CLEAR INJECTED AND NONINJECTED TUMORS

¹Matthew Giacalone, ¹Katherine Reil*, ¹Shingo Tsuji, ¹Kinsey Nelson, ²Elsa Molina, ³Kathleen McGuire. ¹Vaxion Therapeutics, San Diego, CA, USA; ²University of California San Diego, San Diego, CA, USA; ³San Diego State University, San Diego, CA, USA

Background Immunologically “cold” tumors, which lack tumor infiltrating lymphocytes (TILs), are minimally responsive to immune checkpoint blockade (ICB). VAX014 is a novel clinical stage targeted oncolytic agent based on recombinant bacterial minicells and previous preclinical work demonstrated intratumoral (i.t.) administration of VAX014 increased TILs and led to effective lymphocyte-dependent clearance of immunologically cold tumors.^{1,2} When combined with systemic ICB against PD-1 (α PD-1) and CTLA-4 (α CTLA-4) (tripartite combination), this treatment effect was enhanced and systemically expanded to control or eliminate distal noninjected tumors in most mice. Here, we more deeply explored the underlying immune mechanisms in injected and noninjected tumors following VAX014 treatment alone and in combination with systemic ICB by evaluating tumor immunotranscriptomes, TIL populations/phenotypes, and the potential development of protective immunologic memory.

Methods The syngeneic B16F10 model (immune desert phenotype) was used for these studies. Initial changes in immunotranscriptomes of injected tumors were evaluated 24 hours following i.t. treatment with VAX014 in mice bearing a single intradermal (i.d.) tumor. A bilateral variation of the i.d. B16F10 model was then used to systematically evaluate changes in immune gene signatures in both injected and noninjected tumors after addition of systemic α CTLA-4, and again after the further addition of α PD-1. Noninjected tumors from the same series of combination treatment groups were then evaluated by flow cytometry to assess and compare changes in TIL populations/phenotypes. Finally, mice surviving tripartite combination treatment were rechallenged with a second round of i.d. B16F10 tumors to evaluate protective long-term immunologic memory.

Results Immunotranscriptome analysis of injected tumors following i.t. treatment of VAX014 resulted in upregulation of multiple immune gene networks, including Type I/II interferon, dendritic cell function/activation, Natural Killer cell function/activation, antigen processing/presentation, and T cell lymphotaxis and effector function. In distal noninjected tumors, the dual combination of VAX014 with α CTLA-4 resulted in slower tumor growth, upregulation of the same pathways, but also indicated upregulation of *Pdcd1* (PD-1). Addition of α PD-1 to the treatment regimen led to clearance of noninjected tumors, coinciding with an increased cytotoxic cell gene signature and increased cytotoxic and effector memory CD8+ TILs. Finally, mice exhibiting complete response following tripartite combination treatment could limit tumor growth or completely protect against B16F10 tumor rechallenge.

Conclusions VAX014 stimulated rapid local immune activation and lymphocyte-mediated clearance of injected tumors following i.t. administration. When combined with systemic ICB blockade, this treatment effect was systemically expanded to control or eliminate distal noninjected tumors while promoting protective antitumor immunologic memory.

REFERENCES

1. Tsuji S, Reil K, Nelson K, Proclivo VH, McGuire KL, Giacalone MJ. Intravesical VAX014 synergizes with PD-L1 blockade to enhance local and systemic control of bladder cancer. *Cancer Immunol Res* 2022. e-pub ahead of print; doi:10.1158/2326-6066.CIR-21-0879
2. Reil K, Tsuji S, Nelson K, McGuire KL, Giacalone MJ. Intratumoral treatment with VAX014 facilitates in situ immunization leading to systemic antitumor responses that enhance systemic immune checkpoint blockade. *Can Res*. 2022; **82** (12_Supplement):4182.

Ethics Approval All animal studies were conducted in accordance with protocols approved by the Institutional Animal Welfare and Use Committee at San Diego State University

<http://dx.doi.org/10.1136/jitc-2022-SITC2022.1124>

1125 **INTRATUMORAL ADMINISTRATION OF SARS-COV-2 REDUCES TUMOR PROGRESSION AND ALTERS THE TUMOR IMMUNE MICROENVIRONMENT SIMILAR TO THAT OF THE SEASONAL INFLUENZA VACCINE**

Eileena Giurini*, Kajal Gupta. *Rush University Medical Center, Chicago, IL, USA*

Background A significant challenge in using immunotherapies to treat solid tumors is that these treatments are largely ineffective due to lack of immune cell infiltration or are dominated by suppressive immune cell populations. To overcome this, we previously demonstrated that intratumoral administration of influenza converts an immune barren tumor to a tumor that is loaded with inflammatory factors, thus can be targeted by the immune system. With the onset of the COVID-19 pandemic, and there being several shared characteristics between the influenza and SARS-CoV-2 we sought to determine the cancer immunotherapeutic potential of SARS-CoV-2. Here, we have shown that inactivated SARS-CoV-2 can reduce tumor growth in murine tumor models and can shift composition of the tumor microenvironment paralleling that of treatment using the influenza vaccine.

Methods To determine the anticancer response, 4T1 breast cancer and B16 melanoma tumors were induced in BALB/C and C57BL/6 mice, respectively. Tumors were treated with inactivated SARS-CoV-2, seasonal influenza vaccine, or PBS via intratumoral injection. Tumor growth was evaluated via caliper measurements. Determination of immune cell population changes within the tumor following each treatment was determined via flow cytometry analysis.

Results Intratumoral injection of inactivated SARS-CoV-2 and the influenza vaccine showed significant reduction in tumor growth compared to a PBS control ($p < 0.001$) in both 4T1 and B16 tumor models. Within B16 tumors, both SARS-CoV-2 and influenza vaccine increased CD45+ cell populations ($p < 0.0001$) compared to PBS. Notably, both B16 and 4T1 tumors treated with SARS-CoV-2 and influenza experienced a significant increase in CD8+ T-cell infiltration ($p < 0.05$, $p < 0.01$). Additionally, CD11b+ Ly6G/Gr-1+ myeloid derived suppressor cell populations were decreased in B16 melanoma tumors following inactivated SARS-CoV-2 or influenza vaccine treatment.

Conclusions These findings indicate that introducing inactivated SARS-CoV-2 into the tumor microenvironment reduces tumor progression and is able to shift the immune profile of a tumor from an immune-suppressed to a more inflamed, immunologically targeted status. Further, the changes in immune cell populations within the tumor as well, paralleling those of influenza vaccine treated tumors.

<http://dx.doi.org/10.1136/jitc-2022-SITC2022.1125>

1126

MOLECULAR MECHANISMS OF DC ACTIVATION BY MELANOMA CELLS RESPONDING TO LTX-315

¹Xiao-Qing Li, ²Takahiro Yamazaki*, ¹Tianzhen He, ¹Md Masud Alam, ¹Jia Liu, ¹Anna Trivett, ³Baldur Sveinbjörnsson, ³Øystein Rekdal, ²Lorenzo Galluzzi, ¹De Yang, ¹Joost Oppenheim. ¹NCI Center for Cancer Research, Frederick, MD, USA; ²Weill Cornell Medical College, New York, NY, USA; ³Lytix Biopharma, Oslo, Norway

Background Oncolytic peptides are emerging as attractive candidates for the development of novel anticancer regimens¹, reflecting broad cytolytic activities against a variety of malignant (but not normal) cells and a pronounced potential for immunostimulation.² LTX-315 is a synthetic nonameric cationic peptide derived from bovine lactotransferrin³ that has been associated with a pronounced capacity to elicit tumor-targeting immune responses in various preclinical models of cancer.² Specifically, LTX-315 has been shown to (1) cause immunogenic cell death (ICD)⁴ coupled to the release of immunostimulatory cytokines and damage-associated molecular patterns (DAMPs)^{5,6}, (2) deplete the tumor microenvironment (TME) of immunosuppressive cells such as CD4⁺CD25⁺FOXP3⁺ regulatory T (T_{REG}) cells and myeloid-derived suppressor cells (MDSCs)⁷, and (3) synergize with immunogenic chemotherapy⁸ or immune checkpoint inhibitors (ICIs)⁷ in the control of syngeneic mouse tumor models. However, the effects of tumor cells responding to LTX-315 on dendritic cells (DCs) remain to be precisely elucidated.

Methods Human A375 and mouse B16F10 cells were used as models of melanoma, *in vitro* (A375, B16F10) and *in vivo* (B16F10) upon subcutaneous injection in immunocompetent C57BL/6 mice. Flow cytometry, ELISA, RT-PCR and immunoblotting were used to assess DC maturation *in vitro* and *in vivo*, immunoblotting was employed to investigate the molecular mechanisms underlying DC activation, knockout and knockdown systems were harnessed to demonstrate mechanistic involvement. Therapeutic assays with B16F10 melanoma cells growing in immunocompetent vs *Myd88*^{-/-} mice coupled to tumor rechallenge were employed to confirm activation of tumor-targeting immunity coupled to the establishment of immunological memory.

Results LTX-315 mediated the release of immunostimulatory DAMPs and nucleic acids (NAs) from melanoma cells that drove robust DC activation as monitored by surface immunophenotyping for CD80, CD83, CD86 and MHC class II and cytokine (TNF, IL-1 β) secretion. This immunostimulatory effect mechanistically depended on TLR9 (detecting LTX-315-DNA complexes), TLR8 (detecting LTX315-RNA complexes) and TLR7 (which was activated by LTX-315 per se), as well as on the common TLR signal transducer MYD88. Accordingly, the *in vivo* anticancer activity of LTX-315 against B16F10 melanoma cells was significantly reduced in *Myd88*^{-/-} mice, and *Myd88*^{-/-} mice eradicating B16F10 tumors upon LTX-315 treatment remained susceptible to a rechallenge with B16F10 cells.

Conclusions In addition to induce immunogenic cell death, LTX-315 also activates DC via MYD88-dependent pathways that mediate optimal immunostimulatory effects coupled to the establishment of cancer-specific immunological memory in preclinical melanoma models.

REFERENCES

1. Camilio KA, Berge G, Ravuri CS, Rekdal O, Sveinbjörnsson B. Complete regression and systemic protective immune responses obtained in B16 melanomas after treatment with LTX-315. *Cancer Immunol Immunother* 2014;**63**(6):601–613.

2. Camilio KA, Wang MY, Mauseth B, *et al.* Combining the oncolytic peptide LTX-315 with doxorubicin demonstrates therapeutic potential in a triple-negative breast cancer model. *Breast Cancer Res.* 2019;**21**(1):9.
3. Eike LM, Yang N, Rekdal Ø, Sveinbjörnsson B. The oncolytic peptide LTX-315 induces cell death and DAMP release by mitochondria distortion in human melanoma cells. *Oncotarget* 2015;**6**(33):34910–34923.
4. Kepp O, Marabelle A, Zitvogel L, Kroemer G. Oncolysis without viruses – inducing systemic anticancer immune responses with local therapies. *Nat Rev Clin Oncol* 2020;**17**(1):49–64.
5. Kroemer G, Galassi C, Zitvogel L, Galluzzi L. Immunogenic cell stress and death. *Nat Immunol* 2022;**23**(4):487–500.
6. Vitale I, Yamazaki T, Wennerberg E, *et al.* Targeting cancer heterogeneity with immune responses driven by oncolytic peptides. *Trends Cancer* 2021;**7**(6):557–572.
7. Yamazaki T, Pitt JM, Vétizou M, *et al.* The oncolytic peptide LTX-315 overcomes resistance of cancers to immunotherapy with CTLA4 checkpoint blockade. *Cell Death Differ.* 2016;**23**(6):1004–1015.
8. Zhou H, Forveille S, Sauvat A, *et al.* The oncolytic peptide LTX-315 triggers immunogenic cell death. *Cell Death Dis* 2016;**7**(3):e2134.

Ethics Approval This study was approved by Weill Cornell Medicine IACUC.

<http://dx.doi.org/10.1136/jitc-2022-SITC2022.1126>

1127 **CALCIUM PHOSPHATE BIOMATERIALS ENHANCE IMMUNOTHERAPEUTIC MRNA DELIVERY IN MELANOMA**

Hannah Martin*, Joshua Choe, Iris Baurceanu, William Murphy. *University of Wisconsin-Madison, Madison, WI, USA*

Background Messenger ribonucleic acid (mRNA) is a powerful tool for transferring genetic information. Its advantages include potent but transient gene expression without risk of genomic insertion, tailorable immunogenicity to match therapeutic application, and the potential for efficient, scalable manufacturing.¹ The recent success of mRNA-based SARS-CoV-2 vaccines has inspired interest in mRNA as a cancer therapy to deliver immunostimulatory molecules and tumor antigens. However, clinical translation is limited by mRNA instability at physiological conditions and inefficient *in vivo* delivery.² A reliable, non-toxic, and stabilizing *in vivo* delivery system for immunotherapeutic mRNA would help to advance mRNA as a viable cancer therapy. Here, we utilized calcium phosphate mineral-coated microparticles (MCMs) as a delivery system for mRNA-lipid complexes (lipoplexes) to transfect melanoma cells.

Methods MCMs were prepared as previously described³ by suspending β -tricalcium phosphate particles in modified simulated body fluid under rotation for 7 days at 37°C, refreshing the media daily. MCMs were then washed in deionized water and freeze dried. Custom-synthesized reporter or therapeutic mRNA constructs were complexed with a lipidic transfecting agent through mixing, then resulting lipoplexes were incubated briefly with MCMs to facilitate electrostatic binding to the porous CaP coating (figure 1a). Loaded MCMs or soluble lipoplexes were added to B16F10 murine melanoma cell culture, and transfection was measured through various assays, including fluorescence microscopy, bioluminescence, and enzyme-linked immunosorbent assays.

Results Scanning electron microscopy was used to verify plate-like, porous coating morphology following MCM fabrication (figure 1b). MCMs enhanced transfection of B16F10 melanoma cells compared to soluble mRNA lipoplex delivery. This was demonstrated with reporter constructs encoding enhanced green fluorescent protein (eGFP, figure 1c) and Gaussia luciferase (G-Luc), as well as with a therapeutic construct encoding interleukin 15 (IL-15), a T cell growth factor. Timelapse imaging also revealed more rapid transfection with MCMs. A close proximity of cells to MCMs was observed as necessary for transfection.

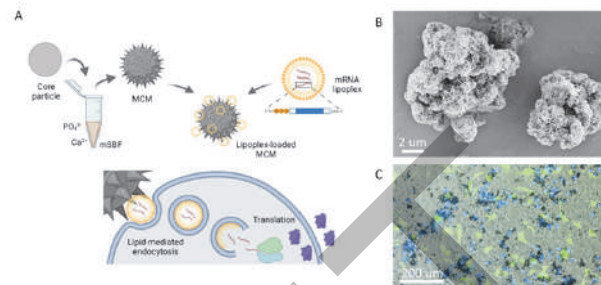
Conclusions We demonstrated that MCMs efficiently and locally deliver mRNA lipoplexes to melanoma cells and cause elevated levels of protein expression compared to soluble lipoplex delivery. This enhanced delivery profile makes MCMs a potential drug delivery platform for future *in vivo* tumor studies and clinical translation.

Acknowledgements The research presented was supported under NIH award TL1TR002375. The content is solely the responsibility of the authors and does not necessarily represent the official views of the National Institutes of Health. Thank you to Michael and Mary Sue Shannon for their generous gift towards this project. Artwork in Fig. 1A created on BioRender.com.

REFERENCES

1. Kowalski P, Rudra A, Miao L, and Anderson D. Delivering the messenger: Advances in technologies for therapeutic mRNA delivery. *Mol Ther* 2019;**27**(4):710-728.

2. Beck J, et al. mRNA therapeutics in cancer immunotherapy. *Mol Cancer* 2021;**20**(1):69.
3. Yu X, et al. Nanostructured mineral coatings stabilize proteins for therapeutic delivery. *Adv Mater.* 2017;**29**(33):1701255.



Abstract 1127 Figure 1 Mineral-coated microparticles (MCMs) as an efficient mRNA lipoplex delivery vehicle. (A) Fabrication, loading, and cellular delivery mechanism of MCMs. (B) Scanning electron microscopy image of the surface topography of MCMs (scale bar = 2 μm). (C) Representative fluorescence micrograph of B16F10 melanoma cells transfected with MCMs carrying enhanced green fluorescent protein (eGFP) mRNA lipoplexes. eGFP+ cells are shown in green, while nuclei are blue (Hoechst) (scale bar = 200 μm).

<http://dx.doi.org/10.1136/jitc-2022-SITC2022.1127>

1128

NEW VIRAL-DELIVERY OF GLYCAN-MODIFYING SIALIDASE INDUCES ANTI-TUMOR IMMUNITY

¹Natalia Rodrigues Mantuano*, ¹Michael Sandholzer, ¹Andreas Zingg, ²Heinz Läubli.
¹University of Basel, Basel, Switzerland; ²University Hospital Basel, Basel, Switzerland

Background Recent advancements in the stimulation of the immune microenvironment and anticancer immune responses with immune checkpoint inhibitors (ICI) has improved the outcome of cancer patients. However, primary and acquired resistance significantly diminish the success of ICI and only a minority of patients benefit. Thus, new strategies are urgently needed in order to induce long-term remissions with cancer immunotherapy. Changes of glycosylation have a significant impact on cancer biology and cancer progression. New therapies that aim to remodel the tumor glycosylation and reactivate the immune system are being explored. In particular, approaches that target the sialoglycan-Siglec glyco-immune checkpoint showed very promising results in pre-clinical animal models and are currently under investigation in early clinical trials.

Methods An adeno-associated virus (AAV) was constructed to express influenza sialidase under a CMV promoter (AAV-sia). Efficacy of sialidase production in transduced cells and the sialidase activity were tested in *in vitro* assays and mouse tumor models after intratumoral injection. In addition, efficacy of immune reactivation against tumors and cancer control was tested in various transplantable, syngeneic mouse models. Immune reactions were further characterized by flow cytometry and single cell RNA sequencing.

Results Upon AAV-sia treatment, cancer cells express sialidase on the cell surface and are able to cleave sialic acid in the tumor microenvironment in mouse models. We are further able to show an inhibitory effect on tumor growth and survival in syngeneic tumor models responsive and unresponsive to PD-1 blockade. Furthermore, a relevant synergism combining AAV-sia and anti-PD-1 treatment was observed. Mechanistic studies demonstrate an increased activation of CD8⁺ T cells, a polarization of myeloid cells towards a less immunosuppressive phenotype and an increase in conventional dendritic cell infiltration. In addition, scRNAseq data shows an increase in a macrophage population that up-regulate M1-like genes as TNF- α , CD80, MHCII, NOS2, IL1- β and CXCL9. Despite local injection and desialylation, we observed also a growth inhibition on distant tumor sites and an increase in tumor-specific T cells suggesting a systemic immune activation.

Conclusions Taken together, AAV-sia removes the immune-suppressant carbohydrate sialic acid from the tumor microenvironment and cancer cells rendering them more vulnerable for destruction by immune cells.

Ethics Approval All mouse experiments were approved by the local ethics committee (Approval 3036, Basel Stadt, Switzerland) and performed in accordance with the Swiss federal regulations

<http://dx.doi.org/10.1136/jitc-2022-SITC2022.1128>

1129 **A NOVEL CPG MOTIF INTRODUCED INTO A BISPECIFIC AM003 COMPOUND FOR THE TREATMENT OF SOLID TUMORS**

Neta Zilony- Hanin, Erez Lavi, Zohar Pode, Sapir Dahan, Vitaliy Buravenkov, Leeron Shefet Carasso, Ido Bachelet, Raanan Berger, Irit Carmi Levy*. *Aummune, Tel Aviv, Israel*

Background Despite clinical activity of immunotherapy agents in a broad range of cancer indications, there is still a substantial percentage of patients who fail to respond to those therapies, and hence, an unmet need to address mechanisms of tumor immune resistance. One of the most promising approaches is to turn a “cold” tumor into “hot” tumor.

CpG motif is a DNA sequence rich in unmethylated Cytosine-phosphate Guanine (CpG) nucleotides, prevalent in bacterial DNA, eliciting host immune reaction.

AM003 is a Bispecific Personalized Aptamer comprised of a T cell engager arm and a tumor-targeting arm, which is the outcome of Aummune’s innovative tailored therapeutic platform that identifies functional aptamers capable of killing tumor target cells. The two ssDNA aptameric arms of AM003, when hybridized, are designed to form a novel immunostimulant CpG motif

Methods In vitro evaluation of the AM003 CpG mode-of-action was performed using B cell and dendritic cells (DC) flow cytometry analyses, cytokines measurements and co-culture assays. Moreover, in vivo immunologic effects were investigated in syngeneic mice tumor models.

Results The AM003 CpG motif induced a potent stimulation of antigen presenting cells. Stimulated dendritic cells (DC) had an increased cell surface expression of different co-stimulatory receptors and elevated TNF- α secretion.

DC cultured with AM003 demonstrated enhanced CD4 T cells stimulation in a mixed lymphocyte reaction (MLR) model with higher levels of IFN- γ detected. Furthermore, anti-PD1 led to a synergistic effect when combined with AM003 in the MLR assay, where IFN γ levels were further elevated, compared with both single agents.

In line with the observed results of innate immune stimulation, in vivo, intratumoral injection of AM003 effectively transformed the immune landscape of the injected tumor, with increased infiltration of CD8+ CD4+ T cells and of B cells.

Conclusions Our findings suggest that AM003 addresses the challenges of immune resistance by activating the innate immune system, improving T cell infiltration and enabling a follow-on effective T cell activation by the compound’s T cell engager arm.

These data provide a framework for the clinical development of this novel personally tailored immunotherapy. Aummune has initiated a first-in-human clinical study of AM003 in subjects with solid tumors.

Ethics Approval

TLV medical center ethics committee TLVMC – IL – 2205 – 113 – 5 (Animals study)

Helsinki approval number 0297-15-TLV (Buffy coat)

<http://dx.doi.org/10.1136/jitc-2022-SITC2022.1129>

1130 INVESTIGATING MACROPHAGE MODULATION IN A MURINE MODEL OF SOFT TISSUE SARCOMA

Kurt Hildebrand*, Karys Hildebrand, Franz Zemp, Carolina Salazar Arcila, Michael Monument. University of Calgary, Calgary, Canada

Background Soft tissue sarcomas (STSs) are a heterogeneous group of malignancies that arise from mesodermal tissue. Generally, STSs are treated with morbid surgical resection and radiation therapy.¹ The STS tumour microenvironment (TME) contains an abundance of macrophages² and few lymphocytes.³ In many malignancies, macrophages can be associated tumour progression⁴ and suppression of lymphocytes.⁵ The role of macrophages in STSs needs further investigation. Therefore, the purpose of this study was to modulate macrophages in an immune competent model of STS, and assess the changes in tumour growth and the immune landscape.

Methods Two models were used to modulate macrophages in an immune competent murine STS model; the Macrophage Fas-Induced Apoptosis (MaFIA) model⁶, and the C-C chemokine receptor-2 Knockout (CCR2 KO) model.⁷ MaFIA mice express a transgene and can be given a pharmacological agent to induce cell death in CSF1R+ cells. The CCR2 KO model shows a deficiency in recruiting monocytes to inflamed tissue. Both models have reduced tumour macrophages in other murine models.^{8, 9} MaFIA and CCR2 KO mice were engrafted with STS cells in the right hindlimb.¹⁰ Tumour volume, macrophages (CD45⁺, CD11b⁺, F4/80⁺, and CD80⁺ or CD206⁺), as well as lymphocytes (CD45⁺, CD3e⁺, and CD4⁺ or CD8⁺) were assessed using flow cytometry.

Results MaFIA mice showed a ~84% decrease ($p < 0.01$) in tumour volume, whereas the CCR2 KO mice and control mice showed no differences in tumour volume. MaFIA mice showed a significant reduction of CSF1R+ macrophages (53%; $p < 0.01$) and CSF1R+, CD206+ macrophages (54%; $p < 0.05$), but no changes to total macrophages. Interestingly, the CCR2 KO mice showed a significant decrease in tumour macrophages (47%; $p < 0.01$), as well as CD206+ macrophages (41%; $p < 0.01$). The MaFIA model showed no differences in lymphocytes, but the CCR2 KO model showed a significant increase in CD8 T cells (360% increase; $p < 0.01$). Interestingly, CSF1R+ ablative treatment was associated with an increased expression of PD1 in the MaFIA model (211%; $p < 0.01$).

Conclusions Both CSF1R and CCR2 modulation diminished macrophage subtypes, but CSF1R modulation did not diminish the total macrophage population. However, only the CCR2 KO model improved lymphocyte (CD8 T cell) infiltration, which did not improve disease outcome. Additionally, CSF1R modulation was associated with an increased PD1 expression. Thus, modulating the CCR2 axis influenced the TME but did not change tumour burden. The CSF1R axis diminished STS tumour burden and macrophage subtypes, and could potentially also sensitize STS tumours to anti-PD1 therapy.

REFERENCES

1. Cormier JN, Pollock RE. Soft tissue sarcomas. *CA Cancer J Clin*;2004;**54**(2):94–109.
2. Sawa-Wejksza K, Kandefer-Szerszen M. Tumor-associated macrophages as target for antitumor therapy. *Archivum immunologiae et therapeuticae experimentalis*, 2018;**66**(2):97–111.
3. Sorbye SW, et al. Prognostic impact of lymphocytes in soft tissue sarcomas. *PLoS One* 2011;**6**(1):e14611.
4. Lin Y, Xu J, Lan H, Tumor-associated macrophages in tumor metastasis: biological roles and clinical therapeutic applications. *J Hematol Oncol* 2019;**12**(1):76.

5. Peranzoni E, et al. Macrophages impede CD8 T cells from reaching tumor cells and limit the efficacy of anti-PD-1 treatment. *Proceedings of the National Academy of Sciences* 2018;**115**(17):E4041–E4050.
6. Burnett SH, et al. Conditional macrophage ablation in transgenic mice expressing a Fas-based suicide gene. *Journal of Leukocyte Biology* 2004;**75**(4):612–623.
7. Boring L, et al. Impaired monocyte migration and reduced type 1 (Th1) cytokine responses in CC chemokine receptor 2 knockout mice. *The Journal of Clinical Investigation* 1997;**100**(10):2552–2561.
8. Gabrusiewicz K, et al. Macrophage ablation reduces M2-like populations and jeopardizes tumor growth in a MAFIA-based glioma model. *Neoplasia* 2015;**17**(4):374–384.
9. Sanford DE, et al. Inflammatory monocyte mobilization decreases patient survival in pancreatic cancer: a role for targeting the CCL2/CCR2 axis. *Clinical Cancer Research* 2013;**19**(13):3404–3415.
10. Hildebrand KM, et al. The Kras G12D; Trp53 fl/fl murine model of undifferentiated pleomorphic sarcoma is macrophage dense, lymphocyte poor, and resistant to immune checkpoint blockade. *PLoS One* 2021;**16**(7):e0253864.

Ethics Approval Studies involving animals were conducted according to the Canadian Council on Animal Care guidelines. Ethics approval was obtained from the University of Calgary Health Sciences Animal Care Committee (AC19-0072, 6/25/2021). All mice are housed at the University of Calgary Foot-hills Campus in a level 2 containment facility.

<http://dx.doi.org/10.1136/jitc-2022-SITC2022.1130>

1131

GRWD5769: A FIRST-IN-CLASS INHIBITOR OF ERAP1, GENERATING NOVEL CANCER ANTIGENS TO DRIVE DE NOVO ANTI-TUMOR T CELL RESPONSES

¹Peter Joyce*, ¹Andrew Leishman, ²Asolina Braun, ¹Mitul Patel, ¹Michael Pinggera, ¹Jessica Sette, ¹Kate Anderton, ³Edd James, ¹Valeriya Shunina, ²Anthony Purcell, ⁴Nicola Temette, ⁵Jason Shiers, ¹Martin Quibell, ⁴Wayne Paes, ¹Tom McCarthy. ¹Grey Wolf Therapeutics, Oxford, UK; ²Monash University, Melbourne, Australia; ³University of Southampton, Southampton, UK; ⁴University of Oxford, Oxford, UK; ⁵Signature Discovery, Nottingham, UK

Background Immune checkpoint inhibitors (ICI) have changed the cancer treatment paradigm, yet significant unmet need remains. Clinical data demonstrates increased antigen presentation diversity, genomic instability, tumor mutational burden and HLA diversity are all factors that improve clinical response to ICI.^{1,2,3} Further, the effectiveness of ICI is limited by the permanent exhaustion of pre-existing cytotoxic T cells, caused by chronic cancer antigen stimulation.⁴ Endoplasmic reticulum aminopeptidase 1 (ERAP1) trims peptides loaded into classical and nonclassical MHC Class I.⁵ In cancer, knockout or inhibition of ERAP1 changes a proportion of the antigen repertoire, generating and up-regulating cancer antigens.^{6,7} This leads to the activation of de novo anti-tumor T cell responses, causing tumour growth inhibition and bypassing a key resistance mechanism in immuno-oncology (IO), T cell exhaustion. We report the preclinical development, characterisation and mechanistic analysis of the first-in-class ERAP1 inhibitor, GRWD5769.

Methods Immunopeptidomics was used to assess the impact of ERAP1 inhibition on the cancer antigen repertoire, thus determine proof of mechanism. T cell receptor (TCR) repertoire sequencing, RNAseq and immunohistochemistry established the ability of ERAP1 inhibition to drive a differentiated T cell response in syngeneic mouse models and primary human immune cell co-cultures.

Results Extensive analysis of the immunopeptidomes of diverse cancer cell lines robustly showed that GRWD5769 modulates the cancer-related antigen repertoire across genotypes and cancer-type backgrounds. Novel or upregulated neoantigens generated by ERAP1 inhibition are conserved across cancer cell types and genetic backgrounds. ERAP1 inhibition diversified the TCR repertoire, up-regulated prognostic immune gene markers in the tumor, including markers for recently activated (thus non-exhausted) T cells, and drove infiltration of T cells into syngeneic mouse model tumours. ERAP1 inhibition is efficacious across syngeneic models, including different mouse strains. Importantly, the effects of ERAP1 inhibition on the T cell response correlate with efficacy. Further, ex vivo human T cell co-cultures demonstrate that novel and upregulated neoantigens generated by ERAP1 inhibition drive tumour cell killing.

Conclusions Grey Wolf Therapeutics' first-in-class, ERAP1 inhibitor clinical candidate, GRWD5769, drives novel anti-tumor T cell responses through neoantigen creation, circumventing T cell exhaustion, a key resistance mechanism in IO. GRWD5769 has completed GLP toxicology studies, has a very good safety profile and clear path forward to first patient dosed. Extensive biomarker development has resulted in development of proof of mechanism and proof of principle biomarkers that will be used to establish the activity and efficacy of GRWD5769 in patients in 2023.

REFERENCES

1. Rizvi N, Hellmann MD, Snyder A, *et al.* Mutational landscape determines sensitivity to PD-1 blockade in non-small cell lung cancer. *Science*. 2015;**348**(6230):124–128.
2. Chowell D, uc G T Morris LGT,2 3, Grigg CM *et al.* Patient HLA class I genotype influences cancer response to checkpoint blockade immunotherapy. *Science* 2018;**359**(6375):582–587
3. Chowell D, Chirag Krishna, Federica Pierini *et al.* Evolutionary divergence of HLA class I genotype impacts efficacy of cancer immunotherapy. *Nature Medicine* 2019;**25**(11):1715–1720
4. Oliveira G, Stromhaug K, Klaeger S, *et al.* Phenotype, specificity and avidity of antitumour CD8+ T cells in melanoma. *Nature* 2021;**596**:119–125
5. Shastri N, Nagarajan N, Lind KC, *et al.* Monitoring peptide processing for MHC class I molecules in the endoplasmic reticulum. *Curr Opin Immunol*. 2014;**26**:123–127.
6. James E, Bailey I, Sugiyarto G, *et al.* Induction of protective antitumor immunity through attenuation of ERAAP function. *J Immunol*. 2013;**190**(11):5839–5846.
7. Manguso RT, Pope, HW, MD Zimmer *et al.* In vivo CRISPR screening identifies Ptpn2 as a cancer immunotherapy target. *Nature* 2017;**547**(7664):413–418

<http://dx.doi.org/10.1136/jitc-2022-SITC2022.1131>

1132

IMPACT OF INTRALESIONAL ONCOLYTIC VIRAL THERAPY TARGETING *IN SITU* ACTIVATION OF CD40 AND TYPE 1 INTERFERON SIGNALING PATHWAYS ON THE TME AND SYSTEMIC T CELL IMMUNITY IN MURINE MODELS AND CANCER PATIENTS

¹Andreas Saltos*, ¹Hong Zheng, ²Christy Arrowood, ²Georgia Beasley, ²James Ronald, ¹Ghassan El-Haddad, ²Uzma Khan, ¹Luiziane Guerra-Guevara, ²Steven Wolf, ²Lin Gu, ²Xiaofei Wang, ³Mark Cantwell, ²Scott Antonia, ¹Amer Beg, ²Neal Ready. ¹Moffitt Cancer Center, Tampa, FL, USA; ²Duke University, Durham, NC, USA; ³Memgen, Inc, Meadow Vista, CA, USA

Background Oncolytic viral therapies are thought to act through both direct killing of tumor cells and activation of conventional dendritic cells (cDCs), resulting in an enhanced T cell response. However, cDC activation has not been optimized with current therapies. MEM-288 is a conditionally-replicative oncolytic adenovirus encoding transgenes for human interferon beta (IFN β) and a recombinant membrane-stable form of CD40-ligand (MEM40), two potent activators of the immune response and cDCs.

Methods We evaluated intralesional adenoviral delivery of MEM40 and IFN β to activate cDCs in mouse melanoma and lung tumor models. Flow cytometry and scRNA-seq were used to determine treatment impact on cDCs and T cells. Clinical translational research also investigated the immune response of intralesional administration of MEM-288 in patients with select solid tumors in an ongoing Phase 1 dose-escalation, multi-center, open-label trial (NCT05076760). Patient pre- and on-treatment tumor biopsies and peripheral blood were collected before and after MEM-288 treatment for immunologic evaluation.

Results In preclinical studies, MEM40 and IFN β in situ co-expression induced higher cDC activation than either molecule alone, in addition to a dramatic increase in lymph node migration, a systemic anti-tumor CD8⁺ T cell response, and regression of established tumors in a manner dependent upon type 1 cDCs. MEM40 and IFN β expression enhanced generation of both Granzyme B⁺ CD8⁺ T cell effectors as well as TCF1⁺ stem-like CD8⁺ T cells that are known to be strongly associated with response to immune checkpoint inhibitors (ICIs). Intralesional therapy with MEM40 and IFN β expressing adenovirus synergized with ICIs, leading to effective control of distant tumors and lung metastases. Notably, these preclinical results are translating into the clinical setting. Pre- and on-treatment biopsies from the initial 2 non-small cell lung cancer (NSCLC) patients on study were evaluated for TME impact of MEM-288 treatment. A single intralesional injection of low dose cohort MEM-288 (1e10 viral particles) resulted in shrinkage of the injected tumor (-31 and -53%), concomitant with substantial increases in overall CD8⁺ T cells and TCF1⁺ stem-like CD8⁺ T cells. Studies to determine systemic effects on T cells are ongoing.

Conclusions MEM40 and IFN β expression induces strong remodeling of the TME in both murine models and solid tumor patients. Preliminary safety, antitumor, and immune response data in the ongoing MEM-288 clinical trial is also encouraging. Following completion of the monotherapy study, an expansion arm is planned where MEM-288 will be combined with anti-PD1 antibody in patients with advanced NSCLC refractory to ICI.

Ethics Approval The studies described received IRB approval (Moffitt: Adverra IRB, # Pro00060205, Duke: DUHS IRB, #Pro00109517) prior to commencement, and in the clinical

trial described all participants gave informed consent before taking part.

<http://dx.doi.org/10.1136/jitc-2022-SITC2022.1132>

1133

REMODELING THE IMMUNOSUPPRESSIVE TUMOR MICROENVIRONMENT WITH ONCOLYTIC VIRUS-MEDIATED DELIVERY OF A POTENT TGF- β INHIBITOR

Kristin DePeaux*, Dayana Rivadeneira, Kevin Quann, Konstantinos Lontos, Andrew Hinck, Greg Delgoffe. University of Pittsburgh, Pittsburgh, PA, USA

Background Checkpoint blockade often fails due to a lack of pre-existing immune response. Oncolytic viruses (OVs) induce inflammation and generate a tumor specific immune response which is critical for patients with immune desert or excluded tumors. Further, OVs can be engineered to deliver therapeutic cargo in the tumor microenvironment. However, mechanisms of resistance to OVs are not well understood. To study OV resistance, we developed derivatives of the head and neck cancer line MEER: one sensitive to oncolytic vaccinia virus (VV, MEER^{VV^S}), and one resistant to VV (MEER^{VV^R}). Using these, we determined mechanisms which suppressed the anti-tumor immune response and engineered a new VV to target them.

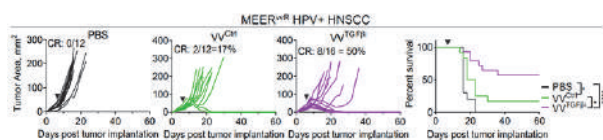
Methods A MEER^{VV^S} tumor that grew out post-treatment was passaged in mice with a single intratumoral dose of VV given at each passage. This was repeated until a VV-resistant line was generated. For flow-cytometric tumor infiltrating lymphocyte analysis, MEER^{VV^R} and MEER^{VV^S} tumors were implanted in mice, treated with a single dose of VV^{ctrl}, VV^{TGF β i}, or PBS, and harvested 7-days post-treatment.

Results After VV treatment, we found increased T cell infiltration in both tumor types; however, MEER^{VV^S} infiltrate had significantly increased function, suggesting local suppressive mechanisms may define VV resistance. Indeed, in mice bearing both MEER^{VV^R} and MEER^{VV^S} we found the regulatory T (Treg) cells in the sensitive tumors had lower Nrp1 expression and higher STAT1 signaling, suggesting they may be primed for fragility. Resistant tumors were characterized by high intratumoral TGF β , a driver of resistance to VV. We found TGF β increased Nrp1 on Treg cell surface and led to maintained Treg suppression in the presence of IFN γ . We then generated a VV expressing a TGF β inhibitor (VV^{TGF β i}), which outcompetes TGF β for receptor binding, preventing receptor signaling. When MEER^{VV^R} were treated with VV^{TGF β i} there was a significant increase in tumor clearances and survival compared to VV^{ctrl} (figure 1). Response to VV^{TGF β i} was linked to a fragile Treg cell phenotype. Further, VV^{TGF β i} synergized with PD1-blockade in a melanoma model resistant to either therapy alone.

Conclusions Our data suggest that a TGF β -rich microenvironment is a main driver of VV resistance, due in part to stabilization of Treg cells. Targeting TGF β using an inhibitor-armed virus can overcome this resistance. Importantly, virally-encoded TGF β inhibition is local, carrying no toxicity associated with systemic routes. Taken together, our findings confirm TGF β as a major player in immunotherapeutic resistance and that OVs are an attractive means to deliver TGF β inhibition to synergize with other immunotherapies.

represent four independent experiments. Each line represents an individual mouse. * $p < 0.05$, ** $p < 0.01$, *** $p < 0.001$, **** $p < 0.0001$ by Mantel-Cox test. ns, non-significant.

<http://dx.doi.org/10.1136/jitc-2022-SITC2022.1133>



Abstract 1133 Figure 1 Growth Curve and Survival Tumor growth (left) and survival (right) of MEERwR-bearing C57BL/6 mice treated with an intratumoral injection of PBS, VV-ctrl or VV-TGF β i (black arrow) at 2.5x10⁶ PFU/mouse. CR = complete response. Data

1134

DYNAMIC ANALYSES OF TUMOR MICROENVIRONMENT MODULATION BY CAN-2409 TREATMENT USING KAEDE PHOTOCONVERTIBLE TRANSGENIC MICE

<http://dx.doi.org/10.1136/jitc-2022-SITC2022.1134>

¹David Withers*, ²Anne Diers, ¹Zhi Li, ¹Suaad Idris, ¹Claire Willis, ²Paul Peter Tak, ²Francesca Barone. ¹University of Birmingham, Birmingham, UK; ²Candel Therapeutics, Needham, MA, USA

Background CAN-2409 is a replication-defective adenovirus that delivers the HSV-thymidine kinase gene. Intratumoral administration of CAN-2409 followed by prodrug results in the formation of a toxic metabolite able to induce immunogenic cell death, exposure of tumor-associated antigens, and activation of local and systemic immune responses. Use of state-of-the-art preclinical tools for dynamic assessment of the lymphocyte response in vivo will enable assessment of the evolution of the anti-tumor immune response induced by CAN-2409 and provide the immunological rationale for potential therapeutic combinatory approaches.

Methods We utilized a dynamic labeling model¹ where MC38 tumor cells were implanted subcutaneously into photoconvertible Kaede mice; violet light was used to simultaneously label the entire tumor microenvironment (TME), enabling the discrimination of cells retained within the tumor (Kaede Red+) versus newly entering cells (Kaede Green+) and the ability to assess real-time changes occurring in the immune compartment of the TME. CAN-2409 was administered intratumorally on day 10 after tumor inoculation followed by prodrug (ganciclovir, 50mg/kg IP QD on days 11 to 14). Photoconversion occurred on day 12, and analysis was performed 48h later. Dynamic of MC38-tumor specific T cell clones was evaluated by flow cytometry. We also explored the effect of CAN-2409 in combination with immune checkpoint inhibition (ICI).

Results Administration of CAN-2409 led to control of tumor growth and a significantly increased effector CD8 T cell response. Photolabeling of the TME revealed that rather than enhancing recruitment of T cells to the tumor, CAN-2409 altered the TME such that newly entering, but also retained CD8 T cell were significantly more proliferative. Amongst the retained population, terminally exhausted neoantigen-specific CD8 T cells showed evidence of reinvigoration, adopting a CX3CR1+ GZMB+ phenotype. There was also enhanced proliferation within the PD-1+ stem-like compartment of newly recruited cells and we observed expansion of a population of non-activated, likely less suppressive, Tregs. The combination of CAN-2409 and anti-CTLA-4 (clone 9H10) treatment further improved control of tumor growth and remodeled the Treg compartment to further skew the Treg:CD8 ratio in favor of the effector response.

Conclusions CAN-2409 alters the TME such that newly entering CD8 T cells expand and retain key effector functions while the exhausted CD8 compartment is reinvigorated, likely reducing Treg-mediated suppression. Collectively, these data suggest at least two temporally distinct pathways underpinning CAN-2409 action that overcome cell exhaustion and decreased immune suppression, supporting the rationale for the use of CAN-2409 either as monotherapy or in combination.

REFERENCE

1. Zhi Li, Zewen K Tuong, Isaac Dean *et al.* In vivo labeling reveals continuous trafficking of TCF-1+ T cells between tumor and lymphoid tissue. *J Exp Med* 2022;**219**(6):e20210749. doi: 10.1084/jem.20210749

Ethics Approval All in vivo experiments were conducted in accordance to UK HO guidelines on an approved PPL

1135

SINGLE CELL RESOLUTION OF IMMUNE RESPONSES TO ONCOLYTIC HERPES SIMPLEX VIRUS C134 IN PRECLINICAL MEDULLOBLASTOMA MODELS

¹Jack Hedberg*, ¹Adam Studebaker, ²Luke Smith, ¹Chun-Yu Chen, ¹Jesse Westfall, ¹Maren Cam, ¹Amy Gross, ¹Ryan Roberts, ¹Timothy Cripe, ¹Elaine Mardis, ¹Kevin Cassady, ¹Jeffrey Leonard, ¹Katherine Miller. ¹Nationwide Children's Hospital, Columbus, OH, USA; ²Ohio State University, Columbus, OH, USA

Background Medulloblastoma is the most common malignant brain tumor in children.¹ Despite recent advances in our understanding of its tumor biology, one-third of affected children do not survive this disease. Even amongst survivors of medulloblastoma, there are significant issues with treatment-related health sequelae, and thus more effective and safer therapies are urgently needed. Oncolytic herpes simplex viruses (oHSV), which exploit the dysregulated cellular programs in malignant cells as a replicative advantage, also evoke innate immune responses. As such, they provide an increasingly appealing option for treating many malignancies, including brain cancers.

Methods Here, we studied the effects of the oHSV C134 in two syngeneic medulloblastoma mouse models, one that aligns with the sonic hedgehog (SHH) subtype (MYCN) and another that aligns with group 3 subtype tumors (CMYC).^{2,3} We treated intracranial tumors with C134 or vehicle to evaluate changes in overall survival, then applied single cell RNA-sequencing (scRNA-seq) and flow cytometry to study tumor samples across multiple post-treatment timepoints and characterize the immune responses evoked by C134 treatment.

Results Treatment with C134 increased survival in C57BL/6 mice bearing tumors for the CMYC model (C134 median = 38.5 days, range = 24-75 days, n = 10 vs. vehicle median = 19 days, range = 17-24 days, n = 10, p<0.0001) as well as the MYCN model (C134 median = 17.5 days, range = 14-23 days, n = 10 vs. vehicle median = 13 days, range = 10-14 days, n = 10, p<0.0001). Flow cytometry demonstrated similarities in immunophenotypic response to C134 between the two models including increased M1-like macrophages, CD4+ T cells, CD8+ T cells, NKT cells, and myeloid-derived suppressor cells. Collectively these data provided evidence for a complex immune response. scRNA-seq data analysis allowed higher resolution immune response characterization, indicating over twenty cell types (figure 1). Here, we identified statistically significant (FDR < 0.05) increases in proportions of macrophages, monocytes, lymphocytes, and dendritic cells after C134 treatment. Differential gene expression revealed that cytokines, MHC class I, Ib, and II genes, and interferon-response genes exhibited marked expression changes in lymphocytes, macrophages, microglia, and dendritic cells in response to C134.

Conclusions Our findings suggest a multifaceted immune response contributes to the efficacy of C134 oHSV treatment to prolong survival in two mouse models of medulloblastoma. A wide array of gene expression changes occurs in response to C134 treatment across immune cell types, time points, and medulloblastoma models, illuminating potential mechanisms involved in C134's antitumor effects.

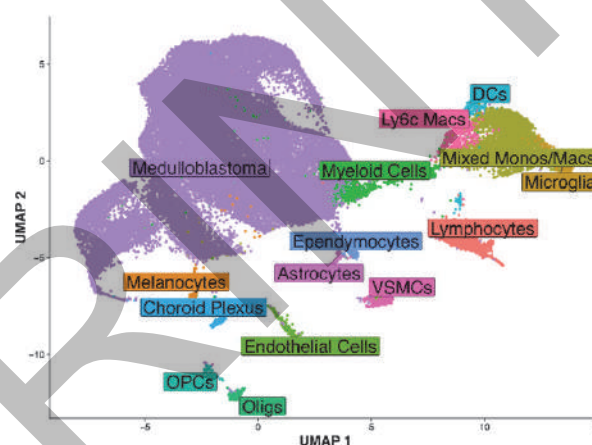
Acknowledgements The authors would like to acknowledge the following support: Nationwide Children's Hospital start-up funds (J.R.L.); CancerFree KIDS Pediatric Cancer Research Alliance Award (A.W.S.) and the Nationwide Insurance Innovation Fund. The authors would like to acknowledge Dr. Martine Roussel and Dr. Frederique Zindy (St. Jude Children's Research Hospital, Memphis, TN) for the syngeneic mouse

medulloblastoma models, as well as Dr. Matt Cannon for computational support.

REFERENCES

1. Northcott PA, Robinson GW, Kratz CP, et al. Medulloblastoma. *Nat Rev Dis Prim* 2019;**5**:1–20.
2. Zindy F, Uziel T, Ayrault O, et al. Genetic Alterations in Mouse Medulloblastomas and Generation of Tumors De novo from Primary Cerebellar Granule Neuron Precursors. *Cancer Res* 2007;**67**:2676–2684.
3. Kawauchi D, Robinson G, Uziel T, et al. A Mouse Model of the Most Aggressive Subgroup of Human Medulloblastoma. *Cancer Cell*. 2012;**21**:168–180.

Ethics Approval All animal experiments were approved by the Nationwide Children's Hospital Institutional Animal Care and Use Committee (AR17-00039).



Abstract 1135 Figure 1 Single Cell RNA Sequencing of Medulloblastomas UMAP plot showing combined sample dataset and annotated cell types identified by single cell RNA sequencing of eight murine medulloblastomas of subgroup MYCN or CMYC, treated with C134 oHSV or vehicle, and at post-treatment day two or day six.

<http://dx.doi.org/10.1136/jitc-2022-SITC2022.1135>

1136

INDUCTION OF TERTIARY LYMPHOID STRUCTURES IN NON-SMALL CELL LUNG CANCER IMPROVES B AND T CELL ANTI-TUMOR IMMUNITY

¹Hye Mi Kim*, ²Dongyan Liu, ¹Ayana Ruffin, ²Alexandra McDonough, ²Caleb Lampenfeld, ²Sheryl Kunning, ²Ashwin Somasundaram, ²Laura Stabile, ²Tullia Bruno. ¹University of Pittsburgh School of Medicine, Pittsburgh, PA, USA; ²UPMC Hillman Cancer Center, Pittsburgh, USA

Background Tertiary lymphoid structures (TLS) are lymphoid aggregates that often form locally in tissues with chronic infection, autoimmune disease, and cancer. As such, TLS correlate with favorable prognosis in patients with solid tumors, including non-small-cell lung cancer (NSCLC). Further, TLS have recently been associated with superior response to immune checkpoint blockade (ICB).^{1, 2, 3} B cells are predominantly located within TLS and correlate with improved survival and ICB response.⁴ Despite the therapeutic promise of B cells and TLS, they have not been investigated as immunotherapeutic targets. Moreover, a mechanistic understanding of TLS formation and function in cancer is lacking.

Methods Our studies aim to interrogate unique factors that promote or inhibit TLS formation. First, we studied TLS in human lung adenocarcinoma using multispectral imaging and spatial transcriptomics (Nanostring Digital Spatial Profiler) to uncover known and unknown pathways that could improve TLS formation and subsequently B and T cell function. We paired these studies with murine models of lung adenocarcinoma. Specifically, we utilized a physiologically relevant, carcinogen (4-(methylnitrosamino)-1-(3-pyridyl)-1-butanone; NNK) induced murine model of lung cancer that spontaneously forms TLS. A syngeneic tumor line derived from this model that can be orthotopically injected into the murine lung also forms high B cell infiltrate and TLS. We utilized these models to test if TLS induction and maturation were increased with an oncolytic virus that targets known TLS-initiating factors.

Results According to spatial transcriptomics, tumor-associated TLS have decreased TLS-initiating and maturation factors such as CXCL13, IL-21, CD40, and LTbeta/LIGHT in comparison to normal lymphoid tissues. Further, as TLS proximity to the tumor increases, there is an increased immune regulation surrounding TLS formation. Thus, using an oncolytic virus that targets CXCL13, IL-21, CD40 and LTbeta ligation or LIGHT, we observed increased TLS induction and tumor reduction.

Conclusions These studies will increase our understanding of TLS formation for improved immunotherapies in NSCLC patients and will potentially provide therapeutic interventions that could be administered prior to cancer development.

Acknowledgements This work is supported by funding from the Mark Foundation for Cancer Research (Endeavor Award). We would like to thank Rebecca A. Elsner from Mark J. Shlomchik's lab for critical comments and acknowledge KaliVir Immunotherapeutics for providing oncolytic virus.

REFERENCES

1. Di Caro G, Bergomas F, Grizzi F, Doni A, Bianchi P, Malesci A, Laghi L, Allavena P, Mantovani A, Marchesi F. Occurrence of tertiary lymphoid tissue is associated with T-cell infiltration and predicts better prognosis in early-stage colorectal cancers. *Clinical Cancer Research* 2014;**20**(8):2147–2158.
2. Cabrita R, Lauss M, Sanna A, Donia M, Skaarup Larsen, M, Mitra S, Johansson I, Phung B, Harbst K, Vallon-Christersson J, van Schoiack A, Lövgren K, Warren S, Jirstrom K, Olsson H, Pietras K, Ingvar C, Isaksson K, Schadendorf D, Jönsson, G. Tertiary lymphoid structures improve immunotherapy and survival in melanoma. *Nature*. 2020;**577**(7791):561–565.
3. Ukita M, Hamanishi J, Baba T, Murakami R, Abiko K, Mandai M. Clinical significance of tertiary lymphoid structures (TLS) and tumor-infiltrating plasma cells in ovarian cancer. *Tumor Biology*. 2018;Abstract 1021.

4. Fridman W, Petitprez F, Meylan M, Chen T, Sun C, Roumenina L, Saue`s-Fridman C. B cells and cancer: To B or not to B?. *Journal of Experimental Medicine*. 2021;**218**(1)

Ethics Approval This study is approved by University of Pittsburgh and UPMC Hillman Cancer Center; IACUC protocol 20118291.

<http://dx.doi.org/10.1136/jitc-2022-SITC2022.1136>

1137 **SUPERNOVA1 (SNV1), A NOVEL ONCOLYTIC-CELL BASED PLATFORM FOR CANCER THERAPY**

¹Duong Nguyen*, ²Mohamed Hammad, ²Rachael Mooney, ¹Forrest Neuharth, ¹Ashley Alamillo, ¹Ivelina Minev, ¹Israel Romero, ¹Stephanie Songco, ¹Emma Kedl, ¹Yunyi Kang, ²Hoi Ngai, ²Marisa McDonald, ²Linda Flores, ²Dae Kim, ²Jacqueline Lara, ³Thomas Herrmann, ³Barbara Härtl, ³Laura Edith, ³Daniela Kleinholz, ¹Boris Minev, ²Karen Aboody, ¹Antonio Santidrian. ¹Calidi Therapeutics, San Diego, CA, USA; ²City of Hope, Duarte, CA, USA; ³StemVAC, Bernried, Germany

Background The therapeutic potential of the oncolytic virotherapy is severely restricted by multiple innate and adaptive immune barriers. To overcome this obstacle, we utilized adipose-derived stem cells (AD-MSC) loaded with tumor selective CAL1 oncolytic vaccinia virus to generate a new therapeutic agent called SNV1 (SuperNova-1). Intratumoral injection of SNV1 inhibited drastically tumor growth of multiple human cancer xenograft models at significant low virus titers. In syngeneic immunocompetent models, SNV1 showed a robust tumor growth inhibition and immune cell recruitment of both the local injected tumors and distant non-injected tumors.

Methods SNV1 was tested for its ability to resist humoral immunity-mediated virus inactivation in cell culture. In tumor-bearing mouse models, tumor growth inhibition of multiple human xenografts and murine syngeneic was examined by using either single or three dose regimens. Additionally, in bilateral tumor-bearing mouse models, immune profiles at different time courses of both treated and untreated tumors as well as lymph nodes were analyzed by flow cytometry. Antiviral and anti-tumor immunity was analyzed by ELISPOT.

Results Data showed that SNV1 was more resistant to rapid inactivation by humoral immune system as compared to naked CAL1 virus leading to a significant and robust improvement of oncolytic virus therapeutic efficacy in human melanoma (MeWo), head and neck (Fadu) and triple negative breast (MDA-MB-231) cancer cells. Furthermore, SNV1 significantly inhibited the growth of the tumors even at the very low dose of 1.5×10^3 cells containing 1.6×10^4 PFU. In a bilateral colon cancer tumor-bearing immunocompetent mouse model CT26, data showed both one (1) and three (3) administrations of SNV1 significantly inhibit tumor growth of injected tumors in comparison with the naked CAL1 virus or controls. However, significant systemic therapeutic efficacy was only achieved by three (3) but not one (1) intratumoral administrations of SNV1 suggesting multiple intratumoral administrations of SNV1 were required to induce robust systemic activation of the immune system. Furthermore, tumor infiltrating lymphocytes (TILs) from both treated and untreated tumors showed increased CD4 and CD8 T-cell infiltrations while suppressing frequency of Tregs. Early recruitment of innate populations was observed in tested models.

Conclusions The SNV1 stem cell-based platform protects and potentiates oncolytic vaccinia virus by circumventing humoral innate and adaptive immune barriers, resulting in enhanced anti-cancer effects in tumor-bearing mouse models. SNV1 provided instantly active viral particles for immediate infection in the injected tumors which help transforming tumor environment from “cold” to “hot” locally and systemically.

<http://dx.doi.org/10.1136/jitc-2022-SITC2022.1137>

1138

ENGINEERED ONCOLYTIC VIRUSES EXPRESSING IMMUNOMODULATORY GENES ENHANCED ANTI-TUMOR IMMUNE RESPONSES *IN VITRO*

Zhongbao Song*, Limin Tian, Guangxu Ding, Ka Fung Noi, Jie Xu, Qingyang Gu. *WXi ApTec, Nantong, China*

Background While chemo- and radio-therapies were considered the first-line treatment for most cancers, their serious side effects have led to continuous innovation and discovery of new cancer therapies. Oncolytic viruses (OVs), either naturally occurred or genetically engineered to selectively target and lyse cancer cells without harming normal tissues, have emerged as the next remarkable wave in cancer immunotherapy. OVs possess a magnitude of mechanisms to elicit anti-tumor immune response, including the infection in cancer cells causing the viral replication and cell lysis. In addition to OVs innate cytotoxicity, further anti-tumor enhancement can be achieved *via* inserting tumor-associated antigen (TAA)/immunomodulatory genes by genetic engineering technology, leading to the release of inflammatory and immunoregulatory cytokines. This in effect, causes the tumor to become “hot” and detectable by other immune cells, which are subsequently stimulated to eradicate tumor. Our recent study assessed the effect of modified OVs (mOVs) engineered with immunomodulatory genes in the *in vitro* assays with various immune cells including T, natural killer (NK) and monocyte-derived dendritic cells (moDC).

Methods • The expression of exogenous immunomodulatory genes, in different tumor cells infected with mock or mOV, was detected by flow-cytometry and ELISA.

- Cytotoxicity of mOV on different tumor cell lines were evaluated by CCK-8 and plaque assays.
- The apoptosis induced by mOV in different tumor cells was analyzed by flow-cytometry.
- The activation of T cells in co-culture with mOV-infected tumor cells was evaluated by the ELISA detection of IFN- γ .
- T or NK cells were treated with supernatants from the culture of mOV-infected tumor cells. Released IFN- γ was detected by ELISA.
- CD8⁺ T cells were co-cultured with mOV-treated moDC cells, and the T cell activation was evaluated by flow-cytometry and ELISA.

Results A susceptible cell line was identified for mOV infection, which had high expression efficiency of exogenous immunomodulatory genes.

mOV induced a cytotoxicity on the susceptible cells through apoptosis effect.

mOV-infected tumor cells and the harvested supernatants significantly promoted the activation of T or NK cells.

mOV treatment promoted the maturation of moDCs and the secretion of IFN- γ by CD8⁺ T cells.

Conclusions Modified OV significantly induced cytotoxicity on the susceptible tumor cells, and promoted the activation of T, NK and moDC immune cells with increased inflammatory cytokine secretion. Our study suggested an effective approach for the development and validation of the next generation of oncolytic viruses being more potent in both the direct tumor killing and immune activation.

<http://dx.doi.org/10.1136/jitc-2022-SITC2022.1138>

1139 **VIROTHERAPY WITH CODALYTIC™, A CODON-MODIFIED INFLUENZA VIRUS, INDUCES AN ANTI-TUMOR IMMUNE MICROENVIRONMENT ACROSS PRECLINICAL MODELS WITH DIFFERENT IMMUNE CONTEXTURES**

Marcin Stawowczyk, Yiwen Zhao, Katie Pfeffer, Juliana Tafrova, Nusrat Jahan, James Rodriguez, Chen Yang, Sybil Tasker, Steffen Mueller, J Robert Coleman, Johanna Kaufmann*. *Codagenix Inc., Farmingdale, NY, USA*

Background Multiple oncolytic viruses have been shown to induce beneficial changes in the tumor microenvironment (TME) by increasing immune cell infiltration and activating stimulatory immune responses, which ultimately support induction of anti-tumor immunity and efficacy. We have previously demonstrated that CodaLytic™, a codon-modified influenza virus, can activate the cancer immunity cycle at various steps in EMT6, a murine triple-negative breast cancer model with moderate responsiveness to immunotherapies, leading to 67% complete tumor regressions. Here, we are confirming the mechanisms of action of the virus alone and in combination with immune checkpoint inhibition in several murine models and human tumor explants with different baseline immune contexture.

Methods Efficacy after intratumoral injection of 10⁸ PFU CodaLytic 3x/week for up to 12 doses as a monotherapy and/or in combination with systemic anti-PD-1 checkpoint blockade was determined in EMT6 breast cancer, CT26 colon cancer and B16F10 melanoma mouse models. Pharmacodynamic changes in the TME after treatment were characterized using flow cytometry. Anti-tumor immune memory was assessed by interferon-γ ELISpot in splenocytes of long-term survivors. Human breast cancer tumoroids maintaining the original patient TME were incubated *ex vivo* with 10⁸ PFU CodaLytic, 10 μg/ml pembrolizumab or both. Tumor cell killing (TCK) was detected by high-content imaging at 72h and the TME was characterized by flow cytometry, cytokine release and RNA sequencing at 24h and 48h.

Results CodaLytic monotherapy led to significant tumor growth inhibition (TGI) across tumor models, including 76% in EMT6 with moderate, immunologically active infiltration [1] and 69% TGI in poorly infiltrated B16F10 melanoma resistant to PD-1 blockade. In this model, efficacy further improved to 86% with addition of anti-PD-1. In all models, CodaLytic treatment increased infiltration of CD45+ leukocytes, CD8+ T cells and cross-presenting dendritic cells. *Ex vivo* recall responses to tumor cell lysate (EMT6) or AH1 peptide (CT26) were observed in long-term survivors, confirming generation of an anti-tumor T cell response. Efficacy of the CodaLytic/anti-PD-1 combination was confirmed in well-infiltrated human breast cancer tumoroids (51% TCK vs 24% with pembrolizumab alone, 6% with CodaLytic alone, and 2% in poorly-infiltrated tumoroids), a system in which priming and immune cell recruitment from a systemic reservoir are absent.

Conclusions CodaLytic treatment induced favorable changes in multiple murine tumor models independently of their intrinsic immune contexture and sensitized B16F10 melanomas to PD-1 blockade. Ongoing work investigates correlates of TCK in human tumoroid cultures beyond baseline immune infiltration to support future development of CodaLytic for immunovirotherapy.

Acknowledgements We would like to thank Soner Altioek, MD, PhD and the team and Nilogen Oncosystems for their expert support of this work.

REFERENCE

1. Yu JW, Bhattacharya S, Yanamandra N, *et al.* Tumor-immune profiling of murine syngeneic tumor models as a framework to guide mechanistic studies and predict therapy response in distinct tumor microenvironments. *PLoS ONE*. 2018;**13**(11): e0206223.

Ethics Approval The animal work in this study was approved after MisPro Biotech Services IACUC review, protocols 2019-01-17-COD-1 and 2022-COD-02.

The human tissue component of this study was approved by Vanderbilt University's Ethics review board; approval no. 031078.

<http://dx.doi.org/10.1136/jitc-2022-SITC2022.1139>

1140

CANCER STEM CELLS AND PD-L1-EXPRESSING EXOSOMES SUPPRESS ANTI-TUMOR EFFECTOR B CELLS

Ying Xin*, You Qin, Max Wicha, Alfred Chang, Qiao Li. *University of Michigan, Ann Arbor, USA*

Background We have identified anti-tumor effector B cells in adaptive immunotherapy. We also reported that cancer stem cell (CSC) vaccination induces CSC-specific T and B cell responses associated with the therapeutic efficacy which can be enhanced by anti-PD-L1 administration. Tumor cells were reported to suppress T cell function *via* secretion of exosomes that express PD-L1. However, the role of exosomal PD-L1 in CSC-B cell interaction is unknown.

Methods 4T1 and CT26 tumor-bearing mice were administered with anti-CD20 mAb to deplete B cells prior to anti-PD-L1 mAb administration. We isolated exosomes from D5 tumor cell culture media. To investigate if exosomal PD-L1 contributes to immunosuppression of B cells, we generated Rab27a^{ko} D5 cells to delete exosomes and PD-L1^{ko} D5 cells by CRISPR/Cas9 gene editing system.

Results *In vivo* B cell depletion significantly abrogated the efficacy of anti-PD-L1 with more aggressive tumor growth, indicating the anti-tumor effect of anti-PD-L1 involves host B cells. We detected upregulated expression of PD-1 on activated B cells, and higher PD-L1 expression on ALDH^{high} CSCs than on ALDH^{low} non-CSCs. ALDH^{high} CSCs directly suppressed IgG production by purified normal spleen B cells in culture and the suppression could be blocked by anti-PD-L1 in a dose-dependent manner. Anti-PD-L1 also rescued CSC suppression on the IgG production by B cells isolated from the spleen of tumor-bearing mice. Administration of anti-PD-L1 partially recovered the humoral immune response, confirming the PD-L1/PD-1 pathway involvement in B cell suppression by CSCs. D5-derived exosomes suppressed B cell proliferation and IgG production *in vitro*, and administration of these exosomes promoted tumor growth and reduced animal survival, indicating the role of tumor-derived exosomes in B cell immunosuppression. Tumor-derived exosomes expressed PD-L1, but PD-L1 was absent in the exosomes isolated from the PD-L1^{ko} tumor cells as evident by western blot and flow cytometry. Deletion of Rab27a or PD-L1 did not affect the proliferation of the tumor cells *in vitro*. However, Rab27a^{ko} or PD-L1^{ko} resulted in significantly enhanced host anti-tumor immunity evident by reduced 4T1 tumor growth *in vivo* compared with the WT tumor. Furthermore, anti-PD-L1 therapy significantly reduced Rab27a^{ko} or PD-L1^{ko} 4T1 tumor growth and prolonged animal survival *vs.* the WT tumor control.

Conclusions PD-L1-expressing CSCs and exosomes suppress B cells *via* the PD-L1/PD-1 axis. Isolation of Rab27a^{ko} ALDH^{high} CSCs will help further characterize the suppression of CSC-derived exosomes on host B cells as well as T cells.

<http://dx.doi.org/10.1136/jitc-2022-SITC2022.1140>

1141

DKN-01 DEMONSTRATES IMMUNE MODULATORY ACTIVITY AND ROBUST EFFICACY IN COLORECTAL CANCER MODELS

¹Michael Haas*, ¹Michael Kagey, ¹Walter Newman, ²James Rottman, ³Milad Moloudizargari, ³Ajay Goel, ¹Cynthia Sirard, ¹Jason Baum, ¹Leap Therapeutics, Cambridge, MA, USA; ²Athenaeum Pathology Consulting, LLC, Sudbury, MA, USA; ³Beckman Research Institute, Duarte, CA, USA

Background Colorectal cancer (CRC) is the third most prevalent cancer and the second leading cause of cancer-related death worldwide. CRC has elevated Wnt signaling activity in which DKK1 plays a regulatory role. DKN-01 is an IgG4 clinical stage antibody that specifically neutralizes DKK1. Fluorouracil (5FU)-based therapies are the standard backbone treatment for CRC and have demonstrated clinical activity in combination with DKN-01 in gastroesophageal adenocarcinoma (GEA). DKK1 expression has been shown to correlate with 5FU resistance in CRC tumors and cell lines. We evaluated the efficacy of DKN-01 alone and in combination with 5FU in parental and 5FU-resistant HCT116 and SW480 xenograft models. Further, given the established role of DKK1 on TME modulation, we also explored treatment with DKN-01 as a monotherapy and in combination with anti-PD-1 in a CT26 syngeneic CRC model.

Methods For the xenograft models, athymic nude mice were inoculated subcutaneously (SC) with either parental or 5FU-resistant colon carcinoma cell lines. Once tumors reached 50mm³, dosing was initiated with either isotype control, DKN-01, 5FU, or the combination. For the CT26 syngeneic model, BALB/c mice were inoculated SC with CT26 mouse colon carcinoma cells. Once tumors reached 50mm³, dosing initiated with either isotype control, a murinized version of DKN-01 (mDKN-01), anti-PD-1, or the combination.

Results In the parental HCT116 model, 30%, 39%, and 55% tumor growth inhibition (TGI) were observed in the DKN-01, 5FU, and combination treatment groups compared to isotype controls. Strikingly, in the HCT116 5FU-resistant model, 5FU had a negligible effect on TGI compared to DKN-01 monotherapy; and combination treatment groups in both 5FU-resistant models experienced 100% tumor regression. In the CT26 syngeneic model, mDKN-01 monotherapy resulted in 71% TGI with 47% of the group experiencing tumor regression at study termination unlike the anti-PD-1 monotherapy which had negligible TGI. The effect of mDKN-01 was further enhanced by the combination resulting in an additional 58% TGI with 73% of the group experiencing tumor regression. Notably, a robust inflammatory infiltrate was observed in the tumors of mDKN-01 monotherapy and combination groups, correlating with the level of necrosis. In addition, a significant increase in PD-L1 staining occurred with mDKN-01 monotherapy.

Conclusions In multiple models of CRC, DKN-01 showed strong anti-tumor effects. This included tumor regression in a 5FU-resistant setting reflective of second line CRC, as well as significant monotherapy efficacy and synergy with anti-PD-1.

<http://dx.doi.org/10.1136/jitc-2022-SITC2022.1141>

Arthur Liu*, Michael Curran. *UT MD Anderson Cancer Center, Houston, TX, USA*

Background Pancreatic cancer patients remain largely unresponsive to single agent immune checkpoint blockade (ICB) therapy. This refractory state originates from PDAC's unique immunosuppressive microenvironment that is densely populated by suppressive myeloid cells, exhibits poor vascularity, and is highly hypoxic. We previously showed that the hypoxia-activated prodrug TH-302 (Evoxofosamide) reduces intratumoral hypoxia through a tissue remodeling process, initiates tumor vasculature reorganization, and sensitizes aggressive, spontaneous murine models of prostate cancer to ICB.¹ In a clinical trial testing the combination of TH-302 with cytotoxic T-lymphocyte-associated protein (CTLA-4) blockade (NCT03098160) a subset of metastatic, immune checkpoint blockade refractory patients showed prolonged progression free survival.² While these studies highlight hypoxia as therapeutically tractable, we lack complete understanding of the contribution of the tumor vasculature to hypoxia reduction therapy, as well as the downstream consequences of hypoxia reduction on the cellular composition of the tumor microenvironment and the associated sensitivity, or lack thereof, to immunotherapy. We hypothesized that anti-angiogenic therapy and Evoxofosamide could cooperate to normalize tumor vasculature and diminish hypoxia.

Methods TH-302 and a vascular endothelial growth factor receptor-2 (VEGFR-2) blocking antibody were used to treat several syngeneic murine models, including orthotopic pancreatic cancer and a transplantable model of prostate cancer. Immunofluorescence and flow cytometry were used to assess intratumoral hypoxia, vessel normalization, and tumor immune infiltrate. RNA-sequencing analysis of bulk tumor samples was done to determine changes in gene signatures.

Results We find that Evoxofosamide with anti-VEGFR-2 (DC101) significantly extends mouse survival. Combination therapy reduces intratumoral hypoxia, improves vessel integrity, and increases intratumoral DNA damage. In response to the improved metabolic microenvironment, CD8 T cells gain enhanced effector function and lose expression of exhaustion-associated features. Like other anti-angiogenic regimens, combination DC101 and TH-302 leads to an increased frequency of PD-L1 expressing cells within the tumor, however blockade of PD-1 failed to prolong survival. Bulk-tumor RNA sequencing and tumor infiltrating lymphocyte analysis implicates immature myeloid cells as mediators of therapy resistance.

Conclusions Evoxofosamide and DC101 utilize unique yet complementary mechanisms to improve the survival of mice challenged with pancreatic or prostate tumors. This combination relieves hypoxic stress and simultaneously reinvigorates T cell function, but may facilitate de novo MDSC infiltration. Future work will determine the underlying factors that shape the tumor immune microenvironment and influence immunotherapy responses.

REFERENCES

1. Jayaprakash P, Ai M, Liu A. Targeted hypoxia reduction restores T cell infiltration and sensitizes prostate cancer to immunotherapy. *J Clin Invest.* 2018;**128**(11):5137–5149.
2. Hegde A, Jayaprakash P, Couillault CA. A Phase I Dose-Escalation Study to Evaluate the Safety and Tolerability of Evoxofosamide in Combination with Ipilimumab in Advanced Solid Malignancies. *Clin Cancer Res.* 2021;**27**(11):3050–3060.

1143 **5T4-CD40 BISPECIFIC ANTIBODIES ACTIVATE IMMUNE RESPONSES IN A 5T4-DEPENDENT MANNER**

Fang Liu*, Wenci Gong, Yuanyuan Yang, Zhijian Cai, Feifei Cui, Lei Fang, Wenqing Jiang.
Concept To Medicine Biotech Co.,Ltd, Shanghai, China

Background CD40 is a key costimulatory molecule expressed on professional antigen presenting cells (APCs) and functions to bridge innate and adaptive immunity. CD40 primes dendritic cells (DCs) to upregulate the expression of other costimulatory molecules such as CD80 and CD86 that further activates CD8+T cells. CD40 activation on B cells increases their activation and proliferation that further promotes anti-tumor effects. Agonistic CD40 monoclonal antibodies displayed clinical response, however, the further development was hampered by dose-limiting toxicities possibly due to the systemic activation. To overcome this issue, we have developed a conditional CD40 bispecific antibody which was only activated in 5T4-expressing tumor cells. 5T4 is a oncofetal protein rarely expressed in normal adult tissues, however, the expression is upregulated in multiple cancers. Therefore, we hypothesized that CD40 crosslinking by engagement of 5T4 on the cancer cells could boost the immune response in the tumor microenvironment while minimizing the risk of peripheral toxicity.

Methods To achieve maximal agonistic effect, we have generated a panel of 5T4 x CD40 bispecific antibodies in different formats. 5T4 x CD40 bispecific antibodies were evaluated in CD40 reporter cells and cocultured with target cells expressing 5T4. The potency was further confirmed by measuring IL12 production from primary DCs and CD80 and CD86 expression on the DC and B cells. The anti-tumor efficacy was determined in CD40-humanized C57BL/6 mice bearing MC38-hu5T4 tumor.

Results 5T4 x CD40 bispecific antibodies activated CD40 signaling in a 5T4-dependent manner. Similarly, DCs and B cells were activated only when cocultured with 5T4-expressing cells. Interestingly, we have identified an optimal format that showing superiority to other formats in inducing more potent CD40 agonism while remained silent in 5T4-negative cells. Treatment of 5T4 x CD40 displayed a more potent anti-tumor efficacy, compared to an equivalent dose of clinical benchmark CD40 monospecific antibody. Furthermore, tumor-free mice were resistant to tumor rechallenge, indicating an established long-lasting memory response. The *ex vivo* analysis suggested a focused immune activation in the tumor and no peripheral activation.

Conclusions We have generated bispecific antibodies specific to both CD40 and 5T4 that could achieve APC activation only in 5T4-expressing tumor microenvironment and demonstrate anti-tumor efficacy without inducing systemic toxicity. The preclinical data warrant further development of 5T4 x CD40 bispecific antibody as a potential therapeutic option for solid tumor.

<http://dx.doi.org/10.1136/jitc-2022-SITC2022.1143>

1144

IL17-PRODUCING $\gamma\delta$ T CELLS PROMOTE RESISTANCE TO CDK4/6 INHIBITORS IN HR⁺HER2⁻ BREAST CANCER

¹Giulia Petroni, ²Kenneth Gouin, ¹Claudia Galassi, ¹Aitziber Buqué, ¹Norma Bloy, ¹Takahiro Yamazaki, ¹Ai Sato, ¹Carlos Jiménez-Cortegana, ³Alexander Kirchmair, ⁴Chiara Massa, ⁵Carlos Eduardo De Andrea, ²Belén Navarro, ⁵Irantzu Serrano, ⁶Esther Navarro Manzano, ³Francesca Finotello, ¹Xi Zhou, ⁶Elena García-Martínez, ⁷María Rodríguez-Ruiz, ⁴Barbara Seliger, ⁸Victor Sánchez-Margalet, ⁸Luis de la Cruz-Merino, ²Heather McArthur, ¹Silvia Formenti, ²Simon Knott, ¹Lorenzo Galluzzi*. ¹Weill Cornell Medicine, New York, NY, USA; ²Cedars-Sinai Medical Center, Los Angeles, CA, USA; ³Medical University of Innsbruck, Innsbruck, Austria; ⁴Martin Luther University Halle-Wittenber, Halle, Germany; ⁵Clinica Universidad de Navarra, Pamplona, Spain; ⁶Hospital Universitario Morales Meseguer, Murcia, Spain; ⁷CIMA Universidad de Navarra, Pamplona, Spain; ⁸Universidad de Sevilla, Sevilla, Spain

Background CDK4/6 inhibitors are approved in combination with hormone therapy as a first-line intervention against advanced/metastatic hormone receptor (HR)⁺ HER2⁻ breast cancer, reflecting their ability to extend progression-free survival (PFS) and overall survival (OS) in this patient population.¹⁻³ Nonetheless, >50% of women with HR⁺ breast cancer receiving CDK4/6 inhibitors ultimately progress and succumb to their disease, owing to hitherto poorly characterized mechanisms of acquired resistance.¹⁻³ While CDK4/6 inhibitors have been conceived to inhibit the proliferation of cancer cells, accumulating preclinical and clinical evidence indicates that they also mediate numerous immunostimulatory effects that may contribute to efficacy.^{4,5} These observations suggest that hitherto unidentified immunological mechanisms may promote resistance to CDK4/6 inhibitors in patients with HR⁺HER2⁻ breast cancer.

Methods We harnessed a unique immunocompetent mouse model that closely recapitulates the immunobiology of human HR⁺HER2⁻ breast cancer – including a cold tumor microenvironment (TME) coupled to poor sensitivity to PD-1 blockers⁶ – along with scRNAseq, functional assays and blocking/neutralization experiments to dissect the immunological mechanisms underlying resistance to CDK4/6 inhibitors. The Cancer Genome Atlas (TCGA) was interrogated by *in silico* analysis. Moreover, immunohistochemistry, multispectral immunofluorescence, and circulating immunophenotyping were performed on samples from 3 independent cohorts of patients with HR⁺HER2⁻ breast cancer (including longitudinal samples obtained before, during and after CDK4/6 inhibition).

Results Interleukin 17 (IL17)-producing $\gamma\delta$ T cells are recruited to mouse HR⁺HER2⁻ mammary tumors upon CDK4/6 inhibition through a CCL2-dependent mechanism. In this model, circulating IL17 levels correlate with poor OS, and blocking the $\gamma\delta$ TCR, neutralizing IL17 or CCL2 equally improve the therapeutic activity of CDK4/6 inhibitors. Patients from the TCGA with a signature of IL17 signaling have poor OS and signs of immunosuppression in the TME. In diagnostic biopsies from patients with HR⁺HER2⁻ breast cancer, $\gamma\delta$ T cell infiltration correlate with tumor grade, and $\gamma\delta$ T cells reside in the proximity of PD-L1⁺ tumor cells and macrophages. Patients with high activated $\gamma\delta$ T cells in the circulation have reduced PFS on CDK4/6 inhibitors as compared to their low counterparts. Circulating CCL2 levels augment during CDK4/6 therapy in progressing patients. Finally, tumor-infiltrating $\gamma\delta$ T cells increase as compared to baseline in patients relapsing on CDK4/6 inhibitors.

Conclusions Our findings prompt the initiation of clinical trials comparing standard-of-care CDK4/6 inhibition plus letrozole vs CDK4/6 inhibition plus letrozole and an IL17 blocker

(at least three of which are currently approved for psoriasis treatment) in patients with HR⁺HER2⁻ breast cancer.

Acknowledgements This work has been partially sponsored by the 2019 Laura Ziskin Prize in Translational Research (#ZP-6177, PIs: Formenti, McArthur) from the Stand Up to Cancer (SU2C).

REFERENCES

1. Im SA, Lu YS, Bardia A, Harbeck N, Colleoni M, Franke F, Chow L, Sohn J, Lee KS, Campos-Gomez S, Villanueva-Vazquez R, Jung KH, Chakravarty A, Hughes G, Gounaris I, Rodriguez-Lorenc K, Taran T, Hurvitz S, Tripathy D. Overall survival with ribociclib plus endocrine therapy in breast cancer. *N Engl J Med* 2019;**381**(4):307–316.
2. Turner NC, Slamon DJ, Ro J, Bondarenko I, Im SA, Masuda N, Colleoni M, DeMichele A, Loi S, Verma S, Iwata H, Harbeck N, Loibl S, André F, Puyana Theall K, Huang X, Giorgetti C, Huang Bartlett C, Cristofanilli M. Overall survival with palbociclib and fulvestrant in advanced breast cancer. *N Engl J Med* 2018;**379**(20):1926–1936.
3. Slamon DJ, Neven P, Chia S, Fasching PA, De Laurentis M, Im SA, Petrakova K, Bianchi GV, Esteva FJ, Martín M, Nusch A, Sonke GS, De la Cruz-Merino L, Beck JT, Pivot X, Sondhi M, Wang Y, Chakravarty A, Rodriguez-Lorenc K, Taran T, Jerusalem G. Overall survival ribociclib plus fulvestrant in advanced breast cancer. *N Engl J Med* 2020;**382**(6):514–524.
4. Petroni G, Buqué A, Zitvogel L, Kroemer G, Galluzzi L. Immunomodulation by targeted anticancer agents. *Cancer Cell* 2021;**39**(3):310–345.
5. Petroni G, Formenti SC, Chen-Kiang S, Galluzzi L. Immunomodulation by anti-cancer cell cycle inhibitors. *Nat Rev Immunol* 2020;**20**(11):669–679.
6. Buqué A, Bloy N, Perez-Lanzón M, Iribarren K, Humeau J, Pol JG, Levesque S, Mondragon L, Yamazaki T, Sato A, Aranda F, Durand S, Boissonnas A, Fucikova J, Senovilla L, Enot D, Hensler M, Kremer M, Stoll G, Hu Y, Massa C, Formenti SC, Seliger B, Elemento O, Spisek R, André F, Zitvogel L, Delaloge S, Kroemer G, Galluzzi L. Immunoprophylactic and immunotherapeutic control of hormone receptor-positive breast cancer. *Nat Commun* 2020;**11**(1):3819

Ethics Approval Mouse experiments were approved by WCM IACUC (#2019-0022). All human studies were on retrospective, fully deidentified samples collected upon informed consent at respective Institutions.

<http://dx.doi.org/10.1136/jitc-2022-SITC2022.1144>

1146

NKG2D CO-STIMULATION VIA ANTI-SMIC/MIC TARGETING ANTIBODY ENHANCES CD8 T CELL FUNCTIONAL HETEROGENEITY AND MEMORY DEVELOPMENT IN MOUSE PROSTATE TUMORS

¹Tyler Smith*, ¹Sizhe Liu, ²Lisha Zhu, ¹Jennifer Wu. ¹Northwestern University Feinberg, Chicago, IL, USA; ²University of Chicago, Chicago, IL, USA

Background Effective co-stimulation of CD8 T cells is critical for anti-tumor effector responses and maintenance of antigen-specific TCF-1⁺ memory CD8 T cells necessary for long-term tumor control. NKG2D co-stimulation of CD8 T cells via binding of stress ligands such as membrane-bound MIC enhances CD8 T cell effector functions and is important for promoting memory development. Cancer cells often shed MIC into a soluble form (sMIC) that inhibits CD8 T cell activation. Humanized TRAMP/MICB prostate tumor mice treated with anti-sMIC/MIC targeting antibody develop potent anti-tumor responses by CD8 T cells by 1) sequestering sMIC and 2) inducing NKG2D pathway signaling, thereby re-invigorating CD8 T cell immunity. However, the mechanistic underpinnings of CD8 T cell reprogramming by NKG2D co-stimulation in the tumor microenvironment are poorly understood. In this preliminary study, we used scRNA-seq of CD8 TILs from TRAMP/MICB mice treated or untreated with the anti-sMIC/MIC targeting antibody B10G5 to investigate the hypothesis that B10G5 differentially reprograms CD8 T cells at the transcriptional and epigenetic level via sustained NKG2D pathway co-stimulation, thereby optimizing TCR-dependent effector and memory responses.

Methods Adult TRAMP/MICB mice were treated with 200µg B10G5 intraperitoneally twice per week for 4 weeks. Prostate tumors from B10G5-treated mice, untreated mice with well-differentiated tumors, and untreated mice with poorly differentiated tumors were collected, and their CD45⁺ cells isolated via FACS for scRNA-seq. Subclusters specific to CD8 T cells were the focus of subsequent transcriptomic analyses.

Results Prostate tumors from mice treated with anti-sMIC/MIC antibody B10G5 revealed enhanced functional heterogeneity of CD8 T cell subtypes compared to tumors from untreated mice. In contrast to tumors from untreated mice that were populated with primarily effector CD8 T cells expressing CD226^{hi}, CXCR3^{hi}, GZMB^{hi} and/or NKG7, tumors from B10G5-treated mice were enriched in TCF7^{hi} IL7R⁺ EOMES^{hi} stem-like memory CD8 T cells and EOMES⁺ CD27^{hi} PD-1⁺ effector memory CD8 T cells. These memory populations upregulated epigenetic modifiers (KMT2A/E) and transcription factors (NR4A1/2/3) important in metabolic reprogramming and memory CD8 T cell differentiation.

Conclusions These results establish a groundwork for identifying targets for epigenetic and metabolic alteration of CD8 T cells via NKG2D co-stimulation within the tumor microenvironment.

Ethics Approval All animal studies were approved by the Institutional Animal Care and Use Committee (IACUC) committee of Northwestern University.

<http://dx.doi.org/10.1136/jitc-2022-SITC2022.1146>

Abstracts

1147 DIFFERENCES IN CO-EXPRESSION OF T CELL CO-INHIBITORY AND CO-STIMULATORY MOLECULES WITH PD1 ACROSS DIFFERENT HUMAN CANCERS

¹Ahmad Tarhini*, ²Dale Hedges, ¹Aik Choon Tan, ¹Paulo Rodriguez, ³Vineeth Sukrithan, ⁴Aakrosh Ratan, ⁵Martin McCarter, ⁶John Carpten, ⁷Howard Colman, ⁸Alexandra Ikeguchi, ⁹Igor Puzanov, ¹⁰Susanne Arnold, ²Michelle Churchman, ¹Patrick Hwu, ¹Jose Conejo-Garcia, ²William (Bill) Dalton, ¹¹George Weiner. ¹Moffitt Cancer Center and Research Inst., Tampa, FL, USA; ²M2GEN, ORIEN, Tampa, FL, USA; ³The Ohio State University, Bronx, OH, USA; ⁴University of Virginia, Charlottesville, VA, USA; ⁵University of Colorado Cancer Center, Aurora, CO, USA; ⁶USC Norris Comprehensive Cancer Center, Los Angeles, CA, USA; ⁷Huntsman Cancer Institute, Salt Lake City, UT, USA; ⁸Stephenson Cancer Center, Oklahoma City, OK, USA; ⁹Roswell Park Comprehensive Cancer Center, Buffalo, NY, USA; ¹⁰Markey Cancer Center, Lexington, KY, USA; ¹¹University of Iowa Holden Cancer Center, Iowa City, IA, USA

Background PD1 immune checkpoint inhibitors (ICIs) have resulted in significant improvements in the care of patients with advanced malignancies. PD1 based combinations including with CTLA4 and LAG3 represent the future of ICI immunotherapy and there is a need to better understand the rationale for investigating combinations involving other immune modulator therapeutic candidates across cancer types.

Methods We utilized real-world clinical and transcriptomic data collected under the Total Cancer Care Protocol (NCT03977402) and Avatar® project within the Oncology Research Information Exchange Network (ORIEN) of 18 cancer centers to which all included subjects provided an IRB-approved written informed consent at their participating institutions. Using RSEM we analyzed mRNA co-expression levels of PD-1 with 12 immune checkpoints including the co-inhibitory receptors LAG3, CTLA4, TIGIT, TIM3 (HAVCR2), VISTA (VSIR), BTLA and the positive co-signaling molecules CD28, OX40 (TNFRSF4), GITR (TNFRSF18), CD137 (TNFRSF9), CD27, HVEM (TNFRSF14) as well as PD-L1 (CD274). Pearson's R coefficients and associated P values were calculated using SciPy 1.7.0. We defined Pearson's coefficient > 0.5 and p < 10E-10 as significant correlation.

Results Co-expression of PD1 along with the 12 immune checkpoints and PD-L1 across select malignancies included in our analysis is shown in (table 1), including Pearson's correlation and the associated P values, sorted by the level of correlation. In cutaneous melanoma, in terms of co-inhibitory receptors that suppress T cell activation, the expression of PD1 was significantly correlated with four molecules: LAG3, TIM3, TIGIT and VISTA; and only significantly correlated with one costimulatory molecule CD137. For urothelial carcinoma, there were 4 co-inhibitory (TIGIT, CTLA4, LAG3 and VISTA) and 4 co-stimulatory (OX40, CD27, CD137 and HVEM) molecules statistically correlated with PD1 expression. For pancreatic adenocarcinoma, only CD28 was deemed to be correlated with PD1 expression. No immune checkpoints were deemed significantly correlated with PD1 expression in the ovarian cancer cohort. Overall, in melanoma and to a certain extent in urothelial carcinoma, the co-expression of co-inhibitory molecules with PD1 was more dominant reflecting late exhausted T cells, as compared to co-stimulatory molecules likely more dominant in ovarian and pancreatic carcinomas reflecting less differentiated T cells.

Conclusions With PD1 blockade as a backbone for immune checkpoint targeting combinations, our interrogations of pan-cancer transcriptomic data provide support for multiple potential combination strategies in the tested malignancies that warrant further investigation. Melanoma and urothelial carcinoma as more immunogenic tumors reflected a PD1

+immunoinhibitory dominant phenotype, while less immunogenic ovarian and pancreatic carcinomas reflected a trend toward a PD1+immunostimulatory phenotype.

Acknowledgements We are grateful to the participating patients and their family members as well as all research staff supporting the conduct of the Total Cancer Care protocol.

Trial Registration NCT03977402

Ethics Approval We utilized real-world clinical and transcriptomic data collected under the Total Cancer Care Protocol (NCT03977402) and Avatar® project within the Oncology Research Information Exchange Network (ORIEN) of 18 cancer centers to which all included subjects provided an IRB-approved written informed consent at their participating institutions.

Abstract 1147 Table 1 Co-expression PD1 with select co-inhibitory molecules and PDL1

Table 1. Co-expression PD1 with select co-inhibitory and co-stimulatory molecules and PDL1.

Cutaneous Melanoma N=235			Ovarian Cancer N=725			Pancreatic Adenocarcinoma N=648			Urothelial Carcinoma N=360		
Gene	Pearson R	P-value	Gene	Pearson R	P-value	Gene	Pearson R	P-value	Gene	Pearson R	P-value
PD1	1	—	PD1	1	—	PD1	1	—	PD1	1	—
LAG3	0.646	3.87E-29	CD27	0.217	3.72E-09	CD28	0.524	2.22E-48	TIGIT	0.679	5.04E-50
TIM3	0.605	7.66E-25	VISTA	0.135	7.45E-04	TIGIT	0.415	1.00E-30	CTLA4	0.67	3.50E-48
CD27	0.583	7.87E-23	TIGIT	0.209	3.40E-03	PDL1	0.423	2.11E-30	LAG3	0.602	6.38E-47
CD27	0.559	1.12E-20	BTLA	0.107	3.77E-03	CD27	0.42	6.71E-30	OX40	0.544	4.68E-49
PD1	0.524	5.49E-18	CD28	0.107	4.04E-03	VISTA	0.384	6.11E-25	CD27	0.526	5.43E-47
VISTA	0.464	5.95E-14	CTLA4	0.105	4.52E-03	TIM3	0.372	2.42E-23	VISTA	0.526	5.85E-47
GITR	0.325	3.61E-07	CD137	0.105	4.79E-03	BTLA	0.345	1.35E-19	CD137	0.516	7.37E-46
CTLA4	0.300	2.64E-06	TIM3	0.09	1.66E-02	HVEM	0.313	1.29E-16	HVEM	0.506	7.74E-45
CD28	0.197	2.43E-03	LAG3	0.089	1.66E-02	CTLA4	0.309	3.31E-16	CD28	0.472	2.24E-41
PDL1	0.184	1.19E-02	HVEM	0.087	5.64E-02	GITR	0.296	5.37E-15	TIM3	0.458	4.28E-40
TIGIT	0.178	6.51E-03	PDL1	0.066	7.55E-02	CD137	0.283	1.00E-13	BTLA	0.400	2.78E-35
OX40	0.174	3.99E-02	GITR	0.055	1.38E-01	OX40	0.276	6.74E-10	GITR	0.374	1.51E-13
BTLA	0.116	7.46E-02	OX40	0.052	1.63E-01	LAG3	0.193	4.69E-07	PDL1	0.186	3.92E-04

<http://dx.doi.org/10.1136/jitc-2022-SITC2022.1147>

1148

SIGNAL-REGULATORY PROTEIN ALPHA (SIRP α) CONFERS TUMOR CELL RESISTANCE TO ANTI-TUMOR IMMUNITY

¹Chien-Huan Weng*, ¹Linda Hamadene, ²Shabnam Eghbali, ¹Divya Venkatesh, ¹Sébastien Monette, ¹Levi Mangarin, ¹Fadi Samaan, ¹Cailian Liu, ³Pamela Holland, ⁴Jedd Wolchok, ⁴Taha Merghoub. ¹Memorial Sloan-Kettering Cancer Center, New York, NY, USA; ²Weill Cornell Medical College, New York, NY, USA; ³Alpine Immunescence, Seattle, WA, USA; ⁴MSKCC and Cornell University, New York, NY, USA

Background The expression and function of signal-regulatory protein alpha (SIRP α ; also known as PTPNS1, SHPS-1, CD172a, and P84) is well characterized in myeloid effector cells (e.g.: monocytes, macrophages, neutrophils, dendritic cells and microglia),¹⁻³ where it contributes to tissue homeostasis and regulation of erythrocyte, platelet, and hematopoietic stem cells (HSC). In addition, it regulates synaptic pruning during neuronal development.⁴⁻⁷ Another important feature of SIRP α is that, upon engagement by cluster of differentiation 47 (CD47), a trans-membrane protein ubiquitously expressed on all cells and overexpressed on tumor cells,⁴ it activates ITIM and ITSM domains to recruit the SH2-domain-containing protein tyrosine phosphatases SHP-1 and SHP-2, thereby inhibiting phagocytosis of tumor cells by myeloid effector cells.^{8, 9} Based on its anti-phagocytic property, CD47 is well recognized as a “don’t eat me” signal,¹⁰ together with other anti-phagocytic surface proteins, including programmed cell death ligand 1 (PD-L1),¹¹ beta2 micro-globulin subunit of the major histocompatibility class I complex (B2M)¹² and CD24.¹³ Therapeutic blockade of the CD47 – SIRP α pathway has therefore become a promising strategy to enhance innate immune clearance of tumor cells and subsequent invigoration of anti-tumor immunity.

Methods

Experimental Procedures Our analysis using publicly available datasets published in Human Protein Atlas¹⁴ and the Cancer Cell Line Encyclopedia¹⁵ confirmed that SIRP α is expressed in human melanoma and renal cell carcinoma.¹⁶ To explore the role of tumor SIRP α , we designed gRNAs to CRISPR out the SIRP α region that interacts with CD47. Our study using SIRP α -knockout (hereinafter, SIRP α -KO) B16 melanoma cells show that SIRP α -KO B16 cells proliferate comparably to the control SIRP α -wild type (WT) B16 cells in vitro; however, upon implantation in immune-competent (C57BL/6j; B6) mice, but not immune-deficient (i.e., RAG^{null}) mice, SIRP α -KO B16 tumors grow significantly slower than the control SIRP α -WT B16 tumors. Intriguingly, SIRP α -KO B16 tumors exhibit significantly more activated infiltrating lymphocytes (e.g., CD8+ T cells and macrophages) than SIRP α -WT B16 tumors as evidenced by flow cytometry analysis, immunohistochemistry (IHC) and our single cell RNA-sequencing (scRNA-seq) data analysis. Analysis of our bulk RNA-seq of unstimulated, cultured SIRP α -WT and SIRP α -KO B16 cells allows us to identify Cxcl10, Ccl5 and several other genes and pathways that potentially contribute to the observed growth inhibition of SIRP α -KO B16 tumors in immune competent mice.

Results Our recent work characterized a novel role of tumor SIRP α in suppressing the anti-tumor adaptive immunity.

Conclusions SIRP α expression on tumor cells confer resistance to anti-tumor immunity.

REFERENCES

1. Adams S, et al. Signal-regulatory protein is selectively expressed by myeloid and neuronal cells. *J Immunol* 1998;**161**(4):1853–9.

- Seiffert M, et al. Human signal-regulatory protein is expressed on normal, but not on subsets of leukemic myeloid cells and mediates cellular adhesion involving its counterreceptor CD47. *Blood* 1999;**94**(11):3633–43.
- Veillette AE, Thibaudeau, and S. Latour, High expression of inhibitory receptor SHPS-1 and its association with protein-tyrosine phosphatase SHP-1 in macrophages. *J Biol Chem* 1998;**273**(35):22719–28.
- Jaiswal S, et al. CD47 is upregulated on circulating hematopoietic stem cells and leukemia cells to avoid phagocytosis. *Cell* 2009;**138**(2):271–85.
- Lehrman EK, et al. CD47 Protects Synapses from Excess Microglia-Mediated Pruning during Development. *Neuron* 2018;**100**(1):120–134 e6.
- Lutz HU, Bogdanova A, Mechanisms tagging senescent red blood cells for clearance in healthy humans. *Front Physiol* 2013;**4**:387.
- Yamamoto T, et al. Negative regulation of platelet clearance and of the macrophage phagocytic response by the transmembrane glycoprotein SHPS-1. *J Biol Chem* 2002;**277**(42):39833–9.
- Willingham SB, et al. The CD47-signal regulatory protein alpha (SIRP α) interaction is a therapeutic target for human solid tumors. *Proc Natl Acad Sci U S A* 2012;**109**(17):6662–7.
- Logtenberg MEW, Scheeren FA, Schumacher TN. The CD47-SIRP α Immune Checkpoint. *Immunity*, 2020;**52**(5):742–752.
- Majeti R, et al. CD47 is an adverse prognostic factor and therapeutic antibody target on human acute myeloid leukemia stem cells. *Cell* 2009;**138**(2):286–99.
- Gordon SR, et al. PD-1 expression by tumour-associated macrophages inhibits phagocytosis and tumour immunity. *Nature* 2017;**545**(7655):495–499.
- Barkal AA, et al. Engagement of MHC class I by the inhibitory receptor LILRB1 suppresses macrophages and is a target of cancer immunotherapy. *Nat Immunol* 2018;**19**(1):76–84.
- Barkal AA, et al. CD24 signalling through macrophage Siglec-10 is a target for cancer immunotherapy. *Nature* 2019;**572**(7769):392–396.
- Yanagita T, et al. Anti-SIRP α antibodies as a potential new tool for cancer immunotherapy. *JCI Insight* 2017;**2**(1):e89140.
- Uhlen M, et al. A human protein atlas for normal and cancer tissues based on antibody proteomics. *Mol Cell Proteomics* 2005;**4**(12):1920–32.
- Barretina J, et al. The Cancer Cell Line Encyclopedia enables predictive modelling of anticancer drug sensitivity. *Nature* 2012;**483**(7391):603–7.

Ethics Approval All mice were maintained in microisolator cages and treated in accordance with the NIH and American Association of Laboratory Animal Care regulations. All mouse procedures and experiments for this study were approved by the MSKCC Institutional Animal Care and Use Committee (IACUC).

<http://dx.doi.org/10.1136/jitc-2022-SITC2022.1148>

1149 **TARGETING REGULATORY T CELLS WITH CTM033, A NOVEL ANTI-CCR8 ANTIBODY, INHIBITED TUMOR GROWTH**

Yuanyuan Yang*, Yuehua Chen, Feifei Cui, Wenqing Jiang, Lei Fang. *Concept To Medicine Biotech Co.,Ltd, Shanghai, China*

Background Regulatory T cells (Tregs) are potent suppressors of immune activation in the periphery and tumor microenvironment and high density of Tregs are associated with poor response to immune oncology (IO) therapies. CCR8 was selectively expressed on tumor infiltrating Tregs across multiple cancer types, but its expression on peripheral Tregs or other proinflammatory effector T cells was negligible. Moreover, CCR8+ Tregs were identified as a highly suppressive cell population within tumors which hampered the efficacy of immunotherapy. Recent studies also showed the CCR8 and its ligand CCL1 potentiated Tregs via an autocrine loop, implying CCL1-CCR8 axis may play a pivotal role in restraining anti-tumor immunity.

Methods The binding activity and specificity of anti-CCR8 antibody CTM033 was determined by a panel of flow cytometry based assays. Antagonistic activity of CTM033 against CCL1-CCR8 signaling was assessed by β -arrestin, calcium flux and migration assay. Antibody-dependent cell-mediated cytotoxicity (ADCC) function was evaluated by reporter assays and primary cells mediated killing against tumor infiltrating Tregs. The anti-tumor efficacy of CTM033 was evaluated in a MC38 syngeneic mouse model where the murine CCR8 gene was replaced by its human counterpart. Finally, Biacore and ADCC assay was performed to determine the ADCC-enhancing strategies.

Results CTM033 specifically bound to human CCR8 with subnanomolar activity and did not bind to closely related chemokine receptors and other unrelated proteins. CTM033 also potently inhibited CCL1-mediated β -arrestin recruitment, calcium flux, and migration of hCCR8+ cells. Furthermore, to maximize ADCC effect, different strategies were screened to determine the best approach for efficient Treg depletion. In vivo efficacy study suggested CTM033 monotherapy showed significant inhibition of tumor growth with evidence of intratumoral Treg depletion while sparing peripheral Treg subset.

Conclusions CTM033 is a humanized antibody against CCR8 with high affinity. CTM033 efficiently blocked CCL1-CCR8 pathway and induced ADCC function to deplete Tregs in the tumor microenvironment. Targeting CCR8+ Treg by CTM033 showed single agent activity in a preclinical model. Therefore, current data support anti-CCR8 is a promising approach for the cancer treatment that warrants further development.

<http://dx.doi.org/10.1136/jitc-2022-SITC2022.1149>

1150 **ATG-101, A TETRAVALENT PD-L1×4-1BB BSAB, DEMONSTRATES POTENT *IN VIVO* ANTI-TUMOR EFFICACY IN ICI-RESISTANT OR REFECTORY MOUSE TUMOR MODELS**

¹Hui Yuwen, ¹Tengteng Li, ¹Yijing Ren, ²Jay Mei, ²Bo Shan, ²Bing Hou*. ¹Antengene Corporation Limited, Shanghai, China; ²Antengene Corporation Limited, Shaoxing, China

Background Immune checkpoint inhibitors (ICIs), has revolutionized the treatment landscape of malignancies. However, many patients present with or develop resistance to them. Tumors with little anti-tumor immune cell infiltration or lack of pre-existing antitumor immune responses are defined as immunologically “cold” tumor. Patients with these tumors have a poor prognosis following PD-(L)1 blocking therapy.¹ On the other hand, malignancies that initially respond well to ICIs may develop acquired drug resistance, in part as a result of a condition known as T cell exhaustion.² ATG-101 is a tetravalent PD-L1×4-1BB bispecific antibody (BsAb), which activates 4-1BB signaling upon PD-L1 crosslinking. In this study, we evaluated the potential of ATG-101 in treating ICI-resistant or refractory diseases using mouse syngeneic tumor models. **Methods** To assess the efficacy of ATG-101 on exhausted T cells, human T cells were isolated, and the cell exhaustion was induced through consistent strong activation with anti-CD3/CD28 beads for up to 6 days. The *in vivo* efficacy of ATG-101 was tested in 4-1BB humanized mouse bearing syngeneic B16F10 (Melanoma), EL4 (Lymphoma) or Pan02 (Pancreatic) tumors, all of which have been suggested to be ICI-resistant. To evaluate ATG-101 efficacy in tumors progressing after anti-PD(L)1 treatment, mice bearing MC38 colorectal tumors were treated with anti-PD-L1 initially to achieve tumor growth inhibition, and half of the mice switched to ATG-101 upon disease progression. TIL was analyzed using flow cytometry or multiplex IHC.

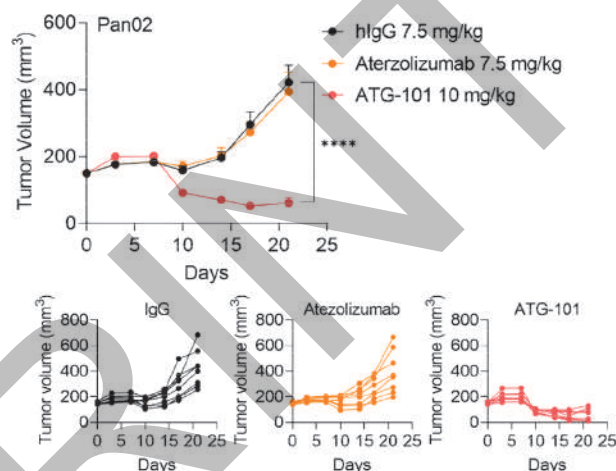
Results In the presence of PD-L1 positive cells, ATG-101 enhanced the IL2 and INF- γ production by the terminally exhausted T cells and progenitor exhausted T cells. In Pan02 murine pancreatic model, Atezolizumab (anti-PD-L1) did not show anti-tumor efficacy at 7.5mg/kg. While ATG-101 at molar-equivalent 10 mg/kg was well tolerated and significantly inhibited tumor growth, with a TGI value of 78.48% (figure 1). ATG-101 also demonstrated significant tumor growth inhibition in EL4 and B16F10 model compared with control. Furthermore, ATG-101 induced growth inhibition or regression in MC38 tumors that had progressed on Atezolizumab, revealing a significant survival advantage over Atezolizumab or the control group. TIL analysis suggested that ATG-101 increases the infiltration, proliferation and activation of CD8+ T cells, the infiltration of natural killer T cells and the CD8+/Treg ratio in TILs (figure 2).

Conclusions ATG-101 activates exhausted T cells upon PD-L1 crosslinking and exhibits effectiveness against ICI-resistant diseases, a significant unmet medical need. A phase I, multicenter, dose-escalating clinical trial evaluating ATG-101 in patients with solid tumors and hematologic malignancies is ongoing.

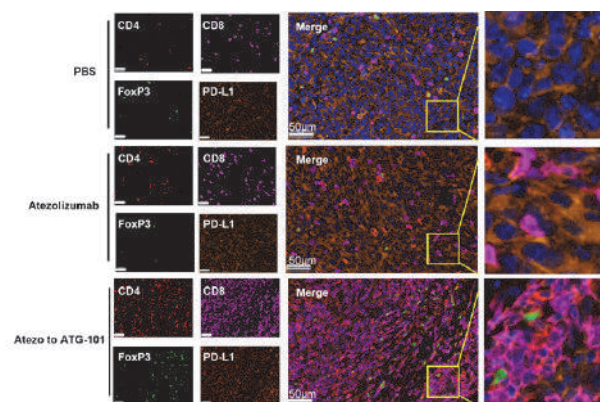
REFERENCES

1. Chen DS, Mellman I, Elements of cancer immunity and the cancer-immune set point. *Nature* 2017;**541**,321–330.
2. Pauken KE, Sammons MA, Odorizzi PM, Manne S, Godec J, Khan O, Drake AM, Chen Z, Sen DR, Kurachi M, Barnitz RA, Bartman C, Bengsch B, Huang AC, Schenkel JM, Vahedi G, Haining WN, Berger SL, Wherry EJ. Epigenetic stability of exhausted T cells limits durability of reinvigoration by PD-1 blockade. *Science* 2016;**354**,1160–1165.

Ethics Approval The protocol and any amendment(s) or procedures involving the care and use of animals in this study were reviewed and approved by the Institutional Animal Care and Use Committee (IACUC) of CrownBio to execution with an AUP number or IACUC approval number for each animal study. During the study, the care and use of animals were conducted in accordance with the regulations of the Association for Assessment and Accreditation of Laboratory Animal Care (AAALAC). All studies were conducted following an approved IACUC protocol. AUP NO.:2004-12-1465, 2004-12-1000, 2104-09-1895



Abstract 1150 Figure 1 ATG-101 demonstrates *in vivo* efficacy in Pan02 model. Average tumor growth curves (top panel) and individual tumor growth spaghetti plots (bottom) of Pan02.



Abstract 1150 Figure 2 ATG-101 increased the anti-tumor immunity in the TME

Representative images of multiplex immunohistochemistry (IHC) staining of samples collected from mouse bearing MC38 tumors that had progressed on Atezolizumab. Mice were treated with PBS, 10mpk atezolizumab only or mice initially treated with 10mpk atezolizumab and switched to 13mpk ATG-101 upon disease progression (Atezo to ATG-101). The tumor slices were stained for CD4 (helper T cell, red), CD8 (effector T cell, green), Foxp3 (Treg, purple), and PD-L1 (cancer cells, dark orange). Nucleus were labeled with DAPI (blue). Areas highlighted in the merged images are enlarged. Scale bars are 50 μ m.

<http://dx.doi.org/10.1136/jitc-2022-SITC2022.1150>

1151 REVEALING NOVEL THERAPEUTIC INDICATIONS THROUGH PROFILING OF IMMUNE MODULATORY PROPERTIES BY ULILEDLIMAB

Yanni Zhang*, Zhen Sheng, Xinyun Zhu, Yanling Niu, Yuan Meng, Zhengyi Wang, Andrew Zhu. I-MAB Biopharma, Shanghai, China

Background The adenosine pathway is associated with immunosuppressive tumor microenvironment, and CD73 is a rate-limiting enzyme for adenosine production. Uliledlimab is a differentiated CD73 antibody that binds to a unique epitope to achieve complete inhibition of CD73 and its anti-tumor activity is currently being evaluated in clinical studies in combination with checkpoint inhibitors. Here we investigated the immune modulatory mechanism of uliledlimab in different cell subsets and pathways to explore new therapeutic combinations of uliledlimab for cancer treatment.

Methods Gene expression of anti-CD3 stimulated human PBMCs in the presence of AMP with or without uliledlimab was measured using NanoString platform. Association of CD73 and immune signature pathways regulated by uliledlimab was analyzed in multiple cancer types in TCGA database. In vitro cytotoxicity by T cells or NK cells or phagocytosis by macrophages in the presence of uliledlimab alone and in combination with PD-1 antibody were evaluated by co-culture of CD73⁺ tumor cells and PBMCs or purified macrophages. Anti-tumor activity of uliledlimab combination was examined subsequently in xenograft tumor models.

Results Expression of cell lineage markers in immuno-suppressive cell subsets was up-regulated in human PBMCs cultured with AMP. Notably, the expression of various co-inhibitory checkpoint receptors was induced in T cells, including PD-L1 and CTLA-4, myeloid cells, including LILRB and SIGLEC1, and NK cells, including KIR and KLRD1. Signature genes involved in the recruitment of immuno-suppressive cells and angiogenesis were also up-regulated. The induction of these genes was inhibited by uliledlimab. Similar to PD-L1, a panel of angiogenesis signature genes regulated by uliledlimab were found to positively correlate with CD73 expression in multiple solid tumors ($p < 0.05$), and concurrent high expression of CD73 and VEGFA was associated with poor prognosis ($p < 0.05$). Uliledlimab treatment led to increased cytotoxic activity of T cells and NK cells and phagocytic activity of macrophage in tumor killing. When combined with a PD-1 antagonist, uliledlimab elicited enhanced anti-tumor activity in vitro and in vivo through the regulation of infiltrating immune cells in tumor.

Conclusions Our study has delineated the immune regulatory properties of uliledlimab as evident by its down-regulation of immuno-suppressive pathways and restored activity of cytotoxicity and phagocytosis of various effector cells. In addition to the current combination therapy of uliledlimab with PD-L1 inhibitor, identification of selected pathways regulated by uliledlimab and their co-expression with CD73 that serves as a negative prognosis factor provides much needed scientific rationale to explore new combination therapies of uliledlimab in cancers.

<http://dx.doi.org/10.1136/jitc-2022-SITC2022.1151>

1152

**IN VITRO ANTICANCER AND IMMUNOMODULATORY
ACTIVITIES OF A NOVEL MOLECULAR GLUE COMPOUND
NBT-018**

¹Sophia Zhang, ²Magdalena Dragan, ²Nicole Potter, ²Everett Henry, ²Harris Zhang*.
¹Mountain Lakes High School, Mountain Lakes, NJ, USA; ²Picolimmune Co., Whippany, NJ, USA

Background Targeted protein degradation is a rapidly exploding drug discovery strategy which uses small molecules to recruit disease-causing proteins for rapid destruction via the ubiquitin-proteasome pathway. It shows great potential for treating diseases such as cancer, autoimmune, infectious, inflammatory, and other diseases, especially for those with “undruggable” pathogenic protein targets. Here we report one ‘molecular glue’ type of protein degrader NBT-018, which binds cereblon (CBRN) and has selective anti-cancer and immunomodulatory activities.

Methods NBT-018 was screened out from our chemical library. Its biological activity was examined using cancer cell survival assays and immunological assays with various types of human cells including various cancer cell lines, PBMCs and enriched immune cells including NK, CD4+ T cells and CD14+ derived macrophages, as well as dg T cells. Luminex-based immunoassay was used to measure cytokine release from immune cells. Automatic western blot was used to quantify degradation of targeted proteins in sensitive cells.

Results NBT-018 selectively inhibited proliferation of leukemia and myeloma cells such as H292, HL-60, Jurkat cells in *in vitro* experiments (IC₅₀ 7.3, 0.12, 1.2 μM respectively); while it had little inhibitory effects on other cancer cells tested including lymphoma, breast cancer, colorectal carcinoma and glioblastoma cells (RIVA, Granta-529, RL, Farage, HCT116, U87, T98G, A172, MCF-7, IC₅₀ > 100 μM). NBT-018 also enhanced production of T cell cytokines (such as IL-2, IFN-γ, etc) from anti-CD3/CD28 stimulated normal human PBMC or from mixed culture of allotypic PBMCs. At 100 nM NBT-018 significantly enhanced SLP76 (Ser376) phosphorylation in Jurkat cells stimulated with anti-CD3/CD28 for 15 min; or in the coculture of Jurkat and HCT116 cells in the presence or absence of a bispecific T-cell engager. In addition, NBT-018 modulated production of inflammatory cytokines from PBMC stimulated with toll-like receptor agonists including LPS (TLR4), resiquimod (TLR7 and TLR8) and Poly (I:C) (TLR3). Furthermore, NBT-018 enhanced killing activities of human NK and dg T cells against K562 cells. However, NBT-018 had no appreciable effect on phagocytosis of CD14-derived macrophages, THP-1 monocytic cells and immortalized microglial cells (IMG). Finally, NBT-018 was found to bind CRBN and cause the degradation of IKZF1/2/3 in several lines of leukemia cells.

Conclusions Our data showed that NBT-018, a novel ‘molecular glue’, had anticancer and immunomodulatory activities such as modulation of expression of cytokines in immune cells and induction of cancer cell-killing activities of NK and dg T cells. NBT-018 could be a promising cancer immunotherapeutic agent targeting both cancer cells and immune cells.

<http://dx.doi.org/10.1136/jitc-2022-SITC2022.1152>

1153

PRECLINICAL ACTIVITY OF C-C CHEMOKINE RECEPTOR 2 (CCR2)-TARGETED IMMUNE STIMULATING ANTIBODY CONJUGATE (ISAC), MOTIVATING CLINICAL TESTING OF TAK-500

Vicky Appleman*, Atsushi Matsuda, Michelle Ganno, Angel Maldonado Lopez, Emily Rosentrater, Camilla Christensen, Samantha Merrigan, Hong Myung Lee, Min Young Lee, Linlin Dong, Jian Huang, Natasha Iartchouk, Dong Mei Zhang, Jianing Wang, He Xu, Tomoki Yoneyama, Konstantin Piatkov, Carole Harbison, Adnan Abu-Yousif*. Takeda Development Center Americas, Inc. (TDCA), Lexington, MA, USA

Background Increasing evidence suggests that myeloid populations are among the most sensitive to Stimulator of Interferon Genes (STING) agonism and downstream interferon (IFN) production and could augment activity of α -PD-1, radiation, and other therapies. We present preclinical data with a murine surrogate ISAC, mTAK-500, designed to selectively deliver the STING agonist, TAK-676, to CCR2+ cells. This approach enables systemic delivery and is designed to achieve enhanced activity through prolonged exposure and selective targeting of CCR2+ cells.

Methods mTAK-500 was evaluated in preclinical *in vitro* and *in vivo* systems to characterize potency, exposure, mechanism, and antitumor activity alone and in combination with radiation or α -PD-1 treatment.

Results CCR2-mediated delivery of TAK-676 triggered dose-dependent activation of the STING signaling pathway and STING induced gene expression, as well as robust activation of innate and adaptive immune activity both *in vitro* and *in vivo*. Following systemic administration of mTAK-500 in preclinical studies, plasma exposure of total antibody and conjugated TAK-676 was observed beyond 24 hours. Characterization of exposure in the tumor revealed that systemic administration resulted in accumulation of mTAK-500 and liberation of TAK-676 in the tumor microenvironment (TME), however, TAK-676 was below limit of detection in plasma. Collectively, these observations demonstrate that CCR2-targeted delivery of TAK-676 prolongs exposure in the TME. In syngeneic mouse models, a transient decrease in peripheral monocytes along with dose-dependent activation of dendritic cells in the TME, lymph node, and periphery was observed. Further, mTAK-500 treatment caused increases in frequency, proliferation, and activation of peripheral CD8 T cells, ultimately resulting in accumulation and activation of CD8 T cells in the TME resulting in antitumor activity. The combination of 8 Gy radiation and mTAK-500 also resulted in increased frequency of CD8 tetramer specific T cells accompanied by an increase in antitumor activity observed in CT26 tumor bearing mice. In MC38 tumor bearing mice, treatment with a single dose of mTAK-500 treatment alone achieved strong antitumor activity, including a durable complete response (CR). Single agent α -PD-1 treatment also resulted in a 12.5% CR rate, however, when combined, mTAK-500 and α -PD-1 treatment achieved enhanced anti-tumor response with a 37.5% CR rate.

Conclusions Nonclinical antitumor activity and mechanistic insight have motivated design and clinical testing of TAK-500, a CCR2-targeted STING ISAC comprising the clinical stage STING agonist TAK-676 and a high-affinity antibody targeting human CCR2, as a single agent and in combination with pembrolizumab in adults with select locally advanced or metastatic solid tumors (NCT05070247).

<http://dx.doi.org/10.1136/jitc-2022-SITC2022.1153>

1154

HIGH-POTENCY SYNTHETIC STING AGONISTS REWIRE MYELOID SUBSETS IN THE TUMOUR MICROENVIRONMENT TO DISMANTLE IMMUNOSUPPRESSIVE STROMA IN REFRACTORY PANCREATIC DUCTAL ADENOCARCINOMA

¹Akash Boda*, ²Casey Ager, ³Kimal Rajapakshe, ¹Krithikaa Rajkumar Bhanu, ¹Spencer Lea, ¹Michael Curran. ¹UT MD Anderson Cancer Center, Houston, TX, USA; ²Columbia University, New York, NY, USA; ³Baylor College of Medicine, Houston, TX, USA

Background Pancreatic ductal adenocarcinoma (PDAC) is clinically unresponsive to immune checkpoint blockade (ICB) immunotherapy.^{1,2} Dense immunosuppressive myeloid stroma (MS) and consequent T cell exclusion from the tumour microenvironment renders PDAC resistant to immune-based therapies³⁻⁷ Innate immune activation of the MS via cyclic dinucleotide (CDN) agonists of the STING (Stimulator of Interferon Genes) pathway can trigger T cell infiltration into cold tumours leading to robust anti-tumour immunity.⁸⁻¹¹ Despite proven therapeutic efficacy in preclinical models, the cellular and molecular mechanisms of how CDNs reprogram the suppressive MS to sensitise tumours to ICB is poorly understood.

Methods Using flow cytometry, multi-omic profiling followed by pathway analyses of MDSCs and M2 Macrophages of human and murine origin, we compared the ability of synthetic STING agonist, IACS-8803, with natural CDN, 2'3'-cGAMP to rewire these populations from immunosuppressive to immune-permissive phenotypes. To that end we investigated targets and pathways associated with c-Myc signaling, energy metabolism, and cell cycle. Furthermore, we describe the effects of IACS-8803 on apoptosis and Myc-dependent cell proliferation in these cells. We utilised Seahorse assays and CYTO-ID autophagy assays to characterise the metabolic reprogramming of myeloid cells upon treatment with IACS-8803 and CDN agonists.

Results Flow cytometry, RNA-Seq and protein array data on MDSCs and M2 Macrophages of human and murine origin show that IACS-8803 rewire these populations from immunosuppressive to immune-permissive phenotypes in part through inhibition of c-Myc signaling, energy metabolic modulation, and antagonism of cell cycle. IACS-8803 but not 2'3' cGAMP significantly reduces c-Myc gene expression in M2c macrophages and MDSCs. Further, these cells undergo reduced proliferation and enhanced apoptosis in response to IACS-8803 treatment. Metabolically, IACS-8803 rewires M2 Macrophages and MDSCs to a hypometabolic state marked by diminished ATP levels. Seahorse MitoStress analyses on these cells further showed reduced OCR and Spare Respiratory Capacity. Concomitantly, we observe elevated autophagic induction in the MS following IACS-8803 treatment, likely as a salvage pathway to maintain energy and survival.

Conclusions This study uncovers molecular and cellular mechanisms by which STING agonists drive proinflammatory conversion of tumour myeloid stroma. We are the first to report that synthetic CDN STING agonists affect MDSC and M2 macrophage repolarization through downregulation of c-Myc signalling and alterations in energy metabolism. Thus, high potency synthetic STING agonists remodels the MS in an aggressive orthotopic tumour model of PDAC through proinflammatory repolarization of myeloid cells, limiting their proliferation in the TME and forcing them into a hypometabolic state.

REFERENCES

1. Royal RE, Levy C, et al. Phase 2 trial of single agent Ipilimumab (anti-CTLA-4) for locally advanced or metastatic pancreatic adenocarcinoma. *J Immunother* 2010;**33**(8):828-33.
2. Brahmer JR, Tykodi SS, et al. Safety and activity of anti-PD-L1 antibody in patients with advanced cancer. *N Engl J Med* 2012;**366**(26):2455-65.
3. Karakhanova S, Link J. Characterization of myeloid leukocytes and soluble mediators in pancreatic cancer: importance of myeloid-derived suppressor cells. *Oncimmunology* 2015;**4**:e998519.
4. Dallal RM, Christakos P, et al. Paucity of dendritic cells in pancreatic cancer. *Surgery*. 2002;**131**:135-138.
5. Yamamoto T, Yanagimoto H, et al. Circulating myeloid dendritic cells as prognostic factors in patients with pancreatic cancer who have undergone surgical resection. *J Surg Res* 2012;**173**:299-308.
6. Hegde S, Krisnawan V, et al. Dendritic cell paucity leads to dysfunctional immune surveillance in pancreatic cancer. *Cancer Cell* 2020;**37**(3):289-307.
7. Beatty GL, Winograd R, et al. Exclusion of T cells from pancreatic carcinomas in mice is regulated by Ly6Clow F4/80+ Extratumoral Macrophages. *Gastroenterology* 2015;**149**(1):201-210.
8. Baird JR, Friedman D, et al. Radiotherapy combined with novel STING-targeting oligonucleotides results in regression of established tumors. *Cancer Res* 2016;**76**(1):50-61.
9. Ager CR, Reilley MJ, et al. Intratumoral STING activation with T-cell checkpoint modulation generates systemic antitumor immunity. *Cancer Immunol Res* 2017;**5**(8):676-84.
10. Smith TT, Moffett HF, et al. Biopolymers codelivering engineered T cells and STING agonists can eliminate heterogeneous tumors. *J Clin Invest* 2017;**127**(6):2176-91.
11. Jing W, McAllister D, et al. STING agonist inflames the pancreatic cancer immune microenvironment and reduces tumor burden in mouse models. *J Immunother Cancer* 2019;**7**(1):115.

<http://dx.doi.org/10.1136/jitc-2022-SITC2022.1154>

1155

ONM-501, A POLYVALENT STING AGONIST, EXHIBITS ANTI-TUMOR EFFICACY WITH INCREASED TUMOR T-CELL INFILTRATION IN MICE AND IS WELL TOLERATED IN RATS AND NON-HUMAN PRIMATES

¹Zirong Chen*, ¹Jason Miller, ²Wei Li, ²Katy Torres, ¹Qingtai Su, ²Gang Huang, ¹Yasser Saud O Albaroodi, ¹Rachel Morsch, ¹Teresa McElvaney, ¹Fiona Stavros, ¹Don Kruppa, ¹Tian Zhao, ²Jinming Gao, ¹Ruolan Han, ¹Zirong Chen. ¹Onconano Medicine, Southlake, TX, USA; ²University of Texas Southwestern Medical, Dallas, TX, USA

Background The Stimulator of Interferon Genes (STING) plays a crucial role in the innate immune response.¹ Several small molecule STING agonists have demonstrated effectiveness against cancer in preclinical models. In clinical trials, however, they showed limited therapeutic efficacy. We developed ONM-501, a dual-activating STING agonist that employs PC7A, a synthetic polymer that induces polyvalent STING condensation and prolongs innate immune activation.^{2,3} ONM-501 encapsulates the endogenous STING agonist 2',3'-cGAMP with the PC7A micelles offering dual 'burst' and 'sustained' STING activation. The mechanism and effectiveness of ONM-501 as an immunotherapy against solid tumors has been demonstrated in multiple preclinical models.^{3,4} Here we report in vivo efficacy and pharmacodynamic (PD) analysis of ONM-501 as a monotherapy and in combination with anti-PD1 in multiple murine tumor models and the safety evaluation in rats and primates.

Methods Anti-tumor efficacy of ONM-501 was evaluated by tumor growth inhibition and survival in tumor-bearing mice as a monotherapy or combined with anti-PD1. Immune activation and tumor microenvironment changes were evaluated by FACS analysis in tumors and draining lymph nodes and cytokine analysis in peripheral blood. STING activation was evaluated by expression of IFNB1, IRF7 and CXCL10 in tumors and draining lymph nodes using qPCR. Safety and tolerability were evaluated in rats and primates by single- and multiple-dose subcutaneous injections in naïve animals up to the highest feasible dose.

Results ONM-501 demonstrated broad anti-tumor efficacy both as monotherapy and combined with anti-PD1 in multiple models including A20, CT26, MC38 and B16F10. FACS analysis showed significantly increased tumor-infiltrating T-cells after ONM-501 mono- and combo- therapies in the B16F10 tumors. ONM-501 upregulated PD-L1 expression in tumor tissue. STING activation was confirmed by the increased IRF7 and CXCL10 mRNA levels in tumor and draining lymph nodes after monotherapy and anti-PD-1 combination. In the single- and multiple-dose toxicology studies, Sprague-Dawley rats and cynomolgus monkeys were well tolerated without severe or irreversible systemic toxicities up to the maximum feasible dose (30mg/kg). Dose-dependent increases in lymphocytes and cytokines, consistent with STING activation, were also observed.

Conclusions ONM-501 demonstrated marked anti-tumor efficacy as a monotherapy and in combination with anti-PD1 in murine syngeneic tumor models. The in vivo PD analysis confirmed STING activation, enhanced tumor T-cell infiltration and PD-L1 upregulation by ONM-501. Toxicology studies in rats and primates demonstrated a strong safety profile and large therapeutic window. The novel dual STING agonist ONM-501 is a promising therapeutic candidate for clinical evaluation in solid tumors.

Acknowledgements This work is partially funded by the Product Development Award DP190066 from the Cancer Prevention and Research Institute of Texas (CPRIT) to OncoNano

Medicine. The work at UT Southwestern is supported by a sponsored research award from OncoNano Medicine.

REFERENCES

1. Afsaneh Amouzegar, Manoj Chelvanambi, *et al.* STING agonists as cancer therapeutics. *Cancers* 2021,**13**(11):2695.
2. Zachary Bennett, Suxin Li, *et al.* Polyvalent design in the cGAS-STING pathway. *Seminars in Immunology*. 2021.p101580.
3. Suxin Li, Min Luo, *et al.* Prolonged activation of innate immune pathways by a polyvalent STING agonist. *Nature Biomedical Engineering* 2021,**5**:455–466.
4. Suxin Li, Jian Wang, *et al.* ONM-501: A polyvalent STING agonist for oncology immunotherapy. *Cancer Research* 2022,**82**(12 Supplement):4234.

Ethics Approval All animal experiments were performed with ethical compliance and approval from Institutional Animal Care and Use Committee of the University of Texas Southwestern Medical Center, Labcorp Early Development Laboratories Inc and ITR Laboratories Canada Inc.

<http://dx.doi.org/10.1136/jitc-2022-SITC2022.1155>

1156

STING ACTIVATION IN SARCOMA: ASSESSING TRANSLATIONAL THERAPEUTIC STRATEGIES

Karys Hildebrand*, Kurt Hildebrand, Kayla Marritt, Carolina Salazar Arcila, Michael Monument. *University of Calgary, Calgary, Canada*

Background Undifferentiated pleomorphic sarcoma (UPS) is a highly aggressive and metastatic soft tissue sarcoma that is resistant to most conventional systemic therapies and immunotherapies.¹⁻⁵ Activation of the STimulator of INterferon Genes (STING) pathway is an emerging immunotherapeutic strategy that can be used to recruit effector lymphocytes into the TME to induce tumour eradication.⁶⁻⁹ In a murine model of UPS, we have demonstrated that intra-tumoural (i.t.) administrations of a murine-specific STING agonist, DMXAA, results in profound immune mediated tumour clearance.¹⁰ The objective of this study is to evaluate the anti-tumour potential of three STING agonists that can activate both murine and human STING receptors as monotherapies and in combination with immune checkpoint blockade (ICB) therapy in a murine model of UPS to assess translational feasibility.

Methods Immune competent mice were orthotopically engrafted with a syngeneic murine UPS cell line in the hindlimb muscle. UPS bearing mice in the monotherapy groups were treated with a single i.t. dose of 1) CDN, 2) MSA-2, 3) E7766 or 4) DMXAA. Mice treated in combination with ICB therapy received monoclonal anti-PD1 in addition to a single dose of CDN, MSA-2, or DMXAA. Tumour volume measurements and bioluminescence were measured over time. Surviving mice were re-challenged with UPS in the contralateral limb. Flow cytometry and transcriptomics were completed 24hrs, 72hrs, and 1-week after STING monotherapy treatment.

Results Unlike DMXAA, monotherapy with CDN or MSA-2 failed to eradicate UPS tumours. Survival studies with E7766 have shown UPS clearance in 18-40% of E7766 treated mice. 100% of the surviving E7766 and DMXAA treated mice completely rejected the re-challenge inoculation of UPS cells. Immune profiling of CDN, MSA-2, and DMXAA treated tumours at multiple timepoints post-treatment showed similar inflammatory changes and increased lymphocytic infiltration. STING+ICB therapy significantly improved survival outcomes in CDN+ICB treated tumours, as 14% of CDN+ICB treated mice eradicated their UPS tumours. In DMXAA monotherapy and DMXAA+ICB combination therapy, there were no significant differences in survival. Unfortunately, there were no survivors in the MSA-2+ICB group, but survival was significantly extended compared to MSA-2 monotherapy.

Conclusions STING activation is a promising immunotherapeutic strategy for UPS. We have demonstrated that the human and murine compatible STING agonist, E7766, can be used to elicit immune mediated UPS clearance and adaptive immune protection against UPS re-challenge. Ultimately, this study demonstrates the potential opportunity for clinical translation of STING as an immunotherapy for UPS which could significantly improve outcomes for this patient demographic.

REFERENCES

1. Vodanovich DA, MC PF. Soft-tissue sarcomas. *Indian J Orthop* 2018;**52**(1):35-44.
2. Hoffmann D, et al. Evaluation of twenty human adenoviral types and one infectivity-enhanced adenovirus for the therapy of soft tissue sarcoma. *Hum Gene Ther* 2007;**18**(1):51-62.
3. Steen S, Stephenson G. Current treatment of soft tissue sarcoma. *Proc (Bayl Univ Med Cent)* 2008;**21**(4):392-6.

4. Tawbi HA, et al. Pembrolizumab in advanced soft-tissue sarcoma and bone sarcoma (SARC028): a multicentre, two-cohort, single-arm, open-label, phase 2 trial. *The Lancet Oncology* 2017;**18**(11):1493-1501.
5. Paoluzzi L, et al. Response to anti-PD1 therapy with nivolumab in metastatic sarcomas. *Clinical sarcoma research* 2016;**6**(1):1-7.
6. Corrales L, et al. Direct activation of STING in the tumor microenvironment leads to potent and systemic tumor regression and immunity. *Cell reports* 2015;**11**(7):1018-1030.
7. Sivick KE, et al. Magnitude of therapeutic STING activation determines CD8+ T cell-mediated anti-tumor immunity. *Cell reports* 2018;**25**(11):3074-3085.e5.
8. Pan B-S, et al. An orally available non-nucleotide STING agonist with antitumor activity. *Science* 2020;**369**(6506).
9. Huang, K-C, et al. Discovery and characterization of E7766, a novel macrocycle-bridged STING agonist with pan-genotypic and potent antitumor activity through intravesical and intratumoral administration. 2019, AACR.
10. Marritt K, et al. Sting activation as an immunotherapeutic strategy for soft-tissue sarcoma. In orthopaedic proceedings. 2021. The British Editorial Society of Bone & Joint Surgery.

<http://dx.doi.org/10.1136/jitc-2022-SITC2022.1156>

1157

DISCOVERY OF A NOVEL, POTENT SMALL MOLECULE INHIBITORS OF ENPP1 ENHANCES ANTI-TUMOR EFFICACY IN COMBINATION WITH IMMUNE CHECK INHIBITORS

Juhyeon Kim, Pyoung Oh Yoon, A-Ram Lee, Eunji Son, Young Cheol Lee, Eunmi Jung, HyoungRae Kim, YeonHee Lee, SoEun Park, Dae-Yon Lee, Chul-Woong Chung, Pyoung Oh Yoon*. *LegochembiScience, Daejeon, Korea, Republic of*

Background The cGAS-STING (cyclic GMP-AMP synthase-stimulator of interferon genes) signaling pathway has led to significant innate immune responses in cancer immunotherapy. 2'3'-cGAMP, the second messenger in the cGAS-STING signaling pathway, binds to STING and promotes the production of various pro-inflammatory cytokines such as type I interferon (IFN). Therefore, activated STING pathway has been considered an important target for cancer immunotherapy. However, STING agonists excessively activate the STING pathway, causing side effect due to hyper-accumulation of cytokines. Here we show that targeting ENPP1 is emerging as a promising target of STING regulation in immunotherapy, because it indirectly activates the STING pathway. Ecto-nucleotide pyrophosphatase/phosphodiesterases 1 (ENPP1), highly expressed membrane-bound enzyme in cancer cells, modulates cGAMP levels by hydrolyzing 2',3'-cGAMP to alter the inflammatory milieu. In this study, we present our potent ENPP1 inhibitors, which show highly improved enzymatic activities, immune cell related immune responses in vitro and CT-26 syngeneic mouse model.

Methods We discovered potent ENPP1 inhibitors with highly potent activities in various cell-based assay systems. The in vivo antitumor efficacy was assessed as monotherapy and in combination with Anti-PD-L1 (immune checkpoint inhibitor) by monitoring tumor growth for 15 days, in a CT-26 syngeneic mouse model.

Results Our two candidates showed excellent inhibitory activity of nanomolar level in a non-cell-based in vitro ENPP1 inhibition assay using pNP-TMP (artificial substrate) and cGAMP as substrates, respectively. In vitro THP-1 dual reporter assay demonstrated the potency and efficacy of the compounds that induce STING-mediated type I IFN release. In addition, one of the two candidates exhibited good PDE and kinase panel selectivity as well as good in vivo pharmacokinetic properties.

Finally, both candidates exhibited good anticancer efficacy in the CT-26 colorectal cancer syngeneic mouse model. IV administration of one candidate at 25 mg/kg demonstrated a TGI of 53% as monotherapy and a TGI of 81% in combination with anti-PD-L1 treatment. In contrast, another candidate, when administered orally at 25 mg/kg, provided a TGI of 39% as monotherapy and a TGI of 86% in combination with anti-PD-L1 antibody treatment. Therefore, our candidates demonstrated a much better efficacy profile in combination with Anti-PD-L1 antibody.

Conclusions Taken together, our study demonstrates that a novel and potent small molecule inhibitor that inhibits extracellular ENPP1 has been designed. Our candidates with desirable drug properties, were evaluated for activity in the syngeneic mouse tumor model CT-26. As a result, these candidates were well tolerated and demonstrated significant antitumor activity when combined with anti-PD-L1 antibody.

<http://dx.doi.org/10.1136/jitc-2022-SITC2022.1157>

1158

HIGH POTENCY STING AGONISTS INDUCE ADAPTIVE-IMMUNITY DEPENDENT CURATIVE RESPONSES IN CHECKPOINT-REFRACTORY GLIOBLASTOMA MODELS

Spencer Lea*, Michael Curran, Chao-Hsien Chen. *University of Texas MD Anderson Cancer Center, Houston, TX, USA*

Background Glioblastoma (GBM) is the most common and aggressive adult primary brain malignancy, with a median overall survival of 15 months post-diagnosis. Clinically, GBM is refractory to T cell immune checkpoint blockade (ICB), which may be attributable to its immunosuppressive tumor microenvironment enriched in glioma-associated myeloid cells (GAM) and lacking in effector T cells.^{1,2} This phenotype is reflected in the *Qki*^{-/-} *Pten*^{-/-} *P53*^{-/-} (QPP8) tumor model,³ which we show is ICB-refractory but sensitive to agonists of the Stimulator of Interferon Genes (STING) innate immune sensing pathway. While we have shown that STING agonists potently repolarize *in vitro* generated suppressive myeloid cells towards more T cell supportive phenotypes,^{4,5} their function in the context of the GBM myeloid compartment remains poorly understood.

Methods Using the synthetic cyclic di-nucleotide STING agonist IACS-8803 we treated orthotopic QPP8 tumors intratumorally. We then analyzed survival and performed high parameter flow cytometry profiling of the tumor immune microenvironment following STING agonist treatment. To assess the contribution of adaptive immunity to STING agonist therapeutic efficacy, we treated orthotopic QPP8 tumors implanted in RAG1 KO mice and monitored survival.

Results We found that STING agonist therapy cured murine orthotopic QPP8 tumors, in contrast to ICB that showed no survival benefit. In RAG1^{-/-} mice bearing QPP8 tumors STING agonist therapy extended survival, however, the curative effect observed in wild-type mice was lost in the absence of adaptive immunity. STING agonist-treated QPP8 tumors displayed increased counts of CD8 T cells and NK cells, and decreased CD8 T cell PD1 expression. Infiltration of STING-treated gliomas by Ly6C⁺ F4/80⁺ Mono-MDSC substantially increased; however, these cells expressed reduced CD206 and CD163 and increased CD86, suggestive of a more proinflammatory state. Finally, in the cervical lymph node of QPP8-treated mice the frequency and CD86 expression of cDC1 cells increased.

Conclusions We found that STING agonists induce adaptive immunity-dependent curative responses in ICB-refractory murine QPP8 GBM tumors. Increased frequencies of cDC1 dendritic cells in the draining lymph node, as well as augmented CD8 T cell densities within treated tumors likely help drive regression of these established gliomas. While STING agonist therapy also increased the frequency of cells classically defined as monocytic MDSC, their suppressive capacity may have been reduced, similar to previous publications on expanded Ly6C⁺ F4/80⁺ populations in other STING-treated tumors.⁶ Together these results indicate that STING activation induces proinflammatory repolarization of the murine GBM myeloid stroma that drives rejection of established, ICB-refractory tumors.

REFERENCES

1. Gabrusiewicz K, Rodriguez B, Wei J, *et al.* Glioblastoma-infiltrated innate immune cells resemble M0 macrophage phenotype. *JCI Insight* 2016;**1**(2).
2. Quail DF, Joyce JA. The microenvironmental landscape of brain tumors. *Cancer Cell* 2017;**31**(3):326–41.

3. Shingu T, Ho AL, Yuan L, *et al.* Qki deficiency maintains stemness of glioma stem cells in suboptimal environment by downregulating endolysosomal degradation. *Nat Genet* 2017;**49**(1):75–86.
4. Ager CR, Boda A, Rajapakse K, *et al.* High potency STING agonists engage unique myeloid pathways to reverse pancreatic cancer immune privilege. *J Immunother Cancer* 2021;**9**(8).
5. Ager CR, Reilley MJ, Nicholas C, *et al.* Intratumoral STING Activation with T-cell Checkpoint Modulation Generates Systemic Antitumor Immunity. *Cancer Immunol Res* 2017;**5**(8):676–84.
6. Ohkuri T, Kosaka A, Ishibashi K, *et al.* Intratumoral administration of cGAMP transiently accumulates potent macrophages for anti-tumor immunity at a mouse tumor site. *Cancer Immunol Immunother* 2017;**66**(6):705–16.

<http://dx.doi.org/10.1136/jitc-2022-SITC2022.1158>

1159

USE OF SMALL MOLECULE STING AGONIST IMMUNOTHERAPY FOR CANINE SOFT TISSUE SARCOMA: A CROSS-SPECIES ANALYSIS

¹Ye-Jean Park*, ²Joseph Kendal, ¹Carolina Salazar Arcila, ¹Karys Hildebrand, ¹Max Labrecque, ¹Michael Monument. ¹University of Calgary, Calgary, Canada; ²University of California Los Angeles, Los Angeles, CA, USA

Background Soft tissue sarcomas are rare connective tissue malignancies that are highly resistant to traditional systemic therapies.¹ Sarcomas are relatively common in dogs, yet few studies have previously investigated anti-sarcoma immunotherapies in this species.^{2,3} In this study, we sought to investigate several small molecule STING (STimulator of Interferon Genes) agonists' dose toxicities and pathway inductions via canonical cytokine responses in canine macrophage and sarcoma lines, as compared to murine and human macrophage and sarcoma lines. We further aimed to assess the efficacy of a selected small molecule STING agonist without species specificity (ADU-S100) as an intra-tumourally administered drug in two canine patients with soft tissue sarcoma.

Methods To assess the cytotoxicity of STING agonists DMXAA, ADU-S100, and MSA-2, an in-vitro MTT cell viability assay was used. Murine, canine, and human macrophages and sarcoma cells were exposed to the following conditions: media, vehicle control, or 0.1, 1, 10, and 100µg/mL of treatment (up to 200µg/mL of treatment for ADU-S100). 6, 12, and 24-hours post-exposure to the conditions, cell viability was assessed via formazan absorbance values. STING-pathway induced interferon-dependent cytokine production (IFN-β, TNF-α, CXCL-10) in cells was assessed via the Luminex cytokine assay. All cells were treated with 177nmol/L of the STING agonists, and cytokine release 2- and 6-hours post-exposure were quantified. Clinical efficacy of ADU-S100 was further evaluated in vivo for two canine STS patients (1 hindlimb, 1 forelimb). Serial intra-tumoural doses further ranged from 200µg to 2.0mg of ADU-S100. Tumour volumes were calculated from caliper measurements of tumour length, width, and depth.

Results DMXAA and ADU-S100 were not cytotoxic below 100 and 200µg/mL, respectively, and MSA-2 was cytotoxic above 10µg/mL. All STING agonists effectively stimulated the interferon-dependent STING pathway in murine macrophage cells. In addition, ADU-S100, MSA-2, and E7766 stimulated the canine and human interferon-dependent STING pathways. Our subsequent in vivo pilot study demonstrated that the intra-tumoural administration of ADU-S100 led to a 3.5-fold and 2.3-fold reduction of canine patients' tumour volumes over the course of 6-weeks, respectively (from 594cm³ to 172cm³ for patient 1, and from 420cm³ to 180cm³ for patient 2).

Conclusions Overall, our findings suggest that STING agonists – in particular, ADU-S100 – possess potential as a novel and effective therapeutic approach for canine STS. As sarcomas are highly metastatic and commonly fatal in dogs, further evaluating STING agonist therapy in canines may provide therapeutic insights into similar challenges for treating human disease using a comparative biology approach.

Acknowledgements We would like to acknowledge the McCaig Bone and Joint laboratory at the University of Calgary, and the Alberta Cancer Foundation and COREF for their support.

REFERENCES

1. Corrales L, Glickman LH, McWhirter SM, Kanne DB, Sivick KE, Katibah GE, *et al.* Direct activation of STING in the tumor microenvironment leads to potent and systemic tumor regression and immunity. *Cell Rep* 2015;**11**(7):1018–30.
2. Motedayen Aval L, Pease JE, Sharma R, Pinato DJ. Challenges and opportunities in the clinical development of STING agonists for cancer immunotherapy. *J Clin Med* 2020;**9**(10).
3. Séguin B. Canine soft tissue sarcomas: can being a dog's best friend help a child? *Front Oncol* 2017;**7**:285.

Ethics Approval All experiments were approved by the canine patients' respective owners and their informed consent, along with the approval and expertise of veterinary medicine specialists who assisted with conducting the trials.

<http://dx.doi.org/10.1136/jitc-2022-SITC2022.1159>

1160

STING SIGNALING COMPENSATES FOR MUTATION BURDEN-LOW TUMORS TO STIMULATE THE IMMUNE RESPONSE

Jiayi Tan*, Colt Egelston, Weihua Guo, Peter Lee. *City of Hope, Duarte, CA, USA*

Background Tumor mutation burden (TMB) is known to predict the immune response, especially tumor-infiltrating lymphocytes (TILs) in various tumor types. Besides, it's also one of the most well-accepted biomarkers to select responsive patients for immunotherapy. However, increasing evidence indicates the complex association between TMB and immune infiltration, and the overall response rate to immunotherapy selected based on TMB in clinical trials was not satisfied.

Methods Bulk RNA-seq and somatic mutation datasets from The Cancer Genome Atlas (TCGA) of 10 major cancer types were downloaded to investigate the role of TMB and other determinants in immune response. Unsupervised patient clustering analysis with UMAP using major immune components and TMB was performed to further identify different types of tumor microenvironment (TME).

Results Mutation burden was found poorly correlated with active immune response in various cancer types. The unsupervised clustering analysis revealed the tumor group with low mutation burden but inflamed TME as well as the group with high mutation burden but poor immune response. Notably, the stimulator of interferon genes (STING) signaling was upregulated in that low TMB group to enhance the immune response. In contrast, the tumors harboring high mutation burden with robust proliferation and DNA damage repair machinery failed to stimulate STING signaling leading to poor immune activation, which may result from minimal cell death and apoptosis to release tumor DNA.

Conclusions This study demonstrates the non-linear relationship between TMB and inflamed TME. High mutation burden in tumors is not always necessary for the active immune response which instead may lead to non-inflamed TME. Moreover, this study emphasizes the initial step of tumor apoptosis to stimulate either antigen-presenting cells (APCs) to uptake tumor antigens or STING signaling for further immune activation. Together these data suggest the application of STING agonist in high mutation burden tumors with non-inflamed TME to interrupt the aggressive replication cycle and enhance the immune response.

<http://dx.doi.org/10.1136/jitc-2022-SITC2022.1160>

1161

SYNTHETIC CD206 TARGETED CONSTRUCTS CARRYING PACLETAXEL OR NOVEL BISPSPHONATE PAYLOADS ALTER MACROPHAGES TOWARDS PRO-INFLAMMATORY PHENOTYPES; THE PACLETAXEL CONSTRUCT IMPROVES THE EFFICACY OF ANTI-CTLA4 IN CT26 TUMORS

David Ralph*, Jeffrey Arnold, Michael Rosol. *Navidea Biopharmaceuticals, Dublin, OH, USA*

Background Tumor associated macrophages (TAMs) promote an immunosuppressive and protumor immune microenvironment reducing the efficacies of cancer immunotherapies. Altering TAM phenotypes from immunosuppressive to proinflammatory should stimulate TAMs directly and lymphocytes indirectly to attack cancer cells and potentially increase the efficacies of check point inhibitor therapies, like anti-CTLA4. Mannosylated Amine Dextrans (MADs) are synthetic ligands for CD206 that can carry small molecule payloads on degradable linkers to CD206 expressing cells, i.e. TAMs. Three MAD constructs were made carrying payloads of paclitaxel or one of two novel bisphosphonates and were evaluated in human GM-CSF macrophages for their abilities to durably alter macrophage phenotypes towards pro-inflammatory. The paclitaxel MAD was tested in the CT26 tumor model with or without anti-CTLA4.

Methods >Human monocytes from 3 donors were differentiated to CD206+ macrophages in GM-CSF supplemented RPMI1640 with 10% FBS (fresh medium) for 5 days.

>Medium was replaced with fresh media with varying concentrations of MAD + drug constructs or molar equivalents of free drugs or zoledronate and incubated for 24 hours.

>Saline or MAD without payload were controls.

>Drug containing media were replaced with fresh medium and incubated for 3 days (for durable responses)

>Cells were assessed by flow cytometry (MFI) for viability, CD206, CD163, CD80, CD86, MHC1, MHC2, SIRPalpha, and PD1.

>CT26 tumors implanted in Balb/c mice, treatment began when tumors were 100mm².

>Mice treated with MAN-Paclitaxel (127 micrograms/dose), free paclitaxel, saline, or MAD no payload twice/week for 5 doses. Tumor volumes measured with calipers were the output.

Results Cell/FlowAssays

>None of the constructs reduced macrophage viability significantly.

>All three MAD-Drug constructs reduced expression of CD206 and CD163 (immunosuppression markers) and increased expression of CD80 and CD86 (pro-inflammatory markers).

>PD1 expression increased.

>MHC1 and MHC2 expression was not significantly changed.

>Both MAD-bisphosphonates – but not free drugs or MAD-paclitaxel – significantly reduced expression of SIRPalpha (p<.0001).

CT26 Studies

>MAD-Paclitaxel and free paclitaxel were equally effective at tumor growth reduction.

>MAD-Paclitaxel plus anti-CTLA4 reduced tumor growth by 76%. Anti-CTLA4 alone by 52%.

Conclusions > All 3 MAD-drug constructs shifted macrophage phenotypes towards pro-inflammatory and more effectively the free drugs.

> Both MAD-Bisphosphonated constructs significantly reduced expression of SIRPalpha (checkpoint)

>MAD-paclitaxel and free paclitaxel increased the efficacy of anti-CTLA4, but

>CD206 targeted delivery can avoid off target toxicities of paclitaxel.

Shifting TAM phenotypes towards a pro-inflammatory state in a targeted fashion has the potential to increase the efficacies of other immunotherapies to reduce tumor burdens.

Acknowledgements Macrophage cell culture assays were performed at Discovery Life Sciences (Huntsville, AL). CT26/Balb/c studies were performed by Charles River Laboratories (North Carolina).

Ethics Approval All studies performed at Charles River Laboratories were reviewed and approved by an institutional IACUC committee.

<http://dx.doi.org/10.1136/jitc-2022-SITC2022.1161>

1162

A NECTIN-4 TARGETED TLR9 AGONIST ANTIBODY CONJUGATE INDUCES ROBUST IMMUNE CELL ACTIVATION AND ANTI-TUMOR RESPONSES

Amy Chen*, Min Li, Maja Bonacorsi, Emma Sangalang, Danielle Fontaine, Ons Harrabi, Mingrui An, Tiffany Chou, Laura Doyle, Janet Sim, Bora Han, Hong Wan, Tracy Kuo, Maria Jose Costa, Pavel Strop. *Tallac Therapeutics Inc, Burlingame, CA, USA*

Background Novel therapies that engage both innate and adaptive immune responses may engender durable anti-tumor immunity. Activation of Toll-Like Receptor 9 (TLR9) by unmethylated CpG oligonucleotides promotes innate inflammatory responses and the induction of adaptive immunity. Several CpG-based TLR9 agonists have demonstrated clinical activity in melanoma by inducing a pro-inflammatory tumor microenvironment (TME), when administered intratumorally.¹ However, intratumoral delivery has various development challenges that need to be addressed, including limited tumor indications, injection site variability and poor pharmacokinetics. A systemically delivered TLR9 agonist with favorable safety profile has potential to provide innate and adaptive anti-tumor immunity across multiple tumor types. We developed a Toll-like Receptor Agonist Antibody Conjugate (TRAAC) comprised of a CpG oligodeoxynucleotide conjugated to a novel Nectin-4-targeting antibody for systemic administration and TME delivery of a potent TLR9 agonist. Nectin-4 is a cancer associated antigen over-expressed in many solid tumor types with limited expression in normal tissues. Additionally, Nectin-4 over-expression correlates with poor prognosis.² Activation of myeloid cells via TLR9 signaling within the TME may promote pro-inflammatory signals countering immunosuppressive pathways, thereby resulting in initiation and enhancement of anti-tumor responses.³ Here we present preclinical data demonstrating that Nectin-4 TRAAC triggers TLR9 signaling, induces myeloid and dendritic cell activation, phagocytosis, cytokine production and lymphocyte activation, resulting in potent anti-tumor efficacy.

Methods *In vitro* activity of Nectin-4 TRAAC was evaluated using human peripheral blood mononuclear cells (PBMCs) co-cultured in presence of Nectin-4 expressing cancer cells. The anti-tumor efficacy of Nectin-4 TRAAC as a monotherapy was evaluated using syngeneic models.

Results Nectin-4 TRAAC induced both innate and adaptive anti-tumor immune mechanisms in human PBMC co-cultured with Nectin-4-expressing cancer cell lines. Nectin-4 TRAAC potently activated myeloid cells, leading to enhanced phagocytosis, increased expression of co-stimulatory molecules, secretion of pro-inflammatory cytokines and B, T and NK cell activation. In both immunogenic and checkpoint inhibitor (CPI) refractory syngeneic tumor models, single agent Nectin-4 TRAAC treatment led to durable tumor regression and eradication across a range of Nectin-4 expression levels. Animals in which Nectin-4 TRAAC treatment led to tumor clearance were protected from tumor growth upon rechallenge, demonstrating that Nectin-4 TRAAC induces potent anti-tumor immunological memory.

Conclusions The preclinical data shown here provide a strong rationale for pursuing Nectin-4 TRAAC for the treatment of Nectin-4-expressing solid tumors, including those that are refractory to CPI therapy.

REFERENCES

1. Hamid O, Ismail R, Puzanov I. Intratumoral immunotherapy-update 2019. *Oncologist* 2020;**25**(3):e423–e438.

2. Chatterjee S, Sinha S, Kundu CN. Nectin cell adhesion molecule-4 (NECTIN-4): a potential target for cancer therapy. *Eur J Pharmacol* 2021;**911**:174516.
3. Liu M, O'Connor R, Trefely S, Graham K, Snyder NW, Beatty GL. Metabolic rewiring of macrophages by CpG potentiates clearance of cancer cells and overcomes tumor-expressed CD47-mediated 'don't eat me signal'. *Nat Immunol* 2019;**20**(3):265–275.

<http://dx.doi.org/10.1136/jitc-2022-SITC2022.1162>

1163

A UNIQUE DENDRITIC CELL ACTIVATION STATE UTILIZES INFLAMMASOMES TO STIMULATE MEMORY T CELL RESPONSES IN HUMANS

Jon Chow*, Veronica Komoroski, Emily Gosselin, Andrew Cornforth. *Corner Therapeutics, Watertown, MA, USA*

Background Dendritic cells (DCs) represent the primary drivers of new T cell responses that defend against cancer and infection. In order to execute this task, DCs must be stimulated in a manner that induces several T cell stimulatory activities. These activities include the ability of DCs to 1) present tumor or microbial antigens, 2) express T cell co-stimulatory molecules, 3) express cytokines that induce effector T cell differentiation, 4) migrate in high numbers to lymph nodes and 5) produce the memory T cell inducing cytokine IL-1 β . Diverse approaches have been undertaken to stimulate these DC activities in a clinical or pre-clinical setting, with common strategies targeting Toll-like Receptors, STING or inflammasomes. These approaches are based on the general concept—permeating the literature for over 30 years—that infection-like signals are sufficient to stimulate DC-mediated instruction of adaptive immunity. However, the therapeutic success of these strategies remains elusive.

Methods Herein, we demonstrate that the aforementioned approaches are unable to elicit all 5 of the aforementioned activities in human DCs. This observation may explain the ineffectiveness of these approaches in generating protective immunity to cancer. We report a distinct means of stimulating DCs, using molecular signals that mimic infection and tissue injury, that elicit all DC activities needed to stimulate adaptive immunity. We devised proprietary chemical mimics of infection and tissue injury that induce a new DC activation state termed hyperactive.

Results Primary human DCs that have been stimulated with hyperactivators far exceed the capacity of other DCs to stimulate Th1-biased memory T cell activities, by a process dependent on inflammasomes and the cytokine IL-1 β .

Conclusions These studies reveal a unique DC activation state, and chemical agonists that elicit this state, as key determinants of T cell mediated immunity. DC hyperactivating chemicals represent a means to expand the opportunities in immunotherapy, and may enable durable T cell immunity to be elicited in a clinical setting.

<http://dx.doi.org/10.1136/jitc-2022-SITC2022.1163>

1164

SYSTEMIC ADMINISTRATION OF AXA-042, A NOVEL TLR2/6 AGONIST, RESHAPES THE TUMOR MICROENVIRONMENT, AS REVEALED BY SINGLE CELL SEQUENCING ANALYSIS

<http://dx.doi.org/10.1136/jitc-2022-SITC2022.1164>

¹Bedrich Eckhardt, ¹Kellie Mouchemore, ¹Yang Liao, ¹Wei Shi, ²Francesca Mercuri, ³Phil Kearney, ¹Robin Anderson, ³Anna Galkin*, ¹Olivia Newton-John Cancer Research Institute, Heidelberg, Australia; ²ENA Respiratory, Melbourne, Australia; ³Axelia Oncology, Melbourne, Australia

Background Treatment approaches that engage both the innate and adaptive immune response have the potential to transform anti-cancer therapy, especially in settings of checkpoint inhibitor insensitivity. Toll-like receptors (TLRs) mediate the initial cellular response to external pathogens or endogenous alarmins, activating downstream pro-inflammatory cascades associated with innate cell activation and recruitment. AXA-042 is a novel synthetic TLR2/6 agonist designed for systemic delivery to re-engage the innate immune response to help overcome tumor immune escape. Once-a-week treatment with AXA-042 led to 87% growth inhibition of syngeneic EMT6 tumors. Single cell sequencing analysis was completed to characterize the immediate impact of systemic TLR2/6 activation on the tumor microenvironment.

Methods Female Balb/c mice bearing orthotopic EMT6.5 mammary tumors received a single intravenous treatment of saline or AXA-042 (10 µg/mouse). Equal numbers of viable cells were recovered by flow cytometry from collagenase-digested tumors (n=3/group) 24 hours after treatment and pooled prior to loading onto a Chromium Single Cell Chip. 10x Genomics single-cell transcriptome libraries were prepared from each sample and sequenced with Illumina NextSeq 550 sequencing platform. Cell type annotation based on the ImmGen database was determined using the SingleR package. Differential gene expression analyses were completed to identify AXA-042 responsive gene signatures in cell subsets that included at least 10 cells. The identified genes were required to be expressed in at least 3 cells.

Results AXA-042 treatment decreased the total number of tumor-associated macrophages, monocytes, fibroblasts, endothelial, epithelial and stromal cells within 24 hours of treatment. A parallel increase in neutrophils, B cells, NKT and activated CD4 and CD8 T cells was observed. Re-clustering of myeloid populations revealed AXA-042-induced shifts in the macrophage, monocyte and neutrophil clusters. Differential expression analysis within the TLR2 positive myeloid cells demonstrated AXA-042-mediated engagement of pathways associated with antigen processing and presentation, Fc receptor signaling and immune hypersensitivity in monocytes; granulocyte chemotaxis, lipid metabolism and iron sequestration in neutrophils; and cellular response to bacterial lipopeptide, stress response to metal ions and arginine metabolism in macrophages

Conclusions Systemic AXA-042 treatment led to a reorganization of the tumor microenvironment within 24 hours of treatment. AXA-042 altered the myeloid cell subset profiles, promoted the influx of activated T cells and reduced tumor cell viability. AXA-042 has completed GLP toxicology studies and is currently undergoing evaluation in a Phase 1 clinical trial (ACTRN12622000993796) in advanced solid tumors.

Trial Registration ACTRN12622000993796

Ethics Approval The study was approved by the Austin Health Animal Ethics Committee, approval number 05640.

1165 **IMPACT OF SD-101, A TOLL-LIKE RECEPTOR 9 CLASS C (TLR9C), AGONIST ON MYELOID DERIVED SUPPRESSOR CELLS**

Chandra Ghosh*, Steven Katz, Chandra Ghosh. *Trisalus Life Sciences, Westminster, CO, USA*

Background Specific immunosuppressive pathways, including unique programming of myeloid derived suppressor cells (MDSC), may limit the success of immunotherapy in the liver. SD-101, a TLR9C agonist delivered via intravascular Pressure Enabled Drug Delivery™ (PEDD™), is currently under study in combination with systemic checkpoint inhibition across multiple intrahepatic tumor indications (NCT04935229, NCT05220722). There are multiple classes of TLR9 agonists, with differential effects on plasmacytoid DC (pDC) IFN α production, B and NK cell activation, and other immune cell populations. TLR9C agonists have relatively broad immunologic effects, but the impact on MDSC is less clear. We investigated the impact on myeloid cells by various TLR agonists (TLR4, TLR7, TLR9B and TLR9C) to expand our understanding of their differential effects on MDSC and potential to immunomodulate liver tumor microenvironments (TME)

Methods Peripheral Blood Mononuclear Cells (PBMCs) obtained from healthy donors were cultured in IL6+GMCSF (20ng/ml) to induce MDSCs and treated with various TLR agonists. Flow cytometry was performed to evaluate MDSCs (CD33⁺CD11b⁺HLADR⁻), subtypes of MDSCs (monocytic/granulocytic CD14⁺/CD15⁺MDSCs), M1 macrophages (CD14⁺CD86⁺), and monocytic dendritic cells (CD14⁺CD11C⁺CD123⁻). Nanostring analysis (n=3) was performed on total RNA isolated from day 2 samples, verified by qRT-PCR. Bone marrow (BM) murine MDSCs (CD11b⁺GR-1⁺) were treated for 72h with GMCSF and effects on MDSC were evaluated by flow cytometry.

Results SD-101, a TLR9C agonist, significantly inhibited MDSC expansion compared to vehicle (Veh), TLR9B, TLR4 and TLR7 agonists on day 2 (p<0.01; n=11). Similar results were obtained with murine BM derived MDSCs (p<0.001; n=5). SD101 significantly reduced the human M/G MDSC ratio as compared to Veh, TLR4, TLR7 and TLR9B agonists (p<0.05; n=11). In addition, SD101 shifted DC towards a myeloid program compared to Veh, TLR4 and TLR7 agonists (p<0.05; n=6). Nanostring gene expression analysis revealed that SD101 induced higher adaptive immunity, innate immunity, immunometabolism scores compared with Veh and TLR9B agonist (p<0.05; n=3). There was greater induction of TLR, Th1, NF κ B and lymphocyte activation signatures in SD101 as compared to Veh and TLR9B agonist (p<0.05; n=3). SD101 induced more PD-L1, IFN γ and IP10 gene expression compared to Veh and TLR9B (p<0.05; n=6), in addition to B and NK cell expansion compared to Veh (p<0.05; n=6).

Conclusions SD101 inhibited MDSC expansion and enhanced polarization towards M1 macrophages. The favorable impact on MDSC, in addition to broad immune activating effects, suggests that TLR9C agonists, if delivered effectively, have the potential to enable better performance of other immunotherapy agents within hostile liver TMEs.

<http://dx.doi.org/10.1136/jitc-2022-SITC2022.1165>

1166

PROFILING THE EFFECTS OF TARGETED TLR9 STIMULATION WITHIN SPONTANEOUSLY ARISING BREAST TUMORS

Caitlyn Miller*, Idit Sagiv-Barfi, Patrick Neuhofer, Debra Czerwinski, Carolyn Bertozzi, Jennifer Cochran, Ronald Levy. *Stanford University, Mountain View, CA, USA*

Background Tumor-localized delivery of immune-stimulants, such as Toll-like receptor (TLR) agonists, is a promising strategy to treat various cancer types, including immunologically “cold” tumors that lack T cell infiltration. Immunostimulants can elicit anti-tumor immunity by promoting immune activation in the tumor microenvironment (TME), thereby counteracting tumor immunosuppression and driving adaptive responses against tumor antigens available at the tumor site. However, the majority of preclinical studies investigating these therapies are performed in implanted murine tumor models, which do not fully recapitulate the TMEs of naturally-arising tumors. In this work, we performed comprehensive immune profiling studies to understand how tumor-localized TLR9 stimulation remodels the TME of spontaneously-arising tumors during an effective anti-tumor immune response.

Methods Serving as an immunologically “cold” spontaneous cancer model, we utilized female MMTV-PyMT transgenic mice, which spontaneously develop multiple breast tumors throughout their lives. To enable immunostimulant delivery to every tumor site, we employed a systemically-administered tumor-targeting immunostimulant (PIP-CpG), which is comprised of a tumor-targeting peptide (PIP) conjugated to an immune-stimulating TLR9 agonist (CpG).¹ This fully synthetic PIP-CpG conjugate is cross-reactive between mouse and human receptors and enables targeting to most types of solid tumors. To investigate how PIP-CpG therapy modulates the TME, we evaluated cytokine/chemokine profiles in the tumors via Luminesx analysis (48-plex) and performed spectral flow cytometry (24-color) to characterize various tumor-infiltrating immune populations and their activation status.

Results We demonstrate tumor-localized TLR9 stimulation via PIP-CpG therapy elicited a systemic anti-tumor immune response that effectively inhibited tumor growth and prolonged survival in an aggressive autochthonous breast cancer model. Immune profiling studies revealed that systemic PIP-CpG treatment dramatically amplified chemokine and cytokine production in the TME and promoted recruitment and expansion of many innate and adaptive immune cells. In addition to transforming the cellular landscape of the TME, PIP-CpG therapy also elicited diverse immune phenotypes that indicate changes in immune activation, cellular maturation, antigen presentation capacity, and inhibitory checkpoint expression. These immune-modulating effects ultimately enabled a T cell-mediated immune response against shared tumor antigens, which promoted regression of existing tumors and also delayed growth of independent newly-arising tumors.

Conclusions Intravenous delivery of a tumor-targeted TLR9 agonist transforms the immune microenvironment of spontaneously-arising malignancies to enable effective T cell-mediated immunity.

REFERENCE

1. Miller CL, Sagiv-Barfi I, Neuhofer P, *et al.* Systemic delivery of a targeted synthetic immunostimulant transforms the immune landscape for effective tumor regression. *Cell Chem Biol* 2022;**29**:451–462.e8. doi:10.1016/j.chembiol.2021.10.012

Ethics Approval All mouse experiments were performed in accordance with protocols approved by the Stanford Administrative Panel on Laboratory Animal Care.

<http://dx.doi.org/10.1136/jitc-2022-SITC2022.1166>

1167

APR003, AN ORAL LIVER- AND GI-TARGETED TLR7 AGONIST, ELICITS A ROBUST TYPE I INTERFERON RESPONSE IN ADVANCED COLORECTAL CANCER PATIENTS

¹Andrew Miller*, ²Trinh Le, ³Jaymes Holland, ³Ron Weitzman, ¹Tom Wu. ¹*Apros Therapeutics, San Diego, CA, USA*; ²*Collaborative Clinical Research Consult., Carlsbad, CA, USA*; ³*Weitzman Consulting Group, Los Altos Hills, CA, USA*

Background The potential of toll-like receptor (TLR) agonists to induce anti-tumor immunity has been limited by toxicities associated with systemic administration. Recently, intratumoral TLR agonists (CMP-001, SD-101) have shown promising responses in melanoma as single agents and in combination with checkpoint blockade. Building on the concept of localized innate activation to induce systemic anti-tumor immunity and increased safety window, APR003 is a small molecule TLR7 agonist designed to concentrate in the GI/liver upon oral administration for treatment of metastatic GI malignancies. Studies in mice and monkeys demonstrated robust Type-1 Interferon pathway activation with good tolerability compared to benchmark TLR7 agonists. APR003 is also efficacious in several models of liver and colon cancer, both as single agent and in combination with anti-PDL1.¹ APR003 is currently being evaluated in an ongoing Phase 1 dose escalation trial (NCT04645797) in relapsed/refractory colorectal cancer (CRC) patients with hepatic metastasis.

Methods APR003 was administered to patients orally once weekly either at 25 mg or 50 mg in 21-day cycles. Peripheral blood was collected at various time points post-dose on Cycle 1/Day 1 (C1D1), Cycle 1/Day 15 (C1D15), and Cycle 2/Day 1 (C2D1). Plasma was analyzed for pharmacokinetics. Plasma cytokines, including IFN α , IP-10, IL-6, and TNF α , were quantified by SIMOA[®] technology.

Results Between the 25 mg (n=6) and 50 mg (n=4) dose cohorts, APR003 plasma levels were low, with no dose-dependent increase in exposure. APR003 induced a transient yet robust cytokine response peaking around 6-8 hours post-dose and declining by 24 hours. After a week of recovery, all cytokines returned to baseline before the subsequent weekly dose. Cytokine induction in plasma also revealed no dose-dependency. The dose cohort combined geometric mean maximum fold induction over pre-dose of IFN α , IP-10, IL-6, and TNF α were 41-, 21-, 5-, and 2-fold on C1D1 and 107-, 28-, 6-, and 3-fold on C1D15, respectively. Comparing the cytokine levels at 6 hours on the plasma sampling days indicated slightly diminished response on C2D1 compared to C1D1; no APR003 plasma exposure accumulation or reduction was observed on C2D1.

Conclusions In an ongoing Phase 1 dose escalation trial, oral administration of APR003 elicited a strong type I interferon response (IFN α and IP-10) over the pro-inflammatory response (IL-6 and TNF α) at well tolerated doses. The results suggest our tissue-targeted oral TLR7 agonist may have an increased safety window compared to prior (non-targeted) agents of the same class, thereby achieving Proof-of-Drug Design and warrants further investigation.

Trial Registration This study is registered on Clinicaltrials.gov: NCT04645797

REFERENCE

1. Miller AT, Rodrigo E, Corpuz M, Plouffe D, Wu T Y-H. Gastrointestinal/liver-targeted TLR7 agonist for treatment of colorectal and liver cancers. AACR 2020 poster 684.

Ethics Approval The studies described were approved by the Institutional Review Boards of the respective clinical sites.

Consent Each patient provided consent to participate in this clinical trial.

<http://dx.doi.org/10.1136/jitc-2022-SITC2022.1167>

1168 **A NOVEL IMMUNOSTIMULATORY TLR7/8 AGONIST IS CURATIVE AS A MONOTHERAPY IN LEWIS LUNG CARCINOMA AND SYNERGIZES WITH ANTI-PD-1 IN B16F10 AND MC38 TUMOR MODELS**

Shannon Miller*, Caleb Beyer, Danielle Talbot, Konner Jackson, Margaret Whitacre, Janine Ward, Roman Schoener, Helene Bazin, David Burkhart. *Inimmune Corp, Missoula, MT, USA*

Background Over the past 130 years, the field of immunotherapy has progressed to the use of cytokines and of immune checkpoint inhibitors, namely anti-PD-1 and anti-CTLA4. Despite these advances, response rates remain stubbornly low. New immunotherapies that stimulate the immune system in different ways and can synergize with and expand the population of patients who respond to existing immunotherapies are urgently needed. Inimmune has developed and evaluated a novel TLR7/8 agonist as an immunotherapy for cancer.

Methods To test the activity of our novel TLR7/8 agonist, fresh human peripheral blood mononuclear cells (hPBMCs) were collected from healthy adult donors and stimulated with TLR7/8 agonist for 24 hours. Supernatants were then analyzed for cytokine production by ELISA. For pre-clinical murine studies to determine the efficacy of our novel TLR7/8 agonist as a cancer immunotherapy, LLC, B16F10, or MC38 tumor cells were implanted in the flank of C57BL/6 mice. Our novel TLR7/8 agonist was injected IV, SC, IP, or IT on days 5 and 12 post-implantation. For experiments where anti-PD-1 was used, anti-PD-1 was administered via IP injection on days 3, 6, and 9 post-implantation. To investigate changes in immune cell populations in the TME post-treatment, B16F10 tumors were treated with TLR7/8 agonist on days 5 and 12 post-implantation, or anti-PD-1 on days 3, 6, and 9 post-implantation, or both, and were harvested on day 12 post-implantation. Untreated tumors were harvested on day 12 post-implantation as controls. Tumors were disaggregated to single cell suspensions, stained with phenotyping antibodies, and analyzed by flow cytometry.

Results The lead formulation of our novel TLR7/8 agonist was able to eliminate Lewis Lung Carcinoma (LLC) flank tumors in 80% of mice after just two treatments. Further, as a monotherapy, our novel TLR7/8 agonist slowed growth of MC38 and B16F10 flank tumors and synergized with anti-PD-1 therapy, leading to a 100% rejection rate in MC38 flank tumors and a 75-100% rejection rate in B16F10 tumors when both treatments were used in combination depending on the route of administration and dose schedule. Mechanistically, the combination of our TLR7/8 agonist plus anti-PD-1 lead to increases in monocytes, B cells, and CD8 T cell populations in the TME of B16F10 flank tumors when compared to treatment with TLR7/8 agonist or anti-PD-1 alone.

Conclusions As we advance our novel synthetic TLR7/8 agonist to Phase I clinical trials, these data suggest potential efficacy as a monotherapy or in combination with checkpoint inhibitors in patients with solid tumors.

<http://dx.doi.org/10.1136/jitc-2022-SITC2022.1168>

1169

SYSTEMIC ADMINISTRATION OF TLR7/8 AGONIST MICELLES TRIGGERS A POTENT ANTI-TUMOR RESPONSE MEDIATED BY NEUTROPHILS AS PRIMARY EFFECTOR CELLS FOLLOWED BY ESTABLISHMENT OF AN IMMUNE MEMORY RESPONSE

¹Simon Jensen*, ²Esben Christensen, ¹Morten Just Petersen, ²Anders Hansen, ²Martin Bak, ²Camilla Stavnsbjerg, ¹Svetlana Panina, ²Thomas Andersen. ¹MonTa Biosciences, Lyngby, Denmark; ²Danish Technical University, Lyngby, Denmark

Background Clinical use of TLR7/8 agonists is currently restricted to topical application of Imiquimod for treatment of superficial basal cell carcinoma since systemic administration is a challenge due to dose-limiting toxicity. Here, we present data to overcome this challenge using a novel micelle-based drug delivery technology containing a lipid-anchored TLR7/8 agonist for intravenous administration. The MBS8 formulation shows good efficacy in mouse cancer models, is well tolerated in rodents and non-human primates and is currently being tested in clinical studies (NCT04855435).

Methods MBS8 was tested in 12 syngeneic mouse cancer models as monotherapy or in combination anti-PD-1 and anti-PD-L1 antibodies. MBS8 was administered IV as slow bolus on up to 5 occasions with different time schedules. Tumors and spleens were analysed using histology, immunohistochemistry, ELISPOT and flow cytometry. Phenotyping of tumor immune microenvironment was done using flow cytometry and Nanostring analyses. Safety and tolerability were tested in mice, rats and cynomolgus monkeys.

Results In several syngeneic mouse tumor models, MBS8 led to complete eradication of established tumors. The complete responders showed tumor rejection upon re-challenge. In these mice, a CD8⁺-dependent tumor-specific immune memory response was evident. Tumors demonstrated a massive tissue necrosis (>80%) within 24-48h after the first drug administration and showed massive neutrophil infiltration 6h after dosing. Antigen specific CD8⁺ T-cells were detected in tumors 24 hours after treatment with increased CD8⁺:T_{reg} cell ratio and enhanced antigen presentation in tdLN.

MBS8 showed both additive and synergistic effect when combined with anti-PD-1 or anti-PD-L1 antibody treatment. Moreover, in tumors being resistant to anti-PD-1 treatment, co-administration of MBS8 reverted sensitivity to anti-PD-1 treatment in a synergistic manner.

Conclusions MBS8 showed significant anti-cancer activity in multiple *in vivo* solid tumor models when administered either as monotherapy or in combination with ICIs.

MBS8 demonstrated a novel mode of action with neutrophils playing a central role as primary effector cells causing a rapid killing of tumor cells. Further, an adaptive immune response was initiated including generation of tumor antigen-specific CD8⁺ cells and establishment of immune memory response.

MBS8 was well tolerated in rodents and cynomolgus monkeys at dose levels above therapeutic effective doses identified in mice, thus providing a good therapeutic window.

<http://dx.doi.org/10.1136/jitc-2022-SITC2022.1169>

1170 **EGFR-TA:RNA: MULTIMODAL MECHANISM OF ACTION POTENTIATES IMMUNE CHECKPOINT INHIBITOR ACTIVITY**

¹Babette Schade, ¹Derrick Broka, ¹Caroline De Feyter, ²Shoshana Klein, ²Alexei Shir, ²Alexander Levitzki, ¹Davor Bajic, ¹Lucia D'Amico, ¹David Colecchia, ¹Eric Kitas, ¹Anita Jarzebinska, ¹Esteban Pombo-Villar, ¹Maya Zigler*. ¹TargImmune Therapeutics AG, Basel, Switzerland; ²The Hebrew University of Jerusalem, Jerusalem, Israel

Background The discovery and development of immune checkpoint inhibitors (ICIs) revolutionized cancer treatment and cancer immunotherapy. However, the majority of patients with metastatic disease do not achieve durable response following treatment with ICIs, highlighting the unmet need for effective cancer therapeutics. TargImmune's novel platform technology, Ta:RNAs, consists of targeted nanoparticle drugs, in which polyinosinic polycytidylic acid (pIC), a Pattern Recognition Receptor (PRR) agonist, is formulated with a non-viral vector. The non-viral vector comprises linear polyethyleneimine (LPEI) and polyethylene glycol (PEG), linked to the tumor-targeting moiety EGF. Unlike other PRR inducers under development, which are delivered intratumorally or intramuscularly, the Ta:RNA polyplex is designed for systemic administration: the nanoparticles are targeted to tumors that overexpress EGFR, and the pIC enters the cancer cells by receptor-mediated internalization. Furthermore, while other PRR agonists act as adjuvants, the Ta:RNA polyplex has strong cytotoxic and immunomodulatory effects, displaying a multimodal mode of action that harnesses the body's antiviral defenses to fight cancer.

Methods The anti-tumor efficacy and complex mode of action of EGFR-targeted Ta:RNA polyplex (EGFR-Ta:RNA) were extensively studied *in vitro* and *in vivo*. *In vitro*, EGFR-Ta:RNA potency and specificity was established by comparing the responses of high-EGFR-expressing cancer cells versus low-EGFR-expressing control cells using a cytotoxicity assay. The effects of EGFR-Ta:RNA alone or in combination with Nivolumab on human PBMC activation were also measured. *In vivo* efficacy was studied in an aggressive syngeneic experimental lung metastasis mouse model overexpressing human EGFR, in which EGFR-Ta:RNA alone was compared to the combination of EGFR-Ta:RNA with anti-PD-1 antibody treatment.

Results

Our EGFR-TA RNA nanoparticles induced cytotoxicity and proinflammatory cytokine (RANTES/CCL5, IP-10) secretion selectively in EGFR-overexpressing cancer cells, *in vitro*. Supernatant from EGFR-overexpressing cancer cells treated with EGFR-Ta:RNA enhanced the activation of human PBMCs, and this was further potentiated by combination treatment with anti-PD-1 antibody Nivolumab, demonstrated by increased INF γ secretion. Systemic administration of EGFR-Ta:RNA in the experimental lung metastasis mouse model led to potent anti-tumor activity, while anti-PD-1 antibody as a single therapy did not have any effect on mouse survival. In contrast, the combination of EGFR-Ta:RNA with an anti-PD-1 antibody exerted a profound effect and further increased the survival of the mice in comparison to EGFR-Ta:RNA alone.

Conclusions

EGFR-Ta RNA nanoparticles provide a multimodal anti-tumor approach by inducing targeted tumor cytotoxicity and anti-tumor immunity. This approach has been shown to potentiate anti-PD-1 antibodies in an experimental lung metastasis mouse model.

Ethics Approval This study was approved by the Hebrew University of Jerusalem Institutional Animal Care and Use Committee, approval number: NS-20-16089-5

<http://dx.doi.org/10.1136/jitc-2022-SITC2022.1170>

1171

CAN1012: A SELECTIVE AND POTENT TLR7 AGONIST WITH STRONG ANTITUMORAL PROPERTIES MEDIATED BY LOCALIZED INNATE IMMUNE ACTIVATION

¹Henry Yu, ²Hong-Ming Hu*, ¹Rongliang Lou, ¹Wanping Geng, ¹Sanlong Wang, ³William Redmond, ³Yoshinobu Koguchi, ¹Baotian Qin, ⁴John Mao, ⁵Shaoshan Wang. ¹Canwell Pharma Inc, Newton, MA, USA; ²UbiVac, Portland, OR, USA; ³Providence Cancer Institute, Portland, OR, USA; ⁴JWM Pharma, San Francisco, CA, USA; ⁵CanWell Pharma In, Newton, MA, USA

Background Toll-like receptors (TLRs) are commonly expressed on innate immune cells such as macrophages and dendritic cells (DC), and they play crucial roles in 1) mediating the first-line innate immune response against a wide variety of pathogens and 2) promoting adaptive immunity involving T and B cells. The TLR family consists of 10 subtypes (TLR1-TLR10) in humans and 12 (TLR1-TLR9, TLR11-TLR13) in mice. CAN1012 was developed as a selective TLR7 agonist uniquely designed for intratumoral (IT) administration.

Methods CAN1012 was evaluated by *in vitro* cell-based assays and *in vivo* animal models. Its DMPK, safety and toxicology properties were also studied.

Results Based on the receptor screening study, CAN1012 has been proved to have a significant stimulatory effect (NF- κ B activation) via human and mouse TLR7. In addition, CAN1012 stimulated significant IFN- α release from human PBMC at low concentrations (nM), whereas TNF- α secretion required a relatively high concentration.

Most importantly, CAN1012 induced a robust production of IFN- α exclusively by plasmacytoid DCs in human PBMC. When given intratumorally, CAN1012 exposure in tumor tissues was over 1,000-fold higher than in blood, resulting in much less systemic toxicity. The antitumoral effects of IT-administered CAN1012 monotherapy or combined with other therapeutical agents were investigated in mouse SCC7, CT26, and MC38 syngeneic tumor models. The results showed that CAN1012 possessed significant anti-tumor growth effects in a dose-dependent and schedule-dependent manner, and antitumoral effects could be augmented when combined with other agents. Pharmacodynamic studies revealed that IT administration of CAN1012 increased CD4⁺ and CD8⁺ T cell infiltration but decreased the number of myeloid-derived suppressor cells (MDSCs) and tumor-associated macrophages (TAMs) in the tumor microenvironment (TME). CAN1012 has a favorable ADME/PK profile when administered subcutaneously in mice, rats and monkeys, and its pharmaceutical properties have also been optimized for IT administration.

Conclusions In conclusion, CAN1012 is a potent, safe, and selective TLR7 agonist and could be a best-in-class agent for cancer immunotherapy. A first-in-human Phase I clinical study in advanced cancer patients is ongoing in the US (NCT04987112).

Trial Registration NCT04987112

Ethics Approval Anjaml studies had been approved by the ethics review committee at the institution at which the studies were conducted

<http://dx.doi.org/10.1136/jitc-2022-SITC2022.1171>

1172

A UNIQUE DENDRITIC CELL ACTIVATION STATES UTILIZES INFLAMMASOMES TO STIMULATE ANTI-TUMOR IMMUNITY IN MICE

Dania Zhivaki*, Kelsy Finn, Emily Gosselin, Holly Concepcion, Dania Zhivaki, Andrew Cornforth, Caitlin Sullivan. *Corner Therapeutics, Watertown, MA, USA*

Background Dendritic cells (DCs) represent the primary drivers of new T cell responses that defend against cancer and infection. In order to execute this task, DCs must be stimulated in a manner that induces several T cell stimulatory activities. These activities include the ability of DCs to 1) present tumor or microbial antigens, 2) express T cell co-stimulatory molecules, 3) express cytokines that induce effector T cell differentiation, 4) migrate in high numbers to lymph nodes and 5) produce the memory T cell inducing cytokine IL-1 β . Diverse approaches have been undertaken to stimulate these DC activities in a clinical or pre-clinical setting, with common strategies targeting Toll-like Receptors, STING or inflammasomes. These approaches are based on the general concept—permeating the literature for over 30 years—that infection-like signals are sufficient to stimulate DC-mediated instruction of adaptive immunity. However, the therapeutic success of these strategies remains elusive.

Methods Herein, we demonstrate that the aforementioned approaches are unable to elicit all 5 of the aforementioned activities in murine DCs. This observation may explain the ineffectiveness of these approaches in generating protective immunity to cancer. We report a distinct means of stimulating DCs, using molecular signals that mimic infection and tissue injury, that elicit all DC activities needed to stimulate adaptive immunity. We devised proprietary chemical mimics of infection and tissue injury that induce a new DC activation state termed hyperactive.

Results Primary murine DCs that have been stimulated with hyperactivators far exceed the capacity of other DCs to migrate to skin draining lymph node and stimulate antigen specific T cell activities in mice. When combined with a tumor-derived antigen source, we find that DC hyperactivators induce T cell responses that prevent the growth of tumors that are otherwise resistant to checkpoint inhibitor therapies.

Conclusions These studies reveal a unique DC activation state, and chemical agonists that elicit this state, as key determinants of T cell mediated anti-tumor immunity. DC hyperactivating chemicals represent a means to expand the opportunities in immunotherapy, and may enable durable T cell immunity to be elicited in a clinical setting.

<http://dx.doi.org/10.1136/jitc-2022-SITC2022.1172>

1173

ST101, A PEPTIDE ANTAGONIST OF NOVEL I/O TARGET CEBP β , REPROGRAMS MDSC POLARIZATION AND DECREASES TUMOR-ASSOCIATED TREGS, SUGGESTING AN IMMUNE COMPONENT TO OBSERVED CLINICAL RESPONSES

¹Claudio Scuoppo, ²Gerald Falchook, ²Elisa Fontana, ²Anja Williams, ³Nehal Lakhani, ⁴Jeff Evans, ⁵Fabio Iwamoto, ²Meredith McKean, ⁶Stefan Symeonides, ⁴Alistair McLaren, ²Jason Henry, ¹Gina Capioux, ⁷Robert Michel, ⁷Stephen Kaesshaefer, ¹Alice Bexon, ¹Jim Rotolo*. ¹Sapience Therapeutics, Harrison, NY, USA; ²Sarah Cannon Research Institute, Denver, CO, USA; ³START Midwest, Grand Rapids, MI, USA; ⁴University of Glasgow, Glasgow, UK; ⁵Columbia University, New York, NY, USA; ⁶University of Edinburgh, Edinburgh, UK; ⁷Bexon Clinical Consulting, LLC, Montclair, NJ, USA

Background CCAAT/Enhancer Binding Protein β (C/EBP β) is a basic leucine zipper (bZIP) transcription factor that causes aberrant gene activation in many cancers. Upregulated or over-activated C/EBP β drives oncogenesis by promoting tumor survival and proliferation¹ and is a critical regulator of the immunosuppressive environment.² Specifically, C/EBP β regulates macrophage differentiation, promoting the expression of M2 myeloid-derived suppressor cells (MDSCs) that contribute to suppression of antitumor immunity and correlate with poor prognosis.³ Reprogramming tumor-associated macrophages (TAMs) from M2 to M1 phenotype represents a potential strategy to enhance antitumor immunity. ST101 is a novel peptide antagonist that prevents C/EBP β dimerization and inhibits C/EBP β -dependent gene expression. Confirmed responses in melanoma and other tumors prompted evaluation of ST101 impact on macrophage differentiation.

Methods Primary human macrophages were cultured from peripheral blood mononuclear cells (hPBMCs) and activated toward the M1 or M2 phenotype by LPS and IFN γ (M1) or IL-4 (M2), respectively, in the presence of ST101. Macrophage M1 (CD80, CD86) and M2 (CD163, CD206) expression were analyzed by flow cytometry and rtPCR. Paired biopsy tissue from the ST101 Phase 1-2 clinical study in patients with advanced unresectable and metastatic solid tumors were collected during screening (prior to ST101 exposure) and within 24 hrs of ST101 administration during cycle 2 of therapy. Nanostring gene expression analysis was performed to determine differential gene expression and the impact of ST101 on the tumor microenvironment.

Results Treatment with pharmacologically relevant concentrations of ST101 (2.5, 5 or 10 μ M) resulted in dose-dependent reduction in M2+ macrophage and corresponding induction of M1+ macrophage. At the highest ST101 concentration, a 12-fold reduction in the M2 to M1 ratio was observed without substantial impact on cell viability. Paired patient biopsy tissue from the ST101 Phase 1-2 clinical study indicates a decrease in C/EBP β target gene IL-6 signaling, an important driver of the M2 macrophage phenotype. Decreased IL-6 signaling resulted in an increase in the tumor-infiltrating macrophage vs. tumor-infiltrating lymphocyte (TIL) ratio, and a decrease in the regulatory T cell (Treg) vs. TIL ratio in tumor samples of treated patients.

Conclusions Overall, these results validate the potential of ST101 in reprogramming M2 macrophages to M1, support a novel, macrophage-driven mechanism of action for ST101 as an anticancer agent and support future exploration of ST101 in immune-oncology therapeutic strategies.

Trial Registration ClinicalTrials.gov Identifier: NCT04478279

REFERENCES

1. Homma J, Yamanaka R, Yajima N, Tsuchiya N, Genkai N, Sano M, Tanaka R. Increased expression of CCAAT/enhancer binding protein β correlates with prognosis in glioma patients. *Oncology Reports* 2005;**15**:595–601.
2. Ruffell D, Mourkioti F, Gambardella A, Kirstetter P, Lopez RG, Rosenthal N, Nerlov C. A CREB-C/EBP β cascade induces M2 macrophage-specific gene expression and promotes muscle injury repair. *PNAS* 2009;**106**:17475–17480.
3. Marigo I, Bosio E, Solito S, Mesa C, Fernandez A, Dolcetti L, Ugel S, Sonda N, Biccato S, Falisi E, Calabrese F, Basso G, Zanovello P, Cozzi E, Mandruzzato S, Bronte V. Tumor-induced tolerance and immune suppression depend on the C/EBP β transcription factor. *Immunity*. 2010;**32**:790–802.

Ethics Approval ST101 study sites all have obtained ethics approval prior to study start. All participants gave consent prior to starting the study. Advarra's IRB Organization (IORG) Number is 0000635; Columbia University Medical Center Institutional Review Board FWA# 00002636; North East – Newcastle & North Tyneside 1 Research Ethics Committee DUKE UNIVERSITY HEALTH SYSTEM Institutional Review Board for Clinical Investigations.

<http://dx.doi.org/10.1136/jitc-2022-SITC2022.1173>

1174

MULTI-EPILOPE DNA VACCINE TARGETING CANCER NEOANTIGENS ENHANCES EFFICACY OF ANTI-PD1 THERAPY

¹Pratik Bhojnagarwala*, ²Alfredo Perales-Puchalt, ¹Ebony Gary, ²Niranjan Sardesai, ¹David Weiner. ¹Wistar Institute, Philadelphia, PA, USA; ²Geneos Therapeutics, Philadelphia, PA, USA

Background Immune checkpoint inhibition (ICI) has revolutionized cancer therapy and significantly improved survival of patients across several cancer types. However, ICI is only effective in some patients and most patients don't respond to ICI.^{1, 2} Neoantigens are tumor specific antigens derived from either point mutations or gene/RNA fusions in cancer cells, and can be recognized by the host immune system as foreign antigens. Several studies have shown that the success of ICI is linked to the number of neoantigens in the patient's tumor^[3]^[4]. Here, we demonstrate that DNA immunogens designed to target 40 neoantigens derived from MC38 mouse model of colon cancer synergizes with anti-PD1 antibody and improves the efficacy of anti-PD1 therapy.

Methods We performed whole exome sequencing on MC38 tumors to identify neoantigens. Through the sequencing data, we identified 40 neoantigens based on predicted affinity to class I MHC binding. All 40 neoantigens were encoded into a single plasmid vector, we designed each neoantigen separated by a furin cleavage site. Immune responses were measured in C57/Bl6 mice via IFN- γ ELISPOT assay and flow cytometry. Finally, we tested immunization with MC38vax to impact tumors *in vivo* and whether co-treatment with anti-PD1 antibody treatment further impacted tumor control.

Results In ELISPOT data, we observed that 11/40 neoantigens generated immune responses in mice. We also studied immune response to WT peptides and observed that the immune response was specifically induced against mutated peptides. Using flow cytometry, we observed that the vaccine induced predominantly CD8+ T cell responses, although CD4+ T cell responses were also observed. In a therapeutic tumor challenge, both anti-PD1 antibody and MC38vax as single treatment partially controlled the growth of MC38 tumors. However, co-treatment with both therapies was synergistic, demonstrating a 100% tumor control rate and improved animal survival.

Conclusions Large collections of neoantigens in a DNA immunization platform drive CD8+ T cell immunity against a diverse set of tumor antigens resulting in significant impact on tumor growth and improving survival. In combination with anti-PD1 these vaccines allow for tumor clearance and 100% survival from challenge, significantly improving the outcome of anti-PD1 therapy alone. These studies establish the importance and feasibility of improving patient specific T cell immunity, providing new tools for improving immunotherapy of, in this case colon adenocarcinoma, that is worth considering in other cold tumors that respond poorly to ICI.

Acknowledgements This work is supported in part by a grant from Geneos Therapeutics

REFERENCES

1. Robert C, Ribas A, Wolchok JD, Hodi FS, Hamid O, *et al.* Anti-programmed-death-receptor-1 treatment with pembrolizumab in ipilimumab-refractory advanced melanoma: a randomised dose-comparison cohort of a phase 1 trial. *Lancet* 2014;**384**(9948):1109–17
2. Robert C, Schachter J, Long GV, Arance A, Grob JJ, *et al.* Pembrolizumab versus ipilimumab in advanced melanoma. *N Engl J Med.* 2015;**372**(26):2521–32

3. Goodman AM, Kato S, Bazhenova L, Patel SP, Frampton GM, *et al.* Tumor mutational burden as an independent predictor of response to immunotherapy in diverse cancers. *Mol. Cancer Ther* 2017;**16**(11):2598–608
4. Cristescu R, Mogg R, Ayers M, Albright A, Murphy E, *et al.* Pan-tumor genomic biomarkers for PD-1 checkpoint blockade-based immunotherapy. *Science.* 2018;**362**(6411):eaar3593

<http://dx.doi.org/10.1136/jitc-2022-SITC2022.1174>

Abstracts

1175

MEMORY T CELLS ELICITED BY MICROORGANISMS CROSS-REACT WITH TUMOR-ASSOCIATED ANTIGENS

Luigi Buonaguro, Maria Tagliamonte*, Beatrice Cavalluzzo. *National Cancer Institute "Pascale", Naples, Italy*

Background Individuals are exposed to intracellular pathogens (i.e. viruses and intracellular bacteria) and intestinal microbiota, collectively microorganisms (MOs), which enter the body during the host's lifetime. Altogether, MOs are a natural source of non-self antigens (MoAs) expressed by host's cells in the context of the HLA class I molecules, inducing a wide pool of specific memory CD8⁺ T cell clones. Such MoAs may share sequence and structural homology with cellular self-antigens (molecular mimicry), possibly inducing autoimmune reactions leading to autoimmune diseases (ADs). We have recently shown that a molecular mimicry may be found also to self-antigens presented by cancer cells (i.e. tumor-associated antigens, TAAs). Consequently, memory CD8⁺ T cell clones specific for the MoAs may turn out to be a natural "anti-cancer vaccination" if a nascent tumor lesion should express TAAs similar or identical to MoAs.

Methods In the present study we looked for homology between published TAAs and non-self MoAs. Blast search for sequence homology was combined with extensive bioinformatics analyses. Ex vivo immunological validations have been performed by screening with DNA barcode labeled pMHCs strategy and confirmation by tetramer and dextramer staining procedure.

Results Several TAAs and MoAs show sequence and structural similarities as well as comparable patterns of contact with HLA and TCR α and β chains (figure 1 and 2). The predicted average affinity to HLA molecules of MoAs is very high (<100nM). The structural conformation of MoAs is, in general, highly similar to the corresponding TAA. In some cases, it is identical and contact areas with both HLA and TCR chains are indistinguishable. Moreover, the spatial conformation of TCR-facing residues can be identical in paired TAA and microbiota-derived epitopes, with exactly the same values of planar as well as dihedral angles. Importantly, CD8⁺ lymphocytes are able to cross-react against paired TAAs and MoAs supporting the concept that the same T cell can recognise similar peptides.^{1,2}

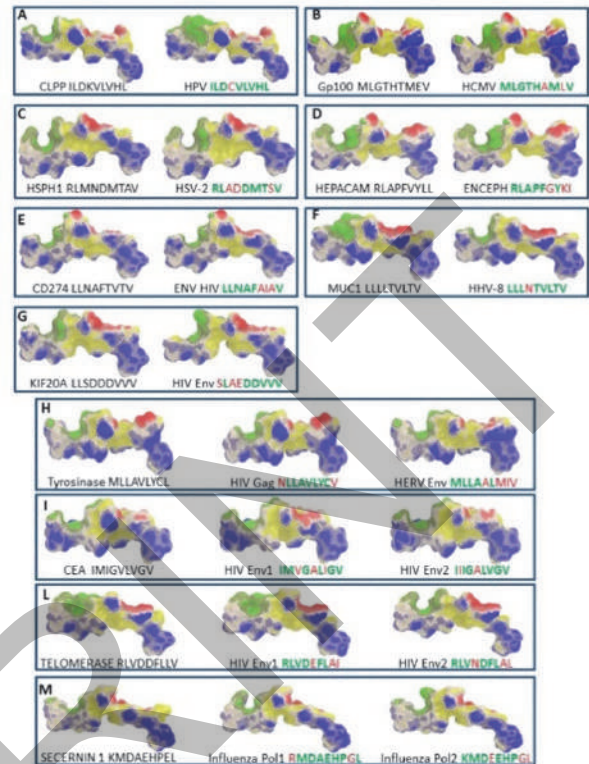
Conclusions Here we report for the first time 1) the molecular mimicry between TAAs and MoAs; and 2) cross-reacting CD8⁺ T cell responses. Therefore, the T cell memory elicited by MoAs may turn out to be an anti-cancer T cell memory, able to control the growth of cancer developed during the lifetime if the expressed TAA is similar to MoAs. This may ultimately represent a relevant selective advantage for cancer patients and lead to novel preventive

REFERENCES

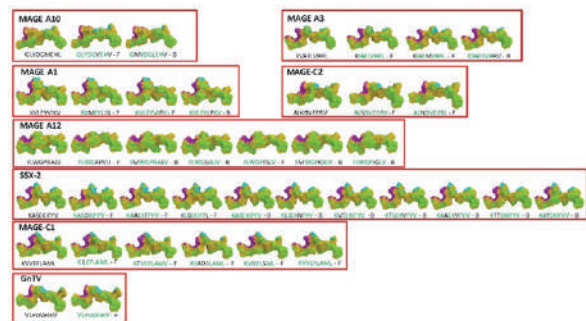
1. Ragone C, et al. Identification and validation of viral antigens sharing sequence and structural homology with tumor-associated antigens (TAAs). *J Immunother Cancer* 2021;**9**(5):e002694. doi:10.1136/jitc-2021-002694. PMID: 34049932; PMCID: PMC8166618.
2. Ragone C, Manolio C, et al. Molecular mimicry between tumor-associated antigens and microbiota-derived epitopes. *J Transl Med* 2022;**20**(1):316. doi:10.1186/s12967-022-03512-6. PMID: 35836198; PMCID: PMC9281086.

Ethics Approval The study obtained ethics approval by the ethics committee of the National Cancer Institute "Pascale" (Registry Nr. 8 of Oct.2, 2013 and following addendum). All Participants gave informed consent before taking part.

Fig. 2



Abstract 1175 Figure 1 Homology between viral antigens and TAAs



Abstract 1175 Figure 2 Homology between microbiota antigens and TAAs

<http://dx.doi.org/10.1136/jitc-2022-SITC2022.1175>

1176 **OPTIMIZING IMMUNIZATION SCHEDULES FOR THERAPEUTIC VACCINATION**

Yushe Dang*, Denise Cecil, Lauren Corulli, Erin Rodmaker, Mary Disis. *University of Washington, Seattle, WA, USA*

Background Most cancer vaccines will not generate high levels of T-cell immunity with only one immunization. Even vaccines against foreign antigens, such as COVID, may require three or four immunizations spaced some months apart to achieve protective levels of immunity in cancer patients. The use of cancer vaccines in the therapeutic setting, as single agents or as part of a combination regimen to treat established cancers, would require high levels of T-cells to be generated quickly. We evaluated immunization schedules with a 5-antigen, multi-epitope plasmid DNA vaccine, STEMVAC, targeting cancer stem cell associated proteins. The vaccine is immunogenic in patients with advanced breast cancer (NCT02157051) and the majority of patients can develop high levels of STEMVAC specific type I T-cells after 3 priming and 2 booster immunizations. Using a murine model, we questioned whether we could more rapidly achieve high levels of antigen specific Type I T-cells with STEMVAC immunization.

Methods Six-week-old FVB mice were used for experiments. A dose of 300ug of STEMVAC plasmid with 5ug of rm-GM-CSF as an adjuvant was given in 4 immunizations using three different schedules; (1) every 3-4 days, (2) once a week, and (3) every 2 weeks (standard). Immunogenicity was evaluated two weeks after the last vaccine using IFN-gamma ELISPOT quantitating responses to each of the 5 antigens in the vaccine. Parameters studied included magnitude, incidence, and breadth of the T-cell response. Ten mice were included/group with empty plasmid and PBS as controls.

Results All three immunization schedules could generate a significant IFN-gamma response to at least one of the antigens encoded in STEMVAC as compared to controls. Vaccines given every two weeks elicited the greatest magnitude immune response among the three schedules (vs. 3-4 days, $p=0.001$; vs. 1 week, $p=0.01$). Of note, although the total magnitude of immune response elicited was lower, the weekly immunization schedule resulted in a significantly greater number of mice responding to vaccination as well as a greater breadth of response with all mice responding to at least 2 antigens and 50% to 3-5 antigens.

Conclusions Varying the time between immunizations can significantly impact the quality of the T-cell response to a multi-antigen plasmid-based vaccine. Further studies are ongoing to correlate these differences to anti-tumor activity.

<http://dx.doi.org/10.1136/jitc-2022-SITC2022.1176>

1177

IDENTIFICATION OF AND VACCINATION WITH ANTIGEN SPECIFIC TH1 SELECTIVE EPITOPES IN BLADDER CANCER: A STEP TOWARDS A MULTI-ANTIGEN VACCINE FOR BLADDER CANCER PREVENTION

¹Yushe Dang*, ¹Lauren Corulli, ¹Erin Rodmaker, ¹Denise Cecil, ¹Yi Yang, ¹Carissa Walsh, ¹Will Gwin, Jonathan Wright, ¹Jennifer Childs, ²Shizuko Sei, ¹Mary Disis, ¹Yushe Dang. ¹University of Washington, Seattle, WA, USA; ²National Cancer Institute, Bethesda, MD, USA

Background Bladder cancer is a frequently diagnosed malignancy. Half of patients responding to standard therapy develop recurrence within 5 years. Vaccination for secondary prevention of bladder cancer could reduce recurrence. We developed an epitope identification approach for vaccine construction from non-mutated tumor associated proteins combining in silico prediction of Class II epitopes with functional screening to edit out sequences inducing regulatory responses. The method allows the identification of Th1 selective epitopes which elicit an antigen specific IFN-gamma response without IL-10 secretion. We aimed to identify bladder cancer antigens and determine Class II binding peptides for use in a multi-antigen Th1 selective vaccine.

Methods Seven datasets (GEO); 38 normal bladder, 229 NMIBC and 86 muscle invasive non-metastatic bladder cancers were studied. Genes with at least 2-fold upregulation in cancer compared to normal with a corrected p-value < 0.1 and found in >50% of cancer samples were identified (n=159). We prioritized those upregulated in >75% of cancers (n=15). Nine genes encoded proteins with known overexpression in human bladder cancer; CDC20, TOP2A, CCNB2, MAPK13, CDK1, AURKA, CEP55, PRC1, and MELK. We evaluated expression by IHC in OH-BBN induced mouse bladder tumors. Eight proteins were expressed in tumors and the murine MB49 bladder cancer cell line. Using a multi-algorithm approach, we selected 24 putative class II epitopes, associated with high binding affinity across multiple MHC class II alleles, derived from these proteins. All epitopes had >88% homology between species.

Results We screened PBMC (12 donors/9 bladder cancer patients) by IFN-g/IL-10 ELISPOT. Th1 selective epitopes were identified for 5 antigens, CDC20, TOPO2A, CCNB2, CDK1, and CEP55. We evaluated immunogenicity of single-antigen vaccines in C57BL6 mice to identify any epitopes inducing selective Th1 immunity. Five peptides generated significant antigen-specific Th1 with no evidence of Th2. To evaluate anti-tumor activity, single-antigen vaccines were given four times, two weeks apart, with CFA/IFA. Two weeks after vaccination, mice were implanted with MB49. All vaccines could significantly inhibit tumor growth as compared to PBS control; CDC20 (p=0.0001), TOPO2A (p<0.0001), CCNB2 (p<0.0001), CDK1 (p<0.0001), and CEP55 (p<0.0001). We admixed epitopes into a single vaccine, BLADVAC, immunizing mice to discern epitope competition. Significantly elevated levels of antigen-specific IFN-g secreting T-cells were detected for all epitopes except CDK1 (p<0.001 compared to HIV control).

Conclusions We identified bladder cancer antigens covering the majority of tumors with clinically effective Th1 selective vaccines constructed. Prevention trials in the OH-BBN model are ongoing.

<http://dx.doi.org/10.1136/jitc-2022-SITC2022.1177>

1178 DELIVERY OF DNA ORIGAMI CANCER VACCINE USING ALGINATE MICROPARTICLES

Amani Djouadi*, Niksa Roki, Carlos Castro. *The Ohio State University, Powell, OH, USA*

Background Deploying the immune system to seek out and destroy cancer cells is a rapidly developing strategy for cancer treatment and prevention. This is accomplished via vaccination against tumor antigens to elicit an antigen-specific anti-cancer immune response. DNA origami nanodevices (DO) have shown enhanced antigen and adjuvant delivery to antigen-presenting cells (APCs) and stimulation of antigen-specific CD8⁺ T cells. This enhancement is due to DO's unique properties, including size, shape, modular nature, and programable payload capacity.¹ Despite these features, free DO-based vaccine (DO-VAC) faces a harsh physiological environment within the lymphatic system and the periphery that compromises its integrity and longevity once injected subcutaneously. Previous work demonstrated that alginate-mediated release of vaccines is advantageous to traditional vaccines due to prolonged release of antigen, payload protection, and promoting adequate delivery of payload to lymph nodes.² Therefore, it is believed that DO-VAC delivery can be further enhanced by encapsulation in alginate microparticles. . Encapsulation could address the rapid clearance of DO-VAC, produce a strong persistent immune response, and remove the need for booster shots in clinical settings.

Methods We have constructed a rod-shaped DO (92 x 12 x 15nm) using M13 scaffold DNA devoid of endotoxin with standard DO construction methods. To construct the DO-VAC, DO was hybridized to 65 CpG adjuvant molecules and K10-OVA peptides. Alginate particles were manufactured using 2% endotoxin-free alginate and cross-linked in 2% calcium chloride solution using a syringe pump and pressurized nitrogen gas to create microparticles (10 uM – 100 uM). Alginate encapsulated DO was incubated for 28 days at 37°C in PBS in sink conditions and at 4°C in storage conditions. TEM image samples were prepared with standard methods. Agarose gel electrophoresis was used to characterize DO.

Results Agarose gel and TEM imaging demonstrate that DO retains structural stability once released from alginate particles. Based on release studies, alginate encapsulated DO exhibits sustained release properties in release conditions and stability in storage conditions.

Conclusions The sustained release property of encapsulated DO and stability of released DO indicate encapsulation in alginate microparticles is a promising strategy for future vaccine delivery. This delivery platform could be used to promote vaccine payload stability and protection while promoting a robust tumor-specific immune response.

REFERENCES

1. Liu S, Jiang Q, Zhao X, *et al.* A DNA nanodevice-based vaccine for cancer immunotherapy. *Nat Mater.* 2021;**20**(3):42–430. doi:10.1038/s41563-020-0793-6
2. Sarei F, Dounighi NM, Zolfagharian H, Khaki P, Bidhendi SM. Alginate nanoparticles as a promising adjuvant and vaccine delivery system. *Indian J Pharm Sci* 2013 Jul;**75**(4):442–9. doi: 10.4103/0250-474X.119829.

<http://dx.doi.org/10.1136/jitc-2022-SITC2022.1178>

1179 **EFFICACY STUDY OF STC-1010 ANTITUMOR VACCINE ASSOCIATED WITH STANDARD CHEMOTHERAPIES ON MC 38 SYNGENEIC COLON CANCER TUMOR MODEL**

¹Corinne Tortorelli, ²Celine Gongora*, ³Doriane Mathe, ¹Benoit Pinteur, ¹Lionel Chalus, ¹Paul Bravetti, ⁴Nicolas Gadot, ⁴Sylvie Lantuejoul, ⁵Charles Dumontet, ⁶François Ghiringhelli. ¹Brenus Pharma, Issoire, France; ²Brain and Spine Institute (ICM), Paris, France; ³Antinéo, Lyon, France; ⁴Centre de Lutte Contre le Cancer Lyon, Lyon, France; ⁵Inserm, Lyon, France; ⁶Centre Georges François Leclerc Dijon, Dijon, France

Background Metastatic colorectal cancer(mCRC) is a major cause of death. Unmet medical need in immunotherapy is high for MSS patients and still present for MSI-H/dMMR patients. STC-1010 (Brenus Pharma) therapeutic vaccine is developed by tumor cells stimulation to induce overexpression of tumor associated antigens and neoantigens to mimic mCRC resistant cancer cells. The aim is to educate the immune system to target patient's tumor cells harboring the same resistance factors. We report efficacy results of three (3 CL-S) cell lines S=stimulated by irradiation and heat shock versus three cell lines (6 CL-S) physically and chemically stimulated (irradiation, heat shock and chemotherapies), both haptenized (H) and administrated with immunostimulant (IS=cyclophosphamide and mGM-CSF) associated w/o to standard chemotherapy FOLFOX or FOLFIRI.

Methods Female C57BL6 mice were subcutaneously grafted with 1.10^6 MC38 tumor cells. 7 groups (15 mice/group) were allocated to: Control, FOLFOX, FOLFIRI (intra-peritoneal injection to D5, D8 and D11 post-tumour injection), 3 CL-SH, 6 CL-SH, 6 CL-SH + FOLFOX and 6 CL-SH + FOLFIRI groups. Subcutaneous vaccine injections (3CL-SH or 6 CL-SH) were associated to IS once a week for 3 weeks. Overall survival (OS) and tumor growth (TG) were recorded until 1600 mm³ or tumor necrosis. We conducted automated immunohistochemical analysis (HALO IndicaLabs software) on 5 tumor groups (n=35) to evaluate the correlation between response and immune population (number of cells/mm²) including: CD3, CD4, CD8, FOXP3 T cells and M1/M2 macrophages.

Results At Day16, all groups treated by 6CL-SH had a significant reduction of the mean tumor volume compared to the control group (p=0,0011), as well as for 6CL-SH+ FOLFIRI versus FOLFIRI alone (p=0,0024).

The necrotic tumors in the 3CL-SH, 6CL-SH and 6CL-SH +FOLFIRI groups are denser (weight/volume) than the control group. Tumors treated by 6CL-SH+FOLFIRI were also denser than the FOLFIRI ones (p=0,0052).

Grafted mice treated by FOLFOX alone had dramatic weight loss and some had to be sacrificed.

HALO analysis showed that adding 6CL-SH to FOLFOX increase CD8 infiltration in comparison with FOLFOX alone (> 200 cells/mm³) and a recruitment of immune cells within the tumor. Among treated groups, M1/M2 ratio >7 was main criteria correlated with a long survival.

Conclusions This third preclinical study confirms efficacy and safety of Brenus STC vaccine stimulated and haptenized alone or with standard chemotherapies associated to immunostimulant. This significant anticancer effect in mice could be explained by mobilization of CD3, CD8, CD4 T cells within the tumors and oriented M1 macrophage immune responses.

<http://dx.doi.org/10.1136/jitc-2022-SITC2022.1179>

1180 **LISTERIA-BASED IMMUNOTHERAPY SCULPTS CD8⁺ T CELL RESPONSE IN THE TUMOR MICROENVIRONMENT TO CONTROL RENAL CELL CARCINOMA**

Mariam Oladejo*, Laurence Wood. *Texas Tech University Health Sciences Center, Abilene, TX, USA*

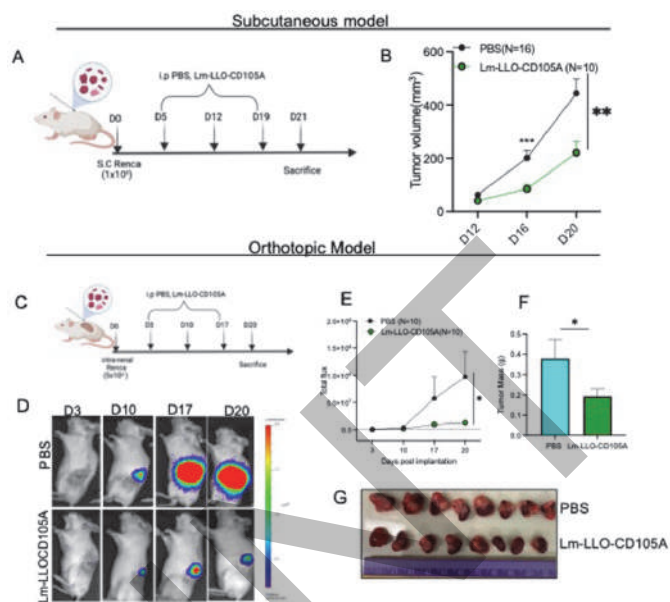
Background Agents that modulate the tumor microenvironment (TME) to promote anti-tumor effects are desirable for the therapy of solid tumors. Recombinant Listeria-monocytogenes vaccine consisting of the fusion protein of truncated Listeriolysin O and tumor-associated antigen (TAA) is an established strategy to improve antigen-specific T cell response for cancer immunotherapy. CD105 is a co-receptor for the TGF-beta signaling cascade. Due to its elevated expression in many cancer types, including renal cell carcinoma (RCC), CD105 is characterized as a TAA of therapeutic potential. Here we evaluated the efficacy and immunomodulatory effects of a Listeria-based vaccine encoding CD105 (Lm-LLO-CD105A) for the therapy of renal cell carcinoma (RCC) in a murine model.

Methods Murine RCC cell line (Renca) cells were implanted subcutaneously or orthotopically into male Balb/c mice. Subsequently, mice were vaccinated with PBS, Lm-LLO-CD105A, or Control Lm weekly for three weeks, and tumor progression was routinely monitored. Splenocytes and subcutaneous and orthotopic tumor tissues were immunophenotyped by flow cytometry. Lymphocyte depletion experiments were carried out in subcutaneous and orthotopic models to evaluate the immune subset responsible for the anti-tumoral effect of the recombinant Listeria-based vaccine.

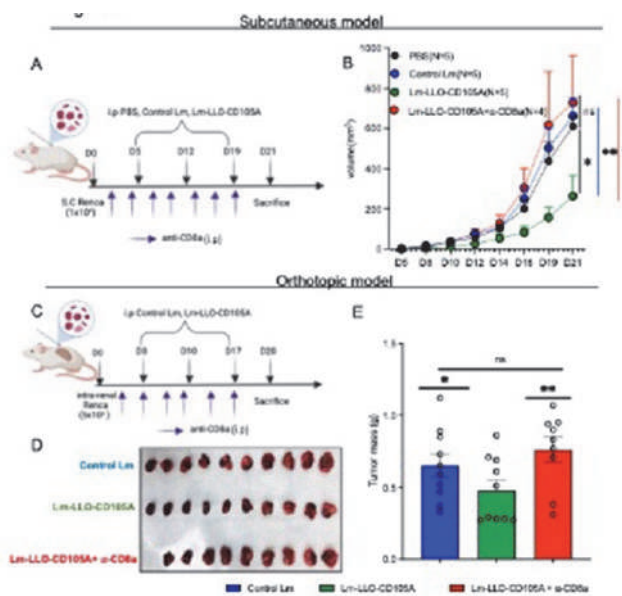
Results In both models, vaccination with Lm-LLO-CD105A led to significant control of tumor growth compared to placebo and Control Lm (figure 1). This antigen-specific vaccine promoted tumor control by significantly improving the infiltration of effector CD8⁺ T and CD4⁺T cells into the TME. The CD8⁺ T cells are polyfunctional and characterized by profound production of inflammatory cytokines, including IFN-g, IL-2, and TNF-a, but the functionality of the CD4⁺ T cells was not as robust. Similarly, the systemic cytotoxic response demarcated by IFN-g⁺IL-2⁺ TNF-a⁺ producing splenic CD8⁺ T cells was highly potent upon Lm-LLO-CD105A vaccination. Further, in both subcutaneous and orthotopic models, the TME was polarized from an immunosuppressive phenotype to an inflamed phenotype characterized by a reduction in the CD4⁺ Foxp3⁺Treg population and a reduced population of MDSCs (CD11b⁺Gr1⁺) in the kidney TME. Not surprisingly, the antitumor effect was completely abrogated when Lm-LLO-CD105A was utilized in the presence of a CD8⁺ T cell-depleting antibody (figure 2)

Conclusions Lm-LLO-CD105A effectively controlled subcutaneous and orthotopic kidney tumors. This efficacy depended on the profound infiltration of cytokine-producing CD8⁺ T cells and the reduction of suppressive immune subsets in the TME. Altogether our data suggest that tumor targeting with a Listeria-based approach is an effective strategy to modulate the TME for effective control of renal cell carcinoma.

Ethics Approval All studies involving animals were carried out in accordance with ethical standards of the Texas Tech University Health Sciences Center under the IACUC protocol number 17018



Abstract 1180 Figure 1 Lm-LLO-CD105 controls RCC tumor growth (A) vaccination schedule for subcutaneous tumor challenge (B) longitudinal tumor growth curve of subcutaneous tumor challenge (C) vaccination schedule for orthotopic tumor challenge (D) representative bioluminescence imaging of kidney tumor burden (E) graphical representation of longitudinal luciferase flux (F) tumor mass of diseased kidney (G) image of final kidney tumor burden. Number of animals are depicted in the plots. Data were analysed using unpaired t-test. *P < 0.05, **P < 0.01, ***P < 0.001. All error bars are shown as mean ± SEM.



Abstract 1180 Figure 2 CD8⁺ T cells are responsible for the therapeutic efficacy (A) experimental schedule for subcutaneous CD8⁺ depletion studies (B) longitudinal tumor growth curve (C) experimental schedule for orthotopic CD8⁺ depletion studies (D) Representative image of diseased

Abstracts

kidney (E) final kidney mass. Number of mice for A-B is depicted in the plots. Number of animals for (C-E) Control Lm=10, Lm-LLO-CD105A=10, Lm-LLO-CD105A+ α -CD8a=9 Data were analyzed using unpaired t-test for subcutaneous model (B) and Mann Whitney U test for orthotopic model (E). *P < 0.05, **P < 0.01, ***P < 0.001. All error bars are shown as mean \pm SEM.

<http://dx.doi.org/10.1136/jitc-2022-SITC2022.1180>

PREPRINT

1181

THERAPEUTIC VACCINES CONSISTING OF CANCER GERMLINE ANTIGEN-BASED SYNTHETIC LONG PEPTIDES ARE IMMUNOGENIC IN HUMAN HEPATOCELLULAR CARCINOMA PATIENTS

¹Yannick Rakké*, ²Marij Schoenmaekers-Welters, ¹Lisanne Noordam, ²Sanne Boekestijn, ¹Luc Magre, ¹Robbie Luijten, ¹Rachelle van Gemerden, ¹Monique de Beijer, ¹Michael Doukas, ¹Jeroen Demmers, ³Anna-Sophia Wiekmeijer, ³Willem-Jan Krebber, ³Cornelis Melief, ¹Jan Ilzermans, ¹Jaap Kwekkeboom, ²Sjoerd van der Burg, ¹Sonja Buschow, ¹Dave Sprengers. ¹Erasmus MC University Medical Center, Rotterdam, Netherlands; ²Leiden University Medical Center, Leiden, Netherlands; ³ISA Pharmaceuticals B.V., Oegstgeest, Netherlands

Background In melanoma, cancer germline antigen (CGA)-directed vaccination has shown to induce objective clinical responses accompanied by strong anti-tumor immune responses.¹ As CGAs are immunogenic and highly expressed by hepatocellular carcinoma (HCC) tumor cells, these have demonstrated to be attractive targets to be implemented in therapeutic anti-liver cancer vaccination as well.² Synthetic long peptide (SLP) vaccination has proven to elicit efficient anti-tumor CD4⁺ and CD8⁺ T cell responses and to have promising clinical effects.³ We aimed to develop an SLP vaccine targeting HCC-restricted CGA-epitopes covering at least five different HLA super types that are highly prevalent globally.

Methods We applied an integrative pre-clinical approach of *in silico* epitope prediction, immunopeptidomics, and *in vitro* tools to select GSAs and validate CGA-SLPs in HCC patient-derived tumor infiltrating lymphocytes (TILs) and peripheral blood mononuclear cells (PBMCs).

Results Out of a set of 13 CGAs, previously shown to be expressed in primary human HCC tissues, two CGAs (i.e., CGA-A and -B) demonstrated no healthy tissue expression and covered >75% of HCC patients collectively (N = 55). Immunopeptidome analysis of human HCC-derived hepatocytes (N = 12), together with *in silico* CGA-related epitope predictions according to epitope immunogenicity, enabled identification of 196 and 220 potential epitopes for CGA-A and -B, respectively. HLA-A*02:01 binding of these epitopes was validated *in vitro* using a HLA-A2 stabilization assay and ranked accordingly. Six SLPs were designed incorporating 54 HLA-A*02:01, 25 HLA-A*01:01, 24 HLA-A*03:01, 27 HLA-A*24:01, and 15 HLA-B*07:02 predicted and/or validated CGA-A- and -B-related epitopes. Top three-ranked epitopes were selected to validate *ex vivo* intra-tumor immune reactivity using corresponding peptide-HLA-A*02:01 dextramers in human HCC-derived TILs. Tumors of 8/11 patients contained CGA-A- and CGA-B-specific TILs that were characterized by a tumor reactive phenotype. Upon *in vitro* enrichment, SLP immunogenicity was demonstrated through Interferon gamma ELISPOT in 2/3 of human HCC-derived PBMCs using an *in vitro* co-culture system with autologous antigen presenting cells.

Conclusions Here, we describe the intelligent design of a set of immunogenic SLPs comprising CGA-related epitopes for the global population that can be further exploited for the development of an off-the shelf anti-cancer vaccine to treat HCC.

REFERENCES

1. An RNA vaccine drives immunity in checkpoint-inhibitor-treated melanoma. *Nature* 2020;**585**(7823):107–112.
2. Expression of cancer testis antigens in tumor-adjacent normal liver is associated with post-resection recurrence of hepatocellular carcinoma. *Cancers (Basel)* 2021;**13**(10):2499.
3. Vaccination against HPV-16 oncoproteins for vulvar intraepithelial neoplasia. *N Engl J Med.* 2009;**361**(19):1838.

Ethics Approval All study procedures were approved by the local ethics committee (Medische Ethische Toetsings Commissie Erasmus MC Rotterdam; NL58534,078.16). Patients had given informed consent for tissue and blood donation as well as usage of personal data.

Consent Patients had given informed consent for tissue and blood donation as well as usage of personal data.

<http://dx.doi.org/10.1136/jitc-2022-SITC2022.1181>

1182

MODULATING THE TUMOR MICROENVIRONMENT BY A TARGETING TGFB1 WITH VACCINE-INDUCED IMMUNE RESPONSES

Brian Weinert*, Tine Hannibal, Preeyam Patel, Evelina Martinenaite, Marion Chapellier, Marco Carretta, Alireza Alavi, Ayako Pedersen, Muhammad Al-Hajj. *IO Biotech, Copenhagen, Denmark*

Background Recent clinical results¹ provide a rationale for cancer immunotherapy based on activation of “anti-regulatory” T cells. Anti-regulatory T cells recognize antigens expressed by immunosuppressive cells and thereby target pro-inflammatory signals to the tumor microenvironment.² TGFB1 promotes immune suppression in diverse cancers. We hypothesize that activating T cells against TGFB1 may allow targeting of pro-inflammatory immune response to TGFB1-expressing tumors while avoiding the toxicities associated with TGFB1 pan-inhibition. TGFB1-specific T cells are frequently detected in humans.³ Vaccination with a TGFB1 peptide ameliorates fibrosis in a model of chronic colitis⁴ and enhances the anti-tumor activity of an HPV16 E7-specific vaccine⁵, indicating a therapeutic potential of a TGFB1 vaccine. Here we sought to enhance the specificity anti-TGFB1 immune responses and identify peptides with high TGFB1 selectivity (vs TGFB2/3), thereby mitigating potential off-target toxicities. To understand the TGFB1 landscape in human tumors we performed a multiplexed IHC analysis of TGFB1 expression on tumor cells and the multiplicity of cells in the tumor microenvironment.

Methods PBMCs were assayed by ELISPOT to measure responses to peptides from TGFB1, TGFB2, and TGFB3. TGFB1 expression was examined by multiplex immunofluorescence in a tissue microarray panel of tumor indications with hyperplexed visualization of markers on a single section. Vaccination is evaluated in mouse models expressing TGFB1. Tumor growth monitored, organs and tumor samples collected. Histopathological examination is performed on multiple tissues. Vaccine activity is determined and immune infiltrate analysis conducted by FACS and RNAseq.

Results Healthy human donors exhibited robust immune responses to TGFB1 peptides selected for improved TGFB1-specificity. Stimulation of PBMCs with TGFB1 peptides did not result in cross-reactivity to homologous TGFB2 or TGFB3 peptides. Analysis of TGFB1 expression showed widespread TGFB1 expression in cancers and provides a rationale for targeting TGFB1 in selected indications. Anti-TGFB1 T cell clones functional activity and TGFB1-specificity were confirmed. Therapeutic activity of TGFB1 vaccine in mouse models and in addition to the cellular and molecular analysis of the tumors in the various cohorts will be presented.

Conclusions A TGFB1 vaccine is an attractive new approach for cancer immune therapy. Optimal synthetic long peptides able to elicit robust and highly selective TGFB1-immune responses were developed. These peptides showed ability to change an immune suppressive TME to a pro-inflammatory state and drive efficacy in mouse models. These data support the preclinical development of an TGFB1 vaccine for the treatment of multiple solid tumors.

REFERENCES

1. Kjeldsen JW, Lorentzen CL, Martinenaite E, Ellebaek , Donia M, Holmstrom RB, Klausen TW, Madsen CO, Ahmed SM, Weis-Banke SE, Holmstrom MO, Hendel HW, Ehrnrooth E, Zocca MB, Pedersen AW, Andersen MH, Svane IM. A phase 1/2 trial of an immune-modulatory vaccine against IDO/PD-L1 in combination with nivolumab in metastatic melanoma. *Nat Med* 2021;**27**(12):2212–2223.
2. Andersen MH. The T-win(R) technology: immune-modulating vaccines. *Semin Immunopathol* 2019;**41**(1):87–95.

3. Holmstrom MO, Mortensen REJ, Pavlidis AM, Martinenaite E, Weis-Banke SE, Aaboe-Jorgensen M, Bendtsen SK, Met O, Pedersen AW, Donia M, Svane IM, Andersen MH. Cytotoxic T cells isolated from healthy donors and cancer patients kill TGFBeta-expressing cancer cells in a TGFBeta-dependent manner. *Cell Mol Immunol* 2021;**18**(2):415–426.
4. Ma Y, Q Guan, Bai A, Weiss CR, Hillman CL, Ma A, Zhou G, Qing G, Peng Z. Targeting TGF-beta1 by employing a vaccine ameliorates fibrosis in a mouse model of chronic colitis. *Inflamm Bowel Dis* 2010;**16**(6):1040–50.
5. Chu X, Li Y, Huang W, Feng X , Sun P, Yao Y, Yang X, Sun W, Bai H, Liu C, Ma Y. Combined immunization against TGF-beta1 enhances HPV16 E7-specific vaccine-elicited antitumor immunity in mice with grafted TC-1 tumours. *Artif Cells Nanomed Biotechnol* 2018;**46**(sup2):1199–1209.

<http://dx.doi.org/10.1136/jitc-2022-SITC2022.1182>

Immuno-Conjugates and Chimeric Molecules

1183 ASKG915 – AN ANTI-PD-1 ANTIBODY-IL-15 PRODRUG FUSION MOLECULE WITH ENHANCED THERAPEUTIC POTENTIALS

¹Kurt Shanebeck*, ¹Chunxiao Yu, ¹Shiguang Yu, ²Jieye Sun, ²Dongfang Wang, ¹Jeanine Luiz, ¹Ming Li, ¹Ray Chuang, ¹Jing Chen, ¹Samantha Luiz, ¹Lynwel Cunanan, ¹Stone Shi, ¹Matt Hsu, ²Yong Wen, ¹Jeff Lu, ¹Yuefeng Lu. ¹AskGene Pharma Inc., Camarillo, CA, USA; ²Aosaikang Biotherapeutics Co Ltd, Nanjing, China

Background AskGene has established a proprietary cytokine prodrug platform (Smartkine[®]) to achieve its overarching objective of modulating immune reactions at a disease site in a selective and controlled manner. Cytokines are potent molecules, yet their broad application as therapeutics has been hampered due to short PK, severe systemic toxicity, and narrow therapeutic window. To improve the therapeutic potential of cytokines, AskGene has developed several antibody-cytokine prodrug fusion molecules using its proprietary SmartKine[®] platform.

Methods The in vitro activities of ASKG915 were evaluated using reporter cell line and PBMC-based assays. Peripheral immune activation was evaluated in a GvHD model with human PBMC-engrafted NSG mice. Anti-tumor activities were tested in a human PBMC-engrafted tumor xenograft model and a syngeneic tumor model. The PK/PD properties and safety profiles of ASKG915 were assessed in non-human primates (NHPs) following three IV injections every two weeks.

Results ASKG915 showed minimal activity prior to protease-dependent activation and significantly enhanced activity after protease-dependent activation in vitro. Specifically, it has significantly higher activities stimulating PD-1⁺ immune cells, presumably through “cis activation”. In in vivo efficacy studies, it showed similar potency as a reference anti-PD-1-IL-15 fusion molecule (not masked) while having a better safety profile. In addition, in a GvHD study, ASKG915 at 10 mg/kg i.p. induced lower interferon gamma levels in the periphery at Day 4 compared to the reference molecule at 1 mg/kg i.p. These results showed that, compared to the reference molecule, ASKG915 had comparable immune stimulation in the tumor while having significantly reduced immune stimulation in the periphery. In NHPs, ASKG915 demonstrated prolonged and antibody-like PK profiles. More importantly ASKG915 was well tolerated at the highest dosage tested in NHP, with no cytokine release syndrome (CRS) and minimal immune reaction at injection sites.

Conclusions Activated ASKG915 showed selective stimulation for PD-1⁺ immune cells in in vitro assays with human PBMC. ASKG915 in vivo showed tumor-selective activation compared to a reference molecule. In addition, it had extended antibody-like PK in NHPs and was well tolerated at the highest dosage tested in the GLP PK/PD study. It also showed a significantly expanded therapeutic window. An IND filing is planned in the second half of 2022. To our knowledge, ASKG915 is the first anti-PD-1 antibody-IL-15 prodrug fusion molecule moving into clinical development.

Ethics Approval The use of the animals in the studies have been approved by the ethics committees of the research contract organizations (CRO).

<http://dx.doi.org/10.1136/jitc-2022-SITC2022.1183>

1184

SYN101, A FIRST IN CLASS, IMMUNE CELL TARGETED TGF-BETA INHIBITOR THERAPY, SELECTIVELY BLOCKS IMMUNE SUPPRESSION AND DRIVES TUMOR CLEARANCE IN VITRO AND IN VIVO

Dori Thomas-Karyat*, Robert Lutz, Douglas Burtrum. *Synthis Therapeutics, New York, NY, USA*

Background TGF- β is both a validated pro-tumorigenic pathway and a fundamental immunosuppressive cytokine that is overexpressed in virtually all solid tumors. In cancer patients, elevated TGF- β levels limit T cell activation and drive resistance to immune checkpoint inhibitors.¹ Preclinically, mice with a genetic blockade of TGF- β signaling only in T cells reject multiple tumors, including melanoma, lymphoma and colorectal cancers.² However, because TGF- β is also essential in maintaining host tissue homeostasis, systemic TGF- β therapies, such as the TGF- β receptor I/ALK5 inhibitors, cause significant host toxicity and have fallen far short in clinical efficacy.³ Novel, targeted TGF- β therapies are required to improve safety and increase patient response rates.

Methods To improve immune function, efficacy and safety relative to systemic TGF- β therapies, Synthis has developed a first in class, immune cell targeted TGF- β therapy, SYN101, for cancer patients. Utilizing proprietary antibody drug conjugate (ADC) components, SYN101 is comprised of an immune cell specific antibody linked to a potent ALK5 inhibitor payload to selectively block TGF- β signaling in immune cells.

Results As a monotherapy, SYN101 reversed TGF- β mediated immune suppression in primary human T cells and increased expression by 3-4 fold of critical T cell functions required for tumor clearance, such as Granzyme B in cytotoxic killer CD8 + T cells and IFN γ levels and fully restored T cell proliferation. In combination studies, SYN101 plus antiPD1 increased IFN γ expression by 4-fold, compared to only 2-fold with monotherapy treatment. In the EMT6 breast tumor model, SYN101 + antiPD1 combination led to >93% tumor regression in vivo, with 3/5 complete and 1/5 partial responders ($p=0.0003$, versus antiPD1 alone). Mice with complete responses to SYN101 combination therapy were resistant to subsequent tumor rechallenge, demonstrating immunological memory. In circulating immune cells, combination therapy significantly increased pharmacodynamic markers, CD69 and Ki67+ (CD4+ and CD8+ T cell activation and expansion, respectively), relative to antiPD1 alone ($p<0.05$), correlating with tumor clearance. Similar in vivo efficacy and PD markers were observed with colorectal tumor models, CT26 and MC38.

Conclusions Synthis is the only company developing a non-cytotoxic ADC therapeutic that inhibits TGF- β induced immune suppression and drives tumor clearance in vivo. Current studies will expand in vivo efficacy studies and demonstrating improved safety. Safer, more effective TGF- β therapies, like SYN101, will provide novel monotherapy options for cancer patients. Additionally, because TGF- β sets the overall threshold for T cell activation, SYN101 could improve the efficacy of a variety of therapies, including checkpoint inhibition, radiation and NK/CAR-T therapies.

REFERENCES

1. Derynk R, Turley S, Akhurst R. TGF β biology in cancer progression and immunotherapy. *Nat Rev Clin Oncol* 2021;**18**:9–34.
2. Gorelik L, Flavell R. Immune-mediated eradication of tumors through the blockade of transforming growth factor- β signaling in T cells. *Nat Med* 2001;**7**:1118–1122.

3. Ciardiello D, Elez E, Tabemero J, Seoane J. Clinical development of therapies targeting TGF β : current knowledge and future perspectives. *Annals Oncol* 2020;**31**:1336–1349.

<http://dx.doi.org/10.1136/jitc-2022-SITC2022.1184>

1185 OPTIMIZATION OF PURINE-BASED TLR7 AGONISTS AS PAYLOADS FOR IMMUNE-STIMULATING ANTIBODY CONJUGATES (ISACS)

¹Graham Garnett*, ¹Katina Mak, ¹Renee Duan, ¹Truman Hirakala-Schaefer, ¹Manuel Lasalle, ¹Nichole Escalante, ¹Joy Guedia, ²Kara Moyes, ¹Sam Lawn, ¹Raffaele Colombo, ¹Jamie Rich, ¹Stuart Barnscher. ¹Zymeworks, Vancouver, Canada; ²Nuvation, Vancouver, Canada

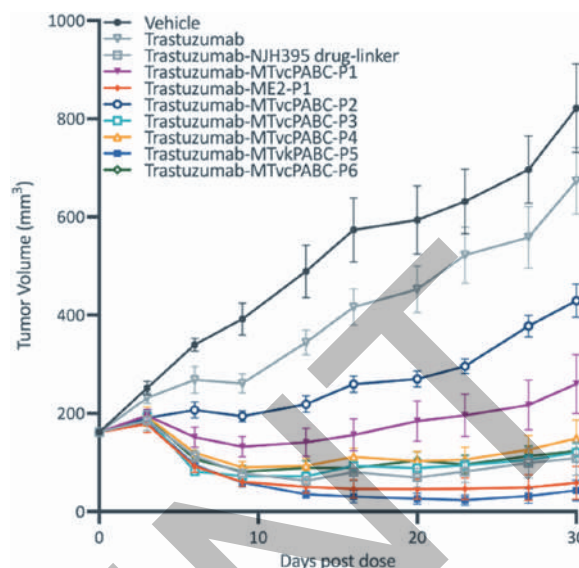
Background Immune-stimulating antibody conjugates (ISACs) consist of antibodies conjugated to immune stimulants and are designed to induce antitumor immune response. Despite promising preclinical results, ISAC clinical development has been hampered by systemic toxicities or lack of efficacy. Substituted purines have previously been identified as a privileged scaffold to elicit TLR7 activation. Here, we demonstrate newly designed purine-based TLR7 agonists conjugated to trastuzumab which show significant tumor volume reduction in a HER2-high gastric cancer xenograft model without associated body weight loss (BWL) in healthy mice.

Methods A library of TLR7 agonists was generated by varying substituents at C2- and N9-positions of a common 6-amino-8-hydroxy-purine scaffold, and the structure-activity relationship was studied *in vitro* using human and mouse TLR7 reporter gene assays (RGAs) as well as measuring cytokine secretion from human peripheral blood mononuclear cells (PBMCs) and mouse splenocytes. Lead TLR7 agonists were conjugated to trastuzumab, and the resulting ISACs were evaluated *in vitro* for their abilities to induce the production of interleukin-6 (IL-6) from human PBMCs or mouse splenocytes co-cultured with NCI-N87 tumor cells. Selected ISACs were tested for efficacy (single iv injection at 2.5 mg/kg) in mice bearing NCI-N87 tumors (figure 1) and for tolerability (single iv injection at 3, 15, and 45 mg/kg) in healthy mice (figure 2).

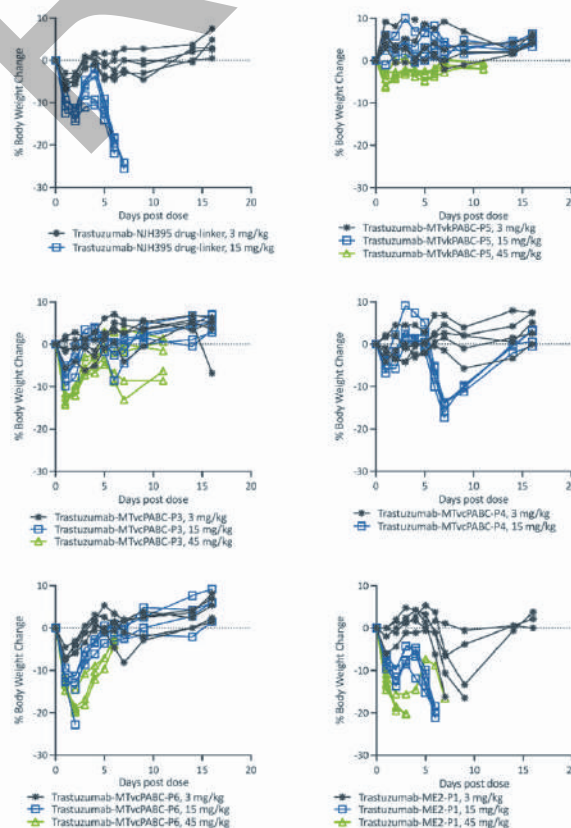
Results We prepared ~220 new TLR7 agonists with different substituents at C2- and N9-positions of the purine scaffold. Compounds with IC50 <100 nM in both human and mouse TLR7 RGAs were further screened for their abilities to induce production of cytokines in PBMCs and mouse splenocytes. Certain substituents were found to be highly immunostimulatory in both human and murine settings. Lead TLR7 agonists were conjugated to trastuzumab with a drug-to-antibody ratio of ~4 using cleavable or non-cleavable linkers. ISACs capable of inducing IL-6 production from PBMCs or splenocytes co-cultured with tumor cells were further tested in an NCI-N87 xenograft model in comparison to unconjugated trastuzumab and trastuzumab conjugated with the same linker-payload as NJH395, a clinical benchmark ISAC. Selected ISACs were tested for tolerability in healthy mice with a lead ISAC (Trastuzumab-MTvkPABC-P5) identified, capable of inducing tumor regression without causing BWL.

Conclusions We demonstrated the potential of using novel purine-based TLR7 agonists as payloads for ISACs. In contrast to other TLR7-agonist conjugates, our lead ISAC appears to have a sufficiently wide therapeutic window displaying efficacy in an NCI-N87 xenograft model at 2.5 mg/kg without causing BWL in healthy mice at 45 mg/kg.

Ethics Approval All animal studies were performed in accordance with Institutional Animal Care and Use Committee (IACUC)-approved protocols.



Abstract 1185 Figure 1 Antitumor activity of selected purine-based TLR7 agonist conjugated to trastuzumab (DAR = 4) in a NCI-N87 tumor cell-line derived xenograft model, following single intravenous administration of 2.5 mg/kg of the respective ISACs or control articles



Abstract 1185 Figure 2 Body weight change over time of healthy mice following single intravenous administration of 3, 15, or 45 mg/kg of the respective ISACs or control articles

<http://dx.doi.org/10.1136/jitc-2022-SITC2022.1185>

1186

SGN-B6A INDUCES IMMUNOGENIC CELL DEATH AS A SECONDARY MECHANISM OF ACTION

Robert Lyon*, Vivian Trang, John Gosink, Michelle Ulrich, Allana Ubben, Sean Allred, Li-Ya Huang, Kelly Hensley, Piper Treuting, Kerry Klussman, Shaylin Higgins, Patrick Younan, Roma Yumul, Natalya Nazarenko. *Seagen, Bothell, WA, USA*

Background SGN-B6A is a novel investigational antibody-drug conjugate (ADC) directed to integrin beta-6 and uses the clinically validated vedotin drug-linker platform that delivers the microtubule disrupting agent, monomethyl auristatin E (MMAE).¹ SGN-B6A is designed to bind and internalize the integrin beta-6/ADC complex from the surface of malignant cells and release the cytotoxic payload MMAE. We have previously demonstrated the antitumor activity of SGN-B6A in cell line-derived xenograft models originating from multiple carcinomas as well as patient-derived xenograft models of non-small cell lung cancer (NSCLC).² Other ADCs delivering the MMAE payload (including vedotin ADCs using the antibodies brentuximab, enfortumab, ladiratuzumab, and tisotumab) have been shown to induce immunogenic cell death (ICD) in preclinical models³⁻⁷ and have demonstrated promising clinical activity in combination with immunotherapy.⁸⁻¹⁰ Since the induction of ICD appeared to be a consequence of the activity of MMAE, and is independent of the antibody that delivers it, we hypothesized that this mechanism of action may also apply to SGN-B6A.

Methods In vitro and in vivo assessment of ICD was performed in cell lines derived from pancreatic carcinoma. Induction of ICD markers were assessed using plate-based assays, flow cytometry, and immunoblotting. ICD was also assessed in vivo using RNA sequencing and immunohistochemistry (IHC) on cell line-derived xenografts.

Results Consistent with this hypothesis we observed that tumor cells treated with SGN-B6A in vitro showed key hallmarks of immunogenic cell death, including markers of endoplasmic reticulum (ER) stress, exposure of calreticulin, and release of ATP and high mobility group protein B1 (HMGB1). Further, in vivo studies demonstrated that treatment with SGN-B6A led to immune activation and recruitment of immune cells to the tumor environment.

Conclusions Preclinical models suggest that, like other vedotin ADCs, SGN-B6A induces immunogenic cell death which then promotes activation and recruitment of immune cells to the tumor. These data provide a strong rationale for the combination of SGN-B6A with immunotherapies, which may further lead to enhanced antitumor activity and can be utilized as a potential treatment for integrin-beta-6-expressing tumors including NSCLC, head and neck squamous cell carcinoma, and esophageal carcinoma. Altogether, our preclinical results support the current evaluation of SGN-B6A in an ongoing phase 1 study (NCT04389632).

REFERENCES

1. Lyon RP, Schmitt MW, Jonas M, et al. SGN-B6A: A new MMAE ADC targeting integrin beta-6 in multiple carcinoma indications [abstract]. *Cancer Res* 2020;**80**(Suppl 16):Abstract 2906.
2. Lyon RP, Gosink JJ, Hale CS, et al. Activity of SGN-B6A in patient-derived xenograft models of non-small cell lung cancer [abstract]. *Cancer Res* 2021;**81**(Suppl 13): Abstract 914.
3. Cao AT, Law CL, Gardai SJ, et al. Auristatin-based Antibody Drug Conjugates Activate Multiple ER Stress Response Pathways Resulting in Immunogenic Cell Death and Amplified T-cell Responses [abstract]. *Cancer Res* 2016;**76**(Suppl 14): Abstract 4914.
4. Cao AT, Law CL, Gardai SJ, et al. Brentuximab vedotin-driven immunogenic cell death enhances antitumor immune responses, and is potentiated by PD1 Inhibition in vivo [abstract]. *Cancer Res.* 2017;**77**(Suppl 13):Abstract 5588.

5. Cao AT, Law CL, Gardai SJ, et al. Additional mechanisms of action of ladiratuzumab vedotin contribute to increased immune cell activation within the tumor [abstract]. *Cancer Res* 2018;**78**(Suppl 13):Abstract 2742.
6. Liu BA, Olson D, Snead K, et al. Enfortumab vedotin, an Anti-Nectin-4 ADC demonstrates bystander cell killing and immunogenic cell death anti-tumor activity mechanisms of action in urothelial cancers [abstract]. *Cancer Res* 2020;**90**(Suppl 16): Abstract 5581.
7. Gray E, Hensley K, Allred, S, et al. Tisotumab vedotin shows immunomodulatory activity through induction of immunogenic cell death [abstract]. *J Immunother Cancer* 2020;**8**(Suppl 3):Abstract 653.
8. Pusztai L, Lu H, Hale C, et al. Systemic administration of ladiratuzumab vedotin alone or in combination with pembrolizumab results in significant immune activation in the tumor microenvironment in metastatic breast cancer patients [abstract]. *J Immunother Cancer* 2020; **8**(Suppl 3): Abstract 349.
9. Rosenberg JE, Flaig TW, Friedlander TW, et al. Study EV-103: Preliminary durability results of enfortumab vedotin plus pembrolizumab for locally advanced or metastatic urothelial carcinoma [abstract]. *J Clin Onc* 2020;**38**(Suppl 6): 441.
10. Herrera, AF, Moskowitz, AJ, Bartlett NL, et al. Interim results of brentuximab vedotin in combination with nivolumab in patients with relapsed or refractory Hodgkin lymphoma. *Blood* 2018;**131**(11):1183-1194.

Ethics Approval All animal studies were conducted in accordance with protocols reviewed and approved by the Institutional Animal Care and Use Committee at Seagen or the external testing facility that conducted the studies.

<http://dx.doi.org/10.1136/jitc-2022-SITC2022.1186>

1187

ENFORTUMAB VEDOTIN INDUCES IMMUNOGENIC CELL DEATH, ELICITS ANTITUMOR IMMUNE MEMORY, AND SHOWS ENHANCED PRECLINICAL ACTIVITY IN COMBINATION WITH IMMUNE CHECKPOINT INHIBITORS

¹Devra Olson, ¹Patrick Younan, ¹Bernard Liu, ¹Gabriele Blahnik-Fagan, ¹John Gosink, ¹Katie Snead, ¹Elena Tenn, ¹Kelly Hensley, ¹Disha Sahetya, ¹Albina Nesterova, ¹Margo Zaval, ¹Anthony Cao, ¹Christine O'Day, ¹Ryan Heiser, ¹Timothy Lewis, ¹Shyra Gardai, ²Taisuke Nakazawa, ³Masashi Shimazaki, ¹Christopher Carosino, ¹Sharsti Sandall*. ¹Seagen, Inc., Bothell, WA, USA; ²Astellas Pharma Inc., Tsukuba, Ibaraki, Japan; ³Astellas Research Institute of America, Northbrook, IL, USA

Background Enfortumab vedotin (EV) is a first-in-class Nectin-4-directed antibody-drug conjugate (ADC) with demonstrated improved overall survival in patients with previously treated advanced-stage urothelial carcinoma.¹ EV is comprised of a fully human Nectin-4-directed monoclonal antibody conjugated to the microtubule-disrupting agent monomethyl auristatin E (MMAE) by a protease cleavable maleimidocaproyl-valine-citrulline linker. EV has a multifaceted mechanism of action. Previously, we demonstrated that EV induces antitumor activity in vitro via direct cytotoxicity on Nectin-4-expressing malignant cells and indirect bystander activity on neighboring Nectin-4 negative cells, both of which are mediated by MMAE release within target cells. Here, we expand upon the mechanism of action and show EV induces tumor cell killing in a manner leading to immunogenic cell death (ICD) and improves antitumor responses when combined with checkpoint inhibitors.

Methods The ability of EV to induce hallmarks of ICD was evaluated in vitro in Nectin-4-expressing human urothelial carcinoma cell lines. Immune activation associated with ICD was assessed in vitro in monocytes co-cultured with EV-treated tumor cells and in vivo by immunohistochemistry, RNA-seq, flow cytometry, and immune cytokine profiling. The effects of EV plus anti-PD-1 on tumor growth inhibition, the tumor microenvironment, and immune memory were evaluated in syngeneic mouse models engineered to express human Nectin-4. Antitumor immune memory was also assessed in mice vaccinated with EV-treated cells.

Results In vitro, EV induced ICD via MMAE-mediated microtubule disruption and concomitant endoplasmic reticulum (ER) stress, as evidenced by increased phosphorylation of JNK, extracellular release of inflammatory mediators ATP and HMGB1, and cell surface exposure of calreticulin. Xenograft tumors treated with EV demonstrated upregulation of MHC genes as well as genes involved in ER stress, autophagy, and type I interferon response. Additionally, there were noted increases in both macrophages and dendritic cells along with cytokines involved in chemoattraction and T-cell stimulation. Consistent with ICD induction, vaccination with EV-treated Nectin-4-expressing tumor cells promoted antitumor immunity and provided protection against tumor rechallenge. Lastly, the combination of EV with PD-1 inhibition improved antitumor activity and durable immunity in vivo, consistent with complementary modes of action of these two anticancer agents.

Conclusions These data provide insight into the clinical activity observed with EV and bolster the scientific rationale to combine EV with checkpoint inhibitors, which is currently an area of active clinical investigation across multiple studies.²⁻⁶

REFERENCES

1. Powles T, Rosenberg JE, Sonpavde GP, Loriot Y, Duran I, Lee JL, *et al.* Enfortumab Vedotin in Previously Treated Advanced Urothelial Carcinoma. *N Engl J Med.* 2021;**384**(12):1125–35. Epub 2021/02/13. doi:10.1056/NEJMoa2035807. PubMed PMID: 33577729; PubMed Central PMCID: PMCPCMC8450892.

- Friedlander TW, Milowsky MI, Bilen MA, Srinivas S, McKay RR, Flaig TW, *et al.* Study EV-103: Update on durability results and long term outcome of enfortumab vedotin + pembrolizumab in first line locally advanced or metastatic urothelial carcinoma (la/mUC). *Journal of Clinical Oncology* 2021;**39**(15_suppl):4528. doi: 10.1200/JCO.2021.39.15_suppl.4528.
- Galsky MD, Necchi A, Shore ND, Plimack ER, Jia C, Sbar E, *et al.* KEYNOTE-905/ EV-303: Perioperative pembrolizumab or pembrolizumab plus enfortumab vedotin (EV) and cystectomy compared to cystectomy alone in cisplatin-ineligible patients with muscle-invasive bladder cancer (MIBC). *J Clin Oncol.* 2021;**39**(6_suppl):TP5507. doi: 10.1200/JCO.2021.39.6_suppl.TP5507.
- Heijden MSVD, Gupta S, Galsky MD, Derleth CL, Lee S, Kataria RS, *et al.* Study EV-302: A two-arm, open-label, randomized controlled phase 3 study of enfortumab vedotin in combination with pembrolizumab versus chemotherapy in previously untreated advanced urothelial carcinoma (aUC) (trial in progress). *J Clin Oncol* 2022;**40**(6_suppl):TP5589. doi: 10.1200/JCO.2022.40.6_suppl.TP5589.
- Hoimes CJ, Bedke J, Loriot Y, Nishiyama H, Fang X, Kataria RS, *et al.* KEYNOTE-B15/EV-304: Randomized phase 3 study of perioperative enfortumab vedotin plus pembrolizumab versus chemotherapy in cisplatin-eligible patients with muscle-invasive bladder cancer (MIBC). *J Clin Oncol* 2021;**39**(15_suppl):TP54587. doi: 10.1200/JCO.2021.39.15_suppl.TP54587.
- ClinicalTrials.gov [Internet] Bethesda (MD): U.S. National Library of Medicine. 2000 – . ClinicalTrials.gov Identifier: NCT04960709. Treatment Combination of Durvalumab, Tremelimumab and Enfortumab Vedotin or Durvalumab and Enfortumab Vedotin in Patients With Muscle Invasive Bladder Cancer Ineligible to Cisplatin or Who Refuse Cisplatin (VOLGA). 2021 Jul 14 [cited 2022 Jul 22]. Available from: <https://clinicaltrials.gov/ct2/show/NCT04960709>.

Ethics Approval All animal studies were conducted in accordance with protocols reviewed and approved by the Institutional Animal Care and Use Committee at Seagen, Astellas, or the external testing facilities that conducted the studies.

<http://dx.doi.org/10.1136/jitc-2022-SITC2022.1187>

Abstracts

1188

ANTIBODY SUBSTRATE OLIGONUCLEOTIDE CONJUGATES (ASOCs): A NEW CLASS OF IMMUNOTHERAPEUTIC AGENTS TO INHIBIT METASTASIS OF TUMOR CELLS AND BLOCK CHECKPOINT INHIBITION

¹Beverly Packard*, ²Akira Komoriya. ¹OncoArrestin, LLC, Gaithersburg, MD, USA; ²Oncolmmunin, Inc., Gaithersburg, MD, USA

Background Armed monoclonal antibody (mAb)-based therapeutics, e.g., antibody-drug conjugates (ADCs) or antibody-oligonucleotide conjugates (AOCs), can be highly effective for patients with gene-amplified or protein-overexpressing tumors. However, many tumor cells do not overexpress surface antigens recognized by mAbs and, for these patients, armed mAb therapies are often poorly effective. Additionally, expression of checkpoint molecules on tumor infiltrating lymphocytes (TILs) can vary with disease progression. ASOCs are a new class of modified mAb that enable delivery of oligonucleotides into targeted cells without requiring overexpression of the antigen or internalization of the mAb (figure 1).

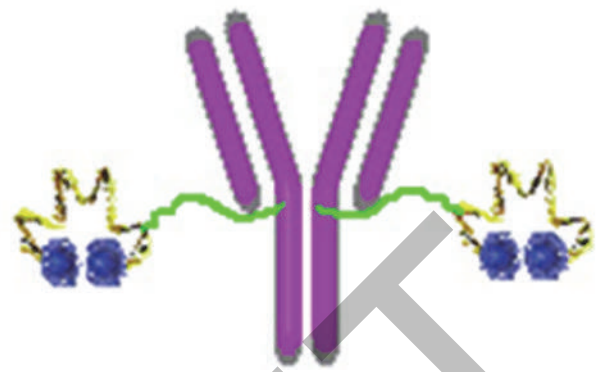
Methods We have covalently modified mAbs such that they are linked to protease substrates specific for proteases that enable metastasis; the latter are also covalently linked to oligonucleotides bearing H-type excitonic dimers. The substrates can be cleaved by proteolytic enzymes on a tumor cell surface essential for metastasis, e.g., matrix metalloproteases (MMPs). Cleavage of the protease substrates results in localization of oligonucleotides at a targeted cell surface. Oligonucleotides (both single strand DNA and double strand RNA) are then able to diffuse into the tumor cell or lymphocyte and inhibit translation of targeted mRNAs.

Results Oligonucleotides cleaved from ASOCs by cell surface proteases enter cells *via* the delivery mechanism we have previously used to block HIV proliferation in CD4⁺ T cells.¹ Thus, ASOCs differ from the current armed mAb-based therapies, e.g., antibody-drug conjugates (ADCs) or antibody-oligonucleotide conjugates (AOCs), in that delivery of the oligonucleotides into the cytoplasm does not require internalization of the mAb or endosomal processing; additionally, off-target toxicity will be reduced by release at the cell surface of the payload (the oligonucleotide). With this approach, using an MHC-Class I mAb (KE-2) or the antiCD20 mAb Rituxan we have delivered antisense oligonucleotides targeting β -Actin and *KRAS* into the following tumor cell lines: Raji (Burkitt's lymphoma), A549 (NSCLC), COLO205 (colon), MB-MDA231 (breast), and Caki (kidney). Additionally, anti-PD-1 and anti-PD-L1 mAbs can be derivatized to block checkpoint inhibition. Proof of delivery of oligonucleotides into cells was confirmed by confocal imaging after binding of mAbs to the cell surface with quantitation by flow cytometry.

Conclusions ASOCs represent a unique immunotherapeutic structural class that overcomes the previous requirements of: (1) internalization of the mAb and (2) delivery of the payload (oligonucleotides) through intracellular degradative organelles, e.g., lysosomes. Additionally, off-target toxicity is minimized.

REFERENCE

1. Packard, BZ, Wrightson, JA, Komoriya A. An oligonucleotide delivery platform to enable assessment of intracellular transcripts in live cells by flow cytometry. *Cytometry A* 2020;**97**:94–54.



Abstract 1188 Figure 1 Structure of ASOCs: mAbs (purple) are covalently linked to protease substrates (green) specific for proteases that enable metastasis; the latter are also covalently linked to oligonucleotides (yellow) bearing H-type excitonic dimers (blue)

<http://dx.doi.org/10.1136/jitc-2022-SITC2022.1188>

1189

A GPC2 ANTIBODY-DRUG CONJUGATE REPROGRAMS THE NEUROBLASTOMA IMMUNE MILIEU TO ENHANCE MACROPHAGE-DRIVEN THERAPIES

¹Guillem Pascual-Pasto*, ¹Brendan McIntyre, ¹Rawan Shraim, ¹Samantha Buongervino, ²Amy Erbe, ³Dontcho Jeleu, ¹Anna Giudice, ¹Daniel Martinez, ⁴Laura Garcia-Gerique, ³Dimitar Dimitrov, ²Paul Sondel, ¹Kristopher Bosse. ¹The Children's Hospital of Philadelphia, Philadelphia, PA, USA; ²University of Wisconsin, Madison, WI, USA; ³University of Pittsburgh, Pittsburgh, PA, USA; ⁴Wistar Institute, Philadelphia, PA, USA

Background Antibody-drug conjugates (ADCs) have emerged as an effective and safe anticancer therapy. ADCs may induce immunogenic cell death (ICD) that promotes additional endogenous antitumor immune responses. We have identified GPC2 as a target in neuroblastoma and developed an anti-GPC2 pyrrolobenzodiazepine (PBD) dimer-bearing ADC (D3-GPC2-PBD). Here, we explored whether the D3-GPC2-PBD ADC induces ICD, reprograms the neuroblastoma tumor immune microenvironment (TIME) and synergizes with other immunotherapies.

Methods Mouse neuroblastoma cell lines NXS2 and 9464D were engineered to express GPC2 to study D3-GPC2-PBD immunoregulatory properties. Induction of ICD was evaluated *in vitro* by quantifying calreticulin and HSP70/90 membrane translocation and HMGB1 and ATP release, and *in vivo* performing vaccination/re-challenge experiments. ADC modulation of the neuroblastoma TIME was studied using RNA-seq, cytokine profiling, CyTOF, and flow cytometry. ADC efficacy was tested alone and in combination with anti-CD40 agonists and anti-CD47 antagonists. We also studied ADC-mediated ICD in human neuroblastoma cells *in vitro* and elucidated synergy with macrophages and CD47 blockade *in vitro* and *in vivo* in a neuroblastoma patient-derived xenograft (PDX).

Results In GPC2-expressing murine neuroblastoma cells, the GPC2 ADC induced markers of ICD (mean ICD marker fold-change of 5.3 vs vehicle-treated controls). *In vivo*, subcutaneous vaccination with ADC-treated NXS2-GPC2 cells prevented tumor growth in 72% and 70% of mice re-challenged with naïve GPC2 isogenic and empty-vector NXS2 cells, respectively. Transcriptomic and immunophenotypic analyses of ADC-treated NXS2-GPC2 allografts revealed reprogramming of the TIME to a pro-inflammatory state. By RNA-seq, ADC-treated tumors showed upregulation of genes related to immune cell recruitment and activation (e.g., *Ccl2*, *Cd40*, *Cd80*, or *Cd69*) and cytokine arrays showed upregulation of CXCL16, CD40 and CCL12. By CyTOF and flow cytometry, ADC increased intratumor infiltration of activated CD40⁺, MHCII⁺ macrophages and CD69⁺, CD8⁺ T-cells. In this model, inhibition of antitumor macrophages and T-cells impaired ADC efficacy, whereas combination of GPC2 ADC plus CD40 agonist antibodies induced 100% of complete responses. In human neuroblastoma cells, ADC treatment induced phagocytosis of NB-EbC1 ($P=0.0004$) but not SMS-SAN cell lines, which correlated with higher calreticulin translocation in NB-EbC1 cells. The addition of CD47 blockade increased ADC-mediated phagocytosis of SMS-SAN cells ($P=0.0001$). Finally, we observed that low doses of the D3-GPC2-PBD ADC combined with CD47 antagonist antibodies significantly increased survival of mice bearing neuroblastoma PDXs compared to ADC treatment alone ($P=0.012$).

Conclusions We elucidated the immunoregulatory properties of GPC2-targeted ADCs and showed robust efficacy of this ADC in combination with rationally selected antibodies that modify host macrophage anti-tumor immunity.

Acknowledgements We thank the DNA sequencing, Human Immunology, and CyTOF core facilities at the University of Pennsylvania for their work on plasmid verification, human monocyte isolation, and mass spectrometry analysis, respectively. We also would like to thank the Pathology and Small Animal Imaging facility cores at The Children's Hospital of Philadelphia. Additionally, we appreciate the Cancer Genomics Laboratory at Sidney Kimmel Cancer Center (Thomas Jefferson University) for their work on RNA-sequencing. Finally, we thank Drs. Takuya Ohtani, Allie Greenplate, and Divij Mathew for their technical advice on CyTOF studies.

Ethics Approval Animal experiments were conducted using protocols approved by the CHOP Institutional Animal Care and Use Committee (IACUC; Approved IACUC Protocol #643) with adherence to the NIH guide for the Care and Use of Laboratory Animals accredited by the Association for Assessment and Accreditation of Laboratory Animal Care (AAALAC).

Consent For human samples, donors provided informed consent through the University of Pennsylvania Immunology Core.

<http://dx.doi.org/10.1136/jitc-2022-SITC2022.1189>

1190

SGN-B7H4V INDUCES IMMUNOMODULATORY CHANGES TO THE TUMOR MICROENVIRONMENT AND PAIRS WELL WITH AN ANTI-PD1 AGENT IN A PRECLINICAL MODEL

Michelle Ulrich, Angela Epp, Kelly Hensley, Julie Hahn, Sean Allred, John Gosink, Piper Treuting, John Hernandez Villanueva, Sarah Anderson, Alyson Smith, Jason Schrum, Natalya Nazarenko, Shyra Gardai*, Elizabeth Gray. *Seagen, Bothell, WA, USA*

Background SGN-B7H4V is an investigational vedotin antibody-drug conjugate (ADC) directed to B7-H4, an immune checkpoint ligand with elevated expression on multiple solid tumor types, including breast, ovarian, and endometrial tumors.¹ SGN-B7H4V is composed of an anti-B7-H4 human monoclonal antibody conjugated to the microtubule disrupting agent monomethyl auristatin E (MMAE) via a protease-cleavable peptide linker. This vedotin drug linker system has been clinically validated in multiple ADC programs, including brentuximab vedotin, enfortumab vedotin, and tisotumab vedotin. SGN-B7H4V is designed to bind the immune checkpoint ligand B7-H4, internalize the ligand/ADC complex from the surface of B7-H4-expressing tumor cells and release the cytotoxic payload, MMAE, within the cell. SGN-B7H4V demonstrates strong antitumor activity in preclinical models through multiple potential mechanisms including direct MMAE-mediated cytotoxicity as well as antibody-mediated functions including antibody-dependent cellular cytotoxicity (ADCC) and phagocytosis (ADCP) *in vitro*.¹ Vedotin ADCs can elicit MMAE-mediated immunomodulatory changes to the tumor microenvironment (TME) via induction of immunogenic cell death²⁻⁴ which may position vedotin ADCs to uniquely synergize with checkpoint inhibitors. This is supported by clinically meaningful responses observed when vedotin ADCs are paired with anti-PD1 agents.^{5,6} Here, we use an immunocompetent mouse model to characterize SGN-B7H4V-mediated immunomodulatory activity along with antitumor activity and induction of immune memory in combination with an anti-PD1 agent.

Methods Immunomodulatory changes in SGN-B7H4V-treated tumors were characterized by RNAseq and immunohistochemistry. The antitumor activity of SGN-B7H4V as a monotherapy and in combination with an anti-PD1 agent was evaluated using a murine B7-H4-expressing Renca syngeneic tumor model. Finally, tumor rechallenge experiments were performed to evaluate immune memory.

Results Treatment of B7-H4-expressing syngeneic tumors with SGN-B7H4V led to immunomodulatory changes in the TME, including recruitment of multiple immune cell types and upregulation of immune-related genes that have been previously associated with response to anti-PD(L)1 agents. Moreover, SGN-B7H4V drove robust antitumor activity as well as durable immune memory as a monotherapy and in combination with an anti-PD1 agent.

Conclusions In preclinical models, SGN-B7H4V demonstrates robust antitumor activity accompanied by immunomodulatory changes in the TME. Moreover, SGN-B7H4V in combination with an anti-PD1 agent led to improved antitumor activity and elicited durable immune memory. Altogether, these non-clinical data further support the evaluation of SGN-B7H4V as a monotherapy in the ongoing Phase 1 Study of SGN-B7H4V in Advanced Solid Tumors (NCT05194072) and potential future clinical combinations with immunotherapies.

REFERENCES

1. Gray E, *et al.* 854 SGN-B7H4V, a novel, investigational vedotin antibody-drug conjugate directed to the T cell checkpoint ligand B7-H4, shows promising activity in preclinical models. *Journal for ImmunoTherapy of Cancer* 2021;**9**:A895–A895.
2. Puzstai LL, Hale H, Grosse-Wilde C, Specht A, Modi J, Han S, Cortes H, Oliveira J, Garfin H, Wang P, Onsum ZM. Systemic administration of Iadiratuzumab vedotin alone or in combination with pembrolizumab results in significant immune activation in the tumor microenvironment in metastatic breast cancer patients. *Journal for ImmunoTherapy of Cancer* 2020;**8**.
3. Liu BAOD, Snead K, Gosink J, Tenn E-T, Zaval M, Cao A, Sahetya D, Nesterova A, Hensley K, Cochran J, Gardai S, Lewis TS. Enfortumab vedotin, an anti-Nectin-4 ADC demonstrates bystander cell killing and immunogenic cell death anti-tumor activity mechanisms of action in urothelial cancers. *Cancer Research*, 2020;**80** (16_Supplement):5581.
4. Gray EHK, Allred S, Trueblood E, Gosink J, Thurman R, Smith K, Jacquemont C, Bieda M, Gow J, Harris J, Brady L, Soumaoro I, Jain S, Nicacio L, Gardai S. Tisotumab vedotin shows immunomodulatory activity through induction of immunogenic cell death. *Journal for ImmunoTherapy of Cancer* 2020;**8**.
5. Rosenberg JEF, Friedlander TW, Milowsky MI, Srinivas S, Petrylak DP, Merchan JR, Bilen MA, Carret A-S, Yuan N, Sasse C, Hoimes CJ. Study EV-103: Preliminary durability results of enfortumab vedotin plus pembrolizumab for locally advanced or metastatic urothelial carcinoma. *Journal of Clinical Oncology* 2020;**38**(6):441–441.
6. Advani RH, *et al.* Brentuximab vedotin in combination with nivolumab in relapsed or refractory Hodgkin lymphoma: 3-year study results. *Blood* 2021;**138**(6):427–438.

Ethics Approval All animal studies were conducted in accordance with protocols reviewed and approved by the Institutional Animal Care and Use Committee at Seagen or the external testing facility that conducted the studies.

<http://dx.doi.org/10.1136/jitc-2022-SITC2022.1190>

1191 **STRO-003 IS A NOVEL ROR1-TARGETED ADC FOR BREAST AND LUNG CANCER**

¹Alice Yam*, ¹Jeff Hanson, ¹Krishna Bajjuri, ¹Sihong Zhou, ¹Dayson Moreira, ¹Jennifer Smith, ²Cristina Abrahams, ³Xiaofan Li, ¹Grace Lee, ¹Stephanie Armstrong, ¹Amandeep Gakhal, ¹Daniel Calarese, ¹Young Park, ¹Miao Wen, ¹Gang Yin, ⁴Simon Chivers, ¹Faye Hsieh, ¹Guifen Xu, ¹Werner Rubas, ¹Andreas Maderna, ¹Kristin Bedard, ¹Trevor Hallam. ¹Sutro Biopharma, South San Francisco, CA, USA; ²Seagen, South San Francisco, CA, USA; ³Sutro Biopharma, Inc., South San Francisco, CA, USA; ⁴ibilogix, Basel, Switzerland

Background Receptor tyrosine kinase-like orphan receptor 1 (ROR1) is a cell-surface, oncofetal protein whose expression is correlated with oncogenic properties such as enhanced proliferation, survival, and chemoresistance. Despite its prevalence across many cancer indications, ROR1 has restricted expression in adult tissues, making it an ideal target for targeted therapies.

Methods We have designed a novel ROR1-targeted ADC, STRO-003, which is composed of an anti-ROR1 human IgG1 antibody (SP11285) conjugated to an exatecan warhead via a stable, β -glucuronide linker (SC3417) with a drug-to-antibody ratio (DAR) of 8. SP11285 was discovered using Fab ribosome display as a selective and high affinity ROR1 antibody that exhibits favorable internalization activity upon cell binding, consistent with an ADC mechanism of action. The exatecan payload is a potent topoisomerase I inhibitor of the camptothecin class and has anti-proliferative activity against a variety of cancer cell lines *in vitro*. The SC3417 linker-payload releases exatecan upon glucuronidase linker cleavage and is site-specifically conjugated using strain promoted alkyne-azide cycloaddition (SPAAC) to form a stable, homogeneous ADC.

Results The anti-Ror1 antibody SP11285 binds with high affinity to the ROR1 immunoglobulin domain and is cross-reactive to both rodent and monkey ROR1. Unlike other camptothecin analogs, exatecan is resistant to overexpression of Pgp, and therefore has reduced risk of multi-drug resistance. Exatecan also induces immunogenic cell death, thereby providing an avenue for engaging the immune system and enriching the anti-tumor response. STRO-003 has exhibited potent and specific activity in xenograft models for TNBC and lung cancer, and importantly, elicited significant anti-tumor suppression in a panel of NSCLC PDx models, including those with low ROR1 expression. In nonclinical safety studies conducted in cynomolgus monkeys, STRO-003 was tolerated up to 45 mg/kg without signs of hematological toxicity or tissue-specific lesions. By comparison, a similar exatecan-ADC with a cathepsin-sensitive linker was more poorly tolerated and elicited signs of inflammation in the lung.

Conclusions Our data suggests that STRO-003 is a promising clinical candidate for solid tumor indications and we have initiated IND-enabling studies.

Ethics Approval All *in vivo* procedures were conducted in compliance with the guidelines of the Institutional Animal Care and Use Committee (IACUC) at Sutro Biopharma or commissioned contract research organization (CRO).

<http://dx.doi.org/10.1136/jitc-2022-SITC2022.1191>

1192

IDENTIFICATION OF ONCOGENE-INDUCED SURFACE PROTEIN IL1RAP AS AN IMMUNOTHERAPY TARGET IN MULTIPLE CANCERS

¹Hai-Feng Zhang*, ²Wei Li, ³Christopher Hughes, ⁴Rajesh Kumar, ¹Alberto Delaidelli, ³Yue Zhou Huang, ³Michael Lizardo, ⁴Rimas Orentas, ²Dimitar Dimitrov, ¹Poul Sorensen. ¹University of British Columbia, Vancouver, Canada; ²University of Pittsburgh, Pittsburgh, PA, USA; ³BC Cancer Research Centre, Vancouver, Canada; ⁴Seattle Children's Research Institute, Seattle, WA, USA

Background Adoptive and antibody-based immunotherapies are highly successful in the clinic for the treatment of certain malignancies. However, effective immunotherapy targets remain elusive for various cancers, in particular metastatic diseases. Certain existing targets often encounter antigen loss, leading to tumor relapse. Thus, it is crucial to discover novel cell surface targets that are essential for tumor sustenance and metastasis, and thus less prone to immunotherapeutic escape.

Methods To uncover crucial cell surface proteins that drive anoikis-resistance and metastasis, we performed an integrated analysis of the global proteome and acute transcriptome in distinct oncogene-transformed and non-transformed cells in 3D cultures. Anoikis-resistance *in vitro* and metastasis *in vivo* were measured by 3D spheroid cultures and a murine renal subcapsular implantation metastasis model, respectively. Candidate surface targets from the screens were evaluated by immunohistochemistry using tissue microarrays (TMAs) of multiple human cancers, and TMAs consisting various adult and pediatric normal tissues. Phage-display biopanning was performed to identify single-domain VH binders, based on which CAR-T cells and a panel of humanized IgG1 antibody-drug conjugates (ADCs) were engineered. The CAR-T cells and ADCs were tested both *in vitro* and *in vivo* using murine tumor xenograft models.

Results The screens identified that distinct oncoproteins such as mutant KRas^{G12V}, KRas^{G13D}, ETV6-NTRK3, and EWS-FLI1 each upregulate IL1RAP (IL-1 receptor accessory protein) to suppress tumor cell anoikis. IL1RAP is highly expressed on cell surface in multiple malignancies, including Ewing sarcoma (EwS), melanoma, pancreatic ductal adenocarcinoma, high-grade astrocytoma, glioblastoma, and ALK+ anaplastic large cell lymphoma. Genetic *IL1RAP* inactivation in EwS triggers anoikis and ferroptosis *in vitro* and impedes metastasis *in vivo*. Importantly, IL1RAP is minimally expressed in pediatric and adult normal tissues and blood cells, nominating IL1RAP as a promising surface target for immunotherapy. We identified a panel of novel and highly specific IL1RAP binders via phage-display biopanning, and engineered IL1RAP CAR-T cells and anti-IL1RAP ADCs conjugated to cytotoxic payloads such as pyrrolbenzodiazepine (PBD) dimer and Duocarmycin SA. IL1RAP CAR-T cells and anti-IL1RAP ADCs induced massive cell killing in a panel of EwS cells *in vitro*. Although the efficacy of IL1RAP CAR-T cells in murine EwS xenografts was limited by an immune suppressive tumor microenvironment, the anti-IL1RAP ADCs effectively limited EwS tumor progression at low doses such as 0.1mg/kg.

Conclusions Therefore, we have defined surface IL1RAP as an immunotherapy target in EwS and potentially other human malignancies, and our pre-clinical studies suggest anti-IL1RAP ADCs as a highly promising immunotherapy strategy.

Acknowledgements We thank the funding support from the NIH U54 Pediatric Immunotherapy Discovery and Development Network (1U54CA232568-01), a St. Baldrick's Foundation/American Association for Cancer Research/Stand Up to Cancer Pediatric Dream Team Translational Research Grant

(SU2C-AACR-DT-27-17), and a St. Baldrick's Foundation/Martha's Better Ewing Sarcoma Treatment (BEST) Grant (#663113). H.-F. Zhang is funded by a fellowship from the Canadian Institutes of Health Research (#415377) and a trainee award from the Michael Smith Foundation for Health Research partnered with the Lotte and John Hecht Memorial Foundation (#18569).

<http://dx.doi.org/10.1136/jitc-2022-SITC2022.1192>

1193 **INDUCING IMMUNOGENIC CELL DEATH AND ANTITUMOR ACTIVITY IN RESPONSE TO RADIOIMMUNOTHERAPY**

Denis Beckford*, Jason Li, Caroline Jennings, Megan McCloskey, Le-Cun Xu, Debbie Lewis, Patrik Brodin, Amanda Chin, Monideepa Roy, Mary Chen, Helen Kotanides. *Actinium Pharmaceuticals, Inc, New York, NY, USA*

Background Conventional cancer therapies, such as chemotherapy and external beam radiation therapy, are known to induce the release of damage-associated molecular patterns (DAMPs) that stimulate an antitumor immune response. Radioimmunotherapy (RIT) offers a unique opportunity by delivering cytotoxic energy specifically to target-expressing cancer cells. However, the immunomodulatory properties of RIT are not well characterized. Hence, we hypothesized that tumor cell cytotoxicity induced by radiolabeled antibodies (ARCs) can activate an immune response by releasing DAMPs. Herein we investigated the effects of alpha or beta emitting ARCs (^{225}Ac and ^{177}Lu) on DAMP induction and engagement of the innate immune response *in vitro*. Furthermore, we evaluated the antitumor effects of ^{225}Ac and ^{177}Lu ARCs *in vivo*.

Methods ^{225}Ac or ^{177}Lu ARCs (CD33, HER2 and HER3) were prepared using p-Bn-SCN-DOTA. ARCs were evaluated for target-binding using human recombinant proteins and receptor positive tumor cell lines. The cytotoxic effect of ARCs was determined by XTT, flow cytometry and clonogenic assays. DAMP induction was investigated in cells treated with ^{225}Ac or ^{177}Lu ARCs and levels of CRT, HSP70, and HMGB1 were measured by flow cytometry and ATP concentrations determined by ELISA. The influence of ARC treatment on the innate immune response was evaluated by flow cytometry. The antitumor effects of ^{225}Ac or ^{177}Lu ARCs was examined in mice bearing human NCI-H1975 NSCLC xenograft tumors.

Results The ^{225}Ac and ^{177}Lu ARCs showed cytotoxicity and inhibited colony formation in target expressing cancer cells *in vitro*. DAMP levels in ^{225}Ac ARC treated cells was induced, including CRT translocation to cell surface, increased ATP release and HSP70 upregulation. Furthermore, an enhanced innate immune response was observed following ^{225}Ac ARC treatment. Contrastingly, treatment with ^{177}Lu ARCs did not show significant DAMP induction compared to untreated cells in the dose ranges studied. However, the efficacy study testing ^{225}Ac and ^{177}Lu ARCs in mouse xenograft model of NSCLC revealed that both ARCs had similar antitumor efficacy *in vivo*.

Conclusions The observations from this study suggest that ^{225}Ac radionuclide-based ARCs as part of their mechanism of action can induce immunogenic cell death by the release of DAMPs whereas beta radionucleotides such as ^{177}Lu may utilize different damage response pathways. These findings could be explained by DNA double stranded breaks caused by alpha radiation. Importantly, both ^{225}Ac and ^{177}Lu ARCs showed *in vivo* antitumor activity that warrants their further evaluation as warheads for RIT.

<http://dx.doi.org/10.1136/jitc-2022-SITC2022.1193>

1194

DISCOVERY AND PRE-CLINICAL DEVELOPMENT OF A NOVEL AND DIFFERENTIATED EPHA2-TARGETED ANTIBODY IN MULTIPLE BISPECIFIC FORMATS

<http://dx.doi.org/10.1136/jitc-2022-SITC2022.1194>

Maryam Bhatti, Michael Weiss, Amanda Haltom, Jessica Finn, Annie Gai, Anne Ye, Danhui Zhang, Cathrin Czupalla, Andreea Stuparu, Yvonne Leung, Erin Wechsler, Iraz Aydin, Daniel Emerling, Amy Manning-Bog, Nikhil Vad, Alexander Scholz, Philippe Marguet, Shaun Lippow*. *Atreca, Inc., San Carlos, CA, USA*

Background Eph proteins are the largest family of receptor tyrosine kinases in humans and are normally involved in cell-to-cell communication, plasticity, and patterning. EphA2 represents an attractive therapeutic target due to its overexpression in many cancers. Unfortunately, to date, clinical efforts to target EphA2 have demonstrated limited efficacy or significant toxicity.

Methods We sequenced the antibody chains expressed by single plasmablast B cells from patients with cancer and identified antibodies selectively binding to non-autologous human tumor tissues. The target and epitope of an antibody of interest were identified by FACS, yeast display, and crystallography methods. Lead optimization used sequence- and structure-based rational mutations, combined with selections from high-throughput yeast display screening. Optimized leads were engineered into several weaponized formats and tested for safety and anti-tumor activity.

Results An anti-EphA2 antibody was identified from plasmablasts of a patient with lung cancer after treatment with nivolumab. This antibody binds to the surface of tumor cell lines and selectively to human tumors compared with normal tissue. The antibody binds a novel conformational epitope on the most membrane-proximal fibronectin type-II domain, and this epitope is conserved across relevant model species. The epitope targeted is non-overlapping with biologics previously or currently in clinical development exhibiting neither agonist nor antagonist activity.

Antibody engineering yielded leads with significantly improved potency and developability, exhibiting single-digit picomolar activity in cell-based assays. Optimized leads demonstrated tumor-selective binding across multiple tumor types and labeling of plasma membranes and cytoplasmic puncta.

Antibody weaponization in multiple formats delivered potent anti-tumor activity in vivo without safety signals. A novel 4-1BB bispecific significantly enhanced therapeutic index compared with untargeted 4-1BB agonist antibodies. A weak 4-1BB agonist paired with tumor targeting drove cross-linking and activation at the tumor and dose-dependently inhibited tumor growth while avoiding the alanine transaminase increases observed with a urelumab surrogate. In addition, a CD3-bispecific T-cell engager was generated that exhibited sub-picomolar potency in vitro and robust tumor reduction in vivo. Separately, an antibody–drug conjugate version, ATRC-301, is entering IND-enabling studies and is described elsewhere.

Conclusions Our EphA2 program leverages a patient-derived antibody and a novel epitope to deliver differentiated biologics for this potentially high-value target. Optimized leads with high potency and developability exhibit anti-tumor activity in multiple formats, including a 4-1BB bispecific. These data demonstrate the power of our antibody discovery platform to uncover unique antibodies and their epitopes.

Acknowledgements Jiang Liu, Niv Chowdhury, Tapan Shah, Mark Whidden, Bamini Balaji, Shayla Wyman, Kelsey Hart, Alan Liu, Ming Han Ho, Jason Tong, Jason Heisler, Gary Bolton, Lance Kates, Blair Cain

1195

GENERATION OF A HIGHLY POTENT, CIS-SIGNALING PD1-IL2 IMMUNOCYTOKINE USING A NOVEL CHEMICAL SYNTHESIS AND CONJUGATION PLATFORM

Jean Carralot*, Matilde Arévalo Ruiz, Rubén Alvarez Sanchez, Robert Tam, Lilian Gremlich, Andrew Chi, Vijaya Pattabiraman Bertolt Kreft. *Bright Peak Therapeutics, Basel, Switzerland*

Background Immunocytokines (IC) provide the opportunity to simultaneously address distinct and complementary mechanisms of action and to deliver cytokine payloads to specific immune cells (“cis-signaling”) resulting in enhanced antitumor activity. To generate ICs, we developed an entirely different approach based on the site-specific, chemical conjugation of cytokines to existing antibodies (Ab) taken “off-the-shelf”. Using an anti PD-1 Ab that is in advanced stages of clinical development, we generated a PD1-IL2 IC to target an “alpha-dead” IL-2 to tumor resident PD-1^{high} effector T cells while simultaneously releasing PD-1-mediated immune suppression.

Methods Our novel protein engineering platform allows the generation of enhanced and conjugatable cytokines that can be used as “payloads” to create ICs. Enhanced cytokine payloads can be chemically conjugated to existing Abs in a site-specific manner without prior Ab engineering yielding ICs with a defined drug-Ab ratio. Using various IL-2 variants that lack IL-2Ra binding (“alpha-dead”), we created PD1-IL2 ICs with different payload potencies. PD1-IL2 ICs were characterized *in vitro* and subsequently *in vivo* determining PK/PD profiles and antitumor efficacy in tumor-bearing transgenic mice expressing human PD-1.

Results Chemical conjugation was found to have no impact on the potency and selectivity of the cytokine payload nor to alter Ab properties such as antigen recognition or binding to either Fc gamma receptors or the neonatal Fc receptor. PD1-IL2 IC shows superior potency *in vitro* due to *cis*-signaling on PD-1^{high} CD8+ T cells and, compared to a non-PD1 targeted control IL-2 IC, it exhibits increased tumor over plasma exposure levels. This translates into strong immune stimulation resulting in superior antitumor efficacy compared to the naked PD-1 Ab, the non-PD1 targeted IL-2 IC, and to the combination of both agents.

Conclusions Bright Peak has developed a unique, chemical conjugation process that enables the generation of ICs via rapid conjugation of synthetically engineered cytokines to the Fc domain of existing human Abs. We generated a PD1-IL2 IC with significantly enhanced potency in PD-1^{high} versus PD-1^{low} T cells. In mice, PD-1-targeting and *cis*-signaling results in high tumor exposure, potent immune stimulation, and strong antitumor efficacy. These results demonstrate the ability of our cytokine engineering platform to generate potent, multi-modal IC therapeutics that synergize complementary mechanisms of action.

<http://dx.doi.org/10.1136/jitc-2022-SITC2022.1195>

1196

STREAMLINING T CELL ENGAGER DEVELOPMENT WITH A DIVERSE PANEL OF FULLY HUMAN CD3-BINDING ANTIBODIES, BISPECIFIC ENGINEERING TECHNOLOGY, AND AN INTEGRATED DISCOVERY ENGINE

Lindsay DeVorkin, Juntao (Matt) Mai, Kate Caldwell, Tim Jacobs, Raffi Tonikian, Karine Herve, Yuri Hwang, Cristina Faralla, Wei Wei, Emma Lathouwers, Rhys Chappell, Stefan Hannie, Katherine Lam, Harveer Dhupar, Tran Tran, Melissa Cid, Lena Bolten, Tova Pinsky, Ping Xiang, Courtenay Lai, Ahn Lee, Patrick Chan, Jasmine Chin, Aaron Yamniuk, Kush Dalal, Bryan Barnhart*. *AbCellera, Vancouver, Canada*

Background CD3 T cell engagers have the potential to be a cornerstone of immuno-oncology. However, a limited pool of CD3-binding antibodies and technological challenges in engineering bispecifics have hindered development. Discovering effective T cell engagers requires two target-binding arms — a CD3 arm that fine-tunes T cell activation and a tumor arm with high specificity for cancer cells — optimized as a whole to work in concert with each other. Beginning with diverse panels of antibodies increases the probability of finding appropriately potent and developable T cell engagers and reduces the need for downstream engineering.

Methods We used microfluidic technology to screen more than 3.5 million single cells from humanized mice and identified >200 CD3-specific antibodies. Using high-throughput assays, we determined affinity for CD3 $\epsilon\delta$ and CD3 $\epsilon\gamma$, cross-reactivity to human and cyno primary T cells, CD3 binding kinetics, and epitope bins. We assessed T cell activation by measuring CD25 and CD69 expression by flow cytometry. We then used our bispecific engineering platform, OrthoMab™, to generate a proof-of-concept panel of CD3 x EGFR bispecific antibodies. Developability properties were assessed, including hydrophobicity (aHIC), self-association (AC-SINS), polyspecificity (BVP-ELISA), stability (nanoDSF), and aggregation (aSEC). CD3 T cell engager potencies were measured using an NFAT reporter T cell activation assay and an xCELLigence tumor cell killing assay, and cytokine release was assessed by FLEX-MAP CD.

Results We identified hundreds of fully human CD3-specific antibodies that are diverse, developable, and validated. The antibodies displayed a wide range of CD3 binding affinities ($K_D \sim 1$ nM to 1 μ M), binding kinetics, and T cell activation potencies ($EC_{50} \sim 6$ to 190 nM). Data on this novel panel includes epitope binning, which revealed human and cyno CD3-binders that are distinct from previously described cross-reactive antibodies. The antibodies were assessed using a range of biophysical assays and have favorable developability properties. In an expanded proof-of-concept study, we used OrthoMab™ to generate a panel of CD3 x EGFR bispecific antibodies. The resulting bispecifics had favorable developability properties, and displayed a wide range of antigen-dependent T cell activation ($EC_{50} \sim 2$ pM to 2 nM) and tumor cell killing potencies ($EC_{50} \sim 0.01$ to 1 nM). From this panel, we identified potent T cell engagers that achieved >90% tumor cell killing with low levels of cytokine release.

Conclusions By integrating our panel of CD3-binding antibodies with our bispecific engineering and high-throughput antibody assessment capabilities, we identified developable CD3 T cell engagers with potent tumor cell-killing activity and minimal cytokine release.

<http://dx.doi.org/10.1136/jitc-2022-SITC2022.1196>

1197

OPTIMIZING A T CELL-ENGAGING BISPECIFIC ANTIBODY TARGETING THE HIGHLY RECURRENT P53 R175H NEOANTIGEN VIA AFFINITY MATURATION

<http://dx.doi.org/10.1136/jitc-2022-SITC2022.1197>

Sarah DiNapoli*, Emily Hsiue Wright,, Brian Mog, Sandra Gabelli, Kenneth Kinzler, Bert Vogelstein, Shibin Zhou. *Johns Hopkins Univ. School of Medicine, Baltimore, MD, USA*

Background Targeting mutation-associated neoantigens (MANAs) is a highly-cancer specific strategy to selectively eliminate cells harboring common driver mutations in genes encoding intracellular proteins such as Ras and p53.^{1, 2} T cell-engaging bispecific antibodies targeting MANAs redirect T cells to kill cancer cells presenting mutant peptides on human leukocyte antigens (pHLA). However, T cell-redirecting therapies' efficacy can be limited by the low antigen density of these MANAs on the cell surface. Here, we investigate whether increasing the affinity of a T cell-engaging bispecific antibody (clone H2) targeting the p53 R175H MANA (HMTEVVRHC) presented on HLA-A*02:01 (R175H/A2) improves its efficacy *in vitro* and *in vivo*.

Methods To identify higher affinity variants, we screened a phage display library consisting of 1159 single-amino acid variants at 61 sites in the six complementarity determining regions of the H2 single chain variable fragment targeting R175H/A2. Variants retaining R175H/A2 specificity were selected over multiple rounds of panning followed by affinity enrichment via thiocyanate elution. Selected variants were compared to the original H2 bispecific antibody in co-cultures with primary human T cells and cancer cell lines expressing endogenous levels of HLA-A*02:01 and the mutant p53-R175H protein or isogenic control cell lines. For *in vivo* comparison, NSG mice inoculated with KMS26 or Nalm6 cells and human T cells were treated with a continuous infusion of bispecific antibody for 14 days.

Results Three variant bispecific antibodies were identified with higher affinity and retained specificity for R175H/A2 (KD of 12.9 nM, 6.8 nM, 3.3 nM vs. the original KD of 29.5 nM). The highest affinity variant was a double mutant incorporating two top single variants. Each higher affinity variant elicited greater T cell activation as measured by interferon gamma release and cytotoxicity in co-cultures with cell lines expressing endogenous levels of the R175H/A2 pHLA. *In vivo* testing demonstrated that the higher affinity bispecific antibodies had improved tumor control in xenograft models compared to the lower affinity bispecific, particularly at a lower treatment dose (0.075 mg/kg/d).

Conclusions Increasing affinity for the p53 R175H/A2 pHLA to the low nanomolar range yields increased T-cell activation and cancer cell killing without sacrificing specificity for the R175H mutation.

REFERENCES

1. Hsiue EH, Wright KM, Douglass J, Hwang MS, Mog BJ, Pearlman AH, Paul S, DiNapoli SR, Konig MF, Wang Q, Schaefer A, Miller MS, Skora AD, Azurmendi PA, Murphy MB, Liu Q, Watson E, Li Y, Pardoll DM, Bettegowda C, Papadopoulos N, Kinzler KW, Vogelstein B, Gabelli SB, Zhou S. Targeting a neoantigen derived from a common TP53 mutation. *Science* 2021;**371**:eabc8697.
2. Douglass J, Hsiue EH, Mog BJ, Hwang MS, DiNapoli SR, Pearlman AH, Miller MS, Wright KM, Azurmendi PA, Wang Q, Paul S, Schaefer A, Skora AD, Molin MD, Konig MF, Liu Q, Watson E, Li Y, Murphy MB, Pardoll DM, Bettegowda C, Papadopoulos N, Gabelli SB, Kinzler KW, Vogelstein B & Zhou S. Bispecific antibodies targeting mutant RAS neoantigens. *Sci Immunol* 2021;**6**:eabd5515

Ethics Approval Animal studies were approved by the Johns Hopkins University Animal Care and Use Committee, #MO18M79.

1198

A DUAL TARGETING CD33/CD123 NANOBODY® T-CELL ENGAGER WITH POTENT ANTI-AML ACTIVITY AND A MANAGEABLE SAFETY PROFILE

¹Melissa Dullaers*, ¹Geert Deschamps, ²Helene Bonnevaux, ²Stephane Guerif, ¹Veronique De Brabandere, ²Celine Amara, ¹Ann Brige, ¹Eline Dejonckheere, ²Angela Virone-Oddos, ²Marielle Chiron, ¹Annelies Roobrouck. ¹Sanofi Ghent, Zwijnaarde, Belgium; ²Sanofi RandD, Vitry, France

Background Novel therapies are needed for effective treatment of Acute Myeloid Leukemia (AML). Relapse is common and salvage treatment with cytotoxic chemotherapy is rarely curative. CD123 and CD33, two clinically validated targets in AML, are jointly expressed on blasts and leukemic stem cells in >95% of AML patients. However, their expression is heterogeneous between subclones and between patients which may impact the efficacy of single-targeting agents in some patient populations. We present here a dual targeting CD33/CD123 NANOBODY® T-cell engager (TCE) that was designed to decrease the risk of relapse from single antigen-negative clones and to increase coverage within and across patients.

Methods TCE-driven redirected T cell killing was evaluated *in vitro* against cells lines with different expression levels of both tumor antigens: MOLM-13, U-937 and KG1a. *In vivo* efficacy was addressed in a MOLM-13 disseminated CDX mouse model. PK, PD and safety were studied in an exploratory single-dose study in cynomolgous monkeys. Cytokine release was measured in an *in vitro* autologous PBMC setup.

Results The CD33/CD123 TCE killed AML tumor cells expressing one or both antigens *in vitro*. Compared to single-targeting control compounds, the CD33/CD123 TCE conferred equal or better *ex vivo* killing of AML blasts in most primary AML samples tested, suggesting a higher patient coverage. In a disseminated CDX mouse model of AML, the multispecific CD33/CD123 TCE cleared cancer cells in long bones as well as in soft tissues. As cytokine release syndrome is a well-documented adverse effect of TCE, the compound was tested in a cytokine release assay and shown to induce less cytokines compared to CD123 single-targeting control.

In an exploratory single-dose non-human primate study, the CD33/CD123 TCE revealed a favorable PK profile. Depletion of CD123 and CD33 expressing cells was observed at 0.04µg/kg, without associated cytokine release syndrome nor signs of clinical toxicity.

Conclusions Taken together, the CD33/CD123 dual-targeting NANOBODY® TCE exhibits potent and safe anti-AML activity and promises a broad patient coverage.

Ethics Approval All *in vivo* experiments were approved by the Sanofi Ethical Committee and conducted in accordance with local and institutional Laws, Ethics and guidance in AAALAC accredited facilities.

<http://dx.doi.org/10.1136/jitc-2022-SITC2022.1198>

1199

COMPARISON OF FOUR IN VITRO CYTOTOXICITY ASSAYS FOR ASSESSING THE POTENCY OF CD3-BISPECIFIC ANTIBODIES REDIRECTING T CELLS TO KILL TUMOR TARGET CELLS

¹Jun Guan*, ¹Charlie Kang, ¹Alejandro Amador Arjona, ¹Ricardo Macarron, ¹Patrick Mayes, ²Yao-Bin Liu. ¹Incyte Research Institute, Wilmington, DE, USA; ²Incyte Corporation, Wilmington, DE, USA

Background Evaluation of cytotoxicity is a critical step in the selection of CD3-bispecific antibodies (BsAbs) for cancer immunotherapy. The objective of this study was to compare sensitivities, strengths, and limitations of four commonly used in vitro cytotoxicity assays to determine potency of CD3 BsAbs in a co-culture system composed of tumor target cells and human CD3⁺ T cells.

Methods

Lactate dehydrogenase (LDH) Release Assay 786-O renal cancer cells were co-cultured with human CD3⁺ T cells in the presence of tool CD3 BsAbs or control antibodies. LDH release from membrane-damaged cells was measured using a fluorometric method (Promega). **IncuCyte-based Assay:** Co-culture plates as prepared for the LDH release assay were scanned by IncuCyte S3 system with 5 images captured per well; phase object confluence was measured. **Killing Immune-Lysis Reaction (KILR) Assay:** 786-O KILR cell pool generated by transduction of KILR retroparticles into the parental 786-O cells was co-cultured with human T cells. The release of tagged KILR reporter proteins from dying cells was detected by a luminescence method (Eurofins). **Flow Cytometry-based Assay:** U266 myeloma target cells were co-cultured with effector T cells. CD3 BsAbs-induced T-cell cytotoxicity, proliferation, and activation marker expression were evaluated using Intellicyte iQue flow cytometer. Cytokine secretion from activated T cells in the co-culture systems was measured using Meso Scale Discovery assays.

Results All 4 in vitro cytotoxicity assays consistently demonstrated that tool CD3 BsAbs induced T cell-mediated tumor cytotoxicity in a dose-dependent and time-dependent manner. This was in agreement with other T-cell activation parameters in terms of INF- γ secretion, surface expression of CD25 and CD69, and T cell proliferation. The KILR assay was the most sensitive and specific assay. The fluorescence produced in LDH release assay was mainly contributed by the dead 786-O target cells with minimum contribution from the dead T cells. Automated imaging and phase object confluence analysis by IncuCyte selectively quantified tumor cell death in real-time without labeling the target cells. The flow cytometry-based assay was relatively time consuming, but allowed for measurement of multiple T-cell activation biomarkers simultaneously.

Conclusions All 4 in vitro cytotoxicity assays evaluated are suitable to assess the efficacy of CD3 BsAbs redirecting T-cell cytotoxicity against tumor cells. The LDH release assay, IncuCyte-based assay, and KILR assay may be more robust for screening of CD3 BsAbs, while flow cytometry-based assay is beneficial for confirmation of the lead clones.

Acknowledgements Thanks to Christine Gardiner, Darlise DiMatteo, and Sundee Dees for technical assistance.

<http://dx.doi.org/10.1136/jitc-2022-SITC2022.1199>

1200

A CLINICALLY VALIDATED PH-SENSITIVE NANOMEDICINE PLATFORM FOR ENCAPSULATING THERAPEUTIC BISPECIFIC T CELL ENGAGERS FOR TUMOR SPECIFIC DELIVERY AND ACTIVATION

Stephen Gutowski*, Qingtai Su, Austin Burcham, Irina Kalashnikova, Ashley Campbell, Zirong Chen, Bhargavi Allu, Jason Miller, Tian Zhao. *OncoNano Medicine, Inc., Southlake, TX, USA*

Background Bispecific antibodies (BsAbs) are an important class of therapeutics for immune-oncology applications. T cell engagers (TCEs) target tumor-associated antigens and cytotoxic T cells to eradicate antigen-expressing tumor cells. Blinatumomab (CD19 X CD3 bispecific) is approved for CD19-positive B cell acute lymphoblastic leukemia,¹ but its toxicity may be limiting, with one-third of patients in the pivotal Phase 3 study requiring treatment interruption for adverse events.² TCEs for solid tumors have likewise demonstrated encouraging clinical efficacy but shown dose-limiting toxicities due to on-target/off-tumor effects^{3,4} For instance, patients receiving solitomab (EpCAM X CD3 bispecific) experienced severe gastrointestinal toxicity which precluded its further development.⁵ To minimize the off-tumor effects, we have developed ON-BOARD, an ultra-pH sensitive nanoparticle platform, has shown utility in cytokine and monoclonal antibody encapsulation and targeted delivery to the acidic tumor microenvironment.^{6,7} The clinical safety and feasibility of ON-BOARD has been demonstrated by effective delivery of fluorophores to solid tumors for imaging of multiple tumor types in Phase I and II clinical trials with pegsitacianine.⁸ Herein we expand the utility of ON-BOARD platform for the encapsulation and pH-specific activation of bispecific antibodies with potential for anticancer therapy.

Methods A panel of BsAbs (including biosimilar equivalents of blinatumomab, solitomab, and others) was used to demonstrate encapsulation by the ON-BOARD platform and pH-dependent activation. Formulations of ON-BOARD with BsAbs were purified by size exclusion chromatography and the encapsulation efficiencies were quantified by HPLC. Particle size and uniformity were studied by dynamic light scattering. ON-BOARD/BsAb formulations were assessed *in vitro* under neutral pH or acid-activated conditions to determine target engagement by ELISA, bio-layer interferometry. The target-specific bioactivity and therapeutic window was determined by TDCC assays in multiple models.

Results ON-BOARD nanoparticles successfully encapsulated bispecific antibodies across a wide range of tumor-associated antigens (TAAs), including HER2, EpCAM, CEACAM5, CD19, and CD20, and structural configurations (tandem scFv and Fc-fusion). ON-BOARD formulations were stable nanoparticles with narrow size distribution (<70 nm), good encapsulation efficiency (up to 98%) and drug loading (up to 8%). Acid-mediated release and target engagement of both TAA-targeting and CD3-targeting arms was demonstrated using *in vitro* binding assays with >100-fold activation window. Further pH-specific cell killing was confirmed by TDCC assays in multiple *in vitro* models including Burkitt lymphoma, breast cancer, colorectal cancer, and lung cancer.

Conclusions The ON-BOARD pH-sensitive nanoparticle platform demonstrated potential as an effective and universal tool for solid tumor specific activation and delivery of bispecific antibody therapeutics, potentially minimizing systemic side effects.

REFERENCES

1. Goebeler ME, Bargou R. T cell-engaging therapies — BiTEs and beyond. *Nat Rev Clin Oncol* 2020;**17**:418–34.
2. Kantarjian H, et al. Blinatumomab versus chemotherapy for advanced acute lymphoblastic leukemia. *N Engl J Med* 2017;**376**:836–847.
3. Zhou S, Liu M, Ren F, Meng X, Yu J. The landscape of bispecific T cell engager in cancer treatment. *Biomark Res*. 2021;**9**:38.
4. Edeline J, Houot R, Marabelle A, Alcantara M. CAR-T cells and BiTEs in solid tumors: challenges and perspectives. *J Hematol Oncol*. 2021;**14**:65.
5. Kebenko M, et al. A multicenter phase 1 study of solitomab (MT110, AMG 110), a bispecific EpCAM/CD3 T-cell engager (BiTE[®]) antibody construct, in patients with refractory solid tumors. *Onc Immunology* 2018;**7**:8.
6. Ding X, Miller J, Su Q, et al. ONM-400, a novel approach for interleukin-2 therapy using a pH-activated nanoparticle targeting metabolic acidosis in solid cancers. *J Immunother Cancer* 2020;**8**(Suppl 3) A345.
7. Bharadwaj G, Su Q, Gutowski S, et al. Encapsulating therapeutic antibodies for tumor specific activation and delivery using a clinically validated pH-sensitive nanoparticle platform. *Cancer Res* 2022;**82**(12_Supplement):1734.
8. Voskuil FJ, Steinkamp PJ, Zhao T, et al. Exploiting metabolic acidosis in solid cancers using a tumor-agnostic pH-activatable nanoprobe for fluorescence-guided surgery. *Nat Commun*. 2020;**11**:3257.

<http://dx.doi.org/10.1136/jitc-2022-SITC2022.1200>

1201

SGN-BB228 IS A FIRST-IN-CLASS CD228-TARGETED COSTIMULATORY ANTIBODY ANTICALIN[®] BISPECIFIC DELIVERING POTENT AND CONDITIONAL 4-1BB COSTIMULATION TO TUMOR-SPECIFIC T CELLS

Ryan Heiser*. Seagen Inc., Bothell, WA, USA

Background Agonist antibodies targeting 4-1BB (CD137) effectively costimulate cytotoxic T cells and are active in preclinical models of cancer. However, clinical development of these agents has been hampered by limited efficacy and/or poor tolerability at active doses.^{1,2} To overcome the efficacy and safety limitations of this approach, SGN-BB228, a first-in-class, investigational CD228/4-1BB Antibody Anticalin[®] bispecific was created. SGN-BB228 targets CD228 (melanotransferrin, p97), a glycosylphosphatidylinositol-anchored membrane protein with limited normal tissue expression, but high and prevalent expression in melanoma, mesothelioma, lung cancer and other tumor types.^{3,4} SGN-BB228 is designed to provide a potent costimulatory bridge between tumor-specific T cells and tumor cells, improving and constraining T cell mediated cytotoxicity to tumors, potentially expanding the therapeutic window for 4-1BB agonism.

Methods Here we describe the expression profile of CD228 in cancer and normal tissues and preclinical activity of SGN-BB228 across reporter cell and primary T cell-based assays.

Results SGN-BB228 is comprised of a hinge-stabilized (S228P), Fc-null (FALA) fully human IgG4 antibody specific for CD228 connected to 4-1BB-targeting Anticalin[®] proteins⁵ via C-terminal heavy-chain fusions. The proposed mechanism of action (MOA) for SGN-BB228 is CD228-conditional clustering of 4-1BB on antigen experienced tumor-specific T cells, resulting in enhanced activation and cellular cytotoxicity. Expression analysis across cancer and normal tissues demonstrates CD228 is a tumor associated antigen prevalent in melanoma, mesothelioma, lung cancer and other tumor types with minimal normal tissue expression. Preclinical testing of SGN-BB228 in vitro shows potent CD228-conditional 4-1BB stimulation and cytotoxic T cell activation across a range of assay systems. In the presence of CD228-expressing tumor cells, but not CD228-negative tumor cells, SGN-BB228 drove dose-dependent amplification of NFκB signaling using a 4-1BB reporter cell system. SGN-BB228 also consistently drove potent CD228-conditional costimulatory activity in assays using primary T cells or whole peripheral blood mononuclear cells (PBMCs) receiving different forms of T cell receptor stimulation. The CD228-conditional activity of SGN-BB228 consistently outperformed a clinical benchmark antibody, even in the presence of antibody-clustering FcγRs expressed by PBMC. **Conclusions** Together these data introduce SGN-BB228, a first-in-class, investigational CD228/4-1BB costimulatory Antibody Anticalin[®] bispecific with potent and CD228-conditional 4-1BB costimulatory activity with therapeutic potential in multiple solid tumor types. These data support future clinical study of SGN-BB228 in a first-in-human Phase 1 trial.

REFERENCES

1. Segal NH, Logan TF, Hodi FS, et al. Results from an integrated safety analysis of urelumab, an agonist anti-CD137 monoclonal antibody. *Clin Cancer Res.* 2017;**23**(8):1929–36.
2. Segal NH, He AR, Doi T, et al. Phase I study of single-agent utomilumab (PF-05082566), a 4-1BB/CD137 agonist, in patients with advanced cancer. *Clin Cancer Res* 2018;**24**(8):1816–23.
3. Brown JP, Nishiyama K, Hellström I, Hellström KE. Structural characterization of human melanoma-associated antigen p97 with monoclonal antibodies. *J Immunol* 1981;**127**(2):539–546.

4. Smith LM, Nesterova A, Alley SC, Torgov MY, Carter PJ. Potent cytotoxicity of an auristatin-containing antibody-drug conjugate targeting melanoma cells expressing melanotransferrin/p97. *Mol Cancer Ther* 2006;**5**(6):1474–1482.
5. Hinner MJ, Aiba RSB, Jaquin TJ, et al. Tumor-localized costimulatory T-cell engagement by the 4-1BB/HER2 bispecific antibody-anticalin fusion PRS-343. *Clin Cancer Res.* 2019;**25**(19):5878–89.

<http://dx.doi.org/10.1136/jitc-2022-SITC2022.1201>

Abstracts

1202 TRI-SPECIFIC KILLER ENGAGERS TARGET NATURAL KILLER CELLS TOWARDS MESOTHELIOMA

¹Philippa (Pippa) Kennedy, ¹Quinlan Kile, ¹Blake Jacobson, ¹Brianna Ettestad, ¹Nicholas Zorko, ¹Caroline Hallstrom, ¹Behiye Kodal, ¹Deborah Todhunter, ¹Daniel Vallera, ²Gregory Berk, ¹Jeffrey Miller, ¹Manish Patel, ¹Martin Felices*. ¹University of Minnesota, Minneapolis, MN, USA; ²GT Biopharma, Dover, MA, USA

Background Mesothelioma is a rare but deadly malignancy of cells lining internal organs. It is most commonly found in the pleura (cells lining the lung), but also in the peritoneum. Between 2015 and 2019, half of all mesotheliomas diagnosed were at a distant site, where five-year survival was as low as 9%. Immunotherapy is emerging as a viable systemic therapy both as a first-line and second-line treatment, but there is still room for improvement. We hypothesized that natural killer (NK) cells could be mobilized to contribute to immune control. We set out to test our Tri-specific Killer Engager (TriKE[®]) platform in the context of mesothelioma. TriKEs consist of a single chain variable fragment (scFv) or camelid nanobody targeting a tumor antigen and camelid nanobody targeting Fc receptor CD16 on NK cells, linked by an IL-15 moiety. We tested two different TriKEs, one targeting mesothelin (cam1615SS1), commonly found on epithelioid mesothelioma, and a second TriKE targeting B7H3 (GTB-5550), a common tumor antigen.

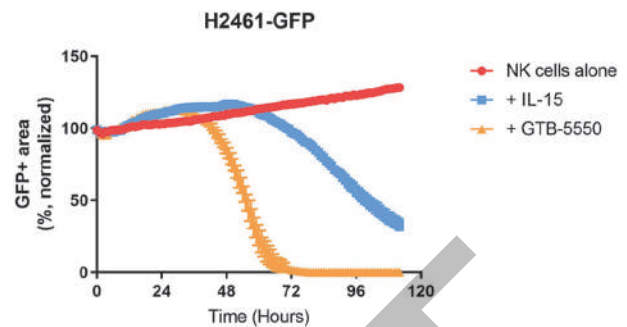
Methods Three pleural mesothelioma lines, H2373, H2596 (both sarcomatoid) and H2461 (epithelioid), and four peritoneal mesothelioma lines, ROB, YOU, HAY and ORT (all epithelioid), were assessed for mesothelin and B7H3 surface expression by flow cytometry. NK cells were isolated from human blood and challenged with these lines in the presence of TriKE or IL-15 as a control. NK cell degranulation and cytokine production were assessed by flow cytometry and tumor cell control was assessed by live cell imaging in three dimensional spheroid cultures.

Results The peritoneal mesothelioma lines had detectable mesothelin and cam1615SS1 induced NK cell degranulation and cytokine responses against these cells. The pleural mesothelioma lines had low levels of surface mesothelin, so although cam1615SS1 triggered NK cell degranulation, it failed to control the tumor in three dimension cultures. B7H3 was expressed on all mesothelioma lines, regardless of subtype, and GTB-5550 induced robust degranulation and cytokine responses in NK cells. Levels of B7H3 and mesothelin did not change with overnight interferon gamma treatment to mimic an inflammatory tumor environment. In long-term spheroid assays, GTB-5550 induced NK cell destruction of tumor spheroids more rapidly than IL-15 treatment (figure 1).

Conclusions GTB-5550 drove NK cell responses towards all mesothelioma subtypes, while cam1615SS1 successfully targeted epithelial peritoneal mesothelioma. In future studies we aim to combine TriKE with immune checkpoint inhibitors to test their potential to drive innate immune responses in the context of currently approved therapies.

Acknowledgements Ira Pastan (NIH) kindly provided the sequence for the anti-mesothelin scFv, SS1. Raffit Hassan (NIH) kindly provided the peritoneal mesothelioma lines. This project was supported in large part by the Meso Foundation and also by the Department of Defense (CA200922) and National Institutes of Health (R35 CA197292, P01 CA111412).

Ethics Approval This study was deemed not to constitute human research as determined by the University of Minnesota Institutional Review Board.



Abstract 1202 Figure 1 NK cells with GTB-5550 decrease the survival time of H2461 spheroids. Live imaging tracks the survival of three-dimensional spheroids made from GFP+ mesothelioma cells over 5 days. The relative two-dimensional area observed in widefield microscopy images is plotted against time for one donor, representative of four.

<http://dx.doi.org/10.1136/jitc-2022-SITC2022.1202>

1203

ANTIGEN TARGETED BUTYROPHILIN HETERODIMER-BASED BISPECIFIC ENGAGERS INDUCE V γ 9 δ 2⁺ T CELL-MEDIATED ANTI-TUMOR ACTIVITY

Derek Franklin*, Anne Lai, Faraha Brewer, Arpita Patel, Kinsley Evans, Mahmud Hussain, Louis Gonzalez, Keith Wilson, George Fromm, Taylor Schreiber, Suresh De Silva. *Shattuck Labs, Durham, NC, USA*

Background Decreased antigen expression and antigen presentation via major histocompatibility complexes (MHCs) evades $\alpha\beta$ T cell recognition. $\gamma\delta$ T cells recognize stressed cells in an MHC-independent manner, and consequently, may be exploited to overcome immunotherapy resistance. The butyrophilin (BTN) 2A1/3A1 heterodimer specifically activates V γ 9 δ 2⁺ T cells, the predominant subtype in peripheral blood. BTN2A1 directly binds to the V γ 9 chain of the $\gamma\delta$ T cell receptor (TCR), but only activates the $\gamma\delta$ T cell if phosphoantigen-sensing BTN3A1 forms a heterodimer complex with BTN2A1. To mimic BTN-mediated activation of $\gamma\delta$ T cells, we generated bispecific $\gamma\delta$ T-cell engagers (GADLEN) containing heterodimeric BTN2A1 and BTN3A1 extracellular domains fused via inert Fc linkers to scFv domains targeting a tumor antigen. We previously reported that in the presence of costimulatory signals from either a cytotoxicity receptor (NKG2D) or T-cell co-stimulatory receptor (CD28), GADLEN compounds activated V γ 9 δ 2⁺ T cells to facilitate antigen-dependent tumor cell killing. The specificity of $\gamma\delta$ TCR/BTN interactions and dependence upon a secondary co-stimulatory signal suggests that GADLENS could be used to redirect V γ 9 δ 2⁺ T cells against hematologic and solid tumors, with a lower risk of off-target activation common with other bispecific engagers. Here, we report the functional characterization of CD20- and B7H3-targeting GADLEN compounds for targeting heme malignancies and solid tumors, respectively.

Methods Specificity of CD20- and B7H3-targeting GADLENS were evaluated using ELISA and cell-based assays by flow cytometry. The functionality of the compounds to activate V γ 9 δ 2⁺ T cells and mediate killing of tumor cells was assessed *in vitro* in tumor co-cultures using flow cytometry and live cell imaging, as well as *in vivo* in murine xenograft models.

Results CD20- and B7H3-targeting GADLENS bound to human cells expressing CD20 or B7H3 and to V γ 9 δ 2⁺ T cells with low nanomolar affinity. GADLEN compounds activated V γ 9 δ 2⁺ T cells in *in vitro* co-culture assays resulting in degranulation and apoptosis of CD20+ or B7H3+ tumor cells, respectively. Importantly, GADLEN treatments induced the secretion of pro-inflammatory cytokines suggesting the potential of both direct and indirect tumor killing mechanisms via additional immune cell subset activation and recruitment. Introduction of CD20-GADLEN into NSG-hIL15 mice engrafted with human PBMCs efficiently depleted human CD20+ B cells in the blood and spleen. Similarly, coadministration of GADLEN with V γ 9 δ 2⁺ T cells reduced tumor growth in tumor xenografts.

Conclusions These results provide proof of concept for *in vivo* manipulation of $\gamma\delta$ T cells using antigen targeted GADLENS for the treatment of hematologic and solid tumor malignancies.

<http://dx.doi.org/10.1136/jitc-2022-SITC2022.1203>

Abstracts

1204

ENHANCING NK CELL FUNCTION IN THE 'COLD' TUMOR MICROENVIRONMENT OF PROSTATE CANCER WITH A NOVEL TRI-SPECIFIC KILLER ENGAGER AGAINST PROSTATE-SPECIFIC MEMBRANE ANTIGEN (PSMA)

Shee Kwan Phung*, Yvette Soignier, Nicholas Zorko, Trygve Nelson, Joshua Walker, Philippa (Pippa) Kennedy, Jeffrey Miller, Martin Felices. *University of Minnesota, Minneapolis, MN, United States*

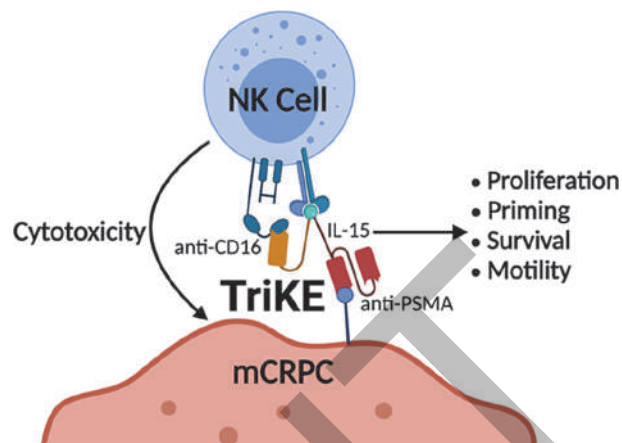
Background Natural killer (NK) cell effector function is suppressed in the tumor microenvironment (TME) of metastatic castration-resistant prostate cancer (mCRPC), the lethal form of prostate cancer. This is largely due to the inherently 'cold' nature of the TME of mCRPC that is immunosuppressive, hypoxic and lacks cytolytic lymphocyte infiltration. To improve NK cell anti-tumor responses against mCRPC in the TME, we designed a novel tri-specific killer engager (TriKE[®]) molecule that consists of three parts: an arm that engages with CD16, an activating receptor of NK cells, an arm that binds to prostate-specific membrane antigen (PSMA) that is highly and specifically expressed on mCRPC, and an interleukin (IL)-15 moiety that is essential for NK cell survival, proliferation, priming and motility (figure 1).

Methods Flow cytometry-based functional and dye dilution proliferation assays were used to compare activation and proliferation of NK cells treated with PSMA TriKE or IL-15. NK cell cytolytic capacity against C4-2, a PSMA-expressing prostate cancer cell line, was measured using IncuCyte live cell imaging. In various assays, hypoxic (1% oxygen) culture condition and cytokine-induced myeloid-derived suppressor cells (MDSC) were incorporated to better examine PSMA TriKE function in the physiological setting of mCRPC.

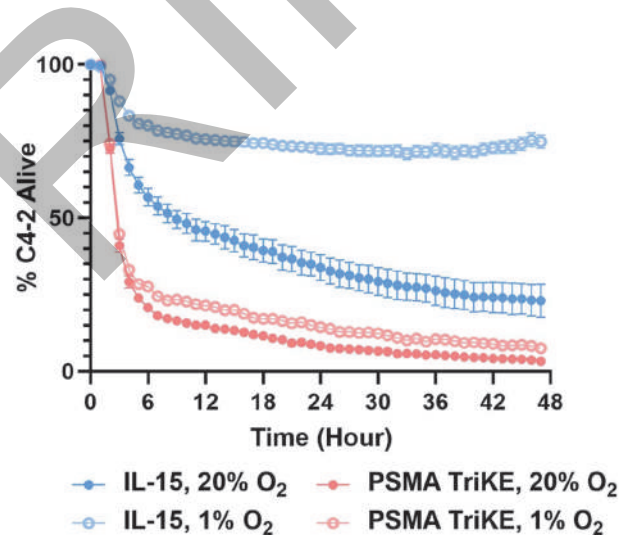
Results PSMA TriKE significantly enhanced expansion of peripheral blood NK cells derived from healthy donors up to 10 folds (N=9). This effect was specific to NK cells and not T cells. Additionally, PSMA TriKE induced NK cell degranulation (up to 60%) and intracellular IFN γ and TNF α buildup (up to 50%) when compared to IL-15 and no treatment groups after incubation with C4-2 (N=6). This result was not observed when PSMA knockout C4-2 were used as target cells. NK cell incubation in hypoxia for 7 days severely impacts cytotoxicity, some of which can be improved with IL-15. However, PSMA TriKE treatment markedly improved NK cell cytolytic capacity against C4-2 in hypoxia (N=5) (figure 2). Similarly, MDSCs suppressed NK cell degranulation in the presence of IL-15 alone but not with PSMA-TriKE treatment (N=4) (figure 3).

Conclusions PSMA-TriKE induces specific NK cell proliferation and activation against PSMA+ tumor cells. Efficient delivery of IL-15 to NK cells by PSMA-TriKE robustly relieves NK cells from suppression induced by hypoxia and MDSCs. These results demonstrate promising potential of PSMA TriKE in overcoming suppression of NK cells in the TME of mCRPC.

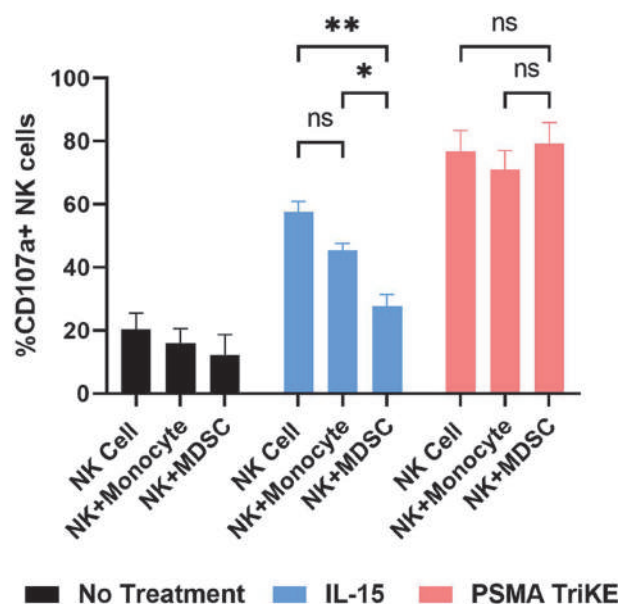
Acknowledgements This work was funded by the Department of Defense (DoD). Figure 1 was made using Biorender.com.



Abstract 1202 Figure 1 Structure of a PSMA TriKE molecule. A PSMA TriKE molecule consists of a humanized anti-CD16 single domain antibody (sdAb) derived from camelid, an anti-PSMA single chain variable fragment (scFv) and an IL-15 molecule. IL-15, interleukin-15; mCRPC, metastatic castration-resistant prostate cancer; PSMA, prostate-specific membrane antigen; TriKE, tri-specific killer engager



Abstract 1202 Figure 2 PSMA TriKE relieves suppressed NK cell cytotoxicity induced by hypoxia. NK cells were incubated with 0.06nM IL-15 or 3nM PSMA TriKE (at equifunctional concentrations) in normoxia (20% oxygen) or hypoxia (1% oxygen) for 7 days then harvested and plated at effectors to targets (E:T) ratio of 2:1 for 48 hours in normoxia to assess NK cell cytotoxicity against C4-2 using IncuCyte live cell imaging. Representative data of N=5. IL-15, interleukin-15; O₂, oxygen; PSMA, prostate-specific membrane antigen; TriKE, tri-specific killer engager



Abstract 1202 Figure 3 PSMA TriKE overcomes suppressed NK cell degranulation induced by MDSCs. NK cells were cultured alone or co-cultured with allogeneic monocytes or MDSCs at 1:1 ratio with no treatment, 0.06nM IL-15 or 3nM PSMA TriKE (at equifunctional concentrations) for 5 days. Flow cytometry was used to assess NK cell degranulation (measured by CD107a) after 5 hours incubation with C4-2 as target cells with no treatment, 0.06nM IL-15 or 3nM PSMA TriKE. Monocytes were CD14+ selected from peripheral blood mononuclear cells and MDSCs were differentiated from monocytes for 7 days using 10ng/mL of IL-6 and granulocyte monocyte-colony stimulating factor (GM-CSF). N=4; mean \pm SEM (Two-way ANOVA with Tukey's multiple comparison test); * $p < 0.05$, ** $p < 0.01$. IL-15, interleukin-15; MDSC, myeloid-derived suppressor cells; PSMA, prostate-specific membrane antigen; TriKE, tri-specific killer engager

<http://dx.doi.org/10.1136/jitc-2022-SITC2022.1204>

1205

SELECTIVE BLOCKADE OF CD47-SIRP ALPHA "DON'T EAT ME" SIGNALING WITH A HER2-CD47 BISPECIFIC ANTIBODY-DERIVATIVE

Yuzhu Qi*, Harm Lourens, Gerwin Huls, Edwin Bremer. *University Medical Center Groningen, Groningen, Netherlands*

Background Human epidermal growth factor receptor 2–positive (HER2+) breast cancer accounts for ~25% of breast cancer cases. Trastuzumab improves clinical outcomes by targeting HER2, but recurrences still occur. Targeting the CD47-SIRP α interaction alone or in combination with therapeutic antibodies such as Trastuzumab contributes to cancer cell elimination, but ubiquitous CD47 blocking associates with toxicity. Here, we designed a bispecific antibody fragment aimed to selectively block CD47 on HER2-positive breast cancer cells (BC) in order to reduce off-tumor binding and limit toxicity towards normal CD47-positive cells, while increasing efficacy against cancer cells.

Methods A novel HER2-CD47 bispecific single chain fragment (HER2-CD47 bs-scFv) antibody with HA tag was produced in HEK293 cells and purified using Anti-HA affinity purification. The HER2-CD47 bs-scFv comprised a CD47-targeting scFv and a Her2-targeting trastuzumab-derived scFv fragment. For binding experiments, BC cells were incubated with HER2-CD47 bsAb in the presence (or absence) of either trastuzumab or anti-CD47 or both, whereupon binding was detected using anti-HA staining. Her-2 restricted blocking activity of the HER2-CD47 bs-scFv was assessed using recombinant human SIRP- α -Fc. For phagocytosis experiments, cancer cells were labelled with CFSE and then incubated with differentiated macrophages (derived from peripheral blood mononuclear cells). Phagocytosis was measured by flow cytometry.

Results The HER2-CD47 bispecific selectively bound to CD47 +/Her2+ cells, but only marginally to single CD47 positive cancer cells. Binding of the HER2-CD47 bs-scFv was partially reduced by trastuzumab or epitope-competing CD47 antibody. Furthermore, incubation with HER2-CD47 blocked the binding of recombinant human SIRP α -Fc only on CD47+/Her2+ cells, demonstrating that functional blocking of SIRP- α /CD47 interaction is restricted to HER2+ cells. Importantly, HER2-CD47 selectively enhanced macrophage-mediated phagocytic removal of CD47+/Her2+ BC cells cancer cells by up to 30%. In contrast, similar treatment did not significantly increase phagocytosis of CD47+/Her2- BC cells.

Conclusions The HER2-CD47 bs-scFv blocked CD47 "don't eat me" signaling in a HER2-restricted manner with essentially only activity towards Her2 and CD47 double-positive cancer cells. This HER2-CD47 bs-scFv may provide a new strategy for the treatment of Her2+ breast cancers.

<http://dx.doi.org/10.1136/jitc-2022-SITC2022.1205>

1206

DISCOVERY AND PRECLINICAL PHARMACOLOGY OF BISPECIFIC ANTIBODIES TARGETING AN HLA-A2 RESTRICTED TUMOR-ASSOCIATED ANTIGEN

¹Alejandro Ramirez, ²Nora Guidotti, ¹John Leonard*, ¹Olivier Dalmas, ¹Jake Kleiner, ¹Joshua Goldsmith, ¹Greg Tuffy, ¹Jason Romero, ¹Bindu Hegde, ¹Tina Giese, ¹Lisa Kirkemo, ²Rafaella Truffer, ²Oralea Buchi, ²Nadine Uebersax, ²Philipp Wild, ²Rohan Eapen, ¹Joanna Dreux, ¹Alaina Cagalingan, ¹Lena Flood, ¹Kyle Pelot, ¹Nathan Katz, ¹Marvin Gee, ¹Venita De Almeida, ²Johannes Schilling, ²Patrik Forrer, ¹Leah Sibener, ¹John Leonard. ¹3T Biosciences, South San Francisco, CA, USA; ²Athebio, Zurich-Schlieren, Switzerland

Background T cell engagers (TCEs) are bi-functional biologics that bind a target on tumor cells and the CD3 of the TCR-complex on T cells to induce immune-mediated killing of tumors expressing the epitope of interest. While most TCEs on the market and in development target cell surface antigens with tumor- or lineage-specific expression, this approach cannot exploit the tumor-specific expression of intracellular proteins, which make up the majority of the human proteome. However, peptides derived from virtually all intracellular proteins are presented on the cell surface by Human Leukocyte Antigen (HLA) and can be targeted therapeutically to exploit the tumor-specific expression of intracellular proteins. A key safety concern for therapeutics targeting peptide-HLA complexes is cross-reactivity, as unintended binding of peptides expressed on healthy tissues can lead to lethal off-target toxicity.

Methods Here, we utilize Athebody® DARPins (Designed Ankyrin Repeat Proteins), engineered proteins based on an ankyrin repeat scaffold, to generate highly specific binders against an epitope from the cancer-germline antigen MAGE-A4 bound to HLA-A2. Using our proprietary 3T-TRACE™ platform, we perform a global cross-reactivity assessment to identify potential off-target liabilities, many of which are sequence-dissimilar to the intended MAGE-A4 epitope and would therefore be undetectable by traditional methods. The interplay of this cross-reactivity risk evaluation, informing tailored binder selection, allowed us to identify leads of unparalleled efficiency and safety profiles. TCEs armed with these Athebody® DARPins induce high potency killing of MAGE-A4-expressing cancer cell lines with no detectable killing of antigen-negative cells. We further tune the format of these molecules to retain high killing activity while minimizing cytokine release, a key determinant of dose-limiting toxicity in the clinic.

Conclusions These optimized TCEs express at high titers and display a favorable developability profile. The work presented here demonstrates a novel approach to develop TCEs with excellent potency and specificity against tumor-restricted intracellular targets.

<http://dx.doi.org/10.1136/jitc-2022-SITC2022.1206>

1207

NKP46 ENGAGING BICYCLE® NK-TICA™ DRIVES TARGETED TUMOR CYTOTOXICITY

Alexandra Rezvaya*, Fay Dufort, Christopher Leitheiser, Hannah Gardner, Tucker Ezell, Lihong Chen, Peter Brown, Philip Brandish, Michael Skynner, Kevin McDonnell, Nicholas Keen. *Bicycle Therapeutics, Lexington, MA, USA*

Background Natural killer (NK) cells are immune cells that can detect and eliminate tumor cells and bridge innate to adaptive immune responses. Bicycles are small (ca. 1.5 kDa), chemically synthetic, structurally constrained peptides discovered via phage display and optimized using structure-driven design and medicinal chemistry approaches. We have now applied this technology to identify Bicycles that bind specifically to a key activating receptor, Nkp46. We term this new class of fully synthetic molecules Natural Killer tumor-targeted immune cell agonists (NK-TICA™) and herein we will describe their in vitro evaluation.

Methods Using our unique phage display screening platform, we have identified high affinity, selective binders to Nkp46. By conjugating the Bicycle® NK cell-engaging binders to model tumor antigen EphA2-binding Bicycle®, we have developed a bifunctional Bicycle® NK-TICA™ molecule. In in vitro functional assays, we evaluated the ability of the Bicycle® NK-TICA™ to induce NK cell activation and proliferation as well as cell-mediated cytotoxicity and cytokine production in NK-tumor co-culture assays. We similarly evaluated changes in EphA2 tumor binding affinity of the Bicycle® NK-TICAs in their ability to enhance NK immune response.

Results We have developed novel modular compounds with high affinity and selectivity to NK cell receptors with specific tumor targeting capability. We demonstrate potent, selective binding of our Bicycles to receptor-expressing cells and the capability of the bifunctional molecule to induce NK cell function. With Bicycle's novel NK-TICA™ compounds, we demonstrate engagement of NK cells, specific activation and function of NK cells, and enhanced tumor cytotoxicity across multiple tumor antigens, in a dose dependent manner. With changes in tumor binding affinity, we found changes in the activation of the NK cells in vitro.

Conclusions We have shown that when chemically coupled to a tumor antigen binding Bicycle®, the result is a bifunctional molecule (NK-TICA™) capable of directing potent and specific NK cell activation and kill in vitro.

<http://dx.doi.org/10.1136/jitc-2022-SITC2022.1207>

1208 **DUOBODY[®]-PD-L1x4-1BB (GEN1046) REVERSES T-CELL EXHAUSTION *IN VITRO***

¹Jordan Blum*, ¹Vanessa Spires, ¹Gregg Masters, ¹Christina Yu, ²Saskia Burm, ²Matt Hancock, ¹Omar Jabado, ¹Brandon Higgs, ³Alexander Muik, ³Kristina Nuernberger, ³Friederike Gieseke, ¹Tahamtan Ahmadi, ¹Kate Sasser, ³Ozlem Tureci, ¹Maria Jure-Kunkel, ³Ugur Sahin, ¹Mark Fereshteh, ²Nora Pencheva. ¹Genmab US, Princeton, NJ, USA; ²Genmab BV, Utrecht, Netherlands; ³BioNTech SE, Mainz, Germany

Background DuoBody[®]-PD-L1x4-1BB (GEN1046) is an investigational, potential first-in-class bispecific immunomodulatory antibody designed to elicit an anti-tumor immune response by simultaneous and complementary blockade of PD-L1 on tumor or immune cells and conditional 4-1BB stimulation on T cells and NK cells. Here we utilized a multi-omics approach to evaluate whether DuoBody-PD-L1x4-1BB could reverse T-cell exhaustion *in vitro*.

Methods An *in vitro* mixed lymphocyte reaction (MLR) assay was developed, optimized, and validated, where healthy donor T cells were exhausted by repeated stimulation with anti-CD3/CD28 beads prior to co-culturing with allogeneic LPS-matured dendritic cells. Publicly available single cell RNA sequencing (scRNAseq) datasets were harmonized across multiple solid-tumor indications (including treatment-naïve and anti-PD-1 and/or anti-CTLA-4 pretreated samples) and analyzed for co-expression of PD-1 and 4-1BB on various immune-cell subsets based on their transcriptome signatures.

Results In the T-cell exhaustion MLR assay, T cells showed increased expression of inhibitory receptors (e.g., TIM-3, LAG-3) and exhibited hyporesponsiveness for both proliferation and cytokine secretion upon restimulation with anti-CD3/CD28 beads, which was partially reversed by PD-1 blockade. DuoBody-PD-L1x4-1BB reinvigorated the exhausted T-cell response *in vitro*, as shown by restored IFN γ secretion. The effect of DuoBody-PD-L1x4-1BB in this assay was roughly two-fold higher to that of PD-1 blockade. When combined, DuoBody-PD-L1x4-1BB showed the potential to synergize with anti-PD-1 antibody treatment as cytokine secretion was further potentiated compared to each agent alone. More extensive molecular profiling from the T-cell exhaustion MLR assay will be presented. Using solid tumor public scRNAseq datasets, we demonstrated co-expression of 4-1BB and PD-1 on exhausted CD8⁺ T cells in the tumor microenvironment. Furthermore, in patients treated with agents that block the PD-1 pathway, an increase in exhausted CD8⁺ T cells expressing PD-1 was observed.

Conclusions PD-1 and 4-1BB are co-expressed on exhausted CD8⁺ T cells within the tumor microenvironment in solid tumors and T cell dysfunction may represent a potential resistance mechanism to checkpoint inhibitors (CPI). DuoBody-PD-L1x4-1BB restored IFN γ secretion by exhausted T cells *in vitro* more potently than PD-1 blockade, which could be further potentiated by the combination with an anti-PD-1 antibody. Together, these results support evaluation of DuoBody-PD-L1x4-1BB in the post-CPI setting and the combination of tumor-targeted 4-1BB co-stimulation with PD-1 checkpoint blockade for the treatment of solid tumors. DuoBody-PD-L1x4-1BB is currently being investigated in an ongoing phase 2 clinical trial in NSCLC patients who have progressed on prior CPI therapy (NCT05117242).

Acknowledgements These experiments were funded by Genmab A/S and BioNTech SE.

<http://dx.doi.org/10.1136/jitc-2022-SITC2022.1208>

Abstracts

1209 ANTIBODY-LECTIN BISPECIFICS FOR GLYCO-IMMUNE CHECKPOINT BLOCKADE

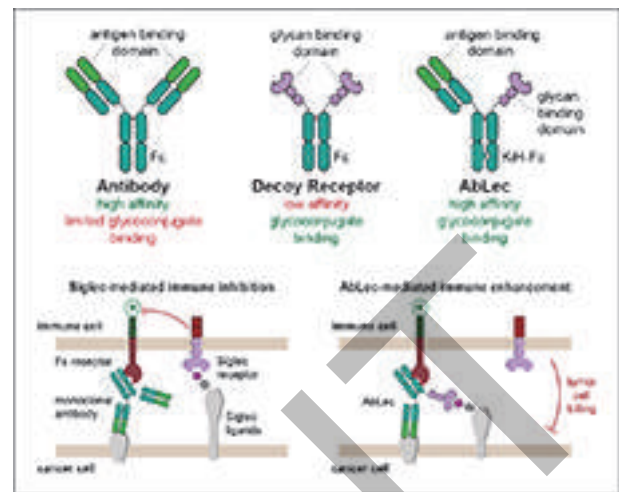
¹Jessica Stark*, ¹Melissa Gray, ¹Simon Wisnovsky, ²Itziar Ibarlucea-Benitez, ¹Nicholas Riley, ¹Mikaela Ribi, ²Jeffrey Ravetch, ¹Carolyn Bertozzi. ¹Stanford University, Stanford, CA, USA; ²The Rockefeller University, New York, NY, USA

Background Cancer immunotherapies, including checkpoint blockade antibodies, represent a breakthrough in cancer treatment with long-term remission observed in select patients. Unfortunately, many tumors remain unresponsive to existing immunotherapies, creating an urgent need to therapeutically target additional immune checkpoints that drive cancer progression. Glyco-immune checkpoints – in which cell-surface biopolymers decorated with sugars, or glycans, engage glycan-binding receptors on immune cells – have emerged as immune modulatory pathways that are misregulated in the context of cancer. In particular, recent evidence suggests that upregulation of the sialic acid monosaccharide on cancer cell surfaces allows tumors to resist treatment by engaging inhibitory receptors called Siglecs on immune cells. However, the lack of glycan-binding reagents with high affinity and selectivity has historically prevented targeting of tumor-associated glycans for cancer immunotherapy.

Methods To address this need, we have developed a new class of antibody-lectin bispecifics (AbLecs) targeting tumor-associated glycans for checkpoint blockade (figure 1). In this approach, glycan-binding domains from immune receptors (e. g., Siglec receptors) are coupled to high-affinity binding domains from FDA-approved antibodies targeting common tumor-associated antigens (e.g., trastuzumab, rituximab, cetuximab) via knobs-into-holes heterodimerization technology.

Results Western blot and mass spectrometry results indicated correct heterodimeric assembly of eight AbLec candidates, demonstrating the feasibility of the AbLec approach. We found that AbLecs bind cancer cell lines at nanomolar concentrations and block cognate Siglec receptor binding via flow cytometry. Finally, we showed that AbLecs enhance antibody-dependent phagocytosis and cytotoxicity of diverse human tumor cell lines by primary immune cells *in vitro* compared to their FDA-approved parent antibodies. Enhancement of *in vitro* tumor cell killing with AbLecs was dependent on the targeted Siglec and was more potent than the combination of the parent monoclonal antibody and a Siglec-blocking antibody.

Conclusions These studies provide proof-of-principle for AbLecs as a first-in-class, modular platform technology enabling blockade of glyco-immune checkpoints for cancer immunotherapy.



Abstract 1209 Figure 1 Graphical abstract

<http://dx.doi.org/10.1136/jitc-2022-SITC2022.1209>

1210 **A HUMAN BISPECIFIC ANTIBODY TARGETING LAG-3 AND PD-1 (INCA32459) POTENTLY ACTIVATES EXHAUSTED T CELLS**

¹Shaun Stewart, ²Floris Fransen, ¹Shane Harvey*, ²Franziska Mortensen, ²Anita Stam, ¹Rahel Awdeh, ¹Arpita Mondal, ¹Christina Stevens, ²Eric Rovers, ²Steeff Engels, ²Melissa Rentrop-Boeijen, ²Linda Hendriks, ²Brenda van Dieren, ¹Rebecca Buonpane, ²Therese Visser, ²Pepijn Schellen, ¹Ashwini Kulkarni, ¹Jonathan Rios-Doria, ¹Jing Zhou, ²Paul Tacken, ¹Lu Lu, ²Vanessa Zondag-van der Zande, ¹Cheng-Yen Huang, ²Renate den Blanken-Smit, ²John de Kruijff, ²Rinse Klooster, ²Simon Plyte, ¹Horacio Nastri, ¹Patrick Mayes. ¹Incyte Research Institute, Wilmington, DE, USA; ²Merus N.V, Utrecht, Netherlands

Background Exhausted T cells are characterized by the expression of negative immune regulatory receptors, including programmed death protein-1 (PD-1) and lymphocyte-activation gene 3 (LAG-3), which inhibit the proliferation and function of T cells and limit antitumor immunity. We describe the generation and characterization of INCA32459, a human IgG1 Fc-silenced bispecific antibody that simultaneously binds to PD-1 and LAG-3 and reverts their inhibitory function.

Methods INCA32459 was generated using the Merus common light chain Biclomics[®] platform. LAG-3 and PD-1 Fab panels were generated through immunization of Merus MeMo[®] mice, and large panels of Biclomics[®] libraries were screened before optimizing lead candidate molecules.

Results INCA32459 binds with high affinity to both human ($K_D=0.39$ nM) and cynomolgus monkey ($K_D=0.44$ nM) PD-1, and human ($K_D=1.15$ nM) and cynomolgus monkey ($K_D=0.20$ nM) LAG-3, as measured by surface plasmon resonance. The monovalent PD-1 arm of INCA32459 blocks PD-1 with similar potency as a bivalent PD-1 antibody (nivolumab analog) in a PD-1/PD-L1 reporter assay. In a loss-of-function reporter assay where luciferase expression increases upon blockade of both LAG-3 and PD-1, INCA32459 significantly induced luciferase expression to a greater extent than either PD-1 (nivolumab analog) or LAG-3 (relatlimab analog) single agent antibody controls, and greater than PD-1 (nivolumab) and LAG-3 (relatlimab) analog antibodies combined. In 2 human primary immune cell assays, a T-cell exhaustion model using chronically SEB-stimulated peripheral blood mononuclear cells (PBMCs), and an antigen recall assay using CEFT MHCII peptide pool-stimulated PBMCs, INCA32459 treatment resulted in higher interleukin-2 and interferon- γ induction, respectively, compared with PD-1 (nivolumab analog) and LAG-3 (relatlimab analog) antibodies combined. In a human MDA-MB-231 breast tumor model in CD34⁺ humanized NSG mice, INCA32459 treatment decreased tumor growth compared with a combination of PD-1 (pembrolizumab) and LAG-3 (relatlimab analog) antibodies. Pharmacodynamic analysis in mice demonstrated a dose-dependent increase in receptor occupancy at 1 and 10 mg/kg. Pharmacokinetic characterization of INCA32459 in cynomolgus monkeys after a single IV infusion at 3 and 30 mg/kg demonstrated an average clearance, steady-state volume of distribution, and mean residence time of 0.515 mL/h/kg, 74.1 mL/kg, and 144 h, respectively.

Conclusions We have developed INCA32459, a potent dual inhibitor of PD-1 and LAG-3 in preclinical models, which induces activation of exhausted T cells to a greater extent than a combination of bivalent monospecific antibodies targeting PD-1 (nivolumab analog) and LAG-3 (relatlimab analog). These data support the clinical evaluation of INCA32459, and a phase 1 study in cancer patients is underway.

<http://dx.doi.org/10.1136/jitc-2022-SITC2022.1210>

1211

DUAL TARGETING OF INNATE AND ADAPTIVE IMMUNE CHECKPOINTS WITH A PD-L1/SIRP α BISPECIFIC MACROPHAGE ENGAGER TO PROMOTE ANTI-TUMOR ACTIVITY

Dawei Sun*, Hongtao Lu, Haixia Jiang, Yanan Geng, Jiahui Hu, Ziqiao Ding, Jinfeng Zhao, Xiang Xu, Wenqiang Lu, Xiaofeng Niu, Rui Gao, Zhihao Wu, Quan Qiu, Zheng Song, Yangsheng Qiu. *Elpiscience Biopharma, Shanghai, China*

Background Tumor-associated macrophages are major component of immune cells in the tumor micro-environment that express an array of effector molecules leading to the inhibition of anti-tumor immune responses. Signal regulatory protein α (SIRP α) is a myeloid-lineage inhibitory receptor that restricts phagocytosis through engagement of its ligand CD47 expressed on tumors and normal tissues. Compared to anti-CD47 therapeutics, targeting myeloid-restricted SIRP α may provide a differential pharmacokinetic, safety, and efficacy profile. Here, we report the construction of a SIRP α antagonist-based bispecific macrophage engager (BiME) called ES019, which uses PD-L1 antibody as a tumor associated antigen (TAA) targeting arm and also as a tool to relieve the inhibition of T cell. The PD-L1/SIRP α bispecific macrophage engager aims to promote macrophage phagocytosis against PDL1 expressing tumor cells, and to activate T cell adaptive immunity resulting in further tumor cell killing.

Methods Through Elpiscience proprietary BiME platform, we have generated a panel of single domain antibody (sdAb) based anti-PDL1/SIRP α bispecific antibodies, including different orientations, ratios, and IgG isotypes of anti-PDL1 arm and anti-SIRP α arm. These bispecific antibodies were evaluated for PDL1, SIRP family homologue binding, PD1-PDL1 and CD47-SIRP α blocking properties by ELISA and FACS. *In vitro* function activity was determined by phagocytosis assay using human monocyte derived macrophage and mouse bone marrow derived macrophage. *In vivo* anti-tumor efficacy was tested in a syngeneic tumor model with hSIRP α knock-in mice. The pharmacokinetic (PK) and safety profile were assessed in hSIRP α knock-in mice or cynomolgus monkeys.

Results In this study, we demonstrated that anti-PDL1/SIRP α bispecific antibodies bound to PD-L1 expressing tumor cell and macrophage simultaneously, effectively inhibited CD47-SIRP α signal and triggered strong macrophage phagocytosis. ES019 showed potent *in vitro* macrophage and T cell tumor killing activity in the presence of peripheral blood mononuclear cells, but without nonspecific killing in PDL1 negative cells. Remarkably, ES019 showed almost 100% tumor growth inhibition in *in vivo* SIRP α knock-in syngeneic models. On the other hand, ES019 did not induce phagocytosis of normal immune cells like activated T cells. In summary, we demonstrated that ES019 exhibited super anti-cancer effects, evidenced by potent phagocytosis *in vitro* and almost complete tumor regression *in vivo*.

Conclusions Using our bispecific macrophage engager (BiME) platform, we have developed a PD-L1/SIRP α bispecific antibody that is capable of activating both macrophages and T cells to kill cancer cells with the potential to overcome the limitations of traditional anti-PD1 therapies.

<http://dx.doi.org/10.1136/jitc-2022-SITC2022.1211>

1212 **AFVT-2101, AN INNATE IMMUNE-CELL ENGAGER THAT SELECTIVELY TARGETS FOLR1 EXPRESSING TUMOR CELLS TO SAFELY HARNESS POTENT ANTI-CANCER RESPONSES**

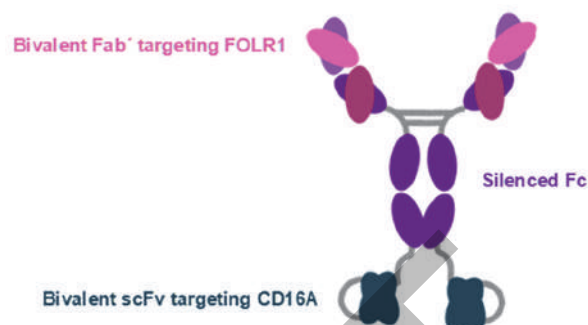
¹Ahmad Trad, ¹Michael Tomaszowski, ¹Josef Caslavsky, ²Robert Freitag, ²Keith Haan, ²Markus Rohrwild, ³Daniel O'Shannessy, ⁴Jana Siegler, ²Sudhir Penugonda, ²Peter Sandy, ²Eric Gaukel, ⁴Daniela Penston, ⁵Zoë Johnson*. ¹Abcheck, Plzen, Czech Republic; ²Roivant Sciences, New York, NY, USA; ³TMDx Consulting LLC, Philadelphia, PA, USA; ⁴Affimed, Heidelberg, Germany; ⁵Affivant Sciences GmbH, Basel, Switzerland

Background Innate Cell Engager (ICE[®]) molecules are designed to bivalently bind CD16A+ natural killer (NK) cells and macrophages and a tumor cell-surface antigen, inducing potent, tumor-directed cytotoxicity via antibody-dependent cellular cytotoxicity (ADCC) and antibody-dependent cellular phagocytosis (ADCP). AFVT-2101 (figure 1) is a tetravalent, bispecific ICE[®] that bridges folate receptor alpha (FOLR1) on tumor cells with innate immune cells, to induce potent and selective targeted tumor cell killing. Herein we describe the structure, mechanism of action and preliminary safety data of AFVT-2101.

Methods Binding of AFVT-2101 to CD16A and human FOLR1 was assessed by ELISA. Binding of AFVT-2101 to NK cells was assessed by flow cytometry in the presence of physiological levels of IgG (10 mg/mL). ADCC was assessed using a 4h- calcein release assay with purified NK cells from healthy donors against a panel of tumor cell lines with different expression levels of FOLR1. ADCP was assessed using a flow cytometry-based method with macrophages derived from healthy donor monocytes and target cell lines with different levels of FOLR1 expression. Quantification of secreted cytokines by healthy donor PBMC cultures in the presence of AFVT-2101 and target cells was assessed after a 24 h incubation using multiplex cytokine quantification.

Results AFVT-2101 binds to CD16A (both 158V and 158F variants) with an apparent avidity of 0.1 nM and to hFOLR1 with an apparent avidity of 0.5 nM. Physiological levels of competing IgG do not alter binding efficacy. AFVT-2101 induces potent and selective ADCC, even on FOLR1^{low} cells. AFVT-2101 is also shown to induce efficient ADCP *in vitro*. Further, AFVT-2101 is demonstrated to be more efficacious and potent in both ADCC and ADCP assays than farletuzumab, an Fc competent monoclonal antibody targeting FOLR1 which shares the same VH/VL sequence as AFVT-2101. Co-culture of PBMCs, tumor cells and AFVT-2101 showed concentration-dependent release of pro-inflammatory cytokines (IFN γ , IP-10, TNF α) and minimal off-target cytokine release.

Conclusions We demonstrate that AFVT-2101 selectively and potently kills tumor cells with a range of expression levels of FOLR1 by two complimentary mechanisms: ADCC and ADCP. The high avidity for CD16A imparts increased potency and efficacy compared to an Fc competent, FOLR1-targeting antibody with the same VH/VL sequence. As AFVT-2101 binds selectively to CD16A outside the IgG binding epitope, physiological levels of IgG do not compete for binding. We show that AFVT-2101 induces moderate concentration-dependent pro-inflammatory cytokine release in a target-restricted manner, confirming a potent but safe *in vitro* profile of AFVT-2101.



Abstract 1212 Figure 1 Structure of AFVT-2101

<http://dx.doi.org/10.1136/jitc-2022-SITC2022.1212>

Abstracts

1213

HYDROPHOBIC INTERACTIONS UNDERLIE RECOGNITION OF A KRAS G12V NEOANTIGEN BY A TCR-MIMIC ANTIBODY

¹Katharine Wright*, ¹Sarah DiNapoli, ²Michele Miller, ¹Sandra Gabelli, ¹P Aitana Azumendi, ¹Jacqueline Douglass, ¹Kenneth Kinzler, ¹Bert Vogelstein, ¹Shibin Zhou, ³Xiaowei Zhao, ³Zhiheng Yu. ¹Johns Hopkins School of Medicine, Baltimore, MD, USA; ²Johns Hopkins University, Baltimore, MD, USA; ³Janeila, Ashburn, VA, USA

Background Antibodies' exquisite specificity enables the development of new targeted immunotherapies for treatment in the fight against cancer. Antibodies can be engineered to target peptides derived from oncogenic proteins that are presented on the cell surface by human leukocyte antigens (pHLA).^{1, 2} Here, we describe the structural basis of recognition of a T cell receptor (TCR)-mimic antibody, termed V2, against the HLA-A*03:01-restricted KRAS^{G12V} epitope (VVVGAVGVGK), highlighting its specificity.

Methods For structural studies, the KRAS^{G12V}-specific full-length antibody (V2-IgG) was expressed in mammalian cells to generate an optimal protein fold. Structure determination of the V2-IgG in complex with KRAS^{G12V}/HLA-A*03:01 was performed by single particle cryo-electron microscopy (cryoEM). Two-dimensional and three-dimensional classifications were performed to produce a final refined map at 3.1 Å resolution. To fully understand determinants of the specificity of the V2 antibody, we determined the X-ray crystal structure of the KRAS^{WT}/HLA-A*03:01 monomer (resolution 2.6 Å). Biophysical characterization included carrying out differential scanning fluorimetry (DSF) and binding kinetics experiments using surface plasmon resonance (SPR). Furthermore, we screened a single variant library of the V2 TCRm antibody to identify key residues for peptide specificity and affinity enhancement.

Results The cryoEM complex structure revealed the V2 TCRm antibody sits on top of the KRAS^{G12V}-HLA-A*03:01 binding groove, making multiple contacts and leaning heavily towards the C-terminus of the KRAS^{G12V} peptide. All contacts made between the V2 TCRm antibody and KRAS^{G12V} peptide were aliphatic and hydrophobic in nature, with no hydrogen bonds made directly with the peptide. Three complementarity determining regions (CDRs) of the V2 TCRm antibody formed a loose cage-like configuration around the G12V neoantigen. Structural alignment of the V2 bound KRAS^{G12V}-HLA-A*03:01 and unbound KRAS^{WT}-HLA-A*03:01 structures revealed the KRAS^{G12V} peptide underwent a conformational change upon antibody binding. This observation is in congruence with the SPR data that showed a two-state binding model. Moreover, the affinity matured process yielded V2 variant antibodies with comparable or enhanced affinity, but none retained both specificity and increased T-cell activation.

Conclusions This complex structure is the first cryoEM structure of an antibody fragment binding a neoantigen-HLA target and the first structures of the KRAS^{WT/G12V} peptides presented by HLA-A*03:01 with or without an antibody in complex. Characterizing how the V2 TCRm antibody recognizes KRAS^{G12V}-HLA-A*03:01 and differences in KRAS^{WT} and KRAS^{G12V} peptide binding to HLA-A*03:01 offers insight into how highly hydrophobic peptide neoantigens can be targeted with antibody-based therapies.

REFERENCES

1. Hsiue EH, Wright KM, Douglass J, Hwang MS, Mog BJ, Pearlman AH, Paul S, DiNapoli SR, Konig MF, Wang Q, Schaefer A, Miller MS, Skora AD, Azurmendi PA, Murphy MB, Liu Q, Watson E, Li Y, Pardoll DM, Bettegowda C, Papadopoulos N, Kinzler KW, Vogelstein B, Gabelli SB, Zhou S. Targeting a neoantigen derived from a common TP53 mutation. *Science*. 2021;**371**:eabc8697.

2. Douglass J, Hsiue EH, Mog BJ, Hwang MS, DiNapoli SR, Pearlman AH, Miller MS, Wright KM, Azurmendi PA, Wang Q, Paul S, Schaefer A, Skora AD, Molin MD, Konig MF, Liu Q, Watson E, Li Y, Murphy MB, Pardoll DM, Bettegowda C, Papadopoulos N, Gabelli SB, Kinzler KW, Vogelstein B & Zhou S. Bispecific antibodies targeting mutant RAS neoantigens. *Sci Immunol*. 2021;**6**:eabd5515.

<http://dx.doi.org/10.1136/jitc-2022-SITC2022.1213>

1214 **A NOVEL ANTI-MSLN X 4-1BB BISPECIFIC ANTIBODY WITH FC EFFECT FUNCTION AUGMENTS THE ANTITUMOR EFFICACY**

Liansheng Cheng, Dayan Zhang*, Dayan Zhang, Lingling Wu, Weiming Zhou, Xiaoli Zeng, Xuejing Dai, Wenting Liu, Qun Zhao. *Hefei Hankemab Biotechnology CO., LTD, Hefei, Anhui, China*

Background Mesothelin (MSLN) is a ~71kDa cell surface glycoprotein that is rarely expressed in normal tissues but over-expressed in a variety of cancers.¹ 4-1BB is not only expressed on the surface of activated T cells and NK cells but also a marker for Treg.² Moreover, 4-1BB shows high selectivity for human tumor-derived Tregs and is associated with worse survival outcomes in patients with multiple tumor types, such as bladder cancer, glioblastoma, prostate cancer, or renal clear cell cancer.³ Here, we developed a IgG1-based bi-specific antibody, HK013-1, targeting both MSLN and 4-1BB to achieve better antitumor therapeutic efficacy.

Methods We tested the binding ability of HK013-1 to tumor cells with different expression levels of MSLN, and tested the killing ability of HK013-1-mediated NK cells against these tumor cells in vitro. Moreover, the 4-1BB agonist activity of HK013-1 was detected using CD8+T cells co-cultured with MSLN+ or MSLN- cells. To confirm the safety of HK013-1, non-specific activation of 4-1BB mediated by Fc receptor and killing potency to CD8+T cells and Tregs induced by HK013-1 was evaluated. In vivo, we verified the ability to inhibit tumor growth of HK013-1 and examined the effects of HK013-1 on spleen and tumor CD8+T cells and Tregs.

Results HK013-1 could bind to various tumor cells that differentially expressed MSLN and induce NK cells to kill these cells. In co-cultured assay, HK013-1 increased IFN- γ production only in the presence of MSLN+ cells. Compared with anti-4-1BB parent antibody and urelumab, HK013 induced weaker Fc γ R-mediated 4-1BB activation. Furthermore, HK013-1 engaged NK cells to kill Treg but not CD8+T cells. In 4-1BB humanized transgenic mice, HK013-1 was revealed to reduce the proportion of Treg cells in tumor but had no effect on CD8+T cells, and CD8+T and Treg cells in the spleen. Compared with IgG4-based bi-specific antibody, IgG1-based HK013-1 showed a more significant anti-tumor effect in MC38/MSLN tumor model.

Conclusions IgG1-based HK013-1 prevents tumor development by directly killing tumor cells and depleting Treg to relieve immunosuppression. Preclinical studies have shown that IgG1-based HK013-1 has good antitumor activity and safety, which may further develop its clinical potential.

REFERENCES

1. Weidemann S, Gorbokon N, Hflmayer D, et al. Abstract 2833: Mesothelin expression in human tumor types: a tissue microarray study on more than 13,000 tumor samples. Proceedings: AACR Annual Meeting 2021; April 10-15.
2. Luu K, Patwardhan MV, Zeng Q, et al. Regulatory T Cells Inhibit T Cell Activity by Downregulating CD137 Ligand via CD137 Trogocytosis. *Cells*. 2021;**10**(2):353.
3. Freeman ZT, Nirschl TR, Hovelson DH, et al. A conserved intratumoral regulatory T cell signature identifies 4-1BB as a pan-cancer target. *The Journal of Clinical Investigation*. 2020;**130**(3).

<http://dx.doi.org/10.1136/jitc-2022-SITC2022.1214>

1215

IGM-7354, AN ANTI-PD-L1/IL-15 IGM IMMUNOCYTOTKINE, ACTIVATES AND EXPANDS NK CELLS AND EFFECTOR MEMORY CD8+ T CELLS IN VIVO

Mélanie Desbois*, Thierry Giffon, Poonam Yakkundi, Sivani Pandey, Rodnie Rosete, Daniel Machado, Marigold Manlusoc, Susan Calhoun, Tasnim Kothambawala, Jey Ananta, Kristina Koyama, Yuan Cao, Dean Ng, Tomas Miranda-Katz, Avneesh Saini, Abhinav Jain, Hongjun Yue, Yang Cai, Miho Oyasu, Liz Bogaert, Roel Funke, Genevive Hernandez, Denise Nagata, Maya Leabman, Eric Humke, Stephen Carroll, Beatrice Wang, Bruce Keyt, Angus Sinclair, Maya Kotturi. *IGM Biosciences, Inc., Mountain View, CA, USA*

Background IGM-7354 is an engineered, humanized high affinity, high avidity anti-PD-L1 pentameric IgM antibody with an IL-15R α chain and IL-15 fused to the joining (J) chain. IGM-7354 was designed to deliver IL-15-mediated stimulation of NK and CD8+ T cells to PD-L1 expressing tumors and antigen-presenting cells, to enhance anti-tumor immune responses.

Methods IGM-7354 has 10 binding sites for human PD-L1 that cross-react with cynomolgus monkey (cyno) PD-L1, but not with rodent PD-L1. The IL-15 component of IGM-7354 binds to human and cyno β chain of the trimeric IL-15 receptor with similar affinities but has weaker affinity to rodent IL-15R β . In vitro activity of IGM-7354 on NK or CD8+ T cells was assessed using PBMCs from healthy donors. In vivo pharmacodynamic studies were conducted in cynos and humanized mice engrafted with human CD34+ cells from cord blood in the absence of tumor (BRGSF-HIS mice) or with human PBMC in MDA-MB-231 human tumor-bearing animals (MHC-/- NSG mice). Immune profiling was done by flow cytometry. Serum cytokines and chemokines were analyzed by ELISA or Luminex assays.

Results Using in vitro assays with human and cyno PBMCs, IGM-7354 dose-dependently enhanced the proliferation of NK and CD8+ T cells. These immune subsets were further phenotypically characterized in vivo in the humanized BRGSF mouse model. Increases in NKp30, Granzyme B, and the proliferation marker Ki67 in NK cells were observed in animals treated with IGM-7354 as low as 1 mg/kg. IGM-7354 also enhanced the proliferation of CD8+ T cells with an increase of serum soluble CD25, suggestive of T cell activation. In MDA-MB-231 tumor-bearing mice engrafted with human PBMCs, the frequencies of proliferating CD8+ T cells, effector memory and CD39+ TCF-1- CD8+ T cells were increased following IGM-7354 treatment. In cynos, intravenous infusion of IGM-7354 was well tolerated at dose levels up to 10 mg/kg, with increased proliferating NK and effector memory CD8+ T cells in blood and lymphoid tissues. Soluble CD25 was also elevated in the serum of treated monkeys.

Conclusions IGM-7354 administration in humanized mouse models and cynomolgus monkeys demonstrated potent activation and expansion of NK cells, effector memory CD8+ T cells, and increased levels of soluble CD25 in the serum. This approach may enhance targeted delivery of the immunostimulatory cytokine IL-15 through high affinity and high avidity binding to PD-L1 potentially improving anti-tumor responses and minimizing toxicity.

Ethics Approval The animal studies were approved by the Testing Facilities' IACUC.

<http://dx.doi.org/10.1136/jitc-2022-SITC2022.1215>

1216

THE CHIMERIC AD5/AD34 FIBER OF ICVB-1042 ONCOLYTIC VIRUS REQUIRES THE CD46 CELL SURFACE RECEPTOR FOR EFFICIENT TUMOR ENTRY

Michael Pokrass*, Peter Rosenthal, Joshua Messinger, Nathaniel Rice, Heba Nowyhed. IcoOVir Bio, San Diego, CA, USA

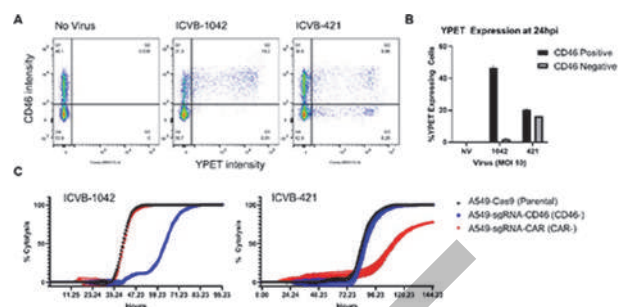
Background Viral entry into target cells through cell surface receptor-viral protein interactions is a crucial step in oncolytic virotherapy. The broad tropism and high transduction efficiency of adenoviruses (Ads) have contributed to their extensive employment in gene therapy and as oncolytic viruses (OVs). The commonly used Ad type-5 (Ad5) utilizes the coxsackie adenovirus receptor (CAR) for cell entry. However, CAR downregulation during cancer progression^{1,2} limits the therapeutic efficacy of OVs reliant on this surface protein. Group B Ads use CD46 (a ubiquitously expressed receptor frequently overexpressed in cancer)^{3,4} for cell entry, thereby presenting an opportunity to equip OVs with chimeric fibers to enhance tropism to malignant cells. We engineered ICVB-1042, a potent, selective, and systemically available OV, with an Ad5/Ad34 chimeric fiber to enable viral entry via CD46 instead of CAR proteins. Here, we demonstrate the cell entry requirements for ICVB-1042 compared to ICVB-421, an Ad5-derived virus with wild-type fiber and capsid.

Methods CD46 and CAR knockout (CD46⁻ and CAR⁻) A549 human lung carcinoma cell lines were generated using CRISPR editing. The cell lines were exposed to ICVB-1042 or ICVB-421, and the yellow fluorescent reporter protein (YPET) expression was analyzed in viable CD46⁺ and CD46⁻ cells. Viral cytotoxicity was measured using cell index, a cell viability surrogate, in CD46⁻, CAR⁻, and CD46⁺ cells. The percentage of cytolysis was quantified relative to controls (no virus). Mouse LL/2 cells expressing transgenic human CD46 were exposed to a replication-independent YPET-expressing vector with the capsid of ICVB-1042 to determine viral entry. **Results** A dramatic increase in YPET expression in CD46⁺ cells was observed post-infection with ICVB-1042, suggesting that CD46 expression is a requisite for ICVB-1042 cell entry (figure 1A-B). ICVB-421 infection was not strongly associated with CD46 expression, indicating that the absence of CD46 did not impair ICVB-421 tumor cell entry. ICVB-1042 infection induced 100% cytolysis in all cell lines faster than ICVB-421 but with a lower rate in CD46⁻ cells (figure 1C), demonstrating that CD46 deficiency induces resistance to ICVB-1042-induced tumor killing. High YPET fluorescence intensity in mouse LL/2 cells harboring human CD46 transgenes was observed, denoting that human CD46 expression by LL/2 cells enabled transduction by a vector version of ICVB-1042 (figure 2A-B).

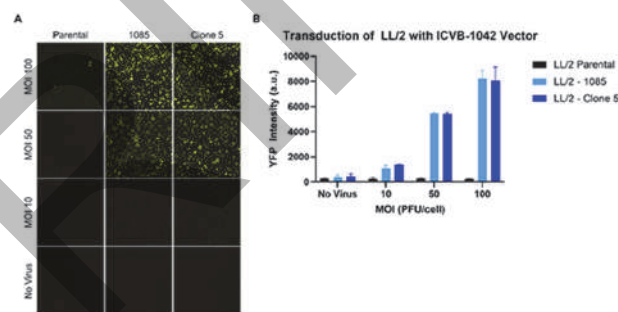
Conclusions These results demonstrate that replacing wild-type fiber with the chimeric Ad5/Ad34 fiber of ICVB-1042 results in a potent OV that relies on CD46 expression for tumor entry.

REFERENCES

1. Sachs MD, Rauen KA, Ramamurthy M, *et al.* Integrin alpha(v) and coxsackie adenovirus receptor expression in clinical bladder cancer. *Urology*. 2002;**60**:531–536.
2. Wunder T, Schmid K, Wicklein D, *et al.* Expression of the coxsackie adenovirus receptor in neuroendocrine lung cancers and its implications for oncolytic adenoviral infection. *Cancer Gene Ther*. 2013;**20**:25–32.
3. Russell S. CD46: a complement regulator and pathogen receptor that mediates links between innate and acquired immune function. *Tissue Antigens*. 2004;**64**:111–118.
4. Elvington M, Liszewski MK, Atkinson JP. CD46 and oncologic interactions: friendly fire against cancer. *Antibodies (Basel)*. 2020;**9**:59.



Abstract 1216 Figure 1 (A) Flow cytometry analysis of YPET expression in CD46 knockout cell lines; the A549 parental cell line with endogenous CD46 expression (CD46⁺) was used as a positive control. (B) Plots showing percentage of YPET-expressing CD46⁺ and CD46⁻ cells (46.5% in CD46⁺ versus 1.9% in CD46⁻ cells; $p=0.0005$, t-test). (C) Cell viability was measured at baseline and every 30 minutes for 144 hours following ICVB-1042 or ICVB-421 infection. MOI: multiplicity of infection; 24hpi: 24 hours post infection.



Abstract 1216 Figure 2 (A) Representative images showing YPET fluorescence in mouse lung carcinoma LL/2 cells (generated via piggyBac transposition) following infection of a replication-independent YPET-expressing vector of ICVB-1042. (B) Plots showing average YPET fluorescence signal intensity (with background fluorescence subtracted). MOI: multiplicity of infection; 1085 and Clone 5 are constructs expressing CD46 isoforms in parental LL/2 cell lines.

<http://dx.doi.org/10.1136/jitc-2022-SITC2022.1216>

1217

EFFICACY AND ADDITIONAL MECHANISM OF ACTION OF SACITUZUMAB GOVITECAN, A TROP-2 DIRECTED ANTIBODY-DRUG CONJUGATE, IN PRECLINICAL MODELS OF NON-MUSCLE INVASIVE BLADDER CANCER

Cih-Chien Chou, Dmytro Korniyev, Becky Yang, Jessica Orf, Hai-Ling Sun, Rutwaj Dave, Yurong Lai, Giuseppe Papalia, Thomas Cardillo, Nathalie Scholler*. *Gilead Sciences Inc., Foster City, CA, USA*

Animals and applicable laws (including the Animal Welfare Act of 1966 and, if applicable, the California Laboratory Animal Use Approval Program).

<http://dx.doi.org/10.1136/jitc-2022-SITC2022.1217>

Background Sacituzumab govitecan (SG, Trodelvy®) is a TROP-2-directed antibody (hRS7) drug conjugate (ADC) coupled to an active form of irinotecan (SN-38) via novel hydrolysable linker (CL2A). SG was approved for adult patients with locally advanced or metastatic urothelial cancers after 2 lines of therapy. TROP-2 is also highly expressed by non-muscle invasive bladder cancers (NMIBC) and treatment options remain limited for BCG-unresponsive NMIBC. We developed model systems to address SG biology and efficacy during short cell exposure and to evaluate SG intravesicular instillations as a treatment option for high-risk NMIBC patients.

Methods Binding affinity of SG and its naked antibody moiety hRS7, was determined by Surface Plasmon Resonance. SN38 release from SG was measured in buffers (pH 6-8) and human urine. SG internalization was visualized by confocal microscopy and Incucyte. SG cytotoxicity after continuous vs. pulse exposure of NMIBC cells was assayed by proliferation assays and DNA damage quantification (γ H2Ax staining). SG efficacy was measured by *in vivo* imaging in sub-cutaneous vs. orthotopic NMIBC xenografts (UM-UC3-hTROP-2⁺-luc⁺) after intraperitoneal injections vs. intravesicular instillations, respectively.

Results hRS7 and SG bound mammalian-expressed human TROP-2 protein with similar affinity ($K_D=0.33$ and 0.36 nM, respectively). Free SN-38 conversion from SG was below 3.5% after 2 hours in buffer pH 6 to 8 and in human urine at 37°C. Loss of cell viability and enhanced DNA damage were demonstrated in TROP-2^{high} NMIBC cells after both continuous and short exposures to SG. In TROP-2^{high} cells, SG 2-fold more potent than control ADC after 2h-pulsed exposure (EC_{50} , $p = 0.0223$) and SG mediated more DNA damage than control ADC after 30 min-pulsed exposure ($p < 0.0001$). Moreover, SG rapidly internalizes in TROP2-positive cells (Incucyte) and, after 1-hr incubation at 37°C of RT112, 5637, and TROP-2-transduced UM-UC-3 NMIBC cells, confocal analysis demonstrated diminishing SG signal at the cell surface and appearance of SG-positive lysosomes (LAMP1⁺) along with vesicles positive for both TROP2 and SG. Finally, SG produced antitumor effects in both subcutaneous and orthotopic xenografts models (vehicle vs. SG $p < 0.0001$).

Conclusions SG colocalization with intracellular TROP-2 and LAMP1 is consistent with prompt SG internalization and SN-38 intracellular release and suggests an additional mechanism of action of SG via TROP-2-dependent endocytosis. Altogether, our results support the hypothesis that intravesicularly-delivered SG can release SN-38 payload in bladder tumor before voiding and indicate that SG instillations in bladder may offer a therapeutic option to high-risk NMIBC patients.

Ethics Approval All animal experiments were approved by the Institutional Animal Care and Use Committee of Gilead Sciences Inc. and carried out by certified staff in an Association for Assessment and Accreditation of Laboratory Animal Care International (AAALACi) accredited facility, in compliance with the institution's Guide for the Care and Use of Laboratory

1218

MSLN-TARGETED IMMUNOTOXIN LMB-100 INDUCES DEVELOPMENT OF TERTIARY LYMPHOID STRUCTURES AND TUMOR REGRESSIONS OF ORTHOTOPIC MESOTHELIOMA

Wenlong Liu*, Chin-Hsien Tai, Xiu-fen Liu, Ira Pastan. *National Institutes of Health, Bethesda, MD, MD, USA*

Background Recombinant immunotoxins (RITs) are chimeric proteins composed of an Fv linked to a toxin and kill cells by arresting protein synthesis. LMB-100 is an RIT that kills mesothelin (hMSLN) expressing cells. Mesothelin is expressed in mesothelioma and many other cancers. Clinically, we observed some patients had delayed responses to LMB-100, suggesting the induction of antitumor immunity. The present study has developed a transgenic mouse model to investigate if LMB-100 monotherapy eradicates orthotopic mesothelioma and induces anti-tumor immunity in mice, and to study the mechanism of this immunity.

Methods To study the immune response induced by LMB-100, we established an immunocompetent transgenic mice model that expresses hMSLN only in the thyroid gland, so that hMSLN-expressed cells won't be rejected. AB1-L9 mouse mesothelioma cells expressing hMSLN were injected into the peritoneal cavity. Mice were treated with LMB-100 (i.p.) and mice with complete responses (CRs) were rechallenged with tumor cells (s.c.) to determine if anti-tumor immunity has developed. Tumors were analyzed by Nanostring and protein arrays, and the distribution of various immune cells was assessed by immunohistochemistry.

Results LMB-100 treatment alone induced CRs in 19/35 mice. Importantly, the CR mice were protected from re-challenge with AB1-L9 cells (17/19 mice), indicating LMB-100 induces anti-tumor immunity in mice. Both non-targeted immunotoxin (LMB-34) and inactive immunotoxin (LMB-255) had no anti-tumor activity, indicating both cell targeting and killing are necessary. The CRs were blocked by antibodies that deplete CD8⁺ T cells, CD4⁺ T cells as well as B cells. We further analyzed regressing tumors and found that pathogen response pathways are activated as early as 12 hours, followed by upregulation of a cascade of immune-related pathways associated with chemotactic-related activities (cytokine & receptors), antigen presentation (DC function), and TIL-based cell killing activities (T cell functions). We observed tertiary lymphoid structures (TLS) with aggregations of B cells developed in the tumor. Genes encoding proteins that are responsible for chemotaxis signals, such as CCL20, CXCL13, and CCL21, were specifically increased in tumors stroma, but not in tumor cells treated *in vitro*.

Conclusions We show RIT monotherapy gives complete regressions of tumors and reprograms the tumor immune microenvironment to trigger anti-tumor immunity. The regression of the primary tumor requires CD8⁺ T cells, CD4⁺ T cells as well as B cells. LMB-100 mediated tumor cell death induces the development of TLS in the solid tumor, probably by upregulating chemotaxis chemokines and cytokines that are associated with TLS formation.

<http://dx.doi.org/10.1136/jitc-2022-SITC2022.1218>

1219

NONCLINICAL SAFETY EVALUATION OF SACITUZUMAB GOVITECAN, A TROP-2-DIRECTED ANTIBODY DRUG CONJUGATE (ADC), FOR NON-MUSCLE INVASIVE BLADDER CANCER

Carrie McMahon*, Lauri Diehl, Laurie Tatalick, Jennifer Boggs, Sunish Mohanan, In Kyoung Mah, Jordan Kardos, Chih-Chien Chou, Congrong Niu, Rutwiji Dave, Nathalie Scholler, Yurong Lai. *Gilead Sciences, Foster City, CA, USA*

Background Trodelvy® (sacituzumab govitecan-hziy, SG) is approved as second-line therapy for patients with locally advanced or metastatic bladder cancers (BC). SG is a TROP-2-directed ADC that delivers an active metabolite of irinotecan (SN-38) to tumors. SG binds to Trophoblast cell-surface antigen 2 (TROP-2), a cell-surface glycoprotein overexpressed in various solid tumors, including non-muscle invasive bladder cancers (NMIBC), and is also expressed in normal epithelial bladder cells. SG cytotoxic payload, SN-38, forms a ternary complex with Topoisomerase 1 (TOP1)-DNA complex. Most BC are diagnosed as NMIBC and treatment options remain limited for BCG-unresponsive patients with high-risk papillary tumors or with carcinoma *in-situ*. We hypothesize that local instillation of SG could offer an alternative to radical cystectomy for the treatment of high-risk NMIBC patients.

Methods Human TROP-2 expression was evaluated in cell lines by flow cytometry and in a bladder cancer tissue panel by IHC and compared to TROP-2 quantification by LC-MS/MS. Normal cynomolgus monkey bladder tissue was similarly analyzed. Human TOP1 RNA expression was quantified and compared across TCGA normal, tumor-adjacent, and tumor tissue panels. SG toxicity for normal epithelial bladder cells and tumor cells was assessed after pulse exposure for apoptosis (annexin V) and DNA damage (p- γ H2AX). SN-38 release from SG in human and monkey urine was determined under various pH conditions. Following two (once weekly) bladder instillations of SG to cynomolgus monkeys, urine cytology and histopathology of uroepithelial tissues were assessed, along with urine and plasma SG exposures.

Results TROP-2 protein detection (IHC) and quantification (LC-MS/MS) were consistent across human bladder cell lines, and human and monkey normal bladder tissues. TROP-2 distribution was differentially localized in normal bladder compared to tumor tissues. TOP1 RNA expression was upregulated in various TCGA tumors compared with normal tissues, consistent with increased SG sensitivity of bladder cancer cell lines compared to normal epithelial bladder cells. Minimal increases in free SN-38 levels in human or monkey urine following 1-hour incubation under physiological conditions with SG were noted. SG was well-tolerated in monkeys with no in-life or histopathological changes following two weekly instillations of 1 hour each, and SG and SN-38 plasma exposures were minimal.

Conclusions Overall, *in vitro* and *in vivo* data suggest that SG intravesicular instillation may provide a favorable safety risk benefit for high-risk NMIBC patients. SG instillation in naïve monkey bladder showed no toxicity at a localized exposure margin of approximately 2.5-fold higher than the projected efficacious dose for NMIBC patients.

Ethics Approval All animal experiments were approved by the Institutional Animal Care and Use Committee of Gilead Sciences Inc. and carried out by certified staff in an Association for Assessment and Accreditation of Laboratory Animal Care International (AAALACi) accredited facility, in compliance with the institution's Guide for the Care and Use of Laboratory

Animals and applicable laws (including the Animal Welfare Act of 1966 and, if applicable, the California Laboratory Animal Use Approval Program).

<http://dx.doi.org/10.1136/jitc-2022-SITC2022.1219>

Immuno-Engineering

1220

DEVELOPMENT OF B CELL MATURATION ANTIGEN (BCMA)-SPECIFIC CD8⁺ CYTOTOXIC T LYMPHOCYTES USING INDUCED PLURIPOTENT STEM CELL TECHNOLOGY FOR MULTIPLE MYELOMA

¹Jooeun Bae*, ¹Shuichi Kitayama, ¹Zach Herbert, ²Laurence Dameron, ¹Nikhil Munshi, ¹Jerome Ritz, ³Shin Kaneko, ¹Kenneth Anderson. ¹Dana-Farber Cancer Institute, Boston, MA, USA; ²Harvard University, Cambridge, MA, USA; ³Kyoto Univ., Kyoto, MA, USA

Background A strategy for reversal of T cell exhaustion is reprogramming of antigen-specific CTL to early lineage memory T cells with selective anti-tumor activities. To accomplish this goal, we epigenetically reprogrammed BCMA-specific CD8⁺ CTL to a pluripotent state through key defined transcription factors, established “induced Pluripotent Stem Cells (iPSC)” exhibiting transcriptional and epigenetic features, re-differentiated them back into antigen-specific CTL and evaluated their properties and functional activities against multiple myeloma (MM).

Methods Functionally active IFN- γ producing HLA-A2 heteroclitic BCMA₇₂₋₈₀ (YLMFLLRKI)-specific CD8⁺ CTL were applied for iPSC via transduction of four reprogramming factors (OCT3/4, SOX2, KLF4, c-MYC). Upon characterization of the BCMA-specific iPSC with high pluripotency potential, embryoid body was formed from the iPSC and further polarized into mesoderm layer development as evidenced by upregulation of transcriptional regulators (ABCA4, BMP10, CDH5, FOXF1, HAND1, PLVAP, SNAI2, TBX3). Next, BCMA-specific embryoid body-derived hematopoietic progenitor cells (HPC; CD34⁺ CD43⁺/CD14⁻ CD235a⁻) were sorted and induced to undergo T cell differentiation in the presence of Fc-DLL4 signaling and retonectin.

Results Our RNAseq analyses demonstrated unique transcriptional profiles of HPC from different iPSC clones committing to CD8⁺ T cells or other cell lineages (monocytes/granulocytes, B lymphocytes/NK cells). Principal component analyses demonstrated a high similarity and low variability of transcription profiles within the replicates of HPC committed to the same cell lineage. In addition, distinct genome-wide shifts and differential gene expression profiles were detected in HPC committed to each specific cell differentiation pathway. Specifically, the HPC commit to CD8⁺ T cells utilized a diverse repertoire of modulators promoting development of T cell maturation, specific immune response regulation, memory T cells, cytotoxicity and interferon induction, which were significantly higher than shown in HPC that differentiate to other cell lineages. In parallel, specific repression genes were identified in the HPC commit to CD8⁺ T cells, which develop TGF- β receptor, rearrangement of Ig heavy chain genes and inhibitory receptors. The T cells differentiated were mainly CD45RO⁺ memory CTL and fully rejuvenated without immune checkpoints expression and regulatory T cells and with high anti-MM activities.

Conclusions These findings identify genetic and epigenetic mechanisms and regulatory elements, which play key roles during lineage specific commitment of HPC developed in iPSC into CD8⁺ CTL and help to further design a next generation of regenerative medicine that provide the appropriate signals for T cell lineage commitment from progenitor cells.

<http://dx.doi.org/10.1136/jitc-2022-SITC2022.1220>

1221 **BP1202-NF2, A NOVEL ADCC-ENHANCING CD39 ANTIBODY, INDUCES DESTRUCTION OF REGULATORY T CELLS AND ENHANCES CYTOTOXIC T LYMPHOCYTES INDUCTION**

Toshifumi Obonai*, Haruka Ban, Motoya Mie, Norihiro Nakamura. *BrightPath Biotherapeutics, Kawasaki, Japan*

Background The immune suppression in the tumor microenvironment (TME) was promoted by the adenosine signaling in metabolites downstream of CD39 (ENTPD1). CD39, an extracellular enzyme, is one of the surface markers of regulatory T cells (Tregs). Tregs were suppressive immune cells that induce inhibitory and anti-proliferative effects on effector cells. Therefore, selective reduction of tumor-infiltrating Tregs is expected to re-invigorate anti-tumor immunity. Here, we describe the development of BP1202-NF2, a novel glycosylation-modified monoclonal antibody (mAb) targeting human CD39 that induces Treg depletion through antibody-dependent cellular cytotoxicity (ADCC) followed by antigen specific cytotoxic T lymphocytes (CTLs).

Methods Anti-human CD39 antibodies were screened by sorting B cells of mice immunized with human CD39 protein. The clones that inhibited the enzyme activity of CD39 were humanized on IgG1. A glycosylation modification was then introduced to the antibody during its production. Binding to human CD39 and Treg was evaluated via surface plasmon resonance (SPR) or flow cytometry. Functional assay was performed by Promega CD16 (V/F variants) ADCC signaling assay. Treg depletion and CTL induction were assayed using peripheral blood mononuclear cells (PBMCs) from healthy donors.

Results The humanized anti-CD39 antibody, BP1202 has a high affinity for the recombinant CD39 protein (K_D : 481 pM) and inhibits the enzyme activity on CD39-expressing cells and human Tregs (IC_{50} : 1 nM). BP1202-NF2, a glycosylation-modified version of BP1202, binds to CD39 on activated Treg with a K_D value in the nano-molar range, and demonstrated a robust ADCC activity in a dose-dependent manner. The ADCC activity was conferred by the glycosylation-modification and peaked at 1 μ g/mL in PBMCs with either of V and F variants of Fc γ RIIIa receptor. By using ADCC assay, BP1202-NF2 selectively depleted CD39^{hi} T cell populations and completely CD39^{hi} Tregs in PBMCs from healthy donors. Further stimulation with CMV peptide robustly induced antigen-specific cytotoxic T lymphocytes. Their exhaustion level was lower than the reference antibodies.

Conclusions The humanized anti-CD39 antibody with glycosylation modification, BP1202-NF2 specifically binds to CD39 and targets CD39^{hi} Tregs for depletion via ADCC and subsequently enhances CTL induction. Our results suggest that BP1202-NF2 modulates the TME to promote immune response in human tumors via Treg depletion and inhibition of CD39 enzymatic activity.

Ethics Approval The present study was approved by the Institutional Ethics Committee of BrightPath Biotherapeutics Co., Ltd. (approved number: ERD-01).

<http://dx.doi.org/10.1136/jitc-2022-SITC2022.1221>

1222 **IN SITU CAR THERAPY USING ORNA™ LIPID NANOPARTICLES REGRESSES TUMORS IN MICE**

Robert Mabry*, Amy Becker, Alex Wesselhoeft, Allen Horhata, Akinola Emmanuel, Thomas Lee, David Soto, Akshi Thakkar, Ramya Elangovan, Magnolia Chinn, Sharmistha Kundu, Kevin Kauffman, Kristen Ott, Trent Stevens, Yessica Wiryawan, Ashley Wong, Ian Langer, Rahul Vungutur, Corey Ciullo, Zifiso Nyoni, Nelson Chau, Thomas Barnes. *Orna Therapeutics, Cambridge, MA, USA*

Background LNP-mediated delivery of long coding RNA has been clinically validated for vaccines and gene editing. We have been developing a novel, synthetic, circular coding RNA platform (oRNA technology) which exhibits significant improvements in production, expression and formulation compared to mRNAs. Lacking the cap structure of mRNA, our oRNA technology uses a proprietary sequence-based IRES element to initiate protein translation in target cells. At the same time, *ex vivo* generated chimeric antigen receptor (CAR) T cell therapies have had tremendous success in treating hematologic malignancies, yet manufacturing, safety and efficacy challenges remain. At Orna Therapeutics, we are combining oRNA technology with novel immunotropic LNPs to address these challenges, by creating off-the-shelf “autologous” *in situ* CAR (isCAR™) therapies.

Methods Orna’s immunotropic LNPs show preferential biodistribution to the spleen, with oRNA reporter expression detected in multiple immune cell subsets, including T cells, macrophages and NK cells. Delivery to immune cells is preserved across mice, rats and non-human primates. *In vitro*, expanding human T cells expressing an anti-human CD19 CAR oRNA show potent and sustained cytotoxicity and pro-inflammatory cytokine production compared to controls. To maximize protein expression, we developed FoRCE (Formulated oRNA Cell-based Evaluation)[AB1] [AW2] : a robust high-throughput platform that enables parallel arrayed synthesis, purification, lipid nanoparticle (LNP) formulation, and cell-based screening of oRNAs. We applied FoRCE to almost 3,000 unique oRNAs containing UTRs extracted from viral genomes and discovered hundreds of IRESs that drive translation from synthetic oRNA in primary human T cells, hepatocytes, and myotubes.

Results Select IRESs from this screen drove high levels of CAR expression in primary human T cells. This elevated CAR expression translated to significantly improved tumor regression in a human PBMC-engrafted NALM6 tumor-bearing mouse model. Tumor regression was dose-dependent, and the novel immunotropic LNP was well tolerated. oRNA-enabled isCAR therapies promise a re-dosable and scalable immune cell therapy.

Conclusions This off-the-shelf treatment does not require leukapheresis or lymphodepletion, and the transient expression of isCAR may provide better management of cytokine release syndrome (CRS) and complexities associated with tumor lysis as compared to conventional autologous cell therapy. Future opportunities exist to expand targeting strategies and leverage a payload capacity (up to 12 kb) well beyond the current cell therapy delivery space.

<http://dx.doi.org/10.1136/jitc-2022-SITC2022.1222>

1223

NG-796A: A T-SIGN VECTOR DESIGNED TO REPROGRAM THE TUMOR MICROENVIRONMENT AND DRIVE ANTI-TUMOR IMMUNITY

Manuela Zonca*, Katy West, Carla Cerqueira, Alice Muntzer, Rochelle Lear, Samuel Hardy, Darren Plumb, Maria Stella Sasso, Eva Vainiute, Tae Hyun Jang, Samantha Bucktrout, Brian Champion. *PsOxus Therapeutics Ltd, Abingdon, UK*

Background T-SIGn virus vectors are transgene-modified variants of enadenotucirev (EnAd), an Ad11p/Ad3 chimeric group B adenovirus, which retain all the functional and epithelial tumor-selectivity properties of EnAd, while also mediating the selective expression of transgenes by infected tumor cells. NG-796A is a vector encoding a single chain variant form of the human interleukin (IL)-12, IL-15, a soluble form of the Sushi domain of IL-15 receptor alpha (IL-15R α), and the chemokine CCL21. Locally produced IL-12 and IL-15 cytokines can synergize to drive T- and NK cell activity within the tumor microenvironment (TME) to promote an effective anti-tumor immunity. Dendritic cells can be recruited by the CCL21 gradient to enhance the uptake and presentation of tumor antigens.

Methods Transgenes were placed under the control of the virus major late promoter (MLP) which is activated following initiation of genome replication in permissive epithelial tumor cells. Tumor cell lines and primary cells derived from surgically-excised patient tumor samples were infected to evaluate the production and activities of the different transgenes. Further functional experiments were run with peripheral blood derived T-cells and NK cells from healthy volunteers. *In vivo* data were obtained in a model of immunodeficient mice bearing human tumor xenografts, and adoptively transferred with tumor antigen specific CAR-T cells.

Results High levels of functionally active IL-12, as well as the other three transgenes, were produced by *in vitro* infected tumor cells. Interestingly, our initial screening of vectors demonstrated that an effective secretion of IL-15 requires co-expression of the Sushi domain of IL-15R α . In NG-796A-infected tumor cells co-cultured with T-cells and NK cells, as well as in primary human tumor cell cultures, sustained IL-12 and IL-15 transgene production synergized potently to drive IFN γ production. In *in vitro* transwell-migration assays, CCL21 produced by NG-796A selectively increased the chemotaxis of dendritic cells. Results obtained using human A549 tumor xenografts in immunodeficient mice, showed that intravenous dosing with NG-796A synergized with adoptively transferred tumor antigen specific CAR-T cells to induce long-term clearance of the tumor mass (an effect not observed in mice dosed with EnAd with or without CAR T-cells). This data is consistent with the encoded transgenes supporting the infiltration and anti-tumor activity of T-cells in this solid tumor setting.

Conclusions Due to its potential to reprogram the TME and support T-cell activity, NG-796A was selected as a candidate for progression into formal preclinical development activities in preparation for clinical evaluation.

<http://dx.doi.org/10.1136/jitc-2022-SITC2022.1223>

1224

CELL-SPECIFIC NANOENGINEERING STRATEGY TO DISRUPT TOLEROGENTIC SIGNALING FROM MYELOID-DERIVED SUPPRESSOR CELLS AND INVIGORATE ANTITUMOR IMMUNITY IN PANCREATIC CANCER

Nilesh Deshpande, Anna Bianchi, Iago De Castro Silva, Babu Surnar, Ifeanyichukwu Ogbuoro, Siddharth Mehra, Samara Singh, Vanessa Garrido, Nipun Merchant, Shanta Dhar, Jashodeep Datta*. *University of Miami Miller School of Medicine, Miami, FL, USA*

Background A defining hallmark of immunosuppression in pancreatic ductal adenocarcinoma (PDAC) is the frequent trafficking of neutrophilic/granulocytic myeloid-derived suppressor cells (gMDSC) which exert their tolerogenic anti-T-cell functions through multiple mechanisms, particularly STAT3-mediated arginase-1 (Arg1) activity. Systemic inhibition of gMDSC trafficking and/or function (e.g., CXCR2, TGF- β , etc.) has been disappointing due to neutropenia, compensatory myelo-poietic adaptations, and off-target effects. We sought to design a novel nanoengineering strategy to abrogate tolerogenic signaling in a gMDSC compartment-specific manner.

Methods We chemically modified AZD5069—a small-molecule inhibitor of the gMDSC surface receptor CXCR2—by conjugating it with polyethylene glycol (PEG) to enhance aqueous solubility. This AZD5069-PEG construct was chemically grafted on an amphiphilic polysaccharide derivative to engineer AZD5069-decorated nanoparticles (NP^{CXCR2}). We encapsulated hydrophobic STAT3i Ruxolitinib in NP^{CXCR2} nanoparticles and compared its effect on inhibition of Arg1 activity from gMDSCs and T-cell activation *in-vitro* and *in-vivo*.

Results To confirm CXCR2 as a gMDSC-specific target, we identified exclusive expression of CXCR2 in gMDSCs in human and murine PDAC via single-cell RNA sequencing and flow cytometric analysis in peripheral blood mononuclear cells derived from treatment-naïve PDAC patients (n=57). NP^{CXCR2} loaded with Cy5.5 dye showed dramatically higher uptake in gMDSC-like promyelocytic J774 cells compared with other PDAC-relevant cells *in-vitro*—KPC6694c2 tumor-cells, cancer-associated fibroblasts (CAF), and M0 macrophages RAW274.1. In *in-vivo* orthotopic *K-ras*^{LSL.G12D/+}; *p53*^{R172H/+}; *Pdx1*^{Cre/+} (KPC) tumor cell:CAF co-injection models, although Cy5.5 dye-loaded non-AZD5069 decorated NP^{CTL} and NP^{CXCR2} both trafficked to tumor sites equally, NP^{CXCR2} but not NP^{CTL} constructs preferentially concentrated in F4/80⁺Ly6G⁺ gMDSCs compared with F4/80⁺ macrophages, F4/80⁺Ly6C⁺ monocytic MDSCs, EpCAM⁺ tumor cells, PDPN⁺ CAFs, CD3⁺ T-cells, and Cd11c⁺ dendritic cells by flow cytometry. Encapsulation of STAT3i Ruxolitinib in NP^{CXCR2} and treatment of endogenous pSTAT3^{hi} J774 cells *in-vitro* showed significantly more durable inhibition of pSTAT3 compared with Ruxolitinib drug treatment alone. Consequently, given that JAK2/STAT3 signaling is the major regulator of Arg1 activity in gMDSCs, Ruxolitinib-NP^{CXCR2} treatment of J774 cells significantly reduced gene expression and enzymatic activity of Arg1 compared with free Ruxolitinib treatment. Co-culture of splenocyte-derived murine CD8⁺ T-cells with J774 treated with Ruxolitinib-NP^{CXCR2} showed significant improvement in T-cell IFN- γ release compared with NP^{CTL} or free Ruxolitinib-treated co-culture conditions. In orthotopic KPC tumor-bearing mice, intravenous delivery of NP^{CXCR2}-encapsulated Ruxolitinib significantly augmented intratumoral trafficking of IFN- γ ⁺CD107a⁺ CD8⁺ T-cells, compared with free Ruxolitinib treatment, without appreciable systemic neutropenia *in-vivo*.

Conclusions Cell-specific delivery of payloads via CXCR2-homing nanoparticles represent a novel immunotherapeutic strategy to target tolerogenic signaling pathways in gMDSCs and invigorate antitumor immunity in PDAC.

Ethics Approval All animal experiments were performed in accordance with the NIH animal use guideline and protocol 21-176 approved by the Institutional Animal Care and Use Committee (IACUC) at the University of Miami.

<http://dx.doi.org/10.1136/jitc-2022-SITC2022.1224>

1225

NCG-SGM3 HUMANIZED MICE – AN IDEAL MODEL FOR HUMAN IMMUNE RECONSTITUTION OF T AND MYELOID CELL LINEAGES

Shiyong Guo, Cunxiang Ju, Hongyan Sun, Mingkun Zhang, Liyou Dong, Mengting Wang, Shuai Li, Dong Li, Huiyi Wang, Santi Suryani Chen, Zhiying Li*, Mark Moore, Jing Zhao, Xiang Gao. *GemPharmatech, Nanjing, China*

Background Immunodeficient mice transplanted with human hematopoietic stem cells (HSC) have been extensively used in immuno-oncology studies to evaluate therapeutic agent's efficacy against cancer cells. However, the lack of human cytokines in these mice provides limited growth support for human immune cells beyond human T cells. Increasing evidence show that myeloid cells, such as macrophages and monocytes, provides critical functions in the immune system's anti-tumor effect.

Methods We established a mouse model, NCG-SGM3, that can support T and myeloid cells in such a way that the evaluation of agents that require the interplay between these two critical immune cell populations can be evaluated appropriately. This model was genetically engineered on the severe immunodeficient strain NCG and can produce human granulocyte/macrophage colony stimulating factor 2 (GM-CSF, also named as CSF2), interleukin-3 (IL-3) and stem cell factor (SCF, also known as KITLG).

Results Upon human CD34⁺ HSC cells transplantation, increased myeloid lineage cells, such as granulocytes, monocytes, neutrophils, macrophages, and dendritic cells, were evident in the NCG-SGM3 cohort compared to NCG. The NCG-SGM3 mouse also supports the development of human T cells, and preliminary data showed increased B cells and NK cells as well.

Conclusions The NCG-SGM3 is an appropriate model for studying therapeutic agents that require human T cells and myeloid cells.

<http://dx.doi.org/10.1136/jitc-2022-SITC2022.1225>

1226 **NCG-hIL15 HUMANIZED MICE – AN EXCELLENT MODEL FOR HUMAN IMMUNE RECONSTITUTION OF NK CELLS**

Xing Liu, Meirong Wu, Huiji Wang, Weiwei Yu, Hongyan Sun, Cunxiang Ju, Hongyu Wang, Zhiying Li, Mark Moore, Jing Zhou, Xiang Gao, Santi Suryani Chen*. *GePharmatech, Nanjing, China*

Background IL-15 is a four α -helix bundle cytokine produced by dendritic cells, monocytes, and epithelial cells. IL-15 is necessary for the development, survival, and activation of natural killer (NK) cells.

Methods Human *IL-15* (*hIL-15*) was knocked into NCG mice to create a model (NCG-hIL15) that can assist the reconstitution of human NK cells.

Results Compared with NCG, hIL-15 expression was significantly increased in NCG-hIL15het and NCG-hIL15homo. The development and function of human NK cells were evaluated in the NCG-hIL15 mouse reconstituted with three different types of human cell sources: (1) purified NK from human PBMC, (2) human PBMC, and (3) human CD34+ hematopoietic stem cells (HSC). In PBMC and CD34+ HSC-reconstituted mice, NK cell development was evident, with approximately 20% of hCD45+hCD56+ NK cells detected in the peripheral blood within weeks of engraftment. The level of hCD45+hCD3+ T cells reached 10 to 30% within 12 weeks of HSC reconstitution, while it reached greater than 80% within 2 weeks of PBMC reconstitution. In the purified NK engrafted cohort, the hCD45+hCD56+ NK cell numbers increased by at least two-fold within the first 3 weeks. Human NK cells were detected in multiple tissues and organs of all reconstituted NCG-hIL15 mice regardless of source of engraftment, except the colon, in the hPBMC-reconstituted NCG-IL15 mice. It was also noted that the level of NK cells post-engraftment varied depending on the donor of the PBMC.

To determine whether the reconstituted NK cells remain functional, purified NK cells from CD34+ HSC engrafted NCG-IL15 were isolated. Data showed that the NK cells could exert cell cytotoxicity when tested in vitro with leukemia cells, Raji, and Rituximab. Similarly, in vivo tumor growth inhibition (TGI= 49%) was observed with Raji.

Conclusions Overall, the addition of human IL-15, via genetic engineering in immunodeficient NCG mice provides excellent support for NK cell development. The NCG-hIL15 is a valuable tool for NK cell research and preclinical agent evaluation that requires NK and T cell activity.

<http://dx.doi.org/10.1136/jitc-2022-SITC2022.1226>

Abstracts

1227

ELIMINATING THE IMMUNOTOXICITY OF INTERLEUKIN-12 THROUGH PROTEASE-SENSITIVE MASKING

¹Jun Ishihara*, ²Aslan Mansurov, ²Jeffrey Hubbell. ¹Imperial College London, London, UK; ²University of Chicago, Chicago, USA

Background Checkpoint inhibitor (CPI) immunotherapy demonstrates modest efficacy against immunologically ‘cold’ or immune-excluded tumors, therefore needs another approach for majority of patients. Although interleukin-12 (IL-12) is a promising antitumor cytokine that enables activation and recruitment of immune cells into tumors, its widespread use in the clinic has been hindered due to severe immune-related adverse events (irAEs). An ideal IL-12 therapy would restrict the proinflammatory effects of IL-12 to the tumor site, while limiting its exposure in the periphery.

Methods Here, we solved the IL-12 toxicity challenge by exploiting the preferential overexpression of proteases (Matrix Metalloproteinases, Serine Proteases) in the tumor to engineer tumor-selective, masked IL-12. A IL-12RB1 receptor-based masking domain was fused to IL-12 p35 domain via a protease-cleavable linker.¹

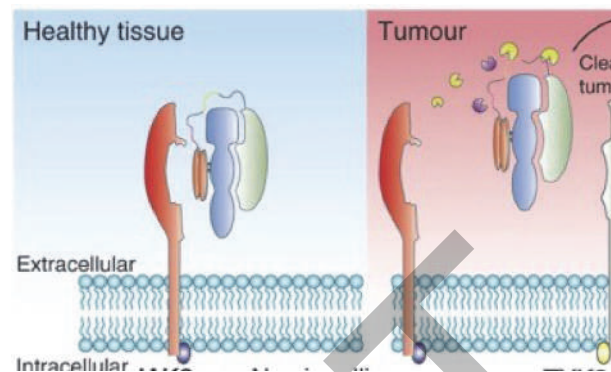
Results Recombinant fusion of masking domain to IL-12 prevented IL-12 from signaling systemically, whereas proteolytic cleavage of the linker domain by tumor-associated enzymes restored the biological activity of IL-12. We demonstrate that intravenously (i.v.) administered, masked IL-12 produces strong therapeutic effects through remodeling the immune-suppressive microenvironment and renders CPI-resistant tumors responsive, while systemic irAEs are eliminated, boosting the therapeutic index of this promising cytokine. In several solid tumour models, the therapeutic effects of masked IL12 were similar to its unmasked wild-type form, yet its toxicity was as low as saline injections. Masked IL-12 synergised with anti-PD-1 antibody for efficacy. We found that addition of human tumour lysates, and not adjacent healthy tissue lysates, cleaved off the mask, induced significant IFN γ production and STAT4 phosphorylation, similar to wild-type IL-12. We made fully humanized masked IL-12 molecule already.

Conclusions Masking approach to IL-12 may solve the toxicity issue of IL-12 observed in 1990s clinical trials, while maintaining extremely high anti-tumor effects in immunologically cold tumors (figure 1).

REFERENCE

1. Mansurov A, Ishihara J, Hubbell JA. Masking the immunotoxicity of interleukin-12 by fusing it with a domain of its receptor via a tumour-protease-cleavable linker. *Nature Biomedical Engineering*, May 2022

Ethics Approval All animal experiments performed in this work were approved by the Institutional Animal Care and Use Committee of the University of Chicago.



Abstract 1227 Figure 1 Masking IL-12 to restrict its activity only in tumor. Schematic of masked IL-12 in healthy tissues (no signalling) and in the tumour, with the mask being cleaved by various tumour-associated proteases.

<http://dx.doi.org/10.1136/jitc-2022-SITC2022.1227>

1228 **STRUCTURAL BASIS FOR LAG3 ENGAGEMENT OF IMMUNOMODULATORY LIGANDS AND ANTIBODIES**

¹Qianqian Ming, ¹Daiana Celas, ²Chao Wu, ²Aidan Cole, ¹Srishti Singh, ¹Charlotte Mason, ³Shen Dong, ¹Timothy Tran, ²Gaya Amarasinghe, ¹Brian Ruffell, ¹Vincent Luca*. ¹Moffitt Cancer Center, Tampa, FL, USA; ²Washington University School of Medicine, St. Louis, MO, USA; ³UCSF, San Francisco, CA, USA

Background Lymphocyte activation gene 3 (LAG3) was recently validated as a target for next-generation immune checkpoint inhibitors. However, unlike PD-1 and CTLA-4, we have a poor molecular-level understanding of the LAG3 immunosuppression mechanism. We determined the structure of the LAG3 ectodomain to gain insight into its architecture and assembly on the surface of T cells.¹ Subsequent functional studies identified key interfaces that mediate LAG3 engagement of antagonist antibodies and its cellular ligands Fibrinogen-like 1 (FGL1) and MHC class II.

Methods To facilitate structural studies of unstable LAG3 proteins, we used yeast display to evolve a human LAG3 variant with improved biochemical properties. This variant (named LAG3*) contains a single conservative M171I mutation and had increased expression yield, stability, and ligand-binding affinity compared to WT LAG3. The LAG3* protein was co-crystallized with an antagonist antibody fragment and the structure was determined to 3.7-angstrom resolution. Mutational mapping identified the binding sites of FGL1 and multiple antagonist antibodies on the LAG3 protein. We also used x-ray crystallography to map the LAG3-binding site of the FGL1 protein, and we used confocal microscopy to visualize LAG3-FGL1 complex formation on the surface of Jurkat T cells.

Results The structure of LAG3* revealed an elongated “X-shaped” architecture and a dimer interface formed by domain 2 (D2) of the LAG3 extracellular domain (ECD). A potent neutralizing antibody blocked LAG3 interactions with both FGL1 and MHCII and bound to a flexible “loop 2” region within LAG3 domain 1 (D1). This loop is distinct from the “loop 1” region previously implicated in MHCII binding and suggests that dual-ligand blockade can be achieved by targeting the loop 2 epitope. Structural modeling and microscopy studies revealed that FGL1 binding to LAG3 induces clustering on the cell surface, which may be important for disrupting proper immune synapse formation.

Conclusions Our structural studies enabled us to finally “see” how LAG3 proteins are organized on the surface of T cells. Subsequent structural analyses revealed multiple potential targets for LAG3 antagonist drugs, including a potent neutralizing epitope linked to dual-inhibition of FGL1 and MHCII binding.

REFERENCE

1. Ming Q, *et al.* LAG3 ectodomain structure reveals functional interfaces for ligand and antibody recognition. *Nat. Immunol.* 2022;**23**:1031–1041.

<http://dx.doi.org/10.1136/jitc-2022-SITC2022.1228>

Abstracts

1229

IMMUNOTHERAPY IN THREE DIMENSIONS: THE TUMOR MICROENVIRONMENT, IMMUNE CELLS, AND TUMOR INVASION

¹W Gregory Sawyer*, ¹Duy Nguyen, ²Ryan Smolchek, ²Jack Famiglietti, ²Stephanie Warrington. ¹University of Florida, Gainesville, FL, USA; ²Aurita Bioscience, Gainesville, FL, USA

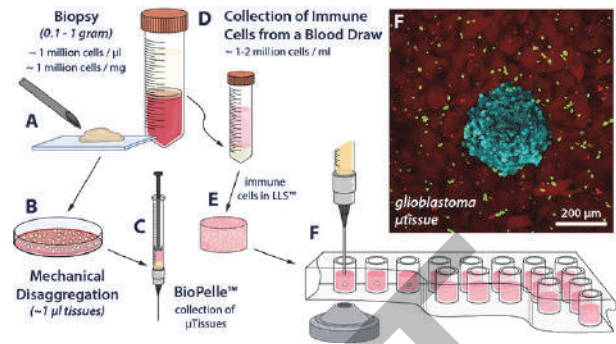
Background Cancer is a complex and heterogeneous disease, an ecosystem architecture that involves far more than just cancer cells. We have developed a 3D ex vivo culture platform that enables the controlled delivery of media and removal of waste metabolites via perfusion in Liquid-Like Solids (LLS) medium that acts as both a 3D support medium and an open porous network mimicking a capillary-bed for fluid transport and cell motility. Using integrated fast scanning laser confocal microscopy we collect in situ spatiotemporal measurements of cytokine concentrations, track immune cells in the tumor microenvironment, and study tumor invasion dynamics in 3D.

Methods Glioblastoma patient derived tumor microexplants (200-400 μm) and PBMCs were co-cultured in 3D LLS. Spatiotemporal cytokine profiles were measured by 3D printing arrays of ELISA beads across the experiment to measure local concentrations of cytokines in situ. Modeling the bead kinetics (cytokine on-rates and off-rates), coupled with measurements of each bead's fluorescence at a specific time and position from the tumor periphery were fit to spatiotemporal reaction-diffusion models quantifying the tumor's production rate, concentrations, and the immuno-regulatory micro-environment (figure 1). 3D imaging of immune and cancer cells created movies that were analyzed frame-by-frame to track 3D positions, motion, proliferation, action, cell death, and elimination as well as quantify tumor evolution-dynamics, and T cell killing. Surface conjugation of the LLS microgels with type 1 collagen (COL1-LLS) enabled cell adhesion to the LLS and cancer invasion studies. Cell tracking used novel AI algorithms from astrophysics data processing (figure 2).

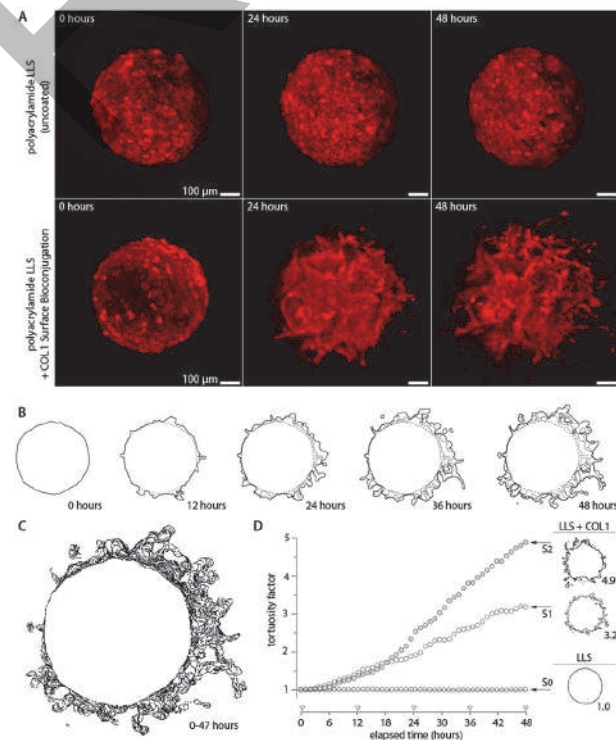
Results Fitting spatiotemporal data of cytokine concentrations revealed production rates of 2 IL8 molecules per cell per second giving tumor margin concentrations of over 2ng/ml after 10 hours (figure 3). Invasive fronts of the micro-tumor protruded into interstitial space and analysis of these invasive paths revealed super-diffusive behavior of these fronts. Off-lattice agent based computational simulations reveal that the interstitial space guided tumor invasion by restricting available paths resulting in super-diffusive behavior. COL1 bioconjugation reveals that glioblastoma cancer cells utilize anchorage-dependent migration to explore their surroundings, and geometrical cues guide 3D tumor invasion along the accessible paths. Tracking revealed both chemotaxis and chemokinetics of CD8+ cells: average migration speed of > 2.8 μm/min, and average killing rates ~3 cancer cells/h decreasing monotonically to ~1 cancer cell/h over 12 hours.

Conclusions The in vitro immuno-oncology platform with in situ fast scanning fluorescence microscopy was able to quantify spatiotemporal concentrations of cytokines, T Cell motions and activity, and tumor invasion dynamics.

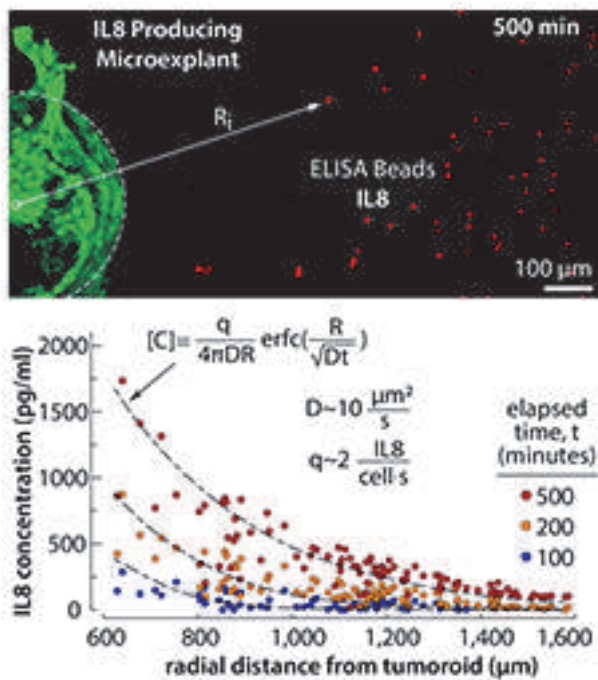
Consent Written informed consent was obtained from the patient for publication of this abstract and any accompanying images. A copy of the written consent is available for review by the Editor of this journal.



Abstract 1229 Figure 1 Schema for in vitro immunotherapy assays (A) Biopsied tissue sample and blood draw from properly consented donor. (B) The tissue sample is mechanically disaggregated into microexplants on the order of 1μl each. (C) Microexplant samples are collected in the BioPelle, a custom micromanipulator mounted on a microscope, for dispensing into sample wells. (D) Immune cells are separated from the blood draw, sorted for CD8+ and CD4+ T cells and stained with CFSE prior to dispersing in LLS and being dispensed into culture wells. (E) Microexplants are placed into a 3D dispersion of immune cells in LLS in each culture well and a liquid cover is added atop the LLS layer. (F) Maximum intensity projection image of glioblastoma microexplant (cyan) in a field of immune cells (green) within the LLS microgel bed (red).



Abstract 1229 Figure 2 Tumor invasion (A) Glioblastoma microexplant over the course of 48 hours in inert polyacrylamide LLS (top) and Collagen-1 coated polyacrylamide LLS (bottom). Where Collagen-1 context is provided, invasion outward into the surrounding regions is seen while the microexplant without Collagen context remains adherent to self. (B) Outlines of the microexplant cultured in Collagen-1 coated LLS over the course of 48 hours. (C) Microexplant outline progression over duration of the experiment (48 hours). (D) Tortuosity index over time showing monotonic increases in LLS with COL functionalization.



Abstract 1229 Figure 3 Cytokine Gradients Spatiotemporal measurements of cytokine concentrations using distributed arrays of ELISA beads allow for in situ measurements that can be fit to reaction-diffusion equations to give production rates and diffusivity for specific cytokines, such as IL8.

<http://dx.doi.org/10.1136/jitc-2022-SITC2022.1229>

1230

VIVOVEC LENTIVIRAL VECTOR PARTICLES SURFACE-ENGINEERED WITH T CELL ACTIVATING AND CO-STIMULATORY LIGANDS ENHANCE *IN VIVO* CAR T CELL GENERATION AND ANTITUMOR ACTIVITY

Chris Nicolai*, Jim Qin, Way Wu, Mollie McDonnell, Erica Shirazi, Greyson Hamilton, Max Chen, Don Parrilla, Susana Hernandez, Kathryn Michels, Shon Green, Andrew Scharenberg, Laurie Beitz, Ryan Larson, Byoung Ryu, Wai-Hang Leung. *Umoja Biopharma, Seattle, WA, USA*

Background Autologous chimeric antigen receptor (CAR) T cell therapies have revolutionized the treatment of B cell malignancies, leading to long-term remission in 30-40% of certain patient populations. Despite the promising clinical efficacy of CAR T cells in hematologic malignancies, major limitations hinder their widespread application, including challenges for patient access, complex manufacturing, and high cost.

Methods To overcome these challenges, we have developed VivoVec, a surface-engineered lentiviral vector-based platform harboring a CAR transgene that is being developed for off-the-shelf use for the generation of CAR T cells *in vivo*. To achieve specific and efficient *in vivo* T cell transduction, VivoVec particles are pseudotyped with the Cocal fusion glycoprotein and an anti-CD3 single chain variable fragment (scFv), and we have previously shown that these first-generation particles generate CAR T cells *in vivo* that mediate antitumor activity.

Results We have advanced the VivoVec platform through incorporating costimulatory molecules into the particle surface, in addition to the anti-CD3 scFv and Cocal fusion glycoprotein. These second-generation VivoVec particles exhibit enhanced T cell binding and activation, resulting in increased transduction and greater numbers of CAR+ T cells *in vitro*. In addition, CAR T cells generated with second-generation VivoVec particles exhibited a less-differentiated, central memory-like phenotype and enhanced CAR-antigen-specific polyfunctionality, including cytokine production, proliferation, and tumor cell killing. Finally, in a humanized NSG mouse model of B cell malignancy we observed that second-generation VivoVec particles generated greater numbers of CAR T cells in the blood, resulting in enhanced antitumor activity at lower doses compared to first-generation particles. Our results indicate that incorporation of costimulatory molecules onto the surface of VivoVec particles increases both the overall number and functionality of the resulting CAR T cells, greatly augmenting VivoVec mediated CAR T cell generation and antitumor activity *in vivo*.

Conclusions Overall, these data demonstrate that second-generation VivoVec particles efficiently generate large numbers of highly functional CAR T cells able to mediate durable tumor control in a preclinical model of B cell malignancy. VivoVec particles have the potential to overcome many of the limitations associated with the current class of CAR T cell therapies.

<http://dx.doi.org/10.1136/jitc-2022-SITC2022.1230>

1231

VIRUS-FREE, TARGETED INSERTION OF LONG TRANSGENES WITHIN PRIMARY NATURAL KILLER CELLS USING CRISPR-CAS9

Keerthana Shankar*, Isabelle Zingler-Hoslet, Christian Capitini, Krishanu Saha. *University of Wisconsin-Madison, Madison, WI, USA*

Background Natural killer (NK) cells are innate cytotoxic lymphocytes capable of killing virally infected cells and malignant tumors. Unlike T cells, NK cells are human leukocyte antigen (HLA)-agnostic and cause little to no Graft vs. Host Disease in allogeneic transfusions, making them excellent candidates for off-the-shelf therapies. However, current techniques to insert a chimeric antigen receptor (CAR) gene into NK cells primarily employ viral vectors. Viral methods can give rise to complications such as insertional mutagenesis, which can lead to gene silencing or oncogene activation.¹ Here we have developed a CRISPR genome editing strategy to modify primary NK cells and report the targeted virus-free CAR integration within peripheral blood NK cells.

Methods In our strategy, the transgene (e.g., CAR) is encoded in a linear double stranded DNA (dsDNA) template and produced by polymerase chain reaction (PCR). The template includes homology to the intended target for insertion that is defined by nuclease mediated double strand break formation by a Cas9-single guide RNA (gRNA) ribonucleoprotein complex (figure 1A).²

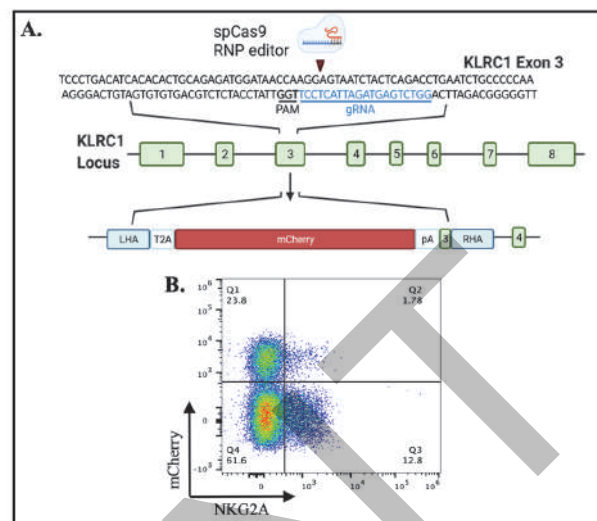
Results We show efficient (>80%) CRISPR knock-out of the inhibitory NKG2A receptor encoded by the *KLRC1* gene within primary NK cells. Optimization of electroporation timing showed that delivery of 3 mg of donor DNA on day 4 of *ex vivo* expansion results in gene knock-in rates of up to 24% for the transgene (figure 1B). Lastly, we report that the use of K562-mbIL15-41BBL feeder cells improves expansion of CRISPR edited cells by approximately twenty-fold.

Conclusions These data provide a proof-of-principle for on-target integration of long transgenes, including CAR, without viral vectors within primary NK cells via CRISPR-Cas9 genome editing. Overall, this virus-free manufacturing strategy could enable the development of novel genetically-programmed NK immunotherapies.

REFERENCES

- Shankar K, Capitini CM, Saha K. Genome engineering of induced pluripotent stem cells to manufacture natural killer cell therapies. *Stem Cell Res Ther.* 2020;**11**.
- Roth TL, Puig-Saus C, Yu R, *et al.* Reprogramming human T cell function and specificity with non-viral genome targeting. *Nature.* 2018;**559**:405–409.

Ethics Approval The study was approved by the IRB at University of Wisconsin-Madison, approval number 2018-0103.



Abstract 1231 Figure 1 Knock-in via CRISPR-Cas9 at the *KLRC1* locus

(A) Schematic showing 2.5kb transgene encoding mCherry fluorescent protein and genome editing strategy. (B) Flow cytometry results showing 23.8% knock-in of a transgene into the *KLRC1* locus in human primary NK cells 14 days after nucleofection of CRISPR reagents. RNP: ribonucleoprotein. NKG2A is encoded by the *KLRC1* locus

<http://dx.doi.org/10.1136/jitc-2022-SITC2022.1231>

1232 **ENGINEERING A PSEUDOTYPED LENTIVIRAL PLATFORM TO ENABLE LINEAGE-SPECIFIC TRANSDUCTION OF IMMUNE CELLS**

¹Blake Smith*, ¹Stephanie Dougan, ²Michael Birnbaum. ¹Harvard Medical School, Boston, MA, USA; ²MIT, Cambridge, MA, USA

Background Cell-specific transduction remains one of the next frontiers for virally-delivered gene therapy. Efforts to achieve cell-specific transduction have largely been limited to borrowing of preexisting viral glycoproteins and pseudotyping viral surface envelopes to result in altered tropism. VSVG is derived from vesicular stomatitis virus (VSV) and is one of the most commonly used lentiviral (LV) pseudotype glycoproteins as its cognate receptor (LDLR) is present on nearly all dividing and non-dividing cells, enabling broad tropism of VSVG-pseudotyped LVs.

Methods Our lab recently developed a “receptor-blinded” version of VSVG, in which point mutations (K47Q, R354A) of this glycoprotein results in a mutated VSVG with inability to bind and infect LDLR-expressing cells. This mutant viral glycoprotein, which we call “VSVGmut”, thereby loses its broad tropism, but critically retains its fusogen ability, enabling co-display of a new LV pseudotype ligand to drive LV tropism.

Results Initial experiments displaying high-affinity anti-CD19 scFvs alongside VSVGmut on the LV surface demonstrated infection of CD19+, but not CD19- cells. Subsequent work using endogenous ligands (CD80), Fabs (a-CD3e), cytokines (IL-13), viral glycoproteins (SARS-CoV-2 RBD), and peptide MHCs (pMHCs) revealed the modularity of this platform for achieving potent transduction of on-target cells, with minimal infection of bystander cells, across a range of affinities (pM to uM) and at frequencies as low as 1 in 100,000. This technology allowed for library on library screening of 96 viral pMHC-displaying LVs against a repertoire of >450,000 TCRs in pool, which accurately uncovered EBV- and Flu-specific TCRs through scRNA sequencing.

Conclusions The VSVGmut platform has resulted in our lab's ability to pair pMHCs with cognate TCRs and viral surface antigens with cognate BCRs, in addition to achieving lineage-specific transduction of T and B cell subsets, setting the stage for cell-specific gene therapy.

Acknowledgements Connor S. Dobson who initially developed the VSVGmut platform.

<http://dx.doi.org/10.1136/jitc-2022-SITC2022.1232>

1233 **REPROGRAMMING PRIMARY MELANOMA CELLS TO DENDRITIC CELL FATE ENHANCES TUMOR IMMUNOGENICITY**

¹Marta Velasco Santiago*, ²Olga Zimmermannova, ¹Morten Hansen, ³Fabio Rosa, ³Cristiana Pires, ¹Özcan Met, ³Carlos-Filipe Pereira, ¹Inge Marie Svane. ¹National Center of Cancer Immune Therapy (CCIT-DK), Herlev, Denmark; ²Molecular Medicine and Gene Therapy, Lund, Sweden; ³Asgard Therapeutics, Lund, Sweden

Background Direct cell reprogramming is characterized by the use of defined factors to rewire the transcriptional and epigenetic network of one cell-type into one of a different lineage. We have recently identified the transcription factors PU.1, IRF8, and BAFT3 (PIB) as sufficient to induce a type 1 conventional dendritic cell (cDC1) fate in both somatic and cancer cells.^{1,2} cDC1 is a rare dendritic cell subset with unique ability to initiate *de novo* T cell responses after migrating to the tumor site. Several studies have shown that higher levels of cDC1s within the tumor microenvironment strongly correlate with good prognosis and responsiveness to immunotherapy for patients with melanoma.³ Therefore, we hypothesized that PIB factors could reprogram primary melanoma cells into functional antigen presenting cDC1s capable of presenting tumor antigens and restoring anti-tumor immunity.

Methods Primary melanoma cells from eight patients were reprogrammed into cDC1-like cells through transduction with lentivirus constitutively expressing PIB. Reprogrammed cells were profiled at multiple time-points to characterize reprogramming efficiency, phenotype, and functional properties including cytokine secretion and the capacity to prime T cells.

Results All eight PIB-transduced melanoma cells progressively acquired a cDC1 surface phenotype characterized by the expression of CD45 and HLA-DR, marking the acquisition of hematopoietic and antigen presentation phenotype. The cell reprogramming process was consistent across all cell lines. Induced cDC1s also expressed CD11c, the cDC1-specific markers CLEC9A and CD141 as well as the costimulatory molecules CD40, CD80 and CD86. Functionally, cDC1-like melanoma cells at day 9 secreted the human cDC1-specific cytokines IL12p70 and IL-29 upon stimulation with Poly(I:C). After pulsing with a 9mer MART-1 peptide restricted to HLA-A2, cDC1-like melanoma cells were able to prime allogeneic HLA-A2 matched naïve CD8+ T cells and resulted in expansion of MART-1-specific T-cells after an eight-day co-culture with IL-2 and IL-7. Moreover, autologous tumor-infiltrating lymphocytes (TILs) were more reactive (higher expression of CD107a, CD137, IFN-gamma, and TNF-alpha) and cytotoxic towards cDC1-like melanoma cells compared to the original tumor cells.

Conclusions Here, we demonstrated that melanoma cells from multiple patients can be efficiently reprogrammed into cDC1-like cells and present tumor-associated antigens. These results lay the groundwork for the development of cDC1 reprogramming as an innovative cancer immunotherapy to counteract immune escape and reactivating anti-tumor immunity.

REFERENCES

1. Rosa Fábio F, et al. Direct reprogramming of fibroblasts into antigen-presenting dendritic cells. *Science Immunology*. 2018;**3**(30):eaau4292.
2. Rosa Fábio F, et al. Single-cell transcriptional profiling informs efficient reprogramming of human somatic cells to cross-presenting dendritic cells. *Science Immunology*. 2022;**7**(69):eabg5539.
3. Tucci Marco, et al. Immune system evasion as hallmark of melanoma progression: the role of dendritic cells. *Frontiers in Oncology*. 2019;**9**:1148.

<http://dx.doi.org/10.1136/jitc-2022-SITC2022.1233>

1234

NCG-MHC DKO MICE – AN EXCELLENT MODEL FOR PBMC RECONSTITUTION AND PHARMACODYNAMIC EVALUATION IN THE ABSENCE OF GVHD

Huiyi Wang, Cunxiang Ju, Mark Moore*, Jun Xing, Jialu Fan, Huanhuan Hou, Santi Suryani Chen, Zhiying Li, Jing Zhao, Xiang Gao. *GePharmatech, Nanjing, China*

Background Human immune cell reconstitution (PBMC or CD34⁺ hematopoietic stem cell; HSC) is commonly done in immunodeficient mouse lines such as NCG, NSG or NOG. The use of PBMC over CD34⁺ HSC is preferred for multiple reasons, including faster engraftment, lower cost, and the presence of mature immune cell populations. One major limitation of human PBMC reconstituted models is the acute Graft-versus-Host Disease (GvHD) that set in within weeks of PBMC injection, leading to a high mortality rate. While donor-to-donor variations exist and specific donors can be selected, the symptoms of GvHD typically occur within 4 weeks. This significantly limits the study window required for appropriate evaluation of the agents, such as cancer immunotherapies. GvHD is an immune reaction triggered mainly by donor T cells identifying the mouse MHC class I and class II as foreign and attacking the host cells and organs. Removing MHC molecules from the host seems a viable approach to avoiding GvHD.

Methods We used CRISPR-Cas9 to knockout the mouse H2-K1, H2-D1 and H2-Ab1 genes. We first generated two KO strains for H2-K1 and H2-Ab1 respectively. After identifying the correctly engineered strain targeting the H2-K1 gene, we generated H2-K1 and H2-D1 double KO strains by knocking out the H2-D1 gene in the embryos of the H2-K1 KO strain. In the final step, we generated the triple KO strain by cross-breeding the H2-K1 and H2-D1 double KO strain with the H2-Ab1 KO strain.

Results While the deletion of $\beta 2M$ (NCG- $\beta 2M$ -KO) reduces the occurrence of GvHD, this model knocked out not only the MHC class I subunit but also the FcRn subunit, which shortens the half-life of IgG, making it unsuitable for IgG antibody agent evaluation. In addition, deletion of MHC class I or class II alone resulted in low or high CD4/CD8. Compared with the existing NCG- $\beta 2M$ or other $\beta 2m$ null mouse models, the NCG-MHC dKO significantly prolonged survival and reduced GvHD occurrences when reconstituted with PBMC.

Conclusions Based on our preliminary data, the NCG[SSC1] - MHC dKO is a promising model for antibody and cell therapy agent evaluation, determining therapeutic-related cytokine release syndrome, and long-term toxicity evaluation of cell therapies.

<http://dx.doi.org/10.1136/jitc-2022-SITC2022.1234>

1235 TARGETING THE SECRETORY PATHWAY OF T CELLS TO BOOST THE EFFICACY OF CANCER IMMUNOTHERAPY

¹Anthea Wirges*, ¹Armin Rehm, ¹Mario Bunse, ¹Jara J Joedicke, ²Eric Blanc, ³Venugopal Gudipati, ¹Michael Moles, ²Dieter Beule, ³Johannes Huppa, ¹Uta Hoepken, ¹Anthea Wirges. ¹MDC Berlin, Berlin, Germany; ²BIH Berlin, Berlin, Germany; ³Medical University Vienna, Vienna, Austria

Background The efficiency of adoptive immunotherapy correlates with the ability of the transferred T cells to release effector molecules. Furthermore, T cell memory formation is important to ensure a long lasting anti-tumor effect and thus, to prevent tumor relapse. Here, we optimized the efficacy of adoptive immunotherapy by silencing EBAG9, a negative regulator of cytolytic enzyme release from CD8⁺ T cells.

Methods Using a retroviral vector that includes an intronically located EBAG9-targeting miRNA, we equipped T cells with defined TCR or CAR specificities and, simultaneously, knocked down EBAG9. *In vitro*, cytotoxicity as well as cytokine release assays were employed. Kinetics of tumor cell killing and the sensitivity of CAR activation were determined by microscopy-based methods. Knockout mice, cytotoxicity assays and xenotransplantation models served as tools to study EBAG9 functionality *in vivo*. Furthermore, T cell memory formation, *in vivo* target cell killing and tumor growth after adoptive transfer of engineered T cells were investigated.

Results EBAG9 knockdown in mouse CTLs resulted in a significant increase of antigen-specific *in vivo* killing activity. Granzyme A release from engineered human TCR and CAR CD8⁺ T cells was increased after EBAG9 silencing, while cytokine secretion was not altered. Enhanced granzyme release translated into strongly improved killing capability and kinetics without leading to faster exhaustion. Adoptively transferred EBAG9-silenced BCMA CAR T cells exhibited an extended control of multiple myeloma growth, even at low effector cell numbers. Upon leukemia challenge of *Ebag9*^{-/-} mice, the enhanced CD8⁺-mediated cytotoxicity was associated with increased commitment to the CD8⁺ T cell memory lineage. Single cell RNA sequencing revealed a preferential expression of the memory-related transcription factors *Zeb1*, *Id3*, and *Stat3* as well as anti-apoptotic genes like *Traf1* in *Ebag9*^{-/-} CD8⁺ cells.

Conclusions Targeting EBAG9 has a promising therapeutic potential when applied to adoptive immunotherapy of leukemia and multiple myeloma and represents a platform technology that can be favorably combined with variable CAR or TCR specificities. We suggest a strategy to boost the efficacy of engineered T cells that, concomitantly, facilitates an optimized manufacturing combined with the need for a lower therapeutic dose. From *Ebag9*-KO mice we infer that an enhanced primary immune response leads to improved memory formation and, thus, lowers the risk for tumor relapse. Gain of cytolytic efficacy by EBAG9 silencing does not come at the expense of adverse effects, such as faster exhaustion or release of inflammatory cytokines.

<http://dx.doi.org/10.1136/jitc-2022-SITC2022.1235>

1236

SELECTIVE DELIVERY OF LOW-AFFINITY IL-2 TO PD-1+ T CELLS REJUVENATES ANTITUMOR IMMUNITY WITH REDUCED TOXICITY

¹Zhenhua Ren*, ²Anli Zhang, ²Yang-Xin Fu. ¹Changping Laboratory, Beijing, China; ²UT Southwestern Medical Center, Dallas, TX, USA

Background Increased levels of tumor-infiltrating lymphocytes (TILs) are associated with improved survival in patients with cancer. Anti-PD-1/PD-L1-based cancer immunotherapies have revolutionized the treatment of cancers, and TIL abundance can be used as a prediction marker for immunotherapy responsiveness. Even though PD-1/PD-L1 blockade can release the brake on the T cell response, T cells are not fully functional and are limitedly expanded in the tumor. Most patients either fail to respond or develop adaptive resistance after an initial response. Importantly, the role of T cell-associated cytokines in the tumor microenvironment for anti-PD-1/PD-L1 responsiveness has not been fully studied. It is possible that additional T cell-driven cytokine therapy might overcome PD-1 therapy resistance. IL-2 is an important T cell growth factor for T cell proliferation. How to target IL-2 to tumor-specific T cells remains a challenge in IL-2 cancer immunotherapy.

Methods Here, we designed a fusion protein (IL-2 linked to an anti-PD-1 antibody) to target TILs, as TILs express more PD-1 than other cells. To reduce the binding of IL-2 to Tregs, we selected a lowaffinity IL-2 (laIL-2) that has greatly reduced binding to both IL-2R α and IL-2R β . We linked laIL-2 to an anti-PD-1 antibody (generating PD-1-laIL-2) to increase its avidity to intratumoral CD8+ T cells.

Results We fortuitously observed that anti-PD-1 therapy depends on IL-2 signaling, which raises the possibility that a lack of IL-2 limits anti-PD-1-induced effector T cell expansion. To selectively deliver IL-2 to PD-1+CD8+ tumor-infiltrating lymphocytes (TILs), we engineered a low-affinity IL-2 paired with anti-PD-1 (PD-1-laIL-2), which reduced affinity to peripheral Treg cells but enhanced avidity to PD-1+CD8+ TILs. PD-1-laIL-2 exerted better tumor control and lower toxicity than single or mixed treatments. Mechanistically, PD-1-laIL-2 could effectively expand dysfunctional and tumor-specific CD8+ T cells. Furthermore, we discovered that presumably dysfunctional PD-1+TIM3+ TILs are the dominant tumor-specific T cells responding to PD-1-laIL-2.

Conclusions Collectively, these results highlight that PD-1-laIL-2 can target and reactivate tumor-specific TILs for tumor regression as a unique strategy with stronger efficacy and lower toxicity.

<http://dx.doi.org/10.1136/jitc-2022-SITC2022.1236>

1237

IN VIVO PROGRAMMING OF MYELOID CELLS BY MRNA MEDIATED DELIVERY OF NOVEL FCA FUSION RECEPTOR ACTIVATES ANTI-TUMOR IMMUNITY

Yuxiao Wang*, Hongyun Zhao, Edward Cochran, Michael Gorgievski, Thomas Prod'homme, Bruce McCreedy, Daniel Getts. *Myeloid Therapeutics, Cambridge, MA, USA*

Background Immunotherapy has revolutionized cancer treatment. However, for the majority of patients with advanced solid tumors, sustained clinical benefit has yet to be achieved. Myeloid cells such as monocytes and macrophages readily accumulate in tumors, in some cases contributing up to 75% of the tumor mass. Reprogramming circulating and tumor associated myeloid cells to activate their ability to elicit anti-tumor adaptive immunity by phagocytosis, cytokine secretion and antigen presentation is an attractive approach to harness and orchestrate systemic anti-tumor immunity. It remains challenging to specifically target and activate myeloid cells in vivo.

Methods To overcome this hurdle, we have developed a novel in vivo myeloid cell engineering platform: Fca Receptor Fusion Constructs. Unlike other chimeric antigen receptors (CARs) the construct was engineered by fusing a tumor recognition scFv with the alpha chain of human Fc receptors. The stable expression and function of these receptors requires endogenously expressed Fc receptor gamma chain, a protein with limited expression to immune cells, mostly myeloid cells. Here, we present that intravenous infusion of lipid-nanoparticle (LNP) encapsulating the Fca Receptor Fusion Construct mRNA results in the uptake and expression of the construct by myeloid cells. In immunodeficient xenograft models of hepatocellular carcinoma and triple negative breast cancer, delivery of LNP mRNA encoding for GPC3 or TROP2 targeted Fca Receptor Fusion Constructs resulted in tumor killing, confirming the ability of this approach to program myeloid cells. Furthermore, in the B16 syngeneic melanoma model, treatment with the melanoma antigen GP75 targeted Fca Receptor Fusion Constructs was also associated with the initiation of broad systemic immune responses, characterized by tumoral accumulation of activated CD8+ T cells, reduced tumor associated Tregs and activation of antigen presenting cells in spleen. Together these studies highlight the potential of Fca Receptor Fusion Construct delivered directly in vivo to program myeloid cells to recognize and kill cancer.

http://dx.doi.org/10.1136/jitc-2022-SITC2022_1237

Abstracts

1238

SEPARATING THE WHEAT FROM THE CHAFF: ENGINEERING CARTS WITH SUPERIOR METABOLIC ATTRIBUTES AGAINST SOLID TUMORS

Yufan Zhou, Andre Kelly, Andrew Frisch, Decheng Song, Saba Ghassemi, Carl June, John Scholler, Roddy O'Connor*. *University of Pennsylvania, Philadelphia, PA, USA*

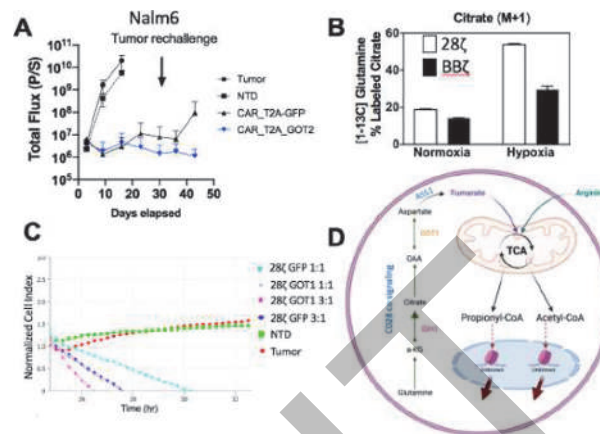
Background For cellular immunotherapies, clinical outcomes depend on the proliferative potency and metabolic fitness of the therapeutic product. For their most successful indications, CAR T cells are effective ‘serial killers,’ each T cell recognizing and eliminating many target cells. What fuels CAR T cell serial killing is unknown. Two critical events define the efficiency of T cell serial killing: migration and immune synapse formation/cytolysis. Importantly, each event is influenced by the local metabolic milieu.

Methods Using a specialized CAR T cell conditioning regimen, the goal of this research is to determine the relative energy cost of migration versus cytolysis using innovative eSIGHT RTCA technology. Our project will reveal how the spare respiratory capacity (SRC), supports CAR T cell migration and/or cytolysis, founded on the hypothesis that cells that can replenish their SRC in repetitive antigen stimulation models, are more efficient serial killers.

Results Our data sheds light on critical metabolic states that impair CAR T cell cytolytic activity. We also use multi-omic approaches to identify arginosuccinate synthase 1 (ASS1), a gene distinguishable at the metabolic (Seahorse), transcriptional (RNAseq), epigenetic level (ATAC seq), and functional (tumor clearance in vivo) in

CAR T cells. Supporting the premise of our work, we show that ASS1 supports high SRC levels despite frequent antigen encounter in repetitive stimulation models in vitro. In parallel work, we provide data that reductive glutamine metabolism is enhanced in 28zCARTs, suggesting mechanisms for why 28zCARTs outperform BBz CARTs in some hypoxic tumor models (figure 1B). We also show that expressing isoforms of the GOT family of amino transaminases enhance CAR T cell anti-tumor function (figure 1A&C). Given the prior link connecting reductive glutamine metabolism and GOT1 in Jurkat cells we hypothesize a fundamental link, involving reductive glutamine metabolism, GOT1-mediated aspartate replenishment, and fumarate production via ASS1, to support mitochondrial function and serial killing in CAR T cells (figure 1D).

Conclusions Our findings reveal unique conditioning and genetic strategies to arm CAR T cells with unique metabolic attributes against solid tumors.



Abstract 1238 Figure 1 A model for enhancing CART metabolic activity(A) Serial quantification of tumor burden in Nalm6 tumor-bearing mice treated with CAR T cells. CARTs with a superior ability to replenish aspartate (GOT2) demonstrate superior tumor control, even after tumor cell re-challenge (day 31). Data are means ± SEM from starting cohorts (n=5 mice per treatment arm), from a single experiment. (B) Lentivirally transduced CAR T cells (SS1-CAR-28z vs SS1-CAR-BBz) were expanded for 9 days until restdown. These cells were restimulated with mesothelin-fc, that was previously conjugated to dynabeads. At 5 of re-stimulation, the cells were treated with [1-13C] glutamine that distinguishes reductive gln metabolism overnight at 20% O₂ or 1% O₂. Citrate labeling (m+1 isotopologue) is accentuated in 28z CARTs. Data are means ± SEM from two independent studies with separate donors. (C) Aspartate replenishment via GOT1 enhances CAR T cell cytolytic potency as assessed by eSIGHT impedance assay. SY5Y-CD19 target cells were adhered to the well. 24 hr later, CARTs were added at various E:T ratios as indicated. Data are means ± SEM from a single experiment. (D) A novel model proposing how 28z signaling drives the vectorial flux of glutamine to citrate, which replenishes OAA, is converted to aspartate which supports TCA anaplerosis (fumarate) by ASS1.

<http://dx.doi.org/10.1136/jitc-2022-SITC2022.1238>

1239

OVEREXPRESSION OF THE CHEMOKINE RECEPTOR CCR7 CONFERS ANTI-CXCR5 CAR T CELLS WITH INCREASED HOMING TO LYMPH NODES AND ENHANCED CYTOTOXICITY TOWARD B CELL LYMPHOMA

Maria Zschummel, Jara Joedicke, Anca Margineanu, Susanne Blachut, Eric Lindberg, Norbert Hübner, Armin Rehm, Uta Höpken*. *Max-Delbrück-Center for Molecular Medicine (MDC), Berlin, Germany*

Background The efficacy of CAR T cell therapy correlates with the ability of the transferred therapeutic T cells to traffic to the respective tumor niche. We observed that engineered T cells downregulate the lymphoid homing receptor CCR7 during the manufacturing process. Consequently, *in-vitro* and *in-vivo* migration of CAR T cells toward the corresponding chemokine ligands was severely impaired. To improve nodal CAR T cell trafficking and anti-lymphoma efficacy of B-NHL-targeting anti-CXCR5 CAR T cells, we engineered CAR T cells which co-expressed the homing receptor CCR7.

Methods The anti-human CXCR5 CAR and anti-mouse CXCR5 CAR, encoded within a retroviral MP71 backbone, were generated essentially as described.¹ In case of the human and mouse CXCR5 CAR-CCR7 vectors, hCCR7 or mCCR7 cDNAs without stop codons were introduced upstream of the CXCR5 CAR cassette via P2A linkage. To test the functionality of CCR7-engineered CAR T cells *in-vitro*, transwell migration, cytotoxicity, and cytokine release assays were employed. CAR T cell killing dynamics were determined by microscopy-based methods. Mouse leukemia and lymphoma models served as tools to study *in-vivo* CCR7-modulated CAR T cell homing to lymph nodes and target cell killing.

Results CCR7 overexpression on human and mouse anti-CXCR5 CAR T cells restored their migratory capacity and improved lymph node homing. In addition, we observed an enhanced killing capacity of CCR7-equipped CAR T cells *in-vitro*, which is likely supported by the costimulatory role of CCR7 in the formation of an immunological synapse. We showed that CCR7 accumulated in mature CAR synapses, an observation that is supported by the transcriptional upregulation of genes associated with cytoskeletal rearrangement, relevant for immunological synapse formation and migration in CCR7-engineered CAR T cells.

Conclusions Therapeutically, CCR7-enforced nodal recruitment and enhanced killing kinetics of CAR T cells conferred improved lymphoma eradication in a mouse lymphoma model. Beyond improved anti-tumor responses in nodal hematological malignancies, we envisage that this CCR7-engineering approach might be useful to improve CAR T cell therapies that specifically target solid tumor entities metastasized to lymph nodes.

Acknowledgements This work was funded by grants from the HGF "Zukunftsthema Inflammation & Immunology".

REFERENCE

1. Bunse M, Pfeilschifter J, Bluhm J, *et al.* CXCR5 CAR-T cells simultaneously target B cell non-Hodgkin's lymphoma and tumor-supportive follicular T helper cells. *Nat Commun.* 2021;**12**:240.

<http://dx.doi.org/10.1136/jitc-2022-SITC2022.1239>

Immunotherapy Toxicities

1241

IL-1 BLOCKADE PREVENTS CARDIAC TOXICITY AND IMPROVES IMMUNOTHERAPY EFFICACY IN MOUSE MODELS OF PANCREATIC CANCER

¹Rakesh Jain, ²Nilesh Talele*, ²Heena Kumra, ²Igor Gomes Dos Santos, ²Sylvie Roberge, ²William Ho, ²Patrik Andersson, ²Sampurna Chatterjee, ²Marie Siwicki, ²Dan Duda, ³Mikael Pittet, ²Dai Fukumura, ²Rakesh Jain. ¹Edwin L. Steele Laboratories, MGH, Boston, MA, USA; ²Massachusetts General Hospital/Harvard Medical School, Boston, MA, USA; ³University of Geneva/Geneva University Hospitals, Geneva, Switzerland

Background Immune checkpoint blockers (ICBs) have revolutionized cancer treatment, but they are often associated with severe immune related adverse events (irAEs). These severe irAEs are more often seen in patients with obesity or concomitantly treated with cytotoxic therapies.

Methods We aimed to understand the mechanisms of ICB-induced irAEs, in the context of obesity [FD1] and ICB/chemotherapy combinations. We used a mouse model of cardiac irAEs, which is the most fatal type of irAE in ICB-treated cancer patients, with clinically relevant features: (i) an ICB-resistant cancer (pancreatic ductal adenocarcinoma or PDAC), (ii) obesity induced with high-fat diets, and (iii) a combination treatment of ICB (α -PD1 + α -CTLA4) and chemotherapy (FOLFIRINOX)[FD2]

Results Mice with orthotopic PDAC and obesity developed irAEs after treatment with ICB and chemotherapy as compared to [FD1] chow diet. These irAEs recapitulated those observed in patients with cancer and obesity, including cardiac dysfunction consistent with myocarditis, cardiac fibrosis, and increased circulating levels of interleukin-1 beta (IL-1b). IL-1b blockade prevented myocarditis and reduced cardiac fibrosis after immunotherapy. Importantly, IL-1b blockade also enhanced the anti-tumor effects of ICB + FOLFIRINOX combination therapy, and increased mouse survival.

Conclusions Using a translationally relevant mouse model, we discovered that IL-1b mediates ICB-induced cardiotoxicity, which is the most fatal type of irAE in ICB-treated cancer patients. In addition, we found that IL-1b blockers, which are already used in the clinic for other indications[FD1], may both reduce adverse events and enhance the antitumor effects triggered by immunotherapy.

<http://dx.doi.org/10.1136/jitc-2022-SITC2022.1241>

1242

ALTERED INTERACTIONS BETWEEN CIRCULATING AND TISSUE-RESIDENT CD8 T CELLS WITH THE COLONIC MUCOSA DEFINE CHECKPOINT INHIBITOR COLITIS

¹Kamil Slowikowski*, ¹Molly Thomas, ¹Kasidet Manakongtreecheep, ¹Pritha Sen, ¹Jessica Tantivit, ¹Mazen Nasrallah, ¹Leyre Zubiri, ¹Neal Smith, ¹Alice Tirard, ¹Swetha Ramesh, ¹Benjamin Arnold, ¹Linda Nieman, ¹Jonathan Chen, ²Thomas Eisenhaure, ¹Karin Pelka, ¹Katherine Xu, ¹Vjola Jorgji, ¹Christopher Pinto, ¹Tatyana Sharova, ¹Rachel Glasser, ¹PuiYee Chan, ¹Ryan Sullivan, ¹Hamed Khalili, ¹Dejan Juric, ¹Genevieve Boland, ¹Michael Dougan, ¹Nir Hacohen, ¹Bo Li, ¹Kerry Reynolds, ¹Alexandra-Chloé Villani. ¹MGH, Boston, MA, USA; ²Broad Institute, Boston, MA, USA

Background Antibodies targeting immune checkpoint inhibitors (ICIs) CTLA-4 and PD-1/PD-L1 have revolutionized the treatment of metastatic solid tumors. However, their use is limited by a high incidence of immune-related adverse events. The colon is a frequent target of this immune attack seen in up to 45% of patients on dual PD-1 and CTLA-4 blockade. We leveraged a multi-omics strategy to further our understanding of the cellular and molecular drivers giving rise to ICI-associated colitis and nominate treatment solutions that spare anti-tumor immune response.

Methods We collected paired endoscopic colon mucosal biopsies and blood specimens from 13 irColitis patients, 8 healthy individuals, and 8 controls on ICIs, and analyzed them with single-cell/nuclei RNA sequencing with paired TCR and BCR sequencing, multispectral fluorescence microscopy, and secreted factor analysis.

Results Analyses of over 300,000 single epithelial, mesenchymal, and immune single cells revealed that patients with irColitis showed expanded mucosal Tregs, *ITGAE*^{Hi} CD8 tissue-resident memory T cells expressing *CXCL13* and *Th17* gene programs. We also identified two circulating *ITGB2*⁺ CD8 T cell populations associated with irColitis – a *CX3CR1*^{Hi} population predicted to be intravascular and an *EOMES*^{Hi} *KLRG1*^{Hi} population. Comparison of dual anti-PD-1/CTLA-4 versus anti-PD1 monotherapy revealed expansion of those two circulating *ITGB2*^{Hi} CD8 T cell populations, as well as a cytotoxic *GNLY*^{Hi} CD4 T cell subset, and endothelial cells associated with hypoxia gene programs. Cell-cell communication analysis predicted crucial roles for ICAM and CXCR3 ligand-mediated recruitment and retention of these two circulating T cell populations by epithelial, endothelial and myeloid cells during active colitis. In irColitis, we also observed significant epithelial turnover marked by fewer *LGR5*⁺ stem cells, more transit amplifying cells, and upregulation of apoptotic and DNA-sensing programs. Mature epithelial cells with top crypt genes upregulated interferon-stimulated pathways, *CD274* (PD-L1), anti-microbial genes, and MHC-class II genes, and down-regulated aquaporin and solute-carrier gene families, likely contributing to epithelial cell damage and absorptive dysfunction. Transcriptional programs associated with irColitis were distinct from those in the tumor microenvironment, which may have important therapeutic implications. Finally, by examining many drugs in clinical trials for inflammatory bowel disease, we expand the putative therapeutic options for treating irColitis reported to-date.

Conclusions This multi-omics approach nominates novel irColitis therapeutic targets and redefines irColitis as a disease not simply marked by the aberrant expansion of CD8 T cells but rather altered global interactions between immune cells and the colon mucosal epithelial or mesenchymal cells.

Ethics Approval Informed consent was obtained from all patients in accordance with protocols obtained from the Mass General Brigham and/or DANA-Farber/Harvard Cancer

Center Institutional Review Boards (DFCI/HCC 11-181 and 13-416, Mass General Brigham 2015P001333).

<http://dx.doi.org/10.1136/jitc-2022-SITC2022.1242>

1243

**IMMUNE CHECKPOINT INHIBITOR-INDUCED
POLYARTHRITIS: A CASE SERIES**

Megan Smith-Uffen*, Konstantinos Tselios. *McMaster University, Hamilton, Canada*

Background Immune checkpoint inhibitors (ICIs) have revolutionized cancer care. However, their mechanism of action also results in the uncontrolled collateral of ICI-related adverse events (ICI-AEs). Polyarthrititis is a rare ICI-AE. Here we describe two cases of ICI-induced polyarthrititis, induced by nivolumab/ipilimumab and sasanlimab for melanoma and urothelial cancer, respectively.

Results A 64-year-old male received combination immunotherapy with nivolumab and ipilimumab for metastatic melanoma. Within one month of his second cycle of nivolumab alone, he developed polyarthrititis of the small joints of the hands bilaterally, as well as the shoulders and knees; active synovitis; and erosive arthropathy on radiographic findings. He was successfully treated with prednisone at 20mg daily, gradually tapered over several months.

A 43-year-old male with high-grade non-invasive urothelial cell carcinoma received two cycles of adjuvant sasanlimab. Within two months of his second treatment, he developed a large-joint polyarthrititis involving the bilateral knees, ankles, elbows, and the cervical spine. His symptoms resolved with prednisone, initiated at 50mg daily with a recommended slow taper, however resurfaced five days after he abruptly ceased treatment. He was subsequently started on methotrexate in combination with prednisone.

Both patients had a past medical history of non-rheumatological autoimmune disease, developed symptoms within 8 weeks of ICI, had elevated inflammatory markers and negative autoantibodies. Neither had to discontinue their cancer therapy and indeed both had a good tumour responses to their ICI. Both of our patients were initially well-managed prednisone. However, our second patient relapsed after abrupt cessation of his prednisone and required a combination of methotrexate with prednisone to control his symptoms.

Conclusions These cases add to the literature on ICI-induced polyarthrititis, a rare ICI-AE. Clinical manifestations most commonly resemble rheumatoid arthritis, with bilateral inflammation of the small joints. Time to onset tends to be <12 weeks after ICI exposure, and repeated ICI exposure is a risk factor. Most patients have no personal or family history of autoimmune disease, negative autoantibodies, and can be managed well with glucocorticoids. As ICIs become more widely used, rheumatologists and oncologists alike should familiarise themselves with their adverse effects. More research is needed to understand the epidemiology, clinical presentation, and treatment of these adverse events.

Consent Written informed consent was obtained from the patients for publication of this abstract. A copy of the written consent is available for review by the Editor of this journal.

<http://dx.doi.org/10.1136/jitc-2022-SITC2022.1243>

1244

ALLIANCE A151804: ESTABLISHMENT OF A NATIONAL BIOREPOSITORY TO ADVANCE STUDIES OF IMMUNE-RELATED ADVERSE EVENTS

¹David Kozono*, ²Tyler Zemla, ³Elie Dib, ⁴Mark Watson, ⁵Yujia Wen, ⁶Frank Keller, ⁷John Kirkwood, ⁸Gary Lyman, ⁹Jarushka Naidoo, ²Barb Mulhern, ⁵Laura Hoffman, ²Jennifer Le-Rademacher, ¹⁰Andrew Nixon, ¹¹Elad Sharon. ¹Brigham and Women's Hospital, Boston, MA, USA; ²Mayo Clinic, Rochester, MN, USA; ³St. Joseph Mercy Ann Arbor, Sioux Falls, SD, USA; ⁴Washington University, St. Louis, MO, USA; ⁵University of Chicago, Chicago, IL, USA; ⁶Children's Healthcare of Atlanta, Atlanta, GA, USA; ⁷University of Pittsburgh, Pittsburgh, PA, USA; ⁸Fred Hutchinson Cancer Research Center, Seattle, WA, USA; ⁹Johns Hopkins University, Baltimore, MD, USA; ¹⁰Duke, Durham, NC, USA; ¹¹National Cancer Institute, Bethesda, MD, USA

Background Immune-related Adverse Events (irAEs) are rare but serious sequelae of treatment with immuno-oncology (IO) therapeutics. These therapeutics, including monoclonal antibodies targeting programmed cell death protein 1 (PD-1), programmed death-ligand 1 (PD-L1) and cytotoxic T-lymphocyte-associated protein 4 (CTLA-4), have had transformative effects on outcomes for patients with advanced cancers. Although most patients tolerate the therapies well, a few experience irAEs ranging in severity up to life-threatening or fatal. These irAEs involve diverse organs including the heart, kidney, liver and lung, and gastrointestinal, musculoskeletal, central and peripheral nervous systems. Because of the relatively low incidence and wide variety of irAEs due to various immunotherapies for multiple tumor types, establishment of an efficient centralized repository for acquisition and organized distribution of well-annotated biospecimens is vital for translational studies that improve understanding of the molecular pathogenesis and treatment of these significant toxicities.

Methods This multi-institutional study is open at sites across the National Clinical Trial Network. Patients may be pre-registered prior to starting IO therapy, or registered when they experience one or more irAEs. Any patient who has not previously been treated with CTLA-4, PD-1 or PD-L1 inhibitors is eligible for pre-registration. These patients provide blood and stool samples prior to starting IO therapy and again after 1 month. Regardless of whether they were pre-registered, patients who received ≥ 1 IO therapeutics (e.g., CTLA-4, PD-1 or PD-L1 inhibitor) and experienced 1) ≥ 1 grade 3–5 irAEs, 2) ≥ 1 grade 2 dermatologic or rheumatologic irAEs, 3) rare infection, or 4) tumor hyperprogression may be registered to the study. IrAEs of interest include myocarditis, colitis, hepatitis, nephritis, myositis, pneumonitis, meningitis/encephalitis, dermatitis, endocrinopathies, neuropathy, other rheumatological, hematologic cytopenias, and pancreatitis. Patients may be on an NCTN or non-NCTN IO trial or be receiving standard-of-care therapy. Registration must occur ≤ 96 hours after confirmation of the irAE. Clinical data are collected at registration, after 1 month after, and for up to 1 year. Biospecimens include archival tumor blocks, biopsies of inflammatory tissues used to establish irAE diagnosis, blood for isolation of plasma and peripheral blood mononuclear cells, and stool samples. Imaging data are collected for patients with hyperprogression, pneumonitis, or other radiographically-diagnosed irAEs. Accrual goal is 2000 pre-registered and 360 registered subjects. As of June 30, 2022, 485 sites have been approved to participate and 88 subjects have been registered. Biospecimens and data will be made available to investigators following future submission and approval of proposals.

Acknowledgements U10CA180821, U10CA180882, U24CA196171; U10CA180899 (COG); U10CA180820

(ECOG-ACRIN); U10CA180888 (SWOG); U10CA180866 (NRG); <https://acknowledgments.alliancefound.org>
Trial Registration ClinicalTrials.gov NCT04242095
Ethics Approval The study is approved by the National Cancer Institute Central Institutional Review Board.

<http://dx.doi.org/10.1136/jitc-2022-SITC2022.1244>

Abstracts

1245

SAFETY AND EFFICACY OF IMMUNE CHECKPOINT INHIBITORS (ICIS) IN PATIENTS WITH PRE-EXISTING ORGAN DYSFUNCTION

Meghana Kesireddy*, Apar Ganti, Alissa Marr, Makayla Schissel. Univ. of Nebraska Medical Center, omaha, NE, USA

Background ICIs (PD-1 inhibitors, PDL-1 inhibitors, CTLA-4 inhibitors) are increasingly used to treat various malignancies. The percentage of cancer patients in the US who may benefit from ICIs has increased from 1.54% in 2011 to 43.63% in 2018¹. ICIs cause unique side effects called immune-related adverse events (irAEs). There is limited to no data regarding the safety/efficacy of ICIs in patients with pre-existing organ dysfunction, as these patients are frequently excluded from clinical trials. Our study aims to evaluate the effects of ICIs in patients with chronic kidney disease (CKD), cirrhosis, COPD (chronic obstructive pulmonary disease), and congestive heart failure (CHF).

Methods Data were obtained retrospectively for patients over 18 with any solid organ malignancy, who received at least 1 dose of ICI between 1/1/2015- 1/1/2021 and had either CKD (n=90), cirrhosis (n=20), COPD (n=142), or CHF (n=82) at our institution. Patients on chronic immunosuppression were excluded. Descriptive statistics (mean/counts/percentages) were used to summarize patient characteristics, treatment characteristics, irAEs, and outcomes. An independent samples t-test or Wilcoxon Rank Sum test was used to assess differences in continuous variables; Chi-Square or Fisher's Exact test was used to assess differences in categorical variables between patients with irAEs compared to those without irAEs. Progression-free survival (PFS) was assessed using Kaplan-Meier curves, and the log-rank test was used to assess differences in PFS. p < 0.05 was considered statistically significant.

Results In this analysis, 21/90 CKD patients, 4/20 patients with cirrhosis, 34/142 patients with COPD, and 25/82 patients with CHF had a clinically significant irAE (table 1). In each of the 4 cohorts, there were no statistically significant differences in the patient characteristics or treatment characteristics, or outcomes among patients with irAEs compared to those without irAEs (table 2). In the CKD cohort, those with irAE were significantly less likely to die than those without irAE, 52% versus 81%, p=0.009; this difference in survival was not seen in other cohorts. There was no statistically significant difference in the number of heart failure and COPD exacerbations while receiving immunotherapy in the CHF and COPD cohorts, respectively. There was no statistically significant difference in PFS between patients with irAE and without irAE in any of the cohorts (figure 1).

Conclusions Our study showed that ICIs are safe in patients with pre-existing organ dysfunction with a trend towards better PFS (though not statistically significant) in those with irAEs. This is the most extensive study to date assessing ICI in this patient population.

REFERENCE

- 1. Haslam A, Prasad V. Estimation of the Percentage of US patients with cancer who are eligible for and respond to checkpoint inhibitor immunotherapy drugs. JAMA Netw Open. 05 03 2019;2(5):e192535.

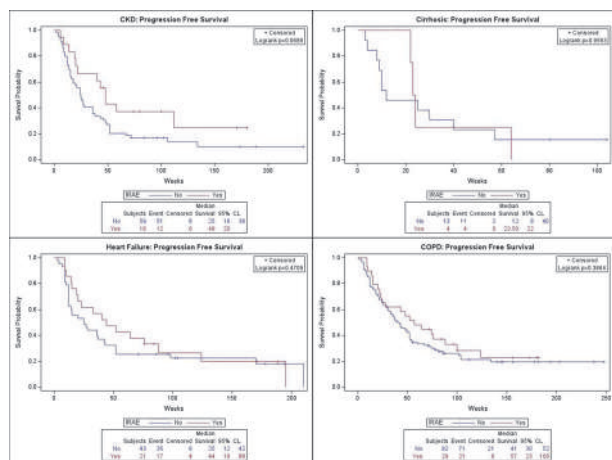
Ethics Approval The study obtained IRB (institutional review board) approval- IRB number # 320-21-EP

Abstract 1245 Table 1 Characteristics of IrAEs in CKD, cirrhosis, COPD, and CHF patients

Table with 5 columns: Cohort (CKD, Cirrhosis, COPD, CHF) and rows for Total number of patients, Number of patients with irAEs, Total number of irAEs, Grade of irAEs, Time in weeks to onset, Treatment response, and No. of patients with autoimmune conditions.

Abstract 1245 Table 2 Patient characteristics, treatment characteristics, and outcomes in patients with IrAE versus those without IrAEs in CKD, cirrhosis, COPD, and CHF patients

Large table with 5 columns: Cohort (CKD, Cirrhosis, COPD, CHF) and rows for Patient Characteristics (Age, Sex, Race, etc.), Treatment Characteristics (Type of ICI, Duration, etc.), and Outcomes (PFS, OS, etc.).



Abstract 1245 Figure 1 Progression-free survival curves of patients with irAE versus those without irAEs in CKD, cirrhosis, COPD, and CHF patients

<http://dx.doi.org/10.1136/jitc-2022-SITC2022.1245>

Abstracts

1246

TROPONIN-T LEVELS AND LONG-TERM SURVIVAL IN IMMUNE CHECKPOINT INHIBITOR ASSOCIATED MYOCARDITIS

Nikhil Dubey*, Daniel Zlotoff, Leyre Zubiri, Kerry Reynolds. *Massachusetts General Hospital, Boston, MA, USA*

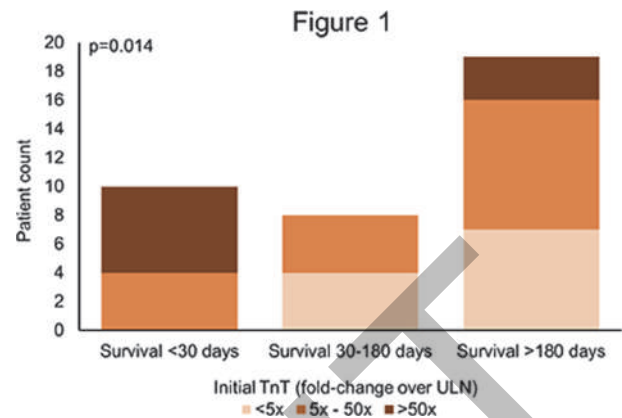
Background Immune checkpoint inhibitor (ICI) associated myocarditis carries a high rate of morbidity and mortality. Despite the clinical consequences, little is known about the relationship between initial troponin-T (TnT) levels at presentation and prognosis or concurrent immune related adverse events (irAEs).

Methods We conducted a retrospective analysis of 37 patients diagnosed with ICI-associated myocarditis at Massachusetts General Hospital in Boston, MA between March 1, 2016, and March 1, 2022. Clinical data including patient demographics, cancer type, ICI regimen, lab values, cardiac tests, immunosuppressive treatment, diagnostic procedures, and survival were obtained from the electronic medical record. Patients were categorized into three groups based on the first measured TnT during the admission for myocarditis: 1) mild elevation (<five-fold the institutional upper limit of normal [ULN]), 2) moderate elevation (five to 50-fold the ULN), and 3) high elevation (>50-fold the ULN). Statistical analyses were performed using the Fisher-Freeman-Halton exact test and Cochran-Armitage test for trend.

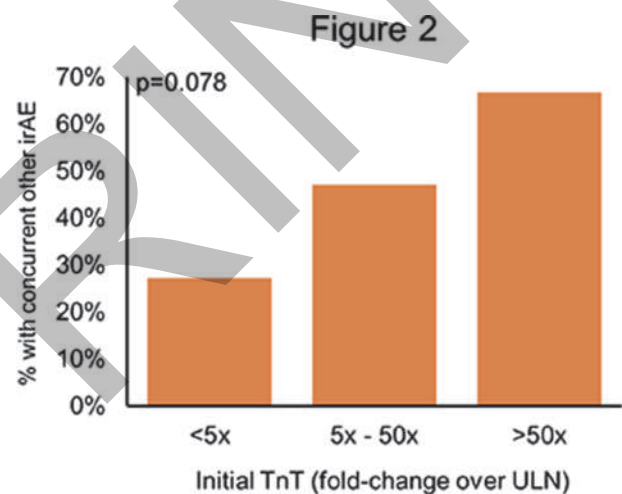
Results This cohort consisted of 29 men and 8 women with a median age of 74.5 years. Cancer types included non-small cell lung cancer (n=11), melanoma (n=9), RCC (n=9), SCC (n=3), and other types of cancer (n=5). The median time of myocarditis onset from the start of ICI was 49.5 days. ICI regimen primarily consisted of pembrolizumab (n=21) and nivolumab (n=12). Concurrent irAEs occurred in 17 patients during their index admission. Of the total cohort, 30% of patients had a mildly elevated TnT, 46% moderately elevated, and 24% highly elevated. 10 patients died within 30 days of myocarditis diagnosis, 8 patients died between 30 and 180 days, and 19 were alive past 180 days. Of those patients that died prior to 30 days from diagnosis, 60% had highly elevated TnT and 40% had moderately elevated TnT; however, of the patients alive past 180 days, 37% had mildly elevated TnT, 47% had moderately elevated TnT, and 16% had highly elevated TnT levels (figure 1; $p=0.014$ for the association of TnT elevation grade with survival category). Furthermore, while concurrent irAEs were diagnosed in 27% of patients with mildly elevated TnT, they were present in 47% of patients with moderately elevated TnT and 67% of patients with highly elevated TnT (figure 2; $p=0.078$ for test of trend).

Conclusions Initial TnT values at time of presentation with ICI-related myocarditis associate with patient survival to at least 180 days from time of diagnosis. Initial TnT values may be related to the presence of concurrent non-myocarditis irAEs.

Ethics Approval The study was approved by Mass General Brigham's Ethics Board, approval number 2017P000501.



Abstract 1246 Figure 1



Abstract 1246 Figure 2

<http://dx.doi.org/10.1136/jitc-2022-SITC2022.1246>

1247

DISTRIBUTION OF IMMUNE-RELATED ADVERSE EVENTS (irAEs) IN SOLID MALIGNANCIES

Dalia Kaakour*, Matthew Slaughter, Armon Azizi, Gianna Kroening, Jennifer Valerin, Nataliya Mar. *UCI, Orange, CA, USA*

Background Checkpoint inhibitors (CPIs) targeting PD-1/PD-L1 and CTLA-4 have dramatically improved outcomes for a range of solid malignancies. irAEs from CPIs affect a wide range of tissues, vary in severity, and are difficult to predict. Multiple studies have reported on incidence of irAEs by immunotherapy type, but few have examined the association of irAEs with tumor histology or with sites of metastasis. This study aims to investigate the association between type and incidence of irAEs with type of solid tumor histology, as well as with sites of cancer metastasis.

Methods We performed a retrospective analysis of all patients with genitourinary (GU), melanoma, gastrointestinal (GI), and lung malignancies treated with CPI monotherapy at the University of California, Irvine using an outpatient oncology pharmacy database. Data was collected from 1/1/2020 to 6/30/2021. Patients were aged 18 years and older. Patients must have received at least one dose of a CPI agent. Patients who received CPI-containing combination therapy with chemotherapy or targeted therapy were excluded.

Results Of 423 patients on unique treatment lines in our data set, 268 patients received CPI monotherapy. irAEs were documented in 133 patients (49.6%). 71 patients (62.8%) required treatment with oral or intravenous steroids, and 42 patients (37.2%) received treatment with other supportive therapy. The incidence of irAEs based on tumor type is listed in table 1. Most common irAEs per tumor type were rash in GU malignancies (26.0%), colitis in melanoma (25.4%), rash in GI malignancies (29.3%), and pneumonitis in lung malignancies (60.0%). In patients with irAEs, 102 (76.7%) had metastatic disease and of those, 18 (17.6%) had an irAE involving a metastatic site (p<0.0001). In patients with irAEs involving the primary site of malignancy, 2 patients (4.7%) with renal cell carcinoma had nephritis, 12 patients (37.5%) with melanoma had dermatitis, and 2 patients (50%) with a lung malignancy had pneumonitis.

Conclusions This study examines the differences in type and incidence of irAEs across GU, melanoma, GI, and lung cancers treated with CPI monotherapy. We found differences in the incidence of irAEs as relevant to tumor histology. Further, there was a statistically significant increased incidence of irAEs involving a metastatic site. Additional studies are needed, including those with a larger sample, combination immunotherapy and chemotherapy, as well as with additional tumor histologies.

Ethics Approval Application #16536 for HS #2021-6843 titled, "Primary Cancer Histology and Sites of Metastatic Disease Correlate with Tissues Affected by Immune-Related Adverse Events" obtained approval by the University of California, Irvine Institutional Review Board. A waiver of consent was obtained as this study involved no more than minimal risk as it was a retrospective chart review.

Abstract 1247 Table 1 Solid Tumor Category and irAE type

irAE type	Solid Tumor Category*			
	GU N = 49	Melanoma N = 48	GI N = 31	Lung N = 5
Dermatologic	26.0%	23.9%	29.3%	0.0%
Colitis	16.9%	25.4%	19.5%	20.0%
Endocrinopathy	16.9%	12.7%	12.2%	0.0%
Pneumonitis	3.9%	8.5%	7.3%	60.0%
Hepatitis	9.1%	7.0%	7.3%	0.0%
Nephritis	3.9%	0.0%	2.4%	0.0%
Myasthenia gravis	1.3%	0.0%	2.4%	0.0%
Encephalitis	2.6%	0.0%	0.0%	0.0%
Myositis	5.2%	4.2%	0.0%	0.0%
Carpal tunnel	1.3%	0.0%	0.0%	0.0%
Peripheral neuropathy	1.3%	0.0%	2.4%	0.0%
Myocarditis	0.0%	1.4%	0.0%	0.0%
Thrombocytopenia	1.3%	2.8%	2.4%	0.0%
Hyperglycemia	0.0%	1.4%	0.0%	0.0%
Arthritis	9.1%	7.0%	0.0%	20.0%
Other	1.3%	5.6%	14.6%	0.0%

*Percents reflect relative percent of specific irAE among all irAEs per solid tumor category

<http://dx.doi.org/10.1136/jitc-2022-SITC2022.1247>

Abstracts

1248

RISK FACTORS AND A RISK-SCORING MODEL FOR SEVERE CHECKPOINT INHIBITOR-RELATED PNEUMONITIS IN LUNG CANCER PATIENTS

¹Haiyi Deng, ²Jiating Deng, ¹Xinqing Lin, ¹Chengzhi Zhou*, ²Yanbin Zhou. ¹Guangzhou Institute of Respiratory Health, Guangzhou, China; ²The First Affiliated Hospital of Sun Yat-sen University, Guangzhou, China

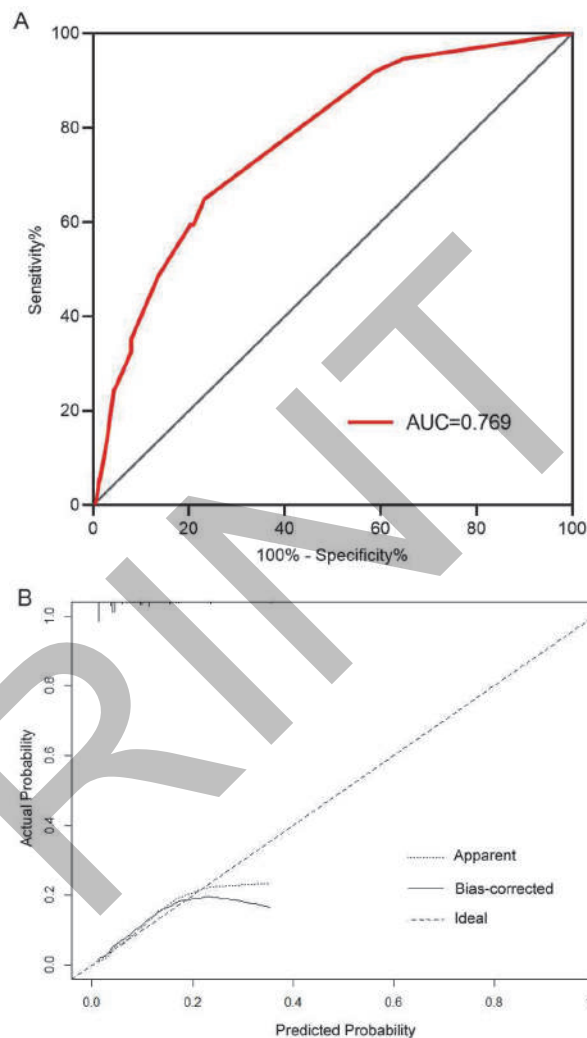
Background Immune checkpoint inhibitors (ICIs) provide enhanced survival benefits for lung cancer patients but can cause potentially fatal adverse events such as checkpoint inhibitor-related pneumonitis (CIP).

Methods This retrospective, case-control study enrolled 666 lung cancer patients receiving ICIs. Patients exhibiting The CIPs were divided into mild (grades 1–2) and severe (grades ≥ 3). Logistic regression identified risk factors for all grade and severe CIP, and a risk score for severe CIP was constructed. The model was validated in a separate patient cohort of 187 patients.

Results In the evaluation cohort, 95 patients developed CIP, of which 37 were severe cases. Multivariate analysis revealed age ≥ 65 years (OR=1.95), current smoking (OR=3.00), chronic obstructive pulmonary disease (COPD, OR=2.49), squamous cell carcinoma (SCC, OR=1.67), prior thoracic radiotherapy (OR=3.12), and extrathoracic radiotherapy during ICI (OR=2.80) were independently associated with CIP events. Five factors, emphysema (OR=2.87), interstitial lung disease (ILD, OR=4.76), pleural effusion (OR=3.00), history of radiotherapy during ICI (OR=4.30), and single agent immunotherapy (OR=2.44) were independently associated with severe CIP and were incorporated into a risk-score model (score ranging 0–17). The area under the model receiver operating characteristic curve for the model was 0.769 in the evaluation cohort and 0.749 in the validation cohort (figure 1).

Conclusions Advanced age, current smoking, COPD, SCC, previous thoracic radiotherapy and extrathoracic radiotherapy during ICI treatment were independent risk factors for CIP incidence. The risk of severe CIP was observed to be independently associated with emphysema, ILD, pleural effusion, radiotherapy during ICI, and immunotherapy alone. The model has a promising predictive capacity for severe pneumonitis.

Ethics Approval This study was approved by the local Ethics Committee of the First Affiliated Hospital of Guangzhou Medical University (No.2021-38).



Abstract 1248 Figure 1 Internal validation of the the risk-scoring model(A) Receiver operating characteristic (ROC) curve analyses the model predicting the occurrence of severe checkpoint inhibitor-related pneumonitis (CIP); (B) Calibration curve of the model for prediction of severe CIP. A perfect model would fully match the 45 ° ideal line.

<http://dx.doi.org/10.1136/jitc-2022-SITC2022.1248>

1249

TREATMENT INTERRUPTIONS FOR IMMUNE RELATED ADVERSE EVENTS AND OVERALL SURVIVAL IN PATIENTS WITH NON-SMALL CELL LUNG CANCER (NSCLC) TREATED WITH FIRST LINE IMMUNE CHECKPOINT INHIBITORS (ICI)

Evelyn Goodyear*, Songzhu Zhao, Mingjia Li, Yihzen Guo, Gabrielle Lopez, Austin Secor, Parthib Das, Nitya Surya, Mariam Husain, Madison Grogan, Daniel Spakowicz, Lai Wei, Kai He, Erin Bertino, Asrar Alahmadi, Regan Memmott, Jacob Kaufman, Carolyn Presley, Peter Shields, David Carbone, Gregory Otterson, Dwight Owen. *The Ohio State University, Columbus, OH, USA*

Background Data from prospective phase 3 trials of anti-PD-1 and anti-CTLA-4 demonstrate durable clinical benefit even in patients who discontinue ICI due to treatment related adverse events. However, outcomes for patients treated with anti-PD-1 therapy alone or with chemotherapy who discontinue treatment due to immune toxicities is unknown.

Methods We retrospectively evaluated patients with stage IV NSCLC treated with first line ICI alone or with platinum-based chemotherapy at a tertiary cancer center between 2017 and 2021. Overall survival (OS) was calculated from the date of ICI treatment initiation to death from any cause or date of last follow-up. Patients still alive were censored at last follow-up. Overall survival was estimated using Kaplan-Meier method.

Results 225 patients were identified and included, mean age 63.5 years, 57% were male, 91% former/current smokers, 17% squamous histology. ICI type was anti-PD-1 alone in 43%, ICI+chemotherapy in 56%, and ICI+ICI in 1%. 42 out of 225 patients had treatment held either temporarily or permanently for irAE (42/225, 19%, table 1). Of these patients, 19 were permanently discontinued from irAE and 22 were resumed on ICI (1 missing due to lost follow up). There was no difference in patient age, race, sex, smoking status, histology, or ICI type among patients with irAE and permanent ICI discontinuation vs not (table 2), however permanent discontinuation was more common in treatment with ICI monotherapy (60% vs 37% in ICI+Chemo vs 0% in ICI+ICI), but not statistically significant (p=0.13). Among all patients with any irAE treatment interruption, the median overall survival (mOS) was 54.1 months (95% CI 26.9, NR). There was no significant difference in mOS among patients who permanently discontinued ICI: 26.9 months (95% CI 3.3, NR) vs 22.8 months (95% CI 16.3, 28.1) for all other patients, p=0.84 (figure 1). Among patients with treatment interruption for irAE, there was no significant difference in mOS among those who resumed treatment vs those who permanently discontinued, though this may have been limited by sample size: 54.1 months (95% CI 26.9, NR) vs 26.9 months (95% CI 3.3, NR) (p=0.07, figure 2).

Conclusions We observed no significant difference in mOS between patients with treatment interruption or discontinuation due to irAE. There appeared to be longer OS in patients who resumed treatment, though this was nonsignificant and likely limited by small sample size. These findings are consistent with continued clinical benefits despite treatment discontinuation in patients treated with first line ICI alone or with chemotherapy.

Ethics Approval The study was approved by the OSU Institutional Ethics Board

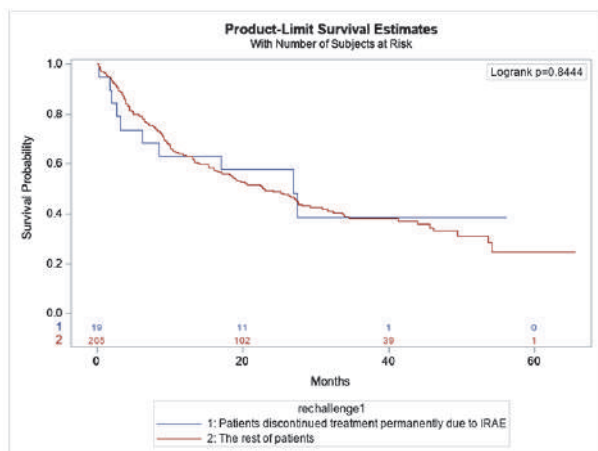
Abstract 1249 Table 1 Demographics of all patients and those with treatment held for irAE

Variable	Level	1: No treatment held for irAE (n=183)	2: Treatment held for irAE (n=42)	Total (n=225)	p-value
Age	Mean (SD) (min, max)	missing=0 63.6 (11.2) (30.2, 92.7)	missing=0 63.3 (9.1) (43.8, 79.4)	missing=0 63.5 (10.8) (30.2, 92.7)	0.8771
	Race	Missing	1	0	1
	Caucasian	157 (79.7%)	40 (20.3%)	197 (88%)	
	Non-Caucasian	25 (92.6%)	2 (7.4%)	27 (12%)	
Sex	Female	73 (75.3%)	24 (24.7%)	97 (43.1%)	0.0567
	Male	110 (85.9%)	18 (14.1%)	128 (56.9%)	
Smoking history	Missing	1	0	1	1.0000
	Never smoker	17 (81%)	4 (19%)	21 (9.4%)	
	Former/current	165 (81.3%)	38 (18.7%)	203 (90.6%)	
Immunotherapy type	1: PD-1/L1 monotherapy	76 (79.2%)	20 (20.8%)	96 (42.7%)	0.0260
	2: ICI+Chemo	107 (84.3%)	20 (15.7%)	127 (56.4%)	
	3: ICI+ICI	0 (0%)	2 (100%)	2 (0.9%)	
Tumor PD-L1 expression	Missing	3	1	4	0.7144
	1: Negative	59 (79.7%)	15 (20.3%)	74 (33.5%)	
	2: Positive	121 (82.3%)	26 (17.7%)	147 (66.5%)	
Histology	Missing	1	0	1	0.4912
	Non-squamous	150 (80.2%)	37 (19.8%)	187 (83.5%)	
	Squamous	32 (86.5%)	5 (13.5%)	37 (16.5%)	
ECOG PS	Missing	2	1	3	0.8483
	0-1	131 (81.9%)	29 (18.1%)	160 (72.1%)	
	>=2	50 (80.6%)	12 (19.4%)	62 (27.9%)	
BMI	Mean (SD) (min, max)	missing=1 26.7 (6.1) (14.7, 49.1)	missing=0 26.4 (5.3) (16.3, 40.4)	missing=1 26.6 (6) (14.7, 49.1)	0.7621

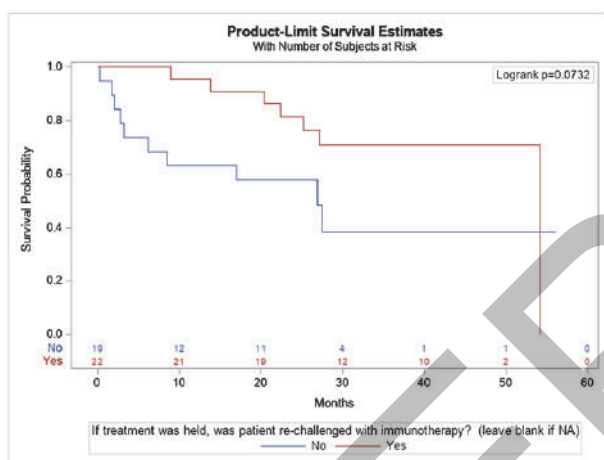
Abstract 1249 Table 2 Demographics of patients with treatment held for irAE comparing those where ICI was resumed vs those where ICI was not resumed

Variable	Level	Permanently discontinued ICI (n=19)	Resumed ICI therapy (n=22)	Total (n=41)	p-value
Age	Mean (SD) (min, max)	missing=0 65.1 (9.4) (48, 79.4)	missing=0 61.4 (8.7) (43.8, 73.9)	missing=0 63.1 (9.1) (43.8, 79.4)	0.1953
	Race	4	19 (48.7%)	20 (51.3%)	39 (95.1%)
	Non 4	0 (0%)	2 (100%)	2 (4.9%)	
Sex	Female	8 (34.8%)	15 (65.2%)	23 (56.1%)	0.1220
	Male	11 (61.1%)	7 (38.9%)	18 (43.9%)	
Smoking history	No	1 (25%)	3 (75%)	4 (9.8%)	0.6099
	Yes	18 (48.6%)	19 (51.4%)	37 (90.2%)	
Immunotherapy type	1: PD-1/L1 monotherapy	12 (60%)	8 (40%)	20 (48.8%)	0.1281
	2: ICI+Chemo	7 (36.8%)	12 (63.2%)	19 (46.3%)	
	3: ICI+ICI	0 (0%)	2 (100%)	2 (4.9%)	
Tumor PD-L1 expression	Missing	0	1	1	0.3329
	1: Negative	5 (35.7%)	9 (64.3%)	14 (35%)	
	2: Positive	14 (53.8%)	12 (46.2%)	26 (65%)	
Histology	All others	17 (47.2%)	19 (52.8%)	36 (87.8%)	1.0000
	Squamous cell carcinoma	2 (40%)	3 (60%)	5 (12.2%)	
ECOG PS	Missing	1	0	1	0.4977
	0-1	12 (41.4%)	17 (58.6%)	29 (72.5%)	
	2 or higher	6 (54.5%)	5 (45.5%)	11 (27.5%)	

Abstracts



Abstract 1249 Figure 1 Survival curves of patients who permanently discontinued ICI due to irAE compared to all other patients



Abstract 1249 Figure 2 Survival curves of patients who permanently discontinued ICI due to irAE compared to those who resumed ICI after irAE

<http://dx.doi.org/10.1136/jitc-2022-SITC2022.1249>

1250

A NOVEL IN VIVO PBMC HUMANIZED MOUSE PLATFORM FOR LONG-TERM ANALYSIS OF EFFICACY AND TOXICITY OF T CELL-BASED IMMUNOTHERAPY DRUGS

Guoxiang Yang*, Hongyuan Yang, Li-Chin Yao, Leonard Shultz, Danying Cai, James Keck, Mingshan Cheng. *The Jackson Laboratory, Sacramento, CA, USA*

Background Immune cell-based therapies, such as bispecific T cell engagers (BiTE), have been developed for treatment of malignancies. However, the current overall success rate of anti-tumor drugs during clinical development remains low. One prominent reason is that the existing animal models in preclinical studies often do not accurately predict the clinical outcomes. The differences between human and mouse immune systems hamper the development of new cancer therapeutic approaches. Herein, we developed a novel humanized mouse model with solid tumor that can allow long-term evaluation of the effectiveness and risk of unwanted toxicity for bispecific immune drugs.

Methods We utilized two human cancer cell lines in this study: 1) Breast cancer cell MDA-MB-231 (MDA, expressed EGFR); 2) B cell lymphoma Raji (Raji, expressed CD19). To establish the breast tumor model, MDA cells were implanted in NSG-MHC class I/II double knock-out (DKO) mouse via mammary fat pad (MFP) 2 days before humanized mice with human peripheral blood mononuclear cells (PBMCs). The same MDA cells were then intravenously (IV) implanted 3 days before EGFRxCD3 BiTE administration. Similarly, subcutaneous (SC) solid lymphoma model was established and treated with CD19xCD3 BiTE. Following BiTE dosing tumor burden was quantified by a Xenogen imaging system. To evaluate the toxicity levels in response to BiTE therapy, serum inflammatory cytokine levels were analyzed. Clinical observation, mouse clinical score, and body weight change were also monitored for drug toxicity assessment.

Results PBMC-humanized model with solid tumors were successfully established. Either MFP MDA tumor or SC B cell lymphoma could keep growing for more than one month in the mice. Low dose BiTE treatment did suppress tumor cell growth in the mouse lungs but did not inhibited solid tumor growth. Increased dosage significantly inhibited MFP or SC solid tumor growth. The mice with BiTE treatment exhibited elevated serum levels of human inflammatory cytokines. This cytokine production was dose-dependent and was associated with an increase of toxicity.

Conclusions This model provides a growth environment like that of the patients with solid tumor and can be used for both short-term and long-term data analysis of efficacy, toxicity, and dosing requirements of immunotherapy drugs. We emphasize that the solid tumor model using both IV and SC/MFP co-engraftment is a promising preclinical platform for simultaneously evaluating long-term efficacy and predictive safety of any T cell-based immunotherapies to define optimal approaches for clinical treatment.

<http://dx.doi.org/10.1136/jitc-2022-SITC2022.1250>

Abstracts

1251

IMMUNE CHECKPOINT INHIBITOR-INDUCED TYPE 1 DIABETES MELLITUS IS ASSOCIATED WITH LONG-TERM RESPONSE AND SURVIVAL IN PATIENTS WITH MELANOMA

¹John Marsiglio*, ²Magdalena Kovacovics, ²Xuechen Wang, ¹Sheetal Hardikar, ²Arabella Young, ²Jennifer Doherty, ²John Hyingstrom, ²Jordan McPherson, ²Ben Haaland, ²Siwen Hu-Lieskovan. ¹University of Utah, Salt Lake City, UT, USA; ²Huntsman Cancer Institute, Salt Lake City, UT, USA

Background Type 1 diabetes mellitus (T1DM) is a rare but serious immune-related adverse event (irAE) of immune checkpoint inhibitors (ICIs).¹ Our goal was to characterize treatment outcomes with ICI-induced T1DM through analysis of clinical and immunological data.

Methods This was a single-center case series of patients with solid tumors at Huntsman Cancer Institute (HCI) who received ICIs and subsequently had a new diagnosis of T1DM. The enterprise data warehouse at the University of Utah used ICD codes (ICD-10-CM E10 and ICD9CM 250.01) to identify patients for chart review to confirm ICI-induced T1DM. Serial blood specimens were studied for pro-teomic and immunophenotypic changes.

Results Between April 14, 2011 and July 15, 2021, 37 of 2745 patients who received ICIs at HCI had a T1DM diagnosis after the first cycle. 8 were confirmed to have ICI-induced T1DM (0.3%), including 3 with melanoma. An additional 5 cases with melanoma were identified by chart review only (table 1). Average age at onset was 54.5 years. 10 of 13 patients received anti-PD1 monotherapy (6 pembrolizumab, 4 nivolumab), 2 received pembrolizumab plus chemotherapy or enzalutamide, and 1 received ipilimumab plus nivolumab. Only 1 received prior ICI (ipilimumab). Median time to onset was 6.4 months (range 0.7-13.7). 10 patients presented with diabetic ketoacidosis (77%) (table 2). Of 6 patients who had autoantibodies tested at onset, only one had elevated anti-glutamic acid decarboxylase. At median follow-up of 24.3 months (range 13.1-66.4), no melanoma patients had progressed nor died, including 6 who received adjuvant and 2 who received active treatments (1 complete response, 1 partial response). Median progression free survival and overall survival were not reached. The 5 patients with other cancers received active treatments (1 partial response, 2 stable disease and 2 disease progression), and 3 died. All patients became permanently insulin-dependent. Further analysis by Olink and CyTOF of serial blood (baseline, pre-irAE, peak-irAE) from 3 ICI-induced T1DM patients, and baseline blood from 6 patients who received anti-PD1 but did not develop irAE, is ongoing and will be presented. Preliminary data suggest lower IL6 and OSMR (in IL-6 signaling) in baseline samples from patients who developed T1DM, among other changes.

Conclusions Despite ICI-induced T1DM, patients with melanoma displayed excellent clinical response and survival. All cases were treated with anti-PD1 antibodies, highlighting the importance of PD-1 blockade in the pathogenesis of ICI-induced T1DM. Most of these patients had negative autoantibodies, suggesting a distinct mechanism of this irAE.²

REFERENCES

- Barroso-Sousa R, Barry WT, Garrido-Castro AC, Hodi FS, Min L, Krop IE, Tolaney SM. Incidence of endocrine dysfunction following the use of different immune checkpoint inhibitor regimens: a systematic review and meta-analysis. *JAMA Oncol.* 2018;**4**(2):173–182. doi:10.1001/jamaoncol.2017.3064. PMID: 28973656; PMCID: PMC5838579.
- de Filette JMK, Pen JJ, Decoster L, Vissers T, Bravenboer B, Van der Auwera BJ, Gorus FK, Roep BO, Aspeslagh S, Neyns B, Velkeniers B, Kharagjitsingh AV.

Immune checkpoint inhibitors and type 1 diabetes mellitus: a case report and systematic review. *Eur J Endocrinol.* 2019;**81**(3):363–374. doi:10.1530/EJE-19-0291. PMID: 31330498; PMCID: PMC6709545.

Abstract 1251 Table 1 Clinical Data

Patient	Sex	Age at Onset	Diagnosis	ICIs	Time to Onset	Diabetic Ketoacidosis	Autoantibodies	Survival
1	M	54	Melanoma	anti-PD1	6.4	Yes	NA	24.3
2	F	55	Melanoma	anti-PD1	1.2	Yes	NA	13.1
3	M	54	Melanoma	anti-PD1	1.2	Yes	NA	13.1
4	M	54	Melanoma	anti-PD1	1.2	Yes	NA	13.1
5	M	54	Melanoma	anti-PD1	1.2	Yes	NA	13.1
6	M	54	Melanoma	anti-PD1	1.2	Yes	NA	13.1
7	M	54	Melanoma	anti-PD1	1.2	Yes	NA	13.1
8	M	54	Melanoma	anti-PD1	1.2	Yes	NA	13.1
9	M	54	Melanoma	anti-PD1	1.2	Yes	NA	13.1
10	M	54	Melanoma	anti-PD1	1.2	Yes	NA	13.1
11	M	54	Melanoma	anti-PD1	1.2	Yes	NA	13.1
12	M	54	Melanoma	anti-PD1	1.2	Yes	NA	13.1
13	M	54	Melanoma	anti-PD1	1.2	Yes	NA	13.1

Abstract 1251 Table 2 T1DM Presentation Data

Patient	Diabetic Ketoacidosis at Presentation	A1c (%)	Peak Blood Glucose (mg/dL)	Bicarbonate (mEq/L)	Anion Gap (mEq/L)	Urine Ketones	C-peptide (ng/ml)	Autoantibodies
1	yes	8.1	572	22	16	positive	NA	NA
2	no	8.4	375	20	14	NA	0.2	NA
3	no	6.6	277	24	9	NA	NA	NA
4	yes	7.7	341	24	18	positive	0.4	GAD, IA2, insulin, ZnT8 negative
5	yes	10.3	1021	20	17	positive	NA	NA
6	yes	11.4	800	8	21	positive	0.1	NA
7	no	9.2	780	21	12	NA	0.1	GAD, IA2, ICA, ZnT8 negative
8	yes	10.4	460	6	10	positive	0.5	GAD, IA2, ICA, ZnT8 negative
9	yes	8.7	475	5	20	positive	NA	GAD elevated, IA2, ICA, ZnT8 negative
10	yes	8.7	475	5	20	positive	NA	NA
11	yes	11.2	813	5.5	17	NA	NA	IA2, GAD negative
12	yes	8	594	NA	17	NA	0.1	GAD, IA2, ICA, ZnT8 negative
13	yes	8	NA	NA	NA	NA	NA	NA

<http://dx.doi.org/10.1136/jitc-2022-SITC2022.1251>

1252

IMMUNE-CHECKPOINT INHIBITOR INDUCED AUTOIMMUNE DIABETES IS A HETEROGENEOUS DISEASE WITH DISTINCT CLINICAL AND IMMUNE PHENOTYPES

¹Karina Ruiz-Esteves*, ²Kaitlyn Shank*, ¹Caitlin Colling, ¹Tianqi Ouyang, ¹Leyre Zubiri, ¹Chloe Villani, ¹Kerry Reynolds, ¹Meghan Sise, ¹Michelle Rengarajan. ¹Massachusetts General Hospital, Boston, MA, USA; ²Brigham and Women's Hospital, Boston, MA, USA

Background Immune checkpoint inhibitors (ICIs) can lead to immune-related adverse events (irAEs). One such irAE, ICI-induced autoimmune diabetes (ICI-DM), affects approximately 1% of ICI recipients. Most reports suggest resemblance to fulminant type 1 diabetes, with low or absent endogenous insulin production at presentation.^{1,2} However, more recent reports have revealed milder cases, suggesting a heterogeneous disease entity.³ We identified distinct clinical phenotypes of ICI-DM that could allow for better optimization of insulin therapy.

Methods We performed a retrospective chart review of 16,582 patients treated with anti-PD1, anti-PDL1, anti-CTLA4, or combination between 2010 and 2022 at a multi-centered academic hospital system. Criteria for inclusion were new diagnosis of type 1 diabetes or drug-induced diabetes and new prescription for insulin following ICI therapy; cases were confirmed by two board-certified endocrinologists. To phenotype ICI-DM based on endogenous insulin production, we reviewed patients with ICI-DM and a C-peptide level, allowing us to classify 45 cases of ICI-DM based on endogenous insulin production and autoantibody status. We are characterizing ICI-DM in these patients at both initial presentation and up to 30 months of follow-up.

Results We identified three distinct clinical phenotypes of ICI-DM based on initial presentation: patients with preserved endogenous insulin production (insulin+) and patients with decreased or absent endogenous insulin production (insulin-), with the latter divided into autoantibody positive (Ab+) and negative (Ab-) patients. Insulin+ ICI-DM patients have high levels of pre-existing insulin resistance, longer time-to-diagnosis (median 175 days), higher A1c at presentation (median 9.8%) and lower likelihood of presenting in diabetic ketoacidosis (DKA). Insulin-Ab+ patients have lower levels of insulin resistance, the lowest time-to-diagnosis (median 65 days), intermediate A1c at presentation (median 8.2%), high rates of DKA and nearly universal hospitalization at presentation. Insulin-Ab- had no pre-existing insulin resistance, a longer time-to-diagnosis (median 154 days) with a relatively low A1c at presentation (median 7.6%) and moderate rates of DKA and hospitalization. As expected, insulin- patients had higher total daily insulin needs compared to insulin+ patients.

Conclusions Our study examined the largest data set to date of deep clinical phenotyping of patients with ICI-DM. We define at least two distinct subsets of ICI-DM, with antibody-positive, islet negative patients being most similar to cases of ICI-DM initially described. However, patients with a milder form of ICI-DM (islet positive patients) may require simpler insulin regimens that could profoundly improve their quality of life. Our findings may also suggest distinct underlying mechanisms for ICI-DM with implications for other irAEs.

REFERENCES

1. de Filette JMK, Pen JJ, Decoster L, Vissers T, Bravenboer B, Van der Auwera BJ, Gorus FK, Roep BO, Aspeslagh S, Neyns B, Velkeniers B, Kharagjitsingh AV. Immune checkpoint inhibitors and type 1 diabetes mellitus: a case report and systematic review. *Eur J Endocrinol*. 2019; **181**(3):363-374.
2. Tsang VHM, McGrath RT, Clifton-Bligh RJ, Scolyer RA, Jakrot V, Guminski AD, Long GV, Menzies AM. Checkpoint Inhibitor-Associated Autoimmune Diabetes Is

Distinct From Type 1 Diabetes. *J Clin Endocrinol Metab*. 2019; **104**(11):5499-5506.

3. Chen X, Affinati AH, Lee Y, Turcu AF, Henry NL, Schiopu E, Qin A, Othus M, Clauw D, Ramnath N, Zhao L. Immune checkpoint inhibitors and risk of type 1 diabetes. *Diabetes Care*. 2022; **45**(5):1170-1176.

Ethics Approval This study was approved by the Mass General Brigham Institutional Review Board, Protocol #2017P000501. There was no direct interaction with patients or their samples so individual consent was not deemed necessary by the IRB.

<http://dx.doi.org/10.1136/jitc-2022-SITC2022.1252>

Abstracts

1253

RETROSPECTIVE ANALYSIS OF IMMUNOTHERAPY TOXICITIES REQUIRING HOSPITALIZATION IN LUNG CANCER PATIENTS

¹Ayo Falade*, ²Leyre Zubiri, ²Kerry Reynolds, ²Meghan Mooradian. ¹MGB Salem Hospital, Salem, MA, USA; ²Massachusetts General Hospital, Boston, MA, USA

Background Immune checkpoint inhibitors (ICI) are associated with a distinct spectrum of toxicities. Data on irAE hospitalization rates and clinical course of patients with thoracic malignancies are lacking.

Methods Patients with advanced thoracic malignancy treated with ICI (2/2016 – 6/2021) were retrospectively identified. Demographic and clinical data of confirmed irAE hospitalizations were extracted from the medical record and a descriptive analysis was performed.

Results From February 2016 to June 2021, 1,312 patients with thoracic malignancy received ICI (monotherapy, combination with 2nd ICI or other agents) with 102 patients (7.7%) hospitalized for irAEs. Treatment intent was first-line therapy with ICI in most patients (N= 50, 49%) and adjuvant ICI in 9% (N =9). 59% (N =60) received ICI alone, 32% (N =33) chemo plus immunotherapy, and 7% (N =7) dual ICI. The average age on admission was 68 years in both genders. The median time between ICI initiation and admission was 64 days (1-935). The most common evidenced irAEs were pneumonitis (N = 38, 37%), hepatitis (N = 20, 20%), myocarditis (N = 14, 14%) and colitis (N = 13, 13%). Nearly half (N = 18, 47%) of patients with pneumonitis were treated with prior thoracic radiation and received first line (N = 22, 58%) ICI. Pneumonitis cases had the highest 60-day readmission rate (37%, N = 14) with a 60-day mortality rate of 53% (N = 20). 60-day re-admission and mortality rates were 19% (N = 17) and 29% (N = 26), respectively, among the rest of the cohort. Multi-organ toxicity occurred in 36% (N = 37) of patients. Myocarditis patients often had a concomitant irAE (79%; 11/14) with 36% (N = 5) presenting overlapping neuromuscular toxicity. Overall, 64% (N = 65) received IV corticosteroids for a median duration of 42.5 days (0-527) and 18% (N = 18) required second line immunosuppression. irAEs solved to grade 1 or less after immunosuppression in 63 patients. Seven patients (7%) experienced a grade 5 event while admitted. ICI rechallenge occurred in 14 patients. Median OS was 360 days; (16 – 2219, table 1).

Conclusions Severe irAE requiring inpatient admission, though infrequent, results in considerable morbidity, mortality, and healthcare utilization. Pneumonitis was the most common irAE requiring inpatient management in our lung cancer population with a significant risk of mortality despite the use of guideline-directed systemic immunosuppression. This study highlights the continued need for prospective research to optimally manage severe toxicities, particularly pneumonitis.

Ethics Approval The study obtained IRB approval.

Protocol #: 2017P000501.

Abstract 1253 Table 1 Characterization of patients and toxicities

Patient Characteristics (N= 102)	No. (%)
Male sex	58 (57)
Smoking Status	
Current	16 (16)
Former	78 (76)
Never	8 (8)
Histologic Features	
Adenocarcinoma	75 (74)
Squamous cell carcinoma	20 (20)
Small cell lung cancer	7 (7)
ECOG PREDATING ADMISSION	
0	17 (17)
1-2	80 (78)
3-4	2 (2)
Unkn	3 (3)
Baseline Autoimmune disease	23 (23)
Hypothyroid:	12
Others*	11
Baseline Immunosuppression (mainly steroids)	9 (9)
Treatment Type	
PD-1/PD-L1 monotherapy	60 (59)
Chemotherapy + Immunotherapy	33 (32)
ipilimumab/ Nivolumab	7 (7)
ICI + Investigational agent **	2 (2)
Line of Therapy	
Adjuvant	9 (9)
First metastatic	50 (49)
Second metastatic	23 (23)
Third or beyond	20 (20)
Characterization of toxicity	
Pneumonitis	38 (37)
Hepatitis	20 (20)
Myocarditis	14 (14)
Colitis	13 (13)
Multiple toxicity (N=37)	
Pneumonitis	10 (26)
Hepatitis	11 (55)
Myocarditis	11 (79)
Colitis	7 (54)
Mortality rate within 60 days	
Pneumonitis	20 (53)
Hepatitis	6 (30)
Myocarditis	5 (36)
Colitis	3 (23)
Number rechallenged with ICI	
Pneumonitis	2 (5)
Hepatitis	4 (20)
Myocarditis	1 (7)
Colitis	3 (23)

Table 1: Characterization of patients and toxicity

*Others: Crohn's disease: 1, Adrenal Insufficiency: 1, Rheumatoid Arthritis: 3, Ulcerative Colitis: 1, Psoriasis: 3, Scleroderma: 1, Eczema: 1

** One patient received concurrent mRNA vaccine, one avelumab monotherapy

<http://dx.doi.org/10.1136/jitc-2022-SITC2022.1253>

1254

DISTINGUISHING T-CELL RESPONSES IN PAIRED HEART AND TUMOR SAMPLES FROM PATIENTS WITH IMMUNE CHECKPOINT-RELATED MYOCARDITIS

¹Steven Blum*, ²Neal Smith, ²Daniel Zlotoff, ²Jaimie Barth, ²Swetha Ramesh, ²Isabela Kemin, ²Leyre Zubiri, ²John McGuire, ²Alice Tirard, ²Dejan Juric, ²Ryan Sullivan, ²Genevieve Boland, ²Mari Mino-Kenudson, ²James Stone, ²Molly Thomas, ²Kerry Reynolds, ²Thomas Neilan, ²Chloe Villani. ¹Massachusetts General Hospital/Dana-Farber Cancer Institute, Boston, MA, USA; ²Massachusetts General Hospital, Boston, MA, USA

Background The relationship between severe immune-related adverse events (irAE) and anti-tumor efficacy resulting from the use of immune checkpoint inhibitors (ICI) is poorly understood. ICI-related myocarditis (irMyocarditis) is among the most serious toxicities and is fatal in 25-50% of cases.¹ Reports of shared T-cell clones in irAE and tumor suggest that common antigens or epitopes may couple anti-tumor immunity and irAE biology.^{2, 3} To test this hypothesis and account for potential nonspecific “bystander” T cells,⁴ we examined the T-cell receptor (TCR) repertoire of matched human heart, tumor, and control tissues to identify T cells enriched in tumor or irMyocarditis.

Methods Five autopsy cases with matched irMyocarditis, tumor, and histologically normal tissue adjacent to tumor (“control”) were identified. FFPE slides were stained for H&E, and marked regions of interest were macroscopically dissected in serial unstained slides to isolate gDNA. Bulk TCR β chain sequencing of the CDR3 region was performed.⁵ Expanded TCRs were defined as those comprising >0.5% of the TCR β repertoire from a given tissue. For each expanded clone, a Fisher’s exact test was used to determine if the TCR β sequence was enriched in irMyocarditis tissue compared to control tissue and in tumor tissue compared to control tissue.

Results Four tumor histologies were captured: melanoma (n=2), renal cell carcinoma, cholangiocarcinoma, and prostate cancer. TCR β sequencing recovered tumor-enriched clones in four of five samples (range: 0-18 clones) and irMyocarditis-enriched clones in all five samples (range: 2-8). Across all patients, 17% (11/63) of tumor-enriched clones and 29% (11/37) of the irMyocarditis-enriched clones were enriched in both tissues. In two patients, the most abundant TCR β sequence in irMyocarditis was not enriched in tumor tissue.

Conclusions TCRs enriched in ICI-treated tumors and irMyocarditis heart tissue are often distinct, suggesting that T-cell responses causing severe irAEs and anti-tumor immunity may not be driven by common antigens or epitopes, as has been previously suggested in other settings.^{2,3} We are currently analyzing these data together with our unpublished single-cell RNA sequencing and TCR data from peripheral blood and heart, which encompass 25 patients and ~300,000 cells.⁶ This effort could identify pathologic T cells that are distinct from tumor-reactive clones or nominate biomarkers for patients with irMyocarditis. Differentiating the T-cells responses driving irMyocarditis and anti-tumor immunity may be the first step towards developing clinical strategies that can maximize ICI efficacy while mitigating irAEs.

Acknowledgements We are grateful to the patients and their families whose generosity with their samples and time have made this study possible.

REFERENCES

1. Palaskas N, Lopez-Mattei J, Durand JB, Iliescu C, Deswal A. Immune checkpoint inhibitor myocarditis: pathophysiological characteristics, diagnosis, and treatment. *J Am Heart Assoc.* 2020;**9**(2):e013757.

- Johnson DB, Balko JM, Compton ML, Chalkias S, Gorham J, Xu Y, Hicks M, Puzanov I, Alexander MR, Bloomer TL, Becker JR, Slosky DA, Phillips EJ, Pilkinton MA, Craig-Owens L, Kola N, Plautz G, Reshef DS, Deutsch JS, Deering RP, Olenchok BA, Lichtman AH, Roden DM, Seidman CE, Koralnik IJ, Seidman JG, Hoffman RD, Taube JM, Diaz LA Jr, Anders RA, Sosman JA, Moslehi JJ. Fulminant myocarditis with combination immune checkpoint blockade. *N Engl J Med.* 2016;**375**(18):1749–1755.
- Berner F, Bomze D, Diem S, Ali OH, Fässler M, Ring S, Niederer R, Ackermann CJ, Baumgaertner P, Pikor N, Cruz CG, van de Veen W, Akdis M, Nikolaev S, Läubli H, Zippelius A, Hartmann F, Cheng HW, Hönger G, Recher M, Goldman J, Cozzio A, Früh M, Neeffes J, Driessen C, Ludewig B, Hegazy AN, Jochum W, Speiser DE, Flatz L. Association of checkpoint inhibitor-induced toxic effects with shared cancer and tissue antigens in non-small cell lung cancer. *JAMA Oncol.* 2019;**5**(7):1043–1047. doi: 10.1001/jamaoncol.2019.0402. Erratum in: *JAMA Oncol.* 2019 Jul 1;**5**(7):1070.
- Simoni Y, Becht E, Fehlings M, Loh CY, Koo SL, Teng KWW, Yeong JPS, Nahar R, Zhang T, Kared H, Duan K, Ang N, Poidinger M, Lee YY, Larbi A, Khng AJ, Tan E, Fu C, Mathew R, Teo M, Lim WT, Toh CK, Ong BH, Koh T, Hillmer AM, Takano A, Lim TKH, Tan EH, Zhai W, Tan DSW, Tan IB, Newell EW. Bystander CD8+ T cells are abundant and phenotypically distinct in human tumour infiltrates. *Nature.* 2018;**557**(7706):575–579. doi: 10.1038/s41586-018-0130-2.
- Sherwood AM, Desmarais C, Livingston RJ, Andriessen J, Haussler M, Carlson CS, Robins H. Deep sequencing of the human TCR γ and TCR β repertoires suggests that TCR β rearranges after $\alpha\beta$ and $\gamma\delta$ T cell commitment. *Sci Transl Med.* 2011;**3**(90):90ra61.
- Blum SM, Zlotoff DA, Smith NP, Ramesh S, Kernin I, Sen P, Zubiri L, Tirard A, Nasrallah M, Tantivit J, Barth JL, Juric D, Sullivan RJ, Boland GM, Mino-Kenudson M, Stone J, Thomas M, Reynolds KL, Neilan TG, Villani AC. Single-cell profiling of human heart and blood in immune checkpoint inhibitor-associated myocarditis. *J Clin Oncol.* 2022;**40**(16_suppl): 2507-2507.

Ethics Approval Patients involved in this study were consented to Dana-Farber Cancer Institute/Harvard Cancer Center collection protocols #11-181 and #13-416.

<http://dx.doi.org/10.1136/jitc-2022-SITC2022.1254>

1255

IMPACT OF IMMUNE CHECKPOINT INHIBITORS ON BONE TURNOVER IN CANCER PATIENTS: PROSPECTIVE CLINICAL STUDY AND PRECLINICAL CORRELATES

¹Tamara Gassner*, ¹Sonia Vallet, ¹Christina Chittilappilly, ¹Theo Pirich, ¹Judith Lind, ¹Osman Aksoy, ¹Vincent Sunder-Plassmann, ¹Klaus Hackner, ¹Elisabeth Zwickl-Traxler, ¹Peter Erhalt, ²Martin Pecherstorfer, ¹Klaus Podar. ¹Karl Landsteiner University of Health Sciences, Ober-Grafendorf, Austria; ²University Hospital Krems, Krems, Austria

Background Treatment-induced bone loss is a risk factor for skeletal morbidity in cancer patients. Despite the widespread use of immune checkpoint inhibitors (ICIs) their impact on bone health is still poorly defined. Here, we prospectively analyzed bone turnover markers (BTM) in patients receiving single-agent PD1 or PD-L1 inhibitors and we evaluated direct effects of ICI on bone cell homeostasis in vitro.

Methods Patients with advanced cancer and no evidence of bone metastases assessed per bone scan or PET-CT were enrolled. Serum markers of bone resorption (C-terminal telopeptide (CTX)) and bone formation (osteocalcin (OCN) and procollagen type I N-propeptide (PINP)) were measured before each ICI application, as well as parameters of bone metabolism. Dose-dependent effects of PD1 and PD-L1 inhibitors on osteoclast and osteoblast differentiation in vitro were evaluated by morphological and functional assays.

Results A total of 53 samples were collected from 10 patients receiving PD1 (n=5) and PD-L1 (n=5) inhibitors for a median of 15 weeks (range 7 to 31). 80% of the patients were male, median age was 71 years (range 58-77). Three weeks after the first ICI application we observed a significant decrease in CTX levels (mean CTX 0,51 ng/ml \pm 0,42 at baseline to 0,42 \pm 0,37 at week 3; p = 0,017), which remained below baseline at 15 weeks (mean 0,36 ng/ml \pm 0,25, p= NS). No significant changes in OCN, PINP and parameters of bone metabolism were detected. Interestingly, changes in CTX at 3 weeks correlated with treatment response and a decrease above 20% was associated with a longer progression-free survival (PFS) (median PFS 68,7 months vs 15,8 months, p < 0,003). In vitro studies confirmed inhibition of osteoclast differentiation (OC number decreased to 26% and 18% of control in the presence of 1000 ng/ml PD-L1 and PD1 inhibitors, respectively) as well as function (resorbed area 8% in the control vs < 0,2%) in the presence of ICI. In contrast, no direct effect of ICI was observed on osteoblasts.

Conclusions Despite the small number of patients included, our study demonstrates for the first time that ICIs inhibit bone resorption in cancer patients by directly impairing osteoclastogenesis. Further analyses are ongoing to elucidate the molecular mechanisms responsible for the anti-catabolic effects ICIs.

Ethics Approval Ethic: GS4-EK-4/606-2019, NÖ Ethikkommission

<http://dx.doi.org/10.1136/jitc-2022-SITC2022.1255>

1256

RELATIONSHIPS BETWEEN IRAES AND CHECKPOINT INHIBITOR RESPONSE IN RADIOHEAD: A LARGE PROSPECTIVE PAN-TUMOR COHORT OF STANDARD-OF-CARE PATIENTS WITH CLINICAL ANNOTATION, MOLECULAR AND IMMUNE PROFILING

¹Anastasia Lucas*, ¹Samantha Liang, ¹Diane Da Silva, ²Arabella Young, ³Zoe Quandt, ⁴Silvia Boffo, ⁴Lisa Salvador, ¹Lacey Padron, ³Mark Anderson, ¹Christine Spencer, ¹Marshall Thompson. ¹Parker Institute for Cancer Immunotherapy, San Francisco, CA, USA; ²Huntsman Cancer Center at the University of Utah, University of Utah, Salt Lake City, UT, USA; ³University of California, San Francisco, San Francisco, CA, USA; ⁴Bristol Myers Squibb, Princeton, NJ, USA

Background Checkpoint immunotherapies (CPI) have resulted in long lasting responses in subsets of cancer patients. Despite this, responses come with the risk of immune-related adverse events (irAEs) which can limit the overall benefit of CPI. Associations with response, such as the correlation between development of irAE and better overall survival (OS), are well characterized in clinical trials but less understood in standard of care settings with wide varieties of patient profiles. Thus, real-world evidence cohorts are integral to bridging the gap between clinical trials reports and clinical practice. The RADIOHEAD study is a pan-tumor, prospective cohort study of 1,200 individuals on standard of care first-line CPI treatment regimens aiming to identify drivers of irAEs and clinical response.

Methods To capture a comprehensive profile of each patient, we prospectively collected blood samples and clinical features at pretreatment, early on treatment, and 6 and 12 month timepoints via case report forms and electronic medical records from 52 community oncology clinics across the United States. Patients who experienced irAEs had additional samples and clinical data collected at analogous time intervals from the irAE onset. Clinical data were structured and harmonized and unbiased statistical analysis was performed to identify clinical predictors of OS.

Results A total of 3951 samples and associated clinical data points were collected over the course of participants' treatment. Patients with any irAE (25%) had significantly longer OS in the pan-tumor cohort (n=1061, HR=0.4, 95% CI=[0.3, 0.6]). The association between irAE and survival held in the largest tumor sub cohorts, non-small cell lung cancer (NSCLC) (N = 397) and melanoma (N = 128), when adjusting for age, and in multivariable analysis. Patients who reported already taking steroids at the time of their pretreatment blood draw had significantly shorter survival than those who did not (HR=1.5 [1.2, 2]); this association appeared more pronounced in patients taking systemic steroids. Comparing NSCLC and melanoma to all other tumor types in this standard of care dataset, patients with melanoma had significantly longer (HR=0.4 [0.3,0.6]) OS.

Conclusions Results from this cohort study of standard of care patients support previously identified variables associated with CPI response. In the future, the potential for molecular profiling of samples collected in the RADIOHEAD cohort provides an opportunity to elucidate the potential mechanistic link between irAE and clinical response to CPI, as well as identify clinically actionable mechanisms for immunotherapy resistance via integrated analyses of multi-omic datasets to be generated from longitudinal patient samples.

Acknowledgements Juvenile Diabetes Research Foundation
The Leona M. and Harry B. Helmsley Charitable Trust
Bristol Myers Squibb
XCancer

Patients who participated in the study

REFERENCES

1. Robert, C. A decade of immune-checkpoint inhibitors in cancer therapy. *Nat Commun.* 2020;**11**:3801. <https://doi.org/10.1038/s41467-020-17670-y>
2. Pasello G, Pavan A, Attili I, Bortolami A, Bonanno L, Menis J, Conte P, Guarneri V. Real world data in the era of Immune Checkpoint Inhibitors (ICIs): Increasing evidence and future applications in lung cancer. *Cancer Treat Rev.* 2020;**87**:102031. doi: 10.1016/j.ctr.2020.102031. Epub 2020 May 16. PMID: 32446182.
3. Das S, Johnson DB. Immune-related adverse events and anti-tumor efficacy of immune checkpoint inhibitors. *Journal for Immunotherapy of Cancer.* 2019;**7**:306. doi: 10.1186/s40425-019-0805-8
4. Maher VE, Fernandes LL, Weinstock C, Tang S, Agarwal S, Brave M, Ning YM, Singh H, Suzman D, Xu J, Goldberg KB, Sridhara R, Ibrahim A, Theoret M, Beaver JA, Pazdur R. Analysis of the association between adverse events and outcome in patients receiving a programmed death protein 1 or programmed death ligand 1 antibody. *J Clin Oncol.* 2019;**37**(30):2730–2737. doi: 10.1200/JCO.19.00318. Epub 2019 May 22. PMID: 31116675.

<http://dx.doi.org/10.1136/jitc-2022-SITC2022.1256>

1257

SINGLE CELL IMMUNOLOGIC DISSECTION OF CHECKPOINT INHIBITOR HEPATITIS AND AUTOIMMUNE HEPATITIS REVEALS INSIGHTS INTO IMMUNE TOLERANCE IN THE HUMAN LIVER

¹Molly Thomas*, ¹Tos Chan, ¹Neal Smith, ¹Marc Sherman, ¹Swetha Ramesh, ¹Alice Tirard, ¹John McGuire, ¹Mazen Nasrallah, ¹Kasidet Manakongtreecheep, ¹Jessica Tantivit, ¹Leyre Zubiri, ¹Dejan Juric, ¹Ryan Sullivan, ¹Genevieve Boland, ¹Georg Lauer, ²Nir Hacohen, ¹Kery Reynolds, ¹Chloe Villani. ¹MGH, Boston, MA, USA; ²Broad Institute, Cambridge, MA, USA

Background The emergence of monoclonal antibodies targeting PD-1 and CTLA-4 to treat solid tumors has revolutionized the field of immuno-oncology. However, immune checkpoint blockade (ICB) is limited by frequent immune-related adverse events. ICB-induced hepatic toxicity (irHepatitis) occurs in approximately 1-17% of patients. While these adverse events are usually mild, they often delay cancer treatment and require initiation of immunosuppressive therapy, which may compromise anti-tumor immune responses. irHepatitis shares clinical and histologic features with autoimmune hepatitis (AIH). As such, the study of irHepatitis is important not only for the care of oncology patients but also for the understanding how immune tolerance is lost across a spectrum of inflammatory liver diseases.

Methods To characterize the cellular and molecular pathways underpinning hepatic injury in irHepatitis, we used single-cell and single-nuclei RNA sequencing (scRNAseq/snRNAseq) with paired T-cell receptor (TCR) and B-cell receptor (BCR) sequencing to characterize ~300,000 cells from the liver and blood of 23 patients – 9 patients with irHepatitis, 4 patients with AIH, 3 controls on ICB, and 7 controls not on ICB. irHepatitis was defined by a hepatocellular or cholestatic rise in LFTs often with centrilobular histiocytic liver injury requiring treatment with steroids. Control patients had drug-induced liver injury, hepatic steatosis, non-alcoholic steatohepatitis, primary biliary cirrhosis, or venous outflow obstruction that did not require immunosuppressive therapy.

Results In irHepatitis we detected liver T cells expressing *CXCL13* and expanded cycling and cytotoxic CD8 T cells spanning effector to exhausted phenotypes. TCR repertoire analysis demonstrated clonal expansion of CD8 T cell subsets specific to irHepatitis. Parallel analysis of tissue immune cells from patients with AIH and irHepatitis enabled the identification of cell types and states both common and unique to each type of immune-mediated liver injury. For all patients, matched blood samples were also analyzed by scRNAseq to determine how cellular and transcriptional signatures in the liver tissue microenvironment were mirrored in circulating immune cells. Lastly, analysis of hepatocytes, cholangiocytes, and mesenchymal cells revealed specific inflammatory signatures in irHepatitis and AIH that suggested significant liver parenchymal dysfunction.

Conclusions In defining the cellular and transcriptional programs that are altered in irHepatitis, we have identified novel pathways that could be therapeutically targeted to treat liver inflammation in this context and have determined how PD-1 and CTLA-4 signaling may contribute to immune tolerance in the liver.

Ethics Approval This study was approved by the Dana-Farber/Harvard Cancer Center Institutional Review Boards (DFCI/HCC 11-181 and 13-416, Mass General Brigham 2010P001242).

<http://dx.doi.org/10.1136/jitc-2022-SITC2022.1257>

1258

PBMC HUMANIZED MOUSE MODEL WITH CLINICAL RELEVANCE IN ASSESSING THE SAFETY PROFILE OF 4-1BB AGONISTS UTOMILUMAB AND URELUMAB

¹Destanie Rose*, ²Wenqian He, ²Bernard Buetow, ²Allison Vitsky, ²Maggie Lui, ¹Jiwon Yang, ¹Guoxiang Yang, ¹James Keck, ²Bart Jessen. ¹The Jackson Laboratory, Sacramento, CA, USA; ²Pfizer, San Diego, CA, USA

Background Immunotherapy is an important tool that can be used to stimulate a patient's own immune system against cancer. 4-1BB agonists were designed to target costimulatory molecules on a patient's immune cells to activate anti-tumor activity. Two 4-1BB agonists were recently investigated in clinical trials. Urelumab demonstrated clinical efficacy but also induced severe liver toxicity while utomilumab was well tolerated. Preclinical toxicity evaluations were unable to predict the clinical safety profile of urelumab.

Methods We developed a PBMC humanized mouse model to better meet the needs of preclinical toxicity evaluations. This model can be used to test a variety of therapeutics that target human immune cells, including both monoclonal and bispecific antibodies, and induce acute or systemic cytokine release responses which can manifest within hours or days later resulting in tissue damage and lethality of the mice. For this study PBMC humanized mice were dosed with 10 or 1 mg/kg of urelumab or utomilumab. Mice were evaluated on a daily basis for bodyweight loss and clinical evaluation scores. Toxicity was also evaluated by liver histology and terminal serum clinical chemistry.

Results Mice dosed with 10 mg/kg of urelumab experienced body weight loss, met the clinical criteria for early euthanasia, and showed marked liver necrosis compared to utomilumab treated animals and PBS controls. Serum levels of AST, ALT and GLDH were also significantly higher in urelumab treated mice. Cytokine analysis of terminal serum revealed similarities with those found to be increased in urelumab clinical trials, including elevated IFN γ , IP-10, MIG, and MIP-1 α and MIP-1 β .¹ Toxicity of urelumab could be reduced by lowering the dose to 1 mg/kg, while utomilumab was safe at both 10 mg/kg and 1mg/kg doses.

Conclusions The data generated in PBMC humanized mice were similar to findings from the clinical trials of utomilumab and urelumab and suggest that our model could identify the clinically relevant toxicity profile induced by 4-1BB agonists. The use of PBMC humanized mouse models for preclinical safety assessments could become an important part of novel immunotherapeutic development for both patient safety and reducing drug development costs.

REFERENCE

1. Segal NH, Logan TF, Hodi FS, McDermott D, Melero I, Hamid O, Schmidt H, Robert C, Chiarion-Sileni V, Ascierto PA, Maio M, Results from an integrated safety analysis of urelumab, an agonist anti-cd137 monoclonal antibody integrated safety analysis of urelumab. *Clinical Cancer Research*. 2017;**23**(8):1929–36.

Ethics Approval The Jackson Laboratory Institutional Animal Care and Use Committee and institutional review board approved all protocols used.

<http://dx.doi.org/10.1136/jitc-2022-SITC2022.1258>

Abstracts

1259 REAL WORLD EXPERIENCE OF IMMUNOTHERAPY IN AN ELDERLY TRIAL-INELIGIBLE COHORT OF PATIENTS WITH ADVANCED CUTANEOUS SQUAMOUS CELL CARCINOMA

Luke Mclean, Annette Lim, Angela Pizzolla, Benjamin Solomon, Danny Rischin. *Peter MacCallum Cancer Centre, Parkville, Australia*

Background Elderly patients are often underrepresented in clinical trials owing to exclusionary comorbidities which are more common with age, frailty and a poorer overall performance status.^{1, 2} Chemotherapy is poorly tolerated in elderly comorbid advanced cutaneous squamous-cell carcinoma (CSCC) patients however little is known on the efficacy and tolerability of immunotherapy in this population. To our knowledge this is the largest dedicated report on a cohort of elderly trial-ineligible patients with advanced CSCC treated with immunotherapy to date. The cemiplimab registrational study, which established immunotherapy as the standard of care for advanced CSCC, enrolled patients with a median age of 71 years (73% over 65 years, n=43).³

Methods This study was a single-centre retrospective review of elderly patients (aged 70 years or more) with locally advanced (not amenable to curative surgery or radiotherapy) or metastatic CSCC who were deemed ineligible for clinical trials and received immunotherapy via a compassionate access scheme between August 2017 and January 2022. Patient demographics, tumor characteristics, treatment history and toxicity data were collected. Disease control rates (DCR), overall response rates (ORR), median overall survival (OS), disease specific survival (DSS) and median progression-free survival (PFS) were assessed. Response assessments for patients with imaging available post commencement of immunotherapy were performed as per RECIST1.1 and/or PERCIST1.0 criteria as appropriate. Kaplan-Meier analysis was performed and descriptive statistics were used.

Results 53 patients ≥ 70 years old receiving immunotherapy were analyzed. Median age was 81 years (range 70-96); 81% were male; 34% immunocompromised; and 34% ECOG 2 or higher. 15% patients had distant metastatic disease (see table 1). All patients were treatment naïve. Average Charlson Comorbidity Index including and excluding solid organ cancer was 9 and 5 respectively. 33% developed an immune-related adverse event (IRAE) but only 2 patients experienced a grade 3 IRAE and 6 patients discontinued due to toxicity with no treatment related deaths. 34 patients were followed with FDG-PET with an ORR of 59% and DCR of 76%. Response assessments are summarised in table 2. With a median follow up of 7.9 months, median OS was 20.5 months (95%CI 11-NA) (Figure 1) and median DSS 25.6 months (95%CI 20.5-NA) (Figure 2).

Conclusions Immunotherapy is effective and well tolerated among elderly trial-ineligible patients with advanced CSCC with no increase in toxicity and a comparable efficacy to what has been demonstrated in current clinical trials.

REFERENCES

- Denson AC, Mahipal A. Participation of the elderly population in clinical trials: barriers and solutions. *Cancer Control*. 2014;**21**(3):209–14.
- Sedrak MS, Mohile SG, Sun V, Sun CL, Chen BT, Li D, *et al*. Barriers to clinical trial enrollment of older adults with cancer: A qualitative study of the perceptions of community and academic oncologists. *J Geriatr Oncol*. 2020;**11**(2):327–34.
- Migden MR, Rischin D, Schmults CD, Guminski A, Hauschild A, Lewis KD, *et al*. PD-1 blockade with cemiplimab in advanced cutaneous squamous-cell carcinoma. *New England Journal of Medicine*. 2018;**379**(4):341–51.

Ethics Approval The study was approved by the Peter MacCallum Cancer Centre Human Research and Ethics Committee HREC/76580/PMCC (21/124).

Consent The study was approved by the Peter MacCallum Cancer Centre Human Research and Ethics Committee HREC/76580/PMCC (21/124) with a waiver of consent granted.

Abstract 1259 Table 1 Basic Demographics

Basic Demographics		n = 53
Median age (years)		81
Sex		
Male		43 (81%)
Female		10 (19%)
Immunocompromised		
Yes		18 (34%)
ECOG performance status		
0		19 (36%)
1		16 (30%)
2		14 (26%)
3		4 (8%)
Average Charlson Comorbidity Index		
Including solid organ malignancy		9
Excluding solid organ malignancy		5
Comorbidities		
Cardiac		25 (47%)
Cerebrovascular		2 (4%)
Dementia		3 (6%)
Chronic airways disease		8 (15%)
Connective tissue disease		5 (9%)
Peptic ulcer disease		1 (2%)
Diabetes mellitus		17 (32%)
Chronic kidney disease		13 (25%)
Haematological malignancy		13 (25%)
Site of primary lesion		
Head and neck region		47 (87%)
Limbs		4 (8%)
Unknown primary		2 (4%)
Extent of disease at immunotherapy commencement		
Locally advanced		39 (74%)
Regional nodal metastasis		24 (45%)
Distant metastasis		8 (15%)

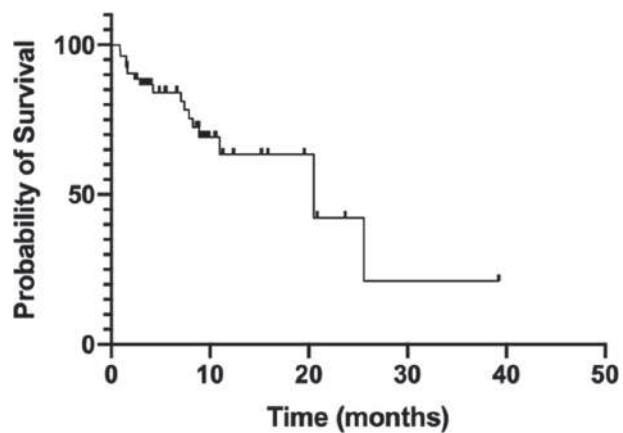
Abstract 1259 Table 2 Response Assessments

Response Assessments*		N = 34
Best response on FDG-PET as per PERCIST1.0		
Progressive metabolic disease		8
Stable metabolic disease		6
Partial metabolic response		10
Complete metabolic response		10
ORR (%)		59%
DCR (%)		76%
Best response as per RECIST1.1		N = 15
Progressive disease		3
Stable disease		6
Partial response		1
Complete response		5
ORR (%)		40%
DCR (%)		80%

* 10 patients were not evaluable

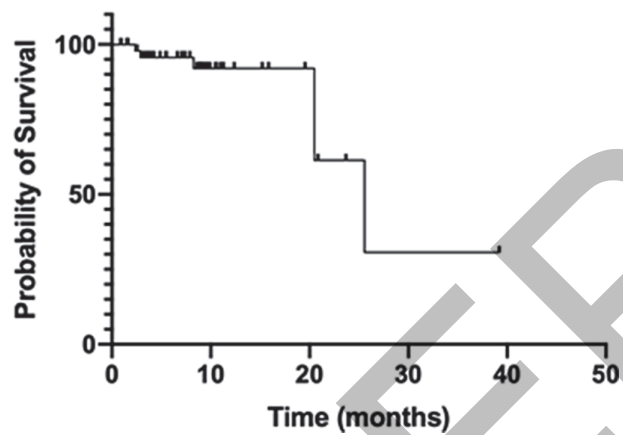
FDG-PET: fluorodeoxyglucose-positron emission tomography; ORR: overall response rate; DCR: disease control rate

Overall Survival



Abstract 1259 Figure 1 Overall Survival

Disease Specific Survival



Abstract 1259 Figure 2 Disease Specific Survival

<http://dx.doi.org/10.1136/jitc-2022-SITC2022.1259>

Abstracts

1260

COMPARATIVE SAFETY AND EFFECTIVENESS OF IL6R INHIBITORS, TNF INHIBITORS AND METHOTREXATE FOR THE TREATMENT OF IMMUNE CHECKPOINT INHIBITOR-ASSOCIATED ARTHRITIS

¹Anne Bass*, ³Noha Abdel-Wahab, ⁴Jeffrey Sparks, ⁵Pankti Reid, ⁶Cassandra Calabrese, ²Deanna Jannat-Khah, ⁷Divya Rajesh, ²Nilasha Ghosh, ⁸Komal Mushtak, ⁸Farah Al Haj, ⁴Lydia Gedmintas, ³Adewunmi Falohun, ⁴Lindsey Macfarlane, ⁹Michael Postow, ³Adi Diab, ¹⁰Ami Shah, ¹⁰Clifton Bingham, ²Karmela Chan, ¹⁰Laura Cappelli. ¹Hospital for Special Surgery/Weill Cornell Medicine, New York, NY, USA; ²Hospital for Special Surgery/Weill Come, New York, NY, USA; ³MD Anderson Cancer Center, Houston, TX, USA; ⁴Brigham and Women's Hospital, Boston, MA, USA; ⁵University of Chicago, Chicago, IL, USA; ⁶Cleveland Clinic, Cleveland, OH, USA; ⁷Hospital for Special Surgery, New York, NY, USA; ⁸Detroit Medical Center, Detroit, MI, USA; ⁹Memorial Sloan Kettering, New York, NY, USA; ¹⁰Johns Hopkins, Baltimore, MD, USA

Background Immune checkpoint inhibitor associated arthritis (ICI-A) affects 4% of ICI-treated cancer patients and often persists, even after ICI cessation. Given its long duration, it is important to identify effective treatments that do not interfere with cancer responses. No studies have compared the safety or effectiveness of disease-modifying antirheumatic drugs (DMARDs) for ICI-A.

Methods We performed a retrospective multicenter observational study. Inclusion criteria were 1) diagnosis of ICI-A and 2) treatment with a DMARD, specifically an interleukin 6 receptor inhibitor (IL6Ri), tumor necrosis factor inhibitor (TNFi), or methotrexate (MTX). Patients with preexisting autoimmune diseases, and patients who received an IL6Ri or TNFi in combination with MTX were excluded. The primary outcome was cancer progression. The secondary outcome was arthritis control, defined as grade 1 arthritis (mild pain, not interfering with function) and prednisone 10 mg daily, within the first 90 days of DMARD treatment. Demographic and clinical features were compared between DMARD groups with Fisher's exact test, Chi-square tests, T-Tests, Wilcoxon rank sum tests and ANOVA as appropriate. Cox proportional hazard models were performed to determine hazard ratios for cancer progression and arthritis control by DMARD treatment, adjusted for confounders (age, sex, cancer type and stage, ICI type, and steroid duration).

Results One hundred sixteen patients from 6 institutions were included, mean(SD) age 62(12) years, 63(54%) male. DMARD treatment was IL6Ri in 43(37%), TNFi in 25(22%), and MTX in 48(41%) (table 1). Kaplan-Meier curves showing time from ICI initiation to cancer progression by DMARD treatment and time to arthritis control are shown in figures 1&2. Compared to patients treated with MTX, patients treated with an IL6Ri had a shorter time to cancer progression (HR 3.67, 95%CI 1.13-11.9, p=0.03) but also a shorter time to arthritis control (HR 3.98, 95%CI 1.21-13.1, p=0.02) in adjusted Cox models. Patients treated with TNFi similarly had a shorter time to cancer progression and arthritis control compared to patients treated with MTX, but these differences were not statistically significant: cancer progression (HR 3.17, 95%CI 0.95-10.5, p=0.06); arthritis control (HR 3.33, 95% CI 0.99-11.1, p=0.051).

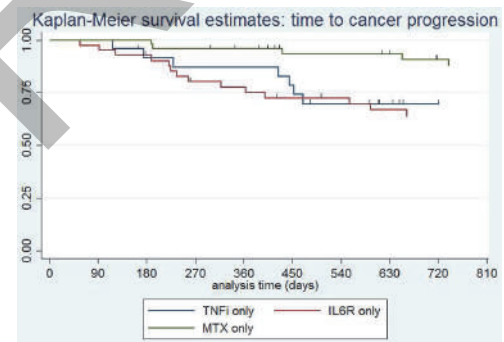
Conclusions In this retrospective cohort study, ICI-A treatment with an IL-6i was associated with a shorter time to cancer progression but more rapid arthritis control compared to MTX. Results for TNFi were similar to those for IL6Ri but were not statistically significant likely due to sample size. A prospective randomized controlled trial is needed to confirm these findings and to optimize management of patients with high-grade ICI-A.

Ethics Approval This study was approved by the Hospital for Special Surgery IRB # 2017-1898 as well as the IRBs of all participating sites.

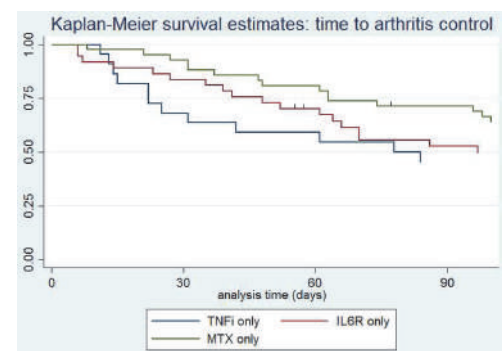
Abstract 1260 Table 1 Patient characteristics Characteristics of cancer patients with checkpoint inhibitor-associated arthritis who were treated with methotrexate, an IL6R inhibitor or a TNF inhibitor

Table 1: Patient characteristics					
N (%) or Median (IQR)	Total	TNFi	IL6Ri	MTX	p-value
Age, mean (SD)	62 (12)	57 (15)	62 (13)	63 (9)	0.40
Sex (male)	63 (54)	16 (64)	29 (67)	19 (40)	0.023
Race (white)	106 (93)	23 (92)	40 (98)	42 (88)	0.56
Smoker (ever)	60 (62)	13 (52)	22 (51)	25 (52)	0.84
Cancer type					<0.001
Melanoma	42 (36)	12 (48)	19 (44)	10 (21)	
RCC	18 (15)	3 (12)	11 (26)	4 (8)	
NSCLC	12 (10)	1 (4)	0 (0)	11 (23)	
Bladder	7 (6.0)	0 (0)	6 (14)	1 (2)	
Other	37 (32)	9 (36)	7 (16)	22 (46)	
Cancer Stage					0.31
II	3 (3)	2 (8)	0 (0)	1 (2)	
III	18 (15)	4 (16)	6 (14)	7 (14)	
IV	95 (82)	19 (76)	37 (86)	40 (83)	
Brain metastases present	14 (12)	1 (4)	6 (14)	7 (15)	0.37
Immunotherapy type					0.17
CTLA4 monotherapy	1 (1)	0 (0)	1 (2)	0 (0)	
PD(L)1 monotherapy	82 (71)	17 (68)	31 (72)	34 (71)	
Combination	30 (26)	6 (24)	11 (26)	13 (27)	
Concomitant chemotherapy	14 (12)	6 (24)	2 (5)	6 (13)	0.063
Concomitant targeted therapy	15 (13)	2 (8)	9 (21)	5 (10)	0.12
Total ICI duration, days	328 (175, 672)	309 (172, 596)	336 (196, 720)	351.5 (175, 594)	0.62
Maximum arthritis grade					0.81
1	2 (2)	0 (0)	1 (2)	1 (2)	
2	57 (49)	12 (48)	20 (47)	25 (52)	
3	52 (45)	13 (52)	21 (49)	18 (38)	
ICI held for arthritis	23 (20)	6 (24)	9 (21)	8 (17)	0.79
ICI discontinued for arthritis	45 (39)	10 (40)	15 (35)	20 (42)	0.75
Maximum steroid dose, mg*	40 (20, 60)	45 (40, 75)	40 (20, 60)	20 (15, 50)	0.004
Steroid duration, days	293 (129, 483)	257 (112, 466)	293 (122, 483)	343 (139, 606)	0.66
Concomitant iAE	45 (39)	15 (60)	10 (23)	20 (42)	0.010

ICI = immune checkpoint inhibitor; NSCLC = non-small cell lung cancer; RCC = renal cell carcinoma; TNFi = TNF inhibitor; IL6Ri = IL6R inhibitor; MTX = methotrexate; ICI = immune checkpoint inhibitor; iAE = immune related adverse event.
*Prednisone dose equivalent



Abstract 1260 Figure 1 Time to cancer progression Kaplan Meier curve showing time to cancer progression in patients treated with methotrexate, IL6R or TNF inhibitors for checkpoint inhibitor-associated arthritis



Abstract 1260 Figure 2 Time to arthritis control Kaplan Meier curve showing time to checkpoint inhibitor-associated arthritis control during the first 90 days of treatment with methotrexate, an IL6R inhibitor or a TNF inhibitor

<http://dx.doi.org/10.1136/jitc-2022-SITC2022.1260>

1261

INCREASED CONCENTRATIONS OF S100B AND NEUROFILAMENT LIGHT CHAIN IN SERUM INDICATE CHECKPOINT INHIBITOR-INDUCED CNS INFLAMMATION

¹Sara Bjursten*, ¹Ankur Pandita, ¹Zhiyuan Zhao, ²Joel Simirén, ²Henrik Zetterberg, ³Anna Rudin, ¹Lars Ny, ¹Max Levin. ¹Sahlgrenska University Hospital, Gothenburg, Sweden; ²Institute of Neuroscience and Physiology, Gothenburg, Sweden; ³Institute of Medicine, Sahlgrenska, Gothenburg, Sweden

Background Checkpoint inhibitor (CPI)-induced CNS inflammation is a severe neurological adverse event.^{1, 2} CPI-induced CNS inflammation can be difficult to diagnose because symptoms indicate more common conditions such as tumor progression or infection.³⁻⁵ There is a clinical need for blood tests to facilitate diagnosis of CPI-induced CNS inflammation.

Our objective was to evaluate if increased concentrations of brain damage markers S-calcium-binding protein B (S100B) and neurofilament light chain (NfL) in serum indicate CPI-induced CNS inflammation.

Methods Medical records and laboratory data were examined in patients with metastatic melanoma or metastatic renal cell carcinoma. The patients were treated with double checkpoint inhibition (nivolumab and ipilimumab) between March 2018 and April 2022 (n=197) at Sahlgrenska University Hospital, Sweden. In patients with suspected CNS-inflammation, brain MRI and analysis of cerebrospinal fluid were performed and brain damage markers S100B and NfL in serum were analyzed repeatedly. S-100B has a dual function as it is secreted by some melanoma metastases as well as damaged astrocytes.^{6, 7} S-100B concentrations in patients with melanoma metastases that do not secrete S-100B (n=29) and renal cell carcinoma patients (n=10) were used as double checkpoint inhibitor treated controls. As controls for NfL, we analyzed frozen plasma from melanoma patients treated with double checkpoint inhibition (ipilimumab + nivolumab) or monotherapy nivolumab (n=49).

Results Nine out of 197 patients had a verified CPI-induced CNS inflammation (4.6%) within 200 days from the first double checkpoint inhibitor treatment (table 1). S100B and NfL in serum increased during CNS inflammation (figure 1A-D and F) and normalized when patients were treated with immunosuppression (figure 1A-C, E and G). S100B concentration in serum increased early in patients with CPI-induced CNS inflammation (figure 1A-C), whereas NfL increased later (figure 1A-C). The sensitivity of an increased S100B and NfL to detect a CPI-induced CNS inflammation was 100% for S100B and 79% for NfL and the specificity was 89% for S100B and 74% for NfL (figure 2).

Conclusions The combined analysis of S100B and NfL in serum is a tool for early detection and monitoring of CPI-induced CNS inflammation. Early diagnosis of CPI-induced CNS inflammation may save lives, prevent long-term hospitalization, and reduce neurological complications.

REFERENCES

1. D Dubey *et al.* Severe Neurological Toxicity of Immune Checkpoint Inhibitors: Growing Spectrum. *Ann Neurol.* 2020;**87**(5):659–669. doi: 10.1002/ana.25708.
2. S Bjursten *et al.* Early rise in brain damage markers and high ICOS expression in CD4+ and CD8+ T cells during checkpoint inhibitor-induced encephalomyelitis. *J Immunother Cancer.* 2021;**9**(7). doi: 10.1136/jitc-2021-002732.
3. JR Brahmer *et al.* Management of Immune-Related Adverse Events in Patients Treated With Immune Checkpoint Inhibitor Therapy: American Society of Clinical Oncology Clinical Practice Guideline. *J Clin Oncol.* 2018;**36**(17):1714–1768. doi: 10.1200/JCO.2017.77.6385.
4. J Haanen *et al.* Management of toxicities from immunotherapy: ESMO Clinical Practice Guidelines for diagnosis, treatment and follow-up. *Ann Oncol.* 2018;**29** (Suppl 4):iv264–iv266. doi: 10.1093/annonc/mdy162.

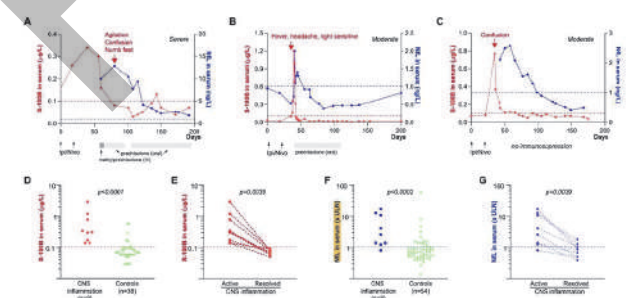
5. I Puzanov *et al.* Managing toxicities associated with immune checkpoint inhibitors: consensus recommendations from the Society for Immunotherapy of Cancer (SITC) Toxicity Management Working Group. *J Immunother Cancer.* 2017;**5**(1)95. doi: 10.1186/s40425-017-0300-z.
6. HD Abraha, LC Fuller, AWPDU Vivier, EM Higgins, and RA Sherwood. Serum S100 protein: a potentially useful prognostic marker in cutaneous melanoma. *British Journal of Dermatology.* 1997;**137**:381-385.
7. R Gerlach *et al.* Active secretion of S100B from astrocytes during metabolic stress. *Neuroscience.* 2006;**141**(4):1697–701. doi: 10.1016/j.neuroscience.2006.05.008.

Ethics Approval The study was approved by the Regional Ethics Board (151-16, 477-18, 2021-04093)

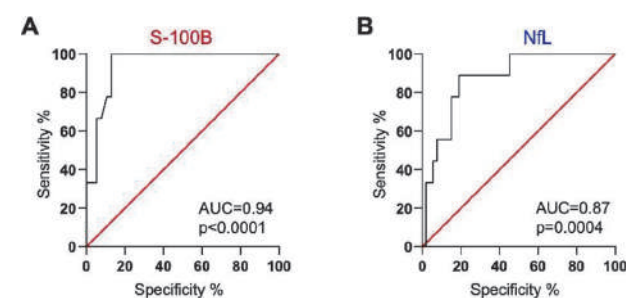
Abstract 1261 Table 1 Checkpoint inhibitor-induced CNS inflammation

Case #1*	Case #2	Case #3	Case #4	Case #5	Case #6	Case #7	Case #8	Case #9	Case #10
Severe Drowsy Headache Fever Focal epilepsy and signs	Severe Fever Headache Focal epilepsy and signs	Severe Fever Headache Focal epilepsy and signs	Severe Fever Headache Focal epilepsy and signs	Severe Fever Headache Focal epilepsy and signs	Severe Fever Headache Focal epilepsy and signs	Severe Fever Headache Focal epilepsy and signs	Severe Fever Headache Focal epilepsy and signs	Severe Fever Headache Focal epilepsy and signs	Severe Fever Headache Focal epilepsy and signs
Peak Handshake Disorientation Focal epilepsy and signs	Peak Handshake Disorientation Focal epilepsy and signs	Peak Handshake Disorientation Focal epilepsy and signs	Peak Handshake Disorientation Focal epilepsy and signs	Peak Handshake Disorientation Focal epilepsy and signs	Peak Handshake Disorientation Focal epilepsy and signs	Peak Handshake Disorientation Focal epilepsy and signs	Peak Handshake Disorientation Focal epilepsy and signs	Peak Handshake Disorientation Focal epilepsy and signs	Peak Handshake Disorientation Focal epilepsy and signs
Brain MRI/CT	Peak Normal	Peak Normal	Peak Normal	Peak Normal	Peak Normal	Peak Normal	Peak Normal	Peak Normal	Peak Normal
CNS	Brain damage markers S100B peak 1.4 ULN NfL peak 12.8 ULN Recovery: Normal	Brain damage markers S100B peak 1.4 ULN NfL peak 12.8 ULN Recovery: Normal	Brain damage markers S100B peak 1.4 ULN NfL peak 12.8 ULN Recovery: Normal	Brain damage markers S100B peak 1.4 ULN NfL peak 12.8 ULN Recovery: Normal	Brain damage markers S100B peak 1.4 ULN NfL peak 12.8 ULN Recovery: Normal	Brain damage markers S100B peak 1.4 ULN NfL peak 12.8 ULN Recovery: Normal	Brain damage markers S100B peak 1.4 ULN NfL peak 12.8 ULN Recovery: Normal	Brain damage markers S100B peak 1.4 ULN NfL peak 12.8 ULN Recovery: Normal	Brain damage markers S100B peak 1.4 ULN NfL peak 12.8 ULN Recovery: Normal
Serum	Brain damage markers S100B peak 1.4 ULN NfL peak 12.8 ULN Recovery: Normal	Brain damage markers S100B peak 1.4 ULN NfL peak 12.8 ULN Recovery: Normal	Brain damage markers S100B peak 1.4 ULN NfL peak 12.8 ULN Recovery: Normal	Brain damage markers S100B peak 1.4 ULN NfL peak 12.8 ULN Recovery: Normal	Brain damage markers S100B peak 1.4 ULN NfL peak 12.8 ULN Recovery: Normal	Brain damage markers S100B peak 1.4 ULN NfL peak 12.8 ULN Recovery: Normal	Brain damage markers S100B peak 1.4 ULN NfL peak 12.8 ULN Recovery: Normal	Brain damage markers S100B peak 1.4 ULN NfL peak 12.8 ULN Recovery: Normal	Brain damage markers S100B peak 1.4 ULN NfL peak 12.8 ULN Recovery: Normal

*Patient described in detail in ref. case #1, PMID: 3421509. Abbreviations: S100B, calcium-binding protein B; NfL, neurofilament light chain; ULN, upper limit of normal; GAD65, gliadin antibody; S100B, calcium-binding protein B; S100B, calcium-binding protein B.



Abstract 1261 Figure 1 Neurological Symptoms and Serum Concentrations of Brain Damage Marker S100B and NfL in Patients with or without CPI-induced CNS inflammation



Abstract 1261 Figure 2 Receiver-Operating Characteristic (ROC) Curves

<http://dx.doi.org/10.1136/jitc-2022-SITC2022.1261>

Abstracts

1262

ELEVATED SERUM TNF- α IS A CANDIDATE PROGNOSTIC BIOMARKER FOR IMMUNE CHECKPOINT INHIBITOR MYOCARDITIS

¹Rebecca Caldwell, ¹Gaspar Pina, ¹Praise Oderinde, ¹Abdelrahman Ali, ²Jensen Garrett, ¹Bilal Siddiqui, ¹Sumit Subudhi, ¹Cezar Iliescu, ¹Syed Wamique Yusuf, ¹Efstratios Koutroumpakis, ¹Ihab Hamzeh, ¹Shaden Khalaf, ¹Anita Deswal, ¹Nicolas Palaskas*. ¹UT MD Anderson Cancer Center, Houston, TX, USA; ²Texas AandM College of Medicine, Houston, TX, USA

Background Immune checkpoint inhibitors (ICI) can cause a myriad of immune related complications, including myocarditis which has a mortality of 25 to 50%.¹ The impact of peripheral cytokine levels on prognosis and treatment of ICI myocarditis has not been well described.

Methods This was a retrospective cohort of patients with ICI myocarditis treated at MD Anderson Cancer Center between January 2011 and May 2022. ICI myocarditis was defined by the adjudication criteria of myocarditis in the setting of cancer therapeutics.² Cytokine levels were obtained during the index hospitalization with ICI myocarditis and measured by two clinical laboratory improvement amendments (CLIA)-certified assays. If cytokine levels were measured more than once, the peak value was used. Major adverse cardiovascular events (MACE) were defined as a composite of heart failure with/without cardiogenic shock, arterial thrombosis (myocardial infarction, stroke, lower limb ischemia), life-threatening arrhythmias (asystole, pulseless electrical activity, third degree heart block, sustained ventricular tachycardia, ventricular fibrillation), pulmonary embolism, and sudden cardiac death. Kaplan Meier curves for MACE free and all-cause mortality with censoring at 90 days and log rank test for comparing survival were used.

Results Ninety-nine patients were identified with ICI myocarditis. The mean age was 67.8 \pm 12.7 years and majority were male (70%) and Caucasian (83%). The most common cancer groups were genitourinary (32%), melanoma (22%), and lung (17%). MACE occurred in 13% of patients with the most common being heart failure (62%), life threatening arrhythmia (38%), and sudden cardiac death (31%). Tumor necrosis factor- α (TNF- α), Interferon γ (IFN- γ), and Interleukin (IL)-6 were checked in 65 of the 99 patients. TNF- α and IL-6 were elevated in 69% and 82% of patients, respectively. IFN- γ was elevated in 31% of patients. Other cytokine levels were elevated in less than 20% of patients, except for IL2 receptor at 62% (table 1). MACE and overall mortality of patients with TNF- α levels above the median level of 32.5 pg/mL was higher compared to those with TNF- α in the lower 50% percentile (p-value 0.031) (figure 1). The administration of infliximab showed similar MACE free and overall survival between all patients and those with elevated TNF- α (p-value 0.698 and 0.830 respectively).

Conclusions Elevated TNF- α may be a sign of worse prognosis in patients with ICI myocarditis. However, the selective use of infliximab in this patient group did not improve outcomes. Therefore, peripheral cytokine levels may aid in prognostication but their use to guide myocarditis therapy is limited.

REFERENCES

- Palaskas N, Lopez-Mattei J, Durand JB, Iliescu C, Deswal A. Immune checkpoint inhibitor myocarditis: pathophysiological characteristics, diagnosis, and treatment. *J Am Heart Assoc.* 2020;9(2):e013757. doi: 10.1161/JAHA.119.013757. Epub 2020 Jan 21. PMID: 31960755; PMCID: PMC7033840.
- Bonaca MP, Olenchock BA, Salem JE, Wiviott SD, Ederhy S, Cohen A, Stewart GC, Choueiri TK, Di Carli M, Allenbach Y, Kumbhani DJ, Heinzlering L, Amir-

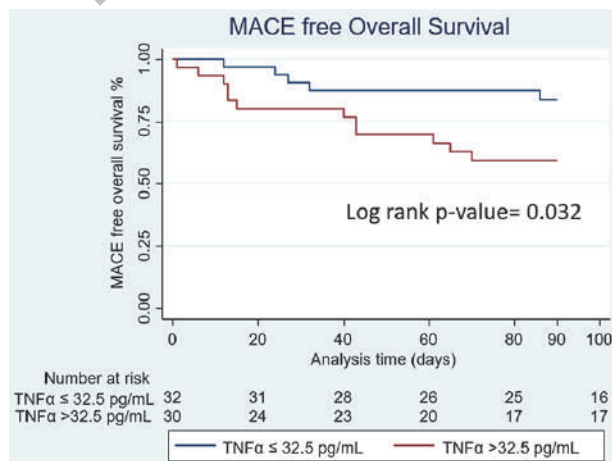
Kordestani L, Lyon AR, Thavendirathan P, Padera R, Lichtman A, Liu PP, Johnson DB, Moslehi J. Myocarditis in the setting of cancer therapeutics: proposed case definitions for emerging clinical syndromes in cardio-oncology. *Circulation.* 2019;140(2):80–91. doi: 10.1161/CIRCULATIONAHA.118.034497. PMID: 31390169; PMCID: PMC6779326.

Ethics Approval This study was approved by the institutional review board 4.

Consent A waiver of informed consent was provided by the institutional review board for this retrospective chart review study.

Abstract 1262 Table 1 Cytokine Levels in Patients with Immune Checkpoint Inhibitor Myocarditis

	Number with elevation/Number with levels measured (% positive) Median (Interquartile Range)
TNF- α normal \leq 22 pg/mL	45/65 (69.2) 32.5 (21-52.5)
IFN- γ Normal \leq 5 pg/mL	20/65 (30.7) 11 (8-18.5)
IL-6, Normal \leq 5 pg/mL	53/65 (81.5) 30 (16-89)
IL-2, Normal \leq 12 pg/mL	7/35 (20.0) 12 (5-66)
IL-1 β , Normal \leq 36 pg/mL	0/35 (0.0) 10 (7-10.1)
IL-10, Normal \leq 18 pg/mL	6/34 (17.7) 10.85 (6-16)
IL-12, Normal \leq 6 pg/mL	2/34 (5.9) -
IL-13, Normal \leq 5 pg/mL	4/34 (11.8) 11.5 (5.5-35.7)
IL-17, Normal \leq 13 pg/mL	3/34 (8.8) 38.9 (29-72)
IL-2 receptor, Normal \leq 1033 pg/mL	21/34 (61.8) 1476 (869-2167)
IL-4, Normal \leq 5pg/mL	2/34 (5.9) -
IL-5, Normal \leq 5 pg/mL	1/34 (2.9) -
IL-8, Normal \leq 5 pg/mL	1/34 (2.9) -



Abstract 1262 Figure 1 Kaplan Meier Curves of Major Adverse Cardiovascular Event Free and Overall Survival

<http://dx.doi.org/10.1136/jitc-2022-SITC2022.1262>

1263

DERMATOLOGIC IMMUNE RELATED ADVERSE EVENT DISEASE DEFINITIONS: A MULTI-INSTITUTIONAL DELPHI CONSENSUS PROJECT PRESENTED ON BEHALF OF THE ONCODERMATOLOGY WORKING GROUP

¹Steven Chen*, ²Nicole LeBoeuf, ¹Kerry Reynolds, ¹Yevgeniy Semenov. ¹MGH, Boston, MA, USA; ²DFCI, Boston, MA, USA

Background The accurate diagnosis and management of Dermatologic immune related adverse events (D-irAEs) from immune checkpoint inhibitors (ICI) are challenging because of the lack of specific, standardized disease definitions and severity grading criteria that capture the heterogeneity of possible manifestations of immune toxicity. However, determining the rash subtype is critical for effective treatment and future irAE risk and management.

Our group sought to develop D-irAE subtype definitions for diagnosis and severity grading developed through a modified Delphi consensus process.

Methods A working group of oncodermatologists drafted a classification system with guidance statements and disease definitions to support the work-up, diagnosis and severity grading of D-irAEs. Core diagnoses for the draft were chosen based on available literature on the presentation and frequency of D-irAEs, choosing the ten most commonly reported D-irAEs. The proposed system of diagnosis and severity grading was then reviewed by a panel of dermatologists, oncologists, oncodermatologists and irAE subspecialists. A modified Delphi consensus process was used, with 2 rounds of anonymous ratings by panelists and 2 virtual meetings to discuss controversial areas. Consensus based on numeric ratings was determined using the RAND/UCLA Appropriateness Method. The Delphi process was exempted by the Massachusetts General Hospital IRB.

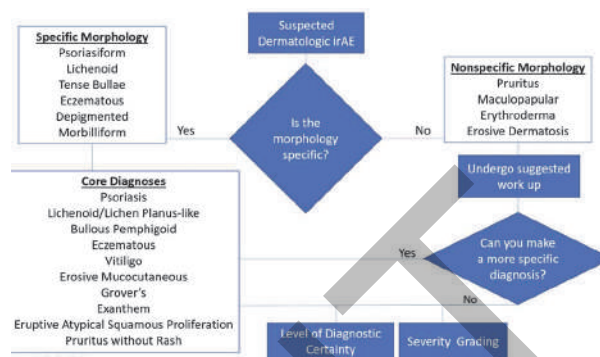
Results The panel consisted of 34 members (of 35 invited) who accepted invitations to participate in the modified Delphi consensus process. Participants represented 16 different centers including US medical centers in the northeast (5), mid-west (2), south/southeast (5), and west (3), as well as 1 international clinicians and subject matter experts.

Over two rounds of voting, the panel identified unmet needs for D-irAE disease definitions and reached consensus on a variety of statements related to D-irAE, including the proposed approach (figure 1), typical timing, and other important factors in the work up of these immune toxicities. A standard work up was also proposed and found to be in agreement for all potential D-irAEs (median 8, range 6-9) (figure 2). Finally, the disease definitions, work up considerations, and diagnostic criteria for 10 predetermined D-irAE subtypes were developed and reached consensus.

Conclusions By properly identifying the patient's D-irAE, the clinician is able to tailor treatment and understand implications about the patient's cancer therapy and toxicities. The proposed system herein allows for a standard algorithm for work-up and investigation that may lead to a core D-irAE diagnosis. We are hopeful that the implementation of said system in clinical trials will allow for more granular adjudication of data.

Acknowledgements Thank you to Project DataSphere (Johnathan Rine, Jon McDunn, Bill Louv, Teillo Schaller) for their assistance and motivation. Thank you to Carina Storrs for her assistance with the drafting of the manuscript and abstract). Our gratitude as well for our colleagues who participated in the Delphi process. We are grateful for our patients and their

families for their willingness to allow for our continued research in this field.



Abstract 1263 Figure 1 Proposed algorithm for D-irAE workup toward core diagnosis

Abstract 1263 Table 1 Standard work up proposed for all potential D-irAEs

STANDARD D-irAE WORK UP	
Common:	
1. Full skin exam by an experienced clinician	
2. Full skin exam by a board-certified dermatologist	
3. Skin biopsy for H&E	
4. Laboratory evaluation to assess of evidence of systemic hypersensitivity reaction (CBC with differential, CMP, UA).	
Possible:	
1.	Skin biopsy for direct immuno-fluorescence
2.	ELISAs for Bullous Pemphigoid antibody titers
3.	ANA, ENA if photo-sensitivity component is noted
Uncommon/Usually Unnecessary:	
For certain subtypes of D-irAE, there are other specific tests that may be considered. These include:	
1.	Joint exam
2.	Indirect immunofluorescence with salt-split skin
3.	Serum IL-6 levels

<http://dx.doi.org/10.1136/jitc-2022-SITC2022.1263>

Abstracts

1264

A SET OF EASY AND STRINGENT CRITERIA TO IDENTIFY IMMUNE-RELATED ADVERSE EVENTS (IRAE SCORING SYSTEM, ISS) IMPROVES CORRELATION WITH OUTCOME IN A PHASE 1–2 TRIAL POPULATION

Luca Mazzarella*, Federica Giugliano, Eleonora Nicolo', Edoardo Crimini, Jacopo Uliano, Chiara Corti, Paolo d'Amico, Pamela Trillo Aliaga, Carmine Valenza, Matteo Repetto, Gabriele Antonarelli, Liliانا Ascione, Grazia Vivanet, Pierpaolo Berton Giachetti, Ida Minchella, Carmen Belli, Angela Esposito, Marzia Locatelli, Carmen Crisciello, Giuseppe Curigliano. *European Institute of Oncology, Milan, Italy*

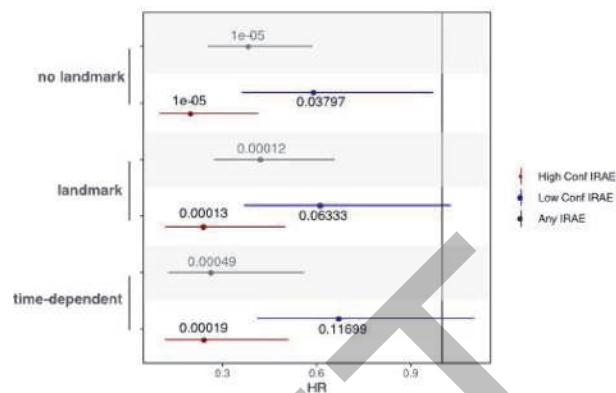
Background The benefit from immune checkpoint inhibitors (IO) is tempered by immune-related adverse events (IrAEs), which involve diverse organs, have varying biology, onset time, and severity. Several reports have found correlation between IrAE and better outcome, suggesting they may even serve as a surrogate of response, but studies are conflicting on the magnitude and significance of this correlation. Estimating the true incidence of IrAEs is particularly important in the early phase 1/2 trial setting, in order to avoid the risk of both over- and under-estimation. A key issue is the lack of IrAE diagnostic criteria, necessary to discriminate pure IrAEs from other treatment-related adverse events not sustained by an autoimmune process.

Methods Of 421 patients enrolled in phase 1-2 trials, we identified patients treated with immune-oncology (IO) drugs and analysed clinical characteristics, temporal dynamics and correlation with survival of treatment-related events, identifying “High Confidence IrAEs” (HC IrAE) by careful reconsideration of available clinical parameters. We developed an IrAE Scoring System (ISS) based on 5 parameters, each ranging 0-2: available biopsy or specific test, response to immunosuppression, temporal correlation, evidence ruling out alternative cause, known IO relationship. Correlation with Overall Survival was explored by multivariate Cox proportional hazard analysis including multiple covariates (BMI, Age, tumor type, NLR, prior IO, prior Autoimmune disease, PS, baseline disease burden). To mitigate immortal time-bias, analyses were conducted i) at 2-month landmark and ii) modeling IrAEs as time-dependent covariate.

Results 204 patients were treated with IO agents (41 with anti-PD(L)1 alone, 33 with non-PD(L)1 agents, 130 with combinations). 53 (25.9%) patients developed ≥ 1 treatment-related adverse event (85 total events). ISS score ranged from 0 to 8; by ROC analysis, a cutoff ≥ 5 achieved 100% specificity and 90% sensitivity to identify bona fide IrAEs. Based on this, we identified 3 groups of patients: 151 never experiencing an IrAE (“no-IrAE”), 33 low-confidence IrAE with ISS score 0-4 (“LC-IrAE”) and 20 high-confidence IrAE with ISS 5-8 (“HC-IrAE”). Compared to no-IrAE, patients experiencing HC-IrAEs had significantly lower Hazard ratio (HR) both in landmark analysis (HR=0.242, 95% CI 0.117-0.500, $p=0.0001$) and IrAE as time-dependent covariate analysis (HR=0.244, 95% CI 0.116-0.511, $p=0.0001$); HR for patients experiencing LC IrAE, instead, was not statistically significant (figure 1).

Conclusions ISS criteria provide a simple system to identify high confidence IrAEs, leading to more reliable estimates of IrAE incidence with significant impact on survival.

Ethics Approval The study was approved by the local ethics committee with number UID 3560



Abstract 1264 Figure 1 Forest plot with Hazard Ratios (points) with 95% CI and p values of patient groups classified by IrAE definition

<http://dx.doi.org/10.1136/jitc-2022-SITC2022.1264>

1265

VEDOLIZUMAB PLUS ANTI-PD1 ANTIBODY IN ADVANCED MELANOMA PATIENTS WITH INFLAMMATORY ENTEROCOLITIS

Asad Javed, Michele Freesmeier, Yousef Zakharia, Mohammed Millhem. *University of Iowa, Iowa City, IA, USA*

Background Use of immune checkpoint inhibitors in advanced melanoma is challenging in patients with a history of immune therapy related colitis or pre-existing inflammatory bowel disease (Crohn’s disease or ulcerative colitis).¹ Vedolizumab is a gut-selective, anti-integrin antibody that binds to the $\alpha4\beta7$ integrin on circulating leukocytes and inhibits their trafficking into the intestinal epithelium (figure 1).² There is limited clinical experience of using Vedolizumab in combination with anti-PD1 antibody in melanoma patients with inflammatory enterocolitis.³ We present outcomes of a cohort of advanced melanoma patients with inflammatory enterocolitis who concurrently received Vedolizumab and anti-PD1 antibody.

Methods In this retrospective single-institution study, records of advanced melanoma patients with a history of inflammatory enterocolitis were reviewed. Patients who received anti-PD1 antibody (Pembrolizumab, Nivolumab), concurrently with Vedolizumab were selected for analysis.

Results Nine patients with stage III/IV cutaneous melanoma and pre-existing enterocolitis received Vedolizumab plus anti-PD1 antibody (table 1). A total of 96 doses of anti-PD1 antibody were administered concurrently with Vedolizumab (56 doses), with each patient receiving at least 7 doses of anti-PD1 antibody. Vedolizumab was administered intravenously (300 mg at weeks 0, 2 and 6 weeks and then every 8 weeks) along with Pembrolizumab (200 mg every 3 weeks) or Nivolumab (240 mg every 2 weeks or 480 mg every 4 weeks). Patients had a history of grade 3-4 colitis from prior checkpoint inhibitor therapy (n=4), Crohn’s disease (n= 4), and ulcerative colitis (n= 1). Seven patients were negative for BRAF V600 mutation. Six patients had no recurrence of colitis symptoms while on anti-PD1 antibody therapy. Three patients with recurrence of colitis had a prior history of Crohn’s disease (n=2), and grade 3 check-point inhibitor related colitis (n=1). All patients with recurrence of colitis symptoms did not have melanoma progression while receiving Vedolizumab plus anti-PD1 antibody. Overall, seven patients did not experience melanoma progression on therapy. One patient had a complete response. Two patients were able to complete adjuvant treatment with anti-PD1 antibody, without melanoma recurrence on follow-up. Vedolizumab infusions were well tolerated, and no treatment related side effects were noted.

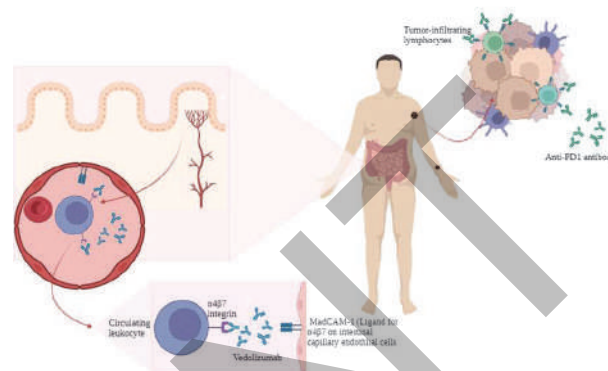
Conclusions Concurrent Vedolizumab appears to allow treatment with anti-PD1 antibody in advanced melanoma patients with pre-existing inflammatory enterocolitis. Prospective studies are needed to definitively determine the safety and anti-melanoma efficacy of this combination.

REFERENCES

1. Abu-Sbeih H, Faleck DM, Ricciuti B, *et al.* Immune Checkpoint Inhibitor Therapy in Patients With Preexisting Inflammatory Bowel Disease. *J Clin Oncol.* 2020;**38**:576–583.
2. Luzentales-Simpson M, Pang YCF, Zhang A, *et al.* Vedolizumab: potential mechanisms of action for reducing pathological inflammation in inflammatory bowel diseases. *Frontiers in Cell and Developmental Biology.* 2021;9.
3. Frohne CC, Llano EM, Perkovic A, *et al.* Complete response of metastatic melanoma in a patient with Crohn’s disease simultaneously receiving anti-alpha4beta7 and anti-PD1 antibodies. *J Immunother Cancer.* 2019;**7**:1

Ethics Approval This study was reviewed and approved by the University of Iowa Institutional Review Board IRB 01, under IRB# 202202583. A waiver of informed consent was granted by the IRB per 45 CFR 46.116 (f)(3)

Concurrent Vedolizumab and anti-PD1 antibody in advanced melanoma



Abstract 1265 Figure 1 Concurrent Vedolizumab plus anti-PD1 in advanced melanoma

Abstract 1265 Table 1 Advanced melanoma patients with inflammatory enterocolitis receiving Vedolizumab plus anti-PD1 therapy

Patient	Melanoma stage	Pre-existing enterocolitis	No. of PD-1 Ab doses	No. of Vedolizumab doses	Recurrence of colitis	Objective Response on therapy
1	IIIB	UC	14	7	No	No recurrence
2	IV*	CD	16	7	No	No recurrence
3	IV	ICI Colitis (G3)	8	6	No	SD
4	IV	ICI Colitis (G4)	9	6	No	SD
5	IV	CD	7	2	No	PD
6	IV	ICI Colitis (G4)	12	7	No	PD
7	IV	CD	7	5	Yes	SD
8	IV	CD	13	10	Yes	CR
9	IV	ICI Colitis (G3)	10	6	Yes	SD

CR: Complete response; SD: Stable Disease; PD: Progressive disease; UC: Ulcerative colitis; CD: Crohn’s disease; ICI: Immune checkpoint inhibitor; G3: Grade 3; G4: Grade 4

<http://dx.doi.org/10.1136/jitc-2022-SITC2022.1265>

Abstracts

1266

TOXICITY PROFILES OF WEIGHT-BASED 2-WEEKLY AND FLAT-DOSE 4-WEEKLY NIVOLUMAB REGIMEN – A REAL-WORLD AUSTRALIAN CENTRE EXPERIENCE

Sang Yoon Kim*, Prajwol Shrestha, Andre van der Westhuizen. *Calvary Mater Newcastle, Macquarie University, Australia*

Background Anti-PD1 inhibitor nivolumab gained US FDA approval in 2014 using a weight-based, 2-weekly regimen (Q2W). In 2018, US FDA approved a flat-dose, 480mg 4-weekly regimen (Q4W) based on quantitative pharmacokinetic modelling.^{1,2} Whilst the Q4W regimen has since been widely adopted, real-world data on safety across various tumour types remain lacking, with anecdotal reports of differing toxicity profiles due to increased drug exposure.

Methods We conducted a single-centre, retrospective analysis on adults receiving nivolumab for any tumour or treatment intent in Calvary Mater Newcastle between Jan 2015 and July 2020, collecting information on treatment and immune-related serious adverse events (SAEs). Those receiving concurrent systemic therapy other than nivolumab were excluded. Toxicity profiles, including incidence rate, types of events, and timing of onset, were compared, as were SAEs' impact on nivolumab treatment intention long term.

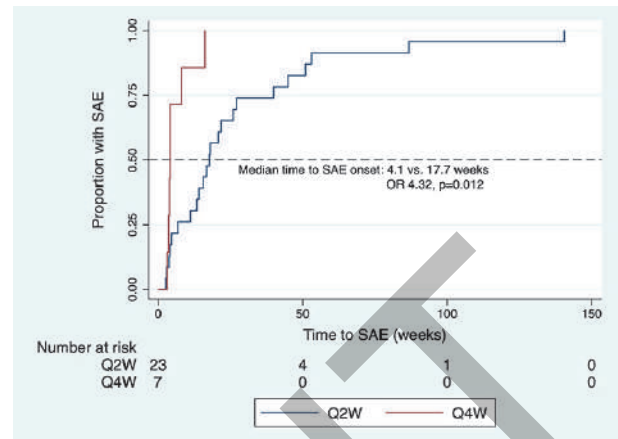
Results 137/43/35 patients received nivolumab on Q2W/Q4W/Q2W switch to Q4W (Q2-4W) regimen. Baseline characteristics were unequal, particularly the dominant tumour types (78% NSCLC in Q2W, 74% melanoma in Q4W) and treatment intention (palliative intent 96% in Q2W vs. 37% in Q4W). Q4W cohort received 29% higher nivolumab dose per week of treatment than Q2W. 23 (17%) and 7 (16%) patients experienced 24 and 9 SAEs on Q2W/Q4W, respectively. SAE per 100 person-weeks on nivolumab was higher in Q4W than in Q2W (0.99 vs. 0.64, OR 1.55), but the difference was statistically insignificant (95% CI 0.63-3.44, p=0.26, table 1). Q4W was associated with significantly earlier SAE onset than Q2W (4.1 vs. 17.7 weeks, OR 4.32, p=0.012, figure 1). Q4W was associated with more colitis (44 vs. 21%) with earlier onset (4.1 vs. 11 weeks). SAEs caused more nivolumab discontinuation in the Q2W cohort, but the difference was statistically insignificant (83% vs. 43%, OR 1.93, p=0.29). Choice of nivolumab regimen did not influence the rate of SAEs in those receiving radiotherapy. Most SAEs required systemic corticosteroid therapy (20/23 vs. 6/7) and hospitalisation (18/23 vs. 7/7), but the majority resolved within six months at a similar rate (71% vs. 75%). The SAE rate was low in the Q2-4W (6%), with no treatment discontinuation.

Conclusions Q4W nivolumab regimen was not associated with an increased incidence of SAE compared to Q2W but was associated with earlier onset with a penchant for colitis. Further research may identify unique toxicity signatures associated with different scheduling and help individualise patient treatment.

REFERENCES

1. Zhao X, Suryawanshi S, Hruska M, et al. Assessment of nivolumab benefit-risk profile of a 240-mg flat dose relative to a 3-mg/kg dosing regimen in patients with advanced tumors. *Ann Oncol* 2017;**28**(8):2002–8.
2. Zhao X, Shen J, Ivaturi V, et al. Model-based evaluation of the efficacy and safety of nivolumab once every 4 weeks across multiple tumor types. *Ann Oncol* 2020;**31**(2):302–9.

Ethics Approval Hunter New England Human Research Ethics Committee provided consent to collect and analyse data as the study involved pre-existing, non-identifiable data (authorisation 2020/STE03882)



Abstract 1266 Figure 1 Kaplan-Meier failure estimates of patients experiencing SAE according to nivolumab regimen

Abstract 1266 Table 1 SAE characteristics stratified by nivolumab regimen

	Q2W cohort (24 events)	Q4W cohort (9 events)	Q2-4W cohort (2 events)
Time to SAE onset (weeks)	17.7 (9.0-33.4)	4.1 (3.7-6.1)	69 (67.6-70.4)
SAE by grade*:			
Grade 3	19 (79%)	8 (89%)	2 (100%)
Grade 4	4 (17%)	1 (11%)	0
Grade 5	1 (4%)	0	0
SAE by type:			
Hepatitis†	3 (13%)	2 (22%)	0
Pneumonitis	4 (17%)	0	0
Colitis	5 (21%)	4 (44%)	1 (50%)
Nephritis	2 (8%)	1 (11%)	0
Skin toxicity‡	3 (13%)	0	0
Endocrinopathy§	2 (8%)	1 (11%)	1 (50%)
Nervous system¶	2 (8%)	1 (11%)	0
Others**	3 (13%)	0	0
SAE amongst recent EBRT	3 (13%)	1 (11%)	0
SAE presence 6 months post onset			
Yes	6 (26%)	1 (11%)	0
No†	17 (74%)	3 (43%)	2 (100%)
Unknown	0	3 (43%)**	0

Data are median (IQR), or n (%).

* As per CTCAE v5
† Including alanine aminotransferase (ALT) and aspartate aminotransferase (AST) rise, hepatic failure
‡ Including rash maculopapular, psoriasis
§ Including adrenal insufficiency, hypo/hypertthyroidism, hyperglycaemia, hypophosphitis
¶ Including encephalopathy, Guillain-Barre syndrome, glossopharyngeal nerve disorder
** Data cut-off pre-dating 6 months post SAE onset

<http://dx.doi.org/10.1136/jitc-2022-SITC2022.1266>

1267

THE EFFECT OF IMMUNOSUPPRESSION DURING ANTI-PD-1 TREATMENT FOR STAGE III MELANOMA

Andrew Knight*, John Kirkwood, Lilit Karapetyan, Xi Yang, Sneha Rajendran, Na Bo, Hong Wang, Cindy Sander. *University of Pittsburgh, Pittsburgh, PA, USA*

Background Anti-PD-1 therapy improves recurrence-free survival in patients with resectable Stage III/IV melanoma. Immune-related adverse events (irAEs) represent a challenge for patient care especially in the setting of adjuvant management and may serve as a predictor for therapeutic benefit. We sought to evaluate the incidence of immune related adverse events (irAEs) in melanoma patients receiving adjuvant anti-PD-1 therapy and assess the impact of corticosteroid and non-corticosteroid-based therapy on recurrence-free and overall survival at the University of Pittsburgh Medical Center (UPMC) cohort.

Methods This retrospective, single-center study reviewed adult patients undergoing treatment for Stage III melanoma between 1996 and 2021 who received either pembrolizumab or nivolumab. Patients were further excluded if they did not receive adjuvant treatment with anti-PD-1 therapy, had prior exposure to immunotherapy or BRAF inhibitors, or did not have sufficient follow-up to allow necessary data collection. The resulting 231 patients were stratified into two cohorts – those treated with >10mg prednisone equivalent for longer than two weeks during anti-PD-1 therapy, and those who were not.

Results Of 231 patients reviewed, 123 (53%) developed an irAE of any grade; 57 patients required systemic steroids during adjuvant therapy, with 11 (5%) patients that received steroids and another immunosuppressing agent. Use of steroids did not reduce OS (HR = 1.037, 95% CI 0.4517, 2.381; p=0.93) or RFS (HR = 1.026, 95% CI 0.6198, 1.699; p=0.92). Development of irAEs was associated with improved OS (HR = 0.3698, 95% CI 0.1682, 0.8127; p=0.010), and melanoma specific survival (HR 0.3608, 95% CI: 0.145, 0.8974; p=0.022), but not RFS (HR = 0.8908, 95% CI 0.5659, 1.402; p=0.62). In a multivariable analysis adjusting for age, sex, and stage development of irAEs remained significantly associated with increased overall survival (HR = 0.4079, 95% CT 0.1826, 0.9112; p=0.0288).

Conclusions IrAEs are common in patients treated with adjuvant anti-PD-1 and frequently require treatment with systemic corticosteroids. The development of irAEs during adjuvant therapy is associated with improved OS, but not RFS. Exposure to systemic steroids during adjuvant therapy did not have an impact on OS or RFS. These results provide reassurance that the use of systemic steroids during adjuvant treatment of fully-resected stage III melanoma does not have a negative impact on disease recurrence or survival.

Ethics Approval Approved by the University of Pittsburgh Institutional Review Board under Study ID: STUDY21080074.

<http://dx.doi.org/10.1136/jitc-2022-SITC2022.1267>

Abstracts

1268

INCREASED RISK OF CUTANEOUS IMMUNE-RELATED ADVERSE EVENTS IN PATIENTS TREATED WITH TALIMOGENE LAHERPAREPVEC AND IMMUNE CHECKPOINT INHIBITORS: A MULTI-INSTITUTIONAL COHORT STUDY

¹Bonnie Leung*, ¹Guihong Wan, ¹Nga Nguyen, ¹Shijia Zhang, ¹Wenxin Chen, ¹Sonia Cohen, ¹Genevieve Boland, ¹Ryan Sullivan, ¹Riley Fadden, ¹Howard Kaufman, ¹Shawn Kwatra, ²Nicole LeBoeuf, ¹Yevgeniy Semenov. ¹Massachusetts General Hospital, Boston, MA, USA; ²Dana-Farber Cancer Institute, Boston, MA, USA

Background Previous studies have shown that combining immune checkpoint inhibitors (ICIs) with Talimogene Laherparepvec (TVEC) may improve antitumor responses for metastatic melanoma.¹ However, the risk of developing cutaneous immune-related adverse events (cirAEs) in patients treated with ICI and TVEC has not been studied. We aim to evaluate the differences in cirAE development between patients treated with ICI with or without TVEC.

Methods In this multi-institutional retrospective cohort study, patients with cutaneous malignancy receiving ICI with or without TVEC therapy at the Massachusetts General Brigham healthcare system between September 12, 2014, and May 31, 2022 were included. CirAE development, time from ICI initiation to cirAE, cirAE grade, cirAE morphology, and survival were analyzed. Manual chart review was conducted by two independent trained research analysts to determine cirAE development based on timing, morphology, competing risk factors, and histologic confirmation. To compare the cohorts, Pearson's chi-squared test or Fisher's exact test for categorical variables and t-test or Kruskal-Wallis test for continuous variables were used. To account for immortal time bias, we performed time-varying Cox proportional hazards models, adjusting for sex, race/ethnicity, age at ICI initiation, ICI type, Charlson Comorbidity Index, and cancer type. Hazard ratios (HRs) and 95% confidence intervals were calculated for all variables.

Results A total of 892 cutaneous malignancy patients treated with ICI and/or TVEC therapy were included in this study, among which 93 patients were treated with both ICI and TVEC (ICI+TVEC). While 799 patients were treated with ICI alone. The rate of cirAE development was 33.2% and 38.7% for ICI only and ICI+TVEC, respectively (table 1). After adjusting for covariates, ICI+TVEC was associated with a 2-fold increased risk of cirAE development (HR: 1.96, p=0.009), when compared to patients receiving ICI therapy alone (table 2).

Conclusions These findings underscore the elevated risk of cirAE in those receiving ICI+TVEC and highlight potential opportunities for dermatologists and oncologists in counseling and monitoring patients who are considering or receiving ICI and TVEC. More individualized education and management can improve decision-making and quality of life for patients and caregivers. Limitations of this study include its retrospective nature and limited sample size from a tertiary-level academic healthcare system.

REFERENCE

- Collins JM, Redman JM, Gulley JL. Combining vaccines and immune checkpoint inhibitors to prime, expand, and facilitate effective tumor immunotherapy. *Expert Rev Vaccines*. 2018;**17**:697–705.

Ethics Approval Reviewed and approved by Mass General Brigham Institutional Review Boards; protocol # 2020P002307

Abstract 1268 Table 1 Baseline characteristics of study cohort

Table 1. Baseline characteristics of study cohort

	ICI and TVEC (N=93)	ICI alone (N=799)	P-value
CirAE			
No	57 (61.3%)	534 (66.8%)	0.34
Yes	36 (38.7%)	265 (33.2%)	
ICI Initiation to CirAE (days)			
Median [IQR]	123 [32, 298]	56 [21, 161]	0.018
CirAE Severity Grade			
Median [IQR]	1 [1, 2]	2 [1, 2]	0.066
CirAE Morphology			
Acne	0 (0%)	7 (0.9%)	0.216
Bullous Dermatitis	1 (1.1%)	7 (0.9%)	
Drug Hypersensitivity	0 (0%)	14 (1.8%)	
Eczematous Dermatitis	3 (3.2%)	10 (1.3%)	
Lichen Planus	4 (4.3%)	17 (2.1%)	
Maculopapular	8 (8.6%)	60 (7.5%)	
Pruritus	8 (8.6%)	36 (4.5%)	
Psoriasis	0 (0%)	11 (1.4%)	
Non-specified Rash	12 (12.9%)	82 (10.3%)	
Vitiligo	0 (0%)	17 (2.1%)	
Other	0 (0%)	7 (0.9%)	
Age at ICI Initiation			
Median [IQR]	68.2 [61.7, 77.4]	65.1 [56.4, 74.3]	0.002
Cancer Type			
Melanoma	78 (83.9%)	765 (95.7%)	<0.001
Other Skin Malignancy	15 (16.1%)	34 (4.3%)	
ICI Type			
CTLA4	2 (2.2%)	46 (5.8%)	0.016
PD-1	57 (61.3%)	574 (71.8%)	
PD-L1	3 (3.2%)	18 (2.3%)	
Combination	31 (33.3%)	161 (20.2%)	
Charlson comorbidity index			
0	1 (1.1%)	3 (0.4%)	0.336
1-2	72 (77.4%)	568 (71.1%)	
3-4	16 (17.2%)	163 (20.4%)	
>=5	4 (4.3%)	65 (8.1%)	
Sex			
Female	44 (47.3%)	307 (38.4%)	0.121
Male	49 (52.7%)	492 (61.6%)	
Race			
White	90 (96.8%)	778 (97.4%)	0.225
Other	0 (0%)	10 (1.3%)	
Unknown	3 (3.2%)	11 (1.4%)	
Mortality Status			
Alive	49 (52.7%)	462 (57.8%)	0.403
Dead	44 (47.3%)	337 (42.2%)	
Duration of Follow-up			
Median [IQR]	795 [454, 890]	1103 [396, 1648]	0.004

Abstract 1268 Table 2 Multivariate modeling of the association between TVEC use, cirAE development, and mortality

Table 2. Multivariate modeling of the association between TVEC use, cirAE development, and mortality

Time-varying CoxPH model on cirAE status				Time-varying CoxPH model on mortality status			
Characteristic	HR*	95% CI ^b	P-value	Characteristic	HR	95% CI	P-value
TVEC	1.96	1.18, 3.25	0.009	TVEC	2.21	1.60, 3.05	<0.001
ICI Type				ICI Type			
CTLA4	Ref ^c	Ref		CTLA4	Ref	Ref	
Combination	1.63	0.94, 2.83	0.084	Combination	1.59	0.98, 2.57	0.062
PD-1	0.90	0.53, 1.53	0.7	PD-1	0.73	0.46, 1.17	0.2
PD-L1	0.66	0.24, 1.85	0.4	PD-L1	0.75	0.34, 1.66	0.5
Age at ICI Initiation	1.00	0.99, 1.01	0.8	Age at ICI Initiation	1.03	1.02, 1.04	<0.001
Cancer Type				Cancer Type			
Melanoma	Ref	Ref		Melanoma	Ref	Ref	
Other Skin Malignancy	1.21	0.74, 1.98	0.4	Other Skin Malignancy	2.09	1.43, 3.06	<0.001
CCI^d				CCI			
>=5	Ref	Ref		>=5	Ref	Ref	
3-4	0.68	0.40, 1.17	0.2	3-4	0.51	0.35, 0.74	<0.001
1-2	1.00	0.62, 1.62	>0.9	1-2	0.41	0.29, 0.58	<0.001
0	4.08	1.35, 12.3	0.013	0	0.21	0.03, 1.52	0.12
Race				Race			
White	Ref	Ref		White	Ref	Ref	
Other	0.58	0.14, 2.36	0.4	Other	1.29	0.48, 3.50	0.6
Unknown	0.33	0.08, 1.31	0.11	Unknown	0.48	0.15, 1.50	0.2
Sex				Sex			
Female	Ref	Ref		Female	Ref	Ref	
Male	1.10	0.87, 1.40	0.4	Male	0.80	0.65, 0.98	0.035

Multivariate time-varying Cox proportional hazards model; *HR: Hazard Ratio; ^bCI: Confidence Interval; ^cRef: Reference; ^dCCI: Charlson comorbidity index

<http://dx.doi.org/10.1136/jitc-2022-SITC2022.1268>

Machine Learning, Artificial Intelligence and Computational Modeling

1269

PRETREATMENT PREDICTION OF ANTI-PD-1 IMMUNOTHERAPY RESPONSE USING MACHINE LEARNING IN PATIENTS WITH METASTATIC MELANOMAS USING TARGETED TRANSCRIPTOMICS IN CIRCULATING CD8 CELLS

Fahad Ahmed*. ALGHORISMUS, LLC, Detroit, MI, USA

Background The aim of this study is to assess the role of machine learning in identifying patients that will respond to anti-PD1 from expression data from circulating CD8 T-cells in patients with metastatic melanoma.

Methods Normalized RNA expression data was obtained from gene expression omnibus (GEO) a public functional genomics data repository.¹ All project files for GSE166181 were downloaded in clinical, RNA sequencing data, and metadata for each of these patients. Pretreatment data were extracted for each patient labeled "T0" which was used in the prediction. All normalized expression data that had no values were deleted and a final profile of the expression profiles was obtained. The expression of these genes was assigned as high or low. The patients were divided into 70/30 for training and test set. The overall accuracy of each cell and total accuracy for individual patients.

Results A total of 20 patients with 11 responders and 9 non-responders a total of 18250 cells were identified at the pretreatment stage. A training set of 9 responders and 6 non-responders was used to train the deep learning algorithm for the test set 3 responders and non-responders each were kept out. A 5-layer deep learning algorithm was trained. In the test set, a total of 2237 cells were classified with a total of 1085 cells (48.5%) correctly identified among all test-set patients. In total 3 out of 6 patients (50%) were correctly identified with a threshold of 50% cells were correctly identified see table 1. Two patients were non-responders and 1 was a responder. While the one non-responder and two responders were.

Conclusions The algorithm was partially successful in identifying non-responders in the pretreatment group in this small cohort of patients. However, a larger dataset is required to train and test to develop a more accurate algorithm for patients that will or will not respond to anti-PD-1 treatment prior to treatment.

REFERENCE

1. De Biàsi S, Gibellini L, Lo Tartaro D, Puccio S *et al.* Circulating mucosal-associated invariant T cells identify patients responding to anti-PD-1 therapy. *Nat Commun* 2021;**12**(1):1669. PMID: 33723257

Abstract 1269 Table 1 Test set cellular classification

	Non-responders			Responders		
	Patient 3	Patient 30	Patient 5	Patient 13	Patient 23	Patient 7
Correct	225(56.9%)	57(50.5%)	349(47.9%)	154(55%)	195(44.7%)	105(38.2%)
Incorrect	179(44.2%)	56(49.6%)	390(52.2%)	126(45%)	242(55.4%)	170(61.9%)
Total	403(100%)	113(100%)	729(100%)	280(100%)	437(100%)	275(100%)

<http://dx.doi.org/10.1136/jitc-2022-SITC2022.1269>

Abstracts

1270

PRETREATMENT PREDICTION OF NON-RESPONDERS TO PD-1 AXIS INHIBITORS IN ADVANCED UROTHELIAL CARCINOMAS USING A HYBRID MULTIMODAL DEEP LEARNING ALGORITHM

Fahad Ahmed*. ALGHORISMUS, LLC, Detroit, MI, USA

Background Post-FDA approval immune therapy for cancer becomes widely used for locally advanced or metastatic urothelial carcinomas. There are patients that may suffer severe side effects from these immune checkpoint blockades (ICBs). The aim of this study was to identify patients that will achieve response or those who do not achieve response to these ICBs.

Methods Pretreatment normalized ribonucleic acid (RNA) Sequencing (Seq), clinical and other data for patients with advanced UC receiving PD-1 axis inhibitors were downloaded from gene expression omnibus (GEO) datasets project PRJNA735749.¹ This data also included responses to treatment data. Responders were categorized as patients with either complete response (CR), partial response (PR), or stable disease (SD) while non-responders comprised patients with progressive disease (PD). The data set was split 70/30 for training and test sets for the deep-learning algorithm. Four distinct algorithms were developed using a complete gene expression profile, targeted normalized RNA or high vs low RNA expression (upper or lower than the 75 percentile) with non-RNA Seq data; total mutational burden (TMB), clinical characteristics of the patient (including age, TNM staging, etc.) and FGFR mutational status. The performance of each of the algorithms was assessed by comparing a matrix of test set accuracy, sensitivity, specificity, positive predictive values (PPV), negative predictive values (NPV), and area under the receiver-operating curves.

Results A total of 89 patients of were selected from a total of 103 that had complete RNASeq, DNA and clinical data. The complete RNASeq + non-RNASeq data showed test set; accuracy (18.5%), sensitivity (100%), specificity (0.0%), PPV (25%), NPV (undefined*). The targeted RNASeq + non-RNA Seq data showed test set; accuracy (70.4%), sensitivity (0.0%), specificity (100%), PPV (undefined), NPV (70.4%). The targeted RNASeq (Hi/Low cutoff) + non- RNASeq data using a Multilayer Perceptron (MLP) classifier showed test set; accuracy (81.5%), sensitivity (20.0%), specificity (95.5%), PPV (50.0%), NPV (84.0%). The targeted RNASeq (Hi/Low cutoff) + non-RNASeq data using a TensorFlow (TF) classifier showed test set; accuracy (77.8%), sensitivity (20.0%), specificity (90.9%), PPV (33.3%), NPV (83.3%) see table 1.

Conclusions The MLP/deep-learning classifier for targeted normalized high vs low RNA expression with TMB, clinical characteristics, and FGFR mutational status shows better overall results compared to other algorithms. However, we can these results need external validation and with a larger dataset, we may also be able to predict responders.

REFERENCE

1. Rose TL, Weir WH, Mayhew GM, Shibata Y *et al.* Fibroblast growth factor receptor 3 alterations and response to immune checkpoint inhibition in metastatic urothelial cancer: a real-world experience. *Br J Cancer.* 2021;**125**(9):1251–1260. PMID: 34294892

Abstract 1270 Table 1 Experiment details

Study	Experiment Type	Split	Total patient characteristics	Training set accuracy (%)	Test set					
					Accuracy (%)	Sensitivity (%)	Specificity (%)	PPV (%)	NPV (%)	AUROC (%)
1	Complete RNASeq + TMB + FGFR mutation + Clinical	70/30	16424	24.19	18.52	100	0.00	25	UD*	-
	Targeted RNASeq + TMB + FGFR mutation + Clinical	70/30	236	81.57	70.37	0.00	100	UD*	70.37	0.783
3	Targeted RNASeq + TMB + FGFR mutation + Clinical	70/30	236	100	81.48	20.00	95.46	50.00	84.00	0.518
	Upper 25th vs Lower 75th Quanta (Hi vs Low) MLP classifier	70/30	236	100	81.48	20.00	95.46	50.00	84.00	0.518
4	Targeted RNASeq + TMB + FGFR mutation + Clinical	70/30	236	100	77.78	20.00	90.91	33.33	83.33	0.536
	Upper 25th vs Lower 75th Quanta (Hi vs Low) TensorFlow	70/30	236	100	77.78	20.00	90.91	33.33	83.33	0.536

UD* represents Un-Defined (x/0) because each of these values were divided by a zero (0).

<http://dx.doi.org/10.1136/jitc-2022-SITC2022.1270>

1272

PROBABILISTIC MIXTURE MODELS IMPROVE CALIBRATION OF PANEL-DERIVED TUMOR MUTATIONAL BURDEN IN THE CONTEXT OF BOTH TUMOR-NORMAL AND TUMOR-ONLY SEQUENCING

¹Jordan Anaya, ²John-William Sidhom, ¹Alexander Baras*. ¹Johns Hopkins, Baltimore, MD, USA; ²Mount Sinai, Baltimore, MD, USA

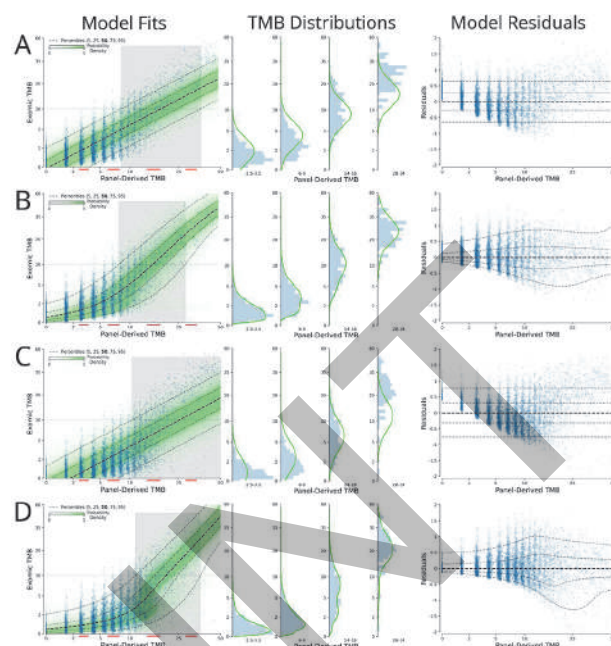
Background Tumor mutational burden (TMB) has been investigated as a biomarker for immune checkpoint blockade (ICB) therapy. Increasingly, TMB is being estimated with gene panel-based assays (as opposed to full exome sequencing) and different gene panels cover overlapping but distinct genomic coordinates, making comparisons across panels difficult. Previous studies have suggested that standardization and calibration to exome-derived TMB be done for each panel to ensure comparability. However, these studies often propose to use The Cancer Genome Atlas (TCGA) for calibration despite this data having a matched normal to remove germline variants while many labs perform tumor-only sequencing. We suggest this approach has the potential to bias TMB estimates and we propose the use of an alternative dataset for calibration of tumor-only sequencing. Current approaches also propose linear models for TMB calibration. We demonstrate why linear models are inappropriate for this data and provide an alternative model.

Methods Our approach to calibration of panel-derived TMB to exomic TMB proposes the use of deep learning to model the probability distribution of the label. We found that a mixture of lognormal distributions can model the nonlinear relationship between panel inputs and TMB as well as the complex error distributions. Using our model we examined the effect of different panel inputs, including nonsynonymous, synonymous, and hotspot counts along with genetic ancestry. To generate a tumor-only version of the TCGA data we reintroduced the germline variants from the matched-normal samples and filtered the data using gnomAD.

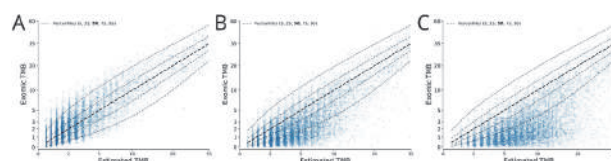
Results We were able to model accurately the distribution of both tumor-normal and tumor-only data with our mixture model while a linear model could not (figure 1). Applying a model trained on tumor-normal data to tumor-only input produced biased TMB predictions (figure 2). Including synonymous mutations resulted in better regression metrics across both data types, but ultimately a model able to dynamically weight the various input mutation types exhibited optimal performance. Including genetic ancestry improved model performance only in the context of tumor-only data. Using the probability distribution can help achieve a given positive predictive or negative predictive value.

Conclusions A probabilistic mixture model approach capable of accurately characterizing the distribution of expected exomic TMB from panel inputs better models the nonlinearity and heteroscedasticity of the data. Synthetic tumor-only panel data can allow for the calibration of tumor-only panels to exomic TMB. Leveraging the confidence of the point estimates better informs cohort stratification in terms of TMB.

Acknowledgements The results here are in whole or part based upon data generated by the TCGA Research Network. NGS gene panel assay coordinates were used from the AACR GENIE consortium. This research was supported by the Mark Foundation for Cancer Research (19-035-ASP), and the philanthropy of Susan Wojcicki and Dennis Troper in support of Computational Pathology at Johns Hopkins.



Abstract 1272 Figure 1 Different modeling strategies for tumor-normal and tumor-only data. Model Fits: Input vs model output scatter plots with overlaid model distribution probabilities (green) along with model uncertainty (95% confidence) of estimate being different from exomic TMB of 10 (grey); TMB Distributions: Histogram of observed distribution of exomic TMB with overlaid model output distribution at the midpoint of the designated range; Model Residuals: conventional residuals plot. (A) tumor-normal data with linear model, (B) tumor-normal data with proposed mixture model, (C) stringent tumor-only data with linear model, (D) stringent tumor-only data with proposed mixture model.



Abstract 1272 Figure 2 Effect of tumor-only sequencing. Prediction versus true plots for a model trained on tumor-normal data and applied to (A) tumor-normal data, (B) tumor-only stringently filtered data, and (C) tumor-only permissively filtered data.

<http://dx.doi.org/10.1136/jitc-2022-SITC2022.1272>

Abstracts

1273

COMBINING MULTIPLE IMMUNOTHERAPY STUDIES AND REAL-WORLD DATA IMPROVES PREDICTION OF IO TREATMENT EFFICACY AND HIGHLIGHTS KEY DRIVING FEATURES

Gustavo Arango*, Etai Jacob, Elly Kipkogei. *AstrZeneca, Arlington, MA, USA*

Background Despite the clinical success of immune checkpoint blockade therapies, many patients do not respond to treatments or become resistant. Previous attempts to predict treatment efficacy suffered from limited accuracy and deficiency to uncover determinants of response. Here, we introduce an AI framework which addresses these issues.

Methods We present a new explainable deep learning framework based on transformer architecture^{1, 2} which combines data with different feature sets (including sparse date) and clinical endpoints for survival prediction or classification. This framework includes: (1) A new loss function based on a sigmoid approximation of Harrell’s concordance-index.³ (2) Explainability module providing feature importance and similarity score between features based on mutual contribution to predictions. (3) Transfer learning strategy to enable leveraging diverse clinical datasets in the public or private domain.

Results We utilized seven data sets comprising of more than 140,000 patients from IO, targeted and Chemotherapy treatments to benchmark our prediction models (table 1) in addition to 10 train/test splits performance evaluations.

Consistently, our framework outperformed other methods previously described in the literature, including CoxPH⁴ and random survival forest.^{5, 6} For example, using the concordance index, our framework achieved 0.66 (0.04) vs. 0.60 (0.04) of the second-best method (Random survival forest in all cases) on MYSTIC IO arms clinical data. This improvement was a result of including transfer learning in the training process (table 2) which also achieved better performance in less training steps (figure 1).

Utilizing our Explainability module, we identified key features driving response prediction consistent with previous publications. For example, in *Chowell et al.* dataset, we identified Albumin, NLR, Chemo-before-IO-treatment and TMB as the most important features (figure 2). We also identified in sparse mutation calls of 469 genes from *Samstein et al.* dataset, functional modules of several genes only, each with a strong predictive power. For example, the functional module comprising of the genes: AKT2, BTK, CDC73, HLA-B, IKBKE, INPPL1, RFWD2, TRAF2 and WHSC1, related to adaptive immunity, stratified patients to two groups with a Hazard Ratio of 0.58 for the *Samstein* dataset and 0.42 for the validation dataset (figure 3).

Conclusions We propose a new framework with state-of-the-art performance in survival prediction and potential to uncover biological and clinical insights related to patient response and resistance. Importantly, our framework simplifies the process of translating complex AI models to clinical practice and may accelerate the benefit immunotherapy can bring to patients.

REFERENCES

1. Vaswani Ashish, et al. Attention is all you need. *Advances in Neural Information Processing Systems*. 2017;30.
2. Devlin Jacob, et al. Bert: Pre-training of deep bidirectional transformers for language understanding. arXiv preprint arXiv:1810.04805 (2018).
3. Schmid Matthias, Marvin N Wright, and Andreas Ziegler. On the use of Harrell’s C for clinical risk prediction via random survival forests. *Expert Systems with Applications* 2016;63:450–459.

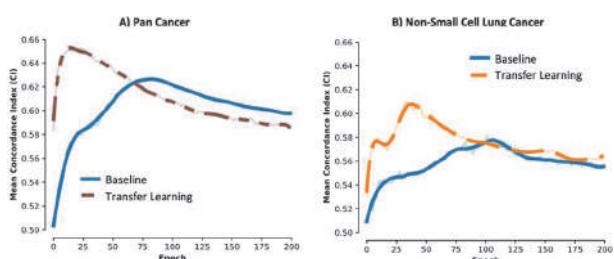
4. Cox, David R. Regression models and life-tables. *Journal of the Royal Statistical Society: Series B (Methodological)*. 1972;34(2):187–202.
5. Ishwaran Hemant, et al. Random survival forests. *The Annals of Applied Statistics*. 2008;2(3):841–860.
6. Chowell Diego, et al. Improved prediction of immune checkpoint blockade efficacy across multiple cancer types. *Nature Biotechnology*. 2022;40(4):499–506.
7. Rizvi Naiyer A, et al. Durvalumab with or without tremelimumab vs standard chemotherapy in first-line treatment of metastatic non-small cell lung cancer: the MYSTIC phase 3 randomized clinical trial. *JAMA oncology*. 2020;6(5):661–674.
8. Rittmeyer Achim, et al. Atezolizumab versus docetaxel in patients with previously treated non-small-cell lung cancer (OAK): a phase 3, open-label, multicentre randomised controlled trial. *The Lancet*. 2017;389(10066):255–265.
9. Samstein Robert M, et al. Tumor mutational load predicts survival after immunotherapy across multiple cancer types. *Nature Genetics*. 2019;51(2):202–206.
10. Thorsson Vésteinn, et al. The immune landscape of cancer. *Immunity*. 2018;48(4):812–830.
11. AACR Project Genie Consortium, et al. AACR Project GENIE: powering precision medicine through an international consortium. *Cancer Discovery*. 2017;7(8):818–831.
12. Miao Diana, et al. Genomic correlates of response to immune checkpoint blockade in microsatellite-stable solid tumors. *Nature Genetics*. 2018;50(9):1271–1281.

Abstract 1273 Table 1 Description of the datasets used to train and evaluate the clinical transformer

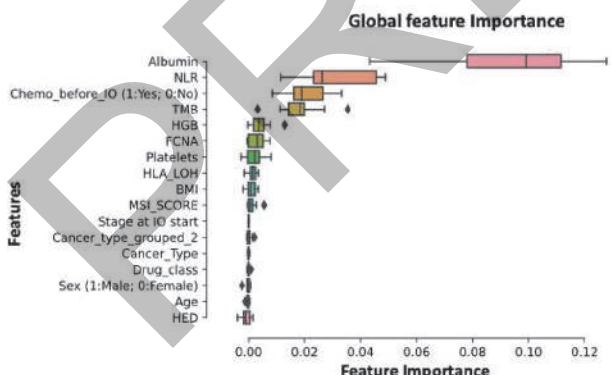
Dataset	Cancer Type	Description	Task	Samples	Arm	Features
Mystic [7] NCT02453282	NSCLC	Stage IV NSCLC treatment naïve anti-PDL1 and CTLA-4 combo. Only considering patients with all available features (e.g., with available tissue TMB and HLA typing).	Survival	150	IO	15
OAK [8] NCT02008227	NSCLC	Stage IV NSCLC patients treated with anti-PDL1 after failing chemotherapy	Survival	396	IO	418
Chowell et al 2021 [6]	Pan Cancer	Patients treated with anti-PDL1/PDL1 and combo in multiple cancer types. This dataset consists of 17 features (e.g., TMB, HLA LOH, MSI, Albumin, NLR)	Survival	1,479	IO	17
Samstein et al - Pan Cancer 2019 [9]	Pan Cancer	Response to IO (anti-PDL1/PDL1 and combo) in a pan cancer setting. This dataset includes molecular data (mutations and copy numbers) and demographic features	Survival	1,610	IO	474
Thorsson et al 2018 [10]	Pan Cancer	The Immune landscape of cancer. A study on the TCGA data that derives features associated with the TME	Survival	6,012	SOC	49
AACR Project GENIE [11]	Pan Cancer	AACR Project GENIE is a publicly accessible international cancer registry of real-world data assembled through data sharing between 19 of the leading cancer centers in the world	Transfer learning	136,000	NA	2,290
Miao et al 2018 [12]	Pan Cancer	Whole-exome sequencing (WES) of 249 tumors from patients with clinically annotated outcomes to immune checkpoint therapy	Validation dataset	249	IO	>10,000

Abstract 1273 Table 2 Clinical transformer improves patient survival prediction across multiple datasets. Model performance is evaluated using the concordance index across 10 random training/testing splits for consistency. ++Transfer learning from GENIE dataset and applied to Samstein et al. +Transfer learning from Chowell et al., dataset and applied to Mystic trial. High Collinearity: Multivariable CoxPH model did not run because of high collinearity among the input features.

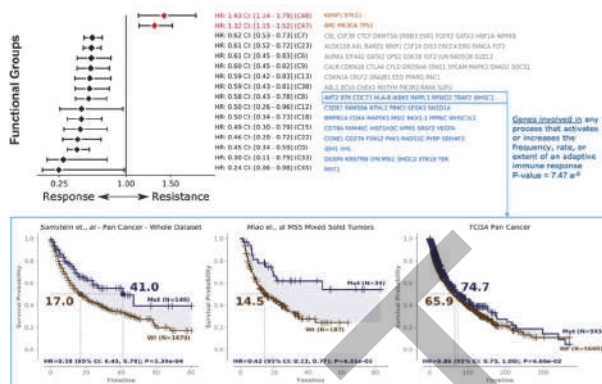
	Mystic Trial – AstraZeneca	OAK Trial - Genentech	Chowell et al 2021	Samstein et al - Pan Cancer 2019	Thorsson et al 2018
Clinical Transformer	0.664* (±0.04)	0.669 (±0.04)	0.721 (±0.01)	0.652** (±0.02)	0.734 (±0.01)
Multivariable Cox PH regression	0.599 (±0.03)	High Collinearity	0.709 (±0.01)	High Collinearity	0.690 (±0.01)
Random Survival Forest	0.606 (±0.04)	0.664 (±0.05)	0.714 (±0.01)	0.638 (±0.01)	0.722 (±0.01)
TMB	0.589 (±0.05)	0.543 (±0.05)	0.550 (±0.02)	0.538 (±0.02)	0.624 (±0.01)



Abstract 1273 Figure 1 Transfer learning positively impact patient response to IO in a pan-cancer and cancer specific settings. A) Prediction of patient response to immunotherapy in a pan-cancer dataset (TMB and Immunotherapy Samstein et., al). Pre-training modeling is performed using self-supervision over the GENIE dataset. Then, to predict patient response to immunotherapy, weights from GENIE pretrained model are transferred to a survival prediction model. Each learning curve describes how the model learnt across different epochs and each line indicates the baseline and transfer learned model. B) Transfer learning impact for predicting response to Immunotherapy in Non-Small Cell Lung Cancer (NSCLC). Learning curves describe the impact of different pre-training iterations over the survival outcome prediction.



Abstract 1273 Figure 2 Model feature importance across 10 random training/testing splits shows consistency on relevant features associated to response to IO. Feature importance is computed by perturbing each feature and computing its effect on the model performance across 10 training/testing splits.



Abstract 1273 Figure 3 Top 16 functional groups associated with response/resistance to treatment discovered using the Samstein et al., dataset with 10 training/testing splits. The forest plot shows the effect on patient survival of mutated/non-mutated functional groups. Pathway analysis indicates that the C8 functional group is associated with adaptive immune response (p-value=7.47e-9) and it has a positive effect on the prediction of response to IO in the training/testing dataset (Left Kaplan Meier plot) and in an independent validation dataset (Miao et., al, Middle Kaplan Meier plot). Interestingly, this pattern is not observed in TCGA pan cancer dataset using the same cancer types (Right Kaplan Meier Plot).

<http://dx.doi.org/10.1136/jitc-2022-SITC2022.1273>

1274

IDENTIFICATION AND CHARACTERIZATION OF IMMUNE CHECKPOINT INHIBITOR INDUCED IMMUNE-RELATED ADVERSE EVENTS FROM ELECTRONIC HEALTH RECORDS USING NATURAL LANGUAGE PROCESSING TECHNIQUES

¹Hannah Barman, ²Sriram Venkateswaran, ²Antonio Del Santo, ¹Krishna Rao, ¹Bharathwaj Raghunatha, ¹Unice Yoo, ³Lisa Kottschade, ³Matthew Block, ²G Scott Chandler, ¹Tyler Wagner, ²Rajat Mohindra*. ¹Inference, Cambridge, MA, USA; ²F. Hoffmann-La Roche, Basel, Switzerland; ³Mayo Clinic, Rochester, MN, USA

Background Immune checkpoint inhibitors (ICIs) have revolutionized cancer treatment, yet their use is associated with immune-related Adverse Events (irAEs). Estimating prevalence and patient impact of these irAEs in the Real-World Data (RWD) setting is critical for further characterizing the benefit/risk profile of ICI therapies beyond the clinical trial population. Studies using International Classification of Diseases (ICD) codes have aimed to understand the safety and effectiveness of drugs. However, this approach does not comprehensively illustrate a patient's care journey, sub-optimally captures patients' concurrent medical conditions, and offers no insight into drug-AE causality. The present study aims to more accurately capture the relationship between ICIs and irAEs by using Augmented Curation (AC), a natural language processing (NLP) based innovation, on unstructured data in Electronic Health Records (EHRs).¹⁻⁴

Methods In a cohort of approximately 6,000 patients treated with ICIs at Mayo Clinic, we compared the prevalence of irAEs using ICD codes and AC which leverages SciBERT to perform downstream tasks including entity extraction, classification, and relationship extraction. Each task was performed by a bespoke AC model that was trained using clinical scientist annotated datasets from Mayo's EHRs.¹⁻⁴ These models were orchestrated together to create an ensemble workflow that detected mentions of drug-AE pairs in clinical notes with implied textual causality. Finally, select irAEs with high patient impact- myocarditis, encephalitis, pneumonitis and SCAR (MEPS) were analyzed further. AC-extracted corticosteroid/immunosuppressive administration and therapy discontinuations were used as proxies of severity.

Results For all irAEs, only 28.5% of the patients found by AC were also identified with structured codes. For MEPS, only 30.5% of patients found by AC were also identified by ICD codes. Using pneumonitis as an example, AC achieved a sensitivity of 0.94, while ICD codes achieved only 0.26. MEPS patients were found to receive corticosteroids for their respective irAE 69% of the time and subsequently discontinued the ICI due to the irAE 48% of the time.

Conclusions Overall, the AC model identified additional irAEs not detected by ICD codes, and the positive sentiment-based approach helped assess the drug-irAE relationships in unstructured clinical notes thus supporting assessment of causal association with use of ICI therapies. The use of AC to accurately detect key irAEs allows physicians to leverage EHRs to discover risk factors for specific irAEs in RWD settings, as well as to review clinical outcomes to identify best practices in treating irAEs.

REFERENCES

1. Murugadoss K, Rajasekharan A, Malin B, Agarwal V, Bade S, Anderson JR, Ross JL, Faubion WA Jr, Halamka JD, Soundararajan V, Ardhanari S. Building a best-in-class automated de-identification tool for electronic health records through ensemble learning. *Patterns (NY)*. 2021;**2**(6):00255. PMID: 34179842
2. Beltagy I, Lo K, Cohan A. SciBERT: A pretrained language model for scientific text. arXiv preprint arXiv. 2019;1903.10676

3. Pawlowski C, Venkatakrishnan AJ, Ramudu E, Kirkup C, Puranik A, Kayal N, Berner G, Anand A, Barve R, O'Horo JC, Badley AD, Soundararajan V. Pre-existing conditions are associated with COVID-19 patients' hospitalization, despite confirmed clearance of SARS-CoV-2 virus. *Eclinical Medicine*. 2021;**34**:100793. PMID: 33778434
4. Wagner T, Shweta F, Murugadoss K, Awasthi S, Venkatakrishnan AJ, Bade S, Puranik A, Kang M, Pickering BW, O'Horo JC, Bauer PR, Razonable RR, Vergidis P, Temesgen Z, Rizza S, Mahmood M, Wilson WR, Challenger D, Anand P, Liebers M, Doctor Z, Silvert E, Solomon H, Anand A, Barve R, Gores G, Williams AW, Morice WG 2nd, Halamka J, Badley A, Soundararajan V. Augmented curation of clinical notes from a massive EHR system reveals symptoms of impending COVID-19 diagnosis. *Elife*. 2020;**9**:e58227. PMID: 32633720

Ethics Approval This study was approved by the Mayo Clinic Institutional Review Board; approval number 22-002906.

<http://dx.doi.org/10.1136/jitc-2022-SITC2022.1274>

1275

MAPPING THE HETEROGENEOUS COLORECTAL TUMOR MICROENVIRONMENT WITH MULTIPLEXED IMAGING AND MACHINE LEARNING

¹Blanca Cabrera Gil, ²Laura Gui Levy, ²Mario Kreutzfeldt, ³Joanna Kowal*, ³Giusy Procopio, ³Deniz Eroglu, ²Doron Merkle, ¹Andrew Janowczyk, ³Diego Dupouy, ¹Aitana Neves, ²Thomas McKee. ¹Swiss Institute of Bioinformatics, Geneva, Switzerland; ²Hôpitaux universitaires de Genève, Geneva, Switzerland; ³Lunaphore Technologies SA, Tolochenaz, Switzerland

Background Colorectal carcinoma (CRC) represents a major worldwide health burden and shows an increasing incidence particularly in younger patients. The majority of metastatic CRC (microsatellite stable, MSS) do not respond to current immunotherapies in contrast to the small subset of microsatellite unstable (MSI) patients. However, responses to immunotherapy were recently observed in subsets of primary MSS tumors indicating their potential vulnerability to such therapeutic approaches. Here, we use multiplex imaging coupled with powerful image analysis tools to highlight important phenotypic differences between MSI and MSS.

Methods 100 human CRC sections (30MSI, 70 MSS) were examined on the COMET™ platform (Lunaphore) with a multiplex sequential immunofluorescence (seqIF) panel of 12 biomarkers (CD3, CD31, CD4, CD8, FoxP3, TCF-1, TOX, EOMES, CK, CD45RO, S100, D2-40).

Images were preprocessed by background subtraction and local contrast enhancement.¹ Cell segmentation was done with the Stardist algorithm.² Cell phenotypes (CT) were defined by threshold-based classifiers. The epithelium was detected based on CK expression. The density of CT was assessed per area of interest. Cell neighborhoods (CN) were defined as the composition of the 10 closest CTs within 300µm. CNs were clustered into CN-classes using DB-SCAN.³

Results Cell segmentation and phenotyping algorithms resulted in precise cell detection (figure 1). We compared CT infiltration patterns in MSI vs MSS in the tumor-epithelium and epithelium-stroma interfaces. While we observed no significant differences in CT densities at the interface, CD3 cell density was significantly higher in MSI vs MSS patients in the tumor-epithelium (figure 2), with MSS more heterogeneously distributed with CD3-high and CD3-low outliers.

Differences in cell interactions CRC patients were examined using CN analysis. We observed a CN composed of CD3, CD8 cytotoxic T cells, CD3+CD8+ and tumor cells to be differentially enriched between MSI and MSS patients (figure 3).

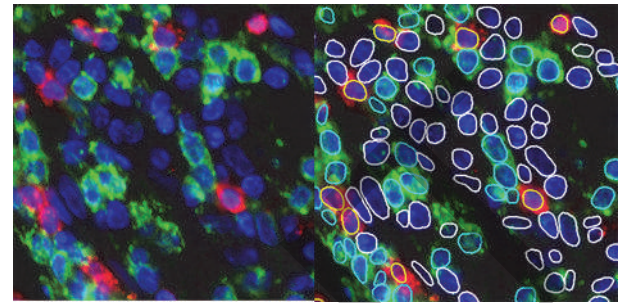
Conclusions A more precise characterization of the immune response to cancers is essential to leverage the advantages of immune modulations in the treatment of cancers. We confirm here important differences between MSI and MSS CRCs in part systematic due to the higher antigen load in MSI CRCs but also highlight heterogeneity amongst the MSS tumors. Characterization of the phenotype of the T-lymphocyte population and its localization with respect to elements such as epithelial cells and tertiary lymphoid structures may help to define both the prognosis of tumors and the possibility of a response to immune checkpoint therapy.

REFERENCES

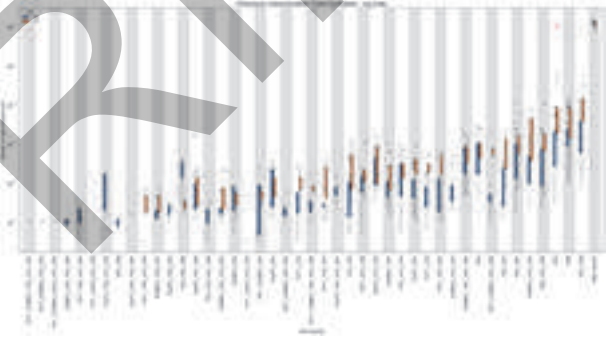
1. SM Pizer, *et al.* Computer Vision, Graphics, and Image Processing 39, 1987.
2. U Schmidt, *et al.* MICCAI, 2018.
3. Martin Ester, Hans-Peter Kriegel, Jörg Sander, and Xiaowei Xu. 1996. A density-based algorithm for discovering clusters in large spatial databases with noise. In Proceedings of the Second International Conference on Knowledge Discovery and Data Mining (KDD'96). AAAI Press, 226–231.

4. Massey FJ 1951. The Kolmogorov-Smirnov Test for Goodness of Fit. *Journal of the American Statistical Association.* 1951;**46**(253):68–78.
5. Cohen J 1988. Statistical power analysis for the behavioral sciences (2nd ed.). Hillsdale, NJ: Lawrence Erlbaum Associates.

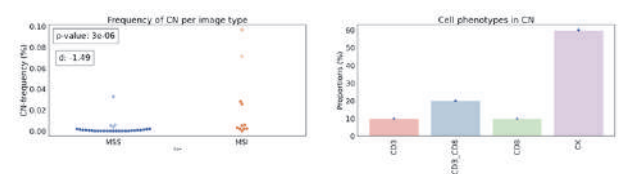
Ethics Approval The study has been approved by HUG.



Abstract 1275 Figure 1 Example results from cell segmentation and phenotyping. Left: Original image patch. Blue: DAPI, green: CD4, red: CD8. Right: Patch with nuclei segmentation (all contours), CD4+ cells (cyan) and CD8+ cells (yellow)



Abstract 1275 Figure 2 CT analysis of the tumor epithelium region. Each boxplot represents the cell density distribution of a CT in MSS and MSI patients. CD3 cell density is observed to be significantly higher in MSI vs MSS patients, with MSS more heterogeneously distributed with CD3-high and CD3-low outliers



Abstract 1275 Figure 3 Cell neighborhood-class consisting of CD3, CD8, and CD3_CD8 cell types is significantly more frequent in MSI vs MSS patients. a) CN frequency in MSI vs MSS patients (KS-test [4] p-value and Cohen d [5] effect size). b) Proportion of CTs in this CN-class

<http://dx.doi.org/10.1136/jitc-2022-SITC2022.1275>

Abstracts

1276

FROM TCR-PMHC BINDING KINETIC CHARACTERISTICS TO TCR PHOSPHORYLATION AND INITIATION OF SIGNAL TRANSDUCTION

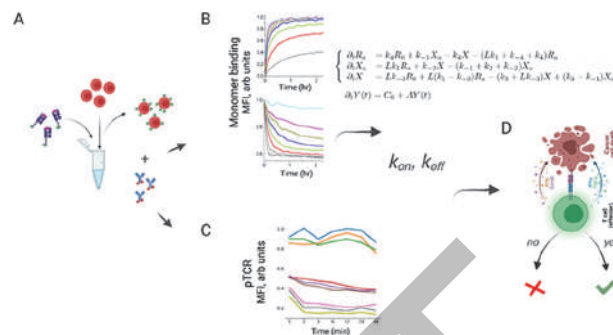
Jonathan Desponds, Mayra Cruz Tleugabulova, Jeanne Cheung, Shirley Ng Palace, Martine Darwish, Geraldine Strasser, Andrey Shaw, Ira Mellman, Andrei Chernyshev, Darya Orlova*. *Genentech, South San Francisco, CA, USA*

Background The development of adoptive cell therapy has made the understanding of T-cell target recognition and activation crucial to cancer treatment. Indeed, the success of many of these therapies directly depends on our ability to predict or measure the specificity of T-cell receptors (TCR) to neoantigens and understand how these specificities translate into activation. While the dynamics of TCR-pMHC binding have been under careful scrutiny for a long time, many fundamental unknowns remain regarding the aspects of the dynamics that relate to immune function. Among the key factors that have impeded progress is the fact that most experimental approaches have relied on using soluble TCRs, as opposed to receptors properly assembled in the plasma membrane.

Methods To overcome these limitations, we developed a cell-based assay (figure 1A) to monitor the binding and unbinding of whole CD8 T-cells to a variety of target peptide-MHC monomers in solution using flow cytometry (figure 1B). Using anti-CD8 antibodies, we also measured the contribution of co-receptors to the formation and stability of the TCR-pMHC complex. In parallel, we measured the phosphorylation of CD3 ζ (figure 1C) to quantify the first step of T-cell activation (figure 1D) and its relation to the TCR occupancy and TCR-pMHC binding kinetics. Using a mix of deterministic and stochastic mathematical tools, we developed a minimal model that captures the kinetics of TCR-pMHC interaction.

Results We find that binding kinetics exhibit complex, peptide- and concentration-dependent non-linear behavior that is time-sensitive. Our minimal effective model succeeded at separating peptides based on the strength of the interaction (including functional avidity) and recapitulating the key features of binding dynamics. Importantly, that model is able to extrapolate experimental measurements to other ranges of concentrations for a given TCR, making it a precious tool for the selection of optimal cognate TCRs. We explored hypotheses regarding mechanistic interpretation of the observed dynamics. In particular, using blocking anti-CD8 antibodies, we separated effects of TCR binding from those of co-receptor binding. We also examined the connection between TCR occupancy and TCR-pMHC binding kinetic rates and the phosphorylation of the CD3 ζ chain.

Conclusions Our unique approach, combining novel experimental methods and mathematical modeling, can extract biomolecular TCR-pMHC interaction rates from TCRs assembled in the plasma membrane. It captures the complexity of TCR-pMHC interactions and connects it to the intracellular signal transduction.



Abstract 1276 Figure 1 Outline of the TCR-pMHC quantitative assessment workflow Cell-based monomer assay (A) measurement of TCR-pMHC binding (B) and TCR phosphorylation (C) combined with mathematical modeling to understand and predict T-cell activation (D)

<http://dx.doi.org/10.1136/jitc-2022-SITC2022.1276>

1277

IDENTIFICATION OF CLINICALLY RELEVANT SPATIAL TISSUE PHENOTYPES IN LARGE-SCALE MULTIPLEX IMMUNOFLOUORESCENCE DATA VIA UNSUPERVISED GRAPH LEARNING IN NON-SMALL CELL LUNG CANCER

¹Robert Egger*, ²Andrew Fisher, ¹Michael Drage, ²Jimena Trillo-Tinoco, ¹John Abel, ²Andrew Browne, ¹Deepta Rajan, ²Tai Wang, ¹Jake Conway, ²Catherine King, ¹Jacqueline Brosnan-Cashman, ²Anne Lewin, ²Arnaud Amzallag, ²Thomas Lila, ²Tyler Simpson, ¹Mike Montalto, ²Benjamin Chen, ¹Benjamin Glass, ²Vipul Baxi. ¹PathAI, Boston, MA, USA; ²Bristol Myers Squibb, Cambridge, MA, USA

Background Multiplex immunofluorescence (mIF) allows simultaneous spatial interrogation of multiple cell- and tissue-based biomarkers from patient cohorts at scale using whole-slide images (WSI). Identification of spatially-derived insights is limited by conventional approaches that reduce spatial data into human-derived feature sets (e.g., nearest neighbor), necessitating new methods for surveying spatial patterns in full. Here, we utilized a graph neural network (GNN) to identify clinically-relevant, spatially-defined tissue phenotypes with distinct immunogenic profiles in non-small cell lung cancer (NSCLC) and compare this method to traditional approaches.

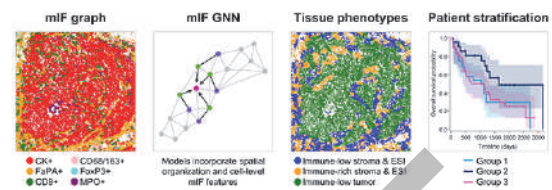
Methods To identify relevant cancer, stromal, and immune cell types, mIF for cytokeratin, CD8, FoxP3, myeloperoxidase, CD68/CD163, and fibroblast activation protein-A was performed with a DAPI counterstain on clinical NSCLC specimens (N=165). From the same cohort, we extracted bulk mRNAseq and proteomic signatures. mIF images were acquired and spectrally unmixed using the Phenoptic platform and Inform software (Akoya). A convolutional neural network was trained to segment regions of cancer epithelium, stroma, and necrosis, while a pretrained network segmented all cells (HALO-AI, Indica Labs). Cells were converted into graphs, and a GNN autoencoder was trained to discover tissue patterns defined by spatial arrangement and mIF cell/tissue phenotypes. Hierarchical clustering identified patient subsets based on tissue patterns, and Cox proportional hazard models assessed overall survival (OS) (figure 1).

Results Segmentation and post-processing of 165 mIF WSIs resulted in graphs describing 243,646 cells/WSI (mean; range: 3,279-1,552,934). Training the GNN autoencoder on this dataset revealed three tissue phenotypes: (1) cancer epithelium, (2) cancer stroma and epithelial-stromal interface (ESI) with high inflammation, and (3) cancer stroma and ESI with low inflammation. Samples were then classified based on the relative abundance of these phenotypes. While conventional analyses (e.g., nearest neighbor) failed to identify subgroups with prognostic value, our model revealed prolonged OS (HR=0.46 [0.22, 0.96]) in patients with abundant phenotype 2. Furthermore, patients in this subgroup displayed significant overexpression of the MHC-I antigen presentation pathway and downregulation of a general immune exclusion signature, potentially increasing intrinsic anti-tumor immunity to improve prognosis.

Conclusions We developed a novel, unsupervised deep-learning-based GNN for analysis of WSI mIF data in NSCLC. This method identified interpretable tissue phenotypes with clinically-relevant differences in anti-tumor immunity and prognosis. These data show the utility of unsupervised spatial deep-learning methods, compared to traditional approaches, for data-driven discovery of complex patterns in large-scale multiplex images.

Ethics Approval This study was performed in accordance with the Bristol Myers Squibb Bioethics policy (<https://www.bms.com/about-us/responsibility/position-on-key-issues/bioethics>-

policy-statement.html) and adhered to the World Medical Association Declaration of Helsinki for Human Research.



Abstract 1277 Figure 1 Study workflow. From left to right: Graphs are constructed from cell locations, morphology, mIF and tissue features. An unsupervised GNN learns to identify characteristic tissue phenotypes defined by these features and the spatial arrangement of cells. Finally, relative abundance of the different phenotypes is used to stratify patients into groups. Notably, these groups are associated with differences in overall survival

<http://dx.doi.org/10.1136/jitc-2022-SITC2022.1277>

1278

CROSSDOME: AN INTERACTIVE R PACKAGE TO PREDICT T-CELL CROSS-REACTIVITY RISK ON IMMUNOPEPTIDOMICS DATABASES

Andre Fonseca*, Dinler Antunes. *University of Houston, Houston, TX, USA*

Background T cell-based immunotherapy is unquestionably a promising strategy against cancer. Regardless, the efficacy of T-cell therapies depends on mitigating off-target effects during the treatment. Off-target toxicity is associated with T-cell cross-reactivity (CR), i.e., therapeutic T-cell receptors (TCR) recognizing undesirable targets, leading to an auto-immune response. In this context, predicting CR risk remains an unsolved challenge. Here we present Crossdome, a tool that performs peptide screening and predicts cross-reactivity risk based on multi-omics data.

Methods Crossdome was developed by leveraging data from peptide-loaded Human Leukocyte Antigen (pHLA) complexes and TCR molecules, including biochemical properties, immunopeptidomics data, and three-dimensional fingerprints/interactions. Together these data were used i) to predict peptides that are biochemically similar to desirable targets, i.e., putative off-target candidates; and ii) to highlight TCRpHLA interactions associated with shared hotspots among the target and other peptides-HLA. Furthermore, we integrate functional data to evaluate immunogenic potential and expression associated with the putative candidates. As proof-of-principle, we benchmark our approach using well-known cross-reactivity cases, such as MAGEA3, NY-ESO-1, AFP, and TMEM161A.

Results Biochemical properties (BP) can be applied to calculate relatedness between peptides. The validated CR cases were found among the best-scored hits into thousand putative candidates ($p\text{-value} \leq 0.01$). Particularly, on the MAGEA3 screening, the known cross-reactive peptide ESDPIVAQY (TITIN) was listed as a best-scored candidate, position 20th out of ~25.000 eluted peptides. Other cross-reactivity peptides were also enriched among the highly similar candidates, including MAGEA3 paralogs and synthetic peptides from yeast-displayed experiments ($p\text{-value} \leq 0.05$). To strengthen our predictions, we implemented a penalty system based on the MAGEA3-specific TCR fingerprint. The hotspot positions were uncovered by molecular dynamics. Positions 1, 4, 5, 7, and 8 were used to recalculate the relatedness scores among the target and candidates. The combination between BP and fingerprints improved the CR predictions to 83%. Finally, we focus on functional characterization among the cross-reactivity candidates associated with the MAGE3A peptide. CR candidates have shown a large variability related to immunogenic prediction and expression pattern, spanning from dangerous to harmless profiles. On the dangerous profile, TITIN and LCAT have shown a high immunogenic level and expression-biased to heart and lung organs, respectively. Curiously, YTDVGVLY (LCAT) peptide was not reported in previous studies.

Conclusions Crossdome is an interactive R package to predict cross-reactivity risk among peptide databases. Additionally, our method can integrate TCR repertoire data to improve the predictions. Currently, we are focusing our efforts on experimental validation and new antigens discovery.

<http://dx.doi.org/10.1136/jitc-2022-SITC2022.1278>

1279

A NOVEL GRAPHICAL DEEP NEURAL NETWORK LEARNING APPROACH UTILIZING MOLECULAR DATA FOR OPTIMIZING PATIENT SELECTION FOR TREATMENT WITH IMMUNE CHECKPOINT INHIBITORS: AN ORIEN PAN-CANCER STUDY

¹Issam El Naqa, ¹Payman Ghasemi, ¹Aik Choon Tan, ²James Chen, ³Aakrosh Ratan, ⁴Martin McCarter, ⁵John Carpten, ⁶Howard Colman, ⁷Alexandra Ikeguchi, ⁸Igor Puzanov, ⁹Susanne Arnold, ¹⁰Michelle Churchman, ¹Patrick Hwu, ¹Jose Conejo-Garcia, ¹⁰William (Bill) Dalton, ¹¹George Weiner, ¹²Ahmad Tarhini*. ¹Moffitt Cancer Center and Research Inst., Tampa, FL, USA; ²The Ohio State University, Columbus, OH, USA; ³University of Virginia, Charlottesville, VA, USA; ⁴University of Colorado Cancer Center, Aurora, CO, USA; ⁵USC Norris Comprehensive Cancer Center, Los Angeles, CA, USA; ⁶Huntsman Cancer Institute, Salt Lake City, UT, USA; ⁷Stephenson Cancer Center, Oklahoma City, OK, USA; ⁸Roswell Park Comprehensive Cancer Center, Buffalo, NY, USA; ⁹Markey Cancer Center, Lexington, KY, USA; ¹⁰M2GEN, ORIEN, Tampa, FL, USA; ¹¹University of Iowa Holden Comprehensive, Iowa City, IA, USA; ¹²H. Lee Moffitt Cancer Center and Research Institute, Tampa, FL, USA

Background Immune checkpoint inhibitors (ICIs) have made significant improvements in the treatment of cancer patients (pts), but many continue to experience primary or secondary resistance. Here, we leveraged clinical and genomic data to identify prognostic biomarkers in pts treated with ICIs utilizing a pan-cancer approach.

Methods Patients were enrolled to the Total Cancer Care protocol (NCT03977402) across 18 cancer centers within the Oncology Research Information Exchange Network® (ORIEN). All included subjects provided an IRB-approved written informed consent at their participating institutions. RNA-seq was performed on tumors following the RSEM pipeline and gene expressions were quantified as Transcript Per Million (TPM) and were logarithmically normalized. A graphical neural network (GNN) architecture was developed based on the prior knowledge of genes and pathways. For comparison, immunoscore for each patient was calculated based on the estimated densities of tumor CD3+ and CD8+ T cells (Galon et. al., 2020) utilizing CIBERSORTx. The quality of overall survival (OS) predictions was assessed using Harrell’s concordance index (C-index). Log-rank test was used to assess stratified group differences (by ICI or cancer histology) along with Kaplan-Meier (KM) survival analysis of GNN and immunoscore.

Results Patients (n=522) with 4 cancer types including melanoma (n=125), renal cell carcinoma (n=149), non-small cell lung cancer (n=128) and head and neck cancer (n=120) treated with 6 ICI regimens were included in this analysis. ICI regimens were nivolumab (n=219), pembrolizumab (n=202), ipilimumab+nivolumab (n=69), ipilimumab (n=30), avelumab (n=1) and cemiplimab (n=1). Table 1 summarizes the overall C-index and associated 95% CIs and log-rank P values for the entire cohort (regardless of histology) resulting from our proposed GNN and the separate estimated immunoscore categorization. The corresponding KM plots showed significantly wider separations of the survival curves in favor of our proposed GNN relative to the immunoscore with more than 30% improvement in prediction power. Table 2 presents the summary of GNN top selected pathways alongside their hazard rate and their univariate Cox p-value.

Conclusions GNN analysis is a promising tool to identify relevant prognostic biomarkers in cancer patients treated with ICI. This may lead to novel therapeutic predictive signatures and identification of mechanisms of ICI resistance. Our GNN gene expression signature was significantly prognostic and outperformed the estimated CD3+, CD8+ T Cell immunoscore.

Further refinements to our prediction power are ongoing along with more advanced neural network architectures to elucidate related functional pathways. Validation and functional studies will follow.

Acknowledgements We are grateful to the participating patients and their family members as well as all research staff supporting the conduct of the Total Cancer Care protocol.

Trial Registration NCT03977402

Ethics Approval Patients were enrolled to the Total Cancer Care protocol (NCT03977402) across 18 cancer centers within the Oncology Research Information Exchange Network® (ORIEN). All included subjects provided an IRB-approved written informed consent at their participating institutions.

Abstract 1279 Table 1 Prediction performance comparison between the GNN a

	Avg. C-index	95% CI	Log-rank test p-value
GNN	0.643	(0.580, 0.727)	2.3 e-19
Immunoscore	0.54	(0.493, 0.599)	0.0008

Abstract 1279 Table 2 Top pathways selected by graphical neural network

Pathways	HR	HR lower 95%	HR upper 95%	Cox p-value
Formation of the cornified envelope	1.303	1.185	1.432	<0.001
Apoptotic cleavage of cell adhesion proteins	1.325	1.213	1.448	<0.001
MET activates PTK2 signaling	1.458	1.255	1.694	<0.001
Phosphorylation of CD3 and TCR zeta chains	0.790	0.705	0.886	<0.001
Translocation of ZAP-70 to Immunological synapse	0.813	0.730	0.904	<0.001
Polo-like Kinase mediated events	1.368	1.167	1.604	<0.001
PD-1 signaling	0.809	0.716	0.916	<0.001
Syndecan interactions	1.399	1.180	1.657	<0.001
Elastic fibre formation	1.346	1.138	1.591	<0.001
Condensation of Prometaphase Chromosomes	1.240	1.081	1.423	0.002
Collagen formation	1.398	1.177	1.661	<0.001
Cholesterol biosynthesis, squalene 2,3-epoxide => cholesterol	1.545	1.313	1.819	<0.001
Laminin interactions	1.367	1.189	1.572	<0.001
Keratinization	1.478	1.267	1.724	<0.001
GRB2 events in ERBB2 signaling	1.498	1.219	1.839	<0.001
MET promotes cell motility	1.468	1.235	1.744	<0.001
Asthma	0.726	0.601	0.878	<0.001
Regulation of TP53 Activity through Association with Co-factors	1.434	1.201	1.713	<0.001
MET activates RAS signaling	1.319	1.088	1.599	0.004
Cell junction organization	1.714	1.372	2.142	<0.001

<http://dx.doi.org/10.1136/jitc-2022-SITC2022.1279>

1280

RADIOMIC AND CLINICAL PREDICTION OF OVERALL AND ORGAN-SPECIFIC RESPONSE TO IPILIMUMAB-NIVOLUMAB IN MELANOMA

Zane Gray*, Alexandra Tompkins, Rebekah Dadey, Serafettin Zenkin, Afsaneh Amouzegar, Priyadarshini Mamindla, Vishal Peddagangireddy, Murat Ak, Ryan Augustin, Rivka Colen, Riyue Bao, Jason Luke. *University of Pittsburgh, Pittsburgh, PA, USA*

Background Radiomics converts medical images into quantitative features and has potential in development of non-invasive biomarkers for cancer treatment. Radiomic models have not been described for ipilimumab+nivolumab (I+N) on a patient level or on an organ-specific level.

Methods The Hillman Cancer Center registry (2015-2020) was queried for patients with melanoma treated with I+N. Clinical data was abstracted and radiographic outcomes were calculated by RECIST as well as organ-specific response. Lesions were segmented into discrete volumes-of-interest (VOI) with 400 radiomics texture features extracted. Feature filtering and selection were performed in training set independent of test set after proper normalization. XGBoost was used to construct machine learning models to predict patient level response with training/test split and 5-fold cross validation, or LOOCV in the case of organ-specific models.

Results Of 1106 patients with melanoma, 95 were treated with I+N with 276 individual metastases. Baseline demographics included 47% female, median age of 59, 83% cutaneous (4% uveal), 51% BRAF mutant, 27% M1c (visceral non-lung), and 43% M1d (brain). Patients had a median baseline eosinophil count of 134, neutrophil-to-lymphocyte ratio (NLR) 3.29, and 78% had elevated LDH. 39% had response (CR+PR+SD) and 57% had PD, with mixed response patterns being reported more frequently in PD. Among responders, lung metastases experienced the greatest median reduction in size (-71%) whereas lymph nodes displayed the least regression (-43%). Conversely, liver metastases experienced the greatest median progression in non-responders (+39%). For patients with multiple same-organ target lesions, liver demonstrated the highest inter-lesion heterogeneity. Of the 95 patients, 84 with high-quality images were kept for radiomics model construction. XGBoost models consisting of a 16-feature radiomic signature successfully classified responders from non-responders with an AUC of 0.72. Integration of clinical variables (Age, BMI, Sex, AJCC stage M category, BRAF status, pre-treatment eosinophil, LDH, NLR) to the radiomic signature achieved an AUC of 0.87 (p=0.027). Organ-specific predictive models demonstrated similar performance as the overall response models, for example an AUC of 0.74 in lymph nodes (43 lesions) and 0.77 for liver metastases (22 lesions).

Conclusions In this population of high-risk patients with metastatic melanoma (due to high levels of hepatic/brain involvement and non-cutaneous histology), differential organ-specific response was observed with the greatest benefit in lung, least benefit in hepatic metastases, and highest within-organ heterogeneity in liver. Integrating clinical factors with radiomics signatures improved overall response prediction suggesting priority development of these models for immunotherapy.

Ethics Approval UPitt STUDY20020107

<http://dx.doi.org/10.1136/jitc-2022-SITC2022.1280>

1281

RECURRENCE PREDICTION IN CUTANEOUS MELANOMA PATIENTS BY EXPLOITING DEEP LEARNING ON H&E SLIDE IMAGES

¹Michele Guida, ²Maria Colomba Comes*, ²Livia Fucci, ²Sabino Strippoli, ²Samantha Bove, ²Ivana De Risi, ²Annarita Fanizzi, ²Martina Milella, ²Fabio Mele, ²Alfredo Zito, ²Raffaella Massafra. ¹IRCCS Istituto Tumori, Bari, Italy; ²IRCCS Istituto Tumori Giovanni Paolo II, Bari, Italy

Background Cutaneous melanoma is one of the most aggressive forms of skin cancer with a high mortality rate.¹ A prognosis improvement in cutaneous melanoma patients is crucial to better plan personalized treatments. Currently, clinical prognosis methods for the evaluation of the risk of recurrence includes multiple parameters, such as Breslow tumor thickness, mitotic rate, ulceration, local or nodal metastasis, which are at the basis of the American Joint Committee on Cancer (AJCC) pathologic tumor stage.²⁻⁴ Despite routinely applied in clinical practice, these methods have some pitfalls.⁵ Thus, predicting the risk of recurrence in melanoma patient is urgent.

Methods In this study, we propose a deep learning model, that exploits convolutional neural networks, which mimic the functioning of human brain, to extract features from hematoxylin and eosin (H&E) slide images with the final goal of predicting 1-year disease-free survival (DFS) in patients with I-III stage cutaneous melanoma. H&E images referred to a cohort of 43 patients from Clinical Proteomic Tumor Analysis Consortium Cutaneous Melanoma (CPTAC-CM) public database (31 DF cases, 12 non-DF cases)⁶ were firstly analyzed to design the predictive model (table 1). Then, the model was validated on H&E images referred to a validation cohort of 11 cutaneous melanoma patients (table 2), which was provided by our Institute (8 DF cases, 3 non-DF cases). Basically, we developed a computerized system to automatically extract information that are usually evaluated manually and visually by pathologists.

Results The median Area Under the Curve (AUC) and accuracy values in the patients from the CPTAC-CM public dataset were 69.5% and 72.7%, respectively, by implementing a 5-fold cross validation scheme for 5-rounds. AUC and accuracy values in the validation cohort of patients were 66.7% and 72.7%, respectively, by using the CPTAC-CM dataset as training set and the validation cohort as test set.

Conclusions Our model proved to be robust and generalizable. The promising results obtained in this preliminary work suggest that our proposal, after further validation on a larger cohort of patients, may have the potential to better define the risk of recurrence for each patient and better tailor adjuvant therapy.

Acknowledgements Public data used in this study were generated by the National Cancer Institute Clinical Proteomic Tumor Analysis Consortium (CPTAC): <https://wiki.cancerimagingarchive.net/display/Public/CPTAC-CM#33948224bcab02c187174a288dbcbf95d26179e8>

REFERENCES

1. Ali Z, Yousaf N, Larkin J. Melanoma epidemiology, biology and prognosis. *Eur J Cancer*. 2013;Suppl 11:81–91. <https://doi.org/10.1016/j.ejcsup.2013.07.012>
2. Hyams DM, Cook RW, Buzaid AC. Identification of risk in cutaneous melanoma patients: Prognostic and predictive markers. *J Surg Oncol*. 2019;**119**:175–186. <https://doi.org/10.1002/jso.25319>
3. Trinidad CM, Torres-Cabala CA, Curry JL, et al. Update on eighth edition American Joint Committee on Cancer classification for cutaneous melanoma and overview of potential pitfalls in histological examination of staging parameters. *J Clin Pathol*. 2019;**72**:265–270. <https://doi.org/10.1136/jclinpath-2018-205417>

4. Ascierto PA, Borgognoni L, Botti G, et al. New paradigm for stage III melanoma: From surgery to adjuvant treatment. *J Transl Med*. 2019;**17**:1–8. <https://doi.org/10.1186/s12967-019-2012-2>
5. Renner P, Torzewski M, Zeman F, et al. Increasing Morbidity with Extent of Lymphadenectomy for Primary Malignant Melanoma. *Lymphat Res Biol*. 2017;**15**:146–152. <https://doi.org/10.1089/lrb.2016.0018>
6. National Cancer Institute Clinical Proteomic Tumor Analysis Consortium (CPTAC). Radiology data from the clinical proteomic tumor analysis consortium cutaneous melanoma [CPTAC-CM] collection [Data set]. *The Cancer Imaging Archive*. 2018. <https://doi.org/10.1186/s12967-019-2012-2>

Ethics Approval The study was conducted according to the guidelines of the Declaration of Helsinki and approved by the Scientific Board of Istituto Tumori ‘Giovanni Paolo II’ (Bari, Italy).

Consent This study was determined by the Scientific Board to not require written consent from subjects, as it is retrospective and involves minimal risk.

Abstract 1281 Table 1 Clinical data referred to CPTAC-CM public database For categorical variables, absolute (abs.) and percentage (%) counts are reported. For continuous values, the median and standard deviation (sd.) values are indicated.

Characteristic	Distribution
Outcome	
DF cases (abs.; %)	31 (72.1%)
non-DF (abs.; %)	12 (27.9%)
Gender	
Male (abs.; %)	21 (48.8%)
Female (abs.; %)	22 (51.2%)
Tumor site	
Trunk (abs.; %)	20 (46.6%)
Face and neck (abs.; %)	1 (2.3%)
Extremities (abs.; %)	11 (25.6%)
Head & neck (abs.; %)	1 (2.3%)
Lymph nodes (abs.; %)	5 (11.6%)
Other (abs.; %)	5 (11.6%)
Stage	
I (abs.; %)	5 (11.6%)
II (abs.; %)	27 (62.7%)
III (abs.; %)	10 (23.1%)
T	
T0 (abs.; %)	2 (4.7%)
T1 (abs.; %)	3 (6.9%)
T2 (abs.; %)	10 (23.1%)
T3 (abs.; %)	4 (9.1%)
T4 (abs.; %)	22 (51.2%)
Age	
Median (sd.)	64.0 (14.9)
Tobacco consumption	
Current smoker	2 (4.7%)
Current non-smoker	4 (9.3%)
Non-smoker	35 (81.0%)
No available	1 (2.3%)

Abstract 1281 Table 2 Clinical data referred to the validation cohort For categorical variables, absolute (abs.) and percentage (%) counts are reported. For continuous values, the median and standard deviation (sd.) values are indicated.

Characteristic	Distribution
Outcome	
DF cases (abs.; %)	8 (72.7%)
non-DF (abs.; %)	3 (27.3%)
Gender	
Male (abs.; %)	3 (27.3%)
Female (abs.; %)	8 (72.7%)
Tumor site	
Trunk (abs.; %)	5 (45.5%)
Extremities (abs.; %)	3 (27.3%)
Head & neck (abs.; %)	1 (9.1%)
Other (abs.; %)	2 (18.2%)
Stage	
I (abs.; %)	2 (18.2%)
II (abs.; %)	8 (72.7%)
NA (abs.; %)	1 (9.1%)
T	
T2 (abs.; %)	2 (18.2%)
T3 (abs.; %)	4 (36.4%)
T4 (abs.; %)	5 (45.5%)
Age	
Median (sd.)	56.0 (13.2)
Tobacco consumption	
Non-smoker	9 (81.8%)
No available	2 (18.2%)

<http://dx.doi.org/10.1136/jitc-2022-SITC2022.1281>

1282

CONCORDANCE ANALYSIS OF AI-POWERED CD8 QUANTIFICATION AND AUTOMATED CD8 TOPOLOGY WITH MANUAL HISTOPATHOLOGICAL ASSESSMENT ACROSS SEVEN SOLID TUMOR TYPES

¹Maria Guramare*, ¹Nishant Agrawal*, ²George Lee, ¹Adam Stanford-Moore, ¹Abhik Lahiri, ¹Diksha Meghwal, ¹Aryan Pedawi, ¹Darren Fahy, ¹Raymond Biju, ¹Archit Khosla, ²Dimple Pandya, ³Scott Ely, ²Jimena Trillo-Tinoco, ²John Wojcik, ²Falon Gray, ²Benjamin Chen, ¹Sergine Brutus, ¹Benjamin Glass, ¹Cyrus Hedvat, ¹Ilan Wapinski, ¹Michael Montalto, ¹Andrew Beck, ¹Charles Biddle-Snead, ²Vipul Baxi. ¹PathAI, Boston, MA, USA; ²Bristol Myers Squibb, Princeton, NJ, USA

Background The degree of CD8+ lymphocyte infiltration into the tumor microenvironment, as well as the distribution of lymphocytes within the tumor and surrounding stroma (inflamed, excluded, or desert immunophenotypes), are key determinants for the potential efficacy of immunotherapy. Thus, accurate characterization of the tumor immune microenvironment is essential. However, manual histopathological assessment of CD8 topology is subject to many challenges, including subjectivity and reproducibility. We developed machine learning (ML)-based models for the identification and quantification of CD8+ lymphocytes and CD8-based CD8 topology classifiers across seven cancer types: urothelial carcinoma (UC), head and neck squamous cell carcinoma (HNSCC), non-small cell lung cancer (NSCLC), gastric cancer (GC), colorectal cancer (CRC), pancreatic cancer (PC), and hepatocellular carcinoma (HCC).

Methods ML algorithms were developed to quantify CD8+ lymphocytes in UC, HNSCC, NSCLC, GC, CRC, PC, and HCC specimens from clinical trials and commercial sources (N=1603) using CD8+ cell detection models trained on digitized whole slide images of CD8 immunohistochemistry (Agilent-Dako clone C8/144b, Agilent). Annotations were provided by the PathAI network of expert pathologists to train algorithms for classifying tissue regions (including parenchyma and stroma) and cell types. To evaluate the performance of the CD8+ cell model, AI-predicted counts were compared to a consensus count from five independent pathologists for representative fields of view (frames) using Pearson correlation. Inter-pathologist agreement was also calculated. Using a distinct cohort of samples from each cancer type (N=1655), a simple, two-parameter CD8 topology classifier was trained using pathologist-provided CD8 topology scores and CD8 model-derived features. Classifier-predicted immunophenotype scores were compared to pathologist-generated scores using unweighted Cohen's kappa.

Results ML-based quantitation of CD8+ lymphocytes yielded counts with high concordance to manual pathologist consensus counts. Frames-based validation of CD8+ counts on held-out test sets from each cancer type confirmed this high correlation (table 1). For scoring CD8 topology, the performance of the CD8 topology classifier was comparable to that of individual pathologists (table 2), indicating non-inferiority of our models with pathologist-generated scores. Overall, our models met pre-determined success criteria for all seven cancer types.

Conclusions ML model-predicted CD8+ cell counts are highly concordant with pathologist-generated counts across seven solid tumor types, and tumor CD8 topologies were predicted with a simple and highly interpretable two-parameter classifier. These data demonstrate the power of AI-powered digital pathology for accurate and reproducible quantitation of CD8+ lymphocytes and automated immunophenotyping in clinical samples, further confirming the potential for AI-based biomarker measurements in immuno-oncology.

Acknowledgements We thank Mevlana Gemici and Aryan Pedawi for their contributions to this study.

Trial Registration Samples from the following clinical trials were used in this study: CA209-275 (NCT02387996), CheckMate 274 (NCT02632409), CV202-103 (NCT03184870), Checkmate 9LA (NCT03215706), CA224-020 (NCT01968109), CheckMate 227 (NCT02477826), CheckMate 141 (NCT02105636), CheckMate040 (NCT01658878), CV202-103 (NCT03184870).

Ethics Approval Clinical trial protocols were approved by local institutional review boards or independent ethics committees and were conducted in accordance with the Declaration of Helsinki and Good Clinical Practice Guidelines, defined by the International Conference on Harmonisation of Technical Requirements for Pharmaceuticals for Human Use. All enrolled patients provided written informed consent based on Declaration of Helsinki principles prior to enrollment. This study was performed in accordance with the Bristol Myers Squibb Bioethics policy (<https://www.bms.com/about-us/responsibility/position-on-key-issues/bioethics-policy-statement.html>) and adhered to the World Medical Association Declaration of Helsinki for Human Research.

Abstract 1282 Table 1 Frames-based quantitative validation of CD8+ cell model performance. For each cancer type, quantitation of CD8+ lymphocytes was measured between pathologists and between our model and the consensus score. Pearson correlation and 95% confidence intervals are shown for each cancer type.

Cancer Subtype	Inter-pathologist (Mean Pathologist vs. Consensus) [Pearson, 95% CI]	PathAI Model vs. Consensus [Pearson, 95% CI]
UC	0.93 [0.90 - 0.95]	0.95 [0.92 - 0.97]
HNSCC	0.95 [0.92 - 0.97]	0.95 [0.92 - 0.97]
NSCLC	0.95 [0.92 - 0.97]	0.96 [0.93 - 0.97]
GC	0.89 [0.82 - 0.93]	0.91 [0.86 - 0.95]
CRC	0.95 [0.92 - 0.96]	0.95 [0.92 - 0.97]
PC	0.91 [0.87 - 0.94]	0.92 [0.88 - 0.95]
HCC	0.94 [0.90 - 0.96]	0.96 [0.94 - 0.98]

Abstract 1282 Table 2 Quantitative feasibility assessment of CD8 topology scoring. For each cancer type, concordance of CD8 topology was assessed between our model and individual pathologists, as well as between pathologists. Cohen's Kappa and 95% confidence intervals are shown for each cancer type.

Cancer Subtype	Inter-pathologist (Pairwise) [Kappa, 95% CI]	PathAI Model vs. Individual Pathologist (Pairwise) [Kappa, 95% CI]
UC	0.47 [0.39 - 0.56]	0.48 [0.41 - 0.56]
HNSCC	0.37 [0.32 - 0.42]	0.41 [0.35 - 0.46]
NSCLC	0.39 [0.33 - 0.47]	0.47 [0.41 - 0.53]
GC	0.45 [0.37 - 0.53]	0.41 [0.31 - 0.51]
CRC	0.35 [0.28 - 0.42]	0.38 [0.29 - 0.46]
PC	0.30 [0.18 - 0.43]	0.25 [0.14 - 0.36]
HCC	0.33 [0.25 - 0.41]	0.39 [0.31 - 0.46]

<http://dx.doi.org/10.1136/jitc-2022-SITC2022.1282>

1283

APPLYING MACHINE VISION TO EMPOWER PRECLINICAL DEVELOPMENT OF IMMUNOTHERAPIES IN PATIENT-DERIVED ORGANOID MODELS OF SOLID TUMORS

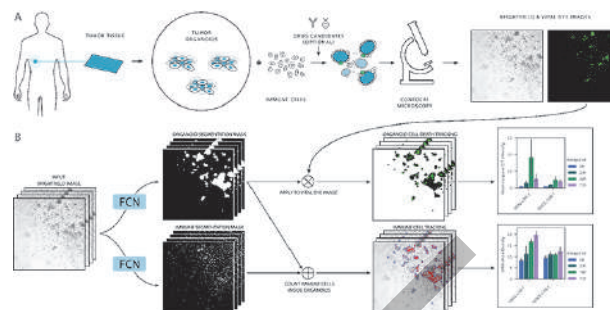
Chi-Sing Ho*, Sonal Khare, Madhavi Kannan, Michael Streit, Timothy Lopez, Luca Lonini, Brian Larsen, Brandon Mapes, Jenna Shaxted, Martin Stumpe, Ameen Salahudeen, Jagadish Venkataraman. *Tempus Labs, Redwood City, CA, USA*

Background Paradigm shifting next-generation immuno-oncology therapeutics such as CAR-T cells and bispecific engagers are rapidly gaining interest as investigational therapies. However, the discovery and preclinical development of these therapies involve 2-D cell line based assays that require differential labeling, often with fluorescent dyes or transgenic fluorescent proteins. These conventional approaches are limited by cumbersome labeling, optimization for each tumor cell line, and dysregulation of effector cell function including primary immune cells. In this work, we build upon a patient-derived tumor organoid (TO) platform to measure TO-specific responses to next-gen immunotherapies using brightfield-only segmentation models. We utilize machine vision on time-lapse microscopy to obtain multiparameter kinetic readouts of tumor cell death, enabling dissection of mechanisms of both CAR-T cells and effector cell engaging bispecifics. The assay co-localizes target and effector cells spatiotemporally without the need for differential labeling, affording insights into therapeutic potency or resistance. Overall, the automated segmentation and co-localization pipeline enables a highly scalable and high-throughput imaging assay for rapid discovery and validation of candidate next-gen immunotherapies across all solid tumors. **Methods** TOs were co-cultured with immune effector cells, optionally in the presence of a drug candidate, and imaged via a confocal microscope as a series of time-lapse images (figure 1A). We independently trained two fully-connected networks (FCNs) to segment the TOs and the immune cells directly from the brightfield channel. We then applied the TO masks to a registered vital dye channel to quantify TO cell death. Simultaneously, we used the TO masks, in conjunction with the immune cell masks from the second FCN, to quantify immune cells surrounding and infiltrating the TOs as a function of time (figure 1B).

Results We find that the rate of immune cell co-localization and infiltration is correlated with TO cell death over time, lending strong biological interpretability to the effectiveness of immunotherapies. We observe a differentiation of response between HER2-targeted and untargeted CAR-T lines, where targeted CAR-T lines exhibit higher infiltration rates with higher corresponding cell death rates. These correlations generate label-free insights into the pharmacokinetics and mechanisms for specific immune therapies.

Conclusions We present an effective solution for scalable, label-free quantification of TOs and immune cells from brightfield images to understand their dynamics in time-lapse imaging. Our machine vision platform enables high-throughput immune oncology preclinical studies to screen and mechanistically probe therapeutic candidates across dozens to hundreds of unique TO models, accelerating their evaluation as immuno-oncology therapeutic candidates in cancer patients.

Ethics Approval Human biospecimens and effector cells were obtained from third parties under IRB approved research protocols.



Abstract 1283 Figure 1 Overview of patient-derived TO-immune co-culture assay. A) Brightfield and vital dye images are collected over time series imaging measurements. B) A cascaded approach consisting of 2 FCN segmentation models and downstream quantification is applied to detect both TOs and immune cells to measure TO-specific cell death along with immune cell clustering and infiltration over time

<http://dx.doi.org/10.1136/jitc-2022-SITC2022.1283>

1284

BIOLOGY-GUIDED DEEP LEARNING PREDICTS PROGNOSIS AND CANCER IMMUNOTHERAPY RESPONSE

¹Yuming Jiang, ²Zhicheng Zhang, ³Wei Wang, ¹weicai Huang, ¹Chuanli Chen, ⁴Sujuan Xi, ²M Usman Ahmad*, ²Yulan Ren, ²Shengtian Sang, ⁵Jingjing Xie, ⁶Wenjun Xiong, ¹Tuanjue Li, ¹Zhen Han, ¹Qingyu Yuan, ¹Yikai Xu, ²Lei Xing, ²George Poulosides, ¹Guoxin Lin, ²Ruijiang Li. ¹Southern Medical University, Guangzhou, China; ²Stanford University, Stanford, CA, USA; ³Sun Yat-sen University, Guangzhou, China; ⁴Sun Yat-sen University, Shenzhen, China; ⁵University of California Davis, Davis, CA, USA; ⁶Guangzhou University of Chinese Medicine, Guangzhou, China

Background Substantial progress has been made in using deep learning for cancer detection and diagnosis in medical images.¹⁻¹⁰ However, a significant hurdle for clinical translation of current data-driven deep learning models is lack of interpretability, often attributable to a disconnect from the underlying pathobiology.¹¹⁻¹⁴ Here, we propose a biology-guided deep learning framework in which a multi-task model is trained to simultaneously predict tumor microenvironment (TME) status and treatment outcomes from radiology images.

Methods 348 patients with gastric adenocarcinoma were used as a training cohort to develop a machine learning algorithm combining radiologic imaging, clinicopathologic data, TME class using ImmunoScore of Gastric Cancer and protein expression of periostin, treatment information, and response to treatment. The model was internally validated with two cohorts of 202 and 636 patients in China. The model was further evaluated with an external validation cohort including 125 and 1062 patients at another Chinese academic medical center. The model was further validated in an American academic medical center cohort consisting of 57 patients. A final immunotherapy cohort of 253 patients was evaluated with advanced gastric cancer undergoing treatment with Anti-PD1 therapy.

Results A total of 2,749 patients were evaluated across training, internal validation, and external validation cohorts. Over 51% of patients with Stage II/III disease received adjuvant chemotherapy. All patients in the immunotherapy cohort had Stage IV disease with 94% harboring mismatch repair deficiency or microsatellite instability-high status. Biology-guided deep learning model was able to accurately predict four distinct TME classes based on computed tomography (CT) imaging 0.81 (95% CI: 0.769-0.851), 0.83 (0.780-0.884), 0.83 (0.780-0.884), and 0.84 (0.776-0.904) which were linked to disease free survival (DFS) and overall survival (OS). The benefit of chemotherapy in DFS and OS was associated with deep learning model and TME class 1-3 ($p < 0.05$), but not class 4. Assessing the effect of immunotherapy (figure 1), combined positive score (CPS) with predicted TME class outperformed CPS alone (Area Under the Curve: 0.805, 95% CI 0.75-0.85 vs 0.642 95% CI 0.58-0.70).

Conclusions Machine learning algorithms trained with pathobiology of tumors may successfully predict TME using only CT imaging in gastric cancer. These algorithms may be prognostic for adjuvant chemotherapy. In addition, use of algorithms may improve prognostication of response to PD-1 therapy despite mismatch repair deficiency and microsatellite instability-high status with use of CPS score of PD-1 expression.

Acknowledgements This project would not have been possible without the assistance and collaboration of staff, faculty, and students of four academic medical centers in China and the United States.

REFERENCES

1. Rajkomar A, Dean J & Kohane I. Machine Learning in Medicine. *The New England journal of medicine*. 2019;**380**:1347–1358.
2. Rajpurkar P, Chen E, Banerjee O & Topol EJ. AI in health and medicine. *Nat Med*. 2022;**28**:31–38.
3. Bhinder B, Gilvary C, Madhukar NS & Elemento O. Artificial intelligence in cancer research and precision medicine. *Cancer Discov*. 2021;**11**:900–915.
4. Esteva A, et al. Dermatologist-level classification of skin cancer with deep neural networks. *Nature*. 2017;**542**:115–118.
5. Ardila D, et al. End-to-end lung cancer screening with three-dimensional deep learning on lowdose chest computed tomography. *Nat Med*. 2019;**25**:954–961.
6. McKinney SM, et al. International evaluation of an AI system for breast cancer screening. *Nature*. 2020;**577**:89–94.
7. Lotter W, et al. Robust breast cancer detection in mammography and digital breast tomosynthesis using an annotation-efficient deep learning approach. *Nat Med*. 2021;**27**:244–249.
8. Yala A, et al. Optimizing risk-based breast cancer screening policies with reinforcement learning. *Nat Med*. 2022;**28**:136–143.
9. Lambin P, et al. Radiomics: the bridge between medical imaging and personalized medicine. *Nat Rev Clin Oncol*. 2017;**14**:749.
10. Wiens J, et al. Do no harm: a roadmap for responsible machine-learning for health care. *Nat Med*. 2019;**25**:1337–1340.
11. Quail DF & Joyce JA. Microenvironmental regulation of tumor progression and metastasis. *Nat Med*. 2013;**19**:1423–1437.
12. Bejarano L, Jordao MJC & Joyce JA. Therapeutic Targeting of the Tumor Microenvironment. *Cancer Discov* 2021;**11**:933–959.
13. Junttila MR. & de Sauvage FJ. Influence of tumour micro-environment heterogeneity on therapeutic response. *Nature*. 2013;**501**:346–354.
14. Fridman WH, Zitvogel L, Sautes-Fridman C & Kroemer G. The immune contexture in cancer prognosis and treatment. *Nat Rev Clin Oncol*. 2017;**14**:717–734.

Ethics Approval Ethical approval was obtained from the institutional review board of the four participating centers.

Consent Informed consent was waived for this retrospective analysis.

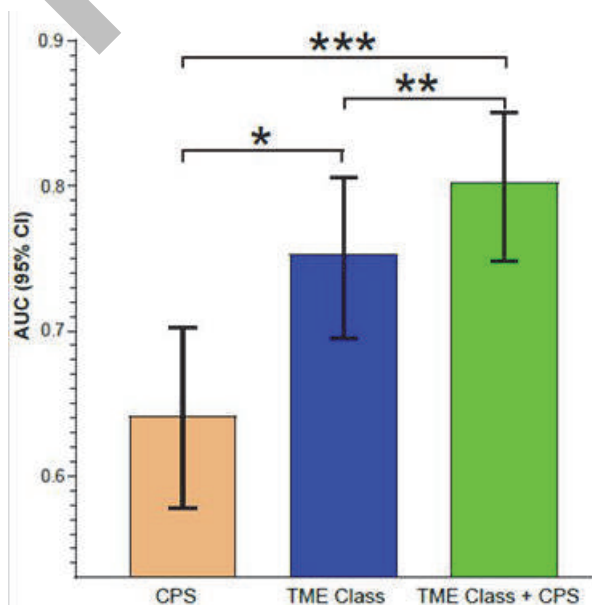


Figure 1: Prediction of objective response with combined positive score and predicted tumor microenvironment

Abstract 1284 Figure 1 Prediction of objective response with combined positive score and predicted tumor microenvironment

<http://dx.doi.org/10.1136/jitc-2022-SITC2022.1284>

1285

SPATIAL ANALYSIS OF TUMOR-INFILTRATING LYMPHOCYTES (TILS) BASED ON HER2 EXPRESSION ACROSS MULTIPLE CANCER TYPES

Sukjun Kim*, Seulki Kim, Yoojoo Lim, Gahee Park, Sanghoon Song, Heon Song, Seonwook Park, Jeongun Ryu, Sergio Pereira, Donggeun Yoo, Kyunghyun Paeng, Chan-Young Ock. *Lunit Inc., Seoul, South Korea*

Background Newer strategies of targeting HER2 such as novel HER2-targeted agents and combination with immune checkpoint inhibitors (ICIs) call for development of newer biomarkers based on deeper understanding of biology. To understand the immune microenvironment of HER2-expressing tumors, we performed spatial analysis of TIL in association with HER2 status, in the The Cancer Genome Atlas (TCGA) pan-carcinoma set.

Methods Hematoxylin and eosin (H&E)-stained slides, copy number alterations, and mRNA expression levels of HER2 for 7,322 patients across 22 cancer types and immunohistochemistry (IHC) results for 622 breast cancer patients were obtained from the TCGA data set. Spatial analysis of TIL distribution was done by an artificial intelligence-powered H&E analyzer, Lunit SCOPE IO. Intratumoral TIL (iTIL) and stromal TIL (sTIL) densities were defined as the number of TILs in each 1mm² grid of cancer area and stromal area. The HER2 amplified cancers were classified as per annotation of TCGA. Receiver operating characteristic (ROC) analysis was used to determine the optimal thresholds of mRNA expression showing maximal value of sensitivity and specificity, to discriminate HER2-expressed ($\geq 1+$) against HER2-negative (0) using IHC results. These thresholds were subsequently used in pan-cancer analysis, to define HER2-expressed vs. HER2-negative.

Results Overall, iTIL and sTIL densities of HER2 amplified cancers were lower than those of non-amplified cancers in the TCGA data set. Also, the iTIL and sTIL densities were mostly decreased in HER2-expressed cancers by the RNA-seq-based threshold. However, when breaking down into individual cancer types, TIL densities increased in endometrial cancer (UCEC) and ovarian cancer (OV). In UCEC (n = 148), iTIL density increased from 74.5 \pm 75.6 (mean \pm standard deviation) in HER2-negative to 167.17 \pm 322.30 in HER2-expressed and sTIL density increased from 649.2 \pm 517.2 to 875.2 \pm 1172.0, respectively. In OV (n = 70), although iTIL density was slightly increased from 50.5 \pm 53.6 to 52.9 \pm 63.5, sTIL density was notably increased from 243.6 \pm 215.6 to 540.9 \pm 563.9, respectively. Among the HER2-expressed cancers, the iTIL and sTIL levels were higher in those expressing PD-L1 or having high-tumor mutational burden (TMB). The differences were notable in urothelial carcinoma (TMB, PD-L1); breast cancer, cervical cancer, lung cancer, and thyroid cancer (PD-L1).

Conclusions HER2 amplification or expression was associated with lower immune infiltration in the pan-cancer cohort, consistent with previous data.¹ Further investigation in individual tumor types may further identify possible responders for combination therapy with HER2-targeted agents and ICIs.

REFERENCE

1. Ock CY, Hwang JE, Keam B, Kim SB, Shim JJ, Jang HJ, Park S, Sohn BH, Cha M, Ajani JA, Kopetz S, Lee KW, Kim TM, Heo DS, Lee JS. Genomic landscape associated with potential response to anti-CTLA-4 treatment in cancers. *Nat Commun.* 2017;**8**(1):1050.

<http://dx.doi.org/10.1136/jitc-2022-SITC2022.1285>

1286

**STRUCTURE-BASED PREDICTION OF NEOANTIGENS
PAIRED WITH T CELL RECEPTORS ON PHENOTYPE-
SELECTED CD8+ TUMOR-INFILTRATING LYMPHOCYTES**

Bo Ryeong Lee*, Sungsik Kim*, Sung-min Kim*, Woong-Yang Park. *Geninus Inc., Seoul, South Korea*

Background Vaccination by tumor neoantigens are promising immunotherapy by providing more tumor-reactive T cell pool, which could be boosted by anti-PD-1. Identification of neoantigens cognate to tumor-reactive tumor-infiltrating lymphocytes (TILs) is critical for clinical efficacy of neoantigen vaccines. Here, we developed *in silico* neoantigen prediction platform by structure-based pairing with T cell receptors (TCR) on pre-existing CD8+ TILs selected by single-cell transcriptome profiles. Neoantigens derived by our strategy reflect *in vivo* immunogenicity and tumor reactivity.

Methods Tumor resections from solid cancer patients are subject to whole exome and transcriptome sequencing. In addition, TILs from the patients are subject to scRNAseq/scTCRseq to stratify TCRs of TILs into target TILs and non-target TILs by single-cell transcriptome profiles. Neoantigen epitopes are filtered with HLA binding/immunogenicity and prioritized by tricomplex (TCR-peptide-HLA) structure-based TCR binding score from our platform Vacinus. To evaluate the immunogenicity of selected neoantigens, the neoantigen peptides are tested for *in vitro* IFN γ ELISPOT assay using peripheral blood mononuclear cells (PBMCs) from the same patients, which sensitively detects antigen-experienced T cells.

Results We have screened the immunogenicity of 286 neoantigens derived from Vacinus platform for 34 solid cancer patients. In particular, we could detect the immunogenic neoantigens in the majority of Hepatocellular carcinoma (HCC) patients (13/14) which had low mutational burden with median 95 (46-373) non-synonymous mutations. Single-cell transcriptome of CD8 TILs from HCC revealed that TILs had primarily exhausted/cytotoxic phenotype (target TIL) and non-exhausted memory phenotypes (non-target TIL). We applied TCRs derived from target or non-target TILs to select cognate neoantigens predicted by Vacinus platform, which are tier1 and tier2 neoantigens, respectively. Interestingly, when those neoantigens were tested for immunogenicity with IFN γ ELISPOT assay, higher T cell responses were detected in tier1 (31%) than tier2 neoantigens (17%), reflecting tier1 neoantigens have more capability to induce *in vivo* immunogenicity in cancer patients. Using mouse tumor models, we are investigating therapeutic efficacy of tier1 neoantigens.

Conclusions It is feasible to develop cancer neoantigen vaccine in HCC which has low mutational burden. Neoantigens paired with TILs in an activated state were identified to have greater immunogenicity compared to TILs in a memory state, underscoring the selection of target TILs. Neoantigen prediction by structure-based pairing of neoantigens and phenotype-selected TILs showed promising potential to better select therapeutically-relevant cancer vaccines.

Ethics Approval The study with samples from HCC patients was approved by the Asan Medical Center Institutional Review Board (IRB) (2022-0263)

<http://dx.doi.org/10.1136/jitc-2022-SITC2022.1286>

1287

RADIOMICS AND DELTA-RADIOMICS SIGNATURES TO PREDICT RESPONSE AND SURVIVAL IN PATIENT WITH NON-SMALL CELL LUNG CANCER TREATED WITH IMMUNE CHECKPOINT INHIBITORS

François Cousin, Thomas Louis, Mariaelena Occhipinti, Wim Vos*, Julien Guiot, Roland Hustinx. *University Hospital of Liège, Liège, Belgium;* ²*Radiomics, Liège, Belgium*

Background Accurate and early selection of patients with advanced non-small cell lung cancer (NSCLC) who would benefit from immunotherapy is of the utmost clinical importance. The aim of our study was to determine the potential role of CT-based radiomics and delta-radiomics signatures in predicting treatment response and survival in patients with advanced NSCLC treated with programmed death-1 (PD-1) or programmed death ligand-1 (PD-L1) inhibitors. Moreover, we compared the results obtained with both signatures to early RECIST v1.1 assessment (first follow up visit).

Methods In this retrospective multi-centric study, we included 188 patients with NSCLC treated with PD-1/PD-L1 inhibitors who underwent a pre-treatment and at least one follow-up CT scans. The training dataset was composed of 146 patients and the external validation dataset of 42 patients. All the lesions, both target and non-target, according to RECIST v1.1 criteria, were manually segmented by experienced reader. Radiomics analysis was performed on both single and multiple target lesions per patient. A delta-radiomics analysis was also conducted on a subset of 160 patients who underwent a follow-up CT after 2 to 4 treatment cycles. Radiomic features were selected by the Minimum Redundancy Maximum Relevance method. Linear and Random Forest (RF) models were tested to predict response at 6 months and overall survival (OS). Performances of the models were expressed in term of Area Under the Curve (AUC) and survival prediction with Cox concordance index.

Results The baseline CT radiomics signatures did not show any significant results for prediction of treatment response or survival. The RF delta-radiomics model showed the best performance for treatment response prediction with an AUC of 0.81 (95% CI: 0.66-0.95). The GLM delta-radiomics model was the most accurate at predicting survival with a concordance index of 0.68 (95% CI: 0.56-0.80) ($p=0.02$). The comparison between the delta radiomics signatures and early RECIST v1.1 assessment showed a clear improvement in survival prediction with an AUC of 0.66 (95% CI:0.54-0.78) for early RECIST against an AUC of 0.77 (95% CI: 0.61-0.93) and 0.81 (GLM and RF signatures respectively) for delta radiomics signature and a concordance index of 0.56 (95% CI: 0.47-0.65) on the validation dataset.

Conclusions Our delta radiomics models were able to early identify patients with advanced NSCLC who were more likely to benefit from immunotherapy.

Ethics Approval This study received approval from institutional review board of University Hospital of Liège, and the need for informed consent was waived based on its retrospective design.

<http://dx.doi.org/10.1136/jitc-2022-SITC2022.1287>

Abstracts

1288

SPATIAL TRANSCRIPTOMICS-ENABLED INTEGRATED MORPHOLOGY-TRANSCRIPTOME TUMOR CELL PHENOTYPING USING MACHINE LEARNING

¹Nga Luong*, ¹Wei Yan, ²Jeffrey Lim, ²Yuezhen Xue, ¹Abu Bakr Azam, ²Joe Poh Sheng Yeong, ²Mai Chan Lau, ¹Yiyu Cai. ¹Nanyang Technological University, Singapore, Singapore; ²A*STAR, Singapore, Singapore

Background In routine cancer diagnosis, pathologists manually characterize tumor cells based on hematoxylin and eosin (H&E)-stained images. On the other hand, transcriptomic-based tumor molecular subtypes were shown to be associated with important clinical features including tumorigenesis and prognosis. Leveraging recent development of spatial transcriptomics (ST) which allows in-situ transcriptomic profiling of tissues,¹ we aim to develop a first-of-its-kind machine learning (ML)-enabled integrated morphology-transcriptome tumor single-cell phenotyping approach.

Methods Two tissue sections each from tumor and adjacent-normal areas collected from a hepatocellular carcinoma (HCC) patient were profiled using 10× Visium ST platform. Using the companion H&E image, individual epithelial cells were segmented (StarDist algorithm) with 53 morphological and staining features extracted (QuPath v0.3.2). These cells were unsupervisedly clustered using encoder-based ensemble method where the optimal clustering solution was determined based on a consensus score of three clustering metrics. Phenotypic gene signatures of the cell clusters were determined through deconvoluting the ST data. Gene ontology (GO) analysis was done using single sample gene set enrichment, based on the molecular signatures database.

Results At the optimal clustering setting, 4 epithelial cell clusters, characterized by differential nuclear size, were detected individually in each HCC tissue (figure. 1). Manual inspection by a pathologist (YZ) confirmed that the tumor epithelial cells demonstrated different nuclear sizes and revealed that the two smaller cell clusters looked relatively more well-differentiated, and ~1% found outside the tumor nest, suggesting potential epithelial to mesenchymal transition (EMT) activity. Whereas the two larger clusters were moderately-differentiated and demonstrated hyperchromatic nuclei and pleomorphism. GO analysis confirmed the upregulation of EMT in the smallest cluster, in both tumor tissues. While epithelial cells in the two normal-adjacent tissues appeared morphologically non-cancerous, the corresponding cell clusters contributed to similar cell fractions as that of the tumor tissues; two smaller clusters contributed to ~70% of the total cells across all tissues (figure. 2). Cell clusters with similar nuclear size shared 30%-65% of the top 20 pathways across tissues, indicating inter-tissue phenotypic consistency. Cells were found near cell-type of its own followed by cell-type of similar size, suggesting preferential cell clustering of similar phenotypes (figure 3).

Conclusions Our ML approach revealed four morphologically-transcriptomically distinct tumor cell subsets in the HCC tissues, with the smallest cells appeared EMT-like. We revealed intra-patient tumor cell heterogeneity yet phenotypic consistency across tissue sampling sites. Altogether, our proposed approach would enable more refined tumor cell phenotyping, advancing our understanding of tumor biology.

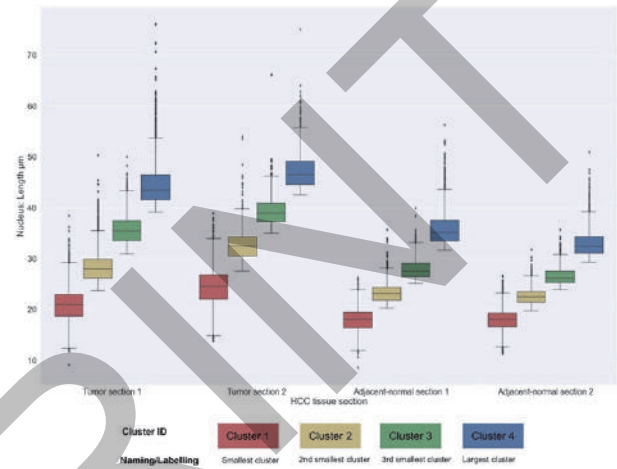
Acknowledgements I would like to thank NTU Undergraduate Research Experience on Campus (URECA) program for giving me opportunity to work on this project for the past year.

REFERENCE

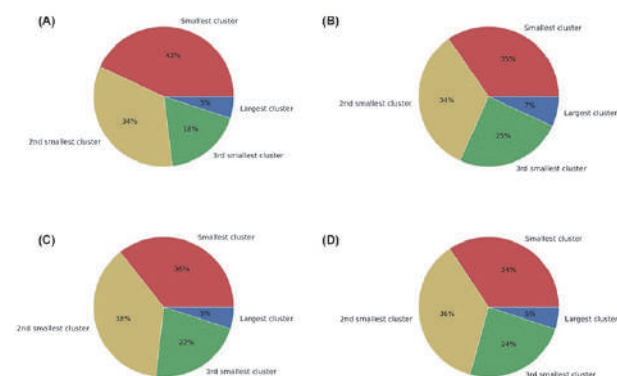
1. Nerurkar SN, Goh D, Cheung CCL, Nga PQY, Lim JCT, Yeong JPS. Transcriptional spatial profiling of cancer tissues in the era of immunotherapy: the potential and promise. *Cancers*. 2020;**12**:2572.

Ethics Approval This study was approved by the SingHealth Centralized Institutional Review Board (reference numbers: 2018/3045 and 2019/2653).

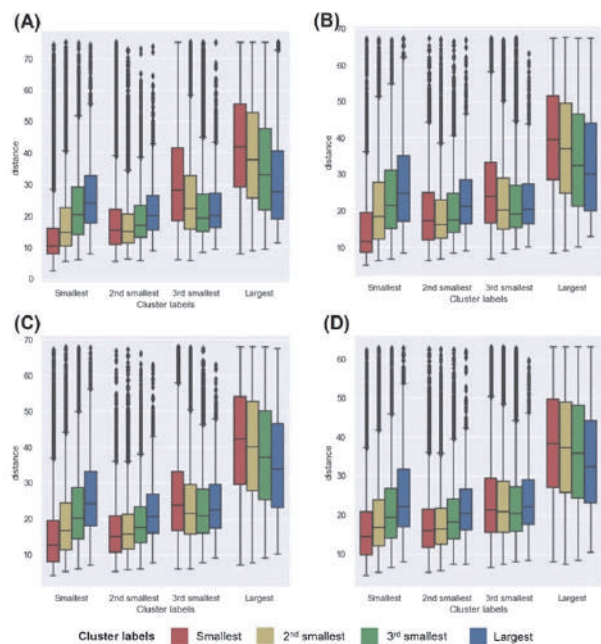
Consent The patients provided their written informed consent to participate in this study.



Abstract 1288 Figure 1 Distribution of nuclear areas (micrometer) of the 4 identified epithelial cell clusters in the 4 tissue sections. The 4 clusters are labelled: 'Smallest cluster', '2nd smallest cluster', '3rd smallest cluster', and 'largest cluster' according to their nucleus size.



Abstract 1288 Figure 2 Cell abundance distribution of the 4 identified epithelial cell clusters in (A) tumor section 1, (B) tumor section 2, (C) adjacent-normal section 1, and (D) adjacent-normal section 2.



Abstract 1288 Figure 3 Distribution of the nearest neighbor distance of cells within a cluster to all 4 clusters, respectively in (A) tumor section 1, (B) tumor section 2, (C) adjacent-normal section 1, and (D) adjacent-normal section 2.

<http://dx.doi.org/10.1136/jitc-2022-SITC2022.1288>

Abstracts

1289

PREDICTING RESPONSE TO IMMUNE CHECKPOINT INHIBITORS (ICI) IN NON-SMALL-CELL LUNG CANCER (NSCLC) BY COMBINING SPATIAL ANALYSIS OF CELLS AND RNA SEQUENCING DATA FROM BIOPSIES USING DEEP LEARNING (DL)

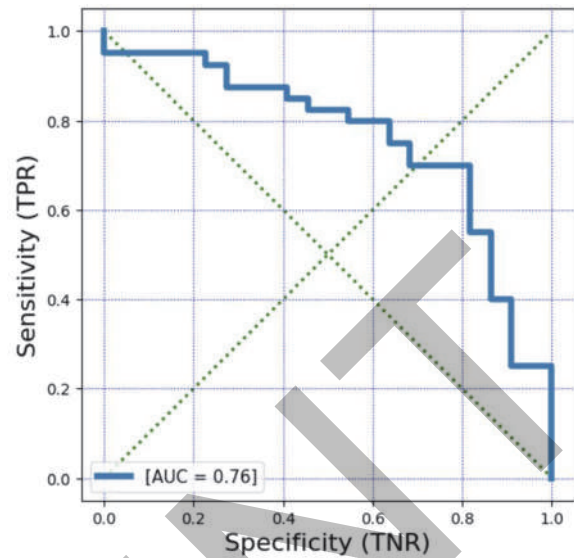
¹Ettai Markovits*, ²David Soong, ¹Becky Arbiv, ¹Alon Groisman, ¹Maya Lipinsky, ¹Yoni Yedidia, ¹Yoad Cohen, ¹Yuval Gabay, ¹Yuval Shachaf, ¹Eyal Oren, ¹Roman Gluskin, ¹Ido Weiss, ²Hisham Hamadeh, ²Kate Sasser, ¹Gali Golan, ²Brandon Higgs, ²Suzana Couto, ¹Ori Zelichov. ¹Nucleai, Tel Aviv, Israel; ²Genmab, Princeton, NJ, USA

Background ICI have transformed treatment of metastatic NSCLC, however, only a small proportion of patients respond. Spatial biology plays a significant role in further understanding the complexities of the tumor microenvironment and drivers of response to ICI. Here, we utilized DL to analyze whole slide images (WSI) of sequential biopsies stained for H&E and five IHC stains and combined it with RNA sequencing data to identify features associated with response to ICI.

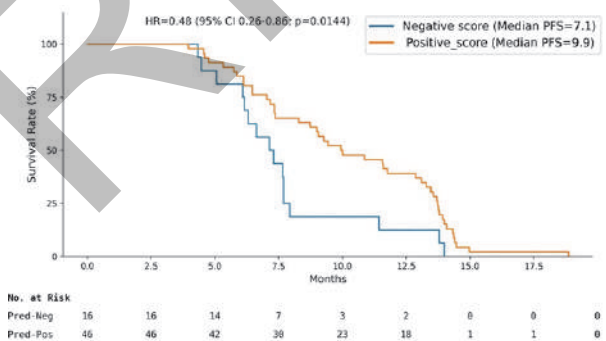
Methods 103 NSCLC patients treated with second line ICI were procured. For each patient, a total of 12 WSI from pre- and post-treatment biopsies, sequentially stained for H&E, CD3, CD8, CD163, CD137 and PD-L1 IHC were analyzed. RNA sequencing data of pre-treatment biopsies from 81 patients were also analyzed. Endpoints included overall response rate (ORR) and progression-free survival (PFS). DL models were trained to classify tumor cells, lymphocytes, fibroblasts, and tumor versus stromal areas from H&E, and positivity of IHC markers per cell. Based on biological hypotheses, 362 spatial and 72 RNA features were pre-defined and calculated for each patient. Univariate analysis identified features associated with clinical outcomes and the best performing features were selected to generate a binary classifier for response prediction. Cross-validation was performed.

Results Multiple spatial and RNA features were significantly correlated with ORR and PFS. Responders had greater density of CD3 in the invasive margin and closer proximity between PD-L1+ tumor cells and CD8+ cells in pre-treatment biopsies compared to non-responders ($p < 0.01$). Gene set enrichment analysis identified upregulation of hallmark TNF-alpha signaling and IFN gamma response genes in responders to ICI pre-treatment ($p < 0.0001$). When comparing pre- and post-treatment biopsies, responders had greater increases in density of CD8+ cells in the tumor microenvironment following ICI ($p = 0.02$). The resulting classifier combined 7 spatial and 3 RNA features and reached an AUC=0.76 when correlated with ORR (figure 1). 62 patients with both RNA and spatial features were classified as positive ($n=46$) or negative ($n=16$). In a Kaplan-Meier (KM) analysis, PFS was significantly longer in positive-scored compared to negative-scored patients (HR=0.48, 95% CI 0.26-0.86, $p < 0.02$) (figure 2).

Conclusions DL for spatial analysis of cells combined with pathway modulation, as measured by RNA sequencing can elucidate unique tumor contexture relevant for response to ICI in NSCLC.



Abstract 1289 Figure 1 AUC and ROC curve of the predictive binary classifier



Abstract 1289 Figure 2 KM analysis of PFS in patients with positive vs. negative prediction score

<http://dx.doi.org/10.1136/jitc-2022-SITC2022.1289>

1290

A DEEP LEARNING ANALYSIS PIPELINE FOR MULTIPLEX IMAGING IDENTIFIES SPATIAL FEATURES ASSOCIATED WITH CLINICAL OUTCOME IN COLORECTAL CANCER

Ettai Markovits*, Roman Gluskin, Tomer Dicker, Ido Weiss, Sun Dagan, Ron Elran, Amit Bart, Oleg Kuybeda, Becky Arbiv, Ori Zelichov. *Nucleai, Tel Aviv, Israel*

Background Multiplex immunofluorescence (mIF) can provide invaluable insights on spatial biology and the complexities of the immune tumor microenvironment (iTME), however, current analysis methods are laborious and user dependent. We applied a novel end-to-end deep learning (DL) pipeline (figure 1) to mIF tumor-microarray (TMA) images, to investigate associations between iTME composition and clinical outcome.

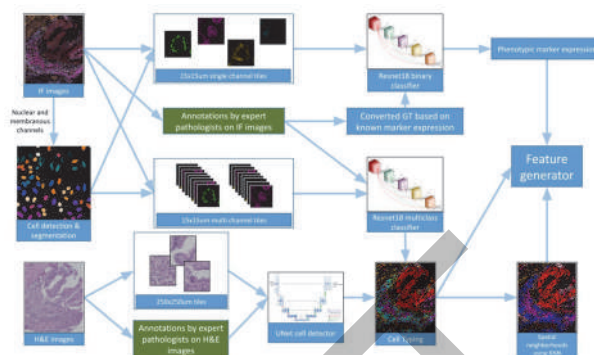
Methods A publicly available CODEX dataset,¹ consisting of 140 tissue cores from 35 colorectal cancer (CRC) patients stained with 56 protein markers and matched H&E slides was analyzed. 7,000 cell annotations on 57 tissue cores were used to train DL models to segment cells and classify them to 13 subpopulations (figure 2). Performance was evaluated quantitatively on 1,800 annotations from 14 test cores, and qualitatively on all cores by expert pathologists. In addition, positivity for 8 immunomodulatory markers was predicted per cell, using a DL binary classifier trained on 100,000 binary single channel annotations, which were automatically extracted from the 7,000 cell annotations by prior knowledge of lineage marker expression. The model performance was evaluated on novel annotations for each phenotypic marker. H&E slides were utilized to annotate tumor and stromal areas and identify fibroblasts and marker-negative tumor cells. 12 Cell neighborhoods were identified by clustering the 10 nearest-neighbors for each cell (figure 3). Over 600 spatial features were calculated and correlated with good vs. bad prognosis defined by 2-year OS cutoff.

Results Cell typing model reached a 91.9% accuracy (figure 4) and good performance (>75% accuracy) by qualitative assessment in 97.7% of cores, thus markedly outperforming existing clustering-based cell typing approaches showing 65.9% accuracy (figure 5). Phenotypic marker classification demonstrated 93.5% accuracy (figure 6). Stromal abundance of a plasma cell-enriched neighborhood was associated with bad prognosis (p=0.009), while higher fraction of LAG3+ (p=0.01) and VISTA+ (p=0.004) plasma cells in the same neighborhood was associated with good prognosis. In addition, LAG3+CD4 + T-cells upregulation in a CD8+ enriched neighborhood was also associated with better prognosis (p=0.006, figure 7 and table 1). Taken together, we demonstrate the importance of complex spatial features, which capture cell type, neighborhood and functional state information for clinical outcome prediction.

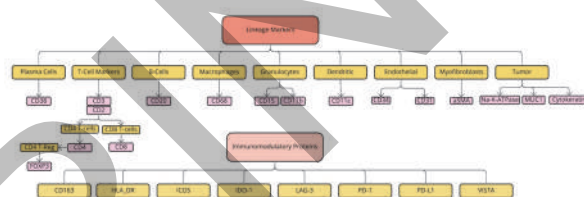
Conclusions A novel DL pipeline for mIF analysis demonstrated high accuracy in classifying cell types and phenotypic markers, thus enabling the identification of multiple cellular and spatial features associated with prognosis in CRC.

REFERENCE

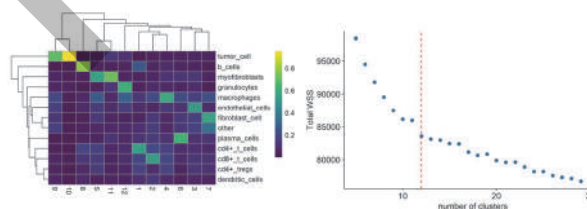
- Schürch CM, Bhaté SS, Barlow GL, *et al.* Coordinated cellular neighborhoods orchestrate antitumoral immunity at the colorectal cancer invasive front [published correction appears in *Cell*. 2020 Oct 29;183(3):838]. *Cell*. 2020;182(5):1341–1359.e19. doi:10.1016/j.cell.2020.07.005



Abstract 1290 Figure 1 A deep learning analysis pipeline for multiplex imaging

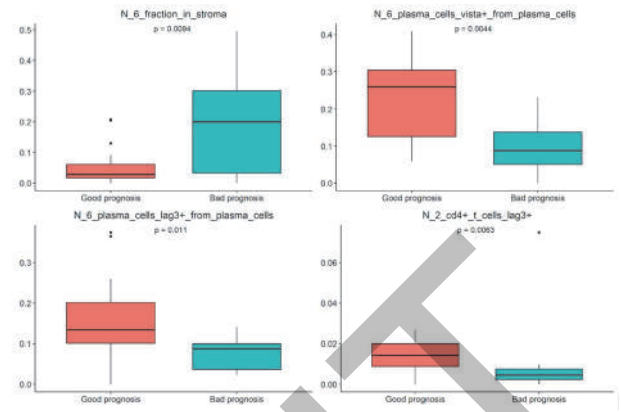
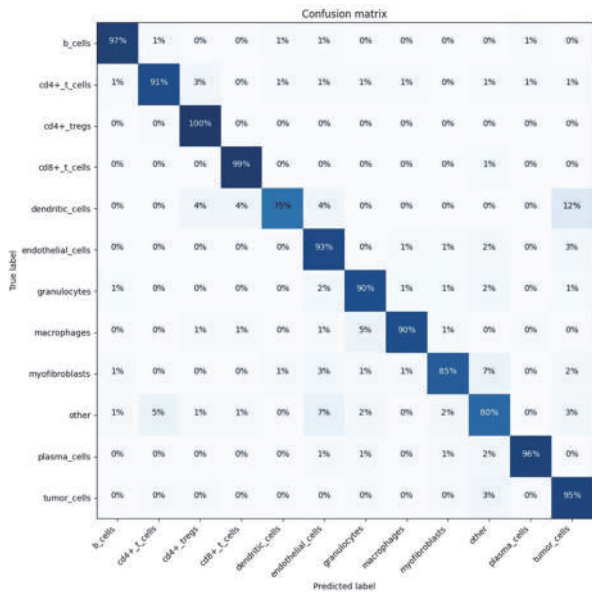


Abstract 1290 Figure 2 Quantification and cell typing methodology



Abstract 1290 Figure 3 Cell neighborhoods

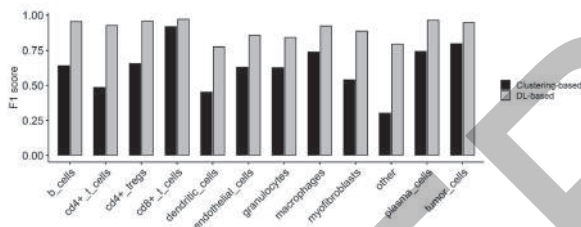
Abstracts



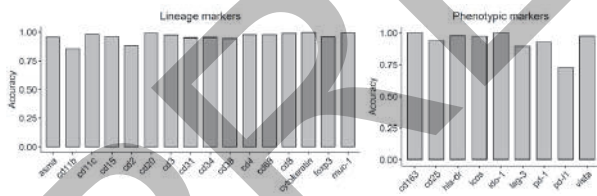
Abstract 1290 Figure 7 Association between the spatial features and clinical outcome

<http://dx.doi.org/10.1136/jitc-2022-SITC2022.1290>

Abstract 1290 Figure 4 Evaluation of mIF-based classifier on test cores annotations



Abstract 1290 Figure 5 Comparison between DL and clustering-based cell typing approaches



Abstract 1290 Figure 6 Phenotypic markers classifier accuracy in test cores

Abstract 1290 Table 1 Top 10 differential features between patients with good and bad prognosis

feature	Good prognosis mean	Bad prognosis mean	diff	pval
N_6_plasma_cells_vista+_from_plasma_cells	0.226	0.106	0.12	0.004
N_2_cd4+_t_cells_lag3+	0.014	0.01	0.004	0.006
N_6_plasma_cells_vista+	0.098	0.049	0.049	0.008
N_6_fraction_in_stroma	0.053	0.193	-0.14	0.009
N_2_cd4+_t_cells_lag3+_from_cd4+_t_cells	0.163	0.115	0.048	0.011
N_6_plasma_cells_lag3+_from_plasma_cells	0.164	0.077	0.087	0.011
N_4_cd4+_tregs_lag3+	0.013	0.005	0.007	0.013
N_1_plasma_cells_fraction	0.036	0.083	-0.047	0.013
N_6_plasma_cells_lag3+	0.073	0.036	0.038	0.013
N_9_macrophages_cd163+	0.033	0.012	0.021	0.013

1291

A MULTI-TUMOR MACHINE LEARNING MODEL TO IDENTIFY TERTIARY LYMPHOID STRUCTURES IN HISTOPATHOLOGICAL H&E IMAGES AS A POTENTIAL CLINICAL BIOMARKER

¹Vanessa Matos-Cruz*, ¹Rachel Sargent, ²Varsha Chinnabireddy, ²Maryam Pouryahya, ¹George Lee, ²Darren Fahy, ²Christian Kirkup, ²Kathleen Supto, ²Sai Gullapally, ²Jacqueline Brosnan-Cashman, ²Archit Khosla, ²Nishant Agrawal, ²Benjamin Glass, ²Sergine Brutus, ²Limin Yu, ¹Benjamin Chen, ²Vipul Baxi, ¹Scott Ely. ¹*Bristol Myers Squibb, Princeton, NJ, USA*; ²*PathAI, Boston, MA, USA*

Background Tertiary lymphoid structures (TLS) are ectopic lymphoid structures that develop in benign and tumor tissues with chronic inflammation. TLS are highly organized structures composed of B cells, T cells, and supportive cells within a structural matrix. They are classified as lymphoid aggregates (LA), immature TLS (imTLS), or mature TLS (mTLS) with the presence of a germinal center (GC). The presence and maturity of TLS have been associated with favorable outcomes in multiple tumor indications and with immune-checkpoint inhibitor (ICI) efficacy. We aimed to develop a digital pathology method to quantify TLS presence, prevalence, and localization as a predictive biomarker of ICI clinical outcome. We developed a machine-learning (ML) algorithm trained on hematoxylin and eosin (H&E)-stained whole slide images (WSIs) to: (1) accurately and reproducibly identify LAs and TLS; (2) to predict TLS subregions and maturity; and (3) extract TLS model-derived features.

Methods A multi-tumor ML-based TLS detection model was trained by expert pathologists to predict mTLS/GCs, imTLS, and LAs in H&E-stained WSIs (N=2777) from TCGA bladder cancer (BLCA), breast cancer (BRCA), stomach adenocarcinoma (STAD), lung adenocarcinoma (LUAD), and lung squamous cell carcinoma (LUSC). Pre-trained indication-specific tissue segmentation models were applied to distinguish cancer, cancer-associated stroma, and necrosis from normal tissue. Features quantitatively derived from TLS and tissue regions were extracted, and correlations with an RNA-seq-derived TLS-associated gene expression signature were calculated. Log-rank analysis was performed to assess the impact of TLS on prognosis.

Results Our model accurately and reproducibly detected and distinguished LA, imTLS, and mTLS/GC in five indications and performed comparably to manual pathologist-derived annotation. Four model-derived TLS features (proportional area of LA, proportional area of imTLS, proportional area of mTLS, and mean perimeter of imTLS) correlated with a published TLS-gene signature, and three gene-expression clusters were found to be concordant with TLS maturity. The proportional area of mTLS was significantly associated with improved progression-free survival in BRCA (p=0.01) and overall survival in LUAD (p=0.04).

Conclusions We developed a robust ML-based algorithm that can accurately distinguish and classify TLS structures across five indications. We demonstrated that novel TLS model-derived features correlated with gene expression and survival in several indications. These data highlight the promise of ML-based approaches for the accurate and reproducible evaluation and potential implementation of prognostic TLS biomarker assays in oncology.

Ethics Approval The trial protocols were approved by site institutional review boards or independent ethics committees and conducted according to Good Clinical Practice guidelines, per the International Conference on Harmonisation. Patients

provided written informed consent based on Declaration of Helsinki principles.

Consent Patients provided written informed consent based on Declaration of Helsinki principles.

<http://dx.doi.org/10.1136/jitc-2022-SITC2022.1291>

1292

A REPRODUCIBLE PIPELINE FOR ANALYSIS OF MULTIPLEX IMAGING (MIBI) DATA WITH APPLICATION TO UNCOVERING NOVEL FEATURES OF THE TUMOR-IMMUNE MICROENVIRONMENT

¹Jessica Maxey*, ¹Marshall Thompson*, ²Katie Campbell, ¹Benjamin Kamphaus, ¹Zaid Bustami, ¹Sandra Santulli-Marotto, ¹Daniel Wells, ³Silvia Boffo, ³Lisa Salvador, ²Philip Scumpia, ¹Christine Spencer, ⁴Adam Schoenfeld, ²Antoni Ribas, ¹Lacey Kitch. ¹*Parker Institute for Cancer Immunotherapy (PICI), San Francisco, CA, USA;* ²*University of California Los Angeles (UCLA), Los Angeles, CA, USA;* ³*Bristol Myers Squibb, Princeton, NJ, USA;* ⁴*Memorial Sloan Kettering Cancer Center, New York, USA*

Background Although immune checkpoint inhibition (ICI) has been transformational, tumor-associated factors regulating response have not been elucidated. High-dimensional spatial profiling technologies have enabled simultaneous investigation of many protein targets on individual cells within the spatial context of the tumor microenvironment (TME). Analysis of these data to uncover immune and tumor profiles relies on identification of individual cells and characterization of their specific marker expression to classify lineage and functional state. However, robust automated cell type assignment remains a key challenge in multiplex image data analysis. Here, we describe a reproducible pipeline for single cell identification and typing from multiplex ion beam imaging (MIBI) data utilizing lineage protein expression, which has applications in the context of precision immunotherapy and beyond.

Methods Biopsies from melanoma (n = 80) or non-small cell lung cancer (NSCLC, n = 38) patients treated with anti-PD-1 were profiled by MIBI for spatial analysis of 32 protein markers. Following cell segmentation, an automated pipeline was developed to assign cell types based on bootstrap sampling of lineage-specific marker expression within each region of interest (n = 395), on a per-pixel basis. This pipeline was further optimized by integrating marker lineage-specificity to improve the identification and segmentation of cells with irregular shapes or sizes (e.g. fibroblasts, macrophages) by expanding cell outlines based on pixel type identity. The overall approach was benchmarked against existing automated and manual methods. Feature extraction and downstream harmonization with clinical and other molecular data was facilitated by our multi-omic data integration platform (CANDEL).

Results Our cell typing and segment expansion approach outperformed several alternatives in proportion of cell types confidently assigned, increasing the proportion of identified segments by 15-55% across all samples tested. The additional improvement in segmentation demonstrated by the pixel expansion method enabled clearer visualization of TME context and cellular structure, increasing the overall inclusion of macrophage and fibroblast markers by 14.9% and 30.47%, respectively. Exploration of the association between image features and clinical response to anti-PD-1 is currently underway.

Conclusions Multiplex imaging data can provide new insights into mechanisms, targets, and biomarkers for cancer immunotherapy. These insights depend on reliable segmentation and cell typing, and manual methods can be unreliable and do not scale. Our toolchain provides a foundation for reliable and scalable analysis of high-dimensional spatial profiling data. These analytical improvements will facilitate generation of new insights into mechanisms of PD-1 resistance and features of the TME that correlate with clinical outcomes.

Trial Registration NCT03033576, NCT02350764

<http://dx.doi.org/10.1136/jitc-2022-SITC2022.1292>

1293

ESTABLISHING THE PRECLINICAL PKPD RELATIONSHIP FOR NM32-2668 A ROR1 TARGETING T CELL ENGAGER

¹Hitesh Mistry, ¹Fernando Ortega*, ²Bithi Chatterjee, ²Nicole Bassler, ²Niels Kirk, ²Julia Tietz, ²Belinda Wickihalder, ²Simone Muntwiler, ²Simon Carnal, ²Daniel Snell, ¹Christophe Chassagnole. ¹Physiomics, Oxford, UK; ²Numab Therapeutics, Wädenswil, Switzerland

Background NM32-2668 is a fragment-based multispecific antibody therapeutic¹ that has been designed to activate T-cells (via CD3) in the presence of tumour antigen receptor tyrosine kinase-like orphan receptor 1 (ROR1). The objective of this work was to build a mathematical model to establish a PKPD relationship using both *in vitro* and *in vivo* data for NM32-2668.

Methods Data were collected from *in vitro* studies measuring CD4/8 activation and cytotoxicity from a panel of cell lines and patient samples to increasing concentrations of NM32-2668, and from *in vivo* tumour growth inhibition (TGI) data from a humanised mouse model in one cell line with two different donors with increasing doses of NM32-2668. Nonlinear mixed-effects models were used to assess the variability in cytotoxicity as a function of drug concentration and immune system activation. The translatability of *in vitro* potency values for immune system activation was assessed by linking PK to *in vitro* data and to TGI *in vivo* data.

Results The combination of ROR1 expression and CD8 activation fully explained the variance in cytotoxicity across all *in vitro* data. The estimated *in vitro* potency for CD8 activation could successfully be used to provide a link between PK and TGI *in vivo*.

Conclusions A PK-PD-Efficacy model based on the *in vitro* data was established showing that the cytotoxicity response was strongly correlated to ROR1 expression and CD8 activation. Building on this *in vitro* model, we developed an *in vivo* PK-TGI model that can link immune system activation to TGI.

REFERENCE

1. Egan TJ, Diem D, Weldon R, Neumann Y, Meyer S, Urech DM. Novel multispecific heterodimeric antibody format allowing modular assembly of variable domain fragments. *MABS*. 2017;**9**(1):68–84

<http://dx.doi.org/10.1136/jitc-2022-SITC2022.1293>

1294

AN AUTOMATED MACHINE LEARNING FRAMEWORK FOR RAPID QUANTIFICATION AND ANALYSIS OF MULTIPLEXED ION BEAM IMAGES (MIBI)

Raghav Padmanabhan, Mate Nagy, Stanislaw Nowak, Peng Si, Sweta Bajaj, Mate Nagy*, Monirath Hav. Ionpath Inc., Menlo Park, CA, USA

Background Multiplexed Ion Beam Imaging (MIBI) offers high-parameter tissue imaging that is well suited for describing complex immuno-spatial features in tissues, including the enumeration of various cell phenotypes, expression of immune checkpoint proteins, and quantitative description of spatial distributions between different populations.¹ The high imaging resolution combined with the rich mass spectral information in each image allows for the quantification of up to 40 biomarkers in a single slide and enables immediate processing without the need for additional imaging rounds. Leveraging this, we outline an automated machine learning framework that enables rapid, deep phenotypic and spatial profiling of tissues at the subcellular level.

Methods Our framework consists of five steps, linked together using Apache Airflow with Kubernetes. The five steps are: 1) Background correction, 2) Cell and region segmentation, 3) Cell classification, 4) Expression quantification, and 5) Spatial analysis. Background correction defines each channel in the staining panel by ensuring that there are no image artifacts that will interfere with subsequent steps. Segmentation is based on deep learning models that leverage multiple biomarker channels to delineate cells, including challenging ones that lack dsDNA signal in the plane of imaging. Cell classification uses deep learning models that leverage staining patterns alongside known phenotypic hierarchies to first define major cell lineages, then further divide them into specific sub phenotypes. Expression quantification calculates the expression levels for each checkpoint or inducible marker of interest and computes counts and densities of each cell phenotype. Lastly, spatial analysis allows for the quantitation of immune infiltration and various cell-to-cell and cell-to-region proximity features.

Results We demonstrate end-to-end analysis of multiple tissue types with diverse morphology and tissue architecture. The robust algorithms adapt to a wide range of tissue background and noise and achieve a high degree of accuracy in segmentation and classification. This obviates the need for multiple iterations and parameter tuning to optimize algorithm performance. The high-quality results generated by the framework have been used to discover interesting associations and spatial patterns of immune cells in the tumor microenvironment.

Conclusions We introduce an automated machine learning based framework for deep tissue profiling from MIBI images. The combination of pre-trained deep learning models connected through Airflow's directed acyclic graphs on a Kubernetes cluster, leads to a rapid and scalable bioinformatics solution for MIBI images that can be used to uncover novel biology.

Acknowledgements The authors would like to acknowledge Ablimit Keskin and Murat Aksoy for their contributions to the development of the framework.

REFERENCE

1. Keren L, Bosse M, Thompson S, Risom T, Vijayaragavan K, McCaffrey E, *et al.* Mibi-TOF: A multiplexed imaging platform relates cellular phenotypes and tissue structure. *Science Advances*. 2019;5(10).

<http://dx.doi.org/10.1136/jitc-2022-SITC2022.1294>

1295

SYSTEMS BIOLOGY ANALYSIS OF ANTI-TUMOR IMMUNITY

¹Mohammad Nikmaneshi*, ²James Baish, ¹Timothy Padera, ¹Lance Munn. ¹*Massachusetts General Hospital, Boston, MA, USA;* ²*Bucknell University, Lewisburg, PA, USA*

Background Initiation of an immune response requires activation of one or more naïve T cells. Each naïve T cell has a unique T cell receptor, and these cells traffic through the blood and lymphatic vasculatures, visiting each of the ~500 lymph nodes in search of matching antigen. If a match is made, then the naïve T cell activates and proliferates. This process is potentially rate-limiting, given the few naïve T cells capable of recognizing tumor antigen and the random nature of their entry into each lymph node. We propose that stochastic nature of this process affects the probability of T cell activation and may contribute to the poor response to ICB therapy seen in most patients.

Methods Here, we use multiscale computational modeling to identify potential reasons for clinical failure of immune checkpoint therapies and develop strategies for improving naïve T cell activation and tumor killing. The model provides a mechanistic framework for optimizing cancer immunotherapy and developing testable solutions to unleash anti-tumor immune responses for more patients with cancer.

Results The results show that tumor antigen production rate is a critical parameter, and that patients with low tumor antigen production rate need additional treatment to enhance antigen level and improve immune checkpoint inhibition therapy.

Conclusions The co-localization of antigen with appropriate naïve T cells is a critical step in immune activation, and affects the anti-tumor response in the context of immune checkpoint therapy.

<http://dx.doi.org/10.1136/jitc-2022-SITC2022.1295>

Abstracts

1296

RADIOMICS-BASED MULTI-MODAL PREDICTION OF TREATMENT RESPONSE TO PD-1/PD-L1 IMMUNE CHECKPOINT INHIBITOR (ICI) THERAPY IN STAGE IV NON-SMALL CELL LUNG CARCINOMA (MNSCLC)

¹Ravi Parikh*, ²Petr Jordan, ²Rita Ciaravino, ²Ryan Beasley, ³Arpan Patel, ⁴Dwight Owen, ⁵Arya Amini, ⁶Brendan Curti, ⁷Ray Page, ⁸Aurelie Swalduz, ⁹Jean-Paul Beregi, ¹⁰Jan Chrusciel, ³Eric Snyder, ¹¹Pritam Mukherjee, ¹¹Heather Selby, ¹²Soohee Lee, ¹³Roshanthi Weerasinghe, ¹²Shwetha Pindikuri, ¹⁴Jakob Weiss, ¹⁵Andrew Wentland, ¹⁶Anish Kirpalani, ⁵An Liu, ¹¹Olivier Gevaert, ¹⁷George Simon, ^{2,14}Hugo Aerts. ¹University of Pennsylvania, Philadelphia, PA, USA; ²Onc.AI, San Carlos, CA, USA; ³University of Rochester Medical Center, Rochester, NY, USA; ⁴The Ohio State University, Columbus, OH, USA; ⁵City of Hope, Duarte, CA, USA; ⁶Providence Cancer Institute, Portland, OR, USA; ⁷The Center for Cancer and Blood Disorders, Fort Worth, TX, USA; ⁸Centre Léon Bérard, Lyon, France; ⁹CHU Nîmes, Nîmes, France; ¹⁰Centre Hospitalier de Troyes, Troyes, France; ¹¹Stanford University, Palo Alto, CA, USA; ¹²Providence Health and Services, Renton, WA, USA; ¹³Providence St. Joseph Health, Portland, OR, USA; ¹⁴Massachusetts General Brigham, Boston, MA, USA; ¹⁵University of Wisconsin, Madison, WI, USA; ¹⁶University of Toronto, Toronto, Canada; ¹⁷Moffitt Cancer Center, Tampa, FL, USA

Background Currently approved biomarkers that predict response to ICIs in mNSCLC are limited to PD-L1 expression levels by immunohistochemistry (IHC) and tumor mutation burden (TMB). However, the predictive performance of PD-L1 IHC and TMB are limited, and rates of testing are suboptimal. Radiomic biomarkers may offer an automated and scalable method to predict ICI response.^{1,2} We developed and validated multi-modal models predicting responses to ICIs in mNSCLC. In contrast to previously published models, our work focuses on generalizable models using a large multi-institutional “real-world” dataset and combines radiomics features with demographic, molecular, and laboratory values routinely available in patients’ electronic medical records [EMR].

Methods We analyzed radiomic characteristics of 6,028 primary and metastatic lesions from 1,169 mNSCLC patients treated with anti-PD-1/anti-PD-L1 ICIs from 8 institutions across the US and Europe. Data were randomly split into training (N=707 patients, n=3,625 lesions) and validation (N=462 patients, n=2,403 lesions) sets. Baseline and follow-up CT scans were manually annotated by board-certified radiologists using RECIST 1.1 criteria and all lesion volumes were manually segmented. We developed two predictive models using gradient-boosted decision tree algorithms, using 1) only manually curated baseline radiomic features quantifying textural heterogeneity and spicularity; and 2) a multi-modal model with radiomic features combined with known demographic, molecular (e.g. PD-L1 IHC), and laboratory (e.g. neutrophil-to-lymphocyte ratio) predictors of ICI response. Primary endpoints were 3- and 6-month radiological progression, defined by a 20% increase in lesion diameter. The primary evaluation metric was the area under the receiver operating characteristic curve (AUC). Models predicting response of lung lesions and lymph nodes were validated on two cohorts: ICI monotherapy and ICI plus concurrent chemotherapy. Patients with unavailable PD-L1 IHC, imaging follow-up, or oncogenic driver mutations were excluded from analysis.

Results The radiomics model showed predictive accuracy comparable to tissue-based PD-L1 IHC for both endpoints and patient cohorts (tables 1, 2). However, the multi-modal model predicted lung and lymph node radiological progression with significantly higher AUC than PD-L1 IHC in all cohorts and endpoints, with 3- and 6-month progression AUCs of 0.86 (P=.00007) and 0.79 (P=.00001) in lung lesions and 0.78 (P=.003) and 0.80 (P=.002) in lymph nodes.

Conclusions Radiomics-based multi-modal prediction of ICI response is feasible and accurate and may provide an opportunity for more personalized management, such as risk-based escalation/de-escalation of concurrent chemotherapy in mNSCLC patients. We will evaluate this methodology in prospective studies.

REFERENCES

- 1. Trebesch S, Drago S, Birkbak N, Kurilova I, Celin A, Delli Pizzi A, Lalezari F, Lambregts D, Rohaan M, Parmar C, Rozeman E, Hartemink K, Swanton C, Haanen J, Blank C, Smit E, Beets-Tan R, Aerts H. Predicting response to cancer immunotherapy using noninvasive radiomic biomarkers. *Ann. Oncol.* 2019; **30**(6): 998–1004.
- 2. Sun R, Limkin E, Vakalopoulou M, Derclé L, Champiat S, Han SR, Verlingue L, Brandao D, Lancia A, Ammari S, Hollebecque A, Scozaec J, Marabelle A, Massard C, Soria J, Robert C, Paragios N, Deutsch E, Ferté C. A radiomics approach to assess tumour-infiltrating CD8 cells and response to anti-PD-1 or anti-PD-L1 immunotherapy: an imaging biomarker, retrospective multicohort study. *Lancet Oncol.* 2018; **19**(9): 1180–1191.

Ethics Approval Ethics approval for US data:

The study was conducted under IRB-approved procedures using de-identified data for patients diagnosed with Stage-IV NSCLC and treated between Jan. 1, 2017 and December 31, 2021. All records were de-identified per HIPAA guidelines at the institution level. Upon transfer, the data was quarantined and then re-inspected by authorized personnel prior to ingestion to ensure compliance and that no PHI was present in the records.

Ethics approval for EU data:

The study was conducted under IRB-approved procedures using de-identified data for patients diagnosed with Stage-IV NSCLC and treated between Jan. 1, 2017 and December 31, 2021. All records were de-identified per GDPR requirements at the institution level. The patients were also notified that their de-identified data would be part of a study and were given the required time and opportunity to respond if they had any objection. Upon transfer, the data was quarantined and then re-inspected by authorized personnel prior to processing to ensure compliance and that no PHI was present in the records.

Consent N/A

Abstract 1296 Table 1 Lung lesion assessment.

Biomarker	ICI monotherapy (N=125, n=232)		ICI plus chemotherapy (N=108, n=207)	
	3-month PFS AUC (95% CI)	6-month PFS AUC (95% CI)	3-month PFS AUC (95% CI)	6-month PFS AUC (95% CI)
Multi-modal	0.86** (0.79-0.92)	0.79** (0.72-0.86)	0.72** (0.63-0.82)	0.72** (0.63-0.82)
Radiomics	0.77 (0.68-0.86)	0.74 (0.66-0.83)	0.72* (0.60-0.83)	0.68 (0.57-0.78)
PD-L1 IHC	0.74 (0.69-0.80)	0.67 (0.60-0.74)	0.57 (0.52-0.63)	0.58 (0.54-0.63)

*/** indicates statistical significance of comparison to clinical standard (PD-L1 IHC) at the 5%/1% level under the two-tailed DeLong test.

Abstract 1296 Table 2 Lymph node assessment.

Biomarker	ICI monotherapy (N=99, n=285)		ICI plus chemotherapy (N=89, n=266)	
	3-month PFS AUC (95% CI)	6-month PFS AUC (95% CI)	3-month PFS AUC (95% CI)	6-month PFS AUC (95% CI)
Multi-modal	0.78** (0.70-0.87)	0.80** (0.72-0.88)	0.76** (0.65-0.86)	0.71* (0.60-0.81)
Radiomics	0.73 (0.62-0.84)	0.73 (0.63-0.83)	0.72 (0.58-0.85)	0.63 (0.50-0.76)
PD-L1 IHC	0.67 (0.57-0.76)	0.69 (0.60-0.77)	0.53 (0.42-0.63)	0.58 (0.51-0.65)

*/** indicates statistical significance of comparison to clinical standard (PD-L1 IHC) at the 5%/1% level under the two-tailed DeLong test.

http://dx.doi.org/10.1136/jitc-2022-SITC2022.1296

1297

UNCOVERING THE HIDDEN STRUCTURE OF T CELL COMPOSITIONS IN PERIPHERAL BLOOD AFTER IMMUNE CHECKPOINT INHIBITOR

Xiyu Peng*, Jasme Lee, Matthew Adamow, Colleen Maher, Margaret Callahan, Katherine Panageas, Ronglai Shen. *Memorial Sloan Kettering Cancer Center, New York, NY, USA*

Background Immune checkpoint inhibitors (ICIs) are a promising treatment option for many cancer patients, however heterogeneous outcomes within and across cancer types are a challenge in guiding treatment decisions. Additional biomarkers to guide the selective use of ICI would address an unmet clinical need. We have shown that pre-treatment peripheral blood immune characteristics detected by flow cytometry are related to clinical outcomes after ICI¹. Our goal is to further mine high-parameter flow cytometry data from blood samples obtained longitudinally during ICI treatment to explore ICI's immunological mechanisms and pharmacodynamics in cancer patients. However, the current field lacks effective statistical and computational approaches to take full advantage of this complex dataset.

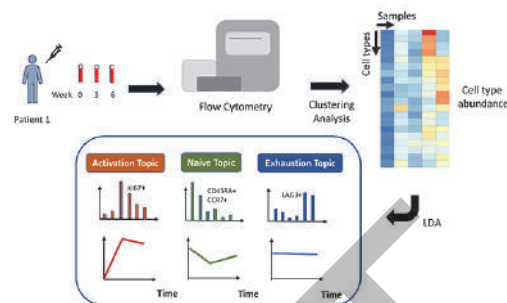
Methods We adapt a Latent Dirichlet Allocation (LDA) model, widely applied for topic discovery in text mining analysis, to explore the temporal evolution of T cell compositions from longitudinal single-cell flow cytometry data (figure 1). The LDA model considers cells as words, patient samples as documents, and biological processes as topics. With an analysis involving ~17 million T cells obtained from 138 pre- and on-treatment samples, we show the model's utility in delineating immune cell compositions and tracking dynamic changes over time in the peripheral blood from a cohort of 51 melanoma patients receiving combination CTLA-4 and PD-1 blockade. Without providing prior domain knowledge, LDA explores the hidden structure and identifies latent topics with great interpretability, allowing the discovery of possible clinical biomarkers.

Results We applied LDA and identified three latent topics in an unsupervised fashion; based on the topic contents, we labeled them the activation topic, naive topic, and exhaustion topic. The activation topic is mainly contributed by memory T cell clusters, which capture the major pattern of T cell expansion after ICI. The naive and exhaustion topics consist of naive T cell clusters and terminally differentiated T cell clusters, respectively. Patients with a large proportion of naive topics were shown to be more likely to experience severe ICI-related toxicity ($P = 0.02$). Moreover, the exhaustion topic is strongly related to the LAG⁺ immunotype, which has been linked to poor clinical outcomes in the earlier study¹.

Conclusions Here, we present a novel statistical and computational framework for investigating temporal dynamics of T cell compositions with the potential to characterize pharmacodynamics under ICI. We demonstrated LDA is effective in deconvoluting the high-parameter flow cytometry data and characterizes immunological topics that provide novel biological insights.

REFERENCE

1. Shen R, Postow MA, Adamow M, *et al.* LAG-3 expression on peripheral blood cells identifies patients with poorer outcomes after immune checkpoint blockade. *Sci Transl Med.* 2021;**13**:eabf5107.



Abstract 1297 Figure 1 LDA reveals hidden structures in flow cytometry data

<http://dx.doi.org/10.1136/jitc-2022-SITC2022.1297>

Abstracts

1298

A WEAKLY SUPERVISED DEEP LEARNING FRAMEWORK TO PREDICT KRAS-STK11 AND KRAS-TP53 CO-MUTATIONS IN LUNG ADENOCARCINOMAS USING H&E TISSUE SECTIONS

¹Daniel Jiménez-Sánchez*, ¹Carlos De Andrea, ¹Álvaro López-Janeiro, ¹María D Lozano, ²Carlos Ortiz-de-Solórzano, ¹Aida Romano-Martínez, ¹Cristina Sainz, ²Luis Montuenga, ¹Ignacio Melero, ²Ruben Pio. ¹Clinica Universidad de Navarra, Pamplona, Spain; ²Cima University of Navarra, Pamplona, Spain

Background Lung adenocarcinomas (LUAD) with co-mutations in KRAS (K-only) and the SKT11/LKB1 (KS) or TP53 (KP) genes define patient subgroups with distinct responses to anti-PD1/PD-L1 immunotherapy. In fact, multicentric studies showed that objective response rates to PD-1 blockade differed significantly among KS (7.4%), KP (35.7%), and K-only (28.6%) subgroups.¹ The association of such specific genetic profiling with morphological patterns assessed on routine H&E tissue slides may contribute to a better selection for personalized immunotherapy treatments.²

Methods We developed a weakly supervised deep learning³ (WSDL) model to predict the mutational status of LUAD patients using routine H&E tissue slides. N=125 KRAS-mutated patients with genomic profile available were obtained from two public databases (CPTAC⁴ and TCGA)⁵ and one in-house cohort (Clinica Universidad de Navarra). 59 patients were K-only, 36 KS, and 30 KP. Our developed model was composed of two neural networks. A convolutional neural network that learns cellular features from 90x90 pixel image patches unsupervisedly, and a graph neural network that learns patient-specific patterns using only the patient mutational status. Abundances of these patterns predict the patient's mutation type. To assess the predictive value of our WSDL model a five-fold cross-validation scheme was used. A Mann-Whitney test was applied to associate learned tissue patterns with patient mutations.

Results Figure 1(a) shows the ROC curves of the model for predicting patient co-mutations. AUC for K-only vs. KP mutations was 0.76 with a 95% CI of [0.66,0.86]. AUC for K-only vs. KS was 0.64 with a 95% CI of [0.54,0.75]. KP vs. KS was 0.78 with a 95% CI of [0.67,0.88]. Figure 1(b) shows, as an example, four WSDL-identified tissue patterns consisting of image patches containing acinar tumor, acinar tumor margin, stromal lymphocytes, and stroma. Figure 1(c) shows abundances of the total of tissue patterns learned showing the complex tumor heterogeneity across patient co-mutations. Figure 1(d) shows a tumoral stroma with absence of immune infiltration pattern that was associated with KS compared to KP (p=0.046). Figure 1(e) shows a mucinous pattern and tumor glands more frequent in KS compared to KP and K-only (p=0.008 and p=0.013, respectively).

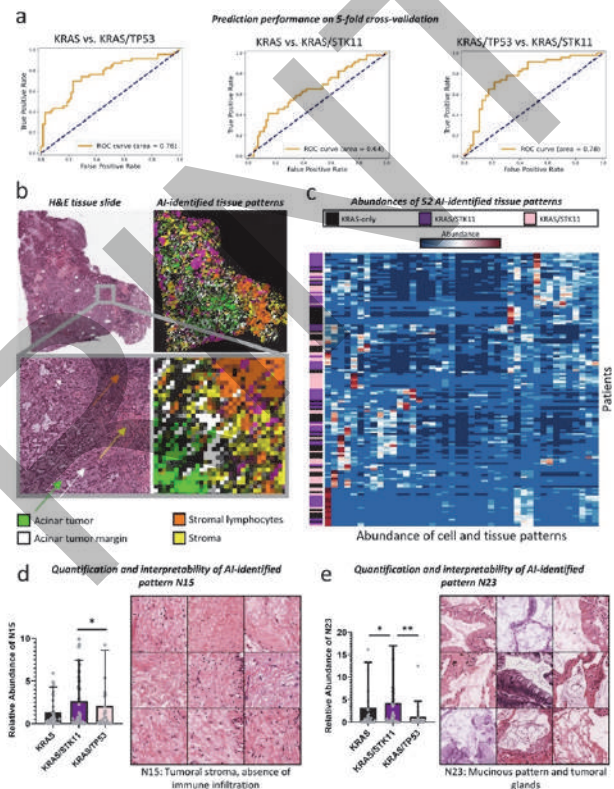
Conclusions WSDL learns tissue patterns without the requirement of manual expert annotations, potentially revealing previously unappreciated or underappreciated facets of the tumor linked to specific mutation types. This model can be especially useful in complex tasks such as the determination of LUAD co-mutations from H&E tissue slides. A validation study in two independent cohorts is ongoing.

REFERENCES

- Skoulidis F, Goldberg ME, Greenawalt DM, et al. STK11/LKB1 Mutations and PD-1 Inhibitor Resistance in KRAS-Mutant Lung Adenocarcinoma. *Cancer Discov.* 2018;**8**(7):822–835.
- Chen M, Zhang B, Topatana W, Cao J, Zhu H, Juengpanich S, Mao Q, Yu H, Cai X. Classification and mutation prediction based on histopathology H&E images in liver cancer using deep learning. *NPJ Precis Oncol.* 2020;**4**:14.

- Jiménez-Sánchez D, Ariz M, Chang H, Matias-Guiu X, de Andrea CE, Ortiz-de-Solórzano C. NaroNet: Discovery of tumor microenvironment elements from highly multiplexed images. *Med Image Anal.* 2022;**78**:102384.
- Gillette MA, Satpathy S, Cao S, et al; clinical proteomic tumor analysis consortium. proteogenomic characterization reveals therapeutic vulnerabilities in lung adenocarcinoma. *Cell.* 2020;**182**(1):200–225.e35.
- Cancer Genome Atlas Research Network. Comprehensive molecular profiling of lung adenocarcinoma. *Nature.* 2014 Jul 31;511(7511):543-50. doi: 10.1038/nature13385. Epub 2014 Jul 9. Erratum in: *Nature.* 2014 Oct 9;514(7521):262. Rogers, K [corrected to Rodgers, K]. Erratum in: *Nature.* 2018;**559**(7715):E12.

Ethics Approval The study was approved by the University of Navarra Ethics Board, approval number 2019.111



Abstract 1298 Figure 1 A framework to predict KRAS-STK11 and KRAS-TP53 mutations

(a) Receiver operating characteristic curves for pairs of patient mutations (k-only vs. KP, K-only vs. KS, and KP vs. KS). (b) H&E tissue slide and corresponding AI-identified tissue patterns, where colors represent patches assigned to different tissue patterns. (c) Abundance heatmap, where rows are patients and columns are tissue patterns, representing the complexity and heterogeneity of LUADs. (d,c) Quantifications of two tissue patterns across patient types, and the nine patches assigned to the tissue pattern with the highest confidence value. Useful to interpret tissue patterns learned by the model.

<http://dx.doi.org/10.1136/jitc-2022-SITC2022.1298>

1299

PREDICTING CD8+ CELL DENSITY AND TUMOR-IMMUNE PHENOTYPES IN NON-SMALL-CELL LUNG CANCER (NSCLC) FROM STANDARD H&E SLIDES USING DEEP LEARNING (DL)

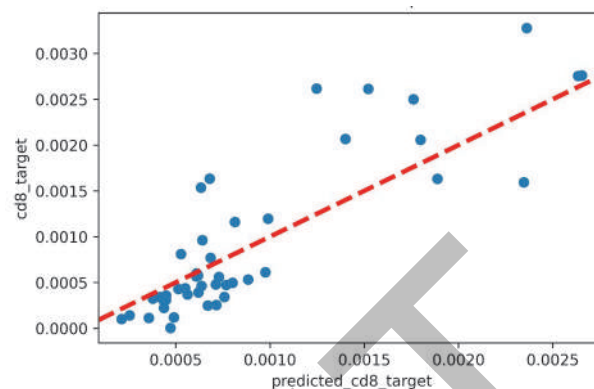
¹David Soong*, ²Becky Arbiv, ²Ettai Markovits, ²Alon Groisman, ²Yuval Shachaf, ²Tomer Dicker, ²Yoni Yedidia, ¹Hisham Hamadeh, ¹Kate Sasser, ²Gali Golan, ¹Brandon Higgs, ¹Suzana Couto, ²Ori Zelichov. ¹Genmab, Princeton, NJ, USA; ²Nucleai, Tel Aviv, Israel

Background Tumor infiltrated lymphocytes (TIL), namely CD8 + TILs play a major role in antitumor immunity and tumor cell eradication. High-density infiltration of CD8+ cells in the tumor, in contrast to CD8+ cell excluded regions, is associated with improved prognosis and response to immunotherapy in multiple cancer types, however, CD8 evaluations require IHC staining, often not performed routinely in clinical practice. Here, we used DL to predict CD8+ cell density and immune phenotypes from standard H&E slides.

Methods 188 pairs of H&E slide and a sequential CD8 stained slide from 103 patients with metastatic NSCLC were procured. DL models were trained to classify tumor cells, lymphocytes, fibroblasts, and tumor versus stromal areas on H&E, as well as positivity of CD8 per cell by IHC. 354 spatial features were calculated from the H&E slides and CD8+ density in the whole tumor region from IHC slides. A training (n=143) and test (n=45) cohort was created and linear regression modeling predicted CD8 density from H&E features. Two board certified pathologists classified IHC slides into immune phenotypes: inflamed, desert and excluded, based on CD8 density (table 1) and a multinomial logistic regression model was train to predict these phenotypes from the H&E images.

Results The H&E features most predictive of CD8 density were related to lymphocyte densities, tumor-lymphocyte proximity in the invasive margin, and lymphocyte density in the tumor area. Correlation using this 3 H&E feature model on the test set was r=0.87 (p<0.0001, figure 1). The H&E features most predictive to immune phenotype were proximity between lymphocytes and tumor cells or granulocytes, as well as lymphocyte:fibroblast density ratio. Model accuracy on the test set reached an accuracy of 74% (95% CI 57%-85%, p<0.0001) in classifying slides to the correct immune phenotypes.

Conclusions Spatial analysis of immune and tumor cells from standard H&E slides using DL can accurately predict CD8 cell density and identify immune phenotypes. By only requiring H&E images, these biomarkers important for checkpoint inhibitor therapy can be measured in clinical practice without the requirement of IHC staining.



Abstract 1299 Figure 1 Correlation between test set predicted CD8 density from H&E analysis and real test set CD8 density calculated on IHC slides

<http://dx.doi.org/10.1136/jitc-2022-SITC2022.1299>

Abstract 1299 Table 1 Criteria for Immune Phenotyping

Immune phenotype	Criteria
Inflamed	Density of CD8 positive lymphocytes in the tumor cell area > 5%
Excluded	CD8+ lymphocyte presence in >50% of the invasive margin in a non-inflamed slide
Desert	Criteria for inflamed or excluded do not apply

Abstracts

1300

CT SCAN NORMALIZATION TO IMPROVE RADIOMICS GENERALIZABILITY AND ASSESS PROGRESSION-FREE SURVIVAL IN PATIENTS WITH ADVANCED NON-SMALL CELL LUNG CANCER TREATED WITH IMMUNE CHECKPOINT INHIBITORS: A MULTICENTRIC STUDY

¹Marion Tonneau*, ²Kim Phan, ²Cécile Low-Kam, ²Francis Dutil, ³Suzanne Kazandjian, ⁴Davy Vanderweyten, ³Justin Panasci, ¹Julie Malo, ⁵François Coulombe, ¹Arielle Elkrief, ¹Wiam Belkaïd, ²Lisa Di Jorio, ⁵Michèle Orain, ⁶Nicole Bouchard, ³Thierry Muanza, ²Kam Kafi, ²Florent Chandelier, ³Philippe Joubert, ¹Bertrand Routy. ¹CRCHUM, Montréal, Canada; ²Imagia Canexia Health, Montreal, Canada; ³Jewish General Hospital, Montreal, Canada; ⁴Centre Hospitalier de Sherbrooke, Sherbrooke, Canada; ⁵IUCPQ, Québec, Canada; ⁶CHUS, Sherbrooke, Canada

Background Recent development in the field of artificial intelligence suggests that radiomics may represent a promising non-invasive biomarker to predict response to immune checkpoint inhibitors (ICI). Nevertheless, validation of radiomics algorithms in independent cohorts remains a challenge in part due to variations in image acquisition and reconstruction. Using radiomics as a biomarker for ICI response in non-small cell lung cancer (NSCLC) patients, we investigated the importance of scan normalization as part of a broader statistical framework to enable model external generalizability.

Methods Discovery cohort was composed of pre-ICI CT scans of 514 advanced NSCLC patients from three academic centers (n=223 CHUM, n=130 JGH and n=161 IUCPQ). A validation cohort included 144 patients from a fourth center (CHUS). Power calculation for the validation cohort was determined with an AUC threshold of 0.67 in the discovery cohort to predict progression-free survival at 6 months (PFS-6), alpha-risk was 0.10, leading to n=140 patients. Radiomics features were extracted from original clinical scans using the established open source PyRadiomics, and a proprietary DeepRadiomics technology (leveraging deep learning). We harmonized images to account for variations in reconstruction kernels, slice thicknesses, and device manufacturers. Multivariable models, evaluated using leave-one-center-out cross validation, were used to estimate the predictive value of clinical variables (ECOG, line of treatment, stage, smoking), PD-L1 expression, and PyRadiomics or DeepRadiomics for PFS-6.

Results In this cohort, the best prognostic factor for PFS-6 excluding radiomics, was combination of clinical + PD-L1 expression with an AUC of 0.66 and 0.62 in the discovery and validation cohort. Without image harmonization, combining clinical + PyRadiomics or DeepRadiomics, AUC were 0.69 and 0.69 respectively in the discovery cohort, but depicting significant drops to 0.57 and 0.52, respectively in the validation cohort. This lack of generalizability was consistent with observations in principal component analysis clustering by center. Subsequently, image harmonization eliminated these clusters and when combining clinical + DeepRadiomics model, we obtained an AUC of 0.67 and 0.63 in the discovery and validation cohort, respectively. The combination of clinical + PyRadiomics failed generalizability validations, with AUC of 0.66 and 0.59, without improvement with the addition of PD-L1 (table 1).

Conclusions We demonstrated that a risk prediction model that combined clinical + DeepRadiomics was generalizable and had similar performances to clinical + PD-L1, when scan harmonization methods were in place. Altogether, this study showed the strong potential of radiomics as a future non-invasive strategy to predict ICI response in advanced NSCLC.

Ethics Approval Number of the approval: MP-02-2019-8091

Abstract 1300 Table 1 Area under the curve (AUC) and confident interval of clinical, clinical + PD-L1, clinical + PyRadiomics and clinical + DeepRadiomics models, in the discovery and validation cohorts, before and after scans harmonization.

Table 1 – Area under the curve (AUC) and confident interval of clinical, clinical + PD-L1, clinical + PyRadiomics and clinical + DeepRadiomics models, in the discovery and validation cohorts, before and after scans harmonization.

	Before scans harmonization		After scans harmonization	
	Discovery cohort	Validation cohort	Discovery cohort	Validation cohort
Clinical	0.64 95%CI [0.59-0.69]	0.58 95%CI [0.49-0.69]	-	-
Clinical + PD-L1	0.66 95%CI [0.61-0.70]	0.62 95%CI [0.51-0.71]	-	-
Clinical + PyRadiomics	0.69 95%CI [0.64-0.74]	0.57 95%CI [0.48-0.67]	0.66 95%CI [0.61-0.70]	0.59 95%CI [0.49-0.68]
Clinical + DeepRadiomics	0.69 95%CI [0.65-0.74]	0.52 95%CI [0.43-0.62]	0.67 95%CI [0.63-0.72]	0.63 95%CI [0.53-0.73]

<http://dx.doi.org/10.1136/jitc-2022-SITC2022.1300>

1301 **CONDITIONAL BISPECIFIC T CELL ENGAGER DESIGN AND DOSING OPTIMIZATION VIA MECHANISTIC MODELING**

Jess Wu*, Michael Vilkhovoy, Sara Shum, Johara Chouitar, Patrick LeRoy, Leticia Fridman, Eilene Kwok, Glendon Wu, Matyas Ecsedi, Antara Banerjee, Dean Bottino. *Takeda Pharmaceuticals, Inc., San Diego, CA, USA*

Background Conditionally activated bispecific T cell engagers (TCEs) have the potential to provide a larger therapeutic window by reducing off-site on-target toxicity. Conditionally Bispecific Redirected Activation (COBRAs) are novel TCEs designed to be activated preferentially in the tumor microenvironment (TME).^{1,2} The conditionality of the COBRA prodrug is mediated upon binding of the high affinity target binding domain to the tumor antigen and by cleavage of the prodrug by matrix metalloproteases such as MMP9/2. The cleavage of the prodrug results in the release of the inactive CD3e VH/VL domains leading to the formation of the active dimer, responsible for tumor killing. In order to understand the dependence of treatment effect on drug and patient properties for this novel modality, we developed a mathematical model of COBRA's mechanism of action.

Methods A mechanistic model was developed to describe the preclinical pharmacokinetics, target engagement and immune synapse formation in the TME, and tumor volume change due to resulting T-cell dependent tumor cell-mediated cytotoxicity (TDCC). Unknown parameters were optimized using *in vitro* TDCC data and *in vivo* efficacy data. Sensitivity analyses were conducted to investigate the influence of molecule- and TME-specific characteristics on synapse formation and treatment effect.

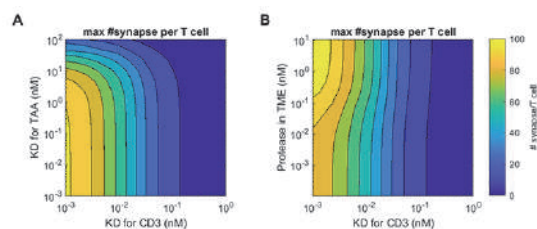
Results The model recapitulates the experimental data *in vitro* and *in vivo*. We used the model to identify parameters that govern the synapse formation and treatment outcome, such as COBRA affinity to TAA and CD3 (figure 1A), and the active protease concentration in the TME (figure 1B). The model also suggests that the drug-induced antigen internalization along with the abundance of target cells and effector T cells can impact the predicted treatment effect of COBRA and that COBRA concentration-synapse formation relationship does not exhibit the bell-shaped TCE concentration-synapse profile due to its conditionality on homodimerization once cleaved.

Conclusions The model framework was used to integrate pre-clinical datasets and project the short-term treatment response in human. This work demonstrates the impact of conditionality of the COBRA design on its dose-response relationship. Importantly, factors such as target abundances and protease activity in the TME can strongly influence synapse formation and the resulting anti-tumor effect, and therefore may serve as baseline biomarkers for patient stratification.

REFERENCES

1. Dettling DE, Kwok E, Quach L, Datt A, Degenhardt JD, Panchal A, *et al.* Regression of EGFR positive established solid tumors in mice with the conditionally active T cell engager TAK-186. *J Immunother Cancer.* 2022;**10**(6). Epub 2022/06/22. doi: 10.1136/jitc-2021-004336. PubMed PMID: 35728872.
2. Panchal A, Seto P, Wall R, Hillier BJ, Zhu Y, Krakow J, *et al.* COBRA: a highly potent conditionally active T cell engager engineered for the treatment of solid tumors. *MAbs.* 2020;**12**(1):1792130. Epub 2020/07/21. doi: 10.1080/19420862.2020.1792130. PubMed PMID: 32684124; PubMed Central PMCID: PMC7531513.

Ethics Approval The animal study protocol received ethics approval by In-Vivo Technologies, Inc Institutional Animal Care and Use Committee IVT-17-002-Y6.



Abstract 1301 Figure 1 Local sensitivity analysis showing the effect on the maximal number of synapses formed by varying KD for CD3 and A) KD for the TAA or B) the active protease concentration in the TME

<http://dx.doi.org/10.1136/jitc-2022-SITC2022.1301>

Abstracts

1302

SPATIAL ANALYSIS OF THE TUMOR MICROENVIRONMENT USING MACHINE LEARNING-ENABLED INTEGRATED MORPHOLOGY-TRANSCRIPTOMIC CELL PHENOTYPES

¹Wei Yan*, ¹Nga Luong, ²Jeffrey Lim, ²Yuezhen Xue, ¹Abu Bakr Azam, ²Joe Poh Sheng Yeong, ²Mai Chan Lau, ¹Yiyu Cai. ¹Nanyang Technological University, Singapore, Singapore; ²Institute of Molecular and Cell Biology, Singapore, Singapore

Background In recent years, immunotherapy has advanced the cancer field by achieving more durable patient response with a relatively tolerable toxicity. However, the overall response rates remain low (< 20%),¹ mainly due to a lack of understanding of the underlying tumor-immune interactions that determine patient responsiveness. Existing tissue-based assays are restricted to dozens of known transcriptomic or proteomic markers, limiting their usefulness in generating new immunological insights. While recently emerged spatial transcriptomics (ST) technology enables an unbiased whole-transcriptomic profiling, it does not provide single-cell resolution read-outs,² leading to potential masking of rare cell signals and loss of cell-to-cell spatial information. Here, we propose a machine learning (ML) approach to characterize single-cell phenotypic traits, through integrating haematoxylin and eosin (H&E) histology and ST data.

Methods One tumor and one adjacent-normal tissue section collected from a hepatocellular carcinoma (HCC) patient were profiled using 10× Visium ST platform. Using the companion H&E image, tissue regions were categorized as tumor epithelium and stroma, and individual cells were segmented (StarDist) with 53 histological features extracted (QuPath v0.3.2). Unsupervised cell clustering and cluster-specific gene signatures were determined simultaneously whereby genetic algorithm was used for feature selection and gene signatures were obtained by deconvoluting ST. Optimal clustering results were determined through maximizing clustering quality and cell-type specificity for individual clusters, where single-sample gene set enrichment on PanglaoDB database was used for cell-type annotation.

Results More immune cells infiltrated into epithelium in the adjacent-normal tissue (18.2% of total 17,480 stromal cells) as compared to that of the tumor tissue (11.6% of total 10,807 stromal cells). Cell clusters with strong T-cell and B-cell signatures were detected in both tissues (figure 1), with higher tumor infiltration in the adjacent-normal tissue (~16% of the total T or B cells, respectively; figure 2) than in the tumor tissue (~5% of the total T or B cells, respectively). Despite the same morphological feature, i.e., nucleus-to-cell area ratio, was selected in both tissues, comparable values were observed in T and B-cells (~0.56) within the adjacent-normal tissue, whereas an average higher area ratio of B-cells (~0.52) than T-cells (~0.47) within the tumor tissue (figure 3).

Conclusions Our data suggests that, during tumorigenesis, T-cells might undergo morphological changes, and reduced T and B-cells infiltration into the epithelium. Our proposed ML approach not only allows single-cell spatial analysis of tumor-immune interactions, but also provides more refined cell phenotypes defined by both morphology and transcriptomic features.

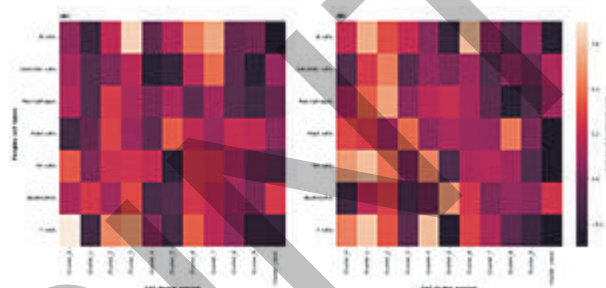
Acknowledgements We would like to acknowledge the funding support from Nanyang Technological University – URECA Undergraduate Research Programme for this research project.

REFERENCES

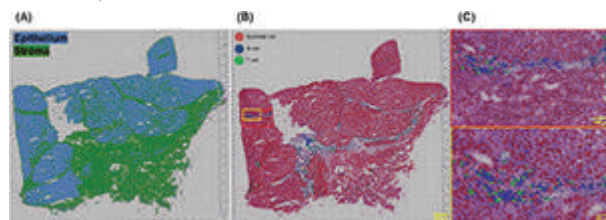
1. Jiang P, Gu S, Pan D, *et al.* Signatures of T cell dysfunction and exclusion predict cancer immunotherapy response. *Nat Med.* 2018;**24**(10):1550–1558. doi:10.1038/s41591-018-0136-1
2. Yang Y, Shi X, Liu W, *et al.* SC-MEB: spatial clustering with hidden Markov random field using empirical Bayes. *Brief Bioinform.* 2022;**23**(1):bbab466. doi:10.1093/bib/bbab466

Ethics Approval This study was approved by the SingHealth Centralized Institutional Review Board (reference numbers: 2018/3045 and 2019/2653)

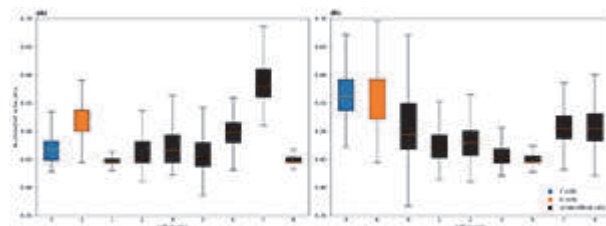
Consent The patients provided their written informed consent to participate in this study.



Abstract 1302 Figure 1 Heat maps of single-sample gene set enrichment (ssGSEA) scores of cell clusters identified at the optimal setting. (A) In the HCC tumor tissue, cluster 0 and cluster 3 demonstrated strong T-cell and B-cell signatures, respectively. (B) in the HCC adjacent-normal tissue, cluster 4 and cluster 6 demonstrated moderate T-cell and B-cell signatures, respectively. Other clusters demonstrated mixed signatures of multiple cell-types



Abstract 1302 Figure 2 Spatial localization of morphology-transcriptome-defined T cells, B cells and epithelial cells in the HCC adjacent-normal tissue. (A) ML-classified epithelial and stromal regions. (B-C) Cellular location of the epithelial, T, and B cells within the tissue space



Abstract 1302 Figure 3 Distribution of morphological feature, nucleus-to-cell area ratio, across the identified cell clusters in (A) the tumor tissue, and (B) adjacent-normal tissue

<http://dx.doi.org/10.1136/jitc-2022-SITC2022.1302>

1303 **PREDICTION OF BEST RESPONSE FOR NSCLC PATIENTS RECEIVING IMMUNOTHERAPY BY MACHINE LEARNING MODELS**

¹Yili Zhang*, ¹Samir Gupta, ¹Anas Belouali, ¹Shaked Lev-Ari, ²Neil Shah, ¹Kanchi Krishnamurthy, ¹Micheal Serzan, ¹Adil Alaoui, ¹Peter McGarvey, ¹Michael Atkins, ¹Subha Madhavan. ¹Georgetown University, Washington DC, DC, USA; ²Memorial Sloan Kettering Cancer Center, New York, NY, USA

Background Immune checkpoint inhibitors (ICIs) have been used to treat many distinct cancers, including non-small cell lung cancer (NSCLC). Better tools are needed to predict which patients will benefit from ICI therapy. This study aims to use machine learning (ML) models to predict the tumor response of patients with NSCLC to immunotherapy.

Methods The Georgetown-Lombardi Comprehensive Cancer Center has developed a centralized Immuno-Oncology (IO) registry encompassing patients treated with ICI within the MedStar Health hospital system from 2011 until April 2018. Data on demographics, immunotherapy information, and lab tests after diagnosis for 220 NSCLC patients were collected from the registry. Responses included complete response (CR), partial response (PR), progressive disease (PD), and stable disease (SD) at 12 weeks from starting the immunotherapy. In this study, we predicted if patients responded to the immunotherapy (CR and PR) or not (PD and SD). Ten ML models were employed for binary prediction with five-fold cross-validation adopted. The area under the receiver-operating curve (AUROC) was used to assess ML model, and important features affecting the model were subsequently analyzed.

Results Among curated patients, 74 (33.64%) responded to the immunotherapy. Nivolumab was used in 107 (48.38%) patients, followed by carboplatin + pembrolizumab + pemetrexed in 20 (9.09%) patients. Ten ML models were performed such as logistic regression, support vector machine, naive Bayesian (NB), random forest, and Bernoulli NB. The AUROC values for the top three performing models were logistic regression (77.91%), naive Bayesian (73.93%), and random forest (73.88%). The 3 most important features selected from the logistic regression model are A/G ratio, line of therapy, and pre-treatment ECOG PS. Features considered unimportant include age, sex, BMI, ALT (SGPT), AST (SGOT).

Conclusions This study leveraged ML algorithms to predict the tumor response to ICI therapy for patients with NSCLC. This novel approach utilizing EMR in the computational models can help predict the outcome of ICI therapy in patients with NSCLC. The best prediction model had an AUROC score of 77.91%. The limitations of this study are the relatively small sample size and the lack of molecular information. These will be addressed with the updating and expansion of the IO registry participation of other institutions and linking to a growing collection of omics data together leading to more robust ML models.

<http://dx.doi.org/10.1136/jitc-2022-SITC2022.1303>

Microbiome and Other Environmental Factors

1304

DIETARY PATTERNS ASSOCIATED WITH INCREASED ABUNDANCE OF *AKKERMANSIA MUCINIPHILA* POTENTIATES ANTI-PD-L1 IMMUNE CHECKPOINT BLOCKADE RESPONSE IN TRIPLE-NEGATIVE BREAST CANCER

Kenysa Clear*, Elizabeth Stirling, Adam Wilson, David Soto-Pantoja, Katherine Cook. Wake Forest School of Medicine, Winston-Salem, NC, USA

Background Immune checkpoint blockade (ICB) therapies targeting programmed cell death protein 1 pathway (PD-1/PD-L1) have advantageously impacted triple-negative breast cancer (TNBC) patient survival; however, there remains a need to improve responses. Recent studies associated gut *Akkermansia muciniphila* as an ICB-response related microbe in other cancer types. As diet is a main modifier of the gut microbiome, we investigated whether diet-gut microbiome interactions potentiate ICB response in TNBC.

Methods Using EMT-6 (n=5-7/group) and E0771 (n=8-10/group) syngeneic models of TNBC, tumor-bearing mice consuming low-fat control, high-fat Western, or a Mediterranean diet were treated with 200 µg of IgG or anti-PD-L1 antibodies and response to therapy was determined by tumor progression. To assess modulation on the gut bacterial microbiome by diet and ICB, 3M read depth metagenomic sequencing was performed on DNA isolated from fecal samples from both models. To further implicate the microbiome, we performed a fecal microbiota transplant (FMT) model (n=8-10/group), where mice consuming a control diet were supplemented via oral gavage with either a control diet-derived FMT, a Western diet-derived FMT, or Mediterranean diet-derived FMT. EMT-6 bearing-mice on each FMT were treated with IgG or PD-L1. Immune response (F4/80 macrophages, granzyme B, and CD8 + cytotoxic T cell infiltrate) in the tumor microenvironment (TME) were examined in residual tumor tissue by immunohistochemistry (n=9/group). Regulation of PD-L1 protein by diet was assessed by Western blot hybridization in tumor sample lysates (n=3/group). Short chain fatty acid (SCFA) analysis was measured in plasma (n=8/group) by LC/MS-MS metabolomics.

Results In EMT-6 bearing-mice, PD-L1 treatment and consumption of a Western or Mediterranean diet significantly reduced both tumor volume and tumor weight when compared to control diet-fed mice (p<0.05). In E0771 bearing-mice, consumption of a Western diet and PD-L1 treatment resulted in a modest increase in ICB response (56%), with the highest efficacy observed in Mediterranean diet-fed mice (70%), when compared with IgG control animals. Western and Mediterranean-fed mice displayed a 25-45% increase in gut *Akkermansia muciniphila* proportional abundance. Anti-PD-L1 therapy in mice given an *A. muciniphila* enriched FMT showed enhanced ICB responsiveness (p<0.05, 70-80%). Mediterranean-diet fed animals treated with anti-PD-L1 antibodies showed elevated plasma butyrate SCFA metabolites. E0771 model results show Western and Mediterranean diet intake regulated expression of PD-L1, macrophages, and cytotoxic T cell function proteins in the TME.

Conclusions Taken together, these data indicate PD-L1 response in TNBC is potentiated by diet-microbiota

interactions and suggests increasing levels of *Akkermansia* may enhance ICB efficacy.

Acknowledgements Kenysa YJ. Clear 1, BS, Elizabeth R. Stirling 1, MS, PhD, Adam S. Wilson 1, David R. Soto-Pantoja 1,2, PhD, Katherine L. Cook 1,2, PhD

1 Department of Surgery, Wake Forest University School of Medicine, Winston-Salem, NC, USA

2 Comprehensive Cancer Center, Wake Forest University School of Medicine, Winston-Salem, NC, USA

Ethics Approval Animal studies were approved by the Institutional Animal Care and Use Committee (IACUC) of Wake Forest University Health Sciences, protocol number(s) A18-088 and A20-010.

<http://dx.doi.org/10.1136/jitc-2022-SITC2022.1304>

1305

IMPACT OF TET2-MUTANT CLONAL HEMATOPOIESIS ON SOLID TUMOR IMMUNOLOGY AND RESPONSE TO CHECKPOINT BLOCKADE

Shelley Herbrich*, Swetha Anandhan, Padmanee Sharma. MD Anderson Cancer Center, Houston, TX, USA

Background Clonal hematopoiesis (CH) is an age-related phenomenon characterized by the overrepresentation of blood cells arising from a single, mutant clone and is detectable in 10-20% of individuals over 70.¹ CH has now been implicated in a variety of non-hematological disorders, such as cardiovascular diseases and Covid-19 infections, by exacerbating the innate inflammatory response.²⁻⁴ However, the impact of CH in solid tumors and response to immune checkpoint blockade (ICB) is unknown.

Methods To assess the prevalence and role of CH in patients with solid tumors, we analyzed publicly available data from the MSKCC-IMPACT study.^{5, 6} To mechanistically study CH in solid tumors, we established an orthotopic model of pancreatic adenocarcinoma (PDAC) in mice with *Tet2*^{+/-} CH. CH and WT mice were treated with either ICB (α CTLA-4 + α PD-1) or vehicle control. Single-cell (sc-) RNAseq was performed on tumor infiltrating lymphocytes (n=3/group) while remaining mice were observed for disease progression and overall survival (n=10/group).

Results Analyzing CH frequencies in a cohort of patients with solid tumors, we observed that the prevalence of CH was approximately 5 times higher in patients with cancer when compared to healthy age-matched controls. Further, patients with detectable CH clones had significantly worse overall survival (figure 1A). *In vivo*, sc-RNAseq data revealed that myeloid cells present within the pancreatic tumors of mice with *Tet2*^{+/-} CH were significantly enriched for both type I and type II interferon (IFN) signaling (figure 1B). Further, these IFN+ myeloid cells were ablated after ICB therapy in *Tet2*^{+/-} WT mice but persisted in mice with *Tet2*^{+/-} CH (figure 1C). PDAC tumors from mice with *Tet2*^{+/-} CH had approximately half the total number of infiltrating CD8 T cells at baseline when compared to those from *Tet2*^{+/+} WT mice. Upon ICB treatment, CD8 effector cells only expanded in the tumors from *Tet2*^{+/+} WT mice. Functionally, this translated to more rapidly progressing tumors, resistance to ICB, and reduced overall survival in mice with *Tet2*^{+/-} CH (figure 1D).

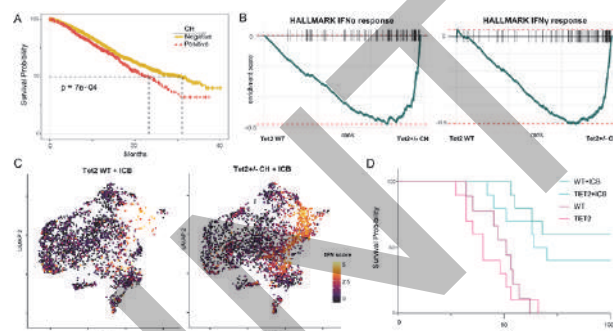
Conclusions CH is present in upwards of 30% of patients with solid tumors and is associated with significantly worsened prognosis. Modeling PDAC in the presence of *Tet2*^{+/-} CH *in vivo* revealed distinct alterations in the tumor microenvironment that ultimately influenced tumor progression and response to ICB. This proposed research bridges the fields of solid tumor immunology and clonal hematopoiesis to address novel mechanisms of immunotherapy resistance that will span cancer type and, ultimately, improve patient care.

REFERENCES

1. Steensma DP, Bejar R, Jaiswal S, *et al*. Clonal hematopoiesis of indeterminate potential and its distinction from myelodysplastic syndromes. *Blood* 2015;**126**(1):9-16.
2. Jaiswal S, Natarajan P, Silver AJ, *et al*. Clonal hematopoiesis and risk of atherosclerotic cardiovascular disease. *N Engl J Med* 2017;**377**(2):111-21.
3. Jaiswal S, Fontanillas P, Flannick J, *et al*. Age-related clonal hematopoiesis associated with adverse outcomes. *N Engl J Med* 2014;**371**(26):2488-98.
4. Bolton KL, Koh Y, Foote MB, *et al*. Clonal hematopoiesis is associated with risk of severe Covid-19. *Nat Commun* 2021;**12**(1):5975.
5. Bolton KL, Ptashkin RN, Gao T, *et al*. Cancer therapy shapes the fitness landscape of clonal hematopoiesis. *Nat Genet* 2020;**52**(11):1219-26.

6. Coombs CC, Zehir A, Devlin SM, *et al*. Therapy-related clonal hematopoiesis in patients with non-hematologic cancers is common and associated with adverse clinical outcomes. *Cell Stem Cell* 2017;**21**(3):374-82 e4.

Ethics Approval All mice were housed in accordance with the Association for Assessment and Accreditation of Laboratory Animal Care and NIH standards. Experiments were conducted according to protocol 00000893-RN02 and approved by the University of Texas MD Anderson Cancer Center Institutional Animal Care and Use Committee.



Abstract 1305 Figure 1

<http://dx.doi.org/10.1136/jitc-2022-SITC2022.1305>

Abstracts

1306

PREVENTION OF ANTIBIOTIC-INDUCED DYSBIOSIS IN HUMAN VOLUNTEERS BY DAV132 AND PRESERVATION OF RESPONSIVENESS TO ANTI-PD-1 THERAPY DEMONSTRATED BY TRANSPLANTATION OF HUMAN FECES INTO TUMOR-BEARING MICE

¹Meriem Messaoudene*, ²Nathalie Saint-Lu, ²Frédérique Sablier-Gallis, ²Stéphanie Ferreira, ²Clément Le Bescop, ²Thomas Loppinet, ¹Mayra Ponce, ³Céline Féger, ²Antoine Andreumont, ²Jean De Gunzburg, ¹Bertrand Routy. ¹CRCHUM – Centre de recherche du CHUM, Montreal, Canada; ²Da Volterra, Paris, France; ³EMI Biotech, Paris, France

Background Antibiotics (ATB) induce intestinal dysbiosis and decrease the efficacy of immune checkpoint inhibitors (ICI).^{1,2} DAV132 is an orally administered colon-targeted ATB adsorbent designed to prevent ATB-induced dysbiosis.³ We investigated whether DAV132 co-administered with ATB could protect gut microbiota diversity and composition. Moreover, in murine avatar tumor model, we assessed anti-PD-1 efficacy through fecal microbiota transplantation (FMT) in germ-free (GF) or antibiotic-treated specific pathogen-free (SPF) mice.

Methods Twenty-four human healthy volunteers (HV) were randomized to receive either ceftazidime-avibactam (CZA, 2g/0.5g q8h IV for 5 days) or CZA+DAV132 (12g PO tid for 7 days). CZA plasmatic and fecal pharmacodynamic levels were measured using HPLC-MS/MS. Microbiome was profiled with 16S and shotgun metagenomics at different timepoints. FMT in GF or ATB-treated SPF mice was performed using fecal samples from 3 HV and 2 HV respectively, in each group before (D1) or after 6 days (D6) of CZA+/-DAV132; subsequently mice were inoculated with MCA-205 tumor and treated intraperitoneally with anti-PD-1, 4 times every 3 days. Immunological population of tumor infiltrating lymphocytes were analyzed by flow cytometry.

Results DAV132 did not impact plasmatic CZA concentrations, but significantly reduced ceftazidime concentration in feces compared to HV treated with CZA alone (p<0.001). DAV132 significantly prevented the reduction in microbiota alpha-diversity at D6 (p=0.0019) and was associated with a more rapid return to baseline microbiota composition (figure 1). Significantly more bacteria associated with better response to ICI were preserved in the DAV group compared to CZA, among which *Faecalibacterium prausnitzii* and several *Alistipes spp.* FMT in GF mice transplanted with feces collected at D1 exhibited a significant anti-PD-1 activity. This anti-tumor response was inhibited in mice transplanted with D6 feces from any of the 3 CZA-treated HV. Conversely, the anti-tumor response was maintained in mice transplanted with D6 feces from any of the 3 HV treated with CZA + DAV132 (figure 2). Similar results were observed upon FMT using samples from HVs into ATB-treated SPF mice. Flow cytometry on tumor T cell infiltrates demonstrated that CZA decreased CD8⁺T cell infiltration and CD8⁺/Tregulatory ratio, compared to CZA + DAV132 treated HVs (figure 3).

Conclusions DAV132 strongly prevented CZA-induced dysbiosis in HV without influencing plasmatic concentrations. In avatar mice FMT from HV treated with CZA+DAV132 was able to preserve anti-PD-1 cancer efficacy. These results provide rationale to launch clinical trials combining DAV132 in patients on ATB amenable to ICI.

Acknowledgements This work was funded by Da Volterra, a French biotech company, through the sharing of fecal samples and a collaboration agreement with Pr. Routy's lab.

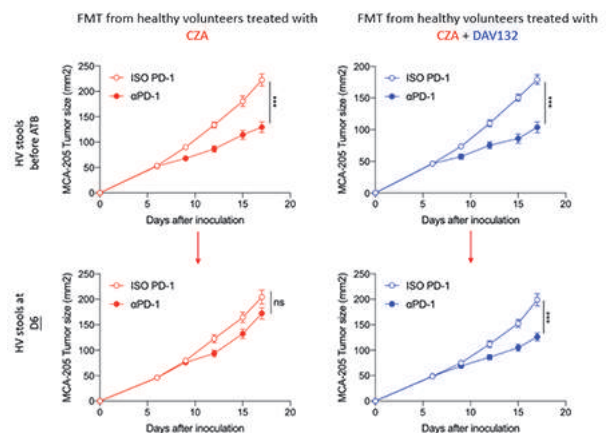
REFERENCES

1. Derosa L, Routy B, Desilets A, Daillère R, Terrisse S, Kroemer G, Zitvogel L. Microbiota-centered interventions: the next breakthrough in Immuno-Oncology? *Cancer Discov.* 2021;**11**(10):2396–2412.
2. Routy B, Le Chatelier E, Derosa L, Duong CPM, Alou MT, Daillère R, Fluckiger A, Messaoudene M, Rauber C, Roberti MP, Fidelle M, Flament C, Poirier-Colame V, Opolon P, Klein C, Iribarren K, Mondragón L, Jacquetot N, Qu B, Ferrere G, Clémenson C, Mezquita L, Masip JR, Naltet C, Brossseau S, Kaderbhai C, Richard C, Rizvi H, Levenez F, Galleron N, Quinquis B, Pons N, Ryffel B, Minard-Colin V, Gonin P, Soria JC, Deutsch E, Loriot Y, Ghiringhelli F, Zalcman G, Goldwasser F, Escudier B, Hellmann MD, Eggermont A, Raoult D, Albiges L, Kroemer G, Zitvogel L. Gut microbiome influences efficacy of PD-1-based immunotherapy against epithelial tumors. *Science.* 2018;**359**(6371):91–97.
3. Vehrenchild MJGT, Ducher A, Louie T, Cornely OA, Feger C, Dane A, Varastet M, Vitry F, de Gunzburg J, Andreumont A, Menétré F, Wilcox MH. An open randomized multicenter Phase 2 trial to assess the safety of DAV132 and its efficacy to protect gut microbiota diversity in hospitalized patients treated with fluoroquinolones. *J Antimicrob Chemother.* 2022;**77**(4):1155–1165.

Ethics Approval All animal studies were approved by the Institutional Animal Care Committee (CIPA) and carried out in compliance with the Canadian Council on Animal Care guidelines (Ethics numbers: C18029BRs).

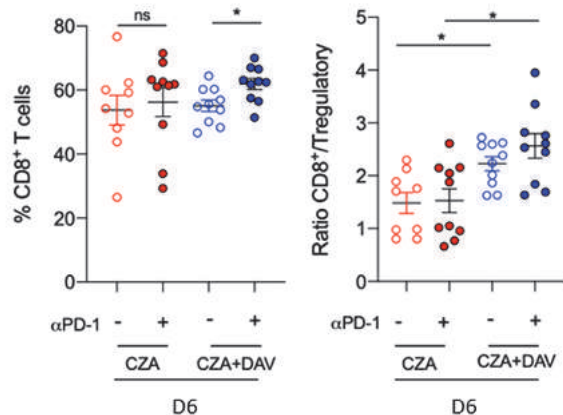


Abstract 1306 Figure 1 Intestinal microbiota composition in CZA ± DAV132 groups Heatmap of hierarchical clustering of microbiota composition represented by 16S rRNA profiling in 24 healthy volunteers treated with ceftazidime-avibactam ± DAV132



Abstract 1306 Figure 2 Anti-tumor response preserved by DAV132 DAV132 prevents antibiotic-induced loss of anti-tumor response in murine germ-free cancer model transplanted with healthy volunteers treated with ceftazidime-avibactam ± DAV132. *** p < 0.001, Mann-Whitney U Tests. Stools from 3 healthy

volunteers selected from each group of treatment (CZA ± DAV132) were transplanted in 10 germ-free mice, 5 being treated with ISO-PD-1 and 5 with aPD-1. Statistics at sacrifice were performed on n=15 mice except for the groups CZA+DAV132/ISO-PD-1 (n=14) and CZA+DAV132/aPD-1 (n=11) before treatment and the group CZA+DAV132/ISO-PD-1 (n=14) at D6.



Abstract 1306 Figure 3 DAV132 preserves local immune responseAntibiotic-depressed anti-tumor CD8+ response and CD8+/Treg ratio are preserved by DAV132.
* p < 0.05, Mann-Whitney U Tests. Statistics were performed on n = 10 mice (from 2 healthy volunteers) per group.

<http://dx.doi.org/10.1136/jitc-2022-SITC2022.1306>

1307

THE MICROBIOME-DERIVED METABOLITE TMAO DRIVES IMMUNE ACTIVATION AND BOOSTS RESPONSE TO IMMUNE CHECKPOINT BLOCKADE IN PANCREATIC CANCER

<http://dx.doi.org/10.1136/jitc-2022-SITC2022.1307>

¹Gauri Mirji*, ¹Alison Worth, ¹Sajad Bhat, ¹Mohamed El Sayed, ¹Toshitha Kannan, ¹Aaron Goldman, ¹Hsin Yao Tang, ¹Qin Liu, ¹Noam Auslander, ¹Chi Dang, ¹Mohamed Abdel-Mohsen, ¹Andrew Kossenkov, ²Ben Stanger, ¹Rahul Shinde. ¹Wistar Institute, Philadelphia, PA, USA; ²University of Pennsylvania, Philadelphia, PA, USA

Background Pancreatic ductal adenocarcinoma (PDAC) is a highly lethal cancer with poor prognosis. Although pancreatic tumors exhibit prominent leukocyte infiltrates, immunotherapy has so far failed to improve clinical outcomes in patients with PDAC. The immunotherapy responses can be improved through strategies that shift the PDAC tumor microenvironment (TME) from an immunosuppressive state to a more immune-activated state. The composition of the gut microbiome controls innate and adaptive immunity and has emerged as a key regulator of tumor growth and the success of immune checkpoint blockade (ICB) therapy. However, the underlying mechanisms remain unclear.

Methods The main objectives of this study were to elucidate how the gut microbe-derived metabolite trimethylamine N-oxide (TMAO) influences the host immune responses in PDAC TME, to determine if TMAO would synergize with immune checkpoint therapy to reduce tumor growth, and to assess whether there is a clinical correlation between TMAO production and survival in cancer patients. The overall design did employ some *in vitro* approaches but relied on *in vivo* mouse model systems, including orthotopic tumor implantation, to achieve the first two objectives; to test for a clinical correlation, we assessed datasets of bacterial species generated by three other groups. We employed flow cytometry and multiomic approaches to determine the impact of TMAO on phenotype of immune infiltrates in the TME.

Results Using a non-targeted, LC-MS/MS-based metabolomic screen, we identified that TMAO enhanced anti-tumor immunity to PDAC. Delivery of TMAO intraperitoneally or via a dietary choline supplement to orthotopic PDAC bearing mice reduced tumor growth and was associated with an immunostimulatory tumor-associated macrophage (TAM) phenotype and activated effector T cell response in the tumor microenvironment. Mechanistically, TMAO potentiated the type-I interferon (IFN) pathway and conferred anti-tumor effects in a type-I IFN-dependent manner. Notably, delivering TMAO-primed macrophages intravenously produced similar anti-tumor effects. Combining TMAO with ICB (anti-PD1 and/or anti-Tim3) in a mouse model of PDAC significantly reduced tumor burden and improved survival beyond TMAO or ICB alone. Finally, the levels of trimethylamine (TMA)-producing bacteria and of the CutC gene (an enzyme that generates TMA, the TMAO precursor) expression correlated with improved survival and response to anti-PD1 in cancer patients.

Conclusions Our study demonstrated that the microbial metabolite TMAO enabled TAMs to become immunogenic and promote effector T cell activity, transformed the TME to an immune activated state, and rendered PDAC sensitive to checkpoint immunotherapy, suggesting that strategies that alter levels of TMAO could be a promising clinical intervention to manage PDAC.

Ethics Approval Mouse experiments were performed following National Institutes of Health (NIH) guidelines and were approved by the Institutional Animal Care and Use Committee (IACUC) of The Wistar Institute.

1308

BACTERIA SPECIFIC IL-10 SECRETING T-CELLS DERIVED FROM THE GUT ARE CROSS-REACTIVE WITH TUMOR ANTIGENS AND ACCELERATE TUMOR GROWTH IN MOUSE MODELS

¹Denise Cecil, ²Jean Feng, ²Alex Paynter, ²Jessica Perry, ²Noah Simon, ²Nicholas Drovetto, ²Lauren Corulli, ²Erin Rodmaker, ³Susan Strenk, ³David Fredricks, ¹Mary Disis*. ¹UW Medicine Cancer Vaccine Institute, Seattle, WA, USA; ²University of Washington, Seattle, WA, USA; ³Fred Hutch Cancer Center, Seattle, WA, USA

Background We developed a method of CD4 epitope identification that includes selecting Class II interacting sequences via a multi-algorithm followed by functional phenotyping. We have evaluated 152 epitopes from 17 non-mutated tumor antigens (TA) and demonstrated Class II restricted epitopes could be identified which elicit either a selective Type I (IFN-gamma) or Type II (IL-10) response across multiple human PBMC (n=40). IL-10 inducing TA epitopes often shared a >50% identity and cross reactivity with multiple gut bacterial species. We questioned how prevalent these bacteria-tumor antigen (BAC-TA) cross reactive T-cells were in humans and whether these cells had any effects in cancer.

Methods IL-10 ELISPOT quantified BAC-TA T-cells in human PBMC, murine spleen, and tumor infiltrating lymphocytes (TIL). Human and murine T-cell lines were tested against bacteria, TA, and controls to show cross reactivity and specificity. Murine BAC-TA T-cells were used for adoptive transfer. T-cells were characterized by cytokine array, PCR, and flow cytometry. The C3(1)-Tag transgenic model of mammary cancer was used to assess effects of BAC-TA T-cells on tumor growth.

Results Measurable BAC-TA T-cells occurred in in up to 90% of PBMC. TA epitopes with the highest incidence of response shared significant sequence homologies with greater than 10 bacterial species. TA specific T-cell lines from multiple donors showed significant reactivity to homologous bacteria and recombinant TA protein, but not unrelated bacteria and protein. Human BAC-TA T-cells secreted IL-6 and IL-10, were memory T-cells, and expressed genes similar to intraepithelial lymphocytes. Similar BAC-TA T-cells were identified in mice. *P. aeruginosa*-specific T-cells generated from FVB mice secreted significantly more IL-10 when stimulated with the 70% homologous peptide YB1-p82-96 as compared to HIV peptide; p=0.0004. We implanted a syngeneic tumor cell line into C3(1)-Tag. After tumor was established, fluorescently-labeled *P. aeruginosa*-YB1 specific T-cells were injected. Significantly increased fluorescence was seen in 100% of tumors and no fluorescence in mice injected with labeled naïve splenocytes (p<0.0001). Tumor volume 20 days after transfer was increased 55% in mice receiving *P. aeruginosa*/YB1-T-cells compared to splenocytes (p<0.0001). When C3(1)-Tag developed spontaneous tumors (500±75 mm³) TIL analysis revealed numerous IL-10-secreting BAC-TA T-cells that had migrated from blood to tumor.

Conclusions A select group of bacteria are associated with the majority of homologies driving generation of BAC-TA T-cells. We have also identified bacteria never associated with TA homologies. These data lay the foundation for precision probiotics designed to reduce the BAC-TA memory T-cell pool.

Acknowledgements This work was funded by the Department of Defence Breast Cancer Program, the Kuni Foundation, WIngs of Karen, and the Helen B Slonaker Professorship.

Ethics Approval University of Washington Institutional Approval was obtained for all animal work shown here (#2878-01). All blood samples were obtained with written informed

consent by the University of Washington Human Subjects Division (Protocol #7721).

<http://dx.doi.org/10.1136/jitc-2022-SITC2022.1308>

1309

DIFFERENTIAL MICROBIAL ENRICHMENT IS ASSOCIATED WITH ORAL CANCER AND PERINEURAL INVASION

¹August Culbert, ²Adrian Chow, ³Raad Gharaiabah, ³Naseer Sangwan, ³Mohammed Dwidar, ²Rachel Newsome, ³Jin Dai, ³Siming Ma, ²Kristiann Fredenburg, ³Emrullah Yilmaz, ³Shlomo Koyfman, ³Daniel McGrail, ³Jamie Ku, ²Christian Jobin, ¹Natalie Silver*. ¹Cleveland Clinic Lerner College of Medicine, Cleveland, USA; ²University of Florida, Gainesville, USA; ³Cleveland Clinic, Cleveland, USA

Background Advanced oral cavity squamous cell carcinoma (OSCC) is an aggressive disease, with 5-year overall survival rates below 50%.¹ While smoking and alcohol are the most established risk factors, there is growing evidence implicating the role of the oral microbiome in promoting immunosuppressive states in OSCC.²⁻⁶ The objective of this study was to evaluate the taxonomic profile of oral bacteria in advanced OSCC patients and correlate with clinicopathologic features.

Methods The Institutional Review Board approved this prospective study of patients diagnosed with OSCC treated surgically from 2016-2020. Samples were taken from tumor and paired adjacent normal tissues at the time of surgery and snap frozen. Demographics, clinical and pathologic information was collected. DNA from 51 samples was isolated and 16S rRNA gene sequencing was performed after PCR amplification of the V1-V3 regions of the 16S rRNA gene for paired samples. 16S rRNA sequences were processed using DADA2, implemented in QIIME2 package, and taxonomic assignments were made using RDA classifier using the Human Oral Microbiome Database V15.22 as the reference database. Sequencing reads processing, denoising, dereplicating, chimeras filtering, and amplicon sequence variants (ASVs) generation was done using DADA2. The association between clinicopathological factors and bacterial profiles was evaluated using R Software.

Results In our cohort, the most common OSCC subtypes were oral tongue (47%) and floor of mouth (25.5%), with 83.4% of patients at advanced stage. The median age was 68 years old, and 84% were either current or former smokers. 16S rRNA gene sequencing and analysis revealed 9 ASVs that were significantly enriched in cancer samples and 22 enriched in normal samples using LEfSe (Linear discriminant analysis effect size). On the genus level, *Fusobacterium* (a known pathobiont), *Lactobacillus*, and *Bacteroides* were enriched in tumor samples, while *Rothia* and *Streptococcus* were enriched in normal tissue samples. Beta diversity was significantly different in cancer vs. normal tissue samples ($p=0.03$, PERMANOVA). Normal tissue had significantly higher alpha diversity than tumor tissue ($p=0.003$, Chao1 GLS). Interestingly, decreased alpha diversity was associated with more aggressive perineural invasion ($p=0.03$, Chao1 GLS).

Conclusions Among patients with OSCC, the bacterial diversity of primary tumor tissues was found to be significantly reduced compared to normal tissue in the same patients. For patients with decreased alpha diversity, there was increased likelihood of tumor perineural invasion, but no other associations found with aggressive pathologic factors. Additional studies are needed to further elucidate the role of microbes in oral cancers.

REFERENCES

1. Bray F, et al. Global cancer statistics 2018: GLOBOCAN estimates of incidence and mortality worldwide for 36 cancers in 185 countries. *CA. Cancer J. Clin.* 2018;**68**:394–424.
2. Almangush A, Leivo I, & Mäkitie AA. Biomarkers for Immunotherapy of Oral Squamous Cell Carcinoma: Current Status and Challenges. *Front. Oncol.* 2021;**11**.
3. Mager LF, et al. Microbiome-derived inosine modulates response to checkpoint inhibitor immunotherapy. *Science.* 2020;**369**:1481–1489.

4. Riquelme E, et al. Tumor Microbiome Diversity and Composition Influence Pancreatic Cancer Outcomes. *Cell.* 2019;**178**:795–806.e12.
5. Kostic AD, et al. *Fusobacterium nucleatum* Potentiates Intestinal Tumorigenesis and Modulates the Tumor-Immune Microenvironment. *Cell Host & Microbe.* 2013;**14**:207–215.
6. Michikawa C, et al. *Fusobacterium* is enriched in oral cancer and promotes induction of programmed death-ligand 1 (PD-L1). *Neoplasia.* 2022;**31**:100813.

Ethics Approval This study obtained insitutional review board approval (#IRB202001062) and all participants gave informed consent.

<http://dx.doi.org/10.1136/jitc-2022-SITC2022.1309>

1310

DIETARY TRYPTOPHAN CATABOLITE RELEASED BY INTRATUMORAL *LACTOBACILLUS REUTERI* FACILITATES ANTI-PD-L1 THERAPY

<http://dx.doi.org/10.1136/jitc-2022-SITC2022.1310>

¹Alex McPherson*, ¹Mackenzie Bender, ¹Catherine Phelps, ¹Mohit Rana, ¹Surya Pandey, ¹Jake Shapira, ¹Angela Gocher-Demske, ¹Steven Mullett, ¹Stacy Wendell, ²Diwakar Davar, ¹Reinhard Hinterleitner, ¹Dario Vignali, ¹Alok Joglekar, ²Hassane Zarour, ¹Marlies Meisel. ¹University of Pittsburgh, Pittsburgh, PA, USA; ²UPMC Hillman Cancer Center, Pittsburgh, PA, USA

Background The use of probiotic supplementation by cancer patients is increasing, including amongst those undergoing immune checkpoint inhibitor (ICI) therapy. While probiotic supplementation has been identified as an important factor influencing cancer patient responses to ICI therapy in melanoma, the underlying mechanisms of how gut probiotics shape systemic tumor immunity and thereby modulate ICI therapy efficacy remain poorly understood.

Methods We used a preclinical melanoma model to identify various probiotic bacteria capable of suppressing tumor growth, and identified the mechanism by which the host-microbial crosstalk enables the most potent tumor-suppressing strain, *Lactobacillus reuteri*, to bolster a strong spontaneous antitumor immunity and increase anti-PD-L1 therapy efficacy. We interrogated the clinical relevance of our findings in a cohort of advanced melanoma patients that either responded or failed to respond to ICI therapy.

Results Probiotic bacterium, *L. reuteri*, induces antitumor immunity and promotes ICI therapy in B16 preclinical melanoma via inducing interferon-gamma production by CD8 T cells. *L. reuteri* translocates to, colonizes and persists within melanoma tumors, and this intra-tumoral localization of *L. reuteri* is both necessary and sufficient to mediate antitumor effects in melanoma. *L. reuteri*-mediated tumor suppression occurs in a tumor- and *L. reuteri*-antigen independent fashion. The mechanism by which *L. reuteri* induces this antitumor response is via catabolization of a dietary tryptophan catabolite, indole-3-aldehyde (I3A). I3A is required and sufficient to promote antitumor immunity and facilitate ICI therapy efficacy, and it mediates antitumor immunity via activation of aryl hydrocarbon receptor (AhR) within CD8 T cells. The translational relevancy of I3A's impact on clinical melanoma is supported by our evidence for a role of I3A in promoting anti-PD-1 immunotherapy efficacy and survival in advanced melanoma patients.

Conclusions We show that probiotic bacterium *L. reuteri* can translocate to gut-distal melanoma tumors and reveal that its presence within the tumor is required to promote antitumor Tc1 cell immunity and facilitate ICI therapy in preclinical melanoma. Collectively, our findings elucidate a critical microbial-host crosstalk between the microbial released AhR agonist I3A and CD8 T cells within the tumor microenvironment that potently enhances spontaneous antitumor immunity and facilitates ICI therapy efficacy in preclinical melanoma.

Ethics Approval Animal care and experimentation were conducted in accordance with NIH guidelines and approved by the Institutional Animal Care and Use Committee at the University of Pittsburgh. Approval to treat patients was obtained from the University of Pittsburgh's Hillman Cancer Center (HCC) Institutional Review Board (No. PRO14030075), and authors attest that signed informed consent was obtained from all patients involved in the study.

Consent N/A- no sensitive or identifiable information is included in this study.

Abstracts

1311

THE MELANOMA TUMOR MICROBIOME AS A PREDICTOR OF OUTCOMES IN PATIENTS WITH METASTATIC DISEASE TREATED WITH IMMUNE CHECKPOINT INHIBITORS

¹Caroline Wheeler*, ¹Rebecca Hoyd, ²Aik Choon Tan, ³Neli Ulrich, ¹Gabriel Tinoco, ¹Dwight Owen, ³Jennifer Ose, ⁴Martin McCarter, ¹Vineeth Sukrithan, ⁵Alexandra Ikeguchi, ⁶Carlos Chan, ⁷Yousef Zakharia, ⁷Rebecca Dodd, ³Sheetal Hardikar, ⁷George Weiner, ²Youngchul Kim, ¹Ning Jin, ¹Yunzhou Liu, ¹Nicholas Denko, ¹Mariam Husain, ⁸John Carpten, ⁹Eric Singer, ²Lary Robinson, ¹⁰William (Bill) Dalton, ¹⁰Michelle Churchman, ¹Daniel Spakowicz, ²Ahmad Tarhini. ¹The Ohio State University, Columbus, OH, USA; ²Moffitt Cancer Center, Tampa, FL, USA; ³University of Utah, Salt Lake City, UT, USA; ⁴University of Colorado, Aurora, CO, USA; ⁵The University of Oklahoma, Oklahoma City, OK, USA; ⁶University of Iowa, Iowa City, IA, USA; ⁷University of Iowa, Holden Cancer Center, Iowa City, IA, USA; ⁸University of Southern California, Los Angeles, CA, USA; ⁹Rutgers Cancer Institute of New Jersey, Belle Mead, NJ, USA; ¹⁰M2Gen, Tampa, FL, USA

Background Emerging evidence supports an important role for the tumor microbiome in relation to oncogenesis, cancer immune phenotype, cancer progression and treatment outcomes in a number of malignancies. In this study, we investigated the metastatic melanoma tumor microbiome and potential roles in association with clinical outcomes, such as survival, in patients with metastatic disease treated with immune checkpoint inhibitors (ICIs).¹⁻³

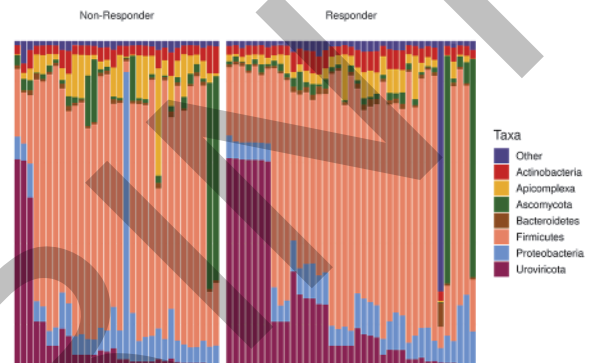
Methods Baseline tumor samples were collected from 71 patients with metastatic melanoma prior to treatment with ICIs. Bulk RNA-seq was conducted on the FFPE tumor samples. Clinical outcome following ICI treatment was evaluated as overall survival (> 24 versus < 24 months). The RNA-seq reads were processed to carefully identify exogenous sequences using ExoTIC (Exogenous sequences in Tumor and Immune Cells).^{4,5} Reads that did not align to the human reference genome were filtered of (1) common laboratory contaminants, (2) taxa that inversely correlate with input RNA quantity, and (3) taxa commonly found in the negative controls of microbiome experiments. DESeq2 was used to perform a differential abundance analysis on the comparison groups at every taxonomic level.

Results The 71 patients with metastatic melanoma ranged in age from 24 to 83 years, 59% were male, and 55% survived > 24 months following the initiation of ICI treatment. Exogenous taxa were identified in the tumor RNAseq, including bacteria, fungi, and viruses (figure 1). Within the tumors responsive to immunotherapy (> 24 months survival), we found a significant enrichment of several microbes, including *Fusobacterium nucleatum*, *Porphyromonas asaccharolytica*, *Nocardia mangyaensis*, and *Mollivirus sibericum*. Comparatively, the cohort of non-responsive tumors (< 24 months survival) was found to have a significant intra-tumoral enrichment of Fungi, as well as the bacteria *Delftia lacustris*, *Enterobacter hormaechei*, *Pseudomonas fluorescens*, and *Moraxella osloensis* (figure 2).

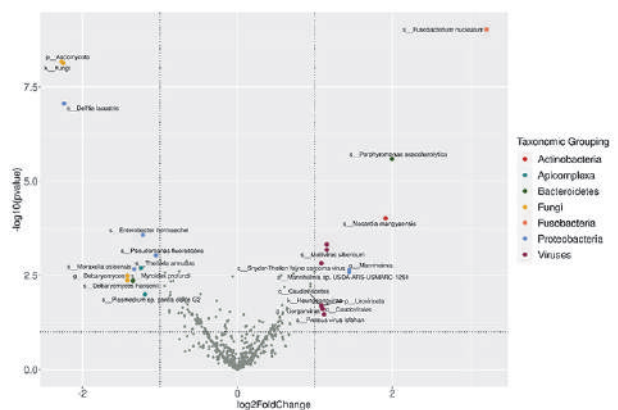
Conclusions In investigating the melanoma tumoral microbiome utilizing baseline tumors (prior to initiating ICI) we found significant variations in the exogenous taxa associated with patient outcomes following ICI treatment. Our findings warrant further investigations and potentially support therapeutic strategies to modify the tumor microbiome in order to improve treatment outcomes with ICIs. Ongoing research is evaluating whether these correlations are causally associated with outcomes and evaluating their effect on the tumor immune microenvironment and immune cell infiltration.

REFERENCES

1. Geller LT, Barzily-Rokni M, Danino T, Jonas OH, Shental N, Nejman D, et al. Potential role of intratumor bacteria in mediating tumor resistance to the chemotherapeutic drug gemcitabine. *Science*. 2017;**357**:1156–60.
2. Nejman D, Livvyatan I, Fuks G, Gavert N, Zwyang Y, Geller LT, et al. The human tumor microbiome is composed of tumor type-specific intracellular bacteria. *Science*. 2020;**368**:973–80.
3. Poore GD, Kopylova E, Zhu Q, Carpenter C, Fraraccio S, Wandro S, et al. Microbiome analyses of blood and tissues suggest cancer diagnostic approach. *Nature*. 2020;**579**:567–74.
4. Malalur PG, Mo X, Hoyd R, Carbone DP, Spakowicz D. Intra-tumoral microbes and overall survival in colorectal cancer patients. *J Clin Oncol*. 2020;**38**:4083–4083.
5. Malalur PG, Mo X, Hoyd R, Hays JL, Carbone DP, Spakowicz D. Investigating intra-tumor microbes, blood microbes, and CEA for development of non-invasive biomarkers in colorectal cancer. *J Clin Oncol*. 2021;**39**:3551–3551.



Abstract 1311 Figure 1 A stacked bar plot showing the relative abundances of exogenous taxa found in tumor RNAseq. Taxa are shown on the phylum level and are ordered by the relative abundance of \log_2 relative abundance.



Abstract 1311 Figure 2 Differential abundance analysis of taxa found within tumor RNAseq data by the exotic pipeline. Colored points represent significantly (p -value < 0.05) enriched taxa with a high (>1.00) fold-difference in abundance between the groups

<http://dx.doi.org/10.1136/jitc-2022-SITC2022.1311>

1312 GUT DYSBIOSIS SUPPRESSES ANTI-TUMOR ILC2S IN PANCREATIC CANCER

Abderezak Zebboudj*, Masataka Amisaki, Pablo Guasp, Luis Rojas, Zachari Sethna, Waters Theresa, Adrienne Chandra, Rebecca Yu, Zagaa Odgerel, Kevin Soares, Vinod Balachandran. Memorial Sloan Kettering Cancer Center, New York, NY, USA

Background Symbiotic microbes that colonize gut promote host immunity.¹ Cancer disrupts this homeostasis to alter microbial populations (“dysbiosis”) that suppresses anti-cancer immunity. Yet, the mechanisms of how dysbiosis suppresses anti-tumor immunity remain unclear. Group 2 innate lymphoid cells (ILC2s) are innate lymphocytes that reside in tissues including the gut, respond to the alarmin interleukin-33 (IL-33), and maintain microbial homeostasis in barrier surfaces.² ILC2s also activate anti-tumor immunity in multiple cancers.³⁻⁷ Yet, links between dysbiosis, ILC2s, and anti-tumor immunity, remain unexplored.

Methods To investigate if cancer dysbiosis modulates ILC2s, we examined dysbiosis in pancreatic ductal adenocarcinoma (PDAC), where dysbiosis correlates with fewer intratumoral T cells and worse survival.^{8,9} PDAC is also infiltrated by anti-tumor ILC2s.⁷ Briefly, we analyzed dysbiosis by 16S-rRNA gene sequencing in fecal samples of PDAC mice deficient or not for ILC2s or IL33. To study the effect of dysbiosis on ILC2s, we ablated dysbiosis using antibiotics or reconstituted it in germ-free mice, we explored ILC2s migration using parabiosis.

Results We found that PDAC induced *Bacteroidetes* overgrowth, thus phenocopying PDAC dysbiosis in patients.^{8,10,11} Interestingly, PDAC-dysbiosis suppressed intestinal ILC2s frequencies, as dysbiosis ablation with antibiotics increased, and fecal transplantation in germ-free mice conversely decreased intestinal ILC2 frequencies. Reciprocally, we found that ILC2 and IL33-deficient mice evidenced *Bacteroidetes* overgrowth at steady state, thus phenocopying the PDAC-induced dysbiosis. Interestingly, ILC2 and IL33-deficient mice also evidenced accelerated PDAC growth, and worse survival compared to wild-type mice (WT). Thus, PDAC-dysbiosis suppresses intestinal ILC2s that serve to maintain optimal gut homeostasis.

We next investigated how dysbiosis-induced ILC2s suppression modulates tumor growth. We previously reported that IL-33 responsive ILC2s infiltrate PDAC to activate antigen-specific CD8⁺T cells.⁷ We identified these anti-tumor ILC2s as unique migratory ILC2s that traffic to tumors. We thus hypothesized dysbiosis may promote tumors by modulating ILC2s migration from the intestine reservoir. Consistently, in parabiotic mice, recombinant IL-33 (rIL-33) induced ILC2s to migrate hematogenously to PDACs in different tissues, and antibiotic ablation of dysbiosis lowered donor-derived ILC2s frequencies in recipient blood and intestine. Thus, dysbiosis modulates anti-tumor ILC2s frequencies in circulation and gut reservoirs. Interestingly, in WT PDAC mice, rIL-33 expanded intestinal ILC2s, restored microbiome composition, increased tumor-infiltrating ILC2s, and reduced PDAC growth.

Conclusions We find that cancer dysbiosis suppresses anti-tumor immunity by suppressing gut-derived ILC2s. Moreover, rIL-33 expands ILC2s in the gut and circulation to restore dysbiosis-suppressed ILC2s and controls PDAC. We thus introduce the therapeutic potential of IL33-based immunotherapies to reverse the dysbiotic state in cancer.

REFERENCES

1. Thaïss CA, Zmora N, Levy M, Elinav E. The microbiome and innate immunity. *Nature*. 2016;**535**(7610):65–74.

2. Monticelli LA, Osborne LC, Noti M, Tran S V, Zaiss DMW, Artis D. IL-33 promotes an innate immune pathway of intestinal tissue protection dependent on amphiregulin-EGFR interactions. *Proc Natl Acad Sci U S A*. 2015;**112**(34):10762–7.

3. Ikutani M, Yanagibashi T, Ogasawara M, Tsuneyama K, Yamamoto S, Hattori Y, et al. Identification of Innate IL-5–Producing Cells and Their Role in Lung Eosinophil Regulation and Antitumor Immunity. *J Immunol*. 2012 Jan 15;**188**(2):703–13.

4. Kim J, Kim W, Moon UJ, Kim HJ, Choi H-J, Sin J-I, et al. Intratumorally Establishing Type 2 Innate Lymphoid Cells Blocks Tumor Growth. *J Immunol*. 2016;**196**(5):2410–23.

5. Saranchova I, Han J, Zaman R, Arora H, Huang H, Fenninger F, et al. Type 2 innate lymphocytes actuate immunity against tumours and limit cancer metastasis. *Sci Rep*. 2018;**8**(1).

6. Jacquelot N, Seillet C, Wang M, Pizzolla A, Liao Y, Hediye-zadeh S, et al. Blockade of the co-inhibitory molecule PD-1 unleashes ILC2-dependent antitumor immunity in melanoma. *Nat Immunol [Internet]*. 2021;**22**(7):851–64. Available from: <http://dx.doi.org/10.1038/s41590-021-00943-z>

7. Moral JA, Leung J, Rojas LA, Ruan J, Zhao J, Sethna Z, et al. ILC2s amplify PD-1 blockade by activating tissue-specific cancer immunity. *Nature [Internet]*. 2020;**579**(7797):130–5. Available from: <http://dx.doi.org/10.1038/s41586-020-2015-4>

8. Riquelme E, Zhang Y, Zhang L, Montiel M, Zoltan M, Dong W, et al. Tumor microbiome diversity and composition influence pancreatic cancer outcomes. *Cell [Internet]*. 2019;**178**(4):795–806.e12. Available from: <https://doi.org/10.1016/j.cell.2019.07.008>

9. Pushalkar S, Hundeyin M, Daley D, Zambirinis CP, Kurz E, Mishra A, et al. The pancreatic cancer microbiome promotes oncogenesis by induction of innate and adaptive immune suppression. *Cancer Discov*. 2018;**8**(4):403–16.

10. Half E, Keren N, Reshef L, Dorfman T, Lachter I, Kluger Y, et al. Fecal microbiome signatures of pancreatic cancer patients. *Sci Rep*. 2019;**9**(1):1–12.

11. Ren Z, Jiang J, Xie H, Li A, Lu H, Xu S, et al. Gut microbial profile analysis by MiSeq sequencing of pancreatic carcinoma patients in China. *Oncotarget*. 2017;**8**(56):95176–91.

<http://dx.doi.org/10.1136/jitc-2022-SITC2022.1312>

Novel Single-Agent Immunotherapies

1313

CHARACTERIZATION OF THE ANTI-TUMOR IMMUNE ACTIVATION POTENTIAL OF AUR107, A NOVEL SMALL MOLECULE P300/CBP BROMODOMAIN INHIBITOR

Girish Dagainakatte*, Chandrasekhar Abbineni, Saravanan Thiyagarajan, Mamon Dey, Aravind Basavaraj, Amit Dhudashiya, Sivapriya Marappan, Sandeep Sadashiv Patil, Naveen Kumar R, Raghavendra NR, Avinash Kumar, Uma Bharathi B V, Girish Renukappa, Venkata Siva Reddy, Amith A, Lavanya CS, Subhendu Mukherjee, Samiulla DS, Thomas Antony, Rajesh Eswarappa, Kavitha Nellore, Shekar Chelur, Murali Ramachandra, Susanta Samajdar. *Aurigene Discovery Technologies Ltd, Bangalore, India*

Background Ubiquitously expressed histone acetyl transferases (HAT), E1A binding protein (p300) and its paralog CREB binding protein (CBP or CREBBP) are critical regulators of gene expression in both tumor and immune cells. Conditional deletion of either p300 or CBP in mouse Tregs or inhibition of their HAT activity resulted in impairment of Treg suppressive function, reduced peripheral Treg generation, and Treg apoptosis. These effects led to allograft rejection and decreased murine tumor growth. We have identified a novel small molecule p300/CBP bromodomain inhibitor, AUR107, as therapeutic agent for solid and hematological cancers. AUR107 has significant activity in a broad range of cancer cell lines with good selectivity. Here, we demonstrate the relevance of CBP/p300 bromodomain inhibition by AUR107 on function of Tregs cells and modulation of T helper cells in addition to its potent activity against various haematological and solid tumour models.

Methods AUR107 was profiled in human Treg differentiation assay, human Th17 assay and MDSC proliferation assay. AUR107 combination efficacy studies with anti-PD-1/anti-CTLA-4 antibodies are in progress in syngeneic models

Results Inhibition of CBP/p300 bromodomains by AUR107 resulted in decrease in differentiation of human Tregs in an *ex vivo* assay. AUR107 caused dose-dependent increase in the CD127⁺CD25⁺FoxP3⁻ effector cells with corresponding decrease in the CD127⁺CD25⁺ cells in the differentiated CD4⁺ cells population. In the human PBMC assay, AUR107 caused increase in Th1 cell population with decrease in Th2 cell population. These observations indicate that inhibition of CBP/p300 bromodomains affects the function of regulatory T cells. Recruitment of regulatory T cells to tumors is known to be one of the major mechanisms of immune evasion by cancer cells, and hence AUR107 is expected to produce antitumour immunity. These results demonstrate that CBP/p300 bromodomain inhibition could be a novel approach for cancer immunotherapy in addition to their development as direct anti-cancer agents

<http://dx.doi.org/10.1136/jitc-2022-SITC2022.1313>

1314 **TRILACICLIB, AN INTRAVENOUS CYCLIN-DEPENDENT KINASE 4/6 INHIBITOR, ENHANCES ANTITUMOR RESPONSES BY MODULATING T CELLS**

Sarah Ahn*, John Yi, Subing Cao. *G1 Therapeutics, Inc., Research Triangle Park, NC, USA*

Background Cyclin-dependent kinase (CDK)4/6 inhibitors, including trilaciclib, have been shown to augment antitumor immunity.^{1,2} In an open-label, phase 2 trial in patients with metastatic triple-negative breast cancer (mTNBC), administration of trilaciclib prior to gemcitabine plus carboplatin improved overall survival, potentially through protection and direct activation of immune function.^{3,4} Here, we report the effects of transient, trilaciclib-mediated CDK4/6 inhibition on immune function *in vitro*.

Methods Peripheral blood mononuclear cells (PBMCs) or naïve CD4⁺ and CD8⁺ T cells were purified from 6 healthy human donors and activated with CD2/3/28 beads with or without trilaciclib. To visualize phenotypic and functional changes, trilaciclib was added to naïve CD4⁺ and CD8⁺ T cells 0-, 1-, and 3-days post-activation. Activated T cells were collected and stained for flow cytometric analyses 3-, 7-, and 14-days post-activation. Supernatant from activated PBMCs was harvested after 72 hours and added to human breast cancer cells. Following 24 hours' incubation, levels of programmed death-ligand 1 (PD-L1) and human leukocyte antigen (HLA) class I and II were quantified by flow cytometry, and CXCL9 and CXCL10 chemokines by enzyme-linked immunosorbent assay.

Results Irrespective of when trilaciclib was added to CD4⁺ and CD8⁺ T cells, significant increases in the frequency of CD45RO⁺ memory T cells were observed. Within CD45RO⁺ memory T cells, T cells incubated with trilaciclib had increased frequencies of CD62L^{lo}CD69^{hi} effector CD4⁺ and CD8⁺ T cells, with increases in CD62L^{lo}CCR7^{lo} effector memory T cells also observed. Furthermore, trilaciclib significantly increased CXCL9 and CXCL10 levels (*P*=0.0001). Surface expression of PD-L1 and HLA class I and II was increased in breast cancer cell lines cultured with supernatant from T cells activated in the presence of 50 and 100 nM of trilaciclib, resulting in a greater frequency of cells being double-positive for HLA class I and II or HLA class I and PD-L1.

Conclusions Trilaciclib may enhance antitumor immunity by modulating essential steps in the cancer-immunity cycle. Our data suggest trilaciclib may increase antigen presentation by promoting HLA class I and II expression and the recruitment of T cells to the tumor site via CXCL9 and CXCL10. Trilaciclib also augments the differentiation of T cells by promoting the formation of memory T cells. These data support a role for trilaciclib in improving antitumor efficacy, as observed in the phase 2 trial in mTNBC, and provide a rationale to combine trilaciclib with immunotherapy to enhance immunogenicity within the tumor microenvironment.

Acknowledgements We thank Dr. Jason Grayson for immune profiling services.

REFERENCES

1. Lai AY, Sorrentino JA, Dragnev KH, *et al.* CDK4/6 inhibition enhances antitumor efficacy of chemotherapy and immune checkpoint inhibitor combinations in pre-clinical models and enhances T-cell activation in patients with SCLC receiving chemotherapy. *J Immunother Cancer*. 2020;**8**:e000847.
2. Goel S, DeCristo MJ, Watt AC, *et al.* CDK4/6 inhibition triggers anti-tumour immunity. *Nature*. 2017;**548**:471–475.
3. Tan AR, Wright GS, Thummala AR, *et al.* Trilaciclib plus chemotherapy versus chemotherapy alone in patients with metastatic triple-negative breast cancer: a multi-centre, randomised, open-label, phase 2 trial. *Lancet Oncol*. 2019;**20**:1587–1601.

4. Tan AR, Wright GS, Thummala AR, *et al.* Trilaciclib prior to chemotherapy in patients with metastatic triple-negative breast cancer: final efficacy and subgroup analysis from a randomized phase II study. *Clin Cancer Res*. 2022;**28**:629–636.

Ethics Approval This study was approved by the Wake Forest University School of Medicine's Ethics Board under IRB #00080511.

<http://dx.doi.org/10.1136/jitc-2022-SITC2022.1314>

1315 **MVDELTA C, A NEW THERAPEUTIC VACCINE
DEMONSTRATES PROMISING PRECLINICAL IMMUNO-
ONCOLYTIC ACTIVITIES**

¹Aleksandr Barinov, ²Chantal Combredet, ²Claude Ruffié, ²Valérie Najburg, ³Nicolas Boisgerault, ¹Marc Gregoire, ¹Véronique Riebbels, ¹Jean-François Le Bigot, ¹Frederic Tangy*. ¹Oncovita, Paris, France; ²Institut Pasteur, Paris, France; ³Inserm, Nantes, France

Background Oncovita, a biotech company spin-off from Institut Pasteur, is developing a therapeutic vaccine in oncology based on Measovir[®], a proprietary technology derived from the safe and highly immunogenic measles attenuated vaccine virus (MV). MV is a paramyxovirus with a negative strand RNA genome. The MV specific tropism for cancer cells is due to the overexpression of its entry receptor CD46 on the surface of most cancer cells.

Methods We constructed MVdeltaC, a genetically modified MV by deletion of its virulence factor C. We evaluated its immuno-oncolytic activity *in vitro* on over 40 human tumoral cell lines, including mesothelioma, lung adenocarcinoma, bladder, ovarian, cervical cancer and hepatocarcinoma, and *in vivo* by i.p. or i.t. administration in different patient-derived xenograft (PDX) mesothelioma and bladder models, and finally in a syngeneic model of neuroblastoma in immunocompetent A/J mice. The mode of action (MOA) has been investigated *ex vivo* using human primary immune cells.

Results *in vitro*, MVdeltaC exhibited a strong oncolytic capacity which was 2 to 3 times greater than standard MV against a series of human tumor cell lines. MVdeltaC was active in more than 70% of the tested cell lines. *In vivo*, a single low dose given intraperitoneally in NOD/SCID mice grafted with human malignant mesothelioma induced a strong reduction of tumor mass two weeks after treatment. This potential was confirmed in PDX models of mesothelioma and bladder tumors by weekly administration of MVdeltaC. Finally, in immunocompetent A/J mice, only three i.t. administrations resulted in tumor regression and even total disappearance in 66% of mice. The animals that completely rejected the tumors were re-challenged on the other flank 3 months later with the same amount of tumor cells. No tumor growth was observed, suggesting an immune protection. In *ex-vivo* MOA experiments with human autologous primary cells, we demonstrated that the infection of cancer cells by MVdeltaC triggers the release of danger signals and tumor associated antigens (TAA), activation of mDC and pDC, phagocytosis of dying cancer cells and cross-presentation of TAA to autologous T lymphocytes.

Conclusions MVdeltaC demonstrated a very efficient immuno-oncolytic activity. Based on these promising preclinical data, Oncovita plans to initiate a FIH trial in patients with solid tumors. The activity on CPI resistant tumors will be of particular interest to investigate. We have already improved the mode of production of genetically stable MVdeltaC.

<http://dx.doi.org/10.1136/jitc-2022-SITC2022.1315>

1316 **A NOVEL CLASS OF T CELL-ACTIVATING ANTIBODY THAT SELECTIVELY TARGETS THE TCR B CHAIN TO PROMOTE ANTITUMOR ACTIVITY THROUGH ACTIVATION AND EXPANSION OF A NOVEL, POLYCLONAL EFFECTOR MEMORY T CELL SUBSET**

¹Andy Bayliffe*, ¹Zhen Su, ²John Wherry, ¹Jonathan Hsu, ¹Madan Katraggada, ¹Jacques Moisan, ¹Gurkan Guntas, ¹Karunya Srinivasan, ¹Jessica Lowry, ³Rajesh Chopra, ¹Roya Servattalab, ¹Wei Huang, ¹Jian Tang. ¹Marengo Therapeutics, Cambridge, MA, USA; ²University of Pennsylvania, Philadelphia, PA, USA; ³Apple Tree Partners, London, UK

Background Limitations with agents that enhance endogenous T cell responses to cancer, particularly in solid tumors, supports the study of alternative approaches. Directly targeting the variable (V) regions of the T cell receptor (TCR) is a novel approach to inducing T cell activation. STAR0602 is a bispecific antibody-fusion molecule that selectively activates and expands a subset of human $\alpha\beta$ T cells expressing the germline-encoded Vb6 and Vb10 TCRs that are enriched in tumor infiltrating lymphocytes. STAR0602 simultaneously engages a novel, non-clonal mode of TCR activation with cytokine co-stimulation.

Methods The effects of STAR0602 on activation and expansion of primary human T cells was assessed *in vitro* by flow cytometry, homogeneous time-resolved fluorescence, TCRseq, and NanoString. A murine surrogate (mSTAR0602) was tested in murine syngeneic tumor models with tumor re-challenge and cellular depletion studies to assess potential for long-term protection and cell-specific activities, respectively. EMT6 tumors were excised for IHC staining and phenotyping of tumor-infiltrating lymphocytes (TILs) using flow cytometry and scRNAseq/TCRseq.

Results *In vitro*, STAR0602 induced TCR signalling and IL-2R pathway activation in human T cells that preceded expansion of Vb6/Vb10 T cell subsets to 80-90% of the T cell compartment. Compared to controls, 80-90% of STAR0602-stimulated human T cells adopted a novel, activated central memory (T_{CM}) phenotype. In multiple syngeneic murine tumor models, mSTAR0602 monotherapy eradicated tumors, or led to substantial regressions (60-70% tumor growth inhibition) with long-term protection from tumor rechallenge. *In vivo* anti-tumor activity was dependent on the accumulation of Vb T cell subsets, and analysis of TILs showed expanded Vb T cells were almost exclusively polyclonal effector memory T cells (T_{EM}) or T_{CM} cells with minimal exhausted T cells or Tregs and were associated with a novel gene signature with upregulation of memory and effector programs, and downregulation of exhaustion pathways.

Conclusions STAR0602 is a first-in-class bi-specific fusion molecule that selectively binds and activates subsets of the germline TCR repertoire. *In vitro*, STAR0602 promotes a novel T cell phenotype with hallmarks of both effector and central memory cells, and *in vivo* mSTAR0602 demonstrates potent and durable single-agent anti-tumor activity in several solid tumor models that is dependent on expanded Vb T cells. The modulation of the tumor microenvironment (TME), striking increase in TCR diversity, and functional immune memory observed in murine models suggests that STAR0602 could remodel the adaptive immune response to solid tumors that are refractory to checkpoint inhibitor therapy, and thus represents a novel therapeutic strategy for patients.

<http://dx.doi.org/10.1136/jitc-2022-SITC2022.1316>

1317

CITRULLINATED GLUCOSE-REGULATED PROTEIN 78 IS A NOVEL CANDIDATE TARGET FOR CANCER IMMUNOTHERAPY

Victoria Brentville, Jia Chua, Peter Symonds, Anne Skinner, Ian Daniels, Katherine Cook*, Lindy Durrant. *Scancell, Nottingham, UK*

Background Post translational modification of proteins produces altered epitopes and can play a significant role in immune recognition. Citrullination is the modification of the positively charged arginine amino acid to a neutral charged citrulline residue. This modification is mediated by PAD enzymes and is increased during cellular stress (autophagy). Citrullination results in altered epitopes that can be presented upon MHC class II molecules for recognition by CD4 T cells. Citrullination also occurs in tumour cells as a result of continuous environmental stresses and increased autophagy. We have shown in animal models that the efficient stimulation of citrullinated epitope specific CD4 T cells results in dramatic elimination or regression of tumours. The ER chaperone glucose-regulated protein 78 (GRP78) is required for stress-induced autophagy and is directly linked to autophagosome formation. GRP78 is known to be highly expressed by many tumour types. In this study we investigated the potential of targeting citrullinated GRP78 for cancer therapy.

Methods *In vivo* experiments were performed with HLA-transgenic mice under an approved home office licence. Mice were immunised with citrullinated peptides in combination with CpG/MPLA adjuvant. Immune responses were determined using IFN γ ELISpot. Anti-tumour studies were carried out by implanting HLA-matched mouse tumour cells subcutaneously and immunising as above. Mass spectrometry analysis was performed to assess peptides presented on tumour cells. Blood samples from healthy individuals were obtained under ethical approval from the University of Nottingham. PBMC responses to citrullinated peptide were assessed using flow cytometry and proliferation assays.

Results Five peptides were selected for screening in HLA-transgenic mouse models. One citrullinated GRP78 peptide was identified that gives a CD4 T cell response that is restricted through the HLA DP*0401 and HLA-DR*0101 alleles. In addition, this peptide is detected by mass spectrometry in B16 melanoma grown *in vivo*. Anti-tumour studies demonstrated that the citrulline modification-specific CD4 response to this epitope mediates efficient therapy of established B16 melanoma tumours ($p < 0.0001$) in a HLA-transgenic HHDII/DP4 mouse model. Finally, the existence of a repertoire of responses to the citrullinated GRP78 peptide in healthy individuals has been demonstrated with 13/17 (76%) of healthy individuals showing a response to the peptide ($p = 0.0023$).

Conclusions Together this data leads us to propose that citrullinated GRP78 is a candidate tumour antigen and that vaccination against citrullinated GRP78 may provide a promising approach for future tumour therapy.

<http://dx.doi.org/10.1136/jitc-2022-SITC2022.1317>

1318

A NEXT GENERATION DNA VACCINE CODING FOR THE IMMUNODOMINANT SEQUENCE OF ALPHA-ENOLASE WITH ENHANCED ABILITY TO INDUCE EFFECTOR T CELL RESPONSES TO CURE PANCREATIC CANCER

¹Silvia Brugiapaglia*, ¹Claudia Curcio, ²Daniele Giordano, ²Rosella Spadi, ²Ennia Dametto, ²Monica Berrino, ¹Alessandro Scagliotti, ¹Antonio Amoroso, ¹Paola Cappello, ¹Francesco Novelli. ¹University of Turin, Turin, Italy; ²A.O.U. Città della Scienza e della Salute di Torino, Turin, Italy

Background Pancreatic ductal adenocarcinoma (PDA) is one of the most aggressive malignancies with a 5-year survival rate of 11%.¹ Only the 15% of patients have a resectable disease eligible for surgical resection followed by adjuvant chemotherapy to reduce the risk of relapse.² The glycolytic enzyme alpha-Enolase (ENO1) has been identified as PDA associated antigen.^{3,4} A non-integrating plasmid DNA vaccine encoding for full-length human ENO1 (FL-ENO1 vaccine) was able to slow tumor progression, inducing an integrated anti-tumor immune response, in mice engineered to spontaneously develop PDA (KPC).⁵ However, in FL-ENO1 vaccinated mice myeloid derived suppressor cells and regulatory T cells arose again, leading eventually to tumor recurrence. To optimize the ENO1 vaccine, we focused the research on the identification of the most immunogenic long epitopes widely presented by HLA molecules.

Methods A library of 14 peptides covering the sequence of ENO1 was synthesized to screen healthy donors and PDA patients for their capacity to recognize fractions of ENO1 through the stimulation of T cells with ENO1 peptides. According to the proliferative response and the cytokine release, the most immunogenic sequences of ENO1 were identified and cloned into the pVax plasmid (ENO3PEP vaccine). KPC mice were vaccinated at 8 weeks and every two weeks for a total of four rounds and sacrificed at 18 weeks of age either with empty, FL-ENO1 or ENO3PEP vaccine. The presence of anti-ENO1 specific antibodies and the number of specific T cells secreting IFN-gamma in response to ENO1 were assessed respectively by ELISA and ELISpot. Pancreas tumoral areas were analyzed on hematoxylin and eosin-stained sections, while the immune infiltrate was characterized through immunohistochemistry.

Results Three portions of ENO1 emerged as immunodominant as T cells from healthy donors and PDA patients stimulated with the related peptides showed the highest proliferation index and ratio of secreted IFN-gamma/IL-10 both compared to those stimulated with full-length ENO1. In KPC mice, the ENO3PEP vaccine i) significantly reduced the pancreatic tumor lesions, ii) increased the production of anti-ENO1 antibodies, iii) enhanced the secretion of IFN-gamma by ENO1-stimulated T cells, iv) recruited more T cells at tumor site compared to FL-ENO1 vaccine.

Conclusions The ENO3PEP vaccine, coding for the most immunogenic sequences of ENO1, was able to efficiently delayed tumor progression, inducing a strong integrated humoral and cellular response, emerging as potential next generation DNA vaccine suitable for immunotherapy in virtually all PDA patients.

REFERENCES

1. Siegel RL, Miller KD, Fuchs HE, Jemal A. Cancer Statistics, 2022. *CA. Cancer J. Clin.* 2022;**72**:7–33.
2. Park W, Chawla A, O'Reilly EM. Pancreatic Cancer: A Review. *JAMA.* 2021;**326**:851.
3. Cappello P, Tomaino B, Chiarle R, Ceruti P, Novarino A, Castagnoli C, Migliorini P, Perconti G, Giallongo A, Milella M, et al. An integrated humoral and cellular

- response is elicited in pancreatic cancer by a-enolase, a novel pancreatic ductal adenocarcinoma-associated antigen. *Int. J. Cancer.* 2009;**125**:639–648.
4. Tomaino B, Cappello P, Capello M, Fredolini C, Sperduti I, Migliorini P, Salacone P, Novarino A, Giacobino A, Ciuffreda L, et al. Circulating autoantibodies to phosphorylated a-enolase are a hallmark of pancreatic cancer. *J. Proteome Res.* 2011;**10**:105–112.
 5. Cappello P, Rolla S, Chiarle R, Principe M, Cavallo F, Perconti G, Feo S, Giovarelli M, Novelli F. Vaccination with ENO1 DNA prolongs survival of genetically engineered mice with pancreatic cancer. *Gastroenterology.* 2013;**144**:1098–1106.

Ethics Approval The ENOAPA study for human samples was approved by A.O.U. Città della Salute e della Scienza di Torino Ethics Board; approval number 0011110, February 2nd, 2021. The study “Utilizzo della vaccinazione a DNA in combinazione con anticorpi monoclonali, inibitori chimici e chemioterapia per inibire la crescita e la metastatizzazione dell'adenocarcinoma pancreatico” for animal samples was approved by Ministero della Salute; approval number 597/2019-PR, July 30th, 2019.

<http://dx.doi.org/10.1136/jitc-2022-SITC2022.1318>

1319 **NEXT-GENERATION TCR BISPECIFICS (TCER[®]) TARGETING PEPTIDE-HLA ANTIGENS FOR THE TREATMENT OF PATIENTS WITH SOLID TUMORS**

¹Sebastian Bunk*, ¹Martin Hofmann, ¹Gabriele Pszolla, ¹Meike Hutt, ¹Felix Unverdorben, ¹Frank Schwoebel, ¹Nadine Aschmeit, ¹Claudia Wagner, ¹Maïke Jaworski, ¹Christoph Schraeder, ¹Heiko Schuster, ¹Sarah Missel, ²Toni Weinschenk, ¹Dominik Maurer, ²Carsten Reinhardt. ¹Immatix Biotechnologies GmbH, Tuebingen, Germany; ²Immatix N. V., Tuebingen, Germany

Background T cell engaging bispecifics have emerged as a promising therapeutic opportunity for patients with solid cancers. However, challenges related to target specificity and drug safety profiles remain and many efforts are being made to generate optimized molecules with improved pharmacodynamic characteristics while reducing T cell engager-associated toxicities. We have developed a pipeline of novel bispecific molecules comprising a T cell receptor (TCR) for giving access to intracellular tumor antigens presented as peptide-HLA molecules and a unique T cell recruiting antibody aiming at conferring a favorable safety profile.

Methods We designed a novel TCR-incorporating bispecific format, called T cell engaging receptor (TCER[®]). TCER[®] molecules targeting different peptide-HLA antigens and using different recruiting moieties were generated and assessed for preclinical characteristics such as *in vitro* efficacy, *in vitro* safety and anti-tumor responses in tumor xenograft models.

Results Based on comparative preclinical testing of different TCR bispecific formats and T cell recruiting antibodies, we have developed a next-generation bispecific (TCER[®]) consisting of a high-affinity TCR capable of targeting tumor-specific peptide antigens and a low-affinity T cell recruiter designed to maximize efficacy while minimizing toxicity. The TCER[®] format harbors an effector function-silenced Fc part for the extension of serum half-life and improved manufacturability. For the development of different TCER[®] candidates, TCRs with promising functional avidity and high target-specificity are identified from the human repertoire and matured via yeast surface display to enhance TCR stability and to increase TCR affinity towards the target-peptide by at least 1,000-fold while retaining the target-specific binding pattern. TCER[®] molecules built with the matured TCRs show *in vitro* activity at picomolar concentrations against tumor cell lines presenting the target peptide at similar copy numbers as found on patient tumors. Further, the TCER[®] molecules demonstrate consistent tumor regression including complete remissions in tumor xenograft models in mice and thereby also uncovered an essential role for the type of T cell recruiting antibody. For our clinical lead TCER[®] candidates we confirmed a favorable *in vitro* safety profile with a broad therapeutic window between tumor and normal cell reactivity against more than 20 different human normal tissue cell types.

Conclusions We have developed a next-generation, half-life extended TCR Bispecific format that in preclinical tests demonstrated higher potency than multiple other established formats. By incorporating an innovative T cell recruiter we aim to reduce the risk for toxicities, specifically CRS, in patients. For each TCER[®] candidate we generate a robust preclinical data package before entering clinical development.

<http://dx.doi.org/10.1136/jitc-2022-SITC2022.1319>

1320

NON-CLINICAL CHARACTERIZATION OF CYT-303 FLEX-NK™ ENGAGER ANTIBODY SUPPORTS CLINICAL EVALUATION

Liang Lin*, Vishal Khairnar, Harish Potu, Hao-Ming Chang, Elisabetta Burchi, Armin Rath, Stanley Frankel, Jean Kadouche, Daniel Teper, Wei Li, Antonio Arulanandam. *Cytovia Therapeutics, Natick, MA, USA*

Background CYT-303 is a multifunctional bispecific NK engager (NKE) targeting NK cell activating receptor NKp46 and tumor antigen Glypican-3 (GPC3) expressed in HCC (hepatocellular carcinoma). Cytovia's proprietary FLEX-NK™ platform utilizes a novel FLEX-linker and human IgG1 back bone to allow for simultaneous binding to targeted cancer cells and NK cells. We evaluated additional CYT-303 Fc effector functions and the impact of CYT-303 when added to peripheral blood NK cells (PBNK) in Hep3B tumor spheroid cytolysis and Hep3B tumor serial killing assays. CYT-303 pharmacokinetics and safety in non-human primates were also evaluated.

Methods CYT-303 Fc effector function against Hep3B tumors was evaluated for antibody dependent cellular phagocytosis (ADCP) using human macrophages differentiated from purified monocytes isolated from peripheral blood and for complement dependent cytotoxicity (CDC) in the presence of rabbit complement. Hep3B tumor spheroids were established in special U-bottom adhesive plates and tumor spheroid killing assays were conducted with PBNKs and CYT-303 using the Incucyte™ Live Cell Analysis System. Serial killing assays were conducted by repeatedly adding the same PBNK cells to fresh tumor cells and CYT-303 following each round of tumor killing. CYT-303 single dose range finding pharmacokinetics and safety and 4-week repeat dose safety studies were conducted in cynomolgus monkeys by intravenous infusion dosing at 6, 20 and 60 mg/kg doses.

Results CYT-303 showed dose dependent ADCP by human macrophages against Hep3B tumors that was maximal at 0.4 ug/ml. CYT-303 also showed maximal CDC against Hep3B tumors at 0.4 – 2 ug/ml concentrations. CYT-303 in the presence of freshly isolated PBNKs showed increased time dependent killing of Hep3B tumor spheroids that peaked at 2-3 days following initiation of killing. This killing was enhanced in the presence of CYT-303 in a dose dependent manner. Furthermore, PBNK serial killing of Hep3B tumors was also enhanced by CYT-303. In the CYT-303 single dose range finding pharmacokinetics study in cynomolgus monkeys the C_{max} and AUC_{0-168h} values increased with dose and increases were approximately dose-proportional. CYT-303, half-lives ($T_{1/2}$) ranged from 39 to 47.6 hrs and exposures persisted up to 1-week. No evidence for any cytokine release was observed. In the 4-week repeat dose toxicity study no CYT-303 related toxicities were observed, enabling CYT-303 clinical development.

Conclusions CYT-303 demonstrated potent ADCP and CDC against Hep3B tumors as well as Hep3B tumor spheroid and serial killing activities in the presence of PBNKs. Preclinical pharmacokinetics and safety study results in cynomolgus monkeys support CYT-303 clinical development.

<http://dx.doi.org/10.1136/jitc-2022-SITC2022.1320>

1321

A BIPARATOPIC ANTI-HER2 ANTIBODY ENABLED WITH CONDITIONAL 4-1BB AGONISM INDUCES POTENT ANTI-TUMOR EFFICACY

¹Liandi Chen, ²Weifeng Huang, ¹Xiaoni Miao, ²Shaogang Peng, ¹Chao Wang, ¹Yao Yan, ¹Chuan-Chu Chou*, ¹Andy Tsun, ¹Yi Luo. ¹Biotheus Inc., Zhuhai, China; ²Biotheus (Suzhou) Co., Ltd., Suzhou, China

Background HER2 is a well-established therapeutic target that is overexpressed in multiple cancers. Monoclonal antibodies (mAbs) targeting HER2 such as Herceptin (trastuzumab) and Perjeta (pertuzumab) have been used in the clinic for many years. Despite good outcomes, there remains an unmet medical need that requires the further development of novel agents for recurrent or metastatic patients. The combination of HER2 mAbs have shown synergistic activity with improved clinical benefit. Moreover, biparatopic antibodies that are composed of trastuzumab and pertuzumab binding domains have shown promising results in the clinic. 4-1BB is a potent stimulator of T cells and NK cells, and when activated, can improve effector and/or memory responses. However, inherent hepatotoxicity has been observed during the clinical development of 4-1BB agonists. PM1234 is a trisppecific antibody that binds to two different epitopes of HER2 (ECD4 and ECD2), and the CRD4 domain of 4-1BB. PM1234 stimulates immune cells such as T cells via HER2-mediated cross-bridging and 4-1BB activation, which results in potent anti-tumor efficacy. Moreover, Fc-effector function was shown to be essential for the *in vivo* anti-tumor efficacy of PM1234.

Methods PM1234 was generated as a biparatopic heterodimeric (1+1) IgG-like antibody composed of both trastuzumab and pertuzumab binding domains with anti-4-1BB VHHs fused to the C-terminus of the Fc. The immunomodulatory functions of PM1234 were evaluated using luciferase reporter cell assays, PBMC/primary T cell activation assays, and human 4-1BB KI mouse tumor models.

Results PM1234 displayed strong HER2 binding and signal inhibition activity due to its biparatopic binding nature. The binding mode of PM1234 may allow up to double the available HER2 binding domains that can facilitate 4-1BB cross-linking and activation and was thus more potent than non-biparatopic anti-HER2 x 4-1BB bispecifics (trastuzumab x 4-1BB and/or pertuzumab x 4-1BB). PM1234 retained Fc effector function towards HER2 but with negligible activity towards the 4-1BB-targeting arm. PM1234 showed more potent activity in *in vivo* CT26 and MC38 tumor models than the control molecules containing Fc-silencing mutations, the combination of trastuzumab and pertuzumab, and anti-HER2-ADC. Importantly, PM1234 induced immune memory and potent anti-tumor efficacy to both HER2+ primary tumors and distal tumors without HER2 expression.

Conclusions PM1234 exhibited potent anti-tumor activity with the induction of strong immunological memory to suppress both primary HER2+ tumors and distal tumors. The differentiation of PM1234 shows the next-generation potential of HER2-targeted therapies in this competitive space and provides an insight into further improvements for benefiting patients with HER2+ tumors.

Ethics Approval All mice were maintained under specified pathogen-free conditions, and all studies were approved by the Animal Care and Use Committee of HUST-Suzhou Institute for Brainmatics.

<http://dx.doi.org/10.1136/jitc-2022-SITC2022.1321>

1322 **TARGETING IMMUNOSUPPRESSIVE MACROPHAGES AND TREGS BY REPURPOSING METABOLIC DRUGS**

¹Shipeng Chen*, ¹Ana Milena Vizcaino, ²Yuzhen Gao, ¹Baukje Nynke Hoogenboom, ¹Toos Daemen, ³Cesar Oyarce. ¹University Medical Center Groningen, University of Groningen, Groningen, Netherlands; ²Sir Run Run Shaw Hospital, Zhejiang University School of Medicine, Hangzhou, China; ³Amsterdam University Medical Center, University of Amsterdam, Amsterdam, Netherlands

Background Accumulating evidence demonstrates that the immunosuppressive tumor microenvironment (TME) contributes to tumor progression and invasion, and hampers response to cancer therapies. Among the immune suppressive cells and mediators in the TME, regulatory T cells (Tregs) and M2-like tumor-associated macrophages are known to suppress tumor-specific CD8⁺ T cells activity and contribute to the development of an immunosuppressive TME. The differentiation/function of Tregs and the phenotype/activity of macrophages are related to their metabolism. Thus, we hypothesized that metabolic drugs could be repurposed to target these immune suppressive cells.

Methods Clinically relevant metabolic drugs were selected to target different metabolic pathways (glutaminolysis, fatty acid oxidation, and mitochondrial respiration) of human peripheral blood mononuclear cells (PBMCs)-derived Tregs/macrophages and murine bone-marrow-derived macrophages. The effect of the drugs on the differentiation and polarization of Tregs/macrophages was determined by flow cytometric analysis. And the cytotoxic activity of re-polarized macrophages was measured by co-culturing with tumor cells.

Results It was demonstrated that targeting fatty acid oxidation or mitochondria of M2-like macrophages, resulted in M2-to-M1 polarization with strong tumor-cytotoxic activity. Moreover, targeting mitochondria or glutaminolysis inhibited the differentiation of T cells to Tregs, reduced the number of the differentiated Tregs, and decreased the expression of the immunosuppressive marker without affecting the proliferation and activation of CD4⁺ and CD8⁺ conventional T cells.

Conclusions These results demonstrate that targeting the metabolism of Tregs and tumor-associated macrophages could reverse the immune suppressive tumor microenvironment into an environment that could support cancer immunotherapies. This study opens a new avenue to repurpose clinically available metabolic drugs for metabolic reprogramming of the tumor microenvironment.

<http://dx.doi.org/10.1136/jitc-2022-SITC2022.1322>

1323

CUE-102 SELECTIVELY ACTIVATES AND EXPANDS WT1-SPECIFIC T CELLS FOR THE TREATMENT OF PATIENTS WITH WT1+ MALIGNANCIES

Natasha Girgis*, Yu Christie, Zohra Merazga, Steven Hatfield, Alex Histed, Fan Zhao, Raymond Moniz, Kristin Yeung, Fulvio Diaz, Wynona Bautista, John Ross, Saso Cemerski, Anish Suri, Matteo Levisetti, Steven Quayle. *Cue Biopharma, Boston, MA, USA*

Background Wilms' Tumor 1 (WT1) was ranked as the highest priority antigen for therapeutic targeting in an effort by the National Cancer Institute. Development of novel modalities targeting WT1 provide a significant opportunity to address high unmet medical need in WT1-positive malignancies, including AML, ovarian, endometrial, breast, lung, colorectal and pancreatic cancer. Leveraging the Immuno-STAT™ platform of targeted IL-2 therapies, and the ongoing development of CUE-101, CUE-102 is being developed as a novel therapeutic fusion protein to selectively activate tumor antigen-specific T cells to treat WT1-expressing cancers. CUE-102 consists of two human leukocyte antigen (HLA) molecules presenting a WT1 peptide, four affinity-attenuated human interleukin-2 (IL-2) molecules, and an effector attenuated human immunoglobulin G (IgG1) Fc domain.

Methods Cellular activity and specificity of CUE-102 were demonstrated in human PBMCs, while the in vivo activity of CUE-102 was assessed in HLA-A2 transgenic mice. HLA-A2/WT1-specific TCRs were validated and expressed in primary human CD8+ T cells. Antigen-specific cells were identified by flow cytometry using tetramer staining, activation markers and cytokine production.

Results Multiple in vitro assessments demonstrated that CUE-102 selectively binds, activates, and expands naturally occurring WT1₃₇₋₄₅-specific CD8+ T cells from PBMCs of healthy and cancer patient donors, consistent with its design. These CD8+ T cells exhibit polyfunctional and cytotoxic responses upon challenge with WT1-presenting target cells. In addition, significant functional attenuation of the IL-2 components of CUE-102 was shown, similar to preclinical results obtained with CUE-101. In vivo studies in HLA-A2 transgenic mice confirmed that CUE-102 elicits and expands polyfunctional WT1-specific CD8+ T cells from naïve and previously immunized mice without significantly altering the frequencies of other immune lineages. The WT1-specific CD8+ T cells expanded in vivo exhibit polyfunctional cytokine responses upon restimulation and selectively kill target cells presenting WT1 peptide in vivo. WT1-specific CD8+ T cells elicited in vivo by CUE-102 were detectable for >180 days following the last CUE-102 treatment, demonstrating the establishment of a long-term memory response to this tumor antigen.

Conclusions CUE-102 elicits selective expansion of WT1-specific cytotoxic CD8+ T cells both in vitro and in vivo. These results, together with its similarity to CUE-101, support its anticipated tolerability profile and potential for clinical efficacy in an ongoing Phase 1 clinical trial (NCT05360680).

Ethics Approval Studies using animals were conducted in accordance with guidelines established by the Smart Labs Institutional Animal Care and Use Committee under protocol 21SL09-0007.

<http://dx.doi.org/10.1136/jitc-2022-SITC2022.1323>

1324

INHIBITION OF ACID SENSING BY GPR65 NORMALISES GENE EXPRESSION IN MACROPHAGES, INCREASES IMMUNE CELL INFILTRATION IN TUMORS, AND RESTRAINS SUBCUTANEOUS MC38 GROWTH IN MICE

¹Alastair Corbin*, ¹Stuart Hughes, ²Mussa Quareshy, ³Tobias Bopp, ¹Barbara Cipriani, ¹David Miller, ¹Alan Naylor, ²Gavin Milne, ⁴Darryl Turner, ²Barbara Young, ⁴Anastasia Nika, ⁴Preeti Singh, ²Rupert Satchell, ²Sourav Sarkar, ⁴Gavin Knox, ³Toszka Bohn, ¹Tom McCarthy. ¹Pathios Therapeutics Ltd., Oxford, UK; ²Sygnature Discovery Ltd., Nottingham, UK; ³University Medical Centre Mainz, Mainz, Germany; ⁴Malvern Panalytical, Edinburgh, UK

Background High frequencies of Tumor Associated Macrophages (TAMs) are related to poor patient prognosis. The Tumor Microenvironment (TME) is characterised by resource scarcity, toxic metabolic by-products, and low pH, together creating an immunosuppressive environment which polarises TAMs towards a pro-tumorigenic state.

Methods We identified the proton-sensing G-Protein-Coupled Receptor 65 (GPR65) as a key determinant of low-pH-induced immunosuppression in human cancers, specifically via modulating TAM phenotype in response to the acidic TME. The importance of GPR65 in human cancers is highlighted by three key findings: (1) cancer patients homozygous for the hypomorphic I231L variant exhibit a pronounced survival benefit, (2) GPR65 and downstream pathway genes are highly expressed in innate immune cells from all human solid tumors when assessed by single cell RNA sequencing, and (3) low pH treatment of macrophages *in vitro* leads to a marked suppression of inflammatory genes and an upregulation of a tissue repair signature.

Results We have identified potent and selective small-molecule antagonists of human GPR65 that inhibit the low pH-induced accumulation of cAMP in recombinant cell systems and primary human macrophages with single-digit nanomolar potencies. These compounds dose-dependently prevent the low pH-driven suppression of inflammatory cytokine and chemokine genes and counteract the upregulation of pro-tumorigenic and tissue repair genes in both human and mouse macrophages.

Oral administration of our exemplar compound PTT-3213 in subcutaneous MC38 tumor-bearing mice caused gene expression changes consistent with those observed in primary macrophages *in vitro*, indicative of a dramatic impact on the TME. Weekly dosing of PTT-3213 significantly reduced MC38 Tumor Volume (TV) compared to vehicle (46%). This monotherapy activity was comparable to bi-weekly administration of anti-PD1, whilst combination of PTT-3213 and anti-PD-1 led to a more pronounced curtailment of TV vs vehicle-treated animals (61%). In accordance with the increased expression of chemokine genes, PTT-3213 monotherapy in MC38-bearing mice markedly elevated the frequency of tumor-infiltrating NK cells (up to 22-fold). There was also an increase in the CD8⁺/CD4⁺ T cell ratio which attained statistical significance in combination with anti-PD-1.

Conclusions Taken together, we have identified GPR65 as a key innate immune checkpoint and therapeutic target in solid tumors and propose that macrophage conditioning via GPR65 inhibition may provide an efficacious strategy to counteract the immunosuppressive action of the acidic TME on TAMs in patients.

Ethics Approval Protocols or procedures involving the care and use of animals in studies in China were reviewed and approved by the Institutional Animal Care and Use Committee of Crown Bioscience. During studies, the care and use of animals was conducted in accordance with the regulation of the

Association for Assessment and Accreditation of Laboratory Animal Care

Studies involving the welfare and use of animals within the UK complied with the UK Animals Scientific Procedures Act 1986 (ASPA) in line with Directive 2010/63/EU of the European Parliament and Council of 22/September/2010 on the protection of animals used for scientific purposes and UK Home Office guidance on the implementation of the Act and applicable codes of practice for the care and housing of laboratory animals.

<http://dx.doi.org/10.1136/jitc-2022-SITC2022.1324>

1325

PRECLINICAL ACTIVITY AND SAFETY PROFILE OF JANX007, A NOVEL PSMA-TARGETING TUMOR-ACTIVATED T CELL ENGAGER FOR TREATMENT OF METASTATIC CASTRATION-RESISTANT PROSTATE CANCER

Thomas DiRaimondo, Natalija Budimir, Simon Shenhav, Hua Wu, Vanessa Cicchini, Renee Jocić, Lina Ma, Fabreze Roup, Calvin Campbell, Carolina Caffaro, Hans Aerni, Ugur Eskioçak, Wayne Godfrey, Charles Winter, Marc Nasoff, Neil Gibson, David Campbell, Shahram Salek-Ardakani*. *Janux Therapeutics, San Diego, CA, USA*

Background Metastatic castration-resistant prostate cancer (mCRPC) remains an incurable disease. Bispecific T cell engagers (TCEs) targeting prostate-specific membrane antigen (PSMA) and CD3 on T cells showed great clinical potential for the treatment of mCRPC. However, cytokine release syndrome (CRS) and poor pharmacokinetic (PK) profile hinder their further development. To overcome these challenges, Janux has developed JANX007, a tumor-activated T cell engager (TRACTr) with enhanced safety and PK properties. JANX007 is a humanized trispecific protein that contains PSMA- and CD3-binding domains, an albumin binding domain to extend circulating half-life, and a CD3 inhibitory peptide mask fused to the molecule through tumor protease cleavable linker. Only when tumor-resident proteases cleave the TRACTr and enable mask separation can the resulting active molecule bind CD3. This cleavage-dependent CD3 agonism can potentially limit systemic toxicity associated with broad T cell activation.

Methods Peptide masks against the CD3 binding domain were identified via phage display. Mask efficiency was evaluated using human CD3 ELISAs. Masking and cleavable linker stability was characterized in human (healthy and mCRPC donor) and cynomolgus monkey serum. JANX007-induced cleavage-dependent activation of T cells was evaluated in human PBMC/prostate tumor cell in vitro co-culture assays. The pharmacokinetic and safety profile of JANX007 was evaluated in non-human primate (NHP) studies.

Results Engagement of CD3 target by JANX007 was shown to be cleavage dependent where masking reduced CD3 binding by >600x. In vitro, JANX007 exhibited a ~500x decrease in potency to activate T cells and induce T cell-mediated tumor cell killing relative to non-masked TCE. JANX007 was highly stable in healthy and mCRPC human donor serum, with ≤1% cleavage per day. While proteolytic cleavage of JANX007 in the tumor microenvironment is expected to drive anti-tumor activity, the maintenance of masking in the blood compartment is expected to mitigate the safety risks associated with potential off-tumor toxicity and CRS. JANX007 was found to be highly stable in NHPs with minimally detectable cleavage. The lack of TCE accumulation in NHPs mitigated on-target healthy tissue toxicities and minimized CRS. Clinical chemistry, hematology, and pathology data package support No-Observed-Adverse-Effect-Level (NOAEL) ≥1.5 mg/kg/dose. Finally, the cleavable albumin-binding domain extended the circulating half-life of JANX007 to ~120h in NHPs, relative to the 2h half-life of non-masked TCE, supporting its projected once-weekly clinical dosing.

Conclusions Cleavage-dependent activity, half-life extended PK, the potential for superior safety and manufacturability properties of JANX007 support its further development as an attractive mCRPC therapeutic.

Acknowledgements We acknowledge Marque Todd for providing insightful comments and help with the interpretation of NHP safety studies.

Ethics Approval All animal experiments were approved by the Institutional Animal Use and Care Committee of the institutions conducting the studies and in compliance with the Animal Welfare Act, the Guide for the Care and Use of Laboratory Animals, and the Office of Laboratory Animal Welfare.

<http://dx.doi.org/10.1136/jitc-2022-SITC2022.1325>

1326

A BIFUNCTIONAL TUMOR ACTIVATED IMMUNOMODULATOR (TRACIR) TARGETING PD-L1 AND CD28 IS A POTENT ENHANCER OF T CELL-MEDIATED ANTI-TUMOR ACTIVITY

Thomas DiRaimondo, Natalija Budimir, Lina Ma, Simon Shenhav, Vanessa Cicchini, Robert Navert, Hua Wu, Renee Jocić, Cuiling Yu, Diane Aceveda, Hannah Best, Clara Prentiss, Kai Muskat, Jason Chang, Farhad Dastmalchi, Fabreze Roup, Carolina Caffaro, Hans Aerni, Wayne Godfrey, Charles Winter, Marc Nasoff, Neil Gibson, David Campbell, Shahram Salek-Ardakan*. *Janux Therapeutics, San Diego, CA, USA*

Background While PD-(L)1 blocking antibodies have demonstrated unprecedented clinical response rates, most patients fail to respond. Preclinical studies have shown that CD28 costimulatory pathway is essential for effective PD-(L)1 therapy. However, the first phase 1 clinical trial of the CD28 agonistic antibody TGN1412 failed due to an unexpected and rapid systemic proinflammatory cytokine response. To overcome the limitation of PD-(L)1 blockade, toxicity of systemic CD28 agonism, and potential healthy tissue toxicity, we engineered a Tumor Activated Immunomodulator (TRACIr). The TRACIr is a tri-specific protein that contains PD-L1- and CD28-binding domains, an albumin-binding domain that extends circulating half-life, and an inhibitory peptide mask bound to the CD28-binding domain via a tumor protease cleavable linker. Only when tumor-resident proteases cleave the TRACIr and enable mask separation can the resulting active molecule bind CD28. This cleavage-dependent CD28 agonism can potentially limit systemic toxicity while enhancing the activity of T cells in the tumor.

Methods Peptide masks against the CD28 binding domain were identified via phage display. Mask efficiency was evaluated using CD28-specific ELISAs. The functional engagement of TRACIr binding arms was evaluated in bioluminescent PD-L1/CD28 cell reporter assays. TRACIr-induced T cell activation was evaluated in human PBMC/tumor cell co-culture assays. Functional activity was confirmed in human renal (RCC) and non-small cell lung cancer (NSCLC) patient-derived TILs. In a mouse model of triple-negative breast cancer (TNBC; MDA-MB231), the cleavage-dependent antitumor activity of TRACIr was demonstrated in combination with CD3 stimulation. The pharmacokinetic and safety profile of TRACIr was evaluated in non-human primate studies.

Results Non-masked PDL-1xCD28 bispecific molecule exhibited potent binding to PD-L1 (1 nM KD) and CD28 (3 nM KD). While the presence of the mask decreased binding to CD28 by >1,000x, PD-L1 binding remained unaffected. PD-L1 blocking activity was comparable with atezolizumab, avelumab, nivolumab, and pembrolizumab. In contrast, CD28 agonistic activity was significantly compromised by the presence of the mask. Moreover, the TRACIr enhanced activation of peripheral blood T cells and TILs was signal 1- and cleavage-dependent and superior in magnitude compared to anti-PD-(L)1 and anti-CD28 monoclonal antibodies. In the TNBC tumor model, TRACIr dramatically enhanced the antitumor activity of a CD3 targeted bispecific antibody in a cleavage-dependent manner. Finally, TRACIr was well tolerated in NHPs at high doses and exhibited half-life extended pharmacokinetics.

Conclusions Preclinical activity and safety profiles of PDL1xCD28 TRACIr support its further development as an attractive bifunctional T cell modulator.

Acknowledgements We acknowledge Marque Todd for providing insightful comments and help with interpretation of NHP safety studies.

Ethics Approval All animal experiments were approved by the Institutional Animal Use and Care Committee of the institutions conducting the studies and in compliance with the Animal Welfare Act, the Guide for the Care and Use of Laboratory Animals, and the Office of Laboratory Animal Welfare.

<http://dx.doi.org/10.1136/jitc-2022-SITC2022.1326>

1327

NOVEL GCN2 MODULATOR HC-7366 DECREASES PULMONARY METASTASES AND REDUCES MYELOID-DERIVED SUPPRESSOR CELLS

¹Jeremy Drees*, ¹Anissa SH Chan, ¹Yunfang Li, ¹Takashi Kangas, ¹Weiyu Zhang, ¹Maria Fumagalli, ¹Iman Dewji, ¹Kathryn Biegging-Rolett, ¹Sho Fujisawa, ¹Sharon Huang, ¹Ben Harrison, ¹Ashley LaCayo, ¹Xiaohong Qiu, ¹Nick Collette, ¹Gemily Wang, ¹Feven Tameire, ¹Paulina Wojnarowicz, ¹Crissy Dudgeon, ²Eric Lightcap, ¹David Surguladze, ¹Nandita Bose. ¹HiberCell, Inc., Roseville, MN, USA; ²HiberCell, Boston, MA, USA

Care and Use Committee of University of Minnesota. IACUC protocol: 2009A38458

<http://dx.doi.org/10.1136/jitc-2022-SITC2022.1327>

Background General controlled nonderepressible 2 (GCN2) is a central kinase in the integrated stress response (ISR) that responds to amino acid deprivation. Cancer cells can utilize the ISR for survival, but prolonged or hyperactivation of the ISR reduces proliferation and induces apoptosis. We are developing HC-7366, a First-in-Class, First-in-Human GCN2 modulator that activates GCN2, resulting in anti-tumor activity. HC-7366, currently in a phase 1 trial (NCT05121948), has demonstrated robust efficacy in multiple pre-clinical solid tumor and AML models.

Myeloid-derived suppressor cells (MDSC) inhibit anti-tumor T cell immunity and promote metastatic spread. Immature myeloid cells are also marked by ISR activation. We hypothesized that HC-7366 treatment could further activate the ISR in MDSCs, leading to cell death or reduced suppressive function and improving anti-tumor immunity. To test this, we used the 4T1 murine breast cancer model, which is characterized by expansion of MDSCs that facilitate lung metastasis.

Methods 4T1 cells were orthotopically transplanted into BALB/c mice. Tumor volume was monitored, and tissues or blood were collected at various timepoints for flow cytometry, IHC, or JESS analysis. Mouse bone marrow derived MDSCs were cultured with T-cells in the presence of HC-7366 *in vitro*, and anti-proliferative function was evaluated.

Results HC-7366 treatment showed consistent anti-metastatic efficacy, reducing lung metastases by an average of ~75% across multiple studies. Primary tumors and metastases in treated mice demonstrated GCN2 pathway activation by increases in downstream signaling proteins, including the amino acid biosynthesis proteins ASNS and PSAT1. Anti-tumor efficacy was correlated with significantly decreased Ly6G+ PMN-MDSC frequency in the lungs, spleen, and blood. Additionally, significantly increased expression of the activation markers CD86 and MHCII was observed on PMN-MDSC in both lungs and spleen. Lungs also showed significantly increased T-cell and NK-cell infiltration, activation, and proliferation as measured by increased expression of IL-2, Ki67, Tbet, and Granzyme B. HC-7366 treatment also significantly reduced the S100A8/A9 calcium binding proteins in CD11b+ cells in both metastatic and normal lung tissue, which have been implicated in facilitating MDSC recruitment and proliferation. Reductions in S100A8/A9 were also detectable in PBMCs isolated from peripheral blood and plasma. *In vitro* suppression assays of bone marrow derived MDSCs co-cultured with T-cells in the presence of HC-7366 showed reduced Arginase 1 expression and T-cell inhibition.

Conclusions Collectively, these data demonstrate the anti-metastatic efficacy of HC-7366 and its inhibitory effects on MDSCs, outlining its potential as a monotherapy and in combination with other immunotherapeutics to treat MDSC-enriched metastatic cancers.

Ethics Approval All *in vivo* experimental procedures were performed in accordance with the NIH Guide for Care and Use of Animals and were approved by the Institutional Animal

1328

A NOVEL HUMANIZED T CELL-ENGAGING CD24XCD3 BISPECIFIC ANTIBODY FOR CD24-POSITIVE SOLID TUMORS

Madelyn Espinosa-Cotton*, Hong-fen Guo, Nai-Kong Cheung. *Memorial Sloan Kettering Cancer Center, New York, NY, USA*

Background CD24 is a small, heavily-glycosylated glycosylphosphatidylinositol (GPI)-anchored protein.¹ It is overexpressed in a variety of adult solid tumors, including breast, ovarian, pancreatic, and colorectal cancers, as well as pediatric cancers such as neuroblastoma, Wilms tumor, and desmoplastic small round cell tumor (DSRCT).² In normal tissue, CD24 is expressed transiently during development but is largely absent from mature, differentiated cells.¹ Functionally, CD24 serves as a “don’t eat me” signal to macrophages, binding to Siglec-10 and preventing phagocytosis.³ It is known as a marker of cancer cell stemness and dysregulates numerous signaling pathways involved in proliferation, invasion, and metastasis.⁴ The presence of CD24 has been strongly correlated to poor clinical outcome for multiple tumor types.⁴⁻⁷ For these reasons, CD24 is a strong candidate for targeting with T cell-engaging bispecific antibodies (BsAbs).

Methods We used immunohistochemical (IHC) staining on patient specimens and flow cytometry on cancer cell lines to evaluate CD24 expression in a variety of tumor types. We then generated a panel of CD24xCD3 BsAbs of different formats including a humanized IgG-[L]-scFv BsAb and assessed purity and stability using high-performance liquid chromatography. To evaluate the ability of the BsAbs to engage T cells against CD24-expressing tumor cell lines, we performed standard chromium release assays. We used immunocompromised mice bearing luciferase-transduced intraperitoneal xenografts to test the ability of the BsAbs to redirect T cells to CD24-expressing tumor cells *in vivo*, and monitored tumor growth using *in vivo* bioluminescent imaging.

Results CD24 was found to be strongly expressed by DSRCT, NB, rhabdomyosarcoma, Ewing sarcoma, mesothelioma, liver cancer, breast cancer, ovarian cancer, and pancreatic cancer. CD24xCD3 BsAbs had high purity (<90%) and were stable for several weeks at 40 C. The humanized CD24xCD3 IgG-[L]-scFv BsAb retained binding ability, indicating that the humanization process did not affect its affinity for CD24 on tumor cells. All the CD24xCD3 BsAbs induced T cell-mediated cytotoxicity against DSRCT cell lines *in vitro*. However, as we have shown previously with BsAbs targeting other tumor antigens,⁸ the IgG-[L]-scFv format is superior *in vivo*, completely ablating established intraperitoneal DSRCT and ovarian cancer xenografts.

Conclusions CD24 is expressed on a variety of solid tumors and is a viable target for T cell-engaging BsAbs. A novel humanized CD24xCD3 BsAb built on an IgG-[L]-scFv platform is effective at clearing disseminated intraperitoneal CD24-positive xenograft tumors. This strategy warrants further study and could eventually be tested in human trials for patients with advanced tumors.

REFERENCES

1. Poncet C, V Frances, R Gristina, *et al.* CD24, a glycosylphosphatidylinositol-anchored molecules is transiently expressed during the development of human central nervous system and is a marker of human neural cell lineage tumors. *Acta Neuropathol.* 1996;**91**(4):400–8.
2. Fang X, P Zheng, J Tang, *et al.* CD24: from A to Z. *Cellular & Molecular Immunology.* 2010;**7**(2):100–103.

3. Barkal AA, RE Brewer, M Markovic, *et al.* CD24 signalling through macrophage Siglec-10 is a target for cancer immunotherapy. *Nature.* 2019;**572**(7769):392–396.
4. Nakamura K, Y Terai, A Tanabe, *et al.* CD24 expression is a marker for predicting clinical outcome and regulates the epithelial-mesenchymal transition in ovarian cancer via both the Akt and ERK pathways. *Oncol Rep.* 2017;**37**(6):3189–3200.
5. Shah MM and CN Landen. Ovarian cancer stem cells: are they real and why are they important? *Gynecol Oncol.* 2014;**132**(2):483–9.
6. Sagiv E, A Starr, U Rozovski, *et al.* Targeting CD24 for treatment of colorectal and pancreatic cancer by monoclonal antibodies or small interfering RNA. *Cancer Res.* 2008;**68**(8):2803–12.
7. Sun F, T Wang, J Jiang, *et al.* Engineering a high-affinity humanized anti-CD24 antibody to target hepatocellular carcinoma by a novel CDR grafting design. *Oncotarget.* 2017;**8**(31):51238–51252.
8. Santich BH, JA Park, H Tran, *et al.* Interdomain spacing and spatial configuration drive the potency of IgG-[L]-scFv T cell bispecific antibodies. *Sci Transl Med.* 2020;**12**(534).

Ethics Approval Patients who provided tumor specimens used in IHC experiments provided consent for their tissues to be used in research, and approval for these experiments was obtained from MSKCC’s IRB under protocol 21-282. Animal experiments were approved by MSKCC’s IACUC under protocol 09-05-010.

<http://dx.doi.org/10.1136/jitc-2022-SITC2022.1328>

Abstracts

1329 ULTRA-PH SENSITIVE NANOPARTICLES INCREASE THERAPEUTIC INDEX OF IL-2-FC

¹Qiang Feng*, ¹Gang Huang, ¹Raymundo Pantoja, ¹Zhichen Sun, ¹Wei Li, ¹Katy Torres, ¹Jonathan Wilhelm, ²Zirong Chen, ²Tian Zhao, ²Ruolan Han, ¹Jinming Gao. ¹University of Texas Southwestern Medical Center, Dallas, TX, USA; ²OncoNano Medicine Inc, Southlake, TX, USA

Background Aldesleukin (IL-2) is clinically approved for the treatment of melanoma and renal cancer, but its use is restricted by short half-life and dose limiting toxicities. Protein engineering and prodrug approaches are under extensive investigation but with limited success.¹ Fc fusion of bivalent IL-2 (IL-2-Fc) increases the half-life and efficacy of IL-2 when administered intravenously, but also elevates toxicity compared to IL-2. We developed ON-BOARD, an ultra-pH sensitive nanoparticle technology for tumor-targeted delivery of drug payloads, including biologics to acidic tumor microenvironment (TME).^{2, 3} The clinical safety and feasibility of ON-BOARD has been demonstrated by the effective delivery of fluorophores to solid tumors for imaging of multiple cancer types in Phase I/II clinical trials by pegsitacianine.⁴ Herein we report ONM-405, an ON-BOARD-encapsulated IL-2-Fc, which is designed to mask toxicity in normal tissues after systemic administration, while achieving pH-activable release of IL-2-Fc at the tumor site against solid cancers.

Methods ONM-405 was formulated through non-covalent self-assembly. pH-dependent protein release was analyzed by fast protein liquid chromatography. Anti-tumor efficacy was evaluated by tumor growth inhibition and survival in murine cancer models. Toxicity was evaluated through bodyweight loss, cytokine release syndrome, lung edema and major organ histology in mice and cynomolgus macaques.

Results ONM-405 shows pH-dependent protection and release of IL-2-Fc. Intravenous injection of ONM-405 in mice demonstrates dramatically reduced toxicity and similar antitumor efficacy compared to IL-2-Fc (figure 1). The maximum tolerated dose (MTD) of IL-2-Fc was determined as 2.1 mg/kg, Q2D×3. Using the same IL-2-Fc equivalent dose, mice treated with ONM-405 show no bodyweight loss, >100-fold reduction in systemic IFN- γ compared to unencapsulated IL-2-Fc, and undetectable lung edema. At 9-fold higher doses over the MTD of IL-2-Fc (i.e., equivalent IL-2-Fc dose of 18.9 mg/kg), ONM-405 only displayed minor, reversible adverse responses such as temporary bodyweight loss. In tumor-bearing mice, ONM-405 inhibited tumor growth at 0.14 mg/kg in immune hot MC38 tumors and 0.7 mg/kg in cold B16F10 tumors, which are comparable to IL-2-Fc. At a dose of 6.3 mg/kg (3-fold higher than MTD of IL-2-Fc), ONM-405 achieved complete response in 5/7 MC38-bearing mice. ONM-405 has significantly widened therapeutic window (>135-fold, 0.14-18.9 mg/kg) compared to IL-2-Fc (15-fold, 0.14-2.1 mg/kg). The enhanced safety profile of ONM-405 is further validated in non-human primates.

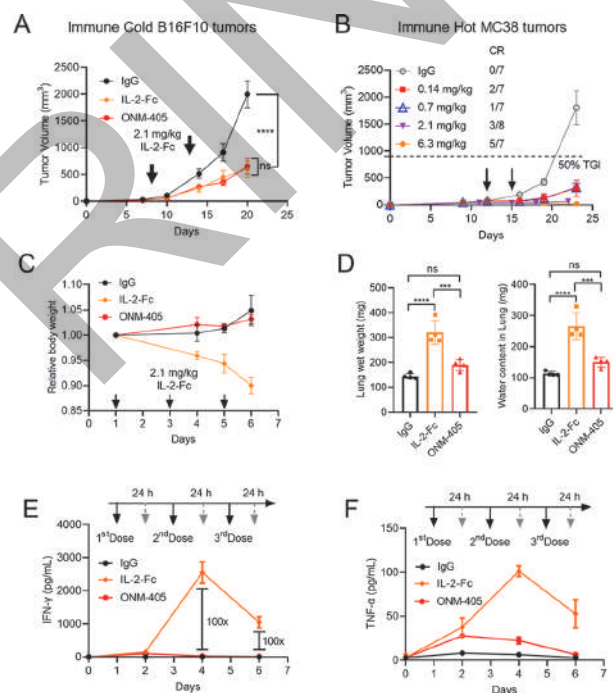
Conclusions ON-BOARD technology offers an effective tumor-directed on/off switch achieving antitumor efficacy in solid tumors in response to the acidic TME, while minimizing systemic toxicity of IL-2-Fc in normal tissues.

Acknowledgements This work is supported by a Cancer Moonshot U54 Center Award (U54 CA244719) by the National Cancer Institute and a sponsored research award from OncoNano Medicine Inc. for the scalable formulation of IL2-Fc loaded micelles for non-human primate studies.

REFERENCES

1. Bristol Myers Squibb and Nektar Announce Update on Phase 3 PIVOT 10-001 Trial [https://news.bms.com/news/details/2022/Bristol-Myers-Squibb-and-Nektar-Announce-Update-on-Phase-3-PIVOT-10-001-Trial-Evaluating-Bempegaldesleukin-BEMPEG-in-Combination-with-Opdivo-nivolumab-in-Previously-Untreated-Unresectable-or-Metastatic-Melanoma/default.aspx]
2. Bharadwaj G, Su Q, Gutowski S, et al. Encapsulating therapeutic antibodies for tumor specific activation and delivery using a clinically validated pH-sensitive nanoparticle platform. *Cancer Res.* 2022;**82**:1734.
3. Huang T, Feng Q, Wang Z, Li W, Sun Z, Wilhelm J, Huang G, Vo T, Sumer D, Gao J, Tumor-Targeted Inhibition of Monocarboxylate Transporter 1 Improves T-Cell Immunotherapy of Solid Tumors. *Adv. healthcare mater.* 2021;**10**:2000549.
4. Voskuil FJ, Steinkamp PJ, Zhao T, van der Vegt B, Koller M, Doff JJ, Jayalakshmi Y, Hartung JP, Gao J, Sumer BD, Witjes MJ. Exploiting metabolic acidosis in solid cancers using a tumor-agnostic pH-activatable nanoprobe for fluorescence-guided surgery. *Nature comm.* 2020;**11**:1-10.

Ethics Approval All animal experiments were performed with ethical compliance and approval from Institutional Animal Care and Use Committee of the University of Texas Southwestern Medical Center (APN 2017-102331).



Abstract 1329 Figure 1 ON-BOARD polymer encapsulation achieves anti-tumor efficacy while significantly reducing the toxicity of IL-2-Fc. (A) Tumor growth curve of B16F10 tumors treated with IL-2-Fc and UPS encapsulated IL-2-Fc (ONM-405) intravenously. (B) Dose escalation studies of ONM-405 in MC38 tumor models after intravenous injection. Significant tumor growth inhibition was observed, and 5/7 complete responses was achieved at 6.3 mg/kg IL-2-Fc equivalent dose. CR: complete remission. Arrows indicate the dosing time in A and B. C, Change of body weight over 6-day treatment at 2.1 mg/kg IL-2-Fc equivalent dose. Arrows indicate the dosing time. D, Lung wet weight and water content on Day 6. Same dose and treatment regimen were used as C. Serum IFN- γ (E) and TNF- α (F) during 6-day treatment with IL-2-Fc or ONM-405 at 2.1 mg/kg IL-2-Fc equivalent dose. Statistical significance was analyzed by two-way or one-way ANOVA. ***P<0.001, ****P<0.0001, ns: not significant.

<http://dx.doi.org/10.1136/jitc-2022-SITC2022.1329>

1330

CHARACTERISING THE IMMUNOTHERAPEUTIC CAPABILITIES OF BACTERIAL OUTER-MEMBRANE VESICLES

¹Jack Firth*, ²Jingjing Sun, ²Jiandong Huang, ¹Kent Gustafsson, ¹Mona Bajaj-Elliott. ¹UCL, London, UK; ²University of Hong Kong, Hong Kong, Hong Kong

Background Outer-membrane vesicles (OMVs) are highly immunogenic particles shed by Gram-negative bacteria, utilised for a variety of functions from nutrient acquisition to antibiotic resistance. Their potent immunogenicity, in combination with an inability to replicate, has led to these vesicles being developed as a novel class of vaccines. Increasing evidence also suggests that the innate immune activation stimulated by OMVs can facilitate the recognition and destruction of malignant cells, inducing a sustained elimination of tumours in various animal models.¹ At present however, the mechanistic pathways underlying the anti-tumour response remains poorly understood. Herein, we sought to investigate OMV-mediated immune interactions, elucidating key cells able to be leveraged in the context of a potential immunotherapy.

Methods OMVs were isolated from a hypervesiculating *E.coli* K-12 MG1655 strain expressing penta-acylated LPS, achieved via *pal* and *lpxM* deletions. Co-cultures were performed using peripheral blood mononuclear cells (PBMCs) from healthy donors, with cytokine and cell marker expression determined using ELISA and flow cytometry. Negatively-isolated OMV-activated lymphocytes were co-cultured with various cancer cell lines, and cytotoxicity investigated using the MTS assay and flow cytometry.

Results Our findings demonstrate that MG1655 $\Delta pal \Delta lpxM$ OMVs induce a broad increase in activation markers on NK cells, β T cells and $\gamma\delta$ T cells. We observed a concordant release of IFN- γ and granzyme B, suggesting the cells exhibit a cytotoxic phenotype upon OMV stimulation. $\gamma\delta$ T cells were found to be the predominant cell type to proliferate, expanding from 3% to 40% of the total lymphocyte population. Noticeably, the majority of $\gamma\delta$ T cells were of the V γ 9V δ 2 type, which possess the ability to respond to both bacterial metabolites as well as stress markers present on malignant cells. Since V γ 9V δ 2 T cells present an MHC-independent innate-like activation mechanism, they are well positioned to respond to OMV stimulation whilst maintaining oncolytic capabilities. Indeed, we observe robust cytolytic activity of V γ 9V δ 2 T cells against both breast cancer and leukaemia cell lines (SkBr3 and Nalm6 respectively) after OMV-mediated expansion. These data therefore identify V γ 9V δ 2 T cells as able to directly respond to OMV-stimulus whilst maintaining anti-tumour capabilities.

Conclusions Our findings support the hypothesis that V γ 9V δ 2 T cells are a crucial component of the OMV-mediated anti-tumour immune response, cells that may be used to improve future immunotherapies.

REFERENCE

1. Kim OY, Park HT, Dinh NTH, Choi SJ, Lee J, Kim JH, *et al.* Bacterial outer membrane vesicles suppress tumor by interferon-gamma-mediated antitumor response. *Nat Comms.* 2017;**8**.

Ethics Approval Human PBMC were purchased from Cambridge Bioscience. According to their site, Cambridge Bioscience source human material in partnership with Research Donors, an HTA-licensed clinic, based in London, dedicated to the collection and processing of human blood and fresh leukopaks for research purposes. Research Donors is ISO

9001 2015 certified with Research Ethics (REC) approval as a Research Tissue bank, and participates in the UK NEQAS QA scheme.

<http://dx.doi.org/10.1136/jitc-2022-SITC2022.1330>

Abstracts

1331 DUAL BLOCKADE OF THE EP2 AND EP4 PGE2 RECEPTORS WITH TPST-1495 IS AN OPTIMAL APPROACH FOR DRUGGING THE PROSTAGLANDIN PATHWAY

¹Justine Lopez, ¹Anja Holtz, ¹Dave Freund, ¹Dara Burdette, ²Dingzhi Wang, ²Raymond Duboise, ¹Sam Whiting, ¹Thomas Dubensky, ¹Brian Francica*. ¹Tempest Therapeutics, South San Francisco, CA, USA; ²MUSC, Charleston, SC, USA

Background Prostaglandin E2 (PGE2) is a bioactive lipid produced by tumor cells that drives disease progression through stimulating tumor proliferation, enhancing angiogenesis and suppressing immune function in the TME. PGE2 is also a mediator of adaptive resistance to immune checkpoint inhibitor therapy via the upregulation of cyclooxygenase-2 (COX-2). While the role of PGE2 signaling in cancer is clear, how best to inhibit PGE2 for cancer treatment remains under investigation. Inhibition of COX-1 and/or COX-2 has shown promising results in observational studies and meta-analyses, but inconsistent results in prospective studies. While COX-2 and single EP inhibitors continue to be developed, the nature of PGE2 signaling supports our rationale to inhibit PGE2 by dual antagonism of the pro-tumor EP2/EP4 receptors, while sparing the pro-immune EP1/EP3 receptors. To our knowledge, TPST-1495 is the first clinical-stage dual inhibitor of both the EP2 and EP4 receptors.

Methods We utilized in vitro murine and human whole blood assays to isolate individual effects of EP inhibitors, as well as multiple syngeneic, xenograft, and GEM models to elucidate the effects of PGE2 pathway antagonism in vivo.

Results In mouse and human blood assays, dual blockade of EP2 and EP4 receptors with TPST-1495 reversed PGE2-mediated suppression of T cells and monocytes, while single receptor antagonists were unable to block suppression at higher PGE2 concentrations. In vivo, TPST-1495 monotherapy significantly reduced tumor outgrowth in five of seven syngeneic, xenograft and genetically engineered mouse models. CT26-bearing mice treated with TPST-1495 showed significant increases immune cell infiltration by CD8+, CD4+ and NK cells, and increased M1:M2 ratio among macrophages. APC-min/+ mice treated with TPST-1495 displayed almost complete reduction in tumor burden, which was not observed with other PGE2 pathway inhibitors, and increased in immune cell presence as demonstrated by histopathology. Transcriptional analysis of resected tumors demonstrated an increase in interferon gamma signature, as well as an increase in a gene profile associated with PGE2 inhibition.

Conclusions These results demonstrate the redundancy of EP2 and EP4 receptor signaling and the requirement for EP2 and EP4 to be blocked to achieve full therapeutic effect of PGE2 inhibition in tumors. The data further define the simultaneous effect of TPST-1495 on immune and non-immune compartments that lead to tumor regression. TPST-1495 is currently being evaluated in an ongoing Phase 1 first-in-human study (NCT04344795) to characterize PK, PD, safety, and to identify a recommended phase 2 dose for expansion cohorts in key indications and biomarker-selected patients.

REFERENCES

1. Pelly VS, Moeini A, Roelofsen LM, *et al.* Anti-inflammatory drugs remodel the tumor immune environment to enhance immune checkpoint blockade efficacy. *Cancer Discov.* 2021;**11**(10):2602–2619. doi: 10.1158/2159-8290.CD-20-1815.
2. Tury S, Becette V, Assayag F, *et al.* Combination of COX-2 expression and PIK3CA mutation as prognostic and predictive markers for celecoxib treatment in breast cancer. *Oncotarget.* 2016;**7**(51):85124–85141. doi: 10.18632/oncotarget.13200.

3. Zelenay S, van der Veen AG, Böttcher JP, *et al.* Cyclooxygenase-Dependent Tumor Growth through Evasion of Immunity. *Cell.* 2015;**162**(6):1257–70. doi: 10.1016/j.cell.2015.08.015.

Ethics Approval All murine studies were performed in accordance with human animal protocols guided by an IACUC.

<http://dx.doi.org/10.1136/jitc-2022-SITC2022.1331>

1332

ANTI-CD161 ANTIBODY IMT-009 IS A NOVEL IMMUNOTHERAPEUTIC AGENT THAT REINVIGORATES T AND NK CELL FUNCTION AND ANTI-TUMOR EFFICACY THROUGH BLOCKING INTERACTION OF CD161 WITH ITS LIGAND CLEC2D

Alexandria Fusco, Elizabeth Scanlon, Frano Irvine, Flavian Brown, Jeffrey Colbert, Andy Tu, Stephanie Gaerlan, Kelly Nichols, Teresse de Rham, Matthew Huggins, Kendall Dionne, Ming Tang, Heather Flick, Alison Tisdale, Seng-Lai Tan, Shruti Malu*. *Immunitas Therapeutics, Waltham, MA, USA*

Background The CLEC2D/CD161 axis is a novel ligand-receptor pathway for immunotherapeutic intervention. IMT-009 is a monoclonal, aglycosylated human IgG1 antibody directed against CD161, a C-type lectin-like receptor, which is broadly expressed on NK cells and subsets of both CD4+ and CD8+ T cells [Mathewson et al. 2021]. Its cognate ligand, CLEC2D (LLT1), is expressed on the surface of both malignant cells and immune cells, including activated B cells and myeloid cells.

Methods Functional inhibition of CD161 by IMT-009 was demonstrated by using several in vitro pharmacological and cellular assays which assessed NK cell degranulation, cytokine production and cellular cytotoxicity towards tumor targets, as well as T cell receptor signaling and polyfunctionality using primary antigen-specific human T cells. To prioritize indications that will likely benefit from CD161 blockade therapy, multiplexed immunofluorescence analysis of over 30 solid tumor types was performed.

Results IMT-009 binds CD161 with high affinity and selectivity, blocking its interaction with CLEC2D at an IC₅₀ of 0.94 nM. In presence of CLEC2D-expressing target cells K562, NK cell degranulation, cytokine production and cellular cytotoxicity towards tumor targets is highly suppressed; IMT-009 can overcome this inhibition with an EC₅₀ of 0.2 nM. Similarly, IMT-009 reversed CLEC2D-mediated inhibition and restored T cell receptor signaling and cytokine production in a Jurkat cell reporter system (EC₅₀ = 3.5 nM), as well as enhanced polyfunctionality of primary antigen-specific human T cells, including secretion of TNF- α , IL2, and IFN γ (EC₅₀ = 0.2 nM, 0.4 nM, and 1.4 nM, respectively), and direct T cell mediated cytotoxicity. IMT-009 also released CD161-mediated suppression on effector memory CD161+ CD4+ T cells, resulting in an increased frequency of IFN- γ + cells and an increase in their proliferation indicative of a stronger recall response to antigen. Finally, multiplexed immunofluorescence data of over 30 solid tumor types showed the highest density of CLEC2D+ and CD161+ cells in the following indications: NSCLC-squamous cell carcinoma, NSCLC- adenocarcinoma, Head and Neck squamous cell carcinoma (HNSCC), Triple negative breast cancer (TNBC), Cutaneous squamous cell carcinoma and Colorectal carcinoma.

Conclusions These results support the development of IMT-009 as a novel cancer immunotherapy for application in several solid tumor indications.

REFERENCES

1. Mathewson N, Ashenberg O, Tirosh I, Inhibitory CD161 receptor identified in glioma-infiltrating T cells by single-cell analysis. *Cell*. 2021;184:1281–1298.
2. Iliopoulou IG, Karamouzis M-V, Missitzis I, Increased Frequency of CD4+ Cells Expressing CD161 in Cancer Patients. *Clin Cancer Res* 2006;12:6901-6909.

<http://dx.doi.org/10.1136/jitc-2022-SITC2022.1332>

1333 DEVELOPMENT OF IMGS-001, A NOVEL ANTI-PD-L1/PD-L2 DUAL SPECIFIC, MULTI-FUNCTIONAL ANTIBODY, TO TREAT IMMUNE EXCLUDED TUMORS

<http://dx.doi.org/10.1136/jitc-2022-SITC2022.1333>

¹Christine Gagliardi*, ¹Federica Peride, ¹Ahmad Salameh, ¹Paul Blezinger, ²Michael Curran. ¹ImmunoGenesis, Inc., Houston, TX, USA; ²MD Anderson Cancer Center, Houston, TX, USA

Background Interruption of the programmed cell death-1 (PD-1) inhibitory pathway by binding PD-1 or its ligand PD-L1 is an effective treatment for various cancers,¹ although resistance is common.² PD-1 has a second ligand, PD-L2, that can be expressed by a variety of immunosuppressive stromal cells, endothelial cells, and tumor cells.³ IMGS-001 is a dual specific monoclonal antibody designed to bind PD-L1 and PD-L2 and block their engagement with PD-1. The Fc region is engineered to induce robust cell-mediated cytotoxicity, enabling depletion of PD-L1⁺ and PD-L2⁺ immunosuppressive cells throughout the tumor microenvironment. Here we describe the development of IMGS-001, including potency, specificity, cytokine release potential, pharmacokinetics (PK), and repeat-dose toxicity

Methods Affinities were measured with the Octet system. Reporter cell assays assessed PD-1 pathway blockade, antibody-dependent cellular cytotoxicity (ADCC), and antibody-dependent cellular phagocytosis (ADCP). Specificity was evaluated by Retrogenix microarray technology. Potential for spontaneous cytokine release was measured by co-culturing with healthy donor peripheral blood mononuclear cells. PK was measured in mice and in cynomolgus monkeys. In a GLP toxicity study, IMGS-001 was dosed weekly over 4 weeks at 10, 50, or 100mg/kg with a 4-week recovery.

Results The affinity of IMGS-001 to monomeric PD-L1 and PD-L2 is 7.62nM and 1.90nM, respectively. Dimer affinities are 1.28nM and 600pM. It has an EC₅₀ of 0.3-1.1nM in a PD-1 blockade assay, the same range as pembrolizumab and avelumab. IMGS-001 has an EC₅₀ of <0.5nM in ADCC and ADCP assays. Specificity screening showed no relevant off-target binding and there was no evidence of specific cytokine release. Mouse PK showed drug exposure of ~1.0x10⁴ µg-hr/ml at the efficacious dose. Half-life was 3.2 days in mice, and 3.7 days in cynos. Repeat-dose toxicity showed mild to moderate hematological and pathological changes, all of which had evidence of reversal within the recovery period. IMGS-001 was manufactured with a titer of 5.95g/L, 98.9% monomer, and 98% purity in the first GMP batch.

Conclusions These data indicate that IMGS-001 binds PD-L1 and PD-L2 and functions per its design. It shows no biologically relevant off target effects, was administered up 100 mg/kg without toxicity, and has a viable PK profile for human administration. Its mechanisms of elimination of immunosuppressive cells with PD-1 pathway blockade could benefit patients that are resistant to existing PD-(L)1 drugs by restoring immune driven anti-tumor activity. IMGS-001 is poised to enter clinical trial in immune excluded tumors by the end of 2022.

REFERENCES

1. Alsaab HO, Sau S, Alzhrani R, Tatiparti K, Bhise K, Kashaw SK, & Iyer AK. PD-1 and PD-L1 Checkpoint Signaling Inhibition for Cancer Immunotherapy: Mechanism, Combinations, and Clinical Outcome. *Front Pharmacol.* 2017;**8**:561.
2. Syn NL, Teng M, Mok T, & Soo RA. (2017). De-novo and acquired resistance to immune checkpoint targeting. *Lancet. Oncol.* 2017;**18**(12):e731–e741.
3. Yearley JH, Gibson C, Yu N, Moon C, Murphy E, Juco J, Lunceford J, Cheng J, Chow L, Seiwert TY, Handa M, Tomassini JE, & McClanahan T. (2017). PD-L2 Expression in Human Tumors: Relevance to Anti-PD-1 Therapy in Cancer. *Clin Cancer Res.* 2017;**23**(12):3158–3167.

1334 AVA-ADR-001 SUPPRESSES TUMOR GROWTH AND INDUCES ANTI-TUMOR IMMUNITY BY SELECTIVELY INHIBITING ADAR1 P150

Arun B Pappiah, Avijit Goswami, Sandeep Goyal, Kawaljit Singh, Princy Khurana, Aditya Kulkarni*. Avammune Therapeutics Inc., Levittown, PA, USA

Background Adenosine deaminase, RNA specific (ADAR1), catalyzes the hydrolytic deamination of adenosine (A) to inosine (I) in double-stranded (ds) RNAs. There are 2 isoforms of ADAR1 (p110 in the nucleus; p150 in cytoplasm) and both modify self dsRNA in coding and non-coding regions. The ADAR1 p150 isoform is expressed from an interferon (IFN)-response promoter and has a Z-DNA/Z-RNA binding domain at the N-terminus. ADAR1 p150 edits 3'-untranslated region dsRNAs comprising of inverted *Alu* repeats and thereby suppresses MDA5-MAVS-IFN signaling. ADAR1 is commonly overexpressed in multiple myeloma, breast, lung, liver, skin and esophageal cancer where it promotes cancer progression. Inhibition of ADAR1 has promising anti-tumor efficacy as monotherapy and in combination with checkpoint inhibitors, radiotherapy and chemotherapeutic modalities. Herein, we outline the discovery of a potential first-in-class ADAR1 inhibitor for cancer immunotherapy.

Methods AVA-ADR-001 was identified through a high throughput p110 knockout cell-based assay. The ability of AVA-ADR-001 to induce interferons was confirmed in various cell lines like A549 p110 KO, HCT116 and B16F10. Finally, the anti-tumor efficacy of AVA-ADR-001 was evaluated in B16F10 syngeneic melanoma mice model as monotherapy and in combination with anti-PD-1.

Results We have identified a first-in-class small molecule inhibitor of ADAR1, which shows significant IFN response *in vitro* in an MDA5 dependent manner. *In vitro* binding studies have confirmed direct binding of AVA-ADR-001 with the Z α domain of ADAR1 thus confirming its selectivity to the p150 isoform. AVA-ADR-001 demonstrates micromolar EC50 and anti-tumor efficacy against B16F10 melanoma syngeneic mouse model. 100 μ g of AVA-ADR-001 treatment resulted in 45% tumor growth inhibition (TGI), 1.5x superior to Anti-PD1 treatment. Combining AVA-ADR-001 with Anti-PD1 demonstrated a synergistic effect 2x superior to Anti-PD1 alone. Additionally, several interferon stimulated genes like IFIH1, IFN- β and CXCL-10 were significantly upregulated in the tumor samples of the AVA-ADR-001 monotherapy and combination groups.

Conclusions To our knowledge no selective small molecule inhibitors of ADAR1 have been reported so far and AVA-ADR-001 is the first disclosure of such an inhibitor. AVA-ADR-001 is a potent and selective first-in-class ADAR1 inhibitor which has shown significant IFN induction in various cancer cell lines and *in vivo* in the tumor microenvironment resulting in substantial tumor growth inhibition as monotherapy and synergistically in combination with Anti-PD1. Considering the immune-suppressive and pro-metastatic role of ADAR1, AVA-ADR-001 serves as a promising starting point for novel ADAR1 inhibitors as therapeutic modalities in cancer immunotherapy.

<http://dx.doi.org/10.1136/jitc-2022-SITC2022.1334>

1335 **AVA-NP-695 POTENTLY AND SELECTIVELY INHIBITS ENPP1 TO ACTIVATE STING PATHWAY AND ABROGATE TUMOR METASTASIS IN 4T1 BREAST CANCER SYNGENEIC MOUSE MODEL**

Aditya Kulkarni*, Avijit Goswami, Sandeep Goyal, Princy Khurana, Arun Papaiah. Avammune Therapeutics Inc., Levittown, PA, USA

Background Innate immune modulators such as STING agonists have become attractive approaches to improve the efficacy of Immune Checkpoint Inhibitors (ICI) due to their ability to turn cold tumors hot. Owing to the modest clinical efficacy of STING agonists, there is a need for other approaches for activating the cGAS-STING pathway for cancer immunotherapy. One such approach is through the inhibition of the enzyme ENPP1, a negative regulator of the STING pathway which directly hydrolyses 2'3'- cGAMP. *ENPP1* is overexpressed in several tumor cells like human astrocyte tumors and TNBC cells like 4T1 and MDA-MB-231, and plays a key role in tumor progression and block T cell infiltration in breast and lung cancer patients. ENPP1 not only abolishes the cGAS-STING mediated immune activation but also produces adenosine, an immune suppressor which promotes cell migration. AVA-NP-695 is a highly potent orally available ENPP1 inhibitor being developed for cancer immunotherapy.

Methods The inhibition potency of AVA-NP-695 was confirmed by enzymatic assays using various substrate like p-Nitrophenyl-5'-TMP, cGAMP and ATP. The efficacy of AVA-NP-695 was depicted in 4T1 Tumor bearing BALB/c mice as monotherapy and in combination with anti-PD-L1, Olaparib and Paclitaxel. Efficacy of AVA-NP-695 in combination with radiation (6.2Gy X 4) was also evaluated in ENPP1 overexpressing ANV5 tumors.

Results Herein, we demonstrate that AVA-NP-695, a selective and potent ENPP1 inhibitor showed no adverse effect at 1000mg/kg BID in 7 Day repeated dose in BALB/C mice, thereby demonstrating an excellent therapeutic window?. Results from in vivo studies have shown superior tumor growth inhibition (TGI) and impact on tumor metastasis by AVA-NP-695 (6mg/kg BID) compared to Olaparib and Anti-PD1 in a syngeneic 4T1 breast cancer mouse model. Subsequently, combination of AVA-NP-695 with Anti-PDL1, Olaparib and Paclitaxel and demonstrated encouraging combinatorial efficacy of AVA-NP-695 along with Paclitaxel. Monotherapeutic arm for Paclitaxel and AVA-NP-695 depicted 40% and 44% TGI respectively, however their combined treatment resulted in ~60% TGI. Additionally, the AVA-NP-695 treatment alone showed 50% enhanced mean survival time followed by 68%, 68% and 72% when given in combination with anti-PD-L1, Olaparib and Paclitaxel respectively. Finally, AVA-NP-695 showed complete tumor ablation of ANV5 ENPP1 overexpressed tumors when given in combination with radiation. Combination group showed significantly delayed recurrence compared to only radiotherapy.

Conclusions The potent anti-tumor efficacy of AVA-NP-695 both as monotherapy and combination along with its safety profile provides a strong rationale for the therapeutic potential of AVA-NP-695 against solids tumors, particularly breast cancer.

<http://dx.doi.org/10.1136/jitc-2022-SITC2022.1335>

1336

DPX-BASED IMMUNE EDUCATION RECRUITS AND ACTIVATES UNIQUE SUBSETS OF ANTIGEN PRESENTING CELLS TO DRIVE IMMUNOGENICITY OF PEPTIDE ANTIGENS

<http://dx.doi.org/10.1136/jitc-2022-SITC2022.1336>

Brennan Dirk*, Moamen Bydoun, Ava Vila-Leahey, Erin Kelly, Olga Hrytsenko, Jeremy Graff. *IMV inc., Dartmouth, Canada*

Background For peptide-based cancer vaccines, successful eradication of tumors relies on the effective and persistent delivery of antigenic peptides to antigen presenting cells (APCs) to prime potent antigen-specific, cytotoxic T cells. Peptide-based vaccines have historically been either; (1) water-based formulations, which provide short exposure of peptides to immune cells; or (2) oil-in-water emulsions that provide longer peptide exposure but can elicit dysfunctional and exhausted T cell phenotypes. By contrast, the DPX® technology is a non-aqueous, lipid-in-oil, immune-educating therapeutic delivery platform. Antigenic peptides formulated in DPX elicit a robust, targeted, and persistent tumor antigen-specific T cell response that for our lead DPX product, Maveropepimut-S, has translated into clinical benefit in multiple cancer indications, including DLBCL and ovarian cancer.

Methods Herein, we compare DPX to aqueous and emulsion-based formulations for the dynamics of immune cell recruitment to the site of injection (SOI), peptide antigen consumption, and trafficking by immune cells. Immune cell composition and antigen uptake at the SOI were assessed by multi-parameter flow cytometry and confocal microscopy using model peptide antigens administered in C57/Bl6 mice. Antigen-specific immune responses were assessed in draining lymph nodes and/or spleens by IFN- γ ELISPOT.

Results These data reveal that aqueous formulations were poorly able to retain lymphocytes at SOIs and consequently did not elicit a detectable IFN- γ ELISPOT response. Both formulations containing an oil component (DPX and emulsion) were superior in recruiting APCs cells to the SOIs and inducing antigen-specific immune responses. Significant increases in immune cell infiltration were detected as early as 2 days post DPX injection. Antigen uptake was confirmed using confocal microscopy. Both DPX and emulsion platforms induced a prompt increase in antigen presentation in the context of MHC. However, antigen presentation driven by the DPX platform had a distinct profile enriched in CD11b⁺CD11c⁺MHCII⁺ APCs co-expressing the CD80, CD86, and CD40 activation/costimulatory markers. The recruitment and activation of this subset was evident regardless of whether a peptide was present in DPX. By contrast, the emulsion incites a distinctly different CD11b⁻CD11c⁻ population. Interestingly, CD11b⁺CD11c⁺ cells have tendency to express higher number of peptide-MHC complexes per cell compared to the CD11b⁻CD11c⁻ population.

Conclusions Collectively these findings highlight quantitative, qualitative, and temporal differences in immune cell recruitment amongst three delivery platforms and show the unique character of the immune response triggered by the DPX platform typified by the recruitment of CD11b⁺CD11c⁺ APCs that have intrinsically higher capacity for antigen uptake, presentation, and activation.

Ethics Approval Experiments were conducted in accordance with ethics protocols approved by the University Committee on Laboratory Animals at Dalhousie University, Halifax, N.S., Canada.

1337

PRECLINICAL EVALUATION OF STAR0602, A NOVEL, FIRST-IN-CLASS ANTI-TCR V β TARGETED BISPECIFIC ANTIBODY WITH POTENT ANTI-TUMOR ACTIVITY FOR PD-1 REFRACTORY SOLID TUMORS

¹Zhen Su, ^{2,3}James Gulley*, ²Jeffrey Schlom, ⁴Lillian Siu, ⁵Ryan Sullivan, ⁶E John Wherry, ¹Ke Liu, ³Renee Donahue, ¹Madan Katraggada, ⁷Rajesh Chopra, ¹Jacques Moisan, ¹Jonathan Hsu, ³Yo-Ting Tsai. ¹Marengo Therapeutics, Cambridge, MA, USA; ²NCI, Bethesda, MD, USA; ³NIH, Bethesda, MD, USA; ⁴Princess Margaret Cancer Center, Toronto, Canada; ⁵MGH, Boston, MA, USA; ⁶UPENN, Philadelphia, PA, USA; ⁷Marengo Therapeutics, London, UK

Background Despite recent advancements with immune checkpoint inhibitors (e.g., anti-PD1 inhibitors) many cancer patients develop treatment resistance, which supports the study of alternative approaches to induce potent and safe anti-tumor T cell responses. STAR0602 is a bifunctional antibody-fusion molecule that selectively activates and expands a sub-set of human $\alpha\beta$ T cells expressing variable (V) b6 and b10 regions of the T cell receptor (TCR). STAR0602 simultaneously engages a novel, non-clonal mode of TCR activation with cytokine co-stimulation.

Methods The prevalence of STAR0602-targeted V β T cells in tumor-infiltrating lymphocytes (TILs) from human tumor tissues was investigated by flow cytometry and by interrogating TIL TCRseq data from a large cancer database. The effects of STAR0602 on T cells from healthy donors and cancer patients were assessed *in vitro* by flow cytometry and NanoString. Using high tumor mutational burden (TMB) and anti-PD1-insensitive murine and human models, we investigated anti-tumor activity, mechanism of action, and an enrichment strategy for patient trials. Finally, the pharmacokinetics (PK) and pharmacodynamics (PD) of IV STAR0602 were investigated in Cynomolgus monkeys.

Results Presence of STAR0602-targeted V β T cells were confirmed in tissue from a range of human tumors, and present as 10-12% of TILs. Stimulation of T cells with STAR0602 resulted in potent expansion with ~80% adopting a novel memory phenotype, and significant boosting of antigen-specific T cells. In human autologous tumor organoid models, STAR0602 induced potent expansion of TILs and killing of tumors, including several PD1 refractory tumors. Dose-related anti-tumor activity (100% cure rate with a murine surrogate (mSTAR0602)) in EMT6-bearing mice correlated with expansion of memory V β CD8⁺ T cells. In Cynomolgus monkeys, IV STAR0602 induced robust expansion of V β CD8⁺ T cells in blood, with limited cytokine release or expansion of Treg. These data were used to build a PK/PD model to simulate human pharmacology and design a first-in-human trial with an enriched patient population.

Conclusions STAR0602 is a first-in-class T cell activator that targets subsets of the germline TCR repertoire that are enriched in TILs. STAR0602 potently expands both naive and antigen-specific human T cells. In PD1 refractory human and murine tumor models with a high TMB, STAR0602 and mSTAR0602 induce potent anti-tumor activity as monotherapy, mediated by selective expansion of V β CD8⁺ memory T cells. This pharmacology was translated into monkeys with IV dosed STAR0602 and supports the design of a novel Phase 1/2 precision-oncology trial with STAR0602 planned to commence in 2022.

<http://dx.doi.org/10.1136/jitc-2022-SITC2022.1337>

1338

SRF114, AN AFUCOSYLATED ANTI-CCR8 ANTIBODY, DEPLETES INTRATUMORAL TREG CELLS AND REDUCES TUMOR GROWTH

Robert Haines*, Marisella Panduro, Andrew Lake, Vito Palombella, Jonathan Hill, James Mohan. *Surface Oncology, Cambridge, MA, USA*

Background Intratumoral regulatory T (Treg) cells promote an immunosuppressive tumor microenvironment, and their increased frequency correlates with poor clinical prognosis.¹⁻⁴ Gene expression profiling has identified chemokine receptor 8 (CCR8) as being highly upregulated by intratumoral Treg cells compared to their lymphoid tissue and blood counterparts, as well as other immune cell types.^{5,6} Because of this restricted expression, using anti-CCR8 antibodies capable of inducing antibody-dependent cellular cytotoxicity (ADCC) and antibody-dependent cellular phagocytosis (ADCP) to deplete intratumoral Treg cells represents an attractive therapeutic hypothesis for cancer treatment. Treatment of mouse cancer models with anti-CCR8 antibodies depleted intratumoral Treg cells and reduced tumor growth.^{7,8} Furthermore, anti-CCR8 treatment can synergize with anti-PD-1 treatment in anti-PD-1-susceptible and -resistant cancer models, highlighting the therapeutic potential of anti-CCR8 antibodies.

SRF114 is a fully human, afucosylated anti-CCR8 antibody designed to preferentially deplete CCR8⁺ Treg cells within the tumor microenvironment. Here, we explore the ability of SRF114 to activate effector immune cells associated with ADCC and ADCP, deplete Treg cells, and reduce tumor growth in a mouse cancer model.

Methods Surface expression of CCR8 on human intratumoral and peripheral immune cells was characterized by flow cytometry. Human peripheral blood mononuclear cells (PBMCs) and dissociated tumor cells (DTCs) were cultured with SRF114 to examine immune cell activation and Treg cell depletion. The efficacy of SRF114 was assessed in MC38 tumor-bearing human CCR8 knock-in (hCCR8 KI) mice.

Results CCR8 surface expression was highest on intratumoral Treg cells compared with peripheral Treg cells and other immune cells. In PBMC cultures, Fc gamma receptor (FcγR)-expressing cells, including natural killer (NK) cells and monocytes, exhibited dose-dependent activation from SRF114 bound to CCR8⁺ cells. DTC cultures treated with SRF114 also displayed dose-dependent NK cell activation and selective Treg cell depletion, with marginal impacts on effector T cell populations. The potency of SRF114 to activate FcγR⁺ cells in DTCs was enhanced compared with that in PBMCs due to increased CCR8 expression on Treg cells. In a syngeneic tumor model, hCCR8 KI mice treated with SRF114 exhibited a significant reduction in tumor growth and depletion of intratumoral Treg cells, with minimal impact on their peripheral counterparts.

Conclusions SRF114 can induce ADCC and/or ADCP pathways to deplete CCR8⁺ Treg cells in vitro. Demonstrated depletion of intratumoral Treg cells and reduction of tumor growth in vivo support SRF114 as a therapeutic candidate to deplete intratumoral Treg cells and drive antitumor immunity in human cancer patients.

REFERENCES

1. Plitas G, Rudensky AY. Regulatory T cells in cancer. *Annu Rev Cancer Biol.* 2020;**4**:459–477.
2. Fu J, Xu D, Liu Z, *et al.* Increased regulatory T cells correlate with CD8 T-cell impairment and poor survival in hepatocellular carcinoma patients. *Gastroenterology.* 2007;**132**(7):2328–2339.

3. Petersen RP, Campa MJ, Sperlazza J, *et al.* Tumor infiltrating Foxp3+ regulatory T-cells are associated with recurrence in pathologic stage I NSCLC patients. *Cancer.* 2006;**107**(12):2866–2872.
4. Shen Z, Zhou S, Wang Y, *et al.* Higher intratumoral infiltrated Foxp3+ Treg numbers and Foxp3+/CD8+ ratio are associated with adverse prognosis in resectable gastric cancer. *J Cancer Res Clin Oncol.* 2010;**136**(10):1585–1595.
5. Alvisi G, Brummelman J, Puccio S, *et al.* IRF4 instructs effector Treg differentiation and immune suppression in human cancer. *J Clin Invest.* 2020;**130**(6):3137–3150.
6. Haruna M, Ueyama A, Yamamoto Y, *et al.* The impact of CCR8+ regulatory T cells on cytotoxic T cell function in human lung cancer. *Sci Rep.* 2022;**12**(1):5377.
7. Campbell JR, McDonald BR, Mesko PB, *et al.* Fc-optimized anti-CCR8 antibody depletes regulatory T cells in human tumor models. *Cancer Res.* 2021;**81**(11):2983–2994.
8. Van Damme H, Dombrecht B, Kiss M, *et al.* Therapeutic depletion of CCR8+ tumor-infiltrating regulatory T cells elicits antitumor immunity and synergizes with anti-PD-1 therapy. *J Immunother Cancer.* 2021;**9**(2):e001749.

<http://dx.doi.org/10.1136/jitc-2022-SITC2022.1338>

1339

ALD2510: NEXT GENERATION FC-ENHANCED, T_{REG}-SELECTIVE AND IL-2-SPARING ANTI-CD25 ANTIBODY WITH PROMISING POTENTIAL FOR THE TREATMENT OF GYNECOLOGICAL CANCERS

<http://dx.doi.org/10.1136/jitc-2022-SITC2022.1339>

¹Jemila Houacine, ¹Riad Abes, ²Anne Marie-Cardine, ¹Aude LeRoy, ³Jérôme Giustiniani, ⁴Anne-Sophie Chrétien, ⁴Stéphane Fattori, ⁴Laurent Gorvel, ²Armand Bensussan, ⁵Daniel Olive, ¹Arnaud Foussat*. ¹Alderaan Biotechnology, Paris, France; ²INSERM U976, Hôpital Saint Louis, Paris, France; ³INSERM U955, Hôpital Henri Mondor, Créteil, France; ⁴Institut Paoli Calmettes, Marseille, France; ⁵Institut Paoli Calmettes, INSERM UMR1068, Marseille, France

Background Regulatory T cells (T_{REG}) inhibit immune responses in many solid cancers and are associated with worse prognosis when they infiltrate tumours. ALD2510 is a low-fucose IL-2-sparing anti-CD25 antibody designed for the selective depletion of T_{REG}, allowing the boost of immune effector functions within the tumor micro-environment (TME) and making it a promising candidate for therapy of solid tumors.

Methods ALD2510 potency and mechanisms of action were investigated in T_{REG} depletion, ADCC, ADCP and trogocytosis assays and in syngeneic or humanized animal models of cancer. Characterization of T_{REG} subpopulations within the TME was achieved by flow and mass cytometry followed by t-sne analysis using biopsies from gynecological cancer patients. ALD2510 safety, tolerability and pharmacokinetic (PK) profile were determined in cynomolgus monkey, with doses up to 100mg/kg. ALD2510 manufacturability was assessed through fed-batch production and analytical characterization.

Results ALD2510 showed strong T_{REG} depletion, ADCC and ADCP activities, while sparing CD4⁺ and CD8⁺ T cell compartments, demonstrating its selectivity for T_{REGS} and a mode of action involving multiple effector cell types. ALD2510 also promoted trogocytosis of induced T_{REG}, suggesting that tumour-infiltrating neutrophils may contribute to its function. In vivo, as monotherapy, ALD2510 confirmed selective and potent T_{REG} depletion together with significant tumor growth inhibition, which could be further improved when combined with checkpoint inhibitors, leading to complete tumor regressions.

Immunophenotyping of tumor biopsies and related PBMCs from gynecological cancer patients and further t-sne analysis allowed the identification of four T_{REG} subsets. That with the highest CD25 expression was shown to be tumour specific and presented the most immunosuppressive phenotype, thus constituting a preferential target for ALD2510.

In a cynomolgus exploratory toxicology study, ALD2510 showed excellent safety and tolerability with doses up to 100mg/kg. PK and exposition parameters were found in line with those of typical humanized IgG1 in NHP.

The manufacturability of the ALD2510 CHO cell line was demonstrated through 10L fed-batch production, where productivity reached ~4g/L. Analytical characterization of purified ALD2510 materials revealed excellent purity and activity, together with very low levels of process/cell-related impurities.

Conclusions ALD2510 is a next generation Fc-enhanced, T_{REG}-selective and IL-2-sparing anti-CD25 mAb showing *in vitro* and *in vivo* efficacy, fully satisfactory safety and tolerability in NHP and excellent manufacturability. ALD2510 thus appears as a promising candidate for treatment of solid tumor patients, especially those suffering from gynecological malignancies, where highly immunosuppressive CD25^{high} T_{REGS} were identified in the TME.

1340

BT7455, A FULLY SYNTHETIC BICYCLE TUMOR-TARGETED IMMUNE CELL AGONIST[®], LEADS TO POTENT EPHA2-DEPENDENT CD137 AGONISM AND ROBUST ANTI-TUMOR EFFICACY

Kristen Hurov*, Lia Luus*, Johanna Lahdenranta, Punit Upadhyaya, Heather Cohen, Chinmayee Shah, Julia Kristensson, Peter Brown, Gemma Mudd, Carly Campbell, Elizabeth Repash, Eric Haines, Sailaja Battula, Mike Kelly, Phil Jeffrey, Paul Beswick, Lihong Chen, Kevin McDonnell, Philip Brandish, Nicholas Keen. *Bicycle Therapeutics, Lexington, MA, USA*

Background To address the limitations of antibody-based agonists of immune costimulatory receptors, we have developed a new class of modular synthetic drugs, termed *Bicycle*[®] tumor-targeted immune cell agonists (*Bicycle*[®] TICAs), which are multifunctional molecules comprised of constrained bicyclic peptides (*Bicycles*).¹ The first molecule of this class, BT7480, a Nectin-4-dependent CD137 (4-1BB) agonist, entered clinical trials in 2021 in patients with solid tumors associated with Nectin-4 expression. Compelling preclinical data characterizing BT7480² led us to develop a second *Bicycle* TICA[™] molecule, BT7455, which is designed to deliver highly potent CD137 agonism to Ephrin receptor A2 (EphA2)-positive cancers. EphA2 is a receptor tyrosine kinase overexpressed in several human cancers and its high expression correlates with poor clinical prognosis in certain cancer types.^{3, 4}

Methods BT7455 bioactivity was assessed *in vitro* using a CD137 reporter assay and by measuring proinflammatory cytokine production in human PBMC/tumor cell co-cultures. BT7455 *in vivo* pharmacological activity was evaluated in efficacy studies in syngeneic EphA2-positive mouse tumor models and pharmacodynamic studies using transcriptional profiling of the tumor immune microenvironment by NanoString.

Results BT7455 engages EphA2 and CD137 with high affinity resulting in picomolar potency in co-culture assays consisting of EphA2-expressing tumor cells and CD137-expressing Jurkat NF-κB-luciferase reporter cells. Moreover, BT7455 led to EphA2-dependent production of interleukin-2 (IL-2) and interferon gamma (IFNγ) in primary human PBMC/tumor cell co-culture assays. Treatment of MC38 tumors in immunocompetent mice with BT7455 with an intermittent dosing regimen led to robust anti-tumor activity, including complete responses. Gene expression profiling of BT7455-treated tumors revealed modulation of the tumor immune microenvironment, including a rapid increase in cytokine expression (both myeloid and T cell origin) and an increase in cytotoxic cell scores. The kinetics and extent of the immune microenvironment modulation differentiated BT7455 from both a checkpoint inhibitor (anti-mouse PD-1) as well as an anti-CD137 agonist antibody (Urelumab analogue). BT7455 treatment also led to the increase in checkpoint gene expression, suggesting that combination with checkpoint inhibitor therapy may be effective. BT7455 exhibits linear pharmacokinetics in non-human primates and appears well-tolerated at exposures more than the predicted efficacious exposure in humans without significant elevation of cytokines or liver enzymes.

Conclusions BT7455 is a highly potent EphA2 expression-dependent CD137 agonist with optimal target binding, pharmacologic, and pharmacokinetic properties that enable intermittent dosing for curative effect through modulation of the tumor immune microenvironment in syngeneic mouse models. BT7455 is currently being evaluated in IND-enabling safety studies.

REFERENCES

1. Upadhyaya P, Lahdenranta J, Hurov K, *et al.* Anticancer immunity induced by a synthetic tumor-targeted CD137 agonist. *JITC.* 2021;**9**:e001762.
2. Hurov K, Lahdenranta J, *et al.* BT7480, a novel fully synthetic Bicycle tumor-targeted immune cell agonist[™] (Bicycle TICA[™]) induces tumor localized CD137 agonism. *JITC.* 2021;**0**:e002883.
3. Campbell C, *et al.* A survey of EphA2 expression by immunohistochemistry (IHC) in tumor tissue microarrays (TMAs) to support BT5528 indication selection. *Cancer Res.* 2020;**80**(16_Supplement):5300.
4. Xiao, *et al.* Targeting EphA2 in cancer. *Journal of Hematology & Oncology.* 2020;**13**:114.

Ethics Approval All the procedures related to animal handling, care and treatment in the studies were performed according to the guidelines approved by the Institutional Animal Care and Use Committee of WuXi AppTec (Beijing, China), following the guidance of the Association for Assessment and Accreditation of Laboratory Animal Care.

<http://dx.doi.org/10.1136/jitc-2022-SITC2022.1340>

1341

CD27 AN EMERGING IMMUNO-ONCOLOGY TARGET AT THE CROSS-ROADS OF INNATE AND ADAPTIVE ANTI-TUMOR IMMUNE RESPONSES

Thierry Guillaudeux*, Shawn Iadonato, Jessica Cross, Nathan Eyde, Emily Frazier, Neda Kabi, Chen Katz, Remington Lance, Yulia Ovechkina, Kurt Lustig, David Peckham, Shaarwari Sridhar, Carla Talboux, Isabelle Tihista. *Kineta Inc., Seattle, WA, USA*

Background CD27 is a member of the TNF-Receptor superfamily expressed on CD4+ and CD8+ T cells, on NK and NKT cells and on B cells. It promotes T cell co-activation, proliferation, clonal expansion and differentiation into antigen specific cytotoxic and memory T cells after stimulation with its ligand CD70. Its stimulatory signal is mediated via the NF κ B pathway, but also via the phosphatidylinositol 3 kinase and the protein kinase B. Moreover, CD27 signaling influences the innate immune response via a direct activation of NK cells and a subsequent secretion of interferon-gamma (IFN- γ). CD27 plays a central role in immunological responses and by promoting T cell and NK cell activation it contributes to anti-tumor immunity. Previous studies have demonstrated tumor growth inhibition with anti-CD27 agonistic monoclonal antibodies in different mice models for solid and hematological tumors. This mechanism of action can be partly explained by the recruitment of IFN- γ producing CD8+ T cells within the tumor. CD27 is a promising target for antitumor therapy.

Methods Kineta has generated a library of 147 fully human anti-CD27 monoclonal antibodies after immunization of Tri-anni mice.

Results From this library, a lead candidate with strong agonistic properties has been selected. This anti-CD27 antibody originates from a unique clade after alignment of the variable heavy chains. Kineta's lead candidate demonstrates selectivity and cross-reactivity with Non-Human Primate (NHP)-CD27 but not with the mouse-CD27. It also induces strong NF κ B signaling in a Jurkat T cell-reporter, either soluble or cross-linked. It also induces T cell proliferation and secretion of pro-inflammatory cytokines *in vitro*. This T cell activation occurs only in the presence of a TCR engagement preventing future risks of spontaneous activation of naïve T cells *in vivo*. Our lead antibody also induces direct activation of NK cells demonstrated by the expression of CD69 on their surface. We have evaluated the anti-tumor properties of our lead antibody as a single agent *in vivo* in human CD27 Knock-In (KI) mice. Our anti-CD27 candidate induces a significant anti-tumor activity in the EG7 thymoma model. We have also demonstrated the anti-tumor efficacy of this lead candidate in Raji cells implanted in Scid mice. Preliminary experiments performed in human CD27 KI mice have demonstrated a long half-life of our antibody at different concentrations.

Conclusions Epitope characterization, NHP pharmacokinetic analysis and additional *in vivo* studies of our lead anti-CD27 antibody in different tumor models use as a single agent and in combination with different check-point inhibitors are ongoing.

<http://dx.doi.org/10.1136/jitc-2022-SITC2022.1341>

1342

THERAPEUTIC TARGETING OF MARCO WITH PY265 ANTIBODY PROMOTES MYELOID CELL REPROGRAMMING AND UNLEASHES ANTI-TUMOR IMMUNITY

<http://dx.doi.org/10.1136/jitc-2022-SITC2022.1342>

Linnea Haegglblom*, Subhadra Dash, Yelena Vayn, Josh Rudolph, Rachael Palmer, Xi Yang, Sergio Lacayo, Cesar Juarez, Erin Mayes, Rachel Greathouse, Kara Mojica, Carlos Santamaria, Johanna Ramoth, Ranna Mehta, Maryam Yousefi, Nadine Jahchan, Svetlana Gratch, Amy-Jo Casbon, Joshua Pollack, Marc Chamberlain, Leonard Reyno, Matthew Myers, Vladislava Juric, Linda Liang, Kristen Pierce, Kevin Baker, Nadine Jahchan. *Pionyr Immunotherapeutics, South San Francisco, CA, USA*

Background The tumor microenvironment (TME) contains immunosuppressive myeloid cells that contribute to checkpoint inhibitor (CPI) resistance. One approach as part of Pionyr Immunotherapeutics' Myeloid Tuning™ strategy is to reprogram immunosuppressive myeloid cells to acquire an immunostimulatory anti-tumor phenotype. Macrophage Receptor with a Collagenous Structure (MARCO) is an attractive target for myeloid reprogramming, considering its immunomodulatory function and expression on tumor-associated macrophages (TAMs) and monocytic myeloid derived suppressor cells (mMDSCs) in the TME. Pionyr has developed a humanized IgG1 k anti-MARCO monoclonal antibody, PY265, to investigate the potential of MARCO modulation as an anti-cancer immunotherapeutic strategy.

Methods MARCO expression on TAMs and mMDSCs from multiple solid tumor indications was determined by single-cell RNA sequencing and by using immunohistochemistry (IHC). PY265 activity on human monocyte derived macrophages (hMDMs) in vitro was evaluated by transcriptional profiling, phosphoprotein array, flow cytometry, and cytokine/chemokine measurements. In vivo efficacy and pharmacodynamic studies using a surrogate anti-mouse MARCO antibody, PY265m, as single agent or in combination with anti-PD-1, were evaluated using syngeneic mouse tumor models.

Results MARCO is specifically enriched in a cluster of TAMs and mMDSCs that correlates with immunosuppressive signatures in multiple solid tumor types. Moreover, IHC profiling shows that MARCO is commonly expressed in the TME of these tumors, and maintain expression in metastatic lesions, as well as in chemo- and CPI-treated tumors. PY265 induces reprogramming in hMDMs in vitro through induction of rapid phosphorylation events, transcriptional activation of pro-inflammatory pathways, production of cytokines and chemokines, and upregulation of cell surface activation receptors. PY265m demonstrates significant anti-tumor activity in syngeneic mouse models as single agent in CPI-sensitive models and in combination with anti-PD-1 in CPI-resistant models. Pharmacodynamic studies suggest that PY265m induces immune activation by reprogramming pro-tumorigenic, M2-like TAMs and mMDSCs to pro-inflammatory anti-tumor M1-like macrophages and monocytes, leading to an increase in infiltration of effector cells in the tumor, spleen, and tumor draining lymph nodes. In a non-human primate toxicokinetic study, PY265 was generally well tolerated at all dose levels tested.

Conclusions Our study demonstrates that targeting MARCO reprograms myeloid cells and remodels the TME to unleash anti-tumor immunity and convert CPI-resistant tumors into treatment responsive tumors. Collectively, these preclinical data support PY265 immunotherapy, alone or in combination with a CPI, in cancer patients resistant or refractory to CPI therapies, to potentially improve both the overall response rate as well as durability of response. First-in-human testing of PY265 will be initiated in 2023.

1343

ANTITUMOR EFFECT OF DA-4507, A NOVEL GCN2 INHIBITOR AS AN IMMUNOTHERAPY IN THE TUMOR MICROENVIRONMENT

cells independent of environmental amino acid sensing. *Cell Rep.* 2016;17(9):2247–2258

<http://dx.doi.org/10.1136/jitc-2022-SITC2022.1343>

Youngjee Jeong*, Jun-Hwan Moon, Ik-Soo Jang, Kyu Hwan Kim, Na Yeon Park, Hyung Ki Lee, Cheonhyoung Park, Tae-Hun Kim, Do Young Choi, Ha Yoon Kim, Ki Moon Ryu, Min Jung Lee, Hyounmie Doh. *Dong-A ST, Yong-in, Korea, Republic of*

Background General control nonderepressible 2 (GCN2) kinase is an integrated stress response (ISR) kinase that responds to amino acid deficiency.¹ Activation of GCN2 in tumor microenvironment (TME), where nutrients are scarce, leads to suppression of immune system and upregulation of translation of proteins for amino acid replenishment.² In this study, it was investigated whether immune cells whose function was suppressed in the tumor microenvironment were recovered through selective pharmacological inhibition of GCN2 and whether antitumor effects were exhibited through this. Also, inhibition effects of the tumor intrinsic signaling of GCN2 was evaluated using several cancer cell lines. Taken together, we have shown that inhibition of GCN2 activity could exert anti-tumor efficacy in various ways in the tumor environment.

Methods We have discovered a novel small molecule GCN2 inhibitor, DA-4507, that is highly potent and selective *in vitro*. Recovery of effector T cell function and macrophage polarization by DA-4507 were evaluated using mouse primary immune cells under tryptophan-deprived condition. T cell rescue was evaluated using co-culture system with MDSCs accumulated in tumor tissues of syngeneic mouse model. Tumor-intrinsic activities were validated *in vitro* in human leukemia, melanoma, breast cancer, and colorectal cancer cell lines. Also, antitumor effects of DA-4507 were evaluated in the murine syngeneic colorectal, breast cancer and human xenograft leukemia models.

Results DA-4507 exhibited high potency (IC₅₀=5 nM) and selectivity for GCN2 over other ISR kinases. DA-4507 restored proliferation of cytotoxic T cells and suppressed differentiation of regulatory T cell in low-tryptophan media, where proliferation of T cell was reduced and differentiation of regulatory T cell was increased. DA-4507 also mitigated the suppressive function of MDSCs on T cells and induced macrophage polarization toward inflammatory macrophage phenotype (M1). By blocking the tumor-intrinsic activity, DA-4507 showed anticancer effects in various cancer cell lines in a context-dependent manner. Oral administration of DA-4507 induced a significant reduction of the tumor growth in several murine syngeneic mouse models and a human leukemia xenograft model and decreased ATF4 and phospho-eIF2 α in tumor tissues. We also confirmed that the antitumor effect of DA-4507 is CD8⁺ T cell-dependent.

Conclusions The activation of GCN2 is known to result in functional suppression of the immune cells and activation of survival pathway of cancer cells in the TME. Our results show that DA-4507, a potent and selective GCN2 inhibitor restores T cell suppression and promotes antitumor activity, demonstrating that GCN2 is a promising therapeutic target for cancer treatment.

REFERENCES

1. Halaby MJ, Hezaveh K, Lamorte S, Ciudad MT, Kloetgen A, MacLeod BL, Guo M, Chakravarthy A, Medina TDS, Ugel S, Tsigos A, Bronte V, Munn DH, Pugh TJ, DeCarvalho DD, Butler MO, Ohashi PS, Brooks DG, McGaha TL. GCN2 drives macrophage and MDSC function and immune suppression in the tumor microenvironment. *Sci Immunol.* 2019;4(42):1–35.
2. Velde LAV, Guo XZJ, Barbaric L, Smith AM, Oguin III TH, Thomas PG, Murray PJ. Stress kinase GCN2 controls the proliferative fitness and trafficking of cytotoxic T

1344

PRECLINICAL PK/PD PROFILE, BIOMARKER IDENTIFICATION AND RATIONALE FOR INDICATION SELECTION OF EXOASO-STAT6™, A SELECTIVE TUMOR-ASSOCIATED MACROPHAGE TARGETING CANDIDATE

Sushrut Kamerkar*, Charan Leng, Kelvin Zhang, Olga Burenkova, Su Chul Jang, Tong Zi, Sílvia Sisó, Kyriakos Economides, Karl Schmidt, Timothy Soos, Dalia Burzyn, Sriram Sathyanarayanan. *Codiak Biosciences, Cambridge, MA, USA*

Background exoASO-STAT6™ is an investigational therapeutic candidate consisting of exosomes loaded with an antisense oligonucleotide (ASO) targeting STAT6. By leveraging exosome tropism to tumor-associated macrophages (TAM), exoASO-STAT6™ is the first systemically administered exosome designed to selectively silence STAT6 in TAMs, inducing their reprogramming from ‘M2’ immunosuppressive to ‘M1’ proinflammatory phenotype, resulting in the induction of an antitumoral immune response and potent monotherapy activity in mouse models. A Phase I study in hepatocellular carcinoma (HCC) patients is currently enrolling.

Methods Here, we evaluated Pharmacokinetics (PK) and Pharmacodynamics (PD) of systemically dosed exoASO-STAT6 in mouse and non-human primates (NHP), identified PD biomarkers with clinical translatability and generated bioinformatic-based rationale for the selection of tumor indications in the clinic.

Results PK analysis in mice and NHP treated with a single IV dose of exoASO-STAT6 (mouse: 0.2-1.5 mg/kg; NHP: 0.3-2.7 mg/kg) suggested rapid clearance of ASO from the plasma within hours. exoASO-STAT6 accumulated in the liver in a dose-proportional manner and was detectable for up to 28 days at all dose levels. Repeated (weekly) administration of exoASO-STAT6 resulted in increased ASO exposure in the liver. PD analysis of STAT6 mRNA expression in liver tissue after a single IV dose showed dose-dependent and durable target gene knockdown (KD) that persisted for up to 28 days with maximal KD between days 4 and 7 in mouse (1.5 mg/kg dose: $69.2 \pm 0.7\%$ KD, $p < 0.0005$ vs. control), and at day 9 in NHP (first timepoint measured) (2.7 mg/kg dose: $50 \pm 3\%$ KD, $p < 0.0001$ vs. control). The extent of STAT6 KD in the liver is proportional to liver exposure, demonstrating a direct relationship between exoASO-STAT6 dose and PD response. Gene expression analysis from NHP liver showed durable modulation of several genes, including IL-4 receptor (IL4R), a gene directly regulated by STAT6 (day 9, 2.7 mg/kg dose: $58 \pm 7\%$ KD, $p < 0.0001$ vs. control). Histological analysis confirmed that STAT6 and IL4R are expressed by TAMs in human HCC tumors, supporting the rationale to use these two biomarkers in the clinic. Analysis of The Cancer Genome Atlas database identified several tumor indications in which high expression of a macrophage-STAT6 signature correlates with poor survival, including HCC, stomach, and bladder cancer ($p = 0.012$, $p = 0.00056$, and $p = 0.0021$, respectively).

Conclusions In summary, we demonstrated that exoASO-STAT6 has a durable PK/PD profile in the liver of preclinical species, identified PD biomarkers with good clinical translational potential and described a rationale for selecting cancer subtypes that could benefit from treatment with exoASO-STAT6.

<http://dx.doi.org/10.1136/jitc-2022-SITC2022.1344>

1345

EXOASO-C/EBPβ™: AN ENGINEERED EXOSOME THERAPEUTIC THAT SELECTIVELY TARGETS MDSCS AND INDUCES POTENT SINGLE-AGENT ANTI-TUMOR ACTIVITY IN CHECKPOINT REFRACTORY TUMOR MODELS

<http://dx.doi.org/10.1136/jitc-2022-SITC2022.1345>

Sushrut Kamerkar*, Charan Leng, Olga Burenkova, Su Chul Jang, Kelvin Zhang, Samuel Kasera, Tong Zi, Sanah Langer, Silvia Siso, Timothy Soos, Dalia Burzyn, Sriram Sathyanarayanan. *Codiak BiSciences, Cambridge, MA, USA*

Background Myeloid-derived suppressor cells (MDSCs) are pathologically activated monocytes and neutrophils that promote an immunosuppressive milieu by inhibiting T-cell activation and recruitment, leading to resistance to immune checkpoint therapies and poor clinical outcomes. C/EBPβ is a critical transcription factor that regulates the immunosuppressive state of MDSCs and is activated by prostaglandin E2 (PGE2) and interleukin 10 (IL10). Both PGE2 and IL10 are involved in MDSC development, accumulation and functional stability.

Methods We have developed a proprietary engineered exosome loaded with antisense oligonucleotides (ASO) targeting C/EBPβ (exoASO-C/EBPβ™), that selectively delivers ASOs to MDSCs, thereby inhibiting C/EBPβ expression, promoting the immune-modulation of MDSCs to a pro-inflammatory phenotype, and demonstrating single agent anti-tumor activity in checkpoint refractory tumor models.

Results Human MDSCs were generated and characterized *in-vitro* using a combination of putative cell surface markers: CD11b, CD33, HLA-DR, CD14 and CD15. Exosome surface glycoproteins enabled preferential delivery of ASO to MDSCs, as demonstrated by a 3-fold improvement in delivery with exoASO vs free ASO. Treatment of MDSCs with exoASO-C/EBPβ resulted in a dose-dependent target gene knockdown, and a cytokine secretion profile consistent with a proinflammatory phenotype. Biodistribution in tumor-bearing mice of systemically administered exoASO demonstrated up-to 11-fold improvement in selective ASO delivery as compared to free ASO, in MDSCs and other myeloid cells in the tumor, blood, and bone marrow. Administration of exoASO-C/EBPβ as a single agent demonstrated significant anti-tumor activity and survival benefits in multiple MDSC rich, checkpoint refractory tumor models: E0771-breast cancer (30% complete responses (CRs)), MB49-bladder cancer (70% CRs) and 4T1-breast cancer (44% Tumor growth inhibition (TGI)). Combination treatment with anti-PD1 further increased the anti-tumor efficacy, while the complete responders were resistant to tumor re-challenge, demonstrating immunological memory associated with exoASO-C/EBPβ treatment. In a lung metastasis model of B16F10 with disseminated tumors in the abdominal cavity, IV administration of exoASO-C/EBPβ significantly attenuated tumor growth (92% TGI with monotherapy, 98% TGI with a combination with anti-PD1), as observed with ex-vivo IVIS imaging. Additionally, exoASO-C/EBPβ treatment resulted in a significant infiltration of cytotoxic CD8 T cells in the lung and tumor. Finally, a myeloid cell specific C/EBPβ/PGE2/IL10 gene signature was generated to identify cancer indications where exoASO-C/EBPβ therapy may have the most therapeutic significance.

Conclusions exoASO-C/EBPβ is a novel therapeutic that selectively targets and attenuates a critical transcription factor in immunosuppressive myeloid derived suppressor cells, resulting in their immune-modulation and potent anti-tumor activity across multiple MDSC rich tumor models.

1346

ANTIBODIES AGAINST GLYCOTARGETS AS NOVEL PLATFORM APPROACH TO ADDRESS UNMET NEEDS IN CANCER THERAPY

Patrik Kehler*, Theresa Neumann, Anika Jaekel, Manon Weis, Johanna Gellert, Antje Danielczyk, Evelyn Hartung, Timo Lischke, Stephanie Gurka, Naomi Kast, Manon Weiske. *Glycotope GmbH, Berlin, Germany*

Background Highly potent therapeutic approaches require clean targets. However, the majority of antibodies in clinical development or approved for cancer therapy address protein targets that are only overexpressed in cancer and yet often show significant expression in healthy organs. Besides protein expression, glycosylation is strongly altered in cancer, reflecting changes in tumor metabolism. Aberrant glycosylation is reasoned by mutated or mislocated glycosyltransferases, glycosidases, substrates and chaperones, giving rise to truncated or highly fucosylated or sialylated glycans.¹ Therefore, tumor-associated carbohydrates like the Thomsen-Friedenreich (TF), Thomsen novelle (Tn) or sialylated Tn (sTn) antigen are expressed on proteins in different carcinomas, leukemias, lymphomas and their metastases.²

To increase the tumor-selectivity of protein-targeting antibodies, we developed antibodies against protein/carbohydrate combined epitopes (GlycoTargets), which bind their protein target only in presence of tumor-associated carbohydrates and thereby avoid binding to the protein if it is expressed in healthy tissues.

Methods The general presence of tumor-associated carbohydrates in cancerous tissues was analyzed using immunohistochemistry. HPLC and mass spectrometry (MS) or bioinformatic prediction was applied to further confirm their presence on specific proteins. Different cell lines were developed and characterized by ELISA and MS to recombinantly express proteins carrying distinct carbohydrates. These GlycoTargets were used for immunization and antibody discovery. Specificity, glycosylation dependency and cell binding properties of antibody lead candidates were characterized by ELISA, flow cytometry and immunohistochemistry on tumor and healthy tissues.

Results We have identified 220 potential GlycoTargets using bioinformatic predictions or cellular screenings. Using our proprietary cell lines as toolbox for antigen production, we were able to generate highly pure and fully characterized GlycoTargets for tailored immunization approaches and antibody screenings. Two case studies show that our approach is suitable to generate antibodies that bind to the protein of interest only if a specific tumor-associated glycosylation is present and do not cross-react with the non-glycosylated protein or the glycan on irrelevant carrier-proteins. Due to this glycan dependency, our antibodies show markedly decreased off-tumor binding. We will show that our antibodies lack unwanted binding to healthy immune cells in contrast to conventional anti-protein antibodies and stain different cancer indications but not related normal tissues.

Conclusions Our approach is suitable to target protein/carbohydrate combined epitopes with specific antibodies. With proper tools for target identification, antigen production, immunization and screening, a platform was installed to generate antibodies with markedly decreased off-tumor binding. The increased tumor selectivity may improve safety for highly potent therapeutic approaches like ADCs, CARs or radiopharmaceutics.

REFERENCES

1. Pinho SS, Reis CA. Glycosylation in cancer: mechanisms and clinical implications. *Nat Rev Cancer*. 2015;**15**(9):540–55.
2. Kudelka MR, Ju T, Heimburg-Molinaro J, Cummings RD. Simple sugars to complex disease—mucin-type O-glycans in cancer. *Adv Cancer Res*. 2015;**126**:53–135.

<http://dx.doi.org/10.1136/jitc-2022-SITC2022.1346>

1347 **TARGETING OF A CANCER-ASSOCIATED LYPD3 GLYCOFORM FOR TUMOR THERAPY**

Patrik Kehler*, Theresa Neumann, Anika Jaekel, Johanna Gellert, Antje Danielczyk, Lisa Weiß, Luisa Willmann, Stephanie Gurka, Naomi Kast, Manon Weiske. *Glycotope GmbH, Berlin, Germany*

Background LYPD3 (C4.4A) is a glycosylphosphatidylinositol (GPI)-anchored, highly glycosylated cell surface protein that was first described as a metastasis-associated protein.¹ Since then, it has been associated with carcinogenesis in several different cancers and is reported to be overexpressed in squamous cell carcinoma (SCC) of the head and neck, esophageal SCC, colorectal cancer as well as non-small cell lung cancer. However, it is also highly expressed in healthy epithelia of the proximal digestive tract, female reproductive organs as well as skin keratinocytes.² This may cause unwanted side effects in cancer therapy with an antibody unable to discriminate between cancer-associated LYPD3 and LYPD3 in normal tissue.

One of the most drastic changes in cancer is the altered glycosylation of proteins and lipids, giving rise to truncated or highly fucosylated and highly sialylated glycans which are almost absent on normal cells.³ Therefore, targeting protein/carbohydrate combined epitopes (GlycoTargets) comprising these specific glycans offers reduced off tumor toxicity, which is key for highly potent therapies. We have developed an antibody which binds to tumor-associated LYPD3 in an O-glycosylation-dependent manner and shows superior tumor specificity compared to conventional protein-binding anti-LYPD3 antibodies.

Methods The specificity of our antibody for glycosylated LYPD3 was determined using differentially glycosylated proteins in an ELISA format and confirmed using cell lines with specific glycosylation patterns as well as tumor cell lines expressing varying levels of LYPD3. Furthermore, binding to healthy and tumor tissues was analyzed by immunohistochemistry.

Results We have generated an anti-LYPD3 antibody that binds to its target protein only if a specific tumor-associated carbohydrate is present. It does not cross-react with non-glycosylated LYPD3 or the carbohydrate structure on other carrier-proteins. The carbohydrate-dependent anti-LYPD3 antibody called GT-002 binds to various tumor cell lines and stains tumor tissues of different cancer indications. Notably, GT-002 elicits markedly reduced binding to normal human tissues compared to anti-LYPD3 polyclonal control antibodies or Lupatumab, an anti-LYPD3 antibody previously in clinical development as ADC (BAY1129980).

Conclusions By using our expertise in cancer-associated glycosylation, we successfully generated GT-002, a highly tumor-specific anti-LYPD3 antibody that targets neither glycan nor LYPD3 protein alone, but only the combination thereof – a tumor-specific protein/carbohydrate combined epitope on LYPD3. By using this approach, we were able to develop an anti-LYPD3 antibody that stains cancer tissue of various indications while showing drastically reduced off-tumor binding towards healthy LYPD3-positive tissues. We believe that this highly specific antibody is exceptionally suitable for potent therapies like ADCs, radio-conjugates and CARs.

REFERENCES

1. Hansen LV, Gårdsvoll H, Nielsen BS, Lund LR, Danø K, Jensen ON, Ploug M. Structural analysis and tissue localization of human C4.4A: a protein homologue of the urokinase receptor. *Biochem J.* 2004;**380**(Pt 3):845–57.

2. Würfel J, Seiter S, Stassar M, Claas A, Kläs R, Rösel M, Marhaba R, Savelyeva L, Schwab M, Matzku S, Zöller M. Cloning of the human homologue of the metastasis-associated rat C4.4A. *Gene.* 2001;**262**(1-2):35–41.
3. Pinho SS, Reis CA. Glycosylation in cancer: mechanisms and clinical implications. *Nat Rev Cancer.* 2015;**15**(9):540–55.

<http://dx.doi.org/10.1136/jitc-2022-SITC2022.1347>

1348

BDC-3042: A DECTIN-2 AGONISTIC ANTIBODY FOR TUMOR-ASSOCIATED MACROPHAGE-DIRECTED IMMUNOTHERAPY

Justin Kenkel*, Rishali Gadkari, Jess Nolin, Fang Xiao, Po Ho, Cindy Kreder, Laughing Bear Torrez, David Ormstead, Katelynn McEachin, Jason Ptacek, Lu Xu, Duy Nguyen, Karla Henning, Steven Chapin, David Dornan, Michael Alonso, Shelley Ackerman. *Bolt Biotherapeutics Inc, Redwood City, CA, USA*

Background Tumor-associated macrophages (TAMs) generally support tumor progression through their immunosuppressive effects on the tumor microenvironment (TME) and are the predominant immune cell population in most cancers. TAMs express the pattern recognition receptor Dectin-2 (*CLEC6A*), an activating C-type lectin receptor (CLR) that binds to high-mannose glycans on fungi and other microbes and induces protective immune responses against infectious disease. Dectin-2 ligation mediates enhanced phagocytosis, antigen processing and presentation, and proinflammatory cytokine production. Agonism of Dectin-2 on TAMs using naturally derived ligands drives potent anti-tumor immunity in syngeneic mouse tumor models. Given these findings, we developed a human Dectin-2-targeted agonistic antibody, BDC-3042, which is capable of robustly activating TAMs as a novel approach to myeloid-directed immunotherapy.

Methods Dectin-2 expression was assessed by flow cytometry, immunohistochemistry, and using public databases. Human whole blood, monocyte-derived macrophages, and single-cell suspensions from dissociated human tumors were stimulated overnight with BDC-3042. Activation was assessed through cytokine analysis. Immune profiling and anti-tumor efficacy were assessed in vivo utilizing MDA-MB-231 tumor-bearing CD34+ HSC engrafted mice (huNOG-EXL, Taconic Biosciences).

Results Dectin-2 is expressed by TAMs across many tumor types, including breast, colon, and lung cancers, but exhibits minimal expression in most normal tissues. BDC-3042 binds to recombinant Dectin-2 and Dectin-2-expressing cells with low-nanomolar affinity. BDC-3042 elicits robust activation of primary TAMs and in vitro-generated macrophages, leading to secretion of proinflammatory mediators characteristic of tumor-destructive “M1” macrophages, such as TNF α , IL-1 β , and CCL3/4. Low levels of BDC-3042 binding are detected on blood monocytes, with minimal binding to other peripheral immune cells. Importantly, BDC-3042 elicits little to no activation of peripheral monocytes or cells in whole blood. BDC-3042 activity is dependent on both Dectin-2 and Fc γ R s , as indicated by the increased activation of macrophages elicited with an Fc-enhanced IgG1 backbone. Systemically administered BDC-3042 activates TAMs and mediates anti-tumor efficacy in mice with humanized immune systems.

Conclusions The data presented demonstrate the therapeutic potential of targeting Dectin-2 expressed by TAMs with the agonistic antibody BDC-3042 as a novel pan-cancer approach for myeloid cell-directed tumor immunotherapy.

<http://dx.doi.org/10.1136/jitc-2022-SITC2022.1348>

Abstracts

1349 TROCEPT MEDIATED *IN-TUMOR* DELIVERY OF IMMUNE CHECKPOINT INHIBITORS REDUCES SYSTEMIC TOXICITY RISKS AND BOOSTS IMMUNE ACTIVATION

¹David Cole, ¹Rahul Khanolkar, ¹James Davies, ¹Alexander Baker, ¹Thomas Webb, ²Alicia Teixeira Crespo, ²Hanni Uusi-Kerttula, ³Lucy Williams, ¹Samantha Moore, ¹Johanne Pentier, ¹Bent Jakobsen, ¹Alan Parker, ¹Jez Gerry*. ¹Accession Therapeutics LTD, Oxford, UK; ²Cardiff university, Cardiff, UK; ³Accession Therapeutics LTC, Cardiff, UK

Background Immune checkpoint inhibitors (ICIs) have revolutionized immunotherapy, but their efficacy is limited to certain cancers, and response rates are largely dependent on the ability of the patients T cells to recognize and activate against tumor antigens. Additionally, systemic delivery can lead to dose limiting toxicity.¹

TROCEPT is a novel tumor-selective delivery technology, based on type 5 adenovirus, engineered not enter normal human tissues. The removal of normal tissues tropisms addresses the main limitation of other viral therapies, which show limited efficacy due to rapid removal by the liver.² TROCEPT has been further engineered to specifically bind to a tumor marker expressed on most carcinomas.³ The TROCEPT platform can be loaded with transgenes encoding protein-based drugs for *in-tumor* delivery (i.e., TROCEPT can deliver the transgene into the cancer cell, turning the cancer cell into a drug factory, which releases the payload into the local tumor environment). TROCEPT-01 enables tumor-localized generation of high concentrations of ICI payloads (figure 1).

Methods Selective cell entry of TROCEPT-01 was assessed *in vitro* using infectivity assays in target-positive and -negative tumor and healthy cell lines. Further *in vitro* assays confirmed the production of ICIs in multiple tumor cell lines, and functionality of the *in-tumor* generated ICI was confirmed using primary T cell activation experiments. Finally, an immune-deficient murine model, engrafted with a human tumor, was used to assess biodistribution of TROCEPT-01, after intravenous delivery, using a bioluminescence *in vivo* imaging system (IVIS[®]) and qPCR.

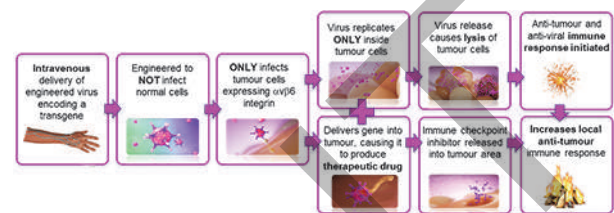
Results *In vitro* testing confirmed TROCEPT-01's exquisite selectivity for tumor cells and demonstrated functional production of ICIs from treated tumor cells. *In vivo* experiments demonstrated tumor-localized biodistribution of TROCEPT-01, with a low amount of TROCEPT-01 detected in healthy organs (including the liver) and peripheral blood.

Conclusions TROCEPT's tumor selective transgene delivery and *in-tumor* production of ICIs enables high local dosing only in the tumor, addressing systemic toxicity and potentially increasing efficacy. Additionally, several pre-clinical studies have demonstrated that oncolytic viruses can induce anti-viral immunity against infected tumor cells, recruiting cytotoxic T cells and other pro-inflammatory cell types.⁴ Thus, TROCEPT delivery of ICIs has the potential to generate a synergistic effect, first attracting and activating T cells, and then delivering tumor-localized ICIs at high concentrations to boost the anti-tumor T cell response and increase response rates in several tumor types. TROCEPT has the potential for delivery of new and powerful therapeutic drugs for the *in-tumor* treatment of cancer.

REFERENCES

1. Watanabe E, Nishida O, Kakihana Y, Odani M, Okamura T, Harada T, Oda S. Pharmacokinetics, Pharmacodynamics, and Safety of Nivolumab in Patients With Sepsis-Induced Immunosuppression: A Multicenter, Open-Label Phase 1/2 Study. *Shock*. 2020;**53**:686–694.DOI: 10.1097/SHK.0000000000001443.

- Baker A, Aguirre-Hernández C, Haldén G, Parker A. Designer Oncolytic Adenovirus: Coming of Age. *Cancers (Basel)*. 2018;**10**:201.DOI: 10.3390/cancers10060201.
- Uusi-Kerttula H, Davies JA, Thompson JM, Wongthida P, Evgin L, Shim KG, Bradshaw A, et al. Ad5 NULL -A20: A Tropism-Modified, $\alpha v \beta 6$ integrin-selective oncolytic adenovirus for epithelial ovarian cancer therapies. *Clinical Cancer Research*. 2018;**24**:4215–4224.DOI: 10.1158/1078-0432.CCR-18-1089.
- Kuryk L, Møller A-SW, Jaderberg M. Combination of immunogenic oncolytic adenovirus ONCOS-102 with anti-PD-1 pembrolizumab exhibits synergistic antitumor effect in humanized A2058 melanoma huNOG mouse model. *Oncol Immunology*. 2019;**8**:e1532763.DOI: 10.1080/2162402X.2018.1532763.



Abstract 1349 Figure 1 Schematic of the mode of action of TROCEPT-01 encoding an immune checkpoint inhibitor

<http://dx.doi.org/10.1136/jitc-2022-SITC2022.1349>

1350

AI/ML-DRIVEN DISCOVERY OF COLLAGEN TRIPLE HELIX REPEAT-CONTAINING 1, CTHRC1, A NOVEL PROTEOGLYCAN FOR DISRUPTION OF STROMAL BARRIERS AND ENHANCEMENT OF IMMUNOTHERAPY RESPONSES IN DESMOPLASTIC TUMORS

Elizabeth Koch, Amy Berkley, Sean Phippen, Max London, Kerry White, Amanda Hanson, Sam Cooper, Christopher Harvey, Michael Briskin*. *Phenomic AI, Toronto, Canada*

Background While checkpoint inhibitors (CPIs) such as anti-CTLA-4 and anti-PD-1/L1 have demonstrated efficacy in many solid tumor indications, those with high stromal presence have been difficult to treat. We aimed to use a proprietary machine learning/artificial intelligence platform to identify novel stromal targets that, upon targeting, will relieve this immunosuppressive barrier and increase CPI responsiveness in difficult-to-treat indications.

Methods Based on bioinformatic analysis using a large single-cell RNA atlas, we assessed cancer-associated fibroblasts (CAFs)/fibroblastic cells in cancer tissue for the identification of novel targets, including proteoglycans. Antibodies were generated by immunization of humanized mice. Lead antibodies demonstrated potent *in vitro* activity in inhibiting cell adhesion and reducing survival of pancreatic cancer cells in CAF conditioned media. We assessed efficacy and PD (flow cytometry and IHC) in the EMT6 orthotopic tumor model in immunocompetent mice.

Results Analysis of a large single-cell RNA atlas spanning many solid tumors identified CTHRC1 as one of the most upregulated CAF targets in the genome. CTHRC1 was also highly associated with CAFs from immune-excluded and desert-like tumor samples. Finally, we also find that CTHRC1 is highly expressed by both cancer cells and CAFs within the tumor, in key indications such as breast, ovarian, and pancreatic, with the potential for Fc-mediated depletion of both tumor and fibroblast cells. Profiling by scRNAseq of syngeneic tumor cells identified EMT6 breast cancer model as representative of human tumor, mirroring both CAF and tumor CTHRC1 expression. Assessment of efficacy demonstrated monotherapy activity with strong combination activity and enhanced survival when we combined anti-CTHRC1 mAbs with anti-PD-1.

Conclusions We have identified CTHRC1 as a novel proteoglycan expressed by both CAFs and tumor cells that appears to be an ideal target for inhibiting of stromal barrier function with therapeutic monoclonal antibodies that may also serve as ideal for targeting payloads to the tumor microenvironment. These data demonstrate the power of large scRNA atlases for novel target ID and show the potential of breaking down stromal barriers in opening up tumor microenvironments to immune attack.

Ethics Approval Animal studies were conducted in accordance with an Animal Use Protocol 6323.3 approved by the University Health Network Animal Care Committee.

<http://dx.doi.org/10.1136/jitc-2022-SITC2022.1350>

1351

PRECLINICAL MECHANISM OF ACTION AND PHARMACODYNAMIC BIOMARKER STUDIES OF DUOBODY®-CD3XB7H4 IN SOLID CANCER MODELS

<http://dx.doi.org/10.1136/jitc-2022-SITC2022.1351>

¹Louise Koopman*, ¹Madelon Paauwe, ¹Laura Smits-de Vries, ¹Frosso Karaiskaki, ¹Marcel Brandhorst, ¹Patrick Franken, ¹Theo Plantinga, ¹Stefanie De Poot, ¹Mischa Houtkamp, ²Kate Sasser, ¹Esther Breijl. ¹Genmab B.V., Utrecht, Netherlands; ²Genmab US, Inc., Princeton, NJ, USA

Background The immune checkpoint protein B7H4 is expressed on malignant cells in various solid cancers, whereas expression is highly restricted in normal tissue. DuoBody-CD3xB7H4 (GEN1047) crosslinks CD3 on T cells with B7H4 on tumor cells, thereby inducing T-cell mediated cytotoxicity in B7H4-expressing tumor cells. Here, we evaluated the prevalence of B7H4 expression in solid cancers and investigated the preclinical mechanism of action (MoA) and pharmacodynamic (PD) markers associated with DuoBody-CD3xB7H4 biological activity *in vitro* and *in vivo*.

Methods B7H4 protein expression was determined by immunohistochemistry in human tumor biopsies, and by semi-quantitative flow cytometry for tumor cell lines. T-cell mediated cytotoxicity was assayed *in vitro* using co-cultures of B7H4+ tumor cells and healthy donor T cells. Antitumor activity *in vivo* was tested in a patient-derived xenograft (PDX) screen using several tumor models engrafted subcutaneously in mice with a humanized immune system (HIS). Antitumor activity and exploratory biomarkers were further evaluated in a follow-up study in ovarian cancer PDX HIS mice.

Results In tissue microarrays of primary NSCLC-SCC, ovarian, endometrial, and breast cancer, over 25% of the tumor biopsies contained at least 50% B7H4-positive tumor cells. *In vitro*, DuoBody-CD3xB7H4 induced target-specific, dose-dependent, and complete tumor cell kill in a panel of tumor cell lines expressing varying levels of B7H4, while B7H4 expression levels correlated with the EC₅₀. DuoBody-CD3xB7H4 demonstrated antitumor activity in ovarian and breast cancer PDX models with high B7H4 expression. Antitumor activity of DuoBody-CD3xB7H4 in an ovarian cancer PDX model was confirmed in a dose-response study and was associated with the number of circulating human CD3⁺ T cells before randomization, an indicator of the humanization rate of the HIS mice. In the periphery, DuoBody-CD3xB7H4 treatment was associated with a transient decrease in circulating immune cells, increased T-cell activation, and elevated levels of granzyme B and cytokines. In the tumor, DuoBody-CD3xB7H4 treatment increased the number of tumor-infiltrating lymphocytes.

Conclusions High prevalence of B7H4 expression was observed in primary NSCLC-SCC, ovarian, endometrial, and breast cancer tissue. *In vitro*, DuoBody-CD3xB7H4 showed antitumor activity across a range of B7H4 expression levels. DuoBody-CD3xB7H4 showed dose-dependent antitumor activity *in vivo*, associated with increased numbers of intratumoral T cells and peripheral PD biomarkers of T-cell activation and cytokine production. Currently, DuoBody-CD3xB7H4 is being investigated in a first-in-human clinical trial for the treatment of solid tumors known to express B7H4 (NCT05180474), in which the MoA and PD, including biomarkers of response, will be clinically explored.

Ethics Approval Animal experiments were performed according to the guidelines of the Institutional Animal Care and Use Committee (IACUC) and in accordance with the regulations of the Association for Assessment and Accreditation of Laboratory Animal Care (AAALAC).

1352

SELECTIVE SMALL MOLECULE INHIBITOR OF INTEGRIN $\alpha_V\beta_8$ AND $\alpha_V\beta_1$ HAS SINGLE AGENT ACTIVITY AND POTENTIATES IMMUNE CHECKPOINT BLOCKADE THERAPY

<http://dx.doi.org/10.1136/jitc-2022-SITC2022.1352>

Vishal Kothari*, Colin Magowan*, Darren Finkelstein, Gail Lee, Chun Chen, Tim Hom, Manuel Muñoz, Dennis Monteleone, Subramanian Karur, Marta Bogaczynska, Erin Budi, Prerna Kotak, Shamra Martin, Katherine Jenkins, Simon Wong, Timothy Machajewski, Fernando Rock, Scott Turner. *Pliant Therapeutics, South San Francisco, CA, USA*

Background Across several cancer types, activated transforming growth factor- β (TGF β) helps support an immuno-suppressive microenvironment that contributes to immune checkpoint blockade (ICB) resistance and treatment failure. Alpha-V integrins, specifically $\alpha_V\beta_8$, $\alpha_V\beta_6$ and $\alpha_V\beta_1$, are the primary activators of TGF β from the latent complex. These integrins have a limited cell-expression profile that make them potential targets to safely and potently inhibit the activation of TGF β in cancer. Targeting $\alpha_V\beta_8$ has recently emerged as a promising approach to realizing the potential of anti-TGF β therapies to address ICB resistance. In the stroma, integrin $\alpha_V\beta_1$ is the major source of activated TGF β . Here, we describe the development of PLN-1095, a dual small molecule inhibitor of $\alpha_V\beta_8$ and $\alpha_V\beta_1$ and characterize this approach in ICB-resistant mouse tumor models.

Methods In vivo efficacy and activities of a dual $\alpha_V\beta_8$ and $\alpha_V\beta_1$ integrin inhibitor, PLN-1095, in combination with anti-programmed death receptor-1 antibody (anti mPD-1) was evaluated in EMT6, Pan02, and CT26 cancer syngeneic mouse models by monitoring animal survival, tumor growth, gene expression, and infiltrating CD8+ lymphocytes. In addition, PLN-1095 single agent proinflammatory and antifibrotic activities was assessed using mouse EMT6 tumors in vivo and human breast tumor tissues *ex vivo*.

Results PLN-1095 showed selective inhibition of integrins $\alpha_V\beta_8$ and $\alpha_V\beta_1$ at nanomolar concentrations. Treatment of mice bearing EMT6 tumors with PLN-1095 alone and in combination with anti-mPD-1 significantly reduced tumor growth. Anti-mPD-1 treatment showed a peripherally restricted CD8+ and CD4+ pattern, whereas PLN-1095 treatment significantly increased intra-tumoral CD8+ T cell infiltration. PLN-1095 treatment, both alone and in combination with anti-mPD-1 was associated with elevated gene expression of CXCL9 and other pro-inflammatory cytokines, enhanced expression of genes involved in antigen presentation, reduced TGF β signaling, diminished expression of pro-fibrogenic and angiogenic transcripts across the models tested. A significant increase in granzyme B positive T cells was observed in human breast cancer tissues treated with PLN-1095 *ex vivo*.

Conclusions PLN-1095 sensitized immunologically cold murine tumors to anti mPD-1 ICB. PLN-1095-mediated inhibition of integrins $\alpha_V\beta_8$ and $\alpha_V\beta_1$ effectively reduced the immunosuppressive effects of TGF β by activating the immune system thereby promoting CD8+ cytotoxic T cell infiltration in the tumors. Based on these results, a first-in-human clinical trial investigating the effects of PLN-1095 is being planned.

Ethics Approval All the animal Studies were approved by Pliant IACUC protocol # PLI-010-2019. Fresh breast tumor samples were collected from the Biological Resource Center of the Centre Léon Bérard by Marie's laboratory, according to the institutional review board and ethics committee and with fully informed patient consent (French Ministry of Research agreement number: AC-2013-1871 and AC-2019-3426).

1353

TARGETING COMPLEMENT FACTOR H MEDIATED TUMOR IMMUNE AND COMPLEMENT EVASION AS A NEXT GENERATION APPROACH

<http://dx.doi.org/10.1136/jitc-2022-SITC2022.1353>

Matthew Kraman*, Carlo Zimarino, Danielle Minns, Jorge Dias, Chelsea Povall, Helen Graves, Bradley Holub, Ralph Minter, Jacob Galson, Jane Osbourn, Donna Finch. *Alchemab Therapeutics, Cambridge, UK*

Background The complement system plays a crucial part in innate immunity, aiding the destruction of pathogens and removing anomalous cells. Complement Factor H (CFH) regulates the complement system through interactions with C3b (both soluble and membrane associated) to prevent unwarranted activation. This forms the basis of a self-versus non-self-recognition process, which in certain cancers, aberrant expression, or abnormal levels of CFH may protect and promote growth of tumors by impairing the activation of the complement system. An analysis of human antibody repertoire data retrieved convergent sequence clusters amongst both viral and cancer (pancreatic, prostate and melanoma) patient cohorts, and led to identification of human derived antibodies that are naturally tolerated with unique properties^{1,2,3}. A representative heavy chain from this cluster was paired with an appropriate light chain and engineered for desirable biophysical characteristics. Target identification revealed CFH, as a potential antigen.

Methods In this study, we tested the ability of human derived antibodies to CFH to activate direct cell killing via complement deposition, and to alter immune cell responses (potentially via alterations in complement receptor activation). This was performed using human in vitro co-culture, immunomodulatory assays, and in vivo syngeneic mouse systems. Additionally, pharmacokinetics and associated measurements were assessed to understand basic tolerability and exposure.

Results Anti-CFH resulted in increased CD11b+ cell tumor infiltration and subsequent C3d deposition in a B16/F10 syngeneic model. Macrophages adopted an inflammatory phenotype characterised by cytokine release profiles and lymphocyte activation.

Immune cell co-culture with tumor cells resulted in myeloid activation, altered cell populations, indirect activation of additional immune cell types, and reduction in viable cancer cells. Both single and dose range pharmacokinetic studies confirmed a lack of binding to circulating CFH, and unaffected levels of C3 that might be associated with systemic complement activation. In a preliminary assessment, no safety issues were identified in the study. Monotherapy in high CFH syngeneic models, suggests a unique epitope recognised by anti-CFH which is primarily associated with membrane associated C3b. Interfering with this binding uniquely enables localised inflammation associated with the alternative pathway of the complement system. Additional mechanistic studies are ongoing.

Conclusions A human derived antibody cluster against CFH is convergently present in various disease state patient groups and has novel immunostimulatory function through engagement of myeloid cells and the complement cascade.

REFERENCES

1. Ehrhardt SA, et al. Polyclonal and convergent antibody response to Ebola virus vaccine rVSV-ZEBOV. *Nat Med.* 2019;**25**(10):1589–1600.
2. Davis CW, et al. Longitudinal Analysis of the Human B Cell Response to Ebola Virus Infection. *Cell.* 2019;**177**(6):1566–1582.e17.
3. Galson JD, et al. Deep Sequencing of B Cell Receptor Repertoires From COVID-19 Patients Reveals Strong Convergent Immune Signatures. *Front Immunol.* 2020;**11**:605170.

1354

CBL-B INHIBITION SHOWED DIFFERENTIATED EFFECTS IN A MIXED LYMPHOCYTE REACTION VERSUS OTHER IMMUNO-ONCOLOGY TARGETED APPROACHES

Yilin Qi*, Jun Kuai, Yingzhi Bi, Huadong Sun, David Greco, Ken Carson, Timothy Reilly, Geraldine Harriman, Fang Wang. *Hotspot Therapeutics, Boston, MA, USA*

Background The mixed lymphocyte reaction (MLR) mimics an immune reaction between T cells and antigen presenting cells and has been used to assess a variety of immune-oncology (I-O) agents as a potential predictor of clinical effects. Inhibition of the E3 ligase, Casitas B-Lineage Lymphoma Proto-Oncogene B (CBL-B), is a novel I-O approach shown to lower the threshold for antigen-specific T cell activation, even in the absence of co-stimulatory signaling or in the presence of an immunosuppressive environment. Moreover, genetic ablation of CBL-B and functional inactivation of its E3 ligase activity in mice or primary human T cells enhanced immune-mediated anti-tumor effects. Previously, Hotspot has disclosed a series of allosteric CBL-B inhibitors (CBL-Bi) with potent *in vitro* effects on T cells and NK cells and immune-mediated anti-tumor effects *in vivo*.

Methods A human allogenic MLR assay was applied to compare the effects of CBL-Bi and antibodies directed against PD1, CTLA4, LAG3, TIGIT and TIM3 on cytokine release and T cell proliferation, followed by evaluation of CBL-Bi effects on dendritic cells maturation and antigen specific CMV response.

Results CBL-Bi significantly enhanced interferon-gamma production comparable to anti-PD1 treatment, with an additional profound effect on CD8 T cell proliferation. Antibodies directed against CTLA4, LAG3, TIGIT and TIM3 had no effect on either endpoint in this assay format. The effects of CBL-Bi extended to CD4 T cells and interleukin-2 (IL-2) production; anti-PD1 also showed similar effects on IL-2. CBL-Bi effects were concentration-dependent, suggesting potential to optimize the extent of desired immune enhancement. The combination of CBL-Bi plus anti-PD1 demonstrated additive or possibly synergistic effects on both cytokine release and T cell proliferation. Combination of CBL-Bi plus other I-O agents did not show any enhancement. Mechanistically, CBL-Bi promoted immature dendritic cell activation and increased the sensitivity to antigen-specific T cell activation in a CMV challenge assay. An integrated literature review further suggested that the MLR assay has been generally correlated with clinical effects of I-O agents as monotherapy and/or in combination with anti-PD1.

Conclusions In summary, CBL-Bi had robust single agent effects on both cytokine release and T cell proliferation in the human MLR assay. These effects were differentiated from a range of other I-O mechanisms and CBL-Bi plus anti-PD1 showed substantial combination effects. These data support the potential for CBL-Bi to drive anti-tumor immunity in patients as both monotherapy and in combination with anti-PD1 standard of care therapy.

<http://dx.doi.org/10.1136/jitc-2022-SITC2022.1354>

1355

NOVEL PHARMACOLOGICAL APPROACH TO INDUCE DIRECT KILLING OF CANCER AND ACTIVATED ANTITUMOR IMMUNITY VIA INHIBITION OF MONOCARBOXYLATE TRANSPORTERS

Sambad Sharma*, Nicole Bowman, Sanath Wijerathna, Maolin Yu, Jennifer Duffy, Jaime Escobedo, Nelly Kuklin, Vincent Sandanayaka. *Nirogy Therapeutics, Framingham, MA, USA*

Background Tumor progression and metastasis is driven by metabolic rewiring of cancer cells as well as cell types involved in the tumor microenvironment (TME). One key hallmark of tumor progression is the aberrant increase in glycolytic flux which creates a TME rich in lactate. The abundance of lactate in the TME serves as a great source of energy to immunosuppressive cell populations, such as Tregs and MDSCs, that thrive on lactate. Increase in immunosuppressive cells in tumors diminish the cytotoxic/effector function of CD8+ T cells thereby converting tumors to be immune-cold and resistant to therapies. Therefore, simultaneous blockade of lactate export by cancer cells and lactate import by suppressive immune cells is a novel therapeutic strategy to treat cancer.

Methods Cytotoxicity was evaluated in cancer cells by MTS assay. Lactate import/export was quantified using Lactate-glo assay (Promega). *In vivo* efficacy in CDX and PDX models was evaluated in NOD/SCID mice model. 4T1 and MC38 syngeneic tumor models were used to study synergistic effect of NGY-091 in combination with immune checkpoint blockade therapies. Activated/differentiated human CD4 T, CD8 T, MDSCs and Tregs were analyzed for markers/cytokines/viability by flow cytometry.

Results NGY-091 exhibited a potent cytotoxicity in cancer cells *in vitro* by modulating transport of monocarboxylates. The mode of action of NGY-091 involved the blockade of lactate import through MCT1 and MCT4-mediated lactate export. Furthermore, NGY-091 demonstrated significant direct killing of cancer cells *in vivo* in human CDX and PDX models. In syngeneic models of 4T1 and MC38 murine tumors, NGY-091 treatment showed synergistic tumor growth inhibition when combined with immune checkpoint inhibitors, in addition to a significant tumor growth reduction by NGY-091 treatment alone. Immune profiling of 4T1 tumors by flow cytometry indicated a robust activation of antitumor immunity. Specifically, increases in effector T cell populations, CD8/Treg ratio and tumor-suppressive M1 macrophages was evident in NGY-091 treated tumors. On the other hand, tumor supporting M2 macrophages were found to be downregulated. These observations were further validated by *in vitro* studies using human immune cells where NGY-091 treatment strongly increased and activated effector CD4 and CD8 T cells. Importantly, NGY-091 significantly reduced the growth and functionality of Treg and MDSCs.

Conclusions Therefore, NGY-091 intervenes with two key hallmarks of cancer – metabolism and immunity and has a strong therapeutic utility in cancer treatment.

<http://dx.doi.org/10.1136/jitc-2022-SITC2022.1355>

1356

TRANSCRIPTIONAL PROFILING OF *BICYCLE*[®] TUMOR-TARGETED CD137 AGONIST-TREATED MOUSE TUMORS REVEALED AN EARLY AND RAPID ACTIVATION OF MYELOID CELLS FOLLOWED BY INFILTRATION OF CYTOTOXIC T CELLS INTO THE TUMOR

Johanna Lahdenranta*, Kristen Hurov, Heather Cohen, Punit Upadhyaya, Kevin McDonnell, Phillip Brandish, Nicholas Keen. *Bicycle Therapeutics, Lexington, MA, USA*

Background CD137 (4-1BB) is an immune costimulatory receptor that has been recognized for its potential as an immunotherapy drug target in cancer alongside checkpoint inhibitors.¹⁻² We have developed a new class of modular synthetic drugs, termed *Bicycle*[®] tumor-targeted immune cell agonists (*Bicycle*[®] TICAs), which are multifunctional molecules comprised of constrained bicyclic peptides.³ The first molecule of this class, BT7480, a Nectin-4-dependent CD137 agonist, entered clinical trials in 2021. Preclinical data demonstrates that BT7480 induces highly potent, tumor localized CD137 agonism leading to tumor regressions and immunogenic memory in a syngeneic mouse model.⁴

Methods In vivo pharmacodynamic responses to treatment with CD137 *Bicycle*[®] TICAs in a huCD137 MC38 syngeneic tumor mouse model were evaluated using mRNA in situ hybridization (ISH), NanoString, and scRNA sequencing.

Results NanoString RNA profiling of tumors excised from mice treated with BT7480 at multiple timepoints revealed a two-step process – an early and rapid increase of genes relating to myeloid cell activation that precedes the upregulation of cytotoxicity-related genes. These data indicate that a wider reprogramming of the immune microenvironment beyond T cells may occur early after BT7480 administration. These pharmacodynamic changes were also observed following treatment with an EphA2/CD137 *Bicycle* TICA™ (BT7455), indicating a common feature of targeted CD137 *Bicycle*[®] TICAs. To better understand the cellular mechanism of action of CD137 *Bicycle*[®] TICAs, we used mRNA ISH to attempt to identify the source of Ccl17 and Ccl22 mRNAs, which ruled out Cd3 and Itgam mRNA positive cells as the source of the chemokine expression. Depletion of CD8+ T cells from the mice prior to CD137 *Bicycle* TICA™ treatment did not alter the early increase in gene expression of distinct chemokines, further indicating the involvement of other immune cell types than just effector T cells. To pinpoint the cells responsible for the early burst of signaling activity, we next turned to single cell RNA sequencing of CD137 *Bicycle* TICA™-treated tumors, which highlighted the involvement of other cell populations such as dendritic cells in the early steps of CD137-driven anti-tumor immunity by CD137 *Bicycle*[®] TICAs.

Conclusions Altogether, these data highlight that CD137 *Bicycle*[®] TICAs like BT7480 and BT7455 impact immune cell populations beyond T cells. This suggests that abundant T cell infiltrates may not be required for *Bicycle*[®] CD137 agonists to initiate tumor rejection, which broadens the patient population that may benefit from CD137 *Bicycle* TICA™ treatment to also include myeloid-rich tumors with lower T cell infiltration (“colder” tumors).

REFERENCES

1. Chester C, Sanmamed MF, Wang J, et al. Immunotherapy targeting 4-1BB: mechanistic rationale, clinical results, and future strategies. *Blood*. 2018;**131**:49–57.
2. Etxeberria I, Glez-Vaz J, Teijeira Alvaro, et al. New emerging targets in cancer immunotherapy: CD137/4-1BB costimulatory axis. *ESMO Open*. 2020;**4**:e000733.
3. Upadhyaya P, Lahdenranta J, Hurov K, et al. Anticancer immunity induced by a synthetic tumor-targeted CD137 agonist. *J Immunother Cancer*. 2021;**9**:e001762.

4. Hurov K, Lahdenranta J, et al. BT7480, a novel fully synthetic Bicycle tumor-targeted immune cell agonist™ (*Bicycle* TICA™) induces tumor localized CD137 agonism. *J Immunother Cancer*. 2021;**9**:e002883.

Ethics Approval All the procedures related to animal handling, care and treatment in the studies were performed according to the guidelines approved by the Institutional Animal Care and Use Committee of WuXi AppTec (Beijing, China), following the guidance of the Association for Assessment and Accreditation of Laboratory Animal Care.

<http://dx.doi.org/10.1136/jitc-2022-SITC2022.1356>

1357

REVERSIBLE CHEMICAL MODULATION OF ANTIBODY EFFECTOR FUNCTION MAINTAINS ANTI-TUMOR ACTIVITY WHILE MITIGATING PERIPHERAL IMMUNE ACTIVATION

<http://dx.doi.org/10.1136/jitc-2022-SITC2022.1357>

Matthew Levengood*, Chris Leiske, Noah Bindman, Xinqun Zhang, Nicole Duncan, Weiping Zeng, Serena Wo, Abbie Wong, Clark Henderson, Karalyne Crowder, Haley Neff-LaFord, Django Sussman, Shyra Gardai, Philip Moquist. *Seagen, Inc., Bothell, WA, USA*

Background Antibody effector functions including antibody-dependent cellular cytotoxicity (ADCC) and phagocytosis (ADCP) are mediated through the interaction of the antibody Fc region with Fc gamma receptors present on immune cells. Several approaches have been used to modulate antibody Fc-Fc gamma receptor interactions with the goal of driving an effective antitumor immune response. One such approach is removal of fucose on the antibody core glycan to increase binding to Fc gamma receptor IIIa (CD16a) and drive increased ADCC and immune agonism. However, robust antibody Fc engagement and immune cell binding of non-fucosylated antibodies in the periphery can lead to unwanted induction of systemic cytokine release and other dose-limiting infusion-related reactions. Identifying a balance between effective engagement of Fc gamma receptors that can induce antitumor activity without incurring systemic immune activation is an ongoing challenge in the field of antibody and immunoncology therapeutics.

Methods A method for the reversible modulation of antibody Fc interactions was designed and applied to a series of non-fucosylated antibodies. This methodology utilizes chemical conjugation of polyethylene glycol (PEG) linkers to the interchain disulfides of an antibody to initially impair binding to Fc gamma receptors on peripheral cells upon administration but allow for restoration of antibody effector function through de-conjugation over time. Impacts of PEGylation on Fc gamma receptor binding, signaling, and restoration of function were assessed in vitro and in vivo.

Results In vitro binding and signaling assays with various loaded conjugates were used to identify a preferred linker format that reduces binding and activity of non-fucosylated antibodies to the level of fucosylated parent antibodies. Plasma stability experiments demonstrated that the preferred linker technology can partially de-conjugate over time, allowing for restoration of Fc binding and function in a time-dependent manner. The lead technology was applied to an agonist CD40 antibody, which resulted in significant reductions in cytokine production in human CD40 mice and non-human primates, while demonstrating retained efficacy and improved pharmacokinetics compared to the parent antibody.

Conclusions A simple, modular approach using chemical conjugation can reversibly attenuate Fc gamma receptor binding and antibody-driven acute systemic immune activation. This approach can be rapidly applied to antibodies that suffer from systemic immune activation that occurs due to peripheral Fc binding immediately upon infusion. As a proof of concept, the technology was applied to an agonist CD40 antibody and resulted in significantly decreased pro-inflammatory cytokine production despite higher plasma concentrations and the same antitumor activity to the parent antibody.

Acknowledgements We would like to thank Bianka Haro and Jamie Mitchell for conjugation support.

Ethics Approval All animals studies were conducted in accordance with protocols reviewed and approved by the Institutional Animal Care and Use Committee at Seagen.

1358 **NOVEL EGFR/PI3K DUAL-TARGETING NANOPARTICLES INDUCE IMMUNOGENIC CELL DEATH IN BLADDER CANCER**

¹Zheng Zhu*, ²Xiangdong Xue, ³Gang Zhou, ⁴Zewen Song, ⁵Guoyin Li. ¹Harvard Medical School, West Roxbury, MA, USA; ²Shanghai Jiao Tong University, Shanghai, China; ³Fourth Military Medical University, Xi'an, China; ⁴Central South University, Changsha, China; ⁵Zhoukou Normal University, Henan, China

Background Bladder cancer (BCa) is one of the most common malignancies worldwide. Epidermal Growth Factor Receptor (EGFR) overexpression is seen in up to 74% of BCa tissue specimens, however, current EGFR-based target therapy shows little benefit for BCa patients as the EGFR downstream pathways could be circumvented by other receptor tyrosine kinases (RTKs). Dual targeted therapy, which can bind and inhibit the EGFR and its downstream PI3K to affect tumor progression, could be a potential strategy for BCa treatment.

Methods Herein, we identified two natural products triptolide (TPL) and hesperidin (HSP), dual targeting EGFR and PI3Kin BCa by network pharmacology and molecular modeling. By applying a succinic acid linker was added between these two products, we synthesized amphiphilic TPL-HSP-EGFR targeting prodrug (THE) which further self-assembles into nanoparticles (THE NPs). Once binding to the EGFR on BCa surface, THE NPs could be internalized into BCa cells and released into lysosome to achieve further biofunctions.

Results THE NPs harbor the high drug-loading (91.99%) and low toxicity properties in utilizing natural products as tumor therapeutics. THE NPs could target BCa cells and internalized into lysosome. After hydrolyzed in low pH environment, THE NPs could release TPL and HSP targeting and inhibiting EGFR and PI3K. Immunogenic cell death markers HMGB1 and CRT levels were evaluated both in vitro and in vivo after treatment so as to inhibit BCa proliferation and tumor growth.

Conclusions Dual targeting nanoparticle may emerge as a novel paradigm in BCa treatment, providing a new approach for inducing immunogenic cell death in BCa care.

<http://dx.doi.org/10.1136/jitc-2022-SITC2022.1358>

1359 **HALF-LIFE EXTENDED ENGINEERED IL18 VARIANTS THAT ESCAPE THE NEGATIVE REGULATION OF IL18BP**

¹Xiaofan Li*, ²Cristina Abrahams, ¹Amandeep Gakhal, ¹Junhao Yang, ¹Kevin Brar, ¹Daniel Calarese, ¹Robert Henningsen, ¹Grace Lee, ¹Katie Neighbors, ¹Jennifer Smith, ¹Andrew McGeehan, ¹Millicent Embry, ¹Abigail Yu, ¹Alan Nguyen, ¹Krishna Bajjuri, ¹Miao Wen, ¹Young Park, ¹Cuong Tran, ¹Mary Rose Masikat, ¹Gang Yin, ¹Alice Yam, ¹Kristin Bedard, ¹Trevor Hallam. ¹Sutro Biopharma, Inc., South San Francisco, USA; ²Seagen, South San Francisco, CA, USA

Background Interleukin-18 (IL18) is a proinflammatory cytokine secreted by monocytes and macrophages to promote T and NK cells activation. While wild type IL18 was shown to be efficacious in inhibiting tumor growth in animal models, limited efficacy was observed for recombinant wild type IL18 in clinical trials. IL18 binding protein (IL18BP) is a decoy receptor for IL18 that binds to IL18 with much higher affinity than IL18 receptors (IL18Ra and IL18Rb). IL18BP is up-regulated upon IL18 treatment and acts as a negative feedback for IL18 signaling pathway, which likely contributes to the limited efficacy observed for wild type IL18 in clinic.

Methods Engineered IL18 that escape the negative regulation of IL18BP could greatly improve the efficacy of IL18 in clinic. Sutro's ribosome display technology and XpressCF expression platform enabled fast engineering and testing cycles of IL18 variants. Ribosome display library was constructed based on site directed mutations and selected for IL18Ra binding in the presence of IL18BP. The resulting IL18 variants were further screened for IL18 pathway activation and thermostability. To increase the half-life of IL18 variants, a non-natural amino acid was introduced at an optimized site in the sequence to enable conjugation to a PEG molecule. Additional protein engineering was also employed to improve the expression, stability and PK profile of our IL18 variants.

Results IL18 variants that maintained binding to IL18Ra in the presence of IL18BP were identified from the ribosome display library. In biacore binding assay, the variants showed higher binding affinity to IL18 receptor (IL18Ra) compared to wild type IL18, while no binding observed to IL18BP. The identified IL18 variants induced potent IFN γ secretion by human PBMCs from healthy donors, which was not affected by high concentration of IL18BP. Conjugation of PEGs to the nnAA inserted into an optimized site in the IL18 sequence enabled half-life-extension. Additional mutations were introduced on the IL18 variants to stabilize the molecule, which also improved the expression, thermal stability and serum clearance profile in mice. The final Sutro IL18 lead activates T and NK cells in the presence of high concentration of IL18BP and exhibited favorable PK profile in mice.

Conclusions Sutro's engineered IL18 variant induces potent T and NK cells activation without the negative regulation of IL18BP. The favorable immune stimulation, pharmacokinetics and adjustable half-life extension make it a compelling product concept for future cytokine therapy in broad oncology indications.

Ethics Approval All in vivo procedures were conducted in compliance with the guidelines of the Institutional Animal Care and Use Committee (IACUC) at Sutro Biopharma

<http://dx.doi.org/10.1136/jitc-2022-SITC2022.1359>

1360 PHARMACODYNAMICS OF JNJ-70218902, A TMEFF2 × CD3 BISPECIFIC ANTIBODY, IN CYNOMOLGUS MONKEY

¹Cassandra Lowenstein, ²Subhasree Basu*, ²Joshua Rusbuldt, ³Sathya Venkataramani, ²Robin Ernst, ²Steve Jarantow, ²Scott Brodeur, ⁴Daniel Rubio, ²Pharavee Jasiprasart, ²Margaret Yu, ²Brent Rupnow, ¹Michael Russell. ¹*Proteovant Therapeutics, King of Prussia, USA*; ²*Janssen RandD, Spring House, USA*; ³*Amgen, Inc, Thousand Oaks, USA*; ⁴*EQRx International, Inc, Cambridge, USA*

Background TMEFF2 is a transmembrane protein with epidermal growth factor-like and 2 follistatin-like domains. The enriched expression of TMEFF2 in prostate cancer and its restricted expression in healthy brain and prostate make it an attractive candidate for targeted prostate cancer therapy. JNJ-70218902 (JNJ-902) is a bispecific TMEFF2 × CD3 antibody that binds to human TMEFF2 on prostate cancer cells and to human CD3 on T cells to promote T cell-mediated killing of tumor cells. Given the 100% sequence homology and analogous biodistribution of TMEFF2 in humans and monkey, the pharmacodynamics of JNJ-902 was studied in cynomolgus monkeys.

Methods Two dosing regimens of JNJ-902 were evaluated in cynomolgus monkeys: single, fixed dosing (0.075 mg/kg) and step-up dosing (0.075 mg/kg followed by 0.3 mg/kg 1 week later). Blood, serum, and prostate tissue were collected for flow cytometry to assess number of T cell infiltrates and myeloid cells, and surface markers of T cell function (activation, proliferation, and suppression).

Results An approximately dose proportional increase in JNJ-902 exposure was observed in this study. Both dosing regimens increased CD4+ and CD8+ T cell infiltration in the prostate, including activation and proliferation of CD4+ and CD8+ T cells (measured by granzyme B, CD25, CD69, and Ki-67), and in the periphery, minimal suppressive biomarkers (CD4+CD25hi Foxp3+) were observed. Interestingly, greater infiltration of CD8+ T cells was observed with step-up dosing. Both dosing regimens led to an influx of pro-inflammatory cells (dendritic cells, myeloid cells, macrophages, and B cells) into the prostate.

Conclusions Redirecting T cell activity to TMEFF2-expressing tumors by JNJ-902 is a promising immunotherapy for prostate cancers. In cynomolgus monkeys, treatment with JNJ-902 induced the infiltration of activated and proliferating T cells and inflammatory cells into the prostate, suggesting the potential to mediate an effective immune response. The clinical evaluation of JNJ-902 is currently underway in a phase 1 dose escalation trial in patients with metastatic castration-resistant prostate cancer (NCT04397276).

Ethics Approval The procedures involving the care and use of animals in this study were reviewed and approved by CR-MWN Institutional Animal Care and Use Committee before conduct (Testing Facility Study Number 886-526). During the study, the care and use of animals were conducted with guidance from the guidelines of the USA National Research Council.

<http://dx.doi.org/10.1136/jitc-2022-SITC2022.1360>

1361

HBM1022: AN AFUCOSYLATED ANTI-CCR8 ANTIBODY, DEPLETES SPECIFICALLY TUMOR INFILTRATING TREGS AND INHIBITS TUMOR GROWTH WITH EXCELLENT SAFETY PROFILE IN PRECLINICAL STUDIES

Shuang Lu*, Yiping Rong, Xin Gan, Joe Zhao. *Harbour biomed, Shanghai, China*

Background Tumor-infiltrating lymphocyte-Treg cells (TIL-Tregs) contribute to establishment of an immunosuppressive tumor microenvironment (TME). Several immunotherapies, such as anti-CD25 antibodies, are designed to target this type of cells. However, the possibility of undesirable targeting Treg cells in peripheral blood hampers their clinical benefits. CCR8 is a chemokine receptor selectively upregulated on TIL-Tregs from cancers such as clear cell renal cell carcinoma (ccRCC), breast, and bladder cancers, but rarely on Tregs in peripheral blood. This tumor specific expression of CCR8 provides us with an opportunity to develop an immunotherapy targeting TIL-Tregs selectively.

Methods

Results

Conclusions HBM1022 is a novel Fc-optimized CCR8 antibody with a high affinity to both human and cynomolgus monkey CCR8. It acts through dual mechanisms of action (MOA). HBM1022 recognizes patient-derived TIL-Tregs, and potently depletes CCR8+Treg cells via enhanced antibody-dependent cellular cytotoxicity (eADCC) activity. Furthermore, it inhibits CCL1-CCR8 signaling pathway and blocks CCL1 induced cell migration. HBM1022 exhibits a potent antitumor activity as monotherapy and in combination with anti-PD (L)1 antibodies. HBM1022 has favorable pharmacokinetic properties and an excellent safety profile in cynomolgus monkey, which suggests a potential good safety profile in human.

<http://dx.doi.org/10.1136/jitc-2022-SITC2022.1361>

1362

NONCLINICAL CHARACTERIZATION OF ICVB-1042, A NOVEL E2F-TUMOR SELECTIVE ONCOLYTIC VIRUS WITH THE POTENTIAL TO TREAT SOLID TUMORS

<http://dx.doi.org/10.1136/jitc-2022-SITC2022.1362>

Michael Lyman*, Jessica Field, Joshua Messinger, Nathaniel Rice, Matthew Lanahan, Alex Kato, Michael Pokrass, Heba Nowyhed. *IcoOVir Bio, San Diego, CA, USA*

Background A major challenge in oncolytic virotherapy is to engineer potent tumor-killing viruses that can be delivered systemically for treatment of metastatic disease while leaving normal cells unharmed. Here we report the nonclinical characterization of ICVB-1042, an optimized E2F-dependent oncolytic adenovirus rationally engineered with specific genomic modifications to confer tumor selective replication and enhanced tumor cell killing. ICVB-1042 has been further engineered with a chimeric fiber to enhance its tumor tropism and a modified capsid hexon protein to allow intravenous (IV) delivery. This combination of rationally designed modifications enables ICVB-1042 to be used for the treatment of a wide range of solid tumor types.

Methods Using a proprietary iterative adenovirus design and screening platform, IcoOVir has engineered ICVB-1042, a potent, tumor selective oncolytic adenovirus. A multi-faceted nonclinical strategy was designed to characterize key therapeutic properties of ICVB-1042 through *in vitro* and *in vivo* studies. Tumor cell selectivity was assessed by testing the replication of ICVB-1042 in a comprehensive panel of primary normal human cells compared to tumor cells. Anti-tumor efficacy was evaluated in multiple human xenograft immunocompromised mouse models. Tolerability, biodistribution and PK were assessed in human CD46 transgenic mice where particle-mediated toxicity and effects on host immune response could be assessed. Biodistribution and pharmacokinetics were evaluated in human tumor xenograft models and in CD46 transgenic mice.

Results ICVB-1042 displayed replication and cell killing against a broad range of human tumor cell lines including breast, prostate, bladder, lung, and glioblastoma. However, replication was tumor selective, and the multiplicity of infection required to kill primary normal cells was 100 to >10,000-fold greater than the concentration of virus required to kill tumor cells. The anti-tumor activity of IV-dosed ICVB-1042 was demonstrated in several subcutaneous and orthotopic models. ICVB-1042 virus particles increased in both tumors and plasma over time suggesting virus replication in tumors, which correlated with efficacy. IV dosing of ICVB-1042 was well tolerated in CD46 transgenic mice. ICVB-1042 distributed throughout CD46 transgenic mice and cleared to less than 0.1% of the administered dose by Day 15 post first dose. There was no preferential distribution into the liver over other organs.

Conclusions ICVB-1042 is a novel, potent, tumor selective, systemically administrable oncolytic virus with the potential to treat a broad range of solid tumors. The *in vitro* and *in vivo* results presented demonstrate ICVB-1042's selective replication in tumor cells compared to quiescent primary normal cells, broad tumor tropism, and safety and anti-tumor efficacy with IV dosing.

Ethics Approval All procedures carried out were conducted in compliance with the applicable laws, regulations and guidelines of the National Institutes of Health (NIH) and with the approval of Labcorp Drug Development PCO's Animal Care and Use Committee. Labcorp Drug Development (Greenfield) is an AAALAC accredited facility.

1363

EVALUATION OF THE ANTI-TUMOR ACTIVITY OF ICVB-1042, A NOVEL E2F-TUMOR SELECTIVE ONCOLYTIC VIRUS, SELECTIVELY TARGETING TUMOR CELLS IN AN ESTABLISHED HUMAN GLIOBLASTOMA MOUSE MODEL

Michael Lyman*, Jessica Field, Jinkil Jeong, Valentino Gantz, Nathaniel Rice, Heba Nowyhed. *IcoVir Bio, San Diego, CA, USA*

Background A major challenge in oncolytic virotherapy is to engineer potent tumor-killing viruses that can be delivered systemically for the selective treatment of metastatic disease while leaving normal cells unharmed. ICVB-1042 is a novel E2 transcription factor (E2F)-dependent oncolytic adenovirus rationally designed with genomic modifications to confer tumor selective replication, allow intravenous delivery, enhance potency and tumor tropism, and aid in screening clinical samples. The goal of this study was to compare anti-tumor activity and tumor selectivity of ICVB-1042 to that of ICVB-940, an Ad5-based oncolytic virus (OV) engineered with a 24 base pair deletion in E1A and an RGD-4C motif in HI loop of the fiber knob (D24RGD). ICVB-940 is similar to another D24RGD Ad5 OV that has been evaluated in clinical trials in glioblastoma patients.^{1,2} This analysis, performed *in vitro* on a panel of glioblastoma tumor cell lines and *in vivo* in an established nonobese diabetic/severe combined immunodeficiency gamma mouse-based human glioblastoma model, showed overall enhanced activity of ICVB-1042.

Methods The replication and cell killing of ICVB-1042 and ICVB-940 were compared in primary astrocytes and in glioblastoma tumor cell lines to evaluate baseline killing in primary brain cells versus tumor cells *in vitro*. Both viruses were compared *in vivo* at doses of 1.00E+08 or 2.00E+08 plaque forming units administered intratumorally in the human glioblastoma model with time to progression (TTP) and mean tumor volume for the treated versus control groups (median $\Delta T/\Delta C$) as endpoints.

Results ICVB-1042 demonstrated enhanced tumor cell killing over ICVB-940 in 11 of 13 human glioma tumor lines *in vitro*. ICVB-1042 showed significant decreases in tumor volume and significant increases in TTP between treated and control animals at both doses. ICVB-940 showed significant decreases in tumor volume but nonsignificant increases in TTP at the high dose; no significant differences in tumor volume or TTP at the low dose were observed. Comparison between ICVB-1042 and ICVB-940 at the low dose resulted in significant decreases in Day 38 tumor volume and significant increases in TTP for ICVB-1042 over ICVB-940. All treatments were well-tolerated, resulting in no deaths or group mean body weight loss in the treatment window.

Conclusions ICVB-1042, a novel E2F-tumor selective rationally designed OV engineered with enhanced tropism and tumor killing potency, produced higher anti-tumor activity *in vitro* and *in vivo* in GBM tumors compared to the D24RGD virus ICVB-940.

REFERENCES

1. Lang FF, Conrad C, Gomez-Manzano C, Yung WKA, Sawaya R, Weinberg JS, et al. Phase I study of DNX-2401 (Delta-24-RGD) oncolytic adenovirus: Replication and immunotherapeutic effects in recurrent malignant glioma. *J Clin Oncol* 2018;**36**:1419–1427.
2. van Putten EHP, Kleijn A, van Beusechem VW, Noske D, Lamers CHJ, de Goede AL, et al. Convection enhanced delivery of the oncolytic adenovirus delta24-RGD in patients with recurrent GBM: A Phase I clinical trial including correlative studies. *Clin Cancer Res*. 2022;**28**:1572–1585.

Ethics Approval All procedures were conducted in compliance with the applicable laws, regulations and guidelines of the National Institutes of Health (NIH) and with the approval of Labcorp Drug Development PCO's Animal Care and Use Committee. Labcorp Drug Development (Greenfield) is an AAALAC accredited facility.

<http://dx.doi.org/10.1136/jitc-2022-SITC2022.1363>

1364

BISPECIFIC ANTIBODIES THAT BLOCK TIM-3 AND CD39 INDUCE ANTI-TUMOR EFFICACY AND IMMUNE RESPONSE BY BLOCKING MULTIPLE SUPPRESSIVE MECHANISMS

<http://dx.doi.org/10.1136/jitc-2022-SITC2022.1364>

Noriko Matsumoto*, Yuji Mishima, Kanto Nakajima, Takahiko Aramaki, Mamoru Shiraiishi, Haruka Matsumura, Norihiro Nakamura. *BrightPath Biotherapeutics Co., Ltd., Kawasaki, Japan*

Background TIM-3 and CD39 are co-expressed in tumor-infiltrating T cells and antigen-presenting cells and considered to act as negative regulators of anti-tumor immunity. TIM-3 has multiple ligands including galectin-9, phosphatidylserine, CEA-CAM-1 and HMGB1. Although galectin-9 induces apoptosis in T cells via TIM-3, most of the TIM-3 antibodies under clinical development only partially block the galectin-9-binding to TIM-3. Adenosine is an immunosuppressive metabolite that suppresses T and NK cells. Inhibition of ATP-hydrolysis by purinergic ectoenzyme CD39 may recover anti-tumor immunity through reducing adenosine level in tumor microenvironment. We report herein BP1210, a novel TIM-3 biparatopic antibody (BpAb), that blocks the binding of multiple ligands including galectin-9 and BP1212, a bispecific antibody (BsAb) against TIM-3 and CD39, that blocks TIM-3-signaling and adenosine-mediated immune suppression.

Methods The antibodies against TIM-3 and CD39 were cloned from mice immunized with recombinant proteins. Optimal combinations of clones were selected by functional assay for BpAb and BsAb, then the CDRs were grafted to human framework in effector null scFv-Fc format with knobs-into-holes mutations. Binding affinities and blocking/inhibiting activities were analyzed using recombinant proteins and cells endogenously expressing TIM-3 or CD39. The proliferation and cytokine production of T cells induced by antibodies were determined using human peripheral blood mononuclear cells (PBMCs). Anti-tumor efficacy of BP1210 was investigated in tumor models in huTIM-3 knock-in mice or in NOG mice transplanted with PBMCs.

Results BP1210 BpAb that fully blocks the interaction of TIM-3 to both galectin-9 and phosphatidylserine, enhanced the activation of T cells stimulated by the antigen. i.e., BP1210 increased the population of IFN γ ⁺ T cells, the production of cytokines, and suppressed the apoptosis of T cells, which are higher than other TIM-3 antibodies that fully blocks the binding to phosphatidylserine but not to galectin-9. *in vivo* studies showed that BP1210 retards the tumor growth and enhances the tumor-growth suppression by anti-PD-L1 antibody. BP1212 BsAb preferentially bound to the CD39⁺TIM-3⁺ cells (exhausted T cells and APCs) and effectively blocked the enzymic activity of CD39 and binding to TIM-3 ligands in these cells. BP1212 augmented the proliferation and cytokine production of T cells, suggesting that BP1212 enhances the T cell immunity even in immunosuppressive tumor microenvironment.

Conclusions BP1210 and BP1212 show the advantages over conventional TIM-3 and CD39 antibodies in T cell-mediated tumor immunity. Our engineered antibodies with novel combinations of antibody clones against immune checkpoints will provide new therapeutic options of tumor immunotherapy.

Ethics Approval The present study was approved by the Institutional Ethics Committee of BrightPath Biotherapeutics Co., Ltd.(approved number: ERD-01). Animal studies were approved by the Institutional Animal Care and Use Committee (approved number: 22012A and 22014A).

1365

AN ACTIVE SITE PTPN2/N1 SMALL MOLECULE INHIBITOR PROMOTES ANTI-TUMOR EFFICACY BY SENSITIZING TUMOR CELLS TO INFLAMMATORY SIGNALS AND ENHANCING IMMUNE CELL ACTIVITY

¹Kathleen McGuire*, ¹Christina Baumgartner, ¹Carey Backus, ¹Rebecca Mathew, ¹Kelly Klinge, ¹Joseph Klahn, ²Prasanthi Geda, ¹Kyle Halliwill, ¹Jacqueline Aguado, ¹Liang Mu, ¹Ryan Duggan, ¹Cara Hrusch, ¹Elliot Farney, ¹Zhaoming Xiong, ¹Marinka Bulic, ¹Patricia Trusk, ¹Loren Lasko, ³Hakimeh Ebrahimi-Nik, ³Kathleen Yates, ³Robert Manguso, ¹Keith Hamel, ⁴Marcia Paddock, ¹Jennifer Frost, ¹Phillip Kym. ¹Abbvie Inc, North Chicago, IL, USA; ²Bristol Myers Squibb, Summit, NJ, USA; ³Broad Institute of MIT and Harvard, Cambridge, MA, USA; ⁴Calico Life Sciences LLC, South San Francisco, CA, USA

Background The tyrosine phosphatases PTPN2 and PTPN1 are important negative regulators of immune signaling pathways and genetic deletion of these proteins in tumor or immune cells has been shown to overcome unresponsiveness to checkpoint blockade and increase anti-tumor immunity *in vivo*. Thus, these proteins should be promising immunotherapy targets, but drugging phosphatases has proven difficult.

Methods Here, we demonstrate that our active site PTPN2 and PTPN1 small molecule inhibitor, ABBV-CLS-484 (AC-484), promotes anti-tumor immunity in several syngeneic mouse tumor models upon oral administration. This first-in-class PTPN2/N1 inhibitor sensitizes tumor cells to inflammation and augments the activity of a variety of immune cell subsets *in vitro* and *in vivo*.

Results Specifically, AC-484 sensitizes tumor cells to inflammation by augmenting interferon signaling, leading to enhanced growth arrest and antigen presentation. AC-484 also promotes T cell activation and function upon TCR stimulation and enhances activity of dendritic cells and macrophages *in vitro*. Consistent with our *in vitro* findings, immunophenotyping and single-cell RNA sequencing analyses demonstrate AC-484 treatment leads to a more inflamed tumor microenvironment characterized by increased abundance of inflammatory macrophages producing pro-inflammatory chemokines such as IP-10, which are important for immune cell recruitment. Further, AC-484 leads to an increased abundance and activation of intratumoral NK and CD8 T cells not only in inflamed but also in less inflamed tumors. Interestingly, PTPN2/N1i also decreased the frequency of dysfunctional/exhausted T cells and increased the frequency of polyfunctional CD8 T cells. To directly confirm these effects on exhausted T cells, we assessed how AC-484 affected T cell dysfunction under T cell exhaustion conditions *in vitro*. Consistent with our *in vivo* findings, AC-484 reduced the frequency of exhausted T cells and promoted polyfunctional T cells with improved cytotoxic activity under chronic antigen stimulation.

Conclusions Taken together, PTPN2/N1 inhibition appears to promote anti-tumor activity by acting on tumor cells directly and promoting the anti-tumor activity of several immune cell subsets including dysfunctional CD8 T cells, which are enriched in the tumor microenvironment. This two-pronged mechanism leads to efficacy in murine tumor models unresponsive to PD-1 pathway blockade. Based on our preclinical data on this novel and efficacious therapeutic approach, ABBV-CLS-484 is currently under Phase I clinical evaluation in cancer patients with solid tumors.

Acknowledgements We thank Geoff Halvorsen (deceased AbbVie employee) for his integral part in the discovery and synthesis of ABBV-CLS-484.

<http://dx.doi.org/10.1136/jitc-2022-SITC2022.1365>

1366 ANTI-PD-1/IL-7V BISPECIFIC ANTIBODY PROMOTES TCF1 + STEM LIKE T CELLS EXPANSION AND LONG-LASTING IN VIVO EFFICACY

Aurore Morello*, Margaux Seite, Justine Durand, Isabelle Girault, Geraldine Teppaz, Virginie Thepenier, Vanessa Gauttier, Caroline Mary, Nicolas Poirier. *OSE Immunotherapeutics, Nantes, France*

Background Immunocytokines can strengthen anti-PD-(L)1 therapy by promoting T-cell survival, but their shortened half-life and systemic toxicity limit their clinical development. We propose to selectively deliver IL-7 to PD-1⁺ T-cells using a bispecific anti-PD1/IL-7v mutein fused to reinvigorate PD1⁺IL-7R⁺ tumor-specific T cells and sustain long-term response. RNAseq and TILs scRNAseq analyses illustrate that IL-7R and IL-7R pathway gene expression is significantly correlated with better long-term OS and/or PFS across several cancers Higher IL-7R and IL-7R pathway expression by tumor-specific T-cell clonotype is significantly correlated with ICI response, higher stemness & proliferative signature, lower exhaustion and apoptosis markers, providing a strong rationale of co-targeting IL-7 to PD-1 to sustain durable tumor-specific T-cells response. Despite low IL-7R expression on Tumor-specific T-cell clonotype a high concentration of IL-7 can rescue them. We propose with the anti-PD-1/IL-7v to cis-target and provide a survival/proliferative specific signal.

Methods Proliferation, IL-7R signaling assays were tested to determine the mechanism. For the suppressive assay, CD4 Treg and autologous CD8 Teff were co-cultured. In vivo experiments were performed in hPD-1KI immunocompetent mice.

Results A high-affinity antagonist anti-PD-1 mAb was fused to a single IL-7 mutein (IL7v) having lower affinity to IL-7R complex allowing a preferential and optimal cis-potential of PD-1+ T-cells. Anti-PD1/IL7v restores proliferation and maintains long-term survival of chronically stimulated human T-cells in vitro (over 5 stimulation). scRNAseq and FACs analyses demonstrated that anti-PD1/IL7v triggers the expansion of TCF1+ stem-like memory T-cells (CCR7+PD1+Ki67+), whereas IL-2 and IL-15 promote differentiation of T-cells into exhausted T-cells (TCF1-Tim3+Ki67+). Furthermore, anti-PD1/IL7v preferentially stimulated T_{eff} over T_{reg} as opposed to IL-2 & IL-15 and abrogated the T_{reg} suppression by restoring IFN-γ secretion and proliferation of CD8 T_{eff}.

In vivo, anti-PD1/IL-7v has impressive monotherapy efficacy in PD-1 sensitive model (orthotopic mesothelioma, >90%CR) and in a PD-1 resistant model (orthotopic HCC, >65% CR) in which anti-PD-1 or IL-7 has no effect. Further analyses in HCC model demonstrate that anti-PD1/IL7v enhanced quality and biodistribution of T-cells by promoting intratumoral TCF1 +CD8+stem-like T-cells proliferation and favoring T-cell migration into the tumor nest whereas anti-PD-1 promotes T-cell exclusion. Combination with sorafenib chemotherapy in HCC model further enhances in vivo efficacy.

Conclusions Our data validate the rational of selective delivery of IL-7 to tumor-specific T-cells to sustain long-lasting response, proliferation, and survival of these key effectors upon ICI therapy. Anti-PD1/IL-7v preferentially cis-potentiates PD1+-tumor-specific-T-cells limiting the risk of I-O/I-O immunotoxicity and induces the expansion of stem-like T-cell capable to strengthen PD-1 therapy efficacy.

<http://dx.doi.org/10.1136/jitc-2022-SITC2022.1366>

1367

A HIGHLY-SELECTIVE HPK1 INHIBITOR ENHANCES T CELL RECEPTOR SIGNALING AND T CELL ACTIVATION POTENTIAL, INCREASING ANTIGEN RECOGNITION AND EFFICACY OF PD-1 THERAPY

¹Andrew Nager*, ²David Schaer, ¹Rebecca Gallego, ¹Eleanore Hendrickson, ¹Sergei Timofeevski, ¹Manqing Li, ¹Allison Rohner, ¹Ruth Seelige, ¹Samuel Stoner, ¹Christopher Dillon, ¹Paulina Cuenca, ¹Cynthia Jones, ¹Sarah Firdaus, ¹Robert Amezquita, ¹Clifford Restaino, ¹Derek Bartlett, ¹Timothy Fisher. ¹Pfizer, San Diego, CA, USA; ²Bayer, New York, NY, USA

Background Recognition of neoplastic transformed cells as foreign is the cornerstone to effective immune surveillance of cancer. Neo-antigens generated by mutations that accumulate in tumors are the basis of immune rejection, and higher levels correlate with responses to PD1 blockade. Unfortunately, most patients have insufficient tumor mutation burden (TMB) to benefit from current immunotherapies, and/or their mutations do not produce sufficiently robust antigens that can break central immune tolerance. Enhancing the ability of a patient's immune system to respond to existing TMB is paramount to overcoming primary resistance to PD1 blockade.

The HPK1 kinase is critically involved in T cell receptor (TCR) signaling, initiating a negative-feedback loop that raises the threshold of stimulus required for T cell responses. Genetic ablation of HPK1 kinase activity has been shown to increase T cell responsiveness to antigen stimulus and improve activity of PD-1 blockade in preclinical models, making HPK1 an attractive target for immunotherapy. However, the high homology of the HPK1 active site with other kinases, including kinases necessary for productive TCR signaling, results in off target liabilities that can limit small-molecule inhibitors from unlocking the full-potential of HPK1 inhibition.

Methods Through structure-based drug design and optimizing for enhanced T cell proliferation, we identified the highly-selective HPK1 inhibitor PF-07265028. Kinome selectivity of PF-07265028 was verified through biochemical profiling and in-cell chemical probes.

Results Treatment of primary human T cells from multiple human donors with PF-07265028 shows a dose-dependent inhibition of SLP76 phosphorylation (pSLP76) while increasing proliferation following suboptimal TCR stimulation. By virtue of HPK1 selectivity, PF-07265028 maintains the ability to enhance immune responses at concentrations well-above that required for 90% inhibition of pSLP76. Inhibition of HPK1 with PF-07265028 increased both CD8 and CD4 cytokine recall responses to MHC-presented peptides, and enabled resistance to immunosuppressive metabolites (PGE₂ and adenosine) that can otherwise activate HPK1 through their receptors. Combination of PF-07265028 with an anti-PD-1 antibody in co-cultures of human T cells and cancer cells led to increased tumor cell killing through synergistic enhancements of T cell activation and cytokine production. PF-07265028 displayed immunostimulatory activity in non-human primates including markers of T cell activation.

Conclusions Based on its ability to enhance multiple axes of T cell activation, PF-07265028 has the potential to improve anti-tumor responses in patients resistant to immunotherapy. Therefore, a phase one study has thus been initiated to evaluate the safety and efficacy of PF-07265028 alone and in combination with PD-1 blockade in patients with advanced solid tumors.

Trial Registration

NCT05233436

<http://dx.doi.org/10.1136/jitc-2022-SITC2022.1367>

1368

A NOVEL BISPECIFIC BCA356 TARGETING TUMOUR ANTIGEN CAIX CONJUGATED TO AN ATTENUATED IL12 DEMONSTRATES PRE-CLINICAL EFFICACY WITH POTENTIAL FOR LIMITED SYSTEMIC TOXICITY

¹Pradip Nair*, ¹Arvind Goswamy, ¹Jaya Bhatnagar, ¹Srinivas Boreddy, ¹Reshmi Nair, ¹Shiv Krishn, ¹Anshu Kuriakose, ¹Prashanth Pandey, ¹Hanumant Kulkarni, ¹Kishore Punmath, ¹Milind Sagar, ¹Prashanthakumara V, ¹Thulasi TK, ¹Abhishek Sinha, ¹Ravindra DR, ²Rachel Salazar. ¹Biofusion therapeutics, Bangalore, India; ²Bicara Therapeutics, Boston, MA, USA

Background IL-12 is a potent cytokine linked to activation of innate and adaptive immune system for anti-tumour immunity.¹ The clinical development of IL-12 therapy has been constrained with severe toxicity reported from systemic administration of IL-12. Toxicity is attributed to poor pharmacokinetics of IL-12, necessitating frequent dosing, and nonspecific distribution. Recently, there has been a renewed interest in IL-12 therapy with various strategies to improve half-life and reduce toxicity, with lead candidates in preclinical and early clinical stages of development.² Here, we describe novel bispecific BCA356 with an affinity matured humanized anti-CAIX antibody and attenuated IL-12 subunits fused to each of the heavy chains at the C-terminus by a linker in a knob-in-hole format.

Methods *In silico* mutational screening was performed on the p40 and p35 subunits of IL-12 to identify optimally attenuated IL-12 variants (IL-12vs). CAIX as a tumour-targeting antigen was selected based on high expression of CAIX across several solid tumour types. Expression of cellular and soluble CAIX across tumour types was evaluated by immunohistochemistry (IHC) on tissues and ELISA on tumour-matched plasma. BCA356 was identified after IL-12vs were screened in a HEK-Blue™ IL-12 assay (figure 1) followed by phosphorylated STAT4 expression on CD8⁺ T cells and IFN γ release by PHA-stimulated PBMCs/IL-2 primed NK-cells. In *in vitro* 2 and 3D co-culture assays with CAIX-overexpressing cell line and PBMCs, cytotoxicity and cytokine/chemokine release were assessed across days. Efficacy and safety of BCA356 were evaluated in PBMC-based humanized mice models and human IL-12 and IL-12 receptor gene knock-in transgenic mice.

Results IHC studies confirmed high CAIX expression in clear cell renal carcinoma³ and multiple other tumour types, a significant number of samples, expressed high and moderate CAIX expression (figure 2). BCA356 significantly attenuated IFN γ release by stimulated PBMCs, activated NK-cell and pSTAT4 expression in CD8 T cells as compared to IL-12(wt). In co-culture assays, BCA356 showed cytotoxicity of cancer cells comparable to IL12(wt) (figure 3) without significant cytokine release unlike IL12(wt) (figure 4). Finally, efficacy studies in PBMC-based humanized mice models and transgenic mice models confirm that BCA356 is efficacious and safe in CAIX-overexpressing tumour bearing mice.

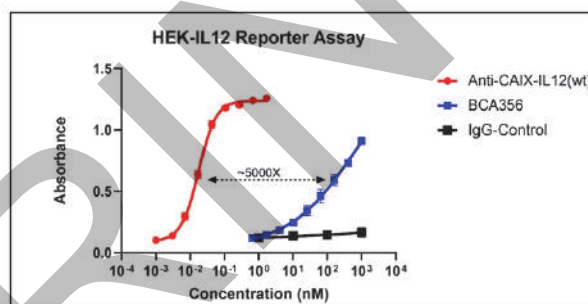
Conclusions BCA356 specifically targets CAIX-expressing tumour cells and similar to wild type IL-12 cytokine, has the potential to reduce tumour proliferation with optimal activation of pro-inflammatory cytokines. Through these *in vitro* and *in vivo* studies, we demonstrate that BCA356 by its CAIX-targeted IL-12v delivery approach is both efficacious and safe.

Acknowledgements The authors would like to acknowledge the help extended by Biocon Limited in running this study. We would also acknowledge the assistance provided by personnel at Syngene vivarium facility for supporting the animal studies at their dedicated vivarium.

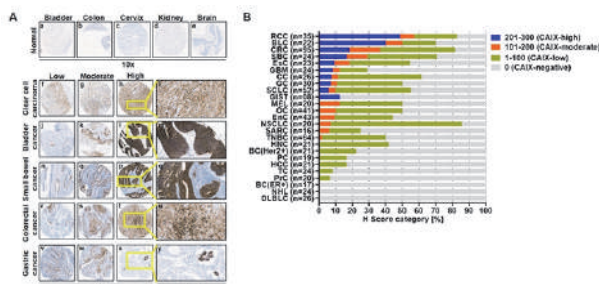
REFERENCES

1. Mirelkar B, Pylayeva-Gupta Y. IL-12 family cytokines in cancer and immunotherapy. *Cancers (Basel)* 2021;**13**.
2. Holder PG, Lim SA, Huang CS, Sharma P, Dagdas YS, Bulutoglu B, et al. Engineering interferons and interleukins for cancer immunotherapy. *Adv Drug Deliv Rev* 2022;**182**:114112
3. Pastorekova S, Gillies RJ. The role of carbonic anhydrase IX in cancer development: links to hypoxia, acidosis, and beyond. *Cancer Metastasis Rev* 2019;**38**:65–77

Ethics Approval Mice were maintained as per the regulations of Committee for the Purpose of Control and Supervision of Experiments on Animals (CPCSEA), Government of India and Association for Assessment and Accreditation of Laboratory Animal Care (AAALAC) guidelines. All animal experiments were approved by institutional ethical committee and performed under approved protocols. All animals were maintained at dedicated Syngene vivarium

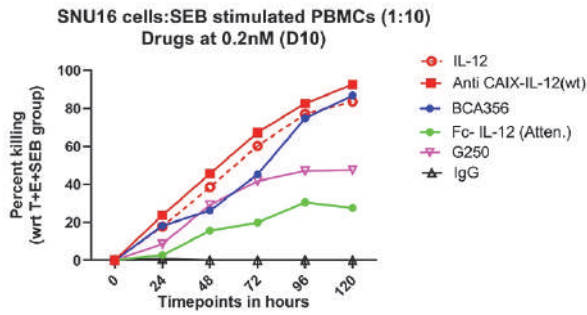


Abstract 1368 Figure 1 Evaluating IL-12 activity by HEK-IL-12 reporter assay. The binding of IL-12 to the IL-12R on the surface of HEK-Blue™ IL-12 cells (Invivogen) triggers a signaling cascade leading to the activation of STAT-4 with the subsequent production of SEAP. HEK-IL-12 cells were incubated with different concentrations of test compounds for 18-24 hours, and IL-12 activity was measured by addition of Quanti-Blue solution. Anti-CAIX-IL-12(wt) showed similar activity as rh-IL-12.

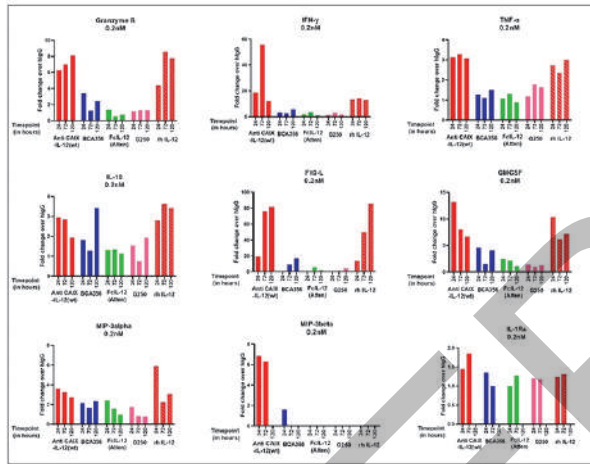


Abstract 1368 Figure 2 CAIX expression in normal and cancer tissues. (A) Upper panel: CAIX expression in normal tissues. (A) Lower panel: Representative images of heterogeneous CAIX expression in different cancer types. (B) For each cancer type (Y axis), percentage of cases corresponding to CAIX-high (201-300), CAIX-moderate (101-200), CAIX-low (1-100), and CAIX-absent (0) H Score category (X axis). BC (Her2+): Breast Cancer(Her2+), BC(ER+): Breast Cancer(ER+), BLC: Bladder Cancer, CC: Cervical Cancer, CRC: Colorectal Cancer, DLBLC: Diffuse Large B-Cell Lymphoma, EnC: Endometrial Cancer, EsC: Esophageal/GEJ Cancer, GBM: Glioblastoma, GC: Gastric Cancer, GIST: Gastrointestinal Stromal Tumour, HCC: Hepatocellular Carcinoma, HNC: Head & Neck Cancer, MEL: Melanoma, NHL: Non-Hodgkin Lymphoma, NSCLC: Non-Small Cell Lung Cancer, OC: Ovarian Cancer, PC: Pancreatic cancer, PrC: Prostate Cancer; RCC: Renal Cell Carcinoma, SARC: Sarcoma, SBC: Small Bowel Cancer, SCLC: Small Cell Lung Cancer, TC: Thyroid Cancer, TNBC: Triple Negative Breast Cancer.

Abstracts



Abstract 1368 Figure 3 Real time tumour cell killing by BCA356. SNU16 target cells were seeded with SEB(0.5 pg/mL) stimulated PBMC at T:E ratio of 1:10. Plates were kept in Incucyte and scanned for 120h to measure cytotoxicity over time. Cytotoxicity is a representative graph from two independent experiments.



Abstract 1368 Figure 4 Cytokine release by BCA356. SNU16 target cells were seeded with SEB (0.5 pg/mL) stimulated PBMC at T:E ratio of 1:10. Cytokines were evaluated at 24h, 72h and 120h using Luminex. Criteria used for shortlisting of key cytokines: 2-fold increase in Anti CAIX-IL-12(wt) over Human IgG and $\geq 20\%$ reduction in BCA356 over Anti CAIX-IL-12(wt). Cytokine release is from a single experiment.

<http://dx.doi.org/10.1136/jitc-2022-SITC2022.1368>

1369

CD64-DIRECTED SCFV FUSION PROTEIN EXHIBITS CYTOTOXICITY AND IS A TOOL FOR SITE-SPECIFIC DIAGNOSIS OF ACUTE MYELOID LEUKEMIA

¹Siew Tai, ²Sikozile Ncembu*, ²Stefan Barth, ²Sue Harrison. ¹Stellenbosch University, Stellenbosch, South Africa; ²University of Cape Town, Cape Town, South Africa

Background Cancer immunotherapy is a promising innovative and effective treatment for many forms of cancer. Among haematological malignancies, acute myeloid leukemia (AML) remains an unmet medical need as it is mainly treated with chemotherapy, which is associated with serious side effects.^{1,2} Therefore, antibody-based targeted therapy is preferred as it can target and specifically eliminate malignant cells. An immunotoxin (IT) is a chimeric molecule consisting of a targeting molecule and a toxic component that specifically kills target cells. H22(scFv) ETA' is an immunotoxin consisting of a humanised single-chain fragment (scFv) antibody that targets CD64, which is overexpressed on the surface of AML cells and a truncated version of *Pseudomonas* exotoxin A (ETA') that kills CD64-positive AML cells.³ CD64 is highly expressed on monocytic blast cells in patients with AML and not on normal haematopoietic stem cells, making it a suitable target antigen.⁴

Methods H22(scFv) ETA' was recombinantly expressed in *E. coli* BL21 (DE3) and channelled into the periplasmic space and purified by metal ion affinity chromatography and size exclusion chromatography. The cytotoxic efficacy of H22(scFv) ETA' was assessed by the Annexin V bioassay and binding assays were assessed using flow cytometry. A diagnostic fusion protein version of H22(scFv) ETA' was constructed in which the toxic component ETA' was removed and replaced with the protein SNAP tag to generate H22(scFv) SNAP. SNAP tag enables efficient tumour targeting and diagnosis of molecular biomarkers for cancer.

Results This study showed that H22(scFv) ETA' is cytotoxic to AML cancer cells expressing CD64. H22(scFv) ETA' showed significant toxicity in vitro against CD64-positive cell lines HL-60 and U937. Binding studies showed specific binding to both cell lines HL-60 and U937. Specific binding of H22(scFv) SNAP to HL-60 and U937 was also demonstrated.

Conclusions The results described show promising results in vitro not only for the treatment of AML, but also provide technology for the effective diagnosis of AML. The development of successful scale-up production of H22(scFv) ETA' and H22(scFv) SNAP is critical for large-scale production to enable further preclinical/clinical studies. The current phase of this study is focused on optimizing productivity and large-scale production of both fusion proteins described above.

Acknowledgements The authors would like to thank the South African Department of Science & Innovation (DSI) & National Research Foundation (NRF) through South African Research Chair Initiative (SARChI) for funding this study.

REFERENCES

1. Yu J, Jiang PY, Sun H, Zhang X, Jiang Z, Li Y, and Song Y. 2020. Advances in targeted therapy for acute myeloid leukemia. *Biomarker Research*, **8**(1):1–11.
2. DeSantis CE, Lin CCRL, Stein KD, Kramer JL, Alteri R, Robbins AS, and Jemal A. 2014. Cancer treatment and survivorship statistics. *CA: A Cancer Journal for Clinicians*, 2014;**64**(4):252–271.
3. Wolf P and Elsässer-Beile U. *Pseudomonas* exotoxin A: from virulence factor to anti-cancer agent. *International Journal of Medical Microbiology*, 2009;**299**(3): 61–176.
4. Rader RA. (Re) defining biopharmaceutical. *Nature*, 2008;**26**(7):743.

<http://dx.doi.org/10.1136/jitc-2022-SITC2022.1369>

Abstracts

1370

DISTINCT ANTI-TUMOR RESPONSE TO LISTERIA-BASED VACCINES BETWEEN ORTHOTOPIC AND SUBCUTANEOUS SYNGENEIC MOUSE MODELS OF RENAL CELL CARCINOMA

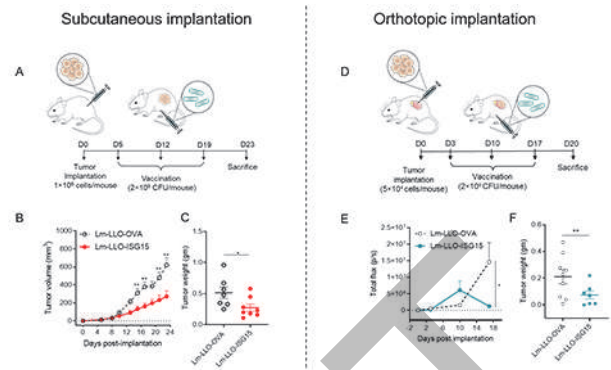
Hong-My Nguyen*, Laurence Wood. *Texas Tech University Health Sciences Center, Abilene, TX, USA*

Background In the past few decades, subcutaneous tumors have been used extensively in vivo studies to test the therapeutic efficacy of several forms of anti-cancer agents including immunotherapy. However, the recent growing demand for pre-clinical models that reflect human diseases more accurately, has led to the attention of orthotopic tumor models. There is a growing body of evidence demonstrating the difference in response to immunotherapy between orthotopic and subcutaneous mouse models. Our work illustrated the distinct anti-tumor response to immunotherapy between subcutaneous versus orthotopic syngeneic mouse models of renal cell carcinoma (RCC).

Methods For subcutaneous studies, 1×10^6 Renca cells were implanted subcutaneously (s.c.) into the right hind flank and mice were subsequently vaccinated i.p. on day 5, 12, and 19 with Lm-based vaccines. For orthotopic studies, 5×10^4 Renca cells expressing luciferase (Renca-luc) were implanted directly into the right kidney as previously described and mice were subsequently vaccinated i.p. on day 5, 12, and 17 with Lm-based vaccines. All mouse experiments were performed in accordance with the regulations of the Institutional Animal Care and Use Committee (IACUC) at the TTUHSC. For flow cytometry analysis, tumor tissues were harvested to prepare single-cell suspensions and stained with appropriate fluorochrome-conjugated anti-mouse monoclonal antibodies. Data were acquired on BD Fortessa and analyzed with FlowJo software version 10.7.0. All statistical analysis was done with Prism 8 GraphPad software version 8.3.0., using unpaired student t-test.

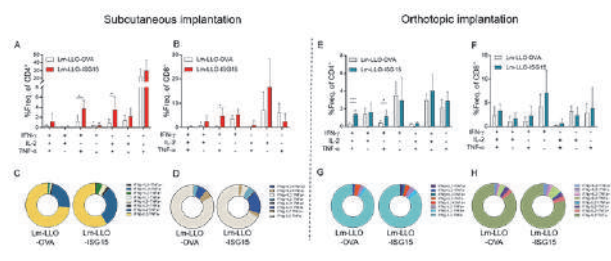
Results Listeria-based vaccines targeting interferon-stimulated gene 15, Lm-LLO-ISG15, significantly controlled tumor burden in both subcutaneous and orthotopic models as compared to that of controlled Lm (figure 1). Interestingly, while anti-tumor efficacy of Lm-LLO-ISG15 in the subcutaneous model was associated with activation of both CD8+ and CD4+ T cells, anti-tumor response in orthotopic models was mainly engaged by the activation of CD4+ T cells. The multi-cytokines producing T cells were higher in subcutaneous tumors as compared to that of orthotopic models (figure 2). In addition, treatment with Lm-LLO-ISG15 increased a higher influx of total myeloid cells as well as both monocytic- and polymorphonuclear-monocytic-derived suppressor cells (MDSCs) to the tumor microenvironment (TME) compared to Lm-LLO-OVA in subcutaneous tumors. In contrast, total myeloid cells, m-MDSCs, and pmn-MDSCs were significantly lower in Lm-LLO-ISG15 group compared to controlled Lm in orthotopic models (figure 3).

Conclusions Vaccination with Lm-LLO-ISG15 significantly controlled RCC tumor burden in both subcutaneous and orthotopic models, as compared to that of controlled Lm. Interestingly, treatment with Lm-LLO-ISG15 resulted in distinct anti-tumor responses in subcutaneous versus orthotopic RCC tumors.



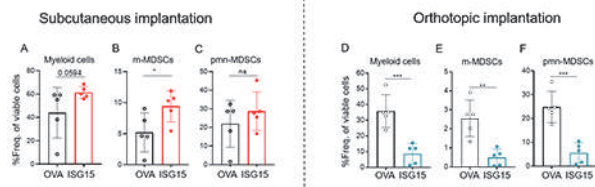
Abstract 1370 Figure 1 Listeria-based vaccines is efficacious against RCC tumors

Listeria-based vaccines is efficacious against both subcutaneous and orthotopic tumors. (A) Experimental schema for subcutaneous studies. Briefly, 1×10^6 Renca cells in 100 μ l PBS were implanted subcutaneously into the right hind flank and mice were subsequently vaccinated i.p. with Lm-based vaccines. (B) Tumor kinetic curve throughout the course of the experiment and (C) final tumor mass at the end of the experiment of both Lm-based vaccines. (D) Experimental schema for orthotopic studies. Briefly, 5×10^4 Renca cells expressing luciferase (Renca-luc) were implanted directly into the left kidney and mice were subsequently vaccinated i.p. with Lm-based vaccines. D-luciferin (150mg/kg, Perkin Elmer) was injected i.p. to the mice and bioluminescence signals was detected by IVIS Imaging system at 10 min post-injection. (E) The tumor kinetic curve was plotted by using total flux (photon/sec) of the region of interest (ROI). (F) Final tumor mass at the end of the experiment of both Lm-based vaccines. All statistical analysis was done with Prism 8 GraphPad software version 8.3.0., using unpaired student t-test. * $p < 0.05$, ** $p < 0.01$. i.p. : intraperitoneal, Lm-LLO-OVA: Listeria-based vaccine targeting non-specific antigen, i.e., chicken ovalbumin. Lm-LLO-ISG15: Listeria-based vaccine targeting interferon-stimulated gene 15 (ISG15)



Abstract 1370 Figure 2 Distinct T cell response between s.c. and orthotopic tumors

Distinct T cell response between subcutaneous and orthotopic tumors to Lm-LLO-ISG15. Data obtained from flow cytometry analysis for subcutaneous (A-D) and orthotopic studies (E-H). Briefly, tumor tissues were harvested, and minced, and single-cell suspensions prepared. Tumor cells were stimulated with Cell Activation Cocktail kit (423303, Biolegend) for 5-6 hours and processed as normal samples. (A, C). Distribution of multi-cytokine produced by live CD4+ in subcutaneous tumors. (B, D). Distribution of multi-cytokine produced by live CD8+ in subcutaneous tumors. (E, G). Distribution of multi-cytokine produced by live CD4+ in orthotopic tumors. (F, H). Distribution of multi-cytokine produced by live CD8+ in orthotopic tumors. All statistical analysis was done with Prism 8 GraphPad software version 8.3.0., using unpaired student t-test. * $p < 0.05$, ** $p < 0.01$, *** $p < 0.001$. Lm-LLO-OVA: Listeria-based vaccine targeting non-specific antigen, i.e., chicken ovalbumin. Lm-LLO-ISG15: Listeria-based vaccine targeting interferon-stimulated gene 15 (ISG15), IFN- γ : interferon-gamma, IL-2: interleukin-2, TNF- α : tumor necrosis factor-alpha



Abstract 1370 Figure 3 Distinct MDSC response between s.c. and orthotopic tumors

Distinct myeloid-derived suppressor cells (MDSCs) response between subcutaneous and orthotopic tumors to Lm-LLO-ISG15. Data obtained from flow cytometry analysis for subcutaneous (A-C) and orthotopic studies (D-F). Briefly, tumor tissues were harvested to prepare single cell suspension, and stained with appropriate fluorochrome-conjugated anti-mouse monoclonal antibodies. Frequency of (A). total myeloid cells, (B). m-MDSCs, and (C). pmn-MDSCs from total viable cells in subcutaneous tumors. Frequency of (D). total myeloid cells, (E). m-MDSCs, and (F). pmn-MDSCs from total viable cells in orthotopic tumors. All statistical analysis was done with Prism 8 GraphPad software version 8.3.0., using unpaired student t-test. * $p < 0.05$, ** $p < 0.01$, *** $p < 0.001$. OVA: Listeria-based vaccine targeting non-specific antigen, i.e., chicken ovalbumin. ISG15: Listeria-based vaccine targeting interferon-stimulated gene 15 (ISG15), m-MDSCs: monocytic myeloid-derived suppressor cells, pmn-MDSCs: polymorphonucleic myeloid-derived suppressor cells

<http://dx.doi.org/10.1136/jitc-2022-SITC2022.1370>

Abstracts

1371 IDENTIFICATION OF VASOACTIVE INTESTINAL PEPTIDE (VIP)-SPECIFIC SINGLE-CHAIN ANTIBODY FRAGMENTS (SCFVS) VIA YEAST SURFACE DISPLAY

David Zaharoff, Khue Nguyen*. NC State University and UNC, Chapel Hill, Raleigh, NC, USA

Background Vasoactive intestinal peptide (VIP) is a 28-amino acid neuropeptide expressed in various tissues including the pancreas, intestines and central nervous system.^{1, 2} The over-expression of VIP and its receptors is associated with increased growth and metastasis of breast, prostate, and lung malignancies.³ In addition, the interaction of VIP with its receptors on activated T cells results in immune suppression which further supports tumor growth.^{4, 5} Furthermore, tumor-supporting regulatory T cells have been found to be promoted by VIP-dependent mechanisms.⁶ Altogether, prior literature implies that blockade of VIP signaling may inhibit tumor-mediated immune suppression and augment antitumor immune responses. Recent preclinical studies in acute myeloid leukemia and T lymphoblastic leukemia demonstrated that VIP receptor antagonists increase T cell-dependent anti-tumor responses.² Unfortunately, the short-half lives of peptide antagonists limit their clinical utility. A more translatable approach is the development of long circulating antibodies that bind VIP and inhibit its immunosuppressive activities.

Methods In this study, we utilized a yeast display of a non-immune human single-chain variable fragment (scFv) library to identify VIP-binding scFvs.⁷⁻⁹ VIP binders were screened by several rounds of selection using magnetic-activated cell sorting (MACS) and fluorescence-activated cell sorting (FACS). The enriched binder population was cloned into single colonies of yeast cells by limited dilution. The binding affinities of VIP-binding clones were evaluated via flow cytometry by titrating fluorescence-labeled VIP. Clones with high binding affinity ($K_d < 500$ nM) were selected for sequencing (figures 1-5).

Results Sequences of the isolated scFv revealed that a unique section of complementarity-determining region 3 (CDR3) of the heavy chain played an important role in VIP binding. Multiple clones with similar but distinct CDR3 sequences produced a useful range of binding affinities for further development (figure 6).

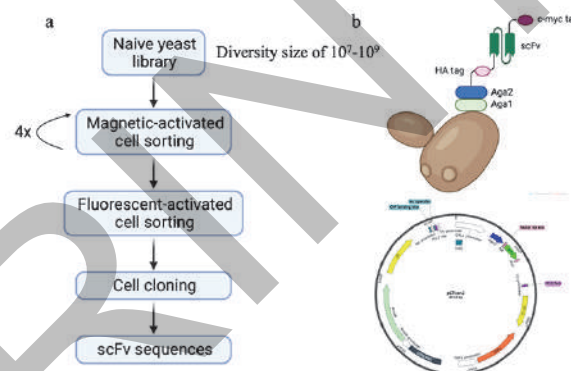
Conclusions Yeast display is an effective technology for identifying human scFvs that bind to the immunosuppressive neuropeptide, VIP. CDR3 of scFv heavy chains were influential in VIP recognition. Ongoing studies are focused on the production, purification, and validation of novel anti-VIP human antibodies.

Acknowledgements We thank Dr. K. Dane Wittrup (Massachusetts Institute of Technology) for kindly providing yeast libraries, Drs. Edmund K. Waller and Jens Wrangmert (Emory University) for helpful discussions and comments, and Dr. Ryan W. Paerl (North Carolina State University) for technical advice on cell sorting.

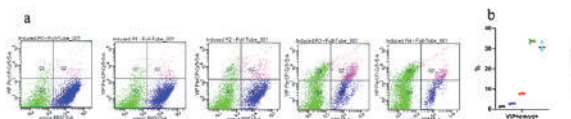
REFERENCES

- Petersen CT, Li JM, Waller EK. Administration of a vasoactive intestinal peptide antagonist enhances the autologous anti-leukemia T cell response in murine models of acute leukemia. *Oncoimmunology*. 2017;**6**(5):e1304336. Epub 2017/06/24.
- Li JM, Darlak KA, Southerland L, Hossain MS, Jaye DL, Josephson CD, et al. VIPhyb, an antagonist of vasoactive intestinal peptide receptor, enhances cellular antiviral immunity in murine cytomegalovirus infected mice. *PLoS One*. 2013;**8**(5):e63381. Epub 2013/06/01.
- Moody TW, Nuche-Berenguer B, Jensen RT. Vasoactive intestinal peptide/pituitary adenylate cyclase activating polypeptide, and their receptors and cancer. *Curr Opin Endocrinol Diabetes Obes*. 2016;**23**(1):38–47. Epub 2015/12/26.

- Forghani P, Petersen CT, Waller EK. Activation of VIP signaling enhances immunosuppressive effect of MDSCs on CMV-induced adaptive immunity. *Oncotarget*. 2017;**8**(47):81873–9. Epub 2017/11/16.
- Liu L, Yen JH, Ganea D. A novel VIP signaling pathway in T cells cAMP→protein tyrosine phosphatase (SHP-2)→JAK2/STAT4→Th1 differentiation. *Peptides* 2007;**28**(9):1814–24. Epub 2007/04/28.
- Delgado M, Chorny A, Gonzalez-Rey E, Ganea D. Vasoactive intestinal peptide generates CD4+CD25+ regulatory T cells in vivo. *J Leukoc Biol* 2005;**78**(6):1327–38. Epub 2005/10/06.
- Angelini A, Chen TF, de Picciotto S, Yang NJ, Tzeng A, Santos MS, et al. Protein engineering and selection using yeast surface display. *Methods Mol Biol* 2015;**1319**:3–36. Epub 2015/06/11.
- Feldhaus MJ, Siegel RW, Opresko LK, Coleman JR, Feldhaus JM, Yeung YA, et al. Flow-cytometric isolation of human antibodies from a nonimmune *Saccharomyces cerevisiae* surface display library. *Nat Biotechnol*. 2003;**21**(2):163–70. Epub 2003/01/22.
- Kelly RL, Le D, Zhao J, Wittrup KD. Reduction of Nonspecificity Motifs in Synthetic Antibody Libraries. *J Mol Biol*. 2018;**430**(1):119–30. Epub 2017/12/01.

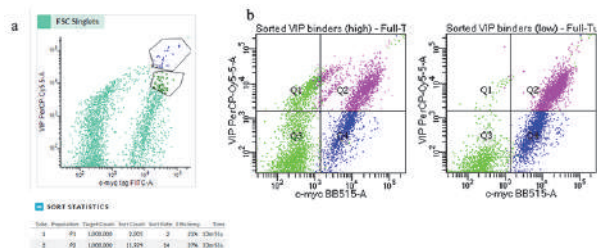


Abstract 1371 Figure 1 Isolation process of anti-VIP scFv utilizing yeast display a) Workflow illustrating the process for isolating protein binders from large combinatorial libraries on yeast using magnetic bead separation followed by flow cytometry-based selection. (b) Illustration of protein scaffolds displayed on the surface of yeast and a related plasmid map.

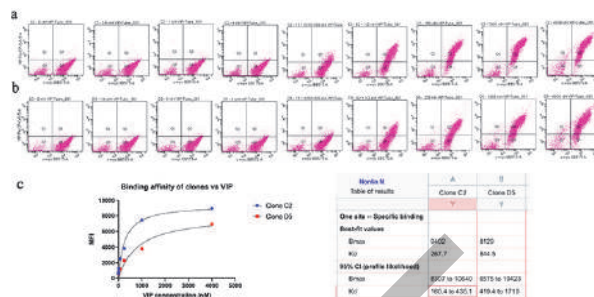


Abstract 1371 Figure 2 Four enrichment rounds of VIP binders using MACS selection

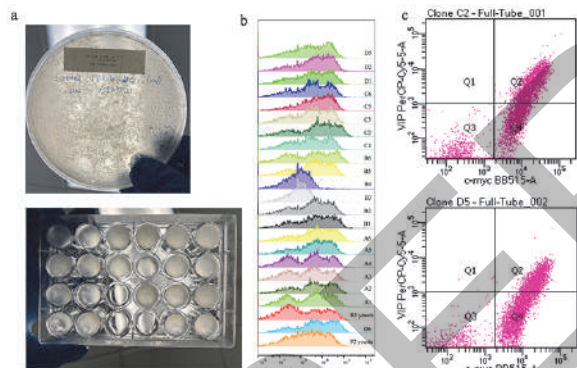
(a) Dot plots show the binding events of VIP to yeast library analyzed by flow cytometry. VIP binders were selected by MACS in four rounds. Selections include a brief incubation of yeast library and VIP-magnetic beads, then binders were pulled out using a magnet. Selected yeasts were expanded and induced by specific culture media before analyzed by flow cytometry. Flow cytometry experiments were performed as staining each round of yeast library by anti-c-myc antibody-FITC (RMYC45FZ, Immunology Consultants), VIP-biotin (P001353, Aapptec), and Streptavidin PerCP-Cyanine5.5 Conjugate (45431782, Invitrogen). Stained cells were analyzed by BD FACSCelesta flow cytometer. (b) Dot plot shows representative binding percentages of VIP+c-myc+ events from 4 rounds of enrichment.



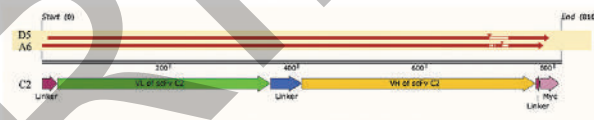
Abstract 1371 Figure 3 Isolation of VIP binders (round 3) by FACS sorting
 (a) VIP binders after 3 rounds of selection (R3 yeasts) were subjected to a FACS sorting. Cells were stained with anti-c-myc antibody-FITC (RMYC45FZ, Immunology Consultants), VIP-biotin (P001353, Aapptec), and Streptavidin PerCP-Cyanine5.5 Conjugate (45431782, Invitrogen). FACS sorting was performed on a BD FACSMelody Cell Sorter. Two populations of VIP high signal and low signal were collected. Sorted yeasts were expanded and induced by specific culture media before analyzed by flow cytometry. (b). Comparison of VIP binding between VIP high signal (left) and low signal(right) populations. Flow cytometry experiments were performed as staining yeast cells by anti-c-myc antibody-FITC (RMYC45FZ, Immunology Consultants), VIP-biotin (P001353, Aapptec), and Streptavidin PerCP-Cyanine5.5 Conjugate (45431782, Invitrogen). Stained cells were analyzed by a BD FACSCelesta flow cytometer.



Abstract 1371 Figure 5 Comparison of VIP-binding affinity between clones C2 vs D5
 Cells of clone C2 (a) and D5 (b) were incubated with a gradient of VIP concentrations before stained and analyzed by flow cytometry. (c) Mean fluorescent intensity (MFI) of VIP+c-myc+ events were analyzed and used to calculate the Kd values of each clone by Prism 9.0. Flow cytometry experiments were performed as staining yeast cells by anti-c-myc antibody-FITC (RMYC45FZ, Immunology Consultants), VIP-biotin (P001353, Aapptec), and Streptavidin PerCP-Cyanine5.5 Conjugate (45431782, Invitrogen). Stained cells were analyzed by a BD FACSCelesta flow cytometer.



Abstract 1371 Figure 4 Cloning of VIP binders using limited dilutions
 (a.top) Yeast cells from low signal population (P2 yeasts) were streaked onto an agar plate using limited dilutions. Single colonies were then picked and cultured in single wells of a 24 well plate (a.bottom). Cells were then expanded and induced by specific culture media. (b). VIP+ signals of different clones analyzed by flow cytometry. (c). Comparison of VIP binding between clone C2 (top) and clone D5 (bottom). Flow cytometry experiments were performed as staining yeast cells by anti-c-myc antibody-FITC (RMYC45FZ, Immunology Consultants), VIP-biotin (P001353, Aapptec), and Streptavidin PerCP-Cyanine5.5 Conjugate (45431782, Invitrogen). Stained cells were analyzed by a BD FACSCelesta flow cytometer.



Abstract 1371 Figure 6 Comparison of DNA sequences of different VIP binder clones
 DNA plasmids of 3 clones (C2, A6, and D5) were purified from yeast cells, then they were transformed into E. coli for expansion. Plasmids were purified from E. coli, subjected to Sanger sequencing, and analyzed by SnapGene. The DNA sequence of scFv clone C2 was used as a template to compare with clone D5 and A6. The isolated scFv sequences indicated that a specific region in the heavy chain's complementarity-determining region 3 (CDR3) played a key role in VIP binding.

<http://dx.doi.org/10.1136/jitc-2022-SITC2022.1371>

1372

XMAB143, AN ENGINEERED IL18 HETERODIMERIC FC-FUSION, FEATURES IMPROVED STABILITY, REDUCED POTENCY, AND INSENSITIVITY TO IL18BP

Alex Nisthal*, Sung-Hyung Lee, Christine Bonzon, Ruschelle Love, Kendra Avery, Rumana Rashid, Panida Lertkiatmongkol, Nicole Rodriguez, Sher Karki, Norman Barlow, Seung Chu, Gregory Moore, John Desjarlais. *Xencor, Monrovia, CA, USA*

Background Interleukin-18 (IL18) is a proinflammatory cytokine that modulates both innate and adaptive immune responses. Mature IL18 promotes the expansion, survival, and cytotoxicity of T and NK cells expressing the heterodimeric IL18 receptor. Preclinical studies with recombinant IL18 have demonstrated anti-tumor activity in animal models, including impressive synergy with both immune checkpoint inhibitors and CAR-T therapy. However, clinical development as a single agent exhibited poor pharmacokinetics and an overall lack of efficacy despite heavy dosing. IL18 participates in a negative feedback loop with IL18 binding protein (IL18BP), a very high affinity natural inhibitor induced by IFN γ . As IL18BP upregulation was observed in early phase clinical trials, it likely limited the efficacy of recombinant IL18.

Methods Prior work at Xencor demonstrated that reduced-potency IL15/IL15R α -Fc fusion proteins exhibited superior pharmacokinetics, pharmacodynamics, and safety in non-human primates through reduction of receptor-mediated clearance. Following that principle, we generated monovalent IL18-Fc fusions upon our XmAb[®] heterodimeric Fc platform and introduced substitutions that could modulate IL18 stability, affinity toward the IL18 heterodimeric receptor, and affinity toward IL18BP.

Results To address IL18's poor native stability, we engineered a disulfide bridge into the cytokine's structure which increased the thermal denaturation temperature from 45 °C to 65 °C. This had beneficial effects on the cytokine's yield and solution behavior, and translated into a significant improvement of PK in mice. Variants at IL18 positions along the IL18 receptor and IL18BP interfaces were explored in vitro by measuring PD-L1 induction on KG-1 cells, with and without a high concentration of IL18BP. Recombining hits generated a potency series with variants exhibiting over a 2,000-fold reduction in PD-L1 induction potency as compared to WT IL18-Fc. Importantly, we identified variants that no longer detectably bound IL18BP, relieving natural inhibition of our engineered IL18-Fc. In vivo immune-mediated inflammation by our lead IL18-Fc, XmAb143, was explored in human PBMC engrafted mouse models of graft versus host disease (GvHD). We observed dose-dependent exacerbation of GvHD, with corresponding dramatic increases in the numbers, activation, and IFN γ release of T and NK cells as compared to a human PBMC only control. Conversely, XmAb143 pharmacodynamics in cynomolgus monkey pilot tox studies was observed only at higher doses, and serum half-life improved from hours to days over WT IL18-Fc.

Conclusions XmAb143, our engineered monovalent IL18-Fc fusion demonstrates insensitivity to IL18BP inhibition, robust inflammation activity in vivo, and improved pharmacokinetics in mice and cynomolgus monkeys.

<http://dx.doi.org/10.1136/jitc-2022-SITC2022.1372>

1373

STC-15, AN ORAL SMALL MOLECULE INHIBITOR OF THE RNA METHYLTRANSFERASE METTL3, INHIBITS TUMOUR GROWTH THROUGH ACTIVATION OF ANTI-CANCER IMMUNE RESPONSES AND SYNERGISES WITH IMMUNE CHECKPOINT BLOCKADE

¹Yaara Ofir -Rosenfeld, ¹Oliver Rausch, ¹Jerry McMahon*, ¹Lina Vasiliauskaite, ¹Claire Saunders, ¹Alexandra Sapetschnig, ¹Georgia Tsagkogeorga, ¹Mark Albertella, ²Marie Carkill, ²Jezrom Self-Fordham, ¹Josefin-Beate Holz. ¹Storm Therapeutics, Cambridge, UK; ²Charles River Laboratories, Portishead, UK

Background METTL3 is an RNA methyltransferase responsible for the deposition of N-6-methyladenosine (m⁶A) modification on mRNA and long non-coding RNA (lncRNA) transcripts, to regulate their stability, splicing, transport and translation. Small molecule inhibitors of METTL3 catalytic activity have previously demonstrated direct anti-tumour efficacy in models of acute myeloid leukemia (AML). Here we present pre-clinical data showing that STC-15, an orally bioavailable small molecule inhibitor of METTL3, restrains cancer growth and induces anti-cancer immunity

Methods To characterise transcriptomic changes following METTL3 inhibition, RNA sequencing studies were performed on several cancer cell lines treated with STC-15. Induction of specific genes was validated by qPCR and Western Blots. The functional consequence of the upregulation of innate immune pathways was investigated in vitro using a co-culture system of SKOV3 ovarian cancer cells and human peripheral blood mononuclear cells (PBMC) or purified primary CD8+ T-cells, and animal studies using subcutaneous A20 and MC38 mouse syngeneic tumour models

Results Inhibition of METTL3 by STC-15 in cancer cell lines leads to prominent upregulation of genes associated with innate immunity, including type-I and type-III IFNs, as well as many interferon stimulated genes. Cells treated with STC-15 accumulated double-stranded RNA suggesting that activation of IFN signalling is triggered by innate pattern recognition sensors.

In an in vitro co-culture system, STC-15 demonstrated strong and dose-dependent enhancement of PBMC-mediated killing of cancer cells. Similar results were obtained when replacing PBMC with purified CD8+ T-cells.

In MC38 colorectal and A20 lymphoma syngeneic models, oral treatment of immune-competent tumour bearing mice with STC-15 significantly inhibited tumour growth. In vivo depletion of CD8+ T-cells abrogated the response to STC-15.

Combination of STC-15 with anti-PD1 antibody resulted in tumour regression in both models, with mice remaining tumour-free long after treatment ceased. When regressed mice from the A20 model were re-challenged with a new batch of A20 cells, no new tumour growth was observed, further demonstrating the induction of durable anti-tumour immunity

Conclusions In pre-clinical cancer models, STC-15 treatment results in activation of innate immune pathways, inhibits tumour growth via activation of CD8+ T-cell mediated tumour cell killing, and enhances the anti-tumour properties of anti-PD1 therapy to generate a durable anti-tumour immune response. These data provide the rationale for the development of STC-15 both as monotherapy and in combination with checkpoint inhibition for the treatment of solid tumour malignancies. A Phase I, First-in-Human clinical trial is planned to begin in 2022

Ethics Approval Animal welfare for this study complies with the UK Animals Scientific Procedures Act 1986 (ASP) in line with Directive 2010/63/EU of the European Parliament and

the Council of 22 September 2010 on the protection of animals used for scientific purposes.

<http://dx.doi.org/10.1136/jitc-2022-SITC2022.1373>

1374 **CHARACTERIZATION AND VALIDATION OF A HUMANIZED LEAD ANTIBODY AGAINST OX003, A NOVEL IMMUNO-ONCOLOGY TARGET**

¹Arnim Bisht, ¹Murray Cox, ²Antonn Cheeseman, ¹Christian Rohlf, ¹Chander Peddaboina*, ¹Abderrahim Fandi. ¹Oxford BioTherapeutics Inc, San Jose, CA, USA; ²University of Manchester, Manchester, UK

Background Immunotherapy, an approach to target or manipulate the immune system, has changed the field of oncology and cancer treatment. Antibodies targeting checkpoint proteins CTLA-4, PD-1, and PD-L1 have shown great success, at the same time some of these checkpoint inhibitors are known to eventually induce immunotherapy resistance in several cancers leading to poor treatment prognosis.¹At Oxford BioTherapeutics, using the proprietary OGAP database, novel targets on TILs (Tumor infiltrating Lymphocytes) have been identified that can lead to a breakthrough in the field of cancer immunotherapy. From proteomic analysis, OX003 is identified as a surface protein on T cells with a co-stimulatory function. OX003 is expressed on most lymphocytes with TILs showing the highest expression.

Methods Immunohistochemistry technique is used to evaluate the expression of OX003 in TILs and wide variety of solid tumors. *In vitro* evaluation of OX003 expression on T cells is performed using flow cytometry technique. A fully humanized agonistic mAb is developed against OX003 and its functional activity on T cells is evaluated *in vitro*. T cell proliferation measured by CFSE dye dilution, IFN γ (interferon gamma) cytokine and Granzyme B secretion via ELISA, Perforin accumulation via flow cytometry, ELISpot assay, and 1-way Mixed lymphocyte reaction (MLR) assays are used for T cell functional activity.

Results Evaluation of OX003 by immunohistochemistry shows abundant expression on TILs, and in a variety of solid tumors. OX003 positive TILs are observed both intratumorally and in the stromal components of the TME (Tumor micro environment). *In vitro* evaluation of OX003 expression on T cells shows upregulation upon activation of naïve T cells which persists between activated and exhausted phenotypes and decreases upon resting, closely following the time course of activation and exhaustion markers. This humanized antibody against OX003 shows a strong agonistic effect in a dose-dependent manner on CD8⁺ T cells promoting proliferation, IFN γ cytokine secretion, Granzyme B release and Perforin accumulation indicating a strong cytolytic ability. In an allogenic one-way MLR setup, it enhances functional activity of T cells in co-culture with PBMC as stimulators, showing dose-dependent increase in IFN γ release compared to an isotype control. Ex vivo assays conducted with the antibody on fresh tumor samples showed increased IFN γ release as compared to Isotype as measured by the ELISpot assay.

Conclusions This data show that OX003 is a novel immunostimulatory receptor on CD8⁺ T cells and the lead agonistic antibody targeting OX003 enhances T cell functional activity critical for successful immunotherapy response.

REFERENCES

1. Havel JJ, Chowell D, Chan TA. The evolving landscape of biomarkers for checkpoint inhibitor immunotherapy. *Nat Rev Cancer* 2019 Mar;**19**(3):133–150.

<http://dx.doi.org/10.1136/jitc-2022-SITC2022.1374>

1375 **A HORMONE-BASED BISPECIFIC T CELL ENGAGER (BiTE)-LIKE MOLECULE FOR THE TREATMENT OF NEUROENDOCRINE TUMORS**

¹Eleonora Pelle*, ²Mauro Cives, ¹Elliot Medina, ¹Charlotte Mason, ¹Sebastian Snedal, ¹Xiomar Bustos Perez, ¹Leticia Tordesillas, ¹Miguel Gomez Fontela, ¹Renata Rossetti, ³Gabriele Maiorano, ¹Vincent Luca, ¹Patrick Hwu, ¹Daniel Abate-Daga, ¹Jonathan Strosberg. ¹Moffitt Cancer Center, Tampa, FL, USA; ²University of Bari Aldo Moro, Bari, Italy; ³National Research Council, Lecce, Italy

Background We designed a novel bispecific T-cell engager (BiTE) targeting the somatostatin receptor (SSTR), which is overexpressed by well-differentiated neuroendocrine tumors (NETs). In our BiTE, the single chain variable fragment (scFV) based anti-SSTR domain is replaced by 2 molecules of somatostatin-14 (SST14), the hormone that physiologically activates the SSTR.

Methods The sequence of the SST14-scFV anti-CD3 BiTE was optimized and cloned into a pAcGP67avector. The recombinant protein was expressed by *Trichoplusia ni* (High Five) using Baculovirus and isolated from the supernatant using nickel affinity chromatography. The binding potential of the BiTE towards CD3 and SSTR was determined by flow cytometry and confocal microscopy. The SSTR-specific T cell activation and the BiTE-induced cytotoxicity were measured after coincubation of CD3⁺ T cells isolated from the peripheral blood of healthy donors with 293T cells stably transduced to concurrently express SSTR and GFP, in presence of the BiTE. The same conditions in absence of BiTE or with the SSTR⁻ parental 293T were used as negative control, while anti-CD3/CD28 beads were added as a positive control. The BiTE-induced cytotoxicity was assessed by real-time quantitative live-cell imaging using the Incucyte system. The BiTE-induced T cell activation was evaluated measuring the secretion of IFN- γ , and granzyme-B by ELISA.

Results At a concentration of 100 nM, the BiTE bound the CD3 receptor of approximately 85% of T cells. By confocal microscopy, the BiTE was found to coat SSTR⁺293T cells. When added to SSTR⁺293T cell cultures, the BiTE by itself exerted antiproliferative activity ($p < 0.0001$), possibly as result of an agonist activity on the SSTR. Such a cytotoxic effect was significantly more pronounced when T cells were also present in the cultures ($p < 0.0001$). IFN- γ and granzyme-B secretion was significantly higher when the T cells were co-cultured with SSTR⁺293T cells in the presence of the BiTE as compared with parallel preparations with SSTR⁻293T cells or without the BiTE, suggesting that the BiTE-induced T cell activation is specific.

Conclusions To our knowledge, this is the first BiTE to incorporate a hormone in one binding site. Our preclinical data indicate that the BiTE specifically engages the SSTR, the T cell receptor and induces a high level of cytotoxicity in the presence of T cells.

<http://dx.doi.org/10.1136/jitc-2022-SITC2022.1375>

1376

**NOVEL, BRAIN PENETRANT SMALL MOLECULE
INHIBITOR OF PD-L1 FOR TARGETING GLIOBLASTOMA
AND BRAIN METASTASIS**

Dhanalakshmi Sivanandhan, Sridharan Rajagopal*, Sridharan Rajagopal, Chandru Gajendran, Naveen Sadhu M, Mohammed Zainuddin, Ramachandraiah Gosu, Luca Rastelli. *Jubilant Therapeutics Inc, Bedminster, NJ, USA*

Background The PD-1/PD-L1 molecular pathway is one of the primary mechanisms of immune evasion deployed by cancer cells. Activation of PD-1/PD-L1 pathway induces anergy and exhaustion of cytotoxic T-cells and enhances the function of regulatory T-cells causing an immune suppressive environment. Therefore, blocking this pathway restores T-cell proliferation and enhanced tumor cell killing. Approved monoclonal antibodies targeting PD-1/PD-L1 pathway require intravenous injections and have a long half-life that could contribute to the well-documented drug-related adverse effects. Also, efficacy of these antibodies appears to be marginal in malignancies associated with CNS due to poor brain penetrance. Therefore, small molecule inhibitors of the PD-1/PD-L1 pathway with oral bioavailability, better tumor and brain penetrance and shorter half-life will be highly valuable in cancer therapy. In this regard, JBI-2174 shows excellent ADME properties, brain exposure, pharmacokinetics and comparable efficacy as approved mAbs in preclinical studies.

Methods Structure based drug design was used to design PD-L1 inhibitors; potency of these inhibitors was assessed in an *in-vitro* TR-FRET assay. Reporter assays and *ex-vivo* co-culture assays were used to assess T-cell proliferation and function. Pharmacokinetics were performed in multiple pre-clinical species to derive at bioavailability and brain penetration. *In vivo* efficacy was assessed in partially humanized mice efficacy models.

Results JBI-2174 showed strong *in vitro* IC₅₀ of 1.5 nM in TR-FRET assay that measures interaction between PD-1 and PD-L1 and led to stabilization of PD-L1 as measured by thermal shift assay. This molecule also augmented T-cell co-inhibitory signalling as observed by Jurkat cell/SHP-1 assay. Competition study between anti-PD-L1 blocking antibody and x-ray crystal structure studies clearly demonstrated that JBI-2174 leads to dimerization of PD-L1. More importantly, JBI-2174 showed excellent oral bioavailability across pre-clinical species and strong and sustained (up to 24 h) brain exposure (0.66 to 2.1 fold plasma vs. brain ratio). JBI-2174 showed comparable or better efficacy to the anti-PD-L1 antibody Atezolizumab in hPD-L1/MC38 syngeneic and brain orthotopic models by oral administration with a concomitant increase in tumor infiltrating lymphocytes. Toxicological studies conducted in non-human primates clearly show that the molecule is well tolerated at exposures much higher than efficacious exposure.

Conclusions Oral administration and brain exposure of these small molecule PD-L1 inhibitors provides an attractive option to be used in the treatment of glioblastoma and other solid tumors with brain metastasis. IND enabling studies are being initiated for this molecule to initiate clinical trials in humans.

<http://dx.doi.org/10.1136/jitc-2022-SITC2022.1376>

1377

PRECLINICAL CHARACTERIZATION OF D3L-001, A NOVEL BISPECIFIC ANTIBODY THAT ENHANCE PHAGOCYTOSIS AND ERADICATION OF HER2 POSITIVE SOLID TUMOR VIA HER2 AND CD47 DUAL BLOCKADE

¹Haopeng Rui*, ²Siwei Nie, ²Jiaxiang Shao, ¹Xiaofeng Yang, ¹Jiahao Chen, ¹Jia Wang, ²Zhiqiang Zheng, ¹Jingtao Lu, ¹Allison Wang, ³Jin Hong, ³Xiaosong Chen, ³Kunwei Shen, ¹George Chen. ¹D3 Bio (Wuxi) Co. Ltd., Shanghai, China; ²WuXi Biopharmaceuticals Shanghai Co. Ltd, Shanghai, China; ³Ruijin Hospital, Shanghai, China

Background HER2 is overexpressed in different solid tumors, including 15-20% of breast cancer. The advent of HER2-targeted drugs, including antibodies (Ab), TKI and ADC, have revolutionized HER2+ cancer treatment; however, the disease will eventually recur in most patients. Recent studies have suggested efficacy of HER2 target antibodies (Ab) therapy could be further enhanced by antibody-dependent cellular phagocytosis (ADCP) principally regulated by antiphagocytic “don’t-eat-me” CD47 signals. CD47 is overexpressed in many HER2+ cancers, which suppresses phagocytosis through binding to SIRP α .

In this study, an internally discovered anti-HER2 \times CD47 bispecific antibody (bsAb), D3L-001, demonstrated synergistic anti-tumor effect by HER2 guided CD47 co-blocking. It enhances macrophage mediated phagocytosis and significantly suppresses *in vivo* tumor growth while sparing hematological toxicities, which are typically induced by anti-CD47 antibodies.

Methods SK-BR-3, HCC1954 and Jurkat cells were used. Cellular binding and *in vitro* blocking of CD47 and SIRP α interaction by Abs were measured by FACS. Monocytes were isolated from PBMC and differentiated into macrophages, which were then used for ADCP assays. Abs *in vivo* efficacy were examined in HER2+ tumor models.

Results D3L-001 was designed to have higher HER2 affinity ($K_D < 1$ nM) than that of CD47 ($K_D > 10$ nM). With this unique design, D3L-001 showed preferential binding to HER2/CD47 double positive tumor cells as compared to CD47 single positive cells (figure 1). This preferential binding prevents D3L-001 from inducing red blood cell hemagglutination *in vitro*. Moreover, its binding to HER2+ tumor cells wasn't affected by whole blood cell pre-culture treatment, indicating low systemic CD47 antigen sink effect. Intriguingly, we found that D3L-001 can block the interaction between SIRP α and CD47 on HER2+ tumor cells very effectively, probably due to the avidity effect induced by the addition of HER2 binding arm (figure 2). This potent blocking translated well into enhanced *in vitro* phagocytosis ability. D3L-001 showed stronger anti-tumor effect than trastuzumab in a panel of HER2+ tumor models. We observed significant tumor growth inhibition and regression in trastuzumab resistant xenograft models in a dose-dependent manner. D3L-001 demonstrated better efficacy than combination of trastuzumab and magrolimab, indicating synergistic effect of co-blocking HER2 and CD47 in bispecific form. In addition, the combination of D3L-001 with pertuzumab also showed synergistic *in vivo* efficacy.

Conclusions D3L-001 is a novel HER2 \times CD47 bsAb which demonstrated potent and synergistic anti-tumor effect via HER2 guided CD47 co-blocking in both *in vitro* and *in vivo* models. D3L-001 might provide a novel treatment approach for HER2+ cancers and overcome their resistance to current therapies.

Fig. 1A

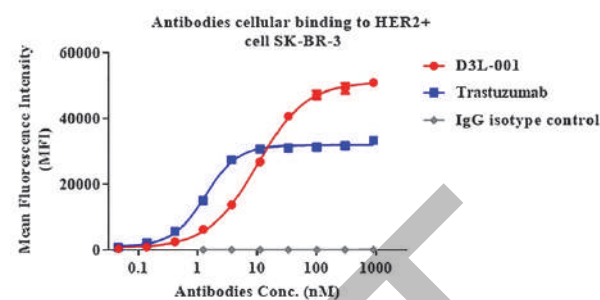
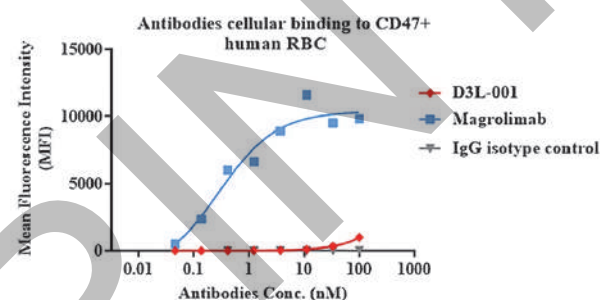
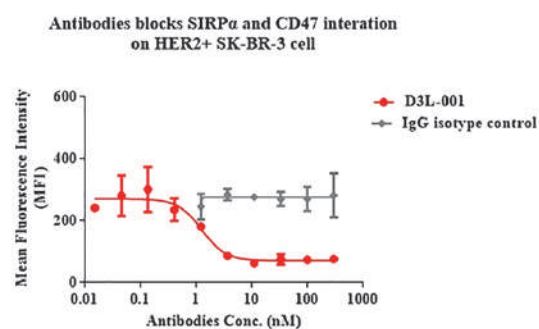


Fig. 1B



Abstract 1377 Figure 1 In vitro cellular binding of D3L-001 to HER2/CD47 double positive SK-BR-3 cell (A) and CD47 single positive red blood cell (B).

Fig. 2



Abstract 1377 Figure 2 In vitro cellular blocking of SIRP α and CD47 interaction by D3L-001

<http://dx.doi.org/10.1136/jitc-2022-SITC2022.1377>

1378

PRECLINICAL CHARACTERIZATION OF IMGS-001, A DUAL ANTAGONIST ANTI-PD-L1, ANTI-PD-L2 ANTIBODY WITH EFFECTOR FUNCTION, TO TREAT PATIENTS RESISTANT TO IMMUNE CHECKPOINT BLOCKADE

¹Ahmad Salameh*, ¹Federica Pericle, ¹Christine Gagliardi, ¹Paul Blezinger, ²Michael Curran. ¹ImmunoGenesis, Inc., Houston, TX, USA; ²MD Anderson Cancer Center, Houston, TX, USA

Background Antibody drugs which block engagement of the T cell co-inhibitory receptor programmed cell death-1 (PD-1) or its cognate ligand programmed death-1 ligand-1 (PD-L1) are a key pillar of modern oncology. While the impact of these drugs has been profound, their efficacy remains limited to cancers with pre-existing immune infiltration and/or higher numbers of mutational neoantigens. To expand the percentage of cancer patients that benefit from immunotherapy, drugs are needed which can diminish multi-modal immune suppression in immune excluded tumors to the extent that T cells can accumulate and expand sufficiently to benefit from PD-1 pathway blockade. Thus, we characterized IMGS-001, a human monoclonal antibody against PD-L1 and PD-L2 with effector functions, developed in collaboration with MD Anderson. IMGS-001 is being tested *in vitro* and *in vivo* to support clinical development in patients resistant or naïve to immunotherapy (IO) treatment.

Methods *In vivo* dose-regimen anti-tumor activity was analyzed using syngeneic mouse models of colon cancer (CT26-expressing mouse PD-L2, MC38) and melanoma (B16F10 expressing mouse PD-L2). Tumor-bearing mice were treated with IMGS-001 at 5-10-20 mg/kg twice a week for 3 weeks. In addition, IMGS-001 mediated antibody dependent cellular cytotoxicity (ADCC) was assessed in immune-competent and immune-deficient mice (nu/nu) injected with CT26-PD-L2 and MDA-MB-231, respectively. In both studies, mice were treated with IMGS-001 twice a week for 3 weeks while a second group (only CT-26-PD-L2 model) was first depleted of natural killer (NK) cells.

Results IMGS-001 significantly inhibited CT26-PD-L2 tumor growth compared to PBS treatment ($p=0.0239$) and extended survival ($p=0.0007$) with an optimal dose of 10 mg/kg. Against MC38, 70% of animals treated with ≥ 10 mg/kg IMGS-001 were alive with no evidence of tumor 70 days post-inoculation. IMGS-001 (10mg/kg) showed 90% inhibition of B16F10-PD-L2 tumor volume compared to the control ($p<0.0001$). In mice lacking T cells, IMGS-001 significantly inhibited MDA-MB-231 tumor growth at 10 mg/kg, indicating a mechanism of action driven by ADCC. Moreover, in NK-depleted immune-competent mice, IMGS-001 lost activity against CT26-PD-L2 ($p=0.0403$).

Conclusions These data suggest 10 mg/kg of IMGS-001 being the optimal dose to induce a strong anti-tumor activity *in vivo*. Moreover, IMGS-001 displayed a mechanism of action driven by the cytoreduction of immune suppressive stroma *in vivo* via ADCC. These results, with a favorable PK, the absence of off-target activity and a clean toxicology profile, support the clinical development of IMGS-001. IMGS-001 would increase the benefit of IO therapy for patients with immune-infiltrated tumors and could mediate significant clinical responses against immune-excluded cancers.

<http://dx.doi.org/10.1136/jitc-2022-SITC2022.1378>

1379

ENGINEERED TOXIN BODY TARGETING TIGIT DEPLETES TREGS IN THE TUMOR MICROENVIRONMENT AND REDUCES TUMOR BURDEN IN MICE

Elizabeth Saputra, Amit Chaudhary, Desirae Martinez, Jennifer Mitchell, Rebecca Martin, John Majercak, Joseph Dekker, Chris Moore, Swati Khanna, Swati Khanna*. *Molecular Templates Inc., Austin, TX, USA*

Background TIGIT (T cell immunoreceptor with Ig and ITIM domains) is an immune inhibitory receptor, which is known to be over-expressed on Tregs in the tumor microenvironment (TME) of multiple solid tumors and functions as an immunological checkpoint. TIGIT is often co-expressed with PD-1 on Tregs and CD4+ and CD8+ T cells in the TME.¹⁻³ Monoclonal antibodies (mAb) blocking TIGIT have shown little efficacy as a monotherapy or in combination with α PD-L1 mAb in clinical studies.⁴⁻⁵ We have shown previously that TIGIT targeting Engineered Toxin Bodies (ETBs) show cytotoxicity in vitro on TIGIT over-expressing cell lines and TIGIT expressing immune cells, including Tregs.⁶ Here, we demonstrate the efficacy and pharmacodynamic (PD) effects of TIGIT ETB in a hTIGIT/PD-1 expressing humanized mouse model. Contrary to mAbs, which function by steric hinderance of the TIGIT-CD155 axis, TIGIT ETBs function by direct cell kill of TIGIT expressing cells and represent a novel approach to targeting TIGIT expressing cells in cancers.

Methods MC38 tumor bearing humanized mice (hTIGIT/PD-1) were treated with TIGIT ETB as a monotherapy and in combination with α PD-1 mAb. The effect of TIGIT ETB was compared with α PD-1 and α TIGIT mAbs used alone or in combination. Tumor volumes were measured during the study and all tumors were harvested at study conclusion on day 18 for evaluation of test article effects on tumor immunophenotype.

Results TIGIT ETB monotherapy resulted in the best overall reduction in tumor burden and was comparable with the α PD-1 mAb group. Strikingly, TIGIT ETB monotherapy worked better than the α TIGIT+ α PD-1 mAb combination. TIGIT ETB+ α PD-1 mAb showed similar effects on tumor growth as the α TIGIT+ α PD-1 mAb combination. These effects on tumor growth coincided with significant reduction in Tregs and increased CD8:CD4 ratio in the TME across all TIGIT ETB treatment groups. This TME Treg depletion was not observed with α TIGIT+ α PD-1 mAb combination.

Conclusions These data demonstrate that targeting TIGIT using our Engineered Toxin Body platform promotes tumor regression through elimination of TIGIT/PD-1 co-expressing immune cells within the TME. Our data supports using ETB as a monotherapy to target TIGIT and represents a wholly novel approach for modulating TIGIT within the TME.

REFERENCES

1. Jinhua X, Ji W, Shouliang C, Liangfeng Z. Expression of immune checkpoints in T cells of esophageal cancer patients. *Oncotarget* 2016; **7**(39):1–10.
2. Blessin NC, Simon R, Kluth M, Fischer K, et al. Patterns of TIGIT expression in lymphatic tissue, inflammation and cancer. *Dis Markers* 2019; **2019**: 1–13
3. Johnston RJ, Comps-Agrar L, Hackney J, Yu X, et al. The immunoreceptor TIGIT regulates anti-tumor and antiviral CD8(+) T effector function. *Cancer Cell* 2014; **26**(6): 923–927.
4. Bendell JC, Bedrad P, Bang Y-J, LoRusso P, et al. Phase Ia/Ib dose-escalation study of the anti-TIGIT antibody Tiragolumab as a single agent and in combination with atezolizumab in patients with advanced solid tumors. Proceedings: AACR Annual Meeting 2020; April 27-28, 2020 and June 22-24, 2020; Philadelphia, PA.
5. Roche News Release. Roche reports interim results for the phase III SKYSCRAPER-01 study in PD-L1-high metastatic non-small cell lung cancer. *News Release*. May 11, 2022. <https://bit.ly/39e8QY4>.

6. Saputra E, Cornelison G, Mitchell J, et al. 884 Engineered toxin body mediated depletion of TIGIT expressing immune cells for cancer immunotherapy. *Journal for ImmunoTherapy of Cancer* 2021;**9**: doi: 10.1136/jitc-2021-SITC2021.884.

Ethics Approval Biocytogen Inc.
IACUC #2018N001

<http://dx.doi.org/10.1136/jitc-2022-SITC2022.1379>

Abstracts

1380

SYNERGISTIC ANTI-TUMOR EFFECT OF ALLOCETRA-OTS, A CELLULAR IMMUNE-THERAPY, IN COMBINATION WITH IMMUNE CHECKPOINT INHIBITORS/ CHEMOTHERAPY/CAR T, THROUGH IN-VIVO REPROGRAMMING OF MACROPHAGES

¹Dror Mevorach*, ²Barak Reicher, ²Oren Hershkovitz, ²Yehudit Shabat. ¹Hadassah-University Hospital, Jerusalem, Israel; ²Enlivex Therapeutics, Jerusalem, Israel

Background Immune checkpoint inhibitors (ICI) revolutionized solid tumor treatment, however, in many tumors only partial response is achieved. Allocetra-OTS has an immune modulating effect on macrophages¹ and showed an excellent safety profile in patients including patients with sepsis.² Here we investigated the anti-tumoral effect of Allocetra-OTS cellular therapy, in solid tumor animal models.

Methods Allocetra-OTS is manufactured from enriched mononuclear fractions and induced to undergo early apoptosis.

In an immunocompetent model, Balb/c mice were inoculated intraperitoneally (IP) with AB12 (mesothelioma) with pLenti-PGK-V5-Luc-Neo and treated with anti-CTLA4 with or without Allocetra-OTS. Mice were monitored daily for clinical score and weekly using IVIS. Kaplan-Meier log rank test was done for survival. For Allocetra-OTS preparation, enriched mononuclear fractions were collected by leukapheresis from healthy eligible human donors and induced to undergo early apoptosis. To follow tumor growth in vivo, HeLa-CD19 cells were stably transduced with pLenti-PGK-V5-Luc-Neo. For CAR preparation, fresh mononuclear cells (MNC) were transfected with CD19-CAR plasmids. SCID-Bg mice were injected IP with human HeLa-CD19 or HeLa-CD19-luciferase cells, 10×10 allocetraOTS or vehicle, and 10×10 CD19-CAR T cells or mock T cells.

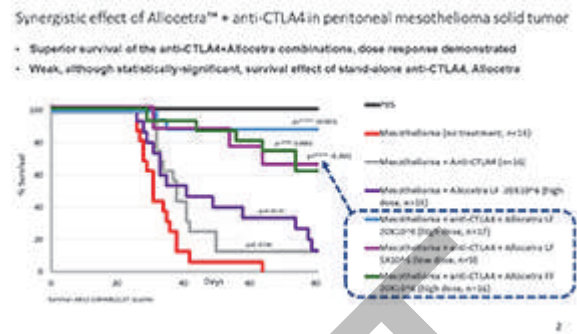
Results In immune competent Balb/c mesothelioma model, anti-CTLA4 standalone therapy significantly improved survival from mean 34±9 to 44.9 ±20 days (p<0.05). Similarly, Allocetra-OTS standalone therapy improved survival to 52.3 ±20 days (p<0.02). However, anti-CTLA4 + Allocetra-OTS combination therapy, ameliorated survival to 86.7±20 days (p<0.0001) with complete cancer remission in 60-100% of mice (figure 1 & 2). Similar anti-tumoral effects of Allocetra-OTS were seen in mesothelioma model in a combination therapy with either anti-PD1 or cisplatin.

In the CAR-T model, SCID-Bg mice were sacrificed or died from tumor progression in 30±5 days (range 27–37). CAR T cell therapy significantly improved survival to 55±11 days (p < 0.05 vs MOCK) but Allocetra-OTS further improved survival to 75±10 (p < 0.001) with 20-40% complete remission. **Conclusions** During IP tumor progression, Allocetra-OTS as a standalone therapy or in combination with ICI, cisplatin or CAR-T therapy, significantly reduced tumor size and resulted in complete remission in up to 100% treated mice.

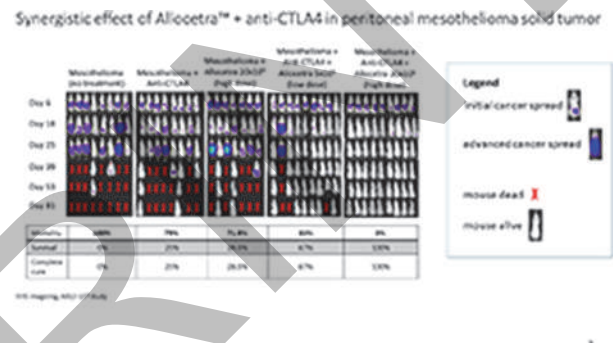
Based on excellent safety profile in > 40 patients treated in prior clinical trials for sepsis and Covid-19, Phase I/II clinical trial of Allocetra-OTS plus chemotherapy has started and first patient already recruited. A second Phase I/II clinical trial of Allocetra-OTS plus anti-PD1, as a second- and third-line therapy in various cancers, is planned for Q4 2022.

REFERENCES

1. Trahtemberg U, Mevorach D. Apoptotic cells induced signaling for immune homeostasis in macrophages and dendritic cells. *Front Immunol* 2017 Oct 25;8:1356.
2. Van-Heerden V, Abitbol A, Mevorach D. Allocetra-OTS for sepsis associated cytokine storm. *Frontiers in Immunology, Front Immunol.* 2021 Sep 30;12:718191.



Abstract 1380 Figure 1 CTLA4 and Allocetra



Abstract 1380 Figure 2 CTLA4 and Allocetra

<http://dx.doi.org/10.1136/jitc-2022-SITC2022.1380>

1381 **LACTATE MODULATION IN CANCER AND IMMUNE CELLS IS ASSOCIATED WITH ANTITUMOR EFFICACY OF DUAL MCT1/MCT4 INHIBITOR NGY-091**

Nicole Bowman*, Sambad Sharma, Jennifer Duffy, Sanath Wijerathna, Nelly Kuklin, Jaime Escobedo, Vincent Sandanayaka. *Nirogy Therapeutics, Framingham, MA, USA*

Background Metabolic profiles of cells in the tumor microenvironment (TME) are known to be altered during the onset and progression of a tumor. Lactate is a key metabolic end-product of glycolysis that plays an important role in tumor progression and antitumor immunity. NGY-091, our first-in-class inhibitor of lactate transporters MCT1 and MCT4, has demonstrated a strong *in vitro* and *in vivo* antitumor efficacy.

Methods Cytotoxicity was evaluated in cancer cells by MTS assay. Lactate level was quantified to demonstrate on-target activity of NGY-091 in both cancer and immune cell types present in the TME by lactate glo assay (Promega). Human CD4+ T, CD8+ T and Treg cells were activated in the presence or absence of NGY-091, and expression of activation markers/cytokines and viability were assessed by flow cytometry. Human monocytes were differentiated to MDSCs followed by treatment with NGY-091. MDSC function and viability were examined by flow cytometry.

Results NGY-091 displayed a blockade of lactate import through MCT1 and lactate export through MCT4. The cytotoxic effect of NGY-091 was mediated by lactate import inhibition through MCT1 and the subsequent decrease in mitochondrial respiration. When studying the phenotypic effect of NGY-091 in immune cells under culture conditions mimicking the TME, we found that CD4+ and CD8+ T cells were strongly activated without affecting their proliferative ability. In contrast, viability and function of suppressive immune cells, Treg and MDSCs, were significantly reduced by NGY-091. In CD4+ and CD8+ T cells, NGY-091 treatment increased accumulation of intracellular lactate and subsequently decreased extracellular lactate that indicated blockade of glycolysis. We examined lactate import by MDSCs and Tregs, as these cells are known to utilize lactate as a source of energy, and found that NGY-091 strongly decreased lactate import in these cells.

Conclusions NGY-091 modulates lactate transport to induce direct cytotoxicity in cancer and activate robust antitumor immunity.

<http://dx.doi.org/10.1136/jitc-2022-SITC2022.1381>

1382

DKK1 IS A BIOMARKER AND IMMUNOTHERAPEUTIC TARGET FOR BONE METASTASES IN MALIGNANT CANCERS

Tao Shi*, Kaijie Liang, Xiaoyu Zhou, Xueru Song, Hanbing Wang, Yipeng Zhang, Lixia Yu, Baorui Liu, Jia Wei. *The Comprehensive Cancer Centre of Nanjing Drum Tower Hospital, The Affiliated Hospital of Nanjing University Medical School, Nanjing, China*

Background Malignant tumors with bone metastases seriously threaten the survival of cancer patients. However, the understanding of bone-tumor microenvironment remains poor, and currently, there is no effective therapeutic target for bone metastases.

Methods Serum Dickkopf-1 (DKK1) expression from healthy donors and gastric cancer (GC) patients were detected. Mouse GC and breast cancer bone metastasis model was established by intro-caudal artery (CA) GC cell injection, and *in vivo* efficacy of DKK1 blockade with murine DKK1 antibody (mDKN-01) was evaluated by micro-CT, MRI and IHC staining modalities. The bone-tumor immune microenvironment (bone-TIME) was analyzed via flow cytometry and immunofluorescence.

Results Serum DKK1 expressions were increased in GC patients (n=63) than in healthy donors (n=25), and stage IV GC patients (n=42) had higher serum DKK1 levels than stage II-III patients (n=21), with bone-metastatic patients (n=22) displaying the highest DKK1 level. Also, serum DKK1 levels are increased in patients with progressive disease (PD), while decreased in patients who had complete response (CR)/partial response (PR) to treatments. DKK1 blockade by mDKN-01 obviously reduced the tumor burden of bone metastases, and significantly inhibited osteoclast activation and alleviates bone destruction in different bone metastasis models. Moreover, the bone-TIME was improved after DKK1 blockade, with increased proportions of CD8⁺ T cells, M1-like macrophages, and activated dendritic cells (DCs).

Conclusions Our study suggests DKK1 as a potential predictor to bone metastasis and progressive disease in cancer patients. Blockade of DKK1 brings an improved bone-TIME, therefore, DKK1 could be considered as a novel and promising immunotherapeutic target for bone metastases.

<http://dx.doi.org/10.1136/jitc-2022-SITC2022.1382>

1383

REMODELING HOST IMMUNE RESPONSE IN HEAD AND NECK CANCER WITH PERSONALIZED THERAPEUTIC MRNA NANO-VACCINES

¹Natalie Silver*, ²Rekha Garg, ²Hector Mendez-Gomez, ²Paul Castillo, ²Carlos Souza, ²Lana Fagman, ²John Ligon, ²Sadeem Qdaisat, ²Frances Weidert, ²Jonathan Chardon-Robles, ¹Jin Dai, ³Siming Ma, ³Jessica Geiger, ³Emrullah Yilmaz, ³Shlomo Koyfman, ³Jamie Ku, ¹Daniel McGrail, ³Timothy Chan, ²Duane Mitchell, ²Elias Sayour. ¹Cleveland Clinic Lerner College of Medicine, Cleveland, OH, USA; ²University of Florida, Gainesville, FL, USA; ³Cleveland Clinic, Cleveland, OH, USA

Background The translational pipeline for novel immunotherapeutics is often stymied due to the lack of relevant immune-competent pre-clinical animal models, which can facilitate the path to human clinical trials. Our group has developed a novel tumor-specific mRNA-vaccine and nano-liposome platform capable of delivering increased mRNA payload and inducing antigen-specific immunity.^{1,2} In order to assist clinical translation, we investigated the feasibility, anti-tumor activity, and immunogenicity of therapeutic personalized RNA-nanovaccines in head and neck cancer pre-clinical murine models and client-owned felines with spontaneously occurring oral cancer.

Methods 1) C57B/6 mice were injected with syngeneic mouse oral cancer cell lines MOC1 or MOC2 orthotopically (tongue) or subcutaneously (flank). Mice were treated with tumor-derived mRNA nano-vaccines intravenously weekly, x3 weeks. Tumor volumes and survival was recorded. Immune cell infiltration of tumors and spleens were analyzed using flow cytometry. 2) A client-owned feline clinical trial was initiated (UF College of Veterinary Medicine, protocol #IACUC20220000077) to treat pet cats with spontaneously occurring oral squamous cell carcinoma. Tumor biopsies were obtained from enrolled felines (N=4), and tumor-specific mRNA-nano-vaccines were generated from the surgical specimen. The felines were administered three cycles of biweekly vaccines administered intravenously. The cats were monitored for adverse events and followed for clinical outcomes. Flow cytometry was performed to evaluate immune responses.

Results 1) Mice treated with tumor-derived mRNA-nanovaccines had significantly decreased tumor volumes when compared with controls in both MOC1 and the more aggressive MOC2 cell lines ($p < 0.001$). Orthotopic models for MOC1 tumors were more responsive to RNA nano-vaccine administration than subcutaneous (flank) models. Treatment response was characterized by intra-tumoral and systemic activated CD4+ ($p = 0.027$) and CD8+ (0.041) T-cell infiltration as well as decreased intra-tumoral immunosuppressive myeloid cell infiltration compared to controls. 2) Feline subjects (N=4) experienced no toxicities or adverse events. Profound CD8+ and CD4+ T cell activation was noted in blood following vaccine administration (4h). There was significant survival benefit with 0/6 untreated felines surviving, while 3/4 of the treated pets are living with either stable or undetectable disease.

Conclusions Personalized RNA-nanovaccines are effective and safe in preclinical murine and feline models of oral cancer demonstrating safety in a large animal study and immune activity. This agent is currently in clinical trials for human brain cancer (NCT04573140). Data from studies in both large and small preclinical models will inform our human clinical trial design for head and neck cancer patients with recurrent/metastatic disease.

REFERENCES

1. Sayour EJ, Grippin A, De Leon G, Stover B, Rahman M, Karachi A, Wummer B, Moore G, Castillo-Caro P, Fredenburg K, Sarkisian MR, Huang J, Deleyrolle LP,

Sahay B, Carrera-Justiz S, Mendez-Gomez HR, Mitchell DA. Personalized Tumor RNA loaded lipid-nanoparticles prime the systemic and intratumoral milieu for response to cancer immunotherapy. *Nano Lett.* 2018;**18**(10):6195–206. Epub 20180927. doi: 10.1021/acs.nanolett.8b02179. PubMed PMID: 30259750; PMCID: PMC6597257.

2. Sayour EJ, De Leon G, Pham C, Grippin A, Kemeny H, Chua J, Huang J, Sampson JH, Sanchez-Perez L, Flores C, Mitchell DA. Systemic activation of antigen-presenting cells via RNA-loaded nanoparticles. *Oncoimmunology* 2017;**6**(1):e1256527. Epub 2017/02/16. doi: 10.1080/2162402X.2016.1256527. PubMed PMID: 28197373; PMCID: PMC5283636.

<http://dx.doi.org/10.1136/jitc-2022-SITC2022.1383>

1384

NOVEL, IMMUNE AGONISTIC CEACAM1/5 ANTIBODY (YB-200) DEMONSTRATES ANTI-TUMOR EFFICACY AND SIGNIFICANTLY INCREASES B-CELL RESPONSE IN SYNGENEIC LIVER HEPA1-6 TUMOR MICROENVIRONMENT

²Michel Janicot, ¹Katrin Rupalla*, ³Alexej Schmidt, ⁴Iris Helfrich, ⁵Bernhard B Singer. ¹Ymmunobio AG, Riehen, Switzerland; ²JMI ONConsulting, Ukkel, Belgium; ³University of Umea, Umea, Sweden; ⁴Ludwig-Maximilians University, Munich, Germany; ⁵University Hospital Essen, Essen, Germany

Background Carcinoembryonic antigen-related cell adhesion molecule 1 (CEACAM1) and 5 (CEACAM5, CEA) are members of the carcinoembryonic antigen (CEA) family. CEACAM1 is expressed on a variety of immune cells and acts as a cell-cell communication molecule. The signal transduction process is associated with immune cell activation, apoptosis, proliferation and differentiation. In the pathophysiological stage, CEACAM1 and 5 are dysregulated in various malignancies including, for instance, breast, lung, and gastrointestinal cancer. This seems associated with poor prognosis linked to a novel checkpoint blockade mechanism mediated by homophilic CEACAM1-1 and heterophilic CEACAM1-5 interaction between immune and tumor cells, respectively. YB-200 is a novel IgG1 antibody targeting CEACAM 1/5, which has shown to preserve the immune agonistic function of CEACAM1 on leukocytes in addition to potentially inhibiting both the homophilic and heterophilic checkpoint blockade of CEACAM1 and 5 on tumor cells. The present study was designed to test the *in vivo* anti-tumor activity of YB-200 and its effect on immune cells.

Methods Anti-tumor activity of YB-200 was assessed using the validated ReactionBiology's SubQperior[®] experimental syngeneic liver Hepa-1-6 tumor model. The tumor cells were injected into the mammary fat pad of C57BL/6 mice. On Day 5 after tumor cell injection, animals were randomized (median tumor size ~50 mm³) in two groups and treatment started. Mice were treated i.p. BIWx3 with either isotype control or YB-200 at 10 mg/kg/administration. Animals were euthanized on Day 20, and tumors harvested for flow cytometry analysis. Flow cytometry for immune-cell profiling was performed using the ReactionBiology All-in-one[®] staining panel.

Results Treatment with YB-200 induced statistically significant tumor growth inhibition by ~80% compared to isotype control, at well-tolerated dose. Flow cytometry analysis revealed that YB-200 led to a 10-fold increase in B-cells in the tumor micro-environment compared to the isotype control. In addition, a statistically significant increase in CD3+ and CD4+ T-cells was observed while granulocytes decreased.

Conclusions This study demonstrates that treatment with YB-200 induced statistically significant tumor growth inhibition compared to isotype control in a validated hepatocellular carcinoma model. Consistent with the role of CEACAM1 as cell-cell communication molecule the anti-tumor activity of YB-200 was correlated with a strong modulation of the immune cell compartment in the tumor micro environment.

Ethics Approval This animal study has been approved by the Ethics Committee for Animal Experimentation and is registered by the regional board Freiburg, Germany. Mice were handled according to the German animal welfare law and the GV-SOLAS guidelines.

<http://dx.doi.org/10.1136/jitc-2022-SITC2022.1384>

1385

DIVERGENT THERAPEUTIC OUTCOMES OF STING AGONIST ADU-S100 IN INTRATUMORAL AND INTRAVESICAL TREATMENT REGIMENS IN SYNGENEIC MURINE MB49 AND IN THE N-METHYL-N-NITROSOUREA (MNU) RAT MODEL OF UROTHELIAL CARCINOMA

¹Kara Lombardo, ¹Monali Praharaj, ¹Andres Matoso, ¹William Bishai, ²Trinity Bivalacqua, ²Alok Singh*. ¹Johns Hopkins Medicine, Baltimore, MD, USA; ²University of Pennsylvania, Philadelphia, PA, USA

Background STING agonist ADU-S100 as an intratumoral (IT) therapeutic regimen shows excellent CD8+T cells-mediated antitumor immunity. Rapid absorption from IT sites, short terminal half-life and treatment related adverse outcomes caused withdrawal of ADU-S100 from clinical trials. We developed BCG-STING, a preclinical candidate for non-muscle invasive bladder cancer (NMIBC) that overexpresses a STING agonist (c-di-AMP) and confers superior antitumor immunity over BCG-WT by increasing tumor infiltrating CD4+ and CD8+ T cells and inflammatory macrophages.¹ Due to similarities in the mechanism of action, comparative antitumor efficacies of BCG-STING and ADU-S100 were examined in an IT and intravesical (IV) dosing regimen.

Methods Syngeneic MB49 flank tumors in C57BL/6 female mice were given IT treatment of BCG-WT, BCG-STING (5×10^6 CFU) or ADU-S100 (100, 50 or 25 mg). End-point measurements included tumor volume and flow-cytometry based tumor immune infiltrate analyses (at 100 mg). MNU carcinogen rat model of NMIBC and the standard IV administration regimen was used for BCG-WT or BCG-STING (5×10^6 CFU, 6x weekly) or ADU-S100 (25 mg, 6x weekly). Histopathological analyses of MNU rat bladders were performed for tumor involvement index (TII) and pathological tumor staging.

Results IT administration of ADU-S100 in MB49 tumor showed greatest tumor regression over BCG-WT or BCG-STING even at lowest dose (25 mg). ADU-S100 caused strongest infiltration of TNF-a+MHCII+F4/80+CD11b+ macrophages and IFN-g+CD8+ T cells as compared to BCG-STING or BCG-WT. We did observe a significant increase in immunosuppressive IL-10+ and ARG-1+ Ly6C^(hi)Ly6G⁽⁻⁾ monocytic myeloid-derived suppressor cells (M-MDSCs) in MB49 tumors treated with ADU-S100 and BCG-WT, but not BCG-STING. In contrast to MB49 model, IV induction course of BCG-STING in MNU rat model showed the greatest antitumor effects with only 5% residual TII compared to 30% in ADU-S100 or 42% in BCG-WT. Tumor staging revealed residual T1 (50%), CIS (25%) and Ta (25%) tumors in ADU-S100 group, BCG-WT treated group showed a lower degree of invasion to the lamina propria with CIS (50%), T1 (25%) and Ta (25%) residual tumors. BCG-STING IV therapy resulted in 60% of rat bladders showing complete tumor regression while 40% had minimal residual non-invasive tumors.

Conclusions Divergent therapeutic outcomes of IT vs IV treatment regimens of ADU-S100 over BCG-STING or BCG-WT in different urothelial carcinoma models indicate the critical role of tumor microenvironment and dosing regimens on relative efficacy. Induction of immunosuppressive M-MDSCs by ADU-S100 or BCG-WT suggests unique advantages of BCG-STING. The therapeutic targeting of M-MDSCs as combination may improve clinical efficacies of BCGs.

Acknowledgements National Institute of Health, Maryland Tedco, Willowcroft Foundation, and Cigarette Restitution Fund

REFERENCES

1. Singh AK, Praharaj M, Lombardo KA, *et al.* Re-engineered BCG overexpressing cyclic di-AMP augments trained immunity and exhibits improved efficacy against bladder cancer. *Nat Commun* 2022;**13**:878. <https://doi.org/10.1038/s41467-022-28509-z>

Ethics Approval All protocols involving animals strictly adhered to US NIH guidelines and were approved by the Johns Hopkins Medical Institutions Animal Care and Use Committee under the protocols: MO18M58, MO20M20, and RA17M332.

<http://dx.doi.org/10.1136/jitc-2022-SITC2022.1385>

1386

NOVEL GUT-RESTRICTED SMALL MOLECULE INHIBITOR OF PD-L1 FOR TARGETING GI CANCERS

Dhanalakshmi Sivanandhan*, Sridharan Rajagopal, Chandru Gajendran, Naveen Sadhu M, Mohammed Zainuddin, Ramachandraiah Gosu, Luca Rastelli. *Jubilant Therapeutics Inc, Bedminster, NJ, USA*

Background The PD-1/PD-L1 molecular pathway is one of the primary mechanisms of immune evasion deployed by cancer cells and several anti-PD-L1 monoclonal antibodies (mAbs) have been approved for the treatment of multiple cancers, including cancers of the GI tract and liver. In such cancers, one of the issues observed is broad-spectrum autoimmune toxicities, including pneumonitis, and others, primarily owing to their long systemic half-life. Therefore, small molecule inhibitors of PD-L1 with gut restricted exposure should potentially be able overcome these toxicities. JBI-1527 is a small molecule PD-L1 inhibitor with similar binding and mechanism of action as anti-PD-L1 antibodies that shows much higher exposure in gastrointestinal tract and liver as compared to plasma. It shows comparable efficacy as approved mAbs in preclinical studies.

Methods Structure based drug design was used to design PD-L1 inhibitors; potency of these inhibitors was assessed in an in-vitro TR-FRET assay. Reporter assays and ex-vivo co-culture assays were used to assess T-cell proliferation and function. Pharmacokinetics studies were performed in multiple pre-clinical species to assess tissue distribution. In vivo efficacy was assessed in partially humanized mice efficacy models.

Results JBI-1527 showed strong in vitro IC_{50} of 2.9 nM in TR-FRET assay that measures interaction between PD-1 and PD-L1 and led to stabilization of PD-L1 protein as measured by thermal shift assay. This molecule also augmented T-cell co-inhibitory signalling as observed by Jurkat cell/SHP-1 assay. Competition study between anti-PD-L1 blocking antibody suggested that JBI-1527 finger-printing on PD-L1 is similar to mAbs. X-ray crystal structure studies clearly demonstrated that JBI-1527 caused dimerization of PD-L1. More importantly, JBI-1527 showed favourable gastrointestinal localised pharmacokinetic profile with high exposure in colon, jejunum, duodenum, ileum (11 to >280 fold vs. plasma) as compared to plasma in preclinical species when dosed orally. JBI-1527 showed comparable efficacy to the anti-PD-L1 antibody Atezolizumab in hPD-L1/MC38 syngeneic and orthotopic models by oral administration and is well tolerated at efficacious doses.

Conclusions Gastrointestinal localised pharmacokinetic profile of JBI-1527 provides an attractive option to be used in the treatment of colon cancer, HCC and other GI-related cancers with minimal systemic toxicity as compared to mAbs.

<http://dx.doi.org/10.1136/jitc-2022-SITC2022.1386>

1387

INHIBITION OF THE CD47-SIRP α AXIS FOR CANCER THERAPY A META-ANALYSIS OF EMERGING CLINICAL DATA

Ji Son*, Rodney Cheng-En Hsieh, Heather Lin, Kate Krause, Ying Yuan, Amadeo Biter, James Welsh, Michael Curran, David Hong. MD Anderson Cancer Center, Houston, TX, USA

Background CD47 interaction with SIRP α acts as a “do not eat me” signal, which is exploited by cancer cells to downregulate immune surveillance. Given mounting evidence regarding the pivotal role of this axis in bridging the innate and adaptive immunity, there has been intense interest to develop a mechanism of blockade for therapeutic purposes. Preliminary data from clinical trials are now being reported, and we aimed to summarize and analyze these findings.

Methods We performed a comprehensive systematic review of relevant databases and conference abstracts. Eligible studies included clinical trials using CD47 and/or SIRP α inhibitors in cancer treatment reporting oncologic outcome or toxicity data. Nonlinear mixed models were applied for comparison of response, with study as a random effect.

Results We retrieved 317 articles, 24 of which were eligible. These included a total of 771 response-evaluable patients with hematologic (47.1%) and solid tumors (52.9%). Of these, 6.4% experienced complete response, 10.4% partial response, and 26.1% stable disease for a 16.7% objective response rate (ORR), 42.8% disease control rate (DCR), and 4.8-month median duration of response (table 1). ORR was significantly higher for hematologic cancers (25.3%) than solid cancers (9.1%, $p=0.042$). Seven CD47 inhibitors and six SIRP α inhibitors were given alone or combined with checkpoint inhibitors, targeted therapy, and/or chemotherapy. In solid cancers, SIRP α inhibitors had a higher ORR (16.2%) than CD47 inhibitors (2.8%, $p=0.079$). This was particularly true for combination therapies using SIRP α inhibitors (ORR 28.3% vs 3.0% in CD47 inhibitors, $p=0.010$). Response was seen in head and neck, colorectal, endometrial, ovarian, hepatocellular, non-small cell lung, and HER2+ gastroesophageal cancers. Dose-limiting toxicity (DLT) was seen in 3.3% of patients (5.4% CD47 inhibitors, 1.4% SIRP α inhibitors; $p=0.01$). The frequency of treatment-related adverse events (TRAEs) \geq grade 3 was 18.0% and was similar between the two groups ($p=0.082$) and mostly laboratory abnormalities. For CD47 inhibitors, the most common toxicities included grade 1-2 fatigue (27.2%), headache (21.0%), anemia (20.5%), and infusion-related reaction (IRR, 17.6%). For SIRP α inhibitors, these included grade 1-2 IRR (23.1%), and fatigue (15.8%). CD47 inhibitors were significantly more likely than SIRP α inhibitors to cause grade 1-2 fever, chills, nausea/vomiting, headache, and anemia.

Conclusions CD47-SIRP α inhibition shows promise in cancer therapy. SIRP α inhibitor combination therapies have higher response rates in solid tumors than CD47 inhibitor combination therapies. Hematologic changes were the main TRAEs, and SIRP α inhibitors seemed to have a better grade 1-2 toxicity profile. Overall, treatment was well-tolerated with minimal DLTs.

Abstract 1387 Table 1 Patient-level data on the efficacy of CD47-SIRP α inhibitors

	Total	CD47 inhibitor	SIRP α inhibitor	p value
Total (n)	771	341	430	
ORR (%)	16.7	12.6	20.0	0.11
DCR (%)	42.8	32.6	50.9	0.19
Hematologic cancer (n)	363	124	239	
ORR (%)	25.3	29.8	23.0	0.48
DCR (%)	56.7	54.0	58.2	0.69
Solid cancer (n)	408	217	191	
ORR (%)	9.1	2.8	16.2	0.079
DCR (%)	30.4	20.3	41.9	0.058
Monotherapy in solid cancer (n)	201	116	85	
ORR (%)	2.0	2.6	1.2	0.51
DCR (%)	21.4	11.2	35.3	0.081
Combination in solid cancer (n)	207	101	106	
ORR (%)	15.9	3.0	28.3	0.01*
DCR (%)	39.1	30.7	47.2	0.28

* $p<0.05$
ORR, objective response rate; DCR, disease control rate

<http://dx.doi.org/10.1136/jitc-2022-SITC2022.1387>

1388

UTILITY OF HUMANIZED ANIMAL MODELS FOR IN VIVO EVALUATION OF NK TICA™ NOVEL BICYCLE® TUMOR TARGETED IMMUNE CELL AGONISTS® BICYCLE TICA™ DESIGNED TO ENGAGE NK CELLS

Lukas Stanczuk*, Johanna Lahdenranta, Fay Dufort, Christopher Leitheiser, Punit Upadhyaya, Kevin McDonnell, Philip Brandish, Nicholas Keen. *Bicycle Therapeutics, London, UK*

Background The use of humanized animal models in preclinical evaluation of immunotherapeutics is often dictated by lack of homology between mouse and human target or divergence in the biology of studied immune cell subtypes. A target expressed on NK cells, NKp46 is a key activating receptor contributing to cytolytic function of NK cells. Bicycle® peptides are small (~1.5 kDa), chemically synthetic, structurally constrained bicyclic peptides discovered using phage display. NKp46-binding Bicycles conjugated to a tumor antigen-binding Bicycle® directed human NK cells to kill the tumor cells expressing the target antigen, and we term these molecules NK tumor-targeted immune cell agonists (NK-TICA™). Due to low homology of NKp46 ectodomain between mouse and human (~63% by NCBI BLAST), we evaluated different approaches to animal humanization to establish the most suitable model for in vivo evaluation of NK-TICA™. The main selection criteria included the number of circulating NKp46+ human NK cells as well as expression of activating and inhibitory receptors.

Methods Distinct approaches to animal humanization were employed: 1) reconstitution of human immune system (HIS) with CD34+ hematopoietic stem cells (HSCs) in NCG mice with hIL-15 hydrodynamic injection (HDI); 2) reconstitution of HIS with CD34+ HSCs in NCG.hIL-15 transgenic mice; 3) infusion of human PBMC-derived NK cells in NCG.hIL-15 transgenic mice. Characterization of NK populations in blood was conducted by multiplex flow cytometry.

Results Immunophenotyping analysis revealed striking differences in numbers of circulating NKp46+ NK cells between different humanized models. The lowest number was observed in mice engrafted with HSCs with transient expression of hIL-15 and the highest in mice infused with PBMC-derived NK cells in a transgenic model constitutively expressing hIL-15. We also observed expansion of NK cells over time in mice with transgenic expression of hIL-15 but not in mice treated with single hIL-15 HDI. Despite these differences, the proportion of NKp46+ NK cells expressing activation receptor NKG2D or activation marker CD69 was similar between all three study designs. In contrast, expression of NKp30 and NKG2A was different across tested models.

Conclusions Transgenic mice with constitutive expression of hIL-15 showed the highest numbers of NKp46+ NK cells in blood and a better expression profile of NK activating and inhibitory receptors making it a more suitable model for in vivo evaluation of NK-TICAs™.

Ethics Approval These studies were approved by the Institutional Animal Care and Use Committee (IACUC). The care and use of animals was conducted in accordance with regulations of the Association for Assessment and Accreditation of Laboratory Animal Care (AAALAC).

<http://dx.doi.org/10.1136/jitc-2022-SITC2022.1388>

1389

GIGA-564 A THIRD GENERATION ANTI CTLA 4 WITH MINIMAL ABILITY TO BLOCK CTLA 4 BINDING TO B7 LIGANDS HAS ENHANCED EFFICACY BUT REDUCED TOXICITY COMPARED TO IPILIMUMAB IN PRECLINICAL MODELS

¹Erica Stone*, ¹Kyle Carter, ¹Ellen Wagner, ¹Michael Asensio, ¹Emily Benzie, ¹Yao Chiang, ¹Gary Coles, ¹Chelsea Edgar, ¹Bishal Gautam, ¹Ashley Gras, ¹Jackson Leong, ¹Renee Leong, ¹Vishal Manickam, ¹Rena Mizrahi, ¹Ariel Niedecken, ¹Jasmeen Saini, ¹Savreet Sandhu, ¹Jan Fredrick Simons, ¹Kacy Stadtmiller, ¹Brendan Tinsley, ²LaRee Tracy, ¹Nicholas Wayham, ¹Yoong Wearn Lim, ¹David Johnson, ¹Adam Adler. ¹*GigaGen, San Diego, CA, USA*; ²*Phastar, San Diego, CA, USA*

Background Anti-CTLA-4 antibodies such as ipilimumab were among the first immuno-oncology agents to show significantly improved outcomes for patients. However, existing anti-CTLA-4 therapies fail to induce a response in a majority of patients and can induce severe, immune-related adverse events. It has been assumed that checkpoint inhibition, i.e., blocking the interaction between CTLA-4 and its ligands, is the primary mechanism of action for current anti-CTLA-4 therapies.¹ Here we present evidence that anti-CTLA-4 therapies with minimal blocking activity can be efficacious in pre-clinical models.

Methods Mice expressing human CTLA-4 were used to investigate the mechanism of action of anti-CTLA-4 therapies including ipilimumab and GIGA-564. These and other humanized mice were also used to investigate the efficacy and toxicity of GIGA-564.

Results GIGA-564, a third generation anti-CTLA-4 with limited ability to block CTLA-4 binding to its B7 ligands, has increased ability to induce in vitro FcR signaling and in vivo depletion of intratumoral Tregs and induces less proliferation of remaining Tregs. In agreement with this, GIGA-564 has superior anti-tumor activity compared to ipilimumab in a murine model. Further experiments showed that the enhanced FcR activity of GIGA-564 likely contributes to its enhanced anti-tumor activity. Importantly, we also showed that GIGA-564 was associated with lower toxicity in murine models.

Conclusions Our work shows that in pre-clinical models GIGA-564 has enhanced efficacy but reduced toxicity compared to ipilimumab.

REFERENCES

1. Stone EL, Carter KP, Wagner EK, Asensio MA, Benzie E, Chiang YY, Coles GL, Edgar C, Gautam BK, Gras A, Leong J, Leong R, Manickam VA, Mizrahi RA, Niedecken AR, Saini J, Sandhu SK, Simons JF, Stadtmiller K, Tinsley B, Tracy L, Wayham NP, Lim Y, Adler AS, Johnson DS. Lack of blocking activity in anti-CTLA-4 antibodies reduces toxicity, but not anti-tumor efficacy. *bioRxiv*. 2021, <https://doi.org/10.1101/2021.07.12.452090>.

Ethics Approval Murine experiments were done in compliance with all relevant ethical regulations and approved by the Institutional Animal Care and Use Committee of Crown Bioscience.

<http://dx.doi.org/10.1136/jitc-2022-SITC2022.1389>

1390

RNA NANOPARTICLE VACCINES OVERCOME THE IMMUNOSUPPRESSIVE TUMOR MICROENVIRONMENT OF METASTATIC OSTEOSARCOMA

¹John Ligon*, ¹Brian Stover, ¹Hector Mendez-Gomez, ¹Adam Grippin, ¹Frances Weidert, ¹Lana Fagman, ¹Jonathan Chardon-Robles, ¹Paul Castillo, ²Natalie Silver, ¹Joanne Lagmay, ³Rowan Milner, ¹Duane Mitchell, ¹Elias Sayour. ¹University of Florida, Gainesville, FL, USA; ²Cleveland Clinic, Cleveland, USA; ³UF College of Veterinary Medicine, Gainesville, FL, USA

Background We previously developed a complex of tumor-derived mRNA (whole tumor transcriptome) with a liposomal nanoparticle to allow systemic delivery of tumor-specific antigens to antigen presenting cells for induction of antigen specific T cell immunity.¹⁻³ We tested this approach to circumvent the lack of specific targets, overcome antigenic heterogeneity, and reprogram the immunosuppressive tumor microenvironment (TME)⁴ present in osteosarcoma, where immunotherapy has not yet been effective.

Methods Total-tumor mRNA was amplified from tumor cell lines or tumor biopsy tissue before complexation in lipid nanocarriers/cationic lipids, generating an RNA-nanoparticle (RNA-NP) for systemic administration. We also developed non-specific RNA-NPs to measure the anti-tumor effect of an “off-the-shelf” immunomodulator. Preclinical murine models were generated using K7M2, KHOS or 143B osteosarcoma cells in either C57Bl/6, BALB/c or BALB/c SCID mice inoculated by tail vein injection to mimic minimal residual metastatic disease from pulmonary osteosarcoma. We launched a comparative oncology clinical trial for client-owned canine patients (pet-dogs) with osteosarcoma through collaboration with the UF College of Veterinary Medicine (UF IACUC#202111376, PI: Milner).

Results In mice inoculated with pulmonary osteosarcoma, total-tumor RNA-NPs elicit significant anti-tumor efficacy in the K7M2 model with long term survivor benefits (7/8 treated mice). These total-tumor RNA-NPs reprogram the TME with significantly less tumor associated macrophages and myeloid-derived suppressor cells ($p < 0.01$). RNA-NPs localize to the perivascular region of the TME, transfect CD45+ myeloid cells, and induce upregulation of genes such as BATF3 known to be related to myeloid reprogramming into activated dendritic cells. Furthermore, monotherapy with non-specific pp65 RNA-NPs generated significant anti-tumor effect in SCID mice ($p < 0.05$). Long-term survivor outcomes from tumor loaded mRNA-NPs correlates with an increase in intratumoral central memory T cells (not observed in animals vaccinated with GFP RNA-NPs). In our first three canine subjects with osteosarcoma, total-tumor RNA-NPs were safe and immunologically active with changes in peripheral blood markers of dendritic cell and T cell activation within 6 hours of vaccine administration.

Conclusions RNA-NPs redirect immunosuppressive myeloid cells which are a hallmark of the osteosarcoma TME[4], resulting in an immune activated state and leading to increased intratumoral central memory T cells. These vaccines bypass MHC restriction and can be made readily available for all patients/canines providing a renewable antigen resource that can be used to continuously vaccinate patients. This agent, which is FDA-IND approved (BB-19304, Sayour) and in human clinical trials for patients with brain tumors (NCT04573140), may be a promising potential novel therapy for patients with recurrent pulmonary metastatic osteosarcoma.

Acknowledgements John A. Ligon and Brian Stover contributed equally to this work and are co-first authors.

REFERENCES

1. Sayour EJ, Grippin A, De Leon G, Stover B, Rahman M, Karachi A, Wummer B, Moore G, Castillo-Caro P, Fredenburg K, Sarkisian MR, Huang J, Deleyrolle LP, Sahay B, Carrera-Justiz S, Mendez-Gomez HR, Mitchell DA. Personalized Tumor RNA loaded lipid-nanoparticles prime the systemic and intratumoral milieu for response to cancer immunotherapy. *Nano Lett.* 2018;**18**(10):6195–206.
2. Sayour EJ, Mendez-Gomez HR, Mitchell DA. Cancer vaccine immunotherapy with RNA-loaded liposomes. *Int J Mol Sci* 2018;**19**(10):2890.
3. Sayour EJ, De Leon G, Pham C, Grippin A, Kemeny H, Chua J, Huang J, Sampson JH, Sanchez-Perez L, Flores C, Mitchell DA. Systemic activation of antigen-presenting cells via RNA-loaded nanoparticles. *Oncoimmunology.* 2017;**6**(1):e1256527.
4. Ligon JA, Choi W, Cojocar G, Fu W, Hsiue EH, Oke TF, Siegel N, Fong MH, Ladle B, Pratilas CA, Morris CD, Levin A, Rhee DS, Meyer CF, Tam AJ, Blosser R, Thompson ED, Suru A, McConkey D, Housseau F, Anders R, Pardoll DM, Llosa N. Pathways of immune exclusion in metastatic osteosarcoma are associated with inferior patient outcomes. *J Immunother Cancer.* 2021;**9**(5):e001772.

Ethics Approval Studies approved by UF IACUC 202111376 and 202009941

<http://dx.doi.org/10.1136/jitc-2022-SITC2022.1390>

1391

ZM008 A FIRST IN CLASS MONOCLONAL ANTI LLT1 ANTIBODY DEMONSTRATED CLINICAL POTENTIAL IN MULTIPLE SOLID CANCERS

Maloy Ghosh*, Anurag Tiwari, Ashvini Dubey, Sanghamitra Bhattacharjee, Yogendra Manjunath, Shalini Kashipathi, Subith Krishna. *Zumutor Biologics, Bangalore, India*

Background Lectin-like transcript 1 (LLT1/CLEC2D) interaction with CD161 on NK cells facilitates tumor immune escape.^{1, 2, 3} Others and we have shown that anti LLT1 antibody disrupts LLT1-CD161 interaction to release the break on NK cells, activate NK cells, improve immune cell infiltration and enhance tumor cell cytotoxicity.^{4, 5, 6} Present work describes a novel anti LLT1 antibody ZM008, its mode of action, GLP safety and toxicity studies, in vivo and ex vivo anti-tumor effects.

Methods Cytokine release and immune cell activation were monitored using human PBMC. PC3 xenografted HuNOG-EXL mice were treated with ZM008 to monitor anti-tumor effects and tumor IHC was performed to study the TME. 4 weeks repeat dose GLP study in Cynomolgus monkey was conducted to determine safety and toxicity of ZM008 at 10-125mg/kg dosing. 3D ex vivo culture of patient biopsies from NSCLC and muscle invasive bladder cancer (MIBC) were used to determine efficacy of ZM008.

Results ZM008 induced CD69 activation and perforin/granzyme B expression on cytotoxic CD8+ T cells and CD16+ NK cells and promoted release of IFN γ and TNF α from immune cells. In HuNOG-EXL-PC3 xenograft mice, ZM008 treatment resulted in ~48% tumor growth reduction and significant tumor infiltration of CD8+ T cells, CD56+ NK cells and NKG2D+ cells was observed. Additionally, low Ki67 and high caspase 3 expression after ZM008 treatment indicates antitumor effects (figure 1). ZM008 exposure was maintained over the treatment period with no mortality or toxicity and was well tolerated in 4 weeks repeat intravenous dosing in Cynomolgus monkeys. No ZM008 related gross pathological findings, organ weight changes or histologic lesions were observed. 3D tumoroid culture from biopsies of NSCLC and MIBC patients were treated with ZM008 monotherapy and Pembrolizumab combination therapy revealed >50% reduction of tumoroids. High-content imaging of the tumoroid clearly shows disintegration of TME and infiltration of immune cells (figure 2).

Conclusions This is the first report describing anti LLT1 antibody efficacy in patient biopsy samples. Tumoroids derived from lung cancer and bladder cancer biopsies revealed significant growth reduction and immune cell infiltration with ZM008 treatment. ZM008 disrupts LLT1-CD161 pathway and transforms the TME to immune responsive "Hot" tumor by activation of immune cells, cytokine secretion, granzyme B/perforin release, and tumor cytotoxicity. GLP safety and toxicity studies in Cynomolgus monkey support future clinical application of ZM008. Overall, the data suggests ZM008 drug product is poised to initiate phase 1 trial (monotherapy and combination with Pembrolizumab) in multiple solid cancers.

REFERENCES

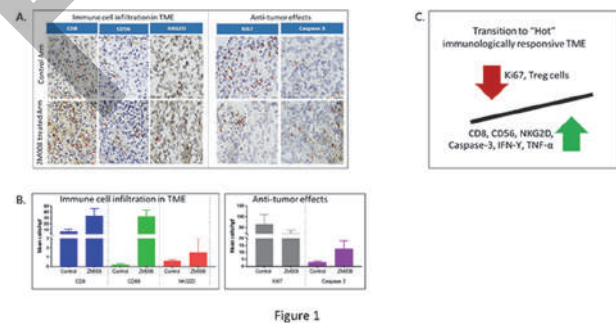
1. Rosen DB, Bettadapura J, Alsharifi M, Mathew PA, Warren HS and Lanier LL. Cutting edge: Lectin-like transcript-1 is a ligand for the inhibitory human NKR-P1A receptor. *J Immunol* 2005;**175**(12): 7796–7799. PMID: 16339513. DOI: 10.4049/jimmunol.175.12.7796
2. Boles KS, Barten R, Kumaresan PR, Trowsdale J and Mathew PA. Cloning of a new lectin-like receptor expressed on human NK cells. *Immunogenetics* 1999;**50**(1-2):1–7. PMID: 10541800. DOI: 10.1007/s002510050679

3. Mathew PA, Chuang SS, Vaidya SV, Kumaresan PR, Boles KS and Pham HT. The LLT1 receptor induces IFN-gamma production by human natural killer cells. *Mol Immunol* 2004;**40**(16):1157–1163. PMID: 15104121. DOI: 10.1016/j.molimm.2003.11.024
4. Mathew SO, Chaudhary P, Powers SB, Vishwanatha JK and Mathew PA. Overexpression of LLT1 (OCIL, CLEC2D) on prostate cancer cells inhibits NK cell-mediated killing through LLT1-NKRP1A (cd161) interaction. *Oncotarget* 2016;**7**(42): 68650–68661. PMID: 27626681. DOI: 10.18632/oncotarget.11896
5. Braud VM, Meghraoui-Kheddar A, Elaldi R, Petti L, Germain C and Anjuère F. LLT1-CD161 interaction in cancer: promises and challenges. *Front Immunol* 2022;**13**:847576. doi: 10.3389/fimmu.2022.847576
6. Gosh M, Rodrigues KI, Maity S, Bhattacharjee S, Manjunath Y, Chakrabarty SP, Dubey AK, Tiwari A, Murugesan S, and Halan V. Novel monoclonal antibody therapeutics for metastatic castration resistant prostate cancer. *J. Clin. Oncol.* 2019;**37**:e14222. <https://doi.org/10.1200/JCO.2019.37.15>.

Ethics Approval Ethics Approval of preclinical study: This study was approved by the Institutional Animal Ethics Committee IAEC Protocol Approval No: SYNGENE/IAEC/1140/02-2020. Institutional Animal Care and Use Committee (IACUC) responsible for the Testing Facility's compliance with applicable laws and regulations concerning the humane care and use of laboratory animals.

Ethics Approval for GLP safety and toxicity study: "This study is approved by Altasciences Preclinical Services Institutional Animal Care and Use Committee (IACUC protocol number – 162822-01)

Ethics Approval for Ex Vivo study: "This study was approved by the National Bioethics Committee in Romania, approval number 9S/4 from 25.11.2019."



Abstract 1391 Figure 1

Transformation of tumor microenvironment (TME) in HuNOG-EXL mice bearing PC3 tumors upon ZM008 treatment

PC3 xenografted HuNOG-EXL mice were treated with 10 mg/kg ZM008 and vehicle control intraperitoneally. In vivo efficacy of ZM008 revealed nearly 48% tumor growth reduction in animals treated with ZM008. Animals were humanely sacrificed intermittently to observe effects of ZM008 on TME. Immunohistochemistry (IHC) of cryopreserved tumor sections were carried out to determine infiltration of human CD8+, CD56+ and NKG2D+ immune cells. In addition, the tumor sections were stained with antibodies against Ki67 and Caspase 3. Critical cytokines and chemokines were also evaluated from peripheral blood of these animals.

A. Tumor IHC images from ZM008 treated animals suggest significant infiltration of CD8+ T cells, CD56+ NK cells and NKG2D+ immune cells (red arrows) compared with control arm. In addition, low Ki67 and high caspase 3 staining (red arrows) were observed in these tumors indicating anti-tumor effects of ZM008 treatment.

B. Bar diagram showing increased infiltration of CD8+ T cells and CD56+ NK cells and NKG2D+ immune cells whereas significant reduction of Ki67 and caspase 3 on the tumor cells.

C. Cartoon showing overall changes observed in the TME of animals treated with ZM008. The representation indicates transition to "Hot" immunologically responsive TME as evidenced by increased infiltration of CD8+, CD56+, NKG2D+ immune cells and decreased Treg cells; low

Abstracts

Ki67 and high Caspase-3 levels in tumor cells; release of proinflammatory cytokines like $\text{IFN}\gamma$ and $\text{TNF}\alpha$ after ZM008 treatment.

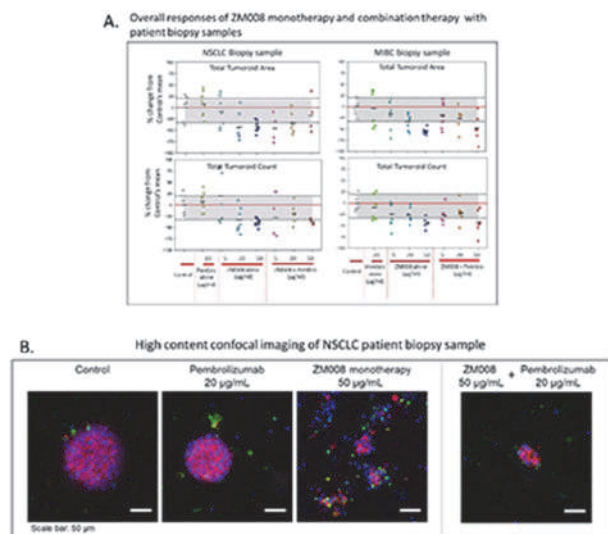


Figure 2

Abstract 1391 Figure 2

Efficacy of ZM008 was determined as monotherapy or in combination with Pembrolizumab using Ex Vivo Clinical Trial's (EVCT) Platform. Freshly isolated patient biopsy samples from Non-Small Cell Lung Cancer (NSCLC) and muscle invasive bladder cancer (MIBC) indications were co-cultured with labeled autologous PBMCs. 3D cell culture system was used to culture the tumoroid in presence or absence of ZM008 or Pembrolizumab. Pembrolizumab was used at 20 $\mu\text{g}/\text{mL}$ and ZM008 was used at 5, 20 and 50 $\mu\text{g}/\text{mL}$ concentrations. Separate wells were used to test the effects of ZM008 and Pembrolizumab combinations. Quantitative image analysis of tumoroid area and tumoroid count were performed to evaluate the effects of ZM008 treatment.

A. Overall responses of ZM008 monotherapy and combination therapy with Pembrolizumab in terms of tumoroid area and tumoroid count in NSCLC and MIBC biopsy samples. The data is represented as percentage change from mean value of the control set (red line). The upper dotted line represents 20% increase of tumoroid area and count, responses above this line indicates tumor progression. The lower dotted line represents 33% decrease in tumoroid area and count, below this line could be considered as partial response to ZM008. The grey shaded area represents no significant change in tumoroid area and count, could be considered similar to stable response. Analysis of the data suggests ZM008 monotherapy and combination therapy with Pembrolizumab revealed significant reduction of tumoroid area and count. This indicates anti-tumor effects of ZM008 on patient biopsies in solid cancers.

B. Few samples were chosen for high content image analysis using confocal microscopy. Tumor cells in the tumoroid structures were indicated by actin staining (red), autologous PBMCs were stained with Cell tracker (green) and nuclei were stained with DAPI (blue). Images represent maximum projection of confocal stacks taken with 20X water immersion (WI) objective and images were processed using ImageJ. Representative image analysis showing significant reduction in tumoroid area upon treatment with ZM008 monotherapy at 50 $\mu\text{g}/\text{mL}$ as well as in combination with Pembrolizumab. Reduction in size of tumoroid was monitored by disintegration of actin signal. Immune cell infiltration was represented by presence of green cells within the tumoroid structures in samples treated with ZM008 monotherapy as well as ZM008 + Pembrolizumab combination therapy.

<http://dx.doi.org/10.1136/jitc-2022-SITC2022.1391>

1392

AN ATYPICAL CENTRAL MEMORY LIKE PHENOTYPE CAN BE INDUCED IN HUMAN T CELLS BY INNATE TCR $\alpha\beta$ ENGAGEMENT

¹Khiyam Hussain*, ¹Pierre Vantourout, ¹Maria Poole, ¹Josephine Eum Eum, ¹Thomas Hayday, ¹Adam Laing, ²Seb Battaglia, ³Madan Katragadda, ³Jessica Lowry, ³Jonathan Hsu, ¹Adrian Hayday. ¹King's College London, London,, UK; ²Bridge Informatics, Salem, MA, USA; ³Marengo Therapeutics, Cambridge, MA, USA

Background The $\alpha\beta$ T cell receptor (TCR) has immense diversity, primarily for peptide-MHC (pMHC) complexes that clonally interact with complementarity-determining region (CDR) 3 motifs assembled by quasi-random somatic gene rearrangement of TCR α and TCR β gene segments. This adaptive biology is shown to an even greater extent by TCR $\gamma\delta$ with its ligands being qualitatively more diverse than pMHC. However, TCR $\gamma\delta$ can also function as an innate receptor whereby germline-encoded variable γ residues are sufficient to engage butyrophilin (BTN) or BTN-like (BTNL) that drive a variety of phenotypic outcomes distinct from clonal CDR3-mediated interactions. This broadened perspective on TCR biology has not hitherto been systematically extended to $\alpha\beta$ T cells.

Methods A panel of human TCR variable β (TCRV β) chain targeting antibodies was assembled, and their binding motifs determined. Using multi-colour flow cytometry and single-cell RNA sequencing, the impact of these antibodies on peripheral blood T cells was assessed by comparison with the impacts of anti-CD3 ϵ reagents, including OKT3.

Results Antibodies engaging germline-encoded regions of human TCRV β chains consistently activated primary human T cells towards an atypical central memory (TCM)-like phenotype distinct from those induced by anti-CD3 ϵ stimulation. Although the cells show myriad surface markers associated with chronic stimulation, they are not exhausted but are highly proliferative with strong cytolytic/Tc1 effector profiles, including expression of T-bet and IRF4. Strikingly, this phenotype can be induced in cells previously driven toward effector memory (T_{EM}) and effector memory T cells re-expressing CD45RA (T_{EMRA}) states.

Conclusions In sum, the use of TCR $\alpha\beta$ as an innate receptor offers new insight into T cell biology and an approach in which antibody mediated TCR agonism may be relevant to distinct clinical settings.

Acknowledgements This work was supported in part by funds provided by Marengo Therapeutics.

Ethics Approval Anonymized leukocyte cones were sourced from healthy adult donors attending blood donation clinics at the National Blood Service (London, UK). Use of human samples was approved by local ethical committees, in accordance with the Declaration of Helsinki.

<http://dx.doi.org/10.1136/jitc-2022-SITC2022.1392>

1393

BEYOND CCR8 KEY EPITOPES TARGETING DYNAMIC CCR8 CONFORMATIONAL STATES AND A DIVERSITY OF MONOCLONAL ANTIBODIES TO MODULATE THE TUMOR MICROENVIRONMENT FOR THE TREATMENT OF CANCERS

Claudine Vermot-Desroches, Iseulys Richert, Malaury Schappler, Alice Gentil Dit Maurin, Mégane Jeannelle, Solène Rose, Luc Baron, Quentin Ruet, Camille Dietsch, Pauline Urquia, Safia Ayachi, Orphée Blanchard, Christel Franchet, Stephan Schann, Xavier Leroy*. *Domain Therapeutics, Illkirch, France*

Background Chemokine (C-C motif) receptor 8 (CCR8) belongs to the G protein-coupled receptor (GPCR) family. Based on the transcriptional landscape of tumor infiltrating T regulatory cells, it has been found that CCR8 positive tumor infiltrating T regulatory cells (TITR) were highly immune suppressive and defined as a specific signature molecule. Generation of functional antibodies against integral membrane proteins such as the G-protein coupled receptor CCR8 is technically challenging for several reasons, including the coverage of epitope diversity related to transcriptional and post-transcriptional regulation CCR8 transmembrane protein and its dynamic conformational according to activation cellular state or immunosuppressive cell subsets.

Methods Domain Therapeutics has generated wide monoclonal antibodies (mAbs) libraries targeting a diversity of separate and non-overlapping CCR8 epitopes. Using different sources of native CCR8 positive cell subsets, distinct mAbs cellular reactivity profile has been also determined. Using different approaches (BRET, ELISA, FCM, ...), mAb activities were characterized in binding and several functional assays, including the inhibition of different G-proteins and B-arrestin 2 recruitment. A deep molecular and pharmacological characterization of each mAb was also performed by taking account the kinetic exposure and the nature of targeted CCR8 ligand. Some experiments were also conducted mimicking the tumor microenvironment conditions.

Results A panel of antibodies targeting human CCR8 was successfully generated. A wide diversity related to targeted epitopes was obtained, combined with high affinity binding properties. The requirement to target, or not, selective post-translational modifications (PTM) was also documented to trigger the highest inhibition level of CCR8 signaling. In parallel, treatment of tumor-bearing mice with cell-depleting anti-CCR8 antibody indeed eradicated established tumors with induction of potent tumor-specific effector/memory T cells. Thus, specific depletion of clonally expanding tumor Tregs is clinically instrumental for evoking effective tumor immunity without autoimmune adverse effects.

Conclusions Due to the high and relatively specific expression of CCR8 on tumor infiltrating Tregs, CCR8 represents an attractive immunotherapeutic target. Up to date, targeting selective CCR8 epitopes mimicking dynamic conformational CCR8 stage according to CCR8 positive cell subset or activation cellular state will be a key issue and differentiate therapeutic approach for the TME modulation in the treatment of cancer. Moreover, the use of depleting anti-CCR8 mAb with enhanced cytotoxic activity (i.e., ADCC, CDC, ADCP) can also reduce the number of CCR8 immune suppressive cells in a tumor.

<http://dx.doi.org/10.1136/jitc-2022-SITC2022.1393>

1394

PRECLINICAL CHARACTERIZATION OF BIODEGRADABLE INJECTABLE ANTIGEN PRESENTING NANOPARTICLES AIM INJ FOR IN VIVO TREATMENT OF SOLID TUMORS

Haiyun Liu*, Aniket Wadajkar, Sophia Zhang, Christian Wirick, Duong Nguyen, Daniel Dembrow, Sojung Kim, Mathias Oelke. *Nelmmune Inc., Gaithersburg, MD, USA*

Background NexImmune's artificial immune modulation (AIM™) technology is designed to direct T cell function and drive a T cell-mediated response. AIM antigen-specific immunotherapies rely on a nanoparticle-based artificial antigen presenting cell (aAPC) platform. The off-the-shelf injectable nanoparticles (INJ) are developed using biodegradable PLGA-PEG or PLA-PEG core materials and designed to mimic the function of natural APCs. AIM INJ nanoparticles present (i) an antigen-specific recognition signal delivered by an MHC molecule loaded with an antigenic peptide (Signal 1), and (ii) a co-stimulatory signal (anti-CD28, Signal 2) to induce expansion of the T cells activated through Signal 1.

Methods AIM INJ nanoparticles were synthesized by nanoprecipitation method on the Ignite NanoAssemblr™ microfluidic system. Murine AIM INJ nanoparticles were formulated by conjugating murine protein Signal 1 and 2, and then loading with tumor-specific peptides. Physicochemical characterization, stability, and in vitro functional tests were performed to assess antigen-specific CD8⁺ T cell proliferation, expansion, and cytokine production upon nanoparticle exposure. In vivo biodistribution and efficacy studies were performed in B16-F10 melanoma model by s.c. injection of AIM INJ nanoparticles. Biodistribution studies were conducted using ⁸⁹Zr radiolabeled nanoparticles. For the efficacy study, on day 7 after nanoparticle injection, tumor tissues were harvested and stimulated ex vivo to measure the expression of CD107a and cytokines IFN-γ, TNF-α, IL-2 by the tumor infiltrating lymphocytes (TILs).

Results PLGA-PEG based AIM INJ nanoparticles, with ~100nm diameter, PDI < 0.2, and close-to-neutral surface charge, have round morphology and were stable in liquid formulation over 6-months. The peptide-loaded murine AIM INJ nanoparticles activated CD8⁺ T cells in antigen-specific manner by promoting cell proliferation, expansion, and poly-functionality. The biodistribution studies showed a significantly higher amount of AIM INJ nanoparticle accumulation in the tumor (24 hours) and draining lymph node (96 hours) compared to naked nanoparticles (no proteins/peptides). In an in vivo treatment study, we demonstrated that the peptide-loaded AIM INJ nanoparticles induced significant amounts of poly-functional CD8⁺ TILs in a B16-F10 melanoma model. In addition, we will present data from ongoing studies using different sizes and formulations of AIM INJ nanoparticles.

Conclusions We demonstrated that biodegradable AIM INJ nanoparticles can activate and expand multiple antigen-specific CD8⁺ T cells in vitro and in vivo to induce anti-tumor activity. These studies along with other in vivo pre-clinical characterization will be used to support multiple INDs and advance AIM INJ into Phase 1 studies for various solid tumors.

<http://dx.doi.org/10.1136/jitc-2022-SITC2022.1394>

Abstracts

1395

CLN 619 A CLINICAL STAGE MICA B SPECIFIC IGG1 ANTIBODY WHICH RESTORES THE MICA B-NKG2D AXIS REQUIRES FC FUNCTION FOR POTENT ANTI-TUMOR ACTIVITY

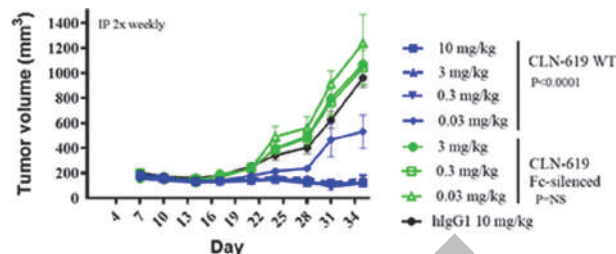
¹Kerry Whalen*, ¹Mehta Naveen, ¹Kristan Meetze, ²Neil Gibson, ¹Jennifer Michaelson, ¹Patrick Baeuerle. ¹Cullinan Oncology, Inc., Cambridge, MA, USA; ²COI Pharmaceuticals, Inc., San Diego, CA, USA

Background MICA and MICB are stress-inducible, highly polymorphic, surface glycoproteins that are expressed on a wide variety of human tumors but restricted in normal tissues. Engagement of MICA/B by NKG2D on natural killer (NK) cells and certain T cell subsets stimulates immune cell activation and subsequent target cell lysis. In cancer patients, tumor cells can escape NKG2D-mediated lysis by shedding MICA/B from the cell surface via proteases in the tumor microenvironment. High concentrations of shed MICA have been observed in serum from patients across multiple tumor types, correlating with poor survival. CLN-619 is a humanized anti-MICA/MICB monoclonal IgG1 antibody being developed for the treatment of multiple cancer indications. It has broad reactivity across MICA/B alleles, prevents shedding of MICA/B from the tumor cell surface, enhances the interaction of MICA with NKG2D, and engages Fcγ receptors on effector cells to collectively drive potent anti-tumor activity. We herein describe the significance of Fc functionality for the therapeutic activity of CLN-619.

Methods MICA/B levels were measured in supernatants by ELISA and on the cell surface by flow cytometry. The Promega ADCC Bioassay Complete Kit was used to evaluate ADCC. MICA binding to NKG2D was measured by flow cytometry. In vitro killing was assessed in a co-culture assay of donor PBMC and MICA-expressing tumor cells. In vivo studies were conducted in human xenograft tumor models.

Results CLN-619 inhibited the shedding of MICA/B shedding and enhanced the interaction of MICA with NKG2D. The latter was mediated by CLN-619 Fc effector function as well as by intrinsic enhancement of MICA-NKG2D binding by CLN-619. A functional Fc domain was also found necessary for CLN-619 induced immune-mediated cell killing of MICA/B expressing cells in vitro and for efficacy in mice bearing subcutaneous HCC1534 human xenograft tumors (figure 1). An Fc-silenced version of CLN-619 had no anti-tumor activity in HCC1534 at 3 mg/kg whereas CLN-619 showed significant tumor control even at 0.03 mg/kg.

Conclusions CLN-619 treatment resulted in robust anti-tumor activity in mice bearing MICA/B-expressing xenograft models. Activity of CLN-619 was dependent on a functional Fc domain. Simultaneous stimulation of the NKG2D-MICA/B axis and ADCC by CLN-619 may uniquely synergize in activating the lytic potential of NK cells. CLN-619 is currently in a Phase 1 clinical trial for the treatment of patients with advanced malignancies (ClinicalTrials.gov Identifier: NCT05117476).



Abstract 1395 Figure 1 Efficacy of CLN-619 depends on a functional Fc-domain

BALB/c SCID mice were inoculated subcutaneously with HCC1534 human lung cancer xenograft cells (N=10/group). Treatment was administered 2X weekly for four weeks intraperitoneal. Statistics were analyzed by one-way ANOVA adjusted for multiple comparisons.

<http://dx.doi.org/10.1136/jitc-2022-SITC2022.1395>

1396

ANTIBODY BLOCKADE OF THE IMMUNOINHIBITORY RECEPTOR SIGLEC 10 POLARIZES TUMOR ASSOCIATED MYELOID CELLS AND PROMOTES ANTI-TUMOR IMMUNITY

¹Julia Schanin*, ¹Thuy Luu, ¹Robert Sanchez, ¹Milene Peterson, ²Lisa McEwan, ²Evan Henneberry, ¹Katherine Chang, ¹Wouter Korver, ¹John Leung, ¹Bradford Youngblood. ¹Allakos Inc, San Carlos, CA, USA; ²LM Biostat Consulting Inc., British Columbia, Canada

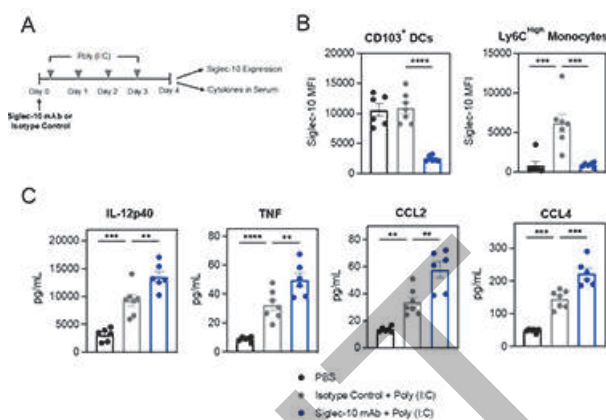
Background Myeloid cells are the most abundant immune cells within the tumor microenvironment (TME) where they play important roles regulating anti-tumor immunity. Targeting myeloid-specific inhibitory receptors to modulate the TME represents an attractive strategy to improve the therapeutic outcome of current cancer immune therapies. Siglec-10 is an inhibitory receptor expressed on tumor-associated macrophages (TAMs) and dendritic cells that regulates immune cell activation via immunoreceptor tyrosine-based inhibitory motifs. Recently, Siglec-10 was shown to induce immunosuppression and promote tumor immune escape through interaction with CD24. Similarly, CD52 and vascular adhesion protein-1 have been shown to drive immunosuppression via Siglec-10, indicating that Siglec-10 functions as an inhibitory receptor through multiple ligands. Here, we report that Siglec-10 expression is upregulated in human tumors and blockade of Siglec-10 with a monoclonal antibody (mAb) enhances proinflammatory responses and delays tumor growth in vivo by modulating myeloid cell function.

Methods Siglec-10 expression was evaluated in human tumors by flow cytometry and RNA-sequencing. Anti-human Siglec-10 mAbs were generated using hybridoma technology and recombinantly produced on mouse IgG1 backbones. Internalization and function of Siglec-10 mAbs were evaluated in vitro by flow cytometry and cytokine production using isolated human CD16⁺ monocytes. To assess the in vivo activity of a Siglec-10 mAb, transgenic mice expressing Siglec-10 were generated and challenged with poly I:C. Anti-tumor activity of a Siglec-10 mAb was determined using the MC38 syngeneic mouse model.

Results RNA-sequencing data revealed high expression of Siglec-10 across multiple tumors compared to normal tissues, including glioblastoma, colorectal carcinoma, and kidney renal clear cell carcinoma. Specifically, Siglec-10 was found to be highly and selectively expressed on intratumor dendritic cells and macrophages. Siglec-10 mAb treatment blocked ligand binding, induced complete receptor internalization, and significantly enhanced TLR-mediated human monocyte activation in vitro. Similarly, in vivo administration of a Siglec-10 mAb induced receptor internalization and enhanced TLR-mediated inflammation as evidenced by increased levels of cytokines, such as TNF and IL-12p40 (figure 1). To assess the potential of a Siglec-10 mAb as an anti-cancer immunotherapy, we established a colon carcinoma model in Siglec-10 transgenic mice. Siglec-10 mAb blockade polarized myeloid cells towards an inflammatory phenotype, enhanced adaptive immune cell activation and promoted anti-tumor activity.

Conclusions Siglec-10 is highly expressed on tumor-associated myeloid cells and antibody blockade promotes anti-tumor immunity through activation of TAMs and dendritic cells. Our findings highlight Siglec-10 as a promising myeloid cell target for enhancing anti-tumor immunity in solid tumors.

Ethics Approval All legal and ethical requirements have been met with regards to the humane treatment of animals described in this study.



Abstract 1396 Figure 1 Anti-Siglec-10 treatment induces receptor internalization and enhances proinflammatory responses in a model of TLR-mediated lung inflammation in Siglec-10 transgenic mice. (A) Schematic of experimental TLR-mediated lung mouse model. (B) Siglec-10 expression levels on CD103⁺ DCs and Ly6Chigh MHC⁺ inflammatory monocytes in lung tissue from mice intranasally challenged with poly (I:C) and dosed with a Siglec-10 mAb (blue) or isotype control (gray) compared to PBS challenged mice (black). (C) Levels of cytokines and chemokines in serum of mice challenged intranasally with poly (I:C) or PBS control. Data are plotted as means +/- SEM for individual mice (n=6-7/group). ** p = <0.01; *** p = <0.001; **** p = <0.0001 as determined by one-way ANOVA with Tukey's multiple comparisons

<http://dx.doi.org/10.1136/jitc-2022-SITC2022.1396>

Abstracts

1397

ATG 027 A FIRST IN CLASS B7 H3 PD L1 BISPECIFIC ANTIBODY SHOWS POTENT T CELL ACTIVATION CAPABILITY AND IN VIVO ANTI TUMOR EFFICACY

¹Hui Yuwen, ¹Tengteng Li, ¹Yijing Ren, ²Linjie Tian*, ³Jay Mei, ⁴Bo Shan, ³Bing Hou. ¹Shanghai Antengene Corporation Limited, Shanghai, China; ²Antengene Biotech LLC, Doylestown, PA, USA; ³Antengene Corporation Co., Ltd, Shaoxing, China; ⁴Antengene Corporation Co., Ltd., Shanghai, China

Background Programmed death-ligand 1 (PD-L1) and programmed cell death protein 1(PD-1) blockade therapy has been approved for the treatment of many malignancies whereas the majority of patients with solid tumors do not respond well.¹ B7-H3, another newly identified immune checkpoint molecule, has limited expression in normal human tissues while highly expressed on cancer cells and tumor-infiltrating antigen-presenting cells (APCs), which is associated with T-cell exhaustion in cancer patients. In addition, B7-H3 is overexpressed by the tumor-associated vasculature and stromal fibroblasts, and contributes to the development of cancer through both immune-dependent and nonimmune routes.² However, clinical therapeutic antibodies targeting B7-H3, such as Enobituzumab, have not shown an immune checkpoint blockade effect. ATG-027, a novel B7-H3/PD-L1 bispecific antibody, was designed to exert the anti-tumor efficiency through reinforcing T cell activation by dual-blocking of B7-H3 and PD-L1, antibody-dependent cellular cytotoxicity (ADCC), complement dependent cytotoxicity (CDC), and antibody-dependent cellular phagocytosis (ADCP).

Methods ATG-027 was developed by introducing high-affinity PD-L1 scFv into a human IgG1 B7-H3 monoclonal antibody (mAb). The bispecific antibody employed wild type Fc domain which enables ADCC and ADCP effects. A series of in vitro studies were performed to evaluate the immune regulating function and anti-tumor efficacy of ATG-027. The in vivo efficacy of ATG-027 was evaluated in mice bearing syngeneic MC38 colorectal cancer cells overexpressing human B7-H3 (MC38-hB7-H3).

Results In the cell-based assay, ATG-027 binds with nanomolar affinity to both B7-H3 and PD-L1 expressing cells. ATG-027 demonstrated higher ADCC/CDC activity compared with anti-PD-L1 and anti-B7-H3 parental antibodies. ATG-027 also demonstrated greater ADCP potency than anti-PD-L1, anti-B7-H3, or the combination. Interestingly, in a Mixed Lymphocyte Reaction (MLR) experiment to assess the T cell activation, the B7-H3 parental antibody (30-C7) or the Fab region of 30-C7 (30-C7-Fab) induced robust IL-2 and IFN γ production, indicating T cell activating function, whereas Enobituzumab showed no effect in the experiment (figure 1). ATG-027 also demonstrated superior in vivo anti-tumor activity in mouse MC38-hB7-H3 models compared to parental antibodies. Biweekly dosing of 7.5mg/kg ATG-027 induced tumor shrinkage or complete tumor regression.

Conclusions By binding to a specific epitope of B7-H3, ATG-027 blocks the protein's inhibitory function, leading to strong T cell activation. ATG-027 can also inhibit the interaction between PD1/PD-L1 to rescue T cell activity suppression. ATG-027's dual T cell activation function and powerful ADCC, CDC, and ADCP properties contribute to its promising anti-tumor efficacy in preclinical models.

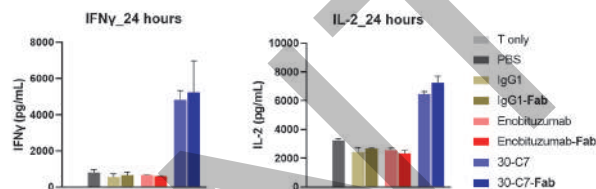
REFERENCES

1. Cai D, J Li, D Liu, S Hong, Q Qiao, Q Sun, P Li, N Lyu, T Sun, S Xie, L Guo, L Ni, L Jin, and C Dong. Tumor-expressed B7-H3 mediates the inhibition of

antitumor T-cell functions in ovarian cancer insensitive to PD-1 blockade therapy. *Cellular & Molecular Immunology* 2020;**17**: 227–236.

2. Zhou WT, and WL Jin. B7-H3/CD276: An Emerging Cancer Immunotherapy. *Frontiers in Immunology* 2021;**12**: 701006.

Ethics Approval The protocol and any amendment(s) or procedures involving the care and use of animals in this study were reviewed and approved by the Institutional Animal Care and Use Committee (IACUC) of CrownBio to execution with an AUP number or IACUC approval number for each animal study. All studies were conducted following an approved IACUC protocol. AUP NO. 2104-09-2186.



Abstract 1397 Figure 1 B7H3 Mab 30-C7 activates T cells in MLR assay

Human T cells were isolated and co-cultured with mature DCs (mDC), ATG-027 parental anti-B7-H3 antibody (30-C7) or Fab region of 30-C7 induced potent IFN γ (left) and IL2 (right) production after 24 hours of co-culturing. Enobituzumab or IgG1 control showed no effect.

<http://dx.doi.org/10.1136/jitc-2022-SITC2022.1397>

1398

PERSONALIZED IMMUNOTHERAPEUTIC PLATFORM WITH EVIDENCE OF CLINICAL ACTIVITY IN GLIOBLASTOMA PROTECTS MICE AGAINST OVARIAN LIVER AND BLADDER CANCER TUMOR CHALLENGES

¹Amelia Zellander*, ¹Christopher Uhl, ¹Christopher Cultrara, ¹Kenneth Kirby, ¹Essam Elrazaq, ²Charles Scott, ¹David Andrews, ¹Jenny Zilberberg, ¹Mark Exley. ¹Imvax, Philadelphia, PA, USA; ²CBS Squared, Philadelphia, PA, USA

Background Imvax is developing a novel personalized immunotherapeutic platform combining irradiated, patient-derived tumor cells and Insulin-Like Growth Factor Type-1 Receptor antisense oligonucleotide (IMV-001) in biodiffusion chambers (BDC; 0.1-micron pores). The combination product IGV-001 was recently evaluated in a newly diagnosed glioblastoma (GBM) phase 1b clinical trial.¹ Median overall survival of highest exposure IGV-001-treated ‘Stupp-eligible’ patients² was 38.2 months compared with 16.2 months in recent standard-of-care-treated patients (P=0.044).¹ We have now found activity with the equivalent murine approach in multiple cancer models, highlighting the transformative potential of this immunotherapeutic platform beyond glioblastoma.

Methods We utilized the ID8-luciferase (-Luc) intraperitoneal ovarian cancer, the orthotopic Hepa1-6-Luc hepatocellular carcinoma model and orthotopic MBT-2 urothelial murine cancer models. BDCs containing saline or 1x10⁶ IMV-001-treated tumor cells (hereon IOC-001, IHC-001, and IUC-001 respectively) were implanted in flanks of mice and explanted 48 h later, as per glioblastoma clinical protocol. Primary tumor challenge was conducted 28d after chamber implantation. Intra-mammary rechallenge in the Hepa1-6 model was conducted 102 days after orthotopic challenge alongside naive controls, since no primary controls were still alive. Mice were monitored for survival and tumor growth. Cytokine analysis and immunophenotyping were conducted.

Results 60% of IOC-001-treated mice survived to end of study at 58d post-tumor challenge, compared to only 19% of mice in the saline control group (MST=37d, P=0.004). Circulating IFN γ was significantly higher in IOC-001-treated mice compared to controls on 1d post-tumor challenge (p<0.001) and trended higher in those receiving IHC-001 14d after tumor challenge. In the Hepa1-6 model, 50% of IHC-001-treated mice survived beyond 110d post-tumor (MST = 60.5d at end of study); Hepa1-6 intramammary rechallenge at 102d demonstrated durable systemic immunity in survivors. There were no survivors in the primary control group beyond 28d (MST = 18d; P=0.004). In the MBT-2 model, 42% of IUC-001-treated mice survived up to 90d post-tumor challenge (MST=33d at end of study); all control mice expired by 37d (MST=21d; P=0.0163). Low end of life bladder weights in surviving IUC-001-treated mice suggested minimal tumor burden. Further Immunological and Pathology data will be provided.

Conclusions These data support the durable antitumor activity of Imvax’s immunotherapeutic platform in multiple cancers beyond glioblastoma. Results suggest that efficacy is associated with a systemic immunological response, resulting in generation of Th1 antitumor cytotoxic T cells. Future studies are seeking additional biomarkers of response using phenotypic evaluation of T cell activation/exhaustion markers and Th1/Th2 responses.

REFERENCES

1. D Andrews, K Judy, C Scott, S Garcia, L Harshyn, L Kenyon, K Talekar, A Flanders, K Atsina, L Kim, N Martinez, W Shi, M Werner-Wasik, H Liu, M Prośniak,

- M Curtis, R Kean, D Ye, E Bongiorno, S Sauma, M Exley, K Pigott and D Hooper. Phase 1b Clinical Trial of IGV-001 for Patients with Newly Diagnosed Glioblastoma, *Clin Cancer Res*, vol. 27, no. 7, pp. 1912-1922.
2. R Stupp, W Mason, M van den Bent, M Weller, B Fisher, M Taphoorn, K Belanger, A Brandes, C Marosi, U Bogdahn, J Curschmann, R Janzer, S Ludwin, T Gorlia, A Allgeier, D Lacombe, J Cairncross, E Eisenhauer and R Mirmanoff. Radiotherapy plus Concomitant and Adjuvant Temozolomide for Glioblastoma, *N Engl J Med*, 2005;**352**:987–996.

<http://dx.doi.org/10.1136/jitc-2022-SITC2022.1398>

1399

**ZL 1218 TARGETS THE MOST SUPPRESSIVE
INTRATUMORAL TREG SUBPOPULATION TO AVOID
PERIPHERAL TOXICITIES**

¹Jing Zhang*, ¹Linda Liu, ¹Grace Wang, ¹Joshua Zeng, ¹Tao Geng, ¹Chakrapani Tripathi, ²Lei Wang, ¹Zai Lab (US) LLC, Menlo Park, CA, USA; ²Zai Lab (China) LLC, Shanghai, China

Background Accumulating evidence demonstrates that the removal of Treg cells is able to evoke and enhance anti-tumor immune response. However, systemic depletion of Treg cells may concurrently elicit deleterious autoimmunity. CCR8, a chemokine receptor expressed by tumor infiltrating Treg cells, is associated with poor cancer prognosis. We have recently reported that ZL-1218, a humanized therapeutic antibody targeting CCR8, exerts its anti-tumor effect as a monotherapy and in combination with PD-1 blockade treatment. In the current study, we aimed to understand the underlying biology of CCR8⁺ regulatory T cells and the mechanism of action of ZL-1218.

Methods Human and mouse dissociated tumor cells (DTCs) were immuno-profiled using multi-color flow cytometry. The CCR8 expression was quantified by both flow cytometry and immunohistochemistry (IHC)/ISH assay. The 10x Genomics single cell RNAseq (scRNAseq) was conducted, and the data was analyzed using unsupervised K-means clustering. nTreg cells were isolated from human buffy coat using EasySep™ Human CD4⁺CD127^{low}CD25⁺ Treg Isolation Kit.

Results We demonstrated that CCR8 is highly expressed on intratumoral FoxP3⁺ Treg cells in multiple cancers and is absent on other major intratumoral immune cell populations or any immune cell population in the peripheral blood. The percentage of CCR8⁺ Treg cells and CCR8 expression level indicated large donor-to-donor variations. In vitro anti-CD3/28 stimulation of nTregs suggested that Treg activation could be a trigger for CCR8 expression. Next, we assessed whether CCR8 is part of a larger Treg activation program using the scRNAseq analysis of selected DTC samples. CCR8⁺ tumor infiltrating Tregs indeed showed a significantly higher surface expression level of Treg activation markers such as GITR, OX-40, 4-1BB, CTLA-4 and TIGIT, which are also the markers for a highly suppressive Treg subpopulation. This implies that CCR8⁺ Treg cells represent a highly activated and suppressive Treg population. Importantly, we further demonstrated that ZL-1218 depleted about 50% Treg cells from selected DTC samples, which is consistent with the percentage of CCR8⁺ Treg cells in these samples. Additionally, in human CCR8 knock-in mice, ZL-1218 treatment depleted comparable intratumoral Tregs leading to increased CD8T/Treg ratios without affecting peripheral Tregs. The toxicology study of ZL-1218 in non-human primates following 5 weekly intravenous infusion administrations demonstrated no safety concerns up to 100 mg/kg.

Conclusions These findings suggest that ZL-1218 antibody may deliver optimal tumor-targeted Treg depletion in the clinic while limiting peripheral toxicities to avoid autoimmune response.

Ethics Approval The study was approved by IACUC committee in Zai Lab (US) LLC (Protocol approval number 2020-11_1).

<http://dx.doi.org/10.1136/jitc-2022-SITC2022.1399>

1400

DM919: A POTENT ANTI-MICA B ANTIBODY REINFORCES NKG2D MICA B AXIS AND PROMOTES ANTI TUMOR ACTIVITIES IN PRECLINICAL MODELS

Guangan Hu, Quanju Zhao, Lai Shi, Xiaochun Chen, Xiaodong Jiang, Sheng Yin, Nan Bing, Dong Zhang*. *D2M Biotherapeutics Inc, Natick, MA, USA*

Background Genome-wide association studies have identified MICA/B proteins as a causal factor for multiple cancers. Membrane MHC-I related MICA/MICB are stress-responding proteins and trigger the cytotoxic effector activity of NK cells and co-stimulatory activation of CD8⁺ T cells through NKG2D receptor. Many human tumors develop immune escape mechanism via proteolytic cleavage of MICA/B from the cell surface. Shedding of MICA/B leads to lack of recognition by NKG2D. Soluble shed MICA/B not only are natural decor of NKG2D, but also downmodulate NKG2D receptor and inhibit NK cell function. DM919, a potent anti-MICA/B antibody, prevents MICA/B shedding and stabilizes surface MICA/B, and presents shed MICA/B to activate NKG2D on NK or T cells and mediates ADCC.

Methods Mice were immunized with recombinant proteins of a3-domain from multiple alleles of MICA/B proteins to maximize allotype coverage in human population (~99.1%). Resulted IgG H&L chain variable regions were PCR amplified from plasma cells and built into yeast displayed scFv libraries. The libraries were screened for specifically binding to multiple alleles of MICA/B and evaluated for ability to prevent the shedding of MICA/B and activate NK and T cells via NKG2D. The selected anti-MICA/B hits were humanized, and affinity maturation was carried out using yeast display technology. Optimized hits were further screened and characterized in series of assays to evaluate functional activities and physicochemical properties. The lead candidate DM919 was identified based on its desirable characteristics and further evaluated in multiple syngeneic and xenograft mouse tumor models.

Results DM919 binds specifically to multiple alleles of MICA/B proteins with sub nanomolar affinities. DM919 inhibits the MICA/B shedding and stabilizes their surface expression. DM919 captures soluble MICA/B and activate NK cells and co-stimulate T cells through NKG2D. DM919 enhances the activation and degranulation of primary human NK cells and increases the cytotoxicity of human NK cells to lyse tumor cells. DM919 demonstrated excellent stability in vitro and in vivo. DM919 significantly inhibited xenograft tumor growth in vivo in SCID mice. DM919 inhibited in vivo growth of syngeneic mouse tumor cells transgenically expressing human MICA/B in a dose dependent manner. DM919 treatment reduced serum soluble MICA/B, which is a pharmacodynamic biomarker.

Conclusions DM919, a high affinity and potent the anti-MICA/B antibody has been developed. DM919 has demonstrated desirable functional and physicochemical characteristics in vitro. DM919 has shown significant antitumor activities in multiple syngeneic and xenograft tumor models. The data support further development of DM919 as an immunotherapeutic for solid tumor malignancies.

Ethics Approval All animal studies and procedures were approved by the Institutional Animal Care and Use Committee (IACUC) of Worcester polytechnic Institute. The protocol ID is #21-134.

Consent Written informed consent was obtained from the patient for publication of this abstract and any accompanying

images. A copy of the written consent is available for review by the Editor of this journal.

<http://dx.doi.org/10.1136/jitc-2022-SITC2022.1400>

1401

**SIGLEC15 INDUCES MONOCYTE APOPTOSIS AND AN
SIGLEC15 ANTIBODY ES012 REVERSES MYELOID CELLS
DRIVEN IMMUNOSUPPRESSION**

Maofa Zheng*, Dawei Sun, Yanan Geng, Rui Gao, Jinfeng Zhao, Zhihao Wu, Xiaoyan Zheng, Jingfeng Yu, Quan Qiu, Chunnian Wang, Yangsheng Qiu, Yingchao Liu, Yefeng Lu, Zheng Song, Mei Shi, Hongtao Lu. *Elpscience Biopharma, Shanghai, China*

Background Siglec15 (S15) is a glycan-recognition proteins belongs to the Siglec family, preferentially recognizing the Neu5Aca2–6GalNAc– structure. Siglec15 is induced by MCSF and is highly expressed on TAM and many tumor cells, which inhibits T cell activity. The detailed mechanism of S15 function on T cells and myeloid cells, however, remains unclear. In this study, we seek to investigate Siglec15 biology and generate anti-Siglec15 antibodies for therapeutic use.

Methods The binding and function of Siglec15 on different cell subsets from healthy donor PBMC were evaluated. Siglec15 antibodies were screened and characterized by antigen binding, ligand blocking assay, rescue of monocyte apoptosis, reversion of monocyte inhibition and PBMC T cell activation assay. Selected leads underwent epitope binning by Bio-layer interferometry (BLI) and mapping by hydrogen deuterium exchange mass spectrometry (HDX-MS), they were then evaluated in MC38/hS15 bearing human S15 knock-in B6/C57 mice for PK profile and in vivo efficacy. Finally, the selected chimeric antibody (ES012) was humanized and undergone pre-clinical assessment, including potential acute toxicity study in cynomolgus monkeys and the pharmacokinetics (PK) study.

Results S15 expresses on human monocyte cells, M2 macrophage and DC cells but not on M1 macrophage. S15 also mainly binds to myeloid cells (including monocytes, M1 and M2 macrophage and THP-1 cell lines). S15-Fc dose-dependently inhibited OKT3-driven T cell proliferation in a PBMC culture, but not T cell proliferation driven by either PMA plus ionomycin, PHA or CD3/CD28 beads, all of which imply that S15-Fc probably does not directly suppress T cell activity; instead, this T cell inhibitory effect is probably through the inhibition on monocyte. We found that S15 dose-dependently induced the apoptosis of subsets of monocyte and down-regulated the surface expression of CD86, HLA-DR and CD14.

ES012 is a S15 humanized monoclonal antibody with strong blocking activity between S15 and multiple ligands including SiaTn and LRRC4C. ES012 dose-dependently rescued S15-mediated monocyte apoptosis, reversed S15-mediated monocyte inhibition, and rescued S15-mediated T cell inhibition. ES012 exhibited a good PK profile and showed excellent anti-tumor activity in a hS15 KI syngeneic mice model with 100% CR at dose of 5mg/kg.

Conclusions In summary, we found that siglec15 has a major effect on myeloid cells (inducing monocyte apoptosis and inhibiting monocyte activation) and an indirect inhibitory effect on T cell function. Based on this newly discovered S15 biology, we have developed a potent, functional anti-Siglec15 mAb ES012 that has great potential to reverse immune suppression in the TME to promote anti-tumor immunity.

<http://dx.doi.org/10.1136/jitc-2022-SITC2022.1401>

1402

**PH 894: AN INTASYL SELF-DELIVERING SIRNA
TARGETING BRD4 HAS DUAL FUNCTIONS TO SENSITIZE
TUMOR CELL KILLING AND ACTIVATE CD8 T CELLS**

Shenghua Zhou*, Benjamin Cui, Melissa Maxwell, Dingxue Yan, Brianna Rivest, Andrew Boone, James Cardia, Simon Fricker. *Phio Pharmaceuticals Corp., Marlborough, MA, USA*

Background Bromodomain containing proteins such as BRD4 play critical roles during cancer development and progression. BRD4 regulates oncogenes such as MYC and contributes to escape from immunosurveillance by decreasing tumor cell immunogenicity. Therefore, BRD4 is an attractive target for cancer therapy. Current clinical studies have focused on small molecule inhibitors of BRD4, however, these are not selective for BRD4 but inhibit other BRD proteins and are associated with toxicity and development of resistance. PH-894 is a self-delivering RNAi compound that specifically silences the BRD4 gene. We previously demonstrated potent antitumor activity of PH-894 in syngeneic mouse tumor models. Here we use B16ova melanoma cells which express ovalbumin peptide (OVA) and OT-1 T cells which recognize OVA to further explore the antitumor mechanism of PH-894.

Methods OT-1 T cells were stimulated with irradiated EG7 cells, followed by treatment with either PH-894 or a chemically matched non-targeting RNAi control (NTC). Seventy-two hours post-treatment, the levels of secreted IFN- γ were assayed by ELISA and BRD4 protein expression determined by flow cytometry. B16ova tumor cells were pre-treated with IFN- γ for 18 hours, followed by treatment with PH-894 or NTC for 3 days, and BRD4 protein expression assessed. To investigate whether PH-894 pretreatment could sensitize the killing of B16ova cells by OT-1 T cells, B16-OVA cells treated with IFN- γ were pre-treated with PH-894 or NTC-647 for 3 days. The treated B16ova cells were cocultured with anti-CD3-activated OT-1 CD8⁺ T cells for 20 hours. OT-1 T cells were removed and B16ova cell viability was measured using CellTiter-Glo. Specific killing activity was calculated by normalizing luminescence in wells with cocultured B16ova/OT-1 T cells to those with B16ova cells only.

Results The expression of BRD4 was downregulated by PH-894 in both IFN- γ treated B16ova tumor cells and EG7 activated OT-1 T cells. Treatment with PH-894 resulted in a significant increase of IFN- γ production by the OT-1 cells. PH-894 pretreatment of the B16ova tumor cells significantly increased cell killing activity of the tumor cells by activated OT-1 T cells (90.8% killing activity with PH-894-treated B16ova cells compared to 68% in untreated cells).

Conclusions We demonstrate that PH-894 potentially activates CD8⁺ T cells, and PH-894 pretreatment of tumor cells can sensitize tumor cell killing by CD8⁺ T cells. These data provide additional mechanistic insight and support further development and clinical investigation of PH-894 as a new class of antitumor therapeutic.

<http://dx.doi.org/10.1136/jitc-2022-SITC2022.1402>

Abstracts

Other

1403 **OUTCOMES FOLLOWING FIRST-LINE IMMUNOTHERAPY WITH OR WITHOUT CHEMOTHERAPY STRATIFIED BY KRAS MUTATIONAL STATUS – A REAL WORLD ANALYSIS IN PATIENTS WITH ADVANCED NSCLC**

¹Charu Aggarwal, ²Halla Nimeiri, ²James Chen, ³Iker Hueriga, ⁴Leora Horn, ⁴Nataliya Trunova, ⁵Jyoti Patel*. ¹University of Pennsylvania, Philadelphia, PA, USA; ²Tempus, Chicago, IL, USA; ³Tempus and AstraZeneca, Chicago, IL, USA; ⁴AstraZeneca, Chicago, IL, USA; ⁵Northwestern University, Chicago, IL, USA; ⁶Robert H Lurie Comprehensive Cancer Cent, Chicago, IL, USA

Background Recent meta-analysis from 12 registrational studies¹ in patients with advanced non-small cell lung cancer (NSCLC) with KRAS mutations (mt), including G12C, evaluated efficacy outcomes of chemotherapy (CTx), immune checkpoint inhibitors (ICI), or ICI with CTx in the first line (1L) setting. Treatment with ICI + CTx provided superior efficacy, independent of KRAS and PD-L1 status and use of ICI + CTx was suggested as the preferred comparator arm in future 1L trials for patients with KRASmt. Herein, we report the largest, multimodal real world data (RWD) analysis for outcomes with 1L therapy in patients with advanced NSCLC stratified by KRASmt status.

Methods Deidentified multimodal RWD was accessed via the Tempus Lens database to retrospectively analyze 2,680 advanced 1L NSCLC patients. Patients were diagnosed between January 1, 2017 – December 31, 2021, had Tempus xT genomic sequencing and received CTx, ICI, or ICI + CTx. Patients were stratified by KRAS status: mutant (mt), G12C, or wildtype (wt). Median overall survival (mOS) was estimated using Kaplan-Meier methods. Subgroup analyses were performed using Cox model stratified by KRAS status, PD-L1 status [High (TPS ≥ 50), Low (TPS ≥ 1- 49), Negative (TPS < 1)] and pathogenic alterations in STK11, KEAP1 and TP53.

Results KRASmt were identified in 31.4% (840/2680), 11.3% (303/2680) were G12C. Proportion of patients with PD-L1 TPS ≥ 50% was highest in KRASmt and G12C groups compared to wt (30%, 31% vs 20% respectively). Demographics were balanced across all subgroups, except for a higher% of squamous histology (wt 25% vs 4% mt) and never-smokers (wt 14% vs. 5% mt). The prevalence of pathogenic variants between mt vs. wt groups were: STK11 (16% vs 10%), KEAP1 (9% vs 8%) and TP53 (48% vs 37%). OS results are shown in (table 1). In the mt subgroup, the greatest benefit was seen in PDL-1 ≥ 50%; mOS (months): High: 27.56, Low: 15.26, Negative: 14.1. Notably, the G12C + PDL-1 high group displayed the longest mOS (47.4). Patients with co-mutations had the worst outcome: KRASmt/STK11 (OS 11.53m) or KEAP1 (OS 11.33m) (table 2).

Conclusions Our analysis suggests that advanced NSCLC patients with KRASmt, including G12C with high PD-L1, had the best outcomes when treated with 1L ICI including ICI alone. Outcomes were significantly worse when STK11/KEAP1 co-mutations were present. This implies that patients with KRASmt NSCLC may represent a heterogeneous group requiring a tailored 1L trial design to account for variabilities in outcome.

REFERENCES

1. Erica C Nakajima, Yi Ren, Jonathon Joseph Vallejo, Oladimeji Akinboro, Pallavi Shruti Mishra-Kalyani, Erin A. Larkins, Nicole Lauren Drezner, Shenghui Tang, Richard Pazdur, Julia A. Beaver, Harpreet Singh. Outcomes of first-line immune

checkpoint inhibitors with or without chemotherapy according to KRAS mutational status and PD-L1 expression in patients with advanced NSCLC: FDA pooled analysis. Meeting Abstract | 2022 ASCO Annual Meeting

Abstract 1403 Table 1 OS of patients stratified by therapy + KRAS status

Efficacy (95% CI)	KRASmt N = 840			KRASwt N = 1,840			KRAS G12C N = 303		
	ICI+CTx (n = 533)	ICI (n = 225)	CTx (n = 82)	ICI+CTx (n = 1120)	ICI (n = 451)	CTx (n = 269)	ICI+CTx (n=192)	ICI (n=79)	CTx (n = 32)
mOS (months)	15.86	25.73	9.73	18.86	24.1	12.73	16.76	30.43	12.46

Overall Survival of 1L NSCLC patients Stratified by KRAS mutational status and therapy

Abstract 1403 Table 2 OS of patients stratified by co-mutations

	KRASwt N = 1285 Median OS (months)	KRASmt N = 645 Median OS (months), Hazard Ratio (95% CI)	KRAS G12C N=226 Median OS (months), Hazard Ratio (95% CI)
PD-L1 High	24.16	27.56 0.97 (0.74 - 1.28) p = 0.87	34.8 0.81 (0.54 - 1.20) p = 0.29
PD-L1 Low	19.93	17.13 1.15 (0.90 - 1.46) p = 0.26	19.93 0.98 (0.69 - 1.41) p = 0.04
PD-L1 Negative	17.03	12.96 1.21 (0.98 - 1.51) p = 0.07	11.3 1.69 (1.28 - 2.35) p = 0.0017
TP53			
TP53mt	16.8	17.6 0.95 (0.80 - 1.13) p = 0.575	17.76 0.92 (0.69 - 1.22) p = 0.56
TP53wt	20.47	16.76 1.18 (0.98 - 1.41) p = 0.06	18.56 1.09 (0.84 - 1.40) p = 0.51
STK11			
STK11mt	15.93	11.53 1.35 (0.99 - 1.84) p = 0.052	11.66 1.20 (0.78 - 1.87) p = 0.4
STK11wt	19.2	20.26 0.96 (0.84 - 1.10) p = 0.61	21.23 0.92 (0.75 - 1.13) p = 0.45
KEAP1			
KEAP1mt	17.53	11.33 1.26 (0.83 - 1.89) p = 0.26	9.53 1.99 (1.08 - 3.66) p = 0.026
KEAP1wt	18.26	17.6 1.02 (0.89 - 1.16) p = 0.73	20.73 0.93 (0.77 - 1.14) p = 0.51

Overall Survival of 1L advanced NSCLC patients stratified by PDL1 status, KRAS, STK-11, KEAP-1, and TP53 alterations

<http://dx.doi.org/10.1136/jitc-2022-SITC2022.1403>

1404

HPV33-DRIVEN OROPHARYNGEAL SQUAMOUS CELL CARCINOMAS ARE INCREASING IN PREVALENCE AND ARE CHARACTERIZED BY LOW CD8 INFILTRATION AND EPITOPE PRESENTATION DEFICIENCIES

¹Shilpa Bhatia*, ¹Brinda Vijaykumar, ¹Qiaomu Tian, ¹Yanbo Sun, ²Charles Quinn, ²Sean Donnelly, ²Ravindra Uppaluri, ²Ann Marie Egloff, ¹Daniel Pregibon, ¹Lakshmi Srinivasan, ¹Anthony Coyle, ²Glenn Hanna, ¹Christine McInnis. ¹*Repertoire Immune Medicines, Cambridge, MA, USA*; ²*Dana Farber Cancer Institute, Boston, USA*

Background The evolving dynamics of human papillomavirus (HPV) genotypes has the potential to impact the prognosis of HPV-associated malignancies. HPV33+ oropharyngeal squamous cell carcinoma (OPSCC) patients in particular may have inferior survival rates compared to the other high-risk HPV subtypes. Despite heterogeneity in disease biology and varying clinical outcomes, ambiguity exists for the optimal clinical management of non-HPV16 high-risk subtypes. Here, we interrogated tumor from HPV33+ HNSCC patients to gain an in-depth understanding of cellular heterogeneity, identify high-risk MHC alleles, and explore disease-relevant targets that may inform strain-specific disease management.

Methods Treatment-naïve HPV+ OPSCC patients (n=19) were prospectively enrolled under an institutional review board (IRB)-approved tissue collection protocol (DF/HCC#09-472) for collection of surgical specimens. Subtype was assessed using TTMV-HPV DNA. Multiplexed, barcoded peptide-MHC-I tetramer libraries containing epitopes derived from the HPV33 genome were used to probe dissociated tumors followed by single cell RNA sequencing using the 10x Genomics platform. SingleR and published gene marker sets were used to phenotype and perform broad lineage assignment. Bulk RNA-sequencing data from additional HNSCC dataset was interrogated to validate select findings.

Results Our cohort (Total patients n=237; HPV33+ n=17, 7.2%) showed a ~2.4 fold higher rate of HPV33-driven OPSCC compared to published reports (3%). Single cell RNA-seq of tumor cells revealed that HPV33+ tumors exhibited a distinct HPV gene expression profile compared to HPV16+ tumors. HPV33+ tumors showed evidence of less infiltration of cytotoxic T-cells, exhausted T-cells and overall CD8+ T-cells. Interrogation of an independent HPV+ OPSCC cohort confirmed an overrepresentation of A*02:01 allele in HPV33 + OPSCC patients compared to HPV16+ OPSCC. Comparative epitope prediction analysis revealed that HPV33 lacks a key epitope found in HPV16 that is known to play a key role in immune recognition in A02:01+ patient samples.

Conclusions Targeted therapeutic trials have focused on HPV16+, rather than other high-risk HPV subtypes such as HPV33. Our data highlight reduced CD8+ T cell infiltrates as a potential correlate to poor outcomes in these patients. In addition, the observed A*02:01 ratios demonstrates potential immunoeediting in HPV16+ patients. Increasing prevalence underscores an unmet need and presents a unique opportunity to design novel precision-based immunotherapeutic approaches for HPV33+ malignancies and potentially improve clinical outcome in this growing patient subpopulation.

<http://dx.doi.org/10.1136/jitc-2022-SITC2022.1404>

Abstracts

1405 A CRISPR-CAS9 SCREEN IDENTIFIES NOVEL EPIGENETIC REGULATORS OF T CELL EXHAUSTION

¹Gayathri Bommakanti, ¹Elizabeth Jaensch, ¹Aparna Gorthi, ²Sin Lih Tan, ²Verena Brucklacher-Waldert, ¹Steven Criscione, ¹Deanna Mele*, ¹Astrazeneca PLC, Waltham, MA, USA; ²Horizon Discovery, Waterbeach, UK

Background Exhausted T cells (Tex) represent a distinct cell state, with a unique transcriptional and chromatin accessibility profile compared to their functional effector counterparts. Terminally exhausted T cells are epigenetically committed and non-responsive to checkpoint blockade therapies.^{1,2} With the aim to identify epigenetic factors which contribute to T cell exhaustion, we carried out a CRISPR screen in an in vitro T cell exhaustion system.

Methods In vitro exhausted T cells were generated by repeated stimulation of human T cells (isolated from healthy donor leukopaks) with anti-CD3 and anti-CD28 antibodies over a period of 10 days. In vitro Tex were characterized by flow cytometry, cytokine secretion, RNA Seq and ATAC Seq. An arrayed CRISPR screen was carried out by Horizon Discovery in this Tex model targeting 829 genes (focused on the human epigenome) for KO in T cells from 3 donors (3 biological replicates). IFN γ , IL-2, TNF α and cell titer glo (viability readout) were used to assess functional ability of KO cells after the final stimulation.

Results We first established an in vitro T cell exhaustion system and showed that it recapitulated phenotypic, functional, transcriptomic and epigenetic features of exhausted T cells (figure 1). An epigenome focused CRISPR screen was then performed in the Tex model to evaluate the role of different epigenetic factors in T cell exhaustion (figure 2). Hits were identified as genes which when knocked out were able to increase cytokine secretion across at least 2 donors. From the screen, we identified previously established^{3,4} and novel regulators of T cell exhaustion (figure 3). We validated the role of ikaros, a top hit from the screen, in T cell exhaustion using functional cytokine and T cell mediated tumor killing assays (figure 4).

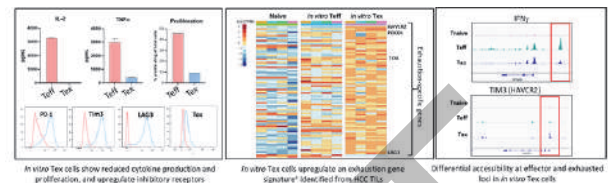
Conclusions A positive control (CBLB) used in the screen and other previously reported factors were hits in the screen. Several novel regulators of T cell exhaustion were also identified. Hits from the screen could potentially be targeted to reinvigorate exhausted T cells and expand responses to check point therapies. We identified a novel role for ikaros in controlling T cell exhaustion, perhaps supporting a possibility in treating solid tumors. The therapeutic target of IMiDs are the Ikaros family of transcription factors which are approved drugs for the treatment of multiple myeloma and other hematological malignancies.

REFERENCES

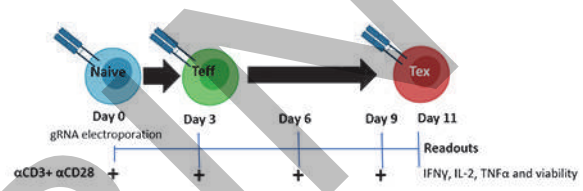
1. Pauken KE, Sammons MA, Odorizzi PM, Manne S, Godec J, Khan O, Drake AM, Chen Z, Sen DR, Kurachi M, Barnitz RA, Bartman C, Bengsch B, Huang AC, Schenkel JM, Vahedi G, Haining WN, Berger SL, Wherry EJ. Epigenetic stability of exhausted T cells limits durability of reinvigoration by PD-1 blockade. *Science* 2016 Dec 2; **354**(6316):1160–1165.
2. Miller BC, Sen DR, Al Abosy R, Bi K, Virkud YV, LaFleur MW, Yates KB, Lako A, Felt K, Naik GS, Manos M, Gjini E, Kuchroo JR, Ishizuka JJ, Collier JL, Griffin GK, Maleri S, Comstock DE, Weiss SA, Brown FD, Panda A, Zimmer MD, Manguso RT, Hodi FS, Rodig SJ, Sharpe AH, Haining WN. Subsets of exhausted CD8+ T cells differentially mediate tumor control and respond to checkpoint blockade. *Nat Immunol* 2019 Mar; **20**(3):326–336. doi: 10.1038/s41590-019-0312-6.
3. Prinzing B, Zebley CC, Petersen CT, Fan Y, Anido AA, Yi Z, Nguyen P, Houke H, Bell M, Haydar D, Brown C, Boi SK, Alli S, Crawford JC, Riberdy JM, Park JJ, Zhou S, Velasquez MP, DeRenzo C, Lazzarotto CR, Tsai SQ, Vogel P, Pruett-Miller SM, Langfitt DM, Gottschalk S, Youngblood B, Krenciute G. Deleting DNMT3A in

CAR T cells prevents exhaustion and enhances antitumor activity. *Sci Transl Med* 2021 Nov 17; **13**(620).

4. Zheng C, Zheng L, Yoo JK, Guo H, Zhang Y, Guo X, Kang B, Hu R, Huang JY, Zhang Q, Liu Z, Dong M, Hu X, Ouyang W, Peng J, Zhang Z. Landscape of Infiltrating T Cells in liver cancer revealed by single-cell sequencing. *Cell*. 2017 Jun 15; **169**(7):1342–1356.

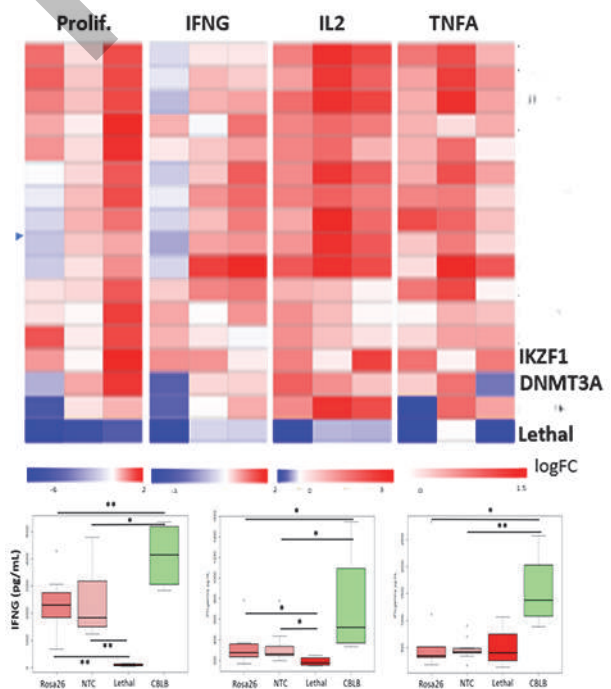


Abstract 1405 Figure 1 In vitro exhausted T cells show phenotypic and epigenetic hallmarks of exhaustion



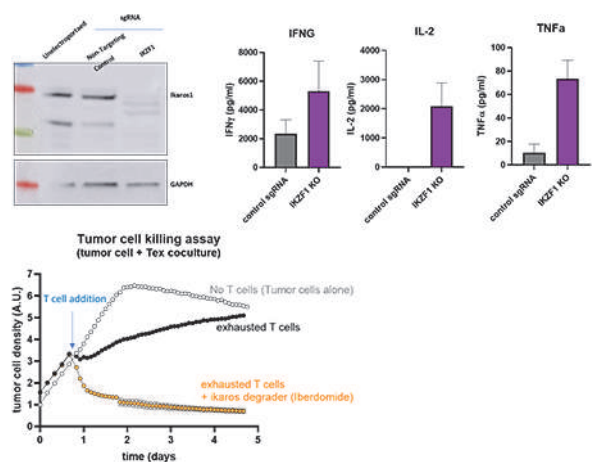
Abstract 1405 Figure 2 Overview of the screen

A) Top screen hits



B) A positive control, CBLB, rescued cytokine secretion by Tex cells

Abstract 1405 Figure 3 Top hits from the screen included known regulators of T cell exhaustion as well as novel regulators



Abstract 1405 Figure 4 Role of a top hit (IKZF1/Ikaros1) in T cell exhaustion validated using. A) rescue of cytokine secretion and B) tumor cell killing

<http://dx.doi.org/10.1136/jitc-2022-SITC2022.1405>

Abstracts

1406 ASSESSMENT OF ADDED ACTIVITY OF AN ANTITUMOR AGENT

Zhiping Sun, Eric Rubin, David Weinstock, Emmett Schmidt, Cong Chen*. *Merck and Co., Inc., Rahway, NJ, USA*

Background Growing clinical evidence shows that treatment effect of most approved combination therapies can be largely explained by the independent drug action model (IDA), i.e., the benefit a patient receives from a combination therapy is driven by the drug component his or her tumor is most sensitive to. IDA has been successfully used to predict objective response rate (ORR), progression-free-survival (PFS), and duration of response (DoR) for many combination therapies.¹⁻⁵ We built upon the model to develop a simple index to measure the added activity of a new drug when combined with any other drug to shed light on oncology drug development.

Methods When IDA is applied to ORR (aka Bliss model⁶), the ORR of the combination therapy is expected to be the sum of ORRs from Drug 1 and Drug 2 minus the product of the two (figure 1). When IDA model is applied to DoR, those who potentially respond to both drugs will have the best duration to a drug component. ORR or DoR alone is not adequate to capture the overall antitumor activity but jointly may.⁷⁻⁸ Integrating results from the two, the added activity from Drug 2 to combination is:

$$\text{ORRxDoR of Drug2} \times (1 - \text{ORRxDoR of Drug1}) / \text{Sum of DoRs of Drug1 and Drug2}$$

Clearly, any new drug with single-agent ORR too low or DoR too short is unlikely to add much activity to the combination.

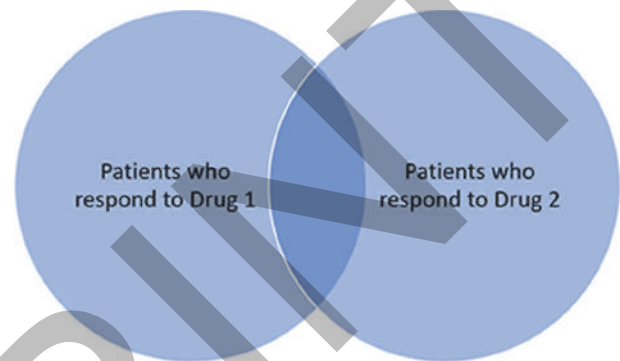
Results Further inspection of the index suggests that DoR of Drug 2 is more impactful than ORR. It also reveals that it is more impacted by ORR than by DoR of Drug 1, implying that there is more room for improvement over standard-of-care with lower ORR (but longer DoR) than with shorter DoR (but higher ORR). When Drug 2 has a superior DoR than Drug 1, the benefit of Drug 2 is largely retained after combination, which explains why some immune checkpoint inhibitors are successful after combining with chemotherapies. Conversely, when Drug 1 has a superior DoR than Drug 2, the benefit of Drug 2 is largely derived from those who do not respond to Drug 1, predicting the challenges in developing new drugs with short DoR for combining with established immune checkpoint inhibitors.

Conclusions We have derived a simple index to help researchers make early Go-No Go decisions on combination therapies. It is insightful, and, assisted with proper analysis method [9-10], it can potentially play a critical role in executing FDA's forthcoming Project FrontRunner.

REFERENCES

1. Palmer AC, Sorger PK. Combination cancer therapy can confer benefit via patient-to-patient variability without drug additivity or synergy. *Cell* 2017; **171**:1678–91 e13.
2. Plana D, Palmer AC, Sorger PK. Independent drug action in combination therapy: implications for precision oncology. *Cancer Discov* 2022; **12**:606–24.
3. Schmidt E, Chisamore MJ, Chaney MF, et al. Assessment of Clinical Citivity of PD-1 checkpoint inhibitor combination therapies reported in clinical trials. *JAMA Network Open* 2020; **3**(2): e1920833.
4. Chen C, Liu F, Ren Y, Sun Z, Shentu Y, Schmidt EV. Independent drug action and its statistical implications for development of combination therapies. *Contemporary Clinical Trials* 2020; 106126.
5. Sun LZ, Wu C, Li X, Chen C, Schmidt EV. Independent Action Models and Prediction of Combination Treatment Effects for Response rate, Duration of Response and Tumor Size Change in Oncology Drug Development. *Contemporary Clinical Trials* 2021; 106434.

6. Bliss CI. The toxicity of poisons applied jointly. *Ann. Appl. Biol* 1939; **26**:585–615.
7. McCaw ZR, Tian L, Wei L. Appropriate analysis of duration of response data in cancer trials. *JAMA Oncol* 2020; **6**(12):1978. doi:10.1001/jamaoncol.2020.4657.
8. Chen H, Wang M, Wu C, Zhou H, Chen C, Diede S. Comparison of duration of response vs conventional response rates and progression-free survival as efficacy end points in simulated immuno-oncology clinical trials. *JAMA Network Open* 2021. doi:10.1001/jamanetworkopen.2021.8175.
9. Huang B, Tian L, Talukder E, Rothenberg M, Kim DH, Wei LJ. Evaluating treatment effect based on duration of response for a comparative oncology study. *JAMA Oncol*. 2018; **4**(6):874–876. doi:10.1001/jamaoncol.2018.0275.
10. Huang B, Tian L, McCaw ZR, et al. Analysis of response data for assessing treatment effects in comparative clinical studies. *Ann Intern Med* 2020; **173**(5):368–374. doi:10.7326/M20-0104.



Abstract 1406 Figure 1 ORR based on the independent drug action model

The overall area represents the patients who may respond to the combination therapy. Patients potentially responding to both drug components (overlapping area) will have longer DoR than patients only responding to one.

<http://dx.doi.org/10.1136/jitc-2022-SITC2022.1406>

1407

UNDERSTANDING THE DEFINITION OF HYPERPROGRESSIVE DISEASE (HPD) AND ITS INCIDENCE – A NEW PATH FORWARD

¹Trie Ami Djunadi, ¹Youjin Oh, ¹Liam Il-Young Chung, ²Timothy Hong, ³Soowon Lee, ¹Zunairah Shah*, ¹Joo Hee Park, ¹Sung Mi Yoon, ¹Young Kwang Chae. ¹Feinberg School of Medicine, Northwestern University, Chicago, IL, USA; ²Northwestern University, Evanston, IL, USA; ³Baylor University, Waco, TX, USA

Background Hyperprogressive disease (HPD) is a phenomenon where tumors grow exponentially following immunotherapy. Multiple definitions have been proposed, and the incidence of HPD varies from 5.9% to 43.1% depending on the definition.¹ As HPD is associated with worse patient outcomes, it is important to have a clear definition of HPD to identify and prevent such cases.^{2,3} There is much discussion about how to best define HPD as RECIST criteria only considers the target lesions.⁴ iRECIST and irRECIST have been newly proposed to incorporate new lesions. This study proposes a new, modified definition for HPD using RECIST 1.1 and taking the sum of new lesions into consideration.

Methods This study retrospectively analyzed 128 lung cancer patients' data (N of patients = 128) and 144 total number of regimens (N of regimens = 144) at a large metropolitan academic medical center. This study compares the incidence of hyperprogression using different definitions including Champiat, Saada-Bouزيد, and Ferrara et al.⁵⁻⁷ As a modification to these definitions, the new lesions were included into the sum of lesions. The difference of incidence between original and modified definitions was evaluated with Chi-squared test.

Results The incidence rate of hyperprogression ranged from 5% to 15%, depending on the original definitions and modified definitions. Among the 144 treatment regimens, hyperprogression was detected in 5% (N=7), 10% (N=14), and 0% (N=0) using the original Champiat, Saada-Bouزيد, and Ferrara et al. definitions respectively. The incidence of hyperprogression increased when new lesions were included in the definition. The incidence rate with modified Champiat, Saada-Bouزيد and Ferrara et al. definitions were 11% (N=16), 15% (N=21) and 6% (N=9) respectively (table 1). Incorporating new lesions enabled the detection of more HPD cases, and the change in the sum of lesions are depicted in figure 1. The difference in incidence between original and modified definitions was statistically significant only for the Champiat et al. (X² = 3.0, p=0.05).

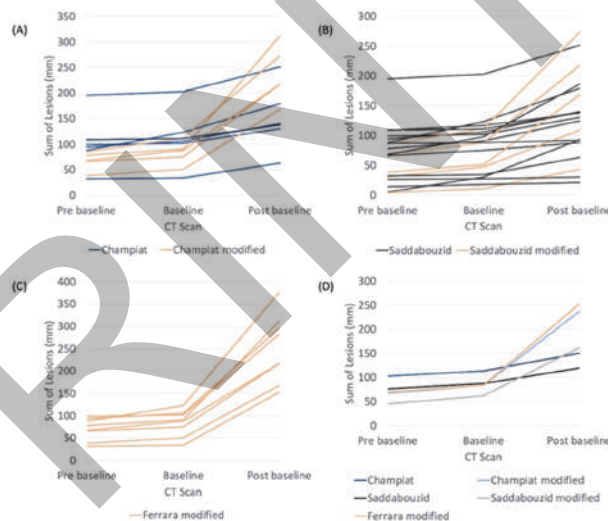
Conclusions Incorporation of new lesions in the definition of hyperprogression resulted in an increase in HPD incidence for all three definitions. However, statistically significant difference was observed only for the Champiat et al. definition. There are limitations of utilizing RECIST 1.1 in the identification of HPD as it does not take new lesions into consideration. This study highlights the importance of including new lesions when defining HPD to accurately capture HPD.

REFERENCES

1. Park HJ, Kim KW, Won SE, Yoon S, Chae YK, Tirumani SH, et al. Definition, incidence, and challenges for assessment of hyperprogressive disease during cancer treatment with immune checkpoint inhibitors: a systematic review and meta-analysis. *JAMA Netw Open* 2021 Mar 1;**4**(3):e211136.
2. Frelaut M, Le Tourneau C, Borcoman E. Hyperprogression under Immunotherapy. *Int J Mol Sci*. 2019 May 30;**20**(11):2674.
3. Sabio E, Chan TA. The good, the bad, and the ugly: hyperprogression in cancer patients following immune checkpoint therapy. *Genome Med*. 2019 Jul 24;**11**(1):43.
4. Champiat S, Besse B, Marabelle A. Hyperprogression during immunotherapy: do we really want to know? *Ann Oncol*. 2019 Jul 1;**30**(7):1028–31.

5. Champiat S, Dercle L, Ammari S, Massard C, Hollebecque A, Postel-Vinay S, et al. Hyperprogressive Disease Is a New Pattern of Progression in Cancer Patients Treated by Anti-PD-1/PD-L1. *Clin Cancer Res Off J Am Assoc Cancer Res*. 2017 Apr 15;**23**(8):1920–8.
6. Saada-Bouزيد E, Defaucheux C, Karabajakian A, Coloma VP, Servois V, Paoletti X, et al. Hyperprogression during anti-PD-1/PD-L1 therapy in patients with recurrent and/or metastatic head and neck squamous cell carcinoma. *Ann Oncol Off J Eur Soc Med Oncol*. 2017 Jul 1;**28**(7):1605–11.
7. Ferrara R, Mezquita L, Texier M, Lahmar J, Audigier-Valette C, Tessonier L, et al. Hyperprogressive disease in patients with advanced non-small cell lung cancer treated With PD-1/PD-L1 inhibitors or with single-agent chemotherapy. *JAMA Oncol* 2018 Nov;**4**(11):1543–52.

Ethics Approval The study was approved by Northwestern University's Institutional Review Board, study number STU00207117.



Abstract 1407 Figure 1 The changes of sum of lesions depending on patients with hyperprogression according to different definitions of hyperprogression and modification.

Abstract 1407 Table 1 A summary of the incidence of hyperprogression according to main different definitions of hyperprogression and modified definitions

Component	Source		
	Champiat et al ^[5] , November 2016	Saada-Bouزيد et al ^[6] , April 2017	Ferrara et al ^[7] , November 2018
Definitions*	RECIST progression and TGR-exp/ TGR-ref >2	TGK-exp/ TGK-ref >2	RECIST progression and TGR-exp - TGR-ref >50
Modified Definition	The modification was made to include new lesions on CT scans into the sum of lesions.		
Single	n=128		
RECIST 1.1	6 (5%)	11 (9%)	0 (0%)
Modification	15 (12%)	19 (15%)	9 (7%)
Multiple	n=144		
RECIST 1.1	7 (5%)	14 (10%)	0 (0%)
Modification	16 (11%)	21 (15%)	9 (6%)

*Indexes are calculated using TGR and TGK values before (ref) and during (exp) therapy.

<http://dx.doi.org/10.1136/jitc-2022-SITC2022.1407>

Abstracts

1408

RISK FACTORS FOR HYPERPROGRESSIVE DISEASE IN LUNG CANCER PATIENTS USING TWO DIFFERENT DEFINITIONS

¹Trie Ami Djunadi, ¹Youjin Oh, ¹Liam Il-Young Chung, ²Timothy Hong, ³Soowon Lee, ¹Zunairah Shah*, ¹Joo Hee Park, ¹Sung Mi Yoon, ¹Young Kwang Chae. ¹Feinberg School of Medicine, Northwestern University, Chicago, IL, USA; ²Northwestern University, Evanston, IL, USA; ³Baylor University, WACO, TX, USA

Background Hyperprogressive disease (HPD) is the accelerated growth of tumor size after treatment with immunotherapy. As HPD is associated with poorer outcomes, it is important to understand the risk factors (RF) to prevent HPD.^{1,2} Some RF for HPD include age, primary lesion size, and presence of metastases in the contralateral lung, pleura, liver, and bone.³ Others identified Eastern cooperative oncology group scale of performance status (ECOG PS) >1, having more than two metastasis sites, and liver metastasis as significant RF.⁴ With existing findings showing varying results, this study aims to complement and identify potential RF for HPD in lung cancer patients.

Methods This study retrospectively analyzed 128 patients' data (N of patients = 128) and 144 total number of regimens (N of regimens = 144) at a large metropolitan academic medical center. Multiple variables were analyzed using chi-squared tests and t-tests to identify RF using two definitions of HPD by Champiat and Saada-Bouzid et al.^{5,6} The variables that were analyzed are treatment line, regimen, immunotherapy type, histology, PD-L1 status, tumor mutational burden (TMB), diagnosis age, sex, smoking status, ECOG PS, neutrophil-to-lymphocyte ratio (NLR), TNM staging, platelets, number of metastases, and the presence of metastases in the brain, bone, and liver.

Results Among the 144 cases, immunotherapy was used as the first line in 27% (N=34), second line in 51% (N=65), and third or more line in 23% (N=29). Immunotherapy was used as a single agent in 77% of cases (N=111) and as a combination with other chemotherapy, targeted therapy in 23% of cases (N=33).

Using the Champiat et al. definition of HPD, immunotherapy only regimen, non-adenocarcinoma histology of tumor (histology was classified as adenocarcinoma, squamous cell carcinoma, small cell lung cancer and other), and bone metastasis were associated with HPD (table 1). Using the Saada-Bouzid et al. definition, histology and immunotherapy only regimen was shown to be marginally associated with HPD. However, no associations were identified between HPD and other clinicopathological variables, including, but not limited to, age, the number of sites of metastatic disease, genomic alterations, and peripheral blood biomarkers, including the NLR.

Conclusions Bone metastasis, non-adenocarcinoma histology, and immunotherapy only regimens were associated with HPD. Given the small sample size, further investigation is warranted to elucidate the correlation with hyperprogression and other clinicopathologic and genomic features.

REFERENCES

1. Frelaut M, Le Tourneau C, Borcoman E. Hyperprogression under Immunotherapy. *Int J Mol Sci.* 2019 May 30;20(11):2674.
2. Sabio E, Chan TA. The good, the bad, and the ugly: hyperprogression in cancer patients following immune checkpoint therapy. *Genome Medicine* 2019 Jul 24;11(1):43.
3. Choi YJ, Kim T, Kim EY, Lee SH, Kwon DS, Chang YS. Prediction model for hyperprogressive disease in non-small cell lung cancer treated with immune checkpoint inhibitors. *Thorac Cancer* 2020 Oct;11(10):2793–803.

4. Chen Y, Hu J, Bu F, Zhang H, Fei K, Zhang P. Clinical characteristics of hyperprogressive disease in NSCLC after treatment with immune checkpoint inhibitor: a systematic review and meta-analysis. *BMC Cancer.* 2020 Jul 29;20(1):707.
5. Champiat S, Derle L, Ammari S, Massard C, Hollebecq A, Postel-Vinay S, et al. Hyperprogressive disease is a new pattern of progression in cancer patients treated by anti-PD-1/PD-L1. *Clin Cancer Res.* 2017 Apr 15;23(8):1920–8.
6. Refae S, Gal J, Brest P, Giaccherio D, Borchelliini D, Ebran N, et al. Hyperprogression under Immune Checkpoint Inhibitor: a potential role for germinal immunogenetics. *Sci Rep.* 2020 Feb 27;10:3565.

Ethics Approval The study was approved by Northwestern University's Institutional Review Board, study number STU00207117.

Abstract 1408 Table 1 A summary of association between clinical, pathologic, tumor mutational burden features, and hyperprogression defined by two main definitions

		Champiat et al.		P-value	Saada-bouzid et al.		P-value
		Non-HPD (N=137)	HPD (N=7)		Non-HPD (N=130)	HPD (N=14)	
Treatment Line	1st	34 (24.8%)	1 (14.3%)	0.648	31 (23.8%)	4 (28.6%)	0.303
	2nd	88 (64.2%)	3 (42.9%)		86 (69.2%)	4 (28.6%)	
	3rd	38 (27.7%)	3 (42.9%)		35 (28.2%)	6 (42.9%)	
Regimen	IO only	105 (76.6%)	6 (85.7%)	0.015	98 (75.4%)	13 (92.9%)	0.057
	IO + chemo	26 (19.0%)	0 (0.0%)		26 (20.0%)	0 (0.0%)	
	IO + targeted	5 (3.6%)	0 (0.0%)		5 (3.8%)	0 (0.0%)	
Immunotherapy	other	1 (0.7%)	1 (14.3%)	0.826	1 (0.8%)	1 (7.1%)	0.987
	PD-1*	43 (31.4%)	3 (42.9%)		41 (31.5%)	5 (35.7%)	
	other	96 (68.6%)	4 (57.1%)		89 (68.5%)	9 (64.3%)	
Histology	Adeno	93 (67.9%)	3 (42.9%)	0.002	90 (69.2%)	6 (42.9%)	0.058
	Sq	16 (11.7%)	0 (0.0%)		14 (10.8%)	2 (14.3%)	
	SCLC	3 (2.2%)	2 (28.6%)		3 (2.3%)	2 (14.3%)	
PD-L1 Status (%)	other	25 (18.2%)	2 (28.6%)	0.698	23 (17.7%)	4 (28.6%)	0.411
	≥50	21 (25.9%)	0 (0.0%)		20 (16.7%)	1 (7.1%)	
	1-49	33 (40.7%)	1 (50.0%)		26 (34.7%)	2 (25.0%)	
Tumor Mutational Burden (mut/Mb)	0-1	27 (19.3%)	1 (50.0%)	1.000	29 (38.7%)	5 (62.5%)	0.290
	≤4	4 (15.4%)	0 (0.0%)		3 (13.0%)	2 (50.0%)	
	>4	22 (84.6%)	1 (100.0%)		20 (87.0%)	2 (50.0%)	
Diagnosis Age	Years	67.5 ± 10.9	63.9 ± 6.6	0.387	67.5 ± 10.8	66.4 ± 9.6	0.530
	Female	78 (54.7%)	8 (57.1%)		71 (54.6%)	8 (57.1%)	
	Male	62 (45.3%)	3 (42.9%)		59 (45.4%)	6 (42.9%)	
Smoking Status	Current	8 (5.8%)	0 (0.0%)	0.781	8 (6.2%)	0 (0.0%)	0.595
	Never	23 (16.8%)	1 (14.3%)		22 (16.9%)	2 (14.3%)	
	Former	106 (77.4%)	6 (85.7%)		100 (76.9%)	12 (85.7%)	
ECOG Status	1-2	125 (91.2%)	7 (100.0%)	0.907	118 (90.8%)	14 (100.0%)	0.497
	3-4	12 (8.8%)	0 (0.0%)		12 (9.2%)	0 (0.0%)	
	1	3 (2.2%)	0 (0.0%)		3 (2.3%)	0 (0.0%)	
TNM Staging	II	2 (1.5%)	0 (0.0%)	0.620	1 (0.8%)	1 (7.1%)	0.256
	III	23 (16.8%)	0 (0.0%)		21 (16.2%)	2 (14.3%)	
	IV	109 (79.6%)	7 (100.0%)		105 (80.8%)	11 (78.6%)	
Neutrophil-to-Lymphocyte Ratio	<5	67 (48.9%)	4 (57.1%)	0.970	63 (48.5%)	8 (57.1%)	0.737
	≥5	29 (21.1%)	3 (42.9%)		27 (20.7%)	6 (42.9%)	
	Platelets (x10 ⁹ /L)	≤450	126 (92.0%)		5 (71.4%)	120 (92.3%)	
Number of Metastatic Lesions	>450	11 (8.0%)	2 (28.6%)	0.240	10 (7.7%)	3 (21.4%)	0.225
	<3	107 (78.1%)	6 (85.7%)		102 (78.5%)	11 (78.6%)	
	≥3	30 (21.9%)	1 (14.3%)		28 (21.5%)	3 (21.4%)	
Brain Metastases	(-)	94 (68.6%)	7 (100.0%)	0.995	88 (67.7%)	13 (92.9%)	1.000
	(+)	43 (31.4%)	0 (0.0%)		42 (32.3%)	1 (7.1%)	
	(-)	94 (68.6%)	2 (28.6%)		90 (69.2%)	6 (42.9%)	
Bone Metastases	(+)	43 (31.4%)	5 (71.4%)	0.075	40 (30.8%)	8 (57.1%)	0.099
	(-)	107 (78.1%)	4 (57.1%)		102 (78.5%)	9 (64.3%)	
	(+)	39 (29.9%)	3 (42.9%)		38 (29.2%)	5 (35.7%)	
Liver Metastases	(-)	107 (78.1%)	4 (57.1%)	0.409	102 (78.5%)	9 (64.3%)	0.387
	(+)	39 (29.9%)	3 (42.9%)		38 (29.2%)	5 (35.7%)	

(IO; Immunotherapy, PD-1*; PD-1 inhibitors, Adeno; Adenocarcinoma, Sq; squamous, SCLC; small cell lung cancer.)

<http://dx.doi.org/10.1136/jitc-2022-SITC2022.1408>

1409 REGULATION AND ROLES OF THE POLYAMINE-HYPUSINE AXIS IN CD8⁺ T-CELL FATE AND FUNCTIONS

Aya Elmarsafawi*, John Cleveland, Rebecca Hesterberg. *Moffitt Cancer Center, Tampa, FL, USA*

Background CD8⁺ T cells play central roles in tumor immune surveillance and are major effectors in adoptive cell therapy. Thus, strategies that enhance their functions are an urgent clinical need. Metabolic reprogramming determines T cell fate and function.¹ The roles of amino acid catabolism in controlling CD8⁺ T cell fate and function are less well understood.^{2,3} Glutamine is essential for nucleotide biosynthesis and as an anaplerotic fuel source for the tricarboxylic acid (TCA) cycle.

Methods Isotope tracing experiments with ¹³C glutamine or ¹³C arginine

Pharmacologic inhibition of ODC and DHPS

Results Pharmacologic inhibition of Odc using difluoromethylornithine (DFMO), or inhibition of hypusination using the pharmacologic inhibitor of Dhps, GC7, augments cytokine production in activated CD8⁺ T cells, including IFN- γ and TNF- α . Indeed, inhibition of Odc or Dhps augments other TRM phenotypes, including increases in CD69^{high};S1PR1^{low}; CD62L^{low} cells that define the tissue resident memory (TRM) CD8⁺ T cells that play key roles in tissue and anti-tumor immunity anti-tumor reactivity. In addition, ACT of DFMO treated CD8⁺ T cells augments their survival in vivo and augments the generation of CD69⁺CD103⁺CD69⁺CXCR6⁺ and Ly6C⁺ TRMs in the bone marrow. Finally, DFMO or GC7 treatment enhances IFN- γ and TNF- α production in human CD8 T cells.

Conclusions We conclude that polyamine-hypusine axis is a metabolic check point in CD8⁺ TRM generation and are an actionable target to improve the anti-tumor immunity of T-cell based immunotherapies.

Acknowledgements Metabolomics and Flow cytometry core at Moffitt Cancer Center

REFERENCES

1. Sugiura A, and JC Rathmell. Metabolic Barriers to T Cell Function in Tumors. *J Immunol*, 2018;**200**(2): 400–407.
2. Geiger R, et al. L-Arginine Modulates T cell metabolism and enhances survival and anti-tumor activity. *Cell* 2016. 167(3): 829–842.e13.
3. Hesterberg RS, JL Cleveland, and PK Epling-Burnette. Role of polyamines in immune cell functions. *Med Sci (Basel)*, 2018;**6**(1).

<http://dx.doi.org/10.1136/jitc-2022-SITC2022.1409>

1410

ESSENTIAL ROLE OF INNATE EFFECTOR IMMUNE RESPONSES FOR THE THERAPEUTIC EFFICACY OF PEPTIDE VACCINE TO TREAT HPV+ TUMORS

<http://dx.doi.org/10.1136/jitc-2022-SITC2022.1410>

¹Venkatesh Hegde, ¹Madison O'Hara, ¹Ananta Yanamandra, ²Gloria Sierra, ¹Jagannadha Sastry*. ¹MD Anderson Cancer Center, Houston, TX, USA; ²CARsgene Therapeutics Corporation, Bellaire, TX, USA

Background High-risk type human papillomaviruses (HPV) are associated with genital and oral cancers, and the incidence of head and neck squamous cell cancers is fast increasing in the USA and worldwide. Survival rates for patients with locally advanced disease are poor after standard of care chemoradiation treatment, while immune therapeutic strategies including vaccines that target the virus-encoded E6 and E7 oncoproteins have mostly been ineffective in inducing regression of established HPV+ tumors despite promoting antigen-specific adaptive immunity. Therefore, vaccination strategies to significantly enhance antitumor immune responses with multiple effector functions to overcome the prevailing immunosuppressive tumor microenvironment are necessary to achieve curative efficacy against established HPV+ tumors. We present here pre-clinical evidence for the essential role of innate immune effector responses induced by a therapeutic HPV peptide vaccine incorporating two clinically relevant adjuvants QS-21 and CpG-ODN to induce sustained, complete regression of oral HPV tumors.

Methods We used mEER and TC-1, two mouse tumor cell lines expressing HPV-16 E6 and E7 along with h-Ras for tumor induction in the tongue and vaginal mucosa in syngeneic C57BL/6J mice. All animal studies were pre-approved and carried out in accordance with the University of Texas MD Anderson Cancer Center Institutional Animal Care and Use Committee (IACUC) guidelines. At days 5 and 11 following tumor implantation vaccine was administered via intranasal route and tumor growth monitored by MRI (for oral mEER) and IVIS (for vaginal TC-1). Around 15 or 16d post-tumor challenge, mice were euthanized and TIL analyses was performed to determine correlates of protection.

Results Vaccination resulted in robust induction of antigen-specific anti-tumor CD8 effector T cell responses along with expanded repertoire of innate cytotoxic effector responses that included unique natural killer cell subsets. The therapeutic efficacy of the vaccine was dependent on CD8 T cells and in addition required NK cells subsets as shown by in vivo antibody depletion and adoptive transfer to HPV peptide vaccine non-responsive oral tumor bearing mice. The combined poly-functional populations of cytotoxic CD8 and NK cell subsets producing IFN γ and granzyme B significantly outnumbered suppressive immune cell repertoire. Notably, the vaccine was effective in treating HPV tumors at both the vaginal and oral mucosal tissues.

Conclusions Overall, these data provide strong support for therapeutic strategies promoting innate immune responses along with antigen-specific immunity, as evidenced by the therapeutic HPV peptide vaccine formulation in the present investigation, for potential clinical assessment in patients with HPV + cancers.

Acknowledgements The research was supported by Cancer Prevention and Research Institute of Texas (CPRIT RP180472) and HPV Moonshot grant awards to KJS. The MD Anderson Cancer Center Advanced Cytometry and Sorting Core Facility and Small Animal Imaging facility are both supported under NIH/NCI award number P30CA016672

1411 BREAST CANCER IMMUNOPEPTIDOMES CONTAIN NUMEROUS SHARED TUMOR ANTIGENS

¹Eralda Kina*, ¹Jean-Philippe Laverdure, ¹Chantal Durette, ¹Joël Lanoix, ¹Mathieu Courcelles, ¹Qingchuan Zhao, ¹Anca Apavaloaei, ¹Jean-David Larouche, ¹Marie-Pierre Hardy, ¹Krystal Vincent, ¹Patrick Gendron, ¹Leslie Hesnard, ¹Maria Virginia Ruiz Cuevas, ²Gregory Ehx, ¹Pierre Thibault, ¹Claude Perreault. ¹University of Montreal, Montreal, Canada; ²University of Liege, Liege, Belgium

Background Hormone-receptor-positive breast cancer (HR+) is an immunologically cold cancer that has not benefited from advances in immunotherapy. In contrast, triple-negative breast cancer (TNBC) displays high levels of leukocytic infiltration and responds to immune checkpoint inhibitors. CD8 T cells, the main effectors of anti-cancer responses, recognize MHC I-associated peptides (MAPs). Our work aimed to characterize the repertoire of MAPs presented by HR+ and TNBC tumors.

Methods Using a proteogenomic approach relying on mass spectrometry, we identified 57 094 unique MAPs in 26 primary breast cancer samples (14 HR+, 12 TNBC).

Results MAP source genes showed a high overlap between both subtypes (>70%). We identified 25 tumor-specific antigens (TSAs) derived from various genomic regions, of which 24 were unmutated. TSAs were mainly identified in TNBC samples (70%) and were more highly shared among TCGA TNBC than HR+ samples. In the TNBC TCGA cohort, the predicted number of TSAs positively correlated with leukocytic infiltration ($p < 0.05$) and overall survival ($p < 0.05$, figure 1), suggesting that these TSAs are immunogenic in vivo. We also identified 49 overexpressed tumor-associated antigens (TAAs), some of which derived from cancer-associated fibroblasts. FEST assays confirmed the in vitro immunogenicity of our TSAs and TAAs.

Conclusions Well-defined antigens were identified in both subtypes of breast cancer and represent attractive targets for cancer immunotherapy. The higher prevalence and immunogenicity of TSAs in TNBC tumors provide a molecular rationale for the responsiveness of TNBC to immune checkpoint inhibitors.

Ethics Approval Approved by the comity for clinical research of University of Montreal (CERC-20-012-D)

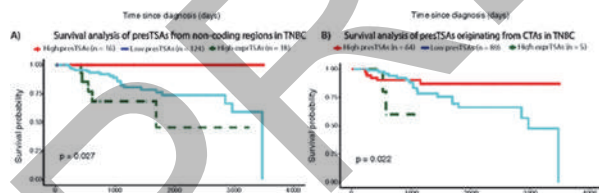


Figure 1. Aberrantly expressed TSAs predicted presentation confers a survival advantage to patients with TNBC tumors. For each individual tumor, TSAs were considered presented (preTSAs) if their coding sequence and an adequate HLA allele for presentation were expressed. High groups (red) correspond to the first quartile of patients with the highest number of preTSAs. Low groups (black) correspond to the 2nd to 4th quartile. **A-B)** High levels of pre-TSAs originating from non-coding regions and CTAs confer a survival advantage to patients with TNBC tumors. To distinguish the impact of expression as opposed to presentation of aeTSAs, an additional curve was computed with expressed antigens who lacked an appropriate HLA allele for presentation (exprTSAs). High expression of aeTSAs alone, without potential presentation, was insufficient to reiterate a survival benefit.

Abstract 1411 Figure 1 Aberrantly expressed TSAs predicted presentation confers a survival advantage to patients with TNBC tumors

<http://dx.doi.org/10.1136/jitc-2022-SITC2022.1411>

Abstracts

1413 THE OVERALL SURVIVAL (OS) AND PROGRESSION-FREE SURVIVAL (PFS) OF HYPERPROGRESSIVE DISEASE (HPD) IN LUNG CANCER PATIENTS

¹Youjin Oh, ¹Trie Ami Djunadi, ¹Liam Il-Young Chung, ²Soowon Lee, ³Timothy Hong, ¹Zunairah Shah*, ¹Joo Hee Park, ¹Sung Mi Yoon, ¹Richard Duan, ¹Young Kwang Chae. ¹Feinberg School of Medicine, Northwestern University, Chicago, IL, USA; ²Baylor University, WACO, TX, USA; ³Northwestern University, Evanston, IL, USA

Background Hyperprogressive disease (HPD) is the acceleration of tumor growth observed in patients treated with immunotherapy. HPD was seen to be negatively associated with the overall survival (OS) and progression-free survival (PFS) when compared to patients without HPD.¹⁻⁵ Various definitions of HPD have been used to evaluate the relationship between HPD and OS/PFS.^{2,6-11} This study uses two HPD definitions from Champiat and Saada-Bouzid et al. to evaluate the association between HPD and OS/PFS in lung cancer patients.^{8,11}

Methods This study retrospectively analyzed 128 patients (N=128) and 144 regimens (N=144) at a large metropolitan academic medical center. The overall survival (OS) and progression free survival (PFS) were analyzed using cox regression to produce a hazard ratio. Clinicopathologic variables were controlled for.

Results Among the 128 patients that were analyzed in this study, immunotherapy was used as the first line in 27% (N=34) and second line in 51% (N=65) of them. Immunotherapy was also used as a single agent in 77% (N=111) of all 144 regimens. In a survival analysis, the presence of hyperprogression was strongly negatively associated with PFS and OS in both definitions (figure 1.) Using the Champiat et al. definition, patients with HPD were about 20 times more likely to show future progression [Hazard ratio (HR) 22.30; 95% confidence interval (CI) 7.84-63.42, p<0.001]. Also, OS was greater in patients without hyperprogression [HR 2.69; 95% CI 1.11-6.5, p=0.029, table 1]. This trend was also seen with the Saada-Bouzid et al. definition, revealing a higher risk of future progression [HR 4.46; 95% CI 1.78-11.18, p<0.001] and death [HR 3.17, 95% CI 1.61-6.2, p<0.001] among patients with HPD (table 2). According to the Champiat et al. definition, patients who were female or had Eastern cooperative oncology group scale of performance status (ECOG PS) 3-4 were more likely to experience future disease progression. The Saada-Bouzid et al. definition showed that patients who were female, ECOG PS 3-4, or had immunotherapy as third line treatment or beyond resulted in a higher chance of future disease progression.

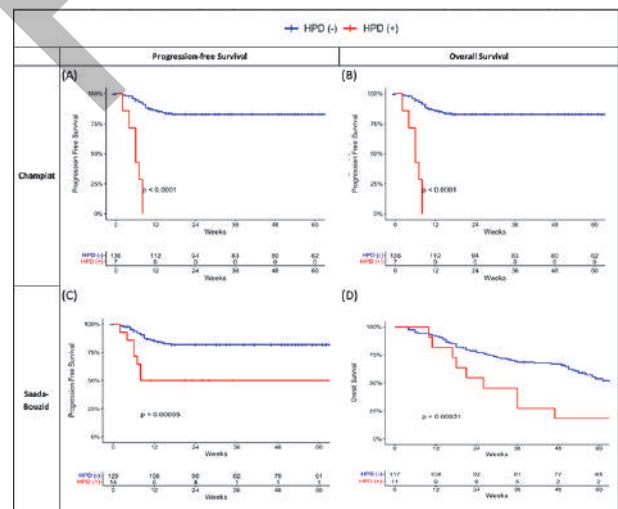
Conclusions Both definitions of HPD were associated with worse OS and PFS in lung cancer patients even after adjusting for confounding variables. Given its clinical importance associated with the poorer prognosis of patients, further attention and efforts are needed to identify hyperprogression and prevent its detrimental effects. Further studies with larger cohorts are warranted.

REFERENCES

- Popat V, Gerber DE. Hyperprogressive disease: a distinct effect of immunotherapy? *J Thorac Dis* 2019 Mar;**11**(Suppl 3):S262-5.
- Ferrara R, Mezquita L, Texier M, Lahmar J, Audigier-Valette C, Tessonier L, et al. Hyperprogressive disease in patients with advanced non-small cell lung cancer treated With PD-1/PD-L1 inhibitors or with single-agent chemotherapy. *JAMA Oncol*. 2018 Nov;**4**(11):1543-52.
- Tachihara M, Nishimura Y. Who will suffer from hyperprogressive disease in patients with advanced non-small cell lung cancer treated with PD-1/PD-L1 inhibitors. *J Thorac Dis*. 2019 May;**11**(Suppl 9):S1289-91.

- Arasanz H, Zuazo M, Bocanegra A, Chocarro L, Blanco E, Martínez M, et al. Hyperprogressive disease: main features and key controversies. *Int J Mol Sci*. 2021 Apr **3**;**22**(7):3736.
- Park JH, Chun SH, Lee YG, Chang H, Lee KW, Kim HR, et al. Hyperprogressive disease and its clinical impact in patients with recurrent and/or metastatic head and neck squamous cell carcinoma treated with immune-checkpoint inhibitors: Korean cancer study group HN 18-12. *J Cancer Res Clin Oncol*. 2020 Dec **1**;**146**(12):3359-69.
- Kato S, Goodman A, Walavalkar V, Barkauskas DA, Sharabi A, Kurzrock R. Hyper-progressors after Immunotherapy: Analysis of Genomic Alterations Associated with Accelerated Growth Rate. *Clin Cancer Res*. 2017 Aug **1**;**23**(15):4242-50.
- Singavi AK, Menon S, Kilari D, Alqwasmii A, Ritch PS, Thomas JP, et al. 1140PD - Predictive biomarkers for hyper-progression (HP) in response to immune checkpoint inhibitors (ICI) - analysis of somatic alterations (SAs). *Annals of Oncology*. 2017 Sep **1**;**28**:v405.
- Saàda-Bouzid E, Defaucheux C, Karabajikian A, Coloma VP, Servois V, Paoletti X, et al. Hyperprogression during anti-PD-1/PD-L1 therapy in patients with recurrent and/or metastatic head and neck squamous cell carcinoma. *Ann Oncol*. 2017 Jul **1**;**28**(7):1605-11.
- Matos I, Martin-Liberal J, García-Ruiz A, Hierro C, Ochoa de Olza M, Viaplana C, et al. Capturing hyperprogressive disease with immune-checkpoint inhibitors using RECIST 1.1 Criteria. *Clin Cancer Res*. 2020 Apr **15**;**26**(8):1846-55.
- Kas B, Talbot H, Ferrara R, Richard C, Lamarque JP, Pitre-Champagnat S, et al. Clarification of Definitions of Hyperprogressive Disease During Immunotherapy for Non-Small Cell Lung Cancer. *JAMA Oncol* 2020 Jul;**6**(7):1039-46.
- Champiat S, Derclé L, Ammari S, Massard C, Hollebecque A, Postel-Vinay S, et al. Hyperprogressive Disease Is a New Pattern of Progression in Cancer Patients Treated by Anti-PD-1/PD-L1. *Clin Cancer Res* 2017 Apr **15**;**23**(8):1920-8.

Ethics Approval The study was approved by Northwestern University's Institutional Review Board, study number STU00207117.



Abstract 1413 Figure 1 Overall survival and progression free survival between hyperprogression (HPD) and non-HPD patients defined by Champiat et al. and Saada-Bouzid et al.

Abstract 1413 Table 1 Multivariate Analysis of overall survival and progression free survival including hyperprogression defined by Champiat et al.

Dependent	PFS			OS		
	HR	95%	p	HR	95%	p
Diagnosis Age	0.97	6.50-50.27	<0.001	1	0.98-1.0	0.627
Sex						
Female				Reference		
Male	0.32	0.14-0.72	0.006	0.75	0.51-1.1	0.15
Hyperprogression	18.08	6.50-50.27	<0.001	2.88	1.2-6.9	0.018
ECOG						
1-2				Reference		
3-4	4.12	1.26-13.48	0.019	1.49	0.70-3.2	0.302

Abstract 1413 Table 2 Multivariate Analysis of overall survival and progression free survival including hyperprogression defined by Saada-Bouزيد et al.

Dependent	PFS			OS		
	HR	95%	p	HR	95%	p
Diagnosis Age	0.97	0.93-1.00	0.081	1	0.98-1.0	0.828
Sex	Reference					
Female	Reference					
Male	0.4	0.17-0.91	0.025	0.77	0.51-1.2	0.223
Hyperprogression	3.92	1.55-9.88	0.004	2.76	1.40-5.4	0.003
Line of Immunotherapy	Reference					
1st line	Reference					
2nd line	1.82	0.59-5.56	0.294	0.92	0.55-1.5	0.751
3+ line	3.19	1.04-9.80	0.043	1.97	1.09-3.6	0.025
ECOG	Reference					
1-2	Reference					
3-4	3.28	1.01-10.64	0.048	1.76	0.81-3.8	0.151

<http://dx.doi.org/10.1136/jitc-2022-SITC2022.1413>

PREPRINT

1414

RACIAL ETHNIC DIFFERENCES IN TREATMENT OF ADVANCED NON-SMALL CELL LUNG CANCER WITH IMMUNE CHECKPOINT INHIBITORS: ANALYSIS OF A LARGE REAL-WORLD DATASET

¹Laura Oswald*, ¹L Robert Gore, ¹Melanie Buhlmann, ²Naomi Brownstein, ¹Kea Turner, ¹Andreas Saltos, ¹Jhanelle Gray, ³Shirish Gadgeel, ¹Clement Gwede, ¹Susan Vadaparampil, ¹Brian Gonzalez, ¹Heather Jim. ¹Moffitt Cancer Center, Tampa, FL, USA; ²Medical University of South Carolina, Charleston, SC, USA; ³Henry Ford Cancer Center, Detroit, MI, USA

Background Immunotherapy is a promising treatment for advanced non-small cell lung cancer (advNSCLC), with several immune checkpoint inhibitors (ICIs) FDA-approved since 2015. As ICI indications expand, disparities in treatment selection could result in disparate lung cancer mortality. This study examined differences in ICI treatment by race/ethnicity using a large cohort of real-world advNSCLC patients.

Methods This study used the nationwide Flatiron Health electronic health record-derived de-identified database.^{1,2} Data included individuals diagnosed with advNSCLC between 2011-2021 with available treatment information. Logistic regression analyses assessed the likelihood of receiving an ICI (any line of therapy) by race/ethnicity before FDA-approval of the first ICI for advNSCLC (2011-2014) and after (2015-2021). Patients aged <65 years (younger) and 65+ (older) were assessed separately due to changes in Medicare eligibility at age 65. Significant racial/ethnic differences in ICI treatment accounting for covariates are reported as adjusted odds ratios (OR) with 95% confidence intervals. Covariates were: diagnosis year, geographic region, practice setting (academic/community), gender, age, insurance coverage within 90 days of treatment, smoking history, ECOG performance status within 60 days of diagnosis, documented biomarker testing (before ICI treatment/none), and PDL1 expressed (<1%/1%+).

Results Of 52,031 patients, most were non-Hispanic White (NHW) (68.7%) followed by unknown race/ethnicity (9.2%), Black/African American (AA) (8.6%), other race/ethnicity (8.1%), Hispanic/Latino (3.1%), and Asian (2.2%). Of patients treated before FDA-approval of ICIs for advNSCLC (N=16,219), 11.8% received ICI treatment. Relative to younger or older NHWs respectively, likelihood of ICI was higher among younger Asians (OR=1.94, 1.24-3.05) and lower among younger and older patients with unknown race/ethnicity (OR=0.50, 0.32-0.79; OR=0.45, 0.32-0.63, respectively). Of patients treated after FDA-approvals (N=35,812), 59.1% received ICI treatment. Relative to younger or older NHWs respectively, likelihood of ICI was lower among younger and older Asians (OR=0.48, 0.37-0.62; OR=0.64, 0.53-0.77, respectively), younger and older patients with unknown race/ethnicity (OR=0.83, 0.72-0.96; OR=0.77, 0.70-0.84, respectively), older Hispanic/Latinos (OR=0.85, 0.73-1.00), and older patients with other race/ethnicity (OR=0.90, 0.81-1.00).

Conclusions Most racial/ethnic disparities in ICI treatment were observed among older advNSCLC patients in the years after FDA-approval. Among younger patients, Asians were more likely than NHWs to receive an ICI before FDA-approvals, but this association reversed thereafter. Though not assessed, this was possibly due to differences in prevalence of EGFR mutations. There were no differences in likelihood of ICI treatment between Black/AAs and NHWs. These results suggest a need for concerted effort to offer all patients appropriate ICI treatment irrespective of race/ethnicity and/or age.

REFERENCES

1. Ma X, Long L, Moon S, Adamson BJS, Baxi SS. Comparison of Population Characteristics in Real-World Clinical Oncology Databases in the US: Flatiron Health, SEER, and NPCR. medRxiv. 2020:2020.03.16.20037143.
2. Birnbaum B, NN Seidl-Rathkopf K, Agrawal M, Estevez M, Estola E, et al. Model-assisted cohort selection with bias analysis for generating large-scale cohorts from the EHR for oncology research 2020 [Available from: <https://arxiv.org/abs/2001.09765>].

Ethics Approval Institutional Review Board approval of the study protocol was obtained prior to study conduct and included a waiver of informed consent (WCG IRB; IRB00000533).

<http://dx.doi.org/10.1136/jitc-2022-SITC2022.1414>

1415

A FLUORESCENT BIOSENSOR METHOD FOR QUANTIFYING ANTIBODY BINDING AND INTERNALIZATION INTO EFFECTOR CELLS AND TARGET CELLS IN A CO-CULTURE SYSTEM

Shu Mao, Yu-Lin Su, Frank Delfino, Craig Meagher, Jason Giurleo, Dangshe Ma, Travis Shaffer*. *Regeneron Pharmaceuticals, Tarrytown, NY, USA*

Background Antibody-mediated delivery of agonists into the tumor microenvironment to selectively activate intracellular targets in immune cells (effector cells) relative to tumor cells (target cells) is not well understood. Here we develop a method using a fluorescent biosensor to quantitatively assess the number of antibodies binding to a cell and frequency of internalized antibodies per cell in both tumor and immune cells in co-cultures by utilizing quantitative spectral flow cytometry.

Methods A hIgG1, anti-HER2 monoclonal antibody (HER2-mAb) or isotype-matched control antibody (Iso-mAb) were conjugated with a fluorescent biosensor consisting of Alexa Fluor 568 (AF568) and Alexa Fluor 647 (AF647) separated by a cathepsin B-cleavable peptide linker. AF568 fluorescence is quenched until the biosensor is cleaved inside cells, while AF647 is fluorescent pre- and post-cleavage. Quantitative flow cytometry calibration curves were prepared to calculate the number of fluorophore molecules per cell and antibody molecules per cell using the measured median fluorescent intensity (MFI).

Murine effector cells, RAW264.7 and RAW309 (macrophage) and MutuDC1940 (dendritic), were plated in 96-well plates 24 hours prior to the addition of target cells expressing variable levels of HER2: JIMT-1, N87, and SKBR3, pre-loaded with pHrodo green cell tracker. Target cells and biosensor-conjugated mAb were added simultaneously to effector cells at 37 °C for 0, 1, 4, or 24 hours. At each designated time point, cells were stained with CD11b-BV785, and flow cytometry was conducted with at least three independent runs.

Flow gates were placed on live single cells of either pHrodo green positive tumor cells, CD11b-BV785 positive immune cells, or double-positive cells. The AF568 and AF647 MFI values were converted to the number of fluorophore molecules or antibodies bound per cell allowing for the number of antibody molecules and% internalized antibody per cell to be determined.

Results Target cells expressing HER2 were required for appreciable HER2-mAb binding and internalization into effector cells. Antibody binding on effector cells correlated with increased HER2 expression across the three tumor cell lines. Importantly, the HER2-mAb-biosensor showed rapid and increased internalization into immune cells with 40-60% of antibody internalized by 1 hour in contrast to <10% internalization into tumor cells.

Conclusions This in vitro quantitative flow cytometry allowed determination of both the number of antibodies and the% internalized antibodies per cell, important parameters for modeling delivery of antibody-mediated immunostimulatory agonists. The demonstrated methodology can be applied to in vivo models to optimize therapeutic agonist delivery.

<http://dx.doi.org/10.1136/jitc-2022-SITC2022.1415>

Regulatory, Financial and Access Considerations

1416

METHODS FOR GATHERING PATIENT-RELEVANT CONCEPTS: THE USE OF THE PATIENT QUALITATIVE ASSESSMENT OF TREATMENT (PQATV2) IN EARLY ONCOLOGY DEVELOPMENT

Nneka Onwudiwe* Keri Brady, Jane Wells, Catherine Coulouvat, Vicky DiBiasi, Christelle Lorenzato, Giovanni Abbadessa, Peter Adamson. *Sanofi, Washington, DC, USA*

Background The importance in measurement and analysis of patient-reported outcomes (PROs) in early oncology development as toxicity and efficacy endpoints— particularly with the emergence of targeted therapies and immunotherapies, has been recognized among researchers.¹⁻⁶ Recently, more attention has been directed towards considerations for applying PROs to early oncology development by the FDA in public workshops.^{7,8} Despite their recognized value, methods for collecting, analyzing, and interpreting early phase PRO data are complex, leading to infrequent use in early oncology trials. The aim of this abstract is to conduct a scoping review of PRO usage in early oncology trials and highlight the novelty of a Sanofi-developed PRO measure, Patient Qualitative Assessment of Treatment version 2 (PQATv2).

Methods To validate our approach to PQATv2 implementation, we sought to identify early phase industry-sponsored oncology trials reporting PRO endpoints registered with ClinicalTrials.gov between January 1, 2009, to July 20, 2022—a start date to coincide with the publication of the 2009 FDA PRO Guidance for Industry. The PQATv2 is a 6-item, generic PRO measure. The PQATv2 includes: two 11-point numeric rating scales assessing participant-perceived treatment benefits and disadvantages (0 = not at all beneficial/disadvantageous to 10 = extremely beneficial/disadvantageous); an item assessing participants' willingness to continue treatment after the trial (yes/no); a 7-point Likert-type item assessing participants' overall benefit/risk ratio perceptions (-3 = 'disadvantages of the drug I received significantly outweighs the benefits' to 3 = 'the benefits of the drug I received significantly outweigh the disadvantages'); and three free-text items assessing participant-perceived treatment benefits, disadvantages, and reasons why the participant would be willing or unwilling to continue the treatment after the trial.

Results Of the 78 early phase studies reporting PRO endpoints and registered with ClinicalTrials.gov, Phase 1 oncology trials accounted for 33.3% (n=26) and Phase 1|2 at 66.7% (n=52). The PQATv2 is being included in several of our early oncology studies. Recognizing the need to enrich traditional efficacy and safety endpoints, Sanofi believes the PQATv2 is a novel and important approach to identifying salient and important concepts that guide the identification of future PRO measures in later phases.

Conclusions The PQATv2 is a novel exploratory measure aimed at generating additional hypotheses to guide selection of fit-for-purpose PROs in later phases. Further analysis of the utility of PROs in early phase oncology, and their impact in guiding preparation of PROs for later stage studies will be conducted as we gain more experience.

REFERENCES

1. Henon C, Lissa D, Paoletti X, Thibault C, Le Tourneau C, Lanoy E, Hollebecque A, Massard C, Soria JC, Postel-Vinay S. Patient-reported tolerability of adverse events in phase 1 trials. *ESMO Open*. 2017;**2**(2).

2. Minasian L, Rosen O, Auclair D, Rahman A, Pazdur R, Schilsky RL. Optimizing dosing of oncology drugs. *Clin Pharmacol Ther* 2014; **96**(5): 572–579.
3. Anota A, Boulin M, Dabakuyo-Yonli S, Hillon P, Cercueil JP, Minello A, Jouve JL, Paoletti X, Bedenne L, Guiu B, Bonnetain F. An explorative study to assess the association between health-related quality of life and the recommended phase II dose in a phase I trial: idarubicin-loaded beads for chemoembolisation of hepatocellular carcinoma. *BMJ Open* 2016;**6**(6).
4. Mendoza TR. Understanding the Toxicity of Cancer Immunotherapies: Use of Patient-Reported Outcomes. *Journal of Immunotherapy and Precision Oncology* 2018; **1**(1):38–45
5. Bossi P, Botta L, Bironzo P, Sonetto C, Musettini G, Sbrana A, Di Giannantonio V, Locati LD, Di Maio M, Antonuzzo A. Systematic review of adverse events reporting in clinical trials leading to approval of targeted therapy and immunotherapy. *Future Oncology*. 2019;**15**(21):2543–53.
6. Safa H, Tamil M, Spiess PE, Manley B, Pow-Sang J, Gilbert SM, Safa F, Gonzalez BD, Oswald LB, Semaan A, Diab A, Chahoud J. Patient-Reported Outcomes in Clinical Trials Leading to Cancer Immunotherapy Drug Approvals From 2011 to 2018: A Systematic Review. *J Natl Cancer Inst* 2021;**113**(5):532–542.
7. US Food and Drug Administration (FDA) Clinical Outcome Assessment in Cancer Clinical Trials (COA-CCT). Workshop: 7th Annual Clinical Outcome Assessment in Cancer Clinical Trials Workshop. Virtual June 29th 2022.
8. US Food and Drug Administration (FDA) American Society of Clinical Oncology (ASCO). Getting the Dose Right: Optimizing Dose Selection Strategies in Oncology. Virtual Workshop May 3-5th 2022.

<http://dx.doi.org/10.1136/jitc-2022-SITC2022.1416>

1417

**UTILIZATION OF IMMUNE-BASED RESPONSE CRITERIA
IN NCI-CTEP SPONSORED IMMUNOTHERAPY CLINICAL
TRIALS**

<http://dx.doi.org/10.1136/jitc-2022-SITC2022.1417>

Sarah Shin*, Alice Chen, Martha Kruhm, David Loose, Geraldine O, Naoko Takebe, Elad Sharon. *NIH/NCI, Bethesda, MD, USA*

Background Immune modulation with immunotherapy in various tumor types has resulted in pattern of responses unique from chemotherapy or targeted therapy, suggesting the need to modify established response criteria to accurately assess and interpret responses to immunotherapy regimens. Multiple iterations of immune-based response criteria adapted from the RECIST criteria have been proposed to date, with the development of the irRC in 2009, followed by the irRECIST criteria in 2013, iRECIST in 2017,¹ and imRECIST in 2018. However, the extent of use of modified response criteria in clinical trials is unknown. We evaluated the trends in the inclusion of immune-based response criteria as an objective in immunotherapy-based CTEP-sponsored clinical trials.

Methods We conducted a retrospective analysis of all NCI-CTEP sponsored investigational clinical trials initiated by the data cut-off date of April 28, 2022. Trials for patients with solid tumors in which an immunotherapy agent was administered in at least one treatment arm were included in the analysis. Stated objectives for each trial were extracted and assessed for utilization of an immune-based response criteria.

Results A total of 160 solid-tumor trials were identified in the CTEP database to have immunotherapy as at least one of the treatment arms. Thirty (19%) of the trials incorporated immune-based criteria to assess response as an objective: 12 iRECIST (40%), 3 irRECIST (10%), 10 irRC (33%), 3 iRANO (10%), 2 “immune RECIST”, unspecified (7%). Sixteen of 97 randomized trials (16%) and 14 of 63 non-randomized trials (22%) used an immune-based response criteria. Of the 16 randomized trials utilizing an immune-related response criteria, 4 trials had incongruous arms comparing an immunotherapy-based regimen with a non-immunotherapy regimen. The remaining 12 randomized trials utilizing an immune-based response criteria had immunotherapy agents in all treatment arms. Forty-nine (92%) of the 53 randomized trials with a non-immunotherapy comparator treatment arm and 32 (73%) of the 44 randomized trials with immunotherapy in all treatment arms did not use immune-based response criteria.

Conclusions Our analysis demonstrates that only a small percentage of immunotherapy-based clinical trials utilized immune-based response criteria. Randomized trials with non-immunotherapy comparator treatment arm(s) tended to avoid inclusion of immune-based response criteria in the objectives, likely in favor of maintaining consistent response criteria for all arms. However, both randomized and non-randomized trials had similar rates of usage of immune-based response criteria, indicative of a generally low level of uptake of these novel response endpoints on immunotherapy clinical trials.

Acknowledgements Thank you to Dr. Howard Streicher and Dr. Helen Chen at the Cancer Therapy Evaluation Program (CTEP) at the NIH/NCI for their expertise and guidance.

REFERENCE

1. Seymour L, Bogaerts J, Perrone A, Ford R, Schwartz LH, Mandrekar S, Lin NU, Litière S, Dancy J, Chen A, Hodi FS, Therasse P, Hoekstra OS, Shankar LK, Wolchok JD, Ballinger M, Caramella C, de Vries EGE; RECIST working group. iRECIST: guidelines for response criteria for use in trials testing immunotherapeutics. *Lancet Oncol.* 2017 Mar;**18**(3):e143-e152. doi: 10.1016/S1470-2045(17)30074-8. Epub 2017 Mar 2. Erratum in: *Lancet Oncol.* 2019 May;**20**(5):e242.

1418 **EXPLORING RWE RWD-BACKED REGULATORY DECISIONS IN IMMUNO-ONCOLOGY**

Valerie Limasi, Amin Osmani, Sheila Galan*. *Cedience Inc, Toronto, Canada*

Background Real-world data (RWD) and real-world evidence (RWE) has long been used in drug development programs: to help generate hypotheses and assess the feasibility of clinical trials, or for post-marketing surveillance purposes. There is a wealth of RWD sources; data can be gathered from medical records, registries and wearables, among others. This data is then analysed to obtain RWE. Today, RWD/RWE is also increasingly being used to support regulatory decisions, especially during market authorisation approval for new drugs or new indications. A number of immuno-oncology drug products have owed their approval to the use of RWD/RWE.

Methods The objective of this experiment is to identify and trace the regulatory history of selected immuno-oncology products to understand how RWD/RWE has been applied in their drug development programs to market, and the perspective of the regulators at the time of review. Using Cedience, we identify the RWD/RWE-generating trials used in an immuno-oncology drug's submission. Cedience is a next-generation regulatory intelligence platform that allows a user to answer regulatory precedent questions, monitor topics of interest, and analyse past development strategies by using a database of documents compiled from various regulatory agencies. We have previously used Cedience to identify drug products associated with RWD/RWE and reconstruct a timeline of said drug products by collecting correspondence letters from the FDA.

Results Using Cedience, case studies were built that show the timeline of a drug's regulatory history; a picture of the drug's journey through development. This timeline focuses on RWD/RWE-generating trials used to examine the immuno-oncology drug, as well as the evidence available prior to said trials. In the context of these regulatory submissions, RWD/RWE functions to support randomised clinical trials by providing a second source of data that is more generalisable to the wider population.

Conclusions From this data, an analysis of how RWD/RWE was used in the real world could be seen: what percentage of FDA approvals are RWD/RWE-backed, the clinical evidence that can be generated from RWD/RWE, and what type of study designs are appropriate for the generation of RWD/RWE. The regulator's perspective could be seen as well: how they evaluate RWD/RWE, and whether any issues or concerns are raised.

<http://dx.doi.org/10.1136/jitc-2022-SITC2022.1418>

Tumor and Stromal Cell Biology

1419 HIGH PREVALENCE OF IMMUNE EXCLUSION IN EPITHELIAL TUMORS

¹Antoine Italiano, ²Jean-Philippe Guégan*, ³Xinwei Sher, ³Laura Dillon, ³Tamas Oravecz, ³Thomas Schürpf, ³Guy Clifton. ¹Institut Bergonie, Bordeaux, France; ²Explicyte, Bordeaux, France; ³Parthenon Therapeutics, Inc, Boston, MA, USA

Background Immune infiltrated tumors have high levels of lymphocytes in contact with tumor cells and are more responsive to immune checkpoint inhibitors. Tumors with a paucity of lymphocytes contacting tumor cells can be divided into immune deserted and immune excluded phenotypes. Immune exclusion is characterized by lymphocytes restricted to the periphery of cancer nests, typically to the peritumoral stroma. Mechanisms that prevent lymphocyte infiltration in immune exclusion may be distinct. Understanding the immune phenotype landscape across tumors is necessary to ensure novel therapies targeting immune exclusion are directed at optimal indications.

Methods Samples from colorectal cancer (CRC), non-small cell lung cancer (NSCLC), ovarian cancer (OC), pancreatic cancer (PDAC), triple-negative breast cancer (TNBC), leiomyosarcoma (LMS), and undifferentiated pleomorphic sarcoma (UPS) were evaluated. Slides were stained with a multiplex IHC assay for CD8 and CK and evaluated by two pathologists who characterized the tumors as: deserted, characterized by a paucity/absence of CD8+ T cells (<1%); excluded, characterized by the presence of CD8+ T cells that do not penetrate the tumor parenchyma; and infiltrated, characterized by the presence within the tumor parenchyma of CD8+ T cells.

Results Overall, 143 samples were evaluated with 18.9% of tumors defined as deserted, 46.9% as excluded, and 34.3% as infiltrated (Table 1). In the 103 epithelial tumors, 19.4% (n=20) were defined as deserted, 63.1% (n=65) as excluded, and 17.4% (n=18) as infiltrated. Of the 40 sarcoma samples, 17.5% (n=7) were defined as deserted, 5% (n=2) as excluded, and 77.5% (n=31) as infiltrated. Immune exclusion was highest in CRC (70.0%), PDAC (71.4%), and TNBC (71.4%).

Conclusions Immune exclusion is the most prevalent immune phenotype in CRC, NSCLC, OC, PDAC, and TNBC. LMS and UPS have a low rate of immune exclusion and are predominantly infiltrated. Further research is warranted to understand and target the mechanisms underlying immune exclusion.

Ethics Approval Ethics approval obtained at Institut Bergonie

Abstract 1419 Table 1 Prevalence of immune phenotypes across evaluated cancer types

Tumor Type	n	Desert (%)	Excluded (%)	Infiltrated (%)
Colorectal	20	3 (15.0)	14 (70.0)	3 (15.0)
NSCLC	21	6 (28.6)	12 (57.1)	3 (14.3)
Ovarian	20	3 (15.0)	9 (45.0)	8 (40.0)
PDAC	21	5 (23.8)	15 (71.4)	1 (4.7)
TNBC	21	3 (14.3)	15 (71.4)	3 (14.3)
LMS	20	3 (15.0)	1 (5.0)	16 (80.0)
UPS	20	4 (20.0)	1 (5.0)	15 (75.0)
Total	143	27 (18.9)	67 (46.9)	49 (34.3)

<http://dx.doi.org/10.1136/jitc-2022-SITC2022.1419>

1420

TARGETING ENDOPLASMIC RETICULUM STRESS-RESPONSIVE PERK IN MELANOMA ELICITS PARAPTOSIS-MEDIATED IMMUNOGENIC CELL DEATH AND INDUCTION OF TYPE I INTERFERON-DEPENDENT ADAPTIVE ANTITUMOR IMMUNITY

¹Jessica Mandula*, ²Shiun Chang, ³Eslam Mohamed, ²Rachel Jiminez, ²Rosa Sierra-Mondragon, ²Darwin Chang, ²Alyssa Obermayer, ²Carlos Moran-Segura, ²Das Satyajit, ²Julio Vazquez-Martinez, ²Karol Pierto, ²Ann Chen, ²Keiran Smalley, ²Brian Czerniecki, ²Peter Forsyth, ⁴Richard Koya, ²Brian Ruffell, ³Juan Cubillos-Ruiz, ⁶David Munn, ²Timothy Shaw, ²Jose Conejo-Garcia, ²Paulo Rodriguez. ¹Moffitt Cancer Center, Tampa, FL, USA; ²H. Lee Moffitt Cancer Center and Research, Tampa, FL, USA; ³California North State University, Elk Grove, CA, USA; ⁴University of Chicago, Tampa, FL, USA; ⁵Sandra and Edward Meyer Cancer Center, Weill Cornell Medicine, Ithica, NY, USA; ⁶Georgia Cancer Center, Augusta University, Augusta, GA, USA

Background In order to survive the hostile tumor microenvironment, cancer cells activate endoplasmic reticulum (ER) stress-associated response proteins, including the protein kinase R (PKR)-like endoplasmic reticulum kinase (PERK). Although intrinsic adaptation to chronic ER stress via PERK has been reported to limit the antitumor potential of immune cells, whether PERK activation in melanoma cancer cells contributes to immune evasion remains poorly understood and therapeutically untargeted.

Methods To establish the mechanistic role and therapeutic potential of targeting PERK in melanoma, we utilized both genetic and pharmacological approaches in both syngeneic transplantable and autochthonous inducible melanoma murine models. To substantiate these findings in a clinical context, we also leveraged bioinformatic interrogation of multiple independent human cohorts and tissue microarray analysis of human melanoma samples.

Results After the elimination or inhibition of PERK, melanoma cells undergoing ER stress activated a process characterized by the accumulation of misfolded proteins, ER enlargement, massive cytoplasmic vacuolation, and elevation of reactive oxygen species, which culminated in paraptosis and release of immunogenic cell death (ICD) mediators. Induction of paraptosis in PERK-ablated melanoma cells was dependent on factor SEC61b. Injection of PERK-null melanoma cells into mice or treatment of melanoma-bearing mice with PERK inhibitors resulted in the accumulation of ICD mediators, dramatic antitumor responses, robust protective T cell immunity, and activation of abscopal responses. Notably, we detected the expansion of monocyte-derived dendritic cells (MoDC) in PERK-null tumor beds, which produced Type I IFNs in response to the accumulated ICD mediators. Subsequently, MoDC-derived IFN β 1 directed CCR2 driven recruitment of splenic common monocyte progenitors (cMoPs) which further developed into MoDCs and perpetuated the development of anti-tumor immunity. Blockade of Type I IFN receptor, elimination of IFN β , or deletion of STAT1, prevented the differentiation of cMoPs into MoDC. Additional studies in human settings substantiated the clinical impact of the activation of PERK signaling in melanoma. Higher expression of active PERK in cancer cells from human melanoma tumors correlated with limited intra-tumoral T cell frequency. In addition, elevated expression of a PERK-activation signature in different human melanoma cohorts corresponded to lower overall survival and impaired response to immunotherapy. Consistently, inhibition or ablation of PERK in murine melanoma tumors augmented response to checkpoint immunotherapy.

Conclusions Collectively, our findings underline the immunotherapeutic potential of targeting PERK in melanoma, support

further development of ER-targeted treatment approaches in cancer and reinforce the benefit of combining ER-stress targeted therapies with checkpoint immunotherapy in cancer.

<http://dx.doi.org/10.1136/jitc-2022-SITC2022.1420>

1421

ELK3 MODULATES THE IMMUNE LANDSCAPE AND IMMUNE RESPONSE TO NATURAL KILLER CELLS IN TRIPLE NEGATIVE BREAST CANCERS

¹Joo Dong Park*, ²Kwang-Soo Kim, ¹Dae-Keum Lee, ¹Seung Hee Choi, ¹Hae-Yun Jung, ¹Kyung-Soon Park. ¹CHA University, Seongnam-Si, Korea, Republic of; ²Northwestern university, Chicago, IL, USA

Background Due to its aggressive behavior and frequent development of chemotherapy resistance, triple negative breast cancer (TNBC) is the most lethal subtype of breast cancer.¹ Although natural killer (NK) cell-based immunotherapy is a promising strategy for overcoming treatment barriers,² the therapeutic efficacy of NK cells against TNBC falls short of expectations. ELK3, an E26 transformation-specific transcription factor, is highly expressed in TNBCs and acts as a master regulator of the epithelial-mesenchymal transition.^{3, 4}

Methods Two representative human TNBC cell lines, MDA-MB231 and Hs578T, were engineered with ELK3-targeting shRNA or ELK3-expressing plasmid. A combination of gene expression profiling and molecular analysis was used to identify ELK3's downstream target genes. The role of ELK3 in determining TNBC immunosensitivity to NK cells was studied in vitro and in vivo in terms of mitochondrial fission-fusion transition and reactive oxygen species concentration. With syngeneic mouse model of Elk3 knockout 4T1 cells, tumor infiltrated immune cells were analyzed.

Results The status of ELK3-dependent mitochondrial fission-fusion in TNBCs was linked to the concentration of mitochondrial superoxide and was a major determinant of NK cell-mediated immune responses. In TNBCs, we discovered that mitochondrial dynamics proteins of 51 (Mid51), a major mediator of mitochondrial fission, is a direct downstream target of ELK3. In addition, we found that ELK3 expression correlated inversely with Mid51 expression, and that the ELK3-Mid51 axis is directly related to mitochondrial dynamics and immune response to NK cells. With a syngeneic mouse TNBC model, we found that ELK3 expression in TNBC is associated with a landscape of immune cells derived from both innate and adaptive immunity that infiltrate the tumor.

Conclusions Taken together, these findings suggest that ELK3 in TNBCs regulates mitochondrial dynamics, which is directly linked to tumor immunosensitivity. Targeting ELK3 in TNBCs is anticipated to shed new light on strategies for improving the efficacy of NK cell-based immunotherapy for TNBC (figure 1).

Acknowledgements This study was supported by the Basic Science Research Program through the National Research Foundation of Korea (NRF), funded by the Ministry of Education (2019R1A6A1A03032888, NRF-2022R1A2C1003390).

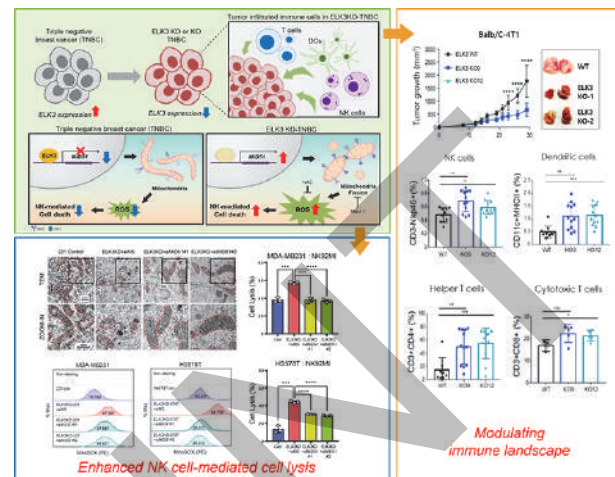
REFERENCES

1. Bianchini G, et al. Treatment landscape of triple-negative breast cancer – expanded options, evolving needs. *Nature reviews. Clinical Oncology* 2022;**19**(2):91–113.
2. Abdel-Latif M, et al. Why natural killer cells in triple negative breast cancer? *World Journal of Clinical Oncology* 2020;**11**(7):464–476.
3. Kong SY, et al. The ELK3-GATA3 axis orchestrates invasion and metastasis of breast cancer cells in vitro and in vivo. *Oncotarget* 2016;**7**(40):65137–65146.
4. Cho HJ, et al. ZEB1 Collaborates with ELK3 to Repress E-Cadherin Expression in Triple-Negative Breast Cancer Cells. *Molecular Cancer Research: MCR* 2019;**17**(11):2257–2266.

Ethics Approval All animal works were approved by the Institutional Animal Care and Use Committee of the laboratory animal research center at CHA University. Primary natural killer cells were isolated from peripheral blood mononuclear

cells obtained from healthy donors. This research was reviewed and approved by the institutional review board of CHA University.

Consent All healthy blood donors provided informed consent.



Abstract 1421 Figure 1

<http://dx.doi.org/10.1136/jitc-2022-SITC2022.1421>

1422

CYTOKINES IMPACT FIBROBLAST ACTIVITY AND TUMOR FIBROSIS IN PANCREATIC DUCTAL ADENOCARCINOMA

Neel Nissen*, Morten Karsdal, Nicholas Willumsen. *Nordic Bioscience, Herlev, Denmark*

Background Pancreatic ductal adenocarcinoma (PDAC) is a devastating disease. The five-year survival is only 11%. One hallmark of PDAC is the excessive fibrotic reaction in the tumor microenvironment surrounding the tumor cells. Tumor fibrosis is characterized by an increased activity of fibroblasts and turnover of collagens. Unfortunately, this leads to reduced drug-uptake, impaired immune cell activity and as a result reduced survival in patients. Cytokines in clinical cancer immunotherapy, either as monotherapy or in combination with check-point inhibitors have gained much attention as anti-cancer drugs. Some cytokines have been shown to possess pro- and anti-fibrotic properties and could therefore provide additive value to the anti-cancer efficacy. TGF- β , PDGF-AB, IL-1 α , IL-1 β , IL-8 and IL-15, are six cytokines highly investigated in clinical trials as monotherapies or in combination with immunotherapies. In this study, we investigated the pro- and anti-fibrotic effects of these cytokines in molecular crowding pancreatic fibroblast culture assays in combination with collagen biomarkers measuring formation of type I, III and VI collagen (PRO-C1, PRO-C3 and PRO-C6, respectively).

Methods Humane pancreatic fibroblasts were cultured in Ficoll-media. Fibroblasts were treated w/wo TGF- β (1ng/mL), PDGF-AB (100 ng/mL), IL-1 α (10 ng/mL), IL-1 β (10 ng/mL), IL-8 (10 ng/mL) and IL-15 (10 ng/mL). The fibrotic activity of the fibroblasts was investigated by measuring PRO-C1, PRO-C3 and PRO-C6 in the supernatant at days 3, 6, 9 and 12. Cell-viability was evaluated by Alamar-blue.

Results The formation of type I collagen (PRO-C1) was significantly increased when fibroblasts were treated with TGF- β , IL-1 α and IL-1 β , but not PDGF, IL-8 and IL-15 at days 6, 9 and 12. The formation of type III collagen (PRO-C3) was significantly increased when fibroblasts were treated with TGF- β , IL-1 α and IL-1 β , but not PDGF, IL-8 and IL-15 at days 6, 9, compared to no treatment. At day 12 PRO-C3 was significantly increased in supernatant from fibroblasts treated with TGF- β , IL-1 α , IL-1 β and IL-8, but not IL-15, compared to no treatment. Interestingly, the formation of type VI collagen (PRO-C6) was only increased when fibroblasts were treated with PDGF-AB compared to no treatment at days 3, 6, 9 and 12. There were no differences in cell viability between treatments.

Conclusions TGF- β , PDGF-AB, IL-1 α , IL-1 β , IL-8 and IL-15 have differential effects on the pro-fibrotic activity of pancreatic fibroblasts. This is important knowledge when developing cytokine drugs for clinical cancer immunotherapy trials, suggesting that tumor fibrosis needs to be accounted for when designing and evaluating such studies.

<http://dx.doi.org/10.1136/jitc-2022-SITC2022.1422>

1423 **BREAST TUMOR CELL HEME METABOLISM ALTERS
MACROPHAGE IMMUNE SUPPRESSION AND FUNCTION
TO SUPPORT LUNG METASTASIS**

Michelle Williams*, Sabrina Hafeez, Jessica Christenson, Nicole Spoelstra, Kathleen O'Neill, Li-Wei Kuo, Lyndsey Crump, Jill Slansky, Jennifer Richer. *University of Colorado Anschutz Medical Campus, Aurora, CO, USA*

Background Bilirubin, a metabolite of the heme degrading enzyme heme oxygenase-1 (HO-1/HMOX1), is commonly believed to be a waste product. Studies in other diseases revealed that bilirubin can alter normal immune cell function including macrophage antigen presentation and phagocytosis. However, the effects of bilirubin on the tumor microenvironment (TME) remain unknown. We hypothesized that tumor cell-HO-1 activity and subsequent bilirubin secretion enhance triple-negative breast cancer (TNBC) metastasis by supporting immune suppressive, pro-tumor macrophage function.

Methods We tested the impact of tumor cell-HO-1 and bilirubin on macrophage immune suppression and efferocytic capacity (engulfment of dead tumor cells) using qRT-PCR, flow cytometry and live cell imaging. Human and mouse macrophages were analyzed after treatment with exogenous bilirubin or bilirubin-depleted conditioned medium collected from tumor cells treated with tin mesoporphyrin (SnMP), an FDA approved HO-1 enzymatic inhibitor. Primary tumor growth, lung metastatic burden and macrophages were observed in immunocompetent mice harboring 66Cl-4 mammary tumors without and with HO-1 genetic depletion (shHO1). Human TNBC specimens were analyzed via CIBERSORT to predict immune cell abundance in patients with high versus low levels of HMOX1.

Results Macrophages cultured with conditioned medium from tumor cells treated with the HO-1 inhibitor SnMP demonstrated a 35-65% decrease in immune suppressive genes (Arg1, Cd274, Tgfb1) and a 25% increase in the efferocytosis gene *Mertk* compared to those treated with control conditioned medium. This effect was rescued by exogenous treatment with 2.5 μ M bilirubin. Direct bilirubin treatment enhanced macrophage PD-L1 mRNA and protein expression by over 6-fold. In contrast, bilirubin decreased expression of *Mertk* by at least 50% and nearly ablated macrophage efferocytic capacity. To test whether bilirubin supports tumor progression via modulation of macrophages, we evaluated tumor growth and metastasis after tumor cell-HO-1 genetic depletion. While mice with shHO1 tumors had enhanced primary tumor growth compared to shCnt tumors, HO-1 depletion decreased lung metastatic capacity. Flow cytometry revealed that macrophages from shHO1 primary tumors had decreased expression of suppressive markers including PD-L1 and CD206 than control tumors. In human TNBC specimens, CIBERSORT analysis revealed that tumors with high levels of HMOX1 have a significant increase in the abundance of suppressive M2-like macrophages compared to those with low HMOX1.

Conclusions Tumor cell-HO-1 may support immune cell suppression and dysfunction during TNBC metastasis via bilirubin. Since HO-1 inhibitors including SnMP are FDA approved for treatment of other diseases, these findings could rapidly be translated to provide an alternative or companion immunotherapy for metastatic TNBC.

<http://dx.doi.org/10.1136/jitc-2022-SITC2022.1423>

Abstracts

1424

M⁶A REGULATORS RELATED TO MOLECULAR FEATURE, IMMUNE MICROENVIRONMENT AND PROGNOSIS IN LUNG ADENOCARCINOMA

Zhibo Tan, Min Chen, Yujie Zhao, Feng Peng, Ying Li, Mengqi Yang, Lei Zhang, Xin Li, Pengfei Yang, Zhe Zhang, Daming Li, Zhaoming Peng, Yajie Liu. *Peking University Shenzhen Hospital, Shenzhen, China*

Background The dynamic changes of N⁶-methyladenosine controlled by m⁶A regulators are vital for cancer biology.¹ However, the role of m⁶A regulators in lung adenocarcinoma (LUAD) remains unclear. This study aimed to gain a deeper insight into the roles of m⁶A regulators in LUAD by bioinformatics.

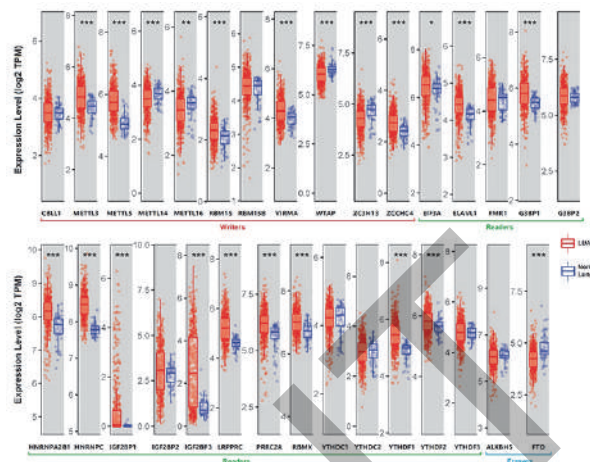
Methods 31 m⁶A regulators were retrieved from previous literature. The expression levels of the 31 regulators were investigated by TIMER2.0. The association between the 31 regulators and overall survival (OS) were explored via K-M plotter and Cox regression. Next, mutations status and copy number alterations of the 31 regulators were probed through cBioPortal. Moreover, the interaction between the 31 regulators were revealed via principal component analysis (PCA), protein-protein interaction (PPI), and Metascape enrichment by R programming, STRING 11.5, Cytoscape, and Metascape. Then, the immune microenvironment including immune score, specific immune cells infiltration, and expressions of immune-related gene families were probed via ESTIMATE, TIMER2.0, TIMER, and R programming. Next, LUAD samples were divided into 3 clusters based on the expression patterns of the 31 regulators by k-means method. The differences of OS, gene enrichment, immune microenvironment of the 3 clusters were compared by Log-rank test, GSVA, ESTIMATE, and CIBERSORTx. Moreover, a m⁶A Score Model was constructed using stepwise regression in this study. The predicting ability of the m⁶A Score Model was verified by GEO LUAD dataset and TCGA Pan- adenocarcinoma dataset.

Results 22 out of 31 regulators showed differential expression levels between LUAD and normal lung (figure 1). 28 out of 31 regulators were linked with OS (figure 2). The frequency of mutation and copy number alterations were 26.6% and 29.1% respectively (figure 3). PCA revealed the 31 m⁶A regulators displayed almost completely distinct distribution patterns between LUAD and normal lung (figure 4). PPI and Metascape enrichment indicated the 31 m⁶A regulators displayed close interrelation (figure 5). Between high and low expression groups of 20, 20 and 29 regulators, tumor purity, immune score, immune cells infiltrations exhibited statistical difference (figure 6). Moreover, 3 clusters displayed distinct OS, gene enrichment, and immune microenvironment (figure 7). Notably, a m⁶A Score Model was built up upon 15 m⁶A regulators (figure 8). The model was associated with OS for LUAD and pan-adenocarcinoma (figure 9).

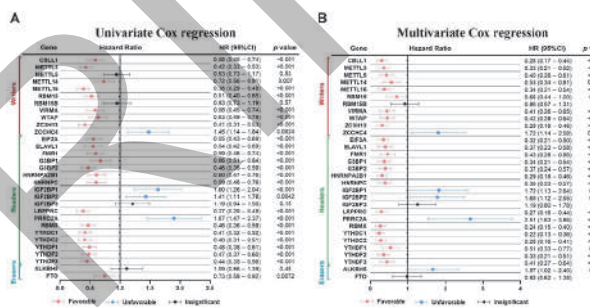
Conclusions m⁶A regulators are associated with molecular features, immune microenvironment and prognosis in LUAD. m⁶A Score could be used as a reference to immunotherapy and a prognostic index for LUAD.

REFERENCE

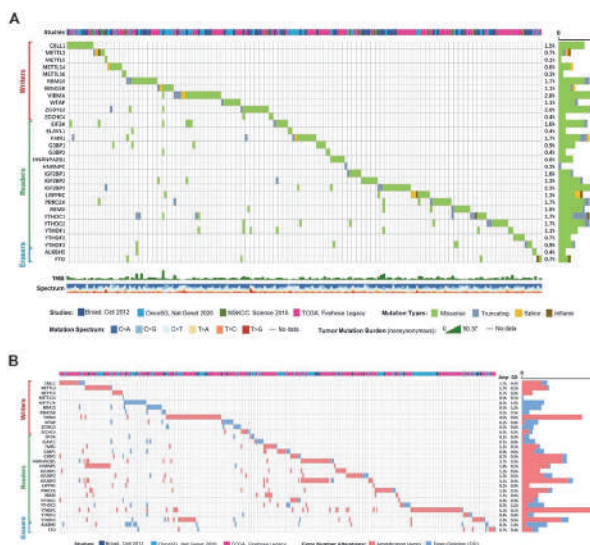
1. Nombela P, Miguel-López B, Blanco S. The role of m6A, m5C and ? RNA modifications in cancer: Novel therapeutic opportunities. *Mol Cancer* 2021;20:18.



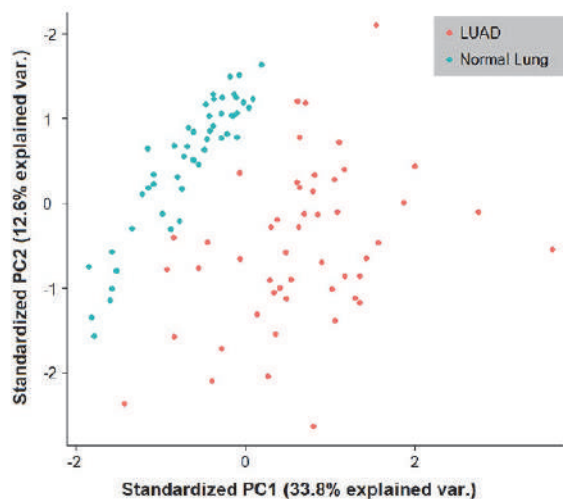
Abstract 1424 Figure 1 The mRNA expression levels of 31 m6A regulators in lung adenocarcinoma and normal lung tissue via TIMER2.0



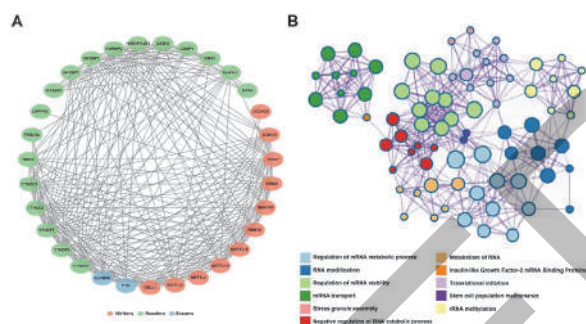
Abstract 1424 Figure 2 (A) The relationship between each m6A regulator and the overall survival in lung adenocarcinoma analyzed by univariate Cox regression via Kaplan-Meier plotter. (B) The relationship between each m6A regulator and the overall survival in lung adenocarcinoma analyzed by multivariate Cox regression via Kaplan-Meier plotter.



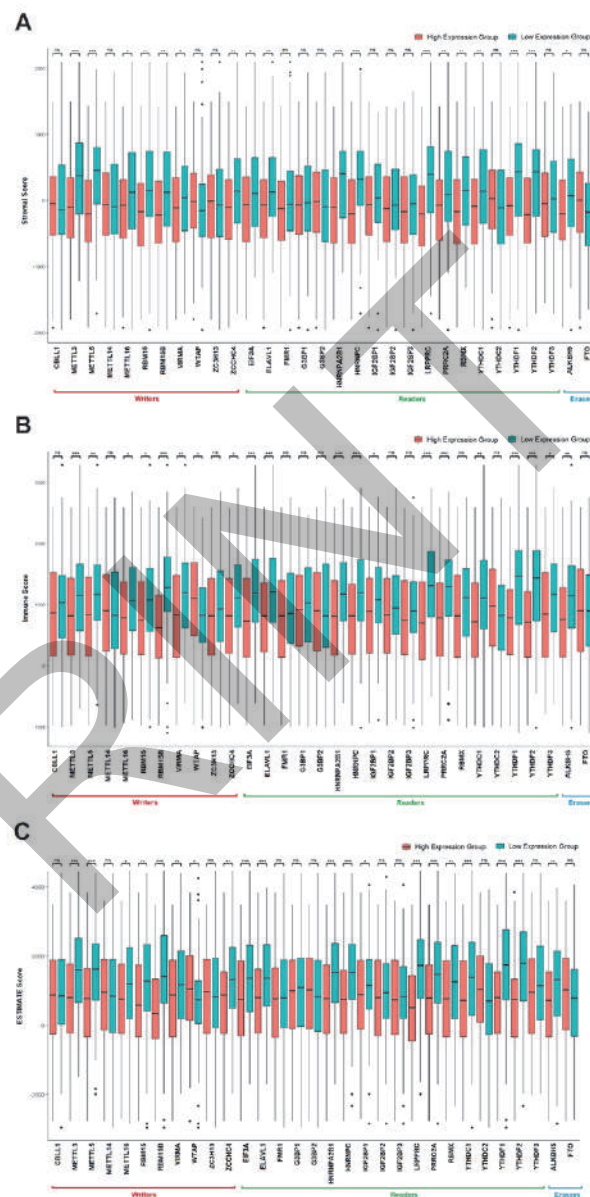
Abstract 1424 Figure 3 (A) Mutations of 31 m6A regulators in 751 lung adenocarcinoma patients from 8 studies via cBioPortal. (B) Copy number alterations frequency of 31 m6A regulators in 1000 lung adenocarcinoma patients from 8 studies via cBioPortal.



Abstract 1424 Figure 4 Principal component analysis of 31 m6A regulators in 50 lung adenocarcinoma samples and 50 normal lung tissue samples from TCGA LUAD cohort.

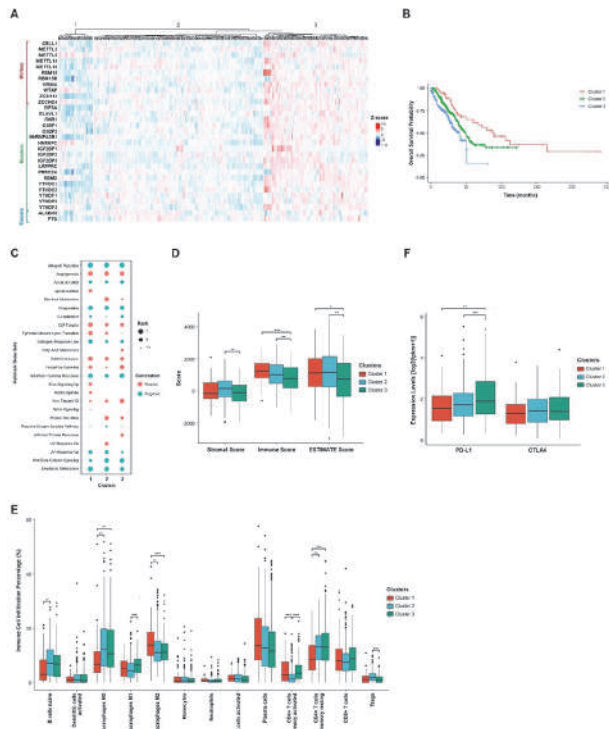


Abstract 1424 Figure 5 (A) Protein-protein interaction network of 31 m6A regulators. (B) Metascape enrichment network of 31 m6A regulators.

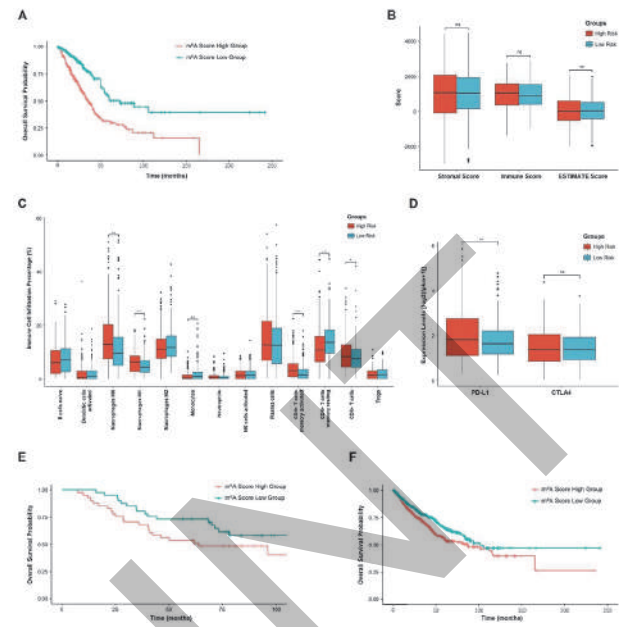


Abstract 1424 Figure 6 (A) Stromal score in high and low expression level groups of each of 31 m6A regulators. (B) Immune score in high and low expression level groups of each of 31 m6A regulators. (C) ESTIMATE score in high and low expression level groups of each of 31 m6A regulators. *** p-value < 0.001, ** p-value < 0.01, * p-value < 0.05, ns: no significance.

Abstracts



Abstract 1424 Figure 7 (A) 3 clusters established according to the expression patterns of the 31 m6A regulators. (B) Overall survival plot of the 3 clusters. (C) Top 10 positively and top 10 negatively enriched hallmark gene sets of the 3 clusters. (D) Comparison of stromal score, immune score, and ESTIMATE score of the 3 clusters. (E) Comparison of specific immune cells infiltrations of the 3 clusters. (F) Comparison of PD-L1 and CTLA4 expression levels of the 3 clusters. *** p-value < 0.001, ** p-value < 0.01, * p-value < 0.05.



Abstract 1424 Figure 9 (A) Overall survival of high and low m6A score groups in training set named TCGA LUAD dataset. (B) Comparison of stromal score, immune score, and ESTIMATE score in high and low m6A score groups. (C) Comparison of specific immune cells infiltrations in high and low m6A score groups. (D) Comparison of PD-L1 and CTLA4 expression level in high and low m6A score groups. (E) Overall survival of m6A score high and low groups in lung adenocarcinoma test set named GSE13213. (F) Overall survival of high and low m6A score groups in pan-adenocarcinoma patients test set named adenocarcinoma subset of TCGA Pan-Cancer dataset. *** p-value < 0.001, ** p-value < 0.01, * p-value < 0.05.

<http://dx.doi.org/10.1136/jitc-2022-SITC2022.1424>



Abstract 1424 Figure 8 Nomogram of m6A to predict overall survival in lung adenocarcinoma.

1425

IN VIVO CRISPR SCREENS IDENTIFY HDAC1 AS AN IMMUNE SENSITIZER REVERSING IMMUNE RESISTANCE DRIVEN BY STK11 LOSS

¹Chengyin Min*, ²Wenrong Zhou, ¹Yi Yu, ¹Shangtao Liu, ¹Xuewen Pan, ¹Jennifer Tsoi, ¹Matthew Goldstein, ¹Alan Huang. ¹Tango Therapeutics, Cambridge, MA, USA; ²WuXi Apptec, Shanghai, China

Background Immunotherapy with checkpoint blockade is effective in only a subset of cancer patients and additional treatment strategies are needed. Here we used a pooled in vivo CRISPR-based genetic screening approach to discover cancer cell intrinsic regulators of immune resistance and sensitization. A two-step approach was taken to uncover tumor suppressor gene loss driving immune evasion as step one, and immune sensitizers specifically reversing the immune evasion driven by certain tumor suppressor loss as step two. Through this approach, we are determined to identify genetic context specific immune sensitizers, also known as synthetic lethal immune targets.

Methods We first performed a pooled CRISPR-Cas9-based in vivo genetic screen targeted to a pre-defined set of tumor suppressor genes to mimic loss-of-function mutations in syngeneic tumor models. CRISPR edited tumor cells were implanted into immune-deficient or immune-competent C57BL/6 mice, a subset of which were treated with anti-PD1 to simulate increased immune pressure in vivo. Tumor samples at the end-point were subjected to next generation sequencing and statistical analysis to identify tumor suppressor genes driving immune evasion. Furthermore, a second pooled CRISPR-Cas9-based in vivo genetic screen targeted to a set of potentially druggable genes was performed in MC38/STK11^{-/-} model vs MC38 wild type model in the presence of increasing immune pressure in vivo. Next generation sequencing and statistical analysis were conducted to uncover STK11 loss specific immune sensitizers.

Results The screen confirmed previously identified immunotherapy targets such as CD47 as well as known drivers of immune resistance in the interferon signaling and antigen presentation pathways. Importantly, STK11 loss was identified as a driver of immune evasion in MC38 and 3LL models. STK11 knockout in MC38 or 3LL tumor cells significantly accelerated tumor growth in immune-competent mice and in these mice treated with anti-PD1. Tumor infiltrating lymphocyte profiling suggests that STK11 knockout induces an immune suppressive tumor microenvironment. Our second step target identification screen discovered HDAC1 as an immune sensitizer specific for STK11 loss context.

Conclusions CRISPR-based in vivo genetic screen is an effective approach to identify tumor cell-intrinsic drivers of immune resistance and sensitization. HDAC1 was identified as an immune sensitizer specifically reversing immune resistance driven by STK11 loss. STK11 mutations are found in ~15% of non-squamous non-small cell lung cancer and have been reported as a predictor of primary resistance to PD-1 blockade. Inhibitors selectively targeting HDAC1 & 2 in combination with anti-PD1 represent a promising therapeutic opportunity for non-small cell lung cancer patients with STK11 mutations.

<http://dx.doi.org/10.1136/jitc-2022-SITC2022.1425>

1426 **COMPREHENSIVE ANALYSIS OF A NOVEL ANTI-PDL1 RESISTANT SARCOMA MOUSE MODEL**

¹Alban Bessede*, ¹Jean Philippe Guegan, ¹Imane Nafia, ¹Assia Chaibi, ¹Christophe Rey, ¹Oren Ngouala, ²Florent Peyraud, ²Antoine Italiano. ¹Explicyte, Bordeaux, France; ²Institut Bergonié, Bordeaux, France

Background Soft Tissue Sarcoma (STS) is known to be resistant to cancer immunotherapy including the prototypical immune checkpoint inhibitor (ICI) anti-PD1 (1). It's therefore crucial to develop innovative strategies aiming at improving current clinical benefit. To this end, a well-characterized sarcoma preclinical model that mimics resistance to immunotherapy is needed. Starting from the anti-PD(L)1-sensitive MCA205 sarcoma mouse model, we therefore aimed at developing and characterizing a novel model resistant to anti-PD1.

Methods Anti-PDL1 antibody was first administered to the ICI-sensitive MCA205 mouse sarcoma model (MCA205-S) and tumor growth was followed overtime. Tumor from a “non-responder” animal – tumor growth profile being similar as in the vehicle group – was then retrieved and processed for tissue dissociation and cell culture. Tumor cells were then amplified and inoculated into immunocompetent C57BL/6 mice that were exposed or not to anti-PD1 antibody, and tumor growth was monitored for a 8-week period. In addition, tumor samples from satellite animals were collected and processed for intratumoral immune landscape characterization by multiparametric flow cytometry as well as for gene expression analysis by RNA sequencing and spatial transcriptomics.

Results While anti-PD1 antibody demonstrated a strong anti-tumor effect in MCA205-S tumor-bearing mice, administration of anti-PD1 to the mice inoculated with the non-responder mouse-originating MCA205 cells did not yield to a significant anti-tumor effect thereby validating the resistant profile of this new MCA205-R cell line. Flow cytometry analysis of tumor-infiltrated immune cells revealed a higher abundance of macrophages (defined as CD11b+/F4:80+) in MCA205-R when compared to the MCA205-S model, which more likely harbor a M2 phenotype. Also, anti-PD1 treatment favored an important MCA205-R tumor infiltration by gMDSC which was more limited in the MCA205-S model. Data from gene expression analysis and spatial transcriptomics will be presented at the meeting.

Conclusions We developed and validated a novel preclinical mouse model of sarcoma (MCA205-R) characterized by its resistance to anti-PD1 and a high tumor infiltration by macrophages. This model – more reflecting the clinic in terms of immunotherapy sensitivity – can thus serve to evaluate novel immunotherapeutic regimens either alone or in combination with reference ICI, to ultimately translate into clinical benefit for STS patients treated with immunotherapy.

<http://dx.doi.org/10.1136/jitc-2022-SITC2022.1426>

1427

COMPARATIVE ANALYSIS OF HUMAN IMMUNE SUBSETS AND RITUXIMAB ANTITUMOR RESPONSE ACROSS MULTIPLE NSG STRAINS ENGRAFTED WITH HUMAN HEMATOPOIETIC STEM CELLS

¹Wonyoung Kang, ²Sunitha Bachawal, ²Anandaroop Mukhopadhyay, ¹Ilian Radichev, ¹Li-Chin Yao, ¹Mingshan Cheng*, ¹James Keck. ¹The Jackson Laboratory, Sacramento, CA, USA; ²Bristol-Myers Squibb, Redwood City, USA

Background Although humanized NSG mice engrafted with hematopoietic stem cells (HSCs), constituting a human immune system, are a robust *in vivo* platform for analyzing effectiveness of novel immune modulators in cancer, inter and intra-experimental variability in immune subsets and anti-tumor response, resulting from utilization of diverse HSC donors, adds complexity to the data, making analysis challenging. To reduce variability, we acquired a significant amount of HSCs from the same donor and humanized six different NSG strains. Frequency and diversity of human immune subsets were characterized across non-tumor bearing humanized mice strains, and treatment effects of Rituximab on tumor burden and immune profiles in Raji-tumor bearing humanized mice were investigated.

Methods The six different NSG strains (NSG, NSG-IL15, SGM3, SGM3-IL15, NSG-TLR4, and NSG-FLT3) were engrafted with 0084 HSCs. Immune subsets in the periphery were assessed by high-dimensional cytometry. Furthermore, the humanized mice in NSG, NSG-IL15, SGM3 and SGM-IL15 strains were implanted with Raji cells subcutaneously and treated with Rituximab two or three times a week for 3 weeks, whole blood and tumors were collected, and the human immune subsets were profiled by flow cytometry.

Results Although the levels of hCD45 engraftment were comparable across the six different humanized strains, CD3⁺ T cells were more enriched in SGM3, SGM3-IL15 and NSG-FLT3, while higher frequency of CD56⁺ NK cell was observed in NSG-IL15, SGM3-IL15 and NSG-FLT3. Furthermore, the human FLT3 transgene expression improved myeloid development in the periphery (NSG-FLT3L ~11.7% vs. NSG ~1%). Interestingly, administration of Rituximab resulted in significant Raji tumor growth inhibition in NSG-IL15, SGM3 and SGM3-IL15 mice, but not in the NSG strain. While CD19⁺ B cells diminished in all humanized strains, trends in CD3 increases in tumor microenvironment were only observed in strains which demonstrated tumor growth inhibition.

Conclusions Humanization of NSG strains engrafted with HSCs from the same donor not only provided an effective platform to assess the influence of different human transgenes on degree and diversity of human immune subsets, but also allowed for investigating Rituximab response in multiple tumor bearing strains with no donor variability. Interestingly, robust anti-tumor effect upon rituximab treatment was observed in NK rich NSG-IL15 and SGM3-IL15 mice suggesting a possible NK driven antibody-dependent cell-mediated cytotoxicity mechanism contributing to tumor growth inhibition. Additionally, antitumor response also seemed to track with an increase in CD3⁺ T cell however the mechanism of action of Rituximab mediated by T cells requires further investigations.

<http://dx.doi.org/10.1136/jitc-2022-SITC2022.1427>

1428

MELANOCYTE-INTRINSIC PDL1 PROMOTES TUMORIGENESIS AND PROGRESSION IN A NOVEL AUTOCHTHONOUS MELANOMA MODEL

¹Carlos Ontiveros*, ¹Yilun Deng, ¹Anand Kornepati, ¹Clare Murray, ²Mary Jo Turk, ¹Harshita Gupta, ¹Alvaro Padron, ²Tyler Curiel. ¹UT Health San Antonio, San Antonio, TX, USA; ²Dartmouth College, Lebanon, NH, USA

Background Tumor PDL1 signals extrinsically to immune cell PD1 to evade antitumor immunity and is highly expressed on distinct cancers.¹⁻⁷ Aside from tumor-extrinsic functions, we and others discovered various pathologic tumor-intrinsic PDL1 signals in distinct cancers, including melanoma.^{2 7 8} We found that melanocytes (the melanoma cell-of-origin) do not express PDL1 but exhibit a gradual progression of PDL1 expression as cells transform from benign nevi to malignant melanomas, suggesting a role for PDL1 in melanomagenesis. We now investigate melanocyte-intrinsic PDL1 signaling, to distinguish bona-fide PDL1 signaling influence on melanomagenesis in the absence of potentially confounding compensatory mechanisms in prior genetic PDL1^{KO} studies in established tumors. We hypothesized that melanocyte-intrinsic PDL1 signals drive melanomagenesis and progression through immune and non-immune mechanisms.

Methods To test melanocyte-intrinsic PDL1 signals during melanomagenesis, we developed an autochthonous, tamoxifen-inducible, UV accelerated, Nras-driven mouse model where mice develop melanomas that are Nras^{Q61R} mutant and lack PDL1 specifically only in melanocytes versus littermates. Mice were induced with tamoxifen on post-natal days 2-3 ± distinct UV exposures and monitored for tumor growth. We established transplantable cell lines from derived tumors and SQ challenged into WT BL6 mice for in vivo treatment studies and studied PDL1 signaling in vitro.

Results Melanocyte PDL1 promotes melanomagenesis in a UV dose-dependent manner. Tumor latency was significantly increased in PDL1^{KO} TN^{Q61R} mice versus littermates at 2 kJ/m² UV (p<0.02) suggesting an immune latency contribution. At 4.5 kJ/m² UV, PDL1^{KO} TN^{Q61R} versus littermate melanoma latencies were indistinguishable, but faster than respective cohorts at 2 kJ/m² possibly from immunosuppression at higher UV doses. Genetic PDL1^{KO} in B16 melanoma induces synthetic lethality to small molecule Chk1 inhibitors by destabilizing Chk2 protein through increased ubiquitination, an effect phenocopied in vitro and in vivo in tumors from PDL1^{KO} TN^{Q61R} versus littermates. Tumors from PDL1^{KO} TN^{Q61R} versus littermates transplanted into WT recipients were resistant to αPD1, αPD1, αPD2, and CD122-biased IL2 immunotherapies, differing from B16 melanomas that are sensitive to all these treatments. Notably, tumor PDL1 suppresses ERK signaling, a downstream target of Nras, in TN^{Q61R} cell lines, suggesting PDL1 control of Nras-mediated oncogenesis.

Conclusions Our novel model dissociates bona-fide cell-intrinsic PDL1 signals from potential genetic PDL1^{KO} compensation confounding effects, allows studies of earliest PDL1 signals in melanomagenesis and progression, helps understand if PDL1 affects Nras-driven oncogenesis, and helps test immunotherapy and small molecule treatment effects. A parallel bladder cancer model was also developed, to be reported later.

Acknowledgements This research was funded by the NIH T32GM113896 (STX MSTP) Award (C.O.). The Clayton Foundation (no grant number) and the NCI (CA204965, CA054515) supported Curiel.

REFERENCES

1. Clark CA, Gupta HB, Curiel TJ: Tumor cell-intrinsic CD274/PD-L1: A novel metabolic balancing act with clinical potential. *Autophagy* 2017;**13**(5):987-988.
2. Clark CA, Gupta HB, Sareddy G, Pandeswara S, Lao S, Yuan B, Drerup JM, Padron A, Conejo-Garcia J, Murthy K, et al: Tumor-Intrinsic PD-L1 Signals Regulate Cell Growth, Pathogenesis, and Autophagy in Ovarian Cancer and Melanoma. *Cancer Res* 2016;**76**(23):6964-6974.
3. Gupta HB, Murray C, Deng J, Mohammad TAS, Zhang X, Wu B, Clark C, Sareddy G, Chen Y, Vadlamudi R, et al: Tumor-intrinsic PD-L1 regulates tumor initiating cell virulence and stemness genes, and TCF1+ stem-like T cells through Raptor in ovarian cancer, which correlates with survival in high grade serous ovarian cancer. *Journal of Immunology* 2019;**202**:195.129.
4. Kornepati AV, Zhang D, Padron AS, Boyd JT, Deng Y, Osta EG, Reyes RM, Shen H, Wang J, Kari S, et al: Tumor cell-intrinsic PD-L1 signals promote DNA damage responses that mediate resistance to Chk1 and PARP inhibitors in vivo. *Journal of Immunology* 2020;**204**:241.233.
5. Hambricht HG, Gupta HB, Padrón Á, Vadlamudi R, Chen Y, Osmulski PA, Curiel TJ: Surface and cytoplasmic tumor cell PD-L1 differentially mediate virulence in ovarian cancer and melanoma through mTOR activation. *Journal of Immunology* 2019;**202**:195.195.
6. Kornepati AVR, Boyd JT, Murray CE, Saifetyarova J, de la Pena Avalos B, Rogers CM, Bai H, Padron AS, Liao Y, Ontiveros C, et al: Tumor-intrinsic PD-L1 promotes DNA repair in distinct cancers and suppresses PARP inhibitor-induced synthetic lethality. *Cancer Res* 2022;**82**(11):2156-2170.
7. Kornepati AVR, Vadlamudi RK, Curiel TJ: Programmed death ligand 1 signals in cancer cells. *Nat Rev Cancer* 2022;**22**(3):174-189.
8. Gupta HB, Clark CA, Yuan B, Sareddy G, Pandeswara S, Padron AS, Hurez V, Conejo-Garcia J, Vadlamudi R, Li R, et al: Tumor cell-intrinsic PD-L1 promotes tumor-initiating cell generation and functions in melanoma and ovarian cancer. *Signal Transduct Target Ther* 2016;**1**(1):1-9.

Ethics Approval All animal studies were approved by the UT Health San Antonio Institutional Animal Care and Use Committee and each experiment was conducted in accordance with the standards required by the UT Health San Antonio Department of Laboratory Animal Resources. Approval number: 09128

<http://dx.doi.org/10.1136/jitc-2022-SITC2022.1428>

1429

IMMUNE RECEPTOR PIRB DELETION IMPACTS PANCREATIC CANCER GROWTH AND ANTI-TUMOR IMMUNE RESPONSE

¹Alessandro Scagliotti*, ¹Claudia Curcio, ¹Silvia Brugiapaglia, ¹Giorgia Tiberi, ¹Francesco Novelli, ²Toshiyuki Takai, ¹Paola Cappello. ¹University of Turin, Torino, Italy; ²Tohoku University, Sendai, Japan

Background Paired immunoglobulin-like receptor B (PIRB), the murine ortholog of human leukocyte immunoglobulin-like receptor B 2 and 3 (LILRB2/3), is an inhibitory receptor expressed on the surface of macrophages, granulocytes, dendritic cells and B lymphocytes, in which it down-regulates their principal functions.¹ The peculiarity of this protein is the presence of three intracellular Immunoreceptor Tyrosine-based Inhibitory Motives, able to recruit Src homology 2 domain-containing protein tyrosine phosphatases (SHP-1/2) when the receptor is activated by contacting its principal ligands, major histocompatibility complex class I molecules.² Previous studies have underlined how PIRB loss is associated with i) the presence of hypersensitive B cells, which display a higher production of antibodies,³ ii) increased cytotoxic T cells² and iii) less suppressive myeloid cells polarized toward an M1-like anti-tumoral phenotype.⁴ In the light of this, we wanted to better characterize extrinsic role of PIRB in modulating the anti-tumoral immune response in mouse models of pancreatic ductal adenocarcinoma (PDA), as well as the intrinsic role.

Methods To this, mice lacking PIRB gene (*Pirb*^{-/-}) were crossed with genetically engineered mice (GEM) that spontaneously develop pancreatic cancer. Histological and immunohistochemical analyses of pancreatic tissues were performed to measure tumor lesions and characterize the immune infiltrate. To investigate the ability to mount a memory response, OVA-expressing PDA cells were used as immunizer. ELISPOT experiment was performed to assess IFN γ and IL17 secretion. ELISA assay was performed on sera to investigate anti-tumor humoral response. MTT and soft agar assay were performed to investigate proliferative and colony formation ability of wild-type and *Pirb*^{-/-} PDA cell lines respectively.

Results PIRB ablation significantly improved survival rate of GEM compared to the *Pirb* proficient counterpart, and this correlated with a reduced percentage of transformed ducts. Immunohistochemical analyses of pancreatic tissues demonstrated increased frequency of effector immune cells inside the tumor microenvironment. The absence of PIRB significantly delayed OVA-expressing PDA cell engraftment after immunization with OVA and increased also both antigen specific T and B cell response. Concerning the intrinsic role, in vitro experiments showed a lower proliferation rate and a lower colony formation ability by *Pirb*^{-/-} PDA cell line.

Conclusions Overall, PIRB represents a promising target to improve the anti-tumor immune response and deserves further characterization to design novel immunotherapy strategies for the treatment of PDA.

REFERENCES

1. Kang X, Kim J, Deng M, John S, Chen H, Wu G, Phan H, Zang C, Inhibitory leukocyte immunoglobulin-like receptors: Immune checkpoint proteins and tumor sustaining factors. *Cell Cycle* 2016;**15**:25-40
2. Endo S, Sakamoto Y, Kobayashi E, Nakamura A, Takai T, Regulation of cytotoxic T lymphocyte triggering by PIR-B on dendritic cells. *PNAS* 2008;**105**:14515-14520
3. Ujike A, Takeda K, Nakamura A, Ebihara S, Akiyama K, Takai T, Impaired dendritic cell maturation and increased TH2 responses in PIR-B^{-/-} mice. *Nat Immunol* 2002;**3**:542-548

4. Ma G, San P, Eisenstein S, Divino C, Chen S, Paired Immunoglobulin-like Receptor-B Regulates the Suppressive Function and Fate of Myeloid-Derived Suppressor Cells. *Immunity* 2011;**34**:385-395

Ethics Approval The animal study was approved by the Italian Ministry of Health; approval number 624/2020-PR

<http://dx.doi.org/10.1136/jitc-2022-SITC2022.1429>

1430

THE IMMUNOLOGICAL AND GENOMIC PROFILING OF COLORECTAL AND BREAST CANCER CELL LINES CAN DISTINGUISH STEM LIKE FROM DIFFERENTIATED TUMOR CELLS: IMPLICATIONS FOR CANCER IMMUNOTHERAPY

¹Neha Gopinath, ²Tanwir Habib, ¹Mohammed Toufiq, ¹Alice Turdo, ¹Asma Al-Sulaiti, ¹Ishita Gupta, ¹Rebecca Mathew, ¹Harshitha Shobha Manjunath, ³Matilde Todaro, ³Giorgio Stassi, ¹Sara Tomei, ⁴Soldano Ferrone, ⁵Ira Skvortsova, ¹Cristina Maccalli*. ¹Sidra Medicine, Doha, Qatar; ²Weill Cornell Medicine, Doha, Qatar; ³University of Palermo, Palermo, Italy; ⁴MGH, Pittsburgh, PA, USA; ⁵University of Innsbruck, Innsbruck, Austria

Background Rare cells endowed with “stemness” and tumor initiating properties, cancer stem cells (CSCs), are considered responsible of metastatization and resistance to therapy, including immunotherapy. The aim of this study is to identify the molecular mechanisms regulating the immunological properties of CSCs isolated from solid tumors.

Methods CRC (N=15) and BC (N=21) cell lines), including differentiated tumor cells and CSCs, and, for BC cell lines, selected in vitro for radioresistance or invasiveness were used for this study. The expression of HLA molecules and the components involved in the antigen processing machinery (APM) was assessed through flow cytometry. DNA and RNA were isolated from these cell lines. The nCounter platform (Nanostring) was utilized to assess the hybridization with 800 probes for miRNAs and the RNA seq-based transcriptomic profile was also assessed. The methylation profiling of cancer cell lines was investigated through Infinium EPIC arrays (Illumina). In addition, the co-culture of tumor cells with HLA-matched lymphocytes, either with or without the treatment with immunomodulatory or epigenetic agents, was performed to assess the ability of the CRC and BC cells to elicit antigen-specific T cell responses.

Results A general impairment of the expression of HLA and APM (e.g., LMPs, TAP and tapasin) molecules was observed in CRC and BC lines. The down-modulation of the expression of HLA and APM was superior in “stem-like” cells as compared to the differentiated tumor cells. The treatment of these cells with immunomodulating or epigenetic agents could only partially restore the expression of these molecules. The induction in vitro of anti-tumor T cell responses through the co-culture of tumor cells with PBMCs, was suboptimal and with variability depending on the subtype of cells and the pre-treatment or not of tumor cells with either immunomodulating or epigenetic agents.

Differential miRNAs, transcriptomic and methylation profiles ($p < 0.05$) were identified in either CRC or BC cells with stemness properties vs. differentiated cells, and in different subtypes of cells. These includes genes and their regulators involved in immunological functions.

The integration analyses among methylation, miRNAs and transcriptomic profiles is under investigations, although preliminary results are available showing the differential involvement in CSCs vs. differentiated tumor cells of immune related pathways.

Conclusions The immunological and genomic profiles of CRC and BC are associated with cell subtypes. These investigations will contribute to understand the mechanisms regulating the biological and immunological properties of tumor cell endowed with variable cell fate and their susceptibility to immunotherapy.

Acknowledgements This study was funded by QNRF; grant # NPRP10-0129-170277

Ethics Approval The study obtained ethics approval from both Sidra Medicine #1805024172, and Hamad Medical Corporation #MRC-03-17-150 institutional review boards; participants gave informed consent before taking part to the study.

<http://dx.doi.org/10.1136/jitc-2022-SITC2022.1430>

1431 **INTRATUMORAL PH 109 INTASYL™ SELFDELIVERING RNAI TARGETING CONNECTIVE TISSUE GROWTH FACTOR PROVIDES EFFICACY IN VIVO IN A MOUSE MODEL OF METASTATIC BREAST CANCER**

Benjamin Cui^{ffo*}, Melissa Maxwell, Dingxue Yan, Andrew Boone, Brianna Rivest, Shenghua Zhou, James Cardia, Simon Fricker. *Phio Pharmaceuticals, Marlborough, MA, USA*

Background Breast cancer is the most diagnosed cancer and the second leading cause of cancer-related deaths globally among women, frequently due to metastatic disease. CTGF orchestrates diverse multicellular processes including embryonic development, wound healing, and tissue repair. CTGF promotes inflammatory diseases and contributes to cancer cell proliferation, migration, invasion, metastasis, and epithelial-mesenchymal transition. High CTGF is associated with poor prognosis in breast cancer. CTGF-inhibition has shown promise in decreasing metastatic dissemination and sensitizing to cancer cells to chemotherapy in preclinical models. PH-109 is a self-delivering RNAi compound built on proprietary INTASYL™ technology, designed to silence human CTGF with high specificity and without need for specialized formulations or drug delivery systems. PH-109 was originally developed and approved as an investigational new drug (IND) for treatment of dermal hypertrophic scarring (Phase 2; NCT02246465) and subretinal fibrosis (Phase 1/2; NCT02599064). Treatment resulted in a statistically significant reduction of CTGF mRNA and protein at the treatment site, with no significant toxicity or adverse effects. Here we present proof-of-concept (POC) in vivo data showing efficacy of intratumorally administered PH-109 in an orthotopic 4T1 model of metastatic mammary cancer.

Methods PH-109 mediated mRNA silencing of CTGF was validated in 4T1 cells in vitro by RT-qPCR. In vivo, 4T1 cells were implanted into the mammary fat pad of BALB/c mice. When tumors reached threshold volume (150 mm³), animals were randomized into treatment groups; test treatments were administered intratumorally (IT) on Days 1, 4, 7, 10 and 13. Vehicle (PBS), a chemically-identical non-targeting control (NTC) INTASYL or PH-109 at two dose concentrations (0.5 mg; 2 mg) were administered IT; doxorubicin chemotherapy (5 mg/kg) was administered intraperitoneally on Days 1, 7, 13. Tumor volumes and body weights were recorded longitudinally. Primary tumors were resected from each animal at ~500 mm³ in survival surgeries and stained with anti- α -SMA to assess stromal content by immunohistochemistry. Three weeks post-resection animals were euthanized and lungs insufflated with India ink and lung macrometastases enumerated.

Results PH-109 provided concentration-associated silencing of CTGF in vitro. In vivo, IT PH-109 elicited antitumor efficacy and improved outcome compared with vehicle- or NTC-treated tumors. In contrast to doxorubicin, PH-109 showed no evidence of toxicity as indicated by weight loss.

Conclusions PH-109 was previously evaluated in over 150 patients without significant toxicity. This, combined with these data in a clinically relevant orthotopic mouse model of metastatic breast cancer, could support accelerated clinical investigation of PH-109 as an anticancer therapeutic.

Ethics Approval Animal studies were performed at Pharma Models LLC, Marlborough, MA 01752, under standard protocol approved by their IACUC.

<http://dx.doi.org/10.1136/jitc-2022-SITC2022.1431>

1432 **DISCOVERY OF HIO 3 A TUMOR-PRODUCED PROTEIN THAT BINDS THE HUMAN IGG1 FC CH3 DOMAIN AND SUPPRESSES ANTIBODY DEPENDENT CELLULAR CYTOTOXICITY AND COMPLEMENT DEPENDENT CYTOTOXICITY**

Nicolas Nicolaides, Luigi Grasso, Brad Kline*. *Navrogen Inc., Cheyney, PA, USA*

Background Human cancers employ a number of mechanisms to evade host immune responses against novel antigens generated from aberrant over-expression, mutations and/or epigenetic alterations. Humoral immunity utilizes antibodies and immune-effector cells as well as molecular immune complexes involving the complement system to mediate the killing of dysregulated cancer cells. We refer to these anti-cancer mechanisms as Humoral Immuno-Oncology (HIO). Suppression of HIO is mediated by tumor-produced proteins called HIO factors. One such factor is CA125, which was previously shown to bind IgG-type antibodies and inhibit their antibody dependent (ADCC) and complement dependent (CDC) cellular cytotoxic activities. Using a combination of experimental screening and literature searches, we screened a number of proteins that have been produced by tumors and associated with a variety of cancer indications to determine if they could impact HIO. Herein, we describe the initial characterization of soluble ICAM-1 (sICAM-1), a tumor antigen capable of binding IgG-type antibodies that inhibits their immune-effector activity.

Methods Deletion and site-directed mutagenesis of the heavy constant domain of IgG1 was performed and constructs expressed as GST fusions in 293F cells. Recombinant proteins were then used in direct binding and competition ELISA formats to determine amino acid residues essential for binding of HIO-3. Constant region mutants that lost HIO-3 binding were then generated to whole IgG constructs for in vitro characterization of HIO-3 resistance.

Results Amino acid substitutions in this domain were able to abrogate sICAM-1 binding and overcome ADCC suppression.

Conclusions These findings highlight yet another mechanism by which tumors can suppress the host's immune system for survival and offers new concepts for developing antibody-based therapies that can aid in the treatment of various cancer indications. Moreover, the findings here offer clinical design opportunities to improve upon existing approved immune-mediated therapies for which this factor is present.

<http://dx.doi.org/10.1136/jitc-2022-SITC2022.1432>

1433

CHARACTERIZATION OF THE SPATIAL AND TEMPORAL DISTRIBUTION OF TUMOR RESIDENT IMMUNE CELL POPULATIONS IN A 3DEXPLORE HUMAN TUMOROID MODEL AND ASSESSMENT OF RESPONSE TO IMMUNOTHERAPEUTICS EX VIVO

Seth Currllin*, Sharon Camacho, Angie Rivera, Jared Ehrhart, Soner Altioik. *Nilogen Oncosystems, Tampa, FL, USA*

Background Tumor cells cause significant chemical, cellular and physical alterations to surrounding tissue. The resulting tumor microenvironment (TME) includes a diverse population of immune and stromal cells contributing to tumor development and response to immunotherapeutic drugs. The 3D-EXplore ex vivo tumoroid platform enables high-throughput drug discovery within human tumor samples with intact TME for improved clinical translation. The work herein provides an in-depth assessment of the heterogenous TME for multiple cellular populations including immune, stromal and tumor cells, as well as non-cellular components of the extracellular matrix (ECM) in a tumor 3D tumoroid platform using fresh patient tumor tissue.

Methods Tumoroids from fresh RCC tumor samples measuring 150 μm in size were generated using a proprietary mechanical process without any enzymatic digestion or propagation. This study was approved by Vanderbilt University Ethics Board, approval number 031078. An array of multiplexed immunofluorescent panels including lymphoid and myeloid markers were applied at timed endpoints with drug treatments ex vivo to highlight dynamic changes among tumor, immune and stromal components of the TME. Samples were then imaged with confocal microscopy.

Results In this study we analyzed the interaction between the tumor cells (CA9), cancer-associated fibroblasts (FAP), and endothelial cells (CD31) in patient renal cell carcinoma tumoroids. Systematical mapping of the immune landscape in tumoroids treated ex vivo with a STING agonist alone or in combination with nivolumab with a cGAS-STING pathway activation allowed characterization of the spatial and temporal distribution of tumor resident T-cells (CD3, CD4 and CD8), B-cells (CD20), and macrophages (CD68, CD163, and CD11b) in the intact tumor microenvironment. These findings were correlated with treatment-mediated changes in tumor cell killing. To further document treatment mediated changes in the tumor immune microenvironment, we performed 17-plex cytokine release assays (GM-CSF, scd137, ifn γ , sfas, sfasl, Granzyme A, Granzyme B, IL-2, IL-4, IL-5, IL-6, IL-10, IL-13, MIP-1 α , MIP-1 β , TNF- α , Perforin) with supernatants collected from ex vivo treated tumoroid cultures.

Conclusions In this comprehensive multiplexed immunofluorescence 3D tumoroid study we demonstrated that the 3D-EXplore ex vivo platform supports an intact tumor microenvironment, ideal for monitoring treatment-induced changes in the tumor resident immune cell populations and their interaction with the epithelial and stromal components of the tumor.

Ethics Approval All tissues in this study were collected under proper patient consent and approved by the Institutional Ethics Board, approval number Pro00014313

<http://dx.doi.org/10.1136/jitc-2022-SITC2022.1433>

1434 **INTERPLAY BETWEEN THE TUMOUR AND GUT MICROBIOME AND THE TUMOUR IMMUNE MICROENVIRONMENT IN COMPLETE RESPONDER CANCER PATIENTS**

¹Nicola Annels*, ¹Tyler Wooldridge, ¹Kate Relph, ¹Anna Krukowsha, ²Izhar Bagwan, ¹Hardev Pandha. ¹University of Surrey, Guildford, UK; ²Royal Surrey NHS Foundation Trust, Guildford, UK

Background The most important insights into mechanisms of tumour rejection, and how these could be exploited therapeutically, is likely to come from patients displaying the best responses. Those individuals with complete and sustained anti-tumour responses, without maintenance therapy, will provide the best evidence of genuine disease modification. Despite much speculation as to how these exceptional responses are generated there is increasing evidence for an immune basis which may be influenced by the tumour microbiome underlying the mechanism for sustained tumour rejection.

Methods To focus on individuals with complete and sustained metastatic disease resolution, we designed a pilot study, the Continuum Long-Term Survivor study, to evaluate patients with the best outcomes, where disease modification may have occurred. The study targeted only those patients (n=50) with a sustained (>5 years) complete clearance of metastatic cancers, without requiring maintenance therapy. Matched controls comprised patients unable to generate an initial response, or those who relapsed within 12 months. DNA extracted from tumour samples was analyzed by 16S BENCHMARK™ microbial amplicon sequencing (Diversigen) to profile the tumour microbiome, whilst the microbial composition of stool samples was determined using BoosterShot Shotgun Sequencing. In parallel mRNA expression from the tumour tissue was evaluated using NanoString's PanCancer IO360 gene expression panel. From a homogeneous subgroup of bowel cancer long-term survivors and their matched controls, multiplex IHC using a panel of 8 immune markers to identify tertiary lymphoid structures (TLS) was performed on the tumour tissues and imaged using a PhenoImager (AkoyaBiosciences).

Results Results will be presented comparing tumour and gut-derived microbial species diversity between long-term vs. short-term survivor matched controls using alpha diversity estimates as well as differential abundance analysis. This will define the microbial species that are more likely to be associated with long-term survivorship. Characterization of the immune gene transcriptional patterns within the tumour microenvironment (TME) from long-term survivors vs controls will also be reported along with any observed differences from the multiplex IHC analysis of immune infiltrates in corresponding patient tissue. To explore any connections of the tumour-microbiome on the TME, an integrated analysis of the microbiome and tumour immune transcriptome will be presented.

Conclusions This study will reveal whether changes in TME influenced by the tumour microbiota may be important factors associated with long-term survivorship. Understanding the precise mechanisms of total tumour rejection in patients, and their evaluation may be game-changing in terms of design of new molecular, biological and immune therapies.

Ethics Approval This study was approved by the University of Surrey Ethics Board; approval number 266581.

<http://dx.doi.org/10.1136/jitc-2022-SITC2022.1434>

1435

COMPARISON OF THE CYTOKINE AND CHEMOKINE SECRETOME OF BENIGN AND MALIGNANT PERITONEAL FLUID IDENTIFIES FGF AND IL 1R ALPHA AS POTENTIAL DRIVERS OF TUMOR GROWTH

¹Patrick Wagner*, ²Vera Donnenberg, ¹Christian Cruz Pico, ²Albert Donnenberg, ¹David Bartlett. ¹Allegheny Health Network Cancer Institute, Pittsburgh, PA, USA; ²University of Pittsburgh School of Medicine, Pittsburgh, PA, USA

Background Peritoneal fluid, in patients with carcinomatosis, constitutes a fluid phase tumor microenvironment that could contribute significantly to tumor progression in the peritoneal cavity. Little is known of the changes in cytokine or chemokine concentration (i.e., the secretome) along the spectrum from benign physiologic peritoneal fluid to fluid from patients with localized abdominal malignancy to those with frank carcinomatosis. In this study, we compare the peritoneal fluid secretome from participants in each of these categories to identify potential drivers of tumor growth and dissemination in the peritoneal fluid tumor microenvironment.

Methods In this pilot study, we compared the normal peritoneal secretome (n=5, derived from patients undergoing elective surgery for benign conditions) with that of abdominal cancer patients (colon, stomach, cholangial, liver, appendix, pancreas cancers), either with (n=29) or without (n=21) carcinomatosis. The peritoneal secretome of patients without carcinomatosis was also compared to that of their serum (n=22). The peritoneal fluid secretome was defined as quantitative assessment of cytokine and chemokine concentrations from fluid specimens, as determined using the Luminex 38plex panel plus IL-6Ralpha and TGF-beta.¹

Results The secretomes of benign physiologic fluid and peritoneal fluid collected from patients with cancer but without carcinomatosis were indistinguishable, but differed from serum in having markedly upregulated FGF2 and IL1Ralpha concentrations. The secretome of peritoneal fluid from patients without carcinomatosis had higher FGF2(1983 pg/mL) than either serum (400-fold, p=0.000000) or malignant ascites (50-fold elevation, p=0.000002). However, the peritoneal fluid from patients with carcinomatosis had significantly elevated levels of GRO, EGF, EOTAXIN, TGFalpha, sCD40L, CCL22, CX3CL1, CXCL10, GM-CSF, TGFbeta, TNFalpha, VEGF, MCP3, MIP-1beta, IL-1beta, IL-6, IL-6Ralpha, IL-10 and IL-12.

Conclusions Physiologic peritoneal fluid contains markedly elevated levels of FGF2 and IL1Ralpha, which may contribute to tumor progression by driving the epithelial to mesenchymal transition or through down regulation of E-cadherin,² among other mechanisms. We identified characteristic secretome abnormalities of peritoneal fluid derived from patients with carcinomatosis, compared with physiologic fluid or patients with localized cancers. The secretome profile described here could find utility both in developing biomarkers of advanced disease status and in identifying potential targets for directed immunotherapeutic interventions in patients with peritoneal malignancy.

REFERENCES

1. Donnenberg AD, Luketich JD, Donnenberg VS, Secretome of pleural effusions associated with non-small cell lung cancer (NSCLC) and malignant mesothelioma: therapeutic implications. *Oncotarget* 10 (2019) 6456-6465.
2. Lau M-T, So W-K, Leung PCK, Fibroblast Growth Factor 2 Induces E-Cadherin Down-Regulation via PI3K/Akt/mTOR and MAPK/ERK Signaling in Ovarian Cancer Cells. *PLoS one* 8 (2013) e59083.

Ethics Approval The study was approved by the Institutional Review Board of Allegheny Health Network (Protocol 2021-085). Informed consent was obtained from all study participants.

<http://dx.doi.org/10.1136/jitc-2022-SITC2022.1435>

1436

MODULATION OF CYTOKINE SECRETION AND MACROPHAGE DIFFERENTIATION IN A 3D HETEROTYPIC SPHEROID MODEL OF COLON CANCER

Jacqueline Bersano, Hiren Gosh, Eva Oswald, Kanstantsin Lashuk, Julia Schueler*. *Charles River Laboratories, Freiburg, Germany*

Background The tumor's immunogenicity is modulated by the tumor microenvironment (TME), which mostly turns out to be immunosuppressive, thereby promoting disease progression. To better understand the crosstalk between tumor, immune and stromal cells we developed an in vitro system enabling the interaction of the different cell types in a 3D environment.

Methods We cultivated three different colorectal cancer cell lines HCT-116, HT-29 and CXF269, two fibroblast lines, human dermal fibroblasts (HDF) or cancer associated fibroblasts (CAFs) and macrophages from healthy donors as mono-, co- and triple cultures in a matrigel-collagen matrix in a 96-well format. Analysis of the secreted cytokines in the supernatant as well as the differentiation of the macrophages was performed after 10 days of culture. We analyzed 45 cytokines in duplicates by using a multiplex bead-based assay. The macrophage differentiation was determined by flow cytometry (FC) based on the expression of CD45, CD11b, CD86 and CD209.

Results The macrophages in monoculture displayed a M1/M2 ratio of 1.39 after 10 days of culture. The co-culture with HDF did not change the phenotype dramatically whereas the cell-cell contact with CAFs induced a marked increase in M1 leading to a ratio of 3.36. A similar diverse pattern was seen in co-culture with tumor lines. Whereas HT29 did not influence the ratio remarkably, HCT116 reduced the ratio to 1.14 and CXF269 increased the M2 fraction clearly, leading to a M1/M2 ratio of 0.85. The triple culture with CAFs presented an additive effect on the macrophage polarization: CAFs led to an increase in the M1 population which was most pronounced in HT29 and least distinct with CXF269. The triple culture with HDF supported the M2 population most prominent in the CXF269 (M1/M2 ratio: 0.77). The presence of fibroblasts induced an enhanced secretion of IL-6, CCL2 and CCL3 in all settings. All tumor lines secreted high levels of VEGF-A and SDF-1 in mono- and co-culture with fibroblasts. However, the secretion was down regulated in the presence of macrophages. Finally, the addition of macrophages to any co-culture induced an increase of IL-1R α in the supernatant. A cluster analysis of the cytokine data defined two major clusters mainly separated by the presence or absence of macrophages.

Conclusions The modular nature of the 3D heterotypic spheroid model enables the deconvolution of the different players in the TME. This flexible mid throughput platform will hopefully help to shed more light into the complex role of tumor associated macrophages in cancer progression.

<http://dx.doi.org/10.1136/jitc-2022-SITC2022.1436>

1437

SINGLE CELL PROFILING OF PANCREATIC DUCTAL ADENOCARCINOMA TUMOR MICROENVIRONMENT IN RESPONSE TO FLT3 LIGAND REVEALS MOLECULAR AND CELLULAR INTERACTION BETWEEN DENDRITIC CELL LINEAGE AND CANCER ASSOCIATED FIBROBLASTS

¹Pratha Budhani*, ¹Brianna Flynn, ¹Robert Norgard, ¹Joshua Tagore, ¹Lucinda Thiede, ¹John Holt, ²Shengyang Wu, ²Chris Kang, ¹Xiaobin Wang, ¹Jessica Potts, ¹Charlie Cote, ¹Greg Peet, ¹Ruby Wasti, ¹Mohanapriya Kamalakannan, ¹Varenka Rodriguez DiBlasi, ¹Sarah O'Brien, ¹Abhishek Kashyap, ¹Kang Liu. ¹Boehringer Ingelheim, Ridgefield, CT, USA; ²Analytical Biosciences, Beijing, China

Background Pancreatic ductal adenocarcinoma (PDAC) has an environment characterized by heterogeneity in cancer associated fibroblasts (CAF) as well as an immune desert phenotype. It is well-established that dendritic cells (DCs) which are often dysfunctional in the PDAC tumor microenvironment (TME), are crucial in priming and sustaining T cell immunity. It is speculated that this immune dysfunction is potentially caused by crosstalk between DCs or their progenitors with tumor or CAF, but this mechanism is not well characterized. Flt3L is known to drive expansion and mobilization of DCs, in particular, the cross-presenting DC1s into the tumor.

Methods We utilized a magnetic bead-based method to capture the tumor, immune and stromal components of the KPCY (Pdx-1-Cre, KRAS^{G12D}, p53^{-/-}, YFP⁺) TME in response to Flt3L injection followed by scRNAseq profiling to examine overall changes.

Results As expected, Flt3L injection induced increased DC numbers in the TME. Interestingly we observed several genes downregulated in tumor cells and a change in the CAF subpopulation upon Flt3L treatment. Because tumor and CAF cells do not express Flt3, our observation suggests this change results from the cross-talk between Flt3-induced DC lineage with tumor and/or CAF subpopulations. Using differential expression of gene (DEG), pathway and ligand-receptor analysis, we characterized molecular interactions between Flt3L-responsive DC lineage with tumors and CAF cells in the TME.

Conclusions Our results highlight the impact of these DCs on tumors and TME stroma as an additional function to shape immune response, thereby providing a rationale to modify TME with Flt3 agonism.

<http://dx.doi.org/10.1136/jitc-2022-SITC2022.1437>

1438 **INTEGRATIVE ANALYSIS OF SINGLE CELL MULTIOMICS DATA USING DEEP LEARNING TO IDENTIFY IMMUNE RELATED BIOMARKERS IN A PATIENT DERIVED 3D EX VIVO TUMOROID PLATFORM**

¹Sarah Carl, ¹Juana Flores-Candia, ²Jeremy Staub, ²Jasmin D'Andrea, ²Brittney Ruedlinger, ²Kate Shapland, ²Jared Ehrhart*, ²Soner Altioik. ¹Scailyte AG, Basel, Switzerland; ²Nilogen Oncosystems, Tampa, FL, USA

Background Our previous studies demonstrated that multiple types of omics data obtained from Nilogen's comprehensive 3D-EXplore ex vivo drug testing platform using tumoroids with intact tumor microenvironment prepared from unpropagated fresh patient tumor samples can reveal cellular mechanisms that are active in individual tumors. This approach allows classification of tumors into subtypes for response to immunotherapeutic drug treatments. Here we aimed to utilize Scailyte's cluster-free, unbiased, and highly sensitive AI platform ScaiVision to better understand the cellular and molecular mechanisms of cGAS-STING activation alone or in combination with an anti-PD-1 treatment to discover clinically relevant biomarker signatures.

Methods For the 3D-EXplore ex vivo platform, tumoroids measuring 150 µm in size were prepared from procured fresh tumor tissue of renal cell carcinoma (RCC) and colorectal carcinoma (CRC) patients. The study was approved by the Institutional Ethics Board, approval number Pro00014313. Tumoroids were generated using a proprietary mechanical process without any enzymatic digestion or propagation and were treated ex vivo with STING agonists ADU-S100 and 2'3'cGAMP alone or in combination with nivolumab. Treatment-mediated changes in the tumor immune microenvironment were analyzed using Cellular Indexing of Transcriptomes and Epitopes by sequencing (CITE-seq), multicolor flow cytometric analysis, and multiplex cytokine release assays.

Results Here we present the results from the integrative analyses of multiomic data generated from the treatment of fresh patient tumor samples in the ex vivo assays. To identify cellular and molecular mechanisms associated with ex vivo responses to the cGAS-STING pathway activation and PD-1/PD-L1 checkpoint blockade therapy we used a supervised machine learning algorithm (ScaiVision) that trains a convolutional neural network with a single layer to predict sample-level labels using single-cell data as inputs. This approach allowed an in-depth characterization of the tumor resident immune cell subsets in the patient tumoroids before and after ex vivo drug treatment to reconstruct cell-type-specific signaling responses to identify cell populations associated with response to immunotherapeutics ex vivo.

Conclusions Our results revealed that the ScaiVision platform allows the integration of high-parameter single-cell data together with multiple types of omics data derived from Nilogen's 3D-EXplore platform to better understand molecular and cellular mechanisms of drug mode of action that may allow the discovery of new clinically-relevant immune-related biomarkers to predict clinical outcome of immunotherapy.

Ethics Approval All tissues were collected under proper patient consent and the study approved by the Institutional Ethics Board, approval number Pro00014313

<http://dx.doi.org/10.1136/jitc-2022-SITC2022.1438>

1439

TERMINALLY EXHAUSTED CD8⁺TILS PROMOTE AGGRESSIVE CANCER STEM CELLS WHILE CONCURRENTLY EVADING ANTI PD1 THERAPY

¹Sukanya Dhar, ¹Saurav Bera, ²Kamalika Roy, ³Abhipsa Sinha, ¹Anirban Sarkar, ¹Shayani Dasgupta, ¹Avishek Bhuniya, ¹Akata Saha, ¹Saptak Banerjee, ¹Neyaz Alam, ¹Manisha Vernekar, ²Chiranjib Pal, ³Dipak Dutta, ¹Rathindranath Baral, ¹Anamika Bose, ¹Mohona Chakravarti*. ¹Chittaranjan National Cancer Institute, Kolkata, India; ²West Bengal State University, Barasat, India; ³CSIR Central Drug Research Institute, Lucknow, India

Background Tumor-infiltrated CD8⁺T cell (TIL) heterogeneity is serving as one of the major hurdles in successful PD1 therapy. According to recent reports, among two subpopulations of exhausted CD8⁺TILs, (progenitor-exhausted, CD8⁺T_{PEX}; terminally-exhausted, CD8⁺T_{TEX}), CD8⁺T_{TEX} do not respond to anti-PD1 therapy.¹⁻³ However, functional status of intra-tumoral-CD8⁺T_{TEX} remains elusive. Whether and how they participate in tumor advancement holds immense clinical importance. Given the prominence of Cancer Stem Cells (CSCs) in establishing metastatic cancer progression by evading therapies, we became interested to study CD8⁺T_{TEX} behaviour in terms of CSC regulation.

Methods CD8⁺T_{TEX} (Lin⁻PD1⁺TCF1⁻) and CSC (Lin⁻CD44⁺CD24⁻CSCs) frequency and their co-relation in regards to tumor advancement were analysed in human carcinomas (n=33; from 22 breast and 11 ovarian carcinoma patients). Furthermore, MACS-isolated CD8⁺T-cells from human-PBMC or murine-spleenocytes were repeatedly exposed to tumor-lysate and tumor-supernatant in presence of antigen-loaded DCs for 120h to obtain CD8⁺T_{TEX} (PD1⁺TIM3⁺TCF1⁻CXCR5⁺IFN γ ^{low}) in-vitro. These CD8⁺T_{TEX} were co-cultured with MCF7, MDAMB-231 and 4T1 cells respectively to study the influence of CD8⁺T_{TEX} on CSCs. RT-PCR, colony-formation assay, matrigel-invasion-assay, tumour-sphere assay and in-vivo tumorigenicity assay with Crl:NU-Foxn1nu athymic nude mice were utilized to characterise CD8⁺T_{TEX} influenced CSCs. ELISA, Western-blot, flow-cytometry, immune-staining, pharmacological inhibition or genetic knockdown by in-vitro and in-vivo si-RNA silencing were used to study mechanism behind CD8⁺T_{TEX}-CSC cell-interaction.

Results Screening of human primary tumors disclosed that CD8⁺T_{TEX} cells remain strongly enriched across cold (low-TIL frequency) advanced-carcinomas, compared to hot (high-TIL frequency) advanced-carcinomas (p<0.001). Additionally, CD8⁺T_{TEX} cells positively correlated with CSC frequency (r = 0.8809) throughout cold-advanced carcinomas; suggesting their interdependency on tumor advancement. Furthermore, in-vitro co-culture assay as well as in-vivo adoptive transfer of CD8⁺T_{TEX} resulted in increment of intra-tumoral CSC frequency. However, this upregulation was not brought down by anti-PD1 therapy (p<0.001). Additionally, CD8⁺T_{TEX}-influenced-CSCs exhibited increased tumorigenic and metastatic potential in athymic-nude mice. They showcased invasive and migratory phenotype with long invadopodia by overexpressing CXCR4, MMP7 and Cofilin (figure 1). These CSCs remained sustained by overexpressing OCT4, SOX2, KLF4 and NANOG. Involvement of LAMP3/NRP1-VEGFR2 axis in CD8⁺T_{TEX}-CSC crosstalk was also observed (figure 2).

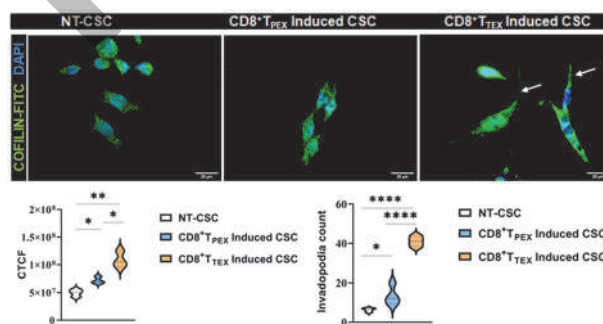
Conclusions Cumulative results counsel against indiscriminate use of anti-PD1 therapy. Rather a prior screening of CD8⁺TIL and CD8⁺T_{TEX} frequency in carcinoma patients would be beneficial. Additionally, LAMP3, NRP1 and VEGFR2 could be utilized as prospective therapeutic targets against CD8⁺T_{TEX}-influenced aggressive CSCs at advanced carcinoma patients with cold-tumor stroma.

Acknowledgements We thank Director, Chittaranjan National Cancer Institute, Kolkata, India, for providing institutional facilities. Special thanks to Dr. Abhijit Rakshit, Head, Animal Facilities, CNCI, Kolkata. We also wish to thank all members of our respective laboratories for their technical support for this work.

REFERENCES

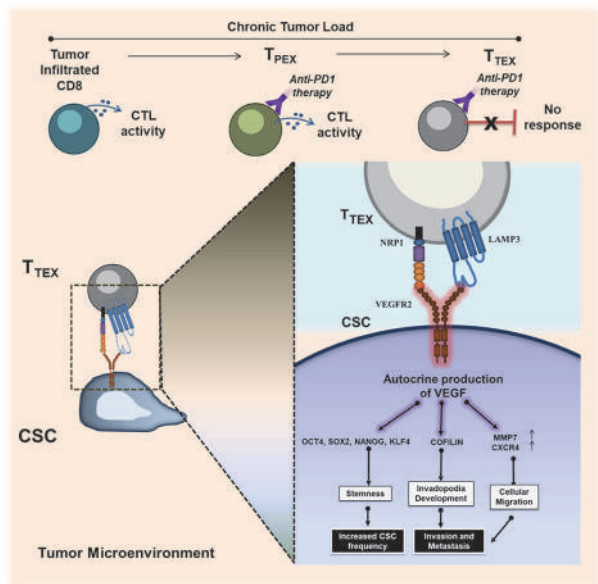
1. Miller BC, Sen DR, Al Abosy R. Subsets of exhausted CD8⁺ T cells differentially mediate tumor control and respond to checkpoint blockade. *Nat Immunol.* 2019;**20**:326–36.
2. Siddiqui I, Schaeuble K, Chennupati V. Intratumoral Tcf1+PD-1+CD8⁺ T Cells with Stem-like Properties Promote Tumor Control in Response to Vaccination and Checkpoint Blockade Immunotherapy. *Immunity* 2019;**50**:195-211.e10.
3. Im SJ, Ha S-J. Re-defining T-Cell Exhaustion: Subset, Function, and Regulation. *Immune Netw.* 2020;**20**.

Ethics Approval All human and animal experiments were approved by Institutional Human and Animal Ethical Committee of Chittaranjan National Cancer Institute, Kolkata, India. Approval numbers are CNCI-IEC-RB-2019-6, IAEC-1774/RB-15/2017/2 and IAEC-1774/RB-19/2017/15. All patients included gave informed consent before taking part in the study.



Abstract 1439 Figure 1 CD8⁺T_{TEX} induce invasive CSC generation Representative immune-fluorescence micrographs at 100x magnification for CSCs stained with Cofilin-FITC. Invadopodia are demarked by white arrows. Corrected total cell fluorescence intensity (CTCF) and number of invadopodia were quantified and displayed as violin graphs (mean±SD). Statistical alpha value was calculated from unpaired t-test (n=4).

Abstracts



Abstract 1439 Figure 2 Model proposing CD8+TTEX mediated aggressive CSC generation
Due to chronic tumor load, CD8TILs undergo terminal exhaustion and generate CD8+TTEX cells which does not respond to anti-PD1 therapy. These CD8+TTEX cells however take part in tumor advancement by generating an invasive and aggressive CSC variant through LAMP3/ NRP1-VEGFR2 axis.

<http://dx.doi.org/10.1136/jitc-2022-SITC2022.1439>

1440

ARGINASE-1 PEPTIDE-BASED VACCINE IS AN EXCITING APPROACH TO MODULATE THE TUMOR MICROENVIRONMENT AND DRIVE EFFICACY IN PRECLINICAL TUMOR MODELS

Marion Chapellier*, Marco Carretta, Ines Lecoq, Evelina Martinenaite, Tine Hannibal, Preeyam Patel, Brian Weinert, Alireza Alavi, Muhammad Al-Hajji, Ayako Pedersen. *IO Biotech, Copenhagen, Denmark*

Background Arginase-1 (ARG1) regulates tumor cells immune escape through various mechanisms in the tumor microenvironment (TME) and is being targeted experimentally in the clinic. However, selective and efficacious inhibitors of ARG1 remain elusive. Vaccination against TME targets have shown to be an exciting therapeutic approach where an IDO1/PD-L1 dual vaccine has shown substantial activity in early trials in melanoma¹ (and confirmatory Ph3 trial underway NCT05155254). We previously showed that vaccination against ARG1 increases anti-tumor activity preclinically.² Here we set out to develop a biological rationale for an ARG1 vaccine as a monotherapy or in combination with other immune therapies and understand the underlying mode of action of the treatment.

Methods ARG1 expression was examined by multiplex immunofluorescence in a tumor microarray (TMA) panel of cancer indications with a hyperplexed visualization of multiple markers on a single section. Vaccination was evaluated in mouse models expressing ARG1. Mice were inoculated with tumor cells and treated with ARG1 peptides. Tumor growth was monitored, organs and tumor samples were collected. Histopathological examination was performed on multiple tissues. Vaccine activity was determined per IFN γ Elispot assay on splenocytes. Tumor samples were processed, RNA sequencing and flow cytometry analysis of the immune infiltrate were conducted.

Results The TMA analysis confirmed ARG1 expression in the TME and revealed that a distinct immune suppressive population of cells in the TME expresses it independently of IDO1/PD-L1 providing a rationale for combining the vaccines. ARG1 surrogate peptides of 20 amino acids (ARG1₂₆₁₋₂₈₀, ARG1₁₉₁₋₂₁₀) were identified and selected based on the induction of ARG1-specific IFN γ recall responses in BALB/c or C57BL/6 animals. Both peptides demonstrated anti-tumor activity in vivo. This was associated with increased infiltration of CD45⁺ cells, CD3⁺ and CD4⁺ T-cells at tumor site. The anti-tumor effect was enhanced when ARG1 treatment was combined with anti-PD-1 mAb, and/or in combination with a the dual IDO1/PD-L1 vaccine. Detailed efficacy results in the models will be discussed in addition to the cellular and molecular analysis of the tumors in the various cohorts and treatments elucidating the mode of action of the treatment.

Conclusions ARG1 is an attractive TME target and vaccination against it drove efficacy in vivo by increasing the recruitment of immune cells at tumor site thus changing from an immunosuppressive to a pro-inflammatory microenvironment. These data support the preclinical development of an ARG1 vaccine for the treatment of multiple solid tumors.

REFERENCES

1. Kjeldsen JW, Lorentzen CL, Martinenaite E, Ellebaek E, Donia M, Holmstrom RB, Klausen TW, Madsen CO, Ahmed SM, Weis-Banke SE, Holmström MO, Hendel HW, Ehrnrooth E, Zocca MB, Pedersen AW, Andersen MH, Svane IM. A phase 1/2 trial of an immune-modulatory vaccine against IDO/PD-L1 in combination with nivolumab in metastatic melanoma. *Nat Med* 2021 Dec;27(12):2212-2223.
2. Aaboe Jørgensen M, Ugel S, Linder Hübbe M, Carretta M, Perez-Penco M, Weis-Banke SE, Martinenaite E, Kopp K, Chapellier M, Adamo A, De Sanctis F, Frusteri

C, Iezzi M, Zocca MB, Hargbøll Madsen D, Wakatsuki Pedersen A, Bronte V, Andersen MH. Arginase 1-Based Immune Modulatory Vaccines Induce Anticancer Immunity and Synergize with Anti-PD-1 Checkpoint Blockade. *Cancer Immunol Res.* 2021 Nov;9(11):1316-1326.

Ethics Approval All animal experiments were reviewed and approved by the Danish Animal Experimentation Council and performed under license number 2018-15-0201-01395.

<http://dx.doi.org/10.1136/jitc-2022-SITC2022.1440>

1441

A POTENT AND SELECTIVE SMALL MOLECULE ANTAGONIST OF CD73 ABSK051 REVERSES IMMUNOSUPPRESSION THROUGH REDUCTION OF ADENOSINE PRODUCTION

Haibing Deng, Wenqun Xin, Weiling Pan, Zhixuan Zhu, Mei Ning, Hongping Yu, Zhui Chen, Haiyan Ying*. *Abbisko Therapeutics, Shanghai, China*

Background CD73, an ecto-5-nucleotidase involved in ATP metabolism, converts AMP into adenosine, thereby plays a critical role in immunosuppression in tumor microenvironment. Overexpression of CD73 has been observed across cancer types and correlated with poor prognosis. Therefore, targeting CD73 enzymatic activity can potentially rescue the immunosuppression induced by adenosine and bring clinical benefits to cancer patients. Unlike antibodies, small molecule modulators may offer potential advantages in dosing regimen, tumor penetration, and others. In this study, we investigated the *in vitro* and *in vivo* function of ABSK051, a novel small molecule antagonist of CD73 discovered by Abbisko, and also its anti-tumor efficacy as a potent immune modulator.

Methods The effects of ABSK051 on adenosine production were evaluated using cell based luciferase assay. Its function in rescuing AMP induced immunosuppression was investigated by monitoring activation levels of CD8+ T cells. For *in vivo* studies, tumor-bearing syngeneic mice were treated with ABSK051 and its inhibition on plasma CD73 activity and tumor growth were measured. In addition, humanized tumor models were also developed using several human cancer cell lines and utilized to evaluate the efficacy of ABSK051

Results ABSK051 demonstrated strong *in vitro* inhibition of CD73 enzymatic activity, thereby effectively rescued the immune inhibition induced by adenosine. It also demonstrated *in vivo* anti-tumor efficacy as a single agent in various preclinical tumor models and in combination with other immunology agents.

Conclusions Taken together, these data demonstrated desirable preclinical biological profile of ABSK051 against CD73 and in regulating tumor growth, paving the road for further development of it as a preclinical drug candidate and potential clinical evaluation as an immune agent for cancer patients.

<http://dx.doi.org/10.1136/jitc-2022-SITC2022.1441>

1442

INVESTIGATING THE TUMOUR IMMUNE MICROENVIRONMENT OF BREAST IMPLANT ASSOCIATED ANAPLASTIC LARGE CELL LYMPHOMA USING SINGLE CELL RNA SEQUENCING

¹Harini de Silva, ¹Niko Thio, ¹Piers Blombery, ¹Ella Thompson, ²Anand Deva, ¹Miles Prince, ¹Paul Neeson, ¹Criselle DSouza*. ¹Peter MacCallum Cancer Centre, Melbourne, Australia; ²Macquarie University, Melbourne, Australia

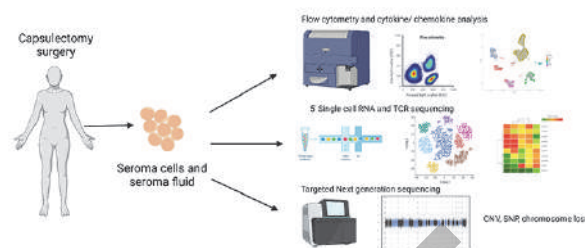
Background Breast implant-associated anaplastic large cell lymphoma (BIA-ALCL) is a newly recognised T cell lymphoma that occurs in women with textured implants and is mostly limited to the periprosthetic seroma space. However, it is not clear how this ALCL forms and whether the tumour microenvironment (TME) plays a key role in ALCL survival and proliferation in breast tissue. To address these issues, we investigated the immunobiology of both the ALCL and endogenous immune cells within the breast seroma from a cohort of patients.

Methods We established a multi-centre national cohort study, and received breast implant seroma samples [benign (n=10) and BIA-ALCL (n=23)] via cosmetic and reconstructive surgeons. We performed single cell CITEseq, RNAseq to characterise the endogenous immune cells and ALCL cells; and abTCRseq and TCRVb deep sequencing to explore their clonal relationship. Finally, we analysed the microenvironment by investigating the seroma cytokine and chemokine levels, and performed an interactome analysis to provide putative cell-cell interactions (figure 1). We also performed targeted sequencing of BIA-ALCL samples to define mutations present.

Results scRNAseq data showed ALCL cells clustered together for individual patients, however their gene expression profile was distinct between patients. ALCL cells expressed common gene signature genes such as BATEF3, SERPIN family genes, TNFSFR8, and IL2RA; along with genes unique to each patient. Endogenous T cells from the BIA-ALCL seroma displayed an activated/exhausted phenotype, immune checkpoints and endogenous T cell clonal expansion. In contrast, benign seroma endogenous T cells had a Th1/Th17 profile and limited T cell clonal expansion. Myeloid clusters were abundant in the BIA-ALCL seroma, but not the benign seroma. TME studies showed a significant increase in BIA-ALCL seroma for cytokines IL13, TNF, IL10 and secretory-PDL1. The single cell interactome analysis described potential unique cell-cell interactions in the BIA-ALCL TME including tumour-tumour, tumour-myeloid DC and tumour-CD8⁺ T effector memory cells. Mutational analysis revealed novel JAK1 mutations and STAT3 mutations along with chromosome 20 loss consistent with previous studies.

Conclusions BIA-ALCL cells are different between patients and from the endogenous immune cells. Furthermore, BIA-ALCL seroma is characterised by endogenous T cells with an exhausted profile and clonal expansion, increased IFN-g and TNF levels suggesting these T cells are responding to TME antigens. In addition, the BIA-ALCL TME has high levels of IL-13 and IL-10 which are generated via tumour-tumour and tumour-myeloid cell interactions.

Ethics Approval This study was approved by Peter MacCallum Cancer Centre human research ethics committee (Reference no. 44068) or by Macquarie University human research ethics committee (Reference No. 5201600427). Informed consent was obtained from all participating patients.



Abstract 1442 Figure 1 Study schema

<http://dx.doi.org/10.1136/jitc-2022-SITC2022.1442>

Abstracts

1443

SUPPRESSION OF HUMAN GAMMA DELTA T CELL ACTIVATION BY SOLUBLE FACTORS PRODUCED BY PANCREATIC DUCTAL CANCER ORGANOTYPIC CULTURE

Johnathan Ebben*, Nicholas Hess, Zachary Mayhew, Jeremy Kratz, Christian Capitini, Melissa Kinney. *University of Wisconsin-Madison, Madison, WI, USA*

Background Pancreatic ductal adenocarcinoma (PDAC) is highly resistant to immunotherapies. Gamma delta (gdT) cells play a key role in driving immunosuppression within the tumor microenvironment.¹ In PDAC, the tumor microenvironment is heavily infiltrated with immunosuppressive gdT cells.² However, the mechanism by which circulating gdT cells acquire an immunosuppressive phenotype within the tumor microenvironment specific to PDAC remains unknown. We hypothesized that secretory cues produced by PDAC act on infiltrating gdT cells to drive immunosuppressive phenotypes. **Methods** PDAC organoids were generated from surgical specimens obtained with IRB approval (UW-Madison B00000976). Organoids were cultured in defined media in serum-free conditions. Conditioned media was collected at passaging. Whole blood was collected, and samples were enriched for T cells (RosetteSep, Stem Cell Technologies), followed by magnetic gdT cell isolation. gdT cells were cultured in conditioned media from two separate patient-derived organoid lines, versus control base media for 72 hours. Cells were then activated with anti-CD3/CD28/CD2 beads in the presence of GolgiStop cocktail. These cells were subjected to intracellular cytokine phenotyping by flow cytometry.

Results After 72 hours of incubation in PDAC conditioned media, production of IFN-gamma and TNF-alpha, indicative of a Th1 antitumor phenotype, are significantly diminished (71% IFN-g+ in control vs 48% in PDAC1 media, 56% in PDAC2 media; $p < 0.002$) in conditioned media cultured gdT cells versus control (figure 1B-C). In a separate series of experiments, we evaluated the specificity of this suppression. Interestingly, there is increased suppression of gdT activation relative to either CD4+ or CD8+ ab T cells, with 40% reduction in IFNg producing gdT cells versus 10% reduction in IFNg producing cells amongst CD4 and CD8+ abT cells (preliminary data).

Conclusions Our work demonstrates for the first time a specific effect of a secreted mediator produced by PDAC that preferentially drives gdT cell immunosuppression. We demonstrate that circulating gdT cells from healthy donors produce significantly less Th1 cytokines after TCR stimulation, following incubation in conditioned media derived from multiple, independent human PDAC organoids. Our next steps include scRNAseq of conditioned gdT cells as well as bulk RNAseq of PDAC organoids to identify ligand-receptor interactions between tumor and gdT cells, aiming to use proteomics approaches to validate and modulate these candidates in the tumor microenvironment. In the broader clinical context, this may suggest a new axis that drives immunosuppression in PDAC, with our work identifying new targets for therapeutic modulation.

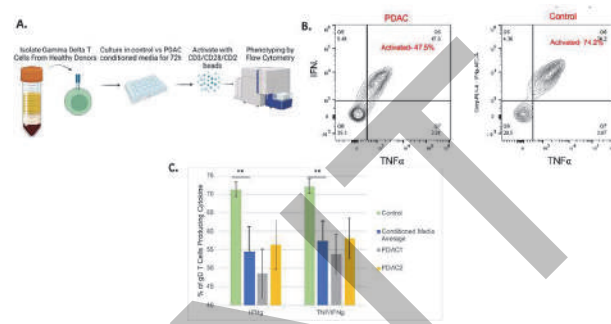
Acknowledgements We are unspeakably grateful to the patients who agreed to donate tissue to establish pancreas ductal adenocarcinoma organoids that made this work possible.

REFERENCES

1. Reis BS, Darcy PW, Khan IZ, et al. TCR-V δ usage distinguishes protumor from antitumor intestinal δ T cell subsets. *Science* 2022;**377**(6603):276-284. doi:10.1126/science.abj8695

2. Daley D, Zambirinis CP, Seifert L, et al. δ T Cells Support Pancreatic Oncogenesis by Restraining $\alpha\beta$ T Cell Activation [published correction appears in *Cell*. 2020 Nov 12;183(4):1134-1136]. *Cell*. 2016;**166**(6):1485-1499.e15. doi:10.1016/j.cell.2016.07.046

Ethics Approval University of Wisconsin-Madison IRB B00000976



Abstract 1443 Figure 1 gdT cell activation is attenuated by pancreas tumor

A. Experimental schema; gdT are isolated from healthy donors, cultured for 72h in PDAC organoid media, activated with CD3/CD28/CD2 beads as described in the Methods section, and subjected to flow cytometry analysis.

B. Representative flow cytometry for gated gdT cells. Right panel= gdT cultured for 72h with PDAC conditioned media, which results in decreased IFNg and TNF α production versus gdT cultured in control media (left).

C. Quantification of flow cytometry evaluating IFNg and TNF α production using two different PDAC organoid conditioned medias versus control media (gdT incubation and activation after 72h of culture).

** $p < 0.02$

<http://dx.doi.org/10.1136/jitc-2022-SITC2022.1443>

1444

TARGETING SIALIC ACID ON STROMAL CELLS REVERSES T CELL SUPPRESSION IN THE COLORECTAL TUMOUR MICROENVIRONMENT A NEW TUMOUR STROMAL CELL IMMUNE CHECKPOINT

¹Aideen Ryan*, ¹Oliver Treacy, ¹Kevin Lynch, ²Kim De Veirman, ²Karin Vanderkerken, ¹Laurence Egan, ¹Thomas Ritter, ¹Aisling Hogan, ³Keara Redmond, ¹Sean Hynes, ³Emma Kerr, ¹Michael O'Dwyer, ¹Philip Dunne, ¹Niamh Leonard, ¹Hannah Egan. ¹*NUI Galway, Human Biology Building, NUI Galway, Ireland;* ²*Vrije Universiteit Brussel, Brussels, Belgium;* ³*Queens University Belfast, Belfast, UK*

Background Hypersialylation of cancer cells induces an immunosuppressive microenvironment. The binding of sialic acid by siglec receptors expressed on immune cells initiates a downstream response via immunoreceptor tyrosine-based inhibitory motif (ITIM) signalling. Cancer associated fibroblasts (CAFs) in the colorectal cancer (CRC) microenvironment are highly immunosuppressive and associated with poor survival. The role of sialylation in stromal cell-mediated immunosuppression, however, is unknown. Here, we investigated if sialylation of CAFs contributed to their potent immunosuppressive properties.

Methods Tumour cell secretome (TCS) from multiple CRC cell lines was used to condition primary human and mouse bone marrow-derived stromal cells, as CAF precursors. Normal and CAFs were isolated from colon tumour resections. Stromal cells were cultured with stimulated splenocytes (mouse) or PBMCs (human) and their immunosuppressive properties were assessed by flow cytometry. An in vivo mouse model of CT26 CRC was used to assess the role of highly sialylated stromal cells in tumour development. Mice were injected subcutaneously with CT26 cells alone, or co-injected with TCS-conditioned stromal cells, either control or de-sialylated. 14 days post induction, tumour, draining lymph nodes and spleen were assessed for frequency and expression of T cell activation markers.

Results Tumour conditioning resulted in significantly higher expression of both $\alpha 2,6$ -linked sialic acid and specific Siglec ligands on stromal cells. CAFs were significantly more sialylated than stromal cells isolated from adjacent normal associated tissue (NAFs) (figure 1). Following co-culture, CAFs induced significantly higher levels of CD8+ T cells with an exhausted phenotype as determined by TIM-3 and PD-1 expression. Siglec-7 and -9 receptors were induced by CAFs on CD8 T cells. Furthermore, de-sialylation of CAFs, specifically, prior to co-culture resulted in a significant reduction in exhausted CD8+ T cells and attenuation of their immunosuppressive ability (figure 2).

14d post tumour induction in vivo, mice with TCS-conditioned, stromal-dense tumours had significantly fewer activated CD4+ and CD8+ CD25-expressing T cells, both intratumourally and distally in the draining lymph nodes and spleen. They also had low levels of cytotoxic granzyme B-expressing CD8+ T cells. Interestingly, this suppression was sialylation-dependent. De-sialylation of TCS-conditioned stromal cells led to restoration of activated T cell levels in tumours and peripheral lymphoid tissues, as well as a marked increase in cytotoxic T cells (figure 3).

Conclusions These results demonstrate, for the first time, that tumour stromal cells suppress activated T cells through sialic acid dependent interactions. We show that targeting stromal cell sialylation may represent a novel immune checkpoint to reactivate anti-tumour immunity.

Ethics Approval The animal study was approved by the Animals Care Research Ethics Committee of the National

University of Ireland, Galway (NUIG) and conducted under individual and project authorisation licenses from the Health Products Regulatory Authority (HPRA) of Ireland (AE19125/P077). The study using human samples was approved by University Hospital Galway Ethics committee under an ethically approved protocol (Clinical Research Ethics Committee, Ref: C.A. 2074).

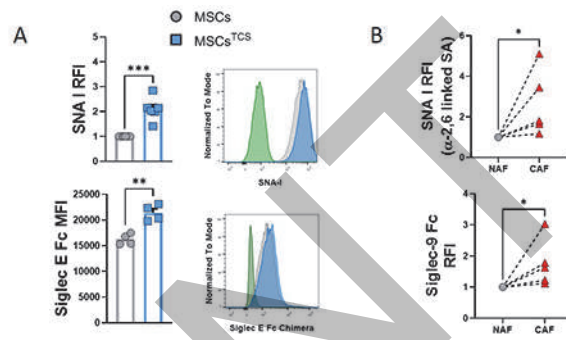


Figure 1. Exposure of stromal cells to tumour cell secretome or microenvironment increases sialic acid and specific Siglec ligand expression. (A) Mouse bone marrow-derived mesenchymal stromal cells (MSCs) have elevated SNA I ($\alpha 2,6$ sialic acid) and Siglec E ligand expression following exposure to tumour cell secretome from CT26 murine colon cancer cells (MSC^{TCS}). Isotype control is shown as green histogram. (B) Cancer-associated fibroblasts (CAFs) isolated from colorectal cancer patient biopsies express higher levels of SNA I and Siglec 9 ligand compared to fibroblasts isolated from non-cancerous (NAF), adjacent intestinal tissue. Data are mean \pm SD; * $p < 0.05$, ** $p < 0.01$, and *** $p < 0.001$ using (A) unpaired t-test and (B) ratio paired t-test. $n = 4$ biological replicates.

Abstract 1444 Figure 1 Exposure of stromal cells to tumour cell secretome or microenvironment increases sialic acid and specific Siglec ligand expression. (A) Mouse bone marrow-derived mesenchymal stromal cells (MSCs) have elevated SNA I ($\alpha 2,6$ sialic acid) and Siglec E ligand expression following exposure to tumour cell secretome from CT26 murine colon cancer cells (MSC^{TCS}). Isotype control is shown as green histogram. (B) Cancer-associated fibroblasts (CAFs) isolated from colorectal cancer patient biopsies express higher levels of SNA I and Siglec 9 ligand compared to fibroblasts isolated from non-cancerous (NAF), adjacent intestinal tissue. Data are mean \pm SD; * $p < 0.05$, ** $p < 0.01$, and *** $p < 0.001$ using (A) unpaired t-test and (B) ratio paired t-test. $n = 4$ biological replicates.

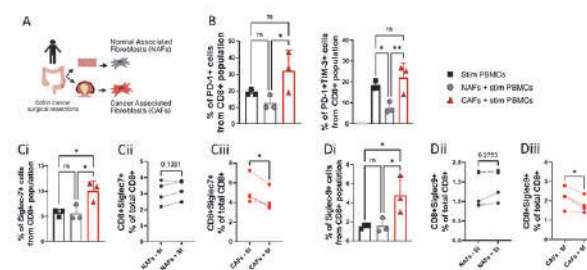


Figure 2. CAFs induce an exhausted phenotype in CD8+ T cells which is reversible by de-sialylation. (A) Schematic overview depicting the process of NAFs and CAFs isolation. (B) Frequency (%) of CD8+PD-1+ and CD8+PD-1+Tim-3+ T cells after co-culture with NAFs or CAFs. (C) Frequency (%) of CD8+Siglec-7+ T cells after co-culture with NAFs or CAFs. (D) Frequency (%) of CD8+Siglec-7+ T cells after co-culture with NAFs or CAFs pre-treated or not with a sialyltransferase inhibitor (SI). (E) Frequency (%) of CD8+Siglec-9+ T cells after co-culture with NAFs or CAFs. (F) Frequency (%) of CD8+Siglec-9+ T cells after co-culture with NAFs or CAFs pre-treated or not with SI. Data are mean \pm SD; * $p < 0.05$ and ** $p < 0.01$ using (B, C and D) one-way ANOVA with a Tukey post hoc test and (E, F, Dii, Diii) ratio paired t-test. $n = 3-4$ biological replicates.

Abstract 1444 Figure 2 CAFs induce an exhausted phenotype in CD8 + T cells which is reversible by de-sialylation. (A) Schematic overview depicting the process of NAFs and CAFs isolation. (B) Frequency (%) of CD8+PD-1+ and CD8+PD-1+Tim-3+ T cells after co-culture with NAFs or CAFs. (C) Frequency (%) of CD8+Siglec-7+ T cells after co-culture with NAFs or CAFs. (D) Frequency (%) of CD8+Siglec-7+ T cells after co-culture with NAFs or CAFs pre-treated or not with a sialyltransferase inhibitor (SI). (E) Frequency (%) of CD8+Siglec-9+ T cells after co-culture with NAFs or CAFs. (F) Frequency (%) of CD8+Siglec-9+ T cells after co-culture with NAFs or CAFs pre-treated or not with SI. Data are mean \pm SD; * $p < 0.05$ and ** $p < 0.01$ using (B,

Abstracts

Ci and Di) one-way ANOVA with a Tukey post hoc test and (Cii, Ciii, Dii and Diii) a ratio paired t test. n = 3-4 biological replicates

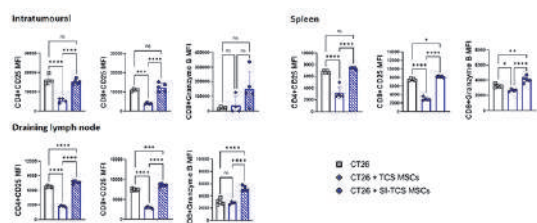


Figure 3. TCS-conditioned stromal cells inhibit T cell activation and cytotoxicity in vivo and these effects can be reversed by targeting stromal cell sialylation. 8-12 week old female Balb/c mice were injected subcutaneously with 5×10^5 CT26 colon cancer cells with or without 1.5×10^5 TCS MSCs or Sialyltransferase inhibited TCS MSCs (SI-TCS) where indicated. 13 days post-injection, tumours, draining lymph nodes and spleens were harvested and analysed for the presence of specific immune cell markers by flow cytometry. Tumour conditioned stromal cells suppress T cell activation in the tumour, spleen and draining lymph node, as determined by CD4/CD8 CD25 expression, which is reversed by targeting stromal cell sialylation. Granzyme B expressing cytotoxic T cells are suppressed by stromal cells in the TME. The stromal mediated immunosuppressive effects on cytotoxic CD8 T cells are restored in the draining lymph and spleen – and partially restored in the tumour. Data are mean \pm SD; * $p < 0.05$, ** $p < 0.01$, *** $p < 0.001$ and **** $p < 0.0001$ using one-way ANOVA with a Tukey post hoc test. n = 4-5 biological replicates.

Abstract 1444 Figure 3 TCS-conditioned stromal cells inhibit T cell activation and cytotoxicity in vivo and these effects can be reversed by targeting stromal cell sialylation. 8-12 week old female Balb/c mice were injected subcutaneously with 5×10^5 CT26 colon cancer cells with or without 1.5×10^5 TCS MSCs or Sialyltransferase inhibited TCS MSCs (SI-TCS) where indicated. 13 days post-injection, tumours, draining lymph nodes and spleens were harvested and analysed for the presence of specific immune cell markers by flow cytometry. Tumour conditioned stromal cells suppress T cell activation in the tumour, spleen and draining lymph node, as determined by CD4/CD8 CD25 expression, which is reversed by targeting stromal cell sialylation. Granzyme B expressing cytotoxic T cells are suppressed by stromal cells in the TME. The stromal mediated immunosuppressive effects on cytotoxic CD8 T cells are restored in the draining lymph and spleen – and partially restored in the tumour. Data are mean \pm SD; * $p < 0.05$, ** $p < 0.01$, *** $p < 0.001$ and **** $p < 0.0001$ using one-way ANOVA with a Tukey post hoc test. n = 4-5 biological replicates.

<http://dx.doi.org/10.1136/jitc-2022-SITC2022.1444>

1445

AIM2 MODULATES AZACYTIDINE-INDUCED ANTITUMOR IMMUNITY IN LUNG CANCER

¹Naoki Furuya*, ¹Sumei Lu, ¹Tamio Okimoto, ¹Yi Wang, ¹No Joon Song, ¹Anqi Li, ²Hong Dong, ²Bao Zhao, ¹Ju Hwan Cho, ¹David Carbone, ¹Zihai Li, ²Haitao Wen, ¹Kai He.

10.1136/jitc-2022-SITC2022.1

¹Ohio State University Comprehensive Cancer Center, Columbus, OH, USA

²The Ohio State University College of Medicine, Columbus, OH, USA

Background Immune checkpoint inhibition (ICI) has been established as an essential treatment for lung and other cancers. Preclinical studies revealed that DNA-demethylating agents induced type I interferon (IFN-I) response and primed the tumor microenvironment (TME) to enhance antitumor immunity.^{1,2} However, this promising effect has not been successfully demonstrated in clinical trials of combined treatments of ICI and DNA hypomethylation agents in lung cancer.³ We hypothesize that azacytidine (AZA), a DNA hypomethylation agent and a broad-spectrum epigenetic programmer, might inevitably also activate key immune suppression mediator(s). We demonstrated that absent melanoma 2 (AIM2), a DNA sensing component of inflammasome, negatively impacts AZA-induced antitumor immunity in non-small cell lung cancer (NSCLC) by modulating IFN-I response and T effector cell tumor infiltration.

Methods We tested gene expression upregulated by AZA in lung cancer cell lines and used genetic modeling to identify the mechanism mediating AZA-induced AIM2 expression. Aim2-deficient (Aim2^{-/-}) tumor cells (CMT167 and LLC) were established with the CRISPR/Cas9 system. We adopted an immune-competent syngeneic mouse tumor model to investigate the impacts of AIM2 on TME and tumor growth. We measured tumor growth and analyzed tumor samples with flowcytometry (FCM) and immunohistochemistry staining (IHC).

Results AIM2 expression was highly synergistically induced by AZA and IFN- γ in multiple human and mouse lung cancer cell lines. We demonstrated that AZA upregulated AIM2 expression through a RNA sensing mechanism. Analysis of AIM2 expression in 1925 NSCLC patients with KM-Plotter (<https://kmplot.com/analysis/>)⁴ showed that high AIM2 expression was associated with significantly shorter overall survival in NSCLC. We showed that AZA and IFN- γ induced IFN-I response was enhanced in Aim2^{-/-} CMT167 cells comparing to Aim2^{+/+} cells. Using Aim2^{-/-} and Aim2^{+/+} CMT167, and the immune-competent syngeneic mouse model, AZA treatment induced significant growth suppression of Aim2^{-/-} tumors, but not Aim2^{+/+} tumors. FCM of the tumor tissue demonstrated that the number of CD8⁺ T cells was significantly increased after AZA treatment in both Aim2^{-/-} and Aim2^{+/+} tumors, whereas IHC revealed AZA promoted significantly more CD8⁺ T cell infiltration into the TME in Aim2^{-/-} tumors than in Aim2^{+/+} tumors. We demonstrated that CD8 depletion negated AIM2's effect on AZA-treated tumor growth in vivo and indicated that the impact of AIM2 on tumor growth would depend on CD8⁺ T cells.

Conclusions AIM2 is a key negative regulator for AZA-induced antitumor immunity and a potential novel therapeutic target in optimizing epigenetic and immune therapy in NSCLC.

REFERENCES

1. Chiappinelli KB, Strissel PL, Desrichard A, Li H, Henke C, Akman B, *et al.* Inhibiting DNA Methylation Causes an Interferon Response in Cancer via dsRNA Including Endogenous Retroviruses. *Cell*. 2015;**162**(5):974-986.
2. Roulois D, Loo Yau H, Singhania R, Wang Y, Danesh A, Shen SY, *et al.* DNA-Demethylating Agents Target Colorectal Cancer Cells by Inducing Viral Mimicry by Endogenous Transcripts. *Cell*. 2015;**162**(5):961-973.
3. Levy BP, Giaccone G, Besse B, Filip E, Garassino MC, Domine Gomez M, *et al.* Randomised phase 2 study of pembrolizumab plus CC-486 versus pembrolizumab plus placebo in patients with previously treated advanced non-small cell lung cancer. *Eur J Cancer*. 2019;**108**:120-128.
4. Lániczky A, Györfy B. Web-Based Survival Analysis Tool Tailored for Medical Research (KMplot): Development and Implementation. *J Med Internet Res* 2021;**23**(7):e27633.

<http://dx.doi.org/10.1136/jitc-2022-SITC2022.1445>

Abstracts

1446

MULTIPLEXED ION BEAM IMAGING IDENTIFIES B-CELL ENRICHMENT IN THE RHAMM-HIGH INVASIVE NICHE OF BREAST CANCER

¹Yuyu He*, ¹Grant Barthel, ²Raghav Padmanabhan, ¹Colleen Forster, ¹Hanna Root, ²Mate Nagy, ²Stanislaw Nowak, ¹James McCarthy, ¹Kathryn Schwertfeger, ¹Andrew Nelson. ¹University of Minnesota, Minneapolis, MN, USA; ²Ionpath Inc, Menlo Park, CA, USA

Background Receptor for hyaluronan (HA) mediated motility (RHAMM) has been shown to work cooperatively with CD44 to mediate tumor progression,¹ but its specific roles in breast cancer are still unclear. In our previous studies, we have shown tumor cell RHAMM deletion significantly inhibits cancer progression in xenograft models and that RHAMM is heterogeneously expressed within human breast tumors.² We propose that focal RHAMM upregulation creates an invasive niche and have identified an RHAMM-dependent signature in this niche that is associated with poor prognosis of breast cancer patients.² Importantly, we found that Type II Interferon signaling and MHC Class I & Class II Antigen Presentation pathways are co-enriched in the RHAMM high invasive niche. This indicates that RHAMM might be involved in regulating immune responses. Herein we characterize the immune infiltrates associated with the RHAMM high invasive niche using a mass spectrometry-based proteomic imaging technique.

Methods FFPE tissues from 5 breast cancers were analyzed by multiple ion beam imaging (MIBI). Sections were stained with 20 antibodies simultaneously, including biomarkers to define immune cell phenotypes. Fields of views (FOVs) were selected from RHAMM high regions and RHAMM low regions. Novel machine-learning-based algorithms were applied to segment the images into spatially resolved single-cell data and to classify immune cell populations in RHAMM-high and RHAMM-low regions.

Results In triple-negative breast cancer (TNBC), the RHAMM-high tumor invasive margin (TI-high) shows a high level of intra-tumoral immune cells compared to the RHAMM-low tumor core (TC-low), wherein immune cells are largely restricted to the peri-tumoral stroma (figure 1). The RHAMM-low invasive margin (TI-low) is fibrotic and only sparsely populated by macrophages. Segmented single-cell data from our novel machine learning-based algorithms show high levels of infiltrating B cells in the TI-high region (figure 2A-B). The invasive margin overall is characterized by higher levels of cytotoxic T-cells, T-helper cells, and macrophages vs. the core (figure 2C-F). Notably, the B-cell-rich TI-high region has fewer cytotoxic T cells than the TI-low region.

Conclusions Our data highlights potentially novel interactions between RHAMM expression/function and B-cell infiltrates in TNBC. Given the dynamic roles of B-cells in cancer immunology,³ this suggests new possible avenues for immune modulation to inhibit RHAMM-supported breast cancer progression. On-going work is confirming this linkage in additional TNBC and expanding the analysis to other molecular subtypes of breast cancer.

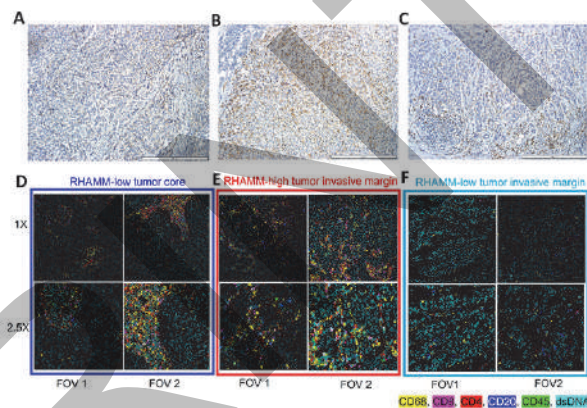
Acknowledgements This work was funded in part by grants from the University of Minnesota Department of Laboratory Medicine & Pathology-Molecular Genomic Pathology Division and the Masonic Cancer Center.

REFERENCES

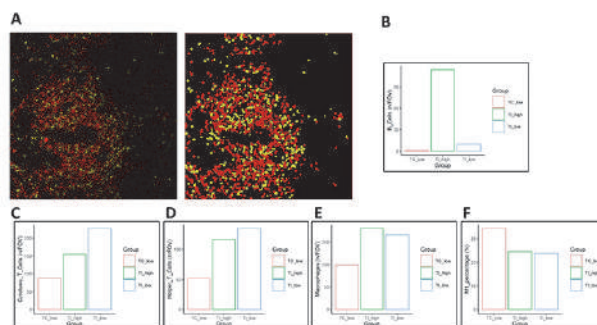
1. Hamilton SR, Fard SF, Paiwand FF, Tolg C, Veisoh M, Wang C, ... Turley EA. The hyaluronan receptors CD44 and Rhamm (CD168) form complexes with ERK1, 2 that sustain high basal motility in breast cancer cells. *J Biol Chem.* 2007;**282** (22):16667-16680.

2. Tarullo SE, He Y, Daughters C, Knutson TP, Henzler C, Price M, ... Nelson AC. Receptor for Hyaluronan-Mediated Motility (RHAMM) defines an invasive niche associated with tumor progression and predicts poor outcomes in breast cancer patients. *bioRxiv.* 2022.
3. Yuen GJ, Demissie E, Pillai S. B lymphocytes and cancer: a love-hate relationship. *Trends in Cancer* 2016;**2**(12):747-757.

Ethics Approval FFPE tumor tissues (IRB Approval Study# 1409E53504) were collected from archived pathology tissue blocks with de-identified clinical data in compliance with HIPAA regulations and institutional policies. All participants had agreed to the institution's standard consent for research participation.



Abstract 1446 Figure 1 Immune profiling in RHAMM-associated invasive niche. A: Representative images showing the MIBI raw staining (left panel, red for CD8, yellow for CD4) and its corresponding segmentation (right panel, red for CD8+ T cells, yellow for CD4+ T cells). B-F: Quantification of B cells, cytotoxic T cells, helper T cells, macrophages, and M1 macrophage percentages. TC_low: RHAMM-low tumor core region; TI_high: RHAMM-high tumor invasive margin; TI_low: RHAMM-low tumor invasive margin.



Abstract 1446 Figure 2 Immune profiling in RHAMM-associated invasive niche. A: Representative images showing the MIBI raw staining (left panel, red for CD8, yellow for CD4) and its corresponding segmentation (right panel, red for CD8+ T cells, yellow for CD4+ T cells). B-F: Quantification of B cells, cytotoxic T cells, helper T cells, macrophages, and M1 macrophage percentages. TC_low: RHAMM-low tumor core region; TI_high: RHAMM-high tumor invasive margin; TI_low: RHAMM-low tumor invasive margin.

<http://dx.doi.org/10.1136/jitc-2022-SITC2022.1446>

1447

A 30 PDX PANEL OF 3D IN VITRO TUMOR MODELS IDENTIFIES RESPONDERS TO PEMBROLIZUMAB AND SOLITOMAB

<http://dx.doi.org/10.1136/jitc-2022-SITC2022.1447>

¹Kolin Hribar*, ¹Bin Xue, ¹Christopher Harrod, ²Julia Schuler. ¹Cypré Inc, South San Francisco, CA, USA; ²Charles River Laboratories, Freiburg, Germany

Background Immunotherapies are emerging as a novel approach to combat cancer. Among them, checkpoint inhibitor treatment has found success in a subset of cancer patients by reversing T cell dysfunction and unleashing their cytolytic potential in the immunosuppressive tumor microenvironment (TME).¹ Nevertheless, many tumors which constitutively express these targets fail to respond to checkpoint inhibitors due to a range of issues – lack of T cell infiltrate, alternative dysfunction pathways, exhaustion and others.² Thus, there is a critical need to assay antitumor effects of novel immunotherapies or combinations across a range of target expression status and tumor indications. Here, we describe a 3D Tumor Panel of 30 patient-derived xenograft (PDX) in vitro models for rapid and scalable screening of immunotherapy. The models incorporate tumor cells, fibroblasts, and peripheral blood monocytes (PBMCs) in a hydrogel matrix to recreate the complex TME and are screened for antitumor effects using high content image analysis.

Methods Thirty PDX-derived tumor cell lines and human dermal fibroblasts (HDF) were grown in a hydrogel matrix³ in 96-well plates. The PDX histotypes included lung, renal, colon, gastric, breast, head and neck, liver, uterus, pancreatic, pleura-mesothelioma, sarcoma, melanoma, and ovary. PBMCs along with test compounds – Pembrolizumab (anti-PD-1) and Solitomab (EpCAM/CD3 bispecific antibody) – were later added to wells in a six-dose, serially diluted fashion. Response was detected at day four endpoint using high content image analysis of tumor size (Hoechst nuclear stain) and killing (DRAQ7 cell death and Caspase 3/7 apoptosis markers).

Results A subset of tumors responded to Pembrolizumab after four days of treatment, where the strongest responders resided in colon, lung and renal cancer. Interestingly, Solitomab responded in pancreatic tumors where Pembrolizumab failed to respond, however, oppositely, Solitomab did not respond in 75% of renal tumors on the Panel. In both compounds, anti-tumor effect was principally observed by tumor size and total tumor area reduction.

Conclusions A robust and diverse 3D PDX tumor panel comprising various solid tumor indications was developed in a hydrogel matrix platform. The PDX cells were grown along with fibroblasts and PBMCs to mimic the tumor, stromal and immune compartments of the TME. Endpoints including tumor size and killing highlighted PDX responders to both Pembrolizumab and Solitomab. These data highlight the ability to screen various immunotherapy compounds in a standardized 3D PDX in vitro panel for determining antitumor effect in drug discovery and translational research to enhance patient outcomes.

REFERENCES

1. Bagchi S, Yuan R, Engleman EG, Immune Checkpoint Inhibitors for the Treatment of Cancer: Clinical impact and mechanisms of response and resistance. *Annu Rev Pathol.* 2021;**16**:223-249.
2. Jenkins RW, Barbie DA, Flaherty KT, Mechanisms of resistance to immune checkpoint inhibitors. *Br J Cancer.* 2018;**118**:9-16.
3. Hribar KC, Wheeler CJ, Bazarov A, Varshneya K, Yamada R, Buckley P, Patil CG, A simple three-dimensional hydrogel platform enables ex vivo cell culture of patient and pdx tumors for assaying their response to clinically relevant therapies. *Mol Cancer Ther.* 2019;**18**:718-725.

ALTERED MYELOID MEMORY FUNCTION BY BMP SIGNALING IN BREAST CANCER BONE METASTASES

¹Claire Ihle*, ¹Desiree Strain, ²Johana Canari, ¹Kathleen Torkko, ¹Kathryn Zolman, ¹Erin Smith, ¹Philip Owens. ¹University of Colorado Anschutz Medical Campus, Aurora, CO, USA; ²Case Western Reserve University, Cleveland, OH, USA

Background Metastatic breast cancer (mBC) patients exhibit a 5-year survival rate of only 29% and metastasis most commonly occurs in the bone.¹⁻² Myeloid progenitors in the bone marrow can undergo trained innate immune responses, resulting in long-lasting inflammatory myeloid memory.³⁻⁴ Myeloid memory has been shown to promote anti-tumorigenic myeloid functions in the tumor microenvironment (TME).⁵⁻⁶ The TME in bone includes unique myeloid cells which are dynamically regulated by bone morphogenetic proteins (BMPs).⁷⁻⁸ We investigated myeloid memory in the context of BMP signaling in the mBC bone TME. Identifying the driver of myeloid functions distinct to mBC bone metastases will advance the understanding of potential immunotherapies to overcome incurable mBC bone lesions.

Methods A cohort of human mBC bone metastases and matched patient primary tumors and bone metastases were assembled and profiled. Gene expression analysis was performed on patient bone metastases and matched primary tumors using nCounter immune-oncology gene expression probes. Clinical bone metastasis regional protein expression was analyzed with GeoMx Digital Spatial Profiling (DSP). Single cell protein expression and spatial analysis was measured in matched patient primary tumors and bone metastases with Akoya Polaris panels. Syngeneic mouse models of MMTV-PyMT orthotopic tumors and intratibial bone metastases were treated with beta-glucan to induce trained innate immunity and/or LDN-193189-2HCl to inhibit BMP signaling. Mouse model readouts included tumor measurements, mBC progression by histology and circulating blood analysis, and myeloid memory function by circulating blood and Akoya Polaris analysis.

Results Differential nCounter gene expression analysis of clinical mBC bone metastases revealed a subset of patient samples with a high myeloid gene signature. High myeloid gene signature patients exhibited enhanced inflammatory gene pathways and BMP signaling. Regional DSP and single cell Polaris protein expression analysis of this patient cohort showed elevated myeloid cell infiltration and heterogeneity as well as myeloid memory phenotypes in the high myeloid gene signature samples. Analysis of matched patient primary tumor and bone metastases with nCounter gene expression panels exhibited enhanced BMP signaling and myeloid cell infiltration in bone samples compared to primary tumors. Syngeneic mouse models of mBC showed beta-glucan induced myeloid memory restricted primary tumor growth. mBC mouse models of bone metastases treated with beta-glucan and LDN-193189-2HCl revealed BMP signaling is required for myeloid memory anti-tumor functions in bone metastases.

Conclusions Distinct bone metastasis patients exhibited myeloid memory and BMP signaling which could allow for precision immunotherapy treatments to prevent myeloid suppression in mBC.

Acknowledgements We would like to thank Sabrina Wright-Hobart for her collaboration and metastatic breast cancer patient advocacy. We thank Ryan Orbus, Cheryl Tan, Liang Zhang, Yan Liang, Wenjie Xu, and Doug Hinerfeld of NanoString Inc. and Jeremy Rahkola of Department of Veterans

Affairs for technical assistance. We would like to thank the University of Colorado Cancer Center Tissue Biobanking and Histology Shared Resource (P30CA046934) as well as the U.S. Department of Veterans Affairs Shared Equipment Evaluation Program (IS1BX003572) for experimental support. We also thank our funding sources NIH TOTTs TL1TR002533 (CLI) and VA 1KBX00002929 (PO).

REFERENCES

1. Xiong Z, Deng G, Huang X, Li X, Xie X, Wang J, Shuang Z, Wang X. Bone metastasis pattern in initial metastatic breast cancer: a population-based study. *Cancer Manag Res.* 2018;**10**:287-95. Epub 2018/02/23. doi: 10.2147/cmar.S155524. PubMed PMID: 29467583; PMCID: PMC5811177.
2. Siegel RL, Miller KD, Fuchs HE, Jemal A. Cancer statistics, 2022. *CA: A Cancer Journal for Clinicians.* 2022;**72**(1):7-33. doi: <https://doi.org/10.3322/caac.21708>.
3. Mitroulis I, Ruppova K, Wang B, Chen LS, Grzybek M, Grinenko T, Eugster A, Troullinaki M, Palladini A, Kourtzelis I, Chatzigeorgiou A, Schlitzer A, Beyer M, Joosten LAB, Isermann B, Lesche M, Petzold A, Simons K, Henry I, Dahl A, Schultze JL, Wielockx B, Zamboni N, Mirtschink P, Coskun Ü, Hajishengallis G, Netea MG, Chavakis T. Modulation of Myelopoiesis Progenitors Is an Integral Component of Trained Immunity. *Cell.* 2018;**172**(1-2):147-61.e12. Epub 2018/01/13. doi: 10.1016/j.cell.2017.11.034. PubMed PMID: 29328910; PMCID: PMC5766828.
4. Netea MG, Dominguez-Andrés J, Barreiro LB, Chavakis T, Divangahi M, Fuchs E, Joosten LAB, van der Meer JWM, Mhlanga MM, Mulder WJM, Riksen NP, Schlitzer A, Schultze JL, Stabel Benn C, Sun JC, Xavier RJ, Latz E. Defining trained immunity and its role in health and disease. *Nature Reviews Immunology* 2020;**20**(6):375-88. doi: 10.1038/s41577-020-0285-6.
5. Geller AE, Shrestha R, Woeste MR, Guo H, Hu X, Ding C, Andreeva K, Chariker JH, Zhou M, Tieri D, Watson CT, Mitchell RA, Zhang H-g, Li Y, Martin li RCG, Rouchka EC, Yan J. The induction of peripheral trained immunity in the pancreas incites anti-tumor activity to control pancreatic cancer progression. *Nature Communications* 2022;**13**(1):759. doi: 10.1038/s41467-022-28407-4.
6. Kalafati L, Kourtzelis I, Schulte-Schrepping J, Li X, Hatzioannou A, Grinenko T, Hagag E, Sinha A, Has C, Dietz S, de Jesus Domingues AM, Nati M, Sormendi S, Neuwirth A, Chatzigeorgiou A, Ziogas A, Lesche M, Dahl A, Henry I, Subramanian P, Wielockx B, Murray P, Mirtschink P, Chung KJ, Schultze JL, Netea MG, Hajishengallis G, Verginis P, Mitroulis I, Chavakis T. Innate Immune Training of Granulopoiesis Promotes Anti-tumor Activity. *Cell.* 2020;**183**(3):771-85.e12. Epub 2020/10/31. doi: 10.1016/j.cell.2020.09.058. PubMed PMID: 33125892; PMCID: PMC7599076.
7. Ihle CL, Strain DM, Provera MD, Novitskiy SV, Owens P. Loss of Myeloid BMPRI1 Alters Differentiation and Reduces Mouse Prostate Cancer Growth. *Front Oncol.* 2020;**10**. doi: 10.3389/fonc.2020.00357.
8. Lefort S, Maguer-Satta V. Targeting BMP signaling in the bone marrow microenvironment of myeloid leukemia. *Biochem Soc Trans.* 2020;**48**(2):411-8. Epub 2020/03/14. doi: 10.1042/bst20190223. PubMed PMID: 32167132.

Ethics Approval All studies were done with approval by the University of Colorado COMIRB. Samples were IRB exempt as all protected health information was removed for the investigators.

<http://dx.doi.org/10.1136/jitc-2022-SITC2022.1448>

1449

LEVERAGING CRISPR CAS9 SCREENING PLATFORM FOR DISCOVERY OF NOVEL TUMOR INTRINSIC PHAGOCYTOSIS MODULATORS

Grace Trombley*, Chengyin Min, Lei Ji. *Tango Therapeutics, Cambridge, MA, USA*

Background Targeting “don’t eat me” signaling has achieved profound responses in clinical trials for hematologic malignancies, highlighting the potential therapeutic value of macrophage-mediated phagocytosis for cancer treatment. In recent years, CRISPR-Cas9 based in vitro co-culture screens have significantly expanded our knowledge of the key tumor-intrinsic mechanisms mediating cytotoxic lymphocyte killing. However, the interactions between tumor cells and macrophages remain elusive. To illuminate the tumor-intrinsic biology governing the interactions between tumor cells and macrophages, we developed both positive and negative screening strategies, and deployed multiple primary bone marrow-derived macrophages (BMDM) or macrophage cell line-based co-culture screens.

Methods DLD1 and MDA-MB-231 cancer lines were infected with a whole-genome CRISPR-Cas9 library and co-cultured with Raw264.7 or J774A.1 in the presence or absence of the therapeutic antibodies magrolimab or cetuximab. MC38 syngeneic cancer cells were infected with a library of 3000 immune-related genes and co-cultured with primary BMDM. For negative selection, the macrophages were selectively killed off post co-culture and the tumor cells were collected for next generation sequencing (NGS) and statistical analysis. For positive selection, macrophages and tumor cells were fully dissociated from the plate post co-culture, and the mixture of cells was subjected to a CD11b positive selection column. Macrophages and tumor cells were enriched separately for downstream analysis.

Results Bioinformatic analysis revealed that CD47 knockout in tumor cells strongly sensitized macrophage-mediated clearance of target cells both from naïve and cetuximab-treated conditions. Furthermore, CD47 or EGFR knockout conveyed growth advantage in co-culture upon treatment with magrolimab or cetuximab, respectively. For the positive screen, we developed a method to sequence bar-coded DNA from tumor cells engulfed by macrophages. Consistently, CD47 sgRNAs were significantly enriched inside macrophages in the naïve condition and were depleted upon treatment with magrolimab. Together, these findings demonstrated the robustness of our phagocytosis-based CRISPR screening platform. In addition to validating the role of CD47 in this system, we discovered and validated a group of novel tumor intrinsic regulators of macrophage-mediated phagocytosis.

Conclusions We successfully established and implemented multiple macrophage and tumor cell co-culture screening platforms, and systematically revealed tumor intrinsic regulators of phagocytosis, uncovering multiple known and novel therapeutic targets regulating vulnerability of tumor cells to macrophage-mediated phagocytosis. Our proprietary high-throughput phagocytosis CRISPR screening platform provides an unbiased and rapid solution to study macrophage and tumor cell interactions and discover novel targets for cancer therapy.

<http://dx.doi.org/10.1136/jitc-2022-SITC2022.1449>

1450

TGF β DEPENDENT LRRC15⁺ MYOFIBROBLASTS DICTATE THE TUMOR FIBROBLAST SETPOINT TO PROMOTE CANCER IMMUNOTHERAPY RESISTANCE

Justin Shyer, Akshay Krishnamurthy*, Minh Thai, Vineela Gandham, Matthew Buechler, Rachana Pradhan, Soren Muller, Shannon Turley. *Genentech, South San Francisco, CA, USA*

Background Single cell transcriptomics has led to the generation of large-scale atlases to understand cellular heterogeneity across both healthy and diseased tissues at the highest resolution. Such atlases have allowed for in silico inferences of fibroblast ontogeny and function, but without in vivo substantiation are limited in their utility to inspire novel fibroblast-directed therapies to improve disease outcome. In cancer, single cell studies identified the emergence of a myofibroblast population, in both mice and humans, uniquely marked by a highly restricted leucine rich repeat containing protein, LRRC15. This cancer-associated myofibroblast population expresses a multitude of extracellular matrix (ECM) associated and immunosuppressive genes. Clinically, high expression of an LRRC15⁺ CAF gene signature in bulk RNAseq data from cancer patients correlated with lack of response to anti-programmed death ligand-1 (aPDL1) checkpoint blockade therapy. It remains unclear if LRRC15⁺ CAFs are the cause of this lack of response, or if they represent a read-out of tumor-intrinsic features driving the association. Also missing are in vivo substantiation of the cellular and molecular signals driving LRRC15⁺ myofibroblast development and the direct impact LRRC15⁺ CAFs have on anti-tumor immunity.

Methods To address these gaps, we paired newly developed preclinical genetic tools in murine tumor models of pancreatic cancer with a large clinical dataset of human stromal cell-sorted expression data from 159 cancer patients across 13 tumor types to understand LRRC15⁺ CAF development and function.

Results In mouse models of pancreatic cancer, we provide in vivo genetic evidence that TGF β 2 signaling in healthy Dermatopontin (DPT)⁺ universal fibroblasts is essential for development of tumor-associated LRRC15⁺ myofibroblasts. Analysis of tumors from 159 patients across 13 indications revealed a conserved axis from universal fibroblasts to LRRC15⁺ myofibroblasts. This axis is the predominant driver of fibroblast lineage diversity in human cancers. Using newly developed Lrrc15-Diphtheria toxin receptor knock-in mice to selectively deplete LRRC15⁺ CAFs, we show loss of this population markedly reduced total tumor fibroblast content and recalibrated the CAF composition towards universal fibroblasts. This, in turn, relieved direct suppression of tumor-infiltrating CD8⁺ T cells to enhance their effector function and significantly augmented tumor regression in response to anti-PDL1 immune checkpoint blockade.

Conclusions Collectively, these findings demonstrate that TGF β -dependent LRRC15⁺ CAFs dictate the tumor-fibroblast setpoint to promote tumor growth, directly suppress CD8⁺ T cell functionality, and limit responsiveness to checkpoint blockade. Development of treatments that restore the homeostatic fibroblast setpoint by diminishing pro-disease LRRC15⁺ myofibroblasts may improve patient survival and response to immunotherapy.

<http://dx.doi.org/10.1136/jitc-2022-SITC2022.1450>

1451

THE IMPACT OF THE TUMOR MICROENVIRONMENT ON B CELL INFILTRATE AND TERTIARY LYMPHOID STRUCTURES IN HIGH GRADE SEROUS OVARIAN CANCER PATIENTS

¹Ian MacFawn*, ¹Ayana Ruffin, ²Sheryl Kunning, ¹Grant Magnon, ²Rinda Soong, ³Caleb Lampenfeld, ¹Huda Atiya, ²Taylor Orellana, ¹Lan Coffman, ¹Tullia Bruno. ¹University of Pittsburgh, Pittsburgh, PA, USA; ²UPMC, Pittsburgh, PA, USA; ³Other, Pittsburgh, USA

Background B cell infiltrate is a common feature of High Grade Serous Ovarian Cancer (HGSOC) and ~15% of patients contain B and T cell-rich tertiary lymphoid structures (TLS) which organize adaptive immunity and correlate with immunotherapy response in other cancer types. Increased B cells, plasma cells, and TLS correlate with improved prognosis in HGSOC. Sadly, current immunotherapies have exhibited poor response in ovarian cancer (~10%), highlighting the need for synergistic or complementary strategies. This research aims to identify underlying stromal and tumor-intrinsic factors promoting TLS formation and maturation in the ovarian tumor microenvironment. We hypothesize that pro-tumorigenic cancer associated mesenchymal stem cells (CA-MSc) hinder TLS, while BRCA mutant tumors promote TLS via DNA damage response. Increasing number and maturity of TLS could boost the poor response of HGSOC patients to immunotherapy.

Methods HGSOC clinical samples were obtained with patient consent through the Pitt Biospecimen Core and clinician collaboration. Original Vectra MoTIF multiplex immunofluorescence panels were designed to capture immune phenotypes and consensus markers of TLS maturity. Digital image analysis was used to analyze TLS presence and maturity and CA-MSc to MSc ratios. These features are correlated with clinical annotations. Digital Spatial Profiling (DSP) using whole transcriptome libraries was conducted on n=16 HGSOC samples to provide a spatially resolved transcriptional signature of TLS, B cells, other immune cells and stroma. Analysis was performed in collaboration with the HCC Cancer Bioinformatics Services.

Results We report the development of a new TLS scoring strategy which relies on multiplex immunofluorescence and spatial transcriptomics. This approach was applied to a large cohort of HGSOC patient samples. Using multiplex immunofluorescence panels, we report the frequency, composition and maturity of TLS across HGSOC anatomical sites (fallopian tube, ovary, omentum), noting an unexpected enrichment of mature structures in tumors residing in the fallopian tubes. Additionally, this analysis reveals a role for BRCA mutations in TLS dynamics. We also quantified CA-MSc burden within tumors using a novel multiplex panel, allowing correlation of CA-MSc to MSc ratio with TLS presence. Complementing this imaging data, we used spatial transcriptomics (DSP) to produce highly precise transcriptional signatures of TLS, TLS-resident versus non-resident B lymphocytes, and TLS-adjacent versus TLS-distal stromal signatures.

Conclusions This work contributes a comprehensive and widely applicable TLS scoring strategy. Its application reveals stromal and tumor-intrinsic factors involved with TLS maturation, revealing plausible strategies for promoting the development of these anti-tumor structures, with the ultimate goal of increasing immunotherapy efficacy, and extending patient survival.

Acknowledgements

Mike Meyer Hillman Cytometry Facility

Hillman Cancer Center Bioinformatics Services DSP interpretation.

Marion Joy image analysis and scanning.

University of Colorado HIMSR: multiplex immunofluorescence optimization.

Ethics Approval This study obtained ethics approval under IRB: STUDY19060197. Specifically; "Prognostic Marker: Acquisition of Blood Samples and Tissue for Research Purposes (UPCI 07-058)". Patient samples utilized were collected with patient consent.

<http://dx.doi.org/10.1136/jitc-2022-SITC2022.1451>

1452

IMAGING MASS CYTOMETRY IDENTIFIES NOVEL NATURAL KILLER CELL INTERACTIONS IN THE PANCREATIC DUCTAL ADENOCARCINOMA TUMOR MICROENVIRONMENT

¹Zoe Malchiodi*, ¹Ivana Peran, ²Elana Fertig, ²Won Jin Ho, ¹Robert Suter, ²Ludmila Danilova, ²Atul Deshpande, ¹Sandra Jablonski, ¹Louis Weiner. ¹Georgetown University, Washington, DC, USA; ²Johns Hopkins University, Baltimore, USA

Background Pancreatic ductal adenocarcinoma (PDAC) has a 5-year survival rate of less than 10%,¹⁻³ which is due in part to its dense desmoplastic and immunosuppressive stroma, caused by cancer-associated fibroblasts (CAFs).⁴⁻⁶ T cell function has been extensively explored in many cancers; however, natural killer (NK) cells of the innate immune system are relatively understudied in PDAC. Interestingly, we have previously shown that fibroblasts express known NK cell ligands and hypothesized that CAFs interact with NK cells as a potential immunosuppressive mechanism in PDAC.⁷ To further examine immune-stromal cell interactions in the PDAC tumor microenvironment (TME), we utilized Imaging Mass Cytometry (IMC), a novel multiplex imaging system that uses up to 40 metal-conjugated antibody markers to gain information of both tissue structure and single-cell data to conduct higher order proteomic single cell analysis.⁸ This novel technology will provide a deeper understanding of the immune architecture in PDAC.

Methods We designed a 34 metal-conjugated antibody panel for known immune, epithelial, and stromal cells, and various immune synapses, cytokines/chemokines, and activation markers. IMC was performed on a human PDAC tissue microarray generated at the Lombardi Comprehensive Cancer Center. IMC image data was pre-processed, segmented, and feature extracted to generate single-cell data,⁹ and downstream analysis was performed using R. Single cells were clustered using Seurat-based clustering approaches to identify known cell populations based on the immune, epithelial, and stromal cell antibody markers. Identified cell clusters were spatially annotated on IMC images using the cytomap R package.⁹

Results IMC images and single-cell analysis preliminarily identified that NK cells are: 1) present within the PDAC TME and 2) surprisingly, co-localize with malignant PDAC cells. This has not been previously reported.

Conclusions Using IMC, we have identified potentially novel interactions between NK cells and malignant epithelial cells in PDAC. Downstream cell neighborhood analysis will reveal further details on immune-stromal interactions in the PDAC TME and identify potential cell populations in further exploit in PDAC.

Acknowledgements Andrew Quong and Eric Swanson (Standard BioTools Inc.), and the Lombardi Comprehensive Cancer Center's Shared Resources, including Histopathology and Tissue Shared Resource, Flow Cytometry Shared Resource, and the Mass Spectrometry and Analytical Pharmacology Shared Resource.

REFERENCES

1. Balachandran VP, Beatty GL, Dougan SK. Broadening the impact of immunotherapy to pancreatic cancer: challenges and opportunities. *Gastroenterology* 2019;**156**(7):2056-72.
2. Shi M, Yu DH, Chen Y, Zhao CY, Zhang J, Liu QH, et al. Expression of fibroblast activation protein in human pancreatic adenocarcinoma and its clinicopathological significance. *World J Gastroenterol.* 2012;**18**(8):840-6.
3. Swayden M, Soubeyran P, Iovanna J. Upcoming revolutionary paths in preclinical modeling of pancreatic adenocarcinoma. *Front Oncol.* 2019;**9**:1443.

4. Karamitopoulou E. Tumor microenvironment of pancreatic cancer: immune landscape is dictated by molecular and histopathological features. *Br J Cancer.* 2019;**121**(1):5-14.
5. Phillips P. Pancreatic stellate cells and fibrosis. In: Grippo PJ, Munshi HG, editors. *Pancreatic Cancer and Tumor Microenvironment.* Trivandrum (India)2012.
6. Yu Y, Yang G, Huang H, Fu Z, Cao Z, Zheng L, et al. Preclinical models of pancreatic ductal adenocarcinoma: challenges and opportunities in the era of precision medicine. *J Exp Clin Cancer Res.* 2021;**40**(1):8.
7. Malchiodi ZX, Fitzgerald A, Galvano E, Weiner LM. Abstract 6169: Identification of molecules mediating natural killer cell-pancreatic stellate cell interactions. *Cancer Res* 2022.
8. Elaldi R, Hemon P, Petti L, Cosson E, Desrues B, Sudaka A, et al. High dimensional imaging mass cytometry panel to visualize the tumor immune microenvironment contexture. *Front Immunol.* 2021;**12**:666233.
9. Windhager J, Bodenmiller B, Eling N. An end-to-end workflow for multiplexed image processing and analysis. *bioRxiv.* 2021:2021.11.12.468357.

Ethics Approval This study was approved by the Lombardi Comprehensive Cancer Center's Biospecimen Use Committee (approval number: GU21-0929).

<http://dx.doi.org/10.1136/jitc-2022-SITC2022.1452>

1454

MULTIOMICS AND MULTIMODAL ANALYSIS APPROACH TO CONSTRUCT A DIFFUSE LARGE B CELL LYMPHOMA ATLAS OF TUMOR MICROENVIRONMENT FOR PREDICTIVE MODELING

¹Mike Mattie, ²Regis Perbost, ²Sarah Turcan, ²Corinne Danan, ³Frederick Locke, ⁴Sattva Neelapu, ⁵David Miklos, ⁶Caron Jacobson, ⁷Lazaros Lekakis, ⁸Yi Lin, ⁹Armin Ghobadi, ¹Jenny Kim, ¹Zixing Wang, ¹Allen Xue, ¹Simone Filosto, ¹Nathalie Scholler, ¹⁰Jérôme Galon*. ¹Kite, a Gilead Company, Santa Monica, CA, USA; ²Veracyte, Marseille, France; ³Moffitt Cancer Center, Tampa, FL, USA; ⁴MD Anderson Cancer Center, Houston, TX, USA; ⁵Stanford University School of Medicine, Stanford, CA, USA; ⁶Dana-Farber Cancer Institute, Boston, MA, USA; ⁷University of Miami Health System, Sylvester Comprehensive Cancer Center, Miami, FL, USA; ⁸Mayo Clinic, Rochester, MN, USA; ⁹Washington University School of Medicine, St. Louis, MO, USA; ¹⁰Veracyte, INSERM, Sorbonne Université, Université de Paris, Centre de Recherche des Cordeliers, Equipe Labellisée Ligue Contre le Cancer, Laboratory of Integrative Cancer Immunology, Marseille, Paris, France

Background Expansion of therapeutic strategies against diffuse large B-cell lymphoma (DLBCL) offers new opportunities to fight aggressive non-Hodgkin's lymphoma. To unveil mechanisms driving cancer evolution and tumor immune contexture from a personalized medicine and diagnostic assay perspective, we sought to build a first-in-class reference database. Using a high-quality testing and innovative multimodal and integrative approach, the first Veracyte Biopharma Atlas for DLBCL evaluated thousands of parameters across more than 150 pre-treatment DLBCL lesions and enabled us to precisely map the spectrum of tumor microenvironments across samples and to establish a robust unsupervised descriptive model. By projecting new specimens associated to relevant clinical information and sample data onto the referential map, Atlas analysis provides a detailed description of the tumor microenvironment and facilitates the development of predictive and prognostic tools.

Methods Veracyte Biopharma Atlas characterizes the tumor microenvironment by analyzing information from 3 different modalities: (i) proteomics (Brightplex[®] panels), (ii) transcriptomics (RNA sequencing and hybridization using Nanostring technology), (iii) genomics (somatic mutations by exome sequencing and/or the rearrangement of the V(D)J regions of the CDR3 receptor of T cells). The specificity, complexity and volume of the information generated required the development of mathematical and bioinformatics processing to extract relevant biological information. The Veracyte Biopharma Atlas innovative approach combines linear (multimodal factor analysis) and non-linear (self-organizing map) approaches with graphical representation of the data. Finally, the incorporation of clinical annotation, either from samples used to generate the map or from clinical specimens projected onto the Atlas, made it possible to identify specific patterns predictive of a clinical parameter of interest (eg, response or toxicity).

Results Gene expression profiling, genomic analysis and proteomics by multiplex spatial technology were performed on more than 150 DLBCL samples collected at diagnosis. Using a centralized multi-omics integrative approach, data were analyzed to capture DLBCL immune contexture. Multimodal analysis allowing multifactor integration was used to derive a unique Atlas map and identify key features. Baseline and screening samples from axicabtagene ciloleucel (axi-cel) anti-CD19 chimeric antigen receptor (CAR) T-cell treated patients from the pivotal ZUMA-1 trial were analyzed with the same multi-omics integrative approach. Projection of ZUMA-1 immune contexture data onto the Atlas map revealed actionable information related to patients receiving CAR-T-cell treatment.

Conclusions Projection of CAR-T clinical trial data highlighted the Veracyte Biopharma Atlas as a powerful tool to stratify patients and identify key immune biomarkers linked to response to CAR T-cell therapy.

Ethics Approval The study protocol for the single-arm, multi-center, registrational ZUMA-1 study of axi-cel in patients with relapsed LBCL was previously described.^{1 2} Each study site's institutional review board reviewed and approved the study protocol and amendments, and all patients provided written informed consent. The study was done according to the International Conference on Harmonisation Good Clinical Practice guidelines. Patients in the ZUMA-1 study did not receive compensation for their participation in the study.

REFERENCES

1. Jensen MC, Riddell SR. Design and implementation of adoptive therapy with chimeric antigen receptor-modified T-cells. *Immunological Reviews* 2014;**257**:127-144.
2. Yang JC, Rosenberg SA. Adoptive T-cell therapy for cancer. *Adv Immunol* 2016;**130**:279-294.

<http://dx.doi.org/10.1136/jitc-2022-SITC2022.1454>

1455

EFFECTIVE CO-TARGETING OF FIBROTIC AND IMMUNE MICROENVIRONMENTS TO IMPROVE THE OVERALL ANTI-TUMOUR RESPONSE IN MODELS OF ADVANCED PANCREATIC CANCER

Benjamin McLean, Diego Chacon Fajardo, Aji Istadi, Sean Porazinski, Marina Pajic, Marina Pajic*. *Garvan Institute of Medical Research, Sydney, Australia*

Background Pancreatic ductal adenocarcinoma (PDA) has a 5-year survival of only 10% and persists as the 3rd most common cause of cancer-related death in Western societies. New treatment options are urgently needed. We have previously defined specific molecular subgroups of PDA associated with pre-clinical and clinical response to select tailored treatment strategies.¹⁻² One such molecular-guided therapy, RXC004, a potent and selective inhibitor of the Wnt/ β -Catenin pathway regulator porcupine, is being investigated in a Ph2 study in patients with pancreatic cancer (NCT04907851). We have previously demonstrated interesting effects of tumour-cell targeted therapies on the environment of PDA.²⁻⁴

Methods We determined the preclinical efficacy and detailed antistromal effects of RXC004 and selective ROCK2 inhibitors in a range of patient derived and genetically-defined PDA models, including clinically relevant combinations with standard of care (SoC) chemotherapy and immunotherapy. Mechanistic assessment of alterations in tumour cell-stromal cell cross-talk was performed using comprehensive transcriptomics and immunofluorescence approaches.

Results In addition to reducing tumour growth and improving overall survival in patient-derived models of aggressive PDA, RXC004 demonstrated striking antifibrotic effects *in vivo*, with changes in cancer-associated fibroblast phenotype, accompanied by decreased levels of extracellular matrix components (fibronectin, periostin) and their organisation (collagen). Moreover, treatment with RXC004 as part of 'priming' combination therapy or 'maintenance' regimen significantly improved *in vivo* chemosensitivity. We also demonstrate that titrated modulation of fibrotic elements *in vivo* via ROCK2 targeting and as part of clinically-applicable therapeutic regimens, can lead to improved outcomes in diverse highly fibrotic and chemoresistant *in vivo* settings. Importantly, selective modulation of ROCK2 or Wnt signalling within the microenvironment of the immunocompetent LSL-KrasG12D/+; LSL-Trp53R172H/+; Pdx1-Cre (KPC) model of metastatic PDA revealed significant positive modulation of distinct immune components. These alterations include decreased level of immunosuppressive regulatory T cells, improved CD8+ and CD4+ T cell infiltration and increased presence of M1 pro-inflammatory macrophages in KPC tumours post-treatment, evident both within the tumour body and the invasive edge.

Conclusions These data demonstrate that therapeutic efficacy of RXC004 and select anti-fibrotics in preclinical development may be the result of targeting both tumour cells and key aspects of the fibrotic and immune PDA microenvironment and in addition provide scientific rationale for the design of future SoC chemotherapy as well as immunotherapy-based combinations in pancreatic cancer.

REFERENCES

1. Waddell N, Pajic M, *et al.* Whole genomes redefine the mutational landscape of pancreatic cancer. *Nature* 2015;**518**(7540):495.
2. Chou A, *et al.* Tailored First- and Second-Line CDK4-Targeting Treatment Combinations in Mouse Models of Pancreatic Cancer. *Gut* 2018;**67**(12):2142.
3. Vennin C, *et al.* Transient tissue 'priming' via ROCK inhibition uncouples pancreatic cancer progression, sensitivity to chemotherapy and the onset of the metastatic niche. *Science Translational Medicine* (2017) pii: eaai8504

4. Murphy KJ, *et al.* Merlin status guides epithelial versus stromal targeting of FAK in pancreatic cancer: improving outcome in personalized medicine. *Science Advances* 2021;**7**(40):eabh0363.

Ethics Approval This study has been approved by the Garvan Institute of Medical Research/St Vincent's Hospital Animal Ethics Committee.

<http://dx.doi.org/10.1136/jitc-2022-SITC2022.1455>

1456

CHARACTERIZATION OF INTER AND INTRA TUMOR HETEROGENEITY IN PRIMARY MELANOMA AND MELANOMA BRAIN METASTASES

¹Alberto Mendoza Valderrey, ¹Daria Kessler, ¹Sierra Thompson, ²Xinmin Li, ¹Kai Rau, ¹Stacey Stern, ³Nicole Rudkin, ⁴Kim Margolin, ³Steven Kolker, ¹Maria Ascierto*, ¹Saint John's Cancer Institute, Santa Monica, CA, USA; ²UCLA, Los Angeles, CA, USA; ³Saint John's Health Center, Santa Monica, CA, USA; ⁴Saint John's Cancer Institute, Santa Monica, CA, USA

Background Melanoma often metastasizes to the brain,¹ usually with a lethal outcome. Recent studies have reported that systemic immunotherapies (IOT) are effective in patients (pts) with melanoma brain metastases (MBM).²⁻³ Nevertheless, the failure of IOT in nearly half of patients with MBM leads to the urgency to deeper investigate mechanisms of intrinsic and acquired resistance. The aim of this study is to deeply characterize the tumor microenvironment (TME) of primary melanoma (PM) and MBM and to assess inter- and intra-tumor heterogeneity in order to identify potential strategies able to increase the success of IOT in pts with MBM.

Methods Formalin-fixed, paraffin-embedded (FFPE) tumor biopsies were derived from 7 PM and 14 MBM biopsies from different pts. RNA was isolated from tumor regions and subjected to whole gene expression profiling (GEP). Ingenuity Pathway Analysis (IPA) was performed for enrichment assessment, and Microenvironment Cell Populations-counter (MCP-counter) method was used to estimate the abundance of immune and stromal infiltrated cell subpopulations. Selected transcripts including mRNA for CD163, CD45 and CD20 were evaluated by immunohistochemistry (IHC). Inter- and intra-tumor immune heterogeneity of n=59 selected immune protein was also determined in PM and MBM by digital spatial profiling (DSP) using Nanostring GeoMx technology.

Results Whole GEP revealed 888 transcripts differentially expressed between PM and MBM ($p \leq 0.01$). We observed an increased expression of genes involved in glycolysis (i.e. ALDOA, ENO2, PKM), immune checkpoint signaling (i.e. TIM3), macrophage activity (i.e. MARCO, CD14), complement signaling (i.e. C1QA/B/C) and chemotaxis (i.e. CCL3) in PM vs. MBM. Conversely, overexpression of genes involved in epithelial signaling (i.e. KRT1), wound healing (i.e. WNT3), stem cell proliferation (i.e. YAP, TP63) and immunosuppressive cytokines and chemokines (i.e. CXCL21, CXCL19) was found in MBM vs. PM. Interestingly, by evaluating the protein expression of immunotherapy drug targets, pan-tumor targets, myeloid targets and immune activation targets using IHC and DSP, we found important inter- and intra-tumor immune heterogeneity in PM and MBM tumors.

Conclusions If confirmed in a larger cohort and correlated with therapy outcomes, our results might lead to the development of novel therapeutic strategies able to increase the success of systemic IOT therapy in patients with advanced melanoma who develop metastases at sites including, but not limited to, the brain.

Acknowledgements We gratefully thank the Rosalie and Harold Rae Brown Cancer Immunotherapy Research Program and the Borstein Family Melanoma Program for their financial support.

REFERENCES

1. Sloan AE, Nock CJ, Einstein DB. Diagnosis and treatment of melanoma brain metastasis: a literature review. *Cancer Control* 2009;**16**:248-255.
2. Tawbi HA, Forsyth PA, Algazi A, Hamid O, Hodi FS, Moschos SJ, Khushalani NI, Lewis K, Lao CD, Postow MA, Atkins MB, Ernstoff MS, Reardon DA, Puzanov I, Kudchadkar RR, Thomas RP, Tarhini A, Pavlick AC, Jiang J, Avila A, Demelo S,

Margolin K. Combined nivolumab and ipilimumab in melanoma metastatic to the brain. *N Engl J Med*. 2018;**379**:722-730.

3. Tawbi HA, Forsyth PA, Hodi FS, Algazi AP, Hamid O, Lao CD, Moschos SJ, Atkins MB, Lewis K, Postow MA, Thomas RP, Glaspy J, Jang S, Khushalani NI, Pavlick AC, Ernstoff MS, Reardon DA, Kudchadkar R, Tarhini A, Chung C, Ritchings C, Durani P, Askelson M, Puzanov I, Margolin KA. Long-term outcomes of patients with active melanoma brain metastases treated with combination nivolumab plus ipilimumab (CheckMate 204): final results of an open-label, multicentre, phase 2 study. *Lancet Onco* 2021;**22**:1692-1704.

Ethics Approval Samples were procured under studies approved by Providence Saint Joseph Health Institutional Review Board or Western Copernicus Group Institutional Review Board. All specimens evaluated were derived from consenting patients.

<http://dx.doi.org/10.1136/jitc-2022-SITC2022.1456>

1457 THE ROLE OF CD26 IN PANCREATIC DUCTAL ADENOCARCINOMA

¹Brandon Ware, ¹Jacklyn Hammons, ¹Isaac Karpovsky, ¹Megan Wyatt, ²Thomas Mace, ¹Shishir Maithel, ³Bassel El-Rayes, ¹Chrystal Paulos, ¹Gregory Lesinski, ¹Maggie Phillips*. ¹Emory University, Atlanta, GA, USA; ²OSUMC, Columbus, OH, USA; ³UAB, Atlanta, GA, USA

Background Pancreatic ductal adenocarcinoma (PDAC) features a dense, fibrotic stroma that obstructs infiltration of immune cells. Our group investigates methods to improve immunotherapy efficacy in PDAC by targeting and manipulating the PDAC stroma. We hypothesize that dysregulated CD26/DPP4 enzymatic activity in PDAC contributes to constrained efficacy of immunotherapy. In addition, we postulate that in vivo pharmacological targeting of CD26 enzyme activity in PDAC, via inhibitors that are FDA-approved for adult patients with Type 2 Diabetes Mellitus, can influence immune cell infiltration and enhance responses to immune checkpoint blockade in murine models of PDAC.

Methods CD26 protein expression was evaluated in immortalized CAFs and PDAC cells by immunoblot and flow cytometry, while soluble CD26 was measured in supernatants by ELISA. In vivo studies used immune-competent C57BL/6 mice orthotopically implanted with syngeneic luciferase-expressing KPC-tumor cells into the pancreas. Tumor establishment was verified by bioluminescence imaging (BLI). Mice were randomized to the following treatment groups: sitagliptin (75mg/kg in drinking water, CD26/DPP4 inhibitor), anti-PD-L1 Ab (200 ug 3x/week), or both combined for 9 days. Controls received vehicle and/or isotype control Ab. BLI monitored tumor growth throughout the study. Tumors were harvested and weighed at study endpoint (day 9 of treatment) and immune cell infiltration was evaluated by flow cytometry. An additional in vivo study was performed to assess differences in efficacy of concurrent versus consecutive administration (2 weeks) of sitagliptin (75mg/kg) and anti-PD-L1 Ab by measuring BLI and pancreas weight at study endpoint.

Results CD26 protein expression was observed in both immortalized human CAFs (HT137 and h-iPSC-PDAC-1) and PDAC cells (HPAC and PANC1) through immunoblot and flow cytometry, however soluble CD26 was only detected in CAF supernatants. Concurrent administration of sitagliptin and anti-PD-L1 Ab limited tumor progression and increased tumor infiltrating CD4+ T cells ($p=.0302$, $p=.0208$ vs isotype control and anti-PD-L1, respectively), CD8+ T cells ($p=.0336$ vs anti-PD-L1), and macrophages compared to vehicle, sitagliptin, and anti-PD-L1 Ab alone. Further studies showed no significant difference in efficacy between concurrent and consecutive administration of sitagliptin together with anti-PD-L1 Ab.

Conclusions Our results reveal that CD26 enzyme inhibition (sitagliptin), augments anti-tumor activity of anti-PD-L1 Ab in PDAC tumor-bearing mice. This work identifies immune cell populations, including T cells and macrophages, that provide insight into mechanisms of efficacy in orthotopic murine models of PDAC. Continued investigations will evaluate the versatility of CD26 inhibition and its capacity to modulate immune checkpoint molecules, thus, broadening efficacy studies across other targets with relevance to PDAC.

<http://dx.doi.org/10.1136/jitc-2022-SITC2022.1457>

1458

REGULATION OF NEOANTIGEN SPECIFIC T CELL INFILTRATION AND SPATIAL TUMOR IMMUNE ARCHITECTURE OF MYELOMA AND ITS PREMALIGNANT PRECURSORS

¹Nancy Villa*, ¹Hope Robinson, ¹David Jaye, ¹Ajay Nooka, ¹Alyssa Duffy, ¹Samuel McCachren, ¹Julia Manalo, ¹Jeffrey Switchenko, ¹Ava Horvat, ¹Vaunita Parihar, ²Jingjing Gong, ²Yan Liang, ¹Geoffrey Smith, ¹Gupta Vikas, ¹Lawrence Boise, ¹Jonathan Kaufman, ¹Craig Hofmeister, ¹Joseph Nisha, Sagar Lonial, ¹Kavita Dhodapkar, ¹Madhav Dhodapkar. ¹Emory University, Atlanta, GA, USA; ²Nanostring Technologies, Seattle, USA

Background Entry of neoantigen-specific T cells into tumors is critical for immunotherapy but underlying mechanisms are poorly understood. Spatial aspects of immune infiltration impact outcome in solid tumors, but the impact of spatial immune patterns in hematologic malignancies such as multiple myeloma is unknown.

Methods We combined several high dimensional spatial analysis platforms with in-vitro/in-vivo modeling in humanized mice of human MM and its precursor monoclonal gammopathy of undetermined significance to gain mechanistic insights into entry of neoantigen-specific T cells into MM tumors.

Results Multiplex immune fluorescence immunohistochemistry (mIF-IHC) analysis of bone marrow biopsies from 95 patients with plasma cell malignancy or its precursor states (MGUS n=13, SMM n=12 and MM n=70) revealed a decline in TCF1+ stem memory like cells and increase in granzymeB+ effector T cells in transition from MGUS to MM. Spatial analyses of tumor/immune infiltration identified formation of microclusters with areas of T cell exclusion in MM but not MGUS. Multifocal growth of MM but not MGUS was reproduced in humanized MISTRG6 mice, indicating this as an intrinsic property associated with malignancy. Consistent with IHC data, MM tumors were resistant to entry of T cells in vitro. In these systems, T cells entry required T cell activation and was enhanced upon CD28-mediated costimulation. T cell entry also required CD2/CD58 interaction and was abrogated upon disruption of these interactions. Importantly, entry of neoantigen-specific T cells into antigen-expressing tumors required in situ stimulation with antigen-presenting dendritic cells (DCs). Upon adoptive transfer into humanized mice, while neoantigen-specific T cells selectively enrich at tumor site, entry of these T cells into tumor masses in vivo again depends on tumor-associated DCs. Spatial analysis of IHCs from MM biopsies revealed that T cell infiltration follows a gradient from CLEC9A+ DCs. Nanostring analyses revealed that CLCC9^{high} regions are enriched for immune activation genes. Patterns of T and myeloid infiltration also correlated with both overall and progression free survival in multivariable analyses.

Conclusions These data identify several distinct aspects of spatial immune alterations that correlate with evolution of malignancy and outcome in MM. They also demonstrate that entry of neoantigen-specific T cells into MM tumors depends on target recognition, costimulation, CD2/58 axis and in situ antigen presentation by tumor-associated DCs. These data therefore identify a novel role for specific antigen presentation by tumor-associated DCs in the effector phase of cancer immunity cycle, with broad implications for immunotherapy and T cell redirection.

Acknowledgements This work was supported in part by funds from NIH R35CA197603 (to MVD). KMD is supported in part by funds from NIH CA238471, AR077926. MVD, KMD, SL and LHB are also supported in part by funds from

Specialized Center for Research (SCOR) award from the Leukemia and Lymphoma Society and from Paula and Roger Riney Foundation. Authors also acknowledge support of the Cancer Tissue and Pathology, immune monitoring and Biostatistics Shared Resources of Winship Cancer Institute of Emory University and NIH/NCI under award number P30CA138292.

Ethics Approval Animal studies including injections of patient samples into mice were approved by the institutional animal care committee at Emory University.

For patients samples, the participants gave informed consent before taking part.

<http://dx.doi.org/10.1136/jitc-2022-SITC2022.1458>

Abstracts

1459

CHARACTERIZATION OF TUMOR BUDDING AND THE TUMOR MICROENVIRONMENT IN COLORECTAL CANCER USING HYPERPLEX IMMUNOFLUORESCENCE

¹Cansaran Saygili Demir*, ¹Mauro Gwerder, ²Deniz Eroglu, ²Marco Cassano, ²Maria Giuseppina Procopio, ²Joanna Kowal, ²Diego Dupouy, ¹Inti Zlobec. ¹University of Bern, Bern, Switzerland; ²Lunaphore, Tolochenaz, Switzerland

Background Current colon cancer classification, prognostication, and therapy decisions are based mainly on cancer staging.¹⁻² However, additional biomarkers are needed to improve patient stratification and complement treatment decision-making strategies. Tumor budding is recognized as an independent prognostic factor in a variety of solid cancers.³⁻⁴ Tumor buds (TBs) are isolated single tumor cells or groups of up to four tumor cells, located both peri- and intra-tumorally. A higher tumor bud count correlates with poor prognosis in colorectal cancer (CRC), and it is hypothesized that a subset of TBs represents, at least in part, an Epithelial-Mesenchymal Transition (EMT) state.⁵ To explore this hypothesis further, we developed a sequential immunofluorescence (seqIFTM)-based panel for a more spatial approach to characterizing TBs and the tumor microenvironment.

Methods Human CRC sections from different cohorts underwent initial pre-processing on PT ModuleTM (Thermo Fisher) followed by automated cycles of seqIF and imaging performed on COMETTM (Lunaphore Technologies). Hyperplex panels consisting of >20 protein biomarkers were generated using off-the-shelf antibodies and served to characterize the tumor-stroma interactions in a preliminary cohort of samples. In a second stage, the spatial screening was performed on larger cohorts of neoadjuvantly treated vs. untreated CRC patient samples. The final characterization of TBs and their interaction with the surrounding milieu was performed by downstream image analysis of the stained tissues.

Results With COMETTM we built an optimized panel including >20 biomarkers for characterization of the tumor and the surrounding stroma. The panel robustness was tested in 15 different CRC cases and resulted in outstanding staining quality with high signal-to-background ratio and elution efficiency (>98%) for all biomarkers. The developed panel allowed the visualization of inter- and intra-tumoral heterogeneity of stained cases and the identification of cell populations including immune cells, cancer-associated fibroblasts, and tumor cells. In line with previously described EMT phenotype of TBs,⁶⁻⁷ our observations showed loss of EpCAM and E-Cadherin in a group of TBs verifying decreased epithelial phenotype (figure 1).

Conclusions The >20-plex panels generated on COMET allowed (i) to discriminate TBs signatures within the depth of tumor-stroma interactions and (ii) to extract valuable TBs features in terms of marker expression. Next, crucial info about TBs phenotypes and their cellular neighborhood will be obtained through an unsupervised analysis approach. This will finally serve to better identify novel immunograms of these cellular entities, thus better defining their therapeutic potential for a personalized medicine approach.

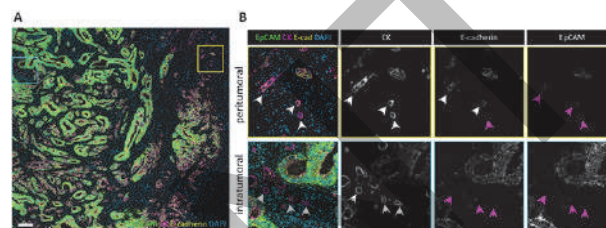
Acknowledgements This study is funded by the Innosuisse grant 51906.1 IP-LS.

REFERENCES

1. Brierley JD, Gospodarowicz MK, Wittekind C. TNM Classification of Malignant Tumours. 8th edition. Wiley Blackwell, 2017.
2. Amin MB, et al. (eds). AJCC Cancer Staging Manual. 8th edition. Springer, 2017.
3. Berg KB, Schaeffer DF. Tumor budding as a standardized parameter in gastrointestinal carcinomas: more than just the colon. *Mod. Pathol* 2018;**31**:862-872.

4. Almgush A, Salo T, Hagstrom J, Leivo I. Tumour budding in head and neck squamous cell carcinoma – a systematic review. *Histopathology* 2014;**65**:587-594.
5. Rogers AC, et al. Systematic review and meta-analysis of the impact of tumour budding in colorectal cancer. *Br. J. Cancer* 2016;**115**:831-840.
6. Grigore AD, et al. Tumor budding: the name is EMT. Partial EMT. *J. Clin. Med.* 2016;**5**(5):51.
7. De Smedt L, et al. Expression profiling of budding cells in colorectal cancer reveals an EMT-like phenotype and molecular subtype switching. *Br. J. Cancer* 2017;**116**:58-65.

Ethics Approval The study was approved by Kantonale Ethikkommission Bern, approval number KEK#2017-01803.



Abstract 1459 Figure 1 Loss of epithelial markers in peri- and intra-tumor

A. Selected composite panel showcasing the loss epithelial markers with remarkable loss of EpCAM in the tumor front. Scale bar is 200 μ m. B. Zoom-in images of representative areas for peri- and intra-tumoral buds. Tumor buds are shown with arrowheads and the TBs with loss of E-cadherin or EpCAM are highlighted with magenta-colored arrowheads.

<http://dx.doi.org/10.1136/jitc-2022-SITC2022.1459>

1460

TREATMENT WITH SMALL MOLECULE NSC243928 IN MOUSE MAMMARY TUMOR MODEL INDUCES CHANGE IN TUMOR MICROENVIRONMENT ASSOCIATED WITH ANTI-TUMOR IMMUNE RESPONSES

¹Benson Selvanesan, ²Alvaro De Mingo Pulido, ¹Sheelu Varghese, ¹Daniel Hupaló, ³Yuriy Gusev, ⁴Sara Contente, ⁵Matthew Wilkerson, ⁶Clifton Dalgard, ⁵Geeta Upadhyay, ⁷Geeta Upadhyay*. ¹Henry Jackson Foundation, Bethesda, MD, USA; ²Moffitt Cancer Center, Tampa, FL, USA; ³Innovation Center for Biomedical Inform, Washington DC, DC, USA; ⁴Pathology, Uniformed Services University, Bethesda, USA; ⁵Uniformed Services University of Health, Bethesda, MD, USA; ⁶Center for Military Precision Health, Bethesda, MD, USA; ⁷Uniformed Services University of Health Sciences, Bethesda, MD, USA

Background Previously, we identified that NSC243928 induces cell death in triple negative breast cancer cells in a LY6K dependent manner. NSC243928 has been reported as an anti-cancer agent in NCI small molecule library. The molecular mechanism of NSC243928 as an anti-cancer agent in the treatment on tumor growth in the syngeneic mice model is not established. With the success of immunotherapies, novel drugs which may elicit an anti-tumor immune response in addition to effecting cancer cell death are of high interest for developing novel drugs to treat solid cancer.

Methods We focused on studying if NSC243928 may elicit an anti-tumor immune response in the in vivo mammary tumor models of 4T1 and E0771.

Results We observed that treatment with NSC243928 induced in vivo tumor mass reductions. The bulk RNA seq analysis of tumor isograft samples showed that NSC243928 generates anti-tumor immune responses in both models. NSC243928 induced cell surface calreticulin expression, indicative of immunogenic cell death in both tumor cell lines at the micromolar concentrations. NSC243928 treatment led to reduced MDSCs in the peripheral blood and increased levels of intra-tumoral immune cells namely- patrolling monocytes and MHC II positive tumor associated macrophages in both mouse models. We observed that NSC243928 showed intra-tumoral immune response such as increased NKT cells, decreased PMN-MDSCs and increased B1 cells in the E0771 mouse model.

Conclusions Taken together we conclude that NSC243928 induces a superior immune response in the E0771 mouse mammary tumor model. Further studies are required to understand the link of NSC243928 associated anti-tumor immune response to determine the adequate molecular signature associated NSC243928 efficacy could be identified, which will be beneficial to future drug development.

Acknowledgements NIH, NCI, R01 CA227694.

DOD, USUHS, VPR-NFP-74-9824.

NIH, NCI, R21 CA256424.

Biomedical Instrumentation Center, USUHS.

The American Genome Center, USUHS.

National Cancer Institute, National Institute of Health.

Disclaimer The opinions expressed herein are those of the authors and are not necessarily representative of the official policy of the Uniformed Services University of the Health Sciences (USUHS), the Department of Defense (DOD), the United States Army/Navy/Air Force, or the U.S. Government or any other funding agencies herein.

<http://dx.doi.org/10.1136/jitc-2022-SITC2022.1460>

1461

DISCOIDIN DOMAIN RECEPTOR 1 EXPRESSION IS ASSOCIATED WITH STROMAL TGF BETA SIGNALING IN SELECTED CANCERS

Xinwei Sher, Ziyin Wang, Thomas Schürpf, Laura Dillon, Tamas Oravecz, Laurent Audoly, Guy Clifton*. *Parthenon Therapeutics, Inc, Boston, MA, USA*

Background Discoidin Domain Receptor 1 (DDR1) has been implicated in cancer prognosis, invasion, and metastases in multiple tumor types.¹ More recently, DDR1 has also been implicated in immune exclusion.² However, the relationship between DDR1 and TGF beta-mediated immunomodulatory pathways is less clear and may vary by tumor type.

Methods The Cancer Genome Atlas (TCGA) was queried for the association between an 80-gene TGF beta pathway activation signature³ and DDR1 gene expression in all tumors and by individual histologic types. To further understand role of the DDR1/TGF beta interaction, TGF beta isoforms (TGFB1, TGFB2, TGFB3) and binding proteins (LTBP1, LTBP3, LRRC32, NRROS) were compared to DDR1 expression by indications with a strong/moderate relationship between TGF beta signature and DDR1 compared to those with a weak or no relationship between the two.

Results DDR1 gene expression and TGF beta signaling expression are not correlated in a pan-tumor analysis ($r=0.12$). In individual indications, there is a strong relationship ($r>0.75$) in thymoma ($r=0.79$); moderate relationship ($0.75>r>0.5$) in papillary renal cell carcinoma ($r=0.57$), and thyroid cancer (0.52); a weak relationship ($0.5>r>0.25$) in testicular ($r=0.49$), prostate ($r=0.49$), hepatocellular carcinoma ($r=0.47$), endometrial ($r=0.44$), ovarian, lung squamous cell carcinoma ($r=0.27$), lung adenocarcinoma ($r=0.29$), rectal ($r=0.32$), cholangiocarcinoma ($r=0.36$), cervical ($r=0.36$), head and neck ($r=0.30$), esophageal cancers ($r=0.30$), glioblastoma ($r=0.27$); No relationship (<0.25) in all others. There was a strong, direct relationship ($r=0.76$, figure 1) between LTBP3 expression and DDR1 expression in indications with a strong/moderate correlation between TGF beta signaling signature and DDR1 and no relationship ($r=0.17$) in those with a weak or no relationship. All other correlations between DDR1 and TGF beta isoforms or binding proteins were weak or nonexistent ($r<0.5$).

Conclusions DDR1 expression is correlated with TGF beta signaling expression in multiple cancer types, but with varying strength of correlation. In indications with a strong or moderate relationship, DDR1 is also strongly correlated with latent-transforming growth factor beta-binding protein 3 (LTBP3) gene expression, suggesting a common stromal-mediated interaction.

REFERENCES

1. Gao Y, Zhou J, Li Jin. Discoidin domain receptors orchestrate cancer progression: A focus on cancer therapies. *Cancer Sci.* 2021;**112**:962-969.
2. Sun X, Wu B, Chiang HC, Deng H, Zhang X, Xiong W, Liu J, Rozeboom AM, Harris BT, Blommaert E, Gomez A, Garcia RE, Zhou Y, Mitra P, Prevost M, Zhang D, Banik D, Isaacs C, Berry D, Lai C, Chaldeckas K, Latham PS, Brantner CA, Popratiloff A, Jin VX, Zhang N, Hu Y, Pujana MA, Curiel TJ, An Z, Li R. Tumour DDR1 promotes collagen fibre alignment to instigate immune exclusion. *Nature* 2021;**599**:673-678.
3. Teschendorff AE, Gomez S, Arenas A, El-Ashry D, Schmidt M, Gehrman M, Caldas C. Improved prognostic classification of breast cancer defined by antagonistic activation patterns of immune response pathway modules. *BMC Cancer.* 2010;**604**:1-20.

<http://dx.doi.org/10.1136/jitc-2022-SITC2022.1461>

1462

ADRENERGIC SIGNALING AUGMENTS CYTOTOXIC T CELL ANTI TUMOR ACTIVITY IN P53 DEFICIENT CANCERS BY CXCL10 RELEASE

¹Deborah Silverman*, ²Sara Leahey, ¹Shamima Akhter, ¹Tong Xie, ¹Simone Anfossi, ¹Jennifer Covello, ¹Frederico Netto, ¹Elien Doorduyn, ²Yunfei Wang, ³Emily Ashkin, ¹Jeffrey Myers, ¹George Calin, ²Patrick Hwu, ¹Moran Amit. ¹MD Anderson Cancer Center, Houston, TX, USA; ²Moffitt Cancer Center, Tampa, FL, USA; ³Stanford University, Palo Alto, CA, USA

Background Harnessing the immune system through the attenuation of immune checkpoints has led to durable tumor rejection in a subset of tumors. However, the majority of epithelial cancers remain resistant to existing immunotherapies. It is imperative to understand how these resistant tumors escape the immune system in order to design more efficacious therapies. Often, nonresponsive tumor types, such as pancreatic cancer and head and neck cancers (HNCC), possess a complex tumor microenvironment (TME) infiltrated by immune and stromal cells, as well as nerve fibers arising from the peripheral nervous system. In comparison with other members of the TME, the role of tumor-infiltrating nerve fibers in oncogenesis and treatment resistance is understudied. Studies across murine models of prostate and pancreatic cancer have shown that ablation of portions of the peripheral nervous system prevents cancer progression.^{1 2} We recently showed that existing nerves sprout and undergo reprogramming to an adrenergic-like phenotype as a result of orchestrated microRNA shuttling from cancer cells to neurons, resulting in activation of transcriptional programs that establish new neuronal identity.³ Given that activated T-cell subsets express high levels of adrenergic receptors, we hypothesized that adrenergic signaling may also influence tumor-infiltrating T-cell function.

Methods We used murine models of HNCC to discern the effect of adrenergic signals on overall immune infiltration, tumor growth, and efficacy in combination with immune checkpoint inhibitors. We correlated our findings with patient cohorts using immunohistochemistry. We studied intratumoral and intra-T-cell pathway changes by RNA sequencing.

Results In T-cell cytotoxicity studies, a variety of adrenergic agonists, particularly β_2 agonists, enhanced T-cell activity against tumor cells. Adrenergic agonists exerted this effect on T-cells not directly on adrenergic receptors on the T-cells themselves, but indirectly on adrenergic receptors on the cancer cells, forcing an increased release of cytokines and chemokines, most notably CXCL10. This dysregulation in immune signaling promoted not only recruitment but also activation/exhaustion pathways within CD8⁺ T-cells. Intriguingly, this signaling axis was dependent on p53 loss within the cancer cell.

Conclusions These results describe a new mechanism for p53's regulation of cancer, and contrast with the known role of adrenergic signaling in cancer. Although nerve-cancer crosstalk drives cancer progression, tumor innervation may also play a positive role in regulating the host's adaptive immune response. Therapeutic approaches targeting this critical component of tumor biology may lead to new efficacious, personalized treatments, expanding the use of immunotherapy and/or combination therapies in new cancer types and ultimately improving patient survival.

REFERENCES

1. Magnon C, Hall S, Lin J, Xue X, Gerber L, Freedland S, Frenette P. Autonomic nerve development contributes to prostate cancer progression. *Science*. 2013;**341**:1236361.

2. Saloman J, Albers K, Li D, Hartman D, Crawford H, Muha E, Rhim A, Davis B. Ablation of sensory neurons in a genetic model of pancreatic ductal adenocarcinoma slows initiation and progression of cancer. *PNAS*. 2016;**113**:3078-3083.
3. Amit M, Takahashi H, Dragomir M, Lindemann A, Gleber-Netto F, Pickering C, Anfossi S, Cai Y, Wong R, Knutsen E, Shimizu M, Ivan C, Rao X, Wang J, Silverman DA, Tam S, Zhao M, Caulin C, Zinger A, Tasciotti E, Dougherty P, El-Naggar A, Calin GA, Myers JN. Loss of p53 drives neuron reprogramming in head and neck cancer. *Nature*. 2020;**578**:449-454.

Ethics Approval MD Anderson IACUC Study #00001522-RN02

<http://dx.doi.org/10.1136/jitc-2022-SITC2022.1462>

1463

ADDITION OF LOSARTAN TO FOLFIRINOX AND CHEMORADIATION DOWNREGULATES PRO-INVASION AND IMMUNOSUPPRESSION ASSOCIATED GENES IN LOCALLY ADVANCED PANCREATIC CANCER

¹Rakesh Jain, ¹Yves Boucher, ¹Jessica Posada, ²Spencer Rosario, ¹Liqun Gu, ¹Ashwin Kumar, ¹Heena Kumra, ¹Mari Mino-Kenudson, ¹Nilesh Talele, ¹Dan Duda, ¹Dai Fukumura, ¹Jennifer Wo, ¹Jeffrey Clark, ¹David Ryan, ¹Carlos Fernandez-del Castillo, ¹Theodore Hong, ³Mikael Pittet, ¹Sonu Subudhi*. ¹Massachusetts General Hospital, Boston, MA, USA; ²Roswell Park Comprehensive Cancer Center, Buffalo, NY, USA; ³University of Geneva, Geneva, Switzerland

Background Adding losartan to FOLFIRINOX (FFX) chemotherapy followed by chemoradiation (CRT) resulted in 61% R0 surgical resection in our phase II trial in patients with locally advanced pancreatic cancer (LAPC). Here we identify potential mechanisms of benefit by assessing the effects of neoadjuvant losartan+FFX+CRT versus FFX+CRT on the stromal tumor microenvironment.

Methods We performed a gene expression analysis of RNA extracted from pancreatic cancer tissue sections and immunohistochemistry (IHC) for cancer cells and immune cells using archived surgical samples from patients treated with losartan+FFX+CRT (NCT01591733), FFX+CRT (NCT01591733) or surgery upfront, without any neoadjuvant therapy. We then assessed whether certain gene sets could stratify the overall survival (OS) of patients.

Results Neoadjuvant losartan+FFX+CRT and FFX+CRT increased the expression of genes linked to vascular normalization, transendothelial migration of leukocytes, T cell activation and cytolytic activity, and dendritic cell (DC) related genes versus no neoadjuvant treatment. In comparison to FFX+CRT, losartan+FFX+CRT downregulated pro-invasion, immunosuppression, and M2 macrophages-related genes, and upregulated genes associated with tumor suppression, including the p53 pathway. Furthermore, immunostaining revealed significantly less residual disease in lesions treated with losartan+FFX+CRT versus FFX+CRT. Losartan+FFX+CRT also reduced CD4⁺FOXP3⁺ regulatory T cells in PDAC lesions with a complete/near-complete response. OS was associated with DC and antigen presentation genes for patients treated with FFX+CRT, and with immunosuppression and invasion genes or DC- and blood vessel-related genes for those treated with losartan+FFX+CRT.

Conclusions Adding losartan to FFX+CRT reduced pro-invasion and immunosuppression-related genes, which were associated with improved treatment outcomes in patients with LAPC. We have shown in murine models of pancreatic ductal adenocarcinoma that the angiotensin receptor 1 blocker losartan improves the delivery and efficacy of cytotoxic agents. Our phase II trial – stemming from our preclinical findings – in patients with LAPC showed that losartan plus FFX chemotherapy followed by CRT led to high rates of complete surgical resection. Here, we identified the potential mechanisms of benefit of neoadjuvant losartan+FFX+CRT. We show that both losartan+FFX+CRT and FFX+CRT improved the expression of genes linked to vascular normalization, transendothelial migration of leukocytes, T cell activation, cytolytic activity and dendritic cell maturation, effects mediated by chemotherapy. In addition, losartan+FFX+CRT downregulated immunosuppression and pro-invasion-related genes, likely mediated by losartan. These findings suggest that losartan potentiates the benefit of FFX+CRT by reducing immunosuppression and invasion, and thus, may help overcome resistance to immunotherapy.

Ethics Approval The study was approved by institutional review board (IRB) of Mass General Brigham (IRB protocol number: 2022P001372).

<http://dx.doi.org/10.1136/jitc-2022-SITC2022.1463>

1464

KNOCKOUT OF COLLAGEN TYPE I IMPEDES TUMOR GROWTH AND SUPPORTS IMMUNE CELL INFILTRATION IN A MURINE MODEL OF PANCREATIC CANCER

²Marco Carretta, ²Anne Mette Rømer, ³Christina Jensen, ²Dorota Kuczek, ²Astrid Johansen, ²Klaire Fjaestad, ³Nicholas Willumsen, ²Mads Andersen, ²Daniel Hargboel Madsen, ¹Marie-Louise Thorseth*. ¹Herlev Hospital, Herlev, Denmark; ²Center for Cancer Immune Therapy, Copenhagen, Denmark; ³Nordic Bioscience, Herlev, Denmark

Background A key characteristic of cancer progression is remodeling of the extracellular matrix (ECM). This remodeling results in a tumor-specific ECM which is often of high density and rich in collagen. The high collagen density of the tumor ECM correlates with a poor prognosis in many types of cancer and with low infiltration of immune cells. The direct effects of increased intratumoral collagen on tumor progression are not yet fully understood. In this study, the role of collagen on tumor growth and immune cell infiltration were directly investigated in vivo using transgenic murine models allowing for manipulation of collagen levels.

Methods Two transgenic murine models were used to study the effects of the level of intratumoral collagen type I; a conditional knockout mouse model with decreased collagen deposition and a collagenase-resistant mouse model with increased collagen deposition. Changes in the level of collagen type I synthesis and content were demonstrated using qRT-PCR, ELISA, and histological staining. Collagen-mediated effects on immune cell infiltration were investigated using flow cytometry analyses, qRT-PCR, and immunohistochemistry. All animal studies were following institutional guidelines and were approved by the Danish Animal Experiments Inspectorate.

Results Collagen type I expression and deposition was significantly decreased in the conditional knockout mouse model. Knockout of collagen led to impeded growth of Pan02 pancreatic carcinomas. This was accompanied by increased infiltration of immune effector cells, including an increase in the amount of NK cells and an increased CD8/CD4 ratio. These results were backed up by employing the collagenase-resistant mouse model with increased collagen deposition. In these mice, tumor growth was increased and there was a higher CD4/CD8 ratio and an increased amount of immunosuppressive myeloid cells.

Conclusions The results of this study demonstrate pronounced effects of collagen on tumor progression and on the tumor immune microenvironment. The potential immunosuppressive role of collagen type I provides a rationale for extending future research in cancer immunotherapy to include focus on the ECM and in particular collagen type I.

<http://dx.doi.org/10.1136/jitc-2022-SITC2022.1464>

1465

SOX2 EXPRESSION IN NSCLC MEDIATES CHANGES IN THE TUMOR MICROENVIRONMENT IMPAIRING T CELL INFILTRATION AND PROMOTING RESISTANCE TO CHECKPOINT BLOCKADE THERAPY

Stefani Spranger, Arjun Bhutkar, Kim Nguyen, Sally Weng, Ellen Duong, Sarah Blatt, Elen Torres-Mejia*. *Koch Institute at MIT, Cambridge, MA, USA*

Background Immunotherapies such as checkpoint blockade therapy (CBT) can be an effective approach to treat patients with metastatic tumors. In non-small cell lung cancer (NSCLC), four major immune subsets have been described, (a) the CBT-sensitive with T cell infiltration and PD-L1 expression, (b) the immune cell desert that lacks CD8+ T cell infiltration, (c) the non-functional T cell phenotype comprising T cells yet no PD-L1 expression, and (d) the T cell excluded phenotype, characterized by effector T cells surrounding the tumor.¹ Patients with a non-T cell-infiltrated tumor microenvironment (TME) correlate with a poor response to CBT.² Data from our lab showed that NSCLC patients can be classified into T cell-infiltrated and non-T cell-infiltrated using a T cell gene signature. Interestingly, we observed that Sox2 upregulation correlates with a lack of T cell infiltration. Using a syngeneic mouse model, we aim to investigate how tumor cell-intrinsic expression of Sox2 mediated immune evasion in NSCLC.

Methods We used a lung adenocarcinoma cell line (KPCt) derived from a *Kras*G12^{D/+} and *Tp53*^{-/-} mouse to overexpress Sox2 (KPS2). Subcutaneous or lung tumors were treated with anti-PD-L1 and anti-CTLA-4 blocking antibodies and analyzed for tumor burden. Tumor infiltration of T cells was evaluated by fluorescence microscopy. To characterize tumor-specific T cell responses, we engineered the KPCt and KPS2 cell lines to express the model antigen SIY. Finally, we performed a bulk RNA-seq analysis of KPCt.SIY and KPS2.SIY cell lines and subcutaneous tumors to determine candidate genes downstream Sox2 that could negatively affect T cell infiltration into the tumor.

Results We found that Sox2 overexpression induces resistance to CBT mediated by T cell exclusion from the tumor core. Analyses of tumor-reactive T cells indicated that T cell priming and differentiation into cytotoxic effector T cells were not affected, yet, cytotoxic T cells failed to infiltrate KPS2 tumors while enriched in the peritumoral regions. Bulk RNA-seq data showed that Sox2 overexpression changed the composition of the extracellular matrix. Furthermore, we observed in KPS2.SIY tumors an increase in endothelial vessel density; however, the size of the vessels was significantly reduced compared to KPCt.SIY tumors.

Conclusions Our results show that tumor cell-intrinsic activation of Sox2 in NSCLC promotes immune evasion and contributes to immunotherapy resistance by inducing changes in the TME. Understanding the molecular and immunological mechanisms mediating T cell exclusion from the lung TME will facilitate the development of novel combination treatment strategies for NSCLC patients.

Acknowledgements This work was supported by the Ludwig Center for Molecular Oncology at MIT and by the SITC-Nektar Therapeutics Equity and Inclusion in Cancer Immunotherapy Fellowship.

REFERENCES

1. Herbst RS, Soria JC, Kowanzet M, Fine GD, Hamid O, Gordon MS, Sosman JA, McDermott DF, Powderly JD, Gettinger SN, Kohrt HE, Horn L, Lawrence DP, Rost S, Leabman M, Xiao Y, Mokatrin A, Koeppen H, Hegde PS, Mellman I, Chen DS,

Hodi FS. Predictive correlates of response to the anti-PD-L1 antibody MPDL3280A in cancer patients. *Nature* 2014;**515**:563-567. doi:10.1038/nature14011

2. Chen DS, Mellman I. Elements of cancer immunity and the cancer-immune set point. *Nature* 2017;**541**:321-330, doi:10.1038/nature21349

Ethics Approval Animal procedures were approved by the Committee on Animal Care (CAC/IACUC) at MIT, DHHS Animal Welfare Assurance # D16-00078

<http://dx.doi.org/10.1136/jitc-2022-SITC2022.1465>

1466

NOVEL CELL PHENOTYPES CORRELATED WITH CHECKPOINT IMMUNOTHERAPY RESPONSES IDENTIFIED IN THE TUMOR AND IMMUNE MICROENVIRONMENT OF PATIENTS WITH METASTATIC MELANOMA

Brian Thompson, Ann Strange, Jonathan Hester-McCullough, David Woods, Carol Amato*. University of Colorado Denver AMC, Aurora, CO, USA

Background Visualizing and profiling cells within the tumor microenvironment (TME) is an important component of translational studies, particularly with the advent of immunotherapies. Successful optimization and utilization of multiplex immunofluorescence (mIF) allows researchers to identify cell populations and interactions involved in cancer biology. In separate publications, we describe novel immunophenotypes in the peripheral blood or tumors of patients with metastatic melanoma receiving immunotherapy.^{1, 2} These populations include ectoenzyme expressing Tcells (CD38 and CD39), and melanoma cells that express CD83, a marker for dendritic cells. The aim of this current study is to create an mIF panel capable of interrogating the TME of melanoma samples for these phenotypes.

Methods Using the Vectra Polaris platform, a nine-parameter immunofluorescence panel was designed and optimized to detect distinct cell phenotypes in paraffin tissues (CD3, CD4, CD8, SOX10S100, KI67, CD38, CD39, and CD83). We implemented this panel to identify unique population(s) of cells within FFPE specimens from patients with melanoma undergoing anti-PD1 immunotherapy. Thirty-four samples from 23 patients were analyzed (including 11 responders and 12 non-responders). Based on specimen availability, we assessed a variety of tissue types collected across anatomic location and/or time points (ie primary or metastatic lesion; before or on-treatment). inForm and phenopt software was used to discern tumor versus stroma compartments and distinguish phenotypes.

Results We detected the previously described immunophenotypes (CD3+/CD4+/CD38+/CD39+, CD3+/CD8+/CD38+/CD39+, and SOX10S100+/CD83+) in all 34 specimens. After cell segmentation, the frequency of CD3+/CD4+/CD38+/CD39+ cells were higher in the tumor compartment compared to stroma ($p=0.0045$). The frequency of CD3+/CD4+/CD38+/CD39+ cells was positively correlated with the frequency of Tregs in the tumor compartment of patients that were non-responsive to immunotherapy (no statistical significance; $R^2=0.16$, $p=0.2$). We also identified CD83-expressing Tcells (CD3+/CD8+/CD83+ and CD3+/CD4+/CD83+) and their frequencies were positively correlated in the stroma compartment of patients that responded favorably to immunotherapy ($R^2=0.98$, $p<0.000001$). Within the stroma compartment of the same patient cohort, similar increases in frequencies are seen with SOX10S100+/CD83+ cells and the two CD83-expressing Tcells phenotypes.

Conclusions We designed an mIF panel that identifies novel immunophenotypes and validated these populations in the TME of patients with metastatic melanoma. Notably, we detected populations that express CD83, a molecule often overlooked in solid tumors. Here we show CD83 expression on melanoma cells and Tcells, and their presence are associated with response to anti-PD1 therapy.

REFERENCES

1. Woods D, et al. Nivolumab and ipilimumab are associated with distinct immune landscape changes and response-associated immunophenotypes. *JCI Insight*. 2020;5(11):e137066.

2. Amato C, et al. Pre-Treatment Mutational and Transcriptomic Landscape of Responding Metastatic Melanoma Patients to Anti-PD1 Immunotherapy Cancers (Basel). 2020 Jul 17;12(7):1943.

<http://dx.doi.org/10.1136/jitc-2022-SITC2022.1466>

1467

AN HOLISTIC AND INTERGRATED APPROACH FOR INVESTIGATING THE BACTERIAL MICROBIOME, GENE EXPRESSION PROFILE AND IMMUNE CELL PROFILE IN THE NON-MUSCLE INVASIVE BLADDER CANCER TUMOUR MICROENVIRONMENT

¹Tyler Woodridge*, ¹Charles Rayner, ¹Sunny Sunshine, ²Matthew Perry, ²Izhar Bagwan, ¹Nicola Annels, ¹Hardev Pandha. ¹University of Surrey, Guildford, UK; ²Royal Surrey NHS Foundation Trust, Guildford, UK

Background Bladder cancer (BC) is the 10th most common cancer world-wide with an estimated 570,000+ people being diagnosed in 2020.¹ It has been shown that communities of bacteria (bacterial microbiome) exist in both normal and cancerous tissues and can impact treatment efficacy (e.g. metabolising chemotherapeutics).²⁻³ We investigated the microbiome in formalin fixed paraffin embedded (FFPE) tumour tissue across different stages of BC compared to adjacent normal tissue to investigate differentially expressed (DE) bacteria. We also investigated DE bacteria between Bacillus Calmette Guerin (BCG) treatment responders vs non responders. These findings were then correlated to differential host immune gene expression and infiltrating immune cell profiles and spatial relationships within the tumour microenvironment (TME).

Methods Bacterial signatures within urine (n=56) and FFPE tissues (n=66), (matching patients n=44), derived from the Royal Surrey Country Hospital, Guildford, UK, were determined using 16s rRNA sequencing (V3-V4). Sequencing data were processed through QIIME2 and clustered into operational taxonomic units (OTUs). Alpha (Shannon and observed) and Beta (Bray-Curtis, weighted and unweighted uniFrac) diversity analysis was performed, with non-parametric statistics for determining significance. RNA extracted from FFPE BC tissues generated gene expression data using the Nanostring IO360 panel (a 770 gene CodeSet) and was correlated to tumour microbiome profiles using SparCC analysis. 9 colour multiplex immunohistochemistry (mIHC) using Phenoimager HT (Akoya Biosciences) was also performed to investigate and spatially define immune cell types (CD4, CD8, CD68, CD57, FOXP3, GRZB, PD-L1, PANCK, DAPI), within tumour tissues (n=71).

Results BC bacterial microbiome showed decreased diversity and composition with disease progression ($P < 0.01$). The bacterial profiles between urine and FFPE cancer tissues revealed independent groups ($P < 0.01$), showing urine is not an accurate proxy. The bacterial microbiome of cancerous and normal tissue, and between responders vs non responders shared mostly similar bacteria, though differentially expressed bacteria were found. Immune cell profiles and spatial relationships determined via mIHC, showed differences between stromal and tumour regions, and low grade (LG) and high grade (HG) disease. Analysis has also shown links between bacteria, immune gene expression and immune cells populations.

Conclusions The analysis of the microbiome in BC has clearly shown differentially expressed bacteria going from low grade to high grade disease. Further investigation of bacteria influencing immune cell phenotype is currently being performed. The potential influence these bacteria have on the tumour immune microenvironment and thus disease and treatment outcomes will provide the rationale for pursuing approaches to modulate the tumour microbiome for improved therapeutic outcomes.

REFERENCES

1. Sung H, Ferlay J, Siegel R, Laversanne M, Soerjomataram I, Jemal A, Bray F. Global Cancer Statistics 2020: GLOBOCAN Estimates of Incidence and Mortality Worldwide for 36 Cancers in 185 Countries. 2021;(3):209-249.
2. Geller L, Barzily-Rokni M, Danino T, Jonas O, *et al.* Potential role of intratumor bacteria in mediating tumor resistance to the chemotherapeutic drug gemcitabine. 2017;**357**(6356):1156-1160.
3. Liu F, Liu A, Lu X, Zhang Z, Xue Y, *et al.* Dysbiosis signatures of the microbial profile in tissue from bladder cancer. 2019;**8**(16): 6904-6914.

Ethics Approval Patient derived Formalin fixed paraffin embedded (FFPE) tissue and urine samples for analysis were received with ethical approval (ethical reference 12/LO/1661).

<http://dx.doi.org/10.1136/jitc-2022-SITC2022.1467>

Late-Breaking Abstracts

Biomarkers, Immune Monitoring and Novel Technologies

1468

FIRST DATA READOUT OF STANDARDIZED TRANSCRIPTIONAL PROFILING FOR OPTIMIZING CELLULAR THERAPIES: A MULTI-CENTER PICI-NANOSTRING COLLABORATION

¹Sarah Church*, ¹Christina Bailey, ¹Phi Phan, ¹Andrew White, ²Lisa Butterfield, ²Samantha Liang, ²Tim Howes. ¹NanoString Technologies, Seattle, WA, USA; ²Parker Institute, San Francisco, CA, USA

Background The field of cellular therapy remains one of the most promising areas for the development of new cancer treatments. To make improvements, it is imperative to broadly understand cell therapy products at the molecular level and to identify factors that contribute to their safety and efficacy. NanoString and the Parker Institute for Cancer Immunotherapy (PICI) have established a ground-breaking collaboration to characterize up to 1,000 apheresis and cellular therapy infusion products with the primary goal of identifying molecular pathways and features that correlate with optimal cellular therapies.

Methods Using a large and diverse sample cohort collected from four (and eventually 8 in Phase II) PICI network Cell Therapy Centers, we are studying Gene Expression Profiles (GEPs) that correlate with optimal apheresis and downstream cellular products, identifying biomarkers and signatures for clinical response and toxicity. We are exploring both cancer-specific and general characteristics associated with effective chimeric antigen receptor (CAR) T cells. Samples are being characterized using the standardized set of genes included in the nCounter CAR-T Characterization Panel, which measures essential features of CAR-T products, including metabolic fitness, TCR diversity, toxicity, activation, persistence, exhaustion and cell type abundances, along with individual transgene expression.

Results We are presenting the initial phase of gene expression analysis for multiple CAR-T cell products across both primary and metastatic hematological and solid tumors. Meta-analysis will be performed using the aggregated set of data alongside individual site-specific analyses. We will explore associations between manufacturing conditions, gene expression and outcomes, and we will examine differences across cancer types and target types.

Conclusions This is the first data output for this one-of-a-kind study characterizing GEPs in CAR-T cells. We anticipate that this information will prove useful across many aspects of the development, manufacturing and clinical application of cellular therapies, and we hope that the findings will lead to improvements in the safety and efficacy of cell therapy products. Data from this project will be made publicly available to the scientific community.

<http://dx.doi.org/10.1136/jitc-2022-SITC2022.1468>

Clinical Trials Complete

1469

A PHASE II BASKET TRIAL OF DUAL ANTI-CTLA-4 AND ANTI-PD-1 BLOCKADE IN RARE TUMORS (DART SWOG 1609 COHORT 47) IN PATIENTS WITH GESTATIONAL TROPHOBLASTIC DISEASE

¹Sandip Patel*, ²Megan Othus, ³Young Kwang Chae, ¹Michael Dennis, ⁴Sarah Gordon, ⁵David Mutch, ⁶Wolfram Samlowski, ⁷Elad Sharon, ⁸Christopher Ryan, ⁹Melissa Plets, ¹⁰Charles Blanke, ¹¹Razelle Kurzrock. ¹University of California San Diego, Moores Cancer Center, La Jolla, CA, USA; ²SWOG Statistics and Data Management Center, Fred Hutchinson Cancer Center, Seattle, WA, USA; ³Northwestern University Feinberg School of Medicine, Chicago, IL, USA; ⁴Thomas Jefferson University/Sidney Kimmel Cancer Center, Richmond, VA, USA; ⁵Washington University School of Medicine, St. Louis, MO, USA; ⁶Comprehensive Cancer Centers of Nevada, Las Vegas, NV, USA; ⁷National Cancer Institute, Cancer Therapy Evaluation Program, Bethesda, MD, USA; ⁸Oregon Health and Science University Knight Cancer Institute, Portland, OR, USA; ⁹Fred Hutchinson Cancer Center, Seattle, WA, USA; ¹⁰SWOG Group Chair's Office, Knight Cancer Institute, Oregon Health and Science University, Portland, OR, USA; ¹¹Medical College of Wisconsin Froedtert Cancer Center, Milwaukee, WI, USA

Background Immune checkpoint blockade has improved outcomes across tumor types; little is known about the efficacy of these agents in rare tumors. We report the results of the gestational trophoblastic disease (GTD) cohort of SWOG S1609 dual anti-CTLA-4 and anti-PD-1 blockade in rare tumors (DART).

Methods We performed a prospective, open-label, multicenter phase II clinical trial of ipilimumab plus nivolumab across multiple rare tumor cohorts, with the GTD cohort reported here. Eligible patients had progressed following at least one line of standard systemic therapy. All participants received nivolumab 240 mg i.v. every 2 weeks and ipilimumab 1 mg/kg i.v. every 6 weeks on a continuous schedule. The primary endpoint was overall response rate [ORR; complete response (CR) and partial response (PR)] by quantitative serum β -hCG; secondary endpoints included progression-free survival (PFS), overall survival (OS), stable disease >6 months, and toxicity.

Results Four eligible patients were enrolled and received therapy. The median number of prior lines of therapy was 2.5 (range 2-4). The median follow-up duration was 11 months. Three of the four patients had a response to therapy [ORR = 75% (CR, 25%, n=1; PR, 50%, n=2) (table 1)], including patients with: malignant gestational trophoblastic neoplasm (n=1, CR, PFS 11+ months), gestational choriocarcinoma (n=1, PR, PFS 10+ months), and choriocarcinoma (n=1, PR, PFS 6+ months). One patient with epithelioid trophoblastic tumor had progression as the best response to therapy. The 6-month PFS was 75% (95% CI 43-100%); all 4 patients were alive at the last follow-up. There were two treatment-related adverse events (TRAEs) of grade 3-4 toxicity: arthralgia and colitis (each observed once), both were immune-related; there were no grade 5 events. No patients discontinued treatment due to TRAEs.

Conclusions Ipilimumab plus nivolumab is well tolerated and demonstrated a 75% ORR in patients with GTD

Acknowledgements This study was funded by NIH/NCI grants U10CA180888, U010CA180819; and in part by Bristol-Myers Squibb Company.

Trial Registration

ClinicalTrials.gov Identifier, NCT03498378

Ethics Approval This study was conducted in accordance with the Declaration of Helsinki ethical principles, Good Clinical Practices, principles of informed consent, and requirements of public registration of clinical trials (ClinicalTrials.gov Identifier,

NCT03498378). The protocol and all amendments were approved by SWOG, the NCI, the NCI central institutional review board (CIRB), and the regulatory committees at the participating institutions. Written informed consent was obtained from each subject at enrollment.

<http://dx.doi.org/10.1136/jitc-2022-SITC2022.1469>

1470

COMBINING THE ANTIGEN-PRESENTING CELL ACTIVATOR EFTILAGIMOD ALPHA (SOLUBLE LAG-3) AND PEMBROLIZUMAB: EFFICACY RESULTS FROM THE 1ST LINE NON-SMALL CELL LUNG CANCER COHORT OF TACTI-002 (PHASE II)

¹Wade Iams*, ²Enriqueta Felip, ³Margarita Majem, ⁴Bernard Doger, ⁵Tim Clay, ⁶Enric Carcereny, ⁷Igor Bondarenko, ⁸Julio Peguero, ⁹Manuel Cobo-Dols, ¹⁰Martin Forster, ¹¹Gyngorii Ursol, ¹²Ewa Kalinka, ¹³Gema Garcia Ledo, ¹⁴Laia Vila Martinez, ¹⁵Matthew Krebs, ¹⁶Begona Campos Balea, ¹⁷Joanna Kefas, ¹⁸Christian Mueller, ¹⁹Chrystelle Brignone, ¹⁹Frederic Triebel. ¹Vanderbilt Ingram Cancer Center, Nashville, TN, USA; ²Vall d'Hebron University Hospital, Barcelona, Spain; ³Hospital de la Santa Creu i Sant Pau, Barcelona, Spain; ⁴Fundación Jiménez Díaz, Madrid, Spain; ⁵St John of God Subiaco Hospital, Perth, Australia; ⁶Catalan Institute of Oncology Badalona, Badalona, Spain; ⁷City Clinical Hospital "4" of Dnipro, Dnipro, Ukraine; ⁸Oncology Consultants, P.A., Houston, USA; ⁹Regional Universitario de Málaga, Málaga, Spain; ¹⁰UCL/University College London NHS, London, UK; ¹¹St. Luke's Hospital, Kropyvnytskyi, Ukraine; ¹²Instytut Centrum Zdrowia Matki Polki, Lodz, Poland; ¹³HM Universitario Sanchinarro, Madrid, Spain; ¹⁴Parc Tauli Sabadell Hospital Univ., Barcelona, Spain; ¹⁵University of Manchester and Christie NHS, Manchester, UK; ¹⁶Hospital Lucus Augusti, Lugo, Spain; ¹⁷Univ. College London Hospitals NHS Trust, London, UK; ¹⁸Immutep GmbH, Berlin, Germany; ¹⁹Immutep S.A.S., Chateaufort, France

Background Eftilagimod alpha (E) is a soluble LAG-3 protein binding to a subset of MHC class II molecules to mediate antigen-presenting cell (APC) activation & T-cell (CD4/CD8) recruitment/activation. By stimulating APCs with E, T cells are recruited, possibly leading to stronger anti-tumor responses than with pembrolizumab (P) alone, especially in tumors not overexpressing PD-L1. Herein we report results of the 1st line non-small cell lung carcinoma (NSCLC) cohort in the TACTI-002 ("Two ACTIVE Immunotherapies") trial.

Methods Pts with measurable, 1st line metastatic NSCLC unselected for PD-L1 were recruited. The objective response rate (ORR) by iRECIST was the primary endpoint (EP). Secondary EPs include ORR by RECIST 1.1, ORR by blinded independent central read (BICR), duration of response (DoR), progression-free survival (PFS), overall survival (OS), PD-L1 and IFN-gamma, safety & tolerability. Pts received 30mg E SC q2w for 8 cycles (1 cycle= 3 weeks) & then q3w for up to 1 year with P (200 mg IV q3w for up to 2 years). Imaging was done every 8 weeks & assessed by investigator. PD-L1 was assessed centrally (22C3 antibody). The study was powered to detect a 52% increase in ORR compared to historical results for P 80% power & 1-sided alpha of 2.5%. Planned recruitment=110 pts.

Results From Mar 2019-Nov 2021, 114 pts were enrolled. Median follow-up was 13 mo (data cut-off Jul 1st 2022). Median age was 67 yrs (44-85) & 74% were male. ECOG PS was 0 & 1 in 37% & 63% of pts. Pts presented with squamous (35%) or non-squamous (63%) carcinoma and 93% had metastatic disease. All PD-L1 subgroups were represented (table 1). Pts received median 9.0 (range 1–18) P & 13.0 (1-22) E. 11 (9.6%) pts discontinued due to related adverse events (AEs). Common (≥15%) AEs were dyspnea (35%), asthenia (33%), decreased appetite (25%), cough (25%), anemia (23%), fatigue (21%), pruritus (21%), constipation (18%), nausea (17%), hemoptysis (16%) & diarrhea (16%).

ORR by iRECIST (primary EP) was 39.5% (95% CI 30.5-49.1) & median PFS was 6.9 mo (95% CI 4.9-9.3). Responses were observed in all PD-L1 subgroups (table 1). ORR (iRECIST) for squamous & non-squamous were 37.5% & 38.9%. Median duration of response was 21.6 mo. Results acc. to RECIST 1.1 were comparable. Early & sustained increases of circulating CXCL-10 & IFN-gamma levels were observed.

Abstract 1470 Table 1

Table 1.

Efficacy (iRECIST)	ORR, % [95% CI]	Median PFS, mo [95% CI]
ITT (N=114), investigator read	39.5 [30.5-49.1]	6.9 [4.9-9.3]
By PD-L1 (centrally tested; 22C3)		
<1% (N=32)	31.1 [16.1-50.0]	4.2 [3.6-6.1]
1-49% (N=38)	44.7 [28.6-61.7]	8.3 [4.4-15.7]
≥50% (N=20)	55.0 [31.5-76.9]	11.4 [4.0-16.8]
≥1% (N=58)	48.3 [35.0-61.8]	9.3 [6.3-15.7]

Conclusions E + P is safe & shows encouraging antitumor activity in 1st line metastatic NSCLC patients unselected for PD-L1, warranting late-stage clinical investigation.

Acknowledgements We thank all the participating patients & their families.

We thank the dedicated clinical trial investigators & their team members.

Merck Sharp & Dohme LLC, a subsidiary of Merck & Co., Inc., Rahway, NJ, USA provided pembrolizumab for the study. Sponsored by Immutep.

Trial Registration The trial identifiers are TACTI-002 (sponsor code), IMP321-P015 (Sponsor code), Keynote-PN798 (MSD code), 2018-001994-25 (EudraCT) and NCT03625323 (ClinicalTrials.gov).

Ethics Approval This has been approved by relevant Competent Authorities, Ethics Committees, and Institutional Review Boards.

<http://dx.doi.org/10.1136/jitc-2022-SITC2022.1470>

Abstracts

1471

PHARMACODYNAMIC AND PREDICTIVE BIOMARKERS ASSOCIATED WITH RESPONSE IN CANCER PATIENTS TREATED WITH TPST-1120: A FIRST-IN-CLASS, SMALL MOLECULE ANTAGONIST OF PEROXISOME-PROLIFERATOR ACTIVATED RECEPTOR-ALPHA

Nathan Standifer*, Yonchu Jenkins, Sam Whiting, Thomas Dubensky. *Tempest Therapeutics, South San Francisco, CA, USA*

Background TPST-1120 is a first-in-class, small molecule antagonist of peroxisome-proliferator activated receptor-alpha (PPAR- α), a transcriptional regulator of fatty acid oxidation and mediator of immune suppression. TPST-1120 was well tolerated and showed signs of activity in a phase I trial as monotherapy (53% disease control rate) and in combination with nivolumab (NCT03829436). In combination cohorts the objective response rate (ORR) was 23%, including 30% (3/10, all partial responses) in subjects treated at the two highest TPST-1120 doses. Responses included two subjects with renal cell carcinoma previously refractory to anti-PD-1 and one subject with late line cholangiocarcinoma.¹ We assessed gene expression changes in post-treatment whole blood and performed baseline mutational analysis on ctDNA to identify potential biomarkers.

Methods Differential expression of 780 genes in 30 subjects receiving 100 mg to 600 mg TPST-1120 BID was assessed using the nCounter[®] PanCancer Immune Profiling panel (NanoString Inc.) supplemented with 30 PPAR- α target genes. Associations between expression change magnitudes and TPST-1120 exposure levels on study day 8 were calculated, and genes exhibiting a False Discovery Rate p-value < 0.05 and effect size > 0.5 were categorized as potential pharmacodynamic biomarkers. Putative clinical response biomarkers were identified using linear discriminant analysis (LDA) with best objective response as categorical discriminants to identify genes differentially expressed by partial response (PR) patients ($p < 0.05$ by Mann-Whitney U Test). Mutational analysis of ctDNA was performed using the PredicineCARE[™] assay (Predicine Inc.).

Results Seven of 780 genes assessed were modulated by TPST-1120 exposure ($p < 0.05$), including genes associated with enhanced immune responsiveness (*CXCL16*, *TNFRSF1A*), monocytes or macrophages (*ITGAX*, *FCGR2A*) and PPAR- α blockade (*NCF4*). Similar TPST-1120 exposure-biomarker associations were observed among monotherapy and combination therapy patients. LDA performed on combination therapy patients revealed that those with PR demonstrated significant elevations ($p < 0.05$) in multiple genes including those associated with Th17 development (*RORC*), lipid transport (*APOE*) and down-regulation of CD155, a TIGIT ligand. Mutational analysis revealed that patients with PR or stable disease were more likely to bear mutations in isocitrate dehydrogenase (*IDH*) and phosphatase and tensin homolog (*PTEN*) compared to patients with progressive disease.

Conclusions TPST-1120 induces pharmacodynamic changes in circulating blood consistent with PPAR- α blockade and reversal of PPAR- α immune suppressive activities. Patients with PR demonstrated gene expression changes that implicate immune activation and alleviation of immune suppression as potential biomarkers of clinical benefit. Increased frequencies of responding patients bearing PI3K pathway or *IDH* mutations may reveal populations likely to benefit from treatment with TPST-1120.

Trial Registration TPST-1120 as Monotherapy and in Combination With Nivolumab in Subjects With Advanced Cancers (NCT03829436)

REFERENCE

1. Yarchoan M, Powderly JD, Bastos BR, Karasic TB, Crysler OV, Munster PN, McKean M, Emens LA, Saenger YM, Ged Y, Stagg R, Goutopoulos A, Moon A, Jenkins Y, Prasi P, Dubensky TW, Whiting SH, Ulahannan SV. A phase 2 study of TPST-1120 as a single agent and in combination with nivolumab in patients with advanced solid tumors. *Jour. Clin. Onc* 2022; **40**(16) suppl.

Ethics Approval The designated study was conducted with adherence to the ethical principles based on the Declaration of Helsinki, International Council for Harmonisation guidelines for current Good Clinical Practice and applicable national and local laws and regulatory requirements. Before the study began, the protocol, the informed consent form, other written materials provided to participants, and any other relevant study documentation was approved by the Institutional Review Board associated with each clinical site with enrolled patients. All participants provided written informed consent prior to initiation of any procedures.

Consent No identifiable information included.

<http://dx.doi.org/10.1136/jitc-2022-SITC2022.1471>

1472

ASSESSING THE CORRELATION BETWEEN CD8 CELL PET IMAGING WITH 89-ZR-CREFMIRLIMAB BERDOXAM AND CD8 CELL IMMUNOHISTOCHEMISTRY IN PATIENTS WITH ADVANCED CANCER RECEIVING IMMUNOTHERAPY

¹Michael Postow*, ¹Audrey Mauguén, ²Michael Farwell, ³Michael Gordon, ^{4,5}David Hays, ⁵Jeffrey Wong, ⁵Sumanta Pal, ⁶Delphine Chen, ⁷Gary Ulaner, ⁸Jonathan McConathy, ⁹Michael Graham, ¹⁰Anthony Shields, ¹¹Annick Van Den Abbeele, ¹²Marcus Butler, ¹³Jacob Thomas, ¹⁴Przemyslaw Twardowski, ^{15,6}Jayant Narang, ¹⁵Aman Singh, ¹⁵Agnish Dey, ¹⁶Kevin Maresca, ¹⁶Edmund Keliher, ¹⁶Feng Liu, ¹⁷Guillaume Potdevin, ¹⁷Guenter Schmidt, ¹⁸Michael Ferris, ¹⁸William Le, ¹⁸Ian Wilson, ¹⁹Ron Korn, ¹Neeta Pandit-Taskar, ¹⁴Kim Margolin. ¹Memorial Sloan Kettering Cancer Center, New York, NY, USA; ²University of Pennsylvania, Philadelphia, PA, USA; ³Honor Health, Scottsdale, AZ, USA; ⁴CARTI, Little Rock, AR, USA; ⁵City of Hope, Duarte, CA USA; ⁶University of Washington, Seattle, WA, USA; ⁷Hoag Hospital, Newport, CA, USA; ⁸University of Alabama, Birmingham, AL, USA; ⁹University of Iowa, Iowa City, IA, USA; ¹⁰Karmanos Cancer Institute, Detroit, MI, USA; ¹¹Dana Farber Cancer Institute, Boston, MA, USA; ¹²Princess Margaret Hospital, Ontario, Canada; ¹³HOAG, Los Angeles, CA, USA; ¹⁴St. John's Cancer Institute, Santa Monica, CA, USA; ¹⁵Takeda Pharmaceuticals, Cambridge, MA, USA; ¹⁶Pfizer, Cambridge, MA, USA; ¹⁷AstraZeneca, Munich, Germany; ¹⁸Imaginab, Bracknell, UK; ¹⁹Imaging Endpoints, Scottsdale, AZ, USA

Background CD8 T-cells (CD8s) mediate the effects of most cancer immunotherapies. CD8s are typically assessed by biopsy which is inherently limited by sample availability, intratumoral and inpatient heterogeneity, and difficulty with repeated, longitudinal assessment. Non-invasive CD8 PET imaging with 89-Zr-Crefmirlimab Berdoxam (crefmirlimab) could circumvent these barriers and has previously demonstrated feasibility and safety.

Methods We conducted a Phase II, prospective multicenter study to test the correlation between crefmirlimab PET signal and CD8 cell quantity by immunohistochemistry (IHC) in patients with solid tumors receiving standard of care immunotherapy. Patients underwent a baseline CD8 PET scan within 1 week prior to starting immunotherapy. A second crefmirlimab PET scan was performed 4-6 weeks after starting immunotherapy. Pre-treatment tissue and a biopsy 4-6 weeks on-treatment were used for CD8 IHC assessment by SP-57 antibody stain. Bone biopsies and those with <5% tumor were excluded. The primary endpoint was the correlation between PET uptake in the biopsied tumors [SUV_{max}, SUV_{mean}, SUV_{peak}; normalized to reference tissue] and CD8 IHC results [CD8 cells/mm²] using the Spearman's correlation coefficient.

Results Among 52 enrolled patients with ≥1 crefmirlimab scan and corresponding biopsy, 48 patients had 35 baseline biopsies and 34 on-treatment biopsies evaluable for the primary endpoint. Eight solid tumor types were represented with renal cell carcinoma (RCC, n=21 samples), melanoma (n=23), and non-small cell lung cancer (NSCLC, n=17) being the most common. Among the examined imaging parameters, SUV_{mean} of the biopsied tumor, normalized to Aorta (SUV_{mean}/SUV_{Aorta}) provided the best correlation. For all 69 biopsied lesions, the SUV_{mean}/SUV_{mean} aorta correlated with CD8 cell density [cells per mm²] by IHC with a Spearman's correlation coefficient of 0.58 (95% CI: 0.385 - 0.697). For the 35 baseline biopsies the correlation was 0.66 (95%CI: 0.387 - 0.825), and for the 34 on-treatment biopsies the correlation was 0.48 (95% CI: 0.148 - 0.713). The correlation for RCC, melanoma, and NSCLC was 0.77 (95% CI: 0.552 - 0.913), 0.55 (95% CI: 0.084 - 0.727), and 0.54 (95% CI: -0.121 - 0.774), respectively. The mean SUV_{mean} lesion/SUV_{mean} aorta and mean CD8 cell density were 1.71 (IQR: 0.93-1.55) and 509 (IQR:114-461) at baseline and 2.43 (IQR: 0.80-3.60) and 759 (IQR:158-963) post-treatment respectively.

Conclusions Non-invasive CD8 PET scanning with crefmirlimab correlates with CD8 assessment by IHC and permits whole patient, longitudinal CD8s assessment. Crefmirlimab imaging is under investigation as a biomarker for immunotherapy responsiveness in ongoing trials (NCT05013099) and could ultimately provide a useful tool for immunotherapy drug development and clinical management.

Trial Registration NCT03802123

Ethics Approval The study was conducted in accordance with the Declaration of Helsinki and the International Conference on Harmonization Guidelines for Good Clinical Practice (ICH-GCP) All patients provided written informed consent.

<http://dx.doi.org/10.1136/jitc-2022-SITC2022.1472>

1473

MECHANISM OF ACTION OF BEMPEGALDESLEUKIN (BEMPEG) PLUS NIVOLUMAB (NIVO) IN PATIENTS WITH UNRESECTABLE OR METASTATIC MELANOMA FROM THE PHASE 3 RANDOMIZED OPEN-LABEL PIVOT IO-001 CLINICAL TRIAL

¹Celeste Lebbe*, ²Shruthi Ravimohan, ²Antara Datta, ²Aparna Chhibber, ³Eva Muñoz Couselo, ⁴Caio Pereira, ⁵Shahneen Sandhu, ²Ming Zhou, ⁶Brendan Curti, ⁷Nikhil Khushalani, ⁶Matthew Taylor, ⁸Alfonsus Van Den Eertwegh, ⁹Ute Hoch, ¹⁰Georgina Long AO, ²Yull Arriaga, ¹¹Adi Diab, ¹²Helen Gogas. ¹Greater Paris University Hospitals, Paris, France; ²Bristol Myers Squibb, Princeton, NJ, USA; ³Vall d'Hebron Barcelona Hospital and Vall d'Hebron Institute of Oncology, Barcelona, Spain; ⁴Fundação Pio XII – Hospital de Câncer de Barretos, Barretos, Brazil; ⁵Peter MacCallum Cancer Centre, Melbourne, Australia; ⁶Providence Cancer Institute of Oregon, Portland, OR, USA; ⁷Moffitt Cancer Center, Tampa, FL, USA; ⁸Amsterdam UMC, Amsterdam, Netherlands; ⁹Nektar Therapeutics, San Francisco, CA, USA; ¹⁰The Melanoma Institute Australia; The University of Sydney; Royal North Shore and Mater Hospitals, Wollstonecraft, Australia; ¹¹MD Anderson Cancer Center, Houston, TX, USA; ¹²National and Kapodistrian University of Athens, Medical School, Athens, Greece

Background BEMPEG is a pegylated interleukin-2 (IL-2) cytokine prodrug engineered to deliver a controlled and sustained IL-2 pathway stimulation, with the goal of preferentially expanding CD8+ T and natural killer (NK) cells over immunosuppressive regulatory T cells (Tregs) in the tumor microenvironment. In the phase 3 PIVOT IO-001 clinical trial (NCT03635983), BEMPEG+NIVO demonstrated no added clinical benefit over NIVO. This first disclosure of comprehensive biomarker analysis from a randomized controlled trial comparing a next-generation IL-2 agonist+NIVO with NIVO aims to gain mechanistic insights underlying the efficacy results.

Methods Patients with previously untreated, unresectable, or metastatic melanoma were randomized 1:1 to receive BEMPEG 0.006 mg/kg+NIVO 360 mg IV Q3W or NIVO 360 mg IV Q3W. Longitudinal changes within Cycle 1 (C1) and 5 (C5) in CD4+ and CD8+ T, NK, and Treg (CD4+CD25+FOXP3+) cell counts, and proliferating (Ki67+) populations, were characterized in blood by flow cytometry. Changes in systemic cytokines, including interferon gamma (IFN γ), were also evaluated. Changes in% tumor cell PD-L1 expression,% CD8+ tumor-infiltrating lymphocytes (TILs), and% FOXP3+ cells from baseline to C1 Day 21 (C1D21) were assessed in tumor biopsies by immunohistochemistry.

Results In peripheral blood, BEMPEG+NIVO mediated statistically significant increases in CD8+ and CD4+ T, NK, and Treg cell counts, as well as IFN γ levels, from baseline to day 8 of C1 and C5, with limited changes observed with NIVO. Compared with NIVO, BEMPEG+NIVO led to significant increases in proliferating Tregs and NK cells from baseline to D8 of C1 and C5. While significant increases in proliferating CD8+ and CD4+ T cells were observed in C1 and C5 following BEMPEG+NIVO, these effects were attenuated in C5. Systemic IFN γ increases, although significant, were attenuated in C5 with BEMPEG+NIVO. Changes in biomarkers measured in the tumor, including increases in CD8+ TILs, from baseline to C1D21 were similar between treatment arms.

Conclusions Observations in peripheral blood demonstrated that, in comparison with limited changes with NIVO, BEMPEG+NIVO increased all immune cell subsets interrogated. Despite greater expansion of peripheral CD8+ T cells within C1 following BEMPEG+NIVO vs NIVO, there was no substantive difference in CD8+ TIL increase between the two arms, suggesting no synergistic/additive tumor activity for BEMPEG+NIVO over NIVO. These observations, together

with attenuation of peripheral T-cell proliferation over time, potentially explain the lack of added clinical benefit for BEMPEG+NIVO vs NIVO in PIVOT IO-001. Results from this study should be taken into consideration and interrogated further as next-generation IL-2 agonists are developed.

Acknowledgements The authors would like to thank the patients who participated in this trial and their families; the investigators, study coordinators, and study teams; and Lisa Panting and Yongliang Sun for their flow cytometry work. Editorial support was provided by Emily Motola, PharmD, of Spark Medica Inc.

Trial Registration NCT03635983

Ethics Approval The trial protocols were approved by site institutional review boards or independent ethics committees and conducted according to Good Clinical Practice guidelines, per the International Conference on Harmonisation. Patients provided written informed consent based on Declaration of Helsinki principles.

Consent Not applicable – no patient-identifiable data reported in this abstract

<http://dx.doi.org/10.1136/jitc-2022-SITC2022.1473>

1474

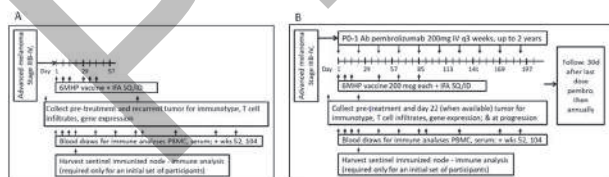
CANCER VACCINE PLUS PD-1 BLOCKADE PROMOTES INFILTRATION OF MELANOMA METASTASES BY VACCINE-INDUCED T LYMPHOCYTES

Christine Tran*, Gabrielle Schwartzman, Walter Olson, Kelly Smith, Jennifer Bryant, Craig Slingluff. University of Virginia, Charlottesville, VA, USA

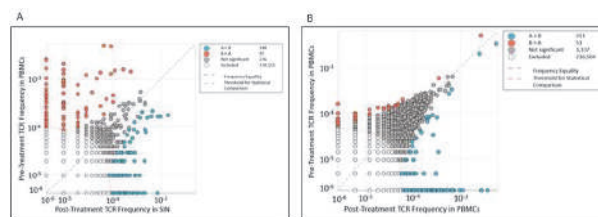
Background T lymphocytes reactive to melanoma antigens can cause regression of advanced melanoma and mediate long-term immunologic memory. However, immune control of melanoma depends on the ability of T cells to infiltrate sites of melanoma deposits. The objective of this study was to determine whether 6 synthetic melanoma helper peptides (6MHP) vaccine plus pembrolizumab increased infiltration of vaccine-induced T cells into tumor metastases compared to 6MHP vaccine alone.

Methods Patients in Mel64 (NCT02515227) received 6MHP vaccines on days 1/8/15/43/64/85. Pembrolizumab was administered intravenously every three weeks, beginning on day 1. Patients also provided blood samples, and sentinel immunized node (SINs) biopsies if available, at specific time points for immune analyses. Tumor biopsies were collected on days 1 (pre-treatment) and 22. Patients in a prior trial, Mel41 (NCT00089219), served as controls, who received 6MHP vaccines on days 1/8/15/29/36/43. Tumor biopsies were collected pre-vaccination and post-vaccination at time of tumor recurrence (figure 1). Across both trials, DNA was extracted from peripheral blood mononuclear cells (PBMCs) pre-treatment, and PBMCs/SINs at time of peak T cell response to 6MHP. These were submitted for high throughput T cell receptor (TCR) sequencing to assess for T cell clonotypes that were significantly increased in number post-treatment or novel clonotypes evident de novo post-treatment. Tumor biopsies were sampled, from which DNA was extracted and submitted for TCR sequencing. These sequences were cross referenced against those in PBMCs/SINs for those that overlapped and were present in tumor post-treatment, but not pre-treatment.

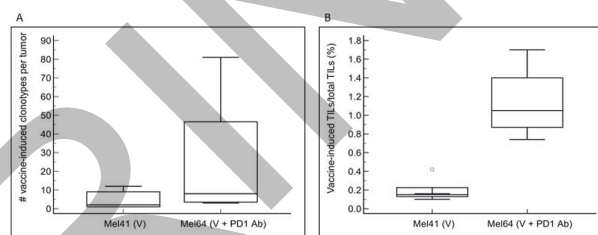
Results Patients across both trials (Mel41 n = 5; Mel64 n = 4) had expanded circulating vaccine-induced T lymphocytes in PBMCs/SINs post-treatment compared to pre-treatment (figure 2). All patients had novel T cell clonotypes in tumor post-treatment compared to pre-treatment, with Mel64 patients having upward trends of the number of vaccine-induced tumor infiltrating T cell clonotypes compared to Mel41 patients (figure 3A). The fraction of vaccine-induced tumor infiltrating lymphocytes (VITILs) of total tumor infiltrating lymphocytes (TILs) was significantly increased in Mel64 patients compared to that in Mel41 patients (p = 0.0159) (figure 3B).



Abstract 1474 Figure 1 Clinical Trial Designs for A) Mel41; B) Mel64



Abstract 1474 Figure 2 Single patient comparisons of TCR clonotypes in PBMCs pre-treatment vs. PBMCs/SINs post-treatment. Sequences in blue appear in higher frequency post-treatment vs. pre-treatment. Sequences present on the x-axis are present post-treatment but not pre-treatment. A) Patient 1 of Mel41: the high number of clonotypes present and increased in pre-treatment PBMC vs. post-treatment SIN is explained by circulating memory cells that are under represented in SIN, while clonotypes appearing in SIN post-treatment are related to vaccination. B) Patient 6 of Mel64.



Abstract 1474 Figure 3 A) Number of Vaccine-Induced Clonotypes per Tumor in Mel41 vs. Mel64; B) Fraction of Vaccine-Induced TILs/Total TILs in Mel41 vs. Mel64. V = Vaccine; PD1 Ab = pembrolizumab

Conclusions These findings suggest that adding pembrolizumab may enhance infiltration of melanoma metastases by vaccine-induced T lymphocytes compared to 6MHP vaccine alone. This treatment combination holds promise in the management of advanced melanoma, and additional interventions may further enhance tumor infiltration of vaccine-induced T cells.

Trial Registration These clinical trials were conducted at the University of Virginia and registered with Clinicaltrials.gov (Mel41 NCT00089219, Mel64 NCT02515227).

Ethics Approval These clinical trials were performed with the University of Virginia Institutional Review Board (IRB), previously known as the Human Investigations Committee (HIC), approval (Mel41 HIC #10464, Mel64 IRB #18174). All participants provided their informed consent before taking part in these clinical trials.

<http://dx.doi.org/10.1136/jitc-2022-SITC2022.1474>

Clinical Trials In Progress

1475

A PHASE 1 STUDY TO CHARACTERIZE THE SAFETY AND TOLERABILITY OF MP0317, A TUMOR TARGETING FAP DEPENDENT CD40 AGONIST DARPIN, IN PATIENTS WITH RELAPSED/REFRACTORY SOLID TUMORS

¹Hilde De Winter*, ¹Elena Fernandez, ¹Vaia Stavropoulou, ¹Nina Stojcheva, ¹Paul Baverel, ²Carlos Gomez-Roca, ³Eelke Gort, ⁴Neeltje Steeghs, ¹Kyriaki Ioannou, ¹Ana Maria Florescu, ¹Jennifer Krieg, ¹Patrick Mossi, ¹Vladimir Kirkin, ¹Philippe Legenne, ⁵Philippe Cassier. ¹Molecular Partners AG, Schlieren, Switzerland; ²IUCT-Oncopole, Marseille, France; ³UMC Utrecht, Utrecht, Netherlands; ⁴Netherlands Cancer Institute, Amsterdam, Netherlands; ⁵Centre Léon Bérard, Lyon, Rhone, France

Background The development of CD40 agonists in immunoncology has been hampered by dose-limiting toxicity (DLT) mainly caused by systemic CD40 activation and peripheral target-mediated drug disposition. By targeting fibroblast activating protein (FAP), our FAP/CD40 directed DARPIn, MP0317, selectively activates CD40 within the tumor microenvironment, while precluding CD40 activation in the periphery. Here we present emerging data from the first-in-human trial (NCT05098405).

Methods This is a Phase 1, first-in-human, multicenter, open label, dose escalation study followed by a safety expansion part, evaluating the safety, tolerability, pharmacokinetics (PK), pharmacodynamics (PD) and preliminary antitumor activity of MP0317 in adult patients with advanced solid tumors. The dose escalation scheme uses an adaptive Bayesian logistic regression model guided by the escalation with overdose control principle to determine the recommended dose. Up to 6 cohorts receive intravenous MP0317 3-weekly until disease progression, unacceptable toxicity, or other discontinuation criteria are met. Dose selection was guided by a translational PK/PD model that accounted for baseline FAP and CD40 expression levels and turnover rates.

Primary endpoints are incidence of DLTs and adverse events. Secondary and exploratory endpoints include PK/PD parameters, response rate (per RECIST and iRECIST), progression free and overall survival.

Results At time of submission, cohort 4 was enrolled, and cohorts 1-3 had completed the study, with no DLT observed. The most frequent AE were grade 2 infusion related reactions in 3/12 dosed patients.

The 7 patients in cohorts 1-3 received ≥ 2 (range 2-8) doses (range 0.03–0.3 mg/kg) of MP0317 and completed the 28-day DLT period. Preliminary PK data show sustained MP0317 serum levels across the dosing interval with evidence of target-mediated drug disposition.

Exposure in the tumor was confirmed with MP0317 co-localizing with FAP and CD40 in 3 out of 5 evaluable paired biopsies. No systemic toxicities were observed and there were no signs of systemic CD40 activation based on circulating PD markers and immunophenotyping data. A PD signal consistent with a tumor-localized myeloid cell activation was observed in cohort 3. Although limited clinical efficacy is expected in monotherapy setting, one heavily pre-treated patient maintained stable disease for 8 cycles.

Conclusions The preliminary clinical and biomarker data provide early evidence of the tumor-targeted CD40 activation mechanism of action of MP0317. As of submission, no DLTs had been observed. Enrollment in dose cohorts covering the projected therapeutic dose range is ongoing to further characterize MP0317 mechanisms of action and safety profile.

Trial Registration NCT05098405 and EudraCT : 2020-005516-22

Ethics Approval This study received ethics approval in France from ETHICS COMMITTEE SUD-OUEST ET OUTRE-MER II initially on 23 July 2021 (and most recently on 27 June 2022) (Dossier: 21.00452.000006) and in The Netherlands from NedMec Medisch-Ethische Toestingscommissie initially on 1 September 2021 (METC21.0653/M21MPA) and most recently on June 10, 2022, (PE/mk/22/500340). All Patients gave written informed consent before taking part in the study. **Consent** N/A at this point

<http://dx.doi.org/10.1136/jitc-2022-SITC2022.1475>

1477

FIRST EFFICACY AND MULTI-OMIC ANALYSIS DATA FROM PHASE 1 CLINICAL TRIAL OF ONCOLYTIC VIRAL IMMUNOTHERAPY WITH CAN-2409 + VALACYCLOVIR IN COMBINATION WITH NIVOLUMAB AND STANDARD OF CARE IN NEWLY DIAGNOSED HIGH-GRADE GLIOMA

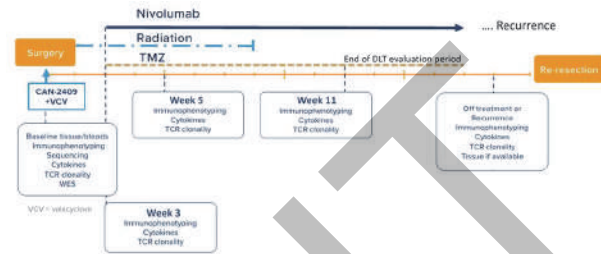
¹Patrick Wen*, ²Caroline Duault, ²Edgar Gonzalez-Kozlova, ²Kevin Brennan, ²Tyson Holmes, ²Seunghye Kim-Schulze, ²Kai Nie, ²Kimberly Argueta, ²Jacques Fehr, ²Mina Pichavant, ²Diane Del Valle, ²Andrew Gentles, ²Sacha Gnjatic, ²Holden Maecker, ³Xiaobu Ye, ¹David Reardon, ¹Wenya Linda Bi, ¹Pierpaolo Peruzzi, ¹Nirav Patel, ⁴Roy Strowd, ⁴Stephen Tatter, ⁵Ian Lee, ⁵Tobias Walbert, ⁵James Snyder, ⁶Steven Brem, ⁶Arati Desai, ⁶Stephen Bagley, ⁷Nduka Amankulor, ⁷Frank Lieberman, ⁷Megan Mantica, ⁸Lenika Lopez, ⁸Susan Bell, ⁸Andrea Manzanera, ¹Sean Lawler, ⁹Lixian Jin, ³Neeraja Danda, ¹⁰Serena Desideri, ¹¹L Burt Nabors, ¹⁰Stuart Grossman, ¹E Chiocca, ⁸Paul Tak, ⁸Francesca Barone. ¹Dana-Farber Cancer Institute, Boston, MA, USA; ²CIMAC Consortium, Stanford, CA, USA; ³Adult Brain Tumor Consortium, Baltimore, MD, USA; ⁴Wake Forest Baptist Health, Winston-Salem, NC, USA; ⁵Henry Ford Health, Detroit, MI, USA; ⁶University of Pennsylvania Hospital, Philadelphia, PA, USA; ⁷University of Pittsburgh Medicine, Pittsburgh, PA, USA; ⁸Candel Therapeutics, Nedeham, MA, USA; ⁹Bristol-Meyers Squibb, Lawrenceville, NY, USA; ¹⁰Adult Tumor Brain Consortium, Baltimore, MD, USA; ¹¹University of Alabama, Birmingham, AL, USA

Background High-grade glioma (HGG) is characterized by a highly immunosuppressive tumor microenvironment and poor prognosis. Limited advances have been made in HGG standard of care (SoC) treatment, with immunotherapy failures reported in this indication. CAN-2409 is a replication-defective adenovirus that delivers HSV thymidine kinase to cancer cells, resulting in local conversion of oral valacyclovir into a toxic metabolite inducing immunogenic cell death. Preclinical data in a mouse model of HGG suggest CAN-2409 potential synergy with anti-PD1 agents.¹ An ongoing phase 1 clinical trial is evaluating safety, initial efficacy and immunological biomarkers associated with the combination of CAN-2409/valacyclovir with nivolumab plus SoC in patients with newly diagnosed HGG.

Methods Forty-one patients with HGG were recruited from February 2019 to March 2021. CAN-2409 was injected into the resection bed during neurosurgery, followed by valacyclovir and SoC chemoradiation. Nivolumab was initiated on day 15 and administered every 2 weeks for up to 52 weeks. Tumor and peripheral blood samples were longitudinally collected (figure 1) from 35 patients (evaluable population). Immune profiling was performed by the CIMAC network including plasma proteomics, multidimensional flow cytometry by CyTOF, whole exome sequencing (WES), TCR analysis and RNA sequencing.

Results Median OS (mOS) for patients with methylated MGMT promoter was 30.6mo for patients undergoing gross total resection (GTR) and 12.6mo for patients undergoing sub-total resection (STR). mOS for patients with unmethylated MGMT was 13.2mo (GTR) and 15.9mo (STR). Propensity score matching analysis is ongoing to evaluate mOS, controlling for known prognostic factors. Plasma proteomics at 3-week post-treatment identified increases in CXCL9, CCL11, GZMA, IFNG, CCL19, MCP1, and MCP3 concentrations (LogFC>1, FDR<0.05). Nivolumab treatment associated with significant increases in CXCL9, IL10, and PDCD1 concentrations (LogFC>1, FDR<0.05) and a trend towards elevated LAMP3, CXCL13, CXCL1, and TNFRSF9 concentrations (logFC>0.5, FDR<0.05 at week 5). Patients with methylated MGMT promoter displayed (at weeks 5 and 11) a significant increase in IL-5, IL-7, IL-10, CD4, CD27, CD40, CD38, CFS-1 and ICOSLG concentrations (FDR<0.05). Baseline concentrations of TIE2 correlated with survival (FDR<0.05). CyTOF analysis unveiled significant post-treatment changes,

including increase in activated CD4 (p 0.0011; week 5), CD8 (p 0.0189; week 5), CD69+ gamma delta T cells (p0.0324; week 5), and plasmacytoid dendritic cells (p=0.0327, p=0.0020 at week 5 and 11). Additional biomarker analysis and canonical correlation analysis with clinical responses are ongoing.



Abstract 1477 Figure 1 Schema of treatment and biomarker timepoints

Conclusions Combination treatment of CAN-2409/valacyclovir plus nivolumab and SoC induces profound immunological changes and appears to associate with encouraging survival data.

Acknowledgements We would like to thank the Adult Brain Tumor Consortium for oversight on the study and the participating patients and their families, as well as site research and clinical staff.

Trial Registration NCT03576612

REFERENCE

1. Speranza MC, Passaro C, Ricklefs F, Kasai K, Klein SR, Nakashima H, Kaufmann JK, Ahmed AK, Nowicki MO, Obi P, Bronisz A, Aguilar-Cordova E, Aguilar LK, Guzik BW, Breakefield X, Weissleder R, Freeman GJ, Reardon DA, Wen PY, Chiocca EA, Lawler SE. Preclinical investigation of combined gene-mediated cytotoxic immunotherapy and immune checkpoint blockade in glioblastoma. *Neuro Oncol* 2018;**20**(2):225–235.

Ethics Approval The protocol was reviewed by the FDA and the Institutional Review Boards at participating institutions. All study participants provided written informed consent before enrollment.

Consent All patients provided informed consent for this trial.

<http://dx.doi.org/10.1136/jitc-2022-SITC2022.1477>

1478

A PHASE I STUDY OF PERSONALIZED ADOPTIVE TCR T CELL THERAPY IN PATIENTS WITH SOLID TUMORS: SAFETY, EFFICACY, AND T CELL TRAFFICKING TO TUMORS OF NON-VIRALLY GENE EDITED T CELLS

¹Susan Foy, ¹Kyle Jacoby, ²Daniela Bota, ¹Theresa Hunter, ³Adam Schoenfeld, ¹Zheng Pan, ¹Eric Stawiski, ¹Yan Ma, ¹William Lu, ¹Songming Peng, ¹Clifford Wang, ¹Benjamin Yuen, ¹Olivier Dalmás, ¹Katharine Heeringa, ¹Barbara Sennino, ¹Andy Conroy, ¹Michael Bethune, ¹Ines Mende, ¹William White, ¹Monica Kukreja, ¹Swetha Gunturu, ¹Emily Humphrey, ¹Adeel Hussaini, ¹Duo An, ¹Boi Quach, ⁴Alphonsus Ng, ⁴Yue Lu, ¹Chad Smith, ⁵Katie Campbell, ¹Daniel Anaya, ¹Lindsey Skrdlant, ¹Eva Huang, ¹Ventura Mendoza, ¹Jyoti Mathur, ¹Luke Dengler, ¹Bhamini Purandare, ¹Robert Moot, ¹Michael Yi, ¹Roel Funke, ¹Alison Sibley, ¹Todd Stallings-Schmitt, ⁶David Oh, ⁵Bartosz Chmielowski, ⁷Mehrdad Abedi, ⁸Yuan Yuan, ⁹Jeff Sosman, ¹⁰Sylvia Lee, ¹¹Claire Williams, ¹¹Sean Kim, ¹¹Matthwe Keefe, ¹¹Michael Leon, ¹¹Youngmi Kim, ¹¹Jason Reeves, ¹¹Wes Goldman, ¹²David Baltimore, ⁴James Heath, ¹Alex Franzusoff, ⁵Antoni Ribas, ¹Arati Rao*, ¹Stefanie Mandl. ¹PACT Pharma, South San Francisco, CA, United States; ²University of California, Irvine, Orange, CA, United States; ³Memorial Sloan Kettering Cancer Center, New York, NY, United States; ⁴Institute for Systems Biology, Seattle, WA, United States; ⁵University of California, Los Angeles, Los Angeles, CA, United States; ⁶University of California, San Francisco, San Francisco, CA, United States; ⁷University of California, Davis, Sacramento, CA, United States; ⁸City of Hope National Medical Center, Duarte, CA, United States; ⁹Northwestern University, Chicago, IL, United States; ¹⁰Fred Hutchinson Cancer Research Center, Seattle, WA, United States; ¹¹Nanostring, Seattle, WA, United States; ¹²California Institute of Technology, Pasadena, CA, United States

Background NeoTCR-P1 is a personalized autologous T cell therapy for treatment of patients with solid tumors. Neoantigen-specific T cell receptors (neoTCRs) were isolated from the patients' own circulating CD8 T cells using the imPACT Isolation Technology[®], followed by non-viral precision genome engineering into an autologous apheresis product for infusion back into the patient.

Methods This phase 1 trial is a first-in-human, multi-center, dose-escalation study to evaluate the safety, tolerability, and manufacturing feasibility of NeoTCR-P1 alone or in combination with IL-2 in solid tumors.

Patients with TCRs identified at screening and meeting eligibility criteria underwent apheresis to manufacture personalized NeoTCR-P1 cell product. Lymphodepleted patients received a single dose of up-to-three distinct NeoTCR cell products at dose levels of 0.4, 1.2, or 4×10⁹ NeoTCR-edited T cells.

Pre- and post-treatment blood and biopsy samples were collected to evaluate NeoTCR-P1 pharmacokinetics, tumor trafficking, signs of T cell engagement or potential mechanisms of resistance.

Results Sixteen patients were infused with NeoTCR-P1 T cells including patients with MSS-colorectal cancer (11), breast cancer (2), ovarian cancer (1), melanoma (1), or non-small cell lung cancer (1). Four of the sixteen patients were treated with NeoTCR-P1 + IL-2.

Two patients experienced toxicities associated with NeoTCR-P1 cell infusions: a grade 1 CRS and a grade 2 ICANS. Five patients had stable disease as their best response at their first tumor assessment (day 28).

NeoTCR+ T cells detected in the peripheral blood had an average peak of 3.6% (range 0.9-7.3%) for DL1, 11.7% (7.7-20.8%) for DL2, and 19.8% (12.0-37.3%) for DL3. Increases in NeoTCR T cells were observed at higher dose levels, stronger lymphodepletion, or higher gene editing rates of the infused product.

Eight post-infusion biopsies were available for sequencing and imaging analysis; 17 of 22 neoTCR-T cells were detected in post-infusion biopsies with 12 neoTCRs among the top 4% of CDR3 sequences detected. The targeted neoantigens were

detected in 7 of 8 post-treatment biopsies (15 of 22 targets), and personalized ctDNA confirmed targeting of a predicted sub-clonal mutation. An APOBEC signature and HLA-LOH were identified as potential mechanisms of resistance. By single-cell, spatial molecular imaging, neoTCR-T cells were visualized in post-treatment biopsies and found to differentially express potential markers of engagement.

Conclusions This study demonstrates the feasibility of isolating and manufacturing NeoTCR-T cells using non-viral precision genome engineering, the safety of infusing up-to-three gene edited NeoTCR-T cell products, and T cell persistence and trafficking to a variety of solid tumors.

Trial Registration NCT03970382

Ethics Approval Ethics approvals have been obtained from each clinical site enrolling patients: City of Hope, Duarte California; University of California Los Angeles, Los Angeles California; University of California, Irvine Medical Center, Orange, California; University of California, Davis, Sacramento California; University of California, San Francisco, San Francisco California; Northwestern University Medical Center, Chicago Illinois; Memorial Sloan Kettering Cancer Center, New York, New York; Tennessee Oncology, Nashville, Tennessee; and Fred Hutchinson Cancer Research Center, Seattle, Washington.

<http://dx.doi.org/10.1136/jitc-2022-SITC2022.1478>

The number next to the author indicates the page number, not the abstract number.

- A Amith, 1313
Aab Alar, 1054
Aanur Praveen, 767
Abadier Michael, 708
Abaid Lisa, 562, 565
Abassi Yama, 12, 188
Abate-Daga Daniel, 1375, 225, 286, 357, 672, 975
Abbadessa Giovanni, 1416
Abbassi-Ghadi Nima, 966
Abbate Franco, 710
Abbate Danilo, 268
Abbineni Chandrasekhar, 1313
Abbott Charles, 119, 146
Abbott Rachel, 312, 343
Abdallah Wassim, 437
Abdelfattah Nouran, 63
Abdelmaksoud Abdalla, 350
Abdel-Mohsen Mohamed, 1307
Abdelrahim Maen, 480, 502, 621
Abdel-Wahab Noha, 1260, 437
Abdou Yara, 633, 634
Abdul-Karim Raghad, 767
Abdullah Shaad, 620
Abdulrahman Ziena, 161, 163
Abed Afaf, 577
Abel John, 1277
Abera Abenezer, 183
Abes Riad, 1339
Aboeella Nada, 796
Aboody Karen, 1137
Abou-Alfa Ghassan, 552, 591, 778
Aboubakar Nana Frank, 437
Abousoud Jawad, 174
Abraham Christopher, 624
Abraham Edith, 617
Abraham-Miranda Julieta, 193
Abrahams Cristina, 1191, 1359
Abrahams Dominique, 191
Abrahmsen Lars, 903
Abrams Scott, 981
Abramson Sascha, 194, 318, 371
Abril-Rodriguez Gabriel, 123
Abu Ghazal Batool, 437
Abu-Amna Mahmoud, 136
Abudayyeh Ala, 502
Abujarour Ramzey, 304, 341
Abulizi Abudukadier, 1060
Abu-Yousif Adnan, 1153
Acero-Bedoya Santiago, 978
Aceveda Diane, 1326
Achar Sooraj, 350, 401
Achour Ikbel, 579, 73
Ackbarali Tariqa, 930
Ackerman Joseph, 1003
Ackerman Shelley, 1348
Acklam Frances, 1046
Acuna-Villaorduna Ana, 589
Adabi Elham, 345
Adada Mohamad, 414
Adam Ammar, 888
Adam Stacey, 29
Adamow Mathew, 587
Adamow Matthew, 1297
Adams Bruce, 924
Adams Gregor, 316
Adams Mark, 118
Adams Micki, 52, 71
Adams Philipp, 137
Adams Sarah, 1112
Adams Scott, 110
Adamson Peter, 1416
Adang Anton, 686
Addeo Alfredo, 437
Adderkin Alison, 850
Adebanjo Tolani, 657
Adebola Serifat, 350
Adedimeji Adebola, 932
Adelberg David, 544
Adelmann Charles, 882
Adeshina Anuoluwapo, 418
Adewoye Adebayo, 659
Adey Andrew, 899
Adhikary Sabina, 687
Adib Deyaa, 760
Adib Elio, 437
Adkins Douglas, 503, 681
Adkins Irena, 716
Adler Adam, 1389
Adler Christina, 576
Adler Leah, 523
Adrianowycz Sarah, 862
Adstamongkonkul Team, 187
Aerni Hans, 1123, 1325, 1326
Aerts Hugo, 1296
Afeyan Alexander, 503
Aftab Blake, 198, 203, 246, 247
Agarwal Neeraj, 558, 664
Agarwal Veena, 25
Agarwal Yash, 1087
Agatsuma Toshinori, 808
Agbarya Abed, 136
Agbedia Owhofasa, 296
Agensky Laura, 636, 681
Ager Casey, 1154
Aggarwal Arpit, 61
Aggarwal Charu, 1403, 635
Aggarwal Vaishali, 952
Aggen David, 661
Aghlara-Fotovat Samira, 1094, 1095, 363
Aghmesheh Morteza, 763
Aglietta Massimo, 190
Agostinelli Veronica, 91
Agrawal Nishant, 1282, 1291
Agrawal Smita, 531, 922
Agrawal Sonia, 835
Aguado Jacqueline, 1365
Agudo Judith, 947
Aguiló Nacho, 1072
Aherm Elizabeth, 763
Ahlin Cecilia, 709
Ahmad M. Usman, 1284
Ahmadi Tahamtam, 1070
Ahmadi Tahamtam, 1208
Ahmed Eiman, 1053
Ahmed Fahad, 1269, 1270
Ahmed Muneeb, 1110
Ahmed Nabil, 412, 816
Ahn Daniel, 660
Ahn Eugene, 764
Ahn Myung-Ju, 635
Ahn Sae Jeong, 1077
Ahn Sarah, 1314, 471
Ahn Sujin, 1058
Ahnert Rodon Jordi, 623
Ahronian Leanne, 444
Ai Xiaohong, 673
Aicher Lauri, 110
Aiken Taylor, 874
Ait-Mohamed Ouardia, 1003
Ajami Nadim, 590, 618
Ajani Jaffer, 445, 553
Ajayi Babajide, 418
Ak Murat, 1280
Akagi Keiko, 374
Akai Satoru, 125
Akaike Takenori, 737
Akbay Esra, 891, 906
Akerley Wallace, 580
Akhter Shamima, 1462
Akpriaye Emmanuel, 803
Aksoy Arman, 369, 390
Aksoy Osman, 1255
Aksu Michael, 513
Al Haj Farah, 1260
Al Kait, 614
Al Sulaiti Asma, 411
Alaguthurai Thanussuyah, 972, 986
Alahmadi Asrar, 1249
Alam Md Masud, 1126
Alam Neyaz, 1439
Alamillo Ashley, 1137
Alanko Tuomo, 715
Alaoui Adil, 1303
Alasonyallilar Demirel Aylin, 324
Alassadi Okba, 312
Alavi Alireza, 1182, 1440
Alayli Farah, 587, 607
Albacker Lee, 29, 584
Albarello Luca, 268
Albarmawi Husam, 797
Albaroodi Yasser Saud O, 1155
Al-Batran Salah-Eddin, 578
Albertella Mark, 1373
Albertini Mark, 862
Albregues Jean, 997
Alcantara Marice, 810, 880
Aldrich Jessica, 159
Aldridge Kelly, 483
Aldrighetti Luca, 268
Aleckovic Masa, 953, 954
Aleksseev Sayan, 1116
Alenazy Sanaalarab, 1001
Alese Olatunji, 134, 636
Alessi Joao Victor, 451, 512, 528
Alexander Melannie, 454
Alexander Nicholas, 265
Alexander Peter, 209
Alfano Benedetta, 21
Algazi Alain, 763
Al-Hader Ahmad, 437
Al-Hajj Muhammad, 1182, 1440
Alhalabi Omar, 661
Ali Abdelrahman, 1262, 749
Ali Ashfaq, 1054
Ali Johannes, 191
Ali Lestat, 1004, 939
Ali Omar, 252
Alici Evren, 1068
Alimadadi Ahmad, 397
Alistar Angela, 636
Alizadeh Darya, 351

Author index

- Alka FNU, 940
Allaire Kathryn, 1002
Allen Alex, 313
Allen E. Kaitlynn, 348
Allen Stephanie, 47, 48
Allison James, 590
Allred Sean, 1186, 1190
Allu Bhargavi, 1200
Almudhar Niran, 221
Alonso Guzman, 631
Alonso Marta, 836
Alonso Michael, 1348
Alonso-Diez Angela, 1120
Alonso-Miguel Daniel, 1120
Al-Sulaiti Asma, 1430
Alt Jesse, 1119
Altan Mehmet, 1050
Altan-Bonnet Grégoire, 350, 401
Alteber Zoya, 504
Altinas Isil, 1070
Altiok Soner, 1433, 1438, 157
Altman Sharoni Efrat, 322, 358
Altorki Nasser, 965
Altreuter Jennifer, 362, 397
Alvarado Diego, 317, 596
Alvarez Andres, 264
Alvarez Freile Jimena, 989
Alvarez Maite, 267
Alvarez Sanchez Rubén, 1080, 1195
Alvarez-Rodríguez Ruben, 776
Alvarez-Rodríguez Rubén, 282, 781
Amador Arjona Alejandro, 1199
Amann Joseph, 585
Amara Celine, 1198
Amarasinghe Gaya, 1228
Amaravadi Ravi, 656
Amato Carol, 1040, 1466, 285, 925
Ambarkhane Sumeet, 35, 714
Ambrogio Chiara, 317
Ambrose Christine, 175
Ambrosio Maria, 706
Amemiya Kenjie, 444
Ames Tyler, 1118
Amezquita Robert, 1367
Amin Asim, 430
Amini Arya, 1296
Amisaki Masataka, 1312
Amit Inbar, 775
Amit Moran, 1462
Ammatuna Emanuele, 995
Amoor Rafet, 333
Amoozgar Zohreh, 907, 911
Amoroso Antonio, 1318
Amouzegar Afsaneh, 1280
Amouzgar Meelad, 587
Amrhein Scott, 919
Amrstrong Blair, 382
Amzallag Arnaud, 1277
An Duo, 123
An Hee-Jung, 886
An Mingrui, 1162
An Xiaoyu, 106, 40, 491
An Xingyue, 1060, 402
An Yuri, 125
Anagnostou Valsamo, 538
Anand Navneet, 277
Anand Neel, 422
Anandhan Swetha, 1305, 505
Ananta Jey, 1215
Anaya Jordan, 1272
Anbunathan Hima, 119
Anderl Janet, 422
Anders Robert, 711
Andersen Mads, 1464
Andersen Rikke, 1013, 524
Andersen Thomas, 1169
Anderson Amy, 991
Anderson Ana, 896, 964
Anderson Courtney, 219
Anderson Jennifer, 490
Anderson Kenneth, 1220, 812
Anderson Mark, 1256
Anderson-Marlisa, 755
Anderson Matthew, 885
Anderson Nicholas, 194
Anderson Robin, 1164
Anderson Ronald, 84, 96, 97
Anderson Sarah, 1190
Andersson Patrik, 1241, 907
Anderton Judith, 895
Anderton Kate, 1131
Ando Yuta, 229
Andoni Alma, 339
André Thierry, 544
Andremont Antoine, 1306
Andresson Thorkell, 350
Andrews Alec, 219
Andrews Alex, 1031, 1044
Andrews David, 1398
Andrews Lawrence, 811, 952
Andrianova Svetlana, 570
Andrup Kristensen Claus, 675
Anfossi Simone, 1462
Angell Helen, 155
Angelo Laura, 685
Angelos Mathew, 633, 634
Anghileri Elena, 648
Anguelov Marilyn, 275
Angus-Hill Melinda, 1, 2
Annavarapu Srinivas, 933
Annels Nicola, 1434, 1467, 966
Annino Donald, 503
Annis James, 940
Annunziata Christina, 405, 55, 637
Ansstas George, 624
Anthoney Alan, 622
Antonakos Brandon, 888
Antonarelli Gabriele, 1264
Antonia Scott, 1132, 699
António Patrícia, 355, 961
Antony Anuja, 122, 976
Antony Grace, 670
Antony Thomas, 1313
Antras Jesus, 743, 744
Antunes Dinler, 1278
Ao Zheng, 390
Aoki Tomohiro, 103
Apavaloaei Anca, 1411
Apfel Abraham, 608
Apodaca Kimberly, 309
Apollon Audrey, 295
Apostol Colleen, 711
Apostolaki Angeliki, 41, 71
Appendino Giovanni, 1121
Appleman Vicky, 1153
Appleton Kathryn, 162
Aragon-Ching Jeanny, 663
Aramaki Takahiko, 1364
Aramburu Tomas, 262
Aranda-Orgilles Beatriz, 217
Arango Gustavo, 1273
Arantes Lidia, 490, 535
Araujo Dejka, 600, 713
Arballo Alex, 378
Arbitman Steve, 895
Arbiv Becky, 1289, 1290, 1299
Archibald Vincent, 1111
Ardizzoni Andrea, 800
Arena Sabrina, 213
Arends Roel, 495
Arévalo Ruiz Matilde, 1195
Arias-Pulido Hugo, 1120
Ariizumi Hirotsugu, 46
Arlen Philip, 55, 637, 724
Armaghani Avap, 645
Armendariz Debra, 189
Armstrong Stephanie, 1103, 1191
Arnaout Angel, 545
Arnold Benjamin, 1242
Arnold Cassidy, 366
Arnold Dirk, 650
Arnold Jeffrey, 1161
Arnold Susanne, 1147, 1279, 54
Arnold Suzanne, 570
Aroldi Andrea, 317
Arora Aakriti, 437
Arora Arshi, 997
Arrieta Victor, 830
Arrowood Christy, 1132
Arslan Shukaib, 685
Arthur Corazon, 476
Arthur Laura, 195
Arulanandam Antonio, 1320, 177, 323
Arvidson Lisa, 1
Aryal Aditi, 269
Aschmoneit Nadine, 1319
Ascierto Maria, 1456, 508
Ascierto Paolo, 112, 21, 592, 606, 774, 842
Ascione Liliana, 1264
Asensio Michael, 1389
Asher Anthony, 1033
Ashitey Naa, 511
Ashkin Emily, 1462
Ashok Preeti, 177, 323
Ashworth Tamera, 980
Asimakopoulos Fotis, 981
Askmyr David, 102
Assenmacher Charles-Antoine, 291
Assis Nadine, 1108
Asuelime Grace, 263
Atieh Anas, 474
Atiya Huda, 1451
Atkins Michael, 1303
Atkins Reginald, 193
Atkinson Kathleen, 1022
Atkinson Victoria, 743, 744
Atmaca Akin, 578, 700
Atwal Gurinder, 576
Atwell Thomas, 689
Au Melinda, 210
Au Qingyan, 87
Audia Alessandra, 1001
Audigier-Valette Clarisse, 701
Audoly Laurent, 1461
Augustin Ryan, 1280, 588
Aung Thazin, 127, 133
Aunins John, 607
Aurisicchio Luigi, 820
Aurora-Garg Deepti, 544
Ausec Luka, 159

- Ausejo Iker, 836
Auslander Noam, 1307
Austen Matthias, 337
Autio Karen, 555, 559
Au-Yeung Amelia, 475
Aversa Catherine, 500
Avery Kendra, 1067, 1073, 1079, 1372
Avigdor Lilach, 860
Avitia Jose, 668
Avniel Amir, 819
Avramis Earl, 259
Avril Stefanie, 1043, 61
Awad Mark, 451, 512, 528
Awad Walid, 348
Awan Arif, 545
Awdew Rahel, 1210
Axel Amy, 449
Ayachi Safia, 1393
Aycock Jeff, 781, 787
Aydin Iraz, 1194
Ayello Janet, 303, 802
Aynajyan Anahit, 423
Azad Nilofer, 710, 711
Azam Abu Bakr, 1288, 1302
Azameera Aruna, 198, 203
Azarianpour-Esfahani Sepideh, 61
Azaro Analia, 708
Aziz Usman, 742
Azizi Armon, 1247
Azqueta Gavaldon Monica, 155
Azumendi P. Aitana, 1213
- B Papaiah Arun, 1334
B V Uma Bharathi, 1313
Baardman Sjoerd, 215
Babadi Elham, 689
Babaei Sepideh, 1019
Bacelli Irène, 484
Bachawal Sunitha, 1427
Bachelet Ido, 1129
Bachu Mahesh, 987
Backert Linus, 713
Backus Carey, 1365
Badalucco Lauren, 483
Baden Lindsey, 437
Bader Andreas, 201, 261, 294
Badri Ti, 167
Bae Donggoo, 488
Bae Joeeun, 1220, 812
Bae Kyoungwhwa, 660
Baecher Kirsten, 506
Baehner Rick, 159
Baek Eunhye, 658
Baek Jina, 196
Baek SeungJae, 658
Baeuerle Patrick, 1061, 1395
Bagchi Atrish, 203, 247
Bagge Nate, 219
Bagwan Izhar, 1434, 1467, 966
Bahary Nathan, 437
Bahjat Rena, 1067, 1079
Bai Haiyan, 453
Bai Xue, 150
bai xueli, 694
Bai Yulong, 605
Baichoo Priya, 378
Baichwal Vijay, 151
Bailey Keith, 180
Bailey Stefanie, 269
Bain Gerard, 834
- Bais Carlos, 475
Baish James, 1295
Baishya Tutumoni, 90
Bajaj Aung, 742
Bajaj Sweta, 1294, 89
Bajaj-Elliott Mona, 1330
Bajic Davor, 1170
Bajjuri Krishna, 1103, 1191, 1359
Bajor David, 763
Bajpai Geetika, 477
Bak Martin, 1169
Bakalov Veli, 437
Baker Alexander, 1349
Baker Kevin, 1342
Baker Suzanne, 231
Bakker Alice, 1097
Bala Krithi, 945
Balachandran Vinod, 1312
Balasubrahmanyam Priyanka, 362, 397
Balasubramaniyan Veerakumar, 1001
Balayya Saroja Kotegar, 411
Baldominos Pilar, 947
Balestrieri Chiara, 268
Baleviic Stephen, 699
Balkissoon Jaikrishna, 314
Balko Justin, 107, 1109
Ball Lauren, 1031
Ball Michael, 315, 371
BALLINGER Elaine, 409
Ballinger Marcus, 435
Ballman Madison, 438
Balmanoukian Ani, 778
Balsevicius Lukas, 551
Bampton Darryn, 721
Ban Haruka, 1221
Ban Yi, 965
Banchereau Romain, 435, 523
bandey irfan, 402
Bandla Arunajyothi, 510
Bandyopadhyay Abira, 232
Bane Octavia, 688
Banerjee Antara, 1301
Banerjee Hridesh, 1020, 1041, 490
Banerjee Saptak, 1439
Banerji Udaj, 622
Bang Won Seon, 365
Banicki Andrew, 221, 228
Bankapur Anand, 437
Banks Lauren, 218
Bansal Divyam, 296
Bao Leyuan, 282
Bao Musheng, 477
Bao Riyue, 1000, 1280, 490, 588, 605, 845, 908
Bao Xiaoyan, 123
Bao Xuanwen, 197
Baral Rathindranath, 1439
Baranda Joaquina, 728
Barandiaran Alexia, 264
Baras Alexander, 1272
Barbara Kalinowska Barbara, 358
Barber Brittany, 19
Barber Glen, 912
Barbie David, 1006, 295
Barbour Mark, 1046
Barbu Alina, 739, 748
Barca Taylor, 198
Barcella Matteo, 648
Bardonneau Clélia, 707
Bar-Ephraim Yotam, 180
Barilla Rocky, 964
- Barinov Aleksandr, 1315
Barlesi Fabrice, 135, 701
Barletta Giulia, 437
Barlow Norman, 1073, 1079, 1372
Barman Hannah, 1274
Barnes Thomas, 1222
Barnett Reagan, 140
Barnhart Bryan, 1196
Barnscher Stuart, 1185
Baron Luc, 1393
Barone Francesca, 1134
Barragan Jessica, 243
Barré Patricia, 701
Barrera-Lopez Irving, 115
Barretina-Ginesta Maria-Pilar, 670
Barrett Carl, 583, 835
Barrett David, 335
Barrett J. Carl, 155, 586
Barrett Ronald, 1097, 625
Barrett Scott, 449
Barrichello Adriana, 512, 528
Barron Luke, 264
Barry Walter, 183
Barsan Valentin, 508
Barschesht Yiftah, 860
Barslesi Fabrice, 1107
Barsoumian Hampartsoum, 869
Bart Amit, 1290
Barth Jaimie, 1254
Barth Stefan, 1369
Bartha Gabor, 691, 692
Barthel Grant, 1446
Bartkowiak Todd, 111
Bartlett David, 1435, 179, 361
Bartlett Derek, 1367
Bartlett John, 545
Bartolini Wilmin, 661, 680
Barton Debora, 633, 634
Barve Minal, 771, 780
Basak Nandini, 142
Basak Sayantani, 128
Basavaraj Aravind, 1313
Baselga Ignacio, 123
Bashir Babar, 661
Bashir Saira, 719
Baskar Reema, 362, 397
Bass Anne, 1260
Bassan David, 316
Bassler Nicole, 1293
Basso Andrea, 635
Basten Sander, 199
Basu Bristi, 774, 850
Basu Gargi, 159
Basu Sreyashi, 590
Basu Subham, 147
Basu Subhasree, 1360
Bates Paul, 373
Batrina Felix, 653, 722
Battaglia Seb, 1392
Battula Sailaja, 1076, 1340
Baudhuin Jeremy, 81
Bauer Kylynda, 1019
Bauer Steven, 344
Baugh Lauren, 242
Baum Alina, 851
Baum Jason, 1141, 553
Bauman Julie, 681
Baumgartner Christina, 1365
Baumgartner Corrine, 328, 413
Baurceanu Iris, 1127

Author index

- Bautista Wynona, 1323
Baxi Vipul, 1277, 1282, 1291
Baxter Bryan, 625
Bayegan Amir, 926
Bayliffe Andrew, 1316
Bayliffe Andy, 1316
Bazargan Sarah, 191
Bazin Helene, 1168
Beagle Brandon, 726, 727, 755
Beasley Aaron, 577
Beasley Georgia, 1132, 22, 827
Beasley Mary, 629
Beasley Ryan, 1296
Beato Francisca, 882
Beaton Nigel, 602
Beatty Matthew, 191, 387
Beaumont Kristin, 946
Becher Oren, 836
Bechter Oliver, 706
Beck Andrew, 1282
Beck Thaddeus, 705
Beckabir Wolfgang, 560
Becker Amy, 1222
Becker Marie, 931
Becker William, 813
Beckett Travis, 232
Beckford Denis, 1193
Becklund Bryan, 1077
Bedaj Marija, 1046
Bedard Kristin, 1103, 1191, 1359
Bedard Melissa, 370
Bedognetti Davide, 1053
Beechem Joseph, 147, 951, 99
Beg Amer, 1132
Beghi Silvia, 318, 572
Behbehani Gregory, 881
Behr Sarah, 721
Behren Andreas, 192
Beijersbergen Roderick, 979
Beirne Emily, 569
Beiss Veronique, 1120
Beitz Laurie, 1230, 366, 375
Bejanyan Nelli, 685
Bejnood Alborz, 444
Bekaii-Saab Tanios, 636, 717
Bekkenk Marcel, 88
Belanger Karl, 614
Belani Rajesh, 728
Belette Allison, 519
Belhe Yash, 554
Belkaid Wiam, 1300
Bell Bryan, 113, 5
Bellemare Sarah, 932
Belli Carmen, 1264
Bellon Steven, 888
Belouali Anas, 1303
Belshaw Erin, 758
Beltran Antonio, 355, 961
Beltran Himisha, 112
Belvin Marcia, 1078
Belz Gabrielle, 79, 923
Belzie Jean-Philippe, 1066
Ben Amar Martine, 1003
Ben Baruch Bar, 200
Ben Cheikh Bassem, 116, 79
Ben David Yonit, 200
Benaroch Philippe, 1003
Benatar Tania, 201, 294
Benchaaben Assil, 957
Bendall Sean, 362, 397
Bender James, 387
Bender Lewis, 545, 710
Bender Mackenzie, 1310
Bender Matthew, 906
Bendle Gavin, 239, 241
Benjamin Jonathan, 717
Benjamin Laura, 159
Benlahrech Adel, 619
Benmebarek Mohamed-Reda, 1019
Benmebarek Reda, 419
Benn Carol, 96, 97
Bennion Kelsey, 506
Benos Panayiotis, 1049
Ben-Shachar Rotem, 132
Benson Beverly, 671
Benson Micah, 255, 297
Bensussan Armand, 1339
Bentebibel Salah-Eddine, 782
Benton Alexander, 1024, 202
Benzaoui Mehdi, 327
Benzie Emily, 1389
Beqiri Marilda, 262
Bera Saurav, 1439
Berardi Rossana, 91
Beregi Jean-Paul, 1296
Berezhnoy Alexey, 1078
Bergaggio Elisa, 317
Berger Allison, 569
Berger Raanan, 1129
Bergin Rachel, 208
Bergler-Klein Jutta, 655
Berglund Anders, 912
Berglund Sofia, 654
Bergmann Michael, 655
Berk Gregory, 1202
Berkhout Ben, 137
Berkley Amy, 1350
Berlin Jordan, 717
Bermingham Candy, 756
Bernard Brady, 940, 959
Bernareggi Davide, 336
Bernatchez Chantale, 782
Bennett Matthew, 1067, 1079
Bernicker Eric, 480, 838
Bernstein Howard, 224, 638
Berraondo Pedro, 267
Berrien-Elliott Melissa, 195
Berrien-Elliott Melissa, 729
Berrino Monica, 1318
Bersanelli Melissa, 112, 437, 91
Bersano Jacqueline, 1436
Bertelsen Lisbeth, 1013, 524
Berthelot Karine, 81
Berthoin Lionel, 332
Bertino Erin, 1249, 585
Bertolet Genevieve, 869
Berton Giachetti Pierpaolo, 1264
Bertoni Francesco, 889
Bertozi Carolyn, 1166, 1209
Berz David, 733
Berzofsky Jay, 557, 813
Besneux Matthieu, 822
Bessede Alban, 135, 141, 1426
Best Andrew, 318
Best Hannah, 1326
Beswick Paul, 1340
Bethune Michael, 123, 210
Betof Allison, 783, 791
Beule Dieter, 1235
Beumer Jan, 588
Beurskens Frank, 1070
Beutner Karl, 639, 77
Bever Katherine, 711
Bexon Alice, 1173
Bexon Martin, 743, 744
Beyer Caleb, 1168
Beymer Michael, 959
Beztsinna Nataliia, 199, 69
Bhagat Milan, 118
Bhagelu Achyut, 173
Bhagwandin Vikash, 875
Bhandarkar Vidit, 1023, 129
Bharanikumar Ramit, 43
Bhardwaj Nina, 364, 555, 559, 62, 946
Bhardwaj Vikas, 257
Bhardwaj Vinnu, 712
Bhaskar Aishwarya, 601
Bhat Arun, 198, 203, 246, 247
Bhat Krishna, 1001
Bhat Sajad, 1307
Bhatia Dimple, 25
Bhatia Shilpa, 1404, 86
Bhatia Vipul, 308
Bhatnagar Jaya, 1368
Bhatta Ankit, 378
Bhattacharjee Sanghamitra, 1391
Bhatti Maryam, 1194
Bhide Shruti, 146
Bhinder Bhavneet, 1117, 446
Bhoi Sujata, 455
Bhoj Vijay, 572
Bhojnagarwala Pratik, 1174, 388
Bhuiyan Enamul, 688
Bhuniya Avishek, 1439
Bhutkar Arjun, 1465, 994
Bhuva Dharmesh, 923
Bhuyan Seema, 90
Bi Lynn, 150
Bi Timothy, 1045
Bi Yingzhi, 1354, 424
Bialucha Uli Carl, 841
Bian Zhen, 969
Biancalana Matthew, 122
Bianchi Anna, 1224
Bianchini Justin, 262
Biancolini Donatella, 268
Biancotto Angelique, 81
Biasco Luca, 514
Biddle-Snead Charles, 1282
Bie Jun, 652
Biediger Ronald, 603
Bieging-Rolett Kathryn, 1327
Bierly Allison, 657
Biermann Jana, 830
Bies Laura, 241
Biesova Zuzana, 485, 856
Biju Raymond, 1282
Bilemjian Vrouyr, 26
Bilen Mehmet, 478, 848
Bilgrami Sameera, 1089
Bindman Noah, 1357
Bing Nan, 1400
Bingaman-Steele Jamie, 823
Bingham Clifton, 1260
Birditt Brian, 147
Birnbaum Michael, 1232, 967
Bischof Sarah, 653, 722
Bishai William, 1385
Bishnoi Sarwan, 632
Bishop Andrew, 542

- Bisht Arnima, 1374
Bisignani Mikayla, 535
Bisso Andrea, 215
Biswas Nidhan, 955
Biter Amadeo, 1387
Bittermann Clemens, 655
Bivalacqua Trinity, 1385
Bivalacqua Trinity Bivalacqua, 666
Bjordahl Ryan, 204, 288, 300, 326, 341, 727
Bjursten Sara, 1261
Blachut Susanne, 1239
Black Cheryl, 244
Black Christopher, 454, 798, 799
Black Graeme, 93
Black Keith, 116
Blackton Michael, 361
Blaga Milena, 669
Blagden Sarah, 719, 777, 850
Blagovic Katarina, 321
Blaha Laura, 313
Blahnik-Fagan Gabriele, 1187
Blanc Eric, 1235
Blanchard Lucas, 507
Blanchard Orphée, 1393
Blaney Martha, 770
Blank Christian, 88, 979
Blasberg Ronald, 904
Blasco Rafael, 317
Blatt Roni, 860
Blatt Sarah, 1465
Blaukat Andree, 497
Blauvelt Jamie, 191
Blayo Anne-Laure, 814
Bleakley Marie, 93
Bleisch Matthias, 968
Blezinger Paul, 1333, 1378
Blick Tony, 923
Block Matthew, 1274, 785
Blombery Piers, 1442
Bloom Debra, 187
Bloy Norma, 1144, 446
Blueml Stephan, 655
Blum Jordan, 1208, 987
Blum Robert, 204, 288
Blum Steven, 1254, 441
Blumenthal Daniel, 194, 318
Bo Na, 1267
Bobilev Dmitri, 605
Bockorny Bruno, 651, 778, 780
Boda Akash, 1154, 866
Boeckstijn Sanne, 1181
Boersema Paul, 495
Boffo Silvia, 1256, 1292, 656
Bogaczynska Marta, 1352
Bogaert Liz, 1215
Bøgevang Jensen Marianne, 551
Boggs Jennifer, 1219
Bognar Ernest, 566
Bohac Chet, 659
Bohn Toszka, 1324
Boi Shannon, 1098, 358
Boise Lawrence, 1458
Boisen Mogens, 138
Boisgerault Nicolas, 1315
Bojja Krishna, 1001
Bokemeyer Carsten, 713
Bokhari Raza, 112
Bol Kalijn, 88
Boland Genevieve, 1242, 1254, 1257, 1268, 150, 441, 607, 916
Bolanos Elixabet, 267
Bold Richard, 1008
Boldajipour Bijan, 185, 232, 252
Bolivar Ana, 28, 36
Bollard Catherine, 176
Bolten Lena, 1196
Bolyard Chelsea, 1064, 839, 920
Bommakanti Gayathri, 1405
Bommareddy Praveen, 508, 610, 611
Bonacorsi Maja, 1162
Bonald Dennis, 295
Bonanno Bruno, 262
Bondarenko Igor, 582
Bone Jennifer, 361
Bonfiglio Silvia, 268
Bonini Chiara, 268, 411
Bonnevaux Helene, 1198
Bonny Christophe, 642
BONNY Christophe, 641
Bono Petri, 709
Bonora Giancarlo, 164
Bontekoe Emily, 374
Bonzon Christine, 1067, 1073, 1079, 1372
Bookhardt Sam, 5
Boone Andrew, 1402, 1431, 493, 537
Boor Patrick, 883
Boorjian Stephen, 140
Bopp Tobias, 1324
Borad Mitesh, 229, 263, 639, 77
Borde Shambhavi, 319
Bordignon Pino, 37, 38
Bordoloi Devivasha, 388
Bordoni Rodolfo, 596
Boreddy Srinivas, 1368
Borges Luis, 262, 265
Borji Mehdi, 115
Bornschelegl Svetlana, 689
Boroughs Angela, 181
Borrebaeck Carl, 1054
Borriello Frank, 632
Borrman Tyler, 712
Bortone Dante, 124, 508, 927
Bory Pierre, 701
Bos Remco, 386
Bose Anamika, 1439
Bose Nandita, 1327, 884
Boss Jeremy, 212
Bosse Kristopher, 1189
Bosson Nicolas, 481, 853
Bostick Magnolia, 320
Bot Adrian, 687
Bottino Dean, 1301
Bottrel Nicole, 987
Bouchard Nicole, 1300
Boucher Lauren, 576
Boucher Yves, 1463
Bouchlaka Myriam, 498
Boudot Antoine, 182, 389
BOUDRIBILA Asmaa, 741
Bouhlal Jonas, 1006
Bouisset Florilene, 589
Boumelha Jesse, 509
Bourass Sarah, 354
Bourayou Nawel, 677, 723
Bourin Clotilde, 497
Bousquet Julien, 337
Bousquet Paula, 669
Boussiotis Vassiliki, 1110
Boustany Leila, 1078
Bouvier Riemke, 760
Bouzekri Alexandre, 104
Bouزيد Rachid, 883
Bove Samantha, 1281
Bower Mark, 437
Bowles Tawnya, 610, 611
Bowman Christine, 991
Bowman Isaac, 661
Bowman Maytal, 182, 389
Bowman Nicole, 1355, 1381
Boyd Marley, 445
Boyd-Kirkup Jerome, 532, 623
Boyer Arnaud, 701
Boyken Scott, 185
Boyle Glen, 1121
Boyle Sean, 119, 146, 51
Boyle Theresa, 672
Boyne Alex, 323
Boyne Alexander, 217
Bradbury Angela, 644
Bradley Linda, 1030
Brady Kelly, 607
Brady Keri, 1416
Brady Mallory, 255
Braem Steven, 215
Brahmer Julie, 57
Brajkovic Saska, 37, 38
Brake Rachael, 815
Brambilla Valentina, 648
Bramson Jonathan, 261
Brana Irene, 675
Brandenberger Ralph, 381
Brandenburg John, 1065
Brandhorst Marcel, 1351
Brandish Philip, 1207, 1340, 1356, 1388, 980
Branicky Andrei, 1043
Branka Manuela, 653, 722
Brant Boris, 860
Branthoover Holly, 387
Brar Kevin, 1359
Brate Ashley, 321
Braubach Oliver, 116, 120, 79
Braun Angela, 345
Braun Asolina, 1131
Braun David, 115, 295
Braun Monika, 337
Braverman Erica, 205
Bravetti Paul, 1179, 949
Bray Mark, 750
Breij Esther, 1070, 1351
Bremer Edwin, 1205, 26, 989, 995
Bremholm Hansen Lasse, 551
Brennick Ryan, 29
Brentjens Renier, 347
Brentville Victoria, 1317
Brett Sara, 232
Breuning Johannes, 232
Brewer Faraha, 1203
Bridgeman John, 282
Bridgen Devin, 224
Brieu Nicolas, 579, 583
Brige Ann, 1198
Brilc Paola, 474
Briones Jessica, 252
briskin michael, 1350
Britten Cedrik, 713
Britton Cameron, 140
Britton-Rivet Camille, 619
Brix Liselotte, 30
Brock Rebecca, 412, 816
Brockman Asa, 111

Author index

- Brodeur Sarah, 588, 908
Brodeur Scott, 1360
Brodin Patrik, 1193
Brodin Heather, 1096
Brody Joshua, 595
Brody Pierce, 206
Brog Rachel, 329
Brogdon Jennifer, 260
Broggi Maria, 835
Brohl Andrew, 604
Broijl Annemiek, 686
Broit Natasa, 1121
Broka Derrick, 1170
Bronevetsky Yelena, 398
Bronson Steven, 492
Brook Lyn, 934
Brookhouser Nicholas, 288, 304, 341
Brooks Cory, 169
Brooks Jennifer, 130
Brosnan-Cashman Jacqueline, 1277, 1291
Brown Carl, 147
Brown Christine, 351
Brown Emily, 147, 951
Brown Erica, 1024
Brown Flavian, 1332
Brown Harrison, 205
Brown Jacqueline, 478
Brown Matthew, 62
Brown Peter, 1207, 1340
Brown Robert, 671
Browne Andrew, 1277
Browner Ilene, 711
Browning Erica, 617
Brownstein Naomi, 1414
Bruce Zara, 1121
Bruchez Marcel, 408
Brucklacher-Waldert Verena, 1405
Bruderer Roland, 602
Brueck Patrick, 700
Brugiapaglia Silvia, 1318, 1429
Bruhns Matthias, 1019
Bruins Slot Karsten, 669
Bruix Jordi, 770
brun scott, 566
Brun Sinne, 524
Brunak Søren, 138
Brune Patrick, 720
Brunet Maxime, 135
Bruni Sofia, 877
Bruno Peter, 63
Bruno Tullia, 1049, 1136, 1451, 490, 818, 908, 973
Brutus Sergine, 1282, 1291, 554
Bruzzone Maria Grazia, 648
Bryan Jeffrey, 1016
Brzezicha Bernadette, 154
Bteich Fernand, 932
Buatois Vanessa, 853
Buchberger David, 456
Bucheit Leslie, 140, 6
Bucher Christoph, 631
Bucher Sydney, 262
Buchholz Christian, 137, 345
Buchi Mélanie, 434
Buchi Oralea, 1206
Buchwald Zachary, 1033, 848
Buck Alicia, 295
Bücklein Veit, 266, 897
Bücklein Veit Leonhardt, 281
Buckorny Bruno, 731
Bucksot Jesse, 976
Bucktrout Samantha, 1223, 555, 559, 587, 656
Buckup Mark, 688
Budde Elizabeth, 558
Budha Nageshwar, 768
Budhani Pratha, 1437
Budhu Sadna, 903, 904, 997
Budi Erin, 1352
Budillon Alfredo, 21
Budimir Natalija, 1123, 1325, 1326
Budka Justin, 301
Buechler Markus, 355, 961
Buechler Matthew, 1450
Buenostro Denise, 93
Buetow Bernard, 1258
Buffa Alexa, 647, 649
Buffa Francesca, 996
Bugel Madison, 391
Buhlmann Melanie, 1414
Bui Jack, 984
Bujanover Nir, 316
Bulic Marinka, 1365
Bullaughay Chiamin, 265
Bullock Andrea, 778
Bullock Bonnie, 651, 778
Bulut Mustafa, 551
Bunch Brittany, 191
Bunk Sebastian, 1319
Bunka Stefan, 653, 722
Bunse Mario, 1235
Buonaguro Luigi, 1175
Buongervino Samantha, 1189
Buonpane Rebecca, 1210
Buqué Aitziber, 1144
Buqué Martinez Aitziber, 446
Buravenkov Vitaliy, 1129
Burcham Austin, 1200
Burchi Elisabetta, 177, 323, 1320
Burdette Dara, 1331
Burenkova Olga, 1344, 1345
Burga Rachel, 369, 390
Burger Michael, 642
BURGER Michael C., 641
Burgess Earle, 663
Burkard Nathaniel, 72
Burke James, 666
Burke Kelly, 1038
Burke Paulo, 925
burke shannon, 835
Burke Thomas, 933
Burkhardt David, 1168
Burks Jared K, 782
Burleigh Katelmy, 382
Burm Saskia, 1208
Burns Brian, 613
Burns Connor, 569
Burns Ethan, 480
Burri Stuart, 1033
Burriss Howard, 774
Burt Bryan, 363
Burtness Barbara, 133, 681
Burton Elizabeth, 607
Burton Jeremy, 614
Burtrum Douglas, 1184
BURZYN DALIA, 1344, 1345
Buschow Sonja, 1181, 883
Bushey Ryan, 699
Bushman Frederic, 395
Bustami Zaid, 1292
Bustillos Christian, 186
Bustos Matias, 962
Bustos Perez Xiomar, 1375
Bustos Xiomar, 286, 975
Buti Sebastiano, 112, 91
Butler Marcus, 787
Butler Samuel, 254
Butt Omar, 624
Butterfield Lisa, 555, 559, 587, 656
BV Manjula, 142
BV Prakash, 142
Bydoun Moamen, 1336
Byers Lauren, 523, 697
Byersdorfer Craig, 205
Bykova Katrina, 1067
Bylsma Sophia, 67
Byraredy Siddappa, 526
Byrd Dan, 894
Byrd Kaelan, 899
Byrne Lauren, 817
Byun Sang Soon, 751
C S Lavanya, 1313
Cabanov Alexandra, 420
Cabanski Christopher, 555, 559, 587, 607, 656
Cabart Mathilde, 135
Cabrera Gil Blanca, 1275
Caffaro Carolina, 1123, 1325, 1326
Cafferata Allison, 1047
Cagalingan Alaina, 1206
Cahal Shay, 860
Cai Danying, 1250
Cai Na, 1078
Cai Winson, 347
Cai Yang, 1215
Cai Yiyu, 1288, 1302
Cai Zhijian, 1143
Cairns Bradley, 664
Cairo Mitchell, 303, 802, 881
Calabrese Cassandra, 1260
Calapre Leslie, 577
Calarese Daniel, 1103, 1191, 1359
Caldwell Kate, 1196
Caldwell Rebecca, 1262, 749
Calhoun Susan, 1215
Caligiuri Michael, 186
Calin George, 1462
Callahan Margaret, 1297, 772
Calloud Sebastien, 481
Calnan Conor, 255, 297
Calvo Aller Emiliano, 589
Calvo Emiliano, 592, 631, 731
Calzone Frank, 316
Cam Maren, 1135
Camacho Luis, 710
Camacho Sharon, 1433
Cambell Calvin, 1123
Campa Michael, 699
Campanati Loraine, 304
Campbell Ashley, 1200
Campbell Calvin, 1325
Campbell Carly, 1340
Campbell David, 1123, 1325, 1326
Campbell Jean, 1022
Campbell Katie, 1292, 529
Campbell Martin, 244
Campbell Matthew, 663
Campbell Ryan, 183
Campbell Shauna, 456
Campbell Thomas, 130
Campian Jian, 624

- Campion Liam, 262, 265
Campolucci Carla, 91
Can Ismail, 324
Can Ismail Can, 414
Canard Luc, 81
Canari Johana, 1448
Candelli Andrea, 180
Cannarile Michael, 27
Canter Robert, 1008, 272, 520, 534
Cantini Luca, 91
Canton David, 617
Cantwell Mark, 1132
Cao Anthony, 1187, 809
Cao Jingjing, 296
Cao Lizhi, 772
Cao Pham Hong Anh, 866
Cao Subing, 1314, 471
Cao Yuan, 1215
Capiaux Gina, 1173
Capillo Tonya, 203
Capitini Christian, 1231, 1443, 373, 391, 981
Capone Mariaelena, 842
Capotondo Alessia, 648
Cappabianca Dan, 391
Cappelli Laura, 1260
Cappello Paola, 1318, 1429
Cappuccini Fabio, 562, 565
Cappuzzello Elisa, 377
Capuano Jared, 1117
Caraballo-Galva Leidy, 206
Caracó Corrado, 21
Carbajo Daniel, 292
Carbone Carmine, 1093
Carbone David, 1249, 136, 1445, 58, 585, 660
Card Deb, 544
Cardell Lars Olaf, 974, 998
Cardell Lars-Olaf, 942
Cardello Carly, 1049, 811, 818, 952
Cardenas Demetrio, 304
Cardenas Maria, 1033
Cardia James, 1402, 1431, 409, 493, 537, 788
Cardillo Thomas, 1217
Carell Thomas, 266
Carias Rafael, 702
Carisey Alexandre, 412
Carkill Marie, 1373
Carl Sarah, 1438
Carlisle Anne, 168, 928
Carlsson Malin, 714
Carmi Levy Irit, 1129
Carmona Guillaume, 1094
Carnal Simon, 1293
Carneiro Ana, 714
Carneiro Benedito, 596, 647, 708
Caroline Gomes de Lima Sarah, 391
Caron Christine, 984
Carosino Christopher, 1187
Carotenuto Claudiopietro, 1093
Carpenter Esme, 972, 986
Carpten John, 1147, 1279, 1311
Carpton John, 54
Carrabba Matteo, 648
Carralot Jean, 1080, 1195
Carrasco Sebastian, 843
Carreno Beatriz, 309
Carretta Marco, 1182, 1440, 1464
Carrizosa Anderson Ana, 514
Carroll Stephen, 1215
Carson Dennis, 861
Carson Ken, 1354, 424
Carson Kenneth, 132
Carson William, 943
Carter Alun, 195
Carter Carly, 894
Carter Kyle, 1389
Carter Laura, 855
Carthon Bradley, 478, 848
Carton Jill, 265
Caruso Joseph, 399
Carvajal Richard, 592, 713
Carvalho Carlos, 355, 961
Casanova-Acebes Maria, 629
Casbon Amy-Jo, 1342
Cascais Sara, 355, 961
Cascone Tina, 590
Casey Denise, 757
Casey Kerry, 735
Caslavsky Josef, 1212
Casorati Giulia, 268
Casper Corey, 110
Cassady Kevin, 1135, 802, 881
Cassano Marco, 1459, 842
Cassier Philippe, 589
Castanon Eduardo, 592
Castañón Eduardo, 708
Castillo Bertha, 363
Castillo Paul, 1383, 1390
Castillo-Martin Mireia, 355, 961
Castine Michael, 705
Castro Brandyn, 830
Castro Carlos, 1178
Castro Daniela, 880
Castro Julio, 585
Casucci Monica, 411
Catino Annamaria, 112
Caudell Jimmy, 682, 684
Caushi Justina, 538, 57
Cavalcanti Ernesta, 21
Cavalloni Giuliana, 190
Cavalluzzo Beatrice, 1175
Cavanaugh Christopher, 771
Cazzamalli Samuele, 900
Ceccarelli Jake, 387
Cecil Denise, 1176, 1177, 1308, 546
Cedeño Oderay, 702
Célias Daiana, 1228
Cella Marina, 833
Cemerski Saso, 1323
Centore Richard, 888
Cerqueira Carla, 1223, 208
Cervantes Andrés, 746
Cervera-Carrascon Victor, 715
Cesar Martins Urbano Paulo, 551
Cesario Jeff, 544
Cha Su Min, 1055
Chacon Fajardo Diego, 1455
Chaddha Udit, 629
Chae Yooree, 927
Chae Young Kwang, 13, 14, 1407, 1408, 1413, 519
Chaft Jamie, 57
Chagin Karen, 335
Chahoud Jad, 742
Chai Jitian, 207
Chai Shengjie, 124
CHAIBI Assia, 1426
Chaim Neta, 316
Chaisson Selena, 819
Chakraborty Arjun, 142
Chakraborty Papia, 320
Chakraborty Tirtha, 334
Chakravarthy Karthik, 839, 920
Chakravarti Mohona, 1439
Chalise Prabhakar, 1109
Challagundla Kishore, 526
Chalus Lionel, 1179, 949
Chamberlain Christopher, 1021
Chamberlain Marc, 1342
Chamberland John, 372
Chambers Andrea, 177, 323
Chambless Lola, 111
Chamourin Maité, 957
Champiat Stephane, 716, 720
CHAMPION BRIAN, 1223, 208
Chan Anissa, 884
Chan Anissa SH, 1327, 884
Chan Carlos, 1311
Chan Isaac, 993
Chan Ivan, 381
Chan Joseph, 523
Chan Karmela, 1260
Chan King, 350
Chan Kok Fei, 192
Chan Nay, 127
Chan Patrick, 1196
Chan Phillip, 430
Chan PuiYee, 1242
Chan Szeman (Ruby), 326
Chan Timothy, 1383, 479
Chan Tos, 1257
Chan Tristan, 351
Chan Vivien, 368
Chand Dhan, 372, 470, 501, 778, 941
Chand Thakuri Bal Krishna, 287
Chandelier Florent, 1300
Chandler G. Scott, 1274
Chandra Adrienne, 1312
Chandra Shilpi, 304
Chandran Smita, 218
Chandrasekaran Ramya, 39, 498
Chaney Marya, 657, 759
Chang Alfred, 1140
Chang Alice, 277
Chang Baoping, 673
Chang Chia-Wei, 204, 300, 326
Chang Christie, 543
Chang Darwin, 1420, 944
Chang Han, 608
Chang Hao-Ming, 1320, 177, 323
Chang Hewitt, 1002
Chang Hyeyoun, 220, 510
Chang Jae Woong, 392
Chang Jason, 1326
Chang Jihoon, 1090
Chang Kai-Hsin, 313
Chang Katherine, 1396
Chang Kyle, 6
Chang Matthew, 295
Chang Mingjin, 257
Chang Patrick, 475
Chang Ruixia, 725
Chang Shiun, 1420
Chang Thomas, 1086
Chang Xue, 514
Chang Yuzhou, 1064, 839
Chanthey Yvan, 203, 246
Chantranuvatana Kan, 147
Chantzoura Eleni, 322, 358
Chao Joseph, 553, 633, 634
Chao Ma Marshall, 177, 323

Author index

- Chapellier Marion, 1182, 1440
Chapin Steven, 1348
Chapman Jocelyn, 361
Chappa Prasanthi, 1033
Chappel Scott, 489
Chappell Rhys, 1196
Chapuis Aude, 244, 342, 93
Chardon-Robles Jonathan, 1383, 1390
Charo Israel, 499
Chasalow Scott, 608
CHASSAGNOLE CHRISTOPHE, 1293
Chatel Laurence, 481
Chater Jack, 650
Chatterjee Ankita, 955
Chatterjee Bithi, 1293
Chatterjee Fiona, 994
Chatterjee Gourab, 60
Chatterjee Manik, 713
Chatterjee Sampurna, 1241
Chaturvedi Nagendra, 526
Chaturvedi Pallavi, 724
Chau Nelson, 1222
Chauchet Xavier, 481
Chaudagar Kiranj, 878, 879
Chaudhary Amit, 1379
Chaudhry Arvind, 838
Chaussabel Damien, 411
Chauvin Joe-Marc, 605
Chava Srinivas, 526
Che Jenny, 772
Chean Borom, 333
Chebib Ivan, 916
Chee Cheng-Ean, 850
Cheeseman Antonn, 1374
Chehrazi-Raffle Alexander, 810, 880
Chelur Shekar, 1313
Chelvanambi Manoj, 590, 618, 988
Chen Alice, 1417
Chen Amy, 1162
Chen Ann, 1420
Chen An-Ping, 323
Chen Benjamin, 109, 1277, 1282, 1291
Chen Bing, 571
Chen Brandon, 1002
Chen Cecil, 591
Chen Cen, 491
Chen Chao-Hsien, 1158
Chen Christopher, 772
Chen Chuanli, 1284
Chen Chun, 1352
Chen Chun-Yu, 1135
Chen Cong, 1406
Chen Dan, 564, 594
Chen Dih-Yih, 750
Chen Dongqi, 652
Chen Fei, 1057, 1075, 115, 477
Chen George, 1377
Chen Hui, 564
Chen Huidong, 834
Chen Inna, 138
Chen James, 1279, 1403, 54
Chen Jeffrey, 259
Chen Jessie, 1092
Chen Jiahao, 1377
Chen Jiajia, 150
Chen Jianji, 147
Chen Jie, 673, 683
Chen Jie-Yu, 32
Chen Jing, 1183
Chen Jon, 181
Chen Jonathan, 1242, 956
Chen Jo-Pai, 805
Chen Kenian, 993
CHEN LEI, 771
Chen Li, 186
Chen Liandi, 1321
Chen Lioping, 167
Chen Lili, 590
Chen Lihong, 1207, 1340
Chen Longyun, 32
Chen Luping, 220, 510
Chen Mary, 1193
Chen Max, 1230
Chen Min, 1424
Chen Ming, 698
Chen Naifei, 652
Chen Pei-Ling, 617
Chen Peng, 482
Chen Qingfang, 477
Chen Raymond, 878
Chen Richard, 119, 146, 51, 559, 587, 692
Chen Ridong, 355, 961
Chen Rui, 209
Chen San-chi, 1102
Chen Sandra, 1081, 1088, 1104
Chen Shipeng, 1322
Chen Steven, 1263
Chen Victor, 1057
Chen Wei, 694
Chen Wenxin, 1268
Chen Xi, 384, 406, 417, 452
Chen Xiang, 401
Chen Xiaobo, 40
Chen Xiaochun, 1400
Chen Xiaoru, 708
Chen Xiaosong, 1377
Chen Yi, 694
Chen Yian Ann, 617
Chen Yi-Jing, 496
Chen Yuehua, 1149
Chen Yulong, 505
Chen Zhiqiang, 1377
Chen Zhui, 1441, 905, 985
Chen Zirong, 1155, 1200, 1329
Chenchik Alex, 3
CHENE Laurent, 641
Cheng Hanning, 964
Cheng Hsinyuan, 210
Cheng Huijun, 673
Cheng Jason, 435
Cheng Liansheng, 1056, 1214
Cheng Li-Chun, 44
Cheng Lili, 1081, 1104
Cheng Mingshan, 1250, 1427, 382
Cheng Pingyan, 1085
Cheng Rebecca, 433
Cheng Xiaoyun, 296
Cheng Xin, 910
Cheng Yang, 1022
Cheng Yun-Chih, 496
Cheng Zih-Fei, 251
Cherala Ganesh, 777
Cherifi Yacine, 144
Chernock Rebecca, 503
Chernyshev Andrei, 1276
Chery Grace, 123
Cherryholmes Greg, 41
Cheshuk Valerii, 675
Chesney Jason, 610, 611, 727, 783, 789
Cheung Alexander, 1002, 252
Cheung Alice, 379
Cheung Christina, 243
Cheung Hung Kam, 688
Cheung Jeanne, 1276
Cheung Keith, 1065
Cheung Laurene, 374
Cheung Lawrence, 867
Cheung Nai-Kong, 1328
Chevalier Sarah, 561
Chheda Milan, 624
Chi Andrew, 1080, 1195
Chian David, 232, 243
Chiang Eugene, 475
Chiang Jun, 64
Chiang Yao, 1389
Chiappori Alberto, 697
Chiariotti Rebecca, 91
Chiarle Roberto, 317
Chielie Saskia, 88
Chien Chih-Yen, 433
Chien Chris, 401
Chien Christopher, 327, 350
Chiffolleau Elise, 484
Chih-Hsin Yang James, 635
Chilakamarti Ramana, 90
Childs Daniel, 140
Childs Jennifer, 1177, 546, 549
Chin Amanda, 1193
Chin Brandon, 483
Chin Diana, 265
Chin Jasmine, 1196
Chin Michael, 1092
Chin Renee, 4
Chin S. Michael, 1083
Chin Shu Shien, 1060
Chinn Magnolia, 1222
Chinnaobireddy Varsha, 1291
Chinta Pearley, 221
Chiocca Antonio, 896
Chioh Florence, 292
Chiron Marielle, 1198
Chisamore Michael, 658, 666, 738, 773, 838
Chitre Avantika, 435
Chittilappilly Christina, 1255
Chiu Christopher, 987
Chiu Joanne, 635
Chivers Simon, 1191
Chizari Shahab, 123
Chmielowski Bartosz, 123, 610, 611, 659, 717, 787
Cho Byoung Chul, 475, 718
Cho Christina, 167
Cho Eun Ji, 488
Cho Hana, 217
Cho Hyun-Il, 250
Cho Hyun-jun, 899
Cho Jae-Won, 295
Cho Jaeyong, 658
Cho Ju Hwan, 1445
Cho Nam Woo, 511
Cho Sean, 854
Cho Soolck, 918
Cho Sukjoo, 519
Cho Sung Yoo, 349
Cho Sunglim, 306
Cho Yongbum, 66
Choe Joshua, 1127
Choi Ashley, 444, 70
Choi Do Young, 1343
Choi Donghoon, 837
Choi Eugene, 264, 392

- Choi Hyejin, 997
Choi Hyeongryeol, 235
Choi Minji, 467
Choi Seung Hee, 1421, 211
Choi Sun Shim, 837
Choi Yoonha, 475
Choi Younghwan, 515
Chokshi Chirayu, 852
Chol Mary, 822
Chon Hong Jae, 753
Chong Elise, 572
Chong Leslie, 305, 368, 847
Choo Su Pin, 867
Chopra Rajesh, 1316, 1337
Chou Chih-Chien, 1217, 1219
Chou Ching-Heng, 348
Chou Chuan-Chu, 1321, 197, 207, 725, 821
Chou Jeffrey, 204, 726, 727, 755
Chou Justin, 687
Chou Tiffany, 1162
Choucair Khalil, 112
Choudhury Arkopal, 1086
Choueiri Toni, 295, 437, 556, 742
Chouitar Johara, 1301
Choukrani Ghizlane, 995
Chow Adrian, 1309
Chow Andrew, 915, 997
Chow Huiyanangel, 895
Chow Jacky, 470, 778, 941
Chow Jon, 1163
Chow Lyndah, 840
Chowanec Eilidh, 1109
Chowdhury Md Raihan, 1110
Chrétien Anne-Sophie, 1339
Christensen Camilla, 1153
Christensen Elyse, 310
Christensen Esben, 1169
Christenson Eric, 739, 746
Christenson Jessica, 1423
Christian Judith, 675
Christiano Melissa, 315
Christie Tanisha, 113
Christie Yu, 1323
Christopoulos Petros, 136
Chrusciel Jan, 1296
Chu Fuliang, 296
Chu Haiyan, 375
Chu Hui-Yi, 204, 259, 300
Chu Phillip, 276, 288, 304
Chu Quincy, 750
Chu Seung, 1372
Chu Yaya, 303, 881
Chu Yu-Waye, 204, 726, 727, 755
Chua Benson, 274, 857
Chua Corrine Ying Xuan, 83
Chua Jia, 1317
Chua Mary, 181
Chua Melvin, 1035
Chua Yen Leong, 283
Chuang Ray, 1101, 1183
Chugh Priti, 586
Chung Christine, 681
Chung Chul-Woong, 1157
Chung Dongjun, 839
Chung Douglas, 999
Chung Hyejin, 1058
Chung Liam Il-Young, 13, 14, 1407, 1408, 1413
Chung Luke, 747
Church Candice, 1045, 50
Church Sarah, 117, 951
Churchman Michelle, 1147, 1279, 1311, 54
Chvatal Stacie, 380
Cianciotti Beatrice, 268
Cianne Junior, 286
Ciaravino Rita, 1296
Cicala Alexander, 981
Ciccaglione Kerri, 194
Cicchini Vanessa, 1123, 1325, 1326
Cicccone David, 460
Ciceri Fabio, 648
Cichocki Frank, 288
Cichutek Klaus, 137
Cid Melissa, 1196
Cieniewicz Brandon, 378
Cifuentes Anokhi, 485, 856
Cillo Anthony, 1049, 818
Cimen Bozkus Cansu, 62
Cinamon Guy, 474
Cioli Eleonora, 21
Cipriani Barbara, 1324
Cirauqui Beatriz, 676
Circelli Jacob, 160
Cirella Assunta, 267, 982
Cirelli Kimberly, 182
Cisneros Napravnik Tatiana, 674
Ciullo Corey, 1222
Cives Mauro, 1375
Claassen Manfred, 1019
Claassen Yvonne, 241
Clack Aaron, 611
Clancy-Thompson Eleanor, 461, 469
Clark Amy, 644
Clark Jeffrey, 1463
Clark Matthew, 834
Clark Paul, 1051
Clarke Jeffrey, 699, 699
Clarke Raedun, 288, 304
Clayburgh Daniel, 569
Clear Kenysha, 1304
Cleaver Maureen, 732
Clemence Demerle, 1107
Clements Miranda, 307
Cleveland John, 1409
Clifton Guy, 1419, 1461
Clinton Steyen, 82
Cloarec Nicolas, 701
Clor Julie, 991
Clynes Raphael, 667, 668
Cobb Dustin, 399
Cobbold Mark, 461, 469
Coccia Jennifer, 238
Cochran Edward, 1237, 393
Cochran Jennifer, 1166, 352
Codd Amy, 110
Codó Paula, 784, 786
Coello Melissa, 743, 744
Cofano Egidio, 275
Coffey Jennifer, 595
Coffey Matt, 548, 650
Coffin Robert, 610, 611
Coffman Lan, 1451
Cogdill Alexandria, 508
Cognigni Valeria, 91
Cohen Emily, 57
Cohen Ezra, 676, 677, 678, 728
Cohen Frederick, 331, 824
Cohen Gadi, 860
Cohen Heather, 1340, 1356
Cohen Julia, 739
Cohen Justine, 759
Cohen Kaitlyn, 558
Cohen Michael, 98
Cohen Sigal, 200
Cohen Sonia, 1268
Cohen Yoad, 1289
Cohn Allen, 570
Cojocar Gady, 659
Cojocar Gady, 504
Colangelo Jaqlyn, 367
Colbert Jeffrey, 1332
Colbert Lauren, 674
Cole Aidan, 1228
Cole Anna, 212, 407
Cole Christopher, 637
Cole David, 1349
Cole Hunter, 778
Colecchia David, 1170
Coleman J Robert, 1139
Coleman Robert, 566
Colen Rivka, 1280
Coles Garry, 1389
Colevas Dimitrios, 681
Collette Nick, 1327, 884
Collienne Maïke, 650
Collignon Aurelie, 957
Colling Caitlin, 1252
Collins Craig, 520, 534
Collins Laura, 619, 620
Collinson-Pautz Matthew, 227
Collison Eric, 656
Colloca Stefano, 706
Colman Howard, 1147, 1279, 54
Colombo Anthony, 103
Colombo Raffaele, 1185
Colonna Marco, 833
Colton Maggie, 80
Colwell Kerri, 1025
Comberlato Alice, 38
Combredet Chantal, 1315
Comes Maria Colomba, 1281
Commisso Cosimo, 1030
Compagnone Mirco, 820
Concepcion Holly, 1172
Condamine Thomas, 194, 315, 318, 371, 376, 633, 634
Concurso Heather, 483, 945
Conejo-Garcia Jose, 1147, 1279, 1420, 54, 609, 672, 944
Conerty Amanda, 306
Confino Hila, 819
Conforti Antonella, 820
Cong Xin, 158
Conley Anthony, 1042
Connelly Jim, 935
Connolly Wendy, 475
Connor Sydney, 538
Conroy Andrew, 123, 320
Conroy Jeffrey, 15, 152, 173
Cons Laura, 481
Constant Nick, 297
Contente Sara, 1460
Contessotto Paolo, 42
Conteras Atahualpa, 221
Conteras Cristina, 362, 397, 996
Conway Jake, 1277, 552, 554
Cooch Neil, 691, 692, 693
Cook Colin, 305, 368, 847
Cook Daniel, 122, 976
Cook Danielle, 384, 406, 417
Cook Katherine, 1304, 1317, 178

Author index

- Cook Natalie, 719, 850
Cook W, 329
Cooley Sarah, 204
Coomans Chris, 215
Cooney Matheww, 132
Cooper Aaron, 181, 332
Cooper Caroline, 117, 79
Cooper Matthew, 195
Cooper Sam, 1350
Copeland Christopher, 967
Copeland Ron, 739, 748
Copik Alicja, 1005, 1009
Copland John, 324
Corbellari Riccardo, 1093
Corbin Alastair, 1324
Corcoran David, 1031
Cordes Lisa, 766
Cordo-Russo Rosalia, 877
Corey Daniel, 378
Coricor George, 954
Corigleano Ellie, 600
Cornforth Andrew, 1163, 1172
Coronella Julia, 728
Corr Bradley, 562, 565
Corral Elena, 631
Correa Arianna, 218
Corrie Pippa, 787
Cortellini Alessio, 112, 437, 512, 91
Cortese Marco, 213
Cortes-Lavaud Xabier, 1046
Cortez Czrina, 997
Cortez Maria, 869
Corti Chiara, 1264
Coruh Ceyda, 7
Corulli Lauren, 1176, 1177, 1308
Costa Maria Jose, 1162
Costa Ricardo, 645
Costanzo Silvio, 631
Costello Joseph, 80
Cote Charlie, 1437
Cottman Rebecca, 228
Cottrell Tricia, 57
Cotugno Gabriella, 706
Couillault Coline, 462
Coulombe François, 1300
Coulouvrat Catherine, 1416
Coulter Don, 526
Coupe Nicholas, 745
Couper Nicole, 131
Courcelles Mathieu, 1411
Cousin François, 1287
Cousin Sophie, 135
Couto Suzana, 1289, 1299
Couturier Aurelie, 838
Coveler Andrew, 546
Covello Jennifer, 1462
Coward Jim, 743, 744
Cowen Benjamin, 831
Cox Michelle, 324
Cox Murray, 1374
Coy Jesse, 899
Coyle Anthony, 1098, 1404, 86
Crawford Aaron, 1046
Crawford Jeffrey, 699
Crawford Jeremy, 348
Crenshaw Aubrey, 480
Creus Immaculada, 406
Crew Linda, 596
Crimini Edoardo, 1264
Cripe Timothy, 1135, 802, 881
Criscione Steven, 1405
Criscitiello Carmen, 1264
Crisman Ryan, 366
Crisostomo Jeanette, 280
Crisostomo Jeannette, 685
Cristescu Razvan, 635
Croom-Perez Tayler, 1005, 1009
Crosby Shadarra, 542
Cross Jessica, 1341
Croteau Nicole, 101, 59
Crowder Karalyne, 1357
Crowley Michael, 965
Crowther Michael, 343
Crump Lyndsey, 1423
Cruz Bryan, 195
Cruz Pico Christian, 1435
Cruz Sylvia, 1008
Cruz Tleugabulova Mayra, 1276
Cruz-Rangel Silvia, 535
Csiki Ildiko, 691, 692, 693
Cubillos-Ruiz Juan, 1420, 965
Cuccarini Valeria, 648
Cuenca Paulina, 1367
Cugno Chiara, 411
Cui Feifei, 1143, 1149
Cui Jian, 1049, 811
Cui Jiuwei, 652
Cuiffo Benjamin, 1402, 1431, 493, 537, 788
Culbert August, 1309
Culhane Aedin, 295
Cullen Jason, 1121
Culley Georgia, 957
Culp William, 1008
Cultrara Christopher, 1071, 1398
Cumberbatch Marie, 118
Cummings Craig, 584
Cunanan Lynwel, 1183
Cunha Andre, 945
Cunnea Paula, 627
Curcio Claudia, 1318, 1429
Curiel Tyler, 1428, 453, 501
Curigliano Giuseppe, 1264, 707, 774
Curran Michael, 1116, 1142, 1154, 1158, 1333, 1378, 1387, 462, 472, 831, 866
Currlin Seth, 1433
Curti Brendan, 1296, 772
Cushing Daniel, 315, 633, 634
Cusnir Mike, 789
Cusumano Zachary, 739, 748
Cwirla Steven, 1097, 625
Cygan Kamil, 690
Czerniecki Brian, 1420, 248, 645
Czerwinski Debra, 1166
Czupalla Cathrin, 1194
D S Samiulla, 1313
D'Amico Lucia, 1170
D'Angelo Sandra, 600
D'Souza Marjorie, 1121
Da Costa Mark, 42
da Cunha Andre, 483
Da Silva Diane, 1256, 559, 587, 607, 656
DA SILVA Jordan, 1122
Da Tong, 291
D'accordio Giulia, 377
Dacoba Tamara, 129
DaCosta Karma, 339
DaCosta Yvonne, 320
Dadey Rebekah, 1280, 908
Dadgar Maisam, 224
Dadi-Mehmetaj Saida, 851
Dadkhal Kimia, 1019
Dadone-Montaudon Berengère, 135
Daemen Toos, 1322
Dagan Sun, 1290
Daggumati Pallavi, 475
Daginakatte Girish, 1313
Dahan Sapir, 1129
Daheron Laurence, 1220
Dahlem Charlotte, 1116
Dahut Madeline, 909
Dai Chunlei, 1017
Dai Jin, 1309, 1383
Dai Rory, 277
Dai Ruby, 753
Dai Shuang, 821
Dai Tong, 761
Dai Xuejing, 1214
Daigle Scott, 552
Dailey Thomas, 204, 279, 288, 326
Daisley Brendan, 614
Daita Kalyani, 895
Dakhal Plaza Sheila, 900
Dalal Kush, 1196
D'Alessandris Giorgio, 648
D'Alessio Antonio, 512, 850
Dalgard Clifton, 1460
D'Alise Anna, 706
Dalla Pieta Anna, 377
Dalla Pria Alessia, 437
Dalmas Olivier, 1206, 123
Dalton William (Bill), 1147, 1279, 1311, 54
Dama Paola, 627
Damania Ashish, 590, 618
Dametto Ennia, 1318
d'Amico Paolo, 1264
Damo Martina, 948
Damstrup Lars, 589
Danaher Patrick, 99
Danan Corinne, 1454
Danao Jay, 223
Dandapat Abhijit, 313
D'Andrea Alice, 213
D'Andrea Jasmin, 1438, 157
Danek Tyler, 77
Dang Chi, 1307
Dang Minghao, 1001
Dang Ton, 499
Dang Yushe, 1176, 1177
D'angelo Grazia, 21
D'Angelo Sandra, 600, 601, 604
Dangl Markus, 337
Daniel Dylan, 1078
Daniel Jeannie, 622, 734, 774
Daniel Krista, 264
Danielczyk Antje, 1346, 1347
Daniel-MacDougall Carrie, 618
Daniels Gregory, 787
Daniels Ian, 1317
Danilova Ludmila, 1452
Danlos Francois-Xavier, 720
Danloss François-Xavier, 788
Dao Tram, 214
Dapash Mark, 830
Dar Henia, 558
Darcy Phillip, 385
Dardalhon Valérie, 350
Daroy Ryan, 1065
Darville Lancia, 56
Darwish Martine, 1276

- Das Bikul, 90
Das Biswajit, 142
Das Nikitha, 444
Das Parthib, 1249
Das Shipra, 217, 325
Dasgupta Shayani, 1439
Dash Asim, 713
Dash Pradyot, 253, 287
Dash Subhadra, 1342
Dashevsky Olga, 1006
DaSilva Diane, 1084, 555, 561
Dastmalchi Farhad, 1326
Datta Jashodeep, 1224
Datta Meenal, 911
Daubeuf Bruno, 481, 853
Daud Adil, 705, 767
Davar Diwakar, 1000, 1310, 588, 592, 605, 716, 721, 763, 838
Dave Rutwij, 1217, 1219
Davenport Huyer Locke, 876
Daviaud Camille, 447
David Cfir, 860
Davies James, 1349
Davies Matthew, 312
Davies Michael, 914
Davies Rupert, 738
Davila Gonzalez Daniel, 83
Davila Marco, 672
Davis Matthew, 660
Davis Melissa, 117, 923
Davis S Lindsey, 898
Davis Tina, 902
Davis Zachary, 288
Davoodi Shabnam, 369
Davydov Iakov, 27
D'Cruz Osmond, 599
De Almeida Venita, 1206
De Andrea Carlos, 1298, 844
De Aquino Deanryan, 617
De Arkendra, 52
De Azevedo Ricardo Alexandre, 866
de Beijer Monique, 1181
De Bono Johann, 720, 777
De Brabandere Veronique, 1198
De Castro Silva Iago, 1224
De Feyter Caroline, 1170
de Gassart Aude, 354, 720
de Gautard Victor, 37
De Giglio Andrea, 800
de Groot Anne, 100
de Groot John, 1001
de Gruijl Tanja, 686
De Gunzburg Jean, 1306
de Henau Olivier, 997
De Jesus Aribet, 16
De Jong Rob, 1070
de Joode Karlijn, 88
de Kok Pita, 343
de Kruijff John, 1210
de la Cerda Jorge, 4
de la Cruz-Merino Luis, 1144
De La Motte Rouge Thibault, 707
De La Vega Francisco, 132
de Laat-Arts Karin, 495
De Lalla Claudia, 268
De Luca Roberto, 1074, 1093, 640, 900
de Man Saskia, 69
De Martino Mara, 447, 877
De Matos Simoes Ricardo, 1006
De Mingo Pulido Alvaro, 1460, 882
de Miranda Noel F.C.C., 163
De Munari Sonia, 647, 649
De Poot Stefanie, 1351
de Rham Teresse, 1332
De Risi Ivana, 1281
De Siddhartha, 603
de Silva Harini, 1442
De Silva Suresh, 1203
De Sousa Eric, 355, 961
de Souza Paul, 769, 775
De Veirman Kim, 1444
de Vos van Steenwijk Peggy J., 163
Dea Steven, 51
Deban Livija, 822
DeBarge Rachel, 511
Deboever Nathaniel, 1050, 590
Decato Benjamin, 697
DeDe Kniya, 401
Deering Raquel, 541, 576
Dees E. Claire, 633, 634
DeFrancesco Melissa, 370
Degefu Hanna, 1032
Degheidy Heba, 344
deGoma Emil, 769
Degos Clara, 1107
Dehghani Amirabad Azim, 1010
Deitrick Christopher, 1000
Deitrick Christopher, 605
Dejonckheere Eline, 1198
Dekker Joseph, 1379, 736, 764
del Balzo Luke, 1033
del Priore Giuseppe, 257
Del Valle Diane, 629
Delafontaine Brant, 734, 774
Delaidelli Alberto, 1192
Delaitte Patricia, 706
Delaney Conor, 964
Delano Dave, 146
Delebecq Sandra, 990
Delepine Chloe, 470, 778
Delfino Frank, 1415
Delgado-Martin Cristina, 422
Delgoffe Greg, 1133, 330, 408, 970
Della Fera Brian, 220, 510
Dellabona Paolo, 268
Delman Keith, 613
Delon Camille, 1080
DeLong Sabrina, 194, 318
Delord Jean-Pierre, 741
DeLuca Steven, 262, 265
Demaria Sandra, 1117
Dembrow Daniel, 1394
Demeester Elena, 259
Demichele Gross Angela, 644
Demin Jr Oleg, 481
Demmers Jeroen, 1181
den Blanken-Smit Renate, 1210
Den Robert, 428
Deng Haibing, 1441
Deng Haiyi, 1248
Deng Jiating, 1248
Deng Min, 482
Deng Nan, 28, 36
Deng Yilun, 1428, 453, 501
Denholtz Matthew, 276
Denic Kristina, 785
Deniger Drew, 227
Denko Nicholas, 1311
Dennis Michael, 67
Densmore Julie, 555, 559, 607
Deola Sara, 411
DePeaux Kristin, 1133
DePietro Paul, 173
Dequeant Mary Lee, 558
DeRenzo Christopher, 348
DeRose Yoko, 44
Derry Jonathan, 569
Desai Aakash, 427
Desai Anjali, 783
Desai Anupam, 767
Desai Jyaysi, 883
Desai Kush, 932
Desbois Mélanie, 1215
Deschamps Geert, 1198
Deshpande Atul, 1452
Deshpande Niles, 1224
Desjardins Christopher, 607
Desjarlais John, 1067, 1073, 1079, 1372
Despas Fabien, 337
Desponds Jonathan, 1276
DesRochers Tessa, 162
Desselle Ariane, 484
Deswal Anita, 1262, 749
DeTomaso David, 332
Deutsch Samuel, 1084
Deva Anand, 1442
Devgan Vik, 147, 99
DeVito Nicholas, 22, 513, 533
DeVorkin Lindsay, 1196
DeWall Stephen, 780
Dewji Iman, 1327, 884
Dexheimer Sarah, 508, 927
Dey Mamon, 1313
Dhabaan Layla, 848
Dhar Payal, 1011
Dhar Shanta, 1224
Dhar Sukanya, 1439
Dhar Swati, 657
Dharani Sonal, 325
Dharmadhikari Bhushan, 532, 623
Dhere Vishal, 1033
Dhindwal Sonali, 1060
Dhodapkar Kavita, 134, 1458
Dhodapkar Madhav, 134, 1458
Dhudashiya Amit, 1313
Dhupar Harveer, 1196
Dhupar Rajeev, 973
Di Blasi Daniela, 631
Di Conza Giusy, 889
Di Federico Alessandro, 451, 528, 800
Di Giacomo Anna Maria, 774
Di Jorio Lisa, 1300
Di Lullo Giulia, 268
Di Meco Francesco, 648
Di Nicola Massimo, 774
Di Nitto Cesare, 1093
Diab Adi, 1260, 756, 782
Diab Maria, 134, 850
Diamant Rachel, 200
DiAndreth Breanna, 263
Diao Lixia, 450
Dias Jorge, 1353
Diaz Fulvio, 1323
Diaz Juan, 1067, 1073
Dib Elie, 1244
DiBiaso Vicky, 1416
Dicke Betty, 109
Dicker Adam, 136
Dicker Tomer, 1290, 1299
Dickey Andrea, 59

Author index

- Diebold David, 410
Dieffenthaler Thomas, 1005, 1009
Diehl Lauri, 1219
Diers Anne, 1134
Dietmann Gabriele, 27
Dietrich Catherine, 471
Dietsch Camille, 1393
Dietz Allan, 689
Dietz Kevin, 797
Diurio Alexa, 483, 945
Diken Mustafa, 1070
Dikov Mikhail, 585
Dikshit Anushka, 128
Dillman Robert, 562, 565
Dillon Christopher, 1367
Dillon Laura, 1419, 1461
Dillon Stacey, 738
Dilmac, Nejmi, 177
Dilmac Nejmi, 323
Dima Danai, 437
DiMascio Leah, 623
Dimitriadis Petros, 979
Dimitrov Dimiter, 1189, 1192, 303
Dimou Anastasios, 785
DiMuzio Jillian, 823
DiNapoli Sarah, 1197, 1213
Ding Guangxu, 1138
Ding Huiwen, 241
Ding Jian, 219
Ding Kaiyang, 571
Ding Liren, 457
Ding Liya, 910
Ding Quanquan, 605
Ding Ziqiao, 1211
Ding Ziyun, 875
Dinh Huyen, 498
Dinter Teresa, 1023
Diolaiti Daniel, 281
Dionne Kendall, 1332
DiRaimondo Thomas, 1123, 1325, 1326
DiRenzo Daniel, 801, 854
Dirk Brennan, 1336
Disis Mary, 1176, 1177, 1308, 546, 549
DiStasi Antonio, 685
Dittus Christopher, 437
Diwanji Neha, 393
Dixey Cynthia, 882
Dixit Apurva, 158
Dixon Chantel, 217
Dixon Karen, 896
Dizman Nazli, 437, 810, 880
Djouadi Amani, 1178
Djunadi Trié Arni, 13, 1407, 1408, 1413
Djuretic Ivana, 1083, 1092
Do Khanh, 767
Dobbs Ryan, 437
Dockery Peter, 42
Dodd Rebecca, 1311
Dodson Anne, 255
Doger de Spéville Bernard, 675
Doglioni Claudio, 268
Doh Hyounmie, 1343
Doh Junsang, 66
Doherty David, 1086
Doherty Jennifer, 1251
Dohnal Alexander, 653, 722
Doi Toshihiko, 737
Dokter Wim, 495
Dolfi Sonia, 606
Dolgoter Alex, 559
Domankevich Vered, 428
Domchek Susan, 644
Domingo-Musibay Evidio, 787, 789
Domingues Ana, 459
Dominguez Ana, 189
Dominquez Adrian, 898
Domonkos Celesztina, 1096
Dona Chathu, 109
Donahue Amber, 781
Donahue Renee, 1337, 438, 695, 766
Dong Chengguo, 422
Dong Haidong, 689, 977
Dong Hong, 1445
Dong Juan, 971
Dong Lauren, 347, 904
Dong Linlin, 1153
Dong Liyou, 1225
Dong Shen, 1228
Dong Xinyue, 911
Dong Zhiwan, 677
Donia Marco, 1021, 715
Donini Chiara, 190
Donkor Moses, 25
Donnelly Sean, 1404, 297, 86
Donnenberg Albert, 1435, 179
Donnenberg Vera, 1435, 179
Donthireddy Laxminarasimha, 610
Doolittle Emerald, 128
Doonan Bentley, 1111
Doorduijn Elien, 1462
Dore-Hansen Johan, 139, 143
Dorff Tanya, 561, 668
Dornan David, 1348
Doroshov Deborah, 595, 629, 717
Doshi Kshama, 1103
Dotti Gianpietro, 317
Doucet Michele, 487
Dougan Michael, 1004, 1242
Dougan Stephanie, 1004, 1232, 939
Douglass Jacqueline, 1213
Doukas Michael, 1181
Dow Steven, 840
Dowdell Taylor, 320
Dowell Alexa, 113
Dower Chris, 262
Dower William, 1097
Dowlati Afshin, 132, 731, 754
Dowling Elizabeth, 626
Dowling John, 823, 823
Downward Julian, 509
Doxie Deon, 134
Doyle Laura, 1162
Doyon Brian, 444
DR Ravindra, 1368
Dragan Magdalena, 1152
Drage Michael, 1277
Draghi Arianna, 1021
Dragovich Matthew, 1073
Drain Allison, 342
Drakaki Alexandra, 587
Drake Charles, 326
Dranoff Glenn, 260
Draper Amber, 848
Drapkin Benjamin, 891, 906
Drazba Judith, 1043
Dredge Keith, 721
Drees Jeremy, 1327, 884
Dreno Brigitte, 715
Drent Esther, 215
Dreux Joanna, 1206, 403
Drever Matt, 332
Driessen-Engels Lilian, 495
Drilon Alexander, 218
Drolen Claire, 437
Drouin Marion, 484
Drovetto Nicholas, 1308
Drusbosky Leylah, 140, 6
Druta Mihaela, 601
Dryg Ian, 168, 928
D'Souza Anishka, 561
D'Souza Criselle, 1442, 385
D'Souza Jimson, 600, 601
Du Aidan, 80
Du Fangfang, 1057
Du Pan, 164
Du Qiumei, 477
Du Xianghui, 698
Duàn Hanna, 1006
Duan Raina, 369
Duan Renee, 1185
Duan Richard, 1413
Duault Caroline, 362, 397
Dubbel Lena, 995
Dubensky Thomas, 1331
Dubey Ashvini, 1391
Dubey Nikhil, 1246
Duboise Raymond, 1331
Duchateau Philippe, 323, 325
Duda Dan, 1241, 1463
Dudgeon Crissy, 1327, 884
Duecker Jason, 410
Duffy Alyssa, 1458
Duffy Jennifer, 1355, 1381
Dufort Fay, 1207, 1388
Dufour Celeste, 195
Dufva Olli, 1006
Dugan Ute, 555, 559, 587, 656
Duggan Ryan, 1365
Duhén Rebekka, 959, 997
Duhén Thomas, 959
Dukaj Livio, 182
Dukes Joseph, 312, 343
Dulak Austin, 489
Dullaers Melissa, 1198
Dumbrava Ecaterina, 659, 728, 760
Dumontet Charles, 1179
Dunai Cordelia, 272, 520, 534
Dunaway Dwayne, 147
Duncan Nicole, 1357
Duncan Sheila, 542
Dunham Kimberly, 557
Dunkle Alexis, 475
Dunlap Carolyn, 499
Dunlap Daniel, 973
Dunn Andrew, 945
Dunn Gavin, 503
Dunn II Robert, 1078
Dunn Lara, 503, 681
Dunne Philip, 1444
Duong Bao, 902
Duong Ellen, 1465, 994
Duose Dzifa Y, 782
Dupouy Diego, 1275, 1459, 37, 38, 78, 842, 85
Duprey Haley, 841
Duquette Mark, 911
durand justine, 1366, 826
Durette Chantal, 1411
Durgin Joseph, 395
Durham Jennifer, 711
Durham Nicholas, 339, 708, 835

- Durrant Lindy, 1317
Duru Adil, 245
DuSold Justyn, 350
Dutil Francis, 1300
Dutta Dipak, 1439
Dutta Upasana, 146
Dutta Gupta Priyanka, 795
Duvivier Herbert, 764
Duvvuri Umamaheswar, 535, 683
Duzagac Fahriye, 28, 36
Dwidar Mohammed, 1309
Dwivedi Alka, 327
Dwivedi Bhakti, 556
Dwivedi Sanyog, 171
Dwyer Connor, 1096, 407
Dystrhe Matthew, 328, 394, 413, 816
- Eagle Catherine, 719
Eapen Rohan, 1206
Ebben Johnathan, 1443
Eberle Christoph, 429
Eberlein Jens, 180
Ebrahimi-Nik Hakimeh, 1365
Ebrahimzadeh Walead, 913
Ebsworth Karen, 499, 769
Echeandia-Marrero Alesandra, 816
Eckelman Brendan, 1077
Ecker Chris, 304
Eckhardt Bedrich, 1164
Eckholdt Kathryn, 400
Eckles Andrew, 1077
Economides Kyriakos, 1344
Economopoulou Panagiota, 133
Ecsedi Matyas, 1301
Eddy James, 927
Edenfield William, 622
Edgar Chelsea, 1389
Edgerton Arden, 265
Edith Laura, 1137
Edmonds Nicole, 11
Eduardo De Andrea Carlos, 1144
Eduardo Rodrigo, 355, 961
Edwards Austin, 1052
Efrati Margalit, 428
Egan Hannah, 1444
Egan Jack, 724
Egan Laurence, 1444
Egea Josune, 267
Egeblad Mikala, 997
Egelston Colt, 1160
Egger Robert, 1277
Eghbali Shabnam, 1148
Eglenen-Polat Buse, 906
Egli Nicole, 1099
Egloff Ann Marie, 1404, 503, 529, 86
Eguren-Santamaria Iñaki, 267
Ehrhart Jared, 1433, 1438, 157
Ehx Gregory, 1411
Eickhoff Jens, 862
Eickhoff Regina, 578
Eigentler Thomas, 784, 786
Eimerman Patrick, 159
Einstein David, 647
Eisele Nick, 1065
Eisenbeisz Elaine, 555, 559
Eisenhaure Thomas, 1242
Eitas Tim, 485, 856
Eitler Jiri, 216
Eiva Monika, 1024, 202
Ekmekcioglu Suhendan, 782
- Ekstedt Sandra, 998
El Farouk Samira, 741
El- Khoueiry Anthony, 647
El Naqa Issam, 1279, 54
El Sayed Mohamed, 1307
El Zarif Talal, 437
Elabed Noha, 320
El-Am Edward, 437
El-Anbari Mohammed, 411
Elangovan Ramya, 1222
ElBadri Salma, 719
El-Deiry Wafik, 112
Eleftheriadou Ioanna, 601
Elemento Olivier, 1117, 446
Elford Alisha, 234
El-Haddad Ghassan, 1132
Elhanati Yuval, 843
Elinton Lee, 528
Elisseeff Jennifer, 515, 876
Elitzin Vassil, 444
Elizalde Patricia, 877
El-Kalay Mohammad, 336
El-Khoueiry Anthony, 591, 708, 710, 746, 756, 772, 778, 850
Elkrief Arielle, 1300, 614
Ellebaek Steensgaard Eva, 715
Elledge Stephen, 63
Elliott Tyler, 1111
Elliott Andrew, 112
Elmark Peter, 35, 714
Elonen Pekka, 1006
Elmarsafawi Aya, 1409
Elmore Ugo, 268
Elran Ron, 1290
El-Rayes Bassel, 134, 1457
Elrazaq Essam, 1071, 1398
Elrod Ashley, 162
Elsayed Abdullah, 1074, 1093
Ely Scott, 1282, 1291
Elzein Elfatih, 960
Emami Nia, 215
Embry Millicent, 1103, 1359
Emerling Daniel, 1194
Emig Michael, 729, 746
Eminizer Margaret, 57
Emmanuel Akinola, 1222
Emmanuel Rafi, 200
Emu Brinda, 437
Enel Smith Karin, 714
Enell Smith Karin, 35
Enfield Katey, 509
engels steef, 1210
Engle Elizabeth, 57
Enstrom Amanda, 738
Eoli Marica, 648
Eom Iseul, 349
Eom Jaehyun, 1058
Epp Angela, 1190
Epshtein Yana, 819
Epstein Natalie, 292
Erbe Amy, 1113, 1189, 45, 72, 874
Erdmann Michael, 784, 786
Erhardt Joseph, 326
Erler Piriil, 217
Ermolieff Jacques, 444
Ermani Vinicius, 703
Ernst Robin, 1360
Ernst Scott, 614
Eroglu Deniz, 1275, 1459
Eroglu Zeynep, 617
- Errhalt Peter, 1255
Ertl Linda, 499
Escalante Nichole, 1185
Escobar Giulia, 514, 964
Escobedo Jaime, 1355, 1381
Esguerra Vince, 442
Eshghi Shawdee, 242
Eshuis Sander, 239
Eskander Ramez, 562, 565
Eskew Jeff, 728
Eskiocak Ugur, 1123, 1325
Esmail Abdullah, 480, 502, 621
Espinari Javier, 437
Espinosa Nicole, 57
Espinosa-Cotton Madelyn, 1328
Esposito Angela, 1264
Esquerré Michael, 337
Eswarappa Rajesh, 1313
Etemad-Gilbertson Bijan, 489
Eto Danelle, 855
Ettestad Brianna, 1202, 465
Ettxeberria Inaki, 218, 844
Ettxeberria Iñaki, 267
Euesden Jack, 232
Eugenia Ortega Maria, 675
Eum Josephine Eum, 1392
Evandro Bezerra, 324
Evans Alysa, 310
Evans Elizabeth, 613, 645
Evans Jeff, 1173, 777, 850
Evans Joanne, 512
Evans Katrina, 1007
Evans Kinsley, 1203
Evans Shane, 44
Evans Thomas, 787
Evans Tiffany, 41
Even Caroline, 589
Evilevitch Vladimir, 762
Evoyan Levon, 423
Evrard Bérangère, 484
Exley Mark, 1071, 1398, 647, 649
Eyde Nathan, 1341
Eyles Jim, 708
Eyquem Justin, 323
Ezell Tucker, 1207
- F. Sanmamed Miguel, 267
Fabbri Giulia, 155
Faber Matthew, 1067
Fabrizio David, 29, 584
Facciabene Andrea, 572
Fadden Riley, 1268
Fagan Ailis, 445
FAGERBERG Jan, 641, 642
Fagman Lana, 1383, 1390
Fahl Shawn, 1025
Fahy Darren, 1282, 1291
Fairchild Justin, 555, 559, 587, 607, 656, 745
Fairve Thea, 706
Fakih Marwan, 639, 778
Falade Ayo, 1253
Falahat Rana, 912
Falchero Lionel, 701
Falchook Gerald, 1173
Falcon Daniel, 1112
Falk Martin, 784, 786
Fallahi Sara, 404
Falohun Adewunmi, 1260, 437
Famiglietti Jack, 1229
Fan Andrea, 422

Author index

- Fan Bin, 476
Fan Jialu, 1234
Fan Lei, 571
Fan Peidong, 960
Fan Pingchen, 499
Fan Timothy, 1016
Fan Xiang-Shan, 32
Fan Zenghua, 1002
Fandi Abderrahim, 1374
Fang Bin, 1085
Fang Bruno, 570
Fang Lei, 1143, 1149
Fang Tian, 694
Fang Weijia, 197
Fang Ying, 422
Fang Zhaohui, 452
Fanizzi Annarita, 1281
Fanny Manoussa, 841
Fantini Massimo, 55, 637
Fanton Christie, 1086
Farahani Navid, 95
Faralla Cristina, 1196
Farber Leonard, 682, 684
Fardy Melissa, 223
Farghaly Ramadan Mohamed, 1110
Farina Francesca, 648
Farkas Adam, 946
Färkkilä Anniina, 910
Farley Lauren, 1008, 272
Farney Elliot, 1365
Farrajota Neves da Silva Pedro, 974
Farrell Alison, 353
Fasano Julie, 595
Faso Hannah, 1030
Fattah Farjana, 159
Fattori Stéphane, 1339
Faucheux Andrew, 919
Favalli Nicholas, 1093
Favari Elda, 91
Fay Brittany, 383
Fay Nicole, 1084
Fayanju Oluwadamilola, 644
Fayed Atef, 295
Fazio Nicola, 604
Fearley Amber, 1060
Féger Céline, 1306
Feher Kristen, 923
Fehlings Michael, 292
Fehniger Todd, 729
Fei Jian, 106
Fei Raymond, 310
Feig Barry, 542
Feils Arika, 1113, 72
Felices Martin, 1202, 1204, 288, 465, 724
Felip Enriqueta, 475, 635
Fellermeier-Kopf Sina, 1070
Feltquate David, 772
Feng Chuan, 1091
Feng Hui, 1081
Feng Jean, 1308
Feng Jun, 277, 332
Feng Mingye, 795
Feng Qiang, 1329
Feng Zheng, 164
Fenocchio Elisabetta, 190
Fenton Keenan, 705
Fereshteh Mark, 1208, 987
Ferguson Andrew, 660
Ferguson Blake, 1121
Ferguson Sarah, 585, 999
Fera Valeria, 648
Ferlin Walter, 481, 707, 853
Fernández García-Hierro José, 702
Fernandez Rodriguez Laura, 434
Fernandez-del Castillo Carlos, 1463
Fernandez-Salas Ester, 991
Ferrando-Martinez Sara, 657, 849
Ferrari de Andrade Lucas, 204
Ferraro Gino, 907
Ferrarotto Renata, 568
Ferre Pierre, 504
Ferreira Carolina, 870
Ferreira Claudia, 27
Ferreira Stéphanie, 1306
Ferreria Carolina, 893
Ferris Robert, 1037, 1049, 490, 535, 683, 908
Ferroli Paolo, 648
Ferrone Soldano, 1430, 148
Ferrusi Ilia, 445
Ferry Shannon, 329
Fertig Elana, 1452
Fesneau Olivier, 959
Festag Julia, 434
Festin Stephen, 429
Festino Lucia, 21, 842
Fett Craig, 320
Fetzko Stephanie, 328, 394
Fiaschi Nathalie, 541, 576, 690
Ficial Miriam, 295
Fiel Maria Isabel, 629, 688
Field Jessica, 1362, 1363
Fields Hannah, 292
Fiering Steven, 1120, 829
Fieschi Jacques, 701, 957
Fieschi-Meric Jacques, 1107
Figueredo Rene, 1028, 464
Fijanoski Brian, 147
Filetti Marco, 112
Filosto Simone, 1454, 301
Finch Donna, 1353
Finckenstein Friedrich, 783, 789
Fine Jay, 1060
Fink Katja, 292
Finkelstein Darren, 1352
Finkler Jessica, 70
Finley Faith, 485, 856
Finn Jessica, 1194
Finn Kelsy, 1172
Finnegan Peter, 924
Finnes Heidi, 785
Finnigan John, 364
Finocchiaro Gaetano, 648
Finocchiaro Giovanna, 635
Finotello Francesca, 1144
Fiorante Alexa, 57
Fiore Ann, 429
Fiore Frederic, 1107
Fiorentini Guido, 268
Fioretos Thoas, 1054
Firdaus Sarah, 1367
Firth Jack, 1330, 293
Fischer Nicolas, 707, 853
Fischer Ryan, 187
Fiset Stephan, 646, 913
Fisher Andrew, 1277
Fisher Chris, 352
Fisher Fernando, 229
Fisher George, 656
Fisher Terrence, 613, 645
Fisher Timothy, 1367
Fitzgerald Allison, 1012
Fitzgerald Bailey, 437
Fitzgerald Brian, 73
Fitzgerald Kelly, 563
Fjaellskog Marie-Louise, 709
Fjaestad Klaire, 1464
Flaherty Keith, 150, 916
Flamand Odile, 81
Flanagan Eimear, 719
Flandes Aldeyturriaga Javier, 702
Flegel Teresa, 754
Fleischman Jessica, 218
Fleming Gini, 659
Fleming Jason, 387, 882
Fleury Devan, 60
Fleury Michelle, 219
Flick Heather, 1332
Flies Dallas, 739, 748
Fling Steven, 1045, 94
Flood Lena, 1206
Flores Elsa, 882
Flores Linda, 1137
Flores Raja, 629
Flores-Candia Juana, 1438
Florin Lawrence, 1089
Florou Vaia, 437
Floudas Charalampos, 766
Flynn Brianna, 1437
Flynn Patrick, 899
Flynn Peter, 306
Fnu Tenzin Passang, 310
Fogarty Zachary, 109
Foley Gavin, 270
Foloppe Johann, 835
Fong Lauren, 288, 304, 341
Fong Lawrence, 1002, 555, 559, 635, 735
Fong Ryan, 181
Fong Yuman, 305, 368, 847
Fonkoua Lionel, 414
Fonseca Andre, 1278
Fontaine Danielle, 1162
Fontana Elisa, 1173
Fontela Miguel, 357
Foo Wai Chin, 587
Foord Orit, 316
Forbes Shaun, 6
Ford Cayla, 547
Ford Mandy, 506
Forde Patrick, 538, 57, 700
Forgie Alison, 676, 678
Formenti Silvia, 1117, 1144, 446
Ferrer Patrik, 1206
Forster Colleen, 1446
Forster Martin, 675
Forsyth Peter, 1420, 248
Fosso Bruno, 486
Foster Mark, 195, 729
Fotheringham Michael, 57
Fotopoulou Christina, 627
Foulke John, 220, 510
Fountaine Thomas, 335
Fousek Kristen, 909
Foussat Arnaud, 1339
Fowler Kevin, 449
Fox Bernard, 113, 409, 5, 8
Fox Ray, 39, 498
Fox Stephen, 350
Foy Susan, 123
Fradette Jared, 450
Fraenkel Paula, 708

- Fraietta Joseph, 335, 644
Frakes Jessica, 682, 684
Frampton Adam, 627
Franceskin Lobo Maria, 989
Franchet Christel, 1393
Francica Brian, 1331
Francis Deneise, 766
Francis Joshua, 244
Franco Charlotte, 264, 392
Frank Richard, 564
Frankel Lizzie, 1113
Frankel Nicholas, 221
Frankel Stanley, 1320, 177, 323
Franken Patrick, 1351
Franklin Derek, 1203
Fransen Floris, 1210
Franta Kristina, 785
Franzin Alberto, 648
Franzsoff Alex, 123
Fraser Amy, 889
Frazier Emily, 1341, 425
Frazier Jason, 569
Fredenburg Kristiann, 1309
Frederick Dennie, 150, 916
Frederick Joshua, 767
Fredericks Christine, 754
Frederico Stephen, 222
Fredricks David, 1308
Fredriksen Agnete, 669
Freedman Gary, 644
Freeman Dory, 437
Freeman Gordon, 295, 489
Freeman Ruby, 310, 347
Freesmeier Michele, 1265
Freile Jimena, 995
Freire-Benítez Verónica, 312
Freitag Robert, 1212
Frenkel Lisa, 110
Frentzas Sophia, 768, 775
Freudenberg Kristin, 216
Freudemann Lena, 713
Freund Dave, 1331
Frey Noelle, 572
Freyberg Justesen Tobias, 551
Fricker Simon, 1402, 1431, 409, 493, 537, 788
Fridman Leticia, 1301
Fridman Wolf, 590
Friedlander Terence, 555
Friedman Claire, 592
Friedman Richard, 562, 565
Friedrich Tyler, 898
Frieling Jeremy, 286
Friend Richard, 625
Frigault Matthew, 301, 639
Frikha Ahmed, 701
Frimannsson Daniel, 1084
Frisch Andrew, 1238, 330
Fritsche Jens, 713
Fritzsche Anna, 404
Frohna Paul, 354, 720
Fromm George, 1203
Fromm Jonathan, 19
Frost H, 329
Frost Jennifer, 1365
Frye Alexandra, 959
Fu Benjamin, 439, 440
Fu Jingxin, 503
Fu Pingfu, 61
Fu Qiang, 1081, 1088
Fu Siqing, 739, 750
Fu Yang-Xin, 1236
Fucci Livia, 1281
Fucikova Jitka, 446
Fuereeder Thorsten, 722
Fueyo Juan, 836
Fuhrman Jessica, 277
Fuhrmann David, 713
Fujisawa Sho, 1327
Fukuda Rachel, 232
Fukumura Dai, 1241, 1463, 907, 911
Fulcher Nicole, 454
Fulgenzi Claudia, 112, 512, 850
Fuller Clifton, 568
Fulton Ben, 851
Fumagalli Maria, 1327, 884
Funchain Pauline, 437
Fung Megan, 1038
Funke Roel, 1215
Funt Jason, 449
Furness Andrew, 787, 789
Furqan Muhammad, 727
Furuya Naoki, 1445
Fury Matthew, 735
Fusaro Gina, 608
Fusco Alexandria, 1332
Fu-Sum Emily, 252, 340
Futran Neal, 19
Futreal Phillip Andrew, 542
Fyvie Gayle, 627, 838
Gabay Yuval, 1289
Gabbasov Rashid, 194, 371
Gabelli Sandra, 1197, 1213
Gabitova Linara, 318
Gabrail Nashat, 596, 636, 681, 763, 771
GabreLOW Grant, 229
Gabusnia Khatuna, 572
Gacerez Albert, 223
Gad Ahmed, 412
Gadde Saikrishna, 663
Gadgeel Shirish, 1414, 732, 734
Gadiot Jules, 241
Gadkari Rishali, 1348
Gadot Nicolas, 1179
Gaerlan Stephanie, 1332
Gaertner Bjoern, 276, 288, 300
Gafvelin Guro, 654
Gagliardi Christine, 1333, 1378
Gagliardi Filippo, 648
Gai Annie, 1194
Gaillard Stephanie, 711
Gainer Marcus, 221
Gainor Justin, 738, 780, 956
Gaipl Udo, 18
Gajendran Chandru, 1376, 1386
Gajewski Thomas, 420, 828, 978
Gakhil Amandeep, 1191, 1359
Galan Sheila, 1418
Galand Claire, 470
Galassi Claudia, 1114, 1144
Galeazzi Simone, 1093
Galletta Domenico, 112
Galletto Roman, 217
Galindo Casas Meritxell, 370
Galkin Anna, 1164
Gallagher Kathleen, 301
Gallagher Shannon, 77
Gallego Rebecca, 1367
Galli Giulia, 91
Galligan Carole, 743
Gallotta Marilena, 331, 824
GALLUZZI LORENZO, 1071, 1114, 1118, 1126, 1144, 446
Galon Jerome, 957
Galon Jérôme, 1454
Galsky Matthew, 555, 559, 663, 946
Galsong Jacob, 1353
Galvagno Federica, 190
Galvan Diana, 259
Galvan Eva, 453
Galvani Elena, 835
Galvao Vladimir, 731
Galvin Brendan, 332
Gamboa Alicia, 103
Gameiro Sofia, 766
Gamelas Magalhaes Joao, 641
Gan Lu, 780
Gan Qiong, 31
Gan Xin, 1057, 1361
Gandara David, 101, 136, 29, 584, 59
Gandham Vineela, 1450
Gandhi Nimisha, 320
Gandhi Saamil, 869
Gandhi Shipra, 547
Gandolfi Sara, 1006
Gandy Evelyn, 1031
Gane Edward, 691, 692, 693
Ganesh MS, 142
Gangadhar Tara, 723, 774
Ganguly Suddipto, 487
Ganju Vinod, 763
Ganno Michelle, 1153
Gannon Hugh, 255
Ganti Apar, 1245
Gantz Valentino, 1363
Ganzinelli Monica, 91
Gao Dingcheng, 965
Gao Jiming, 1155, 1329
Gao Peng, 1031, 1044, 323
Gao Rang, 768
Gao Rui, 1211, 1401, 426, 793
Gao Shuang, 15, 152
Gao Wentao, 605
Gao Xiang, 1225, 1226, 1234
Gao Xin, 588
Gao Yinjie, 43
Gao Yuzhen, 1322
Gaofeng Cui, 324
Garasa Saray, 267, 844, 982
Garassino Marina, 586
Gárate-Carrillo Alejandra, 336
Garbe Christopher, 366
García Alex, 326
García Andrew, 461
García Bradley, 45
García Jordan, 876
García Myrna, 453, 501
García Zoe, 115
García-Batres Carlos, 999
García-Brocana Pilar, 470
García-Garijo Andrea, 406
García-Gerique Laura, 1189
García-Martínez Elena, 1144
García-Moure Marc, 836
García-Reyes Kirema, 629
Gardai Shyra, 1187, 1190, 1357, 281
Garden Adam, 568
Gardner Hannah, 1207, 980
Gardner Heather, 840
Garg Rekha, 1383

Author index

- Garg Saurabh, 609
Gargosky Sharron, 632
Garland Gaby, 227
Garmezy Benjamin, 647, 667, 742
Garnett Graham, 1185
Garnett-Benson Charlie, 50, 606
Garon Edward, 229, 263, 635, 639, 77
Garralda Elena, 406, 592, 708, 716
Garrett Gerald, 685
Garrett Jensen, 1262
Garrido Greta, 361
Garrido Vanessa, 1224
Garrido-Castro Ana, 939
Garrido-Shaqfeh Stefan, 854
Gärtner Ulrike, 746
Garulli Céline, 354
Gary Ebony, 1174
Garyantes Tina, 759
Garzia Irene, 706
Garzone Pamela, 672
Gascoigne Nicholas, 274, 283, 857
Gasmí Billel, 997
Gassner Tamara, 1255
Gastman Brian, 787, 849
Gaukel Eric, 1212
Gautam Bishal, 1389
Gauttier Vanessa, 1366, 484
Gavil Noah, 1027
Gavilá Joaquín, 548
Gavrielatou Niki, 127, 133
Gawdzik Joseph, 500
Gay Carl, 523
Gay Jason, 831
Gayán Sukanya, 90
Gaynor Lilian, 651
Gazi Md, 796
Geda Prasanthi, 1365
Gedmintas Lydia, 1260
Gee Kelly, 480
Gee Marvin, 1206, 403
Geeraerts Xenia, 790
Geiger Jessica, 1383, 456
Geisburger Jill, 760
Geiss Gary, 147, 951
Geller Melissa, 724
Gellert Johanna, 1346, 1347
Gelpi Ellen, 655
Gelsomino Francesco, 800
Gendron Patrick, 1411
Geng Tao, 1399
Geng Wanping, 1171
Geng Yanan, 1211, 1401
Genova Carlo, 112, 437
Genovese Rebecca, 262, 265
Gentil Dit Maurin Alice, 1393
Gentile Angela, 276, 279, 304
Gentner Bernhard, 648
George Mariam, 791, 903
George Mridula, 760
George Rohini, 922
George Thomas, 564
Georges Mer, 324
Georgoudaki Anna-Maria, 245
Georgy Angela, 764
Gerber Allison, 895
Gerber Lorenz, 292
Gerhardt Lara, 1028
Gerhold-Ay Aslihan, 554
Gerken Ian, 834
gerralda elena, 631
Gerry Jez, 1349
Gerstenberg Amandine, 527
Geschwindt Ryan, 774
Getgano Jared, 313
Getts Daniel, 1237, 393
Getz Gad, 301
Geva Ravit, 767
Gevaert Olivier, 1296
Ghabach Bassam, 580
Ghaedi Maryam, 999
Ghahramanyan Nerses, 423
Ghani Sofia, 1095
Ghanta Ravi, 363
Gharaibah Raad, 1309
Ghasemi Payman, 1279
Ghasemi Saghand Payman, 54
Ghassemi Saba, 1238, 395
Gheeya Jinesh, 82
Ghezali Lamia, 701
Ghilardi Guido, 572
Ghimire Bishwa, 1006
Ghimire Niranján, 270
Ghiringhelli Francois, 642
Ghiringhelli Francois, 1179, 641, 949
Ghobadi Armin, 1454, 776
Ghobrial R. Mark, 502
Ghobrial Rafik, 621
Ghosal Suman, 448
Ghose Mitali, 255, 297
Ghosh Arnab, 955
Ghosh Chandra, 1165
Ghosh Maloy, 1391
Ghosh Nilasha, 1260
Giacalone Matthew, 1124
Giangarra Valeria, 174
Gianino Nicole, 148
Giardino Torchia Maria Letizia, 339
Gibbons Don, 450, 697
Gibbs David, 927
Gibney Geoffrey, 787
Gibson Berit, 44
Gibson Michael, 681
Gibson Neil, 1123, 1325, 1326, 1395
Gicobi Joanina, 977
Giese Tina, 1206
Gieseke Friederike, 1070, 1208
Giffon Thierry, 1215
Gigoux Mathieu, 997
Gil Bazo Ignacio, 475
Giladi Moshe, 860
Gilarioni Ettore, 900
Gilbert Jonathan, 224
Gilbert Lucy, 670
Gileadi Uzi, 745
Gilfillan Susan, 833
Gill Saar, 371, 395, 634
Gillanders William, 184
Gillig Marc, 333
Gilligan Riale, 489
Gillison Maura, 374, 568
GillMartin Marta, 641, 642
Gilmour Cassandra, 1043, 463, 479
Giltane Jennifer, 435
Giordani Victoria, 289
Giordano 3rd Thomas, 238
Giordano Daniele, 1318
Girard Jean-Philippe, 507
Girard Luc, 891
girault isabelle, 1366, 484, 826
Girda Eugenia, 671, 735
Girgis Natasha, 1323
Girsch James, 414
Gitto Sarah, 885
Giudice Anna, 1189
Giugliano Federica, 1264
Giurini Eileena, 1125
Giurleo Jason, 1415
Giusti Raffaele, 112
Giustiniani Jérôme, 1339
Gjeci Brikena, 334
Gjyshi Olsi, 674
Gladney Whitney, 335
Glanville Nicholas, 822
Glaser Charles, 951
Glaser Charlie, 147
Glasgow Eric, 1012
Glass Benjamin, 1277, 1282, 1291
Glass David, 94
Glasser Rachel, 1242
Glatt Dylan, 758
Glaudemans Dirk, 495
Gleba Justyna, 324
Gleber-Netto Frederico, 917
Glez-Vaz Javier, 267
Gliser Camelia, 552
Glitza Oliva Isabella, 607
Gloria Olivier, 324
Gluskin Roman, 1289, 1290
Gnad-Vogt Ulrike, 784, 786
Gnjatic Sacha, 541, 543, 595, 629, 688, 690
Go William, 229, 263, 639, 77
Gobessi Stefania, 215
Gocher Angela, 1048
Gocher-Demske Angela, 1310
Godfrey Wayne, 1123, 1325, 1326
Godwin James, 778
Goedegebuure S. Peter, 184
Goekkurt Eray, 650
Goel Ajay, 1141
Goel Apollina, 636, 681
Goel Shom, 471
Goepfert Arnaud, 1080
Goepfert Ryan, 568
Goetze Thorsten O., 578
Gogas Helen, 608
Gögenur Ismail, 551
Gögenur Mikail, 551
Gogishvili Miranda, 582
Gogov Sven, 706
Goguen Laura, 503
Goh Angeline, 284
Goh Jeffrey, 632
Goins William F., 896
Golan Gali, 1289, 1299
Golan Karin, 1082
Golan Talia, 770
Goldfinger Valentina, 713
Goldman Aaron, 1307
Goldman Alicia, 1001
Goldman Jonathan, 586
Goldrath Ananda, 1047
Goldschmidt Jerome, 933
Goldsmith Joshua, 1206
Goldstein Mark, 564
Goldstein Matthew, 1425
Gomes Dos Santos Igor, 1241
Gomes-Santos Igor, 907
Gomez Fontela Miguel, 1375, 225
Gomez Raquel, 241
Gomez Romo Jose, 331, 824

- Gomez-Manzano Candelaria, 836
Gomez-Roca Carlos, 770, 774
Gomez-Roca Carlos-Alberto, 589
Gong Chundan, 725
Gong Gyung Yub, 1029, 338
Gong Gyungyub, 1034, 196, 236, 249, 75, 963
Gong Hua, 809
Gong Jingjing, 1458
Gong Jun, 636
Gong Wenci, 1143
Gong Xinjiang, 197
Gong Zimu, 480
Gongora Celine, 1179
Gonsalves Caryn, 336
Gonye Anna, 150
Gonzalez Brian, 1414
Gonzalez David, 300
Gonzalez Ericsson Paula, 107
Gonzalez Guerrico Anatlilde, 689
Gonzalez Junca Alba, 221
Gonzalez Louis, 1203
GONZALEZ Macarena, 641
González Macarena, 642
Gonzalez Marina, 784
Gonzalez Ricardo, 617
Gonzalez-Cao Maria, 570
González-Gomariz Jose, 267
Gonzalez-Kozlova Edgar, 543
Gonzalez-Menendes Pedro, 350
González-Navarro E.Azucena, 548
Goodfield Laura L., 980
Gooding Hayley, 1046
Gooding William, 588
Goodman Amy, 588
Goodman Oscar, 733
Goodman, Jr. Oscar, 668
Goodridge Jode, 326, 341
Goodwin Louise, 719
Goodyear Evelyn, 1249
Goon Jack, 657
Gopinath Neha, 1430
Gordley Russell, 221, 228
Gordon Michael, 596, 638, 778
Gordon Sean, 6
Gordon Victoria, 1121
Gore L. Robert, 1414
Gore Suraj, 1313
Gorgievski Michael, 1237, 393
Gorgulho Carolina, 355, 961
Gorman Wesley, 228
Gorthi Aparna, 1405
Gorvel Laurent, 1107, 1339
Gosh Hiren, 1436
Gosh Mithun, 886
Gosink John, 1186, 1187, 1190
Gosling Jennifa, 824
Gosselin Emily, 1163, 1172
Gostissa Monica, 483, 945
Gosu Ramachandraiah, 1376, 1386
Goswami Avijit, 1334, 1335
Goswami Meghali, 695
Goswami Sangeeta, 505
Goswamy Arvind, 1368
Gotliv Ira, 200
Goto Daisuke, 798, 799
Gottfried Maya, 136
Gottlin Liz, 699
Gouin 3rd Kenneth, 1144
Goulding John, 204, 288
Gouttefangeas Cecile, 642
GOUTTEFANGEAS Cécile, 641
Goverse Gera, 69
Govindarajan Ameish, 880
Goyal Lipika, 552
Goyal Sandeep, 1334, 1335
Goyal Subir, 1033, 478
Gozo Maricel, 855
Graddis Tom, 39, 498
Graf Ryon, 58
Graff Jeremy, 1336, 646, 913
Graff Julie, 555
Graham Charlotte, 301
Graham Donna, 774
Graham Rosalind, 972, 986
Grandi Paola, 666
Granit Roy, 504
Grant Joy, 276, 304
Grant Nicole, 223
Gras Ashley, 1389
Grasso Luigi, 1432
Gratch Svetlana, 1342
Grattoni Alessandro, 83
Graves Helen, 1353
Gravina Adriano, 670
Gray Elin, 577
Gray Elizabeth, 1190
Gray Falon, 1282
Gray Jhanelle, 1414, 56
Gray Melissa, 1209
Gray Zane, 1280
Gray-Gaillard Elise, 515, 876
Gray-Gaillard Sophie, 616
Greathouse Rachel, 1342
Greco David, 1354, 424
Green Benjamin, 1019, 57
Green Dave, 854
Green Kevin, 498
Green Shon, 1230, 366
Greenbaum Benjamin, 843
Greenberg David, 819
Greenberg Philip, 244, 342
Greene Emily, 134
Greenshields Watson Alexander, 619, 620
Greer John, 123, 320
Greer Renee, 1083
Gregoire Marc, 1315
Gregorc Anze, 159
Gregory Mark, 923
Greiff Lennart, 102
Greillier Laurent, 1107, 701
Grell Peter, 716
Gremlich Lilian, 1195
Grenley Marc, 569
Greten Layla, 1019
Greten Tim, 1019, 419
Grewal Jaspreet, 763
Greystoke Alastair, 581, 719
Griffin Deric, 16
Griffith Malachi, 123, 184
Griffith Obi, 123
Griggs Anastasia, 373
Grigoryan Hayk, 423
Grillet Fanny, 199
Grimaud Marion, 295
Grimm Lisa, 987
Grippin Adam, 1390
Grivas Petros, 665
Grivel Jean-Charles, 411
Grob Jean-Jacque, 608
Grob Jean-jaques, 604
Groff Brian, 341
Grogan Madison, 1249
Groisman Alon, 1289, 1299
Grönlund Hans, 654
Gros Alena, 123, 406
Groschen Susan, 561
Gross Amy, 1135
Gross Neil, 568
Grossman Joseph, 470, 651, 778
Grossmann Kenneth, 607
Grote Hans, 554
Gruber Joshua, 623
Grudman Steven, 217
Grudzinski Joseph, 870
Gruyters Ezogelin, 135
Gryaznov Sergei, 892
Gschweng Eric, 210, 282
Gu Guowei, 227
Gu Jialin, 197
Gu Lee Yung, 572
Gu Lin, 1132, 699
Gu Liqun, 1463
Gu Qingyang, 1017, 1138, 311
Gu Ying, 105
Gu Zhizhan, 220, 510
Guadagnolo B. Ashleigh, 542
Guan Johnny, 209
Guan Jun, 1199
Guan Xiangnan, 475
Guan Xiaowen, 770
Guancial Elizabeth, 661
Guasp Pablo, 1312
Guatam Shikha, 587, 607
Gubens Matthew, 635
Gudipati Venugopal, 1235
Guedan Sonia, 267
Guedia Joy, 1185
Guedj Mickael, 684
GUEGAN Jean Philippe, 135, 141, 1426
Guégan Jean-Philippe, 1419
Guenther Silke, 665
Guerrif Stephane, 1198
Guerossov Serge, 70
Guerra-Guevara Luiziane, 1132
Guerrero Carlo, 480
Guerrero Valerie, 367
Guerrertaz Lisa, 306
Guess Jamey, 150
Gugenberger Romana, 653, 722
Guglietta Silvia, 486
Gui Levy Laura, 1275
Guida Michele, 1281
Guidotti Nora, 1206
Guiducci Cristiana, 331, 824
Guijen Cecile, 883
Guillaudeux Thierry, 1341, 425
Guimaraes Fernando, 923
Guinney Justin, 132
Guiot Julien, 1287
Guitard Geoffrey, 1107
Gulati Roman, 308
Gulati Shuchi, 589
Guldberg Sophia, 511
Guler Gulfem, 7
Gulina Kurban, 673
Gulla Stefano, 1098
Gulley James, 1337, 438, 695, 766
Gullo Giuseppe, 582
Gumin Joy, 1001
Gümüş Mahmut, 582

Author index

- Gunasekaran Ganesh, 629
Gunderson Andrew, 5
Gundurao Smitha, 198, 203, 246, 247
Gunn Gary, 568
Guntas Gurkan, 1316
Guo Chunguang, 690
Guo Hong-fen, 1328
Guo Jun, 725
Guo Rong, 482
Guo Ruifeng, 109
Guo Sheng, 40
Guo Shiyong, 1225
Guo Weihua, 1160
Guo Xiaoli, 793
Guo Xuan, 270
Guo Ye, 725
Guo Yihzen, 1249
Guo Yunfeng, 452
Gupta Amit, 73
Gupta Ashok, 579, 591, 73
Gupta Harshita, 1428
Gupta Ishita, 1430
Gupta Kajal, 1125
Gupta Namita, 576, 690
Gupta Pravesh, 1001
Gupta Samir, 1303
Gupta Saurabh, 556
Gupta Shilpa, 767
Gupta Subash, 526
Gupta Sumati, 664
Gupta Suprit, 499
Guramare Maria, 1282
Gurary Ellen, 558
Gurer Cagan, 182, 389
Gurka Stephanie, 1346, 1347
Gurung Buddha, 262, 265
Gusev Yuriy, 1460
Gustafson Heather, 382
Gustafsson Kenth, 1330, 293
Gutierrez Alma, 300
Gutierrez Martin, 592, 622, 635, 726, 727, 739, 748, 755
Gutierrez Norma, 397
Gutowski Stephen, 1200
Güzel Gülsüren, 604
Guzman Ayala Marcela, 228
Guzman Wilson, 841
Guzzi Lisa, 990
Gwede Clement, 1414
Gwerder Mauro, 1459
Gwin Will, 1177
Gwin William, 546
Gyllenbäck Elin, 145
- Ha Jung-Min, 250
Ha Ngoc-Han, 340
Ha Patrick, 679
Haabeth Ole, 1084
Haake Kathrin, 337
Haaland Ben, 1251
Haan David, 7
Haan Keith, 1212
Haanen John, 558, 88
Haas Michael, 1141
Haber Adi, 860
Haber Tom, 623
Habib Nagy, 850
Habib Robert, 850
Habib Tanwir, 1430
Habibzade Timursah, 578
- Hackett Maria, 1060
Hackett Michael, 1073, 1079
Hackner Klaus, 1255
Hacohen Nir, 1242, 1257, 150, 916, 956
Haddad Rami, 681
Haddad Robert, 503, 677
Hadrava Vanova Katerina, 448
Haeggblom Linnea, 1342
Haeryfar Mansour, 614
Hafeez Sabrina, 1423
Haffner Michael, 308
Hagan Christy, 1109
Haggerty Agnes, 47, 48
Hahn Julie, 1190
Hahn Noah, 665
Haigis Marcia, 1038
Hailemichael Yared, 603, 914
Haines Eric, 1340
Haines Robert, 1338
Haining Nicholas, 181
Haining W Nicholas, 332
Hair Gleicy, 798
Haj Khalil Tharwat, 860
Hakobyan Karapet, 423
Hakobyan Yervand, 423
Halawani Hefez, 580
Halbert Matthew, 159
Halin Cornelia, 1074, 1093
Hall Amy, 191
Hall Andrew, 1046
Hall Brett, 449
Hall David, 159
Hall Elizabeth, 182, 389
Hall Evan, 437
Hall MacLean, 387
Hallam Trevor, 1103, 1191, 1359
Hallanger Johnson Julie, 56
Hallemeier Christopher, 689
Hallet Damien, 244
Halliday Alexa J., 374
Halliwill Kyle, 1365
Hallstrom Caroline, 1202
Haltom Amanda, 1194
Ham Mina, 718
Hamada Akinobu, 8
Hamada Kazuyuki, 46
Hamadane Linda, 997
Hamadeh Hisham, 1289, 1299
Hamadene Linda, 1148, 791
Hamaidi Imene, 1085
Hambitzer Felix, 1004
Hamburger Agi, 263
Hamdad Chafik, 701
Hamel Damon, 1086
Hamel Keith, 1365
Hametner Simon, 655
Hamid Anis, 753
Hamid Omid, 607, 705, 708, 750, 787, 789
Hamidi Habib, 523
Hamilton Ashley, 232
Hamilton Erika, 659, 750
Hamilton Greyson, 1230
Hamm John, 564, 647
Hammad Mohamed, 1137
Hammell Amy, 592
Hammer Bonnie, 500
Hammerbacher Jeffrey, 364
Hammet Andrew, 192
Hammill Joanne, 261
Hammond Paula, 129
- Hammond Scott, 461, 469, 835, 895
Hammond Terese, 649
Hammons Jacklyn, 1457, 613
Hamon Pauline, 541, 629, 688, 690
Hampton Alina, 1113, 72
Hamza Bashar, 264
Hamzeh Ihab, 1262, 749
Han Bora, 1162
Han Celine, 556
HAN DO YEON, 338
Han Dong Wook, 468
Han Haiyong, 470
Han Hong, 852
Han Hye Rim, 751
Han Hyo, 645
Han Hyunsil, 735
Han Jin, 515, 876
Han Joy, 475
Han Kyungmi, 1105
Han Ruolan, 1155, 1329
Han SeongJun, 999
Han SeungHee, 1063
Han Zhen, 1284
Hancockmann Eva, 495
Hancock Bryan, 204, 288
Hancock Matt, 1208
Hand Julia, 71
Handoko Herlina, 1121
Hänel Gerulf, 281
Hang Ke, 106
Hanifi Arezoo, 87
Hanke Bethany, 724
Hanks Brent, 22, 513, 533, 827
Hanna Diana, 710, 778
Hanna Ehab, 568
Hanna Glenn, 1404, 297, 503, 589, 604, 86
Hanna Jonathan, 617
Hannibal Tine, 1182, 1440
Hannie Stefan, 1196
Hanning Cheng, 514
Hannunen Tiina, 1006
Hansen Anders, 1169
Hansen Gwenn, 331, 824
Hansen Morten, 1233, 612
Hansen Thomas Birkballe, 615
Hansen Torben, 1013, 1013, 524, 524
Hanson Amanda, 1350
Hanson Jeff, 1191
Hao Dapeng, 1001
Hapanowicz Olivia, 629
Harada Tomohiko, 598
Haradhvala Nicholas, 301
Haradon Danielle, 528
Harari Steinfeld Rona, 277
Harari-Steinfeld Rona, 181
Harbison Carole, 1153
Harbst Katja, 1021
Harder Nathalie, 339
Hardikar Sheetal, 1251, 1311
Hardiman Gary, 486
Hardy Marie-Pierre, 1411
Hardy Samuel, 1223
Harel Michal, 136
Hari Parameswaran, 783, 789
Hariri Robert, 270, 847
Harkin Timothy, 629
Härkönen Jouni, 1006
Harman Benjamin, 823
Harms Carson, 370
Harrabi Ons, 1162, 756

- Harries Mark, 787
Harriman Geraldine, 1354, 424
Harrington Brittney, 405
Harrington Kevin, 610, 611, 626, 676, 678
Harris Benjamin, 340, 370
Harris David, 299
Harris Maisha, 265
Harris Rayna, 272
Harrison Ben, 1327, 884
Harrison Simon, 558
Harrison Sue, 1369
Harrod Christopher, 1447
Härtl Barbara, 1137
Hartman Byron, 99
Hartman Douglas, 605
Hartman Zachary, 1109
Hartmann Jessica, 137
Hartmann Sarah, 898
Hartsough Lucas, 242
Hartung Evelyn, 1346
Harutyunyan Agnes, 613
Harutyunyan Lusine, 423
Harvey Christopher, 1350
Harvey Shane, 1210
Hasan Md Faqul, 1005, 1009
Hasegawa Takahiro, 598
Hashambhoy-Ramsay Yasmin, 945
Hashemi Sadraei Nooshin, 697
Hashikawa Koichi, 146
Hassel Jessica, 604, 789
Hastings Richard, 1109
Hatcher Sandra, 875
Hatfield Steven, 1323
Hatton Beryl, 702
Hauke Ralph, 596
Hauser Paul, 400
Hav Monirath, 1294, 89
Havunen Riikka, 715
Hawkins Peter, 576
Hawkins Robert, 787
Hawley Jessica, 665
Hay Joanne, 1046
Hayama Ken, 341
Hayashi Shinko, 808
Hayashi Tae, 121
Hayashi Tomoko, 861
Hayday Adrian, 1392
Hayday Thomas, 1392
Hayes Madeline, 111
Hayim Rubi, 862
Haykal Tarek, 22, 437, 533, 827
Haymaker Cara, 1042, 1050, 508, 657, 782, 838
Hayman Jonathan, 705
Hays John, 564
Hays Priya, 516
Hayward James, 820
Hazen Kyle, 7
He Alwu, 206
He Bai, 571
He Eric, 270
He Gong, 936
He Hailey, 1065
He Henry, 1081, 1088, 1104
He Jiang, 504
He Jin, 182
He Jinqiu, 477
He Kai, 1249, 1445, 564, 585, 594, 770, 783
He Shanshan, 951, 99
He Shuyang, 847
He Tianzhen, 1126
He Wenqian, 1258
He Xianfei, 106, 491
He Xingyue, 244, 342
He Xinrong, 521
He Xuanyao, 582
He Xue-Yan, 997
He Yukai, 206
He Yun, 1057, 477, 858
He Yuyu, 1446
Healy Connor, 44
Heath James, 123
Heaton Alexa, 72
Hebbar Nikhil, 231
Hebertson Alexandra, 988
Hecht Andrew, 1094
Hecht J. Randolph, 229, 263, 639, 77
Hectors Stefanie, 688
Hedberg Jack, 1135
Hedge Shweta, 462
Hedges Dale, 1147
Hedrick Catherine, 397
Hedvat Cyrus, 1282
Hedvat Michael, 1073
Heeg Maximilian, 1047
Heeringa Katharine, 123
Hefazi Mehrdad, 414
Hegde Bindu, 1206, 403
Hegde Meenakshi, 412, 816
Hegde Venkatesh, 1410
Heil-Chapdelaine Richard, 1
Heimann Carolina, 927
Heimberger Amy, 1001
Hein Sascha, 137
Heinäniemi Merja, 1006
Heineman Thomas, 548, 650
Heineman Thomas C., 548
Heininen-Brown Mari, 155
Heinrich Bernd, 1019
Heiser Ryan, 1187, 1201
Helbling Paul, 485
Helfrich Iris, 1384
Heller Astrid, 27
Heller Elizabeth, 934
Hellmann Matthew, 522, 635
Helm Dominika, 1109
Hellmann Tyler, 184
Helming Laura, 497
Helmink Beth, 988
Helsen Christopher, 201, 261, 294
Hemberg Martin, 295
Hemmerle Teresa, 640
Hemminki Akseli, 715
Henderson Clark, 1357
Hendrickson Eleanore, 1367
Hendrickx Wouter, 1053
Hendriks Linda, 1210
Hendriks Natasja, 163
Henick Brian, 660, 772
Henitz Erin, 987
Henley Robert, 95
Henn Mathew, 607
Henneberry Evan, 1396
Hennequin Clotilde, 629
Hennessy Marlene, 1086
Henning Karla, 1348
Henningsen Robert, 1359
Henry Everett, 1152
Henry Jason, 1173, 728, 756
Hensel Janine, 95
Hensler Michal, 446
Hensley Kelly, 1186, 1187, 1190
Hentemann Martin, 888
Hentzen Stijn, 112
Henze Janina, 786
Heo Junhyeok, 1105
Herati Ramin, 616
Herbert Zach, 1220
Herbrand Ulrike, 299
Herbrich Shelley, 1305, 505
Herbst Roy, 29, 584, 635
Hermes Alex, 64
Hermosilla Samayoa Cecilia, 614
Hernandez Andrea, 1094, 1095, 363
Hernandez Genevive, 1215
Hernandez Reinjer, 870, 893
Hernandez Susana, 1230, 366
Hernandez Villanueva John, 1190
Hernández-Osuna Reyes, 836
Herndon James, 699
Herreracarrillo Elena, 137
HERRLINGER Ulrich, 641, 642
Herman Marissa, 198, 203, 246, 247
Herrmann Thomas, 1137
Hershkovitz Oren, 1380
Herting Cameron, 134
Hervas-Stubbs Sandra, 267
Herve Karine, 1196
HERVIEU Alice, 641
Herzig Eytan, 223
Herzog Thomas, 566
Hesnard Leslie, 1411
Hess Nicholas, 1443
Hessel Harald, 155, 579
Hestdal Kjetil, 494
Hesterberg Rebecca, 1409
Hester-McCullough Jonathan, 1466, 285
Hether Tyler, 951
Heymach John, 523, 590, 697
Heyman Liezl, 96, 97
Heyne Kirk, 480, 621
Hiam-Galvez Kamir, 511
Hickey John, 256
Hicklin Daniel, 1096
Hicks Nathan, 607
Hidalgo Manuel, 651
Hidalgo-Vargas Melanie, 193
Hieromnimon Hanna, 879
Higgins Doreen, 549
Higgins Kristin, 1033
Higgins Shaylin, 1186
Higgs Brandon, 1208, 1289, 1299, 987
Higgs Emily, 828, 978
Highfill Steven, 350
Hildebrand Karys, 1130, 1156, 1159
Hildebrand Kurt, 1130, 1156
Hill Elizabeth, 1044
Hill Jonathan, 1082, 1338
Hilton Traci, 113, 5
Hinck Andrew, 1133
Hinds John, 238
Hinterleitner Reinhard, 1310
Hintzen Gabriele, 729, 746
Hippe Daniel, 992
Hirankarn Nattiya, 33
Hiranuka Kazushi, 121
Hiraragi Hajime, 232, 243, 252
Hirasawa Yuya, 46
Hirayama Alexandre, 93
Hirkala-Schaefer Truman, 1185
Hirsch Fred, 29

Author index

- Hirsch Heather, 646, 913
Hirschhorn Daniel, 791, 997
Hirsi Lea, 474
Hirz Taghreed, 879
Histed Alex, 1323
Hjaltelin Jessica, 138
Hlatshwayo Nomsa, 97
Hnat Nataliya, 666
Ho Chien_Hsin, 496
Ho Chi-Sing, 1283
Ho Gregory, 829
Ho Kevin, 442
Ho Naphang, 345
Ho Po, 1348
Ho Richard, 935
Ho William, 1241, 658
Ho Won Jin, 1452
Hoag Jess, 159
Hoang Hai, 303, 802
Hoang Kimberly, 1033
Hoang Song-My, 180
Hoang Tsvetelina, 280, 685
Hoang-Minh Lan, 1111
Hochhauser Daniel, 777
Hodgdon Christine, 993
Hodi F. Stephen, 168, 606, 608, 928
Hodi Stephen, 587
Hoefges Anna, 45, 72
Hoefsmid Esmee, 979
Hoeller Christoph, 608
Hoepken Uta, 1235
Hoffgaard Franziska, 713
Hoffman Laura, 1244
Hoffman-Censits Jean, 661, 665
Hoffmann Jens, 154
Hoffmann Michele, 244
Hoffmann Michelle, 342
Hofland Tom, 343
Hofmann Martin, 1319
Hofmeister Craig, 1458
Hofmeister Robert, 219
Hogan Aisling, 1444
Hogson Rose, 850
Hogue Stephanie, 56
Hojgaard Martin, 622
Hok Rosanna, 20
Holderried Tobias, 713
Holland Aliya, 997
Holland Jaymes, 1167
Holland Pamela, 1148
Hollebecque Antoine, 731
Hollingsworth Michael, 169
Hollingsworth Robert, 336
Hollman Travis, 587, 997
Holloran Sean, 1109
Holman Kori, 233
Holt John, 1437
Holtz Anja, 1331
Holtzinger Audrey, 337
Holub Bradley, 1353
Holz Borch Troels, 612
Holz Josefin-Beate, 1373
Hom Tim, 1352
Hominal Stéphanie, 701
Hong Chibo, 80
Hong Cho Rong, 338
Hong Christina, 878
Hong Chun Pyo, 349
Hong David, 1387, 726, 727, 732, 740, 755
Hong Enping, 228
Hong Ilene, 519
Hong Jin, 1377
Hong Jong Moo, 1029, 75
Hong Kyu, 747
Hong Megan, 464
Hong Ruey-Long, 433
Hong Sa Deok, 886
Hong Seung Pyo, 519
Hong Theodore, 1463
Hong Timothy, 13, 14, 1407, 1408, 1413
Hong Yudan, 1081
Honikel Mackenzie, 396
Hont Amy, 176
Hoogenboom Baukje Nynke, 1322
Hoon Dave, 962
Hoopes Matthew, 203, 247
Hoorntje Rachel, 1053
Hoos William, 184, 656
Hoover Jonaathan, 123
Hope Chelsea, 981
Hope Jennifer, 1030
Höpken Uta, 1239, 1239
Hopkins Bei, 131, 149
Hopkins Megan, 545
Hopland Kelsey, 347
Horak Ivan David, 240, 284
Horhata Allen, 1222
Horiike Atsushi, 46
Horn Leora, 1403
Horn Lucas, 909
Hornick Noah, 948
Hornung Veit, 266
Hornyak Thomas, 615
Horowitz Amir, 946
Horowitz Neil, 563
Horsager Alan, 810, 880
Horton Brendan, 1052, 1087, 517
Horvat Ava, 1458
Horvath Staci, 566
Hose Dirk, 707, 853
Hosein Peter, 778
Hosking Martin, 276, 300, 304
hospers Geke, 88
Hossain Farhana, 972, 986
Hossain Mofazzal, 236
Hostetter Daniel, 367
Hou Bing, 1150, 1397, 482, 76
Hou David, 230, 830
Hou Huanhuan, 1234
Hou Jeannie, 610, 611
Hou June, 733
Hou Ming, 571
Hou Yafei, 230
Hou Ying-Yong, 32
Houacine Jemila, 1339
Houg Demi, 241
Houghton Alan, 791
Houke Haley, 231
Houlton Jeffrey, 19, 569
Housseau Franck, 538
Hout David, 101, 59
Houtkamp Mischa, 1351
Howard Raleigh, 817
Howe Jason, 734
Howes Tim, 555, 559
Howes Timothy, 559
Howie Lynn, 740
Hoyd Rebecca, 1311
Hribar Kolin, 1447, 299
Hrusch Cara, 1365
Hrycyniak Laura, 187
Hrytsenko Olga, 1336
Hsiao Ching-Wen, 251
Hsiao Shih-Chia, 251
Hsiao Stephanie, 841
Hsieh Edward, 1066
Hsieh Faye, 1191
Hsieh Rodney Cheng-En, 1387, 866
Hsien Matthew, 753
Hsin Jing-Ping, 229
Hsiue Emily, 1197
Hsu Ethan, 869
Hsu Jer-Yuan, 833
Hsu Jingmei, 685
Hsu JoAnn, 810, 880
Hsu Jonathan, 1316, 1337, 1392
Hsu Karl, 809
Hsu Matt, 1183
Hu Changyun, 483
Hu Dandan, 417
Hu Dongfang, 3
Hu Guangan, 1400
Hu Guoqiang, 197, 725
Hu Hong-Ming, 113, 1171, 5
Hu Jiahui, 1062, 1211, 793
Hu Peirong, 253, 287
Hu Ruozhen, 475
Hu Xiao, 855
Hu Yanfen, 1062
Hu Yu, 571
Hu Yun, 869
Hua Michael, 1088, 1104
Hua Tony, 221
Hua Xing, 29
Huang Ailing, 869
Huang Alan, 1425, 444, 70
Huang Alexander, 644
Huang Bing, 1057, 858
Huang Cheng-Yen, 1210
Huang Danny, 1088, 1104
Huang Elizabeth, 277
Huang Gang, 1155, 1329
Huang Jiaming, 437
Huang Jian, 1153
Huang Jiandong, 1330
Huang Jianing, 1081, 1088, 1104
Huang Jiawei, 476
Huang Jiayi, 624
Huang Jinglai, 458
Huang Julie, 114
Huang Kai-Wen, 850
Huang Linglin, 964
Huang Li-Ya, 1186
Huang Patrick, 1019
Huang Peigen, 907
Huang Richard, 58
Huang Ruiqi, 768
Huang Sharon, 1327
Huang Shu-Pang, 608
Huang Tao, 747
Huang Wei, 1316
Huang weicai, 1284
Huang Weifeng, 1321, 207, 821
Huang William, 487
Huang Xi, 652
Huang Xiao-Wu, 384
Huang Xiaoyong, 694
Huang Yanzhou, 346
Huang Yi, 725
Huang Yina, 329

- Huang Yue Zhou, 1192
Huang Yueyi, 812
Huang Yusheng, 652
Huang Zhaoliang, 521
Huang Zoey, 1088, 1104
Huangfu Yuhao, 376
Hubbell Jeffrey, 1227
Huber Christoph, 1099, 631
Hübner Norbert, 1239
Huerga Iker, 1403
Hufner Pam, 335
Huggins Matthew, 1332
Hughes Brett, 117, 678
Hughes Christopher, 1192
Hughes Stuart, 1324
Hugo Willy, 643
Hukelmann Jens, 713
Hulen Thomas, 343
Hu-Lieskovan Siwen, 1251, 44, 594
Huls Gerwin, 1205, 989, 995
Hultin-Rosenberg Lina, 150
Humke Eric, 1215
Hummer Gerhard, 889
Humpel Andreas, 281
Humphries Timothy, 756
Hund Stephanie, 71
Hundal Jasreet, 123
Hung Chia-Yang, 887
Hung Michelle, 221, 228
Hunt Elizabeth, 1031, 1044
Hunt Kelly, 542
Hunter Theresa, 123
Hupalo Daniel, 1460
Huppa Johannes, 1235
Hupple Clinton, 139, 143
Hurd Drew, 605
Hurov Kristen, 1340, 1356
Hurst Katie, 1031, 1044
Hurwitz Michael, 558
Husain Marium, 1249, 1311
Hussain Abraham, 1077
Hussain Khiyam, 1392
Hussain Mahmud, 1203
Hussein Mohamed, 206
Hustinx Roland, 1287
Hutcheson Katherine, 568
Hutson Alan, 929
Hutt Meike, 1319
Huuhtanen Jani, 1006
Huynh Truc, 324
Huynh Truc Huynh, 414
Hwang Hyung Ju, 74
Hwang Jun-Eul, 658
Hwang Sujin, 344
Hwang Yoon ha, 467
Hwang Yuri, 1196
Hwu Patrick, 1147, 1279, 1375, 1462, 189, 54, 782
Hynes Sean, 1444
Hyngstrom John, 1251, 44
Hyon Min-Kyong, 349

Iadonato Shawn, 1341, 425
Iams Wade, 638
Iartchouk Natasha, 1153
Iavarone Antonio, 1001
Ibanez Jorge, 231
Ibarlucea-Benitez Itziar, 1209
Ibbett Paul, 322, 358
Ibekwe Ugochi, 227

Ibitokou Samad, 326
Ibrahim Ramy, 656
Iche Marina, 720
Ichikawa Kana, 888
Idank Kaitlin, 262, 265
IDBAIH Ahmed, 641, 642
Iding Jeff, 702
Idossa Dame, 437
Idris Suaad, 1134
Iglesias Victoria, 686
Ihle Claire, 1448
Ihrie Rebecca, 111
Ijsselsteijn Marieke, 1053
Ijzermans Jan, 1181
Ikeguchi Alexandra, 1147, 1279, 1311, 54
Ilano Arielle, 1002
Iliescu Cezar, 1262, 749
Im Sun Woo x, 1063
Imbert Caroline, 354
Imianowski Charlotte, 1069
Imle Andrea, 1070
In Gino, 610, 611
Inekci Dilek, 30
Ingala Nicholas, 333
Ingallinera Timothy, 777
Ingersoll Sarah, 1086
Ingham Matthew, 710
Ingram Davis, 1042, 542
Ingram Piers, 532, 623
Inoue Toshikazu, 901
Invrea Federica, 213
Ioan-Facsinay Andreea, 1070
Ioannidis Sonia, 677
Ionta Nicholas, 538
Iorgulescu Bryan, 115
IP Philbert, 201, 261, 294
Ira Douglas, 1095
Iranpur Khurshid, 1008
Irie Hanna, 595
Iriguchi Nana, 46
Irish Jonathan, 111
Irizarry Adriana, 1117
IRSHAD SHEEBA, 972, 986
Irvine Darrell, 317
Irvine Frano, 1332
Isaacs Jordan, 1032
Isakoff Steven, 717
Isgrò Maria Antonietta, 21
Ishida Saori, 808
Ishiguro Jun, 808
Ishiguro Tomoyuki, 46
Ishihara Jun, 1227, 308
Ishikawa Larissa, 318
Ishimoto Yoko, 808
Ishizuka Andrew, 364
Islas Laura, 94
Ismail Nesreen, 1096
Ismaili Taylor, 855
Isnard-Petit Patricia, 144
Isomi Mari, 290
Istadi Aji, 1455
Isumi Yoshitaka, 808
Italiano Antoine, 135, 141, 1419, 1426, 475, 734
Ivanova Elena, 295
Ivison Geoffrey, 559
Iwamoto Fabio, 1173
Iwamoto Noriko, 113, 8
Iyer Janani, 552
Iyer Seema, 159
Izar Benjamin, 830

Izzo Kaitlyn, 313

J Hillary, 265
Jaakkola Marjut, 715
Jabado Omar, 1208, 987
Jablonski Sandra, 1012, 1452
Jackson Donald, 1010, 926
Jackson Konner, 1168
Jackson Ryan, 503
Jacob Etai, 1273
Jacob Lisa, 989
Jacob Natalia, 665
Jacob Shana, 411
Jacobovitch Sara, 860
Jacobs Tim, 1196
Jacobsen Kivin, 30
Jacobson Blake, 1202, 465
Jacobson Caron, 1454, 301, 639, 687
Jacoby Kyle, 123
Jacquelot Nicolas, 999
Jaeger Elke, 578
Jaeger Samira, 424
Jaekel Anika, 1346, 1347
Jaensch Elizabeth, 1405
Jaffe Sarah, 483, 945
Jaffee Elizabeth, 711
Jafri Amir, 1089
Jaganathan Kowshik, 142
Jagasia Madan, 783, 789
Jagdale Mrunali, 313
Jagga Zeenia, 25
Jahan Kenneth, 182
Jahan Nusrat, 1139
Jahchan Nadine, 1342
Jain Abhinav, 1215
Jain Amit, 101, 1035
Jain Rakesh, 1241, 1463, 907, 911
Jain Renu, 807
Jain Rita, 769
Jain Suyog, 554
Jain Vaibhav, 513
Jaiswal Ashvin, 461, 462
Jakobsen Anders, 1013, 524
Jakobsen Bent, 1349
Jakub James, 785
Jalkanen Juho, 709
Jamal Rahima, 614
Jamali Arezoo, 137, 345
Jamboretz Kate, 381
James Edd, 1131
James Nicola, 576
Jameson Katherine, 777
Jana Jessica, 408
Janes Julie, 1065
Janesick Amanda, 95
Jang Do Soo, 349
Jang Hee-Jin, 363
Jang HyeHyeon, 349
Jang Ik-Soo, 1343
Jang Myoung Ho, 718
Jang Myung Ho, 349
Jang Sekwon, 119
Jang Su Chul, 1344, 1345
Jang Tae Hyun, 1223, 208
Jangalwe Sonal, 182
Jani Ashesh, 848
Jani Saumya, 50
Janicot Michel, 1384
Janicova Lucia, 1046
Janjigian Yelena, 930

Author index

- Jankowitz Rachel, 644
Jannat-Khah Deanna, 1260
Janowczyk Andrew, 1275
Jansen Caroline, 1033
Jarantow Steve, 1360
Jarrell Dillon, 366
Jarvis Maria, 1094
Jaryno-Daly Stacy, 770
Jarzebinska Anita, 1170
Jaschinski Frank, 434
Jasiprasart Pharavee, 1360
Jaume Clemence, 957
Javed Asad, 1265
Javle Milind, 552
Jaworski Maike, 1319
Jayakar Sangeeta, 435
Jayaprakash Priyamvada, 472, 831
Jayaram Anuradha, 598
Jayaraman Pushpa, 772
Jaye David, 1458
Jazaeri Amir, 1094, 713
Jdey Wael, 1114
Jeannelle Mégane, 1393
Jeevan Jeevitha, 254, 361
Jefferson Vicki, 312
Jeffery Ian, 627
Jeffrey Phil, 1340
Jelicic Mark, 304
Jeleu Dontcho, 1189
Jenkins Justin, 99
Jenkins Katherine, 1352
Jenkins Liam, 1115
Jenkins Russell, 150
Jenkins Wendy, 569
Jennings Caroline, 1193
Jennings Emily, 708
Jennings Jordan, 59
Jennings Julia, 638
Jennings Rebecca, 295
Jensen Christina, 1464, 23, 574
Jensen Helle, 232
Jensen Malene, 455
Jensen Sam, 1
Jensen Simon, 1169
Jeon Hee Joon, 74
Jeon Yeonjin, 24
Jeong Eunjeong, 467
Jeong Jinkil, 1363
Jeong Joseph H., 1063
Jeong Sam, 355, 961
Jeong Se, 576
Jeong Youngjee, 1343
Jeong YunHee, 718
Jessen Bart, 1258
Jethon Annalise, 265
Jethwa Sangeeta, 631
Jha Jayanti, 153
Jhatakia Amy, 592
Jhaveri Aashna, 362, 397
Jhaveri Niyati, 116, 79
Jhingran Anuja, 674
Ji Hongkai, 538
Ji Lei, 1449, 70
Ji Qunsheng, 1017
Ji Rui Ru, 638
Ji Yongling, 698
Jia Beibei, 652
Jia Dongya, 401
Jia Gezi, 858
Jia Xingxing, 477
Jiang Aixiang, 103
Jiang Bin, 76
Jiang Bo, 374, 568
Jiang Haixia, 1211, 793
Jiang Hong, 832
Jiang Jenny, 1081, 1088, 1104
Jiang Lulu, 76
Jiang Ming, 571
Jiang Peng, 536
Jiang Tao, 910
Jiang Wenqing, 1143, 1149
Jiang Xiaodong, 1400
Jiang Xiaotao, 206
Jiang Yizhou, 776, 781, 787
Jiang Yongji, 1091
Jiang Yuming, 1284
Jiang Zhi-Gang, 856
Jilani Sameeha, 123
Jilesen Zachary, 404
Jim Heather, 1414
Jimena Andrew, 232, 252
Jimenez Jessica, 483
Jimenez Marcelo, 702
Jimenez Rachel, 944
Jiménez-Cortegana Carlos, 1144
Jiménez-Sánchez Daniel, 1298
Jimeno Antonio, 638, 767
Jimenez Rachel, 1420
Jin Chuan, 571
Jin Chunshan, 521
Jin Chunsheng, 42
Jin Fan, 544
Jin Feng, 676, 678, 756
Jin Ge, 452
Jin Guixian, 1060
Jin Lixian, 742
Jin Ning, 1311
Jin Tao, 346
Jin Tingting, 1106
Jin Wonjong, 1051
Jin Xinxin, 1106, 458
Jin Xinyan, 694
Jing Lichen, 50
Jing Weiqing, 1016
Jo Suyoung, 468
Jo Vickie, 503
Joanny Jean-François, 1003
Jobin Christian, 1309
Jochems Caroline, 695, 766
Jocic Renee, 1123, 1325, 1326
Joedicke Jara, 1239
Joedicke Jara J., 1235
Joerger Markus, 631
Joglekar Alok, 1037, 1310
Johal Sukhvinder, 581
Johannessen Liv, 888
Johanns Tanner, 624
Johansen Astrid, 138, 1464
Johansen Lisa, 767
Johns Jenny, 1121
Johnson Benny, 660
Johnson Bryce, 373
Johnson Catrina, 353
Johnson Christin, 187
Johnson Daniel, 679, 782
Johnson David, 1389
Johnson Douglas, 112, 437
Johnson Erika, 1085
Johnson Faye, 681
Johnson Jason, 568
Johnson Jennifer, 264, 392, 732
Johnson Melissa, 475, 581, 591, 633, 634, 660, 727, 732, 735, 761, 772, 780
Johnson Parker, 841
Johnson Sarah, 590, 721, 988
Johnson ZOE, 1212, 889
Johnson Zoë, 1212
Johnston Jim, 316
Johnston Robert, 475
Joly Anne-Laure, 654
jonas oliver, 890
Jonathan Serody, 371
Jones Cinthia, 1367
Jones Dennie, 589
Jones Derek, 559
Jones Jeremy, 636
Jones Kristen, 295
Jones Kyle, 1077
Jonjic Stipan, 474
Jönsson Göran, 1021
Jonsson Vanessa, 9
Joo Donghyun, 227
Jooss Karin, 660
Jordan Kimberly, 898
Jordan Petr, 1296
Jorgji Vjola, 1242
Joseph Jacinth, 233
Joseph Sujith, 412
Josephs Steven, 1089
Joshi Bharat, 344
Joshi Bishnu, 358
Joshi Dinesh, 187
Joshi Ira, 1095
Joshi Nikhil, 948
joshi omkar, 1065
Joshi Prarthana, 1097
Joshi Rohit, 564, 632
Joubert Philippe, 1300
Joubert Warren, 632
Jouffroy Zeller Claire, 741
Jouffroy-Zeller Claire, 814
Joyce Cailin, 470, 941
Joyce Peter, 1131
Joyner Melissa, 674
Ju Christine, 676, 678
Ju Cunxiang, 1225, 1226, 1234, 491
Ju David, 229
Ju Mikyeong, 1058
Ju Wei, 307
Ju Yawen, 780
Juan Manel, 548
Juarez Cesar, 1342
Juco Jonathan, 41
Judge Jennifer, 1038
Judge Sean, 1008, 272
Juillerat Alexandre, 217, 323
Julian Ricklie, 681
Jun Susie, 332
June Carl, 1238, 291, 335, 572
Juneja Vikram, 1038
Jung Eunmi, 1157
Jung Hae-Yun, 1421
Jung Ho Sun, 356
Jung Hyunjin, 740
Jung Jaeho, 1058
Jung Sung Wook, 1034
Juo Zong Sean, 496
Jure-Kunkel Maria, 1208
Jurewicz Mollie, 182, 389
Juric Dejan, 1242, 1254, 1257, 441

- Juric Vladislava, 1342
Juričić Paula, 37
Jurzak Mirek, 432
Just Petersen Morten, 1169
Juteau Susanna, 715
- K Gowri Shankar, 142
K Vasanth, 142
Kaakour Dalia, 1247
Kabi Neda, 1341, 425
Kacena Katherine, 661, 680
Kaczanowska Sabina, 307, 362, 397, 996
Kaczorowska Malgorzata, 700
Kaczynski Heather, 601
Kadara Humam, 590
Kadel Sapana, 322
Kadouche Jean, 1320, 177
Kaesshaefer Stephen, 1173
Kafi Kam, 1300
Kagehara Hideaki, 737
Kagey Michael, 1141, 553
Kageyama Robin, 587
Kai Kang, 849
Kakkassery Helen, 972, 986
Kala Smriti, 139, 143, 60
Kalada John, 919
Kalaitidou Milena, 282
Kalashnikova Irina, 1200
Kalbasi Alireza, 611
Kaliaperumal Valarmathy, 913
Kalinski Pawel, 547
Kalogjeri Dorina, 503
Kalos Denise, 617
Kalpakoff Megan, 71
Kamalakannan Mohanapriya, 1437
Kamalia Shubhangi, 182
Kamat Ashish, 666
Kamat Nikhil, 308
Kamb Alexander, 229, 263
Kamerkar Sushrut, 1344, 1345
Kamiki Jéssica, 355, 961
Kaminker Patrick, 757
Kamiya-Matsuoka Carlos, 1001
Kamphaus Benjamin, 1292, 607
Kamphorst Alice, 541, 576, 690
Kan Tal, 860
Kanazawa Takayuki, 598
Kane Grainne, 621
Kane Lawrence, 1020, 1041, 490
Kaneko Shin, 1220
Kaneko Yuichiro, 754
Kanellopoulou Chrysi, 748
Kaneva Kristiyana, 132
Kang Charlie, 1199
Kang Chris, 1437
Kang Christine, 147, 99
Kang Chung-Hyo, 250
Kang Hyunjin, 718
Kang Hyunseok, 679
Kang Jiman, 1019
Kang Lin, 270
Kang Minsil, 886
Kang Wonyoung, 1427
Kang Yeon-Woo, 837
Kang Yunyi, 1137
Kangas Takashi, 1327, 884
Kankainen Matti, 1006
Kankeu Fonkoua Lionel, 689
Kannan Madhavi, 1283
Kannan Toshitha, 1307
- Kanodia Jitendra, 667
Kanska Justyna, 193
Kanstrup Fiehn Anne-Marie, 551
Kao Pei-Lun, 255
Kao Steven, 768
Kapil Ansh, 339, 583
Kapiteijn Ellen, 88
Kaplan Angelo, 991
Kaplan Daniel, 833
Kaplan Rosandra, 307, 362, 397, 996
Kapoor Gurpreet, 600, 601
Karaiskaki Frosso, 1351
Karapetyan Lilit, 1267, 818
Karasic Thomas, 774
Karasiwicz Kathy, 847
Kardos Jordan, 1219
Karim Christopher, 777
Karki Sher, 1372
Karkwal Shalu, 470
Karlsson Jens-Jakob, 763
Karlsson Niclas, 42
Karlsson-Parra Alex, 386
Karp Hayden, 1060
Karpovsky Isaac, 1457
Karsdal Morten, 1422, 23, 556, 574
Karsten Verena, 558
Karthik Vivin, 182
Karunamurthy Arivarasan, 1000, 605, 818
Karur Subramanian, 1352
Karyampudi Lavakumar, 306, 645
Kaseb Ahmed, 713
Kasera Samuel, 1345
Kashipathi Shalini, 1391
Kashyap Abhishek, 1437
Kashyap Seema, 153
Kasiwicz Melissa, 803
Kask Angela, 549
Kassab Cynthia, 1001
Kassambara Alboukadel, 701, 957
Kassim Yasmin, 116
Kassiotis George, 343, 509
Kast Martin, 561
Kast Naomi, 1346, 1347
Kast W. Martin, 1084
Kastrunes Gabriella, 295
Kasumova Gyulnara, 150
Kater Arnon, 686
Kates Meghan, 234
Kato Alex, 1362
Kato Shumei, 639
Katragadda Madan, 1392
Katraggada madan, 1316, 1337
Katsumata Toru, 359
Katumba Ruth, 624
Katuwal Nar Bahadur, 886
Katz Chen, 1341, 425
Katz Nathan, 1206, 403
Katz Steven, 1165
Katz Sydney, 874
Katzenelson Rivka, 136
Kaubisch Andreas, 932
Kauffman Kevin, 1222
Kauffman Andrew, 629
Kauffman Dan, 336
Kauffman Howard, 1076, 1268
Kauffman Jacob, 1249
Kauffman Jonathan, 1458
Kauffmann Johanna, 1139
Kaur Ramandeep, 198, 203, 246, 247
Kavecansky Juraj, 937
- Kaveri Deepika, 228
Kaviany Saara, 935
Kawaguchi Kosuke, 907
Kawaida Reimi, 808
Kawamura Yoko, 125
Kawasaki Norihito, 808
Kaya Neslihan, 867
Kays Sarah-Katharina, 784
Kaytal Priya, 11
Kazandjian Suzanne, 1300
Kazaryan Marina, 423
Ke Hang, 491
Keam Bhumasuk, 676, 678
Keane Sean, 972, 986
Kearl Tyce, 373
Kearney Phil, 1164
Kearns Michael, 910
Keating Shelby, 262, 265
Keck James, 1250, 1258, 1427, 382
Kedei Noemi, 1019
Kedl Emma, 1137
Keefe Robert, 275
Keegan Hannah, 304
Keen Nicholas, 1207, 1340, 1356, 1388, 980
Keenan Bridget, 1002, 850
Keerthipati Pooja Smruthi, 367
Kefauver Cheryl, 561
Kehinde-Ige Mercy, 206
Kehler Patrik, 1346, 1347
Kehoe Haixing, 1065
Kehren Alexandre, 37
Keidel Sarah, 606
Keisari Yona, 428
Keith Justin, 358
Keler Tibor, 555, 559, 596
Kell Sariah, 758
Keller Frank, 1244
Kelley J, 896
Kelley Robin, 1002, 552
Kelley Shana, 17
Kellis Manolis, 916
Kelly Andre, 1238
Kelly Erin, 1336
Kelly Karen, 29
Kelly Mike, 1340
Kelly Tracy, 646
Kelson Itzhak, 428
Kelton Christie, 432
Kendal Joseph, 1159
Kendell Rick, 316
Kenderian Saad, 324, 414
Kendra Kari, 442
Kenkel Justin, 1348
Kennedy Ann Marie, 780
Kennedy Audrey, 787
Kennedy Barry, 913
Kennedy Eugene, 652
Kennedy Paul, 688
Kennedy Philippa (Pippa), 1202, 1204, 465
Kennedy Stephanie, 304
Kent Michael, 1008, 272
Kernin Isabela, 1254
Kerr Caroline, 1051
Kerr Emma, 1444
Kersch Kristopher, 41
Kerschbaumer Randolph, 1059
Kershaw Michael, 385
Kersten Marie José, 687
Kesireddy Meghana, 1245
Keskin Derin, 812

Author index

- Kesling Michael, 7
Kessler Daria, 1456
Kethar Harini, 378
Kettlun Leyton Claudia, 869
Keung Emily, 542, 590, 618
Keyhanian Kianoosh, 545
Keyt Bruce, 1215
Kgakolo Mahlatse, 84
Khadilkar May, 403
Khairnar Vishal, 1320
Khaki Ali Raza, 427
Khalaf Shaden, 1262, 749
Khalil Danny, 587, 596, 656
Khalili Hamed, 1242
Khamhoung Annie, 264
Khammari Amir, 715
Khan Aly, 43
Khan Jonathan, 347
Khan Mohammad, 1033
Khan Nayel, 535
Khan Saad, 570, 587
Khan Salar, 334
Khan Shawez, 1021, 343
Khan Uqba, 508
Khan Uzma, 1132
Khanna Nikhita, 1068
Khanna Swati, 1379, 736, 764, 817
Khanolkar Rahul, 1349
Khintakova Darya, 833
Khare Sonal, 1283
Khattar Mithun, 369, 390
Khedkar Aditya, 367
Khendu Tenzing, 70
Khodoudoust Michael, 94
Khong Hung, 645
Khorrami Mohammadhadi, 73
Khosla Archit, 1282, 1291
Khouri Lara, 919
Khuat Lam, 520, 534
Khurana Princy, 1334, 1335
Khurana Sudha, 717
Khushalani Nikhil, 789
Kiecker Felix, 604
Kiel Rasmussen Anne-Christine, 1021
Kiemle-Kallee Joachim, 716
Kieser Ryan, 480
Kilari Deepak, 780
Kilcoyne Michelle, 42
Kile Quinlan, 1202, 465
Killick Saadettin, 582
Killingbeck Emily, 923
Kim Albert, 95
Kim Chan Hyuk, 235
Kim Chang, 126, 381
Kim Chul, 112, 437, 589
Kim Dae, 1137
Kim Dae Hee, 837
Kim Dae Won, 636, 639
Kim Daeun, 1105
Kim Do Yeon, 349
Kim Donggeon, 1090
Kim Dongsu, 1090
Kim Edward, 629
Kim Eun Ji, 511
Kim Geona, 1105
Kim Gil-Jung, 349
Kim Ha Yoon, 1343
Kim Haemi, 488
Kim Honesty, 118
Kim Huijeong, 918
Kim Hye Jeong, 466
Kim Hye Mi, 1136, 973
Kim Hye-Jung, 907, 910
Kim Hyojin, 306
Kim HyoungRae, 1157
Kim In-Ho, 553
Kim Jaegil, 601
Kim Jae-Sung, 873
Kim Jayden, 134, 613
Kim Jayoung, 488
Kim Jenny, 1454, 687
Kim Ji-Hae, 837
Kim Jisoo, 718
Kim Jong Hyeok, 236
Kim Joseph, 623
Kim Juhyeon, 1157
Kim Junhwan, 1058, 467
Kim Kei, 1066
Kim Kevin, 1100
Kim Ki Dae, 751
Kim Kwang Hee, 1029
Kim Kwanghee, 75
Kim Kwang-Soo, 1421, 470
Kim Kyoung-Jin, 488
Kim Kyu Hwan, 1343
Kim Leesul, 13
Kim Michelle, 150
Kim Min Jeong, 519
Kim Mi-Ok, 679
Kim Peter, 237
Kim Richard, 657
Kim Sang Yoon, 1266
Kim Sarang, 468
Kim Sean, 99
Kim Segi, 235
Kim Seulki, 1285
Kim Seungwon, 683
Kim Sojung, 1394, 353
Kim Suji, 75
Kim Sukjun, 1285
Kim Sungjune, 1085
Kim Sung-min, 1286, 74
Kim Sungsik, 1286, 74
Kim Sunnie, 756, 898
Kim Tae Hoen, 886
Kim Tae-Hun, 1343
Kim Taewan, 658
Kim Tai-Gyu, 250
Kim Tanya, 316
Kim William, 560
Kim Youngchul, 1311, 56, 609
Kim Youngmi, 923, 99
Kim Yusun, 306
Kimble Erik, 93
Kimmelman Alec, 656
Kim-Schulze Seunghee, 595, 629
Kina Eralda, 1411
King Catherine, 1277
King Chloe, 373
King Martin, 563
King Paula, 629
King Peter, 449
King Ryan, 1010
Kingsley Edwin, 731
Kinjyo Ichiko, 1112
Kinkhabwala Milan, 932
Kinneer Krista, 895
Kinney Melissa, 1443
Kinrot Seon, 406, 417
Kinzler Kenneth, 1197, 1213
Kipkogei Elly, 1273
Kirby Kenneth, 1071, 1398
Kirby Maurice, 649
Kirchhammer Nicole, 434
Kirchhoff Tomas, 88
Kirchmair Alexander, 1144
Kirk Allison, 348
Kirk Christopher, 422
Kirk Niels, 1293
Kirkemo Lisa, 1206
Kirkup Christian, 1291
Kirkwood John, 1000, 1244, 1267, 588, 605, 789, 818
Kirpalani Anish, 1296
Kirschner Jessica, 851
Kirtane Kedar, 229, 263, 639, 77
Kiru Louise, 198
Kischel Roman, 266
Kiselyov Kirill, 535
Kishi Hiroyuki, 121
Kishton Rigel, 340
Kislinger Thomas, 852
Kissick Haydn, 1033, 134, 407, 848
Kis-Toth Katalin, 483, 945
Kitas Eric, 1170
Kitayama Shuichi, 1220
Kitch Lacey, 1292, 643
Kitko Carrie, 935
Kivimae Saul, 1086
Klagges Jorge, 578
Klahn Joseph, 1365
Klaman Irina, 27
Klar Richard, 434
Klaskin Danielle, 1060
Klebanoff Christopher, 218
Klein Daryl, 317
Klein Paula, 595
Klein Roger, 173
Klein Shoshana, 1170
Kleiner David, 1019
Kleiner Jake, 1206
Klein-Goldberg Anat, 860
Kleinholz Daniela, 1137
Kleist Sierra, 1032
Klempler Samuel, 150, 553
Kleschenko Yuliya, 856
Klichinsky Michael, 194, 315, 318, 371, 376, 633, 634
Klievink Jay, 1006
Kliger Yossef, 504
Kline Brad, 1432
Kline Janine, 801, 991
Klinge Kelly, 1365
Klinghoffer Richard, 569
Klippel Kelena, 1111
Klobuch Sebastian, 558
Klohe Erika, 600
Klooster Rinse, 1210
Klopp Ann, 674
Klop-Packel Nory, 967
Kluger Harriet, 127, 789
Klussman Kerry, 1186
Klymyshyn Dmytro, 116, 79
Knickerbocker Aron, 775
Knight Andrew, 1267
Knochelmann Hannah, 212, 407, 89
Knollman Hayley, 644
Knott Simon, 1144
Knox Gavin, 1324
Knuttsdottir Hildur, 993

- Ko Andrew, 656
Ko Dongwoo, 349
Ko Eun-Su, 211
Ko Hayden, 277
Ko Myat, 904
Kobayashi Yuta, 962
Kobie Julie, 635
Kobzik Lester, 3
Koch Elizabeth, 1350
Koch Ina, 136
Koch Joachim, 729
Kodal Behiye, 1202
Kodali Sudha, 621
Kodumudi Krithika, 248
Koelle David, 50
Koeppen Hartmut, 435
Koguchi Yoshinobu, 113, 1171, 8
Koh Andrew, 983
Koh Clara Kai Ting, 274, 283
Koh Xin Yu, 284
Kohanbash Gary, 222
Köhler Florian, 713
Kohler Minna, 441
Kohlhas Laura, 729, 746
Kohli Manish, 664
Kohlmiller Heather, 476
Kohlway Andrew, 174
Koirala Pratirodh, 238
Kok Lianne, 239
Kokubu Yuko, 290
Kolitz Sarah, 449
Kolker Steven, 1456
Kolodziej Andrew, 815
Kolsari Deepa, 724
Koltun Bella, 860
Komoriya Akira, 1188
Komoriya Kaoru, 125
Komoroski Veronica, 1163
Kondo Makoto, 290
Kondo Shunsuke, 737
Kondo Taisuke, 350
Konen Jessica, 450
Koneru Mythili, 685
Kong Connie, 320
Kong Xiangjun, 239
Kong Ya, 76
Koning Ryan, 366
Kononen Juha, 715
Konstantinopoulos Panagiotis, 563, 910
Koo Hyunmo, 1058
Koopman Louise, 1351
Kooreman Loes F.S., 163
Kooski Mitra, 178, 492
Kopetz Scott, 229, 263, 639, 77
Korangy Firouzeh, 1019
Kornepati Anand, 1428, 453
Korniyev Dmytro, 1066, 1217
Korpisaari Riitta, 715
Korski Konstanty, 27
Kortylewski Marcin, 795, 810, 880, 887
Korukonda Mithra, 147
Korver Wouter, 1396
Kosaka Yoko, 899
Kosco Balazs, 369
Koseki Haruhiko, 290
Kosharek Andrew, 862
Koshkin Vadim, 663
Kossenkov Andrew, 1307
Kotak Prerna, 1352
Kotaniides Helen, 1193
Kotecha Rupesh, 703
Kotecki Nuria, 622, 734, 741, 774
Kothambawala Tasnim, 1215
Kothari Nishi, 781
Kothari Vishal, 1352
Kottschade Lisa, 1274, 785
Kotturi Maya, 1215
Kou Baijun, 690
Kouakanou Leonce, 351
Kouri Fotini, 232
Koutroumpakis Efstratios, 1262, 749
Kovacsovic Magdalena, 1251, 44
Kowal Joanna, 1275, 1459, 78, 85
Kowalewski Daniel, 713
Kowash Ryan, 891
Koya Richard, 1420
Koyama Kristina, 1215
Koyama Motoko, 1121
Koyama Takafumi, 737
Koyfman Shlomo, 1309, 1383, 456
Kozaily Elie, 437
Kozono David, 1244, 29, 584
kraehenbuehl Lukas, 997
Kraman Matthew, 1353
Kramer Robert, 745
Kratz Jeremy, 1443
Krause Kate, 1387
Kraynyak Kimberly, 559
Kreber Willem-Jan, 1181
Krebs Matthew, 777
Kreder Cindy, 1348
Kreft Bertolt, 1080, 1195
Kreiter Sebastian, 1070
Krell Jonathan, 427, 627
Kremp Madison, 315
Krenciute Giedre, 231
Kreuger Joshua, 392
Kreutzfeldt Mario, 1275
Krieg Arthur, 605
Krieg Carsten, 486
Kriegbaum Mette, 763
Krieger Laurence, 663
Krieger David, 762
Krijgsman Oscar, 241
Krimm Michael, 1078
Krimsky William, 702
Krishn Shiv, 1368
Krishna Subith, 1391
Krishnamurthy Kanchi, 1303
Krishnamurthy Akshay, 1450
Krishnan Kavita, 876
Krishnan Manoj, 857
Krishnan Shanmugarajan, 470, 907, 941
Krissteleit Rebecca, 774
Kristensson Julia, 1340
Kritikou Joanna, 370
Kroemer Alexander, 1019
Kroening Gianna, 1247
Kroon Paula, 239
Krug Lee, 591
Kruiger Ryan, 888
Kruhm Martha, 1417
Krukowsha Anna, 1434
Krumppoch Megan, 834
Kruppa Don, 1155
Kruse Arnold J., 163
Ku Jamie, 1309, 1383
Ku Jong Beom, 349
Ku Manching, 332
Kua Lindsay, 240, 284
Kuai Jun, 1354, 424
Kuang Shao qing, 296
Kuboki Yasutoshi, 737
Kubota Yutarō, 46
Kuchroo Vijay, 896, 964
Kucuk Omer, 478
Kuczek Dorota, 1464
Kudchadkar Ragini, 506
Kueberuwa Gray, 282
Kuehrer Irene, 655
Kuhl Niklas, 266
KUHNE MICHELLE, 1066, 807
Kuilmann Thomas, 241
Kuiper Emily, 238
Kuklin Nelly, 1355, 1381
Kulangara Karina, 41, 71
Kulasinghe Arutha, 117, 118, 120, 79, 923
Kulikauskas Rima, 50, 992
Kulkarni Abhijeet, 388
Kulkarni Aditi, 1037, 490, 683
Kulkarni Aditya, 1334, 1335
Kulkarni Ashwini, 1210
Kulkarni Gauri, 369, 390
Kulkarni Hanumant, 1368
Kulkarni Neeraja, 292
Kulkarni Rohan, 402
Kulp Daniel, 388
Kulu Askin, 655
Kulusich Joseph, 854
Kumar Amit, 672
Kumar Ashwin, 1463
Kumar Avinash, 1313
Kumar Dinesh, 555, 559, 587, 643
Kumar Manu, 1092
Kumar Nandita, 1035
Kumar Nikhil, 153
Kumar Rajesh, 1192
Kumar Vijay, 95
Kumar Vodnala Suman, 340
Kumlien Georén Susanna, 942, 974, 998
Kummar Shivaani, 758, 767
Kumra Heena, 1241, 1463
Kundu Kunal, 690
Kundu Samit, 312
Kundu Sharmistha, 1222
Kunkel Eric, 320
Kunning Sheryl, 1049, 1136, 1451, 818, 973
Kunwar Pratima, 353
Kunzke Thomas, 583
Kunzmann Volker, 720
Kuo Li-Wei, 1423
Kuo Pan-Hsien, 496
Kuo Paula, 1069
Kuo Sung-Hsien, 805
Kuo Tracy, 1162
Kuo Ya-Huei, 795
Kuo Yi-Chiu, 251
Kuppen Peter, 1053
Kurcon Tomasz, 217
Kuriakose Anshu, 1368
kurokawa cheyne, 835
Kurtov Daria, 192
Kurupati Prathiba, 312
Kurzman Ilene, 862
Kutach Alan, 833
Kuttke Mario, 653, 722
Kuybeda Oleg, 1290
Kuzel Timothy, 705
Kwan Cheryl, 320
Kwarta Vineet, 632

Author index

- Kwatra Shawn, 1268
Kwekkeboom Jaap, 1181, 883
Kwofie Luyanda, 84, 97
Kwok Darwin, 80
Kwok Eilene, 1301
Kwon Byoung S., 1063, 466
Kwon Eugene, 140
Kwon Hyunwoo, 839
Kwong Wesley, 643
Kym Philip, 1365
Kyratsous Christos, 851
Kyriazopoulou Panagiotopoulou Sofia, 181, 332
Kyung Taeyoon, 242
- La Placa Chris, 41
Laajala Essi, 1006
Labanieh Louai, 352
LaBelle James, 983
Laberiano- Fernández Caddie, 31
Labiano Sara, 836
Labo Haley, 595
Laborde Lilian, 701
Labrecque Max, 1159
LaCayo Ashley, 1327, 884
Lacayo Sergio, 1342
Lachance Kristina, 992
Lack Justin, 419
Lacroix Ruben, 979
Lad Latesh, 1066
Ladwa Rahul, 118, 79
Laengle Friedrich, 655
Laengle Johannes, 655
Lagebro Vilma, 942, 974
Lagmay Joanne, 1390
Lahav Coren, 136
Lahdenranta Johanna, 1340, 1356, 1388, 980
Lähdesmäki Harri, 1006
Laheru Daniel, 711
Lahiri Abhik, 1282
Lahn Michael, 889
Lahr David, 888
Lahr Walker, 392
Lahtela Jenni, 1006
Lai Alicia, 1036
Lai Anne, 1203
Lai Courtenay, 1196
Lai Jason, 532
Lai Yi-Shin, 304
Lai Yurong, 1217, 1219
Lai Zengzu, 1060
Lai Zhongwu, 586
Laing Adam, 1392
Lajoie Marc, 185
Lajoie Scott, 278, 369, 390
Lake Andrew, 1338
Lake Ross, 1033
Lakhani Nehal, 1173, 661, 735, 738
Lakins Matthew, 1069
Lal Girdhari, 1014
Lal Prabha, 201, 261, 294
Laliberte Jason, 835
Lam Alan, 293
Lam Christina, 182
Lam Helen, 114
Lam Hubert, 244, 342
Lam Katherine, 1196
Lam Viola, 243
Lam Viola C., 232
Lam Wei-Sen, 635
Lamarque Brandon, 12, 188
- Lamb Andrew, 927
Lamb McKenna, 489
Lambert Caroline, 614
Lamberti Giuseppe, 437, 451, 512, 528
Lameris Roeland, 686
Lamers-Kok Nina, 245
Lamm Donald, 666
Lammers Marshall, 1008, 272
Lammerts van Bueren Jeroen, 883
Lampenfied Caleb, 1136, 1451, 361
Lamping Elizabeth, 766
Lamtire Gauri, 198, 246, 247
Lan Ruth, 1083, 1092
Lanahan Matthew, 1362
Lance Remington, 1341
Landers Gregory, 635
Landers Mark, 159
Landi Daniel, 412
Landi Annick, 191
Landlinger Christine, 1059
Landoni Elisa, 317
Landri Marcellin, 701
Landstrom Tova, 714
Lane Maureen, 761
Lane Nina, 139, 143, 60
Lang Frederick, 1001
Lang Julie, 898
Lang Lixin, 544
Langan David, 353
Langer Corey, 703
Langer Ian, 1222
Langer Sanah, 1345
Langer Timothy, 387
Langermann Solomon, 739, 748
Langley Meghan, 278, 369, 390
Lango Miriam, 568
Lanis Jordi, 898
Lanoix Joël, 1411
Lanroue Danielle, 646
Lantuejoul Sylvie, 1179
Lapointe Rejean, 614
Lapuyade Nicole, 1078
Lara Jacqueline, 1137
Laramore George, 19
Larkin James, 608, 789
Larouche Jean-David, 1411
Larque Ana, 916
Larsen Brian, 1283
Larson Annaleah, 44
Larson Ryan, 1230, 366, 375
Larson Sarah, 639
Lasalle Manuel, 1185
Lashuk Kanstantsin, 1436, 968
Lasko Loren, 1365
Laspidea Virginia, 836
Lassahn Katy, 162
Lastrapes Matthew, 590
Lata Jennifer, 555
Latak Robert, 626
Lathers Deanne, 772
Lathouwers Emma, 1196
Lau Mai Chan, 1288, 1302, 867
Lau Rainbow W H, 702
Lau Sally, 639
Läubli Heinz, 1128, 631
Lauer Georg, 1257
Lauer Ulrich M., 628
Launonen Inga-Maria, 910
Laura Peña Laura, 1120
Laurie Scott, 750
- Laux Douglas, 763
LaVallee Theresa, 555, 559, 587, 607, 656
Laverdure Jean-Philippe, 1411
Lavi Erez, 1129
Lavoie Sara, 767
Law Aariah, 187
Law Vincent, 248
Lawler Brendan, 367
Lawn Sam, 1185
Lawrence Donald, 787
Lawson Devon, 1007
Lazar Alexander, 542, 618
Lazarevic Dejan, 268
Lazetic Sasha, 381
Le Ann-Elizabeth, 168, 928
Le Berichel Jessica, 629
Le Bescop Clément, 1306
Le Bigot Jean-François, 1315
Le Brian, 855
Le Catherine, 520
Le Dung, 711, 739
Le Floch Anne-Charlotte, 354
Le Gall John, 776, 781, 787
Le Loarer François, 135
Le Maitre Erwan, 654
Le Moulec Sylvestre, 135, 141
Le Ray Maryannick, 701
Le Scolan Erwan, 1078
Le Tonqueze Olivier, 322, 358
Le-Tourneau Christophe, 741, 774
Le Trinh, 1167
Le Xiuning, 568
Lea Spencer, 1154, 1158
Leabman Maya, 1215
Leach Emma, 620
Leahy Sara, 1462
Leal Alexis, 898
Lear Rochelle, 1223, 208
Lebas Louisiane, 701
Lebbe Celeste, 784, 786
Lebbé Celeste, 604
LeBlanc Michael, 29
LeBoeuf Nicole, 1263, 1268
Leca Vanina, 701
Lecagoonporn Srisuda, 782
Lechner Melissa, 437
Leclerc Giles, 724
Lecoq Ines, 1440
Ledy Lee, 1044
Lederer Jim, 632
Lee Ahn, 1196
Lee Alee, 1119
Lee Anna, 568
Lee A-Ram, 1157
Lee Benjamin, 1082
Lee Betty, 476
Lee Bo, 93
Lee Bo Eun, 468
Lee Bo Ryeong, 1286, 74
Lee Boah, 804
Lee Byoung, 1090
Lee Byung, 624
Lee Byung Ha, 657, 679, 849
Lee Calvin, 984
Lee Chen-Ting, 221
Lee Chia-Yun, 251
Lee Dae-Keum, 1421
Lee Dae-Yon, 1157
Lee Dahea, 1090
Lee Daniel, 399

- Lee David, 1002
Lee Dean, 1006, 303, 881
Lee Derrick, 221
Lee Elizabeth, 563
Lee Eunjung, 1058, 467
Lee Eun-Jung, 1058
Lee Frank, 603
Lee Gail, 1352
Lee Gary, 370
Lee George, 1282, 1291
Lee Grace, 1103, 1191, 1359
Lee Hanbyul, 1058
Lee Hanna, 1063
Lee Hee Jae, 1055, 365
Lee Hee Jin, 1029, 1034, 1055, 196, 236, 24, 249, 338, 365, 75, 963
Lee Hee-Ra, 468
Lee Hyeon Jin, 338
Lee Hyeonjin, 1034
Lee Hyo, 718
Lee Hyun, 196, 236, 249, 963
Lee Hyung Ki, 1343
Lee Hyun-Sung, 363
Lee Jack, 568
Lee Jacob, 1066
Lee Jae Lyun, 718
Lee Jasmie, 1297
Lee Jeeyun, 658
Lee Jenny, 743, 744
Lee John, 308
Lee Jong-Seok, 635
Lee Joon Sang, 926
Lee Joong Won, 466
Lee Joycelyn Jie Xin, 867
Lee Jun-Young, 1105
Lee Karin, 469
Lee Kelly, 228
Lee Kelvin, 396
Lee Keun-Wook, 553, 658, 676
Lee Kimberley, 645
Lee Kun-Joo, 837
Lee Larissa, 563
Lee Max, 277
Lee Meng-Na, 1102
Lee Min Jung, 1343
Lee Min Young, 1153
Lee Minji, 837
Lee Miseon, 963
Lee Narae, 467
Lee Patrice, 908
Lee Peter, 1160
Lee Philip, 228
Lee Preston, 984
Lee Sadie, 182
Lee Sang-Eun, 250
Lee Seulgi, 804
Lee Seung-Woo, 837
Lee Siyoung, 657
Lee Somin, 911
Lee Soohee, 1296
Lee Soohyeon, 740
Lee Soowon, 13, 14, 1407, 1408, 1413
Lee Su Bin, 349
Lee Suat Ying, 867
Lee Sue, 754
Lee Sumin, 918
Lee Sung-Hyung, 1372
Lee Sunhwa, 235
Lee Taeseob, 657
Lee Thomas, 1222
Lee Tom, 204, 259, 276, 288, 300, 304, 326, 341
Lee Valerie, 711
Lee Wen-Hua, 229
Lee Weon Sup, 751
Lee Won, 382
Lee Wooyul, 718
Lee Yangsoon, 1058
Lee YeonHee, 1157
Lee Yi-Hsuan, 496
Lee Young Cheol, 1157
Lee Younghee, 1042
Lee-Chang Catalina, 830
Lee-Hoeflich Si-Tuen, 780
Leelatian Nalin, 111
Leelayuwatanakul Nophol, 33
Lefranc Celine, 81
Lefrançais Emma, 507
Legnani Federico, 648
Legrand Margaux, 481
Lehrer Julian, 9
Lei Gangjun, 1109
Lei Pin-Ji, 907
Leibman Rachel, 770
Leibowitz Raya, 136
Leidner Rom, 113, 677
Leidy Sara, 233
Leishman Andrew, 1131
Leiske Chris, 1357
Leistriz-Edwards Del, 86
Leit Silvana, 460
Leitheiser Christopher, 1207, 1388
Leitner Elizabeth, 228
Lekakis Lazaros, 1454
Leleti Manmohan, 801, 854
Lelis Felipe, 63
Lemar Hadia, 381, 902
LeMar Sara, 736
Lemech Charlotte, 743, 744
Lemmens Edward, 1084
Lenehan John, 614
Lenehan Patrick, 1004
Leng Charan, 1344, 1345
Leng Pei-Ju, 251
Leng Yumei, 63
Lenne Nathalie, 814
Lenz Heinz-Josef, 747, 762, 778
Leon Michael, 923
Leonard Jeffrey, 1135
Leonard John, 1206, 403
Leonard Niamh, 1444
Leone Robert, 1119
Leong Jackson, 1389
Leong Meredith, 1084
Leong Renee, 1389
Leonhardt Ralf, 312
Leoni Guido, 706
Leontovich Alexey, 109
LePage Carol, 1078
Le-Rademacher Jennifer, 1244
Lerias Joana, 355, 961
LeRoy Aude, 1339
LeRoy Patrick, 1301
leroy xavier, 1393, 814
Lertkiatmongkol Panida, 1073, 1372
Lesimple Thierry, 734
Lesinski Gregory, 134, 1457, 212, 407, 613, 89
Leslie Isla, 610
Lesniak Jan, 583
Lesniak Maciej, 830
Lesnier Adeline, 481
Lesser Glenn, 492
Letai Anthony, 269
Leto Simonetta, 213
Leuci Valeria, 190
Leung Bonnie, 1268
Leung Cheuk, 568, 590
Leung Irene, 1079
Leung Isabel, 375
Leung John, 1396
Leung Lawrence, 932
Leung Wai-Hang, 1230, 366
Leung Yvonne, 1194
Leuschner Carola, 869
Lev-Ari Shaked, 1303
Levengood Matthew, 1357
Levey Daniel, 470
Levin Max, 1261
Levin Noam, 237
Levin Zurit, 504
Levine Ellis, 547
Levine Lauren, 511
Levisetti Matteo, 1323, 636, 681
Levitan Diane, 544
Levitsky Victor, 615
Levitzki Alexander, 1170
Levy Pierre, 406
Levy Ronald, 1166
Levy Samuel, 7
Levy-Kanfo Limor, 316
Lewin Anne, 1277
Lewis Debbie, 1193
Lewis Karl, 789
Lewis Lionel, 603, 761
Lewis Matthew, 898
Lewis Timothy, 1187
Lewis Zachary, 147, 951
Ley Jessica, 503
Li Ai, 753
Li Aileen, 252
Li Anqi, 1064, 1445, 839, 920
Li Ao, 859
Li Aofei, 818
Li Bailiang, 119
Li Baiyong, 521, 571
Li Bin, 384
Li Bo, 1242
Li Chuck, 229
Li Daming, 1424
Li Dan Jun, 278, 369
Li Daneng, 753, 850
Li Dong, 1225
Li Ella, 1088, 1104
Li Fei, 571
li gerald, 58
Li Guangyuan(Frank), 926
Li Guiling, 725
Li Guoyin, 1358
Li Haiqing, 795
Li Haojia, 61
Li Hao-Kang, 251
Li Henry, 106, 40, 491
Li Housaiyin, 1037, 490, 683
Li Huajiang, 667
Li Jack, 779
Li Jason, 1193
Li Jianying, 943
Li Jianzhuo, 1001
Li Jun, 556
Li June, 838
Li Li, 673

Author index

- Li Lianjie, 576
Li Manqing, 1367
Li Marguerite, 878
Li Mei, 197
Li Min, 1162
Li Ming, 1101, 1183
Li Mingjia, 1249, 437, 442, 82
Li Ning, 384, 652
Li Ou, 1084
Li Peng, 32
Li Qiao, 1140
Li Qi-Jing, 209
Li Qin, 73
Li Robin, 146
Li Roger, 666
Li Ruijiang, 1284
Li Ruitong, 964
Li Ryan, 569
Li Shijie 'Chris', 499
Li Shuai, 1225
Li Shuqiang, 115
Li Si, 209
Li Siyu, 735
Li Stephen, 104
Li Tengeng, 1150, 1397
Li Tianhong, 564, 594
Li Tianzhe, 4
Li Tongqing, 317
Li Tony, 1002
Li Tuanjue, 1284
Li wantong, 943
Li Wei, 1155, 1192, 1320, 1329, 177, 303, 323
Li Wenda, 773
Li Xiaofan, 1103, 1191, 1359
Li Xiaoling, 571
Li Xiao-Qing, 1126
Li Xiaoyan, 260
Li Xin, 1424
Li Xinmin, 1456
Li Xun, 652
Li Yalin, 197
Li Yan, 477
Li Yanyun, 587, 997
Li Yen-Cheng, 496
Li Ying, 1424, 689
Li Yongsheng, 725
Li Yongshuai, 402
Li Yunfang, 1327, 884
Li Yunmin, 398
Li Yunxia, 673
Li Yuping, 457
Li Yuwei, 694
Li Ze-Hua, 295
Li Zhi, 1134
Li Zhiyao, 186
Li Zhiying, 1225, 1226, 1234
Li Zhiyuan, 197, 207
Li Zihai, 1064, 1445, 82, 839, 920, 943
Liadis Nicole, 122
Liang 4Yan, 1458
Liang Colin, 444
Liang Genqing, 253
Liang Jinsheng, 244, 342
Liang Kaijie, 1382
Liang Linda, 1342
Liang Pan, 985
Liang Samantha, 1256, 643
Liang Tingbo, 694
Liang Tingting, 652
Liang Xiaofei, 4
Liang xiaoyan, 254, 361
Liang Xingmei, 694
Liang Yan, 147, 951
Liang Yu, 504
Liang Zhiyong, 32
Liao Angela, 300, 326
Liao Charlene, 747
Liao Chih-Yi, 660
Liao Jay, 19
Liao John, 546, 776
Liao Linda, 545
Liao Rosy, 983
Liao Sida, 182
Liao Yang, 1164
Liaw Kevin, 388
Libbra Chiara, 1093
Liberg David, 145
Licht Anna, 980
Lichtlen Peter, 732
Licican Albert, 1066
Lieb David, 150
Liebner David, 601
Liechty Kirstin, 639
Liedberg Fredrik, 1054
Liefertink Cor, 979
Lien Ming-Yu, 433
Lieu Christopher, 898
Lightcap Eric, 1327, 884
Ligon John, 1383, 1390
Ligon Keith, 896
Ligtenberg Maarten, 979
Lih Tan Sin, 1405
Lila Thomas, 1277
Lillie Thomas, 656
Lillie Tom, 762
Lim Annette, 1259, 676
Lim Chae Lyul, 365
Lim Chae-Lyul, 196, 236, 249
Lim Chun Jye, 867
Lim Ho Yeong, 753
Lim James, 398
Lim Jeffrey, 1288, 1302, 867
Lim Joanna Kristyn, 284
Lim Laura, 181
Lim Sam, 139, 143, 49, 98
Lim Sora, 349
Lim Tony Kiat Hon, 867
Lim Wendell, 410
Lim Xinru, 867
Lim Yi Chieh, 1121
Lim Yoojoo, 1285, 918
Lim Yoong Wearn, 1389
Lim Yu Jin, 873
Lima Sierra, 111
Limasi Valerie, 1418
Lin Danni, 694
Lin Guoxin, 1284
Lin Hanna, 1088, 1104
Lin Han-Nan, 433
Lin Heather, 1387, 310
Lin Jessica, 759
Lin Jia-Ren, 916
Lin John, 851
Lin Liang, 1320, 177, 323
Lin Lillie, 674
Lin Mary, 554
Lin Pei-Yu (Kate), 16, 184
Lin Sharon, 255, 297
Lin Wan-Ying, 1102
Lin Wen Hong, 747
Lin Xinqing, 1248
Lin Xu-Alan, 105
Lin Yang-Liang, 251
Lin Yi, 1454, 639, 689
Lin Yusheng, 995
Lin Ziyang, 910
Linch Mark, 598
Lind Evan, 899
Lind Judith, 1255
Lindberg Eric, 1239
Linder Andreas, 266
Linderhof Lexe, 279, 304
Lindpaintner Klaus, 158
Lindstedt Malin, 102, 35
Linette Gerald, 309
Lingaraj Trupti, 661, 680
Linnemann Carsten, 239, 241
Lione Lucia, 820
Lior Izhar Lior, 200
Lipinsky Maya, 1289
Lippa Blaise, 834
Lippow Shaun, 1194
Lipson Evan, 606, 931
Lischke Timo, 1346
Lisi Steve, 819
Lisbeth Oliva Jacqueline, 1050
Littrell Joshua, 52
Liu An, 1296
Liu Andrea, 332
Liu Arthur, 1116, 1142, 866
Liu Baorui, 1382
Liu Bernard, 1187
Liu Bin, 542, 988
Liu Cailian, 1148, 997
Liu Chang, 952
Liu Cheng, 368
Liu Cindy, 977
Liu David, 150, 916
Liu demi, 491, 950
Liu Dongyan, 1136, 973
Liu Edwin, 229
Liu Eugene, 1081
Liu Fang, 1143
Liu Feng, 726
Liu Guizhong, 753, 773
Liu Haiyan, 673
Liu Haiyun, 1394, 510
Liu Hien, 645
Liu Hong, 452
Liu Hongchuan, 1081
Liu Hongtao, 685
Liu Howard, 79
Liu Hsuan-Chen, 83
Liu Jia, 1126
Liu Jin, 867
Liu Jing, 725
Liu Jingwei, 296
Liu Jonna, 1075
Liu Joyce, 563, 910
Liu Kang, 1437
Liu Ke, 1067, 1337
Liu Lan, 780
Liu Liang, 704
Liu Ligen, 571
Liu Lihong, 571
Liu Linda, 1399
Liu Linying, 160
Liu Lulu, 197
Liu Ning, 117, 923
Liu Patrick, 1091

- Liu Qin, 1307
Liu Qinying, 462
Liu Rachel, 99
Liu Samantha, 1004
Liu Shangtao, 1425, 70
Liu Siyang, 452
Liu Sizhe, 1011, 1146
Liu Song, 929
Liu Sophia, 115
Liu Stephen, 112, 523
Liu Tao, 477
Liu Tianbing, 3
Liu Tongrui, 310
Liu Weiqun, 1084
Liu Wenlong, 1218
Liu Wenting, 1056, 1214
Liu Xikui, 855
Liu Xing, 1226
Liu Xingguo, 458
Liu Xiu-fen, 1218
Liu Yajie, 1424
Liu Yang, 362, 397, 564, 594
Liu Yao-Bin, 1199
Liu Ying, 546
Liu Yingchao, 1401, 426
Liu Yuan, 1091, 969
Liu Yun, 482
Liu YunZhou, 1311
Liu Zhang-Xu, 561
Liu Zheng, 673
Livak Ken, 115
Livingston John, 1042
Livingston Natalie, 256
Lizardo Michael, 1192, 303
Lizee Gregory, 374
Lizée Gregory, 782
Lizotte Patrick, 503
Llosa Nicolas, 711
Lloveras Pauline, 481
Lloyd Jessica, 617
Lloyd Peter, 743, 744
Lo Russo Giuseppe, 91
Lobb Roy, 175
LoBello Janine, 159
Lobo Aurelio, 646, 913
Locatelli Marzia, 1264
Locke Darren, 131, 149
Locke Frederick, 1454, 193, 229, 639, 645, 687
Locke Ken, 315
Lockyer Heather, 101, 59
Lofgren Michael, 219
Loftus Loretta, 645
Logan Diane, 614
Logan Suzanna, 1033
Loghmani Houra, 548, 650
Loh Christina, 104, 49, 98
Loh Lauren, 498
Lombardo Kara, 1385
Lomi Neiwete, 153
London Cheryl, 840
London Max, 1350
Long AO Georgina, 437, 606, 608
Long Jacklyn, 1038
Longworth Aaron, 1007
Lonial, Sagar, 1458
Lonini Luca, 1283
Lontos Konstantinos, 1133, 330, 408
Loo Christopher, 607
Look Thomas, 1093, 640
Loose David, 1417
Lopesco Yael, 316
Lopetegui Lia Nerea, 437
López de Rodas Miguel, 148
Lopez Gabrielle, 1249, 442
Lopez Juanita, 631, 719, 731, 746
Lopez Justine, 1331
Lopez Katrina, 562, 565
Lopez Natalia, 767
Lopez Ozuna Vanessa, 545
Lopez Timothy, 1283
Lopez-Giraldez Francesc, 167
López-Janeiro Álvaro, 1298
lopez-lago miguel, 257
López-Pousa Antonio, 675
Lopez-Ramos Dorys, 122, 976
Loppinet Thomas, 1306
Lorentsen Michael, 437
Lorentzen Torben, 1021
Lorenzato Christelle, 1416
Loriot Yohann, 135
Lorusso Patricia, 626, 748, 759, 770
Losch-Beridon Taryn, 732
Lotem Michal, 136
Loter Lorraine, 304
Lotfi-Emran Sahar, 1027
Lotlikar Shalaka, 988
Lotze Michael, 254, 361, 671
Lou Ge, 673
Lou Rongliang, 1171
Lou Sheila, 232, 252, 340
Loughhead Scott, 224, 321, 638
Louis Thomas, 1287
Lourens Harm, 1205
Lourens Harm Jan, 989, 995
Love Colin, 611
Love J, 1052, 517
Love Ruschelle, 1073, 1372
Low Lionel, 240, 284
Lowe Dana, 753, 773
Lowe Michael, 506, 613
Lowenstein Cassandra, 1360
Low-Kam Cécile, 1300
Lowry Jessica, 1316, 1392
Lowy Israel, 576, 735
Loya Matthew, 987
Loyola Jose, 57
Lozac’hmeur Ariane, 639, 77
Lozano Maria D., 1298
Lu Alexander, 363
Lu An, 227
Lu Ann, 398
Lu Binfeng, 1104
Lu Cailin, 903
Lu Charles, 568
Lu Dan, 259
Lu Han, 64
Lu Hongtao, 1062, 1211, 1401, 426, 793
Lu Jeff, 1101, 1183
Lu Jia, 243, 252
Lu Jiacheng, 694
Lu Jingtao, 1377
Lu Kun-Hui, 471
Lu Lu, 1210
Lu Shuang, 1361
Lu Sumei, 1445
Lu Timothy, 221, 228
Lu Ting, 186
Lu victor, 652
Lu Wei-Chen, 805
Lu Wenqiang, 1211
Lu William, 123, 320
Lu Yang, 749
Lu Yao, 477
Lu Yefeng, 1401, 426, 793
Lu Yi-Hsuan, 496
Lu Yong, 258
Lu Yuefeng, 1101, 1183
Lu Zailian, 1057
Luber Jacob, 1038
Luca Vincent, 1228, 1375
Lucas Aimee, 62
Lucas Anastasia, 1256
Lucas Natalie, 629
Lucey Vanessa, 555
Luche Herve, 1107
Lucia Barreno Lucia, 1120
Ludeña Maria, 702
Ludwig Joseph, 1042
Luecke Stephan, 628
Lueoend Fabiana, 260
Luft Alexander, 635
Luheshi Nadia, 895
Lui Maggie, 1258
Luigi Naldini, 648
Luijten Robbie, 1181
Luiten Rosalie, 88
Luiz Jeanine, 1183
Luiz Jeannie, 1101
Luiz Samantha, 1183
Lukacs Jordan, 792
Luke Jason, 1000, 1280, 588, 605, 661, 713, 721,
732, 754, 772, 845, 908
Luketich James, 179
Lukic Ana, 654
Lukowski Samuel, 312
Lulu Amanda, 399
Lundberg Kristina, 1054
Lundgren Karen, 823
Lundy Joanne, 769
Luning Prak Eline, 1024
Lunn Shannon, 724
Luo Hong, 725
Luo Jiamei, 482
Luo Jingquin, 624
Luo Jun, 571
Luo Peter, 753, 773
Luo Ren, 868, 872
Luo Suxia, 652, 725
Luo Wen, 303, 802
Luo Xiaoyong, 673
Luo Yanping, 335
Luo Yi, 1321
Luong Diamond, 1002
Luong Nga, 1288, 1302
Lupo Kyle, 319
Lurain Kathryn, 437
Luri Carlos, 982
Luri-Rey Carlos, 267
Luster Andrew, 441
Lustig Kurt, 1341, 425
Luther Alexandra, 182
Lutz Emi, 1023
Lutz Robert, 1184
Lutzky Jose, 787
Luu Irene, 361
Luu Thuy, 1396
Luus Lia, 1340, 834
Lv Dongqing, 725
Lv Xiaocheng, 1057, 1075
Lv Xiaodong, 457

Author index

- Ly Natasha, 369
Lybaert Willem, 675
Lycan Thomas, 919
Lyden David, 984
Lyle John, 146, 692
Lyman Gary, 1244
Lyman Jaclyn, 656
Lyman Michael, 1362, 1363
Lynam Reena, 636, 681
Lynch Conor, 286
Lynch Kelsey, 375
Lynch Kevin, 1444
Lynch Michael, 295, 315
Lyngby Rasmus, 139, 143
Lynn Erica, 674
Lynn Geoffrey, 364
Lynn Rachel, 243
Lynn Rachel C., 232
Lyon Robert, 1186
Lythgoe Mark, 427, 627
Lyu Haoxiang, 115
- M Naveen Sadhu, 1376, 1386
M Oliyarasi, 142
M Rajashekar, 142
Ma Anjun, 943
Ma Anna, 558
Ma Brigitte, 750
Ma Chi, 1019
Ma Dangshe, 1415
Ma Dennis, 1007
Ma Hong, 432
Ma Honglian, 698
Ma hu, 18
Ma Hua, 635
Ma Jinyan, 311
Ma Leyuan, 317
Ma Lichun, 1019
Ma Lina, 1123, 1325, 1326
Ma Ning, 120
Ma Qin, 1064, 839, 943
Ma Siming, 1309, 1383
Ma Tao, 694
Ma Vincent, 172, 34, 705
Ma Wen, 636
Ma Yan, 123
Ma Zhengyu, 383
Maack Eden, 934
Maaske André, 434
Mabry Robert, 1222
Macarron Ricardo, 1199
Macarulla Teresa, 552
MacBeath Gavin, 182, 389
Maccalli Cristina, 1430, 411
MacDermaid Chris, 778
MacDermaid Christopher, 470, 941
MacDonald Gerry, 812
MacDonald Kyle, 261
MacDonald Lisa, 646, 913
Mace Emily, 1012
Mace Joshua, 242
Mace Thomas, 1457
Macfarlane Lindsey, 1260
MacFawn Ian, 1451
MacGregor Heather, 201, 261, 294
Machado Almeida Pedro, 842, 85
Machado Daniel, 1215
Machajewski Timothy, 1352
Machiels Jean-Pascal, 676, 678, 734, 741, 770
Machold Klaus, 655
- Mackall Crystal, 352, 362, 397
MacKay Abi, 628
Mackert Jessica, 178, 492
Maclean Kirsteen, 60
Macleod Dan, 292
MacMillan Hugh, 1035
MacPherson Kevin, 899
Macpherson Michelle, 139, 143, 60
Madabhushi Anant, 61, 73
Madakamutil Loui, 354
Madala Hanumantha Rao, 841
Maddock Stephen, 555, 656
Maderna Andreas, 1191
Madhavan Subha, 1303
Madlensky Lisa, 67
Madonna Gabriele, 842
Madsen Daniel, 138
Madsen Daniel Hargboel, 1464
Maecker Holden, 362, 397
Ma-Edmonds Manling, 987
Maeng Hoyoung, 557
Maeurer Markus, 355, 961
Maffezzoli Michele, 91
Magalhaes-Silverma Margarida, 685
Maganti Swetha, 1030
Magen Assaf, 541, 543, 576, 690
Magistrelli Giovanni, 481, 853
Magnon Grant, 1451
Magowan Colin, 1352
Magre Luc, 1181
Mah In Kyoung, 1219
Mahadevan Daruka, 778
Mahajan Nitin, 195
Mahalingam Devalingam, 553, 850
Mahaz Kayani, 598
Mahdi Haider, 61
Maher Colleen, 1297
Maheshri Narendra, 242
Maheshwari Atul, 1001
Maheshwari Shamoni, 174
Mahipal Amit, 660, 689
Mahmoud Ahmed, 140
Mahmud Hasan, 253
Mahoney Doug, 852
Mai Juntao (Matt), 1196
Maia Ana, 641, 642
Maia Andreia, 355, 961
Maizarana Jimmy, 935
Maiorano Gabriele, 1375
Mairesse Maelle, 720
Maithel Shishir, 134, 1457
Maitra Arindam, 955
Majeed Sophia, 758
Majercak John, 1379, 817
Majocchi Sara, 853
MAJUMDER ADITI, 356
Majumder Partha, 955
Majzner Robbie, 352
Mak Katina, 1185
Makhanov Mikhail, 3
Makowsky Mallory, 591
Malchiodi Zoe, 1452
Maldonado Lopez Angel, 1153
Malek Karim, 661, 680
Maleki Saman, 1028, 464, 614
Malhotra Deepali, 469
Malhotra Kanam, 485, 856
Malhotra Ritu, 142
Malinee Madhu, 952
Malinga Nonkululeko Z., 84
- Malinge Pauline, 481, 853
Malissen Bernard, 1107
Malka Jessica, 645
Malkoun Richard, 701
Mallardo Domenico, 21
Mallardo Mario, 21
Mallon Emma, 1046
Mallow Crystal, 613
Malmberg Karl-Johan, 341
Malo Julie, 1300
Maloney David, 229, 263, 639, 77
Maloney Michael, 321
Malu Shruti, 1332
Mamdani Hirva, 699
Mamindla Priyadarshini, 1280
Mammadova Najiba, 47, 48
Mamonkin Maksim, 341
Manakongtreecheep Kasidet, 1242, 1257, 441
Manalo Julia, 1458
Manax Victoria, 1089
Mandelboim Ofer, 474
Mandeli John, 629
Mandl Stefania, 123, 320, 712
Mandula J, 944
Mandula Jessica, 1420
Manfredi Francesco, 268
Mangani Davide, 514, 964
Mangarin Levi, 1148, 904
Mangla Ankit, 437
Manguso Robert, 1365
Manickam Vishal, 1389
Maniyar Rachana, 843
Manjunath Yogendra, 1391
Manlusoc Marigold, 1215
Mann Karen, 882
Manna Edward, 52
Manning Luisa, 566
Manning-Bog Amy, 1194
Manriquez Roman Claudia, 324
Manry Diane, 263
Mansfield James, 117, 118, 139, 143, 60, 85
Manso Luis, 548
Mansour Mena, 503
Mansurov Aslan, 1227
Mao Hai-Quan, 256
Mao John, 1171
Mao Linlin, 105
Mao Rui, 206
Mao Shu, 1415
Mao Shuang, 417
Mapes Brandon, 1283
Mar Nataliya, 1247
Marabelle Aurelien, 544, 716
Marabelle Aurélien, 135
Marappan Sivapriya, 1313
Marasco Wayne, 295
Marathe Himangi, 929
Marathi Upendra, 603
Marchiano Emily, 19
Marcinek Anetta, 281
Marco-Sanz Javier, 836
Marcucci Guido, 795
Marczak Ryan, 52
Marder Sandra, 485
Mardiros Armen, 229, 263, 639, 77
Mardis Elaine, 1135, 881
Margineanu Anca, 1239
Margolin Gregori, 942, 974, 998
Margolin Kim, 1456, 767, 778
Margossian Steven, 636, 681

- Marguet Philippe, 1194
Marhefke Nathan, 187
Mariathasan Sanjeev, 475
Marie-Cardine Anne, 1339
Marinheiro Bernardo, 355, 961
Marino Fabio, 312
Mariño Karina V., 267
Marjanovic Nemanja, 964
Marjoncu Dennis, 233
Mark-Adjeli Princess, 637
Markham Merry-Jennifer, 564
Markiewicz Mary, 1109
Markman Janet, 737
Markov Spas, 326
Markovic Svetomir, 109, 785
Markovits Etti, 1289, 1290, 1299
Markowitz Geoffrey, 965
Markowitz Joseph, 609
Markson Samuel, 1038
Marleau Annette, 1089
Marques Marilyn, 264
Marr Alissa, 1245
Marrache Sean, 924
Marritt Kayla, 1156
Maron Thomas, 437, 541, 543, 576, 595, 629,
688, 690, 692, 693, 708, 767
Marshal Nicholas, 500
Marsiglio John, 1251, 44
Marszalek Joseph, 831
Marte Jennifer, 695, 766
Martell Robert, 20, 761
Martens Uwe, 650
Martin Aaron, 229
Martin Alex, 761
Martin Alexander, 20
Martin Amber, 321
Martín Carlos, 1072
Martin Christopher, 728
Martin Gaele, 144
Martin Hannah, 1127
Martin John, 108
Martin Justin, 617
Martin Kea, 1080
Martin Laura, 1117
Martin Mitchell, 965
Martin Philip, 708
Martin Rebecca, 1379, 817
Martin Shamra, 1352
Martin Virginie, 701
Martin William, 100
Martincic Danko, 665
Martincuks Antons, 910
Martinaite Evelina, 1182, 1440
Martinez Daniel, 1189
Martinez Desirae, 1379
Martinez Francisco, 288, 304
Martinez- Gili Luara, 614
Martinez Kodi, 689
Martinez Planes Elena, 357
Martinez Rowena, 232, 243, 252
Martinez Stephanie, 701
Martinez-Morilla Sandra, 127
Martin-Jeantet Perrine, 144
Martin-Liberal Juan, 706, 784
Martins Renato, 19
Martire Sara, 229
Martz Ashley, 739
Marubayashi Sachie, 854
Mary caroline, 1366, 484
Marzano Marinella, 486
Masabanda Julio, 10
Masakayan Reed, 322, 358, 372
Mashru Sandeep, 705
Masi Giulia, 312, 343
Masia Ricard, 1082
Masikat Mary Rose, 1359
Maslyar Daniel, 114
Mason Charlotte, 1228, 1375
Mason David, 85
Mason James, 562, 565
Masopust David, 1027
Masrourpour Fatemeh, 869
Massa Annamaria, 190
Massa Chiara, 1144
Massafra Raffaella, 1281
Massey Christopher, 870
Master Viraj, 478, 848
Masternak Krzysztof, 481, 853
Masters Gregg, 1208, 987
Mastrian Steve, 159
Matar Sittana, 494
Matasci Mattia, 1093
Matei Irina, 984
Mathe Doriane, 1179
Mathers Nicholas, 45
Mathew Grace, 542
Mathew Pretty, 227
Mathew Rebecca, 1365, 1430
Mathews Cara, 670
Mathias Melissa, 735
Mathijssen Ron, 88
Matho Michael, 1089
Mathur Siddhartha Krishan, 544
Mathyer Mary, 195
Matich Erica, 1111
Matis Louis, 1060
Matkowskyj Kristina, 981
Matos-Cruz Vanessa, 1291
Matosevic Sandro, 1018, 214, 298, 319
Matoso Andres, 1385
Matsubara Nobuaki, 663
Matsuda Atsushi, 1153
Matsumoto Noriko, 1364
Matsumura Haruka, 1364
Mattaar Ellen, 495
Matthews Sydney, 736
Mattie Mike, 1454, 193, 301
Matulonis Ursula, 563, 910
Maués Julia, 993
Maughan Benjamin, 664
Mauldin Ileana, 11
Maurer Barbara, 1059
Maurer Deena, 596, 656
Maurer Dominik, 1319
Mauro David, 605
Mauro Florencia, 877
Maus Marcela, 269, 301, 639
Maus Rachel, 109
Mavroukakis Sharon, 55, 637
Maxey Jessica, 1292
Maxwell John, 444
Maxwell Melissa, 1402, 1431, 493, 537
mayall Tim, 275
Mayer Aaron, 118, 559
Mayer Julia, 1059
Mayes Erin, 1342
Mayes Patrick, 1199, 1210, 723
Mayhew Zachary, 1443
Maynard Rachael, 1012
Mazières Julien, 701
Mazor Yariv, 461, 469
Mazrimas Sara, 400
Mazzarella Luca, 1264
Mazzaschi Giulia, 91
Mazzoleni Stefania, 648
Mbofung Rina, 341
McAdams Meredith, 438
McAdory John, 666
McAlister Sean, 1078
McArthur Heather, 1144
McBride Kevin, 542, 590, 988
McCachren Samuel, 1458
McCaigne Joanne, 728
McCallen Justin, 1019
McCallum Robin, 685
McCann Mondona, 344
McCarren Patrick, 444
McCarter Martin, 1147, 1279, 1311, 54
McCarthy Elizabeth, 1002
McCarthy James, 1446
McCarthy Tom, 1131, 1324
McClintock Greta, 478
McCloskey Megan, 1193
McClymont Karen, 131
McCormick Laura, 500
McCoy Ann, 637
McCoy Gabrielle, 689
McCreedy Bruce, 1237, 393
McCreery Chloe, 1052
McCurry Dustin, 1000
McDaniel Lee, 119
McDermott David, 489, 556
McDevitt Jennifer, 332
McDonald Marisa, 1137
McDonnell Glenna, 5
McDonnell Kevin, 1207, 1340, 1356, 1388, 980
McDonnell Mollie, 1230
McDonough Alexandra, 1136
McEachin Katelynn, 1348
Mcelvain Michele, 229
McElvaney Teresa, 1155
McEwan Lisa, 1396
McFarland Jesse, 953, 954
McGarvey Peter, 1303
McGee Heather M., 508
McGeehan Andrew, 1359
McGettigan Melissa, 672
McGinnis Lisa, 475
McGrail Daniel, 1309, 1383, 782
McGraw Timothy, 965
Mcgregor Bradley, 742
McGregor Kimberly, 59
Mcguckin Charlotte, 932
McGuire John, 1254, 1257, 441
McGuire Kathleen, 1124, 1365
McHugh Claire, 123, 320
McIlwain Sean, 45
McInnis Christine, 1404, 86
McIntyre Brendan, 1189
McKay Rana, 437, 668
McKean Meredith, 1173, 661, 705, 738, 767, 780
McKee Thomas, 1275
McKeever Joshua, 983
McKinlay Colin, 1084
McKinley Jessica, 760
McKinnon Karen, 560
McLane Michael, 160
McLaren Alistair, 1173
McLean Benjamin, 1455
McLean Luke, 1259

Author index

- McLeroy Jeffrey, 776
McMahon Carrie, 1219
McMahon Frank, 59
McMahon Jerry, 1373
McMahon Tracey, 1121
McMillan Brian, 444
McMullen Timothy, 1007
McNally Krista, 223
McNeel Douglas, 271, 473, 870, 893
McPherson Alex, 1310
McPherson Jordan, 1251
McWilliams Robert, 785
Meaddough Erika, 203, 247
Meagher Craig, 1415
Medico Enzo, 213
Medina Carlos, 44
Medina Elliot, 1375
Medina Theresa, 787, 789
Medioni Jacques, 707
Medvedev Dmitry, 57
Medvedev Sergey, 885
Meehan Robert, 767
Meehl Michael, 945
Meehl Michaela, 231
Meerten Tom, 995
Meesters Niels, 199
Meetze Kristan, 1061, 1395
Meghwal Diksha, 1282
Mehdi Ahmed, 118
Mehra Navi, 47, 48
Mehra Siddharth, 1224
Mehran Reza, 1050
Mehrotra Shikhar, 407
Mehta Amit, 259, 276, 304
Mehta Arnav, 150, 916
Mehta Kritika, 743
Mehta Ranna, 1342
Mei Jay, 1150, 1397, 482, 76
Mei Shenglin, 879
Meier Samuel, 444, 70
Meier Stefanie, 587
Meijer Menno, 215
Meisel Marlies, 1310
Meitei Heikrujam Thoihen, 1014
Mejia Oneto Jose, 953, 954
Mejias Joscelyn, 876
Mejun Nuthchaya, 33
Mele Deanna, 1405
Mele Fabio, 1281
Melero Ignacio, 1298, 267, 844, 982
Meleza Cesar, 854
Melhem Ramzi, 779
Melief Cornelis, 1181
Melief Sara, 215
Melik-Andreasyan Marina, 423
Meliksetyan Karen, 423
Mellinger Staci, 646
Mellman Ira, 1276, 475
Mello Marielle, 1107
Melms Johannes, 830
Melotti Barbara, 800
Memmott Regan, 1249
Memon Danish, 522
Menchel Brett, 194, 318
Mender Ilgen, 892, 906
Mendez-Gomez Hector, 1383, 1390
Mendonca Mark, 265
Mendoza Valderrey Alberto, 1456
Meng Raymond, 475
Meng Ryan, 113
Meng Wenzhao, 1024
Meng Yuan, 1151
Menges Meghan, 193
Meniawy Tarek, 734, 768
Menon-Singh Lakshmi, 445
Menter Alexander, 937
Mentrasti Giulia, 91
Mentzer Michaela, 834
Menzies Alexander, 437
Meoded Roy, 1080
Merad Miriam, 541, 543, 576, 595, 629, 688, 690
Merazga Zohra, 1323
Mercadal Margaux, 701
Merchant Akil, 103
Merchant Fahar, 743, 744
Merchant Melinda, 362, 397
Merchant Nina, 743, 744
Merchant Nipun, 1224
Mercogliano Maria, 877
Mercuri Francesca, 1164
Meredith Rhonda, 147
Merghoub Taha, 1148, 218, 347, 791, 843, 903, 904, 997
Merieu Emmanuel, 484
Meritet Nicole, 81
Merkler Doron, 1275
Merone Rossella, 706
Merrell Angela, 569
Merrigan Samantha, 1153
Meschi Francesca, 95
Mesko Paul, 1083
Messaadene Meriem, 1306, 614
Messersmith Wells, 727, 898
Messier Cameron, 329, 503
Messina Jane, 617
Messinger Joshua, 1216, 1362
Met Özcan, 1233, 343
Metcalf Robert, 675
Metovic Jasna, 317
Mettetal Jerome, 1115
Meuter Leah, 448
Mevorach Dror, 1380
Meyer Adam, 242
Meyer Christina, 945
Meyer Pieter, 84, 97
Meyer Thomas, 405
Meyer Tim, 850
Meza Luis, 810, 880
Meza Miguel, 204, 288
Miao Benchun, 150, 916
Miao Eric, 1015
Miao Shichang, 499
Miao Shichiang, 769
Miao Xiaoni, 1321
Miao Zhenhua, 499
Micarelli Elisa, 706
Micciché Arianna, 245
Michael Christina, 108
Michaelson Jennifer, 1061, 1395
Michalski Joel, 742
Michaud William, 150
Michel Robert, 1173
Michel Sven, 434
Michelet Xavier, 322, 358, 372, 470, 649
Michels Judith, 903
Michels Kathryn, 1230
Michelson Glenn, 750
Michor Franziska, 362, 397
Middendorp Sabine, 215
Middleton Mark, 610, 611, 745
Mie Motoya, 1221
Mignault Andre, 444
Mignot Jonathan, 78
Mihalek Robert, 429
Mikkelsen Tarjei, 332
Miklos David, 1454, 639, 687
Mikolajewicz Nick, 852
Milani Pamela, 146
Milberg Oleg, 767
Mildenberger Iris, 641, 642
Milella Martina, 1281
Miles David, 762
Miles Dillon, 801
Milhem Mohammed, 1265, 610, 611
Millar Quinn Hillary, 262
Millard Daniel, 380
Miller Andrew, 1167
Miller Caitlyn, 1166
Miller Caroline, 461
Miller David, 1324
Miller Elizabeth, 576, 688
Miller Erin, 324
Miller James, 324
Miller Jason, 1155, 1200
Miller Jeffrey, 1202, 1204, 288, 465, 724
Miller Katherine, 1135
Miller Kathy, 770
Miller Martin, 522
Miller Michele, 1213
Miller Sarah, 465
Miller Shannon, 1168
Miller Wilson, 614
Millerchip Karen, 838
Miller-Moslin Karen, 606
Millrud Camilla, 145
Millward Michael, 577
Milne Gavin, 1324
Milner Rowan, 1390
Milo Jay, 71
Milone Michael, 395
Milowsky Matthew, 560
Min Bokyoung, 306
Min Chengyin, 1425, 1449, 444, 70
Min Jing, 521
Minchella Ida, 1264
Minev Boris, 1137
Minev Ivelina, 1137
Ming Qianqian, 1228
Minghwa Liang Ben, 820
Minn Andy, 644
Minna John, 523, 891
Minns Danielle, 1353
Mino-Kenudson Mari, 1254, 1463, 956
Minter Ralph, 1353
Miranda Miguel, 581
Miranda Noel, 1053
Miranda-Katz Tomas, 1215
Mirazee Justin, 327, 401
Mirenda Michela, 337
Mirji Gauri, 1307
Mirkina Irina, 1059
Miselis Nathan, 638
Mishima Yuji, 1364
Mishra Aditya, 590, 618
Mishra Kaushal, 606
Miska Jason, 830
Missel Sarah, 1319
Mistry Akshitkumar, 111
Mistry Hitesh, 1293
Mita Alain, 623, 759

Mita Monica, 623, 759
Mitchell Alan, 158
Mitchell Duane, 1111, 1383, 1390
Mitchell Jennifer, 1379
Mitiku Selome, 353
Mitra Abhisek, 835
Mitra Ankita, 1040
Mitra Shirsajit, 90
Mitsiades Constantine, 1006
Mittag Diana, 883
Mittal Arjun, 845
Mittal Vivek, 965
Mittelsteadt Kristen, 366, 375
Mittra Arjun, 437
Miyahara Yoshihiro, 121
Miyashita-Lin Emily, 1065
Miyazaki Takahiro, 1086
Mizrahi Rena, 1389
Mo Clifton, 647
Mobley Bret, 111
Mock Jacqueline, 900
Mody Kabir, 646
Mody Kinjal, 767
Moffat Jason, 852
Moffett Howell, 185
Mog Brian, 1197
Mognol Giuliana, 7
Mohamed Ahmed, 140
Mohamed Eslam, 1420, 944
Mohamed Toufiq, 411
MohamedKhan Shybi, 719
Mohamoud Yusuf, 172, 34
Mohan James, 1338
Mohan Suruchi, 411
Mohan Sunish, 1219
Mohindra Rajat, 1274
Mohr Peter, 608
Mohrdieck Nicholas, 373
Mohrs Markus, 851
Moine Valery, 481
Moine Valéry, 853
Moisan Jacques, 1316, 1337, 497
Moiset Gemma, 299
Mojadidi Michelle, 282
Mojica Kara, 1342
Mok Lydia, 9
Mokhtari Ali, 613
Mokhtari Mojgan, 61
Molden Nandini, 475
Moles Michael, 1235
Molgora Martina, 833
Molina Elsa, 1124
Molina Julian, 229, 263, 639, 77
Molloy Michael, 761
Molodtsov Aleksey, 834
Moloudizargari Milad, 1141
Momin Noor, 1052, 1087
Momose Fumiyasu, 359
Monberg Tine, 715
Mondal Arpita, 1210
Monette Anne, 508, 9
Monette Sébastien, 1148
Monge Cecilia, 419
Moniz Raymond, 1323, 636, 681
Monjazebe Arta, 520, 534
Monk Bradley, 566
Monkman James, 117, 118, 120, 923
Monroy Isabel, 305, 368, 847
Monson Jedidiah Mercer, 819
Montalto Michael, 1282
Montalto Mike, 1277
Montalvo Melisa, 402
Montane Heather, 785
Monteiro Natalie, 131, 149
Monteleone Dennis, 1352
Montesion Meagan, 29, 584
Montler Ryan, 409
Montoya Amanda, 227
Montuenga Luis, 1298
Monument Michael, 1130, 1156, 1159
Monville Florence, 701
Mony Jyothi, 12
Moody Gordon, 339, 469
Moogk Duane, 261
Moon Dain, 837
Moon Jun-Hwan, 1343
Moon Yong, 886
Mooney Rachael, 1137
Mooradian Meghan, 1253, 696
Moore Alex, 1025
Moore Chris, 1379, 736, 764, 817
Moore Finola, 264
Moore Gregory, 1073, 1372
Moore Jonni, 555, 559
Moore Kathleen, 670
Moore Mark, 1225, 1226, 1234
Moore Raymond, 109
Moore Samantha, 1349
Moore Tamson, 403
Moosman Philipp, 1080
Moot Robby, 332
Moot Robert, 123
Moquin Deanna, 71
Moquist Phillip, 1357
Morales-Espinosa Daniela, 746
Moran-Segura Carlos, 1420, 944
Morawski Aaron, 739, 748
Mordecai Scott, 313
Moreira Dayson, 1191, 810, 880
Morelli Maria Pia, 229, 263, 637, 639, 77
morello Aureo, 1366, 826
Moreno Amy, 568
Moreno Henry, 264
Moreno Victor, 589, 770
Moreno-Gonzalez Alicia, 702
Moreo Lapieza Eduardo, 1072
Moretti Marco, 91
Morgan Duncan, 1023, 1052, 517
Morgan Martin, 929
Morgensztern Daniel, 589
Morgese Francesca, 91
Mori Kameron, 483
Moriarity Branden, 392
Morin Benjamin, 651
Morin Bret, 306
Morin Michael, 823
Moros Spencer, 265
Morris Ben, 979
Morris Jessica, 412
Morris Luc, 503
Morris Nick, 409
Morris Stefanie, 523
Morris Tom, 455
Morris Van, 713
Morris Zachary, 1051, 862, 874
Morrison Robert, 605
Morriss Julia, 115
Morrow Brittany, 472, 831
Morrow Matthew, 555
Morrow Michelle, 1069
Morsch Rachel, 1155
Morse Barry, 265
Morse Michael, 437
Mortazavi Amir, 82
Mortensen Franziska, 1210
Mortier Laurent, 604
Mortini Pietro, 648
Morton Cienne, 719
Morvan Maelig, 221
Moseman Jena, 473
Moser Justin, 180, 430, 638, 778
Moses Jake, 409
Moshier Erin, 595
Moshyk Andriy, 430
Moskowitz Mor, 136
Moskowitz Darrian, 322, 372, 649
Moss Kara, 760
Moss Rebecca, 608
Mota Ines, 317
Mott Frank, 568
Motzer Robert, 556, 742
Mouchemore Kellie, 1164
Moudgil Tarsem, 113, 409, 5
Mouhieddine Tarek, 437
Moussa Marwan, 1110
Mouton Julie, 631
Moxon Nicole, 646
Moyes Kara, 1185
Moynihan James, 461
Moynihan Kelly, 1083, 1092
Mpekris Fotios, 108
Mrowiec Thomas, 554
Mu Liang, 1365
Muanza Thierry, 1300
Muchamuel Tony, 422
Muchhal Umesh, 1079
Mudd Gemma, 1340
Muehleisen Hannes, 653, 722
Mueller Amy, 483, 945
Mueller Daniel W., 578
Mueller Scott, 118
Mueller Steffen, 1139
Muhsen Ibrahim, 480
Muik Alexander, 1070, 1208
Muiru Gladys, 1066
Mukherjee Arnab, 485, 856
Mukherjee Pritam, 1296
Mukherjee Sarbajit, 534
Mukherjee Subhendu, 1313
Mukherjee Sudip, 1094
Mukhi Shivani, 713
Mukhopadhyay Anandaroop, 1427, 592
Mule James, 609, 912
Mulgrew Kathy, 461, 469, 895
Mulhern Barb, 1244
Muller Carolyn, 759
Muller Soren, 1450
Müller Sören, 435
Müller Thomas, 623
Mullett Steven, 1310
Mullish Benjamin, 614, 627
Mumford Ben, 217
Munn David, 1420
Munn Lance, 1295
Muñoz Manuel, 1352
Munshi Neru, 700
Munshi Nikhil, 1220, 812
Muntwiler Simone, 1293
Muntzer Alice, 1223, 208
Murad John, 360

Author index

- Muralidhar Anusha, 893
Muralidharan Sujatha, 238
Muramatsu Tomoaki, 616
Murano Aubrey, 721
Murer Patrizia, 1099
Murphy Ann, 728
Murphy Briana, 483
Murphy John, 454
Murphy Sarah, 99
Murphy Susan, 855
Murphy William, 1008, 1127, 272, 520, 534
Murray Clare, 1428, 453, 501
Murray Evan, 115
Murray Kristen, 182
Murt Megan, 232
Murter Benjamin, 1020, 1041
Murthy Pranav, 254, 361
Murty Tara, 362, 397
Murugesan Karthikeyan, 58
Mushtak Komal, 1260
Musial Shawn, 1032
Musial Thomas, 361
Muskat Kai, 1326
Mustjoki Satu, 1006
Muth Amelie, 897
Muthuswamy Ravikumar, 894
Mutlu Yasa, 179
Muzaffar Farzonai, 183
Myers Jeffrey, 1462, 568, 917
Myers Jeremy, 1060
Myers Matthew, 1342
Myint Han, 739, 748
Mylavarapu Charisma, 480
Myojin Yuta, 1019, 419
Myrthil Nadia, 748
Myung Lee Hong, 1153
- N R Raghavendra, 1313
Na Hye Young, 488
Näätänen Anna, 1006
Nabar Namita, 129
Nabell Lisle, 675
Nabet Barzin, 435, 475, 523, 584
Nabhan Chadi, 112
Nabisi Nancy, 389
Nadal Lisa, 1093
Nader Noor, 973
Nadler Eric, 454
NAFIA Imane, 1426, 814
Nagata Denise, 1215
Nager Andrew, 1367
Nagy Mate, 1294, 1446, 89
Naidoo Jarushka, 1244
Naika Gajendra, 498
Naiman Brian, 469
Naiman Zachary, 855
Naing Aung, 657, 747
Nair Pradip, 1368
Nair Praveen, 449
Nair Reshmi, 1368
Naitmazi Lawrence, 228
Najburg Valérie, 1315
Najdawi Fedaa, 552
Najjar Amer, 400
Najjar Yana, 1000, 508, 588, 605, 721
Nakai Takashi, 359
Nakajima Kanto, 1364
Nakamura Koji, 901
Nakamura Norihiro, 1221, 1364
Nakayama John, 361, 671
- Nakazawa Taisuke, 1187
Nakhaei Peyman, 445
Nalbandian Ruppen, 339
Naldini Matteo Maria, 648
Nalle Sam, 114
Nam Andy, 951
Nam Daeun, 223
Nam Dong Hyun, 1067
Namini Hamid, 728
Nampe Daniel, 229
Nandakumar Srinand, 671
Napoli Marco, 882
Naqash Abdul Rafah, 437
Naqash Rafah, 112
Naradikian Martin, 263
Narasappa Nell Namitha, 361
Narayan Vivek, 668
Narayanan Babu, 531, 922
Nardin Alessandra, 292
Nardozi Joanathan, 1098
Nareddy Pradeep, 854
Nash Amanda, 1094, 1095, 363
Nasir Apsra, 1012
Naso Michael, 262, 265
Nasoff Marc, 1123, 1325, 1326
Nasrallah Mazen, 1242, 1257, 441
Nassar Amin, 437
Nassif Elise, 542, 590, 618
Nastri Horacio, 1210
Natale Christopher, 759
Natanael Hazel, 514
Nater Jenny, 301
Nath Sangeeta, 1084
Nathenson Michael, 601
Naumovski Allison, 738
Navai Shoba, 412
Nava-Parada Pilar, 729, 746
Navarrete-Galvan Lydia, 736
Navarro Belén, 1144
Navarro Fabio, 119, 146
Navarro Manzano Esther, 1144
Navas Christopher, 232
Naveen Mehta, 1061, 1395
Navert Robert, 1326
Navin Ishwar, 328, 394, 413
Navin Nicholas, 1001
Nawas Zeid, 412
nayak anupma, 644
Nayak Saparya, 123
Nayar Ribhu, 182
Nayler Simon, 97
Naylor Alan, 1324
Nazarenko Natalya, 1186, 1190, 731
Nazha Bassel, 478
Ncembu Sikozile, 1369
Nduom Edjah, 1033
Neal Joel, 930
Nebhan Caroline, 112, 437
Necchi Andrea, 663
Nederby Line, 1013, 524
Needels Michael, 1097
Neelapu Sattva, 1454, 296
Neely Jaclyn, 574
Neeson Paul, 1442, 385
Neff-LaFord Haley, 1357
Neighbors Katie, 1359
Neilan Thomas, 1254
Neilan Tomas, 696
Nejo Takahide, 80
Nellore Kavitha, 1313
- Nelson Andrew, 1446
Nelson Kinsey, 1124
Nelson Megan, 739, 748
Nelson Peter, 308
Nelson Trygve, 1204
Nemunaitis John, 566
Nenclares Pablo, 610
Neri Dario, 1074, 1093, 640, 900
Neskey David, 1044, 89
Nesline Mary, 15, 152, 173
Nesmith Ken, 918
Nesterova Albina, 1187
Netto Frederico, 1462
Neuharth Forrest, 1137
Neuhoefer Patrick, 1166
Neumann Theresa, 1346, 1347
Neuzil Jiri, 448
Neves Aitana, 1275
Nevin James, 964
Newcomer Kathleen, 964
Newell Evan, 1035, 1045, 110, 94
Newman Jenna, 364
Newman Matthew, 899
Newman Ryan, 1094
Newman Walter, 1141
Newsom-Davis Thomas, 512
Newsome Rachel, 1309
Newton Michael, 862
Neyns Bart, 790
Ng Calvin S H, 702
Ng Chee Hoe, 240
Ng David, 997
Ng Dean, 1215
Ng Eric, 229, 263, 639, 77
Ng Juliana Chi Kei, 1016
Ng Kevin, 509
Ng Palace Shirley, 1276
Ngai Hoi, 1137
Nghiem Paul, 1045, 50, 604, 992
Ngo Tran, 913
NGOUALA Oren, 1426
Nguyen Alan, 1359
Nguyen Annie, 363
Nguyen Anton, 277
Nguyen Beverly, 260
Nguyen Diana, 123
Nguyen Duong, 1137, 1394
Nguyen Duy, 1229, 1348, 210
Nguyen Evelyn, 915
Nguyen Helen, 515, 876
Nguyen Henry, 1083
NGUYEN HONG-MY, 1370
Nguyen Hue, 1371
Nguyen Kim, 1465, 882, 967
Nguyen Linh, 378, 750
Nguyen Michelle, 332
Nguyen Nga, 1268
Nguyen Phuoc Quang Huy, 871
Nguyen Phuong, 348, 855
Nguyen Quang-De, 295
Nguyen Quynh, 869
Nguyen Quynhanh, 1047
Nguyen Y-Van, 513, 533
Ni Irene, 1083, 1092
Ni Min, 576
Nicastri Daniel, 629
Nicholls Joanna, 850
Nichols Kelly, 1332
Nicholson Benjamin, 841
Nicolai Chris, 1230, 366

Nicolaides Nicolas, 1432
Nicolaisen Berit, 669
Nicolescu Chris, 823
Nicolò' Eleonora, 1264
Nie Siwei, 1377
Niedecken Ariel, 1389
Niedermann Gabriele, 868, 872
Niederst Matthew, 260
Niedzielska Magda, 358
Niehoff Nicole, 430
Nielsen Dorte, 138
Nielsen Megan, 874
Nielsen Tyler, 101, 59
Nieman Linda, 1242, 956
Nievera Christian, 151
Nika Anastasia, 1324
Nikiforow Sarah, 639, 812
Nikitin Pavel, 823
Nikmaneshi Mohammad, 1295
Nikolic Jovan, 1003
Nikota Jake, 387, 404
Nilsson Johan, 102
Nilsson Ola, 654
Nimeiri Halla, 1403
Ning Franklin, 405
Ning Mei, 1441
Ning Yuhong, 7
Ninkov Marina, 614
Nip Lisa, 182
Nippgen Johannes, 597
Nirschl Christopher, 1096
Nirschl Thomas, 1119
Nisha Joseph, 1458
Nishimoto Kevin, 198, 203, 246, 247
Nishimura Toshinobu, 262
Nishino Mizuki, 528
Nishri Yossi, 428
Nissen Neel, 1422, 23
Nisthal Alex, 1372
Nistor Gabriel, 562, 565
Nitya-Nootan Thanyashanthi, 201, 294
Niu Congrong, 1219
Niu Jiaxin, 610, 611, 682, 684
Niu Shuhuai, 452
Niu Xiaofeng, 1062, 1211, 426, 793
Niu Yanling, 1151
Nixdorf Daniel, 266, 281
Nixon Andrew, 1244, 699
Nobuyuki Ide, 598
Noel Marcus, 850
Noelle Randolph, 761
Noff Maya, 200
Noi-Ka Fung, 1138, 311
Nolin Jess, 1348
Nomaru Hiroko, 125
Nonato Taylor, 437
Nooka Ajay, 1458
Noon Jason, 477
Noordam Lisanne, 1181
Noordam Lissane, 883
Nord Matthew, 449
Nordquist Luke, 668
Norell Haakan, 215
Norgard Robert, 1437
Norris Gregory, 122
Norris Kris, 797
Northcott Josette, 692
Norton Dan, 692
Notari Luigi, 654
Nourain Shirin, 1094
Nouveau Lise, 853
Novak Bryan, 218
Novelli Francesco, 1318, 1429
Novik Amit, 504
Novitski Sif, 138
Nowak Stanislaw, 1294, 1446
Nowyhed Heba, 1216, 1362, 1363
Nuciforo Paolo, 729
Nuermberger Kristina, 1208
Nuesch Manuel, 317
Nunes Cecilia, 371
Nunez Angela, 264
Nunns Harry, 87
Nürnberg Kristina, 1070
Nurmukhambetova Saule, 287
Ny Lars, 1261, 622
Nyakas Martha, 615
Nygren Petra, 1006
Nyhus Christa, 1013, 524
Nyman Jackson, 964
Nyoni Zifiso, 1222
Nyugen-Mau Sao-Mai, 301
O Geraldine, 1417
O'Brien Shaun, 592
O'Connell Ryan, 388
O'Donnell Rebekah, 841
O'Donnell-Tormey Jill, 587
O'Gorman Bill, 475
O'Gorman William, 435
O'Hara Madison, 1410, 674
O'Neil Bert, 742
O'Neil Jennifer, 841
O'Neill Rachel, 739
O'Toole Caitlin, 841
Oaknin Ana, 670
Obeidat Akram, 474
Oberg Fredrik, 455
Oberholzer Jose, 1094
Oberley Matthew, 112
Obermayer Alyssa, 1420, 944
Oberst Michael, 835
Obonai Toshifumi, 1221
O'Brien Cathy, 586
O'Brien James, 770
O'Brien Sarah, 1437
Obrocea Mihail, 892
O'Byrne Ken, 120
O'byrne Kenneth, 117, 118
Ocasio Jennifer, 231
Occhipinti Mariaelena, 1287
Ochoa Maria, 844
Ochs Greg, 187
Ochsenreither Sebastian, 784, 786
Ochyl Lukasz, 1079
Ock Chan-Young, 1285, 657, 918
O'Connor Rachel, 489
O'Connor Roddy, 1238, 395
O'Connor Tracey, 547
Oda Shannon, 342
O'Day Christine, 1187
O'Day Steven, 470, 778
Oderinde Praise, 1262, 749
Odgerel Zagaa, 1312
O'Donnell Peter, 663
O'Donnell Timothy, 364
O'Donnell-Tormey Jill, 555, 559, 656
Odunsi Kunle, 748, 929
O'Dwyer Michael, 1444
Oelke Mathias, 1394, 353
Oelvang Madsen Cecilie, 612
Ofir -Rosenfeld Yaara, 1373
O'Flanagan Stephen, 1027
Ofran Yanay, 775
Ogale Sarika, 797
Oganessian Artem, 423
Oganessian Vaheh, 461
Ogbodo Ekene, 324, 414
Ogbourne Steven, 1121
Ogoburo IfeanyiChukwu, 1224
Ogurtsova Aleksandra, 57
Oguz Cihan, 419
Oh David, 587, 728
Oh Do-Youn, 552, 553, 658
Oh Sang Cheul, 658
OH Seung Eon, 365
Oh Se-Woong, 1058, 467
Oh Steve, 293
Oh Youjin, 13, 14, 1407, 1408, 1413, 519
Oh Youngsik, 837
O'Hara Mark, 592, 596, 656
O'Hara Sam, 366
Ohashi Pamela, 234, 999
Ohkuma Ryotaro, 46
Ohri Rachit, 333
Ohtani Yumi, 371, 376, 823
Ohtsuka Toshiaki, 808
Okada Hideho, 410, 80
Okada Seiji, 794, 846
Okada Yohei, 754
Okal Abood, 737
Oke Oluwatobiloba, 822
Okera Meena, 632
Okimoto Tamio, 1445
Okkes Daniel, 69
Okrah Kwame, 587
Oladejo Mariam, 1180
Olagunju Damilola, 411
Olcina Monica, 486
Olejniczak Scott, 396
Oliner Jonathan, 187
Oliva Jacqueline, 1042
Olive Daniel, 1107, 1339, 354, 720
Olive Marion, 957
Oliveira Giacomo, 503
Oliveira Jillian, 182
Olivera Irene, 267
Olivi Alessandro, 648
Olkhanud Purevdorj, 557, 813
Ols Michelle, 278, 369, 390
Olsen Kelly, 124
Olsman Hugo, 495
Olson Brian, 613, 878
Olson Daniel, 754, 760, 767, 781, 787
Olson Devra, 1187
Olson Jeffrey, 1033
Olson Michael, 269
Olsson-Brown Anna, 610, 611
Olszanski Anthony, 615, 710, 735, 787
Oluwole Olalekan, 687
Olwenyi Omalla, 526
O'Malley David, 564
Omar Bilal, 469, 895
Omilusik Kyla, 304
Omran Dalia, 885
Omstead David, 1348
O'Neill Kathleen, 1423
O'Neill Vincent, 25
Ong Giang, 147
Ong Irene, 45, 862

Author index

- Ong June, 274
Ong June Xu Hui, 283
Ong Mathew, 1089
Ong Richard, 240
Ontiveros Carlos, 1428, 453, 501
Onwudiwe Nneka, 1416
Onyshchenko Kateryna, 868, 872
Oosting Sjoukje, 676, 678
Ophir Eran, 504, 659
Opitz Christiane, 165
Oppelt Peter, 503
Oppenheim Joost, 1126
Opresko Patricia, 408
Opyrchal Mateusz, 547
Orain Michèle, 1300
Oran Betul, 685
Oravec Tamas, 1419, 1461
Orbanic Doriana, 42
O'Reilly Eileen, 656
Orellana Taylor, 1451
Oren Eyal, 1289
Orentas Rimas, 1192
Orf Jessica, 1217
Orlandella Rachael, 736, 764
Orlando Andrea, 9
Orloff Marlana, 759, 789
Orlova Darya, 1276
O'Rourke Matthew, 335
Ortega Fernando, 1293
Ortega Nathalie, 507
OrtegoFranco Ana, 719
Ortiz Montero Paola, 216
Ortiz-de-Solórzano Carlos, 1298
Ortiz-Otero Nerymar, 661, 680
Ortuzar Feliu Waldo, 778
Ortuzar Waldo, 649
Osborn Jane, 1353
Ose Jennifer, 1311
O'Shannessy Daniel, 1212
Osman Abdullah, 917
Osmani Amin, 1418
Ospina Victor, 182, 389
Ostergard Kayla, 941
Ostertag Eric, 728
Ostrowska Simone, 192
Ostrowski Dana, 595
Oswald Eva, 1436
Oswald Laura, 1414
Ota Sadao, 125
Otero Dennis, 1030
Ott Cavin, 1025
Ott Kristen, 1222
Ott Martina, 1001, 713
Ott Patrick, 607
Otterson Gregory, 1249, 442, 585
Ottesen Lone, 615
Ou Jiayu, 417
Ouali Kaissa, 716
Oubihy Zahra, 208
Ouerfelli Ouathak, 903
Ouladan Shaida, 49
Oum Chiyoon, 918
Oumzil Ismael, 367
Ouwerkerk Wouter, 88
Ouwongprayoon Pongsakorn, 33
Ouyang Tianqi, 1252
Ovechkina Yulia, 1341
Overman Michael, 659, 660, 930
Overstreet Michael, 469
Overwijk William, 603
Owen Dwight, 1249, 1296, 1311, 437, 442, 585
Owens Peter, 42
Owens Philip, 1448
Oxnard Geoff, 29
Oxnard Geoffrey, 58
Oyarce Cesar, 1322
Oyasu Miho, 1215
Oyer Jeremiah, 1005, 1009
Oza Kesha, 1019
Özgur Colak Nesibe, 551
Ozguroglu Mustafa, 582, 591
Özkazanc Didem, 245
Ozmadenci Duygu, 288
Paauwe Madelon, 1351
Pabla Sarabjot, 15, 152, 173
Pabla Simarjot, 392
Pacak Karel, 448
Pacey Simon, 777
Pacheco Kaithlen Zen, 352
Pachhal Sagarika, 257
Pachynski Russell, 1100
Packard Beverly, 1188
Packiam Vignesh Packiam, 666
Paddock Marcia, 1365
Padel Thomas, 583
Padera Timothy, 1295
Padmanabhan Raghav, 1294, 1446, 89
Padron Alvaro, 1428, 453, 501
Padron Lacey, 1256, 555, 559, 587
Padrón Lacey, 656
Paeng Kyunghyun, 1285, 657
Paes Wayne, 1131
Page David, 646
Page Ray, 1296, 580
Pagel Mark, 4
Pagès Oliveras Joan, 514
Pagliano Ornella, 605
Pai Sara, 1022, 681
Paidhungat Madan, 1078
Paillasse Michael, 337
Pajic Marina, 1455
Pal Bidisha, 90
Pal Chiranjib, 1439
PAL PRADIPTA, 1014
Pal Sumanta, 558, 561, 667, 810, 880
Palaia Jennell, 430, 439, 440
Palaskas Nicolas, 1262, 749
Palcza John, 635
Palena Claudia, 438, 909
Palermo Miguel, 221
Paleta Ashley, 1030
Pallan Lalit, 787
Pallini Roberto, 648
Palmer Nicole, 209
Palmer Rachael, 1342
Palmerini Pierangela, 377
Palomares Karina, 304
Palombella Vito, 1082, 1338
Palombo Fabio, 820
Palova Jelinkova Lenka, 716
Palti Yoram, 860
Pamintuan Breanna, 232
Pan Cassie, 19
Pan Hongjie, 477
Pan Liulu, 147, 923, 951
Pan Weiling, 1441
Pan Xuwen, 1425, 70
Pan Yijia, 204, 276, 304, 326, 341
Pan Zheng, 123, 320, 712
Panaampon Jutatip, 794, 846
Panageas Katherine, 1297, 997
Panagi Myrofora, 108
Panagioti Eleni, 896
Panasci Justin, 1300
Pandey Bhakti, 57
Pandey Prashanth, 1368
Pandey Sivani, 1215
Pandey Surya, 1310
Pandey Tushar, 976
Pandey Veethika, 1024, 885
Pandha Hardev, 1434, 1467, 966
Pandit Abhay, 42
Pandit Rajay, 1077
Pandita Ankur, 1261
Panduro Marisella, 1338
Pandya Dimple, 1282
Pandya Susan, 552
Panella Denise, 245
Pang Xinghua, 521
Pang Yu, 859
Pangilinan Andy, 528
Paniello Randal, 503
Panina Svetlana, 1169
Panousis Constantinos, 275
Pant Shubham, 838
Pantoja Raymundo, 1329
Papadas Athanasios, 981
Papadatos-Pastos Dionysis, 598
Papadopoulos Kyriakos, 659, 750, 759
Papaiah Arun, 1335
Papalia Giuseppe, 1217
Papastois Gregory, 1076
Papotti Mauro, 317
Pappalardo Angela, 144
Pappas Danielle, 1092
Paradé Marc, 495
Paranthaman Nindhana, 797
Paras Shah, 666
Parashar Kaustubh, 991
Pardoll Andrew, 1119, 487, 50, 515, 538, 57, 711, 876
Parihar Robin, 328, 394, 413, 816
Parihar Vaunita, 1458
Parikh Milan, 150
Parikh Rahul, 838
Parikh Ravi, 1296
Paris Sebastien, 1122, 682, 869
Pariva Tiffany, 308
Park Anthony, 305, 368, 847
Park Chae Gyu, 488
Park Cheon Ho, 751
Park Cheonhyoung, 1343
Park Choi, 235
Park Dan Bee, 349
Park Daniel, 388
Park David, 754
Park Gahee, 1285
Park Haeseong, 727, 762
Park Heungrok, 488
Park Hyun Jung, 605
Park Inkyung Angie, 1097, 625
Park Jae Chan, 349
Park Jeehun, 66
Park Jewel, 14
Park Ji Soo, 488
Park Jin Sung, 1063
Park Jin Young, 126
Park John, 431, 675, 753
Park Jong Chul, 638, 678, 681, 767

- Park Joo Dong, 1421, 211
Park Joo Hee, 13, 1407, 1408, 1413
Park Ju Young, 1058
Park Jung-Wook, 1055
Park Kyeongsu, 1058
Park Kyong Hwa, 126
Park Kyung-Soon, 1421, 211
Park Na Yeon, 1343
Park Ryan, 150
Park Sean, 689
Park Seonwook, 1285
Park Seung Ju, 804
Park Seungtae, 74
Park SoEun, 1157
Park Sungmin, 1063
Park Terrence, 1092
Park Woong-Yang, 1286, 74
Park Wungki, 508
Park Ye-Jean, 1159
Park Yeonggyeong, 519
Park Yeonhee, 172, 34
Park Young, 1191, 1359
Park Young Bong, 1058, 467
Park Young Hyun, 349
Parker Alan, 1349
Parker Douglas, 613
Parker Jefferson, 761
Parkes Matthew, 745
Parks Rachael, 94
Parnell Erinn, 87
Parra Edwin, 31, 838
Parren Paul, 686
Parrilla Don, 1230
Parsons James, 244
Parsons Peter, 1121
Parsonson Andrew, 431
Parthasarathy Pannaga, 246, 247
Parvathaneni Kalpana, 572
Parvathaneni Upendra, 19
Parvathy Seema Nair, 614
Parwani Anil, 82
Pascual Tomás, 548
Pascual-Pasto Guillem, 1189
Passaro Austin, 380
Passaro Carmela, 369
Pastan Ira, 1218, 557
Pastor Danielle, 766
Pastor Sonia, 1107
Pasziewicz Konrad, 532
Patanè Monica, 648
Patchv Sridevi, 296
Patel Anuj, 64
Patel Arpan, 1296
Patel Arpita, 1203
Patel Bhavika, 47, 48
Patel Bindi, 854
Patel Hinel, 335
Patel Jaymin, 470, 651, 778
Patel Jigar, 45
Patel Jimmy, 848
Patel Jyoti, 1403
Patel Kirtesh, 1033
Patel Manish, 1202, 465, 659, 724, 726, 754, 755, 767
Patel Meera, 623
Patel Minesh, 762
Patel Mitul, 1131
Patel Nirja, 823
Patel Preeyam, 1182, 1440
Patel Pretesh, 1033, 848
Patel Radhika, 308
Patel Sagar, 558
Patel Sandip, 229, 263, 639, 67, 708, 755, 77, 772, 781
Patel Sapna, 705, 759
Patel Yogin, 340, 370
Pattera Rosina, 648
Pathak Lekhika, 90
Pathania Anup, 526
Patil Namrata, 435, 475, 523
Patilea-Vrana Gabriela, 731
Patiño-Garcia Ana, 836
Patnaik Akash, 878, 879
Patnaik Amita, 597, 659, 731, 738
Patnaik Sachin, 1043, 463
Patricio Czarina, 561
Patrick Michael, 951, 99
Patrikidou Anna, 716
Pattabiraman Vijaya, 1080, 1195
Patton Gregory, 454
Patz Edward, 699
Paucarmayta Ana, 895
Pauken Kristen, 1038
Paul Somnath, 988
Paul Sourav, 1014
Paulos Chrystal, 1044, 134, 1457, 212, 407, 506, 613, 89
Paulson Kelly, 50
Paulucci David, 608
Paustian Christopher, 5
Pavlick Anna, 430, 439, 440, 610, 611
Paweletz Cloud, 295, 503
Pawlitzy Inka, 709
Paynter Alex, 1308
Paz Keren, 474
Paz Rom, 860
Paz-Ares Luis, 586
Pazdrak Barbara, 782
Peabody Phillip, 123
Pearce Edward, 1119
Pearson Gray, 1012
Peball Bernhard, 653, 722
Pecci Federica, 451, 512, 528, 91
Pecherstorfer Martin, 1255
Peck Nicole, 1084
Peckham David, 1341, 425
Pedawi Aryan, 1282
Peddaboina Chandher, 1374
Peddagangireddy Vishal, 1280
Pedersen Ayako, 1182, 1440
Pedersen Gitte, 92
Pederzoli-Ribeil Magali, 841
Pedita Federica, 268
Pedro Kyle, 390
Pedrosa Elizabeth, 252
Peeper Daniel, 979
Peet Greg, 1437
Pegliasco Hervé, 701
Peguero Julio, 675
Peisert Frederik, 1074, 1093
Pelka Karin, 1242
Pelle Eleonora, 1375
Pellegrino Christian, 900
Pelot Kyle, 1206
Pels Nana Adjoa, 1060
Pelster Meredith, 638, 747
Peltola Katriina, 715
Peltz Lindsay, 71
Pelz Benjamin, 78, 842, 85
Pena Rhoneil, 1086
Pencheva Nora, 1208
Peng Feng, 1424
Peng Kah-Whye, 851
Peng Li, 772
Peng Shaogang, 1321, 207, 821
Peng Songming, 123
Peng Stanford, 738
Peng Wei, 753
Peng Weiyi, 1094
Peng Xiyu, 1297
Peng Yibing, 206
Peng Zhaoming, 1424
Pengam Sabrina, 484
Pennell Nathan, 933
Penston Daniela, 1212
Pentier Johanne, 1349
Penugonda Sudhir, 1212
Perales Renzo, 691, 692, 693
Perales-Puchalt Alfredo, 1174, 388, 691, 692, 693
Peralta Eigen, 259, 276, 300, 304
Peran Ivana, 1452
Perbost Regis, 1454
Pereira Carlos-Filipe, 1233
Pereira Daniel, 500
Pereira Gavin, 538
Pereira Nikhil, 500
Pereira Sergio, 1285
Perets Ruth, 592, 767
Perez Cesar, 756
Perez Oscar, 160
Perez-Alenza Maria Dolores, 1120
Perez-Garcilaso Ivan, 123
Perez-Villarroel Patricio, 912
Pericle Federica, 1333, 1378
Pérol Maurice, 701
Perpinello Sara, 377
Perrault Julie, 350
Perreault Claude, 1411
Perrone Fabiana, 91
Perry Christopher, 656
Perry Jessica, 1308
Perry Matthew, 1467
Perry Trinity, 461
Peters Joann, 691, 692, 693
Peters Solange, 731
Petersen Laetitia, 1099
Peterson Bret, 1065
Peterson Joseph, 122, 976
Peterson Milene, 1396
Petrenko Natalia, 504
Petricevic Branka, 655
Petroni Giulia, 1144, 446
Pettersen Rolf, 494
Petti Consalvo, 213
PEYRAUD Florent, 135, 141, 1426
Peyronnier Arnaud, 949
Pfaender Stefanie, 337
Pffaff Kathleen, 168, 503, 928
Pfeffer Katie, 1139
Pfeiffer John, 122
Pfeiffer Shannon, 587
Pfundt Adam, 315
Pferdekamper AnneMarie, 855
Pfister Sophia, 875
Pfister Thomas, 104, 49, 98
Pham Oanh, 1065
Pham Thinh, 475
Phan Giao, 789
Phan Jack, 568
Phan Joseph, 147

Author index

- Phan Kim, 1300
Phan-Everson Tien, 147
Phelan Stefan, 147, 951
Phelps Catherine, 1310
Phelps Mitch, 609
Philip Lloyd Martin, 339
Philipp Nora, 281, 897
Phillips Caroline, 719
Phillips Maggie, 1457
Phillips Marc, 708
Phillips Sophia, 277
Phillips Tierney, 7
Phippen Sean, 1350
Phoon Yee Peng, 849
Phung Shee Kwan, 1204
Piatkov Konstantin, 1153
Piazza Erin, 147
Piazza Gary, 796
Picarella Dominic, 264
Piccirillo Jay, 503
Pichavant Mina, 362, 397
Pickering Curtis, 917
Pickering Jennifer, 280, 685
Pickford Emily, 627
Pico de Coaña Yago, 35
Piek Jurgen M.J., 163
Pieke Brooke, 760
Piel Brandon, 295
Piening Brian, 113, 8
Pienta Kenneth, 636, 681
Pierce Kristen, 1342
Pierce Robert, 485, 856
Pierini Stefano, 194, 371
Pierog Piotr, 244
Piersiala Krzysztof, 942, 974, 998
Piersma Sytse, 1015
Pierto Karol, 1420
Pietrzak Maciej, 82
Pietzko Kerstin, 729, 746
Pignon Jean-Christophe, 483, 945
Piha-Paul Sarina, 723, 731, 734, 774
Pikiel Joanna, 670
Pikor Larissa, 404
Pilataxi Fernanda, 708
Pillai Rashmi, 188
Pilling Melissa, 123
Pilon-Thomas Shari, 191, 387, 912
Pina Gaspar, 1262, 749
Pinapati Richard, 45
Pinato David, 112, 437, 512, 622, 774, 850
Pindikuri Shwetha, 1296
Pineo-Cavanaugh Psalm, 410
Pinggera Michael, 1131
Pinsky Tova, 1196
Pinteur Benoit, 1179, 949
Pinto Christopher, 1242
Pinto Eleonora, 820
Pinzan Rossi Moira, 322, 358
Pio Ruben, 1298
Piovesan Dana, 801
Pipkorn Patrik, 503
Pirati Sailaja, 261
Pires Cristiana, 1233
Pirich Theo, 1255
Piro Geny, 1093
Pisupati Radhika, 439, 440
Pittet Mikael, 1241, 1463
Pitts Todd, 898
Pizzo Angelina, 255
Pizzolla Angela, 1259
Pizzutilo Pamela, 112
Plantinga Theo, 1351
Platero Suso, 156
Plebanek Michael, 513, 533
Ploucha Darcy, 588
Pluda James Michael, 738
Plumb Darren, 1223
Plummer Joshua, 988
Plummer Ruth, 622, 719, 777, 850
Plüss Louis, 1074
Plyte Simon, 1210
Poch Michael, 191
Podar Klaus, 1255
Pode Zohar, 1129
Poh Chek Meng, 284
Pointing Daniel, 159
Poirier Nicolas, 1366, 484, 826
Poirot Laurent, 217, 325
Poitevin Yves, 481, 853
Pokharel Sapana, 372
Poklepovic Andrew, 588
Pokrass Michael, 1216, 1362
Polite Blase, 660
Politi Katerina, 981
Pollack Ian, 222
Pollack Joshua, 1342
Pollack Seth, 1016
Pollacksmith Daniel, 182
Pollan Sara, 87
Pollard Jack, 1010, 81, 926
Pollastri Federico, 583
Pollizzi Kristen, 461, 469
Pollo Bianca, 648
Pölonen Petri, 1006
Poltoratskiy Artem, 784, 786
Polyak Dina, 277
Polydorides Alexandros, 62
Poma Eric, 736, 817
Pombo-Villar Esteban, 1170
Pomeroy Emily, 392
Ponce Francisco, 71
Ponce Mayra, 1306
Pond Gregory, 545
Ponek Ronni, 228
Pong Erik, 1067
Pongtornpipat Praechompoo, 1097
Pons Jaume, 676, 678
Ponzoni Adele, 527, 990
Poole Maria, 1392
Poon Edmund, 1069
Poon Song Ling, 433
Popa Teodora, 57
Popat Vinita, 508
Popis Martyna, 322, 358
Porazinski Sean, 1455
Porceddu Sandro, 79
Poreta Tayla, 430
Porosnicu Mercedes, 628
Porter David, 572
Porter Ely, 384, 406, 417
Ports Michael, 326
Posada Jessica, 1463
Posch Alexander, 41
Posner Marshall, 595
Postelnek Jennifer, 606
Postow Michael, 1260
Potenza Alessia, 268
Potluri Hemanth, 870
Potluri Shobha, 232, 243, 252, 340, 370
Potter Nicole, 1152
Potts Jessica, 1437
Potu Harish, 1320
Pouliot Yannick, 132
Poultides George, 1284
Poursine-Laurent Jennifer, 1015
Pouryahya Maryam, 1291
Pourzia Alexandra, 269
Poussin Mathilde, 202
Pouzolles Marie, 1019, 350, 401
Povall Chelsea, 1353
Powderly John, 204, 636, 717, 747, 757, 764, 770, 773
Powell Daniel, 1024, 202, 885
Powell Jonathan, 1119
Powell Mark, 762
Powell Steven, 592, 764
Powers Janine, 777
Powers Jay, 854
Powles Thomas, 663, 665
Pozorski Vincent, 172, 34
Prabha Amritha, 142
Prabhu Roshan, 1033
Pradhan Rachana, 1450
Prager Gerald, 653, 722
Praharaaj Monali, 1119, 1385
Prakash C Jaya, 142
Prasad Ranjeeta, 192
Pratapa Aditya, 120
Prathipati Phillip, 526
Preciado Julian, 99
Pregibon Daniel, 1404, 86
Prenen Hans, 622, 734, 774
Prentiss Clara, 1326
Presley Carolyn, 1249, 442, 585
Presti Mario, 1021
Preston Shaun, 966
Previs Rebecca, 173
Prevosto Claudia, 822
Pribadi Mochtar, 204, 276, 300, 326
Pribitzer Beate, 653, 722
Price Leo, 199, 69
Priceman Saul, 305, 308, 360, 368, 634, 847
Priddy Leslie, 953, 954
Pride Cameron, 326
Priess Michelle, 483, 945
Prieto Karol, 882
Primack Benjamin, 278, 369, 390
Prince Miles, 1442
Prince Steve, 1089
Prins Robert, 643
Prins Ruben, 1084
Prinzi Natalie, 604
Prioli Reggie, 1
Prior Wei Wei, 1083
Probst Peter, 498
Procopio Giusy, 1275
Procopio Maria Giuseppina, 1459
Prod'homme Thomas, 1237, 393
Prodi Eleonora, 1093
Proia Theresa, 1115
Proietti Cecilia, 877
Prokhnjevskaja Nataliya, 1033
Proment Alessia, 190
Proost Natalie, 215
Prosser Suzanna, 201, 294
Proto Claudia, 91
Protzer Ulrike, 346
Pryts Stacy, 461, 469
Psyrrri Amanda, 133
Pszolla Gabriele, 1319

- Ptacek Jason, 1348
Pu Chengfei, 652
Puca Emanuele, 1074, 1093, 640, 900
Puebla Osorio Nahum, 869
Pugazenthi Aarthi, 363
Puhalla Shannon, 179
Puig Saus Cristina, 123
Puigdelloses Montserrat, 836
PuiYee Chan Elaina, 441
Pulini Jennifer, 622
Pullarkat Shalini, 93
Pulliam Thomas, 1045, 50, 992
Pulukkunat Dileep, 500
Punnath Kishore, 1368
Puram Sidharth, 503
Purandare Bhamini, 123
Purbhoo Marco, 647, 649
Purcell Anthony, 1131
Purdon Terence, 347
Puri Kamal, 39, 498
Puri Raj, 344
Puri Sonam, 437
Purwanti Yovita, 292
Puzanov Igor, 1147, 1279, 54, 772
Pyke Rachel, 119, 51
Pyun Jung-Hoon, 467
- Qdaisat Sadeem, 1383
Qi Chuan, 105, 771
Qi Hui, 1017
Qi Jing, 1067, 1073
Qi Jonathan, 1019
Qi Yilin, 1354, 424
Qi Yuzhu, 1205, 989, 995
Qian Changli, 910
Qian David, 848
Qian Xiaoyan, 95
Qian Xueming, 105
Qian Yu, 422
Qian Zhengzi, 571
Qiang Li, 1004
Qin Baotian, 1171
Qin Haiyan, 909
Qin Haiying, 350
Qin Jim, 1230
Qin Vicky, 385
Qin Yanru, 725
Qin You, 1140
Qin Yu, 372
Qiu quan, 1062, 1211, 1401, 793
Qiu Xiangguo, 206
Qiu Xiaohong, 1327, 884
Qiu Yangsheng, 1062, 1211, 1401, 426, 793
Qiu Yuting, 1062
Qu Hongjing, 244, 342
Quach Boi, 123
Quamine Aicha, 373
Quandt Zoe, 1256
Quann Kevin, 1133
Quareshy Mussa, 1324
Quatch Phi, 1086
Quayle Steve, 636, 681
Quayle Steven, 1323
Queirolo Paola, 437
Queiroz Rayner, 312
Quek Ruben, 582
Quemeneur Eric, 835
Quereshi Rehman, 371
Qui Yushi, 324
Quibell Martin, 1131
- Quill Timothy, 931
Quinn Charles, 1404, 297, 86
Quinn David, 561
Quinn Marie, 547
Quinson Anne-Marie, 628
Quintanilla Milton, 16, 184
Quintero Silvia, 685
Quintini Gianluca, 784
Quong Andrew, 139, 143, 60
Qureshi Rehman, 315, 318, 634
- R Naveen Kumar, 1313
Raab Christa, 746
Rabia Lilia, 817
Rabinovich Brian, 1068
Rabinovich Gabriel, 267
Rackwitz Wiebke, 216
Rader Janet, 670
Raderer Markus, 653, 722
Radford Maluki, 112
Radhakrishnan Prakash, 169
Radichev Ilian, 1427
Radvyani Lazlo, 545
Rae Christopher, 1084
Raeymaeckers Steven, 790
Rafiq Sarwish, 310
Raghavan Rumya, 916
Raghunatha Bharathwaj, 1274
Rahimian Shah, 694
Rahman Justin, 259
Rahman Nafees, 381
Raimo Monica, 245
Rais Rana, 1119
Raith Stefanie, 434
Raitman Irene, 270
Rajagopal Sridharan, 1376, 1386
Rajamanickam Venkatesh, 959
Rajan Arun, 438
Rajan Cynthia, 636, 681
Rajan Deepta, 1277
Rajapakshe Kimal, 1154
Rajendran Sneha, 1267
Rajesh Christabelle, 169
Rajesh Divya, 1260
Rajkovic Erich, 729
Rajkumar Aarthi, 437
Rajkumar Bhanu Krithikaa, 1154, 831
Rajkumar Jonathan, 430
Rakhmilevich Alexander, 500, 72, 874
Rakhra Kavya, 1061
Rakké Yannick, 1181
Ralph David, 1161
Ram Priyanka, 851
Ramachandra Murali, 1313
Ramadoss Nitya, 203, 247
Ramakrishna Sneha, 362, 397
Ramakrishnan Karthik, 454, 798, 799
Raman Jai, 242
Ramar Rubentiran, 32
Ramasamy Selvi, 1098
Ramaswami Ramya, 437
Ramchurren Nirasha, 1045, 94
Ramello Cecilia, 357
Ramesh Swetha, 1242, 1254, 1257
Rameshbabu Srikrishnan, 878
Ramirez Alejandro, 1206
Ramirez Noah, 47, 48
Ramkissoon Shakti, 173
Ramos Carlos, 1050, 838
Ramos Claudia, 779
- Ramos Corinne, 527, 990
Ramos Hilario, 500
Ramos Jason, 10
Ramothe Johanna, 1342
Ramsdell Danielle, 182
Ramsey Manda, 205
Rana Hemlata, 270
Rana Mohit, 1310
Ranade Koustubh, 619, 620
Rand Jamie, 763
Randhawa Ritu, 294
Randolph Sophia, 676, 678
Rangel Rivera Guillermo, 1044, 212, 407
Rangel Roberto, 917
Rangell Linda, 435
Ranger Ann, 238
Ranheim Erik, 862
Ranjan Kishu, 148
Ranucci Serena, 331, 824
Rao Disha, 979
Rao Krishna, 1274
Rao Qunxian, 673
Rapaport Franck, 1010
Rapicavoli Nicole, 95
Rapoport Bernardo, 84, 96, 97
Rasco Drew, 659, 758, 764
Rashid Rumana, 1067, 1073, 1079, 1372
Rasmussen Erik, 697
Rastelli Luca, 1376, 1386
Rastogi Ichwaku, 271
Ratan Aakrosh, 1147, 1279, 54
Rath Armin, 177, 323, 1320
Rau Kai, 1456
Rau Mary, 387
Raue Andreas, 260
Raulf Nina, 850
Rausch Matthew, 489
Rausch Oliver, 1373
Ravenstijn Paulien, 729, 746
Ravetch Jeffrey, 1209
Ravi Neeraja, 51
Ravi Vinod, 1042
Ravindran Palanikumar, 592
Ravindranathan Sruthi, 310
Ravn Ulla, 481, 853
Rawal Bhupendra, 778
Ray Adrian, 834
Ray Debleena, 532
Ray Patrice, 701
Ray Sydney, 747
Rayaji Rameshwari, 854
Raymon Heather, 306
Rayner Charles, 1467, 966
Raza Qanber, 49, 98
Razak Albiruni, 758, 770
Razimbaud Cecile, 295
Razmara Aryana, 1008, 272
Ready Neal, 1132, 699
Reagan Patrick, 767
Reardon David, 115, 641, 642
Rebhun Robert, 1008, 272
Rech Andrew, 335
Recio-Boiles Alejandro, 717
Reck Martin, 523
Reddell Paul, 1121
Reddy Jay, 568
Reddy Prasanth, 173
Reddy Sangeetha, 993
Redegalli Miriam, 268
Redman Jason, 766

Author index

- Redman Mary, 29, 584
Redman Rebecca, 764
Redmond David, 997
Redmond Keara, 1444
Redmond William, 113, 1171, 8, 803
Reebye Vikash, 850
Reed Alexandra, 437
Reeves Jason, 147, 951, 99
Regan Dan, 840
Regan Kevin, 689
Regev Aviv, 964
Rehani Peter, 72
Rehbein Bettina, 729
Rehm Armin, 1235, 1239
Reichard Chad, 132
Reicher Barak, 1380
Reid Anna, 577
Reid Joel, 785
Reid Pankti, 1260, 936
Reijers Irene, 979
Reil Katherine, 1124
Reilly Christine, 613
Reilly Timothy, 1354, 424
Reinhardt Carsten, 1319
Reinieren-Beeren Inge, 495
Reinmuth Niels, 136
Reisinger Sarah, 920
Reiss Kim, 633, 634
Reiter Lukas, 602
Rekdal Øystein, 1126
Relph Kate, 1434
Remeniuk Bethany, 131, 149
Ren Jun, 907, 911
Ren Lili, 384
Ren Tiger, 223
Ren Xiaoxin, 489
Ren Xiubao, 704
Ren Yijing, 1150, 1397
Ren Yue, 1082
Ren Yulan, 1284
Ren Zhenhua, 1236
Renart-depontieu Florence, 144
Rengarajan Michelle, 1252
Rennert Paul, 175
Renouf Daniel John, 592
Renovanz Mirjam, 641, 642
Rentrop-Boeijen Melissa, 1210
Renukappa Girish, 1313
Repash Elizabeth, 1340
Repetto Matteo, 1264
Reshef Ran, 713
Resseguier Noémie, 701
Restaino Clifford, 1367
Restifo Nicholas, 370
RESZKA-BLANCO NATALIA, 834
Rethy Agnes, 764
Rettig Matthew, 668
Rettig Michael, 624
Reuben Alexandre, 28, 36
Reusch Uwe, 729
Reuschel Emma, 555
Reuss Joshua, 57
Revenko Alexey, 472
Revsine Mahler, 1019
Rey Christophe, 135, 141, 1426
Reyes Daniel, 924
Reyes Uribe Laura, 28, 36
Reyno Leonard, 1342
Reynolds Gary, 441
Reynolds Kelsi, 1064, 920
Reynolds Kerry, 1242, 1246, 1252, 1253, 1254, 1257, 1263, 441, 696
Reynolds Warren, 362, 397
Rezvan Ali, 402
Rezvaya Alexandra, 1207
Rha Sun Young, 658
Rhead Brooke, 132
Rhee John, 721
Rhee Paul, 658
Rhode Peter, 724
Rhodes Michael, 147, 923, 951, 99
Rhodes Terence, 610, 611
Ribas Antoni, 123, 1292
Ribeiro Renata, 303
Ribi Mikaela, 1209
Ricca Jacob, 997
Ricciuti Biagio, 451, 512, 528
Rice David, 1050
Rice Meghan, 831
Rice Nathaniel, 1216, 1362, 1363
Rich Benjamin, 601
Rich Jamie, 1185
Rich Jason, 503
Richard Corentin, 614
Richard Guilhem, 100
Richards Allison, 617
Richards Lori, 775
Richardson Gary, 753, 769
Richartz Nina, 494
Richer Jennifer, 1423
Richert Iseulys, 1393
Richter Kirsten, 1099, 631
Richtig Erika, 784, 786
Ricker Melissa, 772
Riddell Stanley, 881
Ridgway Benjamin, 708
Ridker Paul, 696
Riebbels Véronique, 1315
Riechert Vanessa, 137
Riedl Thilo, 686
Riesenberg Brian, 1031, 1044, 839
Rietschel Petra, 582
Rifman Julia, 273
Rigau Marc, 192
Riley Maria, 442
Riley Nicholas, 1209
Rimaila Kristen, 227
Rimm David, 127, 133
Rinella Sean, 373
Ringel Alison, 1038
Rios Lindsay, 277
Rios Peter, 1094, 1095
Rios-Doria Jonathan, 1210
Rischin Danny, 1259
Ritter Anna, 500
Ritter Thomas, 1444
Ritz Jerome, 1220, 812
Rivadeneira Dayana, 1133, 408
Rivera Angie, 1433
Rivera Lee, 476
Rivera-Reyes Amalia, 212
Rivest Brianna, 1402, 1431, 493, 537
Rizo Alejandro, 981
Rizvi Zain, 19
Rizwan Ahsan, 768
Rizwan Numair, 427
Rizzuto Gabrielle, 997
Ro Gabrielle, 1004
Roach Charlotte, 52
Robbins Paul, 787
Roberge Sylvie, 1241, 911
Roberson Brenda, 557
Robert Caroline, 608, 788
Robert Marie, 734
Robert Nicholas, 430
Roberts Amy, 335
Roberts Lewis, 689
Roberts Ryan, 1135
Roberts Thomas, 910
Roberts Zachary, 781, 787
Robertson Jane, 719
Robertson Susan, 545
Roberts-Thomson Emily, 750
Robinson Hope, 1458
Robinson Jennifer, 52
Robinson Kaitlyn, 1077
Robinson Lary, 1311, 56
Robinson Mark, 486
Robinson Matthew, 823
Robinson Scott, 797
Robinson Sean, 1041
Robison Keith, 242
Robitschek Emily, 916
Robles Rockelle, 562, 565
Robles-Carrillo Liza, 1005, 1009
Rocconi Rodney, 566
Roche Daniel, 223
Rochestie Sarah, 691, 692, 693
Rock Fernando, 1352
Rockstein Lena, 995
Roda Julie, 833
Roda-Perez Desamparados, 770
Rodig Scott, 168, 503, 528, 928
Rodmaker Erin, 1176, 1177, 1308
Rodon Jordi, 759, 761
Rodrigues Mantuano Natalia, 1128
Rodriguez Abreu Delys, 475
Rodriguez B. Leticia, 450
Rodriguez Canales Jaime, 155
Rodriguez Chevez Haroldo, 992
Rodriguez Cristina, 19, 681
Rodriguez DiBlasi Varenka, 1437
Rodriguez James, 1139
Rodriguez Julio, 1060
Rodriguez Nicole, 1079, 1372
Rodriguez Paulo, 1147, 1420, 944
Rodriguez Rebeca, 1042
Rodriguez Rivera Ildefonso Ismael, 728
Rodriguez-Cabello José Carlos, 42
Rodriguez-Rosario Alanis, 917
Rodriguez-Ruiz Maria, 1144
Roe Caroline, 111
Roelands Jessica, 1053
Roerden Malte, 967
Rogalski Mark, 596
Rogers Bruce, 834
Rogers Paul, 306
Rogers Seema, 671
Roguev Assen, 221
Rohleff Ina, 968
Rohlf Christian, 1374
Rohner Allison, 1367
Rohrbacher Lisa, 281
Rohrwild Markus, 1212
Rojas Luis, 1312
Roki Niksa, 1178
Roland Christina, 542, 590, 618
Rolf Andreas, 242
Roller Andreas, 27
Roman Claudia, 414

- Romano Emanuela, 707
Romano-Martínez Aida, 1298
Romee Rizwan, 1006
Rømer Anne Mette, 1464
Römer Michael, 713
Romero Israel, 1137
Romero Jason, 1206
Romine Kyle, 899
Ronald James, 1132
Ronczka Amy, 633, 634
Rong Yiping, 1057, 1075, 1361, 477, 858
Roobrouck Annelies, 1198
Roof Logan, 456
Rooney Cliona, 328, 394
Root Hanna, 1446
Roovers Rob, 686
Rosa Fabio, 1233
Rosado Hector, 1020
Rosario Spencer, 1463, 534
Rosati Riccardo, 268
Rosato Antonio, 377
Rosato Pamela, 1032
Rose Amy, 588, 605, 721
Rose Destanie, 1258
Rose Solène, 1393
Rose Thierry, 1003
Rose Tracy, 560
Rosen Jamie, 335
Rosen Lee, 762
Rosenberg Ari, 682, 684
Rosenberg Steven, 237
Rosenbloom Alyssa, 147
Rosenfeld Aaron, 1024
Rosenthal Arnon, 114
Rosenthal Katherine, 470, 778
Rosenthal Peter, 1216
Rosentrater Emily, 1153
Rosete Rodnie, 1215
Rosfjord Edward, 895
Roskes Jeffrey, 57
Rosol Michael, 1161
Ross Alison, 361
Ross David, 959
Ross Douglas, 101, 59
Ross Jeffrey, 58
Ross John, 1323
Ross Theresa, 278, 369, 390
Rossetti Renata, 1375
Rossi Francesca, 91
Rossi John, 850
Rostock Lida, 713
Roth Jennifer, 1006
rothstein raymond, 835, 895
Rotolo Jim, 1173
Rotolo Ramona, 190
Rotta Giulia, 900
Rottey Sylvie, 570
Rottman James, 1141
Roubaud Guilhem, 135
Roudier Martine, 308
Rouits Elisabeth, 589
Rouleau Melanie, 303
Roumani Sara, 428
Roumieux Marie, 701
Rountree Ryan, 331, 824
Roup Fabre, 1123, 1325, 1326
Roussos Torres Evanthia, 993
Routh Eric, 53
Routier Emilie, 788
Routy Bertrand, 1300, 1306, 614
Rouwendal Gerard, 495
Rovers Eric, 1210
Roviš Tihana, 474
Rowe Jared, 1038
Rowe Jenny, 429
Rowell Sean, 812
Rowinsky Eric, 623
Rowland Teisha, 366
Roy Chowdhuri Sinchita, 31
Roy Christian, 244
ROY DIA, 479
Roy Kamalika, 1439
Roy Monideepa, 1193
Roy Sreeja, 1030
Roychoudhuri Rahul, 1069
Roychowdhury Sameek, 660
Roymoulik Ipsita, 224
Rozeman Elisa, 979
Rozenblatt-Rosen Orit, 964
Ruan Kexin, 457
Rubas Werner, 1086, 1191
Ruben Jurjen, 686
Rubin Eric, 1406
Rubinstein Mark, 407, 920
Rubinsteyn Alexander, 124, 364
Rubió Casadevall Jordi, 675
Rubio Daniel, 1360
Rucevic Marijana, 150
Ruchinskas Allison, 1019
Ruchirawat Mathuros, 1019
Rudin Anna, 1261
Rudin Charles, 523, 586, 915
Rudkin Nicole, 1456
Rudolph Josh, 1342
Rudoy Dmytro, 308
Rudqvist Nils-Petter, 1117, 374, 508, 568, 9
Ruedlinger Brittney, 1438, 157
Ruella Marco, 572
Ruet Quentin, 1393
Ruf Benjamin, 1019, 419
Ruff Michael, 414
Ruffell Brian, 1228, 1420
Ruffié Claude, 1315
Ruffin Ayana, 1136, 1451, 973
Ruggiero Eljana, 268
Ruggiero Nicole, 100
Rui Haopeng, 1377
Ruiz Cuevas Maria Virginia, 1411
Ruiz-Esteves Karina, 1252
Runyon Jessica, 151
Rupalla Katrin, 1384
Rupnow Brent, 1360
RUPP Christian, 154
Ruppin Eytan, 536
Rusan Zeid, 146
Rusbultd Joshua, 1360
Rush Elizabeth, 818
Russell Greg, 919
Russell Jason, 500
Russell Michael, 1360
Russell Stephen, 851
Russo Carlo, 648
Ruta Anna, 515, 876
Rutigliani Carola, 514
Ruzza Valentino, 706
Ryan Aideen, 1444
Ryan Brid, 850
Ryan David, 1463
Ryan Jeremy, 269
Ryu Byoung, 1230, 232, 366, 375
Ryu Heeju, 1045
Ryu Jeongun, 1285
Ryu Ki Moon, 1343
Ryu Min Hee, 658
Ryu Soomin, 1090
Rzepecka Justyna, 1046
Saal Talia, 1022
Saaryan Miranush, 423
Saatcioglu H. Duygu, 552
Saavedra Santa Gadea Omar, 746
Saba Nabil, 681
Sabath Niv, 504
Sablier-Gallis Frédérique, 1306
Sabri Shan, 332
Sacco Joseph, 610, 611
Sacher Adrian, 558
Sachs Christian, 583
Sachse Richard, 716
Saco Justin, 123
Sadashiv Patil Sandeep, 1313
Saddier Axe Dorothee, 807
Sade Hadassah, 155, 583
Sade-Feldman Moshe, 150
Sadeghirad Habib, 117
Sadek Ramses, 206
Sadik Ahmed, 165
Saeed Anwaar, 112, 437
Saeed Azhaar, 112
Saeed Khalid, 1006
Saeed Muhammad, 1100
Saeedi Arash, 402
Saenger Yvonne, 636, 932
Saenz Javier, 484
Safa Houssein, 782
Sagar Milind, 1368
Sagar Satish, 169
Sagiv-Barfi Ildit, 1166
Saha Akata, 1439
Saha Krishanu, 1231, 391
Sahaf Bitu, 362, 397
Saharia Ashish, 502, 621
Sahdeo Sunil, 855
Sahebjam Solmaz, 774
Sahetya Disha, 1187
Sahin Ugur, 1070, 1208, 700
Sahlender Daniela, 589
Sahoo Narayan, 869
Sahtout Mohammad, 770
Sahu Arvind, 1014
Sahu Sombeet, 381
sai.gullapally@pathai.com Sai, 1291
Saibil Sam, 234
Saibil Samuel, 760
Said Patricia, 682, 684
Said Sara, 123
Saikia Partha, 90
Saini Avneesh, 1215
Saini Jasmeen, 1389
Saini Marco, 648
Saini Neeraj, 296
Saini Uksha, 881
Saint-Lu Nathalie, 1306
Sainz Cristina, 1298
Saito Shin, 529
Sakamura Reona, 414
Sakellariou Christina, 102
Sakemura Reona, 324
Sakkal Leon, 430
Sakthi Vale Previtha Dawn, 274

Author index

- Salahudeen Ameen, 1283
Salama April, 112, 22, 705, 827
Salameh Ahmad, 1333, 1378
Salazar Andres, 595
Salazar Arcila Carolina, 1130, 1156, 1159
Salazar Rachel, 1368
Salcedo Estefania, 215
Saleem Rabia, 437
Saleh Mona, 62
Salek-Ardakan Shahram, 1326
Salek-Ardakani Shahram, 1123, 1325, 1326
Salgado-Pires Susana, 481
Sallets Adrienne, 1084
Salmeron Andres, 1096
Saltman David, 101, 59
Saltos Andreas, 1132, 1414
Salum Michael, 203, 246, 247
Salvador Fernando, 548
Salvador Lisa, 1256, 1292, 555, 559, 587
Salvatori Erika, 820
Samaan Fadi, 1148
Samajdar Susanta, 1313
Samaraweera Leleesha, 570
Samlowski Wolfram, 430
Samouëlian Vanessa, 670
Samoylenko Igor, 784, 786
Samson Adel, 610, 611
Samson Kimberly, 959
Samstein Robert, 62
San Miguel Tisha, 263
Sanabria Angelica, 1077
Sanber Khaled, 538
Sanborn Rachel, 596, 647, 731, 778
Sanchez Perez Vicky, 631
Sanchez Robert, 1396
Sanchez Violeta, 107
Sanchez-Gregorio Sandra, 844
Sánchez-Margalet Victor, 1144
Sandall Sharsti, 1187
Sandanyaka Vincent, 1355, 1381
Sandberg Mark, 229
Sander Cindy, 1267, 818
Sandholzer Michael, 1128
Sandhu Savreet, 1389
Sandoval Salemiz, 123
Sandoval Tito, 965
Sands Arthur, 254, 331, 361, 824
Sands Jacob, 58
Sandy Beth, 934
Sandy Peter, 1212
Sanfridson Annika, 145
Sang Shengtian, 1284
Sangalang Emma, 1162
Sanghavi Darpan, 554
Sangiolo Dario, 190
Sangwan Naseer, 1309
Sanjuan Nelson, 409
Sankaran Satish, 142
Sanmamed Miguel, 610, 611
Santamaria Carlos, 1342
Santidrian Antonio, 1137
Santillan Beatriz, 227
Santillana Sergio, 661, 680
Santo Antonio Del, 1274
Santomaso Tyler, 221
Santorelli Melissa, 933
Santoro Armando, 570, 774
Santoro Stephen, 332
Santos Joao, 715
Santos May Delos, 284
Santos Patricia, 1037, 683
Santostefano Katherine, 262
Santulli-Marotto Sandra, 1292, 555, 559, 587, 643
Sapetschnig Alexandra, 1373
Sapisochin Gonzalo, 621
Sapra Puja, 835
Saputra Elizabeth, 1379, 736
Saran Shashank, 155
Sarantopoulos John, 597
Sarbjana Tina, 581
Sardesai Niranjan, 1174, 691, 692, 693
Sargent Rachel, 1291
Sarkar Anirban, 1439
Sarkar Korok, 1045
Sarkar Mohosin, 1060
Sarkar Sourav, 1324
Sarker Debashis, 719, 850
Sarmiento Juan, 134
Sarnaik Amod, 285, 617, 783, 787, 789
Sarra Pauline, 483
Sasaki Koichi, 308
Sasser Kate, 1070, 1208, 1289, 1299, 1351, 987
Sasso Maria Stella, 1223, 208
Sastry Jagannadha, 1410
Sastry Jagannadha K, 674
Sasu Barbra, 210
Satam Swapna, 713
Satchell Rupert, 1324
Satelli Arun, 713
Sater Houssein A., 508
Sather Blythe, 232
Sathyanaryanan Sriram, 1344, 1345
Satijn David, 1070
Satish Aditi, 142
Sato Ai, 1144, 446
Satyajit Das, 1420, 944
Sauer Tim, 394
Saunders Claire, 1373
Saunders Harmony, 1109
Saunders Kaitlyn, 993
Saunders Shani, 83
Sautois Brieuc, 675
Savage Neil, 852
Savina Ariel, 135
Savitsky David, 470
Savoldo Barbara, 317
Sawada Atsushi, 901
Sawhney Paramvir, 598
Sawyer W Gregory, 1229
Sawyer W. Gregory, 1229
Saxena Uma, 601
Sayad Azin, 999
Saygili Demir Cansaran, 1459
Sayour Elias, 1383, 1390
Sbarrato Thomas, 701
Scagliotti Alessandro, 1318, 1429
Sally Christopher, 618
Scanlon Elizabeth, 1332
SCARSELLI ELISA, 706
Schaaf Marina, 578
Schabla Max, 336
Schachter Michael, 643
Schad Sara, 997
Schade Babette, 1170
Schadendorf Dirk, 606, 608
Schaefer Eric, 580
Schaefer Rachel, 160
Schaer David, 1367
Schall Thomas, 499, 769
Schalper Kurt, 148
Schanin Julia, 1396
Schann Stephan, 1393
Schann Stéphan, 814
Schappler Malaury, 1393
Scharenberg Andrew, 1230, 366, 375
Scharping Nicole, 1047, 970
Schary William, 603
Schaub Richard, 723
Schauer Nathan, 569
Scheel Andreas, 337
Scheel Birgit, 784
Scheidegger Adam, 242
Scheinflug Philine, 337
Schell Monika, 434
Schell Thomas, 700
Schellen Pepijn, 1210
Schenk Desiree, 660
Scherer Julian, 334
Scheuempflug Juergen, 164
Schick Kendall, 324
Schick Markus, 155, 339, 583
Schillaci Roxana, 877
Schilling Johannes, 1206
Schimke Jill, 109, 785
Schina Aimiia, 1021, 343
Schinagl Alexander, 1059
Schissel Makayla, 1245
Schiza Aglaia, 622
Schjetne Karoline, 669
Schlabach Michael, 255
Schladenhauffen Jake, 1094
Schlechter Benjamin, 760
Schlechter Benjamin, 778
Schlom Jeffrey, 1337, 438, 695, 766, 909
Schmidberger Rosemarie, 656
Schmidt Alexej, 1384
Schmidt Emmett, 1406
Schmidt Guenter, 155, 579, 583
Schmidt Karl, 1344
Schmidt Maike, 758
Schmidt Mark, 5
Schmidt Michael, 1076
Schmierer Maggie, 315
Schmitt Nicole, 535
Schmitt Thomas, 244, 342
Schmitt-Bormann Beate, 784, 786
Schmohl Michael, 626
Schnair Caitlin, 316
Schneck Jonathan, 256
Schneider Alexis, 150
Schneider Dina, 253, 287
Schneider Fabian, 117, 118, 139, 143, 60, 85
Schneider Reva, 747
Schoen Brianna, 429
Schoenberger Stephen, 861
Schoenenberger Andreu, 716
Schoener Roman, 1168
Schoenfeld Adam, 1292, 776
Schoenfeld Jonathan, 503
Schoenfeld Sara, 441
Schoenmaekers-Welters Marij, 1181
Scholler John, 1238, 291, 572
Scholler Nathalie, 1217, 1219, 1454
Scholz Alexander, 1194
Schoor Oliver, 713
Schopf Allison, 874
Schottelius Arndt, 729
Schröder Christoph, 713
Schraeder Christoph, 1319
Schreiber Robert, 1015, 1083, 1092, 476

- Schreiber Taylor, 1203
Schretzenmair Richard, 555
Schrikkema Bo, 241
Schrock alexa, 58
Schroder David, 997
Schroeder Kaleb, 1051
Schrum Jason, 1190
Schubbert Suzanne, 1079
Schueler Julia, 1436, 968
Schuetze Scott, 601
Schuler F. William, 4
Schuler Julia, 1447, 299
Schulz Lena, 714
Schulze Isabell, 997
Schulz-Knappe Peter, 165
Schumacher Ton, 1083, 1092, 241
Schürpf Thomas, 1419, 1461
Schuster Heiko, 1319, 713
Schuster Stephen, 572
Schütz Daniel, 746
Schoorman Janine, 1070
Schwalie Petra, 27
Schwartz Gary, 778
Schwartz Lauren, 885
Schwartz Myron, 541, 543, 576, 629, 688, 690
Schwartz Ross, 391
Schwartz Taylor, 797
Schwarz Benjamin, 183
Schwarze Julia Katharina, 790
Schweitzer Brock, 101, 59
Schweitzer Catherine, 585
Schweizer Michael, 335, 668, 734
Schwertfeger Kathryn, 1446
Schwoebel Frank, 1319
Scoaazec Jean-Yves, 135
Scott Andrew, 822
Scott Charles, 1398
Scott Ellen, 1048
Scott Jamie, 899
Scott Lizett, 1079
Scott Milcah, 1027
Scotti Giulia, 268
Scribano Christina, 187
Scumpia Phillip, 1292
Scuoppo Claudio, 1173
Seager R.J., 15, 152
Searles Stephen, 984
Seaton Brandon, 93
Seckinger Anja, 707, 853
Secor Austin, 1249
Seebach Frank, 735
Seeberger Sonja, 665
Seelige Ruth, 1367
Segal Neil, 735
Segal Robert, 1089
Seger Clara, 434
Segeber Felix, 155, 579
Seguin Bernard, 1016
Seh Cheah Chen, 240
Sehgal Kartik, 731
Sei Shizuko, 1177
Seibel Tobias, 784
Seidel-Dugan Cynthia, 1096
Seite Margaux, 1366, 826
Seitz Lisa, 991
Seitz Rob, 101, 59
Seiwert Tanguy, 681, 682, 684
Sekacheva Marina, 784, 786
Sekhavati Farzad, 583
Selby Heather, 1296
Self-Fordham Jezrom, 1373
Selfridge J. Eva, 636
Seliger Barbara, 1144
Selvadurai Hayden, 312, 343
Selvanesan Benson, 1460
Semaan Roy, 973
Semenov Yevgeniy, 1263, 1268
Semiletova Yuliya, 784, 786
Sen Pritha, 1242
Sen Rupashree, 487
Sen Triparna, 915
Sena Laura, 1119
Senbabaoglu Yasin, 9
Seng Judy, 781
Sengupta Sadhak, 201, 261, 294
Sennino Barbara, 123, 404
Senosain Maria-Fernanda, 15, 152
Senra Joana, 312
Sentman Charles, 329
Senzer Neil, 566
Seo Jeong-Han, 1034, 1055
Seo Jung Han, 338
Sepesi Boris, 1050, 590
Serda Rita, 415
Serganova Inna, 904
Sergeeva Oksana, 1060
Serie Daniel, 158
Serody Jonathan, 53, 560, 634
Serrano Irantzu, 1144
Serrano-Serrano Martha, 27
Serre Antoine, 701
Servattalab Roya, 1316
Serzan Micheal, 1303
Seth Sameer, 1001
Sethi Dhruv, 278, 369
Sethna Zachari, 1312
Sette Jessica, 1131
Sette Paola, 275
Severgnini Mariano, 761
Severson Eric, 173
Sewastianik Tomasz, 244
Sewell Jared, 264, 392
Sezer Ahmet, 582
Sfakianos John, 946
Shabat Yehudit, 1380
Shachaf Yuval, 1289, 1299
Shafaattalab Sanam, 229
Shaffer Travis, 1415
Shah Ami, 1260
Shah Brinda, 194
Shah Chinmayee, 1340
Shah Chintan, 552
Shah Khatera, 749
Shah Manan, 228
Shah Monil, 305, 368, 847
Shah Neil, 1303, 437, 742
Shah Nirali, 289, 327, 350
Shah Nirzari, 369
Shah Nisha, 780
Shah Payal, 644
Shah Pritom, 889
Shah Satish, 748
Shah Shivan, 480
Shah Vishal, 437
Shah Zunairah, 1407, 1408, 1413
Shahar Nir, 200
Shahi (De) Ankita, 1113
Shahi Payam, 924
Shahid Osmaan, 1038
Shahim Tara, 280, 685
Shahini Greis, 245
Shai Amit, 428
Shaik Jahangheer, 748
Shailete Siwele, 84
Shames David, 435, 475, 523, 584
Shan Bo, 1150, 1397, 482, 76
Shan Feng, 1049, 818
Shanebeck Kurt, 1101, 1183
Shang Jin, 773
Shang Limin, 481, 853
Shank Kaitlyn, 1252
Shankar Keerthana, 1231
Shankara Narayanan Jayanth, 861
Shanmugam Vignesh, 115
Shao Jiaxiang, 1377
Shao Kevin, 123, 320
Shao Weng Tan Daniel, 635
Shao Zuoyi, 689
Shapira Jake, 1310
Shapira-Frommer Ronnie, 592, 767
Shapiro Gary, 244, 342
Shapiro Irina, 1061
Shapland Kate, 1438
Sharathchandra Akshay, 403
Sharbi-Yunger Adi, 316
Shareef Muhammed, 688
Sharei Armon, 224, 638
Sharfman William, 711
Sharif Ehesan, 801, 854
Sharma Anjali, 558
Sharma Himani, 851
Sharma Manish, 659, 750, 772
Sharma Padmanee, 1305, 505, 587, 590, 623
Sharma Ricky, 875
Sharma Sagar, 361
Sharma Sambad, 1355, 1381
Sharma Shruti, 263
Sharon Elad, 1244, 1417
Sharova Tatyana, 1242, 916
Sharp Adam, 777
Sharp Fiona, 255, 297
Sharpe Arlene, 1038
Shaver Laura, 201, 261, 294
Shaw Andrey, 1276
Shaw Kenna, 542
Shaw Timothy, 1420, 944
Shaxted Jenna, 1283
Shay Jerry, 892, 906
Shchelokov Dmitry, 481
Shea Amanda, 1051
Shearman Mark, 313
Shedlock Devon, 728
Sheehan Kathleen, 1015
Shefet Carasso Leeron, 1129
Sheffer Michal, 1006
Shehwana Huma, 1001, 979
Shelansky Robert, 95
Sheldon Brenna, 1002
Shelley Daniel, 1121
Shen Bin, 985
Shen Binzhang, 70
Shen Colette, 682, 684
Shen Fan, 1119
Shen Fang, 823
Shen Guodong, 1056
Shen Kunwei, 1377
Shen Rhine, 301
Shen Ronglai, 1297
Shen Tong, 781
Shen Tsai-Kuei, 496

Author index

- Shen Yanan, 694
Shen Zhirong, 768
Shenderov Eugene, 757
Sheng Michael, 520
Sheng Zhen, 1151
Shenhav Simon, 1123, 1325, 1326
Shenker Sol, 255
Shenoy Tanu, 210
Shepard Dale, 659
Shepphird Jennifer, 351
Sher Joel, 182
Sher Xinwei, 1419, 1461
Sherman Marc, 1257
Sherman Marika, 776
Sherry Lorcan, 131
Shestova Olga, 371, 634
Sheth Rahul, 1094
Shetty Swati, 261
Shi Alvin, 916
Shi Guoming, 694
Shi Huidong, 206
Shi Jueping, 985
Shi Kristine, 753, 773
Shi Lai, 1400
Shi Lei, 969
Shi Mei, 1401
Shi Michael, 105, 771
Shi Shirley, 1081, 1088, 1104
Shi Stone, 1183
Shi Tao, 1382
Shi Wei, 1164, 530
Shi Wen, 789
Shi Xiaohua, 32
Shi Xiaojin, 581
Shi Yang, 768
Shi Yewen, 917
Shiao Stephen, 1027
Shibata Hirofumi, 529
Shiebout Courtney, 329
Shieh Christine, 123, 181
Shields Peter, 1249, 585, 920
Shiers Jason, 1131
Shigemura Tomonari, 489
Shigeura Tomokuni, 290
Shiku Hiroshi, 121, 359
Shim Byoung, 718
Shim Byoung Yong, 553, 658
Shimada Takashi, 113, 8
Shimazaki Masashi, 1187
Shimizu Toshio, 737
Shimoboji Tsuyoshi, 359
Shin John, 916
Shin Sang, 718
Shin Sang Joon, 753
Shin Sangjoon, 740
Shin Sarah, 1417
Shin Seunghwan, 918
Shin Seungjin, 375
Shin Yuri, 468
Shinde Rahul, 1307
Shinde Vaishali, 815
Shinglot Himaly, 1016
Shinners Nicholas, 361
Shir Alexei, 1170
Shiraishi Mamoru, 1364
Shirasaki Ryosuke, 1006
Shirazi Erica, 1230
Shirinbak Soheila, 276, 300, 304
Shiyanbola Oyewale, 862
Shmulevich Ilya, 927
Shobha Manjunath Harshitha, 1430
Sholevar Cyrus, 1008
Sholl Lynette, 528
Shorr Jolene, 668
Shorrock Clay, 820
Short Kirsty, 923
Shotts Kristin, 555, 559
Shoushtari Alexander, 615
Shraim Rawan, 1189
Shrestha Anura, 187
Shrestha Bishwas, 276, 304
Shrestha Prajwol, 1266
Shrestha Yashaswi, 586
Shrewsbury Alexandria, 645
Shukla Halley, 823
Shulman Jonah, 595
Shultz Leonard, 1250
Shum Sara, 1301
Shumilov Anatoliy, 583
Shunina Valeriya, 1131
Shyer Justin, 1450
Si Han, 987
Si Peng, 1294, 89
Siani Loredana, 706
Sibener Leah, 1206, 403
Siddiqui Bilal, 1262, 749
Sidhom John-William, 1272
Siebert Stefan, 252, 340
Siegler Elizabeth, 324, 414
Siegler Jana, 1212
Sierra Gloria, 1410
Sierra-Mondragon Rosa, 1420, 944
Sigal Natalia, 44
Signoretti Sabina, 295
Sikaroodi Shohreh, 204, 288, 304
Sikora Andrew, 917
Sikorski Eden, 823
Silva Andrea, 321
Silva John, 475
SILVA Jordan, 869
Silver Natalie, 1309, 1383, 1390, 456
Silverman Deborah, 1462
Silverman Michael, 614, 668
Silvestre Nathalie, 835
Sim Don, 240
Sim Hajin, 256
Sim Janet, 1162
Simeone Diane, 229, 263, 639, 77
Simeone Ester, 21
Simeoni Fabio, 268
Simic Milos, 410
Simmons Jacinta, 1121
Simmons Julissa, 227
Simon George, 1296, 699, 762
Simon Noah, 1308
Simonelli Matteo, 707
Simons Jan Fredrick, 1389
Simper Melissa, 988
Simpkins Fiona, 885
Simpson Tyler, 1277
Simrén Joel, 1261
Sims Amanda, 232
Sims Candace, 232, 243, 252
Sincic Viktor, 1054
Sinclair Angus, 1215
Singel Stina, 763
Singer Bernhard B, 1384
Singer Eric, 1311
Singer Meromit, 1038, 964
Singh Alok, 1119, 1385
Singh Aman, 737
Singh Hardeep, 64
Singh Harshabad, 656
Singh Jagjit, 605
Singh Jaskirat, 991
Singh Kawaljit, 1334
Singh Lata, 153
Singh Maneesh, 815
Singh Mithalesh, 153
Singh Monisha, 480
Singh Neeraj, 531
Singh Nishant, 967
Singh Parminder, 437
Singh Preeti, 1046, 1324
Singh Rajesh, 854
Singh Samara, 1224
Singh Satwinder Kaur, 386
Singh Sheila, 852
Singh Shweta, 367
Singh Srishti, 1228
Singleterry Will, 180
Singson Tiffany, 776
Singson Victoria, 367
Sinha Abhipsa, 1439
Sinha Abhishek, 1368
Sinha Krishna, 28, 36
Sinha Tanisha, 310
Sinnaeve Justine, 111
Sirard Cynthia, 1141, 553
Sirichoke Tim, 277
Sirpilla Olivia, 414
Sise Meghan, 1252
Siso Silvia, 1345
Sisó Silvia, 1344
Sissons James, 476
Sit Rene, 332
Siteni Silvia, 892, 906
Sitrin Jonathan, 476
Siu Lillian, 1337, 710
Siva Reddy Venkata, 1313
Sivanandhan Dhanalakshmi, 1376, 1386
Siwicki Marie, 1241
Skah Seham, 494
Skala Melissa, 72
Skeate Joseph, 392
Skinner Anne, 1317
Skinner Heath, 908
Skinner Jordan, 217
Skipper James, 855
Skłodowski Kamil, 602
Skokos Dmitris, 735
Skolariki Aglaia, 719
Skolnik Jeffrey, 555
Skoog Petter, 145
Skopelja-Gardner Sladjana, 501
Skvortsova Ira, 1430
Skyenner Michael, 1207
Slanetz Alfred, 183
Slangen Brigitte F.M., 163
Slansky Jill, 1423
Slaughter Matthew, 1247
Slingluff Craig, 11
Slipek Nicholas, 392
Sloas Chris, 376
Slomba Ronald, 547
Slowikowski Kamil, 1242
Slukvin Igor, 356
Slusher Barbara, 1119
Smalley Keiran, 1420
Smallridge Robert, 324

- Smeland Knut, 622
Smit Marie-Anne, 697
Smit Teresa, 84, 96, 97
Smith 2Geoffrey, 1458
Smith Alyson, 1190
Smith Anastasiya, 280, 685
Smith Aubrey, 212, 407
Smith Blake, 1232
Smith Carolyne, 321
Smith Casey, 1025
Smith Chad, 712
Smith Christof, 124
Smith Derek, 754
Smith Eric, 280, 685
Smith Erin, 1448
Smith Jeffrey, 483, 945
Smith Jenessa, 277
Smith Jennifer, 1191, 1359
Smith Jillian, 176
Smith Keira, 934
Smith Kellie, 374, 50, 538, 57, 9
Smith Layton, 276, 279, 304
Smith Luke, 1135
Smith Michael, 1, 2, 585
Smith Neal, 1242, 1254, 1257, 441
Smith Neil, 164
Smith Oghenetajiri, 526
Smith Olivia, 1027
Smith Racehl, 470
Smith Rachel, 358, 649
Smith Sean, 278, 369
Smith Tyler, 1011, 1146
Smith-Boeck Morgan, 198, 203, 246, 247
Smith-Uffen Megan, 1243, 431
Smits-de Vries Laura, 1351
Smolchek Ryan, 1229
Smole Anze, 202
Smythe Kimberly, 992
Snead Katie, 1187
Snedal Sebastian, 1375, 225
Sneiderman Chaim, 222
Snell Daniel, 1293, 732
Snider Justin, 834
Snider Silvia, 648
Snowden Meg, 208
Snyder Alexandra, 635
Snyder Colin, 248
Snyder Eric, 1296
Soares Kevin, 1312
Soarnil Manuel, 241
Sobiesk Anne Marie, 606
Sobti Aastha, 102, 35
Sodergren Mikael, 850
Sodre Laino Andressa, 767
Sofjan Katri, 255
Soh Kah Teong, 501, 941
Sohn Hyun-Jung, 250
Soignier Yvette, 1204
Sokolowski Kevin, 663
Soliman Hatem, 645
Solis Luisa, 838
Solis Sabrina, 616
Soloff Adam, 973
Solomon Benjamin, 1259, 660
Somaiah Neeta, 1042, 542, 590, 601, 618
Somarakis Antonios, 163
Somasundaram Ashwin, 1136
Sommaggio Roberta, 377
Sommer Cesar, 210
Sommerhalder David, 727
Sommermeyer Daniel, 337
Son Eunji, 1157
Son HyunTae, 1063
Son Ji, 1387
Son Wonjun, 1058
Sonabend Adam, 470
Sonawane Poonam, 315, 634
Sonbol Mohamad, 553
Sondak Vernon, 617
Sondel Paul, 1113, 1189, 45, 500, 72, 862, 874
Sõnego Fabiane, 144
Song Chiwoo, 519
Song Decheng, 1238
Song Ha Won, 837
Song Hannah, 350
Song Heon, 1285
Song In-Sil, 250
Song Lijie, 673
Song Lisa, 185
Song No Joon, 1445
Song No-Joon, 1064, 839, 920
Song Paul, 1068
Song Qinghua, 687
Song Sanghoon, 1285
Song Xianmin, 571
Song Xueru, 1382
Song Yongping, 652
Song Youngchul, 260
Song Yuqin, 571
Song Zewen, 1358
Song Zheng, 1211, 1401, 426, 793
Song Zhengbo, 698
Song Zhongbao, 1138
Songco Stephanie, 1137
Soni Nital, 733
Sonnemann Heather, 782
Sonpavde Guru, 437
Sontakke Pallavi, 339, 583
Soong David, 1289, 1299, 987
Soong Rinda, 1451
Soos Timothy, 1344, 1345
Sorensen Poul, 1192, 303
Sorensen Rasmus, 139, 143
Soria Jean Charles, 135
Soria Rivas Ainara, 675
Soriano Ferdie, 801, 991
Sorich Joan, 595
Sormunen Jorma, 715
Sorn Shannon, 320
Sorrentino Antonio, 842
Sorsa Suvi, 715
Sotelo Aldo, 221
Sotillo Elena, 352
Soto David, 1222
Soto-Castillo Juan José, 786
Soto-Diaz Sigfredo, 57
Soto-Pantoja David, 1304, 178, 492
SOUBEYRAN Isabelle, 141
Soukharev Serguei, 754
Sousares Michaela, 817
Southard Matthew, 483
Souza Carlos, 1383
Sowalsky Adam, 1033
Soyano Aixa, 645
Spaapen Robbert, 241
Spadi Rosella, 1318
Spaggiari Dany, 589
Spagl Sophia, 653, 722
Spahr Kellie, 970
Spakowicz Daniel, 1249, 1311, 82
Spanholtz Jan, 245
spanjaard emma, 199
Sparano Francesca, 21
Sparano Joseph, 595
Sparks Jeffrey, 1260
Spasic Marko, 555, 587, 607, 656
Spasova Darina, 855
Spaulding Vikki, 483, 945
Spears Melanie, 545
Specht Jennifer, 93
Speiser Daniel, 123
Speltz Elizabeth, 203, 247
Spencer Christine, 1256, 1292, 508, 607
Spencer Kristen, 774
Sperandi Francesca, 800
Speth Kelly, 687
Spiegelman Dan, 72
Spiga Martina, 268
Spigel David, 58, 764
Spille Jeremy, 59
Spira Alexander, 660, 732, 747, 750, 763
Spires Vanessa, 1208
Spitzer Matthew, 44, 511, 679
Spitzmüller Andreas, 155
Spoelstra Nicole, 1423
Sponheimer Monika, 281
Spranger Stefani, 1023, 1052, 1087, 129, 1465, 420, 517, 967, 994
Spreafico Anna, 750
Sprecher Emmett, 150
Sprengers Dave, 1181, 883
Spurrell Maxwell, 956
Sridhar Shaarwari, 1341
Srinivasamani Anupallavi, 462
Srinivasan Apoorva, 158
Srinivasan Karunya, 1316
Srinivasan Lakshmi, 1404, 86
Srinivasan Ramji, 44
Srinivasan Sangeetha, 953, 954
Srivastava Minu, 523, 584
Srivats Shyam, 475
Srour Samer, 558
St. Paul Michael, 234
St.Jean Samantha, 843
Stabile Laura, 1136
Stadler Guido, 16, 184
Stadtmitter Kacy, 1389
Staeble Sina, 729
Staedler Nicolas, 27
Stagnaro Enzo, 991
Stam Anita, 1210
Stanbery Laura, 566
Stanczuk Lukas, 1388
Stanford-Moore Adam, 1282
Stanger Ben, 1307
Stanhope Sarah, 619, 620
Stanslowski Nancy, 130
Stanton Kelsey, 309
Stanton Sasha, 546, 549, 646, 646, 940
Stapleton Lance, 1066
Stark Jessica, 1209
Starkhammar Magnus, 998
Stasi Lorena, 268
Stassi Giorgio, 1430
Staub Jeremy, 1438
Stauber Jonathan, 527, 990
Stavnsbjerg Camilla, 1169
Stavros Fiona, 1155
Stawiski Eric, 320, 712
Stawowczyk Marcin, 1139

Author index

- Stebbing Justin, 778
Stecklum Maria, 154
Steel Helen, 84, 96, 97
Steenmans Daniëlle, 245
Stegmeier Frank, 255, 297
Steimle Brittany, 287
Stein Alexander, 650
Stein Julie, 605
Stein Mark, 668
Stein Michelle, 43
Steinberg Gary, 100, 666
Steinberg Marcos, 855
Steinberg Seth, 557
Steiner Madeline, 1116
Steiner Philipp, 1096
Steinmetz Nicole, 1120
Stelljes Erin, 392
Stemmer Salomon, 767
Stern Stacey, 1456
Stuert Zoe, 1096
Stevens Christina, 1210
Stevens Don, 647, 649
Stevens Latoya, 790
Stevens Patrick, 82
Stevens Trent, 1222
Stevenson Alex, 838
Stevenson Alexander, 627
Stewart Carli, 324, 414
Stewart Praphaporn, 1121
Stewart Ross, 583, 586
Stewart Shaun, 1210
Sticco-Ivins Maura Aliezah, 295
Stiedl Christian, 103
Stift Anton, 655
Stinchcombe Thomas, 699
Stirling Elizabeth, 1304, 178, 492
Stish Bradley, 140
Stivers Katlin, 515
Stoffel Kevin, 520, 534
Stoffroff Merrill, 1019
Stojdl David, 404
Stokes Michael, 884
Stone Erica, 1389
Stone Geoffrey, 833
Stone James, 1254
Stone Sarah, 463, 479, 971
Stoner Samuel, 1367
Storer Alex, 264
Stott Ryan, 174
Stouten Imke, 1053
Stover Brian, 1390
Stradella Agostina, 641, 642
Straign Desiree, 1448
Strand Jamie, 489
Strange Ann, 1040, 1466, 285, 925
Strange Chad, 1050
Strassburger Hannah, 898
Strasser Geraldine, 1276
Strauss Bryan, 1108, 459
Strauss Julius, 695, 766
Strein Klaus, 853
Streit Michael, 1283
Strenk Susan, 1308
Stringer Bas, 241
Strippoli Sabino, 1281
Strome Scott, 348
Stromhaug Kari, 503
Stroncek David, 557
Strop Pavel, 1162
Strosberg Jonathan, 1375
Strumane Kristin, 1070
Stuart Joshua, 9
Stubbington Micheal, 924
Stucchi Riccardo, 640, 900
Studebaker Adam, 1135
Stueber Gabriella, 187
Stueve Theresa, 320
Stumpe Martin, 1283
Stunnenberg Johanna, 979
Stuparu Andreea, 1194
Styles Rachel, 596
Stylianopoulos Triantafyllos, 108
Stylli Harry, 969
Su Lihe, 175
Su Ling, 327
Su Qingtai, 1155, 1200
Su Yu-Lin, 1415, 795
Su Yu-Wen, 433
Su Zhen, 1316, 1337
Su Zhenbo, 209
Suárez-Redondo María, 1120
Subbiah Vivek, 708, 762
Subklewe Marion, 266, 281, 897
Subramanya Disha, 70
Subramanyam Varun, 1019
Subudhi Sonu, 1463, 907
Subudhi Sumit, 1262, 555, 559, 749
Suchindran Sunil, 600, 601
Sucipto Kathleen, 1291
Sudhagoni Ramu, 570
Sudhakar Rakesh, 320
Sue Cate, 181
Sue Mayumi, 808
Suijkerbuijk Karijn, 88
Sukari Ammar, 681
Suknuntha Kran, 356
Sukrithan Vineeth, 1147, 1311
Sukthankar Meghana, 1083
Sullivan Caitlin, 1172
Sullivan Denise, 380
Sullivan Jenna, 1096
Sullivan Kathleen, 499, 769
Sullivan Ryan, 1242, 1254, 1257, 1268, 1337, 150, 195, 441, 607, 659, 767, 916
Sultan Hussein, 1083, 1092
Sultana Sharmin, 932
Sulur Giri, 789
Sulzmaier Florian, 1077
Suman Shankar, 585
Suman Vera, 785
Sun Dawei, 1211, 1401, 793
Sun Dexue, 278, 369
Sun Grace, 351
Sun Hai-Ling, 1217
Sun Hongyan, 1225, 1226
Sun Huadong, 1354, 424
Sun James, 609
Sun Jie, 605
Sun Jieye, 1101, 1183
Sun Jingjing, 1330
Sun Jun, 1062
Sun Kai, 480
Sun Lu, 643
Sun Nancy, 432
Sun Nuo, 943
Sun Ruilin, 106
Sun Tao, 116
Sun Wei-Tse, 496
Sun Xiaopeng, 107
Sun Xiuhua, 571
Sun Yan, 470, 731
Sun Yanbo, 1404, 86
Sun Yang, 1002
Sun Yongkui, 597
Sun Yuhua, 820
Sun Zhichen, 1329
Sun Zhiping, 1406
Sundar Purnima, 232, 243, 252, 340, 370
Sunder-Plassmann Vincent, 1255
Sung Eric, 259
Sungnam cho, 782
Sunshine Joel, 57
Sunshine Sunny, 1467, 966
Sunwoo John, 639
Suppa Gabrielle, 987
Surace Michael, 155
Surguladze David, 1327, 884
Suri Anish, 1323
Suri Vipin, 264, 392
Surnar Bapu, 1224
Surya Nitya, 1249
Suryani Chen Santi, 1225, 1226, 1234
Sussman Django, 1357
Suteja Lida, 867
Suter Robert, 1452
Suzuki Akiko, 783
Suzuki Ken-ichi, 290
Suzuki Risako, 46
Svane Inge, 1021, 343, 715
Svane Inge Marie, 1233, 612
Sveinbjörnsson Baldur, 1126
Swaby Ramona, 315, 633, 634
Swain Joanna, 1098
Swalduz Aurelie, 1296
Swami Umang, 664
Swanton Charles, 509
Sweeney Robert, 543
Sweere Jolien, 44
Sweis Randy, 763, 767, 780
Sweis Randy F., 508
Swider Cezary, 823
Swift Shannon, 438
Switchenko Jeffrey, 1458
Sykes David, 879
Sykorova Martina, 282
Sylvestre Meilyn, 498
Sym Sun Jin, 553
Symeonides Stefan, 1173, 622, 706
Symonds Peter, 1317
Symons Jessica, 623
Synder Michael, 119
Szabo Peter, 204, 341, 726, 727, 755
Szalay Alexander, 57
Szelinger Szabolcs, 159
Sznol Mario, 772
Szyldergemajn Sergio, 682, 684
Szymczak-workman Andrea, 1041
Szymonowicz Klaudia A., 374
Ta Hieu, 479
Tabachnick-Cherny Shira, 992
Tabachnikova Alexandra, 543
Tabak Sarit, 316
Tabar Viviane, 347
Tabatabai Ghazaleh, 641, 642
Tabrizian Parissa, 629
Tabriziad Maryam, 198
Tabuena-Frolli Siena, 41, 71
Tachkov Ilian, 850
Tacken Paul, 1210, 883

- Tadjalli Mehr Keyvan, 665
Tadros Jenny, 389
Tae Nara, 837
Tafrova Juliana, 1139
Tagliamonte Maria, 1175
Taglienti Cherie, 596
Tagore Joshua, 1437
Taherally Sarah, 1003
Tai Chin-Hsien, 1218
Tai David, 867
Tai Siew, 1369
Tai Wei-Tien, 317
Tak Paul Peter, 1134
Takahashi Chikara, 435, 475
Takai Toshiyuki, 1429
Takaiva Aki, 901
Takayanagi Daisuke, 46
Takebe Naoko, 1417
Takeda Kazuyoshi, 46
Takeuchi Yoshiko, 476
Takimoto Jeffrey, 1068
Takis Panteleimon, 614
Takizawa Masaomi, 754
Talbaux Carla, 1341
Talbot Danielle, 1168
Talebian Vida, 545
Talele Nilesh, 1241, 1463
Tam Ada, 1119, 538
Tam Eric, 1060
Tam Robert, 1195
Tamegnon Auriole, 31
Tameire Feven, 1327
Tan Aik Choon, 1147, 1279, 1311, 54
Tan Alan, 661
Tan Andy Hee-Meng, 379
Tan Chin Wee, 117, 923
Tan Choon Ping, 850
Tan Jia Chi, 274
Tan Jiayi, 1160
Tan Jin Wei, 240, 284
Tan Joanne, 902
Tan Kar Wai, 240, 284
Tan Michelle, 332
Tan Nicholas, 292
Tan Seng-Lai, 1332
Tan Vivian, 857
Tan Vivian Jia Yi, 274, 283
Tan Wei, 768
TAN ZHIBO, 1424
Tandon Prateek, 51
Tandon Sapna, 16
Tang Haiyang, 652
Tang Hsin Yao, 1307
Tang Jenny, 775
Tang Jian, 1316
Tang Liang, 875
Tang Mei, 594, 754
Tang Min, 566
Tang Ming, 1332
Tang Sai-Wen, 251
Tang Tracy, 606, 608
Tang Wilson, 810, 880
Tang Xinyan, 809
Tang Xuzhen, 1017
Tang Yongfu, 296
Tang Zequn, 667
Tangy Frederic, 1315
Taniguchi Hirokazu, 915
Tanne Antoine, 470
Tannir Nizar, 558, 838
Tantivit Jessica, 1242, 1257, 441
Tanzmann Andreas, 653, 722
Tao Yu, 624
Taouli Bachir, 688
Tapia-Rico Gonzalo, 769
Tapper Erin, 324
Tarantelli Chiara, 889
Tarantolo Stefano, 754
Tarihini Ahmad, 1147, 1279, 1311, 54, 617, 780
Tariq Marvi, 506
Tarrowx Dorian, 507
Tasker Sybil, 1139
Tassi Elena, 268
Tatalick Laurie, 1219
Tatari Nazanin, 852
Tate Taylor, 542
Taube Janis, 57, 605
Taunk Neil, 644
Taurelle Julien, 484
Tavakoli Jahan, 937
Tavarez Diamile, 965
Tawbi Hussein, 606, 607, 608
Tay Rong En, 907
Taylor Brandie, 107
Taylor Devon, 469
Taylor Jake, 841
Taylor Meadows Kristen, 855
Taylor Naomi, 289, 327, 350, 401
Taylor Sarah, 174, 95
Tchaicha Jeremy, 278, 369, 390
Tchou Julia, 291, 644
Teague Alexander, 203, 246, 247
Teer Jamie, 387
Teijeira Alvaro, 267, 844, 982
Teijeira Crespo Alicia, 1349
Tejani Mohamedtaki, 553
Tekin Burak, 109
Telford William, 1019, 419
Telli Melinda, 623
Tempel-Brami Catherine, 860
Teng Han-Feng, 496
Teng Teng, 70
Tenn Elena, 1187
Tennant Megan, 1031, 1044
Tenney Daniel, 608
Tenn-McClellan Austin, 331, 824
Tentori Augusto, 64
Teong Kah, 470
Teper Daniel, 1320, 323
Teppaz Geraldine, 1366
Teppaz Géraldine, 484
Tepper Daniel, 177
Tepper Ella, 136
ter Meulen Jan, 278, 369, 390
Terabe Masaki, 557
Teran Evelyn, 1060
Teranishi Kazuki, 125
Ter-Grigoryan Anahit, 423
Terheyden Patrick, 784, 786
Ternette Nicola, 1131
Ternus Nathan, 760
Terrett Jonathan, 367
Teschmichael Dahlia, 172, 34
Tesmer Laura, 889
Tessarollo Nayara, 459
Testori Marco, 155
Tetzlaff Michael, 587
Thaagard Jeppe, 117, 118
Thagaard Jeppe, 139, 143, 60
Thai Minh, 1450
Thakkar Akshi, 1222
Thakkar Dipti, 532, 623
Thakkar Pratik, 608
Thalheimer Frederic, 345
Thalhofer Colin, 409
Thambi Merline, 713
Thamm Doug, 840
Thanos Christopher, 1065
Thaxton Jessica, 1031, 1044, 407
Theile Susann, 138
Theivanthiran Balamayooran, 22, 513, 533
Thell Kathrin, 653, 722
Theodoropoulos Jason, 1006
Theodos Debebe, 1119
Thepenier Virginie, 1366
Thépenier Virginie, 484
Theresa Waters, 1312
Theron Annette, 97
Theuerkauf samuel, 137
Thiam Kader, 144
Thibault Pierre, 1411
Thiede Lucinda, 1437
Thiele Michael, 1059
Thio Niko, 1442, 385
Thisted Thomas, 485, 856
Thistlethwaite Fiona, 787
Thiyagarajan Saravanan, 1313
Thomas Alison, 878
Thomas Ioannis, 784, 786
Thomas Jacob, 710, 778
Thomas Jamie, 181
Thomas Joice, 854
Thomas Molly, 1242, 1254, 1257, 441
Thomas Paul, 348, 9
Thomas Roby, 588, 668
Thomas Sajeve, 787, 789
Thomas Stacy, 1024
Thomas Sunil, 378
Thomas-Karyat Dori, 1184
Thomas-Toth Anika, 983
Thompson Angela, 140
Thompson Brian, 1040, 1466, 285, 925
Thompson David, 745
Thompson Elizabeth, 1119
Thompson Ella, 1442
Thompson Frank, 297
Thompson Jonathan, 783
Thompson Marshall, 1256, 1292
Thompson Morgan, 483, 945
Thompson Reid, 111
Thompson Sierra, 1456
Thomson James, 356
Thorlacius-Ussing Jeppe, 23
Thorne Steve, 894
Thorseth Marie-Louise, 1464
Thorsson Vesteinn, 508, 9
Thorsson Vesteinn, 927
Thosar Sanjana, 408
Throsby Mark, 215
Thurston Gavin, 541, 576, 690, 851
Tian Fang, 220, 510
Tian Limin, 1138
Tian Linjie, 1397
Tian Meijuan, 881
Tian Mengxi, 221
Tian Qiaomu, 1404, 86
Tiberi Giorgia, 1429
Tibrewal Nidhi, 854
Tidwell Keshanti, 353
Tiede Simon, 889

Author index

- Tietz Julia, 1293
Tighe Robert, 219
Tihista Isabelle, 1341
Tijtgat Jens, 790
Tillmanns Sascha, 716
Tilston Craig, 719
Timmer John, 1077
Timmis Helen, 719
Timms Richard, 63
Timofeevski Sergei, 1367
Timothy Marissa, 661, 680
Timpug Patricia, 278, 369
Ting Marc, 123
Ting Mark, 320
Tinker Anna, 670
Tinoco Gabriel, 1311
Tinoco Julio, 1109
Tinsley Brendan, 1389
Tippins Katharine, 373
Tirard Alice, 1242, 1254, 1257, 441
Tisdale Alison, 1332
Titov Anton, 432
Tiwari Anurag, 1391
Tiwari Gayatri, 687
TK Thulsi, 1368
To Minh, 743, 744
Todaro Matilde, 1430
Todhunter Deborah, 1202
Tognetti Marco, 602
Toh Han Chong, 867
Tohmé Mira, 902
Toiyama Yuji, 121
Tokatljan Talar, 263
Toker Aras, 1070
Tolaney Sara, 939
Tolba Khaled, 29, 58, 584
Tolcher Anthony, 753, 770, 771, 772, 773
Toledo Rodrigo, 406
Tollefson Matthew, 140
Tollenaar Rob, 1053
Tomasini Pascale, 774
Tomaszowski Michael, 1212
Tomczak Katarzyna, 1042, 1050
Tomei Sara, 1430
Tompkins Alexandra, 1280
Ton Kathy, 951
Tong Jiandong, 673
Tong Zhou, 197
Tonikian Raffi, 1196
Tonn Torsten, 216
Tonneau Marion, 1300
Tonon Giovanni, 268
Tookman Laura, 627
Tooley Katherine, 514, 964
Topalian Suzanne, 50, 711
Topp Max, 687
Torabi Damoun, 378
Torchiaro Erica, 213
Tordellas Leticia, 1375, 286, 975
Torkko Kathleen, 1448
Torres Ana, 1051
Torres Katy, 1155, 1329
Torres Keila, 542, 618
Torres Mylin, 1033
Torres-Mejia Elen, 1052, 129, 1465, 420
Torretti Elisebeth, 1077
Torrey Heather, 646, 913
Torrez Laughing Bear, 1348
Tortora Giampaolo, 1093
TORTORELLI Corinne, 1179, 949
Touat Mehdi, 641, 642
Toufiq Mohammed, 1430
TOUSSAINT Hélène, 641
Tow Clara, 932
Toy Pamela, 1066
Tyouura Masayoshi, 901
Tracy LaRee, 1389
Trad Ahmad, 1212
Trager James, 381, 902
Tran Ben, 277, 558
Tran Cuong, 1359
Tran Eric, 113, 409, 8, 959
Tran Michelle, 946
Tran Nam, 87
Tran Ngoc, 253, 287
Tran Nguyen, 689
Tran Stella, 277
Tran Timothy, 1228
Tran Tran, 1196
Tran Tri, 287
Tran Tuan, 1001
Tran Tuan-Anh, 763
Trang Vivian, 1186
Traore Tary, 182, 389
Trapani Joe, 385
Trauger Richard, 548, 650
Travesa Anna, 449
Traweek Raymond, 618
Treacy Oliver, 1444
Treonor Louise, 260
Tremblay Jack, 390
Trent Jonathan, 778
Treuting Piper, 1186, 1190
Tribble Sara, 1065
Triebe Frederic, 675
Trieu Vuong, 599
Trillo Aliaga Pamela, 1264
Trillo Jimena, 944
Trillo-Tinoco Jimena, 1277, 1282
Trinh Alex, 957
Triozzi Pierre, 178, 492
Tripathi Chakrapani, 1399
Trivedi Shubhendu, 25
Trivedi Vrunda, 1111
Trivett Anna, 1126
Trojaniello Claudia, 21
Trombley Grace, 1449
Tronconi Francesca, 91
Trotter Benjamin, 554
Trsan Tihana, 833
TRUE Lawrence, 308
Truffer Rafaela, 1206
Trump Saskia, 165
Trunova Nataliya, 1403
Truong Thach-Giao, 937
Truong Thuy, 1073
Trusk Patricia, 1365
Trusz Guillaume, 462
Tsagkogeorga Georgia, 1373
Tsai Alice, 444
Tsai FuNien, 924
Tsai Katy, 610, 611
Tsai Kenneth, 617, 882
Tsai Pei-Lun, 496
Tsai Yo-Ting, 1337, 695
Tsang Kwong, 55, 637
Tsao Annabelle, 308
Tsao Anne, 1050, 703
Tsao-Wei Denice, 561
Tsarovsky Noah, 72
Tschernia Nicholas, 508, 9
Tselios Konstantinos, 1243
Tseng Chi-Ling, 496
Tseng Wan-Yu, 454
Tsiatis Athanasios, 676, 678
Tsimberidou Apostolia, 587, 713, 778
Tso Matthew, 953, 954
Tsoi Jennifer, 1425
Tsou Pei-Yi, 1102
Tsubaki Takuya, 808
Tsubouchi Asako, 125
Tsuda Masanao, 259
Tsuji Shingo, 1124
Tsukerman Pini, 474
Tsun Andy, 1321, 197, 207, 821
Tsunoda Takuya, 46
Tsurui Toshiaki, 46
Tu Andy, 1332
Tu Eric, 339
Tu Xiaolong, 491
Tubb Vanessa, 239
Tucker Lue-Yen, 937
Tuerci Oezlem, 1070, 700
Tuffanelli Marilena, 21
Tuffy Greg, 1206
Tuinhof Ilse, 686
Tun Han, 324
Tunblad Karin, 455
Tuncel Jon, 288
Tung Navpreet, 851
Tunuguntla Ramya, 123
Turcan Sarah, 1454
Turdo Alice, 1430
Tureci Ozlem, 1208
Turek Michelle, 862
Turicek David, 289
Turk Mary Jo, 1428
Turley Shannon, 1450
Turner Broderick, 866
Turner Darryl, 1046, 1324
Turner Joel, 193
Turner Kea, 1414
Turner Madison, 168, 928
Turner Scott, 1352
Turnier Refika, 557
Turpaz Yaron, 504
Turtle Cameron, 93
Tuyaerts Sandra, 790
Tyan Pavel, 682, 684
Tye Emily, 312
Tykodi Scott, 776
Tyo Kevin, 220, 510
Tyroller Karin, 665
Tyzoonn Nomanbhoj, 889
Ubben Allana, 1186
Ubink Ruud, 495
Uboha Nataliya, 636
Uchio Edward, 666
ud Deen Imad, 148
Udyavar Akshata, 1065
Uebersax Nadine, 1206
Ueno Naoto, 633, 634
Ugolkov Andrey, 20
Uher Ondrej, 448
Uhl Christopher, 1071, 1398
Uhlik Mark, 159
Ulahannan Susanna, 717
Uldrich Adam, 192
Uldrick Thomas, 110

- Uliano Jacopo, 1264
Ullenhag Gustav, 714
Ulrich Franziska, 1074
Ulrich Michelle, 1186, 1190
Ulrich Neli, 1311
Umarale Sanjana, 686
Umiker Ben, 945
Umoru Godsfavour, 480
Underwood Dennis, 941
Ungerechts Guy, 650
Unniyampurath Unnikrishnan, 857
Unverdorben Felix, 1319
Uong Nguyen Thanh Tung, 871
Upadhyay Geeta, 1460
Upadhyaya Punit, 1340, 1356, 1388
Uppaluri Ravindra, 1404, 503, 529, 86
Urakami Akane, 290
Uranga Santiago, 1072
Urban Julie, 588
Urban Maria, 653, 722
Urech David, 732
Uribe-Herranz Mireia, 572
Uronis Hope, 553
Urquia Pauline, 1393
Uslu Ugur, 291
Uttam Sonali, 57
Uusi-Kerttula Hanni, 1349
Uyehara Rachel, 862
- V Prashanthakumara, 1368
V Syamkumar, 142
Vad Nikhil, 1194
Vadaparampil Susan, 1414
Vadas Oscar, 889
vader willemijn, 199
Vaena Daniel, 659
Vahrenhorst Dominik, 784
Vail David, 862
Vaillant Brian, 1001
Vainiute Eva, 1223, 208
Vaishampayan Ulka, 780
Vakharia Jehan, 999
Valamehr Bahram, 288, 326
Valamehr Bob, 204, 259, 276, 279, 300, 304, 341, 726, 727, 755
Valdes-Albini Frances, 717
Valdez Joseph, 16, 184
Valdivia Guillermo, 1120
Vale Nolan, 237
Valentin Emmanuel, 720
Valenza Carmine, 1264
Valerin Jennifer, 1247
Vallaster Markus, 244
Valle Juan, 552
Vallera Daniel, 1202
Vallet Sonia, 1255
Valpione Sara, 508
Valton Julien, 217, 325
van Beekhuizen Heleen, 163
Van Besien Koen, 649
Van Blarcom Thomas, 210
Van Cutsem Eric, 734, 774
van de Sande Anna J.M., 163
van de Ven Marieke, 215
van de Weg Sander, 215
van den Berg Timo, 495
van der Burg Sjoerd, 1181, 343
van der Burg Sjoerd H., 161, 163
van der Heijden Erik H F M, 702
Van der Heijden Michiel, 663
- van der Horst Edward, 485, 856
van der Lee Miranda, 495
van der Meer Donny, 199
Van der Veen Lars, 889
Van Der Veken Pieter, 1012
van der Veldt Astrid, 88
van der Vleuten Monique, 495
Van der Vliet Hans, 686
van der Westhuizen Andre, 1266
van Dieren Brenda, 1210
Van Dijk Marc, 322, 358, 372, 941
van Doorn Remco, 88
van Dyk Nydia, 461
van Esch Edith M.G., 163
van Gemerden Rachele, 1181
van Heijst Jeroen, 239
van Helden Mary, 495
van Loenen Marleen, 215
Van Nest Samantha, 1117
van Poelgeest Mariette I.E., 161
Van Riet Ivan, 790
Van Roey Erik, 15, 152
van Royen Paula, 979
Van Tine Brian, 601, 636, 764
van Vliet Amanda, 245
van Waardenburg Youri, 245
van Wijk Daniëlle, 495
Vander Mijnsbrugge An-Sofie, 790
Vander Pol Robin, 83
Vanderkerken Karin, 1444
VanderLaan Paul, 702
Vanderslice Peter, 603
VanderWalde Ari, 610, 611
Vanderweyen Davy, 1300
VanDuzer Josh, 315
Vanella Vito, 21, 842
Vanhille Laurent, 701
Vani Urvi, 991
Vannella Vito, 112
Vanpouille-Box Claire, 447
Vantourout Pierre, 1392
Van-Voorthuysen Martine, 595
Varadarajan Navin, 402
Varga Matthew, 101, 59
Varghese Sheelu, 1460
Varshine ankita, 835
Vasehus Schou Jakob, 1021
Vasiliauskaitė Lina, 1373
Vasista Anuradha, 431
Vasquez Jesse, 41
Vasse Théo, 701
Vasselli James, 775
Vassiliadou Julia, 850
Vasudevan Anu, 277
Vathiotis Ioannis, 127, 133
Vatz Victor, 512
Vayn Yelena, 1342
Vaz Victor, 451, 528
Vazquez-Martinez Julio, 1420, 944
Veenendaal Tomas, 69
Vega-Crespo Agustin, 123
Veisoh Omid, 1094, 1095, 363
Velasco Santiago Marta, 1233, 612
Velasquez Paulina, 231
Velazquez Leandra, 62
Velcheti Vamsidhar, 73
Velegraki Maria, 839
Velez Lujan Juliana, 292
Vellano Christopher, 831
Venantzi Francesco, 91
- Veneris Jennifer, 670
Venkataraman Jagadish, 1283
Venkataramani Sathya, 1360
Venkatesetty Divea, 933
Venkatasubramanian Prashanna Balaji, 483, 945
Venkatesh Divya, 1148, 903
Venkateswaran Sriram, 1274
Vensko Steven, 124, 508, 927
Ventura Annavera, 377
Venturini Nicholas, 629
Venugopal Chitra, 852
Vera Juan, 280, 685
Verdegaal Elizabeth (Els), 343
Vereide David, 366
Verheijden Gijs, 495
Verma Svena, 904
Vermont Sophie, 299
Vermot-Desroches Claudine, 1393
Vernekar Manisha, 1439
Verweij Dagmar, 215
Vesely Matthew, 167
Vezys Vaiva, 1027
Viallet Jean, 949
Vick Logan, 520, 534, 534
Victor David, 621
Vidal Gregory, 101
Vidal Veronica Calvo, 884
Vieito Maria, 641, 642
Vieito Villar Maria, 589
Vigna Elisa, 190
Vignali Dario, 1048, 1049, 1310, 811, 818, 952
Vignini Arianna, 91
Vigolo Emilia, 377
Vijaykumar Brinda, 1404, 86
Vikas Gupta, 1458
Vila-Leahey Ava, 1336
Vilar-Sanchez Eduardo, 28, 36
Vilchez Evelyn, 320
Vilkhovoy Michael, 1301
Villa Nancy, 1458
Villalba Maria, 844
Villani Alexandra-Chloé, 1242
Villani Chloe, 1252, 1254, 1257, 441
Villaruz Liza, 588, 721
Villasamil Ocando Alonso, 390
Vina Estefania, 507
Vinayanuwattikun Chanida, 33
Vincent Benjamin, 124, 508, 53, 560, 9, 927
Vincent Krystel, 1411
Vincent Loic, 244, 342
Vincent Sylvia, 470
Viola Patrizia, 512
Virbasius Amy, 182
Virone-Oddos Angela, 1198
Viscount Brian, 820
Visich Jennifer, 735
Visser Marten, 343
Visser Nienke, 995
Visser Therese, 1210
Viswanath Dixita, 83
Viswanathan Vidya Sankar, 73
Vita Francesca, 190
Vitale Maria Grazia, 21
Vitale Rosa, 706
Vitali Letizia, 190
Vitenshtein Alon, 474
Vítoc Vlad, 892
Vitsky Allison, 1258
Vivanet Grazia, 1264
Vivar Omar, 682, 684

Author index

- Viveiros Matthew, 442
Viviers Louis, 622, 734
Viyacheva Milena, 241
Vizcaino Ana Milena, 1322
Vlierberghe Ronald, 1053
Vo Buu Cathy, 738
Vodnala Suman Kumar, 370
Voena Claudia, 317
Vogelstein Bert, 1197, 1213
Volkmoth Wayne, 7
Vollbrecht Thomas, 924
Volodin Alexandra, 860
Voloshin Tali, 860
vom Baur Elmar, 732
Vom Berg Johannes, 1120
Von Bergwelt-Baildon Michael, 897
Von Essen Magdalena, 312
von Heydebreck Anja, 604
von Massow Georg, 293
Von Roemeling Christina, 1111
von Roemeling Reinhard, 20, 761
Vonderheide Robert, 656
Vos Wim, 1287
Voskanyan Astghik, 423
Voss Tiffany, 869
Voutouri Chrysovalantis, 108
Voutsinas Jenna, 19
Vu Peter, 639
Vucci Kristina, 316
Vuilleminot Brian, 1086
Vujanovic Lazar, 1037, 490, 683
Vuko Miljenka, 155
Vultur Adina, 335
Vungtutur Rahul, 1222
Vyas Avani, 535
- Wabitsch Simon, 1019
Wada Satoshi, 46
Wada Teiji, 808
Wadajkar Aniket, 1394
Wagatsuma Keisuke, 125
Wagner Claudia, 1319
Wagner Ellen, 1389
Wagner Maike, 713
Wagner Nadja, 337
Wagner Patrick, 1435
Wagner Tyler, 1274
Wahi Praneet, 1014
Wai Katherine, 511
Wainberg Zev, 553, 656
Walker David, 262
Walker Joshua, 1204
Walker Julia, 241
Walker Laura, 543
Walker Nigel, 991
Walker Phillip, 112
Walker Quinn, 185, 232, 252
Walker Ross, 778
Wallace Emily, 1031
Wallberg Hans, 455
Waller Edmund, 310
Wallet Mark, 262, 265
Wallis Stephanie, 762
Wallraven Gladice, 566
Walsh Carissa, 1177
Walsh Meghan, 264, 392
Walter Adam, 566
Walters Ian, 545, 710, 745
Walters Kylie, 401
Walters Matt, 854
- Walters Matthew, 801, 991
Walther Wolfgang, 154
Wan Guihong, 1268
Wan Hong, 1162, 756
Wang Adele, 1066
Wang Allison, 1377
Wang Beatrice, 1215
Wang Ben, 223
Wang Binbin, 536
Wang Cankun, 943
Wang Chang, 652
Wang Chao, 1101, 1321, 821
Wang Chelsia Qiuxia, 379
Wang Chunnian, 1062, 1401, 426, 793
Wang Chunyan, 673, 725
Wang Cliff, 320
Wang Clifford, 123
Wang Daniel, 623
Wang Daphne, 57
Wang Daqing, 815
Wang Dingzhi, 1331
Wang Dongfang, 1183, 795, 810, 880
Wang Ena, 361
Wang Fang, 1354, 424
Wang Gemily, 1327
Wang Grace, 1399
wang haitao, 18
Wang Haixia, 277
Wang Haiying, 793
Wang Hanbing, 1382
Wang Hanmin, 351
Wang Hao, 711
Wang Hong, 1267, 605, 721
Wang Hong-Fan, 496
Wang Hongyu, 1226
Wang Hsin, 1078
Wang Hsing-Hui, 560
Wang Huiyi, 1225, 1226, 1234
Wang Izzie, 1075
Wang Jason, 263
Wang Jia, 1377
Wang Jianing, 1153
Wang Jianming, 771
Wang Jie, 905, 985
Wang Jiin-Tarnq, 496
Wang Jing, 450, 673, 869
Wang Jing Gennie, 442
Wang Jingfen, 725
Wang Jingjing, 40, 491
Wang Jinhai, 422
Wang Judy, 750
Wang Juncheng, 490
Wang Junwen, 689
Wang Karrie, 685
Wang Katherine, 203
Wang Ke, 673
Wang Kun, 536
Wang Lei, 1399
Wang Leo, 351
Wang Li, 1043, 463, 479, 971
Wang Ling, 201, 261, 294
Wang Linghua, 1001
Wang Liqun, 868, 872
Wang Liya, 454, 798, 799
Wang Mengting, 1225
Wang Ming, 779
Wang Min-Hsuan, 1085
Wang Nancy, 907
Wang Panwen, 689
Wang Peng, 197
- Wang Qi, 869
Wang Qianxia, 869
Wang Qiwei, 910
Wang Rong, 1091
Wang Ruipeng, 353
Wang Sanlong, 1171
Wang Shaoshan, 1171
Wang Tai, 1277
Wang Tiantian, 311
Wang Wei, 1284, 576, 690
Wang Wei-Lien, 542, 618
Wang Xia, 673
Wang Xiao, 232
Wang Xiaobin, 1437
Wang Xiaofei, 1132
Wang Xiaoxu, 1119
Wang XiaoZhe, 554
Wang Xin, 1019, 1104
Wang Xinan, 528
Wang Xinwei, 773
Wang Xuechen, 1251
Wang Xuefeng, 672
Wang Xueyin, 229, 77
Wang Yan, 32, 949
Wang Ye, 444
Wang Yi, 1064, 1445, 839, 920
Wang Yifan, 182, 389
Wang Yikun, 463
Wang Yin, 530
Wang Yinghong, 112
Wang Yiyang, 330
Wang Yizhuo, 652
Wang Yongqiang, 1075, 477, 858
Wang Youhong, 477
Wang Youlei, 694
Wang Yu, 606
Wang Yue, 469
Wang Yufei, 295
Wang Yuhua, 477
Wang Yunfei, 1462, 189
Wang Yupeng, 330
Wang Yuxiao, 1237, 393
Wang Zhe, 32
Wang Zhengyi, 1151, 859
Wang Ziming, 534
Wang Zixing, 1454
Wang Ziyin, 1461
Wang Zongjie, 17
Wangen Rose, 724
Wani Khalida, 542, 782
Wani Snehal, 555
Wapinski Ilan, 1282
Ward Janine, 1168
Ward Jeffrey, 776, 781
Ward Katarzyna, 343
Ward Stephen, 629, 688
Ware Brandon, 1457
Ware Michael, 657
Wargo Jennifer, 542, 590, 607, 618, 988
Wargowski Ellen, 187
Warmuth Stefan, 732
Warner Jeremy, 427
Warner Kathrin, 999
Warrell Jonathan, 127, 133
Warrington Stephanie, 1229
Wasti Ruby, 1437
Watanabe Noriko, 1364
Watanabe Tsubasa, 754
Watchmaker Payal, 410
Waterhouse Jasmin, 598

- Watson Mark, 1244
Wayham Nicholas, 1389
Weaver Kyle, 111
Webb Jason, 503
Webb Jessica, 244
Webb Thomas, 1349
Webber Beau, 392
Weber Jeffrey, 1040, 285, 608, 609, 767, 789
Weber Lukas, 486
Wechsler Erin, 1194
Wee Felicia, 867
Wee Jon, 295
Weems Omari, 380
Weerasinghe Roshanthi, 1296
Wehn Amy, 544
Wehrli Marc, 301
Wei Guyue, 694
Wei Jia, 1382
Wei Junping, 1109
Wei Kevin, 295
Wei Lai, 1249, 442, 585
Wei Teng, 384
Wei Wei, 1196
Wei Wendy, 723
Wei Yao, 489
Wei Yi, 576
Wei Zhixia, 673
Weichert Jamey, 870, 893
Weickhardt Andrew, 775
Weidert Frances, 1383, 1390
Weinberg Andrew, 409, 959, 997
Weinberg Benjamin, 717
Weinberg Uri, 860
Weinberger Leehee, 316
Weiner Brian, 607
Weiner David, 1174, 388, 693
Weiner George, 1147, 1279, 1311, 54
Weiner Louis, 1012, 1452
Weinert Brian, 1182, 1440
Weinschenk Toni, 1319, 713
Weinstock David, 1406
Weipert Caroline, 6
Weirather Jason, 168, 928
Weis Manon, 1346
Weishaar Kristen, 840
Weiske Manon, 1346, 1347
Weiss Ido, 1289, 1290
Weiss Jakob, 1296
Weiss Jared, 682, 684
Weiß Lisa, 1347
Weiss Michael, 1194
Weiss Tobias, 1093, 640
Weissferdt Annikka, 1050
Weist Brian, 807
Weist Michael, 316
Weitzman Ron, 1167
Weitzner Brian, 185
Welch John, 229, 263, 639, 77
Welch Schwartz Rene, 862
Weller Kevin, 1064, 920
Weller Michael, 1093, 640
Welling Theodore, 229, 263, 639, 77
Welliver Tim, 676, 678
Wells Daniel, 1292, 508
Wells Jane, 1416
Welm Alana, 1036
Wels Winfried, 216
Welsch Dean, 831
Welsh James, 1387, 869
Welters Marij J.P., 161
Wen Haitao, 1445, 943
Wen Miao, 1191, 1359
Wen Patrick, 642
WEN Patrick Y, 641
Wen Sara, 1013
Wen Yong, 1101, 1183
Wen Yujia, 1244
Wendell Stacy, 1310
Weng Chien-Huan, 1148
weng jinsheng, 296
Weng Sally, 1465
Wengenmayer Peter, 784
Wenham Robert, 671, 672
Wennerberg Erik, 508
Wentland Andrew, 1296
Wentworth Chuck, 454
Wentzel Kristopher, 555, 559
Wermke Martin, 713, 720, 789
Werner Lauryn, 1109
Weroha John, 717
Wesemann Duane, 63
Wesevich Austin, 936
Wessel Kristin, 307
Wesselhoeft Alex, 1222
West John, 146
West Katy, 1223, 208
Westfall Jesse, 1135
Weterings Ashgard, 69
Wetterhorn Karl, 483
Wetzel Leslie, 895
Weyu Eyob, 1027
Whalen Giles, 710
Whalen Kerry, 1395
Whang Jennifer, 422
Whang Michael, 381
Wheeler Caroline, 1311
Whelan Sarah, 671, 777
Wherry E. John, 1337
Wherry John, 1316
Whitacre Margaret, 1168
White James, 476
White Katie, 1
White Kerry, 1082, 1350
White Michael, 590, 988
White Rebekah, 861
White Tracey, 159
Whiteley Erik, 381
Whiteside Theresa, 1000
Whiting Chan, 1065
Whiting Junmin, 609
Whiting Sam, 1331
Whitman Darbie, 39, 498
Whitman Eric, 564, 787, 789
Wicha Max, 1140
Wichmann Christian, 281
Wick Antje, 641, 642
Wick Wolfgang, 641, 642
Wickihalder Belinda, 1293
Wiederschain Dmitri, 483, 945
Wieduwild Elisabeth, 354
Wiekmeijer Anna-Sophia, 1181
Wieland Elizabeth, 747
Wiersma Valerie, 995
Wiest Lauren, 308
Wijerathna Sanath, 1355, 1381
Wijeyesinghe Sathi, 1027
Wild Philipp, 1206
Wilga-Savitski Anna, 280, 685
Wilhelm Emmanuelle, 484
Wilhelm Jonathan, 1329
Wilkens Margaret, 470
Wilkerson Matthew, 1460
Wilkinson Alec, 560
Wilkinson Scott, 1033
Wilky Breelyn, 647, 778
Williams Alan, 341
Williams Anja, 1173, 777
Williams Blake, 1097
Williams Kayla, 1025
Williams Leila, 255, 297
Williams Lucy, 1349
Williams Michelle, 1423, 568
Williams Sarah, 934
Williams Stephen, 174
Williams William, 257
Willis Claire, 1134
Willmann Luisa, 1347
Willumsen Nicholas, 1422, 1464, 23, 556, 574
Wilson Adam, 1304, 178, 492
Wilson Dawn, 772
Wilson Keith, 1203
Wilson Matt, 1115
Wilson Melissa, 787
Wilson Nicholas, 592
Win Justin, 320
Wind-Rotolo Megan, 608
Wingert Susanne, 729
Winkler Michelle, 866
Winkowski Dan, 60
Winn Glenn, 914
Winograd Benjamin, 686
Winski Shannon, 908
Winston William, 1096
Winter Charles, 1123, 1325, 1326
Winter Michael, 1078
Winters Aaron, 263
Wirges Anthea, 1235
Wirick Christian, 1394
Wiryanwan Jessica, 1222
Wise-Draper Trisha, 610, 611, 638, 783
Wiseman Charles, 257
Wisnovsky Simon, 1209
Wisskirchen Karin, 346
Withana Nimali, 368, 847
Withers David, 1134
Witness Præst Jensen Agnete, 1021
Witt Russell, 590, 618, 988
Wittrup K., 1023, 1052, 1076, 1087
Wittrup Karl, 1061
Wittstock Keith, 439, 440
Witty Alec, 259, 276
Wiwczar Jessica, 500
Wo Jennifer, 1463
Wo Serena, 1357
Wogen Jenifer, 445
Wohlfahrt Martin, 232
Wojcik John, 1282, 606
Wojnarowicz Paulina, 1327
Wolchok Jedd, 1148, 218, 347, 608, 615, 791, 843, 903, 904, 997
Wolf Andrew, 629
Wolf Ido, 136, 819
Wolf Steven, 1132
Wolfarth Alexandra, 849
Wolff Jacquelyn, 503
Wolff Robert, 656
Won Jonghwa, 1058
Wong Abbie, 1357
Wong Alexander, 442
Wong Ashley, 1222

Author index

- Wong Deborah, 123
Wong Fiona, 240, 284
Wong Hing, 724
Wong Jodie, 321
Wong Jonathan, 198, 203, 247
Wong Karrie, 255, 297
Wong Kenneth, 1078
Wong Lilly, 341
Wong Lu-Min, 229
Wong Matthew, 590
Wong Michael, 32
Wong Michael Thomas, 433
Wong Nicole, 242
Wong Philip, 587
Wong Priscilla, 228
Wong Simon, 1352
Wong-Rolle Abigail, 438
Woo James, 80
Woo Yena, 848
Wood Lauren, 557
Wood Laurence, 1180, 1370
Woodard Gavitt, 167
Woodard Paul, 747
Woodcock Mark, 53, 560
Woodcock Simon, 719
Woodford Rachel, 437
Woods David, 1040, 1466, 285, 925
Woods Elliot, 150
Woodside Darren, 603
Woody Neil, 456
Wool Assaf, 504
Wooldridge James, 605
Wooldridge Tyler, 1434, 1467, 966
Woolston David, 93
Worden Francis, 681
Worel Nina, 653, 722
Workman Creg, 1048, 1049, 811, 952
Worth Alison, 1307, 194, 371
Wortman Jennifer, 607
Wortmann Philipp, 339
Wright Deborah, 322, 358
Wright Harold, 779
Wright Jocelyn, 93
Wright Katharine, 1197, 1213
Wright Jonathan, 1177
Wu Andy, 125
Wu Catherine, 115, 295, 503
Wu Chang-Chih, 232, 375
Wu Chang-Jiun, 1050
Wu Chao, 1228
Wu Chia-Chin, 590
Wu Darong, 287
Wu Gary, 572
Wu Glendon, 1301
Wu Haoyi, 450
Wu Hsin-Jung, 888
Wu Hua, 1123, 1325, 1326
Wu Jennifer, 1011, 1016, 1146
Wu Jess, 1301
Wu Kan Xing, 292
Wu Kathy, 629
Wu Kwan-Ling, 402
Wu Lan, 175
Wu Liangzhe, 274, 283, 857
Wu Ling, 274, 283, 857
Wu Lingling, 1214
Wu Li-Ting, 308
Wu Meirong, 1226
Wu Michael, 29
Wu Qian 'Vicky', 19
Wu Ruohan, 585
Wu Shengyang, 1437
Wu Tai-Sheng, 251
Wu Tom, 1167
Wu Way, 1230, 366
Wu Xianzhu, 254, 361
Wu Xiao, 783, 789
Wu Xiaodong, 1057, 1075, 858
WU Xiaohua, 673, 771
Wu Xiaolin, 327
Wu Xiaoyu, 457
Wu Xingjun, 839
Wu Xinyu, 298
Wu Xinyuan, 444
Wu Yang, 763
Wu Yizhe, 1106, 458
Wu Yu-Chen, 496
Wu Yuling, 708
Wu Zhao, 652
Wu Zhihao, 1062, 1211, 1401, 426, 793
Wucherpennig Kai, 204
Wulf-Goldenberg Annika, 154
Wyant Timothy, 775
Wyatt Megan, 1457, 212, 407, 506
Wyman Margaret, 444
Xi Sujuan, 1284
Xia Ark, 1081
Xia Huiming, 123
Xia Huiqun, 694
Xia Lingfang, 673
Xia Yu, 521, 571
Xia Zhenzhong, 105
Xiang Hong, 747
Xiang Ping, 1196
Xiao Fang, 1348
Xiao Frank, 1103
Xiao Lei, 652
Xiao Miao, 694
Xiao Weihong, 374, 568
Xiao Zemin, 673
Xiao Zhan, 469
Xie Bryan, 403
Xie Changqing, 419
Xie Jingjing, 1284
Xie Mingchao, 155, 586
Xie Ming-Hong, 381
Xie Pin, 346
Xie Tong, 1462
Xie Tongxin, 917
Xie Wanling, 437
Xin Gang, 1064, 943
Xin Wang, 1081
Xin Wenqun, 1441, 905
Xin Ying, 1140
Xing Jun, 1234
Xing Lei, 1284
Xing Weimei, 1066
Xing Yan, 717
Xiong Guangyan, 368
Xiong Lingxin, 491
Xiong Wenjun, 1284
Xiong Zhaoming, 1365
Xu Alexander, 103
Xu Allison, 320
Xu Arron, 555
Xu Chong, 309
Xu Chunxiao, 432, 497
Xu Fenghua, 571
Xu Fiona, 742
Xu Gege, 158
Xu Guifen, 1086, 1191
Xu Han, 229
Xu He, 1153
Xu Hongmei, 1017
Xu Jiaqiong, 480
Xu Jie, 1138, 311
Xu Katherine, 1242
Xu Ke, 592, 859
Xu Lan, 888
Xu Le-Cun, 1193
Xu Lily, 993
Xu Lin, 993
Xu Lu, 1348
Xu Mei, 425
Xu Mengshu, 1066
Xu Nucleus, 644
Xu Peng, 352
Xu Qikai, 182, 389
Xu Richie, 937
Xu Sophie, 181
Xu Stacey, 201, 261, 294
Xu TengTeng, 266
Xu Wenxi, 104
Xu Xia, 350
Xu Xiang, 1211
Xu Yikai, 1284
Xu Yiyang, 16, 184
Xu Yujin, 698
Xuan Jiekun, 384
Xue Allen, 1454
Xue Bin, 1447, 299
Xue Hongwei, 571
Xue Jia, 40
Xue Xiangdong, 1358
Xue Yuezhen, 1288, 1302
Yabuuchi Kohei, 359
Yachnin Jeffrey, 622, 714, 850
Yadav Shalini, 623
Yadav Vinod, 834
Yakkundi Poonam, 1215
Yalamanjali Anirudh, 456
Yalamanchili Sreeni, 667
Yalavarthi Sireesha, 497
Yam Alice, 1103, 1191, 1359
Yam George, 320
Yamamoto Noboru, 737
Yamamura Amy, 449
Yamane Makiko, 121
Yamano Shizuka, 1006
Yamashiro Livia, 801
yamazaki takahiro, 1118, 1126, 1144, 446
Yamniuk Aaron, 1196
Yan Dingxue, 1402, 1431, 409, 493, 537
Yan Han, 768
Yan Jian, 691, 692, 693
Yan John, 932
Yan Karen, 1104
yan kuan, 199, 69
Yan Longjun, 821
Yan Wei, 1288, 1302
Yan Xuefei, 950
Yan Yao, 1321, 207
Yan Yiyi, 785
Yanamandra Ananta, 1410
Yang Becky, 1217
Yang Bi-Huei, 300, 326
Yang Bitna, 306
Yang Chen, 1139

- Yang Chunning, 461, 469
Yang De, 1126
Yang Fei, 905
Yang Guoxiang, 1250, 1258
Yang Hai, 1002
Yang Hongyuan, 1250
Yang Hsiu-Ping, 251
Yang James, 732
Yang Jiwon, 1258, 382
Yang Junhao, 1359
Yang Li, 1017
Yang Lily, 310
Yang Lu, 346
Yang Mengqi, 1424
Yang Ming, 859
Yang Mingxing, 1081, 1088
Yang Pengfei, 1424
Yang Se Hwan, 624, 657, 679
Yang Sen-Han, 251
Yang Wei, 951
Yang Xi, 1267, 1342
Yang Xiang-Hong, 32
Yang Xiaofeng, 1377
Yang Xiao-Yi, 1109
Yang Xue (Cher), 198
Yang Yanhong, 347
Yang Yan-ou, 723
Yang Yi, 1177, 549
Yang Yu, 1082
Yang Yuanquan, 82
Yang Yuanyuan, 1143, 1149
Yang Yunxing, 858
Yang Zhenzhou, 652
Yankelevitz David, 629
Yantorni Lauren, 478
Yao Anzhi, 332
Yao Jenny, 771
Yao Jin, 574
Yao Joyee, 276
Yao Li, 668, 733
Yao Li-Chin, 1250, 1427
Yao Lina, 960
Yao Ning, 301
Yao Xue, 1018
Yao Zhifang, 571
Yap Pei-Yi, 1121
Yap Timothy, 780
Yarchoan Mark, 691, 692, 693, 711
Yarla Nagendra, 22, 513, 533
Yashin Ed, 181
Yates Bonnie, 350
Yates Kathleen, 1365
Yavari Arash, 743, 744
Ye Anne, 1194
Ye Chun Jimmie, 1002
Ye Fan, 1081, 1088, 1104
Ye Jiang Feng, 867
Ye Jordan, 777
Ye Qiuping, 809
Ye Yanzhen, 417
Ye Yijing, 673
Yedidia Yoni, 1289, 1299
Yee Jacqueline, 511
Yee Jarrod, 984
Yegnasubramanian Srinivasan, 1119
Yeh Wen-I, 204, 300
Yeku Oladapo, 781
Yellin Michael, 555, 559, 595, 596
Yen Chia-Jui, 433
Yendamuri Sai, 534
Ye Siok Ping, 284
Yeong Joe Poh Sheng, 1035, 1288, 1302, 867
Yeung Andy, 1083, 1092
Yeung Cecilia, 110, 93
Yeung Kristin, 1323
Yi Hye Son, 147
Yi Jason, 316
Yi Jiaqing, 809
Yi John, 1314, 471
Yi Michael, 123, 210
Yi Wei, 105
Yigit Burcu, 322, 358, 372, 647, 649
Yilmaz Emrullah, 1309, 1383, 456
Yim Christina, 1118
Yim Leon, 1052
Yin Gang, 1103, 1191, 1359
Yin Ming, 82
Yin Sheng, 1400
Yin Yongmei, 673, 725
Ying Cheng, 725
Ying Haiyan, 1441, 905
Yingst Ashley, 366
Yizhak Keren, 150
Yoffe Liron, 965
Yokoyama Jason, 185
Yokoyama Kotoko, 8
Yokoyama Wayne, 1015
Yoneyama Tomoki, 1153
Yonezawa Atsushi, 8
Yoo Donggeun, 1285
Yoo Jongman, 468
Yoo Steven, 740
Yoo Unice, 1274
Yoon Charles, 115
Yoon Mee Sun, 871
Yoon Meesun, 302
Yoon Myeong Jin, 488
Yoon Na Ri, 74
Yoon Pyoung Oh, 1157
Yoon Sung Mi, 13, 1407, 1408, 1413
Yoon Woong Hee, 1105
Yoon Yi Na, 873
Yoshida-Court Kyoko, 674
Yoshimura Kiyoshi, 46
Youkharibache Philippe, 401
Younan Patrick, 1186, 1187, 472
Young Arabella, 1251, 1256
Young Barbara, 1324
Young Geneva, 483, 945
Young Kristina, 646
Young Regina, 291
Young Stephen, 991
Young Violet, 278, 369
Youngblood Bradford, 1396
Yousefi Maryam, 1342
Ysebaert Loïc, 337
Yu Abigail, 1359
Yu Christina, 1208
Yu Chunxiao, 1101, 1183
Yu Culling, 1326
Yu Danni, 1086
Yu Evan, 663
Yu Guohua, 571
Yu Haijuan, 106
Yu Henry, 1171
Yu Hongping, 1441
Yu Hua, 910
Yu Jia, 555, 559
Yu Jia Xin, 656
Yu Jianhua, 186
Yu Jingfeng, 1401, 793
Yu Juan, 32
Yu Kenny Kwok-Hei, 347
Yu Limin, 1291, 554
Yu Lixia, 1382
Yu Maolin, 1355
Yu Margaret, 1360
Yu Qiang, 962
Yu Rebecca, 1312
Yu Shiguang, 1101, 1183
Yu Steven, 105, 771
Yu Wei, 410
Yu Weiwei, 1226
Yu Wenhan, 461
Yu Xu, 63
Yu Yi, 1425, 444, 70
Yu Yun Suk, 126
Yu Zhiheng, 1213
Yuan Changqing, 1060
Yuan Daniel, 1049
Yuan Jianda, 635
Yuan Karen, 1081
Yuan Qingyu, 1284
Yuan Xu, 288, 304
Yuan Ying, 1387
Yuan Yuan, 633, 634
Yuan Zhijun, 821
Yue Bella, 1088, 1104
Yue Hongjun, 1215
Yue Huibin, 769
Yuen Benjamin, 123, 320
Yuen Gavin, 234
Yuet Amy, 764
Yumul Roma, 1186
Yun Hongruo, 277
Yun Jeong Mi, 349
Yun Jing-Ping, 32
Yun Kun, 414
Yun Nari, 718
Yunan Mona, 592
Yushak Melinda, 613
Yusuf Isharat, 855
Yusuf Syed Wamique, 1262, 749
Yuwen Hui, 1150, 1397, 76
Zabinyakov Nick, 49
Zacharek Sima, 767
Zager Jonathan, 617
Zagorulya Maria, 1052, 1087
Zaharoff David, 1371
Zahi Sarah, 701
Zahm Christopher, 187
Zahn Sam, 361
Zahrah George, 564
Zainuddin Mohammed, 1376, 1386
Zajic Stefan, 601
Zakharia Yousef, 1265, 1311
Zaki Anjum, 55, 637
Zaky Wafik, 400
Zalavadia Ajay, 1043
Zalevsky Jonathan, 1086
Zamarin Dmitriy, 708
Zambanini Andrew, 648
Zamora Anthony, 348
Zamora Izabella, 1052
Zampieri Alexandre, 229
Zandberg Dan, 588, 683
Zang Dae Young, 658
Zang Mingfa, 106, 491
Zang Peter, 561

Author index

- Zang XingXing, 489
Zang Yan, 1000
Zapata Francisco, 498
Zappasodi Roberta, 508, 843, 9, 903, 904
Zarif Jelani, 1119
Zarour Hassane, 1000, 1310, 605, 721
Zarubica Ana, 1107
Zauderer Marjorie, 761
Zauderer Maurice, 613, 645
Zaval Margo, 1187
Zayed Hany, 738
Zebboudj Abderezak, 1312
Zebertavage Lauren, 874
Zeidan Stephanie, 739, 748
Zeiger Jennifer, 1060
Zeiner Gus, 223
Zekeri Amin, 971
Zelazowska Monika, 542, 988
Zelichov Ori, 1289, 1290, 1299
Zellander Amelia, 1071, 1398
Zemer-Tov Efrat, 860
Zemla Tyler, 1244
Zemp Franz, 1130, 852
Zemka Olga, 1086
Zen Jane, 969
Zeng Joshua, 1399
Zeng Lingmin, 727
Zeng Veronica, 1073
Zeng Weiping, 1357
Zeng Xiaoli, 1056, 1214
Zeng Yibin, 499
Zeng Zexiang, 503
zeng zhaopie, 597
Zeng Zhen, 538
Zengin Zeynep, 810, 880
Zenkin Serafettin, 1280
Zer Alona, 136
Zerefa Luann, 295
Zerr Patricia, 741, 814
Zeskind Benjamin, 449
Zetterberg Henrik, 1261
Zevallos Jose, 503
Zha Dongxing, 462
Zha Jiping, 753, 773
Zhai Tianhang, 821
Zhai Weiwei, 867
Zhang Ailin, 308
Zhang Ali, 1016
Zhang Anli, 1236
Zhang Bin, 795
Zhang Boyang, 538
Zhang Chenxin, 932
Zhang Danhui, 1194
Zhang Dayan, 1056, 1214
Zhang Dong, 1400
Zhang Dong Mei, 1153
Zhang Faming, 491
Zhang Feng, 725
Zhang Hai-Feng, 1192, 303
Zhang Hangyu, 197
Zhang Hao, 995
Zhang Harris, 1152
Zhang Henan, 689
Zhang Huajun, 206
Zhang Jiacheng, 985
Zhang Jiajia, 50, 538, 57
Zhang Jian, 771
Zhang Jianjun, 1050, 697
Zhang Jianying, 186
Zhang Jie, 905
Zhang Jing, 1399
Zhang Jingwei, 384
Zhang Jue, 356
Zhang Jun, 480
Zhang Ke, 346
Zhang Kelvin, 1344, 1345
Zhang Keman, 479, 971
Zhang Kristen, 210
Zhang L. Harris, 1152
Zhang Lei, 1424, 186, 491
Zhang Li, 1002, 793
Zhang Liang, 951
Zhang Liangliang, 58
Zhang Lilin, 553
Zhang Lin, 1085
Zhang Max, 902
Zhang Ming, 894
Zhang Mingkun, 1225
Zhang Minjie, 444
Zhang Nannan, 985
Zhang Penglie, 499, 769
Zhang Qianying, 452
Zhang Qingming, 673
Zhang Qingyuan, 571
Zhang Rugang, 388
Zhang Ruohan, 943
Zhang Shengle, 173
Zhang Shenyu, 383
Zhang Shijia, 1268
Zhang Sophia, 1152, 1394
Zhang Tian, 1067, 931
Zhang Tuo, 1117
Zhang Wei, 178, 663
Zhang Weiyu, 1327, 884
Zhang Xiaotao, 618
Zhang Xiaoyu, 188, 348
Zhang Xiaron, 973
Zhang Xin, 490
Zhang Xinqun, 1357
Zhang Xijuli, 184
Zhang Yang, 1057
Zhang Yanni, 1151, 859
Zhang Yawei, 610
Zhang Yijuan, 1030
Zhang Yili, 1303
Zhang Ying, 439, 440
Zhang Yipeng, 1382
Zhang Yongxian, 905
Zhang Yumeng, 56
Zhang Yun, 768
Zhang Yuqi, 480
Zhang Yurun, 875
Zhang Zhe, 1424
Zhang Zhenqing, 207
Zhang Zhicheng, 1284
Zhao Bao, 1445, 943
Zhao Chen, 438
Zhao Dawen, 492
Zhao Di, 530
Zhao Edward, 147
Zhao Enxu, 757
Zhao Fan, 1323
Zhao Hao, 227
Zhao Hongyuan, 1237
Zhao Jay, 817
Zhao Jean, 910
Zhao Jianxun, 1057
Zhao Jinfeng, 1062, 1211, 1401, 426, 793
Zhao Jing, 1225, 1234
Zhao Jiuqiao, 1057, 1075
Zhao Joe, 1361, 477
Zhao Junfei, 830
Zhao Lei, 1091
Zhao Liang, 1119
Zhao Lingling, 652
Zhao Lixia, 209
Zhao Lora, 232, 252, 340
Zhao Min, 571
Zhao Niky, 769
Zhao Qingchuan, 1411
Zhao Quanju, 1400
Zhao Qun, 1214
Zhao Ronghua, 694
Zhao Sharon, 854
Zhao Sidi, 123
Zhao Siji, 242
Zhao Songzhu, 1249, 442
Zhao Tian, 1155, 1200, 1329
Zhao Xiaowei, 1213
Zhao Yiwen, 1139
Zhao Yue, 384, 417
Zhao Yujie, 1424
Zhao Zhen, 629
Zhao Zheng, 571
Zhao Zhifeng, 311
Zhao Zhiyuan, 1261
Zharkova Olga, 532
Zheng Grace, 332
Zheng Hao, 768
Zheng Hong, 1132, 673
Zheng Jing, 457
Zheng Maofa, 1401
Zheng Ningbo, 258
Zheng Pan, 564, 594
Zheng Songmao, 753, 773
Zheng Xiaoyan, 1062, 1401
Zheng Xiaoyi, 257
Zheng Yi, 160
Zheng Zhiqiang, 1377
Zhivaki Dania, 1172
Zhong Jim, 1033
Zhong Tingting, 521
Zhong Ziyang, 1081, 1088, 1104
Zhou Alice, 624
Zhou Chelsea, 739, 748
Zhou Chengzhi, 1248
Zhou Diansong, 591
Zhou Feng, 677
Zhou Gang, 1358, 796
Zhou Haiying, 809
Zhou Hui, 571
Zhou Jian-Guo, 18
Zhou Jianya, 457
Zhou Jianying, 457
Zhou Jing, 1210, 1226
Zhou Keshu, 571
Zhou Liye, 503, 529
Zhou Mi, 560
Zhou Nicolas, 1050
Zhou Qi, 673
Zhou Shenghua, 1402, 1431, 493, 537
Zhou Shibin, 1197, 1213
Zhou Shihui, 821
Zhou Sihong, 1191
Zhou Weiming, 1214
Zhou Wenrong, 1425
Zhou Xi, 1117, 1144
Zhou Xiao, 1042
Zhou Xiaoyu, 1382
Zhou Xingliang, 282

Zhou Xinglu, 1106, 458
Zhou Xueyuan, 1068
Zhou Yanbin, 1248
Zhou Yufan, 1238
Zhu Andrew, 1151, 859
Zhu Hehuan, 1053
Zhu Huang, 336
Zhu Jianqing, 673
Zhu Jiman, 673
Zhu Joe Jiang, 385
Zhu Jun, 571
Zhu Lili, 767
Zhu Lisha, 1011, 1146
Zhu Lvyu, 753
Zhu Mingrui, 891, 906
Zhu Qingfeng, 711
Zhu Ruihong, 652
Zhu Xinyun, 1151
Zhu Xizhou, 388
Zhu Yanling, 673
Zhu Yi, 597
Zhu Zheng, 1358
Zhu Zhixuan, 1441, 985
Zhu Zhu, 295
Zhuang Tony, 478
Zi Tong, 1344, 1345
Zielinski Dirk, 156
Zigler Maya, 1170
Zilberberg Jenny, 1071, 1398
Zilony- Hanin Neta, 1129
Zimarino Carlo, 1353
Zimmer Jessica, 442
Zimmerman Stephanie, 951
Zimmermann Barbara, 1120
Zimmermann Johannes, 155
Zimmermannova Olga, 1233
Zingg Andreas, 1128
Zingler-Hoslet Isabelle, 1231
Zippelius Alfred, 434
Zito Alfredo, 1281
Zlobec Inti, 1459
Zlotoff Daniel, 1246, 1254, 441, 696
Zografos Eleftherios, 670
Zolman Kathryn, 1448
Zolp Andrew, 830
Zonca Manuela, 1223, 208
Zondag-van der Zande Vanessa, 1210
Zorko Nicholas, 1202, 1204, 288
Zorro Manrique Soraya, 189
Zou David, 177, 323
Zou Hui, 779
Zou Wei, 435
Zschummel Maria, 1239
Zsiros Emese, 671, 748
Zubair Abba, 324
Zubiri Leyre, 1242, 1246, 1252, 1253, 1254, 1257, 441
Zuck Meghan, 498
Zuleger Cindy, 862
Zuno-Mitchell Patricia, 422
Zuo Haoxiao, 386
Zwarthoff Seline, 495
Zwickl-Traxler Elisabeth, 1255
Zwirtes Ricardo, 638

Late-Breaking Abstracts

Abedi Mehrdad, 1478
Amankulor Nduka, 1477
An Duo, 1478
Anaya Daniel, 1478
Argueta Kimberly, 1477
Arriaga Yull, 1473

Bagley Stephen, 1477
Bailey Christina, 1468
Baltimore David, 1478
Barone Francesca, 1477
Baverel Paul, 1475
Bell Susan, 1477
Bethune Michael, 1478
Bi Wenya Linda, 1477
Blanke Charles, 1469
Bondarenko Igor, 1470
Bota Daniela, 1478
Brem Steven, 1477
Brennan Kevin, 1477
Brignone Chrystelle, 1470
Bryant Jennifer, 1474
Burdette Dara, 1479
Butler Marcus, 1472
Butterfield Lisa, 1468

Campbell Katie, 1478
Campos Balea Begona, 1470
Carcereny Enric, 1470
Cassier Philippe, 1475
Chae Young Kwang, 1469
Chen Delphine, 1472
Chen Valerie, 1479
Chhibber Aparna, 1473
Chioccia E, 1477
Chmielowski Bartosz, 1478
Church Sarah, 1468
Clark Ryan, 1479
Clay Tim, 1470
Cobo-Dols Manuel, 1470
Conroy Andy, 1478
Cope Jamie, 1479
Curti Brendan, 1473

Dalmas Olivier, 1478
Danda Neeraja, 1477
Datta Antara, 1473
De Winter Hilde, 1475
Del Valle Diane, 1477
Dengler Luke, 1478
Dennis Michael, 1469
Desai Arati, 1477
Desideri Serena, 1477
Dey Agnish, 1472
Diab Adi, 1473
Doger Bernard, 1470
Duault Caroline, 1477
Dubensky Thomas, 1471, 1479

Farwell Michael, 1472
Fehr Jacques, 1477
Felip Enriqueta, 1470

Fernandez Elena, 1475
Ferris Michael, 1472
Florescu Ana Maria, 1475
Forster Martin, 1470
Foy Susan, 1478
Francica Brian, 1479
Franzussoff Alex, 1478
Freund Dave, 1479
Funke Roel, 1478

Garcia Ledo Gema, 1470
Gentles Andrew, 1477
Gnjatic Sacha, 1477
Gogas Helen, 1473
Goldman Wes, 1478
Gomez-Roca Carlos, 1475
Gonzalez-Kozlova Edgar, 1477
Gordon Michael, 1472
Gordon Sarah, 1469
Gort Eelke, 1475
Graham Michael, 1472
Grossman Stuart, 1477
Gunturu Swetha, 1478

Hays David, 1472
Heath James, 1478
Heeringa Katharine, 1478
Hoch Ute, 1473
Holmes Tyson, 1477
Holtz Anja, 1479
Howes Tim, 1468
Hsieh David, 1479
Huang Eva, 1478
Humphrey Emily, 1478
Hunter Theresa, 1478
Hussaini Adeel, 1478

Iams Wade, 1470
Ioannou Kyriaki, 1475

Jacoby Kyle, 1478
Jenkins Yonchu, 1471
Jin Lixian, 1477
Johnson Henry, 1479

Kalinka Ewa, 1470
Keefe Matthwe, 1478
Kefas Joanna, 1470
Keliher Edmund, 1472
Khushalani Nikhil, 1473
Kim Sean, 1478
Kim Youngmi, 1478
Kim-Schulze Seunghee, 1477
Kirkin Vladimir, 1475
Korn Ron, 1472
Krebs Matthew, 1470
Krieg Jennifer, 1475
Kukreja Monica, 1478
Kurzrock Razelle, 1469

Lawler Sean, 1477
Le William, 1472
Lebbe Celeste, 1473
Lee Ian, 1477

Author index

Lee Sylvia, 1478
Legenne Philippe, 1475
Leon Michael, 1478
Liang Samantha, 1468
Lieberman Frank, 1477
Liu Feng, 1472
Long Georgina, 1473
Lopez Lenika, 1477
Lu William, 1478
Lu Yue, 1478

Ma Yan, 1478
Maecker Holden, 1477
Majem Margarita, 1470
Mandi Stefanie, 1478
Mantica Megan, 1477
Manzanera Andrea, 1477
Maresca Kevin, 1472
Margolin Kim, 1472
Mathur Jyoti, 1478
Mauguen Audrey, 1472
McConathy Jonathan, 1472
Mende Ines, 1478
Mendoza Ventura, 1478
Moot Robert, 1478
Mossi Patrick, 1475
Mueller Christian, 1470
Muñoz Couselo Eva, 1473
Mutch David, 1469

Nabors L Burt, 1477
Narang Jayant, 1472
Ng Alphonsus, 1478
Nie Kai, 1477

Oh David, 1478
Olson Walter, 1474
Othus Megan, 1469

Pal Sumanta, 1472
Pan Zheng, 1478

Pandit-Taskar Neeta, 1472
Patel Nirav, 1477
Patel Sandip, 1469
Peguero Julio, 1470
Peng Songming, 1478
Pereira Caio, 1473
Peruzzi Pierpaolo, 1477
Phan Phi, 1468
Pichavant Mina, 1477
Plets Melissa, 1469
Postow Michael, 1472
Potdevin Guillaume, 1472
Prasit Peppi, 1479
Purandare Bhamini, 1478

Quach Boi, 1478

Rao Arati, 1478
Ravimohan Shruthi, 1473
Reardon David, 1477
Reeves Jason, 1478
Ribas Antoni, 1478
Ryan Christopher, 1469

Samanta Saheli, 1479
Samlowski Wolfram, 1469
Sandhu Shahneen, 1473
Schmidt Guenter, 1472
Schoenfeld Adam, 1478
Schwartzman Gabrielle, 1474
Sennino Barbara, 1478
Sharon Elad, 1469
Shields Anthon, 1472
Sibley Alison, 1478
Singh Aman, 1472
Skrdlant Lindsey, 1478
Sjlingluff Craig, 1474
Smith Chad, 1478
Smith Kelly, 1474
Snyder James, 1477
Sosman Jeff, 1478

Stallings-Schmitt Todd, 1478
Standifer Nathan, 1471
Stavropoulou Vaia, 1475
Stawiski Eric, 1478
Steeghs Neeltje, 1475
Stojcheva Nina, 1475
Strowd Roy, 1477

Tak Paul, 1477
Tatter Stephen, 1477
Taylor Matthew, 1473
Thomas Jacob, 1472
Tran Christine, 1474
Triebel Frederic, 1470
Twardowski Przemyslaw, 1472

Ulaner Gary, 1472
Ursol Grygorii, 1470

Van Den Abbeele Annick, 1472
Van Den Eertwegh Alfonsus, 1473
Vila Martinez Laia, 1470

Walbert Tobias, 1477
Wang Clifford, 1478
Wen Patrick, 1477
White Andrew, 1468
White William, 1478
Whiting Sam, 1471
Williams Claire, 1478
Wilson Ian, 1472
Wong Jeffrey, 1472

Ye Xiaobu, 1477
Yi Michael, 1478
Yuan Yuan, 1478
Yuen Benjamin, 1478

Zhou Ming, 1473

- Adoptive immunotherapy 1005, 1006, 1009, 1029, 1034, 1047, 1100, 1140, 1175, 1176, 1177, 1192, 121, 1225, 1226, 123, 1232, 1234, 1235, 1236, 1238, 1239, 1276, 1278, 1283, 1374, 1402, 1409, 1421, 16, 162, 17, 175, 176, 177, 179, 180, 181, 182, 183, 184, 185, 186, 188, 189, 190, 191, 192, 193, 195, 196, 197, 198, 201, 203, 204, 205, 206, 209, 210, 212, 213, 214, 215, 218, 220, 221, 222, 227, 229, 231, 232, 233, 234, 235, 236, 237, 240, 243, 244, 245, 246, 247, 248, 249, 250, 251, 254, 255, 256, 259, 261, 262, 263, 264, 265, 267, 272, 274, 275, 276, 277, 278, 282, 283, 284, 285, 286, 290, 291, 292, 294, 295, 296, 297, 30, 300, 302, 304, 305, 306, 307, 308, 309, 311, 312, 313, 314, 315, 318, 320, 321, 323, 325, 327, 328, 330, 331, 336, 337, 338, 340, 341, 342, 343, 344, 346, 348, 349, 350, 351, 352, 355, 356, 357, 358, 359, 360, 361, 362, 364, 365, 366, 367, 368, 370, 371, 373, 374, 376, 377, 378, 379, 381, 382, 384, 385, 386, 387, 390, 393, 395, 398, 402, 403, 404, 406, 407, 409, 410, 411, 413, 417, 493, 506, 548, 572, 578, 601, 612, 632, 639, 645, 649, 652, 654, 672, 674, 685, 689, 697, 70, 712, 713, 715, 722, 726, 727, 728, 75, 751, 755, 77, 775, 781, 783, 787, 789, 792, 796, 819, 832, 837, 849, 852, 857, 871, 881, 883, 886, 911, 929, 93, 939, 944, 947, 950, 951, 959, 961, 965, 975,
- Angiogenesis 1142, 1151, 418, 42, 457, 507, 515, 643, 664, 704, 725, 736, 885, 907, 911,
- Antibody 10, 1011, 1018, 104, 1056, 1059, 106, 1062, 1063, 1067, 1068, 1069, 1070, 1074, 1075, 1077, 1079, 1080, 1083, 1088, 1090, 1093, 1098, 1099, 1104, 1105, 1123, 1140, 1141, 1143, 1146, 1149, 1151, 1153, 1162, 1184, 1186, 1188, 1189, 1191, 1192, 1194, 1195, 1196, 1197, 1208, 1209, 1210, 1212, 1213, 1215, 1219, 1221, 1226, 1228, 1234, 1246, 1260, 1287, 1316, 1320, 1321, 1325, 1326, 1328, 1332, 1333, 1337, 1338, 1339, 1341, 1346, 1347, 1348, 1349, 1350, 1351, 1357, 1360, 1361, 1364, 1369, 1371, 1374, 1377, 1378, 1384, 1391, 1392, 1393, 1395, 1396, 1397, 1399, 1400, 1401, 1415, 1432, 144, 1447, 1449, 145, 147, 154, 169, 204, 206, 207, 262, 270, 281, 296, 3, 306, 31, 346, 35, 354, 37, 373, 377, 38, 388, 39, 41, 425, 426, 432, 438, 45, 461, 462, 465, 466, 469, 47, 470, 474, 477, 48, 482, 483, 485, 488, 489, 491, 492, 494, 497, 498, 501, 506, 507, 52, 521, 53, 532, 542, 543, 55, 553, 571, 574, 578, 582, 589, 592, 596, 604, 607, 616, 619, 623, 631, 637, 640, 663, 667, 668, 675, 699, 707, 709, 71, 714, 717, 72, 725, 726, 727, 729, 731, 732, 733, 735, 739, 74, 740, 746, 748, 751, 753, 755, 756, 757, 758, 761, 764, 770, 771, 773, 775, 778, 779, 78, 782, 793, 794, 8, 80, 802, 807, 808, 809, 815, 816, 817, 821, 823, 833, 836, 839, 843, 846, 853, 856, 858, 859, 869, 877, 885, 891, 900, 901, 950, 973, 98, 988, 989, 991,
- Antigen presenting cells 1001, 102, 1020, 1033, 1035, 1052, 1054, 1065, 1071, 1072, 1083, 1086, 1126, 1129, 1131, 1135, 1137, 1139, 1143, 1153, 1160, 1161, 1162, 1163, 1168, 1171, 1172, 1178, 1181, 1185, 1213, 1233, 1237, 1257, 1315, 1336, 1348, 1365, 1394, 1415, 1420, 1430, 1437, 1458, 16, 163, 180, 183, 184, 194, 220, 224, 227, 237, 256, 257, 271, 28, 30, 315, 318, 321, 361, 378, 404, 470, 477, 483, 484, 504, 569, 572, 578, 588, 63, 638, 656, 675, 676, 689, 700, 714, 751, 778, 782, 790, 793, 80, 808, 828, 836, 861, 866, 895, 903, 907, 910, 941, 944, 951, 967, 969, 973, 979, 981, 982, 989, 991,
- Autoimmunity 1243, 1252, 1257, 1260, 1263, 274, 3, 438, 439, 44, 440, 441, 616,
- B cell 1, 104, 11, 1136, 1140, 1143, 1168, 1194, 1218, 1291, 1302, 134, 1384, 1426, 1427, 1429, 1446, 1451, 146, 147, 212, 245, 271, 3, 30, 35, 383, 39, 435, 460, 468, 509, 53, 542, 543, 590, 610, 613, 616, 618, 619, 702, 717, 756, 782, 819, 823, 830, 843, 913, 924, 948, 951, 972, 973, 974, 988,
- Bioinformatics 100, 1000, 1007, 1010, 102, 1021, 103, 1038, 1049, 1055, 111, 124, 1242, 1269, 127, 1270, 1273, 1274, 1276, 1278, 1281, 1287, 1288, 1290, 1292, 1294, 1296, 1297, 1298, 13, 1300, 1302, 1303, 1311, 133, 136, 1399, 14, 1411, 1424, 1438, 1452, 1454, 1461, 1463, 15, 151, 152, 161, 163, 164, 165, 168, 171, 174, 227, 24, 245, 27, 272, 301, 312, 320, 340, 36, 374, 40, 418, 44, 508, 51, 522, 523, 53, 536, 538, 54, 542, 559, 579, 583, 6, 63, 64, 643, 690, 712, 74, 76, 80, 804, 818, 826, 845, 85, 86, 867, 9, 908, 916, 92, 925, 926, 927, 928, 929, 939, 941, 943, 944, 945, 98, 987, 988, 99, 993, 999,
- Biomarkers 10, 100, 1006, 101, 1013, 102, 103, 1033, 1035, 1040, 1043, 1045, 1049, 105, 107, 108, 11, 111, 112, 113, 1134, 114, 1141, 1147, 115, 117, 1179, 118, 1188, 119, 120, 1212, 1215, 1216, 1217, 1219, 122, 123, 124, 1244, 1246, 1251, 1254, 1255, 126, 1261, 1264, 1269, 127, 1270, 1272, 1273, 1277, 1279, 1280, 1281, 1282, 1285, 1287, 1289, 1290, 1291, 1292, 1294, 1296, 1297, 1298, 1299, 13, 1300, 1304, 131, 132, 133, 1332, 1342, 1344, 135, 1351, 136, 1360, 1369, 1371, 1374, 138, 1382, 14, 140, 1400, 1403, 141, 142, 1422, 1424, 143, 1430, 1432, 1436, 1445, 1446, 145, 1454, 1456, 1459, 147, 148, 149, 150, 151, 153, 155, 156, 159, 16, 160, 163, 164, 165, 167, 168, 169, 172, 18, 180, 187, 19, 199, 2, 20, 21, 22, 23, 24, 249, 25, 26, 27, 28, 281, 285, 289, 29, 296, 3, 30, 315, 32, 33, 333, 335, 339, 34, 36, 37, 374, 38, 39, 41, 43, 433, 438, 44, 45, 451, 47, 474, 478, 48, 480, 49, 502, 506, 508, 51, 510, 512, 513, 516, 517, 52, 523, 524, 527, 528, 530, 531, 534, 54, 541, 542, 544, 545, 55, 552, 554, 556, 559, 56, 560, 566, 568, 569, 57, 574, 576, 577, 579, 58, 580, 583, 584, 586, 587, 59, 6, 60, 600, 601, 602, 606, 607, 608, 609, 61, 611, 612, 613, 614, 616, 62, 623, 63, 635, 64, 650, 653, 656, 657, 659, 661, 663, 669, 67, 675, 680, 685, 687, 688, 695, 697, 7, 701, 708, 709, 71, 713, 714, 717, 719, 722, 73, 731, 733, 739, 74, 745, 748, 759, 76, 761, 767, 768, 777, 78, 782, 784, 79, 8, 800, 81, 818, 82, 834, 838, 842, 843, 845, 85, 859, 867, 87, 877, 879, 88, 880, 890, 894, 9, 90, 91, 92, 923, 929, 93, 930, 94, 941, 949, 95, 957, 97, 987, 99, 990, 992,
- Bispecifics 1018, 1057, 1058, 106, 1061, 1063, 1067, 1069, 1074, 1079, 1083, 1123, 1129, 1143, 1150, 1183, 1194, 1196, 1197, 1198, 1199, 1200, 1201, 1202, 1203, 1204, 1205, 1206, 1208, 1209, 1210, 1211, 1212, 1213, 1214, 1225, 1226, 1234, 1250, 1283, 1293, 1301, 1316, 1319, 1321, 1325, 1326, 1328, 1337, 1340, 1351, 1356, 1360, 1364, 1366, 1368, 1375, 1377, 1397, 1415, 1422, 144, 1447, 154, 177, 180, 197, 207, 208, 266, 305, 377, 388, 399, 461, 462, 467, 468, 469, 481, 491, 500, 521, 619, 620, 667, 668, 686, 707, 713, 723, 725, 729, 732, 733, 735, 746, 771, 821, 837, 853, 858, 895, 897,
- CAR T cells 1020, 1192, 1222, 1223, 1226, 1230, 1234, 1235, 1238, 1239, 1283, 1380, 1454, 16, 162, 175, 181, 185, 187, 188, 190, 193, 197, 198, 200, 201, 202, 203, 205, 206, 208, 209, 210, 213, 217, 220, 223, 224, 225, 229, 230, 231, 233, 238, 240, 242, 243, 244, 246, 247, 250, 252, 253, 258, 259, 260, 261, 262, 263, 267, 269, 274, 276, 277, 278, 279, 284, 286, 287, 288, 289, 290, 291, 294, 295, 296, 299, 300, 301, 304, 305, 308, 309, 310, 311, 314, 316, 317, 322, 324, 325, 326, 327, 329, 330, 332, 334, 335, 339, 341, 344, 345, 347, 350, 351, 352, 357, 358, 360, 362, 366, 367, 368, 375, 379, 380, 381, 382, 383, 385, 391, 395, 396, 397, 398, 399, 400, 401, 402, 410, 411, 412, 414, 558, 572, 633, 634, 639, 652, 672, 687, 697, 728, 737, 760, 77, 796, 816, 832, 847, 852, 902, 911, 929, 93, 935, 975,
- Carcinogenesis 110, 1428, 1459, 1460, 16, 325, 418, 446, 5, 64, 792, 940,
- Checkpoint blockade 100, 1000, 1002, 1005, 1009, 101, 1013, 1015, 1019, 1023, 1037, 1038, 1040, 1041, 1045, 1046, 1052, 1057, 1062, 1064, 1065, 1066, 1069, 107, 1072, 1073, 1074, 1079, 1080, 1082, 1086, 1088, 1089, 1099, 11, 1102, 1104, 1110, 1111, 1114, 1115, 112, 1121, 1124, 1128, 1134, 1139, 1140, 1141, 1142, 1147, 1151, 1154, 1156, 1157, 1158, 1168, 117, 1174, 118, 1183, 1184, 1187, 1188, 119, 1190, 1195, 1208, 1209, 1210, 1211, 122, 1228, 1229, 123, 1234, 1236, 1241, 1242, 1243, 1244, 1245, 1246, 1248, 1251, 1253, 1254, 1256, 1257, 1259, 1260, 1261, 1263, 1264, 1265, 1266, 1267, 1268, 1269, 127, 1270, 1274, 1279, 1280, 1284, 1289, 1296, 1297, 1304, 1305, 1306, 1307, 1313, 1315, 132, 1326, 133, 1332, 1333, 1335, 1337, 1342, 1349, 135, 1350, 1352, 1354, 1355, 136, 1361, 1364, 1366, 1367, 1373, 1376, 1378, 1379, 138, 1380, 1384, 1386, 1387, 1389, 1391, 1393, 1397, 140, 1401, 1403, 141, 142, 1426, 1428, 1439, 1444, 1450, 1455, 1462, 1465, 1466, 148, 149, 15, 150, 154, 157, 158, 162, 164, 167, 172, 178, 19, 199, 20, 21, 216, 22, 225, 268, 270, 288, 29, 311, 325, 33, 34, 346, 347, 363, 37, 371, 373, 39, 4, 406, 41, 412, 415, 418, 420, 422, 423, 424, 425, 426, 427, 428, 429, 43, 430, 431, 432, 433, 434, 435, 437, 438, 439, 44, 440, 441, 442, 444, 445, 447, 448, 449, 450, 451, 452, 453, 455, 456, 457, 458, 459, 460, 461, 462, 463, 464, 465, 466, 467, 468, 469, 470, 471, 472, 473, 474, 475, 476, 477, 478, 479, 480, 481, 482, 483, 484, 485, 486, 488, 489, 49, 490, 492, 493, 494, 495, 496, 497, 498, 499, 50, 500, 501, 502, 503, 504, 505, 506, 507, 508, 509, 51, 510, 511, 512, 513, 514, 515, 516, 517, 519, 52, 520, 521, 522, 523, 524, 527, 528, 529, 53, 530, 531, 532, 534, 535, 537, 538, 541, 542, 543, 544, 554, 556, 559, 56, 560, 563, 564, 568, 569, 57, 570, 571, 574, 576, 578, 579, 580, 581, 582, 583, 584, 586, 587, 588, 589, 59, 590, 591,

Subject index

- 592, 594, 595, 596, 599, 6, 604, 606, 607, 608, 609, 611, 613, 614, 615, 616, 617, 618, 62, 622, 623, 626, 628, 629, 635, 637, 638, 643, 644, 650, 651, 653, 656, 657, 659, 663, 664, 665, 666, 668, 67, 670, 673, 675, 676, 677, 681, 682, 683, 684, 688, 690, 692, 693, 695, 698, 7, 701, 703, 704, 706, 707, 709, 710, 711, 715, 716, 717, 718, 72, 722, 723, 725, 726, 727, 73, 732, 733, 734, 735, 736, 738, 739, 740, 742, 745, 746, 751, 753, 755, 757, 758, 759, 761, 764, 766, 767, 768, 769, 771, 772, 773, 774, 778, 779, 782, 783, 788, 790, 791, 792, 793, 796, 798, 799, 800, 804, 805, 807, 808, 810, 811, 813, 814, 816, 817, 818, 819, 821, 822, 823, 827, 830, 831, 834, 838, 841, 842, 843, 844, 849, 850, 851, 853, 854, 856, 860, 862, 866, 868, 869, 876, 878, 879, 88, 882, 883, 884, 885, 888, 889, 89, 891, 892, 895, 896, 897, 898, 899, 9, 903, 904, 905, 906, 91, 910, 914, 915, 916, 917, 918, 92, 920, 927, 930, 931, 932, 933, 934, 937, 939, 94, 941, 942, 946, 952, 960, 964, 965, 966, 968, 977, 979, 982, 988, 989, 997, Chemokine 1018, 1021, 1029, 1120, 1144, 1171, 1218, 1223, 1239, 128, 1342, 1348, 1365, 1393, 1396, 1436, 1439, 145, 1462, 1463, 148, 199, 211, 276, 301, 304, 322, 338, 349, 405, 547, 548, 658, 724, 76, 761, 768, 777, 807, 81, 823, 882, 910, 914, 917, 94, 962, Chemotherapy 1108, 1114, 1118, 1141, 1142, 1241, 1284, 1335, 1387, 145, 1455, 164, 191, 199, 24, 276, 341, 354, 423, 435, 445, 451, 452, 453, 454, 455, 457, 480, 545, 560, 578, 58, 582, 599, 61, 640, 651, 656, 676, 704, 705, 791, 796, 798, 799, 800, 801, 802, 803, 804, 807, 808, 809, 872, 874, 90, 905, 953, 972, 991, Clinical study 101, 112, 1132, 1244, 1246, 1255, 1264, 1267, 1273, 13, 1303, 1309, 136, 1387, 14, 1406, 1407, 1408, 1413, 1416, 1417, 164, 172, 197, 327, 362, 397, 433, 437, 445, 452, 457, 47, 470, 478, 50, 503, 508, 512, 522, 538, 541, 542, 543, 544, 558, 561, 564, 574, 576, 578, 59, 592, 595, 606, 607, 608, 609, 615, 621, 623, 624, 626, 628, 629, 631, 632, 633, 634, 636, 639, 647, 649, 651, 652, 653, 658, 661, 663, 667, 668, 67, 670, 674, 675, 680, 681, 685, 687, 691, 695, 696, 700, 701, 702, 703, 706, 707, 709, 713, 715, 716, 719, 720, 721, 722, 724, 725, 731, 732, 733, 739, 741, 745, 748, 750, 751, 753, 754, 756, 760, 761, 762, 763, 766, 768, 769, 773, 775, 776, 777, 778, 780, 781, 784, 785, 786, 787, 789, 790, 800, 827, 848, 850, 932, 935, 94, Clinical trial 1082, 114, 1171, 1173, 1264, 1387, 1416, 1417, 1418, 145, 1454, 165, 187, 219, 244, 27, 301, 327, 361, 362, 391, 405, 425, 474, 50, 503, 508, 542, 545, 546, 547, 548, 549, 551, 553, 554, 555, 556, 557, 558, 559, 560, 562, 563, 564, 565, 566, 568, 569, 570, 571, 576, 578, 581, 583, 584, 585, 586, 587, 588, 589, 591, 592, 594, 595, 596, 597, 598, 599, 600, 601, 603, 604, 605, 606, 607, 608, 612, 613, 616, 617, 620, 621, 622, 625, 626, 627, 628, 629, 632, 633, 634, 635, 636, 637, 638, 639, 640, 642, 643, 644, 645, 647, 649, 650, 652, 653, 654, 655, 656, 657, 658, 659, 660, 661, 663, 664, 665, 666, 667, 668, 669, 671, 672, 674, 675, 676, 677, 678, 679, 680, 681, 682, 683, 684, 685, 686, 687, 689, 692, 693, 694, 697, 698, 699, 700, 702, 703, 705, 708, 709, 710, 711, 712, 713, 714, 715, 717, 718, 723, 725, 726, 727, 728, 731, 732, 733, 734, 736, 737, 738, 739, 740, 741, 742, 743, 744, 745, 746, 747, 748, 750, 753, 754, 755, 756, 757, 758, 759, 763, 764, 766, 767, 769, 770, 771, 772, 773, 774, 775, 776, 777, 778, 779, 781, 782, 783, 784, 786, 787, 788, 789, 790, 800, 800, 92, 930, 939, 953, 987, Coinhibition 1025, 1046, 1208, 1211, 1255, 1326, 1332, 135, 1379, 1380, 477, 485, 489, 506, 517, 535, 651, 676, 738, 757, 778, 779, 804, 813, 814, 84, 854, 879, 880, 896, 906, 96, 97, Costimulation 1023, 1025, 1052, 1056, 1057, 1060, 1063, 1069, 1070, 1074, 1076, 1077, 1084, 1107, 1126, 1143, 1146, 1147, 1155, 1168, 1183, 1194, 1201, 1203, 1204, 1208, 1214, 1293, 1321, 1326, 1340, 1341, 1354, 1356, 1368, 1374, 1384, 1415, 1422, 207, 242, 250, 252, 259, 281, 282, 342, 385, 396, 412, 424, 456, 464, 465, 470, 501, 506, 541, 678, 714, 738, 767, 775, 776, 81, 813, 836, 84, 855, 860, 951, 96, 97, COVID and Immunotherapy 1286, 480, 63, 649, 919, 920, 922, 923, 924, Cytokine 1014, 1018, 1020, 1021, 1023, 1028, 1042, 1048, 1052, 1059, 1065, 1069, 1070, 1076, 1077, 1078, 1079, 1080, 1081, 1082, 1083, 1084, 1085, 1086, 1087, 1088, 1089, 1090, 1091, 1092, 1093, 1094, 1095, 1096, 1097, 1098, 1099, 1100, 1101, 1102, 1103, 1104, 1105, 1118, 1120, 1122, 1125, 1126, 1127, 1138, 1152, 1157, 1159, 1163, 1168, 1171, 1172, 1183, 1185, 1187, 1195, 1196, 1199, 1202, 1203, 1207, 1215, 1218, 1223, 1227, 1236, 1241, 1258, 1262, 128, 1293, 1312, 1323, 1329, 1342, 1348, 1351, 1356, 1359, 1366, 1368, 1372, 1392, 1396, 1405, 1410, 142, 1436, 144, 148, 150, 162, 179, 183, 184, 186, 187, 193, 202, 21, 211, 221, 223, 225, 235, 267, 278, 281, 282, 287, 314, 327, 329, 335, 345, 363, 366, 369, 376, 378, 38, 382, 391, 393, 405, 425, 438, 460, 465, 488, 511, 520, 561, 598, 606, 624, 625, 629, 631, 636, 640, 649, 657, 679, 681, 714, 715, 718, 719, 720, 724, 736, 737, 743, 744, 750, 76, 760, 761, 762, 767, 768, 769, 770, 775, 777, 826, 829, 837, 841, 854, 857, 868, 871, 880, 881, 882, 900, 917, 949, 952, 962, 983, 991, 994, 995, 999, Dendritic cell 102, 1033, 104, 1052, 1054, 1070, 1071, 1072, 1124, 1126, 1129, 1132, 1138, 1143, 1153, 1161, 1162, 1171, 1172, 1179, 1208, 1225, 1233, 1237, 1315, 1336, 1365, 1382, 1394, 1396, 1397, 1401, 1415, 1420, 1421, 1437, 1458, 163, 184, 234, 248, 271, 35, 361, 372, 386, 461, 468, 470, 483, 484, 504, 513, 529, 541, 555, 557, 559, 562, 565, 595, 645, 675, 678, 689, 700, 745, 782, 790, 793, 822, 828, 836, 838, 861, 872, 941, 947, 949, 953, 960, 978, 979, 980, 981, 991, 994, Epidemiology 1246, 1256, 13, 14, 1407, 1408, 1413, 1414, 433, 442, 478, 937, Epigenetics 1050, 1113, 1146, 1313, 1421, 1424, 1425, 1430, 1445, 164, 351, 370, 444, 531, 664, 7, 80, 888, 912, 915, 916, Extracellular vesicles/exosomes 1330, 1344, 1345, 984, Gene expression 1006, 101, 1021, 1034, 1049, 1050, 1051, 1054, 1055, 1108, 1113, 1117, 112, 1127, 1135, 1146, 1147, 115, 1151, 1159, 1164, 1182, 1187, 119, 121, 1219, 1223, 1231, 1242, 126, 1269, 127, 1270, 1277, 1278, 1279, 1285, 1286, 1288, 1302, 1307, 1324, 133, 1340, 1344, 1345, 1356, 1373, 1392, 1421, 1424, 1430, 1438, 1451, 1454, 146, 1463, 1467, 148, 15, 151, 153, 159, 165, 167, 173, 174, 208, 210, 223, 227, 229, 245, 25, 263, 27, 301, 312, 327, 340, 343, 35, 365, 38, 390, 40, 406, 411, 428, 434, 438, 448, 459, 46, 470, 478, 490, 493, 50, 504, 508, 510, 517, 522, 523, 538, 54, 545, 560, 569, 59, 601, 608, 639, 64, 643, 660, 666, 712, 75, 76, 77, 784, 818, 86, 913, 916, 917, 92, 923, 924, 926, 927, 929, 941, 944, 945, 95, 951, 955, 961, 962, 965, 971, 983, 987, 99, 996, 999, Genetic polymorphism 229, 263, 448, 461, 758, 759, 77, 978, Glycoproteomics 1346, 1347, 1444, 772, 852, 981, Granulocyte 1164, 1169, 1224, 1384, 1387, 146, 1464, 19, 211, 356, 472, 511, 533, 629, 701, 840, 998, Immune adjuvant 1070, 1078, 1105, 1110, 1111, 1120, 1121, 1124, 1125, 1129, 1158, 1163, 1166, 1167, 1171, 1172, 1178, 1185, 1267, 1281, 1315, 1348, 1385, 1392, 1410, 266, 308, 386, 430, 446, 478, 541, 546, 547, 555, 603, 688, 790, 827, 849, 894, 912, 937, Immune contexture 1001, 1011, 1033, 104, 1059, 109, 11, 111, 1139, 116, 1160, 118, 120, 128, 1282, 1289, 1290, 1299, 131, 133, 135, 139, 1419, 142, 1420, 1429, 143, 1435, 1439, 1442, 1452, 1454, 1456, 146, 1461, 149, 155, 160, 168, 211, 27, 362, 37, 397, 419, 48, 504, 514, 523, 527, 545, 554, 569, 57, 584, 60, 72, 775, 78, 79, 83, 836, 842, 85, 867, 87, 893, 894, 898, 916, 927, 945, 955, 956, 957, 972, 981, 99, 999, Immune monitoring 1020, 1021, 1022, 1035, 104, 1065, 107, 1095, 110, 1113, 1120, 1125, 113, 1140, 1147, 1179, 121, 124, 125, 1251, 1284, 1297, 130, 1303, 134, 1361, 139, 141, 1411, 142, 1421, 1422, 1426, 143, 1433, 1451, 1456, 1458, 150, 155, 156, 16, 162, 165, 184, 187, 21, 218, 220, 23, 27, 28, 289, 3, 30, 31, 324, 34, 36, 362, 374, 397, 4, 418, 419, 420, 44, 448, 47, 48, 49, 50, 502, 504, 510, 512, 520, 53, 538, 541, 542, 545, 546, 55, 560, 576, 580, 609, 610, 611, 613, 617, 621, 64, 641, 642, 656, 659, 667, 675, 685, 69, 691, 692, 693, 695, 708, 715, 719, 720, 761, 782, 784, 8, 81, 826, 83, 836, 838, 844, 85, 862, 873, 89, 891, 898, 90, 923, 935, 94, 940, 942, 949, 957, 961, 97, 974, 98, 986, 987, 989, 996, Immune suppression 1000, 1007, 1013, 1015, 1017, 1019, 1032, 1036, 1040, 1042, 1043, 1049, 1052, 1054, 1062, 1064, 1065, 1082, 1089, 1109, 111, 1112, 1128, 1133, 1140, 1142, 1144, 1148, 1151, 1154, 1165, 1182, 1184, 1202, 1204, 1221, 1224, 1228, 1260, 1267, 1304, 1305, 1307, 1308, 1309, 1312, 1322, 1324, 133, 1331, 1338, 1342, 1343, 1353, 1364, 1370, 1371, 1376, 1379, 1386, 1399, 1401, 141, 1419, 1420, 1423, 1426, 1432, 1436, 1439, 1440, 1441, 1443, 1444, 145, 1450, 1455, 1461, 1463, 149, 150, 157, 159, 165, 178, 187, 189, 199, 225, 228, 231, 24, 276, 281, 304, 325, 329, 358, 360, 376, 385, 398, 413, 414, 425, 426, 434, 437, 445, 446, 447, 450, 465, 472, 474, 477, 479, 48, 483, 485, 487, 490, 494, 498, 502, 505, 506, 510, 511, 513, 52, 522, 523, 526, 530, 533, 551, 56, 57, 574, 587, 588, 599, 60, 604, 610, 62, 621, 623, 637, 683, 69, 701, 712, 736, 771, 772, 793, 801, 807, 808, 810, 813, 814, 815, 817, 822, 830, 831, 832, 833, 834, 84, 855, 856, 857, 873, 877, 878, 879, 889, 891, 893, 894, 896, 898, 899, 90, 905, 910, 912, 913, 914, 917, 935, 942, 946, 950, 955, 957, 960, 962, 964, 970, 974, 989, 992, 995, 999,

Immune tolerance 100, 1050, 1069, 1112, 1113, 1150, 1210, 1253, 1257, 1303, 1308, 1343, 1353, 141, 1443, 1462, 210, 274, 341, 446, 599, 807, 815, 834, 848, 964,
Immune toxicity 1020, 1076, 1083, 1090, 1098, 1103, 1196, 1200, 1227, 1236, 1242, 1244, 1245, 1246, 1247, 1248, 1249, 1250, 1251, 1252, 1253, 1254, 1255, 1257, 1258, 1259, 1260, 1261, 1262, 1263, 1264, 1265, 1266, 1267, 1268, 1274, 1293, 1329, 1386, 1399, 1407, 1408, 1413, 1415, 144, 19, 202, 207, 211, 223, 299, 301, 316, 325, 34, 382, 402, 403, 419, 437, 438, 44, 441, 442, 472, 480, 598, 616, 621, 655, 667, 67, 687, 696, 719, 749, 785, 83, 889, 900, 918, 919, 930, 932, 934, 935, 936, 939,
Immunoscore 1033, 104, 1053, 1279, 1284, 135, 1424, 1454, 1456, 171, 27, 29, 50, 54, 584, 587, 850, 869, 957,
Inflammation 1020, 1032, 1072, 1078, 1089, 1118, 112, 1133, 1141, 1148, 1152, 1156, 1166, 1172, 1224, 1243, 1254, 1257, 1258, 1260, 1262, 128, 1291, 1315, 1359, 1372, 138, 1385, 1386, 1445, 1463, 1464, 149, 15, 153, 161, 19, 21, 3, 301, 376, 418, 42, 441, 442, 478, 486, 511, 551, 580, 610, 611, 643, 649, 687, 702, 749, 767, 796, 832, 840, 882, 90, 917, 946, 961, 981,
Leukemia/Lymphoma 1006, 103, 1152, 1198, 1203, 1225, 1226, 1230, 1234, 1239, 1313, 1369, 1427, 1454, 16, 175, 205, 210, 220, 233, 240, 245, 25, 251, 253, 260, 266, 269, 274, 280, 281, 296, 300, 306, 323, 334, 336, 351, 353, 354, 402, 411, 423, 494, 685, 687, 755, 795, 824, 889, 897, 899, 902, 935, 98, 995,
MDSC 1, 114, 1142, 1154, 1158, 1165, 1171, 1173, 1204, 1224, 1229, 1313, 1327, 1345, 1370, 1381, 1385, 1410, 1460, 1464, 157, 171, 191, 394, 425, 444, 462, 472, 483, 511, 513, 546, 623, 629, 701, 736, 745, 751, 810, 822, 831, 838, 850, 873, 877, 893, 971, 992,
Metabolism 1000, 1020, 1031, 1042, 1044, 1096, 1116, 1119, 1146, 1154, 1238, 1307, 1322, 1343, 1355, 1381, 141, 1423, 178, 188, 189, 2, 205, 211, 214, 223, 234, 238, 267, 330, 350, 370, 398, 4, 407, 408, 463, 607, 72, 79, 831, 879, 904, 91, 965, 970, 975, 976, 977, 98,
Microbiome 1175, 1304, 1306, 1307, 1308, 1309, 1310, 1311, 1312, 1434, 1467, 486, 572, 590, 607, 614, 618, 627, 656, 961,
Monocyte/Macrophage 1, 1000, 1001, 1002, 1003, 1004, 1019, 104, 1054, 1062, 1065, 1082, 111, 1119, 112, 1130, 115, 1153, 1154, 1158, 1161, 1162, 1164, 1165, 1168, 1173, 1179, 1189, 1205, 1209, 1211, 1212, 1225, 1237, 1257, 1304, 1307, 1322, 1324, 1331, 1338, 1342, 1344, 1345, 1348, 1352, 1353, 1359, 1360, 1365, 1377, 1380, 1382, 1384, 1385, 1390, 1393, 1396, 1401, 1420, 1423, 143, 1433, 1436, 1440, 1446, 1448, 1449, 1456, 1464, 147, 150, 163, 19, 194, 301, 315, 318, 328, 329, 337, 345, 363, 371, 372, 376, 378, 393, 397, 405, 414, 425, 466, 467, 468, 472, 476, 477, 482, 484, 485, 487, 492, 494, 496, 498, 505, 52, 523, 532, 555, 559, 629, 633, 634, 648, 69, 701, 707, 721, 764, 793, 794, 802, 808, 810, 816, 822, 838, 840, 85, 850, 852, 853, 856, 859, 873, 877, 879, 884, 901, 910, 917, 943, 944, 945, 946, 951, 962, 971, 984, 991, 992, 995, 996,
Myeloid cells 1, 1001, 1003, 1007, 1019, 102, 1025, 104, 1054, 1062, 1065, 1082, 1083, 1086, 109, 111, 1119, 1128, 1130, 114, 1151, 1153, 1154, 1158, 1162, 1168, 1185, 1204, 1209, 1211, 1224, 1225, 1237, 129, 1307, 1322, 1327, 134, 1342, 1344, 1345, 1348, 1360, 1365, 1369, 1381, 1383, 1385, 139, 1396, 1401, 1410, 1420, 1442, 1448, 145, 1464, 149, 150, 157, 161, 19, 191, 194, 307, 315, 318, 328, 345, 35, 372, 376, 378, 379, 393, 397, 405, 425, 428, 462, 467, 468, 472, 474, 475, 476, 477, 483, 485, 487, 49, 495, 498, 505, 565, 613, 629, 633, 634, 643, 648, 676, 678, 69, 701, 719, 745, 747, 751, 793, 795, 796, 808, 810, 822, 831, 833, 838, 840, 856, 877, 878, 879, 880, 883, 884, 887, 893, 910, 941, 943, 945, 946, 969, 971, 978, 98, 991, 992, 995, 996,
Neoantigens 100, 1015, 1037, 1086, 110, 1117, 113, 1131, 1172, 1179, 119, 121, 1213, 123, 1232, 1233, 1276, 1286, 1317, 1394, 1411, 183, 184, 218, 227, 230, 237, 241, 244, 256, 28, 282, 292, 320, 321, 342, 348, 359, 36, 364, 384, 387, 43, 45, 46, 464, 476, 5, 51, 529, 53, 538, 55, 560, 562, 565, 62, 63, 637, 652, 660, 691, 692, 693, 706, 712, 74, 783, 789, 80, 820, 851, 861, 892, 949, 959, 967,
NK/NKT cell 1, 1005, 1006, 1007, 1008, 1009, 1010, 1011, 1012, 1013, 1014, 1015, 1016, 1017, 1018, 1025, 104, 1054, 1056, 1059, 1061, 1067, 107, 1072, 1075, 1076, 1081, 1097, 1099, 1100, 1101, 1104, 1138, 1151, 1153, 1157, 1183, 12, 1202, 1204, 1207, 1212, 1215, 1223, 1226, 1231, 1320, 1324, 1332, 1338, 1341, 1359, 1365, 1368, 1372, 1384, 1388, 1391, 1395, 1400, 1410, 1421, 1422, 1427, 1433, 1452, 1464, 147, 177, 186, 195, 200, 204, 210, 211, 213, 214, 216, 221, 228, 245, 259, 264, 265, 272, 273, 281, 290, 298, 302, 303, 306, 309, 313, 314, 319, 322, 323, 328, 333, 336, 341, 349, 358, 366, 372, 373, 381, 386, 392, 394, 398, 413, 432, 460, 465, 467, 474, 489, 490, 493, 513, 548, 631, 632, 647, 649, 659, 66, 686, 716, 718, 724, 726, 727, 743, 745, 746, 755, 778, 792, 794, 809, 824, 859, 871, 881, 886, 891, 902, 909, 913, 960, 986,
Pediatric tumors 1113, 1135, 1189, 1192, 1328, 1390, 176, 222, 231, 274, 303, 307, 317, 327, 328, 348, 356, 362, 373, 391, 394, 397, 399, 400, 413, 464, 526, 802, 836, 874, 881, 935, 996,
Post-translational modifications 1085, 1313, 1317, 1424, 158, 223, 23, 42, 55, 569, 592, 602, 609, 637,
Proteomics 1019, 1047, 113, 116, 117, 1181, 1192, 120, 1275, 130, 1359, 136, 139, 1422, 1459, 150, 165, 168, 211, 24, 312, 37, 38, 42, 45, 559, 574, 580, 602, 659, 687, 74, 79, 80, 842, 852, 87, 923, 94, 945, 975, 98,
Radiotherapy 1033, 1051, 1117, 1122, 1144, 1335, 138, 272, 302, 423, 428, 442, 447, 452, 454, 456, 555, 559, 561, 563, 568, 595, 644, 655, 682, 684, 689, 698, 72, 862, 867, 868, 869, 870, 871, 872, 873, 874, 875, 893,
Regulatory T cell (Treg cell) 100, 1000, 1017, 1048, 1049, 1052, 1064, 1069, 1087, 1091, 1096, 1098, 1109, 1112, 1133, 1134, 1149, 1150, 1221, 1236, 1313, 1338, 1339, 1343, 1352, 1355, 1361, 1371, 1376, 1379, 1384, 1386, 1389, 1392, 1393, 1399, 142, 1421, 147, 165, 301, 31, 329, 44, 444, 460, 464, 468, 475, 479, 500, 546, 57, 631, 637, 658, 702, 718, 719, 750, 768, 770, 778, 807, 815, 817, 821, 824, 839, 857, 873, 875, 889, 898, 904, 913, 914, 966, 983,
RNA 10, 101, 1010, 1084, 1117, 1127, 1146, 1170, 126, 1269, 127, 1270, 128, 1288, 129, 1311, 1315, 1344, 1373, 1383, 1390, 1402, 1430, 1431, 15, 151, 159, 173, 174, 183, 223, 267, 3, 312, 321, 343, 360, 38, 411, 493, 537, 543, 59, 616, 638, 660, 700, 76, 784, 786, 788, 92, 940, 944, 95, 951, 962, 987,
Solid tumors 1, 1001, 1002, 101, 1011, 1012, 1013, 1015, 1016, 1017, 1018, 1019, 102, 1022, 1025, 1027, 1030, 1031, 1032, 1040, 1041, 1042, 1047, 105, 1050, 1052, 1054, 1056, 1059, 106, 1061, 1062, 1066, 1067, 1068, 107, 1070, 1072, 1074, 1075, 1076, 1079, 108, 1080, 1081, 1082, 1083, 1084, 1086, 1087, 1088, 109, 1091, 1100, 1103, 1104, 1106, 1107, 1108, 1110, 1113, 1114, 1118, 1119, 112, 1121, 1123, 1124, 1125, 1126, 1127, 1128, 1129, 1130, 1131, 1132, 1133, 1134, 1136, 1137, 1139, 1141, 1143, 1144, 1146, 1147, 1148, 1149, 1154, 1155, 1156, 1158, 1159, 116, 1162, 1166, 1168, 1169, 117, 1170, 1172, 1179, 118, 1181, 1186, 1187, 1188, 1190, 1191, 1192, 1195, 1196, 12, 120, 1200, 1201, 1202, 1203, 1208, 121, 1211, 1212, 1213, 1214, 1216, 1217, 1218, 1219, 122, 1223, 1225, 1226, 1227, 1229, 123, 1233, 1234, 1237, 1238, 1241, 1245, 1247, 1250, 1253, 1254, 1256, 1259, 1264, 1267, 1268, 127, 1270, 1274, 1276, 1280, 1284, 1286, 1287, 1288, 1289, 129, 1290, 1291, 1293, 1295, 1296, 1298, 1299, 1301, 1305, 1307, 1308, 1309, 1312, 1313, 1315, 1316, 1318, 1319, 132, 1320, 1324, 1325, 1326, 1327, 1328, 1329, 133, 1331, 1332, 1334, 1335, 1338, 1339, 134, 1340, 1342, 1344, 1346, 1347, 1348, 1349, 1350, 1351, 1352, 1355, 1356, 1357, 1358, 1359, 136, 1360, 1362, 1363, 1365, 1368, 1373, 1374, 1375, 1376, 1377, 1378, 138, 1380, 1383, 1385, 1386, 1387, 1389, 139, 1390, 1391, 1393, 1394, 1398, 140, 1400, 1401, 1402, 1404, 1411, 1414, 1417, 1419, 142, 1420, 1421, 1422, 1423, 1424, 1425, 1429, 143, 1430, 1431, 1434, 1436, 1439, 1443, 1445, 1449, 145, 1450, 1451, 1455, 1459, 1462, 1463, 1464, 1465, 1466, 1467, 148, 149, 15, 150, 151, 152, 153, 154, 155, 16, 160, 162, 164, 167, 168, 171, 173, 174, 176, 179, 180, 181, 182, 183, 184, 189, 19, 190, 194, 197, 199, 2, 20, 201, 202, 203, 204, 206, 207, 208, 211, 212, 213, 215, 217, 218, 219, 22, 220, 221, 222, 223, 224, 225, 227, 228, 229, 23, 230, 231, 232, 235, 237, 238, 241, 243, 244, 246, 247, 250, 252, 256, 257, 259, 261, 262, 263, 264, 267, 268, 269, 270, 272, 273, 276, 277, 278, 279, 282, 285, 286, 287, 288, 291, 292, 294, 295, 296, 299, 3, 300, 303, 304, 305, 306, 307, 308, 31, 310, 311, 312, 313, 315, 316, 317, 318, 319, 32, 320, 324, 325, 326, 329, 33, 332, 333, 336, 337, 340, 342, 343, 346, 347, 348, 349, 352, 353, 355, 356, 36, 360, 361, 362, 364, 366, 368, 369, 37, 370, 371, 372, 373, 374, 375, 376, 377, 378, 379, 38, 380, 385, 389, 39, 390, 391, 392, 393, 394, 395, 397, 399, 402, 404, 405, 406, 407, 409, 41, 410, 412, 413, 414, 417, 420, 425, 426, 427, 428, 429, 430, 433, 438, 44, 445, 447, 448, 45, 450, 451, 453, 454, 455, 458, 459, 460, 462, 464, 465, 467, 468, 47, 470, 471, 474, 476, 477, 478, 48, 481, 483, 486, 487, 488, 49, 494, 496, 497, 498, 499, 5, 50, 501, 503, 504, 505, 507, 511, 513, 515, 516, 517, 52, 524, 527, 53, 530, 531, 532, 535, 537, 543, 544, 546, 548, 549, 552,

Subject index

- 554, 556, 558, 559, 56, 560, 561, 563, 568, 569, 57, 570, 578, 58, 580, 581, 583, 585, 587, 589, 59, 590, 591, 592, 594, 595, 596, 597, 598, 600, 601, 604, 606, 607, 610, 618, 620, 622, 626, 627, 628, 629, 631, 632, 633, 634, 635, 637, 638, 639, 644, 646, 647, 648, 650, 651, 652, 654, 656, 657, 658, 659, 66, 661, 663, 664, 666, 667, 668, 67, 670, 671, 672, 675, 676, 677, 678, 680, 682, 684, 688, 689, 690, 691, 692, 693, 694, 695, 697, 699, 700, 702, 703, 705, 707, 708, 71, 710, 711, 712, 713, 715, 716, 717, 718, 719, 72, 720, 721, 723, 724, 725, 726, 727, 728, 729, 73, 731, 732, 733, 734, 736, 737, 738, 739, 740, 741, 742, 744, 745, 746, 747, 748, 754, 755, 756, 757, 758, 759, 760, 761, 762, 763, 766, 767, 768, 769, 77, 770, 771, 772, 774, 775, 776, 777, 778, 779, 78, 781, 782, 783, 784, 786, 787, 788, 789, 790, 793, 797, 798, 799, 802, 803, 808, 809, 813, 814, 819, 82, 821, 822, 823, 827, 828, 829, 83, 830, 832, 836, 837, 838, 841, 842, 844, 845, 846, 847, 85, 851, 852, 853, 858, 859, 86, 860, 861, 862, 866, 869, 87, 870, 873, 878, 879, 881, 883, 884, 885, 889, 890, 891, 892, 893, 894, 896, 898, 900, 901, 903, 907, 908, 909, 91, 910, 914, 917, 92, 920, 930, 931, 932, 934, 936, 937, 939, 944, 945, 949, 953, 955, 956, 959, 96, 960, 961, 965, 966, 967, 968, 97, 972, 973, 974, 978, 981, 985, 986, 99, 990, 991, 992, 994, 996, 998, 999,
Stem cell/cancer-initiating cell 1024, 1140, 1191, 1220, 1430, 1439, 319, 323, 516, 546, 562, 565, 852, 871, 90,
Surfaceome 113, 1131, 1192, 1216, 308, 485, 987,
Surgery 1309, 1463, 291, 515, 542, 545, 618, 644, 788, 861, 876, 966,
Systems biology 1006, 1019, 1022, 103, 1049, 111, 1242, 1254, 1257, 127, 1273, 1276, 1285, 1292, 1295, 1301, 136, 139, 143, 1454, 225, 27, 384, 406, 411, 44, 508, 522, 541, 611, 63, 69, 70, 74, 818, 926, 927, 929, 941, 956, 976, 987, 99,
T cell 1, 100, 1000, 1002, 1014, 1019, 102, 1020, 1021, 1022, 1023, 1024, 1025, 1027, 1028, 1029, 1030, 1031, 1032, 1033, 1034, 1035, 1036, 1037, 1038, 104, 1040, 1041, 1042, 1043, 1044, 1045, 1046, 1047, 1049, 1050, 1051, 1052, 1053, 1054, 1057, 1058, 1061, 1062, 1063, 1064, 1065, 1066, 1067, 1068, 1069, 107, 1070, 1071, 1072, 1073, 1074, 1075, 1076, 1077, 1079, 1080, 1081, 1083, 1084, 1085, 1087, 1088, 1092, 1094, 1095, 1096, 1097, 1098, 1099, 11, 110, 1100, 1101, 1104, 1105, 1106, 1107, 111, 1112, 1113, 112, 1123, 1124, 1125, 1127, 1128, 113, 1131, 1132, 1133, 1134, 1137, 1138, 1140, 1141, 1146, 1147, 1151, 1152, 1153, 1156, 1157, 1158, 1163, 1166, 1171, 1175, 1176, 1177, 1178, 1180, 1181, 1182, 1183, 1184, 1188, 1195, 1196, 1197, 1198, 1199, 1200, 1201, 1203, 1208, 121, 1210, 1211, 1213, 1214, 1215, 1220, 1221, 1222, 1223, 1226, 1228, 1229, 123, 1230, 1232, 1234, 1235, 1236, 1238, 125, 1257, 1258, 126, 1269, 1275, 1276, 128, 1282, 1286, 1290, 1291, 1293, 1295, 1297, 1299, 1301, 1302, 1304, 1308, 1310, 1313, 1314, 1315, 1316, 1317, 1318, 1319, 1322, 1323, 1325, 1326, 1327, 1328, 1330, 1331, 1332, 1336, 1337, 1338, 134, 1340, 1341, 1342, 1343, 1348, 1349, 135, 1351, 1354, 1355, 1359, 1360, 1364, 1365, 1366, 1367, 1368, 1370, 1371, 1372, 1373, 1374, 1375, 1376, 1379, 1381, 1384, 1385, 1386, 1389, 1392, 1393, 1394, 1396, 1397, 1402, 1405, 1409, 1410, 1411, 142, 1420, 1422, 1426, 1429, 143, 1433, 1439, 144, 1440, 1442, 1443, 1444, 1446, 1447, 146, 1462, 1464, 1465, 147, 148, 149, 153, 157, 16, 162, 163, 165, 167, 17, 171, 175, 176, 179, 180, 181, 182, 183, 184, 185, 187, 188, 189, 191, 192, 193, 196, 197, 198, 199, 2, 200, 201, 203, 206, 208, 209, 210, 212, 215, 218, 219, 222, 223, 224, 225, 227, 229, 230, 231, 232, 234, 235, 236, 239, 240, 241, 242, 243, 244, 246, 247, 249, 251, 252, 253, 254, 255, 256, 257, 258, 259, 261, 262, 263, 266, 267, 268, 269, 27, 274, 275, 276, 28, 280, 282, 283, 284, 285, 286, 287, 288, 291, 292, 293, 294, 296, 297, 3, 30, 300, 301, 304, 308, 309, 310, 312, 314, 320, 321, 327, 33, 330, 331, 332, 340, 342, 343, 344, 345, 346, 348, 35, 350, 352, 353, 354, 355, 357, 359, 36, 360, 361, 362, 363, 364, 369, 37, 370, 372, 374, 378, 379, 38, 382, 383, 384, 389, 390, 391, 395, 397, 402, 403, 404, 405, 406, 407, 408, 409, 411, 414, 417, 418, 419, 420, 422, 424, 426, 428, 435, 44, 441, 444, 445, 447, 450, 460, 461, 462, 463, 464, 468, 469, 47, 470, 471, 472, 473, 474, 475, 477, 479, 48, 485, 488, 489, 49, 491, 50, 500, 503, 504, 506, 507, 508, 51, 510, 511, 514, 517, 52, 520, 532, 534, 535, 536, 537, 538, 54, 546, 548, 549, 551, 557, 558, 560, 568, 57, 574, 576, 586, 588, 60, 601, 610, 613, 614, 616, 618, 619, 62, 620, 624, 625, 63, 631, 632, 636, 639, 641, 642, 647, 649, 650, 652, 654, 657, 658, 659, 660, 667, 672, 674, 675, 676, 677, 678, 681, 682, 683, 685, 686, 688, 69, 691, 692, 693, 695, 697, 70, 700, 701, 702, 706, 708, 712, 713, 714, 715, 718, 719, 72, 720, 723, 732, 733, 734, 735, 737, 738, 74, 743, 75, 751, 754, 758, 760, 762, 764, 769, 77, 772, 774, 775, 776, 777, 778, 781, 783, 787, 796, 80, 804, 807, 808, 81, 811, 812, 813, 814, 817, 818, 819, 821, 824, 826, 828, 830, 831, 837, 838, 839, 842, 843, 845, 847, 849, 85, 850, 853, 854, 855, 856, 857, 858, 86, 860, 862, 867, 868, 869, 87, 870, 872, 873, 878, 882, 883, 884, 887, 891, 892, 893, 895, 897, 899, 9, 903, 904, 906, 907, 908, 911, 912, 913, 914, 920, 924, 939, 94, 940, 942, 948, 950, 951, 952, 953, 954, 956, 959, 960, 961, 964, 965, 966, 967, 968, 970, 975, 976, 977, 978, 979, 98, 981, 982, 983, 985, 986, 987, 989, 992, 994, 997,
T cell lineages 1, 1019, 1021, 1023, 1027, 1030, 1033, 1036, 1040, 1043, 1047, 1051, 11, 1144, 115, 1163, 1172, 1225, 1232, 1235, 1257, 1269, 1299, 1314, 135, 1389, 139, 1426, 143, 163, 17, 183, 190, 196, 207, 227, 238, 262, 285, 293, 30, 378, 379, 391, 411, 418, 49, 514, 517, 520, 548, 57, 600, 622, 625, 650, 702, 714, 74, 767, 821, 896, 898, 914, 920, 939, 942, 948, 952, 965, 970, 975, 978, 983, 986, 987,
Targeted therapy 1015, 105, 1058, 1059, 1068, 1070, 1073, 1074, 1075, 1077, 1079, 1080, 1093, 1098, 1104, 1111, 1112, 1140, 1142, 1152, 1153, 1161, 1162, 1166, 1170, 1181, 1184, 1186, 1188, 1190, 1191, 1192, 1193, 1195, 1196, 1197, 1198, 1201, 1204, 1205, 1206, 1210, 1212, 1213, 1214, 1216, 1217, 1219, 1220, 1221, 1227, 1230, 1232, 1237, 1246, 1249, 1284, 1293, 1313, 1319, 1321, 1328, 1333, 1336, 1339, 1340, 1345, 1346, 1347, 1349, 1351, 1356, 1357, 1360, 1361, 1362, 1363, 1368, 1369, 137, 1371, 1373, 1378, 1379, 1387, 1388, 1391, 1392, 1394, 1395, 1396, 1398, 1399, 1423, 1431, 144, 1462, 158, 159, 164, 169, 182, 194, 197, 199, 20, 200, 201, 203, 207, 216, 220, 225, 228, 232, 237, 243, 244, 247, 248, 253, 257, 261, 264, 266, 274, 277, 281, 282, 283, 287, 288, 290, 292, 294, 296, 300, 312, 317, 320, 322, 323, 324, 332, 343, 344, 353, 356, 360, 375, 377, 381, 383, 388, 389, 391, 393, 402, 406, 41, 423, 431, 432, 444, 448, 449, 450, 453, 454, 461, 469, 478, 485, 496, 502, 510, 52, 537, 55, 553, 554, 570, 586, 588, 589, 6, 600, 604, 606, 612, 616, 621, 622, 636, 637, 640, 652, 661, 663, 664, 665, 666, 667, 671, 672, 677, 680, 681, 686, 697, 705, 707, 709, 71, 713, 717, 723, 729, 731, 734, 74, 741, 742, 746, 750, 754, 757, 759, 76, 760, 764, 774, 775, 792, 80, 808, 817, 829, 832, 835, 842, 846, 847, 852, 853, 877, 878, 879, 880, 881, 882, 883, 884, 885, 889, 892, 893, 895, 898, 900, 902, 903, 906, 910, 913, 915, 924, 93, 939, 943, 945, 952, 961, 985, 989, 997,
TLR 1065, 1126, 1162, 1163, 1164, 1165, 1166, 1167, 1168, 1169, 1170, 1171, 1172, 1178, 1185, 1330, 1396, 1410, 359, 360, 378, 393, 415, 533, 547, 595, 605, 721, 756, 763, 784, 786, 795, 810, 82, 822, 84, 887, 96,
Tumor antigens 100, 1018, 1022, 1032, 1035, 1037, 1045, 1059, 1063, 1071, 1075, 1086, 1093, 110, 1117, 113, 1131, 1134, 1137, 1138, 1160, 1162, 1174, 1175, 1176, 1177, 1178, 1179, 1181, 1186, 1187, 1190, 1191, 1192, 1196, 1197, 1198, 1202, 1203, 1206, 1207, 121, 1212, 1213, 1214, 1220, 1232, 1237, 124, 1276, 1278, 1286, 1293, 1308, 1317, 1318, 1319, 1321, 1323, 1328, 1346, 1351, 1357, 1367, 1368, 1369, 1370, 1374, 1394, 1402, 1411, 1430, 1432, 1433, 148, 16, 169, 17, 182, 183, 184, 190, 197, 201, 203, 207, 209, 218, 219, 220, 221, 222, 227, 229, 237, 241, 244, 245, 246, 247, 256, 261, 263, 270, 281, 282, 292, 294, 3, 308, 310, 312, 320, 321, 329, 340, 342, 343, 356, 364, 372, 374, 375, 378, 379, 384, 388, 389, 390, 393, 403, 404, 406, 414, 428, 432, 45, 46, 464, 465, 467, 5, 50, 51, 52, 53, 532, 543, 546, 55, 557, 560, 566, 572, 598, 619, 62, 63, 638, 639, 641, 652, 656, 660, 685, 691, 692, 693, 700, 707, 713, 77, 776, 80, 809, 820, 832, 835, 851, 852, 853, 855, 86, 861, 866, 891, 895, 903, 907, 912, 940, 949, 959, 967, 968, 973, 988, 989, 997,
Tumor evasion 100, 1006, 1007, 1015, 1020, 1036, 1052, 1062, 107, 1086, 1109, 1112, 1113, 1128, 1133, 1144, 1147, 1148, 1153, 1154, 1184, 1188, 122, 1229, 1295, 1313, 1353, 1374, 1379, 1382, 1420, 1425, 1426, 1428, 1430, 1432, 1455, 1460, 1462, 1463, 148, 15, 157, 167, 178, 21, 216, 219, 229, 260, 263, 269, 276, 304, 320, 325, 329, 399, 402, 418, 450, 46, 47, 492, 494, 510, 511, 52, 522, 526, 533, 535, 604, 610, 62, 620, 639, 66, 690, 691, 693, 768, 77, 795, 817, 828, 839, 866, 877, 880, 891, 896, 908, 909, 911, 912, 916, 917, 947, 957, 967, 989,
Tumor infiltrating lymphocytes (TILs) 1, 1000, 1011, 1014, 1015, 1016, 1017, 1018, 102, 1021, 1022, 1024, 1025, 1027, 1028, 1030, 1031, 1032, 1033, 1036, 1037, 1041, 1042, 1043, 1044, 1045, 1047, 1048, 1049, 1050, 1053, 1054, 1055, 1056, 1057, 1058, 1061, 107, 1070, 1072, 1073, 1074, 1077, 1079, 1080, 1083, 1086, 1088, 109, 1095, 1096, 11, 1103, 1104, 1109, 111, 1110, 1112, 1113, 1114, 1116, 1118, 112, 1121, 1124, 1128, 1129, 1133, 1134, 1135, 1136, 1137, 1139, 1141, 1143, 1146, 1147, 1149, 1151, 1154, 1155, 1156, 1158, 1160, 1166, 1168, 1169, 1179, 1180, 1181, 1188, 119, 1195, 1203, 1208, 121, 1214, 1218,

1223, 1225, 1226, 1229, 123, 1232, 1234, 1236, 1275, 1276, 128, 1282, 1283, 1284, 1285, 1286, 1289, 1293, 1298, 1299, 1304, 1307, 131, 1310, 1312, 1316, 1321, 1322, 1324, 1331, 1337, 1338, 1339, 135, 1356, 1360, 1361, 1365, 1370, 1372, 1373, 1374, 1376, 1379, 1385, 1386, 1389, 139, 1391, 1393, 1394, 1399, 141, 1410, 1411, 1419, 142, 1421, 1426, 1427, 1429, 1433, 1434, 1436, 1438, 1439, 1440, 1442, 1443, 1444, 1445, 1451, 1457, 1458, 1459, 146, 1460, 1462, 1465, 147, 152, 153, 154, 157, 160, 161, 162, 163, 167, 17, 171, 179, 187, 191, 192, 196, 197, 199, 20, 206, 207, 211, 214, 218, 222, 224, 227, 236, 237, 238, 24, 241, 249, 254, 255, 259, 26, 267, 268, 278, 282, 283, 285, 297, 30, 31, 314, 320, 325, 329, 331, 338, 340, 343, 348, 355, 361, 364, 365, 369, 370, 374, 384, 387, 390, 391, 40, 404, 406, 407, 409, 417, 420, 428, 429, 450, 455, 461, 462, 463, 464, 466, 469, 47, 470, 472, 473, 474, 477, 479, 48, 489, 49, 490, 497, 50, 503, 504, 505, 506, 507, 511, 514, 523, 529, 534, 536, 538, 54, 541, 543, 551, 57, 574, 576, 587, 60, 606, 608, 61, 610, 611, 612, 613, 615, 62, 636, 638, 643, 650, 657, 659, 671, 676, 678, 679, 683, 691, 692, 693, 701, 709, 710, 714, 715, 72, 720, 751, 754, 756, 767, 776, 781, 783, 787, 789, 792, 803, 804, 807, 810, 811, 813, 815, 817, 819, 821, 828, 83, 830, 831, 832, 837, 839, 841, 842, 845, 849, 851, 855, 856, 859, 86, 860, 861, 866, 869, 87, 870, 873, 877, 878, 883, 885, 893, 894, 898, 9, 901, 904, 908, 911, 912, 939, 944, 945, 947, 949, 952, 953, 954, 956, 957, 961, 964, 965, 966, 970, 972, 978, 98, 981, 983, 988, 997, 999, Tumor microenvironment 1, 10, 1000, 1001, 1003, 1004, 101, 1010, 1014, 1015, 1017, 1018, 1019, 102, 1020, 1022, 1025, 1027, 103, 1031, 1032, 1033, 1037, 1041, 1042, 1043, 1044, 1046, 1048, 1055, 1059, 1062, 1065, 107, 1070, 1072, 1074, 1076, 1078, 108, 1081, 1082, 1083, 1086, 1087, 1088, 109, 1090, 1093, 1095, 1096, 11, 110, 1100, 1101, 1102, 1103, 1104, 1109, 111, 1110, 1111, 1112, 1113, 1114, 1116, 112, 1120, 1122, 1124, 1125, 1126, 1128, 1132, 1133, 1134, 1135, 1136, 1139, 1141, 1143, 1144, 1146, 1147, 1148, 1149, 115, 1150, 1153, 1154, 1157, 1158, 116, 1160, 1161, 1162, 1164, 1165, 1166, 1169, 117, 1170, 1171, 1173, 1179, 118, 1180, 1182, 1183, 1187, 1188, 1189, 1193, 1196, 12, 120, 1200, 1202, 1204, 1208, 1211, 1212, 1218, 1221, 1223, 1224, 1225, 1226, 1229, 1234, 1237, 1239, 125, 126, 127, 1273, 1275, 1277, 1279, 1284, 1285, 1289, 1290, 1291, 1292, 1293, 1298, 1299, 130, 1301, 1302, 1304, 1305, 1307, 1309, 131, 1310, 1311, 1312, 1315, 1318, 1321, 1322, 1326, 1327, 133, 1331, 1333, 1334, 1335, 1338, 1339, 134, 1341, 1342, 1343, 1344, 1348, 135, 1350, 1355, 1356, 1360, 1361, 1364, 1365, 1370, 1374, 1375, 1376, 1378, 1379, 1380, 1382, 1383, 1384, 1385, 1386, 1389, 139, 1390, 1391, 1393, 1396, 1401, 141, 1410, 1419, 142, 1420, 1421, 1422, 1424, 1426, 1427, 1428, 1429, 143, 1432, 1433, 1434, 1435, 1436, 1437, 1438, 1439, 1440, 1441, 1442, 1443, 1444, 1445, 1446, 1447, 1448, 1449, 145, 1450, 1451, 1452, 1454, 1455, 1456, 1457, 1458, 1459, 1460, 1462, 1463, 1464, 1465, 1466, 1467, 147, 148, 149, 15, 150, 151, 152, 155, 156, 157, 159, 160, 161, 162, 163, 165, 167, 168, 169, 178, 179, 183, 187, 188, 189, 192, 197, 199, 2, 20, 200, 207, 208, 217, 219, 221, 223, 23, 24, 255, 259, 264, 266, 268, 27, 276, 277, 278, 281,

282, 287, 288, 290, 299, 304, 307, 308, 31, 310, 320, 322, 328, 329, 330, 333, 337, 342, 346, 358, 360, 369, 37, 372, 374, 375, 376, 379, 38, 380, 385, 388, 391, 393, 394, 398, 4, 40, 405, 408, 413, 414, 418, 419, 420, 424, 425, 428, 429, 43, 434, 445, 446, 447, 448, 453, 462, 463, 465, 466, 467, 47, 471, 472, 478, 479, 48, 482, 483, 485, 487, 488, 49, 490, 492, 497, 499, 500, 501, 503, 504, 505, 507, 513, 514, 519, 521, 522, 523, 526, 527, 532, 534, 536, 538, 54, 541, 542, 547, 548, 55, 551, 552, 554, 555, 569, 57, 574, 587, 588, 59, 597, 599, 60, 606, 607, 608, 61, 610, 611, 613, 615, 618, 62, 620, 621, 623, 633, 634, 637, 64, 643, 648, 650, 656, 658, 659, 66, 661, 680, 681, 683, 69, 690, 702, 708, 710, 712, 714, 715, 716, 72, 725, 73, 732, 736, 737, 739, 745, 751, 754, 762, 764, 767, 779, 78, 784, 788, 79, 792, 796, 801, 802, 803, 804, 807, 810, 814, 815, 816, 817, 818, 82, 822, 823, 829, 83, 830, 831, 832, 836, 837, 839, 84, 840, 841, 842, 843, 845, 849, 85, 850, 852, 856, 857, 86, 866, 867, 869, 87, 870, 873, 875, 877, 878, 879, 882, 883, 884, 885, 887, 889, 89, 890, 892, 893, 894, 896, 898, 90, 900, 901, 904, 908, 909, 910, 911, 912, 913, 914, 916, 917, 92, 926, 927, 928, 929, 94, 944, 945, 946, 947, 948, 949, 95, 952, 953, 954, 955, 956, 957, 959, 96, 960, 961, 962, 963, 964, 966, 97, 970, 972, 973, 976, 98, 981, 983, 984, 985, 989, 99, 990, 991, 992, 993, 998, 999, Tumor stroma 1000, 101, 102, 1025, 1074, 1078, 1093, 1110, 1124, 117, 1218, 127, 1277, 1284, 1288, 1290, 131, 1311, 133, 135, 1350, 1352, 1378, 139, 141, 1422, 1424, 143, 1431, 1433, 1436, 1437, 1439, 1444, 1446, 1447, 1448, 145, 1450, 1451, 1452, 1457, 1459, 1460, 1462, 1464, 1465, 147, 149, 160, 161, 167, 168, 2, 23, 325, 358, 37, 375, 38, 47, 48, 483, 49, 507, 515, 523, 554, 569, 574, 59, 60, 61, 633, 634, 640, 710, 739, 762, 78, 815, 836, 84, 85, 894, 90, 914, 928, 947, 953, 954, 957, 96, 97, 972, 981, 99, 990, Vaccine 1032, 1071, 1072, 1100, 1120, 1125, 113, 1137, 1172, 1174, 1175, 1176, 1177, 1178, 1179, 1181, 1182, 1286, 1315, 1317, 1318, 1323, 1336, 1370, 1383, 1385, 1390, 1394, 1410, 1411, 1440, 161, 184, 224, 257, 271, 28, 312, 321, 343, 359, 373, 374, 388, 415, 473, 5, 506, 546, 549, 551, 555, 557, 559, 562, 565, 566, 595, 598, 62, 638, 641, 642, 643, 645, 646, 660, 669, 689, 691, 692, 693, 695, 700, 706, 72, 74, 790, 80, 813, 820, 832, 851, 862, 870, 894, 896, 913, 92, 922, 940, 949,

Late-Breaking Abstracts

Adoptive immunotherapy 1468, 1478, Antibody 1470, Antigen presenting cells 1470, Autoimmunity 1468, Bioinformatics 1478, Biomarkers 1468, 1470, 1471, 1472, 1473, 1477, CAR T cells 1468, Checkpoint blockade 1469, 1470, 1471, 1473, 1474, 1477, Clinical study 1470, 1471, 1472, 1477, Clinical trial 1469, 1470, 1471, 1473, 1474, 1475, 1477, 1478, Cytokine 1473, 1479, Dendritic cell 1470, Gene expression 1468, 1471, Immune contexture 1472, Immune monitoring 1468, 1470, 1472, 1477, 1478, Inflammation 1479, Leukemia/Lymphoma 1468, Metabolism 1468, Monocyte/Macrophage 1479, Myeloid cells 1479, Neoantigens 1478, NK/NK T cell 1473, Regulatory T cell (Treg cell) 1473, RNA 1468, Solid tumors 1468, 1469, 1470, 1472, 1474, 1477, 1478, 1479, T cell 1470, 1472, 1473, 1474, 1477, 1478, 1479, Targeted therapy 1475, 1479, Tumor antigens 1474, 1478, 1479, Tumor evasion 1478, 1479, Tumor infiltrating lymphocytes (TILs) 1472, 1474, 1478, Tumor microenvironment 1472, 1473, 1474, 1475, 1479, Vaccine 1474,